

VOLUME 1



UPSTREAM INDUSTRIAL BIOTECHNOLOGY

Expression Systems and Process Development

MICHAEL C. FLICKINGER, EDITOR

WILEY

UPSTREAM INDUSTRIAL BIOTECHNOLOGY

UPSTREAM INDUSTRIAL BIOTECHNOLOGY

Edited By

MICHAEL C. FLICKINGER

Golden LEAF Biomanufacturing Training and Education Center (BTEC)
Department of Chemical and Biomolecular Engineering
North Carolina State University, Raleigh
North Carolina, USA



A JOHN WILEY & SONS, INC., PUBLICATION

Copyright © 2013 by John Wiley & Sons, Inc. All rights reserved

Published by John Wiley & Sons, Inc., Hoboken, New Jersey
Published simultaneously in Canada

No part of this publication may be reproduced, stored in a retrieval system, or transmitted in any form or by any means, electronic, mechanical, photocopying, recording, scanning, or otherwise, except as permitted under Section 107 or 108 of the 1976 United States Copyright Act, without either the prior written permission of the Publisher, or authorization through payment of the appropriate per-copy fee to the Copyright Clearance Center, Inc., 222 Rosewood Drive, Danvers, MA 01923, (978) 750-8400, fax (978) 750-4470, or on the web at www.copyright.com. Requests to the Publisher for permission should be addressed to the Permissions Department, John Wiley & Sons, Inc., 111 River Street, Hoboken, NJ 07030, (201) 748-6011, fax (201) 748-6008, or online at http://www.wiley.com/go/permission.

Limit of Liability/Disclaimer of Warranty: While the publisher and author have used their best efforts in preparing this book, they make no representations or warranties with respect to the accuracy or completeness of the contents of this book and specifically disclaim any implied warranties of merchantability or fitness for a particular purpose. No warranty may be created or extended by sales representatives or written sales materials. The advice and strategies contained herein may not be suitable for your situation. You should consult with a professional where appropriate. Neither the publisher nor author shall be liable for any loss of profit or any other commercial damages, including but not limited to special, incidental, consequential, or other damages.

For general information on our other products and services or for technical support, please contact our Customer Care Department within the United States at (800) 762-2974, outside the United States at (317) 572-3993 or fax (317) 572-4002.

Wiley also publishes its books in a variety of electronic formats. Some content that appears in print may not be available in electronic formats. For more information about Wiley products, visit our web site at www.wiley.com.

Library of Congress Cataloging-in-Publication Data:

Upstream industrial biotechnology / edited by Michael C. Flickinger.
v. cm
Includes bibliographical references and index.
Contents: volume 1. Expression Systems and Process Development–volume 2. Equipment, Process Design, Sensing, Control and cGMP Operations.
ISBN 978-1-118-13123-7 (set : hardback) 1. Biotechnology. I. Flickinger, Michael C., editor of compilation. II. Encyclopedia of industrial biotechnology. Selections.
TP248.2.U675 2013
660.6–dc23
2012030697

Printed in the United States of America

10 9 8 7 6 5 4 3 2 1

CONTENTS

VOLUME I: EXPRESSION SYSTEMS & PROCESS DEVELOPMENT

PREFACE xi

CONTRIBUTORS xiii

PART I INTRODUCTION 3

PART II INDUSTRIAL CELL GROWTH AND GENE EXPRESSION SYSTEMS 7

1 Animal Cells, Suspension Culture 9
John R. Birch

2 Baculovirus Expression Systems 19
Robert D. Possee, Richard B. Hitchman, and Linda A. King

3 Baculovirus Kinetics, Insect Culture 33
Leslie Chan, Steve Reid, and Lars Keld Nielsen

4 Cell Culture, Aseptic Techniques 49
John M. Davis and Kevin L. Shade

5 Cell Cycle in Bioprocesses 71
Mariam Naciri and Mohamed Al-rubeai

6 Cell Growth and Protein Expression Kinetics 85
Dhinakar S. Kompala

7 Cell Viability Measurement **97**
Ning Wei and Benjamin Sommer

8 Contamination Detection in Animal Cell Culture **105**
Carol Mclean and Colin Harbour

9 Culture Collections and Biological Resource Centers (BRCs) **131**
David Smith

10 Culture Preservation **153**
Robert L. Gherna

11 Expression and Secretion of Heterologous Proteins, *Bacillus* and Other Gram-Positive Bacteria **163**
Boyke Bunk, Rebekka Biedendieck, Dieter Jahn, and Patricia S. Vary

12 Gene Expression in Human Cells **181**
Marco A. Cacciuttolo, Gene Lee, John Chon, and John Lewis

13 Gene expression in *Pichia* and other methylotroph yeast **195**
Koti Sreekrishna

14 Gene Expression in Recombinant Animal Cells and Transgenic Animals **213**
Richard M. Twyman and Bruce Whitelaw

15 Inoculum Expansion Methods, Animal Cell Lines **297**
Claudia Kloth, Glenn Maclsaac, Haile Ghebremariam, and Alahari Arunakumari

16 Insect Cell Culture **311**
Someet Narang, Erik M. Whiteley, Sunyia Hussain, and Michael J. Betenbaugh

17 Kinetics of Microbial Growth **331**
Nicolai S. Panikov

18 Microalgae, Mass Culture Methods **371**
Emílio Molina Grima, Jose María Fernández Sevilla, and Francisco Gabriel Acién FernáNdez

19 Microbial Growth Measurement **399**
Arthur L. Koch

20 Microbial Media Composition **413**
Rosalie J. Cote

21 Microscopic Characterization of Cells **437**
Erwin Huebner

22 Mycoplasma Contamination of Cell Cultures **467**
Cord C. Uphoff and Hans G. Drexler

23 Protein Glycosylation: Analysis, Characterization, and Engineering **489**
Mikael R. Andersen, Jong Hyun Nam, and Susan T. Sharfstein

24 Secretion of Heterologous Proteins, Gram Positive Bacteria **543**
Eric Morello, Isabelle Poquet, Philippe Langella

25 Soluble Protein Expression in Bacteria **557**
Catherine H. Schein

PART III MEDIA, CELL LINES AND PROCESS DEVELOPMENT **579**

26 Animal Cell Culture Media **581**
Natarajan Vijayasankaran, Jincai Li, Robert Shawley, Aaron Chen, Masaru Shiratori, Martin Gawlitzek, Feng Li, Robert Kiss, and Ashraf Amanullah

27 Animal Cell Culture, Effects of Osmolality and Temperature **599**
James C. Warren and Shyamsundar Subramanian

28 Animal Cell Stability **617**
Martin S. Sinacore, Timothy S. Charlebois, Denis Drapeau, Mark Leonard, Scott Harrison, and S. Robert Adamson

29 Animal Cell Types, Hybridomas **635**
K. Heilmann and B. Micheel

30 Antibody Production, Human Recombinant **645**
Stefan Dübel

31 Antifoams and Pluronic Polyols, Cell Protection **663**
David W. Murhammer

32 Biominiaturization of Bioreactors **669**
Michael A. Hanson and Govind Rao

33 Inoculum Preparation **699**
Craig J.L. Gershater

34 Microcarrier Culture **711**
Susan T. Sharfstein and Christian Kaisermayer

35 Monoclonal Antibody Production, Cell Lines **733**
Julia F. Markusen and David K. Robinson

36 Plant Cell Culture, Laboratory Techniques **747**
Mark Richard Fowler

37 Scale-Up of Biotechnological Processes **759**
Marko Zlokarnik

VOLUME II: EQUIPMENT, PROCESS DESIGN, SENSING, CONTROL, AND cGMP OPERATIONS

PREFACE ix

CONTRIBUTORS xi

PART IV BIOREACTOR DESIGN, ENGINEERING, PROCESS SENSING AND CONTROL 789

38 Aeration, Mixing, and Hydrodynamics in Animal Cell Bioreactors 791
Ruben Godoy-Silva, Claudia Berdugo, and Jeffrey J. Chalmers

39 Biocatalytic Membrane Reactors 821
Lidietta Giorno and Enrico Drioli

40 Bioreactor Scale-Down 847
Laura A. Palomares, Alvaro R. Lara, and Octavio T. Ramírez

41 Bioreactor Scale-Up 863
Laura A. Palomares and Octavio T. Ramírez

42 Bioreactors: Airlift Reactors 887
J.C. Merchuk and F. Garcia Camacho

43 Bioreactors, Continuous Culture of Plant Cells 955
H.J.G. Ten Hoopen

44 Bioreactors, Fluidized-Bed 963
Winfried Storhas

45 Bioreactors, Gas-Treatment 979
Graham Andrews and William Apel

46 Bioreactors, Perfusion 995
Wei Wen Su

47 Bioreactors: Rotating Biological Contactors 1013
Susana Cortez, Pilar Teixeira, Rosário Oliveira, and Manuel Mota

48 Bioreactors, Stirred Tank for Culture of Plant Cells 1031
Pauline M. Doran

49 Cell Immobilization, Engineering Aspects 1069
Ronnie Willaert

50 Fermenter/Bioreactor Design 1101
Marvin Charles and Jack Wilson

51 Gas-Holdup in Bioreactors 1137
Christian Sieblist and Andreas Lübbert

52 Immobilization of Proteins and Enzymes, Mesoporous Supports **1147**
Martin Hartmann and Dirk Jung

53 Immobilized Cells **1179**
Manojlović Verica, Bugarski Branko, and Nedović Viktor

54 Immobilized Enzymes **1201**
Jose M. Guisan, Lorena Betancor, and Gloria Fernandez-Lorente

55 Impeller Selection, Animal Cell Culture **1219**
Alvin W. Nienow

56 Mammalian Cell Bioreactors **1233**
Weichang Zhou, Gargi Seth, Maria J. Guardia, and Wei-Shou Hu

57 Mammalian Cell Culture Reactors, Scale-Up **1245**
J. Bryan Griffiths

58 Mass Transfer **1261**
Yusuf Chisti

59 Oxygen Transfer Rate Determination Methods **1303**
Felix Garcia-Ochoa and Emilio Gomez

60 Photobioreactors **1327**
Mario R. Tredici, Graziella Chini Zittelli and Liliana Rodolfi

61 Rheological Behavior of Fermentation Fluids **1347**
Colin R. Thomas and Grainne L. Riley

62 Rheology of Filamentous Microorganisms, Submerged Culture **1359**
Maria Papagianni

63 Sampling and Sample Handling for Process Control **1377**
Bo Mattiasson and Martin Hedström

64 Solid State Fermentation, Kinetics **1387**
David A. Mitchell, Deidre M. Stuart, and Robert D. Tanner

65 Solid Substrate Fermentation, Automation **1413**
Mario Fernández-fernández and J. Ricardo Pérez-correa

66 Stainless Steels **1427**
C.P. Dillon

67 Static Mixing, Fermentation Processes **1435**
Radu Z. Tudose and Maria Gavrilescu

68 Transfer Phenomena in Multiphase Systems **1451**
Rodica-Viorica Roman

PART V PROCESS ANALYTICAL TECHNOLOGIES (PAT) **1469**

69 Bioprocess and Fermentation Monitoring **1471**
Michael Pohlscheidt, Salim Charaniya, Marco Jenzsch, Christopher Bork, Tim L. Noetzel, and Andreas Luebbert

70 Flow Injection Analysis in Industrial Biotechnology **1493**
Elo Harald Hansen and Manuel Miró

71 Fluorescence Techniques for Bioprocess Monitoring **1511**
Fabienne Anton, Carsten Lindemann, Bernd Hitzmann, Kenneth F. Reardon, and Thomas Scheper

72 Off-Line Analysis in Animal Cell Culture **1523**
Heino Büntemeyer

73 Process Analytical Technology: Strategies for Biopharmaceuticals **1543**
Anurag S. Rathore and Gautam Kapoor

74 Vent Gas Analysis **1567**
David Pollard and Jens Christensen

PART VI UPSTREAM cGMP OPERATIONS **1585**

75 Antibody Manufacture, Disposable Systems **1587**
Regine Eibl and Dieter Eibl

76 Bioreactor Operations **1595**
David R. Gray

77 Bioreactors, Cell Culture, Commercial Production **1635**
Tan-Che Zhou, Wen-Wen Zhou, Weiwei Hu, and Jian-Jiang Zhong

78 Biotransformation, Process Optimization **1665**
Lutz Hilterhaus, Andreas Liese, and Udo Kragl

79 Foam Formation and Control in Bioreactors **1679**
Frank Delvigne and Jean-Paul Lecomte

80 Pilot Plants, Design and Operation **1695**
Beth H. Junker

81 Shear Sensitivity **1719**
Yusuf Chisti

82 Sterilization and Decontamination, Bioprocess Equipment **1763**
Peter L. Roberts

INDEX **1781**

PREFACE

Upstream Industrial Biotechnology is a compilation of essential in depth articles, organized topically and listed in alphabetical format, for biopharmaceutical, bioprocess and biologics process scientists, engineers and regulatory professionals from the comprehensive seven volumes of the *Encyclopedia of Industrial Biotechnology*. Process development for the manufacture of complex biomolecules involves solving many scientific, compliance and technical problems quickly in order to support pilot, preclinical and clinical development, technology transfer and manufacturing start-up. Every organization develops new processes from accumulated process knowledge. Accumulated process knowledge has a very significant impact on accelerating the time to market (and reducing the financial resources required) of products manufactured using recombinant DNA and living microbes, cells, transgenic plants or transgenic mammals. However, when an entirely new upstream platform is needed, there are few books that will quickly provide the depth of industry-relevant background. *Upstream Industrial Biotechnology* can fill this void as a 2 volume advanced desk reference. These volumes include relevant biology, protein purification and engineering literature with abundant process examples provide by industry subject matter experts (SMEs) and academic scholars. This desk reference will also be useful for advanced biomanufacturing students and professionals to quickly gain in depth knowledge on how to design processes (and facilities) capable of being licensed to manufacture enzymes, biopharmaceutical intermediates, human and veterinary biopharmaceuticals or vaccines. The opportunity is yours to leverage the combined knowledge from scores of industry professionals from around the world who have contributed to *Upstream Industrial Biotechnology* to reduce the time and cost to deliver engineered proteins, biomolecules and cost-effective biologics to the market and especially to millions of patients worldwide.

Professor Michael C. Flickinger, Editor

Golden LEAF Biomanufacturing Training and Education Center (BTEC)
Department of Chemical and Biomolecular Engineering
North Carolina State University
Raleigh, North Carolina, 27695-7928, USA

Contributors

S. Robert Adamson, Genetics Institute, Andover, Massachusetts, USA

Mohamed Al-rubeai, University College Dublin, Belfield, Dublin, Ireland

Ashraf Amanullah, Oceanside Process Research & Development, Genentech. Inc, Oceanside, California, USA

Mikael R. Andersen, Technical University of Denmark, Department of Systems Biology, Lyngby, Denmark

Graham Andrews, MMBD Consulting, Gresham, Oregon, USA

Fabienne Anton, Institut für Technische Chemie, Gottfried Wilhelm Leibniz Universität Hannover, Hannover, Germany

William Apel, Idaho National Engineering and Environmental Laboratory, Idaho Falls, Idaho, USA

Alahari Arunakumari, Medarex, Inc., Bloomssbury, New Jersey, USA

Heino Büntemeyer, Institute of Cell Culture Technology, University of Bielefeld, Bielefeld, Germany

Claudia Berdugo, The Ohio State University, Columbus, Ohio, USA

Lorena Betancor, Instituto de Catalisis, CSIC, Madrid, Spain

Michael J. Betenbaugh, Johns Hopkins University, Baltimore, Maryland, USA

Rebekka Biedendieck, Protein Science Group, University of Kent, Canterbury, Kent, United Kingdom

John R. Birch, Lonza Biologics plc, Berkshire, United Kingdom

Christopher Bork, Genentech Inc., Manufacturing Science and Technology, Oceanside, California, USA

Bugarski Branko, University of Belgrade, Belgrade, Republic of Serbia

Boyke Bunk, Institute of Microbiology, Technische Universität Braunschweig, Braunschweig, Germany

Marco A. Cacciuttolo, Percivia LLC, Cambridge, Massachusetts, USA

F. Garcia Camacho, Universidad de Almeria, Almeria, Spain

Jeffrey J. Chalmers, The Ohio State University, Columbus, Ohio, USA

Leslie Chan, Australian Institute for Bioengineering and Nanotechnology, University of Queensland, Brisbane, Australia

Salim Charaniya, Genentech Inc., Manufacturing Science and Technology, Oceanside, California, USA

Timothy S. Charlebois, Genetics Institute, Andover, Massachusetts, USA

Marvin Charles, Lehigh University, Bethlehem, Pennsylvania, USA

Aaron Chen, Oceanside Process Research & Development, Genentech. Inc, Oceanside, California, USA

Yusuf Chisti, School of Engineering, Massey University, School of Engineering, Palmerston North, New Zealand

John Chon, Percivia LLC, Cambridge, Massachusetts, USA

Jens Christensen, Merck & Co. Inc, Rahway, New Jersey, USA

Susana Cortez, Institute for Biotechnology and Bioengineering, Centre of Biological Engineering, University of Minho, Braga, Portugal

Rosalie J. Cote, Becton Dickinson Microbiology Systems, Sparks, Maryland, USA

Stefan Dübel, Technische Universität Braunschweig, Institute of Biochemistry and Biotechnology, Spielmannstr, Braunschweig, Germany

John M. Davis, School of Life Sciences, University of Hertfordshire, Hatfield, Hertfordshire, United Kingdom

Frank Delvigne, Fond de la Recherche Scientifique (FRNS-FRS), Bruxelles, Belgium; Faculté Universitaire des Sciences Agronomiques, Unité de Bio-industries/CWBI, Gembloux, Belgium

C.P. Dillon, C.P. Dillon & Associates, Hurricane, West Virginia, USA

Pauline M. Doran, Monash University, Australia

Denis Drapeau, Genetics Institute, Andover, Massachusetts, USA

Hans G. Drexler, DSMZ-German Collection of Microorganisms and Cell Cultures, Braunschweig, Germany

Enrico Drioli, Institute on Membrane Technology, ITM-CNR, At University of Calabria, Rende, Italy

Dieter Eibl, Zurich University of Applied Sciences, School of Life Sciences and Facility Management, Institute of Biotechnology, Wädenswil, Switzerland

Regine Eibl, Zurich University of Applied Sciences, School of Life Sciences and Facility Management, Institute of Biotechnology, Wädenswil, Switzerland

Mario Fernández-Fernández, Universidad de Talca, Talca, Región del Maule, Chile

Gloria Fernandez-Lorente, Instituto de Catalisis, CSIC, Madrid, Spain

Mark Richard Fowler, Leicester School of Pharmacy, De Montfort University, Leicester, United Kingdom

Francisco Gabriel Acién Fernández, Department of Chemical Engineering, University of Almería, Almería, Spain

Felix Garcia-Ochoa, Facultad Quimicas, Universidad Complutense, Madrid, Spain

Maria Gavrilescu, Research Centre for Antibiotics, Iaşi, Romania

Martin Gawlitzek, Late Stage Cell Culture, Genentech, Inc., San Francisco, California, USA

Craig J.L. Gershater, S.B. Pharmaceuticals, Harlow, Essex, England

Haile Ghebremariam, Medarex, Inc., Bloomssbury, New Jersey, USA

Robert L. Gherna, American Type Culture Collection, Rockville, Maryland, USA

Lidietta Giorno, Institute on Membrane Technology, ITM-CNR, At University of Calabria, Rende, Italy

Ruben Godoy-Silva, The Ohio State University, Columbus, Ohio; Department of Chemical and Environmental Engineering, Universidad Nacional de Colombia, Bogotá, Colombia

Emilio Gomez, Facultad Quimicas, Universidad Complutense, Madrid, Spain

David R. Gray, Chiron Corporation, Emeryville, California, USA

J. Bryan Griffiths, Scientific Consultancy & Publishing, Salisbury, United Kingdom

Emílio Molina Grima, University of Almería, Almería, Spain

Maria J. Guardia, Camino De Purchill, Puleva Biotech Department of Process Engineering, Granada, Spain

Jose M. Guisan, Instituto de Catalisis, CSIC, Madrid, Spain

Elo Harald Hansen, Department of Chemistry Technical University of Denmark Lyngby, Denmark

Michael A. Hanson, Bio-Manufacturing Sciences Group, Pfizer, New York, USA

Colin Harbour, University of Sydney, NSW, Australia

Scott Harrison, Genetics Institute, Andover, Massachusetts, USA

Martin Hartmann, University of Augsburg, Augsburg, Germany

Martin Hedström, Lund University, Lund, Sweden

K. Heilmann, University of Potsdam, Institute of Biochemistry and Biology, Potsdam, Germany

Lutz Hilterhaus, Institute of Technical Biocatalysis, Hamburg University of Technology, Hamburg, Germany

Richard B. Hitchman, Oxford Expression Technologies Ltd., Oxford Brookes University, United Kingdom

Bernd Hitzmann, Institut für Technische Chemie, Gottfried Wilhelm Leibniz Universität Hannover, Hannover, Germany

H.J.G. Ten Hoopen, Delft University for Technology, Delft, The Netherlands

Wei-Shou Hu, University of Minnesota, Minneapolis, Minnesota, USA

Weiwei Hu, Cell Culture Development, Biogen Idec Inc., San Diego, California, USA

Erwin Huebner, University of Manitoba, Winnipeg, Manitoba, Canada

Sunyia Hussain, Johns Hopkins University, Baltimore, Maryland, USA

Dieter Jahn, Institute of Microbiology, Technische Universität Braunschweig, Braunschweig, Germany

Marco Jenzsch, Roche Diagnostics GmbH, Pharma Biotech, Penzberg, Germany

Dirk Jung, Advanced Materials Science, Department of Physics, University of Augsburg, Augsburg, Germany

Beth H. Junker, Bioprocess R&D, Merck Research Laboratories, Rahway, New Jersey, USA

Christian Kaisermayer, Project Manager Cell Culture Applications & Support, GE Healthcare, Vienna, Austria

Gautam Kapoor, Department of Chemical Engineering, Indian Institute of Technology, Hauz Khas, New Delhi, India

Linda A. King, School of Life Sciences, Oxford Brookes University, United Kingdom

Robert Kiss, Late Stage Cell Culture, Genentech, Inc., San Francisco, California, USA

Claudia Kloth, Medarex, Inc., Bloomssbury, New Jersey, USA

Arthur L. Koch, Indiana University, Bloomington, Indiana, USA

Dhinakar S. Kompala, University of Colorado, Boulder, Colorado, USA

Udo Kragl, Rostock University, Rostock, Germany

Andreas Lübbert, Institute of Biotechnology; Centre of Bioengineering, Martin-Luther-University Halle-Wittenberg, Weinbergweg, Halle (Saale), Germany

Alvaro R. Lara, Departamento de Procesos y Tecnología, Universidad Autónoma Metropolitana-Cuajimalpa, Cuernavaca, México

Philippe Langella, Unité d'Ecologie et Physiologie du Système Digestif (UR910), INRA, Jouy-en-Josas, France

Jean-Paul Lecomte, Dow Corning S.A., Seneffe, Belgium

Gene Lee, Percivia LLC, Cambridge, Massachusetts, USA

Mark Leonard, Genetics Institute, Andover, Massachusetts, USA

John Lewis, Crucell NV, Leiden, The Netherlands

Feng Li, Oceanside Process Research & Development, Genentech. Inc, Oceanside, California, USA

Jincai Li, Oceanside Process Research & Development, Genentech. Inc, Oceanside, California, USA

Andreas Liese, Institute of Technical Biocatalysis, Hamburg University of Technology, Hamburg, Germany

Carsten Lindemann, Boehringer Ingelheim Pharma GmbH & Co. Biberach/ Riß, Germany

Andreas Luebbert, Martin Luther University, Halle, Germany

Glenn Maclsaac, Medarex, Inc., Bloomssbury, New Jersey, USA

Julia F. Markusen, Bioprocess Research & Development, Merck Research Laboratories, Rahway, NJ

Bo Mattiasson, Lund University, Lund, Sweden

Carol Mclean, Protein Fractionation Centre, Scottish National Blood Transfusion Service, Edinburg, Scotland

J.C. Merchuk, Ben-Gurion University of the Negev Beer-Sheva, Israel

B. Micheel, University of Potsdam, Institute of Biochemistry and Biology, Potsdam, Germany

Manuel Miró, University of the Balearic Islands Carretera de Valldemossa, Illes Balears, Spain

David A. Mitchell, Universidade Federal do Parana, Curitiba, Brazil

Eric Morello, Unité Biologie Moléculaire du Gène chez les Extrêmophiles, Institut Pasteur, Paris, France

Manuel Mota, University of Minho, Portugal

David W. Murhammer, University of Iowa, Iowa City, Iowa, USA

Mariam Naciri, University College Dublin, Belfield, Dublin, Ireland

Jong Hyun Nam, Rensselaer Polytechnic Institute, Department of Chemical and Biological Engineering, Troy, New York, USA

Someet Narang, Johns Hopkins University, Baltimore, Maryland; MedImmune, Inc. Gaithersburg, Maryland, USA

Lars Keld Nielsen, Australian Institute for Bioengineering and Nanotechnology, University of Queensland, Brisbane, Australia

Alvin W. Nienow, University of Birmingham, School of Chemical Engineering, Birmingham, United Kingdom

Tim L. Noetzel, Roche Diagnostics GmbH, Pharma Biotech, Penzberg, Germany

Rosário Oliveira, Institute for Biotechnology and Bioengineering, Centre of Biological Engineering, University of Minho, Braga, Portugal

J. Ricardo Pérez-Correa, Chemical and Bioprocess Engineering Department, Pontificia Universidad Católica de Chile, Santiago, Chile

Laura A. Palomares, Universidad Nacional Autónoma de México, Cuernavaca, México

Nicolai S. Panikov, Northeastern University, Boston, Massachusetts, USA

Maria Papagianni, Aristotle University of Thessaloniki, Greece

Michael Pohlscheidt, Genentech Inc., Manufacturing Science and Technology, Oceanside, California, USA

David Pollard, Merck & Co. Inc, Rahway, New Jersey, USA

Robert D. Possee, Centre for Ecology and Hydrology, Oxford, United Kingdom

Isabelle Poquet, Unité des Bactéries Lactiques et pathogènes Opportunistes (UR888), Jouy-en-Josas, France

Octavio T. Ramírez, Universidad Nacional Autónoma de México, Cuernavaca, México

Govind Rao, Center for Advanced Sensor Technology, University of Maryland Baltimore County, Baltimore, Maryland, USA

Anurag S. Rathore, Department of Chemical Engineering, Indian Institute of Technology, Hauz Khas, New Delhi, India

Kenneth F. Reardon, Colorado State University, Fort Collins, Colorado, USA

Steve Reid, Australian Institute for Bioengineering and Nanotechnology, University of Queensland, Brisbane, Australia

Grainne L. Riley, School of Chemical Engineering, University of Birmingham, United Kingdom

Peter L. Roberts, R&D Department, Bio Products Laboratory, Elstree, Hertfordshire, United Kingdom

David K. Robinson, Bioprocess Research & Development, Merck Research Laboratories, Rahway, NJ

Liliana Rodolfi, CNR, Istituto per lo Studio degli Ecosistemi, Firenze, Italy

Rodica-Viorica Roman, Chemical Pharmaceutical Research Institute, Iaşi, Romania

Catherine H. Schein, Sealy Center for Structural Biology and Molecular Biophysics, Sealy Center for Vaccine Development, University of Texas Medical Branch, Galveston, Texas, USA

Thomas Scheper, Institut für Technische Chemie, Gottfried Wilhelm Leibniz Universität Hannover, Hannover, Germany

Gargi Seth, Genentech, Inc., 1 DNA way, South San Francisco, California, USA

Jose María Fernández Sevilla, University of Almería, Almería, Spain

Kevin L. Shade, Novartis Vaccines and Diagnostics, Speke, Liverpool, United Kingdom

Susan T. Sharfstein, Center for Biotechnology and Interdisciplinary Studies, Rensselaer Polytechnic Institute, Troy, New York, USA

Susan T. Sharfstein, University at Albany, College of Nanoscale Science and Engineering, Albany, New York, USA

Robert Shawley, Late Stage Cell Culture, Genentech, Inc., San Francisco, California, USA

Masaru Shiratori, Late Stage Cell Culture, Genentech, Inc., San Francisco, California, USA

Christian Sieblist, Institute of Biotechnology; Centre of Bioengineering, Martin-Luther-University Halle-Wittenberg, Weinbergweg, Halle (Saale), Germany

Martin S. Sinacore, Genetics Institute, Andover, Massachusetts, USA

David Smith, CAB International Europe United Kingdom, Egham, United Kingdom

Benjamin Sommer, Faculty of Technology, Fermentation Engineering, University of Bielefeld, Bielefeld, Germany

Koti Sreekrishna, Procter & Gamble Co., Cincinnati, Ohio, USA

Winfried Storhas, Mannheim University of Applied Sciences, Mannheim, Germany

Deidre M. Stuart, Queensland University of Technology, Brisbane, Australia

Wei Wen Su, University of Hawaii, Honolulu, Hawaii, USA

Shyamsundar Subramanian, Merck & Co. Inc., West Point, Pennsylvania, USA

Robert D. Tanner, Vanderbilt University, Nashville, Tennessee, USA

Pilar Teixeira, Institute for Biotechnology and Bioengineering, Centre of Biological Engineering, University of Minho, Braga, Portugal

Colin R. Thomas, School of Chemical Engineering, University of Birmingham, United Kingdom

Mario R. Tredici, Università degli Studi di Firenze, Firenze, Italy

Radu Z. Tudose, Technical University Gh.Asachi Iaşi, Iaşi, Romania

Richard M. Twyman, John Inness Centre, Norwich, United Kingdom

Cord C. Uphoff, DSMZ-German Collection of Microorganisms and Cell Cultures, Braunschweig, Germany

Patricia S. Vary, Northern Illinois University, DeKalb, Illinois, USA

Manojlović Verica, University of Belgrade, Belgrade, Republic of Serbia

Natarajan Vijayasankaran, Late Stage Cell Culture, Genentech, Inc., San Francisco, California, USA

Nedović Viktor, University of Belgrade, Belgrade, Republic of Serbia

James C. Warren, Merck & Co. Inc., West Point, Pennsylvania, USA

Ning Wei, Faculty of Technology, Fermentation Engineering, University of Bielefeld, Bielefeld, Germany

Bruce Whitelaw, Roslin Institute, Roslin, Midlothian, United Kingdom

Erik M. Whiteley, Geron Corporation, Menlo Park, California, USA

Ronnie Willaert, Flanders Interuniversity Institute for Biotechnology, Vrije Universiteit Brussel, Brussels, Belgium

Jack Wilson, ABEC, Inc., Allentown, Pennsylvania, USA

Jian-Jiang Zhong, Key Laboratory of Microbial Metabolism, Ministry of Education, School of Life Sciences & Biotechnology, Shanghai Jiao Tong University, Shanghai, China; State Key Laboratory of Bioreaetor Engineering, School of Bioechnology, East China University of Science and Technology, Shanghai, China

Tan-Che Zhou, Molecular Biochemical Engineering Group, Key Laboratory of Microbial Metabolism, Ministry of Education, School of Life Sciences & Biotechnology, Shanghai Jiao Tong University, Shanghai, China

Wen-Wen Zhou, Molecular Biochemical Engineering Group, Key Laboratory of Microbial Metabolism, Ministry of Education, School of Life Sciences & Biotechnology, Shanghai Jiao Tong University, Shanghai, China

Weichang Zhou, Genzyme Corporation, Framingham, Massachusetts, USA

Graziella Chini Zittelli, CNR, Istituto per lo Studio degli Ecosistemi, Firenze, Italy

Marko Zlokarnik, Chemical Process Engineering, University of Köln, Cologne, Germany

Volume 1

Expression Systems & Process Development

PART I

INTRODUCTION

INTRODUCTION

Volume 1: *Expression systems & Process Development*
Volume 2: *Equipment, Process Design, Sensing, Control and cGMP Operations*

Upstream biomanufacturing processes are designated on the basis of volume or surface area (liters, gallons, cubic meters, square meters etc.). As the process is developed and optimized, it is scaled up in volume or area and optimized for biocatalyst specific reactivity to match the market demand for the product. Therefore, close integration of the characteristics of the biological system that produces the product with the engineering and optimal performance of the manufacturing scale bioreactors is essential. This means that engineers, life scientists, and manufacturing operations staff with broad expertise all need to work and communicate effectively as a team to design an upstream process that can be scaled from the laboratory bench and transferred to the manufacturing scale.

Designing the upstream process requires focusing on the biochemistry of the final product (peptide, protein, hormone, and low-molecular-weight metabolic intermediate) *and working backwards* to design living cells or enzymes that will generate the product in the precise form for optimal biological activity or clinical efficacy. Many peptides and proteins are post-translationally modified or are synthesized on a multienzyme complex and the biological catalysts that carry out these modifications differ from cell line to cell line. This results in different degrees of modification or mixtures of partially modified products depending on the choice of cell line used and the growth conditions. The enzymes in some cell lines or microorganisms also inactivate or degrade the product as it is being produced. Fortunately, the range of these modifications can now be minimized or precisely altered by strategic host cell line engineering. These same concepts also apply when the product is more complex such as in the manufacture of biologics (cells, virus particles, virus-like particles, and complex antigens) used as vaccines or artificial tissues. In some cases the products are isolated from living tissues (eggs, blood, whole organs, milk, and fluids from individual patients) and this isolation step is considered as a component of the upstream manufacturing process. Fortunately, the genes encoding many complex biologics can now be cloned from their tissue of origin and expressed in microorganisms, fungi, mammalian or insect cell lines thereby diminishing or eliminating the need for direct tissue isolation. Regardless of their biological source, the precise biochemical characteristics of all of these products must be carefully defined at the beginning of the process design and these characteristics are often expressed as target product profiles (TPPs).

The first section of Volume I of *Upstream* provides indepth information on industrial cell gene expression systems and methods to quantify cell growth in order to design processes that are highly reproducible. Choice of the gene expression platform (host cell line, vector, promoters, the site of protein accumulation, and optimal expression conditions) has a major impact on the overall process design and final product yield. This is often determined by in-house gene expression expertise, existing process equipment as well as intellectual property restraints (composition of matter or process patents, licensing agreements, and freedom to operate).

How cells grow and the extent to which they grow are affected by media composition, growth conditions, and upstream process design (batch, fed-batch, continuous, cell recycle, immobilized biocatalysts, illumination, and heat transfer), which are included in Section III. For some cells

that require attachment to a surface, the chemistry of the surface and the available surface area are critical to optimizing growth. Upstream process design and development, even at the laboratory bench scale, must also consider eventual scale up to manufacturing scale. Scale-up approaches are included in Volume 1 Section III, and in Volume 2 Section IV.

Volume 2 includes important engineering information on the materials and design of specific types of bioreactors that have been found by the industry to be optimal for the growth of specific types of microorganisms and cells. Also included are reactors engineered for immobilized biocatalysts (whole cells, enzymes, and photo reactive cells). Each type of bioreactor must be designed to grow cells at optimal rates to a desired concentration and, therefore, methods for calibrating bioreactors for oxygen transfer, cell illumination, mixing, shear, foam formation, design of aseptic sampling systems, culture fluid rheology and effective sterilization/decontamination are included in Sections IV and VI.

As stated above, the eventual goal of bioreactor design is to scale up to the total volume needed on the manufacturing scale to meet market demand. However, there are critical regulatory considerations that need to be included in upstream process design and process operations for products manufactured under current Good Manufacturing Practice (cGMP) mandated by USFDA federal regulations (CFRs) and guidelines. These include monitoring of the process to obtain detailed process knowledge used to determine multivariant design space for optimal performance of each unit operation. Methods are included for these Process Analytical Technologies (PAT) as well as upstream cGMP operations in Volume 2, Sections V and VI. While these cGMP regulations may vary from country to country, a significant international harmonization effort has resulted in common global guidance documents (ICH, International Conference on Harmonization of Technical Requirements for Registration of Pharmaceuticals for Human Use) referred to in these sections.

Optimal biopharmaceutical product yield is *the mathematical product* of the number of cells used to generate the product, the amount of product produced per cell, *multiplied* (most importantly) by the yield of recovered product in the appropriate final biologically active form and purity. Each upstream process decision impacts downstream product recovery and purification. Therefore, the companion volume *Downstream Industrial Biotechnology* should also be consulted when designing an upstream process.

PART II

INDUSTRIAL CELL GROWTH AND GENE EXPRESSION SYSTEMS

1

ANIMAL CELLS, SUSPENSION CULTURE

JOHN R. BIRCH
Lonza Biologics plc, Berkshire, United Kingdom

1.1 INTRODUCTION

Mammalian cells can be distinguished by their requirement to grow when attached to a surface (anchorage dependence) or in free suspension. The ability to grow in suspension is frequently associated with cell lines that demonstrate an "immortal" or infinite lifespan phenotype. Suspension culture systems are preferred for most large-scale manufacturing processes because scale-up is more straightforward. Relatively homogeneous conditions can be achieved in a suspension bioreactor, allowing efficient monitoring and control of key process parameters.

Suspension culture technology for animal cell culture started in the 1950s, with the demonstration that several types of cells could be grown in simple agitated systems such as tumbling tubes and shaken flasks (1,2). By the end of the decade, methods had been developed for growing cells in magnetically stirred spinner vessels (3,4) and in bioreactors similar to those used for microorganisms (5,6). By the 1960s, pilot plant reactors at scales of hundreds of liters were in operation (7).

The initial drive to develop an industrial process based on mammalian cell suspension culture came from the need to produce very large volumes of vaccines against foot-and-mouth disease (FMD) virus. Processes were developed using baby hamster kidney (BHK) cells growing in stirred-tank reactors up to 3000 L (8–10). Subsequently, stirred-tank reactors of up to 8000 L were used for the production of interferon α from human Namalwa cells (9). The industrial application of animal cell culture has increased significantly over the last 20 years, driven by the need to produce monoclonal antibodies and recombinant proteins in addition to vaccines. It is the demonstration that these products can be made safely in immortal cell lines that has made possible their large-scale manufacture. In the case of monoclonal antibodies, requirements can be as high as hundreds of kilograms or tons per year. To meet this demand, bioreactors with working volumes up to 20,000 L are now used (11) and global reactor capacity is expected to increase from ~2.3 million L in 2004 to ~3.7 million L in 2011 (12).

1.2 TYPES USED FOR LARGE-SCALE PRODUCTION IN SUSPENSION CULTURE

Cell types used for large-scale production in suspension culture and those that are most commonly used industrially are described below.

1.2.1 Cell Types Used for Protein Production

1.2.1.1 CHO. The CHO line is the most commonly used cell type for recombinant protein production. Approximately 70% of all licensed biotherapeutic proteins are produced in this cell line (13). CHO cells have been used to produce a wide range of therapeutic proteins (hormones, growth factors, thrombolytics, blood clotting factors, and immunoglobulins). The choice of the CHO cell is based on several factors: compatibility with efficient gene expression systems leading to good productivity, ability to carry out important posttranslational modifications of proteins, and freedom from detectable pathogenic agents. In addition, the cell type can be grown in large-scale suspension

Upstream Industrial Biotechnology: Expression Systems and Process Development, Volume 1, First Edition. Edited by Michael C. Flickinger.
© 2013 John Wiley & Sons, Inc. Published 2013 by John Wiley & Sons, Inc.

bioreactors. CHO cells can also grow as attached cultures, and in fact, growth in suspension traditionally required a period of adaptation after the production cell line had been created. This requirement for adaptation, which can take several weeks or months, can be circumvented by using host cells for gene transfection that have been preadapted to grow in suspension (14). Kurano *et al*. (15) isolated several anchorage-independent sublines of CHO, one of which grew in suspension even in static flasks. A CHO variant, CHOK1SV, has been described, which grows spontaneously in suspension in chemically defined medium (11). A different approach was taken by Renner *et al*. (16), who demonstrated that expression of recombinant cyclin E (a cell cycle regulator) in CHO cells prevented surface attachment and additionally permitted growth in protein-free medium.

1.2.1.2 Hybridomas and Myeloma Cell Lines. Rodent monoclonal antibodies are typically produced in hybridoma cells, which can be readily grown in suspension culture (see, e.g. Ref. 17). In general, rodent antibodies are used in diagnostic and research applications and are required only in modest quantities. For the vast majority of therapeutic applications, antibodies are now genetically engineered and produced in CHO cells or in mouse lymphoid cell types (particularly NS0 and SP2/0), which, like CHO, can be grown in large-scale suspension culture (13).

1.2.1.3 Other. BHK cells are used for the production of recombinant blood clotting factors VIIa and VIII (18,19). Immortalized human cell lines such as PER.C6® are also being developed for the production of recombinant proteins (20).

1.2.2 Cell Types Used for Vaccine Production

Many vaccines are produced in anchorage-dependent cell systems, but suspension culture is also used, particularly where the scale of production is large. BHK cells have been used for large-scale production of FMD vaccine because of their ability to propagate the virus and their capacity to grow in large-scale suspension culture (10). Rabies vaccine for veterinary use is also manufactured in BHK cells (21).The availability of cell lines that can be grown in large-scale suspension culture is leading to a shift in technology in some key areas of human vaccine manufacture. In the case of influenza vaccine in particular, the new cell culture processes may be an attractive alternative to the traditional egg-based processes (22,23). Examples of cell lines that have been developed for the production of large-scale human vaccine include the PER.C6 cell line derived from human retinal cells by immortalization with adenovirus E1 genes (20), the canine cell line MDCK (23), and EBx™ diploid cell lines derived from avian embryonic stem cells (24). There are also examples of suspension cultures of insect cells being used in the development of virus vaccines (25).

1.2.3 Cell Lines for Transient Production of Proteins

Transient expression technologies are frequently used for the rapid production of research quantities (milligrams to grams) of protein. The human HEK293 cell line has been very widely used for this purpose and suspension culture processes up to 100-L scale have been described (26). A process at similar scale for transiently transfected CHO cells has been described (27). Insect cells are also used for the rapid production of research materials using baculovirus expression technology (e.g. see Ref. 28).

1.3 SUSPENSION CULTURE REACTORS

Bioreactors up to 20,000-L scale are now used in the manufacture of recombinant therapeutic products from mammalian cells (11); the most commonly used systems being based on stirred tanks. Airlift reactors are also used, but much less frequently. The principles underpinning the design and scale-up of animal cell bioreactors have been reviewed by several authors (29–31). In addition to stainless steel systems, a variety of simpler technologies are used at smaller scales (<100 L) including spinner flasks and, more recently, disposable bag reactors.

1.3.1 Stirred Reactors

The majority of products made using large-scale mammalian cell culture are produced in stirred-tank reactors (see Ref. 32 for description of reactors used for a range of licensed products). Stirred bioreactors up to 20,000-L scale are now in use particularly for the production of monoclonal antibodies, which can be required in very large quantities. Birch and Racher (11) provide details of the process flow for 20,000-L scale reactors. Typically, reactors are stainless steel with height-to-diameter ratios in the range 1:1–3:1. In some cases, mammalian cell bioreactors have been developed by retrofitting microbial vessels, usually by changing the agitators and aeration system. Backer *et al*. (17) described the retrofitting of 150- and 1300-L reactors. Rushton impellers were replaced with marine propellers, and the agitator drives were altered to allow operation between 25 and 250 rpm. Air was sparged through a sintered stainless steel sparger with 10-μm pore size. Garnier *et al*. (28) describe the retrofitting of a 150-L microbial bioreactor (height-to-diameter ratio 3). They used two large pitched-blade impellers (45°), three surface baffles, and a polypropylene porous sparger (80-μm pore size). Agitation was controlled at 60–120 rpm. Nienow *et al*. (33) found

that Intermig impellers improved mixing times in a mammalian reactor compared with the Rushton turbines commonly used in microbial reactors. Impellers may be directly driven via a shaft or indirectly driven through a magnetically coupled drive (34,35). Magnetic drives remove the potential for microbial ingress through mechanical shaft seals. The operation of mammalian reactors differs from that of microbial reactors in one very important respect: power inputs are very low to minimize the risk of damage to cells. For an 8000-L reactor, it has been reported (33) that a maximum agitator speed of 1.5 rev/s is used, giving a maximum power input of 30 W/m^3. This is around two orders of magnitude less than the value typically achieved in microbial fermentations. Similarly very low aeration rates are used in animal cell reactors compared with microbial cultures. This combination of low power input and low aeration rate means that particular attention has to be paid to the design (impellers, spargers, and aspect ratio) and operation of vessels to ensure good bulk mixing and adequate mass transfer of gases (especially oxygen and carbon dioxide). Nienow *et al*. (33) describes a study of mixing characteristics and oxygen uptake rates in an 8000-L reactor and discuss ways of improving reactor performance. Ma *et al*. (36) provide an in-depth review of aeration, mixing, and hydrodynamics in bioreactors.

1.3.2 Airlift Reactors

The airlift reactor is used less commonly than the stirred reactor for cell culture and was originally developed for microbial fermentation. Sparging of air or other gas mixtures is used to aerate the culture and to provide mixing. Mixing is achieved by separating the vessel into riser and down comer sections using a draught tube, divider plate, or external recirculation loop. The presence of gas bubbles in the riser section creates a density difference between the riser and the down comer that causes the fluid to circulate, providing mixing. Airlift reactors tend to have larger height-to-diameter ratios than stirred reactors (typically as high as 10:1). Their advantage is simplicity (no mechanical agitators) combined with good mass transfer and low shear characteristics (42,43). A disadvantage of the technology is lack of flexibility in working volume. The basic design features of airlift reactors have been described in reviews (44,45). Airlift reactors have been used for the culture of BHK and human lymphoblastoid cells (46), insect cells (47), and at scales up to 5000 L for a variety of cell types including CHO, hybridomas, and myelomas (48,49).

1.3.3 Disposable Reactor Systems

Increasing use is being made of disposable, plastic film, bioreactors for suspension culture, particularly at small to medium scale where they offer significant flexibility and simplicity of operation compared with conventional stainless steel plants. This is particularly relevant where multiple products are being handled. Farid *et al*. (50) have described a decision-support tool for assessing disposables versus stainless steel plants under different scenarios. Disposable bags up to 500-L scale are increasingly used for small-scale production and for inoculum preparation. One of the most widely used systems (Wave Bioreactor™) exploits wave-induced agitation in disposable bag reactors to maintain cell suspension and oxygen transfer (51). Disposable stirred reactors have also been developed (52,53) at a range of scales up to 1000 L (Table 1.1).

1.4 OPERATING MODES FOR REACTORS

Although the type of vessel used for suspension culture is usually a stirred reactor (occasionally airlift), the mode of reactor operations can vary significantly. Production methods have been developed based on batch, fed-batch, and continuous (perfusion) systems. The choice of process will be dictated by several factors. Batch and fed-batch culture have the advantage of simplicity, reliability, flexibility, and reduced timescales for development and validation (compared with continuous systems). On the other hand, continuous systems may offer an advantage for less stable products, since residence time in the bioreactor is reduced. For most products, the ultimate decision comes down to process economics. Lim *et al*. (54) have described a decision-support tool to help compare the production economics of continuous (perfusion) versus fed-batch.

1.4.1 Batch and Fed-Batch Culture

Batch and fed-batch culture are the most widely used in production processes. Cells and medium are added to the reactor, and the culture is harvested after an appropriate period of culture. The time of harvest will depend on the kinetics of product accumulation and, in some cases, on the stability of product within the reactor. A commonly used variation on this type of culture is repeated batch or "draw and fill" culture. This is a batch culture in which a proportion of the culture is retained in the reactor as an inoculum, and fresh medium is added. This allows repeated batch growth cycles within the reactor, obviating the need to repeatedly clean, sterilize, and reinoculate the vessel. Backer *et al*. (17) described such a system, which was operated for several months at a time, for monoclonal antibody production in a 1300-L reactor. Every 84 h, the reactor was harvested, leaving 10% of the culture in the reactor as inoculum for the next culture.

A further commonly used variant on batch culture is fed-batch culture in which small volumes of selected nutrients are fed to the culture during the growth cycle

TABLE 1.1. Examples of Industrial-Scale Mammalian Cell Suspension Culture Processes

Product	Cell Line	Reactor	References
Foot-and-mouth disease vaccine	BHK 21	3,000 L	Pullen *et al*. (9)
Interferon	Namalwa	8,000 L	Pullen *et al*. (9)
Tissue plasminogen activator (tPA)	CHO	10,000 L	Lubiniecki *et al*. (37)
Factor VIII	BHK 21	Perfused 500-L reactor with cell recycle system	Bödeker *et al*. (19)
Factor VIII	CHO	2,500-L batch refeed	Adamson (38)
Monoclonal antibodies	Hydridoma/myelomas	Perfused 500-L spin filter reactor	Deo *et al*. (39)
Monoclonal antibody	NSO myeloma	2000-L fed-batch reactor	Ray *et al*. (40)
Monoclonal antibody	Hybridoma	1,300-L batch, draw and fill	Backer *et al*. (17)
Monoclonal antibody	Myeloma	2,000-L airlift reactor	Brown *et al*. (41)
Recombinant proteins/antibodies	Various	20,000-L stirred reactor	Birch and Racher (11)

to improve growth and productivity. Feeding strategies can be used to increase maximum cell population density and IVC (time integral of the viable cell concentration in the reactor). On the basis of an understanding of the nutrient requirements and metabolism of cells, feeds have been designed to avoid nutrient depletion and excessive accumulation of toxic by-products such as lactate and ammonia. The approaches taken in developing feeding strategies have been reviewed by Xie and Zhou (55). Progress with fed-batch technology has probably been the single most important factor contributing to the 100-fold increase in recombinant protein titers since the mid-1980s (56). This progress has been driven particularly by the need to produce very large quantities of therapeutic monoclonal antibodies. Initially, feeding methods were based on relatively simple supplementation strategies (reviewed in (57)). Subsequently, more sophisticated methods were developed, including techniques based on a stoichiometric model of the demands of nutrients for growth and product formation. This strategy aimed at providing nutrients based on their rate of utilization and reducing the formation of toxic products of metabolism such as ammonia and lactate, by avoiding excess concentrations of the nutrients that give rise to them. Application of this approach to hybridoma cells was described by Xie and Wang (58). They demonstrated that in fed-batch cultures of hybridoma cells the method resulted in very high cell densities (1.7×10^7 cells/mL), extended culture spans, and a 50-fold increase in monoclonal antibody concentration compared with batch culture (58). Although most methods have been based on off-line measurements, progress has also been made in the use of on-line measurement to estimate nutrient utilization rate and feed stoichiometric amounts of nutrients to support growth and reduce accumulation of toxic metabolites. Zhou *et al*. (59) demonstrated such a system using on-line measurement of oxygen uptake rate to automatically control the feed to a 500-mL hybridoma culture. Maximum cell concentrations were increased ca. sevenfold and lactate production was reduced. Kurokawa *et al*. (60) used on-line HPLC measurement of glucose and glutamine to control the concentration of these nutrients in fed-batch culture at low levels (0.2 and 0.1 g/L, respectively). This strategy reduced the accumulation of lactate and ammonia and gave an approximately twofold increase in cell growth and antibody production.

In the literature, there are now several descriptions of fed-batch strategies applied to culture of recombinant cell lines, particularly those used to make monoclonal antibodies.

A significant number of licensed antibodies are produced in mouse NS0 and SP2/0 cell lines. Burky *et al*. (61) describe a platform fed-batch process for making antibodies in NS0 cell lines using protein and cholesterol-free chemically defined medium and feeds. Optimization of this process led to antibody titers of 2.64 ± 0.19 g/L and volumetric productivity of >200 mg/L-day in a 13-day process for one cell line. Zhou *et al*. (62) reported antibody titers of >2.7 g/L for a fed-batch process using an NS0 cell line. Sauer *et al*. (63) have described a platform fed-batch process for SP2/0 cells.

In the case of CHO cells, antibody titers of >1 g/L are now routinely obtained in manufacturing processes. Birch and Racher (11) described the evolution of a fed-batch process for a GS-CHO cell line making an antibody. A titer of 5.5 g/L was obtained in a protein-free, chemically defined process. Maximum cell population densities in excess of 10^7/ml were realized. A contributory factor in the achievement of this high titer was the introduction of a new cell strain based on a variant of CHO, CHOK1SV, a cell line that grows spontaneously in suspension in chemically defined medium and appears to have improved growth characteristics compared with the parent CHOK1. The authors note that for this particular antibody the titer was a 100-fold increase compared with a CHO suspension process used to make the same antibody in 1990. Growth and product generation during fed-batch culture of a GS-CHO cell line making a recombinant monoclonal antibody are shown in Fig. 1.1.

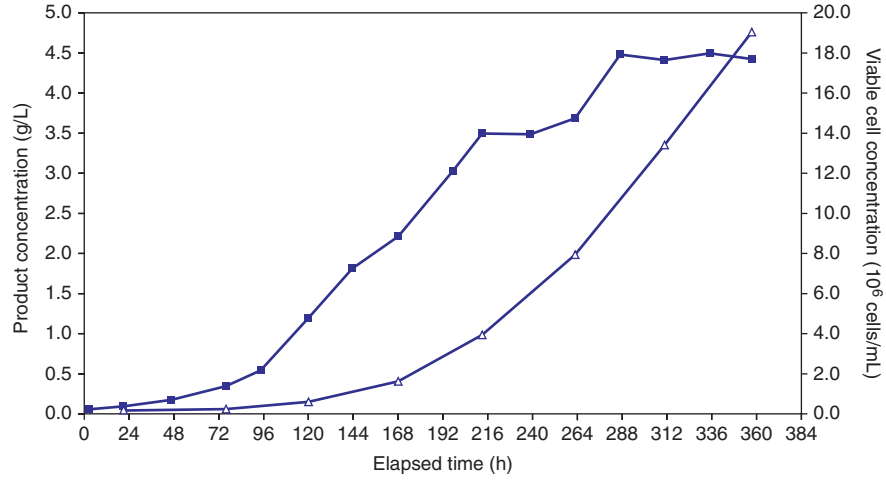


Figure 1.1. Production of a recombinant antibody from a GS-CHO cell line growing in protein-free, chemically defined medium in a bioreactor. (This figure is available in full color at http://onlinelibrary.wiley.com/book/10.1002/9780470054581.)

Although fed-batch technology has been driven significantly by the requirement for monoclonal antibodies, it has been applied to other proteins. Zhou *et al*. (64) described a feeding strategy that led to a 10-fold increase in productivity for large-scale mouse myeloma cultures, producing recombinant mouse and rat growth hormones. Wong *et al*. (65) developed a dynamic on-line fed-batch process for making interferon gamma, based on maintaining low glucose and glutamine concentrations to minimize accumulation of lactate and ammonia. Interferon levels were increased 10-fold compared with batch culture.

1.4.2 Continuous Culture Systems

Continuous (perfusion) suspension culture systems are used in several large-scale manufacturing operations for the production of recombinant proteins including monoclonal antibodies (66). Reactors up to 4000 L are in operation or being constructed (67). For a discussion of perfusion culture technology and the engineering issues involved in designing and operating such systems, the reader is referred to the review by Kompala and Ozturk (66). Perfusion culture uses a continuous supply of culture medium to the reactor and a continuous off take of spent culture fluid containing product. By retaining cells in the reactor (by preventing them leaving the vessel or by an external recycle device), very high cell densities and consequently very high product throughput can be achieved. The earliest device of this kind was the spin filter culture developed by Himmelfarb (68). A spinning filter within the reactor allowed cell retention, and with continuous perfusion of culture medium, cell densities approaching 10^8/mL were achieved. A wide range of cell retention devices have been described in the literature, based on filters, settlers, centrifuges, acoustic resonators, and hydrocyclones. Retention devices have been reviewed in detail by Voisard *et al*. (69) and Kompala and Ozturk (66)

At industrial scale Bodeker (19) describe the use of a perfused 500-L bioreactor with an external cell retention/recycle system to manufacture recombinant factor VIII from BHK cells. This is apparently the first approved biopharmaceutical from recombinant mammalian cells made using perfusion culture. Bodeker discusses the advantages of perfusion culture for factor VIII production, which requires the generation of greater than one million liters of harvest. These advantages include a high degree of culture control compared with batch operation (operates in steady-state conditions) and reduction in reactor size (hence easier to operate, clean, and sterilize). The main disadvantage reported was the extended process validation required. This validation included process stability, stability of product characteristics, and genetic stability of the cell line over the duration of the culture, which was up to 185 days. Several full-length campaigns were run to establish process consistency.

Deo *et al*. (39) described the design and operation of a 500-L perfused spin filter reactor for monoclonal antibody production. They note that continuous perfusion generally gives an ~10-fold greater volumetric productivity in comparison with batch and fed-batch processes. Hence, less reactor capacity is required. At an antibody titer of 400–500 mg/L, the 500-L reactor is capable of producing more than 1 kg of antibody per week, which they estimate would require a 5000- to 10,000-L bioreactor operating in batch or fed-batch mode. Successful operation of spin filter systems depends on careful optimization of the filter system to prevent fouling (39)

Another approach to continuous culture is to use a chemostat in which growth rate is controlled by the supply of a single limiting nutrient. The advantage of this system

is that true physiological steady-state conditions can be maintained indefinitely, allowing very precise control of culture conditions, and this can be extremely valuable in a variety of research applications for studying cell physiology (see, e.g. Refs 70–72). To date, however, the technique has not been applied in industrial processes.

1.5 PROCESS MONITORING AND CONTROL

The key parameters that are usually monitored and controlled in industrial-scale suspension cultures are pH, temperature, and dissolved oxygen. There is also increasing interest in the use of devices that allow real-time monitoring of biomass concentration (73). Such devices will allow improved monitoring and control of fermentations, particularly where fed-batch and perfusion strategies are adopted. Instrumentation and process control of bioreactors has been reviewed by Riley (74).

1.5.1 pH Control

Mammalian cell growth metabolism and productivity can be profoundly influenced by even small changes in pH of the culture. Ozturk and Palsson (75) found that the growth rate for a hybridoma was optimum at pH 7.2 but that the specific antibody production rate increased twofold at pH values below 7.2. They also showed that glucose and glutamine uptake rates and production rates for lactate and ammonia increased at higher pH values. Wayte *et al*. (76) reported that differences in pH of as small as 0.1 units could profoundly affect cell growth and/or productivity of hybridoma and myeloma cell lines. The effects observed were cell line specific. pH may also influence product characteristics, especially glycosylation. Borys (77) showed that pH affected the glycosylation pattern and specific expression rate of a recombinant lactogen protein made in CHO cell culture. Hence, it is essential to establish the optimum pH for a given cell line and to measure and control pH precisely. pH is typically controlled at a value in the range 7.0–7.5. Most cell culture media rely on a bicarbonate–CO_2 buffering system. Hence, when a bioreactor is sparged with air, the pH can be controlled by injecting a controlled flow of CO_2 on demand to maintain a constant pH value. It is frequently found that lactic acid accumulates to levels that cannot be controlled by sparging with air and CO_2; it is then common practice to control the pH by addition of a sterile base solution such as sodium bicarbonate (17) or sodium carbonate (33). Care is needed in designing bioreactors to avoid pH gradients during the addition of base solution. Regions of high pH may arise, especially if the base is added to a poorly mixed zone (often the upper region) in both stirred reactors (33) and airlift reactors (76). The problem can be minimized by adding base to a well-mixed region of the reactor. Osman *et al*. (77,78) studied the response of GS-NS0 cells to pH shifts and perturbations in stirred reactors.

1.5.2 Dissolved Oxygen Concentration

Animal cells have an absolute requirement for oxygen. There are several ways in which it can be provided to cultures, but the most common method is to bubble or "sparge" air or oxygen into the reactor. Dissolved oxygen concentrations can be measured *in situ* with a dissolved oxygen electrode and controlled automatically by adjusting the flow rate of air or oxygen to the reactor. The optimum dissolved concentration varies from one cell line to another, although most cell types will grow over quite a wide range of dissolved oxygen concentrations. Boraston *et al*. (72) found that the growth of a hybridoma cell was relatively unaffected over the range 8–100% air saturation. Ozturk and Palsson (75) showed that growth rates of hybridoma cells were not influenced at dissolved oxygen concentrations in the range 20–80% air saturation. Specific death rates were lowest in the range 20–50% air saturation. Nienow (33) found that a CHO cell line producing recombinant interferon γ grew well and had similar productivity over the range 20–80% saturation, but growth and productivity were reduced at 5% and 100% saturation. The oxygen uptake rate of animal cells is typically in the range 0.05–0.5 mmol $O_2/10^9$ cells/h (79). It is, of course, necessary to ensure that oxygen transfer into the culture is sufficient to meet the uptake rate of the cells, and this becomes an increasingly important issue as higher cell densities are achieved through improvements in process design. Factors influencing oxygen transfer include height-to-diameter ratio for the vessel, sparger and impeller designs, and gas flow rates. Tramper (80) has pointed out that gradients of dissolved oxygen concentration may occur in large bioreactors. It is not clear what impact such gradients have in practice, but they should be borne in mind and minimized when designing reactors. Aeration in cell culture bioreactors has been reviewed in detail by Aunins and Henzler (81).

1.5.3 Dissolved Carbon Dioxide Concentration

In addition to CO_2 added to the culture as part of the pH buffering system, account must be taken of CO_2 generated by cell metabolism. Although systems for *in situ* monitoring and control of CO_2 are not yet commonly used, it is useful to measure CO_2 levels off-line, for example, using a clinical blood gas analyzer. In recent years, it has become apparent that in some large-scale processes CO_2 can accumulate to levels that inhibit cell growth and recombinant product formation (28,79–82). It has been suggested (82) that CO_2 accumulation may be the factor that will ultimately limit the

reactor scale for some processes. Kimura and Miller (83) point out that inhibition may be caused by an effect of CO_2 on intracellular pH (even if the culture pH is controlled). Accumulated CO_2 may also lead to inhibition of growth due to an increase in osmolarity caused by the additional base required to maintain pH.

Gray *et al*. (84), working with CHO cells in a high density perfused process, showed that productivity of a recombinant product was maximized when CO_2 was maintained in the range 30–76 mm Hg. Levels greater than 105 mm Hg resulted in inhibition of growth and productivity. CO_2 concentration may also influence glycosylation of recombinant proteins (83). Aeration systems designed for efficient oxygen transfer will not necessarily be efficient at stripping out CO_2. Gray *et al*. (84) found that sparging with microbubbles of pure oxygen gave very efficient oxygen transfer but was inefficient for CO_2 removal because the bubbles dissolved before reaching the surface of the culture. Sparging with large bubbles (2–3 mm diameter) improved CO_2 removal while retaining adequate oxygen transfer. Zhou *et al*. (64), working with GS cell lines making recombinant mouse and rat growth hormones in a 250-L fed-batch reactor, also found that the use of a sintered steel frit delivering pure oxygen gave good oxygen transfer, but CO_2 accumulated to 200 mm Hg, depressing cell growth. By using a less efficient sparger generating larger bubbles, CO_2 accumulation was reduced to a noninhibitory level. Goudar *et al*. (85) addressed the issue of elevated pCO_2 levels in high density cultures of BHK cells by eliminating bicarbonate addition to the culture. MOPS–Histidine buffer replaced the $NaHCO_3$ in the medium and Na_2CO3 was used in place of $NaHCO_3$ for pH control. The resultant reduction in pCO_2 (by 63–70%) to 68–85 mm Hg led to increased growth rates of 68–123% and increased specific productivity of 58–92%.

1.5.4 Temperature

Temperature is typically controlled at around 37°C. Bloemkolk *et al*. (86) studied the effect of temperature on growth and antibody production of a hybridoma in suspension culture; 37°C was the optimum temperature for cell growth and antibody production. At 39°C growth was completely inhibited. In some instances, the optimum temperature for product accumulation may be below 37°C. The effects of temperature seem to be cell line and possibly product specific. Yoon *et al*. (87) found that lowering the temperature from 37 to 30 or 33°C had no beneficial effect on the production of a recombinant antibody from CHO cells. The result was in contrast to the improved production seen for erythropoietin in the same host cell. It may be advantageous to shift process operating parameters during the period of culture. Trummer *et al*. (88) described a biphasic culture process for Epo-Fc production in CHO cells in which they enhanced volumetric productivity by shifting both pH and temperature.

1.6 CULTURE MEDIA FOR SUSPENSION CULTURE

In general, media for suspension culture are similar to those used for other processes, with the exception that an agent to protect against mechanical damage is frequently added. For reactors that are aerated by sparging, it may also be necessary to use an antifoam agent, which is usually a silicone emulsion (81,89). In some instances, changes in nutritional requirements have been observed in suspension as opposed to static culture. For example, Murakami *et al*. (90) showed that a myeloma cell line in suspension culture had a requirement for a phospholipid component that was not required in static culture.

Significant progress is being made in the optimization of media composition as well as of nutrient feeds for fed-batch culture (see earlier section). Brown *et al*. (41) described how an iterative program of medium development gave a six- to sevenfold improvement in productivity of antibody from a recombinant myeloma cell line. The addition of a feed gave a further twofold increase in productivity. Jo *et al*. (91) increased maximum cell concentrations significantly for several cell lines by increasing the nutrient concentrations in RPMI 1640 medium.

There is an increasing drive to remove animal-derived raw materials from cell culture processes to reduce the risk of inadvertently introducing adventitious agents. Encouraging progress has been made, and there are now several examples in the literature of industrially important cell lines being grown in chemically defined protein-free medium. Keen (92) described the growth of myeloma and hybridoma cell lines in a protein-free medium in shake flask culture and Burky *et al*. (61) described a protein-free fed-batch process for recombinant NS0 cells. Zang *et al*. (93) developed a protein-free culture medium for the growth of CHO cell lines making recombinant proteins. A fed-batch process using protein-free, chemically defined medium for recombinant GS-CHO cells has been described (11).

1.6.1 Protective Polymers

Two mechanisms have been identified that can potentially cause cell damage in bioreactors; the first is the interaction of cells with bubbles in sparged reactors (reviewed by Chisti (94), and the second is the stress created by impellers at high agitation rates in stirred reactors. In practice, given the low impeller speeds used in animal cell reactors, interaction with bubbles is the only likely source of damage in aerated cultures (81,95). It seems probable that damage occurs when cells are attached to bubbles that burst

at the surface of the culture. The energy released by bubble bursting kills cells. The problem is readily overcome by incorporation of a protective polymer such as the nonionic surfactant Pluronic® F68 into the culture medium (96). Protective polymers seem to act by preventing cells from attaching to bubbles.

1.7 CONCLUSIONS

Animal cell suspension culture has become an extremely important industrial technology driven mainly by the need for biopharmaceutical products. With the steadily increasing number of biotechnology products in clinical trial (96), this trend seems set to continue, driven particularly in the short term by the need for large quantities of a significant number of therapeutic antibodies. Developments in other areas including vaccines are likely to expand the use of suspension culture technology even further. The requirement for large volumes of some animal-cell-derived pharmaceuticals, notably antibodies, has been a driver for improving productivity and cost efficiency of production processes. The most frequently used system for therapeutic protein production is the fed-batch bioreactor, which has been scaled up to >20,000 L. For recombinant antibodies, titers of grams per litre are now frequently reported, and protein-free, chemically defined media and feeds have been developed for a number of processes. Continuous perfusion culture is also used at reactor scales up to 4000 L for a number of products and is particularly favored for products that are relatively unstable.

REFERENCES

1. Owens O, Gey MK, Gey GO. Ann N Y Acad Sci 1954; 58: 1039–1055.
2. Earle WR, Schilling EH, Bryant JC, Evans VJ. J Natl Cancer Inst 1954; 14: 1159–1171.
3. Cherry WR, Hull RN. Anat Rec 1956; 124: 483.
4. McLimans WF, Davis EV, Glover FL, Rake GW. J Immunol 1957; 79: 428–433.
5. McLimans WF, Giardinello FR. J Bacteriol 1957; 74: 768–771.
6. Ziegler DW, Davis EV, Thomas WJ, McLimans WF. Appl Microbiol 1958; 6: 305–310.
7. Moore GE, Hasenpusch P, Gerner RE, Burns AA. Biotechnol Bioeng 1968; 10: 625–640.
8. Capstick PB, Telling RC, Chapman WG, Stewart DL. Nature 1962; 195: 1163–1164.
9. Pullen KF, Johnson MD, Phillips AW, Ball GD, Finter NB. Dev Biol Stand 1985; 60: 175–177.
10. Radlett PJ, Pay TWF, Garland AJM. Dev Biol Stand 1985; 60: 163–170.
11. Birch JR, Racher AJ. Adv Drug Deliv Rev 2006; 58: 671–685.
12. Frost and Sullivan Report 2004 quoted by in- Pharma Technologist. Available at www.in-pharmatechnologist.com/news/ng.asp?id=56516-biomanufacturing-at-overcapacity. Accessed 2007 Aug 21.
13. Birch, JR, Onakunle Y. In: Smales CM, James DC, editors. Volume 308, Methods in molecular biology, Therapeutic proteins: methods and protocols. Totowa (NJ): Humana Press; 2005. p 1–16.
14. Sinacore MS, Charlebois TS, Harrison S, Brennan S, Richards T, Hamilton M, Scott S, Brodeur S, Oakes P, Leonard M, Switzer M, Anagnostopoulos A, Foster B, Harris A, Jankowski M, Bond M, Martin S, Adamson SR. Biotechnol Bioeng 1996; 52: 518–528.
15. Kurano N, Leist C, Messi F, Gandor C, Kurano S, Fiechter A. J Biotechnol 1990; 16: 245–258.
16. Renner WA, Lee KH, Hatzimanikatis V, Bailey JE, Eppenberger HM. Biotechnol Bioeng 1995; 47: 476–482.
17. Backer MP, Metzger LS, Slaber PL, Nevitt KL, Boder GB. Biotechnol Bioeng 1988; 32: 993–1000.
18. Jurlander B, Thim L, Klausen NK, Persson E, Kjalke M, Rexen P, Jorgensen TB, Ostergaard PB, Erhardtsen E, Bjorn SE. Semin Thromb Hemost 2002; 27: 373–384.
19. Bodeker BGD, Newcomb R, Yuan P, Braufman A, Kelsey W. In: Spier RE, Griffiths JB, Berthold W, editors. Animal cell technology, products for today, prospects for tomorrow. Oxford: Butterworth-Heinemann; 1994. p 580–583.
20. Yallop C, Crowley J, Cote J, Hegmans-Brouwer K, Lagerwerf F, Gagne R, Coco Martin J, Oosterhuis N, Opstelten D-J, Bout A. In: Knablein J, editor. Modern biopharmaceuticals. Weinheim: Wiley-VCH; 2005. p 779–807.
21. Pay TWF, Boge A, Menard FJRR, Radlett PJ. Dev Biol Stand 1985; 60: 171–174.
22. Sheridan C. Nat Biotechnol 2007; 25: 701.
23. Microbe Magazine. 2006. American Society for Microbiology. www.asm.org/microbe/index.asp?bid=40620. Accessed 2007 Aug 21.
24. Hartshorn J, Guehenneux F, Kolell K, Geng Z-H, Atarod E, Mohabbat T, McCormick C, Sutrave P, Fernandez C, Avery M, Luo S, Mehtali M, Etchberger K. In: Smith R, editor. Cell technology for cell products. Netherlands: Springer; 2007. p 579–581.
25. Palomares LA, Estrada-Mondaca S, Ramirez OT. In: Ozturk SS, Hu W-S, editors. Cell culture technology for pharamaceutical and cell-based therapies. Florida: Taylor & Francis; 2006. p 627–692.
26. Baldi L, Muller N, Picasso S, Jacquet R, Girard P, Thanh HP, Derow E, Wurm FM. Biotechnol Prog 2005; 21: 148–153.
27. Derouazi M, Girard P, van Tilborgh F, Iglesias K, Muller N, Bertschinger M, Wurm FM. Biotechnol Bioeng 2004; 87: 537–545.
28. Garnier A, Voyer R, Tom R, Perret S, Jardin B, Kamen A. Cytotechnology 1996; 22: 53–63.
29. Varley J, Birch J. Cytotechnology 1999; 29: 177–205.
30. Nienow AW. Cytotechnology 2006; 50: 9–33.
31. Fenge C, Lullau E. In: Ozturk SS, Hu W-S, editors. Cell culture technology for pharmaceutical and cell-based therapies. Florida: Taylor & Francis; 2006. p 155–224.
32. Chu L, Robinson DK. Curr Opin Biotechnol 2001; 12: 180–187.
33. Nienow AW, Langheinrich C, Stevenson NC, Emery AN, Clayton TM, Slater NKH. Cytotechnology 1996; 22: 87–94.

34. Cameron J, Godfrey EI. Biotechnol Bioeng Symp 1974; 4: 821–835.
35. Finter NB. In: Lubiniecki AS, editor. Large scale mammalian cell culture technology. New York, Basel: Marcel Dekker; 1990. p 1–14.
36. Ma N, Mollet M, Chalmers JJ. In: Ozturk SS, Hu W-S, Editors. Cell culture technology for pharmaceutical and cell-based therapies. Florida: Taylor & Francis; 2006. p 155–224.
37. Lubiniecki A, Arathoon R, Polastri G, Thomas J, Wiebe M, Garnick R, Jones A, van Reis R, Builder S. In: Spier RE, Griffiths JB, Stephenne J, Crooy PJ, editors. Advances in animal cell biology and technology for bioprocesses. London: Butterworth; 1989. p 442–449.
38. Adamson R. Ann Hematol 1994; 68: S9–S14.
39. Deo YM, Mahadevan MD, Fuchs R. Biotechnol Prog 1996; 12: 57–64.
40. Ray NG, Rivera R, Gupta R, Mueller D. In: Carrondo MJT, *et al*., editors. Animal cell technology. Dordrecht: Kluwer Academic; 1997. p 235–241.
41. Brown ME, Renner G, Field RP, Hassell T. Cytotechnology 1992; 9: 231–236.
42. Katinger H, Scheirer W. In: Spier RE, Griffiths JB, editors. Volume 1, Animal cell biotechnology. London, Orlando: Academic; 1985. p 167–193.
43. Birch JR, Lambert K, Boraston R, Thompson PW, Garland S, Kenney AC. In: Duarte JMC, Archer LJ, Bull AT, Holt G, editors. Perspectives in biotechnology. New York, London: Plenum; 1987. p 97–109.
44. Merchuk KC, Siegel MH. J Chem Technol Biotechnol 1988; 41: 105–120.
45. Onken U, Weiland P. Adv Biotechnol Processes 1983; 1: 67–95.
46. Katinger HWD, Scheirer W, Kromer E. Ger Chem Eng 1979; 2: 31–38.
47. Maiorella B, Inlow D, Shauger A, Harano D. Biotechnology 1988; 6: 1406–1410.
48. Arathoon WR, Birch JR. Science 1986; 232: 1390–1395.
49. Rhodes M, Birch J. Biotechnology 1988; 6: 518–523.
50. Farid SS, Washbrook J, Titchener-Hooker NJ. Biotechnol Prog 2005; 21: 486–497.
51. Singh V. Cytotechnology 1999; 30: 149–158.
52. Hyclone web information. Available at www.hyclone.com/bpc/new_prod/sub.php. Accessed 2007 Aug 21.
53. Xcellerex Inc. Web information. Available at www.xcellerex.com/images/XDR_Brochure.pdf. Accessed 2007 Aug 21.
54. Lim AC, Washbrook J, Titchener-Hooker NJ, Farid SS. Biotechnol Bioeng 2006; 93: 687–697.
55. Xie L, Zhou W. In: Ozturk SS, Hu W-S, editors. Cell culture technology for pharmaceutical and cell-based therapies. Florida: Taylor & Francis; 2006. p 155–224.
56. Wurm FM. Nat Biotechnol 2004; 22: 1393–1398.
57. Bibila TA, Robinson DK. Biotechnol Prog 1995; 11: 1–13.
58. Xie L, Wang DIC. Biotechnol Bioeng 1996; 51: 725–729.
59. Zhou W, Rehm J, Hu W-S. Biotechnol Bioeng 1995; 46: 579–587.
60. Kurokawa H, Park YS, Iijima S, Kobayashi T. Biotechnol Bioeng 1994; 44: 95–103.
61. Burky JE, Wesson MC, Young A, Farnsworth S, Dionne B, Zhu Y, Hartman TE, Qu L, Zhou W, Sauer PW. Biotechnol Bioeng 2007; 96: 281–293.
62. Zhou W, Chen C-C, Buckland B, Aunins J. Biotechnol Bioeng 1997; 55: 783–792.
63. Sauer PW, Burky JE, Wesson MC, Sternard HD, Qu L. Biotechnol Bioeng 2000; 67: 585–597.
64. Zhou W, Bibila T, Glazomitsky K, Montalvo J, Chan C, Di Stefano D, Munshi S, Robinson D, Buckland B, Aunins J. Cytotechnology 1996; 22: 239–250.
65. Wong DCF, Wong KTK, Goh LT, Heng CK, Yap MGS. Biotechnol Bioeng 2005; 89: 164–177.
66. Kompala DS, Ozturk SS. In: Ozturk SS, Hu W-S, editors. Cell culture technology for pharmaceutical and cell-based therapies. Florida: Taylor & Francis; 2006. p 155–224.
67. Genzyme Corporation Website. Available at www.genzyme.be/docs/Genzbe_0906.pdf. Accessed 2007 Aug 21.
68. Himmelfarb P, Thayer PS, Martin HE. Science 1969; 164: 555–557.
69. Voisard D, Meuwly F, Ruffieux P-A, Baer G, Kadouri A. Biotechnol Bioeng 2003; 82: 751–765.
70. Robinson DK, Memmert KW. Biotechnol Bioeng 1991; 38: 972–976.
71. Hayter PM, Curling EMA, Gould ML, Baines AJ, Jenkins N, Salmon I, Strange PG, Bull AT. Biotechnol Bioeng 1993; 42: 1077–1085.
72. Boraston R, Thompson PW, Garland S, Birch JR. Dev Biol Stand 1984; 55: 103–111.
73. Konstantinov K, Chuppa S, Sajan E, Tsai Y, Yoon S, Golini F. Trends Biotechnol 1994; 12: 324–333.
74. Riley M. In: Ozturk SS, Hu W-S, editors. Cell culture technology for pharmaceutical and cell-based therapies. Florida: Taylor & Francis; 2006. p 249–297.
75. Ozturk SS, Palsson BO. Biotechnol Prog 1991; 7: 481–494.
76. Wayte J, Boraston R, Bland H, Varley J, Brown M. Genet Eng Biotechnol 1997; 17: 125–132.
77. Borys, MC, Linzer, DIH, Papoutsakis, ET, Biotechnology 1993; 11: 720–72.
78. Osman JJ, Birch J, Varley J. Biotechnol Bioeng 2001; 75: 63–73.
79. Osman JJ, Birch J, Varley J. Biotechnol Bioeng 2002; 79: 398–407.
80. Fleischaker RJ, Sinskey AJ. Eur J Appl Microbiol Biotechnol 1981; 12: 193–197.
81. Tramper J. Cytotechnology 1995; 18: 27–34.
82. Aunins JG, Henzler H-J. In: Stephanopoulos G, editor. Volume 3, Biotechnology, Bioprocessing. Berlin: VCH; 1993. p 219–281.
83. Zhu MM, Goyal A, Rank DL, Gupta SK, Vanden Boom T, Lee SS. Biotechnol Prog 2005; 21: 70–77.
84. Kimura R, Miller WM. Biotechnol Prog 1997; 13: 311–317.
85. Gray DR, Chen S, Howarth W, Inlow D, Maiorella BL. Cytotechnology 1996; 22: 65–78.
86. Goudar CY, Matanguihan R, Long E, Cruz C, Zhang C, Piret JM, Konstantinov KK. Biotechnol Bioeng 2007; 96: 1107–1117.
87. Bloemkolk JW, Gray MR, Merchant F, Mosmann TR. Biotechnol Bioeng 1992; 40: 427–431.

88. Yoon SK, Kim SH, Lee GM. Biotechnol Prog 2003; 19: 1383–1386.
89. Trummer E, Fauland K, Seidinger S, Schriebel K, Lattenmeyer C, Kunert R, Vorauer-Uhl K, Weik R, Borth N, Katinger H, Muller D. Biotechnol Bioeng 2006; 94: 1045–1052.
90. van der Pol LA, Bonarius D, van de Wouw G, Tramper J. Biotechnol Prog 1994; 9: 504–509.
91. Murakami H, Edamoto T, Shinohara K, Omura H. Agric Biol Chem 1983; 47: 1835–1840.
92. Jo E-C, Kim D-I, Moon HM. Biotechnol Bioeng 1993; 42: 1218–1228.
93. Keen MJ. Cytotechnology 1995; 17: 193–202.
94. Zang M, Trautmann H, Gandor C, Messi F, Asselbergs F, Leist C, Fiechter A, Reiser J. Biotechnology 1995; 13: 389–392.
95. Chisti Y. Trends Biotechnol 2000; 18: 420–432.
96. Papoutsakis ET. Trends Biotechnol 1991; 9: 316–324.
97. PhRMA Report. Medicines in Development, Biotechnology. 2006. www.phrma.org.

FURTHER READING

Farid SS. Process economics of industrial monoclonal antibody manufacture. J Chromatogr B 2007; 848: 8–18.

Knablein J, editor. Modern biopharmaceuticals. Weinheim: Wiley-VCH; 2005.

Ozturk SS, Hu W-S, editors. Cell culture technology for pharmaceutical and cell-based therapies. Florida: Taylor & Francis; 2006.

2

BACULOVIRUS EXPRESSION SYSTEMS

Robert D. Possee
Centre for Ecology and Hydrology, Oxford, United Kingdom
Richard B. Hitchman
Oxford Expression Technologies Ltd., Oxford Brookes University, United Kingdom
Linda A. King
School of Life Sciences, Oxford Brookes University, United Kingdom

2.1 INTRODUCTION

Insect baculoviruses have been developed as successful expression vectors of foreign genes. This owes much to a very late phase of gene expression that is unique to the replication cycles of some insect viruses. In this phase, which occurs after the production of infectious progeny, large quantities of two virus proteins are produced in infected cells. This feature is exploited for expressing recombinant proteins using baculoviruses. They are also highly attractive as a virus-based gene expression system as baculoviruses cannot replicate in mammalian cells, which renders them a very safe system to use in low containment laboratories. Before outlining the baculovirus expression system in more detail, it is worth describing the basic elements of virus replication in insect cells so that the advantages and also the limitations of this vector can be understood more thoroughly.

2.2 BACULOVIRUS STRUCTURE AND REPLICATION

Baculoviruses comprise a family of insect viruses (Baculoviridae) that have large, double-stranded DNA genomes ranging in size from 80 to 170 kb p. They are divided into two genera: the Alphabaculoviruses, which contain the nucleopolyhedroviruses (NPVs) and the Betabaculoviruses containing granuloviruses (GVs) (1). Only NPVs have been extensively developed as expression vectors. All baculoviruses have covalently closed, circular, double-stranded DNA genomes packaged in a rod-shaped nucleocapsid. This structure, usually about 30 nm wide and 100 nm long, appears to be able to expand in length to accommodate more DNA as required. Baculovirus genome size varies considerably from 80 to 180 kbp. The prototype member of the family, *Autographa californica* multicapsid nucleopolyhedrovirus (AcMNPV) has a genome of 134 kbp and is the virus most commonly used as an expression vector. The nucleocapsid is enclosed in a lipoprotein envelope to form virus particles. These may contain more than one nucleocapsid. Numerous virus particles are then occluded within a proteinaceous matrix mostly comprising a 29 kDa polyhedrin protein. These structures are known either as occlusion bodies or polyhedra (2). They are very resistant to degradation and are thought to serve as a survival mechanism for the virus in the environment. This is essential as their susceptible hosts, which are most commonly larvae of various lepidopteran species, are not normally available continuously.

Polyhedra are consumed by insect larvae as they feed on leaf surfaces. In the midguts of these insects, which are highly alkaline, the polyhedra quickly dissolve and liberate the virus particles. These fuse with the midgut epithelial

Upstream Industrial Biotechnology: Expression Systems and Process Development, Volume 1, First Edition. Edited by Michael C. Flickinger.
© 2013 John Wiley & Sons, Inc. Published 2013 by John Wiley & Sons, Inc.

cells and release capsids into the cytoplasm. These move rapidly to the nucleus and release DNA to initiate virus replication. Virus genes are expressed in an ordered cascade of early, late, and very late phases (3). Early genes are transcribed by host RNA polymerase II and encode a number of late expression factors (19 in total), such as a virus-encoded alpha amanitin-resistant RNA polymerase, that are required for late gene expression from about 8 hours postinfection (hpi) (4). Prior to the late phase, however, virus DNA replication must be initiated. This seems to be essential for subsequent high level virus gene expression.

In the late phase, virus structural proteins are produced. These package virus DNA into capsids in the nucleus, which then exit this organelle, move to the plasma membrane, and bud from the cell to spread infection to other cells in the insect. A feature of this budded virus (BV) phenotype is that its envelope contains a major glycoprotein known as *GP64*. This serves as the attachment protein for the virus to bind uninfected cells and subsequently mediate dissemination of virus particles between cells (5). In contrast to the enveloped virus from the polyhedra, the BV does not fuse immediately with the plasma membrane but is taken up by receptor-mediated endocytosis before this vesicle fuses with an endosome. The acidic environment within the resulting structure causes fusion of the virus envelope with that of the endosome to release the capsid into the cytoplasm. This moves to the nucleus and replication continues. Within the original virus-infected cell, however, BV synthesis is replaced very late in infection by production of an enveloped virus form that remains within the nucleus. Although bounded by a lipoprotein envelope, these virus particles lack GP64. They are frequently known as occlusion-derived viruses or ODV. Their envelope contains several ODV-specific proteins, including glycoproteins that appear to be essential for attachment and entry of the virus to the insect gut (6).

From about 15 hpi, the virus-infected cell begins to produce two very late proteins: polyhedrin and *P10* (7). Both are synthesized to very high levels. The polyhedrin protein occludes a number of ODV within a crystalline matrix to form the polyhedron. Each cell nucleus may contain up to 100 polyhedra (Fig. 2.1). The role of the P10 in this process is unclear. If the *p10* gene is deleted from the virus genome, polyhedra are still formed but they appear more fragile and rupture when mechanically agitated (8). They also lack a polysaccharide envelope that normally surrounds them, which may confer on polyhedra their structural integrity (9). When most cells of the insect have been infected, the host dies and in the case of AcMNPV the cadaver liquefies. This process appears to result from the action of virus-encoded chitinase and cathepsin proteins that act in concert to reduce the structural integrity of the insect cuticle (10). The liquefaction process is important for the efficient release of polyhedra from the host. This is assumed to increase the chances of the virus encountering a new host.

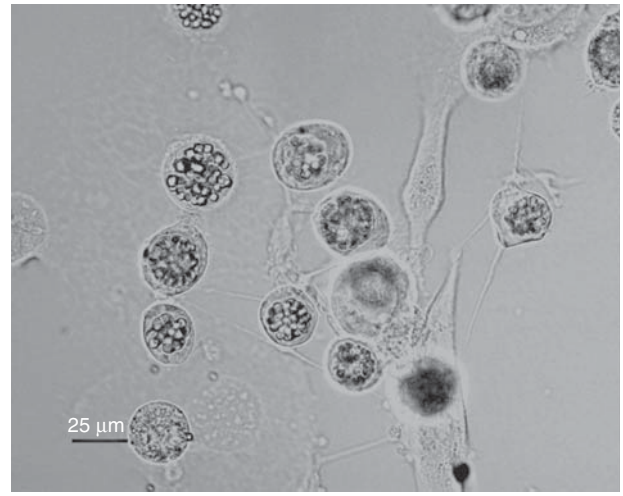


Figure 2.1. *Trichoplusia ni* 368 cells infected with AcMNPV at 60 hpi. Note the polyhedra in cells and how the nuclei have expanded to occupy most of the cytoplasm.

Baculoviruses, therefore, are unusual in that they produce two structural forms of enveloped viruses and an occluded form that packages one of these. The BV is never packaged within polyhedra and serves merely for cell to cell transmission within insects. In cell culture, only the BV phenotype is required to continue the replication cycle. Since there is no mechanism whereby polyhedra can be dissolved at physiological pH to release occluded virus, these structures are redundant in cell culture. By deleting the polyhedrin or *p10* gene coding regions and replacing them with heterologous sequences, it is possible to produce recombinant proteins in virus-infected cells (11,12).

2.3 PRODUCTION OF RECOMBINANT BACULOVIRUSES

Manipulation of baculovirus DNA is complex because of its size, which renders direct insertion of foreign genes in the manner of bacterial plasmids difficult. Despite polyhedrin and P10 proteins being synthesized to similar levels in virus-infected cells, polyhedrin has been most commonly used as a site for the insertion of foreign genes. This is a consequence of its easily visible phenotype of occlusion bodies in virus-infected cells, which is removed after insertion of a foreign coding region to render the virus polyhedrin-negative. Subsequent to this original selection system, a variety of ingenious methods has been developed to facilitate this process and some of these are summarized below.

2.3.1 Circular Virus Genomic DNA

The original methods for producing recombinant baculoviruses required the cotransfection of insect cells with circular AcMNPV DNA and a transfer vector, based on the polyhedrin gene region, which contained a foreign coding sequence (11,12). Homologous recombination between virus DNA and plasmid resulted in the replacement of the polyhedrin coding region with that of the foreign gene. This process was inefficient and required the careful separation of recombinant viruses from parental stock with the use of plaque assays. In insect cells, these can be difficult to perform and isolating a single recombinant virus could take many months of effort. The method was not easy for the nonspecialists and was a significant factor in slowing the wider adoption of the technology by non-virologists. Although p10 has a very effective gene promoter, the lack of a readily identified phenotype associated with the protein rendered it difficult to use as a site for foreign gene insertion. Clearly, if baculovirus expression vectors were to be adopted by a wider user group better methods for recombinant virus production were required.

2.3.2 Rescue of Linear Baculovirus DNA

Baculovirus DNA must be circular to initiate an infection after transfection of insect cells. However, mixing AcMNPV DNA linearized at the polyhedrin gene locus with an appropriate transfer vector resulted in the proportion of recombinant viruses rising to 30% after cotransfection of cells (13). This made their subsequent isolation in a plaque assay relatively simple. The linear virus DNA appeared to be restored to an infectious circular form after recombination with the homologous sequences in the plasmid transfer vector. Whether or not virus gene expression is required for this process is not clear. Although linearization of the virus DNA was estimated to be near 100%, a relatively high background of parental viruses suggested some religation of digested DNA within transfected cells.

This system was improved further by introducing the *Escherichia coli lac*Z coding region in lieu of polyhedrin and adding *Bsu*36I restriction enzyme sites upstream within ORF603 and downstream within ORF1629 (14). There is also a *Bsu*36I site within *lac*Z. Digestion of purified virus DNA (BacPAK6) with *Bsu*36I removed the complete *lac*Z and portions of ORFs 603 and 1629. While the putative ORF603 product is nonessential for virus replication, the protein encoded by ORF1629 is a virus structural protein (p78/80) and must be present for infectious virions to be formed. Hence, digested virus DNA, even if it relegates in transfected cells cannot initiate infectious virus production. When a transfer vector is mixed with *Bsu*36I-digested BacPAK6 DNA prior to cotransfection of insect cells, the resulting progeny virus consists of nearly 100% recombinant expression vectors.

While BacPAK6 almost guaranteed production of a recombinant virus, there was still a need to do a plaque assay and isolate clones to ensure no background contamination with the parental genome. This last obstacle to a plaque assay free recombinant expression vector selection system based on using DNA from virus particles was overcome by using *E. coli* bacmids to amplify a defective AcMNPV genome in bacteria (15,16). Essentially, this comprised the large DNA fragment generated by *Bsu*36I digestion of BacPAK6, inserted into a very low copy number bacmid vector. The bacmid DNA recovered from these cells is unable to produce infectious virus in insect cells unless mixed with a plasmid transfer vector prior to cotransfection. Consequently, all infectious virus recovered is recombinant expression vectors. A further advantage of this approach is that production of recombinant viruses can be automated using robotic liquid handling devices. This modified BacPAK6 DNA is now marketed as *flash*BAC™ by Oxford Expression Technologies, Ltd., Oxford, UK.

2.3.3 Selection of Recombinant Viruses within a Bacterial Host

Prior to the development of *flash*BAC, an alternative technology permitted the production of recombinant baculoviruses without the need to use a plaque assay for selection. A mini-F replicon, selectable antibiotic marker gene and a Tn7 transposition site were inserted into a baculovirus genome to permit low copy amplification of the virus DNA in bacteria (17). A customized plasmid transfer vector encoding Tn7 transposase functions and a foreign gene was then used to transform bacteria containing this modified genome. Transposition of DNA sequences from the plasmid to the virus genome results in foreign gene insertion at the polyhedrin locus of AcMNPV between the left and right arms of Tn7. The recombinant clones are then selected on agar plates containing appropriate antibiotics. Subsequent amplification of the bacteria and recovery of recombinant virus DNA via a simplified alkaline lysis method facilitates transfection of insect cells to produce infectious BV. This system has been a mainstay in many laboratories using baculovirus expression systems for many years. It is marketed as Bac-to-Bac™ by Invitrogen Ltd. The transfer vectors used for transposition in bacteria are not compatible with the systems described above in the section Rescue of Linear Baculovirus DNA.

2.3.4 Manipulation of Baculovirus DNA *In Vitro*

Digestion of baculovirus vectors with restriction enzymes and subsequent direct insertion of foreign genes to place them under the control of the polyhedrin gene promoter

was explored as a method for construction of recombinant viruses (18,19). However, since ligation reactions are rarely 100% efficient, plaque assays of virus progeny was still required to ensure genetic homogeneity of the recombinant expression vector.

The most successful system to date for making recombinant baculovirus genomes *in vitro* is the BaculoDirect, marketed by Invitrogen Ltd. It is also compatible with Gateway® clones since the parental virus contains *att*R sites. The system is based on the use of ganciclovir (9-[1,3-Dihydroxy-2-propoxy)methyl] guanine). Ganciclovir is a nucleoside analog, which is phosphorylated by the product of the herpes virus simplex virus type 1 (HSV-1) thymidine kinase (*tk*) gene. The phosphorylated active analog incorporates into DNA and inhibits DNA replication. If a baculovirus is used to express *tk* in insect cells, virus replication is sensitive to ganciclovir. The parental baculovirus genome contains the *att*R sites for Gateway recombination flanking the HSV1-*tk*, which is regulated by the AcMNPV *ie-0* promoter. This promoter is active in the early phase of virus replication with transcription initiated immediately after entry of virus DNA to the insect cell nucleus. Also flanked by the *att*R sites is a copy of the β-galactosidase coding region regulated by the p10 promoter, which is active in the very late phase of virus gene expression. The BaculoDirect linear DNA is mixed with a donor Gateway vector in a 1 h enzymatic reaction and replacement of both HSV1-*tk* and β-galactosidase with the foreign gene is achieved. Removal of HSV1-*tk* causes the virus to be insensitive to ganciclovir after the genome is used to transfect insect cells (20). Removal of β-galactosidase provides another level of selection. The advantage of this system is that baculovirus genome manipulation is done *in vitro* without the need to use bacterial cells. Plaque assay purification of virus after transfection of insect cells is also not required.

2.4 BACULOVIRUS TRANSFER VECTORS

A very important component of baculovirus expression vectors are the plasmid transfer vectors used to convey the desired foreign gene into the virus genome, either in insect or bacterial cells or *in vitro* via BaculoDirect. These may contain a range of baculovirus gene promoters, sequences encoding peptide tags to aid downstream protein purification, and protease cleavage sites for removal of such tags at the appropriate time. Such regions are flanked by other sequences homologous to the baculovirus genome, so that recombination can direct their insertion into the recipient virus. Most have been developed for use with either circular or linear baculovirus DNA but some of the recombinant virus selection systems, such as Bac-to-Bac and BaculoDirect require a different set of plasmids. Many of the transfer vectors currently available commercially are summarized in Table 2.1. Some of the key vectors are described in the sections below. Care must be taken to use them with the appropriate parental virus DNA. Others were developed in the 1980s and 1990s in academic laboratories but may be difficult to obtain now.

2.4.1 Vectors for Use With Circular or Linear Virus Genomes

The original AcMNPV transfer vectors consisted of partial or complete deletions of the polyhedrin coding region. The polyhedrin gene promoter and transcriptional terminator sequences were left largely intact. However, it is interesting that the very first polyhedrin transfer vector described had all of the promoter removed but was still able to produce recombinant interferon in insect cells (11). Subsequent analysis of the AcMNPV polyhedrin gene promoter showed that it was essential to retain the TAAG motif about 50 nucleotides upstream from the ATG of the native coding region and the intervening sequences to achieve maximum gene expression (22,23). A burst sequence associated with very late gene expression was also identified just upstream of the polyhedrin ATG (24). Generally, if polyhedrin gene-based transfer vectors contain the complete 5′ noncoding gene region then, maximum foreign gene expression will be attained when it is introduced into the parental virus. Some plasmid transfer vectors have gone one stage further in retaining part of the polyhedrin gene coding region, albeit with a mutated ATG (17), which is claimed to enhance foreign gene expression further.

All of the early baculovirus transfer vectors required that the inserted foreign gene coding region donated its own ATG codon to ensure translation initiation. Most only had a single restriction site for the insertion of the recombinant DNA sequences. Later versions of these reagents added multiple cloning sites for more convenient ligation of DNA fragments. Early transfer vectors were also quite large, with ~7 kbp of AcMNPV DNA spanning the polyhedrin gene region inserted into a base vector such as one of the pUC series. This could cause some difficulties in inserting larger foreign genes. The size of these vectors is now much reduced with examples such as pBacPAK8/9 at about 5.5 kbp. There is probably still some scope for reducing this size further.

The use of fusion vectors has also become widespread. These may be composed of plasmids with a short sequence encoding a signal peptide coding region to direct recombinant proteins to the endoplasmic reticulum of recombinant virus-infected cells. Several different signal peptides are in use, which include AcMNPV GP67 (25) and honey bee mellitin (26). Further fusions have been made with peptide tags such as histidine residues at the N or C termini of the protein. These are intended to aid protein purification

TABLE 2.1. Commercially Available Transfer Vectors

Type (Gene Locus)	Vector (Size)	Promoter(s)	Insertion Sites/Other Features	Additional Features	Supplier	Parental Virus (Source)
Single promoter (*polyhedrin*)	pFastBac™1 (4.8 kbp)	*Polyhedrin*	*Bam*H I, *Rsr* II, *Bss*H II, *Eco*R I, *Stu* I, *Sal* I, *Sst* I, *Spe* I, *Not* I, *Nsp*V, *Xba* I, *Pst* I, *Xho* I, *Sph* I, *Kpn* I, *Hin*d III	—	Invitrogen	Bac-to-Bac[a]
	pFastBacHT (4.8 kbp)		ATG, 6x His tag-TEV protease cleavage site, *Nhe* 1, *Nco* I, *Bam*H I, *Eco*R I, *Stu* I, *Sal* I, *Sst* I, *Spe* I, *Not* I, *Nsp* V, *Xba* I, *Pst* I, *Xho* I, *Sph* I, *Kpn* I, *Hin*d III	—		
Multiple promoter (*polyhedrin*)	pFastBacDual (5.2 kbp)	*Polyhedrinp10*	*Bam*H I, *Rsr* II, *Bss*H II, *Eco*R I, *Stu* I, *Sal* I, *Sst* I, *Spe* I, *Not* I, *Nsp* V, *Xba* I, *Pst* I, *Hin*d III*Bbs* I, *Sma* I, *Xho* I, *Nco* I, *Nhe* I, *Pvu* II, *Nsi* I, *Sph* I, *Kpn* I.	Dual expression from polyhedrin and p10 gene promoters		
Single promoter (*polyhedrin*)	pDEST™8 (6.5 kbp)pDEST10 (6.7 kbp)pDEST20 (7.0 kbp)	*Polyhedrin*	Gateway™ entry siteGateway entry site N-term. 6x His tagGateway entry site N-term. Glutathione-S-transferase (GST)	Insert genes from Gateway entry vectors, such as pENTR™		
	pVL1392 (9.6 kbp)	*Polyhedrin*	*Bgl* II, *Pst* I, *Not* I, *Eag* I, *Eco*R I, *Xba* I, *Sma* I, *Bam*H I	—	BD Biosciences Pharmingen	AcMNPV (wild-type virus DNA)BacPAK6 (14)BaculoGold (BD Biosciences Pharmingen)Bac1000Bac2000 Bac3000 The latter two virus DNAs have AcMNPV gene deletions (Novagen) *flashBAC* Cloned version of AcMNPV unable to replicate in insect cells unless rescued with appropriate transfer vector. (Oxford Expression Technologies Ltd.)
	pVL1393 (9.6kbp)	*Polyhedrin*	*Bam*H I, *Sma* I, *Xba* I, *Eco*R I, *Not* I, *Eag* I, *Pst* I, *Bgl* II	—		
	pAcG1 (8.5 kbp)	*Polyhedrin*	ATG, GST, *Bam*H I, *Sma* I, *Eco*R I	—		
	pAcG2 (8.5 kbp)	*Polyhedrin*	ATG, GST, Thrombin cleavage-*Bam*H I, *Sma* I, *Eco*R I	—		
	pAcG3X (8.5 kbp)	*Polyhedrin*	ATG, GST, Factor Xa cleavage, *Bam*H I, *Sma* I, *Eco*R I	—		

(*continued*)

TABLE 2.1. (*Continued*)

Type (Gene Locus)	Vector (Size)	Promoter(s)	Insertion Sites/Other Features	Additional Features	Supplier	Parental Virus (Source)
	pAcGHLT-A (8.7 kbp)	*Polyhedrin*	ATG, GST, *Bam*H I-6x His tag, Protein kinase A site, Thrombin cleavage-*Nde* I, *Eco*R I, *Stu* I, *Nco* I, *Sac* I, *Not* I, *Sse*8387 I, *Pst* I, *Kpn* I, *Sma* I, *Bgl* II	—		
	pAcGHLT-B (8.7 kbp)	*Polyhedrin*	ATG, GST, *Bam*H I, 6x His tag-Protein kinase A site, Thrombin cleavage-*Xho* I, *Eco*R I, *Stu* I, *Nco* I, *Sac* I, *Not* I, *Sse*8387 I, *Pst* I, *Kpn* I, *Sma* I, *Bgl* II	—		
	pAcGHLT-C (8.7 kbp)	*Polyhedrin*	ATG, GST, *Bam*H I, 6x His tag-Protein kinase A site, Thrombin cleavage, *Nde* I, *Xho* I, *Eco*R I, *Stu* I, *Nco* I, *Sac* I, *Not* I, *Sse*8387I, *Pst* I, *Kpn* I, *Sma* I, *Bgl* II	—		
	pAcHLT-A (8.1 kbp)	*Polyhedrin*	ATG, GST, *Bam*H I, 6x His tag, Protein kinase A site-Thrombin cleavage, *Nde* I, *Eco*R I, *Stu* I, *Nco* I, *Sac* I, *Not* I, *Sse*8387 I, *Pst* I, *Kpn* I, *Sma* I, *Bgl* II	A, B, and C represent three different reading frames and also contain slightly different restriction sites		
	pAcHLT-B (8.1 kbp)	*Polyhedrin*	ATG, GST, *Bam*H I, 6x His tag, Protein kinase A site, Thrombin cleavage-*Xho* I, *Eco*R I, *Stu* I, *Nco* I, *Sac* I, *Not* I, *Sse*8387 I, *Pst* I, *Kpn* I, *Sma* I, *Bgl* II			
	pAcHLT-C (8.1 kbp)	*Polyhedrin*	ATG, GST, 6x His tag, Protein kinase A site, Thrombin cleavage site, *Nde* I, *Xho* I, *Eco*R I, *Stu* I, *Nco* I, *Sac* I, *Not* I, *Sse*8387 I, *Pst* I, *Kpn* I, *Sma* I, *Bgl* II			
Multiple promoter (*Polyhedrin*)	pAcUW21 (9.2 kbp)	*Polyhedrin p10*	*Pac* I, *Bgl* II, *Eco*R I	Polyhedrin gene intact; foreign gene expression from *p10* promoter		
	pAcUW51 (5.8 kbp)	*Polyhedrin p10*	*Bam*H I*Bg*l II, *Eco*R I	Dual expression vector from polyhedrin and p10 promoters		
	pAcAB3 (10.1 kbp)	*P10Polyhedrin p10*	*Sma* I, *Bam*H I*Xba* I, *Stu* I*Bgl* II, *Esp* I	Triple expression vector from polyhedrin and 2x p10 promoters		

	pAcDB3 (6.0 kbp)	*P10Polyhedrin p10*	*Sma* I, *Bam*H I*Xba* I, *Stu* I*Bgl* II, *Eco*R I	Triple expression vector from polyhedrin and 2x p10 promoters. Smaller version of pAcAB3	
	pAcAB4 (10.2 kbp)	*Polyhedrinp10 Poly-hedrinp10*	*Bam*H I*Sma* I*Xba* I, *Stu* I*Bgl* II, *Eco*R I, *Esp* I	Quadruple expression vector from 2x polyhedrin and 2x p10 promoters	
Single promoter (*Polyhedrin*)	pBAC-1 (5.3 kbp)	*Polyhedrin*	*Bam*H I, *Stu* I, *Eco*R I, *Sac* I, *Hin*d III, *Eag* I, *Not* I, *Ava* I, *Xho* I, 6x His tag, *Sty* I, *Avr* II, *Bpu* 1102, *Sph* I		Novagen
	pBacgus-1 (7.4 kbp)	*Polyhedrin*	*Bam* HI, *Stu* I, *Eco*R I, *Sac* I, *Hin*d III, *Eag* I, *Not* I, *Ava* I, *Xho* I, 6x His tag, *Sty* I, *Avr* II, *Bpu* 1102, *Sph* I	B-glucuronidase under *p6.9* promoter control to monitor recombinant virus production	
	pBAC-2cp (5.4 kbp)	*Polyhedrin*	*Nco* I, 6x His tag, *Sac* II, thrombin cleavage site, S tag, *Pfl*M I, *Nhe* I, enterokinase cleavage site, Ligation-Independent Cloning (LIC) site, *Sma* I, *Srf* I, *Bse*R I, *Stu* I, *Bam*H I, *Eco*R I, *Sac* I, *Hin*d III, *Eag* I, *Not* I, *Xho* I, 6x His tag, *Avr* II, *Bpu*1102 I, *Sph* I	An LIC version of the vector is available for directional cloning PCR products.	
	pBacgus-2cp (7.6 kbp)	*Polyhedrin*	*Nco* I, 6x His tag, *Sac* II, thrombin cleavage site, S tag, *Pf*M I, *Nhe* I, enterokinase cleavage site, LIC site, *Sma* I, *Srf* I, *Bse*R I, *Stu* I, *Bam*H I, *Eco*R I, *Sac* I, *Hin*d III, *Eag* I, *Not* I, *Xho* I, 6x His tag, *Avr* II, *Bpu*1102 I, *Sph* I	An LIC version of the vector is available for directional cloning PCR products. B-glucuronidase under *p6.9* promoter control to monitor recombinant virus production	
	pBAC-3 (5.5 kbp)	*Polyhedrin*	Gp64 signal peptide, *Nco* I, 6x His tag, *Sac* II, thrombin cleavage site, S tag, *Pfl*M I, *Nhe* I, enterokinase cleavage site, *Sma* I, *Srf* I, *Bse*R I, *Stu* I, *Bam*H I, *Eco*R I, *Sac* I, *Hin*d III, *Eag* I, *Not* I, *Xho* I, 6 x His tag, *Avr* II, *Bpu*1102 I, *Sph* I		

(*continued*)

TABLE 2.1. (*Continued*)

Type (Gene Locus)	Vector (Size)	Promoter(s)	Insertion Sites/Other Features	Additional Features	Supplier	Parental Virus (Source)
Multiple promoter (*polyhedrin*)	pBAC4x-1 (5.9 kbp)	*P10Polyhedrin p10Polyhedrin*	*Bgl* II, *Eco*R I, *Bsu*36 I*Xba* I, *Stu* I*Sma* I, *Spe* I*Bam*H I, *Hin*d III, *Eag* I, *Not* I, *Xho* I 6x His tag, *Sty* I, *Bpu*1102 I, *Sph* I	Quadruple expression vector from 2x polyhedrin and 2x p10 promoters.		
	pBACgus4x-1 (8.1 kbp)	*P10Polyhedrin p10Polyhedrin*	*Bgl* II, *Eco*R I, *Bsu*36 I*Xba* I, *Stu* I*Sma* I, *Spe* I*Bam*H I, *Hin*d III, *Eag* I, *Not* I, *Xho* I 6x His tag, *Sty* I, *Bpu*1102 I, *Sph* I	Quadruple expression vector from 2x polyhedrin and 2x p10 promoters. B-glucuronidase under *p6.9* promoter control to monitor recombinant virus production		
Single promoter (*polyhedrin*)	pBAC-5 (5.5 kbp)	*Gp64*	*Nco* I, 6x His tag, *Sac* II, Thrombin cleavage site, S tag, *Pfl*M I[b], *Nhe* I, enterokinase cleavage site, *Sma* I, *Srf* I, *Bse*R I, *Stu* I, *Bam*H I, *Eco*R I, *Sac* I, *Hin*d III, *Eag* I, *Not* I, *Xho* I, 6x His tag, *Avr* II, *Bpu*1102 I, *Sph* I	Has early/late *gp64* promoter but no signal peptide coding region		
	pBACgus-5 (7.7 kbp)	*Gp64*	*Nco* I, 6x His tag, *Sac* II, Thrombin cleavage site, S tag, *Pfl*M I[b], *Nhe* I, enterokinase cleavage site, *Sma* I, *Srf* I, *Bse*R I, *Stu* I, *Bam*H I, *Eco*R I, *Sac* I, *Hin*d III, *Eag* I, *Not* I, *Xho* I, 6x His tag, *Avr* II, *Bpu*1102 I, *Sph* I	B-glucuronidase under *p6.9* promoter control to monitor recombinant virus production. Has early/late gp64 promoter but no signal peptide coding region		
	pBAC-6 (5.6 kbp)	*Gp64*	GP64 signal sequence, *Nco* I, 6x His tag, *Sac* II, Thrombin cleavage site, S tag, *Pfl*M I[b], *Nhe* I, enterokinase cleavage site, *Sma* I, *Srf* I, *Bse*R I, *Stu* I, *Bam*H I, *Eco*R I, *Sac* I, *Hin*d III, *Eag* I, *Not* I, *Xho* I, 6x His tag, *Avr* II, *Bpu*1102 I, *Sph* I	Has early/late gp64 promoter and signal peptide coding region		

	pBACgus-6 (7.7 kbp)	*Gp64*	GP64 signal sequence, *Nco* I, 6x His tag, *Sac* II, Thrombin cleavage site, S tag, *Pfl*M I[b], *Nhe* I, enterokinase cleavage site, *Sma* I, *Srf* I, *Bse*R I, *Stu* I, *Bam*H I, *Eco*R I, *Sac* I, *Hin*d III, *Eag* I, *Not* I, *Xho* I, 6x His tag, *Avr* II, *Bpu*1102 I, *Sph* I	Has early/late gp64 promoter and signal peptide coding region. B-glucuronidase under *p6.9* promoter control to monitor recombinant virus production		
	pBACsurf-1 (9.4 kbp)	*Polyhedrin*	*Spe* I, gp64 signal sequence, *Pst* I, *Kpn* I, Sma I, gp64 coding region	Designed for incorporating target proteins on the virion surface by utilizing gp64 signal sequence and membrane anchor region		
Single promoter (*p10*)	pAcUW1 (4.6 kbp)	*p10*	*Bg*l II, *Hin*d III	—	(21)	AcUW1.lacZ virus DNA linearized with *Bsu*36 I (21)
Multiple promoter (*p10*)	pAcUW42 (7.1 kbp)	*p10Polyhedrin*	*Bgl* II, *Pst* I, *Not* I, *Xba* I, *Kpn* I, *Sma* I*Bam*H I	—	BD Biosciences-Pharmingen	
	pAcUW43 (7.1 kbp)	*p10Polyhedrin*	*Sma* I, *Kpn* I*Xba* I, *Not* I, *Pst* I, *Bgl* II*Bam*H I	—		

[a]Supplied in *E.Coli* (17: Invitrogen).
[b]Within S tag.

from virus-infected cells. Such fusions leave some extra amino acids at either end of the recombinant protein, hence, other vectors include appropriately sited protease cleavage sites to facilitate postpurification cleavage from the isolated molecules (27).

Most baculovirus transfer vectors are intended for the insertion and expression of single foreign genes within AcMNPV. If more than one gene is to be expressed then, specialized vectors can be used that allow for the insertion of 2–5 foreign genes at the polyhedrin gene locus. These use multiple copies of the polyhedrin or p10 gene promoters assembled in tandem or reverse orientation. Transcription terminators such as those from Simian virus 40 or beta globin are used to minimize polycistronic mRNAs (28).

Although most baculovirus transfer vectors are based on the polyhedrin gene locus, an alternative for the insertion of foreign genes is the *p10* gene region. This has the disadvantage of lacking a readily selectable marker for screening recombinant viruses, but this was circumvented by inserting the lacZ coding region for blue white selection of recombinant plaques. This coding region also contains a *Bsu*36I restriction enzyme site, hence, it is also possible to linearize virus DNA prior to cotransfection with the transfer vector (21). With the use of available transfer vectors it is feasible to insert up to seven genes within the AcMNPV genome.

2.4.2 Transfer Vectors for the Bac-to-Bac System

Transfer vectors for use with Bac-to-Bac are specific for this system. They are incompatible with either circular or linear DNA methods described in the section titled Circular Virus Genomic DNA or Rescue of Linear Baculovirus DNA. The base vector is pFastBac1. A derivative, pFastBacHT, has a histidine tag coding region with a protease cleavage site. The pFastBacDual has both polyhedrin and *p10* gene promoters for coexpression of two genes. All three vectors have a variety of cloning sites for insertion of coding sequences.

2.4.3 Transfer Vectors for Baculo Direct

Unlike other technologies for making recombinant baculoviruses, the use of BaculoDirect requires a slightly different approach. Gene constructs derived via PCR (polymerase chain reaction) are cloned into a Gateway entry vector. These sequences can then be transferred *in vitro* to any of the other compatible plasmids. The introduction of genes into the baculovirus is also done *in vitro*, with subsequent transfection of insect cells with recombinant DNA to make the infectious stock. Despite the ease of use, the system does not have the flexibility of numerous transfer vectors to achieve expression of foreign genes with different peptide tags or promoters. There are three BaculoDirect constructs available. These facilitate N-terminal tagging of proteins with V5-His tags, C-terminal tagging with V5-His tags and a combination of N-terminal V5-His tagging, and an N-terminal honeybee melittin secretion signal for improved protein secretion.

2.5 MODIFYING THE BACULOVIRUS GENOME TO IMPROVE PROTEIN PRODUCTION

Most parental baculovirus genomes used for foreign gene expression are only modified at the polyhedrin gene locus. The remaining 154 potential ORFs are unchanged in the expression vector subsequent to foreign gene insertion. Although the function of some baculovirus genes has been determined, many are uncharacterized with little idea of how their products might affect recombinant protein production. Essentially, many baculovirus expression vectors are simply wild type polyhedrin-negative genotypes containing a foreign gene that are still able to cause the full pathology associated with baculovirus infection in insects.

The discovery that baculoviruses encode chitinase and cathepsin, which result in liquefaction of the insect larval host, suggested that removal of these genes might improve recombinant protein production. Deletion of the cathepsin gene from *Bombyx mori* NPV demonstrated that recombinant protein degradation in virus-infected insects was reduced (29). Chitinase appears to accumulate in the endoplasmic reticulum of AcMNPV-infected cells. Deletion of the chitinase and cathepsin genes from AcMNPV results in greatly improved secretion and stability of recombinant proteins (15). Commercial expression vectors based on these gene deletions are available as flashBACGOLD from Oxford Expression Technologies Ltd., Oxford, UK.

2.6 INSECT CELL CULTURE

Considerable progress in the use of insect cell lines to host production of recombinant proteins with baculovirus expression vectors has been made in recent years. The first continuous insect cell line was derived from *Trichoplusia ni* (30). Since then, over 50 lepidopteran species have been used to establish more cell lines from embryonic, larval, pupal, and adult sources of tissue. For baculovirus expression, the most commonly used cell lines are from *T. ni* (31) or *Spodoptera frugiperda* (32). Originally, these cell lines were cultured in medium containing serum, but more recently many applications have moved to using defined, serum-free media.

2.6.1 Culturing Cells in Serum-Containing Medium

Cell lines from *T. ni* or *S. frugiperda* are most often propagated using medium such as TC100 (33) supplemented with

foetal bovine serum (FBS). This replaced many early insect media formulations that used insect hemolymph as a growth supplement, which was difficult to obtain in large quantities. While the addition of FBS makes the final medium less defined, it does alleviate problems such as the shear sensitivity of insect cells and affords some masking of proteases that can degrade recombinant proteins.

One of the most commonly used insect cell lines for work with baculoviruses is *S. frugiperda* Sf21, which was derived from ovarian tissue (32). This is generally propagated in TC100 containing 10% FBS, although it will tolerate 5% serum. The cells can be grown in monolayers attached to a plastic or glass surface or in suspension as spinner cultures where densities can reach 2×10^6 cells/mL before viability starts to decline. One of the major advantages of many insect cells is that when grown as monolayers they can be readily harvested by scraping from the surface that has supported their growth. Unlike most mammalian cells they do not need to be detached using trypsin. However, a few cell lines such as those from *Heliothis virescens* do need to be removed from a solid support using trypsinization (34). They can also be propagated in suspension and then returned to monolayers for specific experiments. Originally, most recombinant AcMNPV were produced using Sf21 cells. However, one of the perceived disadvantages of these cells is that they consist of a mixed population from the original source of tissue. A cloned cell line was derived from Sf21 cells and designated Sf9 (35). This has become the cell line of choice in many laboratories for working with recombinant baculoviruses.

Adult *T. ni* ovaries were the source of tissue used to derive TN-368 cells (36), which are also commonly used to propagate AcMNPV. A cell line with enhanced characteristics for recombinant protein production was originally isolated from *T. ni* embryonic tissues as BTI-Tn-5B1-28 (31). A clone derived from this was designated BTI-TN5B1-4. This cell line is generally better for producing secreted glycoproteins. More recently, it was designated for commercial purposes as High-Five™ from Invitrogen Ltd. Although cell lines derived from *T. ni* offer significant advantages over others for recombinant protein production, care must be exercised in using them. Serial propagation of AcMNPV in *T. ni* cells in culture results in the rapid selection of virus mutants with either deletions, insertions, or single nucleotide changes in the *FP-25* gene, which encodes a 25K protein (37–39). Such mutations result in the few polyhedra or FP phenotype since transcription from the polyhedrin gene promoter is reduced. Interestingly, transcription of p10 remains unaffected by such mutations in FP-25 (40).

2.6.2 Culturing Insect Cells in Serum-Free Medium

The use of FBS solved many of the earlier problems associated with formulating efficient insect cell culture media. However, it also added a level of uncertainty in that serum can vary in quality from batch to batch, requiring testing prior to purchasing a large stock. Also, as more users needed to purify protein from insect cell cultures infected with recombinant baculoviruses the presence of animal serum was a complicating factor. Even minor traces of serum components are undesirable if the purified protein is to be used to analyze its function or tested in clinical trials. The fears of contamination of serum with agents such as bovine spongiform encephalopies made the development of defined, animal product-free media a priority. Several serum-free media are now available from various suppliers such as Invitrogen and Sigma. Their development began with the formulation of IPL-41 and its derivatives (40,41). Frequently, these media allow higher cell densities ($>10^7$ cells/mL) to be attained in suspension cultures, hence improving the productivity of the baculovirus expression system (42). One of the few problems associated with their use is that Sf9 cells grown as a monolayer are susceptible to shear damage when scraped from a plastic flask. Instead, cells must be removed from the support by vigorous tapping. This is most successful when the cells are confluent.

2.6.3 Modification of Insect Cell Lines to Improve Recombinant Protein Production

While baculovirus-infected cells are able to perform many of the posttranslational modifications to recombinant proteins to confer biological activity, these products may not be identical to the same proteins made in mammalian cells. Although the very high levels of expression of recombinant proteins using the baculovirus system are one of its strengths, it may be difficult for the host cell to process accurately the mass of protein produced. Host cell gene expression is repressed in baculovirus-infected cells (43,44). Hence there may be a diminishing pool of proteins available to modify recombinant molecules very late in virus replication.

A major difference between insect and mammalian cells concerns the production of *N*-glycosylated proteins. In insect cells the *N*-glycans are usually high-mannose in content with no terminal sialic acid residues (45). They are relatively simple and short structures. However, in mammalian cells the original *N*-glycan is extended by glycosyltransferases. The *N*-glycan may also terminate with a sialic acid residue to confer a negative charge. Terminal sialylation blocks the removal of glycoproteins by carbohydrate-specific receptors in mammalian species (46). Consequently, recombinant glycoproteins produced using the baculovirus system, which lack the N-terminal sialic acid are unlikely to persist for long in mammals (47). This would have serious consequences for therapeutic glycoproteins.

These problems with glycoproteins were addressed by genetically modifying the insect host cell so that it constitutively expressed genes encoding mammalian glycosyltransferases. The Sf9 cell line was transformed with a plasmid-based vector containing β1,4-galactosyltransferase coding region under the control of the AcMNPV *ie-1* gene promoter (48). When this cell line was infected with AcMNPV, the virus glycoprotein GP64 contained β-linked galactose residues. Further modification of this cell line with an α2,6,-sialyltransferase gene resulted in the production of GP64 with a terminal sialic acid (49). The system was extended by introducing a range of mammalian glycosyltransferase genes into Sf9 cells to derive SfSWT-1, which was able to produce complex, biantennary *N*-glycans with sialic acid at the α3 branch and galactose at the α6 branch (50). Clearly, there is considerable scope for adapting insect cells to ensure that they produce recombinant proteins that are more similar to their native mammalian form compared to those produced in unmodified hosts.

2.6.4 Scaling Up Insect Cell Cultures

Insect cell lines, particularly Sf9, can be cultured using a wide variety of formats in monolayer or suspension. Prior to the advent of serum-free media, scale up was an issue because early formulations such as TC100 containing FBS proved unable to support culture volumes greater than 1000 ml in spinner/suspension. Insect cells have a high demand for oxygen and the bubbling of gas through the cultures resulted in foaming and shearing of the insect cells. However, present day serum-free media have solved many of these problems and it is now possible to use large (>10 L) bioreactors for producing recombinant proteins. These instruments have sophisticated monitors for pH, temperature, nutrients, and oxygenation to ensure optimal conditions for growing the cells.

On a smaller scale it is possible to use simple shake cultures to propagate virus-infected cells, which may be particularly attractive to the academic user. It is also feasible to use the Wave Bioreactor™ technology (GE Healthcare), where simple sterile plastic bags containing medium are rocked on a wave platform to ensure adequate agitation of cells and oxygenation during growth (51). These bags may contain 100 mL–500 L working volumes, providing considerable flexibility to the user. The bags are disposable and therefore, may be replaced almost immediately when one is harvested. This avoids the need to clean and sterilize a dedicated glass bioreactor system. They may also contain sophisticated controls to regulate growth conditions as described above.

Thus, the baculovirus insect cell culture system can be operated at a wide variety of scales for production of recombinant proteins. Very simple sterile plastic or glass flasks or large volume agitated bioreactors can be employed. Most laboratories with facilities for bacterial or mammalian cell culture can usually adapt their facilities to grow insect cells.

2.7 BACULOVIRUSES FOR GENE EXPRESSION IN MAMMALIAN CELLS

One of the primary features of baculoviruses as biocontrol agents is that they cannot cause an infection in human cells. However, it has been known for many years that AcMNPV BV can enter these cells, although no cytopathic effect has been observed (52,53). Whether or not this counts as an "infection" is debatable. The requirement for a safe way to transduce mammalian cells for gene expression or therapy led to the development of suitably modified baculovirus vectors containing mammalian gene promoters (54,55). BacMam technology is based on the Bac-to-Bac system in *E. coli* (17). The pFastBac transfer vectors used to create recombinant baculoviruses in bacterial cells are modified so as to contain the cytomegalovirus (CMV) immediate early gene (CMV) promoter which is active in mammalian cells. These are then introduced into the baculovirus genome via the normal transposition method and subsequently used to infect insect cells. The resulting BacMam particles are generally concentrated prior to use to improve the efficiency of introducing them into mammalian cells.

BacMams can transduce a wide range of mammalian cells (56) including the commonly used Human embryonic kidney (HEK) 293, Chinese hamster ovary (CHO), COS-1, Sarcoma osteogenic (Saos) -2, and Human Bone Osteosarcoma epithelial (U2-OS) lines as well as nondividing cells (55). However, transduction efficiencies may vary considerably depending on cell type and can be as high as 95% for Baby hamster kidney (BHK) cells or below 10% for mouse embryonic fibroblast (NIH-3T3), or cells of hematopoietic origin (56,57). Entry of baculovirus to mammalian cells is thought to be similar to that of insect cells, by receptor-mediated adsorptive endocytosis. However, the mechanisms responsible for intracellular trafficking and nuclear entry still remain to be elucidated, and it is likely that these are the stages where efficient transduction and recombinant expression are blocked (58). Various methods have been described in the literature to improve delivery and expression of foreign genes by BacMams: for example, using phosphate-buffered saline (PBS) in place of culture media and longer transduction incubation times at lower temperatures (59,60). Treatment of transduced cells with histone deacetylase inhibitors, such as butyrate, trichostatin A (TSA), or valproic acid has also been used to enhance recombinant expression. The observed increase in expression may be the result of an association between the BacMam DNA and histones or histone-like proteins, which can upregulate transcription, depending on their acetylation status (56,61,62), although cytotoxicity is often associated

with the use of these drugs (61). Promoter choice can also play a role. For example, the hybrid CAG promoter, consisting of the chicken β-actin promoter fused to a CMV immediate early enhancer element, showed increased reporter expression in human epithelial cervical carcinoma (HeLa) cell line and COS-1 cells when compared with a CMV promoter (63). It has been speculated that incorporating additional copies of baculovirus genes, such as the AcMNPV homologous region (*hr1*) (64) could be beneficial in enhancing promoter transcriptional activity (65). Indeed, overexpression of the baculovirus GP64 envelope protein showed increased reporter gene expression in Human hepatocellular liver carcinoma (HepG2) cells (66,67). Pseudotyping baculoviruses by introducing heterologous viral envelope proteins such as the vesicular stomatitis virus G protein (VSV G) and the rabies virus G glycoprotein (RVG) have also improved transduction efficiency, probably by augmenting gp64-mediated endosomal release (58,68). Pseudotyping was also used to overcome complement-mediated inactivation, which has removed the primary barrier to using baculoviruses for gene therapy (69). However, regardless of these improvements to the system, there still remains much to be done to universally improve the efficiency of BacMam transduction and expression.

Despite this bottleneck in efficiency, BacMams still offer many advantages over transient transfection and mammalian viral vector-based assays. These include a better biosafety profile (BacMams are inactivated by human complement and classified as Biosafety Level 1), no environmental risk (the vector is polyhedrin-negative), reduced cost (no transfection reagents are required, large-scale plasmid DNA purification etc.), no reagent cytotoxicity (as is observed with many transfection reagents), and no transient expression that facilitates expression of toxic proteins. BacMams are also easily generated and production can be rapidly scaled up, can simultaneously deliver multiple genes (70) for coexpression, and are highly adaptable to high throughput screening assays. It is also possible to control the expression level of the target gene by varying the virus dose applied to the cells (i.e., for modulating receptor coupling). As such, BacMam technology is being increasingly used for the development of pharmacologically relevant assays for drug discovery, particularly for membrane proteins such as G-protein coupled receptors (GPCRs), ion channels, transporters, nuclear receptors, and viral targets (71).

2.8 CONCLUSION

Baculoviruses have provided a durable and reliable system for the production of recombinant proteins in insect cells for over 25 years. Despite the early problems for the nonexperts in insect virology in selecting recombinant viruses, several user-friendly systems are now available that permit rapid and efficient insertion of foreign genes into the baculovirus genome. Many of these are available commercially in kit form. Accompanying developments in insect cell cultures and media mean that very high cell densities can now be achieved with concomitant yields of recombinant protein. These improved cells and media are also very simple to use and require little specialized equipment. Finally, the use of baculoviruses as biological insecticides was founded on the idea that they are nonpathogenic for higher vertebrates. This feature of their safety has been further exploited in the development of vectors for transduction of human cells, where they show great promise as a vector for gene therapy.

REFERENCES

1. Carstens EB, Ball LA. Arch Virol 2009; 154: 1181–1188.
2. Funk CJ, Braunagel SC, Rohrmann GF. In: Miller LK, editor. The baculoviruses. New York, London: Plenum; 1997. p 7–32.
3. Kelly DC, Lescott T. Microbiologica 4: 35–57.
4. Rapp JC, Wilson JA, Miller LK. J Virol 72: 10,197–10,206.
5. Monsma SA, Oomens AGP, Blissard GW. J Virol 1996; 70: 4607–4616.
6. Williams GV, Faulkner P. In: Miller LK, editor. The baculoviruses. New York, London: Plenum; 1997. p 61–107.
7. Lu A, Miller LK. In: Miller LK, editor. The baculoviruses. New York, London: Plenum; 1997. p 193–216.
8. Williams GV, Rohel DZ, Kuzio J, Faulkner P. J Gen Virol 1989; 70: 187–202.
9. Whitt MA, Manning JS. Virology 1988; 163: 33–42.
10. Hawtin RE, Zarkowska T, Arnold K, *et al*. Virology 1997; 238: 243–254.
11. Smith GE, Summers MD, Fraser MJ. Mol Cell Biol 1983; 3: 2156–2165.
12. Pennock GD, Shoemaker C, Miller LK. Mol Cell Biol 1984; 4: 399–406.
13. Kitts PA, Ayres MD, Possee RD. Nucleic Acids Res 1990; 18: 5667–5672.
14. Kitts PA, Possee RD. Biotechniques 1993; 14: 810–817.
15. Possee RD, Hitchman RB, Richards KS, Mann SG, Siaterli E, Nixon CP, Irving H, Assenberg R, Alderton D, Owens RJ, King LA. Biotechnol Bioeng 2008; 101: 1115–1122.
16. Zhao Y, Chapman DAG, Jones IM. Nucleic Acids Res 2003; 31(2): e6.
17. Luckow VA, Lee SC, Barry GF, Olins PO. J Virol 1993; 67: 4566–4579.
18. Ernst WJ, Grabherr RM, Kattinger HW. Nucleic Acids Res 1994; 22: 2855–2856.
19. Lu A, Miller LK. Biotechniques 1996; 21: 63–68.
20. Godeau F, Saucier C, Kourilsky P. Nucleic Acids Res 1992; 20: 6239–6246.
21. Weyer U, Knight S, Possee RD. J Gen Virol 1990; 71: 1525–1534.
22. Matsuura Y, Possee RD, Bishop DHL. J Gen Virol 1986; 67: 1515–1529.
23. Possee RD, Howard SC. Nucleic Acids Res 1987; 15: 3635–3654.

24. Ooi BG, Rankin C, Miller LK. J Mol Biol 1989; 210: 721–726.
25. Stewart LMD, Hirst M, Lopez-Ferber M, Merryweather AT, Cayley PJ, Possee RD. Nature 1991; 352: 85–88.
26. Tessier DC, Thomas DY, Khouri HE, Laliberié F, Vernet T. Gene 1991; 98: 177–183.
27. Harwood S. In: Murhammer DW, editor. Baculovirus and insect cell expression protocols. New York, Humana Press; 2007. p 211–223.
28. Belyaev AS, Hails RS, Roy P. Gene 156: 229–235.
29. Suzuki T, Kanaya T, Okazaki H, *et al*. J Gen Virol 1997; 78: 3073–3080.
30. Grace TDC. Nature 1962; 195: 788–789.
31. Granados RR, Derkson ACG, Dwyer KG. Virology 1986; 152: 472–476.
32. Vaughn JL, Goodwin RH, Thompkins GJ, McCawley P. In Vitro 13: 213–217.
33. Gardiner GR, Stockdale H. J Invertebr Pathol 1975; 25: 363–370.
34. Lynn DE. In: Murhammer DW, editor. Methods in molecular biology 338: baculovirus and insect cell expression protocols, 2/e. Totowa (NJ): Humana Press Inc.; 2007.
35. Summers MD, Smith GE. Texas Agric Exp Stn Bull 1987; 1555: 1–57.
36. Hink WF. Nature 1970; 226: 466–467.
37. Hink WF, Vail PV. J Invertebr Pathol 1973; 22: 168–174.
38. Ramoska WA, Hink WF. J Invertebr Pathol 1974; 23: 197–202.
39. Beames B, Summers MD. Virology 1989; 168: 344–353.
40. Harrison RL, Jarvis DL, Summers MD. Virology 1996; 226: 34–46.
41. Weiss SA, Smith GC, Kalter SS, Vaughn JL. In Vitro Cell Dev Biol 1981; 17: 495–502.
42. Maiorella B, Inlow D, Shauger A, Harano D. Biotechnology 1988; 6: 1406–1410.
43. Ooi BG, Miller LK. Virology 1988; 166: 515–523.
44. Nobiron I, O'Reilly DR, Olszewski JA. J Gen Virol 2003; 84: 3029–3039.
45. Marchal I, Jarvis DL, Cacan R, Verbert A. Biol Chem 2001; 382: 151–159.
46. Szkudlinski MW, Thotakura NR, Tropea JE, Grossmann M, Weintraub BD. Endocrinology 1995; 136: 3325–3330.
47. Grossmann M, Wong R, Teh NG, *et al*. Endocrinology 1997; 138: 92–100.
48. Hollister JR, Sharper JH, Jarvis DL. Glycobiology 1998; 8: 473–480.
49. Hollister J, Jarvis DL. Glycobiology 2001; 11: 1–9.
50. Hillister JR, Grabenhorst E, Nimtz M, Conradt HO, Jarvis DL. Biochemistry 2001; 41: 15093–15104.
51. Singh V. Cytotechnology 1999; 30: 149–158.
52. Volkman LE, Goldsmith PA. Appl Environ Microbiol 1983; 45: 1085–1093.
53. Carbonell LF, Klowden MJ, Miller LK. J Virol 1985; 56: 153–160.
54. Hofmann C, Sandig V, Jennings G, Rudolph M, Schlag P, Strauss M. Proc Natl Acad Sci U S A 1995; 92: 10099–10103.
55. Boyce FM, Bucher NL. Proc Natl Acad Sci U S A 1996; 93: 2348–2352.
56. Condreay JP, Witherspoon SM, Clay WC, Kost TA. Proc Natl Acad Sci U S A 1999; 96: 127–132.
57. Cheng T, Xu CY, Wang YB, Chen M, Wu T, Zhang J, *et al*. World J Gastroenterol 2004; 10: 1612–16118.
58. Kaikkonen MU, Räty JK, Airenne KJ, Wirth T, Heikura T, Ylä-Herttuala S. Gene Ther 2006; 13: 304–312.
59. Hsu CS, Ho YC, Wang KC, Hu. YC. Biotechnol Bioeng 2004; 88: 42–51.
60. Ho YC, Chen HC, Wang KC, Hu YC. Biotechnol Bioeng 2004; 88: 643–651.
61. Hu YC, Tsai CT, Chang YJ, Huang JH. Biotechnol Prog 2003; 19: 373–379.
62. Spenger A, Ernst W, Condreay JP, Kost TA, Grabherr R. Protein Expr Purif 2004; 38: 17–23.
63. Shoji I, Aizaki H, Tani H, Ishii K, Chiba T, Saito I, *et al*. J Gen Virol 1997; 78: 2657–2664.
64. Lo HR, Chou CC, Wu TY, Yuen JP, Chao YC. J Biol Chem 2002; 277: 5256–5264.
65. Viswanathan P, Venkaiah B, Kumar MS, Rasheedi S, Vrati S, Bashyam MD, *et al*. J Biol Chem 2003; 278: 52564–52571.
66. Tani H, Nishijima M, Ushijima H, Miyamura T, Matsuura Y. Virology 2001; 279: 343–353.
67. Tani H, Limn CK, Yap CC, Onishi M, Nozaki M, Nishimune Y, Okahashi N, Kitagawa Y, Watanabe R, Mochizuki R, Moriishi K, Matsuura Y. J Virol 2003; 77: 9799–9808.
68. Barsoum J, Brown R, McKee M, Boyce FM. Hum Gene Ther 1997; 8: 2011–2018.
69. Hüser A, Rudolph M, Hofmann C. Nat Biotechnol 2001; 19: 451–455.
70. Ames RS, Fornwald JA, Nuthulagani P, Trill JJ, Foley JJ, Buckley PT, Kost TA, Wu Z, Romanos MA. Receptors Channels 2004; 10: 99–107.
71. Kost TA, Condreay JP, Ames RS, Rees S, Romanos MA. Drug Discov Today 2007; 12: 396–403.

3

BACULOVIRUS KINETICS, INSECT CULTURE

LESLIE CHAN, STEVE REID, AND LARS KELD NIELSEN
Australian Institute for Bioengineering and Nanotechnology, University of Queensland, Brisbane, Australia

3.1 HISTORY AND CHALLENGE

From the mid-1950s, when the pioneering work of Earle and colleagues (1) enabled routine cell culture, until the emergence of commercial hybridoma and recombinant technologies in the 1980s, cell technology was almost synonymous with viral vaccine production technology. Vaccine production posed a number of unique challenges for research as compared to those faced in microbial fermentation, such as the following:

- the exclusive use of primary cells/tissue and diploid human cell strains rather than cell lines in human vaccine production;
- the predominant use of anchorage-dependent cells;
- the inherent complexity of cell-virus systems;
- the inherent problems of working with human or animal pathogens.

As a result, cell technology research followed a path divergent to microbial fermentation research, which in the same period moved toward bioprocess engineering science, including detailed studies of kinetics. Much work in cell technology was related to "scale-out" technology, that is, ways to handle large numbers of small cultures (e.g. Roux or roller bottles), and the technology surrounding the fermentation process (medium preparation, sterile techniques, downstream processing). Notable exceptions were the development of large-scale BHK (baby hamster kidney) suspension culture for production of Foot-and-Mouth and later, rabies vaccines (2,3) and the development of microcarrier technology for large-scale propagation of anchorage-dependent cells (4).

The 1980s saw the development of large-scale production of polio and rabies vaccines in Vero cell microcarrier cultures and the development of standards for the use of heteroploid cell lines for human vaccine production (5,6). Economy-of-scale, quality control issues, and increasing reticence against the use of animal-derived tissue have resulted in virus production in continuous cell lines becoming the preferred option for new viral-based vaccines, where it was previously limited to animal vaccines. In the past decades, vaccine production has been joined by protein and biopesticide production in insect cells and production gene therapy vectors as bioprocesses relying on virus production.

There is still much to be learned about the kinetics of virus production, even in many of the well-established production systems. This can partly be attributed to a relative lack of academic groups working on the engineering of viral vaccine production and partly due to the inherent complexity of virus processes. Not surprising, most progress has been achieved in the baculovirus/insect cell system, which has several advantages, including the following:

- baculovirus are nonpathogenic in humans and animals;
- insect cells are anchorage-independent and do not produce large amounts of acids, hence quality data can be generated in shaker flasks;
- the infection cycle is extended, which overcomes the problem of overlapping processes in most viral systems.

Mathematical modeling plays a crucial role in building an understanding of the kinetics of virus production. Without models, it is practically impossible to unveil the kinetics underlying the complex, observed dynamics. Consider a

Upstream Industrial Biotechnology: Expression Systems and Process Development, Volume 1, First Edition. Edited by Michael C. Flickinger.
© 2013 John Wiley & Sons, Inc. Published 2013 by John Wiley & Sons, Inc.

typical production process where cells are infected at a low multiplicity of infection (MOI), where initially only a fraction of cells will be infected. In order to describe the behavior of this process, we need the following:

- a model of noninfected growth;
- a model of the physical interaction between virus and cells (attachment and internalization);
- a model of the infection cycle in individual cells to account for changes as cells gradually change from being biomass producers early in the infection cycle to being virus producers late in the cycle;
- a population balance model to take into account the fact that cells may be infected at different point in time and thus at any point in time, the dynamics of the culture is the cumulative effect of the kinetics shown by the cells in various stages of infection;
- a mass-balance model to take into account the physical system, for example describing substrate consumption in a batch culture or the dilution effect in a continuous culture.

In addition, depending on the actual system studied, it may be necessary to include the following:

- a model describing genetic stability of the virus, for example, to account for the accumulation of defective viruses observed in continuous culture;
- a model to describe the effect of multiple infection such as when using multiple virus constructs for multicomponent virus-like particles' production or packaging of gene therapy vectors.

We have previously reviewed three early kinetic models developed for baculovirus infection of insect cells (7) and several models have been proposed more recently (8–14). Several groups, including ours, have developed relatively detailed kinetic models of the baculovirus system. By comparing and contrasting the approaches taken, it is possible to gain insight into what works and what does not. In the remainder of this article, we will describe how to develop kinetic models of virus production using the baculovirus system as the model system. The emphasis is on how to link experiments and model development. The first section provides a brief introduction to baculoviruses. The second section presents the cell yield concept, a highly simplified view of viral processes based on a pseudo mass balance of the process. The cell yield concept provides an objective for process optimization, but does not provide the means for designing the process. For this, we need a kinetic model and this is developed in two stages. First, a model is developed for synchronous infection and this model is then used together with a population balance model and virus attachment kinetics, to formulate a model for asynchronous infection. The usefulness of the developed model is illustrated in the final section, where very low MOI is discussed as a possible production strategy.

3.2 BACULOVIRUS

Baculoviruses and their use as expression vectors have been described in several excellent books and reviews (15–18). Baculoviruses are rod-shaped viruses with ~130 kb of genetic material located on a single double-stranded DNA molecule. Baculoviruses have been isolated from over 500 insect species, mainly of the order Lepidoptera. The biology of *Autographa californica* nuclear polyhedrosis virus (AcNPV) has been studied in great detail and forms the basis of most recombinant expression systems, while *Helicoverpa zea* nuclear polyhedrosis virus (HzNPV) is produced commercially and *Helicoverpa armigera* nuclear polyhedrosis virus (HaNPV) is considered for biopesticide usage.

The individual viruses in NPVs are occluded (embedded) in a paracrystalline matrix composed mainly of a single protein called *polyhedrin*. The occlusion body, called *polyhedron*, protects the enclosed virus particles against the environment. Upon digestion by larvae, the polyhedron will dissolve in the alkaline gut juices and the released viruses will infect the midgut epithelium cells. During the ensuing infection cycle nonoccluded viruses (NOVs) will be formed in addition to the occluded form. NOVs bud through the cell membrane into the hemolymph, where they become responsible for lateral infection (Fig. 3.1).

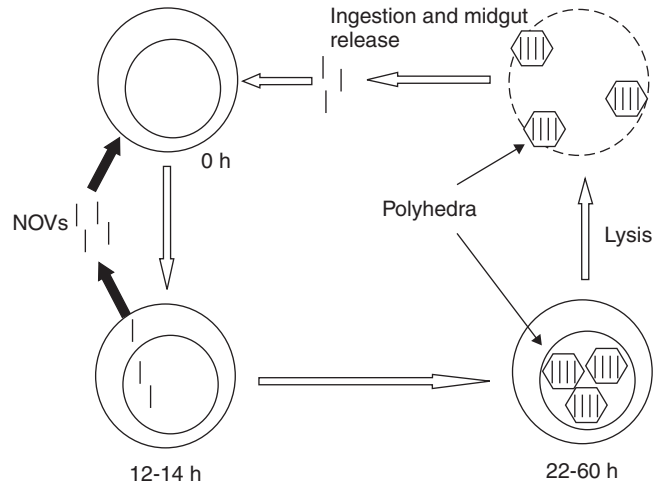


Figure 3.1. Infection cycle of NPV baculoviruses. The open arrows indicate the virus cycle between larvae from ingestion of polyherdra and midgut release of virus to the release by lysis of new polyhedra. The solid arrows indicate lateral infection through nonoccluded viruses (NOVs) released early in the infection cycle.

Several cell lines are available for propagating baculoviruses. AcNPV is typically propagated in suspension cultures of Sf-9 cells, a cell line established from ovarian tissue of *Spodoptera frugiperda* (fall armyworm), while HzNPV can be propagated in cell lines derived from ovarian tissue of *H. zea* (cotton bollworm). Propagation relies on the lateral infection route, that is via NOV infection. This is the basis for the baculovirus expression system, where the highly expressed but nonessential polyhedrin gene is replaced with a gene of interest through homologous recombination. The model system used by many to study recombinant expression in baculovirus is that of β-galactosidase expression. While ideal for gene expression, the fact that polyhedrin is nonessential for *in vitro* culture poses stability problems for biopesticide production, where occlusion bodies are essential for delivery. Typically, baculoviruses will degenerate to low producers in five to ten *in vitro* passages (19), unless a stable isolate has been found (20).

3.3 CELL YIELD CONCEPT

Baculovirus production is greatly affected by a number of process variables, including the design of the fermentation system, cell line (21,22), composition of the medium used for cell growth (23–27), age and condition of the cell population at time of infection (TOI) (28–32), MOI (33–36), and passage number of virus inoculum (37,38). Most of these variables are set early in process development; for example, we have chosen batch fermentation in serum-free medium using the aforementioned cell lines and a low-passage number virus stock.

The two remaining parameters, TOI and MOI, are highly correlated and—combined with the variability of cultures and the relatively inaccurate assays available for virus determination—it proved to be a nontrivial task to resolve their effect empirically. Indeed, prior to the development of kinetic models, descriptions of TOI and MOI effects tended to be inconsistent listings of individual observations. Only through working with a relatively complex model, did we finally develop a conceptual understanding of the system that we termed the *cell yield concept* (39). Like any good concept, it is a simplification with obvious limitations and should only be regarded as a first handle on the system. Importantly, however, it does not rely on baculovirus-specific features and should be applicable to other virus production systems. The cell yield concept is based on an overall pseudo balance for the process:

$$\text{Substrate} \rightarrow \text{cells} + \text{virus/viral products}$$

The process is catalyzed by cells and each cell can support the production of only a limited number of virus particles. The virus yield per cell is highest at low cell density but remains essentially constant up to the point where substrate becomes limiting. Thus, until the point of substrate limitation, the yield of virus will increase nearly proportionally with cell yield (i.e., the total number of cells produced in the process). Once substrate becomes limiting, any further yield in cells comes at the expense of virus and viral product yields.

What is important here is that there is no distinction made based on when the cells were produced: whether they all were produced prior to infection as would be the case at high MOI infection, or whether most were produced in parallel with the infection process as would be the case at very low MOI. In other words, the outcome is ultimately dictated by the total cell yield in the process, not on the combination of TOI and MOI used to achieve this yield. This point is illustrated in Fig. 3.2a for recombinant baculovirus and Fig. 3.2b for HaNPV production. By choosing

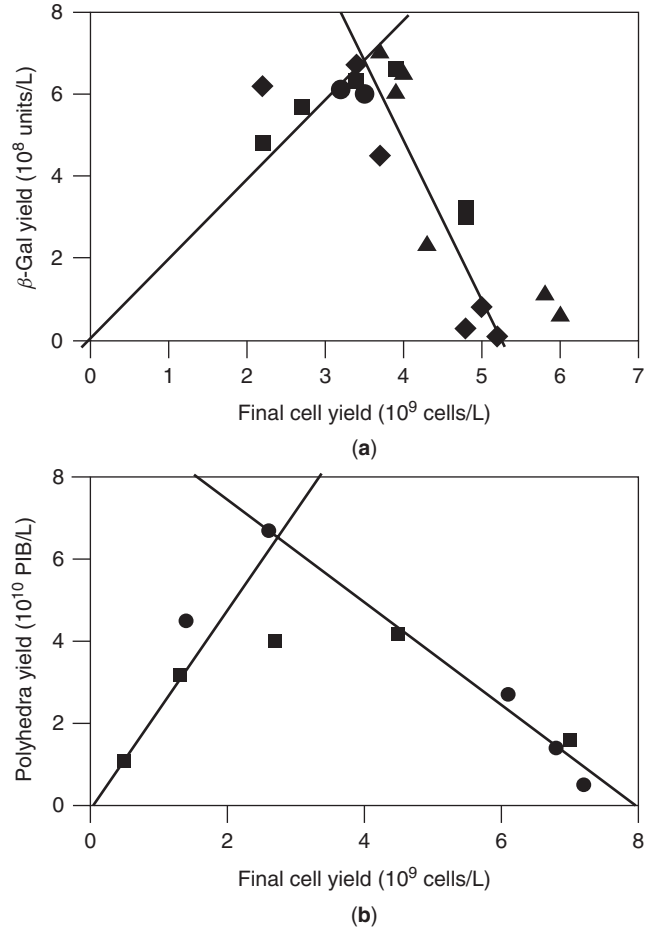


Figure 3.2. The cell yield concept. (a) Total β-galactosidase yield for r β-gal-AcNPV infections of Sf-9 cells in SF(00II medium performed at MOIs of 5 (circle), 0.01 (square), 0.0001 (triangle), and 0.0001 (diamond) in shaker flasks. (b) Polyhedra yield for HaPNV infections of *H. zea* cells in SF-900II + 10% serum medium performed at MOIs of 0.5 (circle) and 1–2 (square) in shaker flasks.

the appropriate TOI it is possible to achieve the optimal cell yield for whatever MOI is chosen.

At high MOI (>5 infective viruses per cell), essentially all cells will be infected immediately and the ensuing infection process will be synchronous. Cell growth halts almost immediately and thus the cell yield is close to the cell density at TOI. Thus, to achieve optimal production, cells should be infected at a cell density close to the optimal cell yield. At lower MOIs, only a fraction of the cells are initially infected (primary infection). It can be assumed that the remainder will continue to grow as noninfected cells. These cells and their progeny will first be infected at some later point (secondary infection) when the cells infected in the primary infection begin to release progeny virus. Hence, the cell yield may be much higher than the cell density at TOI. Thus, to achieve optimal production when using low MOIs, cells should be infected at a cell density lower than the optimal cell yield.

Practically, we obtain the product versus cell yield curve by performing a series of high multiplicity infections at different cell density. For insect cells, we use a bioreactor for cell growth, harvest 100 mL aliquots into shaker flasks at 6–12 h intervals, infect at MOI 5–10, incubate on shaker, and follow the ensuing infection process (Fig. 3.3). Because pH is not a problem in these cultures, the response curve observed in shaker flasks is valid even for controlled bioreactors. In many systems, it may be necessary to perform the infection in bioreactors to match the expected performance in a controlled system.

In suspension insect cell culture, the limiting substrate is a nutrient and the maximum reasonably well-defined. In many virus production systems, cells are anchorage-dependent and the limiting substrate will be surface area. In such systems, the transition could be broader and the decline is not necessarily linear. Even in this case, however, the observed optimum cell yield provides an initial goal to aim for in optimizing the process. It does not, however, indicate how to achieve this cell density if we choose a low MOI. In order to predict this, we need a kinetic model.

3.4 KINETIC MODEL OF VIRAL INFECTION: SYNCHRONOUS INFECTION

All studies of viral kinetics should commence with a study of synchronous infection somewhat below the optimal cell yield. If a batch culture of cells is infected at a high multiplicity (MOI > 5), the ensuing infection process will essentially be synchronous, that is, all cells will go through the infection cycle simultaneously and will—at any given point—be at the same point in the cycle. Under these conditions culture dynamics simply reflect the infection cycle occurring in each cell, amplified by the number of cells.

Synchronous cultures are biphasic in nature. We distinguish between the noninfected (cell-only) phase and the infection phase. During the noninfected phase, time is the independent variable. During the infection phase, we introduce a new independent variable, *infection time*, denoted

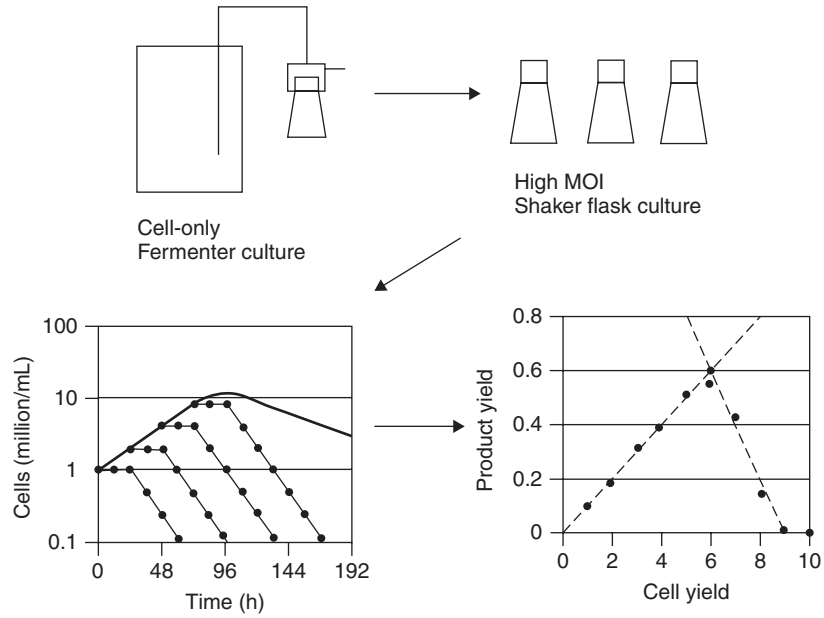


Figure 3.3. Generating the product versus cell yield curve. During a cell-only bioreactor culture, cells are repeatedly harvested straight into shaker flasks and infected at high MOI and the infection ensued. Maximum product and cell yield are used to generate the product versus cell yield curve and the maximum determined by drawing the supporting lines.

as τ and measured in hours postinfection (hpi). This terminology can cause some confusion. Infection time does not automatically follow true time; rather it relates to a reference infection. The reference infection is typically a high MOI infection (e.g. MOI = 10) of cells in the early to mid-exponential phase (i.e. relatively low cell density), and in a given medium. When we say that a cell is at 15 hpi, we are actually not saying that the cell has been infected for 15 h; rather, we are saying that the cell is at the same point of the infection cycle that a cell would be after 15 h in the reference system.

Infection time can be slower or faster than true time. Infection in late exponential phase, for example, often results in slow progression through the infection cycle (discussed later), that is infection time goes slower than real time. For some viral systems, the initial viral load per cell can affect the timing of the infection cycle and in a very high multiplicity infection, infection time may go faster than real time. We define the infection velocity, ν, as

$$\nu = \frac{\mathrm{d}\tau}{\mathrm{d}t} \tag{3.1}$$

and note that for the reference system the infection velocity is one hour of infection time (hpi) per one hour of true time (h).

3.4.1 NonInfected Cell Growth

Any traditional cell growth model could be used to describe cell growth prior to infection. Experience tells us, however, that for most virus production systems, cells must be infected in optimal health, that is in the mid-exponential phase, in order to achieve a reasonable product yield. Thus, all relevant situations can be modeled with a simple exponential growth model

$$\frac{\mathrm{d}N_\mathrm{V}}{\mathrm{d}t} = (\mu_{\max} - k_\mathrm{D})\ N_\mathrm{V} \tag{3.2}$$

where N_V is the concentration of viable cells, $\mu_{\max}$ the maximum specific growth rate, and k_D the specific death rate. The noninfected cell parameters, $\mu_{\max}$ and k_D, can be determined using standard techniques from the number of viable and dead cells during the exponential phase of a noninfected culture.

3.4.2 Infection Cycle: Qualitative Aspects

Typically, the qualitative aspects such as virus attachment mechanism, molecular biology, and general timing of events, are well-established for commercially relevant viruses. This information serves as a sound basis on which mathematical models can be formulated. The starting point may be a graphical representation of the infection cycle as in Fig. 3.4 for recombinant baculovirus (see also Ref. 40) where the first step is virus diffusing to the surface of the cell and (2) attaching to a specific receptor. (3) Baculovirus enter the cytosol via random endosomal activity, (4) followed by pH-regulated fusion with the endosomal membrane. From the cytosol, (5) baculovirus is localized to (6) the nucleus, where the outer protein coat dissolves. All of these processes take place within the first couple of hours of cells being inoculated with the virus. Hereafter follows the "genetic" part of the infection with (7) simultaneous replication of viral DNA, (8) transcription, and (9) translation of viral proteins. The infection cycle is "timed" through sequential protein expression and can be divided into three phases (16):

1. *Early (0–6 h Postinfection).* The viral reproduction apparatus is established and the cellular reproduction apparatus switched off.
2. *Late (8–18 h Postinfection).* Synthesis of nonoccluded virions, which are coated in protein (16) and are capable of budding from the cell surface (17).
3. *Very Late (20–72 h Postinfection).* Polyhedrin or recombinant product is transcribed using a unique, viral-derived RNA polymerase. In wild-type virus, virions are embedded in occlusion bodies composed primarily of polyhedrin.

3.4.3 Infection Cycle: Modeling

There are two approaches that can be taken to describe the infection cycle: an unstructured and a structured, mechanistic approach. In the unstructured approach, the temporal

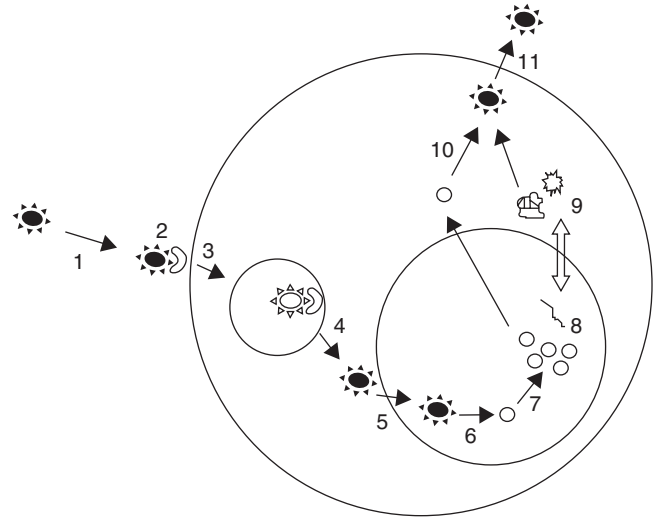


Figure 3.4. The infection cycle in recombinant baculovirus. 1. Diffusion, 2. attachment, 3. internalization, 4. fusion, 5. nuclear location, 6. uncoating, 7. replication, 8. transcription, 9. translation, 10. encapsulation, and 11. budding.

element of the infection cycle is described by a number of time-varying rates. No attempt is made to follow the internal events of the cell. The five existing full models all employ this approach (9,11,36,41,42).

In the structured, mechanistic approach, the infection cycle is described as closely as possible to the true mechanism outlined in Fig. 3.4. For example, separate variables are used to describe viruses at the different locations (free, attached, endosomal, cytosolic, and nuclear) and rate equations are expressed in terms of these variables. Shuler's group has outlined a possible structure for such a model (40) and has developed detailed models up to the point of nuclear location (discussed later). Sanderson *et al*. (14) and Jang *et al*. (12) have developed structured models of batch and fed-batch infections based on Shuler's outline and an animal cell metabolism model (43) which include descriptions of coinfection, metabolic fluxes, and feedback inhibition. Roldao *et al*. (13,44) also developed a structured model, to describe coinfections for the production of three types of Rotavirus-like particles. As a guide to more fundamental research, the mechanistic models obviously excel. Ultimately, they will also prove excellent engineering tools for designing viral production processes. Presently, however, the structured models are too cumbersome and require too much effort to develop, so here we will concentrate on the unstructured models.

The modeling approach described below has three important features:

1. Only directly observable state variables are used.
2. All parameters are graphically verifiable.
3. All parameters are estimated for high MOI.

In order to achieve this simplicity, a number of assumptions have been made. It is assumed that there is no growth after infection. In our experience, the total number of cells does increase on average by 15% postinfection, suggesting that cells may continue to divide through the early phase of infection. Accounting for this growth, however, would involve deciding whether both daughter cells in a division are infected or only one of them. It is possible to determine this based on the MOI for individual cells, but introducing this distinction adds substantially to the numerical effort, and the simplifying assumption of no postinfection growth is made in most models of infection.

Presently, we shall not consider the effects that multiple infection and infection with defective virus particles have on the infection cycle. We will only consider a "standard" infection at relatively high MOI (5–10) producing a single type of infected cell. This corresponds to the approach taken in our 1994 model to describe β-galactosidase production using a recombinant AcNPV to infect Sf-9 cells in suspension culture (42). More advanced models will be described later. For modeling purposes, the time points of interest are those linked with readily observable events, such as

- virus release,
- membrane integrity,
- β-galactosidase production and release.

Extracellular virus is not observed in the culture fluid until around the onset of the very late phase. Electron microscopy observations (unpublished) have confirmed that virus progeny is produced from the beginning of the late phase, τ_E. The newly produced virus progeny were observed on the cell surface and some were observed to readsorb to the cell of origin. Surface presentation of NOV in the late phase could be the means by which lateral infection of proximal cells occurs in the gut cells of insects (15). It is not clear if the release, rather than surface presentation, of virus progeny is linked to the very late phase or is simply a delayed process. Hence, in all three pioneer models of baculovirus kinetics (36,41,42), the commencement of virus release is designated by its own marker, here designated τ_{VRC}. Viruses appear to be released at a relatively constant rate, α_{VR}, and this end after the end of the very late phase at a point designated τ_{VRE}. Thus, the specific rate equation for virus release, r_{VR}, is

$$r_{VR}(\tau) = \begin{cases} 0, & \text{for } \tau \le \tau_{VRC} \\ \alpha_{VR}, & \text{for } \tau_{VRC} < \tau \le \tau_{VRE} \\ 0, & \text{for } \tau \ge \tau_{VRE} \end{cases} \tag{3.3}$$

Since virus binding has finished by the time virus release is observed, the virus titer, V, can be described by

$$\frac{dV}{d\tau} = r_{VR}(\tau)N_V - k_V V \tag{3.4}$$

where the second term accounts for degradation of the virus, which is significant for many viruses. Virus degradation is assumed to follow first order kinetics with the degradation constant, kV. Inserting Equation 3.3 in Equation 3.4 and integrating, we find the solution

$$V^*(\tau) = \begin{cases} 0, & \text{for } \tau \le \tau_{VRC} \\ \dfrac{\alpha_{VR}}{k_V}(1 - e^{-k_V(\tau-\tau_{VRC})}), & \text{for } \tau_{VRC} < \tau \le \tau_{VRE} \\ \dfrac{\alpha_{VR}}{k_V}(1 - e^{-k_V(\tau_{VRE}-\tau_{VRC})})e^{-k_V(\tau-\tau_{VRE})}, & \text{for } \tau \ge \tau_{VRE} \end{cases} \tag{3.5}$$

Membrane integrity can be measured by trypan blue dye exclusion. For noninfected cells, membrane integrity can be used as an indicator of viability. For infected cells, however,

membrane integrity gradually decreases during the late part of the infection rather than spontaneously at the end of infection (36). As viruses and recombinant products are also released gradually, there is no particular need for the model to identify the point of death and lysis. The gradual staining of cells is expressed with an empirically fitted equation giving the fraction of stained cells as a function of τ

$$f_U(\tau) = \begin{cases} 1, & \tau \le \tau_U \\ e^{-\beta_U(\tau-\tau_U)}, & \tau \le \tau_U \end{cases} \tag{3.6}$$

where τ_U is time following infection where staining commences and β_U is the first order rate of staining hereafter. Using a similar approach, de Gooijer *et al*. employed the gradual visual changes in infected cells to follow the progression of infection with wild-type viruses (41).

In the baculovirus expression vector system, the recombinant protein is expressed under the control of the polyhedrin promoter. Thus, recombinant protein expression is directly linked to the expression of the very late genes commencing at τ_L and terminating at τ_{VL}. The production rate is assumed constant, α_{PP}. Both intracellular and extracellular β-galactosidase can be determined experimentally. β-galactosidase is not a secreted product and protein release is assumed to be linked to the leakiness of the membrane as evidenced by trypan blue uptake. Thus, release is assumed to commence at the same time as staining, τ_U. Hereafter, the rate of release is assumed to be proportional to the intracellular concentration (the release constant denoted α_{PR}), that is,

$$r_{PR}(\tau) = k_{PR}(\tau)\, p_i(\tau) \tag{3.7a}$$

where

$$k_{PR}(\tau) = \begin{cases} 0 & \text{for } \tau < \tau_U \\ \alpha_{PR} & \text{for } \tau \ge \tau_U \end{cases} \tag{3.7b}$$

The intracellular concentration, p_i, is given by

$$\frac{dp_i}{d\tau} = r_{PP}(\tau) - r_{PR}(\tau)\, p_i; \quad p_i(0) = 0 \tag{3.8a}$$

where $r_{PP}(\tau)$ is the specific production rate

$$r_{PP}(\tau) = \begin{cases} \alpha_{PP} & \text{for } \tau_L \le \tau \le \tau_{VL} \\ 0 & \text{otherwise} \end{cases} \tag{3.8b}$$

Solving Equation 8, the intracellular concentration can be determined

$$p_i(\tau) = \begin{cases} 0 & \text{for } \tau \le \tau_L \\ \alpha_{PP}(\tau - \tau_L) & \text{for } \tau_L < \tau \le \tau_U \\ \dfrac{\alpha_{PP}}{\alpha_{PR}} + \alpha_{PP}\left(\tau_U - \tau_L - \dfrac{1}{\alpha_{PR}}\right) & \\ \quad e^{-\alpha_{PR}(\tau-\tau_U)} & \text{for } \tau_U < \tau \le \tau_{VL} \\ p_i(\tau_{VL})\, e^{-\alpha_{PR}(\tau-\tau_{VL})} & \text{for } \tau \ge \tau_{VL} \end{cases} \tag{3.9}$$

The extracellular product concentration is given by

$$\frac{dP}{d\tau} = r_{PR}(\tau) N_V - k_P P \tag{3.10}$$

where the second term accounts for decomposition of extracellular product.

The number of parameters in the above model may initially seem large. All parameters, however, can be determined and visually verified using a synchronous infection of cells in the mid-exponential phase and several are determined independently of other parameters. Decomposition parameters, k_V and k_P, are determined from the exponential decay curves observed in cultures in which cells are removed after some viruses and products have been produced. The membrane integrity parameters, τ_U and β_U, are determined by nonlinear regression from synchronous culture cell viability data.

The three viral production parameters—α_{VR}, τ_{VRC}, and τ_{VRE}—are obtained by nonlinear regression on experimental data using Equation 3.4 as illustrated in Fig. 3.5. The timing parameters are visually verifiable, while the production rate is more difficult to confirm due to the effect of degradation. The parameters for product formation are determined in a similar manner.

The protein release model described above is a convenient assumption, especially when moving from synchronous to asynchronous infections. However, it presumes that stained cells (that have lost the ability to

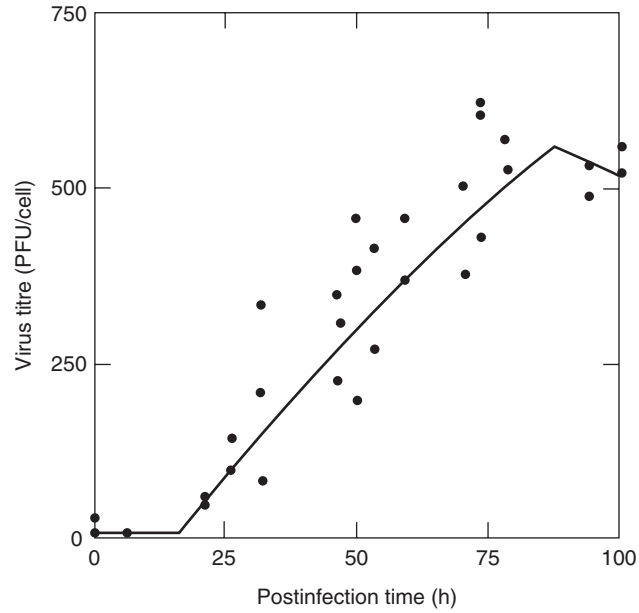


Figure 3.5. Fitting of virus production parameters. Sf-9 cells cultured in serum Sf-900II medium were infected with recombinant baculovirus at a multiplicity of 10 PFU. The datapoints are from three independent experiments and the solid line represents the model fit to data.

exclude trypan blue) are still metabolically active and continue to express protein product, which is unlikely to be true. A more likely scenario is one in which protein product is generated exclusively by unstained (viable) cells while protein leakage occurs only in stained (nonviable) cells. Haas and Nielsen (10) have proposed such a protein release model, by using an empirically fitted normal cumulative probability distribution to describe the change in nonviable cell proportion postinfection, which is paired with a zero-order kinetic model of specific intracellular protein production (by viable cells), to predict the specific extracellular protein level at any point of time postinfection.

3.4.3.1 Substrate Limitation. The simple model outlined above works well when the cell yield is below the optimal cell yield defined earlier. Near the optimal cell yield, however, it is our experience that the infection process slows down and the response is slower than predicted.

In suspension cultures, the limitation appears to be related to the depletion of an essential substrate (31,45). In our 1994 model, we had to overcome several problems in order to describe substrate limitation (42):

1. *Limiting Substrate is Unknown.* The limiting substrate is still to be identified and the model had to assume an arbitrary substrate to be present at 1 unit/L of fresh medium.
2. *Substrate Limitation Causes Complex Changes in Kinetics.* It has been our experience that substrate limitation causes a general slowdown of the growth and infection processes, not only a lowering in production rates as assumed by Licari and Bailey (36). As a simple initial approach, the model was made a simple depletion model, that is, all cellular processes were assumed to occur at maximum rate until depletion of substrate, at which point all cellular processes would stop.
3. *Consumption Pattern Unknown.* The limiting substrate being unknown it was not possible to formulate a consumption profile. Instead the specific consumption rate was assumed constant for noninfected and infected cells. The concept was that substrate consumption remained constant while the end-product would change from cell mass to viral products over the infection.

With these simplifying assumptions the resulting substrate limitation model only required a single parameter to be obtained, namely, the maximum cell density observed in a noninfected culture, Y_S. Mathematically, the model read

$$\frac{dS}{d\tau} = -\frac{\mu}{Y_S N_V}, \tau = 0 : S = 1 - \frac{N_V}{Y_S} \tag{3.11}$$

where S is the substrate concentration and the boundary condition accounts for the amount of nutrients consumed during the cell growth phase.

While this model capture the essence of the cell yield concept (Fig. 3.2), the temporal development remains poorly described around the peak, since the model fails to describe the slowdown in growth and infection when substrate becomes limiting. Moreover, the assumption of constant substrate consumption before and after infection—while fortuitously correct for β-galactosidase production in Sf-9 cells—does not hold for other systems (Table 3.1) (46). This flaw, however, can be corrected by introducing a separate consumption rate after infection $q_S \neq \mu / Y_S$.

One possible solution to address the model's inability to accurately describe substrate limitation is to make the infection velocity, ν, a function of substrate concentration, for example,

$$\nu(S) = \frac{S}{K_S + S} \tag{3.12}$$

Note, that with this definition the "infection time" τ, becomes a marker of the progression through the infection cycle rather than a measure of time. At $S = K_S$, for example, the cell progresses half an "infection hour" for each true hour in culture. If the specific rates of virus 3 and protein production 8b also are multiplied with ν, the result is to stretch out the infection cycle at lower substrate levels without changing the total yields.

If the limiting substrate is the space available, Equation 3.12 can be replaced with a spatial saturation model

$$\nu = \frac{\text{total capacity—capacity taken by noninfected and infected cells}}{\text{total capacity}} \tag{3.13}$$

as was done by Licari and Bailey (36). The approach argued here, however, differs from that used by Licari and Bailey,

TABLE 3.1. Specific consumption rates (mmol per 10^{12} cells per hour) for five amino acids before and after infection[a]

System Phase	Gln	Asn	Leu	Thr	Tyr
Sf9/rAcNPV Uninfected	24	2	8	3	13
Sf9/rAcNPV Infected	18	13	9	4	14
H.zea/HaNPV Uninfected	59	125	16	7	9
H.zea/HaNPV Infected	20	37	2	1	2

The comparison shows that while consumption remains essentially constant after infection in the Sf9/rAcNPV system, there is a significant drop in the *H. zea*/HaNPV system. [a]From Ref. (46).

in that they only took the change in production rate into account, not the prolonging of the infection cycle. The new approach is yet to be tested. The constant K_S will have to be a fitted constant, that is, chosen as the value that gives the best description to a series of high MOI experiments infected at different initial cell density.

3.4.3.2 Multiplicity of Infection. Infected cells continue to bind viruses after the initial infection, yet the proposed model does not take into account possible differences caused by the MOI of individual cells. Conceptually, an increase in multiplicity represents an increase in number of viral templates; hence, at least the early stages of infection should progress faster at high multiplicity. Indeed, increased rate of RNA synthesis was observed during the 2.5 h after infection when BHK cells were infected with an increasing number of Semliki Forrest Virus (47). What remains unclear is to what extent this transient increase affects the overall timing and whether or not total productivity is affected by the multiplicity.

In our experience, the use of an MOI of 10 versus an MOI of 5 in suspension culture does not significantly change the timing of the infection cycle. Furthermore, experiments using two different viruses suggest that any additional viruses compete with the existing viruses within the cell (Table 3.2). When recombinant β-galactosidase AcNPV and VP7 AcNPV viruses were added simultaneously (both at an MOI of 5), virus production for each was ~50% of that observed in the absence of the other virus. When one virus was added earlier, it gained a greater share of the total production at the expense of the other virus, and with 4 h difference the titer of the second virus would only reach about 10% of the normal level. It follows from these two sets of observations, that when a cell is infected with 10 instead of 5 viruses, the productivity *per virus* is essentially halved. Presumably, there is an upper limit on the copy number during the infection cycle and this limit is reached even if a single virus enters the cell.

Although MOI does not appear to affect timing or outcome significantly for baculovirus, there may be other systems where this is an important issue. In particular, timing may be important for viruses with a much shorter cycle than baculovirus, when stochastic aspects may become dominant. Hence, it may be necessary to model the effect of multiplicity. If infection occurs over a short period of time (either due to rapid binding of an available virus or due to deliberate removal of the viral inoculum after a short contact period), the effect of multiplicity can be accounted for by defining separate cell populations, N1, N2, and so on and define separate kinetics for each population. The number of cells in each population can be determined by assuming that viruses get distributed randomly according to the Poisson distribution with MOI as the parameter (9,11,36).

A common error, originating with Licari and Bailey's model (36) but often repeated, is the use of Poisson statistics for continuous models. While infection can be described as a Poisson process, a probability for one or more infections to occur cannot be assigned for the instant. Models employing this approach use the arbitrarily chosen time step used for numerical integration, typically 1 h. As indicated by Table 3.2, there is no evidence that additional infection events cannot occur after 1 h.

If infection occurs over a longer period of time, it becomes necessary to take into account that the first virus bound may have been replicated before later viruses bind. This situation may occur in a system where binding is intrinsically slow or during secondary infection in low MOI infections (discussed later), where the primary infected cells continue to release viruses gradually throughout the secondary infection. This situation can only be dealt with using highly mechanistic models as we would need to know not only the amount of DNA/RNA already present in the infected cell to add the contribution from additional infections, but also the delay between virus attachment and release of DNA/RNA into the cytosolic or nuclear pool.

3.4.3.3 Multiple Virus Infection. The experiment described in Table 3.2 is an example of viral production systems in which cells are infected by several different viruses. Multiple virus infection can be a deliberate process as in packing of replication deficient virus for gene therapy or production of multisubunit proteins (e.g.

TABLE 3.2. The effect of coinfection

	Timing VP7 h	rβgal-AcNPV titer 10^8 pfu/mL (%max)	rVP7-AcNPV titer 10^8 pfu/mL (%max)
Culture 1	−inf	0.00 (0)	0.62 (100)
Culture 2	−4	0.09 (7)	0.55 (89)
Culture 3	−2	0.22 (18)	0.58 (94)
Culture 4	0	0.56 (46)	0.33 (53)
Culture 5	2	0.77 (64)	0.18 (29)
Culture 6	4	0.68 (56)	0.08 (13)
Culture 7	+inf	1.21 (100)	0.00 (0)

Cells were infected with two recombinant AcNPV viruses—one producing β-galactosidase and one producing VP7, a blue tongue virus capsid protein—both at an MOI of 5. The table presents the timing of rVP7-AcNPV virus addition relative to rβgal-AcNPV addition and the resulting virus titers for the two viruses.

virus-like particles (48)). It may, however, also be the inadvertent outcome of defective virus accumulation.

The latter is an important quality control issue in most viral production systems and is frequently termed the *passage effect* (49), because serial passage at high multiplicity leads to defective virus accumulation. For Baculovirus, we can consider two types of viruses: normal infective particles (I-NOVs) and defective interfering particles that lack about 44% of the virus genome (D-NOVs). There is a third type that leads to an abortive infection, but we will ignore this type here for illustration purposes. With the two virus types, three modes of infection can be envisaged (41):

1. Correct infection arising from entry of at least one I-NOV without any D-NOVs. This infection gives rise to I-NOVs and a small number of D-NOVs.
2. Simultaneous infection of a cell by at least one I-NOV and at least one D-NOV. The genetic advantage of the D-NOV results in production of large quantities of D-NOVs and few I-NOVs.
3. The third mode results from infection of a cell with a D-NOV in the absence of an I-NOV. Without the helper effect of the I-NOV, such infections do not produce any virions.

If we assume that infection occurs over a short period of time, we can again consider the statistics of random virus distribution and calculate the probability for each mode of infection. Because of the vast difference in productivity (a single D-NOV will make the cell produce almost exclusively D-NOV progeny), we do not have to consider exactly how many viruses of each type attaches. Infection results in the formation of three populations, N_{I}, $N_{\mathrm{I+D}}$, and N_{D}, and we would define a parameter set for each population.

In general, it would be necessary to subdivide the $N_{\mathrm{I+D}}$ population into many subpopulations to account for differences resulting from different initial amounts of the two viruses. Hu and Bentley (48) developed such a stochastic model for simulating the coinfection of two recombinant baculoviruses encoding four protein products for virus-like particle production. Alternatively, it may again be necessary to consider a structured modeling approach, now with separate pools of DNA and RNA representing each virus. Structured models are also required if the infection process is not instantaneous.

3.5 KINETIC MODEL OF VIRAL INFECTION: ASYNCHRONOUS INFECTION

Asynchronous infection represents a significantly more complex problem than synchronous infection. Firstly, it is necessary at any point in time to keep track of cells at any point of the infection cycle. Secondly, understanding the kinetics of virus attachment and internalization is of paramount importance in asynchronous cultures, whereas in the synchronous culture it is sufficient to assume that all cells were infected simultaneously. The complexity of asynchronous culture dynamics, however, is also the main argument for modeling: it is practically impossible to quantitatively comprehend culture dynamics without the aid of a model. This section outlines how to use the behavior observed at high multiplicity infection—together with a population balance and attachment kinetics—to predict the behavior in low multiplicity infections, where the infection process is asynchronous.

3.5.1 Population Balance for Asynchronous Infection

When cells are infected at an MOI less than 3–5 in a batch culture, the culture will no longer be synchronous. At any point in time, the culture will be composed of noninfected cells and cells at different points in their individual infection cycle. The culture behavior is the cumulative behavior of these individual cells. In a continuous culture, noninfected cells are added continuously and the culture will obviously be asynchronously infected.

In order to keep track of the culture, we introduce the cell density function for infected cells, $n(t, \tau)$, where t is true time and τ is time since infection. Note that $n(t, \tau)\mathrm{d}\tau$ represents the number of cells at true time t, that have been infected for a period between τ and $\tau + \mathrm{d}\tau$ hours. Assuming no postinfection growth (as discussed earlier), the law of conservation for cell numbers reads

$$\begin{pmatrix} \text{change in number} \\ \text{of cells in } [\tau, \tau + \mathrm{d}\tau] \end{pmatrix} = \begin{pmatrix} \text{number of cells} \\ \text{entering } [\tau, \tau + \mathrm{d}\tau] \end{pmatrix} - \begin{pmatrix} \text{number of cells} \\ \text{leaving } [\tau, \tau + \mathrm{d}\tau] \end{pmatrix}$$

$$n(t + \mathrm{d}t, \tau)\mathrm{d}\tau - n(t, \tau)\mathrm{d}\tau = \nu(t, \tau)n(t, \tau)\mathrm{d}t - \nu(t, \tau + \mathrm{d}\tau)n(t, \tau + \mathrm{d}\tau)\mathrm{d}t$$

$$\frac{\partial n}{\partial t} + \nu \frac{\partial n}{\partial \tau} = 0 \tag{3.14}$$

Normally, it will be assumed that $n(0, \tau) = 0$, that is at $t = 0$, no cells are infected. If, furthermore, the infection rate at all times t that is $\mathrm{IR}(t) = \nu n(t, 0)$, is specified, then Equation 3.14 has a unique solution.

3.5.2 Attachment, Internalization, and Infection

The first event of the infection cycle is the attachment of virus to the cell. Wickham *et al*. (50) identified three modes of viral attachment for a number of different animal viruses:

Mode 1: Virus attaches to single receptor and is internalized.

Mode 2: Initial attachment to receptor is followed by reversible attachment to surrounding receptors and the complex is internalized.

Mode 3: Similar to Mode 2, except the number of receptors is so high that spatial saturation of cell surface with virus may occur.

Some insect cells, such as T.ni cells, have sufficient number of binding sites to indicate a possible involvement of spatial saturation, while for others such as *S. frugiperda*, the number of binding sites is too low (38,49). Practically, saturation is likely to be a factor only in low temperature attachment studies, where very high virus titers are used and internalization is minimal (51). Under standard infection conditions, binding is first order with respect to both virus and receptor number and the depletion of extracellular virus (V) due to binding is (52)

$$\frac{dV}{dt} = -k_a N V \tag{3.15}$$

where k_a is the attachment rate constant and N is the total number of cells. Dissociation has been neglected as it is typically slow relative to multivalent bond formation (stabilization) and internalization.

The infection rate, IR(t), differs from the attachment rate in that the former is only concerned with attachment to previously uninfected cells, N_V, rather than all cells. The infection rate is expressed as

$$\mathrm{IR}(t) = -k_a N_V V \frac{\text{cells}}{\text{PFU}} \tag{3.16}$$

where the last part is a unit conversion from viruses to cells.

The interpretation of k_a depends on whether attachment is diffusion- or reaction-limited. The maximum rate of attachment occurs when attachment is diffusion limited and every virus collision with the cell surface results in binding (52). This diffusion limited attachment rate can be calculated from a modified Scoluchowski equation (52)

$$k_{a(\text{diffusion})} = 4\pi r_{\text{cell}} D_v \eta \tag{3.17}$$

where r_{cell} is cell radius, D_v is the diffusion coefficient of the virus, and η is an efficiency factor accounting for the fact that virus can only attach to the cell surface where a receptor is present ($\eta \to 1$ as the number of receptors increases). For binding of AcNPV to *Spodoptera* cell lines (e.g. Sf-9), typical numbers are $r_{\text{cell}} = 9\ \mu\text{m}$, $D_v = 4 \times 10^{-8}\ \text{cm}^2/s$ (at 28°C from Stokes–Einstein equation corrected for rod-shape of virus, 40 nm × 300 nm), and $\eta = 0.5–1$ (50,52). Inserting these values in Equation 3.17, the diffusion limited rate is found to be $k_{a(\text{diffusion})} \sim 1–3 \times 10^{-8}\ \text{cm}^3/\text{cell/min}$.

When attachment is reaction-limited, k_a is equal to $k_f(\alpha N_r)$, where k_f is the intrinsic forward rate constant for binding of a single viral attachment protein to a receptor, α is the number of attachment proteins per virus, and N_r is the average number of receptors per cell.

Equation 3.17 is for cells in suspension (i.e. spheres) and the corresponding equation for cells in a monolayer is $k_{a(\text{diffusion})} = 4r_{\text{cell}} D_v \eta$. Assuming limited spread in the monolayer and assuming that receptors do not localize on the exposed surface, the theoretical ratio of $k_{a(\text{diffusion})}^{\text{suspension}}$ to $k_{a(\text{diffusion})}^{\text{monolayer}}$ is π. For reaction-limited attachment, this ratio is 4, the ratio between exposed surface area in suspension and in monolayer. Hence, $k_{a(\text{diffusion})}^{\text{suspension}} / k_{a(\text{diffusion})}^{\text{monolayer}} \sim 3–4$ can be used as general correlation and a ratio of almost 3 is indeed observed experimentally (52).

The observed attachment rate varies with virus, host, medium, mode of infection, and cell density (or "health" of cells). For Sf-9 cells propagated in serum-free SF900II suspension cultures, we observe attachment rates of $\sim 1.8 \times 10^{-8}\ \text{cm}^3/\text{cell/min}$, that is around the diffusion limit, up to a cell density of $4 \times 10^6\ \text{cells/cm}^3$ (Fig. 3.6), which corresponds to the optimal cell yield for this system (53). The attachment rate for the same virus and cell line in serum containing IPL-41 suspension cultures is only one-fifth, highlighting the sensitivity of attachment to medium composition (54).

Attachment continues after the initial infection. For baculovirus, the attachment rate remains at noninfected level

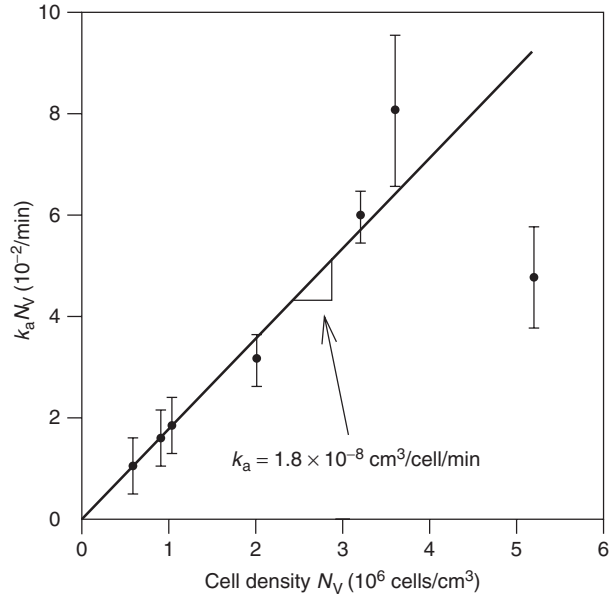


Figure 3.6. Attachment rate of recombinant AcPNV virus to Sf-9 cells in serum-free medium. Suspension cultures were incubated with ~50–100 radioactive labeled virus particles per cell and the attachment determined from the exponential decline in free virus concentration.

for 2–4 h, before falling exponentially until it reaches zero around 15–20 h postinfection (Fig. 3.7) (53). The 2- to 4-h period is consistent with the time it takes for the virus to internalize and commence transcription (52). The exponential decline may be attributed to the effect of natural protein turnover in the absence of new transcription and translation (the virus takes control over RNA and DNA replication, which is ultimately performed by a virus-specific replication apparatus). Mathematically, we can describe the infection rate for infected cells by

$$k_{\mathrm{ai}}(\tau) = \begin{cases} k_{\mathrm{a}}, & \tau \le \tau_{\mathrm{IE}} \\ k_{\mathrm{a}} e^{-\beta_{\mathrm{i}}(\tau - \tau_{\mathrm{IE}})}, & \tau > \tau_{\mathrm{IE}} \end{cases} \tag{3.18}$$

where τ is a measure of how long cells have been infected, k_{a} is the uninfected infection rate, β_{i} is the decline rate, and τ_{IE} is the duration of the immediate early period, that is the postinfection period until cell behavior is affected. The fit of Equation 3.18 to real data is shown in Fig. 3.5.

Internalization follows different routes for different viruses. Baculovirus enters cells through receptor-mediated endocytosis followed by low-pH mediated fusion of the viral and endosomal membrane (52). A similar mechanism is used by orthomyxovirus (e.g. influenza), togavirus (e.g. Semliki Forrest virus, rubella, yellow fever, dengue), and rhabdovirus (e.g. rabies). Internalization is reasonably fast (of the same order or faster than binding) and will not saturate under normal infection conditions (52). Only 50% of AcNPV virus is effectively internalized with the remainder found stuck on the outer membrane (52,53). A similar efficiency has been observed for Semliki Forrest Virus and it appears to reflect the efficiency of endosomal fusion rather than defective virus (51). Indeed, Dee and Shuler have presented evidence that low estimates for infective to total virus particles normally observed for AcNPV (typically 1 in 100–300) is caused by inadequate virus assays rather than truly defective viruses (51). It is possible that all virus particles in a low-passage inoculum are fully functional, but half gets randomly routed from endosomes to the lysosomes and released back to the cell surface following partial degradation.

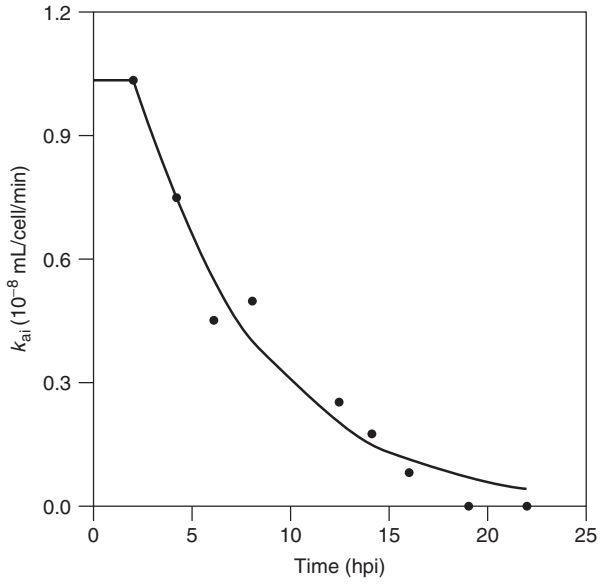


Figure 3.7. Attachment of AcPNV virus to Sf-9 cells in serum-free medium following infection. Cells were infected at 2.3×10^6 cells/mL at an MOI of 5.

Accurate virus titers are crucial to predict the behavior in low multiplicity infections. While it probably matters little for kinetics if cells are infected with 5 or 50 infective viruses (the result is a synchronous infection in both cases), an infection at 0.01 virus per cell will behave very differently from an infection with 0.001 virus per cell. For Equation 3.16 to make any sense, V must represent the true number of infective viruses.

3.5.3 Mass Balances

Mass balances are formed by combining the population balance model with the virus attachment model and infection cycle model. For example, the virus titer in a batch culture is described by the ordinary differential equation

$$\begin{aligned} \frac{\mathrm{d}V}{\mathrm{d}t} = & -k_{\mathrm{a}} N_{\mathrm{V}} V \text{ attachment to non-infected cells} \\ & - \int_{\tau=0}^{\infty} k_{\mathrm{ai}}(\tau) n(t,\tau) \mathrm{d}\tau \text{ attachment to infected cells} \\ & + \int_{\tau=0}^{\infty} r_{\mathrm{VR}}(\tau) n(t,\tau) \mathrm{d}\tau \text{ production} \\ & - k_{\mathrm{V}} V \text{ degradation} \end{aligned} \tag{3.19}$$

where the integrals are used to "sum up" the contributions to binding and production of cells at different stages of infection.

Similarly, for substrate, the mass balance for a batch culture is

$$\begin{aligned} \frac{\mathrm{d}S}{\mathrm{d}t} = & -q_{\mathrm{S}} N_{\mathrm{V}} \text{ consumption by noninfected cells} \\ & - \int_{\tau=0}^{\infty} q_{\mathrm{S}}(\tau) n(t,\tau) \mathrm{d}\tau \text{ consumption by infected cells} \end{aligned} \tag{3.20}$$

3.5.4 Solving the Model

In order to solve the model, the population balance, virus mass balance, and substrate mass balance models must be solved simultaneously. If we use a simple substrate depletion model, the maturation velocity is constant, $\nu = 1$, until

depletion after which, all cellular processes are assumed to cease. Prior to depletion the model is

$$\mathrm{IR}(t) = k_a N_V V \tag{3.21a}$$

$$\frac{dN_V}{dt} = (\mu - k_d)\ N_V - \mathrm{IR}(t) \tag{3.21b}$$

$$\frac{\partial n}{\partial t} + \frac{\partial n}{\partial \tau} = 0 \tag{3.21c}$$

$$\frac{dV}{dt} = -k_a N_V V - \int_{\tau=0}^{\infty} k_{ai}(\tau) n(t,\tau) d\tau + \int_{\tau=0}^{\infty} r_{VR}(\tau) n(t,\tau) d\tau - k_V V \tag{3.21d}$$

$$\frac{dS}{dt} = -q_S N_V - \int_{\tau=0}^{\infty} q_S(\tau) n(t,\tau) d\tau \tag{3.21e}$$

$$N_V(0) = N_0 \quad n(0,\tau) = 0 \quad n(t,0) = \mathrm{IR}(t)$$
$$V(0) = V_0 \quad S(0) = S_0 \tag{3.21f}$$

In this case, Equation 3.21b has the simple solution

$$n(t,\tau) = n(t-\tau, 0) = \mathrm{IR}(t-\tau) \tag{3.22}$$

that is, the number of cells of infection age τ at true time t is exactly the number of cells infected $(-\tau)$ hours earlier. If we introduce the variable, $s = t - \tau$, Equation 3.21c is converted to

$$\frac{dV}{dt} = -k_a N_V V - \int_{s=0}^{t} k_{ai}(t-s)\mathrm{IR}(s) ds + \int_{s=0}^{t} r_{VR}(t-s)\mathrm{IR}(s) ds - k_V V \tag{3.23}$$

The integrals on the right hand side of Equation 3.23 can be calculated at each time point, t, by numerical integration using the infection rates, IR(s), in previous time points as nodes. Thus, the problem can be solved using a standard ordinary differential equation (ODE) solver. We use a variable step-length, improved Euler algorithm, and the trapezoidal rule for integration. It should be stressed that Equation 3.22 holds only when the infection velocity is constant. If we introduce a more accurate description of infection velocity under substrate limitation, such as Equation 3.12, the solution is nontrivial and requires a numerical method for solving the first order partial differential equation and the ODEs simultaneously (e.g. method of lines).

Figure 3.8 illustrates the model's ability to predict the behavior in low MOI experiments. All parameters were obtained from high multiplicity infections in shaker flasks, yet the model adequately predicts the dynamics of a culture infected at a MOI 4 orders of magnitude lower, in which total infection occurs only after tertiary infections.

3.5.5 Using the Model

Having introduced this relatively complex modeling framework, it is important to return to basics such as how does

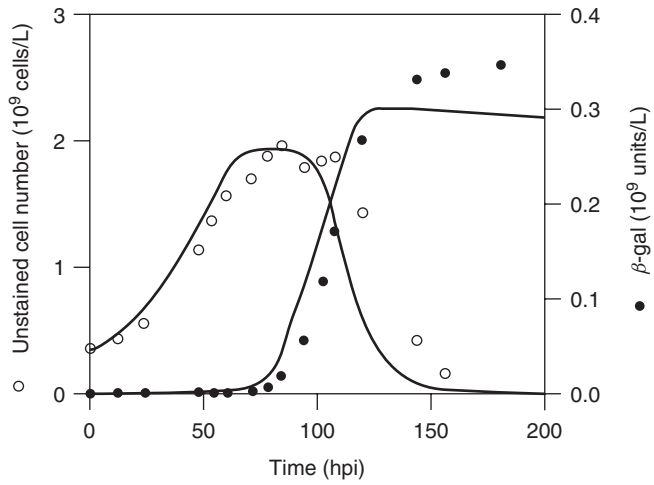


Figure 3.8. Model fit. The model with parameters determined in high MOI shaker flask cultures was used to predict the behaviour in bioreactor cultures, where cells were infected at 0.35×10^6 cells/mL at an MOI of 0.0001.

this help us in developing better viral production processes? This final section will illustrate how we have used the model to develop very low MOI infection processes.

There is substantial commercial incentive to use very low MOIs. The virus titer for a high yielding recombinant baculovirus is $\sim 2 \times 10^{12}$ PFU/L. Thus, to achieve synchronous infection (MOI = 5) in a 10,000-L batch culture infected around the optimal cell yield of 4×10^9 cells/L, we would need 100 L of virus stock. Due to the so-called passage effect (38)—serial passage leading to defective viruses—the virus stock should preferably be derived directly from a well-characterized Master Bank. Assuming that the Master virus stock is stored in 10-mL lots, the 100-L virus inoculum could be produced through 2–3 batch scale-up fermentations. In other words, a process relying on synchronous infection will consist of two parallel scale-up processes: one for cells and one for virus.

A more straightforward strategy is to inoculate the 10,000-L batch reactor directly with the 10-mL virus stock. This would obviously lead to an infection at a very low MOI and total infection would rely on secondary and tertiary infections. According to the cell yield concept, if the right cell density is chosen at TOI, the culture will reach the optimal cell density and yield the optimal product titer. That this actually works was illustrated in Fig. 3.2, where MOIs down to 0.0001 were used. Figure 3.2 does not address two important issues concerning the utility of low multiplicity infection: dispersion and reproducibility.

Intuitively, low MOI infection must lead to dispersion in product release and, hence, an undesirable increased exposure of the product to the culture environment (an important issue with labile viral products). Model simulations, however, revealed that low MOI infections in the baculovirus system do not necessarily result in significant dispersion. The reason for limited dispersion is that only a small fraction of cells are involved in building up the virus titer and that the final surge in virus titer leading to total infection occurs over a short period of time. Interestingly, dispersion does not increase with decreasing MOI. In fact, the highest level of dispersion will occur with an MOI of ~ 0.7 where half the *final* cell number is infected in first round and the other half (after cell growth) in the second round of infection.

These model predictions were confirmed experimentally (Fig. 3.9). Except for a delay in the onset of measurable production, lower MOIs did not alter the β-galactosidase concentration profiles (Fig. 3.9a). For each of the four multiplicities, the production period lasted ~ 36 h, occurred at an identical rate, and yielded approximately the same final β-galactosidase concentration. There is no apparent difference between infecting cells early at a very low MOI or late at a high MOI. This suggests that the final infection in all the experiments infected almost all of the cells and that this infection occurred over a relatively short period. For an MOI of 5, the final infection is also the primary infection and β-galactosidase production commenced at the onset of the very late phase 20–24 hpi. For an MOI of 0.01, only 1% of the cells are infected in the primary infection. The secondary and final infection appears to have occurred around 24 hpi, leaving another 20–24 h until the commencement of the major release period. Similarly, for MOIs of 0.001 and 0.0001 two and three rounds of infections, respectively, seem to have preceded the major final infection. The point is further illustrated by comparing the ratio of intracellular to total β-galactosidase yield for the four MOIs (Fig. 3.9b). In all four cases, the maximum intracellular β-galactosidase level was 50–60% of the total activity obtained at the end of the culture and the time to achieve this level was always 24 h after the onset of production.

The real challenge of performing low MOI infections is to ensure that the final infection reproducibly occurs when the culture has reached the optimal cell yield. In high MOI cultures, we can track the cell density all the

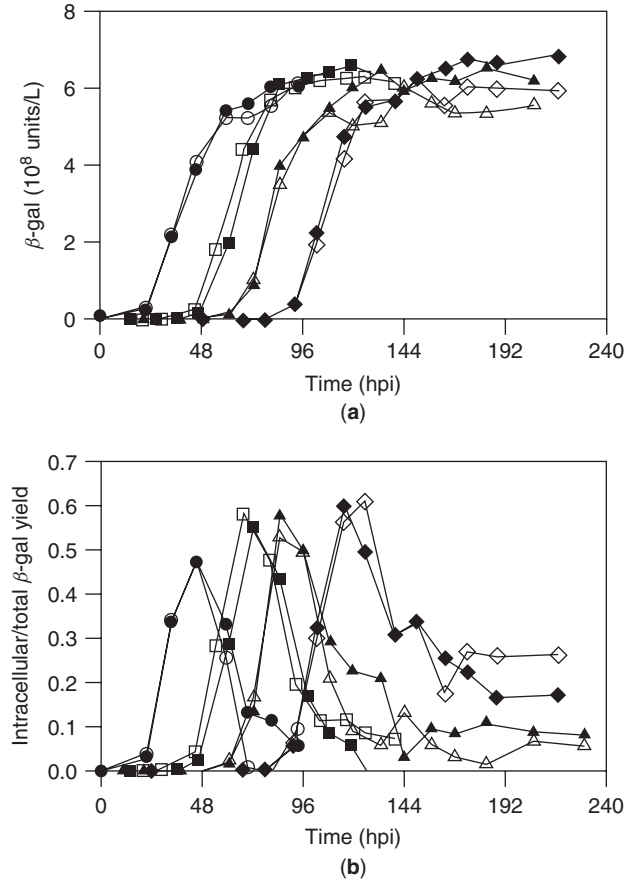


Figure 3.9. β-Gal production profiles for the best infections performed at MOIs of 5 (circle), 0.01 (square), 0.001 (triangle), 0.0001 (diamond) in shaker flasks. The figure shows (a) the total β-gal concentration and (b) the ratio of intracellular on total β-gal concentration.

way and cause infection when the culture reaches the optimal cell density. In contrast, low MOI cultures must be infected long before the optimal cell yield, and we rely on virus production and cell growth to reach the optimal cell density. The optimal cell density at infection, given the MOI, can be predicted using the model as was done in the above experiments and the main issue is to ensure reproducible behavior of the culture. Inherent variability in cell growth and relatively inaccurate assays make these a nontrivial task in the laboratory environment. For example, in our experience the specific growth rate of Sf-9 cells changes over their useful culture lifespan from $\sim$0.026 h^{-1} a month after thawing to 0.032 h^{-1} 3–5 month later, before they rapidly degenerate. In an industrial setting, where cells are taken from a well-characterized Master Bank, this should be less of a problem. Similarly, the low virus inoculum requirement means that the virus is taken directly from a well-characterized Master Bank thereby avoiding variation caused through scale-up processes.

REFERENCES

1. Earle WR, Bryant JC, Schilling EL. Ann N Y Acad Sci 1954; 58: 1000–1011.
2. Pay TWF, Boge A, Menard F, Radlett PJ. Dev Biol Stand 1985; 60: 171–174.
3. Radlett PJ. In: Fiechter A, editor. Volume 34, Advances in biochemical engineering/biotechnology (Vertebrate Cell Culture I). Berlin, Heidelberg: Springer-Verlag; 1987. p. 129–146.
4. van Wezel AL. Nature 1967; 216: 64.
5. Dureux B, Canton P, Gerard A, Strady A, Deville J, Lienard M, Ajjan N. Lancet 1986; 2: 98–98.
6. Montagnon BJ, Fanget B, Vincent-Falquet JC. Rev Infect Dis 1984; 6 Suppl 2:S341–S344.
7. Power JF, Nielsen LK. Cytotechnology 1996; 20: 209–219.
8. Enden G, Zhang YH, Merchuk JC. J Theor Biol 2005; 237: 257–264.
9. Gotoh T, Chiba K, Kikuchi K. J Chem Eng Jpn 2004; 37: 1357–1366.
10. Haas R, Nielsen LK. Biotechnol Bioeng 2005; 91: 768–772.
11. Hu YC, Bentley WE. Chem Eng Sci 2000; 55: 3991–4008.
12. Jang JD, Sanderson CS, Chan LCL, Barford JP, Reid S. Cytotechnology 2000; 34: 71–82.
13. Roldao A, Carrondo MJT, Alves PM, Oliveira R. Comput Chem Eng 2008; 32: 68–77.
14. Sanderson CS, Barford JP, Barton GW, Wong TKK, Reid S. Biochem Eng J 1999; 3: 219–229.
15. Granados RR, Federici BA, editors. Volume 1 and 2, The biology of baculoviruses. Boca Raton (FL): CRC Press; 1986.
16. Miller LK. Annu Rev Microbiol 1988; 42: 177–199.
17. Van Lier FLJ, Vlak JM, Tramper J. Anim Cell Biotechnol 1992; 5: 169–188.
18. Vlak JM, de Gooijer CD, Tramper J, Miltenburger HG, editors. Volume 2, Insect cell culture –fundamental and applied aspects. Dordrecht: Kluwer Academic Publishers; 1996.
19. Potter KN, Faulkner P, Mackinnon EA. J Virol 1976; 18: 1040–1050.
20. Slavicek JM, Mercer MJ, Kelly ME, HayesPlazolles N. J Invertebr Pathol 1996; 67: 153–160.
21. Hink WF, Thomsen DR, Davidson DJ, Meyer AL, Castellino FJ. Biotechnol Prog 1991; 7: 9–14.
22. Wu JY, King G, Daugulis AJ, Faulkner P, Bone DH, Goosen MFA. J Ferment Bioeng 1990; 70: 90–93.
23. Gardiner GR, Stockdale H. J Invertebr Pathol 1975; 25: 363–370.
24. Goodwin RH, Adams JR. In: Kurstak E, Maramorosch K, Dubendorfer A, editors. Invertebrate systems *in vitro*. Amsterdam: Elsevier/North Holland Biomedical Press; 1980. p. 493–509.
25. Vaughn JL, Fan F, Dougherty EM, Adams JR, Guzo D, McClintock JT. J Invertebr Pathol 1991; 58: 297–304.
26. Weiss SA, Gorfien S, Fike R, Disorbo D, Jayme D. In: Proceedings of the 9th Australian Biotechnology Conference; 1990 Sep 24–27; Gold Coast; 1990. p. 220–231.
27. Weiss SA, Whitford WG, Godwin GP, Reid S. In: Workshop on Baculovirus and Recombinant Protein Production Processes; Interlaken; 1992. p. 306–315.
28. Caron AW, Archambault J, Massie B. Biotechnol Bioeng 1990; 36: 1133–1140.
29. Hink WF, Strauss EM, Ramoska WA. J Invertebr Pathol 1977; 30: 185–191.
30. Radford KM, Reid S, Greenfield PF. Anim Cell Technol Basic Appl Aspects 1992; 4: 419–424.
31. Reuveny S, Kim YJ, Kemp CW, Shiloach J. Biotechnol Bioeng 1993; 42: 235–239.
32. Stockdale H, Gardiner GR. J Invertebr Pathol 1977; 30: 330–336.
33. Brown M, Faulkner P. J Invertebr Pathol 1975; 26: 251–257.
34. Dougherty EM, Weiner RM, Vaughn JL, Reichelderfer CF. Appl Environ Microbiol 1981; 41: 1166–1172.
35. Licari P, Bailey JE. Biotechnol Bioeng 1991; 37: 238–246.
36. Licari P, Bailey JE. Biotechnol Bioeng 1992; 39: 432–441.
37. Kool M, Voncken JW, Vanlier FLJ, Tramper J, Vlak JM. Virology 1991; 183: 739–746.
38. Wickham TJ, Davis T, Granados RR, Hammer DA, Shuler ML, Wood HA. Biotechnol Lett 1991; 13: 483–488.
39. Wong KTK, Peter CH, Greenfield PF, Reid S, Nielsen LK. Biotechnol Bioeng 1996; 49: 659–666.
40. Shuler ML, Cho T, Wickham T, Ogonah O, Kool M, Hammer DA, Granados RR, Wood HA. Ann N Y Acad Sci 1990; 589: 399–422.
41. De Gooijer CD, Koken RHM, Vanlier FLJ, Kool M, Vlak JM, Tramper J. Biotechnol Bioeng 1992; 40: 537–548.
42. Power JF, Reid S, Radford KM, Greenfield PF, Nielsen LK. Biotechnol Bioeng 1994; 44: 710–719.
43. Sanderson CS, Barford JP, Barton GW. Biochem Eng J 1999; 3: 203–211.
44. Roldao A, Vieira HLA, Charpilienne A, Poncet D, Roy P, Carrondo MJT, Alves PM, Oliveira R. J Biotechnol 2007; 128: 875–894.
45. Lindsay DA, Betenbaugh MJ. Biotechnol Bioeng 1992; 39: 614–618.
46. Chakraborty S. PhD thesis. Brisbane: The University of Queensland; 1998.

47. Dee KU, Hammer DA, Shuler ML. Biotechnol Bioeng 1995; 46: 485–496.
48. Hu YC, Bentley WE. Biotechnol Bioeng 2001; 75: 104–119.
49. Wickham TJ, Shuler ML, Hammer DA, Granados RR, Wood HA. J Gen Virol 1992; 73: 3185–3194.
50. Wickham TJ, Granados RR, Wood HA, Hammer DA, Shuler ML. Biophys J 1990; 58: 1501–1516.
51. Dee KU, Shuler ML. Biotechnol Prog 1997; 13: 14–24.
52. Dee KU, Shuler ML. Biotechnol Bioeng 1997; 54: 468–490.
53. Wong KTK. PhD thesis. Brisbane: The University of Queensland; 1997.
54. Power JF, Reid S, Greenfield PF, Nielsen LK. Cytotechnology 1996; 21: 155–163.

4

CELL CULTURE, ASEPTIC TECHNIQUES

JOHN M. DAVIS
School of Life Sciences, University of Hertfordshire, Hatfield, Hertfordshire, United Kingdom
KEVIN L. SHADE
Novartis Vaccines and Diagnostics, Speke, Liverpool, United Kingdom

4.1 INTRODUCTION

4.1.1 Microbial Contamination

We live in a world in which we are constantly surrounded by microbes, in our environment as well as upon and within our own bodies. Yet the successful performance of cell culture demands that we be able to maintain and manipulate our cultures free of all microbial contamination. As we cannot sterilize our cultures after manipulating them, we are completely dependent on *Aseptic Technique* to ensure that, in handling our reagents, cells, and all the associated equipment, we maintain the sterile environment that our cultures require.

Aseptic technique is a combination of many procedures all designed with the single goal of *minimizing the probability* of a microbe gaining access to the cell culture environment. It is important to appreciate this concept of minimizing the probability of contamination, as even the best aseptic technique cannot absolutely guarantee the maintenance of sterility (indeed all sterilizing techniques work on this same principle (1)). Thus, a methodical and fastidious approach is required, with attention to each element of each procedure. Dropping an element or cutting corners may not necessarily result in an actual contamination the first time, but will *increase the probability* of a contamination occurring. Consequently, it is essential that all the elements of an aseptic procedure are carried out consistently every time, making sterility breakdowns rare events.

4.1.2 Cellular Cross-Contamination

Cell culture requires more however, than just the type of aseptic technique used for the exclusion of microbes. Our work becomes at best meaningless, and at most potentially dangerous if we are not culturing the cells we think we are. Thus aseptic technique for cell culture must include procedures to minimize the possibility of contaminating one cell line with another. Evidence that such inadvertent cross-contamination could occur was presented in the 1970s when various cell lines from a number of different laboratories were all shown by isoenzyme analysis and/or karyotyping to be, in fact, HeLa cells; these findings were later extended to include contamination involving cells other than HeLa (2–4). Thus the second aim of all aseptic technique used for cell culture is to minimize the probability of contaminating our pure characterized cultures with microbes or other cells.

4.1.3 Biohazards

So far we have concentrated on the role of aseptic technique in protecting the cells that we are culturing. However, there is another element to almost all aseptic techniques used for cell culture, which is the protection of the operator from hazards posed by the cells or (re)agents used in their culture.

Both human and nonhuman cells may carry viruses pathogenic to humans, and at least one actual fatality has

Upstream Industrial Biotechnology: Expression Systems and Process Development, Volume 1, First Edition. Edited by Michael C. Flickinger.
© 2013 John Wiley & Sons, Inc. Published 2013 by John Wiley & Sons, Inc.

been documented, which was caused by inadequacies in the handling of such cells (5). Thus any new or poorly characterized cell line, or any cell line new to a laboratory *must* be handled as if it harbored a potential pathogen. Indeed, although the risk may be less when handling cell lines that have been extensively screened for microbiological contamination, the assays for such contaminants have limitations both in the level of contamination and the range of organisms they can detect. Furthermore, the continual discovery of previously unidentified human viral pathogens—for example, in the last 30 years we have seen the discovery of human retroviruses, and various "new" human herpes and hepatitis viruses—suggests that however extensive our microbiological screening, we can never be certain that a cell line might not contain a potentially dangerous viral "passenger." Moreover the risk is not limited to viruses as other contaminating microbes (such as mycoplasma) could be hazardous, and it may be that the cells themselves could pose a threat if inoculated into an operator via a puncture wound, for example owing to their oncogenic potential (6).

The commonest cell culture *reagent* that could be biohazardous is animal serum, of which the most widely used is fetal calf serum. This can contain a variety of microorganisms, but mycoplasma and bovine viruses are probably the most important. The agent that causes bovine spongiform encephalopathy (BSE) is also of concern, particularly as it appears to be the cause of variant Creutzfeldt–Jakob disease (vCJD) in humans (7–9). The chances of such agents being present in a batch of serum appears to be low (10) and can be minimized by purchasing only from the most reputable suppliers, who can document the source and health of the animals at slaughter and the standard of abattoir procedures, and who process and test the serum to minimize the chance of such agents appearing in the final product. Sourcing from a country where BSE is not endemic is important (see www.oie.int for the latest information), but as there was (and probably still is) a lot of "fake" Australasian and other sera on the market (much of it originating in countries where blue tongue, foot-and-mouth disease, and other viruses are a problem (11)) purchasing from a reputable supplier is doubly important. Further guidance on this topic has been issued by the World Health Organization (10).

Other reagents that may pose a hazard are those intentionally added to cultures, such as viruses that are being propagated or assayed. (Radioisotopes and other harmful chemicals may also pose a risk, but these hazards cannot be addressed by aseptic technique.)

Because of all the potential hazards outlined above, it is essential to carry out a full risk assessment before starting the culture of any cell line (12). The results of this will have a major impact on the aseptic techniques used, and most importantly on the environment in which they are carried out. Reference must always be made to the relevant local and national regulations governing the handling and containment of biological organisms (13).

4.1.4 Cell Culture Environments

The environments in which cell culture may be carried out vary both in the degree of protection given to the cells against external contamination, and the degree of protection afforded to the operator against potential hazards posed by the culture and its manipulation. In the early days of cell culture, procedures were carried out on the open laboratory bench, an environment which did little to protect the culture and nothing to protect the operator. As laminar flow cabinets or hoods—now more correctly termed *unidirectional airflow cabinets* (UDAFs)—and microbiological safety cabinets (MSCs) became available and our understanding of the possible hidden hazards associated with cell culture increased, so the move has been away from the open bench toward a more protective environment. However, cell culture can still be carried out successfully on the open bench, and under circumstances where the risk assessment indicates a minimal risk to the operator, and where using an appropriate MSC is not possible, doing so may still be justified. The vast majority of the principles and aseptic techniques utilized for culture are the same whether they are to be performed on the open bench or carried out within the environment of an MSC. Thus the general principles of aseptic technique for cell culture will be described first, as applied to working on the open bench. This will be followed by an examination of high efficiency particulate air (HEPA) filtration and the range of sophisticated equipment currently available, which employs HEPA filtration and provides protection to the operator and/or the cell cultures, and the adaptations in aseptic technique required to use this equipment safely and successfully. Finally, cleanrooms for use in cell culture will be examined.

4.2 ASEPTIC TECHNIQUE: GENERAL CONSIDERATIONS

4.2.1 Culture Equipment

All materials that come into direct contact with a cell culture *must* be sterile–aseptic technique only aims to maintain that sterility. As a consequence, all equipment such as flasks, bottles, dishes, pipettes, and so on must be treated by a sterilizing technique that gives a very high probability of sterility and is appropriate for the individual piece of equipment and the materials from which it is manufactured. The conditions of subsequent storage prior to use are also important. All sterile cell culture equipment should be stored in a clean, dry environment away from unnecessary airflow, and protected from possible sources of physical, chemical,

or other damage to itself or any of the packaging that maintains its sterile integrity. The integrity of such packaging (e.g. the bags containing single-use pipettes or the autoclave bags containing autoclaved materials) must be confirmed before the equipment is used: any equipment in damaged or inadequate packaging must be discarded, or repackaged and resterilized before use. Sometimes damaged equipment comes in perfectly good packaging; for example, crushed and cracked cell culture flasks can arrive inside a plastic bag that is still airtight. *Never* be tempted to use equipment over which you have the slightest doubt concerning sterility. It may be expensive to discard or resterilize, but not as expensive as your wasted time and the other materials you will waste working on a contaminated culture.

All equipment to be used directly in, or indirectly associated with, aseptic techniques must be carefully chosen with the three aims of aseptic technique constantly in mind:

- protection of the cells from microbes;
- protection of the cells from cross-contamination with other cells;
- protection of the operator from possible associated hazards.

Illustrations could be given relating to almost any piece of equipment, but two are given below:

1. Pipetting aids must always be used to operate pipettes, thereby protecting both the operator and the cells from each other. There are many designs, and the most comfortable and efficient for you and your type of work should be selected; one that is too awkward to use, or takes too long to pipette the volumes you use, will lead to tiredness, and a tired operator is a sloppy operator with poor aseptic technique.
2. An incubator is an essential piece of equipment, but must be kept clean in order to minimize the growth of microbes within it; so one that is easy to clean and has no inaccessible areas that will harbor microorganisms should be chosen. If humidified, the incubator should also have very good control of the humidity, as condensation forming on flasks and dishes can be a major source of microbial contamination. Indeed, persistent contamination can be a major problem in humidified incubators. This problem can be overcome by using a dry incubator (i.e. nonhumidified) so long as this is consistent with the research being undertaken. In the case of incubators maintaining a CO_2 atmosphere, one must check that the CO_2 sensor will operate satisfactorily under nonhumidified conditions. If a humidified incubator must be used, then it must be thoroughly cleaned and decontaminated at frequent and regular intervals, and a suitable microbial growth inhibitor [e.g. Roccal II (Sterling)] added to the humidifying water, which itself should be changed at weekly intervals. Where the incubator has a heat-sterilization cycle, this should be employed (at the highest temperature possible) for decontamination.

4.2.2 Working Area

Whether working in an MSC or not, a suitable working area must be chosen where the environmental flow of potentially contaminating particles can be minimized. A separate room, which is not a thoroughfare and is designated only for use when employing aseptic techniques, is preferable. This should be kept as clean as reasonably possible, with the minimum amount of equipment necessary, and preferably without shelving (which can harbor dust) above the working area. Air movement should be kept to a minimum commensurate with adequate ventilation and temperature control. If a separate room is not available, find a quiet corner of the laboratory where you can get as near as possible to the above conditions. (Siting of MSCs is dealt with further in the section titled Class II Microbiological Safety Cabinets.)

The work surface *must* be kept clean and tidy. Start with a clear surface, and wash it down with 70% ethanol or other liquid disinfectant (1). Then introduce to this clean area *only* those items required for a particular procedure. If these are many, it is better to break the procedure down into a series of steps and change the items in your clean area at suitable points, rather than work in a clutter. Arrange your equipment so that you have easy access to all items without having to reach across one to get to another, and make sure there is a large open space in the center on which to work. Having too many items in your clean area will inevitably lead, sooner or later, to you touching the sterile surface of (e.g.) a pipette against a nonsterile item. Cultivate a sensitivity to such undesired contacts, and always work within the central range of your vision. The same principle applies here as mentioned above: if you are in any doubt about the sterility of an item, don't use it—it is just not worth it.

Should you spill a liquid, mop it up immediately, and swab the surface down with your liquid disinfectant. Finally, when the work is done, remove all items from the work surface and swab down again.

4.2.3 Personal Hygiene

Before Work. Wash your hands. If you have long hair, tie it back or wear a suitable cap to keep it away from your face and the work. (Hair is a good source of microorganisms, particularly yeast, and when working with a Bunsen flame it is not unknown for individuals with long hair worn loose to set it on fire.)

During Work. Never eat, drink, smoke, chew, or apply cosmetics in the laboratory. This is to avoid bringing the hands (which may have hazardous material on them) into contact with the mouth or other mucous membranes, which offer easy access to the body. Similarly, always cover any cuts or cracks in the skin to avoid the ingress of unwanted material.

At the End of Work. Always wash your hands, irrespective of whether you have been wearing gloves or not.

4.2.4 Clothing

Before starting any aseptic handling make sure you are correctly clothed. A clean laboratory coat with long sleeves and close-fitting cuffs is the minimum requirement. Gloves can be useful (if carefully chosen so that they have the minimum adverse effect on manual dexterity and sensitivity), as they may contain any flakes of skin or loosely adherent microbes that may be present on the hands. Furthermore, if pulled up over the cuffs of the laboratory coat, they may contain any flakes of skin or microbes that might otherwise be expelled from the cuffs by currents of air forced down the sleeves by your movements. Nitrile or latex surgical gloves without a powder coating are the best type to use. Gloves should be sprayed or swabbed regularly during use with a liquid disinfectant (preferably 70% ethanol, as it simply evaporates leaving no residue) but, particularly if you are using a Bunsen, do not forget that 70% ethanol is flammable. Gloves also offer you a degree of protection from your cells. Keep an eye on the condition of your gloves, and if they get holed, discard them immediately and replace them with fresh ones. The use of a face mask is also worth considering, particularly if you have a moustache and/or beard (see comments on hair above).

4.2.5 Swabbing/Spraying

As far as possible, the surface of all nonsterile items should be dried (if necessary), then sprayed or swabbed with a liquid disinfectant before being introduced into your clean working area. This is particularly important for items coming from refrigerators, water baths, or humidified incubators, where microbial growth can be rife. Again, don't forget that 70% ethanol is flammable!

4.2.6 Capping

Deep screw caps are preferable to other types of closures for all bottles used routinely in aseptic techniques. They generally offer a good seal when screwed down, and offer a significant degree of protection to a bottle's contents even when only placed loosely in position, a situation that often occurs during aseptic handling. Bottles with International Organization for Standardization (ISO) threads can be used with a variety of caps of different materials, as well as other fittings designed for liquid handling.

4.2.7 Pouring

Pouring from one sterile container to another should be avoided if at all possible. Pouring generates aerosols, and they can carry cells or infectious biological reagents to other cultures or the operator. However, the most common risk is to sterility maintenance, as a bridge of liquid can be formed between the nonsterile outside and the sterile inside of a vessel and act as a conduit for the introduction of microorganisms. It follows that, if pouring *must* be done, then it must be done as a single delivery in one tip; even then it still carries a significant risk.

4.2.8 Flaming

When working on the open bench, it is common to use the flame of a Bunsen or similar burner to flame the necks of the bottles and screw caps before and after use, and glass pipettes before use only. This practice comes from microbiological technique, and its purported mechanism of action (and indeed its usefulness in cell culture) is open to some discussion. Any sterilizing or fixing effect on microbes is restricted to dry surfaces in direct contact with the flame. Some workers claim that if one works close to the flame, an updraught is created that prevents particles settling onto the work; others claim that the convection currents produced are not unidirectional and cause more problems than they solve. Either way, *flaming is not an essential part of sterile technique* even on the open bench, and should be avoided if at all possible when working in UDAFs or MSCs, as it disturbs the airflow and can be a fire hazard.

4.2.9 Pipetting

Pipettes commonly used in cell culture handle volumes from around 1 to 100 mL. Below 1 mL, Gilson- or Eppendorf-type pipettes (sometimes termed *micropipettes*) would normally be used along with single-use sterile disposable plastic tips (although for unmeasured volumes, glass or plastic Pasteur pipettes are also useful). From 1 mL upward, standard glass or disposable plastic pipettes probably represent the easiest way of manipulating measured volumes of liquids. Syringes can be used and are particularly useful for measuring volumes of highly viscous liquids such as glycerol or methylcellulose solutions. However, the hypodermic needles that fit them are not long enough to reach the bottom of most cell culture vessels, would be virtually impossible to use with viscous liquids, and carry the risk of causing needlestick and associated injuries to operators. Mixing needles—basically

a length of plastic tubing connected to a suitable fitting for a syringe—are a better option, will reach the bottom of all except some of the larger vessels, and are available presterilized (e.g. from Henleys Medical Supplies, Welwyn Garden City, Herts, United Kingdom). However, syringes may still prove unsuitable for manipulating some cells, owing to the high shear forces created when liquid passes through the relatively small aperture where the needle is mounted.

As mentioned before, pipettes must only be used in cell culture applications in association with a pipetting aid that must be suitable for the range of pipettes to be used. All pipettes should be fitted with a cotton (or similar) plug to maintain the sterility of the inside of the pipette when used with the (nonsterile) pipette aid. Suitable pipettes may conveniently be purchased as preplugged sterile single-use plastic items, which are discarded after use. Despite this, many laboratories still use glass pipettes, which appear to be a cheaper option in the long run. However, when the cost of unplugging, cleaning, drying, replugging and resterilization are factored in, any financial advantage claimed for glass pipettes is less evident. In addition, safety can be more of an issue with glass pipettes, as they are more prone to breakage, and consequently to injuring the operator if stressed or chipped during use.

When using a pipette, a number of precautions must be taken. The first is when inserting the pipette (particularly if it is a glass pipette) into the pipette aid. The pipette must be held at a point close to the pipette aid and excessive force must be avoided; it is easy to break a pipette, with the broken end then lacerating the hand or arm of the operator. Then, when sucking up liquid into the pipette, it is important that the cotton plug is not wetted. If it is, the pipette may effectively become blocked, or if it is not blocked then microbes can be introduced into the sterile liquid as it is being expelled from the pipette. Finally, in order to reduce the formation of aerosols, liquid should be expelled from the pipette as gently as possible, commensurate with the technique being employed. For the same reason, bubbles should not be blown through cell culture solutions, and the tip of a pipette should never be held above the lip of a vessel while expelling a liquid.

Pipetting aids can potentially harbor and spread contamination, but a little care can minimize this problem. They should be cleaned every time before use and regular decontamination should also be considered (some are designed to tolerate fumigation or autoclaving). In addition, if fitted with an integral filter, this should be changed regularly.

4.3 ASEPTIC TECHNIQUE: BASIC PROCEDURES

The range of aseptic manipulations that may be employed during cell culture is enormous, therefore the following procedure will be used to illustrate the way in which the principles discussed so far are brought together to form an aseptic procedure.

4.3.1 Manipulation of Cells and Liquid Reagents

This is illustrated by a procedure for supplementing a bottle of medium with fetal calf serum and then passaging a suspension cell line on the open bench. In this example, glass pipettes, presterilized within a metal can, are used for manipulating the solutions.

4.3.1.1 Protocol.

1. Bring medium and serum from the refrigerator or freezer, check the caps are secure, and then warm/thaw them in a water bath set at 37°C.

   The water bath should be sited away from the clean working area, as it can be a source of contamination, particularly bacteria and algae. To minimize this, water baths should be emptied, cleaned, and decontaminated on a frequent and regular basis, and preferably left empty when not in use. A contaminated water bath will contaminate any item placed in it. Indeed, such contamination should be assumed to occur every time a water bath is used, therefore items placed in it must be securely closed, and dried and decontaminated before use (see step 3).
2. Prepare your clean area by removing all unnecessary items and spraying/swabbing the bench with liquid disinfectant and allowing the surface to dry.
3. Bring to your working area only the equipment you need for the first step (supplementing the bottle of medium). The pipette can and pipetting aid should be sprayed down with liquid disinfectant before being placed in an easily accessible position within the clean working area. The Bunsen burner should also be introduced to the area; it should be clean, but should *never* be sprayed with ethanol (in case some has not evaporated by the time it is lit). Finally the medium and serum bottles are removed from the water bath, dried, sprayed with liquid disinfectant, and placed in the clean working area.
4. If ethanol or another flammable disinfectant has been used, wait until it has all evaporated before lighting the Bunsen. Open the pipette can and place the lid out of the way but still within the clean working area (i.e. with its mouth neither facing the ceiling nor in contact with the bench).

   In many cases, the lid can be placed under the open end of the pipette can to tilt the can upward at a convenient angle for removing pipettes. This also ensures that the lid is out of the way during subsequent operations.

5. Slacken the caps of the medium and serum bottles.
6. Remove a pipette carefully from the pipette can, touching the top of the pipette as little as possible with the fingers, and allowing the selected pipette to touch the other pipettes as little as possible, particularly near their tops.

   The aim here is not to touch any part of the pipette that will come into contact with your sterile solutions or equipment on the tops of the other pipettes which may have been touched by nonsterile hands or gloves.
7. Insert the pipette carefully into the pipetting aid, then flame the pipette by pushing it length ways through the Bunsen flame, rotating it through 180° (around the long axis of the pipette), then pulling it back through the flame. This should take no more than 3 s.

   Remember to hold the pipette close to its point of insertion into the pipetting aid and not to use excessive force, in order to avoid the dangers associated with breaking a pipette.
8. Pick up the bottle of serum in your free hand.
9. Grasp the lid of the bottle in the crook formed between the little finger and the palm of the hand holding the pipetting aid and unscrew the bottle from the lid.
10. Flame the neck of the bottle, by rotating it briefly in the Bunsen flame, then holding the pipette and bottle at an angle such that the pipetting aid and hand never get positioned vertically above the open mouth of the bottle, insert the pipette into the bottle.

    On the open bench, particles may fall downward from nonsterile items such as hands or pipetting aids onto whatever is underneath. Thus, the open necks of sterile bottles or flasks should never be below such nonsterile items, and this is the reason for working at an angle. This is also the case when working in a hood or cabinet with a vertical (top to bottom) airflow, such as a Class II MSC (see later section).
11. Draw up the required amount of serum into the pipette, then withdraw it from the bottle.
12. Flame the neck of the serum bottle, then bring it to its lid, and place the lid securely on the bottle. Pick up the bottle of medium and repeat steps 9 and 10.
13. Expel the contents of the pipette into the medium, withdraw the pipette, reflame the neck of the bottle, and replace the lid. Finally, discard the pipette into a container of disinfectant.

    To continue the process and use the freshly prepared medium to passage a suspension cell line.
14. Remove the bottle that contained the serum from the clean working area, as it is no longer required.

    This is to keep the working area as uncluttered as possible.
15. Take a new, sterile, plastic cell culture flask out of its sterile wrapping, ensure that it is not damaged and that its cap is secure, and place it in the clean working area.

    When first removed from its wrapping, the flask should be sterile both inside and out, and thus should not need spraying with disinfectant.
16. Pipette an appropriate amount of the freshly prepared medium into the flask using the technique detailed in steps 5–13, but here of course the liquid is withdrawn from the bottle of medium and expelled into the culture flask. It is recommended that the neck of the culture flask is *not* flamed, as the plastic could easily melt or catch fire.
17. Remove from the incubator the flask containing the cells to be passaged, and make sure its cap is secure. If there is any wetness on the outside of the flask, dry it immediately as such moisture is an excellent source of microbes. Spray or swab the outside of the flask with liquid disinfectant if this will not affect the culture (i.e., if the flask is sealed and there is no chance of the disinfectant reaching the cells). Once the flask has dried, introduce the flask to the clean working area.
18. Resuspend the cells and pipette an appropriate volume from the cell-containing flask into the flask containing fresh medium, again using the technique described in steps 5–13, and *not* flaming the necks of the plastic flasks. When expelling the cell suspension into the fresh medium, place the tip of the pipette either against the vessel wall or below the surface of the medium, and once the cells are expelled do not blow bubbles through the medium. Both these precautions are to avoid the formation of aerosols, as described earlier.
19. Place the new flask of cells in the incubator and discard the old flask of cells (to be destroyed by incineration or autoclaving). If the work is now finished, turn off the Bunsen, replace and/or secure any closures (lids on pipette cans, caps on bottles, etc.), remove all items from the clean working area, and spray and wipe down with liquid disinfectant.

4.3.1.2 General Note. Ethanol, including 70% ethanol solution, poses a real fire hazard when used with techniques that employ a Bunsen burner. It is recommended that in this situation a nonflammable disinfectant is used if at all possible.

As far as possible, only one cell line should be handled at a time, and each cell line must have a bottle(s) of medium dedicated for use only with that cell line and clearly labeled to this effect. All cultures and bottles of medium for one cell line must be removed from the working area,

the Bunsen turned off, and the area sprayed/swabbed down with disinfectant before introducing another cell line to the area. This should only be done after a gap of at least 5 min, to allow any possible cell-containing aerosols to dissipate. These precautions are to avoid cellular cross-contamination. Remember that working on the bench offers no protection to the operator from any biohazards present in the cell culture, and should only be undertaken if the risk assessment permits.

4.3.1.3 Working without a Bunsen. When working without a Bunsen, one must be even more fastidious with regard to maintaining the initial sterility of one's equipment. The advantage is that the fire hazard is eliminated, but one loses the comfort that if the outside of a pipette (for example) were to be nonsterile, then passing it through the Bunsen flame *might* sterilize it. Thus, for example, it may be worth using individually wrapped single-use pipettes rather than reusable ones, in order to avoid the potential for contamination when removing the pipette from the pipette can. Individually wrapped pipettes should be opened at the end furthest from the tip, and the open end of the wrapper turned inside out over the wrapping still in place, such that when the pipette is withdrawn it can only touch the inner surface of the wrapping, which should still be sterile. Similar precautions should be taken when removing other sorts of wrapping from sterile equipment.

Provided the maximum precautions are taken to maintain the initial sterility of all equipment, aseptic technique performed without a Bunsen can give at least as good results in terms of sterility maintenance as when using a Bunsen. Indeed, the decreased time of exposure to the environment caused by not having to flame the equipment may be positively advantageous in this respect.

4.3.2 Aseptic Manipulation of Equipment

The above handling guidelines should be sufficient to cover most cell culture operations carried out at the small scale. However, as the scale of operation increases, it may be necessary to aseptically assemble sterile pieces of equipment, for example, connect segments of tubing, or connect tubing to culture or media vessels. This is best achieved by completely covering the equipment to be sterilized in a wrapping that microbes cannot penetrate. Then, once sterilized, the equipment remains sterile until it is unwrapped immediately prior to aseptic assembly. In many cases it may be worth covering the actual assembly points separately to help maintain sterility. Assembly is then simply achieved after discarding the final wrapping on all assembly points. As with the aseptic techniques already described, manipulations are best performed wearing (sterile) gloves, and in an environment that will protect the equipment from airborne contaminants. In this case, that might be a Class II MSC, but could also be a vertical or horizontal *UDAF*, as sterile equipment poses no microbiological risk to the operator.

However, although the actual points of connection must always be sterile, it is not always possible for the whole of each piece of equipment to be sterile. An example of this might be when replacing an empty media vessel with a full one on a pilot-scale culture system, or when sampling from such a system via a septum. Maintenance of sterility during such manipulations may be facilitated by the use of a surface sterilizing reagent such as beta-iodine or 0.2% chlorhexidine gluconate ("Hibitane") in 70% ethanol. As an example, when disconnecting one piece of tubing connected to another by a Luer or similar fitting, and replacing it with a new one, one would proceed as follows:

1. Douse both halves of the existing connection, and both the new connector-half and its cover, plug or sheath, with the liquid surface sterilizing agent. This can be done conveniently by squirting the liquid disinfectant over the area from a squeeze bottle.
2. Using swabs made of segments of sterile butter muslin (or a similar absorbent and autoclavable cloth) soaked in the surface sterilizing agent, wrap the four half-connectors separately. This should be done such that the swab on each half-connector butts up against, but does not overlap, that on the other half. In order that any stray strands from the cut edges of the muslin do not get trapped in the new connection when it is made, these swabs should first be folded in half then placed on the half-connectors such that the folded edges butt together. Leave the swabs in place for at least 3 min to sterilize the covered surface.
3. Rapidly remove the cover, plug, or sheath from the new connector, break the old connection and make the new connection. This is done with the swabs still in place, and they are only discarded after the connection has been completed.

Wearing (sterile) gloves is strongly recommended. Also, note that if any of the tubes already contain liquid then they must be clamped before attempting this procedure.

It should be noted that the swabs soaked in surface sterilizing agent can fulfill two purposes. The first is to sterilize the area surrounding a connection. Thus, if there is any slight inaccuracy in making a connection, then the surrounding area that might be touched will be sterile and not compromise the sterility of the system. The second role is to act as a barrier between one's gloves (which may not be sterile) and the sterile surfaces.

Sampling from a septum is achieved in a similar way, but only the surface of the septum is sterilized using a

soaked swab, and in this case the swab is discarded before penetrating the septum with a sterile needle. (By the term *septum*, here we mean a small unit often marketed as a sterile injection site, not the large industrial type fitted to fermentors and similar equipment.)

As with all aseptic techniques, the surface sterilizing agent/swab technique gives no total assurance of sterility, and the relatively short exposure times and nature of the chemicals involved mean that some organisms may not be inactivated. However, in practice it appears to be an effective technique when used against those organisms commonly found in laboratories. We have run cell cultures in bioreactors using antibiotic-free medium for over 6 months in an ordinary laboratory, with hundreds of aseptic manipulations carried out as described. The cultures tested negative for bacteria, fungi, yeast, and mycoplasma at the end of this period.

4.4 HEPA FILTRATION

4.4.1 Introduction

Although performing aseptic techniques on the open bench can be successful, it offers no protection to the operator from any hazards posed by the work, and the high particulate load in the air of the average laboratory means that the chances of contamination of the work are always significant. These problems can be greatly reduced by performing the work in a suitable environment that incorporates a controlled flow of air from which the vast majority of both inert particles and associated viable contamination has been removed. This is achieved by the use of HEPA filtration.

HEPA filters are defined by their particle removal efficiency and their flow rate. They have a removal efficiency of at least 99.97% and they attain this efficiency when the air velocity through the filter is ~2 cm/s (4 ft/min). Although higher-grade filters have been developed recently [e.g. ultra low penetration air (ULPA) filters], these are intended for the microelectronics industry where contamination of the electronic components with very small particles can be a significant problem. This level of filtration is not normally required for pharmaceutical and biological (including cell culture) applications. Indeed, providing a level of filtration greater than that required can have significant cost penalties, and the associated working practices may make the work unnecessarily difficult and time consuming.

4.4.2 Mechanisms of Filtration

Filtration of a gaseous medium is not a simple process of sieve retention but rather the sum effect of several different mechanisms. The relative contributions of these various mechanisms can vary considerably depending on the size of the particles and the air velocity passing through the filter.

Sieve retention is the simplest mechanism of particle retention and occurs when the particle is larger than the spaces between the fibers of the filter medium. This sieving effect is only of significance for relatively large particle (>2 μm) and these would normally be captured by the coarser and less expensive prefilter placed upstream of a HEPA filter. It would not be cost effective to use HEPA filters to remove large particles.

The three most important particle removal mechanisms of HEPA filters are inertial impaction, diffusive retention, and interception (Fig. 4.1).

4.4.2.1 Inertial Impaction. As the air flows around the fibers of the filter medium (see the section titled Construction of HEPA Filters) the larger particles, because of their inertia, do not follow the airflow but continue in their original direction and become embedded in the fibers. This mechanism is a major factor for particles of >1 μm. As the air velocity through the filter increases, this mechanism becomes more effective.

4.4.2.2 Diffusive Retention. Small particles (<0.1 μm) are retained primarily by impaction resulting from Brownian motion (i.e., randomized movement caused by the particles in question being hit by other small particles or the molecules of the gas in which they are suspended) which causes them to deviate from the direction of the airflow. This random motion results in the impaction of the particles on the fibers of the filter.

4.4.2.3 Interception. Particles of an intermediate size (ca. 0.1–0.5 μm) have less inertia than the larger particles and tend to follow the flow of air around the fibers. If a particle strikes a fiber as it passes it, that is tangentially, or if it approaches one closer than half its diameter it will be captured and retained by it, this mechanism being interception.

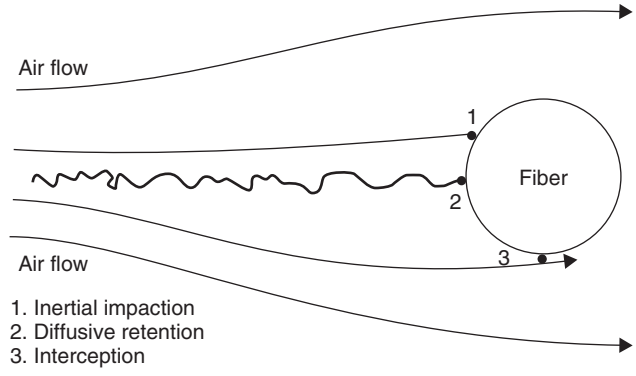


Figure 4.1. Schematic representation of mechanisms of filtration.

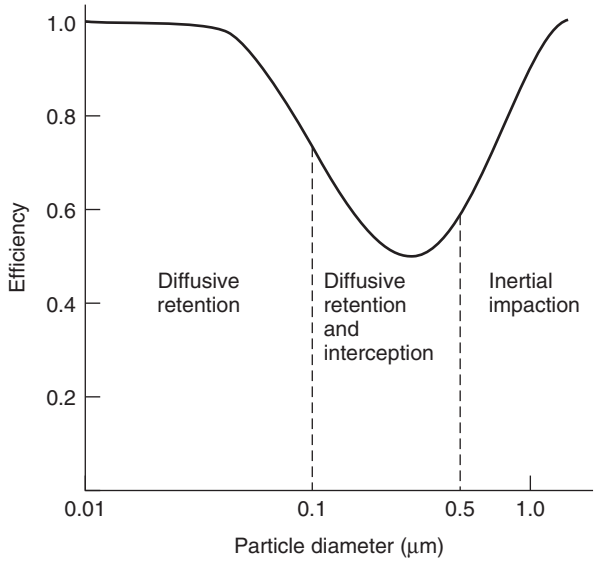


Figure 4.2. Classical efficiency curve for a HEPA filter.

Once a particle has come into contact with the fiber of the filter it is held by surface/surface interactions, such as electrostatic forces, and will become difficult to dislodge. It is the combination of these mechanisms that explains the efficacy of HEPA filters.

4.4.3 Filter Efficiency

Figure 4.2 shows the classical efficiency curve of a HEPA filter, the minimum efficiency being for a particle of about 0.2–0.3 μm, particles both larger and smaller being removed more efficiently. However, the actual minimum efficiency is variable and will depend on the following factors (14):

- the density of the individual particles;
- the velocity and mean free path of the particles;
- the thickness of the medium;
- the velocity, pressure and temperature of the air;
- the sizing and distribution of the fibers within the filter medium.

As penetration is a function of so many variables, the actual shape of the curve and the minimum efficiency will vary. Rather than considering a single most penetrating particle size it has been suggested that it would be better to think in terms of the most penetrating particle range, for example, 0.1–1.0 μm (14).

Filter efficiency decreases with increasing flow rate, conversely the lower the flow rate the more efficiently a filter will retain particles. Airflow velocities of around 90 ft/min, as frequently found in cleanroom situations, should not result in problems due to particle penetration of intact HEPA filters as any upstream particles are likely to be either too small or too large to penetrate to any significant degree. The large surface area of HEPA filters is designed to provide an adequate volume of filtered air at the flow rate required to maintain suitable conditions within the cleanroom or device (e.g. UDAF). It is possible, by increasing the amount of filter medium in a filter, not only to decrease the pressure drop across it but also to increase its efficiency. If the air velocity were reduced sufficiently it could be possible to achieve 99.97% removal of particles in the range 0.1–1.0 μm with a relatively coarse filter. However, the dynamics of filtration is but one factor necessary to achieve suitable air quality in any particular situation. The filtered airflow volume needs to be sufficient to allow adequate flushing of the critical area in order to cope with the particulate and microbiological contamination that may be introduced from the process equipment or the personnel.

4.4.4 Construction of HEPA Filters

The filter medium is a paper formed from fine glass fibrils, the higher the efficiency of the filter the higher the proportion of smaller fibers. The filters can be constructed in a number of ways depending on the nature of the system/room/cabinet and the predefined standards it must meet. Each method is intended to produce a relatively large surface area of filter medium, which is sealed within a rigid frame and with a suitable gasket to prevent the leakage of unfiltered air into the working environment. The filter medium is mounted in the frame, normally in one of the following ways (15):

4.4.4.1 Standard Filters. The sheets of filter medium are folded in parallel pleats, the pleats being separated by corrugated aluminum or Kraft paper separators. The filter medium and separators are assembled and bonded to the frame with a resin. The frame may be constructed of metal, wood/chipboard, or plastic.

For most biological or pharmaceutical applications filters with wooden/chipboard frames would not be considered suitable because these materials can themselves shed particles and because of the potential for microbiological growth on the frame, particularly if they became damp. However in some applications, for example when used in certain chemical or biological processes, the use of wooden frames may be indicated in order to facilitate incineration after use.

4.4.4.2 Mini-Pleat Filters. This format is a modification of the standard filter but without the use of separators; the filter medium is folded in tighter pleats (~2–3 pleats/cm compared to ~1 pleat/cm for standard filters). To allow the air to flow satisfactorily the paper has in-built nylon

cords or molded media that protrude slightly from the paper folds in order to hold them apart. These filters can provide greater volume flow capacity and more uniform face velocities compared to standard filters but they are more expensive. However, as they hold approximately twice the surface area of filter medium when compared to the same size of standard filter unit, they may have advantages where space constraints are a problem or where extended use between filter changes is required.

4.4.4.3 Flanders Filters. This type of filter is constructed from crenellated corrugated filter paper, the surface "texture" acting in lieu of separators to keep the pleats apart. The crenellated surface and the absence of separators result in ~40% more available filtration area compared to standard filters. These filters, however, only fit patented frames. The filter-holding frames have a slot filled with thixotropic gel, which accepts a tongue on the filter edge, achieving an air tight seal without using a compressed gasket [the gaskets on both standard and mini-pleat filters use compressible gaskets made from closed-cell neoprene, polytetrafluoroethylene (PTFE), or molded polyurethane].

4.4.5 Testing of HEPA Filters

Filters are tested by the manufacturers to assign or confirm their particle removal efficiency. In addition, on-site testing after delivery and installation needs to be carried out to verify that no damage has occurred during storage, transportation, or installation. At times confusion has arisen regarding the purpose and intention of this on-site testing.

The tests carried out by the filter manufacturers use relatively sophisticated equipment to control challenge aerosol particle size, airflow rates and so on, and would normally consist of one of the following:

4.4.5.1 Hot DOP (Dioctylphthalate) Test. Thermally generated particles of dioctylphthalate (DOP), of an essentially monodisperse aerosol with a mean diameter of ~0.3 μm, is generated upstream of the filter and the percentage penetration determined by comparing the downstream concentration of particles to the upstream (100%) concentration.

4.4.5.2 Sodium Flame Test. An aerosol of particles of sodium chloride, mainly within the range of 0.02–2.0 μm with a median of 0.6 μm, is generated by atomizing a sodium chloride solution and evaporating the water. By comparing the upstream and downstream concentrations photometrically, the percentage penetration can be determined. The hot DOP and sodium flame tests produce substantially similar size distribution aerosols and the tests give comparable results.

4.4.5.3 Oil Mist Test. This is the basis of the German (DIN 24184) test. The principle of the test is the same as the DOP and sodium flame tests, but the test aerosol is an oil mist with a particle size between 0.3 and 0.5 μm.

The test normally carried out on-site is a cold version of the DOP test or a variant of it using, for instance, a different challenge aerosol such as mineral oil. An aerosol of polydisperse particles in the range 0.1–3.0 μm is generated, usually at ambient temperature, and introduced upstream of the filter, while the downstream filter face is scanned with a photometer to detect any leaks, again by comparing the upstream and downstream concentrations of the aerosol. It is normally accepted that a photometer reading of >0.01% is indicative of an unacceptable leak. There are a number of fundamental differences between this test and the more sophisticated tests used by the filter manufacturers to verify the particle removal efficiency (e.g., particle size distribution, concentration of the aerosol challenge, temperature control, airflow velocity control, etc.). This *in situ* test is intended to be a check of the integrity of the complete filter installation, and is not suitable to verify the particle removal efficiency of the filters.

4.5 HOODS AND CABINETS EMPLOYING HEPA FILTRATION

These can be divided into two categories: UDAFs, where a flow of HEPA-filtered air is used to protect the work from contamination by particulates, but which offer little or no protection to the operator from hazards posed by the work; and MSCs, all of which offer protection to the operator but which may or may not offer protection to the work.

4.5.1 Unidirectional Airflow Cabinets

4.5.2 Horizontal Flow

In these hoods, the flow of HEPA-filtered air is directed from the back of the hood across the work surface toward the operator. Thus these hoods should only be used for the manipulation of clean, preferably sterile, nonhazardous equipment and solutions, and never for cell culture (Fig. 4.3).

4.5.2.1 Vertical Flow. In these hoods the airflow is from top to bottom. Thus, air is not blown directly from the work at the operator as in a horizontal flow hood, but the absence of a front screen and of filtration of the exhaust air means that there is still no significant protection offered to the operator. Thus it is recommended that these hoods are also not used for cell culture (Fig. 4.4).

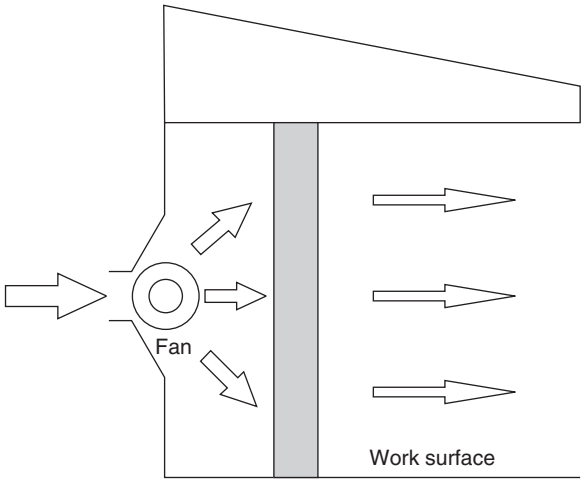


Figure 4.3. Schematic cross-section of a horizontal unidirectional airflow cabinet (arrows indicate airflow; hatched area = HEPA filter).

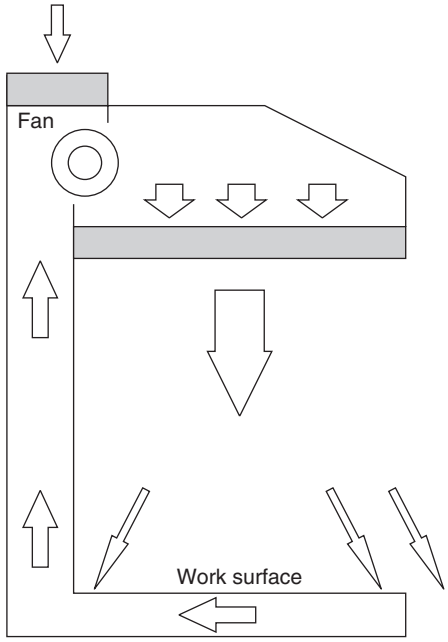


Figure 4.4. Schematic cross-section of a vertical unidirectional airflow cabinet (arrows indicate airflow; hatched areas = HEPA filters).

4.5.3 Microbiological Safety Cabinets

An MSC can be defined as a cabinet intended to offer protection to the user and environment from the aerosol hazards of handling infected and other hazardous biological material, but excluding radioactive, toxic, and corrosive substances, with air discharged to the atmosphere being filtered (16). Some, *but not all* of these cabinets will also offer protection to the work from environmental contaminants.

4.5.3.1 Class I MSCs. These cabinets operate by pulling in a constant stream of air from the room through the working aperture, and passing it through a HEPA filter to exhaust. The inward airflow through the working aperture protects the operator from particulates generated within the cabinet, and these particulates are prevented from escaping to the environment by the HEPA filtration of the exhaust. However, this type of cabinet offers no protection to the work from particles generated outside the cabinet. Class I MSCs are generally used for the handling of viruses and other biological agents that pose a moderate risk to the operator (Fig. 4.5).

4.5.3.2 Class II MSCs. These are the cabinets most commonly used for cell culture, as they are easy to use but offer protection both to the operator from particulates generated inside the cabinet, and to the work from particulates generated outside the cabinet (Fig. 4.6).

The work is protected by the vertical flow of HEPA-filtered air from the top of the cabinet, and by the fact that air entering the front of the cabinet is drawn directly away beneath the work surface without passing over the work. The operator is protected by the inflow of air at the working aperture, which prevents the outflow

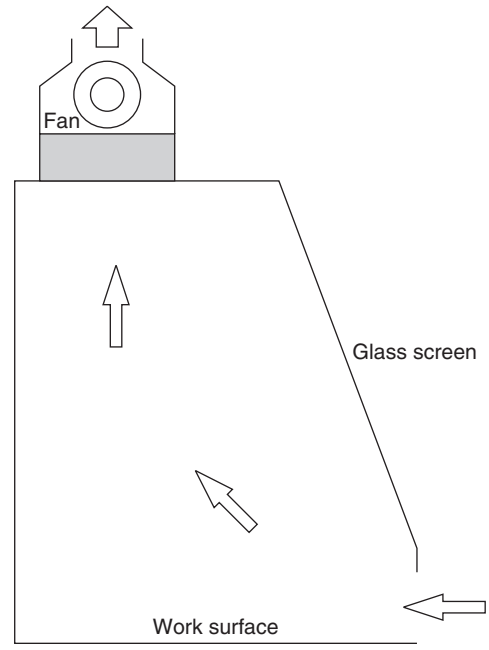


Figure 4.5. Schematic cross-section of a Class I microbiological safety cabinet (arrows indicate airflow; hatched area = HEPA filter).

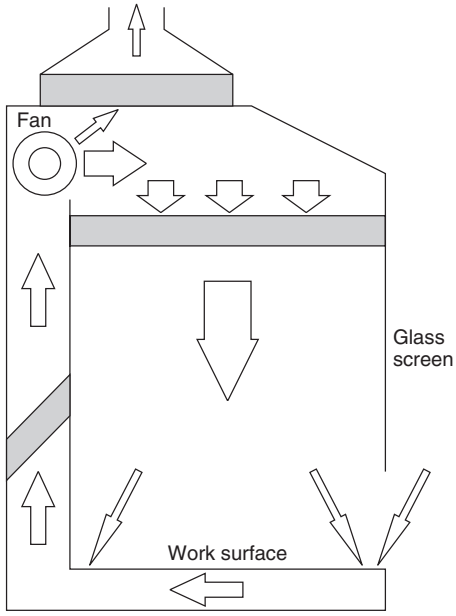


Figure 4.6. Schematic cross-section of a Class II microbiological safety cabinet (arrows indicate airflow; hatched areas = HEPA filters).

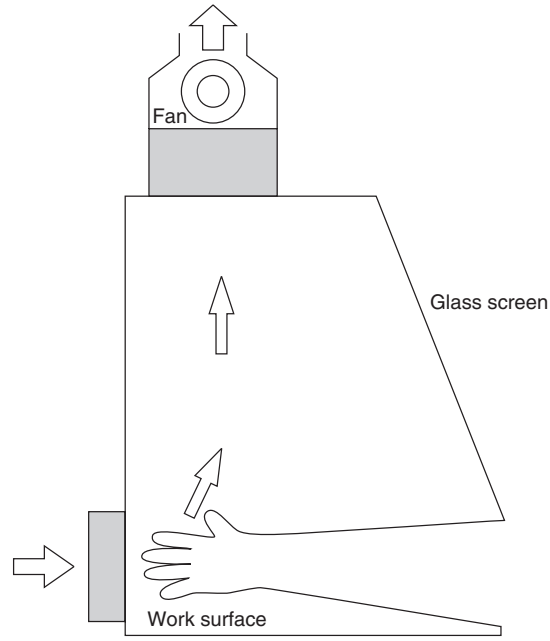


Figure 4.7. Schematic cross-section of a Class III microbiological safety cabinet (arrows indicate airflow; hatched areas = HEPA filters).

of particles from inside the cabinet, and by the fact that all the exhaust air is HEPA filtered before being released to the environment. Only a percentage of the total airfow within the cabinet is sent to exhaust, the amount required being that needed to compensate for the air constantly flowing into the cabinet at the front aperture; the balance of the air is recycled within the cabinet.

4.5.3.3 Class III MSCs. These cabinets offer maximum protection, both to the work and to the operator and environment, but are extremely cumbersome to use and are only normally employed when manipulating dangerous [Hazard Group 3 or 4 (13)] pathogens. In these cabinets, the operator is separated from the work by gloves mechanically attached to the cabinet, and both the inlet and exhaust air have airborne particulates removed by HEPA filtration systems (Fig. 4.7).

4.6 WORKING WITHIN UNIDIRECTIONAL AIRFLOW CABINETS AND MICROBIOLOGICAL SAFETY CABINETS

4.6.1 General

Before use, all cabinets/hoods should be switched on and allowed to run for at least 15 min before use, to establish the correct airflow and clear any airborne particles. When using cabinets that employ a blanking plate for the front aperture (Class I and II MSCs) the blanking plate should be removed immediately before starting the fan and placed on a *clean* surface (not the floor!). It is replaced once the fan has been stopped after use (although many cabinets are designed to run continuously). In all hoods/cabinets, the use of Bunsen and similar burners should be avoided if at all possible as they disturb the airflow pattern and may be a fire hazard. All hoods/cabinets must be kept as clean as possible, and the working surface should be cleaned with a suitable disinfectant before and after every use. Spills should be mopped up immediately and the working surface wiped with disinfectant. If anything should be spilt down the perforations in the working surface of a vertical UDAF or Class II MSC, then the working surface must be removed and the underlying area cleaned and treated with a suitable disinfectant. This should in any case be done at least weekly even if no known spills have occurred.

In order to operate efficiently, the hood/cabinet must be tested regularly (at intervals of not more than 1 year) for HEPA filter integrity, airflow direction and rates, and particulate containment and elimination of external contamination if appropriate (see the section titled Testing of Class I and Class II Microbiological Safety Cabinets). If used for handling level 3 pathogens, testing must be performed more frequently (i.e. at least every 6 months). All hoods/cabinets must be fully tested when first installed and whenever they are relocated within or between laboratories (see the section titled Class II Microbiological Safety Cabinets). Some cabinets may have integral airflow meters that continuously monitor performance, and cabinets should not be used if the meter

indicates that parameters are outside the range required for safe operation. Where such a meter is not incorporated into the cabinet's design, simple and regular (e.g. monthly) in-house testing using an anemometer can help to show consistency of performance, and indicate if, for example, a prefilter needs changing. However, this does not remove the necessity to check the cabinet's operation fully every 6–12 months, and after being installed or moved.

4.6.2 Unidirectional Airflow Cabinets

4.6.2.1 Horizontal Unidirectional Airflow Cabinets. Because the airflow is directed at the operator, these hoods must *never* be used for cell culture or when manipulating any other potentially hazardous material.

The type of aseptic technique described in the section titled Manipulation of Cells and Liquid Reagents should be adopted when working in such hoods. However, it must be modified such that any item that may not be sterile (e.g. hands and pipetting aids) should, instead of not being directly above any sterile openings (e.g. open bottles), not be directly *behind* them.

4.6.2.2 Vertical Unidirectional Airflow Cabinets. General aseptic technique is carried out as described for use on the open bench, without a Bunsen burner.

4.6.3 Microbiological Safety Cabinets

4.6.3.1 Class I Microbiological Safety Cabinets. As stated above, these cabinets are designed to protect the operator from the material being handled, and offer no protection to that material or the work being performed with it. Thus, such a cabinet must be positioned where the incoming air is as clean as possible. In addition, in order not to compromise the containment of particulates within the cabinet, it must be sited where there is minimum air turbulence outside the cabinet—see the next section (on Class II cabinets) for further details. The lack of protection offered to the work means that the amount of work carried out in a Class I cabinet should be kept to a minimum. For example, if performing a virus assay by plaque formation on a cell monolayer, the handling of the (uninfected) cells when preparing the monolayer should be carried out in a Class II cabinet. Only the preparation, dilution, and addition of the virus should be performed in the Class I cabinet.

Performing manipulations within the Class I cabinet is rather different from that described for all the other types of hood or cabinet, as the only way to protect the work from the incoming unfiltered air is to position equipment such that the airflow is directed away from any sterile area, for example open bottles or culture dishes. Thus, when removing material from a bottle, for example, the base of the bottle should be pointed into the airflow with the neck pointing toward the extract filter. In cases where equipment (e.g. Petri dishes or multiwell plates) must remain horizontal when opened, they should be positioned well to the rear of the cabinet away from the front aperture. The length of time that vessels are left open must in all cases be kept to a minimum. In other respects, aseptic technique used in Class I cabinets is the same as that described for use on the open bench in the section titled Manipulation of Cells and Liquid Reagents.

4.6.3.2 Class II Microbiological Safety Cabinets. Protection of both the work and the operator is dependent on the integrity of the inward airflow at the working aperture and its efficient and immediate removal through the perforations/slits in the front of the working surface. Eddies caused by (i) turbulent air outside the cabinet, or (ii) around the arms of the worker, can cause nonsterile incoming air to be directed across the top of the work surface, or air from within the cabinet to escape, unfiltered, to the environment. Two ways to avoid this are as follows:

1. Steps must be taken to reduce to a minimum the turbulence of the air in the vicinity of the front of the cabinet. This means that very careful consideration must be given to the siting of the cabinet in terms of its proximity to building/room structures (walls, columns, and doors), work benches, other cabinets, and routes of movement by other worker (Figs 4.8 and 4.9). Furthermore, in the vicinity of the cabinet the velocity of the air due to the room's ventilation system must be kept to a minimum. It is particularly important that air entering the room via grilles, diffusers, and so on should not discharge directly across or toward the aperture of the cabinet, and every attempt should be made to keep all air velocities in the room below 0.3 m/s. Clearly, when designing a new laboratory the siting of the MSCs must be decided early and incorporated into the design process. Positioning of cabinets in an existing laboratory similarly requires the most careful consideration, and all cabinets must be performance tested once in their new position, even if they have only been moved a short distance within the same room. These requirements apply equally to Class II and Class I cabinets.
2. The operator should avoid rapid movement of his/her arms in the working aperture, and should avoid coughing, sneezing, singing, whistling or, as far as possible, talking or being otherwise disturbed while working. It should always be remembered that the front perforations/slits are a nonsterile area, and thus all work should be performed at least 5 cm away from them. Similarly the perforations/slots at the rear of the working surface should be kept clear so as not to impede the downward flow of air in the cabinet.

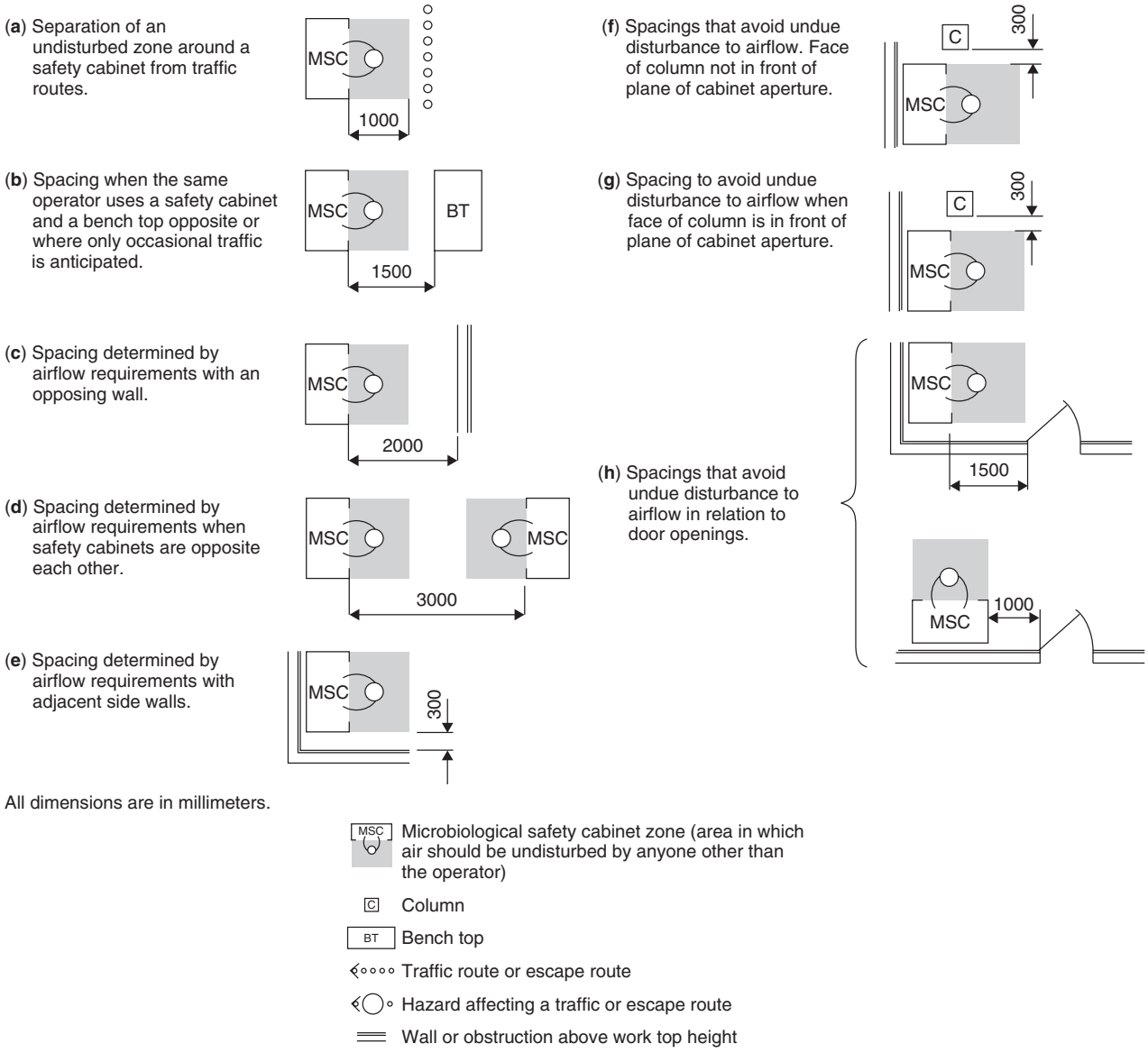


Figure 4.8. Siting of microbiological safety cabinets: recommendations for minimum distances for avoiding disturbance to the safety cabinet and its operator. [Reproduced with permission from BS 5726:2005.]

In all other respects, aseptic technique for use in a Class II MSC is the same as for work on the open bench without a Bunsen. Care must be taken, however, not to place any piece of apparatus in a position where it will obstruct the airflow within the cabinet (e.g. over a grille) or to inadvertently allow a piece of sterile apparatus to come into the nonsterile airflow at the front of the cabinet, for example when removing a pipette from a pipette can.

4.6.3.3 Class III Microbiological Safety Cabinets. These are such specialized pieces of equipment, and used to handle such hazardous materials, that no advice will be offered here. They must only be used after the most thorough and rigorous training.

4.7 TESTING OF CLASS I AND CLASS II MICROBIOLOGICAL SAFETY CABINETS

Class I and Class II MSCs require some common basic tests of function to demonstrate satisfactory performance, but a Class II cabinet also needs additional testing due to its design and method of operation.

The full details of the tests to be carried out and detailed test methods should be obtained from the relevant official

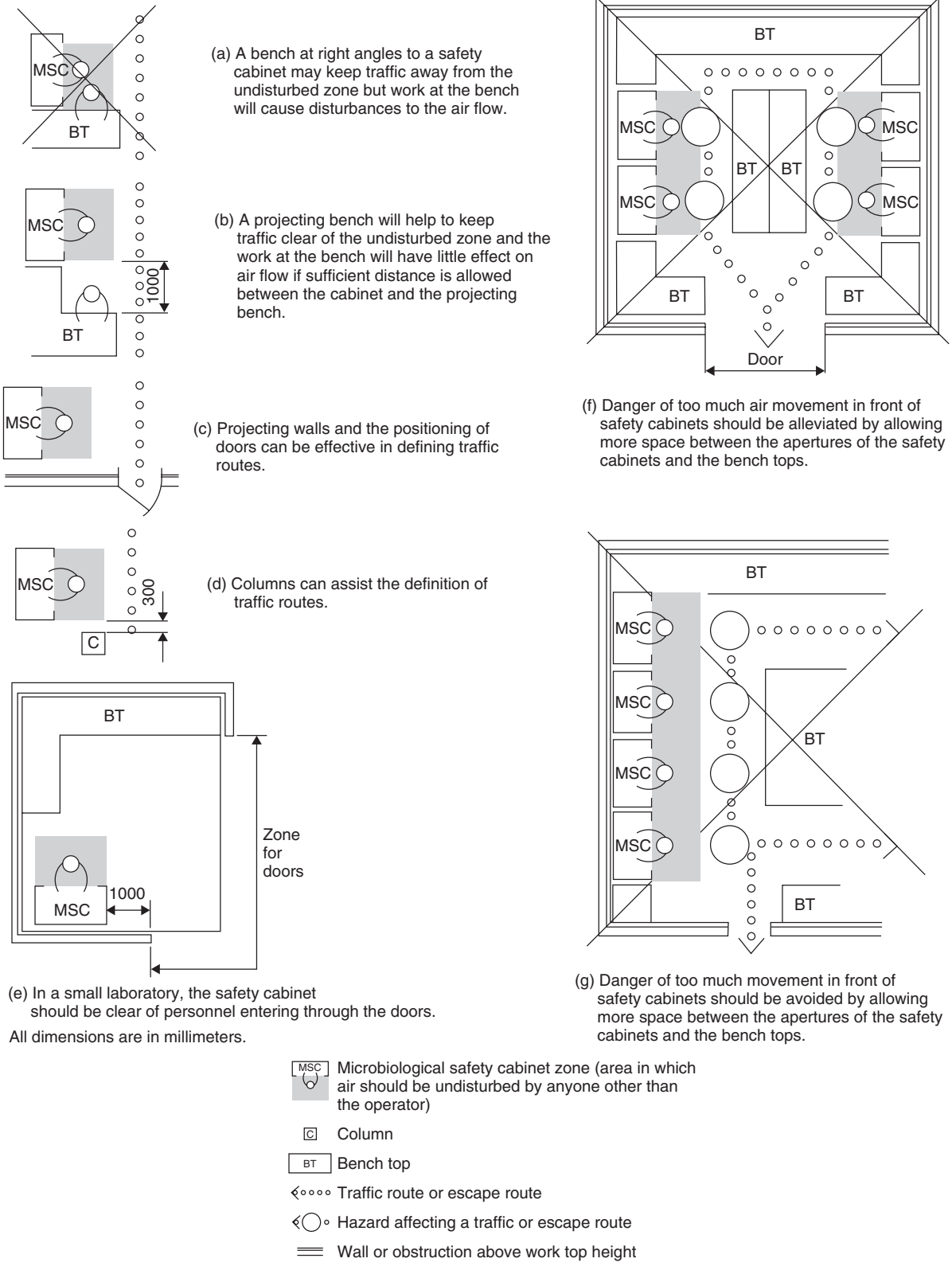


Figure 4.9. Siting of microbiological safety cabinets: Avoiding disturbance due to other personnel. Note: Siting arrangements which should be avoided are overlaid with a cross. [Reproduced with permission from BS 5726:2005.]

standards. However, the following is an overview of the testing requirements for these two types of safety cabinet together with an indication of their relevance.

4.7.1 Performance Tests

Table 4.1 provides a quick reference to the performance tests needed for Class I and Class II cabinets.

4.7.1.1 Operator Protection Tests. Ideally there should be no escape of aerosols from the inside of the cabinet to the external environment. However, with open-fronted cabinets some escape will be inevitable, but this should be within "acceptable" limits in order to minimize any risk to the operator.

This test is intended to quantify the degree of protection offered by the cabinet, and is defined as the ratio of exposure to airborne contamination generated on the open bench to the exposure resulting from the same dispersal of airborne contamination generated within the cabinet (16).

The test basically consists of generating a detectable aerosol within the cabinet and determining the proportion of the aerosol that escapes to the outside of the cabinet through the front aperture. During the test, the airflow entering the cabinet is disturbed in order to simulate the effect of an operator's arm, by introducing a cylinder through the front aperture. A number of different aerosols have been described, some of which have been incorporated into official standards.

4.7.1.1.1 Biological Method. This utilizes a bacterial spore suspension (e.g. *Bacillus subtilis* var. *globigii*) which is generated inside the cabinet using a nebulizer, and determining the number of spores escaping by using microbiological air samplers situated outside the cabinet but close to the open aperture. The protection factor is calculated by comparing the numbers generated inside to those detected outside.

Spraying spore suspensions can be potentially problematical because of the risk of inhalation by the operators, in addition to the problem of contaminating a cabinet that is intended to be used for cell culture work where bacteria-free conditions are needed. Another potential problem that is sometimes overlooked is that the precision of microbiological enumeration methods is not particularly good and can vary according to the type of air sampler used. Any variability in the counting method may well have an effect on the accuracy of the calculated protection factor. Another disadvantage to this method is that the agar plates exposed in the air samplers need to be incubated to allow the bacteria to grow and the result will not, therefore, be available until several days after testing.

4.7.1.1.2 The Potassium Iodide (KI Discus) Test. The arrangement of aerosol generator, cylinder, and samplers is similar to that used in the Biological Test, but in this case the challenge aerosol is produced by dropping a solution of potassium iodide under controlled conditions onto a rapidly rotating disc (17). The aerosol dries rapidly and produces particles in the size range of 3–10 μm. The particles are collected in membrane filter-based air samplers. The filters are then placed in a solution of palladium chloride enabling the particles to be seen and counted under a low-magnification microscope. The biological and potassium iodide methods give comparable results.

Other aerosol materials, such as polystyrene microspheres, have been used with the same kind of nebulizer utilized for spores, and seem to be suitable alternatives to the Biological and KI Discus tests. In addition, in order to enhance the level of particle detection, optical brighteners can be added to the membranes that are used to capture the aerosol (18,19).

The requirement for this test is that no individual protection factor obtained should be less than 1.0×10^5. This means that an operator working in a safety cabinet should be exposed to less than 1/100,000 the level of airborne contamination within the cabinet. Similarly, it means that the operator is exposed to less than 1/100,000 the level of airborne contamination compared to working on an open bench (assuming the same level of aerosol generation).

4.7.1.2 External Contamination Test. This is intended to demonstrate whether the curtain of air descending at the front of a Class II cabinet prevents contamination from

TABLE 4.1. Performance Tests for Class I and Class II MSCs

Test	Class I	Class II
Operator protection test	Yes	Yes
External contamination test	No	Yes
Cross-contamination test (where applicable)	No	Yes
Airflow checks	Yes	Yes
Temperature checks	No	Yes
Tests for leakage	Yes	Yes
Lighting level checks	Yes	Yes
Noise level checks	Yes	Yes

the room entering the working area of the cabinet where it might compromise the work being carried out. A spore suspension and nebulizer, as used in the Biological Operator Protection Method, is used to generate a large aerosol of spores outside the cabinet but close to the open aperture for a period of not less than 4 min, and the number of spores entering the cabinet during this period and for a further 5 min afterward is detected using exposed agar plates that are distributed over the working surface. The challenge aerosol should contain at least 3×10^6 spores.

Both the British and US National Sanitation Foundation standards permit no more than five colonies per test (in total, not per agar plate) and a control test, where the test is repeated but with the cabinet switched off, should have more than 300 colonies present on the agar plates.

This test carries similar problems of potential contamination with bacterial spores as mentioned in the previous section, but the Potassium Iodide Test could be used as a quicker and safer alternative. Another alternative would be to use an electronic particle counter to compare the particle counts both inside and outside the cabinet. However, unless a sufficiently large room particle count is obtained then test sensitivity may be a problem, in which case a particulate aerosol would need to be generated. A disadvantage of employing an alternative method to that specified in the relevant standard is the problem of setting acceptable limits for the test method employed.

4.7.1.3 Cross-Contamination Test. This test is intended to demonstrate whether aerosols generated on one side of the cabinet will contaminate materials at the other side. There are differences in the test methods described in the US and British standards, although the principle is the same. A nebulizer is used to generate a spore aerosol on one side of the cabinet and agar plates are used to detect the degree of contamination on the other side of the cabinet. The problems of bacterial contamination mentioned earlier, that is those of deliberately contaminating a cabinet intended for cell culture work, are equally applicable with this test. However, the relevance of the test needs to be considered carefully as it may not be applicable for most safety cabinet applications. It was originally introduced to test relatively large cabinet installations where more than one operator was working within a single cabinet and to provide some evidence that cross-contamination did not occur between one operation and the other. Where a single operator is working within a cabinet, this type of test is probably not necessary.

4.7.1.4 Airflow Checks. In order to function properly, air must enter Class I and Class II cabinets with a velocity sufficient to retain within the working area any aerosols or particles that may be generated. However, this flow rate should not be so high that turbulence is created within the cabinet; otherwise, there is an increased risk that air will spill out of the open aperture. Air movements into the cabinet can also be influenced by air currents from within the room (e.g. from the ventilation system, other equipment operating in the vicinity, opening and closing of doors, movement of people, etc.). The control of the inward flow of air in Class II cabinets is further complicated by the gain in energy (in the form of heat) of the recirculating air, which can disturb the balance between room air and cabinet air at their interface (20).

For Class I and Class II cabinets it is necessary to measure the inflow, and for Class II cabinets also the downward flow inside the cabinet. The expected airflows should be within the limits given below (Table 4.2).

In addition to velocity measurements, air visualization tests can be useful for checking that air flows inward over the whole of the working aperture. This can be particularly useful for demonstrating any effects caused by air currents within the room under different operating conditions. This can be done relatively simply using commercially available smoke pencils or cotton wool swabs soaked in titanium tetrachloride.

While this test is simple to perform and can provide evidence of satisfactory air movement, it is not particularly sensitive as smoke streams are transient and sometimes difficult to see (21). The use of schlieren photography has been

TABLE 4.2. Airflow Rates for Class I and Class II MSCs

Cabinet Type	Inward Velocity (m/s)	Downward Velocity
Class I	0.7–1.0[a]	N/A
Class II	≥0.4[b]	0.25–0.5[a]

[a] No individual measurement to differ from the mean by more than 20%.

[b] With Class II cabinets the downward flow of air within the cabinet cannot be so easily measured, as the inward flow of air at the open aperture varies in the vertical plane, normally having a higher velocity at the bottom. This also makes it difficult to make meaningful measurements of the inward airflow using anemometer readings at the aperture (or to set limits for a range of readings across this open face). To overcome this problem it is customary to measure the air velocity in the exhaust duct and then calculate the volume of air being extracted; this volume equates to that being drawn in through the front opening. The mean inward velocity can then be calculated by dividing the volume of discharge air by the cross-sectional area of the front aperture (20).

used successfully to visualize airflow patterns and provide more meaningful data on air movements in safety cabinets (22). However, although this is an elegant technique it is a method not available to most testing facilities.

4.7.1.5 Temperature Checks. This is a particular requirement for Class II cabinets because of the potential heat gain referred to earlier. After 4 h of continuous running with the fan(s) and lights on, the air temperature inside the cabinet measured 100 mm above the center of the working space should not rise by more than 8°C above the ambient laboratory temperature (16).

4.7.1.6 Test for Leakage. This test is to demonstrate the absence of any significant leaks through filters, seals, and construction joints. The same principle is used as that described earlier for the *in situ* testing of HEPA filters, using cold DOP or a suitable mineral oil. A test aerosol is generated on the dirty side of the filter, seals, and joints, the clean sides being scanned with a photometer probe.

Again it should be recognized that this test is not suitable for confirming the efficiency rating of the installed HEPA filters, but is only intended to detect leaks that may affect the integrity of the cabinet.

4.7.2 Testing Program

The following is not meant to be a comprehensive list of all the checks and tests to be carried out but is given as broad guidance:

4.7.2.1 Testing after Installation. After a cabinet has been delivered or moved, a number of tests will need to be carried out. Checks should be performed on the integrity of filters, gaskets, and construction joints in order to confirm that no damage or movement, that might affect performance, has occurred during transportation or installation. Performance tests for airflow, operator protection, and, ideally, external contamination should be performed. The test for cross-contamination may be appropriate in some cases. Also, if the cabinet was dismantled for transportation and then reassembled, checks must be made to detect any leakage of the cabinet carcass.

4.7.2.2 Periodic Testing. A suitable regular testing program will have to be put in place but the level and frequency of testing will be a matter of judgment, depending not only on the particular application and the type of work being carried out, but also on the need to satisfy health and safety requirements and whether full compliance to the relevant published standard is required.

In order to confirm continual satisfactory operation, the checks performed ought to include airflow measurements (and possibly air visualization checks), tests of filter and seal integrity, and operator protection tests. As a minimum these tests should be carried out annually, but more frequent testing will be required if high-risk pathogens are handled.

4.8 CLEANROOMS FOR CELL CULTURE USE

Modern cleanroom technology was originally developed for the military and space industries and was quickly utilized in the electronics industry. This technology was then embraced by the pharmaceutical and biological industries for aseptic operations. The basic design, construction, and operation of cleanrooms for different industries and different applications followed similar principles. A significant advance was the development of HEPA filters (23). Following the introduction of the conventional turbulent flow facilities using HEPA-filtered air, the laminar flow room concept developed, although this probably had greater application in the microelectronics industry and generally it was not seen as cost effective or directly applicable for many pharmaceutical cleanroom operations. This basic cleanroom technology was undoubtedly the best available at the time but for pharmaceutical and similar aseptic operations its limitations have become apparent. The direct involvement of people within the cleanrooms introduces a potentially significant particulate and microbiological bioburden to the process (24,25). The problems associated with the control of the personnel activities is becoming increasingly realized and we are now seeing reference to clean zones and the introduction of isolator systems for critical activities, for example filling or the loading of freeze driers. These can give a greater level of protection to the process and can also provide added protection to the staff where the materials they are handling may be toxic or a potential source of infection.

4.8.1 Cleanroom Standards

4.8.1.1 Design and Operation of Cleanrooms. Following the advent of cleanrooms, the need for suitable formal standards against which they could be designed, built and tested became apparent. Over the years, a number of different standards have been produced, but the scope and basis of the classification methods differed and this resulted in considerable confusion.

The standard that became well established and that greatly influenced other cleanroom standards was the US Federal Standard 209 (FS 209). Subsequently, other national standards were produced, but the basis of the particulate classification system adopted for each of them was modeled on FS 209. Some of these standards introduced different terminology, a different basis for classification, differing levels of requirements and so on. The use of these various standards sometimes created

difficulties when companies were operating or trading in different countries and where compliance with different standards was required. These differences undoubtedly combined to create confusion and uncertainty, and this was exacerbated when later versions of FS 209 changed from counts per cubic foot to counts per cubic meter. Thus 100 counts per cubic foot became 3520 counts per cubic meter. On top of this, the FS 209 nomenclature was changed at the same time, to become M followed by the logarithm to the base 10 of the maximum number of particles per cubic meter. Thus the "old" Class 100 became M 3.5, and similarly the "old" Class 10,000 became M 5.5.

As a consequence of the confusion and difficulties in trying to cope with so many different cleanroom standards, a concerted effort was made to harmonize these various standards and this resulted in the publication of ISO 14644—Cleanrooms and Controlled Environments. This was published under the auspices of the ISO and has superseded many of the separate national standards.

ISO 14644 encompasses a range of cleanroom issues such as classification, testing methods to prove compliance, design and construction, operation, requirements for separative enclosures, and so on and comprises the following parts:

Part1: *Classification of air cleanliness*

Part 2: *Specifications for testing and monitoring to prove continued compliance with ISO 14644-1*

Part 3: *Metrology and test methods*

Part 4: *Design, construction and start-up*

Part 5: *Operations*

Part 6: *Terms and definitions*

Part 7: *Separative enclosures (clean air hoods, glove boxes, isolators, and minienvironments)*

Part 8: *Molecular contamination*.

The ISO classification of air cleanliness is based on the following equation:

$$\mathrm{Cn} = 10^{N} \times (0.1/D)^{2.08}$$

where Cn is the maximum permitted concentration (in particles/m^3 of air) of airborne particles that are equal to, or larger, than the considered particle size; N is the ISO classification number; and D is the considered particle size, in micrometers.

In this standard the reference particle size is 0.1 μm. (This particle size was chosen largely for the benefit of the electronics industry, and marks another change from FS 209, which used 0.5 μm. However, the above equation permits interconversion on the basis of the particle size measured.)

Table 4.3 is based on the equation above, and shows the maximum limits for the various particle sizes specified for the different classes in ISO 14644-1.

Table 4.4 shows a comparison between some of the equivalent classes of ISO 14644-1 and the "old" and "newer" versions of FS 209.

The ISO standard has the provision for testing in any of three occupancy states. The "as-built" state refers to the empty cleanroom before the installation of production equipment and with no people present. In this state there

TABLE 4.3. Particle Concentration Limits as Specified in ISO 14644-1

ISO Classification Number	Maximum Concentration Limits (Particles/m^3 of Air) for Particles Equal to and Larger than the Considered Sizes Shown Below					
	0.1 μm	0.2 μm	0.3 μm	0.5 μm	1.0 μm	5.0 μm
Class 1	10	2	—	—	—	—
Class 2	100	24	10	4	—	—
Class 3	1,000	237	102	35	8	—
Class 4	10,000	2,370	1,020	352	83	—
Class 5	100,000	23,700	10,200	3,520	832	29
Class 6	1,000,000	237,000	102,000	35,200	8,320	293
Class 7	—	—	—	352,000	83,200	2,930
Class 8	—	—	—	3,520,000	832,000	29,300
Class 9	—	—	—	35,200,000	8,320,000	293,000

TABLE 4.4. ISO 14644-1 Classes and Corresponding FS 209 Classes

Standard	Class					
ISO 14644-1	3	4	5	6	7	8
"Old" FS 209	1	10	100	1,000	10,000	100,000
"Newer" FS 209	M 1.5	M 2.5	M 3.5	M 4.5	M 5.5	M 6.5

should be a low level of particles that will reflect the quality of air supplied and the operational efficiency of the cleanroom. The "at-rest" state refers to the cleanroom after equipment installation and operation but with no people present. Under these conditions, there will be a higher level of particles. The "operational" state refers to the cleanroom under normal operating conditions. Under these conditions, there will inevitably be an even higher level of particles owing to the presence of people and to the activities being undertaken.

The ISO standard also includes methods for using particle sizes outside the normal size range. The use of "ultrafine" particles (<0.1 μm) in the analysis is intended primarily for the microelectronics industry where smaller particles are a concern. The use of "macroparticles" (>5.0 μm) is intended for use in, for instance, some parts of the medical device industry where smaller particles are not important.

It should be recognized that the particle size distributions defined in cleanroom standards are for classification purposes, and will not necessarily represent the actual size distributions found in any particular cleanroom situation. The source, type, and amount of particulate matter will vary considerably from one facility to another and within an individual facility when different activities take place. Simple idealized particle size distributions with straight line relationships will not always occur in practice, a factor not always recognized by users of cleanrooms or by regulatory authorities.

4.8.1.1.1 Control of Airborne Contamination. The control of airborne contamination in a cleanroom is accomplished by the following means:

1. *Preventing Entry*. This is achieved by filtering the air entering the cleanroom and preventing the ingress of external air by the use of a positive air pressure relative to the external environment.
2. *Purging*. The air handling system changes the air in the room at a sufficient rate to remove or dilute particulate matter generated within the room, from either the process or the personnel.
3. *Minimizing the Generation of Particulate Matter*. Room appointments (floors, walls, equipment, etc.) are chosen for their resistance to particle generation. The number of people admitted to the cleanroom is kept to the minimum that is consistent with the work that must be performed, and cleanroom clothing is made of nonlinting material and designed to minimize the release into the room of particles shed by the personnel (e.g., skin flakes, hair, etc.).
4. Providing localized protection for the product or process from the settling of particulate matter, from product-to-product contamination and for the protection of staff from potential hazards.
5. Providing designated areas for personnel entry, for the entry of equipment, parts, and so on, and for the cleaning of equipment and parts.
6. Controlling the flow of materials through the process steps and controlling the personnel activities.

4.8.1.1.2 Critical Design Parameters. A number of critical parameters need to be addressed in any cleanroom facility; these can be summarized as follows:

- total particulate cleanliness;
- microbiological cleanliness (where necessary);
- HEPA filtration specification;
- room pressurization;
- temperature and humidity;
- air change rates;
- hazards from products and processes;
- disinfection and cleaning procedures.

4.8.1.1.2.1 Total Particulate Cleanliness. This will be dictated by the nature of the work to be carried out. Conventional aseptic filling operations will require an ISO Class 5 (FS 209 Class 100/M 3.5) room, but in most instances cell culture work will probably only require an ISO Class 7 (FS 209 Class 10,000/M5.5) room.

Overspecifying a room needs to be avoided to prevent unnecessary construction and maintenance costs.

4.8.1.1.2.2 Microbiological Cleanliness. Again this will depend on the nature of the work and the need to control this parameter. For aseptic filling operations, a comprehensive microbiological monitoring program would be needed to demonstrate compliance with appropriate standards. The nature of cell culture work probably makes this requirement unnecessary in most cases.

4.8.1.1.2.3 HEPA Filtration Specification. This aspect is dealt with separately earlier in the chapter. However, it should be recognized that the type of grille or diffuser on the filtered air inlet will influence air movement in a conventionally ventilated room (26). Careful consideration will need to be given to the siting of safety cabinets to avoid the disruption of air movement into the cabinet (see the section titled Class II Microbiological Safety Cabinets).

4.8.1.1.2.4 Room Pressurization. The establishment of pressure levels is an important requirement to prevent the ingress of external, unfiltered air into the cleanroom or clean zone. Depending on the size and complexity of the facility, it may be necessary to provide a cascade of differential pressures across rooms or zones within the cleanroom. Room

pressures can also be an indicator of a number of performance characteristics such as air balance stability, HEPA filter blockage, control and fan faults, and so on. It is normal to provide a pressure differential of at least 15 Pa between adjacent areas (the highest pressure being in the most critical area) although some reduction in this figure may have to be accommodated in relatively complex facilities with multiple pressure differentials in order to avoid excessive overpressure relative to the outside (27).

4.8.1.1.2.5 Temperature and Humidity. These parameters need to be controlled to create comfortable conditions for the staff and avoid excessive generation of particles (bearing in mind that under normal conditions the personnel are usually the major source of particulate contamination in cleanrooms). As a general guide the temperature should be around 20°C and the humidity levels not more than 50% RH although there may at times be differences to cater for specific requirements (e.g. low RH for moisture sensitive materials).

4.8.1.1.2.6 Air Change Rates. This determines the quantity of air moving through the classified clean space. It is needed to provide an adequate degree of flushing of the room or zone in order to avoid the buildup of particulate matter. In trying to determine the required air change rate, due allowance will also have to be given to compensate for internal heat gain, process exhaust (e.g. loss of air through safety cabinets), an allowance for loss due to leakage (e.g. through doors), and the air volume required to pressurize the room. Minimum air change rates of 20 room volumes per hour are often quoted but rates of 30–35/h are not uncommon to compensate for the parameters mentioned above.

4.8.1.1.2.7 Hazards from Products and Processes. Many of the potential hazards that may be encountered during cell culture have been dealt with in the sections titled Biohazards and Aseptic Technique: General Considerations. Additional hazards may be posed by large-scale operations or specialized techniques, particularly those capable of producing aerosols. It is essential that a full risk assessment is carried out, and that, where appropriate, measures are put in place in the cleanroom to deal with identified hazards.

4.8.1.1.2.8 Disinfection and Cleaning Procedures. There are many factors that influence the efficacy of disinfectant procedures. The choice of cleaning agents and disinfectants, how they are prepared and used, and the environment in which they are used can have a bearing on their efficacy. There is no compound which has all the characteristics of an ideal disinfectant and the choice of which to use in any particular situation will need to be made carefully, taking into account Health and Safety considerations, the risk of corrosion of treated surfaces and the potential for residues as well as the factors which influence efficacy (1). The choice of which disinfectants to use must be made specifically for each working environment.

Periodic rotation of disinfectants has been advocated by some workers in order to change the selective pressures on microorganisms and avoid the emergence of strains that are less susceptible to the disinfectants. Although regulatory authorities sometimes require some form of rotation, there are arguments for and against this practice. This is a controversial subject and the principle of disinfectant rotation is not universally accepted.

4.8.1.1.3 Process and Personnel Influence. Although the design and maintenance of a cleanroom are undoubtedly important, probably even more important are the activities of the personnel working within it. The cleanroom only provides a suitable environment within which the processes can be operated. The design and control of the processes and the personnel activities need to given very careful consideration. Poor practices within a well-designed and -maintained cleanroom will inevitably result in contamination problems. Good techniques are crucially important; otherwise, all the effort and cost expended in providing the cleanroom facility and associated equipment will be wasted. We have attempted, in some of the earlier sections, to describe some aspects of good technique as applicable to cell culture, and further details can be found elsewhere (28,29).

4.8.2 Acknowledgment

Permission to reproduce extracts from BS 5726:2005 is granted by BSI. British Standards can be obtained from BSI Customer Services, 389 Chiswick High Road, London W4 4AL, UK. Tel: +44 (0)20 8996 9001. Email: cservices@bsi-global.com.

REFERENCES

1. Roberts PL. Sterilization. In: Davis JM, editor. Basic cell culture; a practical approach. Oxford: Oxford University Press; 2002. p 29–67.
2. Nelson-Rees WA, Flandermeyer RR. Science 1976; 191: 96–98.
3. Nelson-Rees WA, Daniels DW, Flandermeyer RR. Science 1981; 212: 446–452.
4. Gold M. A conspiracy of cells. Albany, NY: State University of New York Press; 1986.
5. Hummeller K, Davidson WL, Henle W, LaBoccetta AC, Ruch HL. N Engl J Med 1959; 261: 64–68.
6. Gugel EA, Sanders ME. N Engl J Med 1986; 315: 1487.
7. Hill AF, Desbruslais M, Joiner S, Sidle KCL, Gowland I, Collinge J, Doey LJ, Lantos P. Nature 1997; 389: 448–450.
8. Bruce ME, Will RG, Ironside JW, McConnell I, Drummond D, Suttie A, McCardle L, Chree A, Hope J, Birkett C, Cousens S, Fraser H, Bostock CJ. Nature 1997; 389: 498–501.

9. Asante EA, Linehan JM, Desbruslais M, Joiner S, Gowland I, Wood AL, Welch J, Hill AF, Lloyd SE, Wadsworth JDF, Collinge J. EMBO J 2002; 21: 6358–6366.
10. WHO WHO guidelines on tissue infectivity distribution in transmissible spongiform encephalopathies. Geneva, Switzerland: WHO; 2006. Also available at http://www.who.int/bloodproducts/tse/WHO%20TSE%20Guidelines%20FINAL-22%20JuneupdatedNL.pdf.
11. Hodgson J. Biotechnology 1991; 9: 1320–1324.
12. Stacey G. Risk assessment of cell culture procedures. In: Stacey G, Davis J, editors. Medicines from animal cell culture. Chichester: Wiley; 2007. p 569–587.
13. Advisory Committee on Dangerous Pathogens. Biological agents: managing the risks in laboratories and healthcare premises. Norwich: The Stationery Office; 2005. Also available at http://www.hse.gov.uk/biosafety/biologagents.pdf.
14. Caldwell GH, Whyte W. High efficiency air filtration. In: Whyte W, edtior. Cleanroom design. London: John Wiley & Sons; 1991. p 181–204.
15. Diamond JA, Wrighton M. Parenteral society tutorial no. 3 "Understanding clean rooms". Parenteral Society; 1986.
16. BS EN 12469 Biotechnology. Performance criteria for microbiological safety cabinets. London: British Standards Institute; 2000.
17. Foord N, Lidwell OM. J Hyg 1975; 75: 15–56.
18. Matthews JA. An evaluation of test methods for microbiological safety cabinets. Thesis, Council for National Academic Awards, London; 1985.
19. Kennedy DA. Br Health Saf Soc Newsl 1987; 15: 22–30.
20. Collins CH. Laboratory-acquired infections. Sevenoaks: Butterworth; 1988.
21. Clark RP. Lab Pract 1980; September; 926–929.
22. Clark RP, Mullan BJ. J Appl Bacteriol 1978; 45: 131–135.
23. Tetzlaff R. FDA regulatory inspections of aseptic manufacturing facilities. In: Olson WP, Groves MJ, editor. Aseptic pharmaceutical manufacturing: technology for the 1990's. Interpharm Press; 1987. p 367–401.
24. Austin PR. Contam Control 1966; 5: 26–32.
25. Heuring H. Contam Control 1970; 9: 18–20.
26. Farquharson GJ, Whyte W. The design of cleanrooms for the pharmaceutical industry. In: Whyte W, editor. Cleanroom design. London: John Wiley & Sons; 1991. p 57–84.
27. Farquharson GJ. Clean rooms international. 1992; 18–20.
28. Davis JM, editor. Basic cell culture; a practical approach, 2nd ed. Oxford: Oxford University Press; 2002.
29. Freshney RI. Culture of animal cells: a manual of basic technique. 5th ed. New York: Alan R. Liss; 2005.

5

CELL CYCLE IN BIOPROCESSES

Mariam Naciri and Mohamed Al-rubeai
University College Dublin, Belfield, Dublin, Ireland

5.1 INTRODUCTION

The cell cycle model (G_1-event model) currently accepted by authors of the major cell and molecular biology books (2–5) describes the cell cycle as discrete phases controlled by cell cycle proteins interacting with each other and directing cellular events including DNA synthesis and cell division. However, the validity of this model and the interpretation of many experiments that underpin the current established view of the cell cycle and its regulation have been questioned (6,7). The proposed alternative, the continuum model, suggests that the cell cycle does not exist as currently recognized but takes the form of a continuum from one cell division to the next, rather than discrete phases with discrete groups of regulatory proteins. A hypothetical initiator of DNA replication is synthesized by the cell during all phases of the cell cycle, and its concentration reaches a critical level that initiates DNA synthesis. Thus the cell can control its rate of division by regulating the amount of initiator. Nevertheless, until discussion of these competing models is concluded, with perhaps more work to determine the correctness and applicability of the continuum model, it is only reasonable to accept the weight of evidence for the established view of the cell cycle and its regulation. Thus the established model is summarized here and is the basis for the process biotechnology applications that are described.

The pathways of cell cycle regulation are, unsurprisingly perhaps, shared with another important cell process: apoptosis, or "programmed cell death," which is, in effect, the opposite of the cell proliferation cycle. Because the cell cycle and apoptosis share some common pathways, regulatory imbalance can lead to cancer in multicellular organisms (8). Regulation of the cell cycle is also crucial in embryology and ontogeny, where features such as limb formation, tissue differentiation, and growth are a function of the balance between proliferation and apoptosis. Therefore, much of the cell cycle (and apoptosis) literature is from the field of biomedical science, particularly cancer and anticancer chemotherapy research. General texts, as well as much of what is written here, provide a consensus of information describing a hypothetical typical cell and thus, by implication at least, describe what is true of all eukaryotic cells.

5.2 THE CELL CYCLE

5.2.1 Overview

The cell cycle and its control mechanisms are highly conserved, so most of what is described in general terms for a "typical mammalian cell" is also true for other animals (such as insects) and plant cells, although there is the obvious exception of the cell wall and its effect on cell division. The cell cycle and its control in yeast are essentially similar to but much simpler than the analogous mechanisms in higher eukaryotes; where one protein pair exerts a particular control function in a yeast, several may be required for the same function in an animal cell. As a result of this less complex system and the fortuitous discovery of cell cycle control mutants (*cdc* mutants) in which the cell cycle is inhibited at specific stages, many early discoveries about cell cycle control were made using the budding yeast *Sacharomyces cerevisiae* and the fission yeast *Schizosaccharomyces pombe*. Subsequent research

Upstream Industrial Biotechnology: Expression Systems and Process Development, Volume 1, First Edition. Edited by Michael C. Flickinger.
© 2013 John Wiley & Sons, Inc. Published 2013 by John Wiley & Sons, Inc.

has shown homology between cell cycle control proteins in yeast and those in mammalian cells.

However, the bacterial cell cycle is markedly different from the eukaryotic cell cycle, and its control mechanisms are (to date) less well understood than the analogous processes in eukaryotes. Given a hypothetical typical bacterial cell, its structure and thus the function of its cell cycle are very different from those of a eukaryotic cell. Bacteria, like all cells, are enclosed in a cytoplasmic membrane, but in addition, they have a cell wall outside the cytoplasmic membrane. Within the cell there are no organelles, only free ribosomes and the nucleus which is actually an area that contains DNA but is not segregated from the cytoplasm by a membrane. The entire genome is contained in a single, circular, double-stranded DNA chromosome; one strand is a closed circle and the other is open. There are no histone or similar DNA-associated proteins; instead there is a relatively high proportion of small, basic polyamines whose function may be to counteract the acidity of the DNA. The "joint" in the closed DNA strand, the origin of replication, is attached to a mesosome, an invagination of the cytoplasmic membrane. When DNA replication starts, the 5′ end of the open strand attaches to the cytoplasmic membrane and starts to form a second mesosome; meanwhile, the DNA unwinds in one direction from the origin of replication and splits into two single strands to form a replication fork. As the replication fork progresses along the chromosome, complementary strands of DNA are synthesized until two daughter chromosomes of double-stranded DNA are formed, each with an origin of replication attached to its mesosome. While the chromosome replicates, the cytoplasmic membrane and cell wall are synthesized in the region between the two mesosomes, enlarging the cell. After chromosome replication, a septum forms across the middle of this region, finally separating the two daughter cells. However, it takes about 40 min to duplicate the single chromosome; hence, to allow doubling times as low as 20 min, each daughter chromosome must start to replicate in exactly the same way before the parent has finished replication. Thus, instead of one there will be three origins of replication operating at once. In addition, when the doubling time of a culture is less than about 40 min, DNA synthesis is continuous, so it may be that DNA replication and cell division cycles are independent in bacteria (9). However, despite the essentially continuous DNA synthesis and cell division shown in the fast-growing cultures likely to be used in process biotechnology, it has recently been shown (10) that slow-growing *Escherichia coli* cells (doubling time up to 5 h) display cell cycle phases analogous to eukaryotic G_1, S, and G_2 phases, *vide infra*, followed by cell division. Furthermore it was shown that initiation of DNA replication was related to cell mass. Two genes, *seqA* and *dnaA*, were shown to be involved in the regulation of replication initiation; gene mutants exhibited decreased and increased mass, respectively, at initiation of replication. Recent work with *Caulobacter* (11) described a protein, CtrA, that has sequence homology with response regulatory proteins in other bacteria including *E. coli* and is involved in cell cycle control including cell division and cell cycle–specific transcription. It was proposed that CtrA is part of a phosphorelay signal transduction system responsible for transcriptional-level control of bacterial cell cycle events.

The mammalian cell cycle is best described by illustration (Fig. 5.1a). Starting from a recently divided daughter cell, untransformed, or "normal," cells may enter gap phase 0, or G_0 (12,13). This is an offshoot from the cell cycle in which cells may remain viable and nondividing but retain the potential to divide given the appropriate stimulus (14,15). A cell, depending upon its type, can remain

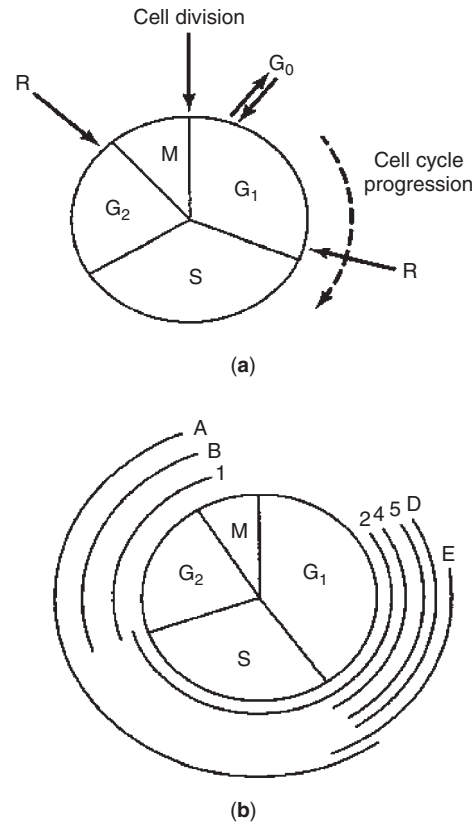


Figure 5.1. (a) A simple diagrammatic representation of the cell cycle. G_0, gap phase 0; G_1, gap phase 1; S, synthesis phase, in which the DNA and cell cytoplasmic components are duplicated; G_2, gap phase 2; M, cell division by mitosis (or meiosis); R, restriction point (check point). (b) A simple diagrammatic representation of cyclin and cyclin-dependent kinase activation during cell cycle traverse. A, cyclin A; B, cyclin B; D, cyclin D; E, cyclin E; 1, cyclin-dependent kinase 1 (homologous to cdc2); 2, cyclin-dependent kinase 2; 4, cyclin-dependent kinase 4; 5, cyclin-dependent kinase 5.

out of the cell cycle, in G_0, for extended periods but can return to gap phase 1, or G_1, due to cell maturation after a certain time has elapsed, after a critical mass or size is reached, or as a response to an external stimulus (16–19). In contrast, cells from continuous (sometimes called *established* or *immortal*) cell lines and transformed cells (which includes most animal cells used in biotechnology) do not enter G_0 after division but restart their cell cycle after mitosis by progressing directly to G_1. During G_1, cells prepare to duplicate themselves. When a cell enters the synthesis, or S phase, it starts to precisely and accurately duplicate its genome by synthesizing DNA and the associated nuclear protein components, so that daughter cells carry a genome identical to each other and to the parent. During this time, ribosomes, mitochondria, endoplasmic reticulum, and all the other subcellular organelles are also replicated in preparation for cell division. Thus by the end of S phase, a normally diploid ($2n$) cell will be tetraploid ($4n$), containing enough DNA (and cellular components) for two cells. After S phase, the cycling cell enters the second gap, or G_2, phase. During G_2 the cell synthesizes the proteins required to direct chromosome segregation and cell division in the following mitosis, or M phase. After mitotic division the daughter cells return to G_1 at the beginning of a new cell cycle or exit the cycle to G_0. In a typical cell cycle of 24-h duration, G_1 would last 10 h, S phase 9 h, G_2 4 h, and mitosis 1 h. However, the duration of the cell cycle varies both between cell lines and between individual cells within the same culture. Variation in cycle time is usually due either to cells exiting the cycle and arresting in G_0 or to a variation in the duration of G_1. It has been suggested that the intercellular variability of the postmitotic early G_1 period is smaller than that seen with initiation of DNA replication (presynthetic late G_1) (20). It is also postulated, by the same author, that cells that make the "yes or no" decision in the postmitotic early G_1 period about whether to proceed through the cell cycle, also have the capacity to decide in the presynthetic late G_1 period, when the cell will enter S phase. Heterogeneity in the duration of G_1 is the main reason why a synchronized culture loses synchrony with time to the extent that the culture is completely asynchronous within three or four cell cycles.

This apparently simple cell cycle is subject to complex control mechanisms. Some of the molecular pathways have been understood only in recent years and there may be others that have not yet been described. Mammalian cells periodically transcribe cell cycle genes that encode proteins directly involved in cell cycle regulation. These include the cyclins and the cyclin-dependent kinase (Cdk) families. The Cdks are phosphorylating enzymes that are inactive when not associated with an appropriate cyclin; it is the associated cyclin that determines the substrate specificity of the complex. The activity of this heterodimeric complex is then regulated by phosphorylation or dephosphorylation of specific activation and/or inhibition sites, as well as by further binding with inhibitory proteins. Many of the cyclins, Cdks, and related regulatory proteins are expressed or form active complexes only during particular cell cycle phases. Cdk4–cyclin D1 drives cells through mid G_1, Cdk2–cyclin E drives late G_1, Cdk2–cyclin A controls entry into S phase, and Cdk1–cyclin B drives the G_2–M transition; their phase-related activities are summarized in Fig. 5.1b and Table 5.1. Others, including Cdk4 (21,22) are expressed throughout the cell cycle. The noncyclic proteins exert their cell cycle-;controlling effects by association with phase-specific cyclins or Cdks, association with Cdk-cyclin inhibitors, and specific amino acid phosphorylation or dephosphorylation to form active complexes in specific phases. A family of genes encoding proteins related to the retinoblastoma susceptibility gene, *RB*, and genes for transcription factors including *BYMB, E2F1*, and *JUN* are all induced in late G_1 or early S phase and have been shown to interact with cell cycle regulatory complexes. In addition, there are restriction points in the cell cycle that, once passed, commit the cell to continuing the division cycle. There are also check points where in effect, the cell ensures that the previous phase has been completed properly before proceeding or that there has been no DNA damage. To continue to mitosis before the genome is properly duplicated, for example, would be catastrophic for the cell; one if not both daughters would not be viable. It has been suggested that induction of the *p53* tumor suppressor gene and its transcriptional activation of the Cdk inhibitor *p21WAF1/CIP1* with subsequent cell cycle arrest, following DNA damage, allows time for DNA repair before entering S phase (23). Activation of *p53* in cells with unrepaired DNA damage may lead to apoptotic cell death.

5.2.2 Gap Phase 1 or G_1

G_1 was originally thought to be a gap in the cell cycle—a resting phase while the cell recovered from division before starting a new cell cycle by synthesizing more DNA—although this is now known to not be so. Rather, complex control processes are preparing the cell to synthesize the cellular machinery required for DNA synthesis in the S phase. There is also a "point of no return" near the end of G_1 called the *restriction point* (R), which is analogous to START in yeast. Once cells pass this point they are committed to the next stages of the cell cycle. Signals for passing this point include adequate cell size and a favorable environment, including the presence of growth factors. The transition at the R point from growth-factor dependence to growth-factor independence in normal cells, as opposed to cancer or transformed cells, is likely to reflect a stringent growth regulatory mechanism that is defective in the latter cell

TABLE 5.1. Cyclin–Cdk Complexes, Stability, and Associated Proteins[a]

Cyclin	Associated Cdk	Cell Cycle Activity	Associated Proteins	Stability	Degradation
A	Cdk2 and cdc2 (Cdk1)	S and G2 → M	p107, E2F, p21, PCNA	Unstable in mitosis	Ubiquitin
B1	cdc2 (Cdk1)	G2 → M	(p21), (PCNA)	Unstable in mitosis	Ubiquitin
B2	—	G2 → M	(p21), (PCNA)	Unstable in mitosis	Ubiquitin
C-type	Cdk X	?	ND	ND	PEST
D1	Cdk4(2, 5, 6)	G1	pRb, p21, p27, PCNA, p16, p15	Rapid turnover	PEST
D2	Cdk4(2, 5, 6)	G1	pRb, p21, p27, PCNA, p16, p15	Rapid turnover	PEST
D3	Cdk4(2, 5, 6)	G1	pRb, p21, p27, PCNA, p16, p15	Rapid turnover	PEST
E	Cdk2	G1 and G1 → S	p107, E2F, p21, PCNA and p27 after TGFβ treatment	Rapid turnover	—
F	—	—	ND	ND	—
G	—	—	ND	ND	—
H	Cdk7	All phases	ND	ND	ND

Note: ND, not determined; PCNA, proliferating cell nuclear antigen; TGFβ, transforming growth factor β; PEST, proteins that contains sequences rich in praline (P), glutamate (E), serine (S), and threonine (T).

[a]From Ref. 24: Hunter and J. Pines, *Cell* **79**, 573-582 (1994), Copyright Cell Press, used with permission.

types. Coordination between cell cycle commitment, START (or R), and cell size, involving the G_1 cyclins, has been suggested as a regulatory mechanism for cell growth in yeast. During early G_1, immediately after G_0, cells are stimulated to reenter the cell cycle; a critical step occurs involving the induction of cell cycle–specific genes including *myc, cyclin D, and fos*, and *Cdk* genes. It is now apparent that Cdk 2, Cdk 4, and Cdk 5, despite constitutive expression of Cdk4 thoughout the cell cycle, start to complex with cyclins D1, D2, and D3 and become active in early to mid G_1 (possibly at a point when or soon after noncycling cells return from G_0). The level of activation of the G_1 Cdk–cyclin complexes peaks at about R; so it is possible that, by reaching a threshold activity, it is these complexes that allow cells to pass R. Cdk2 also forms active complexes with cyclin E starting from mid G_1 and peaking later than the Cdk–cyclin D complexes, in other words, between R and the G_1–S phase transition.

The primary substrate of the cyclin D complexes is the retinoblastoma tumor suppressor gene product pRB. Active, unphosphorylated pRB complexes with and inhibits the transcription factor E2F. When pRB is phosphorylated and inactivated, the complex dissociates, releasing active E2F; the cell cycle is not stopped at the G_1 checkpoint, and cells are allowed to proceed to S phase (25). E2F was originally characterized as an activator of the adenovirus early region 2 transcription unit (25). It is now recognized that E2F promotes the transcription of enzymes associated with DNA synthesis (26,27). It has been proposed that the cyclin E complex also phosphorylates pRB, with similar effects (28).

5.2.3 Synthesis Phase or S

The transition from G_1 to S phase is marked by the transcription (as already described) and activation of the many synthetic enzymes required for cellular duplication including DNA polymerase α, thymidine kinase, and dihydrofolate reductase (DHFR) (29). This is followed by the exact duplication of the genetic material and replication of organelles and structural proteins. At the same time, there is a marked change in the regulatory proteins activated. At the onset of S phase, the activation of the G_1-phase Cdk–cyclin complexes decreases in the same temporal order as it increased and the complexes dissociate. As Cdk2 disssociates from cyclins D and E, it complexes with cyclin A which starts to be synthesized at about the G_1–S transition. The Cdk2–cyclin A complex retains its activity until the end of S phase. Disruption of cyclin A function inhibits DNA synthesis, suggesting that a threshold activity of the Cdk2–cyclin A complex is essential for the maintenance of S phase.

5.2.4 Gap Phase 2 or G_2

As with G_1, G_2 was originally thought to be a gap in the cell cycle, as a resting phase while the cell recovered from DNA synthesis before dividing. This has now been shown to not be so although G_2 remains analogous to G_1 in that once the appropriate control signals are received, genes encoding for the proteins responsible for cell division are transcribed and ready for cell division. At the end of S phase the activity of the Cdk2–cyclin A complex decreases as the components dissociate. Cyclin A and cyclin B then form complexes with Cdk1 (also often referred to as cdc2 because of its homology with the product of *S. pombe* cell division cycle gene 2). It is these complexes, increasing in activity throughout G_2 and continuing into mitosis, that mediate activation of the cell division machinery. At the transition point between G_2 and M is a second check point that, in effect, ensures that the cells are big enough, the environment is favorable, and DNA synthesis has been fully and accurately completed before the cell continues into mitosis and division.

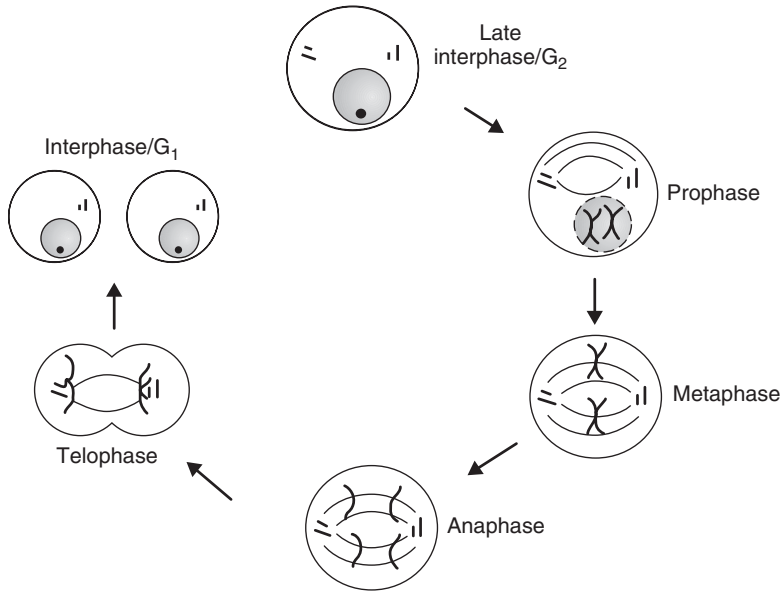


Figure 5.2. A simple diagrammatic representation of mitosis.

5.2.5 Mitosis or M: Cell Division

Mitosis is the division of one normally diploid, or $2n$, somatic cell into two genetically identical (both to each other and the parent) cells. Mitosis, like the cell cycle itself, displays distinct phases that are best represented diagrammatically (Fig. 5.2). When the cell leaves interphase at the end of G_2, it enters prophase. The nucleolus disappears (disperses), and nuclear DNA condenses into chromosomes. Following DNA synthesis in S phase, a normally diploid ($2n$) cell is now tetraploid ($4n$) and contains an identical pair of each chromosome, which is in turn organized as a pair of identical chromatids joined to each other at the centromere. During late prophase, the nuclear envelope is broken down. At the same time, the centrioles divide; one pair migrates to each cell pole with spindle fibers, which are microtubular structures, linking each pair. The transition from prophase to metaphase is marked by alignment of all the chromosome pairs on an equatorial plane, the metaphase plane, with their centromeres connected to each polar centriole pair by spindle fibers. The cell progresses into anaphase when the chromosomes separate and one chromatid from each homologous chromosome pair migrates along the spindle fibers toward each centriole. In the next phase, telophase, when the chromatids (one from each homologous chromosome pair) arrange at each pole, the spindle fibers depolymerize, and cytokinesis (division of cytoplasm) begins as a cytoplasmic cleavage furrow begins to form. Further changes follow: the cytoplasm cleaves completely, chromosomes uncoil, the nuclear envelope re-forms around each nucleus, and the nucleoli reappear to give two genetically identical daughter cells in interphase. The final telophase changes, in which the cytoplasm divides and the cells separate, are markedly different in plant cells and in animal cells due to the constraints of the rigid cellulose cell wall. As with other cell cycle phases, Cdk–cyclin complexes perform a major regulatory function in mitosis. The activity of Cdk1–cyclin A and Cdk1–cyclin B, which started in G_2, continues to increase until the middle of mitosis at the metaphase–anaphase boundary. At this point the activity of both complexes declines abruptly to zero, allowing the cell to complete mitosis. It is also thought that the rapid decrease in G_2 cyclin–Cdk complexes is necessary for cells to start a new cell cycle at G_1.

5.2.5.1 Meiosis. Although unlikely to be encountered in process biotechnology, it is useful to point out that germ cells may undergo an alternative form of division to form zygotes, which may also be considered to be a form of terminal differentiation, called *meiosis*. Assuming a normally diploid ($2n$) cell, initial cell division occurs exactly as in mitosis until the end of anaphase, or in this case the first meiotic anaphase. At telophase the cell may divide or partially divide and enter a brief meiotic interphase comprising two identical diploid ($2n$) daughter nuclei (if not cells). Otherwise the cell progresses directly to the second meiotic prophase. Now there is only a single copy of each chromosome, still comprising two chromatids. During the second meiotic anaphase, the chromatids separate again to each of four poles. The cell then progresses to (the second meiotic) telophase and on to interphase to give four haploid (n) daughter cells instead of the two diploid ($2n$) cells produced by mitosis.

5.2.6 Gap Phase 0 or G_0

The term G_0 was first used in the early 1960s when three types of cells were recognized: static cells, incapable of further division (e.g. a terminally differentiated adult neuron); renewing, constantly dividing cells (e.g. bone marrow cells); and conditionally renewing cells which do not normally divide but can respond to an appropriate extraordinary stimulus (e.g. liver cells starting to proliferate after partial hepatectomy). G_0 is used to describe this last category of cells, which have "opted out" of the cell cycle after a mitosis because of, for example, growth-factor depletion. In this circumstance, in contrast, transformed or tumor cells do not enter G_0 but continue through the cell cycle until they die from nutrient exhaustion, often by apoptosis. It has been argued that G_0 should not be used to describe cells, for example, in the stationary phase of a hybridoma or CHO (Chinese hamster ovary) batch cultures, which are in a pseudo-steady state of growth and death due to nutrient depletion and/or accumulation of toxic metabolites. Unlike normal cells, they have not down-regulated themselves; they have been closed down by their environment. Cells that lose their ability to respond to growth-factor depletion or do not exit the cell cycle to G_0 may have a defective G_1 program which is different from the cyclin-Cdk4-pRB phosphorylation mechanism involved in R regulation in normal cells. However, G_0 is commonly used today, some claim inappropriately, to describe any cell (containing a G_1 amount of DNA) that is not expected to proceed to S phase for any reason, including the result of any means of artificial interference with the cell cycle. Markers of G_0 include reduced RNA, reduced ribosome content, and an absence of cyclins D and E (30).

5.2.7 External (Environmental) Influence on the Cell Cycle

Extrinsic cell cycle regulation may be considered at two levels. At the more basic level is the effect of the physical environment and nutrient availability; the more complex level of extrinsic cell cycle control is through growth factors. The physical environment has a great effect on the cell cycle. When temperature is reduced from the optimum, the length of the cell cycle increases, and growth rates slow down. When temperature exceeds the optimum even by a few degrees, profound changes in cell behavior occur including the expression of heat shock proteins, and cells eventually die. Alternatively, if appropriate nutrients such as amino acids and glucose are not available in the medium, cell cycle duration and even progression will be influenced due to lack of energy and the precursors for protein and DNA synthesis.

Serum starvation, in the presence of appropriate nutrients and physical conditions, may also affect the cell cycle but this is more likely to be caused by the absence of the specific growth factors that serum provides. Most, if not all, cell lines were originally grown in medium containing animal serum, usually newborn or fetal bovine serum. The main contribution to the cell cycle and hence, growth of a culture from these undefined and heterogeneous supplements, is the supply of growth factors that promote or enhance the cell cycle. Thus, because G_0 cells reenter the cell cycle as a result of serum addition, serum is regarded as a source of positive regulatory growth factors. The presence of growth factors in the environment, their binding to specific transmembrane receptor proteins, and subsequent signal transduction, effects changes in cellular processes including the cell cycle. Expression of cyclin D, important in progression through G_1, is induced by growth factors (31). These effects are cell-type dependent because cells do not all express the same growth-factor receptors. Furthermore, different cell types or lines may not only require different individual growth factors but may require a specific cocktail for optimal proliferation. Fibroblast growth, for example, requires growth factors including fibroblast growth factor (FGF), epidermal growth factor (EGF), and platelet-derived growth factor (PDGF). Other growth factors that promote cell division include insulin-like growth factor (IGF) I and II, macrophage–granulocyte colony stimulating factor (G-CSF), and endothelial cell growth factor. Each growth factor stimulates a specific receptor on the plasma membrane, which in turn activates protein kinases, many of which phosphorylate tyrosine residues on their substrates, so they are generically called *tyrosine kinases*. Subsequent signal transduction by phosphorylation or dephosphorylation cascades can lead to an increased rate of protein synthesis, influence the activity of DNA topoisomerase or modify the glucose transport system, all with the similar effect of promoting cell division. Transformed cells are known to have a reduced (or no) requirement for external growth factors when compared with normal cells. However, through adaptation of cell lines and extensive development of medium formulation, many cells can now be grown in a protein-free medium, indicating that it is possible to bring about cell proliferation and support long-term culture in media free of (extrinsic) growth factors, hormones, and other contaminating proteins. This absence of extraneous protein is particularly important in large-scale process biotechnology for facilitating downstream processing and product recovery. However, in addition to the positive growth-promoting (cell cycle-promoting) factors, there are also negative, growth-inhibiting factors, although these may be the same growth factors displaying opposite effects under different conditions. Transforming growth factor $\beta 1$ (TGF-$\beta 1$), in addition to its strong positive stimulatory effect, has been shown to produce a density-independent negative response that prolongs G_1 in the NIH-3T3 mouse embryo cell cycle and has a similar effect on mortal human fibroblasts (32).

It is commonly accepted that the depletion of glucose and amino acids as well as the accumulation of toxic metabolites (ammonia and lactate, e.g.) inhibits culture proliferation.

5.3 METHODS FOR DESCRIBING THE CELL CYCLE

5.3.1 Mitotic Index

There are three main approaches to describing the cell cycle. The first and most historically established approach is to determine the percentage of cells in mitotic cell division. This method, called the *mitotic index*, is simple and can be applied to attached cells grown on a microscope slide or any other appropriate substratum, as well as cells in suspension. There are many fixation and staining methods described in any textbook of cytology, from which a protocol appropriate to animal cell biotechnology can be selected. A generic protocol is as follows. Take cells grown on a glass microscope slide (or coverslip) or prepare a smear of suspended cells on a microscope slide, using an attachment agent such as polylysine if necessary. Fix the cells with a fixative appropriate to the proposed staining method. Stain the cells with either a standard cytological or histological stain that differentiates DNA such as Feulgen staining, or alternatively, stain with a fluorescent DNA stain such as ethidium bromide (EB), Hoechst 33258, or DAPI. Examine stained slides by conventional or fluorescence microscopy, as appropriate. Count the number of nuclei in mitosis and express the result as a percentage of the total. A recent publication investigating mitosis in a hydrodynamically stressed environment, described the use of the fluorescent DNA-intercalating stain propidium iodide (PI) with cells fixed with 3:1 ethanol to glacial acetic acid, followed by fluorescence microscopy (33). A major disadvantage to measuring the mitotic index is that although it gives information about cell division in M phase, it can give no information about the other cell cycle phases or their associated processes. Measuring the mitotic index also exhibits disadvantages common to all manual microscopic methods including sampling error, because a small proportion of the total population is examined and interobserver variation results from subjective discrimination between mitotic and interphase cells. Furthermore, this slow and labor-intensive method is not appropriate for on-line automation or use in integrated process control.

5.3.2 Labeled Nucleotide Uptake in S Phase

An alternative approach for describing the cell cycle is to document the incorporation of labeled nucleotides into nuclear DNA during S phase. This method relies on [^{3}H]thymidine incorporation followed by autoradiography and can be used in one of two ways: continuous labeling, in which the cells are exposed to the label for a fixed time period, usually 24 or 48 h followed by analysis at that time; or pulse-chase labeling, in which the cells are exposed to the label for a short pulse (0.5–1 h) and then analyzed at regular intervals for 24–48 h. Continuous labeling gives information about the growth fraction of a culture, which is the percentage of cells that are in the cell cycle during the labeling period. However, this information is not likely to be of great use to the process biotechnologist because most cells under optimum conditions, when viability is close to 100%, will also have a growth fraction close to 100%. A simple generic protocol for continuous labeling is as follows: [^{3}H]thymidine is added to the culture medium, and the culture continues for a specified period; cells are fixed and subjected to autoradiography; when the autoradiograph has developed, the number of radiolabeled nuclei is counted and expressed as a percentage of the total.

In contrast, pulse-chase labeling is used to determine the average duration of each cell cycle phase. A generic protocol for [^{3}H]thymidine pulse-chase labeling is as follows: [^{3}H]thymidine is added to the culture; after a short period (1–2 h), cells are removed to a fresh medium without [^{3}H]thymidine; the culture is sampled regularly at times greater than the length of one cell cycle (24–48 h); each sample is subjected to autoradiography; and the number of labeled mitoses is counted as a percentage of the total. The average duration of G_2, S, M, and the total cell cycle is measured from the plot of labeled mitoses against time, then G_1 is calculated. Details of using [^{3}H]thymidine incorporation for determining growth fraction and cell cycle phase duration are summarized elsewhere (34). As with the mitotic index, any autoradiographic technique exhibits inherent disadvantages including sampling error because a small proportion of the total cell population is examined; the technique is slow, labor intensive, and not appropriate for on-line automation or use in integrated process control; and the use of radioisotopes requires additional containment and waste disposal facilities.

In recent years the thymidine analogue bromodeoxyuridine (BrdU) has been used as a safer, nonisotopic alternative to [^{3}H]thymidine for DNA labeling. BrdU can be used in exactly the same way as [^{3}H]thymidine, as either a continuous or pulse-chase label. The only difference in the protocol is that BrdU incorporation is detected by immunostaining with fluorescent anti-BrdU antibodies followed by fluorescence microscopy instead of autoradiography, so the method still suffers the disadvantages of any manual microscopic method. Alternatively, BrdU incorporation can be measured by flow cytometry, *vide infra*.

5.3.3 Measuring DNA Content

The third and probably easiest approach to adopt for cell cycle analysis is to measure the DNA content of each cell in a population by flow cytometry and thus determine the proportion of cells in G_0 or G_1, S, and G_2 or M at the time of sampling. A major and obvious advantage to this approach is that heterogeneous nonsynchronized cultures can be analyzed easily and rapidly, with the useful bonus that sub-G_1 apoptotic populations can also be identified. Other advantages include minimizing sample error by analyzing a large number of cells, and minimal interobserver variation because of the objective discrimination between G_1, G_2, and S cells. Furthermore, the method is appropriate for near on-line automation and use in integrated process monitoring or control. Although this approach is not able to resolve G_0/G_1 or G_2/M because DNA content is the same, this is of little concern in most process biotechnology applications because the (transformed) cells commonly used do not enter G_0. Furthermore the G_2 or M cell subpopulation can be resolved, if necessary, by measuring the mitotic index of the population (as already described) to determine the proportion of cells in M phase.

5.3.4 Flow Cytometry for Cell Cycle Analysis

Flow cytometric cell cycle analysis by measuring DNA content may follow any one of many protocols. A generic protocol is as follows: fix or permeabilize the cells; stain with a fluorescent DNA stain; measure stained DNA content by flow cytometry; and analyze data by simple gating or using dedicated cell cycle analysis software. Variations include pretreatment of cells; altered fixation or permeabilization protocols; postfixation treatment of cells; different stains, although stains such as PI or EB which intercalate into double-stranded nucleic acid are commonly used; and methods for data analysis. A typical flow cytometric measurement of PI-stained DNA in ethanol-fixed recombinant CHO cells and the subsequent cell cycle analysis using software based on a polynomial S-phase algorithm with an iterative nonlinear least squares fit, is shown in Fig. 5.3. By fitting the G_1 and G_2 peaks as Gaussian distributions and the S-phase distribution as a Gaussian broadened distribution, the cell cycle phase distribution can be deconvoluted.

Flow cytometry can also be used with BrdU incorporation to measure the growth fraction or to determine average cell cycle phase times. For flow cytometric analysis, BrdU incorporation can be detected by either fluorescent immunostaining or its quenching effect on Hoechst DNA stains. Thus BrdU incorporation can be analyzed simultaneously with DNA content. The advantage of this method is that it can recognize arrested but non-DNA-synthesizing cells during S phase. Cell size and/or protein content can also be analyzed simultaneously to give further related information. Again, there are many variations on a theme,

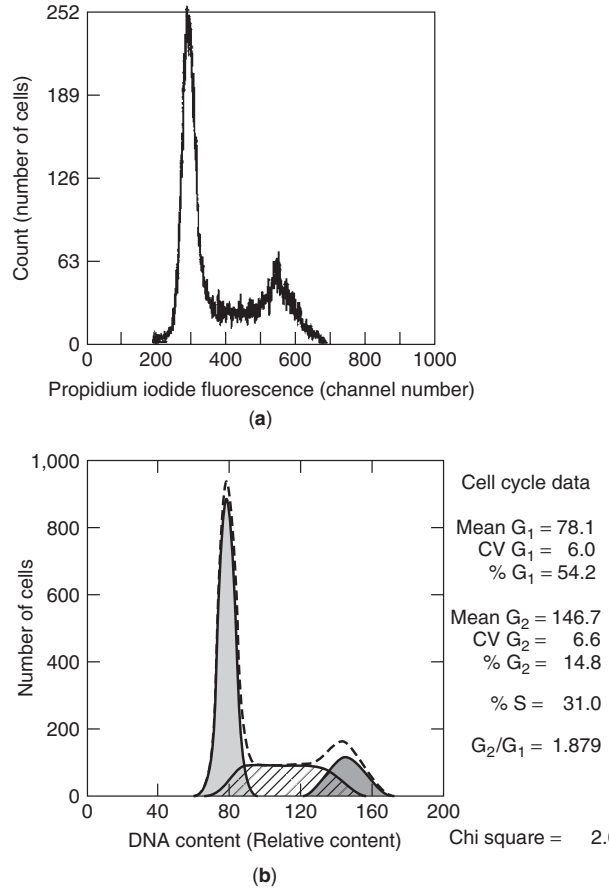


Figure 5.3. (a) Typical flow cytometric measurement of fluorescent (propidium iodide–stained) DNA content in recombinant CHO cells. (b) Resolution of cell cycle fractions from the fluorescent DNA content of recombinant CHO cells, using dedicated cell cycle analysis software (Multicycle®, Phoenix Flow Systems).

details of which and other flow cytometric methods for cell cycle analysis have been summarized elsewhere (35). Flow cytometry is also very useful for analyzing specific cell cycle–related proteins, following appropriate fluorescent immunostaining. For example, the absence of cyclin D or E in G_0 cells, shown by flow cytometry, has been used to distinguish G_0 from G_1 cells (22), and flow cytometric measurement of the Ki67 nuclear antigen has been shown to correlate with [^{3}H]thymidine and BrdU incorporation (36). Multiparameter flow cytometric analysis of G_1 and G_2 cyclin expression and DNA content has also been shown to be a useful tool in cell cycle analysis (37) because G_1 cells can be differentiated from G_0 cells, and cells with unusual karyotypes (e.g. G_1 tetraploid) can be distinguished from G_2 diploid cells. Flow cytometry can also be applied to investigating the relationship between the cell cycle and recombinant protein expression in economically important cell lines as a means of optimizing medium and environmental conditions for successful commercial operation.

5.4 IMPORTANCE OF THE CELL CYCLE IN PROCESS BIOTECHNOLOGY

5.4.1 Culture Proliferation and Growth

The cell cycle is the means by which a culture proliferates. Cell division and cell death, both active programmed cell death (apoptosis) and passive necrosis, are responsible for the change in the number of cells present. In addition to the cell cycle control genes, the transcription of genes coding for proteins involved in nucleotide and DNA synthesis is also cyclic. However, the progress of the cell cycle is costly in nutrient utilization and energy expenditure, particularly during S phase when the nucleic acid content of the cell is duplicated, and also during other phases because regulatory proteins are continuously synthesized and degraded. In theory it should be possible to arrest cells, in other words, stop them from cycling, thus preventing the "wastage" of energy and nutrients that could otherwise be directed into product synthesis. The maintenance energy model (38) states that energy (as adenosine triphosphate or ATP) consumption is divided into that which is needed for cell growth (cell cycle progression, as determined by increase in cell number) and that which is needed for cell maintenance. Based on this model it has been determined that the maintenance energy requirement of a hybridoma is $14.4/10^9$ mmol ATP/cell day, at a specific growth rate (μ) of 0.66 per day (31) corresponding to 62% of the energy (ATP) consumed. These values were confirmed by work that showed that the maintenance energy requirement of the same cells under slightly different nutrient and specific growth rate conditions was $11.4/10^9$ and $12/10^9$ mmol ATP/cell day, again, corresponding to $\sim$60% of the estimated ATP consumption rate (39). These observations agree with the value of 65% which was determined as the proportion of energy consumption used for maintenance by mouse LS cells grown at $\mu = 0.60$ per day (40). Thus it is apparent that about two-third of the energy used by a culture is for its own maintenance, and this proportion is not likely to be readily altered. Consequently, it appears that if the growth (cell cycle progression) requirement was removed, all of the remaining resources could be directed toward product elaboration, or alternatively, cultures would require up to one-third less energy and nutrient resources for the same product yield. However, we have shown recently that the increase in specific productivity of NS0 arrested culture over the proliferated culture cannot only be met by energy diversion alone (unpublished data). The increase in specific recombinant productivity is the result of an overall increase in cell growth (protein synthesis, cellular energy). In addition, the more active mitochondria in the arrested culture mean that the cell now needs more energy, rather than diverting energy.

Three main approaches have been used to prevent cells from cycling. The first is chemical blockade. For example, the addition of thymidine, hydroxyurea, TGF-β or adriamycin to culture medium causes cells to arrest at the G_1-S phase boundary, so cells accumulate in G_1 and specific productivity increases (41,42) . Other cell cycle inhibitors used to enhance productivity include protein synthesis inhibitors [potassium acetate, cycloheximide, aphidicolin, rapamycin, doxorubicin, staurosporine, mimosine, and nocodazole) (43–45)] and RNA synthesis inhibitor (Actinomycin D) (42). However, this production advantage is short-lived because the imbalanced growth state leads to culture death (usually by apoptosis) within a few days of the onset of the chemical blockade. The second approach is not to arrest the cell cycle but to substantially reduce its progression by reducing the culture growth rate. Using a custom-built total cell recycle bioreactor system, where the growth rate of a mouse hybridoma was substantially reduced ($\mu < 0.05$ μ max), Flickinger et al. (46) showed that specific monoclonal antibody secretion remained constant as the specific growth rate decreased. This demonstrated that production could be uncoupled from growth (cell cycle progression), although there was no evidence that the energy saved by substantial (>95%) reduction of growth was diverted into production. However, using this method for production-scale processes may have the advantage of less medium (energy or nutrient) expenditure per unit product, although the total product yield per unit of production (from each bioreactor) would not be increased. Furthermore, questions of product fidelity, especially with respect to glycosylation, are raised when growth is limited by the stress of nutrient deprivation or limitation.

The third approach is to use cell engineering to genetically control proliferation. Cytostatic genes, p21, p27, and IRF-1 have been used to control proliferation in a bioprocessing environment. The induction of p21 and p27 leads to the accumulation of most of the cells in the G_1 phase of the cell cycle while IRF-1 showed aphasic cell cycle arrest (46). In our laboratory NS0 and CHO cell lines have been constructed to inducibly express the $p21^{CIP1}$ cyclin-dependent kinase inhibitor, using the Lacswitch system (47,48). In these studies, arrested cells causing the overexpression of p21 have been shown to increase cell productivity. Long-term perfusion culture of p21 inducible NS0 cells showed that the antibody product could be increased 4-fold upon growth arrest (48). Bi *et al*. (49) found that arrested cells have higher mitochondrial mass, dehydrogenase activity, and ribosomal protein S6, as well as larger cell size indicating the uncoupling of cell growth, energy metabolism, and protein synthesis from cell cycle progression. At a later study (unpublished results; S H G Khoo, PhD thesis), the increased antibody productivity seen in the arrested cells is shown to be directly correlated with the increase in biomass (dry cell weight) and total intracellular protein. The results from various physiological and cellular organization levels have

demonstrated relatively good consistency. The cells are able to shift to a high productivity state by transcriptional and mRNA stability changes to the heavy and light chains, as well as cope with high productivity by a simultaneous increase in the post-translational capacity of the cell, including N-glycan biosynthesis and secretory functions. Energy metabolism remains a critical issue during high antibody productivity. These changes are controlled at the gene transcription level, demonstrating that the cellular objective is altered toward a high productivity state.

Besides having high productivities, it was believed that a decrease in the number of cell divisions reduces the possibility of genetic drift, which is of great importance when using genetically engineered cells for the production of biologics (43). Furthermore, once a high cell density is achieved, cessation of cell growth reduces the accumulation of toxic products, cell lysis and potentially reduces product contamination with cellular debris and product deterioration due to glycosidases and proteases (50).

Recent work tested the use of extracellular nucleotides, nucleosides, and bases as arresting agents. Carvalhal and coworkers (51) have used NADH, NAD, ATP, ADP, AMP, and adenosine to arrest the cell cycle and enhance productivity. AMP has been demonstrated to be the most promising for increasing specific productivity in CHO cells, resulting in cell arrest in the S phase. The authors suggested that a considered use of such natural compounds is required due to the presence of nucleotides and nucleosides in certain media (51). Other interesting approaches to increase productivity via inhibition of cell cycle progression include high osmolarity and low temperature (52,53). Both techniques have been shown to increase specific productivity where in many cases, the latter has been shown to be proportional to proliferation inhibition, but the role of the cell cycle in regulating or determining their effects is still not clear.

5.4.2 Production in Relation to Cell Cycle Phase

It is important not to confuse the relationship between cell cycle phase and productivity, with the relationship between cell cycle arrest and productivity. The substantial increases in productivity from the metabolically engineered transfects just described are most likely to exist because the arrested cells do not need to devote resources to biomass production (54). This section addresses the situation in "simple" recombinant cells that may be grown in standard industrial processes such as batch, continuous, or draw-and-fill semicontinuous culture modes. Determining the relationship between cell cycle phase and productivity is important for developing automated on-line (or near on-line) process control strategies. These strategies will be based on models that, in addition to the basic parameters of pH, dissolved oxygen (dO_2), cell density, and so forth, must incorporate information concerning cell state, including cell cycle phase and its effect on productivity.

It has been shown that specific monoclonal antibody production by a synchronized mouse–mouse hybridoma culture is maximal during G_1; furthermore, the specific activity increases when the cell cycle is arrested and cells are maintained in late G_1 (55). However, apparent specific productivity also increases when the culture declines (viability decreases); this is the result of substantial passive release of intracellular product into the culture medium from dead and dying cells. Phase dependence was also found in recombinant CHO cells transfected with an expression vector containing *dhfr* and *lacZ* genes; the former was controlled by an SV40 (simian virus 40) promoter, and the latter was controlled by the constitutive human cytomegalovirus (hCMV) promoter (56). In this study, the nonsecreted product, β-galactosidase, was produced almost exclusively during the S phase. Furthermore, cell cycle arrest in S phase, by specific inhibition of DNA polymerase, did not inhibit transcription or translation and thus had no effect on β-galactosidase expression.

However, the literature on the relationship between cell cycle and protein expression summarized in Table 5.2, is inconsistent. Different researchers have shown that product expression (or the maximum rate of expression) is related to different cell cycle phases. In addition, others have shown that product expression is aphasic. These observations do not necessarily contradict each other and may be a true reflection of the systems used, because a variety of cells, products, and constructs were studied. Cell cycle–dependent product expression may not be universal and could vary with cell type or cell line, the construction of the expression vector, the nature of the recombinant gene expressed, or the promoter or enhancer used to drive product expression. Other variables may include post-transcriptional regulation (mRNA level), product gene copy number, and even the culture mode (e.g. whether the cells are attached to a substrate or are free in suspension), may be relevant. However, there are two potential flaws in studying cell cycle–related productivity: synchronizing cells using chemical means, such as thymidine block or nutrient starvation, and comparing cells of different phases that are from the same culture but separated in time. The two problems often go together, for example, following a culture for a day after release from the thymidine block. The difficulty with the former is that the chemical stress used (whatever its nature) may, in addition to its desired effect on cell synchrony, directly cause perturbations in productivity that could wrongfully be ascribed to the cell cycle. The difficulty with the latter is simply that if two cell populations from a culture are separated in time, they are also separated in environmental conditions; recent work (57) has shown that the effect of medium condition is dominant to any cell cycle effect on productivity. The effect of temporal separation is made more uncertain following stress synchronization; an early population may have only partially recovered from the stress, whereas a later population may have fully recovered.

TABLE 5.2. Variation in Phase Expression of Different Products with Cell Line and Promoter

Cell Line	Promoter	Product	Phase Expression	References
Mouse leukemia	Endogenous	DHFR	Aphasic	58
CHO	Endogenous	DHFR	Aphasic	59
Human osteosarcoma	Endogenous	DHFR	Aphasic	59
Mouse embryo fibroblast	Endogenous	DHFR	Aphasic	59
Human prostrate epithelium	Endogenous	PSAP	All except early G_1	60
Hybridoma	Endogenous	MAb	G_1/G_0 (mainly)	61
CHO	AMLP	DHFR	G_1 (mainly)	62
Hybridoma	Endogenous	MAb	G_1/S	63
Mouse plasacytoma	Endogenous	Immunoglobulin	Late G_1/early S	64
Human lymphoid cell	Endogenous	Immunoglobulin	Late G_1/S	65
CHO	Endogenous	DHFR	G_1/S	30
Mouse leukemia	Endogenous	TMPS	S	58
CHO	CMV	β-Gal (*lac*Z)	S	57
CHO	SV40	tPA	S (mainly)	62
CHO	SV40	IFN-γ	S	66
Mouse L-cell	MMTV	β-Gal (*lac*Z)	S (predominantly)	66
CHO	Endogenous	DHFR	S	67
Rat adenocarcinoma	Endogenous	tPA	Shortly after S	68
Rat adenocarcinoma	Endogenous	uPA	Shortly after S	68
CHO	Endogenous	PA	G_2/M	69
NS0	CMV	MAb	G_1	58
NS0	CMV	MAb	G_1	64
CHO	GS	MAb	G_1/S and G_2/M	70

Note: DHFR, dihydrofolate reductase; CHO, Chinese hamster ovary; TMPS, thymidine monophosphate synthetase; MAb, monoclonal antibody; PSAP, prostrate-specific acid phosphatase; AMLP, adenovirus major late promoter; CMV, cytomegalovirus; β-Gal (*lacZ*), β-galactosidase (product of the *Escherichia coli lacZ* gene); SV40, simian virus 40; MMTV, mouse mammary tumor virus; NS0, mouse myeloma; GS, glutamine synthetase; tPA, tissue-like plasminogen activator; IFN-γ, interferon-γ; UPA, urokinase-like plasminogen activator; PA, plasminogen activator.

5.4.3 Cell Cycle Analysis as a Proliferation Predictor

Cells may be arrested in G_1 before the restriction point, but once past that point, they are committed to continuing their cycle and dividing unless prevented from doing so by a catastrophe or artificial intervention. Therefore, one can presume that once a cell enters S phase, under normal growth conditions, one single cell will in due course become two cells. This phenomenon can be used to predict culture growth. The growth-enhancing effect of peptone supplementation on hybridoma culture was predicted by cell cycle analysis 5 h after supplementation, although the effect on cell density was not apparent until 16 h later, 21 h after supplementation (71). A similar use of cell cycle analysis was made with CHO cells: the percentage of S-phase cells correlated with the specific growth rate 10.5 h later and the time difference was the average duration of S phase remaining plus the duration of G_2 and M for that population (72). Thus, the proportion of cells in S phase can be used to predict the subsequent proliferation rate of that culture.

5.4.4 Cell Cycle-Related Susceptibility to Hydrodynamic Damage

The effect of hydrodynamic stress as found in stirred and sparged bioreactors, is at least in part related to cell cycle phase, and there may be a role for hydrodynamic cell damage in the induction of apoptosis (73). It has been reported that DNA synthesis (74) and the proportion of the cell population in S phase (75) were increased under conditions of hydrodynamic stress (high sparging and agitation rates). However, the cell number remained low even though the S-phase population correlated with an increase in cell number. The observed reduction in growth rate was shown to be a consequence of a decline in the proportion of G2- and M-phase cells with a corresponding decrease in the cell size of the population, suggesting that the larger G2 cells were particularly susceptible to hydrodynamic damage (73). Subsequently it was shown that mitotic cells, while also being susceptible to hydrodynamic damage due to their size, were even more sensitive to hydrodynamic damage than G2 cells perhaps due to cytoskeletal rearrangements, alteration of plasma membrane fluidity, or morphological changes during mitosis (33).

5.4.5 Cell Cycle and Apoptosis

Apoptosis (active or programmed cell death) is the means by which intrinsic or extrinsic stimuli activate a series of molecular cascades, triggering events that culminate in a particular morphologically, ultrastructurally, and biochemically defined process of cell death that is, in effect, the opposite of the cell cycle. Entry of a cell into apoptosis can be restricted to a particular cell cycle phase (57,66–78) although this cell cycle dependence does not appear to be universal (79). Cell cycle checkpoints appear to link the

cell cycle to apoptosis. Deregulation of the cell cycle components has been shown to induce mitotic catastrophe and to trigger apoptosis (80).

Cell cycle progression and apoptosis are not only opposite in effect, they may also be alternate outcomes from a single cell control mechanism; they are inextricably linked by common components in the signal transduction pathways for both processes. In addition, circumstantial evidence from the induction of apoptosis by DNA damage or cell cycle disruption and the existence of many oncogenes that both promote the cell cycle and induce apoptosis implies that there is an equilibrium between these two antagonistic processes in all eukaryotic cells. It has been demonstrated by several investigators that apoptosis can occur at any stage of the cell cycle (41,81). For an excellent review of the link between apoptosis and cell proliferation, see Ref. 82.

REFERENCES

1. Alvarado-Moreno JA, Mayani H. Gac Med Mex 2007; 143: 149–161.
2. Alberts B, Bray D, Lewis J, Raff M, Roberts K, Watson JD. The molecular biology of the cell. 3rd ed. New York: Garland; 1994.
3. Watson JD, Hopkins NH, Roberts JW, Steitz JA, Weiner AM. Molecular biology of the gene. 4th ed. Melno Park (CA): Benjamin/Cummings; 1987.
4. Lodish H, Baltimore D, Berk A, Zipursky SL, Matsudaira P, Darnell J. Molecular cell biology. 3rd ed. New York: Scientific American Books; 1995.
5. Murray A, Hunt T. The cell cycle: an introduction. New York: Freeman; 1993.
6. Cooper S. Nature 1979; 280: 17–19.
7. Cooper S. J Theor Biol 1988; 135: 393–400.
8. Evan GI, Harrington E, McCarthy N, Gilbert C, Benedict MA, Nuñez G. In: Thomas NSB, editor. Apoptosis and cell cycle control in cancer. Oxford: Bios Scientific; 1996. p 109–129.
9. Holland IB. Cell 1987; 48: 361–362.
10. Boye E, Stokke T, Kleckner N, Skarstad K. Proc Natl Acad Sci U S A 1996; 96: 12206–12211.
11. Quon KC, Marczynski GT, Shapiro L. Cell 1996; 84: 83–93.
12. Schafer KA. Vet Pathol 1998; 35: 461–478.
13. Johnson DG, Walker CL. Annu Rev Pharmacol Toxicol 1999; 39: 295–312.
14. Kohn KW. Mol Biol Cell 1999; 10: 2703–2734.
15. Hay BA, Guo M. Hippo weighs. Dev Cell 2003; 5: 361–363.
16. Bardin AJ, Amon A. Nat Rev Mol Cell Biol 2001; 2: 815–826.
17. Bardin AJ, Boselli MG, Amon A. Mol Cell Biol 2003; 23: 5018–5030.
18. Murray A, Hunt T. The cell cycle: an introduction. Oxford, New York: Oxford University Press; 1993.
19. Pagano M, editor. Cell cycle control. New York, Berlin: Springer-Verlag; 1998. p 149–168.
20. Zetterberg R. In: Thomas NSB, editor. Apoptosis and cell cycle control in cancer. Oxford: Bios Scientific; 1996. p 17–36.
21. Matsuoka M, Kato JY, Fisher RP, Morgan DO, Sherr CJ. Mol Cell Biol 1994; 14: 7265–7275.
22. Kato JY, Matsuoka M, Strom DK, Sherr CJ. Mol Cell Biol 1994; 14: 2713–2721.
23. El-Deiry WS. In: Thomas NSB, editor. Apoptosis and cell cycle control in cancer. Oxford: Bios Scientific; 1996. p 55–75.
24. Hunter T, Pines J. Cell 1994; 79: 573–582.
25. Weinberg RA. Cell 1995; 81: 323–330.
26. Ogris E, Rotheneder H, Mudrak I, Pichler A, Wintersberger E. J Virol 1993; 67: 1765–1771.
27. Pearson BE, Nasheuer HP, Wang TSF. Mol Cell Biol 1991; 11: 2081–2095.
28. Dulic V, Lees E, Reed SI. Science 1992; 257: 1958–1961.
29. Wells J, Held P, Illenye S, Heintz NH. Mol Cell Biol 1996; 16: 634–647.
30. Darzynkiewicz Z, Gong J, Juan G, Ardelt B, Traganos F. Cytometry 1996; 25: 1–13.
31. Sherr CJ. Cell 1993; 73: 1059–1065.
32. Zhang D, Jacobberger JW. Cell Prolif 1996; 29: 289–307.
33. Abdul Majid FA, Al-Rubeai M. In: Carrondo MJT, Griffithsnobreak B, Moreira JLP, editors. Animal cell technology from vaccines to genetic medicine. Dordrecht: Kluwer; 1997. p 731–736.
34. Baserga R. In: Studzinski GP, editor. Cell growth and apoptosis: a practical approach. Oxford: IRL Press at Oxford University Press; 1995. p 1–19.
35. Crissman HA. In: Studzinski GP, editor. Cell growth and apoptosis: a practical approach. Oxford: IRL Press at Oxford University Press; 1995. p 21–43.
36. Gore SD, Weng LJ, Burke PJ. Exp Hematol 1993; 21: 1702–1708.
37. Gong J, Li X, Traganos F, Darzynkiewicz Z. Cell Prolif 1994; 27: 357–371.
38. Pirt SJ. Principles of microbe and cell cultivation. Oxford: Blackwell Scientific; 1975.
39. Miller WM, Wilke CR, Blanch HW. Biotechnol Bioeng 1989; 33: 477–486.
40. Kilburn DG, Lilly MD, Webb FC. J Cell Sci 1969; 4: 645–654.
41. Al-Rubeai M, Emery AN, Chalder S, Jan DC. Cytotechnology 1992; 9: 85–97.
42. Suziki E, Ollis DF. Biotechnology 1990; 6: 231–236.
43. Carvalhal AV, Coroadinha AS, Alves PM, Moreira JL, Hauser H, Carrondo MJT. Enzyme Microb Technol 2002; 30: 95–109.
44. Grosjean F, Batard P, Jordan M, Wurm FM. Cytotechnology 2002; 38: 57–62.
45. Futcher B. Methods Cell Sci 1999; 21: 79–86.
46. Muller A, Maurin L, Bonne C. Gen Pharmacol 1998; 30: 315–318.
47. Watanabe S, Shuttleworth J, Al-Rubeai M. Biotechnol Bioeng 2002; 77: 1–7.
48. Bi J-X, Shuttleworth J, Al-Rubeai M. Biotechnol Bioeng 2004; 85: 741–749.

49. Ibarra N, Watanabe S, Bi JX, Shuttleworth J, Al-Rubeai M. Biotechnol Prog 2003; 19: 224–228.
50. Fussenegger M, Schlatter S, Dätwyler D, Mazur X, Bailey JE. Nat Biotechnol 1998; 16: 468–472.
51. Carvalhal AV, Marcelino I, Carrondo MJT. Appl Microbiol Biotechnol 2003; 63: 164–173.
52. Van Breukelen F, Martin SL. J Appl Physiol 2002; 92: 2640–2647.
53. Al-Fageeh MB, Smales CM. Biochem J 2006; 397: 247–259.
54. Fussenegger M, Mazur X, Bailey JE. Biotechnol Bioeng 1997; 55: 927–939.
55. Al-Rubeai M, Emery AN. J Biotechnol 1990; 19: 67–86.
56. Gu MB, Todd P, Kompala DS. Biotechnol Bioeng 1993; 42: 1113–1123.
57. Lloyd DR, Leelavatcharamas V, Emery AN, Al-Rubeai M. Cytotechnology 1999; 30: 49–57.
58. Matherly LH, Schuetz JD, Westin E, Goldman ID. Anal Biochem 1989; 182: 338–345.
59. Feder JN, Assaraf YG, Seamer LC, Schimke RT. J Biol Chem 1989; 264: 20583–20590.
60. Herz F, Czerniak B, Deitch D, Wersto RP, Simmons DA, Koss LG. Cell Prolif 1991; 24: 321–330.
61. Kromenaker SJ, Srienc F. Biotechnol Bioeng 1991; 38: 665–677.
62. Kubbies M, Stockinger H. Exp Cell Res 1990; 188: 267–271.
63. Garatun-Tjeldst O, Pryme IF, Weltman JK, Dowben RM. J Cell Biol 1976; 68: 232–239.
64. Buell DN, Fahey JL. Science 1969; 164: 1524–1525.
65. Leelavatcharamas V, Emery AN, Al-Rubeai M. In: Funatsu K, Shirai Y, Matsushita T, editors. Volume 8, Animal cell technology: basic and applied aspects. Dordrecht: Kluwer; 1997. p 55–60.
66. Gu MB, Todd P, Kompala DS. Biotechnol Bioeng 1996; 50: 229–237.
67. Mariani BD, Slate DL, Schimke RT. Proc Natl Acad Sci U S A 1981; 78: 4985–4989.
68. Scott FM, Sator de Serrano V, Castellino FJ. Exp Cell Res 1987; 169: 39–46.
69. Aggeler J, Kapp LN, Tseng SCG, Werb Z. Exp Cell Res 1982; 139: 275–283.
70. McTaggart S, Al-Rubeai M. Biotechnol Bioeng 2001; 76: 52–60.
71. Al-Rubeai M, Chalder S, Bird R, Emery AN. Cytotechnology 1991; 7: 179–186.
72. Leelavatcharamas V, Emery AN, Al-Rubeai M. In: Al-Rubeai M, Emery AN, editors. Flow cytometry applications in cell culture. New York: Marcel Dekker; 1996. p 1–15.
73. Al-Rubeai M, Singh RP, Emery AN, Zhang Z. Biotechnol Bioeng 1995; 46: 88–92.
74. Lakhotia S, Bauer KD, Papoutsakis ET. Biotechnol Bioeng 1992; 40: 978–990.
75. Oh S, Al-Rubeai M, Emery AN, Nienow AW. In: Spier RE, Grifiths JB, Berthold W, editors. Animal cell technology products for today, prospects for tomorrow. Oxford: Butterworth Heinmann; 1994. p 405–407.
76. Klucar J, Al-Rubeai M. FEBS Lett 1997; 400: 127–130.
77. Sellins KS, Cohen JJ. J Immunol 1987; 139: 3199–3206.
78. Shih S-C, Stutman O. Cancer Res 1996; 56: 1591–1598.
79. Lazebnik YA, Cole S, Cook CA, Nelson WG, Earnshaw WC. J Cell Biol 1993; 123: 7–22.
80. King KL, Cidlowski JA. J Cell Biochem 2004; 58: 175–180.
81. Furuya Y, Lundmo P, Short AD, Gill DL, Isaacs JT. Cancer Res 1994; 54: 6167–6175.
82. Alenzi FQB. Br J Biomed Sci 2004: 61 .

6

CELL GROWTH AND PROTEIN EXPRESSION KINETICS

DHINAKAR S. KOMPALA
Chemical and Biological Engineering Department, University of Colorado, Boulder, Colorado

6.1 INTRODUCTION

In this article, the experimental observations and mathematical descriptions of mammalian cell growth kinetics, as well as protein expression kinetics, in batch, fed-batch, continuous, and perfusion cultures are summarized. Focusing primarily on the experimental data from freely suspended single-cell cultures, which are being used increasingly in the biotechnology industry because of their simplicity and easy scalability (1), this article discusses the development and utility of mathematical models of mammalian cell growth kinetics in operating and controlling bioreactors. Further, it addresses the different observed patterns of protein expression kinetics as they relate to cell growth kinetics for hybridoma versus recombinant mammalian cells, and discuss the different bioreactor operating strategies necessary to maximize the production of desired proteins from any production pattern.

Mathematical models of animal cell growth kinetics may be classified along the lines of microbial growth models, which are either structured or unstructured and segregated or unsegregated (2). The unstructured cell growth models consider cell mass as a single entity, compositionally uniform and unchanging even at different growth conditions, whereas the structured growth models include some details on the varying composition of intracellular components (ribosomes, proteins, metabolites, etc.). The unsegregated cell models consider all cells identical, whereas the segregated cell growth models allow for cellular variations or different cell types (such as high and low producers, cells at different cell cycle phases, or cells with different target gene copy numbers). Therefore, the unstructured, unsegregated models are simpler in their kinetic expressions and numeric simulations, but can become unrealistic when dealing with complicated growth phenomena. When the models include more details on the intracellular composition of the average cell (structured growth models) or allow for the different cellular types (segregated growth models), the mathematical descriptions become more realistic, but at the same time more difficult for estimating model parameters, independent model verifications, and numerical computations. Therefore, we will focus in this article primarily on the simpler types of mathematical models for simulating or predicting the different cell growth and protein expression kinetics and provide some references to the more complicated mathematical models developed for mammalian cells.

6.2 BATCH CULTURE KINETICS

6.2.1 Experimental Data

Typical batch culture data for cell growth and product expression kinetics of a murine hybridoma cell line grown in homogeneous suspension cultures (3) are shown in Fig. 6.1. The salient features in the cell growth curve include an early exponential cell growth period, a gradual slowdown in cell growth as the viable cell concentration reaches its maximum value because a key nutrient component is depleted or a toxic metabolite has accumulated, and a subsequent cell death period.

Upstream Industrial Biotechnology: Expression Systems and Process Development, Volume 1, First Edition. Edited by Michael C. Flickinger.
© 2013 John Wiley & Sons, Inc. Published 2013 by John Wiley & Sons, Inc.

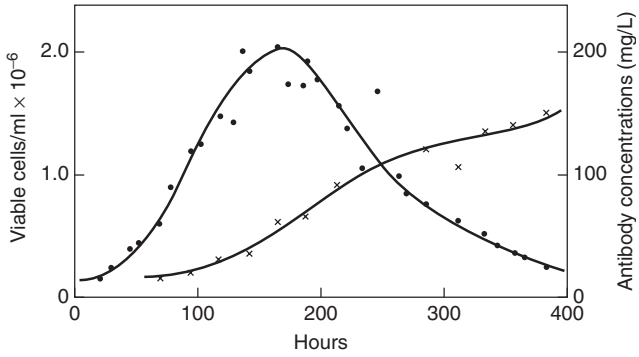


Figure 6.1. Batch culture kinetics of a mouse hybridoma cell line in a 1000-L fermenter, showing viable cell (•) and monoclonal antibody (×) concentrations. [Reproduced from Ref. 3 with permission.]

The product (monoclonal antibody) accumulation curve shows more subtle features, which are harder to interpret. One common observation is that the antibody production rate (the *slope* of the curve marked ×) is maximum when the viable cell concentration is at its maximum, and the production rate is noticeably slower when the viable cell concentration is lower. A second common observation made from these data is that the antibody production rate increases again as more cells die.

The first observation on the antibody production curve suggests that the antibody production rate is proportional to the viable cell concentration, which can be expressed mathematically as

$$\frac{\mathrm{d[MAb]}V}{\mathrm{d}t} = q_{\mathrm{MAb}} X_{\mathrm{v}} V \tag{6.1}$$

where [MAb] is the antibody concentration (mg/mL), t is time (day), V is culture volume (mL), q_{MAb} is the specific (per cell) antibody production rate (mg/cell/day), and X_{v} is the viable cell concentration (cells per milliliter). Assuming constant culture volume (for batch cultures) and a constant specific production rate (as a first guess), this equation can be simplified to give

$$[\mathrm{MAb}] = q_{\mathrm{MAb}} \int X_{\mathrm{v}} \mathrm{d}t \tag{6.2}$$

This equation has been used by different investigators to define the viability index (4), which is also known as the *integral of viable cells* (IVC) (5) and correlates strongly with product titer. This simple relationship immediately suggests some strategies for increasing antibody titers in batch cultures, such as prolonging the viability of the cells, increasing the viable cell concentration, or a combination of the two. These strategies have been implemented easily by strengthening or increasing the concentrations of some medium components to achieve higher viable cell concentrations, and by feeding in concentrated medium intermittently or continuously after about 5 days into batch culture to delay the depletion of key nutrient components in the so-called fed-batch culture operation (6,7).

The second observation on the slight increase in product accumulation during the late culture period, when most cells are dying, has prompted a number of experimental studies to characterize this phenomenon. However, this increase in product accumulation caused by the release of stored products from dying cells is a small fraction of the total product accumulated in the batch or fed-batch cultures (5,8).

6.2.2 Unstructured Kinetic Models

Factors that limit the maximum viable cell concentration and the prolonged viability of these cells were investigated by several investigators (7,9,10). It is commonly found that the growth-limiting substrates are glutamine and glucose and that the toxic metabolic by-products are ammonia and, to a lesser extent, lactic acid. On the basis of these observations, extended Monod saturation kinetic expressions for multiple substrates and inhibitors were proposed (11–13) to describe the specific growth rate μ of hybridoma cells as a function of the concentrations of the limiting nutrients and toxic by-products. A typical expression (12) for μ is

$$\mu = \mu_{\max} \left(\frac{G}{K_G + G}\right)\left(\frac{Gn}{K_{Gn} + Gn}\right) \left(\frac{K_A}{K_A + A}\right)\left(\frac{K_L}{K_L + L}\right) \tag{6.3}$$

where μ is the specific growth rate of hybridoma cells; $\mu_{\max}$ is the maximum specific growth rate; and G, Gn, A, and L are the concentrations of glucose, glutamine, ammonia, and lactate, respectively. The different Ks represent the saturation constants for growth or inhibition by each of these chemicals. A similar multiple saturation kinetic expression has been proposed (11) for the experimentally observed death of these cells in the presence of the two metabolic by-products and in the absence of growth-limiting nutrient:

$$k_{\mathrm{d}} = k_{\mathrm{d,\,max}} \left(\frac{A}{K_{A\mathrm{d}} + A}\right)\left(\frac{L}{K_{L\mathrm{d}} + L}\right)\left(\frac{K_{Gn,\mathrm{d}}}{K_{Gn,\mathrm{d}} + Gn}\right) \tag{6.4}$$

where k_{d} and $k_{\mathrm{d,max}}$ represent the specific death rate and its maximum death rate constant, respectively and the different K_{d}s represent the saturation constants for ammonia, lactate, and glutamine, respectively.

The cell growth and death rate expressions (Eqs 6.3 and 6.4) can be coupled with material balance equations for glucose, glutamine, ammonia, and lactate through the use of yield coefficients Ys and maintenance coefficient m (14)

to describe the dynamic variations of all these chemical and cell concentrations in batch or continuous cultures. Bree *et al*. (11) simulated the dynamics of cell growth and death, consumption of the limiting nutrients, accumulation of by-products, as well as the product antibody concentration in a glutamine-limited serum-supplemented batch culture. The rate expression for intracellular antibody production was proposed as

$$\frac{\mathrm{d[MAb]}}{\mathrm{d}t} = k_{\mathrm{p}} X_{\mathrm{v}} \left(\frac{K_{\mathrm{p}}}{K_{\mathrm{p}} + Gn} \right) \left(\frac{X_{\mathrm{T}}}{K_{\mathrm{XI}} + X_{\mathrm{T}}} \right) \qquad (6.5)$$

where k_{p} is the maximum specific antibody production rate constant, K_{P} is an inhibition constant for glutamine, X_{T} is the total cell concentration, and K_{XI} is an inhibition constant for total cell number. This proposed expression suggests that the specific monoclonal antibody production rate constant q_{MAb} used in Equations 6.1 and 6.2 is not a constant and has to be modified to reduce the specific production rate at high glutamine concentration and at low total cell concentrations. Many of the parameter values, particularly the yield coefficients, saturation coefficients, and the rate constants, were determined from experimental data, and remaining six parameters were adjusted to fit the experimental data. Although the model development and consequently the simulations miss a slight reutilization of lactate in late batch culture period, it is remarkable that this unstructured kinetic model can describe the experimentally measured consumption of glucose and glutamine relatively closely. Model simulations ignore the early batch data, recognizing the well-known difficulty of fitting the initial lag phase with the Monod saturation kinetic expressions. The complexities of animal cell culture, such as the complex media requirements, are manifested in the formulation of multiple saturation or inhibition kinetic expressions and difficulties in determining model parameters.

Dalili *et al*. (15) subsequently developed simpler kinetic expressions for these three rates (cell growth, cell death, and product expression) in glutamine-limited serum-supplemented batch cultures. These model simplifications recognize that glucose is typically in excess and therefore not rate limiting (as recognized by Bree *et al*. as well). Further, ammonia and lactate saturation terms are also eliminated in both growth- and death-rate expressions because these toxic metabolites do not build up to growth-limiting or toxic levels in their batch cultures, but the death rate expression has an additional low constant death rate. A significant difference from the previous model by Bree *et al*. is proposed in the antibody production rate expression. On the basis of their experimental observations of a relatively constant specific antibody production rate for a given initial serum concentration and a reduced production rate as glutamine is depleted, they propose the following rate expression for specific antibody production:

$$q_{\mathrm{MAb}} = m(S_{\mathrm{i}}) \frac{Gn}{K_{\mathrm{MAb}} + Gn} \qquad (6.6)$$

where $m(S_{\mathrm{i}})$ is a production rate constant, which is a function of the initial serum concentration, and K_{MAb} is a saturation constant for antibody production. Most of the simplified model parameters were estimated from a single batch culture experiment, and the glutamine degradation-rate constant was estimated from available literature. With these rate expressions and associated material balance equations, they simulated the dynamic variations in the cell number, glutamine, and monoclonal antibody concentrations in batch cultures with the same initial serum concentration. The model simulations agree reasonably with the set of batch culture data in which glutamine is the limiting nutrient.

Following these early modeling attempts, many other unstructured models (16–21) were proposed with many small differences in their rate equations. Portner and Schafer (22) analyzed about 10 different unstructured kinetic models for hybridoma cell growth and metabolism published in the literature that vary significantly in each of the rate expressions, and compared some model simulations with different sets of experimental data. Though these models were developed on the basis of different sets of experimental data from different hybridoma cell lines growing on different medium formulations and varying serum content, their quantitative comparisons provide some useful general conclusions.

6.2.3 Comparison of Model Simulations with Experimental Data

Despite the use of different rate expressions, many of these models agree well for specific growth rates with experimental data from continuous cultures at different dilution rates. However, significant differences are found between the model simulations and experimental data in the trends of specific death rate, glucose and glutamine consumption rates at low growth rates, and lactate yield from glucose and monoclonal antibody production rate plotted against the specific cell growth rate.

A comparison of the model prediction with experimental data for a specific death rate indicates the adequacy of each proposed rate expression within a limited range of specific growth rates, but shows diverging trends outside that range. These large differences strongly indicate that the proposed expressions for cell death (typically saturation terms with ammonia and lactate and an inhibition term for glutamine) are not quite representative of apoptosis, which is the prevalent mode of gradual cell death due to the buildup of toxic metabolites or depletion of nutrients during the long batch and fed-batch culture times. Necrosis, or sudden traumatic

death more common during excessive sparging or stirring, is not addressed by these proposed rate expressions. Even with these barely adequate specific death rate expressions, these unstructured kinetic model simulations were applied to develop or optimize fed-batch culture strategies (23,24) to increase hybridoma cell densities, prolong their viabilities, and thus increase antibody titers.

Nutrient consumption rate expressions have been typically based on the successful models of microbial growth kinetics. For the simpler microbial growth on a single rate-limiting carbon and energy substrate, the substrate consumption rate in batch cultures is typically modeled as proportional to the cell growth rate, and the proportionality coefficient is usually called the *yield coefficient Y* (grams of cell mass dry weight generated per gram of substrate consumed). In continuous cultures, an additional maintenance coefficient m is necessary (14) to account for the lower observed yield coefficients at low growth rates. For mammalian cell cultures, however, each of the two major required nutrients glucose and glutamine can provide the carbon and energy requirements to different degrees, depending on the availability of the other substrate, as summarized in Fig. 6.2.

The model simulations with the standard method of using a yield coefficient and a maintenance term in each

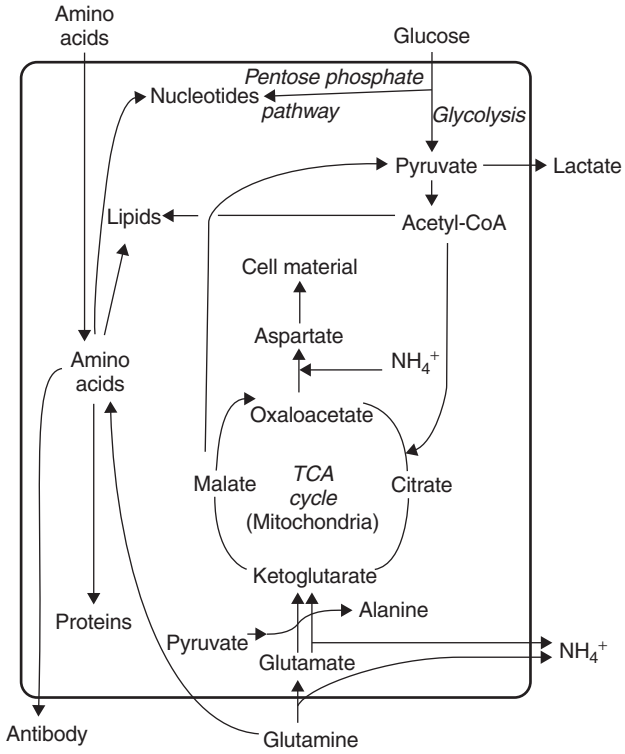


Figure 6.2. Summary representation of metabolic pathways for the utilization of glucose and glutamine in mammalian cells. [Reprinted from Ref. 19] with permission.]

nutrient consumption equation agree with the chemostat data on nutrient consumption rates over a limited range of dilution rates (20). Glucose consumption rates exhibit a saturation-type dependence on residual glucose concentration, even at a constant cell growth rate μ. Therefore, some modelers proposed saturation-type kinetics for nutrient consumption rates as a function of the residual nutrient concentration (18,21,25). However, these different modifications to nutrient consumption rates describe a set of observed data and do not represent the intrinsic flexibility of intracellular metabolism summarized in Fig. 6.2. Observations of multiple steady states through controlled nutrient feeding procedures in fed-batch cultures (26) highlight the feasibility of exploiting metabolic flexibility to minimize the toxic metabolite buildup, and to increase the cellular yield. Such strategies are developed only with a more detailed analysis of intracellular metabolism summarized in Fig. 6.2, and cannot be predicted with any of the simpler unstructured kinetic models discussed before.

Similarly, the two different rate expressions (Eqs 6.5 and 6.6) proposed before for antibody production kinetics in batch cultures represent simplified descriptions of more complex intracellular mechanisms governing synthesis and secretion of monoclonal antibody. Because these expressions do not directly represent the details of intracellular mechanisms, they are expected to be valid mainly in the cases for which they are developed and tested. Subsequent modelers (16–18,22) have used the classical Leudeking–Piret equation for product expression kinetics, typically consisting of a constant (nongrowth-associated) q_{MAb} plus in some cases a growth-associated term, which is proportional to the specific growth rate μ.

6.3 CONTINUOUS CULTURE KINETICS

6.3.1 Experimental Data

In batch cultures, all of the culture conditions such as cell number, nutrient concentrations, and product concentrations change throughout the culture period. Consequently, it becomes difficult to evaluate whether the key metabolic parameters, such as the cell-specific antibody production rate q_{MAb} and the different yield coefficients, remain constant or change systematically with time or nutrient concentrations. This uncertainty contributes significantly to the diversity of rate expressions proposed by different researchers using only batch culture data. More accurate experimental data are obtained from the steady-state conditions obtained over longer periods of continuous cultures. A constant nutrient flow rate F is fed into a bioreactor and the spent medium from the bioreactor is removed along with the cells to the same flow rate to maintain a constant bioreactor culture volume

V. At a constant dilution rate D $(= F/V)$, the continuous culture bioreactor gradually reaches a steady state and hence known as the *chemostat*, wherein the concentrations of chemicals (nutrients, metabolite products) as well as the cells remain constant, even as the cells are actively growing, consuming nutrients, and secreting products. At each steady state, the specific cell growth rate can be easily estimated from the material balances using the measured values of D, X_v, and X_T as

$$\mu = D\frac{X_T}{X_v} \tag{6.7}$$

Similarly, the specific nutrient consumption rates, as well as the antibody production rates, can be estimated through material balance equations and measured concentrations of nutrient and antibody, respectively. Using this method with their steady-state data from continuous cultures of hybridoma cells, Miller *et al*. (12) calculated many metabolic quotients or specific nutrient consumption and product formation rates over a range of cell growth rates or dilution rates.

An interesting highlight from Miller *et al*.'s (12) continuous culture data is that growth rate does not immediately adjust to a change in dilution rate, but changes gradually to reach a new steady state. Consequently, the cell number and nutrient concentrations can go through maxima or minima as cells adapt slowly to the newly imposed dilution rate. Similar dynamic phenomena have been observed repeatedly in microbial cultures as well. The unstructured Monod models are commonly found to be incapable of predicting these dynamics accurately.

6.3.1.1 Inverse-Growth-Associated Production Kinetics. The most surprising result from Miller *et al*.'s (12) steady-state experimental measurements of hybridoma cell metabolism in continuous cultures is that the specific antibody production rate q_{MAb} does not appear to be related to the specific cell growth rate μ according to standard models of growth-associated or nongrowth-associated production kinetics. Instead, the specific antibody production rate appears to follow a new inverse-growth-associated pattern; that is, the specific (per cell) antibody production rate is about two- to threefold higher at lower cell growth rates, as shown in Fig. 6.3.

This inverse-growth-associated production pattern obtained from steady-state data in continuous cultures of murine hybridoma cells has been corroborated by other continuous culture experimental results (17,27,28) and other growth-limiting batch culture conditions (29–31) such as high osmolarity and suboptimal pH and addition of specific growth inhibitors. Although a few experimental studies (20) have observed nongrowth-associated or growth-associated production kinetics, the predominant observation on *monoclonal antibody* production kinetics from *hybridoma* cell cultures has been inverse-growth associated, as shown in Fig. 6.3.

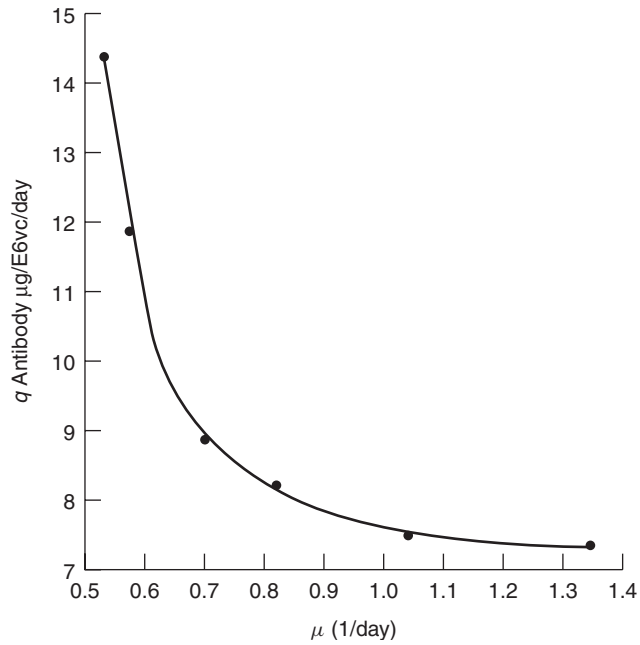


Figure 6.3. Commonly observed inverse-growth-associated production of monoclonal antibody production by murine hybridoma cells. [Reprinted with permission from Ref. 12.]

6.3.1.2 Growth-Associated Production Kinetics. Among the well-characterized exceptions to the commonly observed inverse-growth-associated production kinetics, the production kinetics of humanized chimeric antibodies in transfected myeloma cells have been found to be growth associated in steady-state continuous cultures (32), as shown in Fig. 6.4. These growth-associated production kinetics are commonly observed in the production of recombinant therapeutic proteins, such as γ-interferon and human growth hormone, in batch and continuous cultures of transfected mammalian cells (33,34). An interesting switch in the production pattern has been reported (35) in batch cultures of baby hamster kidney (BHK) cells: although the specific production rates of a secreted recombinant antibody and a secreted reported protein (alkaline phosphatase) are growth associated in suspension cultures, inverse-growth-associated production kinetics are reported for the same cell lines when they are grown attached to microcarriers. However, in the light of the difficulties in getting accurate kinetic results from batch cultures and the added difficulty in estimating the growth rate from attached growth on microcarriers, it is not certain whether this reported switch in the production kinetics on changing the culture environment is reproducible or an experimental artifact.

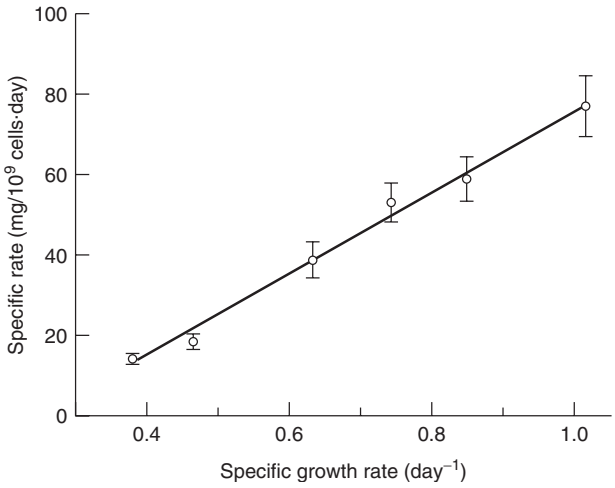


Figure 6.4. Growth-associated production of chimeric antibody by transfected myeloma cells. [Reprinted with permission from Ref. 32.]

In summary, it is well established through continuous suspension culture steady-state results that transfected mammalian cells exhibit growth-associated production kinetics for the synthesis of different recombinant proteins, as shown in Fig. 6.4, whereas the production kinetics for the synthesis of monoclonal antibody from hybridoma cell cultures follows an inverse-growth-associated pattern, as shown earlier in Fig. 6.3.

6.3.2 Structured Kinetic Models

In contrast to the unstructured kinetic models that consider the cells as uniform in composition, the structured kinetic models consider the dynamic variations of some key intracellular metabolic components, such as DNA, RNA, nucleotides, proteins, amino acids, membranes, and lipids. Batt and Kompala (36) developed a structured kinetic modeling framework for simulating the dynamics of cell growth in batch and continuous cultures of mammalian cells. To simplify their structured kinetic model, Batt and Kompala lumped these components into four separate pools and developed different rate expressions in the form of Equation 6.3 for the synthesis of each pool. Then the cell growth rate is simply calculated as the sum of the rate equations of all intracellular pools. With this framework, the model calculates the dynamics of cell growth rate even in the unbalanced growth conditions, such as in the initial lag phase of batch cultures and when the dilution rates are shifted up or down in continuous cultures. The structured growth model has been shown capable of simulating the maxima and minima observed in cell number and nutrient concentrations during the shift-up or shift-down experiments. Therefore, this structured model can be useful for simulating simple batch culture dynamics and steady-state data in continous cultures and also for simulating the dynamics of these cultures due to intermittent additions of nutrients, as well as the fed-batch cultures discussed in a later section.

However, as the single growth rate expression (Eq. 6.3) is now replaced with a rate expression for each of the four intracellular pools, the number of model parameters increases significantly. Although some of these parameter values of lymphocyte metabolism are determined from the literature, many other parameter values were estimated from the same experimental results of Miller *et al*. (12). For the antibody synthesis rate, this structured kinetic model uses a descriptive rate expression based on the experimental data shown in Fig. 6.3 in the absence of an exact mechanistic understanding of this pattern. With a more detailed understanding of the mechanisms involved in determining the inverse-growth-associated production kinetics, it is possible to alter the rate expression within the same structured kinetic modeling framework to enhance the utility of model simulations.

DiMasi and Swartz (37) developed a so-called energetically structured model, focusing on energy metabolism of hybridoma cells, represented by four pseudometabolite pools, such as glycolytic intermediates, metabolites derived from glutamine, energy charge (38) of the cell (ratio of ATP, ADP, and AMP), and the redox state of the cell or the ratio of NADH/NAD. Then the specific nutrient uptake rates and waste product synthesis rates are expressed as combinations of saturation and inhibition terms based on these pseudometabolites. The cell growth rate expression is formulated as a product of multiple exponential saturation terms each based on a single pseudometabolite. Although this approach recognizes the possible variations in the different intracellular metabolites, as in the previous structured kinetic model, the growth rate expression multiplies different saturation terms, as in the unstructured models represented by Equation 6.3. This energetically structured model satisfactorily describes the steady-state data for different nutrients and metabolites from Miller *et al*.'s (12) continuous culture experiments. It is not known if the simulations of the model are equally successful in simulating the dynamic variations in shift-up or shift-down experiments. As in the previous structured kinetic model, incorporating mechanistic detail into the model comes at the cost of additional model parameters, which need to be estimated through independent experiments to test any predictive capabilities.

Because of the increasing availability of detailed mechanistic knowledge, it is becoming possible to develop kinetic models for different metabolic pathways, for example, monoclonal antibody assembly and secretion (39), and regulatory subsystems, for example, intraorganelle pH regulation (40). Because the speed and ease of numerical computations have increased rapidly along with our detailed mechanistic

knowledge, it may indeed be possible to develop a more complete structured kinetic model to describe the complex dynamics of animal cell cultures. Barford and coworkers (41,42) used a modular approach to construct a complex structured kinetic model with three major compartments of cell culture medium, cytoplasm, and mitochondria. However, as the number of parameters increases dramatically to more than a hundred with such detailed mechanistic models describing over 40 model variables, it is increasingly difficult to estimate the parameter values to simulate the cell metabolism on a computer. Therefore, these researchers (43) had to use artificial intelligence methods, such as a hybrid neural network model (44), in conjunction with the metabolic model to optimize the estimation of parameter values so that model simulations agree better with experimental data on the dynamics of metabolite concentrations in batch cultures.

6.3.3 Cell Cycle Models

Suzuki and Ollis (45) proposed a cell cycle model for antibody synthesis by hybridoma cells to explain the repeated observations of inverse-growth-associated production kinetics of monoclonal antibody in continuous cultures of murine hybridoma cells, as shown in Fig. 6.3. On the basis of prior literature on cell cycle-dependent synthesis of antibodies by myeloma or lymphoid cells, they proposed that hybridoma cells secrete monoclonal antibodies primarily in the late G1 and early S phase of the cells. According to the well-established cell cycle models, cells spend more time in the G1 phase during low growth rates in continuous cultures, as well as in growth-limited batch or fed-batch cultures. Consequently, the higher antibody synthesis in the late G1 phase results in a higher specific (per cell) antibody synthesis rate at lower growth rates. At higher growth rates, the cells spend less time in the productive G1 phase, resulting in a reduced specific antibody production rate. This cell cycle model for antibody synthesis by hybridoma cells was investigated experimentally by a number of investigators (46–48) providing significant support for this central hypothesis.

Following Suzuki and Ollis's successful prediction of the inverse-growth-associated antibody production kinetics by hybridoma cells with the cell cycle model, Linardos *et al*. (49) proposed a cell cycle model for apoptotic cell death, which is observed strongly at low cell growth rates. They proposed that apoptotic cell death occurs primarily in cells arrested in the G1 phase of the cell cycle and that the death rate is proportional to the fraction of cells arrested in the G1 phase. This cell cycle model satisfactorily describes the higher cell death rates at low dilution rates in continuous cultures of hybridoma cells.

With these two successful descriptions of antibody productivity and cell death by simpler cell cycle models, Martens *et al*. (50) developed a combined cell cycle and unstructured kinetic model for simulating Miller *et al*.'s (12) continuous culture steady-state data. The cell growth rate expression is similar to Equation 6.3 and the substrate consumption rate equations are based on the yield coefficient and maintenance energy terms described earlier. Although the model simulations follow the trends qualitatively in the steady-state data, the average model parameter values chosen do not fit the experimental data closely enough. Further, the predictions of this unstructured kinetic model for dynamic variations in batch, fed-batch, or continuous culture shift-up or shift-down experiments are expected to be more divergent, as discussed earlier.

The dramatic switch in protein expression kinetics from the inverse-growth-associated production of antibodies by hybridoma cells (Fig. 6.3) to a growth-associated production of recombinant proteins by transfected mammalian cells (Fig. 6.4) has been addressed with a cell cycle model (51). Gu *et al*. (51) assumed that although hybridoma cells produce antibodies primarily in the G1 phase, transfected mammalian cells produce their recombinant proteins primarily in the S phase. Gu *et al*.'s (51) cell cycle model predictions for an intracellular reporter protein accumulation, shown in Fig. 6.5, have an inverse-growth-associated production pattern for the G1-phase-synthesis assumption and a growth-associated or nongrowth-associated production pattern for the S-phase synthesis assumption. The S-phase synthesis assumption is supported by flow cytometric investigations on recombinant protein synthesis in transfected Chinese hamster ovary (CHO) cells (52,53). On the basis of the different cell cycle phase-specific characteristics of recombinant protein expression from different promoters, Kompala and coworkers (54,55) developed different CHO cell lines

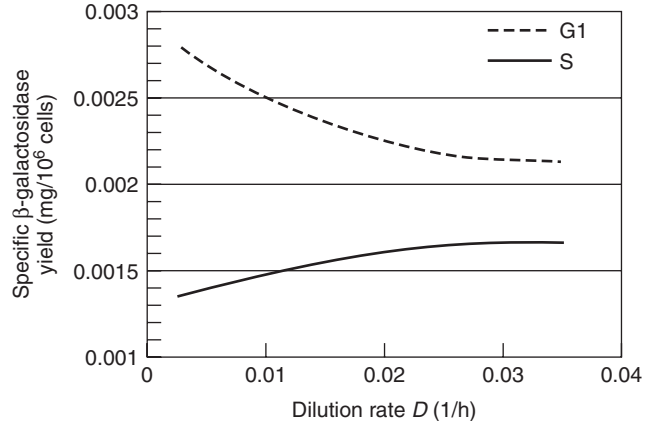


Figure 6.5. Predictions of the previous two production patterns with different assumptions on the cell cycle phase-specific expression for intracellular protein accumulation. [Reprinted with permission from Ref. 51.]

transfected with different expression vectors that contain the same reporter gene (*lac Z*). In continuous cultures of stably transfected CHO cells, the S-phase-specific SV40 promoter-driven expression of β-galactosidase was growth associated (54), whereas the G1-phase-specific adenovirus major late (AML) promoter-driven expression of the intracellular reporter protein was inverse-growth associated (55). If these results yielding the dramatic switch between growth-associated and inverse-growth-associated production kinetics are reproducible with secreted reporter proteins, this phenomenon will have a significant impact on maximizing culture productivities, as discussed in the section on fed-batch cultures.

6.3.4 Segregated Models

Long-term cultures of some hybridoma cell lines have shown a gradual decrease in antibody productivity due to the appearance of faster growing nonproducer hybridoma cells (16). The loss of culture productivity can be modeled only by explicitly recognizing the growth and production kinetics of these two distinct cell lines, producer and nonproducer, in a segregated modeling approach (56). On the basis of a similar approach used successfully to analyze instabilities in recombinant bacterial cultures, new insights have been developed on the rate of conversion from producers to nonproducers and the growth rate difference between two cell types required to generate this culture instability (57). More general segregated models develop single-cell models, along the lines of pH regulation model of CHO cells (40), and integrate them among the whole cell population to develop population balance models (58). The desirability of population balance models for analyzing mammalian cell cultures as well as the difficulties associated with the detailed modeling analysis are discussed in a recent review on modeling of mammalian cells (59). With numerous theoretical and computational difficulties added on top of the difficulties in developing detailed mechanistic models for single cells, the population balance modeling approach is not yet widely used in understanding the kinetics of mammalian cell growth and protein expression.

6.4 FED-BATCH AND PERFUSION CULTURES

6.4.1 Optimization of Monoclonal Antibody Production

Successful exploitation of cell growth and protein expression kinetics has led to systematic development of fed-batch cultures for maximizing monoclonal antibody productivity from hybridoma cells (60). Maximizing the hybridoma cell concentration and maintaining the viability of these cells by careful feeding of medium concentrates, as suggested by Equation 6.2, are the key ingredients in this optimization process. An equally important ingredient in achieving high product titers has been the *inverse-growth-associated* production kinetics, as shown in Fig. 6.3. During the early batch culture period, cells grow at a high rate with a low specific production rate. After high cell densities have been achieved, controlled nutrient feeding reduces the cell growth rate and maintains the cells' viability as long as possible. During this low growth fed-batch culture period, the specific (per cell) antibody production rate is significantly increased, as shown in Fig. 6.3, resulting in a large production of monoclonal antibodies in fed-batch cultures. Similarly, in high cell density perfusion cultures, after high cell densities are achieved through the early batch culture period, the cells are maintained in a lower growth mode once perfusion culture begins. During such a high cell density perfusion operation, the specific production rate increases (61), resulting again in larger antibody titers than in continuous cultures.

6.4.2 Model Simulations for Fed-Batch Cultures

The preceding development of optimal fed-batch and high cell density perfusion cultures to maximize culture productivity has taken place without any significant direct input from model simulations. The unstructured models, based on extended Monod Kinetics, are ill suited for dynamic simulations, even though they have been applied for this purpose in fed-batch (23,24) as well as perfusion (62) cultures. Emborg and coworkers (63) simulated the structured kinetic model of Batt and Kompala (36) in batch and fed-batch culture modes and indeed found the fed-batch cultures better suited for maximizing culture productivity, as confirmed by many experimental studies. Ryszczuk and Emborg (64) subsequently compared the fed-batch simulations of the same structured model (36) with an unstructured model to conclude that the structured model simulations are more responsive to the different fed-batch culture strategies and predict a more significant improvement in antibody production in fed-batch cultures.

6.4.3 Suboptimal Growth-Associated Production Kinetics

Although high cell density fed-batch and perfusion cultures have been successful in maximizing monoclonal antibody production from hybridoma cells, a necessary requirement for this optimization has been *inverse-growth-associated* production kinetics, as shown in Fig. 6.3. However, recombinant protein synthesis kinetics from transfected mammalian cells are typically growth associated, as shown in Fig. 6.4. Some experimental researchers have already

recognized the suboptimal nature of fed-batch cultures for these mammalian cell lines and have used repeated batch cultures (65) to maximize protein synthesis. Unfortunately, these repeated batch cultures are significantly inferior from the perspective of process optimization. During exponential batch cultures where the growth and specific (per cell) production rates are high, the cell concentrations are typically low. After cell numbers reach a high enough value and the cell growth rate slows down, the specific productivity drops enormously, if the cells exhibit growth-associated production kinetics. If the successful paradigms of high cell density fed-batch and perfusion cultures for maximizing the monoclonal antibody synthesis from hybridoma cells are to be applied to recombinant mammalian cell cultures, then it will be necessary to reengineer them to obtain the same inverse-growth-associated production kinetics. The reengineering of CHO cells to achieve inverse-growth-associated production kinetics has so far been demonstrated only for an intracellular reporter protein (54,55).

6.5 CONCLUSIONS

This article highlights the importance of characterizing cell growth and protein synthesis kinetics to maximize culture productivity. Unstructured kinetic models, based on extensions of classical Monod kinetics, yield and maintenance coefficients, and Leudeking–Piret production kinetics, provide the simplest choice for describing the dynamics of cell growth, nutrient consumption, and product expression. Structured kinetic models address more details of cellular metabolism and consequently can describe more accurately cell growth and product expression dynamics in batch, fed-batch, and continuous cultures. With increasing knowledge of animal cell metabolism, it may soon be more feasible to develop more detailed structured kinetic models to enhance our understanding and optimization of mammalian cell cultures.

Protein expression kinetics follow two different patterns, namely, growth-associated and inverse-growth-associated production kinetics. Inverse-growth-associated production kinetics more commonly found for the monoclonal antibody synthesis by hybridoma cells have been successfully exploited to maximize productivity in high cell density fed-batch and perfusion cultures. Growth-associated production kinetics, observed increasingly in the production of therapeutic proteins by recombinant mammalian cells, are more difficult to optimize because repeated batch cultures and continuous cultures are necessary to maintain the high cell growth and specific production rates. It may be possible to employ the successful paradigms of high cell density fed-batch and perfusion cultures to maximize antibody productivities, if recombinant mammalian cells can be engineered to yield inverse-growth-associated production kinetics.

Acknowledgments

The author's research on mammalian cell culture kinetics has been funded by grants BES-9504840, BES-9817249, and BES-0541119 from the National Science Foundation.

NOMENCLATURE

A	ammonia concentration (g/L)
D	dilution rate (day^{-1})
F	nutrient flow rate (mL/day)
G	glucose concentration (g/L)
Gn	glutamine concentration (g/L)
K_d	saturation constant in death rate (g/L)
K_{MAb}	Monod saturation constant for antibody production (g/L glutamine)
K_P	inhibition constant for glutamine (g/L)
K_{XI}	inhibition constant for total cell number (cells/mL)
K_d, $K_{d,max}$	specific death rate and maximum death rate constant (day^{-1})
k_p	maximum specific production rate constant (μg/106 cells/day)
L	lactate concentration (g/L)
[MAb]	antibody concentration (g/L)
m	maintenance coefficient ((g or mM)/day/cells)
$m(S_i)$	specific antibody synthesis rate constant, which is a function of initial serum concentration (μg/106 cells/day)
q_{MAb}	specific (per cell) antibody production rate (μg/106 cells/day)
t	time (day)
V	culture volume (L)
X_T	total cell concentration (cells/mL)
X_v	viable cell concentration (cells/mL)
Y	yield coefficients (cells or g or mM)/(g or mM)
μ, μ_{max}	specific growth rate and its maximum value (day^{-1})

REFERENCES

1. Arathoon W, Birch JR. Large-scale cell culture in biotechnology. Science 1986; 232(4756): 1390–1395.
2. Ramkrishna D, Fredrickson AG, Tsuchiya HM. Dynamics of microbial propagation: models considering inhibitors and variable cell composition. Biotechnol Bioeng 1967; 9(2): 129–170.

3. Birch JR, Boraston R, Wood L. Bulk production of monoclonal antibodies in fermentors. Trends Biotechnol 1985; 3(7): 162–166.
4. Luan YT, Mutharasan R, Magee WE. Effect of various glucose/glutamine ratios on hybridoma growth, viability and monoclonal antibody formation. Biotechnol Lett 1987; 9(8): 535–538.
5. Renard JM, Spagnoli R, Mazier C, Salles MF, Mandine E. Evidence that monoclonal antibody production kinetics is related to the integral of viable cells curve in batch systems. Biotechnol Lett 1988; 10(2): 91–96.
6. Luan YT, Mutharasan R, Magee WE. Strategies to extend longevity of hybridomas in culture and promote yield of monoclonal antibodies. Biotechnol Lett 1987; 9(10): 691–696.
7. Reuveny S, Velez D, Macmillan JD, Miller L. Factors affecting cell growth and monoclonal antibody production in stirred reactors. J Immunol Methods 1986; 86: 53–56.
8. Velez D, Reuveny S, Miller L, Macmillan JD. Kinetics of monoclonal antibody production in low serum growth medium. J Immunol Methods 1986; 86(1): 45–52.
9. Butler M. Growth limitations in high-density microcarrier cultures. Dev Biol Stand 1985; 60: 269–280.
10. Low K, Harbour C. Growth kinetics of hybridoma cells: 2. The effects of varying energy-source concentrations. Dev Biol Stand 1985; 60: 73–79.
11. Bree MA, Dhurjati P, Geoghegan RF, Robnett B. Kinetic modeling of hybridoma cell growth and immunoglobulin production in a large scale suspension culture. Biotechnol Bioeng 1988; 32(8): 1067–1072.
12. Miller WM, Blanch HW, Wilke CR. A kinetic analysis of hybridoma growth and metabolism in batch and continuous suspension cultures - effect of nutrient concentration, dilution rate and pH. Biotechnol Bioeng 1988; 32(8): 947–965.
13. Glacken MW, Adema E, Sinskey AJ. Mathematical descriptions of hybridoma culture kinetics: 1. Initial metabolic rates. Biotechnol Bioeng 1988; 32(4): 491–506.
14. Pirt SJ. Principles of microbe and cell cultivation. Cambridge: Blackwell Scientific; 1975.
15. Dalili M, Sayles GD, Ollis DF. Glutamine-limited batch hybridoma growth and antibody production - experiment and model. Biotechnol Bioeng 1990; 36(1): 74–82.
16. Frame KK, Hu WS. Kinetic study of hybridoma cell growth in continuous culture: 1. A model for nonproducing cells. Biotechnol Bioeng 1991; 37(1): 55–64.
17. Linardos TI, Kalogerakis N, Behie LA. The effect of specific growth rate and death rate on monoclonal antibody production in hybridoma chemostat cultures. Can J Chem Eng 1991; 69(2): 429–438.
18. De Tremblay M, Perrier M, Chavarie C, Archambault J. Optimization of fed-batch culture of hybridoma cells using dynamic programming - single and multi feed cases. Bioprocess Eng 1992; 7(5): 229–234.
19. Gaertner JG, Dhurjati P. Fractional factorial study of hybridoma behavior: 2. Kinetics of nutrient uptake and waste production. Biotechnol Prog 1993; 9(3): 309–316.
20. Harigae M, Matsumura M, Kataoka H. Kinetic study on HBS-MAB production in continuous cultivation. J Biotechnol 1994; 34(3): 227–235.
21. Portner R, Bohmann A, Ludemann I, Markl H. Estimation of specific glucose uptake rates in cultures of hybridoma cells. J Biotechnol 1994; 34(3): 237–246.
22. Portner R, Schafer T. Modelling hybridoma cell growth and metabolism: a comparison of selected models and data. J Biotechnol 1996; 49(1–3): 119–135.
23. Glacken MW, Adema E, Sinskey AJ. Mathematical descriptions of hybridoma culture kinetics: 3. Simulation of fed-batch bioreactors. J Biotechnol 1989; 10(1): 39–65.
24. De Tremblay M, Perrier M, Chavarie C, Archambault J. Fed-batch culture of hybridoma cells - comparison of optimal control approach and closed loop strategies. Bioprocess Eng 1993; 9(1): 13–21.
25. Zeng AP, Deckwer WD. Mathematical modeling and analysis of glucose and glutamine utilization and regulation in cultures of continuous mammalian cells. Biotechnol Bioeng 1995; 47(3): 334–346.
26. Hu WS, Zhou WC, Europa LF. Controlling mammalian cell metabolism in bioreactors. J Microbiol Biotechnol 1998; 8(1): 8–13.
27. Reuveny S, Velez D, Miller L, Macmillan JD. Comparison of cell propagation methods for their effect on monoclonal-antibody yield in fermenters. J Immunol Methods 1986; 86(1): 61–69.
28. Dean RC, Karkare SB, Ray NG, Runstadler PW, Venkatasubramanian K. Large-scale culture of hybridoma and mammalian-cells in fluidized-bed bioreactors. Ann N Y Acad Sci 1987; 506: 129–146.
29. Ozturk SS, Palsson BO. Growth, metabolic, and antibody-production kinetics of hybridoma cell-culture.2. Effects of serum concentration, dissolved-oxygen concentration, and medium Ph in a batch reactor. Biotechnol Prog 1991; 7(6): 481–494.
30. Ozturk SS, Palsson BO. Effect of medium osmolarity on hybridoma growth, metabolism, and antibody-production. Biotechnol Bioeng 1991; 37(10): 989–993.
31. Takahashi K, Tereda S, Ueda H, Makishima F, Suzuki E. Growth-rate suppression of cultured-mammalian-cells enhances protein productivity. Cytotechnology 1994; 15(1–3): 57–64.
32. Robinson DK, Memmert KW. Kinetics of recombinant immunoglobulin production by mammalian-cells in continuous culture. Biotechnol Bioeng 1991; 38(9): 972–976.
33. Mitchell CA, Beall JA, Wells JRE, Gray PP. Growth and protein-production kinetics of a murine myeloma cell-line transfected with the human growth-hormone gene. Cytotechnology 1991; 5(3): 223–231.
34. Hayter PM, Curling EMA, Gould ML, Baines AJ, Jenkins N, Salmon I, Strange PG, Bull AT. The effect of the dilution rate on CHO cell physiology and recombinant interferon-gamma production in glucose-limited chemostat culture. Biotechnol Bioeng 1993; 42(9): 1077–1085.
35. Racher AJ, Moreira JL, Alves PM, Wirth M, Weidle UH, Hauser H, Carrondo MJT, Griffiths JB. Expression of recombinant antibody and secreted alkaline-phosphatase in mammalian-cells-influence of cell-line and culture system upon production kinetics. Appl Microbiol Biotechnol 1994; 40(6): 851–856.
36. Batt BC, Kompala DS. A structured kinetic modeling framework for the dynamics of hybridoma growth and monoclonal-antibody production in continuous suspension-cultures. Biotechnol Bioeng 1989; 34(4): 515–531.
37. Dimasi D, Swartz RW. An energetically structured model of mammalian-cell metabolism.1. Model development

and application to steady-state hybridoma cell-growth in continuous-culture. Biotechnol Prog 1995; 11(6): 664–676.

38. Atkinson DE. Energy charge of adenylate pool as a regulatory parameter. Interaction with feedback modifiers. Biochemistry 1968; 7(11):4030–403–.
39. Bibila T, Flickinger MC. A structured model for monoclonal-antibody synthesis in exponentially growing and stationary phase hybridoma cells. Biotechnol Bioeng 1991; 37(3): 210–226.
40. Wu P, Ray NG, Shuler ML. A computer-model for intracellular Ph regulation in Chinese-hamster ovary cells. Biotechnol Prog 1993; 9(4): 374–384.
41. Barford JP, Phillips PJ, Harbour C. Simulation of animal-cell metabolism. Cytotechnology 1992; 10(1): 63–74.
42. Sanderson CS, Phillips PJ, Barford JP. Structured modelling of animal cells. Cytotechnology 1996; 21(2): 149–153.
43. Fu PC, Barford JP. A hybrid neural network - first principles approach for modelling of cell metabolism. Comp Chem Eng 1996; 20(6–7): 951–958.
44. Karim MN, Rivera SL. Comparison of feedforward and recurrent neural networks for bioprocess state estimation. Comp Chem Eng 1992; 16:S369–S377.
45. Suzuki E, Ollis DF. Cell-cycle model for antibody-production kinetics. Biotechnol Bioeng 1989; 34(11): 1398–1402.
46. Ramirez OT, Mutharasan R. Cell cycle-dependent and growth phase-dependent variations in size distribution, antibody productivity, and oxygen-demand in hybridoma cultures. Biotechnol Bioeng 1990; 36(8): 839–848.
47. Alrubeai M, Emery AN, Chalder S, Jan DC. Specific monoclonal-antibody productivity and the cell cycle-comparisons of batch, continuous and perfusion cultures. Cytotechnology 1992; 9(1–3): 85–97.
48. Richieri RA, Williams LS, Chau PC. Cell-cycle dependency of monoclonal-antibody production in asynchronous serum-free hybridoma cultures. Cytotechnology 1991; 5(3): 243–254.
49. Linardos TI, Kalogerakis N, Behie LA. Cell-cycle model for growth-rate and death rate in continuous suspension hybridoma cultures. Biotechnol Bioeng 1992; 40(3): 359–368.
50. Martens DE, Sipkema EM, Degooijer CD, Beuvery EC, Tramper J. A combined cell-cycle and metabolic model for the growth of hybridoma cells in steady-state continuous-culture. Biotechnol Bioeng 1995; 48(1): 49–65.
51. Gu MB, Todd P, Kompala DS. Analysis of foreign protein overproduction in recombinant CHO cells: effect of growth kinetics and cell cycle traverse. Ann N Y Acad Sci 1994; 721: 194–207.
52. Mariani BD, Slate DL, Schimke RT. S Phase-specific synthesis of dihydrofolate-reductase in Chinese-hamster ovary cells. Proc Natl Acad Sci U S A Biol Sci 1981; 78(8): 4985–4989.
53. Kubbies M, Stockinger H. Cell cycle-dependent DHFR and t-PA production in cotransfected, Mtx-amplified CHO cells revealed by dual-laser flow-cytometry. Exp Cell Res 1990; 188(2): 267–271.
54. Banik GG, Todd PW, Kompala DS. Foreign protein expression from S phase specific promoters in continuous cultures of recombinant CHO cells. Cytotechnology 1996; 22(1–3): 179–184.
55. Lee FWF, Elias CB, Todd P, Kompala DS. Engineering Chinese hamster ovary (CHO) cells to achieve an inverse growth associated production of a foreign protein, beta-galactosidase. Cytotechnology 1998; 28(1–3): 73–80.
56. Lee GM, Varma A, Palsson BO. Application of population balance model to the loss of hybridoma antibody productivity. Biotechnol Prog 1991; 7(1): 72–75.
57. Kromenaker SJ, Srienc F. Stability of producer hybridoma cell-lines after cell sorting - a case-study. Biotechnol Prog 1994; 10(3): 299–307.
58. Ramkrishna D, Mahoney AW. Population balance modeling. Promise for the future. Chemical Engineering Science 2002; 57(4): 595–606.
59. Sidoli FR, Mantalaris A, Asprey SP. Modelling of mammalian cells and cell culture processes. Cytotechnology 2004; 44(1–2): 27–46.
60. Bibila TA, Robinson DK. In pursuit of the optimal fed-batch process for monoclonal-antibody production. Biotechnol Prog 1995; 11(1): 1–13.
61. Batt BC, Davis RH, Kompala DS. Inclined sedimentation for selective retention of viable hybridomas in a continuous suspension bioreactor. Biotechnol Prog 1990; 6(6): 458–464.
62. Pelletier F, Fonteix C, Dasilva AL, Marc A, Engasser JM. Software sensors for the monitoring of perfusion cultures - evaluation of the hybridoma density and the medium composition from glucose-concentration measurements. Cytotechnology 1994; 15(1–3): 291–299.
63. Hansen HA, Madsen NM, Emborg C. An evaluation of fed-batch cultivation methods for mammalian-cells based on model simulations. Bioprocess Eng 1993; 9(5): 205–213.
64. Ryszczuk A, Emborg C. Evaluation of mammalian fed-batch cultivations by two different models. Bioprocess Eng 1997; 16(4): 185–191.
65. Seewoster T, Lehmann J. Cell size distribution as a parameter for the predetermination of exponential growth during repeated batch cultivation of CHO cells. Biotechnol Bioeng 1997; 55(5): 793–797.

7

CELL VIABILITY MEASUREMENT

NING WEI AND BENJAMIN SOMMER
Faculty of Technology, Fermentation Engineering, University of Bielefeld, Bielefeld, Germany

7.1 INTRODUCTION

Cell viability is a fundamental physiological characteristic of a cell, and has been one of the general interests in biology and biotechnology since the microscopic discovery of cells, because it is the basis of various kinds of cell-based biological research and applications. Cell viability has a direct impact upon the productivity and quality of biological production, as well as the performance of biological systems. Diverse assays have been invented for assessing viability. The major categories of these methods include permeability assays, functional assays, flow cytometry, and physical methods. The assumption that only viable cells possess an intact cytoplasmic membrane that prevents normally impermeable matters from passing through the membrane is made for all kinds of permeability assays. In functional assays, the activity of intracellular enzymes, ATP level, RNA level etc., are investigated. Flow cytometry can be described as automated microscopy, in which a single file of cells are formed in a sheath flow and presented in front of a focused light beam. Multiple optical characteristics of the cells are investigated simultaneously. Methods based on various physical properties of cells have also been developed for the determination of cell viability.

7.2 PERMEABILITY ASSAYS

Since long it has been known that cells are surrounded by a barrier labeled as the cell membrane. Therefore, since the beginning of the twentieth century various cell viability assays have been developed on the basis of the test of the permeability, or integrity of the cytoplasmic membrane. Permeability assays can be classified into three different groups: exclusion, inclusion, and release.

7.2.1 Exclusion

It is evident that upon cell damage, bulky, charged molecules that are normally excluded by a cell are able to access the cytoplasm through the compromised membrane. If the molecules added have special light-absorbing or fluorescent properties, the damaged cells can be readily identified. These molecules are named *stains.* For mammalian cells the classical stain is trypan blue (1,2). Under bright field microscopy, damaged or dead cells appear purple-violet, whereas live cells are not stained. Methylene Blue is widely used for the determination of yeast viability (3). Nevertheless, this stain is notoriously inaccurate when the yeast viability is below 95%. Therefore, an alternative stain, Methylene Violet is recommended (4). The applicable stains can also have special fluorescent characteristics. For instance, Propidium Iodide (PI) is a common fluorescent stain that binds to nucleic acids. In dead cells, the intensity of the red fluorescence from PI is much higher than that in live cells. For identifying the bacterial viability, a dual stain composed of two fluorescent dyes, SYTO 9 and PI, is used. SYTO 9 penetrates all bacterial membranes and stains the cells green, while PI only penetrates cells with damaged membranes, and the combination of the two stains produces red fluorescing cells (5). Besides, the use of Acridine Orange (AO), Alcian Blue (6), Congo Red (7), Ethidium Bromide (EB) (8), and SYTOX Green (9) for assessment of viability is based on the same principle.

Upstream Industrial Biotechnology: Expression Systems and Process Development, Volume 1, First Edition. Edited by Michael C. Flickinger.
© 2013 John Wiley & Sons, Inc. Published 2013 by John Wiley & Sons, Inc.

7.2.2 Inclusion

The converse of dye exclusion is dye inclusion. The nonfluorescent esterase substrate fluorescein diacetate (FDA) is used commonly in assessing viability of mammalian cells and yeasts (10,11). FDA diffuses into cells, where it is cleaved by cellular esterase to yield a fluorescent product, fluorescein. Fluorescein is an impermeable, charged molecule, thus, will be retained in viable cells, and stain the cells green. However, FDA will leak from cells with damaged membranes, therefore, damaged or dead cells fluoresce only weakly. FDA is not an ideal fluorescent substrate for bacteria, as they retain fluorescein poorly, resulting in low S/N (signal to noise) ratio (12). Leakage of probe to the external environment may be reduced by using FDA derivatives with additional functional groups. For instance, carboxyfluorescein diacetate (CFDA) (13), chloromethylfluorescein diacetate (CMFDA) (14), Calcein-AM (15), and 7′-bis-(carboxyethyl)-5 (6)-carboxyfluorescein-pentaacetoxymethylester (BCECF-AM) (16).

7.2.3 Release

The release of specific molecules or intracellular enzymes can also be used to measure cell viability. Typical assays in this aspect include the assessment of the release of ^{51}Chromium (17) and lactate dehydrogenase (LDH) for mammalian cells (2,18–20), magnesium, phosphate, and potassium for microbial cells (21–23). In addition, iododeoxyuridine (^{125}I-UDR) (24,25), [^{3}H]praline (26), [^{75}Se]selenomethionine, and [^{3}H]uridine (27) have been used to assess cell viability by measuring the incorporation of these compounds into DNA (^{125}I-UDR), RNA ([^{3}H]uridine), and proteins ([^{3}H]praline and [^{75}Se]selenomethionine) of the cells.

^{51}Cr is a γ-emitting radioisotope. It is known to bind tightly to intracellular proteins. The disadvantage of using ^{51}Cr as an indication of cell viability is a high spontaneous release rate of the ^{51}Cr-labeled proteins. In comparison, use of ^{125}I-UDR, [^{3}H]praline, [^{75}Se]selenomethionine, and [^{3}H]uridine is less problematic, since they are directly incorporated into the DNA, RNA, and proteins of the cells. Nevertheless, the above radioactive compounds may be toxic to the cells, and thus limit the sensitivity of the assay.

7.3 FUNCTIONAL ASSAYS

7.3.1 Bioluminescence Assay

Bioluminescence occurs in biological systems when a biochemical reaction produces an electronically excited unit, which emits a photon so as to return to the ground state. The basis of the assay is the measurement of intracellular ATP, a universal energy unit in all living cells. When a cell dies, the intracellular ATP is rapidly degraded by ATPases and the ATP levels decline quickly. ATP-dependent oxidation of the substrate luciferin in the presence of luciferase produces oxyluciferin, carbon dioxide, adenosine monophosphate (AMP), inorganic phosphate, and light. One photon is produced per molecule of hydrolyzed ATP. The amount of light emitted is directly correlated with the amount of ATP present (2,28–30).

7.3.2 Tetrazolium Assay

Instead of direct measurement of ATP content, activity of enzymes involved in the production of ATP can also be examined for assessment of cell viability. Tetrazolium dyes are most widely used to measure activity of mitochondrial reductases. Tetrazolium dyes act as electron acceptors and are reduced to formazan products. These have special optical properties, hence, they are readily identified. The most frequently used tetrazolium dyes are 3-(4,5-dimethylthiazol-2-yl)-2,5-diphenyltetrazolium bromide (MTT) (2,31) and 5-cyano-2,3-ditolyl tetrazolium chloride (CTC) (32).

MTT is widely used in assessment of viability of mammalian cells. In viable cells, MTT is reduced to a formazan product, which strongly absorbs light at a typical wavelength of about 560 nm. Usually a solution, for example, dimethyl sulfoxide, is used to dissolve the purple insoluble formazan product, and the absorbance of this colored solution can be quantified by a spectrophotometer. CTC is widely used in assessing viability of microbial cells. CTC has an advantage that the formazan product is fluorescent, which enormously enhances the sensitivity of the assay.

7.3.3 FISH Methods

Fluorescent *in situ* hybridization (FISH) is a cytogenetic technique. It uses oligonucleotides that bind to intracellular DNA, RNA, or chromosome. The binding sites are located where they show a high degree of sequence similarity. These oligonucleotides are usually designed for specific target and must be tagged with fluorophores, so that FISH can be observed and analyzed with either fluorescence microscopy or flow cytometry. If a selective oligonucleotide probe binds specifically to intracellular rRNA's, the intensity of fluorescence can then be correlated to viability (33,34). By contrast, antibody-labeling methods often fail in viability assessment. The reason therefore, may be the short half-life of rRNA within nonviable cells.

7.3.4 Membrane Potential Assay

In microorganisms a potential is present across the cytoplasmic membrane of viable cells, whereas absent from nonviable cells. This potential is principally generated by

the extrusion of H^+ ions by H^+ ATPase or the electron transfer chain. Some stains for assessing viability are based on this fact. Cells that have a membrane potential (generally negative inside) accumulate positively charged dyes, such as rhodamine 123 (35), whereas negatively charged dyes, such as those from the oxonol group (36,37), are excluded. As a result, rhodamine 123 stains viable cells, while oxonol will stain nonviable cells. These dyes can be excited by a laser with a central wavelength of about 490 nm and emit green fluorescence. They have been used successfully for bacteria and yeasts. In eukaryotic cells, rhodamine 123 accumulates preferentially in the mitochondria, which possess a high membrane potential. This may result in toxicity to the cells.

7.3.5 RT-PCR Methods

Methods based on polymerase chain reaction (PCR) have been developed for detecting the presence of specific nucleic acids as indicators of cell viability. DNA is highly stable even in dead cells and may still be detected after a long term by PCR. Thus, it is hardly suitable for the detection of viable cells. RNA, in contrast, is prone to chemical degradation due to the susceptibility to hydrolysis of the ribose 2′-hydroxyl group, as well as the rapid nucleolysis by cellular ribonucleases. Therefore, RNA was found to be unstable in dead cells and favorable for viability assessment in comparison to DNA (38).

Various attempts to prove the suitability of RNA detection by RT-PCR (reverse transcriptase PCR) methods for an estimation of cell viability have been made so far (39–43). It was found that during incubation at room temperature subsequent to cell killing, RNA could only be detected for a certain time by RT-PCR, indicating its degradation *postmortem* and its eligibility as a target substance for the detection of viable cells (43). However, the time passing until the RNA target may no longer be detected from a population of dead cells only, needs to be determined prior to analyses of unknown samples. Moreover, the incubation time required until the target is completely abolished depends on the RNA type investigated (43,44). mRNA is supposed to be the least stable among the RNA species and therefore the ideal target substance.

Moreover, the choice of the RNA target molecule, particularly its stability, as well as the sequence and length of the PCR amplicon must be considered carefully to prove its suitability as an indicator of live cells prior to analysis of unknown samples (43,45).

Since common RT-PCR is generally not quantitative, this method does not yield the absolute amount of viable cells in an analyzed specimen (46). Therefore, a quantitative estimation of RNA molecules by real-time RT-PCR (quantitative RT-PCR, qRT-PCR) was found to allow a more precise determination of the viable cell quantity because of a direct correlation between the PCR signal (RNA copy-number) and the viable cell concentration (38,47).

The CT (number of cycles at which fluorescence reaches the threshold) values of a qRT-PCR assay were observed to strongly correlate with the amount of viable cells (as determined by reproductive methods) employed to the reaction (38), as shown in Fig. 7.1.

As stated above, a positive RT-PCR signal does not necessarily report a viable cell; it may also result from a cell that has died only recently, with the target RNA not being degraded in time. Thus, the qRT-PCR CT values solely allow statements about the maximum number of putative viable cells in a sample, rather than the actual live cell titre.

7.3.6 FUN-1 Assay

A new fluorescent probe has been recently developed exclusively for assessing the viability of yeasts (48). This

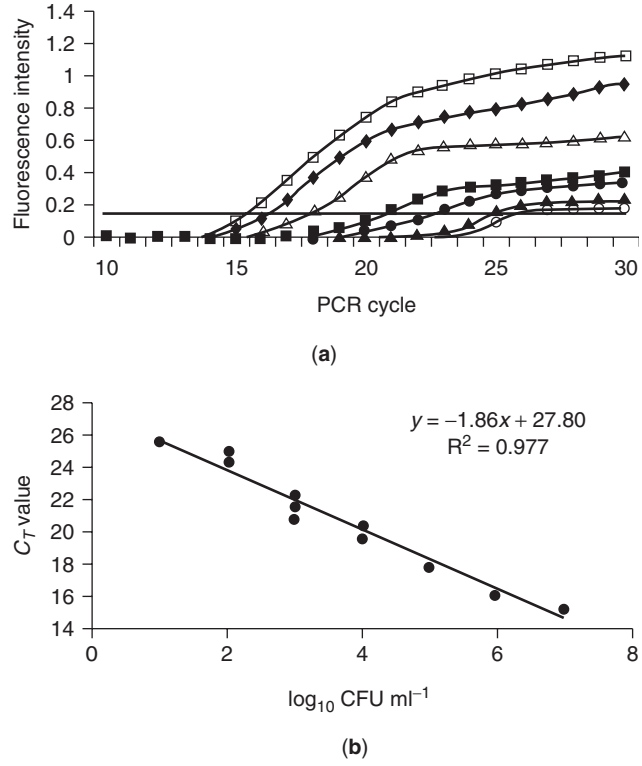


Figure 7.1. Correlation qPCR (Ct)<-> viable cells (CFU). Real-time RT-PCR assays of serial dilutions of mixed cultures of yeasts and molds. (**a**) Increase in fluoresence intensity with the number of PCR cycles. Fungal contaminations were present at 7( ), 6( ), 5( ), 4( ), 3( ), 2( ), and 1(◦) $\log_{10}$ CFU mL^{-1}. The straight horizontal line indicates the threshold value. (**b**) C_T values plotted against the $\log_{10}$ CFU mL^{-1} derived from, the plate count; three repetitions for each dilution are indicated. [Source: Fig. 3 of Ref. 38.]

membrane-permeant and nucleic acid-binding dye is named *FUN-1*. It has been found to give rise to cylindrical intravacuolar structures (CIVS) in *Saccharomyces cerevisiae*. Biochemical processing of the dye by active yeasts yields CIVS that are markedly red-shifted in fluorescence emission and therefore, spectrally distinct from the nucleic acid-bound form of the dye. Generally, in presence of FUN-1, live cells are marked clearly with orange fluorescent CIVS, whereas dead cells exhibit extremely bright, diffuse, green-yellow fluorescence.

7.3.7 DNA Gel Electrophoresis for Apoptosis Analysis

There are in general, two distinct sorts of cell death: necrosis and apoptosis. While necrosis is a passive form in which cell die from acute cellular injury, and apoptosis is rather a *programmed* intracellular process which involves a series of biochemical events leading to a characteristic cell morphology and death.

During apoptosis DNA is cleaved at the internucleosomal sections to produce low molecular DNA fragments of 180–200 pb. Therefore, DNA Gel Electrophoresis (DGE) can be performed to detect a characteristic "laddering" pattern of these smaller DNA fragments on agarose gels after electrophoresis (49) if the cells have undergone an apoptosis.

7.4 FLOW CYTOMETRY

Flow cytometry is a technique, by which the measurements of physical and/or chemical characteristics of single cells or other particles are made when they pass through a measuring apparatus, flow cytometer, in a fluid stream. Measurements of optical properties of single cells (or other particles) are by far the most common in flow cytometry, although other properties, for example, electrical and acoustic properties, can be also measured. When a flow cytometer is equipped with an electrical and/or mechanical mechanism diverting cells (or other particles) according to the range of values of their measured characteristics, it becomes a cell sorter (50,51).

Flow cytometry can be described as automated microscopy, in which cells are injected into a fast flowing fluid stream termed as *sheath flow*. The slow moving cells are hydrodynamically focused at the central line of the sheath flow, creating a single file of cells that move into the measuring apparatus termed as *cytometer*. In the cytometer, optical characteristics of cells are measured as they are presented in front of a focused light beam. Usually, a fluorescent stain is applied upon the cells, and the emitted fluorescence is detected for cell analysis. Besides, forward and side scatter is also measured. In modern instruments the fluorescent emission is measured normally by multiple detectors at different spectral regions, for instance, three detectors for red, orange, and green fluorescence, respectively. In data processing, multivariate analysis methods are generally applied. The most frequently used is a binary plot, by means of which, two selective optical characteristics of the cells are depicted as visually separable data clouds.

In the past decade, flow cytometry has been employed extensively in the field of biotechnology (52–58). Some typical applications are determination of cell parameters (e.g. measuring viability, apoptosis, proliferative activity, and DNA content), functional screening of genetic libraries for drug target discovery, screening of combinatorial protein libraries, vaccine analysis, isolation of human chromosomes, etc. In most of the applications, fluorescent reagents are required to label the cells.

Flow cytometry is also commonly used for determination of viability. Because of the variety of cell types in biotechnology it may need different reagents for specific assays of cell viability. For instance, viability of mammalian cells can be determined through the exclusion of PI or EB by the intact membrane of viable cells. However, this approach is less useful with bacteria (59,60). In flow cytometry, for bacteria viability measurements, it has been found that rhodamine 123 is an effective reagent (61,62). Alternative approaches are based on the facts that lipophilic cations are accumulated by microbial cells and nonfluorescent substrates are converted to fluorescent products by the metabolic activities of viable cells (63). In the research of Caron *et al*. (64), bacteria were classified into different groups according to their specific interactions with fluorescent dyes EB, bis-oxonol (BOX), and PI. Cells that performed exclusion of EB are classified as metabolically active cells; uptake of EB but exclusion of bis-oxonol (BOX) is related to de-energized cells with a polarized cell membrane, and uptake of both dyes related to depolarized cells. Permeabilized cells were identified by PI.

In recent years, ready-made reagent "kits" are also commercially available from specific suppliers. These kits enable rapid development of protocols. For instance, the measurement of bacteria viability can be accomplished using the LIVE/DEAD BacLight bacterial viability kit from Molecular Probes. The FUN-1 kit from the same company will favor the determination of yeast viability.

In Ref. 49, several methods based on flow cytometry have been introduced to investigate apoptosis in commercial cell culture processes. For instance, using high-affinity DNA binding fluorochromes, like PI, apoptosis can be probed with the occurrence of a sub-G1 region of the cell cycle distribution. Another method is on the basis of dual staining with annexin V-FITC and PI. The fundamental hereby is the externalization of phosphatidylserine (PS), which is normally present on the inner surface of an intact membrane, to the outer layer of the surface of an apoptotic

cell, which loses its membrane phospholipids asymmetry. Since necrotic cells in the absence of membrane integrity will also stain positive with annexin V-FITC, dual staining with PI enables the appropriate distinguishment. Moreover, techniques based on TUNEL (TdT-mediated dUTP Nick End Labeling), Rhodamine-123 and detection of Caspase-3 Activation, respectively, have also been introduced in this work.

7.5 PHYSICAL METHODS

7.5.1 *In situ* Microscopy

Characterization of cell populations is normally performed by *ex situ* means, namely, cells are extracted and taken away from the original place (e.g. a bioreactor) and measured in a separate apparatus. However, techniques, which can measure the cells at the original site, have also been developed. One of them is *in situ* microscopy (ISM). Through a microscope, which is directly mounted at one port of the bioreactor, the cell parameters can be determined, and hence, the growth of the cell population can be monitored.

One of the earliest realizations of ISM was accomplished by Bittner (65). In this work a sterilizable sensor with a miniaturized and automated mechanical sampling mechanism is made for monitoring cell concentration and size distribution. Suhr *et al*. constructed their sensor on the basis of fluorescence of intracellular NADP(H) (66). It realized an epifluorescence microscope with a pulsed nitrogen laser as stimulating light source. Because of unknown fluctuations of the camera sensitivity quantitative evaluation of the emitted fluorescence was not enabled. For this reason no information about cell viability was obtained, but only cell concentration can be monitored with this sensor.

In order to realize on-line monitoring of cell viability Wei *et al*. (67,68) developed an ISM probe based on dark field microscopy. With this probe enhanced image contrast and quality were obtained, thus, morphological information of fine intracellular structures could be used in conjunction with advanced machine learning technique. The computer learned from the images of cell populations containing only live or dead cells, and understood the morphological characteristics of live and dead cells, respectively. In this way it was trained and used for evaluation of any given cell images, and gave the determination of the viability. In their work *in situ* measurement of both density and viability of yeast *S. cerevisiae* was realized.

7.5.2 Dielectrophoresis

In electrophoresis, particles or molecules are separated by their net intrinsic charge upon exposure to a uniform direct current (DC) electric field. Separation is achieved by distinct mobility, either caused by nonuniform mass/charge ratios or, if the mass/charge ratios are equal for different specimen, by migration through porous substances that function as particle sieves.

In dielectrophoresis (DEP), particle separation results from the application of nonuniform, alternating current (AC) electric fields. This technique makes use of differences in the polarizability of dissimilar substances and works even if the net charge of a substance is zero. In a DC field, equal and opposite charges ($+q$ and $-q$) are induced at the boundary of the particles, which yields a macroscopic dipole (69).

Equation 7.1 describes the net translational dielectrophoretic force a particle or cell experiences in an electric field E, where α is the effective polarizability of the cell that depends on the cell conductivity and permittivity with respect to the surrounding medium (70). Besides the conductivity of the medium, a furthermore depends on the frequency supplied to a DEP chamber.

$$F_{\mathrm{DEP}} = \alpha \cdot \nabla E^2 \tag{7.1}$$

If α is positive the induced dipole moment is aligned with the applied field and the cell moves toward the strong field region (positive DEP). A negative α results in a dipole moment aligned opposite to the field, and causes a motion toward the weak field region (negative DEP) (69).

The field factor E^2 accounts for the field gradient between the electrodes, the voltage applied, and the distance of the cell from the electrodes.

Since cell death coincides with a break-down of membrane integrity, it permits a free diffusive exchange of intra- and extracellular compounds. The conductivity of dead cells is therefore significantly higher compared to viable cells with an increase by a factor of 10^4 (69). Accordingly, by choosing an appropriate frequency, α may obtain values that allow a separation of viable from nonviable cells by means of positive and negative DEP.

For a gentle separation of live and dead cells, the electrode design is of particular importance. Upon reduction of the electrode distance, a proportionally lower voltage is required to generate an equal dielectrophoretic force. Electrical heating and electrochemical effects are, hence, directly proportional to the electrode scale. Microelectrodes of castellated interdigitated shape are frequently used to spatially segregate viable and nonviable cells (71).

Such electrodes may be loaded with a cell suspension and, provided that an appropriate frequency is applied, allow selective retention of either dead or live cells at the electrode edges. By convective flushing, the nonretained cell type is eluted from the electrode chamber and may be quantified using turbidity measurement, plate counting or staining procedures. This method has been successfully established for different cell types, especially, yeast (71).

Moreover, repeated reversing of the flow direction in phase with activation and inactivation of the applied voltage, renders a possibility for continuous cell sorting (72).

7.5.3 Impedance Measurement

Impedance is a physical characteristic of matters that can be used for studying biological materials. As depicted in the theory of electrical engineering, impedance is complex, consisting of a reactive and a resistive part, which correspond to conductance and capacitance, respectively. Impedance alteration in a medium containing cells can reflect the change of metabolic activity of the cells, hence, measurements of impedance have been used to quantify viable microorganisms (73,74).

7.5.4 Image Analysis

Viability determination based solely on image analysis has recently come into the sight of biotechnologists. Long *et al*. developed a method employing fluorescence microscopy in conjunction with machine learning techniques (75). They used iterative training procedures to choose the most representative samples for determining the correct decision boundary for distinguishing dead cells from live ones.

Wei *et al*., in contrast, developed a machine vision system based on dark field microscopy in conjugation with supervised machine learning and wavelet feature selection (76). This automates the cell viability assessment, and yields comparable results to commonly accepted methods. The eligibility lies in the fact that, according to the research, live cells exhibit morphologically more details and are intracellularly more organized than dead ones, which display more homogeneous and diffuse gray values throughout the cells.

REFERENCES

1. Borner C. Diminished cell proliferation associated with the death-protective activity of Bcl-2. J Biol Chem 1996; 271: 12695–12698.
2. Butler M, Spearman M. Cell counting and viability measurements. In: Portner R, editor. Volume 24, Animal cell biotechnology, methods and protocols. Methods in biotechnology: Publishing: Humana Press: New York; 2007. p. 223–238.
3. Smart KA. Yeast and fermentation the industry's use of methylene blue in assessing yeast viability and vitality and considers alternatives to the norm. Brew Guard 2001; 130: 24–28.
4. Smart KA, Chambers KM, Lambert I, Jenkins C, Smart CA. Use of methylene violet staining procedures to determine yeast viability and vitality. J Am Soc Brew Chem 1999; 57: 18–23.
5. Boulos L, Prevost M, Barbeau B, Coallier J, Desjardins R. LIVE/DEAD BacLight: application of a new rapid staining method for direct enumeration of viable and total bacteria in drinking water. J Microbiol Methods 1999; 37: 77–86.
6. Fukudome K, Sato M, Takata Y, Kuroda H, Watari J, Takashio M. Evaluation of yeast physiological state by alcian blue retention. J Am Soc Brew Chem 2002; 60: 149–152.
7. Kovács A, Foote RH. Viability and acrosome staining of bull, boar and rabbit spermatozoa. Biotech Histochem 1992; 67: 119–124.
8. Maria RD, Lenti L, Malisan F, d'Agostino F, Tomassini B, Zeuner A, Rippo MR, Testi R. Requirement for GD3 ganglioside in CD95- and ceramide-induced apoptosis. Science 1997; 277: 1652–1655.
9. Breeuwer P, Abee T. Assessment of viability of microorganisms employing fluorescence techniques. Int J Food Microbiol 2000; 55: 193–200.
10. Rotman B, Papermaster BW. Membrane properties of living mammalian cells as studied by enzymatic hydrolysis of fluorogenic esters. Proc Natl Acad Sci U S A 1996; 55: 134–141.
11. Van Zandycke SM, Simal O, Gualdoni S, Smart A. Determination of yeast viability using fluorophores. J Am Soc Brew Chem 2003; 61: 15–22.
12. Diaper JP, Tither K, Edwards C. Rapid assessment of bacterial viability by flow cytometery. J Appl Microbiol Biotechnol 1992; 38: 268–272.
13. Breeuwer P, Drocourt P, Rombouts FM, Abee T. Energy-dependent, carrier-mediated extrusion of carboxyfluorescein from Saccharomyces cerevisiae allows rapid assessment of cell viability by flow cytometry. Appl Environ Microbiol 1994; 60: 1467–1472.
14. Palková Z, Váchová L, Valer M, Preckel T. Single-cell analysis of yeast, mammalian cells, and fungal spores with a microfluidic pressure-driven chip-based system. Cytometry 2004; 59A: 246–253.
15. Comasa J, Vives-Rego J. Enumeration, viability and heterogeneity in Staphylococcus aureus cultures by flow cytometry. J Microbiol Methods 1998; 32: 45–53.
16. Obexer W, Schmid C, Brun R. A novel in vitro screening assay for trypanocidal activity using the fluorescent dye BCECF-AM. Trop Med Parasitol 1995; 46: 45–48.
17. Vennström L, Bysell C, Björkelund H, Lundqvist H, Andersson K. Real-time viability assay based on ^{51}Cr retention in adherent cells. Biotechniques 2008; 44: 237–240.
18. (a) Masters JRW, editor. Chapter 7: cytotoxicity and viability assays: Oxford University Press: Oxford, UK; 2000; (b) Smart KA, Chambers KM, Lambert I, Jenkins C, Smart CA. Use of methylene violet staining procedures to determine yeast viability and vitality. J Am Soc Brew Chem 1999; 57: 18–23.
19. Racher AJ, Looby D, Griffiths JB. Use of lactate dehydrogenase release to assess changes in culture viability. Cytotechnology 1990; 3: 301–307.
20. Legrand C, Bour JM, Jacob C, Capiaumont J, Martial A, Marc A, Wudtke M, Kretzmer G, Demangel C, Duval D, Hache J. Lactate dehydrogenase (LDH) activity of the number of dead cells in the medium of cultured eukaryotic cells as marker. J Biotechnol 1992; 25: 231–243.
21. Heggart H, Margaritis A, Stewart RJ, Pilkington M, Sobezak J, Russell I. Measurement of brewing yeast viability and vitality: a review of methods. Tech Q — Master Brew Assoc Am 2000; 37: 409–430.
22. Mochaba FM, O'Connor-Cox ESC, Axcell BC. A novel and practical yeast vitality method based on magnesium ion release. J Inst Brew 1997; 103: 99–102.

23. Mochaba FM, O'Connor-Cox ESC, Axcell BC. Practical procedures to measure yeast viability and vitality prior to pitching. J Am Soc Brew Chem 1998; 56: 1–6.
24. Schneiderman MH, Hofer KG, Schneiderman GS. An in vitro 125IUdR-release assay for measuring the kinetics of cell death. Int J Radiat Biol 1991; 59: 397–408.
25. Gee AP, Rolfe AE, Worthington-White D, Graham-Pole J, Boyle MD. Rapid alternative to the clonogenic assay for measuring antibody and complement-mediated killing of tumor cells. Clin Immunol Immunopathol 1985; 34: 2263–2271.
26. Vázquez MER, Román TD, Cuesta MG, Botta CZ, Ibáñez JS, Díaz SP, Nuñez CA. Viability and histologic structure of porcine valves after cryopreservation. Ann Thorac Surg 2003; 77: 186–190.
27. Hu Y, Mangan JA, Dhillon J, Sole KM, Mitchison DA, Butcher PD, Coates ARM. Detection of mRNA transcripts and active transcription in persistent mycobacterium tuberculosis induced by exposure to rifampin or pyrazinamide. J Bacteriol 2000; 182: 6358–6365.
28. Kaneshiro ES, Collins MS, Cushion MT. Inhibitors of sterol biosynthesis and amphotericin B reduce the viability of pneumocystis carinii f. sp. carinii. Antimicrob Agents Chemother 2000; 44: 1630–1638.
29. McBane RD, Ford MA, Karnicki K, Stewart M, Owen WG. Fibrinogen, fibrin and cross-linking in aging arterial thrombi. Thromb Haemost 2000; 84: 83–87.
30. Chen F, Cushion MT. Use of an ATP bioluminescent assay to evaluate viability of pneumocystis carinii from rats. J Clin Microbiol 1994; 32: 2791–2800.
31. Li J, Liu Y, Ru B. Effect of metallothionein on cell viability and its interactions with cadmium and zinc in HEK293 cells. Cell Biol 2005; 29: 843–848.
32. Nielsen JL, Muro MA, Nielsen PH. Evaluation of the redox dye 5-cyano-2,3-tolyl-tetrazolium chloride for activity studies by simultaneous use of microautoradiography and fluorescence in situ hybridization. Appl Environ Microbiol 2003; 69: 641–643.
33. Smith JJ, Gunasekera TS, Barardi CRM, Veal D, Vesey G. Determination of Cryptosporidium parvum oocyst viability by fluorescence in situ hybridization using a ribosomal RNA-directed probe. J Appl Microbiol 2004; 96: 409–417.
34. Vesey G, Ashbolt N, Wallner G, dorsch M, Williams KL, Veal DA. Asessing Cryptosporidium parvum oocyst viability with fluorescent in situ hybridisation using ribosomal RNA probes and flow cytometry. In: Betts WB, editor. Protozoan parasites and water. Cambridge: Royal Society for Chemistry; 1995. p. 131–138.
35. López-Amorós R, Castel S, Comas-Riu J, Vives-Rego J. Assessment of E. coli and Salmonella viability and starvation by confocal laser microscopy and flow cytometry using rhodamine 123, DiBAC4(3), propidium iodide, and CTC. Cytometry 1997; 29: 298–305.
36. Mason DJ, Lopéz-Amorós R, Allman R, Stark JM, Lloyd D. The ability of membrane potential dyes and calcafluor white to distinguish between viable and non-viable bacteria. J Appl Bacteriol 1995; 78: 309–315.
37. Deere D, Shen J, Vesey G, Bell P, Bissinger P, Veal D. Flow cytometry and cell sorting for yeast viability assessment and cell selection. Yeast 1998; 30: 147–160.
38. Bleve G, Rizzotti L, Dellaglio F, Torriani S. Development of reverse transcription (RT)-PCR and real-time RT-PCR assays for rapid detection and quantification of viable yeasts and molds contaminating yogurts and pasteurized food products. Appl Environ Microbiol 2003; 69: 4116–4122.
39. Bej AK, Ng WY, Morgan S, Jones DD, Mahbubani MH. Detection of viable Vibrio cholerae by reverse-transcriptase polymerase chain reaction (RT-PCR). Mol Biotechnol 1996; 5: 1–10.
40. Cook M, Lynch WH. A sensitive nested reverse transcriptase PCR assay to detect viable cells of the fish pathogen Renibacterium salmoninarum in Atlantic salmon (Salmo salar L.). Appl Environ Microbiol 1999; 65: 3042–3047.
41. Klein PG, Juneja VK. Sensitive detection of viable Listeria monocytogenes by reverse transcription-PCR. Appl Environ Microbiol 1997; 63: 4441–4448.
42. Patel BKR, Banerjee DK, Butcher PD. Determination of Mycobacterium leprae viability by polymerase chain reaction amplification of 71-kDa heat-shock protein mRNA. J Infect Dis 1993; 168: 799–800.
43. Sheridan GEC, Masters CI, Shallcross JA, Mackey BM. Detection of mRNA by reverse transcription-PCR as an Indicator of viability in Escherichia coli cells. Appl Environ Microbiol 1998; 64: 1313–1318.
44. Davis BD, Luger SM, Tai PC. Role of ribosome degradation in the death of starved Escherichia coli cells. J Bacteriol 1986; 166: 439–445.
45. Aellen S, Que YA, Guignard B, Haenni M, Moreillon P. Detection of live and antibiotic-killed bacteria by quantitative real-time PCR of specific fragments of rRNA. Antimicrob Agents Chemother 2006; 50: 1913–1920.
46. Bustin SA. Absolute quantification of mRNA using real-time reverse transcription polymerase chain reaction assays. J Mol Endocrinol 2000; 25: 169–193.
47. Birch L, Dawson CE, Cornett JH, Keer JT. A comparison of nucleic acid amplification techniques for the assessment of bacterial viability. Lett Appl Microbiol 2001; 33: 296–301.
48. Millard PJ, Roth BL, Thi HP, Yue ST, Haugland RP. Development of the FUN-1 family of fluorescent probes for vacuole labeling and viability testing of yeasts. Appl Environ Microbiol 1997; 63: 2897–2905.
49. Ishaque A, Al-Rubeai M. Measurement of apoptosis in cell culture. In: Portner R, editor. Volume 24, Animal cell biotechnology, methods and protocols. Methods in biotechnology: Publishing: Humana Press: New York; 2007. pp. 285–300.
50. Kamentsky LA, Melamed MR. Spectrophotometric cell sorter. Science 1967; 156: 1364–1365.
51. Fulwyler MJ. Electronic separation of biological cells by volume. Science 1965; 150: 910–911.
52. Lorens JB, Sousa C, Bennett MK, Molineaux S, Payan DG. The use of retroviruses as pharmaceutical tools for target discovery and validation in the field of functional genomics. Curr Opin Biotechnol 2001; 12: 613–621.
53. Daugherty PS, Chen G, Olsen MJ, Iverson BL, Georgiou G. Antibody affinity maturation using bacterial surface display. Protein Eng 1998; 11: 825–832.
54. Leary JF. Strategies for rare cell detection and isolation. Methods Cell Biol 1994; 42 (Pt. B): 331–358.
55. Baumgarth N, Roederer M. A practical approach to multicolor flow cytometry for immunophenotyping. J Immunol Methods 2000; 243: 77–97.

56. De Rosa SC, Herzenberg LA, Roederer M. 11-color, 13 parameter flow cytometry: identification of human naive T cells by phenotype, function, and T-cell receptor diversity. Nat Med 2001; 7: 245–248.
57. Sklar LA, editor. Flow cytometry for biotechnology. New York: Oxford University Press; 2005.
58. Shapiro HM. Practical flow cytometry. 4th ed. Hoboken (NJ): Wiley-Liss; 2003.
59. Winson MK, Davey HM. Flow cytometric analysis of microorganisms. Methods 2000; 21: 231–240.
60. Jernaes MW, Steen HB. Staining of Escherichia coli for flow cytometry: influx and efflux of ethidium bromide. Cytometry 1994; 17: 302–309.
61. Diaper JP, Tither K, Edwards C. Rapid assessment of bacterial viability by flow cytometry. Appl Microbiol Biotechnol 1992; 38: 268–272.
62. Kaprelyants AS, Kell DB. Rapid assessment of bacterial viability and vitality by rhodamine 123 and flow cytometry. J Appl Bacteriol 1992; 72: 410–422.
63. Davey HM, Kaprelyants AS, Weichart DH, Kell DB. Estimation of microbial viability using flow cytometry. In: Robinson JP, editor. Current protocols in cytometry: John Wiley & Sons: New York; 2005. Chapter 11, Unit 11.3.
64. Caron GN, Stephens P, Badley RA. Assessment of bacterial viability status by flow cytometry and single cell sorting. J Appl Microbiol 1998; 84: 988–998.
65. Bittner C. In situ mikroskopie-ein neues verfahren zur online-bestimmung der biomasse bei kultivierungsprozessen. PhD Thesis. Hannover: Department of Chemistry of the Hannover University; 1994.
66. Suhr H, Wehnert G, Schneider K, Bittner C, Scholz T, Geissler P, Jähne B, Scheper T. In situ microscopy for on-line characterization of cell-populations in bioreactors, including cell-concentration measurements by depth from focus. Biotechnol Bioeng 1995; 47: 106–116.
67. Wei N, You J, Friehs K, Flaschel E, Nattkemper TW. In situ dark field microscopy for on-line monitoring of yeast cultures. Biotechnol Lett 2007; 29: 373–378.
68. Wei N, You J, Friehs K, Flaschel E, Nattkemper TW. An in situ probe for on-line monitoring of cell density and viability on the basis of dark field microscopy in conjunction with image processing and supervised machine learning. Biotechnol Bioeng 2007; 97: 1489–1500.
69. Pethig R, Markx GH. Applications of dielectrophoresis in biotechnology. Trends Biotechnol 1997; 15: 426–432.
70. Pethig R, Huang Y, Wang XB, Burt JPH. Positive and negative dielectrophoretic collection of colloidal particles using interdigitated castellated microelectrodes. J Phys D Appl Phys 1992; 25: 881–888.
71. Markx GH, Talary MS, Pethig R. Separation of viable and non-viable yeast using dielectrophoresis. J Biotechnol 1994; 32: 29–37.
72. Markx GH, Pethig R. Dielectrophoretic separation of cells: continuous separation. Biotechnol Bioeng 1995; 45: 337–343.
73. Kell DB, Kaprelyants AS, Weichart DH, Harwood CR, Barer MR. Viability and activity in readily culturable bacteria: a review and discussion of the practical issues. Antonie van Leeuwenhoek 1998; 73: 169–187.
74. Noble PA. Hypothetical model for monitoring microbial growth by using capacitance measurements – a mini review. J Microbiol Methods 1999; 37: 45–49.
75. Long X, Cleveland WL, Yao YL. Automatic detection of unstained viable cells in bright field images using a support vector machine with an improved training procedure. Comput Biol Med 2006; 36: 339–362.
76. Wei N, Flaschel E, Friehs K, Nattkemper TW. A machine vision system for automated non-invasive assessment of cell viability via dark field microscopy, wavelet feature selection and classification. BMC Bioinformatics 2008 9: 449.

8

CONTAMINATION DETECTION IN ANIMAL CELL CULTURE

Carol Mclean
Protein Fractionation Centre, Scottish National Blood Transfusion Service, Edinburg, Scotland
Colin Harbour
University of Sydney, NSW, Australia

8.1 INTRODUCTION

This chapter describes the detection of contamination in cell culture by a range of infectious agents, including bacteria, fungi, mycoplasmas, viruses, and prions. The presence of any form of microbial contamination renders the results of scientific studies with that cell culture invalid. In manufacturing processes designed to produce therapeutic biologics from cell culture systems, it is imperative that all possible steps be taken to ensure that the product is free from any infectious agents. This chapter provides a historical perspective to demonstrate how contamination and its detection have affected the development of cell culture as a technology and then describes the current regulatory requirements expected of cell-culture-derived biologics. The regulatory framework is described, in part, to draw attention to the current gulf in cell culture practices with regard to contamination detection required by manufacturers compared to that performed by cell culture workers in institutions devoted to research such as universities. The issues of good manufacturing practice (GMP) and good laboratory practice (GLP), which largely determine the procedures adopted by the former group, are usually ignored by the latter. This is an unacceptable situation and it is our hope that this chapter will indicate what can happen if the detection of contamination is not performed as an essential part of cell culture practice. In addition, the chapter describes appropriate strategies for detecting contamination and thus avoiding the generation of erroneous results in cell culture research and providing the safest possible biologics.

8.2 HISTORICAL PERSPECTIVES

Following the cultivation of nerve cell tissue using the hanging drop technique by Harrison in 1907, the historical development of cell and tissue culture was inhibited by the problem of microbial contamination. Microbes grow rapidly in the enriched media required for cell and tissue growth leading almost inevitably to the destruction of such cultures. Although some practitioners were successful, such as Alexis Carrel who had shown in 1923 that it was possible to culture cells *in vitro* for long periods by employing rigorous aseptic techniques, the problem of microbial contamination was never controlled sufficiently until the introduction of antibiotics in the 1940s. Since then, the introduction of work stations such as laminar air flow cabinets for cell culture manipulations in clean, filtered air, has also contributed enormously to reducing the levels of microbial contamination. Nevertheless, contamination does occur from time to time, and regular screening for the presence of bacteria, fungi, and mycoplasmas should be mandatory practice in all cell culture facilities. This is even more important today when the routine use of antibiotics for cell culture is discouraged because it may make low level contamination difficult to detect, lead to the emergence of

Upstream Industrial Biotechnology: Expression Systems and Process Development, Volume 1, First Edition. Edited by Michael C. Flickinger.
© 2013 John Wiley & Sons, Inc. Published 2013 by John Wiley & Sons, Inc.

resistant micro organisms, and in the production situation, could result in side effects in patients, who receive cell-culture-derived biologics contaminated with trace amounts of antibiotics. The procedures for detecting these microbes are relatively straightforward, and the appropriate protocols are provided in this chapter. By contrast, the detection of viral contamination is more complex, and thus this chapter devotes more attention to this problem.

As stated earlier, the introduction of antibiotics in the 1940s led to rapid advances in cell culture, such as the work of Enders and co-workers who published the first report of growing polio virus in nonneural cells in culture (1). This seminal work, recognized with the award of a Nobel prize, showed that it was feasible to produce viruses and hence viral vaccines in cell culture systems and thus provided the stimulus for the development of cell culture as a technology. Rapid advances were then made resulting in the production of the Salk polio vaccine derived from monkey kidney cells, which was first licensed in 1954, followed by the Sabin polio vaccine (a live vaccine) which was first licensed in 1955 (2,3). Unfortunately, it was recognized then that these early polio vaccines were contaminated with a virus, simian virus 40 (SV40), present in the monkey kidney cells. This finding had a salutary effect on the cell culture "industry" and demonstrated clearly that any material of biological origin can be contaminated with an infectious agent (4,5). Since that discovery, various strategies have been introduced to address the issue of viral contamination, including a wide range of different types of viral assays which are described in this chapter. The problem of viral contamination was also a major driving force in developing more sophisticated cell culture techniques, including the introduction of normal diploid cell lines for producing viral vaccines (6,7). These cells provide the opportunity to establish frozen cell banks and thus the time to perform comprehensive investigations designed to detect microbial contamination. Thus, as a result of these screening procedures, normal diploid cell lines are inherently safer than primary cells in their potential to transmit infectious diseases, but because absolute safety can never be guaranteed, all cell lines must be regularly, monitored. Further advances in cell culture technology and molecular biology have led to the introduction and acceptance of transformed or continuous cell lines for producing a range of biologics for therapeutic use such as interferon (8), monoclonal antibodies, and various recombinant proteins, for example, tissue plasminogen activator (9). Many of these cells are known to express endogenous retroviruses (10–12) which have oncogenic potential, and this issue has been addressed by the introduction of a comprehensive range of screening assays which are described in detail in this chapter.

After summarizing the historical development of cell culture so as to emphasize the move away from the use of primary cells to improve safety regarding transmitting infectious agents, it is somewhat ironic to note that the most recent developments in this field, broadly categorized as cell and/or gene therapy and tissue transplantation involve, in many cases, a return to the use of primary cells with all, of their inherent safety risks (13,14). These primary cells, which may be autologous, allogenic, or xenogenic cells chemically stimulated *in vitro* in some way or even genetically modified, must be administered to a patient as rapidly as possible after treatment because the cells have a limited life span and the patient is more than likely gravely ill. Therefore, it is a necessary to perform all quality control screening procedures as rapidly as possible. For example, by the end of the 14-day period required for a routine sterility test, the patient may have died or become so sick that the treatment would no longer be effective. The sample sizes required for the recommended screening procedures may constitute an unacceptably large proportion of single-patient treatments, and reducing the sample size so as to preserve the treatment dose will obviously lead to a reduced likelihood of detecting infectious agents. These are important issues created by new developments in cell culture technology, and the ways by which they are being addressed are discussed later, as is the prion problem (15). At this time, the latter has become a major challenge for all those involved in manufacturing biologics and is discussed in more detail later in this chapter. The prion, or proteinaceous infectious particle, appears to have crossed the species barrier from cows suffering from bovine spongiform encephalopathies (BSE) and resulted in a new variant of Creutzfeldt–Jakob disease (vCJD) in humans. The prion is the latest discovery of an infectious agent that can infect humans and underlines the continuing need and importance of the screening procedures described in this chapter (16). In the next section the detection of contamination is described in the context of the current regulatory framework which has developed to ensure that cell-culture-derived biologics are as safe as possible.

8.3 REGULATORY ISSUES

Biopharmaceuticals are manufactured from three main sources comprising human tissues or plasma, animal tissues or plasma, and mammalian cell lines. Production of biologics in mammalian cell lines offers the advantage over the other systems that the products can be readily manufactured in large amounts and, compared to biologics prepared from human tissues or plasma, are less likely to be contaminated with human pathogens. Mammalian cell culture systems, however, carry the risk that the cell line or raw materials used in cell cultivation can introduce a viral contaminant of animal origin capable of zoonoses or other microbial contaminants pathogenic

to humans such as *Mycoplasmas*. For example, some cell lines harbor viral sequences integrated into the genomic DNA that are passed vertically from generation to generation such as endogenous retrovirus sequences which are found in cell lines of many species. Integrated viral sequences alternatively originate from virus that was deliberately introduced during establishment of the cell line such as Epstein–Barr virus (EBV) used to immortalize human B cell lines for establishing human hybridomas and human–murine heterohybridoma. Raw materials or ingredients of animal origin used during cell line cultivation or product purification that may introduce adventitious agents include reagents, such as bovine serum used in cultivation of cell lines, and monoclonal antibodies produced in ascites or cell culture used for affinity purification of the product. Manipulation of cell lines, product intermediates, and materials by human operators during manufacturing provides a further source of adventitious agent contamination, for example, via aerosols or by direct contact.

"Notes for guidance" and "points for consideration" have been issued by various national and international agencies, including the CBER (Center for Biologics Evoluation Research) a branch of the Food & Drug Administration of the USA in the United States, the Committee for Proprietary Medicinal Products (CPMP) in the European Commission, and Japanese regulatory authorities, that outline the testing strategy recommendations and requirements for safety evaluation of biological products made in cell line systems (17–21). The strategies recommended vary slightly from one agency to another; therefore integration has been done by the International Committee for Harmonisation (ICH) (18). These guidelines are initially published in draft form and issued to interested parties for comment before being issued as a final version. The final versions of these regulatory documents are not issued simultaneously; therefore when testing cell lines used to produce biologics, the most recent final versions of the relevant regulatory documents, as well as the most recent version of the ICH guidelines, should be consulted.

The regulatory documents mentioned recommend the following strategies as evidence of product safety with respect to viral contamination:

1. Testing cell lines and raw materials for viruses that may be infectious for humans.
2. Testing the product/intermediates at appropriate stages during the production process for viral contaminants.
3. Validation of the production process for its capacity to remove and/or inactivate viral contaminants.

The approach adopted by manufacturers will depend on several factors such as the nature of the particular product, the results obtained during testing (points 1 and 2 above), and will generally be a combination of the three. Some biopharmaceutical products undergo little or no downstream processing and therefore rely on virological testing and characterization of the producer cell line and the final product, for example, replication-incompetent gene therapy vectors (22,23).

When physical and/or chemical purification steps are involved in the manufacture of the final product, validation of the ability of the process to remove or inactivate viral contaminants is performed by process validation studies (also called *virus clearance studies*) (point 3 above) (18,24). These contaminants may be known to exist in the manufacturing process, such as murine endogenous retroviruses in cell lines of murine myeloma lineage used in the manufacture of therapeutic monoclonal antibodies (19,20), or they may be contaminants for which there is a risk in the manufacturing process but for which testing for low levels of such contamination in process samples and raw materials is limited by the sample size.

Process validation studies are done by first establishing a representative downscale version of a specific step in the manufacturer's process that has been identified as known or likely to be effective in removing or inactivating viral contaminants. The downscale version must represent as faithfully as possible the conditions of the manufacturing process with respect to physical and chemical aspects such as flow rate, pH, protein concentration, etc. The downscale process is then spiked with a range of viruses with varying degrees of resistance to physical and chemical methods of inactivation to evaluate the ability of the process to remove and/or inactivate known and/or unknown viral contaminants. The viruses used in process validation studies can be "relevant" or "model" for example, human immunodeficiency virus (HIV) (relevant) and bovine viral diarrhoea virus (BVDV) (a model for Hepatitis C virus), in products manufactured from human plasma. By assaying the viral load in the spiked starting material and processed material, an estimate of the ability of a particular step in the manufacturing process to remove and/or inactivate the virus can be made and consequently provide further assurance of product safety.

When manufacturing a product from a cell line, a seed lot cell bank system must be established, where each bank is comprised of ampoules of cells with uniform composition derived from a cell seed. The master cell bank (MCB) is generally propagated from a selected cell clone under defined conditions, then aliquoted into multiple containers, and stored under appropriate conditions (frozen at or below -100°C). The working cell bank (WCB) is manufactured from one vial of the MCB. Then cells from the WCB (or occasionally the MCB) are propagated to the production cells. A cell bank at the limit of *in vitro* cell age used for production (usually called a *postproduction cell bank (PPCB)* or *extended cell bank (ECB)* is also laid down from

a WCB vial expanded under pilot plant or commercial scale conditions. The number of vials in any MCB and WCB will vary from process to process but is often in the order of 100 per bank, thus enabling long-term supply of material for any one process. The current strategy recommended by the ICH for safety testing cell lines of human or animal origin used to produce biologics (with the exception of inactivated and live vaccines, and genetically engineered live vectors) is outlined in Table 8.1 (18,20). Extensive qualification of the MCB (or WCB) for adventitious agents and identity testing is required, and because the WCB has a low population doubling level beyond the MCB, testing of the WCB is minimal. Testing of the PPCB should be performed at least once to provide assurance that the conditions used during production are unlikely to introduce adventitious agents or activate viral contaminants that may be suppressed at the MCB stage. Therefore testing of the PPCB is repeated if there are changes in the scale or cultivation conditions during production. In-process testing of bulk harvests in the form of cells and fluid harvested from fermenters is also required because, like PPCB testing, this, provides assurance that the conditions used during production do not introduce and/or activate contaminants (18,20).

The use of raw materials from animal origin for the propagation of MCB, WCB, and in production should be avoided if possible. In doing so, characterization of the MCB (or WCB) will provide assurance of the cell bank safety. However, because of the growth characteristics and requirements of cell lines, the use of raw materials such as serum, insulin, transferrin, and trypsin, cannot always be avoided. In such circumstances, raw material must be sourced from suppliers that can provide traceability of their origins, and batches must be sampled and tested for freedom from adventitious agents before their use in manufacturing.

8.4 MANUFACTURING AND SAFETY TESTING STANDARDS

The manufacture of pharmaceutical products must be done in environments that assure the safety, uniformity, efficacy, and quality of the products. A system of principles that lay down the procedures required for production and quality control, including documentation, personnel, environment, equipment, materials, auditing, sampling, and safety, are stipulated by cGMP (25). Testing of biopharmaceuticals for adventitious agents should be performed by laboratories with experience in virological assays and Good Laboratory Practice (GLP) accreditation. International GLP principles have been laid down by the OECD (Organisation for Economic Cooperation Development) (26). These guidelines exist so that safety studies are planned, performed, monitored, recorded, reported, and archived in an organized and controlled manner following approved procedures in a facility with adequate resources so that the quality and validity of the testing are assured.

8.5 EXAMPLES OF VIRAL CONTAMINANTS

Many animal cell lines currently used in producing biologics contain endogenous viruses. For example, cell lines of murine origin can harbor endogenous Type B or Type C retroviruses (oncoviruses), and cell lines of hamster origin express defective Type C and Type R retrovirus particles (27). Table 8.2 lists examples of endogenous retroviruses associated with cell lines commonly used for producing biologics. Exogenous viral infections may be present in cell lines that were acquired by the animal from which the cell line was established, for example, SV40 infection

TABLE 8.1. Testing Strategy for Cell Lines used to Produce Biologics[a]

Test	MCB	WCB	PPCB
Infectious (endogenous viruses)	+	−	+
Electron microscopy	+	−	+
Reverse transcriptase[b]	+	−	+
In vitro assay[c]	+	−	+
In vivo assay[c]	+	−	+
Antibody production assays[d]	+	−	−
Other virus specific tests[e]	As appropriate	−	As appropriate
Mycoplasma	+	+	+
Sterility	+	+	+

[a] Refs. 18 and 20.

[b] Reverse transcriptase assay is not necessary if the cell line is positive for infectious retrovirus.

[c] These assays should be performed on the cells at the limit of *in vitro* cell age generated from the first WCB; for subsequent WCBs a single test can be done either on the WCB or on the cells at the limit of *in vitro* cell age.

[d] These include mouse antibody production assays (MAP), hamster antibody production assays (HAP), and rat antibody production assays (RAP) and are usually applicable only to cell lines of rodent origin.

[e] This includes assays performed on, for example, human cell lines such as PCR assays for the human viruses HBV, HCV, HIV-1, HIV-2, HHV-6, HTLV I and II, EBV, and CMV.

TABLE 8.2. Endogenous Retroviruses Found in Cell Lines Commonly used to Produce Biologics

Cell Line	Retrovirus Particle Type	Infectious
Mouse myeloma/ hybridoma	A, C	Ecotropic and xenotropic
Chinese hamster ovary	C	Noninfectious
Baby hamster kidney	R	Noninfectious
Human/ murine heterohybridoma	A, C	Xenotropic
Human	None	No
Monkey	None	No
Insect	None	No

of Vero cells (4). Alternatively, cell lines may become accidentally infected with an exogenous virus during their establishment and/or development in research laboratories from, for example, another cell line or a laboratory operator. Expression of exogenous or endogenous retroviral infection can in some instances be low or undetectable in normal culturing conditions and can be chemically induced by agents such as 5-bromodeoxyuridine, 5-iododeoxyuridine, sodium butyrate, or 5-azacytidine (28–32).

Current use of replication-deficient virus-based vectors for gene therapy introduces the additional risk of viral contamination by replication-competent viruses which may be generated by recombination between sequences in the viral vector and the packaging cell line. The viruses from which gene therapy viral vectors are constructed are infectious for human cells. Therefore generation of a replication-competent virus may result in disease.

At some point in their histories most if not all cell culture systems have been exposed to raw materials of animal origin such as bovine serum or porcine trypsin, which constitute further potential sources of viral or mycoplasmal contamination. The most common contaminants of bovine serum are BVDV—also called *mucosal disease virus (MDV)*—and bovine polyomavirus (BPyV) (33–36). BVDV is distributed worldwide affecting ~60% of cattle in the United Kingdom and Australia, and is infectious to several even-toed ungulates in addition to cattle, including pigs, sheep, and goats (37). It is therefore probable that a large proportion of bovine products used in cell culture systems is contaminated with either infectious or defective BVDV. The BVDV or BPyV status of bovine raw materials is often not provided, and commonly used filtration techniques used in the manufacture of bovine serum do not efficiently remove these viruses. Some suppliers, however, perform viral inactivation steps such as UV-C or gamma irradiation of serum to provide assurance of product safety (38,39).

Contamination of cell cultures with bovine viruses is of major concern when manufacturing products for use in ruminants because BVDV infection can result in abortion or growth retardation in offspring that are persistently infected (37). Several instances of BVDV contamination have been reported (40–45) which, in cases where the product is a ruminant vaccine, have resulted in livestock growth retardation and death (41,42). Pestivirus RNA has been detected in biopharmaceutical products for human use, although no confirmed symptomatic infections in humans have occurred (45). Bovine serum has also been implicated as the source of epizootic hemorrhagic disease virus (EHDV) in a Chinese hamster ovary (CHO) cell line (46), and the parvovirus, minute virus of mice (MVM), in a baby hamster kidney (BHK) cell line (47). Two similar MVM contamination incidents have been reported in hamster cultures (48,49), one of which was detected in fermenter cultures of CHO cells and the second during production of foot-and-mouth disease vaccine. The source of the contamination in these instances was not identified but in the former case was believed to be from mouse excretions contaminating media or their components during storage.

The main virus of concern in raw materials of porcine origin is porcine parvovirus (PPV) which has widespread distribution, that is, 40% infection has been reported (50), and it has been isolated from commercial trypsin (51). Testing of porcine trypsin for PPV is required by a number of regulatory bodies including the US. Department of Agriculture (9CFR) (52) and the European Pharmacopoeia (53). Examples of exogenous viral contaminants of biopharmaceutical systems are listed in Table 8.3 (54).

8.6 DETECTION OF VIRAL CONTAMINANTS IN CELL LINES

Viral contamination of cell lines can be detected by direct analysis, such as fixation of the cells and examination by electron microscopy, or by polymerase chain reaction (PCR) of nucleic acid extracted from the cell line. Alternatively, viral contaminants can be detected indirectly by examining the effect that the cell line has on a test system, for example, inoculation of a cell extract into a detector cell line or into an animal susceptible to the virus of concern. The effect of a viral contaminant on a cell line or animal test system may be general, producing a cytopathic effect (cpe) in the form of cell or animal death

TABLE 8.3. Examples of Exogenous Viral Contamination in Intermediate and Final Products Manufactured in Cell Culture Systems

Product/Intermediate	Contaminant	Contamination Source	Reference
Polio vaccine	SV40	Infected cell line	4
Vet vaccine	BVDV	Unknown	40
Swine fever vaccine	BVDV or Border Disease virus	Bovine serum or lamb cell culture?	41
Rota-corona vaccine	BVDV	Unknown	42
Final product (IFNα, IFNβ)	BVDV	Bovine serum?	43
Live vet vaccines	BVDV	Bovine serum?	44
Human vaccines (MMR, MR)	BVDV	Bovine serum?	45
CHO cell line	EHDV	Bovine serum?	46
Unprocessed bulk (CHO cell line)	MVM	Medium component?	48
Foot-and-mouth disease vaccine	MVM?	Unknown	49
Vet vaccine	CPV	Unknown	54

or cell morphological change, or may be specific such as in the production of antibodies to a specific virus in mice following inoculation of virally contaminated material. The testing strategies required by the ICH for cell lines used to produce biologics are outlined in Table 8.1. These primarily consist of *in vitro* and *in vivo* testing of the MCB and PPCB for infectious virus and testing using molecular biology techniques and electron microscopy for viruses that may be infectious or defective.

8.6.1 Detection of Retroviruses

Retroviruses are single-stranded RNA viruses, surrounded by a lipid envelope. When examined under thin-section electron microscopy, they are 100–140 nm in diameter and frequently exhibit glycoprotein surface projections. Cell lines of several species, including human, porcine, and murine, contain endogenous retroviral sequences. Murine cell lines of epithelial and myeloma lineages all contain endogenous retrovirus sequences and in many cases express infectious murine leukemia virus (MLV). MLV isolates can show varying tropisms, including ecotropic MLV (E-MLV) which is infectious for cell lines of murine origin or closely related species, and xenotropic MLV (X-MLV) which is infectious for cell lines of species other than of murine origin (37). Xenotropic endogenous retroviruses capable of infecting human cells have been described for murine and porcine cell lines (10,13,55). However the efficiency of murine retroviral infection apparently differs in the few reported incidents. In one study, supernatant was harvested form 17 mouse hybridoma cell lines and inoculated onto the human embryonic lung fibroblast cell line, 7605L. Eight of the 17 supernatants contained type-C retrovirus infectious for the human cells (10). In another study, 18 mouse cell lines of myeloma lineage were assayed for retrovirus by cocultivation with a human cell line, but none were positive (56).

Retroviral vectors used for gene therapy often contain envelope sequences originating from amphotropic MLV (A-MLV), feline leukemia virus (FeLV), or gibbon ape leukaemia virus (GaLV), which have been chosen because they are infectious for human cells (57). Therefore the generation of replication-competent retrovirus (RCR) with human tropism is of concern in such systems. Cell lines of human and simian origin have been used to produce biologics, for example, human–murine heterohybridoma cell lines used to produce monoclonal antibodies. These have the potential to be infected with exogenous human and simian retroviruses such as HTLV, simian retrovirus types 1 and 2, HIV, and simian and human foamy viruses (58–60). Following are details of a number of standard methods for detecting retroviruses which may be encountered in cell lines commonly used in producing biologics. Most of the cell lines and positive control viruses used in these methods are available from the ATCC.

8.6.1.1 Cell Culture Techniques for Retroviral Detection

8.6.1.1.1 Assays for Infectious MLV. Tests for infectious MLV should be performed on cell lines of murine origin on the MCB (or WCB) and again on the PPCB to determine whether there has been any change in the dynamics or tropism of MLV expression. It is also advisable to test samples from at least one fermenter run to monitor the dynamics of infectious retrovirus production during the manufacturing process. Similarly, testing regimes for RCR in retroviral gene therapy systems should include testing the producer cell line (1% or 10^8 of the cells, whichever is least, and 5% of the vector supernatant) (22,23). The following methods outline the procedures for detecting MLV using cell-free supernatant harvested from the cell line under test or fermenter sample. The methods described are so-called direct assay which are quantitative and therefore provide the titer

of virus per unit volume of sample tested. The sensitivity of the direct assay may be increased by serial passage of the inoculated detector cell line and consequently amplification of the retrovirus (61). So-called extended assays are qualitative and can increase assay sensitivity by approximately one log (62). When sampling for retroviral infectivity assays, it is important to harvest supernatant from test cell lines that are actively growing because this is the period during which the retrovirus is normally most highly expressed (63).

8.6.1.1.2 Assays for Ecotropic MLV

8.6.1.1.2.1 XC Assays (64). The XC assays utilize the cell line SC-1 which can be infected with E-MLV without inducing cpe. The virus can subsequently infect cells of the Wilistar rat tumour (XC cell line) in which a prominent syncytial effect is evident. E-MLV cannot infect XC cells directly. The assay should be set up as follows utilizing negative control cultures and positive control cultures infected with a suitable E-MLV for example, Moloney.

1. Plate the SC-1 cells at a density of 10^5 cells per 10 cm^2 plate in Dulbecco's Modified Eagle's Medium (DMEM) containing 10% fetal bovine serum (FBS)(v/v), and incubate at 37°C with 5% CO_2.
2. Examine the cells the following day, and if suitably subconfluent (~20–30%), inoculate with cell-free test material in the presence of polybrene at an effective concentration of 10 μg/mL.
3. Feed the cultures with 4–5 mL of DMEM containing 10% FBS (v/v) following an adsorption period of ~1–2 h at 37°C with 5% CO_2.
4. Maintain the cultures at 37°C with 5% CO_2 until confluent (normally 4–5 days). Then remove the culture medium, and irradiate the cells under UV light for ~1 min to kill the SC-1 cells.
5. Overlay the monolayers with XC cells at a high cell density (~10^6) per plate in DMEM containing 10% FBS, and reincubate the monolayer cultures at 37°C with 5% CO_2.
6. Stain the monolayers, when confluent, with crystal violet. Wash the excess stain from the cells with water, and allow them to dry. Examine the monolayers for infectious centers, identified as holes (plaques) in the XC monolayer. Evidence that the plaques are due to infection by E-MLV is provided by association of the plaque with one or more syncytial cell.

8.6.1.1.2.2 FG10 Assay. The FG10 cell line (also called *D56*) is a 3T3 cell line transformed with murine sarcoma virus (MSV) but does not produce infectious MSV (65). As such the cell line is termed sarcoma positive, leukemia negative (S^+L^-) and can be infected with leukemia virus with the result that the MSV genome is rescued and cell transformation occurs which is manifested as a "focus" at the site of infection. Foci appear as regions of rounded cells in association with a lytic area on the cell monolayer. The murine origin of this cell line permits an assay system for E-MLV. The assay should be set up as follows utilizing negative control cultures and positive control cultures infected with a suitable E-MLV, for example, Moloney.

1. Plate the FG10 cells at a density of 10^5 cells per 10 cm^2 plate in RPMI 1640 medium containing 10% FBS, and incubate overnight at 37°C with 5% CO_2.
2. Examine the cells the following day, and if suitably subconfluent (~20–30%), inoculate with cell-free test material in the presence of polybrene at an effective concentration of 10 μg/mL.
3. Feed the cells with 4–5 mL of RPMI 1640 medium containing 10% FBS (v/v) following an adsorption period of ~1–2 h at 37°C with 5% CO_2.
4. Maintain the cultures at 37°C with 5% CO_2 until confluent (normally 4–5 days). Then examine for foci formation which appear as described before. It is important to maintain the cultures until fully confluent because foci are not easily recognizable in a subconfluent monolayer in which there are many mitotic (rounded) cells and gaps in the monolayer which are similar in morphology to foci.

8.6.1.1.2.3 Mink S^+L^- Assay. The mink lung ($MiCl_1$) cell line is S^+L^- and as such can be infected with leukemia virus resulting in rescue of the MSV genome and cell transformation manifested as a "focus" at the site of infection (66). Confluent monolayers of the $MiCl_1$ cell have a flat morphology, and foci can easily be identified as regions of rounded cells raised above the contact inhibition layer of the monolayer. Focus formation on this cell line from material of origin other than mink indicates the presence of a xenotropic leukemia retrovirus, and thus is an assay system for X-MLV, Fe-LV, and Ga-LV. The assay should be set up as follows utilizing negative control cultures and positive control cultures infected with a suitable xenotropic leukemia virus, for example, X-MLV.

1. Plate the $MiCl_1$ cells at a density of 2.5×10^5 cells per 10 cm^2 plate in RPMI 1640 medium containing 10% FBS (v/v) and incubate overnight at 37°C with 5% CO_2.
2. Examine the cells the following day, and if suitably subconfluent (~20–30%), inoculate with cell-free

test material in the presence of polybrene at an effective concentration of 10 μg/mL.

3. Feed the cultures with 4–5 mL of RPMI 1640 medium containing 10% FBS (v/v) following an adsorption period of ~1–2 h at 37°C with 5% CO_2.
4. Maintain the cultures at 37°C with 5% CO_2 until confluent (normally 8–10 days). Then examine for foci formation which appear as described before. Again, it is important to maintain the cultures until fully confluent because foci are not easily recognizable in a subconfluent monolayer.

8.6.1.1.2.4 PG4 S^+L^- Assay. The PG4 cell line is a feline S^+L^- cell (67) which when infected with leukemia virus, like other S^+L^- cell lines, results in cell transformation manifested as a "focus" at the site of infection. This cell line is susceptible to infection by xenotropic and amphotropic MLV and Ga-LV. Therefore it is useful for detecting RCR in producer cell lines used in gene therapy vector production or in vector supernatant. Foci can be identified on PG4 monolayers as regions of rounded transformed cells adjacent to a lytic region in the cell monolayer. The assay should be set up as follows utilizing negative control cultures and positive control cultures infected with a suitable leukemia virus, for example, A-MLV.

1. Plate the PG4 cells at a density of 2×10^5 cells per 10 cm^2 plate in McCoy's medium containing 10% FBS (v/v), and incubate overnight at 37°C with 5% CO_2.
2. Examine the cells the following day, and if suitably subconfluent (~20–30%), inoculate with cell-free test material in the presence of polybrene at an effective concentration of 10 μg/mL.
3. Feed the cultures with 4–5 mL of McCoy's medium containing 10% FBS following an adsorption period of ~1–2 h at 37°C with 5% CO_2.
4. Maintain the cultures at 37°C with 5% CO_2 until confluent (normally 5–7 days). Then examine for foci formation which appear as described before. It is important to examine the cultures daily because the PG4 monolayer can deteriorate with the formation of holes in the monolayer which makes foci identification difficult.

8.6.1.1.2.5 Mus dunni Assay. The *Mus dunni* tail fibroblast cell line (68) is sensitive to A-MLV, X-MLV, and E-MLV (with the exception of the Moloney strain), and also mink cellfocus-forming viruses. However, acute infection does not result in an obvious cpe (69). This cell line is recommended by regulatory authorities for detecting infectious MLV in production systems using cell lines of murine origin (17,19) and in gene therapy vector systems based on MLV (22,23). Because of the absence of cpe in infected *Mus dunni* cultures, quantitative infection assays ("direct" assay) utilize an immunofluorescence end point. Qualitative assessment of the MLV status of a cell line can be done by inoculating the test material onto *Mus dunni* cells followed by amplification of any infectious MLV present by serial passage of the cells and assay of the *Mus dunni* supernatant for infectious MLV by an appropriate assay such as direct PG4 or direct mink S^+L^- assay described before. The direct and extended *Mus dunni* assays are performed as follows, using negative control cultures and positive control cultures infected with an appropriate virus such as A-MLV.

Direct Assay

1. Seed multichamber slides (slides are commercially available with each well ~4 cm^2) with *Mus dunni* cells at a concentration of 2×10^4 cells/well in DMEM containing 10% FBS (v/v), and incubate the slides overnight at 37°C with 5% CO_2.
2. Examine the cells the following day, and if suitably subconfluent (~50%), inoculate with cell-free test material in the presence of polybrene at an effective concentration of 10 μg/mL.
3. Feed each well with an appropriate volume of DMEM containing 10% FBS (v/v) following an adsorption period of ~1–2 h at 37°C with 5% CO_2.
4. Maintain the cultures at 37°C with 5% CO_2 until confluent (normally 2–4 days). Then fix in cold acetone for 10–15 min.
5. Perform indirect immunofluorescence by placing a suitable volume of anti-MLV antibody into each well (several monoclonal antibodies to MLV are available, e.g. 34, R187, or 548) (70). Place the slide in a humidified chamber at 37°C for a suitable period of time, for examples, 30 min.
6. Wash the slides with phosphate-buffered saline (PBS) to remove the primary antibody. Air dry the slides. Then add antispecies FITC antibody at a suitable dilution to the slides, and allow the antibody to adsorb as before
7. Wash the slides in PBS to remove the secondary antibody, and air dry as before.
8. Examine the slides for fluorescent foci under a suitable fluorescent microscope, and count the foci to give the titer of MLV per unit volume in the test sample.

Extended Assay

1. Seed the *Mus dunni* cells at a density of ~5×10^5 per 25 cm^2 tissue culture flasks in DMEM containing 10% FBS (v/v), and incubate the cultures overnight at 37°C with 5% CO_2.

2. Examine the cells the next day for confluency, and if subconfluent (~50%), inoculate the cells with the test sample in polybrene at an effective concentration of 10 μg/mL. Allow the sample to adsorb for 1–2 h. Then feed the cells with DMEM containing 10% FBS (v/v) and reincubate at 37°C with 5% CO_2.
3. Maintain the cells at 37°C with 5% CO_2, and passage the cultures several times on reaching confluency (normally three to five times is sufficient).
4. MLV can be assayed in the *Mus dunni* cells at this point by several means such as immunofluorescence in which the cells are subcultured into slides and tested as described before for the direct assay. Alternatively, cell-free supernatant can be harvested from the cultures and tested for MLV by the direct infectivity assays described before, or by reverse transcriptase assay.

Little has been published regarding the relative sensitivities of the previously mentioned cell lines for leukemia viruses. However, one study that examined the titers of X-MLV detected in fermenter harvests from a murine plasmacytoma cell indicated that for this particular X-MLV, the *Mus dunni* cell line was the most sensitive, followed by mink S^+L^--cells and PG4 cells were least sensitive (56).

If a cell line used to produce a biologic for human use is positive for a xenotropic retrovirus, it is necessary to determine whether the virus is infectious in human cell lines (19). An alternative approach to assaying cell-free supernatant for infectious retrovirus is by cocultivation of the cell line under test with a detector cell line for a given period of time (e.g. two or three passages) followed by removal of the test cell line and further passage of the detector cell line to amplify any infectious retrovirus present and to dilute any noninfectious retrovirus carried over from the test cell line culture medium. Then the detector cell line can be assayed for the presence of retrovirus by reverse transcriptase assay of the culture supernatant, electron microscopy, or one of the infectivity assays described before. If the cell line under test is nonadherent and the detector cell line is adherent, the test cell lines can be decanted. When both detector and test cell line are adherent, they can be cocultivated in a dish that separates the two cell lines by a transwell membrane which has pores large enough to allow passage of virus but not cells (commercially available transwell dishes normally have membranes with a pore size of 0.4 μm). Human cell lines that have been reported to be susceptible to xenotropic retroviruses include the embryonic lung fibroblast 7605L, the rhabdosarcoma cell line RD, the embryo fibroblast cell line MRC-5, the embryo kidney cell line 293, and the osteosarcoma cell line HOS (10,13,57,62,71).

8.6.1.2 Detection of Retrovirus by Reverse Transcriptase Assay. The presence of the reverse transcriptase enzyme within retroviral particles facilitated the assay for virus (infectious or noninfectious) in supernatant harvested from growing cultures. The reverse transcriptase enzyme synthesizes DNA using an RNA template and therefore can be assayed by including radiolabeled nucleotides in the reaction mixture. The optimum stage for reverse transcriptase detection in cell culture supernatant will depend on the cell line in question. However, in cell lines that produce retrovirus at levels detectable by reverse transcriptase, enzyme activity is normally readily detectable in supernatants harvested from cells that are exponentially growing or have recently stopped growing. The method described here comprises six separate reactions that assay polymerase activity under conditions with an RNA template (poly (rA)), a DNA template (oligo (dT)) or no template, and in the presence of either the magnesium or manganese cation (62). These six conditions control the following: (i) RNA dependent DNA polymerase activity that may arise from contaminating cellular DNA polymerase (higher levels of radiolabeled nucleotide incorporation when the template is DNA indicate that incorporation in the RNA template is likely to be from contaminating DNA polymerase); (ii) failure to separate unincorporated from incorporated radionucleotides (no template control); and (c) distinction between reverse transcriptase enzymes that have a preference for either the magnesium or manganese cation (63,72).

1. Clarify cell-free supernatant (10–20 mL) to remove cell debris by centrifugation at 11,000*g* for 10 min.
2. Pellet the retrovirus in the sample by centrifuging the resultant supernatant at 100,000*g* for 1 h. Then discard the supernatant, and allow the tubes to drain.
3. Disrupt the retroviral particles in buffer (~200 μL) comprising 40 m*M* Tris pH 8.1, 50 m*M* KCl, 20 m*M* DTT, 0.2% NP40.
4. Divide the sample into six 25 μL aliquots, and add an equal volume of one of each of the following six reaction mixtures:
   - 40 m*M* Tris pH 8.1, 50 m*M* KCl, 25 μCi [methyl ^{3}H] TTP, 2 m*M* MnCl, poly r(A) [0.05 A_{260} units].
   - 40 m*M* Tris pH 8.1, 50 m*M* KCl, 25 μCi [methyl ^{3}H] TTP, 2 m*M* $MnCl_2$, oligo (dT) [0.05 A_{260} units].
   - 40 m*M* Tris pH 8.1, 50 m*M* KCl, 25 μCi [methyl ^{3}H] TTP, 2 m*M* $MnCl_2$, 2 m*M* Tris pH 8.1, 30 m*M* NaCl.
   - 40 m*M* Tris pH 8.1, 50 m*M* KCl, 25 μCi [methyl ^{3}H] TTP, 20 m*M* $MgCl_2$, poly r(A) [0.1 A_{260} units].
   - 40 m*M* Tris pH 8.1, 50 m*M* KCl, 25 μCi [methyl ^{3}H] TTP, 20 m*M* $MgCl_2$, oligo (dT)) [0.1 A_{260} units].

– 40 m*M* Tris pH 8.1, 50 m*M* KCl, 25 μCi [methyl ^{3}H] TTP, 20 m*M* $MgCl_2$, 4 m*M* Tris pH 8.1, 60 m*M* NaCl.

5. Incubate the reaction mixtures at 37°C for 1 h to allow RNA-dependent and DNA-dependent DNA polymerase enzyme reactions to occur.
6. Precipitate the DNA or RNA templates onto GF/C filters using 10% trichloroacetic acid (TCA), 1% sodium pyrophosphate.
7. The precipitated nucleic acids with incorporated radiolabeled nucleotides are then measured in scintillation fluid in a scintillation counter.

The background levels of radioactivity obtained by this method are generally of the order of 100–2000 disintegrations per minute (dpm). Levels higher than this in those reactions with a template indicate polymerase activity. However, one can assume RNA-dependent DNA polymerase activity from reverse transcriptase only when the level of incorporation into the DNA template is relatively low, for example, at least half the dpm incorporation into the RNA template. The level of dpm in the reaction mixtures without template should be lower still, for example, half the dpm of the DNA template reaction. Suitable controls for use with this reaction include MLV for reactions that include the manganese cation and maedi-visna virus for reactions that include the manganese cation.

8.6.1.3 Electron Microscopy. Electron microscopy is a direct method of detecting viral contaminants and as such can provide evidence of viral contamination in the absence of any cytopathological effect. It is therefore a useful method for detecting endogenous and exogenous retroviral particles. Cell lines themselves can be examined directly for viral contaminants by thin-section transmission electron microscopy (TEM). Alternatively, the amount of retrovirus in culture fluids sampled from fermenters can be enumerated to determine the retroviral load. Although electron microscopy provides a useful means of detecting and classifying viral contaminants, it is not suitable as a diagnostic method for low levels of contamination because the technique allows examination only of a thin section of a the cell preparation or a small volume of culture supernatant. Quantitation of retroviral particles is required by regulatory authorities for cell lines used to produce monoclonal antibodies (19). The quantity of retrovirus present should be shown to be consistent between lots, and it should be demonstrated in process validation studies that the values obtained are removed or inactivated during product purification.

The retroviral burden in culture or fermenter supernatants can be estimated by negatively staining a virus preparation followed by TEM. However this method can be problematic because retroviruses are fragile and the method may cause structural artifacts that make identification difficult. Following is an outline of a suitable method for quantitating retroviral particles in cell culture or fermenter fluid samples. However, because electron microscopy is a highly specialized technique, the reader is advised to consult more specialized literature before embarking on such methods (71–78).

1. Clarify the culture supernatant by centrifugation at 11,000*g* for 10 min.
2. Pellet the retrovirus from the resultant supernatant by ultracentrifugation at 100,000*g* for 90 min (the conditions required for other virus types will differ).
3. Dilute commercially available latex particles to a concentration of $\sim 10^8$/mL, and mix the concentrated virus preparation with an equal volume of latex particles.
4. Apply the virus/latex particle mix to an EM carbon-coated grid.
5. Wash the EM grid gently with distilled water.
6. Apply a drop of negative stain to the grid (negative stains commonly used include 1–3% phosphotungstic acid (pH 5–8) and 1–2% uranyl acetate (pH 4.4).
7. Following a suitable staining time, remove excess stain from the grid using filter paper.
8. Allow the grid to air dry. Then examine by TEM.
9. The virus concentration in the initial culture supernatant can be determined by the following equation:

$$\text{Concentration of virus} = \frac{\text{Concentration of latex particles} \times 2 \times \text{virus count}}{\text{Latex particle count} \times \text{centrifugation concentration factor}}$$

Culture supernatant preparations from fermenter harvests may have large quantities of cellular debris. This is particularly so for batch fermentation samples. Further purification of the culture supernatant, for example, by sucrose density gradient centrifugation (78) may be necessary to reduce background material that may obscure virus identification.

Direct examination of cell lines by TEM using fixation of a cell pellet and thin-section preparation can be performed as outlined below (75). For detection of retrovirus, the culture should be actively growing.

1. Pellet the cells from a medium-sized culture flask ($\sim 5 \times 10^6$ cells should be harvested) by gentle centrifugation (500*g* for 5 min).
2. Carefully break up the cell pellet into small pieces of about 1 mm^3.

3. Fix the cells in 2.5% glutaraldehyde in phosphate buffer (pH 7.2) for 60 min.
4. Wash the cells three times in PBS (10 min per wash). Then postfix in 1% osmium tetroxide in PBS for 1 h.
5. Wash the cells three times in dH_2O, 10 min per wash. Then dehydrate the cells in a graded ethanol series of 50%, 75%, 95%, and 100% twice (15 min per step).
6. Embed the cells by first placing them in propylene oxide for 10 min: then in a 1 : 1 mix of resin to propylene oxide for 1 h, followed by three 1-h treatments in neat resin.
7. Place the samples in fresh resin, and polymerize the blocks by heating to 60°C for 24 h.
8. One-micrometer sections are then cut from the block using an ultramicrotome; then placed on EM grids and stained in 1% uranyl acetate, then lead citrate, and examined under TEM.

The retrovirus family comprises the oncoviruses, lentiviruses, and spumaviruses. The oncoviruses can be further divided into four groups comprising Type A, Type B, Type C, and Type D. Classification of retroviruses is based on their morphological features and morphogenesis as determined by electron microscopy.

Figure 8.1 illustrates some of the features (micrographs provided by Q-One Biotech Ltd., Glasgow, UK).

8.6.2 *In Vitro* Assays

So-called *in vitro* tests (Table 8.1) are recommended by regulatory authorities for identifying nonendogenous or adventitious viruses in cell banks which may be noncytopathic contaminants of the cell line or were introduced via a raw material or a breach in GMP procedures. The cell lines recommended for such *in vitro* assays by CBER are a human diploid cell line, a monkey kidney cell line, and a cell line of the same species and tissue type as used in production (17). Therefore, cell lines generally employed are the human embryo fibroblast cell line, MRC-5, and the monkey kidney cell line, Vero. The cell line of the same species and tissue type as used in production is as appropriate. CPMP regulations for cell lines producing monoclonal antibodies suggest, in addition, the use of cells capable of detecting a range of human, murine, and bovine contaminants (if relevant) (20). The rationale for the choice of cell lines is to provide a general screening assay that detects a broad range of viral contaminants that may be present in the cell line or in fermenters and may be pathogenic to humans. The assay is performed by examining inoculated detector cell lines for cpe and hemadsorbing agents and therefore has the limitation that it will detect only cytopathic and hemadsorbing viral contaminants that can replicate in the chosen detector cell lines. The specific format of the assay is unspecified by the regulatory guidelines. However, it is stipulated that the assay be examined for cytopathic and hemadsorbing viruses (17,20) and be maintained for a minimum of 14 days with passage of the human diploid cell line for a further 14 days with hemadsorption performed at the end of the cultivation period if the test system can support growth of human cytomegalovirus (17). The nature of the inoculum is specified by ICH as "a lysate of cells and their culture medium" (18). A possible format for such *in vitro* assays would therefore be the following (negative control and suitable positive controls for cpe on each detector cell line used should be tested in parallel):

1. Prepare six-well tissue culture dishes each of MRC-5, Vero, the cell line of the same species and tissue type as used in production (and other cell lines as appropriate) by inoculating 3 mL of cells at $1–2 \times 10^5$ cells/mL in an appropriate growth medium containing 10% FBS (v/v). Incubate the cultures overnight at 37°C with 5% CO_2.
2. Prepare the test sample lysate by harvesting cells and supernatant from a healthy confluent culture grown in a medium-sized flask ($\sim$80 cm^2) (adherent cells can be harvested by first scraping the cells into the spent culture medium with a sterile cell scraper). Clarify the preparation by centrifugation at 500*g* for 5 min. Transfer 70–80% of the supernatant to a fresh container, and place on ice (supernatant 1). Then resuspend the cell pellet in the remaining supernatant, and lyse the cells by freeze/thawing three times. Clarify the resultant lysate by centrifugation as before, and pool this the supernatant (supernatant 2) with supernatant 1 to constitute the sample for inoculation. Preparation of lysate by this method ensures that viruses sensitive to repeated freeze/thawing are represented by inclusion of "supernatant 1," viruses that may be trapped intracellularly are released and present in "supernatant 2," and the presence of intact cells that escaped disruption by freeze/thawing and could potentially interfere with observations for cpe is minimized by clarification of both supernatants 1 and 2. Cell lysates can also be prepared as before for samples taken from fermenters.
3. Inoculate a suitable volume, for example, 1 mL of lysate, into each well of each cell type, and allow the sample to adsorb for 1 h at 37°C with 5% CO_2.
4. Feed the cultures with 3–4 mL of maintenance medium (containing 1% v/v FBS) and incubate at 37°C with 5% CO_2.
5. Examine the cultures every 2–3 days for signs of abnormalities such as cells rounding, syncytia, or cell lysis.
6. Feed the cells as required (after seven days is normally adequate) with an appropriate maintenance

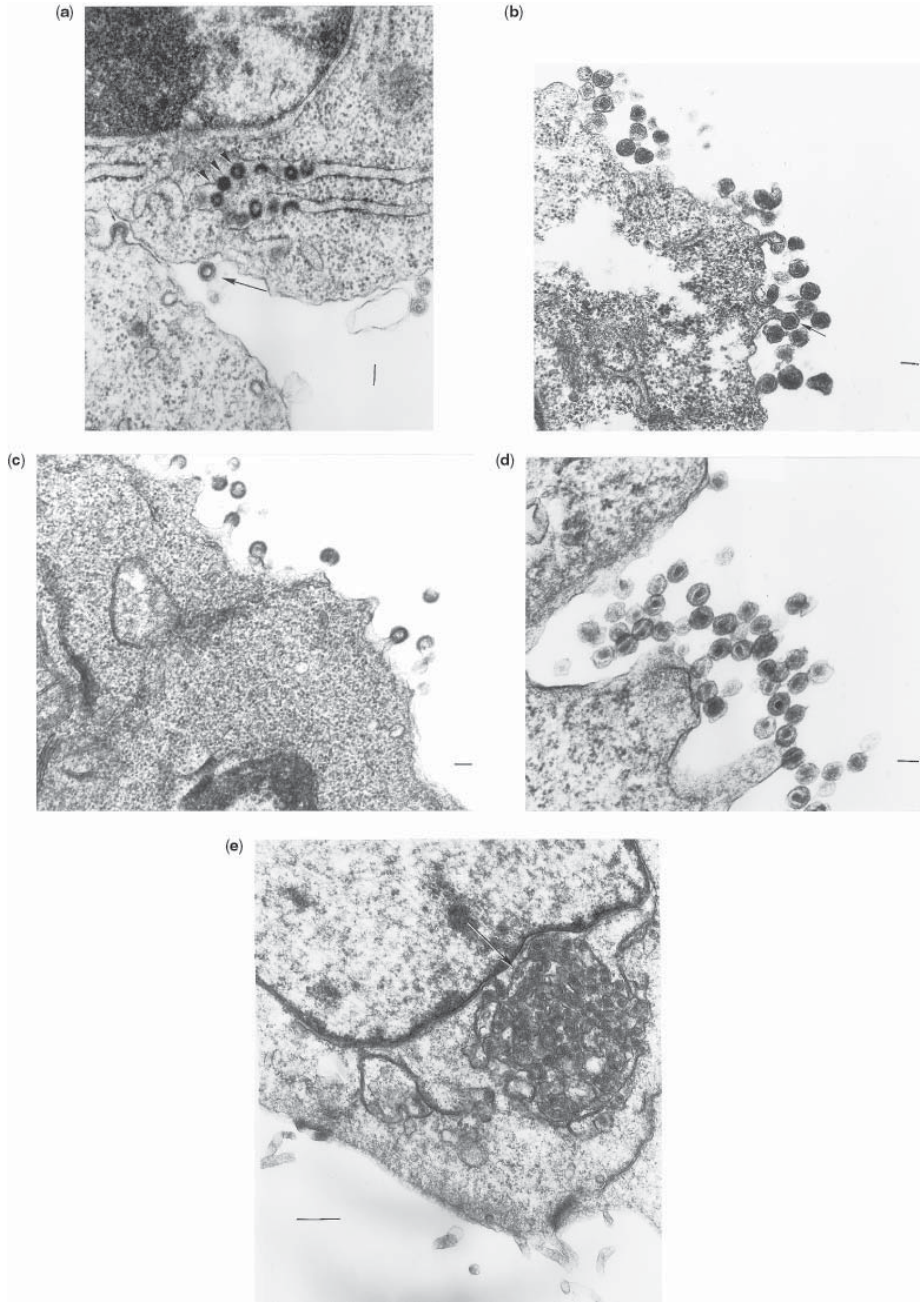


Figure 8.1. TEM micrographs of cells infected with retrovirus. (a) A murine myeloma cell line with an endogenous oncovirus. The large arrow heads indicate Type A particles within the endoplasmic reticulum (ER) characterized by two electron-dense concentric shells surrounding a central area of low electron density. The small arrowheads indicate Type A particles budding into the ER. An immature Type C particle with centrally located core is indicated by the large arrow (in mature Type C particles the core is electron-dense). The small arrow indicates a Type C particle budding from the cell membrane into the intracellular space. Note that the core of Type C particles is formed during budding. The scale bar is 100 nm. (b) Raji cells infected with the Type D oncovirus, squirrel monkey retrovirus (SMRV). Several extracellular Type D particles with electron-dense cores, sometimes tubular in shape, are evident. A budding Type D particle with characteristic preformed core is indicated (arrow). The scale bar is 100 nm. (c) Cells infected with the lentivirus HIV. Several budding particles can be seen characterized, as in Type C particle budding, by simultaneous core assembly. The scale bar is 100 nm. (d) A cell infected with HIV displaying numerous extracellular particles. This micrograph illustrates the characteristic tubularly shaped core of mature lentivirus particles. The scale bar is 100 nm. (e) A monkey kidney cell infected with the spumavirus, simian foamy virus (SFoV). A large group of spumavirus can be seen within the ER of the cell (arrow). The particles are characterized by an electron-dense ring-shaped core with a translucent center surrounded by an envelope with prominent surface projections. The scale bar is 500 nm. All micrographs were provided by Q-One Biotech Ltd., Glasgow, United Kingdom.

medium (Vero and MRC-5 cell lines can normally be maintained in culture in DMEM containing 1% FBS (v/v) without passaging for 14 days. However, if the cell type being used deteriorates during this period, as shown by a negative control culture condition, or assay for hemadsorbing agents on the human diploid cell line (MRC-5) is required at 28 days postinoculation, the cells should be subcultured to prevent this.

7. At 14 days postinoculation (or 28 days for MRC-5 detector cells when the test sample is capable of supporting human CMV growth), perform hemadsorption using guinea pig, human, and chicken red blood cells (rbc's) as follows:
   - Prepare the rbc's by centrifuging at 2000*g* for 10 min. Then wash the pelleted rbc's twice in PBS in tubes with volume markings. Following the second wash, measure the volume of packed rbc's. Then add sufficient fresh PBS to the pelleted cells for a 0.5% preparation of rbc's.
   - Remove the culture medium from the cells, and carefully wash the monolayers with PBS.
   - Overlay duplicate wells of each cell type with 2–3 mL of each of the three rbc species, and incubate the plates at ~4°C for 30–60 min.
   - Remove the rbc's by gentle agitation. Then pipette off. Wash the monolayer gently with PBS two or three times until all the nonadsobed rbc cells are removed.
   - Hemadsorption is indicated by adhesion of the rbc's to the detector cells. A suitable positive control for hemadsorption is parainfluenza type 3 (PI3) which is infectious for both MRC-5 and Vero cell lines.

8.6.3 *In Vivo* Assays

Assays in animals are part of the general safety tests recommended by regulatory authorities for manufacturers of biologics and involve the so-called *in vivo* assay and the antibody production assay (MAP, HAP, or RAP) (Table 8.1). "*In vivo*" assays normally utilize suckling mice, adult mice, guinea pigs, and embryonated eggs. Mice are inoculated intracerebrally, intramuscularly, and intraperitoneally, guinea pigs are inoculated intramuscularly, and embryonated eggs by the yolk sac, allantoic cavity, and amniotic cavity (20,76). The inoculum is normally a small volume of lysate prepared from the cell line under test, and the animals are observed for 3–4 weeks and the eggs for a shorter period of time (refer to refs 20 and 79 for specific durations) for morbidity and mortality. Hemagglutination is performed on fluids harvested from the eggs inoculated vial the allantoic route. The *in vivo* assay is designed to detect a wide range of viral contaminants. Suckling mice are susceptible to many arthropod-borne viruses, Herpes simplex virus, rabies, some arenaviruses, and picornaviruses, including poliovirus, coxsackievirus, echovirus, and encephalomyocarditis virus (adult mice are susceptible to some of these viruses) (77,78); guinea pigs are susceptible to paramyxoviruses, reoviruses, and filoviruses (37), and embryonated eggs are susceptible to poxviruses, paramyxo-, orthomyxoviruses, and Herpes simplex virus (79). Antibody production assays are performed on cell lines of mouse (MAP), rat (RAP) and hamster (HAP) origin to assay for viruses introduced by the source species. These assays are therefore normally performed only on the MCB because a negative result indicates that the cell bank system is free of viruses of the species of origin. In addition, MAP assays are performed on monoclonal antibody preparations made in ascites. The viruses assayed in these tests include hantaan virus, lymphocytic choriomeningitis virus (LCMV), reovirus type 3, and Sendai virus all of which are known to infect humans or primates (20). In these assays, adult mice, rats, or hamsters are inoculated with test cell lysate and held for 4 weeks, then bled, and the serum is tested for antibody to viruses of concern using antibody specific assays such as enzyme-linked immunosorbent assay (ELISA) and indirect immunofluorescence (IF).

8.6.4 Polymerase Chain Reaction (PCR)

PCR is a highly sensitive technique for detecting specific DNA sequences and therefore is important for detecting viral and mycoplasmal contaminants whose genomic sequence is known fully or partially. The reaction involves amplification using repeated thermal cycles of DNA denaturation, primer annealing, and DNA polymerization by *Taq* polymerase of a specific region of DNA defined by the primers. The reaction mass balance alters as the cycles progress resulting in an increase in product (and consequently available template), a decrease of nucleotides and primer (although these two components are greatly in excess in the reaction), and a decrease in the ratio of *Taq* polymerase molecules to available template copies. The reaction therefore reaches a point after 30 cycles or so when production of product is no longer exponential due to limiting *Taq* polymerase and self-annealing of product. The specific conditions employed for any PCR assay depend upon the sequences being amplified, the primers used, the number of initial copies of template in the sample, and the size of the region being amplified. In addition, viruses with RNA genomes must be reverse transcribed before PCR amplification.

PCR is important as a tool for virus adventitious agent detection when a culture system is not available, as is

the case with hepatitis C virus detection, or when detection of infectious virus is limited by the sample size, as is the case with detection of replication-competent virus during monitoring of patients treated with gene therapy constructs. It should be noted, however, that PCR detects infectious, as well as defective virus. Therefore in circumstances where virus is likely to be present but has been inactivated by processing, PCR is less useful, for example, PPV in γ-irradiated trypsin. The specific protocols for viral diagnosis by PCR are beyond the scope of this chapter, and readers interested in the details are advised to consult more relevant literature (80).

8.7 TESTING RAW MATERIALS

8.7.1 Tests for Bovine Viral Contaminants

The most common viral contaminant in raw materials of bovine origin is the pestivirus BVDV because of its prevalence, the large numbers of animals from which a serum batch is prepared, and partial resistance of the virus to standard procedures used to heat inactivate bovine serum for use in tissue culture medium preparations (56°C for 30 min) (81). Some manufacturers of bovine serum reduce the risk of infectious BVDV in bovine serum by irradiation with UV-C (wavelength of 254 nm) or γ- irradiation (38,39). Both techniques are effective inactivators of BVDV and other viruses. However, in the absence of effective virus inactivation treatment of bovine raw material, it is advisable to test for BVDV. The majority of BVDV strains are noncytopathic. Therefore detection of infectious BVDV is most easily done, as outlined in the following protocol, by end-point immunofluorescence using an antibody that recognizes BVDV antigen following inoculation of a susceptible cell line such as the bovine turbinate (BT), bovine trachea (EBTr) cell lines, or the Madin Darby bovine kidney cell line (MDBK). Negative and positive control cultures are tested in parallel. The negative control cultures are cells assayed in parallel and cultured in a medium containing BVDV-free serum. The positive control cultures can either be cells infected with a noncytopathic strain of BVDV (e.g. New York-1) at the same time as the test sample is inoculated, or a subculture of the negative control culture can be infected with a cytopathic strain of BVDV (e.g. NADL) toward the end of the assay.

1. Seed BVDV-free cultures of one of the above cell types into tissue culture flasks to obtain cultures ~70% confluent on the following day.
2. Remove the growth medium the next day, and replace with a culture medium containing 10–15% (v/v) of the test serum as the FBS component (all three cell lines mentioned above grow in DMEM). Alternatively, if the bovine raw material under test is not serum, dissolve the test material in a small volume of BVDV-free medium. Then inoculate this onto the monolayer, and allow it to absorb for 1 h. Feed the cultures with BVDV-free growth medium.
3. Incubate the cultures at 37°C with 5% CO_2, and passage when confluent, (approximately every 3–4 days) for five passages. During subculturing, use a medium containing 10–15% (v/v) of the bovine serum under test.
4. At passage five, prepare the cells for immunofluorescence by subculturing 1×10^5 cells/mL (2 mL per well) onto two chambered tissue culture slides. Reincubate the slides at 37°C with 5% CO_2 until confluent.
5. When confluent, remove the culture medium, and fix the cells by submerging the slides in cold acetone for 10–15 min. At this point, the slides can be stored frozen or tested by immunofluorescence.
6. Perform indirect immunofluorescence using commercially available antibodies to BVDV and commercially available antispecies FITC (fluorescin isothiocyanate) conjugated antibody.
7. Dilute the anti-BVDV antibody to a predetermined working dilution in PBS. Then allow the antibody to adsorb onto the cells by incubation in a humidified chamber at 37°C for a suitable period of time (30 min is normally sufficient).
8. Remove the primary antibody by washing the slides in PBS. Add the secondary antibody (commercially available antispecies FITC conjugated antibody) to each well, and allow this to adsorb as above.
9. Following a suitable adsorption period, wash the slides in PBS to remove the secondary antibody.
10. Examine the slides under a suitable fluorescent microscope. Samples that are positive for BVDV may show varying proportions of positive cells, depending on the strain of BVDV and the number of passages in culture. Figure 8.2 illustrates the pattern of BVDV fluorescence which is predominantly cytoplasmic.

The US Code of Federal Regulations (9CFR) (52) stipulates requirements for testing animal-derived products used as ingredients in producing biologics. In the case of bovine-derived ingredients, specific procedures for viral detection using Vero cells (African green monkey kidney) and a cell line of bovine origin are provided. The method involves cultivating these two cell lines in a medium containing at least 3.75 mL or 15% of the ingredient for 21 days or more with at least two passages during this period. At the final passage, monolayers are set up of specified surface area and assayed 7 days later for viral contaminants by cytological staining, hemadsorption, and IF. Viruses assayed by IF on detector cells of bovine origin are BVDV,

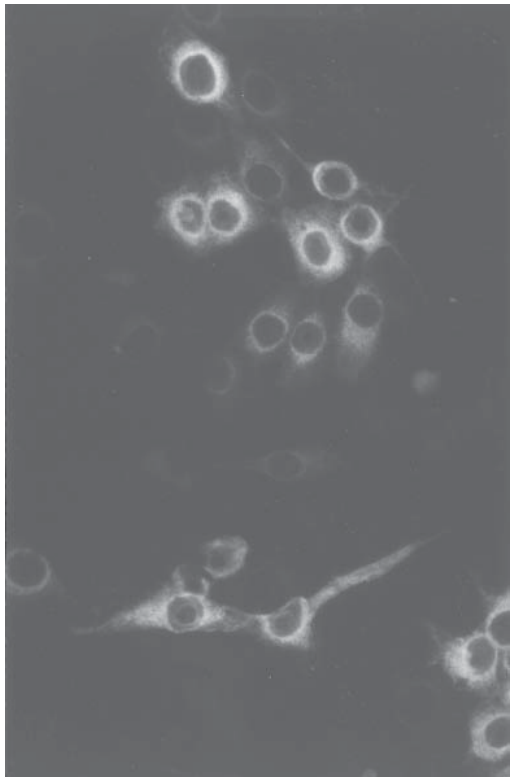


Figure 8.2. BT cells infected with BVDV and assayed for infectivity by indirect immunofluorescence, as described in the text. Cells infected with BVDV display green cytoplasmic fluorescence. Photograph provided by Q-One Biotech Ltd., Glasgow, United Kingdom.

bovine adenoviruses (BAV), bovine parvovirus (BPV), bluetongue virus (BTV), bovine respiratory syncytial virus (BRSV), reovirus, and rabies virus. Vero cells are tested by IF for BVDV, reovirus, and rabies virus.

8.7.2 Tests for Porcine Viral Contaminants

Trypsin is a raw material of porcine origin widely used in cell cultures for dissociating anchorage-dependent cells. The virus of concern in trypsin preparations, as discussed previously, is PPV. As with raw materials of bovine origin, the US Code of Federal Regulations (9CFR) (52) stipulates the method for testing for PPV in trypsin preparations which have not undergone appropriate treatment to inactivate this virus. The following method complies with 9CFR recommendations:

1. Seed duplicate medium-sized tissue culture flasks (75–80 cm^2) of primary porcine kidney cell lines at a density such that at inoculation (the following day) the monolayer is 30–50% confluent. (It is important to inoculate PPV onto mitotically active cells because parvoviruses require the cellular functions available during the S and G phases of the cell cycle for DNA replication (82).
2. The following day, ultracentrifuge the trypsin preparation at 80,000*g* for 1 h to pellet the virus and separate it from trypsin so that monolayer detachment can be avoided (9CFR requires testing 5 g of trypsin is tested and resuspending the resultant pellet in water).
3. Inoculate the resuspended pelleted material into one of the two flasks of primary porcine kidney cells, and incubate for 1 h at 37°C with 5% CO_2 to allow any virus to adsorb. Inoculate the remaining flask with culture medium as a negative control, and incubate as above.
4. Feed the flasks with an appropriate growth medium, and reincubate the culture at 37°C with 5% CO_2.
5. Examine the cultures every 2–3 days for confluency of growth and viral cpe.
6. Maintain the culture for 14 days or more postinoculation, with at least one subculture during this period. It is important to ensure that all subculturing of the primary porcine cells is performed using trypsin that is negative for PPV.
7. At the last subculture (this should fall on or after day seven postinoculation), set up monolayers for immunofluorescence. 9CFR stipulates that these monolayers must be a minimum of 6 cm^2 (commercially available glass or plastic chamber slides are suitable for this purpose). Three sets of 6 cm^2 monolayers are required from the "test material" culture such that two are the "test material" monolayer, and the remaining one is inoculated with PPV as a positive control. Set up one 6 cm^2 monolayer from the negative control culture.
8. One day after subculture, remove the medium from one of the "test material" slides, and inoculate with PPV (100–300 fluorescent units). Allow the virus to adsorb at 37°C with 5% CO_2 for 1 h. Then feed the culture with an appropriate volume (2–3 mL) of fresh medium. Return the slide to a 37°C incubator with 5% CO_2.
9. Examine the cultures every 2–3 days for viral cpe. If cpe is evident on the positive control culture, it can be fixed in cold acetone for 10–15 min. However, a "test material" monolayer must be fixed at the same time. Maintain the negative control and remaining "test material" cultures until at least 7 days post-subculture (i.e. day 14 or later). Then fix with cold acetone as above.
10. Perform indirect immunofluorescence for PPV, as described before for BVDV. Specific fluorescence to PPV is evident from nuclear fluorescence.

PPV cytopathology is often difficult to recognize and requires serial passage before it becomes evident. Therefore, specific end-point assay such as immunofluorescence described before provides conclusive evidence of PPV contamination.

8.8 DETECTION OF MYCOPLASMAS

Mycoplasmas are bacteria that lack the rigid cell wall structure composed of peptidoglycan that is normally associated with bacteria. Thus mycoplasmas have properties that distinguish them from other bacteria. Testing for mycoplasmal contamination requires a different set of assays independent of sterility testing for normal bacteria, and these are described following. The term mycoplasma denotes organisms that belong to the class designated Mollicutes which includes other generic groups referred to as acholeplasma, ureaplasma, and spiroplasma. Many distinct organisms (158 recognized species) are grouped in the class Mollicutes because they lack cell walls due to the absence of the genes for peptidoglycan synthesis (83). Mycoplasmas also differ from other bacteria by incorporating cholesterol and other sterols into their plasma membranes which makes the membranes of mycoplasmas more pliable and more resistant to physiochemical properties than would be predicted (84). This pliability combined with their small size, average diameter of 0.3–0.8 μm, allows them to pass through filtration systems designed to remove bacteria. The most likely source of mycoplasmal contamination in a cell culture facility is a contaminated cell culture, thus emphasizing the need for thorough screening of all new cell lines and appropriate quarantine and storage protocols for all incoming cell cultures. After establishing an infection in a particular cell line, mycoplasma and other microbes are spread by aerosol droplet dispersion via a variety of normal cell culture procedures including pipetting and dispensing of media liquids. The inappropriate use of a common medium bottle or common pipettes between cell cultures and cell lines can lead to contamination of many cell lines in the facility with the same species of mycoplasma (85). Human isolates represent the majority of mycoplasmal contaminants in cell culture. *Mycoplasma orale*, *M. fermentans*, and *M. salivarium* are the most frequently isolated, and *M. buccale*, *M. faucium*, *M. genitalium*, *M. hominis*, *M. pirum*, and *M. fermentans* less frequently. Many species of mycoplasma are known to cross host ranges, and thus isolates from contaminated bovine serum such as *Acholeplasma laidlawii*, *M. arginini* and *My. hyorhinis* represent further cause for concern in cell culture. The consequences of mycoplasmal contamination are too numerous to describe in this chapter. Those interested in a more comprehensive description of the subject are referred to the recent review of mycoplasmal contamination by Lincoln and Gabridge (86). A major problem is that despite heavy microbial contamination, for example, 10^9 colony-forming units per milliliter of culture, the cell cultures often appear to be normal by both macroscopic and microscopic inspection. Thus, due to an undetected mycoplasmal contamination, research results could be distorted and hence erroneous and in a production facility infection could reduce yields of products such as monoclonal antibodies and enzymes.

As a strategy to prevent and control bacterial and mycoplasmal contamination the use of antibiotics in routine cell culture should be avoided wherever possible because they may mask mistakes in aseptic technique and quality control and may also result in the emergence of antibiotic-resistant strains of microorganisms. In any case there is not a single antibiotic which is effective against all bacteria. For example, the inhibitors of peptidoglycan synthesis such as the penicillins and cephalosporins, are clearly ineffective against mycoplasmas, and many antibiotics simply retard or inhibit bacterial growth, that is, they are bacteriostatic agents and do not destroy bacteria. The absence of antibiotics is also a requirement for effective mycoplasmal detection in cell culture. Thus, to summarize this brief background survey of mycoplasmas, it is necessary to perform routine screening for mycoplasmal contamination because mycoplasmas may not cause readily apparent changes in cell culture.

Several direct and indirect procedures are currently used to detect mycoplasmas, but unfortunately, there is not a single, foolproof test that will detect all species. One major problem that has to be addressed in the screening program is the fact that some mycoplasmas will not grow in artificial media and thus must be detected using a cell culture system. The lengthy time required to complete these assays has focused attention on some of the indirect assays, and it is possible that PCR reactions may gain acceptance for these situations, for example, the screening of cells used for *ex vivo* therapies mentioned previously, where a rapid assay is critical. Direct culture methods are the most sensitive but are also the most time-consuming and take up to 28 days for incubation.

Alternative methods for detecting mycoplasmal contamination include PCR reactions, indirect culture methods using DNA fluorochrome stains as described later, DNA probes, ELISAs, biochemical assays, and electron microscopy (87–89). These methods are more rapid than direct assays but less sensitive and vary in their capacities to detect a wide range of species. A thorough review is beyond the scope of this chapter, but readers are referred to a recent publication that details molecular and diagnostic procedures in mycoplasmology, for example, detection by

PCR (90). In points to consider in the characterization of cell lines used to produce biologicals issued by CBER (17), tests for the presence of both cultivable and noncultivable mycoplasmas are recommended. Biological products made in insect cells should be tested for both mycoplasmal and spiroplasmal contamination. If storage is required for samples before assay, then it should be at between 2 and 8°C for 24 h or less and at −60°C or lower for 24 h or more. As specified by CBER (17), mycoplasmal contamination testing must be performed by both the agar and broth media procedures and the indicator cell culture procedure or by a procedure demonstrated to be comparable using the protocols described here.

8.8.1 Cultivation Methods

8.8.1.1 Agar and Broth Procedures

1. Each lot of agar and broth medium should be free of antibiotics, although penicillin G can be present, and each lot of medium should be checked for its mycoplasmal growth-promoting properties. This requires the use of positive cultures that are described below.
2. Inoculate at least 0.2 mL of the sample over the surfaces, of two or more agar plates of one medium formulation. In addition inoculate at least 10 mL of the sample into a flask containing 50 mL of broth medium which is then incubated at 36 ± 1°C.
3. Test 0.2 mL of the broth culture on the third, seventh, and fourteenth days of incubation by subculture onto two or more agar plates of the same medium as that used before.
4. Incubate two of the initial isolation plates and two each of the three subculture plates in 5–10% CO_2 in a nitrogen atmosphere containing no less than 0.5% oxygen during the incubation period. Some laboratories incubate the cultures both aerobically and anaerobically.
5. Incubate all culture agar plates for at least 14 days at 36 ± 1°C, and observe microscopically at 100× magnification for growth of mycoplasma colonies.
6. As positive controls, at least two known mycoplasma species or strains should be used, one of which is a dextrose fermenter, that is, *M. pneumoniae* strain FH or equivalent, and the other an arginine hydrolyzer, that is *M. orale* strain CH 192999 or equivalent species or strains. These positive strains should not be more than fifteen passages from isolation and should be used in a standard inoculum of 100 colony-forming units (CFU) or less. Sterile mycoplasma broth is used as the negative control.

8.8.1.2 Indicator Cell Culture Procedure.

This procedure uses a Vero cell culture known to support the growth of appropriate mycoplasmas. Figure 8.3 illustrates the typical fluorescent pattern observed with normal and mycoplasma-contaminated cultures.

1. Inoculate at least 1 mL of the sample onto two or more indicator cell cultures grown on cover slips, in dishes, or equivalent containers.
2. Incubate the cell cultures for 3–5 days at 36 ± 1°C in 5% CO_2, and then examine by epifluorescence microscopy following staining with a DNA-binding fluorochrome.
3. As positive controls, *M. hyorhinis* strain DBS1050 and *M. orale* strain CH 19299 are recommended using an inoculum of 100 CFU or less.

8.8.1.3 Enhanced Cell Culture Procedure.

Some laboratories employ an enhanced procedure when a test sample interferes with the performance of the direct Vero cell culture assay. Test samples, negative control, and a positive control, that is, *M. hyorhinis*, are inoculated into cultures of Vero cells. T25 flask cultures are appropriate, and the flasks are incubated for 3–5 days. The cells are then removed, and 0.2 mL of each of the cultures is inoculated into each of six wells of Vero cells and then incubated and examined as described in the direct cell culture assay. In evaluating these assays, a sample is considered to meet the requirements of the test for the presence of mycoplasma if mycoplasma, growth does not appear in the sample of inoculated media. In addition all positive cultures must demonstrate appropriate growth, and in all negative cultures growth must not be detected.

8.8.2 Indirect Detection of Mycoplasmas

The direct assays described before are probably beyond the scope of most small cell culture facilities although large production facilities may perform these assays in-house. In contrast some of the indirect assays now available can be performed by any operator because they are available in kit form. An outline of just one of these methods is included here, but a range of indirect methods including PCR reactions is being developed and evaluated.

8.8.2.1 Mycoplasmal Detection using the Gen-Probe System.

This system uses a ^{3}H-labeled DNA probe homologous to mycoplasmal, acholeplasmal and spiroplasmal rRNA. The manufacturers (Gen-Probe Inc.) claim that all species that commonly infect cell cultures can be detected with this probe, which targets the rRNA of the organisms to form a stable RNA to DNA labeled hybrid. The latter

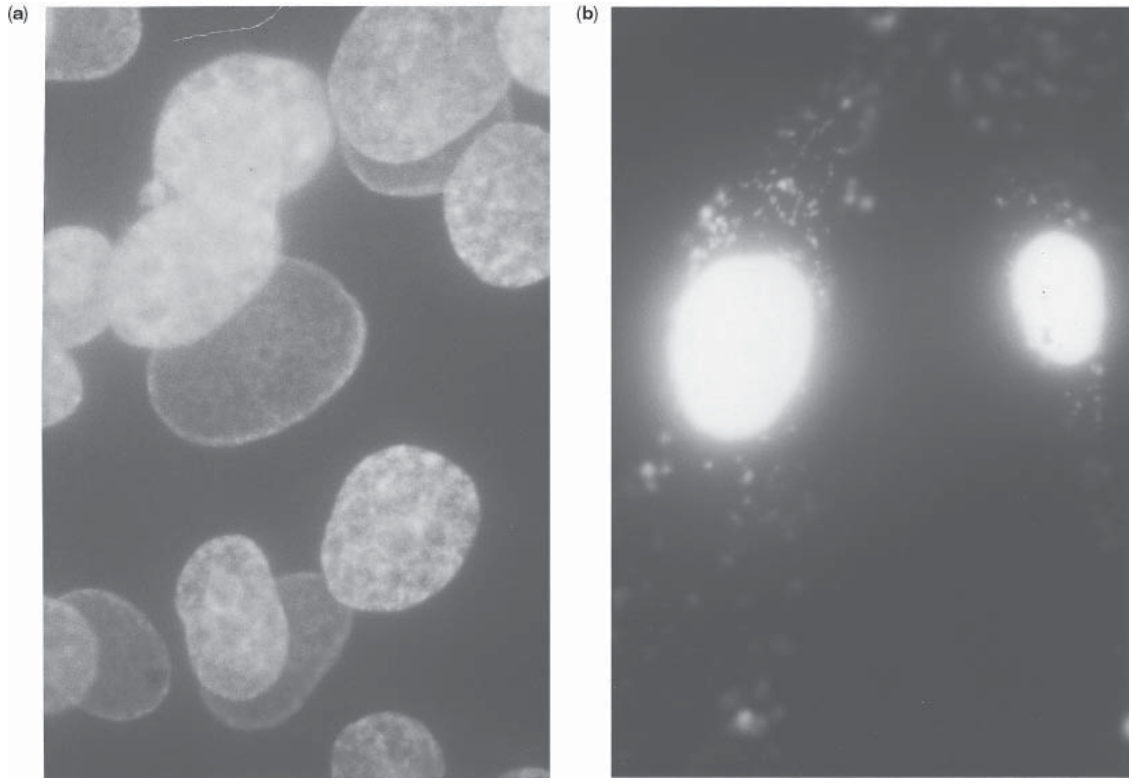


Figure 8.3. Detection of mycoplasmal infection by DNA fluorochrome staining. (a) Cells free of mycoplasmal contamination display only nuclear fluorescence. (b) Cells contaminated with mycoplasma display both nuclear and extranuclear fluorescence.

is separated from a nonhybridized DNA probe using hydroxyapatite, and then the amount present is measured in a scintillation counter. Following is the recommended test procedure:

1. Prepare a background count [in counts per minute (cpm)] on 5 mL of the scintillation fluid used in the scintillation counter programmed to an appropriate parameter to measure ^{3}H activity.
2. Perform a total count determination, that is, the activity of the labeled probe solution, by pelleting a 5 mL suspension of the separation mixture at 500*g* for 1 min (hydroxyapatite in a buffered solution provided in the kit) in a screw-capped scintillation vial. The supernatant is discarded, the pellet is vortexed in 50 μL of the probe solution, and the cpm is determined.
3. Microfuge the test samples, for example, 1.5 mL aliquots of antibiotic-free cell culture medium (in which the test cultures have been grown for a minimum of 3 days), at 12,000*g* for 10 min to pellet any mycoplasmas present.
4. Discard the supernatants, and resuspend the pellets in 200 μL of the probe solution. In addition, prepare positive and negative controls by vortexing 50 μL each of the control solutions provided in the Gen-Probe kit with 200 μL of probe solution.
5. Incubate the preparations overnight at 72°C. Aliquot 5 mL of resuspended suspension into the required number of scintillation vials, and then transfer 200 μL aliquots of incubated sample plus probe solution to the scintillation vials containing the 5 mL of separation solution. Thoroughly mix the solutions by vortexing, and incubate at 72°C for 5 min.
6. Briefly vortex the vials, centrifuge for 1 min at 500*g*, and remove and discard the supernatants. Wash the pellets, reincubate, wash again, centrifuge for 1 min at 500*g*, and remove the supernatant. Rewash the pellets.
7. Add 5 mL of scintillation fluid to each vial, and resuspend the pellets by vortexing. Stand the vials at room temperature for 5 min to minimize background phosphorescence, and then measure ^{3}H activity as described before.

8. The percentage of hybridization of the sample to the probe DNA is

$$\%\text{hybridization} = \frac{\text{Sample cpm} - \text{background cpm}}{\text{Total count cpm}} \times 100\%$$

Controls:

- % hybridization of positive should be >30%;
- % hybridization of negative should be <0.2%.

Providing that the controls are within acceptable limits, a hybridization result of >0.4 is considered positive. This method provides a rapid assessment of mycoplasmal contamination and appears to correlate well with direct culture results which should be used as the gold standard for these indirect assays. The Gen-Probe® system has been used successfully by researchers in the Sydney laboratory, as reported by Thompson (91).

8.9 BACTERIA AND FUNGI

The effects of bacterial and/or fungal contamination on cell culture systems have been long recognized and are well documented in numerous other publications. The risks of such contamination can be reduced by employing rigorous aseptic techniques and using appropriate and regularly maintained and validated equipment, for example, regularly monitoring the performance of all HEPA laminar flow cabinets. Contamination does occur, however, despite the precautions, and thus the kind of protocols for sterility testing recommended by the USA 21 Code of Federal Regulations (92) should be performed regularly on appropriate specimens. The protocol described is applicable to single, bulk, or final product with the recommendation that bulk material should be tested separately from final material and material from each final container should be tested in individual test vessels as follows:

1. Samples are cultured in a fluid thioglycollate medium (THIO) and a soybean-casein digest medium (TSB). Some manufacturers of biologics adopt a more comprehensive approach to sterility testing and also include other media, such as peptone yeast glucose broth and Saboraud dextrose agar slants.
2. The amount of sample tested depends on the nature of the test material. As a guideline, samples from bulk material should be representative of the bulk and be not less than 10 mL. For sterility testing of final containers, it is recommended that samples from at least 20 final containers be taken for each medium used. The volume tested is the entire contents of the final container if it is less than 1 mL and, if 1 mL or greater, then the volume tested should be the largest single dose recommended by the manufacturer or 1 mL, whichever is larger, but not more than 10 mL.
3. Incubate tests using THIO at 30–35°C for no less than 14 days, and examine visually for evidence of growth on the third, fourth, or fifth day, on the seventh or eighth day, and on the last day of the test period. Incubate tests using TSB at 20–25°C, and inspect as described for THIO. If the medium is rendered turbid by the inoculum, thus interfering with visual inspection for microbial growth, then at least 1 mL of the test medium is transferred to additional containers of the medium. It is standard practice to test replicate sets of two tubes of each medium.
4. Positive control strains, for example, *Bacillus subtilis* (ATCC 6633) and *Bacteroides valgatus* (ATCC 8482) for THIO and *Candida albicans* (ATCC 10231) for TSB are used at inoculum levels of less than 100 CFU/inoculum. The viability and purity of these organisms should be verified regularly. A negative control of uninoculated medium serves as the negative control. USP 23 (93) provides more detailed information regarding the nature of the control cultures that should be used in sterility tests, including description of alternative tests, for example, membrane filtration, for samples not readily water soluble.

8.10 OXYGEN UPTAKE RATE

In large-scale cultivation of cells, several parameters can be used to monitor cell growth and metabolism, including oxygen uptake rate (OUR), Eh, pH, glucose uptake, lactate production, glutamine uptake, NH_3 accumulation, and levels of intracellular nucleotide pools. The major limitation is the type of test available to detect the chosen parameter. Recent developments have led to the availability of more on-line detectors, for example, glucose biosensors, which provide a rapid check on the culture condition, and these now augment oxygen and pH probes which have been the major indicators of cell viability and growth to date. For example, in vaccine manufacture the viral infection of some cell types can be monitored by following OUR, which correlates with viral infection (94) because cells have an increasing or constant OUR, during the growth and production phases whereas the OUR drops after viral infection. In a cell culture system contaminated by an aerobic organism, the OUR can increase significantly, whereas the oxygen levels monitored by the oxygen probe often fall to undetectable levels. Thus microbial contamination can often be quickly detected by reference to oxygen levels in the culture, providing that the probes have been calibrated properly. In

addition, pH levels usually fall significantly as a result of lactate production by the microbes, and this can be detected by the pH probe or the rapid change of color of the pH monitoring dye if present in the medium.

8.11 ENDOTOXIN DETECTION

Although endotoxins are not infectious agents, they are derived from the lipopolysaccharide cell wall component of Gram-negative bacteria and could be present even in the absence of viable bacteria. If endotoxin, is present in a therapeutic product administered parenterally, it can induce fever and possibly shock in the recipient. Thus endotoxin testing is incorporated as part of the safety testing protocol of final products. The testing procedure involves either monitoring the rectal temperature of rabbits following injection of a standard amount of product per kilogram of rabbit or using an *in vitro* test known as the *LAL test* in which the lymph material of the horseshoe crab is gelled in the presence of endotoxin. It has been our experience that if endotoxin is present in the cell culture media, it can affect the growth and viability of cell cultures and should always be borne in mind if cells are not growing as expected. This problem can be avoided by using water suitable for injection, which has been pretested for endotoxin, to prepare media if in doubt about the useful water supply.

8.12 STATISTICAL ANALYSIS

In the context of this chapter, statistical analysis of viral contamination in a sample can be at two extremes. First, when assaying raw material or a cell line, the contaminant, if present, is in low amounts and therefore may not be detected. Second, when performing process validations, high titers of virus are spiked into a downscale version of the process, and samples are collected at the start, during, and after processing, and then are assayed for virus titer. Therefore samples generated from process validations can contain high levels of virus or have virus titers close to or below the detection level of the assay. Calculation of virus titers at low concentrations (e.g. in the range of 10–1000 infectious particles per liter) can be made by estimating the minimum detectable level (mdl), whereas estimation of virus titers in samples containing high titer loads can be made by the $TCID_{50}$ assay.

8.12.1 Minimum Detectable Level

There is a discrete probability that a sample that contains a low concentration of virus will produce a negative result when assayed in tissue culture because of random distribution of virus particles and the fact that the sample tested is usually much smaller than the volume available, for example, only a few milliliter sample from 100 to 200 L fermenters is assayed for viral contaminants by *in vitro* assays. The probability P that a sample is negative for viral contamination can be calculated using the following formula:

$$P = \left[\frac{(V - v)}{V}\right]^n$$

where P is the probability that the sample contains no infectious virus, V is the total volume of the material, v is the sample volume, and n is the absolute number of virus particles statistically distributed in V.

When V is much greater than v, the formula can be approximated by the Poisson distribution as

$$P = e^{-cv}$$

where c is the virus titer per unit volume and v is the sample volume.

This equation becomes the following by natural logarithmic (In) conversion:

$$\ln P = -cv$$

or

$$c = \frac{-\ln P}{v}$$

The probability P that the sample is free of virus is normally set at 0.05 or 0.02, that is, in 5% and 2% of cases, respectively, a false-negative result will be obtained; in other words there are 95% or 98% confidence limits, respectively, that the detection limit calculated is correct. Thus, in a sample where virus has not been detected, a minimum detectable limit (mdl) with a set confidence level can be calculated. The following example illustrates the formula

In a solvent detergent process validation study, 450 mL of material was spiked with 50 mL of enveloped virus. One milliliter of the resultant material was assayed for virus, but virus was not detected. By using the above formula and applying a confidence level of virus detection of 98%, the following can be calculated:

$$c = \frac{-\ln P}{v}$$

$$\Rightarrow \quad c = \frac{-\ln 0.02}{1 \text{ mL}}$$

$$\Rightarrow \quad c = 3.9 \text{ virus particles/mL}$$

The mdl of virus in the sample, therefore, is 3.9 virus particles/mL.

The mdl of virus in the process sample, therefore, is

$$\begin{aligned} &3.9 \times \text{total sample volume} \\ \Rightarrow\ &3.9 \times 500\,\text{mL} \\ \Rightarrow\ &1950 \text{ virus particles.} \end{aligned}$$

8.12.2 Quantitation of Virus by $TCID_{50}$

The $TCID_{50}$ (tissue culture infectious dose, 50) is a standard method for infectious virus quantitation defined as the dilution of sample at which 50% of the replicate cell cultures inoculated with the sample become infected. The assay involves serial dilution of a sample and inoculation of equivalent volumes of each dilution onto replicate monolayers of tissue culture cells sensitive to the virus being assayed. At the assay end point, the inoculated cultures are scored as positive or negative for viral infection. In practice, this method involves serial dilution of the sample through an appropriate medium, for example, maintenance medium or PBS, at a dilution factor of normally 3, 5, or 10, and inoculation of a given volume (e.g. 100 μL) into replicate wells of a multiwell plate (e.g. 96-or 24-well plate with eight wells inoculated per dilution). The accuracy of this method can be increased by increasing the numbers of replicate wells inoculated at each dilution and by decreasing the dilution factor. Several formulas may be used to estimate the virus titer in samples assayed by this method, but the method most commonly used is that of Karber expressed by the following equation (95):

$$-m = \log_{10}\text{starting dilution} - \left[\sum p - 0.5\right] \times d$$

where m is the $\log_{10}TCID_{50}$ (per unit volume inoculated per replicate culture), d is the $\log_{10}$ dilution factor, and p is the proportion of wells positive for viral infection.

Thus, in the data shown in Table 8.4, using a fivefold dilution factor, eight replicate wells, and an inoculum volume of 0.1 mL per well, the $TCID_{50}$ can be calculated as follows:

$$\begin{aligned} -m &= -0.7 - (4.875 - 0.5) \times 0.7 \\ -m &= -3.76 \\ TCID_{50} &= 10^{3.76}/0.1\,\text{mL} \end{aligned}$$

Because the value calculated by the Karber formula is a statistical estimate of the titer, the standard deviation s of the $TCID_{50}$ can be calculated using the following equation:

$$s = \sqrt{d}^2 \sum \left[\frac{p1(1-p1)}{(n_1 - 1)}\right]$$

where d is the $\log_{10}$ dilution factor, $p1$ is the observed rate of the reaction, and n_1 is the number of test cultures per dilution.

Therefore, for the example given in Table 8.4, s can be calculated as

$$\begin{aligned} s &= \sqrt{0.49} \times 0.422/7 \\ s &= 0.17 \end{aligned}$$

Using this value for the standard deviation s, the 95% confidence limits can be approximated as $2 \times s$, that is, 0.34.

Calculation of virus titers by these methods is recommended by regulatory authorities for evaluating process validation studies (24). By quantitating virus titers in spiked starting material and processed material by $TCID_{50}$ assay (or mdl calculations for those processes sample with no detectable virus), an estimate of the ability of the process to remove and/or inactivate viruses can be made by the following equation:

$$R = \log_{10}\frac{V_1 \times T_1}{V_2 \times T_2}$$

where R is the reduction factor, V_1 is the volume of starting material, T_1 is the concentration of virus in the starting material, V_2 is the volume of processed material, and T_2 is the concentration of virus in the processes.

TABLE 8.4. Data Used to Calculate $TCID_{50}$ by the Karber Formula

Log Dilution	No. of Positive Wells	Proportion of Wells Positive	Rate of Reaction $[p1(1-p1)]$
−0.7	8	1	0
−1.4	8	1	0
−2.1	8	1	0
−2.8	8	1	0
−3.5	5	0.625	0.234
−4.2	2	0.25	0.188
−4.9	0	0	0
−5.6	0	0	0
		$\sum p = 4.875$	$\sum p1(1-p1) = 0.422$

The 95% confidence limit of the reduction factor can be calculated by the following equation:

$$\pm\sqrt{(s^2 + a^2)}$$

where s is the 95% confidence limit for the titer of virus in the stating material and a is the 95% confidence limit for the titer of virus in the processed material.

8.13 DETECTION OF PRIONS

In recent decades a previously unknown mechanism of disease has been described in humans and animals. Several fatal neurodegenerative diseases, including scrapie in sheep, BSE in cattle, and CJD in humans, are now thought to be caused by the accumulation of a post-translationally modified cellular protein (15,16). CJD may present as a sporadic, genetic, or infectious illness. In the theory proposed by Prusiner, prions are described as transmissible particles that are devoid of nucleic acid and are composed exclusively of a modified protein (PrP^{Sc}). The normal, cellular prion protein (PrP^{c}) is converted to PrP^{Sc} through a post-translational process involving a conformational change whereby the α-helical content decreases while the β-sheet content increases, leading to significant changes in properties. For example, PrP^{c} is soluble in nondenaturing detergents, whereas PrP^{Sc} is not, and PrP^{c} is easily degraded by proteases, whereas PrP^{Sc} is partially resistant. Stanley Prusiner recently received a Nobel prize for his prion studies, and investigations earlier by Carlton Gadjusek led also to the award of a Nobel prize for demonstrating that the neurodegenerative disease known as Kuru found in the Fore people of New Guinea was transmitted from person to person by ritualistic cannibalism and is now recognized as a prion disease (96). Cases of horizontal transmission of CJD were reported in 1974 by Duffy *et al*. (97) who were the first to draw attention to the iatrogenic transmission of CJD following the development of CJD in the recipient of a corneal transplant from a donor who had died from rapidly progressive dementia. Since then, other mechanisms of iatrogenic transmission have been recognized, including contaminated neurosurgical equipment, dura mater homografts, and therapy with human cadaveric pituitary hormones. It is now thought that ~100 deaths worldwide have been caused by growth hormone derived from contaminated pituitary glands (98), and four deaths are associated with the use of pituitary gonadotrophins which appears to be unique to Australia (99). The pituitary hormone program was ended in the mid-eighties following the first reports of deaths, but cases continue to occur after longer and longer incubation periods following exposures that occurred mainly in the 1970s. Another mechanism of CJD transmission was proposed in 1996 by Will *et al*. (100) who reported the deaths of patients who were unusually young for classical CJD and had clinical and neuropathological features different from sporadic CJD; they suggested that it is caused by a novel variant of CJD derived from BSE.

Further cases since then appear to confirm that human disease can be caused as a result of bovine prions passing from BSE or "mad" cows to humans through the consumption of contaminated beef products. This prion disease has been named *new variant* or *variant CJD* (nvCJD or vCJD). This finding, if true, has serious implications for human health in general, particularly in the United Kingdom where "mad cow" disease has had its greatest effect, but it also has enormous ramifications for cell culture practices because bovine-derived products such as serum, transferrin and insulin have long been used to cultivate cells. It is now recognized that strategies designed to reduce the risk of prion transmission via cell culture technology will need to be developed and hence this summary of the prion issue in this chapter.

The prion problem has already impacted on the biologics industry in the United Kingdom where in early 1998 the Government announced that it would impose a ban on the use of all UK-derived human plasma for producing plasma-derived biologics such as albumin, immunoglobulins, and coagulation factors. Although plasma is seen as a very low risk material for transmitting prions because there has not been a case reported to date of CJD transmission via either blood transfusion or blood products, an extremely cautious approach has been taken until more is known about the infectivity of the vCJD agent. It is thought that because the agent has passed from sheep to cows by feeding cows with meat and bone meal derived from scrapie-infected sheep, and then passed to humans, it may have increased virulence if transmitted via biologics derived from humans compared to classical CJD, or perhaps a different distribution within the body leads to a higher level of variant prions in the blood and hence plasma. Until a highly sensitive and reasonably rapid test becomes available for detecting prions, the only strategy available to ensure that biologics are as safe as possible is to avoid using, wherever possible, material likely to be contaminated with bovine, vCJD, and CJD prions. For example, process materials derived from bovine sources, such as Tween 80 used for inactivation of enveloped viruses in the processing of some plasma products, should be replaced by material from nonanimal sources. In addition, excipients, such as albumin, which are often added to stabilize labile biologicals in final products should not be used if there is a risk that they may be contaminated with prions.

The implications for cell culture technology arising from BSE are clearly serious and an international meeting in 1998 under the auspices of the Council of Europe was largely devoted discussing of the prion issue (101). In

summary, the majority opinion from the meeting was to avoid bovine-derived materials for use in cell culture, wherever possible, and in those situations where serum or protein-free culture was not possible, for example, the use of normal cell lines for vaccine production, to use bovine serum from BSE-free areas such as New Zealand, Australia, and the United States and to ensure that the respective government agencies employ a rigorous program to guarantee that particular herds of cattle are disease-free and that pooling or mixing of different serum batches is not allowed. In addition to avoiding the use of contaminated raw materials, it is also necessary to introduce, if possible, measures designed to remove prions from biologics because inactivation is not an option because prions are extremely resistant to physicochemical processes and require sequential treatment of at least 1 h in the presence of 1 M NaOH followed by autoclaving at 121°C to inactivate them (102,103) and an appropriate assay. This brief background to the prion issue has hopefully justified the need for a section on prion assays and demonstrated why this is currently an area of intense investigation.

8.13.1 Prion Assays

8.13.1.1 In Vivo Assays. Prions can be detected *in vivo* by bioassays in susceptible laboratory animals. The practical use of bioassays is restricted due to the existence of a species barrier and long incubation times (several years) for most prion isolate/host combinations. Until recently, it was only possible to work with scrapie prions derived from sheep because this is the only prion material available in plentiful supply. Thus purification processes used to manufacture biologics could be assessed for their capacity to remove scrapie prions following spiking of starting material with large doses of scrapie in scale-down models of the large-scale process. The levels of scrapie prions remaining at different stages of the process are assessed by inoculating specimens into either mice or hamsters. Mouse adapted strains, either ME7, with a 200– to 400-day incubation period, or 22A, with a 300–500 day incubation period, and hamster adapted scrapie, 263 K with a 90– to 200-day incubation period, are the agents which have been used to date for spiking studies. There are clearly disadvantages with assays which generally take >200 days to complete even though they are highly sensitive. The hamster assay is faster than the mouse, assay but housing costs are higher for hamsters with the outcome that the costs for both assays are similar but high. Another major problem is that these studies must assume that the scrapie prion will have properties similar to vCJD and CJD prions, and this is unknown at present. Alternative systems are becoming available, including a mouse-adapted BSE strain for validations and transgenic mice with high levels of expression of human, bovine, or chimeric prion protein (PrP) genes which have an abrogated species barrier and significantly shorter incubation times for prions, compared with natural wild hosts. Thus it is now just becoming possible to quantify prions accurately in the brain and other organs of patients with CJD and cattle with BSE.

8.13.1.2 In Vitro Assays. Because of the high cost and durations of *in vivo* tests they are not appropriate for use in routine screening assays although they will serve as the gold standard by which all *in vitro* tests are assessed for sensitivity and specificity. At present PrP^{Sc} is the only known disease-specific diagnostic marker, and immunoassays have been developed to detect this marker using monoclonal antibodies. This is an area of intense research at present and without doubt rapid advances will occur over the next few years. Currently, Western blotting is the most common method of assay usually involving the following steps:

1. Ultracentrifuge the sample to concentrate the specimen.
2. Perform a protease *K* digest using a method in which the concentration of protease kinase has been optimized to reduce background staining.
3. Denature the preparation, dilute to the end point, and analyze all dilutions by Western blotting.

This assay relies on detecting the protease resistant form of PrP^{Sc} which has been shown to correlate with infectivity. The maximum sensitivity of the assay is $\sim 10^2 - 10^3$ IU, which is less sensitive than the bioassay, but the assay is rapid and cost-effective. At present, immunoassays are limited by the lack of monoclonal antibodies that are effectively specific for the PrP^{Sc} protein and the lack of reagents that can detect the presence of PrP^{Sc} in very low levels in the presence of normal prion PrP. A new assay, DELFIA (a dissociation enhanced lanthanide fluoroimmunoassay), appears to be the most sensitive assay developed to date because it claims that it detects a single infectious unit. At present protease digestion is still required, but it is anticipated that the introduction of reagents that can distinguish between PrP^{c} and PrP^{Sc} will obviate the need for this procedure.

8.14 SUMMARY

This chapter demonstrates that, in some situations at least, the lessons of history can be learned and thus influence current thinking and practices. The problems of virus contamination associated with the initial polio vaccines derived from primary monkey kidney cells described briefly in the historical introduction to this chapter were a major driving force in establishing the comprehensive range of

screening procedures outlined in other sections. These measures have made a major contribution to the excellent safety record for the therapeutic use of biologics derived from mammalian cell culture technology. One cannot be complacent, however, because, as also described in this chapter, new infectious agents continue to be discovered, such as prions, that are considered responsible for BSE and nvCJD and porcine endogenous viruses (PERV). The rapid scientific response to the PERV problem, as measured by the research papers published since 1997 describing highly specific and sensitive assays for detecting these agents (104,105), is reassuring in that it provides evidence that this area of infectious diseases is recognized as important and that the capacity exists for appropriate action in terms of technologies and personnel. These developments augur well for the continued successful screening of cell culture contamination although vigilance is still essential because a new challenge, according to historical precedent, is bound to emerge. The rapid developments in *ex vivo* cell therapies and xenotransplantation involving the use of organs, tissues, or primary cells are a real challenge with regard to the transmission of infectious agents and will clearly need close scrutiny, using protocols described in this chapter, as clinical use of these procedures increases.

REFERENCES

1. J.F. Enders, T.H. Weller, and F.C. Robbins, Science 109: 85–87 (1949).
2. J.E. Salk, Am. J. Public. Health 45: 151–162 (1955).
3. A.B. Sabin, JAMA 164: 1216–1223 (1957).
4. K. Shah and N. Nathanson, Am. J. Epidemiol. 103: 1–12 (1976).
5. B.H. Sweet and M.R. Hilleman, Proc. Soc. Exp. Biol. Med. 105: 420–427 (1992).
6. L. Hayflick and P.S. Moorhead, Exp. Cell Res. 25: 585–621 (1961).
7. J.P. Jacobs, Nature (London) 227: 168–170 (1970).
8. N.B. Finter and K.H. Fantes, in I. Gresser, ed., Interferon, Vol. 2: Academic Press, London, 1981, p. 65–80.
9. S.E. Builder *et al*., in R.E. Spier, J.B. Griffiths, J. Stephenne, and P.J. Crooy, eds., Advances in Animal Cell Biology and Technology for Bioprocesses, Butterworth, Guilford, U.K., 1989, p. 452.
10. R.A. Weiss, N. Engl. J. Med. 307: 1587 (1982).
11. P. Carthew, J. Gen. Virol. 67: 963–974 (1996).
12. C. Harbour and G. Woodhouse, Cytotechnology 4: 3–9 (1990).
13. C. Patience, Y. Takeuchi, and R.A. Weiss, Nat. Med. 3: 282–286 (1997).
14. R.A. Weiss, Nature (London) 391: 327–328 (1998).
15. S.B. Prusiner, Science 252: 1515–1522 (1991).
16. S.B. Prusiner, Science 278: 245–251 (1997).
17. Center for Biologicals Evaluation and Research, Points to Consider in the Characterization of Cell Lines Used to Produce Biologicals, U.S. Food and Drug Administration, Bethesda, Md., 1993.
18. International Committee for Harmonization Topic Q5A, Notes for Guidance on the Quality of Biotechnological Products: Viral Safety and Evaluation of Biotechnology Products Derived from Cell Lines of Human or Animal Origin (CPMP/ICH/295/95). 1997.
19. Center for Biologicals Evaluation and Research, Points to Consider in the Manufacture and Testing of Monoclonal Antibody Products for Human Use, U.S. Food and Drug Administration, Bethesda, Md., 1997.
20. Committee for Proprietary Medicinal Products, Production and Quality Control of Monoclonal Antibodies. (CPMP approved 13 December 1994. Doc. III/5271/94). European Commission, Brussels, 1995.
21. World Health Organization, Requirements for Use of Animal Cells as in vitro Substrates for the Production of Biologicals (Requirements for Biological Substances No. 50). WHO Expert Committee on Biological Standardization, WHO, Geneva, 1997.
22. Center for Biologics Evaluation and Research, Points to Consider in Human Somatic Cell Therapy and Gene Therapy. U.S. Food and Drug Administration, Bethesda, Md., 1991.
23. Center for Biologics Evaluation and Research, Addendum to Points to Consider in Human Somatic Cell and Gene Therapy, U.S. Food and Drug Administration, Bethesda, Md., 1991. Human Gene Therapy. 7, 1181–1190, (1996).
24. Committee for Proprietary Medicinal Products, Notes for Guidance on Virus Validation Studies: The Design, Contribution and Interpretation of Studies Validating the Inactivation and Removal of Viruses (CPMP/BWP/286/95) 1996.
25. Medicines Control Agency, Rules and Guidance for Pharmaceutical Manufacturers, H.M. Stationery Office, London, 1997.
26. Organization for Economic Co-operation and Development, Principles of Good Laboratory Practice, OECD Environmental Health and Safety Publications, Environment Directorate, Paris, 1998.
27. M. Dinowitz, Y.S. Lie, and M.A. Low, Dev. Biol. Stand. 76: 201–207 (1992).
28. J. Hotta and P.C. Loh, J. Gen. Virol. 68: 1183–1186 (1987).
29. M. Schweizer *et al*., Virology 192: 663–666 (1993).
30. N. Teich, D.R. Lowy, J.W. Hartley, and W.P. Rowe, Virology 51: 163–173 (1973).
31. D.R. Lowy, W.P. Rowe, N. Teich, and J.W. Hartley, Science 174: 155–156 (1971).
32. J.C. Olsen and J. Sechelski, Hum. Gene Ther. 6: 1195–1202 (1995).
33. R. Schuurman *et al*., J. Gen. Virol. 72: 2739–2745 (1991).
34. A. Kappeler, C. Lutz-Wallace, T. Sapp, and M. Sidhu, Biologicals 24: 131–135 (1996).
35. E.L. French and W.A. Snowdon. Aus. Vet. J. 40: 99–105 (1964).
36. C. McLean, D. Docherty, and A.J. Shepherd, Eur. J. Parenteral Sci. Biotechnol., Spec. Issue, p. 27–30 (1997).
37. J.S. Porterfield, ed., Andrew's Viruses of Vertebrates, 5th ed., Baillière Tindall, London, 1989.
38. M. Plavsic, Programme and Abstracts, International Conference, Animal Sera, Animal Sera Derivatives and Substitutes used in the Manufacture of Pharmaceuticals: Viral Safety

and Regulatory Aspects, Strasbourg, 1998, Co-organized by European Department for the Quality of Medicines of the Council of Europe and the International Association of Biological Standardization, 1998.

39. J. Kurth *et al*., Programme and Abstracts, International Conference, Animal Sera, Animal Sera Derivatives and Substitutes used in the Manufacture of Pharmaceuticals: Viral Safety and Regulatory Aspects, Strasbourg, 1998, Co-organized by European Department for the Quality of Medicines of the Council of Europe and the International Association of Biological Standardization, 1998.
40. H.A.J.G. Kreeft, I. Greiser-Wilke, V. Moennig, and M.C. Horzinek, Dtsch. Tieraerztl. Wochenschr. 97: 63–65 (1990).
41. G. Wensvoort and C. Terpstra, Res. Vet. Sci. 45: 143–148 (1988).
42. C.H. Lohr, J.F. Evermann, and A.C. Ward, VM/SAC, Vet. Med. Small Anim. Clin. 78: 1263–1266 (1983).
43. R. Harasawa and T. Sasaki, Biologicals 23: 263–269 (1995).
44. R. Harasawa, Vaccine 13: 100–103 (1995).
45. R. Harasawa and T. Tomiyama, J. Clin. Microbiol. 32: 1604–1605 (1994).
46. H. Rabenau *et al*., Biologicals 21: 207–214 (1993).
47. P.F. Nettleton and M.M. Rweyemamu, Arch. Virol. 64: 359–374 (1980).
48. R.L. Garnik, in Development in Biological Standardization. Proceedings of the IABS. International Scientific Conference on Viral Safety and Evaluation of Viral Clearance from Biopharmaceutical Products, Bethesda, Md., 1995, Karger, Basel and New York, 1996.
49. P. Minor, N. Finter, and B. Hughes, in Developments in Biological Standardization. Proceedings of the IABS. International Scientific Conference, on Viral Safety and Evaluation of Viral Clearance from Biopharmaceutical Products, Bethesda, Md., 1995, Karger, Basel and New York, 1996.
50. W.L. Mengeling, in A.D Leman, *et al*., eds., Diseases of Swine, 7th ed., Wolfe Publishing, London, 1992, p. 299–311.
51. D.L. Croghan, A. Matchett, and T.A. Koski, Appl. Microbiol. 26: 431 (1973).
52. Code of Federal Regulations 9. Animal and Animal Products, Part 113.53 Requirements for Ingredients of Animal Origin used for Production of Biologics (1996).
53. European Pharmacopoeia, 3rd ed., Monogr. 0694. 1997. Available from EP Secretariat, BP 907 F6 7029, Strasbourg, Cedex 1, France.
54. M. Senda *et al*., J. Clin. Microbiol. 33: 110–113 (1995).
55. J.A. Levy, Science 182: 1151–1153 (1973).
56. S.J. Froud *et al*., in M.J.T. Carrondo, B. Griffiths, and J.L.P. Moreira, eds., Proceedings of the 14th Meeting of the ESACT, Vilamoura, Portugal, 1996, Kluwer Academic Publishers, Dordrecht, The Netherlands, 1997, p. 681–686.
57. M.A. Sommerfelt and R.A. Weiss, Virology 176: 58–69 (1990).
58. A.J. Shepherd *et al*., Hum. Antibody Hybridomas 3: 168–176 (1992).
59. M. Popovic, V.S. Kalynaraman, M.S. Reitz, and M.G. Sarngadharan, Int. J. Cancer 30: 93–100 (1982).
60. J.J. Hooks and C.J. Gibbs, Bacteriol. Rev. 39: 169–190 (1975).
61. P.N. Blatt, R.O. Jacoby, H.C. Morse, III, and A.E. New, in Methods Virol. 349–388 (1986).
62. A.J. Shepherd and K.T. Smith, Methods Mol. Biol. 9: (in press).
63. D.L. Kacian and S. Speilgelmen, Methods Enzymol. 29: 150–173 (1974).
64. V. Klement, W.P. Rowe, J.W. Hartley, and W.E. Pugh, Proc. Natl. Acad. Sci. U.S.A. 63: 753–758 (1969).
65. R.H. Bassin, N. Tuttle, and P.J. Fischinger, Nature (London) 229: 564–566 (1971).
66. P.T. Peebles, Virology 67: 288–291 (1975).
67. D.K. Haapala, W.G. Robey, S.D. Oroszalan, and W.P. Tsai, J. Virol. 53: 827–833 (1985).
68. S.K. Chattopadhyay *et al*., Virology 113: 465–483 (1981).
69. M.A. Lander and S.K. Chattopadhyay, J. Virol. 52: 695–698 (1984).
70. B. Chesesbro *et al*., Virology 127: 134–148 (1983).
71. G.J. Todaro *et al*., Proc. Natl. Acad. Sci. U.S.A. 70: 859–862 (1973).
72. H.M. Temin and D. Baltimore, Adv. Virus Res. 17: 129–186 (1972).
73. A.B. Maunsbach, in J.E. Celis, ed., Cell Biology: A Laboratory Handbook, Academic Press, San Diego, Califo, 1998, p. 249–259.
74. A. Bremer, M. Haner, and U. Aebi, in J.E. Celis, ed., Cell Biology: A Laboratory Handbook, Academic Press, San Diego, Califo, 1998, p. 277–284.
75. R.A. Killington, A. Stokes, and J.C. Hierholzer, in B.W.J. Mahy and H.O. Kangro, eds., Virology Methods Manual, Academic Press, London, 1996, p. 71–89.
76. Code of Federal Regulations 21. Part 630.35. Test for safety (1996).
77. E.A. Gould and J.C.S. Clegg, in B.W.J. Mahy, ed., Virology: A Practical Approach, IRL Press, Oxford, U.K., 1985, p. 43–78.
78. A.J. Shepherd, in J.H.S. Gear, ed., Handbook of Viral and Rickettsial Hemorrahgic Fever, CRC Press, Boca Raton, Fla., 1988, p. 241–250.
79. N.G. Schmidt and R.W. Emmons, in N.J. Schmidt and R.W. Emmons, eds., Diagnostic Procedures for Viral, Rickettsial and Chlamidial Infections, 6th ed., American Public Health Association, Washington, D.C., 1989, p. 1–36.
80. J.P. Clewley, The Polymerase Chain Reaction (PCR) for Human Viral Diagnosis, CRC Press, Boca Raton, Fla., 1995.
81. P.A. Nuttall, P.D. Luther, and E.J. Stott, Nature (London) 266: 835–837 (1977).
82. P. Tattersall and D.C. Ward, Replication of Mammalian Parvoviruses, Cold Spring Harbor Press, Cold Spring Harbor, N.Y., 1978.
83. J.G. Tully and R.F. Whitcomb, in S. Razin and J.G. Tully, eds., Molecular and Diagnostic Procedures in Mycoplasmology, Vol. I: Academic Press, San Diego, Calif., 1995, p. 137–146.
84. G.J. McGarrity, J. Samara, and V. Vanaman, ASM News 51: 170–183 (1985).

85. A. Smith and J. Mowles, in S. Razin and J.G. Tully, eds., Molecular and Diagnostic Procedures in Mycoplasmology, Vol. 2: Academic Press, San Diego, Calif., 1996, p. 445–451.
86. C.K. Lincoln and M.G. Gabridge, in J.P. Mather and D. Barnes, eds., Animal Cell Culture Methods, Vol. 57: Academic Press, San Diego, Calif., 1998, p. 49–65.
87. G.J. McGarrity, in K. Maramorosch, ed., Advances in Cell Culture, Vol. 2: Academic Press, San Diego, Calif., 1982, p. 99–131.
88. G.K. Masover and F.A. Becker, in S. Razin and J.G. Tully, eds., Molecular and Diagnostic Procedures in Mycoplasmology, Vol. 2: Academic Press, San Diego, Calif., 1996, p. 419–429.
89. C. Veilleux, S. Razin, and L.H. May, in S. Razin and J.G. Tully, eds., Molecular Diagnostic Procedures in Mycoplasmology, Vol. 2: Academic Press, San Diego, Calif., 1996, p. 419–429.
90. S. Razin and J.G. Tully, eds., Molecular Diagnostic Procedures in Mycoplasmology, Vol. 2: Academic Press, San Diego, Calif., 1996.
91. C. Thompson, Ph.D. Thesis, University of Sydney, 1994.
92. Code of Federal Regulations 21. Part 610. 12. Test for the presence of bacteria and fungi (1996).
93. United States Pharmacopeia, Rev. 23. U.S. Pharmacopeial Convention, Rockville, M., 1995, p. 1686–1690.
94. W. Werz, H. Hoffmann, K. Harberer, and J.K. Walter, Arch. Virol. 13: 245–256 (1997).
95. J. Karber, Arch. Exp. Pathol. Pharmakol. 162: 480–483 (1931).
96. D.C. Gajdusek, Science 197: 943 (1977).
97. P. Duffy, J. Wolf, and J. Collins, N. Engl. J. Med. 290: 692–693 (1974).
98. P. Brown, Transfusion 38: 312–315 (1998).
99. S. Collins and C.L. Masters, Med. J. Aust. 164: 598–602 (1996).
100. R.G. Will, J.W. Ironside, and M. Zeidler, Lancet 347: 921–925 (1996).
101. Programme and Abstracts, International Conference, Animal Sera, Animal Sera Derivatives and Substitutes used in the Manufacture of Pharmaceuticals: Viral Safety and Regulatory Aspects, Strasbourg, 1998, Co-organized by European Department for the Quality of Medicines of the Council of Europe and the International Association of Biological Standardization, 1998.
102. D.M. Taylor *et al*., Arch. Virol. 139: 313–326 (1994).
103. D.M. Taylor, K. Fernie, and I. McConnell, Vet. Microbiol. 58: 87–91 (1997).
104. W. Heneine *et al*., Lancet 352: 695–699 (1998).
105. C. Patience *et al*., Lancet 352: 699–701 (1998).

9

CULTURE COLLECTIONS AND BIOLOGICAL RESOURCE CENTERS (BRCs)

DAVID SMITH
CAB International Europe United Kingdom, Egham, United Kingdom

9.1 INTRODUCTION

Culture collections are centers that provide authentic examples of organisms that can be grown or maintained in the laboratory; they normally have a public service role and can provide associated information and services. They can be small and limited in coverage, collected and maintained by single researchers and range through institutional entities to large public service collections covering a broad range of organisms from many sources. They can focus on organism type, for example, fungi or human-derived material and, in some instances, specific genera, on use, for example, industrial enzymes or antimicrobials, on host crops, and they may be linked to a particular sector such as the environment, healthcare, education, or agriculture. Many culture collections have now developed into Biological Resource Centres (BRCs), which give access to high quality biological materials, validated information, and expert services.

9.1.1 Transition toward Biological Resource Centres

The Organisation for Economic Cooperation and Development (OECD) Biological Resource Centre Initiative now defines a Biological Resource Centre (1) as follows:

> Biological Resource Centres are an essential part of the infrastructure underpinning biotechnology. They consist of service providers and repositories of the living cells, genomes of organisms, and information relating to heredity and the functions of biological systems. BRCs contain collections of culturable organisms (e.g. microorganisms, plant, animal, and human cells), replicable parts of these (e.g. genomes, plasmids, viruses, cDNAs), viable but not yet culturable organisms cells and tissues, as well as data bases containing molecular, physiological, and structural information relevant to these collections and related bioinformatics. BRCs should meet the high standards of quality and expertise demanded by the international community of scientists and industry for the delivery of biological information and materials. They should provide access to biological resources on which R&D in the life sciences and the advancement of biotechnology depends.

The OECD BRC initiative to establish the virtual infrastructure Global Biological Resource Centre Network (GBRCN) encourages collections to meet the high quality operational standards required today. In 2007, the results of this seven-year activity were published, *OECD Best Practice Guidelines for Biological Resource Centres* (2). The document delivers the basic rules and best practice as guidance for culture collections. It is intended that BRCs adopt these practices to ensure that users get legitimate and safe access to high quality biological materials and associated information. This best practice brings together the product of decades of research and development. No one single collection can provide the needs of the life sciences and biotechnology. A collaborative approach is necessary with common practices and procedures that allow reproducibility between centers. A global network is under development to improve efficiency by coordinating and driving activities

Upstream Industrial Biotechnology: Expression Systems and Process Development, Volume 1, First Edition. Edited by Michael C. Flickinger.
© 2013 John Wiley & Sons, Inc. Published 2013 by John Wiley & Sons, Inc.

to meet user needs. The BRC has been defined, a global network envisaged, and a capacity building program identified to ensure the functionality of the network and the transition of traditional culture collections to BRCs.

Public service culture collections are charged with several tasks; they are custodians of *ex situ* genetic resources and have a key role to play in their conservation (3). Biologists who collect organisms for their research and publish information on them should deposit key strains in BRCs. This makes them available for confirmation of results and future use in the long term; indeed many scientific journals now require this as a prerequisite to publication. This will aid collections in their major roles of the following:

- the *ex situ* conservation of organisms;
- custodians of national resources;
- provision of living resources to underpin the science base;
- reception of deposits subject to publication;
- safe, confidential, and patent deposit services.

The BRC can support countries establish a means to release the potential of their microbial resources to provide solutions to national economic, environmental, food, and health-care problems and consequently contribute to achieving the Millennium Development Goals. This ambitious agenda for reducing poverty and improving lives can be partially delivered by better management and utilization of biological resources:

- improve livelihoods (Millennium Goal–MG 1);
- provide new sources of food, reduce agricultural losses (MG 2);
- lead to discovery of new drugs and treatments of disease to reduce child mortality and improve maternal health (MG 4, 5, and 6);
- understand and contribute to environmental stability (MG 7);
- develop a global partnership in the conservation and utilization of microbial resources for development (MG 8); and
- resources created from the above can be mobilized to promote gender equality and empower women (MG 3) and achieve universal primary education.

Biotechnology continues to offer a future beyond depletion of our natural resources and can provide a basis for a bioeconomy. More and more natural resource alternatives are being found to provide biofuels, drugs, and neutraceuticals food and beverages. BRCs are knowledge bases necessary to underpin the development of biological based-industries leading to economic development. Research is underpinned by BRCs, an infrastructure that secures the *ex situ* conservation of biodiversity while working in a legal and policy framework to enable access and equitable benefit sharing of biological resources. Collections develop isolation programs, carry out or support organism characterization and screening leading to natural product discovery and added value. Biotechnology is "a global powerhouse with over $60 billion in revenues and hundreds of marketed products, Pharma makes a $6bn spend on candidate compounds with 12% growth each year and Agbio spends $0.6bn" (4). Microorganisms provide an improved route to solutions to several agricultural, environmental, food, forestry, and public health problems, for example, several agents isolated mainly from *Streptomyces* species are in preclinical or clinical development for the treatment of cancer: Rebeccamycin analog (lymphomas and neuroblastoma.); COL-3 (a tetracycline analog) for advanced solid tumors; Bizelesin (a CC1065 analog); UCN-01 (a staurosporine analog); KRN5500 (a spicamycin analog); 17-AAG (17 Allylamino-17-desmethoxy-geldanamycin); and FR 901228 (a bicyclic depsipeptide) (5).

In the field of microbiology and cell culture, there are currently over 520 collections registered with the World Data Centre for Microorganisms (WDCM) and there are countless other collections associated with bioindustry, microbiology laboratories, and research and higher educational establishments (6). A little over 20 WDCM registered collections have some form of independent third-party certification or accreditation to demonstrate the provision of quality services. In other fields, there are similar numbers of collections maintaining other types of biological materials. The OECD Best Practice can be used as a benchmark for culture collections worldwide, and mechanisms to ensure that collections adopt these standards to deliver high quality should be put in place (2). The traditional collection activities are losing pace with technology and user needs, and they require a major shift in their operations and delivery. Advances in molecular biology take authenticity by taxonomy to another level, analytical tools to characterize strain properties are often beyond the reach of the small specialist collections. Access to such expertise and technology might be through partnerships. To achieve access to and utilize the world's biodiversity requires sharing of tasks, and a global network of collections is needed with close links to the user community.

To deliver their services, BRCs preserve their holdings using long-term storage techniques such as cryopreservation and lyophilization depending upon the organism type. Quite often, these techniques require optimization to enable not only survival but also retention of properties. On receipt, a collection should request the depositor to assure that the materials have been collected legitimately and that they are allowed to deposit them. A collection must also have

the expertise and facilities to handle them. There is extensive legislation that impacts upon access to, the safe handling, distribution, and use of biological resources (7–9). A number of culture collection organizations exist to help collections keep up to date in a constantly changing legal framework, notably biosecurity, shipping regulations, and ethical access and use. These include the World Federation for Culture Collections (WFCC) at the global level (10), European Culture Collection Organisation (ECCO) at a regional level (11), and there are several national federations or affiliations.

9.1.2 Sustainability of BRCs

BRCs demonstrate a wide variety of structures and scope, and, consequently, there are differing financial models supporting each. The BRC includes a range of activities directly related to quality control, collection development, and operation that may include opportunities for cost recovery activities. There are the traditional lines of income such as culture supply, identification, and characterization of cultures and private, confidential or patent deposits. Among several potential sources of revenue is the generation of genomics and proteomics data that complement and add value to biological materials themselves. The degree to which such activities may actually provide support sufficient to ensure financial sustainability of a BRC is unproven. However, it is generally expected that most BRCs, whether single larger national centers or smaller distributed or specialized centers, require some degree of core funding by their respective national governments. Other kinds of funding sources include support from industry, grants from agencies that support research, cost recovery through fees-for-service, development of databases, and other tools that compliment the core role of BRCs, and even funding from charitable sources, especially those associated with public health or sustainable development.

As the needs and capacities of individual countries vary, governments should identify collections and centers already capable of or near to being designated as BRCs, and build upon and improve these before starting up new BRCs, especially where resources are limited (1). Similarly, partnerships must be developed among BRCs and appropriate existing agencies, identifying their capacities and interests in terms of support for BRCs. The OECD initiatives ultimate goal is the long-term sustainability of BRCs (1). The OECD task force concluded the following:

- BRCs should be encouraged to coordinate their activities to best serve their essential functions in response to the needs of sectors that depend on their biological resources.
- Governments must be encouraged to provide a baseline of long-term core funding to centers that provide a public service to high standards, to promote their research and development.
- Various foundations and philanthropic or charitable organizations should be asked to extend the level of support.
- Marketable products and services may be developed, including those aimed at meeting regulatory demands and for sale to specialized customers, as long as they do not divert capacity from core activities.
- Industry should be persuaded to take a long-term view of its interests and to offer core support, either through funding or through direct participation in their functioning, provided the latter maintain their independence.

The financial models provided by existing "culture collections" of various types are well recognized and include the following:

- The "General Collection"—often a national/regional facility
  - "popular items" for distribution can guarantee income
  - archive function requires subsidy
- The "specialist collection"—usually more localized
  - the "Institutional Collection"—can provide internal institutional service or wider external community/network service.
  - the "research collection"—provides a service relevant to one or more research interests.

These models vary considerably in the proportion of income derived from the various sources defined below. It must be emphasized, however, that the larger the archiving function carried out for strategic reasons rather than supply, the greater is the need for public and private subsidy.

The OECD Biological Resource Centres Task Force recognized two types of income streams. "Existing" income streams are those that support existing models of culture collections. "Anticipated" income streams represent activities in which BRCs will or may participate and that may generate recoverable income from stakeholders.

9.1.3 Existing Income Streams

- Government support;
- Private industrial support for participation in the functioning of BRCs;
- Private industrial support for internal restricted BRC activities;
- Public and private foundation support;

- Public fundraising;
- Fees for supply of biological resources and technical materials;
- Provision of specialist services and technical consulting expertise;
- Research income (grants and contracts);
- Fees for repository service (safe deposits and patent strain maintenance);
- Provision of technical courses;
- Exploitation of and adding value to genetic resources.

9.1.4 Anticipated Income Streams

- cDNA libraries, genomic libraries, filter sets, clones, plates, PCR products;
- Microarrays and reagents;
- RNAi resources;
- Accreditation/standardization—added value products and services;
- Data storage and retrieval;
- Software development/collaborations—data mining tools;
- Technology development/collaborations—LIMS/robotics;
- Sequence database annotation/phenotypic analysis;
- Linking genomics databases to proteomics;
- MLST (multilocus sequence typing)—population studies.

9.2 CULTURE COLLECTION FUNDING

The World Data Centre for Microorganisms (6) provides key elements of information regarding culture collections, and statistics are summarized annually on the World Federation for Culture Collections (WFCC) website (10). This data demonstrates that governments support 147 of the 525 culture collections registered, which is 20 fewer than 4 years ago, a further 30 (reduced from 33) are semigovernmental, 131 (reduced from 141) are supported by university, 6 are supported by industry, and 18 are private (6, four years ago); over all, the total number of collections have increased by 44 since 2003. It is a fact that availability of governmental funds is reducing, and it is more appropriate that collections should not simply receive core funding but must justify funding by providing services under contract. Collections help meet obligations of governments to the Convention on Biological Diversity and making available biological resources to underpin science, education, and the economy. Collections protect public funding investments in research by preserving the biological materials generated. Government funding is usually balanced against the income received for the various services and products offered by the collection. This leaves very little for investment, to enable the collections to improve their coverage and incorporate new and advancing technologies. Collections need sound and innovative business plans to allow them to keep pace with the ever increasing demands of their users.

The traditional business of collections must be extended by the provision of new products to meet the needs of today's users. Additional products may include DNA, enzymes, metabolites, and other derivatives from authenticated strains. Collections can move beyond this by developing commercial products through the provision of biotechnological solutions through the discovery of active compounds and funding it through public/private investment. The sale of products and services and the delivery of consultancies can be supplemented by research program funding for projects designed to meet donor requirements. The deposit function of collections should also be supplemented by engaging each program funders to protect their investments by paying for deposits in collections and supply of reference strains.

Not only do collections need to find novel ways of funding but they also need to keep abreast and harness new technologies to produce information on the strains, also adding value with the aim to provide today's users with the information they need. Bioinformatics is of increasing importance to the operation of collections and new ways of collecting, storing, analyzing, presenting, and interrogating information are required to make best use of biodiversity information. It is essential, if collections are to survive, that they keep pace with new technologies and user needs, and it is essential that

- BRCs need to function as a strategic, national repository for key academic and industrial research resources, which will in turn provide an income stream.
- Governments and their funding agencies must ensure that products derived from publicly funded research programs are deposited in BRCs as part of the conditions attached to any award.
- BRCs need to provide greater support to researchers in terms of training and advice on standards, quality control, and integrate more with the national activities in key related priority research areas.
- Governments must ensure that infrastructure aspects of the support for research are funded through relevant research programs.
- BRCs must create partnerships with centers of excellence working with and developing new technologies and databases to ensure that linkage is possible

between these leading edge aspects of research and the physical resources held in BRCs.

There is not one financial model that can be applied to all culture collections or BRCs. A combination of governmental funding, income through commercial products and services and research or contract project funding offers the best chance for long-term sustainability.

9.3 OPERATION

BRCs operate to high standards: this includes quality management, compliance with legislation, and, appropriately, the authenticity of biological materials and associated information. The resources a collection provides must meet user needs, be traceable to source, give reproducible performance, and continue to be available over time. BRCs are beginning to publicize their operational management procedures and harmonize their approach by employing common best practices. Here, the World Federation for Culture Collections has provided support with information resources and providing guidance. Full coverage of BRC procedures is presented elsewhere (1,2,7,12); some key elements, long-term preservation, compliance with legislation, quality management, and services provided are presented here.

9.3.1 Preservation of Holdings

The primary objective of preserving and storing an organism is to maintain it in a viable state without morphological, physiological, or genetic change until it is required for future use. Ideally, complete viability and stability should be achieved, especially for important research and industrial isolates. Preservation techniques range from continuous growth methods through to methods that reduce rates of metabolism to the ideal situation where metabolism is suspended (12). Continuous growth techniques involve frequent transfer from depleted to fresh nutrient sources, which initially provide optimum growth conditions; such techniques are not recommended for preservation. The need for frequent subculture can be delayed by storing cultures in a refrigerator, freezer (at -10 to -20°C), under a layer of paraffin oil or in water. Continuous growth techniques are not considered here as they are mainly used for short-term maintenance and they allow deterioration and loss of properties during storage. Drying of the whole cell, propagule, or resting stage of an organism (e.g. spores, cysts, or sclerotia), can be achieved by air drying, in or above silica gel, in soil or sand. Again as such techniques are not always successful and often only allow low numbers of cells to recover; these techniques are not covered here (12).

The methods selected by BRCs must suspend metabolism, which normally involves reducing the water content available to cells by dehydration or cryopreservation. Freeze-drying (lyophilization) is the sublimation of ice from frozen material at reduced pressure and requires storage in an inert atmosphere: either under vacuum or at atmospheric pressure in an inert gas. This technique is not applicable to all cell types. Cryopreservation generally implies storage at temperatures of around -70°C that impede chemical reactions but preferably below -139°C when water structure is normally stable (13). This can be achieved in mechanical deep freezers (some are capable of reaching temperatures of -150°C) or in/above liquid nitrogen (Fig. 9.1).

Desiccation has been used successfully for the preservation of many microorganisms. The removal of water suspends metabolism of the cell. The techniques considered here are freeze-drying and a technique often known as L-drying (12). After a suitable preservation technique is selected and the strains successfully stored, a distribution and seed stock should be kept. An inventory control system should be used to manage stock for distribution and use. After preservation, the viability, purity, and identity should be rechecked and compared with the original results before the culture is made available outside the collection.



Figure 9.1. Cryopreservation in liquid nitrogen. (This figure is available in full color at http://onlinelibrary.wiley.com/book/10.1002/9780470054581.)

The viability, purity, and stability of strains must also be monitored during storage.

No single preservation technique has been successfully applied to all microorganisms, although storage in liquid nitrogen appears to approach the ideal (14). Even this technique can induce changes in physiology, and genetic instability has been observed in some isolates of fungi when suboptimal techniques were applied (15). Preservation protocols often need optimization (16). Organisms that have yet to be cultured in the laboratory, those that require growth on their host, and many delicate organisms can be successfully cryopreserved. In contrast, centrifugal freeze-drying allows only the more robust organisms to survive. In general, it is restricted to some of the microorganisms such as bacteria, fungal spores, viruses, and yeasts. Factors affecting survival are becoming better understood at the subcellular level, but many strains from a wide range of species remain difficult to preserve. Cell growth conditions, suspension media, cryoprotectant, and cooling rates must all be optimized. There is no apparent relationship between survival and taxonomic position, although structure such as thickness and composition of cell wall, volume–surface ratio, and the shape of the cell play an important part; the factors determining survival tend to be strain specific (12). Unfortunately, a preservation method that is satisfactory for one strain of a species may be unsuitable for others. If strain stability is of paramount importance, the choice of maintenance method becomes critical.

Lyo-injury can occur during the cooling and/or drying stages (17). The phase changes encountered during the drying process can cause the liquid crystalline structure of the cell membranes to degenerate to the gel phase, which disrupts the fluid-mosaic structure of the membrane (17). This causes leakage of the membrane, which may culminate in cell damage. Optimal survival can be improved with the use of a suitable lyoprotectant. This medium should be readily available, easy to prepare, and provide protection during the freeze-drying process (i.e. to protect the spores/cells from ice damage during cooling and storage problems such as oxidation). Skimmed milk is a suitable lyoprotectant and is sometimes used in combination with inositol. Saccharides such as trehalose (17,18) protect membranes by attaching to the phospholipids, replacing water and lowering the transition temperature. Other suspending media can be used, for example, Tan *et al*. (18) suggest that a mix of dextran and trehalose improves viability. The recommended final moisture content following drying is between 1 and 2% (w/v). To monitor freeze-drying, a means of measuring vacuum both in the chamber and close to the vacuum pump is required. A pressure rise test can be conducted to determine the end point of the drying process. When the values are equal, water has ceased to evaporate from the material being dried and drying is probably complete. This is confirmed by determining the residual water content, for example, determined by dry weight or by the use of chemical methods (19). The stability of the freeze-dried product is dependent on the stability of the frozen water, a glass, which is the result of the dehydrated lyosolution. The product should be stored below the glass transition temperature, where the solid shifts into the liquid phase.

The technique of centrifugal freeze-drying, which relies on evaporative cooling, can be used successfully for the storage of the bacteria, many sporulating fungi, and yeasts (12). However, this is not a method that can be adapted and changed easily, as it is dependent upon the scope of the equipment. The variety of final freeze-dried product available demonstrates this (Fig 9.2). Optimization of cooling rate to suit the organism being freeze-dried can be applied using a shelf freeze-drier. The sealing of the ampoules or vials is most important, and heat sealed glass is preferred to butyl rubber bungs in glass vials as these leak over



Figure 9.2. There is a vast array of freeze-drying equipment on the market, ranging from laboratory bench models through pilot scale plant to huge industrial installations. (This figure is available in full color at http://onlinelibrary.wiley.com/book/10.1002/9780470054581.)

long-term storage, release toxic gases, and allow deterioration of the freeze-dried organism. There are many advantages of freeze-drying over other methods, including the total sealing of the specimen and protection from infection and infestation. Cultures generally have good viability/stability and can be stored for many years. Ampoules take up little space and can be easily stored. In addition, cultures do not have to be revived before postal distribution. However, there are disadvantages, some isolates fail to survive the process and others have reduced viability and may show genetic change (15,20), though unless high viability is retained it is difficult to differentiate between this and selection of spontaneous mutants by freeze-drying (21). Ampoules of freeze-dried organisms must be stored out of direct sunlight and chilled storage reduces the rate of deterioration and extends shelf-life.

The ability of living organisms to survive freezing and thawing was first realized in 1663 when Henry Power successfully froze and revived nematodes (13). Polge *et al*. (22) became the first "modern-day" scientists to report the freezing of living organisms when they successfully froze and thawed avian spermatozoa in glycerol. Liquid nitrogen is the preferred cooling agent for cryopreservation, although liquid air or carbon dioxide can be used. Lowering the temperature of biological material reduces the rate of metabolism until, when all internal water is frozen, no further biochemical reactions occur, and metabolism is suspended (23). Provided adequate care is taken during freezing and thawing, the culture does not undergo change, either phenotypically or genotypically (24).

Cryoprotection is achieved by the following:

1. noncritical volume loss by the reduction of ice formation;
2. an increase in viscosity that slows down ice crystal growth and formation and solute effects;
3. reduction in the rate of diffusion of water caused by the increase in solutes.

Glycerol 10% (v/v) gives very satisfactory results and is generally the cryoprotectant of choice for most organisms. Dimethyl sulfoxide (DMSO) penetrates rapidly and is often more satisfactory but it can be toxic and mutagenic, and exposure in the unfrozen state must be kept to a minimum (25,26). Sugars and large molecular substances, such as polyvinyl pyrrolidine (PVP) (27), have been used but in general have been less successful (12). Trehalose may be better but is expensive. Establishing the optimum cooling rate has been the subject of much research (12,28,29). Slow cooling at 1°C/min over the critical phase has proved most successful (12), but some less sensitive isolates respond well to rapid cooling, some without protectant. Slow warming may cause damage owing to the recrystallization of ice, therefore rapid thawing is recommended. Slow freezing and rapid thawing generally give high recoveries for many organisms (21).

As with other methods of preservation, cryopreservation, in or over liquid nitrogen, has advantages and disadvantages. Advantages include the length of storage, which is considered to be effectively limitless if storage temperature is kept below −139°C. Most of the organisms survive well, giving the method a greater range of successful application. Organisms remain free of contamination when stored in sealed ampoules. The samples can be stored in the liquid phase, which regulates the low storage temperature better but increases hazards on retrieval and if seals are permeable the liquid can penetrate. If storage is in the gaseous phase above the liquid, temperature can fluctuate but can be stabilized by storing in an inner chamber which is immersed in liquid. Disadvantages of liquid nitrogen storage include the high cost of apparatus such as cryostorage tanks and a continual supply of liquid nitrogen. A regular supply cannot be obtained in some parts of the world and therefore the technique cannot be used. If the supply of nitrogen fails (or the double-jacketed, vacuum-sealed storage vessels corrode and rupture), then the whole collection can be lost. Backup storage is required at a separate site as with all preservation techniques. There are also safety considerations to be made: the storage vessels must be kept in a well-ventilated room equipped with an automatic monitoring device for oxygen content of air, as the constant evaporation of the nitrogen gas could displace the air and asphyxiate workers.

9.3.2 Biological Resource Management and the Law

Organisms are isolated, grown, characterized, preserved, and are transported between laboratories within countries and often across borders or continents. They are sent for identification, reference, research, or for production purposes from colleague to colleague, from and to culture collections. All these actions must be carried out safely and must be compliant with the various legislation and regulations that control these matters. Not only is there legislation in place (Table 9.1) but also from time to time it is changed or added to. Some of the key areas covered are health and safety, quarantine regulations, ownership of Intellectual Property Rights (IPR), the Convention on Biological Diversity, safety information provided to the recipient of biological materials, and regulations governing shipping of dangerous organisms. It is not only in the laboratory that there is cause for concern, as, for example, a microorganism in transit might put carriers, postal staff, freight operators, and recipients at risk, some organisms being relatively hazard free while others are quite dangerous. It is essential that safety and shipping regulations are followed to ensure safe transport. There are several other pieces

TABLE 9.1. Regulatory Control in Microbiology

Action	Requirement	Law, Regulation, Convention	Further information
Collecting in the field	Prior informed consent from a recognized authority	Convention on Biological Diversity	http://www.biodiv.org
	Mutually agreed terms on use	Convention on Biological Diversity	http://www.biodiv.org
	Consent from the land owner	Property law	National sources
Import	Nonindigenous plant pathogens require licenses from country authority	Quarantine regulations	National authorities; Europe: European and Mediterranean Plant, Protection Organisation (EPPO), 1 rue le Nôtre, 75016 Paris, France
	Human, animal, and plant pathogens can often only be imported to specified laboratories	Health and safety	National Authorities e.g. DEFRA in the United Kingdom
Handling: manipulation; growth	Containment dependent on hazard	Control of Biological Agents—Health and Safety EC Directive 2000/54/EEC on Biological Agents	http://eur-op.eu.int/opnews/395/en/r3633.html
Genetic manipulation	Containment of manipulated organisms	EEC Directives 90/219/EEC. Contained use of genetically modified microorganisms (GMO's), *L117 Volume 33, 8 May 1990.	http://www.biodiv.org/biosafety/protocol.asp
		EEC Directives 90/220/EEC. Release of GMO's, *L117 Volume 33, 8 May 1990.	http://biosafety.ihe.be/Menu/BiosEur1.html
		Cartagena Protocol on Biosafety	http://biosafety.ihe.be/Menu/BiosEur1.html
Deposit as part of a patent process	Long-term storage and compliance with the Budapest treaty	Budapest Treaty on the International Recognition of the Deposit of Microorganisms for the Purposes of Patent Procedure	http://www.cnpat.com/worldlaw/treaty/budapest_en.htm
Storage	Appropriate containment	Health and safety Licence to hold pathogens Security	World Health Organisation; National Authorities
Export to another country	Some plant and animal pathogens require export licences	Quarantine regulations	National authorities
	Dangerous organisms with potential for dual use	Export Licences for dangerous organisms, Biological and Toxic Weapon Convention (BTWC)	http://binas.unido.org/binas/regs.php3 http://www.opcw.nl/fact/rel_conv.htm http://www.dfat.gov.au/isecurity/pd/pd_4_96/pd9.html
Distribution	Packaging and transport considerations	IATA Dangerous Goods Regulations (DGR), Universal Postal Union(UPU United Nations Expert Committee on the Transport of dangerous goods	http://www.iata.org/cargo/dg/dgr.htm http://www.upu.int/ http://www.unece.org/trans/danger/danger.htm
	Sovereign rights over the strains	Convention on Biological Diversity	http://www.biodiv.org
	Access and benefit sharing	Bonn Guidelines	http://www.biodiv.org
	Intellectual Property Rights Customer licensed to receive organism?	IPR	National authorities
	Dangerous organisms	EU Council Regulation 3381/94/EEC on the Control of Exports of Dual-Use Goods from the Community	http://eur-op.eu.int/opnews/395/en/r3633.html See national Export Offices

[a] Taken from OECD Best Practice Guide Lines (2).

of legislation that restrict the distribution of microorganisms of which a microbiologist must be aware. The World Federation for Culture Collections (WFCC), the European Biological Resource Centre Network (EBRCN) partners, and the OECD Task Force have drawn together a list of treaties, directives, and legislation that impact on culture collection operations (Table 9.1).

The starting point for correct control procedures is a risk assessment (7,12,30), which must include all hazards involved. For example, with microorganisms, it is not just pathogenicity that is considered, but also other hazards like the production of toxic metabolites and the ability to cause allergic reactions. It is the responsibility of the microbiologist to provide such assessment data to a recipient of a culture to ensure its safe handling and containment.

Best practice involves the following:

- adequate assessment of risks;
- provision of adequate control measures;
- provision of health and safety information;
- provision of appropriate training;
- establishment of record systems to allow safety audits to be carried out;
- implementation of good working procedures.

Various classification systems exist to grade the degree of hazard and risk, which include the definitions for classification by the World Health Organisation (WHO); United States Public Health Service (USPHS); Advisory Group on Dangerous Pathogens (ACDP); European Federation of Biotechnology (EFB); and the European Union. In Europe, the EC Directive (93/88/EEC) on Biological Agents sets a common base line, which has been strengthened and expanded in many of the individual member states. The definition and minimum-handling procedures of pathogenic organisms are set by appropriate authorities in each country and are often the same or similar for all EC countries. Microorganisms are normally classified on their potential to cause disease to humans into four groups (30):

Group 1. A biological agent that is most unlikely to cause human disease.

Group 2. A biological agent that may cause human disease and which might be a hazard to laboratory workers but is unlikely to spread in the community. Laboratory exposure rarely produces infection and effective prophylaxis or treatment is available.

Group 3. A biological agent that may cause severe human disease and present a serious hazard to laboratory workers. It may present a risk of spread in the community but there is usually effective prophylaxis or treatment.

Group 4. A biological agent that causes severe human disease and is a serious hazard to laboratory workers. It may present a high risk of spread in the community and there is usually no effective prophylaxis or treatment.

All strains must be assigned to appropriate risk groups; this includes a positive assignment to risk group 1 unless otherwise considered hazardous. All other groups have lists of species included but there is no such list for those organisms not considered hazardous. Hazard information must be recorded and made available to recipients of this material. It is not only the handling of organisms that harm humans that are controlled. All those who wish to obtain or work with plant or animal pathogens must also be aware that there are regulations that impact on operations. Cultures of nonindigenous plant pathogens require a permit to import, handle, and store from the appropriate Government Department. Under the terms of such a licence, the shipper is required to see a copy of the Ministry permit before such strains can be supplied. It is best practice that the holder of such organisms must ensure that nonindigenous pathogens or controlled indigenous pathogens are not distributed unless the recipient has an appropriate licence. However, this is not always straightforward as not all countries provide lists.

A biologist must first seek permission before collecting biological material; rules for access and benefit sharing may differ from country to country. Terms and conditions for use or further distribution may exist, for example, Intellectual Property Rights or those negotiated with Prior Informed Consent, granted under the Convention on Biological Diversity (CBD). A collector is required to agree to terms on which benefits will be shared should they accrue from the use of the organisms. The benefit sharing may include monetary elements but may also include information, technology transfer, and training. A BRC must ensure transparency retaining the link between the source country and end user of genetic resources. Biological materials must be received and supplied within the spirit of the CBD ensuring material transfer agreements are in place. A BRC must maintain contact and follow recommendations of its national CBD Contact Point (31). When biological material is distributed to others, information should always be provided to enable recipients to comply themselves. This involves data on ownership of IP and must include a safety data sheet indicating which hazard group it belongs to and what containment and disposal procedures are necessary. A safety data sheet accompanying a microorganism should include the following:

- the hazard group of the organism being despatched
- a definition of the hazards and assessment of the risks involved in handling

- requirements for the safe handling and disposal of the organism.
  - containment level
  - opening procedure for cultures and ampoules
  - transport
  - disposal
  - procedures in case of spillage.

When shipping cultures, the International Air Transport Association (IATA) Dangerous Goods Regulations (DGR) may be relevant, which require that shippers of microorganisms of hazard groups 2, 3, or 4 must be trained by IATA certified and approved instructors (every 2 years). They also require shippers declaration forms, which should accompany the package in duplicate and specified labels should be used for organisms in transit by air (32). Essentially, IATA DGR requires that packaging used for the transport of hazard group 2, 3, or 4 meets defined standards of a UN combination package, IATA packing instruction 602 (class 6.2) (32). Packaging must meet EN 829 triple containment requirements for hazard group 1 organisms (33).

There is considerable concern over the transfer of selected infectious agents capable of causing substantial harm to animal, human, and plant health and to the environment. There is potential for such organisms to be passed to parties not equipped to handle them or to persons who may make illegitimate use of them. Of special concern are pathogens and toxins causing anthrax, botulism, brucellosis, plague, Q fever, tularaemia, and all agents classified for work at Biosafety Level 4 (risk group 4). The "Australia Group" of countries has strict controls for movement outside their group but has lower restrictions within. Collections that hold dangerous organisms that are pathogens or produce toxins that could be misused or cause harm must recognize requirements for biosafety and biosecurity. Biosafety concerns the health aspect, the protection of people during normal functioning of a BRC, and biosecurity concerns the legal and regulatory arrangements governing the possession and circulation of biological products reputed to be hazardous, and sanctioning malicious use of such products. The degree of hazard that a biological resource presents must be treated separately to the issue of biosecurity, for example, the prevention of terrorism. The question of biosafety arises wherever biological material and associated information is handled. Biosecurity and biosafety affect many aspects of culture collections, their operation, and their external relations:

- worker safety and health aspects
- security of facilities and transport
- public and environmental protection (containment)
- safeguarding resources
- prevention of bioterrorism.

Hazardous biological material must be available for study to provide public health solutions and tools for protection and therefore collections must be able to store, conserve, and distribute such materials, ensuring that their own development and activity does not increase risks. Access to such resources must be controlled and thus culture collections have a role in enhancing the general level of biosecurity. The OECD BRC Beat Practice (2) has laid down guidance mechanisms that reduce the possibility of misuse; it is critical that such controls do not impede the legitimate use of such agents. Current rules and regulations differ from country to country and demonstrate clear problems of exchange. The OECD Best Practice initiative provides common rules that can be used worldwide. If during an epidemic of a new disease (e.g. SARS), exchanges of materials between laboratories and countries were not possible then the identification of the causative organism and the production of potential treatments would have been impeded. There have to be culture collections to meet the needs of science, but culture collections are inherently vulnerable. There must be a guarantee that they will not serve the purposes of terrorist movements, facilitate theft of hazardous products or endanger confidentiality, staff safety, intellectual property, and so on. Exchanges between collections and users must be traceable, for example, through Material Transfer Agreements (MTAs).

Identifying those organisms that should be controlled is not straightforward because there are so many lists that are not coordinated. The Australia group provides a list of what are considered to be the most dangerous pathogens but individual country lists of these differ. Nevertheless, a collection must follow its national rules, but how does it check the validity of the requestor and the end use of the material to be supplied? Can it rely on the statement of a potential customer? A collection does not have the power or the resources to investigate. The UK National Collections have been set rules so that when the end use or validity of the potential recipient is in doubt, there is a mechanism for the government to investigate.

Governments could in the long run prohibit direct trade in hazardous biological products between unauthorized parties. The purpose of the restrictions of the OECD best practice is to prevent uncontrolled transfers, to monitor distribution, and ensure traceability of products transferred by culture collections—not to interfere with research or with property rights. The obligation for international transfers to go through collections could be an important factor for increasing trust and therefore stimulating trade.

9.4 QUALITY MANAGEMENT

There are numerous sources of information on best practice, guidelines, and protocols for the management of biological resources. They have been compiled by the expertise in individual collections and of organizations such as the WFCC, EU projects such as the European Biological Resource Centres Network (EBRCN), the Common Access to Biological Resources and Information (CABRI) consortium, and the UK National Culture Collection (UKNCC). Such standards have been drawn together by the OECD BRC Task Force (2). However, mechanisms must be adopted to ensure user confidence that these practices are being followed. One system that might be adopted by the national Governments where the BRCs reside might be that of the International Standards Organisation (34). Currently, there are a number of standards or guides that could be used that cover at least part of the activities of BRCs. Several collections have already adopted ISO 9001: 2000 certification (Table 9.2), a system that ensures quality through critical management of processes. The system requires that procedures and practices are documented and that auditing procedures are put in place to ensure that what is said is actually carried out. A key element of the ISO 9001: 2000 is directed at improving customer satisfaction and the implementation of product improvement mechanisms. Examples of standards developed for microbial and cell culture collection*s* are as follows:

- the WFCC *Guidelines for the establishment and operation of collections of microorganisms* (35);
- the Microbial Information Network for Europe (MINE) project standards for the member collections (36);
- UKNCC quality management system (37);
- CABRI guidelines (38);
- the OECD Best Practice Guidelines for Biological Resource Centres (2).

There are also standards that can be applied to microbiology laboratories such as Good Laboratory Practice (GLP), ISO 17025, ISO Guide 34, *General requirements for the competence of reference material producers*, and, as described above, ISO 9001: 2000. Industry is expressing the need for quality control and standards within collections. The UKNCC quality management system set minimum standards (12) and the CABRI electronic catalog project (38) has made available a set of guidelines to aid collections to put best practice in place. These cover critical elements in the handling, storage, characterization, and distribution and handling of associated information. Ultimately, BRCs should adopt the OECD best practice (2) to ensure user satisfaction and reproducibility.

TABLE 9.2. Collections Operating Independent Third-Party Assessed Certification or Accreditation Quality Management Systems

Collection	System
AGO—Arocrete Group Co., Taiwan	ISO 9001:2000
BIOCEN (BioCC)—Centro Nacional de Biopreparados, Cuba	ISO 9001:2000
CABI—CAB International Genetic Resource Collection, UK	Part of services to ISO 17025
CBS—Centraalbureau voor Schimmelcultures	ISO 9001:2000
CCCM—Czech Culture Collection of Microorganisms	ISO 9001:2000
CCRC—Culture Collection and Research Center, FIRDI, Taiwan	ISO 9001:2000
CECT—Coleccion Espanola de Cultivos Tipo, Spain	ISO 9001:2000
CIP—Collection de l′Institut Pasteur, France	ISO 9001:2000
DSMZ—Deutsche Sammlung von Mikroorganismen und Zellkulturen, Germany	ISO 9001:2000
ECACC—European Collection of Cell Cultures, UK	ISO 9001:2000
ICLC—Interlab Cell Line Collection; Italy;	GMP
IFM—Quality Services Pty Ltd, Australia	ISO Guide 34
IHEM—Insitute of Higiene and Epidemiology, Mycology, Belgium	ISO 9001:2000
LMBP—Plasmd collection, Belgium	ISO 9001:2000
LMG—University of Gent, Belgium	ISO 9001:2000
MUCL—Mycology, University Louvain la Neuve, Belgium	ISO 9001:2000
NBRC—NITE Biological Resource centre, Tsukuba, Japan	ISO 9001:2000
NCIMB—National Collection of Industrial, Food, Marine Bacteria, UK	ISO 9001:2000
NCPV—National Collection of Pathogenic Viruses, UK	ISO 9001:2000
NCTC—National Collection of Type Cultures, UK	ISO 9001:2000
NCYC—National Collection of Yeast Cultures, UK	ISO 9001:2000

Best practice demands that the culture collection performs authentication tests and establishes baseline information for in-storage maintenance checks and validation after preservation. The OECD best practice guidelines (2) advise that competent persons carry out such operations and that a maintenance plan for periodic control is put in

place for each organism preserved. The OECD best practice provide guidance at two levels, that applicable to all BRCs holding biological material and a second level that makes domain-specific recommendations. In 2007, the latter covered the microbial domain, being the most advanced followed by the guidelines for human-derived material. At the general level, it is recommended that biological material be preserved by at least two methods but if two distinct methods are not applicable, it is recommended that cryopreserved stocks be maintained in separate locations. It is best practice to lay down master cell banks from which further stocks for distribution can be sourced. The details of the techniques are laid down in the domain-specific criteria (2). The guidance requires that the number of transfers or generations of original material before preservation and storage be kept to a minimum, the master stock be created from the original material, and that sufficient distribution stocks are produced to minimize the need to go back to stocks for replenishment. The material should be stored under environmental parameters that assure the stability of properties, and additionally details of inventory control, lead times, and restocking practices be documented and that duplicate collections be maintained. The guidance requires the validation of methods and the recording of such details. Finally, quality audits and review procedures should be in place. Such practices are becoming more common in collections as automation and technology is developed to help manage such processes. In mycology, data is available on many common species to enable the selection of best protocols and assess stability but it is far from complete. Cryopreservation is by far the best technique for the storage of fungi (12,15) but there is not one protocol for all. Of the 250 species investigated at CABI, 248 had different optimum cooling rates from 0.5 to 200°C/min, although most fungi survive well, albeit with some cell death at 1°/min cooling in 10% glycerol as cryoprotectant. Molecular techniques such as DNA fingerprinting are used to assess stability, and poor technique has been shown to cause polymorphisms (15).

The more specific best practice guidelines for the microorganisms are aimed to ensure that the organisms held and supplied are authentic and of the highest standard. The methods used should be such that the key properties of the microorganisms are retained and should ensure their consistency amongst the BRCs supplying them. To meet requirements, BRCs must put in place documented and audited processes. On receipt, a unique number is assigned to the strain and its identity confirmed using, for example, morphological characteristics, if appropriate or sequencing of the 16S ribosomal RNA or the ITS region of the genome. This adds to the strain data, which can be used as a baseline for monitoring the strain following preservation and storage. Additional characters that can be useful to test stability are growth rates, descriptive data, photomicrographs, metabolic profiles, and genome fingerprinting techniques. Strains must be pure or defined mixtures. The purity of strains should be checked and recorded before preservation, immediately after, and, depending on the method, during storage. For fungi, this is normally done through microscopic examination or growth in broth particularly to detect bacterial contamination. The preferred standard would be that no contamination at all is accepted. There are exceptions where strains cannot be grown without their symbiont, host, or feeder organisms; these are not contaminants but it would be imperative that the components of such mixtures are described, recorded, and defined. Viability of strains, normally expressed as a percentage of propagules to produce colony growth, should be checked and recorded before preservation, immediately after and during storage. The frequency of testing depends upon the method used and the organism involved: cryopreserved strains need testing least frequently, freeze-dried materials more regularly, depending on the storage temperature. The data obtained demonstrates if a strain is deteriorating during storage. Preferred levels of viability are often set according to the organism. In the case of fungi, survival is normally relatively high or nil but in the bacteria titre drops vary and may well be in excess of threefold. Once set, any deviation from the standard requires explanation and must be recorded.

A program of tests to ensure stability of strains must be put in place. Known properties can be checked periodically but full metabolic profile checks are seldom necessary on a regular basis. However, to be able to judge stability, a less stable property should be selected to indicate how well a strain is being maintained. It must always be borne in mind that preservation protocols are not natural and that cells need a period of time to recover. Optimized techniques and standard procedures should be adhered to. It is necessary that procedures are documented, so that all coworkers and their successors can follow them and that in the future the methods and the treatments used can be traced. This would include all measuring and recording techniques from viability and purity checks through preservation methods to characterization and the checking of properties. The accepted level of deviation from measurable parameters must be set and records maintained to show that performance is within the accepted limits. A procedures manual is essential to ensure continuity and new staff must be trained to ensure the attainment of the standards set. Training must not only include how to carry out methods but also the accepted levels of result, monitoring, and what must be recorded and where data is maintained. All equipment used in the BRC must be regularly maintained and calibrated and must operate to set limits. All details must be recorded so that you can ensure traceability and reproducibility.

There is little point in establishing a collection without considering the long-term security of its holdings. If procedures are put in place that cannot be maintained in the future, then a considerable waste of time and resources is inevitable. Freeze-dried collections need little maintenance. A frozen collection needs only to be kept cold. A collection must ensure that there is a backup, organisms should be stored by a minimum of two techniques, and that both working and security stocks are maintained. It is also advisable to keep a duplicate collection in another secure building or site as a reserve. At least all important strains should be stored on another site with all the information about them as a disaster measure. It is essential that adherence to set standards is monitored at every level. The appointment of auditors from other departments, or even from outside the organization (required for many accreditation schemes), is beneficial. The recording of such monitoring is vital to demonstrate competence, and self-checks should be part of a good management system. There are several national and international schemes that can be followed to give a standard of quality assurance accepted by a collection's customers. There is no accreditation scheme that has been specifically designed for culture collections but using the OECD BRC best practice alongside recognized schemes is being explored and deemed appropriate by several accreditation bodies. High standards are required to meet the requirements of the users of microbial resource collections of today. At the very least, this requires set methods and levels of acceptability, recording of results, and an independent monitoring system to enable the long-term security and sustainability of holdings. Underpinning the quality system is the maintenance of the biological resources without change.

The underlying ethos is that the user benefits from the accreditation of culture collections through better access to authentic and reproducible materials in a transparent and traceable way. There must be benefits for the collection to provide incentive to change. There is an ever-increasing demand for authentic reference materials as more and more industries are adopting certification or accreditation as a means to demonstrate quality and competence. This may be the driving force for the business elements of a collection's strategy for long-term sustainability, but it is also an increasing requirement of funders of research who seek high quality science and solutions. The ability to demonstrate the competence to carry out and manage high quality research is being recognized by Research Councils and Government Departments. Third-party evaluation through accreditation or certification may be the only way to demonstrate this.

9.5 SERVICES

A BRC offers other services in addition to supply of biological materials and associated information. Among such services are the identification of organisms, their biochemical and molecular characterization, bioaudits, challenge testing, training and contracting, and consultancies engaging their broad multidisciplinary expertise (12). The individual member collections of the WFCC offer identification by a range of techniques for many organisms including actinomycetes, algae, animal cells, bacteria, cyanobacteria, filamentous fungi, nematodes, protozoa, mycoplasma, and yeasts. Techniques used for strain identification include anatomical and morphological analysis, FAME analysis, several automated commercial systems, biochemical and molecular fingerprinting, and sequencing. The collections that provide the service and methods used are listed on the World Data Centre for Microorganisms (WDCM) website (6) and in Table 9.3.

BRCs strive to optimize preservation protocols and to develop new ones. Most research is aimed at improving cryopreservation methodology with emphasis on species specific criteria. In addition to their culture collection activities, most collections, in association with their parental organizations can offer external organizations

TABLE 9.3. Some Identification Methods Used by Collections for Strain Identification

{PRIVATE} Organism	Technique				
	Morphological	MIDI	BIOLOG	Biochemical	Molecular Fingerprinting and Sequencing
Actinomycetes	+	+		+	+
Algae	+			+	+
Animal cell lines					+
Bacteria	+	+	+	+	+
Cyanobacteria	+			+	+
Filamentous fungi	+			+	+
Nematodes	+				+
Protozoa	+				+
Mycoplasma	+				+
Yeasts	+	+		+	+

TABLE 9.4. Service Activities of Culture Collections

Service/Activity	Benefits
Patent deposit service	A facility for deposition of strains included in patent applications in to meet national legislation and also where applicable in compliance with the Budapest Treaty.
Safe deposit service	Provides the microbe-based industries with a facility to preserve their strains for long- term storage; ensuring a backup strain is kept in a safe and secure facility. Loss of these industrially important strains could mean a tremendous setback in the operations of a company.
Microbial diversity R&D	Contract research, for example, novel microorganisms with potential applications in agriculture, medicine, industry, and so on.
Preservation by lyophilization	Preserving strains for laboratories without such facilities and providing them with the ampoules to store and use.
Human resource development	Training courses and other modes of continuing education contributing to the enhancement of quality of research in areas related to patenting, bioprospecting, and conservation of microorganisms for various applications in the pharmaceutical, food, and other microbiologically based industries. Capability building where gaps exist. Training of trainers, to provide in-country teaching resource,
Supply of cultures	Cultures that are being distributed may be used in the production of certain desirable end-products in the food, pharmaceutical and other microbe-based industries and screened for other properties. Reference strains are a must in microbial systematics work, thus providing authenticated cultures for instruction and research purposes improves the quality of research and teaching. Microbial cultures are also used in strain improvement work to further enhance the organism's desirable traits, foe example, alcohol production, antibiotic production, and so on. Standard test strains with reproducible properties.
Complete microbiological analysis/total count	Providing information on the microbial content of a given sample, which is important in the formulation of microbe-based products like biofertilizers, inoculum, and so on. Knowledge of the right kinds and number of microorganisms is necessary to produce high-quality products for field application to improve yields of agricultural crops and other products. Providing information on the quality of raw materials that will be used in production. Knowledge of the types of microflora in the raw material will enable a producer to decide whether to discard a contaminated raw material or modify their production processes.
Microbiological analyses of food and water	Provides information on the quality of food and water—whether they are safe for human consumption or are suitable for use in the production of certain products requiring high-quality water.
Identification services	Provides value-added information on the morphological, biochemical, and molecular fingerprinting, chemical composition and sequencing; also other properties of an unknown isolate.
photomicroscopy anti microbial sensitivity testing	Information generated by fluorescence microscopy giving indication of organism sensitivity to antimicrobials.
cytotoxicity assays	Information generated on toxicity of cells and their products.
phytosanitary testing	Presence or absence of specific pathogens on crops and commodities.
developing screens	Producing assays to detect properties of strains.
development of diagnostic kits for the early detection of pathogens	To aid in the early detection of animal and human foodborne and water-borne pathogens.

a diverse range of consultancy and contract services (Table 9.4). Areas such as biodeterioration, biodegradation, biological control, biodiversity, ecology, parasitology, pest management, biochemistry, molecular biology, taxonomy, identifications, metabolite and enzyme screening, analytical chemistry, food and beverage microbiology, process development and large-scale culture, stored product microbiology, plant pathology, evaluation of microbial identification kits, and environmental monitoring are covered (6,12).

A range of deposit services are offered, BRCs normally accept deposits of strains that meet their accession criteria and that are of value to the scientific community into their open collections, making them available in their public catalogs. There are other deposit services they may offer, if a depositor wishes to store materials but not make them publicly available collections often offer a confidential safe deposit service. Patents may be taken out to protect Intellectual Property Rights (IPR). In many cases, the organism involved must be part of the disclosure and many countries

either recommend or require by law that a written disclosure of an invention involving the use of organisms be supplemented by the deposit of the organism into a recognized culture collection. Most patent lawyers recommend that the organism is deposited, regardless of it being a requirement, to avoid the possibility of the patent being rejected. To remove the need for deposit of organisms in a collection in every country where patent protection is desired, the "Budapest Treaty on the International Recognition of the Deposit of Micro-organisms for the Purpose of Patent Procedure" was concluded in 1977 and came into force toward the end of 1980 (39). This recognizes named culture collections as "International Depository Authorities" (IDA) and a single deposit made in any one is accepted by every country party to the treaty. Any collection can become an IDA, provided it has been formally nominated by a contracting state and meets certain criteria. There are 32 IDAs around the world (Table 9.5) that accept patent deposits of human and animal cell lines, algae, bacteria, cyanobacteria, fungi, nematodes, nonpathogenic protozoa, plant seeds, and yeasts.

9.5.1 Organization and Information Resources

To meet new and increased demands, collections have recognized the need to network. Culture Collection organizations such as the WFCC and the ECCO act as fora for discussion bringing together a critical mass of collections and users to try and coordinate activities, exchange information, and technologies to facilitate progress in this vital task. This is happening at the national, regional, and global levels.

9.5.2 The World Federation for Culture Collections

The WFCC, a key global organization, was founded in 1970, its roots dating back to 1963, and since 1973 is a multidisciplinary commission of the International Union of Biological Sciences (IUBS) and since the separation of the International Union of Microbiological Societies (IUMS) from IUBS in 1979 it has operated as an interunion commission (10). It seeks to promote activities that support the interests of culture collections and their users. Member collections of the WFCC register with the World Data Center for Micro-organisms (WDCM) and there are currently ~520 registered collections (6) in 67 countries with

TABLE 9.5. Some National Culture Collection Organizations

Acronym	Network	Link
BCCM™	Belgium Co-ordinated Collections of Microorganisms	http://bccm.belspo.be
SBMCC	Brazil - Sociedade Brasileira de Microbiologia Coleções de Culturas	Sociedade Brasileira de Microbiologia Coleções de Culturas : colecao@sbmicrobiologia.org.br Databases : http://www.cria.br
CCCCM	China Committee for Culture Collections of Microorganisms	http://micronet.im.ac.cn
FCCM	Federation of Czechoslovak Collections of Microorganisms	http://www.natur.cuni.cz/fccm/
CCRB	French Comité Consultatif des Ressources Biologiques	http://www.crbfrance.fr
SCCCMOMB	Cuban Culture Collection and other Biological Materials Section;	Contacts: Iglesias: elsie@finlay.edu.cu (President); weng@infomed.sld.cu / ccm@inhem.sld.cu (Vice President); nancy@liorad.quimefa.cu (Secretary); raisi@cecmed.sld.cu (Finances)
KFCC	Korean Federation of Culture Collections	Shinchondong Sodaemunku, Seoul 120-749, Korea
HPACC	UK Health Protection Agency Culture Collections	http://www.hpa.org.uk/business/collections.htm
FORKOMIKRO	Indonesia - Communication Forum for Indonesian Culture Collection Curators	http://www.mabs.jp/kunibetsu/indonesia/indonesia_04.html
JSCC	Japan Society for Culture Collections	http://www.nbrc.nite.go.jp/jscc/aboutjsccc.html
PNCC	Philippines National Culture Collections	Contact: Rosario G. Monsalud, Ph.D., Head, PNCM, rosegm@laguna.net
TNCC	Thailand Network on Culture Collection	http://www.biotec.or.th/tncc/
UKFCC	UK Federation for Culture Collections	http://www.ukfcc.org/
UKNCC	UK National Culture Collection –UK affiliation of national collections	http://www.ukncc.co.uk

over 2000 staff. A congress is held every 3 years to discuss advances in technology and common policies with regard to biodiversity and the role of culture collections. The WFCC keeps its members informed on matters relevant to collections in its Newsletter and has working programs addressing patent depositions, biosafety and biosecurity, safeguard of endangered collections, capacity building, and quality standards. Since 1986, the WFCC has overseen the activities of the World Data Centre (WDCM), which is now the data center for the WFCC and Microbial Resource Centers (MIRCENs) Network. It was established in 1966 and produced the first hard copy volume of the *World Directory of Collections of Cultures of Microorganisms* in 1972, while based at the University of Queensland, Australia. The WDCM relocated in 1986 to RIKEN, Saitama, Japan and then again in 1999 to the National Institute of Genetics, Japan. The WDCM collections hold in excess of 1.7 million strains (Table 9.6), 44% are fungi, 43% bacteria, 2% viruses, 1% live cells, and 10% others (including plasmids, plant, animal cells, and algae).

The WFCC is the largest independent global organization that represents professional individuals and culture collections, which preserve biodiversity and enable their proper use. They target living microorganisms, cell lines, viruses, and parts and derivatives of them. Key values are authenticity and genetic integrity of the material and validity of the information provided. The WFCC supports the professionals, organizations, and individuals with interests in culture collection activities through the following:

- networking, providing information and expertise, and facilitating communication;
- facilitating access to the collection resources;
- providing training and promoting partnerships;
- encouraging the development and implementations of quality and security procedures and the use of common standards and regulations;
- representing member interests in international organizations and fora; and
- promoting the establishment of culture collections, their promotion, and perpetuation.

TABLE 9.6. World Data Centre for Microorganisms (WDCM)

Country	Number of Collections	Number of Strains	% of Total Number of Strains
Africa	11	12,255	0.7
Asia	177	322,195	18
Europe	173	1,005,930	57.3
America	121	326,297	19
Oceania	43	89 786	5
Total	*525*	*1,756,463*	

In the growing bioeconomy, WFCC's members face increasing global demands for worldwide and controlled access to biological resources, public security, industrial quality of their holdings and associated data, and long-term genetic stability of the material. The key to the use of microorganisms from culture collections is the retention of their properties as research and development must be based on authentic and well-preserved biological material. The WFCC have been helping collections in this respect for over three decades and have produced *Guidelines for the Establishment and Operation of Culture Collections* (35). It is a goal that strains of organisms are supplied from member collections with traceability, conforming to national and international regulatory requirements, and that they are preserved in such a way as to retain their full potential.

9.5.3 The Asian Consortium for Microbial Resources

The Asian Consortium for the Conservation and Sustainable Use of Microbial Resources (40) was established by the consensus of representatives of 12 Asian countries during the *10th International Congress of Culture Collection (ICCC-10)* held at Tsukuba in 2004. Head of culture collections and government officers were involved in the meeting along with research microbiologists. The objective of the consortium is to promote collaboration among government or public organizations in Asian countries for the purposes of enhancing conservation and suitable use of microbial resources in Asia. The current member countries are Cambodia, China, Indonesia, Japan, Korea, Laos, Malaysia, Mongolia, Myanmar, Philippines, Thailand, and Vietnam.

The planned activities of the consortium are as follows:

1. development of human resources;
2. promotion of research and development on microbial resources and their application in industrial and other uses;
3. collaboration through the network of biological resource centers;
4. exchange of views and information;
5. enhancement of public awareness on the consortiums activities for the conservation and sustainable use of microbial resources; and
6. organization of scientific meetings (seminars, workshops, etc.) and other related matters

The General Assembly Meeting of the Asian Consortium for Microbial Resources is held annually to set up task forces for Bioresource Information Management and for Human Resource Development.

9.5.4 European Culture Collections' Organization

The European culture collections have collaborated since 1982 when the European Culture Collection Curators Organisation was established to bring together the managers of the major public service collections in Europe to discuss common policy, exchange technologies, and seek collaborative projects. The organization opened itself to staff and users of collections and is now named *the European Culture Collection Organisation (ECCO)*. There are currently 65 members, of which there are 57 collections holding ~350,000 strains. The members have been involved in producing practical approaches to international rules and regulation. Initiatives led by the Belgian Co-ordinated Collections of Microorganisms (BCCM™) have produced a practical code of practice for collections to operate within the Budapest Treaty (41) and the Micro-Organisms, Sustainable Access and use, International Code of Conduct (MOSAICC), which provides guidelines for operation within the spirit of the Convention on Biological Diversity (42). There have been several collaborative projects developed out of discussions between ECCO members that have placed the European Collections at the cutting edge of culture collection activities and research. Examples are the European Biological Resource Centre Network (EBRCN), which followed on from the Common Access to Biological Resources and Information (CABRI) electronic catalogue project. Information on members, activities, and meetings can be accessed via the web site (43).

9.5.5 Microbiological Resource Centres

In 1974 UNEP, UNESCO, and ICRO established the Microbiological Resource Centres (MIRCEN) network. The objectives of this network are to preserve and exploit microbial gene pools, make them accessible to developing countries, and to carry out research and development in environmental microbiology and biotechnology. The 34 MIRCENs carry out various activities that meet these ends including training and provision of information. Further details can be obtained from the MIRCEN Secretariat at the United Nations Educational Scientific and Cultural Organisation (UNESCO), Paris, France (44). The production of MIRCEN News in 1980 helped publicize the activities of the network; this has now broadened in content and is published as the World Journal of Microbiology and Biotechnology.

9.5.6 National Federations and Affiliations

There are several countries that have established national organizations that support, foster, or coordinate culture collection activities (Table 9.7). Among them is the United Kingdom. The UK Federation for Culture Collections (UKFCC) was established at its inaugural meeting on the 10 April 1975 at Imperial College London. Membership of the Federation is open to all those involved with culture collections and the users of cultures including those from academia and commercial organizations.

The Objectives of the UKFCC are as follows:

- aid the establishment and promote the use of culture collections
- facilitate communication between culture collections and their users
- make every effort to save endangered collections of important cultures;
- encourage establishment of special reference collections and identification services;
- promote research in systematics, microbial diversity, and preservation;
- promote the training of personnel in the operation of culture collections;
- encourage distribution of culture data using up-to-date information technology;
- represent culture collections and their users at national and international forums;
- organize conferences and symposia on topics and problems of common interest;
- seek funding possibilities to support UKFCC objectives;
- keep abreast of current and future legislation such as postal regulations, quarantine rules, patent laws, and public health issues; and
- liaise with relevant National Government Departments, funding bodies, and steering groups such as the UK National Culture Collection Steering Group.

Similar objectives are the founding stones of other national organizations that can be found in Belgium, Brazil, China, Cuba, the Czech Republic, France, Indonesia Japan, Portugal, The Philippines, Thailand, and the United States (Table 9.7).

Affiliations of Collections have also been established either as national organizations such as the United Kingdom National Culture Collection (UKNCC) or project consortia. The UKNCC linked 9 collections with over 100,000 strains of algae, bacteria, cell lines, fungi, protozoa, and viruses (37). The online database is easy to use and offers a convenient way to look for materials using a simple interface. The UKNCC secretariat coordinated some of its member's communication and research activities, producing joint catalogues, publicity materials, and the publication, the UKNCC Biological Resource Book (12). The members offer both a culture/cell supply service and an identification service; organisms supplied include actinomycetes, algae, animal cells, bacteria,

TABLE 9.7. Culture Collections Holding 10,000 Strains in the World Data Centre for Microorganisms

Collection	Country	Organism	Number
Agricultural Research Service Culture Collection	USA	Fungi, bacteia	78060
American Type Culture Collection	USA	Bacteria, Archaea, fungi, viruses, plasmids, cell lines	73507
Bioresource Collection and Research Center	Taiwan	Bacteria, fungi, viruses, cell lines	10398
CABI	UK	Fungi and bacteria	29000
Canadian Collection of Fungal Cultures	Canada	Fungi	10000
Centraalbureau voor Schimmelcultures, Fungal and Yeast Collection	Netherlands	Fungi	61000
Center for Fungal Genetic Resources	Korea	Fungi	24531
China General Microbiological Culture Collection Center, Institute of Microbiology, Chinese Academy of Sciences	China	Bacteria, fungi	14433
Culture Collection, University of Goteborg	Sweden	Bacteria, Fungi	40500
DSMZ-Deutsche Sammlung von Mikroorganismen und Zellkulturen GmbH	Germany	Bacteria, Archaea, fungi, viruses, plasmids, cell lines	27360
Department of Medical Sciences Culture Collection	Thailand	Bacteria	10000
European Collection of Cell Cultures	UK	Human and animal cell lines	15400
Fungal Genetics Stock Center	USA	Fungi	16330
IBT Culture Collection of Fungi	Denmark	Fungi	22500
IHEM, Scientific Institute of Public Health	Belgium	Fungi	12282
Institute for Fermentation, Osaka	Japan	Bacteria, Fungi, Cell lines	15784
International Collection of Microorganisms from Plants, Plant Diseases Division DSIR	New Zealand	Bacteria Fungi	10500
Japan Collection of Microorganisms	Japan	Bacteria, Archaea, Fungi	11551
KCTC Korean Collection for Type Cultures	Korea	Bacteria, fungi, cell lines	13155
LMG Bacteria Collection	Belgium	Bacteria	23000
MAFF Genebank, Ministry of Agriculture Forestry and Fisheries	Japan	Bacteria, fungi, viruses, cell lines	19710
Mycotheque de l'Universite catholique de Louvain	Belgium	Fungi	15700
NCCB, the Netherlands Culture Collection of Bacteria (formerly LMD and Phabagen Collection)	Netherlands	Bacteria	11900
Russian National Collection of Industrial Microorganisms	Russia	Bacteria, Fungi, Cell lines	15250
Salmonella Genetic Stock Centre	USA	Bacteria	10060
The Culture and Information Centre of Industrial Microoganisms of China Universities	China	Bacteria, Fungi	13120
The International Escherichia and Klebsiella Centre (WHO)	Denmark	Bacteria	63500
University of Alberta Microfungus Collection and Herbarium	Canada	Fungi, bacteria	10229
28 collections	15 countries	(39% of all strains)	678760

(www.wdcm.ac.jp)

cyanobacteria, filamentous fungi, nematodes, protozoa, mycoplasma, and yeasts. Similar initiatives have brought together Belgian collections, the Belgian Coordinated Collection Collections of Microorganisms (BCCM^{TM}) (45), and European collections through the electronic catalogue Common Access to Biological Resources and Information (CABRI) (38).

9.6 SUMMARY

Despite the 525 collections registered with the World Data Centre for Microorganisms and the 1.7 million strains held by them (Table 9.6), there are still gaps in coverage. Not all species are represented in these collections; currently there are 423,894 fungus names listed by Index Fungorum (46). Published names do not equate to accepted species because fungi will often have different names for the anamorph and teleomorph states and other synonyms. There are currently around 80,000 described fungi and a significantly larger number still to be discovered, which may exceed 1.5 million (47). Considering that many of these cannot yet be grown in culture, collections are doing quite well but there is still some way to go to represent what is in nature. It may not be necessary to ensure all species are represented in collections but at the very least conservation programs for microbes should be established with a balance between

TABLE 9.8. Collections Designated as International Depository Authorities

Collection	Country	Organisms Covered
AGAL, Australian Government Analytical Laboratories	Australia	Microorganisms
BCCM™ IHEM, Scientific Institute of Public Health - Louis Pasteur	Belgium	Fungi, yeasts
BCCM™ LMBP, Universiteit Gent, Vakgroep voor Moleculaire Biologie	Belgium	Plasmids
BCCM™ LMG, Universiteit Gent (RUG), Laboratorium voor Microbiologie, Bacteria Collection	Belgium	Bacteria
BCCM™ MUCL, Mycotheque de l'Universite Catholique de Louvain, Faculté des Sciences Agronomiques (UCL)	Belgium	Fungi, yeasts
CABI Bioscience UK Centre	UK	Bacteria, fungi, nematodes, yeasts
CBS - Centraalbureau voor Schimmelcultures	Netherlands	Bacteria, fungi, yeasts
CCAP, Culture Collection of Algae and Protozoa	UK	Algae, protozoa
CCM, Czech Collection of Microorganisms, Masaryk University	Czech Republic	Bacteria, fungi
CCY, Sláviková, Institute of Chemistry, Slovak Academy of Sciences	Slovakia	Yeasts
CECT, Coleccion Espanola de Cultivos Tipo, Universidad de Valencia, Edificio de Investigacion	Spain	Bacteria, fungi, yeasts
CGMCC, China General Microbiological Culture Center	China	Bacteria
CNCM, Collection Nationale de Cultures de Microorganismes, Institut Pasteur	France	Animal cells, bacteria, phages, fungi, viruses (animal), yeasts
DBVPG, Dipartimento di Biologia Vegetale, Sez. Microbiologia Applicata	Italy	Yeast
DSMZ-Deutsche Sammlung von Mikroorganismen und Zellkulturen GmbH	Germany	Animal cells, bacteria, fungi, phages, plant cells, plasmids, viruses (plant), yeasts
ECACC, European Collection of Animal cells	UK	Animal cells
IAFB, Collection of Industrial Microorganisms	Poland	Microorganisms
ICLC, Interlab Cell Line Collection, Department of Biotechnology, Instituto Nazionale per la Ricerca sul cancro; Advanced Biotechnology Center (ABC)	Italy	Animal cells
IPOD, International Patent Organism Depositary	Japan	Microorganisms
KCCM, Korean Culture Center of Microorganisms	Republic of Korea	Microorganisms
MTCC, Microbial Type Culture Collection and Gene Bank	India	Microorganisms
MSCL, Microbial Strain Collection of Latvia, University of Latvia	Latvia	Bacteria, fungi, yeasts
NBIMCC, National Bank for Industrial Microorganisms and Cell Cultures	Bulgaria	Animal cells, bacteria, fungi, viruses (animal and plant), yeasts
NCAIM, National Collection of Agricultural and Industrial Microorganisms	Hungary	Bacteria, fungi, yeasts
NCIMB, National Collection of Marine, Industrial and Food Bacteria	UK	Bacteria, phages, plasmids
NCTC, National Collection of Type Cultures	UK	Bacteria, plasmids
NCYC, National Collection of Yeast cultures	UK	Yeasts
NMLHC, National Microbiology Laboratory, Health Canada	Canada	Microorganisms
NRRL, Agricultural Research Service Culture Collection	USA	Fungi
PCM, Polish Collection of Microorganisms	Poland	Microorganisms
VKM, All-Russian Collection of Microorganisms, Institute of Biochemistry and Physiology of Microorganisms, Russian Academy of Sciences	Russia	Bacteria, fungi, plasmids, yeasts
VKPM, Russian National Collection of Industrial Microorganisms	Russia	Bacteria, fungi, phages, plasmids, yeasts

in situ and *ex situ* maintenance. The impact of climate change and man's activities affect microorganisms as they do plant and animal life but this hidden resource is often forgotten. There is also an imbalance between where collections are established and where most biological diversity resides. It is often the case that biodiversity rich countries are poor in resources. Table 9.6 demonstrates that 76% of the organisms held are in collections in Europe and the Americas, most of the latter in collections in North America and Canada (Table 9.8). Indeed, the 28 collections (each holding more than 10,000 strains) that are listed in Table 9.8 are from 15 countries and they hold 39% (678,760) of the total numbers of strains held by WDCM registered collections. It is therefore essential that capacity building programs, such as that envisaged by the GBRCN and offered by collections and their organizations such as the WFCC are developed to help establish the facilities and resources to support countries with the greatest need. BRCs offer much needed services to researchers and industry giving access to high quality materials and expertise to ensure their work is based on authentic cultures and validated information.

REFERENCES

1. Biological Resource Centres. Underpinning the Future of Life Sciences and Biotechnology (Online), http://oecdpublications.gfi-nb.com/cgi-bin/oecdbookshop.storefront. Accessed December 01, 2007.
2. Biological Resource Centres. OECD Best Practice Guidelines for Biological Resource Centres (Online), http://www.oecd.org/dataoecd/6/27/38778261.pdf. Accessed December 01, 2007.
3. Kirsop BE, Hawksworth DL. The Biodiversity of Microorganisms and the Role of Microbial Resource Centres. Germany: World Federation for Culture Collections; 1994. ISBN 92 91029 0419.
4. Szaro D. Beyond Borders: Global Biotechnology Report. New York: Ernst & Young; 2006.
5. Newman DJ, Cragg GM. J Nat Prod 2007; 70: 461–477.
6. World Data Centre for Microorganisms (WDCM). Web information available at http://wdcm.nig.ac.jp. Accessed December 01, 2007.
7. Smith D, Rohde C. UK: Society for Microbiology (Online). http://www.sgm.ac.uk/pubs/micro_today/pdf/0299brc.pdf. Accessed November 21, 2007.
8. Smith D, Rohde C. Laboratory manager issue 124. Croner, UK; 2007. pp 6–8.
9. Smith D, Rohde C. Laboratory manager issue 125. Croner, UK; 2008. pp 4–6.
10. World Federation for Culture Collections. Web information available at http://www.wfcc.info. Accessed December 01, 2007.
11. European Culture Collection Organisation (ECCO). Web information available at http://www.eccosite.org. Accessed December 01, 2007.
12. Smith D, Ryan MJ, Day JG. The UK National Culture Collection Biological Resource: properties, maintenance and management. Egham, UK: UK National Culture Collection; 2001.
13. Morris GJ. Cryopreservation: an introduction to cryopreservation in culture collections. Cumbria, UK: Culture Centre of Algae and Protozoa; 1981.
14. Ryan MJ, Smith D, Jeffries P. World J Microb Bio 2000; 16: 183–186.
15. Smith D, Ryan MJ. Mycol Res 2004; 108: 1351–1362.
16. Smith D, Thomas VE. World J Microb Biotechnol 1998; 14: 49–57.
17. Tan CS. Cryptogamie Mycol 1997; 18: 157–163.
18. Tan CS, van Ingen CW, Talsma H, van Miltenburg JC, Steffensen CL, Vlug IA, Stalpers JA. Cryobiology 1995; 32: 60–67.
19. Baker PRW. J Hyg Cambridge 1955; 53: 426–435.
20. Ashwood-Smith MJ, Grant E. Cryobiology 1976; 13: 206–213.
21. Heckly RJ. Adv App Microbiol 1978; 24: 1–53.
22. Polge C, Smith AU, Parkes S. Nature 1949; 164: 666.
23. Franks F. In: Morris GJ, Clarke A, editors. Effects of low temperature of biological membranes. London: Academic Press; 1981. p 3–19.
24. Hubalek Z. Cryopreservation of microorganisms at ultra-low temperatures. Prague: Academy of Sciences of the Czech Republic; 1996.
25. Hwang SW, Howells A. Mycologia 1968; 60: 622–626.
26. Hwang SW, Kwolek WF, Haynes WC. Mycologia 1976; 68: 377–387.
27. Ashwood-Smith MJ, Warby C. Cryobiology 1971; 8: 453–464.
28. Hwang SW. Mycologia 1960; 52: 527–529.
29. Morris GJ, Smith D, Coulson GE. J Gen Microbiol 1988; 134: 2897–2906.
30. WHO. Biosafety manual (Online). http://www.who.int/csr/resources/publications/biosafety/who_cds_csr_lyo_20034/en/.
31. Convention on Biological Diversity. Web information. Available at http://www.biodiv.org. Accessed May 19, 2009.
32. IATA. International ir Transport Association dangerous goods regulations (Online). http://www.iata.org. Accessed December 01, 2007.
33. EBRCN. Information resource (Online). http://www.wfcc.info. Accessed December 01, 2007.
34. International Standards Organisation (ISO). Web information. Available at http://www.iso.ch/iso/en/ISOOnline.frontpage. Accessed December 01, 2007.
35. WFCC. The WFCC guidelines for the establishment and operation of culture collections (Online). http://www.wfcc.info/guideline.html. Accessed December 03, 2007.
36. Hawksworth DL, Schipper MAA. MIRCEN J 1989; 5: 277–281.
37. UK National Culture Collection. Web information. Available at http://www.ukncc.co.uk. Accessed December 01, 2007.
38. Common Access to Biological Resources and Information. Web information. Available at http://www.cabri.org. Accessed December 01, 2007.
39. Budapest Treaty on the International Recognition of the deposit of micro-organisms for the purposes of patent procedure. Web information. Available at http://www.cnpat.com/

worldlaw/treaty/budapest_en.htm. Accessed December 01, 2007.

40. The Asian Consortium for the Conservation and Sustainable Utilisation of Microbial Resources (ACM). Web information. Available at http://www.biotek.lipi.go.id/index.php?option=content&task=view&id=385&catid=120&Itemid=100. Accessed December 01, 2007.
41. Bosschaerts, Marleen, Code of Practice for IDAs Web Information. Europe: IDA Collections. Available at http://bccm.bdlspo.bet/tbu/ida/index.php. Accessed 2007 December 01.
42. Micro-Organisms, Sustainable Access and use, International Code of Conduct (MOSAICC). Web information. Available at http://bccm.belspo.be/projects/mosaicc. Accessed December 01, 2007.
43. The European Culture Collection Organisation. Web information. Available at http://www.eccosite.org. Accessed December 01, 2007.
44. The MIRCEN Secretariat, United Nations Educational Scientific and Cultural Organisation (UNESCO). Web information. Available at http://www.unesco.org/science/life/life1/rcenform.htm. Accessed December 01, 2007.
45. Belgian Coordinated Collection. Collections of microorganisms. Web information. Available at http://www.bccm.belspo.be. Accessed December 01, 2007.
46. Index fungorum web information. Available at http://www.speciesfungorum.org/Names/Names.asp. Accessed December 01, 2007.
47. Hawksworth DL. Mycol Res 2001; 105: 1422–1432.

FURTHER READING

Barnet HL, Hunter BB. Illustrated genera of imperfect fungi. 4th ed. London: Collier Macmillan Publishers; 1998.

Barnett JA, Payne RW, Yarrow D. Yeasts: characteristics and identification. 3rd ed. Cambridge, UK: Cambridge University Press; 2000.

Cannon PF, Kirk PM. Fungal families of the world. Wallingford, Oxon, UK: CABI; 2007.

Day JD, Stacey G. Cryopreservation and freeze-drying protocols. 2nd ed. Totowa, NJ: Humana Press; 2007.

Ellis MB, Ellis JP. Microfungi on land plants an identification handbook. Slough, UK: The Richmond Publishing Co Ltd.; 1997.

Ellis MB, Ellis JP. Microfungi on miscellaneous substrates an identification handbook, Slough, UK: The Richmond Publishing Co Ltd.; 1998.

Gams W, Hoekstra ES, Aptroot A. CBS course of mycology. 4th ed. Utrecht, Netherlands: Centraalbureau voor Schimmelcultures; 1998.

Garrity GM. Bergey's manual of systematic bacteriology. New York: Springer; 2008.

de Hoog GS, Guarro J. Atlas of clinical mycology. Baarn and Delft, The Netherlands: Centraalbureau voor Schimmelcultures; 1995.

Kirk PM, Cannon PF, David JC, Stalpers JA. Ainsworth & Bisby's dictionary of fungi. Wallingford, Oxon, UK: CAB International; 2001.

Kurtzman C, Fell JW. The yeast a taxonomic study. 4th ed. Amsterdam, The Netherlands: Elsevier; 1998.

Sutton BC. The coelomycetes. Wallingford, Oxon, UK: CAB International; 1990.

Swings J, Kurtboke I. Microbial genetic resources and biodiscovery. Wallingford, Oxon, UK: World Federation for Culture Collections; 2000.

Webster J, Weber R. Introduction to fungi. 3rd ed. Cambridge, UK: Cambridge University Press; 2007.

10

CULTURE PRESERVATION

ROBERT L. GHERNA
American Type Culture Collection, Rockville, Maryland

10.1 INTRODUCTION

The ubiquitous presence of microorganisms, as well as their metabolic diversity, has made them important factors in industrial applications and product development. Bacteria, fungi, and yeasts have been used for the production of food, medicinals, solvents, enzymes, and numerous other products. They have also been used as standards for bioassay and bioremediation applications. In addition, advances in bioengineering have enabled the incorporation of genes into microorganisms for the production of mammalian proteins and peptides.

During the past 20 years, cell line technology grew dramatically to enable the isolation and maintenance of a wide variety of tissue lines from any species of interest. The initial use of cell lines for vaccine production was expanded by developments in cell hybridization, transduction and transfection, and genetic manipulation to include the production of monoclonal antibodies, cytokines, and other pharmaceutical products. Lines that have been genetically engineered have been successfully expanded and grown in fermenters for large-scale production.

The development of microbial and cell cultures represents an enormous investment in time and money and is an important asset to industry. These cultures must be protected from accidental loss by means of standardized preservation techniques. The primary aim of culture preservation is to maintain the culture such that it is as close as possible to the original strain or line exhibiting the desired phenotypic or genetic traits. Often, industrial cultures are not analogous to taxonomic strains in that they have been modified to have special properties, either rapid growth, more active metabolic rates, or other features.

Many methods have been used to preserve bacteria and fungi, but not all species respond in a similar way to a given method. Unfortunately there is no universal method that can be applied to all microorganisms. It should be emphasized, however, that the success or failure of any preservation technique also depends on the use of the proper growth medium and cultivation procedures and on the age of the culture at the time of preservation. This is particularly true when working with microorganisms that contain plasmids or recombinant DNA, or that exhibit growth phases such as morphogenesis or spore formation.

The following provides practical information for the maintenance and preservation of bacteria, fungi, yeast, and cell lines. It should be noted, however, that not all microorganisms will be preserved by these methods, and some experimentation with cryoprotective agents and other factors may be necessary for success. Additional information on bacterial, fungal, and cell-line preservation may be found elsewhere (1–3).

10.2 CULTURE AND PRESERVATION OF BACTERIA

10.2.1 Short-Term Preservation

10.2.1.1 Subculture. Most bacteria can be preserved by periodic serial transfer to fresh medium. The period between transfers varies with the organism, medium employed,

Upstream Industrial Biotechnology: Expression Systems and Process Development, Volume 1, First Edition. Edited by Michael C. Flickinger.
© 2013 John Wiley & Sons, Inc. Published 2013 by John Wiley & Sons, Inc.

and the external conditions. In general, minimal media are preferred for subculturing because they lower the metabolic rate of the organism and thus prolong the interval between transfers. In rich media, growth is often much faster, with the accumulation of metabolic products. These compounds may alter environmental conditions such as pH and gas phase and shorten the interval between transfers. Some bacteria such as pathogens need complex media (4) for growth, or their retention of specific physiological properties require the addition of complex compounds to the medium. The subculturing interval for these organisms must be determined by experience.

When preserving bacteria by serial transfer, it is important to use containers that can be securely sealed. Glass test tubes or 6-mL bottles with rubber-lined screw caps are widely used. The bacteria can be grown with slightly loose caps until adequate growth is obtained and then tighten to prevent dehydration. Solid media are preferred to broth because contaminants can be readily seen. Duplicate tubes should be maintained as a precaution against loss, at least until the subculturing interval is determined. The cultures should be examined for purity after each transfer, and abbreviated characterization tests must be run periodically to ensure retention of desired traits. Storage in a refrigerator is the preferred method for subcultures. Many bacteria can be kept for 3–5 months between transfers if proper precautions are taken to avoid dehydration of the medium.

It should be noted, however, that the maintenance of cultures by serial transfer is precarious, time-consuming, and expensive. The frequent transfer of cultures can result in contamination, mislabeling, and the selection of strain variants.

Other methods involve storing cultures at refrigeration temperatures, drying in sterile soil, glass beads, filter paper, and other substrates. Detailed descriptions of these methods can be found in Refs 5–7.

Short-term maintenance and preservation procedures are not recommended for industrial strains because a number of problems can occur using these methods. The main hazards are contamination, population changes through selection resulting in the loss of key genetic and physiological properties, and the expense of maintaining cultures under these conditions.

10.2.1.2 Ordinary Freezing. The use of the freezer compartment of a refrigerator or an ordinary freezer with a temperature range of 0 to -20°C to preserve bacteria is not recommended because the freezing process (see Long-Term Methods, Deep Freeze) damages the cells. In addition, most refrigerators that have a freezer compartment in the range of 0 to -20°C are frost free. The frost-free state is achieved by an alternating warming and cooling cycle, which can result in further damage to the cells and a loss of viability.

10.2.2 Long-Term Methods

10.2.2.1 Freeze-Drying or Lyophilization. Freeze-drying, or lyophilization, is one of the most economical and widely used methods for long-term preservation of bacterial cultures and other microorganisms. Many metabolically diverse bacterial species have been successfully preserved by this technique and have remained viable and unaltered for more than 60 years.

Freeze-drying is a complex process that involves the removal of water and other solvents from a frozen product by sublimation (8,9). Sublimation occurs when a frozen liquid goes directly to a gaseous phase without passing through the liquid phase. There are three stages in the freeze-drying process: (i) prefreezing of the suspension to ensure a solid frozen starting material, (ii) primary drying during which most of the water is removed through sublimation, and (iii) secondary drying to remove the bound water.

The rate of cooling during the prefreezing step and the final temperature of the frozen material can affect the freeze-drying process. The removal of water during the primary drying stage requires an environment that allows the water molecules to migrate from the frozen material. This is achieved by using a vacuum pump. A large-capacity pump must be used to prevent the water vapor load from compromising the efficiency of the system. The procedure also requires a moisture trap or condenser to collect and remove the water molecules before they enter the vacuum system. The condenser temperature must be lower than the frozen material for sublimation to occur. The sublimation rate is dependent on the differential vapor pressure between the frozen material and the condenser. Because the vapor pressure varies with the temperature, heat can be carefully applied to the frozen cell suspension to increase the vapor pressure and promote a faster primary drying rate. Precautions must be taken during the application of heat to prevent the frozen cell suspension from thawing. Most commercial instruments have sophisticated controllers that allow the input of heat to the frozen material to achieve maximum drying rates without damaging the product.

When the primary drying is complete, some bound water remains. This water cannot be eliminated by sublimation and requires the application of external heat to the material under low pressure and low condenser temperature. The moisture remaining in freezed-dried cells is termed residual moisture. A residual moisture content of 1%–3% seems to be required for the long-term shelf life of bacteria. For an in-depth review of the complex freeze-drying process, the reader is referred to several excellent reviews (10–12).

Centrifugal freeze-drying and prefreezing are two of the most commonly used methods of lyophilization of bacteria. In centrifugal freeze-drying, the suspensions are initially frozen by evaporative freezing under a vacuum while centrifuging to prevent frothing due to removal of dissolved

gases. After primary freeze-drying, the vials are constricted using a narrow flame and then placed on a manifold for secondary freeze-drying. A detailed discussion of centrifugal freeze-drying can be found in articles by Rudge (13) and Lapage (14). The prefreezing method employs a controlled rate of cooling to freeze the cell suspension and then a primary drying phase, as discussed earlier.

The simplest system consists of a vacuum pump capable of an ultimate pressure of less than 10 μmHg (a pump rated at 35–50 L/min is usually adequate), a small stainless steel condenser for cooling with dry ice, a thermocouple vacuum gauge to monitor the vacuum system, and heavy-walled vacuum/pressure tubing to connect the components. The connection of these modules into a single system is often termed a component freeze-dryer. The main components are the vacuum pump, thermocouple vacuum gauge, and a condenser that can be attached to several manifolds, to which glass vials can be attached by means of vacuum-tubing nipples, or the manifolds can be connected to a stainless steel pan containing the vials. The manifold system is relatively simple, and it has been used successfully by many laboratories to preserve cultures. A small amount of cell suspension (0.2 mL) containing a cryoprotectant is dispensed into sterile ampules, which are plugged with sterile cotton. A 1-in. piece of nonpowdered amber latex IV tubing is attached to the rim of each ampule (by using a tube stretcher) and then to the manifold. The ampules are then immersed in an ethylene glycol (50%) dry-ice bath at −40°C to freeze the cell suspension. The freeze-drying cycle is initiated by starting the vacuum pump and allowing the temperature of the bath to rise of its own accord to ambient temperature. In general, runs can be started early in the afternoon and allowed to proceed overnight. At the end of the drying cycle, the ampules are sealed using a double-flame air/gas torch and stored at 2–8°C. For specific details on the equipment and methods see articles by Gherna (15) and Simione and Brown (16). Details of other procedures and equipment are given by Haynes *et al*. (17).

The American Type Culture Collection (ATCC) has successfully lyophilized many of the bacteria described in the literature. It currently uses three methods:

1. *Component Freeze-Dryer*. Samples are freeze-dried in cotton-plugged inner vials, which are then sealed in outer vials under vacuum.
2. *Commercial Freeze-Dryer*. Cultures are freezed-dried in the double-vial system in a commercial freeze-dryer.
3. *Preceptrol Cultures*. Cultures are lyophilized in a commercial freeze-dryer using glass serum vials that are sealed with a rubber stopper and metal cap.

It should be noted that after the drying cycle is complete in the commercial freeze-dryer and Preceptrol methods, the vacuum in the drying chamber is replaced with cooled nitrogen gas (2–8°C) that has been passed through a 0.2-μm Pall filter. The condenser temperature must not be allowed to rise above −50°C. The nitrogen gas may have to be passed through a copper coil immersed in liquid nitrogen.

10.2.2.1.1 Culture Preparation. Successful freeze-drying depends on using healthy cells grown under optimum conditions on the medium of choice for each strain, which ensures the retention of the desired features of the bacterium. Bacteria can be grown on agar or in shaken or static broth cultures. The cells are harvested at maximum stability and viability, in the late logarithmic or early stationary phase, and suspended in a medium. The cell suspension should contain at least 10^7–10^{10} cells/mL in order to achieve optimal results. Anaerobic cultures must be grown, harvested, and dispensed under anaerobic conditions (18).

The viability of freeze-dried cultures is greatly influenced by the suspending medium. The choice of suspending medium for freeze-drying depends on the type of bacteria and on the method used.

The ATCC uses two suspending media for the commercial freeze-drying method:

1. Reagent 18
   - 0.75 g trypticase soy broth
   - 10.0 g sucrose
   - 5.0 g bovine serum albumin fraction V
   - 100.0 mL distilled water
   - filter sterilized through a 0.2-μm filter.
2. Reagent 20
   - 10.0 g bovine serum albumin fraction V
   - 20.0 g sucrose
   - 100 mL distilled water
   - filter sterilized through a 0.20-μm filter.

Reagent 18 is more commonly used for freeze-drying bacteria and fungi. Reagent 20 is employed for bacteria that are adversely affected by trypticase soy broth and is added to an equal volume of cell suspension in the broth.

In the component freeze-drying method (double-vial), the additive is a 20% (wt/vol) sterile solution of skim milk, prepared by autoclaving a 20% skim milk solution at 116°C for 20 min in 10-mL tubes. For cultures grown on agar surfaces, the cells are washed off with the 20% skim milk solution. Broth cultures are centrifuged, and the cell pellet is resuspended with the sterile skim milk to give a suspension of 10^8 cells/mL. Skim milk should not be used for bacteria that are inhibited by milk, instead use a 24% (wt/vol) sterile sucrose solution diluted equally with growth medium to yield a 12% (wt/vol) sucrose solution (final concentration) for the single-vial manifold or commercial

freeze-dryer method. As soon as the cell suspension is prepared, it should be dispensed into the ampules. The interval between dispensing and freeze-drying should be kept to a minimum to avoid possible alteration of the culture. Other investigators have used 10% (wt/vol) dextran, horse serum, inositol, raffinose, trehalose, and other cryoprotective chemicals in the suspending medium (19–21).

Most bacteria can be lyophilized using these methods; for those cultures that require special conditions, the reader is referred to Ref. 16. The same methods have been employed successfully to freeze-dry most bacteriophages; exceptions are stored in liquid nitrogen. In general, bacteriophages can be grown in a soft agar layer or in broth. The phages are harvested by scraping off the soft agar with a sterile glass rod or rubber policeman, macerating and dispensing into a sterile centrifuge tube, and centrifuging at low speed to sediment the agar and most of the unlysed bacteria. Broth-gown cultures are centrifuged at low speed to remove the unlysed bacteria. The supernatant is then filtered through a 0.45-μm and then through a 0.2-μm Millipore filter. The filtrate should be titrated to determine the concentration of phages; a titer of 10^8 pfu/mL is desirable. The phage can be freeze-dried using 20% skim milk and the component freeze-dryer method.

Freeze-dried bacteria and bacteriophages can be stored at 2–8°C. A longer shelf life has been obtained when cultures are stored at −30 or −70°C in a mechanical freezer. Freezed-dried cultures should not be stored in a freezer compartment of a frost-free refrigerator because of the alternate heating and freezing cycles, nor should they be stored at room temperature.

Although lyophilization has facilitated the long-term preservation of bacteria, viability checks must be done before and after lyophilization to determine the effectiveness of the process. Quality control procedures must be in place to check for purity, retention of essential characteristics and periodic viability to determine the shelf life of the culture.

10.2.2.2 Deep Freeze. The long-term preservation of bacterial species not amenable to freeze-drying has been achieved through storage in the frozen state at a temperature of −70°C or, more advisable, at the temperature of liquid nitrogen (−196°C) or liquid vapor phase (−150°C).

The freezing process results in several events that can be destructive to the cells. As the bacterial suspension begins to cool, the liquid water turns to ice at 0°C (the exact temperature depending on the nature of the bacterial suspension). Ice formation occurs first in the external aqueous environment, resulting in an increased concentration of solutes outside the cells. The differential osmotic pressure causes water to migrate from the cells. The rate and extent of the water loss are dependent on the rate of cooling and the permeability of the cells. Removal of too much water leads to a concentration of solutes within the cells that may be harmful. If too much water is left in the cells, internal ice crystals may form, which would result in intracellular damage. It is important to maintain the critical balance between the two events by controlling the rate of cooling while freezing the cells, and warming as rapidly as possible when the cells are thawed. Chemical compounds such as glycerol and dimethyl sulfoxide (DMSO) can be added to the cells to minimize the damage caused by freezing. These compounds, labeled cryoprotective agents (see Cryoprotectants), exhibit certain properties that are essential for good cryoprotection (22,23). They must be nontoxic to the cells, show good permeability, and bind either the electrolytes that accumulate or the water molecule to delay freezing.

The physiological condition of the cells plays an important role in survival of freezing. In general, actively growing cultures harvested at the mid to late logarithmic phase of growth will survive the freezing process better than those harvested at an earlier or later phase. The bacteria should be grown under optimum conditions in the appropriate medium that best retains the prominent characteristics of the strain. Bacteria can be grown on broth that is static or shaken, or on agar. Shaken cultures generally reach optimal cell density faster than agar-grown cultures. Some strict anaerobes require prereduced media and anaerobic procedures for harvesting and dispensing.

Cells grown in broth cultures are harvested by aseptic centrifugation, and the resultant pellet is resuspended in sterile broth containing 30–50% (vol/vol) sterile glycerol. Bacteria grown on agar are harvested by aseptically washing the growth with sterile broth containing the cryoprotectant. Dispense 0.4 mL of the cell suspension, containing at least 10^8 cell/mL into each sterile, prelabeled vial. Plastic presterilized screw-capped vials (such as Nunc) are recommended for bacteria. Place the filled vials into a mechanical freezer set at −70°C. The cells are recovered by rapidly thawing the frozen cell suspensions in a 37°C water bath.

A wide variety of bacterial have been successfully preserved at −70°C using glass beads and 15% glycerol as the cryoprotectant (24). The glass beads are prepared as described in Ref. 15, and 30 beads are placed in 2-mL glass screw-cap vials and sterilized for 15 min at 121°C. The vials must be prelabeled with ink that will not come off at ultralow temperatures. Cell suspensions are prepared containing $\sim 10^8$ organisms/mL in sterile 15% glycerol, and 0.5 mL is dispensed into each vial. The vials are shaken gently to ensure that all the beads are wetted with the bacterial suspension, and then the excess liquid is aseptically removed with a sterile pasteur pipette. The vials are placed into a mechanical freezer at −70°C. The cells are recovered by aseptically removing a bead from the vial with a sterile spatula or forceps and placing the bead in sterile broth. It should be noted, however, that the contents of the vial

should not be allowed to thaw; this can be prevented by placing the vial in crushed dry ice and removing the bead after ensuring the beads will remain frozen. This technique has been used to preserve bacteria obtained from extreme environments such as hypersaline pools.

Precautions must be taken against electrical shutdowns and compressor malfunctions. Adequate back-up systems (such as alarms, back-up freezers, or an electrical generator) will help to prevent the loss of a valuable collection. However, additional alarm systems are recommended, such as the sound/off power-temperature monitor (Arthur H. Thomas Co.), which has a temperature range of −75 to +200°C. The unit is battery powered and can be mounted on a wall.

10.2.2.3 Ultrafreezing or Cryopreservation. Although the long-term maintenance of bacteria in liquid nitrogen has been considered expensive, the successful preservation of physiologically diverse bacteria by this method, along with minimal handling and lower labor cost, makes this method feasible to use. The ATCC has successfully preserved many bacteria and bacteriophages, including fastidious ones, in liquid nitrogen for over 36 years without the loss of phenotypic properties.

A large variety of liquid-nitrogen refrigerators are now commercially available, with a wide assortment of features and storage capacities. The sizes range from 10 to 1000 L, allowing storage of 300–40,000 ampules.

The physiological condition of the cultures plays an important role in the survival of bacteria under liquid-nitrogen freezing. Bacteria are grown in the appropriate medium and harvested at mid-late logarithmic phase of growth (25). Cultures grown in broth are harvested by aseptic centrifugation, and the resultant pellet is resuspended with sterile fresh medium containing either glycerol or DMSO. For agar-grown cells, the growth is washed off from the agar surface with sterile broth containing the appropriate cryoprotectant. Cryoprotective agents must be added to the suspending medium to protect cells from freeze damage. Cryoprotectants fall into two main classes: compounds such as glycerol and DMSO, which are permeable and appear to provide both intracellular and extracellular protection against freezing; and agents such as dextran, glucose, lactose, mannitol, polyglycol, polyvinylpyrrolidone, and sucrose, which seem to exert their protective effect external to the cell membrane. The first class of cryoprotectants has proven to be the most effective, and in general, glycerol and DMSO seem to be equally effective in protecting a wide range of bacteria. It is advisable to conduct a tolerance test on new species to ascertain whether the cryoprotectant is toxic or beneficial.

DMSO and glycerol are routinely used at concentrations of 5% (vol/vol) and 10% (vol/vol), respectively, in the proper suspending medium. Glycerol is normally prepared as a double-strength (20%, vol/vol) solution and then mixed with an equal amount of the cell suspension. Glycerol is sterilized by autoclaving at 121°C for 15 min and stored in 6-mL volumes at 2–8°C. DMSO is filter sterilized with a 0.22-μm-pore-size Teflon (polytetrafluoroethylene) membrane (Gelman or Millipore) that has been prewashed with methanol and DMSO, collected in 10- to 15-mL quantities in sterile test tubes, and stored in the frozen state at 5°C (DMSO freezes at 18°C) and protected from light. An opened bottle of DMSO should not be used for more than 1 month because of the accumulation of oxidative breakdown products.

Cell suspensions containing at least 10^8 cells/mL are dispensed into prelabeled sterile vials. There are a variety of vials available commercially, ranging from prescored glass to sterile plastic. With glass vials, care must be taken when sealing and storing because improperly sealed glass vials can explode when retrieved from the liquid nitrogen as a result of the rapid expansion of the liquid nitrogen that enters the vials through microscopic holes. Plastic screw-cap vials that are not properly sealed can fill with liquid nitrogen if stored in liquid phase; retrieval of the vials to a warmer temperature can result in liquid nitrogen expansion, causing the contents of the plastic vials to spray into the laboratory environment. Plastic screw-cap vials should always be stored in the vapor phase. Protective gloves and face shields should be worn when handling frozen liquid-nitrogen vials.

The rate of cooling is important in liquid-nitrogen storage. In general, the best results for preservation of bacteria have been achieved with slow cooling. This step can be controlled using programmable controllers such as the Linde BF 3-2 (Union Carbide Corp.), which has an adjustable cooling rate. The cells are frozen at a controlled rate of 1–3°C/min to −40°C and then at a more rapid rate of 10°C/min to −90°C. After this temperature is reached, the vials are transferred to a liquid-nitrogen tank and stored in the liquid phase at −196°C or above in the vapor phase at −150°C.

If a programmable freezer is not available, slow cooling can be obtained by placing the filled glass or plastic vials in a stainless steel pan at the bottom of a mechanical freezer at −60°C for 1 h and then plunging the vials into a liquid-nitrogen bath for 5 min. The rate of cooling to −60°C is ∼1.5°C/min. The frozen vials can then be stored in the liquid-nitrogen tank in the liquid or vapor phase.

It has been reported that the best recovery of cultures from liquid-nitrogen storage is obtained by rapid thawing (26,27). This has also been the experience with cultures frozen at the ATCC. The events during thawing are complex, and slow warming rates can lead to ice crystal formation; a rapid warming rate of ∼100°C/min will minimize the damage due to ice formation. A rapid rate of warming

can be achieved by quickly immersing the frozen vials in a 37°C water bath with moderate agitation until all the ice melts. This usually takes about 50 s for glass vials and 90 s for polypropylene ones.

Cryopreservation of strict anaerobic bacteria must be performed under anaerobic conditions. Technical details of the procedures involved have been described by Hill *et al*. (28). The reader should consult various sections of *Bergey's Manual of Systematic Bacteriology*, volumes 1–4 (29–32), for information on the maintenance and preservation of representative bacterial genera.

The successful cryopreservation of plasmid-containing bacteria depends on the stability of their plasmids (33). These organisms are less genetically stable and more likely to lose their foreign genetic material (34). In general, bacteria containing unstable plasmids should be grown on antibiotic-containing liquid medium at 30°C, frozen with 10% (vol/vol) glycerol, and stored in the vapor over liquid nitrogen.

10.3 CULTURE AND PRESERVATION OF FUNGI AND YEAST

10.3.1 Short-Term Preservation

10.3.1.1 Subculture. Many filamentous fungi can be successfully maintained by serial transfer on suitable media. It is important, however, to use optimal media and growth conditions to ensure healthy cells that retain their morphological and physiological characteristics. A list of suitable media and incubation temperatures for a variety of fungi is provided by Onions and Pitt (35). In general, a medium that promotes good sporulation is considered to be the most desirable. When possible, it is best to cultivate the fungi on agar slants in test tubes or culture bottles. Transfers should be made only from the growing edges of the culture, taking precautions to ensure that contamination is prevented. Some fungi degenerate when maintained on the same medium for extended periods, thus media should be alternated from time to time. A minimal medium such as potato/carrot agar can often be used to induce sporulation in a culture that has deteriorated (36). Also, the continual transfer of spores from some aging fungal cultures such as *Mucorales* can result in a deterioration of the culture; the transfer of mycelium and spores seems to minimize this problem.

The interval between transfers varies from fungus to fungus; some require transfer every 2–4 weeks, the majority every 2–4 months, while others may survive for 12 months without transfer. Cultures grown on agar slants can be stored at room temperature. Storage in the refrigerator or cold room at 5–8°C can extend the transfer period to 4–6 months. However, there are some fungi, such as the thermophiles, that are sensitive to storage at these temperatures.

The maintenance of fungi by serial transfer has many disadvantages. The most notable are contamination, selection of variants, mislabeling of cultures, infestation with mites, and labor intensity.

Yeasts have been successfully maintained by serial transfer on either solid or liquid media. In general, many yeasts will survive for longer periods when grown on solid media rather than in broth, especially nonfermentative yeast. Fresh medium is inoculated with actively growing cells and incubated at the appropriate temperature. After sufficient growth occurs, the cells are stored at refrigerated temperature (+4°C). The majority of yeast species will remain viable for a least 6 months. The interval between transfers must be determined by experimentation. Serial transfer is not recommended for extended maintenance because genetic drift has been observed. In addition, ascosporogenous strains may sporulate on agar slant media stored for prolonged periods, resulting in strain variability.

Many fungi and yeast can be preserved for years by drying on a suitable menstruum such as soil, silica gel, and filter paper (37), and drying under vacuum from the liquid state (L-drying) (38).

10.3.1.2 Silica Gel. Sterile anhydrous silica gel (6–22 mesh, nonindicator) is prepared by dispensing the gel into growth bottles so that they are one-quarter filled, and sterilizing in an oven at 180°C for 2–3 h. The bottles containing the sterile gel are cooled by placing in a pan containing ethylene gycol and dry ice to the depth of the gel layer or by placing the bottles in water in a mechanical freezer at a temperature of −17 to −24°C. Fungal spores are suspended in a sterile 5% skim milk solution that has been cooled to 4°C. The spore suspension is added to the cooled silica gel until three-quarters of the gel has been moistened. It is important to avoid saturating the gel. The growth bottles are left in the ice bath for ∼20–30 min and then agitated to ensure thorough dispersion of the suspension. The bottles are held at 25°C for ∼1–2 weeks until the crystals easily separate when shaken. Inoculated bottles are sealed with screw caps and stored over indicator silica gel in an airtight container at 4°C. To recover the fungal spores, a few crystals are sprinkled on an appropriate medium and incubated. This method has been used successfully for a variety of fungi (39). This method has produced variable results with yeast; some are not viable after 3 months of storage, whereas other survive after 2–5 years (40).

10.3.1.3 Soil. A variety of fungi have been maintained in soil (41). The method involves the inoculation of ∼1 mL of a spore suspension into soil that has been sterilized by autoclaving twice, 24 h apart, at 121°C for 15 min. The soil is incubated at room temperature for 5–10 days and then stored in a refrigerator at 4–8°C. Cultures are recovered by inoculating a suitable medium with a few grains of soil.

10.3.1.4 Paper. Yeasts have been preserved by drying on paper discs or squares and storage over the desicant silica gel (42). Whatman No. 4 filter paper is cut into small squares or discs about 10 mm across and placed on a small aluminum foil, which is folded into a packet and autoclaved at 121°C for 15 min. The sterile discs or squares are inoculated by immersing into drops of a heavy yeast suspension prepared in 5% skim milk. The packets are dried in a desiccator for 2–3 weeks at 4°C and then placed in an airtight container and stored at 4°C. Cultures are recovered by aseptically removing a piece of filter paper and inoculating the appropriate solid or liquid medium. Yeast maintained in this manner have been viable after 2–3 years.

10.3.1.5 L-Drying. L-drying refers to liquid-state drying in such a way as to prevent freezing. Drying occurs under vacuum at temperatures generally no colder than 5–10°C. The method has been improved and simplified by Malik (43) for the preservation of sensitive microorganisms that are damaged by freezing or freeze-drying. The technique has been used to successfully preserve some yeasts and filamentous fungal spores.

10.3.2 Long-Term Methods

10.3.2.1 Freeze-Drying or Lyophilization. The equipment, cryoprotectants, and theoretical aspects of freeze-drying have already been discussed. Fungi are grown under optimum conditions using media that will produce maximum sporulation. Mature spores are harvested by flooding the agar cultures with ~2 mL of a 20% sterile skim milk solution. The skim milk must be cold when used, and thus it is stored at 2–8°C until required. The spores are gently scraped from the surface of the culture to yield a suspension containing at least 10^6 spores/mL. The spore suspension is pipetted back into the tube containing the remaining milk and mixed thoroughly. If more than one tube is used, repeat the procedure and pool the suspension in one tube to yield a concentration of at least 10^6 spores/mL. The spores of cultures grown in broth medium are centrifuged and resuspended in sterile 20% skim solution. Approximately 0.2 mL of the spore suspension is dispensed into sterile vials for freeze-drying. The interval between harvesting the spores and dispensing must be minimized because many spores begin to germinate when suspended in liquid. Spores should not be in the skim milk for more than 2 h before being processed. Filled vials should be refrigerated while awaiting further processing.

The fungi are freeze-dried using one of the ATCC methods already described. Lyophilized spores can be stored at 2–8°C. Extended shelf life can be achieved by storing the vials at −70°C in a mechanical freezer.

Freeze-dried fungal cultures are rehydrated with 0.5–0.9 mL of sterile water, then transferred to tubes containing 6 mL sterile water and allowed to soak for 50–60 min before transferring to solid medium.

At the ATCC, yeasts are processed in the same manner as bacteria for the component freeze-drying method. Cultures are grown on the appropriate solid medium and suspended in sterile 20% skim milk or reagent 18 to a concentration of at least 10^6 cells/mL. The suspension is mixed thoroughly, and 0.2 mL is dispensed into each vial. The cultures are freezed-dried using the component freeze-drying method described earlier.

10.3.2.2 Ultrafreezing or Cryopreservation. The preservation of fungi at ultralow temperatures of liquid nitrogen (−196°C for liquid phase and −150°C for vapor phase) is presently considered the best method of storage. The method can be applied to both sporulating and nonsporulating strains, as well as those fungi that have been genetically altered or harbor plasmids. The freezing rates and cryoprotective agents described for bacteria are also applicable to the freezing of fungi. Spores or mycelial fragments are harvested by flooding slants or plates with 10% glycerol or 5% DMSO and gently scraping the surface of the cultures. The fungal suspension is dispensed in 0.5-mL amounts into sterile plastic freezing vials and frozen at a controlled rate. Fungi that produce sticky mycelia or whose mycelia grow embedded in the agar can be prepared for freezing by cutting agar plugs containing new growth (hyphyl tips) with a sterile cork borer (5 mm). Three or four plugs are place into each sterile plastic vial with 0.4 mL of 10% glycerol and frozen at a slow controlled rate.

Cultures grown in broth are fragmented in a sterile Waring blender in a biological hood and suspended in equal parts of 20% glycerol and growth medium or equal parts of 10% DMSO and growth medium to give a final concentration of 10% glycerol (vol/vol) or 5% (vol/vol) DMSO, respectively. Some strains must be concentrated by centrifugation in order to obtain sufficient material for freezing. Pathogens must not be macerated in a mechanical blender because of the hazard of aerosol dispersion.

Some cultures, such as *Agaricus* strains, can consist of seeds, grains, or pollen and be frozen without the presence of a cryoprotectant. Slime molds can be preserved by freeze-drying or freezing. Spores, microcysts, and spherules are preserved by a controlled freeze in 10% glycerol and stored in the liquid-nitrogen vapor phase. Thawing of the frozen culture should be done rapidly in a 37°C water bath with moderate agitation. Once the ice melts, the culture can be transferred to a suitable medium.

Yeast cells have been successfully preserved by controlled freezing to liquid-nitrogen temperature (−196°C liquid, −150°C vapor phase). The yeast cultures are handled in the same manner as bacteria and grown as described

in the freeze-drying section for yeast. Cell suspensions are prepared in 10% glycerol to a concentration of at least 10^6 cells/mL. The yeast are frozen under controlled conditions as described in the bacterial section.

Several reports have described the loss of plasmid expression or the induction of respiratory-deficient mutants in yeast as a result of freeze-drying or improper freezing (44). Nierman and Feldblyum (33) reported that when plasmid-containing *Saccharomyces cerevisiae* were preserved by freezing in liquid nitrogen, no loss of viability was observed, and the fraction of plasmid-containing cells was the same before and after freezing. The preservation of plasmid-containing yeast is superior in liquid nitrogen with a controlled freezing rate than by freeze-drying.

10.4 CULTURE AND PRESERVATION OF CELL CULTURES

10.4.1 Long-Term Preservation

10.4.1.1 Ultrafreezing or Cryopreservation. Storage in liquid nitrogen is currently the best method of preserving cultured cells. Cryopreservation methods for a variety of cell lines are well developed and used extensively for culture storage. For a detailed description of standard cryopreservation protocols see reports by Freshney (45) and Hay (46).

The general events that occur during freezing and the effect of the cooling rate, cryoprotective agents, and a controlled rate of cooling have been discussed in the bacterial section.

Cell suspensions are prepared in the same manner used for routine subcultivation; trypsin is added if necessary to produce a uniform suspension. The cell suspension is centrifuged at $\sim 100g$ for 10 min, and the resultant pellet is resuspended in an appropriate amount of fresh medium containing a cryoprotectant. Normally, 5–10% DMSO or glycerol is employed. The freeze medium should be prepared just prior to use by mixing fresh growth medium and the cryoprotective agent and kept at room temperature. The remaining cryoprotectant is discarded because oxidative contaminants can accumulate. A cell suspension containing $\sim 10^6$–10^7 cells/mL is satisfactory. The cell suspension is dispensed in 1-mL amounts into each glass vial or plastic ampule and frozen at a controlled rate of 1°C/min to about −50°C. The vials are immediately transferred into liquid nitrogen for storage in the liquid or vapor phase. Rapid thawing is essential for recovery of frozen cells, thus the frozen vials are immersed directly into a 37°C water bath and agitated until the suspension is completely thawed. The thawed cell suspension is transferred to 10 mL of sterile growth medium and centrifuged at $100g$ for 10 min. The supernatant containing the cryoprotectant is discarded, and the cell pellet is resuspended in fresh medium and propagated using standard procedures.

10.4.1.2 Quality Control. It is important that all preservation methods include standard operating procedures for the determination of culture purity, viability, retention of morphological and physiological characteristics, production of desirable products, and other key attributes. Purity checks must be conducted before and after processing microorganisms for freeze-drying and microorganisms and cell lines for freezing. Generally, the cell suspension is diluted and inoculated into suitable medium and incubated at optimum temperature. After growth appears, the cultures are examined for purity. It is also important to conduct pre- and post-preservation viability checks for freeze-drying and freezing to determine the effectiveness of the process. In addition, periodic viability assays should be performed to ascertain the shelf life of the culture.

Cell lines should also be examined for *Mycoplasma* contamination, because it has been estimated that about 10% of cell lines are contaminated (47). It is also important to conduct tests to verify cell-line identity; several rapid techniques have been developed that use DNA probes to identify the cell lines (48).

10.4.1.3 Documentation. Documentation plays an important role in the maintenance and preservation of cultures. Important data include the identity of the culture, isolation source and methods, the individual who isolated it, geographical location, morphological and physiological characteristics, maintenance data, and other salient features. If the culture was obtained from another investigator, the documentation should include the name of the investigator, culture history if available, and date of acquisition. The greater the amount of data recorded and regularly updated, the greater the value of the culture.

REFERENCES

1. R.J. Heckly, Adv. Appl. Microbiol. 24: 1–53 (1978).
2. D. Smith and J. Kolkowski, in J.C. Hunter-Cevera and A. Belt eds., Maintaining Cultures for Biotechnology and Industry, Academic, New York, 1996, p. 101–132.
3. R.J. Hay, in I. Freshney ed., Animal Cell culture: A Practical Approach, IRL Press, Oxford, England, 1986, p. 71–112.
4. F. Kauffman, The Bacteriology of Enterobacteriaceae, Williams & Wilkins, Baltimore, 1966, p. 1–400.
5. L.R. Hill and B.E. Kirsop eds., Living Resources for Biotechnology, Cambridge University Press, Cambridge, 1991.
6. B.E. Kirsop and J.J.S. Snell eds., Maintenance of Microorganisms: A Manual of Laboratory Methods, Academic, London, 1984.
7. R.E. Miller and L.A. Simmons, J. Bacteriol. 84: 1111–1114 (1962).
8. L.R. Rey, in V.J. Cabasso and R.H. Regamey eds., Development in Biological Standardization. International Symposium

of Freeze Drying of Biological Products, S. Karger, Basel, 1977, 19–27.

9. T.W.G. Rowe and J.W. Snowman, Edwards Freeze-drying Handbook, Edwards High Vacuum, Inc., Grand Island, New York, 1976.
10. R.J. Heckly, Adv. Appl. Microbiol. 3: 1–76 (1961).
11. R.J. Heckly, Dev. Ind. Microbiol. 26: 379–395 (1985).
12. H.T. Merryman, in H.T. Merryman ed., Cryobiology, Academic, New York, 1966, p. 609–663.
13. R.H. Rudge, in B.E. Kirsop and A. Doyle eds., Maintenance of Microorganisms and Cultured Cells, 2nd ed., Academic, London, 1991, p. 31–44.
14. S.P. Lapage, J.E. Shelton, T.G. Mitchell, and A.R. Mackenzie, in J.R. Norris and D.W. Ribbons eds., Methods in Microbiol, vol. 3A, Academic, London, 1970, p. 135–228.
15. R.L. Gherna, in P. Gerhardt, R.G.E. Murray, W.A. Wood, and N.R. Krieg eds., Methods for General and Molecular Bateriology, American Society for Microbiology, Washington, D.C., 1994, p. 278–292.
16. F.P. Simione and E.M. Brown eds., ATCC Preservation Methods: Freezing and Freeze-drying, American Type Culture Collection, Rockville, Md., 1991.
17. W.C. Haynes, L.J. Wickerham, and C.W. Hesseltine, Appl. Microbiol. 3: 361–368 (1955).
18. H. Hippe, in B.E. Kirsop and A. Doyle eds., Maintenance of Microorganisms and Cultured Cells, 2nd ed., Academic, London, 1991, p. 101–113.
19. V.J. Cabasso and R.H. Regamy eds., International Symposium on Freeze-Drying of Biological Products, Dev. Biol. Stand. vol. 36, 1977.
20. H.T. Merryman, in H.T. Merryman ed., Cryobiology, Academic, New York, 1966, p. 1–114.
21. K.F. Redway and S.P. Lapage, Cryobiology 11: 73–75 (1974).
22. G.M. Fahy, Cryobiology 23: 1–13 (1986).
23. H.T. Merryman, Cryobiology 8: 173–183 (1971).
24. R.K.A. Feltham, A.K. Power, P.A. Pell, and P.H.A. Sneath, J. Appl. Bacteriol. 44: 313–316 (1978).
25. M.L. Speck and R.A. Cowan, in H. Iizuka and T. Hasegawa eds., Proceedings of the First International Conference on Culture Collections, Univ. of Tokyo Press, Tokyo, 1970, p. 241–250.
26. A.P. Mackenzie, in V.J. Cabasso and R.H. Regamey eds., International Symposium on Freeze-Drying of Biological Products, S. Kargel AG, Basel, 1977, p. 263–277.
27. P. Mazur, in H.T. Merryman ed., Cryobiology, Academic, New York, 1966, p. 213–315.
28. L.R. Hill, M. Kocur, and K.A. Malik, in L.R. Hill and B.E. Kirsop eds., Living Resources for Biotechnology, Cambridge University Press, Cambridge, 1991, p. 62–80.
29. N.R. Krieg and J.G. Holt eds., Bergey's Manual of Systematic Bacteriology, vol. 1, Williams & Wilkins, Baltimore, 1984.
30. P.H.A. Sneath, N.S. Mair, M.E. Sharpe, and J.G. Holt eds., Bergey's Manual of Systematic Bacteriology, vol. 2, Williams & Wilkins, Baltimore, 1986.
31. J.T. Staley, M.P. Bryant, N. Pfennig, and J.G. Holt eds., Bergey's Manual of Systematic Bacteriology, vol. 3, Williams & Wilkins, Baltimore, 1989.
32. S.T. Williams, M.E. Sharpe, and J.G. Holt eds., Bergey's Manual of Systematic Bacteriology, vol. 4, Williams & Wilkins, Baltimore, 1989.
33. W.C. Nierman and T. Feldblyum, Dev. Ind. Microbiol. 26: 423–434 (1985).
34. T. Imanaka and S. Aiba, Ann. N.Y. Acad. Sci. 36: 1–14 (1981).
35. A.H.S. Onions and J.I. Pitt, in D.L. Hawksworth and B.E. Kirsop eds., Living Resources for Biotechnology, Cambridge University Press, Cambridge, 1988, p. 188–193.
36. D. Smithand J. Kolkowski, in J.C. Hunter-Cevera and A. Belt eds., Maintaining Cultures for Biotechnology and Industry, Academic, San Diego, 1996, p. 101–132.
37. D. Smith, in D.L. Hawsworth and B.E. Kirsop eds., Living Resources for Biotechnology, Cambridge University Press, Cambridge, 1988, p. 75–99.
38. I.C. Tommerup and D.K. Kidby, Appl. Environ. Microbiol. 37: 831–835 (1979).
39. D. Smith, in B.E. Kirsop and J.J.S. Snell eds., Maintenance of Microorganisms: A Manual of Laboratory Methods, Academic, London, 1984, p. 83–107.
40. B.E. Kirsop, in B.E. Kirsop and J.J.S. Snell eds., Maintenance of Microorganisms: A Manual of Laboratory Methods, Academic, London, 1984, p. 109–130.
41. R.G. Atkinson, Can. J. Bot. 32: 542–547 (1953).
42. R.G. Atkinson, Can. J. Bot. 32: 673–678 (1954).
43. K.A. Malik, J. Microbiol. Methods 12: 125–132 (1990).
44. B.M. Pearson, P.J.H. Jackman, K.A. Painting, and G.J. Morris, Cryo-Letters 11: 205–210 (1990).
45. R.I. Freshney, Culture of Animal Cells: A Manual of Basic Technique, 3rd ed., Wily-Liss, New York, 1994.
46. R.J. Hay, in R.I. Freshney ed., Animal Cell Culture: A practical Approach, IRL Press, Oxford, England, 1986, p. 71–112.
47. R.J. Hay, in J.C. Hunter-Cevera and A. Belt eds., Maintaining Cultures for Biotechnology and Industry, Academic, San Diego, 1996, p. 161–178.
48. D.A. Gilbert, Y.A. Reid, M.H. Gail, D. Pee, C. White, R.J. Hay, S.J. O'Brien, Am J. Hum. Genet. 47: 499–514.

11

EXPRESSION AND SECRETION OF HETEROLOGOUS PROTEINS, *BACILLUS* AND OTHER GRAM-POSITIVE BACTERIA

BOYKE BUNK
Institute of Microbiology, Technische Universität Braunschweig, Braunschweig, Germany

REBEKKA BIEDENDIECK
Protein Science Group, Department of Biosciences, University of Kent, Canterbury, Kent, United Kingdom

DIETER JAHN
Institute of Microbiology, Technische Universität Braunschweig, Braunschweig, Germany

PATRICIA S. VARY
Department of Biological Sciences, Northern Illinois University, DeKalb, Illinois

11.1 INTRODUCTION

Several species and strains of the genus *Bacillus* have been used for decades to produce useful products such as α-amylases for food industry, including sweeteners and bread manufacture, and in biofuel production using starch substrates on a very big scale, as well as proteases for laundry detergents. The simple media required for optimum growth and production are well known and many protocols for cultivating the organisms have been optimized over many years. This chapter will review the characteristics of several of the most utilized industrial species, both as enhanced producers of natural products and as hosts for products derived from genetic engineering. Many of the genomes of useful bacilli have been sequenced, which should greatly facilitate their use through new and innovative strategies.

11.1.1 Advantages of Bacilli

Within the Gram-positive bacteria, *Bacillus* represents one of the most interesting genera. Since they lack the outer cell membrane found in Gram-negative bacteria, bacilli are able to secrete large amounts of proteins into their surrounding medium. The secretion of various proteins enables the cell to attack and convert highly polymeric nutrients such as polysaccharides, nucleic acids, peptides, and lipids into monomeric or dimeric building blocks, that are then taken up by the cell. This phenomenon allows *Bacillus* to grow on many simple substrates. The genus also lacks the endotoxins associated with the outer membrane of Gram-negative organisms. Moreover, members of the genus that are used as hosts for the production and secretion of (recombinant) proteins in industry are also nonpathogenic. The major industrial strains are *Bacillus subtilis*, *Bacillus licheniformis*, *Bacillus amyloliquefaciens*, *Bacillus clausii*, *Brevibacillus brevis*, and *Bacillus megaterium*. The first four species are closely related (1). In contrast, *B. brevis* and *B. megaterium* are less related to each other as well as to the others (1). *B. subtilis* and *B. licheniformis* are designated as Generally Recognized As Safe (GRAS) by the Food and Drug Administration of the United States (2).

Upstream Industrial Biotechnology: Expression Systems and Process Development, Volume 1, First Edition. Edited by Michael C. Flickinger.
© 2013 John Wiley & Sons, Inc. Published 2013 by John Wiley & Sons, Inc.

11.1.2 Bacilli in Industry

Bacilli were used for many years in the food and feed industry for the production of proteins and metabolites. Recently, since the industry has become more aware that the oil supplies of the world are not endless, the so-called "white biotechnology" is gaining in importance. "White Biotechnology" stands for the biotechnological production of chemical bulk products and fine chemicals using microorganisms. In 2008, the German company BASF SE (Ludwigshafen, Germany) spent $135 million in research and development in the white biotechnology sector. Within this branch of biotechnology, enzymes of bacilli represent around 60% of the approximately € 2 billion worldwide industrial market of homologous and heterologous enzyme production (3). The genus *Bacillus* has long been used for the production of enzymes including several α- and β-amylases for starch modification in the baking industry and also to a much greater extend for starch processing in general on a level of over 30 millions of tons for ethanol manufacture, and sweetener production (glucose and glucose/fructose syrup) (4,5). Furthermore, the production of penicillin acylases essential for the synthesis of novel β-lactam antibiotics (6), neutral proteases, employed in the leather tanning industry since the early twentieth century and glucose dehydrogenase as well as eukaryotic proteins are major products. Besides the production and secretion of different kinds of proteins, bacilli are known to produce metabolites including pyruvate (7) and vitamin B_{12} (8). Many pharmaceutically and industrially relevant natural and recombinant proteins produced by bacilli are summarized in Table 11.1 (*B. megaterium* products are given in Table 11.5).

11.2 MAJOR INDUSTRIAL STRAINS

11.2.1 *Bacillus subtilis*

Over the last 30 years, *B. subtilis* strain 168 has been the Gram-positive model organism. The first version of

TABLE 11.1. Production Yields of Some Industrially and Pharmaceutically Relevant Proteins which were Successfully Produced in *B. subtilis*, *B. licheniformis*, and *B. brevis*[a]

Recombinant Protein	Bacillus Strain	Yield (mg/L)	Secretion (Yes/No)	References
α-Amylase (*Bacillus amyloliquefaciens*)	*B. subtilis*	1000–3000	Yes	10
α-Amylase (*Bacillus licheniformis*)	*B. licheniformis*	n.d.	Yes	11
	B. brevis	3500	Yes	12
α-Amylase (*Bacillus stearothermophilus*)	*B. brevis*	3000	Yes	12
α-Amylase (human)	*B. brevis*	60	Yes	13
β-Amylase (human)	*B. brevis*	1600	Yes	12
β-Tubulin (*Plasmodium falciparum*)	*B. brevis*	2	Yes	14
Cellulase	*B. brevis*	100	Yes	15
Chitosinase (*Bacillus amyloliquefaciens*)	*B. brevis*	150	Yes	16
Cholera toxin B (*Vibrio cholerae*)	*B. brevis*	1400	Yes	17
Gelatin	*B. brevis*	500	Yes	18
Gramicidin, linear	*B. brevis*	20.3	Yes	19
Epidermal growth factor (human)	*B. brevis*	240	Yes	20
Epidermal growth factor (human)	*B. subtilis*	7	Yes	21
Epidermal growth factor (mouse)	*B. brevis*	50	Yes	22
Mouse/human chimeric Fab′	*B. brevis*	100	Yes	23
Interferon-α2 (human)	*B. subtilis*	0.5–1.0	Yes	24
Interleukin-1 receptor antagonist (human)	*B. brevis*	200	Yes	25
Interleukin-2 (human)	*B. brevis*	120	Yes	26
Interleukin-6 (human)	*B. brevis*	200	Yes	27
Lipase A	*B. subtilis*	600	Yes	28
Penicillin G acylase	*B. subtilis*	n.d.	Yes	29
Pepsinogen (swine)	*B. brevis*	11	Yes	12
Polyhydroxyalkanoate (PHA) depolymerase A (*Paucimonas lemoignei*)	*B. subtilis*	1.9	Yes	30
Proinsulin	*B. subtilis*	1000	Yes	31
Protective antigen (*Bacillus anthracis*)	*B. brevis*	300	Yes	32
Protein disulfide isomerase	*B. brevis*	1100	Yes	33
Single-chain variable fragment (ScFv)	*B. subtilis*	10–15	Yes	34
Staphylokinase	*B. subtilis*	337	Yes	35
Streptavidin	*B. subtilis*	35–50	Yes	36
Subtilisin Carlsberg (*Bacillus licheniformis*)	*B. licheniformis*	n.d.	Yes	37
	B. subtilis	n.d.	Yes	37
Thioredoxin (*Aliciclobacillus acidocaldarius*)	*B. subtilis*	500	Yes	38

[a]Based on Ref. 9, page 217

its genome sequence was published in 1997 (39). In 2009, a revised, resequenced, and reannotated version of this reference genome has been published (GenBank AL009126) (40). Furthermore, easy access to the genome sequence, gene-centered information as well as many reference data are provided to the community by the SubtiList database, and are now integrated in the GenoList database system (41). Due to the broad genetic knowledge and techniques available, *B. subtilis* has been used extensively for industrial production. However, unlike strain 168, most industrial strains are not naturally transformable. In addition, *B. subtilis* has eight extracellular alkaline proteases that degrade secreted heterologous proteins, and further, cannot stably maintain plasmids. These problems have been addressed by constructing a strain that has been finally mutated for all eight proteases (WB800) (42) and by using *Bacillus* θ-replicating plasmid derivatives such as pAMβ1 (43,44). *B. subtilis* genetics, metabolism, and applications have been thoroughly covered in several books and reviews (39,45–47). Some proteins industrially produced with *B. subtilis* are summarized in Table 11.1. As a remarkable example thermostable α-amylases are used in starch hydrolysis at about 105°C in the first process step (4).

11.2.2 *Bacillus licheniformis*

Historically, *B. licheniformis* is one of the first industrial hosts for the production of thermostable enzymes, especially its amylases and alkaline proteases (subtilisin) (11,37). The genome sequences of two identical *B. licheniformis* strains were published in 2004 (ATCC 14580/DSM13: GenBank CP000002 and AE017333), both revealing a very close similarity to *B. subtilis* on the nucleotide level of about 84.6% (48,49). Under anaerobic conditions, *B. licheniformis* is able to grow by a mixed acid fermentation process similar to *B. subtilis* (50). In 2005, Nahrstedt and coworkers described a gene knock-out system for this organism (51). Several mutant strains were constructed which are deficient in sporulation and DNA repair (51) or show UV hypersensitivity (52). Further, mutants deficient in producing some extracellular proteins to enhance secretion of target proteins were developed (53). Industrially relevant proteins produced with *B. licheniformis* are also listed in Table 11.1.

11.2.3 *Brevibacillus brevis* (formerly *Bacillus brevis*)

The genome sequence of *Brevibacillus brevis* (formerly *Bacillus brevis*) was published in 2009 (strain NBRC 100599, GenBank AP008955). With a genome size of almost 6.3 Mbp its genome is one of the largest of all bacilli. It is only distantly related to the *B. subtilis* group (54). *B. brevis* is commonly found in soil, air, and water. Although it is not as well-studied as *B. subtilis*, much research has been done in Japan by Udaka, Yamagata, and coworkers since 1981 (5,12,17,20,33,55). *B. brevis* secretes large amounts of proteins into its environment which are correctly folded, soluble, and active. Yields of secreted protein in industry are between 11 mg and 3.5 g per liter (Table 11.1). Plasmids with high and low copy numbers are available (5,55). *B. brevis* shows very low levels of extracellular protease activity. Based on this, Kajino and coworkers isolated a protease-deficient mutant, in which extracellular protease activity was only about a quarter compared to the parent one (55). Unfortunately, little genetic analysis has been reported for this organism.

11.2.4 *Bacillus amyloliquefaciens*

B. amyloliquefaciens, with a name that was derived from its ability to liquefy amylose (starch), is well known for its amylases used in the baking industry. Moreover, it is used for the production of the alkaline protease subtilisin, as has been mentioned. *B. amyloliquefaciens* is naturally competent. Genetic transformations can easily be done using a modified protocol of *B. subtilis* (56). Many of the enzymes from *B. amyloliquefaciens* are now produced heterologously in other bacilli or *Escherichia coli*, including α-amylase (57) or chitosinase (16) (Table 11.1). The restriction endonuclease *Bam*HI is also derived from this organism. The complete genome sequence was published in 2007 (strain FZB42, GenBank CP000560) and promises to increase its usefulness (56).

11.2.5 *Bacillus clausii*

B. clausii can be isolated from soil and water. The genome sequence of *B. clausii* was published in the beginning of 2005 (strain KSM-K16, GenBank AP006627). On the basis of 16S rRNA, *B. clausii* is very closely related to *B. subtilis* (1). An advantage of *B. clausii* is its ability to tolerate environments with high pH levels. It produces alkaline-tolerant enzymes, particularly alkaline proteases (58). It is reported to have a beneficial effect in the human gut and is being considered for use as a probiotic (59).

11.3 BACILLUS MEGATERIUM

B. megaterium was first described by de Bary more than a century ago (60). Named for its large size of 1.5 × 4 μm, "megat(h)erium" (Greek: "big animal"), this microorganism is one of the largest bacteria (Fig. 11.1). Due to the dimension of the vegetative form and spores, *B. megaterium* is well suited for morphological research, such as cell wall and cytoplasmic membrane biosynthesis, sporulation, spore structure and cellular organization, DNA partitioning, and protein localization (61). In the

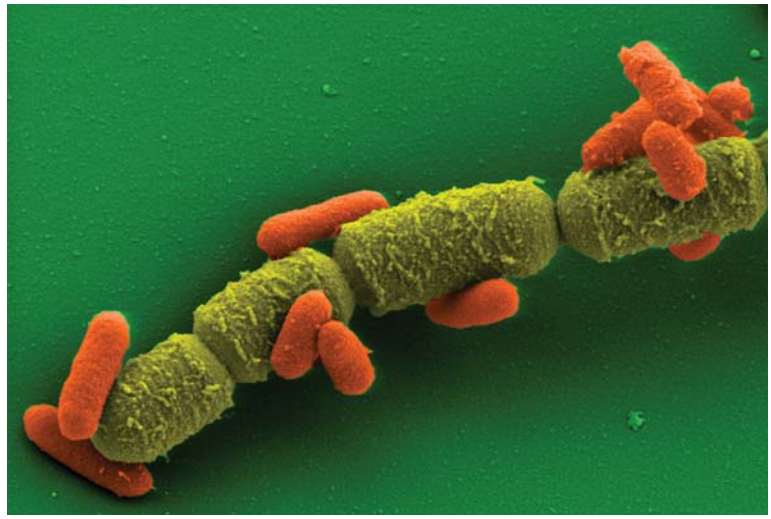


Figure 11.1. Electron microscope image of *Bacillus megaterium* and *Escherichia coli* cells. Large, yellow cells: *B. megaterium*; small, red cells: *E. coli*. Aldehyde-fixed cells were dehydrated with a graded series of acetone, critical-point-dried with liquid CO_2 and sputter-coated with gold. Sample examination was done in a field emission scanning electron microscope (FESM) Zeiss DSM982 Gemini. Magnification × 15,000. Subsequently, cells and background of the picture were stained. (This figure is available in full color at http://onlinelibrary.wiley.com/book/10.1002/9780470054581.)

1960s, *B. megaterium* was *the* model organism for intensive studies on sporulation since it sporulates and germinates very efficiently. Primarily a soil bacterium, *B. megaterium* is also found in diverse environments from rice paddies to dried food, seawater, sediments, fish, normal flora, and even in bee honey (62). Because of its production of several biotechnological relevant substances, *B. megaterium* is of general interest for industry. It produces penicillin acylase used to construct semisynthetic penicillins (e.g. ampicillin) and is the major producer of vitamin B_{12}. It is nonpathogenic; this makes *B. megaterium* useful in the food and pharmaceutical industries.

Two genomes of two *B. megaterium* strains, QM B1551 and DSM319 (further described in the sections "*Bacillus megaterium* Strain QM B1551" and "*B. megaterium* Strain DSM319"), both important for biotechnological use, have currently been sequenced. Their chromosomes are circular and about 5.1 MBp in size. Taxonomically, *B. megaterium* is placed into the *B. subtilis* group of bacilli (62,63), although there is only a small degree of homology in the genome structure between *B. megaterium* and *B. subtilis*. Genome-wide comparisons revealed that only a region of approximately 2 MBp around the origin of replication of the *B. megaterium* chromosome is synthenic to currently sequenced *Bacillus* genomes (in preparation).

The utilization of a wide variety of carbon sources allows this organism to grow on low-cost substances. In contrast to other bacilli, *B. megaterium* can use the glyoxylate pathway as a "shortcut", since isocitrate lyase AceA (EC 4.1.3.1) and malate synthase GlcB (EC 2.3.3.9) are present. Under anaerobic conditions, *B. megaterium* is able to use the mixed acid fermentation pathway as found in *B. subtilis* (50). All key enzymes involved in this fermentation process were identified in *B. megaterium*, especially lactate dehydrogenase Ldh (EC 1.1.1.27), acetolactate synthase AlsS (EC 2.2.1.6), acetolactate decarboxylase AlsD (EC 4.1.1.5), phosphate acetyltranferase Pta (EC 2.3.1.8) and acetate kinase AckA (EC 2.7.2.1). Respiration with nitrate as electron acceptor, from which most other bacilli are able to get their energy under anaerobic conditions, is not possible in *B. subtilis* because it lacks a membrane bound nitrate reductase of the Nar-type. One of the major advantages of *B. subtilis* is that it does not possess any obvious alkaline proteases degrading recombinant gene products. Therefore, a large amount of intact functional protein is produced with little or no degradation products (64,65).

B. subtilis was one of the first biotechnological vitamin B_{12} producers (61,66,67). It is known for its ability to synthesize vitamin B_{12} both, in the presence and absence of oxygen (68). Starting in the early 80s, major parts of the biosynthetic pathway of B_{12} production in *B. subtilis* have been genetically and biochemically characterized (8,62,67–69). The genes for oxygen-independent vitamin B_{12} biosynthesis genes are organized in two distinct, independent operons. The larger one consisting of *cbiW*, *cbiH*, *cbiX*, *cbiJ*, *cbiC*, *cbiD*, *cbiET*, *cbiL*, *cbiF*, *cbiG*, *cbiA*, *cysG*, *cbiY*, and *btuR* has already been described (68,70); the smaller one consists of *cbiB*, *cobU*, *cobS* and *cobC*. This natural ability of *B. subtilis* to

produce vitamin B_{12} was combined using tools developed for this organism (refer "*Bacillus megaterium* Toolbox for Recombinant Protein Production"). Using these experiments, the intracellular yields of vitamin B_{12} were enhanced up to 40-fold. The strategies used illustrate the versatility of the organism. They included recombinant overexpression of single genes and whole operons, integration of strong promoters upstream of genes and operons involved in B_{12} production, directed enzyme engineering to enhance enzyme stability, overproduction of recombinant vitamin B_{12} binding proteins to prevent vitamin B_{12} dependent feedback inhibition, as well as an antisense RNA strategy to inactivate mRNA of genes involved in competing pathways (71).

11.3.1 *Bacillus megaterium* Strain QM B1551

Strain QM B1551 is second only to *B. subtilis* in the amount of genetics and multiply marked, characterized strains, hundreds of which are now available from the Bacillus Genetic Stock Center (BGSC, Ohio State University). It carries seven indigenous plasmids (pBM100-pBM700) with characterized, compatible replicons. These seven indigenous plasmids have different copy numbers and comprise approximately 11% of the total cellular DNA. The size spectrum of the plasmids ranges from only 5.4 kb to over 164 kb (72). The two smallest ones replicate by the rolling circle mechanism, whereas the larger five are θ-replication plasmids, four of which have cross-hybridizing replicons (73). The rolling circle replicons show similarities to sequences on plasmids known from *Bacillus thuringiensis* and *Bacillus anthracis* (74). All five θ-replicons appear to be unique. They may form at least one new class of compatible replicons (75). Beside the replicons, the plasmids of *B. subtilis* QM B1551 carry several interesting genes; for example, genes coding for proteins involved in cell division, in germination, in heavy metal resistance, in cell wall hydrolysis, and in rifampin resistance. Even a complete rRNA operon is located on one of the plasmids (74,75). *B. subtilis* strain PV361, a derivative of strain QM B1551 (76), lacks all seven plasmids. Surprisingly, this plasmidless strain is able to grow on rich and minimal medium and shows no differences in sporulation compared to QM B1551. It does require rich medium for germination, however. Therefore, the plasmids of QM B1551 may play a role in its adaptation to various environmental conditions. The genome of QM B1551 including all seven plasmids has now been completely sequenced and annotated. The QM B1551 genome has no alkaline proteases. Plasmid vectors are stable without selection for over 100 generations (75). Several techniques are available for its manipulation.

11.3.1.1 Transduction. A transducing phage, MP13, was isolated and characterized (77,78) and was used to map over 50 chromosomal loci. A mapping strain kit is also available (79). There are mutants for auxotrophy (80–82), recombination, division, DNA repair (83), antibiotic resistances, sporulation and germination and its neutral protease (84). Many genes have been cloned and characterized over the last few years including ATP synthetase (85), the *spoIIA* and *spoVA* operons (84) and several germination genes (86). Most are available from BGSC as mentioned above. For a more extensive discussion see a previous review (62).

11.3.1.2 Transformation. Although conditions to develop natural competence for the uptake of DNA have not been described for *B. subtilis* so far, other genetic methods to transform this organism, including poly(ethylene) glycol (PEG) protoplast transformation, have been developed (65,87). Recently, successful electrotransformation (ETF) of *B. subtilis* and *B. licheniformis* were reported by Xue and coworkers (1999) (88) and modified by Scott Grayburn for *B. subtilis* QM B1551 (unpublished data) (refer section titled "ETF of *Bacillus megaterium* QM B1551 and Derivatives"). While the frequency of ETF is still low, it is consistent and simple enough to use routinely, and competent cells can be frozen. Minor adjustments of cell density, number of washes, and osmolarity should optimize the protocol and make the technique useful for several other *B. subtilis* strains as well.

11.3.1.3 Integrative Genetics. Transposon Tn917 in several configurations constructed by Youngman, Perkins, and Losick (89) has been successfully integrated into QM B1551 to generate many mutations, assay promoter function, and clone sporulation genes (84,90). Integrative plasmids have also been used to map *ssp* (SASP) genes (76) and vectors that integrate into the *xyl* or *gdh* genes have been constructed (91). A simple, integrative suicide vector, pKV1, is also available (76).

11.3.2 *Bacillus megaterium* Strain DSM319

Beside *B. subtilis* strain QM B1551, much research has been done using strain DSM319 (92). In contrast to QM B1551, this strain naturally does not contain any plasmids. The genome of DSM319 has been sequenced and is available in GenBank.

For many recombinant industrial applications, bacterial strains which are genetically debilitated when released into the environment are required. Several strains of *B. subtilis* DSM319 have been constructed by different genetic approaches. Mutants that have lost their ability to form viable endospores have been made (93) including transposon knock-out mutants (66). Generated mutants are available in the laboratories of Friedhelm Meinhardt (Institute for Molecular Microbiology and Biotechnology, Muenster, Germany) and Wolfgang Hillen (Microbiology, Erlangen,

Germany). Another mutant useful for recombinant gene expression under xylose control is the mutant strain WH323 which is deficient in xylose utilization. Using this strain the inducer xylose cannot be consumed as carbon source (94). *B. subtilis* shows only low overall protease activity. To further lower residual extracellular protease activity, the gene for the major extracellular protease (NprM) was successfully knocked out resulting in strain MS941 (95). Protease activity of the mutant strain was reduced by 98.6% compared to that of the parental wild-type strain (95).

11.3.3 *Bacillus megaterium* Toolbox for Recombinant Protein Production

There are many tools now available to facilitate the cloning, secretion, expression, and purification of recombinant products in *B. subtilis*.

11.3.3.1 Vectors. Several vectors used in a *B. subtilis* host have been used successfully in *B. subtilis*. They are very stable and last for 60–100 generations without selective pressure in *B. subtilis*. These include transposon Tn917 vectors like pLTV1 and pTV1–pTV51 made by Youngman (96). Vector pLTV1 contains a small *E. coli* plasmid with origin, an ampicillin based selection marker and a *lacZ* gene that can be used to make random reporter gene fusions for expression screening and to clone the upstream region. Further, there are other vectors, several of which include the pE194 origin from *Staphylococcus* (97). They have been successfully tested in *B. subtilis* (74). Plasmid pHV33, one of the first *Bacillus* shuttle plasmids, has been used to generate several genomic libraries (Vary, unpublished). The series of defined copy number plasmids including pHT304, pHT315, and pHT3101 (98) generate within the host cell 4, 15, and 101 copies respectively. Plasmid pHT315 has proven to be a good general cloning plasmid. Vector pVG6 is a derivative of pSG1151 (99) that can be used to generate green fluorescent protein (GFP) fusions in *B. subtilis*. pKV1 and pVG6 are being deposited at BGSC.

For several decades, much effort was devoted to optimizing vector systems for recombinant gene expression and protein production in various bacterial organisms. Several of these vector systems are commercially available like the pET-series for *E. coli* (Novagen; pET-System-Manual; 11th edition) or the pMUTIN-series for *B. subtilis* (100). Kaltwasser and coworkers described the construction of six *B. subtilis* vectors allowing the fusion of a target gene to six different epitopes and localization tags. In addition to these epitope tags, like the Myc-epitope (101) and localization tags (99), fusion to further affinity tags for recombinant protein purification is common (102).

In 1991, Rygus and Hillen identified a xylose inducible promoter system in the genome of *B. subtilis*. Using this promoter, they constructed a vector for regulated gene expression in *B. subtilis* which was named pWH1520 (103). Within a few years, many more vectors were designed that are useful for recombinant protein overproduction in this Gram-positive organism. These vectors vary in their origin of replication (*ori*), their antibiotic selection marker gene, and their multiple cloning site (MCS). Moreover, different promoter systems for the recombinant gene expression are used. The vectors differ in the presence or absence of coding sequences for affinity tags upstream or downstream of the MCS and of sequences coding for leader peptides for protein export (Fig. 11.2).

11.3.3.2 Origins of Replication. Several molecular protein production strategies require genes carried on two different, compatible plasmids. For example, in so-called "codon plus" strains of *E. coli*, the coproduction of vector encoded tRNAs for rare codons and the target recombinant protein uses two independently replicating vectors (104). The initial T7-promoter system in *E. coli* was also based on two vectors (105). For the stable parallel replication of two or more vectors, origins of replication (ori) belonging to different compatibility classes are required. The origin of replication *oriU* and the gene *repU* constitute a replicon suitable for *B. subtilis*. This replicon is derived from the plasmid pBC16, a *Bacillus cereus* plasmid, which is replicated by the rolling circle mechanism (106,107). The *oriU* and *repU* genes are localized on the plasmid pMM1520 and all its derivatives (108). Replication of vectors carrying this replicon is not temperature sensitive.

The characterization of seven indigenous plasmid replicons of *B. subtilis* QM B1551 in pBM100 to pBM700 provide seven more compatible plasmids (refer to previous sections "*Bacillus megaterium* Strain QM B1551"). While pBM100 and pBM200 replicate by the rolling circle mechanism, pBM300–pBM700 use θ-replication. The copy numbers of these seven plasmids vary from 1 to 224 (72). Further, the temperature sensitive origin of replication originated from the plasmid pE194 (97) can be used in parallel to pMM1520 and all of the seven pBM100–pBM700 plasmids. This temperature sensitive origin is used for gene knock-out and chromosomal integration experiments in *B. subtilis* (69,71,95). A plasmid carrying the pE194 origin of replication is replicated independently from the genome at a temperature below 37°C. After raising the temperature to 42°C, the plasmid does not replicate. The plasmid can be integrated into desired regions of the chromosome if regions of homology to the chromosomal locus are encoded (69,71,95).

Several plasmid origins of replication useful in *B. subtilis* are listed in Fig. 11.2. Vectors carrying some of these origins are summarized in Table 11.2. In addition, most vectors used in *B. subtilis* also work in *B. subtilis*

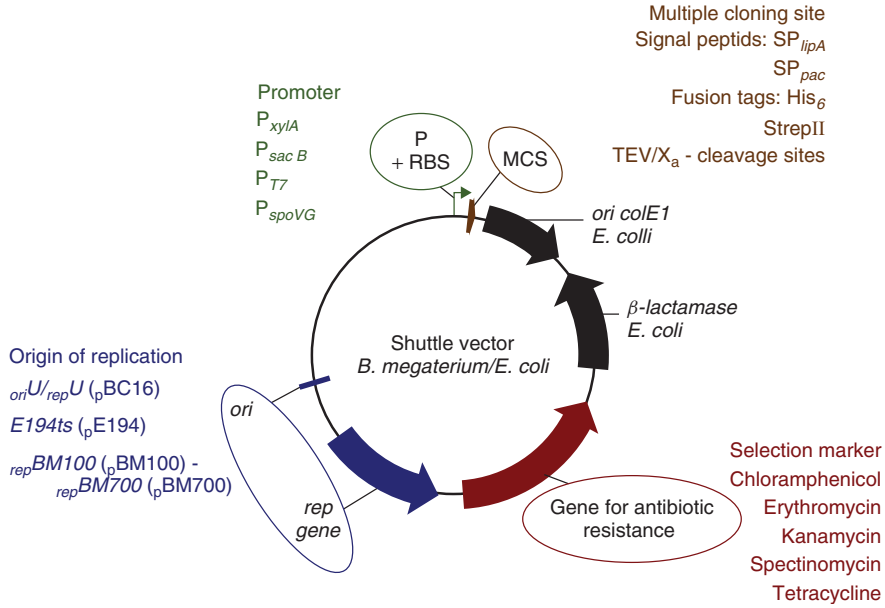


Figure 11.2. Map of a *Bacillus megaterium*/*Escherichia coli* shuttle vector. Characters functional in *B. megaterium* which can be changed modularly are indicated. P_{xylA}: promoter of *xylA*; P_{T7}: T7 RNA polymerase dependent promoter; P_{sacB}: promoter of *sacB*; P_{spoVG}: promoter of *spoVG*; His_6: 6x histidin tag; StrepII: streptavidin II tag; TEV: tobacco etch virus protease cleavage site; X_a: factor X_a protease cleavage site; SP_{lipA}: signal peptide of the lipase A; SP_{pac}: signal peptide of the penicillin G acylase. Characters functional in *E. coli* are indicated as *β-lactamase* (antibiotic resistance gene) and *ori colE1* (origin of replication). (This figure is available in full color at http://onlinelibrary.wiley.com/book/10.1002/9780470054581.)

with the exception of those that require integration into the genome.

11.3.3.3 Antibiotic Resistance Genes. Different antibiotic resistance genes can be used for selection in *B. subtilis*. In 1995, Guérout-Fleury and coworker developed vectors containing so-called "antibiotic-resistance cassettes" for *B. subtilis* which can also be used in *B. subtilis* (112). The genes forming these cassettes have been cloned into the polylinker region of *E. coli* plasmids in a way that they can be recovered by different combinations of restriction enzymes to further clone them into different *B. subtilis* vectors. Among those are genes for resistance to tetracycline (e.g. pWH1520 (103), pMM1520 (108), and derivatives), erythromycin (e.g. pHBintE (69) and derivatives), kanamycin (e.g. pHBintN (71) and derivatives), and spectinomycin. Moreover, chloramphenicol can be used as selection marker in *B. subtilis* (e.g. pYZ11 (109), pKM307 (75), pGB22, and derivatives). Vectors carrying these different marker genes are summarized in Table 11.2.

11.3.3.4 Promoters and Multiple Cloning Sites. In 1991, Rygus and Hillen identified a xylose inducible promoter P_{xylA} with its repressor protein XylR in the genome of *B. subtilis* strain DSM319 (113). Originally, this promoter is located upstream of an operon encoding genes involved in xylose utilization. Based on this xylose inducible promoter, they developed a xylose-dependent plasmid-borne system for the overproduction of recombinant proteins. This plasmid encoded system includes the coding sequences for XylR, the promoter P_{xylA} and the first 195 bp of the *xylA* gene followed by an MCS. The corresponding plasmid was called pWH1520. In further studies, this promoter was modified and further optimized for recombinant gene expression in *B. subtilis*. The catabolite response element (*cre*) sequence was eliminated and an enhanced MCS was inserted (108). In the resulting plasmid pMM1520, glucose, and other sugars present in nutrient rich medium no longer inhibit recombinant gene expression by catabolite control. Moreover, the MCS allows simple cloning of target genes by the use of 15 different DNA restriction enzyme cleavage sites. This MCS was further included in all vectors based on pMM1520 to allow simple subcloning. A major advantage of this system is that the xylose inducible promoter does

TABLE 11.2. Summary of Shuttle Vectors Carrying Different Origins of Replications and Selection Marker Genes for *B. megaterium*

Plasmid Designation	Description	References
pYZ5	Truncated form of pYZ11 (109), shuttle vector for cloning in *E. coli* (Ap^r) and replication in *B. megaterium* (Cm^r) containing a 1.1 kb fragment of pBM100. Ori: *BM100* (pBM100)	(unpublished data)
pGB22	Shuttle vector for cloning in *E. coli* (Ap^r) and replication in *B. megaterium* (Cm^r) containing a fragment coding for the origin of replication of pBM200 in pJM103 (110). Ori: *BM200* (pBM200)	(unpublished data)
pKM307	Shuttle vector for cloning in *E. coli* (Ap^r) and replication in *B. megaterium* (Cm^r) containing a 3.6 kb *Hae*III fragment of pBM300 in pJM103 (110). Ori: *BM300* (pBM300)	75
pKM60	Shuttle vector for cloning in *E. coli* (Ap^r) and replication in *B. megaterium* (Km^r) containing a fragment coding for the origin of replication of pBM400 in pJM103 (110). Ori: *BM400* (pBM400)	109
pDS110	Shuttle vector for cloning in *E. coli* (Ap^r) and replication in *B. megaterium* (Km^r) containing a 2.4 kb fragment of pBM500 in pBEST501. Ori: *BM500* (pBM500)	73
pKM704	Shuttle vector for cloning in *E. coli* (Ap^r) and replication in *B. megaterium* (Cm^r) containing a 6.4 kb *Eco*RI fragment of pBM700 in pJM103 (110). Ori: *BM700* (pBM700)	(unpublished data)
pP_{T7}	Shuttle vector for cloning in *E. coli* (Ap^r) and gene expression under T7 RNA polymerase control in *B. megaterium* (Cm^r); P_{T7}-MCS-Stop-T_{T7}. Ori: *BM100* (pBM100)	111
pMM1520	Shuttle vector for cloning in *E. coli* (Ap^r) and gene expression under xylose control in *B. megaterium* (Tc^r); P_{xylA}-MCS. Ori: *oriU* (pBC16)	108
pWH1520	Shuttle vector for cloning in *E. coli* (Ap^r) and gene expression under xylose control in *B. megaterium* (Tc^r); P_{xylA}-MCS. Ori: *oriU* (pBC16)	103
pVG6	Shuttle vector for cloning in *E. coli* (Ap^r) and replication in *B. megaterium* (Er^r) containing the pE194 1.8 kb origin inserted into pSG1151; used to construct GFP fusion proteins; ori: *E194ts* (pE194)	(unpublished data)
pKV1	Integrative suicide vector for *B. megaterium*, pUC18 derivative, Ap^r removed and Km^r inserted at *Cla*I	(unpublished data)
PHBintE	Shuttle vector for cloning in *E. coli* (Ap^r) and integration and gene expression under xylose control in *B. megaterium* (Er^r). Ori: *E194ts* (pE194)	69
PHBintN	Shuttle vector for cloning in *E. coli* (Ap^r) and integration and gene expression under xylose control in *B. megaterium* (Km^r). *E194ts* (pE194)	71

not show any basal expression in *B. subtilis* in the absence of xylose (114).

To further enhance the toolbox for *B. subtilis*, Gamer and coworkers made use of the fact that two different plasmids belonging to two different compatibility classes can coexist in this organism (refer section on "Antibiotic Resistance Genes") (111). The T7 RNA polymerase (T7 RNAP)-dependent expression system that was developed in the early 1980s for *E. coli* (105) is based on the RNAP of the bacteriophage T7. This expression system combined several advantageous features, such as stringent selectivity of the RNAP toward its cognate promoter and its high processivity. To utilize the system in *B. subtilis*, the expression of the *rnap* gene was put under control of the xylose inducible promoter, while the expression of the gene of interest is controlled by the T7 RNAP. The MCS following the T7 RNAP dependent promoter has the same sequence as found in pMM1520 and derivatives to allow easy subcloning of recombinant genes between different expression vectors. The recombinant expression of the target gene with the T7 RNAP-dependent promoter increases the yield of recombinant protein up to sixfold compared to the xylose inducible one (111).

Another promoter used for recombinant protein production in *B. subtilis* is the promoter of the *B. subtilis* sporulation gene *spoVG* (115). The promoter containing vector pVG1 was combined with the *Bacillus* vector pE194 (116) to construct the multifunctional plasmid pAS5. The heterologous promoter has been used successfully for the recombinant industrial overproduction of the HIV antigen in *B. subtilis* (115).

Sucrose, a very cheap disaccharide, can also be used to induce recombinant protein production under the control of P_{sacB}, a sucrose inducible promoter. In 2007, this promoter was identified in the genome of *B. subtilis* strain DSM319 and cloned. In contrast to the xylose inducible

promoter, this one shows basal activity even in the absence of sucrose (117).

11.3.3.5 Affinity Tags for Protein Purification. The production of recombinant proteins in an apparently pure form for characterization, crystallization, or applications in the pharmaceutical industry has become a major goal in research and application. For this purpose, appropriate expression vectors provide the genetic setup for the in-frame fusion of peptides or proteins with high ligand binding specificity to the target protein. During the last few years, several epitope peptides and proteins have been developed for overproduction and purification of recombinant proteins. These affinity ligands have proven to have a minimal effect on the tertiary structure and the biological activity of the fusion protein. In addition to large fusion peptides like the glutathione *S*-transferase (GST) or the maltose-binding protein (MBP), small peptide tags like polyhistidine (His-tag) or a streptavidin binding polypeptide (Strep-tag) are commonly used (118). Various vector systems are commercially available for *E. coli* (104).

Two different affinity tags, the StrepII-tag (119) and the polyhistidine (His_6-) tag (120), were chosen as N- or C-terminal fusion partners for target proteins produced or/and secreted in *B. subtilis*. They are encoded on the expression plasmids either upstream or downstream of the MCS. For some of the resulting fusion proteins the corresponding N-terminal affinity tag may be removed via protease digestion, either by the tobacco etch virus (TEV) (121) or the factor X_a protease (122). The vectors were successfully tested using GFP as model protein. After cell disruption, between 25–71% of the recombinantly intracellularly produced GFP was recovered after a single purification step (Table 11.3). The secretion of recombinant target protein avoids the need for cell disruption. This protein can be purified directly from the cell-free growth medium by incubation with the affinity purification matrix. In such experiments with a levansucrase as model protein, between 26–43% of affinity tagged secreted enzyme was purified from the cell-free growth medium (123).

Vectors containing the different affinity tags for intra- as well as for extracellular production of recombinant proteins are listed in Table 11.4 and their structure is shown in Fig. 11.3.

11.3.3.6 Signal Peptides for Protein Secretion. In bacilli, 90% of all secreted proteins are transported via the

TABLE 11.3. Comparison of the Recombined Production and Affinity Chromatographic Purification of Green Flourescent Protein (GFP) from *B. megaterium* Using Different Vectors[a]

Protein	Protein Produced		Protein Purified	
	[mg/L Cell Culture]	[mg/g_{CDW}]	[mg/L Cell Culture]	[mg/g_{CDW}]
GFP-His	9.6 ± 0.5	6.8 ± 0.3	2.4 ± 0.1	1.5 ± 0.1
His-TEV-GFP	17.9 ± 0.9	14.0 ± 0.7	5.0 ± 0.3	3.0 ± 0.2
Strep-Xa-GFP	8.4 ± 0.4	6.3 ± 0.3	6.0 ± 0.3	4.0 ± 0.2
Strep-TEV-GFP	13.2 ± 0.7	10.5 ± 0.5	9.0 ± 0.5	6.0 ± 0.3
GFP-Strep	16.0 ± 0.8	11.2 ± 0.6	10.8 ± 0.5	6.9 ± 0.4

[a]From (109). Different affinity tag fusion forms of GFP were recombinantly produced in *B. megaterium*. Protein purification via the StrepII- or the Histidin-affinity tag was performed by using affinity chromatography. CDW, cell dry weight.

TABLE 11.4. Summary of *B. megaterium* Expression Vectors for the Production and Secretion of Recombinant Proteins[a]

Plasmid Designation	Description	References
pMM1522	P_{xylA}-MCS	123
pSTOP1622	P_{xylA}-MCS-Stop	114
pC-HIS1622	P_{xylA}-MCS-His_6-Tag-Stop	114
pN-STREP-Xa1622	P_{xylA}-StrepII-Tag-Xa-MCS-Stop	114
pC-STREP1622	P_{xylA}-MCS-StrepII-Tag-Stop	114
pN-HIS-TEV1622	P_{xylA}-His_6-Tag-TEV-MCS-Stop	114
pN-STREP-TEV1622	P_{xylA}-StrepII-Tag-TEV-MCS-Stop	114
pMM1525	P_{xylA}-SP_{lipA}-MCS	123
pSTREP1525	P_{xylA}-SP_{lipA}-StrepII-Tag-Xa-MCS-Stop	123
pHIS1525	P_{xylA}-SP_{lipA}-MCS-His_6-Tag-Stop	123
pSTREPHIS1525	P_{xylA}-SP_{lipA}-StrepII-Tag-Xa-MCS-His_6-Tag-Stop	123
pRBBm27	P_{xylA}-SP_{pga}-StrepII-Tag-Xa-MCS	(unpublished data)
pP_{T7}	P_{T7}-MCS-Stop-T_{T7}	111

[a]Proteins can be fused to different affinity tags. Secretion of the target protein is possible by using different signal peptides.

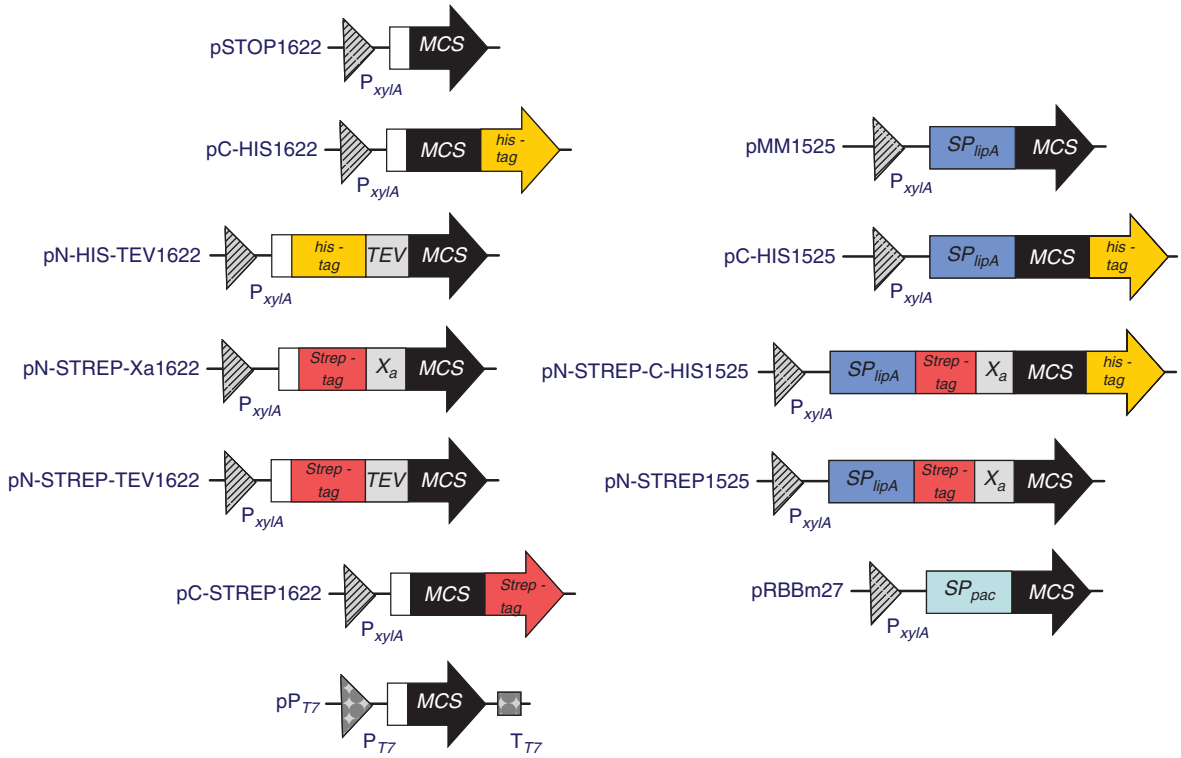


Figure 11.3. Series of expression plasmids for the intra- and extra-cellular production of recombinant proteins by *B. megaterium*. All expression plasmids shown allow parallel cloning of genes of interest into the identical multiple cloning site (MCS). P_{xylA}: promoter of *xylA*; P_{T7}: T7 RNA polymerase dependent promoter; T_{T7}: terminator for T7 RNA polymerase; TEV: tobacco etch virus protease cleavage site; X_a: factor X_a protease cleavage site; SP_{lipA}: signal peptide of the lipase A; SP_{pac}: signal peptide of the penicillin G acylase. (This figure is available in full color at http://onlinelibrary.wiley.com/book/10.1002/9780470054581.)

Sec-dependent pathway demonstrating the major importance of this mechanism for the secretion of proteins. After the protein is synthesized at the ribosomes, the N-terminal signal peptide is recognized by proteins of the Sec system. The newly synthesized protein is kept in an unfolded state and transported through a channel in the cytoplasmic membrane into the space between membrane and cell wall. A special type I signal peptidase anchored at the surface of the cell membrane removes the signal peptide by cleavage at its recognition sequence. Chaperons in the space between cytoplasmic membrane and cell wall assist in protein folding. Finally, the protein diffuses through the cell wall into the growth medium (summarized in Ref. 124).

For the secretion of heterologous proteins into the surrounding growth medium of *B. subtilis*, the toolbox contains sequences for two different signal peptides. The recently discovered extracellular *B. subtilis* esterase LipA was secreted in high amounts into the culture medium of *B. subtilis* (125). The LipA signal peptide consists of 28 amino acids. The three typical regions of an Sec-pathway dependent signal peptide were identified in the LipA signal peptide by the SignalP algorithm (126). Using this signal peptide, 1,800 U/L of heterologously produced penicillin G acylase and 4 mg/L of recombinant levansucrase were secreted. Further, the signal peptide of the extracellular penicillin G acylase Pac, which is also secreted by the Sec pathway, was used to secret up to 1,500 U/L of Pac into the surrounding growth medium (Table 11.5).

11.3.3.7 Codon Usage of the Recombinant Genes. The codon bias of heterologous genes often provides a limiting factor for the expression in a certain host system. Hence, the so-called codon adaptation index (CAI) of a gene for the host is of importance. The CAI permits the calculation of a comparable value for the codon usage. The calculation of this value requires the definition of a set of highly expressed genes of an individual organism (127). The codon usage of all its other genes is calculated with respect to this subset of genes (128).

TABLE 11.5. Proteins Recombinantly Produced in *B. megaterium*

Protein	Origin	Promoter	Location	Yield	References
β-Galactosidase	*Escherichia coli*	P_{xylA}	Intracellular	4.937 Miller U	103
Dextransucrase	*Leuconostoc mesenteroides*	P_{xylA}	Extracellular	28.600 U/L	108
δ-Endotoxin	*Bacillus thuringiensis* subsp. *kurstaki*	vegetative	Intracellular	n. d.	132
Formate dehydrogenase	*Mycobacterium vaccae*	P_{xylA}	Intracellular	0.9 U/mg protein	130
Glucose dehydrogenase	*Bacillus megaterium*	P_{xylA}	Intracellular	101 U/mg protein	103
Green fluorescent protein	*Aequorea victoria*	P_{xylA}	Intracellular	274 mg/L (HCDC)	114
HIV-1 p41 antigen	Eukaryotic	P_{spoVG}	Intracellular	n. d.	115
Keratinase	*Bacillus licheniformis*	P_{xylA}	Extracellular	166.2 U/mL	133
Levansucrase	*Bacillus megaterium*	P_{sacB}	Extracellular	4.252 U/L	117
Levansucrase	*Lactobacillus reuteri*	P_{xylA}	Extracellular	4 mg/L	123
Mannitol dehydrogenase	*Leuconostoc pseudomesenteroides* (codon adapted)	P_{xylA}	Intracellular	2.4 U/mg protein	130
Mutarotase	*Acinetobacter calcoaceticus*	P_{xylA}	Intracellular	73.7 U/mg protein	103
Penicillin G amidase	*Bacillus megaterium*	P_{xylA}	Extracellular	1.800 U/L	134
Protective antigen	*Bacillus anthracis*	P_{xylA}	Extracellular	1 mg/L	135
Urokinase-like plasminogen activator	Human	P_{xylA}	Intracellular	400 U/mL	103
Thermobifida fusca hydrolase	*Thermobifida fusca* (codon adapted)	P_{xylA}	Extracellular	6.098 U/L	129
Toxin A	*Clostridium difficile*	P_{xylA}	Intracellular	500 μg/L	136

An optimal adapted gene shows a CAI value of 1. In several studies, genes encoding the hydrolase TfH from *Thermobifida fusca* (129), the formiate dehydrogenase Fdh from *Mycobacterium vaccae* (130), and a human ceratin binding domain KbdB were expressed before and after adaptation of their codon usages to *B. subtilis*. All of the native genes showed CAI values below 0.3. Very little or none of the recombinant gene product was obtained. This phenomenon was previously described for *E. coli* (131). The design and synthesis of the artificial genes with a CAI > 0.9 for *B. subtilis* resulted in good production of all recombinant gene products in *B. subtilis* (129,130). Rare codons have been found in bacilli coding for leucine, serine, arginine, and proline. The different codon usage for those amino acids is summarized in Table 11.6.

11.3.4 Commercial Protein Production Systems for *Bacillus megaterium*

For several years now, the company MoBiTec (Goettingen, Germany) has been commercializing a vector system for recombinant protein production in *B. subtilis* based on the xylose inducible promoter P_{xylA}. Starting with the vector pWH1520 (103), MoBiTec now markets all production and secretion vectors which are listed in Table 11.4. Using these vectors, recombinant gene products can be produced intra- as well as extracellularly with or without an affinity tag for protein purification. These vectors have been successfully used by several different laboratories to produce recombinant proteins from prokaryotes and eukaryotes. Proteins produced under control of the xylose inducible promoter are summarized in Table 11.5.

11.3.5 Culture Heterogeneity in *Bacillus megaterium*

In 2007, Biedendieck and coworkers described culture heterogeneity during intracellular recombinant protein production with *B. subtilis*. Using the production of GFP under control of the xylose inducible promoter as a model in fluorescent activated cell sorting experiments, it was shown that only around 70% of the genetically homogenous cells in a high cell density cultivation were producing GFP (114). The phenomenon of culture heterogeneity was previously reviewed for *B. subtilis* (137). Dubnau and Losick described the phenomenon that genetically identical bacteria behave differently across the population for the expression of genes involved in competence development, sporulation, swimming, and chaining (137).

11.3.6 Outlook: Genomics and Systems Biotechnology

The availability of the genome sequences of two important *B. subtilis* strains in addition to the establishment of genetic tools offers a promising future for systems biotechnology approaches. Genome-wide comparisons have already shown that just two of the 5.1 MBp of the *B. subtilis* genome are synthenic to other bacilli. Although all genes in the nonsynthenic region (especially those on *B. subtilis* QM B1551 plasmids) were annotated and raw gene names were assigned, most of these genes are lacking clear

TABLE 11.6. Rare Codons in *B. megaterium* QM B1551 and DSM319 Compared to Those from *B. subtilis*

Amino Acid	Codon	*Bacillus megaterium* QM B1551 Codon Counter	Frequency/ Acid	Overall Frequency	*Bacillus megaterium* DSM319 Codon Counter	Frequency/ Acid	Overall Frequency	*Bacillus subtilis* 168 Codon Counter	Frequency/ Acid	Overall Frequency
Leu	CUA	15287	11.00	1.08	15218	10.97	1.08	6059	*5.08*	*0.49*
Leu	CUC	6949	*5.00*	*0.49*	6882	*4.96*	*0.49*	13398	11.24	1.09
Leu	CUG	14880	10.71	1.05	14707	10.60	1.04	28648	24.03	2.32
Leu	CUU	33079	23.81	2.34	33108	23.86	2.35	28534	23.94	2.32
Leu	UUA	52477	37.77	3.72	52558	37.87	3.73	23614	19.81	1.92
Leu	UUG	16260	11.70	1.15	16306	11.75	1.16	18945	15.89	1.54
Pro	CCA	15262	30.72	1.08	15260	30.77	1.08	8582	19.06	0.70
Pro	CCC	3658	*7.36*	*0.26*	3652	*7.36*	*0.26*	3994	*8.87*	*0.32*
Pro	CCG	11167	22.48	0.79	11051	22.28	0.78	19559	43.44	1.59
Pro	CCU	19599	39.45	1.39	19630	39.58	1.39	12891	28.63	1.05
Arg	AGA	11312	21.26	0.80	11245	21.24	0.80	13192	26.27	1.07
Arg	AGG	2782	*5.23*	*0.20*	2777	*5.24*	*0.20*	4698	*9.35*	*0.38*
Arg	CGA	9888	18.58	0.70	9760	18.43	0.69	4957	*9.87*	*0.40*
Arg	CGC	10843	20.38	0.77	10769	20.34	0.76	10390	20.69	0.84
Arg	CGG	2918	*5.48*	*0.21*	2916	*5.51*	*0.21*	7840	15.61	0.64
Arg	CGU	15465	29.07	1.10	15483	29.24	1.10	9149	18.22	0.74
Ser	AGC	15826	17.80	1.12	15666	17.62	1.11	17389	22.55	1.41
Ser	AGU	13962	15.71	0.99	14122	15.89	1.00	8149	10.57	0.66
Ser	UCA	21268	23.92	1.51	21271	23.93	1.51	18225	23.64	1.48
Ser	UCC	6701	*7.54*	*0.47*	6758	*7.60*	*0.48*	9802	12.71	0.80
Ser	UCG	8116	*9.13*	*0.57*	7967	*8.96*	*0.57*	7723	10.02	0.63
Ser	UCU	23026	25.90	1.63	23110	26.00	1.64	15820	20.52	1.28

[a]Codons for all amino acids were counted and their relative frequencies were calculated for one amino acid (frequency/acid) as well as for all codons in the genome (overall frequency). All frequencies are given in percent. Rare codons (with a frequency <10% per acid) are printed in italics. Codon usage was calculated based on the program JCat (128).

functional annotations and biochemical investigations. To overcome this lack of information, comparative and functional genomics in combination with systems biotechnology might provide solutions. Based on the information of the genome sequences, DNA-microarrays were designed and successfully employed (unpublished data).

Along these lines, investigations were made of the responses of a protein-producing *B. subtilis* culture to changes in the cultivation and induction conditions and proteome analyses were performed (138). Furthermore, to complete the picture first metabolome studies were carried out (139,140).

The first steps using *B. subtilis* as a model organism for systems biotechnology have already been taken. Currently, the establishment of bioinformatics models for the prediction of cellular processes with use of these high-throughput data is underway.

11.4 PROTOCOLS FOR BACILLUS MEGATERIUM

Genetic competence is well studied in the Gram-positive model organism *B. subtilis* 168. So far, no conditions have been found for the development of natural competence for *B. subtilis*. The genome data reveals that *B. subtilis* lacks two of the competence genes, *comFB* and *comGG*, found in *B. subtilis* (141,142). Nevertheless, reasonable transformation frequencies are attained using PEG protoplast transformation. Consistent, but low transformation frequencies are now possible by the ETF protocol below. PEG transformation of QM B1551 is more efficient using RHAF medium and is detailed in (73). An ETF protocol for QM B1551 and a PEG transformation protocol for DSM319 are included here.

11.4.1 Electrotransformation of *Bacillus megaterium* QM B1551 and Derivatives

This protocol is based on the electroporation procedure described for *B. subtilis* and *B. licheniformis* by Xue and coworkers (88) and was modified by Scott Grayburn (unpublished data) by increasing the sorbitol and cell density and performing fewer washes.

11.4.1.1 Preparation of Competent Cells.

1. Inoculate 5 mL *growth medium* with cells of *B. subtilis* QM B1551 or derivatives. Grow on a shaker at 225 rpm and 37°C overnight.
2. Use 3 mL of the overnight culture to inoculate 45 mL of preheated (37°C) *growth medium* in a 250 mL

shaking flask and incubate at 225 rpm and 37°C for 1–2 h. Grow the cells to $OD_{600\ nm}$ of 0.85–0.95.

3. Cool the cell suspension in ice water for 10 min.
4. Harvest the cells by centrifugation at 5.000 × *g* for 5 min at 4°C in a prechilled rotor. Decant the supernatant and place tubes in ice.
5. Resuspend the cell pellet in 24 mL (1 volume) of cold (4°C) *electroporation medium* by vortexing. Harvest the cells by centrifugation at 5,000 × *g* for 5 min at 4°C in a prechilled rotor. Wash the pellet in *electroporation medium* a total of two times.
6. Resuspend the cell pellet in 1.2 mL of cold (4°C) *electroporation medium*. Maintain on ice. Any leftover cells can be frozen (refer step 5 of transformation).

11.4.1.2 Transformation. Please note that everything is kept on ice during handling.

1. Prechill 1.5 mL centrifuge tubes and electroporation cuvettes (1 mm gap, Fisher cat. No. FB101) in ice.
2. Mix 60 μL of resuspended cells with 1 μL (100 ng/μL) of plasmid DNA in a prechilled 1.5 mL tube by drawing the cell–DNA mixure into and out of a 200 μL pipette tip three times. Transfer to an electroporation cuvette.
3. Use the BTX electro cell manipulator 600 for electrical pulses (BioRad MicroPulser). Settings for BTX: Mode T 2.5 kV resistance, R5, S = 2 kV*.
4. After the pulses are completed, add 1 mL *recovery medium* directly to the cuvettes on ice. Transfer the liquid to the sides of glass culture tubes. Transfer to a shaker at 37°C and 225 rpm.
5. Make 0.2 mL aliquots of any leftover electrocompetent cells in 1.5 mL tubes and store the cells at −80°C.
6. After 3 h of incubation, pour the entire transformation mixtures onto Lunia-Bertani (LB) plates containing antibiotic and spread the cells evenly across the plate. Allow liquid on the plates to soak into the agar at 37°C then invert the plates and incubate overnight at 37°C.

11.4.1.3 Media and Solutions.

- *10N NaOH*
  - Dissolve 40 g NaOH in water and bring to a final volume of 100 mL.
- *Growth medium (500 mL)*
  - 5 g tryptone
  - 2.5 g yeast extract
  - 5 g NaCl
  - 45.55 g D-sorbitol.

  Adjust the pH by adding 0.25 mL 10N NaOH.
- *Recovery medium (100 mL)*
  - 6.92 g mannitol in 100 mL growth medium.
- *Electroporation medium (500 mL)*
  - 45.55 g D-sorbitol
  - 45.55 g mannitol
  - 50 mL glycerol.

11.4.2 Protoplast Transformation of *Bacillus megaterium* DSM319 and Derivatives

11.4.2.1 Preparation of Protoplasts.

1. Inoculate 50 mL *LB-medium* in a 300 mL shaking flask with cells of *B. subtilis* DSM319 or derivatives. Grow for 16 h at 100 rpm or 8 h at 200 rpm (must not reach stationary phase) at 37°C.
2. Inoculate 50 mL *LB-medium* with 1 mL of preculture in 300 mL buffled flask.
3. Grow the cells to an $OD_{578\ nm}$ of 1 at 37°C and strong shaking (250 rpm).
4. Harvest cells in a sterile 50 mL tube for 15 min at 5000 × g and 4°C.
5. Resuspend the pelleted cells in 5 mL freshly prepared *SMMP*.
6. Fill cell suspension in 15 mL tube and add 50 μL freshly prepared and sterile filtered lysozyme solution (1 mg/mL in *SMMP*).
7. Incubate at 37°C and very soft shaking until 20–80% of cells are protoplasted (microscope).
8. Harvest protoplasted cells by centrifugation for 10 min at 1300 × *g* at room temperature.
9. Remove supernatant very carefully using a pipette and resuspend cells in 5 mL *SMMP*. Cell pellet is soft and fragile, do not vortex! Repeat twice.
10. Add 750 μL 87% (v/v) sterile glycerin, mix softly (rolling) and make aliquots of 500 μL.
11. After freeze at −80°C, protoplast can be kept for about 2 months, but competence will sink gradually.

11.4.2.2 Transformation.

1. Dry 5 μg DNA and resuspend in 10 μL SMMP for 20 min at 37°C.
2. Add 500 μL of protoplasts to the Eppendorf tube with DNA and transfer into 15 mL tube containing 1.5 mL *PEG-P*. Mix softly (rolling).

3. After an incubation for 2 min at room temperature, add 5 mL freshly prepared *SMMP* and mix very carefully (rolling).
4. Harvest cells by centrifugation for 10 min at 1300 × *g* and room temperature.
5. Carefully remove the supernatant by using a pipette. Usually the cell pellet is not visible.
6. Carefully resuspend the cells in 500 μL *SMMP* (do not vortex!) and transfer them into a 1.5 mL Eppendorf tube.
7. Incubate for 90 min at 30–37°C and soft shaking (100 rpm).
8. In the mean time, prepare 2.5 mL of CR5-Topagar in 15-mL tubes and incubate at 43°C in a waterbath.
9. Pipette the cells to the tube containing the topagar and mix gently by rolling.
10. Pour the topagar containing the cells on prewarmed (37°C) antibiotic agar plates.
11. Incubate for 24 h at 30–37°C, separate grown colonies into single colonies and check microscopically.

11.4.2.3 Media and Solutions.

- *LB-medium (500 mL)*
  - 5 g tryptone
  - 2.5 g yeast extract
  - 2.5 g NaCl.
- *2 × AB3 (Antibiotic Medium No. 3) (200 mL)*
  - 7 g AB3 (Difco).
- *2 × SMM (solubilize in the given order) (250 mL)*
  - 1.16 g malic acid
  - 0.8 g NaOH
  - 2.03 g $MgCl_2 \times 6H_2O$
  - 85.58 g sucrose.
    Adjust pH with HCl to 6.5
    Sterilize by filtration.
- *SMM*
  - 2 × AB3 and 2 × SMM 1:1 (freshly prepared!)
- *PEG-P solution (50 mL)*
  - 20 g PEG-6000 in 1 × SMM
    Autoclave 11 min.
- *Solution A (250 mL)*
  - 51.5 g sucrose
  - 3.25 g MOPS
  - 0.3 g NaOH.
    Adjust pH to 7.3 with NaOH
    Sterilize by filtration.
- *Solution B (142.5 mL)*
  - 2 g agar
  - 0.1 g casamino acids
  - 5 g yeast extract.
- *8 × CR5-salts (625 mL)*
  - 1.25 g K_2SO_4
  - 50 g $MgCl_2 \times 6\ H_2O$
  - 0.25 g KH_2PO_4
  - 11 g $CaCl_2$.
- *12% proline (25 mL)*
  - 3 g proline
    Sterilize by filtration.
- *20% glucose (100 mL)*
  - 20 g glucose.
- *CR5-topagar (2.5 mL)*
  - 1.25 mL solution A
  - 0.288 mL CR5-salts
  - 0.125 mL 12% proline
  - 0.125 mL 20% glucose
  - 0.713 mL solution B (after liquefaction).

REFERENCES

1. Stackebrandt E, Swiderski J. In: Fernandez JM, Hoeffler JP, editors. Gene expression systems. San Diego (CA): Academic Press Carlsbad; 1999. pp. 8–22.
2. Schallmey M, Singh A, Ward OP. Can J Microbiol 2004; 50: 1–17.
3. Ferrari E, Miller B. In: Fernandez JM, Hoeffler JP, editors. Gene expression systems. San Diego (CA): Academic Press Carlsbad; 1999. pp. 66–94.
4. Olsen HS. In: Reed G, Nagodawithana TW, editors. Biotechnology Vol. 9. Weinheim: VCH; 1995. pp. 663–736.
5. Udaka S, Yamagata H. Methods Enzymol 1993; 217: 23–33.
6. Panbangred W, Weeradechapon K, Udomvaraphant S, Fujiyama K, Meevootisom V. J Appl Microbiol 2000; 89: 152–157.
7. Hollmann R, Deckwer WD. J Biotechnol 2004; 111: 89–96.
8. Martens JH, Barg H, Warren MJ, Jahn D. Appl Microbiol Biotechnol 2002; 58: 275–285.
9. Terpe K. Appl Microbiol Biotechnol 2006; 72: 211–222.
10. Palva I. Gene 1982; 19: 81–87.
11. Rothstein DM, Devlin PE, Cate RL. J Bacteriol 1986; 168: 839–842.
12. Udaka S, Yamagata H. Antonie Van Leeuwenhoek 1993; 64: 137–143.
13. Konishi H, Sato T, Yamagata H, Udaka S. Appl Microbiol Biotechnol 1990; 34: 297–302.
14. Bell A, Wernli B, Franklin RM. Biochemie 1995; 77: 256–261.
15. Kashima Y, Udaka S. Biosci Biotechnol Biochem 2004; 68: 235–237.

16. Seki K, Kuriyama H, Hashimoto Y, Uchida Y. Bull Fac Agric Saga Univ 2000; 85: 117–121.
17. Ichikawa Y, Yamagata H, Tochikubo K, Udaka S. FEMS Microbiol Lett 1993; 111: 219–224.
18. Kajino T, Takahashi H, Hirai M, Yamada Y. Appl Environ Microbiol 2000; 66: 304–309.
19. Nakai T, Yamauchi D, Kubota K. Biosci Biotechnol Biochem 2005; 69: 700–704.
20. Yamagata H, Nakahama K, Suzuki Y, Kakinuma A, Tsukagoshi N, Udaka S. Proc Natl Acad Sci U S A 1989; 86: 3589–3593.
21. Lam KH, Chow KC, Wong WK. J Biotechnol 1998; 63: 167–177.
22. Wang B, Yang X, Wu R. Protein Expr Purif 1993; 4: 223–231.
23. Inoue Y, Ohta T, Tada H, Iwasa S, Udaka S, Yamagata H. Appl Microbiol Biotechnol 1997; 48: 487–492.
24. Palva I, Lehtovaara P, Kääriäinen L, Sibakov M, Cantell K, Schein CH, Kashiwagi K, Weissmann C. Gene 1983; 22: 229–235.
25. Takii T, Honda H, Sasayama S, Kobayashi T, Ikezawa H, Udaka S, Oomoto Y, Onozaki K. J Interferon Cytokine Res 1999; 19: 1325–1331.
26. Takimura Y, Kato M, Ohta T, Yamagata H, Udaka S. Biosci Biotechnol Biochem 1997; 61: 1858–1861.
27. Shiga Y, Maki M, Ohta T, Tokishita S, Okamoto A, Tsukagoshi N, Udaka S, Konishi A, Kodama Y, Ejima D, Matsui H, Yamagata H. Biosci Biotechnol Biochem 2000; 64: 665–669.
28. Lesuisse E, Schanck K, Colson C. Eur J Biochem 1993; 216: 155–160.
29. Yang S, Huang H, Zhang R, Huang X, Li S, Yuan Z. Protein Expr Purif 2001; 21: 60–64.
30. Braaz R, Wong SL, Jendrossek D. FEMS Microbiol Lett 2002; 209: 237–241.
31. Olmos-Soto J, Contreras-Flores R. Appl Microbiol Biotechnol 2003; 62: 369–373.
32. Rhie G-E, Park Y-M, Chun J-H, Yoo C-K, Seong W-K, Oh H-B. FEMS Immunol Med Microbiol 2005; 45: 331–339.
33. Kajino T, Ohto C, Muramatsu M, Obata S, Udaka S, Yamada Y, Takahashi H. Appl Environ Microbiol 2000; 66: 638–642.
34. Wu S-C, Yeung JC, Duan Y, Ye R, Szarka SJ, Habibi HR, Wong S-L. Appl Environ Microbiol 2002; 68: 3261–3269.
35. Ye R, Kim JH, Kim BG, Szarka S, Sihota E, Wong SL. Biotechnol Bioeng 1999; 62: 87–96.
36. Wu SC, Wong SL. Appl Environ Microbiol 2002; 68: 1102–1108.
37. Jacobs MF. Gene 1995; 152: 69–74.
38. Digilio FA, Morra R, Pedone E, Bartolucci S, Rossi M. Protein Expr Purif 2003; 30: 179–184.
39. Kunst F, Ogasawara N, Moszer I, Albertini AM, Alloni G, Azevedo V, Bertero MG, Bessieres P, Bolotin A, Borchert S, Borriss R, Boursier L, Brans A, Braun M, Brignell SC, Bron S, Brouillet S, Bruschi CV, Caldwell B, Capuano V, Carter NM, Choi SK, Codani JJ, Connerton IF, Danchin A, *et al*. Nature 1997; 390: 249–256.
40. Barbe V, Cruveiller S, Kunst F, Lenoble P, Meurice G, Sekowska A, Vallenet D, Wang T, Moszer I, Médigue C, Danchin A. Microbiology 2009; 155: 1758–1775.
41. Lechat P, Hummel L, Rousseau S, Moszer I. Nucleic Acids Res 2008; 36:D469–D474.
42. Murashima K, Chen CL, Kosugi A, Tamaru Y, Doi RH, Wong SL. J Bacteriol 2002; 184: 76–81.
43. Janniere L, Bruand C, Ehrlich SD. Gene 1990; 87: 53–61.
44. Nguyen HD, Nguyen QA, Ferreira RC, Ferreira LC, Tran LT, Schumann W. Plasmid 2005; 54: 241–248.
45. Fujita Y. Global regulatory networks in bacillus subtilis. Kerala: Transworld Research Network; 2007.
46. Sonenshein AL, Hoch JA, Losick R. Bacillus subtilis and other gram-positive bacteria: biochemistry, physiology, and molecular genetics. Washington (DC): American Society for Microbiology; 1993.
47. Sonenshein AL, Hoch JA, Losick R. Bacillus subtilis and its closest relatives. Washington (DC): American Society for Microbiology; 2001.
48. Rey MW, Ramaiya P, Nelson BA, Brody-Karpin SD, Zaretsky EJ, Tang M, de Leon AL, Xiang H, Gusti V, Clausen IG, Olsen PB, Rasmussen MD, Andersen JT, Jørgensen PL, Larsen TS, Sorokin A, Bolotin A, Lapidus A, Galleron N, Ehrlich SD, Berka RM. Genome Biol 2004; 5:R77.
49. Veith B, Herzberg C, Steckel S, Feesche J, Maurer KH, Ehrenreich P, Baumer S, Henne A, Liesegang H, Merkl R, Ehrenreich A, Gottschalk G. J Mol Microbiol Biotechnol 2004; 7: 204–211.
50. Ramos HC, Hoffmann T, Marino M, Nedjari H, Presecan-Siedel E, Dreesen O, Glaser P, Jahn D. J Bacteriol 2000; 182: 3072–3080.
51. Nahrstedt H, Waldeck J, Grone M, Eichstadt R, Feesche J, Meinhardt F. J Biotechnol 2005; 119: 245–254.
52. Waldeck J, Meyer-Rammes H, Nahrstedt H, Eichstadt R, Wieland S, Meinhardt F. Appl Microbiol Biotechnol 2007; 73: 1340–1347.
53. Waldeck J, Meyer-Rammes H, Wieland S, Feesche J, Maurer KH, Meinhardt F. J Biotechnol 2007; 130: 124–132.
54. Priest FG, Goodfellow M, Todd C. In: Berkeley RCW, Goodfellow M, editors. The aerobic endospore-forming bacteria. London: Academic Press; 1981. pp. 91–103.
55. Kajino T, Kato K, Miyazaki C, Asami O, Hirai M, Yamada Y, Udaka S. J Biosci Bioeng 1999; 87: 37–42.
56. Chen XH, Koumoutsi A, Scholz R, Eisenreich A, Schneider K, Heinemeyer I, Morgenstern B, Voss B, Hess WR, Reva O, Junge H, Voigt B, Jungblut PR, Vater J, Sussmuth R, Liesegang H, Strittmatter A, Gottschalk G, Borriss R. Nat Biotechnol 2007; 25: 1007–1014.
57. Palva I, Pettersson RF, Kalkkinen N, Lehovaara P, Sarvas M. Gene 1981; 15: 43–51.
58. Kobayashi T, Hakamada Y, Adachi S, Hitomi J, Yoshimatsu T, Koike K, Kawai S, Ito S. Appl Microbiol Biotechnol 1995; 43: 473–481.
59. Duc le H, Hong HA, Barbosa TM, Henriques AO, Cutting SM. Appl Environ Microbiol 2004; 70: 2161–2171.
60. De Bary A. Vergleichende morphologie und biologie der pilze, mycetozoen und bacterien. Leipzig: Wilhelm Engelmann; 1884.
61. Vary PS. In: Doi RH, McGloughlin M, editors. Biology of bacilli, applications to industry. Boston (MA): Butterworth-Heinemann; 1992. pp. 251–310.

62. Vary PS. Microbiology 1994; 140: 1001–1013.
63. Priest FG. *Bacillus subtilis* and other gram-positive bacteria. Washington (DC): American Society for Microbioloty; 1993. pp. 3–16.
64. Kim JY. Biotechnol Lett 2003; 25: 1445–1449.
65. von Tersch MA, Robbins HL. FEMS Microbiol Lett 1990; 70: 305–310.
66. Vary PS, Biedendieck R, Fuerch T, Meinhardt F, Rohde M, Deckwer WD, Jahn D. Appl Microbiol Biotechnol 2007; 76: 957–967.
67. Wolf JB, Brey RN. J Bacteriol 1986; 166: 51–58.
68. Raux E, Lanois A, Warren MJ, Rambach A, Thermes C. Biochem J 1998; 335: 159–166.
69. Barg H, Malten M, Jahn M, Jahn D. In: Barredo JL, editor. Microbial processes and products. Totowa (NJ): Humana Press Totowa; 2005. pp. 165–184.
70. Raux E, Lanois A, Rambach A, Warren MJ, Thermes C. Biochem J 1998; 335(Pt 1): 167–173.
71. Biedendieck R, Malten M, Barg H, Bunk B, Martens JH, Derry E, Leech H, Warren MJ, Jahn D. Microb Biotechnol 2010; 3: 24–27.
72. Kieselburg MK, Weickert M, Vary PS. Biotechnology 1984; 2: 254–259.
73. Stevenson DM, Kunnimalaiyaan M, Müller K, Vary PS. Plasmid 1998; 40: 175–189.
74. Scholle MD, White CA, Kunnimalaiyaan M, Vary PS. Appl Environ Microbiol 2003; 69: 6888–6898.
75. Kunnimalaiyaan M, Vary PS. Appl Environ Microbiol 2005; 71: 3068–3076.
76. Sussman MD, Vary PS, Hartman C, Setlow P. J Bacteriol 1988; 170: 4942–4945.
77. Vary PS, Garbe JC, Franzen M, Frampton EW. J Bacteriol 1982; 149: 1112–1119.
78. Vary PS, Halsey WF. J Gen Virol 1980; 51: 137–146.
79. Vary PS, Tao Y-P. In: Ganesan AT, Hoch JA, editors. Genetics and biotechnology of bacilli. New York: Academic Press; 1988. pp. 403–407.
80. Callahan JP, Crawford IP, Hess GF, Vary PS. J Bacteriol 1983; 154: 1455–1458.
81. Garbe JC, Franzen MA, Hess GF, Vary PS. J Bacteriol 1984; 157: 454–459.
82. Lach DA, Sharma VK, Vary PS. J Gen Microbiol 1990; 136: 545–553.
83. English JD, Vary PS. J Bacteriol 1986; 163: 155–160.
84. Tao Y-P, Vary PS. Biochemie 1992; 74: 695–704.
85. Brusilow WSA, Scarpetta MA, Hawthorne CA, Clark WP. J Biol Chem 1989; 264: 1528–1533.
86. Christie G, Lowe CR. J Bacteriol 2007; 189: 4375–4383.
87. Vorobjeva IP, Khmel IA, Alfoldi L. FEMS Microbiol Lett 1980; 7: 261–263.
88. Xue G-P, Johnson JS, Dalrymple BP. J Microbiol Methods 1999; 34: 183–191.
89. Youngman P, Zuber P, Perkins JB, Sandman K, Igo M, Losick R. Science 1985; 228: 285–291.
90. Stevenson DM, Lach D, Vary PS. In: Balla E, Berencsie G, editors. DNA transfer and gene expression in microorganisms. Budapest: Intercept Budapest; 1993. pp. 197–207.
91. Schmiedle D, Vary PS, Jablonski L, Hillen W. Appl Microbiol Biotechnol 1997; 47: 543–546.
92. Stahl U, Esser K. Eur J Appl Microbiol Biotechnol 1983; 17: 248–251.
93. Wittchen KD, Strey J, Bultmann A, Reichenberg S, Meinhardt F. J Gen Appl Microbiol 1998; 44: 317–326.
94. Rygus T, Hillen W. J Bacteriol 1992; 174: 3049–3055.
95. Wittchen KD, Meinhardt F. Appl Microbiol Biotechnol 1995; 42: 871–877.
96. Youngman P, Poth H, Green B, York K, Olmede G, Smith K. In: Smith I, Slepecky RA, Setlow P, editors. Regulation of procaryotic development, structural and functional analysis of bacterial sporulation and germination. Washington (DC): ASM Washington; 1989. pp. 65–88.
97. Gruss A, Ehrlich S. J Bacteriol 1988; 170: 1183–1190.
98. Arantes O, Lereclus D. Gene 1991; 108: 115–119.
99. Lewis PJ, Marston AL. Gene 1999; 227: 101–110.
100. Kaltwasser M, Wiegert T, Schumann W. Appl Environ Microbiol 2002; 68: 2624–2628.
101. Evan GI, Lewis GK, Ramsay G, Bishop JM. Mol Cell Biol 1985; 5: 3610–3616.
102. Terpe K. Appl Microbiol Biotechnol 2003; 60: 523–533.
103. Rygus T, Hillen W. Appl Microbiol Biotechnol 1991; 35: 594–599.
104. Makrides SC. Microbiol Rev 1996; 60: 512–538.
105. Tabor S, Richardson CC. Proc Natl Acad Sci U S A 1985; 82: 1074–1078.
106. Bernhard K, Schrempf H, Goebel W. J Bacteriol 1978; 133: 897–903.
107. Khan SA. Plasmid 2005; 53: 126–136.
108. Malten M, Hollmann R, Deckwer WD, Jahn D. Biotechnol Bioeng 2005; 89: 206–218.
109. Kunnimalaiyaan M, Stevenson DM, Zhou Y, Vary PS. Mol Microbiol 2001; 39: 1010–1021.
110. Perego M, Spiegelman GB, Hoch JA. Mol Microbiol 1988; 2: 689–699.
111. Gamer M, Frode D, Biedendieck R, Stammen S, Jahn D. Appl Microbiol Biotechnol 2009; 82: 1195–1203.
112. Guerout-Fleury AM, Shazand K, Frandsen N, Stragier P. Gene 1995; 167: 335–336.
113. Rygus T, Scheler A, Allmansberger R, Hillen W. Arch Microbiol 1991; 155: 535–542.
114. Biedendieck R, Yang Y, Deckwer WD, Malten M, Jahn D. Biotechnol Bioeng 2007; 96: 525–537.
115. Shivakumar AG, Katz L, Cohen LB, Ginsburgh CL, Paul LS, Vanags RI, (to Abbott Laboratories). US patent 5,726,042. 1998.
116. Gruss A, Ehrlich SD. Microbiol Rev 1989; 53: 231–241.
117. Biedendieck R, Gamer M, Jaensch L, Meyer S, Rohde M, Deckwer WD, Jahn D. J Biotechnol 2007; 132: 426–430.
118. Lichty JJ, Malecki JL, Agnew HD, Michelson-Horowitz DJ, Tan S. Protein Expr Purif 2005; 41: 98–105.
119. Schmidt TG, Koepke J, Frank R, Skerra A. J Mol Biol 1996; 255: 753–766.
120. Porath J, Carlsson J, Olsson I, Belfrage G. Nature 1975; 258: 598–599.
121. Kapust RB, Waugh DS. Protein Expr Purif 2000; 19: 312–318.
122. Nagai K, Thogersen HC. Nature 1984; 309: 810–812.

123. Malten M, Biedendieck R, Gamer M, Drews AC, Stammen S, Buchholz K, Dijkhuizen L, Jahn D. Appl Environ Microbiol 2006; 72: 1677–1679.
124. Tjalsma H, Antelmann H, Jongbloed JD, Braun PG, Darmon E, Dorenbos R, Dubois JY, Westers H, Zanen G, Quax WJ, Kuipers OP, Bron S, Hecker M, van Dijl JM. Microbiol Mol Biol Rev 2004; 68: 207–233.
125. Ruiz C, Blanco A, Pastor FI, Diaz P. FEMS Microbiol Lett 2002; 217: 263–267.
126. Nielsen H, Krogh A. Proc Int Conf Intell Syst Mol Biol 1998; 6: 122–130.
127. Carbone A, Zinovyev A, Kepes F. Bioinformatics 2003; 19: 2005–2015.
128. Grote A, Hiller K, Scheer M, Munch R, Nortemann B, Hempel DC, Jahn D. Nucleic Acids Res 2005; 33:W526–W531.
129. Yang Y, Malten M, Grote A, Jahn D, Deckwer WD. Biotechnol Bioeng 2007; 96: 780–794.
130. Bäumchen C, Roth AH, Biedendieck R, Malten M, Follmann M, Sahm H, Bringer-Meyer S, Jahn D. Biotechnol J 2007; 2: 1408–1416.
131. Jia M, Li Y. FEBS Lett 2005; 579: 5333–5337.
132. Shivakumar AG, Vanags RI, Willcox DR, Katz L, Vary PS, Fox JL. Gene 1989; 79: 21–31.
133. Radha S, Gunasekaran P. J Appl Microbiol 2007; 103: 1301–1310.
134. Yang Y, Biedendieck R, Wang W, Gamer M, Malten M, Jahn D, Deckwer WD. Microb Cell Fact 2006; 5: 36.
135. Berger BJ, Schwandt KE, Radford CL. Defence R&D Canada –Suffield; 2004.
136. Burger S, Tatge H, Hofmann F, Genth H, Just I, Gerhard R. Biochem Biophys Res Commun 2003; 307: 584–588.
137. Dubnau D, Losick R. Mol Microbiol 2006; 61: 564–572.
138. Wang W, Hollmann R, Furch T, Nimtz M, Malten M, Jahn D, Deckwer WD. Proteome Sci 2005; 3: 4.
139. Fürch T, Hollmann R, Wittmann C, Wang W, Deckwer WD. Bioprocess Biosyst Eng 2007; 30: 47–59.
140. Fürch T, Wittmann C, Wang W, Franco-Lara E, Jahn D, Deckwer W-D. J Biotechnol 2007; 132: 385–394.
141. Anagnostopoulos C, Spizizen J. J Bacteriol 1961; 81: 741–746.
142. Chen I, Christie PJ, Dubnau D. Science 2005; 310: 1456–1460.

12

GENE EXPRESSION IN HUMAN CELLS

Marco A. Cacciuttolo, Gene Lee, and John Chon
Percivia LLC, Cambridge, Massachusetts
John Lewis
Crucell NV, Leiden, The Netherlands

12.1 BACKGROUND

12.1.1 The Use of Human Cell Lines in Research

One of the chief appeals of biotechnology products is the ability to give patients medicines that resemble the natural molecules present in the human body as a way to minimize the risk of adverse events or unknown toxicological effects, as opposed to using new and chemically synthesized drugs. The goal of achieving increased fidelity also demands an increase in the complexity of the production process, and the industry has resorted to source these products initially from cadavers, animal and human sera, to more recently recombinant DNA technologies to satisfy the need for solving unmet medical needs, shortages in supply, and safety concerns of these therapeutic products (Fig. 12.1). This progression in the sources for these products is driven not only by the economics of the production process but also by the need to improve the assurance of patients' safety without compromising on quality.

Until recently, a major drawback of using nonhuman recombinant expression systems to express human proteins was the inability to obtain the complete human characteristics of these protein products (1). Even though the safety of "partially true" recombinant human products obtained from nonhuman cell lines (such as BeneFix™) or even transgenic animals (such as Atryn™) were acceptable for approval, in some instances these recombinant molecules are cleared much faster than the plasma-derived ones due to differences to the native human molecule being replaced, requiring higher or more frequent dosing to achieve the intended clinical effect (2).

More recently, technology improvements for making recombinant human proteins from nonhuman sources have been made. For instance, Glycofi's technology (acquired by Merck Inc. in 2006), has engineered human glycosylation pathways in the yeast *Pichia pastoris* (3) in order to express secreted recombinant fully human antibodies. In addition, a multitude of novel research approaches had been recently demonstrated to mimic human pathways in nonhuman expression systems (1) including transgenics (4), and even bacteria have been shown to be able to express full-length, nonglycosylated human antibodies (5). These efforts overcome in part some of the difficulties of expressing complex human proteins in nonhuman expression systems as a way to make these molecules more economical to produce. However, either the inability to obtain the complete protein structure due to, perhaps, differences in protein folding (1) or the lack of commercially viable production yields are still the obstacles to truly achieve the autonomy of producing human biotherapeutics from human sources such as serum plasma, tissues, or even stem cells.

Fundamental research in medical pharmacology is still being carried out using human cells to test the different mechanisms of human disease and interactions between different molecules *in vitro* (6). However, very little progress has been made in facilitating the extrapolation of these

Upstream Industrial Biotechnology: Expression Systems and Process Development, Volume 1, First Edition. Edited by Michael C. Flickinger.
© 2013 John Wiley & Sons, Inc. Published 2013 by John Wiley & Sons, Inc.

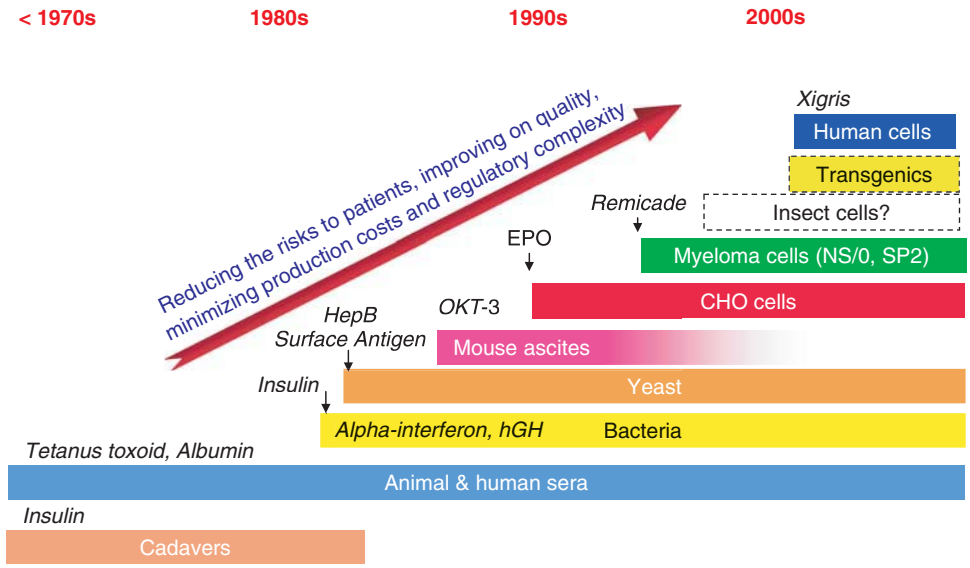


Figure 12.1. The evolution of therapeutic proteins expression systems. (This figure is available in full color at http://onlinelibrary.wiley.com/book/10.1002/9780470054581.)

results to clinical settings by supplying the same human proteins along the clinical development cycle and into commercial production. Typically, once a target has been identified and validated *in vitro* using human cells or tissues, the protein reagent (agonist or antagonist) is then expressed in a nonhuman expression system before going into first-time in human clinical trials in an effort to overcome the economic and/or technical hurdles of obtaining these molecules from their natural sources in large amounts. Historically, this has been circumvented by using animal cells as a close approximation due to the lack of available human cell lines that address safety concerns and achieve industrial performance for robustness and product yields. The industry has been forced to use what is available in research laboratories, even if that meant nonwell characterized animal cell lineages. When expressing human proteins in animal cells (i.e. human amino acid sequence), there is still the potential for either carrying nonhuman posttranslational modifications (PTMs) into the final product or incomplete human PTMs. In either case, both safety and efficacy of the intended protein drug could be suboptimal. Products derived from animal cells are still being approved on the basis that clinical studies show acceptable safety and efficacy in short term clinical studies. Nevertheless, there is evidence suggesting that nonhuman PTMs such as the presence of α-1,3 gal in some of the approved protein products may pose safety risks to humans (7). Mouse cell lines contain α-1,3-galactosyltransferase activity which adds galactose residues to proteins in the α configuration, designated as Gal($\alpha 1 \rightarrow 3$)Gal. Humans indeed recognize this structure as foreign (8) being the main reason for preventing xenotransplantation of animal organs into humans (4).

Even if these antigenic responses by patients to nonhuman proteins or nonhuman components in protein therapeutics may not necessarily carry a safety risk to the patient, it could certainly affect the efficacy of the product as this response may increase the clearance of the protein therapeutic, thereby reducing the bioavailability of the clinically tested dose. In fact, even "fully human" antibodies (such as Humira™) produced in Chinese hamster ovary (CHO) cells show immunological responses to the product (9).

The definition of "fully human" antibody has only considered the amino acid sequence, and not to the rest of the required structures present in the protein molecule. This is important to bear in mind when trying to develop the next generation of safer and more effective therapeutics. Not only the correct molecular moiety but also the correct molecular linkages have to be in place in order to provide true fidelity to the natural protein. And in some cases, evolution has resulted in some subtle but critical differences among the posttranslational modifications different species of mammals will perform on proteins, not to mention among members of the other different animal kingdoms and microorganisms.

For instance, the presence of α-2,6-sialyl-transferase enzyme in humans is particularly critical as a different linkage for the same sugar moiety to a protein immunoglobulin G (IgG) will cause a faster clearance in the human body (1,4,8). In this regard, CHO cells, a widely used recombinant protein expression system, lack this enzyme activity and they add sugars to proteins via 2,3-linkages (4,8). In addition, other typically human glycosylation reactions, such as fucosylation, are much more diminished in CHO cell lines having to resort to engineer these nonhuman

cell lines to accomplish the desired modifications to approach a true human profile in the final molecule by expressing human *N*-acetyl-D-glucosaminyltransferase and α-1,3-fucosyl-transferase III (1). It is worth noticing that in some instances, lower amounts of fucosylation (or lack of it) may lead to improved attributes to products. One remarkable example is the discovery that reduced or absence of fucosylation of antibodies increase their antibody-dependent cell cytotoxicity (ADCC) (10). In other cases, increased sialylation of antibodies has been recently elucidated to be associated to their antiinflammatory effects (11). In this particular case, the linkage of sialic acid is critical for this effect and only 2,6-linkages, typical of human cells and not of animal cells, work.

In addition, nonhuman cell lines can make modifications to proteins which could be immunogenic to humans. For instance, the enzyme CMP-*N*-acetylneuraminic acid hydrolase which glycosylates CMP-*N*-acetylneuraminic acids (NANA) to CMP-*N*-glycolylneuraminic acid (NGNA) is present in CHO cells but not in humans (1,12). This NGNA structure could be immunogenic if injected (1) and it can also be incorporated into human proteins if provided exogenously in the diet (12). The connection between this NGNA structure and human disease is being established (12), thereby increasing the putative risks that CHO-derived protein therapeutics containing this NGNA structure may carry. Eliminating this enzymatic activity by altering the genotype of CHO cells or by using cell lines that do not contain it will certainly alleviate these concerns.

12.1.2 The Use of Human Cell Lines in the Production of Cell Culture Products in Manufacturing

12.1.2.1 Early Products. The first demonstration of using human cell lines for making a human therapeutic is the approval and marketing of Wellferon. Wellferon, a human interferon α, was first approved in 1986 in the United Kingdom for hairy cell leukemia, and produced and marketed by the Wellcome Foundation Ltd. (now part of GlaxoSmithKline PLC) (13). This product was made in Namalwa cells, which are human lymphocytes obtained from an African female who has died of lymphoma (Burkitt's tumor). The production process consisted in stimulating the production of interferon α by infecting these Namalwa cells with Sendai virus. The cell culture contained animal-derived components and this product was manufactured with the standards and testing available in the 1980s and early 1990s. It was subsequently withdrawn from the market in 1999 due to the competition from recombinant products made much more cheaply and arguably more safely in *Escherichia coli*, such as Roferon and Intron. In retrospect, the production process to make Wellferon would not satisfy current demands for safety in the production process, but it did demonstrate the suitability of using human cells for making active and safe protein therapeutics.

In most of the cases illustrated in Table 12.1, the proteins produced in human cells are actually induced. That is, endogenous capability of the host cells is enhanced rather than exogenous transfer of genes to express a given protein. However, this list is provided as evidence of the safety of using human cells for making protein therapeutics. The only two examples of an approved recombinant protein expressed in human cells to date are Elaprase™ and Xigris™. However, the availability of adequate human cell lines specifically developed for their use in commercial production such as the PER.C6® cells, having its history and safety well documented (14) to backup the use of such cell line in making human therapeutics offer a renewed perspective for the production of human therapeutics in human cell lines. The PER.C6 human cells are the only cells developed exclusively for the production of therapeutics such as gene therapy, vaccine, and protein products, and its extensive testing for safety and adequacy is documented in a Biological

TABLE 12.1. Approved Protein Products from Human Cells

Product Name	Protein	Human cell	Sponsor	Date approved
Wellferon	Interferon α	Namalwa	Wellcome Foundation Ltd.	1986 (UK) (withdrawn in 1999 by Glaxo Wellcome)
Xigris	Activated Protein C (recombinant)	HEK 293	Eli Lilly & Co.	2001 (US)
Dynepo	Erythropoietin	Human fibroblast	Shire Pharmaceuticals	2002 (EU)
Replagal	Human alfa galactosidase (agalsidase alfa)	Human fibroblast	Shire Pharmaceuticals	2001 (EU)
Elaprase	Idursulfase (recombinant)	Human fibroblast	Shire Pharmaceuticals	2006 (US)

TABLE 12.2. Clinical Trials of Recombinant Proteins Expressed in Human Cells

Protein	Human Cell Line	Sponsor	Clinical Trial Stage	Indication(s)
Antirabies IgG (cocktail of 2 IgGs)	PER.C6®	Crucell/Sanofi Pasteur	Phase 2	Rabies exposure (prophylaxis and therapy)
Anti-GM-CSF IgG	PER.C6®	Morphosys	Phase 1	Inflammatory diseases
GLP-1	Recombinant mesenchymal stem cell	Biocompatibles International PLC	Phase 1/2	Stroke
Undisclosed	PER.C6®	AME/Lilly	Phase 1	Undisclosed

IgG, immunoglobulin G; GM-CSF, granulocyte monocyte-colony stimulating factor.

Master File with the US Food and Drug Administration (USFDA) (15).

The maturing of the technologies employed in using human cells for gene expression is making it possible currently to achieve record level productivities of IgGs of more than 10 g/L in fed-batch (16) and of more than 25 g/L in continuous processes such as the XD™ technology (17). At the same time, IgM levels are reaching over 3.5 g/L in fed-batch using human cells (18). These yields far exceed the current best practices achieved in other nonhuman cell lines, such as CHO cells due to the intrinsic properties of, for instance, the PER.C6 cells for their use in biopharmaceutical production. Many other human proteins of therapeutic value are also being expressed in human cells due to the intrinsic nature of human cells being the natural host to make these complex proteins requiring the correct PTMs for activity and, possibly, for lowering the risk of immunological responses against these therapeutics. These record yields in productivity provide a very attractive opportunity to decrease the production costs without sacrificing product quality.

These developments are opening a renewed interest in using human cells which is demonstrated by the increasing number of clinical trials of proteins derived from recombinant human cell lines (Table 12.2).

12.1.3 Future Trends in the Expression of Genes in Human Cells

Although the overwhelming majority of therapeutics products and recombinant proteins in clinical trials are currently made in nonhuman cells, it is expected that future use of human cells will increase (15) as this system provides the natural host for making human recombinant therapeutics. Significant efforts have been devoted to modifying *in vitro* some of the human proteins expressed in nonhuman systems (19) in order to achieve the desired "humanness" for these molecules. The alternative path of engineering nonhuman expression systems to mimic human posttranslational modifications, and thereby expressing a truly fully human molecule, need to overcome multiple technical challenges such as achieving expression levels that reach economic feasibility, attaining the proper balance of the enzymes involved in these anabolic pathways (3,20), obtaining stable cell lines expressing the entire array of exogenous enzymes without losing product expression level, and a tolerable level of freedom to operate.

The increase use of human cell lines for making recombinant therapeutic proteins will also make it possible to address the relative differences in safety and efficacy with currently nonhuman recombinant sources, especially for chronic indications where the long-term harmful effects of drugs are hard to evaluate in limited-term clinical trials. For instance, there is already solid evidence that improved amino acid sequences of proteins such as the so-called fully human antibodies (i.e. amino acid sequence) are much better tolerated and more efficacious (stronger binding to antigen) than their chimeric counterparts (21). However, these fully human antibodies when expressed in nonhuman cell lines can carry nonhuman posttranslational modifications and/or immunogenic residues from the host expression cell line, which may lead to immunogenic responses in humans (22). These effects can be avoided not only by engineering nonhuman expression systems, but also by increasing the overall production cost. At the end, safer and efficacious products made economically are to be the goals to aim when pursuing the medicines of the future.

12.2 THE SAFETY AND REGULATORY ASPECTS OF USING HUMAN CELL LINES FOR GENE EXPRESSION

The safety of recombinant protein biologics manufactured using human cell substrates is ensured by a process of regulatory oversight whose codification and maturity have been realized through the last 70 years to support the manufacture and release of viral vaccines for use in humans. The development of the earliest human viral vaccines was sponsored by various US military agencies to offer prophylaxis for US military servicemen deployed to Asian theaters

of combat during World War II where the debilitation of entire units with vector-borne pathogens threatened combat readiness and effectiveness. These early prototypical vaccines were developed with the most unsophisticated *in vivo* culture methods, for example, mouse brain, to propagate the virus for the formalin inactivated Japanese encephalitis virus vaccines, embryonated hens' eggs for the manufacture of the first inactivated influenza virus vaccines (23), and the live attenuated 17D yellow fever virus vaccine from M.Theiler and the Rockefeller Foundation (24). These manufacturing substrates and primitive methods of processing and containment provided theoretical opportunities for the adventitious contamination of the vaccine viruses with other viruses of human or nonhuman origin. Despite these theoretical opportunities for compromise, these prototypical vaccines offered highly favorable equations of benefit and risk supporting widespread administration in epidemiological contexts of endemic infection and morbidity. Indeed similar favorable benefit risk equations supported the development and widespread use of both inactivated and oral polio virus vaccines manufactured on primary monkey kidney cell cultures to control epidemic disease, and live vaccinia vaccines deployed for the global eradication of small pox prepared as lyophilized preparations of lymph fluid (pus) from bovine skin infected by scarification with various vaccinia virus strains.

These early vaccine manufactures using nonhuman substrates were not without incident, most notably the contamination of inactivated and attenuated poliovirus vaccines with Simian Virus 40 propagated in the rhesus monkey cell substrates and the contamination of live virus vaccines manufactured in embryonated eggs with avian leukosis viruses. Although it now appears through long-term prospective studies that the widespread SV40 contaminations resulted in no long-term untoward medical consequences to vaccine recipients (25), these episodes made frighteningly real the theoretical hazards of biologics manufacture with cell substrates from nonhuman sources whose spectrum of virus sensitivity and endogenous viral burdens were not well characterized or understood.

With these hazards in mind, the use of human cell lines for the manufacture of biologics and vaccines would appear to offer the advantages that National Institute of Health (NIH) supported medical science investigations of the last 50 years have been mostly focused on the isolation and thorough characterization of viruses which replicate in humans causing human disease. These investigations have led to the development of numerous assay systems appropriate for the propagation and sensitive detection of adventitious viruses of human origin and tropism and a familiarity beneficial to detection and elimination.

Despite the theoretical advantages of familiarity, to vaccine safety of the use of human cell lines to propagate vaccines and biologicals, the adoption of human cell lines awaited the development of the WI-38 and MRC-5 primary human lung diploid cell strains at the Wistar Institute (26) and National Institutes of Medical Research (27) in the decade of the 1960s, nearly 20 years after the proposal of M. Hilleman to adopt the human cervical carcinoma cell line as a substrate for his manufacture of an inactivated adenovirus vaccines for use in military recruits in 1954 (28). The rejection of the US Armed Forces Epidemiology Board (AFEB) of Hilleman's proposal for HeLa cells to support biologics manufacture owed largely to the ignorance at the time of the etiological role of human viruses in the development of human cancers, especially reasonable and prudent concerns in an era in which retroviruses were shown to be responsible for a range of avian and murine leukemias and solid tumors and subsequently the oncogenicity of the human retroviruses human T-cell leukemia virus type-1 (HTLV-1) and HTLV-2, various human papilloma viruses (HPVs), the human Epstein-Barr virus (EBV), and the Kaposi sarcoma virus–associated human herpes virus (HHV)-8 were shown to be etiological agents of various human cancers.

The adoption of the normal diploid primary WI-38 and MRC5 cell substrates for the manufacture of numerous live attenuated vaccines for both pediatric and adult populations, including measles, mumps, rubella, varicella vaccines, and most recently second generation vaccinia virus vaccines has been attended by impeccable records of safety and manufacturabiity. Moreover, a similarly impressive record of vaccine safety and manufacturability have been recorded with the use of embryonated eggs, primary chick embryo fibroblasts to manufacture influenza virus vaccines and the African green monkey kidney continuous cell line VERO, and both attenuated poliovirus and rotavirus vaccines. This record of safety and consistent large-scale manufacture using cell substrates which are exquisitely sensitive hosts for a wide range of human virus replication, argues compellingly that the use of human cell substrates in contemporary manufacturing settings with human operators poses no special risks to the safety of the human biological product. Indeed, it remains an irony that the only recent example of adventitious viral contamination that compromised the consistency of large-scale biotechnological manufacturing campaigns is the well-described episodes of bioreactor contamination with mouse minute virus (29), contamination introduced not through human agency but presumably through raw material contamination.

The principles of current good manufacturing practice (cGMP) which have emerged through decades of virus vaccine manufacture are described and codified in various regulatory documents, most notably the seminal two documents, *"Points to Consider in the Characterization of Cell Lines Used to Produce Biologicals"* of the USFDA (30) and the International Conference on Harmonization

(ICH) guideline *"Note for Guidance on the Quality of Biotechnological Products; Derivation and Characterization of Cell Substrates Used for the Production of Biotechnological/Biological Products"* (31).

In brief, these documents provide regulatory guidance to manufacturers to ensure the safety of biologicals manufactured in human cell substrates. In short, this is achieved by the combination of: (i) an extensive documentation of the origin and processing of the cell substrate intended for use as a Master Cell Bank, as well as a thorough documentation of all materials of animal origin used for their manufacture, (ii) the manufacture of Master Cell Banks and bulk biological product according to cGMPs in facilities meeting mandated standards of microbiological containment with demonstrated validation and appropriately trained operators, and (iii) an extensive panel of release testing for adventitious microbial and virological agents using a broad panel of nonspecific but highly sensitive *in vivo* and *in vitro* assays to reveal adventitious viral contamination through biological effect supported by biochemical and molecular assays of considerable specificity and sensitivity and breadth for the detection of known human pathogenic viruses.

These principles of manufacture practice have been validated by a long history of successful manufacture of live virus vaccines and with the continued development and refinement of manufacturing facilities and processes, and they can be expected to serve the manufacture of important biologicals and recombinant proteins whose essential attributes are most thoroughly and consistently endowed with the use of human cell substrates.

12.3 GENE EXPRESSION IN HUMAN CELL LINES

In the late nineteenth century, the German zoologist, Wilhelm Roux successfully cultured embryonic chick cells *in vitro* in a simple saline solution, thus establishing the basic principles of tissue culture. Over the following decades, many other scientists were able to propagate a variety of animal cells in culture. The earliest work focused on primary cell cultures, which are derived directly from a specific animal tissue. A large panel of human diploid cell lines (HDCLs), derived from a variety of fetal tissue, was developed at the Wistar Institute in Philadelphia and first described in a paper published by Leonard Hayflick (26). These cell lines were designated WI-1 through 25. Additional HDCLs were later isolated at the Wistar Institute and other laboratories, including the WI-38 line which is still used for virus vaccine production. The FS-4 line, derived from human neonatal foreskin fibroblasts, has been used extensively to study the antiviral and biological functions of human interferons and cytokines (32). The isolation of primary cell lines from human tissue remains an active area of research today, and a number of companies offer the ability to create novel HDCLs. One particular application is to use such cell lines as "biorepositories", for research on a number of human diseases and for clinical pathology. However, a major drawback with primary cell lines is that they have a finite life span, and are often heterogeneous in nature (i.e. comprised of different cell types), which can limit their usefulness as a research tool or production platform (33,34). Transformed cell lines, on the other hand, can be propagated in culture indefinitely, and as such are often referred to as *immortal cell lines*. Cell lines derived from many tumor types exhibit this transformed phenotype. Moreover, as the acquisition of the immortalizing or transformed phenotype is often the result of rare mutation events to the cellular genome, such cell lines are typically clonal, or homogeneous. Currently, such cell lines are in common use as models for studying the origins of the cancer itself, as well as for understanding mechanisms underlying cellular processes such as growth, division, differentiation, and gene expression.

While a number of cell lines have been successfully isolated from patient tumors, the first continuous cancer cell line and perhaps the most widely used cell line in research is the HeLa cell line (35). HeLa cells were isolated in 1951 by George Otto Gey, who was the head of tissue culture research at Johns Hopkins University. HeLa cells exhibit an epithelial morphology, and grow adherently (although suspension-adapted cultures have also been described). The cell line has a fast doubling time, which has been attributed to low levels of the tumor suppressor protein p53. HeLa cells were isolated from a patient with aggressive cervical cancer named *Henrietta Lacks* (the name HeLa is derived from the first two letters of the patient's names). The cells were removed without the patient's knowledge or permission, and were later commercialized. The issue of patient rights sparked a bioethics debate which was noted by the Supreme Court in the case *John Moore v the Regents of the University of California*, in which the court ruled that a deceased person's body or tissue are not their property, and can therefore be commercialized.

One of the earliest uses of the HeLa cell line was in the development and testing of different poliovirus strains, and the HeLa cell was established as a model for testing the new Salk vaccines being developed in the 1950s. This early virus vaccine program, established by the National Foundation for Infantile Paralysis, culminated in the shipment of over 600,000 cultures of HeLa cells to production laboratories at the Tuskegee Institute (35). This use of an immortalized human cell line for the propagation of human disease-causing viruses, and for the development of vaccines, was an early example of biotechnology. However, further use of immortalized human cell lines for this purpose was hindered by the

recommendations from the USAFEB, which stated in 1954 that adenovirus vaccine production for use in the military should use "normal cells" as the substrate, rather than cell lines established from human tumors (i.e. HeLa). The main concerns raised by the board were that cells derived from tumors may be contaminated and may confer oncogenicity to patients, making them susceptible to cancer. These recommendations continue to resonate with regulatory agencies, and the only cultured animal cells currently in use for the production of viral vaccines in the United States are primary cells (derived from monkey, chick, or mouse), continuous animal cell lines (VERO) and nontumorigenic human diploid cell lines (e.g. WI38, MRC-5). Recently, however, there have been attempts to reintroduce immortalized human cells for the production of viral vaccines. Certain viral strains, such as human immune deficiency virus (HIV), cannot be adequately propagated in traditionally accepted cell substrates. The Office of Viral Research and Review (OVRR) and the Center for Biologics Evaluation and Research (CBER) at the FDA have commented on so-called designer cell substrates, which are described as "neoplastic cells derived from normal human cells transformed by defined viral or cellular oncogenes or by immortalizing cellular genes." Specifically, in 2001 the FDA requested to the Vaccines and Related Biological Products Advisory Committee the use of two immortalized human cell lines, HEK293 and PER.C6, for the production of viral vaccines. Both cell lines express the immortalizing E1 genes from adenovirus Ad5. However, OVRR/CBER believes that "there is an extremely low probability that residual DNA from adenovirus 5-transformed human cells could transfer traits that could induce neoplastic development in vaccinees."

In addition to HeLa cells, many other cell lines derived from human cancers are widely used in research laboratories (Table 12.3). Each of these tumor-derived cell lines offers researchers unique attributes and opportunities for study. For example, because such cell lines originate from a variety of tissues, different cell type specific proteins (such as cytokine receptors) may be expressed on the cell surface. Similarly, individual cell lines may respond differently to experimental stimuli. Thus, Jurkat cells may allow a researcher to study T-cell signaling pathways, U937 cells may be used for understanding the behavior of monocytes and macrophages, and K562 cells may be used to study erythrocyte function. The differential responses to stimuli also allow such cells to be used as *in vitro* models for evaluating the functionality and efficacy of new drugs being developed for the treatment of human diseases, particularly those which target specific cell types. The A549 and BxPC-3 cell lines, derived from lung and pancreatic cancers respectively, have been used to test the binding of tissue-specific antibodies being developed for the treatment of these cancers. For all of these aforementioned cell lines, their derivation from human tissues is an important feature, which distinguishes them from cells lines derived from other species. The "humanness" of these cell lines reflects the intrinsic differences across species, encoded within the genome and expressed as differences in the complement of cellular proteins involved in structural, regulatory, enzymatic, and other functions.

TABLE 12.3. Examples of Tumor-Derived Human Cell Lines

Cell Line	Origin Tissue
A-549	Lung carcinoma
BCP-1 cells	PBMC
BR 293	Breast
BxPC3	Pancreatic adenocarcinoma
DU145	Androgen insensitive carcinoma
H1299	Lung
HCA2	Fibroblast
HeLa	Cervical cancer
HepG2	Hepatocellular carcinoma
HL-60	Myeloblast
HT-29	Colon epithelium
Jurkat	T-Cell leukemia
JY cells	Lymphoblastoid
K562 cells	Lymphoblastoid
NALM-1	Peripheral blood
THP1 cell line	Monocyte
U373	Glioblastoma-astrocytoma
U937	Leukemic monocytic lymphoma
WM39	Skin
WT-49	Lymphoblastoid
YAR	B-cell

PBMC, peripheral blood mononuclear cells.

However, not all immortalized human cell lines are derived from human neoplasms. The transformed phenotype can also be induced by oncogenic or transforming viruses, and more specifically by individual genes expressed in the genomes of these viruses. Indeed, the HeLa cell line, while isolated from a cervical carcinoma, was likely derived from normal epithelial tissue that became infected and thereby transformed with HPV. The HPV-16 and -18 gene E6 binds to and inactivates the tumor suppressor protein p53 (36). Other human cell lines have been created by transformation with HPV-16 and -18 DNA, as well as with the DNA from other transforming viruses. HEK293 and PER.C6 cell lines, derived from kidney and retinal tissue respectively, express the adenovirus E1 genes (specifically the Ad5 E1A and E1B genes). The adenovirus E1 protein also binds to (and inactivates) p53, as well as to another tumor suppressor protein, Rb (37,38). Freshly isolated B-cells may be transformed by EBV, although it has been reported that such cell lines are not truly immortalized and have a finite life span (39).

The ability to transform specific cell types with viral genes ("designer cell substrates") offers researchers

additional tools for studying cellular processes in human cells. Such cell lines also provide opportunities for the large-scale biopharmaceutical expression and production of viral vaccines and recombinant proteins. Because such cell lines can be transformed with specific viral genes (and tested for the expression of these genes), and the history of creating such cell lines can be formally documented, regulatory agencies have found the use of these cell lines to be acceptable for the manufacturing of therapeutic products. This has allowed cell lines such as HEK293 and PER.C6 to be used as platforms for the production of recombinant adenoviruses, as well for the production of recombinant proteins such as monoclonal antibodies and blood coagulation factors. Not all virus-transformed human cell lines, however, are suitable for large-scale manufacturing, as other attributes, such as fast growth rates and the ability to grow in suspension culture must also be exhibited.

Such cell lines must also be capable of high level expression in order for them to be competitive with alternative and well established production platforms, such as *E.coli* or CHO cells. A potentially attractive feature of human cell lines for the production of recombinant proteins is that the glycan modifications—carbohydrate side chains that are added to the protein as it is being processed inside the cell—are fully human and therefore less likely to be immunogenic than animal-derived cell lines. In contrast, the glycan structures of proteins expressed in CHO cells such as NGNA (12), host cell proteins (22), or other animal cell lines may be recognized as foreign if introduced to patients. Human cell lines, like other mammalian cell lines, are capable of complex protein folding and disulfide bond formation.

Interestingly, in addition to contributing to the transformed or immortalizing phenotype in human cell lines, the Ad5 E1A and E1B genes may also confer additional phenotypes that make cell lines such as HEK293 and PER.C6 attractive options as industrial production host cell lines—resistance to apoptosis and transactivation of viral promoters, such as human cytomegalovirus (hCMV). These features allow cell lines to achieve high cell densities and high cell-specific productivities, which ultimately leads to very high levels of recombinant protein.

12.3.1 Vectors and Gene Transfer Methods

The wide variety of human cell lines available for study, from both normal and neoplastic tissues, reflects the desire to choose model systems with the appropriate endogenous gene expression or developmental profiles. However, many research programs and industrial applications require heterologous gene expression, also known as *recombinant gene expression*, rather than the expression of endogenous genes. Such applications may range from the use of fluorophore tagged proteins or mRNAs to monitor and track cellular processes to the overexpression and secretion of proteins that can be used therapeutically to treat disease.

Since the early 1990s, when the biotech industry firmly demonstrated the ability to successfully commercialize recombinant therapeutic proteins such as insulin and erythropoietin, the design and development of expression vectors—replicating pieces of DNA that contain the recombinant gene(s) expressed in a cell line—have been the focus of intense study. While much of this work has been done in the context of gene expression in CHO cells (and other cell lines of nonhuman origin), many of the same principles can be applied to the expression of recombinant proteins in human cell lines. Expression vectors that are designed to direct very high levels of gene expression commonly utilize strong viral or cellular promoter sequences upstream of the gene to be expressed. One example of such a promoter is derived from the hCMV. While expression vectors containing the hCMV promoter have been used for recombinant protein expression in CHO cells, such promoters have also been shown to support very high levels of heterologous gene expression in human cell lines such as PER.C6 (ref.). The use of efficient enhancer elements, signal peptides, polyadenylation sequences, and selection markers are also important considerations in the design of expression constructs.

Similarly, methods and technologies developed for the introduction or insertion of the expression vector into CHO cells can generally be applied to human cell lines as well. Common methods in use, nowadays, include lipid or liposome-based transfection and electroporation. Interestingly, one of the earliest methods of transfecting DNA was developed by Frank Graham and Alex van der Eb, who also developed the human transformed cell lines HEK293 and PER.C6. The calcium phosphate method, which delivers DNA complexed with a calcium phosphate precipitate, occurs through a poorly understood process, and is relatively inefficient. However, it is relatively inexpensive, and can be scaled up to transfect large numbers of cells.

12.3.2 Clone Selection Methods

The transfer of genes into cells (as part of an expression vector) and the stable integration of the gene into the host cell genome is an inefficient process. The result is that the majority of cells in culture following a transfection reaction remain untransfected. The ability to isolate (clone) cells, which have been stably transfected must therefore require a means to differentiate transfected cells from untransfected cells. Positive selection methods, such as fluorescence activated cell sorting (FACS), may be used to isolate those clones which exhibit a desired phenotype or attribute (such

as expression of the recombinant protein). Alternatively, untransfected cells may be negatively selected, which will result in a pool of cells that is enriched for transfected subpopulations. This is commonly achieved by coexpressing the gene(s) of interest with a selectable marker, or a gene, which confers resistance to a cytotoxic substance (such as an antibiotic). Such methods have been used for many years in the development of mammalian cell lines and have been successfully adapted for use with industrial cell lines of human origin such as PER.C6.

Following the selection of a number of clones (single cells which express the gene of interest), the clones can be further screened for appropriate phenotypes. Such phenotypes may include growth rate, productivity, and/or product quality attributes. A relatively simple approach is used for cell lines that are generated in PER.C6 cells. Following transfection, cells are cultured in the presence of a selection agent to enrich the population for drug-resistant clones (which also express the gene of interest). The enriched population is plated in 96-well tissue culture plates as single cells, by limiting dilution, and the individual wells can subsequently be assayed for the expression of the secreted protein in the culture supernatant, typically by using an enzyme-linked immunosorbent assay (ELISA)-based method. Cells that express relatively high levels of the protein can then be scaled up to larger culture formats. This method eliminates the need to include serum in the culture media (as is required for many adherent cell types), and allows cell lines to be isolated from a single originator cell, which defines them as monoclonal. Serum, most commonly derived from fetal bovine origin, provides a mixture of nutrients and growth factors, which are favorable for supporting cell growth. However, there has been concern in the industry that serum may also be a potential source of adventitious agents, most notably bovine spongiform encephalopathies (BSEs). Cell culture media have been developed that can support the high density growth of human cell lines in a serum-free formulation (see section titled "Cell Culture Media, Cultivation and Handling Methods"). Cell lines can be further selected for other attributes, such as performance in a fed-batch culture, or specific product quality profiles, by running a comparative study with a number of candidate cell lines.

12.3.3 Cell Culture Media, Cultivation, and Handling Methods

As with other mammalian cell lines, in general, human cell types can be divided into two major categories: those that are able to grow in suspension (anchorage-independent) and those that require a physical support for growth (anchorage-dependent). In either case, the products produced can be secreted into the production medium or can be accumulated inside the cells. The properties of the cells and the location of the produced product dictate the method used for growth and production, and consequently, the selection of a suitable type of bioreactor.

Those human cell lines that require physical support for growth such as A549 and WI-38 fibroblast cells are typically cultured in T-flasks, roller bottles, or on microcarriers in spinners. These cells are typically cultured in standard basal media such as Dulbecco's Modified Eagle's Medium (DMEM) or Ham's F12 supplemented with serum to promote attachment (40). A number of serum-free medium for anchorage-dependent human cell cultures are also available from vendors such as Invitrogen, many of which are based on the molecular, cellular, and developmental biology (MCDB) line of medium developed by Ham *et al*. in the Department of MCDB at the University of Colorado in Boulder, Colorado (41–52). In many cases, however, the individual companies prefer to use their own in-house proprietary medium. These in-house media are usually free of animal-derived components and are often chemically defined.

For industrial applications, cells that grow in suspension are preferred (53–58). Although some of the human cell lines—those with fibroblast-like characteristics in particular are anchorage-dependent, HEK293 and PER.C6 cells have been adapted to grow in suspension. Without the need for a solid substrate on which to anchor, these cells may be more easily handled and expanded using standard suspension cell culture techniques and without the need for any specialized equipment. Similar to suspension-adapted CHO and NS/0 cells, human cell lines such as PER.C6 cells are typically cultured in shake flasks or spinners. These cells may be cultured in standard basal media such as DMEM supplemented with serum. Also, a number of serum-free media for both HEK293 and PER.C6 cells are commercially available from vendors such as HyClone, Invitrogen, and JRH (acquired by Sigma Aldrich Fine Chemicals or SAFC).

In routine culture, cells are allowed to grow to mid-log phase before splitting by dilution. Depending on the growth rate and the medium used for cultivation, this typically occurs between 3 and 5 days after inoculation. This is accomplished by simply inoculating a new culture vessel with the existing culture to achieve between 0.2 and 0.5 million cells/mL. Depending on the growth rate and the medium used for cultivation, the cell concentration from 3 to 5 days after inoculation may be as high as 5 million cells/mL. This means that split ratios of greater than 1:20 is sometimes possible. However, a normal split ratio of 1:10 is more typical. Nevertheless, this illustrates one feature of some human cell lines—namely their ability to grow to high cell densities. If left to continue to grow, some human cell lines may grow to very high densities—much higher than typically observed for CHO or NS/0 cells. For example, PER.C6 cells have been

observed to achieve viable cell concentration greater than 10 to 15 million cells/mL in batch mode without any feeding.

12.3.4 Production Parameters and Methods

Methods typically used for culturing human cell lines for recombinant protein productions in the biotech industry is not appreciably different than those used for other mammalian cell lines, such as hybridomas, CHO or NS/0. As with these cell lines, two main production processes are utilized with human cell lines—fed-batch and continuous perfusion. Fed-batch production process remains the main work horse for recombinant protein production with human cell lines due to its operational simplicity, reliability, and flexibility for implementation in multipurpose facilities (59). Typical feed strategy is based on the metabolic requirement of the specific human cell line for the maintenance of growth and productivity. Feed media are designed by using metabolic characterizations of several cell lines and assembling a nutrient concentrate consisting of glucose, amino acids, vitamins, lipids, trace elements, and growth factors (60,61). Similarly, the feeding schedule involves the addition of the nutrient concentrate based on cell-specific requirements in order to supply the nutrients only as required by the culture and to limit overflow metabolism or the buildup of nutrients or metabolites that may result in reduced process performance and product quality (62–64).

Human cell lines also have been successfully used in perfusion culture systems (60,65,66) to produce commercial recombinant proteins (67). In perfusion systems, fresh medium is continuously added to the bioreactor. Simultaneously, spent medium is continuously removed while the cells are retained in the bioreactor. A number of cell retention devices have been described, which may be internal or external to the reactor, with some being commercially available. The advantages of perfusion systems are many. By continuously adding fresh medium to the bioreactor, the cells are provided with the critical nutrients needed to multiply and for protein synthesis. At the same time, continuous removal of the spent medium from the bioreactor ensures that potentially toxic metabolic by-products do not accumulate. The cell retention device ensures that productive cells remain in the bioreactor, where they continue to produce the desired product. The disadvantages of the system is that large amounts of medium need to be used and the product is being continuously removed from the bioreactor in the spent medium, which results in a large volume of a very dilute harvest. This requires a very intensive concentration and clarification operation, besides the need to store the harvest under sterile conditions until processing. Recently, a modified perfusion system called XDwas described as combining the advantages of fed-batch with perfusion processes by retaining the product in the bioreactor along with the cells throughout the process (17,68). With this process, viable cell concentrations greater than 150 million cells/mL have been achieved using the PER.C6 human cell line. Assuming an average cell diameter of approximately 15 μm, concentration of 150 million cells/mL means that 1 L of working volume contains approximately 270 mL of solid cell mass, which is close to high density microbial fermentation-like condition. By amassing these many cells and retaining the product in the bioreactor, which is the main feature of the XD process, a volumetric productivity of over 27 g/L IgG in 18 days has been reported with this system using PER.C6 cells using only 15 equivalent volumes of bioreactor in cell culture medium (17). Again, spent medium in the XD process is removed directly into waste. In this XD process, the culture viability is always high (over 95%) and product quality is unchanged throughout the process as the cells are under quasi steady-state conditions and growing at their maximum growth rate, and they are also producing product at their maximum specific productivity. Consequently, it is possible to achieve the maximum theoretical volumetric product concentration for a given cell line (for a given specific productivity) once the biomass in the bioreactor has reached the maximum packed cell volume.

12.4 SCALE-UP OF RECOMBINANT HUMAN CELL LINES CULTIVATION

The clinical and commercial success of biologics has led to the need for very large-scale production in mammalian cell culture. This has resulted in rapid expansion of global manufacturing capacity, an increase in size of reactors and a greatly increased effort to improve process efficiency with concomitant manufacturing cost reduction. Like other nonhuman mammalian cell cultures, recombinant human cell lines are typically cultured in stirred tank bioreactors. Human cell lines such as HEK 293 and PER.C6 cells have been cultured at large-scale fed-batch and perfusion modes. For instance, various PER.C6 human cell lines have been used to produce monoclonal antibodies in fed-batch, and XD systems at up to 250 L scale (16) and Xigris™ is produced by HEK293 cells in 500 L bioreactors using a hollow fiber perfusion system (67).

A relatively recent innovation is the use of disposable stirred tank bioreactors. Disposable bioreactors have the advantage of facilitating process validation and allowing users to have flexibility in the facility design and operation (69–78). Until recently, wave bioreactors were the only available disposable system for mammalian cell cultures. However, vendors such as Xcellerex and HyClone (part of Thermo Fisher Scientific) among an ever-growing list of suppliers now offer disposable stirred tank bioreactors with sizes up to 1000 L (HyClone) and 2000 L (Xcellerex). It is

expected that even larger disposable bioreactors will come on market in the near future. Recombinant human cell lines, PER.C6 cells in particular, have been cultured in both stainless steel and disposable stirred tank bioreactors up to 250 L for high yield protein production (16).

Recombinant human cell lines that are anchorage-dependent are most often cultivated on microcarriers at larger scales (79–89). Microcarriers are small solid spherical particles, which can be suspended in liquid culture medium. Porous microcarrier beads are also frequently used with anchorage-dependent cells. The advantage of porous microcarriers is that the surface area to volume ratio is much larger, enabling higher number of cells to be cultured on each bead. By using these porous microcarriers suspended in culture medium, standard stirred tank bioreactors may be used to culture and scale-up anchorage-dependent cells much easier. The disadvantage of culturing cells on microcarriers is that, as they grow into layers, diffusion limitations of nutrients and metabolic waste products develop. Consequently, cells in the inner layers are often nutrient-starved and are not productive. Nevertheless, for anchorage-dependent cultures, microcarrier systems provide the most straightforward method for culturing and scaling-up anchorage-dependent cell lines.

Human cell lines that grow as single cells in suspension may be cultivated and scaled up in much the same manner as nonhuman mammalian cultures such as CHO and NS/0 cell lines used nowadays for the industrial production of most of the approved recombinant protein therapeutics. Human cell lines share much of the same characteristics, limitations, and sensitivities as most nonhuman mammalian cell lines. Consequently, much of the considerations of scaling-up recombinant human cell lines are very similar to those that pertain to the scale-up of nonhuman mammalian cell cultures. These considerations typically include homogeneous mixing, shear, mass transfer (oxygen supply and carbon dioxide removal), and potential damage from bubbles (72–74,90,91). Interestingly, some human cell lines have been demonstrated to be very resistant to shear damage. For example, PER.C6 cells are typically cultured in 5 L-stirred tank bioreactors equipped with two pitch-blade impellers with an agitation rate of up to 300 rpm (16). This translates to a tip speed of approximately 1 m/second, which is approximately three to five times higher than those typically used in CHO or NS/0 cells cultures (56). The advantage of this insensitivity to shear is that much of the typical scale-up limitations typically encountered for other mammalian cultures may be resolved much more easily by using shear resistant cell lines such as PER.C6 cells. For example, efficient mass transfer (k_La) may be maintained during scale-up by increasing agitation rates without the concern of shear-induced damage. This means that need for increasing aeration rates used at larger scale to maintain gas mass transfer (i.e. oxygen supply and carbon dioxide removal) may not be necessary. Consequently, there is less risk of foaming and resultant bubble damage during scale-up (92). Also, with the possibility of using high agitation rates, the cultures are better mixed, resulting in better mass and heat transfer, more homogeneous and evenly mixed systems, and less localized insults to the cells from bolus addition of pH titrants or nutrients that may be toxic at high concentrations. Lastly, due to the high bulk shear associated with high agitation rates, cells tend to clump less even at very high viable cell concentrations (16).

This relative insensitivity to shear-associated insults is especially valuable in perfusion and XD systems where viable cell concentrations can reach extreme levels. With PER.C6 cells, the high mass transfer rate necessary to meet the oxygen demand and CO_2 removal requirement resulting from high viable cell concentration may be met in part by pushing the agitation rate to microbial fermentation-like levels. At extremely high cell densities of, for instance, over 100 million cells per mL, agitation alone is usually not sufficient to increase the mass transfer coefficient (k_La) in order to match the oxygen transfer rate and the oxygen uptake rate by the cells (17). Consequently, the oxygen-sparging rate will also need to be increased, which may lead to foaming issues. Problems with foaming may be avoided by the use of medical grade antifoams—a number of varieties are commercially available from various vendors. Human cell lines generally tolerate the presence of antifoam. However, the use of antifoam is tempered by the difficulties one may encounter during protein purification.

12.5 CONCLUDING REMARKS

The field of biotechnology has proven value to society by providing valuable and unique medicines to solve unmet medical needs. The evolution in the methods for producing these biologicals reflects the constant dialogue that both the industry and regulatory bodies have engaged over the years of product testing and collection of clinical data. Owing to the proven safety record and amenability to industrial production requirements, the advent of using human cell lines is imminent. And judging by the evidence of potentially harmful structures present in products made in animal cells to humans, it is possible that manufacturing methods will have to adopt more natural substrates for expressing and producing human therapeutics.

REFERENCES

1. Bout A, Hateboer G, Verhulst KC, Uytdehaag AG, Schouten GJ. Govert John US patent 7,470,523. 2008 (to Crucell Holland B.V.).

2. Rader RA, editor. Biopharmaceutical Products in the U.S. and European Market. 6th ed. Rockville (MD): BioPlan Assoc. Inc; 2007. pp. 115–120.
3. Li H, Sethuraman N, Stadheim TA, Zha D, Prinz B, Ballew N, Bobrowicz P, Choi B-K, Cook WJ, Cukan M, Houston-Cummings NR, Davidson R, Gong B, Hamilton SR, Hoopes JP, Jiang Y, Kim N, Mansfield R, Nett JH, Rios S, Strawbridge R, Wildt S, Gerngross TU. Nat Biotechnol 2006; 24: 210–215.
4. Brooks SA. Mol Biotechnol 2004; 28: 241–255.
5. Mazor Y, Vlarcom T, Mabry R, Iverson BL, Gerogiou G. Nat Biotechnol 2007; 25: 563–565.
6. Kawashima I, Ozawa H, Kotani M, Suzuki M, Kawano T, Gomibuchi M, Tai T. J Biochem (Tokyo) 1993; 114: 186–193.
7. Chung CH, Mirakhur B, Chan E, Le Q-T, Berlin J, Morse M, Murphy BA, Satinover SM, Hosen J, Mauro D, Slebos RJ, Zhou Q, Gold D, Hatley T, Hicklin DJ, Platts-Mills TAE. N Engl J Med 2008; 358: 1109–1117.
8. Raju TS. Bioproc Int 2003; 1: 44–53.
9. van de Weert M, Moller EH. Biotechnology: pharmaceutical aspects. Immunogenicity of biopharmaceuticals: AAPS Press, N.Y., Springer; 2006. pp. 103.
10. Shields RL, Lai J, Keck R, O'Connell LY, Hong K, Meng YG, Weikert SH, Presta LG. J Biol Chem 2002; 277: 26733–26740.
11. Anthony RM, Nimmerjahn F, Ashline DJ, Reinhold VN, Paulson JC, Ravetch JV. Science 2008; 320: 373–376.
12. Cohen J. Science 2008; 322: 659–660.
13. Rader RA, editor. Biopharmaceutical products in the U.S. and European Market. 6th ed. Rockville (MD): BioPlan Assoc. Inc; 2007. pp. 1255–1257.
14. Morrow KJ, Dorsett P. In: Langer ES, editor. Volume 1, Advances in large-scale biopharmaceutical manufacturing and scale-up production. Washington (DC): ASM Press; 2004. pp. 32–33.
15. Campbell RL. In: Langer ES, editor. Volume 1, Emerging and novel technologies in biopharmaceutical manufacturing, in advances in large-scale biopharmaceutical manufacturing and scale-up production. Washington (DC): ASM Press; 2004. pp. 65.
16. Kral K, Erskine B, Foley M, Powers D, Hoff R, Chon J. Development of a high performance platform fed batch process for the production of monoclonal antibodies using the PER.C6®Human Cell Line (manuscript in preparation).
17. Golden K, Bragg C, Zijlstra G, Nieboer M, Chon J. Extreme monoclonal antibody productivities with PER.C6 human cell line using the XD™ Production Process (manuscript in preparation).
18. Tchoudakova A, Hensel F, Murillo A, Eng B, Foley M, Smith L, Schoenen F, Hildebrand A, Kelter A-R, Ilag LL, Vollmers HP, Brandlein S, McIninch J, Chon J, Lee G, Cacciuttolo M. High level expression of functional human IgMs inHuman PER.C6® cells. MAbs 2009; 1: 163–171.
19. Morrow RKJ, Dorsett P. In: Langer ES, editor. Volume 1, Emerging and novel technologies in biopharmaceutical manufacturing, in advances in large-scale biopharmaceutical manufacturing and scale-up production. Washington (DC): ASM Press; 2004. p. 35.
20. Takamatsu S, Inoue N, Katsumata T, Nakamura K, Fujibayashi Y, Takeuchi M. Biochemistry 2005; 4: 6343–6349.
21. Hutas G. Curr Opin Mol Ther 2008; 10: 393–406.
22. Rup B. 5th Annual PEGS Conference; 2009 Apr 8th; Boston (MA).
23. Francis T Jr, Salk J, Pearson HE, Brown PN. Proc Soc Exp Biol Med 1944; 55: 104.
24. Norrby E. Vacc J Exp Med 2007; 204: 2779–2784.
25. Shah KV. Int J Cancer 2007; 120: 215–223.
26. Hayflick L, Moorhead PS. Exp Cell Res 1961; 25: 585–621.
27. Jacobs J. J Nat 1970; 277: 168.
28. Hilleman MR. Immunol Rev 1999; 170: 7–27.
29. Garnick RL. Dev Biol Stand 1998; 93: 21–29.
30. Points to Consider in the Characterization of Cell Lines Used to Produce Biologicals. 1993 Jul 12.
31. ICH Guidance, Q5D: Derivation and Characterisation of Cell Substrates Used for Production of Biotechnological/Biological Products. 1998 (63 FR 50244; Sept 21).
32. Vilcek J, Havell EA, Gradoville ML, Mika-Johnson M, Douglas WH. Adv Exp Med Biol 1978; 110: 101–118.
33. Shay JW, Wright WE. Nat Rev Mol Cell Biol 2000; 1: 72–76.
34. Cristofalo VJ, Pignolo RJ. Physiol Rev 1993; 73: 617–638.
35. Masters JR. Nat Rev 2002; 2: 315–319.
36. Yoshifumi Nakao NXY, Masatoshi Y, Pater MMPA. Carcinogenesis 1996; 17: 577–583.
37. Liu Y, Colosimo AL, Yang X-J, Liao D. Mol Cell Biol 2000; 20: 5540–5553.
38. Gallimore PH, Turnell AS. Oncogene 2001; 20: 7824–7835.
39. Sugimoto M, Tahara H, Ide T, Furuichi Y. Cancer Res 2004; 64: 3361–3364.
40. Ham RG. Exp Cell Res 1962; 28: 489–500.
41. Ham RG. Science 1963; 140: 802–803.
42. Ham RG. Exp Cell Res 1963; 29: 515–526.
43. Ham RG. Proc Natl Acad Sci U S A 1965; 53: 288–293.
44. Ham RG. J Natl Cancer Inst 1974; 53: 1459–1463.
45. Ham RG. In Vitro 1974; 10: 119–129.
46. Ham RG, Hammond SL, Miller LL. In Vitro 1977; 13: 1–10.
47. Ham RG, McKeehan WL. In Vitro 1978; 14: 11–22.
48. Ham RG, McKeehan WL. Methods Enzymol 1979; 58: 44–93.
49. Ham RG, St Clair JA, Meyer SD. Adv Exp Med Biol 1990; 280: 193–199.
50. Ham RG, St Clair JA, Webster C, Blau HM. In Vitro Cell Dev Biol 1988; 24: 833–844.
51. Hamilton WG, Ham RG. In Vitro 1977; 13: 537–547.
52. Hammond SL, Ham RG, Stampfer MR. Proc Natl Acad Sci U S A 1984; 81: 5435–5439.
53. Wang D, Liu W, Han B, Xu R. Curr Pharm Biotechnol 2005; 6: 397–403.
54. Xie L, Metallo C, Warren J, Pilbrough W, Peltier J, Zhong T, Pikus L, Yancy A, Leung J, Aunins JG, Zhou W. Biotechnol Bioeng 2003; 83: 45–52.
55. Hu WS, Piret JM. Curr Opin Biotechnol 1992; 3: 110–114.
56. Nelson KL, Geyer S. Bioprocess Technol 1991; 13: 112–143.
57. Merten OW, Litwin J. Cytotechnology 1991; 5: 69–82.
58. Hu WS, Oberg MG. Bioprocess Technol 1990; 10: 451–481.

59. Bleckwenn NA, Shiloach J. Curr Protoc Immunol, Appendix 1, Appendix 1U. 2004.
60. Havenga MJ, Holterman L, Melis I, Smits S, Kaspers J, Heemskerk E, van der Vlugt R, Koldijk M, Schouten GJ, Hateboer G, Brouwer K, Vogels R, Goudsmit J. Biotechnol Bioeng 2008; 100: 273–283.
61. Maranga L, Goochee CF. Biotechnol Bioeng 2006; 94: 139–150.
62. Agy PC, Shipley GD, Ham RG. In Vitro 1981; 17: 671–680.
63. al-Rubeai M, Singh RP. Curr Opin Biotechnol 1998; 9: 152–156.
64. Bettger WJ, Ham RG. Adv Nutr Res 1982; 4: 249–286.
65. Berdichevsky M, Gentile MP, Hughes B, Meis P, Peltier J, Blumentals I, Aunins J, Altaras NE. Biotechnol Prog 2008; 24: 158–165.
66. Meuwly F, Ruffieux PA, Kadouri A, von Stockar U. Biotechnol Adv 2007; 25: 45–56.
67. Rader RA, editor. Biopharmaceutical products in the U.S. and European Market. 6th ed. Rockville (MD): BioPlan Assoc. Inc.; 2007. pp. 583–589.
68. Zijlstra GM, Hof RP, Schilder J. WIPO patent Application WO2008/006494 A1. 2008. (to DSM IP Assets, B.V., Holland).
69. Aunins JG, Bader B, Caola A, Griffiths J, Katz M, Licari P, Ram K, Ranucci CS, Zhou W. Biotechnol Prog 2003; 19: 2–8.
70. Eibl R, Eibl D. Adv Biochem Eng Biotechnol 2008.
71. Fontova A, Soley A, Galvez J, Sarro E, Lecina M, Rosell J, Riu P, Cairo J, Godia F, Bragos R. Conf Proc IEEE Eng Med Biol Soc 2006; 1: 632–635.
72. Heath C, Kiss R. Biotechnol Prog 2007; 23: 46–51.
73. Jain E, Kumar A. Biotechnol Adv 2008; 26: 46–72.
74. Kilani J, Lebeault JM. Appl Microbiol Biotechnol 2007; 74: 324–330.
75. Mikola M, Seto J, Amanullah A. Bioprocess Biosyst Eng 2007; 30: 231–241.
76. Okonkowski J, Balasubramanian U, Seamans C, Fries S, Zhang J, Salmon P, Robinson D, Chartrain M. J Biosci Bioeng 2007; 103: 50–59.
77. Singh V. Cytotechnology 1999; 30: 149–158.
78. Terrier B, Courtois D, Henault N, Cuvier A, Bastin M, Aknin A, Dubreuil J, Petiard V. Biotechnol Bioeng 2007; 96: 914–923.
79. Chun BH, Chung SI. Cytotechnology 2001; 37: 1–12.
80. Hu X, Xiao C, Huang Z, Guo Z, Zhang Z, Li Z. Cytotechnology 2000; 33: 13–19.
81. Kong D, Cardak S, Chen M, Gentz R, Zhang J. Cytotechnology 1999; 29: 215–220.
82. Landauer K, Durrschmid M, Klug H, Wiederkum S, Bluml G, Doblhoff-Dier O. Cytotechnology 2002; 39: 37–45.
83. Lock LT, Tzanakakis ES. Med J Malaysia 2008; 63 Suppl A: 5–6.
84. Quesney S, Marvel J, Marc A, Gerdil C, Meignier B. Cytotechnology 2001; 35: 115–125.
85. Serra M, Brito C, Leite SB, Gorjup E, von Briesen H, Carrondo MJ, Alves PM. Ann Anat 2009; 191: 104–115.
86. Varani J, Piel F, Josephs S, Beals TF, Hillegas WJ. Cytotechnology 1998; 28: 101–109.
87. Wang C, Gong Y, Zhong Y, Yao Y, Su K, Wang DA. Biomaterials 2009; 30(12): 2259–2269.
88. Wang Y, Ouyang F. Cytotechnology 1999; 31: 221–224.
89. Zecchini TA, Smith RJ. Cytotechnology 1999; 30: 203–210.
90. Negrete A, Kotin RM. J Virol Methods 2007; 145: 155–161.
91. Junker BH, Wang HY. Biotechnol Bioeng 2006; 95: 226–261.
92. Ma N, Chalmers JJ, Aunins JG, Zhou W, Xie L. Biotechnol Prog 2004; 20: 1183–1191.

13

GENE EXPRESSION IN *PICHIA* AND OTHER METHYLOTROPH YEAST

KOTI SREEKRISHNA
Procter & Gamble Co., Cincinnati, Ohio

13.1 INTRODUCTION

A wide variety of expression systems for production of proteins of interest have become available with the advent of recombinant DNA technology since the 1970s. The various expression systems include those based on bacteria, lower eukaryotes (yeasts and fungi), invertebrates (insect cells and larvae), vertebrates (cells and transgenic animals), and plants (cells and transgenic plants). Each of these systems has unique advantages. Yeasts and fungi have robust growth characteristics like bacteria. They are also readily amenable to genetic manipulation. Furthermore, they can perform many posttranslational modifications found in higher eukaryotes. The purpose of this chapter is to highlight the strategies that have been used for optimal protein expression with the *Pichia* yeast expression system, which in the past few years has turned out to be versatile and impressive yeast for production of proteins.

13.2 BACKGROUND

Pichia pastoris is a methylotrophic yeast. It is able to use methanol as sole carbon source for energy as well as for growth (1,2). It was originally developed by Phillips Petroleum Company (Bartlesville, Oklahoma) as an organism of choice for bioconversion of natural gas (methane) into food (single cell protein). This may sound ironic, because nowadays every one is talking bioconversion of food crops to fuels (biofuels). Phillips Petroleum Company in the 1970s developed an efficient *Pichia* fermentation process [cell density >130 g dry cell weight per liter and biomass productivity >10 g/(L h)] (3,4). Though impressive, it could not compete with the economics of production of soy protein. After this set back, Phillips in the early 1980s directed its future course with *Pichia* into two areas:

1. *Speciality Food or Feed Application.* A rather impressive 100,000 L fermentation plant to churn out tons of *Pichia* for potential speciality food applications was completed in 1988. However, by 1993, the idea to use *Pichia* for speciality food/feed was abandoned as *Pichia* did not have generally regarded as safe (GRAS) status and Phillips Petroleum Company decided to focus on its core business of oil exploration, production, and petrochemicals.
2. *Development of Pichia Expression System for Production of High Value Recombinant Proteins.* *Pichia* possesses a highly regulated pathway for the utilization of methanol (2,4). Synthesis of the enzymes of methanol metabolism are undetectable in the absence of methanol, but increase rapidly when methanol is used as the sole carbon source. The most dramatic effect is seen for alcohol oxidase (AOX1), which accounts for >30% of cellular protein (5). An extensive proliferation of the peroxisomes, known to sequester AOX1 and dihydroxy acetone synthase, is also observed in cells grown on methanol (5–7).

Upstream Industrial Biotechnology: Expression Systems and Process Development, Volume 1, First Edition. Edited by Michael C. Flickinger.
© 2013 John Wiley & Sons, Inc. Published 2013 by John Wiley & Sons, Inc.

Perhaps the decision of Phillips to exploit the above noted unique features of *Pichia* to develoa protein expression system was highly fortuitous, because the molecular genetic tools that had just become available for *Saccharomyces cerevisiae*, such as yeast–*E.coli* shuttle vectors, transformation protocols, and site-specific integrative transformation (8,9) were found to be readily applicable to *Pichia*. With the advent of cloning of *AOX1* promoter (10,11), availability of auxotrophic *Pichia* strain [GS115 (*his4*) developed by George Sperl] and *Pichia* transformation protocols (12,13), successful high level expression of several proteins was readily demonstrated. They include, intracellular expression of Hepatitis B surface antigen particles (14), *E. coli* β-galactosidase (LACZ) (15), human tumor necrosis factor (TNF) (16), as well as greater than gram per liter level of secretion of *S. cervesiae* invertase (SUC2) (17), and human serum albumin (HSA) (18). *Pichia* expression technology patent was granted to Phillips Petroleum Company in 1988 (11) and thus, by the late 1980s, *Pichia* expression system was well on its way to leave the nest.

In the fall of 1988, Phillips Petroleum Company made a conscientious decision to license the system to other companies. Fortunately for Phillips licensing team (Katherine Bartosh, L.V. Benningfield, Mary Jane Hagenson, Jack Phillips, and Koti Sreekrishna), their very first commercial licensee (Glaxo–Wellcome) with just 2 days of training at Phillips produced some impressive expression results (19–23). Phillips was able to license the technology to 20 companies in 4 years. Along side, it also started distributing the *Pichia* expression kit, free of cost to any academic institution that approached the company for the kit. This was getting out of hand, and thus the company transferred distribution rights, free of cost, to Invitrogen Corporation (Carlsbad, California) in 1993. Since then, Invitrogen Corporation (http://www.invitrogen.com) has been aggressively distributing *Pichia* expression kit at reasonable cost and with some user friendly modifications. They are largely responsible for wide usage of *Pichia* technology. In the same year (1993), Phillips sold *Pichia* technology to Research Technology Corporation (Tucson, Arizona) (http://www.rctech.com). They have licensed the technology thus far to 160 companies. To date, >500 proteins have been expressed in the *Pichia* yeast (24) and over 3000 scientific chapters published. There are over 100 publications on fermentation optimization alone.

Hepatitis B vaccine and interferon-α derived from *P. pastoris* have been commercialized in India since 1999 and 2002, respectively, by Shantha Biotechnics (http://www.shanthabiotech.com) (25). Now the company makes >100 million units of hepatitis vaccine per year and sells these vaccines in 50 countries. The cost of vaccine has dropped to 15 cents a dose (24). Recombinant human insulin produced in *Pichia* is also marketed in India since 2003, by joint venture between Shantha Biotechnics and Biocon (http://www.biocon.com) (24,25).

HSA expression technology originally demonstrated at Phillips Petroleum Company (18) and transferred to Green-Cross Corporation (Osaka, Japan) has been further developed and scaled up to produce one million dosage vials (12.5 g per vial) of authentic rHSA/year by Mitsubishi Pharma Corporation (Osaka, Japan) (26,27). This truly is a testimony to the high expression level and scale-up possible with *Pichia* (25). (Please refer to http://www.rctech.com for a more complete list of *Pichia*-produced products under various stages of commercialization.)

13.3 STRATEGIES FOR OPTIMIZATION OF PROTEIN EXPRESSION

The typical *Pichia* expression vectors are all yeast–*E. coli* shuttle plasmids (see "Glossary of *P. pastoris* Vectors"). The most commonly used vectors are based on *AOX1* promoter (10,11) (see section titled "Alternative Promoters for Expression" below for other promoters available for *Pichia* expression). Numerous selectable marker genes available include *HIS4* (His^+ selection) (12), *ARG4* (Arg^+ selection) (28), A*DE1* (Ade^+ selection) (29), and *URA3* and *URA5* (Ura^+ selection) (29,30), which can be used in conjunction with the appropriate *Pichia* auxotrophic strains. Several dominant selection markers that can be used for transformation of any *P. pastoris* strain are also available. These include *SUC2* (allows growth on sucrose) (13), Kan^R (G418/Geneticin selection) (23,31), Zeo^R (Zeocin selection) (32), Bsd^R (Blasticidin selection) (http://www.invitrogen.com), FLD1 (Formaldehyde selection) (33), and Sor^R (Soraphen A selection) (34).

A wide assortment of proteins have been produced in *Pichia*, which include human insulin (35), glucagon-like peptide (GLP) (36), G-protein coupled receptors (GPCRs) (37), Aquaporin (AQP1) (38), as well as correctly assembled human collagen fibers (39) and fibrinogen chains (40). These are among >500 proteins that have expressed in this system (24). Obviously, not all proteins are expressed at multiple grams per liter range. The expression level is largely influenced by inherent properties of a protein. Some proteins are readily expressed at high levels with minimal manipulation, while some proteins barely reach milligram levels, despite tremendous effort. Encouragingly, in many instances, the initial production yield of a protein can be dramatically enhanced by addressing the multiple factors that influence protein expression (41–43). The purpose of this review is to highlight the various expression-optimization strategies.

13.3.1 Cellular State of the Expression Cassette

The expression cassette can be introduced into *Pichia* by way of chromosomal integration or autonomous replication. Chromosomal integration is preferable because of the following advantages: (i) stability of expression cassette; (ii) ability to generate clones that stably maintain multiple copies of the expression cassette (see section titled "Gene Dosage: Exploiting the Clonal Variation of Expression"); (iii) control over the site of integration (for example, *AOX1*, *HIS4*, *ARG4*, *URA3* loci); and (d) ability to engineer different modes of integration (with or without eviction of the *AOX1* coding sequences) (see section titled "Methanol Utilization Phenotype of the Host: Mut^+ or Mut^s").

Plasmids based on autonomous replication sequence (*ARS*) such as pHIL-A1 (see "Glossary of *P. pastoris* Vectors") although can be introduced into *Pichia* cells with a high transformation frequency, they are rapidly lost from the population of dividing cells, and eventually integrate at one or more of the homologous sites on the chromosome (12,13). Owing to their ability of transform *Pichia* at high frequency ($>10^5$ μg^{-1}) and ease of plasmid rescue, the autonomous plasmids are useful for cloning genes in *Pichia* by functional complementation.

13.3.2 Site of Integration of the Expression Cassette

The *AOX1* promoter used in *Pichia* expression vectors is active irrespective of the site of integration (*AOX1*, *HIS4*, *ARG4*, *ADE1*, or *URA3* loci). However, AOX1 locus is the preferred site of integration for stable expression, because integration at the other loci can result in loss of the expression cassette due to intrachromosmal cross over between the mutant and good copy of the gene (unpublished observations). If the vector also contains a dominant selection marker (discussed earlier), then selection pressure can be applied for stable maintenance of expression cassette at those sites.

13.3.3 Methanol Utilization Phenotype of the Host: Mut^+ or Mut^s

Transformation of a *P. pastoris his4* strain (GS115) using linear DNA expression cassette with the ends bearing homology to the 5′ and 3′ regions of the *AOX1* chromosomal locus results in the site-specific eviction of the *AOX1* structural gene at a high frequency (5–20% of the His^+ transformants) (16,28). Such clones can be readily distinguished by replica-plating the colonies from the initial His^+ selection plate on to a minimal methanol (MM) medium plate. The clones that have undergone eviction of *AOX1* grow slower (Mut^S) compared to Mut^+ clones with an intact AOX1 gene, because, in such clones, growth on methanol is dependent on the alcohol oxidase encoded by *AOX2*, which is expressed at much lower level (weaker promoter) (44). The Mut^+ clones arise due to circularization of the linear DNA expression cassette inside the yeast cell prior to integration. Thus, both Mut^S and Mut^+ clones result in the same experiment.

Alternatively, one can use the *Pichia* strain KM71 (*his4 arg4 aox1*Δ*:SARG*), which has been rendered Mut^S by replacing much of the chromosomal *AOX1* with *S. cerevisiae ARG4* (28).

For intracellular expression, it is critical to use Mut^S cells because they will have a lower level of *AOX1* and the expressed protein of interest can be more readily purified. Furthermore, the precious cellular machinery can be more fully utilized for the expression of protein of interest. For protein secretion, the choice of Mut^+ or Mut^S is less stringent and more a matter of preference as the impact is more on feed protocols than the secretion level. In fact, the secretion levels of HSA are similar with both Mut^+ and Mut^S cells (45).

13.3.4 Gene Dosage: Exploiting the Clonal Variation of Expression

Early on a dogma prevailed among the researchers of the *Pichia* system, based on limited experience (14,15), that increasing the gene dosage did not impact expression because of the remarkable strength of the *AOX1* promoter. This dogma was shattered on the Good Friday of March 28, 1986, with my observation of dramatic clonal variation (<1% to >30%) in the expression of human TNF, that was subsequently attributed to gene dosage. Furthermore, the high copy number was stably maintained even after several days of growth in high cell density fermentor. The observation with TNF expression was readily exploited for expression of tetanus toxin fragment C (21), *Bordetella pertussus* pertactin P69 (20), and mouse epidermal growth factor (EGF) (19), and has been a key strategy for successful expression of hundreds of proteins in the *Pichia* system. However, in numerous cases, a single copy of the expression cassette is sufficient and deliberately increasing the copy number had no significant effect on the production (14,15,17,18). In some rare instances, an increase in copy number has a deleterious effect on the production level as has been noted with secretion of human insulin-like growth factor (IGF) (46) and *Necator americanus* (hookworm) secretory protein (Na-ASP1) (47).

Because the effect of gene copy number on expression is unpredictable, it is prudent to examine the production level as a function of gene dosage. The spheroplast method of transformation of *Pichia* results in transformants with a wide range of copy numbers (16,48). Evaluation of as few as 100 individual clones for protein production is generally adequate to arrive at a good producer. Though bit laborious, spheroplast method of transformation yields clones with wide range of gene dosage at a high

frequency (48). If other methods of transformation such as using LiCl or electroporation, which do not yield high frequency of multicopy clones, then one can use more efficient screens. These include use of colony hybridization with DNA probes or using appropriate vectors that would allow selection based on increased level of resistance to one of G418/geneticin (23,31), zeocin (32), formaldehyde (33), blasticidin (http://www.invitrogen.com), or soraphen A (34). Increased drug resistance does not automatically ensure multicopy integration and several dozen resistant colonies must be analyzed for copy number and expression.

Another approach to identify high producers may be to use a visual tag to the protein being expressed. In one instance, C-terminal green fluorescent protein fusion was used as a visual reporter to identify human Mu-opioid receptor expressing clones (49). *Rhizopus oryzae* lipase (ROL) bearing an N-terminal GFP tag was more efficiently secreted in *Pichia* compared to one with a C-terminal GFP tag (50). Recently, a fusion protein ZZ-EGFP consisting of ZZ domain of staphylococcal protein A (SpA) with enhanced green fluorescent protein (EGFP) was also secreted in the *Pichia*, with a hexahistidine tag (51). GFP tag may serve as a visual reporter to readily identify high producing clones. It can also be useful for on-line monitoring of protein production in the fermentor (52) However, on-line monitoring can be complicated by high levels of riboflavin (excitation/emission = 450/530 nm) secreted by *Pichia* (50), which in itself has been used for monitoring biomass production (53). By using a fluorescent protein tag outside the interfering range, one may be able to reliably monitor simultaneously both cell and product yield on-line.

Vectors such as pAO815 (54,55) have also been described that would allow *in vitro* construction of expression cassette concatamers. This approach is useful to accurately correlate copy number to expression level over a narrow range of gene dosage.

13.3.5 Translational Optimization: 5′ Untranslated Region

The nucleotide sequence and the length of the 5′ untranslated region (5′UTR) are detrimental to optimal protein translation. The leader length of the highly expressed *AOX1* mRNA is 114 nucleotides long, and the sequence is A + U rich (10,11). For optimal synthesis of heterologous proteins, it is essential that the 5′UTR should closely resemble that of the *AOX1* mRNA. Ideally, it is preferable to make it identical to that of *AOX1* mRNA. The expression level of HSA is increased >50 fold by optimizing the 5′UTR to mimic that of *AOX1* mRNA (18). Expression plasmids such as pHIL-D7 (42) can be used to make an exact construct. This plasmid has unique *Asu* II and *Eco* RI sites immediately following 5′*AOX1*. The second *Asu* II site that was originally present in 3′*AOX1* has been eliminated. Therefore, the sequence TTCGAAACG can be added immediately upstream of the ATG start codon of the gene of interest, and an *Eco* R I site can be engineered downstream of the stop codon for insertion at *Asu* II–*Eco* RI sites of pHIL-D7 (42).

13.3.6 Transcriptional Optimization

Genes with high A + T nucleotide clusters are poorly transcribed in *Pichia* due to premature termination of the transcription. For example, ATTATTTTATAAA, present in HIV-gp120 has been identified to block transcription in *P. pastoris*, and the premature termination is overcome by altering the sequence to TTTCTTCTACAAG (22). Because we are not aware of all the problematic A + T rich clusters, a general strategy with A + T rich genes is to redesign them using *P. pastoris* preferred codons (48,54), http://www.kazusa.or.jp/codon/) so as to have an A + T content in the range of 30–55%. By using this approach, it has been possible to construct *Pichia* strains for efficient production of several proteins, which include tetanus toxin fragment C (20), *Bacillus sphaericus* BSP1 and BSP2 heterodimeric mosquitocidal toxin (55), anticoagulant protein ghilanten (56), spider silk proteins (57), human endostatin (58), and human lactoferrin (59).

13.3.7 Product Secretion

For a protein which is normally secreted, that is the preferred mode of expression, for multiple reasons. It is easier to recover product from extracellular medium as there will be relatively fewer proteins. Also, many proteins that are normally secreted remain predominantly insoluble when expressed in the intracellular compartment, as has been seen with HSA and salmon growth hormone (unpublished observations). Likewise, a protein that is not normally secreted may be difficult to secrete. However, in some cases, such as human TNF, it is possible to express at high levels in the intracellular compartment (16). Interestingly, the intracellular human tetrameric catalase has successfully been expressed as a secreted protein in *Pichia* (60).

A wide variety of heterologous proteins have been secreted in *Pichia*. In several instances, HSA (18), invertase (17), bovine lysozyme (61), barley alpha amylases (62), cathepsin E (63), and thaumatin (64) the native signal sequence is adequate. In the case of matrix metalloproteinases, although native signal sequences work (41), both secretion and product yield are improved while using the *S. cerevisiae* pre-proalpha mating factor (αMF) secretion signal sequence (65,66). Likewise, with *Candida rugosa* lipase 1, although native signal works, both product stability and yield are tremendously improved with the use of pre-proαMF signal sequence (67). For thaumatin

secretion, native signal works, but not the pre-proαMF signal sequence (64), whereas for human interferon-alpha 2b (IFN-a2b), native signal sequence does not work, but pre-proαMF works (68).

Pre-proαMF secretion signal sequence has worked well for secretion of large variety of proteins, including the smaller-sized products such as aprotinin (69), EGF (19,69), IGF-1 (70), and ghilanten (56). The processing of pre-proαMF secretion signal involves three steps. The first is the elimination of the pre-region by signal peptidase, second, KEX2, and YPS proteinases cleave out the proregion (71,72), and finally, N-terminal Glu–Ala repeats are removed by the action of dipeptidyl-aminopeptidase (Dpap). The efficiency of each processing step depends on amino acid sequence adjacent to the processing site as well as the tertiary structure of the secreted protein. All these factors contribute to incomplete processing and/or reduced yield of mature protein (73–75).

In making αMF signal sequence constructs, it is generally preferable to retain the Glu-Ala spacers adjacent to the Kex2-like protease cleavage site (. . . Val-Ser-Ser-Leu-Glu-Lys-Arg-^{Kex2p}Glu-Ala-^{Dpap}-Glu-Ala-^{Dpap}-fused protein). The presence of Glu-Ala spacers help to alleviate the steric interference imposed by the fused protein, resulting in an efficient cleavage of the prosequence by the *Pichia* Kex2 like protease (69). The Glu-Ala spacer is subsequently cleaved by diamino peptidase (Dpap coded by *STE13*) to yield the protein of interest free of additional N-terminal amino acid residues. Interestingly, it has recently been reported that the pre-proαMF without the Glu-Ala repeats directed the secretion of correctly processed human IFN-a2b at 200 mg/L level, whereas the pre-proαMF having the Glu–Ala spacer, although secreted an equivalent amount of IFN-a2b, the secretion signal was inefficiently processed (68). Thus, ideally all variations must be explored to arrive at the best fit for a given protein.

Other secretion signal sequences used in *Pichia* include those of acid phosphatase (Pho1p), hybrid of Pho1p secretion signal with αMF and Kex2p cleavage site, invertase, lysozyme, HSA, *Phaseolus vulgaris* agglutinin, inulinase, and alpha amylase, glucoamylase, and *S. cerevisiae* killer toxin I (42,59,76).

13.3.8 Choice of the Secretion Signal

Only in a limited number of cases has a thorough comparison been made on the relative efficacies of different signal sequences and variations thereof (for example, (59,64,68,69)). In the case of invertase secretion, both the extent of glycosylation and secretion rate are enhanced when the native signal sequence is substituted with the pre-proαMF signal sequence (69), although both yields are greater than gram per liter level of the product. However, in the case of proteins that are more susceptible to proteolysis, improvement in secretion rate can increase production level as has been noticed with MMP-1 (41,65,66). Based on the relatively high success of pre-proαMF signal sequence, it makes sense to test that signal (and variations there of) first, side by side with the native secretion signal sequence, before exploring other signal sequences.

13.3.9 Production Enhancement by Manipulation of Media and Growth Conditions

More often than not, a secreted protein is rapidly degraded in the *Pichia* medium due to extracellular proteases, cell-bound proteases, as well as by intracellular proteases released to medium due to cell death and cell lysis. Multiple stress factors (especially in high cell density fermentor), which include starvation, pH shift, temperature change, change of carbon source, buildup of toxins, and reactive oxygen species (ROS) are considered to cause cell death and cell lysis (77).

One of the approaches to increase the stability and yield of the secreted protein in the culture medium is by manipulating the pH of the medium to arrive at the optimal pH for blocking a problem protease. Suggested pH range for experimentation is between 2.8 and 8 (see section titled "Media Compositions"). This pH range does not affect the growth significantly. HSA yield was significantly improved by raising the pH from 5.2 to 6, with adequate aeration. The yield was further enhanced by the addition of yeast extract (1%) and peptone (2%) (45,48,78,79). Production of mouse EGF was favored at pH 6 in the presence of casamino acids (19). Casamino acids is preferable to yeast extract + peptone, because the peptide components of peptone (such as collagen fragments) can interfere in product analysis and recovery (41). For both IGF-I (70) and cytokine growth-blocking peptide (80), pH 3 was found to be optimal. Greater than twofold increase in production of cellulose-binding module cellulose 6A and lipase B (CBM-CALB) is noted by reducing the pH from 5 to 4 in a bioreactor run (81).

Hirudin variant 2 (rHV2) secreted in *Pichia* was found to be degraded to four active fractions, including the intact rHV2 (Hir 65) and three C-terminally truncated forms Hir 64, Hir 63, and Hir 62 (82). Degradation of hirudin was reduced by using growth-rate-limiting quantities of methanol (3.09 g/L methanol; specific growth rate maintained at 0.02–0.047 h^{-1}) (82). Degradation of hirudin was also reduced by increasing NH_4^+ to relieve the stress of nitrogen starvation (83). Ascorbic acid (4 mmol/L) was used to quell ROS and improve cell viability. Under these conditions intact and total hirudin production reached 2.90 and 5.03 g/L, respectively, in contrast to 1.75 and 4.70 g/L in the absence of ascorbic acid (84).

Lower cultivation temperature is shown to improve product yield in several instances, which include CBM-CABL (22°C) (81), laccase (20°C) (85), galactose oxidase (25°C)

(86), Rh midkine (20°C) (87), human AFP (23°C) (88), herring proteins (23°C) (89), and human bile salt activated lipase (BSSL, 20°C) (90). *Pichia* cultivated at temperatures as low as 15°C, greatly enhanced the yield of ScFV production due to reduced protease level (91). Secretion level of bivalent T cell immunotoxin A-dmDT390-bisFy(G_4S) was also enhanced at 15°C, which was attributed to reduced protease levels, improved folding, as well as reduced toxicity of the immunotoxin to *Pichia* (92). Thus, we may say that the low temperature expression helps to increase the yield of aggregation-prone, unstable, and toxic products in *Pichia*.

Addition of 5 m*M* EDTA to the medium also improves accumulation of proteins expressed in *Pichia* (41). Supplementation of the induction medium with 0.4 *M* L-arginine, 5 m*M* EDTA, or 2% casamino acids in the BMMY induction medium (see section titled "Media Compositions") increased scFV expression (91). It should be noted that medium manipulation can significantly alter the profile of endogenous protein components in the culture media, such that previously unnoticed proteins accumulate at high levels. For example, we have noticed that addition of 5 m*M* EDTA causes accumulation of a protein of approximately 50 kDa in the extracellular medium (41). This protein has the aa sequence DIIWDYSSEKIMGVNLGGWL. . ., which matches closely with the exo-β-1,3-glucanase of *S. cerevisiae* (93) and *Candida albicans* (94). We have also noticed that overexpression of human tissue inhibitor of matrix metalloproteinase (TIMP1) in *Pichia* leads to greater gram per liter accumulation of a 18–22 kDa *Pichia* protein of sequence ADYMC?GLAIYGAWEC? GPEAGPFDSEC?LLATD (41).

13.3.10 Production Enhancement Using Protease-Deficient Strains

In addition to the optimization of media and growth conditions, the product yield can be further improved by using a protease-deficient *Pichia* strains generated by knocking out a *Pichia* protease or by overexpressing a protease inhibitor (for example, TIMP1 strain as noted above).

Protease-deficient *Pichia* strains SMD1168 (*his4*, *pep4*), SMD1165 (*his4*, *prb1*), and SMD1163 (*his4*, *pep4*, *prb1*) have been constructed (95). These strains have a disruption in the genes encoding proteinase A (*PEP4*) and/or proteinase B (*PRB1*) (56). Proteinase A is a vacuolar aspartyl protease necessary for the activation of vacuolar proteases, such as carboxy peptidase Y and proteinase B. In the absence of proteinase A, *Prb1p* is not fully active. Thus, *pep4* strain (SMD1168) is also expected to have a lower level of Proteinase B activity. The *prb1* strain (SMD1165) lacks proteinase B, whereas *pep4prb1* strain (SMD1163) lacks all three of the protease activities. These strains in general have low storage viability and are less robust (42,43). Nevertheless, these protease-deficient strains, in combination with other strategies to improve product stability, have been used to improve the production yield of IGF-1 (46), ghilanten (56), laccase (96), and human catalase (60). Disruption of *KEX1*, which codes for a carboxy peptidase, resulted in expression of full-length endostatin in *Pichia* (97). Recently, using a gene pop-in/pop-out gene replacement approach (98), the *KEX1* was deleted from a *Pichia* hirudin production strain. This resulted in most significant improvement in intact Hir65 production, which approached 2.4 g/L for the *KEX1* deleted strain compared to 1.1 g/L seen with the strain without *KEX1* deletion (99).

13.3.11 Enhancement of Protein Secretion by Overexpression of Chaperone Proteins

Pichia is able to perform many posttranslational modifications found in higher eukaryotes, which include correct folding, disulfide bond formation. Folding and disulfide bond formation in some cases can be the rate-limiting step in protein expression leading to protein aggregation (100). It is not clear which single chaperone is most important or which combination optimally cooperates in this process.

Overexpression of *Pichia* protein disulfide isomerase (PDI), which is important for protein folding in the endoplasmic reticulum (ER), was able to increase the secretion of Na-ASP1 protein in high copy clones (47). As noted before, high copy clones of Na-ASP1 secreted less material than single-copy constructs, perhaps due to overburdening the *Pichia* secretory/protein folding machinery, which was corrected by PDI overexpression.

A33scFV in *Pichia* is expressed at 4 g/L level, which rose to >10 g/L by overexpression of immunoglobulin binding protein (Bip) (101). The noted impressive increase is attributed to increase in folding capacity. PID overexpression did not have any effect on A33scFV expression. This was unexpected because A33scFV contains disulfide bonds. Furthermore, simultaneous overexpression of both BiP and PDF also did not have any effect in this system. It was also noted that PDI expression in the A33scFV strain caused a six-fold increase in endogenous BiP expression, suggesting that PDI was inducing an unfolded protein response due to excess chaperone and recombinant protein in the ER. In another study it was found that the chaperone combinations YDJiP/PDI, YDJiP/Sec63, and Kar2p/PDI synergistically increase secretion levels 8.7, 7.6, and 6.5 times, respectively (102).

A transcriptomics-based approach to identify novel factors enhancing heterologous protein secretion by analyzing differential transcriptome of a *Pichia* strain overexpressing human trypsinogen versus that of a control strain has identified 524 genes to be significantly impacted. This was narrowed down to 13 genes, all upregulated in the expression strain, as potentially important. The respective *S. cerevisiae* homologs of these genes were cloned and tested. All genes

except one showed a positive effect on Fab fragment secretion, of which *PDI1*, *ERO1*, *SSO2*, *KAR2*, *BiP*, *and HAC1* are previously characterized secretion helpers; the newly identified ones to have role in product secretion are *Bfr2* and *Bmh2* (involved in protein transport); *Ssa4* and *SSe1* (chaperones); *Cup5* (vacuolar ATPase subunit); and *Kin2* (a protein kinase subjected to exocytosis) (103). The chaperone game has just begun and we can foresee exploitation of this approach more fully in the years to come.

13.3.12 Protein Glycosylation and "Humanization" of *Pichia* N-linked Glycosylation

Pichia is able to perform both O-linked and N-linked glycosylation of secreted proteins (17). O-linked glycosylation involves addition of oligosaccharides to the hydroxyl groups of Serine and Threonine residues of the secreted proteins. The O-linked residues in mammalian cells are composed of variety of sugars (*N*-acetyl glucosamine, galactose, sialic acid), whereas in *Pichia* it is solely made up of mannose sugar. There is no defined consensus primary amino acid sequence for O-glycosylation and different hosts may O-glycosylate at different positions of the same protein. Even if a protein is not O-glycosylated in the native host, it may receive O-glycosylation in *Pichia*. For example, IGF-1 is not O-glycosylated in human host, whereas in *Pichia*, about 15% of the IGF-1 produced is O-glycosylated (46).

N-linked glycosylation involves addition of oligosaccharide chains to Aspargine at the recognition sequence Asn-X-Ser/Thr. It begins in the ER with the transfer of a lipid-linked oligosaccharide unit, Glc(3)Man(9)GlcNAc(2) (Glc = glucose; Man = Mannose; GlcNAc = *N*-acetyl glucosamine) to Asn of Asn-X-Ser/Thr (104). This unit is then trimmed to Man(8)GlcNAc(2). At this point onwards, the lower eukaryotes and higher eukaryotes deviate in the subsequent modifications that take place in the Golgi apparatus.

The mammalian Golgi performs a series of trimming and additions leading to three classes of N-linked glycans: "high mannose" [Man(5–6)GlcNAc(2)], "complex" (mixture of several different sugars) and "hybrid" (combination of the high mannose and the complex) with a common core, Man(3)GlcNAc(2). In *Pichia* secreted glycosylated proteins (native as well as heterologous) only "high mannose" kind typically with 8 to 9 mannose residues in length [Man(8–9)GlcNAc(2)] predominate with smaller amounts of chains with more mannose residues. In *S. cerevisiae*, only "hypermannose" kind with 50–150 mannose residues in length [Man(50–100)GlcNAc(2)] are present resulting in a hyperglycosylated protein. *Pichia* appears not to have any terminal α-1,3 linked mannose (105,106) that are unique to fungal glycoproteins and render recombinant proteins produced in fungi unsuitable for human pharmaceutical uses (105). This should not be misconstrued to think that *Pichia*-produced glycoproteins are perfect for human pharmaceutical use, because with only "high mannose" kind, it is a far cry from mammalian-type glycosylation. The high mannose glycans are believed to reduce the half-life of the glycoprotein *in vivo* and may be immunogenic, thus limiting the potential therapeutic value of *Pichia* derived glycoproteins (107). Over the past two decades, several groups have attempted to overcome this problem, yet with limited success. Recently, however, major advances in the glyco-engineering of the *Pichia* yeast have culminated in the production of fully humanized sialylated glycoproteins (108). With the advent of glycoengineered *Pichia* host with humanized N-linked glycosylation potential, the goal of production of authentic human glycoproteins in *Pichia* is getting closer than ever (59,109).

13.3.13 Coexpression of Proteins and Proteins Complexes

Coexpression approach may not only be useful for increasing expression, often it may be necessary to express two or more heterologous proteins at the same time. The first example of coexpression is that of the BSP1 (43 kDa) and BSP2 (52 kDa) components of *B. sphaericus* mosquitocidal toxin (55). Since then, there have been other reports of coexpression (47,101–103,110,111). Many proteins function as members of multicomponent complexes and successful expression strategy necessitates coexpression of subunits (39–41,110). The simplest way to engineer strains for coexpression is by sequential transformation or by cotransformation. Numerous dominant selection markers are available, which can be readily used for introducing multiple constructs at the same time.

13.3.14 Fusion Proteins

Fusion protein expression has many advantages. Often it can help stabilize a protein, and can also be valuable for expression of peptides. The most popular fusion partner is the highly expressed HSA (112). Often therapeutic proteins fused to HSA can be used directly for therapeutic applications. Albuferon is a long-lasting fusion protein between human interferon α-2b and HSA, which is being codeveloped by Human Genome Sciences and Novartis for treatment of Hepatitis C (113). Both fusion configurations HSA–IFN α-2b and IFN α-2b–HSA were expressed in *Pichia*. Although both expressed well, and showed comparable antiviral activity, IFN α-2b–HSA was more homogenous and stable. Heterogeneity and instability of HSA–IFN α-2b was caused by incomplete disulfide bridge formation between Cys^{1} and Cys^{98} of IFNα-2b due to structural perturbation of IFN α-2b by HSA. Other active fusion proteins successfully expressed in *Pichia* include HSA–PTH (1–34,114).

13.3.15 Overcoming Protein Toxicity

Occasionally the protein being expressed may be toxic to *Pichia*. Whether a protein is toxic to *Pichia* can be ascertained by comparing the growth of transformants on 1% sorbitol (or 100 m*M* alanine) as sole carbon source to that on sorbitol or alanine + methanol. Because, sorbitol and alanine are nonrepressive carbon sources (42,115), methanol is able to induce *AOX1* promoter in their presence. The other nonrepressive carbon sources include mannitol and trehalose (115). If the expressed protein is toxic, the growth in the presence of methanol will be drastically impaired. Even if the protein is toxic, it is still possible to express, because of the tight regulation of *AOX1* promoter. A stepwise induction is suggested. First the cell mass is built up using glucose as sole carbon source, taking care to see that glucose is not limiting. Under these conditions *AOX1* promoter remains completely repressed. Subsequent to this, protein production is initiated with methanol feed.

13.3.16 Alternative Promoters for Expression

Although *AOX1* promoter has been used extensively, with great success, several other promoters are available for exploration. The only potential drawback with the *AOX1* promoter, if we may say so is the need for methanol, which is a potential fire hazard especially in quantities needed for megaton plants. Also, the use of methanol may not be appropriate for production of food products. Furthermore, the unique, unsurpassed tight regulatory and highly inducible features of *AOX1* promoter may not be needed in every instance. Thus, promoters that are not induced by methanol may be useful in some instances for expression of certain genes. The following are alternative promoters:

1. The constitutively active *GAP* (glyceraldehyde-3-phosphate dehydrogenase) promoter (116).) The advantages of this promoter is that the protein can be produced more straightforwardly without having to make media shifts and the promoter strength is quite high. It is also convenient for production of isotope labeled proteins for NMR studies. GAP promoter is not a good choice for the production of proteins that may be toxic.
2. Methylamine (or methanol) inducible *FLD1* (formaldehyde dehydrogenase) promoter (117). This retains many of the tight regulatory features of *AOX1* promoter. Promoter strength is quite high. A key advantage is that it can be induced using methylamine, which is inexpensive, as a sole nitrogen source (with glucose as carbon source). It is repressed in medium with glucose and ammonium sulfate.
3. Methanol or oleate inducible *PEX8* (a peroxisomal matrix protein gene) promoter (118). The promoter strength on methanol is considerably weaker than that of *AOX1* or *FLD1* promoters.
4. Constitutively active weak *YPT1* (a GTPase involved in secretion) promoter (119). The YPT1 promoter provides a low but constitutive level of expression in media containing glucose, methanol, or mannitol as carbon sources (119). This may be useful for coexpression of chaperones to enhance protein folding and secretion in production strains.
5. Ethanol and stationary phase inducible ICL1 (isocitrate lyase 1) promoter (120). ICL1 promoter is inducible with ethanol and repressed by glucose in the exponential phase. In the stationary phase ICL1 is expressed even in the presence of glucose.

One aspect that investigators have to keep in mind in using these alternate promoters for commercial applications is that they may have to pay royalty as the patents are still active, unlike *AOX1* promoter patent, which has expired.

13.4 FERMENTATION PROCESS

Typically two-phase fermentation is used. In the first phase (biomass stage), cells are grown until glycerol is depleted. In the second phase (protein production stage), gene expression begins by feeding methanol to the bioreactor. There are numerous factors that impact production yield in a bioreactor, including culture medium composition, strain, pH, temperature, agitation rate, dissolved oxygen, induction condition, and fermentation strategy. Several of these factors have been already discussed (see section titled “Production Enhancement by Manipulation of Media and Growth Conditions”. Basic protocols for *P. pastoris* fermentation have been abundantly described in literature (e.g. (42,121), and http://www.biotechlab.net/UserFiles/File/787348_Ref_Invitrogen2002.pdf.). Improvements which have been made to basic protocol have been recently reviewed (122,123). Few salient features are reviewed here.

13.4.1 Fermentation Media and Operational Conditions

Basal salt medium (BSM) is the most common medium for high cell density fermentation, although it may not be the optimum and may have some important problems (unbalanced composition, precipitates, ionic strength, etc.). Therefore, alternative media such as FM21 (44) and FM22 (121,122) have been described. The BSM medium provides, in general, high concentration of basic elements, all at the upper level of the recommended range proposed by Wegner (3). Conversely, FM21, and the D’Anjou media (123) have a low concentration of chemical elements, around the low limit suggested by Wegner (3). The concentrations of

the elements in FM22 media are similar to BSM with the exception of potassium. One of the most important points in a medium formulation is the nitrogen source. In BSM, and FM21, nitrogen is solely added as ammonium hydroxide when controlling pH. This is also true to a large extent for FM22. However, in the D'Anjou medium all nitrogen is supplied at the initial formulation and it is not added during the culture. Nitrogen starvation starts around 50 g/L of biomass (123). The lack of nitrogen is directly related to the increase in proteolytic activity resulting in the degradation of extracellular protein. Thus, in BSM and FM22 media, where nitrogen is added to control pH, this effect could be present when high biomass concentration is reached. The optimal conditions (medium, pH, temperature, etc.) are dependent on the strain used and thus have to be adjusted accordingly using the guidelines and considerations noted (see section titled "Production Enhancement by Manipulation of Media and Growth Conditions").

13.4.2 Dissolved Oxygen (DO) Control

Dissolved oxygen (DO) is an important factor for protein productivity in a bioreactor. It can be controlled with combination of agitation rate, and the air (or O_2) flow rate. During the glycerol batch phase (20–24 h), the DO is controlled by adjusting the agitation rate up to 800 rpm for a typical 4-L bioreactor, and around 450 rpm for 60-L reactor, and then manually adjusting the air (or O_2) flow rate into bioreactor. Upon exhaustion of glycerol, the DO will rise rapidly. Typically, DO should be maintained around 30%, but need to be further optimized on a case by case basis.

13.4.3 Growth Kinetics

In the methanol unlimited fed-batch and continuous cultures with Mut^+ cells, growth inhibition at high methanol concentration is noted. Specific growth rate increases with methanol concentration up to a maximum value named theoretical maximum specific growth rate μ'_{max}, corresponding to a critical substrate concentration (Scrit), beyond which it declines. Methanol concentration lower than Scrit, represent growth-limited state and for values higher than Scrit, represent the growth inhibited state. A comparison of the kinetic parameters obtained for the different heterologous proteins indicate that the growth rate is influenced by the protein being expressed (123).

13.4.4 Fed-Batch Fermentation Operational Strategy

Fed-batch fermentation protocols include three different phases. A glycerol batch phase (GBP), a transition phase (TP), and finally a methanol induction phase (MIP).

1. *Glycerol Batch Phase (GBP).* The objective of GBP is to rapidly generate biomass prior to protein production. The maximum specific growth rate of wild-type *Pichia* on glycerol (0.18 h^{-1}) is higher than growing on methanol (0.14 h^{-1}) (69) and this methanol μ_{max} is, generally, lower when *Pichia* is producing a heterologous protein. GBP strategy is common for Mut^+, Mut^-, and Mut^S *Pichia* strains and typically 40 g/L glycerol is used; concentration over 40 g/L could inhibit growth. Brierley and coworkers recommended a maximum glycerol concentration of 6% (70) and ethanol levels between 0.5 and 2.4% were detected when glycerol concentration was over 7% (124). The observed biomass to substrate yield (YX/S) (biomass expressed as dry cell weight) is about 0.5. Thus, a final biomass around 20 g/L is obtained at the end of GBP. The glycerol exhaustion (end of batch phase) is indicated by a sharp increase in the DO, which is the most common parameter used for initiation of TP.
2. *Transition Phase (TP).* TP has two objectives, one is to further increase biomass level and the other is to cause de-repression of the *AOX1* promoter due to the absence of excess glycerol prior to MIP. Constant glycerol feeding rate (125) or an exponential glycerol feeding rate is used to reach a growth-limited level. Cell growth predictions, for different exponential feeding profiles have been shown by Zhang and coworkers (126). The maximum glycerol specific consumption rate is 0.0688 g/(g h). The final biomass levels reached at the end of the TP is generally above 30 g/L. During TP, glycerol feeding rate is generally complemented with a methanol feeding rate to augment the de-repression of *AOX1* promoter. With mixed feeding, cultures can be primed for methanol induction, which leads to a substantial reduction in the length of MIP, as has been demonstrated in lipase production (127). Also, the methanol supplement can strongly support cells to synthesize *AOX1* (128). Different methanol profiles have been used for the TP, which include the following:
   - raising methanol feeding rate as a function of response of DO up to a 7.6 mL/(h L) (129);
   - maintaining methanol concentration at set points 4 g/L (125) or 1–2 g/L (130);
   - about 1 h starvation phase prior to MIP to assure that glycerol is completely consumed (131);
   - a decreased glycerol feeding rate and constant methanol feeding rate (132,133).
3. *Methanol Induction Phase (MIP).* The methanol feeding strategy, which also dictates the specific growth rate, is one of the key factors for maximizing protein production (126,128), since protein production is directly or indirectly associated with cell growth (134). Moreover, MIP may depend on the operational conditions (e.g. temperature,

pH, and culture medium), phenotype, and specific characteristics of the heterologous protein produced. The synthesis, processing, and secretion of the protein could also affect cell growth. Different approaches have been proposed to optimize MIP. These strategies are reviewed in (123).

13.4.5 Methods for Monitoring Methanol Concentration

One of the key parameters of *AOX* promoter based *Pichia* expression system is the methanol concentration, which is both a substrate and inducer. High levels of methanol are toxic to the cells and low levels of methanol may not be adequate for induction of expression. For optimal protein production, methanol induction strategy is critical. This has to be implemented keeping in mind the genetic background of the strain (Mut^+, Mut^S, or Mut^-), which has been addressed in the fermentation guidelines provided by Invitrogen Corporation (http://www.biotechlab.net/UserFiles/File/787348_Ref_Invitrogen2002.pdf) and in other published reviews (42,121–123). Keeping a constant methanol concentration during the induction phase is beneficial to optimal protein production (121). DO spike method has been used historically to estimate the methanol concentration. This technique, however, exposes the cells to potentially noninducing levels of methanol and cannot be easily implemented with Mut^- clones or with mixed substrate feeds. Off-line methods for methanol quantification include gas chromatography, HPLC (high performance liquid chromatography), and enzymatic determination, which are used in connection with a batch or fixed preprogrammed methanol addition strategy. A near infrared spectroscopy (NIRS) technique has also been used to model key analytes (biomass, glycerol, methanol, and product concentration) in the production of a therapeutic protein in high cell density culture (135). These off-line methods require a pretreatment of the sample and there will be precious time lapse for implementation. The sequential injection analysis (SIA) developed by Surribas and coworkers is able to measure seven samples per hour with low standard deviation (136). YSI 2700 select analyzer (http://www.ysilifesciences.com/) from Yellow Springs Instruments (Yellow Springs, Ohio) can be readily connected to a bioreactor for SIA. However, continuous extraction of samples increases contamination probability, besides sample loss.

Fortunately, many on-line methanol sensors have been successfully adopted to monitor *Pichia* fermentors (123), which are as follows:

- Raven methanol sensor from Raven Biotech Inc. (Vancouver, BC, Canada), which uses a probe inserted into the bioreactor (http://www.ravebiotech.com/products.html).
- TGS822 sensor for the detection of organic vapors from Fiagro Electronic Co. Ltd (Tahin, China) (http://www.etesters.com/products/details.cfm/part/TGS822/productID/58856492-802e-f41e-d604-2d325dd53216).
- Directly detecting the methanol vapor in the stream gas outlet by diverting it to an MC-168 methanol monitor and controller (PTI Instruments, Inc., Kathleen, Georgia) equipped with a TGS822 methanol sensor.
- Alkosense probe (Frings America, Illinois) (137). This measuring principle is based upon the selectivity of the semipermeable membrane system, which rejects low volatility substances like sugar and glycerin, as well as most organic substances including organic acids. If easily volatilized components are present, that is ethanol and methanol, the system will not be able to differentiate between the various components, and will measure the combined concentrations. (http://www.fringsamerica.com/markets/brewing/alkosens.asp).

If the growth kinetics of a *Pichia* production strain is preestablished, then the methanol feed rate can be adjusted according to the specific growth rate during the induction phase. This can be an effective way to maintain optimal methanol concentration in the bioreactor. In fact, this strategy has resulted in 2.5-fold higher productivity of lipase (127). To improve the expression level, glycerol and methanol were fed simultaneously, followed by a single methanol feed, and resulted in the highest productivity [12,888 U/(L h)], which is 13.6-fold higher than the DO-based strategy. On-line methanol measurement, which permits implementation of closed-loop control algorithm (138) can be more effective than open-loop control strategies or indirect methanol feed rate from other fermentation parameters/variables as specific growth rate in particular, from industrial point of view for a reproducible fermentation at a constant methanol set point.

13.4.6 Methanol Control Schemes

To produce small quantities of heterologous protein, the methanol feeding strategy from http://www.biotechlab.net/UserFiles/File/787348_Ref_Invitrogen2002.pdf or as found in (42) is adequate. When the objective is to reproducibly maximize product yield and for quality control, the selection of the optimal methanol feeding strategy in the induction phase is necessary. When on-line methanol concentration monitoring is not available two different methanol feeding strategies, DO spike method, and an open-loop methanol control strategy are most commonly used (121). Both these strategies and their limitations have been elegantly reviewed (123). In the DO spike method, methanol feeding rate is modified in order to avoid methanol exhaustion as indicated by a sharp increase in dissolved oxygen. Neither methanol concentration nor specific

growth rate are constant in this strategy, and thus it is difficult to study the effect of these variables on the production of the heterologous protein. DO spike method has an additional problem, if an inhibitory methanol level is reached, a sharp increase in DO will be observed, the response of the system will be then to increase the methanol feeding rate leading to methanol accumulation to toxic levels in the bioreactor. In the method based on the methanol control using an open-loop structure, a feeding rate profile derived from mass balance equations to theoretically maintain a constant specific growth rate (μ) is used. This approach is based on simple cell growth models with no on-line information about the system. To implement this method, a constant YX/S for the fed-batch induction phase is considered and, biomass concentration and volume are supposed to be known at the beginning of the preprogrammed feeding strategy. Zhang and coworkers, empirically developed a methanol feeding strategy based on a growth model, obtaining μ to maximize the protein production (126). D'Anjou and Daugulis have demonstrated the usefulness of a rational, model-based approach for improving the productivity by using an exponential feeding strategy with mixed glycerol–methanol substrate in a fed-batch (130). Although open-loop systems could be easy to implement they do not respond to possible perturbations of the system. Simplest closed-loop control strategy is the "on–off" control mode. Some works have been published with apparently satisfactory results (for example, (126,133)). However, due to the complexity of the system, a simple "on–off" control strategy is inadequate for precise control of methanol concentration in the bioreactor leading to fluctuations in methanol concentration around the set point.

13.4.7 Mixed Substrates

One strategy to increase the productivity of *Pichia* expression is the use of a multicarbon substrate in addition to methanol. It is a simple way to augment the energy supply to cells in the culture broth (128,133,139). A mixed feed reduces the induction time, increases cell density, and volumetric productivity (140). The mixed feeding strategy is generally employed for Mut^s *Pichia* fermentations because of the slow methanol utilization, which requires large induction times (above 100 h), although it has also been used for Mut$^+$ strains (141). Glycerol has been the most feeding cosubstrate used at limited rates, ensuring good cell growth while inducing the expression of the heterologous protein. However, although the volumetric productivity increased, the specific productivity of recombinant protein is lower because glycerol represses the *AOX1* promoter (142). Inan and Meagher compared different carbon sources in terms of their ability to support growth and expression of an *AOX1-lacZ* fusion in shake flasks studies of a *P. pastoris* Mut$^-$ strain (115). As predicted, glucose, glycerol, ethanol, and acetate supported growth but repressed the expression of β-gal. On the contrary, growing on media containing alanine, mannitol, sorbitol, and trehalose expressed as much or higher amount of β-galactosidase compared to the Mut$^+$ strain. Recently, lactic acid has also been referred as nonrepressing substrate (142). The use of a less repressing carbon source may result in higher specific production rates, improving overall productivity, and eliminating the need for such tight control of residual substrate levels. Among them, sorbitol is a widely accepted nonrepressive carbon source for *P. pastoris* and methanol can be added to the sorbitol feed at any desired point to initiate induction of expression (41).

13.4.8 Continuous Fermentation

Continuous production mode in comparison to fed-batch fermentation, offers advantages in terms of higher volumetric productivity, product quality, product uniformity, significant reduction in exposure of the product to the proteolytic enzymes, oxidative damage or inactivation, and overall reduction of downtime (143,144). Continuous operation using methanol as sole carbon source under control of *AOX1* promoter is practically limited to Mut$^+$ cells. The low maximum specific growth rate of Mut^s phenotype limits the operational dilution rate and thus, the productivity of the process. However, Boze and coworkers in a continuous process at a dilution rate of 0.012/h with a Mut^s obtained a 6.4-fold higher productivity and 2.3 times higher specific productivity of porcine Follicle-stimulating hormone (FSH) compared to that achieved with fed-batch process (145). As discussed under "mixed substrate" section, one approach to increase the productivity of Mut^s phenotype is the use of a mixed carbon feed. Glycerol and sorbitol are the most commonly used cosubstrates jointly with methanol. With glycerol, the continuous strategy is to select a dilution rate far enough from μmax to ensure that no glycerol is allowed to accumulate in the broth, and also methanol concentrations have to be maintained at levels sufficient to fully induce heterologous protein production, yet not so high as to be inhibitory to cell growth or heterologous protein expression (130). D'Anjou and Daugulis performed a set of continuous stirred tank reactor or CSTR (continuous fermentation) experiments to determine the relationship between the dilution rate (in a range between 0.01 h^{-1} and 0.09 h^{-1}), the specific methanol consumption rate, and the specific production rate in the heterologous production of a sea raven antifreeze protein using mixed methanol–glycerol feed (146). The specific methanol consumption rate as a function of the dilution rate showed a maximum at approximately $D = 0.05$ h^{-1}. Maximum production was achieved at the lowest dilution rate. However, the maximum specific production rate (Q_p) was achieved at the highest dilution rate. This behavior

confirms that product formation is related to growth by a constant yield coefficient. Finally, they demonstrated that a CSTR system will yield a higher productivity compared with a fed-batch system. Readers are directed to Refs (122) and (123) for further discussions on CSTR.

13.4.9 Cyclic Fed-Batch Culture (CFBC)

A simple cyclic fed-batch culture (CFBC) consisting of a constant medium feed with periodic withdrawals of culture resulted in a product yield (13.4 mg HSA/g biomass) similar to that obtained using the complex multiphase industrial production strategy (13.7 mg HSA/g biomass) has been reported (147). Thus, using a much simpler protocol, it is possible to obtain yields comparable to that seen with more complex multiphase feed strategy.

13.4.10 Hypoxic Fed-Batch Cultivation

High cell density fermentation of *Pichia* has to cope with many technical limitations, most importantly the transfer of oxygen. By applying hypoxic conditions to chemostat cultivations of *Pichia* expressing an antibody Fab fragment under the GAP promoter, a 2.5-fold increase of the specific productivity Q_p at low oxygen supply was observed. At the same the biomass decreased and ethanol was produced, indicating a shift from oxidative to oxidofermentative condition. Based on these results a feedback control for enhanced productivity in fed-batch processes, where the concentration of ethanol was kept in the culture at 1% (v/v) by regulated addition of feed medium. This strategy was tested successfully with three different production strains, leading to a three- to sixfold increase in Q_p and threefold reduced fed-batch times. Taken together, volumetric productivity Q_p increased 2.3-fold (148).

13.4.11 Optimization of Trace Metals

A study of trace metals effect on growth and yield of LACZ production in GS115 Mut^+ strain has shown that both Mg and Zn are essential to support growth, but the amount required is considerably lower than the level typically used. Supplementation with Ca, Co, Mo, Fe, Mn, I, and B were not required to sustain cell mass. When the medium was reformulated with only Mg and Zn, the cells grew for 12–15 generations, which are expected for high cell density fed-batch fermentation. Product yields of LACZ was significantly affected by trace metals. When optimizing a fermentation process, the objective is also to decrease production costs, including indirect issues such as compliance to regulatory agency restrictions, impacts to downstream processing steps, effect of the medium components to equipment maintenance, etc. Clearly, reduction or elimination of trace metals potentially impacts all these intangibles (149). This study shows the importance of critically examining and accordingly adjusting the trace metal levels for a given production strain.

13.5 CONCLUSIONS AND FUTURE PERSPECTIVES

Pichia undoubtedly has proven to be a reliable system for expression of a wide assortment of proteins, many of which are expressed at several grams per liter levels. It is impressive to see how enthusiastic researchers from all corners of the world are willing to make it work, because it seems as though a researcher feels, it is his/her own fault, if the protein of interest did not work in *Pichia*! This bears testimony to the grand track record of *Pichia*. With the recent success seen in expression of several membrane proteins, I am sure we will hear many more success stories in that category as well. With the availability of glycoengineered *Pichia*, we can foresee that *Pichia* will gradually replace mammalian cell expression system for production of authentic human pharmaceuticals. *Pichia* surface display has just surfaced (150); we can anticipate all sorts of novel surface display applications in the years to come. *Pichia* expressing fish growth hormone has been directly fed to fish to dramatically impact growth rate (151); *Pichia* expressing *B. sphaericus* mosquitocidal toxins (55) is an effective biopesticide when fed to mosquito larvae, and likewise, *Pichia* expressing garlic lectins (152) shows potent insecticidal activity toward aphids. With wider acceptance of genetically modified organisms, we can foresee wholesome *Pichia* applications in biopesticide (55,152), biocatalysis (153,154), and perhaps even *Pichia* burger—why not? It is able to assemble collagen fibers so efficiently, just clone in that beef savory-peptide; we are on our way to a *Pichia* burger. May be the Phillips Petroleum Company's initial *Pichia*-SCP dream, will be realized after all.

I can see someone out there read *Pichia* genome, create knockout and knockin strains for every *Pichia* ORF, and study their impact on recombinant protein expression in a bioreactor! Thinking of bioreactors, I am a bit puzzled why *Pichia* has not yet been adopted for cultivation in wave bioreactors offered by GE Healthcare (http://www.wavebiotech.com/products/wave_bioreactor/system500/index.html). Wave technology is a completely closed system with disposable bioreactor chamber, scalable to 500 L, easy to operate, and provides controllers for dissolved oxygen, pH, CO_2, O_2, and other optional modules. Designed for R&D, process development and cGMP production use, the Wave Bioreactor is gaining popularity for mammalian and insect cell cultivation and has recently been adopted for *S. cerevisiae* (155). Culture medium and cells only contact a presterile, disposable chamber called a Cellbag that is placed on a special rocking platform. The rocking

motion of this platform induces waves in the culture fluid. These waves provide mixing and oxygen transfer, resulting in a perfect environment for cell growth. The bioreactor requires no cleaning or sterilization, providing the ultimate ease in operation and protection against cross-contamination.

With the expiry of the key *Pichia* patent, and presence of literally hundreds of *Pichia*-experts around the globe, many more industrial outfits will embrace *Pichia* and we can anticipate many more *Pichia* derived proteins and vaccines to be commercialized in the near future. May be we will see *Pichia* engineered to fix CO_2, as well as makes its own O_2, so that we would not have to worry about feeding methanol or oxygen to bioreactors—certainly a sigh of relief!

13.6 MEDIA COMPOSITIONS

Stock solutions (42)

10 × YNB: 13.4 g of yeast nitrogen base without amino acids (YNB) in 100 mL of water and filter sterilize.

500 × B: 20 mg D-biotin in 100 mL water and filter sterilize.

100 × H: 400 mg L-Histidine in 100 mL water (heat if necessary) and filter sterilize.

10 × D: 20 g D-glucose in 100 mL water. Autoclave or filter sterilize.

10 × GY: Mix 10 mL of glycerol with 90 mL water and filter sterilize.

10 × M: Mix 5 mL methanol with 95 mL water and filter sterilize.

Minimal media compositions (42)

MD: Mix 100 mL of 10 × YNB, 2 mL of 500 × B, and 100 mL of 10 × D with 800 mL autoclaved water (include 15 g bacto-agar for plates).

MM: Mix 100 mL of 10 × YNB, 2 mL of 500 × B, and 100 mL of 10 × M with 800 mL autoclaved water (include 15 g bacto-agar for plates).

MGY: Mix 100 mL of 10 × YNB, 2 mL of 500 × B, and 100 mL of 10 × Gy with 800 mL autoclaved water (include 15 g bacto-agar for plates).

Supplemental medium (42)

MDH: Mix 100 mL of 10 × YNB, 2 mL of 500 × B, 100 mL of 10 × D, and 10 mL 100 × H with 790 mL autoclaved water (include 15 g bacto-agar for plates).

MMH: Mix 100 mL of 10 × YNB, 2 mL of 500 × B, 100 ml of 10 × M, and 10 mL 100 × H with 790 mL autoclaved water (include 15 g bacto-agar for plates).

MGYH: Mix 100 mL of 10 × YNB, 2 ml of 500 × B, 100 mL of 10 × MGY, and 10 mL 100 × H with 790 mL autoclaved water (include 15 g bacto-agar for plates).

Complex media composition (42)

YPD: Dissolve 10 g bacto yeast extract, 20 g peptone, and 20 g glucose in water (also include 15 g bacto-agar for plates) and autoclave for 20 min.

YMPD: Dissolve 3 g of yeast extract, 3 g of malt extract, 5 g of peptone, and 10 g of glucose in 1 L of water and autoclave.

YMPGY: Same as YMPD with the exception that 10 mL of 100% glycerol is used instead of 10 g glucose.

Secretion media composition (42)

BMGY: Mix 100 mL of 1 *M* potassium phosphate buffer, pH 6, 100 mL of 10 × YNB, 2 mL of 500 × Biotin, and 10 mL of glycerol. Filter sterilize and add to an autoclaved solution of 10 g yeast extract and 20 g peptone in 788 mL water (15 g bacto-agar is included for plates),

BMMY: Same as BMGY, with the exception that 5 mL methanol is added in the place of 10 mL glycerol.

Note: Yeast extract and peptone in the above media can be replaced by 1% casamino acids.

The following buffers are used to adjust the pH of BMGY and BMMY to desired pH:

Phosphate buffer for pH range 5.7–8

Alanine–HCl buffer for pH range 2.8–3.6

Aconitic acid–NaOH buffer for pH range 3–5.7

Citrate buffer for pH range 3–6.2

Avoid succinate buffer, because succinic acid will repress induction of the *AOX1* promoter.

13.6.1 Fermentation Medium and Reagents

Basal salts medium (BSM) derived from Wegner (3)

For 1 L, mix together the following ingredients:

H_3PO_4 (85%) 26.7 mL

$CaSO_4 \cdot 2H_2O$ 0.93 g

K_2SO_4 18.2 g

$MgSO_4 \cdot 7H_2O$ 14.9 g

KOH 4.13 g

Glycerol 40 g

Water to 1 L

After autoclaving, adjust the pH to 5 with 28% NH_3 (concentrated ammonium hydroxide). It is normal that the medium becomes cloudy at pH 5. The added ammonium hydroxide serves as nitrogen source during fermentation.

FM21 basal salt media, derived from Wegner (3)

For 1 L, mix together the following ingredients:

H_3PO_4 (85%) 3.5 mL

$CaSO_4 \cdot 2H_2O$ 0.15 g

K_2SO_4 2.4 g
$MgSO_4 \cdot 7H_2O$ 1.95 g
KOH 0.65 g
Glycerol 40 g
Water to 1 L

FM22 basal salt media (121)
For 1 L, mix together the following ingredients:
KH_2PO_4 42.9 g
$CaSO_4 \cdot 2H_2O$ 18.2 g
$(NH_4)_2SO_4$ 5 g
K_2SO_4 14.3 g
$MgSO_4 \cdot 7H_2O$ 1.95 g
Glycerol 40 g
After autoclaving pH is approximately 4.5

PTM1 trace salts derived from Wegner (3)
Mix together the following ingredient in 1 L of water:
$CuSO_4 \cdot 5H_2O$ 6 g
NaI 0.08 g
$MgSO_4 \cdot H_2O$ 3 g
$Na_2MoO_4 \cdot 2H_2O$ 0.2 g
H_3BO_3 0.02 g
$CoCl_2$ 0.5 g
$ZnCl_2$ 20 g
$FeSO_4 \cdot 7H_2O$ 65 g
Biotin 0.2 g
H_2SO_4 5 mL
Water to a final volume of 1 L
Filter sterilize and add 4.35 mL/L to the autoclaved starting medium.
Note: There may be a cloudy precipitate upon mixing of these ingredients.
The precipitate does not have any adverse effect on growth of *Pichia*.
If precipitation is a concern, then PTM4 (see section titled "PTM4 Trace Salts"), which has lower amounts of copper, iron, zinc, and sulfuric acid may be used.

PTM4 trace salts (122)
Mix together the following ingredient in 1 L of water:
$CuSO_4 \cdot 5H_2O$ 2 g
NaI 0.08 g
$MnSO_4 \cdot H_2O$ 3 g
$Na_2 \cdot Na_2MoO_4 \cdot 2H_2O$ 0.2 g
H_3BO_3 0.02 g
$CoCl_2$ 0.5 g
$ZnCl_2$ 6.7 g
$FeSO_4 \cdot 7H_2O$ 21.6 g
Biotin 0.2 g
H_2SO_4 1.7 mL
Water to a final volume of 1 L
Filter sterilize and add 4.35 mL/L to the autoclaved starting medium.

5% (w/v) antifoam solution (AF) (122)
Dissolve 25 g of KFO^{TM} 673 antifoam (food grade, KAOB Chemicals, Inc., WY, USA) in 500 mL water, filter sterilize, and add 2 mL/L to the starting medium. Additional amounts may be added as needed to eliminate foam during the fermentation.

13.7 GLOSSARY OF *P. PASTORIS* STRAINS

Y-11430-SC5 (wild type) (NRRL)
X-33 (wild type) Invitrogen
GS115 (*his4*)—this Mut$^+$ strain is also known as GTS115 (54)
KM71 (*his4, aox1::SARG4*)—this is Mut^S strain (28)
PPF1 (*his4, arg4*) (28)
MC100-3 (*aox1::SARG4, aox2::HIS4, his4, arg4*)—this is Mut$^-$ (44)
Protease-deficient strains
SMD 1168 (*his4*, *pep4*) (95)
SMD1165 (*his4*, *prB1*) (95)
SMD 1163 (*his4*, *pep4*, *prB1*) (95).

REFERENCES

1. Ogata K, Nishikawa H, Ohsugi M. Agric Biol Chem 1969; 33: 1519–1520.
2. van der Klei IJ, Yurimoto H, Sakai Y, Veenhuis M. Biochim Biophy Acta 2006; 1763: 1453–1462.
3. Wegner, EH. US Patent 4,414,329. 1983, to Phillips Petroleum Company.
4. Wegner EH, Harder W.. In: Van Verseveld HW, Duine JA, editors. Microbial growth on C1 compounds. Boston (MA): Martinus Nijhoff; 1986. pp 139–149.
5. Couderc R, Baratti J. Agric Biol Chem 1980; 44: 2279–2289.
6. Egli T, van Dijken JP, Veenhuis M, Harder W, Fiechter A. Arch Microbiol 1980; 124: 115–121.
7. Veenhuis M, van Dijken JP, Harder W. Adv Micob Physiol 1983; 24: 1–82.
8. Hinnen A, Hicks JB, Fink GR. Proc Natl Acad Sci U S A 1978; 75: 1929–1933.
9. Szostak JW, Orr–Weaver TL, Rothstein RJ, Stahl FW. Cell 1983; 33: 25–35.
10. Ellis SB, Brust PF, Koutz PJ, Waters AF, Harpold MH, Gingeras TR. Mol Cell Biol 1985; 5: 1111–1121.

11. Stroman DW, Brust PF, Ellis SB, Gingeras TR, Harpold MM, Tschopp JT. US Patent 4,855,231. 1989, to Phillips Petroleum Company.
12. Cregg JM, Barringer KJ, Hessler AY, Madden KR. Mol Cell Biol 1985; 5: 3376–3385.
13. Sreekrishna K, Tschopp JF, Fuke M. Gene 1987; 59: 115–125.
14. Cregg JM, Tschopp JF, Stillman C, Siegel R, Akong M, Craig WS, Buckholz RG, Madden KR, Kellaris PA, Davis GR, Smiley BL, Cruze J, Toregrossa R, Velicelebi G, Thill GP. Biotechnology 1987; 5: 479–485.
15. Cregg JM, Madden KR. Dev Ind Microbiol 1988; 29: 33–41.
16. Sreekrishna K, Nelles L, Potenz R, Cruze J, Mazzaferro P, Fish W, Fuke M, Holden K, Phelps D, Wood P, Parker K. Biochemistry 1989; 28: 4117–4125.
17. Tschopp JF, Svelow G, Kosson R, Craig W, Grinna L. Biotechnology 1987; 5: 1305–1308.
18. Sreekrishna K, Barr KA, Hoard SA, Prevatt WD, Torregrosa RE, Levingston RE, Cruze JA, Wegner GH, Fifteenth International Congress of Yeast Genetics and Molecular Biology, Hague, The Netherlands, Topic number 09-37B; 1990.
19. Clare JJ, Romanos MA, Rayment FB, Rowedder JE, Smith MA, Payne MM, Sreekrishna K, Henwood CA. Gene 1991; 105: 205–212.
20. Romanos MA, Clare JJ, Beesley KM, Rayment FB, Ballantine SP, Makoff AJ, Dougan G, Fairweather NF, Charles IG. Vaccine 1991; 9: 901–906.
21. Clare JJ, Rayment FB, Ballantine SP, Sreekrishna K, Romanos MA. Biotechnology 1991; 9: 455–460.
22. Scorer CA, Buckholz RG, Clare JJ, Romanos MA. Gene 1993; 136: 111–119.
23. Scorer CA, Clare JJ, McCombie WR, Romanos MA, Sreekrishna K. Biotechnology 1994; 12: 181–184.
24. Shekar C. J Chembiol 2008. DOI: 10.1016/j.chembiol.2008.03.002, 15: 201–292.
25. Julien C. Bioprocess International 2006; 4: 22–31.
26. Kobayashi K, Nakamhra N, Sumi A, Ohmuta T, Yokoyama K. Ther Apher 1998; 2: 257–262.
27. Chuang VT, Otagiri M. Drugs Today (Barc) 2007; 43: 547–561.
28. Cregg JM, Madden KR. In: Stewart GG, Russell I, Klein RD, Hiebsch RR, editors. Biological research on industrial yeasts. Boca Raton (FL): CRC Press; 1987. pp 1–18.
29. Cereghino GL, Lim M, Johnson MA, Cereghino JL, Sunga AJ, Raghavan D, Gleeson M, Cregg JM. Gene 2001; 263: 159–169.
30. Nett JH, Gerngross TU. Yeast 2003; 20: 1279–1290.
31. Cereghino JL, Hashimoto MD, Moy A, Castelo J, Orazem CC, Kuo P, Xiong S, Gandhi V, Hatae CT, Chan A, Cereghino GL. Yeast 2008; 15: 293–299.
32. Higgins DR, Busser K, Comiskey J, Whither PS, Purcell TJ, Hoefeler JP. Methods Mol Biol 1998; 103: 41–53.
33. Sunga AJ, Cregg JM. Gene 2004; 330: 39–47.
34. Wan H, Sjolinder M, Schairer HU, Leclerque A. J Microbiol Methods 2004; 57: 33–39.
35. Kjeldsen T. Appl Microbiol Biotechnol 2000; 54: 277–286.
36. Hou J, Yan R, Yang L, Wu Z, Wang C, Ding D, Li N, Ma C, Li M. Biosci Biotehnol Biochem 2007; 71: 1462–1469.
37. Patrick SM, Fazenda ML, McNeil B, Harvey LM. Yeast 2005; 22: 249–270.
38. Nyblom M, Oberg F, Linkvist KP, hallgren K, Findlay H, Wikstrom J, Karlsson A, Hansson O, Booth PJ, Bill MR, Neutze R, Hedalk K. Protein Expr Purif 2007; 56: 110–120.
39. Baez J, Olsen D, Polarek JW. Appl Microbiol Biotechnol 2005; 69: 245–252.
40. Tojo N, Miyagi I, Miura M, Ohi H. Protein Expr Purif 2008; 59: 289–296.
41. Sreekrishna K, Brankamp RG, Kropp KE, Blankenship DT, Tsay JT, Smith PL, Wierschke JD, Subramaniam A, Birkenberger LA. Gene 1997; 190: 55–62.
42. Sreekrishna K. In: Flickinger MC, Drew SW, editors. Encyclopedia of bioprocess technolohy: fermentation, biocatalysis, and bioseparation. Hoboken (NJ): John Wiley & Sons, Inc.; 1999. pp 1971–1986.
43. Ilgen C, Cereghino JL, Cregg JM. In: Gellissen G, editor. Production of recombinant proteins. Novel microbial and eukaryotic expression systems. Weinheim: Wiley-VCH Verlag GmbH & Company KGaA; 2005. pp 143–162.
44. Cregg JM, Madden KR, Barringer KJ, Thill GP, Stillman CA. Mol Cell Biol 1989; 9: 1316–1323.
45. Barr KA, Hopkins SA, Sreekrishna K. Pharm Eng 1992; 12: 48–51.
46. Brierly RA. Methods Mol Biol 1998; 103: 149–177.
47. Inan M, Fanders SA, Zhang W, Hotez PJ, Zhan B, Meagher MM. Methods Mol Biol 2007; 389: 65–76.
48. Sreekrishna K. In: Baltz RH, Hegeman GD, Skatrud PL, editors. Industrial microorganisms: basic and applied molecular genetics. Washington (DC): American Society of Microbiology; 1993. pp 119–126.
49. Sarramegna V, Talmont F, Seree de Roch M, Milon A, Demange P. J Biotechnol 2002; 99: 23–39.
50. Surribas A, Resina D, Ferrer P, Valera F. Microb Cell Fact 2007; 6 . DOI: 10.1186/1475-2859-6-15.
51. Tang JB, Zhu P, Yang HM, Sun LM, Song SL, Ji AG. Biotechnol Lett 2008, 30: 1409–1414.
52. Jones JJ, Bridges AM, Fosberry AP, Gardner S, Lowers RR, James PJ, Hall RM, Jenkins O. J Biotechnol 2004; 108: 115–125.
53. Surribas A, Geissler D, Gierse A, Scheper T, Hitzmann B, Montesinos JL, Valero F. J Biotechnol 2006; 124: 412–419.
54. Sreekrishna K, Kropp KE. Non conventional yeasts in biotechnology. Berlin: Springer; 1996. pp 203–252. pp
55. Sreekrishna K, Prewatt WD, Thill GT, Davis GR, Koutz P, Barr KA, Hopkins SA. US Patent 5,827,684. 1998, to Research Technology Corporation Inc.
56. Brankamp RG, Sreekrishna K, Smith PL, Blankenship DT, Cardin AD. Protein Exp Purif 1995; 6: 813–820.
57. Fahnestock SR, Yao Z, Bedzyk LA. J Biotechnol 2000; 74: 105–119.
58. Su Z, Wu X, Feng Y, Ding C, Xiao Y, Cai L, Feng W, Li X. Appl Microbiol Biotechnol 2007; 73: 1355–1362. DOI: 10.1007/s00253-006-0604-2.
59. Choi BK, Actor JK, Rios S, d'Anjou M, Stadheim TA, Warburton S, Giaccone E, Cukan M, Li H, Kull A Sharkey N, Gollnick P, Kocieba M, Artym J, Zimecki M, Kruzel ML, Wildt S. Glycoconj J 2008. DOI: 10.1007/s10719-008-9123-y.
60. Shi XL, Feng MQ, Shi J, Shi ZH, Zhong J, Zhou P. Protein Expr Purif 2007; 54: 24–29.

61. Degan ME, Lair SV, Brierly RA, Siegel RS, Williams ME, Ellis SB, Kellaris PA, Provow SA, Craig WS, Velicelebi GV, Harpold MM, Thill GP. Biotechnology 1989; 7: 160–164.
62. Juge N, Anderson JS, Tull D, Roepstroff P, Svensson B. Protein Exp Purif 1996; 8: 204–214.
63. Yamada M, Azuma T, Matsuba T, Iida H, Suzuki H, Yamamoto K, Kohli Y, Hori H. Biochim Biophys Acta 1994; 1206: 279–285.
64. Ide N, masuda T, Kitabatake N. Biochem Biophy Res Commun 2007; 363: 708–714.
65. Rosenfield SA, Ross OH, Hillman MC, Corman JI, Dowling RL. Protein Expr Purif 1996; 7: 423–430.
66. Roy N, Smith MM, Navre M, Das G. Current topics in gene expression systems. San Diego (CA): Invitrogen Inc.; 1996. p 28.
67. Brocca S, Schmidt DC, Lotti M, Alberghina L, Schmid RD. Protein Sci 1998; 7: 1415–1422.
68. Ghosalker A, Sahai V, Srivastava A. Protein Expr Purif 2008. DOI: 10.1016/j.pep.2008.02.006 60: 103–109.
69. Thill GP, Davis GR, Stillman C, Holtz C, Brierly R, Engel M, Buckholz R, Kinney J, Provo S, Vedvick T, Siegel RS. Proceedings of the sixth international symposium on genetics of industrial microorganisms. Paris: Societe Francaise de Microbiologie; 1990. pp 477–490.
70. Brierly RA, Davis GR, Holtz GC. US Patent 5,324,639. 1994.
71. Olsen V, Cawley NX, Brandt J, Egel MM, Loh YP. Biochem J 1999; 339: 407–411.
72. Werten MWT, deWolf FA. Appl Environ Microbiol 2005; 71: 2310–2317.
73. Cereghino JL, Cregg JM. FEMS Microbio Rev 2000; 24: 45–66.
74. Daly R, Hearn TW. J Mol Recognit. 2005; 18: 119–138.
75. Kozlov DG, Yagudin TA. Biotechnol Lett 2008. DOI: 10.1007/s10529-008-9738-9 30: 1661–1663.
76. Raemaekers RJM, de Muro L, Gatehouse JA, Fordham-Skelton AP. Eur J Biochem 265: 394–403.
77. Sinha J, Plantz BA, Inan M, Meagher MM. Biotechnol Bioeng 2005; 89: 102–112.
78. Sreekrishna K, Tschopp J, Thill G, Brierly R, Barr KA. US Patent 5,707,828. 1998, to Research Corporation Technology Inc.
79. Prevatt WD, Sreekrishna K. US Patent 5, 330, 901. 1994, to Research Corporation Technology Inc.
80. Koganesawa N, Aizava T, Shimojo H. Prot Expr Purif 2002; 25: 416–425.
81. Jahic M, Gustavsson M, Jansen AK, Martinelle M, Enfors SO. J Biotechnol 2003; 102: 45–53.
82. Zhou XS, Zhang YX. Biotechnol Lett 2002; 24: 1449–1453.
83. Yang JZ, Zhou XS, Zhang YX. Biotechnol Lett 2004; 26: 1013–1017.
84. Xiao AF, Zhou XS, Zhou L, Zhang YX. Appl Microbiol Biotechnol 2006; 72: 837–844.
85. Hong F, Meinander NQ, Johnson LJ. Biotechnol Bioeng 2002; 79: 438–449.
86. Whittaker MM, Whittaker JW. Prot Expr Purif 2000; 20: 105–111.
87. Murasugi A, Tohama-Aiba Y. Prot Expr Purif 2003; 27: 244–252.
88. Li PZ, Gao XG, Arellano RO, Renugopalakrishnan V. Prot Expr Purif 2001; 22: 369–380.
89. Li Z, Xiong F, Lin Q *et al*. Prot Expr Pur 2001; 21: 438–445.
90. Murasugi A, Asami Y, Mera-Kikuchi Y. Prot Expr Purif 2001; 23: 282–288.
91. Shi X, Karkut T, Chamankhah M, Alting-Mees M, Hemmingsen SM, Hegedus D. Prot Expr Purif 2003; 28: 321–330.
92. Woo JH, Liu YY, Stavrou S, Neville DM Jr. Appl Environ Microbiol 2004; 70: 3370–3376.
93. Muthukumar G, Suhng SH, Magee PT, Jewell RD, Primerano DA. J Bacteriol 1993; 175: 386–394.
94. Chambers RS, Broughton MJ, Cannon RD, Carne A, Emerson GW, Sullivan PA. J Gen Microbiol 1993; 139: 325–334.
95. Gleeson MA, White CE, Meininger DP, Komives EA. Methods Mol Biol 1998; 103: 81–94.
96. Jonsson LJ, Saloheimo M, Pentilla M. Curr Genet 1997; 32: 425–430.
97. Boehm T, Sheperd SP, Trinh LB, Shiloach J, Folkman J. Yeast 1999; 15: 563–572.
98. Soderholm J, Bevis BJ, Glick BS. Biotechniques 2001; 31: 306–312.
99. Ni Z, Zhou X, Sun X, Wang Y, Zhang Y. Yeast 2008; 25: 1–8.
100. Hohenblum H, Gasser B, Maurer M, Borth N, Mattanovich D. Biotechnol Bioeng 2004; 85: 367–335.
101. Damasceno LM, Anderson KA, Ritter G, Cregg JM, Old LJ, Batt CA. Appl Microbiol Biotechnol 2007; 74: 381–389.
102. Zhang W, Zhao HL, Xue C, Xiong XH, Yao XQ, Li XY, Chen HP, Liu ZM. Biotechnol Prog 2006; 22: 1090–1095.
103. Gasser B, Sauer M, Maurer M, Stadimayr G, Mattanovich D. Appl Environ Microbiol 2007; 73: 6499–6507.
104. Goochee CF, Gramer MJ, Anderson DC, Bahr JB, Ramussen JR. Biotechnology 1991; 9: 1347–1355.
105. Romanos MA, Scorer CA, Clare JJ. Yeast 1992; 8: 423–488.
106. Montesino R, Garcia R, Quintero O, Cremata JA. Protein Expr Purif 1998; 14: 197–207.
107. Gerngross TU. Nat Biotechnol 2004; 22: 1409–1414.
108. Hamilton SR, Gerngross TU. Curr Opin Biotechnol 2007; 18: 387–392. DOI: 10.1016/jcopbio.2007.09.001.
109. Li H, Sethuraman N, Stadheim N, Zha TA, Printz B, Ballew N, Bobrowicz P, Choi BK, Cook WJ, Cukan M, Houston-Cummings NR, Davidson R, Gong B, Hamilton SR, Hoopes JP, Jiang Y, Kim N, Mansfield R, Nett JH, Rios S, Strawbridge R, Wildt S, Gerngross TU. Nat Biotechnol 2006; 24: 210–215.
110. Choi BK, Actor JK, Rios S, d'Anjou M, Stadheim TA, Warburton S, Giaccone E, Cukan M, Li H, Kull A, Sharkey N, Gollnick P, Kocieba M, Artym J, Zimecki M, Kruzel ML and Wildt S. Glycoconj. J 2008; 6: 581–593.
111. Lalandadze A, Galleno M, Foncerrada L, Strominger JL, Wucherfennig KW. J Biol Chem 1996; 271: 20156–20162.
112. Rosen CA, Haseltine WA. US Patent 6,905,688. 2005, to Human Genome Sciences, Inc.
113. Zhao HL, Xue C, Wang Y, Li XY, Xiong XH, Yao XQ, Liu ZM. J Biotechnol 2007; 131: 245–252.
114. Chen J, Sun HY, Yang Y, Wang XF, Chen SQ. J Zhejiang Univ Med Sci 2008; 37: 126–133.

115. Inan M, Meagher MM. J Biosci Bioeng 2001; 92: 585–589.
116. Waterham HR, Digan ME, Koutz PJ, Lair SV, Cregg JM. Gene 1997; 186: 37–44.
117. Shen S, Sutler G, Jeferies TW, Cregg JM. Gene 1998; 216: 93–102.
118. Liu H, Tan X, Rissell KA, Veenhuis M, Cregg JM. J Biol Chem. 2008; 270: 10940–10951.
119. Sears IB, O'Connor J, Rossanese OW, Glick BS. Yeast 1998; 14: 783–790.
120. Menendez J, Valdes I, Cabrera N. Yeast 2003; 20: 1097–1108.
121. Stratton J, Chiruvolu V, Meagher M. Methods Mol Biol 1998; 103: 107–120.
122. Zhang W, Inan M, Meagher M. Methods Mol Biol 2007; 389: 43–63.
123. Cos O, Ramon R, Montesinos JL, Valero F. Microb Cell Fact 2006; 5: 17. DOI: 10.1186/1475-2859-5-17.
124. Chiruvolu V, Eskridge KM, Cregg JM, Meagher MM. Appl Biochem Biotechnol 1998; 75: 163–173.
125. Curvers S, Brixius P, Klauser T, Thommes J, Weuster-Botz D, Takors R, Wandrey R. Biotechnol Prog 2001; 17: 495–502.
126. Zhang W, Bevins MA, Plantz BA, Smith LA, Meagher M. Biotechnol Bioeng 2000; 70: 1–8.
127. Minning S, Serrano A, Ferrer P, Sola C, Schmid RD, Valero F. J Biotechnol 2001; 86: 59–70.
128. Zhang W, Inan M, Meagher MM. Biotechnol Bioprocess Eng 2000; 5: 275–287.
129. Brierly RA, Bussineau C, Kosson R, Melton A, Siegel RS. Ann NY Acad Sci 1990; 589: 350–362.
130. d'Anjou MC, Daugulis AJ. Biotechnol Bioeng 2001; 72: 1–11.
131. Chen Y, Krol J, Cino J, Freedman D, White C, Komives E. J Chem Technol Biotechnol 1996; 67: 143–148.
132. Cos O, Serrano A, Montesinos JL, Ferrer P, Cregg JM, Valero F. J Biotechnol 2005; 116: 321–335.
133. Katakura Y, Zhang WH, Zhuang GQ, Omasa T, Kishimoto M, Goto W, Suga KI. J Ferment Bioeng 1998; 86: 482–487.
134. Shioya S. In: Fiechter A editor. Advances in biochemical engineering/biotechnology. Berlin: Springer; 1992. pp 111–142.
135. Crowley J, Arnold SA, Wood SA, Harvey LM, MacNeil B. Enzyme Microb Technol 2005; 36: 621–628.
136. Surribas A, Cos O, Montesinos JL, Valero F. Biotechnol Lett 2003; 25: 1795–1800.
137. Hellwig S, Emde F, Raven NP, Henke M, van der Logt P, Fischer R. Biotechnol Bioeng 2001; 74: 344–352.
138. Cos O, Ramon R, Montesinos JL, Valero F. Biotechnol Bioeng 2006; 95: 145–154.
139. Zhang WH, Potter KJ, Plantz BA, Schlegel VL, Smith LA, Meagher MM. J Ind Microbiol Biotechnol 2003; 30: 210–215.
140. Files D, Ogawa M, Scaman CH, Baldwin SA. Enzyme Microb Technol 2001; 29: 335–340.
141. Zhang WH, Sinha J, Smith LA, Inan M, Meagher MM. Biotechnol Prog 2005; 21: 386–393.
142. Xie JL, Zhou QW, Pen D, Gan RB, Qin Y. Enzyme Microb Technol 2005; 36: 210–216.
143. Schilling BM, Goodrick JC, Wan NC. Biotechnol Prog 2001; 17: 629–633.
144. Goodrick JC, Xu M, Finnegan R, Schilling BM, Schiavi S, Hoppe H, Wan NC. Biotechnol Bioeng 2001; 74: 492–497.
145. Boze H, Laborde C, Chamberlin P, Fabien R, Venturin C, Combarnous Y, Moulin G. Process Biochem. 2001; 36: 907–913.
146. d'Anjou MC, Daugulis AJ. Biotechnol Tech. 1997; 11: 865–868.
147. Bushell ME, Rowe M, Avignone-Rossa CA, Wardell JN. Biotechnol Bioeng 2003; 82: 678–683.
148. Baumann K, Maurer M, Dragosits M, Cos O, Ferrer P, Mattanovich D. Biotechnol Bioeng 2008; 100: 177–183.
149. Plantz BA, Nickerson K, Kachman SD, Schlegel VL. Biotechnol Prog 2007; 23: 687–692.
150. Wang Q, Li L, Chen M, Qi Q, Wang PG. Curr Microbiol 2008; 56: 352–357. DOI: 10.1007/s00284-007-9089-1.
151. Acosta J, Morales R, Morales A, Alonso M, Estrada MP. Biotechnol Lett 2007; 29: 1671–1676. DOI: 10.1007/s10529-007-9502-7; DOI: 10.1007/s00253-007-1315-z.
152. Fitches E, Wiles D, Douglas AE, Hinchliffe G, Audsley N, Gatehouse JA. Insect Biochem Mol Biol 2008; 10: 905–915.
153. Pscheidt B, Glieder A. Microb Cell Fact 2008; 7. DOI: 10.1186/1475-2859-7-25.
154. Marx H, Mattanovich D, Sauer M. Microb Cell Fact 2008; 7. DOI: 10.1186/1475-2859-7-23.
155. Mikola M, Seto J, Amanullah A. Bioprocess Biosyst Eng 2007; 30: 231–241. DOI: 10.1007/s00449–00007-0119-y.

FURTHER READING

Cregg JM, editor, Methods in molecular biology, Volume 389, Pichia protocols, 2nd ed. Totowa (NJ): Humana Press Inc., 2007.

Gellisen G, Kunze G, Gaillardin C, Cregg JM, Berardi E, Veenhuis M, van der Klei I. New yeast expression platforms based on methylotrophic *Hansenula polymorpha and Pichia pastoris and on dimorphic Arxula adenivorans and Yarrowia lipolytica* – A comparison. FEMS Yeast Res 2005; 5: 1079–1096.

Ghosalker A, Sahai V, Srivastava A. Optimization of chemically defined medium for recombinant *Pichia pastoris* for biomass production. Bioresour Technol 2008; 99: 7906–7910.

Hartner FS, Glieder A. Regulation of methanol utilization pathway genes in yeasts. Microb Cell Fact 2006; 14: 5–39.

Jahic M, Veide A, Charoenrat T, Teeri T, Emfors S. Process technology for production and recovery of heterologous proteins with *Pichia pastoris*. Biotechnol Prog 2006; 22: 1465–1473.

Jungo C, Marison I, Stockar UV. Regulation of alcohol oxidase of a recombinant *Pichia pastoris* Mut+ strains in transient continuous cultures. J Biotechnol 2007; 136: 236–246.

Maurer M, Kuhleitner M, Gasser B, Mattanovich D. Versatile modeling and optimization of fed-batch processes for the production of secreted heterologous proteins with *Pichia pastoris*. Microb Cell Factories, 2006; 11: 5–37.

Midgett CR, Madden DR. Breaking the bottleneck: Eukaryotic membrane protein expression for high-resolution structural studies. J Struct Biol 2007; 160: 265–274.

Routtinen M, Bollock M, Kogler M, Neubauer A, Krause M, Hamalainen ER, Myllyharju J, Vasala A, Neubauer P. Improved

production of human type II procollagen in the yeast *Pichia pastoris* in shakeflasks by a wireless-controlled fed-batch system. BMC Biotechnol 2008; 27: 8–33.

Tolner B, Smith L, Hillyer T, Bhatia J, Beckett P, Robinson L, Sharma SK, Griffin N, Vervecken W, Contreas R, Pedley RB, Begent RHJ, Chester KA. From laboratory to phase I/II cancer trials with recombinant biotherapeutics. Eur J Can 2007; 43: 2515–2522.

Zhang AL, Zhang TY, luo JX, Chen SC, Guan WJ, Fu CY, Peng SQ, Li HL. Constitutive expression of human angiostatin in *Pichia pastoris* by high-density cell culture. J Ind Microb Biotechnol 2007; 34: 117–122. DOI: 10.1007/s10295-006-0175-3.

14

GENE EXPRESSION IN RECOMBINANT ANIMAL CELLS AND TRANSGENIC ANIMALS

Richard M. Twyman
John Inness Centre, Norwich, United Kingdom
Bruce Whitelaw
Roslin Institute, Roslin, Midlothian, United Kingdom

14.1 INTRODUCTION

The ability of mammalian cells to take up DNA from their surrounding medium was first shown in the early 1960s (1). However, gene transfer to animal cells had been appreciated even since the 1940s, when viruses were first shown to carry their own nucleic acid. It is now known that animal cells can take up DNA naturally from a variety of sources, such as from incompletely hydrolyzed DNA molecules in the digestive tract (2). However, the *predetermined* genetic manipulation of animal cells only became possible at the beginning of the recombinant DNA era. This saw the development of a range of tools and techniques for the cloning and *in vitro* manipulation of particular DNA fragments, permitting the construction of *recombinant DNA* molecules containing novel combinations of sequences from diverse sources. Such techniques facilitated the design of *vectors*, purpose-constructed delivery vehicles used to introduce and establish foreign DNA sequences in animal cells. This, and the inclusion of transcriptional and translational control sequences in vectors to drive foreign gene expression, forms the basis of genetic engineering in animal cells.

In most cases, the underlying aim of a particular gene transfer experiment is to express a protein, either for commercial or research purposes or for gene therapy. In many cases, the recombinant protein is not typically synthesized by the host cell (e.g. it may be a protein from a different species or a protein that is normally restricted to a different cell type), in which case it may be described as a *heterologous protein*. Alternatively, it may be an endogenous protein, but the aim may be to overexpress it, or express it under unusual circumstances. Finally, the recombinant protein may be a particular mutant form of an endogenous protein, or one that has been modified so it is targeted to a different intracellular compartment.

The expression of recombinant proteins in animal cells is now a well-established technology and has been used in a huge variety of experimental systems. As a commercial approach to protein production, large-scale cultures of engineered mammalian cells have been used to synthesize antibodies, hormones, growth factors and cytokines, blood clotting factors, and the surface proteins of numerous viruses for use as recombinant vaccines (3). More recently, the same gene transfer technology has been used to alter endogenous gene expression or make targeted genome rearrangements in host cells. Vectors producing antisense RNA can be used to inhibit the expression of specific endogenous genes. Novel vectors can also be used as insertional mutagens and to facilitate the identification and cloning of genes by reporting their expression patterns. Others can replace endogenous genes by homologous recombination and can even generate specific chromosome rearrangements. The scope of such experiments may be limited to animal cells in culture, but if fertilized eggs, early embryos, or embryonic stem (ES) cells are used as host cells for gene transfer, it is possible to regenerate chimeric or fully transgenic

Upstream Industrial Biotechnology: Expression Systems and Process Development, Volume 1, First Edition. Edited by Michael C. Flickinger.
© 2013 John Wiley & Sons, Inc. Published 2013 by John Wiley & Sons, Inc.

animals expressing recombinant proteins or carrying specific germline alterations. The reintroduction of engineered cells into living animals and gene transfer to animal cells *in vivo* are also becoming established as technologies for gene therapy and the generation of chimeric animals for research.

14.2 OVERVIEW

14.2.1 Animal Cells Used for Genetic Manipulation

For the analysis of animal genes, it is usually beneficial, and in many cases essential, to use animal cells as hosts. Animal cells alone provide the correct genetic and biochemical background for such studies. Furthermore, animal proteins expressed in animal cells are more likely to be correctly processed and modified compared with those expressed in bacteria or microbial eukaryotic systems. For these reasons, there has been an intense effort over the past 20 years to develop efficient vectors and DNA transfer procedures for use with animal cells. Generally, this means *mammalian* cells and cell lines. However, other vertebrate cells are used for specialized purposes (e.g. the chicken DT40 cell line for homologous recombination). Furthermore, insect cell lines are used for the highly efficient baculovirus-based transient expression system, and as they are cheap to maintain, insect cells have recently emerged as hosts for recombinant protein expression in their own right (4). One exception to this apparently polarized exploitation of the diversity within the animal kingdom is in the field of transgenesis. The eggs and early embryos of many animals—nematodes, mollusks, annelids, insects, fish, amphibians, birds, and mammals—have been subjected to gene transfer procedures to produce animals containing transient episomal foreign DNA or carrying stable germline modifications. In addition, the large oocytes and eggs of the South African clawed frog *Xenopus laevis* have been widely exploited as a transient heterologous expression system for the analysis of protein function (5).

14.2.2 Protein Expression

For protein expression, the DNA sequence to be expressed is typically cloned in a bacterial host and then introduced into animal cells either by transfection (direct DNA transfer) or transduction (carried within a virus particle). In each case, cloning and transfer involve the use of specialized vectors carrying all the DNA sequences required for transcription and translation (Table 14.1.). Sometimes such a strategy is chosen because the foreign sequence cannot be expressed in any other host (e.g. if it contains introns that are incorrectly spliced in microbial systems). Characterizing the properties of cloned genes by expression in mammalian cells may also be one route to isolate a particular gene or cDNA sequence from a DNA library, an approach termed *expression cloning*. In many cases, cloned sequences are introduced into animal cells to be subjected to some kind of functional analysis, such as testing various mutant forms of a protein or regulatory element for their activity. Alternatively, protein production may itself be the goal, allowing biochemical and structural analysis and commercial production for research, industrial, or medical use. The exploitation of animal cells is particularly important if correct posttranslational modification is required for efficient protein activity or if the product is intended for human therapeutic use, because incorrect modification often renders recombinant human proteins immunogenic. Where protein synthesis is itself the ultimate aim, a small number of cell lines have been specially developed to complement particular vectors, such as COS-7 cells for simian virus 40 (SV40)-derived replicons, HEK 293 cells for adenoviral vectors, and Sf9 cells for baculovirus vectors. Gene transfer procedures for such cells have been carefully optimized.

Many of the strategies discussed require only transient protein expression. The foreign DNA need only remain intact and functional in the host cell for a short time or the host cell itself need only survive transiently. This type of system is sufficient for protein harvesting if a large amount of protein can accumulate over a short period of time. It is also sufficient for many types of functional analysis, because the given assay can be completed rapidly. In other situations, however, it may be necessary to generate a cell line producing recombinant protein on a long-term basis. This approach is used where a continuous supply of protein is required or where the cell line is used as a basis for further study. Such applications require foreign genes to be stably and permanently maintained in their animal cell hosts. This can be achieved in two ways: first by stable integration of foreign DNA into the genome and second by the use of stably maintained episomal vectors. Stable maintenance and long-term expression are also required where manipulated cells are used to generate transgenic animals or as part of a gene therapy program. Like engineered cells, transgenic animals may be used purely for functional analysis or as novel strains for exploitation in further experiments. Transgenic animals can also be used as living factories, producing correctly modified commercially valuable proteins, for example, in their milk.

14.2.3 Recent Advances in Gene Transfer Technology

While protein expression remains the predominant use for animal cells, attention has recently switched to a powerful set of novel applications that exploit the same gene transfer techniques directly to modify animal genomes or

TABLE 14.1. Reasons for the Genetic Manipulation of Animal Cells

Protein expression	1. For the production of large amounts of a protein that is either naturally scarce or the completely novel product of recombinant DNA technology, especially applicable for the production of biologically active proteins with specific forms of posttranslational modification, which are carried out incorrectly in microbial expression systems 2. For confirmation of the identity of a cloned gene by immunological assay of its product 3. For the study of protein function, transport, localization, and so on within animal cells 4. For the comparison of normal and mutant proteins 5. For the expression of proteins from genomic sequences containing introns, which are not spliced or incorrectly spliced in microbial systems 6. For gene augmentation therapy, the expression of proteins in animal cells to correct a genetic defect in a live animal 7. For the production of transgenic animals expressing a foreign protein
Regulatory analysis	1. For transient analysis of gene regulatory sequences in cells using reporter constructs 2. For the analysis of gene regulatory sequences using reporter constructs in transgenic animals 3. For the cloning and analysis of higher order function elements (origins, centromeres, matrix attachment regions, boundary elements, etc.)
Gene inhibition	1. For the inhibition of endogenous gene function using antisense RNA, ribozymes, intrabodies, or dominant negative alleles either for functional analysis in cells/transgenic animals or for gene inhibition therapy
Mutagenesis and targeting	1. For untargeted gene mutation by random insertional mutagenesis 2. For mutagenesis screening and cloning by tagging or plasmid rescue 3. For the entrapment of genes or regulatory elements 4. For targeted disruption of an endogenous gene (gene knockout) 5. To introduce a subtle mutation (allele replacement) 6. To replace one gene with another (gene knock in)

the expression of endogenous genes. *Gene targeting* is the replacement of one allele with another by homologous recombination, leaving the rest of the genome unchanged. This technique facilitates allele replacement and gene disruption (gene knockout) to create tailor-made mutant cells. The expression of endogenous genes can also be influenced by using expression constructs to generate antisense RNA, sometimes associated with ribozymes. These interact with and destroy cellular mRNAs, and hence block gene expression at the posttranscriptional level. Both gene targeting and antisense RNA strategies are extremely powerful when combined with current methods for generating transgenic animals, because they allow the creation of specific mutants with particular genes interrupted, replaced, altered by subtle mutation, or inhibited. The random insertion of cloned DNA also has many applications, for example, saturation mutagenesis, gene cloning by tagging or plasmid rescue, and the trapping of endogenous genes and regulatory elements using randomly inserted reporter gene constructs. Once again, this technology is most powerful when used in transgenic animals, allowing the isolation of genes and regulatory elements with specific expression patterns or the isolation of genes associated with particular mutant phenotypes.

Of particular interest is the use of site-specific recombination systems from bacteriophage and yeast to control gene expression and generate targeted genome rearrangements, often in an inducible or regulated fashion. The design of fully synthetic or hybrid inducible gene expression systems should eventually allow the experimenter to exercise complete and predictable control over foreign genes transferred to animal cells and in transgenic animals.

14.2.4 Transfer and Fate of DNA Introduced into Animal Cells

DNA can be introduced into cultured animal cells by two routes. The first exploits the natural ability of animal viruses to infect cells and deliver the viral genome either to the cytoplasm (most RNA viruses) or nucleus (most DNA viruses). Recombinant viruses carrying foreign DNA can thus be used to transfer foreign genes into the cell, a process termed *transduction*. Most DNA viruses, as well as the retroviruses (which have a DNA stage of the replication cycle), have been used to deliver foreign genes to the nucleus. Some replicate episomally (e.g. herpes viruses), while others integrate (e.g. retroviruses). Exceptionally, the poxviruses are DNA viruses that replicate in the cytoplasm. They, and some RNA viruses, have been exploited for cytoplasmic gene delivery and expression, which can be advantageous in certain experiments (e.g. for producing antisense RNA). The general advantage of transduction as a gene delivery method is its high efficiency: In certain systems, every cell in a culture dish can receive foreign DNA. It is also possible to exploit the natural tropism of a virus to infect particular cells in a tissue; for example, Epstein–Barr virus (EBV) is

lymphotropic. On the down side, there is often a complex series of manipulations involved in the preparation of recombinant viruses. Most viruses also exhibit cytopathic effects, and there are safety concerns over the use of recombinant human viruses. The alternative and simpler strategy is direct DNA delivery, where the cell is forced to internalize DNA present in the surrounding medium or where there is direct physical delivery of DNA into the nucleus, such as by microinjection. These unnatural DNA uptake routes are grouped under the term *transfection*. Direct delivery is by far the most commonly used strategy due to its simplicity and the requirement for only small, easily manipulable vectors. However, it is much less efficient, and strong selection systems must be used to identify successfully transfected cells.

The fate of the DNA introduced into cells depends on the vector system being used. Many viruses, and plasmids derived from them, carry *cis*-acting elements that facilitate episomal replication, allowing the DNA to be replicated and expressed without integration. Alternatively, foreign DNA may integrate into a random chromosomal site and replicate as a normal part of the genome. Integration generally represents a permanent modification, while episomal maintenance may be permanent or transient, depending on the nature of the replicon and its effect on the cell. Genes carried on vectors with no capacity for episomal maintenance may also be expressed transiently, but are soon diluted from the cell population. In some cases, the use of nonreplicating vectors, or even simple donor DNA without vector, ensures that only cells that have stably integrated the DNA will be selected.

14.3 PLASMID EXPRESSION VECTORS FOR ANIMAL CELLS

14.3.1 Classes of Expression Vector and Common Modular Components

An expression vector contains regulatory elements allowing the expression of any foreign DNA it carries. The simplest expression vectors, *transcription vectors*, allow transcription but not translation of cloned foreign DNA and are designed for *in vitro* use (Fig. 14.1a). They allow the production of large quantities (up to 100μg/reaction) of recombinant RNA and are often equipped with dual, opposing promoters allowing both message sense and antisense RNA to be synthesized, for example, for use as probes in hybridization experiments. Significantly, such vectors utilize the very specific promoters from *Escherichia coli* bacteriophages such as T3, T7, and SP6, which do not function in animal cells. More complex vectors can therefore be designed to incorporate this *in vitro* transcription system without interfering with the function of eukaryotic transcription units in animal cells. Simple transcription vectors lack other regulatory sequences, including transcriptional termination sites. RNA of specified length can therefore be produced from such vectors only by linearization (run-off transcription). Although designed for *in vitro* use, transcription vectors play an essential role in certain protein expression systems.

Typical *protein expression vectors* allow both the transcription and translation of cloned DNA, and thus facilitate the production of recombinant protein (Fig. 14.1b). Such vectors are equipped with transcriptional regulatory sequences and sequences that control RNA processing and

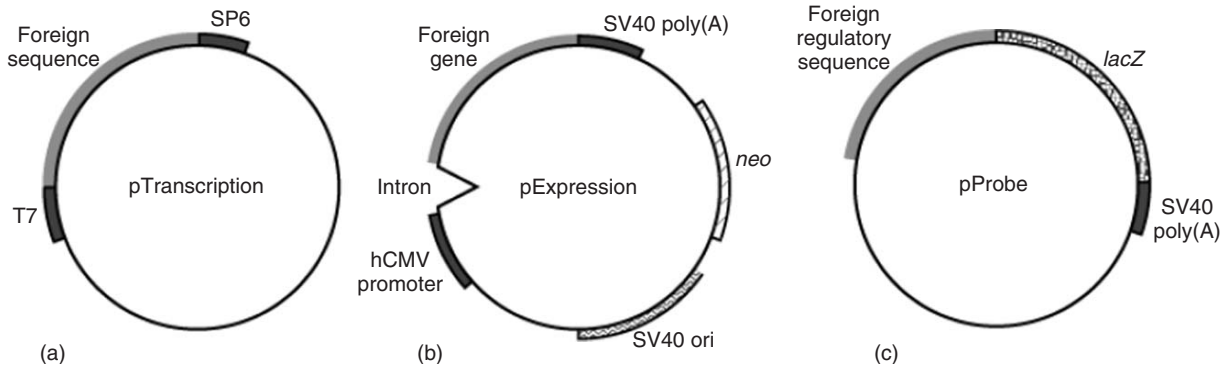


Figure 14.1. Generic maps of different types of expression vector: (a) a transcription vector, which carries promoters allowing the *in vitro* transcription of foreign DNA; (b) a protein expression vector, which contains the regulatory elements (promoter–enhancer, intron, and polyadenylation site) allowing the transcription and translation of foreign DNA; such vectors may also carry a marker gene for selection of transformants or a viral origin of replication for episomal maintenance; (c) a regulatory probe vector, which carries a reporter gene and allows the characterization of cloned regulatory elements.

protein synthesis (6). They are designed for use in both cell culture and *in vivo*. In cases where the objective of the expression experiment is simply to produce as much protein as possible, *overexpression vectors* are used, which are designed to maximize both transcription and translation. Where more moderate protein expression levels are appropriate for the experiment, or where large amounts of protein would be toxic to the cells, inducible regulatory elements may be used. A common fusion strategy is to express recombinant proteins with an N-terminal signal peptide. This allows secretion from host cell, so that the protein can be purified from the growth medium without resorting to cell lysis.

Further expression vectors are designed not for the analysis of cloned gene products, but cloned regulatory elements (7). Such *regulatory probe vectors* carry a screenable marker gene, such as *lacZ*, and allow the insertion of putative regulatory elements that can be used to drive marker gene expression (Fig. 14.1c). Different vectors are available for the analysis of different types of *cis*-acting element. *Promoter probe vectors* carry a reporter gene with an initiation codon but no upstream regulatory sequences and are used for the identification and dissection of putative promoters. *Enhancer probe vectors* carry a reporter gene driven by a minimal promoter, allowing analysis for the upregulation of basal activity. There are also vectors available for the analysis of transcriptional terminator/polyadenylation sites and splice signals. Specialized probe vectors called *entrapment vectors* are used for the identification and isolation of novel regulatory elements following random integration into the genome.

The typical modular components of an expression vector for animal cells can be divided into five major categories (6):

- *Plasmid backbone sequences:* Sequences required for cloning in bacteria and for *in vitro* manipulation
- *Plasmid maintenance sequences:* Many vectors also carry sequences of viral origin that allow episomal replication in animal cells
- *Components of the animal gene transcription unit:* Sequences used for the efficient expression of foreign genes, including promoter and enhancer elements, a polyadenylation site, an intron, sequences for translational control, and sequences for protein targeting in the host cell
- *Marker genes:* Either for visible quantification or characterization of gene expression or for selection of transfected cells
- *Sequences to simplify protein purification:* In overexpression vectors, there may be additional sequences encoding a signal peptide (to facilitate secretion), a protein tag (to allow, e.g. affinity purification of the fusion protein), and a protease cleavage site (to remove the tag after purification).

14.3.2 Plasmid Backbone Sequences

All expression vectors for use in animal cells are *shuttle vectors*; that is, they can be propagated in cells of more than one species. In most cases, the alternative host is *E. coli*, allowing large quantities of plasmid DNA to be prepared and isolated from bacterial culture. Such vectors contain an origin of replication derived from the plasmid ColE1 and a dominant marker for selection in bacterial cells. This marker is usually an antibiotic resistance gene. However, suppressor tRNAs are used in some host–vector systems.

In addition to these basic maintenance sequences, other backbone sequences include those used for *in vitro* manipulation (8). The most important of these is the *multiple cloning site*, a cluster of unique restriction enzyme sites allowing the insertion of foreign DNA, using a variety of subcloning strategies, at a site that does not disturb vector functions. For many vectors, recombinant screening is facilitated by locating the multiple cloning site within a marker gene so that recombinants can be screened for loss of marker activity. The simplest and most popular system is *blue–white selection*. This is based on the marker gene *lacZ*, whose product β-galactosidase converts the chromogenic substrate X-gal (5-bromo-4-chloro-3-indolyl-β-D-galactopyranoside) into a blue pigment. Recombinant vectors, in which the marker is interrupted, lack β-galactosidase activity. Therefore, on X-gal supplemented medium, recombinant colonies appear white and nonrecombinant colonies blue. The best contemporary vectors are extremely versatile and contain a bacteriophage f1 (or similar) origin of replication, facilitating the production of single-stranded DNA for sequencing, *in vitro* mutagenesis, and so on, and opposed bacteriophage promoters allowing the synthesis of sense and antisense RNA corresponding to the insert (e.g. for *in situ* hybridization).

Generally, the bacterial and animal components of shuttle vectors are functionally segregated. The animal DNA does not function in bacteria, and therefore does not interfere with cloning. Similarly, the *E. coli* backbone sequences are not intended for use once the plasmid has been introduced into animal cells, and they do not interfere with maintenance or expression. However, certain plasmid sequences have been shown to inhibit vector function in mammalian cells. The first example was a fragment of the pBR322 backbone that inhibited the activity of the SV40 origin of replication in monkey cells (9). Such *poison sequences* are often poorly defined, but they may be responsible for the varying efficiencies of otherwise similar expression vectors. Occasionally, eukaryotic insert sequences can interfere with cloning in bacteria—this usually involves rearrangement of

the insert due to the presence of repetitive DNA sequences, but can also result in nonrecovery of recombinant vectors from bacterial culture. Some vectors are designed to use certain sequences both in bacterial and animal cells. A recent series of expression vectors from Invitrogen utilizes a single dominant selectable marker for resistance to the antibiotic Zeocin. This can be selected in bacteria and mammalian cells because the gene is controlled by dual tandem promoters (a synthetic bacterial promoter and the human cytomegalovirus promoter), and hence significantly reduces the size of the vector allowing the propagation of larger inserts. Bacterial promoters, such as the T7 promoter and the *E. coli lac* promoter, have also been used as part of animal gene transcription units. They have been exploited as heterologous inducible promoters, allowing efficient inducible expression of cloned genes if the appropriate transcription factors are provided in *trans*.

14.3.3 Plasmid Maintenance Sequences

The transfection of animal cells with bacterial plasmids results in a low frequency of transformation due to stable integration of the DNA into the host genome. Such vectors are not maintained episomally because the bacterial ColE1 origin does not function in eukaryotes. Any extrachromosomal DNA is rapidly diluted and degraded in nontransformed cells. Certain mammalian viruses, however, propagate their genomes as episomal plasmids on either a long-term (latent) or a short-term (lytic) basis. The inclusion of viral origins in recombinant plasmids allows expression vectors to be propagated in the same manner.

Lytic origins, such as the SV40 *ori* and EBV *ori*Lyt, can promote massive extrachromosomal replication of expression vectors if appropriate regulatory proteins are supplied in *trans*. This prolific amplification of the foreign DNA allows high level recombinant protein synthesis, but this rapidly becomes toxic to the host cell, resulting in cell death within a few days. Vectors with lytic origins are thus suitable for transient expression, but not for long-term protein synthesis. Conversely, latent origins, such as EBV *oriP* and the bovine papillomavirus (BPV) origin, allow stable maintenance of expression vectors at a low copy number. This is not toxic to the cell, and such vectors are suitable for long-term propagation and facilitate the stable expression of recombinant proteins.

14.3.4 Regulatory Sequences

All protein expression vectors carry a transcription unit containing the sequences required for efficient gene expression. These comprise transcriptional regulatory sequences, RNA processing signals, and sequences for protein synthesis and targeting. The major components are as follows:

- *Promoter and enhancer sequences:* The promoter is the site where RNA polymerase II binds to the transcription unit, and *cis*-acting elements upstream of the promoter also control its cell-type specificity and induction in response to external signals. Enhancers are *cis*-acting elements that work with endogenous promoters to increase their transcriptional activity; they may also impart cell type and inducible specificity on gene expression. The promoter and enhancer elements chosen for particular expression strategies depend on the experimental parameters. There are three types of systems: (i) endogenous systems, (ii) promiscuous viral systems, and (iii) inducible systems. Where a particular level or pattern of gene expression is required (e.g. when directing gene expression to specific tissues in transgenic mice), an endogenous promoter/enhancer system may be employed. Where high level expression and versatility are required, the strong and promiscuous regulatory elements found in mammalian viruses are often used. These include the SV40 early promoter and enhancer, the human cytomegalovirus promoter/enhancer, and the Rous sarcoma virus long terminal repeat (LTR) promoter/enhancer. These widely used elements function in many cell types, often beyond the scope specified by the host range of the virus, allowing the same expression vectors to be transfected into a range of different cell lines. Where precise control of gene expression is desired, or where the recombinant protein is toxic to the cells, inducible systems may be used. These may be of endogenous origin (e.g. heat induction), in which case endogenous genes may also be activated. Alternatively, they may be heterologous systems that have to be activated by supplying appropriate transcriptional regulators in *trans* (e.g. *E. coli lac* and *tet* systems, the *Drosophila melanogaster* ecdysone system). Both endogenous and heterologous systems may suffer from leakage (high background expression) or a low induction ratio, so there has been an effort to develop hybrid or completely artificial induction systems, for precise control of foreign gene expression.
- *RNA processing sequences:* These include a transcriptional termination/polyadenylation site and often an intron. Termination and polyadenylation sites are essential for stable RNA production. Introns are not necessary for the efficient expression of all genes, but in many cases, the inclusion of an intron has been shown to improve protein expression levels. For some genes, this may be because splicing is required for continued transcription or RNA stability. Alternatively, the recruitment of particular proteins during splicing may facilitate translation when the mRNA is exported from the nucleus.

- *Sequences for efficient translation and protein targeting:* The most important consideration is the Kozak consensus, a sequence surrounding the initiation codon whose context sponsors efficient ribosome scanning and initiation. The size of the 5′ untranslated region (UTR) is also kept as short as possible, as secondary structure in the transcript can inhibit translation. If a 3′ UTR is included into the vector, AU-rich instability sequences are avoided. A further sequence included in some vectors is a picornaviral internal ribosome entry site (IRES), allowing the production and translation of polycistronic mRNAs. Sequences that target recombinant proteins to particular cellular compartments may also be included. Nuclear localization sequences are used to target proteins to the nucleus. Signal peptides target proteins to the secretory pathway, which may be essential for correct posttranslational modification. KDEL retention signals (KDEL specifies a tetrapeptide sequence in the single-letter amino acid code) may be used to favor intracellular protein accumulation.

14.3.5 Marker Genes

A *marker gene* is one conferring a readily identifiable phenotype. Many expression vectors carry marker genes or are introduced along with a second vector carrying a marker gene. Such genes can be divided into two classes serving distinct functions.

Visible or *screenable markers (reporter genes)* provide visible evidence of transfection and gene expression. Under the control of a constitutive promoter, reporter genes can be used to determine transfection efficiency. Such vectors are often used for cotransfection with a series of experimental vectors to provide an internal experimental control. If a reporter gene is linked to a heterologous regulatory element, it can be used to quantify the expression levels and patterns associated with that regulatory element. If a reporter gene is joined to a foreign gene and expressed as a fusion protein, it can be used as a flag to determine protein localization or exploited for protein purification (see the following section). Entrapment vectors, which integrate into the genome and reveal the attributes of proximal genes and regulatory elements by reproducing their expression patterns, can exploit both these principles.

Selectable markers encode products conferring resistance (positive selection) or sensitivity (negative selection or counterselection) to a particular treatment. These are used to select stably transfected cells from a background of nontransfected cells or other rare products of transfection (e.g. cells that have undergone homologous recombination as opposed to those that have integrated the DNA randomly).

14.3.6 Sequences for Protein Purification

The synthesis and accumulation of recombinant protein in the cytoplasm of stably transfected cells has several disadvantages, including toxicity effects and dependence on cell lysis for protein isolation. However, by expressing recombinant proteins with an N-terminal signal peptide, proteins can be secreted from the cell and purified from the medium, reducing toxicity and allowing long-term protein production by repeated passaging. Many current expression vectors include sequences incorporated specifically to simplify the purification of overexpressed proteins (10). These sequences fall into three classes: fusion polypeptides, fusion epitopes, and oligo(amino acid) tails. Each provides a tag with which to purify the protein product of any gene expressed using that vector (Table 14.2.). Fusion polypeptides include β-galactosidase, glutathione-*S*-transferase, and staphylococcal protein A. In each case, there is a particular ligand to which this polypeptide binds, allowing the recombinant fusion protein to be captured and then eluted. Fusion epitopes are short peptides providing a single epitope of a particular protein, such as c-Myc, for recognition by a monoclonal antibody. The advantage of epitopes is that their small size and surface location usually does not interfere with the native folding or activity of the recombinant protein, which is sometimes a problem when using the larger fusion polypeptides. Similarly, a short oligo(amino acid) tail provides an unobtrusive tag, allowing purification by simple chromatographic procedures or again using antibodies. The tail is usually 2–20 residues in length. A further sequence often included in such vectors is a consensus cleavage site allowing the overexpressed protein to be separated from its fusion tag. A number of simple sequences may be chemically or enzymatically cleaved (e.g. cyanogen bromide cleaves after methionine residues). More complex cleavage sites, such as the motif recognized by enterokinase, are useful because they are unlikely to appear within the recombinant protein by chance.

14.4 OTHER DIRECT TRANSFER VECTORS

14.4.1 Yeast Artificial Chromosome Expression Vectors

Simple engineering strategies, such as protein synthesis and transient analysis, can be performed with cDNAs or minigene constructs cloned in plasmid or viral vectors. Although such constructs provide the essential information for protein structure, it is well established that endogenous gene expression is influenced not just by local regulatory elements but also by distant sites that may exert a direct regulatory influence or may control chromatin structure or

TABLE 14.2. Sequences Included in Mammalian Expression Vectors to Simplify the Purification of Overexpressed Proteins

Sequence	Comments
	Secretion
Signal peptide	An N-terminal 15–30 amino acid peptide which, by interacting with a signal recognition particle, causes ribosomes to attach to the ER membrane and pass the nascent polypeptide into the ER lumen for secretion; many signal peptides have been characterized and some exploited in mammalian expression vectors; for example, the mouse Ig-κ chain signal peptide is used in the Invitrogen vector pSecTag
	Fusion polypeptides
β-Galactosidase	Approximately 120-kDa polypeptide, binds to APTG
Glutathione-*S*-transferase	Approximately 30-kDa polypeptide, binds to glutathione
Staphylococcal protein A	Approximately 30-kDa polypeptide, binds to IgG and elutes at low pH
	Fusion polypeptides
c-Myc	11 amino acid epitopes, recognized by mouse monoclonal antibody 9E10; elutes at low pH
FLAG	Hydrophilic eight amino acid epitopes recognized by commercially available antibody anti-FLAG M1/M2
	Oligo(amino acid) tails
$(His)_6$	Purified by metal chelate affinity chromatography or anti-$(His)_6$ antibodies
$(Cys)_4$	Purified by affinity to thiopropyl groups
	Cleavage sites
Collagenase	Cleavage site is -Pro-xxx-↓-Gly-Pro-xxx-↓
Enterokinase	Cleavage site is -$(Asp)_4$–Lys-↓
Factor Xa	Cleavage site is -Ile-Glu-Gly-Arg-↓ at pH 8.0

Abbreviations: APTG, ***p***-aminophenyl-***β***-D-thiogalactopyranoside; ER, endoplasmic reticulum; FLAG, amino acid one-letter code for residues within the "FLAG" epitope.

the extent of DNA methylation. Hence, to reproduce the native expression characteristics of an endogenous gene fully, a transgene may need to be bracketed by hundreds of kilobase pairs of flanking sequence. Inserts >50 kbp cannot be cloned in standard plasmid, cosmid, or viral vectors due to packaging constraints, instability resulting from recombination, the selection of spontaneous deletion mutants, and the likelihood of shearing the DNA during *in vitro* manipulation.

Such limitations have been overcome by developing yeast artificial chromosome (YAC) vectors (11). These are linear vectors carrying the essential *cis*-acting elements of a yeast chromosome and are stably propagated in yeast cells at a low copy number. The components required are a yeast centromere (*CEN*), an origin of replication (autonomous replicating sequence, *ARS*) and telomeres (*TEL*). The vectors also carry a multiple cloning site for the insertion of foreign DNA and selectable markers for stable maintenance (such markers generally restore prototrophy to an auxotrophic yeast strain). Of the various large-capacity vectors developed for use in bacterial and mammalian cells (reviewed in Ref. 11), YAC vectors have many advantages, including their capacity (theoretically up to 2 Mbp, which should enable even the largest mammalian genes to be cloned) and the amenability of yeast for homologous recombination. This allows yeast vector sequences to be replaced by mammalian selectable markers before transfection, a process termed *retrofitting*. It also allows specific mutations to be introduced into the foreign DNA. Recombinant YAC clones are fragile and subject to shear, but several methods have been developed for their efficient transfection into mammalian cells, including lipofection, fusion with yeast spheroplasts, and microinjection into the pronuclei of fertilized eggs (see later). ES cells have been the predominant targets for YAC transfection, and such techniques yield transgenic mice with at least the same efficiency as obtained using more traditional and smaller transgenes.

The generation of YAC transgenic mice is not a trivial process, because recombinant YAC DNA is difficult to purify intact and is highly susceptible to fragmentation once inside the cell. Typically, transgenic animals integrate several YACs, some with terminal deletions reflecting intracellular fragmentation events. Despite these difficulties, YACs have been used to study the expression of a number of human and mouse genes in a transgenic environment, using constructs ranging in size from 40 kbp to over 1 Mbp (11). In most cases, transgene expression was shown to closely mirror the expression of the endogenous gene, suggesting that the inclusion of flanking material can isolate transgenes from position effects, which often influence basic expression constructs. The applications of this technology include mutational analysis, the generation of animal models for human disease, the analysis of *cis*-acting elements in their natural context, and the analysis of higher order genome function (e.g. genomic imprinting and X-chromosome inactivation). YACs have also been used as the basis of one class of mammalian artificial chromosome (MAC), as discussed later.

14.4.2 Targeting Vectors

Some plasmid vectors do not carry the typical components of a eukaryotic transcription unit and are therefore not strictly expression vectors. There are two uses for such constructs: gene targeting and random integration.

Gene targeting is the replacement of specific target DNA sequences with foreign DNA carried in a vector by homologous recombination and/or gene conversion (12). *Targeting vectors* are used to replace genomic DNA sequences, and to replace sequences in viral genomes already in the cell, to generate recombinant viral vectors (see later). Like expression vectors, targeting vectors carry plasmid backbone sequences and selectable markers, but they lack eukaryotic maintenance sequences because the vectors are not designed for amplification or recovery—their sole purpose is delivery of the foreign DNA to the homologous target. For this reason, such vectors are often termed *gene delivery vectors* or *suicide vectors*. The most important feature of a targeting vector is the region of homology with the intended target, as this is an absolute requirement for homologous recombination. The design of the homology region allows either insertion by single crossover or transplacement by double crossover.

14.4.3 Insertional Mutagenesis and Entrapment Vectors

The use of vectors for random integration into genomic DNA serves two purposes. First, integrating vectors can be used to generate mutants. Mutagenesis in classical genetic analysis traditionally involves exposing a population of organisms to high levels of a mutagen, and then recovering mutant offspring by suitable selection and screening. The mutagens employed are either chemical (e.g. ethylmethane sulfonate added to food) or physical (e.g. bombardment with X-rays). More recently, *biological* mutagens have been exploited. These are based on transposable elements, DNA sequences that naturally jump from one site to another in the genome, often happening to interrupt genes. Transposable elements cloned in plasmid vectors can be introduced into animal cells and will jump to random sites in the genome resulting in insertional mutagenesis. This strategy has been widely used to generate *Drosophila* mutants: vectors carrying recombinant *Drosophila* transposons called *P elements* have been microinjected into eggs, leading to the recovery of mutant offspring (13). Transposable elements require both *cis*-acting sequences and *trans*-acting enzymes for mobilization. The strategy used to control P element mutagenesis in *Drosophila* is to coinject eggs with two plasmids, one containing a defective P element (lacking the *trans*-functions) and another containing a helper P element, which has been rendered nonmobilizable by deleting its *cis*-functions (these are termed *wings-clipped elements*). This enables the defective P element to jump once, from the plasmid to a random location in the genome, and then remain stably integrated. Insertional mutants have also been generated in mice, initially by the chance integration of transgenes or retroviral vectors designed for other purposes and later by specially dedicated integration vectors (14).

Second, integrating vectors can be used as *entrapment vectors* to identify local genes and regulatory elements (Fig. 14.2a). In this case, the transposable element contains a reporter gene that responds to local promoter or enhancer elements at the site of integration. The classic example is the *Drosophila enhancer trap* (15). A recombinant P element transferred to the *Drosophila* germline carries *lacZ* under the control of a minimal promoter. The randomly integrated cassette is then influenced by any local enhancer, and the reporter gene expression pattern reveals the expression parameters of the gene normally controlled by the enhancer. *Gene traps* use the same strategy to identify genes. In this case, the reporter gene may be located downstream from an AUG codon or a splice acceptor site. The first type of gene trap is activated on insertion into the first exon of an endogenous gene, while the other is activated if inserted into an intron. Entrapment strategies are widely used in *Drosophila* to identify novel genes on the basis of their expression parameters. More recently, the same approach has been used in other animals, including mice (16), where libraries of ES cells carrying reporter insertions can be used to generate transgenic animals (17). ES cells are the preferred target for such experiments as the interpretation of insertional mutation phenotypes generated by the pronuclear injection of mouse eggs may be complicated by the extensive genome rearrangements that often accompany this procedure. More refined approaches can be used to identify specific classes of genes, for example, the use of a reporter gene that requires an N-terminal signal sequence for expression effectively selects for mutations in genes that encode secreted proteins. Also, a gene trap comprising two selectable markers and designed to express the site-specific recombinase Cre will induce a permanent switch between the markers when integrated adjacent to a constitutive promoter (Cre recombinase is discussed later). This approach can be used to identify genes expressed in a temporally restricted manner through the generation of a cell autonomous marker (no switching of marker genes). The integration of a gene trap vector is generally mutagenic, and depending on the gene, the mutant phenotype may be observed in heterozygotes or homozygotes. Such vectors thus serve a dual role—interesting new genes can be identified both

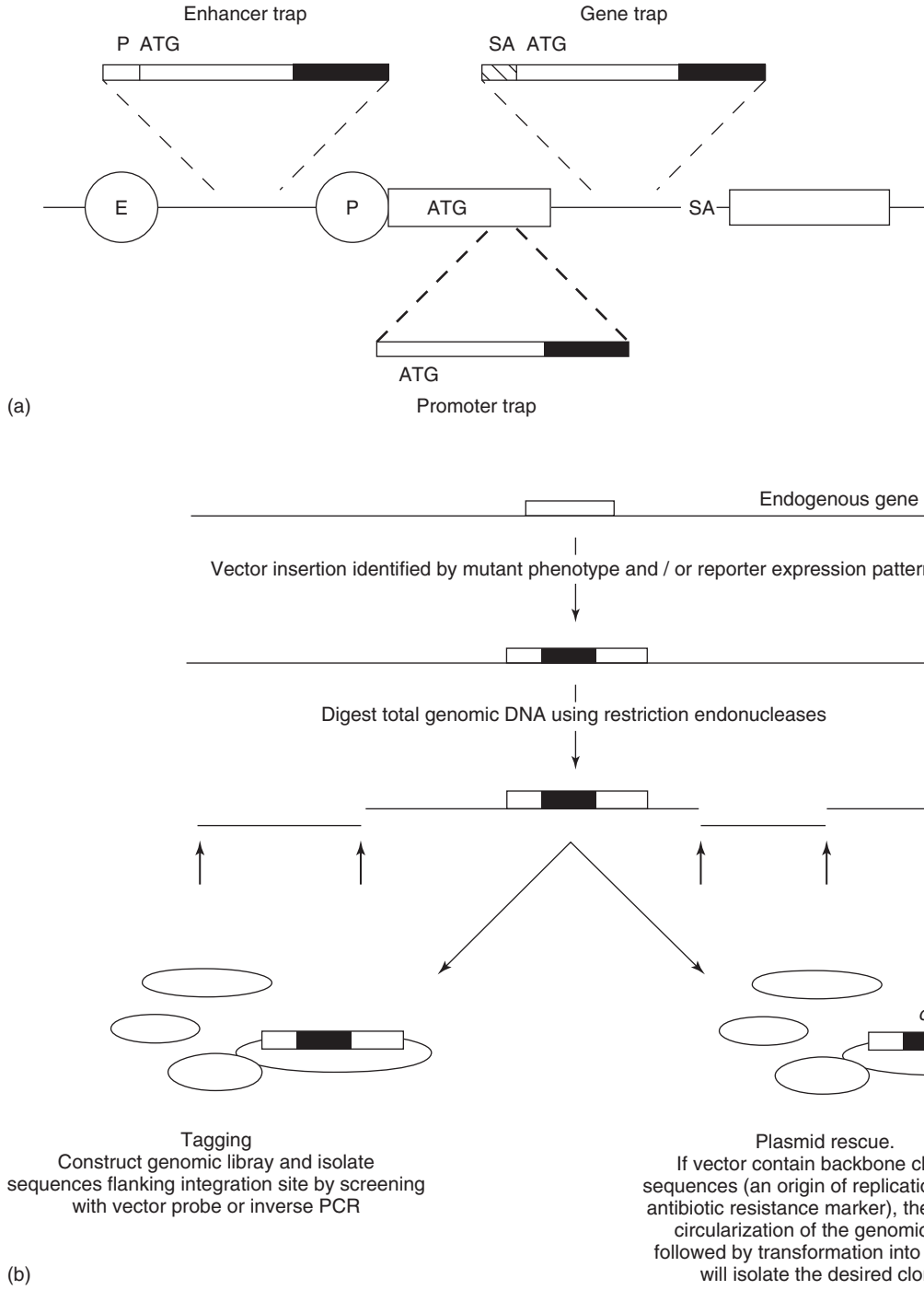


Figure 14.2. Insertional mutagenesis and entrapment vectors: (a) different forms of entrapment vector. The enhancer trap vector carries a minimal promoter, and gene trap vectors may carry a "naked" start codon (this type of vector is also known as a *promoter trap*) or a splice acceptor. (b) Insertional mutagenesis and entrapment vectors may be used to clone local genes either by tagging or plasmid rescue.

by their reporter expression pattern and by their mutant phenotype. Note that retroviruses (see later) are often used for insertional mutagenesis and trapping in mammals. Their unusual mode of replication allows them to be classed as transposable elements as well as viruses; so their activity is very similar to *Drosophila* P element vectors.

Basic integrating vectors do not require any special sequences in addition to the plasmid backbone, and even this can be dispensed with—insertional mutants in mice can be generated by introducing foreign DNA fragments into fertilized eggs without a vector. Entrapment vectors require a marker gene and minimal regulatory elements, but both basic integrating vectors and entrapment vectors lack eukaryotic maintenance sequences, because they are not deigned for amplification or recovery. However, careful design of such vectors can prove very useful. One consideration is the uniqueness of the introduced sequence. In *Drosophila*, the introduction of single P elements into fly strains normally lacking P elements enables genes identified by insertional mutagenesis to be cloned by *tagging*, which involves screening a genomic library generated from the mutant line for the unique sequence of the integrated element (Fig. 14.2b). Any clone isolated by this technique would contain the integrated foreign DNA and surrounding genomic DNA. This could then be used to screen genomic and cDNA libraries from wild-type flies to identify and isolate the noninterrupted version of the gene. This is an extremely convenient reverse genetics approach in the study of gene function (18).

An even more elegant refinement is the technique of *plasmid rescue* (19). In this case, the vector is designed so that the sequence that integrates into the genome contains certain plasmid backbone elements: the origin of replication and a bacterial selectable marker. The isolation of flanking DNA can then be achieved without library construction: Genomic DNA from the mutant line is digested with a restriction endonuclease cutting at a single site in the vector, and the resulting genomic DNA fragments are ligated to form circles. These can be introduced into bacterial cells *en masse*, but only those carrying a plasmid origin and marker will replicate under the selective regime (Fig. 14.2b). Bacterial colonies growing on selective media thus contain circularized genomic fragments carrying the inserted DNA sequence and flanking genomic DNA.

14.5 DIRECT DNA TRANSFER

14.5.1 Overview of Cell Transfection

The direct transfer of DNA into animal cells can be accomplished by a number of techniques that either force the cells to take in DNA by breaching the cell membrane or exploit the natural ability of cells to internalize certain molecules in their environment. The DNA introduced into cells by transfection may be maintained transiently or permanently. In transient transfection, the DNA may be nonreplicative, in which case it is diluted and lost from the population of cells over a few hours, depending on its stability. For plasmids containing an SV40 origin of replication, episomal replication occurs in certain simian cells, but the high replication rate eventually causes cell death. In both the cases, foreign genes may be expressed transiently, with a rapid onset of protein synthesis, but for a limited duration. Transient transfection is useful for expression cloning, rapid assays for protein activity, and establishing the potential of different promoters. Transient transfection is not an efficient method for the overexpression and purification of recombinant proteins on a long-term basis and cannot be used to generate transgenic animals. For stable transfection (also termed *transformation* because the genotype of the cell is altered), foreign DNA must be maintained permanently in the cell. If the exogenous DNA is nonreplicative, stable transfection must occur by integration of the DNA into the genome. Alternatively, the foreign DNA may be carried in an episomal vector, whose moderate replication rate does not cause cell death. Stable transfection is required for the long-term production of foreign proteins, for gene silencing by antisense RNA synthesis, and for the generation of transgenic animals.

What governs whether a given DNA molecule will transiently or stably transfect a cell depends on the type of vector. Those carrying episomal maintenance sequences control their own fate: SV40-based vectors kill simian host cells by high level episomal replication; so stably transfected cells are not recovered. However, vectors carrying the EBV latent origin are stably maintained in permissive cells because their replication rate is moderate and is tolerated by the host. For nonreplicating DNA, however, both transient and stable transfections occur concurrently. The efficiency of transient transfection varies considerably among different cell types and according to the transfection method, but is always several orders of magnitude higher than that of stable integration. Thus, in transient transfection, a small number of cells will also be stably transfected, but these will not generally be noticed in the short experimental timescale. In stable transfection experiments, many cells are initially transiently transfected, but the DNA is soon diluted and destroyed. Selection is used to identify the rare cells where foreign DNA has integrated into the genome, and by this time, the "transient" DNA is no longer present. Stable integration is thought to occur by illegitimate recombination—end-joining between broken chromosomal DNA and vector DNA. In some cells, an alternative to illegitimate recombination is homologous recombination. The efficiency of this process is extremely low in most cells, and even in particularly amenable cells (such as ES cells and the DT40 line), it is still a rare process and occurs several orders of magnitude

less frequently than random integration. Homologous recombination occurs only if the vector carries a homology region, where ectopic pairing can occur between the genome and the vector, facilitating crossing over or gene conversion. Due to the rarity of this event and the relative frequency of random integration, very powerful selective strategies must be employed to identify targeted cells.

14.5.2 Transient Transfection: Nonreplicating Vectors

In transient transfection, DNA is not integrated into the genome. Instead, when taken up by cells, it is transferred to the nucleus, where it remains for a short period of time in an extrachromosomal state (6,20). Almost any vector and any cell line can be used for this type of transient transfection, and recombinant proteins can be synthesized as long as the vector contains a mammalian expression cassette. The onset of protein expression is rapid, but the yield depends not only on the regulatory elements in the vector but also on the transfection efficiency (i.e. how much DNA is taken into each cell) and the stability of the extrachromosomal DNA. Covalently closed circular plasmid DNA survives 12–48 h in many cell lines before it is degraded and diluted, allowing the transient expression of foreign genes from simple vectors lacking eukaryotic maintenance sequences. Some cell lines are renowned for the stability of transfected DNA, allowing survival and foreign gene expression for over 80 h. One example is the adenovirus-transformed human embryonic kidney line 293 (21). Covalently closed and supercoiled plasmid DNA is required for efficient transient transfection. Relaxed DNA (i.e. nicked circles or linear DNA) is a poor template for transcription and is prone to exonucleolytic degradation. Ideally, high quality plasmid DNA, prepared using either cesium chloride equilibrium density gradient ultracentrifugation or anion exchange chromatography, should be used for transient transfection.

14.5.3 Transient Transfection: Runaway Polyomavirus Replicons

The polyomaviruses are a genus of small DNA viruses from the papovavirus family. Each virion comprises a nonenveloped, icosahedral capsid and a circular double-stranded DNA genome of approximately 5 kbp. The best-characterized species is SV40, whose productive host range is limited to certain permissive monkey cells. SV40 was the first animal virus to be exploited as a vector because, like bacteriophage λ, it was considered a model system and its molecular biology was studied in great detail. The first SV40-based vectors were viral transduction vectors. Despite many successes, however, the use of such vectors has been severely curtailed by the limited capacity for foreign DNA (maximum insert size: 2.5 kbp), reflecting the small size of the capsid.

A breakthrough came with the discovery that plasmids containing a polyomavirus origin of replication were propagated in the same way as the virus genome, that is, as episomal replicons in permissive cells (22). Replication also requires the presence of a viral-encoded *trans*-acting regulator termed the *T-antigen*. However, as the polyomavirus replicon is not packaged into viral capsids, there is no effective limit to insert size. A number of polyomaviruses have been exploited to develop episomal vectors, including SV40 for monkey cells, murine polyomavirus for mouse cells, and BK virus for human cells. The related BPV has also been used. BK virus and BPV-derived replicons can be maintained episomally at a moderate copy number and allow long-term protein expression. The replication of SV40- and murine polyomavirus-derived vectors is uncontrolled. In permissive cells, with readily available T-antigen, such vectors can replicate to an astonishingly high copy number (up to 10^5 vector molecules per cell). This facilitates high level recombinant protein synthesis, making such host–vector systems among the most efficient available. Unfortunately, this prodigious replication and gene expression cannot be sustained by the host cell, and cell death occurs within a few days. SV40 and polyomavirus replicons are therefore suitable only for transient transfection because so much DNA is synthesized that the cell cannot survive.

In some polyomavirus vectors, the T-antigen coding sequence is included, enabling propagation in any permissive cell line. Other vectors lack the T-antigen, which must then be supplied in *trans*. The development of the COS cell line simplified the use of SV40-based vectors. This is a derivative of the African Green Monkey cell line CV-1, which is stably transformed with a partial SV40 genome (hence COS: CV-1, origin, SV40). The integrated SV40 origin is mutated and nonfunctional, but the early transcription unit is functional, allowing constitutive expression of the T-antigen. This can stimulate the replication of any SV40 replicon in the same nucleus, and therefore allows the episomal propagation of SV40 vectors lacking their own T-antigen transcription unit (22). A whole series of SV40-based expression vectors has been designed for use in COS cells, some also utilizing SV40 transcriptional regulatory elements, others containing heterologous elements (20). Cell lines have also been developed for the propagation of murine polyomavirus replicons, such as the mouse cell line MOP-8 (23). Some of the most versatile transient expression vectors contain both SV40 and murine polyomavirus origins (e.g. the pcDNA1 vector series). Notably, while the SV40 origin of replication may function only in certain permissive monkey cells, the promoter and enhancer sequences of this and other viruses are extremely promiscuous. SV40 replicons can therefore be used for transient transfection of any mammalian cell type, although protein yields are much lower than for monkey cells because there is

no episomal replication. In nonpermissive cells, SV40 DNA may also integrate into the genome resulting in stable transformation. Recently, it has been possible to generate permissive monkey cell lines stably transformed with episomal SV40-based vectors by using conditionally expressed or temperature-sensitive T-antigens, which have more moderate replication rates (24,25).

14.5.4 Reporter Genes in Transfection Analysis

Transient transfection is often used to study gene expression, function, and regulation in animal cells because it is rapid, repeatable, and simple to perform, allowing the comparative analysis of many different expression constructs simultaneously. The alternative strategy of producing cell lines for each construct is laborious and expensive. In addition, the integrated foreign DNA is subject to random position and dosage effects that may obscure the true relationship between different constructs. Following the introduction of foreign DNA into animal cells, it is possible to study gene expression directly, for example, by northern blot, nuclease protection, RT-PCR, immunological assay, or assay for protein activity. This strategy suffers several disadvantages, including the time-consuming assays, the requirement for gene-specific probes, and the fact that if the transfected gene is similar to an endogenous gene, it may be impossible to discriminate between them.

A reporter gene is a screenable marker gene, that is, a gene whose product is easily detected using a simple assay (7). Reporter genes are often used to detect and characterize gene regulatory elements by inserting the putative elements upstream of the marker in specialized regulatory probe vectors. The recombinant vectors are then introduced into one or more types of animal cell, and quantitative assays for the reporter molecule allow the experimenter indirectly to gauge the level of transcriptional activity conferred by the regulatory elements (26). Inducible regulatory elements can be tested for their response to particular stimuli by measuring the induction of reporter gene expression. Cell type or developmental specificity can be assayed by causing cells to differentiate *in vitro* or by testing reporter constructs in transgenic animals known as *reporter transgenics*. A common strategy is to generate a series of mutated versions of a given reporter construct to narrow down particular *cis*-acting motifs in regulatory elements. Upstream signaling events can also be studied, for example, by addressing the response of reporter genes to the perturbation of specific signaling pathways.

Reporter genes are not used only to analyze regulatory elements. By fusing a reporter gene to the coding region of a second foreign gene, a fusion protein may be generated that generally retains reporter activity. This can be used to study protein localization in the absence of a specific antibody or to simplify protein purification. One of the most important uses of reporter genes in transient transfection is to normalize data for transfection efficiency. The yield of protein obtained from a dish of transiently transfected cells is highly dependent on transfection efficiency, which can vary widely within an experiment according to the transfection method used. When comparing the activities of different constructs, it is necessary to discriminate between variation caused by genuine functional differences between constructs and that caused by fluctuations in transfection efficiency. A reporter gene hitched to a constitutive viral promoter can provide an excellent internal control.

There are many different reporter genes used in animal systems, each with specific advantages and disadvantages (Table 14.3) (27–36). Reporter molecules also differ greatly in their half-lives, an important consideration to study rapid inductive responses and longer term effects. General properties that make ideal reporter genes include the following:

- The availability of rapid, sensitive, and inexpensive product assays
- Minimal background activity
- The reporter assay should be quantitative and have a broad linear range to detect both major and minor differences in activity
- A small coding region, so that expression vectors and fusion proteins are a reasonable size
- The product should not be toxic or otherwise affect the host cell.

14.5.5 Stable Transfection Using Nonreplicating DNA

In stable transfection, transformed *cell lines* are produced, which can synthesize recombinant proteins on a long-term basis, lasting months to years. Stable transfection thus requires foreign DNA sequences to be maintained in the cell in such a manner that the cell can function normally (5,20,37). This can occur in two ways. First, foreign DNA may integrate into the genome, where it is maintained as a new chromosomal locus by endogenous DNA replication. Second, foreign DNA can be maintained episomally on a vector that replicates at a moderate rate and hence does not affect cell viability. In both the cases, transformed cells may be maintained under a selective regime, ensuring that the foreign DNA is still present.

The most popular strategy for generating stable cell lines is the integration of foreign DNA into the genome. This strategy does not require specialized vectors, as the integration mechanism involves illegitimate recombination, where any DNA sequence can serve as a substrate. A foreign gene that has integrated into the host genome is termed a *transgene*. Stable integration has been achieved with many different types of vector, including those with no eukaryotic maintenance sequences. Even linear foreign

TABLE 14.3. Properties of Genetic Reporter Systems Used in Animal Cells

Reporter gene (product)	Comments
lacZ (β-galactosidase) *Activity:* Catalyzes the hydrolysis of β-galactosides, for example, lactose and many specialized derivative substrates for different assay formats *Assays:* β-Galactosidase assays are nonisotopic. *In vitro* assay formats based on colorimetric (with substrate ONPG) or fluorometric (with substrate MUG) detection systems lack sensitivity, but chemiluminescent systems using 1,2-dioxetane derivatives are highly sensitive. High resolution *in vivo* histological assays are also available. The chromogenic substrate X-gal can be used for fixed tissue, and the fluorescent substrate FDG can be used for live cells *Advantages:* Versatile, sensitive and many assay formats available *Disadvantages:* Some mammalian cells have high endogenous β-galactosidase activity *Other comments:* β-Galactosidase is a stable protein *References:* 27, 28	*Source: E. coli*
cat (chloramphenicol acetyltransferase) *Activity:* Catalyzes the transfer of acetyl groups from acetyl coenzyme A to chloramphenicol *Assays: In vitro* assays are isotopic, involving chromatographic separation of acetylated and nonacetylated forms of ^{14}C-chloramphenicol. Such assays have low sensitivity and are expensive, but more recently developed immunological and fluorometric assays are better. *In vivo* CAT assays rarely used due to low resolution *Advantages:* Minimal background activity in mammalian cells *Disadvantages:* Low sensitivity, expense, reliance on isotopic assay format *Other comments:* CAT is a highly stable protein *Reference:* 29	*Source: E. coli* transposon Tn9
SEAP (secreted alkaline phosphatase) *Activity:* Removes phosphate groups from a variety of substrates *Assays:* Nonisotopic, sensitive *in vitro* assays using either colorimetric, fluorometric, or chemiluminescent formats to detect secreted protein. Not used for *in vivo* assays *Advantages:* Secreted protein can be assayed in growth medium without lysing cells, allowing multiple assays for the same culture and further manipulation of cells following assay *Disadvantages:* High endogenous levels of alkaline phosphatase in some mammalian cells (although SEAP is heat tolerant, allowing endogenous enzyme to be inactivated by heat treatment). Reporter system depends on correct function of the secretory pathway *References:* 30, 31	*Source:* Truncated form of human *PLAP*
luc (firefly luciferase) *Activity:* Light produced in the presence of luciferase, its substrate luciferin, oxygen, magnesium ions, and ATP *Assays:* Nonisotopic bioluminescent assays are used *in vitro* and *in vivo*. These are highly sensitive and can be performed in live cells, using lipophilic luciferin esters *Advantages:* Sensitive, minimal background activity in mammalian cells *Disadvantages:* Requires expensive detection equipment, some assay formats have limited reproducibility *Other comments:* Luciferase has a high turnover rate and is thus useful for the study of inducible systems *References:* 28, 32, 33	*Source:* The firefly *Photinus pyralis*
GFP (green fluorescent protein) *Activity:* Intrinsic ability to fluoresce under blue or UV light *Assays:* Nonisotopic. Used for *in vivo* assays in live animals. Allows monitoring of changes of gene expression in real time, and fusion GFPs allow protein sorting events to be followed *Advantages:* Intrinsic activity (no substrate requirements), sensitivity, use in live organisms *Disadvantages:* The signal from *A. victoria* GFP is not intense enough for some systems *Other comments:* Improved GFPs with stronger emission, and emission at different wavelengths, have been generated by mutation allowing multiple studies in a single cell *References:* 33–36	*Source:* The jellyfish *Aequorea victoria*

Abbreviations: ATP, adenosine **5′**-triphosphate; CAT, chloramphenicol acetyltransferase; FDG, fluorescein-di-**β**-D-galactopyranoside; GFP, green fluorescent protein; MUG, 4-methylumbelliferyl-**β**-D-galactoside; ONPG, ***o***-nitrophenyl-**β**-D-galactopyranoside; PLAP, human placental alkaline phosphatase; SEAP, secreted alkaline phosphatase; UV, ultraviolet; X-gal, 5-bromo-4-chloro-3-indolyl-**β**-D-galactopyranoside.

DNA fragments without a vector are suitable substrates for integration. In fact, in contrast to transient transfection, which is more efficient using supercoiled plasmids, the frequency of stable integration is increased using linear DNA because this is a better substrate for illegitimate recombination. The integration mechanism is extremely inefficient, that is, three to four orders of magnitude less efficient than transient transfection and viral gene transfer. Transformants are typically recovered at a frequency of 10^{-5} to 10^{-6}. For this reason, selectable markers must be used to identify and selectively propagate the rare, stably transformed cells.

Another important factor in stable transfection by integration is the random nature of the integration event. Typically, multiple copies of the transfected DNA integrate at a single donor site, following end-to-end ligation to form a transient low complexity structure termed a *transgenome*. Some transfection methods allow a degree of control over copy number (e.g. electroporation parameters can be set to favor single copy integration), while others, such as calcium phosphate-mediated transfection, are not controllable. The position of integration and the number of transgene copies integrated are therefore highly variable, and both can influence transgene expression. This results in varying expression levels between independently derived transformed clones, and the phenomenon of transgene silencing, where even cells with stably integrated and intact transgenes fail to express recombinant proteins.

14.5.6 Selectable Markers Used in Mammalian Cell Lines

Under some circumstances, the foreign DNA introduced into a cell may confer a phenotype that can itself be selected or used as a visible assay for stable transfection. This is unusual, however; so a selectable marker gene is normally introduced along with the nonselectable foreign DNA to allow transformed cells to be propagated under conditions where the high background of nontransformed cells will die. Initially, selectable markers were included on the same vector as the nonselectable foreign DNA, so that the two would cointegrate and selection for the marker would necessarily identify cells carrying the nonselectable gene of interest. However, it was shown that two discrete plasmids cotransfected into mammalian cells also resulted in a high frequency of *cotransformation* (i.e. where the initially unlinked genes were integrated together, usually at the same locus) (38). Typically, a 10:1 ratio of nonselectable to selectable vector is used, so that cells transformed with the marker are highly likely to be cotransformed with the nonselectable DNA. The markers are used to select founder cells that give rise to stably transformed cell lines. Cells are allowed to grow under the appropriate selective regime for about 10 generations. At this point, individual clones of surviving cells are isolated and used to found new lines.

The first selectable marker to be widely used was *Tk*, encoding the enzyme thymidine kinase (TK) (39). This is an *endogenous marker*; it is an activity already present in most mammalian cells, and therefore requires a tk^- cell background for positive selection. Like most endogenous markers, *Tk* encodes a nonessential enzyme involved in nucleotide biosynthesis. Such markers have been developed because there are two alternate nucleotide biosynthesis pathways in mammalian cells, allowing viable mutant cells for each pathway to be isolated and chemical inhibitors of each pathway to be identified. Under normal growth conditions, TK is not required because dTTP can be synthesized from carbamyl phosphate (the *de novo pathway*). However, if cells are grown in medium containing the inhibitor aminopterin, the de novo pathway is blocked and dTTP must be synthesized from thymine (the *salvage pathway*), which requires TK. Other endogenous markers are listed in Table 14.4, and their role in nucleotide biosynthesis is summarized in Fig. 14.3. The problem with such markers is that the number of cell types available for transfection is limited to those where appropriate mutant lines have been developed. Thus, although tk^- mutant cells are easily selected using 5-bromodeoxyuridine, there has been a drive to develop new markers that can be used in all mammalian cells.

Such *dominant selectable markers* (dominant because they are derived from an exogenous source and there is no competing activity in any mammalian cell) are often drug resistance genes of bacterial origin (3,6,20,37). Cells can be propagated in normal medium and then transformed cells can be positively selected by adding the drug at the appropriate concentration. Commonly used dominant selectable markers are listed in Table 14.4. One disadvantage of bacterial markers is that the concentration range over which the selective agents are active is narrow. These markers are not suitable for stepwise selection for increased transgene copy number. *In situ* transgene amplification is one way to overcome position effects and generate high yield transformed cell lines, but this requires markers that can be selected in a stepwise manner over a range of selective conditions (40,41). The predominant example of this type of *amplifiable marker* is *Dhfr*, which encodes the enzyme dihydrofolate reductase (DHFR). Increasing resistance to methotrexate, a competitive inhibitor of DHFR, usually correlates to increased *Dhfr* gene copy number and coamplification of the nonselected donor gene. Amplifiable markers are highly efficient, but *Dhfr* is endogenous, and the background of wild-type cells that express and amplify their wild-type *Dhfr* locus can be a problem. For this reason, such markers tend to be used in mutant cell lines, which again restricts the number of cell types available for transfection.

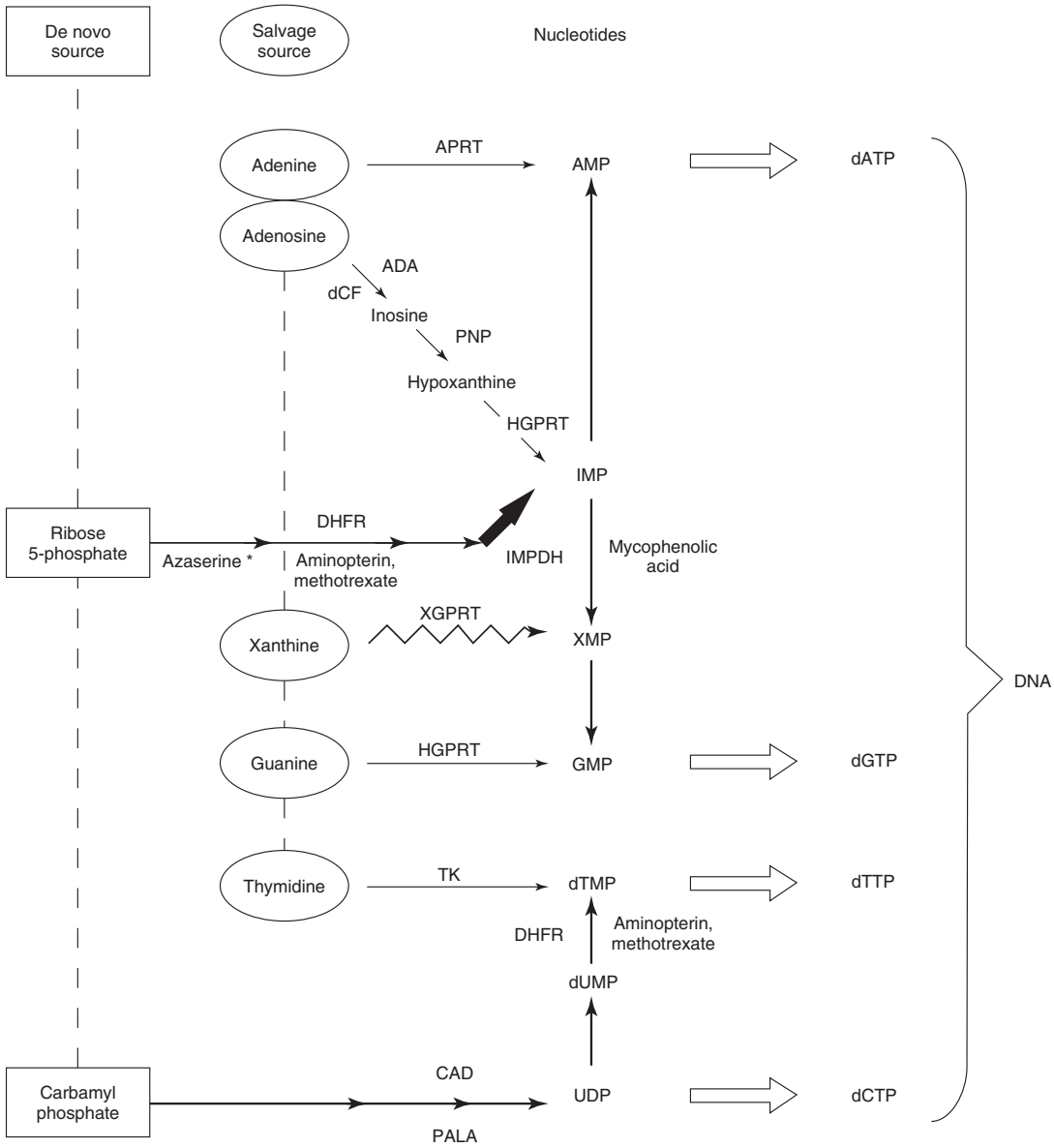


Figure 14.3. Nucleotide biosynthesis and commonly used endogenous selectable markers. De novo nucleotide synthesis (boxed precursors) follows the thick arrows. In the absence of d e novo substrates, or where the d e novo pathway is blocked, the cell can use pyrimidine and purine salvage pathways (circled precursors), following the thin arrows. Mammalian cells cannot convert xanthine to XMP, but this reaction is carried out by the *E. coli* enzyme XGPRT, encoded by the *gpt* gene, allowing this to be used as a dominant selectable marker in mammalian cells (zigzag arrow). The nucleotides are converted into dNTPs (open arrows) and incorporated into DNA. The salvage enzymes are not required for cell growth when d e novo substrates are available; so salvage pathway mutants are viable under normal growth conditions. However, if the d e novo pathway is blocked using any of the inhibitors (shown in bold), genes encoding salvage pathway enzymes can be used as selectable markers when salvage precursors are also provided. For example, *Tk* can be used to circumvent aminopterin-inhibited d e novo dTMP synthesis if the salvage precursor, thymidine, is included in the growth medium. Alternatively, d e novo and salvage inhibitors can be overcome by amplifiable selection, for example, PALA, an inhibitor of d e novo UDP synthesis, can be overcome by amplification of the *Cad* gene, and methotrexate, an inhibitor of several d e novo and salvage reactions, can be overcome by amplification of the *Dhfr* gene. Salvage pathway markers can also be counterselected using toxic base or nucleoside analogs. These are toxic when incorporated into DNA via the salvage pathway, but innocuous if nucleotides are synthesized d e novo. For example, 5-bromodeoxyuridine (bdUr) is a thymidine analog incorporated into DNA following conversion into a nucleotide by TK. In the absence of TK, bdUr is not phosphorylated and is not incorporated into DNA. Azaserine blocks several d e novo reactions, the most important of which is shown. Abbreviations of enzymes and inhibitors: APRT, adenine phosphoribosyltransferase; ADA, adenosine deaminase; CAD, carbamyl phosphate synthase/aspartate transcarbamoylase/dihydroorotase; dCF, deoxycoformycin; DHFR, dihydrofolate reaductase; HGPRT, hypoxanthine–guanine phosphoribosyltransferase; IMPDH, inosine monophosphate dehydrogenase; PALA, *N*-phosphonacetyl-L-aspartate; PNP, purine nucleoside phosphorylase; TK, thymidine kinase; XGPRT, xanthine–guanine phosphoribosyltransferase.

TABLE 14.4. Selectable Markers Used in Animal Cells: Endogenous Markers, Dominant Selectable Markers, and Amplifiable Markers (3,6,20,37,40,41)

Endogenous markers

These markers are involved in nonessential endogenous biosynthetic pathways. Most of the markers are enzymes involved in the nucleotide biosynthesis salvage pathway, and such markers can be used both for positive and negative selection. Positive selection is achieved using salvage pathway mutant cell lines in combination with drugs that block the de novo nucleotide biosynthesis pathway. Negative selection is achieved using toxic base analogs that are incorporated into DNA only if the salvage pathway is used. Alternative endogenous markers are expressed at a low level in animal cells and can be used for selection in the presence of a certain inhibitor. The endogenous functions of the markers and the activity of the inhibitors are summarized in Fig. 14.3

Marker	Product and function	Principles of selection
Ada	ADA; converts adenosine to inosine	Xyl-A (9-β-D-xylofuranosyl adenosine) is an adenosine analog, which is toxic if incorporated into DNA. ADA detoxifies Xyl-A added to the growth medium by converting it to Xyl-I, its inosine equivalent. There is a low background of ADA activity in most mammalian cells and 2′-deoxycoformycin, an ADA inhibitor, is therefore included in the selection medium
Aprt	Adenine phosphoriboyl-transferase; converts adenine to AMP	*Positive selection:* Adenine, and azaserine, to block de novo dATP synthesis, so only cells using salvage pathway survive *Negative selection:* Toxic adenine analogs (e.g. 2,6-diaminopurine) that are incorporated into DNA only in cells with APRT activity
Cad	Carbamyl phosphate synthase; aspartate transcarbamylase; dihydro-oroatase. These are the first three steps in de novo uridine biosynthesis	*Positive selection:* PALA (*N*-phosphonacetyl-L-aspartate) inhibits the aspartate transcarbamylase activity of CAD
Dhfr	DHFR; converts folate to dihydrofolate and then to tetrahydrofolate	*Positive selection:* DHFR is required for several reactions in de novo and salvage nucleotide/amino acid biosynthesis; hence, selection is carried out in nucleotide-free medium. However, *Dhfr* is typically used as an amplifiable marker with the inhibitor methotrexate (see third section of the table)
Hgprt	Hypoxanthine–guanine phosphoribosyl-transferase; converts hypoxanthine to IMP and guanine to GMP	*Positive selection:* Hypoxanthine and aminopterin, to block de novo IMP synthesis; so only cells using salvage pathway survive. Selected on HAT medium* *Negative selection:* Toxic guanine analogs (e.g. azaguanine) that are incorporated into DNA only if there is HGPRT activity in the cell
Tk	TK, converts thymidine to dTMP	*Positive selection:* Thymidine, and aminopterin to block de novo dTTP synthesis; so only cells using salvage pathway survive. Selected on HAT medium* *Negative selection:* Toxic thymidine analogs (e.g. 5-bromodeoxyuridine and ganciclovir) that are incorporated into DNA only if there is TK activity in the cell

Dominant selectable markers

These markers are derived from a different species and confer an alien drug resistance phenotype on the transfected cell

Marker	Product (and source species)	Principles of selection
AS	Asparagine synthase (*E. coli*)	Bacterial enzyme uses ammonia as amide donor unlike mammalian equivalent. Hence, cells transformed with *AS* grow on asparagine-free medium containing the toxic glutamine analog albizziin

(*continued*)

TABLE 14.4. (*Continued*)

ble	Glycopeptide-binding protein (*Streptoalloteichus hindustantus*)	Confers resistance to glycopeptide antibiotics bleomycin and pheomycin (and its derivative, Zeocin™)
gpt	Guanine–xanthine phosphoribosyltransferase (*E. coli*)	Analogous to *Hgprt* in mammals, but possesses additional xanthine phosphoribosyltransferase activity allowing survival in medium containing aminopterin and mycophenolic acid (Fig. 14.3)
hisD	Histidinol dehydrogenase (*Salmonella typhimurium*)	Confers resistance to histidinol
hpt	Hygromycin phosphotransferase (*E. coli*)	Confers resistance to hygromycin-B
neo	Neomycin phosphotransferase (*E. coli*)	Confers resistance to aminoglycoside antibiotics (e.g. neomycin, kanamycin, and G418)
pac	Puromycin *N*-acetyltransferase (*Streptomyces alboniger*)	Confers resistance to puromycin
trpB	Tryptophan synthesis (*E. coli*)	Confers resistance to indole
	Markers used for *in situ* gene amplification	
These markers can be amplified *in situ* by increasing the concentration of a competitive inhibitor in the medium. Many amplifiable markers are also used as endogenous or dominant selectable markers, but in some cases, the drug used for amplification may not be the same as that used for standard selection		
Marker	Product	Amplifying selective drug
Ada	ADA	Deoxycoformycin
AS	Asparagine synthase	β-Aspartylhydroxamate
Cad	Aspartate transcarbamylase	*N*-phosphonacetyl-L-aspartate
Dhfr	DHFR	Methotrexate
gpt	Xanthine–guanine phosphoribosyltransferase	Mycophenolic acid
GS	Glutamine synthase	Methionine sulfoxamine
Hgprt	Hypoxanthine–guanine phosphoriboosyltransferase	Aminopterin
Impdh	Inosine monophosphate dehydrogenase	Mycophenolic acid
Mt-1	Metallothionein 1	Cd^{2+}
M^{res}	Multidrug resistance: P-glycoprotein 170 gene	Adriamycin, colchicine, and others
Odc	Ornithine decarboxylase	Difluoromethylornithine
Rnr	Ribonucleotide reductase	Hydroxyurea
tk^-	TK	Aminopterin
Umps	Uridine monophosphate synthase	Pyrazofurin

14.5.7 Maximizing Transgene Expression by Gene Amplification

When cultured cells are exposed to toxic concentrations of certain drugs, rare individual cells survive because they happen to have undergone a mutation that confers drug resistance. The first such system to be investigated in detail was resistance to the folic acid analog methotrexate, which is a competitive inhibitor of DHFR (42). Resistant cells were shown to fall into three classes: those with reduced methotrexate uptake; those with point mutations in the *Dhfr* gene, making the enzyme less susceptible to inhibition; and those carrying multiple copies of the *Dhfr* locus, allowing the production of enough enzyme to out-compete the inhibitor. This latter class can be selected stepwise by successive increases in drug dosage, resulting in the propagation of clones with highly amplified *Dhfr* gene arrays and allowing cell growth in concentrations of methotrexate up to 10^5 times greater than the dose lethal to wild-type cells. The amplified copies may be maintained as large intrachromosomal tandem repeat units known as *homogeneously staining regions* (HSRs) or as small extra chromosomes termed *double minutes*. The drug does not *induce* gene amplification but facilitates the selection of rare cells that have undergone random amplification.

Cloned copies of the *Dhfr* gene and its cDNA, reintroduced into cells by transfection and randomly integrated into the genome, are also amplified by drug selection. However, it is not just the essential coding region that is amplified. Extensive flanking sequences of up to 10^6 bp of DNA may be coamplified. This amplification of nonselected flanking material can be exploited in gene transfer experiments. Vectors have been constructed in which a gene such as *Dhfr* is included adjacent to the

multiple cloning site where the nonselectable foreign gene is inserted. The stable transfection of this construct allows tandem cointegration of the amplifiable marker and the nonselected gene. Alternatively, the *Dhfr* vector can be cotransfected with a second vector carrying nonselectable foreign DNA. Cotransfected vectors tend to cointegrate at the same locus. Cointegration is followed by a regime of intensifying drug selection, resulting in the propagation of cells containing highly amplified arrays of both the marker and nonselected transgenes (40,41).

This strategy facilitates high level recombinant protein synthesis and can overcome position-dependent transgene silencing because amplification can continue until there are so many transgene copies that the amount of mRNA synthesized is no longer the limiting factor for protein expression. Alternatively, a specific regime of drug treatment can be used to select for transformants where the transgene is not subject to negative position effects. However, because *Dhfr* is an endogenous marker, drug selection can amplify the endogenous *Dhfr* gene as well as transfected copies. *Dhfr* is therefore most advantageous when used in a $dhfr^-$ cell line, so that nontransfected cells are not coselected on the basis of endogenous gene amplification. Several derivatives of the Chinese hamster ovary (CHO) cell line have been described that lack DHFR activity. These include DUKX-B11 (DXB-11), which has one active *Dhfr* gene (43), and DG44, which is a homozygous null cell line (44). Two strategies have been used to extend the range of cell lines available for DHFR selection. First, a mutant form of the *Dhfr* gene, which is highly resistant to methotrexate, can be used to select for methotrexate resistance even in cells carrying two normal copies of the normal *Dhfr* gene. However, the level of amplification is restricted because large doses of methotrexate are required to inhibit the endogenous genes. Second, the *Dhfr* marker can be cotransfected with a dominant selectable marker such as *neo*. Thus, cells can be treated with increasing concentrations of methotrexate, and also selected with constant levels of G418, to counterselect wild-type cells (which would otherwise survive through amplification of the endogenous *Dhfr* gene). *Dhfr* was the first selectable marker to be used for amplification and remains the most popular. Other markers (Table 14.4) have also been used, but they suffer from the prevalence of nonamplified resistance mutants or cytotoxicity at high drug concentrations. Only glutamine synthase has been used as frequently as *Dhfr*.

14.5.8 Stable Transfection Using Episomally Maintained Vectors

Replicating, extrachromosomal vectors for stable transfection possess a number of distinct advantages over integrating vectors. First, recombinant proteins are expressed at a moderate level, which is uniform among independently derived clonal lines. This is because there are no position effects (the construct does not integrate) and no dosage effects (the plasmid reaches a stable episomal copy number, regardless of initial transfection efficiency). Second, stable transfection by episomal maintenance is equivalent in efficiency to transient transfection, that is, up to 10^5 times more efficient than stable transfection by integration. Finally, because the vectors are episomal, they can be separated easily from chromosomal DNA: This is particularly advantageous in techniques such as expression cloning, which rely on the recovery of cloned DNA. While nonreplicating plasmids suffice for stable transfection by integration, episomal plasmids require maintenance sequences derived from viruses whose genomes are also maintained episomally. In addition to SV-40-derived vectors, three other viruses that have been widely exploited to construct episomal vectors are BPV, BK virus (a human polyomavirus), and EBV.

The papovavirus family includes the polyomavirus and papillomavirus genera. SV40 and the related murine polyomavirus have been used to develop a range of transient expression vectors that replicate to high copy number and eventually cause cell death. The human BK polyomavirus is stably maintained at a moderate copy number (approximately 500 copies per cell) in human cells. Plasmid vectors carrying the BK virus origin of replication are maintained as long as the BK virus T-antigen is available, and cell lines stably transformed with such vectors have been continuously propagated for over a year (45). BK virus-derived replicons contain a selectable marker (e.g. *neo*) as well as plasmid backbone sequences, BK virus functions, and the mammalian transcription unit. This allows high level recombinant protein expression to be achieved by increasing the drug concentration in the medium and hence selecting for increased copy number. In this way, stable cell lines carrying up to 9000 copies of the vector can be generated, although the copy number falls when selection is removed. This vector system is extremely versatile: Variants have been described with different promoters and selectable markers, and a number of different host cell lines have been used, including HeLa, COS-7, and 293 (45,46).

The papillomaviruses are related to the polyomaviruses but possess larger, more complex genomes and encode proteins on only one DNA strand. They infect higher vertebrates, including man, and cause benign growths called *papillomas* or *warts*. BPV can infect cultured mouse cells but cannot produce progeny virions. Instead, 50–100 copies of the genome are maintained episomally as plasmids, and it is this property that has been exploited to develop a series of episomal expression vectors. Like SV40 and other polyomaviruses, the early functions of BPV cause growth transformation. The earliest BPV-derived vectors therefore comprised the entire BPV genome cloned in a bacterial plasmid with a mammalian expression

cassette, and transfected cells were identified by their transformation to a continuously proliferative state. The early functions are carried on a 5.5-kbp sector of the BPV genome, which is termed the 69% transforming fragment (BPV_{69T}), and this appears to be sufficient for establishment and maintenance of the episomal state (47). This fragment forms the basis of a more versatile series of expression vectors that also contain a mammalian selectable marker to extend the range of possible host cells (48). The ability of BPV_{69T} vectors to replicate efficiently is increased in some cells by certain mammalian genomic sequences, which are included in the BV-1 vector series (49). BPV vectors can establish long-term, moderate-level foreign gene expression in a broad range of mammalian cell types, such as 3T3 and C127 fibroblasts. There is no limit to insert size, allowing both cDNAs and full genes to be expressed. However, BPV vectors suffer from several limitations. First, although the viral genome is small in comparison to, for example, herpes virus or vaccinia virus, it is still too large (>10 kbp) to manipulate easily *in vitro* and lacks the cloning versatility of other plasmids. Second, there are problems with vector stability (50). Recombinant vectors may undergo recombination or deletion, resulting in the loss of foreign DNA, and in certain cell lines, the vector may integrate into the genome. Recombination between vectors can occur, so that either single plasmids or oligomers may be propagated. These effects are largely unpredictable, depending on multiple parameters such as cell line, vector type, and insert structure. The same parameters also affect replication efficiency; so the episomal copy number may vary from 20 plasmids per cell to over 300 copies.

Due to the instability of BPV replicons, many researchers have turned to EBV as an episomal expression vector (51). EBV is a human herpes virus whose productive host range is limited to primates and a few other mammals (e.g. dogs). The virus is naturally lymphotropic and commonly infects B cells, causing infectious mononucleosis. The virus has a large, double-stranded linear DNA genome that circularizes shortly after penetration by interaction between terminal repeat sequences. In culture, the virus can cause lytic infection, resulting in cell death, but most infected cells are transformed into a proliferative state and the virus genome is maintained as a latent, episomally replicating plasmid, with a copy number under 1000. Although the tropism of the virus is limited by its interaction with a specific receptor found on very few cell types, the circular EBV genome is maintained in many primate cells and thus shows great potential as a broad cellular host-range expression vector. However, the species host range is still limited to primate and dog cells—rodent cell lines are not permissive for episomal EBV replication. Only two regions of the EBV genome are essential for the establishment and maintenance of latent replication: the bipartite origin of replication *oriP* and the gene encoding the *trans*-acting regulator of transcription and replication, EBV nuclear antigen-1 (*EBNA-1*). These sequences form the basis of EBV latent expression vectors, which are maintained at a copy number of 2–50 per cell. A distinct origin, *ori*Lyt, and a different regulator termed *ZEBRA* are required for lytic replication, thus *oriP*/EBNA-1 vectors do not amplify in cells undergoing lytic EBV infection. Recently developed EBV vectors containing both origins can be maintained as low copy-number vectors in latently infected B-cell lines and amplified approximately 500-fold when cells are transfected with constitutively expressed *BZLF-1* (the ZEBRA gene) to induce lytic replication. EBV vectors may contain *oriP* only (in which case EBNA-1 must be supplied in *trans*) or both *oriP* and the EBNA-1 coding region driven by a mammalian promoter (in which case the vectors are helper independent). EBV vectors must also carry a selectable marker, because (i) transformation efficiency is still <10%, and (ii) in the absence of selection, both *oriP* and *oriP*/EBNA-1 vectors are passively lost at the rate of 2–6% of cells per generation. A number of markers have been successfully used, including *Tk, neo*, and *gpt*. Many foreign genes have been successfully expressed using EBV vectors, including those encoding enzymes, growth factors and receptors, structural proteins, and heterologous viral proteins (51). EBV replicons can be recovered intact from mammalian cells, facilitating their use for expression cloning. The EBO series of vectors has been designed for this purpose (52). Furthermore, because of their large capacity, the inclusion of bacteriophage λ cohesive end (*cos*) sites allows such vectors to be maintained in *E. coli* as cosmids (53). The most recent advance in EBV-replicon technology is the development of EBV vectors as human artificial episomal chromosomes. Such vectors represent one of a number of strategies for the design of MACs and can carry up to 350 kbp of genomic DNA (54).

14.6 TRANSFECTION METHODS

14.6.1 Overview

Forcing animal cells to take up DNA from the surrounding medium using a variety of chemical and physical methods is termed *transfection* and can be a highly efficient way to introduce DNA either transiently or stably into cultured cells or cells *in vivo*. When the term *transformation* is applied to animal cells, it usually refers to a stable change in genotype brought about either by incorporation of the transfected DNA into the genome or by its long-term episomal maintenance. However, the same term is also used to indicate *oncogenic* transformation (growth transformation), the change in phenotype resulting from the activation of an oncogene, causing, for example, loss of substrate

dependence, uncontrolled proliferation in the absence of growth factors, and abnormal differentiation.

When DNA transfer to cultured animal cells was first demonstrated (1), the uptake mechanism was unknown. Later it was shown to depend on the formation of a calcium phosphate–DNA coprecipitate, and this was the first of many "chemical transfection" techniques to be described, where cells take up DNA complexed with another molecule by endocytosis. Generally, these techniques result in a significant frequency of transgene mutation due to passage of the DNA through acidic endosomes. Over the years, a number of alternative transfection strategies have been devised (6,20,55) (Fig. 14.4). *Fusion transfection* involves cells taking up DNA by fusion with a natural or artificial lipid membrane containing foreign DNA. *Poration transfection* involves the creation of small pores in the cell membrane through which DNA can be imported. *Physical transfection* involves a mechanical breach of the cell membrane and the direct delivery of DNA either to the cytoplasm or nucleus. All these mechanisms result in direct delivery and avoid endosomal processing of the DNA. By conjugating DNA to a suitable ligand, it can be introduced into specific cell types by receptor-mediated endocytosis (this strategy is particularly applicable for cell targeting in gene therapy). These different transfection mechanisms are summarized in Table 14.5.

The transfection of animal cells in culture is dependent on many parameters such as the quality of the foreign DNA and the health of the target cells. Other parameters are cell-type specific; thus, different cells are transfected with differing efficiencies, and not all cells respond to the same transfection methods. Primary cells are particularly resilient to transfection, using standard methods. Cells that grow as monolayers are easier to transfect than those growing in suspension or as clumps, and quiescent or postmitotic cells are more recalcitrant than rapidly dividing cells. The efficiency of chemical transfection often depends on the composition of the growth medium; the presence of serum tends to inhibit transfection using cationic lipid preparations. Chemical transfection in particular tends to have the most adverse effects. Some cells are badly affected by calcium phosphate transfection because they respond poorly to the precipitate adhering to their surfaces. Conversely, cationic lipids appear to be better tolerated and are suitable for many cells traditionally regarded as difficult to transfect. Transformation protocols have been optimized for the major cell lines used for recombinant protein expression (e.g. CHO, COS-7, HEK 293, and Sf9). Unfortunately, cell lines for transfection cannot always be chosen purely for the ease of DNA transfer. The choice is often made according to other properties, such as the ability of cells to express certain proteins or to use specific regulatory elements efficiently, the ability of cells to differentiate or respond to particular inductive treatments, or because a particular form of posttranslational modification is carried out. Therefore, the first step in a transfection strategy is often to optimize transfection efficiency using a range of protocols and testing the parameters within each transfection method.

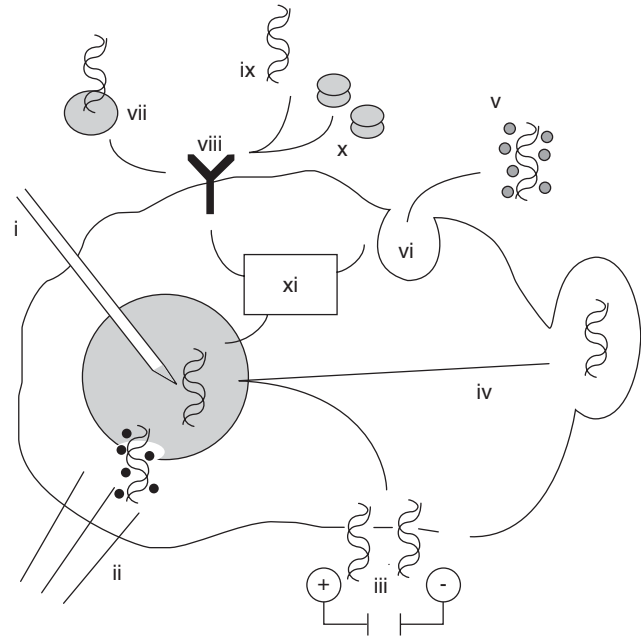


Figure 14.4. Transfection of animal cells and routes to the nucleus. Microinjection (i) or particle bombardment (ii) facilitate the direct delivery of DNA to either the nucleus or cytoplasm. Electroporation (iii) or fusion transfection (e.g. protoplast fusion, liposome fusion (iv)) result in the delivery of DNA to the cytoplasm, and its subsequent transfer to the nucleus. Chemical transfection (v) results in the uptake of DNA–chemical complexes by endocytosis (vi). Ligand-conjugated DNA (vii) is taken up by receptor-mediated endocytosis (viii), which is also thought to be the case for naked DNA (ix) having first interacted with unknown extracellular proteins (x). Following endocytosis, the DNA is transferred to the nucleus through the endosomal pathway (xi). This delivery mechanism is made more efficient using adenoviral capsid proteins, which cause endosomal disruption.

14.6.2 Locally Applied Naked DNA

Naked DNA transfects cultured cells very inefficiently when added to the growth medium, due both to degradation and poor internalization. Similarly, uncomplexed DNA administered intravenously to live animals is rapidly degraded following hepatic uptake (56). The injection of uncomplexed plasmid DNA *in vivo* into muscle results in high efficiency gene transfer and expression (57). This can be exploited to raise a protective immune response against viral and other pathogenic antigens and against tumor proteins (58). The application of naked DNA to other tissues has also resulted in successful transfection (59). DNA has also been injected into the blastocoel cavity of

TABLE 14.5. Properties of the Major Categories of Transfection Methods Used to Introduce DNA into Animal Cells

Category[3]	Examples	Method of Uptake	Route	Transgene Structure
Chemical	Calcium phosphate, DEAE–dextran, polybrene, lipofection	Endocytosis of DNA complexes	Via endosome	Multiple arrays[4]
Poration	Electroporation, laser transfection	Diffusion through transient pores in cell membrane	Directly into cytoplasm	Single transgenes or multiple arrays; highly controllable
Fusion	Liposome/virosome delivery, protoplast fusion	Fusion of DNA-containing lipid vesicle with cell membrane	Directly into cytoplasm	Multiple arrays
Physical	Particle bombardment, microinjection	Mechanical direct transfer of DNA into cell	Directly into cytoplasm or nucleus	Multiple arrays
Receptor mediated	Conjugation to various ligands, naked DNA transfection?	Receptor-mediated endocytosis	Via endosome	?

Note that some methods are suitable for both transient and stable transfection (e.g. calcium phosphate transfection and lipofection), whereas others tend to favor transient transfection (e.g. DEAE–dextran transfection and protoplast fusion) and others tend to favor stable transfection (e.g. nuclear microinjection).

Transgene structure following chemical transfection is dependent on method. Calcium phosphate generates large random arrays if there is carrier DNA, but smaller, concatemeric arrays are generated by other methods. For more details, see the section on Fate of Foreign DNA and Structure of the Transgenome.

mouse embryos, resulting in the generation of transgenic mice, albeit with much lower efficiency than pronuclear microinjection. The mechanism by which naked DNA is taken into muscle cells is entirely unknown. It is thought that the extracellular DNA may become coated with certain extracellular proteins and that these may facilitate receptor-mediated endocytosis.

14.6.3 Calcium Phosphate

Calcium phosphate transfection was first used in 1973 to introduce adenovirus DNA into mammalian cells (60). The first mammalian cell lines stably transfected with nonviral DNA were also produced using this technique (61). Calcium phosphate transfection is probably still the most widely used gene transfer technique because it is inexpensive, highly repeatable, and suitable for both the transient and stable transfection of a wide range of cells (62,63). In transient calcium phosphate-mediated cotransfection, the molar ratio of different plasmids used in the transfection mix appears to be faithfully reproduced in the transfected cell population (64).

There are many variations in the original technique, but all involve mixing DNA, a HEPES-buffered phosphate solution, and calcium chloride, resulting in the immediate formation of a fine DNA/calcium phosphate coprecipitate. This settles onto the cells and is internalized by endocytosis resulting in the transfer of calcium phosphate–DNA complexes to the nucleus (65).

Calcium phosphate transfection is particularly suitable for cells that grow as monolayers, as opposed to cells growing as clumps or in suspension. An alternative technique, using a BES buffer, which allows the precipitate to form gradually over several hours, is up to 100-fold more efficient for stable transfection with high quality plasmid DNA, although equivalent in efficiency to the original HEPES-buffered method for transient transfection or for stable transfection with linear DNA (66,67). The efficiency of transient transfection using the original method may be enhanced by chemical shock; however, this does not increase the efficiency of the BES-buffered method.

14.6.4 Diethylaminoethyl–Dextran

A major disadvantage of the calcium phosphate transfection technique is that certain cell lines are adversely affected by the precipitate, resulting in cell death. A mixture of DNA and diethylaminoethyl (DEAE)–dextran, a *soluble* polycationic carbohydrate, allows the transfection of many cells that respond poorly to calcium phosphate–DNA coprecipitates. The DEAE–dextran technique was originally devised to facilitate the transfer of viral DNA into animal cells and was later adapted as a plasmid transfection method (66,67). DEAE–dextran transfection protocols are based on improved strategies (68,69), which include chemical shock treatments to increase the efficiency of DNA uptake. The DEAE–dextran technique is highly reproducible and simple to carry out. DNA is mixed with 10 mg/mL of DEAE–dextran and added to the cells. The mixture is presumed to contain complexes that

increase the efficiency of endocytosis, and compared with calcium phosphate transfection, a much smaller amount of DNA is required. Plasmid DNA introduced into cells by DEAE–dextran adopts the nucleosome structure typical of endogenous chromosomes, whereas most of the estimated 1 Mbp of DNA entering cells as calcium phosphate coprecipitates remains in an aggregated form (70). Less DNA is introduced into cells using DEAE–dextran, this method is useful only for transient transfection, not for the generation of stably transfected cell lines.

14.6.5 Enhancing Transient Transfection Efficiency

In some transient transfection systems, cotransfection with a plasmid carrying the RNA polymerase III-dependent adenoviral VA_I gene results in an increased efficiency of foreign gene expression (71). VA_I is thought to act at the level of protein synthesis by restoring the activity of the host translational initiation factor eIF2. This factor is inhibited by a protein kinase activated in the presence of double-stranded RNA (dsRNA), which can sometimes arise from dual-strand transcription of transfected plasmid DNA. The adenoviral VA_I gene product is an RNA molecule that specifically interacts with and represses this kinase, the dsRNA-activated inhibitory protein kinase (DAI kinase), and is used to stimulate viral protein synthesis during adenovirus infections. Vectors carrying the adenoviral VA genes are commercially available (e.g. pAdVAntage).

A number of chemical treatments have also been described, which enhance the efficiency of transient transfection. A commonly used procedure is to expose cells to an osmotic shock following transfection, which increases the amount of DNA taken up from the surrounding medium. The shock involves brief exposure of transfected cells to 10–30% solutions of glycerol or dimethylsulfate (68,69). As with other transfection parameters, the optimal concentration and exposure time must be determined empirically. Another transfection enhancer is chloroquine, which inhibits acidification of endosomal vesicles and thus probably protects DNA from degradation (72). Chloroquine is moderately cytotoxic, however, and cells may be exposed to this chemical either during or after transfection, but only for a few hours. Sodium butyrate is also used to increase transfection efficiencies and may be used in conjunction with an osmotic shock (73). The treatment involves adding sodium butyrate (final concentration 10 m*M*) to the growth medium after the shock, leaving cells in contact with it for 24 h.

14.6.6 Electroporation and Laser Transfection

Electroporation is the transfection of cells in culture by exposing them to a transient electric field. This causes nanometer-sized pores to open briefly in the cell membrane, allowing uptake of free DNA from the surrounding medium. This method is ideal for many cells recalcitrant to chemical transfection methods. It is efficient, highly reproducible, and suitable for both stable and transient transfection and has the added advantage that transgene copy number can be controlled (74). Electroporated DNA is transferred directly into the cytoplasm without processing through endocytotic vesicles (75), and the frequency of mutation is much lower than that for chemical transfection methods (76). Electroporation is applicable to most cell types, and once optimal conditions have been determined, it is a very simple procedure—cells are suspended in electroporation buffer in a cuvette and exposed to a brief, high voltage electrical pulse. The exact magnitude and duration of the pulse are the critical parameters, and these must be determined empirically for different cells. Many cells are efficiently electroporated by a brief high voltage pulse (800–1500 V), but others, especially primary cells, may be killed by such treatment and respond better to a longer lasting pulse of 100–300 V. The highest transfection efficiencies typically occur when there is about 50% cell death. The technique was first carried out in 1982 using mouse fibroblasts (77) but was soon adapted to many other cell types (78). Among the few disadvantages of this technique are the requirement for specialized capacitor discharge equipment capable of accurately controlling pulse length and voltage, and the requirement for larger numbers of cells and higher DNA concentrations than that for other procedures (79,80).

Another transfection technology, which has not become widely used, is transfection following laser treatment (81). This technique has been grouped with electroporation because it involves a similar DNA uptake mechanism. Free DNA is taken up directly from the surrounding medium through transient pores created by a finely focused laser beam. Like microinjection, this strategy can be applied only to a small number of cells at a time, but with optimal DNA concentration can result in stable transfection frequencies of $>0.5\%$.

14.6.7 Liposomes, Virosomes, and Lipofection

Gene transfer mediated by liposomes was first described in 1980 (82). *Liposomes* are unilaminar phospholipid vesicles into which DNA can be packaged. When mixed with cells in culture, the vesicles fuse with the cell membrane and deliver DNA directly into the cytoplasm (83). The original liposome transfection techniques were no more efficient than calcium phosphate transfection and suffered the further disadvantage that the preparation of DNA-containing liposomes was complicated and labor intensive. One particular advantage of the method, however, was the ability to transform cells *in vivo* by injecting liposomes into

the bloodstream (84). The efficiency of liposome-mediated gene transfer can be enhanced by incorporating viral proteins that facilitate the active fusion between viral envelopes and cell membranes. Such fusogenic particles have been termed *virosomes*. Virosomes have been prepared from the envelopes of Sendai virus allowing the delivery of DNA to astroglial cultures (85).

A breakthrough came with the development of cationic/neutral lipid mixtures, which spontaneously associate with negatively charged DNA to form complexes (86). Residual positive charge in the complexes then interacts with negatively charged molecules on the cell surface, causing the DNA to be internalized. Technically, this is one of the simplest transfection protocols. Lipid–DNA complexes are prepared by mixing DNA with the lipid preparation in serum-free medium, then the mixture is added to the cells. This facilitates rapid and efficient DNA uptake and is gentle enough to be applicable to both conventional plasmid vectors and YACs (11). The uptake mechanism was originally thought to be similar to liposome fusion (86), but more recent experiments suggest that endocytosis of DNA–lipid complexes occurs (87,88). *Lipofection*, as this technique has become known, is highly reproducible and extremely efficient for both transient and stable transfection. It allows up to 90% of cells in culture to be transiently transfected and demonstrates stable transfection efficiencies up to 20-fold greater than standard chemical transfection methods. One drawback to this approach is that the lipids are very expensive. There are now many different lipid preparations available (89).

14.6.8 Polybrene-Mediated Transfection

Another polycationic chemical, the detergent polybrene, has been used to mediate the transfection of certain cell lines, for example, CHO cells, which resist transfection by calcium phosphate (90). Like DEAE–dextran, polybrene is soluble and may form complexes with DNA to facilitate uptake by endocytosis. For other cell lines, polybrene has been shown to be no more efficient than calcium phosphate as a transfection mediator, and it has not gained widespread use.

14.6.9 Cell or Protoplast Fusion

Polyethylene glycol (PEG) acts as a fusogen causing cell membranes to fuse together. This can be exploited to transfect animal cells by mixing them with other cells containing large amounts of plasmid DNA. Schaffner first successfully used bacterial protoplasts to transfect mammalian cells in culture by treating bacterial cells with chloramphenicol to amplify the plasmid DNA content and lysozyme to remove the cell wall. The protoplasts were then centrifuged onto a layer of mammalian cells and induced to fuse with them, thus delivering the DNA directly into the cytoplasm (91). This is a highly efficient method for transient transfection, but poor for stable transfection and cotransfection. Some investigators have used the hemoglobin-free ghosts of erythrocytes for gene delivery (92). In both the cases, the complexities involved in preparing and delivering the donor cells have hindered the widespread adoption of the method. However, the technique is gentle, allowing it to be applied to the transfection of ES cells with fragile YAC vectors and human chromosome fragments. For YAC delivery, yeast spheroplasts containing recombinant YAC vectors are induced to fuse with ES cells in culture, facilitating the introduction of YAC vector DNA and the eventual generation of YAC transgenic mice. One drawback to this method of YAC transfection is that all the endogenous yeast chromosomes are also introduced into the mouse cells, and these may have unpredictable effects (11). The largest DNA molecules currently transferred to mouse cells are human chromosome fragments, a process involving microcell-mediated gene transfer (93).

14.6.10 Microinjection

The direct microinjection of DNA into the cytoplasm or nuclei of cultured cells is sometimes used as a transfection method, but although highly efficient on an individual cell basis, this procedure is time consuming, and only a small number of cells can be treated. Originally, this technique was used for the transformation of cells that were resistant to any other method of transfection (94). Stable transfection efficiencies are extremely high, in the order of 20%, and very small quantities of DNA are sufficient. Another major advantage of this technique is that direct nuclear delivery avoids exposing the foreign DNA to any cytoplasmic organelle; so it is delivered intact. Microinjected DNA therefore suffers less mutation than DNA delivered by most chemical transfection methods. The most significant use of microinjection is the introduction of DNA into the oocytes and eggs of animals, either for transient expression analysis or to generate transgenic animals. It is suitable for the introduction of YAC vectors into the pronuclei of fertilized mouse eggs, but because DNA delivered in this manner must be very pure, painstaking preparation of the DNA must be carried out to avoid fragmentation. Shearing can also occur in the delivery needle, and YAC DNA is often protected by dissolving it in a high salt buffer and/or mixing it with polyamines.

14.6.11 Particle Bombardment

Particle bombardment (also known as *microballistic* or *microprojectile transfection*) is a relatively recent addition to the range of transfection techniques available to scientists working with animal cells. The procedure

involves coating micrometer-sized gold or tungsten particles with DNA and then accelerating the particles into cells or tissues using a blast of high pressure helium gas or an electrical discharge. The size and total mass of the particles and the force of the bombardment are important parameters that balance efficient penetration against cell damage. The technique was developed for the transformation of maize (95) and is now a method of choice for generating transgenic cereal plants. For animal cells, the technique has been less widely used. The technique has found a role in the transfection of whole organs and tissue slices (96,97) and more recently for the transfer of DNA to surface organs in gene therapy (98). In a variation of the technique, Vahlsing et al. (99) have used a pneumatic gun to drive DNA *solutions* through skin and into muscle. This technique, which is much less efficient than the traditional injection route to *in vivo* muscle transfection, has nevertheless allowed the robust expression of several viral and bacterial antigens, resulting in a particular immune response.

14.6.12 Receptor-Mediated Transfection

A recent development in transfection technology, suitable for gene therapy applications, is the delivery of DNA to particular cells by conjugation to a specific ligand. The ligand interacts with receptors on the cell surface, allowing both it and the attached DNA to be internalized. This strategy was first used to deliver plasmid DNA to liver cells by targeting the liver-specific asialoglycoprotein receptor (100). Plasmid DNA was conjugated to the ligand, asialoorosomucoid protein, using a polylysine bridge. The conjugate was added to cultured cells, and plasmid reporter gene activity was observed in liver cells but not other cell types. Since then, many similar experiments have been performed, and the efficient receptor-mediated transfection of many cell types using various ligands has been reported (58). One problem associated with this technique is that the ligand–DNA complexes are internalized via endocytotic vesicles that generally fuse with lysosomes, resulting in degradation of the DNA and consequent failure of gene expression. Some DNA escapes this fate and finds its way to the nucleus to be expressed. A >1000-fold enhancement of gene expression occurs if the ligand–DNA complexes are joined to adenoviral particles, which are known to disrupt endosomes as part of their infection strategy (101). More recently, adenovirus-derived peptides have been used for the same purpose, because these are less toxic and are less likely to provoke an immune response after *in vivo* delivery. Receptor-mediated transfection is highly efficient in cell culture, resulting in the transfection of up to 90% of cells carrying the appropriate receptor. Less success has been observed for *in vivo* gene transfer, partly because the ligand–DNA complexes are degraded in serum and partly because the size of the particles appears to be a critical parameter for the transfection of different cell types. The attachment of peptides to DNA molecules can serve other purposes in gene delivery. Recently, plasmid DNA has been conjugated to the SV40 T-antigen nuclear localization signal (102), resulting in the accumulation of transfected DNA in the nucleus.

14.7 VIRAL EXPRESSION VECTORS

14.7.1 General Properties

Viruses are natural gene delivery vehicles; so it was inevitable that they should be exploited as vectors for DNA transfer to animal cells, which reflects seven advantageous characteristics of animal viruses:

- They have evolved efficient mechanisms to adsorb to the surface of and gain entry into cells without damaging them.
- They deliver their nucleic acid intact because it is initially packaged in a proteinaceous capsule.
- They tend to block host cell protein synthesis to favor the expression of viral genes (including transduced foreign genes), which simplifies the recovery of recombinant proteins.
- Viral genomes contain strong and promiscuous regulatory elements that drive high level foreign gene expression.
- Many animal viruses have a broad host range and can thus replicate in diverse cell types from a large number of species.
- During lytic infection, viruses replicate to a high copy number and hence facilitate amplification of any foreign gene they carry.
- Many viruses can stably transform cells by integration or latent episomal replication, becoming quiescent in the process and allowing the production of cell lines. The integrated form of a viral genome is a *provirus*.

Many animal viruses have been exploited as vectors, mostly for foreign gene expression in cultured cells, but more recently as gene therapy vectors both *in vitro* and *in vivo*. Four classes of viral vectors—adenovirus, adeno-associated virus (AAV), herpes simplex virus (HSV), and retrovirus—have been used in phase 1 clinical gene therapy trials (103).

Foreign genes inserted into a viral genome are termed *transgenes*. There are three strategies for the incorporation of foreign genes into viral genomes. In two of these strategies, the resulting virus is known as *helper independent* or *replication competent*, meaning that the recombinant virus is able to propagate, even though it carries foreign DNA.

First, foreign DNA can be *added* to the entire viral genome without loss of viral genomic sequences. Vectors designed on this principle are termed *insertion vectors*, and typically, the foreign DNA is inserted between functional viral genes or at the edge of a linear genome. Second, foreign DNA can be used to replace a nonessential viral gene (nonessential, at least, for productive infection in cell culture). Vectors designed on this principle are termed *replacement vectors*, and the wild-type viral DNA fragment that is replaced is termed the *stuffer fragment*. The third strategy also involves replacement, but in this case, one or more *essential* viral genes are replaced with foreign DNA. This renders the recombinant vector *helper dependent* or *replication defective* and missing essential functions must be supplied in *trans*.

Helper-dependent vectors are especially important for gene therapy applications because an obligatory viral infection accompanying gene transfer would be extremely undesirable. The *trans*-functions may be supplied (i) using a *helper virus* (a virus carrying the essential functions, which is cointroduced with the vector) or (ii) using a helper plasmid, which is transfected into the cells infected by the vector. Alternatively, (iii) dedicated cell lines sometimes termed *packaging lines* or *complementary lines* can be used to propagate the vector. These cells are transformed with a deficient viral genome that is itself incapable of replication but supplies helper functions in *trans* to the vector. The extreme form of this strategy uses derivatives that are sometimes termed *amplicons* and sometimes described as *gutted* (or *gutless*): All viral coding sequences are deleted, leaving behind only those *cis*-acting elements required for replication, packaging, and/or proviral integration. The choice of strategy depends on many factors, including genome size, the availability of packaging lines, the number and nature of nonessential genes, and the packaging capacity of the viral capsid. Many viruses (e.g. papovaviruses) package DNA into a preformed capsid and thus have a strictly defined packaging capacity that limits the size of foreign DNA. Others (e.g. the baculoviruses) form the capsid around the genome, and no such limitation exists.

There are a number of techniques for placing foreign DNA into viral genomes. The two most popular are ligation and homologous recombination. In the ligation strategy, restriction enzymes are used to prepare vector and foreign DNA and the two elements are joined *in vitro* using DNA ligase. In the homologous recombination strategy, a plasmid carrying the foreign DNA within a viral homology region is transfected into cells infected with the parental vector, and recombinants are generated by crossing over within the homology region. The homologous recombination strategy is favored for viruses with large genomes, which are difficult to manipulate directly (e.g. baculovirus, herpes virus, and vaccinia virus). In both the cases, various screening and selection strategies may be employed to isolate recombinant vector molecules. The use of helper viruses that are themselves replication defective or that carry mutations allowing counterselection is useful for preparing pure stocks of recombinant vector. Systems are also designed so that two or more entirely independent recombination events are required to generate replication-competent, wild-type virus genomes. Novel strategies involving site-specific recombination and transposition have also been used to generate recombinant viruses.

14.7.2 Adenovirus Vectors

The major advantages of adenoviruses as vectors are the high titer (10^{12}–10^{13} pfu/mL), the efficiency of gene transfer (approaching 100%), the broad species and cellular host range (including postmitotic cells), and the ease of *in vitro* manipulation (104,105). Adenovirus vectors in current use can accommodate up to 8 kbp of foreign DNA, although the theoretical maximum is approximately 30 kbp. One disadvantage of adenoviral vectors is the low efficiency of transformation (10^{-5}). They are therefore useful as transient expression vectors, but not for efficient stable gene transfer. This, together with their tendency to provoke an immune response, may limit their utility for human gene therapy (106,107).

Adenoviruses are, as discussed earlier, exploited in two other areas of gene transfer technology. First, plasmids expressing the adenoviral VA genes may be used to increase foreign gene expression following transient transfection with plasmid vectors. This is because the RNA products of these genes inhibit the activity of DAI protein kinase, an enzyme that blocks protein synthesis in the presence of dsRNA. Second, the presence of adenoviral capsids during receptor-mediated transfection has been shown to increase the efficiency of transgene expression up to 2000-fold. This is because DNA taken up by receptor-mediated endocytosis is delivered to lysosomes, wherein it is degraded, but because the adenovirus disrupts endosomes as a normal part of its infection strategy, the addition of adenovirus particles can increase the survival of internalized DNA and increase foreign gene expression.

14.7.2.1 Adenovirus Molecular Biology. There are approximately 10 transcription units in the linear adenovirus genome, but the number of gene products produced is increased by complex patterns of alternative splicing and protein processing (104,105) (Fig. 14.5). Genes are expressed in two phases, early genes before replication and late genes after replication. E1a proteins are transcriptional regulators. E1b proteins control mRNA export and the inhibition of host cell protein synthesis. E2a and E2b encode proteins for viral DNA replication. E3 proteins help evade the host immune response, and E4 encodes

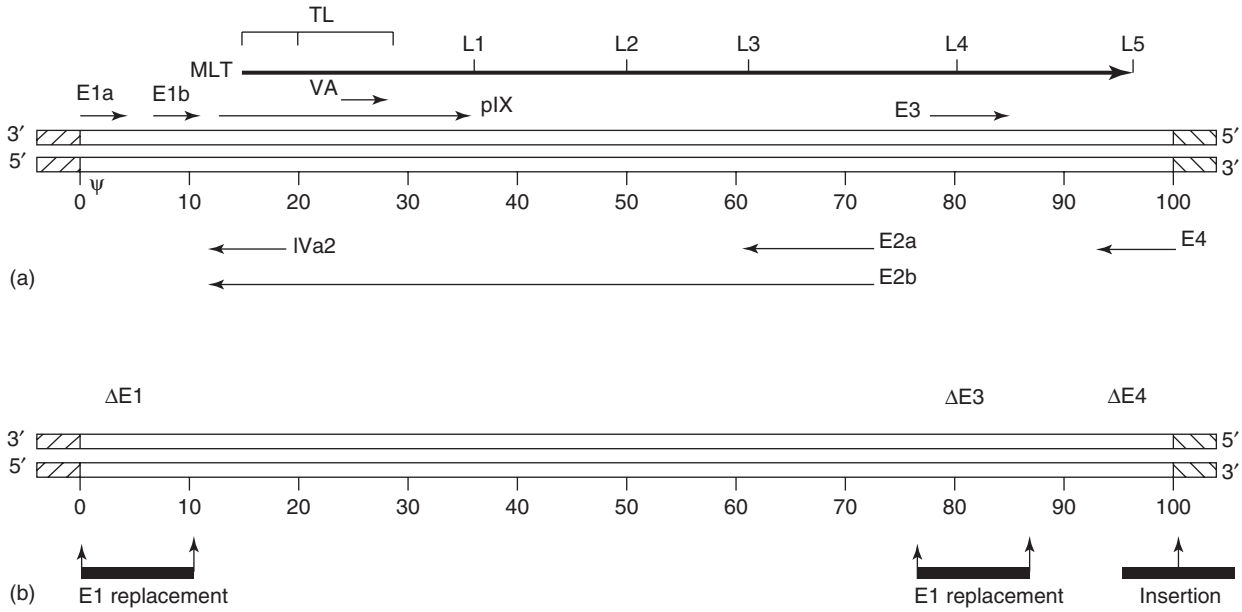


Figure 14.5. (a) The adenovirus 5 (Ad5) genome divided into 100 map units, each representing 360 bp, with inverted terminal repeats (hatched boxes). Arrows represent transcripts, the early transcripts E1–E4, the intermediate transcripts pIX and IVa2, and the major late transcript (MLT). The RNA polymerase III-dependent VA genes are also shown. The MLT is differentially spliced to yield five families of mature transcripts (LI–L5), each beginning with the tripartite leader (TL) and ending where indicated. (b) Strategies for vector development. Foreign genes can be inserted adjacent to the E4 region or used to replace either E1 or E3. E1 replacement vectors are the most widely used, and their capacity may be increased also by deleting the E3 and E4 regions. A further strategy is to delete all internal sequences except the packaging site (ψ), generating an amplicon vector.

further transcriptional regulators. After replication, early gene expression is switched off and transcription initiates from the single *major late promoter*, producing five major families of transcripts. All these late transcripts begin with a *tripartite leader*, an UTR containing two introns, which increases the efficiency of protein synthesis. Late genes encode viral structural proteins and proteins involved in their processing and assembly to form the mature virion.

Although stable integration of adenovirus DNA occurs at low frequency, one of the major reasons for interest in the adenoviruses is their ability to transform cells. The adenoviruses are divided into several subgroups based on their oncogenicity, with subgroup A being the most oncogenic, usually causing tumors when injected into newborn mice. Subgroup B is weakly oncogenic, and subgroups C–F induce tumors only occasionally. All adenoviruses can transform cultured cells; however, this involves stable integration of at least the leftmost 11% of the viral genome. This fragment of the genome contains the E1a and E1b transcription units. Certain products from this region are oncogenic because they inhibit the activity of host cell cycle regulators. E1a inactivates the retinoblastoma protein, whose function is to prevent S-phase transcription, and E1b inhibits the activity of p53, which blocks the cell cycle in response to DNA damage and other signals.

14.7.2.2 Recombinant Adenovirus Vectors. Both replication-competent and replication-deficient adenoviral vectors have been developed (104,105) (Fig. 14.5b). The replication-competent vectors include E3 replacement vectors and insertion vectors (where foreign DNA is added at the right-hand edge of the linear gene map just upstream of the E4 transcription unit). The most widely used adenovirus vectors are replication defective due to deletion of the E1a and E1b transcription units. These E1 replacement vectors are propagated in the complementary human embryonic kidney cell line 293, which is transformed with the leftmost 11% of the adenovirus genome, which supplies the missing functions. E1 replacement vectors may also lack the E3 transcription unit, which increases the maximum capacity of the vector to approximately 8 kbp (108). The further deletion of the E4 region allows foreign DNA of up to 11 kbp to be inserted and has the further advantage of removing adenoviral functions that interfere with host cell physiology. The theoretical maximum capacity of an adenoviral vector is 30 kbp. This

requires the deletion of all adenoviral coding DNA, leaving just the *cis*-acting elements required for packaging and replication—a so-called adenovirus amplicon. Packaging lines such as HEK 293 cannot be prepared for amplicons because the overexpression of adenoviral late proteins is cytotoxic. Current strategies therefore use helper viruses, although there remain problems separating the recombinant vector and helper, and with vector instability. Amplicon vectors have been used successfully to prepare vectors carrying the cystic fibrosis transmembrane receptor cDNA (109) and dystrophin cDNA (110) in 293 cells either cotransfected or coinfected with helper vectors, but yields of the recombinant vector are so far very low.

The production of recombinant adenoviral vectors by homologous recombination is a popular strategy, and a series of plasmid vectors has been produced, containing adenoviral sequences interrupted by a multiple cloning site (104,105). The alternative strategy of recombinant vector production *in vitro* has been facilitated by the development of derivatives of the wild-type adenovirus genome containing unique restriction sites for insertion, or paired sites for excision of E1 or E3 stuffer fragments and their replacement with foreign DNA (104,105). Recombinant adenoviral genomes produced as discussed earlier are infectious and can be introduced into permissive cells by transfection. Evidence of viral infection is seen within a few days, and cell lysates can then be used to infect fresh cells, resulting in the formation of plaques representing viral clones. These can be purified and the DNA analyzed for the presence of the foreign insert by PCR. It is desirable to check for sequence loss and rearrangements, especially if the insert is large and the recombinant genome approaches the maximum packaging size of the virus.

14.7.3 AAV Vectors

The parvovirus family of single-stranded DNA viruses is divided into the autonomous and dependovirus subgroups. The latter includes AAV, which is naturally *defective*, that is, unable to complete its replication cycle in the absence of a helper virus. In this instance, the term *helper virus* does not refer to a replication-competent derivative of the same species. Rather, the dependoviruses require functions supplied by a different virus species for their propagation. Adenovirus is a suitable helper virus; hence, "adeno-associated" but herpes virus is also competent to supply the required functions, and to a lesser extent so is vaccinia virus. The AAV virion is small, with a nonenveloped icosahedral capsid. Either DNA strand is packaged with equal efficiency, and both strands are infectious. AAV has a biphasic infection cycle. In adenovirus-infected cells, it enters the lytic cycle and replicates to a high copy number. In other cells, it enters a latent state where it does not replicate, but instead integrates into the genome. It is this latent state that is currently being exploited for gene transfer, due to the potential for long-term transgene expression. However, if a transformed cell is subsequently infected with adenovirus, the AAV provirus is excised (*rescued*) and lytic infection commences.

AAV has numerous properties that make it a valuable gene transfer and expression vector, particularly for gene therapy (111,112). First, stable integration occurs with great efficiency, and proviral transgenes can be expressed using either AAV or heterologous promoters. Second, the virus has an impressive host range that includes nonproliferating cells. Third, the virus is unusual in that even the wild type does not cause any disease symptom. Fourth, it is very safe to use: Recombinant AAV vectors lacking replication functions require two helper viruses, a helper AAV to supply missing AAV functions, as well as adenovirus. Finally, there is no superinfection immunity; so cells can be transduced with different AAV vectors as many times as necessary. This allows the addition of multiple traits to cells through successive transformations. The host range of AAV has not been fully explored, but it appears to infect and replicate efficiently in all mammalian cell lines if a suitable helper virus is used. The helper virus is the primary determinant of which cells can be productively infected. Integration efficiencies vary from species to species, with human cells the most efficient hosts. This specific targeting could be an advantage in gene therapy, but recombinant AAV vectors tend to integrate randomly, suggesting that the site specificity is conferred by AAV *trans*-functions. AAV has been shown to integrate into the DNA of all human cell lines tested, although the potential of primary cells has not been widely examined. One problem with AAV is the low titer of recombinant viral stocks. Initially, this was as low as 10^4-10^5 transducing units per milliliter, although by careful optimization of preparation methods, this has increased to 10^9.

14.7.3.1 AAV Molecular Biology. The AAV genome is approximately 5 kbp in length. The unique central region of the genome is flanked by 145-bp inverted terminal repeats, which are required for several functions, including replication, gene regulation, and proviral integration (111). The internal region of the genome has been divided into two large sections by genetic analysis (Fig. 14.6a). The *rep* region encodes nonstructural proteins, and mutations within this region generate a replication-deficient phenotype that also lacks certain transcriptional functions. The *cap* region encodes the structural proteins of the capsid, and mutations within this region generate a packaging-deficient phenotype. There are three promoters in the AAV genome (p5, p19, and p40). Rep proteins arise from mRNAs transcribed from the p5 and p19 promoters, while capsid proteins arise from mRNAs transcribed from the p40 promoter.

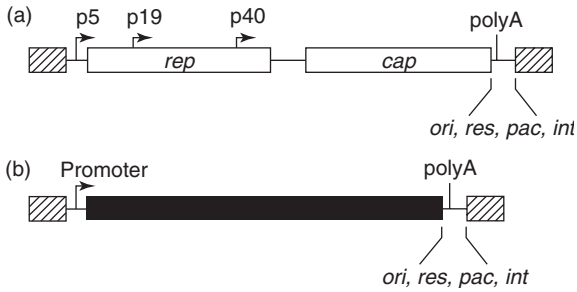


Figure 14.6. (a) Simplified map of the AAV genome showing the *rep* and *cap* regions, the three promoters (p5, p19, and p40), the polyadenylation site, the cluster of *cis*-acting sites (origin of replication, rescue, packaging, and integration), and the inverted terminal repeats (hatched boxes). (b) A recombinant AAV vector. The viral coding sequences have been removed and replaced by a foreign gene under the control of a heterologous promoter. The *cis*-acting sites remain *in situ*.

All transcripts share a common intron and polyadenylation site. The polyadenylation site is adjacent to the origin of replication and *cis*-acting elements required for packaging, integration, and rescue. The regulation of AAV gene expression is complex, involving both helper virus and AAV functions (111).

14.7.3.2 Recombinant AAV Vectors. The first AAV vectors, produced in 1984, were *cap*-replacement vectors. Initially, the *cap* region was replaced with the *E. coli neo* gene. The integrated *neo* gene was expressed at a low level from the endogenous AAV p40 promoter, but levels were sufficient to allow G418 selection of transduced cells. Major improvements to AAV-mediated gene delivery came with the development of vectors where all internal reading frames were deleted, leaving just the polyadenylation site and the *cis*-acting sequences for packaging, integration, and rescue in addition to the terminal repeats (111,112) (Fig. 14.6b). The maximum capacity of the AAV capsid is 110% wild-type genome size; thus, amplicon vectors of this nature allow the insertion of approximately 4.5 kbp of foreign DNA. The removal of the *rep* region provided an additional advantage: AAV Rep proteins control transcription as well as replication and have been shown to interfere with endogenous promoters and enhancers in AAV vectors. However, *rep*$^-$ vectors are not affected in this manner and have been used with several constitutive and inducible eukaryotic promoters, and the patterns of cell type-specific and inducible expression have been faithfully reproduced. Vectors with intact Rep functions are less predictable, although some promoters appear unaffected (e.g. the adenovirus E4 promoter).

One disadvantage of AAV expression vectors is the laborious procedure for producing stocks of recombinant virus. As both a helper virus (adenovirus) and a helper AAV are required to provide missing functions in *trans*, there are two types of contaminants to remove. Wild-type AAV can be used as a helper, but the resulting recombinant stock contains adenovirus and wild-type AAV contaminants, the latter often in great excess to the recombinant virus. Adenovirus can be inactivated by heating (lysates are heated to 60°C for 2 h) and effectively removed by CsCl density centrifugation or other physical methods. Several strategies have been employed to restrict the propagation of wild-type AAV, including the use of packaging-deficient AAV strains, the use of helper plasmids transfected into the cells infected with the parental AAV vector and adenovirus, the use of cell lines with integrated AAV genomes lacking functional rescue sequences, and the use of conditional lethal AAV mutants as helpers. These strategies have reduced the proportion of wild-type virus in the resulting stocks, although the level can still reach 10–50% due to recombination between the recombinant and helper AAV genomes. There is little chance of generating true AAV packaging lines because the overexpression of AAV genes is cytotoxic and so is the overexpression of adenoviral helper functions. The current method for producing essentially pure recombinant AAV is to use two plasmids, one carrying the recombinant AAV genome with all *cis*-acting sites intact, but all *trans*-functions replaced by foreign DNA, and the other carrying the *rep* and *cap* functions, but lacking any *cis*-acting element. These are cotransfected into cells infected with adenovirus. There is no homology between the two plasmids, preventing the production of wild-type AAV by homologous recombination, but with all the required functions supplied in *trans*, the recombinant AAV vector is rescued from the plasmid and packaged. Contaminating adenovirus is then removed as discussed, leaving the recombinant AAV vectors.

AAV vectors are newcomers in the field of gene transfer, and much remains to be learned of their suitability for stable gene expression, especially in gene therapy. In particular, issues that need to be addressed include the nature and efficiency of vector transduction and transgene activity *in vivo*. A number of such studies have been carried out recently (112).

14.7.4 Alphavirus Vectors

The alphaviruses are a group of single-stranded positive-sense RNA viruses with a broad host range, including insects and mammals (113). Alphaviruses have several properties making them suitable as transient expression vectors (113,114). First, they have a broad host range and cell tropism, facilitating gene delivery to many cell types. Second, recombinant alphaviruses deliver their RNA to the cytoplasm, where it is efficiently self-replicated and expressed to yield high levels of recombinant protein

(however, alphavirus genomes can also be cloned as cDNA and expressed from a normal expression vector, resulting in the export of recombinant viral RNA from the nucleus). Third, because the viral structural proteins are encoded on a separate subgenomic RNA, this region can be replaced by foreign DNA without rendering the vector replication defective. Fourth, the delivery of recombinant vector RNA ensures that the virus never integrates into the genome, making this system particularly useful for short-term gene therapy (e.g. cancer therapy). Finally, the two best-characterized alphaviruses—Semliki Forest virus (SFV) and Sindbis virus (SIN)—are transmitted in an asymptomatic manner, so they express foreign DNA in cell culture and *in vivo* without causing cytotoxic effects or disease symptoms. The alphaviruses have been developed as vectors only recently and are so far the only RNA viruses (excluding the retroviruses, which have a DNA stage in their replication cycle) to be commercially exploited as expression vectors. The use of RNA viruses is advantageous because there is no chance of proviral integration, and hence no danger of mutation or transformation. A number of negative-strand RNA viruses have also shown potential for vector development, although at this time, the number of successful gene transfer and expression experiments are limited (115). One potential disadvantage with the use of RNA viruses is the generally low fidelity of the viral replicase enzymes, which results in a higher level of transgene mutation than seen with DNA viruses.

14.7.4.1 Molecular Biology of SFV and SIN. SFV, Sindbis, and other alphaviruses infect cells by receptor-mediated endocytosis. The spike glycoprotein of the virus envelope then causes the viral and endosome vesicles to fuse, releasing the viral nucleocapsid into the cytoplasm. Proteins such as Sindbis spike glycoprotein have been exploited to enhance the efficiency of liposome-mediated transfection by catalyzing the fusion of liposomes and their target cells—such fusogenic DNA-containing particles are known as *virosomes*. Following entry into the cytoplasm, the genomic RNA is released from the nucleocapsid and is immediately translated to yield the viral replicase (Fig. 14.7a). This enzyme produces progeny genomes by first synthesizing a negative-sense antigenomic strand, and then using this as a template to generate positive-sense genomic strands. The replicase also transcribes the subgenomic RNA from an internal promoter, and this encodes a polyprotein containing the viral structural proteins. The polyprotein is cleaved by capsid protein C, which has chymotrypsin-like autoproteolytic activity. The viral proteins associate with naked genomic RNA, and the new nucleocapsids migrate to the cell surface, where they are released by budding, generating new lipid envelopes with spike proteins.

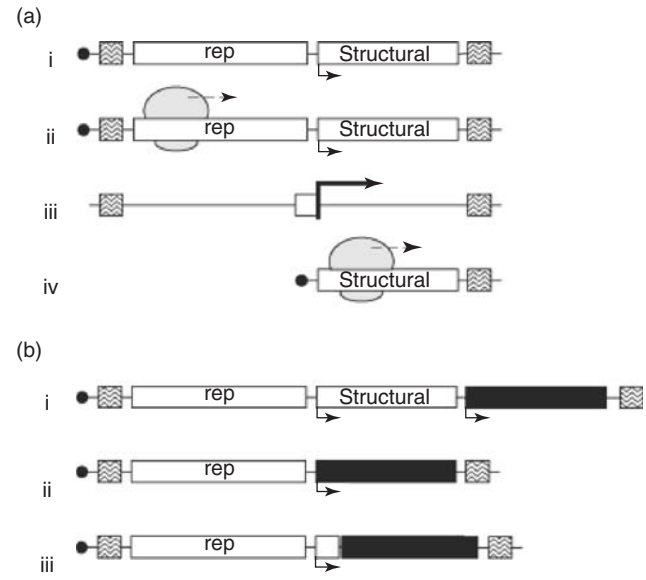


Figure 14.7. (a) Structure and replication of a simplified alphavirus genome. (i) Two genes, one encoding replicase and the other encoding structural proteins. The genome is flanked by replicase binding sequences (wavy lines) and is capped at the 5′ end (black circle). (ii) The 5′ cap allows ribosome binding, resulting in translation of the replicase gene (broken arrow). (iii) Replicase copies the genomic RNA to generate an antigenomic strand. This contains an internal promoter (thick arrow on antigenomic strand, small arrow on genomic strand). (iv) Replicase initiation at the internal promoter facilitates transcription of the subgenomic RNA, which is capped and translated to yield the structural proteins. (b) Alphavirus vectors. (i) Addition vector, where a gene can be added to the full genome under a second internal promoter. (ii) The structural genes can be replaced by foreign DNA. (iii) The foreign DNA can be fused to part of the structural polyprotein gene to take advantage of a translational enhancer.

14.7.4.2 Recombinant SFV and SIN Vectors. One strategy for expressing recombinant proteins from alphavirus vectors is to add a second promoter either upstream or downstream of the structural genes, allowing the insertion of a foreign gene and its expression as an additional subgenomic RNA (113,114). All subgenomic RNAs are capped and can be translated. Alternatively, the insertion of an IRES element between the structural genes and the transgene allows internal translation of the transgene, albeit at a lower efficiency compared with cap-dependent translation. This strategy produces vectors that are not only replication competent but also competent to produce infectious viral progeny. As this is not always desirable, a second strategy is to replace the structural genes with foreign DNA. Such constructs are more efficient than the addition-type vectors, which tend to be unstable (113). Structural gene replacement does not affect replication, but it prevents the formation of infectious virions, and can result in extremely high levels of recombinant protein synthesis, up to 50%

total cellular protein. Foreign DNA can be used to replace the entire structural coding region, but the first 40 amino acid residues include a strong enhancer of protein synthesis, which significantly increases the yield of recombinant protein. In many expression systems, this region is included in the vector, so that the foreign gene is expressed as an N-terminal fusion protein. Alternatively, the entire capsid C protein region can be included. In this case, foreign genes are initially expressed as N-terminal fusion proteins, but autocatalytic cleavage results in the production of native protein (Fig. 14.7b).

As SFV and Sindbis are RNA viruses, *in vitro* manipulation and recombinant vector construction must involve the use of cDNA genome copies (113). These can be used to produce infectious RNA *in vitro*, which can be transfected into cells using many of the methods used for DNA transfection. Sindbis expression vectors are marketed by Invitrogen. The vector pSinRep5 is a plasmid containing bacterial backbone elements, the Sindbis replicase genes and packaging site, and an expression cassette featuring a Sindbis subgenomic promoter, a multiple cloning site, and a polyadenylation site. There is an SP6 promoter upstream of the replicase genes and expression cassette for generating full-length *in vitro* transcripts. There is a second set of restriction sites downstream from the polylinker, allowing the vector to be linearized before *in vitro* transcription. Foreign DNA is cloned in the expression cassette, the vector is linearized and transcribed, and the infectious recombinant Sindbis RNA thus produced is transfected into cells and expressed to generate high levels of recombinant protein. A different approach is to clone the entire alphavirus vector as an expression unit in a conventional plasmid expression vector under the control of a typical mammalian promoter, such as the SV40 promoter. In this case, DNA is transfected into the cell as normal and alphavirus RNA is produced as mRNA and exported to the cytoplasm. Here, it replicates as a virus and produces large amounts of recombinant protein. In both the RNA and DNA transfection strategies, helper functions are not required and recombinant virus particles are not produced.

The introduction of recombinant RNA into cells is unsuitable for gene delivery *in vivo*. In these cases, viral infection of cells is used for gene transfer. The propagation of infectious recombinant viruses requires helper functions (i.e. structural genes) to be supplied in *trans*. A binary approach has been used successfully to produce recombinant viruses. A vector such as that described earlier is used in concert with a second vector carrying the structural genes (113,114). Two *in vitro* transcription reactions are performed and target cells are cotransfected with two RNAs, one expressing replicase and the transgene and the other expressing structural proteins. This facilitates one round of replication and packaging and the production of recombinant viral particles that can be used to infect other cells. There is a risk of replication-competent viruses assembling by promiscuous replication, involving switching between the alternative RNA templates. This has been addressed by developing helper viruses with conditional lethal mutations, but the risks are at present too great for alphaviruses to be considered safe for human gene therapy.

14.7.5 Baculovirus Vectors

The baculoviruses are a diverse group of double-stranded DNA viruses whose productive host range is limited to insects and other arthropods (116). There are no known vertebrate hosts; thus, vectors derived from baculoviruses are among the safest to use. However, baculoviruses are taken up by mammalian cells in culture, and recent studies have shown them to be capable of expressing foreign genes under the control of mammalian viral promoters (117). Baculoviruses are therefore potential vectors for gene therapy.

The main role of baculovirus vectors is the high yield transient expression of foreign proteins in insect cells (118–120). The usefulness of baculoviruses as vectors stems from the unusual infection cycle of one particular subfamily, known as the *nuclear polyhedrosis viruses* (NPVs). The baculoviruses are divided into three subfamilies: the NPVs, the granulosis viruses, and the nonoccluded viruses (116). The NPVs are potentially the most suitable vectors because they produce *nuclear occlusion bodies*, where mature virions are embedded in an abundant proteinaceous matrix. The matrix allows virions to survive in a harsh environment such as the external surface of leaves. The two important features of this system (as concerns vector development) are (i) the matrix consists predominantly of a single virus protein, *polyhedrin*, which is expressed at very high levels, and (ii) the nuclear occlusion stage of the infection cycle is nonessential for viral propagation in insect cell lines. The polyhedrin coding region can therefore be replaced with foreign genes, allowing heterologous gene expression from the polyhedrin promoter, and replacement vectors are replication competent.

Due to the simple procedures involved in laboratory handling and propagation, vector development has concentrated on two species of viruses (119,120). For the production of recombinant proteins in insect cells, the multiple NPV from the alfalfa looper *Autographa californica* has been extensively utilized. This virus [*A. californica* multiple nuclear polyhedrosis virus (AcMNPV)] is propagated in several insect cell lines, the most popular of which are derived from *Spodoptera frugiperda* (e.g. Sf9 and Sf21). Alternative hosts include cell lines derived from *Estigmene acrea, Mamesta brassicae*, and *Trichoplusia ni* (e.g. High Five™). A related virus (BmNPV), which infects the silkworm

Bombyx mori, has been used for the production of recombinant protein in live silkworm larvae.

The baculovirus expression system has two other important advantages in addition to its safety, convenience, and yield. First, the rod-shaped viral capsid is completed after genome packaging, so that the size of the capsid is determined by the length of the genome. This means that any amount of foreign DNA can be accommodated, and multiple genes can be expressed in tandem (121). Second, many types of posttranslational protein modification have been documented in insect cell lines, including proteolytic cleavage, formation of disulfide bonds, N-linked and O-linked glycosylation, and fatty acid acylation (121). Baculoviruses are therefore ideal for overexpressing mammalian proteins, especially those intended for therapeutic use. However, there is some variation in the nature of protein modification, particularly with respect to N-linked glycosylation, between mammalian cells and the baculovirus host cell line Sf9. It has been reported that glycosylation patterns in an alternative cell line derived from *E. acrea* are similar to those in mammalian cells (122). Furthermore, mammalian glycosylation enzymes have been coexpressed with target foreign proteins using baculovirus vectors in Sf9 cells, and this strategy has successfully altered the specificity of the glycosylation pathway to generate correct modifications typical of mammalian proteins (122). For cellular localization studies, it is also notable that most proteins expressed in insect cells using baculovirus vectors are correctly targeted.

14.7.5.1 Molecular Biology of AcMNPV. AcMNPV replicates with a biphasic cycle in susceptible insect cells and produces two distinct forms of viruses (121). The early cycle results in the production of *extracellular budded viruses* (EBVs), single-enveloped virions that are released by budding from the cell membrane and go on to infect other cells. This first phase of the lytic cycle occurs within 20 h following infection and involves the expression of three sets of viral genes. The immediate early (α) genes and the delayed early (β) genes are expressed before DNA replication. The α-genes are expressed immediately after the infecting virus is uncoated, and expression requires no viral gene products; hence, transfected naked AcMNPV genomic DNA is infectious. The β-genes are expressed after the α-genes, and their expression is dependent on α-gene products. The late (γ) genes are expressed after the onset of replication and are thought to encode products involved in ECV structure and assembly. Most of the α-,β-, and γ-genes are essential for productive infection.

After 20-h postinfection, the production of ECVs is dramatically reduced. This corresponds to reduction in the transcription of α-, β-, and γ-genes, and the induction of a fourth set of very late (δ) genes. Importantly, these genes can be regarded as nonessential for productive infection in insect cell lines, although they are essential for the spread of the virus in nature. This establishes a containment system for laboratory-constructed baculovirus vectors.

14.7.5.2 Recombinant Baculovirus Vectors. Most baculovirus vectors involve replacement of the polyhedrin or p10 coding regions (121). The nonessential nature of these δ-gene functions has made them desirable targets for replacement with foreign DNA. There are also vectors that use early promoters, particularly for the production of proteins known to be toxic to insect cells and for baculovirus surface display technology (122).

Polyhedrin replacement vectors are used for prodigious expression of polyhedrin in the late part of the replication cycle (accounting for up to 25% of total cellular protein or 1 mg/10^6 cells). The polyhedrin upstream promoter and 5′ UTR are important for high level foreign gene expression, and these are included in all polyhedrin replacement vectors. Initially, the highest levels of recombinant protein expression were obtained as fusions with at least the first 30 amino acids from the N-terminal region of the polyhedrin protein. This would appear at first to reflect optimization of protein stability, but in fact reflects the presence of additional regulatory elements located downstream of the polyhedrin translation start site. For the production of native proteins, vectors are available where the natural polyhedrin initiation codon is mutated, so that these important "downstream" sequences become part of the 5′ UTR of the foreign gene. However, it has been reported that initiation may still occur at this mutated site; so cloned foreign genes must be trimmed off their own UTRs, and the start codon should be out of frame with respect to the natural polyhedrin start codon.

The major disadvantage of p10 replacement vectors is that p10 mutants are not OB^- and have no easily scorable phenotype. Plaques of both polyhedrin and p10 replacement vectors can be screened for the presence of the insert by hybridization or immunological detection of foreign protein. A number of visual screening strategies have been developed as well as systems for *selecting* recombinant viruses. The *E. coli lacZ* gene has been used to help identify recombinant plaques. The general visibility of plaques is improved by insertion of the *lacZ* gene under an appropriate promoter somewhere in the baculovirus genome, so that *all* plaques turn blue on exposure to X-gal. More refined approaches include exploiting *lacZ* for blue–white selection: By using parental baculovirus strains in which β-galactosidase is expressed from the polyhedrin promoter, recombinants (which replace the *lacZ* gene with the foreign gene to be expressed) form clear plaques, while parental vectors form blue plaques; alternatively, by introducing *lacZ* as a marker alongside the foreign gene, the recombinant vectors form blue plaques, while the wild-type virus

produces clear plaques. Due to the lack of screenable phenotype, p10 expression vectors must incorporate a reporter gene detection system to allow recombinant plaques to be identified. Recently, vectors have been designed with polyhedrin expressed from the p10 promoter, so that the original OB assay can be used.

Baculovirus genomes are large, and although strains have been constructed with unique restriction sites, allowing insertion of foreign DNA by *in vitro* ligation, the favored strategy is homologous recombination using plasmid targeting vectors containing a baculovirus homology region into which foreign DNA has been inserted (119,120). Generally, plasmid and wild-type baculovirus DNAs are cotransfected into the appropriate insect cells by calcium phosphate transfection, lipofection, or electroporation. This strategy generates recombinant vectors at a frequency of 0.5–5%. Linearized baculovirus genomes are noninfectious, but remain recombinogenic, and this can be used to reduce contamination from wild-type virus. The proportion of recombinants can be increased through the use of nonviable deleted derivatives of the wild-type baculovirus genome, which are repaired by homologous recombination with the targeting vector. Derivatives of the wild-type AcMNPV genome, with unique restriction sites added upstream of the polyhedrin gene and within an essential gene found downstream of the polyhedrin locus, can be used to generate linear genome fragments lacking an essential function (e.g. BacPAK6). Compatible targeting vectors span the deletion and provide enough flanking homologous DNA to sponsor recombination between the two elements and generate a viable, recombinant genome. Such approaches result in the production of up to 90% recombinant plaques. Combinatorial approaches using deleted nonviable genomes and targeting vectors incorporating *lacZ* or green fluorescent protein visible screening systems provide very powerful selection for recombinant vectors (122).

Alternative systems, in which the baculovirus genome is maintained and targeted as a low copy-number episome in bacteria (123) or yeast (124), are gaining popularity because they allow the direct isolation of recombinant vectors. Low copy-number maintenance is important to prevent the survival of a background of nonrecombinant vectors. The baculovirus genome can be stably maintained as a low copy-number episome in bacteria if it contains an F-plasmid origin of replication and a bacterial selectable marker such as kanamycin resistance (Bac-to-Bac), which exploits the specificity of the bacterial transposon Tn*7* to introduce foreign genes into the baculovirus/plasmid hybrid, which is called a *bacmid*. The foreign gene is cloned into a bacterial transfer plasmid between two Tn*7* repeats. This is transformed into the appropriate strain of *E. coli*, which contains the bacmid and a helper plasmid supplying Tn*7* transposase. Induction of transposase synthesis results in the site-specific transposition of the transgene into the bacmid, generating a recombinant bacmid that can be cloned and isolated from bacterial culture for transfection into insect cells. The Tn*7* target site in the bacmid is inserted in-frame within the *lacZ* gene, allowing blue–white screening of recombinants.

The baculovirus genome can also be maintained as a low copy-number episome in yeast if it contains a suitable origin of replication, a centromere, and selectable markers: These elements are inserted as a cassette to replace the polyhedrin gene. In the original system, a pair of selectable markers was used, allowing the power of yeast genetics to be applied to vector selection. One marker was used for positive selection of transformed cells, while the other was used for counterselection against nonrecombinant vectors. The *SUP4-o* marker was initially used for counterselection. This is a nonsense suppressor that, in the particular yeast strain used, confers sensitivity to the arginine analog canavanine and the ability to grow in media lacking adenine. Removal of the marker by replacement with homologous DNA confers resistance to canavanine and a requirement for adenine. Plasmid DNA isolated from canavanine-resistant, adenine-requiring yeast cultures was used to transfect insect cells and produce pure recombinant baculovirus. In both bacteria and yeast, the maintenance sequences (origin of replication/centromere and positive selection marker) must stay in the recombinant baculovirus vector. They have been shown to have no effect on baculovirus replication or gene expression in insect cells.

14.7.6 Herpes Virus Vectors

Herpes viruses are large, enveloped viruses with linear, double-stranded DNA genomes varying from 100 to 200 kbp in size. Different herpes viruses differ considerably in their host range and cell tropism. Furthermore, while some cell types undergo only lytic infection, others are also permissive for latent infection, resulting in long-term episomal maintenance of the viral genome. Of the eight known types of human herpesvirus, two have been extensively developed as vectors (51,125). EBV has a narrow host range, and its cell tropism is limited to B-lymphocytes and nasopharyngeal cells displaying the appropriate receptor. Cultured lymphocytes tend to undergo latent viral infection, but many other cell types are also permissive for latent EBV replication following the transfection of naked viral DNA. Hence, the major use of EBV has been the development of episomal plasmid vectors for transfection (51). Conversely, the human HSV-I and HSV-II have a broad host range and cellular tropism because they interact with a near-ubiquitous cell-surface molecule. Many cell types therefore undergo lytic HSV infection, while neurons also undergo latent infection. HSV vectors have thus been developed both

for short-term foreign gene expression in many cell types and for long-term foreign gene expression in neurons (125–128). The vectors show great potential for gene therapy applications, especially genetic intervention in the brain (126). The major advantages of HSV vectors are their broad host range and tropism, their natural ability to cause latent infection of neurons, and their large capacity: Up to 50 kbp of foreign DNA can be incorporated, which may comprise multiple genes.

14.7.6.1 Molecular Biology of HSV-I. HSV-I has a broad host range and cell tropism because it interacts with ubiquitous heparan sulfate molecules on the surface of target cells (129). The viral genome is linear, but after release from the nucleocapsid, it gains entry to the nucleus and immediately circularizes. The capsid also contains a virion host shutoff (VHS) protein that interrupts host protein synthesis and a transcriptional activator termed VP16. During lytic infection, VP16 forms a dimer with the host transcription factor Oct-1 and induces the expression of the five viral immediate early genes: $\alpha 0$, $\alpha 4$, $\alpha 22$, $\alpha 27$, and $\alpha 47$. The immediate early genes are all essential for lytic replication. These encode further regulators that act both on their own genes (in a self-regulatory manner) and on a set of approximately 15 early genes controlling DNA replication. Following replication, approximately 40 late genes are activated, which encode DNA cleavage and packaging proteins and capsid proteins. Progeny genomes are then packaged into virions and transported to the cell surface, where lysis occurs (129).

Lytic infection occurs in many different cell types, but latency is restricted mostly to neurons (129). The switch to latency is thought to reflect the balance of host- and virus-encoded transcriptional regulators in the cell. The immediate early genes are not expressed, and viral activity is restricted to a 152-kbp genomic region that overlaps the $\alpha 0$ immediate early gene in the antisense orientation. This region encodes a set of latency-associated transcripts (LATs). The LATs are also synthesized during lytic infection, although no protein products have been detected (even though LATs are associated with ribosomes). During latency, the LATs remain in the nucleus. The LATs are neither required for the establishment of latency nor its maintenance, but they are required for reactivation of the lytic cycle.

14.7.6.2 HSV Vector Construction. HSV has a large genome, and one simple strategy for generating recombinant HSV vectors is to transfect HSV-infected cells with a targeting vector containing a foreign gene within a viral homology region (103,126). Several HSV genes are nonessential for productive infection and can be replaced with foreign DNA. The resulting viruses are replication competent and infectious. For approaches such as gene therapy, however, HSV vectors must be replication defective. Several derivatives of HSV are now available that carry deletions in one or more of the immediate early genes, and such vectors must be propagated in a complementing cell line or in the presence of a cotransfected helper plasmid. The deletion of immediate early genes is also beneficial because their products are toxic to the host cell. HSV amplicon vectors are also widely used (103,126–128). These comprise the HSV origin of replication and genome packaging site cloned in a plasmid vector along with a mammalian transcription unit. All viral genes are deleted, leaving a vector that can only be packaged in the presence of a helper virus supplying the many missing functions in *trans*. Wild-type HSV-I can be used to supply helper functions, but the wild-type virus often causes lytic infections, resulting in rapid cell death both *in vitro* and in live animals. A number of HSV-I mutants have been developed as helper viruses, as these are nonpermissive for lytic replication (but still induce latent infection when introduced into cultured neurons or injected into the brain). Initially, a temperature-sensitive mutant was used carrying a point mutation in one of the immediate early genes. This was conditionally defective, inducing latent infections in the brain and in cultured neurons at 37°C but lytic infections at 31°C. Unfortunately, its applicability was limited by a significant reversion frequency, resulting in the induction of lytic infections. More recently, defective helper viruses with deletions in one or more of the immediate early genes have been used, providing complementary packaging lines to produce infective recombinant particles. In some cases, the reversion frequency has been reduced to 10^{-7}.

14.7.6.3 HSV Vectors for Prolonged Transgene Expression in Neurons. Due to their ability to cause long-term latent infection of neurons, the major use of HSV-I-derived vectors has been for gene transfer to neurons either *in vitro* or in the central nervous system of living animals (126–128). Neurons have been a difficult gene transfer target because they are postmitotic, and many transfection and viral transduction systems require rapidly dividing cells. The *in vitro* transfection of neurons often yields poor results due to limited uptake as well as the standard problems associated with position and dosage effects. HSV-I vectors possess a number of advantages for gene transfer to neurons, including efficient DNA transfer, a large genome size permitting the transduction of large segments of foreign DNA, and long-term episomal maintenance without viral gene expression. This later property ensures that during latent infection, the host cell physiology is unaffected—in fact, it is thought that most of the human population carries latent herpes virus infections in the absence of disease symptoms. The effect of foreign gene expression can

therefore be studied without considering the background effects of viral gene activity.

Vectors based on pHSVlac have been used to transfer many genes into neurons, including reporter genes, and genes encoding growth factors and their receptors, signal transduction components, and neurotransmitters (127,128). This strategy can be used both for therapeutic intervention and for the experimental study of cell function, for example, through the introduction of novel heterologous genes, the overexpression or constitutive expression of endogenous genes, the expression of dominant negative proteins to generate loss of function effects, and the use of toxins to ablate particular cells. Generally, it has been found that *in vivo* transfer results in relatively long-term foreign gene expression (2 weeks or more) with transformed cells restricted to those surrounding the injection site and more distant cells whose axons project into the site. The duration of transgene expression is strongly influenced by promoter choice. The number of infected cells is influenced by the extent of virion diffusion from the site of injection and the titer of the innoculum. HSV has a broad cell tropism and will infect glia and other nonneuronal cells as well as neurons. There have been a number of successful attempts to restrict the expression of foreign genes carried in HSV vectors using cell type-specific promoters, such as the neurofilament L promoter, which is panneuronal, and the tyrosine hydroxylase promoter, whose activity is restricted to catecholaminergic neurons. Reporter genes driven by IE1, IE3, and IE4/5 promoters have been shown to be active for up to 10 weeks in cultured sensory neurons.

The defective HSV-I vectors described provide a system for therapeutic gene transfer to neurons, which could be used to treat a variety of neurophysiological disorders (126). A number of potentially therapeutic genes have been cloned in this type of vector, including tyrosine hydroxylase for the treatment of Parkinson's disease, nerve growth factor for the treatment of Alzheimer's disease, and brain-derived neurotropic factor for potential repair of neuronal damage. Generally, transgene expression was detected for about 2 weeks following infection under the control of the IE4/5 promoter or other constitutive promoter. The rat brain glucose transporter cDNA has been introduced into the hippocampus of rats by stereotactic injection of HSV amplicon vectors and has successfully reduced neuron loss following kainic acid-induced seizures. However, foreign gene expression was observed for only a few days. Conversely, in a rat Parkinson's disease model, the transfer of tyrosine hydroxylase cDNA in a vector derived from pHSVlac resulted in long-term (>1 year) behavioral recovery.

14.7.6.4 HSV Vectors for Transient Expression in Nonneuronal Cells. The wide cell tropism of HSV provides an opening for its development as a gene delivery and expression vector for many cell types in addition to neurons. Miyanohara et al. (130) carried out successful gene transfer to liver by injecting recombinant herpes virus vectors both directly into the organ and into the portal vein. Although liver cells do not support latent HSV replication, HSV-mediated gene transfer to nonneuronal cells allows short-term recombinant protein expression, which may be sufficient for short-term or repetitive gene therapy, for example, the expression of canine factor IX in liver as a potential therapeutic treatment for hemophilia B. The restriction of HSV-mediated transgene expression to short duration would be an advantage in cancer therapy, as shown by the treatment of experimental glioma by delivering HSV vectors expressing TK, allowing infected dividing cells to be killed by treatment with ganciclovir (131).

14.7.7 Retrovirus Vectors

Retroviruses are RNA viruses whose unusual replication strategy includes reverse transcription of the RNA genome to generate a terminally redundant double-stranded cDNA copy, which integrates into the host genome in a semirandom manner (133). Progeny virions are produced by transcription of the provirus to yield both daughter viral genomes and subgenomic mRNAs encoding enzymes and structural proteins of the viral capsid. The host range and cell specificity of a particular retrovirus species is determined primarily by the envelope proteins, which interact with cell-surface receptors. The envelope proteins of amphotropic murine leukemia virus (MLV) are particularly promiscuous, so this virus has a broad host range and cell tropism and has been extensively developed as a vector for gene transfer to mammalian cells (134–136).

The retroviruses are an obvious choice for vector development, first, because of their natural ability to integrate DNA into the host genome, and second, because some, known as *acute transforming retroviruses*, demonstrate the inherent ability to transduce and express foreign genes. Over 100 acute transforming retroviruses have been described, leading to the discovery of many oncogenes, including those encoding growth factors and their receptors, signal transduction proteins, cell cycle regulators, and transcription factors. In many cases, the viral oncogene is fused to another viral gene so that it is expressed as a fusion protein. If this was an obligatory expression strategy, the construction of recombinant retroviral vectors could be very cumbersome. However, certain retroviruses contain oncogenes whose translation is initiated at a unique start codon (e.g. v-*src* in Rous sarcoma virus), and others carry two oncogenes (e.g. v-*erbA* and the unrelated v-*erbB* in avian erythroblastosis virus), suggesting that a number of alternative transgene integration strategies could be used. Retroviruses are

attractive potential vectors for many reasons (134,135). First, their small genome is no more difficult to manipulate *in vitro* than a standard plasmid vector. Second, they can be propagated to high titers (10^6-10^8 pfu/mL) using appropriate packaging lines. Third, they contain a strong promoter–enhancer complex that can drive high level transgene expression in many cell types. In all naturally occurring acute transforming retroviruses, oncogenes are driven from these LTR promoter–enhancer complexes, but transgenes can also be driven by their own promoters or by heterologous promoters from within the retroviral vector. Fourth, the efficiency of infection *in vitro* can approach 100%. Finally, retroviral integration produces stably transduced cell lines that can express foreign genes on a long-term basis—this makes them particularly suitable for gene therapy (137). The first successful report of human gene therapy, the correction of severe combined immunodeficiency (SCID) by transferring adenosine deaminase (*ADA*) cDNA to cultured hemopoietic stem cells or T-lymphocytes, involved the use of retroviral vectors (138). Similarly, retroviruses can be used for *in vivo* gene transfer simply by injecting recombinant vectors at the appropriate site. A similar concept involves the injection of retroviral vectors into embryos to generate chimeric embryos for the study of cellular interactions during development (139). Retroviral vectors are not used just to generate chimeric animals. Fully transgenic animals can also be produced (140) by retroviral infection of ES cells or preimplantation embryos, followed by the rearing of chimeric animals from which transgenics can be bred. As retroviruses are also transposable elements, retroviral vectors can be used as insertional mutagens. If the appropriate vector components are included, retroviruses can also be used as entrapment vectors and flanking sequences can be isolated by plasmid rescue (14).

14.7.7.1 Molecular Biology of the Retroviruses. Retroviral genome organization is simple and highly conserved between species (133) (Fig. 14.8a). The integrated provirus comprises three major open reading frames (*gag, pol*, and *env*) bracketed by tripartite direct LTRs. A single promoter located in the left LTR is used to transcribe genomic RNA. The *gag* region encodes viral structural proteins (*group antigen*), the *pol* region encodes reverse transcriptase (*polymerase*), integrase and protease, and the *env* region encodes viral *envelope* proteins. The full-length RNA is translated to yield two polypeptides, Gag and Gag-Pol, the latter by occasional programmed read-through of the *gag* termination codon. The full-length RNA also undergoes splicing to eliminate the *gag* and *pol* regions. The splice product is translated to generate the Env polypeptide. The protease encoded by the *pol* region (or occasionally the *gag* region, depending on the virus) cleaves the major gene products to yield approximately 10 mature polypeptides.

The retroviral infection cycle begins by uptake of virions through interaction between virus envelope proteins and the appropriate cell-surface receptors (133). The capsid contains two copies of the RNA genome (i.e. it is diploid) as well as reverse transcriptase. As the packaged RNA genome is transcribed from an integrated proviral cDNA using a promoter within the left LTR and a polyadenylation site within the right LTR, the free genome is truncated at both ends compared with the provirus, and lacks its characteristic LTR structure. Early in the replication cycle, the RNA genome is copied to generate a double-stranded cDNA replica, in a complex process involving two template jumps. It is this process that generates the LTRs. The cDNA genome, complete with redundant LTRs, is integrated into the host DNA using viral integrase. It is then transcribed to generate progeny genomes and mRNAs for translation. Mature viral proteins assemble with the genomic RNAs to form new virions. A specific *cis*-acting packaging site termed ψ is required.

14.7.7.2 Recombinant Retroviral Vectors. Most retroviral vectors are replication defective. Several replication-competent vectors have been developed, but they have a limited insert size and allow the spread of vector DNA throughout the host genome following infection, a consequence that is usually undesirable (134–136). Most naturally occurring acute transforming retroviruses are also replication defective, because the viral oncogene replaces an essential viral function. They require superinfection with a wild-type virus to replicate successfully in the host. An exception is Rous sarcoma virus, which carries the v-*src* oncogene in addition to the entire viral genome. Replication-competent RSV vectors have been developed in which the v-*src* gene is replaced by foreign DNA. These vectors infect avian cells efficiently, but not mammalian cells, unless they have been modified to express the appropriate heterologous receptor. For mammalian cells, replication-competent vectors based on Moloney murine leukemia virus (MoMLV) have also been developed.

Replication-defective vectors are generally amplicons, with most of the viral coding region replaced by foreign DNA (Fig. 14.8b). Such vectors can be propagated only in the presence of helper functions, either using a replication-competent helper virus or a packaging cell line (134–136). The use of helper viruses results in the production of recombinant vector contaminated with the helper virus itself. Packaging cell lines are therefore more suitable for the production of pure, infectious viral particles capable of reverse transcription and integration, but not of further replication. A range of different packaging lines has been developed, differing in the parental virus used to create the line and the extent to which the helper virus genome has been modified and

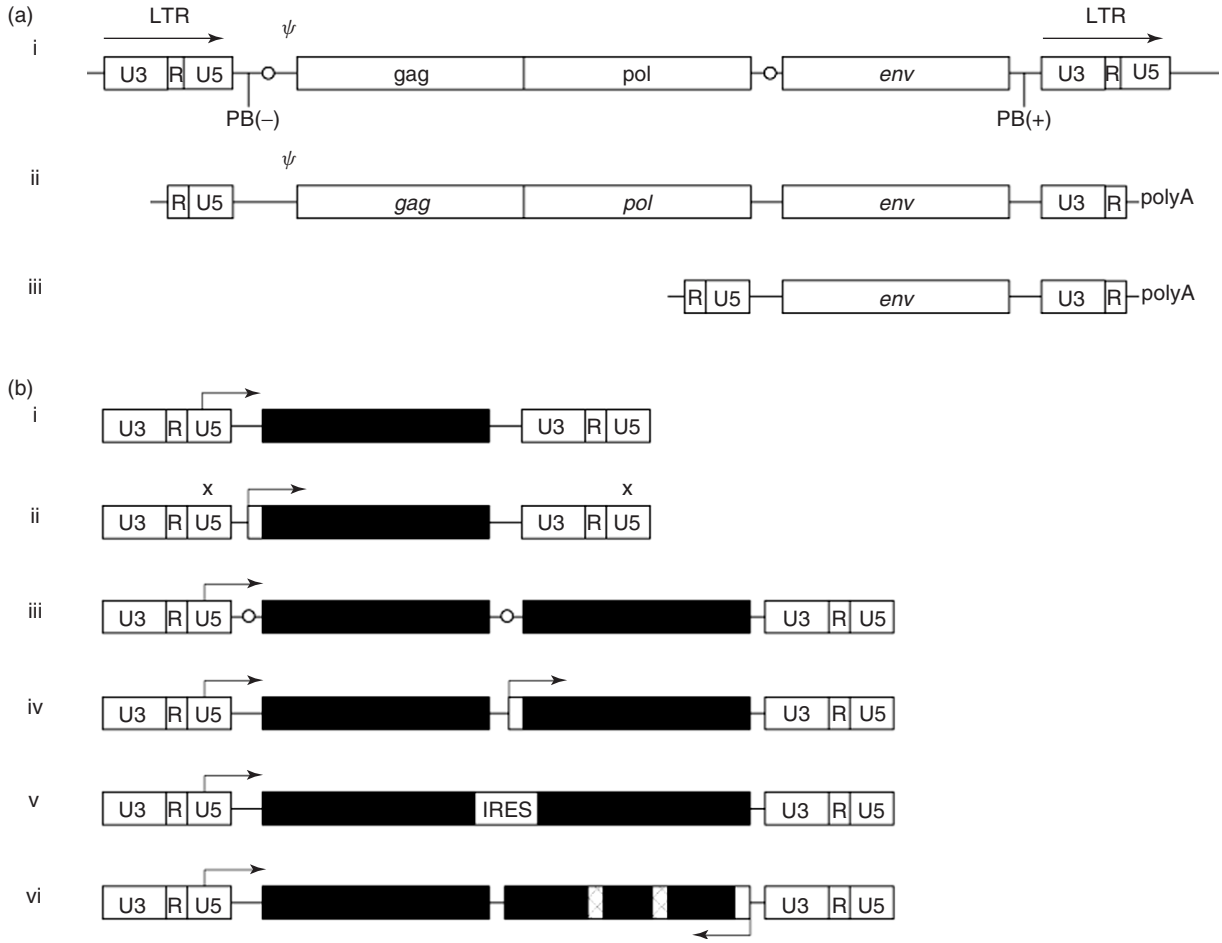


Figure 14.8. (a) Structure of a typical retrovirus genome. (i) Proviral genome is flanked by long terminal direct repeats and with three open reading frames, *gag, pol*, and *env*. The sites marked PB are primer binding sites, where genome replication is initiated. ψ is the packaging site. (ii) The U5 region contains a promoter–enhancer complex that stimulates genomic transcription. The R region contains a polyA site. The maximum transcript thus lacks terminal U3 and U5 elements, which are regenerated during cDNA synthesis. (iii) Splicing between acceptor and donor sites (shown as circles in *1*) generates a subgenomic transcript enabling translation of the *env* coding region. (b) Structure of recombinant retroviral vectors (black bar is foreign gene). (i) Simple vector with transgene driven by LTR promoter. (ii) Vector with transgene driven by an internal heterologous promoter. Such a vector may carry a mutation in the U5 region (x) that abolishes LTR promoter activity. (iii) Double-gene vector where each gene is driven by the LTR promoter by splicing. (iv) Double-gene vector with gene 1 driven by a LTR promoter and gene 2 by its own promoter. (v) Double-gene vector with the downstream gene under the control of an IRES. (vi) Double-gene vector where one transgene contains introns. The intronless transgene is controlled by the LTR promoter, and the other gene is inverted and controlled by an internal promoter.

rearranged. The former property determines the host range of the recombinant vector because it specifies the type of envelope protein inserted into the virion envelope. The most promiscuous vectors are generated using packaging lines derived from amphotropic viruses such as MLV. Many alternative packaging lines are available, which allow the tailoring of vector host range for particular experimental strategies. The latter property determines the extent to which replication-competent viruses are generated by recombination. The most efficient lines contain helper viruses with genomes modified to (i) limit the extent of homologous sequence shared between the helper virus and the vector and (ii) increase the number of independent crossover events required to form a replication-competent genome. One of the most efficient lines in this category is GP + E-86 (141), which contains

split coding regions, point mutations, and deletions, and hence requires three independent recombination events to generate a replication-competent virus.

Various strategies have been used to express foreign genes in retroviral vectors (134,135,138). The simplest strategy is to remove all coding sequences and place the foreign gene between the LTR promoter and the viral polyadenylation site. This results in the high level constitutive production of a single RNA encoding the foreign protein and is useful to synthesize large amounts of protein. However, if a specific expression pattern is required, an internal heterologous promoter can be inserted as part of the transgene. A difficulty with vectors containing internal heterologous promoters (non-LTR promoters) is that the LTR regulatory elements can either positively or negatively affect internal transcription. This problem has been circumvented by the development of *self-inactivating* or *suicide retroviral vectors* (142), with deletions in the 3′ LTR. A mutation in the 3′ LTR is copied to the 5′ LTR during the subsequent round of vector replication, resulting in a virus with inactive LTR promoter and/or enhancer elements, but functional internal promoters.

Selectable markers can be used to identify stably transduced cells to express two genes, the foreign gene and the marker, in the same vector. Many of the selectable markers (Table 14.4) have been used. The dominant markers *neo, hpt, Dhfr*, and *gpt* can be used in any cell, but *Hprt* and *Tk* require gene transfer to $hprt^-$ or tk^- cell lines. The expression of two (or more) genes can be achieved in a number of ways (Fig. 14.8b). An internal promoter can be used so that there are two independent transcription units within the virus. Alternatively, the vector can be modeled on the splicing pattern of a wild-type virus, so that full-length and spliced transcripts are produced. In both the cases, it is essential to allow full-length RNAs to be produced from the recombinant genome in the packaging line; so it is important not to include a polyadenylation site at the end of the first gene, which could terminate (replicative) transcription and result in loss of the second gene. In two-promoter vectors, the lack of a polyadenylation site for the upstream gene can result in read-through transcription and occlusion of the second promoter. This can be alleviated by placing the two genes in opposite orientations, so that the (reversed) polyadenylation site of the transgene is not recognized during full-genome transcription. For alternative splicing vectors, the existence of cryptic splice sites in the upstream gene should be considered. Multiple gene expression with LTR-based, internal promoter-based, and alternative splicing vectors can also be achieved by using IRES. Although the open reading frame downstream of the IRES is usually translated less efficiently than that using the more typical 5′ cap ribosome loading mechanism, it is certainly efficient enough for marker-based selection and reporter-based visible screening.

The interference of introns and polyadenylation signals with the virus replication cycle places certain limitations on the type of sequence that can be expressed in retroviral vectors. cDNAs are the simplest sequences to express because they can be inserted in the same orientation as the viral transcription unit (or they can be reversed with respect to the promoter to generate antisense RNA). Genes are more difficult to express, because the introns and polyadenylation signals may interfere with viral replication and RNA processing. If full, intron-containing genes must be expressed, they need to be placed under the control of an internal promoter, and the whole expression cassette has to be reversed in orientation. This allows intron recognition and splicing (and hence normal translation) from the reversed internal promoter but prevents the introns being spliced during forward, full-genome transcription. The alternative strategy is to remove the introns artificially and insert an intronless minigene into the vector in the forward orientation. Virus titer is reduced by the inclusion of an endogenous polyadenylation site at the end of the intronless minigene, but only by 5- to 10-fold; so infection is still productive.

Recombinant retroviral vectors for mammalian cells are constructed using cloned retrovirus cDNA, containing the essential *cis*-acting sites for the retroviral life cycle but lacking the *gag, pol*, and *env* genes whose products can be supplied in *trans*. The essential elements for high titer virus production are the LTRs, primer binding sites, and the packaging site ψ. Importantly, it has been determined that the ψ site, originally defined as a noncoding sequence 5′ to the *gag* open reading frame, actually extends into the *gag* coding region. Retroviral vectors therefore include this entire sequence (ψ^+) to ensure high titer.

14.7.8 SV40 Vectors

SV40-derived transduction vectors are rarely used these days (132). SV40 is a polyomavirus that infects certain monkey cells. It has a small, icosahedral capsid and a circular, double-stranded DNA genome approximately 5 kbp in size. SV40 was the first animal virus to be characterized in detail at the molecular/genetic level and was hence the first to be developed as a vector.

SV40 lytic infections in monkey cells can be divided into three stages. First, there is a latent stage, where the virus genome is uncoated and transported to the nucleus. This is followed by an "early stage" where early viral genes are expressed and host cell DNA synthesis is stimulated. Finally, in the late stage, the viral genome itself is replicated and progeny genomes are packaged. The host cell is then lysed and progeny virions are released. The SV40 genome has two transcription units known as the *early and late regions*, which have opposite polarities. The transcriptional start sites are located close together, facing outward, and are separated by a complex regulatory

region containing early and late promoters, an enhancer, and the SV40 origin of replication. Both transcription units encode single transcripts that are differentially spliced to yield multiple products. The early transcript produces two mature mRNAs encoding the large T- and small t-antigens (tumor antigens), involved in replication and transcriptional control. The T-antigen is essential for viral replication and must be supplied in *trans* to SV40-derived vectors lacking this function. In addition, the T-antigen also plays a major role in the stimulation of host DNA synthesis by interfering with the regulation of the cell cycle. Hence, cells such as COS-7, which express T-antigen constitutively, are transformed into a continuously proliferating state. The late transcript produces three partially overlapping mRNAs that encode the major coat protein VP1 and the minor coat proteins VP2 and VP3.

In the first SV40 vectors, either the entire early region or the entire late region could be replaced by foreign DNA. As both regions are essential for viral propagation, missing functions had to be supplied in *trans*. This involved coinfection with a helper virus, until the development of the complementary COS cell lines carrying a defective integrated SV40 genome. Such cell lines allowed the propagation of "early replacement" vectors by supplying T-antigen in *trans*. Many recombinant proteins have been produced in CV-1 or COS cells infected with SV40 vectors (132), but they suffer two serious drawbacks, which have limited their use. First, they have a restricted host range (certain permissive monkey cells, such as CV-1 and its derivatives), and most important, the maximum insert size is limited to 2.5 kbp, due to the capacity of the capsid. Such vectors have become obsolete with the discovery that plasmids carrying the SV40 origin of replication can be propagated in just the same way as the virus but without any limit to the insert size.

14.7.9 Vaccinia and Other Poxvirus Vectors

The poxviruses comprise a large family of DNA viruses, with a genome size ranging from 1 to 300 kbp and a host range including vertebrates and invertebrates (143). The most unusual aspect of this DNA virus family is the cytoplasmic site of replication, which means that the virus must encode and package all the enzymes required for replication and transcription. The best-known poxvirus is variola virus, the agent responsible for smallpox. Much interest was therefore generated by the potential use of recombinant vaccinia vectors, carrying genes from other infectious microorganisms, as live vaccines. Vaccinia virus has been used to express several heterologous viral proteins in mammals, including influenza virus hemagglutinin, hepatitis B surface antigen, and HIV envelope protein, and canarypox virus vectors are currently undergoing clinical trials for vaccination of humans (144). Poxviruses represent an advantageous transient expression system due to the wide host range, strong expression levels, and cytoplasmic transcription (145).

14.7.9.1 Molecular Biology of Vaccinia Virus. Vaccinia virus has a complex structure comprising a central core (containing about 100 proteins) and a lipid envelope derived from the Golgi apparatus (containing a further number of unique viral proteins). The envelope is essential for infection and (*in vitro*) plaque formation, and virions containing the envelope are termed *extracellular enveloped viruses* (145). The majority of infectious particles, however, exist as intracellular naked viruses in the cytoplasm. The vaccinia virus genome is double-stranded linear DNA, although the ends of the DNA strands are sealed by hairpins. The genes of the vaccinia virus genome can be divided into four temporal classes: constant, immediate, intermediate, and late. The constant and immediate genes are expressed as infection begins, using the viral RNA polymerase carried in the virion. The immediate genes encode enzymes and other proteins required for replication and exposure of the genome. Expression of most of the immediate and intermediate genes is mutually exclusive; hence, when intermediate gene expression commences after replication, immediate gene expression ceases. The intermediate genes encode, among other products, late gene transcriptional regulators. The constant genes have both early and late promoters and are hence expressed throughout the infection cycle. The late genes encode packaging proteins, capsid components, and enzymes that are carried in the virion and used immediately after infection.

14.7.9.2 Recombinant Vaccinia Virus Expression Vectors. Vaccinia virus is simple to grow because of its broad host range, including both established cell lines and primary cells. However, the efficiency of plating varies according to cell type (145). The genome is too large to manipulate *in vitro*, and because the virus normally carries its own replication and transcription machinery, recombinant genomes introduced into the cell by transfection are not infectious. Although it is now possible to generate infectious recombinant genomes (144), the strategy of choice is to transfect virus-infected cells with targeting vectors carrying a vaccinia promoter/foreign gene expression unit within a vaccinia homology region, allowing the insertion of foreign DNA by homologous recombination (143,145).

As poxviruses encode their own transcriptional apparatus to allow cytoplasmic transcription, endogenous poxvirus promoters must be used to drive the expression of foreign genes. A number of vaccinia promoters have been used, and the gene expression parameters depend on whether early, late, or constant promoters are chosen (143,145). Early expression may be desirable to avoid

the cytopathic effects of the virus, but the highest levels of transcription are provided by late promoters. The P11 promoter is extensively used and can generate over 1μg of protein/10^6 cells. The constant promoter P7.5 is not quite as active as P11 but allows transcription throughout the replication cycle and is widely used. The vaccinia virus early transcriptional apparatus uses a specific transcriptional termination signal with the consensus sequence TTTTTNT; so it is advisable to eliminate such motifs within foreign genes to prevent possible truncation. It is also notable that, due to cytoplasmic transcription, vaccinia virus contains no introns and cannot splice introns present in foreign genes. Therefore, vaccinia vectors must be used to express cDNA sequences or minigenes with introns artificially removed. Higher levels of foreign gene expression can be achieved using a hybrid expression system in which the transgene is driven by the bacteriophage T7 promoter, and the T7 RNA polymerase is expressed from a second vector (146). High level transient expression can be achieved if the T7-expressing vector is a plasmid, transiently present in the cell following transfection. More prolonged expression is achieved by incorporating the T7 gene under the control of a vaccinia promoter in a second recombinant virus vector. For toxic proteins, inducible expression systems have also been designed. One example incorporates a strong vaccinia promoter, such as 4b, combined with the *lac* operator sequence from *E. coli*. The foreign gene is coexpressed with *E. coli lacI*, encoding the Lac repressor, allowing foreign gene expression to be regulated by isopropyl-β-D-thiogalactopyranoside (IPTG).

Vaccinia forms large plaques on permissive cells, and these can be lifted onto nitrocellulose or nylon filters and subjected to hybridization-based screening for the foreign gene. Negative TK selection is used where the foreign gene is inserted into the viral *Tk* locus: tk^- viruses are resistant to the normally lethal effects of 5-bromodeoxyuridine and can be selected on this basis, although naturally occurring tk^- mutants are coselected and true recombinants must still be identified by hybridization. Negative HA selection is used where the foreign gene is inserted into the viral hemagglutinin locus: When chicken erythrocytes are added to the plate, HA plaques are clear, whereas wild-type plaques are red. Selection can also be accomplished by cotransfer of a dominant selectable marker such as *neo* or *gpt* or a visible marker such as *lacZ*. The latter is a popular screening method: Recombinant plaques become blue when incubated in the presence of X-gal, while parental plaques remain clear.

14.7.10 Hybrid Viral Vectors

Individual viruses have certain advantages and disadvantages as vectors, and none is suitable for all applications (103). For instance, herpes virus and adenovirus each has a broad host range, and herpes virus in particular has a large capacity, but neither integrates efficiently into the host genome. Conversely, while AAV integrates with great efficiency, it has a limited capacity. Recently, there has been an effort to design hybrid viral vectors with selected advantageous properties from each of the component viruses. This is one direction in which the field of vector development could expand in the next few years, providing vectors for specific applications, especially for gene therapy (103). Using the example given, a HSV vector carrying inducible AAV *rep* functions could be used to carry recombinant AAV into a broad range of cells, facilitating transfer of the AAV passenger to the genome. The advantage of this strategy is that the AAV genome does not need to be packaged, and there would therefore be no size constraints on the foreign DNA it could carry.

14.8 EXPRESSION PARAMETERS AND OPTIMIZATION—VECTOR AND INSERT SEQUENCES

Sequences in the vector and the insert play a major role in the regulation of foreign gene expression at all levels (transcription, RNA processing, translation, and beyond), and to a large degree, the effect of such sequences is predictable. Much less predicable is the influence of the cellular environment, particularly on integrated transgenes, which are subject to position and dosage effects, and also to variations in the level of DNA methylation.

14.8.1 Transcriptional Initiation: Promoters and Enhancers

Transcriptional initiation is the rate-limiting step in the expression of most higher eukaryotic genes. Control is mediated by *cis*-acting DNA elements that act as binding sites for *trans*-acting regulators termed *transcription factors*. Transcription factors can act positively or negatively and function in one of three ways: (i) by interacting with the transcriptional apparatus to recruit RNA polymerase, and thus influencing the stability of the initiation complex; (ii) by affecting chromatin structure or DNA conformation by displacing a nucleosome or by introducing a kink in the DNA; or (iii) indirectly, by influencing the activity of a second transcription factor.

In animals, many genes are expressed in complex spatial, temporal, and inducible patterns. The manner in which a particular gene is transcribed depends on the combination of *cis*-acting recognition sequences controlling it and the availability of functional transcription factors in the cell (147). Most genes are controlled by at least two functionally distinct elements: a *promoter*, which is located at the 5′ side of the gene and directly interacts with the initiation

complex, and an *enhancer*, which may be located some distance away and interacts with the initiation complex by looping out of the intervening DNA. The promoter is minimally the sequence where RNA polymerase is loaded, and usually consists of an *initiator element* surrounding the transcriptional start site, and/or the *TATA box* located about 25-bp upstream of the start site. The initiator and TATA box are not present in all promoters, but when they are present, they are in the same orientation and on the same strand. Promoters lacking an initiator element typically have multiple start sites because RNA polymerase is not loaded at a unique position. Further motifs are located 5′ to this *basal promoter* and comprise the *upstream promoter elements*. These include (i) the CAAT box, GC-rich boxes, and other elements, which act as binding sites for transcriptional activators; (ii) motifs that bind transcription factors synthesized or activated only in certain cell types and/or at certain developmental stages; and (iii) response elements that bind transcription factors whose activity is inducible or repressible by endogenous and exogenous signals. Enhancers are made up of different motifs, some of which may act generally and some of which may confer cell-type, temporal, or inducible specificity on the gene. Promoters control basal transcription and are therefore orientated so that transcription proceeds only in one direction. Enhancers act to stimulate transcription from a promoter but, because they cannot load RNA polymerase, they have very little promoter activity themselves. Enhancers act in a position-, orientation-, and distance-independent manner and may stimulate transcription up to 1000-fold from a given promoter.

14.8.2 Endogenous and Constitutive Viral Promoters

In the first gene transfer experiments, mammalian transgenes were expressed under the control of their own transcriptional control sequences. As mammalian regulatory elements began to be defined, the use of endogenous promoters continued to impose severe limitations on the range of cells in which foreign genes could be expressed. The rate of recombinant protein expression was wholly dependent on the ability of the cell line chosen to utilize particular promoters and enhancers (20).

The cloning of viral regulatory elements was a breakthrough in gene expression technology. Hence, foreign genes cloned in recombinant viral vectors are often expressed under the control of the most active promoters and enhancers from that viral system, especially as this often represents the most convenient cloning strategy. Examples include the baculovirus polyhedrin and p10 promoters (121), the adenoviral E1 promoter (104), and the vaccinia virus p7.5 promoter (143). Many plasmid overexpression vectors employ the most transcriptionally active promoter/enhancer systems, which maximize the transcription of the cloned gene, and allow expression in a broad range of transfected cells. The most popular systems are the SV40 early promoter and enhancer (148), the Rous sarcoma virus LTR promoter and enhancer (149), and the human cytomegalovirus immediate early promoter (150). These elements function in a broader range of cells because although a virus may not be able to gain entry into all cells due to a lack of appropriate surface receptors, the transcriptional control elements have often evolved to exploit transcription factors present in many cells. While the replication of SV40 is restricted to certain simian cells, the SV40 promoter/enhancer functions in most mammalian cells. Certain cells appear to repress transcription from particular viral promoters; for example, the human embryonic kidney cell line 293, which is widely exploited for propagation of adenoviral vectors, does not support transcription from the SV40 promoter (151).

The advent of transgenic technology and gene transfer to live organisms has resulted in a new requirement for cell- and stage-specific promoters to restrict transgene expression to particular cell types. Examples include the use of cell-specific promoters to ablate particular cell types, the use of milk promoters to obtain high yields of recombinant protein in the milk of transgenic mice and livestock, and the use of neuron-specific promoters to ensure that herpes virus vectors delivered to the brain express transgenes only in neurons and not in glial or epithelial cells.

14.8.3 Inducible Promoters

While high level constitutive protein expression may be suitable for many applications, there are certain situations where the external control of transgene expression is desirable. Where protein overexpression is the aim, external control is required if the recombinant protein is potentially cytotoxic or cytostatic. Furthermore, many experiments require transgenes to be activated at a certain time or for a certain duration.

The earliest experiments involving external transgene regulation took advantage of endogenous inducible systems (152). The best-characterized of these include the heat shock promoter (responsive to elevated temperature) (153), the metallothionein promoter (responsive to the presence of heavy metals such as cadmium and zinc) (154), the mouse mammary tumor virus (MMTV) LTR promoter (responsive to dexamethosone) (155), and the interferon-β promoter (responsive to interferon, viral infection, and dsRNA) (156). A transgene placed under the control of one of these regulatory elements could be stably integrated, and protein expression could be induced by shifting to an elevated temperature or by adding the appropriate inducing substance to the growth medium. These systems suffer from one or more of the following major disadvantages (157): (i) substantial *leakage* (background transgene activity in the noninduced

state); (ii) low *induction ratio* (the ratio of induced to noninduced protein yield); (iii) cytotoxic effects of the inducing agent; and (iv) the concomitant activation of other endogenous genes whose activity may be undesirable or may interfere with the system being studied. For example, activation of the heat shock promoter can induce transgene activity up to 100-fold, but the high temperature causes extensive cell death, blocks protein synthesis, and interferes with protein secretion. Protein synthesis begins when cells are returned to 37°C, but the rate of transcription then drops. Similarly, the metallothionien promoter has a high basal transcription level, an induction ratio of <10, and cadmium is cytotoxic. The glucocorticoid response element of the MMTV LTR promoter provides a more effective system because there is only minimal leakage, but the induction ratio is <10, and other hormone-responsive genes are activated. These promoters have also been used in transgenic animals. In this context, even moderate leakage is unacceptable. A further disadvantage is the unexpected and often undesirable tissue-specific effects of induction, reflecting the tissue-specific distribution of transcription factors or the differential uptake of the inducing agent.

14.8.4 Heterologous, Recombinant, and Artificial Inducible Systems

Many of the problems attributed to the use of endogenous inducible systems can be addressed using systems that are heterologous, recombinant, or totally synthetic. A disadvantage of this approach is that the components of the system (e.g. genes encoding the appropriate *trans*-acting regulators) have to be introduced into the cell along with the target gene and its control sequences. This can be a problem when generating transgenic animals, and for this reason, specific regulator strains of mice have been developed. These can be used to "cross in" heterologous regulatory systems by breeding with transgenic animals carrying the regulatable transgene of interest. Despite this complication, the advantages of nonendogenous systems are manifold (157):

- Transgene induction is specific to exogenously supplied, nontoxic agents.
- Transgene induction does not interfere with any endogenous pathway because no endogenous genes are affected.
- There is no leaking—in the noninduced state, transgene expression is minimal.
- Undesirable cell type–specific effects of induction can be eliminated; alternatively, transgene expression can be induced in specific cell types by design.
- The inducing agent can be chosen to penetrate cells quickly for rapid induction and decay quickly for prompt return to the basal state.

All such systems are designed around a switch principle, where transgene expression is controlled by a heterologous, recombinant, or artificial response element. This is activated (or repressed) by a heterologous, recombinant, or artificial *trans*-acting regulator, whose activity is modulated by a small, exogenously supplied molecule (the inducer). Four major types of system have been exploited (Fig. 14.9): the *E. coli lac* operon (158), the *E. coli tet* operon (159,160), the *Drosophila* molting hormone ecdysone (161), and mammalian steroid hormones (157). Not all inducible switches function at the transcriptional level, and switches at the protein level are discussed later.

The *E. coli lac* system (158) is based on the *lacI* gene, which encodes a transcriptional repressor protein. In the absence of lactose, the LacI repressor binds to operator sites around the transcriptional start site and prevents RNA polymerase initiating transcription. The presence of lactose in the medium results in the synthesis of a metabolic by-product, allolactose. This binds to the repressor, effecting a conformational change that causes it to release the DNA. The same result arises from treatment with a gratuitous inducer, IPTG. Transcription of the genes for lactose catabolism then commences. The strategy for transgene regulation in animal cells is to place a *lac* operator sequence downstream of the transgene transcriptional start site and introduce a second expression construct constitutively expressing the *lacI* gene. Under basal conditions, the transgene is repressed, but if IPTG is added to the medium, the repressor is released from the operator site, allowing transgene expression. This system achieves an induction ratio of about 3–500, up to 100-fold greater than chemical induction systems. However, the number and position of *lac* operator sites in the target gene appears to be critical for correct regulation (159). The original *E. coli tet* system, pioneered in transgenic tobacco plants, was based on a similar principle to the *lac* system. The *tetR* gene encodes a repressor that binds to operator sequences in the *tet* operon when tetracycline is absent. Here, tetracycline itself is the inducer and causes the release of the repressor and induction of the *tet* genes. The operational parameters of the *lac* and *tet* systems in mammalian cells were similar, except that the number and position of *tet* operator sequences was less important for inductive control than the equivalent *lac* operators. The original *lac* and *tet* systems also suffered certain disadvantages. To suppress transgene activity fully, high levels of LacI or TetR proteins were required and were found to be cytotoxic. Furthermore, IPTG and tetracycline levels were slow to decay, resulting in a long time lag before induction.

Some disadvantages of the "repressor"-based systems have been addressed by converting TetR and LacI into activators, by generating fusion proteins in which the repressor is joined to the HSV VP16 transactivator (162,163). In the

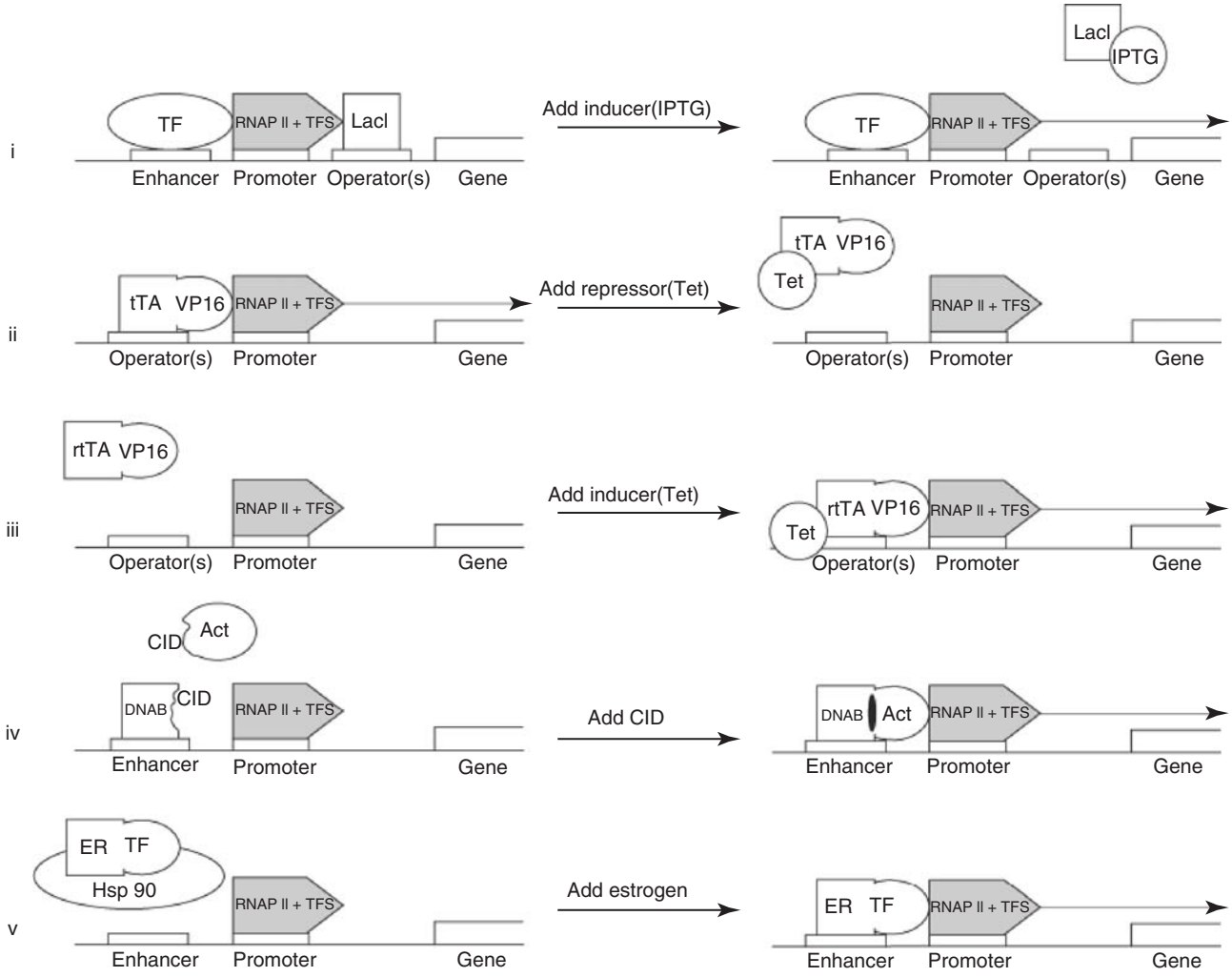


Figure 14.9. Mechanisms of inducible transgene control. (a) Repressor-based system, for example, the Lac switch. The transgene construct contains *lac* operator(s), which bind LacI repressor and prevent transcription. Induction is achieved with IPTG, which binds to and inactivates the repressor, causing it to release the DNA. (b) Activator-based system, for example, tTA. The *E. coli* Tet repressor is fused to a transcriptional activation domain, for example, VP16. The transgene contains *tet* operators that now function as enhancers. Introducing tetracycline into the system inactivates tTA causing transgene repression. (c) Reverse activator-based system, utilizing a mutated Tet repressor–VP16 fusion, which binds to DNA in the presence of tetracycline and releases DNA in its absence. (d) CID system. A transcription factor is expressed as separate DNA-binding and activation domains, each including a binding site for a bivalent ligand such as FKBP12. Introducing the ligand into the system causes dimerization and transcription factor activity. (e) Steroid-based system. A transcription factor is expressed as an estrogen receptor fusion protein. In the absence of estrogen, the fusion protein is sequestered into an inactive complex by Hsp90. Introducing estrogen to the system releases, and hence activates, the transcription factor. *Abbreviations:* TF, transcription factor; RNAP, RNA polymerase; IPTG, isopropyl-β-D-thiogalactopyranoside; Tet, tetracycline; Act, activator domain; DNAB, DNA-binding domain; ER, estrogen receptor.

case of the *tet* system, the fusion product (termed *tTA*) confers constitutive transgene activity in the absence of tetracycline and is suppressible by tetracycline (or its derivative deoxycycline). These systems have a reduced basal transcription level because a eukaryotic enhancer is not required (the operator now provides the enhancer activity) and high levels of repressor protein are unnecessary. This provides an induction ratio in the order of 10^5. One disadvantage, however, is the constant requirement for tetracycline in the growth medium (for cells) or drinking water (for transgenic

animals) to maintain the basal state. This is toxic in many experimental systems, and the unequal distribution of tetracycline results in fluctuation in the basal level of transgene activity, which is intolerable for the regulated expression of some proteins. Furthermore, as induction requires the absence of tetracycline, it is dependent on the rate at which tetracycline can be eliminated. The tTA protein has also proven to be toxic when expressed at high levels, although autoregulatory systems have been designed to optimize tTA expression levels. These problems have been addressed by generating a mutated form of the tTA activator whose DNA-binding activity is improved rather than abolished by tetracycline (164). This protein (termed *rtTA*, reverse tTA) is thus an activator in the presence of tetracycline, removing the requirement for long-term exposure to the inducer. Numerous plasmid- and viral-based delivery vectors have been constructed (157).

The *Drosophila* ecdysone system (161) exploits a steroid hormone signaling pathway endogenous to insect cells but absent from mammalian cells. The steroid hormone ecdysone is responsible for the extensive morphological changes that occur during molting in *Drosophila*. The hormone acts through a heterodimeric transcription factor of the nuclear receptor family, comprising the products of the genes *ecr* (ecdysone receptor) and *usp* (ultraspiracle). This system can be used for transgene regulation by including an ecdysone response element upstream of the transgene and cotransfecting cells with constructs carrying the two *Drosophila* genes encoding the receptor. Transgene induction is achieved by treating cells with either ecdysone or its analog muristerone A. As both the receptor and its response element are insect specific, neither the ligand nor its receptor has any toxic or other physiological effects on mammalian cells. Ecdysone and muristerone A appear to be harmless when injected into mice and are totally eliminated within a few hours. Despite its advantages, the original ecdysone system had a poor induction ratio. This problem has been addressed by introducing mammalian components into the system to generate hybrid receptors recognizing totally artificial response elements. A systems has recently been described in which the Ecr protein is expressed as a fusion with the HSV transactivator protein VP16 and the mammalian glucocorticoid receptor (157). The Usp protein is replaced by its mammalian homolog, the retinoid X receptor. The resulting hybrid recombinant receptor responds to ecdysone and muristerone A and binds to an artificial response element recognized by no other receptor of mammalian or insect origin. This powerful system has minimal background activity and an induction ratio of up to 1000. In addition, because the hormones are eliminated rapidly from cells and animals, this system enables rapid induction and return to the basal state. Perhaps the most promising approach is the construction of a recombinant progesterone receptor carrying the yeast GAL4 DNA-binding domain and the HSV transactivator VP16 (165,166). This receptor is unable to bind progesterone, but can bind the progesterone antagonist RU486, also known as *mifepristone*. Transgenes driven by the yeast GAL4 recognition site are induced by RU486, apparently at levels low enough not to affect endogenous progesterone activity. However, these systems suffer from leakage, low induction ratio, and undesirable physiological effects.

A recently described system of transgene regulation exploits the yeast two-hybrid system. This technique, known as *chemically induced dimerization* (CID), uses a divalent ligand simultaneously to bind and hence aggregate separate DNA-binding and transactivation domains to generate a hybrid transcription factor. This facilitates very tight transgene regulation and shows minimal background effects. The initial system exploited the immunophilin-binding domain of the immunosuppressant drug FK-506. A divalent homodimer of this drug, FK-1012, binds to two immunophilin domains and promotes dimerization (167). A problem with this system is that homodimer transactivators and homodimer DNA-binding domains are generated at high frequency. More recent systems have used heterodimers of FK-506 and rifamycin, so that only two different proteins are able to dimerize, thus preventing such undesirable interactions (168). Unfortunately, while these CIDs penetrate and decay rapidly, they are only active at concentrations causing immunosuppressive side effects.

14.8.5 Transcriptional Termination and RNA Processing

In eukaryotic cells, the primary transcripts of protein-encoding genes are extensively processed before export from the nucleus for translation. The processing steps include the addition of an inverted 7-methylguanosine cap to the 5′ end, the removal of introns by splicing, the cleavage and polyadenylation of the 3′ end, and the methylation of certain internal bases (169). The function of internal methylation is not understood, but the other modification steps are essential for message stability, nuclear export, and efficient translation. These factors must therefore be taken into account when designing expression vectors.

14.8.5.1 Capping. All eukaryotic mRNAs are capped. The capping process occurs immediately following transcriptional initiation, probably because the enzyme responsible (mRNA guanyltransferase) is associated with the initiation complex. Most animal cell mRNAs have a type 1 cap, which is methylated at position G^7 of the cap itself and at position $O^{2'}$ on the ribose moiety of the next residue. The capping reaction occurs automatically;

hence, no special precautions are needed to ensure that vector-encoded transcripts are capped. The cap serves a number of functions—it appears to be required for nuclear export, it prevents 5′ end degradation, and it serves as a recognition site for the factors that initiate translation.

14.8.5.2 Intron Splicing. Most genes in animal cells are interrupted by one or more noncoding segments of DNA, known as *introns*. These are removed from the primary transcript by the recognition of 5′ and 3′ splice sites by a large, *trans*-acting spliceosome assembly. The activities of the spliceosome result in a transesterification reaction that joins the upstream and downstream exons and eliminates the intron. Many vertebrate genes contain large and numerous introns, and the majority of mammalian genes comprise more intron material than exon material, in some cases exceeding 95% of the transcription unit. However, due to the size constraints of many expression vectors, the simplicity of *in vitro* manipulation, the genes are often expressed as cDNAs or as artificial minigenes with all introns removed (20,6,170).

Splicing might be required for efficient mRNA synthesis, prompting the inclusion of an intron in the transcription unit. Many investigators have independently confirmed that cDNA expression is either intron dependent or significantly improved in the presence of an intron, in some cases up to 500-fold (170). However, there have also been numerous reports of cDNAs that are efficiently expressed without an intron. Furthermore, there are a number of mammalian genes that lack introns, and the vast majority of bacterial genes lack introns yet are still efficiently expressed in mammalian cells. However, the presence of an intron has rarely been shown to have adverse effects. Genuine introns include the SV40 small t-antigen intron (used, e.g. in vectors marketed by Invitrogen) and the human growth hormone intron. Improved expression has been documented using hybrid introns, for example, comprising a 5′ splice site from the β-globin gene and a 3′ splice site from an immunoglobulin gene. These are particularly close to the ideal splice signal consensus. In some cases, point mutations have been introduced so that introns match the splice consensus perfectly. The requirement for introns in transgenic animals is more widely accepted, and genomic constructs are generally more efficiently expressed than cDNAs (171).

Early investigations showed that the presence or absence of an intron could control gene expression by affecting the resultant levels of mRNA. The role of introns in the regulation of foreign gene expression has been investigated recently, and a posttranscriptional regulatory mechanism has been identified (172). Primary transcripts are associated with proteins during synthesis, processing, and export from the nucleus to form heterogenous ribonucleoproteins (hnRNPs). It appears that intron-containing and intronless genes expressed in the nucleus end up associated with different sets of proteins and that this ribonucleoprotein architecture may affect translational efficiency. The absence of an intron resulted in a significant amount of posttranscriptional silencing, presumably due to repression by hnRNP structure. An intron placed at the 5′ end of the transcript could alleviate this silencing, but a 3′ intron increased the silencing effect. Although these data were obtained using *Xenopus* oocytes rather than mammalian cells, the study provides evidence that the nature of the transcription unit can affect subsequent levels of gene expression by stimulating the recruitment of particular regulatory proteins. While the evidence from mammalian systems is in some cases contradictory, the presence of a 5′ intron is also favored and may indicate that a similar mechanism is in operation.

Another consideration is the nature of the splice signals and the presence of cryptic splice sites. Generally, eukaryotic primary transcripts are spliced in a predictable fashion, even though all introns carry the same consensus splice signals, which are short enough to occur by chance. The sequence context of the splice sites, the distance between them, and the secondary structure adopted by the nascent transcript or completed primary transcript may dictate how the splicing apparatus and RNA interact to define the introns to be removed. If a normal splice site is mutated, one or more local cryptic splice sites may become active, and these are used efficiently even if there is no "leaky" cryptic splice site usage in the wild-type transcript. This readiness to utilize alternative splice sites should be considered when designing recombinant genes with hybrid introns, as they may not be spliced in a predictable fashion and may produce aberrant transcripts that are not translated.

Finally, the requirement for introns should be considered carefully if a viral gene delivery strategy is favored. The inclusion of sense-orientation introns in retroviral vectors can interfere with the viral replication cycle (134,135). If a cDNA or intronless minigene cannot be expressed efficiently, the intron-containing genes must be inserted in the reverse orientation so that the introns are not recognized during the transcription phase of the replication cycle. Poxviruses are unusual DNA viruses that replicate in the cytoplasm, and no viral genes contain introns because the virus does not have access to the nuclear splicing machinery. Therefore, foreign genes cloned in poxvirus vectors such as vaccinia virus must also lack introns (143).

14.8.5.3 Transcriptional Termination and Polyadenylation. The mechanism of transcriptional termination is thought to occur downstream of the mature 3′ end of the transcript, which is generated by endonucleolytic cleavage of the nascent RNA (169). The cleavage reaction is followed by polyadenylation, the addition of a variable number (approximately 200) of adenylate residues to

generate the so-called poly(A) tail. This occurs 10–30 nucleotides downstream of a highly conserved polyadenylation site, with the consensus sequence AAUAAA. A GU-rich sequence downstream of the polyadenylation site may influence the actual position of cleavage. Cleavage and polyadenylation are carried out by a multimeric complex comprising recognition factors that bind to the polyadenylation site, a dimeric cleavage enzyme, and the enzyme polyadenylate polymerase. Although the precise function of polyadenylation is not known, it appears to increase mRNA stability and control mRNA export. If the polyadenylation site is mutated, the level of protein synthesis can drop by as much as 90%. It is therefore essential to include an authentic polyadenylation site and terminator region in expression vectors, downstream of the foreign gene. A number of polyadenylation sites are commonly used, including those from the SV40 early transcription unit and the mouse β-globin gene. The inclusion of a polyadenylation site within the vector removes any reliance on endogenous polyadenylation sites supplied with foreign genes and cDNAs. This is particularly advantageous for the expression of genes and cDNAs with large 3′ UTRs, because these can be trimmed off, an operation that may also improve transgene expression by increasing mRNA stability (170).

14.8.5.4 Polyadenylation Sites in Cointegrate Vectors. Many gene transfer experiments involve the use of cointegrate vectors, that is, vectors containing multiple genes. A cointegrate vector is usually defined as one where linked genes are under separate transcriptional control and gene transfer experiments involving two or three genes linked on the same vector. In such vectors, it is particularly important to include termination/polyadenylation sequences at the end of each transcription unit. If this is not carried out, it is possible for gene expression to be limited at three levels. First, where transcription from one gene reads through into a second downstream gene, *promoter occlusion* can occur. This involves transcription through the promoter of the downstream gene, preventing the assembly of the transcription complex and blocking gene expression (173). Promoter occlusion occurs if two adjacent genes are in the same orientation. If adjacent genes are in opposite orientation, read-through transcription from one gene generates antisense RNA that can block the expression of the second gene at the posttranscriptional level, a phenomenon termed *antisense suppression*. If both promoters are active, both sense and antisense RNA can be generated. These may associate to generate dsRNA, activating the DAI protein kinase, which phosphorylates and inactivates eIF2, a critical translation initiation factor (71). These problems can be alleviated by preventing read-through transcription, through the inclusion of a terminator and polyadenylation site after each gene.

14.8.6 Protein Synthesis

14.8.6.1 Kozak Consensus. The requirements for high efficiency translation of foreign genes in mammalian cells have been studied in great detail (174,175) and reflect three important properties of the foreign gene: (i) the nucleotide sequence surrounding the translational start site, (ii) codon choice throughout the coding region, and (iii) the structure of the 5′ and 3′ UTRs.

The optimal translational start site sequence was defined by Kozak as 5′ CCRCC*AUG*G 3′, with the italicized sequence representing the initiation codon (R is any purine). The adenosine residue of the initiation codon is defined as position +1 of the coding region and the residue immediately 5′ to that is defined as position −1 (there is no position 0). The two most important residues appear to be the purine at position −3 and the guanosine at position +4. Most expression vectors contain the Kozak sequence, although only proteins with valine, alanine, glutamine, glycine, or aspartate as their second residue can be specified by a coding region with guanosine at position +4. Mutations deviating from the Kozak consensus can reduce protein expression levels by up to 90%.

14.8.6.2 Codon Choice. The genetic code is degenerate; hence, most amino acids are encoded by a family of codons. Some codon families (e.g. those encoding leucine and serine) have as many as six members. The analysis of many gene sequences obtained from different organisms has revealed two important principles of codon usage. First, there is codon bias; that is, particular codons within a family are used more often than others. Second, the codon bias differs from species to species, so that a codon favored in one animal might be different to that favored in another (176). Codon bias can reflect several underlying factors. Degeneracy at first and second base positions is caused by the presence of isoaccepting tRNAs, alternative tRNAs that are charged with the same amino acid but recognize distinct codons. Third base degeneracy reflects the relaxed base pairing rules (the so-called wobble rules) at the third base of the codon and the first base of the anticodon, which reflects the modification of tRNA bases. A further reason for codon bias involves bulk properties of the genome. In GC-rich genomes, guanine- or cytosine-containing codons might be favored over adenine- or thymine-containing codons, while in AT-rich genomes, the opposite bias might apply. Codon choice can influence transgene expression at several levels. The progress of translation can be inhibited if a particular codon is favored in the source organism, but not in the host to which the foreign gene is transferred. The translation machinery may pause at a rare codon. This may reduce the rate of protein synthesis, resulting in a lower yield, or it may cause misincorporation, frameshifting, or truncation. This can be addressed by attempts to match codon preference in the

transgene to that of the host, by introducing translationally neutral mutations into the coding region. However, this can sometimes have unpredictable effects by influencing the stability of the mRNA. It should also be borne in mind that rare codons are occasionally used in a regulatory capacity and that under some special circumstances, they may even misread in a programmed fashion. Examples include frameshifting during the translation of retroviral *gag* and *pol* genes and insertion of the rare amino acid selenocysteine (169).

14.8.6.3 Structure of Noncoding Regions. The structure of the 5′ UTR influences translational efficiency by affecting ribosome assembly and scanning (174,175). Ribosomes comprise two subunits, and initial binding involves only the small subunit, which interacts with proteins assembled at the 5′,7-methylguanosine cap, and scans along the mRNA until the first AUG codon is encountered. If the 5′ UTR contains a significant amount of secondary structure, assembly and scanning can be inhibited. The presence of false AUG codons upstream of the genuine start site is also deleterious, especially if they are followed by in-frame termination codons. Most expression vectors are therefore designed to incorporate minimal *processed* 5′ UTR sequences (there may be an intron in the 5′ UTR, but this would not be represented in the processed mRNA) or a 5′ UTR known to function efficiently in concert with the appropriate promoter–enhancer system. The sensitivity of transgene expression to sequences upstream of the initiation codon means that it is important to ensure that sequences at the 5′ end of the insert do not generate secondary structure or additional start codons when integrated into the vector.

A 3′ UTR is not usually included in expression vectors because it serves no function essential for translation. Endogenous 3′ UTRs may contain regulatory elements, such as AU-rich elements conferring instability on the message resulting in rapid turnover (177). Typically, the entire 3′ UTR is removed from cloned genes or cDNAs before insertion, so that the termination codon of the transgene is more or less adjacent to the polyadenylation site (170).

14.8.6.4 IRESs and Polycistronic Vectors. Multiple genes may be expressed on the same cointegrate vector as independent transcription units, by placing each under the control of an independent promoter and polyadenylation site. Another way to express multiple genes on a single vector is to include several coding regions in the same polycistronic message. The discovery of IRES elements provided a useful strategy for transgene coexpression and selection for high level foreign gene expression (178). A reporter gene such as *lacZ* can be placed downstream of an IRES in the same transcription unit as a given foreign gene. This allows cells expressing the foreign gene to be identified through coexpression of β-galactosidase. This is particularly useful in transgenic animals where expression patterns can be mapped and the effect of heterologous protein expression determined in the same animals (179). In knockout mice, the insertion of an IRES–*lacZ* construct into an endogenous gene facilitates both knockout by insertional mutagenesis and the identification of cells that now lack the targeted gene product (179). The expression of genes downstream of an IRES is much less efficient than normal 5′ cap-dependent genes. This can be exploited to isolate cells expressing foreign genes at high levels. If a selectable marker is placed in the downstream position, only cells with high levels of marker expression will survive, and this will identify cells with elevated levels of foreign gene expression (170).

14.8.7 Posttranslational Events

During or following synthesis, all polypeptides undergo some form of covalent modification before folding to form functional proteins. Such modifications may involve minor chemical changes to specific amino acid side chains or the addition of major chemical adducts such as complex oligosaccharides or lipids. Other proteins are modified by endo- or exoproteolytic cleavage. In some cases, protein modification may be reversible and can be used as a means to regulate protein activity (e.g. phosphorylation of serine, threonine, and tyrosine residues) or can be permanent (e.g. glycosylation and proteolytic cleavage). Certain forms of modification are required for the protein to adopt its correct tertiary or quaternary structure (e.g. the formation of disulfide bonds) or are characteristic of particular protein sorting pathways in the cell; for example, N-linked glycosylation occurs in the endoplasmic reticulum (ER) lumen and O-linked glycosylation occurs in the Golgi network. In some cases, particular modifications are required for protein sorting (e.g. the addition of mannose-6-phosphate groups targets proteins to lysosomes and the cleavage of signal peptides may be required to reveal further targeting motifs, e.g. in mitochondrial import). Finally, some forms of protein modification are involved in the regulation of protein degradation (e.g. ubiquitination of lysine residues).

The secretion of proteins from mammalian cells involves a series of modifications that take place in the ER and Golgi (180,181). Such proteins generally carry an N-terminal signal peptide that causes the ribosome to associate with the ER membrane. The protein is then cotranslationally translocated into the ER lumen, a process termed *vectorial discharge*. In the lumen, the signal peptide is cleaved, and a preformed high mannose oligosaccharide is added to asparagine residues in the "sequon" element with the consensus sequence Asn–Xaa–Ser/Thr (Xaa is any residue except proline). Terminal glucose residues and

probably a single mannose residue are removed, and fatty acylation may also occur, before the part-modified protein is transported to the Golgi network. In the Golgi, further modifications occur to the N-linked glycosyl groups, including the hydrolysis of more mannose residues, and the addition of distinct oilgosaccharide groups such as fucose, galactose, *N*-acetylglucosamine, and sialic acid. De novo O-linked glycosylation may also occur by the transfer of *N*-acetylglucosamine groups to serine and threonine residues. In addition to glycosylation and acylation, other forms of modification also occur in the secretory pathway, such as the O^4-sulfation of tyrosine residues, and various forms of proteolytic processing.

14.8.7.1 Factors Affecting the Processing of Recombinant Proteins. Three major factors affect the processing of recombinant proteins: (i) correct targeting of the protein, (ii) the ability of the protein to fold and undergo proper modification, and (iii) the availability of appropriate enzymes in the host cell. A protein that requires a particular form of posttranslational modification needs to be targeted to the correct intracellular compartment for that processing to occur. Hence, a normally secreted protein whose coding region is truncated so that the signal peptide is no longer translated will likely accumulate in the cytoplasm in a biologically inactive form. Many vectors are available with integral secretory signals to target expressed proteins to the secretory network. Other targeting motifs, such as mitochondrial entry sequences and nuclear localization signals, are also terminal, and the same precautions need to be taken when expressing proteins containing these signals.

The modification of a protein is dependent on the presence of appropriate targeting sequences, the presence of modification consensus sequences (such as the N-linked glycosylation sequon), the sequence context surrounding this motif, and the overall tertiary conformation of the protein. Modification relies not just on the presence of particular motifs in the polypeptide primary structure, but also on the tertiary structural context in which this motif is presented to the processing enzymes and the enzyme positioning (e.g. in the Golgi). Furthermore, where modification occurs in a series of successive steps, each modification may cause the tertiary structure of the protein to change to make it more accessible to the next processing enzyme. Hence, any alteration to the primary structure of a polypeptide may cause a critical deviation from the optimum tertiary conformation, resulting in the failure of a particular modification reaction (182). This is demonstrated by the alteration of, for example, glycosylation patterns following mutations causing nonconservative amino acid changes or following the incorporation of amino acid analogs.

Finally, it has been observed that recombinant proteins may be processed differently in alternative expression hosts, probably reflecting the absence or differential abundance of processing enzymes. Some differences in glycosylation patterns have been observed between alternative mammalian hosts; for example, secreted proteins produced in CHO cells tend to have more terminal sialic acid residues than those produced in COS cells (183,184). Insect cells use a distinct N-linked glycosylation pathway to that found in mammals (185). Proteins expressed in the popular Sf9 cell line cannot produce certain glycosylation intermediates, such as side chains ending in galactose–sialic acid residues, and this is thought to reflect the absence of a key processing enzyme synthesized in mammalian cells, *N*-acetyl-β-glucosidase. However, cell lines derived from the alternative host *E. acrea* do synthesize *N*-acetyl-β-glucosidase and are hence more likely to produce authentic mammalian glycoproteins. Recently, the ability of the baculovirus expression system to coexpress two or more proteins simultaneously has been exploited to alter the endogenous glycosylation pathway of Sf9 cells (186).

14.8.7.2 Many endogenous proteins are processed by cleavage. Some are autoproteolytic, while others, including inactive proenzymes (zymogens), growth factors, and a large number of hormones and neuropeptides (e.g. proinsulin, proglucagon, prorenin, proenkephalin, prodynorphin) require modification in *trans*. The overexpression of such recombinant proteins is often hampered by the low level of endogenous proteases, termed *proprotein convertases*. Recently, a family of proprotein convertases has been extensively characterized and several members have been cloned (187). Several groups have successfully coexpressed the precursor and its cognate proprotein convertase in an attempt to generate high yields of mature recombinant protein, such as insulin in insect cells (188), von Willebrand factor in CHO cells (189), and coagulation factor C in transgenic pigs (190).

14.8.7.3 Inducible Protein Activity. Two promising approaches are the use of steroid-binding fusion proteins (191) and the exploitation of CID (167). The estrogen receptor exists in an inert state in the absence of estrogen because the hormone-binding domain interacts with heat shock protein 90 (Hsp90) to form an inactive complex. When estrogen is present, however, a conformational change causes the release of the receptor, which is then free to dimerize and interact with DNA. The principle of the steroid-based posttranslational switch is that any protein expressed as a fusion with a hormone-binding domain will similarly interact with Hsp90 and form an inactive complex (191). A given heterologous protein can thus be expressed at high levels in an inactive state and can be activated by feeding cells or transgenic animals with estrogen (reviewed in Ref. 192). The kinetics of the switch are rapid, on the order of seconds rather than hours, and can therefore be used to study rapid cellular events

such as those occurring in signal transduction pathways. A more recently developed version of this system uses a modified estrogen receptor, which is highly specific for the ligand 4-hydroxytamoxifen, thus removing many of the pleiotropic effects of estrogen administration (193).

The CID system takes advantage of the ability of ligands to facilitate the dimerization of proteins carrying ligand-binding domains (167). The CID system has already been described as a transcriptional switch, in which separate DNA-binding and transactivation domains expressed as ligand-binding fusion proteins are conditionally dimerized by supplying a divalent ligand. The same idea can be exploited to activate proteins whose normal activation requires a dimerization step or the separately expressed domains of monomeric proteins. CID has been successfully used to regulate the activity of a range of transmembrane receptors and intracellular signaling proteins by conditional activation. It is also possible to use inhibitory proteins to facilitate conditional gene silencing.

14.9 EXPRESSION PARAMETEROPTIMIZATION—CONSEQUENCES OF TRANSGENE INTEGRATION

The integration of foreign DNA into the genome of a host cell is a chaotic and typically random process (194). Certain viral vectors display various degrees of regional specificity, for example, retroviruses may preferentially integrate into actively transcribed DNA (134,135) and wild-type AAV shows definite preference for a particular region of the human genome (111). The existence of preferential integration sites for plasmid DNA transfected into animal cells has been suggested (195). The integration of foreign genes into animal genomes is highly variable among cell lines or transgenic animals generated by independent transformation events. Transgene integration may cause unexpected changes in phenotype. Conversely, transgene expression within a clone of transformed cells, or within a line of transgenic animals, is more likely to be comparable.

As DNA integration is both chaotic and random, several molecular parameters can vary between clones but would be expected to remain the same within clones (194). First, the position of integration can vary, giving rise to the so-called position effects that reflect the influence of the local molecular environment. Second, the number of integrated transgene copies can vary, giving rise to gene *dosage effects*. Third, transgene structure and organization can vary, including factors such as the internal mutation, rearrangement, or truncation of single transgenes and the orientation and arrangement of adjacent transgenes. Finally, transgenes can become de novo methylated, which often causes transgene silencing and may represent a genomic defense mechanism.

14.9.1 Timing of Integration

When DNA is introduced into cultured cells, individual cells are selected on the basis of their ability to express the foreign DNA on a long-term basis, which is an evidence for stable integration. For transgenic animals, however, the timing of integration may play an important role in the behavior of transgenes in different cells and hence determine the characteristics of the whole animal. In mice, DNA introduced into the fertilized egg by pronuclear microinjection often integrates after DNA replication, or after one or more cell divisions, and the resulting embryo may thus be mosaic for transgene insertion. This means that a transgene has to be transmitted through the germline before it is stably inherited.

Mice, and mammals generally, undergo a characteristic form of development where very little material is stored in the egg, and zygotic transcription begins at the two-cell stage. Conversely, animals such as fish and amphibians have large eggs with a stockpile of proteins and RNA. The early embryo undergoes a rapid series of synchronous cleavage divisions followed by an event termed the *mid-blastula transition*, where division becomes asynchronous and zygotic transcription begins. This event is thought to reflect the titration of DNA packaging proteins such as histones. It is the initial surplus of these DNA packaging proteins that may be responsible for the unique behavior of DNA introduced into fish and amphibian eggs. Unlike mammalian systems, where the DNA is soon integrated, exogenous DNA in fish and frog eggs is rapidly concatemerized and subject to extrachromosomal replication (196). As the embryo cleaves, the distribution of transgene copies is arbitrary, resulting in mosaic and variable expression levels between equivalent cells. Although mosaic transgene expression is widely attributed to differential *distribution* of the transgene in cells of the early embryo, there may also be factors causing differential transgene *expression*: This applies to fish, frogs, and mammals (197). Eventually, exogenous DNA is degraded, but at some point, integration may occur. While this is an early event in mouse development, with fish and frogs, integration occurs much later, and the resulting mosaics may contain only a low percentage of transformed cells (reflecting integration after perhaps 12 rounds of cleavage). Consequently, there are different position and dosage effects in different cells of the same animal, and it may also be more difficult to obtain fully transgenic animals.

14.9.2 The Fate of Foreign DNA and the Structure of the Transgenome

Exogenous DNA introduced into animal cells rapidly becomes covalently joined to form larger arrays. The size and structure of the arrays depends on the amount, conformation, and complexity of the source DNA. In

techniques such as calcium phosphate transfection, a large amount of DNA enters the cell. In many cases, at least two independent transgenes are introduced (a selectable marker and one or more nonselected genes) and carrier DNA is used to bring the DNA concentration to optimal levels for coprecipitate formation. Carrier DNA is often sheared or sonicated genomic DNA from a convenient source, such as salmon sperm, and is thus linear and of high complexity. Shortly after transfection, the transgenes and carrier DNA form large, randomly arranged arrays reflecting the arbitrary ligation of DNA fragments. This structure, termed the *transgenome*, usually integrates at a single site. It is sometimes unstable and may be subject to full or partial excision, probably reflecting intrachromosomal recombination events (19,198).

In other transfection methods, and in microinjection, carrier DNA is not used. Less DNA therefore enters the cell and the DNA that does reach the nucleus is relatively simple (and hence repetitive) in its sequence. There are two consequences of using smaller amounts of less complex DNA. First, the transgenome is smaller; hence, the number of integrated transgene copies is reduced. Single or multiple copies can integrate, but rarely more than 30 copies are present at a single site. There may be several sites of integration, and a degree of control can be exercised over transgene copy number by varying the amount of DNA introduced into the cell. Second, smaller amounts of DNA are likely to favor the generation of head-to-tail concatemers rather than randomly arranged arrays. This is because larger amounts of DNA (especially carrier DNA) increase the concentration of free DNA ends, and this can stimulate the synthesis of DNA ligase (199). Large amounts of high complexity DNA thus favor random ligation, while small amounts of low complexity DNA favor homologous recombination. In mammals, linear DNA is integrated five times more efficiently than supercoiled plasmid DNA because it provides a substrate for DNA ligase (78). Supercoiled plasmids presumably have to undergo homologous recombination with each other, or become randomly broken, to generate free ends. Although both linear and circular DNA is concatermerized by homologous recombination in mammals, only circular DNA tends to promote concatemerization in frogs and fish, while linear DNA is more likely to form random arrays. This is presumed to reflect the accumulation of stored DNA ligase in the precleavage embryo, which can use linear but not circular DNA as a substrate (200,201). In fish and frogs, the random ligation of linear DNA is much more rapid than the concatemerization of circular DNA, thus linear DNA is more effective for transient expression, episomal replication, and integration (202).

14.9.3 Position Effects

Position effect is a catch-all term used to describe variability in transgene expression conferred by the position of integration. As the earliest transformation experiments, it has been known that the chromosomal locus of a transgene can influence its expression. For example, when a transgene isolated from an anomalously expressing transgenic mouse is microinjected back into eggs, the secondary transgenic mice may express the transgene in the normal manner (203). This suggests that the anomalous expression profile of the primary transgene was due to the site of transgene integration. Position effects are a major cause of differential transgene expression levels among independently derived transformed cell lines or transgenic animals, and they are also thought to reduce or eliminate copy-number dependence in transgene expression. The position of integration can influence transgene expression through at least three mechanisms (Fig. 14.10): the activity of local regulatory elements, the local chromatin structure, and the local state of DNA methylation. These factors may be interdependent.

A transgene may come under the influence of a local regulatory element, and this causes the most specific position effects (16). If a transgene integrates near an endogenous enhancer, it may come under that enhancer's influence, resulting either in the elevation or depression of transcriptional activity, or in transgenic animals, an altered spatial or temporal expression pattern. The effect of local regulatory elements is succinctly demonstrated by the success of entrapment vectors (16). An enhancer trap consists of a reporter gene linked to a minimal promoter. If this integrates near an endogenous enhancer element, the reporter gene expression pattern reveals the properties of the enhancer. In this case, the position effects are desirable and indeed useful—they can lead to the identification and cloning of a novel gene. Transgenes with weak promoters and enhancers are the most susceptible to such position effects, but local enhancers (and silencers) will affect any transgene construct, even those with strong and specific promoters and enhancers of their own.

Transgenes can also integrate within endogenous genes, in which case they may be influenced by local promoter elements or splice signals (12). Again, there are entrapment vectors that exploit this phenomenon. Such vectors contain either a "naked" reporter gene (i.e. one driven simply by a translational start codon that can respond to adjacent promoter elements) or a splice acceptor site, which enables the vector to function as an ectopic exon when it integrates into an endogenous intron. Transgenes integrating at the 5′ end of a gene may come under the control of the endogenous promoter, or the endogenous and transgene promoter elements may combine in a novel and unexpected manner. Transgenes that integrate into the body of an endogenous gene may be expressed either from their own promoter or as an aberrant hybrid mRNA under the control of the endogenous gene promoter.

Not all position effects result from such specific influences. Gene expression is dependent not only on

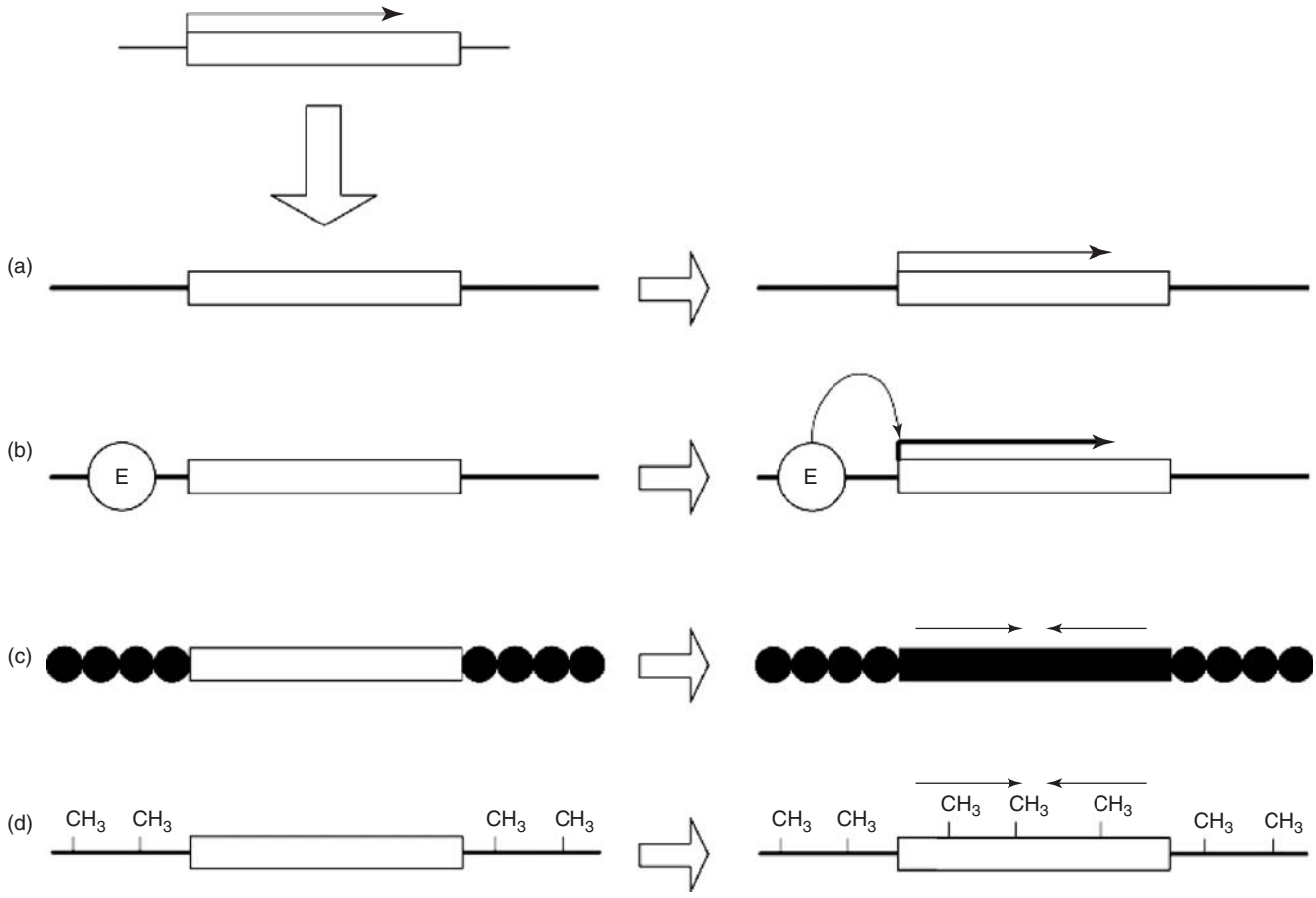


Figure 14.10. Causes of position effects. A transgene under the control of its own promoter (top of figure) integrates into the host genome (left). In (a), there are minimal local influences and the transgene is expressed as expected. In (b), the transgene happens to integrate near an endogenous enhancer; so its expression may be modified by the enhancer. In (c), the transgene integrates into repressed chromatin, while in (d), it integrates into hypermethylated DNA. In either case, the epigenetic structure can spread across the transgene causing silencing.

the availability of specific *cis*-acting sites but also on the local chromatin structure, which may be "open" and transcriptionally active or "closed" and transcriptionally repressed (204). Open and closed chromatin differs in the degree of histone acetylation, the degree of DNA methylation, the presence of certain types of nonhistone protein, and the sensitivity of the DNA to nuclease digestion. A transgene integrating into a region of closed, inactive chromatin (heterochromatin) is often silenced by the spreading of transcriptional repression across the transgene (205). Similarly, if a transgene integrates into hypermethylated DNA, the DNA methylation may also spread across the transgene causing transcriptional silencing. Chromatin structure and DNA methylation are often linked in vertebrates, and indeed, it has been shown recently that methylcytosine-binding proteins exist in a complex with histone deacetylase (206). Certain regions of the genome (e.g. centromeric DNA and the Y chromosome in mammals) consist predominantly of heterochromatin, and transgenes integrating there are likely to be subject to position-dependent silencing. Conversely, other regions of the genome, such as the subtelomeric areas, are highly transcriptionally active, and transgenes integrating there are likely to be efficiently expressed.

Position effects also occur naturally, and in humans, they are often responsible for cancer. If an oncogene is transferred to a new chromosomal locus by a translocation, it may come under the influence of a novel regulatory element, it may fuse with a different gene, or it may find itself integrated into active chromatin, all of which can increase its transcriptional activity, resulting in uncontrolled cell proliferation. In *Drosophila*, a phenomenon often associated with chromosome translocations is *position-effect variegation* (PEV) (207). This occurs when active and repressed chromatin become juxtaposed by a translocation and the transcriptional repression spreads

from the heterochromatin into the active chromatin, but to a different extent in different cells. This reflects the mechanism of heterochromatinization, which is thought to involve the addition of heterochromatin proteins to preexisting heterochromatin. Usually, this occurs until a boundary is reached, but when such a boundary is removed by chromosome rearrangement, the spreading is limited only by the amount of free heterochromatin protein in each cell. Hence, genes near the translocation breakpoint may be inactivated in some cells but remain active in others. This epigenetic state is clonally heritable, causing a variegated pattern resulting from patches of cells with the gene either active or repressed. Similar phenomena occur in transgenic mammals through inconsistent spreading of transcriptional repression from heterochromatin into a transgene. This may cause mosaic transgene activity and is further complicated where there are multiple transgene copies because different numbers of transgenes can be active in different cells. Position effects may therefore cause variable levels of transgene expression, either between individual transgenic animals within a given line or between transgenic lines. For example, discrete patches of transgene-expressing cells surrounded by nonexpressing cells in the mammary gland of transgenic mice expressing β-lactoglobulin transgenes have been observed. It has been proposed that patchy or variegated silencing may be a consequence of the proximity of the transgene array to centromeric heterochromatin (208) or that multicopy transgene arrays may themselves act as the focus for heterochromatin formation (209).

14.9.4 Integration Effects

Position effects describe the influence of the local molecular environment on transgene activity, but the effect may also be reciprocal (2). Transgene integration can generate unexpected phenotypes by influencing the expression of adjacent or even distant genes. The most overt integration effect is insertional mutagenesis, where a transgene integrates into an endogenous gene and generates a mutant phenotype. The phenotype may be apparent immediately if there is only one functional copy of the host gene, if the locus is haploinsufficient, or if the integration event happens to generate a dominant mutant allele. Otherwise, a phenotype may only be observed if the transgene is bred to homozygosity. The effect may be due to simple insertional disruption or through the deletion of cellular DNA surrounding the integration site. This appears to be a totally random process: In some cases, the integration site remains intact; in others, up to 80 kbp of DNA can be deleted. In many cases, insertional mutagenesis by transgene integration has led to the serendipitous isolation of novel interesting genes (14). For example, transgenic mice carrying a tyrosinase transgene were shown to have situs inversus (mirror-image reversal of the left–right axis). This has nothing to do with tyrosinase activity but reveals the functional mutation of a new locus controlling left–right axis specification (210).

More subtle integration effects can also occur. A transgene may cause ectopic activation of a nearby gene that comes under the influence of transgene regulatory elements. This often occurs with retroviral vectors, which carry a strong enhancer–promoter complex in the right-hand LTR. Wild-type retroviruses also show this activity and can occasionally activate an adjacent proto-oncogene causing it to be overexpressed. Specialized "suicide" retroviral vectors have been designed to limit this effect: They have a mutated LTR promoter–enhancer, with transgene expression driven by an internal promoter (142). Another consequence of transgene integration is the alteration of cellular methylation patterns. Surprisingly, the integration of certain sequences can cause the alteration of cellular methylation patterns at sites located a great distance from the integration locus (2).

14.9.5 Copy-Number and Dosage Effects

Foreign DNA may integrate either as a single transgene copy or as multiple copies, and the copy number depends on the transfection method and the amount of DNA used. For conventional transgenes, there appears to be no correlation between transgene copy number and expression. Copy-number dependence may be blocked by position effects. If position effects are abolished, transgene expression often becomes copy number related, if not perfectly correlated. The discrepancy may reflect interaction in *trans* between transgene copies or the unaccounted presence of nonfunctional transgenes in the cluster. The effects of transgene dosage can best be observed where a single gene causes a dose-dependent phenotype in a transgenic animal. Hence, when the *Pax-6* gene was expressed in YAC transgenic mice, a range of eye phenotypes was observed, reflecting varying dosage of this transcription factor (211). Gene amplification strategies, which produce thousands of transgene copies, eventually maximize transgene expression by saturating the protein synthesis machinery, but provide little information concerning the effect of transgene dosage on protein expression levels in a nonsaturated system.

14.9.6 Organization

Several aspects of transgene organization could potentially affect transgene activity, resulting in the production of mutant or aberrant proteins or in the failure of transgene expression (2). Foreign DNA often undergoes point mutation due to damage in transit. This applies especially to transfected DNA, less so to virally transduced DNA and DNA injected directly into the nucleus. Furthermore, the integration event itself is often destructive, resulting in

the deletion of terminal regions of the transgene, internal rearrangement, and transgene fusion. This can result in the production of aberrant, compound, and truncated transcripts.

Transgenes are generally integrated at a single site in pseudotandem arrays (arrays where fragments of host DNA and transgene DNA may be interposed between neighboring transgenes). In cotransfer experiments (i.e. where two or more discrete transgenes are introduced into the cell at the same time), both transgenes tend to integrate at the same site, whether the two genes were originally linked on the same, cointegrate vector or were cotransfected using separate vectors. For cointegrate vectors, the copy number of each transgene is approximately the same within individual cell clones, and the numbers covary between clones. For separate transgenes, the copy numbers of each transgene appear to vary independently between clones, although if one transgene is a selectable marker, there is often less cross-clone variability for that transgene due to selective constraints. Transgenes may integrate at more than one locus, and occasionally, cotransfected transgenes may integrate separately. Adjacent transgenes may also influence each other's expression. Tandem transgenes may cause promoter occlusion by transcriptional read-through, while inverted transgenes may cause antisense suppression. However, while adenoviral VA_I RNA can improve episomal foreign gene expression following transient transfection, stable transgene expression appears not to be affected, suggesting that significant amounts of dsRNA are not synthesized. Some bacterial sequences in transgenic animals have been shown to exert specific negative transcriptional effects in *cis*. Most problems are caused by vector backbone sequences, which can be efficiently separated from the transgene before gene transfer (29). However, the selectable marker *neo* has also been shown to exert undesirable negative effects on adjacent promoters (212), and strategies for generating transgenic animals often incorporate a recombination step, allowing the removal of this marker.

14.9.7 DNA Methylation and Homology-Dependent Gene Silencing

In vertebrate genomes, approximately 10% of cytosine residues in the dinucleotide motif 5′-CG−3′ are methylated. DNA methylation is often correlated with gene silencing (213,214), and transgenes methylated *in vitro* before gene transfer also tend to be silent, in contrast to nonmethylated transgenes of identical sequence. It has been proposed that DNA methylation may be widely used as a form of gene regulation in mammals. The analysis of methylation sites in mammalian DNA suggests that the primary role of DNA methylation may be the silencing of invasive DNA, such as that of viruses and transposable elements. Most naturally occurring methylated cytosine residues in human DNA have been found to lie within *Alu* and LINE elements, two abundant classes of dispersed repetitive DNA corresponding to active and "ghost" (inactivated by mutation) transposable elements (215).

DNA methylation is relevant to animal cell genetic engineering in several ways. First, transgenes introduced into cells and transgenic animals are frequently de novo methylated (2,216), either immediately on integration, or within a few cell generations (in cell lines) or after passing through the germline (in transgenic animals). This type of methylation is different to the methylation spreading phenomenon discussed previously. For example, de novo methylation is position independent and may affect transgenes integrated at known active chromosomal sites. The mechanism of de novo methylation is poorly understood, but the targeting of many unrelated transgenes suggests that a specific sequence is not responsible for initiating methylation (217). The de novo methylation apparatus may scan the genome for unusual structure, such as uncharacteristic chromatin conformation following an integration event. It has also been suggested that transgenes may be identified on the basis of their atypical base composition. Vertebrate genomes are divided into the so-called isochore regions, each with a specific base composition (average % GC content). The different isochores are also characterized by differences in gene density, gene structure, chromatin conformation, replication timing, recombination frequency, and the presence of specific classes of transposable element (218). The base composition is maintained in the genes and the surrounding nontranscribed DNA, and isochore regions are separated by relatively distinct borders containing clusters of repetitive elements. In plants, it has been suggested that the tendency for some transgenes to be consistently expressed and for others to be consistently silenced in a particular host species reflects the degree of cross-species isochore similarity (219). It may therefore be possible to protect transgenes from de novo methylation by matching their base composition to that of the integration site.

A second methylation effect in gene transfer experiments was observed when cells were transformed with either adenoviral or bacteriophage λ DNA (2). Integrated transgenes (in this case the viral genome) often undergo de novo methylation. A more surprising consequence of transgene integration, however, is the alteration of cellular DNA methylation patterns at loci very distant from the integration site, including endogenous genes. DNA hypermethylation generally corresponds to transcriptional repression, so it is possible that the integration of a transgene at one site in the genome can alter endogenous gene expression patterns by causing some genes to be methylated and repressed and others to be demethylated and activated.

In certain plants, multicopy transgene integration often leads to transgene silencing, whereas single copy insertion

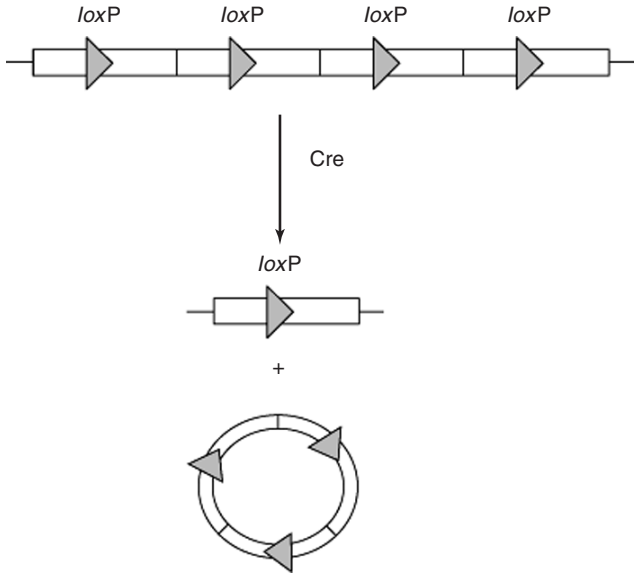


Figure 14.11. Repeat-induced gene silencing by Cre recombinase. If transgenes carry a single Cre recombinase recognition site (*loxP*), the activation of Cre recombinase in a multicopy transgenic animal results in copy number reduction, from four to one. The excised copies are rapidly degraded, and the single-copy transgene is expressed at a much higher level.

results in high level transgene expression (219). This phenomenon is position independent but may be copy number related, and often involves DNA hypermethylation. Homology-dependent silencing occurs at two levels. At the transcriptional level, silencing often occurs if there is homology in the promoter region, and is thought to result from ectopic DNA pairing, which initiates de novo methylation. Cre recombinase (discussed in the following section) has been instrumental in demonstrating that this phenomenon of *repeat-induced silencing*, which has been extensively reported in both plants and *Drosophila*, also occurs in mammals (Fig. 14.11) (220). Silencing can also occur at the posttranscriptional level, requiring homology in the coding region, and may involve the production of aberrant or antisense RNA molecules. Alternatively, a threshold system may be in operation, where a certain mRNA dosage stimulates RNA degradation. A remarkable consequence of posttranscriptional silencing is *cosuppression*: If a transgene is homologous to an endogenous gene, multicopy integration can silence not only the transgene but also the endogenous gene, generating an apparent null phenotype (219). The first cases of cosuppression-like silencing in animals were observed in *Drosophila* (221).

14.9.8 Stability and Transmission

It is also important to consider how transgenes are maintained and transmitted through successive cell divisions following integration. In cells transfected using calcium phosphate, it is not uncommon to see complete or partial transgene excision, resulting in reversion to the nontransformed phenotype. Other forms of transformation are more stable because the transgenome is smaller, but where there are multiple transgene copies, copy number expansion or reduction can occur through unequal crossing over or sister chromatid exchange between tandem repeats. This mechanism is thought to be responsible for generating the large transgene arrays that accompany gene amplification. The maintenance of selection ensures that any cell undergoing reversion is counterselected, and increasing selection pressure selects for those cells with copy number expansions. Integrated transgene arrays and amplified units are often pseudotandemly arranged, containing fragments of host DNA between transgene copies. They also appear to contain unlinked DNA, which may originate a great distance away from the amplification site. It is unknown how this DNA is cointegrated and coamplified, but is presumed to represent chromosomal recombination events resulting from the interaction of distant loci in *trans*.

In transgenic animals, spontaneous transgene loss is also observed. In species such as fish and frogs, the tendency for foreign DNA to be replicated and episomally expressed means that it is not always possible to confirm that integration has occurred. This can be checked by various experimental approaches, including Southern hybridization to genomic DNA, analysis of Mendelian segregation ratios, *in situ* hybridization to chromosomes, and sequencing across integration junctions (196). Only rarely has sustained episomal maintenance been observed in transgenic mice. Very occasionally, the loss of a transgene phenotype may be caused by transgene excision or mutation early in development, so that the resulting mouse is phenotypically and genotypically wild type. More often, the genotype of the animal is unchanged, and changes in phenotype result from transgene silencing through de novo transgene methylation. This may occur after one or more generations and is subject to various controlling factors, including the influence of different genetic backgrounds and the parental route of transgene transmission (222). Transgenes, such as endogenous genes, may be subject to parental imprinting effects. Hence, the offspring of a transgenic male and wild-type female may show a different phenotype to that of a wild-type male and transgenic female, through sex-specific transgene methylation during gametogenesis (223). In mice, particular strains are associated with different forms of transgene behavior. BALB/c and C57BL/6 backgrounds are thought to promote de novo methylation, while inbred lines such as DBA/2 are thought to promote demethylation (224). Hence, crossing a founder transgenic mouse with a BALB/c wild-type mouse may cause transgene silencing in the mixed genetic background. Conversely, crossing to a

DBA/2 mouse often results in continued transgene activity and can also erase transgene parental imprinting effects. Strain-specific methylation, transgene cluster mosaic methylation, cellular mosaicism for transgene methylation, and imprinting may be largely position dependent (222).

14.9.9 Design of Transgenes for Transgenic Animals

With the information presented previously concerning transgene behavior, and the time and expense required for the generation of transgenic animals, it is beneficial to give careful consideration to transgene design. The ability to modify transgene constructs *in vitro* means that sequences from diverse sources can be combined, and completely synthetic genes can be constructed. This is extremely useful when the intention is the ectopic expression of a protein. For example, a protein normally found in blood can be targeted to milk by linking the regulatory DNA elements from a gene normally expressed in the mammary gland to the protein coding sequences of the gene of interest (225). This type of construct is termed a *hybrid transgene*, and the strategy is being exploited to develop transgenic livestock as animal bioreactors for the commercial production of human pharmaceuticals.

Unfortunately, for the majority of genes, the exact location of the regulatory elements required for efficient expression is still unknown. Consequently, for many studies, the sequences included in the transgene and their organization have been determined on an empirical basis. First, all prokaryotic vector sequences should be removed before microinjection (194). Second, transgene design should be as simple as possible. Where hybrid transgenes are used, the sequences from different sources are linked to generate a novel gene, and it is best to keep the number of different sequence fragments as small as possible. A third consideration is whether to use genomic or cDNA sequences. In general, genomic sequences are expressed more efficiently. Many studies have demonstrated that introns facilitate cDNA transgene expression and that intron removal reduces genomic transgene activity (Fig. 14.12), although the mechanisms involved remain to be identified (226). Fourth, if precise transcriptional control elements have not been defined, it is best to use as large a promoter region as feasible. This has been facilitated by the development of methods to introduce large genomic fragments (e.g. YACs) into the mouse germline. Finally, inclusion of dominantly acting

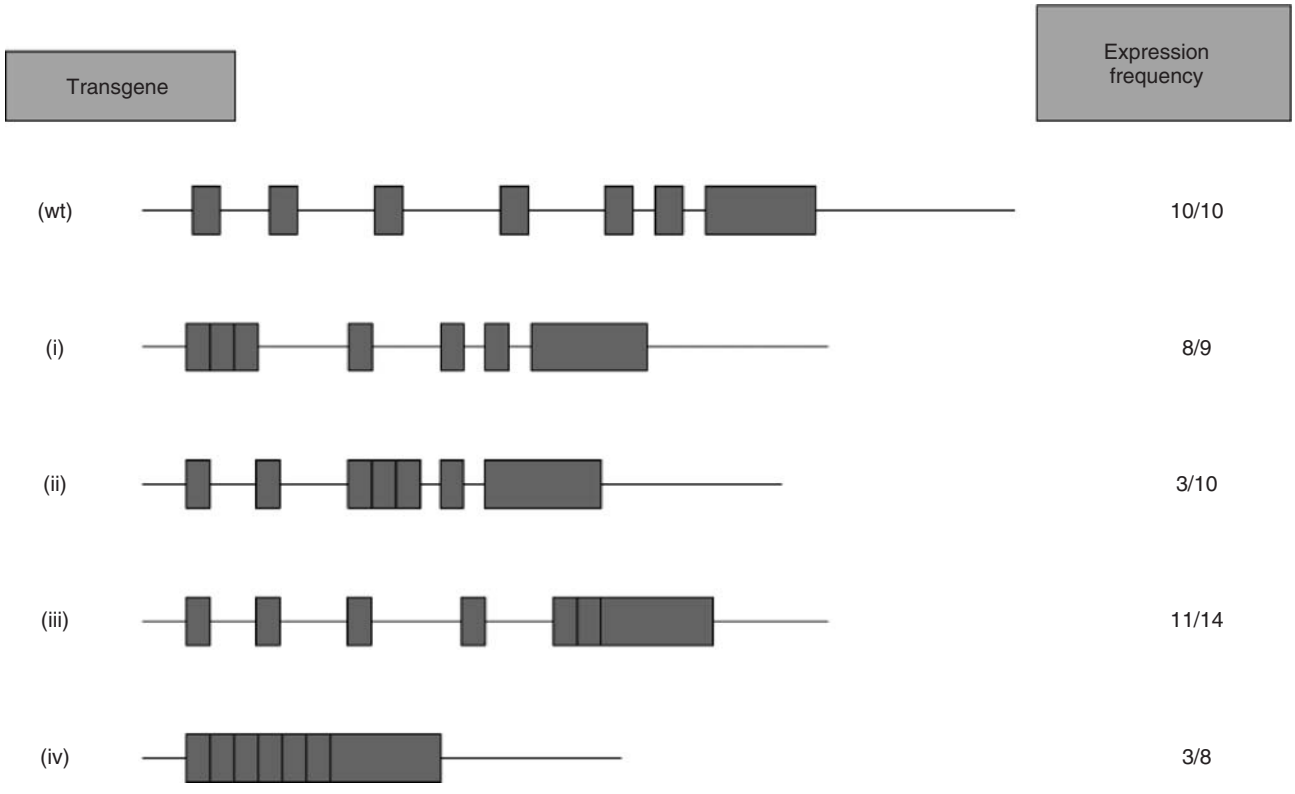


Figure 14.12. Reduction in transgene activity by intron removal. Wild-type (wt) genomic β-lactoglobulin transgenes are expressed in all transgenic lines generated. The removal of any pair of introns reduces the expression frequency (i, ii, and iii), and a construct containing no introns (iv) was expressed in only 30% of transgenic lines.

control elements, such as locus control regions (LCRs), should be considered (227). Unfortunately, this type of element has been identified for only a few genes.

Conventional transgenes have traditionally been small in size. If the desired gene covers a large genomic region, or if several genes (perhaps part of a gene cluster) are to be transferred, larger vectors are required. In this regard, transgenic animals have been produced that carry transgenes derived from bacteriophage P1 vectors and bacterial or YACs (PACs, BACs, and YACs). P1 clones carry inserts of 80–90 kbp, YACs can carry inserts over 1 Mbp, while BACs carry an intermediate insert size (11). The aim now is to generate MAC vectors with the recent description of a YAC-based MAC (228). Alternative approaches have been developed that rely on recombination between two injected fragments to generate a large integrated transgene. The use of these large transgenes is not limited to mice, because transgenic rabbits carrying YACs have also been produced (229). The main use of these large clone transgenes is in positional cloning, specifically in relation to adding functional information to the genetic maps currently being generated for most livestock species. Recently, the potential for introducing even larger genomic fragments has been demonstrated by the generation of transgenic mice carrying human chromosome fragments. This was accomplished by microcell-mediated chromosome transfer (MMCT) into ES cells (93).

14.9.10 Overcoming Position Effects

Position effects can reduce or silence transgene expression or generate ectopic expression patterns. There are four ways to deal with position effects: (i) increase transgene copy number so that the rate of mRNA synthesis is no longer the limiting factor in recombinant protein synthesis, (ii) ensure that the transgene integrates at a site that is not subject to undesirable position effects, (iii) protect the transgene from position effects, and (iv) import positive position effects along with the transgene.

One way to overcome position effects is to amplify the transgene to such a high copy number that even if each transgene copy is transcribed minimally, enough mRNA is produced to ensure that transcription is no longer the limiting step in foreign gene expression (40,41). This is achieved by cotransfecting cells with the experimental transgene and an amplifiable marker such as *Dhfr*, followed by subjecting the transfected cells to stepwise increments in the concentration of the selective drug, in this case methotrexate. This approach is only useful where the aim of the experiment is to maximize yields of recombinant protein and cannot be used for the precise control of transgene expression either in cells or transgenic animals.

The alternative approaches each allow a degree of control over transgene expression and can be used in more refined experiments. The use of site-specific recombination and gene targeting systems to introduce transgenes at specific loci chosen for their favorable position effects has been proposed to avoid transgene silencing and expression variability (230). Such approaches would also be advantageous because isogenic cell clones and transgenic animals could be produced on demand. Transgene targeting to a specific gene locus in transgenic mice has thus been the focus of attempts to identify permissive sites within the genome (231). The existence of position effects suggests that certain sites within the genome may prove more permissive for expression than others for a given transgene. One strategy is to identify lines of mice that efficiently express a transgene and clone the entire transgenic locus, including as much chromosomal flanking sequences as possible. This assumes that sequences relatively close to the site of insertion mediate the effect. Alternatively, neutral sites within the genome, which shield the transgene, can be identified using the appropriate gene targeting construct in ES cells.

A promising approach for overcoming position effects is to protect transgenes from surrounding chromatin in the same way that the cell is thought to isolate active and repressed chromatin domains by using *cis*-dominant boundary elements. It has been observed that genes *in situ* reside within large chromatin domains, which extend many kilobases either side of the transcription unit. Active chromatin domains are biochemically defined by the extent of nuclease sensitivity, and transcription per se is not required for a domain to remain in the open configuration (232). There are several ways to exploit these observations. First, DNA sequences found at the domain borders can be used as artificial insulator elements. Such elements have been isolated, for example, from the chicken lysozyme A gene locus and have been shown to insulate transgenes from the activity of local enhancers and to protect transgenes from position effects in cell lines (233) and transgenic animals (234). Such elements are thought to act by attaching to the nuclear matrix and isolating the transgene as a topologically defined chromatin loop. In animals, it has generally been observed that when such boundary elements protect transgenes from position effects, transgene expression also becomes copy number dependent.

Second, susceptibility to position effects can be suppressed through the incorporation of dominantly acting transcriptional control elements in the transgene (227). The best-studied element is from the human β-globin locus and comprises a set of DNase I hypersensitive sites normally located several kilobases upstream of the β-globin gene. This chromatin element is called the *LCR*. For those β-globin transgenes that harbor the LCR, expression is seen in all transgenic lines and at a level that corresponds to the transgene copy number. Conversely, β-globin transgenes lacking the LCR are often silenced, and where expression occurs, it does so at a low level.

Although a vast literature has accumulated concerning the various protein factor interactions within this region, there is no clear understanding of LCR-mediated transgene regulation (235).

Third, the use of large vectors, such as YACs and chromosome fragments, can also protect transgenes from position effects. YAC transgenes are rarely subject to position effects and tend to show dose-dependent activity, presumably reflecting the inclusion of native dominant transcriptional control elements (LCRs) and/or boundary elements within the construct.

A final strategy for overcoming position effects is termed *transgene rescue*. In this approach, which is particularly suited to cDNA transgenes, the experimental transgene is cotransfected with a second transgene renowned for its strong expression, such as the β-lactoglobulin (*BLG*) gene (236). The *BLG* transgene cointegrates with the experimental transgene, and high level expression of both transgenes is observed. The basis of the "rescue" is thought to reflect a favorable chromatin configuration in the *BLG* transgene spreading into the surrounding chromatin and keeping it in an active state, a phenomenon that can be regarded as an "antiposition effect."

14.10 RECOMBINATION-BASED METHODOLOGY AND GENE INHIBITION STRATEGY

14.10.1 Recombination and Its Use in Genetic Engineering

The term *recombination* refers to the creation of new combinations of preexisting DNA sequences. Two major forms of recombination can be recognized: intergenic recombination (also called *independent assortment*), which refers to the mixing of discrete DNA elements such as complete chromosomes, and intragenic recombination, where DNA fragments are covalently joined together. There are five different classes of intragenic recombination (Table 14.6) (237). Illegitimate recombination, which is responsible for random transgene integration, and homologous recombination, which is exploited for gene targeting, are general recombination mechanisms occurring in all cells. Conversely, site-specific recombination and transposition are controlled by enzymes encoded by particular DNA elements, such as plasmids, viruses, and transposons. As such recombination systems are not ubiquitous, they can be exploited to carry out specific tasks in genetic engineering by transferring them into

TABLE 14.6. Categories of Intramolecular Recombination and Their Use in Genetic Engineering[a]

Category	Properties	Relevance to Genetic Engineering
Illegitimate	Ubiquitous and neither homology nor sequence dependent, although regions of microhomology may be involved. End-joining is a form of illegitimate recombination	Random joining of multiple transgene copies. Transgene integration at random sites
Homologous	Ubiquitous and homology dependent. Not sequence dependent. Often involves long regions of homology	Transgene concatemerization. Gene targeting strategies. Construction of recombinant viral vectors. YAC mutation and retrofitting in yeast
Site-specific	Encoded by specific genetic elements, for example, plasmids and viruses. Dependent on proteins (recombinases) that recognize short consensus sequences in donor and target molecules	Site-specific transgene integration and excision. Transgene engineering *in vivo*. Tissue- and stage-specific transgene (in) activation. Chromosome engineering
Transposition	Encoded by specific genetic elements (transposons). Dependent on proteins (transposases) that recognize short consensus sequences in donor, although target site is relatively nonspecific	Retrovirus integration. Insertional mutagenesis and cloning by tagging or plasmid rescue. Insertion of foreign DNA into viral vectors (e.g. Tn*7* transposase targeting of Bac-to-Bac vectors)
Artificial	Joining DNA molecules with DNA ligase *in vitro*	Preparation of recombinant vectors for gene transfer

[a] Site-specific and homologous recombination are discussed in more detail in the current text. See earlier section on mechanisms and consequences of transgene integration for a discussion of illegitimate recombination, and earlier sections on insertional mutagenesis and entrapment vectors, and construction of recombinant baculovirus vectors for discussion of transposition. Note that Tn*7* transposase is unusual in its preference for particular target sequences, allowing its use for site-specific transgene integration, while insertional mutagenesis and trap vector integration exploit the lower specificity of, for example, P elements and retroviruses.

new host cells. The use of cloned recombination systems from heterologous sources has facilitated *in vivo* transgene manipulation and chromosome engineering.

14.10.2 Inhibition of Endogenous Genes

The major thrust of genetic engineering in animal cells has been to optimize and regulate the expression of recombinant proteins; however, there is now an interest in using the same gene transfer technology to silence endogenous genes and alter the endogenous genome to generate functional mutants (192). With the advent of recombinant DNA technology, it became possible to address gene function by first cloning the gene, then mutating it *in vitro*, and reintroducing it into the source organism to study its function. Until a few years ago, the scope of this so-called reverse genetics approach was limited to the transfer of *in vitro* mutated genes into cells and later transgenic animals to study their effects. Only recently has it become possible to directly modify the genotype of a cell or animal by altering endogenous genes. Silencing is not only useful experimentally to generate mutants for functional studies but also in applied fields to knock out undesirable traits and to correct dominant genetic disorders (a form of gene therapy known as *gene inhibition therapy*).

14.10.3 Homologous Recombination

Homologous recombination in mammals occurs predominantly during meiosis and in some types of DNA repair. Exogenous DNA involved in homologous recombination events is probably used as a substrate by these DNA repair enzymes. Mechanistic parallels between DNA replication, recombination, and transcription are evident (238). There are three possible outcomes of a homologous recombination event (Fig. 14.13). In most cases, the choice is between reciprocal exchange (usually termed a *crossover event*) and nonreciprocal exchange (usually termed *gene conversion*). In the former case, a recombination event occurring between two heterozygous loci will result in the exchange of markers between recombination partners (Fig. 14.13, panel I). In the latter case, recombination results in the unidirectional transfer of information, so that one allele appears to have been converted into the other. This can occur both in the absence (Fig. 14.13, panel II) and in the presence (Fig. 14.13, panel III) of a crossover event involving a third marker. Both crossing over and gene conversion involve the invasion of double-stranded DNA by a single strand, a process often initiated by a single- or double-strand chromosome break in the donor DNA molecule (or the free end of a linearized targeting construct). Homologous recombination then proceeds in a conservative manner with a preponderance of gene conversion over reciprocal recombination. The third possibility is extrachromosomal recombination (Fig. 14.13, panel IV), which occurs nonconservatively and results in the loss of the sequences at the opposite end of the two molecules.

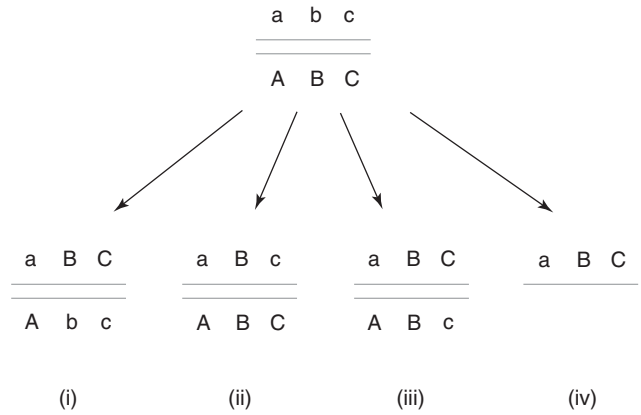


Figure 14.13. Possible outcomes following homologous recombination. The bars represent homologous DNA molecules, and the letters represent three genetic loci, with upper and lower cases indicating different alleles: (i) reciprocal recombination, (ii) gene conversion, (iii) gene conversion with crossover, and (iv) nonconservative recombination.

14.10.4 Development of Homologous Recombination as a Genetic Tool

The development of engineering strategies based on homologous recombination in mammalian cells was preceded by the demonstration that exogenous DNA could participate in extrachromosomal recombination. The mechanism of extrachromosomal recombination differs from that of homologous recombination between exogenous DNA and chromosomal DNA, which is loosely termed *gene targeting*. Extrachromosomal recombination involves a nonconservative recombination event where one of the substrates is lost, while gene targeting usually involves sequence conservation, unless the targeting strategy is specifically designed to remove sequences.

Homologous recombination between similar or identical DNA sequences allows the introduction of any sequence modification into a living cell. Initially, the technology was used to interrupt target genes, a gene silencing strategy popularly, if inaccurately, known as *gene knockout*. However, precise single-base-pair changes can also be generated (239). Alternatively, large-scale genomic rearrangements are possible, including chromosomal translocations (240). A novel exploitation of this technique is to replace one gene with an entirely different gene, a strategy termed *gene knock in*. In each case, the desired mutation is generated in a cloned and *in vitro* modified DNA fragment, while the target homologous sequence representing the gene of

interest resides within a chromosome of the host cell (241). The recombination event is catalyzed by the endogenous general recombination machinery of the cell.

Homologous recombination is a rare event in mammalian cells, with nonhomologous (illegitimate) recombination occurring three to five orders of magnitude more frequently (242). Therefore, it is necessary to incorporate a selectable marker system that will enrich for the targeted integration event. The design of an appropriate targeting construct is a critical step for successful gene targeting. In 1985, a mutation was generated in the human β-globin gene using an insertion vector (243). A targeting frequency of 10^{-3} clones was achieved, but this still represented an inefficient targeting event. The procedure was refined through use of the endogenous *Hprt* marker gene, which could be selectively inactivated by homologous recombination (244). As discussed earlier (Table 14.4), cells *lacking* HPRT activity can be selected by culturing them in the presence of the toxic base analog 6-thioguanine (6-TG) and counterselected in the presence hypoxanthine, aminopterin, and thymidine (using HAT medium). This system allowed studies concerning the variables associated with homologous recombination to be addressed, such as the size of the homology region required and the effects of terminal homology (245).

Homologous recombination strategies in genetic engineering rely on the detection of very rare molecular events, so it is important to optimize the targeting efficiency. The targeting frequency depends on a number of factors (246). First, better targeting efficiencies are achieved with a larger *homology region* (the region of shared homology between the targeting vector and the target itself). Targeting efficiency increases exponentially with the size of the homology region up to about 10–14 kbp, where a plateau is reached. In addition, the degree of similarity between the sequences in the targeting construct and the endogenous locus has a major effect on the recombination efficiency. For example, the frequency of the recombination event can be increased three- to fivefold if the DNA used is from an identical (isogenic) source rather than a different strain of animal (247). Another factor is the actual targeted locus. For as yet unknown reasons (but presumably due to either the specific overall sequence composition or higher order chromosomal structure), some genomic targets are highly resistant to recombination and are thus recalcitrant to gene targeting. Finally, the design of the targeting vector also determines the outcome of the experiment, with targeting strategies reflecting the use of either insertion or replacement vectors (248,249).

14.10.5 Gene Silencing—Targeting Vector Design

There are two classes of targeting vector, termed *insertion vectors* and *replacement* (or *transplacement*) *vectors*. Insertion vectors are linearized *within* the homology region, resulting in the insertion of the entire vector into the target locus (250). This type of vector disrupts the target gene but leads to a duplication of the sequences adjacent to the selectable marker (Fig. 14.14a). This is not always a desirable configuration (251). First, duplication of the target sequences can lead to a leaky phenotype (e.g. if the intention is to disrupt the target gene, the duplicated region can undergo variable splicing event leading to production of wild-type transcript). Second, a subsequent homologous recombination event can occur between the duplicated regions, removing the selectable marker and causing reversion to the wild-type genotype (Fig. 14.14c).

Replacement vectors are designed so that the homology region is collinear with the endogenous target. The vector is linearized *outside* the homology region before transfection, resulting in crossover events in which the endogenous DNA is replaced by the incoming DNA (Fig. 14.14b). With this type of vector, plasmid backbone sequences are not inserted, only sequences within the homology region. Insertional inactivation is thus achieved by interrupting the vector homology region with extra DNA so that it is no longer functional (Fig. 14.14b). To allow identification of targeted cell clones, the homology region is interrupted by a selectable marker such as *neo*. Insertion or replacement thus introduces the selectable marker at the target site, and growing the cells under selection (e.g. neomycin or its more widely used analog, G418) will kill all those cells that do not harbor the appropriate allele, representing the integration event. This strategy produces a disrupted target gene (252) and is termed *positive selection*.

The use of a single selectable marker, although allowing selection for integration events, does not discriminate between targeted events due to homologous recombination and random, nontargeted integrations. What is needed is an enrichment procedure. The most widely used system requires the inclusion of a second, counterselectable marker and is the basis of *positive–negative selection* (Fig. 14.15) (253). The most commonly used system involves inclusion of the HSV TK (*tk*) gene, which will kill transfected cells in the presence of ganciclovir. The counterselectable marker is positioned at one end of the vector, outside the homology region, and will not be inserted by homologous recombination, allowing correctly targeted cells to survive. However, the marker is inserted by random integration, allowing cells carrying randomly integrated constructs to be counterselected with ganciclovir.

Variations on positive–negative selection are available, including a highly efficient system involving a promoterless construct (254). In this case, the selectable marker lacks the sequences required to initiate transcription, and its expression is therefore dependent on insertion into the target gene by homologous recombination. Modifications on this approach include using an IRES, which generates a

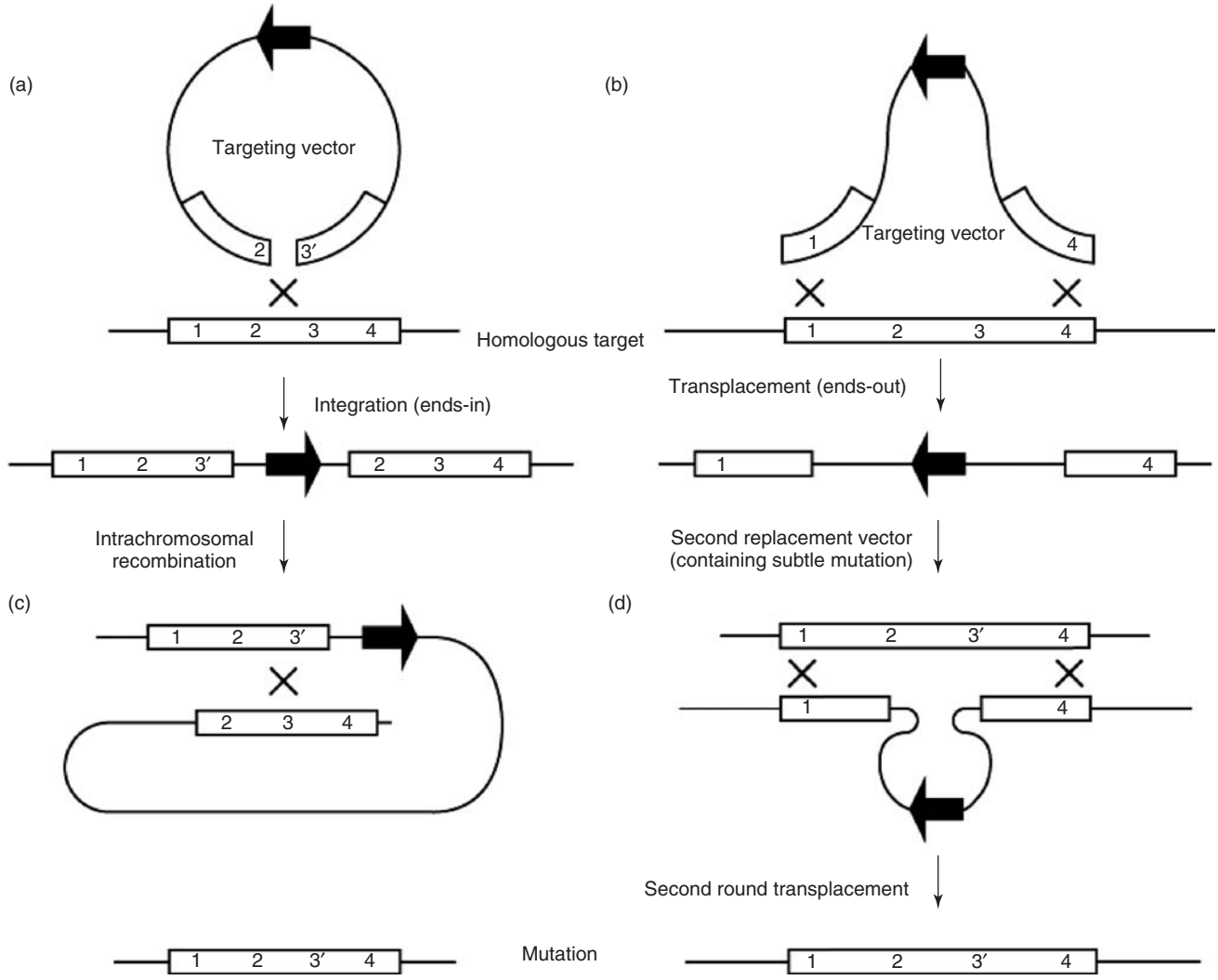


Figure 14.14. Design of targeting vectors and their use for gene knockout and allele replacement. (a) Insertion vector, linearized in the homology region. This undergoes "ends-in" recombination with a single crossover; inserts the entire vector into the targeted locus. (b) Replacement (or transplacement) vector, linearized outside the homology region. This undergoes "ends-out" recombination with a double crossover or gene conversion; replaces the targeted locus with the homologous region of the vector. Gene knockout is achieved by interrupting the vector homology region. (c) Subtle mutation using an insertion vector (hit and run). The first integration generates the hit and inserts the marker(s) (black arrow), which are used for positive selection. The vector homology region carries the desired mutation. Subsequently, intrachromosomal recombination between the tandem homology regions replaces the endogenous gene with the mutant allele with no further intervention from the experimenter. The mutation is represented by (′). Targeted clones can be identified by negative selection, because the second recombination event removes the counterselectable marker. (d) Subtle mutation by transplacement requires two vectors. The first vector is the tag, interrupting the gene and leaving the selectable markers. The second vector carries the desired mutation and facilitates the exchange, replacing the interrupted allele with the desired mutation and removing the counterselctable marker.

bicistronic messenger RNA (179). In addition to providing a very efficient targeting strategy, the IRES also considerably simplifies construction of the vector, because the selectable marker does not have to be inserted in-frame.

14.10.6 Introducing Subtle Mutations

While gene targeting has traditionally been used to disrupt and hence silence specific endogenous genes by introducing large insertions, more refined approaches are now

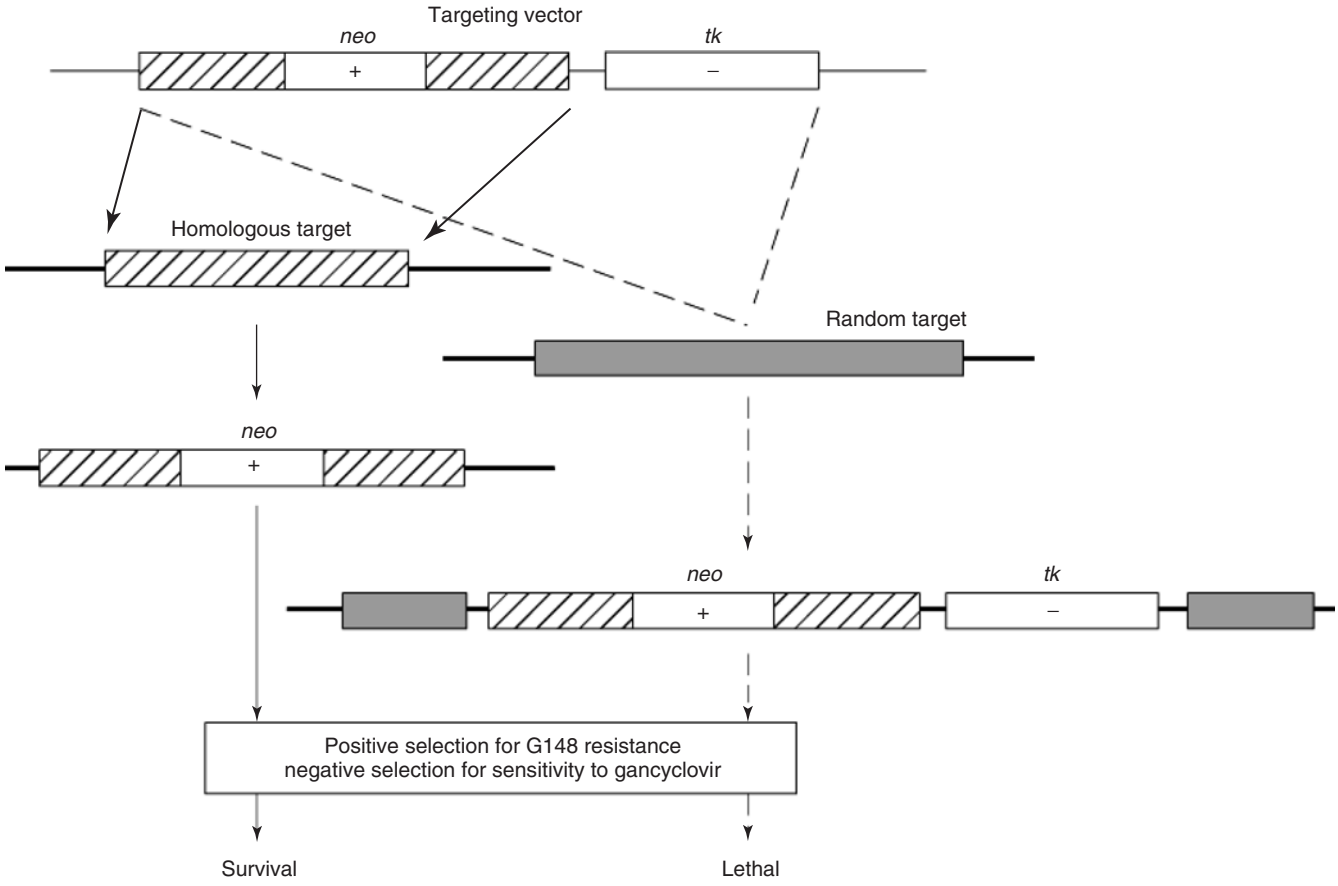


Figure 14.15. Positive–negative selection. Random integration occurs several orders of magnitude more frequently than homologous recombination in mammals, and a single selectable marker cannot discriminate between the two events. Positive–negative selection employs two markers, a selectable marker within the homology region, which is integrated by both recombination and random end-joining, and a counterselectable marker outside the homology region, which is only integrated by random end-joining, not by homologous recombination. Only targeted clones are therefore resistant to both G418 (conferred by *neo*) *and* ganciclovir (conferred by the *absence* of *Tk*).

being used to generate subtle mutations. The precise effects of minor deletions or point mutations cannot be assessed through simple targeting strategies, which necessarily leave the selectable marker, and in some cases the entire targeting vector, integrated at the target site. Two major strategies for introducing *clean mutations* (subtle mutations without markers or foreign sequences) have been devised, each involving two rounds of homologous recombination. These are the "hit-and-run" strategy (Fig. 14.14c), involving a single insertion vector, and the "tag-and-exchange" strategy (Fig. 14.14d) involving two replacement vectors. In each case, the first targeting event introduces a marker or markers for positive–negative selection—this event is identified by positive selection. The second targeting event introduces the mutation and removes the marker(s)—this event is identified by negative selection.

The *hit-and-run* or "in–out" strategy (239,255) involves the use of an insertion vector carrying two selectable markers, such as *neo* and *Tk* (Fig. 14.14c). The insertion event is positively selected by culturing the cells in the presence of G418. As an insertion vector is used, the entire vector is integrated and the homology region is duplicated in the targeted clone. One of these duplicated regions, the one derived from the insertion vector, harbors the desired subtle mutation. The success of this approach relies on a second intrachromosomal homologous recombination event between the duplicated homology regions, which first replaces the endogenous allele with the mutant and second deletes the markers allowing negative selection for ganciclovir resistance. Pending the resolution of this second event, the desired mutation may be left at the target locus. Although elegant in conception, this technique

suffers from one disadvantage, which is that the second homologous recombination event is inefficient.

The *tag-and-exchange* strategy is similar in that it also requires two homologous recombination events, but differs in that it requires two replacement-type vectors (256). The first "tag" vector is designed to mutate the target gene and insert the selectable marker(s). The second vector facilitates the exchange reaction by reintroducing the desired mutation into the target gene, while eliminating the selectable marker(s). Selection for the two events is analogous to that for the hit-and-run approach when two markers such as *neo* and *Tk* are used (Fig. 14.14d). Variations include strategies using a single selectable marker such as *Hgprt*, which can be positively selected or counterselected as appropriate (257).

14.10.7 Target Cells for Homologous Recombination

In theory, any mammalian cell can provide the target for homologous recombination. However, gene targeting in the majority of cells is very inefficient, with ES cells being a notable exception (246). Indeed, the general inefficiency of homologous recombination in mammalian cells remains one of the central limiting factors in the exploitation of this powerful technique. *ES cells* have therefore been used in most gene targeting experiments (Fig. 14.16) (258,259). Furthermore, when handled appropriately, ES cells are pluripotent: They can differentiate into any (all) somatic cell type (241). This means that a genetic modification introduced into ES cells can be incorporated into the germline of an animal. To date, the only animal that has been genetically modified through homologous recombination is mice. This is because only mouse ES cells are currently available (260,261). ES cells are also a valuable cell culture-based resource for studying gene function, especially in development, because they can be induced to differentiate into specific cell lineages in culture (262).

DNA can be introduced into ES cells by a variety of routes, the choice depending on the intended use of the cells. If germline transmission is the desired outcome, the effect of the protocol on the integrity of the ES cell genotype and phenotype must be considered. For example, cells that have undergone chromosomal rearrangements or cells that have differentiated will not contribute to the germline. ES cell transformation was first achieved by retroviral transduction and calcium phosphate-mediated transfection, but electroporation has now replaced these as the method of choice. Electroporation gives a higher transfection efficiency, is relatively simple and reproducible, and is compatible with germline transmission. Alternative methods to introduce DNA into ES cells include microinjection (which is technically very demanding) and lipofection, perhaps best suited for the delivery of large fragments of DNA.

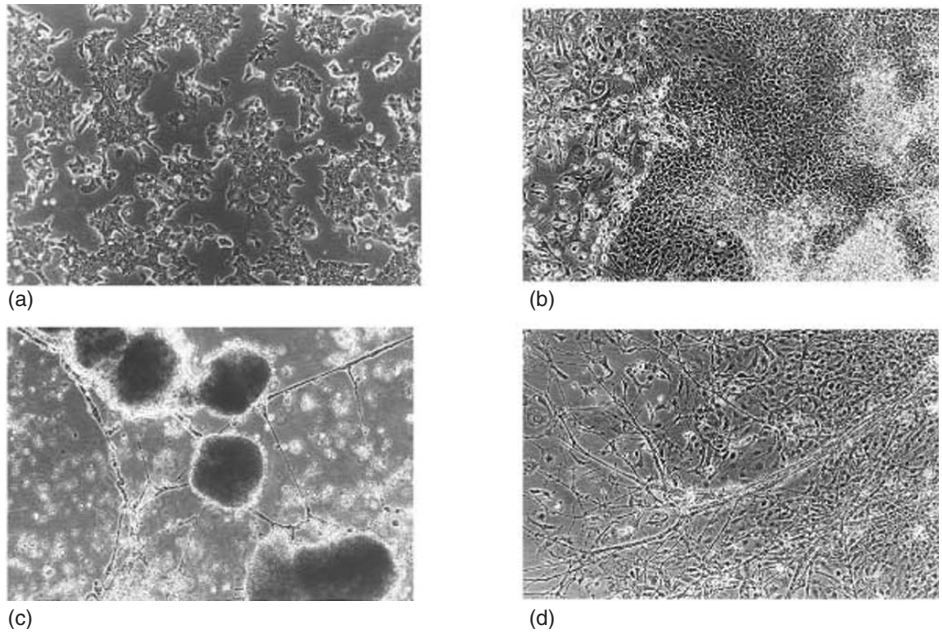


Figure 14.16. ES cells. (a) Recently plated mouse ES cells from strain 129 (note the small cytoplasmic volume relative to nuclear size). (b) In culture, the cells will develop three-dimensional growth characteristics. In the absence of the growth factor LIF, embryoid bodies will be formed. Alternatively, ES cells will differentiate into a variety of cell types, including (c) epithelial and fibroblastoid or (d) neuronal filament-like. Photographs courtesy of Jim McWhir and Ray Ansell (Roslin Institute).

Recently, there has been considerable interest in the potential of primary cells for gene targeting, at least in part due to the development of nuclear transfer techniques in mammalian species. Gene targeting is an inefficient process with individual targeting events in primary and established somatic cells occurring at low frequencies, typically $<10^{-4}$. At this efficiency, thousands of stably transfected clones must be screened to isolate a single homologous recombinant, and this requirement severely limits the use of primary somatic cells as the target for homologous recombination. Primary cells are usually isolated in only small numbers and are capable of only a few rounds of cell division before senescence or crisis. In attempts to overcome this limitation, various enrichment strategies have been developed, including the positive–negative selection system discussed, which can achieve a 30% targeting efficiency. As more experiments have been documented, however, the promoterless vectors have emerged as the most successful. Using these approaches for gene knockout in human primary cells, human gene function can be addressed. For example, disruption of the $p21^{CIP1/WAF1}$ gene in normal diploid human fibroblasts demonstrated its pivotal role in cell senescence (263).

There is also considerable interest in the use of somatic cells for gene targeting. For example, as the means to propagate human somatic cells in the form of lineage-specific stem cells becomes available, gene targeting could be used to correct or remedy genetic defects by interrupting dominant mutant alleles or replacing them with the wild-type allele. The somatic cells could then be used to replace the mutant cells *in vivo*, a form of somatic gene therapy. Alternatively, gene targeting in somatic cells could provide a basis for the genetic modification of animals when used in conjunction with nuclear transfer technology. Gene targeting in the majority of cell lines is an inefficient process compared with ES cells, and the basis of the amenability of ES cells for homologous recombination is unclear. One example is the chicken pre-B cell line DT40. The characterization of the high targeting efficiency of DT40 cells is not understood. Importantly, these cells can be used to direct genetic modification of human cells. For example, by combining gene targeting in DT40 cells and microcell fusion (which allows chromosome shuttling between cells), specific mutations can be introduced into human gene sequences before their functional testing in human cells. Other genetic tricks are possible in these cells, including telomerase-directed truncation, allowing gross modifications of target chromosomes (264).

14.10.8 Site-Specific Recombination Systems

Site-specific recombination involves the recognition of short consensus sequences by specific enzymes (recombinases) that catalyze strand exchange and resolution within small regions of DNA homology. They are encoded by individual bacteria, plasmids, viruses, and transposons and serve many purposes (237). The most extensively used systems are Cre recombinase from bacteriophage P1 (265) and FLP recombinase (flippase) from the *Saccharomyces cerevisiae* 2-μm plasmid (266). These have been shown to function in many heterologous eukaryotic systems, including mammalian cells and transgenic animals. Both recombinases recognize 34-bp sites (termed *loxP* and *FRP*, respectively) comprising a pair of 13-bp inverted repeats surrounding an 8-bp central element. *FRP* possesses an additional copy of the 13-bp repeat sequence, although this is nonessential for recombination. The introduction of these sequences into animal genomes, along with expression constructs driving expression of the recombinase protein, can therefore induce site-specific recombination events in mammals. The activity of Cre recombinase is shown in Fig. 14.17.

14.10.9 Site-Specific Recombination

If two recombination sites are integrated in the same orientation, site-specific recombination between them will excise the intervening DNA. Transgenes flanked by such sites can therefore be introduced into the genome as normal, but excised by supplying the recombinase in *trans*. This "site-specific excision" strategy has many applications (230), including the excision of unwanted sequences from the transgene (e.g. selectable markers and plasmid backbone sequences) and deletion of blocking sequences to allow transgene activation. This last strategy, known as *recombination activation of gene expression* (RAGE), involves the insertion of a blocking element (such as a polyadenylation site) between the transgene and its promoter. RAGE can be used to excise the blocking element, bringing the transgene and promoter into juxtaposition, resulting in transgene activation. Site-specific recombination, in concert with gene targeting, can also be used for endogenous gene silencing. In one strategy, sometimes termed *floxing*, gene targeting is used to introduce recombinase sites flanking an endogenous gene. The term *floxing* is derived from the term *flanking loxP*, but other recombinases are used in an analogous manner. Once the targeting strategy is complete, the introduction of recombinase into the system causes site-specific gene deletion or inversion (as appropriate), resulting in gene silencing. Similar strategies can be used to facilitate the deletion, inversion, or transposition of particular chromosome segments, an approach often used to model human diseases caused by chromosome rearrangements.

Site-specific recombination can also be used for transgene integration. In this strategy, a single recombination site is introduced into a particular chromosomal locus by gene

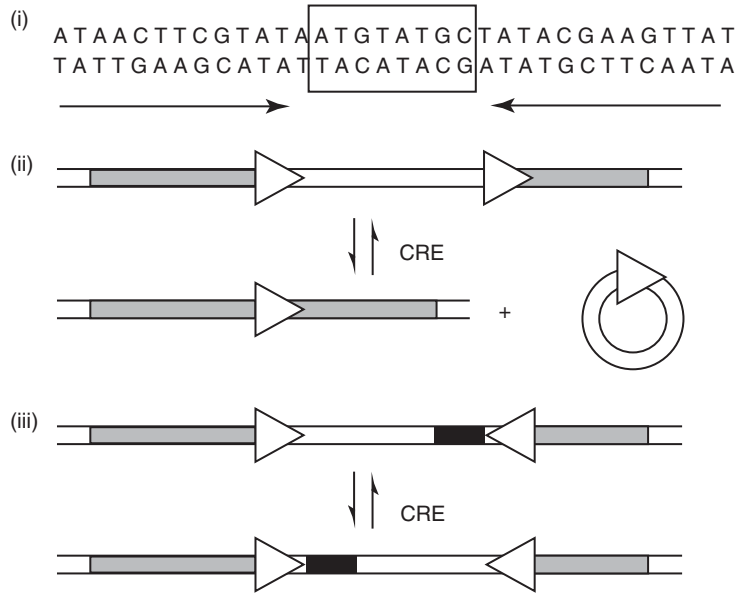


Figure 14.17. Characteristics of Cre recombinase. (a) The *loxP* site recognized by Cre recombinase, comprising 13-bp palindromic sequences (arrows) surrounding an 8-bp core (boxed). (b) Cre recombinase deletes the sequence between two *loxP* sites in the same orientation, and such a sequence is said to be "floxed." (c) When *loxP* sites are inverted with respect to each other, Cre recombinase inverts the DNA sequence between them. In both the cases, the reaction is reversible, but the circular excision product in (b) is quickly degraded, making the reaction effectively irreversible. Floxed linear DNA can integrate at a single *loxP* site in the presence of Cre, but because integration and excision occur with equal frequency, the degradation of the excision product drives the equilibrium of the reaction toward excision. Cre-mediated DNA integration is currently as inefficient as random integration.

targeting, and if recombinase is supplied in *trans*, transgene constructs flanked by recombination sites can be transfected into the cell and persuaded to integrate by site-specific recombination. However, while the constitutive expression of recombinase is sufficient for site-specific excision strategies, a transient burst of recombinase is required for integration because the reaction is easily reversible. The availability of recombinase is difficult to control precisely; thus, site-specific integration is currently only just as efficient as random transgene integration by illegitimate recombination.

14.10.10 Gene Silencing Using Antisense RNA Constructs

Gene targeting and site-specific recombination-based strategies are now well-established technologies for gene silencing. However, the activity of an endogenous gene may also be suppressed if antisense RNA is introduced into a cell. Antisense RNA has a complementary sequence to mRNA and can bind to the sense transcript either in the nucleus or cytoplasm to form a duplex. The mechanism of gene inhibition is unclear and may act at several levels. Protein synthesis is a likely target, either through the prevention of productive pre-mRNA processing and export, or duplex-induced mRNA degradation, or by direct inhibition of ribosome binding, scanning, or translocation. In addition, the presence of dsRNA induces DAI protein kinase, causing a general reduction in the rate of protein synthesis. The effects of injecting or transfecting antisense RNA into a cell are transient because the RNA cannot replicate and is rapidly degraded. However, long-term gene inhibition can be achieved simply by reversing the orientation of a transgene with respect to its promoter and introducing such a construct into cells or transgenic animals through the normal routes. If such a construct integrates and is expressed, the cell has a constant supply of antisense RNA sufficient for long-term gene inhibition. This strategy has been achieved using both transfected plasmid DNA and retroviral vectors. Antisense inhibition has been used in many cell culture experiments and in ES cells to generate transgenic animals. The results have been variable, with mRNA levels reduced by 20% to almost 100% (267). It is not necessary to express full-length antisense RNA for "knockdown" effects to occur. The expression of an approximately 5-kbp antisense RNA corresponding to the *Wnt-1* transcript resulted in 98% reduction, while just 40 bp of antisense RNA corresponding to the mouse $G_{\alpha i}$ transcript resulted in 95% reduction.

Additional sequences can be added to antisense transcription units to increase the inhibitory activity of the molecule. In a few cases, targeting sequences have been used to direct antisense RNA to particular subcellular locations. A popular strategy is to exploit the ability of ribozymes linked to antisense RNA to cleave mRNA in a sequence-dependent manner. Ribozymes are catalytic RNA molecules whose complex tertiary structure allows them to adopt the molecular configurations characteristic of (protein) enzymes and hence to catalyze biochemical reactions. The self-splicing introns found in organelle genomes are autocatalytic (i.e. the RNA facilitates its own excision), whereas other ribozymes are catalytic in the strict sense, because they act in *trans* on a distinct substrate. Ribozymes have a bipartite structure, including a targeting sequence and a catalytic core. The targeting sequence is an antisense RNA that forms base pairs with a specific RNA substrate and holds the catalytic core in the correct position, allowing cleavage of a phosphodiester bond. If the ribozyme catalytic core is fused *in vitro* to a given antisense RNA (268), the ribozyme can be targeted to the mRNA, which will be cleaved. Cleavage destroys the function of the mRNA, and the 3′ fragment (lacking a cap) is rapidly degraded. Critical comparisons of ribozyme constructs and related antisense constructs containing no catalytic core have often revealed similar levels of inhibitory activity (267). This suggests that some ribosome constructs may work simply through their antisense effects rather than by cleaving mRNA.

14.10.11 Gene Silencing Using Inhibitory Proteins

Genetic engineering can be used to interfere with endogenous gene expression at the protein level, as well as at the RNA level. The specificity and affinity of antibodies for their complementary antigens has been widely exploited for identifying, localizing, and purifying proteins (269). Antibodies microinjected into cells have also been used to inactivate proteins (270), but such effects are only transient and cannot readily be applied to whole organisms. A new approach is to stably transform animal cells with antibody-encoding genes. This strategy results in the long-term expression of "intracellular antibodies" known as *intrabodies*, which can be targeted to particular cellular compartments and used to abolish the activity of specific proteins. Intrabodies have been used to generate functional knockouts of important molecules such as growth factor receptors, and their potential role in gene therapy has been explored by targeting oncogenic proteins and the gp120 HIV envelope protein (271). The strategy for expressing intrabodies is complex. Immunoglobulin genes cannot be used for transfection due to their size and the absence of V(D)J recombinase and switch recombinase in most cells. In addition, because *specific* antibodies are required, DNA sequences corresponding to particular mature (rearranged) immunoglobulins must be used. However, the native immunoglobulin assembly pathway occurs very inefficiently in the cytoplasm and attempts to reassemble functional immunoglobulins from distinct heavy and light chains have not succeeded. One strategy is to synthesize single-chain antibodies carrying the antigen-binding domains of both heavy and light chains on a single polypeptide with a flexible intervening linker chain. Such molecules are capable of folding in the cytoplasm and interact with their targets, but they have shorter half-lives than secreted immunoglobulins.

An alternative strategy for gene inhibition at the protein level is to transfect cells with constructs encoding dominant inhibitory proteins. Proteins that function as oligomeric complexes possess domains for interaction with other subunits. It is often possible to identify dominant loss of function alleles (*dominant negatives*) for the genes encoding such proteins. These encode nonfunctional subunits that form stable complexes with the functional wild-type subunits, sequestering them into inactive oligomers. Dominant negative alleles may be generated by point mutations or truncations, and the overexpression of such alleles is useful for generating functional knockout phenotypes. This strategy has been used to inactivate many different types of protein, including receptor tyrosine kinases and cytokine receptors, transcription factors, and other oncoproteins. More recently, dominant negative overexpression has been combined with techniques for conditional gene expression to generate conditional silencing systems for the study of signal transduction, cell cycle, apoptosis, and the function of telomerase (192). The major therapeutic application of dominant negative gene expression has been blocking the HIV replication cycle by interfering with capsid assembly (272).

14.10.12 Transient Gene Silencing with Oligonucleotides

Gene silencing strategies based on the integration and long-term expression of inhibitory transgenes are designed to permanently block the expression of a given endogenous gene. However, a similar but transient effect can be achieved by introducing the inhibitory gene product directly into the cell, such as antisense RNA or antibodies active against specific gene products. Another approach to transient gene silencing is the introduction of short oligonucleotides (15–30 nucleotides) into the cell. Depending on their design, oligonucleotides can block the expression of specific genes at the levels of transcription, RNA processing, translation, or protein function. Pyrimidine-rich oligonucleotides can interact with duplex DNA if there is pronounced pyrimidine/purine strand asymmetry. The oligonucleotide can interact

with the duplex using Hoogsteen pairing. The resulting triple helix is stable and blocks transcription, allowing gene-specific silencing (273). Oligonucleotides for triple-helix gene silencing can be sense or antisense with respect to the target gene, but their use is limited by the stringent pyrimidine-rich sequence requirements. A more general approach is to use antisense oligonucleotides in the same way as antisense RNA. However, because the oligonucleotides are DNA, they are generally more stable than the RNA, and they also form DNA:RNA hybrids that act as substrates for RNaseH and, hence, induce the degradation of the target mRNAs. Antisense oligonucleotides for gene therapy have been validated in animal disease models and are now undergoing clinical trials for human diseases (274). Finally, improvement in oligonucleotide synthesis technology has allowed the production of sets of degenerate oligonucleotides that can be screened for their ability to bind specific proteins. An oligonucleotide binding in such a specific manner is termed an *aptamer*. Current problems with oligonucleotide-mediated gene inhibition include stability and delivery. Oligonucleotides are linear and prone to exonuclease attack, but this can be alleviated by chemical modification of the terminal residues. Cellular uptake of naked oligonucleotides is poor because they are large hydrophilic molecules, and transfection may require cell permeabilization or the use of a gene delivery system such as liposomes or lipofection.

14.10.13 Conditional Gene Silencing

Constitutive and permanent gene silencing are useful techniques, but cannot address complex questions such as the effect of withholding the product of a gene for a specific duration and the function of pleiotropic genes with embryonic lethal null phenotypes. In the latter case, it should be stressed that many genes active in early development also have roles in later development or the adult, and these roles cannot be studied with constitutive knockouts if the animal dies in early development due to loss of an early gene function. Traditional methods for studying such genes include conditional mutants, usually temperature-sensitive mutants, which can be maintained under permissive conditions and then shifted to restrictive conditions at the appropriate time. However, more sophisticated and regulatable strategies for conditional gene silencing can be devised by combining the silencing strategies discussed with the inducible gene expression systems discussed earlier in this chapter.

Gene targeting and site-specific recombination can be used in a number of related strategies to bring endogenous gene expression under exogenous control. In the first strategy, gene targeting is used to flox the endogenous gene, but the recombinase enzyme gene is expressed under a tissue-specific or inducible promoter, or the recombinase enzyme is expressed as, for example, a steroid receptor fusion that can be activated in a ligand-dependent manner. This allows the generation of somatic knockouts, where an endogenous gene present in all cells can be selectively deleted in particular cells or at particular stages of development. It also allows the generation of inducible knockouts, so that the timing of deletion can be controlled by the experimenter. An alternative strategy is to use gene targeting to replace the endogenous gene with a homologous copy containing a blocking element flanked by *loxP* sites. In this case, the supply of recombinase catalyzes the removal of the blocking element, leading to conditional gene activation, a strategy termed *infloxing*. In all conditionally silenced mice generated to date, either inducible or cell type-specific Cre recombinase has been used. The general strategy is to use two strains of mice, a responder carrying the floxed target and a regulator carrying a *cre* gene either under inducible or cell type-specific control. Conditional gene silencing is observed when the two strains of mice are interbred. Although site-specific recombinases offer exciting possibilities for transgene engineering *in vivo*, their activity in transgenic animals is not 100% efficient. There is a low level of background recombination, leading to leaky (in)activation. There is also pronounced and undesirable tissue specificity, resulting in the production of mosaics, and unexpected cell type-preferred transgene (in)activation.

Strategies for conditional gene silencing that do not rely on Cre recombinase have been used most frequently in cell lines as opposed to transgenic animals (conversely, Cre-mediated silencing has not been used for conditional silencing in cell lines). Gene targeting strategies include the replacement of endogenous promoters with inducible ones (192). Conditional silencing can be achieved by the inducible transcription of antisense RNA, and the inducible expression of dominant negative proteins. A final strategy is the conditional expression of a toxic transgene, such as the ricin toxin A chain gene or the diphtheria toxin A chain gene. This strategy has been reported in mammals but has been extensively used in *Drosophila* (275).

14.11 THE PRODUCTION OF TRANSGENIC MAMMALS FROM MANIPULATED CELLS

A *transgenic* animal is one in which every cell carries a fragment of foreign DNA. Initially, the term *transgenic* specifically applied to animals (and plants) carrying genes from a heterologous species. In many cases, the scope of the term can be broadened to include animals carrying, for example, extra or modified copies of endogenous genes, but most researchers stop short of using the term to describe any form of genome modification, because this would include animals carrying subtle mutations (e.g. point mutations)

generated by two rounds of replacement. In the majority of cases, the foreign DNA represents a gene (a *transgene*) or set of transgenes (194). The transgene integrates into one of the host chromosomes, becomes part of that animal's genetic repertoire, and is usually inherited by subsequent generations as a Mendelian trait. The transgene can be derived from any conceivable source, that is, the same species (e.g. an extra copy of an endogenous gene controlled by a heterologous promoter), a related species (e.g. human growth hormone expressed in mice), or an evolutionary distant species (such as bacterial transgenes in sheep). In addition, a hybrid gene may be generated from a variety of sources or a synthetic gene may be produced de novo. Integrated transgenes are often expressed correctly and can have profound phenotypic effects as shown by the greatly increased size of transgenic mice carrying growth hormone transgenes. The abnormal growth resulted from the elevated levels of growth hormone in their serum (276).

A variety of methods have been developed for the production of transgenic animals. All are based on the introduction of the DNA into a single cell that contributes to the development of the animal. In most cases, the cell is a fertilized egg, although cell culture-based approaches (using ES cells or nuclear transfer) are more sophisticated. The advantage of transgenic animals over cell culture studies lies in their ability to show the function of a gene in its normal physiological environment, that of the whole organism (241,246). Transgenic animals permit the study of developmental and physiological events in the context of the natural processes occurring in the animal.

In mammals, the vast majority of transgenic experiments have been performed using mice. Nevertheless, studies have been performed in a number of other mammals (277). Transgenic rats are well suited for experiments involving multiple analyses (e.g. blood sampling) and have been successfully used in studies addressing blood pressure. Transgenic rabbits offer an intermediate between a laboratory species and a farm animal and display a similar lipid metabolism to man and may provide useful models for the study of fat-related diseases (e.g. athersclerosis). However, excluding mice, it has been the generation of transgenic farm animals—pigs, sheep, goats, and cattle—which has received most attention. Certainly, transgenic livestock have provided the incentive for substantial commercial involvement in the discipline of animal genetic engineering.

14.11.1 Pronuclear Microinjection

The most widely used method for introducing genes into the germline of mammals is the direct microinjection of DNA into the pronuclei of fertilized eggs (278). Pronuclear microinjection is a fine needle used to pierce the pronucleus and the DNA is injected (Fig. 14.18). This requires special equipment and a considerable amount of technical expertise and dexterity from the operator. Nevertheless, the majority of research laboratories around the world now have access to such transgenic mouse facilities. By adapting the techniques employed for gene transfer to mice, pronuclear microinjection has been used to generate transgenic farm animals (279).



Figure 14.18. Pronuclear microinjection of a fertilized mouse egg. The two pronuclei are visible within the egg, which is being held by a suction pipette. The DNA is introduced through a fine glass needle. Photograph courtesy of Roberta Wallace (Roslin Institute).

Pronuclear microinjection is relatively inefficient, with only 20–30% of the mice derived from microinjected eggs carrying the transgene. This efficiency drops to 1% for domestic farm animals. It is generally accepted that the DNA integrates at or after the first round of chromosomal DNA replication. This means that the founder embryo is mosaic with regard to transgene status (280), resulting in founder animals with different integration positions and transgene copy numbers in different tissues, due to the mixing and allocation of cells during early embryogenesis. Once transmitted through the germline, however, the transgene copy number is usually stable, and the transgene is then inherited in a Mendelian fashion. There have been a few reports of transgenes undergoing rearrangement, deletion, or amplification, but these appear to be exceptions to the rule. Also, with a few obscure exceptions, the transgene does not appear to be retained extrachromosomally in mammalian species.

Although pronuclear microinjection has provided the main route for the generation of transgenic animals, a variety of other approaches are available. Integration has been observed following cytoplasmic injection or injection into the blastocoel cavity. Both routes proved to be substantially less efficient than pronuclear injection. Attempts to improve the efficiency of these approaches (e.g. using poly-L-lysine) have shown some promise, but remain unreliable (281). Retroviral infection of

preimplantation embryos has been successful, but this method is now used only rarely to generate transgenic animals (140). It has been proposed that adenovirus vectors may be used for germline transformation in the future (282). However, viral transduction as a method for generating transgenic animals suffers from several drawbacks, including the limited amount of foreign DNA that can be incorporated into integrating viral vectors, the effect of viral sequences both on transgene expression and the expression of endogenous genes located near to the transgene insertion site, and the susceptibility of transgenes carried in recombinant proviruses to de novo DNA methylation.

There have also been reports that transgenic animals can be produced using a simple technique in which DNA is mixed with spermatozoa before *in vitro* fertilization. However, a reliable sperm-mediated gene transfer technique in mammals remains to be developed (283).

14.11.2 ES Cells

Mouse ES cells have revolutionized mammalian genetics by providing a route for the directed and sequence-specific alteration of the mouse genome (241,246). ES cells possess a unique combination of useful properties: They are pluripotent (and hence compatible with germline modification), they are amenable to *in vitro* cell culture, and they possess an inherent capacity for homologous recombination (Fig. 14.19). First, the DNA transfected into cultured ES cells integrates into the genome (either randomly or by homologous recombination—gene targeting). Then, the genetically modified cells are introduced into preimplantation stage embryos, either by blastocyst injection or by morula aggregation, to produce chimeras. In some of these chimeric animals, the ES cells will have contributed to the germline, thus providing a source of fully transgenic offspring. One strategy is to use ES cells and preimplantation embryos from mouse strains with different coat color markers. The ES cells often carry a dominant marker such as agouti, while the recipient embryos carry a recessive black coat color. The chimeric founder mice have patchwork black/agouti coats representing cell clones derived from the two genotypes that contributed to the embryo, because the markers are cell autonomous. Chimeric males are then mated to black females, and transgenic offspring are identified by their agouti coats, showing they are entirely derived from the ES cells. This germline modification is then inherited as a Mendelian trait. This simple strategy saves performing Southern blot hybridization or PCR analysis on all offspring to determine their genotype. ES cells offer an attractive route to germline modification when compared with pronuclear injection because DNA alterations can be carried out in cell culture and verified before being introduced into the embryo. The limitations associated with pronuclear injection (technical requirements for working with pronuclear eggs and the lack of preimplantation screening so that transgenic status has to be verified after birth) do not apply to ES cells. ES cells may therefore facilitate more precise genome modifications, especially by exploiting the versatility of gene targeting strategies (239,240).

The injection of ES cells into blastocysts has been developed to improved strategies for ES cell delivery into the embryo. Morula injections are easier and give better results in terms of germline transmission but suffer from very high embryo mortality rates. Alternatively, coculturing ES cells with eight-cell-stage embryos generates blastocysts with an inner cell mass containing ES cells. The *in vitro* derived blastocysts are then reimplanted. This is an appealing method due to its simplicity and has proven effective. However, the resulting animals are still chimeras, and germline transmission is not always achieved. It is also possible to make aggregates between tetraploid morula cells (obtained by electrofusion) and ES cells. As tetraploid cells cannot support development, the postimplantation embryos developing from these aggregates give rise to mice derived entirely from ES cells (284). Under these conditions, chimeric diploid/tetraploid embryos implant and develop to midgestation at high frequency, but the efficiency drops off during later development and few embryos survive to term. However, this *tetraploid rescue* technique is becoming more robust (285).

14.11.3 Primoridal Germ Cells

Nonmurine ES cells are currently available only for mice. The application of the recently developed selection protocol for embryonic cells, which kills differentiated cells while leaving the undifferentiated (and pluripotent) cells to grow, may now provide a route to generate ruminant ES cells (261). The failure to derive ES cells from other species has been the driving force to discover alternative strategies. One alternative approach would introduce the genetic change directly into the germline by gene targeting of primordial germ cells (PGCs) (Fig. 14.20). There have been claims that embryonic germ (EG) cells may be analogous to ES cells. Unfortunately, it has proven difficult to persuade PGCs to contribute to the germline (286), and the technique is not yet routine.

14.12 USES FOR TRANSGENIC ANIMALS

Since the first transgenic mice produced by pronuclear injection in the early 1980s (287), a vast literature has been amassed concerning genetically modified mammals (277). The majority of transgenic mammals are mice. The use of

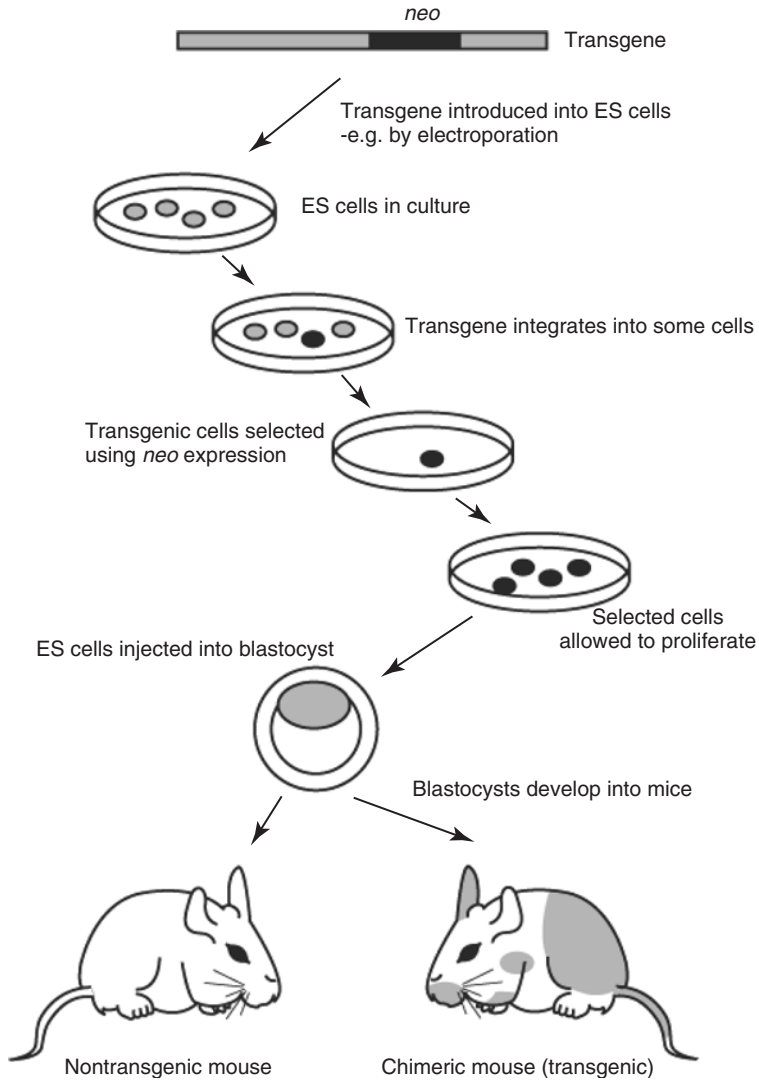


Figure 14.19. Generation of transgenic mice from ES cells modified in culture by transfection or retroviral transduction. Transformants are selected and injected into wild-type blastocysts. A proportion of the mice developing from ES cell-injected blastocysts will be normal, and a proportion will be chimeric for donor- and ES cell-derived tissue. In some of the latter category, the germline will be ES cell derived, and any progeny of these "germline-transformed" mice will be transgenic. The identification of chimeric and transgenic mice is simplified by using donor blastocysts and ES cells carrying different coat color markers and of different sexes. Chimeric mice therefore possess a variegated coat, but transgenic mice will carry the ES coat color marker.

other species has been restricted by technical limitations, cost, the time involved in breeding, and welfare issues. The recent development of nuclear transfer techniques in livestock (288) provides new openings for animal breeding and animal biotechnology (289).

14.12.1 Gene Function Studies

There are two basic expression strategies for studying gene function in transgenic mice. The first involves a gain-of-function by overexpression of the protein of interest. All that is required is the appropriate transcriptional control elements and the coding region of the gene of interest. The gene can be expressed according to its normal cellular parameters or deliberately expressed in an ectopic fashion. In addition, the incorporation of inducible promoters allows overexpression at a defined developmental stage. The transgene can be in the form of either a genomic fragment or a cDNA, although, in general, genomic constructs are the more efficient. An alternative use of this approach has been to facilitate the production

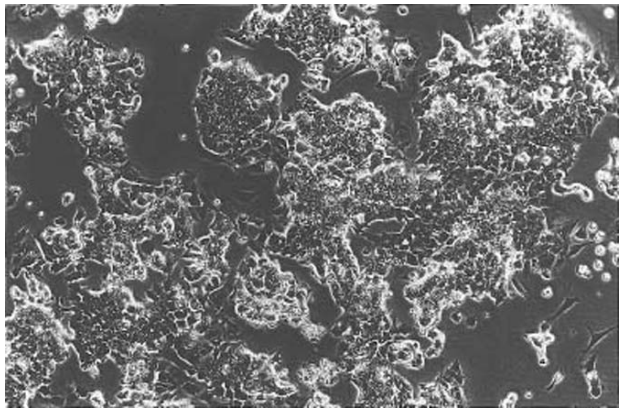


Figure 14.20. Mouse embryonic germ (EG) cells, strikingly similar to ES cells. Photograph courtesy of Ed Gallacher and Jim McWhir (Roslin Institute).

of immortalized cell lines. To do this, a transgene is constructed consisting of the desired promoter linked to a gene capable of immortalizing cells, most commonly the SV40 viral T-antigen (290). Transgenes can be expressed in atypical tissues/stages of development, which can result in inappropriate but informative phenotypes (e.g. mice expressing the HSV *Tk* gene) that are sterile due to the ectopic expression of TK gene in the testes (291). Ectopic expression can be due to influences of the adjacent cellular DNA or to unforeseen interactions between *cis*-acting sequences in hybrid transgenes.

The alternative strategy results in a loss of function. This can be achieved by either gene targeting approaches to generate a knockout (see the following) or directing expression of a transgenes encoding cytotoxic proteins (292). More recent efforts have utilized genes encoding enzymes that convert an inactive prodrug into a cytotoxin. This approach is being developed as a strategy for cancer treatment, termed *gene-directed enzyme prodrug therapy* (GDEPT). One of the most promising examples of this approach is the *E. coli* nitroreductase gene, which offers a number of advantages over the more commonly used HSV *Tk* gene (293). Variations of this strategy include suppressing gene expression through the use of transgenes generating antisense RNA molecules or the overexpression of a dominant negative form of the protein (192).

Another way to use a transgene to study gene function is to use it as a tracer. This can be in the form of a physical genetic marker, because multicopy transgenes can be easily detected by chromosomal *in situ* techniques. Alternatively, transgene expression can be used to trace cell lineages, particularly during development (16).

14.12.2 Knockout (Null) Mice

The most powerful approach used to interfere with the function of a gene is to disrupt one allele by gene targeting in ES cells (241). In conjunction with the established positive–negative selection systems, precise genetic changes can be produced. However, this approach has also revealed the high degree of redundancy in the mammalian genome. In attempts to get around this problem, a variety of spatial and temporal expression vectors have been developed.

Gene targeting has been used successfully to define the function of a number of genes, including many proto-oncogenes (e.g. c-*Myb* and *Wnt*-1) (246). Gene targeting has also made valuable contributions to the understanding of the immune system. Nevertheless, the greatest use of gene targeting has been to identify and characterize developmentally regulated genes. This has been most clearly demonstrated for the *Hox* genes and the transcription factors involved in muscle cell development (294).

The first step in generating a knockout mouse is to introduce the appropriately designed targeting vector into ES cells. In a few cells, the vector is inserted, by homologous integration, into the target gene. This event is identified by positive–negative selection. Subsequent clonal expansion of the target cell then generates an isogenic population of genetically modified cells. These are injected into the blastocoel cavity of a preimplantation mouse embryo. The blastocyst is surgically transferred into the uterus of a foster mother, where development is allowed to continue to term. The resulting offspring are chimeric, and these can be bred to produce transgenic knockout mice in the subsequent generation.

14.12.3 Gene Regulation Studies

Transgenic studies specifically designed to localize and characterize gene regulatory elements have provided important information regarding transcription regulation. The use of enhancer trap and gene trap mice falls into this category. Indeed, gene regulatory elements have been identified *in vivo* through transgenic studies that were not apparent in cell culture studies.

Two classes of transcriptional control elements have been identified by transgenic studies. Both act dominantly to facilitate transgene expression. The first is the human β-globin LCR that overcomes position effects. LCRs enable position-independent, copy-related expression of most genes (227). However, there are genes that even LCRs cannot drive efficiently in transgenic animals (e.g. the *lacZ* reporter gene) (295). The second element is the boundary or insulator element. These loosely characterized sequences appear to protect the transgene from *cis*-acting influences at the site of transgene integration (296). Other aspects of gene regulation have become apparent through transgenic studies. For example, several studies have clearly demonstrated that intronic sequences facilitate gene

expression *in vivo*. Indeed, it has been argued that intron removal per se increases the sensitivity of transgenes to position effects *in vivo* (226).

Transgenes can also provide a valuable tool to look at the mechanisms involved in gene suppression or silencing (297). These include bacterial genes, such as the routinely used *cat* reporter gene encoding chloramphenicol acetyltransferase, and the intronless versions of genomic genes, which are regularly used in expression systems. No robust route to express this type of sequence has been developed, although LCRs and transgene rescue have proved useful. There are now several examples of variegated or patchy transgene expression within a given cell type; that is, not all cells within a given population efficiently express the transgene. This phenomenon is both position and dosage effects (208). It has also been proposed that transgenes present as a multicopy array may themselves direct the formation of heterochromatin (209).

14.12.4 Disease Models

Considerable effort has been directed to the development of transgenic animals as suitable models for human diseases, and there have been a number of successes that should now allow the development of novel therapies. The majority of these animals have been generated using the pronuclear injection method. Such transgenic mice have played a particularly important role in unraveling the consequence of oncogene expression in tumorigenesis. The pronuclear injection technique, however, suffers from the limitations that foreign DNA can only be added, not deleted or altered. The use of homologous recombination in ES cells overcomes this limitation (246,298).

The desire and ability to produce mouse models is clearly demonstrated by the generation of a variety of cystic fibrosis models within 3 years of the isolation of the cystic fibrosis transmembrane conductance regulator (CFTR) gene. This example also shows the limitation of the mouse model, as none of the cystic fibrosis mice clearly reflected the human disease phenotype (i.e. no lung pathology). Although not showing the relevant disease phenotype, these mice do lack CFTR gene activity and therefore are valuable as a model to develop gene therapy strategies to restore the CFTR mRNA levels and hence protein function (299).

To date, all genetically engineered animal disease models have been mice, although it has been suggested that alternative species might be more appropriate models for certain diseases (300). The recent development of nuclear transfer methodology may now allow the development of large animal models of human disease (e.g. sheep genetically modified to provide a model for cystic fibrosis).

14.12.5 Nonmammalian Species as Heterologous Systems

Gene transfer has been accomplished in many nonmammalian animals, including the model invertebrates *D. melanogaster* and the nematode *Caenorhabditis elegans* (275,277), model vertebrates such as the chicken (301), and more recently *X. laevis* (302) and many species of fish (196). In all the cases, DNA transfer is achieved by the microinjection of DNA into oocytes, eggs, or early embryos. In addition to providing valuable information concerning gene function in these species, information relevant to mammalian genes can be generated. For instance, the use of recombinant P elements has facilitated the study of vertebrate regulatory elements such as the β-globin LCR and the chicken lysozyme A boundary elements in *Drosophila* (303). Some nonmammalian species have commercial applications, such as fish, with regard to accelerating growth (304), and birds, with regard to enhanced disease resistance. The latter was brought a step closer with the development of microinjection techniques for chickens (301).

14.12.6 Expression Modeling

Gene regulatory elements not apparent in cell culture have been identified *in vivo* through transgenic studies (305). Furthermore, a comparison of the effect of various regulatory elements showed examples of high efficiency expression *in vitro* and only moderately efficient expression *in vivo*.

These differences can relate to specific transcriptional control elements or more generic differences. For example, molecular analysis of the distal enhancer of the mouse α-fetoprotein gene has shown that mutations affecting specific transcription factor-binding sites caused a 10-fold reduction in enhancer function *in vitro*, whereas in transgenic mice, the same mutation resulted in sporadic tissue-specific expression of the transgene, dependent on the site of integration. In contrast, mutations in the glucocorticoid receptor element of the ovine β-lactoglobulin promoter all abolished expression in transfected cells but had no effect on expression in transgenic mice, as compared with wild-type constructs. The same contrast between *in vitro* and *in vivo* experiments is also observed for the basal transcription machinery. Mutagenesis of the αB-crystallin TATA-box sequence had no effect on promoter activity in transfected lens cells but preferentially reduced promoter activity in the lenses of transgenic mice. Therefore, when comparing cell transfection and transgenic mice, it would seem that regulation of transcription differs *in vitro* from *in vivo* at the levels of both the basal transcription machinery and upstream regulatory elements. There is also considerable evidence to support the hypothesis that a more stringent requirement for

introns exists in transgenic mice than in cell culture. For example, while introns increase transcriptional efficiency of metallothionein-I promoter-driven rat growth hormone gene constructs in transgenic mice, expression in cultured cells seems to be insensitive to the presence of introns (306). This observation led to the proposal that introns facilitate gene expression, but only once the target genes have passed through the germline.

Transcriptional control mechanisms observed *in vivo* are often not consistent with those acting *in vitro*. However, pre-mRNA processing mechanisms observed in cell culture have been shown to correlate with the posttranscriptional modifications observed in transgenic mice. For example, β-lactoglobulin minigene constructs were inefficiently spliced, with the frequency of intron retention similar *in vitro* and *in vivo* (307). This similarity may prove distinctly useful by allowing transgene constructs to be tested for efficient posttranscriptional processing *in vitro* before their use in transgenic livestock.

14.12.7 Transgenic Livestock

Classical animal breeding regimes rely on gene import by cross-breeding and are therefore limited to the improvement of those traits already present in a given species. Transgenic animal technology can overcome these limitations because the exogenous DNA can be derived from a heterologous species and it can be modified *in vitro* before being introduced into the germline.

Working with domestic animals poses a number of technical problems (277). The recovery of adequate numbers of pronuclear eggs, and their successful transfer following microinjection, requires a large number of donor and recipient animals. In addition, the pronuclear eggs of livestock species are delicate and relatively opaque. In pigs and cattle, centrifugation is often necessary before injection to visualize the pronuclei. In sheep, eggs must be observed using a differential interference optics (DIC) microscope to see the pronuclei clearly. These technical hurdles add to the constraints of dealing with large animals with generation intervals of several years.

It has been proposed that transgenesis may allow the generation of farm animals with improved traits, animal models for research, and animal bioreactors. This includes the production of animals with modified growth characteristics and carcass compositions, novel properties of the digestive system, enhanced wool yields, and the production of novel proteins. It is this last opportunity that has seen the most progress over the past decade, with the expression of a variety of proteins targeted to the milk of sheep, cattle, pigs, goats, and rabbits (225). Indeed, this application of gene transfer in livestock is fast approaching commercial success, with the first products currently undergoing clinical trials.

14.12.8 Modulation of Production Traits

The ability to transfer genes into the germline of livestock may well be instrumental in providing an alternative route to satisfying the ever-increasing demand for animal food and products. Productivity traits that may be amenable to modification by transgenesis include growth rate, nutrient composition of food products, quality of wool, and resistance to disease. Initial experiments concentrated on the transfer of growth-related genes (308). These studies were on the whole unsuccessful due to undesirable side effects. The problem was identified as a lack of stringent control over the expression of the transgene. Encouraging results have been obtained with attempts to improve wool production (309). Perhaps the greatest progress has been made in projects aiming to modulate milk composition through the generation of transgenic animal bioreactors (225). In the near future, most progress will perhaps be seen in the area of engineering disease resistance. However, while several strategies addressing disease management have potential, additional research is still required before these approaches can be applied (310).

14.12.9 Animal Bioreactors

To date, the most successful application of gene transfer technology in livestock has been to target the expression of commercially and medically valuable proteins to milk. In the early 1980s, it was speculated that transgenic animals could be used to produce important human proteins for medical use. It was perceived that transgenic animal bioreactors would overcome the limitations of the other recombinant protein production systems and provide proteins with appropriate posttranslational modifications in large amounts (225,311). The first step involves the generation of a hybrid transgene, comprising DNA control elements from a gene normally expressed in the mammary gland linked to the coding region of a valuable gene that is normally expressed in a different tissue, such as the liver.

Clark et al. (312) provided the first demonstration of the feasibility of this approach in large animals. In this study, transgenic sheep were generated that expressed a transgene encoding human clotting factor IX. Unfortunately, in this early experiment, the level of product detected in the milk was very low (25 mg/L). The problem of low yield has now been solved for many proteins, and this general approach has been applied to several animal species, including rabbits, goats, sheep, pigs, and cattle (225). Many different proteins have now been produced in the milk of transgenic animals, although these predominantly reflect model studies in the mouse. These range from relatively simple proteins, such as albumin, to highly complex proteins such as monoclonal IgA antibodies and hexameric fibrinogen (313). The successes in large animals include tissue plasminogen activator in rabbits and goats, antithrombin III in goats,

α-1-antitrypsin and clotting factor IX in sheep, and protein C in pigs. In one of these studies, very high level production was obtained (Fig. 14.21). Tracy, the transgenic ewe, produced human α-1-antitrypsin in her milk at 30 g/L, which approaches half that of the total protein content (314).

It may be that certain species are more appropriate bioreactors for the synthesis of specific proteins. For example, rabbits have been proposed to be appropriate for those products required in small quantities, while the generation of transgenic birds using a DNA microinjection approach opens up the possibility of producing pharmaceuticals in chicken eggs (301). Different tissues may also have particular advantages, for example, because they carry out a specific form of posttranslational modification.

14.13 NUCLEAR TRANSFER TECHNOLOGY

Although to date all gene transfer experiments in livestock have involved the *addition* of genetic material, there is an understandable desire to develop gene targeting strategies. This would open up a vast range of applications in livestock. For example, gene targeting techniques could allow disruption of the prion-related protein gene (*Prp-1*) in cattle and sheep, which could facilitate the production of bovine spongiform encephalopathy (BSE)- and scrapie-resistant animals. In addition, the removal of certain histocompatibility genes would allow the production of animals (pigs) as a source of xenograft organs for transplantation surgery. Furthermore, the ability

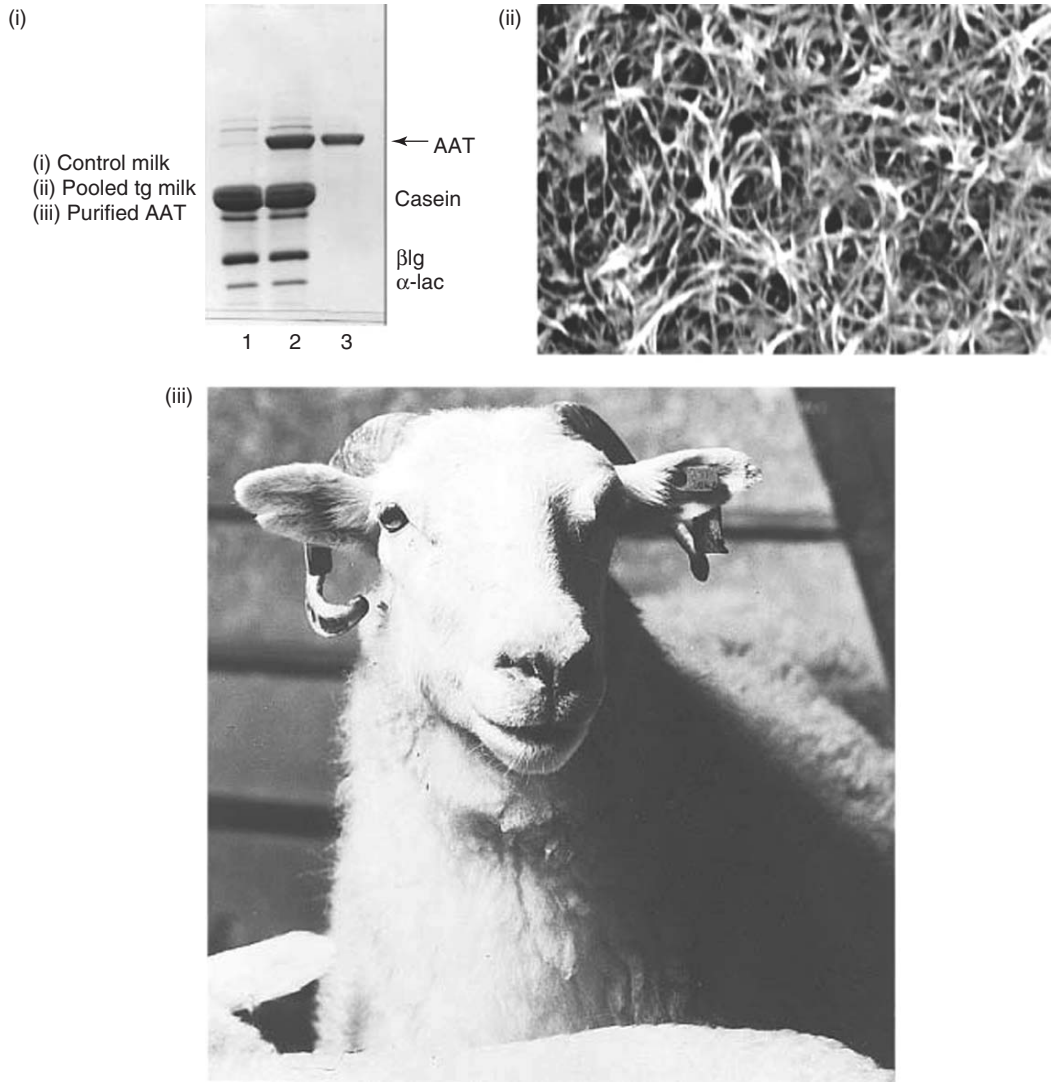


Figure 14.21. Animal bioreactors. (a) Western blot showing production of human α-1-antitrypsin (AAT) and (b) structure of fibrinogen, both products of animal bioreactors. (c) Tracy, the transgenic ewe, expressing AAT in her milk. Photographs courtesy of Ian Garner and April D'Arcy (PPL Therapeutics plc).

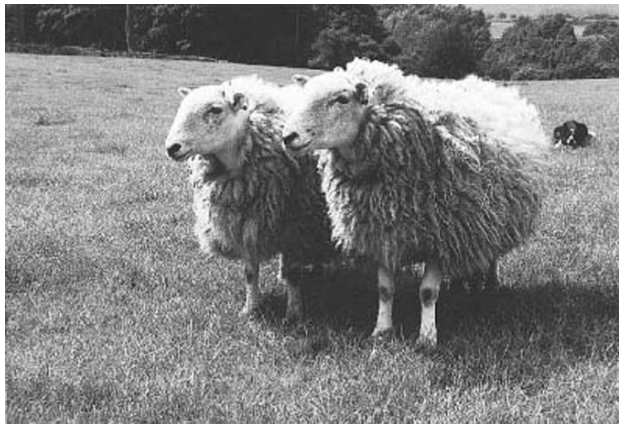


Figure 14.22. Megan and Morag, the first sheep to be produced by nuclear transfer from cultured cells.



Figure 14.23. Dolly, the first mammal produced by nuclear transfer from an adult cell, and her lamb Bonnie.

to derive live animals from cultured cells would provide a more efficient way to produce superior farm animals. Before such strategies become feasible, however, cell lines that can contribute to the germline must be derived from livestock (260,289).

Nuclear transfer was the first cell culture-based procedure used to produce livestock and was achieved by Campbell and colleagues at the Roslin Institute in 1995 with the generation of the cloned sheep Megan and Morag (288) (Fig. 14.22). Two years later, the same group announced the generation of Dolly (Fig. 14.23), who was derived from an adult cell by nuclear transfer (289). Variations on this procedure, including the generation of ruminant ES or EG cells, are being explored and encouraged by the recent demonstration of live births following nuclear transfer in mice (315). Whatever the route to gene targeting in livestock, the inevitable experimental timescale and the unavoidable financial costs will mean that only those projects likely to yield profitable biotechnological or agricultural applications will be undertaken. At present, there would be little public support for the production of genetically modified livestock for the food chain, though this might well change if it could be shown the animals would benefit (e.g. by having improved resistance to disease). Therefore, the first applications of this second-generation transgenic technology will almost certainly concern biotechnology and medicine (e.g. xenotransplantation or the production of therapeutic proteins in milk).

14.13.1 Advantages of Cell-Based Gene Transfer Procedures

There are two driving forces behind the development of cell-based gene transfer procedures in livestock. First, the desire to overcome position and dosage effects (316), and second, the desire to overcome the laborious techniques involved in the production of transgenic livestock by pronuclear microinjection (primarily reflecting the large number of animals required). In addition, microinjection can only add genes. A cell-based method to produce transgenic livestock allows single-copy transgene integrants to be generated at predetermined sites, which should limit problems such as variegated transgene expression. Future transgenic livestock will probably have the transgene integrated into a permissive site, and although such an appropriate genomic site remains to be determined, this approach has been evaluated in the mouse model. The outcome is likely to be more predictable in terms of generating the anticipated transgene expression profile. Expression levels from these single-copy transgenes may need to be enhanced, because multiple-copy transgene loci can generate very high levels of expression. It is likely that many of these issues can be evaluated in cells before generating a transgenic animal.

Targeted integration has been possible in the mouse model through ES cell technology (241). Although there has been considerable effort to generate ruminant ES cells, to date all attempts have been unsuccessful. An alternative approach involves the transfer of nuclear genetic material from cells grown in culture into an unfertilized egg (317). Now, rather than merely evaluating a transgene construct in cell culture, the actual cell is the genetic material from which the transgenic animal is generated. The gateway has been opened for the production of a variety of livestock for both agricultural and biomedical applications. There are many advantages to this technology; for example, all founder animals are transgenic, mosaic founders are not produced, the sex of the founder can be selected, and a flock/herd of clonal animals can be produced within one generation. More important, many aspects of the

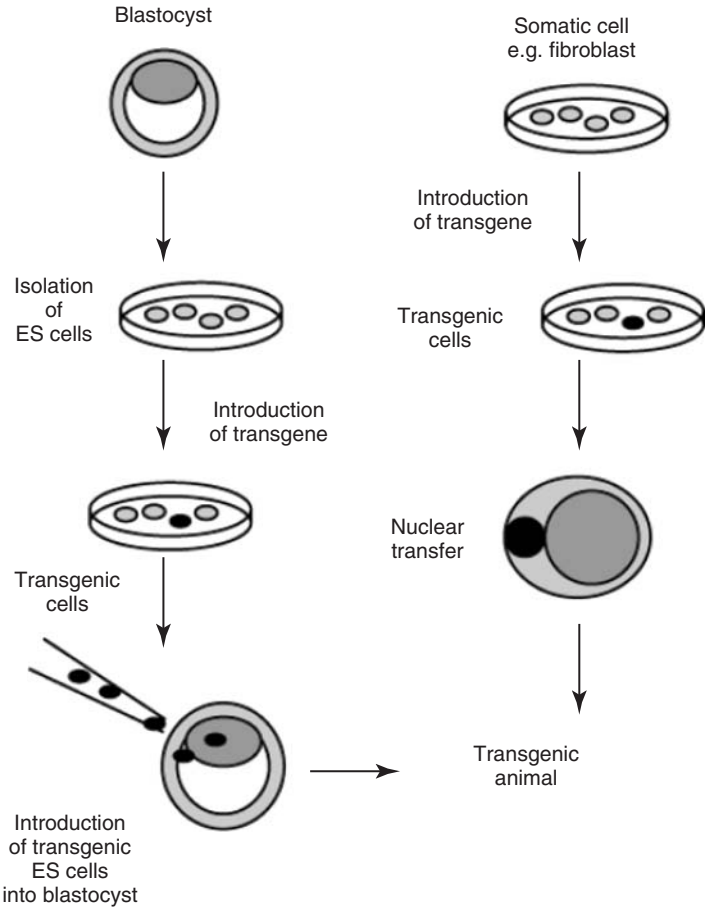


Figure 14.24. A comparison of the ES cell and nuclear transfer routes to generate transgenic livestock. Either procedure is amenable to gene targeting strategies, following introduction of DNA by microinjection, electroporation, or other forms of transfection.

transgene can be analyzed *in vitro* before the generation of an animal. The integrity of the transgene locus can be evaluated, which may be particularly important when large transgenes such as YACs are used. Furthermore, it will be possible to check the expression potential of a transgene before going through the cost of producing the animal. Expression strategies could, for example, involve the transient production of an appropriate transcriptional activator, which could mediate *trans*-induction of transgene expression. The most important point, however, is that it is possible to select for site-specific integration events generated by gene targeting, thus allowing strategies involving gene knockout or replacement to be performed as shown in Fig. 14.24.

14.13.2 Ruminant Embryonic Cells

No ruminant ES or EG cells are currently available. In this regard, there is an ongoing debate about which *in vitro*, environmental, and genetic factors could be responsible for the differences between mice and other mammalian species (261). The rationale behind this approach is that ES cells can be isolated from some mouse strains more efficiently than others. It was proposed that this may reflect the differences in the control of ES progenitor cells by other lineages within the embryo (318). Thus, if these other lineages were removed, the ES cell progenitors might survive. This is indeed the case, at least for some mouse strains nonpermissive for ES cells (Fig. 14.25). This approach is currently being tried in pigs and rabbits. Although encouraging, the selection method is limited by the initial requirement of the appropriate transgenic line. In an attempt to overcome this limitation, transient expression strategies are being developed.

An alternative cell type is the EG cell derived from PGCs. There is some considerable progress in the development of this cell type, and recent advances in PGC isolation and culture, and hence the culture of EG cells, have provided the impetus to develop this approach.



Figure 14.25. Selective ablation of differentiated cells permits isolation of ES cell lines from nonpermissive strains. The photograph shows a germline chimera derived from line 39/1, its albino MF1 mate, together with germline (agouti) and nongermline (albino) littermates. Courtesy of Jim McWhir and Helen Wallace (Roslin Institute).

14.13.3 Nuclear Transfer

Xenopus nuclear transfer was first reported in 1952. Since then, it has been widely used in amphibians, primarily for experiments addressing early development (319). In 1977, a mouse was generated by nuclear transfer using a cell from a very early embryo. The procedure in mice proved to be very difficult. Since then, most research has concentrated on farm animals, driven by the prospect of large financial benefits derived from cloning elite and/or transgenic embryos. In the 1980s, cloned sheep and cattle were generated using early embryo cells as donors. Furthermore, some experiments in the United States showed that live calves could be derived by nuclear transfer using cells from the late blastocyst stage. At this stage of mammalian development, primitive cell types are distinguishable; therefore, this was the first suggestion that nuclear transfer in mammals was possible from at least partially differentiated cells. The major breakthrough came in 1995, when Ian Wilmut and Keith Campbell produced two live lambs—Megan and Morag—by nuclear transfer of embryonic cells grown in culture (288). Within a year, a lamb had been produced from an adult cell (289). This lamb was called *Dolly*. Since then, a number of lambs and calves have been generated using this technology, some of which are transgenic (260,317). The objective is now to expand the number of species where nuclear transfer can be applied. In this regard, the recent demonstration of nuclear transfer in mice should dramatically accelerate the development of this technology (315).

Embryo reconstruction by nuclear transfer involves the transfer of a single nucleus to an unfertilized oocyte or one-cell zygote from which the genetic material has been removed. For livestock, the recipient cell of choice is usually an unfertilized oocyte that has been arrested at metaphase of the second meiotic division. The first step is to enucleate the recipient oocyte. The genetic material is removed using a small glass pipette, a highly skilled procedure. The genetic material from the donor cell is then introduced into the enucleated oocyte, usually by cell fusion using a short electrical pulse, although treatment with PEG or Sendai virus is also possible. The next phase involves the activation of the reconstructed embryo. In nature, this is achieved by fertilization and involves calcium mobilization. Activation can be mimicked by a variety of chemical agents, such as phorbol esters or calcium ionophores. In practice, this step is often simplified, because the electric pulse used to fuse the cells can also activate the embryo. Finally, the embryo is cultured to a stage at which it can be transferred to a synchronized recipient animal for development to term. Some livestock generated by nuclear transfer are shown in Fig. 14.26.

14.13.4 Source of Donor Nuclei

The highly publicized generation of Dolly demonstrated that the donor cell for nuclear transfer could be derived from a differentiated cell. In this case, the source was a cultured mammary cell line, the cells being derived originally from a 6-year-old ewe. However, this experiment was very inefficient with only one animal being produced from about 250 cultured cells (289). The donor cell must be neither aneuploid nor contain any other chromosomal damage. In addition, for technical reasons, it must be easy to handle and manipulate in culture. The most commonly used cell



Figure 14.26. Livestock generated by nuclear transfer. (a) Mr Jefferson, a Holstein calf produced by nuclear transfer from a fetal fibroblast cell line in 1998. (b) Dolly, the first transgenic lamb produced by nuclear transfer, born in 1997. Photographs courtesy of Ian Garner and April D'Arcy (PPL Therapeutics plc).

type is the fetal fibroblast (317). Obviously, if ruminant ES or EG cells become available, they would provide ideal donor cells (260).

One of the main requirements for successful nuclear transfer using ruminant cells is the synchronization of the cell cycle between donor and recipient cells. The outcome of these studies demonstrated that cell cycle arrest in G_0 phase was crucial for the procedure to work. This can be accomplished simply by reducing serum levels in the culture medium, although whether this is the best strategy remains to be investigated. The suitability of the quiescent donor nuclei may reflect a number of factors, such as reduced transcription and translation, low metabolic activity, and condensed chromatin. Presumably these changes render the nucleus and cytoplasm more compatible with the mechanisms of reprogramming.

14.13.5 Reprogramming

Reprogramming refers to the change in differentiation state associated with nuclear transfer. The donor cell is differentiated, to varying degrees, while the egg is not. Before transfer, a variety of cell type-specific genes would be active in the donor nucleus. These must be repressed, and the appropriate genes required for early embryonic development must be activated; that is, the nucleus has to "forget" its history (whether it was taken from a fibroblast, mammary cell, etc.) and take instructions from the cytoplasm of the recipient cell. Reprogramming is anticipated to depend on a large number of factors, the majority of which are undefined and not understood at present. In addition to differences in the levels of various transcription factors, the nucleus itself also changes during development, through chromatin remodeling and DNA methylation, resulting in the silencing of many genes. Such changes also need to be erased before development can be recapitulated by nucleus transferred to a reconstituted embryo. Another important factor is the age of the donor nucleus. The cell used to generate Dolly was derived from a 6-year-old ewe, raising the question of whether Dolly would show signs of premature aging. One anticipated effect is that the telomeres, which protect the chromosome ends, become progressively shorter. A recent study (320) showed that Dolly's telomeres were indeed shorter than expected for a sheep her age. However, this does not appear to have affected the health or reproductive ability of Dolly or any other cloned animal—indeed, Dolly has already had two successful pregnancies. This finding does have important implications for some nuclear transfer strategies, such as sequential cloning.

14.13.6 Xenotransplantation

Over the past few decades, transplantation has become the preferred treatment for human organ failure. However, there is a chronic shortage of donor organs, so that only half of the potential operations are actually performed. If animal organs could be used instead of human organs (xenotransplantation), this shortage would be overcome (321). The major limitation to the use of nonprimate organs in human patients is tissue rejection. As the immune system plays such a critical role in the host defense, there is considerable interest in engineering tissue compatibility into the xenograft donor as opposed to suppressing the patients' immune response. Transgenic animals offer a route to overcome this limitation.

The hyperacute rejection of organs reflects the activity of the host's complement system. One proposed strategy involves the generation of animals that carry transgenes, allowing evasion of the complement system. For example, transgenic pigs have been produced carrying a transgene encoding a complement inhibitory factor that coats the cells (322). At present, further developments are required, including modulation of the antibody response induced by xenotransplantation (323). Here, the ability to remove genes could have a major impact on the success of xenotransplants. Surprisingly, most of the antibodies in our blood that would react against a pig organ recognize a single carbohydrate linkage present on pig cells (324). This disaccharide, Gal-$\alpha 1-3-$Gal, is synthesized by α1,3-galactosyltransferase. Primates do not have a functional α1,3-galactosyltransferase gene and therefore do not recognize this carbohydrate. Elimination of this enzyme in pigs by gene knockout could therefore reduce hyperacute rejection of transplanted organs. This strategy requires the ability to perform germline gene targeting experiments in pigs. This may now be possible with the development of nuclear transfer technology (260,289).

The first experimental transfer of a genetically modified pig's heart was into cynomolgus monkeys (325). None of the 10 hearts was rejected, and the monkeys survived for an average of 40 days. Conversely, hearts from control pigs were rejected within hours. This is encouraging, but the routine use of xenotransplantation by the surgeon will require equally challenging approaches to overcome delayed rejection, such as cellular rejection. Currently, this type of rejection is controlled by immunosuppressive drugs, but here again gene transfer technology may hold the answer. Notwithstanding the technical hurdles required to generate transgenic pigs with the appropriate genetic modifications, there are many ethical issues that need to be debated. In addition, xenotransplantation may well bring novel disease problems, and the potential severity of these issues remains to be examined. For example, the transplantation of a pig heart into a human patient may expose that individual to infection from endogenous retroviruses present in the pig cells (321).

14.13.7 Nuclear Transfer and Somatic Cell Therapy

An alternative approach to *in vivo* gene therapy is to modify cells genetically *ex vivo* and then reintroduce them into the patient. This route overcomes many of the serious problems associated with efficient gene delivery but has been restricted by the ability to isolate the appropriate cells. The development of nuclear transfer using somatic cells grown in culture has provided an new impetus to these studies (289). These pioneering nuclear transfer experiments have demonstrated that a differentiated cell can be programmed to restart development. Once the mechanisms behind this process are understood, it may be possible to reprogram animal cells without resorting to the use of an egg. In the future, this may well allow a patient's own cells to be used for personal gene therapy. This would avoid the expense and uncertainty of tissue matching. In this scenario, cells would be removed from the patient, converted into the desired cell type in the laboratory by nuclear reprogramming, and then reintroduced into the same patient.

14.13.8 Animal Cloning

The cloning of animals provides immediate advantages for both animal breeding and basic research. The main advantage in breeding would not be in the selection programs and in the rapid dissemination of the genetic progress from elite herds to the commercial farmer. There is a risk attached, that of loss of genetic diversity, but this could be avoided, for example, by systems to ensure that breeding companies produce a limited number of clones of each type. Alternatively, nuclear transfer from cultured cells could be of use for species where repeated breeding is impractical or prohibitively expensive. It may also prove useful in providing new approaches for genetic conservation. In the context of research, genetic variation between individuals tends to confound the often subtle responses to test diets or drugs. The advantages of genetic uniformity has been demonstrated in studies with inbred lines of mice and exploited to some extent with the numerous back crosses that provide the basis for many animal genome mapping schemes.

REFERENCES

1. Szybalska EH, Szybalski W. *Proc Natl Acad Sci USA* 1962; 48: 2026–2034.
2. Doerfler W, et al. *Trends Biotechnol* 1997; 15: 297–301.
3. Dawson M, Butler M. In: Butler M, Dawson M, editors. *Cell culture labfax*. Oxford, UK: BIOS Scientific Publishers/Blackwell; 1992. p 177–189.
4. McCarroll L, King LA. *Curr Opin Biotechnol* 1997; 8: 590–594.
5. Colman A. Hames BD, Higgins SJ, editors. *Transcription and translation: a practical approach*. Oxford, UK: IRL Press; 1984. p 271–302.
6. Chisholm V. In: Glover DM, Hames BD, editors. *DNA cloning 4, Mammalian systems: a practical approach*. 2nd ed.. Oxford, UK: IRL Press; 1995. p 1–42.
7. Kain SR, Ganguly S. *Current protocols in molecular biology*. Suppl. 29. New York: Wiley; 1995. p 9.6.1–9.6.12.
8. Messing J, Vieira J. *Gene* 1982; 19: 269–276.
9. Lusky M, Botchan M. *Nature (London)* 1981; 293: 79–81.
10. Grisshammer R, Nagai K. In: Glover DM, Hames BD, editors. *DNA cloning 2, Expression systems: a practical approach*. 2nd ed. Oxford, UK: IRL Press; 1995. p 71–87.
11. Peterson KR, Clegg CH, Li Q, Stamatoyannopoulos G. *Trends Genet* 1997; 13: 61–66.
12. Joyner AL, editor. *Gene targeting: a practical approach*. Oxford, UK: IRL Press; 1993.
13. Cooley L, Berg C, Spralding A. *Trends Genet* 1988; 4: 254–258.
14. Rijkers T, Peetz A, Ruther U. *Transgenic Res* 1994; 3: 203–215.
15. O'Kane CJ, Gehring WJ. *Proc Natl Acad Sci USA* 1987; 84: 9123–9127.
16. Allen ND, et al. *Nature (London)* 1988; 333: 852–855.
17. Evans MJ, Carlton MBL, Russ AP. *Trends Genet* 1997; 13: 370–375.
18. Lowry I, et al. *Cell* 1980; 22: 817–823.
19. Perucho M, Hanahan D, Lipsich L, Wigler M. *Nature (London)* 1980; 285: 207–210.
20. Sambrook J, Fritsch EF, Maniatis T. *Molecular cloning: a laboratory manual*. Cold Spring Harbor, NY: ColdSpring-Harbor Laboratory Press; 1989. p 16.1–16.81.
21. Gorman CM, Gies DR, McCray G. *DNA Protein Eng Tech* 1990; 2: 3.
22. Mellon P, Parker V, Gluzman Y, Maniatis T. *Cell* 1981; 27: 279–288.
23. Muller WJ, Naujokas MA, Hassel JA. *Mol Cell Biol* 1984; 4: 2046–2412.
24. Gerard RD, Gluzman Y. *Mol Cell Biol* 1985; 5: 3231–3240.
25. Rio DC, Clark SG, Tjian R. *Science* 1985; 227: 23–28.
26. Twyman RM, Jones EA. *J Mol Neurosci* 1997; 8: 63–73.
27. Alam J, Cook JL. *Anal Biochem* 1990; 188: 245–254.
28. Bronstein I, et al. *Anal Biochem* 1994; 219: 169–181.
29. Gorman CM, Moffat LF, Howard BH. *Mol Cell Biol* 1982; 2: 1044–1051.
30. Berger J, et al. *Gene* 1988; 66: 1–10.
31. Cullen BR, Malim MH. *Methods Enzymol* 1992; 216: 362–368.
32. Thompson JF, Hayes LS, Lloyd DB. *Gene* 1993; 103: 171–177.
33. Welsh S, Kay SA. *Curr Opin Biotechnol* 1997; 8: 617–622.
34. Chalfie M, et al. *Science* 1994; 263: 802–805.
35. Cubitt AB, et al. *Trends Biochem Sci* 1995; 20: 448–455.
36. Heim R, Tsein RY. *Curr Biol* 1996; 6: 178–182.
37. Kingston RE. *Current protocols in molecular biology*. Suppl. 14. New York: Wiley; 1996. p 9.5.1–9.5.6.
38. Wigler M, et al. *Cell* 1979; 16: 777–785.
39. Littlefied JW. *Science* 1964; 145: 709–710.
40. Kaufman RJ. *Methods Enzymol* 1990; 185: 537–566.

41. Bebbington C. In: Glover DM, Hames BD, editors. *DNA cloning 4, Mammalian systems: a practical approach*. 2nd ed. Oxford, UK: IRL Press; 1995. p. 85–112.
42. Stark G. *Cancer Surv* 1986; 5: 1.
43. Urlaub G, Chasin LA. *Proc Natl Acad Sci USA* 1980; 77: 4216–4223.
44. Urlaub G, Kas E, Carothers AM, Chasin LA. *Cell* 1983; 33: 405–412.
45. Debenedetti A, Rhoads RE. *Nucleic Acids Res* 1991; 19: 1925–1931.
46. Sabbioni M, et al. *Arch Virol* 1995; 140: 335–339.
47. Sarver N, et al. *Mol Cell Biol* 1981; 1: 486–496.
48. Campo MS. In: Glover DM, editor. *DNA cloning: a practical approach*. 1st ed.. Volume 2. Oxford, UK: IRL Press; 1985. p 213–244.
49. D. DiMaio, in NP Salzman and PM Howley, editors. *The papovaviridae: the papillomaviruses*. Volume 2. New York: Plenum; 1987.
50. Mecsas J, Sugden B. *Annu Rev Cell Biol* 1987; 3: 87–108.
51. Margolskee RF. *Curr Top Microbiol Immunol* 1992; 185: 67–95.
52. Margolskee RF, Kavathas P, Berg P. *Mol Cell Biol* 1988; 8: 2837–2847.
53. Kioussis D, et al. *EMBO J* 1987; 6: 355–361.
54. Larin Z. Lemoine NR, Cooper DN, editors. *Gene therapy*. Oxford, UK: Bios Scientific Publishers; 1996. p 113–126.
55. Keown WA, Campbell CR, Kucherlapati RS. *Methods Enzymol* 1990; 185: 527–537.
56. Kawabata K, Takakura Y, Hashida M. *Pharm Res* 1995; 12: 825–830.
57. Wolff JA, et al. *Science* 1990; 247: 1465–1468.
58. Middaugh CR, Chastain M, Caskey CT. Lemoine NR, Cooper DN, editors. *Gene therapy*. Oxford, UK: BIOS Scientific Publishers; 1996. p 11–32.
59. Nabel EG, Pompilli VJ, Plautz GE, Nabel GJ. *Cardiovasc Res* 1994; 28: 445–455.
60. Graham FL, van der Erb AJ. *Virology* 1973; 52: 456–467.
61. Wigler M, Pellicer A, Silverstien S, Axel R. *Cell* 1977; 14: 725–729.
62. Chen C, Okayama H. *Mol Cell Biol* 1987; 7: 2745–2752.
63. Chen C, Okayama H. *Bio/Techniques* 1988; 6: 632–638.
64. Kingston RE, Chen CA, Okayama H. *Current protocols in molecular biology*. Suppl. 17. New York: Wiley; 1996. p 9.1.7–9.1.9.
65. Orrantia E, Chang PL. *Exp Cell Res* 1990; 190: 170–174.
66. McCutchann JH, Pango JS. *J Natl Cancer Inst (US)* 1968; 41: 351–354.
67. Milman G, Hertzberg M. *Somatic Cell Genet* 1981; 7: 161–168.
68. Lopata MA, Cleveland DW, Sollner-Webb B. *Nucleic Acids Res* 1984; 12: 5707–5717.
69. Sussman DJ, Milman G. *Mol Cell Biol* 1984; 4: 1641–1643.
70. Reeves R, Gorman C, Howard B. *Nucleic Acids Res* 1985; 13: 3599–3615.
71. Kaufman R. *Proc Natl Acad Sci USA* 1985; 82: 689–693.
72. Luthman H, Magnusson G. *Nucleic Acids Res* 1983; 11: 1295–1308.
73. Gorman CM, Howard BH. *Nucleic Acids Res* 1983; 11: 7631–7648.
74. Boggs SS, Gregg RG, Bornstein N, Smithies O. *Exp Hematol* 1986; 14: 988–994.
75. Bertling W, Hunger-Bertling K, Cline MJ. *J Biochem Biophys Methods* 1987; 14: 233–232.
76. Drinkwater NR, Klinedinst DK. *Proc Natl Acad Sci USA* 1986; 83: 3402–3406.
77. Wong TK, Neumann E. *Biochem Biophys Res Commun* 1982; 107: 584–587.
78. Potter H, Weir L, Leder P. *Proc Natl Acad Sci USA* 1984; 81: 7161–7165.
79. Potter H. *Anal Biochem* 1988; 174: 361–373.
80. Zaho X. *Adv Drug Delivery Rev* 1995; 17: 257–262.
81. Kurata S, Tsukakoshi M, Kasuya T, Ikawa Y. *Exp Cell Res* 1986; 162: 372–378.
82. Schaefer-Ridder M, Wang Y, Hofschneider PH. *Science* 1982; 215: 166–168.
83. Itani T, et al. *Gene* 1987; 56: 267–276.
84. Scheule RK, Cheng SH. In: Lemoine NR, Cooper DN, editors. *Gene therapy*. Oxford, UK: BIOS Scientific Publishers; 1996. p 93–112.
85. de Fiebre CM, et al. *Neurochem Res* 1993; 18: 1089–1094.
86. Felgner PL, et al. *Proc Natl Acad Sci USA* 1987; 84: 7413–7417.
87. Felgner JH, et al. *J Biol Chem* 1994; 269: 2550–2561.
88. van der Woude I, et al. *Biochim Biophys Acta* 1995; 1240: 34–40.
89. Hawley-Nelson P, et al. *Gibo-BRL Focus* 1994; 15: 3–6.
90. Charney WG, et al. *Somatic Cell Mol Genet* 1986; 12: 237–244.
91. Schaffner W. *Proc Natl Acad Sci USA* 1980; 77: 2163–2169.
92. Wiberg FC, Sunnerhagen P, Bjursell G. *Exp Cell Res* 1987; 173: 218–231.
93. Tomizyka K, et al. *Nat Genet* 1997; 16: 133–143.
94. Capecchi MR. *Cell* 1980; 22: 479–485.
95. Klein TM, et al. *Proc Natl Acad Sci USA* 1988; 85: 2305–2309.
96. Lo DC, McAllister AK, Katz LC. *Neuron* 1994; 13: 1263–1268.
97. Arnold D, Feng L, Kim J, Heintz N. *Proc Natl Acad Sci USA* 1994; 91: 9970–9974.
98. Haynes JR, et al. *J Biotechnol* 1996; 44: 37–42.
99. Vahlsing HL, et al. *J Immunol Methods* 1994; 175: 11–22.
100. Wu GY, Wu CH. *J Biol Chem* 1987; 262: 4429–4432.
101. Curiel DT, Agarwal S, Wagner E, Cotten M. *Proc Natl Acad Sci USA* 1991; 88: 8850–8854.
102. Stebestyen MG, et al. *Nat Biotechnol* 1998; 16: 80–85.
103. Robbins PD, Tahara H, Ghivizzani SC. *Trends Biotechnol* 1998; 16: 35–40.
104. Berkner KL. *Curr Top Microbiol Immunol* 1992; 158: 39–67.
105. Gerard RD, Meidell RS. In: Glover DM, Hames BD, editors. *DNA cloning 4, Mammalian systems: a practical approach*. 2nd ed. Oxford, UK: IRL Press; 1995. p 285–306.
106. Ring CJA. Lemoine NR, Cooper DN, editors. *Gene therapy*. Oxford, UK: BIOS Scientific Publishers; 1996. p 61–76.

107. Kovesdi I, Brough DE, Bruder JT, Wickham TJ. *Curr Opin Biotechnol* 1997; 8: 583–589.
108. Bett AJ, Prevec L, Graham FL. *J Virol* 1993; 67: 5911–5921.
109. Fischer KJ, et al. *Virology* 1996; 217: 11–22.
110. Kochaneck S, et al. *Proc Natl Acad Sci USA* 1996; 93: 5731–5736.
111. Muzyczka N. *Curr Top Microbiol Immunol* 1992; 158: 97–129.
112. Bartlett JS, Samulski RJ. In: Lemoine NR, Cooper DN, editors. *Gene therapy*. Oxford, UK: BIOS Scientific Publishers; 1996. p 77–92.
113. Berglung P, Tubulekas I, Liljestrom O. *Trends Biotechnol* 1996; 14: 130–134.
114. Lundstrom K. *Curr Opin Biotechnol* 1997; 8: 578–582.
115. Garcia-Sastre A. *Trends Biotechnol* 1998; 16: 230–235.
116. Blissard GW, Rohrmann GF. *Annu Rev Entomol* 1990; 35: 127–155.
117. Boyce FM, Butcher NL. *Proc Natl Acad Sci USA* 1996; 93: 2348–2352.
118. Patel G, Jones NC. In: Glover DM, Hames BD, editors. *DNA cloning 2, Expression systems: a practical approach*. 2nd ed. Oxford, UK: IRL Press; 1995. p 205–244.
119. O'Reilley DR, Miller LK, Luckow VA. *Baculovirus expression vectors: a laboratory manual*. San Francisco (CA): Freeman; 1992.
120. King LA, Possee RD. *The baculovirus expression system: a laboratory guide*. London: Chapman & Hall; 1992.
121. Fraser MJ. *Curr Top Microbiol Immunol* 1992; 158: 131–172.
122. Possee RD. *Curr Opin Biotechnol* 1997; 8: 569–572.
123. Luckow VA, Lee SC, Barry GF, Ollins PO. *J Virol* 1993; 67: 4566–4579.
124. Patel G, Nasmyth K, Jones N. *Nucleic Acids Res* 1992; 20: 97–104.
125. Vos J-MH. Vos J-MH, editors. *Viruses in human gene therapy*. Durham, NC/London, UK: Carolina Academic Press/Chapman & Hall; 1995. p 109–140.
126. Vos J-MH, Westphal E-M, Banerjee S. In: Lemoine NR, Cooper DN, editors. *Gene therapy*. Oxford, UK: BIOS Scientific Publishers; 1996. p 127–153.
127. Geller AI, During MJ, Neve RL. *Trends Neurosci* 1991; 14: 428–432.
128. Lim F, et al. In: Glover DM, Hames BD, editors. *DNA cloning 4, Mammalian systems: a practical approach*. 2nd ed. Oxford, UK: IRL Press; 1995. p 263–283.
129. B. Roizman. In: Fields BN, Knipe DK, editors. *Virology*. 2nd ed. New York: Raven Press; 1990. p 1787–1793.
130. Miyanohara A, et al. *New Biol* 1992; 4: 238–246.
131. Boviatsis EJ, et al. *Cancer Res* 1994; 54: 5745–5751.
132. Hentschel CC. In: Spier RE, Griffiths JB, Meignier B, editors. *Production of biologicals from animal cells in culture*. Oxford, UK: Butterworth-Heinemann; 1991. p 287–321.
133. Coffin JM. In: Fields BN, Knipe DN, editors. *Virology*. 2nd ed. New York: Raven Press; 1990. p 1437–1500.
134. Brown AC, Dougherty JP. In: Glover DM, Hames BD, editors. *DNA cloning 4, Mammalian systems: a practical approach*. 2nd ed. Oxford, UK: IRL Press; 1995. p 113–142.
135. Miller AD. *Curr Top Microbiol Immunol* 1992; 185: 1–24.
136. Cepko C. *Current protocols in molecular biology*. Suppl. 17. New York: Wiley; 1996. p 9.10.1–9.10.7.
137. Gunzburg WH, Salmons B. In: Lemoine NR, Cooper DN, editors. *Gene therapy*. Oxford, UK: BIOS Scientific Publishers; 1996. p 33–60.
138. Gaspar HB, Kinnon C. In: Lemoine NR, Cooper DN, editors. *Gene therapy*. Oxford, UK: BIOS Scientific Publishers; 1996. p 225–239.
139. Cepko CL, et al. *Methods Enzymol* 1993; 225: 933–960.
140. Robertson E, Bradley A, Kuehn M, Evans M. *Nature (London)* 1986; 323: 445–448.
141. Markowitz D, Goff S, Bank A. *J Virol* 1988; 62: 1120–1124.
142. Hawley RG, Covarrubias L, Hawley T, Mintz B. *Proc Natl Acad Sci USA* 1987; 84: 2406–2410.
143. Moss B. *Curr Top Microbiol Immunol* 1992; 185: 25–39.
144. Carroll MW, Moss B. *Curr Opin Biotechnol* 1997; 8: 573–577.
145. Mackett M. In: Glover DM, Hames BD, editors. *DNA cloning 4, Mammalian systems: a practical approach*. 2nd ed. Oxford, UK: IRL Press; 1995. p 43–83.
146. Moss B. *Proc Natl Acad Sci USA* 1996; 93: 11341–11348.
147. Twyman RM. *Advanced molecular biology: a concise reference*. Oxford, UK: BIOS Scientific Publishers; 1998. p 443–465. pp.
148. Mulligan RC, Berg P. *Proc Natl Acad Sci USA* 1981; 78: 2072–2076.
149. Gorman CM, Merlino GT, Willingham MC. *Proc Natl Acad Sci USA* 1982; 79: 6777–6781.
150. Boshart M, et al. *Cell* 1985; 41: 521–530.
151. Gorman CM, Gies D, McCray G, Huang M. *Virology* 1989; 171: 377–385.
152. Yarrington GT. *Curr Opin Biotechnol* 1993; 3: 506–511.
153. Bendig MM, Stephens PE, Crocket MI, Hentschel CC. *DNA* 1987; 6: 343–352.
154. Pavlakis GN, Hamer DH. *Proc Natl Acad Sci USA* 1983; 80: 397–401.
155. Lee F, Mulligan R, Berg P, Ringold G. *Nature (London)* 1981; 294: 228–232.
156. McCormick F, et al. *Mol Cell Biol* 1984; 4: 166–172.
157. Saez E, No D, West A, Evans RM. *Curr Opin Biotechnol* 1997; 8: 608–616.
158. Hu MC, Davidson N. *Cell* 1987; 48: 555–566.
159. Gossen M, Bonin AL, Bujard H. *Trends Biochem Sci* 1993; 18: 471–475.
160. Shockett PE, Schatz DG. *Proc Natl Acad Sci USA* 1996; 93: 5173–5176.
161. No D, Yo TP, Evans RM. *Proc Natl Acad Sci USA* 1996; 93: 3346–3351.
162. Labow MA, Baim SB, Shenk T, Levine AJ. *Mol Cell Biol* 1990; 10: 3343–3356.
163. Gossen M, Bujard H. *Proc Natl Acad Sci USA* 1992; 89: 5547–5551.
164. Gossen M, et al. *Science* 1995; 268: 1766–1769.
165. Wang Y, O'Malley BW, Tsai SY, O'Malley BW. *Proc Natl Acad Sci USA* 1994; 91: 8180–8184.
166. Delort JP, Capecchi MR. *Hum Gene Ther* 1996; 7: 809–820.

167. Spencer DM. *Trends Genet* 1996; 12: 181–187.
168. Belshaw PJ, Ho SN, Crabtree GR, Schreiber SL. *Proc Natl Acad Sci USA* 1996; 93: 4604–4607.
169. Twyman RM. *Advanced molecular biology: a concise reference*. Oxford, UK: BIOS Scientific Publishers; 1998. p 411–424. pp.
170. Kaufman RJ. *Methods Enzymol* 1990; 185: 487–511.
171. Palmiter RD, et al. *Proc Natl Acad Sci USA* 1991; 88: 478–482.
172. Matsumoto K, Montzka Wassarman K, Wolffe AP. *EMBO J* 1998; 17: 2107–2121.
173. Cullen BR, Lomedico PT, Ju G. *Nature (London)* 1984; 307: 214–245.
174. Kozak M. *Cell* 1986; 44: 283–292.
175. Kozak M. *Nucleic Acids Res* 1984; 12: 3873–3893.
176. Brown TA, editor. *Molecular biology labfax*. Oxford, UK: BIOS Scientific Publishers/Blackwell; 1991.
177. Shaw G, Kamen R. *Cell* 1986; 46: 659–667.
178. Peabody DS, Berg P. *Mol Cell Biol* 1986; 6: 2695–2703.
179. Mountford PS, Smith AG. *Trends Genet* 1995; 11: 179–184.
180. Kornfield R, Kornfield S. In: Lennarz W, editor. *The biochemistry of glycoproteins and proteoglycans*. New York: Plenum; 1985. p 34–87.
181. Sakaguchi M. *Curr Opin Biotechnol* 1997; 8: 595–601.
182. Dorner AJ, Bole DG, Kaufman RJ. *J Cell Biol* 1987; 105: 2665–2674.
183. Hsieh P, Rosner MR, Robbins PW. *J Biol Chem* 1983; 257: 2548–2554.
184. Williams DB, Lennarz WJ. *J Biol Chem* 1984; 259: 5105–5114.
185. Davies AH. *Curr Opin Biotechnol* 1995; 6: 543–547.
186. Wagner R, et al. *Glycobiology* 1996; 6: 165–175.
187. Seidah NG, Chrétien M. *Curr Opin Biotechnol* 1997; 8: 602–607.
188. Bravo DA, et al. *J Biol Chem* 1994; 269: 25830–25837.
189. Ayoubi TAY, Meulemans SMP, Roebroek AJM, van de Ven WJM. *Mol Biol Rep* 1996; 23: 87–95.
190. Subramanian A, et al. *Ann NY Acad Sci* 1996; 782: 249–255.
191. Picard D. *Curr Opin Biotechnol* 1994; 5: 511–515.
192. Porter A. *Trends Genet* 1998; 14: 73–79.
193. Littlewood TD, et al. *Nucleic Acids Res* 1995; 23: 1686–1690.
194. Palmiter RD, Brinster RL. *Annu Rev Genet* 1986; 20: 465–499.
195. Sutherland HF, Lovell-Badge RH, Jackson IJ. *Gene* 1993; 131: 265–268.
196. Iyengar A, Muller F, Maclean N. *Transgenic Res* 1996; 5: 147–166.
197. Kothary RK, et al. *Biochem Cell Biol* 1992; 70: 1097–1104.
198. Miller OK, Temin HM. *Science* 1983; 200: 606–609.
199. Bishop JO, Smith P. *Mol Biol Med* 1989; 6: 283–298.
200. Stuart GW, Vielkind JR, McMurray JV, Westerfied M. *Development* 1990; 109: 577–584.
201. Endean D, Smithies O. *Chromosoma* 1989; 97: 307–314.
202. Chong SSC, Vielkind JR. *Theor Appl Genet* 1989; 78: 369–380.
203. Al-Shawi R, Kinnaird J, Burke J, Bishop JO. *Mol Cell Biol* 1990; 10: 1192–1198.
204. Elgin SCR, editor. *Chromatin structure and gene expression*. Oxford, UK: IRL Press; 1995.
205. Tsukiyama T, Wu C. *Curr Opin Genet Dev* 1997; 7: 242–248.
206. Bestor TH. *Nature (London)* 1998; 393: 311–312.
207. Eissenberg JC, Elgin SCR, Paro R. In: Elgin SCR, editor. *Chromatin structure and gene expresion*. Oxford, UK: IRL Press; 1995. p 147–171.
208. Dobie K, Mehtali M, McClenaghan M, Lathe R. *Trends Genet* 1997; 13: 127–130.
209. Dorer DR. *Transgenic Res* 1997; 6: 3–10.
210. Yokoyama T, et al. *Science* 1993; 260: 679–682.
211. Schedl A, et al. *Cell* 1996; 86: 71–82.
212. Artelt P, et al. *Gene* 1991; 99: 249–254.
213. Eden S, Cedar H. *Curr Opin Genet Dev* 1994; 4: 255–259.
214. Siegfried Z, Cedar H. *Curr Biol* 1997; 7: R305–R307.
215. Yoder JA, Walsh CP, Bestor TH. *Trends Genet* 1997; 13: 335–340.
216. Jahner D, et al. *Nature (London)* 1982; 298: 623–628.
217. Doerfler W. *Microb Pathog* 1992; 12: 1–8.
218. Gardiner K. *Trends Genet* 1996; 12: 519–534.
219. Meyer P. *Trends Biotechnol* 1995; 13: 332–337.
220. Garrick D, Fiering S, Martin DIK, Whitelaw E. *Nat Genet* 1998; 18: 56–59.
221. Bingham PM. *Cell* 1997; 90: 385–387.
222. Koetsier PA, Mangel L, Schmitz B, Doerfler W. *Transgenic Res* 1996; 5: 235–244.
223. Reik W, Howlett SK, Surani MA. *Development* 1990;(Suppl) 99–106.
224. Sasaki H, et al. *Development* 1991; 111: 573–581.
225. Wilmut I, Whitelaw CBA. *Reprod Fertil Dev* 1994; 6: 625–630.
226. Webster J, et al. *Gene* 1997; 193: 239–243.
227. Kamakaka RT. *Trends Biochem Sci* 1997; 22: 124–128.
228. Vos JMH. *Curr Opin Genet Dev* 1998; 8: 351–359.
229. Brem G, et al. *Mol Reprod Dev* 1996; 44: 56–62.
230. Sauer B. *Curr Opin Biotechnol* 1995; 5: 521–527.
231. Stacey AJ, et al. *Mol Cell Biol* 1994; 4: 1009–1016.
232. Geyer PK. *Curr Opin Genet Dev* 1997; 7: 242–248.
233. Steif A, Winter DM, Stratling WH, Sippel AE. *Nature (London)* 1989; 341: 343–345.
234. McKnight RA, et al. *Proc Natl Acad Sci USA* 1992; 89: 6943–6947.
235. Ellis J, et al. *Nucleic Acids Res* 1997; 25: 1296–1302.
236. Clark AJ, et al. *Philos Trans R Soc London, Ser B* 1993; 339: 225–232.
237. Leach DRF. *Genetic recombination*. Oxford, UK: Blackwell; 1996.
238. Kodadek T. *Trends Biochem Sci* 1998; 23: 79–83.
239. Hasty P, Ramirez-Solis R, Krumlauf R, Bradley A. *Nature (London)* 1991; 350: 243–246.
240. Ramirez-Solis R, Liu P, Bradley A. *Nature (London)* 1995; 378: 720–724.
241. Capecchi MR. *Sci Am* 1994; 270: 34–41.
242. Zhang J, Temin HM. *Science* 1993; 259: 234–248.

243. Smithies O, et al. *Nature (London)* 1985; 317: 230–234.
244. Thompson S, et al. *Cell* 1989; 56: 313–321.
245. Kumar S, Simons JP. *Nucleic Acids Res* 1993; 21: 1541–1548.
246. Hooper ML. *Embryonal stem cells: introducing planned changes into the animal germline*. Chur, Switzerland: Harwood Academic Publishers; 1992.
247. Te Riele H, Maandag ER, Berns A. *Proc Natl Acad Sci USA* 1992; 89: 5128–5132.
248. Hasty P, Rivera-Perez J, Chang C, Bradley A. *Mol Cell Biol* 1991; 11: 4509–4517.
249. Thomas KR, Capecchi MR. *Cell* 1987; 51: 503–512.
250. Smith AJH, Berg P. *Cold Spring Harbor Symp Quant Biol* 1984; 49: 171–181.
251. Fiering S, et al. *Genes Dev* 1995; 9: 2203–2213.
252. Moens CB, et al. *Genes Dev* 1992; 6: 691–704.
253. Mansour SL, Thomas KR, Capecchi MR. *Nature (London)* 1988; 336: 348–353.
254. Jasin M, Berg P. *Genes Dev* 1988; 2: 1353–1363.
255. Valencius V, Smithies O. *Mol Cell Biol* 1991; 11: 1402–1408.
256. Moore RC, et al. *Bio/Technology* 1995; 12: 999–1004.
257. Hormuzdi SG, Pentinen R, Jaenisch R, Bornstein P. *Mol Cell Biol* 1998; 18: 2268–3375.
258. Evans MJ, Kaufman MH. *Nature (London)* 1981; 292: 154–156.
259. Martin GR. *Proc Natl Acad Sci USA* 1981; 78: 7634–7638.
260. Cibelli JB, et al. *Nat Biotechnol* 1998; 16: 642–646.
261. McWhir J, et al. *Nat Genet* 1996; 14: 223–226.
262. Dani C, et al. *J Cell Sci* 1997; 110: 1279–1285.
263. Brown JP, Wei W, Sedivy JM. *Science* 1997; 277: 831–834.
264. Kuroiwa Y, et al. *Nucleic Acids Res* 1998; 26: 2447–2448.
265. Lewandoski M, Martin GR. *Nat Genet* 1997; 17: 223–225.
266. Buchholz F, Angrand PO, Stewart AF. *Nat Biotechnol* 1998; 16: 657–662.
267. Sokol DL, Murray JD. *Transgenic Res* 1996; 5: 363–371.
268. Coutre LA, Stinchcomb DT. *Trends Genet* 1996; 12: 510–515.
269. Harlow E, Lane D. *Antibodies: a laboratory manual*. Cold Spring Harbor, NY: ColdSpringHarbor Press; 1988.
270. Morgan DO, Roth RA. *Immunol Today* 1988; 9: 84–88.
271. Richardson JH, Marasco WA. *Trends Biotechnol* 1995; 13: 306–310.
272. Gibola E, Smith C. *Trends Genet* 1994; 10: 139–144.
273. Chubb JM, Hogan ME. *Trends Biotechnol* 1992; 10: 132–136.
274. Agrawal S. *Trends Biotechnol* 1996; 14: 376–387.
275. Sentry JW, Kaiser K. *Transgenic Res* 1994; 3: 155–162.
276. Palmiter RD, et al. *Nature (London)* 1982; 200: 611–615.
277. Houdebine LM. *Transgenic animals: generation and use*. Chur, Switzerland: Harwood Academic Publishers; 1997.
278. Hogan B, Constantini F, Lacey E. *Manipulating the mouse embryo: a laboratory manual*. Cold Spring Harbor, NY: ColdSpringHarbor Press; 1986.
279. Hammer RE, et al. *Nature (London)* 1985; 315: 680–683.
280. Whitelaw CBA, Springbett AJ, Webster J, Clark AJ. *Transgenic Res* 1993; 2: 29–32.
281. Page RL, et al. *Transgenic Res* 1995; 4: 353–360.
282. Clarke AR. *Nat Biotechnol* 1996; 14: 942.
283. Maione B, Lavitrano B, Spadafora C, Kiessling AA. *Mol Reprod Dev* 1998; 50: 406–409.
284. Nagy A, et al. *Development* 1990; 110: 815–821.
285. Forrester LM, Bernstein A, Rossant J, Nagy A. *Proc Natl Acad Sci USA* 1991; 88: 7514–7517.
286. Labosky PA, Barlow DP, Hogan BLM. *Development* 1994; 120: 3197–3204.
287. Gordon JW, et al. *Proc Natl Acad Sci USA* 1980; 77: 7380–7384.
288. Campbell KHS, McWhir J, Ritchie W, Wilmut I. *Nature (London)* 1996; 380: 64–66.
289. Wilmut I, et al. *Nature (London)* 1997; 385: 810–813.
290. Noble M, et al. *Transgenic Res* 1995; 4: 215–225.
291. Al-Shawi R, et al. *Mol Cell Biol* 1991; 11: 4207–4216.
292. Bernstein A, Breitman M. *Mol Biol Med* 1989; 6: 523–530.
293. Clark AJ, et al. *Gene Ther* 1997; 4: 101–110.
294. Kessel M, Balling R, Grus P. *Cell* 1990; 61: 301–308.
295. Guy LG, et al. *EMBO J* 1996; 15: 3713–3721.
296. Kellum R, Elgin SCR. *Curr Biol* 1998; 8: R521–R524.
297. Clark AJ, Harold G, Yull F. *Nucleic Acids Res* 1997; 25: 1009–1014.
298. Evans GL, Morgan RA. *Proc Natl Acad Sci USA* 1998; 95: 5734–5739.
299. McLachlan G, Porteous DJ. *Transgenic animals: generation and use*. Chur, Switzerland: Harwood Academic Publishers; 1997. p 435–444.
300. Harris A. *Hum Mol Genet* 1997; 6: 2191–2193.
301. Love J, Gribben C, Mather C, Sang H. *Bio/Technology* 1994; 12: 60–63.
302. Gong SG, Etkin LD. *Transgenic animals: generation and use*. Chur, Switzerland: Harwood Academic Publishers; 1977. p 123–127.
303. Chung JH, Whiteley M, Falsenfeld G. *Cell* 1993; 74: 505–514.
304. Devlin RH, Yesaki TY, Donaldson EM, Hew CL. *Nature (London)* 1994; 371: 209–210.
305. Twyman RM, Jones EA. *J Neurogenet* 1995; 10: 67–101.
306. Brinster RL, et al. *Proc Natl Acad Sci USA* 1988; 85: 840–863.
307. Donofrio G, Bignetti E, Clark AJ, Whitelaw CBA. *Mol Gen Genet* 1996; 252: 465–469.
308. Pursel VG, Rexroad CE. *Mol Reprod Dev* 1993; 36: 615–623.
309. Damak S, Su HY, Jay NP, Bullock DW. *Bio/Technology* 1996; 14: 185–188.
310. Muller M, Brem G. *Reprod Fertil Dev* 1994; 6: 605–613.
311. Hughes BO, Huges GS, Waddington D, Appleby MC. *Anim Sci* 1996; 63: 91–101.
312. Clark AJ, et al. *Bio/Technology* 1989; 7: 487–492.
313. Sola I, et al. *J Virol* 1998; 72: 3762–3772.
314. Wright G, et al. *Bio/Technology* 1991; 9: 830–834.
315. Wakayama T, et al. *Nature (London)* 1998; 394: 369–374.
316. Wilson C, Bellen HJ, Gehring WJ. *Annu Rev Cell Biol* 1990; 6: 679–714.
317. Sschnieke AE, et al. *Science* 1997; 278: 2130–2133.

318. Brook FA, Gardner RL. *Proc Natl Acad Sci USA* 1997; 94: 5709–5712.
319. McKinnell RG. *Cloning: of frogs, mice and other animals*, Minneapolis: University of Minnesota Press; 1985.
320. Shiels PG, et al. *Nature (London)* 1999; 399: 316–317.
321. Lanza RP, Cooper DKC, Crick WL. *Sci Am* 1997: 40–45.
322. White DJG, Langford GA, Cozzi E, Young VK. *Xenopus* 1995; 2: 213–217.
323. Greenstein JL, Sachs DH. *Nat Biotechnol* 1997; 15: 235–238.
324. Platt JL, Logan JS. *Transgenic animals: generation and use*. Chur, Switzerland: Harwood Academic Publishers; 1997. p 455–460.
325. White DJG, Langford GA. *Animal breeding: technology for the 21st century*. Amsterdam: Harwood Academic Publishers; 1998. p 229–242.

15

INOCULUM EXPANSION METHODS, ANIMAL CELL LINES

Claudia Kloth, Glenn Maclsaac, Haile Ghebremariam, and Alahari Arunakumari
Medarex, Inc., Bloomssbury, New Jersey

15.1 INTRODUCTION

Genetically engineered mammalian cell lines are the main production systems used for therapeutics as well as diagnostics (1). For such manufacturing processes, the initial process steps of inoculum expansion contribute greatly to the success of the subsequent manufacturing steps, overall process efficiency, and product consistency. Common therapeutic protein products such as Epogen®, Rituxan®, Herceptin®, Avastin®, Humira®, and Vectibix® are manufactured in immortalized Chinese hamster ovary (CHO) cells (1). Other commonly used cell lines for the production of recombinant products are derived from baby hamster kidney (BHK), mouse myeloma (NS0, SP2/0), mouse mammary (C127), human embryonic kidney (HEK-239) and more recently, human primary embryonic retinoblasts (PER.C6®) (2–5).

Hence, in this chapter previous practices as well as state-of-the-art inoculum expansion methods for recombinant mammalian cell lines are summarized. Suspension cell lines are the main focus due to their predominant current and potential usage in large-scale biomanufacturing. Conventional inoculum expansion process operations are discussed including both, small-scale flask expansion and seed bioreactor. In addition, the trend toward applying current disposable technologies in the inoculum trains is also highlighted. This review also covers strategies to reduce the duration of the inoculum expansion process since it can be one of the most time-consuming phases of large-scale manufacturing. In addition, technology transfer of the inoculum expansion and the influence of cell bank quality on a successful vial thaw and inoculum process are addressed.

15.2 INOCULUM EXPANSION PROCESSES

A consistent and robust inoculum expansion method is crucial to initiate a successful manufacturing run. The main objective is to generate large volumes of highly viable cells in the shortest possible time period, for inoculation of the production bioreactor. This is achieved by maintaining the cells in an actively growing state, known as the *exponential phase*, throughout the inoculum expansion.

Conventional inoculum expansion procedures start with thawing the cryopreserved cells, commonly one vial of the Master Cell Bank (MCB) or Working Cell Bank (WCB), followed by cell expansion through multiple cell passages (Fig. 15.1). During expansion, culture medium is added to replenish nutrients and increase cell inoculum volume. Shaker flasks (available in 125 mL to 3 L sizes), T-flasks (T25 to T175), spinner flasks (100 mL to 5 L) and/or roller bottles (500 mL to 2 L) are mostly used for the initial expansion steps. In these flasks, cell inoculum of 10–20 L volume is commonly generated, and can be used to inoculate 40–100 L bioreactors. Beyond this volume, the workload of passaging cells under aseptic conditions and the increased incubator demand renders the flask process laborious and impractical. For larger inoculum volumes, seed bioreactors or seed bioreactor trains are used (refer

Upstream Industrial Biotechnology: Expression Systems and Process Development, Volume 1, First Edition. Edited by Michael C. Flickinger.
© 2013 John Wiley & Sons, Inc. Published 2013 by John Wiley & Sons, Inc.

Step		Description	Duration (days)	Final volume
Vial thaw		Thaw one vial (a) Seed T-flask (b)	0 0	1 mL 50 mL
Inoculum expansion (passages)	P#1	Count cell density/viability Seed spinner flask (c)		150 mL
	P#2	Count cell density/ viability Seed spinner flask (d)	5	600 mL
	P#3	Count cell density/ viability Seed spinner flask (e)	8	3 L
	P#4	Count cell density/ viability Seed spinner flask (f)	11	10 L
Seed bioreactor		Inoculate reactor in perfusion (g) or batch mode	14	35 L
Production bioreactor		Inoculate reactor (s)	19	250 L

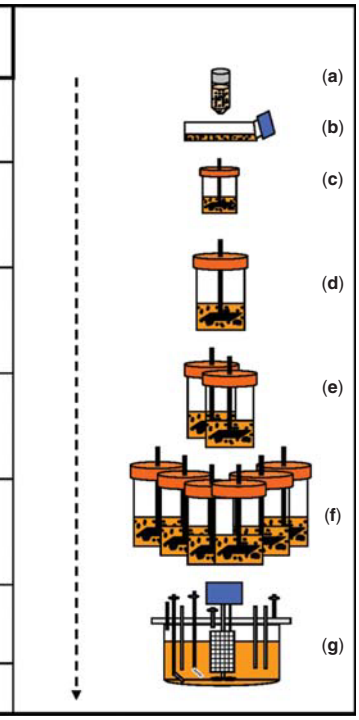


Figure 15.1. Example of inoculum expansion process for a large-scale production bioreactor. (This figure is available in full color at http://onlinelibrary.wiley.com/book/10.1002/9780470054581.)

to section titled "Expansion in Seed Bioreactors"). The expansion steps in flasks require routine opening of culture flasks which present a significant risk of contamination. As a result, the dedicated inoculum preparation room for cGMP manufacturing is segregated and controlled as a Class 10,000 (ISO Class 7) area. Within this room, activities related to cell culture, like sampling and passaging, are conducted in a Class 100 (ISO Class 5) biosafety cabinet. Examples for vial thaw and inoculum expansion processes, also used in cGMP production, are described in the following sections. Contamination risks can be minimized by direct inoculation of bioreactors without the flask expansion process (refer to section titled "Time Reduction").

15.2.1 Vial Thaw

The vial thaw is the first step to commence cell inoculum from cell banks. Cryopreserved cells are removed from vapor phase liquid nitrogen used for long-term storage and are thawed at controlled temperature. Depending on the product development stage, the cells for the inoculum may originate from the MCB or manufacturer's WCBs. The MCB is generally used for early clinical phases of cGMP production, while vials from the WCB are used to initiate commercial manufacturing runs.

All cell banks are prepared from a homogeneous cell source and aliquoted into cryogenic containers, typically vials. The cell bank is frozen slowly using a controlled rate freezing process at around 1–3°C/min, and subsequently stored in the vapor phase of liquid nitrogen (6,7). To protect the cells from freezing related damage such as intracellular ice crystallization and cell lysis during freezing, long-term storage, and cell recovery (8), cryoprotectants such as DMSO are used in the freezing mixture (8). Historically, freezing mixtures have contained a defined amount of heat inactivated serum, like fetal bovine serum (FBS) of 10–95% (v/v) final concentration, along with cryoprotectants like dimethyl sulfoxide (DMSO), glycerol or polyethylene glycol (PEG), sucrose, and conditioned culture medium (9,10). Due to regulatory preferences and the shift to animal component–free processes, FBS is generally avoided in current banking procedures for production of cell lines. Freezing mixtures containing solely DMSO and animal component–free or chemically defined media are successfully used for preparing cell banks.

For highest viable cell recovery during cell revival, literature recommends a rapid thaw above 20°C/min (8), commonly performed in a 37°C water bath. Slow warming should be avoided since it may result in intracellular crystallization which damages fragile cell membranes (11) and may expose the cells to hyperosmotic concentrations of external and internal solutes (12).

Once thawed, cells are immediately re-suspended in culture medium and generally centrifuged to remove the freezing mixture. Centrifugation removes the majority of DMSO, FBS, or other media components in the freezing mixture, and the cell pellet is re-suspended in new culture medium for the first passage at predetermined cell density. The centrifugation step, however, may lead to stress-related loss of cell viability and cells (13). To avoid this loss as well as to ease the thaw process operation, the most desirable thawing procedure appears to be seeding of the cells directly into the culture without centrifugation. This can be easily incorporated when the freezing and inoculum expansion medium are identical or comparable. It is further recommended to sufficiently dilute the thawed cells with culture medium to reduce DMSO below cell inhibitory concentrations. For example, freshly thawed CHO-S cells tolerate up to 0.4% DMSO in the culture medium while maintaining their original doubling time (12), whereas in a case study for a frozen fragile recombinant CHO DG-44 cell line, additional dilution of the DMSO was required; for example to concentrations as low as 0.1% (13).

15.2.2 Cell Expansion for Suspension Cell Cultures

Expansion of cell cultures in a small scale, also referred as passaging, subculturing or splitting the culture, involves transferring a defined number of cells into a new vessel and adding culture medium for further cell propagation. When passaged at well-defined intervals, cells are maintained in a healthy condition for a long period of time. For the biomanufacturing of recombinant proteins in mammalian cell lines, both suspension and adherent cells have been used, though suspension cell cultures are far more common. During inoculum expansion, the suspension cells are maintained in static or agitated cultures or a combination of both. The cultures are generally split using a ratio of cell culture to medium volumes from as low as 1:2 up to 1:10 depending on cell line and culture medium.

15.2.2.1 Static Cultures. In static cultures, cells are grown in flasks without agitation. Here, the shear stress–free environment may be advantageous immediately after thaw. However, even suspension cells tend to attach to plastic surfaces in static conditions, leading to potential cell loss. In addition, cell growth in static culture allows only a limited volume to surface ratio due to ineffective gas diffusion requiring large surface area. Therefore, the inoculum is expanded using either multiple T-flasks or larger systems like Nunc Cell Factories, which provide increased surface areas from 632 cm^2 (one tray) up to 25,280 cm^2 (40 trays, www.nuncbrand.com). Since each tray can handle 200 mL of culture, up to 8 L of cell culture inoculum can be generated using a 40 tray factory. Each Cell Factory is filled and harvested in a single operation which minimizes culture manipulations. Although the 40 tray factory has been described as a challenge to operate manually (14), it can successfully be automated with a manipulator and robot (www.nuncbrand.com).

Most static processes lead to cell aggregation. When these cannot be separated solely by tapping or pipetting, obtaining accurate cell counts remains challenging. Precise cell counts facilitate the specified seeding cell densities for each passage, and are essential for robustness and predictability of the entire cell expansion phase. To limit operator variances due to subjectivity in counting aggregates, the representative cell sample can be pretreated with proteases such as porcine trypsin, or enzyme containing mixtures such as Accumax™ (www.innovativecelltech.com). These agents separate cell aggregates into single cells without altering cell viabilities (www.innovativecelltech.com, 13). For use in cGMP manufacturing, animal component–free agents like Accumax™ are preferred. Reduced cell aggregates are generally observed in agitated systems in comparison to static growth cell cultures.

15.2.2.2 Agitated Cultures. Agitated systems are mainly used in inoculum expansion for clinical and commercial processes. They are superior to static flask cultures through active mixing of the cell culture, maintaining homogenous temperature, improved mixing of nutrients, as well as better gas diffusion. The agitation speed is a crucial process parameter to be optimized for each flask size and culture volume and also includes roller speed, speed of magnetic stir plates, as well as speed and angle of rotation for orbital moving shaker flasks. Though most agitated systems provide sufficient gas transfer through surface aeration, it is also common practice to aerate by active sparging to accommodate increased inoculum volumes in the culture vessels. Adherent cells fixed on porous carriers can also be cultured in agitated cultures, similar to suspension cells (refer to section titled “Cell Expansion for Adherent Cell Cultures”).

15.2.2.3 Process Parameters. For a robust manufacturing process, operational ranges for process parameters need to be established prior to process transfer from process development to clinical and commercial manufacturing. Both static and agitated systems require the maintenance of temperature and carbon dioxide concentration within a defined range to promote optimum cell growth. Incubators are maintained at a physiological temperature of around 37°C at which mammalian cells grow optimally. Lower temperatures reduce cell growth, which in turn prolongs the inoculum expansion time. On the other hand, elevated temperatures may also lead to heat shock and cell death (15,16).

Similarly, culture medium pH plays a crucial role in cell growth. Values of pH between 6.7 to 7.9 support cell growth of most animal cells, though the optimum range depends

upon the specific cell line (17,18). In most cases, buffering components in the medium, such as sodium bicarbonate ($NaHCO_3$) in combination with carbon dioxide (CO_2) in the incubator, are used to control the culture pH. Other media components, like amino acids or HEPES, may also modify the culture medium pH. To establish growth-supporting pH conditions in the cell culture, the amount of selected buffering agents and corresponding CO_2 concentration need to be optimized for each culture medium. The CO_2 gas is introduced into the culture by either pre-gassing a CO_2–air mixture into the flask prior to cap closure or by continuous gas transfer using vented flasks. During vented flask operation, flask caps with integrated filters are used and the flasks are maintained in the humidified incubator chamber with desired CO_2 concentration, which is commonly between 5% and 10%. The most effective way to add CO_2 gas to the cell culture is by actively gassing the CO_2 –air mixture into the culture medium.

For healthy cell cultures, sufficient oxygen supply is required. Agitated systems effectively enhance gas exchange through active mixing, which allows increased working volumes. Even though agitated systems increase the rate of oxygen transfer into the culture, it is still often limited through low agitation speeds used to protect cells from shear forces. As a consequence, flasks still operate with a diminished working volume. To overcome this limitation, agitated systems can be actively sparged using dip tubes, porous spargers, or internal gas permeable membranes to significantly enhance gas transfer. As a result, greatly increased culture volumes can be maintained in these actively sparged flasks (19). In the case of a 3-L spinner flask, up to 1.5 L of cell culture can be supported when maintained in conventional spinner flask operation, and up to 3 L of culture volumes when actively sparged. Advanced designs of disposable flasks such as SuperSpinner (www.sartorius.com) result in even more effective gas transfer using active bubble-free addition of gas mixture through a permeable internal membrane. For this system, a 3.5 times increased volumetric transfer coefficient ($k_L a$) was reported in contrast to other agitated systems (20). This may support growth to higher cell densities than conventional surface-aerated spinners which lead to economically enhanced inoculum expansion processes through decreased flask usage and culture handling (21).

15.2.3 Cell Expansion for Adherent Cell Cultures

Suspension cultures are passaged by diluting cell culture with new medium, whereas for adherent cultures, the cells first need to be detached from the matrix surface before seeding a new culture. Adherent cell cultures, also known as anchorage-dependent cultures, are seeded either in static flasks (e.g. T-flasks), or more commonly, in agitated systems like roller bottles where the cells attach to the flask surface thereby covering greater surface area during cell growth. For inoculum expansion, minimum seed cell densities for around 10% flask confluence are recommended to avoid initial lags in growth. The cell culture should be split prior to reaching confluence to maintain rapidly growing adherent cells. The routine subculturing is performed according to a strict schedule to ensure a reproducible growth pattern. A recommended routine may follow subculturing once a week with a medium change in-between the splits (22). Roller bottles are inoculated with 5–30% of overall volume and slowly rotated. The rotation promotes nutrient and gas supply for the adherent cells. Between the middle of the logarithmic growth phase and the time before entering the plateau phase (confluence), cell passaging commonly occurs. The excess culture medium is typically removed and the cells are detached from the matrix with enzyme mixtures. Historically, a porcine trypsin–EDTA mixture (23) was used, although animal component–free enzyme mixtures such as Accustase™ (www.innovativecelltech.com), Detachin™ (www.genlantis.com) are currently available, and preferably used in cGMP operation. The detached cells are diluted with new culture medium and new flasks are inoculated until sufficient cells are generated to either start the production stage in roller bottles, or inoculate a seed or production bioreactor. The production in roller bottles was successfully automated as shown in the production of erythropoietin (EPO) (24). Here, most of the critical manufacturing steps of bottle handling are performed by robots, including cell seeding, media fill, and harvesting of supernatant. For conventional bioreactor operations, adherent cells are seeded onto microcarriers or porous microspheres and can be maintained in agitated culture (6,25,26), fixed/packed or fluidized bed operations. Cells adhering to microcarriers grow within pores and possibly in multiple layers, which may result in difficulties during the cell removal process and in significant loss of cells during the seed bioreactor phase.

Adherent cells can be transitioned into suspension cells by changing culture conditions and medium composition, such as reducing Ca^{2+} concentration. This transition is often time-consuming, involving the screening of various media and requiring multiple cell passages before the cells have adapted to single-cell suspension. Institutions have generated suspension-based host cells in chosen culture medium to eliminate this adaptation process and to reduce developmental timelines significantly (27). Many of these cell lines are commercially available and can be used immediately for the transfection step to generate the recombinant cell line.

In contrast, suspension cells may convert back to adherent cells, mainly through the choice of culture medium and carrier material. Alternatively, cells can also be entrapped

in fibrous material such as that used in the iCellis™ technology (www.artelis.be), where the perfusion in the fibrous bed relies on cell attachment to the three-dimensional structure. Some of the advantages of the so-called 3D cultures are higher cell densities and higher productivities (28), although the monitoring of cell growth and viability may still be challenging.

15.2.4 Expansion in Seed Bioreactors

For large-scale production of suspension cells at 200 to 20,000 L bioreactor scale, the initial inoculum expansion process continues in seed bioreactors to bridge the gap between culture flasks and production bioreactors. Seed bioreactors of successively larger volumes are used, and their number and scale depends on the final production scale and volume split ratio. Most commonly, the seed reactors in biopharmaceutical production are operated in batch or perfusion mode.

15.2.4.1 Batch Process. The batch process is a simple operation that requires the least amount of culture medium compared to a perfusion process. Once the culture is inoculated, cell growth and viability is monitored for several days until the transfer cell density is reached. Here, the batch process provides only a narrow time window for the transfer of exponentially growing cells with a limited split ratio. Batch-to-batch transfers from small to subsequently larger size bioreactors commonly have split ratios from 1:5 to 1:10. As an example, a 40-L cell inoculum can seed a 200- to 400-L bioreactor. These split ratios are considered during the design of seed bioreactor trains in commercial facilities.

A special case of batch operation is the "feed and bleed process", which is a semicontinuous process. In this case, the cell inoculum is grown to the transfer cell density in the seed bioreactor, and then around 80–90% of the cell culture is removed to inoculate the production bioreactors (29). The remaining 10–20% of cell culture in the seed reactor is replenished with new culture medium to continue the cell expansion and to serve again as cell inoculum for the future production reactors. This cycle can continue until either the maximum population doubling level (PDL) of the cell line is reached, or sufficient production bioreactors are inoculated.

If a cell line in basal medium cannot achieve adequate transfer cell densities in batch operation, the cell culture can be enriched with nutrients to increase overall cell densities. Table 15.1 shows an example where seed reactors were cultured in batch mode as well as with nutrient supplementation on day 0 or day 3. The maximum transfer cell density was set to not exceed 75% of the measured peak cell density. As a result, an approximately 60% increase in peak viable cell density was observed with supplement-enriched conditions in comparison to the batch process independent of the time of supplementation. With the increased peak cell density, the transfer range to the next larger bioreactor was widened, providing additional operational flexibility.

15.2.4.2 Perfusion Process. In comparison to batch operation, a seed bioreactor in perfusion mode is extremely flexible in allowing an extended window of inoculation. Here, the cell culture can be maintained at high cell density and viability for a long period of time, due to continuous perfusion of culture medium and possible cell purge. Since higher cell densities can be achieved in the perfusion mode relative to batch mode, a perfusion seed reactor can inoculate larger reactor volumes or multiple bioreactors simultaneously.

Inoculation ratios up to 1:20 are commonly being reached in perfusion application for example, a 10-L perfusion seed bioreactor can inoculate a 200-L production bioreactor (8). The inoculation ratio can be even extended up to 1:250 by using a novel gravity settling device to achieve high cell density and viability seed cultures (30). In this condition, as little as 0.8 L of cell culture would be sufficient to inoculate a 200-L bioreactor. Although such a perfusion system demonstrates future potential for inoculum expansion, such a device is currently not implemented in large-scale production.

Staggered inoculation of multiple production bioreactors from perfusion seed bioreactors were demonstrated in 5-L

TABLE 15.1. Seed Bioreactor Operation in Batch, Fed-Batch with Nutrient Addition on Days 0 and 3 and Perfusion Mode in 5-L Bioreactor Scale

Mode of Operation	Peak Cell Density ($\times 10^6$ vc/mL)	Maximum Transfer Cell Density ($\times$106 vc/mL)	Maximum Production Bioreactor Volume (L) using 5-L Seed Reactor
Batch Mode			
Basal medium = Control + Feed addition (day 0) + Feed addition (day 3)	2.1	1.6	40
	3.5	2.6	65
	3.4	2.6	65
Perfusion mode			
With basal medium (1RV/d)	4.6	3.5	90

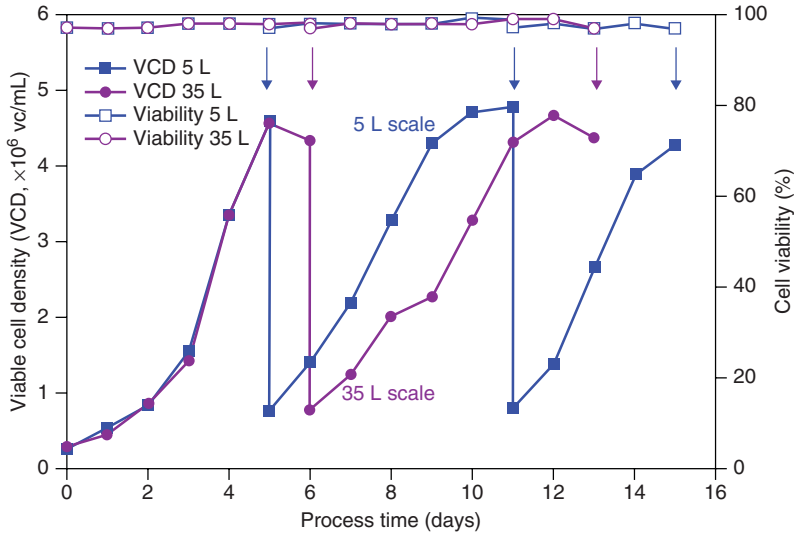


Figure 15.2. Operational flexibility of seed bioreactor in perfusion mode. Perfusion seed bioreactors in 5-L (blue) and 35-L (red) scale. Multiple production bioreactors were inoculated in a staggered fashion as indicated by arrows. (This figure is available in full color at http://onlinelibrary.wiley.com/book/10.1002/9780470054581.)

development and 35-L manufacturing scales (Fig. 15.2). In a staggered fashion, each perfusion bioreactor could inoculate two or three production bioreactors. In both scales, the recommended transfer cell densities were reached on day 5 for a 1:15 to 1:20 inoculation ratio and partial seed culture volumes were sufficient to inoculate the production bioreactors. After inoculation, the seed bioreactor working volume can be replenished with new medium and the perfusion operation continues until additional production bioreactors require inoculattion. All sets of production bioreactors can be inoculated based on the manufacturing schedule since the perfusion operation can easily be modified, that is, maintaining a certain cell density through initiation of cell purge. Clearly, seed bioreactor operations in perfusion mode provide manufacturing flexibility. The inoculation cycle can be repeated multiple times as long as the cell line is stable, resulting in consistent and robust production bioreactor performance in terms of cell growth, product concentration, and quality. On the other hand, the major disadvantages of perfusion are the increased volume of medium usage and the relative complexity of operation (31). In comparison to batch processes, operation in perfusion mode requires additional characterizations of process parameters like cell retention device–related settings, perfusion or biomass removal rates.

Selecting the most appropriate seed bioreactor mode is mainly based on equipment availability, operational knowledge, cell line, and medium-specific performance. Table 15.1 summarizes a study where the seed bioreactor operation was tested in baseline batch mode, batch mode with nutrient supplementation, and perfusion mode. In perfusion mode, the transfer cell densities increased 120% relative to batch performance using one reactor volume per day (1 RV/d) perfusion rate. Here, the peak cell density could be further enhanced by either increasing perfusion rate or supplementing the basal medium with nutrients. In this case study, both modes of seed bioreactor operation, fed-batch and perfusion, fulfilled the inoculation requirements and delivered healthy seeds.

15.2.4.3 Process Parameters. Different seed reactor designs and operations, such as stirred tank and air lift bioreactors, are found in large-scale manufacturing of suspension cells. In recent years, disposable systems including single-use stirred tank bioreactors or wave-mixed bioreactors have been increasingly utilized due to their operational ease and reduced validation requirements (see section titled "Disposable Systems"). Seed bioreactors are operated with process controls analogous to production bioreactors, including dissolved oxygen (DO), pH, temperature, agitation, and aeration besides cell density and cell viability. The latter two are the most crucial expansion parameters and can be monitored regularly through automated sampling systems (e.g. www.grotonbiosystems.com, www.innovatis.com) connected to automated cell counters (e.g. Cedex, www.innovatis.com). Continuous, *in situ* monitoring of these key parameters in a nondisruptive fashion is also enabled using new sensor technologies such as capacitance-based probes monitoring viable biomass (e.g. www.aber-instruments.com, www.fogalebiotech.com). Recent developments in noninvasive optical sensors provide means of

monitoring cell culture performance in disposable systems with single-use sensors (32,33). Such sensors commonly measure DO, pH, and various nutrients although cell density monitoring is also commercially available (e.g. www.aberinstruments.com, www.fogalebiotech.com). Such sensors allow real-time monitoring, resulting in better process understanding and controls and may increasingly be integrated in future production processes. These improvements can lead to successful implementation of process analytical technologies (PAT) in the manufacturing process and support quality by design (QbD) process concepts (34,35).

15.2.5 Inoculum Cell Density and Cell Physiology

Since the main goal of inoculum expansion is to generate healthy and rapidly growing cell cultures, cells should be maintained in exponential growth phase to minimize lag phases. Generally, for the first passage after vial thaw, increased seed cell densities ensure a smooth transition into typical growth pattern. In the case of CHO and HEK293 cell lines, seeding cell densities of $0.3–2.0 \times 10^6$ c/mL supported growth directly out of vial thaw, without lag phase (12). For each individual project, minimum seeding and maximum transfer cell densities are established to avoid lag and stationary phases (36). These ranges can be determined experimentally in a small scale by performing growth studies with various initial seeding cell densities such as 0.1×10^6 vc/mL to 0.8×10^6 vc/mL (Fig. 15.3). By plotting the viable cell densities, the logarithmic growth phase in this case study ranges from 0.25×10^6 vc/mL to maximum transfer cell densities of 2.8×10^6 vc/mL. This range ensures the fastest cell growth rate and the shortest inoculum expansion time.

15.3 IMPACT OF CELL BANKS ON INOCULUM EXPANSION

The quality of cell banks significantly influences the consistency of inoculum expansion. Many factors contribute to the success of the expansion including the physiological state of the cells prior to freezing, the type of freezing mixture, the freezing procedure, storage, and vial transport. Its overall impact can be detected during small-scale characterization studies of MCB and WCB. Growth and productivity profiles over multiple cell generations (37) can reflect on long-term cell culture expansion for large-scale manufacturing.

15.3.1 Influence of Culture Medium

Cell cultures in the exponential growth phase show the best potential to sustain freezing and thawing procedures and to recover them with high cell viability. A bank with a prematurely adapted cell line, or a cell line frozen in a medium different from the medium for inoculum expansion, may lead to inconsistent growth profiles during initial passages, prolonging the already time-consuming inoculation process even further. Therefore, it is recommended to fully adapt the cell cultures to the inoculum expansion medium prior to freezing the banks.

A case study is given in Fig. 15.4 demonstrating the significance of cell adaptation. From Bank #1 two cell banks were prepared, designated as Bank #2 and #3. During bank preparation the cell culture medium was shifted from medium A of Bank #1 to B; medium B also being used during the inoculum expansion phase. Bank #2 was prepared after expanding the cells for limited passages (five passages)

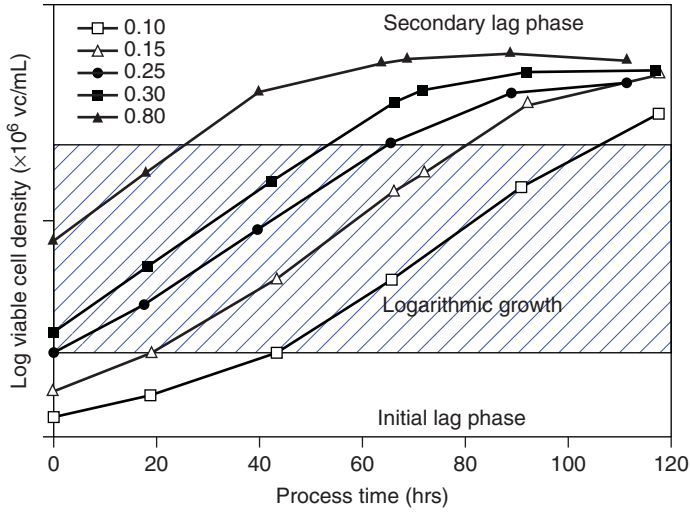


Figure 15.3. Optimization of seeding and transfer cell densities to reduce the inoculum expansion period. The optimum is shown in blue, indicating the exponential growth phase. (This figure is available in full color at http://onlinelibrary.wiley.com/book/10.1002/9780470054581.)

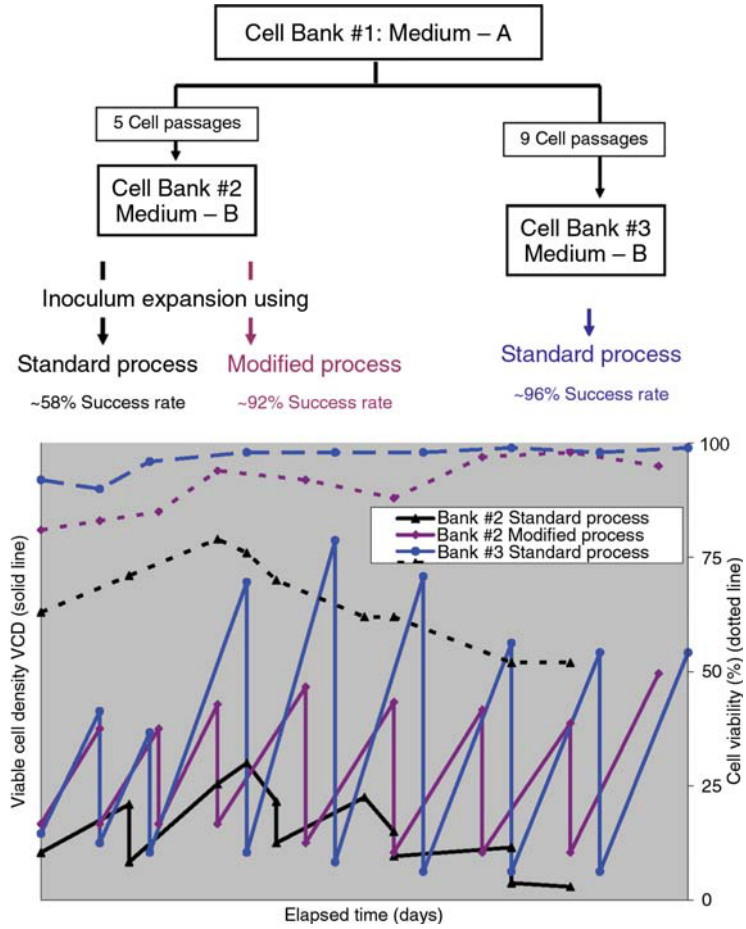


Figure 15.4. Impact of cell adaptation on inoculum expansion. Cell Banks #2 and #3 were prepared from Bank #1 in different medium. Bank #2 was prepared after five passages. The inoculum expansion required further optimization for robust process. Bank #3 was adapted for four additional passages (nine passages) prior cell banking resulting in successful inoculum expansion by standard procedure. Success rate is defined as number of vials reaching seed bioreactor stage. (This figure is available in full color at http://onlinelibrary.wiley.com/book/10.1002/9780470054581.)

in medium B, whereas for Bank #3 it was extended to four additional passages (nine passages). During vial thaw and initial cell expansion, cells from Bank #2 did not recover consistently with high cell viabilities. The low success rate and unpredictable growth pattern of this cell expansion were not practical for a manufacturing process. Therefore, multiple modifications were incorporated for a consistent inoculum expansion using Bank #2. To avoid cell stress during the vial thawing procedure, the cells were settled instead of centrifuged; this increased overall cell recovery and viability. The pH buffering strategy for the culture medium was also changed which resulted in far better cell growth. Medium exchanges were introduced in the beginning phase of the inoculum where the most inconsistent cell growth was observed. Overall, the optimized process led to a robust inoculum expansion with improved success rate (13). In contrast, the vials from Bank #3 were revived and expanded with a very high success rate even using a standard thaw and inoculum expansion process. Therefore, cell adaptation to the appropriate culture medium prior to cell banking is a factor that contributes significantly to successful vial thaw and cell expansion.

The use of one basal medium throughout production cell line generation, selection, banking, and production process is preferable since it minimizes media shifts and cell line adaptation periods (38). Besides reducing cell line developmental timelines, this developmental process generates fully adapted, healthy cells for a robust inoculum expansion.

15.3.2 Maintaining Cell Banks

Frozen cell bank aliquots are preferably stored in the vapor phase of liquid nitrogen (around $-150^{\circ}C$) or at equivalent low temperatures. Maintaining low temperature during

the frozen vial storage is extremely important to guarantee highly viable cells after vial thaw. Temperature variations during short term vial handling and transport should be kept to a minimum. Once vials are removed from storage and exposed to room temperature, the vials warm at a rate of ~10–20°C/min and remaining below −50°C is critical to avoid cell deterioration (22). Sufficient care needs to be employed during frozen vial shipment among different facilities as well as during delivery from the cryostorage area to the inoculum expansion suite prior to vial thaw (39). A common practice in the biotech industry is the extensive validation of cryo-shippers for cell bank transport to ensure a successful transfer under well-defined temperature conditions. To provide evidence of adequate storage, cell bank stability needs to be investigated at predetermined intervals to ensure sufficient cell recovery and viability after thaw (37). These data can be generated every time a vial is thawed that is, during manufacturing campaigns, WCB preparation, or at otherwise predetermined intervals.

15.3.3 Genetic Stability of Cell Lines

The cell line development process is geared toward selecting stable production cell lines. Only stable cell lines can ensure process consistency as well as biochemical equivalency which are directly linked to drug safety, efficacy, and process economics. For fed-batch processes, 60 to 100 cell generations are commonly analyzed to cover cell line stability for up to 20,000-L manufacturing scale. However, for production bioreactors in perfusion mode, additional generations may be required depending on process scale and duration.

The advantage of testing a large number of cell generations is to provide sufficient room for successful manufacturing processes despite unforeseen interruptions. A maximum cell generation number is preferably allocated to the inoculum expansion phase as compared to the production bioreactor in batch or fed-batch operation. For seed bioreactors in perfusion mode, a larger number of PDLs need to be reserved to accommodate multiple staggered inoculations of production bioreactors from one single perfusion bioreactor.

In many cases, it is recommended to maintain the selective pressure during the inoculum expansion phase, to ensure the stability of cell lines in the production process. In the case of CHO dhfr$^-$ cells, significant gene copy losses (40) and decrease in productivity were reported after removal of the selective agent methotrexate (MTX) (41). In these situations, the addition of MTX throughout parts of the manufacturing process might be advantageous to maintain gene stability and avoid significant productivity loss. In the case of the GS expression system, the selective agent methionine sulphoximine (MSX) is added in some instances throughout the inoculum phase in order to maintain cell line stability (42). Upon MSX removal CHO-GS cell lines have shown more cell instability than NSO-GS cell lines (43).

Under special circumstances, titering the concentration of selective agent may add value in maintaining stability in the inoculum expansion process and therefore, the entire production process. It was observed however, that with elevated selection pressure, the cell doubling time may also increase, further prolonging the already time-consuming inoculum expansion (5).

By considering cell line stability as part of the selection and banking process, issues involving cell line instability can be resolved early in the development phase. This is a key to avoid subsequent situations jeopardizing clinical or even commercial manufacturing (44).

15.4 CURRENT TRENDS IN INOCULUM EXPANSION

15.4.1 Disposable Systems

Disposable T-flasks, shaker flasks, and roller bottles are established culture flasks for early inocuum expansion, and disposable spinner flasks have also become available (Fig. 15.5). For seed reactor operation, disposable bioreactors such as single-use stirred bioreactors (STR), for example XDR™ (www.xcellerex.com), BIOSTAT® CultiBag STR (www.sartorius.com) or SUB (http://www.thermo.com), and wave-mixed bioreactors are increasingly used. Several models of wave-mixed bioreactors are commercially available, including BioWAVE® (www.sartorius.com), WAVE Bioreactor™ (www5.gelifesciences.com), BIOSTAT® CultiBag RM (www.sartorius.com), AppliFlex (www.applikon.com), and CELL-tainer® (www.lonzabiologics.com). All have the general principle of waving operation in common which is provided by a rocking platform. Since most of these disposable systems come in sizes between 0.5–1000 L working volume, they are able to completely cover the inoculum expansion phase, starting with vial thaw up to the production bioreactor (21). Other disposable reactor systems, such as hollow-fiber reactors, are used in recombinant protein production in smaller scale (45) but they are not a good fit for the inoculum expansion phase due to their limited predictability of cell density and cell viability, and difficulties in cell harvesting.

Using the wave-mixed bioreactors, the entire inoculum expansion process can be performed in disposable reactors by direct inoculation of a 2-L disposable bag with 0.5-L working volume after cell thaw. The initial culture volume is steadily increased by adding culture medium, and is transferred into the next larger seed reactor once the maximum volume in the bag is reached. Direct inoculation of a disposable reactor after cell thaw simplifies the process

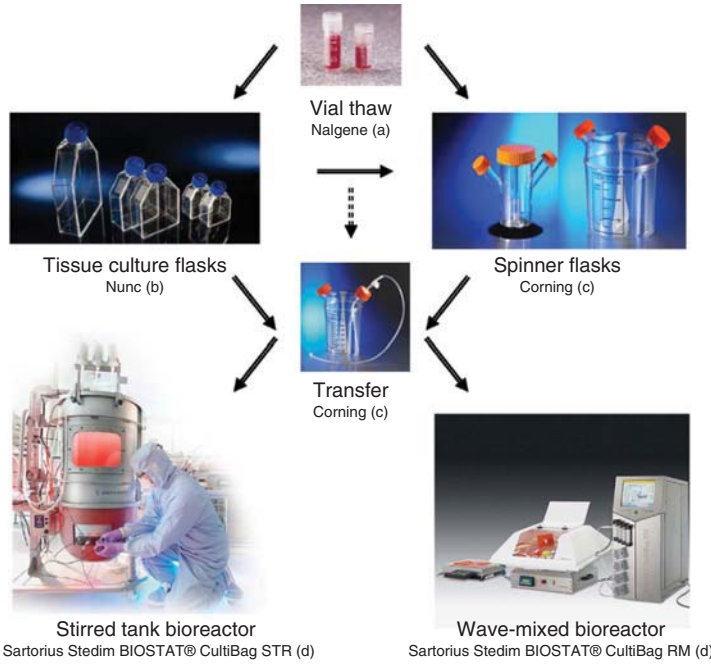


Figure 15.5. Examples of commercially available disposable systems for a complete inoculum expansion process. [Pictures sourced from (a) www.nalgenelabware.com, (b) www.nuncbrand.com, (c) www.corning.com/lifesciences, (d) www.sartorius.com.] (This figure is available in full color at http://onlinelibrary.wiley.com/book/10.1002/9780470054581.)

by carrying only one inoculum pool instead of multiple flasks while generating a homogeneous inoculum. It also decreases the risk of contamination through the use of a closed bioreactor system in comparison to the open operation in the biosafety hood required during conventional inoculum expansion in flasks.

Similar growth performance has been demonstrated in disposable systems relative to glass containers, although sometimes, small adjustments may be required in the operation of disposables including increased inoculum cell density to avoid lag in cell growth (28). Figure 15.6 shows a cell expansion in disposable containers compared to conventional glass spinners and seed bioreactors. Equivalent cell growth and cell densities were achieved in all container operations and seed reactors, and the cells were used to finally inoculate production bioreactors. Here, cell growth and viability profiles as well as final product concentration were comparable, providing evidence for a feasible switch to disposable technologies for the inoculum expansion.

The very first models of disposable WAVE bioreactor™ were not provided with feedback control for pH and DO, and instead, values were manually adjusted. In most cases, even these simple operations were superior relative to a flask inoculum expansion process (28). However, newer disposable systems are equipped with feedback controls to support robust processes throughout cell expansion stages (46). The advancements and sophistication of single-use systems support the paradigm shift to completely disposable solutions in the biomanufacturing industry, and may include production as well as support activities (47). Currently, various vendors (www.sartorius.com, www.xcellerex.com, www.pall.com, and www.millipore.com) offer partial or complete disposable solutions like the FlexFactory™ (www.xcellerex.com). The main advantages of disposable systems are low capital investment, increased flexibility through reduced downtime, reduced validation expense, and up to 87% reduced water usage due to reduced equipment washing and flushing (48,49). The main disadvantages are increased amounts of solid waste and higher material costs. These are commonly outweighed by the overall advantages and it is generally expected that the use of disposables, particularly for inoculum expansion, will continue to increase in the future. Economic models help to determine the benefits of disposable technologies and may vary for each company, product, and process (50).

15.4.2 Automation

During inoculum expansion, the labor-intensive cell maintenance in flasks is an optimal target for automation. Various automated systems are available and include roller bottle operation (www.synthecon.com) as well as T-flask and shake flask scale-up (www.auto-

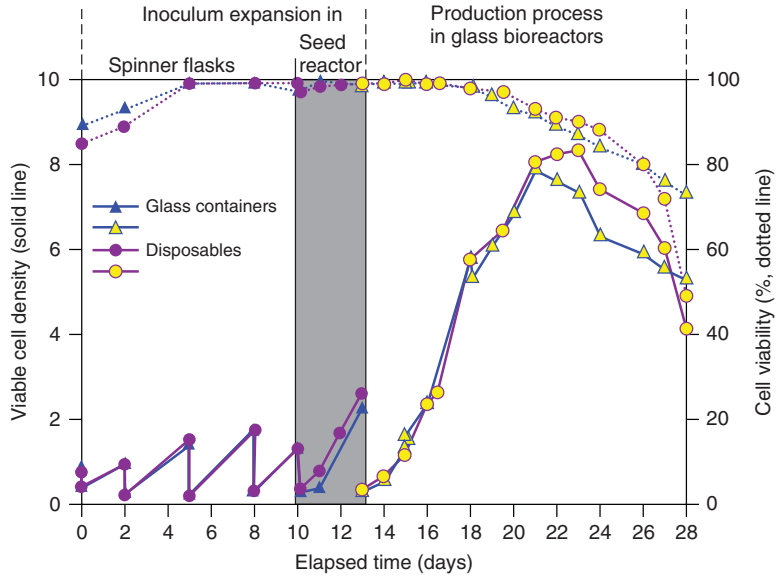


Figure 15.6. Equivalent performances of disposable versus conventional glass equipment during inoculum expansion. Cells were expanded in disposable (disposable spinners and 10-L WAVE reactor) and glass containers (glass spinners and 5-L glass STR). The cells from both systems inoculated glass production bioreactors. (This figure is available in full color at http://onlinelibrary.wiley.com/book/10.1002/9780470054581.)

mationpartnership.com, 51). Due to the complexity and operational specifics, automated systems often require custom-built solutions. Automation of the inoculum expansion, therefore, seems cost-effective for commercial production processes and frequent usage of these systems such as multiple campaigns of the same process or campaigns of similarly operating inoculum processes. In special cases, cell culture handling is feasible only by incorporating robots, that is for the 40-tray Nunc Cell Factory (www.nuncbrand.com, refer to section titled "Static Cultures") and for excessive amounts of roller bottles (as given in "Cell Expansion for Adherent Cell Cultures"). Accuracy, sterility, and round-the-clock operation are the biggest advantages for automating the inoculum expansion. As with all cGMP systems, automated systems and software require 21 CFR Part 11 compliance and validation.

15.4.3 Time Reduction

Generating sufficient biomass from vial thaw to the initiation of the production bioreactor remains a time-consuming process which can take from as little as 1 week up to 6 weeks depending on scale, cell line characteristics, and process (8). A lengthy inoculum expansion process increases manufacturing costs significantly, through additional facility occupancy. Efforts to reduce timelines include the use of multiple cryovials for culture initiation as well as freezing cells at higher cell densities and/or higher volumes in vials or disposable bags to generate frozen seeds. For CHO, BHK, and HEK cells, freezing and thawing conditions were optimized for 50 and 100 mL cell volumes in bags with cell densities between $2-5\times10^7$ c/mL (8,12). Frozen cells from these large volume seed bags enabled direct inoculation of a bioreactor with initial 2-L working volume right after thaw of the frozen cell bulk. This "one-step" inoculum process reduced valuable facility time by 60–70% leading to a more cost-effective and streamlined inoculum expansion process (8). Such high cell density and high volume cell banks are mostly effective and appropriate for the preparation of WCBs used to initiate large-scale production campaigns and commercial production.

Incorporating the high volume bag banks into an existing cGMP cell banking area requires new procedures and equipment for controlled freezing, storage, and thawing of the frozen bags. However, significant process improvements are still attainable without drastically changing the banking procedure and storage equipment (52). Increased volumes and cell densities could be obtained by freezing 9-mL cell volume in 10-mL Nunc vials at higher freezing cell densities, which can directly inoculate 3-L spinner flasks or small disposable bags. Therefore with minimum changes, the inoculum volume was increased 10–30 fold, reducing the expansion time by over 50% (Fig. 15.7).

15.5 TECHNOLOGY TRANSFER

Vial thaw and inoculum expansion is an important part of the process technology transfer which is for the most part

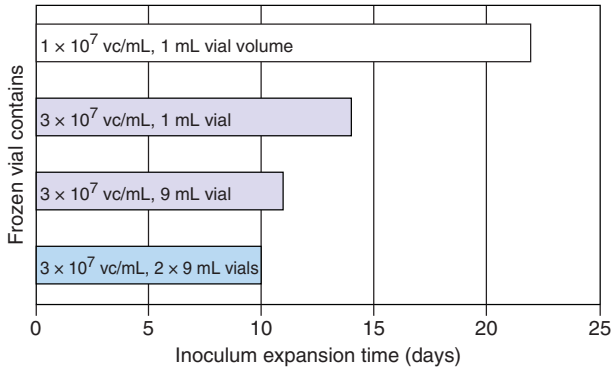


Figure 15.7. Time reduction in inoculum expansion through high cell density and large volume banks. (This figure is available in full color at http://onlinelibrary.wiley.com/book/10.1002/9780470054581.)

quite straightforward in comparison to other process steps. The transfer package includes a detailed description of the expansion process, along with knowledge transfer on cell line stability and characteristics. For a successful technology transfer, the description should contain general parameters like equipment settings, media preparation, media and supplement storage, and expiry. In addition, the maximum number of cell generations for the inoculum expansion and seed bioreactor phase is transferred, to ensure manufacturing within the stability-assessed period (refer to section titled "Genetic Stability of Cell Lines"). Transfer parameters for the flask expansion phase may include container usage, volume ranges, splitting schedule as well as ranges for seeding and transfer cell densities. For seed bioreactor operation in batch mode, the transfer includes process parameter settings, seeding, and transfer cell densities. In comparison, perfusion seed bioreactors need more attention and description of additional process parameters including perfusion rate, specific perfusion rate, and cell retention device–specific settings.

During transfer, limited process modifications might be necessary to adapt to the new facility. In the past, it was observed that different incubator brands may vary in their performance which can result in changed cell growth characteristics mainly due to different pH profiles. Therefore, a proactive approach could include a pH screening in the dedicated incubators during technology transfer (13). This procedure may help to normalize incubator variances between facilities, and CO_2 concentration adjustments can be applied when necessary.

Incorporating a medium-exchange step might be beneficial in the early inoculum expansion phase for certain cell lines. Added as preventative measure, the cells regain vigor and cell growth is restored in case of a slow or halted growth pattern. This method is practical for the expansion robustness of fragile cell lines and can reduce inoculum expansion failures (13).

15.6 CONCLUSION

During the inoculum expansion phases, batch, fed-batch, and perfusion process modes can be used to generate sufficient cells for the inoculation of production bioreactors. Cell line–specific knowledge to maintain the exponential growth phase leads to a rapid and streamlined inoculum expansion process with predetermined cell passaging schedule. In addition, much attention needs to be given at the cell banking process, vial storage, and shipment conditions to ensure healthy cells from the thawed vials.

Process simplification is achieved through the preparation of large volume and high cell density cell banks. This allows the immediate inoculation of seed bioreactors from the frozen bag or vials and may in fact reduce a significant portion or even eliminate the flask inoculum expansion phase in the future. It not only reduces cell handling of multiple flasks but may possibly convert all steps to disposable bioreactor systems. Building the expansion process as a completely disposable train enables the integration of flexible inoculum expansion methods into current manufacturing facilities. Such processes will generally be straightforward and relatively easy to transfer among different facilities.

15.7 PRODUCT WEBSITES

ABER Instruments	www.aberinstruments.com
Applikon	www.applikon.com
Artelis	www.artelis.be
The Automation Partnership	www.automationpartnership.com
Corning	www.corning.com/lifesciences
FOGALE Nanotech	www.fogalebiotech.com
GE Healthcare	www.gelifesciences.com
Genlantis	www.genlantis.com
Groton Biosystems	www.grotonbiosystems.com
HyClone, part of Thermo Fisher Scientific	http://www.thermo.com
Innovative Cell Technologies	www.innovativecelltech.com
Lonza	www.lonzabiologics.com
Millipore	www.millipore.com
Nalgene, part of Thermo Fisher Scientific	www.nalgenelabware.com
Nunc, part of Thermo Fisher Scientific	www.nuncbrand.com
Pall	www.pall.com

Roche Innovatis AG	www.innovatis.com
Sartorius Stedim Biotech	www.sartorius.com
Synthecon Inc	www.synthecon.com
Xcellerex	www.xcellerex.com

REFERENCES

1. Cacciuttolo M, Arunakumari A. In: Levin M, editor. Pharmaceutical process scale-up. 2nd ed. New York: Taylor & Francis; 2006, Chapter 5. pp. 129–160.
2. Anderson D, Krummen L. Curr Opin Biotechnol 2002; 13: 117–123.
3. Chu L, Robinson D. Curr Opin Biotechnol 2001; 12: 180–187.
4. Jones D, Kroos N, Anema R, van Montfort B, Vooys A, van der Kraats S, van der Helm E, Smits S, Schouten J, Brouwer K, Lagerwerf F, van Berkel P, Opstelten DJ, Logtenberg T, Bout A. Biotechnol Prog 2003; 19: 163–168.
5. Birch JR, Racher AJ. Adv Drug Deliv Rev 2006; 58: 671–685.
6. Doyle A, Griffith JB, editors. Cell and tissue cultures: laboratory procedures in the biotechnology. Chichester: John Wiley & Sons, Ltd; 1998.
7. Morrison CB. In: Day JG, McLallan MR, editors. Cryopreservation and freeze drying protocols. New York: John Wiley & Sons, Inc.; 1995, Chapter 18.
8. Heidemann R, Mered M, Wang DQ, Gardner B, Zhang C, Michaels J, Henzler H-J, Abbas N, Konstantinov K. Cytotechnology 2002; 38: 99–108.
9. Day JG, McLallan MR, editors. Cryopreservation and freeze drying protocols. New York: John Wiley & Sons, Inc.; 1995, Chapter 18.
10. Neranov AJ, Bratanov MB, Tsenov IA. Cryobiology 1992; 29: 296–299.
11. Mazur P, Leibo SP, Chu EHY. Exp Cell Res 1972; 71: 345–355.
12. Kleman MI, Oellers K, Lullau E. Biotechnol Bioeng 2008; 100(5): 911–922.
13. Kloth C, MacIssac G, Ghebramariam H, Arunakumari A. Bioprocess Int 2008; 6: 44–50.
14. Mazur-Melnyk M, Doyle A, Griffith JB, editors. Cell and tissue cultures: laboratory procedures in the biotechnology. Chichester: John Wiley & Sons, Ltd; 1998. pp. 254–261.
15. Shuler ME, Kargi F. Bioprocess engineering: basic concepts. Upper Saddle River, NJ: Prentice Hall; 2002. pp. 169–173.
16. Kompala DS, Ozturk SS. In: Ozturk SS, Hu W-S, editors. Cell culture technology for pharmaceutical and cell-based therapies. New York: Taylor & Francis; 2006. pp. 387–411.
17. Vriezen N, Van Dijken JP, Haeggstroem L. In: Ratledge C, Kristiansen B, editors. Basic biotechnology. Cambridge: Cambridge University Press; 2001. pp. 449–470.
18. Wayte J. Presentation at Waterside Conference 2002. Available at http://www.lonza.com/group/en/company/news/publications_of_lonza.-ParSys-0002-ParSysdownloadlist-00-22-DownloadFile.pdf/20_Slides%20Protein-free%20Processes%20for%20Antibody%20Prod.pdf
19. De Jesus MJ, Wurm FM. Bioprocess Int 2009; 7 Suppl 1: 12–17.
20. Heidemann R, Riese U, Luedkemeyer D, Buentemeyer H, Lehmann J. Cytotechnology 1994; 14: 1–9.
21. Eibl R, Eibl D. Bioprocess Int 2009; 7 Suppl 1: 18–23.
22. Freshney RI, editor. Culture of animal cells: a manual of basic techniques. 4th ed. New York: Wiley-Liss; 2000.
23. Phelan MC. In: Ausubel FM, Brent R, Kingston RE, Moore DD, Seidman JG, Smith JA, Struhl K, editors. Current protocols in molecular biology. New York: John Wiley & Sons, Inc.; 1998. pp. A.3F.1–A.3F.14.
24. Mammalian Cell Culture: Production technologies and market overview; 2005, Drug and Market Development Publishing (online). Available at http://www.researchandmarkets.com.
25. Fenge C, Luellau E. In: Ozturk SS, Hu W-S, editors. Cell culture technology for pharmaceutical and cell-based therapies. New York: Taylor & Francis; 2006. pp. 155–197.
26. Hu WS, Meier J, Wang DIC. Biotechnol Bioeng 2006; 95(2): 306–316.
27. Rendall MH, Maxwell A, Tatham D, Kahn P, Gray RD, Kallmeier RC, Wayte JRT, Racher AJ. In: Godia F, Fussenegger M, editors. Animal cell technology meets genomics. Dordrecht: Springer; 2005. pp. 701–704.
28. Heath C, Kiss R. Biotechnol Prog 2007; 23: 46–51.
29. Adamson SR, Leonard M, Drapeau D, Harrison SA, O'Connell BD, Charlebois TS. In: Sofer G, Zabriskie DW, editors. Biopharmaceutical process validation. New York Basel: Marcel Dekker; 2000. pp. 101–127.
30. Wang Z, Tan W, Poptic EJ, Belovich J. Feasibility of using a small-scale perfusion bioreactor with a novel cell retention device to inoculate a large-scale bioreactor. Conference Presentation at the American Chemical Society National Meeting. San Francisco, CA.
31. Cacciuttolo M. In: Butler M, editor. Cell culture and upstream processing. New York: Taylor & Francis Group; 2007, Chapter 9.
32. Junker BH, Wang HY. Biotechnol Bioeng 2006; 95(2): 226–161.
33. Rao G, Moreira A, Brorson K. Biotechnol Bioeng 2009; 102(2): 348–356.
34. ICH Topic Q 8, Pharmaceutical Development, May 2006 and Revision 1 - ICH Topic Q 8 (R1) (Draft 2008).
35. Guidance for Industry, PAT- a framework for innovative pharmaceutical development, manufacturing, and quality assurance, Pharmaceutical cGMP; Sep 2004.
36. Wurm F. High level expression of recombinant proteins by transient and stable expression. Cell Line Engineering Conference; La Jolla, CA. 2007.
37. ICH Topic Q 5 D, Quality of Biotechnological Products: Derivation and Characterization of Cell Substrate Used for Production of Biotechnological/Biological Products, Mar 1998, CPMP/ICH/294/95.
38. Arunakumari A, Dai XP, Goldstein J, Kloth C, Ghebremariam H, MacIsaac G, Wagner M. Biopharm Int 2009; 22(6 Suppl): 4–15.
39. Konstantinov K. Manufacturing support –lessons learned and trends for the future. Presentation at IBC International Conference; 2008 Sep. Anaheim, CA.

40. Kim NS, Kim SJ, Lee GM. Biotechnol Bioeng 1998; 60(6): 679–688.
41. Fann C, Guirgis F, Chen G, Lao MS, Piret JM. Biotechnol Bioeng 2000; 69(9): 204–212.
42. Racher AJ. Cell Line Development and Engineering Meeting. 2005 Nov. (online Available at http://www.lonza.com/group/en/company/tradefairs/biologics_2004_presentations_posters.html)
43. Hassell T, Brand H, Renner G, Westerlake A, Field RP. In: Spier RE, Griffiths JB, MacDonald C, editors. Animal cell technology, developments, processes and products. Oxford: Butterworth-Heinemann; 1992.
44. Heller-Harrison R, Crowe K, Cooley C, Hone M, McCarthy K, Leonard M. Biopharm Int 2009; 22(6 Suppl): 16–27.
45. Brecht R, Sandig V, Marx U, Riedel M, Koch S. Biopharm Int (Online) 2005. Available at http://biopharm-international.findpharma.com/biopharm/article/articleDetail.jsp?id=170702&pageID=1&sk=&date=. Accessed 2009 Dec.
46. Ullah M, Burns T, Beltz H-W, Greller G, Adams T. Biopharm Int 2008; 21(11 Suppl).
47. McLeod LD. Bioprocess Int 2009; 7 Suppl 5: 4–17.
48. D'Aquino R. Chem Eng Prog (Online) 2006 Available at http://www.aiche.org/CEP, 1 May (2006), free subscription http://findarticles.com/p/articles/mi_qa5350/is_200605/ai_n-21392133/?tag=content;col1. Accessed 2009 Jul.
49. Sinclair A, Leeven L, Monge M, Lim J, Cox S. Biopharm Int 2008; 21(7 Suppl): 4–15.
50. Montgomery SA. Bioprocess Int 2009; 7(6): 26–34.
51. Kempner ME, Felder RA. J Assoc Lab Autom 2002; 7(2): 56–62.
52. Arunakumari A. Bioprocess Int 2009; 7 Suppl 1: 48–54.

FURTHER READING

Butler M. Appl Microbiol Biotechnol 2005; 68: 283–291.

Doyle A, Griffith JB. Cell and tissue cultures: laboratory procedures in the biotechnology. Chichester: John Wiley & Sons, Ltd; 1998.

Dutton RL, Scharer JM. Advanced technologies in biopharmaceutical processing. Ames, IA: Blackwell Pub; 2007.

Freshney RI. Culture of animal cells: a manual of basic techniques and specialized applications. 6th ed. New York: Wiley-Blackwell; 2010.

Nusim S. Active pharmaceutical ingredients. Boca Raton, FL: Taylor & Francis Inc.; 2005.

Ozturk SS, Hu W-S. Cell culture technology for pharmaceutical and cell-based therapies. New York: Taylor & Francis; 2006.

Pollard JW, Walker JM. Basic cell culture protocols. 2nd ed. Totowa, NJ: Humana Press; 1997.

Wurm F. Production of recombinant protein therapeutics in cultivated mammalian cells. Nat Biotechnol 2004; 22(11): 1393–1398.

16

INSECT CELL CULTURE

Someet Narang
Johns Hopkins University, Baltimore, Maryland
MedImmune, Inc. Gaithersburg, Maryland

Erik M. Whiteley
Geron Corporation, Menlo Park, California

Sunyia Hussain and Michael J. Betenbaugh
Johns Hopkins University, Baltimore, Maryland

16.1 INTRODUCTION

Owing to their potential as biopesticides in agriculture, substantial knowledge has been obtained over past decades concerning the structure and function of insect viruses. This knowledge has been used to alter the genetic content of these insect-specific viruses in order to incorporate heterologous genes for production of recombinant proteins. Baculoviruses such as the *Autographica californica* nuclear polyhedrosis virus (AcMNPV or AcNPV) have been modified to incorporate foreign genes from a number of other organisms. Insect cells or insect larvae are then infected with these altered viruses in the baculovirus expression vector system (BEVS or BES), which includes both a cell growth and infection stage, to generate recombinant proteins for vaccines, biopharmaceuticals, diagnostics, biopesticides, and structure and function studies. Various insect cell hosts, viral vectors, and expression methodologies are being explored along with alternative media formulations and bioreactors. Fed-batch, semibatch, and continuous processes are available to scale-up production for cells such as *Spodoptera frugiperda* (Sf-9) and *Trichoplusia ni* (High Five™). Alternatively, larval systems with their lower capital costs are also finding wide-spread use. These processes are now being optimized by evaluating insect metabolism using sophisticated analytical techniques in concert with control methods based on complex mathematical models. Metabolic engineering of glycosylation and other posttranslational events are being applied to improve product yields and generate proteins applicable as human therapeutics. Indeed, the future application areas and prospects of BEVS will continue to expand thanks to significant advances in the biology, biochemistry, and engineering of insect cells and insect-culture processes.

16.2 INSECT CELL LINES

Insect cell lines have been established from nearly 100 different species within the following seven orders of Arthropoda: Lepidoptera, Diptera, Homoptera, Hymenoptera, Orthoptera, Hemiptera, and Coleoptera. These lines are isolated from eggs or embryonic, larval, or adult tissues such as hemocytes, ovaries, imaginal discs, testes, midgut, and fat body using methods that are now well known (1). The procedures typically involve the lysis of tissue followed by suspension in a rich serum-containing medium in tissue culture flasks. The nutrients are replaced periodically, and the cultures are monitored until cell division is observed. The cells are then subcultured after one to several weeks to obtain a new cell line. Eventually, the cell lines are screened for desired properties such as

Upstream Industrial Biotechnology: Expression Systems and Process Development, Volume 1, First Edition. Edited by Michael C. Flickinger.
© 2013 John Wiley & Sons, Inc. Published 2013 by John Wiley & Sons, Inc.

short doubling times, virus susceptibility, recombinant gene expression, or posttranslational processing. Clonal isolates can be obtained that have better growth or gene expression properties, as was the case in the development of the Sf-9 clone from the established cell line (IPLB-Sf-21) of the fall armyworm, *S. frugiperda*. Both of these cell lines are now widely used for the replication of AcMNPV and production of recombinant proteins.

The screening of established cell lines led to the identification of a *T. ni* (cabbage looper) cell line (BTI-TN5B1-4), with the trade name High Five™ (Invitrogen, Inc.), which often provides recombinant protein yields on a per cell basis that are superior to those of Sf-9 and Sf-21(2). Originally, an attachment-dependent cell line, High Five cells have been adapted to suspension growth in many laboratories. Adaptation to suspension is aided by the addition of 50–2000 U/cm^3 heparin to prevent clumping, but the heparin should be removed prior to viral infection and expression of products (3,4). Shown in Fig. 16.1 is a micrograph of healthy and AcMNPV-infected Sf-9 and High Five cells. Commercial serum-free media has been developed for High Five, Sf-21, and Sf-9 cell lines. Because the Sf-9 cell line produces higher levels of the extracellular virus (EV), this cell line is often used for virus production, whereas the High Five are used for heterologous gene expression. Although, High Five and Sf-9 are the cell lines of choice for many applications, recombinant protein production from AcMNPV has been achieved in a number of other cell lines such as those isolated from *Heliothis, Lymantria, Plutella*, and *Trichoplusia* (5,6). A smaller variety of cell lines from *Bombyx mori* (silkworm) and *Lymantria dispar* (gypsy moth) are available for infection with *Bombyx mori* nuclear polyhedrosis virus (BmNPV) and *Lymantria dispar* nuclear polyhedrosis virus (LdNPV), respectively.

Cell lines are usually cultured at the laboratory scale in polystyrene culture flasks or roller bottles. Those cell lines that are not anchorage dependent can be grown in shaker flasks or small suspension culture flasks. Cells are monitored for number density and passaged one to two times per week by subculturing into fresh medium. Attachment-dependent cells must be dislodged by agitation, scraping, or enzymatic treatment. Following a lag phase, the cells grow logarithmically with doubling times between 0.5 and 2 days. Maximum cell densities in shake flask cultures are typically in the range of 2–10 million cells/mL. Cell size is in the range of 8–20 μm, and culture temperatures are typically between 25 and 30°C. Stocks of cells can be cryopreserved in liquid nitrogen using medium and dimethylsulfoxide (DMSO). Recovery is achieved by a rapid thaw and can be enhanced by using a serum-bearing medium prior to freezing the cells.

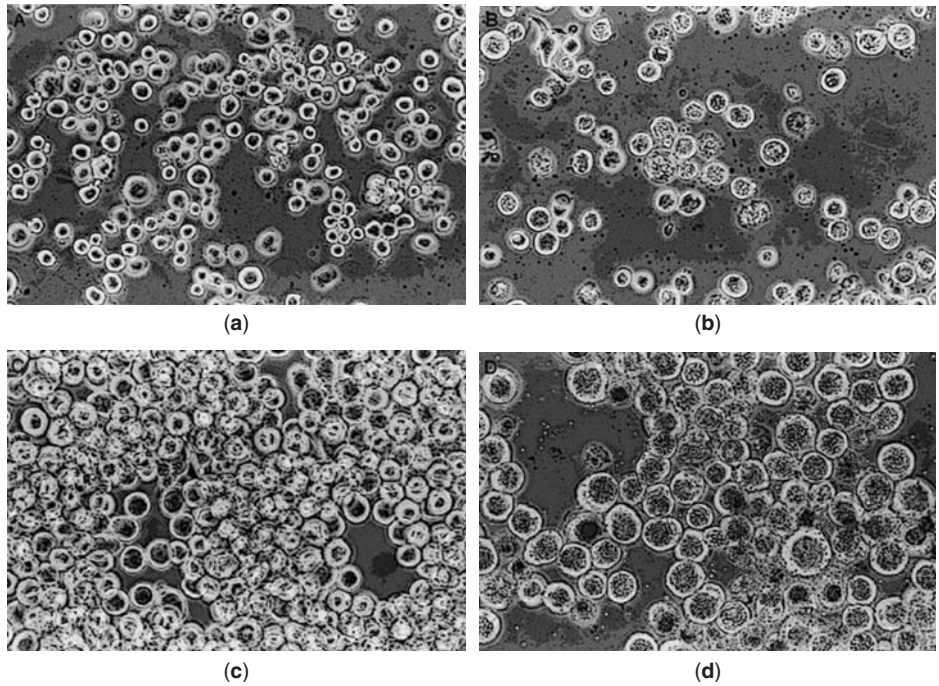


Figure 16.1. Insect cell morphology. (a) Healthy Sf-9 cells grown in insect-culture medium. (b) Sf-9 infected with wild-type AcMNPV baculovirus. (c) Healthy BTI-TN5B1-4. (d) BTI-TN5B1-4 infected with wild-type AcMNPV baculovirus.

16.3 VIRUSES

The most widely studied and utilized insect viruses are the baculoviruses, a helper-independent eukaryotic DNA vector that can infect a wide range of lepidopteran (butterflies and moths) insects and insect cells. *Baculo* refers to the rod-shaped capsid that is characteristic of these viruses, which are 40–50 nm in diameter and 200–400 nm in length. The two most widely studied baculoviruses, AcMNPV and BmNPV, contain DNAs that are approximately 130 kb in length. The relatively large size of the virus allows for the encapsulation of large pieces of foreign DNA in addition to the essential viral DNA.

The infection of a single cell by the baculovirus is illustrated in Fig. 16.2. Baculoviruses are deposited in two forms, budded and occluded, in the infected cells (7,8). During the initial stages of infection (10–14 h postinfection), membrane-enveloped viruses bud from the plasma membrane of an infected host in a form commonly referred to as *extracellular virus (EV)*, *nonoccluded virus* (NOV), or *budded virus* (BV). A second form of the virus, the occluded virus (OV), forms in the nucleus of an infected cell beginning at 20–24 h postinfection. This intracellular virus is enveloped and encased within a crystalline viral protein matrix called *polyhedrin*. These protein crystals, called *occlusion bodies*, *polyhedra*, or *polyhedral inclusion bodies* (*PIB*s), may be as large as 5 μm in diameter and contain many virions as shown in (Fig. 16.3). The OV encased within the polyhedrin protein matrix may contain multiple nucleocapsids within a single envelope for multiple embedded nuclear polyhedrosis viruses (MNPVs), or a single nucleocapsid per envelope for single nuclear polyhedrosis viruses (SNPVs). In addition to nuclear polyhedrosis virus (NPV), a second type of occluded baculovirus, the granulosis virus (GV), includes one or, very rarely, two virions embedded in a much smaller protein matrix called a *capsule* or *granule*. Most baculoviruses used as biopesticides and all baculoviruses used in biotechnology are NPVs, although, a few GVs have shown potential for future applications.

It is the OV that is responsible for transmission of the virus from insect to insect, as shown in the baculovirus life cycle depicted in Fig. 16.4 (8). After death and decomposition of an infected insect, the polyhedra are deposited on vegetation where they are ingested by other feeding insect larvae. Transported with food to the midgut, the

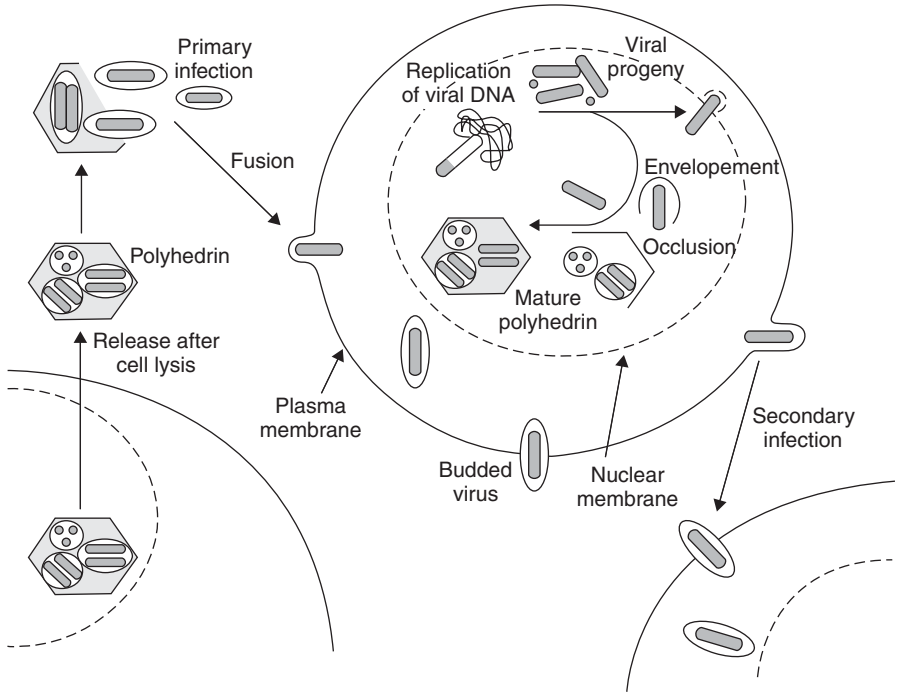


Figure 16.2. Single-cell replication life cycle of the natural baculovirus, AcMNPV. Primary infection by occluded virus occurs upon disintegration of the polyhedrin matrix and subsequent fusion to the plasma membrane. Budded virus produced within the cell proceed to initiate the secondary infection process. Adapted from figure appearing in *Baculovirus Expression Systems and Biopesticides*, M.L. Shuler, H.A. Wood, R.R. Granados, and D.A. Hammer, Wiley-Liss, 1995. Reprinted by permission of John Wiley & Sons, Inc.

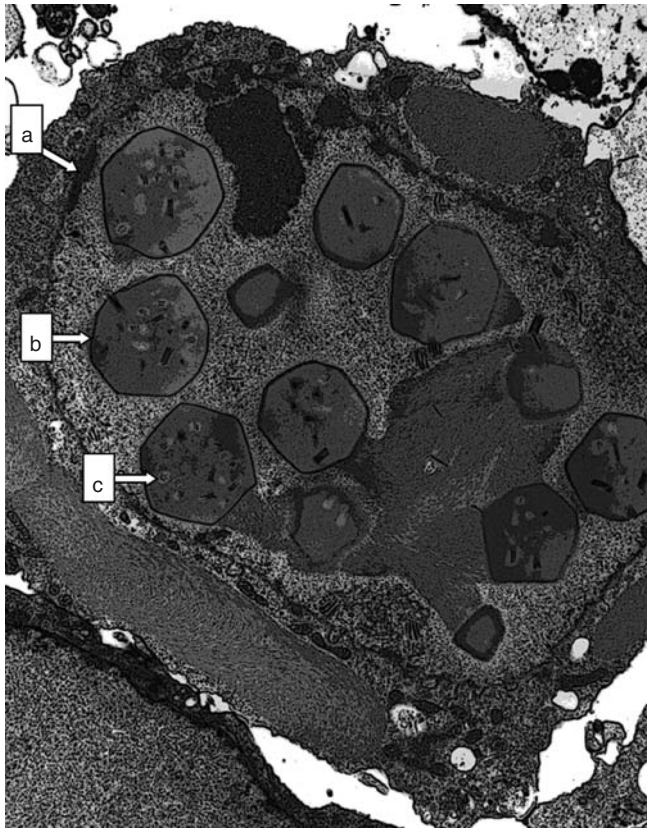


Figure 16.3. Electron micrograph of AcMNPV infection in *S. frugiperda*. (a) Nuclear membrane, (b) polyhedrin inclusion bodies, and (c) virions at 48 h postinfection. Micrograph courtesy of G. Williams.

polyhedra are dissolved in the alkaline environment, subsequently, releasing virions into the lumen of the midgut. These viruses then fuse to the epithelial cells where they cause an infection in the midgut tissue. The infected cells then release BV, which are responsible for secondary infection of other tissues by spreading through the hemolymph and trachea. The infected larva continues to feed for 5–7 days until it becomes listless. The larval cuticle melanizes, and the muscular structure dissolves in a process called *melting* or *wilting*. The larva eventually ruptures, releasing about 25% of its dry weight in the form of PIBs, which are spread over vegetation for consumption by other insects and reinitiation of the infection cycle.

16.4 BACULOVIRUS GENE EXPRESSION

Baculovirus gene expression of viruses such as AcMNPV occurs over four phases: immediate early (α), early (β), late (γ), and very late (δ). During the immediate early phase, viral genes are expressed using host cell factors. The immediate early gene products then control the expression of the early genes, whose products are responsible for cytoskeletal rearrangement and nucleus enlargement. Extensive viral DNA replication occurs about 5–7 h after infection, followed by expression of the late genes. The late phase extends from 6 until 20–24 h postinfection and involves the assembly of nucleocapsids, the transport and release of BV, and the degradation of the host genome. The formation of OV occurs during the very late phase, beginning at about 20–24 h postinfection. The occluded viral particles can accumulate for 3–5 days until the infected cells lyse.

Two genes abundantly expressed during the very late phase are the polyhedrin and p10 genes. The product of the polyhedrin gene (*polh)* is the 29-kDa protein that forms the crystalline matrix of the occlusion particles protecting encased virus nucleocapsids. The product of the p10 gene is a 10-kDa protein that forms large fibrous arrays in the nucleus and, occasionally, in the cytoplasm. In 1983, it was observed that viruses containing deletions in the polyhedrin gene were stable and could be replicated in cells in culture (9). Though, the cells infected with these viruses lack the characteristic occlusion particles, production of BV was unaffected. Furthermore, these BV could be collected from the cell culture media and used to infect other cells in order to passage the altered virus. Because the polyhedrin gene is nonessential for BV infection and propagation in cell culture, the construction of a recombinant baculovirus can be accomplished by replacing the polyhedrin gene with a foreign gene such as interferon β (10). In this way, the foreign gene, now under the control of the very strong polyhedrin promoter, is expressed, instead of the polyhedrin gene at the very late phase of AcMNPV infection. Similarly, it was observed that the disruption of the p10 gene resulted in the disruption of the fibrous matrix, but the formation of BV was not affected. Subsequently, recombinant baculovirus constructs containing foreign genes inserted under the control of the p10 promoter were used to produce heterologous proteins in place of the p10 protein (11). Because the polyhedrin and p10 are very strong late promoters, with as much as 50% of the total stained protein consisting of polyhedrin (12), these promoters have the potential for very high rates of foreign gene expression. One disadvantage of this system is that the production of heterologous protein is accomplished late in the viral infection, at the time when host cell function is deteriorating. Furthermore, the insect host eventually succumbs to the infection, thus, requiring a new batch of insect cells to be grown and infected each time recombinant protein is to be produced.

In an effort to avoid the problems associated with insect cell death because of virus infection, a number of vectors have been developed that allow the stable integration of foreign DNA into insect cell hosts. Stable expression of heterologous proteins using these integrated vectors

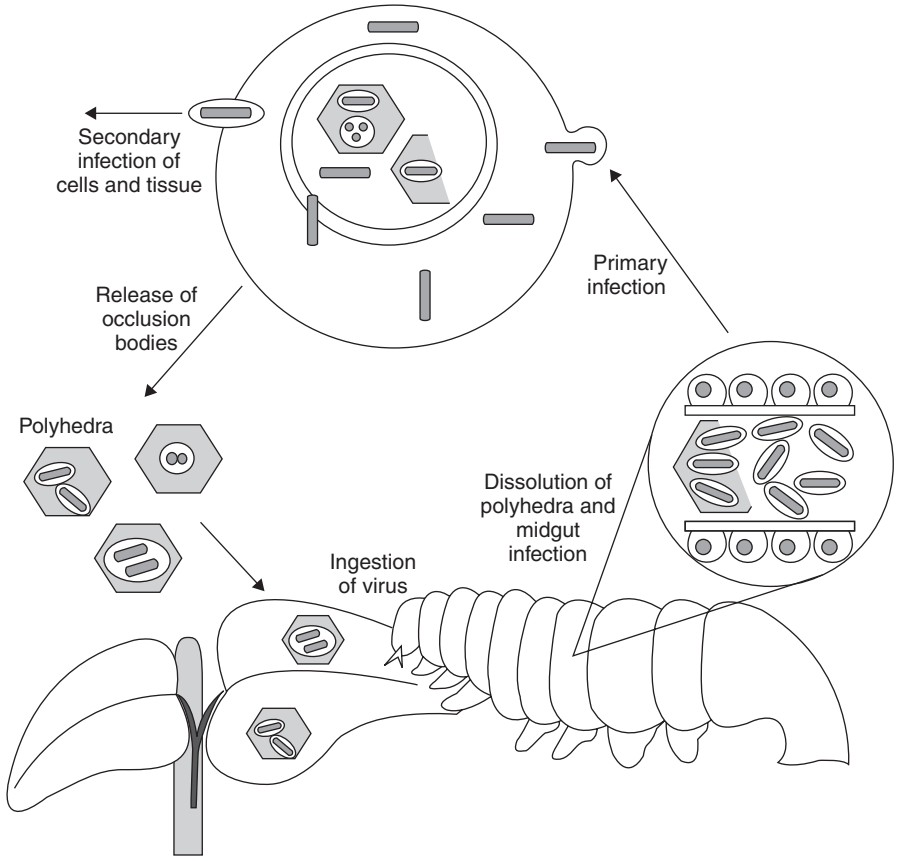


Figure 16.4. Life cycle of the natural baculovirus, AcMNPV. Adapted from figure appearing in *Baculovirus Expression Systems and Biopesticides*, M.L. Shuler, H.A. Wood, R.R. Granados, and D.A. Hammer, Wiley-Liss, 1995. Reprinted by permission of John Wiley & Sons, Inc.

has been achieved in several insect cell lines including Sf-9, *Drosophila* S2, *B. mori, T. ni*, and *Aedes albopictus* (13,14). However, expression levels in most cases are many times lower than baculovirus, so these systems are yet to approach the popularity of BEVS. Stable expression systems are likely to find niche applications when lower expression is acceptable in return for desirable host processing functions.

16.5 CONSTRUCTION OF RECOMBINANT BACULOVIRUSES

More than 500 different baculoviruses of the Baculoviridae family are currently known. For use as a vector to deliver foreign genes into insect cells, the most extensively used is AcMNPV (15). BmNPV (16), LdMNPV (17), and granulosis viruses (18) have also been considered as vectors, but to a much lesser extent. Techniques for manipulating AcMNPV to generate recombinant baculoviruses is discussed here because this subtype is the most widely investigated and the procedures are similar for many other baculoviruses. AcMNPV is a large, double-stranded, circular DNA virus for which the complete nucleotide sequence has been determined (19). Because of the large size of the baculovirus capsid, very large genes (>20 kb) can be inserted into the viral genome, making it a favorable expression system for a wide variety of proteins including huge virus like particles (VLPs). However, the large size of the baculovirus DNA prohibits the typical recombinant DNA manipulations used for cloning with bacterial plasmids. Consequently, an alternative approach involving plasmid transfer vectors and allelic replacement (homologous recombination) was developed and remains the most popular method for foreign gene insertion into the baculovirus. Many improvements have been made for generating recombinant baculoviruses, but almost all are based on homologous recombination.

The first step in allelic replacement involves the manipulation of a transfer plasmid in *Escherichia coli* by cloning the foreign gene downstream from a baculovirus promoter, typically those for polyhedrin or p10. The promoter and gene are also flanked by baculovirus DNA derived from a nonessential locus such as polyhedrin

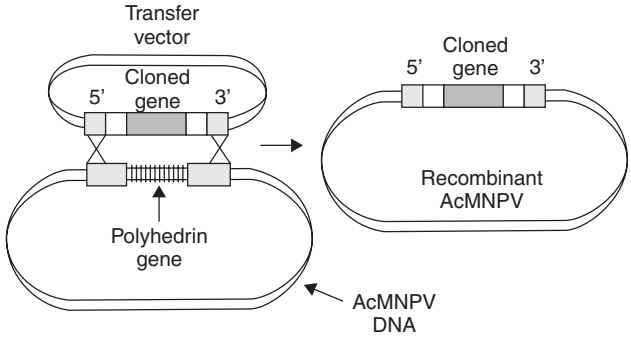


Figure 16.5. Homologous recombination. A baculovirus gene locus (usually p10 or polyhedrin) is targeted for homologous recombination using a transfer vector that includes flanking homologous sequences and, in some cases, encoding a selectable marker. The recombination event (represented here by X's) results in the replacement of sequences flanked by the homologous areas with the sequence of the foreign gene.

or p10 genes. The recombinant transfer plasmid is then mixed with native baculovirus DNA, and the mixture is transfected into insect cells using calcium phosphate or cationic lipids. A small fraction of the baculoviruses will undergo homologous recombination with the transfer plasmid to create a recombinant baculovirus containing a heterologous gene under the control of the appropriate promoter (Fig. 16.5). The recombinant baculovirus constructs may be identified by examining for the absence or presence of a particular baculovirus or plasmid function because of the insertion of the foreign gene.

The initial screening technique involved the identification of plaques of insect cells containing occlusion-minus (*occ*−) infections as a result of the deletion of the polyhedrin gene from the original baculovirus DNA. Occlusion-positive plaques include an opaque light refractile characteristic that can be visually distinguished from the characteristics of *occ*− plaques under the microscope. However, picking an *occ*− clone is a formidable task for inexperienced researchers because young nonrecombinant plaques often show no sign of "occlusion," and recombination frequencies can be as low as 0.1%. These difficulties resulted in the time consuming and tedious isolation of recombinant baculovirus through multiple rounds of plaque purification. The first modification of the system was the use of the bacterial gene *lacZ* (β-galactosidase) to produce chromogenic recombinant plaques that enhance plaque purification (20,21). Significant progress in isolating recombinant baculovirus was achieved by derivatizing the circular, double-stranded wild-type baculovirus into a linear form through the introduction of a unique restriction site (*Bsu36I*) at the polyhedrin locus (22). A higher proportion of recombinant viruses were obtained when the linearized baculovirus genome was cotransfected with a transfer vector, because the infectivity of the linearized virus alone was substantially reduced below wild-type levels. Later, aβ-galactosidase gene flanked with restriction sites (*Bsu36I*) was inserted in the AcMNPV under the polyhedron promoter such that linearizing the viral DNA using the restriction enzyme also removed a part of another essential viral gene (ORF 1629). The missing part of the viral gene was then provided via the transfer vector along with the recombinant gene of interest. As a result, the recircularized AcMNPV DNA without homologous recombination was unable to infect and any nonlinearized parent AcMNPV could be detected using X-Gal because of the expression of β-galactosidase. Conversely, commercial systems are also available that turn on expression of β-galactosidase expression under a second promoter as a positive marker for homologous recombination in combination with reconstruction of ORF 1629 gene needed for viral replication.

A more rapid approach to generate pure recombinant baculovirus in 7–10 days has also been reported (23). This technique uses a baculovirus shuttle vector (bacmid) that can replicate in *E. coli* and infect susceptible lepidopteran insects. The homologous recombination event is performed using site-specific transposition by transforming the gene of interest in recombinant *E. coli* engineered to express the parent bacmid and transposase. The successfully cloned candidates are visually screened (e.g. based on *lacZ* gene) and the high molecular weight bacmid DNA is isolated from the colonies. A recombinant baculovirus is then generated by introducing the composite bacmid into insect cells in culture and harvesting the virus from the medium. This approach eliminates the need for plaque purification because only the recombinant baculovirus is generated during the initial infection.

Other expression vectors are available that provide for the expression of up to four genes in the same baculovirus construct (e.g. pBAC4x-1). These constructs may include one or more polyhedrin, p10, or heat shock promoters to control expression of the foreign genes. Infection of insect cells with several viruses, each containing multiple genes, can provide simultaneous expression of numerous proteins in one insect cell. Constructs containing baculovirus promoters such as IE1 and core that are activated earlier in the infection are also available (24). Specialized vectors that include histidine tags, that help facilitate protein purification, as well as gp64 or melittin fusions, for enhancing protein secretion, are also available. Commercial vectors have also been developed to aid surface display of recombinant proteins on baculovirus particles. A modified baculovirus system, BacMam, has also been developed to enable the use of baculovirus technology to deliver genes or to express recombinant proteins in mammalian cells (25). This is done by either adding a mammalian expression cassette or by

replacing the viral expression cassette with a mammalian expression cassette in the viral DNA.

For a laboratory not experienced with BEVS, it is advisable to employ the linear baculovirus genome with a lethal deletion and selectable marker or the *E. coli* bacmid shuttle vector as the initial method for generating recombinants. Many kits are now commercially available that include the transfer vectors and baculovirus DNA for rapidly generating recombinant baculovirus constructs.

16.6 POSTTRANSLATIONAL PROCESSING

Because insects are eukaryotic organisms, the derived cell lines are capable of performing many of the posttranslational processes including secretion, folding, and glycosylation observed in higher organisms. In fact, insect cells are often the expression system of choice for the rapid generation of functional eukaryotic proteins. However, the posttranslational processing may not be identical to that performed in the native environment. It may be worthwhile to compare the protein expressed in the insect cells with the native protein to determine if significant differences in posttranslational processing exist that will detract from subsequent structural or functional analysis. Some of the posttranslational processing events that are observed in insect cells are described in the following sections.

16.6.1 Glycosylation

A majority of secreted and membrane proteins are glycosylated, and the attached oligosaccharides can play critical roles in cellular targeting, structural stability, resistance to proteolysis, immunogenicity, and circulatory half-life. The oligosaccharide residues are added to the protein at specific amino acids during processing in the endoplasmic reticulum (ER). Subsequently, these oligosaccharides are trimmed and modified during processing in the ER and Golgi compartments. Both N-linked and O-linked glycosylation have been observed in insect cells.

During N-glycosylation in both insect and mammalian cells an initial $Glc_3Man_9GlcNAc_2$ group is added to the Asn residue of the Asn-X-Ser/Thr sequence of a nascently translated protein. Glucose and mannose residues are then trimmed from the $Glc_3Man_9GlcNAc_2$ group. However, the level of trimming and subsequent modifications are likely to be different in insect cells than those observed in mammalian cells. Recent evidence indicates that these differences may depend significantly on the particular insect cell line used. Many initial studies of *N*-glycans from heterologous glycoproteins obtained from Sf-9 or Sf-21 cells indicated the presence of only high mannose type ($Man_{9\text{-}5}GlcNAc_2$) or short, truncated, paucimannosidic ($Man_{3\text{-}2}GlcNAc_2$) oligosaccharides, sometimes including an α(1,6)-linked fucose (26,27).

A comparison of the *N*-glycans of IgG from High Five cells (28) with those attached to an IgG3a from the mammalian NS/0 cells reveals significant similarities and some differences in the glycosylation properties of the two cell lines. A typical endogenous oligosaccharide processing pathway observed in many insect cell lines is shown in Fig. 16.6 (29). The initial mammalian ER pathway, including trimming of the terminal glucose and mannose residues, is operative. Insect cell processing diverges from mammalian cell processing in the pathways leading to the paucimannosidic structures, with the critical step being the cleavage of GlcNAc from the α-(1,3) branch by a hexosaminidase (30–32). Other significant differences in insect cell processing are the α-(1–3)-linked addition of fucose, also observed in the processing pathway of plants, and the absence of any attached sialic acids (28,33,34). Glycoprotein processing in insect cells has now been engineered by expressing mammalian glycosylation enzymes in insect cells in order to generate glycoforms similar to those produced by mammalian cells (24,35). This has been achieved by expressing various glycosyltransferases as well as expressing the cytidine monophosphate (CMP)-sialic acid synthesis pathway enzymes (Fig. 16.6) (36,37).

Several studies on heterologous glycoproteins have indicated that certain insect cell lines can synthesize hybrid and complex oligosaccharides (28,34,36,38,39). For example, analysis of *N*-glycans of heterologous interferon-γ secreted from *Estigmena acrea* (Ea-4) confirmed the presence of complex, hybrid, paucimannosidic, and high mannose N-linked oligosaccharides (34). In contrast, *S. frugiperda* (Sf-9) cells were observed to produce only hybrid, paucimannosidic, and high mannose *N*-glycans. Alternatively, the insect cell line *Danaus plexippus* (DpN1) was observed to produce a combination of *N*-glycans including 26% complex structures, some of which terminated in sialic acid (38).

O-glycosylation, which involves the addition of carbohydrates to hydroxylated amino acids such as serine or threonine residues, has been observed for several recombinant proteins produced by baculovirus-infected insect cells. A pseudorabies viral glycoprotein, gp50, and extracellular domains of the respiratory syncytial virus protein were found to contain the attached monosaccharide GalNAc and lesser amounts of the disaccharide Galβ1-3GalNAc (40). In mammalian cells, only the disaccharide form was observed in the presence or absence of attached sialic acids. Activity levels of the relevant glycosyltransferases in the insect cells and mammalian cells supported the particular distribution patterns observed.

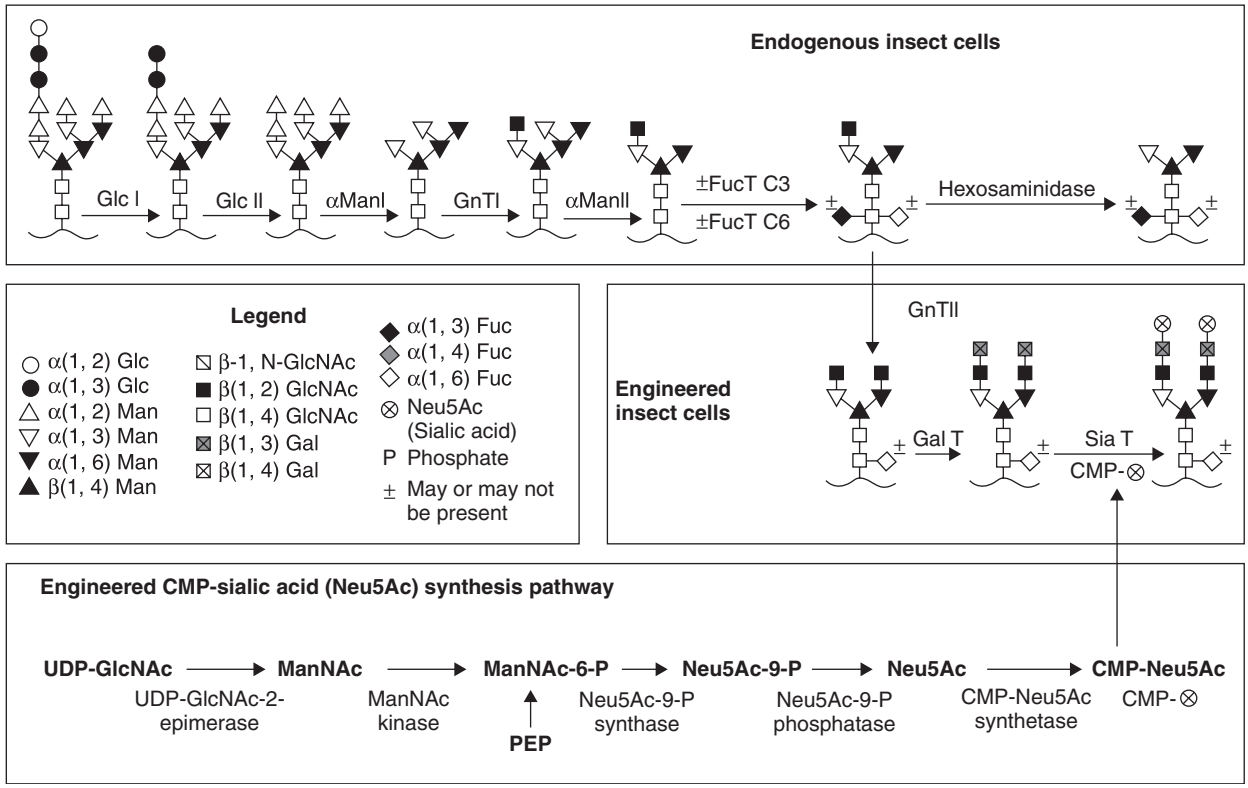


Figure 16.6. Endogenous *N*-glycan processing pathway in insect cells together with efforts to engineer glycosylation and CMP-sialic acid synthesis pathways. Enzymes involved in processing are noted with abbreviated titles.

16.6.2 Other Posttranslational Processes

Many proteins expressed in insect cells are directed to the appropriate cellular compartment including the nucleus, cytoplasm, organelles, plasma membrane, or extracellular space. For secreted proteins, a short (15–40 amino acids) signal peptide is present for translocating polypeptide from the cytoplasm into the ER. This signal peptide, whether from mammalian, plant, or yeast sources, is usually cleaved correctly by the signal peptidases in insect cells. However, signal peptide processing is not always efficient, especially for peptides from plants or other distant eukaryotes. In fact, a complete absence of processing has been observed in at least one case (40). Replacement of the original signal peptide with another signal peptide from a protein such as melittin of honeybee venom (41) or the gp67 and ecdysteroid UDP-glucosyltransferase (EGT) proteins (7) from AcMNPV can help to alleviate this limitation in some cases. Alternatively, the expression of recombinant signal peptidase can also overcome a limitation in the processing capacity of insect cells (42). Sometimes, a substantial fraction of proteins destined for secretion will be retained intracellularly in incorrectly folded forms or as aggregates. Coexpression of chaperones or folding enzymes can reduce aggregation and enhance secretion of recombinant proteins that rely on such folding assistance factors (43,44). Another, undesirable posttranslational processing event that often occurs with insect cell-derived proteins is proteolysis, that releases cellular and baculovirus proteases that can degrade target recombinant proteins. Protein degradation can be minimized through control of culture conditions to limit cell lysis or by addition of protease inhibitors to the medium (45–47). Another approach to limit proteolysis is to delete the proteases genes from the virus (48) or inhibit protease activity in the virus or cells using RNA inhibition (49). Other posttranslational processing steps including phosphorylation, fatty acid acylation, α-amidation, and N-terminal amidation have also been observed in insect cells or insect larvae.

16.7 APPLICATIONS

Baculovirus-infected insect cells often provide high levels of expression of heterologous proteins, leading to the use of this system across a broad spectrum of applications and fields. BEVS has been used for the production of proteins for structure and function studies, vaccines, VLPs, multisubunit assemblies, and diagnostic reagents (50). The

application of BEVS products as human and animal therapeutics and vaccines is also under active development.

The ability to generate vaccines rapidly using this system, makes this a favorable candidate, particularly for producing influenza vaccine in which new variants are generated each year. FluBlok, a trivalent influenza vaccine being developed by Protein Sciences Corp. and UMN Pharma Inc., is one example using the insect cell-baculovirus expression system. This technology will enable production of this vaccine in less than 2 months, and the vaccine is currently under Phase III clinical trails (51). Another approach to generate the influenza vaccine is by using VLPs produced by coexpressing the core matrix protein M1 and various combinations of hemagglutinin, neuraminidase and/or M2 proteins of the influenza virus. Novavax has initiated clinical trials for seasonal influenza VLP vaccine (52) and for a pandemic VLP vaccine (53). In 2007, the European and Australian approval of GlaxoSmithKline's human papillomavirus (HPV) vaccine, Cervarix, produced using the baculovirus expression system reinforced the commercial potential of insect cell-baculovirus technology. In addition, a promising vector for human gene therapy, recombinant adeno-associated virus (rAAV) vectors was produced in large-scale bioreactors using baculovirus expression vectors in insect cell cultures (54).

The use of baculoviruses as biopesticides, the original motivation for studying these viruses, represents another thrust of the technology (4,55). Wild-type baculoviruses have been used as efficacious pest control agents for many years but have a limited host range and can take between 5 and 10 days to debilitate insect larvae. A number of genetic modifications, mostly centered on replacement of polyhedrin or p10 genes with heterologous insect toxins, have been implemented to lower viral killing time and reduce the duration of pest feeding. Some of the heterologous genes that have been considered are listed in Table 16.1. A major concern in the development of baculovirus pesticides is the potential safety of these agents. However, extensive studies have concluded that baculoviruses have a very low range of infectivity and will not infect beneficial insects or mammals. Inclusion of a foreign gene under the control of a baculovirus promoter appears to present little danger as well. Finally, insect cell expression system has been exploited as tools for examining the role of proteins in physiological processes.

16.8 LARGE-SCALE PROCESSING: CELL CULTURE OR LARVAL PRODUCTION

Structural and functional characterization studies, diagnostic reagents, and vaccine production often require product levels beyond the scale of shaker flasks. Biopesticides will require huge amounts of the final product for use in field trials. The production of these large quantities of heterologous proteins or baculoviruses will require the use of large-scale cell culture or insect larvae. Insect cell culture provides an environment in which the process parameters can be carefully controlled and monitored (4,7). It also allows for the utilization of a single-cell line with more uniform posttranslational processing than can be achieved in larvae. Chemically defined animal protein free medium can be used to grow the cells, although, care must me taken to successfully remove any toxic compounds from cell culture medium. Also, the cost of commercial media used in cell culture can become prohibitive for large volumes, and a significant capital investment is required for purchasing large bioreactors. These considerations may warrant the consideration of insect larvae as an alternative method for the production of recombinant proteins. The use of larvae can provide substantial cost advantages and easy scale-up for the production of recombinant proteins and the yields may even be higher. Some posttranslational processing events such as glycosylation, secretion, and carboxy-terminal amidation also may be more efficient in larvae (56). However, larvae may include significant levels of other insect proteins including larval proteases that can degrade the final product. Also, larval purification will require an additional solids handling step for separating the hemolymph from the insect carcass but this step can be automated.

16.8.1 Cell Culture Processes

Increasing the volume and mass of production from a small 100 mL spinner flask to a large 100-L bioreactor is not a simple linear process (13). Many of the process parameters, especially, the delivery of O_2 and mixing, change when production is moved to a large bioreactor. Even so, large-scale production of proteins in BEVS has been achieved in 100-L bioreactors while maintaining cell growth kinetics and productivity. Issues that are relevant to cell culture scale-up are addressed next.

16.8.2 Bioreactors

A number of bioreactor configurations and processing conditions have been applied to the culture of insect cells including both airlift and agitated–sparged (stirred-tank) bioreactors. Stirred-tank bioreactors typically consist of glass, carbonate, or stainless steel vessels containing a marine or paddle impeller driven by an overhead motor. Temperature, oxygen, and pH can be controlled. Temperature control can be maintained by immersion in a water jacket, using circulating cooling and heating coils, or by enclosure in a controlled incubator. Stirred-tank bioreactors typically require the injection of air or oxygen into the bioreactor at a position below the impeller.

TABLE 16.1. Genes Utilized to Increase the Insecticidal Effects of Recombinant Baculoviruses

Name of gene	Effect(s) of expressed gene on host insect	Percentage increase in insect killing
Diuretic hormone	Reduction of hemolymph volume	20
Juvenile hormone esterase	Feeding cessation and blackening	—
Bacillus thuringiensis toxin	Feeding cessation	$(2 \times LD_{50})^a$
Scorpion toxin (AaIT)	Paralysis, body tremors, and dorsal arching	30–40
Mite toxin (Txp-1)	Paralysis	30–40
Wasp toxin (antigen 5)	Premature melanization and low weight gain	—
AcNPV deletion mutant lacking ecdysteroid UDP-glucosyltransferase gene (egt)	Reduces larval feeding times	20% reduction in $ST_{50}{}^b$

[a] LD_{50}, the dose necessary to kill 50% of the larval population.
[b] ST_{50}, the time necessary to kill 50% of the larval population.

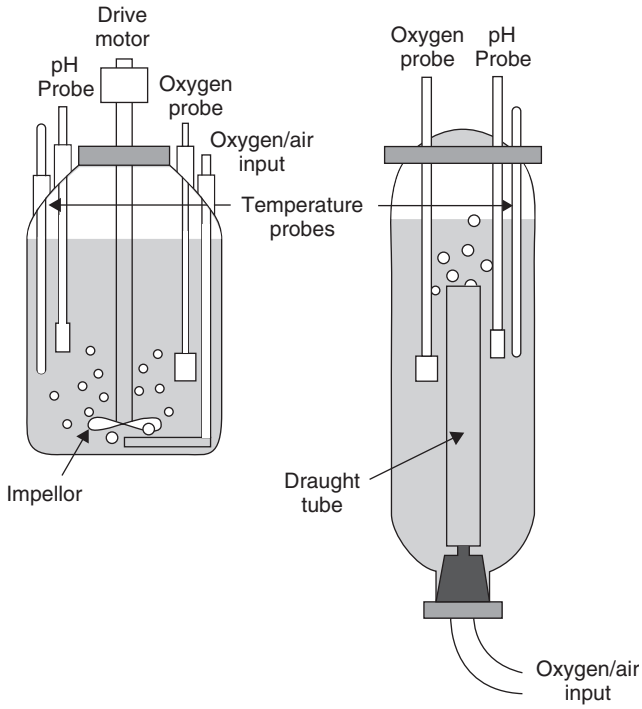


Figure 16.7. Configuration of stirred-tank and airlift reactors.

Air can also be supplied to the headspace in order to limit the amount of oxygen sparged directly into the bioreactor. An alternative to the stirred-tank bioreactor is the airlift bioreactor in which liquid circulation through the bioreactor is driven by the lifting force created by injection of air or oxygen through the bottom of the bioreactor (Fig. 16.7). This bioreactor includes an inner draft tube that carries the air/oxygen and liquid medium up through the bioreactor to the surface of the medium in order to set up circular flow of the medium within the bioreactor.

A side-by-side comparison of a 6-L airlift vessel and an 8-L stirred-tank vessel (5.5-L working volume) containing Sf-9 cells in serum-free medium showed similar growth rates, cell viabilities, and cell densities throughout the cell growth period (57). The stirred-tank fermentation system can be implemented without a commercial vendor, if necessary, by purchasing a large motor and vessel, whereas an airlift system is usually purchased as a single unit from a commercial source.

A number of other bioreactor configurations have also been considered. The NASA designed rotating-wall vessel, which limits shear effects, has been used to culture both Sf-9 and High Five for the production of recombinant proteins and found to be superior to shake flask cultures (58,59). Wave bioreactors have also been used up to the 40-L scale with production yields of rAAV particles equivalent to those obtained in stirred-tank bioreactors (60). Hollow fiber configurations have also been applied for the high density cultivation of *Drosophila* S2 cells for several months allowing the production of multimilligram amounts of recombinant protein with minimal culture maintenance (61).

Clumping of attachment-dependent cell lines in suspension, such as with High Five, is common, so bioreactor configurations that allow attachment-dependent cell growth and infection have also been developed (3,62). These attached cell lines are typically grown in roller bottles or on supporting particles such as glass beads or microcarriers. The supporting particles are then incorporated into immobilized perfusion or airlift bioreactor configurations. In addition, bioreactors in which oxygen is supplied through membrane tubing have been utilized, although not extensively for large-scale cell culture (63).

16.8.3 Process Monitoring Techniques

Cell growth and infection in insect cell bioreactors are usually monitored by following total and viable cell numbers by means of trypan blue staining and counting with a hemacytometer. Cell viability typically drops after several days after baculovirus infection of an insect cell culture. Given the labor-intensive and invasive nature of this assay, other

techniques have been considered for monitoring cell growth and infection, both off-line and on-line (63). Coulter™ particle counters and optical density (OD) measurements taken using a fiber optic probe can speed the cell counting process considerably during the cell growth period. Alternatively, growth can be monitored online through indirect measurements of cellular respiration such as oxygen uptake rate (OUR) using dissolved oxygen probes or carbon dioxide evolution rates (CERs) using infrared detectors (64). Near infrared (NIR) absorption spectroscopy can also be applied as a means to monitor the glucose and glutamine concentrations in bioreactors using noninvasive methods (65).

Monitoring the infection process is much more challenging, although, several techniques are used to supplement trypan blue staining. OUR can track the infection process because an increase in oxygen consumption occurs during the initial stages of the baculovirus infection (66). The CER is also observed to increase up to 24 h postinfection followed by a decline as the virus is released. Relative permittivity (ε), has been also used as an on-line monitor of the different phases of infection in which a plateau is observed between 18 and 24 h postinfection and a peak detected at 48 h postinfection corresponding to active cell lysis (67).

Other tools that have been used to monitor the infection process include epifluorescence microscopy of live and dead cells using fluorescence stains as well as flow cytometry, in which the side scatter parameter can be used to differentiate between infected and noninfected cells (68). The amount of recombinant protein generated during baculovirus infections can be followed by tracking the levels of a secondary protein such as green fluorescent protein (GFP) coexpressed along with the target protein of interest either in bioreactors or in larvae (69–71). The use of a GFP marker will assist in monitoring and optimizing infection conditions and identifying optimal harvesting time for the target protein.

16.8.4 Oxygen Supply

One of the critical nutrients that must be supplied to an insect cell culture during the growth and infection stages is oxygen. Oxygen consumption rates per cell range from 10^{-17} to 10^{-18} mol/cell-s and can increase up to 40% or more during the initial stages of infection (72). Absence of sufficient aeration and oxygen supply during the infection stage can inhibit the viral infection and lower recombinant protein yields several fold (73). Consequently, it is important to monitor the dissolved oxygen level in large-scale insect cell bioreactors using commercially available probes. Some researchers have suggested that dissolved oxygen tension (DOT) be maintained at about 50% saturation to reduce the oxygen sparging that is potentially lethal to insect cells (74). Aeration rates greater than 0.04 vol/vol-min can be inhibitory to cell growth (75). The production of VLPs during the infection stage was reported to be optimal when the oxygen concentration was maintained at 25% saturation with significant declines in productivity observed when dissolved oxygen decreased to 10% or increased above 50% (75).

16.8.5 Cell Damage during Sparging

Oxygen supply to the bioreactors is typically provided through sparging of oxygen or air into the bottom of a stirred-tank or airlift bioreactor. The oxygen is transferred from the gas to the liquid as the bubbles rise up the bioreactor. In order to provide sufficient mass transfer area, the air is bubbled through small openings. Impeller rotation can enhance bubble breakup further to increase the surface area available for mass transfer. The resulting bubble size is typically 1–5 mm in diameter, and the Reynolds number of a rising bubble can vary from 100 to 1000 in conventional bioreactors (76). It is now known that the sparging of oxygen or air can cause significant damage to insect cells as well as mammalian cells in suspension (77–79). This cell damage is principally because of the adhesion of cells to bursting gas bubbles at the gas–liquid interface. In contrast, agitation is likely to be less of a factor in causing cell damage in many sparged bioreactor environments. Suspended cells can often tolerate high agitation rates as long as the gas–liquid interface is removed (80,81). Cell damage from agitation may occur in some cases because of the formation of Kolmogorov eddies on a length scale comparable to the size of a cell (80,81).

High speed video microscopy studies have been used to observe directly cell–bubble interactions during the bubble rise through an insect cell culture medium (78,79). Cells attach independently or in clumps to a rising bubble and are carried upward through the fluid (Fig. 16.8). These cells then accumulate in high concentrations in the foam layer at the surface of the medium. The rupture of bubbles at the gas–liquid interface leads to the formation of upward and downward liquid jets that generate large shear stresses sufficient to damage or kill insect cells attached to the bubbles. The cell concentration in the jets is higher than in the medium, and more than 75% of these cells are killed by bubble rupture and jet formation. Approximately, 1,200 Sf-9 cells can be killed per bubble rupture (76).

Much of the cell damage because of bubble rupture can be prevented by the addition of surfactant polymers such as Pluronic F-68 at concentrations in the range of 0.1–0.2% (78,82–84). The addition of Pluronic F-68 prevents the adhesion of cells to bubbles and eliminates the damage to cells caused by bubble breakup at the liquid surface. The polymeric surfactants may prevent cell adherence to bubbles by lowering the interfacial tension at the

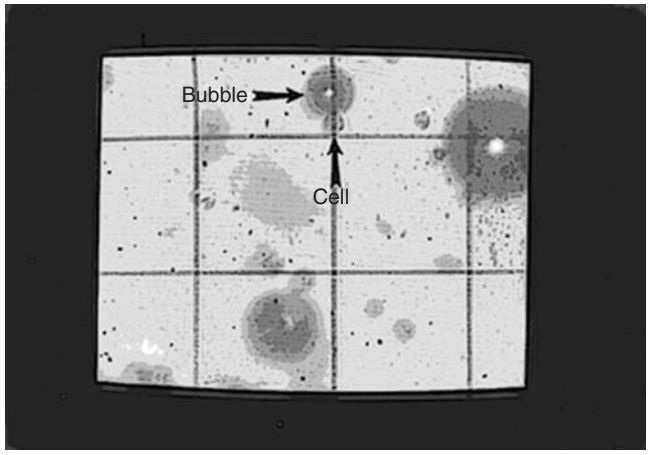


Figure 16.8. Insect cell attachment to bubbles rising through culture medium. Grid spacing is 100 μm. Photograph courtesy of J. Chalmers.

gas–liquid interface. Most commercial serum-free cell culture media for insect and mammalian cells include Pluronic F-68, although, other surfactants such as methylcellulose, serum, carboxymethylcellulose, bovine serum albumin, and dextrans have been considered as well. Unfortunately, only a limited selection of surfactants can be used because the interaction of the surfactants with the cells may affect membrane permeability and cause cell lysis (76).

16.8.6 Media Formulation

Media formulations are derived from elements originally identified in the insect hemolymph and include salts, vitamins, amino acids, sugars, organic acids, and trace elements (85,86). A number of proprietary commercial serum-free media are available for insect cell growth, including HyClone SFX-Insect™, Express Five®, Drosophila-SFM, and Sf-900 III™ from Invitrogen, and EX-CELL® 405 and 420 from Sigma-Aldrich. These media are derivations of noncommercial media such as Grace's, TNM-FH, TC-100, and IPL-41 that were supplemented with 5–20% fetal calf serum and used for many years in the cultivation of insect cells. The serum-free media are supplemented with lipids (cholesterol, α-tocopherol acetate, cod liver oil fatty acid methyl esters, β-sitosterol, and stigmasterol), yeast extract (yeastolate), and Pluronic F-68 in addition to other proprietary alterations (87,88). Antibiotics such as penicillin G and streptomycin are often added to the medium during cell culture.

Media sugars, including glucose, maltose, and fructose, can be partially or completely consumed during insect cell growth and recombinant protein production. Also, a significant fraction of the amino acids, including glutamine, glutamate, serine, asparagine, threonine, aspartate, and arginine, can be consumed during insect cell growth. However, much of this consumption may be devoted to energy use by the cells rather than the production of biomass (86,87).

Because the level of amino acids present in IPL-41 medium is sometimes in excess of that required for biomass production, media alterations that reduce these amino acid levels may lead to more efficient nutrient utilization (88). Furthermore, the amino acids utilized may vary depending on the cell line with some cell lines utilizing more glutamine and other consuming more asparagine (89). Supplementary components such as yeastolate or Primatone RL were observed to improve cell growth and the length of the stationary phases (90). A more detailed characterization of the yeast extract components critical to cell growth may eventually result in the development of a truly defined medium for insect cell culture (85,88). The consumption rates of these nutrient components may change following baculovirus infection (74).

16.8.7 Cell Culture By-Products

A significant amount of carbon dioxide is exhausted because of nutrient oxidation. Metabolites including lactate and other organic acids (pyruvate, α-ketoglutarate, fumarate) can also accumulate during growth and infection. The production of lactate from Sf-9 cells is generally lower than that observed with mammalian cells and poses no significant inhibitory effect on growth, although, lactate levels can increase significantly following dissolved oxygen (DO) limitations (91). The metabolites secreted and nutrients consumed in cell culture may change significantly depending on the cell line and even the specific medium considered.

For example, much higher levels of lactate and/or ammonia are generated by *T. ni* and *B. mori* cells when compared to Sf-9 cells (74,89,92). Likewise the glucose utilization rates and lactate and alanine production rates were found to vary significantly depending on particular commercial medium used for High Five cells (89). Different cell lines will also utilize the cellular energetic pathways in different ratios. Sf-9 cells channel slightly more glucose into the tricarboxylic acid (TCA) cycle than High Five cells (2.7% vs 0.6%) but the High Five cells direct nearly five times more glutamine into the TCA cycle than Sf-9, perhaps explaining the accumulation of higher ammonia and lactate in the High Five cells. In both cell lines, approximately 15% of the remaining glucose is directed to the pentose phosphate (PP) pathway with the bulk of the glucose (83% in both cell lines) metabolized into by-products including lactate, alanine, and others (93). Metabolic engineering can be used to alter the ratios of a substrate devoted to these different energetic pathways (93).

Most insect-culture media are not buffered with carbon dioxide, so there is no need for a CO_2 environment for growth. The optimal pH for growth of most insect cells is

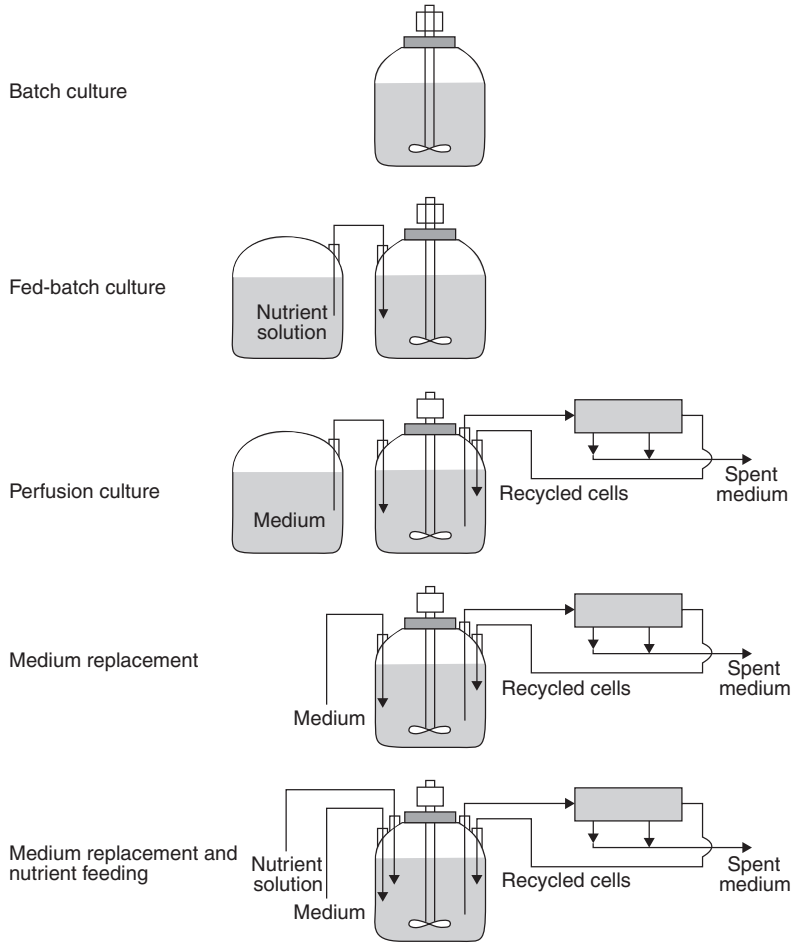


Figure 16.9. Various reactor configurations for batch and fed-batch production strategies.

between 6.2 and 6.3, though the pH of Sf-9 cultures in an uncontrolled medium can reach a minimum value between 5.9 and 6 (63). Because pH variations in the medium will affect both the growth and infection stages (94), pH control is suggested for optimal productivity in large-scale cell cultures. Osmolarity is another variable that should be considered, although, varying the osmolarity from 350 to 385 mOsm/kg did not alter the insect cell growth rate more than 10% (95). Most media osmolarities range from 320 to 375 mOsm/kg.

16.8.8 Batch Production Techniques

Recombinant baculovirus and heterologous proteins have been produced using batch, fed-batch, and continuous production modes. Typical processing of insect cells involves the batch cultivation of cells in a small suspension vessel, followed by a gradual scale-up of the cultures into progressively larger bioreactors. The cells are grown to a maximum cell density in one vessel and then pumped through steam-sterilized lines to increasingly larger vessels containing fresh medium. The optimal growth temperature is usually between 27 and 29°C, with cell doubling times between 17 and 24 h, depending on the cell line and medium utilized. High Five cells typically have a shorter doubling time (13–17 h) than Sf-9 cells (20–24 h) (92). In the final production-scale vessel, the cells are infected with virus during the exponential growth phase, and the virus or recombinant protein is collected at the conclusion of the infection stage (typically, between 48 and 100 h postinfection).

16.8.9 Fed-Batch, Perfusion, and Semibatch/Semicontinuous Production

It is desirable to grow the cells to a high cell density to maximize the productive capacity of the bioreactor. Supplementation of glucose, amino acids, yeastolate, lipids, or a concentrate of multiple nutrients can be used to increase the maximum cell density up to 5×10^7 cells/mL and enhance recombinant productivity (96). These nutrients can be added continuously in a fed-batch mode or added as one or multiple pulse feeds over the growth and infection

stages (97) (Fig. 16.9). As an alternative, fresh medium can be fed continuously in a perfusion mode to replace the spent medium exiting through a hollow fiber or other device (0.4–0.6 vol/day) to provide cell densities up to 3×10^7 cells/mL of bioreactor volume (98). Another approach that has been used to increase cell density is the replacement of 80% of the medium for several consecutive days near the end of the growth stage. Using the same hollow fiber technology (0.2 μm pore size), most of the spent media is removed, and then fresh medium is added to the bioreactor. Similar nutrient supplementation strategies are used to enhance the yields of recombinant proteins during the infection stage because the recombinant product yield is highly dependent on the nutrient levels. One approach that is used to ensure high product yields is to resuspend the cells in fresh medium prior to the infection, or else to add fresh medium to the bioreactor at the beginning and/or during the infection stage (73). Supplementation of limiting nutrients such as glucose, glutamine, and yeastolate can also be used to enhance the infection process (4,99–101), eliminating the costly replacement of the entire medium. Another feeding alternative during the infection stage is to perfuse the bioreactor with fresh medium which will generate a larger volume of spent medium compared with nutrient supplementation but ensure high recombinant protein yields throughout the infection phase (102).

A semibatch operating strategy used for production of recombinant baculoviruses and heterologous proteins can also utilize separate growth and infection reactors (Fig. 16.10) (103). An initial cell growth reactor is followed by single or multiple sequential infection vessels in series. After each cycle, the contents from one infection vessel are pumped to a following infection vessel, while the contents of the final infection vessel are harvested for product. The first infection vessel is then filled with medium and cells from the growth reactor and inoculated with virus. The cell growth reactor is provided with fresh medium, and the growth cycle repeated. Some of the cells from the growth stage may remain in the reactor to serve as an inoculum for the next growth cycle (104,105), and a portion of the contents of the first infection reactor can be left to infect a new batch of cells. However, modeling studies have indicated that the productivity of this sequential system may decline after a number of cycles because of the buildup of mutant viruses known as *defective interfering particles* (DIPs) (see later section) (106). The formation of these mutants is because of the "passage" effect. The recombinant protein productivity of the second and subsequent infection stages must be monitored closely for the buildup of these particles, and the second infection stage must be completely emptied and inoculated with a fresh sample of virus in order to eliminate the DIPs. Semicontinuous operation has been achieved by maintaining a first-growth reactor in a

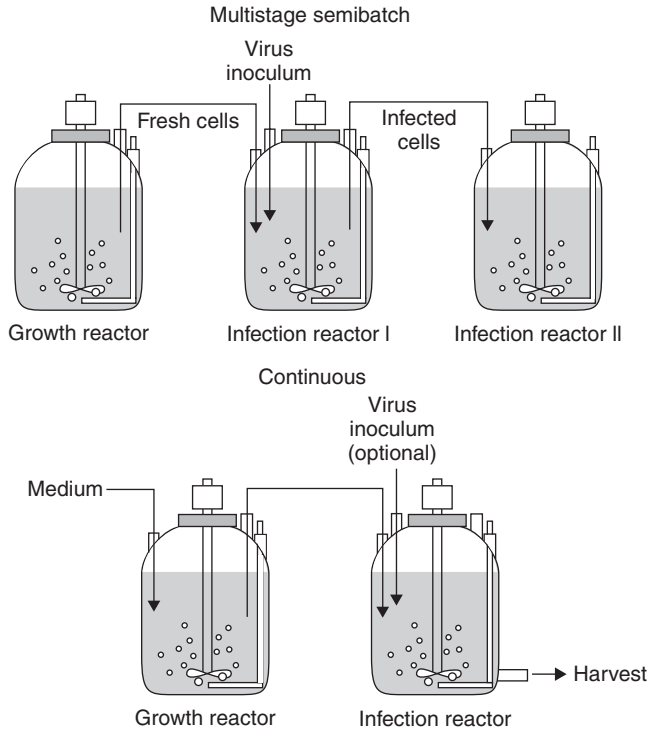


Figure 16.10. Multistage reactor systems. Multistage reactor systems used for the semibatch, semicontinuous, and continuous production of recombinant proteins in insect cell culture using AcMNPV. The initial reactor is primarily used for cell growth, whereas subsequent reactors contain the insect cells infected with the virus.

continuous operating mode and then gradually filling a second reactor (107). Following the filling of the second reactor, virus is added to initiate a batch infection in the second stage. At the end of the infection process, the second stage is emptied in part or completely, and the filling and infection cycle repeated. The medium in the infection reactors may also be supplemented or replaced by separating the cells from spent medium by settling, membrane filtration, or ultracentrifugation. Since the nutrients are often not consumed completely in the infection stage(s), it may not be necessary to replace all the spent media. These semibatch/semicontinuous processes can be achieved with processing times dictated by the exhaustion of nutrients, decline of cell viability, and accumulation of recombinant proteins.

16.8.10 Continuous Production Systems

The release of BV from infected insect cells into the cell culture medium has led to the design and evaluation of continuous-flow stirred-tank reactors for the production of polyhedra and recombinant proteins. The utilization of a continuous system could reduce production costs by 50% when compared with a batch system (108). Batch

systems have the disadvantage of long downtimes as a result of cleaning and sterilization after each run. Continuous systems typically consist of sequential two-stage continuous-flow bioreactors in which the first stage is used for cell growth and the second stage is used for virus production and heterologous gene expression (Fig. 16.10). The effluent of cells from the first stage feeds the second infection stage, and the effluent of the second stage includes the infected cells and associated baculoviruses and/or recombinant product. The BV generated in the second stage are used to infect the feed from the first reactor. In one study (109), a 60 h mean residence time was maintained in each stage, and production of polyhedra and recombinant protein was sustained for approximately, 4 weeks. Because about 200 BVs are produced per cell, there is a gradual accumulation of virus in the second reactor, followed by a severe decline in productivity after 4 weeks because of the formation of DIPs. A model that considers the presence of infectious virus (I-BV), defective virus (DIP), and abortive virus (A-BV) effectively predicted the accumulation of DIPs and the decline of recombinant protein production for a two-stage continuous-infection process (106).

Thus, a continuous reactor system may be problematic for extended production of baculovirus and recombinant protein. However, such a setup may be used for production over shorter periods such as a 30-day cycle prior to the accumulation of DIPs (106). This reactor setup would be analogous to a continuous catalytic reactor that experiences gradual catalyst deactivation during its operation and has to be periodically recharged with new catalyst. This could be accomplished by a complete shut down and restart with fresh virus or else by providing a secondary feed of fresh virus to the second infection reactor. A continuous setup provides for larger processing volumes of insect cell culture and recombinant product than does batch operation, although, the yield of recombinant protein in the effluent may be low compared with batch or fed-batch operation. Another innovation in the continuous culture process has been the sequential combination of a continuous stirred-tank reactor (CSTR) for growth, followed by a tubular reactor for infection. The tubular reactor provides for the continuous introduction of baculovirus at higher multiplicity of infection (MOI) without the negative passage effects present in a two-stage CSTR system (110).

16.8.11 Virus Stocks, Multiplicity of Infection, and Time of Infection

To initiate the infection, an aliquot of virus is added to the cell culture broth. Virus stocks are made from a single viral isolate obtained by plaque assay or end-point dilution. The plaque assay involves the infection of a monolayer of cells with a low concentration of virus, followed by an overlay of agarose-containing medium. Eventually, an isolated region of infected cells, called a *plaque*, is identified, and an agarose plug is collected at this plaque location for generating viral stocks. With the end-point dilution method, the tissue culture medium is diluted to the point at which any infection must result from a single infectious virus. Large stocks of the virus are obtained by infecting a monolayer or suspension cell culture with the agarose plug (from a plaque) or tissue culture medium (from the end-point dilution). The cell culture medium is then collected after 4–5 days, however, it may be necessary to repeat the infection several times in order to generate a viral stock of sufficient titer. The viral titer can determined by several methods, such as, plaque assay method, end-point dilution method, anti-gp64 antibody method or by using flow cytometry.

The viral titer obtained by determining the number of plaque-forming units (PFUs) per milliliter, using the plaque assay, or by finding the 50% tissue culture–infectious dose ($TCID_{50}$) per milliliter using end-point dilution are more commonly used as they selectively provide the concentration of the infectious baculovirus particles. The $TCID_{50}$ dose per milliliter is then multiplied by 0.69 to determine the number of plaque-forming units per milliliter. Staining of baculovirus with a highly fluorescent nucleic acid specific dye such as SYBR Green I combined with flow cytometry can be used as a rapid method to estimate viral titers in as little as 2 h, and the technique may also ascertain baculovirus aggregation in stored viral stocks (111,112). Several master viral stocks are frozen at $-70^{\circ}C$ for long-term storage, with one master stock kept at $4^{\circ}C$ in order to generate working viral stocks. Cells are then infected at a desired MOI, which represents the number of plaque-forming units per viable cell, from the working viral stock. In small shaker-flask cultures, cells are typically infected at an MOI greater than three during the mid to late exponential phase of growth in order to generate a synchronous infection. The Poisson distribution predicts that approximately 9.5, 63.2, and 99.995% of the cells will be infected at MOI of 0.1, 1, and 10 respectively. Infecting the cells at the highest possible cell density and cell viability while still in the exponential growth phase provides high volumetric productivities. However, an efficient infection is also dependent on the presence of adequate nutrient levels in the medium. If the cells are infected at a point near the end of the exponential phase or during the stationary phase, insufficient substrates may be available for the viral infection, and low recombinant product yields will result (73).

In larger bioreactors, infection at a high MOI (>1) may not be feasible or desirable because of the requirements for large amounts of virus stock. If cells are infected at a lower MOI, then the infection of the cells will not be synchronous, and some insect cell growth will occur prior to secondary infection by BV generated during the initial infection (95). If the MOI is too low or cell density too

high, the cells will grow to the late exponential or stationary phase prior to complete infection, and product yields will be lower. Consequently, it is important to optimize both the time of infection (TOI) and MOI to ensure that all cells are infected by virus and that sufficient substrates remain for virus and/or protein production (113). This optimization is facilitated by the use of mathematical models that consider both cell growth and viral infection stages as well as substrate consumption, recombinant protein production, and cell death (114–116), These models are often probabilistic in nature and consider the infection of cells as a Poisson distribution or a stochastic event in which the MOI or another variable is varied in order to maximize production of heterologous proteins (114,117,118). According to some models, high protein yields can be achieved even using very low MOIs although this approach may be difficult to implement in practice because of inaccuracies in viral titers and other parameters (113). Furthermore, infections at low MOI and low cell density may be effective for cell lines such as Sf-9, but the approach may not be as successful for cell lines such as TN-5-B1-4, which produce much lower levels of EV.

16.8.12 Passage Effects and Mutant Virus Formation

The continuous passage of viruses in cell culture often leads to the formation of mutant viruses such as DIPs (119,120). The DIPs will replicate more rapidly than the normal-size viruses, and the concentration of DIPs can rise to as high as 60% of the total virus stock (119,120). These DIPs average about 200–230 nm in size, as compared with the standard 330 nm sized virions (120), and can lack up to 40% of the baculovirus genome because of spontaneous deletions during passaging (119). The deleted segment often includes the polyhedrin gene and at least one other gene necessary for virus replication. Consequently, DIP mutants cannot be plaque purified because they replicate only in cells that are also infected by a normal virus. To avoid the passage effect, viral passage number should be monitored, and a low passage master viral titer stock used to generate working viral titer stocks since DIP mutants can accumulate within two passages of the original viral isolation (121). If contamination with DIPs is suspected, then a plaque assay can be performed to reisolate the infectious virus. Also, low MOI infections can be used to minimize DIP formation, but this approach results in asynchronous infections. Alternatively, baculovirus homologous repeat regions (hours) may be inserted to increase the stability of baculoviral vectors since deletions in the virus are observed to correlate with a low density of hours (122).

Other mutant viruses, such as ones that result in the generation of a few polyhedra (FP), have also been observed. The FP mutants substantially lower the number of polyhedra produced per infected cell and reduce the number of occluded viruses generated (123). These FP mutants may have a selective advantage in cell culture by producing more BV at the expense of polyhedra. Unlike DIPs, FP mutants can be plaque purified. Once again, formation of FP mutants can be minimized by working with low passage viral titers and utilizing a master viral titer stock. Because FP mutants do not include significant virus levels in the polyhedra, insect-to-insect transmission will not include FP mutants, which are not capable of spreading through polyhedra infections.

16.8.13 Larval Production Systems

On the basis of productivity comparisons with polyhedra, approximately, 100–200 larvae will provide a final protein yield approximately equal to 1 L of cells for an intracellular recombinant protein (7). The use of larvae eliminates the need for high capital investments in large-scale bioreactors, but requires the development of systems for insect rearing and infection. Furthermore, purification strategies must be implemented to isolate the proteins from insect parts or hemolymph. Typical species considered include *S. frugiperda*, *T. ni*, *Heliothis virescens*, *Manduca sexta*, and *Hyalaphora cecropia* for AcMNPV infections, and *B*. for BmNPV infections (7,56). Lepidopteran eggs are available from commercial suppliers and hatch 5 days to 1 week after incubation at 25–27°C in a humidified environment under a controlled light cycle. Artificial diets are also available from commercial sources or may be prepared from components in the laboratory. Constituents typically include pinto beans, Brewer's yeast, ascorbic acid, wheat germ, sorbic acid, 14% auromycin, and a vitamin mix. The ingredients are combined with agar and then provided to larvae with periodic replacement to ensure a moist supply of nutrients. It is important to infect the insects at the appropriate developmental stage to provide the maximum yield of baculovirus or heterologous protein. The insects typically molt five or six times as larvae with the last stage being the larval–pupal molt. The intermolt period is the stadium or instar. Optimal infections are typically achieved 1 or 2 days after molting into the last larval instar. Infections are accomplished by feeding the insects with PIBs or by injecting BV directly into the hemolymph. For recombinant baculoviruses that are occlusion negative, injection of the BV is the required method of infection. A small number of mock-infected insects should also be maintained to check for possible contamination problems and to provide a comparison of infected and uninfected larvae. The expression of fluorescent proteins such as GFP in larvae can be used in order to identify optimal infection and harvesting conditions (69,124). Shown in Fig. 16.11a is a photograph of an infected *T. ni* larva expressing GFP as compared with an uninfected larva (69). Fig. 16.11b shows massive

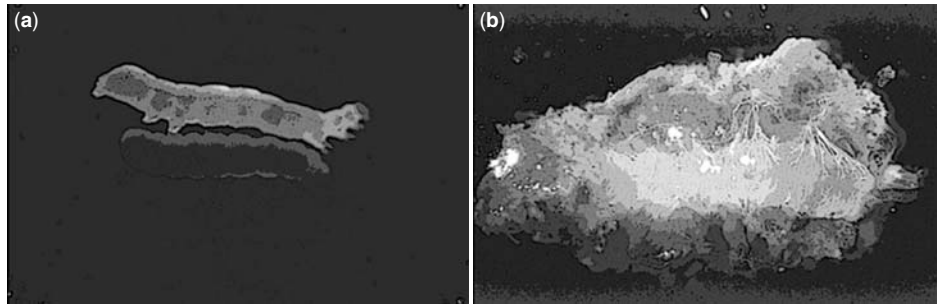


Figure 16.11. (a) Photo of *T. ni* larvae sitting on top of a laboratory UV transilluminator table. The upper larva has been infected (72 h) with a recombinant AcMNPV baculovirus that contains the gene for green fluorescent protein (GFPuv) placed under control of the polyhedrin promoter. The brightness is because of the massive overexpression of GFPuv, which has been shown to reach 26% of the total larvae protein. The lower larva (nonglowing) is the uninfected control. Photograph courtesy of W. Bentley. (b) Micrograph showing AcMNPV-β-galactosidase infection of *T. ni* insect larva at 60 h postinfection. Staining represents β-galactosidase expressed in insect cell tissues. Infection has cleared the midgut and spread to the fat body. Micrograph courtesy of G. Williams.

expression of β-galactosidase in a *T. ni* larva when infected with AcMNPV containing the heterologous *lacZ* gene under the control of the p10 promoter. At 60 h postinfection, the infection has cleared the midgut and entered the fat body. The best time to collect product from infected insects is generally prior to death. For secreted proteins, the product is collected by bleeding the insects to collect hemolymph, whereas nonsecreted proteins are isolated by homogenization of whole insects. Unfortunately, homogenization can result in the release of proteases; these can be minimized by the removal of the insect gut before processing (7,56). Alternatively, a particular metabolically active tissue such as the fat body can be removed from the insect and used as a source of the desired protein (7,56). The number of recombinant proteins expressed in larvae continues to grow because of the low cost and convenience of this method. Furthermore, production has recently been automated and is linearly scaleable with the rearing of more insect larvae giving more recombinant protein (125). Examples of secreted proteins produced and purified from larvae include monoclonal antibody Fab fragments and human granulocyte-macrophage colony-stimulating factor with yields up to 1.1 g/kg larvae (125,126).

16.9 CONCLUSION

The use of the baculovirus–insect cell system for heterologous gene expression and recombinant biopesticides has grown dramatically since its first application in 1983. Commercially available vectors that provide for the rapid selection and screening of recombinant viruses have made this technology accessible in most biotechnological laboratories. The development of serum-free media, the isolation of alternative insect cell lines, and the implementation of efficient bioreactor operating strategies have increased productivities and lowered costs. As a result, insect cells are often the method of choice for rapid and high level production of functional eukaryotic proteins. The use of BEVS is likely to increase even more with the growth of genomics and its associated need for functional characterization of unknown proteins. The use of insect cell-derived proteins as vaccines and pharmaceuticals is now beginning to emerge as another important application of BEVS as a number of clinical approvals are in progress. The future growth of the insect cell culture systems will also be assisted by the modification of posttranslational processing including glycosylation using metabolic engineering approaches. Other promising areas include the use of insect larvae and the development of stable expression systems for *T. ni*, *B. mori*, Sf-9, and *Drosophila* S2 cells (127). With these advances, insects and insect cells are likely to remain a popular choice for the manufacture of recombinant DNA products.

Acknowledgments

The authors are grateful to Greg Williams, Jeffrey Chalmers, and William Bentley for graciously providing photographs for this review.

REFERENCES

1. Lynn DE. J Tissue Cult Methods 1989; 12: 23–29.
2. Davis TR, *et al*. In Vitro Cell Dev Biol 1993; 29A: 388–390.
3. Taticek RA, Hammer DA, Shuler ML. In: Shuler ML, Wood HA, Granados RR, Hammer DA, editors. Baculovirus expression systems and biopesticides. New York: Wiley–Liss; 1995. pp. 131–174.

4. Murhammer DW. Appl Biochem Biotechnol 1996; 59: 199–220.
5. Betenbaugh MJ, Balog L, Lee P-S. Biotechnol Prog 1991; 7: 462–467.
6. Hink WF, Thomsen DR, Davidson DJ, Meyer AL, Castellino FJ. Biotechnol Prog 1991; 7: 9–14.
7. O'Reilly DR, Miller LK, Luckow VA. Baculovirus expression vectors: a laboratory manual. New York: W.H. Freeman and Company; 1992.
8. Shuler ML, Hammer DA, Granados RR, Wood HA. In: Shuler ML, Wood HA, Granados RR, Hammer DA, editors. Baculovirus expression systems and biopesticides. New York: Wiley-Liss; 1995. pp. 1–11.
9. Smith GE, Fraser MJ, Summers MD. J Virol 1983; 46: 584–593.
10. Smith GE, Summers MD, Fraser MJ. Mol Cell Biol 1983; 3: 2156–2165.
11. Vlak JM, Schouten A, Usmany M, Belsham GJ, Klinge-Roode EC, Maule AJ, Van Lent JWM, Zuidema D. Virology 1990; 179: 312–320.
12. Luckow VA, Summers MD. Biotechnology 1988; 6: 47–55.
13. Patterson RM, Selkirk JK, Merreck AB. Environ Health Perspect 1995; 103: 756–759.
14. Farrell PJ, Lu M, Prevost J, Brown C, Behie L, Iatrou K. Biotechnol Bioeng 1998; 60 (6): 656–663.
15. Summers MD, Smith GE. A manual of methods for baculovirus vectors and insect cell culture procedures, Texas Agricultural Experiment Station Bulletin No. 1555. College Station, TX: Texas Agricultural Experiment Station; 1987.
16. Maeda S, Kawai T, Obinata M, Fujiwara H, Horiuchi T, Saeki Y, Sato Y, Furusawa M. Nature 1985; 315: 592–594.
17. Choi O, Tomiya N, Kim JH, Slavicek JM, Betenbaugh MJ, Lee YC. Glycobiology 2003; 13 (7): 539–548.
18. Obregón-Barboza V, Del Rincón-Castro MC, Cabrera-Ponce JL, Ibarra JE. J Virol Methods 2007; 140 (1–2): 124–131.
19. Ayres MD, Howard SC, Kuzio J, Lopez-Feriber M, Possee RD. Virology 1994; 202: 586–605.
20. Pennock GD, Shoemaker C, Miller LK. Mol Cell Biol 1984; 4: 399–406.
21. Vialard J, Lalumiere M, Vernet T, Briedis D, Alkhatib G, Henning D, Levin D, Richardson C. J Virol 1990; 64: 37–50.
22. Kitts PA, Possee RD. Biotechniques 1993; 14: 810–817.
23. Luckow VA, Lee SC, Barry GF, Olins PO. J Virol 1993; 67: 4566–4579.
24. Jarvis DL, Finn EE. Nat Biotechnol 1996; 14: 1288–1292.
25. Kost TA, Condreay JP. Curr Drug Targets 2007; 8 (10): 1126–1131.
26. Marz L, Altmann F, Staudacher E, Kubelka V. In: Montreuil HSJ, Vliegenthart JFG, editors. Glycoproteins. Amsterdam, NL: Elsevier Science B.V.; 1995. pp. 543–563.
27. Altmann F. Trends Glycosci Glycotechnol 1996; 40: 101–114.
28. Hsu T-A, Takahashi N, Tsukamoto Y, Kato K, Shimada I, Masuda K, Whiteley EM, Fan J-Q, Lee YC, Betenbaugh MJ. J Biol Chem 1997; 272: 9062–9070.
29. Ailor E, Takahashi N, Tsukamoto Y, Masuda K, Rahman BA, Jarvis DL, Lee YC, Betenbaugh MJ. Glycobiology 2000; 10 (8): 837–847.
30. Altmann F, Schwihla H, Staudacher E, Gloosl J, Marz L. J Biol Chem 1995; 270: 17344–17349.
31. Léonard R, Rendic D, Rabouille C, Wilson IB, Préat T, Altmann F. J Biol Chem 2006; 281 (8): 4867–4875.
32. Tomiya N, Narang S, Park J, Abdul-Rahman B, Choi O, Singh S, Hiratake J, Sakata K, Betenbaugh MJ, Palter KB, Lee YC. J Biol Chem 2006; 281 (28): 19545–19560.
33. Jarvis DL, Finn EE. Virology 1995; 212: 500–511.
34. Ogonah OW, Freedman RB, Jenkins N, Patel K, Rooney BC. Biotechnology 1996; 14: 197–202.
35. Wagner R, Liedtke S, Kreztschmar E, Geyer H, Geyer R, Klenk H-D. Glycobiology 1996; 6: 165–175.
36. Davidson DJ, Fraser MJ, Castellino FJ. Biochemistry 1990; 29: 5584–5590.
37. Jarvis DL, Harrison RL. Adv Virus Res 2006; 68: 159–191.
38. Palomares LA, Joosten CE, Hughes PR, Granados RR, Shuler ML. Biotechnol Prog 2003; 19 (1): 185–192.
39. Joosten CE, Shuler ML. Biotechnol Prog 2003; 19 (3): 739–749.
40. Iacono-Connors LC, Schmaljohn CS, Dalrymple JM. Infect Immun 1990; 58: 366–372.
41. Tessier DC, Thomas DY, Khouri HE, Laliberte F, Vernet T. Gene 1991; 98: 177–183.
42. Ailor E, Pathmanathan J, Jongbloed JD, Betenbaugh MJ. Biochem Biophys Res Commun 1999; 255 (2): 444–450.
43. Betenbaugh MJ, Ailor E, Whiteley E, Hinderliter P, Hsu T-A. Cytotechnology 1996; 20: 149–159.
44. Ailor E, Betenbaugh MJ. Curr Opin Biotechnol 1999; 10 (2): 142–145.
45. Ikonomou L, Schneider YJ, Agathos SN. Appl Microbiol Biotechnol 2003; 62 (1): 1–20.
46. Gotoh T, *et al*. Appl Microbiol Biotechnol 2001; 56 (5–6): 742–749.
47. Hu YC, Bentley WE. Biotechnol Prog 1999; 15 (6): 1065–1071.
48. Hiyoshi M, *et al*. J Virol Methods 2007; 144 (1–2): 91–97.
49. Kim EJ, *et al*. Biotechnol Bioeng 2007; 98 (3): 645–654.
50. Kidd M, Emery VC. Appl Biochem Biotechnol 1993; 42: 137–159.
51. Clinical Trial: NCT00539864. 2008. Available at http://clinicaltrials.gov/ct2/show/NCT00539864.
52. Clinical Trial: NCT00754455. 2008. Available at http://clinicaltrials.gov/ct2/show/NCT00754455.
53. Clinical Trial: NCT00519389. 2008. Available at http://clinicaltrials.gov/ct2/show/NCT00519389.
54. Negrete A, Kotin RM. Methods Mol Biol 2008; 433: 79–96.
55. Maeda S. Curr Opin Biotechnol 1995; 6: 313–319.
56. Maeda S. Annu Rev Entomol 1989; 34: 351–372.
57. Rice JW, Rankl NB, Guranuss TM, Marr CM, Barna JB, Walters MM, Burns DJ. Biotechniques 1993; 15: 1052–1059.
58. Francis KM, O'Connor KC, Spaulding GF. In Vitro Cell Dev Biol Anim 1997; 33 (5): 332–336.
59. Saarinen MA, Murhammer DW. In Vitro Cell Dev Biol Anim 2000; 36 (6): 362–366.
60. Negrete A, Kotin RM. J Virol Methods 2007; 145 (2): 155–161.
61. Baxter SC, *et al*. Biotechnol Appl Biochem 2006; 45 (Pt 3): 167–172.

62. King GA, Kuzio J, Daugulis AJ, Faulkner P, Bayly D, Goosen MFA. Biotechnol Lett 1988; 10: 683–688.
63. Agathos SN. Cytotechnology 1996; 20: 173–189.
64. Kamen AA, *et al*. Biotechnol Bioeng 1996; 50 (1): 36–48.
65. Riley MR, *et al*. Biotechnol Bioeng 1997; 55 (1): 11–15.
66. Lecina M, *et al*. J Biotechnol 2006; 125 (3): 385–394.
67. Zeiser A, *et al*. Biotechnol Prog 2000; 16 (5): 803–808.
68. Nordstrom T, *et al*. Cytometry 1999; 37 (3): 238–242.
69. Cha HJ, Pham MQ, Rao G, Bentley WE. Biotechnol Bioeng 1997; 56: 239–247.
70. Cha HJ, Bentley WE. Methods Mol Biol 2007; 388: 407–418.
71. Philipps B, *et al*. Protein Expr Purif 2005; 42 (1): 211–218.
72. Kioukia N, *et al*. J Biotechnol 1995; 38 (3): 243–251.
73. Lindsay DA, Betenbaugh MJ. Biotechnol Bioeng 1992; 39: 614–618.
74. Wang MY, Pulliam TR, Valle M, Vakharia VN, Bentley WE. J Biotechnol 1996; 46: 243–254.
75. Cruz PE, *et al*. Biotechnol Bioeng 1998; 60 (4): 408–418.
76. Chalmers JJ. In: Shuler ML, Wood HA, Granados RR, Hammer DA, editors. Baculovirus expression systems and biopesticides. New York: Wiley-Liss; 1995. pp. 175–204.
77. Tramper J, Williams JB, Joustra D. Enzyme Microb Technol 1986; 8: 33–36.
78. Handa A, Emery AN, Spier RE. Dev Biol Stand 1987; 66: 241–253.
79. Bavarian F, Fan LS, Chalmers JJ. Biotechnol Prog 1991; 7: 140–150.
80. Oh SKW, Nienow AW, Al-Rubeai M, Emery AN. J Biotechnol 1989; 12: 45–62.
81. Kunas KT, Papoutsakis ET. Biotechnol Bioeng 1990; 36: 476–483.
82. Handa-Corrigan A, Emery AN, Spier RE. Enzyme Microb Technol 1989; 11: 230–235.
83. Murhammer DW, Goochee CF. Biotechnology 1988; 6: 1411–1418.
84. Murhammer DW. Appl Biochem Biotechnol 1991; 31: 283–310.
85. Fraser MJ. Curr Top Microbiol Immunol 1992; 158: 131–172.
86. Drews M, Paalme T, Vilu R. J Biotechnol 1995; 40: 187–198.
87. Ferrance JP, Goel A, Ataai MM. Biotechnol Bioeng 1993; 42: 697–707.
88. Bhatia R, Jesionowski G, Ferrance J, Ataai MM. Cytotechnology 1996; 20: 33–41.
89. Rhiel M, Mitchell-Logean CM, Murhammer DW. Biotechnol Bioeng 1997; 55 (6): 909–920.
90. Ikonomou L, *et al*. In Vitro Cell Dev Biol Anim 2001; 37 (9): 549–559.
91. Bentley WE, Wang M-Y, Vakharia V. Ann N Y Acad Sci 1994; 745: 336–359.
92. Sugiura T, Amman E. Biotechnol Bioeng 1996; 51: 494–499.
93. Benslimane C, *et al*. Biotechnol Prog 2005; 21 (1): 78–86.
94. Licari P, Bailey JE. Biotechnol Bioeng 1990; 37: 238–246.
95. Zhang J, Kalogerakis N, Behie LA, Iatrou K. J Biotechnol 1994a; 33: 249–258.
96. Elias CB, *et al*. Biotechnol Bioeng 2000; 68 (4): 381–388.
97. Chan LC, Greenfield PF, Reid S. Biotechnol Bioeng 1998; 59 (2): 178–188.
98. Jardin BA, *et al*. Biotechnol Bioeng 2007; 97 (2): 332–345.
99. Nguyen B, Jarnagin K, Williams S, Chan H, Barnett J. J Biotechnol 1993; 31: 205–217.
100. Reuveny S, Kim YJ, Kemp CW, Shiloach J. Biotechnol Bioeng 1993; 42: 235–239.
101. Wang M-Y, Kwong S, Bentley WE. Biotechnol Prog 1993; 9: 355–361.
102. Chico E, Jager V. Biotechnol Bioeng 2000; 70 (5): 574–586.
103. Hink WF, Strauss EM. In: Kurstak E, Maramorosch K, Dubendorfer A, editors. Invertebrate systems in vitro. Amsterdam: Elsevier/North-Holland Biomedical Press; 1980. pp. 27–33.
104. Zhang J, Kalogerakis N, Behie LA, Iatrou K. Biotechnol Bioeng 1993; 42: 357–366.
105. Zhang J, Kalogerakis N, Behie LA, Iatrou K. Biotechnol Prog 1994; 10: 636–643.
106. de Gooijer CD, Koken RHM, van Lier FLJ, Kool M, Vlak JM, Tramper JA. Biotechnol Bioeng 1992; 40: 537–548.
107. van Lier FLJ, van den Hombergh JPTW, de Gooijer CD, den Boer MM, Vlak JM, Tramper J. Enzyme Microb Technol 1996; 18: 460–466.
108. Tramper J, Vlak JM. Ann N Y Acad Sci 1986; 469: 279–288.
109. van Lier FLJ, van Duijnhoven GCF, de Vaan MMJCM, Vlak JM, Tramper J. Biotechnol Prog 1994; 10: 60–64.
110. Hu YC, Wang MY, Bentley WE. Cytotechnology 1997; 24: 143–152.
111. Jorio H, *et al*. J Virol Methods 2006; 134 (1–2): 8–14.
112. Shen CF, Meghrous J, Kamen A. J Virol Methods 2002; 105 (2): 321–330.
113. Wong KTK, Peter CH, Greenfield PF, Reid S, Nielsen LK. Biotechnol Bioeng 1995; 49: 659–666.
114. Hu Y-C, Bentley WE. Chem Eng Sci 2000; 55 (19): 3991–4008.
115. Licari P, Bailey JE. Biotechnol Bioeng 1992; 39: 432–441.
116. Power JF, Reid S, Radford KM, Greenfield PF, Nielson LK. Biotechnol Bioeng 1994; 44: 710–719.
117. Roldão A, Carrondo MJT, Alves PM, Oliveira R. Comput Chem Eng 2008; 32 (1–2): 68–77.
118. Enden G, Zhang YH, Merchuk JC. J Theor Biol 2005; 237 (3): 257–264.
119. Kool M, Voncken JW, van Lier FLJ, Tramper J, Vlak JM. Virology 1991; 183: 739–746.
120. Wickham TJ, Davis T, Granados RR, Hammer DA, Shuler ML, Wood HA. Biotechnol Lett 1991; 13: 483–488.
121. Pijlman GP, *et al*. Virology 2001; 283 (1): 132–138.
122. Pijlman GP, *et al*. Biotechnol Bioeng 2004; 87 (6): 743–753.
123. Fraser MJ, Smith GE, Summers MD. J Virol 1983; 47: 287–300.
124. Kramer SF, Kostov Y, Rao G, Bentley WE. Biotechnol Bioeng 2003; 83 (2): 241–247.
125. O'Connell KP, *et al*. Mol Biotechnol 2007; 36 (1): 44–51.
126. Chen J, Wu XF, Zhang YZ. J Biotechnol 2006; 123 (2): 236–247.
127. Culp JS, Johansen H, Hellmig B, Beck J, Matthews TJ, Delers A, Rosenburg M. Biotechnology 1991; 9:173–177.

17

KINETICS OF MICROBIAL GROWTH

NICOLAI S. PANIKOV
Northeastern University, Department of Biology, Boston, Massachusetts

17.1 INTRODUCTION

Kinetics (Greek $\kappa\iota\nu\varepsilon\tau\iota\kappa o\sigma$, forcing to move) is a branch of natural science that deals with *the rates and mechanisms* of any processes—physical, chemical or biological. Kinetic studies in microbiology cover all dynamic manifestations of microbial life: growth itself, survival and death, product formation, adaptations, mutations, cell cycles, environmental effects and biological interactions. Kinetics provides a theoretical framework for optimal design in biotechnologies based on fermentation and enzyme catalysis, as well as on employment of outdoor activity of natural microbial populations (wastewater treatment, soil bioremediation, etc.)

Contrary to simple rates measurements, kinetic studies require the perception of the underlying basic *mechanisms* of studied processes. We will define mechanistic studies as those that interpret some complex process as an interplay of several simpler reactions, for example, cell growth can be explained through activity of enzymes and microbial community dynamics can be interpreted—through behavior of individual cells and populations. Ideally, mechanistic studies infer the coupling of experimental measurements with analysis of simulating mathematical models. The models formalize postulated mechanisms, so that the comparison of observations and the model's predictions allows one to discard an incorrect hypotheses.

The quantitative studies in microbiology often involve the assessment of *growth stoichiometry*. Stoichiometry (Greek $\sigma\tau\omega\iota\kappa\eta\varepsilon\iota o\nu$, element) is the quantitative relationship between reactants and products in a chemical reaction. In microbiology, stoichiometry stands for a quantitative relationship between substrates and products of microbial processes, including biomass formation (the consequence of complying with mass and energy conservation laws). In practical terms, kinetic and stoichiometry are tightly linked to each other, but stoichiometry mainly addresses problems of a static nature (how much? in what proportion?), whereas kinetics considers the dynamics questions (at what rate? by which mechanism?).

17.2 GROWTH STOICHIOMETRY

17.2.1 Macrostoichiometry of Microbial Growth

By analogy to simple chemical reactions we can represent growth as a conversion of a number of substrates (medium components) into cell mass and products. Growth of aerobic heterotrophic microorganisms can be approximated by the following stoichiometric equation (1,2):

$$\underset{\text{substrates}}{\mathrm{CH_mO_l} + a_1\mathrm{NH_3} + a_2\mathrm{HPO_4}^{2-} + a_3\mathrm{K}^{+} + \ldots + b\mathrm{O_2}} = \underset{\text{biomass}}{Y\mathrm{CH_pO_nN_qP_oK_v}\ldots} + \underset{\text{products}}{a_4\mathrm{CO_2} + a_5\mathrm{H_2O}} \qquad (17.1)$$

Here, microbial biomass is empirically expressed by the gross formula $\mathrm{CH_pO_nN_qP_oK_v}\ldots$, for example, if

Upstream Industrial Biotechnology: Expression Systems and Process Development, Volume 1, First Edition. Edited by Michael C. Flickinger.
© 2013 John Wiley & Sons, Inc. Published 2013 by John Wiley & Sons, Inc.

TABLE 17.1. Selected Macrostoichiometric Equations Describing Growth of Microorganisms with Different Types of Energy Generation

Microbial Process	Substrates		Biomass		Products	Stoichiometric Parameters
Heterotrophic growth and product formation	$CH_mO_1 + a_1O_2 + a_2\ NH_3$	=	$YCH_pO_nN_q$	+	$Y_pCH_rO_sN_t + a_3CO_2 + a_4H_2O$	$a_1 = 0.5(Yn + Y's - l + a_4) + a_3$, $a_2 = Yq + Y't, a_3 = 1 - Y - Y'$, $a_4 = 0.5[m + Y(3q - p) + Y'(3t - r)]$
Phototrophic growth (algae or plant cells)	$CO_2 + a_1H_2O + a_2\ NH_3$	=	$YCH_pO_nN_q$	+	$a_3CH_rO_sN_t + a_4O_2$	$a_1 = 0.5[Y(p - 3n) + (r - 3t)(1 - Y)]$, $a_2 = Y(n - t) + t, a_3 = 1 - Y$, $a_4 = 0.5(2 + a_1 - Y_n - a_3s)$
Hydrogenotrophic methanogenesis	$CO_2 + a_1H_2 + a_2\ NH_3$	=	$YCH_pO_nN_q$	+	$a_3CH_4 + a_4H_2O$	$a_1 = 4 - 0.5Y(4 + 2n + 3q - p)$, $a_2 = Yq, a_3 = 1 - Y$, $a_4 = 2 - Yn$
Nitrification	$YCO_2 + a_1O_2 + a_2NH_4^+$	=	$YCH_pO_nN_q$	+	$a_3NO_3^- + a_4H^+ + a_5H_2O$	$a_1 = 2Y^{-1} - Y[1 + 0.25(p - 2n - 3q)]$, $a_2 = Y^{-1} + Yq, a_3 = Y^{-1}$, $a_4 = 2Y^{-1} + Yq, a_5 = Y^{-1} - 0.5Y(p - 3q)$

some average microbial cell contains per dry cell weight (%) C, 46; H, 7.5; O, 31; N, 11; and P, 1.3, then the biomass formula $CH_{1.9}O_{0.5}N_{0.2}P_{0.01}$. The stoichiometric quotients $a_1 - a_5 \ldots, b$ and Y (biomass yield) specify quantities of substrate and products of microbial growth. If we know biomass yield and gross formulas of all substrates and products, then quotients a_1-$a_6 \ldots$ are easily calculated from conservation conditions. There are at least two such conditions. First, the mass of each element (C, H, O, N, P, K, ...) on the left side of Equation 17.1 should be equal to that on the right side (mass balance). Second, if ionized substances are involved, we should take into account the balance of charges to satisfy the condition of electroneutrality. Table 17.1 demonstrates some examples of stoichiometric growth reactions relevant to biotechnology.

Described formalism is useful as a first step in biotechnological studies aimed at planning and optimizing microbial growth. It estimates how much nutrient should be supplied to the fermentor to obtain the required amount of biomass or target product. However, it should be absolutely clear that stoichiometric equations like Equation 17.1 are no more than an approximation to reality. The most severe deviation stems from the fact that unlike chemical reagents, microbial cells are characterized by changeable composition, and stoichiometric coefficients are not true constants. One task of contemporary microbial stoichiometry is to find out the functional relationships between stoichiometric parameters and internal (physiological) and external (environmental) factors.

17.2.2 Growth Yield: Catabolic and Conserved Substrates

The growth yield is one of the main stoichiometric parameters. It is defined as follows:

$$Y = -\frac{\delta x}{\delta s} \approx -\frac{\Delta x}{\Delta s} \tag{17.2}$$

where Δx is the increase in microbial biomass consequent on utilization of the amount Δs of substrate, and δx and δs are respective infinitely small increments. Rigorous definition of Y as derivative $\delta x/\delta s$ stems from the fact that Y can vary in time, the negative sign being introduced because of x and s vary in opposite senses. Sometimes, it is used as the reciprocal of $Y : \alpha = 1/Y$ which is called *the economic coefficient*. It expresses explicitly the nutrient requirements for growth: how many mass units of a particular substrate should be consumed to produce one unit mass of cell material.

The growth efficiency depends generally on the partitioning of consumed element between new cell biomass and extracellular products. The mass balance is as follows:

total element consumed		incorporated into cell	+	incorporated into extracellular products	
δE_s	=	δE_x	+	δE_p	(17.3)

There are two groups of substrates for microbial growth: (i) *catabolic substrates*, which are sources of energy; and (ii) *anabolic* or *conserved substrates*, which are sources of biogenic elements forming cellular material. Catabolic substrates include H_2 for lithotrophic hydrogen bacteria, NH_4^+ and NO_2^- for nitrifying bacteria, S^0 for sulfur-oxidizing bacteria, oxidizable or fermentable organic substances for heterotrophic bacteria and fungi, and so on. Their consumption is accompanied by oxidation and dissipation of chemical substances into extracellular waste products that are no longer reusable as an energy source ($H_2O, NO_3^-, SO_4^{2-}, CO_2$, etc.) The anabolic substrates after uptake are incorporated into *de novo* synthesized cell components, being conserved in biomass (that is why they are called conserved). Contrary to catabolic substrates, they can be reused (e.g. after cell lysis to be taken up by survived cells). The conserved substrates include nearly all the noncarbon sources of biogenic elements (N, P, K, Mg, Fe, and trace elements), CO_2 for autotrophs, and the indispensable amino acids and growth factors. Most catabolic substrates are used also as a source of biogenic elements. We can assess both these components separately in terms of respective yields Y_E (biomass yield/mass unit of oxidized substrate) and Y_A (biomass yield/mass unit of assimilated substrate), from the experimentally measured yield, Y. For C substrate, Equation 17.4 can be specified as follows:

Total carbon consumed		C incorporated into cell		C oxidized to CO_2 to provide energy		C incorporated into by-products	
δC_s	=	δC_x	+	δC_{CO2}	+	δC_P	(17.4)

Let us neglect the last term δC_P (by assuming that extracellular by-products can be reused and functionally are equivalent to C substrate) and divide the substrate balance by δC_x, which is the amount of biomass C produced, then:

$$\frac{1}{Y} = 1 + \frac{1}{Y_E}, \tag{17.5}$$

where Y = gram of biomass of C/gram substrate of C and $Y_E = gram$ of biomass of C/gram $CO_2 - C$

$$\frac{1}{Y} = \frac{\sigma_x}{\sigma_s} + \frac{12}{Y_E \sigma_s}, \tag{17.6}$$

where Y = grams of CDW/gram substrate, $Y_E = gram$ of CDW/mmol of CO_2, σ_x and σ_s are fractions of carbon in biomass and substrate, respectively. For example, if total measurable yield Y is 0.6 g biomass C/g glucose C, it means that from each gram of consumed C, 0.6 g is incorporated into biomass (assimilated), and 0.4 g is dissimilated (oxidized to CO_2), then $Y_E = 0.6/0.4 = 1.5$. To calculate oxygen demand for aerobic growth (or biomass yield on O_2) we have a balance:

oxygen required to produce 1 g CDW		oxygen required to burn substrate consumed to produce 1 g CDW		oxygen required to burn 1 g CDW	
$1/Y_{x/o}$	=	A/Y	−	B	(17.7)

where A and B are constants estimated from stoichiometry of their respective combustion reactions (see Eq. 17.10 later), for example, the value of A is 33.33 mmol O_2g glucose and B is about 42 mmol O_2/g CDW. The relationship between biomass yields on O_2 and CO_2 is derived from comparison of Equations 17.6 and 17.7:

$$\frac{Y_{x/CO_2}}{Y_{x/o}} = \frac{A - BY}{\sigma_s - \sigma_x Y} \tag{17.8}$$

Now we will go back to the general substrate balance (Eq. 17.3) and derive an expression for conserved substrate. Again, we neglect term δE_P (because extracellular products are assumed to be reusable) and divide the balance by δx, which is the amount of biomass produced:

$$\frac{1}{Y} = \frac{\delta E_x}{\delta x} \approx \sigma_x \tag{17.9}$$

where σ_x is the intracellular content of element incorporated into biomass from consumed substrate. Sometimes σ_x is called the *cell quota*. The values $1/Y$ and σ_x are not identical although they have the same dimension (e.g. milligram N/gram biomass) and very close numeric value. The reciprocal $1/Y$ is characterizing the *process* (the expenditure of conserved substrate to synthesize biomass unit), whereas σ_x is an index of cell composition (the content of intracellular N/biomass unit). Formally $1/Y$ is equal to σ_x value of an infinitely small increment of cell biomass, and σ_x is the averaged value for entire cell. Notice that although σ_x is a slow and $1/Y$ is a rapid variable, their numerical values are exactly the same for balanced steady-state growth and can differ considerably during transients.

17.2.3 Yield Variation as Dependent on the Chemical Nature of Organic Substrates

In this section, we will discuss why biomass yield varies when microorganisms are grown on different C substrates. This problem was best solved within the framework of the *theory of mass and energy balance* (TMEB) (3,4). Evidently, the fraction of C in dry biomass is almost constant. By contrast, the content of carbon in utilized substrates, σ_s, and energetic quality of substrate vary over a broad range (e.g. compare methane vs oxalic acid). To characterize substrate and biomass by a single common measure, TMEB

uses an index of *degree of carbon reduction*, γ related to the internal energy of organic compounds. The heat liberated by biological or chemical oxidation is proportional to oxygen uptake or equally to the number of electrons gained by oxygen from oxidized substrates, according to Payne's term *available electrons* (*ae*) (5). The heat production from an oxidation reaction averages at 27 kcal/*ae* equivalent. A carbon reduction degree, γ is defined as the number of *ae*/carbon atom. Its numeric value can be determined from the stoichiometry of the oxidation reaction:

$$CH_pO_nN_q + bO_2 = CO_2 + 0.5(p\text{-}3q)H_2O + qNH_3, \quad (17.10)$$

$$\gamma = 4b = 4 + p - 2n - 3q \quad (17.11)$$

The *ae* balance for Equation 17.1 can be written as

$$\gamma_s + b(-4) = Y\gamma_x + Y_P\gamma_p \quad (17.12)$$

where γ_s, γ_x, and γ_p are the carbon reduction degree of respectively substrate, biomass, and extracellular product. Dividing both sides of Equation 17.12 by γ_s we obtain the relationship delineating the *ae* distribution between oxygen (*ae* used for respiration), biomass, and the intracellular product:

$$\underset{\text{oxygen}}{\frac{4b}{\gamma_s}} + \underset{\text{biomass}}{\frac{Y\gamma_x}{\gamma_s}} + \underset{\text{product}}{\frac{Y_P\gamma_p}{\gamma_s}} = 1 \quad (17.13)$$

The second term in this equation is the fraction of *ae* transferred to biomass from utilized substrate, termed the *energetic growth yield*.

$$\eta = Y_C\gamma_x/\gamma_s \quad (17.14)$$

The third term designates that fraction of total substrate internal energy that is transferred to the product. It is called the *energetic product yield*.

$$\xi = Y_P\gamma_p/\gamma_s \quad (17.15)$$

Energetic yield η is related to other stoichiometric parameters as follows:

$$\eta = Y_{x/s}\sigma x\ \gamma x/(\sigma s\gamma s)$$
$$\eta = Y_{x/C}\gamma_x/\gamma_s$$

where $Y_{x/s}$ is gram of CDW/gram of substrate and $Y_{x/C}$ is gram of CDW-C/gram of substrate C.

The advantage of using η is that it varies within a much smaller range than other yield expressions. At one and the same efficiency of energy utilization (η), the conventional biomass C yield $Y_{x/C}$ is proportional to substrate reduction degree γ_s and, for example, it is 4 times higher on glucose ($\gamma_s = 4$) than on oxalate ($\gamma_s = 1$), 0.48 and 0.12 g C/g C, respectively (assuming $\eta = 0.5$ and $\gamma_x = 4.2$). The energetic growth yield η is more or less constant (0.5–0.7) for substrates with $\gamma_s \leq 4.2$ (4.2 corresponds to average reduction degree of microbial biomass), and it declines at higher γ_s.

The attractiveness of macrostoichiometry and TMEB is that all growth coefficients are interrelated and could be measured from any available components of the culture mass balance. For example, if you cannot record microbial growth by conventional routine as dry weight biomass (because of presence of solids in broth liquid), you may still calculate it from N or O_2 uptake, CO_2 evolution, pH titration rate, and so on.

17.2.4 Variations in Yield from Energy Source, Maintenance Requirements

To multiply and grow cells require energy, but the opposite is not true: cells do not require growth to spend energy. Sometimes catabolic machinery is entirely wasteful (respiration without cell growth) and always at least some minor part of energy consumption is diverted from growth. To account for this phenomenon, it was postulated that microbes and cells require energy not only for growth but also for other *maintenance purposes*. Certain specific maintenance functions recognized now are turnover of cell material, osmotic work to maintain concentration gradients between the cell and its exterior, and cell motility.

According to conventional definition of maintenance (6), the balance of energy source is

$$\underset{\text{source consumed}}{\text{total energy}} \quad \underset{\text{for cell growth}}{\text{consumption}} \quad \underset{\text{maintenance}}{\text{consumption for}}$$
$$\delta S_E = \delta S_G + \delta S_M \quad (17.16)$$

Let us divide it by δx, the amount of biomass produced, then:

$$\frac{1}{Y} = \frac{\delta S_G}{\delta x} + \frac{\delta S_M}{\delta x} = \frac{1}{Y^{\max}} + \frac{m}{\mu} \quad (17.17)$$

Here $Y^{\max} = \delta x/\delta S_G$ is "true" growth yield, that is, yield under imaginary conditions of maintenance being zero. The maintenance coefficient, m is introduced as the specific (i.e. expressed per unit of biomass) rate of energy consumption for maintenance functions: $m = (1/x)(\delta S_M/\delta t)$. The ratio m/μ on the right side of Equation 17.17 was derived as follows: $m/\mu = [(1/x)(\delta S_M/\delta t)]/[(1/x)(\delta x/\delta t)] = \delta S_M/\delta_x$.

If we divide Equation 17.16 by $x\delta t$ (note that the second term is $\delta S_G/(x\delta t) = [\delta x/(x\delta t)]/[\delta x/\delta S_G] = \mu/Y^{\max}$, then we have:

$$q = \mu/Y^{\max} + m, \quad (17.18)$$

where q is specific rate of energy source consumption, $q = (1/x)(\delta S_E/\delta t)$.

It should be noticed that Y^{max} is a parameter, but not the yield of a real culture that always has some nonzero maintenance requirements. It is a very common mistake in the application of the maintenance concept to a particular organism: to take the real measured Y value and pick up from literature some average m coefficient. The correct way would be either to borrow concurrently two parameters Y^{max} and m or to treat actually observed Y as a variable that is altered along with specific growth rate μ according to Equation 17.17:

$$Y = \frac{\mu Y^{max}}{\mu + mY^{max}} \tag{17.19}$$

There is another way to formulate maintenance requirements by stating that the net growth of cells μ is the difference between true growth (μ_{true}) and endogenous decay of cellular components (specific rate, a):

$$\mu = \mu_{true} - a, \mu_{true} = \mu + a$$

Then, for the rate of energy source uptake, we have

$$\frac{\mu x}{Y} = \frac{\mu_{true} x}{Y^{max}} = \frac{(\mu + a)x}{Y^{max}} \quad \text{or} \quad \frac{1}{Y} = \frac{1}{Y^{max}} + \frac{a}{\mu Y^{max}} \tag{17.20}$$

Comparing Equations 17.17 and 17.20, we see that $a = mY^{max}$.

17.2.5 Experimental Determination of *m*

To practically determine the maintenance coefficient, the microorganisms are grown in chemostat culture limited by energy sources at several dilution rates D (numerically D is equal to specific growth μ if steady state is achieved). At each D, we have to measure steady-state biomass $\tilde{x}$ and residual energy source substrate, $\tilde{s}$ to calculate specific rate of substrate uptake $q_s = (s_0 - \tilde{s})D/\tilde{x}$; q_s measurement may be substituted by any appropriate integral characteristic of catabolic activity, for example, aerobic respiration (O_2 uptake, CO_2 production), anaerobic respiration (release of CH_4, NO_3^-, sulfides, ...), formation of fermentation products, and so on. These data are fitted to Equation 17.17 or 17.18, m and Y^{max} being found as nonlinear regression parameters. An example is presented in Fig. 17.1. Most available experimental data do obey this relationship. However, considerable deviation occurs for slowly growing cells in chemostat running at very low dilution rates or in dialysis culture and chemostat with biomass retention. The experimental Y values for slowly growing cells are higher than predicted by Equations 17.17 and 17.18 (see insets in Fig. 17.1). Thus, maintenance coefficient varies

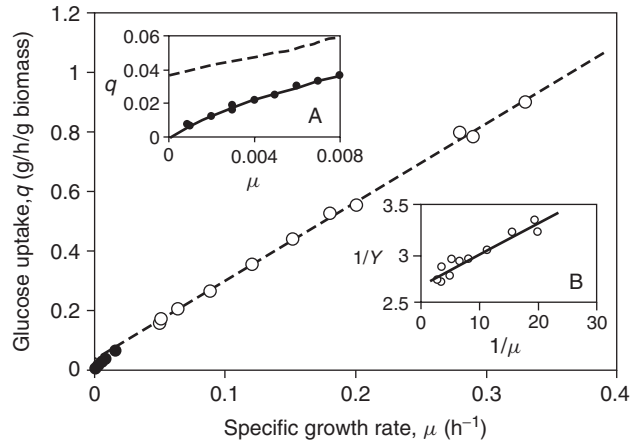


Figure 17.1. Experimental data used to determine maintenance coefficient in continuous culture of microorganisms. Main panel: variation of glucose uptake rate in regular chemostat (open circles) and culture with cell recycle (closed circles) as dependent on specific growth rate. Inset A: data for low growth rates under higher magnification. Inset B: double-reciprocal plot of $1/Y$ versus $1/\mu$ (Eq. 17.17) used for determination of m and Y^{max}. Solid curves were calculated from SCM (2), the dotted curve was calculated from Equation 17.18. Note that it fails at low growth rates (see inset A).

in response to nutritional status and could not be taken as an absolute constant; under substrate deficiency, the cells adjust their maintenance requirements to lower values by reducing turnover rate, osmotic work, and motility (2).

The described experimental technique is indirect because it is based on measurements of μ-dependent Y variation rather than m itself, and there are some assumptions needed to be confirmed (e.g. that m is constant and that maintenance requirements are the only reason of Y variation). However, some components of maintenance requirements are available for direct estimation. In particular, we can assess the total turnover rate of cellular material, a, which is one of the main components of maintenance requirements (Eq. 17.20). The principal cell constituents that are turned over are proteins, nucleic acids, and cell wall polymers. The turnover rate is very close to *endogenous respiration*, which is the oxidation of those compounds produced from the turnover (breakdown) of cellular macrocomponents. Accurate measurements of endogenous respiration need to be made under normal growing conditions. It is known that the simple removal of cells from nutrient broth by filtration with subsequent washing and incubation in buffer renders strong stress and may alter the normal turnover rate (7). To avoid artifacts, we can use a label substitution technique (Fig. 17.2). The chemostat culture is fed alternately from two bottles containing unlabeled and labeled $^{14}C(U)$ substrate respectively. The $^{14}CO_2$ evolution rate is recorded after switching to unlabeled substrate, when the main source of $^{14}CO_2$ are cell components. The calculated a value was

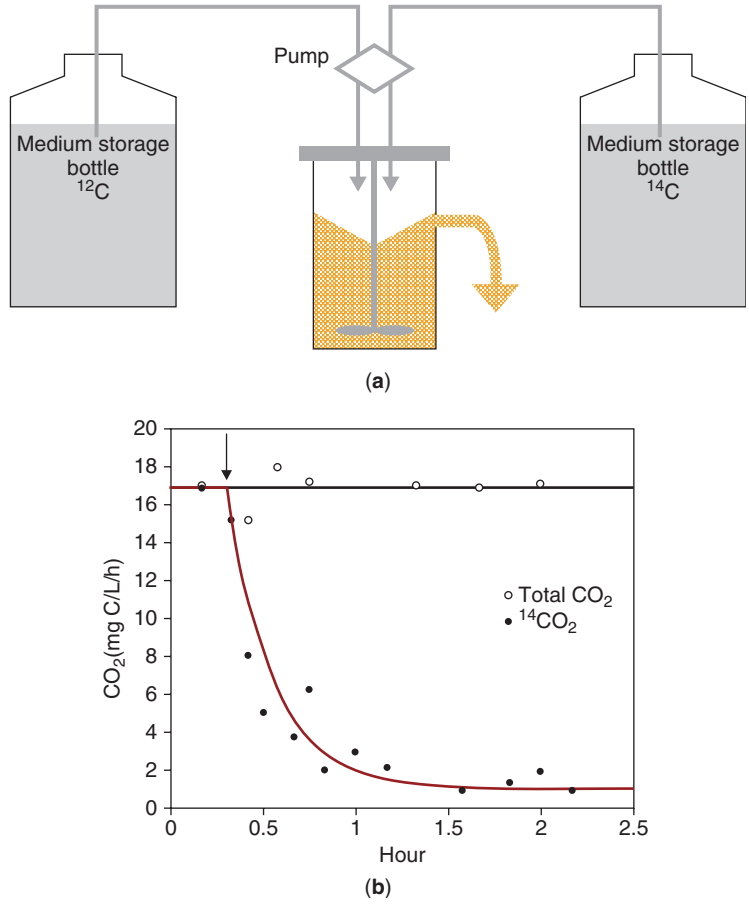


Figure 17.2. Label substitution technique for determination of turnover rate of cellular macromolecules. (a) experimental setup including two medium reservoirs containing ^{14}C- and ^{12}C-glucose pumped into cultivation vessel through two-way valve. (b) example of $^{14}CO_2$ evolution dynamics before and after (arrow) switching of medium feed. Glucose-limited culture of *Pseudomonas fluorescens* 1472, $D = 0.08\ h^{-1}$ (8).

found to be rather high, accounting for the major part of total maintenance determined by the indirect method (2). The endogenous respiration declined at the low growth rate, indicating that under starving conditions, self-adjustment of the maintenance requirement occurs mainly as a reduction in the turnover rate of macromolecules.

Finally, we would like to comment on another method to measure maintenance coefficient which was claimed to be simple and direct (9) but turned out to be too protracted. Principle of this technique agrees well with the formal concept of maintenance: chemostat culture limited by energy source is run with complete cell recycling (Fig. 17.3), growing cells are retained in the vessel and total biomass is expected to increase until a steady-state value, $\tilde{x}$, is reached when maintenance requirements are just met by the limiting substrate addition. Then the maintenance coefficient can be found as $m = D(s_0 - \tilde{s})/\tilde{x}$. However actual behavior of all tested microorganisms in the described recycling system was different (10): instead of approaching steady state, they continued to grow exceeding many times $\tilde{x}$-level, based on prior m-determination in conventional chemostat culture. The only reasonable explanation is that maintenance rate is not constant for particular organism. Chronic starvation triggers expression of stress-response genes, their products have essentially lower maintenance demand. These starvation-adaptive events sometimes are observed as stepwise raises in cell biomass during continuous cultivation reflecting synchronized abrupt decrease in m values from 12 to 5.3, 4.3 and then eventually to 2.5 mg glucose/h/(g biomass) (curve 2, Fig. 17.3). General conclusion is that under chronic starvation (supply of energy source below the maintenance limit) cells may follow one of three routs: (i) to die/lyse, (ii) to enter the state of dormancy, or (iii) to continue slow growth, by reducing maintenance requirements. The fourth route—the maintenance of viability of vegetative cells without their growth—is forbidden.

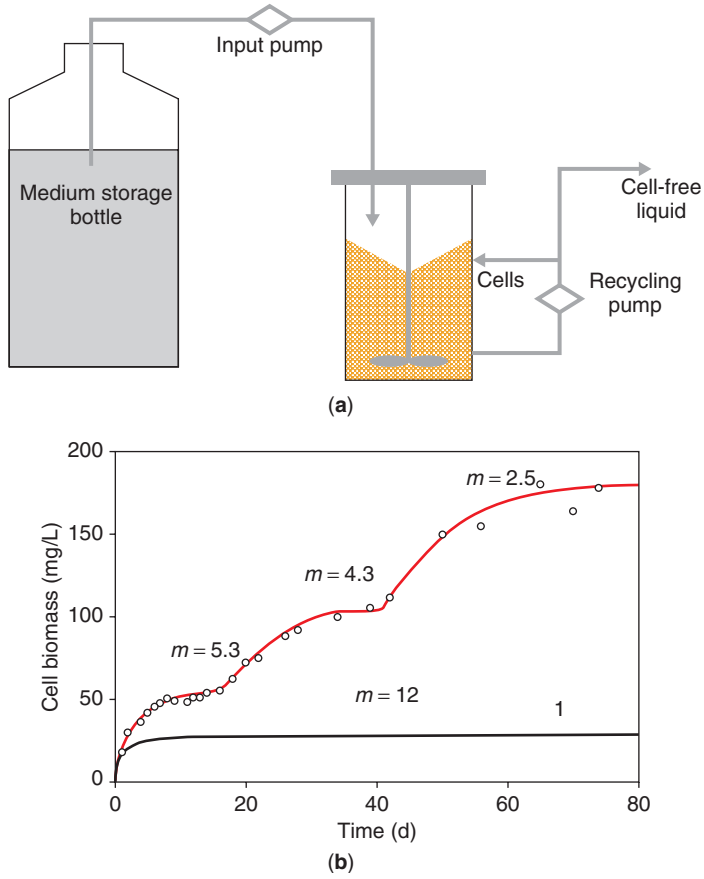


Figure 17.3. Growth dynamics of microorganisms in continuous culture with complete biomass recycling. (a) Experimental design (6,9). (b) The calculated biomass dynamics assuming maintenance requirement ($m = 0.012$ g/h/g DW) as found preliminary in regular chemostat (curve 1) and the actual biomass of yeasts *Debaryomyces vanrijiae* (curve 2) displaying spontaneous stepwise decrease in m from 5.3 to 2.5 mg/h/(g DW) (2).

17.2.6 Maintenance Requirements and Wasteful Catabolism

The described concept of maintenance requirements was the subject of intensive debates (11). One of the strongest arguments against it was an apparent increase in $Y^{\max}$ observed in chemostat cultures limited by P, N, and other conserved substrates under conditions of energy excess. To preserve the constancy of the "true" yield, Pirt (12) had to modify Equation 17.18 in the following way:

$$q = \frac{\mu}{Y^{\max}} + m + m'\left[1 - \frac{\mu}{\mu_m}\right] \qquad (17.21)$$

where $m'(1 - \mu/\mu_m)$ is the second μ-dependent component of maintenance energy that operates under excess of energy substrate.

However, it is better to differentiate maintenance requirements *sensu stricto* as a minor component of the cell energy budget that is observed under energy-limitation and wasteful use of catabolic substrate under energy excess. In physiological terms, these two groups of nonproductive catabolic reactions are completely different. The first reactions are mainly responsible for compensation of turned-over macromolecules and therefore belong to the category of regular primary catabolism. The catabolic reactions of the second group include excretion into environment of partly oxidized substances (*overflow metabolism*), uncoupling of respiration from ATP generation by metabolic inhibitors, functioning of futile cycles, or substrate oxidation through alternative oxidases without ATP generation. These and related phenomena take place in chemostat culture limited by conserved substrates (opposite to limitation by energy source) as well as during lag phase of batch culture started from starving inoculum. We will discuss the mathematical formulation of these phenomena in the section devoted to growth kinetics.

17.2.7 Variation in Biomass Yield from Conserved Substrates

Yield on conserved substrates varies mainly as a result of alterations in biomass chemical composition expressed by parameter σ_s, the intracellular content of deficient element or cell quota (Eq. 17.9). For most of known cases, the content σ_s increases parallel to growth acceleration (Fig. 17.4). As yield and cell quota are inversely related to each other (Eq. 17.9), then Y values decrease with growth rate. The physiological mechanisms of this variation are as follows. The intensive growth requires higher *internal concentration* of some conserved limiting substrates that preserve their chemical identity after uptake (K^+, Mg^{2+}, vitamins). Other conserved substrates (sources of P, N, S, etc.) are incorporated into macromolecular cell constituents (mainly nucleic acids and proteins) whose *intracellular content* also should be kept high at high growth rate. Both types of changes in cellular composition are manifested as σ increase, and both of them require additional maintenance energy (to maintain concentration gradient or compensate turnover of macromolecules). The observed μ-dependent variation in σ is therefore a compromise between biosynthetic requirements and energy conservation that is attained because of optimal metabolic control of cell performance. However, it would be erroneous to consider μ as truly independent variable setting up chemical composition of cells. In fact, both μ and σ are functions of one common independent variable, the limiting substrate concentration in the medium, s. For steady-state chemostat culture we have:

$$\mu = \frac{q}{\sigma} = \frac{1}{\sigma}\frac{Q\tilde{s}}{K_s + \tilde{s}}, \sigma = \sigma_0 + \frac{(\sigma_m - \sigma_0)\tilde{s}}{K_\sigma + \tilde{s}} \qquad (17.22)$$

where μ is specific growth rate and q is specific substrate uptake rates, σ_0 and σ_m are respectively lower and upper limits of σ variation, low limit $\sigma \to \sigma_0$ is attained when $\tilde{s} \to 0$ and upper limits $\sigma \to \sigma_m$ when $\tilde{s} \to \infty$. By excluding $\tilde{s}$ from both these equations, we arrive at following relationship between σ and μ:

$$\mu = \mu_m \frac{\sigma_m(\sigma - \sigma_0)}{\sigma[\lambda(\sigma_m - \sigma_0) + \sigma - \sigma_0]}, \quad \lambda = \frac{K_s}{K_\sigma} \qquad (17.23)$$

Under realistic assumption $\lambda \approx 1$ ($K_s \approx K_\sigma$) we have:

$$\sigma = \frac{\sigma_0}{1 - (1 - \sigma_0/\sigma_m)\mu/\mu_m}, \quad Y = Y_m - (Y_m - Y_0)\frac{\mu}{\mu_m}, \qquad (17.24)$$

where Y_m and Y_0 are respectively upper and lower limits of yield variation ($Y_m = 1/\sigma_0$, $Y_0 = 1/\sigma_m$). As we can see, the linear relationship between Y and μ is normally observed in chemostat culture (Fig. 17.4).

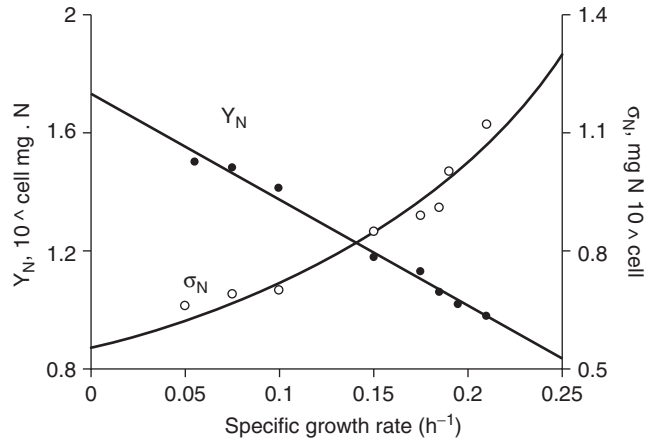


Figure 17.4. Relationship between stoichiometric parameters Y and σ and specific growth rates of *Chlorella vulgaris* grown in chemostat culture limited by nitrogen source. The curves are calculated using Equations 17.23 and 17.24 (13).

17.2.8 Microscopic Approach in Studies of Growth Stoichiometry

Equations 17.1–17.24 exemplify the *macroscopic approach* in studying of microbial growth stoichiometry. Its typical features are the use of gross formulas for biomass and metabolic products, evaluation of total mass balance for chemical elements (C, N, P), and formal description of microbial growth as a single-step conversion of substrate(s) into biomass. By contrast, the *microscopic approach* focuses on the much more complex real metabolic reactions and attempts to account for a limited but still quite large number of individual metabolic intermediates. The final aim of this approach is to organize the biochemical information into a consistent picture of microbial metabolism at the level of entire cell.

The microscopic approach has become possible by virtue of advancements in biochemistry, which has succeeded in establishing a sufficiently full picture of metabolic processes in certain microorganisms. The pioneering work, in this area, was done by Bauchop and Elsden (14), who were able to sum up the balance of ATP for fermenting microorganisms. As a result, a relation was established between the biomass yield (a macroscopic quantity) and the number of generated ATP moles (a stoichiometric characteristic of real catabolic reactions):

$$Y_{\mathrm{ATP}} = MY_{x/s}/n \qquad (17.25)$$

where n = moles of ATP made available to the organism by the metabolism of 1 mol of energy source; M = molecular weight (gram) of energy source. The following example illustrates the Y_{ATP} calculation: if biomass yield of some organisms aerobically grown on glucose is 0.52 g CDW/g, then $Y_{x/s}$ is 1.49 g CDW/g of oxidized

glucose (calculated from Eq. 17.6) or $Y_{x/s} = 1.49 \times 180 = 268$ g CDW/mol (180 is glucose molecular weight); assuming that P/O = 2 (i.e. 2 mol of ATP produced/atom oxygen taken up) and that two ATP moles are produced via glycolysis (substrate phosphorylation) we arrived at $n = 2 + 12 \times 2 = 26$ and $Y_{ATP} = 268/26 = 10.3$ g CDW/mol ATP. Careful determination of n and Y_{ATP} is possible only for anaerobic growth of fermenting microorganisms generating ATP via substrate phosphorylation. The mean value tends to be around 10.5 g CDW/mol ATP (Fig. 17.5). For aerobic growth, we need to make assumptions on the P/O ratio. As soon as the respiratory chain of bacteria differ widely for various organisms and growth conditions, this assumption can never be reliable. To avoid this obstacle, an interesting approach was proposed: microbial culture is grown in a chemostat limited by two carbon-containing energy sources, their ratio is varied while the total carbon feed rate is kept constant; yield measurements should allow one to determine both parameters (P/O and Y_{ATP}) by linear regression (1).

Today, microstoichiometry is quickly progressing as so-called metabolic balancing. Cell growth is viewed as a set of transport and intracellular metabolic reactions known for some particular organisms. As a rule, the produced metabolic networks are composed of a combination of true stoichiometric equations for individual metabolites and empirical gross equations (Table 17.2). The amount of such equations vary in different models from 20 to 30 to more than 100. For example, van Gulik and Heijnen (16) describe yeast growth by a set of more than 90 reactions including glycolysis and the citric acid cycle (14 reactions); phosphoenolpyruvate (PEP) phosphotransferase; pentose phosphate pathway (6 reactions); glyoxylate shunt (2 reactions); oxidative phosphorylation (4 reactions); CO_2 interaction with tetrahydrofolate (THF) (3 reactions); transport of inorganic P, NH_4^+, SO_4^{2-}, acetate, lactate, pyruvate, glucose, gluconate, succinate and citrate (totally 10 transport reactions); amino acid synthesis (15 reactions) and polymerization (2 reactions); nucleotide synthesis (9 reactions); RNA synthesis; ATP consumption for maintenance; fatty acids synthesis (2 reactions); formation of glycogen and polysaccharides; and finally, the biomass formation from proteins, polysaccharides, RNA, fatty acids, and glycerol.

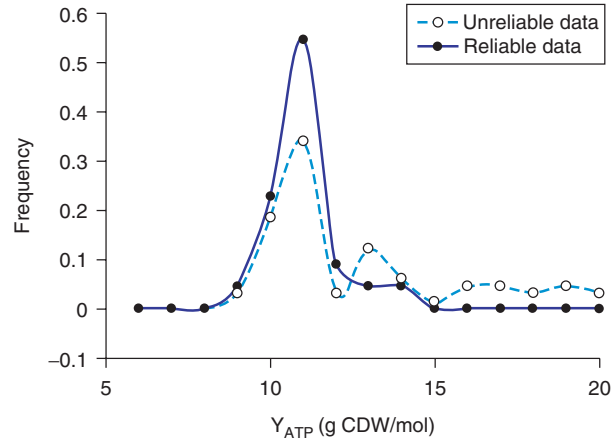


Figure 17.5. Frequency distribution of experimentally measured values of Y_{ATP} at different degree of creditability. The reliable data refer to studies of anaerobic growth with direct measurements of fermentation products (plotted from database in Ref. 15. Note that these data are normally distributed with mean value 10.55, whereas all data display considerable skewness.

For each compound, i, involved in a metabolic system, a mass balance can be defined:

$$\frac{dC_i}{dt} = r_{Ai} + \Phi_i \tag{17.26}$$

where C_i is concentration of ith compound, r_{Ai} and Φ_i denote the net rates of, respectively, i chemical conversion and transport over the boundaries of bioreactor (fluxes of CO_2, O_2, nutrients, cells and products). Most metabolic balancing equations are applied to steady-state growth (which means that no intracellular accumulation of metabolites occurs). In such cases, the differential equations like Equation 17.26 are reduced to linear algebraic ones. Besides, an extensive use of matrix calculus is customarily made to obtain a concise notation. The problem of experimental support of such model is especially important (16). The degree of freedom, df, of

TABLE 17.2. Examples of True Stoichiometric (1–4) and Empirical Gross Equations (17.5) to Represent Cellular Processes

Reaction	Equation	
Glycolysis reaction	Glucose + ATP → Glucose-6-P + ADP + H	(17.1)
	Glucose-6-P → Fructose-6-P	(17.2)
	0.5 Fructose-6-P + 0.5 ATP → Glyceraldehyde-3-P + 0.5 ADP + 0.5 H	(17.3)
Oxidative phosphorylation	NADH + 0.5 O_2 + d_1ADP + d_2Pi + $(1 + d_1)$H → $(1 + d_1)H_2O$ + NAD + d_1ATP	(17.4)
Biomass formation	a_1 Proteins + a_2 Polysaccharides + a_3 RNA + a_4 Lipids → Biomass	(17.5)

the resulting system of linear equations is equal to the total number of unknown rates (both intracellular and exchange reactions) minus the total number of linear equations. To resolve the system, df rates have to be measured, and then the system is fully *determined*. If the number of measured rates is greater than df, then the system is *overdetermined*, and the redundancy of the data can be used for statistical analysis and error minimization. However, it is much more typical to have an *underdetermined* system when the sum of measured rates is less than df. In this case, the number of possible solutions is infinite unless additional constraints are applied (e.g. maximization of biomass yield, minimization of energy expenditure) to find the one and only one solution by the linear optimization technique.

In most studies, flux estimates are obtained using measurements of substrate consumption and product formation. This approach has proved to be efficient in some particular biotechnological cases, such as when only specific pathways need to be considered (17) or if the contribution of flux for cellular growth is weak, as with mammalian or hybridoma cells (18). The more complex microbial systems are turned out to be seriously underdetermined. In such cases, the application of metabolic balancing requires the use of one or another maneuvers: (i) to lump together several sets of reactions (19); (ii) to utilize data from *in vitro* enzyme assays; (iii) to make assumptions on numeric values of some stoichiometric growth parameters, such as Y_{ATP}, P/O, and H^+/e ratios, which are the subject of controversial debates (16).

However, the best solution would be to get direct experimental data on *in vivo* flux and resolve the system. Isotopic tracers are one of the best candidates for such a purpose. We will illustrate this point by one of the early published work (20). *Corynebacterium glutamicum* was grown in chemostat culture continuously fed with [1 $-^{13}$C]-glucose; when steady state was established, the cells were harvested and hydrolyzed and the amino acids were separated by ion-exchange chromatography and analyzed by NMR spectroscopy. NMR provides data on ^{13}C enrichment at each specified carbon position of amino acid. Because metabolic pathways for amino acid synthesis are exactly defined, then the entire central metabolism can be assessed for *in vivo* fluxes, including determination of the forward and back rates of bidirectional reactions. In *C. glutamicum*, the flux through the pentose phosphate pathway turned out to be 66.4% (relative to glucose input flux 1.49 mmol g CDW h); the entry into tricarboxylic acid cycle, 62.2%, and the contribution of the succinylase pathway to lysine synthesis, 13.7%. The total net flux of the anaplerotic reactions (carboxylation of PEP/pyruvate into oxaloacetate/malate) was quantitated as 38%, the true forward flux of C3 $\rightarrow$ C4 being 68.6% (1.8 times of 38%) and a back flux of C4 $\rightarrow$ C3 being 30.6% (0.8 times of 38%).

The metabolic balancing proved to be very promising and useful to identify metabolic constraints for intensive synthesis (overproduction) of products such as amino acids. Last decade flux balancing was efficiently applied to development, testing and optimizing of recombinant strains (21–25). Majority of industrially significant microorganisms are fully sequenced; their gene expression patterns and proteomic data give valuable data on potential size of stoichiometric matrix describing intracellular metabolic reactions. The actual intracellular fluxes depend critically on intracellular concentrations of metabolic intermediates, primarily cofactors such as NAD/NADH (26,27). So far, this approach is restricted to steady-state analysis which is not sufficient to predict microbial performance under real-life transient conditions (28). However, progress in this research direction is amazingly fast and novel computational algorithms are able to deal with nonstationary metabolic fluxes (29).

17.3 KINETICS OF CHEMICAL AND ENZYME REACTIONS

We need to introduce some basic principles of kinetic analysis of chemical and enzymatic reactions. Quantitative description and understanding of microbial growth dynamics and kinetics are impossible without some elementary knowledge in underlying scientific disciplines. Enzymatic and chemical reactions play an essential role in biotechnology, which is one of the most important fields in industrial development.

17.3.1 Order and Molecularity of Chemical Reactions

The molecularity of any chemical reaction is defined by the number of molecules that are altered in the reaction (Table 17.3). The order is a description of the number of concentration terms multiplied together in the rate equation (Table 17.4). Hence, in a first-order reaction, the rate is proportional to one concentration of reactant; in a second-order reaction, it is proportional to two concentrations or to the square of one concentration. For a simple single-step reaction, the order is generally the same as the molecularity. For a complex reaction involving

TABLE 17.3. Molecularity of Chemical Reaction

Molecularity of reaction	Reactants		Product
Unimolecular or monomolecular	S	$\rightarrow$	P
Bimolecular	S + S	$\rightarrow$	P
Or	$S_1 + S_2$	$\rightarrow$	P
Trimolecular or termolecular	S + S + S	$\rightarrow$	P
Or	$S_1 + S_1 + S_2$	$\rightarrow$	P
Or	$S_1 + S_2 + S_3$	$\rightarrow$	P

TABLE 17.4. Kinetic Order of Chemical Reactions

Reaction Order	Differential Equation	Dimension of Rate Constant	Dynamics of Residual Reactant	Dynamics of Product Accumulation
Zero	$\frac{ds}{dt} = -k$	(concentration)(time)$^{-1}$	$s(t) = s_0 - kt$	$p(t) = p_0 + kt$
First	$\frac{ds}{dt} = -ks$	(time)$^{-1}$	$s(t) = s_0 \exp(-kt)$	$p(t) = s_0[1 - \exp(-kt)]$
Second	$\frac{ds}{dt} = -ks^2$	(concentration)$^{-1}$(time)$^{-1}$	$s(t) = \frac{s_0}{1 + ks_0t}$	$p(t) = \frac{s_0^2kt}{2(1 + s_0kt)}$
Second	$\frac{dp}{dt} = -ks_1s_2$	(concentration)$^{-1}$(time)$^{-1}$	$s_1(t) = s_{01} - p(t)\ s_2(t) = s_{02} - p(t)$	$p(t) = \frac{s_{01}s_{02}(1 - \exp[(s_{02} - s_{01})kt])}{s_{01} - s_{02}\exp[(s_{02} - s_{01})kt]}$
Pseudofirst $s_{01} \gg s_{02}$	$\frac{dp}{dt} = -ks_1s_2$	(concentration)$^{-1}$(time)$^{-1}$	$s_2(t) = s_{02}\exp(-ks_{01}t)\ s_1(t) \approx s_{01}$	$p = s_{02}[1 - \exp(-ks_{01}t)]$

[a] t, time; s, reactant concentration; p, product concentration; s_0, reactant concentration at $t = 0$.

a sequence of unimolecular and bimolecular steps, the molecularity is not the same as its order. Reactions of molecularity greater than 2 are common, but reactions of order greater than 2 are very rare. For instance, a trimolecular reaction, such as $A + B + C \rightarrow P$, as a rule proceeds through two elementary steps, $A + B \rightarrow X$ and $X + C \rightarrow P$, each of which are of the second or first order. Very often, bimolecular reactions between S_1 and S_2 occurs under the condition that their respective concentrations $s_2 \gg s_1$ (e.g. if the second reactant S_2 is solvent), then we have a *pseudo first-order* reaction. Some reactions are observed to be of the zero order, that is, the rate appears to be constant, independent of the concentration of reactant. This is a characteristic feature of catalyzed reactions and occurs if reactant is present in such large excess that the full potential of catalyst is realized.

17.3.2 Dimensions of Rate Constants

Knowledge of dimensions is very useful to check the correctness of derived kinetic equations: the left- and right-hand sides of equations must always have the same dimensions. This general rule is applicable to all mathematical models (not only in chemical kinetics). It is incorrect to add or subtract terms of different dimensions, although you may multiply or divide them. For example, if expression "$\ldots(1 + s)$" occurs in an equation, where s has dimension (concentration), then either it is incorrect, or the 1 is a concentration that happens to have a numerical value of 1 unit. The operation rising to power is allowed for only simple dimensionless numbers, for example, expression $e^{2.5t}$, where t is time, is correct only if 2.5 has dimension (time)$^{-1}$. The comparison of velocities of two reactions does make any sense only for kinetic terms of the same dimension. If the kinetic order of inspected reactions is different, then we have to equalize the respective rate of expressions; for example, the second-order rate constant k (time)$^{-1}$ (concentration)$^{-1}$ should be multiplied by instant concentration of reactant s to be compared with the first-order rate constant having dimension (time)$^{-1}$. The dimensions of the zero-, first-, and second-order rate constants are shown in Table 17.4.

17.3.3 Reaction Dynamics

If rate constant and so-called initial conditions [concentrations of reactants at zero-time $(s_{01}, s_{02}, \ldots)$], are known, then it is possible to calculate the time course of reactions either in terms of dynamics of residual reactant concentration, $s(t)$ or product accumulation, $p(t)$. For this purpose, we have to integrate a differential equation under specified initial conditions (see results of integration in Table 17.4). The dynamics of $s(t)$ is linear in the case of a zero-order reaction, exponential in the case of the first order and hyperbolic in the case of the second-order reaction. The difference between the last two dynamic curves can be made visible with a semilogarithmic plot of log (concentration) versus time; it should become linear for the first-order reaction and remain to be curvilinear for the reaction of higher order.

17.3.4 Reaction Half-Time

The reaction half-time ($\mathbf{t_{0.5}}$) is a very popular kinetic parameter. It is easily calculated from integral equations by putting $s = s_0/2$ when $t = t_{0.5}$. A unique feature of the first-order reaction is the constancy of $t_{0.5}$ independently of the initial reactant concentration s_0. However, the half-time of other reactions does depend on s_0; it increases for zero-order reactions and decreases for the second-order reactions with increase in s_0. Thus, it is not recommended to use half-time as a parameter or estimator for reactions other than first-order reactions.

17.3.5 Determination of the Order of Reaction and Numeric Values of Kinetic Constants

If the reaction has an order n and rate constant k, then the reaction rate v and reactant concentration s are related by the equation:

$$v = -\frac{ds}{dt} = \frac{dp}{dt} = ks^n \tag{17.27}$$

The simplest way to find both unknown values (n and k) would be to measure reaction rate v at several concentrations of reactant. Then a plot of log(rate) against log(concentration) gives a straight line with a slope equal to n and intercept equal to $\log(k)$: $\log v = \log k + n \log s$. If there are several reactants, then it is useful to know the order in respect to each one. For this purpose, you need to have several experiments with variation of each reactant concentration while keeping the other concentrations constant.

The most frequent goal is the determination of the first-order rate constants. There are some special methods to determine the values of the first-order rate constants from the experimental curves of product formation or substrate depletion dynamics. Some of them were designed to improve the accuracy of k determination if s_0 is unknown (methods of Guggenheim, Kezdy–Swinbourne, and other, see details in Ref. 30). Today these methods are replaced by computer-aided nonlinear regression (e.g. "Solver" in MS Excel). Apart from being more convenient than graphic methods, the nonlinear regression has higher precision and generates useful statistics (e.g. confidence limits for k and s_0 based on scatter degree of experimental data and selected P-level).

17.3.6 Derivation of Basic Kinetic Equations for Enzymatic Reactions

Contrary to simple chemical reactions, enzyme-catalyzed reactions proceed through *reversible* formation of the dynamic *enzyme-substrate complex* (ESC). The word *reversible* is essential because the ESC can be decomposed into free enzyme E and product P or dissociate back to E and substrate S. There are many ways to simulate mathematically the mechanism of the enzymatic reaction. We will consider here equilibrium, steady-state, and general non-steady-state approaches.

17.3.7 Equilibrium Approach

This approach was used by Michaelis and Menten (31) to describe the effect of sucrose concentration on invertase activity. They assumed that the first step of ESC formation is so rapid that could be represented by an *equilibrium constant* K_s:

$$\overset{e}{\mathrm{E}} + \overset{s}{\mathrm{S}} \overset{K_s}{\longleftrightarrow} \overset{x}{\mathrm{ES}} \overset{k_2}{\longrightarrow} \mathrm{E} + \overset{p}{\mathrm{P}}, \tag{17.28}$$

where e, s, x, and p denote the concentrations of free enzyme, substrate, ESC, and product, respectively. The equilibrium constant, K_s, is defined as $K_s = es/x$. The instantaneous concentrations s and e are not directly measurable, but they could be expressed in terms of the initial, measured concentrations e_0 and s_0, using mass–balance relationships:

$$e_0 = e + x \qquad s_0 = s + x, \qquad x \ll s,\ s \approx s_0 \tag{17.29}$$

The overall reaction rate, v is a simple first-order reaction with rate constant k_2:

$$v = dp/dt = -ds/dt = k_2 x \tag{17.30}$$

The x value can be found from expression for K_s and mass–balance conditions (Eq. 17.29): $x = e_0 s/(K_s + s)$. Substitution of this expression into Equation 17.30 finally produces

$$v = \frac{k_2 e_0 s}{K_s + s} \tag{17.31}$$

17.3.8 Steady-State Approximation

This approach was applied by Briggs and Haldane (32) for the following scheme of enzymatic reaction

$$\mathrm{E} + \mathrm{S} \underset{k_{-1}}{\overset{k_1}{\rightleftarrows}} \mathrm{ES} \xrightarrow{k_2} \mathrm{E} + \mathrm{P} \tag{17.32}$$

This scheme implies the reversibility of ESC formation instead of much more restrictive equilibrium postulate. However, still there was steady-state assumption in respect to ESC formation:

$$dx/dt = k_{+1}(e_0 - x)s - k_{-1}x - k_{+2}x \approx 0 \tag{17.33}$$

Therefore, $x = k_{+1}e_0 s/(k_{+1}s + k_{-1} + k_{+2})$, and substitution of this expression into Equation 17.30 gives:

$$v = -\frac{ds}{dt} = k_{+2}x = \frac{k_{+1}k_{+2}e_0 s}{k_{+1}s + k_{-1} + k_{+2}} = \frac{k_{+2}e_0 s}{\frac{k_{-1}+k_{+2}}{k_{+1}} + s} = \frac{V_s}{K_m + s} \tag{17.34}$$

Equation 17.34 is what usually called the *Michaelis–Menten equation*, the fundamental equation of enzymatic

kinetics. It contains two parameters, K_m, the *Michaelis constant*, and V, the *maximum velocity*. V is the rate of reaction that would occur under full substrate saturation of an enzyme's active sites ($s \gg K_m$). In reality, the V value can be never attained, because extremely high substrate concentrations inhibit enzymes (see later text). It is clear also that V is not a fundamental property of enzyme because it depends upon e_0, the enzyme concentration. More advantageous as a specific enzyme characteristic is the *catalytic constant* or *turnover number'* k_{cat} which is V/e_0. For reaction scheme 32, k_c is identical with k_{+2}, but in general the more noncommittal notation k_{cat} is preferable (e.g. k_{cat} may differ from k_{+2} if the product formation from ESC is a reversible reaction). Numerically, the Michaelis constant, K_m is the substrate concentration that provides half the maximal reaction rate. Contrary to this simple practical definition, the mechanistic interpretation of K_m is not so lucid. Sometimes, K_m is interpreted as a substrate binding constant, K_s, assuming that $k_{+2} \ll k_{-1}$. This is a very dubious assumption. There are very few enzymes for which the individual values of k_{+2} and k_{-1} are known. Ironically, the best-studied examples (e.g. horseradish peroxidase) present just opposite case: $k_{+2} \gg k_{-1}$. It is important that many specific mechanisms (not necessarily Eqs 17.28 and 17.32) generate the same steady-state rate Equation 17.32–17.33. However, the particular expression for K_m should be different for each individual case.

Although undefined in mechanistic terms, the parameters K_m and V are very useful at the first steps of kinetic studies:

1. The use of Equation 17.34 allows the expression of the complex effects with simpler terms.
2. K_m and V are helpful as predictive parameters to design a valid enzyme assay. One practical recommendation is to keep substrate concentration in incubation mixture at the level of 10 K_m or higher.
3. Equation 17.34 permits one to obtain at least rough estimate of *in vivo* enzyme activity provided the internal substrate concentrations are known.

17.3.9 General Non-Steady-State Approach

Reaction scheme 17.32 contains four variables (*s, p, e*, and x) constrained by two mass–balance equations ($e_0 = e + x$, and $s_0 = s + p + x$). Therefore it is enough to integrate just two differential equations (e.g. Eqs 17.33 and 17.34) to characterize the whole system. A typical example of a numeric solution is shown in Fig. 17.6. We can see that enzyme-catalyzed reaction proceeds through three definite phases well separated on the time scale. Each phase is now safe to analyze with simpler mathematical expressions because any assumptions could be tested against the full exact solution.

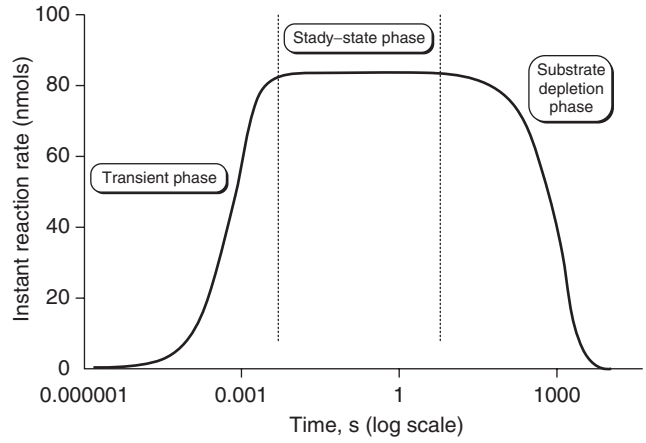


Figure 17.6. Time course of reaction proceeding by the Michaelis–Menten mechanism. Numeric integration of Equations 17.33–17.34: $s_0 = 10^{-4}$ M, $e_0 = 10^{-8}$ M, $k_{+1} = 10^6$ M/s, $k_{-1} = 10^3$ s^{-1}, $k_{+2} = 10^2$ s^{-1}.

1. The first *transient phase* occurs before the steady-state concentration of ESC is reached. It occupies less than 10^{-3} s for most of enzymes. During this phase, the substrate concentration remains fairly constant ($s \approx s_0$) allowing for the following analytical solution:

$$x(t) = \frac{k_{+1}e_0s_0}{A}[1 - e^{-At}],$$
$$v(t) = \frac{Vs}{K_m + s}[1 - e^{-At}],$$
$$A = k_{+1}s_0 + k_{-1} + k_{+2} \qquad (17.35)$$

   As compared with Equation 17.34 it contains a relaxation term $[1 - \exp(-At)]$ that is zero when t is small, but tends to 1 as t increases above $\tau = 1/A$. Accordingly, the rate of enzymatic reaction is initially zero but increases rapidly to the steady-state value as the exponential term decays. Because the relaxation term contains s_0, then the experimentally observed delay depends on substrate concentration. It allows for direct determination of individual rate constants k_{+1} and $(k_{-1} + k_{+2})$ by techniques such as in stopped-flow (33).
2. The second *steady-state phase* is characterized by the constancy of reaction rate due to the exact balance between the rates of ESC formation and breakdown ($dx/dt = 0$) while the substrate concentration remains close to the initial value s_0. This phase proceeds for at least several seconds. As a rule, it is enough to measure the *initial velocity* of enzymatic reactions unaffected by substrate depletion or product accumulation. Steady-state kinetics is the most popular research domain; it is the most accessible and developed and provides the

most kinetic data. However, it fails to determine individual rate constants as fully as the transient and relaxation approaches do. Steady-state equations were derived earlier (Eq. 17.34).

3. The third phase is characterized by considerable changes in the concentrations of substrate and product. Thus, we can no longer assume that $s = s_0$ and should integrate the complete set of Equations 17.32,17.33. However, very good precision provides the quasi–steady state approximation $ds/dt \gg dx/dt \approx 0$. Then we arrive at a relatively simple differential equation that is solved analytically:

$$\frac{ds}{dt} = -\frac{Vs(t)}{K_m + s(t)} \tag{17.36}$$

For initial conditions $s = s_0$, $p = 0$, $t = 0$, we have

$$K_m \ln \frac{s_0}{s} + s_0 - s = Vt \tag{17.37}$$

Equation 17.37 is called the *integrated Michaelis–Menten equation*. It remains to be valid not only for initial rate measurements but for any point within the reaction progress curve.

17.3.10 Experimental Determination of Kinetic Parameters of the Michaelis–Menten Equation

Until recently, most enzyme kinetic experiments have been analyzed by means of one of linear plots (Table 17.5). Linear plots are used to examine an agreement of experimental data with Equation 17.34 as well as to determine numeric values of parameters K_m and V from slopes and intercepts. Today, this graphic approach seems to be too cumbersome as compared with much more efficient computer routines. The main objection is also that any linear transformation introduces some statistical bias (ironically, the highest bias is attributed to the most popular double-reciprocal plot!). In addition, manual line drawing is very arbitrary, so obtained parameters could not be assessed statistically for confidence limits. However, plotting of original or linearized data is useful as an illustration and the first sketchy estimate of enzymatic parameters. For definitive work, it is advisable to avoid all plots and to use a nonlinear regression with following assessment of confidence limit for determined parameters (2).

17.3.11 Reversible Enzymatic Reactions

The majority of biochemical reactions are reversible. To account for this feature, the Michaelis–Menten mechanism

TABLE 17.5. Linear Plots (after Ref. 30)

$\frac{1}{v} = \frac{1}{V} + \frac{K_m}{V}\frac{1}{s}$	Lineweaver–Burk or double-reciprocal plot
$\frac{s}{v} = \frac{K_m}{V} + \frac{s}{V}$	Langmuir–Hanes plot
$v = V - K_m\frac{v}{s}$	Eadie–Hofstee plot
$V = v + \frac{v}{s}K_m$	Direct linear plot

can be modified as follows:

$$\underset{e_0-x-y}{E} + \underset{s}{S} \underset{k_{-1}}{\overset{k_{+1}}{\rightleftarrows}} \underset{x}{ES} \underset{k_{-2}}{\overset{k_{+2}}{\rightleftarrows}} \underset{y}{EP} \underset{k_{-3}}{\overset{k_{+3}}{\rightleftarrows}} \underset{e_0-x-y}{E} + \underset{p}{P} \tag{17.38}$$

Contrary to the basic scheme 17.32, there are two intermediates, one of which is the normal ESC and another is the *enzyme-product complex* (EP). The substrate, S and product, P can interconvert to each other. Application of the steady-state approach to this scheme results in the following equation:

$$\begin{aligned} v &= \frac{V^f s/K_m^s - V^r p/K_m^p}{1 + s/K_m^s + p/K_m^p} \\ V^f &= \frac{k_{+2}k_{+3}e_0}{k_{-2} + k_{+2} + k_{+3}}, \\ K_m^s &= \frac{k_{-1}k_{-2} + k_{-1}k_{+3} + k_{+2}k_{+3}}{k_{+1}(k_{-2} + k_{+2} + k_{+3})}, \\ V^r &= \frac{k_{-1}k_{-2}e_0}{k_{-1} + k_{-2} + k_{+2}}, \\ K_m^p &= \frac{k_{-1}k_{-2} + k_{-1}k_{+3} + k_{+2}k_{+3}}{k_{-3}(k_{-1} + k_{-2} + k_{+2})} \end{aligned} \tag{17.39}$$

where superscripts f and s denotes parameters of forward reaction, while r and p are indicators of reverse reaction.

When a reaction is at equilibrium, the net velocity must be zero and, consequently, if s_∞ and p_∞ are the equilibrium values of s and p, it follows from Equation 17.39 that equilibrium constant K is expressed via kinetic parameters (the *Haldane relationship*):

$$K = p_\infty/s_\infty = V^f {K_m}^p / V^r {K_m}^s \tag{17.40}$$

Equation 17.39 implies that the rate must decrease as the product accumulates, even if the decrease in substrate concentration is negligible. Thus, reversibility is closely associated with and requires the *product inhibition*. In many essentially irreversible reactions (e.g. invertase-catalyzed hydrolysis of sucrose) product inhibition is also significant. It can be explained by scheme 17.38 with only the second step being irreversible. In such a case, the accumulation of product causes the enzyme to be sequestered because of the

EP complex and reaction rate are as follows (compare with Equation 17.39):

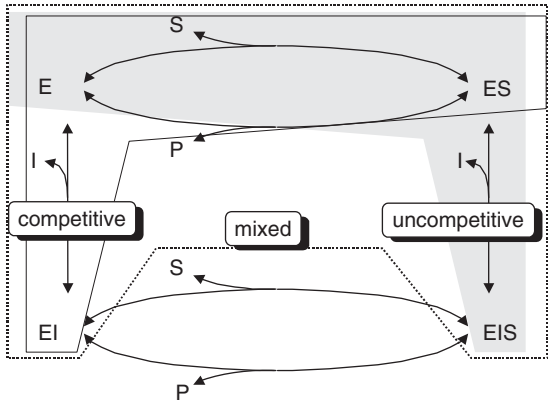
$$v = \frac{V^f s/K_m^s}{1 + s/K_m^s + pK_m^p} = \frac{V^f s}{K_m^s(1 + pK_m^p) + s} \qquad (17.41)$$

17.3.12 Inhibitors and Activators

Compounds that reduce the rate of enzyme-catalyzed reactions when they are added to the reaction mixture are called *inhibitors*. Just opposite effects (increase of reaction rate) are caused by *activators*. Both of them belong to the category of *modifiers*. We will concentrate here on inhibitors as having more practical application and even more specifically on *reversible* inhibitors, which form various dynamic complexes with enzymes. The *irreversible* inhibitors are known as *catalytic poisons* (many heavy metals, such as mercury); their binding to enzyme molecules reduces activity to zero, leaving no room for quantitative analysis.

The reversible inhibitors can form complexes with free enzymes or enzyme–substrate complexes as shown in the scheme of Botts and Morales (30)

There are three major simple (or linear) inhibition mechanisms, which can be generated from this scheme by omitting some of the six involved:



1. *Competitive* inhibition if *EIS* is missing (inhibitor binds to the same site on the enzyme as the substrate forming abortive nonproductive complex *EI*).
2. *Uncompetitive* if *EI* is missing and *EIS* occurs as a dead-end complex; it implies that the inhibitor-binding site becomes available only after the substrate has bound.
3. *Mixed* if *EI* and *EIS* both occur but are not interconvertible (the complex *EIS* does not break down to products; this situation frequently occurs when the inhibitor is reaction product). The particular case of mixed inhibition is *pure noncompetitive inhibition*, which takes place if two inhibitor dissociation constants (for *EI* and *EIS*) are exactly matched to each other.

For all types of inhibition, the Michaelis–Menten equation remains valid: under constant inhibitor concentration, i, the v–s relationship is of the same hyperbolic type as predicted by Equation 17.34, the only difference is that apparent values of K_m and V are now more or less simple functions of I (Table 17.6).

Some parameters (in boldface in Table 17.6) are not affected by inhibitors, whereas others are changed: competitive inhibitors increase K_m, pure noncompetitive inhibitors reduce V, uncompetitive inhibitors decrease at the same degree both V and K_m leaving first-order rate constant V/K_m to be unchanged. In mixed inhibition, there are no unchanged parameters.

One interesting case is so-called substrate inhibition. It occurs when two substrates are bound to the same active site on the enzyme, forming nonproductive triple complex ES_2

$$E + S \overset{K_s}{\longleftrightarrow} \begin{matrix} ES \\ {\scriptstyle K_{ss}\uparrow\downarrow} \\ ES_2 \end{matrix} \xrightarrow{k_2} E + P$$

then enzyme reaction rate is (34):

$$v = \frac{Vs}{K_s + s + s^2/K_{ss}} \qquad (17.42)$$

where K_{ss} is the dissociation constant for complex ES_2.

17.3.13 Cooperativity

Many enzymes respond to changes in metabolite concentrations (substrates, modifiers) with much higher sensitivity as compared with predictions from the classic hyperbolic

TABLE 17.6. Types of Inhibition

Type of Inhibition	V^{app}	$V^{app}/K_m{}^{app}$	$K_m{}^{app}$
Competitive	V	$(V/K_m)/(1 + i/K_i)^a$	$K_m(1 + i/K_i)$
Uncompetitive	$V/(1 + i/K'_i)$	V/K_m	$K_m/(1 + i/K'_i)$
Mixed	$V/(1 + i/K'_i)$	$(V/K_m)/(1 + i/K_i)$	$K_m(1 + i/K_i)/(1 + i/K'_i)$
Pure noncompetitive	$V/(1 + i/K_i)$	$(V/K_m)/(1 + i/K_i)$	K_m

[a] K_i = [I][E]/[EI]. K'_i = [I][ES]/[EIS].

Equations 17.34–17.42. This property is generally known as *cooperativity*, because it is thought to arise from cooperation between the active sites of the polymeric enzymes. As a rule, such enzymes consist of several *subunits* and display so-called sigmoid or S-shaped dependence of rate on substrate concentration. Many cooperative enzymes (but not all!) have *active sites* binding substrate and *allosteric sites* binding effectors. There are *homotropic* and *heterotrophic* cooperative effects caused by interactions between, respectively, identical and different ligands (e.g. substrate and an allosteric effector).

To explain the cooperativity and associated sigmoid kinetics, a number of models have been suggested. The earliest one is the Hill equation, which was originally designed to describe the S-shaped curve of oxygen binding to hemoglobin. It was assumed that each protein molecule E binds n molecules of ligands S in a single step, an amount of other possible forms ($ES_{n-1}, ES_{n-2}, \ldots ES$) being negligible:

$$E + nS \overset{K_h}{\longleftrightarrow} ES_n$$

where K_h is respective equilibrium constant. The fractional saturation of protein (enzyme or hemoglobin), Θ is given as

$$\Theta = \frac{\text{number of occupied binding sites}}{\text{total number of binding sites}} = \frac{[ES_n]}{[E] + [ES_n]} = \frac{[S]^n}{K_h + [S]^n} \tag{17.43}$$

Equation 17.43 can be rearranged into

$$\frac{\Theta}{1-\Theta} = \frac{[S]^n}{K_h}, \quad \log\left[\frac{\Theta}{1-\Theta}\right] = -\log K_h + n \log[S] \tag{17.44}$$

A plot of $\log \Theta/(1-\Theta)$ against log [S] known as *Hill plot*, should be a straight line of slope n (so). This equation is used to fit the experimental binding and kinetic data displaying sigmoid shape. When plotting kinetic measurements, it is assumed that $\Theta = v/V$, maximum velocity V should be known from independent measurements taken at saturation substrate concentration. However, the results of fitting should be interpreted with care. Firstly, Hill equation is empirical and generally provides good agreement only in the Θ range 0.1–0.9 (the discrepancy at extreme s is probably caused by neglecting other forms of ESC apart from ES_n). Secondly, parameter n (*Hill coefficient*) could not be interpreted as the number of subunits in the fully associated protein, rather it is an index of cooperativity.

Monod, Wyman and Changeux (35), proposed a general model explaining cooperativity and allosteric phenomena within a simple set of postulates:

1. Each subunit of enzyme can exist in two different conformations, designated R (relaxed) and T (tense).
2. All subunits of a molecule must occupy the same conformation at any time (e.g. for tetrameric enzyme only R_4 or T_4 are permitted, not R_3T or R_2T_2, etc.).
3. The two states are in equilibrium with constant $L = [R_4]/[T_4]$.
4. The affinity of ligand to subunit depends on conformation state: $K_R = [R][S]/[RS]$, $K_T = [T][S]/[TS]$, $c = K_R/K_T$.

The general equilibrium solution of this scheme is rather bulky, so we demonstrate one particular case of tetrameric protein, if $c = 0$ (i.e. $K_R \ll K_T$, S binds only to the R state), then we have

$$\Theta = \frac{(1 + s/K_R)^3 s/K_R}{L + (1 + s/K_R)^4} \tag{17.45}$$

At high s when $s/K_R \gg L$, we can neglect the term L in the denominator, and the entire expression is converted to no more than simple hyperbolic Langmuir isotherm. At low s, the contribution of L is considerable, so the saturation curve rises slowly from the origin displaying the S-shape.

There are other models describing the mechanisms of cooperativity and allosteric effects, for example, sequential model of Koshland, Nemethy and Filmer, the association–dissociation model Freiden and other (see details in Ref. 30).

17.3.14 Effects of pH

Every enzyme contains a large number of acidic and basic groups. Some of them are either fully deprotonated (aspartate, glutamate) or fully protonated (arginine, lysine). However, several groups with pK_a 5–9 (imidazole group of histidine, thiol sulphydryl group of cysteine) do change their ionization state when pH is varied. Assume as a first approximation that enzyme is represented as a dibasic acid H_2E and only singly ionized complex, HES^-, is able to react to give products:

$$\begin{array}{ccccc} H_2E & & H_2ES & & \\ \uparrow\downarrow K_1^E & & \uparrow\downarrow K_1^{ES} & & \\ S + HE^- & \underset{k_{-1}}{\overset{k_{+1}}{\rightleftharpoons}} & HES^- & \xrightarrow{k_{+2}} & HE^- + P \\ \uparrow\downarrow K_2^E & & \uparrow\downarrow K_2^{ES} & & \\ E^{2-} & & ES^{2-} & & \end{array}$$

Then the reaction rate is dependent on H^+ concentration, h, as follows (30):

$$v = \frac{Vs}{K_m + s}, \quad V = \frac{\widetilde{V}}{\left(\frac{h}{K_1^{ES}} + 1 + \frac{K_2^{ES}}{h}\right)}, \quad \frac{V}{K_m} = \frac{\widetilde{V}/\widetilde{K}_m}{\left(\frac{h}{K_1^{E}} + 1 + \frac{K_2^{E}}{h}\right)}, \quad (17.46)$$

where $\widetilde{V}$ and $\widetilde{K}_m$ are the pH-corrected constants. It is clear that pH-dependent variation of V reflects the ionization of ESC, while V/K_m reflects the ionization of the free enzyme. The pH-effects on K_m is more complicated being affected by both. Generally the dependence of enzyme activity on pH is described by Equation 17.46 as a bell-shaped curve with maximum at $\frac{1}{2}(pK_1 + pK_2)$.

17.3.15 Effects of Temperature

In chemical kinetics, the dependence of reaction rate on temperature is explained by *transition-state theory* developed by Eyring as early as in 1930–1935. It is based on the use of thermodynamics and principles of quantum mechanics. The reaction proceeds through a continuum of energy states and must surpass the state of maximum energy, when transient activated complex is formed. Then the dependence of reaction rate constant k on absolute temperature, T is expressed as follows:

$$\frac{d \ln k}{dT} = \frac{\Delta H^* + RT}{RT^2} \quad (17.47)$$

where R is the gas constant and ΔH^* is the enthalpy of activated complex formation. The classic *Arrhenius* equation may be obtained from Equation 17.47 under a simplified condition $\Delta H^* + RT \approx \Delta H = E_a$ (where E_a is *activation energy*). Most often Arrhenius equation is used in its integrated form

$$\ln k = \ln A - E_a/RT \text{ or } k = A \exp(-E_a/RT) \quad (17.48)$$

where A is the integration constant, interpreted as the frequency of collisions of reacting molecules. Apart from mechanistic derivations, there are a number of empirical expressions relating k and Celsius temperature T_c. The most popular is exponential formula:

$$\ln\ k = \ln\ A - \alpha T_c \text{ or } k = A \exp(\alpha T_c) \quad (17.49)$$

where α is empirical constant related to widely used temperature coefficient $Q_{10} = \exp(10 \times \alpha)$.

All presented mathematical expressions predict exponential or almost exponential increases of chemical reaction rates with temperature. However, enzymatic reactions deviate from this relationship at high temperature because of thermal denaturation of enzymes. Assume that denaturation is reversible with equilibrium constant $K_T = [E']/[E]$, where E is active enzyme molecules and E′ is inactive one. Then the combination of Equation 17.48 with the van't Hoff relationship for $K_T (-RT \ln K_T = \Delta G^\circ = \Delta H^\circ - T\Delta S^\circ)$ results in

$$v = \frac{A \exp(-E_a/RT)}{1 + \exp(\Delta S^\circ/R - \Delta H^\circ/RT)} \quad (17.50)$$

where ΔG°, ΔS°, and ΔH° are the standard Gibbs free energy, enthalpy, and entropy of denaturation reaction, respectively, and v is the observed rate of biological process. This equation produces a curve with single maximum and fits to the most of available experimental data on temperature dependent variation of enzymatic activity.

Sometimes denaturation is irreversible, and there are no possibilities for simple mathematical expressions, because temperature effects are time-dependent. However, still numeric solution of respective differential equations can be used.

17.4 SIMPLE MODELS OF MICROBIAL AND CELL GROWTH

This section deals with simple unstructured models. These models mainly ignore any changes in cell quality (biochemical composition, spectrum of enzymatic activity, etc.) induced by environmental factors.

17.4.1 Main State Variables and Growth Parameters

There are two types of growth models, *deterministic* and *stochastic*. The former describe clear determined and regular processes. The latter deal with random or stochastic processes. The main variables used in deterministic models are the same as in chemical kinetics, concentrations of biomass, substrates, and products, and stochastic models consider instead the probabilities, frequency distributions, variance, and so on. For example, a stochastic model can consider the probability of a single bacteria cell dividing under specified environmental conditions. Although any real-life biotechnological process has both deterministic and stochastic components, most useful growth models are strictly deterministic. In this section, we will concentrate on this type of model, and the stochastic counterparts will be considered only in section titled "Cell Cycle." The major state variables of deterministic models describing cell growth are described in Table 17.7. The concentration of biomass and

TABLE 17.7. Major State Variables of Deterministic Models

Variable	Notation	Dimension (Examples)
Concentration of cell biomass	x	g CDW/liter of cultural liquid
Cell number[a]	N	10^9 cell/mL of cultural liquid
Single-cell mass[a]	m_1	g CDW/cell
Mycelium length[b]	L	meter/liter of cultural liquid
Tips number[b]	n	10^6 tips/mL of cultural liquid
Concentration of limiting substrate	s	gram/liter of cultural liquid
Concentration of product	p	gram/liter of cultural liquid or gram/gram of CDW

[a]For unicellular organisms (bacteria, yeasts).
[b]For filamentous organisms (fungi, actinomycetes).

cell number are related to each other by simple formula:

$$x = m \cdot N \tag{17.51}$$

where conversion factor m is the average dry mass of a single cell. In some studies, it is safe to assume m to be a constant and use both variables x and N as equivalent measures of growth. However, the average size and mass of single cells vary depending on the nature of studied organisms and environmental conditions (see section titled "Cell Cycle"); therefore, it is advisable to make a selection. The biomass, x, has obvious advantage in studies aimed at understanding or control of mass flows, and cell number, N, is preferred in population studies when, for example, mutation or plasmid transfer is an essential factor controlling the efficiency of the biotechnological process.

The choice of method to determine biomass or cell number depends on many factors (6). Today, the preference should be given to those techniques that allow exact and automated measurements (Table 17.8). The most advanced analytical methodology is now available for automatic recording of gaseous or volatile substrates, intermediates, and end products, such as methane, CO_2, O_2, H_2, volatile fatty acids, alcohols, and other fermentation products (infrared and mass spectrometry, gas chromatography, NMR, etc.).

The *primary* state variables that are measured directly in cell culture are usually recalculated into the *secondary* growth characteristics: gross growth rate, $\mathrm{d}x/\mathrm{d}t$; specific growth rate, $\mu = (\mathrm{d}x/\mathrm{d}t)/x$; degree of multiplication, x/x_0; biomass doubling time, $t_\mathrm{d} = \ln 2/\mu$; growth yield, $Y = -\mathrm{d}x/\mathrm{d}s$; product yield, $Y_{p/s} = -\mathrm{d}p/\mathrm{d}s$, $Y_{\mathrm{p/x}} = \mathrm{d}p/\mathrm{d}x$; specific rate of substrate consumption, $q_\mathrm{s} = -(\mathrm{d}s/\mathrm{d}t)/x = \mu/Y$; specific rate of product formation $q_p = (\mathrm{d}p/\mathrm{d}t)/x = \mu Y_{p/x} = \mu(Y_{p/x}/Y)$. Most of the listed secondary growth characteristics are called *specific* rates expressed as a first-time derivatives of measured variable *per unit of cell mass*. The specific rates are not sensitive to variations in total cell biomass, so they can be considered as analogous to enzyme activity in most kinetic derivations. The specific growth rate, μ, may be viewed as the activity of an autocatalytic enzyme producing itself. The specific growth rate, μ, measured from biomass dynamic, x, can differ from that estimated from the increase in cell number, N (denoted as μ_N). It follows from Equation 17.51 that

$$\mu = \frac{1}{x}\frac{\mathrm{d}x}{\mathrm{d}t} = \frac{1}{x}\frac{\mathrm{d}(N \cdot m)}{\mathrm{d}t} = \frac{1}{N \cdot m}\left[N\frac{\mathrm{d}m}{\mathrm{d}t} + m\frac{\mathrm{d}N}{\mathrm{d}t}\right]$$
$$= \frac{1}{m}\frac{\mathrm{d}m}{\mathrm{d}t} + \frac{1}{N}\frac{\mathrm{d}N}{\mathrm{d}t} = \mu_\mathrm{cell} + \mu_N \tag{17.52}$$

If mass of single cell m is constant, then $\mu_\mathrm{cell} = 0$ and $\mu = \mu_N$. Otherwise we have to take into account m-variation.

17.4.2 Validity of Exponential Growth Low

One of the earliest postulates in microbial kinetics is that under optimal nonrestrictive conditions (nutrient media containing all essential components at nonlimiting concentrations, absence of inhibitors, adequate physicochemical parameters, perfect mixing) the increase in biomass ($\mathrm{d}x$) during an infinitely small time interval ($\mathrm{d}t$) is proportional to this time interval and the instant biomass concentration (x), that is

$$\mathrm{d}x = \mu x \mathrm{d}t, \text{ or } \mathrm{d}x/\mathrm{d}t = \mu x \tag{17.53}$$

where μ is the proportionality coefficient. If μ is constant, integration of Equation 17.53 gives

$$\ln x = \ln x_0 + \mu t \Rightarrow x = x_0 \exp(\mu t) \tag{17.54}$$

where x_0 is biomass at zero-time or *inoculum size*.

According to early views, true exponential growth occurs only in the case of symmetrically dividing bacteria with equal probability of subsequent division for the mother and daughter cells. Organisms with asymmetrical multiplication (budding yeasts) were thought to obey the exponential low only approximately, whereas the growth of filamentous organisms (fungi, streptomycetes) was

TABLE 17.8. Methods Used for Determination of Microbial Biomass

Method	Measuring Principle	DL[a]	Advantage	Disadvantages
Dry mass	Mass of separated and dried solids	50	Provides direct unconditional estimate	Interference from dead cells and noncell solids
Wet mass	Mass of separated material	50	Simplicity, quickness	The variation of wet biomass bulk density
Wet biovolume	Linear dimension of pelleted cells or colony	100	Simplicity, quickness	The variation of wet biomass bulk density
Particulate organic carbon	CO_2 after cell separation and combustion	1.0	High precision and sensitivity, provides direct estimate of mass	Interference from dead cells and noncell solids
Biuret proteins	Colorimetric reaction of peptide bonds	1.0	High uniformity	Variation of protein-to-biomass ratio, possible extracellular accumulation
Folin–Ciocalteu protein	Colorimetric reaction of tyrosine and tryptophan	0.1	High sensitivity	Variation of protein-to-biomass ratio and amino acid composition of cell protein, possible extracellular accumulation
DNA	Colorimetric estimation of deoxyribose	1.0	High specificity, constancy of the DNA cellular content	Possible extracellular accumulation
ATP	Bioluminescence assay	10^{-5}	High sensitivity and specificity	Variation of the intracellular ATP pool
Fatty acids	Gas or liquid chromatography, colorimetric reaction	1.0	High specificity, allows identification of composition of mixed culture	Variation of the intracellular content, possible extracellular accumulation
Metabolic potential	Rate of added substrate uptake or product formation	10^{-3}–10	High specificity, quickness	Variation in conversion factor from measured rate to biomass
Opacity	Light scattering	0.1	Simplicity, quickness, automation	Interference from noncell solids, cell aggregation, wall growth
Electrical measurements	Conductivity, capacitance	1	Simplicity, quickness, automation	Variation of conversion factor, interference from electrolytes in the medium
Manual microscopy	Cell count, measuring of hypha length	10^{-5}	Low cost, sensitivity, allows visual assay of biomorphological structure	Time-consuming, low precision
Image analysis	Computer-aided count	10^{-5}	Combined benefit of manual and automated quantification, speed, generation of size distribution	High cost
Coulter counter	Automated count and sizing	10^{-5}	Quickness, automation, generation of size distribution	Interference from noncell solids
Plating	Growing of the colonies on Petri dish	10^{-5}	Low cost, high sensitivity	Time-consuming, low precision

[a]DL = detection limit, the minimum CDW required for an estimation with an error <2% (mg).

deviated considerably. However, direct measurements performed from 1930 to 1960 (see Ref. 6) revealed that exponential growth does occur in all prokaryotes and eukaryotes independent of their biomorphological features, including protozoa, fungi, and homogeneously cultivated plant and animal cells. The deviation is observed only as a result of growth-associated change in the environment. Wang and Koch (36) made very precise measurements of μ dynamics by growing *Escherichia coli* directly in an aerated cuvette of the computer-linked double-beam spectrophotometer. They found temporary slowdowns in the complex peptone plus beef-extract media attributed to diauxie phenomena (e.g. depletion of some preferred oligopeptides) and a gradual increase of the μ value during sequential subculture in succinate minimal medium. Long-term cultivation of microorganisms in continuous turbidostat or pH-auxostat culture (37) revealed that the increase in μ is mainly result of autoselection of mutants having higher maximum specific growth under specified cultivation conditions [see section titled "Population Dynamics (Mutations, Autoselection, Plasmid Transfer)"].

17.4.3 Early Views of Cell Growth

The derivation of the exponential growth equation was done for binary dividing bacteria, based on the geometric progression $2, 2^2, 2^3 \ldots$ (38):

$$N = N_0 2^n \tag{17.55}$$

where n is the number of divisions, $n = t/t_d$.

The growth dynamics were viewed as a succession of distinct phases approximated with empirical formulas (39)

$$N = N_0 \exp[\mu F(t) t] \tag{17.56}$$

where function $F(t)$ undergoes stepwise changes as shown in Table 17.9.

The alternative way to describe growth dynamics was to use *the logistic equation* borrowed from demographic studies (40):

$$\frac{\mathrm{d}N}{\mathrm{d}t} = rN\left(1 - \frac{N}{K}\right) \text{ or } \frac{\mathrm{d}x}{\mathrm{d}t} = rx\left(1 - \frac{x}{x_m}\right) \tag{17.57}$$

TABLE 17.9. Stepwise Changes of Function $F(t)$

Initial Stationary Phase	$F(t) = 0$
Lag phase, $1.56 \le n \le 2.7$	$F(t) = t^{n-1}$
Logarithmic growth phase	$F(t) = 1$
Negative growth acceleration phase	$F(t) = t^{-t-1}$
Maximum stationary phase	$F(t) = 0$
Accelerating death phase, $1.56 \le n \le 2.7$	$F(t) = t^{n-1}$
Logarithmic decrease phase	$F(t) = -1$

where r is the net growth rate (the difference between true growth and death rates) and K or x_m are the upper limits of respectively population density or biomass (K is used preferentially in ecological literature, being called the carrying capacity of the ecosystem). This equation simulates S-shaped growth dynamics frequently observed in natural ecosystems and cell cultures.

Similar (but not identical) equation of cell biomass dynamics would be produced if we assume that the limiting substrate is consumed according to first-order kinetics and is converted to biomass with a fixed yield factor

$$Y = (x - x_0)/(s_0 - s), \tag{17.58}$$

then:

$$\frac{\mathrm{d}s}{\mathrm{d}t} = -ks, \quad s = \frac{x_0 + Ys_0 - x}{Y} = \frac{x_m - x}{Y},$$
$$\Rightarrow \frac{\mathrm{d}x}{\mathrm{d}t} = -Y\frac{\mathrm{d}s}{\mathrm{d}t} = kx_m\left(1 - \frac{x}{x_m}\right) \tag{17.59}$$

17.4.4 Monod's Model

This model still is very popular because of its elegant simplicity. It played an important role in the history of microbial growth kinetics as a first encouraging example when the theoretical development based on mathematical formalisms came before novel experimental designs. As compared with simple exponential Equation 17.53 this model (41) takes into account the mass-conservation condition linking substrate uptake to biomass formation through constant yield factor, Y (Eq. 17.2) and the dependence of the specific growth rate on limiting substrate concentration:

$$\frac{\mathrm{d}x}{\mathrm{d}t} = \mu(s)x = \mu_m \frac{s}{K_s + s}x$$
$$\frac{\mathrm{d}s}{\mathrm{d}t} = -\frac{1}{Y}\frac{\mathrm{d}x}{\mathrm{d}t}. \tag{17.60}$$

By substitution of s by x through Y (Eq. 17.58) we can reduce equation set 60 to a single equation having the analytical solution:

$$\mu_m t = (1 + P)\ln(x/x_0) - P\ln(Q - x/x_0) + P\ln(Q - 1), \tag{17.61}$$

where $P = YK_s/x_m$, $Q = x_m/x_0$, $x_m = Ys_0 + x_0$, while s_0 and x_0 are respectively s and x at $t = 0$.

Equation 17.61 contains three parameters, Y, μ_m, and K_s, that can be thought of as passport data for a particular organism (e.g. for *E. coli* grown on glucose at 30°C $Y = 0.23$, $\mu_{\mathrm{m}} = 1.35\ \mathrm{h}^{-1}$, and $K_{\mathrm{s}} = 4\ \mathrm{mg\ l}^{-1}$) and describe the S-shaped growth dynamics of a batch culture. The initial conditions, s_0 and x_0 are set by the experimenter, who

selects the inoculation dose and medium composition. Thus, knowing the values of all these entities, the growth dynamics can be calculated *prior to the experiment*. Moreover, this model was used as a basis for development of the *chemostat theory* to understand and predict the behavior of microbial cultures in continuous-flow bioreactors before the respective hardware was constructed. For this purpose, original Equation 17.60 was modified as follows (42):

$$\frac{dx}{dt} = (\mu - D)x, \quad \mu = \mu_m \frac{s}{K_s + s} x$$
$$\frac{ds}{dt} = D(s_r - s) - \frac{1}{Y}\mu x, \quad D = \frac{F}{V}, \qquad (17.62)$$

where s_r is the concentration of limiting substrate in the fed fresh medium delivered with pump from reservoir, F is the pumping rate (cubic centimeter/hour), V is culture volume (cubic centimeter), and D is the dilution rate defined as the ratio $D = F/V$ (h^{-1}).

The mathematical analysis of Equation 17.62 allows us to make the following conclusions on the growth kinetics of continuous culture:

1. The described open system attains stable *steady state*, when $dx/dt = 0, ds/dt = 0$, and variables x and s are not changed with time (denoting steady-state concentrations $\tilde{x}$ and $\tilde{s}$ respectively). From the first equation it follows that $\mu = D$, that is, the specific rate of microbial growth is equal to the dilution rate, which is under the full control of the experimenter. From the second equation, we find

$$\tilde{x} = Y(s_r - \tilde{s}), \qquad (17.63)$$

   As compared with Y expression for batch culture (Eq. 17.58), this formula no longer contains the term, x_0, the inoculum size. Thus, a steady-state culture is not dependent on past history, and its properties are determined solely by current cultivation parameters.
2. The dilution rates permitting stable microbial growth (i.e. those D, at which $\tilde{x} > 0$), are confined between 0 and washout point or *critical dilution rate*, D_c

$$D_c = \mu_m s_r/(K_s + s_r) \qquad (17.64)$$

3. The specific growth rate μ does not depend on either s_r or x and is governed solely by the substrate concentration in the cultural liquid. On the other hand, the indirect effect of s_r on μ may be evaluated from the dependence of $\tilde{x}$ on D, as soon as $\tilde{x}$ and $\tilde{s}$ are linked by the conservation condition in Equation 17.63.

The most important biological implication of the chemostat theory was the discovery of the fact that microorganisms can grow endlessly with any rate between 0 and μ_m. Such substrate-limited growth is nevertheless exponential, because two subsequent acts of cell division will be separated by a constant time interval. Earlier, substrate limitation had been observed only transiently at the end of the exponential phase of batch growth. The most important biotechnological implication of the chemostat model was the concept of *controlled cell biosynthesis* which implies the purposeful manipulation of microbial culture to optimize the productivity by such tools as changing the flow rate and the composition of medium in continuous-flow bioreactors.

17.4.5 Derivation of the Monod Equation from Mechanistic Considerations

The equation relating μ and s is known as *Monod equation*:

$$\mu = \mu_m \frac{s}{K_s + s} \qquad (17.65)$$

It was introduced by the author as a purely empirical relationship resembling adsorption isotherm. However, many microbiologists did view the Monod equation as something having deep inherent meaning rather than as just an empirical formula. Below, we shall outline a number of attempts to deduce this equation logically from the conjectured growth mechanisms.

1. *The Bottleneck Concept.* There is an obvious similarity between the Monod and Michaelis–Menten equations. A theoretical "substantiation" for this similarity can be the bottleneck postulate originally put forward by Blackman (43). According to this postulate, the growth rate of a cell is on the whole determined by a single *enzymatic master reaction*. Microbial metabolism is symbolized as a unidirectional chain of reactions of substrate S conversion to cell biomass X′ via some hypothetical intermediates $P_1, P_2 \ldots P_n$:

$$S + X' \xrightarrow{k_1} P_1 \xrightarrow{k_2} P_2 \longrightarrow \ldots \xrightarrow{k_n} P_n \xrightarrow{k_{n+1}} 2X' \qquad (17.66)$$

   Assuming steady state in respect to intermediate concentration $p_i, dp_i/dt = 0$, we arrive at the Monod equation, composite parameters μ_m and K_s being expressed via elementary kinetic constants of individual enzymatic reactions:

$$\frac{dx}{dt} = \mu_m \frac{s}{K_s + s} x; \quad \mu_m = \frac{1}{\sum_{i=2}^{n+1} 1/K_i};$$
$$K_s = \frac{1}{k_1 \sum_{i=2}^{n+1} 1/K_i}, \qquad (17.67)$$

where $x = x' + p_1 + \ldots p_n$. The "bottleneck" idea can now be formulated as follows. If one of the constants $k_j \ll k_i, i = 2, \ldots, n+1, i \neq j$, then $\mu_m = k_j$ and $K_s = k_j/k_1$, and so the jth enzymatic reaction is the master reaction.

The obvious shortcomings of the reaction scheme 17.66 are the unjustified oversimplification of the cell metabolism (which is a network, rather than a simple unidirectional sequence of reactions) and the lack of a definite interpretation of variables x' and p in real biochemical terms. An evaluation of the characteristic times of major intracellular metabolic reactions showed that there could be two possible "bottlenecks": (i) uptake of limiting substrate (processes of active transport, transphosphorylation of sugars, etc.) (44) and (ii) the formation of intracellular protein-synthesizing structures such as rRNA and the ribosomal proteins (45).

2. *Stochastic Considerations.* Microbial populations were assumed to consist of active (which utilize the substrate) and inactive cells (46). The probability of a transition from the inactive state to the active one was supposed to be proportional to s, whereas the probability of the reverse transition was s independent. From these assumptions, a relationship between μ and s, can be inferred, similar to Equation 17.65.
3. *Derivations Based on Mechanistic Considerations of Protein Synthesis (47).* The rate of protein synthesis, dp/dt, is supposed to be determined by rRNA concentration R and by the size of the amino acids pool, A, $dp/dt = kxRA/(K_A + A)$, $k =$ constant. Other conditions are defined as: $R = R_0 + (R_m - R_0)\mu/\mu_m$, $A = bs$, and $P = p/x$, where R_m and R_0 are respectively, the upper and lower limits of R variation, and P and b are constants. For a steady-state chemostat culture, $dp/dt = 0$ and $dx/dt = (1/P)(dp/dt) = 0$, then

$$\mu = (k\ R_m/P)s/(R_m K_A/\beta R_0 + s) = \mu_m s/(K_s + s). \quad (17.68)$$

Here again, the Monod equation is derived through a consideration of underlying intracellular processes.

Needless to say, none of the cited derivations are free from criticism. The Monod equation remains empirical. Any attempts to provide the mechanistic interpretation of this equation inevitably lead to much more complicated mathematical expressions (see section titled "Structured Models").

17.4.6 Biological Meaning and Experimental Determination of Growth Parameters K_s and μ_m

The parameter μ_m, maximal specific growth rate, has very lucid biological meaning: it is the upper limit of μ variation on specified nutrient medium. It could not be attained in reality because of its asymptotic nature: $\mu \to \mu_m$ as $s \to \infty$. However, in practice μ_m is achieved if $s \gg K_s$. It should be remembered that μ_m is not absolute maximum of growth rate, as it depends on the nature of the limiting substrate. For example, *E. coli* has μ_m above 2.5 h^{-1} on complex beef-extract medium and below 1.0 h^{-1} on minimal medium with succinate. Saturation constant, K_s could be defined functionally as such concentration of limiting substrate which provides specific growth rate equal to 0.5 of μ_m. We can say also, that K_s is a measure of cell affinity to substrate: the lower is K_s the better the organism is adapted to consume substrate from diluted solution. Any other definitions are speculative, for example, K_s interpretation as the dissociation constant of ESC of the cellular enzyme involved in the first step of substrate conversion.

There are several ways to determine numeric values of K_s and μ_m:

1. *Batch Culture, Differential Form of Monod Equation.* The biomass dynamics, $x(t)$ are followed from the start of the exponential phase until the complete consumption of the limiting substrate and the attainment of the maximal cell density, x_m. The residual substrate concentration, s is calculated from mass–balance (Eq. 17.58). Yield is calculated as $(x_m - x_0)/s_0$ (the s_0 value should be known) and corresponding $\mu(t)$ values from the slopes $d(\ln x)/dt$. Finally, parameters K_s and μ_m are to be found graphically or from nonlinear regression as in the case of the Michaelis–Menten equation (see below).
2. *Batch Culture, Initial Growth Rates.* The inoculum size, x_0, and the duration of experiment are chosen to minimize the uptake of added substrate: $s \approx s_0$ (48). Typically, bacterial cell density should be of the order 10^{-5} or less, and is measured by such sensitive instruments as the Coulter Counter. The quasi–steady state growth rate is measured at several s_0 values and then fitted to Equation 17.65 as described before. In numerous determinations made at much high cell densities (when we can no longer neglect substrate consumption) it was anyway observed that dependence of μ on s_0 is formally described by Monod equation with s replaced by s_0 (see as example, Ref. 49). The explanation of these results could be made only by more complex structured models; however, the described procedure is not appropriate for K_s and μ_m determination.
3. *Batch Culture, Integral Form of Monod Equation.* The S-shaped curve of biomass dynamics is fitted directly to Equation 17.61 either through preliminary linearization or nonlinear regression (preferential). Sometimes (e.g. when cells are grown in opaque media) it is more convenient to follow the dynamics

of residual substrate, $s(t)$, product formation, $p(t)$, for example, CO_2 evolution, or even dynamics of O_2 uptake (respiration). In these cases, we can integrate the set of differential Equations 17.60 in terms of $s(t)$ or $p(t)$ dynamics taking into account mass–balance relationships (Eqs 17.7,17.8 and 17.58 and similar).

4. *Steady-State Chemostat Culture.* The chemostat provides the opportunity for estimations under steady-state condition which is commonly believed to be more reliable. By running an experiment at different dilution rates, D, the corresponding $\tilde{s}$ values may be measured, and, therefore, the dependence of $\mu = D$ on $\tilde{s}$ can be obtained, in principle, as accurately and carefully as desired. Such an approach, however, may and frequently does encounter serious technical problems because of high affinity to limiting substrate of some microorganisms. There is the need (i) to select highly sensitive analytical techniques to measure extremely low residual concentrations of particular substances, (ii) to develop instant sampling procedures to minimize substrate loss, and (iii) to eliminate apparatus-related artifacts such as nonperfect mixing, fluctuations in nutrient medium supply. This can always be accomplished by use of radio-labeled substrate, some other tips are covered in specific experimental works (50). However, the most essential objection to this method is that organisms at various steady-states do change their kinetic properties which are not accounted by Monod's model (see section titled "Structured Models").
5. *Non-Steady-State Chemostat Culture.* The measurements are made during short-term experiments started by addition of different amounts of limiting substrate to a steady-state chemostat culture. Then substrate uptake or respiration rates are recorded in perturbed culture until the new steady-state is established (2). The opportunity of continuous culture is that the physiological state of cells just before perturbation is well defined and reproducible. On the other hand, these experiments do provide data on affinity to substrate (K_s) and maximal rates of respiration, for example, Q_{CO2}, or uptake, Q_s, which are related but are not identical with μ_m:

$$\mu_m = Y_{p/x} Q_{CO2} = Y_{s/x} Q_s \tag{17.69}$$

where stoichiometric parameters $Y_{p/x}$ and $Y_{s/x}$ should be determined in independent experiments. Immediate assay of μ_m in such an experimental setup is possible as follows: the steady state is perturbed by setting the dilution rate by 20–100% higher than critical value D_c (Eq. 17.64). The washout dynamics is followed and μ_m is determined from approximate relationship (6): $x \approx x(0)\exp[(\mu_m - D)t]$, where $x(0)$ is biomass before perturbation. More rigorous estimate of μ_m could be provided if such washout experiments are made at several (at least two) input substrate concentrations s_0 to account for the fact that s_r is still not infinity.

17.4.7 Modification of the Monod Equation

It was found that not all experimental data could be reasonably well fitted by Equation 17.65. The best-fit hyperbola often passed above experimental points at small s and below them at large s. A better fit was claimed to be provided by using the following, entirely empirical equations (51–53):

$$\mu = \mu_m[1\text{-}\exp(-Ks)] \tag{17.70}$$

$$\mu = \mu_m s^n/(K_s + s^n) \tag{17.71}$$

$$\mu = \mu_m s/(K_s x + s) \tag{17.72}$$

The preference of the first expression, Equation 17.70 is questionable. An expansion of the Monod equation by addition of the third parameter, n in Equation 17.72, or introduction of the second variable, x in Equation 71, does improve the approximation capability of kinetic equations. We can even provide the mechanistic basis for this improvement. Thus, the Moser equation is similar to the Hill equation in enzymology (Eq. 17.43) indicating the cooperativity effects in performance of some "master" reaction of cellular metabolisms. The Contois equation could be interpreted in terms of growth autoinhibition by-products, because under the realistic assumptions [(i) $x \gg x_0$, (ii) $xY_{p/x}/K_p \gg 1$ and (iii) product, p, formation is coupled with growth], the apparent saturation constant K_s^{app} displays linear relationship with biomass x resembling the Contois expression:

$$\begin{aligned} K_s{}^{\text{app}} &= K_s(1 + p/K_p) \\ &= K_s[1 + Y_{p/x}(x - x_0)/K_p] \approx K_s x, \end{aligned} \tag{17.73}$$

An account of maintenance requirements. Powell (54) assumed that substrate uptake rate, q obeys the Michaelis–Menten kinetics, then from Equation 17.18 it follows that

$$q_s = Q_s/(K_s + s) = \mu/Y^{\text{m}} + m \tag{17.74}$$

If μ_m is defined as $\mu_m = Y Q_{\text{s}}$ (6), then

$$\mu = \frac{\mu_m s}{L_s + s} - mY^m = \mu_m \left(\frac{s}{K_s + s} - \frac{s^*}{K_s + s^*} \right),$$

$$s^* = \frac{mY^m}{\mu_m - mY^m} \tag{17.75}$$

If we define $\mu_m = Y^m(Q_s - m)$ (2), then

$$\mu = \mu_m \frac{(s - s^*)}{K_s + s}, \quad s^* = \frac{K_s m Y^m}{\mu_m} \tag{17.76}$$

Equations 17.75 and 17.76 both predict the occurrence of threshold substrate concentration s^*, below which growth is impossible. It yields a substantially better fit to experimental data. The difference is that according to Equation 17.75 the parameter μ_m is the specific growth rate under imaginary conditions of substrate excess and zero maintenance requirements, whereas Equation 17.76 implies the traditional definition of μ_m as the specific growth rate under substrate excess: $\mu \to \mu_{\mathrm{m}}$ when $s \to \infty$.

17.4.7.1 Account for Substrate Leakage. Mathematically identical to Equation 17.76 modification of the Monod equation was proposed for the case of conserved substrates. However, the biological meaning is entirely different: if the specific leakage rate is assumed to be constant, then a decrease in s down to some threshold value s^* will lead to the counterbalance of the two reverse processes (uptake and leakage), so that the net consumption of the limiting substrate will be zero.

17.4.7.2 Account of Inhibitory Effects. A few valuable refinements of the Monod equation were borrowed from enzymology, most often they were noncompetitive and substrate inhibition. The former inhibition mechanism is simulated by the so-called *Monod–Ierusalimsky* equation:

$$\mu = \mu_m \frac{s}{K_s + s} \times \frac{K_p}{K_p + p}, \tag{17.77}$$

The growth retardation with an excess of such substrates as phenol, methanol, and ethanol is described by an analogue of Haldane's equation (55):

$$\mu = \mu_m \frac{s}{K_s + s + s^2/K_{ss}} \tag{17.78}$$

Equation 17.78 simulates a single-peak curve, and so one and the same μ value may be obtained at two different s, one in the substrate-limiting range, $\mathrm{d}\mu/\mathrm{d}s > 0$ (stable), and the other in the substrate inhibition range, $\mathrm{d}\mu/\mathrm{d}s < 0$ (unstable). A sustainable maintenance of a population under conditions of substrate inhibition is possible either in the second stage of a two-stage chemostat or in the case of plentiful wall growth in a conventional chemostat (56).

17.4.7.3 Account of Diffusion Effects. We will present one example of such models (54). The basic assumption is that substrate is taken up by an enzyme that obeys Michaelis kinetics and is localized on the inner side of cell membrane. The actual substrate concentration around the enzyme active centers is smaller than in the solution, because of a limited diffusion rate. By applying a simplified Laplace equation, it was found eventually that

$$\mu = \frac{\mu_m(K_s + L + s)}{2L}\left(1 - \sqrt{1 - \frac{4Ls}{(K_s + L + s)^2}}\right) \approx \mu_m \frac{s}{K_s + L + s}, \tag{17.79}$$

where L is a factor determined by membrane permeability and by the maximum rate of the enzymatic reaction.

17.5 STRUCTURED MODELS

The unstructured models (such as Monod's model or its modifications) are able to predict and describe only simplest manifestation of growth phenomena. Sometimes it is declared that Monod-type models are able to describe only *balanced* and *steady-state* growth. The analysis of more complicated unbalanced and non-steady-state growth requires formulation of structured models.

17.5.1 Definitions

Balanced growth was defined by Campbell (57) as a proportional increase in the amounts of all cell components, in other words, balanced growth produces cells of the same quality without any variation of composition. The terms *steady state* and *non–steady state* stem from chemical and enzyme kinetics. The first one refers to such a regime when the reaction rate remains constant, because of exact balance between formation and breakdown of intermediary products such as the ESC. In microbial culture, the growth is called *steady state* if *specific* rather than *total rates* remain constant. In an open system such as a chemostat, both total ($\mathrm{d}x/\mathrm{d}t$, $\mathrm{d}s/\mathrm{d}t$) and specific rates $\mu = (1/x)\mathrm{d}x/\mathrm{d}t$, $q_s = (1/x)\mathrm{d}s/\mathrm{d}t$ tend to have constant steady-state values. A closed system such as a batch culture should be considered under steady state only during the exponential phase when μ and q_s are constant. The linear growth with a constant total rate ($\mathrm{d}x/\mathrm{d}t = \mu x = \text{const.}$) is characterized by monotonously declining μ, and is not steady-state growth. However, under some conditions (such as in dialysis culture) it may attain *quasi–steady state*, when $\mathrm{d}s/\mathrm{d}t \approx 0$.

The non-steady-state kinetic regimes take place before establishment of steady state or after its perturbation. In enzyme kinetics, non-steady-state measurements are taken

in the millisecond range of time scale. In microbial cultures, similar non-steady-state transient and perturbation processes advance much more slowly, typically during several hours and days. An example is transient process in the chemostat induced by changes in D or s_r (fed substrate concentration). In such growth, μ, q_s, q_p and other metabolic rates exhibit continuous variation in time. The attractiveness of non-steady-state studies for microbiology and biotechnology is obvious:

- They allow a wider range of hypotheses to be tested and yield much more data on the studied objects;
- They have higher practical value in biotechnology, steady-state operation is the exception rather than the common routine because of unavoidable disturbances in cultivation conditions;
- They provide additional tools for optimal regulation of cell performance in the bioreactor, because purposeful non-steady-state growth may display greater efficiency and higher productivity (58).

By *structured*, we mean mathematical models describing growth-associated changes in microbial cell composition. It includes mass balance equations for all assigned intracellular components. Their concentrations can be expressed either per unit volume of fermentor vessel, $(c_1, c_2, .., c_n)$, or per unit cell mass, $(C_1, C_2, .., C_n)$, and, hence, $C_i = c_i/x$. The mass balance equations can be written as follows,

$$\sum_{i=1}^{n} c_i = x, \quad \sum_{i=1}^{n} C_i = 1. \tag{17.80}$$

For each variable C_i a differential equation is written that takes into account all sources, r_+, and sinks, r_-, as well as its dilution from cell mass expansion (growth),

$$\frac{dC_i}{dt} = r_+(s, C_1, \ldots, C_n) - r_-(s, C_1, \ldots, C_n) - \mu C_i \tag{17.81}$$

The simplest structured models with n no more than 2 or 3, are called two or three-compartment models. For example, a model (59) incorporated two compartments, (i) nucleic acids and (ii) proteins combined with other active cell components. The model variables also included concentrations of the limiting substrate and the inhibitor. Compared to Monod's model, the proposed set of four equations was able to account for a much wider range of dynamic patterns. Specifically, it simulated D-dependent changes in the cell composition (chemostat) and all known growth phases of batch culture from the lag to decline. However, the choice of variables in this model was more or less arbitrary, and so it should be regarded more as an interesting illustration rather than a research tool.

During the last two decades, much more realistic structured models based on biochemical data have been developed. The simulation model of *E. coli* growth (60) contains the following dynamic variables: glucose and NH_4^+, as exosubstrates, CO_2 and acetate, as products excreted into the medium, amino acids, ribonucleotides, deoxyribonucleotides, monomeric precursors of cell wall components, rRNA and tRNA, nonprotein polymeric components, glycogen, guanosinetetraphosphate, enzymes transforming ribonucleotides into deoxyribonucleotides, ATP, NAD(H), and protons. Altogether, the dynamic model amounts to a system of 21 differential and 14 algebraic equations. An even more complicated model simulating growth of *Bacillus subtilis* (61) is the set of 39 nonlinear and coupled differential equations containing nearly 200 parameters! These models are able to simulate particular growth features such as changes in cell sizes, shape and composition, as well as the D-dependent variations in replication time brought about by the shifts in glucose concentration. However, the predictive capability of such an intricate dynamic model should be still estimated as modest as compared with invested modeling efforts: they are still a "caricature parody" of real cell but already too complex to be studied by conventional mathematical tools (stability analysis, parameters identification, etc.) or to be used in biotechnological applications. The "best choice" of a mathematical model lies, apparently, midway between unstructured and highly structured models outlined here. One of the known compromises has been found through attempts to express quantitatively the *cell physiological state*.

17.5.2 Physiological State of Chemostat Culture

The term was coined by Malek (62) without giving a clear definition. The impetus for the development of the concept of a physiological state was the evidence on changes in the chemical composition of microorganisms as dependent on dilution rate, D and medium composition in chemostat culture (63). It has been found that some of the studied parameters remained constant (e.g. DNA and total carbon), while others exhibited regular D-dependent variations, either an increase (RNA content, cell sizes) or a decrease (the content of reserved polysaccharides). Those properties, that were D-dependent, were recognized as components of the *vector of the physiological state*.

Powell (54) combined and put on a quantitative mathematical footing three notions, which were beforehand separated and cloudy: (i) physiological state, (ii) past history and (iii) non-steady-state growth kinetics of microbial culture. The specific rate of substrate uptake, q_s, was presented as a product

$$q_s(s) = q'_a(s)S(s) \tag{17.82}$$

where $S(s)$ is a simple saturation function, for example, a Michaelis hyperbola, $S(s) = s/(K_s + s)$, and $q'_a(s)$ is a function associated with the microbial physiological state. The instant value of $q'_a(s)$ is determined by way in which s varies until the given moment (τ h ago), effects of later events contributing more than earlier ones. Transient processes are influenced by the past history of the culture in the following manner. Suppose that a steady-state growth of a chemostat culture is upset and the residual substrate concentration jumps from $s(0)$ to $s(1)$. Immediately, q_s will increase from $Q(0)S[s(0)]$ to $Q(0)S[s(1)]$. If no further changes in $s(1)$ occur, then Q will also eventually attain a new steady-state value equal to $q'_a[s(1)]$. In essence, Q is the potential metabolic activity, that is, the specific rate of a key metabolic process measured just at the moment of relief from substrate limitation. The transient Q dynamics are described as

$$\text{net change} = \text{production} - \text{dilution caused by cell growth}$$

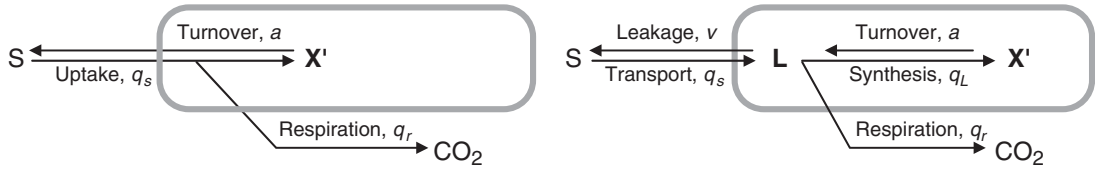
$$\frac{dQ}{dt} = r(Q, s) \qquad - \mu(Q, s)Q \tag{17.83}$$

"Substance Q" may, in reality, be represented by a single enzyme or multienzymatic complexes, as well as by ribosomes or other cell components occupying the bottleneck position. Monod's model, supplemented by Equation 17.83, made possible at least a qualitative understanding of chemostat transient processes triggered by a D switch (64).

17.5.3 Synthetic Chemostat Model (SCM)

The SCM (2) combines Powell's ideas with new molecular data on microbial growth. The basic SCM interprets microbial growth as a conversion of exosubstrate S into cell macromolecules $\mathbf{X}'$ either directly (left) or via a pool of intermediates $\mathbf{L}$ (right).

Macromolecular cell components are susceptible to degradation (turnover), and monomeric metabolites can escape into environment because of leakage. Contrary to simple growth models, the composition of cells is allowed to vary (therefore, X' and $\mathbf{L}$ are vectors) in response to a changing environment because of the adaptive nature of microbial metabolism. At the heart of the SCM are the solution of the problem, how to cope with these variations, and how to describe adaptive changes in cell composition by relative simple models.



All macromolecular cell constituents are divided into two groups: primary cell constituents necessary for intensive growth (P-components), and components needed for cell survival under any kinds of growth restriction (U-components). The characteristic examples of P-components are ribosomes (rRNA and ribosomal proteins) and enzymes of the primary metabolic pathways. Their intracellular content increases parallel to an increase in μ. The contribution of U-components to cell biomass decreases with growth acceleration. Examples are enzymes of the secondary metabolism, protective pigments, reserved substances, and transport systems of high affinity.

The analysis of available data as well as mass-conservation conditions allowed the formulation of several rules of variation of cell components taking place because of optimal control of cell biosynthesis:

1. Amounts of P- and U-components expressed as a fraction of total cell mass (P and U, gram/gram of biomass respectively) vary within the upper ($P^{\max}$, $U^{\max}$) and low ($P^{\min}$, $U^{\min}$) limits, the latter being the constitutive part.
2. An increase of one individual P-component is accompanied by increase of other P-components.
3. The total enlargement of P-sum is accompanied by corresponding decrease of U-sum and *vise versa*.
4. The P/U-ratio is controlled by limiting substrate concentration in environment.

These rules are translated into mathematical terms as follows:

$$\frac{P_1 - P_1^{\min}}{P_1^{\max} - P_1^{\min}} \approx \ldots \approx \frac{P_n - P_n^{\min}}{P_n^{\max} - P_n^{\min}} = r;$$

$$\frac{U_1 - U_1^{\min}}{U_1^{\max} - U_1^{\min}} \approx \ldots \approx \frac{U_m - U_m^{\min}}{U_m^{\max} - U_m^{\min}} = 1 - r;$$

$$\overline{r} = \frac{\overline{s}}{K_r + \overline{s}} \tag{17.84}$$

where variable r (*index of physiological state*) is already scalar (not vector!) function controlled by environmental factors, for example, concentration of the limiting substrate; symbols $\overline{r}$and $\overline{s}$ stand for steady-state concentrations of r

and s respectively. The r values in steady-state chemostat culture change from zero (in culture at almost zero growth rate, when $\overline{s} \to 0$ and all P-components come down to low limits) to 1.0 (in unlimited culture, when $\overline{s} \gg K_s$ and P-components attain maximum). During transients caused by sudden s changes, an instant r value goes toward new steady state (compare with Eq. 17.82):

$$\frac{\mathrm{d}r}{\mathrm{d}t} = \mu \times \left(\frac{s}{K_r + s} - r \right) \tag{17.85}$$

The introduction of the r-variable greatly simplifies the use of structured models, because the adaptive variation of cell composition (and metabolic activity which is determined by the intracellular content of particular enzymes) now could be expressed via one single "master" variable r. For example, the specific rate of substrate uptake q_s is defined as:

$$q_s = r\frac{Qs}{K_s + s} + (1 - r)\frac{Q's}{K'_s + s} \tag{17.85a}$$

where the first and the second terms on the right side stand respectively for low (P-component) and high (U-component) affinity of transport system. Similar r-dependent expressions are derived for other reactions (q_L, ν, a) and stoichiometric parameters. The full set of basic SCM for chemostat culture is given as follows:

$$\begin{aligned}
&\frac{\mathrm{d}s}{\mathrm{d}t} = D(s_r - s) - q_s x, \\
&\qquad q_s = rQ\frac{s}{K_s + s}, \quad \text{or} \quad \text{equation 17.85a} \\
&\frac{\mathrm{d}x}{\mathrm{d}t} = \mu x - Dx, \quad \mu = Y(q_s - m) - a, \\
&\qquad m = m_0 r, \quad a = a_0 r \\
&\frac{\mathrm{d}r}{\mathrm{d}t} = \mu \times \left(\frac{s}{K_r + s} - r \right)
\end{aligned} \tag{17.86}$$

As compared with the Monod model (Eq. 17.62), the SCM contains one additional differential equation for variable r, index of physiological state. This variable reflects the changes of all cellular P-components, but it can be viewed specifically as a total cellular RNA content, easily measurable variable. The saturation constant K_r shows how fast the content of P-components approaches maximum with raising the limiting substrate concentration in chemostat. Other growth parameters remain similar to their equivalents in the Monod model. The only difference is that parameters assumed to be constant in the Monod model (maintenance coefficient, turnover rate, substrate maximal uptake rate and saturation constant) are treated by SCM as functions of slow variable r. The instant maximal substrate uptake rate is given as product rQ, where Q is a true maximal rate measured in a fully established substrate-sufficient continuous culture. The maintenance requirements are given as product $m = m_0 r$, where m_0 is the upper limit of the m-variation. The turnover rate a is introduced as $a = a_0 r$, where a_0 is the upper limit of turnover rate variation.

Originally Equation 17.84 was introduced as a convenient semiempirical relationship satisfying most experimental observations. Its validation recently came from molecular-genetic studies. Several genes and their products were found to play the role of master regulator and metabolic coordinator as dependent on the state of environment. All bacteria have functionally similar but chemically diverse master regulators. In *E. coli* and other γ-proteobacteria, there are two forms of a sigma subunit of RNA polymerase: σ^{S} (*rpoS*) and σ^{70} (*rpoD*) which are expressed under stress and normal growth conditions respectively. While rapidly growing cells contain very little σ^{S}, exposure to many different stresses results in rapid and strong σ^{S} induction which is then followed by transcription of numerous σ^{S}-dependent genes (more than 70) responsible for stress-protective functions. Substrate limitation results in increased *rpoS* transcription, whereas high osmolarity, low temperature, acidic pH, and some late-log-phase signals stimulate the translation of *rpoS* mRNA. In addition, carbon starvation, high osmolarity, acidic pH, and high temperature stabilize σ^{S}, which, under nonstress conditions, is degraded with a half-life of one to several minutes (65–68).

This finding explains the presence of two groups of cellular macromolecules, **P** and **U** (they are eventually products of two cascades initiate respectively by σ^{70} and σ^{S}). Linear approximation of vectors **P** and **U** through scalar r is firmly supported by the fact that sigma factors turn on/off simultaneously the entire group of genes (at least 70 under stress and probably higher number of genes under normal growth conditions). Finally the coupling between starvation and other forms of stress justifies our selection for formulae $r(\overline{s})$ as a main link between the state of environment and cell composition. This fact also explains old observations that any stress-resistance is expressed in a higher degree in starving cells as compared with cells actively growing in a rich nutrient media.

Contrary to all known chemostat models, SCM provides adequate simulation of D-dependent variation of microbial physiological state. Under energy- and C-limited growth, it was expressed as an increase of apparent K_{s}, potential uptake and respiration rates, maintenance ratio, and turnover parallel to increase of D. Under N limitation, a similar trend was complemented by considerable decrease of Y_{N} due to alteration of cell composition in favor of N-rich P-components (Fig. 17.7). SCM adequately describes the transient growth caused by shift-up in chemostat culture. The phenomena of overshoot in substrate concentration and undershoot in biomass during

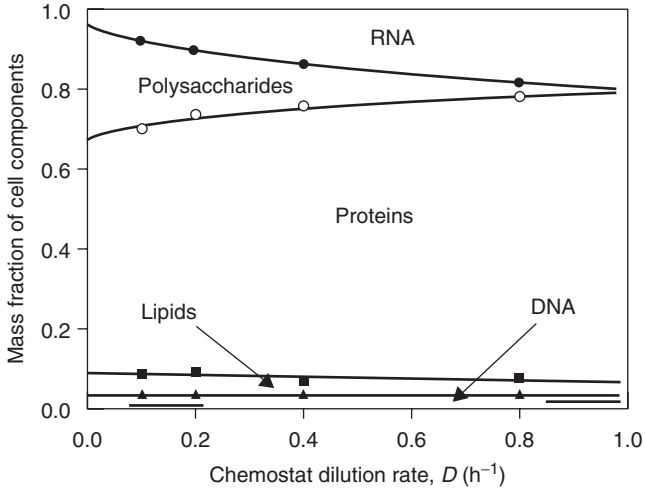


Figure 17.7. Simulation of D-dependent changes in cell composition of *Aerobacter aerogenes* grown in NH_4^+-limited chemostat culture. The curves are calculated from SCM (2), the original experimental data are from Ref. 69.

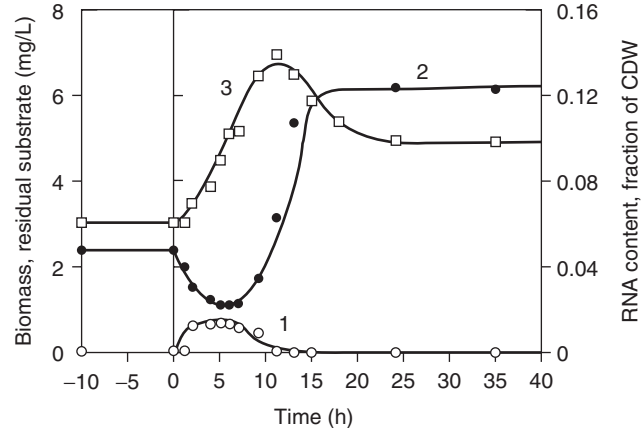


Figure 17.8. SCM simulation of transient growth induced by change of chemostat dilution rate. Residual glycerol concentration (1), biomass (2) and cell RNA content (3). At $t = 0$ dilution rate was shifted from 0.004 to 0.24 h^{-1}. Redrawn from Ref. 2, the original data (69) are for chemostat culture of *A. aerogenes* limited by glycerol.

transient growth are explained by slow adjustment of cell composition (RNA content, respiratory activity) to new growth conditions (Fig. 17.8). Batch culture limited by carbon and energy source was simulated by SCM on the whole from inoculation to death stage; conventional growth phases (lag, exponential, deceleration, stationary, decline) were generated automatically without setting any specific conditions (Fig. 17.9). It is important that SCM realistically describes and predicts not only net growth but also the survival dynamics of starving cells after substrate depletion. During this phase, surviving bacteria sustain very slow cryptic growth at the expense of cell turnover and metabolites leakage. The rate of decline in biomass gradually decreases as the result of buildup of some U-components (parallel to the decrease of such P-components as ribosomes and CN-sensitive respiration enzymes). Batch culture limited by conserved substrate (the source of N, P, Mg, Fe, or other) has an interesting feature: the growth is not stopped after substrate depletion but proceeds at an even higher rate. SCM explains this phenomenon by the partitioning of deficient elements between mother and daughter cells.

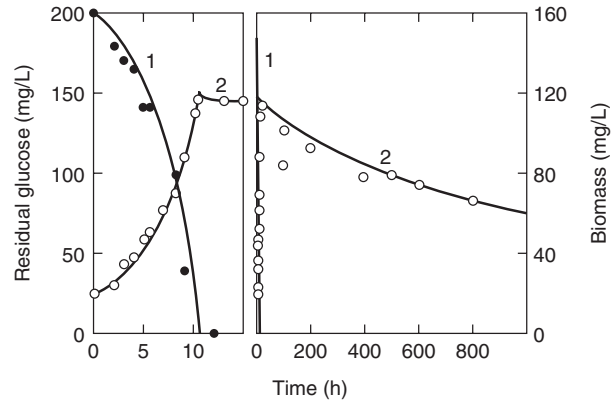


Figure 17.9. SCM simulation of complete dynamic curve of batch culture: residual glucose (1) and biomass (2) of yeasts *D. vanrijiae* (old name *D. formicarius*) grown on glucose-mineral medium (2). Note that contrary to old empirical models (Eq., 17.56, Table 17.9), all growth phases are reproduced automatically without specifying preset time ranges.

17.5.4 Cell Cycle

The term *cell cycle* is used to designate the regularly repeated sequence of events that occur between consecutive *cell divisions*, for example, the formation of two identical daughter cells from one cell, which takes place in most known bacteria. Equivalent cell cycle events include *budding* (most yeasts and budding bacteria), *branching of hypha* (filamentous organisms), *fragmentation* (actinobacteria). The majority of available data have been obtained for rod-shaped bacteria (*E. coli, Salmonella typhimurium, Bacillus cereus*) under steady-state growth conditions when the cell cycle consists of three distinct phases:

1. The growth of the newborn cell without chromosome replication from the initial mass m_0 until some critical initiation mass m^*
2. DNA replication (C period)
3. Separation of daughter cells (D period).

17.5.4.1 Relationship between Cell Size and Specific Growth Rate. The periods C and D are constant and occupy in the case of *E. coli* about 40 and 20 min

respectively independently of environmental conditions. However, the duration of the first phase does depend on cultivation conditions: the time of the single-cell mass increase from m_0 to m^*, is inversely related to the specific growth rate, μ. It is this difference that yields μ-dependent variations of cell sizes, because faster-growing cells produce for the same $\tau = C + D$ time bigger cell mass than do slower growing cells. It became clear from the following simple algebra:

The steady-state growth of an individual cell proceeds exponentially throughout the entire cell cycle [$m = m_0 \cdot \exp(\mu t)$]. At the time of the second part of the cycle it takes exactly τ min for the cell to enlarge from critical mass m^* to $2m_0$: Hence

$$2m_0 = m^* \cdot \exp(\mu\tau) \Rightarrow m_0 = 0.5m^* \cdot \exp(\mu\tau) \quad (17.87)$$

Equation 17.87 remains to be valid for steady-state culture at any μ which can be varied from 0 to μ_m. Assuming that cell critical mass m^* is constant and does not depend on growth rate, we see that Equation 17.87 predicts μ-dependent variation mass of newborn cells m_0 and hence the average mass and size of the bacterial population. This finding is supported by numerous experimental studies from the beginning of this century (70) that displayed the positive correlation between cell size and growth rate. Because the term $\mu\tau$ is rather small ($\mu\tau \leq \mu t_d = \ln 2$), it is difficult to notice the exponential curvature of the experimental curve. Thus, a linear approximation is frequently used to relate the average cell size $\overline{m}$ ($\overline{m} \approx m_0 \cdot 2 \cdot \ln 2$ for rod-shaped bacteria, see derivation below) and μ:

$$\overline{m} = \overline{m}(0) + k\mu \quad (17.88)$$

The regression parameters $\overline{m}(0)$ and k have meaningful biological interpretation: y-intercept, $\overline{m}(0) \approx (\ln 2)m^*$ is equal to approximately 69% of the cell critical mass m^* initiating chromosome replication, and slope $k = [\exp(\mu_m\tau) - 1]/\mu_m \approx \tau$, is close to the duration of C + D periods.

The postulate on the constancy of the critical mass, m^* was derived from the observation that the cell has accurate control over its size-at-division and poorer control over its age-at-division (71). Recently, accurate measurements with flow cytometry (72) revealed that m^* is inversely related to the specific growth rate; slowly growing cells tend to initiate DNA replication at a slightly higher critical mass as compared with intensively growing cells. However, we may safely assume that m^* variation is much smaller than the variation of cell mass during the cell cycle: $dm^*/dt \ll dm/dt$.

17.5.4.2 Simulation of Cell Cycle by Simple Deterministic Structured Model. In biochemical terms, it is difficult to envisage how cell mass *per se* could determine when to initiate replication. A more likely candidate is some mass-related parameter, such as intracellular concentration of some signal metabolite like *initiator protein*, according to the popular model proposed by Helmstetter and Cooper (15,73). It was postulated that the initiation of DNA replication is triggered by a threshold intracellular concentration of protein V^*, this protein is synthesized at a rate proportional to the total growth rate and requires exactly one mass doubling time to reach its threshold concentration again. This mechanism is translated into mathematical form of structured model such as SCM as follows (2):

$$\frac{dV}{dt} = \Theta(\mu + a) - \mu V$$

$$\frac{d\lambda}{dt} = \zeta \begin{cases} \text{if } V \geq V^* \text{ then } \zeta = \zeta_1 > 0 \text{ else } \zeta = 0 \\ \qquad\qquad \text{(initiation)} \\ \text{if } \lambda \geq \lambda^* \quad \text{then} \quad \lambda = \lambda/2, \quad V = 0, \quad m = m/2 \\ \qquad\qquad \text{(division)} \end{cases} \quad (17.89)$$

where Θ is the fractional contribution of protein V to total cell synthesis. The V content is an intrinsically transient entity: even during steady-state growth, it continuously changes between zero (Helmstetter and Cooper postulated the annihilation of the initiator protein after every replication cycle) to an upper threshold value, V^* which is less than the potential steady-state level, $\Theta(\mu + a)/\mu$. The second variable, λ imitates the replicating chromosome: it sets up the discontinuity associated with cell division.

Analysis of coupled equation set 89 reveals that this model is stable toward perturbations. Suppose that by chance, the content of initiator protein has risen to some abnormally high level. The immediate result would be several more frequent cell divisions with smooth reversal to normal multiplication pace. Similar events take place under the opposite situation of V deficiency: several divisions are delayed resulting in production of abnormally long cells, but then steady state is restored. The negative feedback mechanism that brings things back into line is based on the dynamic nature of variable V: it is characterized by unique stable steady state that is approached from different initial conditions.

It may be easily shown that the described model adequately simulates various morphological effects exhibited during non-steady-state growth (Table 17.10).

17.5.5 Statistical Analysis of the Population Distributions

Equations 17.87–17.89 were derived by using deterministic approach, which assumes that all cells in the microbial population are exact copies of each other and their division is

TABLE 17.10. Morphological Effects during Non-Steady-State Growth

Effects	Explanation
The longer lag phase in batch culture when growth is surveyed by cell count rather than biomass measurements	The partial synchronization of cell division is delayed as compared with mass growth until attainment of the value $2m$
The accumulation of enlarged cells during transition from lag to exponential growth phase	The $\mu-m$ relationship (Eq. 17.87) combined with the transient misbalance in V synthesis (Eq. 17.89)
The formation of dwarf cells in starving population	The small cells are produced during very slow cryptic growth of surviving organisms
The accumulation of division potential if division is blocked by inhibitor, then after block release all missing division takes place in quick sequence	This phenomenon is simulated by Equation 89 and explained by overproduction of initiator protein in the presence of inhibitor

completely asynchronous. However, real culture is always heterogeneous, individual cells differ in size, age, metabolic activity and cellular composition. Experimental assessment of heterogeneity became possible due to rapid advance of analytical tools such as computer-aided microscopy, flow cytometry, electronic count and sizing of cells with Coulter counter.

There are two possible approaches to the mathematical description of age heterogeneity: the discrete approach, where several age groups of cells are introduced, and the continuous approach, which utilizes the *distribution function* of cells by age (74). The first approach is usually applied to multicellular organisms (plants and animals) whose individual age can be instantly determined; it is often based on use of matrix notation, for example, Leslie matrices (75,76). For bacteria, direct estimation of individual cell age (i.e. how many minutes ago given cell was born by a binary division) is practically insolvable task. Newborn cells are generally smaller than mature cells just before their division but the cellular sizes depend not only on age but also on the quality of nutrient medium and other factors. Therefore, the most fruitful approach in microbial kinetics is to deal with mathematically derived continuous *age distribution functions* of cells and then relate them to experimentally measured size distribution function based on various hypotheses on cellular division.

McKendrick (77) and later von Foerster (78) introduced the *age density function* $n(t, \tau)$ of bacterial cells as follows: consider population containing $N(t)$ cells. Select all those cells which, at time t, have ages between τ and $\tau + \Delta\tau$. Let their number be $\Delta N_\tau(t)$. Then the age density function is defined as the limit:

$$\lim_{\Delta\tau\to 0} \Delta N_\tau(t)/\Delta\tau = n(t, \tau)$$

It has the property that

$$N(t) = \int_0^\infty n(t, \tau)\, \mathrm{d}\tau$$

The von Foerster equation (78,79) states that

$$\frac{\partial n(t, \tau)}{\partial t} + \frac{\partial n(t, \tau)}{\partial \tau} = -\lambda \cdot n(t, \tau) \tag{17.90}$$

where λ is cell loss function, the initial age distribution $\beta(\tau) \equiv n(0, \tau)$ and cell birth rate $\alpha(t) \equiv n(t, 0)$

von Foerster equation remains too abstract, as it does not show explicitly the effect of environmental conditions, such as limiting substrate concentration. This gap has been filled in by introducing the age distribution function into chemostat model (74):

Modified Von Foerster equation

$$\frac{\partial n}{\partial t} + \frac{\partial n}{\partial \tau} = -(w + D)n(t, \tau) \tag{17.91}$$

Cell proliferation

$$n(t, 0) = 2\int_0^\infty wn(t, \tau)\, \mathrm{d}\tau \tag{17.92}$$

Initial age distribution

$$n(0, \tau) = \Gamma(\tau) \tag{17.93}$$

Total cell concentration

$$\frac{\mathrm{d}N}{\mathrm{d}t} = \int_0^\infty wn(t, \tau)\, \mathrm{d}\tau - DN \tag{17.94}$$

Limiting substrate concentration

$$\frac{\mathrm{d}s}{\mathrm{d}t} = -\int_0^\infty \rho n(t, \tau)\, \mathrm{d}\tau + D(s_r - s) \tag{17.95}$$

where w and ρ are specific rates of cell division and substrate consumption, D is dilution rate and s_r is substrate concentration in the medium feed.

Numeric solution of the normalized set of Equations 17.91–17.95 displays a number of new counterintuitive properties observed in some chemostat experiments but not reproduced by a nonstructured and nondistributed chemostat model (Eq. 17.62 above), such as spontaneous synchronization of cellular divisions and oscillations in residual limiting substrate and cell density after abrupt changes in D.

Equations 17.90–17.95 deal with age distribution of microbial (mostly rod-shaped bacteria) cells. Now we will look to relationship between cellular age and size. If certain conditions are met, the culture is fully desynchronized, cells grow according to some deterministic low, all divide into two and only two identical daughter cells, and there are no cell elimination, then age distribution is given by (71)

$$\phi(\tau)\mathrm{d}\tau = 2\mu e^{-\mu\tau}\mathrm{d}\tau : 0 \le \tau \le \ln 2/\mu = t_d, \qquad (17.96)$$

where μ is specific growth rate, t_d is mean doubling time, τ is the age since birth, and $\phi(\tau)\mathrm{d}\tau$ is the frequency of cells whose ages are between τ and $\tau + \mathrm{d}\tau$.

Assuming that cells grow exponentially between divisions, then the frequency of mass distribution is

$$\phi(m)\mathrm{d}m = 2m_0/m^2\mathrm{d}m : m_0 \le m \le 2m_0, \qquad (17.97)$$

where m_0 is the mass of newborn cell and $\phi(m)\ m + \mathrm{d}m$ is the frequency of cells whose masses are between m and $m + \mathrm{d}m$. The mean cell size is $2m_0 \cdot \ln 2$ (calculated as an integral of $m \cdot \phi(m)\mathrm{d}m$).

If cell growth between two consecutive divisions is linear, then (80):

$$\phi(m)\mathrm{d}m = 4 \cdot \ln 2/m_0 \exp(-m \cdot \ln 2/m_0)\mathrm{d}m : m_0 \le m \le 2m_0, \qquad (17.98)$$

Equations 17.96 and 17.97 are called *canonical* age or mass distributions to emphasize that they are an idealized form applicable when cell division takes place at a precise size. Assuming that momentary distribution of size-at-division of individual cells is *normal* and *random* (not correlated with other cell cycle events), we can obtain computer-simulated curves for any fixed level of noise expressed as the coefficient of variation (CV). As shown in Fig. 17.10, random variations of size-at-division tend to round the corners of the canonical distribution.

Another source of cell size variation can be nonequal separation of mother cells into two daughter cells. It is characterized by the K-distribution which is the distribution of the ratio of daughter cell length to mother cell length. The average values absolutely necessarily equals 0.5, but CV is at best about 4% (e.g. for well-behaved *E. coli* strains) and can attain rather high values for other organisms. The deviation of observed versus predicted size distribution may be caused also by cell death and different kinds of cell pathology (abnormally long or dwarf cells).

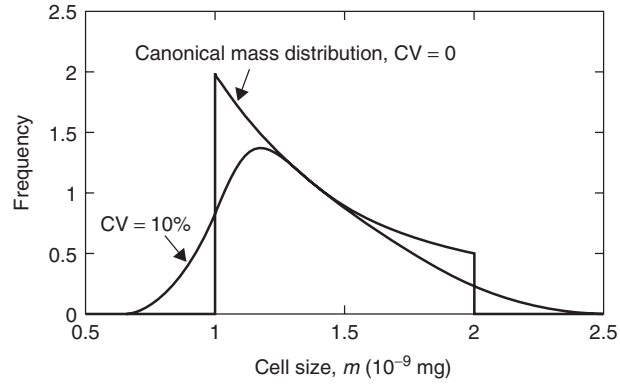


Figure 17.10. Distribution of cell sizes (as single-cell mass) for canonical case where there is no variation in the size-at-division and for the case of normal distribution of size-at-division with CV = 10% (see details in Ref. 71).

Collins and Richmond (81) introduced an entirely different approach based on the use of three distributions:

$$v_m = \mu\left\{2\int_0^m \Psi\mathrm{d}m - \int_0^m \phi(m)\ \mathrm{d}m - \int_0^m \lambda(m)\ \mathrm{d}m\right\}/\lambda(m) \qquad (17.99)$$

where V_m is growth rate of cells of size m, $\lambda(m)$ is the extent population distribution, Ψ is the momentary distribution of dividing cells, and $\phi(m)$ is the momentary distribution of newborn cells. This equation allows the calculation of the mean growth rate of cells of particular size class. Instead of this analytical method, Koch in his work with Shaechter (71) proposed the synthetic approach. Starting from the set of specific postulates of the cell multiplication mechanism (linear or exponential growth of cell mass between divisions, kind of control, the evenness of the division) they derived the size or age distribution which then was compared with the observations.

17.5.6 The Growth Law

Some believe that there should be a general law of cell growth that can be discovered by sensitive methods of analysis. The rate of biomass growth throughout the cell cycle was hypothesized to be linear, bilinear, exponential, double-exponential, and so on. Two limiting cases have generally been considered: the exponential and linear growth models proposed respectively by Cooper and Kubitschek (71). To differentiate between these two mechanisms three classes of experiments have been used:

1. Size measurements of individual cells growing in the microculture by use of phase contrast microscopy

or recently developed confocal scanning light microscopy combined with image analysis.

2. Pulse-chase labeling of cells with their subsequent separation into different phases of the cell cycle. Most frequently, labeled uracil and leucine are used as precursors of RNA and protein synthesis respectively. There are two major sources of errors in this approach: poor resolving power of separation methods and artifacts associated with effects of exogenous compounds on intracellular fluxes (feedback inhibition, pool expansion, label dilution, etc.). One of the best options for separation is probably the "baby machine" based on membrane elution principle (73). To minimize the second source of error, the mutants blocked in the synthesis of the probe compound can be used.
3. Analysis of the frequency distributions of steady-state populations (Eqs 17.91 and 17.92). However, the resolving power of this approach is rather low because linear and exponential models produce similar patterns.

Most of the obtained results are in better agreement with the exponential growth model rather than with the linear model. However there are some serious doubts about whether there is a unique simple mathematical growth law describing bacterial growth during the division cycle. Cooper (73) proposed distinguishing three categories of cell components that are synthesized with a unique pattern:

1. Cytoplasm (proteins, RNA and ribosomes, small molecules) that are accumulated exponentially
2. Cell DNA that is replicated in a linear fashion as a sequence of constant and zero rates
3. Cell surface composed of peptiodoglycan and membranes that are synthesized exponentially during most parts of the cell cycle but immediately before cell division the synthesis accelerates to accomplish new pole formation.

Thus, the growth pattern of the whole cell is the sum of these three patterns. Because the cytoplasm is the major constituent (up to 80% of CDW), the growth of the cell should be approximately exponential.

17.6 POPULATION DYNAMICS (MUTATIONS, AUTOSELECTION, PLASMID TRANSFER)

17.6.1 Description of Mutation and Autoselection

The continuous culture turned out to be very efficient tool to study mutation and autoselection (82). Let N be the total cell concentration, M the concentration of mutants, μ the specific growth rate of the main nonmutated part of the cell population and η the specific growth rate of neutral mutants, then

$$\frac{dM}{dt} = \lambda\mu N + \eta M - DM,$$
$$\frac{dN}{dt} = \mu N - \lambda\mu N - DN \qquad (17.100)$$

where λ is the mutation rate expressed as the ratio of the numbers of mutants to total number of cells formed. If $\lambda \ll 1$ and $\mu = \eta$, in the steady state, we obtain, $\mu = \eta = D$, and

$$\frac{dM}{dt} = \lambda N D \quad \text{or} \quad M = M_0 + \lambda D N t. \qquad (17.101)$$

If $\eta > \mu$, then the original strain will be displaced by the mutant, otherwise, if $\eta < \mu$, M will tend to a lower limit $M^* = \lambda N/(1 - \eta/D)$.

Experimental studies of phage resistant mutants in a tryptophan-limited chemostat culture of *E. coli* showed that the period of linear M increase in accordance with Equation 17.95 was fairly short. Every 20–100 generations there was an abrupt fall in the number of mutants, after which the linear growth resumed at the same rate (82). The observed "sawtooth" dynamics in M were explained by Moser (52) as a combined effect of mutation and selection. The original wild clone gives not a single but a whole array of mutations with subsequent reversions. Let us denote the total cell population in a chemostat culture as N, which is the sum of all subpopulations including original and emerging variants, $N = \sum N_i$. All possible transitions between variants are given by the matrix, $\lambda_{i\to j} (j = 1, \ldots, n; i = 1, \ldots, n; j \neq 1)$. Then the chemostat model takes the following form

$$\frac{dN}{dt} = \sum_{j=1}^{n} \frac{dN_j}{dt} = \overline{\mu}(s)N - DN, \quad \overline{\mu} = \frac{1}{N}\sum_{j=1}^{n} \mu_j N_j,$$
$$\frac{dN_j}{dt} = \mu_j(s)N_j - DN_j - \sum_{i\neq j}^{n} \lambda_{j\to i} N_j + \sum_{j\neq i}^{n} \lambda_{i\to j} N_i, \qquad (17.102)$$
$$\frac{ds}{dt} = D(s_0 - s) - \sum_{j=1}^{n} \mu_j(s) N_j / Y_j,$$
$$\mu_j(s) = \mu_m \frac{s}{K_{sj} + s}$$

Every drop in the "sawtooth" dynamics of neutral mutants detected by their phage-resistance can be interpreted as the appearance of other types of spontaneous mutant with higher growth capabilities. In a chemostat culture, such mutants overcompete and displace all other cells by virtue of their higher affinity to limiting substrate (a decreased K_s value). Let such a mutant be denoted by

the subscript k and $\overline{\mu}(s)$ be the average growth rate of all other subpopulations. The selection pressure for this mutant, σ, is given by

$$\frac{\mathrm{d}(M_k/N)}{\mathrm{d}t} = \sigma\frac{M_k}{N} = [\mu_k(s) - \overline{\mu}(s)]\frac{M_k}{N}. \qquad (17.103)$$

If $K_{sk} < K_{sj} (j \neq k)$, then $\sigma > 0$ until a new equilibrium is established. In this process, the original cells will be displaced by the mutants, and the growth-limiting substrate concentration will decrease from $\overline{s}_1 = DK_{sj}/(\mu_m - D)$ to $\overline{s}_2 = DK_{sk}/(\mu_m - D)$, and the culture density will rise by $Y(\overline{s}_1 - \overline{s}_2)$.

17.6.2 Autoselection in Turbidostat and pH-Auxostat

The affinity to substrate was not always the only driving force of selection outcome. A number of instructive examples were reviewed by Pechurkin (37)

1. In turbidostat and pH-auxostat, autoselection is in favor of mutants with higher maximum specific growth rates, $\sigma = \mu_{mk} - \mu_{mj} > 0$. Because the population density is kept constant instrumentally and the dilution rate is allowed to vary, then autoselection results in the increase in D from μ_{mj} to μ_{mk}.
2. Mutation toward a higher growth efficiency, $Y_k > Y_j$, will lead to the same result as an increase in μ_m : $\sigma = \mu_k - \mu_j = (\mu_{mk} - \mu_{mj})s/(K_{sj} + s)$, as soon as $\mu_k = q_s Y_k$ and $\mu_j = q_s Y_j$.
3. Growth of a mutant with a higher resistance to inhibitory metabolic products can be described by Equation 17.77 with $K_{pk} > K_p$. Under selection pressure $\sigma = \mu_k - \mu = \mu_m \frac{s}{K_s+s}\left(\frac{K_{pk}}{K_{pk}+p} - \frac{K_p}{K_p+p}\right)$ the original population will be completely displaced, and the product concentration will reach a higher steady-state level, $\overline{p} = \mu_m K_{pk}\overline{s}/(K_s + s)D - K_{pk}$.
4. A mutation resulting in enhanced adhesion to fermentor walls will lead to accumulation of slow-growing cells (as the adhesion prevents washout), eventually we have $\sigma = \mu_k + D - \mu_j$.

17.6.3 Extrachromosomal Cell Elements (ECE)

The present-day "hot spot" in microbial population genetics is the study of such ECE as plasmids, phages, transposons, and insertion elements. Normally ECEs do not carry genes, absolutely essential for growth, but they improve stress-resistance of host cells, thus according to SCM (see section titled "Structured models"), ECEs should be identified as U-components. Indeed, experimental data and mathematical simulation of plasmid replication in *E. coli* including turnover of plasmids, transcription and translation activities of the host cell (83) confirmed decrease of plasmid number with growth rate.

The best-studied R-plasmids are responsible for bacterial growth in the presence of antibiotics, but under normal conditions (with no antibiotics present) their synthesis becomes too heavy a burden for the host cell, which is manifested in a decreased growth rate (84). Among more than 100 R-factors studied, about a quarter were found to increase the bacterial generation time by 15% (85). For this reason, plasmid-bearing strains are unable to compete with plasmid-free populations, although there are a few exceptions. Thus, colicin-positive cells carrying respective plasmids are able to withstand the competition with faster-growing plasmid-free strains by virtue of antagonistic inhibition. In recent years, various dynamic models of autoselection have been proposed that take into account the ECE-related effects, including the transfer of ECEs within the population, their segregation loss, changes in μ arising from the ECEs carriage, and so on. Some of these models have interesting biotechnological and medical applications (86).

17.7 MICROBIAL GROWTH IN VARIOUS CULTIVATION SYSTEMS

The array of laboratory cultivation systems that define the dynamic patterns of microbial growth is summarized in Table 17.11. Microbial growth patterns are distinguished by three features:

- Regime of substrate supply (1, continuous supply; and 2, single-term addition)
- Elimination of growing microorganisms (α, yes; β, no)
- Magnitude of spatial gradients (a, homogeneous systems; b, heterogeneous systems).

Each specific cultivation procedure can be represented by a point inside a cube with the axes 1 to 2, α to β, and a to b. The 2b combination is logically forbidden because, any spatial segregation results in protracted substrate utilization and so transforms a batch process into a continuous one. The dynamics of microbial growth in any type of cultivation system can be described by the following mass–balance equations:

$$\begin{aligned} \frac{\mathrm{d}s}{\mathrm{d}t} &= F - G(s) - \mu(s)x/Y - mx, \\ \frac{\mathrm{d}x}{\mathrm{d}t} &= V - H(x)x + \mu(s)x, \end{aligned} \qquad (17.104)$$

where F is the substrate input rate; $G(s)$ is the rate of unused substrate removal from cultivation vessel (washout, leaching, evaporation, etc.); V is the rate of microbial

TABLE 17.11. Matrix of Cultivation Techniques

	Substrate Input			
	Continuous (1)		Single-term (2)	
Spatial Organization	Cell Eliminated (α)	No Elimination (β)	Cell Eliminated (a)	No Elimination (b)
Homogeneous (a)	$1a\alpha$ Chemostat Turbidostat pH-auxostat abd bistat	$1a\beta$ Chemostat with recycle Fed-batch Dialysis culture	$2a\alpha$ Phased culture	$2a\beta$ Simple batch
Heterogeneous (b)	$1b\alpha$ Plug-flow (tubular culture) Colonies	$1b\beta$ Column packed with microbe attached	Forbidden combination	

biomass input, which may be a single-term inoculation or continuous delivery of cells to the fermentor (specially designed or unintentional, e.g. contamination); and $H(x)$ is the rate of microbial elimination, such as washout, death, grazing, or lysis. The rest of the notation is conventional. To simulate microbial growth dynamics in a particular homogeneous system, one has to make the following selection: $F(t) = 0, s_0 > 0$ for a category 2 (batch culture), $F(t) > 0$ for category 1 (continuous cultivations); $H(t) = 0$ for systems retaining cell biomass (dialysis, fed-batch, simple batch, column with immobilized cells), and $H(t) > 0$ when cell elimination occurs (chemostat, turbidostat, phased culture, etc.)

Spatially heterogeneous systems can be simulated either by partial derivatives or compartmental models (e.g. the total biomass x of a microbial colony may be represented as a sum of the peripheral and central components).

17.7.1 $1a\alpha$—Homogeneous Continuous Culture (Continuous-Flow Fermentors with Complete Mixing)

There are two subgroups within this type of cultivation technique. In the first one, steady-state growth is maintained naturally by the microbial culture itself. Self-regulation is performed through negative feedback that originates from the dependence of the growth rate on substrate concentration (chemostat) or on temperature (caloristat). In the second group, electronic devices are used for the automatic adjustment of dilution rate to the instantaneous growth rate of the microbial culture. Electronic control is based on the sensing of cell density or growth-linked products, that is, optical density in turbidostat (87), culture liquid viscosity in viscostat (88), CO_2 concentration in output air in CO_2-auxostat (89), dissolved oxygen tension in pO_2-auxostat (90), culture pH in pH-auxostat (91), and so on.

In theory, the steady-state growth may be established in chemostat between 0 and μ_m, but in practical terms neither very low nor very high values are attainable because of the long time needed to reach the steady state in the first case and the risk of culture washout in the second. The second group of continuous techniques (turbidostat, pH-auxostat, viscostat, etc.) are capable of maintaining steady growth at high s when either $\mu \to \mu_m$ or under substrate inhibition, when $d\mu/ds < 0$. The most popular device among them is definitely pH-auxostat; its advantage is based on the following beneficial features: (i) low cost and availability of pH control, (ii) short response time, (iii) no interference from wall growth (as in turbidostat), (iv) possibility to use clear and opaque media. There is also a potpourri mixed technique known as the *bistat* (92), which combines a chemostat and a pH-auxostat. Bistat provides widest range of cultivation conditions from a limited ($0.05\mu_m < \mu < \mu_m$) to unlimited growth ($\mu \sim \mu_m$) as well as growth under substrate or product inhibition.

The mass–balance equations for the chemostat and its modifications have already been given (Eqs 17.62–17.64). In a simple, complete mixing cultivator, all cells have an equal probability of being washed out, hence $\mu = D$. If there is substantial wall growth, biomass retention, or feedback, then $\mu < D$; this difference increases with the extent of biomass retention in the fermentation vessel. In terms of our scheme, such cultivation systems correspond to points on the edge $1a\alpha$ to $1a\beta$.

In recent years, chemostat has been used under deliberately nonstationary conditions. For example, A-stat (acceleration-stat) was proposed which provides linear increase in dilution rates from minimal values to D_{crit} (93–95). If D-acceleration rate is low enough (from 0.02 to 0.001 h^{-2}), then the entire transition dynamics of continuously growing microorganisms remains smooth which greatly accelerates the full-range screening of studied strains in continuous culture. Moreover, the response of culture to D-changes provides valuable additional information relevant to real-life of biotechnological applications which are seldom maintained under perfectly stationary conditions. Another non-steady-state version of chemists was called D-stat because dilution rate is maintained constant while one of other environmental parameters (temperature, pH, pO_2, concentration of inhibitors, and so on) is varied in linear or nonlinear

fashion (93). Such technique may be useful in modern biotechnological studies aimed at selection of bioagents under extreme conditions.

17.7.2 1$a\beta$—Continuous Cultivation without Cell Washout

This group embraces cultures with batch or continuous dialysis, fed-batch culture (FBC), and batch culture with a supply of limiting substrate via the gas phase (gases and volatile compounds). It also includes the chemostat with complete biomass feedback by means of filtration (9). The limiting substrate is supplied into the dialysis culture through a semipermeable membrane and, in the case of a gaseous nutrient, through the gas–liquid interface. In both cases, mass transfer is reasonably well described by Fick's law. Substrate delivery via dialysis membrane is cheaper but slower than filtration, filters (even with tangential flow) tend to be easily plugged with cells than dialysis membrane—these factors should be considered before a final choice of the cell retention method. The culture volume remains fixed in all systems, with the exception of a FBC. In a FBC, a constant nutrient feed F provides a linear increase of culture volume V during the cultivation span; the dilution rate $D = F/V$ is decreased hyperbolically. The great advantage of these cultivation techniques for biotechnology is that they provide the possibility of realizing very slow continuous growth accompanied with derepression of synthesis of many secondary metabolites. With a constant limiting substrate flux, Fs_r, the absence of cell washout means that at each subsequent moment an equal ration is shared by an increasing microbial biomass, and, as a result, μ eventually falls down to negligible values or even to zero (the maintenance state). Unlike the chemostat, no true steady state is established in this case, but when the substrate is virtually depleted, we have $ds/dt \sim 0$ and the system reaches a quasi–steady state (6). If a quasi–steady state approximation is found to be sufficient, then extremely slow continuous growth can be obtained after a reasonable period of time, perhaps a few weeks, as compared to the several months needed in a chemostat.

17.7.3 2$a\alpha$—Continuous Cultivation with a Discontinuous Supply of Limiting Substrate

Suppose we have a simple chemostat culture fed by nutrient medium lacking just one essential component. This component is added as a small volume of concentrated solution at regular and sufficiently large time intervals, Δt. Then

$$\frac{ds}{dt} = D[s_r(t) - s] - q(s)x, \quad \frac{dx}{dt} = \mu(s)x - Dx, \tag{17.105}$$

$$s_r(t) = \begin{cases} A > 0, & \text{when } t = i\Delta t,\ i = 0, 1, \ldots, n \\ 0, & \text{otherwise} \end{cases}$$

This cultivation method was originally used to obtain synchronized cell division (96). A continuous phased culture (97) is a repeated simple batch culture, that is, at regular intervals, Δt, half of the culture volume is withdrawn and the fermentor is refilled with an equal volume of fresh medium. Under such conditions, repeated batchwise growth proceeds with biomass increasing cyclically from x_0 to $2x_0$. Obviously, the growth dynamics are governed by the time interval between consecutive substrate additions Δt. If $\Delta t < \ln 2/\mu_m$, a sawtooth nonlimited growth takes place as in a turbidostat. With $\Delta t < \ln 2/\mu_m$ the culture should be washed out and, when $\Delta t > \ln 2/\mu_m$, the maximal attainable biomass decreases with increasing Δt because of endogenous biomass decomposition and waste respiration during the lag phase.

17.7.4 2$a\beta$—Simple Batch Culture

Cultivation begins at the initial limiting substrate concentration, s_0, and inoculum size, x_0. The biomass reaches its maximum, x_m, when the limiting substrate is depleted, $s = 0$, and then declines even in the absence of exogenous elimination, so that $x \to 0$ as $t \to \infty$ Description of batch dynamics has been given earlier: specified growth phases are described by simple nonstructured models (Eq 17.56), while entire dynamics—by SCM and other structured models (Eqs 17.84–17.86, Fig. 17.9).

17.7.5 1$b\alpha$—Plug-Flow (Tubular) Culture

The inoculum and the medium are mixed on entry into a long reactor tube and the culture flows in the tube at a constant velocity without mixing. In each small element of culture liquid, moving along the spatial coordinate z at a linear velocity $f = F/A$ (where F is flow rate, cubic centimeter/hour, and A is the cross-section area, cubic centimeter), growth of biomass proceeds as in a simple batch culture. To account for the culture movement *per se*, we have to pass from ordinary to partial derivatives and replace dx/dt by $\partial x/\partial t + f\partial x/\partial z$ ("along-the flow-growth rate"). Allowing in addition for some dispersion of the moving front by diffusion, we can write (98)

$$\frac{\partial s}{\partial t} + f\frac{\partial s}{\partial z} = D_s\frac{\partial^2 s}{\partial z^2} - q(s)x$$
$$\frac{\partial x}{\partial t} + f\frac{\partial x}{\partial z} = D_x\frac{\partial^2 x}{\partial z^2} + \mu(s)x \tag{17.106}$$

where D_s and D_x are the diffusion coefficients of the substrate and microbial cells, respectively.

17.7.6 1$b\beta$—Continuous-Flow Reactors with Microbes Attached

The nutrient solution is pumped through column filled with adsorbent material and is utilized as it moves by growing

immobilized cells. The mass balance equations for a packed column are obtained from Equation 17.106 by simplifying the equation for x,

$$\frac{\partial s}{\partial t} + f\frac{\partial s}{\partial z} = D_s\frac{\partial^2 s}{\partial z^2} - q(s)x(z)$$
$$\frac{\partial x}{\partial t} = \mu(s)x = Y[q(s) - m]x \qquad (17.107)$$

Bacterial cells accumulate faster on the top of the column because of larger $q(s)$ values and as a result, a distinctive spatial biomass distribution develops in the form of an hyperbolic decrease of x with column depth. Growth does not reach steady state with respect to x until cell elimination becomes well expressed (the effects of inhibitory products, endogenous cells decomposition, and leaching).

17.7.7 1*bα*—Colonies

Besides continuous-flow columns, other heterogeneous systems are widely used. Especially popular is plating on solid media made from natural or synthetic gels (agar, PAAG, silica gel, synthetic alumosilicates, etc.) as well as on some porous materials (sand, glass beads, glass fiber). Impregnated with nutrient solution, such materials are used to grow microorganisms in the form of colonies or lawns.

At first glance, it is tempting to consider these techniques as analogies of a simple batch culture with single-term substrate input (type 2*bβ* in Table 17.11). However, a closer look at the mechanism of colony growth reveals a greater resemblance to chemostat culture. Here we will outline our considerations.

The spread of a colony over a solid substrate, for example, a layer of agar, proceeds by the growth of only a peripheral zone with biomass, x_p (Fig. 17.11). Then

$$\frac{ds}{dt} = -q(s)x, \quad \frac{dx}{dt} = \mu_w x_p - ax, \qquad (17.108)$$

where a is the specific decay rate of cellular components. Straightforward geometrical analysis shows that the linear spread rate for a regularly shaped colony (a cylinder, a sphere, or a strip) of size R is given by the following relation (2,6):

$$\frac{dR}{dt} = \mu_w w = K_r, \quad \text{or} \quad R = R_0 + K_R t, \qquad (17.109)$$

where K_r is the colony linear expansion rate, millimeter/hour; μ_w is the microbial specific growth rate within the peripheral zone; and w is the zone width.

In the case of unicellular organisms (e.g. bacteria, yeasts) which are incapable of penetrating into the gel's matrix, the substrate is available through passive diffusion to the peripheral zone from the underlying gel layer. As the colony grows this flux diminishes, K_r decreases, and eventually the growth stops altogether. The filamentous organisms (fungi and actinomycetes) are able to propagate both on the surface

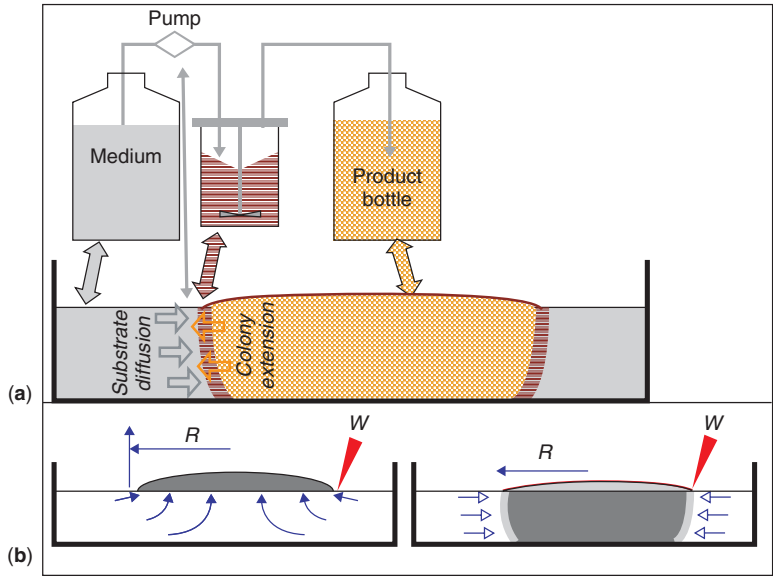


Figure 17.11. Kinetic mechanisms of colony growth (a) Illustration of the similarity between growing colony and chemostat culture (see text for explanation). (b) Schematic illustration of the difference between the growth modes of bacterial (*right*) and fungi (*left*) colonies. Note that unicellular organisms (*bacteria*) do not penetrate into the agar layer as opposed to filamentous fungi. *Arrows* indicate directions of substrate diffusion across concentration gradients. R and w are, respectively, radius and width of the peripheral zone of the colony.

and in the depth of gel. As a result, their growth is not completely dominated by diffusion effects and the colony front advances at a faster rate than substrate is depleted at the boundary zone. The colony spreads at a constant radial rate, K_r, until the Petri dish is filled or the agar deteriorates from dryness. (In the case of rich nutrient media, there are also effects of self-inhibition by metabolic products approximated by Eqs 17.76 and 17.77.)

Thus, the colony growth is (i) continuous, (ii) substrate-limited, (iii) directed, and (iv) spatially ordered. Properties (i) and (ii) suggest a strong similarity between growth of a colony (especially a fungal one) and that of a chemostat culture. If so, a colony's peripheral zone is analogous to the cell culture in the fermentor, and its central part is comparable with the waste cell suspension that is discharged into the product bottle. A steady running of a pump, delivering medium at a rate, F (cubic centimeter/hour), corresponds to the active and uniform substrate utilization by the growing mycelium at a rate $K_r A$ (cubic centimeter/hour, A is the area of colony–medium interface). Finally, both cultivation systems are characterized by the elimination of propagating biomass, that is, by the expulsion of grown cells (mycelium) from further active growth (either by washing out or by the motion of the colony front). In both cases, the elimination rate is equal to biomass growth in the active compartment. The essential deviation from the chemostat lies in properties (iii) and (iv). Spatial differentiation of hypha and the direction of colony expansion are governed by spatial gradients of limiting substrate and, possibly, some metabolic products. Steepness of gradients is partly diminished by the effects of metabolic translocation along hypha over distances of the order of w.

It can be concluded from the previous discussion that colony growth belongs to class $1b\alpha$, and not to $2b\beta$. In general, it is very likely that the $2b$ combination is an empty, logically forbidden combination, because a single-term momentary input of substrate may only be realized in a homogeneous system. Any spatial segregation whatever will actually prolong the consumption of substrate and, therefore, transform a batch process into a continuous one. For this reason, growth on any insoluble substrate (lignocellulose and other plant polymers, oil droplets, grains of sulfur, etc.) should always be treated as a continuous process. The solid-phase fermentation can also not be anything but continuous, whether new portions of substrate are added to the reactor or not (Obviously, this applies to the growth mechanism itself and not to the engineering operation.).

17.7.8 Biofilms

Microbial biofilms represent particular case of colonial growth ($1b\alpha$) on the surface of any solid material. Biofilms grow on nearly every surface that is in contact with water and humid air, even at extremely low nutrient concentrations. Their presence includes negative effects, such as biofouling and biocorrosion, but also positive effects if used in biofilm reactors for the degradation or production of chemical substances (99–101). Most often biofilms as object of biotechnological studies are formed by natural multispecies community, but recently there were reported numerous studies on laboratory biofilms prepared from pure cultures (102).

Biofilms are composed of bacterial cells embedded in extracellular polysaccharide matrix (e.g. linear polymer of *N*-acetyl-D-glucosamine residues in *E. coli*) that mediates intercellular adhesion and attachment to abiotic surfaces. Attachment and detachment of cells in biofilms is also controlled by extracellular signal molecules (quorum-sensing). Young biofilms is presented by the monolayer of cells, further growth leads to a buildup of the multilayered spatially differentiated biofilm: the peripheral surface zone facing incoming nutrients, oxygen and other essential growth factors contain the metabolically active cells, whereas the deeper submerged parts are occupied by dormant and starving and possibly intoxicated cells. The architecture of the mature biofilms can vary from flat, homogeneous biofilms, to highly structured biofilms, characterized by void spaces and towers of cells encased in an extracellular matrix (Fig. 17.12).

Generally growth rate of cells within biofilms is much lower as compared with planktonic form or agitated culture, therefore it is not surprising that gene expression profile of cells from biofilms is close to one found in planktonic cells at stationary phase (103). Many physiological features of bacteria from biofilms resemble ones in stationary phase: decreased cell size, low RNA content, resistance to antibiotics, synthesis of protective extracellular polymers and pigments. To simulate the described physiological state of cells in the biofilm, one should use structured models, for example, SCM and take into account the spatial differentiation, at least into peripheral and deep parts of biofilm.

Until now, the major focus in quantitative/mathematical description of biofilms were mass transfer through water-biofilm boundary, particularly diffusion of O_2 and antibiotics (6,104). Another focus is the modeling of physical factors responsible for observed architecture of mature biofilms. Two major modeling approaches are used: cellular automata (CA) that performs discretization of cell mass along a grid, and individual-based modeling (IbM) that represents cell aggregates as spherical particles which can absorb nutrients, grow and move in response to sheer forcing and other mechanical effects. Hermanowicz (105) used stochastic CA model; detachment of cells at the biofilm/liquid interface occurred with a given probability, defined as function of an overall shear stress and parameter quantifying biofilm strength. The deterministic description

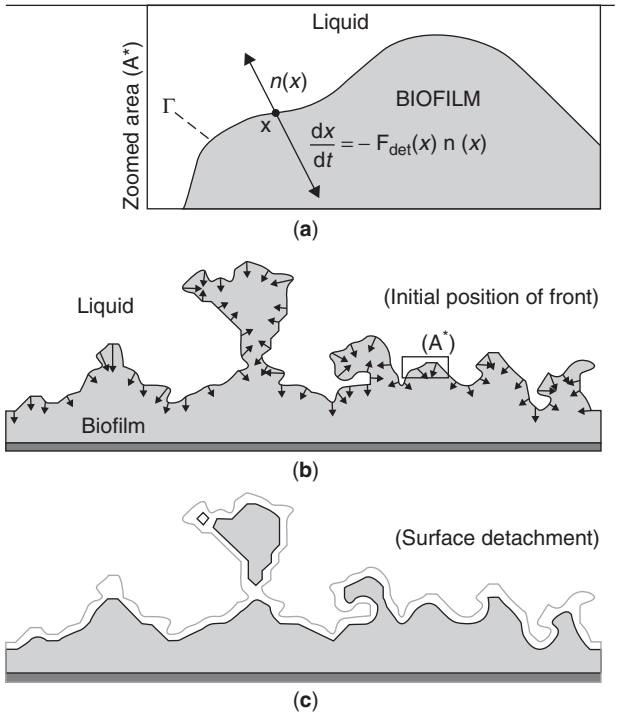


Figure 17.12. Computer simulation of biofilms (100). (a) The zoomed in fragment of biofilms, x is spatial coordinate, F_{det}, is detachment speed function, and $n(x)$ is the vector normal to the surface. (b) Position of the biofilm front before detachment is applied, arrows indicate the detachment speed vectors. (c) The biofilms after application of the surface detachment, loss of biomass clusters by sloughing.

of biomass detachment is based on use of computational fluid dynamics (CFD) (106,107) which generates velocity profiles of the moving liquid and then calculates the propagation of stresses along the elastic biofilm. Detachment occurs when stresses exceeded the local strength of the biofilm. The application of this method allowed the generation of realistic biofilm formation patterns correlated with the flow regime and the substrate load (Fig. 17.12).

REFERENCES

1. Esener AA, Roels JA, Kossen NWF. Biotechnol Bioeng 1983; 25(12): 2803–2841.
2. Panikov NS. Microbial growth kinetics. London: Chapman & Hall; 1995. p. 378.
3. Erickson LE, Minkevich IG, Eroshin VK. Biotechnol Bioeng 1979; 21(4): 575–591.
4. Erickson LE, Minkevich IG, Eroshin VK. Biotechnol Bioeng 2000; 67(6): 748–774.
5. Mayberry WR, Prochazka GJ, Payne WJ. Appl Microbiol 1967; 15(6): 1332–1338.
6. Pirt SJ. Principles of microbe and cell cultivation. Oxford, London, Edinburgh, Melbourne: Blackwell Science; 1975.
7. Marr AG, Nilson EH, Clark DJ. Ann N Y Acad Sci 1963; 102(3): 536–548.
8. Dorofeyev AG, Panikov NS. Microbiology (Moscow) 1995; 64: 601–609.
9. Beyeler W, Rogers PL, Fiechter A. Appl Microbiol Biotechnol 1984; 19: 277–280.
10. Dorofeev AG, Bondarenko TF, Zvyagintsev DG, Panikov NS. Microbiology (Moscow) 1984; 53(2): 271–274.
11. Tempest DW, Neijssel OM. Annu Rev Microbiol 1984; 38: 459–486.
12. Pirt SJ. Arch Microbiol 1982; 133(4): 300–302.
13. Panikov NS, Pirt SJ. J Gen Microbiol 1978; 108(2): 295–303.
14. Bauchop T, Elsden SR. J Gen Microbiol 1960; 23(2): 457–469.
15. Helmstetter CE, Cooper S, Pierucci O, Revela E. Cold Spring Harb Symp Quant Biol 1968; 33: 809–822.
16. van Gulik WM, Heijnen JJ. Biotechnol Bioeng 1995; 48(6): 681–698.
17. Stephanopoulos G, Vallino JJ. Science 1991; 252(5013): 1675–1681.
18. Kashiwaya Y, Sato K, Tsuchiya N, Thomas S, Fell DA, Veech RL, Passonneau JV. J Biol Chem 1994; 269(41): 25502–25514.
19. Vallino JJ, Stephanopoulos G. Biotechnol Bioeng 1993; 41(6): 633–646.
20. Marx A, de Graaf AA, Wiechert W, Eggeling L, Sahm H. Biotechnol Bioeng 1996; 49(2): 111–129.
21. Smolke CD, Martin VJ, Keasling JD. Metab Eng 2001; 3(4): 313–321.
22. Carlson R, Fell D, Srienc F. Biotechnol Bioeng 2002; 79(2): 121–134.
23. Jin YS, Jeffries TW. Metab Eng 2004; 6(3): 229–238.
24. Alper H, Jin YS, Moxley JF, Stephanopoulos G. Metab Eng 2005; 7(3): 155–164.
25. Sanchez AM, Bennett GN, San KY. Metab Eng 2005; 7(3): 229–239.
26. Berrios-Rivera SJ, Bennett GN, San KY. Metab Eng 2002; 4(3): 217–229.
27. Heux S, Cachon R, Dequin S. Metab Eng 2006; 8(4): 303–314.
28. Hjersted JL, Henson MA, Mahadevan R. Biotechnol Bioeng 2007; 97(5): 1190–1204.
29. Young JD, Walther JL, Antoniewicz MR, Yoo H, Stephanopoulos G. Biotechnol Bioeng 2008; 99(3): 686–699.
30. Cornish-Bowden E. Fundamentals of enzyme kinetics. 3rd ed. London: Portland Press; 2004.
31. Michaelis N, Menten MI. Biochem Z 1913; 49: 333–369.
32. Briggs GE, Haldane JBS. Biochem J 1925; 19: 338–339.
33. Burke BJ, Regnier FE. Anal Chem 2003; 75(8): 1786–1791.
34. Haldane JBS. Enzymes. London: Longmans Green; 1930.

35. Monod J, Wyman J, Changeux J. J Mol Biol 1965; 12(1): 88–118.
36. Wang CH, Koch AL. J Bacteriol 1978; 136: 969–975.
37. Pechurkin NS. Populational microbiology. Novosibirsk: Nauka; 1978. p. 277.
38. Rahn O. Physiology of bacteria. Philadelphia: P.Blackiston's Son and Co; 1932. p. 438.
39. Buchanan RE. J Infect Dis 1918; 23(1): 109–125.
40. Verhulst PF. Corresp Math Phys 1838; 10(1): 113–121.
41. Monod J. Recherches sur la croissancu des cultures bacteriennes. Paris: Hermann & C; 1942. p. 210.
42. Monod J. Ann Inst Pasteur (Paris) 1950; 79: 390–410.
43. Blackman FF. Ann Bot (Lond) 1905; 19(74): 281–293.
44. Monod J. Annu Rev Microbiol 1949; 3: 371–394.
45. Ierusalimsky ND. Continuous cultivation of microorganisms. Salisbury: H.M. Stationary Office; 1967. pp. 23–33.
46. Shvytov IA. J Gen Biology 1974; 35(6): 904–910.
47. Romanovsky JM, Stepanova NV, Chernavsky DS. Mathematical biophysics. Moscow: Nauka; 1984. p. 304.
48. Shehata TE, Marr AG. J Bacteriol 1971; 107(1): 210–216.
49. Guady AFJ, Obayashi A, Gaudy ET. Appl Microbiol 1971; 22: 1041–1047.
50. Button DK. Microbiol Rev 1985; 49(3): 270–297.
51. Teissier G. Ann Physiol Physicochem Biol 1956; 12: 527–586.
52. Moser H. The dynamics of bacterial populations maintained in the chemostat. Washington (DC): Carnegie Institution of Washington Publication No. 614; 1958. p. 136.
53. Contois DE. J Gen Microbiol 1959; 21: 40–49.
54. Powell EO. Continuous cultivation of microorganisms. Salisbury: H.M.Stat.Office; 1967. pp. 34–55.
55. Andrews JF. Biotechnol Bioeng 1968; 10: 707–723.
56. Pawlowsky U, Howell SA, Chi CT. Biotechnol Bioeng 1973; 15(5): 905–916.
57. Campbell A. Bacteriol Rev 1957; 21(2): 263–272.
58. Cooney CL. Ann N Y Acad Sci 1979; 326: 295–314.
59. Ramkrishna D, Fredrickson AG, Tsuchiya HM. Biotechnol Bioeng 1967; 9(2): 129–170.
60. Domach MM, Leung SK, Cahn RE, Cacks GG, Shuler ML. Biotechnol Bioeng 1984; 26(2): 203–216.
61. Jeong JW, Snay J, Ataai MM. Biotechnol Bioeng 1990; 35: 160–184.
62. Malek I. Continuous cultivation of microorganisms. A symposium. Prague: Publ.House of Czech.Acad.Sci.; 1958. pp. 11–28.
63. Herbert D. Volume II, A symposium of the society for general microbiology. Cambridge: Cambridge University Press; 1961. pp. 391–416.
64. Agrawal P, Lim HC, Ramkrishna D. J Chem Technol Biotechnol 1983; 33B: 155–163.
65. Klauck E, Lingnau M, Hengge-Aronis R. Mol Microbiol 2001; 40(6): 1381–1390.
66. Hengge-Aronis R. Microbiol Mol Biol Rev 2002; 66(3): 373–395.
67. Hengge-Aronis R. Curr Opin Microbiol 2002; 5(6): 591–595.
68. Weichart D, Querfurth N, Dreger M, Hengge-Aronis R. J Bacteriol 2003; 185(1): 115–125.
69. Tempest DW, Herbert D, Phipps PJ. Continuous cultivation of microorganisms. Salisbury: H.M.Stat.Office; 1967. pp. 240–253.
70. Henrici AT. Morphologic variation and the rate of growth of bacteria. Springfield, IL: C.C.Thomas; 1928. p. 194.
71. Koch AL. Crit Rev Microbiol 1973; 19: 17–42.
72. Wold S, Skarstad K, Steen HB, Stokke T, Boye E. EMBO J 1994; 13: 2097–2102.
73. Cooper S. Res Microbiol 1990; 141(1): 17–29.
74. Minkevich IG, Abramychev AY. Bull Math Biol 1994; 56(5): 837–862.
75. Leslie PH. Biometrika 1945; 38: 183–222.
76. Leslie PH. Biometrika 1948; 35: 213–245.
77. McKendrick AG. Proc Edinb Math Soc 1926; 44: 98–130.
78. Von Foerster H In: Stohlman F Jr. (Hg.), editor. The kinetics of cellular proliferation. New York: Grune and Stratton; 1959. pp. 382–407.
79. Trucco E. Bull Math Biol 1965; 27(2): 285–304.
80. Koch AL. J Gen Microbiol 1966; 45: 409–417.
81. Collins JF, Richmond MH. J Gen Microbiol 1962; 28: 15–33.
82. Novick A. Recent progress in microbiology. Oxford: Blachwell Sci. Publication; 1959. pp. 403–415.
83. Lee SB, Bailey JE. Biotechnol Bioeng 2002; 79(5): 550–557.
84. Velkov VV, Matys VY, Sokolov DM. J Biosci 1999; 24(3): 279–286.
85. Adams J, Kinney T, Thompson S, Rubin L, Helling RB. Genetics 1979; 91(4): 627–637.
86. Freter R, Freter RR, Brickner H. Infect Immun 1983; 39(1): 60–84.
87. Bryson V. Science 1952; 116(1): 48–50.
88. Silman RW, Bagley EB. Biotechnol Bioeng 1979; 21: 173–179.
89. Watson TG. J Gen Microbiol 1969; 59: 83–89.
90. Hospodka I. Biotechnol Bioeng 1966; 8: 117–134.
91. Rice CW, Hempfling WP. Biotechnol Bioeng 1985; 27(2): 187–191.
92. Minkevich IG, Krynitskaya AY, Eroshin VK. Biotechnol Bioeng 1989; 33(9): 1157–1161.
93. Kasemets K, Drews M, Nisamedtinov I, Adamberg K, Paalme T. J Microbiol Methods 2003; 55(1): 187–200.
94. Paalme T, Kahru A, Elken R, Vanatalu K, Tiisma K, Raivo V. J Microbiol Methods 1995; 24(2): 145–153.
95. Van der Sluis C, Westerink BH, Dijkstal MM, Castelein SJ, Van Boxtel AJB, Giuseppin MLF, Tramper J, Wijffels RH. Biotechnol Bioeng 2001; 75(3): 267–275.
96. Goodwin BC. Eur J Biochem 1969; 10(4): 511–514.
97. Dawson PSS. Can J Microbiol 1965; 11: 893–903.

98. Saunders PT, Bazin MJ. Soil Biol Biochem 1973; 5(5): 545–557.
99. Flemming H-C, Tamachkiarowa A, Klahre J, Schmitt J. Water Sci Technol 1998; 38(8–9): 291–298.
100. Baker-Austin C, Wright MS, Stepanauskas R, McArthur JV. Trends Microbiol 2006; 14(4): 176–182.
101. Terada A, Lackner S, Tsuneda S, Smets BF. Biotechnol Bioeng 2007; 97(1): 40–51.
102. Kaplan JB, Ragunath C, Velliyagounder K, Fine DH, Ramasubbu N. Antimicrob Agents Chemother 2004; 48(7): 2633–2636.
103. Fux CA, Costerton JW, Stewart PS, Stoodley P. Trends Microbiol 2005; 13(1): 34–40.
104. Rani SA, Pitts B, Stewart PS. Antimicrob Agents Chemother 2005; 49(2): 728–732.
105. Hermanowicz SW. Math Biosci 2001; 169: 1–14.
106. Picioreanu C, Van Loosdrecht MCM, Heijnen JJ. Biotechnol Bioeng 2001; 72(2): 205–218.
107. Xavier JDB, Picioreanu C, van Loosdrecht MCM. Biotechnol Bioeng 2005; 91(6): 651–669.

18

MICROALGAE, MASS CULTURE METHODS

Emílio Molina Grima, Jose María Fernández Sevilla, and Francisco Gabriel Acién Fernández

Department of Chemical Engineering, University of Almería, Almería, Spain

18.1 INTRODUCTION

Microalgae have been cultured commercially for about 50 years for applications in secondary wastewater treatment (1) and use as animal feeds (2,3) and fertilizers (4), in production of chemicals (5,6), and in secondary metabolites with pharmaceutical potential (7), as well as other purposes. Microalgae can also provide several different types of renewable biofuels. These include methane produced by anaerobic digestion of the algal biomass (8), biodiesel derived from microalgal oil (9), and photobiologically produced biohydrogen (10). The idea of using microalgae as a source of fuel is now being taken seriously because of the escalating price of petroleum and, more significantly, the emerging concern about global warming that is associated with burning fossil fuels (11). However, the major focus of algal mass cultures is on relatively specialized niche applications; nevertheless, progress remains slow relative to biotechnological use of bacteria, yeasts, and animal cells. A cost-effective culture of microalgae requires substantially improved biomass productivity, better utilization of the available light, and more efficient use of carbon dioxide, which is the principal carbon source.

In the past few decades, most of the research in this field has been aimed toward the development of open outdoor mass cultures, resulting in large-scale production facilities currently in operation throughout the world (12). Open outdoor mass culture systems, such as ponds and raceways, typically operate at low cell densities (0.01%–0.06% w/v); consequently, harvesting is expensive and economic returns are low. In addition, species control is difficult in open systems, and much of the incident radiation is wasted. The low productivity of open systems has prompted the development of enclosed photobioreactors(PBRs) (i.e. transparent tubes or containers in which the culture may be circulated by various devices). Enclosed PBRs allow a more controlled culture environment, including improved temperature control. The fact is that most microalgal strains can only be cultured under controlled conditions and protected from the environment. This is only possible with fully closed PBRs (13). The design of closed PBRs must be carefully optimized for each individual algal species, according to its unique physiological and growth characteristics (14). Successful designing of PBRs relies on attaining a proper balance of engineering and biological factors that are interdependent and also depends on the species being cultured. Of course, from a commercial perspective, reliability and the costs of construction and operation are also important. The physical rate processes of concern are the light delivery, the gas–liquid mass transfer, temperature control, fluid dynamics, and mixing. The biological rate processes of concern are photosynthesis, growth, and production of metabolites.

This chapter details the major types of bioreactors used in mass culture of microalgae. The basic requirements for successful outdoor culture are noted, and the physics and biology of mass cultivation are discussed.

Upstream Industrial Biotechnology: Expression Systems and Process Development, Volume 1, First Edition. Edited by Michael C. Flickinger.
© 2013 John Wiley & Sons, Inc. Published 2013 by John Wiley & Sons, Inc.

18.2 BIOREACTORS FOR MICROALGAE MASS CULTURES

Three microalgae—*Chlorella*, *Dunaliella*, and *Spirulina*—are currently produced commercially on a relatively large scale (approximately 1000 tons each per annum). The current commercial production systems for these species are mostly open raceway ponds. Many commercially useful algae are difficult to cultivate in open systems because they require a mild culture environment that is highly susceptible to contamination by other algae, bacteria, protozoa, and fungi. The inability to cultivate desirable algal species that contain valuable products (e.g. astaxanthin, aquaculture feeds, polysaccharides, and polyunsaturated fatty acids) in open ponds has increased interest in closed systems. Closed PBRs are suitable for the production of strains rich in high value products, and also allow taking advantage of the metabolic flexibility of microalgae: the generation rate of the desired product can be enhanced by setting proper culture conditions. Thus, for the successful production of microalgae on an industrial scale, it is necessary to design and use PBRs and production systems that accomplish the requirements of the individual microalgae cells. Two dominant environmental factors require substantial attention: sunlight and temperature (15,16). Also, other design parameters such as light regime, mixing, and heat and mass transfer must be fine tuned for proper operation (17,18).

A variety of closed PBRs has been proposed to suit the particular characteristics of different microalgal strains. Closed systems that have been and are being studied include the following: (i) bags culture, which are widely used for culture of algae for aquaculture (2,19); (ii) alveolar panels and other flat plate reactors of various designs (20–22); (iii) stirred tank reactors with internal illumination (23,24); (iv) bubble-column and airlift reactors (25,26); and (v) tubular reactors (27–29). The most scalable designs correspond to horizontal or helical tubular systems, as well as combinations of vertical flat panels and bubble columns, and therefore these types of PBRs have attracted most interest. Some of the major types of PBRs are discussed in the following text.

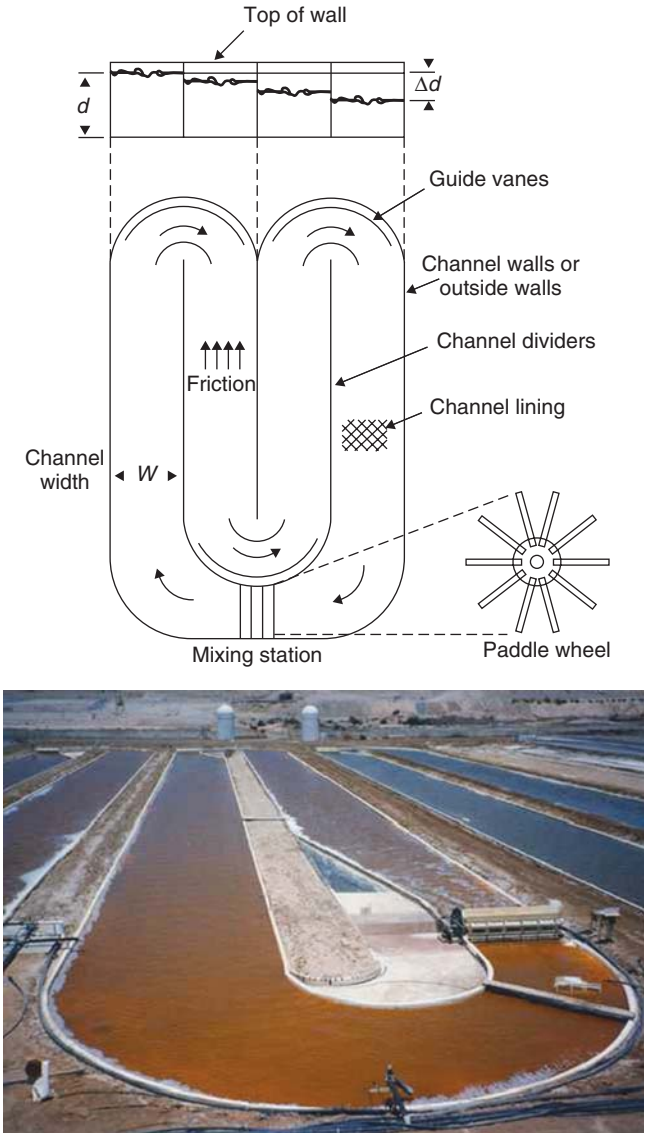


Figure 18.1. Diagram and photograph of an open raceway showing in detail a paddle wheel used for mixing. The channel length is the distance traveled by the culture from the discharge side of the paddle wheel to the entering side. [From Ref. (1). With permission.] (This figure is available in full color at http://onlinelibrary.wiley.com/book/10.1002/9780470054581.)

18.2.1 Open Raceways

Open raceways, or shallow mixed ponds for microalgal production, were introduced in the 1950s and early 1960s by Oswald *et al*. (30). The principles for design and construction of shallow paddle stirred raceways for large microalgal production were reviewed by Doodd (31) as well as Oswald (32). The pond is set in a meandering configuration with channels utilizing various designs of paddle wheel mixers that promote low shear environment. The simplified diagram of an open raceway, showing the nomenclature of the major parts, is depicted in Fig. 18.1.

The selection of a suitable bottom lining and wall construction is important to the success of the open pond. The lining may be made of concrete or sheets of plastic and rubber material. The size of commercial ponds varies from 1000 to 5000 m^2 and stirring is accomplished with one or two paddle wheels per pond. A wheel of large diameter (ca. 2 m) revolving slowly (e.g. 10 rpm) is preferable to smaller diameter wheels that rotate faster and produce excessive shear damage and foam. Under these conditions,

biomass concentrations of up to 1.0 g/L and productivities of 0.1 g/L/day are possible, although only species such as *Dunaliella*, *Spirulina*, or *Chlorella* are suitable for production in these systems (33).

18.2.1.1 Technical Issues

18.2.1.1.1 Supply of Carbon Dioxide. Techniques for the supply of CO_2 represent an important element in the raceway, particularly for species grown near neutral pH. Several systems have been developed, aimed at supplying CO_2 efficiently to shallow suspensions. In most cases, the gas is supplied in the form of fine bubbles. Owing to the shallowness of the suspension, the residence time of the bubbles is not sufficient to allow all the CO_2 to be dissolved; therefore, losses to the atmosphere are difficult to control. The most effective method currently available for transferring CO_2 to algal cultures is counter-current carbonation (32) in which the gas is injected as minute bubbles into a column of culture. The culture velocity is adjusted so that small bubbles of CO_2 rise against the current. Using this technique, Laws *et al*. (34) have reported a 70% efficiency in CO_2 transfer compared to 13%–20% if it is supplied in bubble form (35).

18.2.1.1.2 Mixing. The evolution of the open culture technology is the reflection of the mixing systems that have been developed in parallel with them. Mixing is necessary in order to avoid cells settling and sticking to the bottom and to avoid thermal stratification of the culture. Properly designed paddle wheels are by far the most efficient and durable pond mixers. They discharge all of the culture entering them and are thus highly efficient. The engineering design of a raceway equipped with paddle wheels has been comprehensively described by Oswald (32). With reference to Fig. 18.1, consider culture flowing at depth d in a channel with finite width, w, and unspecified length, L. The channel length, L, which corresponds to the assumed change in depth for a given friction factor and a culture velocity (v) is given (32):

$$L = \frac{\Delta d(dw/(w+2d))^{4/3}}{v^2 \cdot n^2} \tag{18.1}$$

where n is the Manning friction factor (s/m$^{1/3}$), L is the channel length that corresponds to the assumed change in depth (Δd), and w is the channel width. The value of n varies according to the relative roughness of the channel. Experimentally determined n values in algae growth channels vary from 0.008 to 0.030 (32); the former being for smooth plastic-lined channels and the latter for relatively rough earth. The channel velocity, v, effect on the paddle wheel's power requirements, is calculated as:

$$P = \frac{Q \cdot \rho \cdot \Delta d}{\eta} \tag{18.2}$$

where P is the power (kW), Q the culture flow rate in motion (m^3), ρ is the specific weight of culture (kg/m^3), Δd is the change in depth (m), and η is the efficiency of the paddle wheel. Because $\Delta d = s \cdot L$ and taking into account that s, the rate of loss of energy in the channel per unit length, is a function of v^2, the power consumption, P, increases as the cube of velocity. It is therefore worthwhile to minimize velocity whenever energy is a major cost factor. Typical values of flow rates range between 15 and 30 cm/s, whereas the power supply is around 1 W/m^3. Velocities greater than 30 cm/s result in large values of Δd in long channels and may require high channel walls and higher divider walls. Note that, for a finite value of the channel width, w, the permissible mixing channel length, L, and thus the mixable area, $a = L \cdot w$, is a function strongly dependent on depth, d.

The control of contaminants in open pond systems is the most important problem raised by this technology. Additionally, they have many other drawbacks related to temperature control and culture depth. The culture depth cannot be reduced below 12–15 cm; otherwise, a severe reduction of flow and turbulence would occur. This obliges to work with a large areal volume of 120–150 L/m^2 (16), requiring maintenance of rather low cell concentration (around 500 mg/L). A low cell concentration in turn increases the cost of harvesting and of pond maintenance and greatly increases the extent of contamination by foreign species. These problems could, at least in principle, be minimized by PBRs designs that allow shallower cultures, maximize cell densities, allow better process control, and minimize contamination. These objectives can be met with closed PBRs that are described in the next section.

18.2.2 Enclosed Photobioreactors

PBRs can be defined as algal culture systems that do not allow direct exchange of gases (e.g. CO_2, O_2, H_2O) and gross contaminants between the culture and the atmosphere. PBRs generally may be grouped into two classes: tubular and flat plate. These groups can be further classified into several categories: (i) vertical tubular bubble PBR, which are rigid and are placed vertically up to some practical height of few meters; (ii) tube reactors placed horizontally, inclined, in fence-type configuration, or in spiral manners; and (iii) flat plate and alveolar PBRs, which are made of multiple interconnected channels (their cross-sectional area may be rectangular, square, or circular) that constitute flat reactors. Only flat panel and tubular PBRs have been built to sizes exceeding 1000 L (36–38), whereas for column systems a maximum of 125 L has been proposed as optimum (26,39). Summary of the state of the art in close PBRs has been provided (40,41), some of which are in commercial operation. A brief description follows.

18.2.2.1 Bubble Columns. In vertical column reactors, bubble columns or airlift, aeration, and agitation are provided by injection of CO_2-enriched air through an inlet tube at the bottom of the column. Practically speaking, the vertical column can be extended only to a few meters high; otherwise, a prohibitively expensive structure would be needed for support. James and Al-Khars (25) studied the growth and the productivity of *Chlorella* and *Nannochloropsis* in a vertical airlift PBR. Contreras Gómez (42), showed that the average annual volumetric productivity of a draught tube airlift (0.1 m in diameter) was about 1.0 g/L/day in culture of *Phaeodactylum tricornutum*. Sánchez Mirón *et al*. (26) reported an average annual productivity for the same microalgae using a 0.2 m in diameter and 2.1 m tall bubble column (Fig. 18.2) of 0.49 g/L/day.

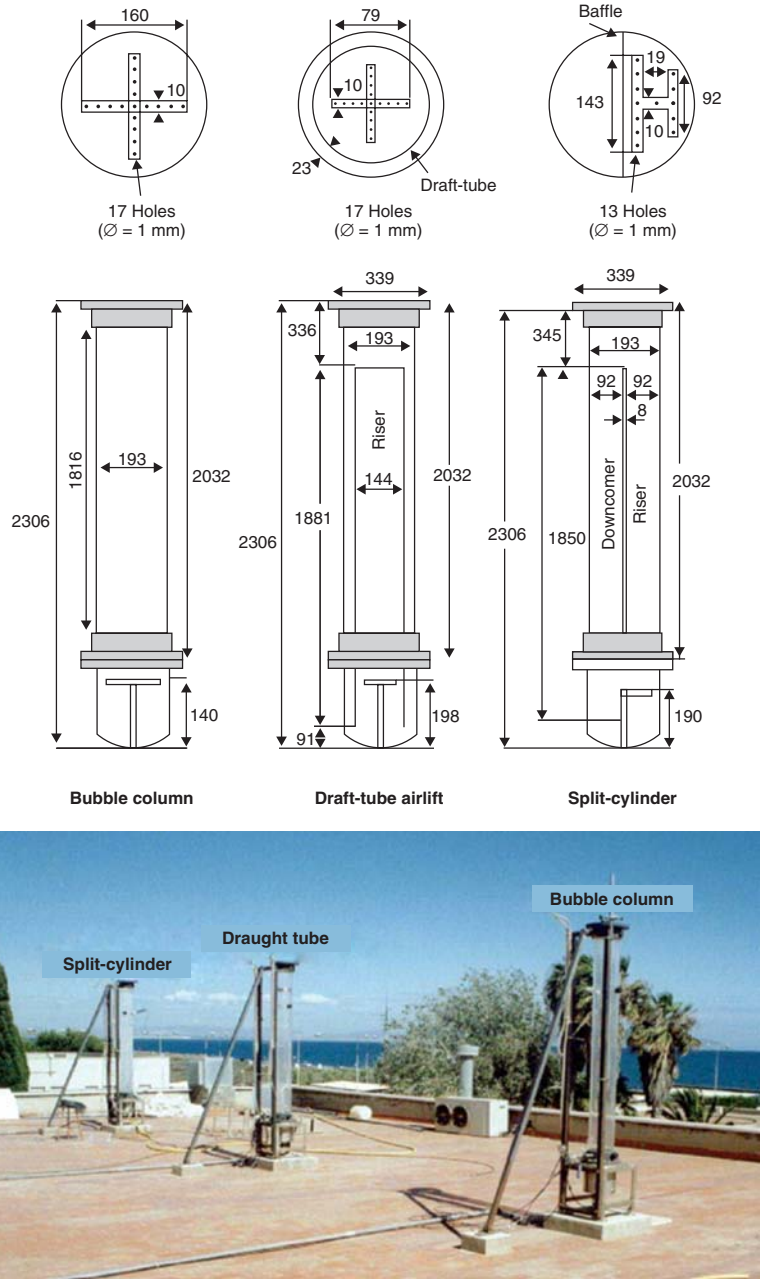


Figure 18.2. Diagram and photograph of several vertical tubular photobioreactors. Different configurations are obtained according to the position of internal walls. Dimensions in mm. [From Ref. 26. With permission.] (This figure is available in full color at http://onlinelibrary.wiley.com/book/10.1002/9780470054581.)

A major advantage of tower reactors is that oxygen does not accumulate in the growth medium because it reaches an outlet after a short path, equivalent to the vertical axis of the reactor, and the sterility to the level demanded in pharmaceutical industry is potentially higher than in other tubular systems. For the usual gas flow rate employed (corresponding to superficial gas velocity of less than 0.05 m/s), the average volumetric mass transfer is about fourfold the estimated value for a horizontal tube with a reported 3% maximum gas holdup (26). In view of this result, vertical tubular PBRs such as bubble columns should easily maintain a dissolved oxygen (DO) level only a little higher than the air saturation value. Consequently, the vertical reactors experience little oxygen inhibition. Because of a reduced level of DO, the photooxidation-associated loss of biomass and product metabolite is lower in bubble-column reactors. Photooxidation occurs especially when high levels of DO combine with an intensely irradiated environment. Also, tower bioreactors are potentially easier to keep sterile compared to other tubular systems. The major drawback with respect to the tubular system, positioned either horizontally or inclined, is that the reactor is always at a large angle to the sun's rays and substantial amount of solar energy is thus reflected at the central hours of the day. Under identical conditions, the volumetric biomass productivity in a bubble column is roughly 60% of that in a horizontally placed serpentine PBR (26,39).

The hydrodynamics of the flow in bubble columns and tubular reactors are generally quite different. The necessarily gas sparged bubble-column and airlift reactors tend to have substantially greater gas holdup than horizontal tubular reactors. The latter are virtually free of gas, and any bubbles present are localized to a narrow zone along the upper portion of the tubes; moreover, the bubbles are relatively small. In contrast, there are many more and larger bubbles in vertical PBRs and the gas–liquid flow is much more chaotic than the highly directional flow in a small diameter horizontal tubular reactor. Differences in gas holdup and the bubble size affect light penetration, gas-liquid mass transfer, mixing, and shear stress level. For best performance, bubble columns need to be operated at the highest feasible aeration rates consistent with the shear tolerance of the microalgae; however, the aeration must not be so high as to produce a gas holdup level that prevents light transmission through the column. Ideally, the culture environment in the column should be manipulated to promote formation of relatively large bubbles ($d_b > 0.006$ m) that rise rapidly. This also contributes to the enhancement of the radial flow into and out of the central dark core and, consequently, the productivity.

18.2.2.2 Tubular Photobioreactors. The first described outdoor tubular reactor was made of a serpentine immersed in a water bath, using a 3-cm-diameter glass tubes, with the total length of illuminated tubes being 33.3 m (i.e. 1 m^2, with the connections consisting of opaque rubber tubing) (43). The culture was recirculated in the system by a motor-driven pump at 15–30 cm/s, and the gas exchange system was a bubble column which injected 5% CO_2 at a rate of 1–1.5 mL/min. The total culture volume was 40 L. This system is essentially identical to other newer systems, particularly those developed by Gudin in France (44)—with tubes placed horizontally on the floor—and Pirt in England (45)—with the tube placed vertically on the floor. In the last two systems, the culture was recirculated, as in the Tamiya concept, by means of pumps. However, they commented on the problems of such pumps when dealing with fragile, shear sensitive cells, and recommended the use of airlifts, for both culture recirculation and CO_2 supply (and O_2 degassing).

Although with a few modifications, the designs of other tubular reactors that have been proposed, namely the two plane tubular reactors (18,46), the near-horizontal tubular reactor (47), the helical bubble reactor (48,49), the α-tubular reactor (50), and the parallel flow tubular PBR (51), are essentially of the same nature as those used in Pirt or Gudin (44,45). Figure 18.3 depicts a scheme of a fully instrumented tubular PBR like that proposed by Gudin *et al*. setup in the authors' laboratory. The PBR consists of a vertical external-loop airlift pump that drives the culture fluid through the horizontal tubular solar receiver. The airlift section (riser, downcomer, and degasser) has a height of 3.5 m. The gas-injected riser and the downcomer sections are extensions of the solar receiver tube. The solar receiver is made of transparent Plexiglas tubes (0.05 m internal diameter, 0.005 m wall thickness) joined into a loop configuration by Plexiglas joints to obtain a total horizontal length of 98.8 m. The solar receiver is submerged (~0.05 m) in a shallow pool of water that is maintained at 21 ± 2°C by cooling with a heat pump when needed. The bottom and the inside walls of the pool are painted white to improve reflectance. The surface area of the pool is 21.4 m^2. The total culture volume of the bioreactor is 0.22 m^3.

For the efficient and reliable large-scale culture of microalgae in PBRs, several operational, environmental, and design variables need to be assessed. The most important design criteria are, likely, the efficiency of light utilization (which, in turn, is related with the productivity of the system), a homogeneous turbulence regime, and the capability of the system to match the conditions required by the particular microalgae through time and in all the reactor volume. From the commercial point of view, the capital cost of construction and operation (directly related to the CO_2 consumption efficiency) are, of course, also critical (51). The on-line data acquisition of DO, pH, and temperature inside the culture allows for

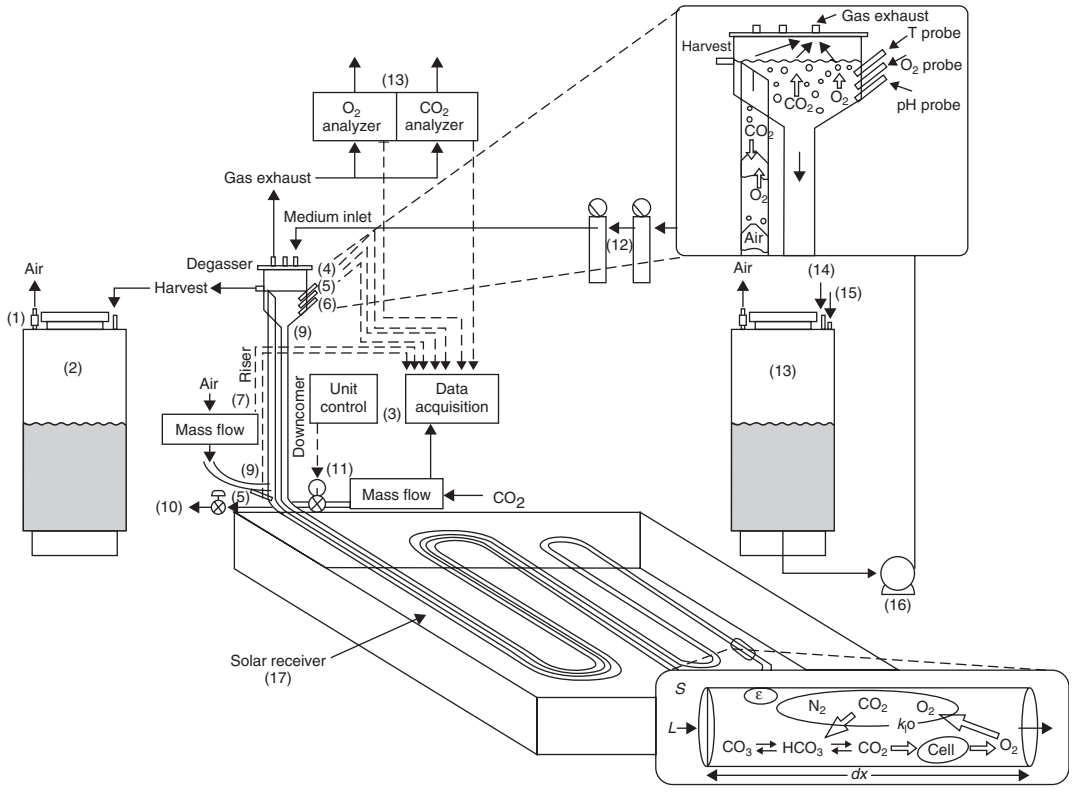




Figure 18.3. Scheme and image of tubular photobioreactor and additional equipment (1 air filter, 2 harvest tanks, 3 control units, 4 temperature sensors, 5 dissolved O2 probes, 6 pH probes, 7 risers, 8 downcomers, 9 air injections, 10 samplers, 11 CO_2, 12 medium sterile filters, 13 fresh mediums, 14 nutrient inlets, 15 sea water inlets, 16 pumps, 17 thermostatic water pools). [From Ref. 52 With permission.] (This figure is available in full color at http://onlinelibrary.wiley.com/book/10.1002/9780470054581.)

rapid characterization of the physiological state of the cells. The measurement of CO_2 and O_2 molar flow at the gas inlet and outlet enables the estimation of the mass transfer capability of the system and the efficiency of CO_2 utilization. The measurement of the biomass concentration and product/s content/s allows the estimation of the biomass and product productivities.

This type of PBR has been extensively used on a pilot scale, biomass productivities of 2.76 g/L/day with *P. tricornutum* (52), of 1.76 g/L/day with *Porphyridium cruentum* (53), and of 0.55 g/L/day with *Haematococcus pluvialis* (54) being reported. This PBR is now applied on an industrial scale. Thus, after an upscaling period of nearly 3 years, an industrial tubular system was established near Wolfsburg, Germany (Fig. 18.4). This closed system is apparently the largest PBR to have gone into successful production. It consists of compact and vertically arranged horizontal running glass tubes of a total length of 500,000 m and a total PBR volume of 700 m^3. In a glasshouse requiring an area of only 10,000 m^2 an annual production of 130–150 tonnes of dry biomass was demonstrated to be economically feasible under Central European conditions (13). Other industrial plants based on tubular PBRs have been also set up in Germany and Spain. In Spain, the Fundación CAJAMAR built a 30-m^3 plant for the production of a proprietary strain (*S. almeriensis*) on a commercial scale, according to good manufacture practices for the food industry (Fig. 18.4). The plant is based on 10 individual tubular-type PBRs (tubes arranged horizontally in a fence configuration), 3 m^3 working volume each, installed in a greenhouse. The production capacity of the plant is 7–10 tonnes of dry biomass per year.

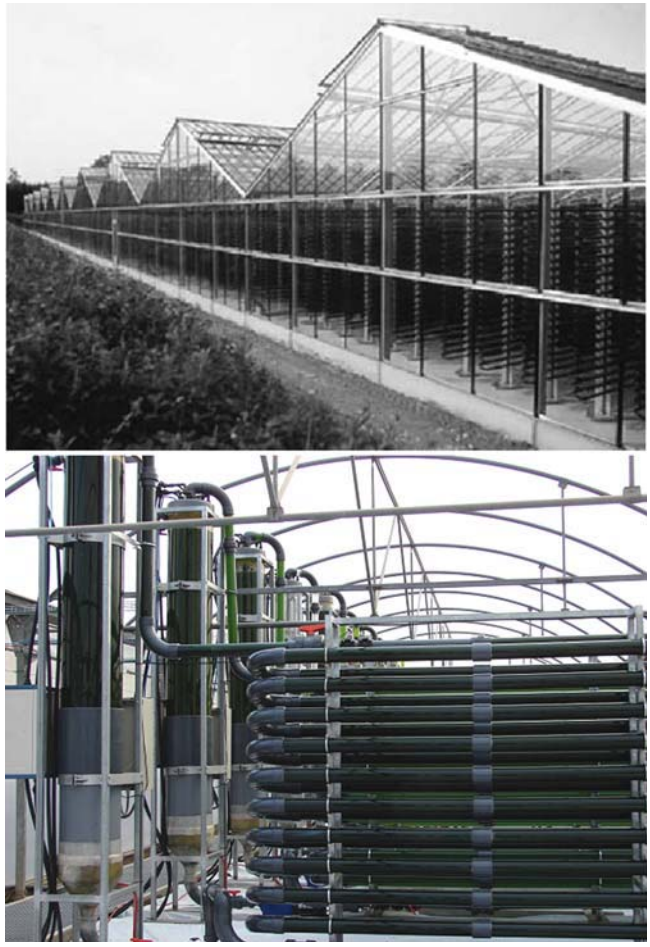


Figure 18.4. Photographs of two industrial-sized tubular photobioreactors. *Top*: 700 m^3 glass tube PBR producing *Chlorella* biomass in Germany. *Bottom*: A 30-m^3 plant for the production of *Scenedesmus almeriensis* in Spain, property of Fundación CAJAMAR. [From Ref. 13. With permission.] [With permission from Ref. 38.] (This figure is available in full color at http://onlinelibrary.wiley.com/book/10.1002/9780470054581.)

18.2.2.3 Flat Panels. Flat-panel PBRs have important advantages for mass production of photoautotrophic microorganisms and may become a standard reactor type for the mass production of several algal species. The construction of flat-plate reactors dates back to the early 1950s (55). Samon and Leduy (20) used vertically translucent flat plates, illuminated on both sides and stirred by aeration. Tredici and Materassi developed this idea (21,56) proposing a rigid alveolar panel. Pulz *et al*. (57) used flat panels with inner walls arranged to promote an ordered horizontal culture flow that was forced by a mechanical pump. The most innovative aspect of the Pulz reactor was that parallel plates were packed together; close enough to attain 6 m^3 of culture volume on 100 m^2 of ground area, with a total illuminated culture surface of ca. 500 m^2. The research of Hu and Richmond (58,59) resulted in a type of flat-plate reactor made of glass sheets, glued together with silicon rubber to make flat vessels. This simple methodology for the construction of glass reactors provided the opportunity to easily build reactors with any desired light path. Zhang *et al*. (60) reported a biomass productivity of 1.0 g/L/day, with *Synechocystis aquatilis* in outdoor flat panels, at aeration rates of 0.05 v/v/min. Tredici *et al*., (21) used a vertical alveolar panel (1.2 cm wide, tilt 25 degrees, south faced, 2.2 m^2) for the production of *Anabaena azollae* and *Spirulina platensis*, attaining biomass productivities of 15 g/m^2/day at air flow rates of 1.0 v/v/min, the maximum biomass productivity obtained being 24 g/m^2/day. Cheng-Wu *et al*., (36) operated a 500-L flat plate reactor, 10-cm light path, using *Nannochloropsis* sp., an annual average productivity of 24 g/m^2/day being reported. Zou and Richmond (61) noted that the optimal light patch for *Nannochloropsis* sp cultures was 10 cm, yielding biomass productivities of 0.5 g/L/day and 50 g/m^2/day in summer, using a flat-panel PBR. Recently a new design of a vertical flat-panel PBR consisting of a plastic bag located between two iron frames

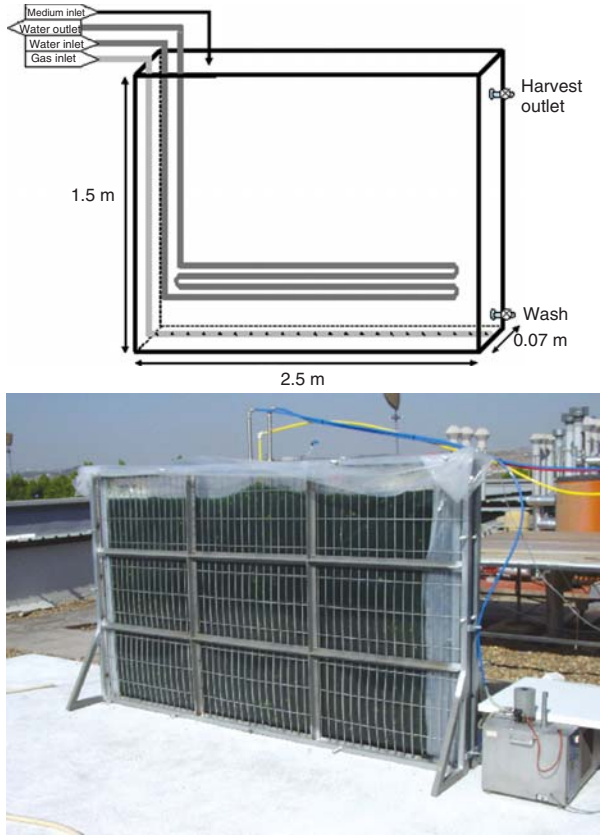


Figure 18.5. Diagram and photograph of a flat-panel photobioreactor. The reactor is equipped with an aeration system, heat exchanger, medium inlet, and harvesting valve for the continuous operation of the photobioreactor. [With permission from Ref. 38.] (This figure is available in full color at http://onlinelibrary.wiley.com/book/10.1002/9780470054581.)

was proposed (62); this brings a substantial cost reduction to this type of reactors (Fig. 18.5). Mass transfer, mixing, and heat transport in flat panel reactors have also been recently studied (63). This last reference demonstrates that the east/west orientation is the most favorable because the total solar radiation intercepted increased by 5%, with regard to horizontal placement, and homogenized the radiation intercepted over the year. The main advantages of this reactor are the low power consumption (53 W/m^3) and the high mass transfer capacity (0.007/s).

18.2.3 Comparison

For the mass cultures of microalgae, open pond systems have mainly been the dominating systems up until now. However, closed systems of light-distributing tube or plate design, known as *photobioreactors*, are now increasingly finding new applications both for high value products in pharmacy and cosmetics as well as for aqua and agricultural uses. Table 18.1 summarizes the advantages and disadvantages of both types of culture systems.

TABLE 18.1. Advantages and Disadvantages of Open and Closed Algal Cultivation Plants

Parameter	Open Ponds	Closed Systems (PBR Systems)
Contamination risk	Extremely high	Low
Space required	High	Low
Water losses	Extremely high	Almost none
CO_2losses	High	Almost none
Biomass quality	Not susceptible	Susceptible
Variability as to cultivable species	Not given, cultivation possibilities are restricted to a few algal varieties	High, nearly all microbial varieties may be cultivated
Flexibility of production	Change of production between the possible varieties nearly impossible	Change of production without any problems
Reproducibility of production parameters	Not given, dependent on exterior conditions	Possible within certain tolerances
Process control	Not given	Given
Standardization	Not possible	Possible
Weather dependence	Absolute, production impossible during rain	Insignificant, because closed configurations allow production also during bad weather
Period until net production is reached after start or interruptions	Long, approximately 6–8 wk	Relatively short, approximately 2–4 wk
Biomass concentration during production	Low, approximately 0.1–0.2 g/L	High, approximately 2–8 g/L
Efficiency of treatment process	Low, time-consuming, large volume flows due to low concentrations	High, short-time, relatively small volume flows

[From Ref. 12. With permission.]

18.3 MAJOR FACTORS GOVERNING THE PRODUCTION OF MICROALGAE

The biomass productivity in any culture system depends on how closely the culture conditions match the requirements of the selected strain. Because mineral nutrient limitation is easily avoided in a microalgal mass culture, light availability inside the PBR and temperature are found to be

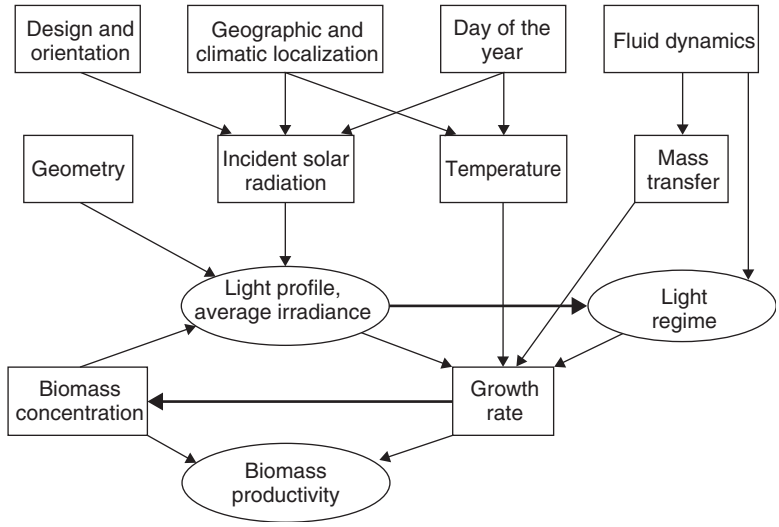


Figure 18.6. Relationship between major factors influencing the biomass productivity of microalgal mass cultures. [From Ref. 70. With permission.]

the main management factors in obtaining optimum system profitability. Thus, when temperature culture is kept within an appropriate interval, light availability is the only factor determining growth. Figure 18.6 shows the relationship between the different factors governing biomass productivity under outdoor conditions. The key factor is the growth rate, which is a function of the light profile within the reactor and the light regime at which the cells are subjected. Once this function is known, it becomes possible to obtain a correlation between biomass productivity and the average irradiance within the reactor, I_{av}. On the other hand, I_{av} is a function of the irradiance impinging on the reactor surface, I_0, which is, at the same time, dependent on geographic and environmental factors. The geographic location and day of the year determine the solar incident radiation and therefore the temperature in the culture. While temperature can be kept within a narrow interval by using suitable thermostatic systems, solar radiation cannot be controlled.

The incident solar radiation, which is a function of climatic and geographic parameters of the facility location (64), as well as the design and orientation of the PBR (50,58,63), determines the maximum energy available for growth. The incident solar radiation, along with the PBR geometry and the biomass concentration, determines a heterogeneous light profile due to cell mutual shading inside the culture (65,66). The light availability or average irradiance inside the culture can be calculated by a volumetric integration of the irradiance profile. The cell metabolism adapts to this light availability and so does the biochemical composition and growth rate (52). However, the PBR fluid-dynamics also determine the mass transfer and the light regime of the cells. The latter is affected by the time the cells spend in zones with a different irradiance level and the frequency of movement into and out of these zones (67–69). This light regime affects the behavior of the cells, determining the extent at which the cells are exposed to the photic and the dark zones of the PBR, and thereby the efficiency of using solar radiation by the cultures. The biomass concentration is in itself influenced by the growth rate, which is a function of the average irradiance, temperature, mass transfer, and light regime. Both, the growth rate and the biomass concentration, determine the final biomass productivity of the system (Fig. 18.6). Thus, in an optimum system where there are no limitations other than light, a direct interrelationship among light availability, rate of photosynthesis, and productivity may be expected. In fact, it seems that other limitations do not only limit growth through their direct effect but also impose a limitation on the ability to utilize the absorbed solar energy. This may result in a photoinhibitory response further limiting the ability of the photosynthetic apparatus to operate at its maximal efficiency (71). The present section considers the above-noted issues that influence biomass productivity in outdoor conditions.

18.3.1 Light Distribution and Average Solar Irradiance Inside Photobioreactors

When considering commercial-scale microalgal culture, the source of light is usually sunlight as artificial light is too expensive for most products. The effects of outdoors illumination in microalgae cultures are not completely clear. This is because just about all the studies concerning the characterization of the photosynthetic response to light (72–75) have been conducted under carefully controlled

laboratory conditions, in which temperature and irradiance were constant and the irradiance used was significantly lower than that of peak solar irradiance prevailing outdoors. Outdoor conditions are very difficult to simulate in laboratory; the impinging irradiance on cultures grown outdoors changes within a few hours from zero at dawn to over 2000 $\mu E/m^2/s$ at noon (i.e. a rate several times above saturation), and within a few additional hours thereafter, declines to zero again as evening sets in. This large and fast change in irradiance during the day may shift the culture from being light limited in the morning to being light inhibited at noon and thereafter light limited once again as light intensity diminishes further in the afternoon and evening.

Information concerning light distribution in microalgal mass culture systems is scant. Existing methods of estimating average illumination employ an approach consisting of the following: (i) estimation of the total photosynthetically active incident radiation at the surface of the PBR, (ii) use of Beer–Lambert's law to determine the radiation level at any depth inside the culture as a function of the concentration of the cells and the light absorption characteristics of the cellular pigments, and (iii) the integration of the local values over the total volume of the culture. Rigorous solutions for different geometries and PBRs have been developed. Thus, Acien Fernández *et al*, (67) developed a comprehensive model for light distribution and average solar irradiance inside a horizontally placed tubular outdoor PBRs. That model has been further generalized for use with bubble-column-type reactors (39). The mathematical model determines the distance traveled by an incident ray of light to any point inside the culture and estimates the local irradiance by taking into account the light attenuation due to biomass. The incident total radiation is divided into direct and disperse radiation.

The model is mathematically complex. For example, the angle of incidence of direct radiation on the PBR surface is a function of five variables: day of the year, solar hour, geographic latitude, surface slope, and surface azimuth angle (i.e. the deviation of the projection on a horizontal plane of the normal to the surface from the local meridian, with zero due south, east negative, and west positive) (76,77). Figure 18.7 shows the local irradiance profiles either in a horizontal or vertical arrangement at 8 and 12 solar hours. As expected, as the solar hour changes, curves of local irradiance at the same internal ratio adjust to the sun's position in both arrangements. In the morning, the vertical reactor facing the sun has much higher direct irradiance values than the opposite side; this difference being lower in the horizontal reactor. However, at noon, the irradiance distribution in the vertical, unlike the horizontal, is practically homogeneous. This profile is because, during midday, the contribution of disperse irradiance to total irradiance in relation to the direct irradiance is very important in the vertical arrangement. Therefore, the level of irradiance for each internal radius and for any hour of the day is higher in the horizontal reactor tube than in the vertical. The irradiance distribution inside the culture and the patterns of cell movement inside the PBRs are also different.

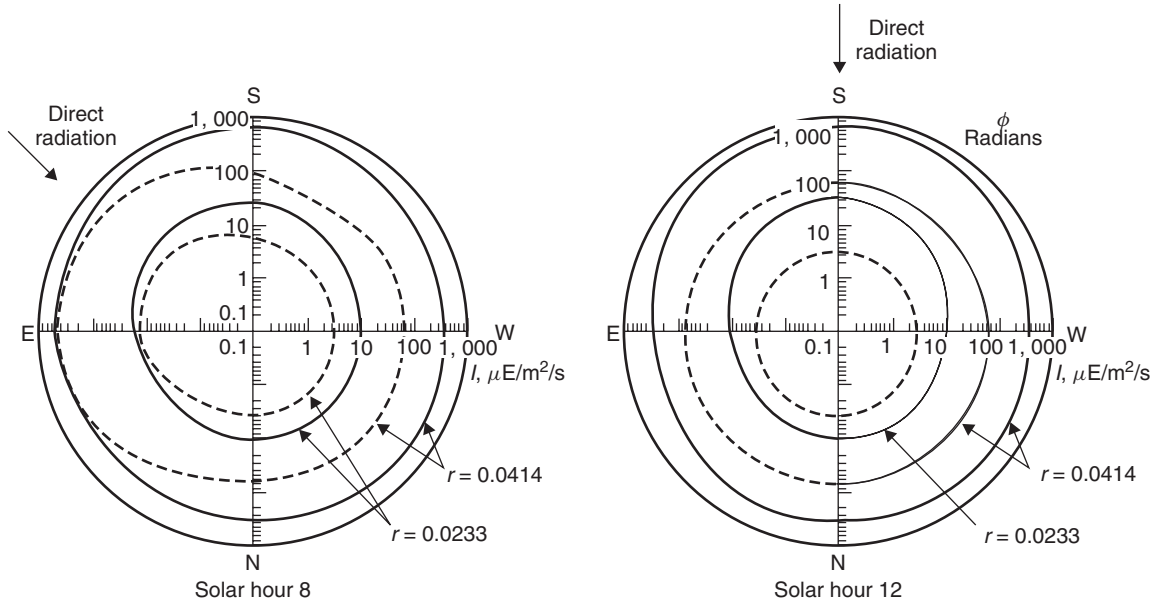


Figure 18.7. Polar plot of irradiance profiles in the cross-section of a bubble-column-type photobioreactor (PBR) (dashed lines) and horizontal loop tubular PBR (solid lines) for the 0.041 m and 0.023 m internal radii at the 8 and 12 solar hours.

Another simplified model to calculate I_{av} (Eq. 18.3) has been also proposed (78). This model is suitable for any combination of disperse and direct light as long as it is impinging uniformly on the reactor surface. According to this model, the average irradiance, I_{av}, is a function of irradiance measured in the center of an empty reactor, I_o, the extinction coefficient of the biomass, K_a, the optical light path, p, and the biomass concentration in the culture, C_b.

$$I_{av} = \frac{Io}{K_a \cdot p \cdot C_b}(1 - \exp(-K_a \bullet p \bullet C_b)) \qquad (18.3)$$

This model has been successfully used to analyze the influence of light on the behavior of indoor and outdoor cultures for different microalgae (52,53).

18.3.2 Light Saturation Constant and the Photoinhibition Phenomenon

Algal growth is related to light intensity. According to Goldman (13), the generalized curve relating algal growth to light intensity has the shape shown in Fig. 18.8. The curve has four main features: (i) at some low growth rate, the growth is balanced by decay, and the net growth rate is zero; (ii) the initial slope of the curve represents the maximum efficiency of growth in response to light; (iii) there is a saturating light intensity at I_s for which $\mu = \mu_{max}$; (iv) at some light intensity $I_p > I_s$, the growth is inhibited and $\mu < \mu_{max}$. Because most algal species become light saturated at a fraction of peak solar-light intensity, much potentially useful solar energy is essentially wasted for photosynthesis. The light saturation constant depicts the intrinsic capacity of cells to utilize light energy, and thus it should be given special attention in mass cultures of photoautotrophs. The selection of algal strains having a high

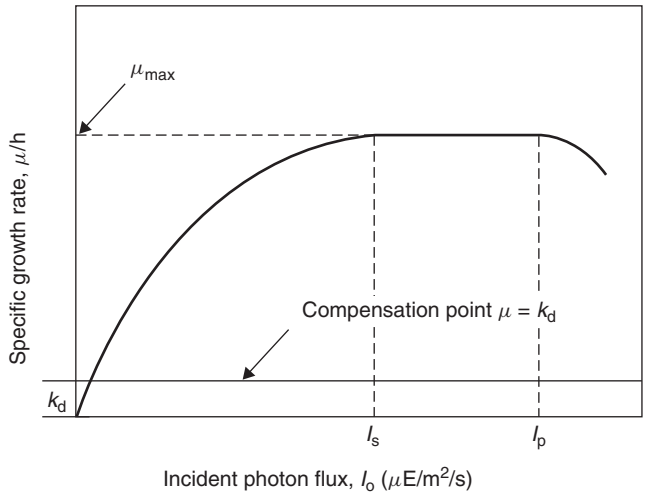


Figure 18.8. Dependence of the growth rate (μ) on the incident photon flux (I_o). [From Ref. 15. With permission.]

I_s value is desirable to avoid the saturation effect. A high saturation constant gives rise to a double advantage on photoautotrophs exposed to high photon flux densities (PFD). It increases the efficiency by which high PFD may be utilized and concomitantly diminishes the occurrence and magnitude of photoinhibition, which would substantially reduce the output rate of sensitive strains in outdoor cultures.

Photoinhibition, which may be defined as depression of the photosynthetic capacity due to supraoptimal light intensities in great excess of that required to saturate photosynthesis (16), has been much studied in algae. Shading the culture by shad nets is a normal practice that provides protection from the light inhibitory effect. The kinetic of photoinhibition and its recovery in *Porphyridium cruentum* was previously studied (79). A linear relationship was found between the specific rate of photoinhibition and the specific light absorption rate. Temperature was found to have a most pronounced modifying effect on photoinhibition. At 15°C, no damage could be detected at 2300 μE/m^2/s, even after 45 min of illumination. In contrast, at 35°C, 84% inhibition of photosynthetic activity was observed within 10 min of exposure to irradiance. *P. cruentum* cells recovered readily when transferred to low light (90 μE/m^2/s) and darkness, the specific rate of recovery was independent of the light intensity to which the cells were exposed during the inhibitory treatment. Photoinhibition in outdoor mass cultures can be detected with high sensitivity from changes in variable chlorophyll fluorescence (80). The Fv/Fm ratio (variable to maximum fluorescence yield) is a convenient measure of the potential maximum quantum yield of PSII, and it has been assumed as a measure of photoinhibition (81).

The existence of photoinhibition in continuous outdoor cultures of *P. tricornutum* has been evidenced (52). Figure 18.9 shows how I_{av} varies with the dilution rate regardless of the tube diameter, hence indicating that the cultures adapt mainly to average irradiance. At D= 0.025/h, I_{av} increased only slightly with increasing I_{wm} (slope = 0.014 ± 0.004); the mean value of I_{av} for the whole range was 84 ± 9 μE/m^2/s. With smaller tube diameter and/or higher external irradiance, I_{wm}, the biomass concentration increased as expected for self-shaded light-limited growth. However, the slight increase in I_{av} with I_{wm} points to some photoinhibition by external irradiance, although this is not very extensive due to the high biomass concentrations. At D = 0.040/h, I_{av} values are higher (163 ± 20 μE/m^2/s) than at D = 0.025/h because of the lower steady-state biomass concentrations. The greater light availability gives rise to a higher specific growth rate as well as photoinhibition, because of the greater increase in I_{av} with I_{wm} (slope = 0.032 ± 0.004). At 0.050/h dilution rate, the exponential increase in I_{av} with I_{wm} caused by the low steady-state biomass concentration, underlines the existence of photoinhibition,

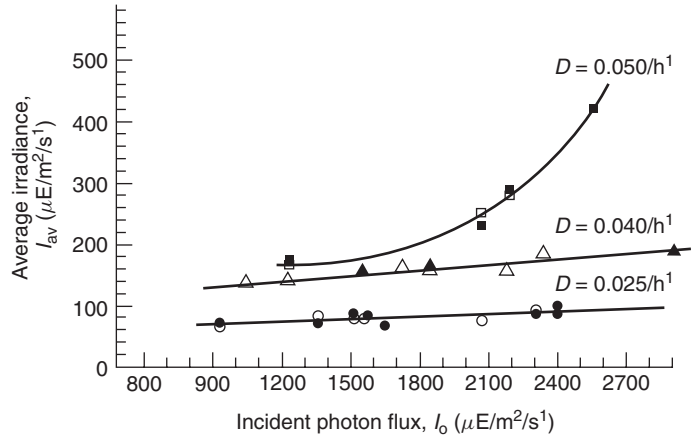


Figure 18.9. Variation in average irradiance I_{av} inside the culture with daily mean photosynthetic irradiance inside the pond I_{wm} for the various dilution rates and the photobioreactors used. [From Ref. 52 With permission.]

and thus the one-to-one relationship between μ and I_{av} no longer applies.

Photoinhibition is caused by oversaturation of photosystem II, which damages the D1 protein that carries the binding site of the electron carrier (82,83). This photoinhibition effect is quite distinct from that of temperature rise that occurs in uncontrolled systems as a function of the PFD. At low light intensities, the few damaged D1 protein molecules are replaced rapidly and the net damage to the photosynthetic apparatus is negligible. Under this situation, a dark period reduces growth rate (photosynthesis) because fewer photons are captured but no gain is obtained from the dark time. In contrast, under conditions of intense illumination, part of the light energy impairs the photosynthetic apparatus. Repair and damage proceed simultaneously and the observed growth is the sum of the two processes. If a dark period is introduced under this situation, the duration of the photosynthetic period declines, but the damaging period is also reduced, while the photon trap repair continues during the dark time. Consequently, during the next light period, a substantially rejuvenated photon trap compensates for the loss in photosynthetic time. Under these circumstances, alternating light/dark periods do not reduce growth, which may in fact be slightly enhanced. Nevertheless, the length of the dark period is important: lengthening the light period beyond an optimal value produces loss of growth. The optimal or critical dark period is not a fixed quantity; instead it depends on the PFD of the previous light period and the fluid residence time in zones of different irradiance.

To explain the influence of light regime in the behavior of microalgal cultures, a mechanistic model of photosynthesis has been recently published (84). The model considers that photosynthesis in microalgal cell occurs only in the photosynthetic unit (PSU), a portion of the thylakoidal membrane that brings together photon receptors, electron carriers, and the enzymes necessary for regenerating NADPH and adenosine triphosphate (ATP). During photosynthesis, a resting-state PSU^o is rapidly activated by absorption of photon, giving activated PSU*, which is deactivated slowly in enzyme-mediated reactions to regenerate PSU^o. However, excess of photons convert functional PSU_f into nonfunctional PSU_{nf}. The kinetics of processes involved in these transitions are modeled and the characteristic parameters determined. Figure 18.10 summarizes the scheme of the mechanism proposed. The proposed model can take into account the influence of the light regime characterized as a frequency, ν, of change from light to dark zones and a so-called "duty cycle," ϕ, that represents the predominance of light or dark zones. The simulated effect of the frequency of changes from light to dark in the photosynthesis efficiency is shown in Fig. 18.11 (expressed in relative terms as ν/β, the ratio of frequency to β, and the microalgae sensitivity to the frequency of changing light; (see Ref. 84 for further detail). Figure 18.11 shows how important it is to have an adequate frequency of renovation from light to dark zones for an efficient use of light and that no matter how high the light availability is (represented on the x-axis as $\phi \cdot I/\alpha$, see reference for details), the photosynthetic response is poor if ν is small compared to β (see line $\nu/\beta = 0.1$ in Fig. 18.11). This dynamic mechanistic model of photosynthesis also accounts for photoadaptation as described by Marra (85) and photoinhibition. The well-known "flashing light effect" is also evident in Fig. 18.11 because, at a fixed light intensity, the photosynthetic response greatly increases with frequency especially for $\phi \cdot I/\alpha$ above 1.0 (which means the microalgae are close to light saturation).

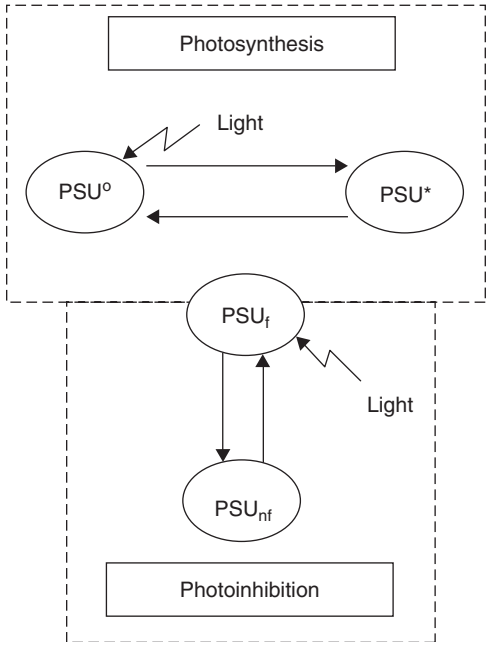


Figure 18.10. Schematic representation of photosynthesis and photoinhibition. A resting PSU° is activated to PSU* by absorption o flight. Excess photons reversibly convert functional PSU_f to nonfunctional PSU_{nf}. [From Ref. 84. With permission.]

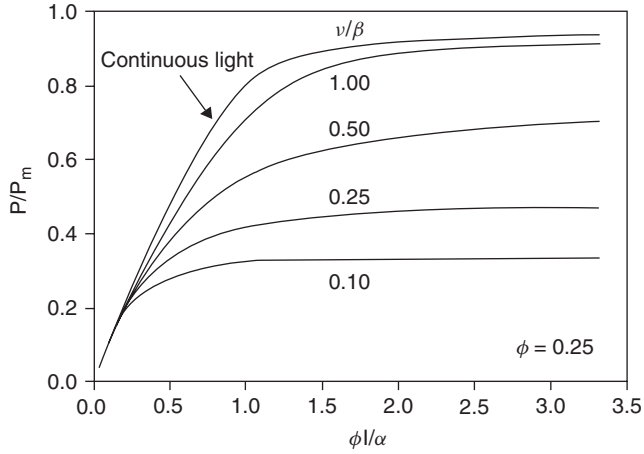


Figure 18.11. Variation in the relative photosynthetic response (P/P_m) with a dimensional light intensity (ϕ/α) at different light regimes of increasing frequency (n). A full photosynthetic response ($P/P_m \approx 1$) is possible only for light regimes with a flashing frequency close to the microalgae characteristic frequency, $\beta(\nu/\beta \approx 1)$. [From Ref. 84. With permission.]

Clearly, therefore, the principal problem of designing or choosing a PBR is assuring, for any species with defined photosynthetic characteristics, that the largest possible fraction of cells experiences optimal exposure to light in the largest possible reactor volume.

18.3.3 Biomass Productivity

Many studies on the influence of environmental variables on biomass productivity have been carried out in the laboratory, but very few have been performed under outdoor conditions. Some models have been proposed specifically for outdoor alga ponds (65,86–88). Incropera and Thomas (64) present a model for determining the mean irradiance in an open pond as a function of climate and geographic location parameters. Starting from estimated irradiance values, a six-parameter growth model, four of which are obtained experimentally, and which does not consider photoinhibition, is proposed. This model, which predicts maximum productivities of about 34 g/m^2/day in June, was not experimentally verified. On the other hand, Sukenik *et al*., (86,87) proposed a five-parameter mathematical model to estimate the biomass productivity in outdoor systems, which considers that the cells adapt to mean irradiance inside the culture. However, they do not take into account the existence of photoinhibition, and their results are not valid at low biomass concentration. In spite of this, the model estimates productivities from 10.2 to 27.2 g/m^2/day, although this has also not been experimentally verified. By using mean temperature and irradiance data, Gutterman *et al*., (88) proposed a growth model for open systems. The model estimates the variation of culture parameters such as DO, temperature, pH, and biomass concentration, by considering empirical linear relationship, and does not consider photoinhibition either. The estimated maximum productivity was 38 g/m^2/day at irradiances of 2500 μE/m^2/s. In all these cases, under no photoinhibition conditions, a one-to-one relationship between the growth rate and the average irradiance is considered. One of the most used equations to relate these variables is the one proposed by Molina Grima *et al*., (65). Studies suggest that growth models that express μ in terms of the average irradiance raised to some power greater than unity better fit experimental observations (78,79).

$$\mu = \frac{\mu_{\max} I_{\mathrm{av}}^{\mathrm{n}}}{I_{\mathrm{k}}^{\mathrm{n}} + I_{\mathrm{av}}^{\mathrm{n}}} \tag{18.4}$$

None of these models consider the effect of photoinhibition, because they estimate that maximum productivities are reached at very low biomass concentration, when the mutual-shading effects are negligible and the culture may be considered light saturated. However, these cultures could not have been carried out, as photoinhibition in the middle of the day decreases growth rate, even leading to culture washout.

To consider the photoinhibition phenomenon, modification of Equation 18.4 has been proposed (Eq. 18.5) (52), where a, b, and c are empirical parameters, whereas I_{k} and I_{i} are the irradiance constant and irradiance of photoinhibition respectively. This equation accounts for photoinhibition and the fact that the dependence of μ on the

average irradiance varies with the incident irradiance level, I_o. This equation was established from outdoor cultures of *P. tricornutum* UTEX 640, carried out during 3 years in two different tube diameters of tubular PBRs (52).

$$\mu = \frac{\mu_{\max} I_{\text{av}}^{\left(b+\frac{c}{I_0}\right)}}{I_k\left(1+\left(\frac{I_0}{I_i}\right)^a\right)^{\left(b+\frac{c}{I_0}\right)} + I_{\text{av}}^{\left(b+\frac{c}{I_0}\right)}} \qquad (18.5)$$

On the basis of this equation, a macromodel has been proposed to estimate the year-long biomass productivity of microalgal cultures, which is useful for outdoor tubular PBRs (52). In this model, the solar irradiance impinging on the reactor surface is determined as a function of the day of the year and location. By taking into account the geometry of the system, the average irradiance to which the cells are exposed inside the culture, I_{av}, is determined. Finally, in order to correlate the growth rate, μ, with I_{av}, the influence of solar irradiance (an environmental variable), tube diameter (a design variable), and dilution rate (an operational variable) on continuous cultures were analyzed in two different tubular PBRs. Thus, the relation between μ, the impinging irradiance on the reactor surface, I_o, and I_{av} has been described for light-limited growth, which at the same time is partially photoinhibited (Eq. 18.5), the characteristic parameter values that reproduced the experimental results being obtained ($\mu_{\max} = 0.063/\text{h}$, $I'_k = 94.3$ $\mu\text{E/m}^2\text{/s}$, $K_I = 768.4$ $\mu\text{E/m}^2\text{/s}$, $n_1 = 3.04$, $n_2 = 1.209$, and $n_3 = 514.6$, $r^2 = 0.9945$). In this form, by the conjunction of the solar irradiance estimation, the estimation of the average irradiance inside the culture, the kinetic model, and the biomass productivity along the year can be estimated (52). The estimated values reproduced the experimental productivities with less than 20% error. Therefore, the biomass productivity over the annual cycle as a function of geographic location and reactor geometry was obtained (Fig. 18.12). This methodology could be extended to other strains. If photoinhibition would not have been considered, as in previous models (65,86–88), the experimental results could be adjusted to the hyperbolic model that only considers photolimitation (Eq. 18.4) (90). The estimated values, in this case, had an error of over 20%, some of them over 45%.

From the previous analysis, several conclusions already emerge and can be used to optimize biomass production in microalgae mass cultures: (i) the optimum dilution

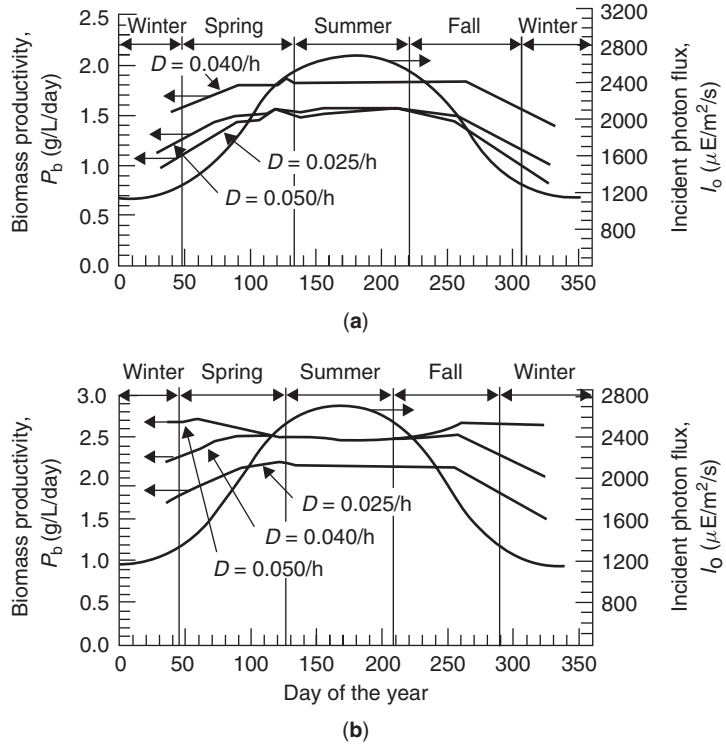


Figure 18.12. Comparison of estimated productivities during the year, with only photolimitation, and with photolimitation plus photoinhibition. (a) Tubular photobioreactor (PBR) 0.06 m tube diameter; (b) tubular PBR tube diameter 0.03 m. [From Ref. 52. With permission.]

rate is not a constant value, but varies over the year as a function of incident radiation and tube diameter, and therefore of average irradiance; (ii) the larger the tube diameter, the more extensive the photoinhibition effect, although the simultaneous existence of photolimitation and photoinhibition permeate the growth to be maintained and thus reaches quasi-steady states; and, (iii) ultimately, the microalgal growth is determined by the photolimitation–photoinhibition regimes in dense cultures.

18.3.4 Temperature

Many studies in both open ponds and closed reactors have shown that temperature is an important factor affecting productivity. The highest biomass growth rate can be obtained only at the optimal temperature for growth. Although there are microalgal strains adapted to extreme temperature conditions, low or high, most microalgae grow optimally at 15–30°C. Below this value, the growth is depressed by the reduction of metabolic kinetics, whereas above this value temperature and oxidative stress appear and the yield of the cultures greatly decreases. Some other strains tolerate higher temperatures, up to 45°C, being adequate for outdoor culture due to lower refrigeration requirements.

Although this effect is obvious and well documented under laboratory conditions, the magnitude of the effect on the annual production of biomass outdoors does not seem to be sufficiently documented. The diurnal variation in temperature that affects cultures in open raceways results in temperature-limited growth during a significant fraction of the day. Lee *et al*., (75) showed that the light yield (g biomass/kJ) increased some three- to fivefold with increasing temperature in cultures of *Chlorella*, an effect that may be easily observed with other microalgae. The response of microalgae to temperature shows a typical behavior of other microorganisms as bacteria, yeast, or fungi, an Arrhenius's type equation being usually used to model this behavior.

$$\mu_{\max} = \mathrm{A} \exp\left(\frac{-\mathrm{B}}{T}\right) \tag{18.6}$$

where A and B are empirically determined constants for a range of temperatures, T. However, in outdoor cultures, the temperature is not constant and varies simultaneously with the solar cycle and the cells adapt to this variation in a process similar to the adaptation phenomena related to the light variation. The temperature of the culture at night is yet another important factor that affects the net output rate of biomass. The effect of temperature on dark respiration is, of course, very well documented (28,46,52).

To maximize the yield of outdoor microalgal cultures, it has been proposed to maintain the cultures cold during the night and to heat them to the temperature of operation just before sunrise, then cool them during the hours of maximum irradiance by water spraying systems to avoid overheating of the cultures (91,92). However, the capacity of these systems is limited and their application is only possible under certain environmental conditions (temperature, humidity, etc.). The other strategy considers the use of heat reservoirs to recirculate cool water trough a heat exchanger inside the PBR, thus homogenizing the temperature of the cultures over the solar cycle and reducing the power consumption.

18.3.5 Fluid Dynamics and Mixing

In order to achieve high productivity, microalgal cultures have to be mixed. The method of providing adequate mixing (turbulence) is, however, critical because many algae are quite sensitive to shear stress (27,93). It has been proposed that, when light is the limiting factor for growth, stirring represents the most practical way to attempt to distribute solar energy evenly to all cells in the culture. Stirring affects the flashing light effect by changing the duration that the cells are exposed in the photic zone and the time they remain in the dark zones inside the reactor (this concept is often referred to as *light regime*, introduced by Richmond, (16)). This field has been intensively investigated by Laws *et al*. (94), who introduced a simple technique for utilizing the flashing light effect in shallow but optically dense outdoor algal cultures by inserting an array of small foil segments across the width of a continuous flume at intervals of 1.2 m along the length of the flume. The wing-shaped foils create a vortex circulation that produces an ordered pattern of vertical stirring. By using these foils, Laws *et al*. (94) obtained averaged photosynthetic efficiencies (based on the photosynthetic active radiation [PAR]) of 9.6 and 7.5, respectively, with and without the foil in place.

In tubular PBRs and ponds, higher flow rates generally enhance productivity. Typical values of flow rates range between 20 and 30 cm/s. This flow can be achieved by using the paddle wheel devices in open reactors, or peristaltic, diaphragm, centrifugal pumps, or airlift devices in closed systems. However, the use of these equipments introduces shear forces in the culture. Airlift systems are generally less damaging to the cells and are most effective. In tubular reactors, the airlift system is the usual method for maintaining a degree of turbulence in the mass culture. The higher velocity in the tube controls the turbulence and shear effects, determines the mixing behavior and the mass transfer capacity, and it greatly influences the axial oxygen concentration profiles in the tube. The liquid velocity, U_{L}, may be estimated by an extension of the well known and widely tested model developed by Chisti (95).

$$U_{\mathrm{L}} = \left[\frac{g h_{\mathrm{d}} \varepsilon_{\mathrm{r}}}{2 C_{\mathrm{f}} \frac{L_{\mathrm{eq}}}{D}} \frac{A_{\mathrm{r}}}{A_{\mathrm{d}}}\right]^{0.5} \tag{18.7}$$

where f is the Fanning friction factor that can be calculated using the Blasius equation.

$$C_f = 0.0791\,\mathrm{R_e}^{-0.25} \tag{18.8}$$

where Re is the Reynolds number, or $(\rho_L U_L \mathrm{D})/\mu$. Here D is the tube diameter, and ρ_L and μ are the density and the viscosity of the liquid respectively. As shown in Equation 18.7, the superficial liquid velocity in the tubular PBR is a function of gas holdup in the riser, ε_r, the height of the dispersion, h_D, and the ratio between the cross-sectional area of both the riser and the downcomer. The gas holdup follows a potential relationship with the power supply (Eq. 18.9) (95), the power supply due to aeration being a function of the density of the liquid, ρ_L, the gravitational acceleration, g, and the superficial gas velocity in the aerated zone, U_G (Eq. 18.10).

$$\varepsilon = 3.32 \cdot 10^{-4} \left(\frac{P_\mathrm{G}}{V_\mathrm{L}}\right)^{0.97} \tag{18.9}$$

$$\frac{P_\mathrm{G}}{V_\mathrm{L}} = \rho_\mathrm{L} g U_\mathrm{G} \tag{18.10}$$

18.3.6 Mass Transfer, Oxygen Accumulation, and Carbon Uptake

Microalgae perform photosynthesis, then oxygen is produced and carbon dioxide is taken up from the environment. If oxygen is not removed from the culture medium, it accumulates. Similarly, carbon dioxide must be provided such that availability of carbon does not become a limiting factor. Removing oxygen and supplying carbon dioxide are problems of gas–liquid mass transfer. Therefore, modeling of an algal reactor must consider gas–liquid mass transfer and how it is affected by hydrodynamics.

Oxygen concentrations above air saturation generally inhibit photosynthesis in microalgae (96). In cultures of *A. azollae* performed in vertical alveolar panels, the yield of the cultures decreases when the DO accumulates up to 400% with respect to saturation with air (21). In *P. tricornutum*, the photosynthetic activity not only decreases at DO concentrations exceeding 100% saturation (i.e. 100% with respect to saturation with air) but also below this value. A maximum photosynthesis rate of 0.0036 $\mathrm{molO_2/m^3/s}$ was measured at 100% saturation, reducing by 15% at DO concentrations of 0% and 300% saturation. At DO concentrations of 475% saturation, the photosynthesis rate declined sharply to 0.0016 $\mathrm{molO_2/m^3/s}$ (55% reduction) (18). Regarding CO_2, Weissman *et al*. (97) reported that CO_2 concentration in bulk liquid of at least 65 mM and pH 8.5 were required for optimal productivity of some marine- and saline-water diatoms. Similarly, Markl and Mather (98) observed a low critical CO_2 for *Chlorella vulgaris*: Concentrations as low as 60 mM enabled unlimited photosynthesis. In principle, CO_2 limitation can be easily avoided by supplying it in excess, but use of carbon dioxide represents a major operational expense of microalgal culture; hence, loss of residual CO_2 in the exhaust gas needs to be minimized.

Whatever the PBR design considered, it is possible to ensure a sufficient mass transfer capacity so that photosynthetically generated oxygen does not accumulate at excessively high concentrations. Thus, considering a maximum biomass productivity of 2.0 g/L/day with 50% carbon content in the biomass and a photosynthesis ratio of 1 $\mathrm{molO_2/molCO_2}$, a mass transfer coefficient of 0.006/s would be needed to prevent DO levels exceeding 300% saturation. To achieve this mass transfer capacity in flat-panel PBRs, the power supply must be 53 $\mathrm{W/m^3}$, as compared to 40 $\mathrm{W/m^3}$ in bubble columns (26,99), and 2400–3200 $\mathrm{W/m^3}$ in tubular PBRs (49,100,101). This shows that oxygen removal into the exhaust gas phase is substantially easier in flat-panel and bubble-column reactors than in tubular ones, although in the latter it was also enough to avoid excessive oxygen accumulation.

To adequately supply CO_2 from a gas phase to the culture, it is necessary to take into account that the dissolved carbon dioxide is in equilibrium with carbonate and bicarbonate species. These equilibria are pH dependent. Loss of dissolved carbon dioxide due to uptake into algal cells is partly compensated by regeneration from carbonates and bicarbonates. Consequently, carbon dioxide uptake is accompanied by changes in pH. The relevant equilibrium and the corresponding equilibrium constants that need to be considered are (100):

$$\mathrm{H_2O} \leftrightarrow \mathrm{H^+ + OH^-}\quad \mathrm{K_w} = [\mathrm{OH^-}] \cdot [\mathrm{H^+}] = 10^{-14} \tag{18.11}$$

$$\mathrm{CO_2 + H_2O} \leftrightarrow \mathrm{H_2CO_3} \leftrightarrow \mathrm{HCO_3^- + H^+}\quad \mathrm{K_1} = [\mathrm{HCO_3^-}] \cdot [\mathrm{H^+}]/[\mathrm{CO_2}] = 10^{-6.381} \tag{18.12}$$

$$\mathrm{HCO_3^-} \leftrightarrow \mathrm{CO_3^{2-} + H^+}\quad \mathrm{K_2} = [\mathrm{CO_3^{2-}}] \cdot [\mathrm{H^+}]/[\mathrm{HCO_3^-}] = 10^{-10.377} \tag{18.13}$$

To ensure a sufficient supply of CO_2, different strategies have been proposed. Lee and Hing (103) have suggested supplying carbon dioxide by diffusion through silicone tubes containing the pure gas. Camacho Rubio *et al*., (100) proposed the use of short-time injections of pure CO_2, whereas Mazzuca *et al*., (104) proposed the injection of CO_2–air mixtures. Although all these strategies reduce the carbon losses with regard to on–off injection, the most advantageous system is the use of model predictive control to adequately inject pure CO_2 into the reactor (105,106). In this way, carbon losses lower than 5% were achieved.

The adequate design and operation of PBRs require both the removal of oxygen and the supply of CO_2. In both cases, the major variable determining it is the mass transfer coefficient. The mass transfer from the gas phase to the culture suspension in open ponds has been extensively studied (98,107).In aerated systems, the volumetric gas–liquid mass transfer coefficient has been referenced to increase potentially with the power supply (Eq. 18.30) (95).

$$K_L a_L = 2.39 \cdot 10^{-4} \left(\frac{P_G}{V_L} \right)^{0.86} \tag{18.14}$$

18.3.7 Power Supply and Stress Damage

Power is supplied to microalgae cultures to increase the mass transfer and avoid toxic levels of DO, to reduce the nutrients gradient in the culture broth, to avoid cell sedimentation in the reactor, and to force the cells to move from dark to light zones, enhancing the photosynthesis. However, excessive aeration and/or agitation by pneumatics and mechanical devices may produce cell damage if the microalgae are susceptible to hydrodynamic and mechanical shear forces, affecting the culture performance. Power supply promotes mass transfer in both directions: CO_2 from the gas phase to the bulk liquid and DO from the bulk liquid to air bubbles. To avoid excessive oxygen levels, the mass transfer capacity of the system must be enough to remove the oxygen generated by photosynthesis (18,101). Power supply also promotes an adequate light–dark cycle regime. In both cases, there is an optimum value of power supply that ensures enough mass transfer to prevent excessive oxygen accumulation and adequate light regimes. However, the optimum could differ for both variables.

All the power supplied to the culture is dissipated, excessive power supply damaging the cells. Factors determining the shear sensitivity are the type of microalgae, the composition, and thickness of the wall cell, when present, the size and morphology of cells—the presence of flagella is a very important factor the intensity and nature of the shear stress (laminar/turbulent regime, presence of pumps, etc.), and finally the growth environment to which the cells are exposed (pH, temperature, irradiance, etc.) (27,108). The energy dissipation rates in the fluid are linked to shear stress, shear rates, the microeddy length scale, and other characteristics of flow (108,110).

In aerated systems, the power supplied may damage cells when the bubbles detach at the sparger, during the eventual breakup or coalescence of the bubbles within the bulk liquid and, above all, when bubbles burst at the culture surface. Bubble bursting has been recognized as the main factor that harms cells in aerated cultures. The mechanism of the bubble rupture and cell damage has been extensively studied. It is well established that small bubbles are more damaging than larger ones and that the higher the aspect ratio of the reactor (height/diameter ratio), the lower is the bubble-associated damage.

On the other hand, either in aerated or in nonaerated systems, the power supply may also damage the cells because of interactions between the wall of the PBR and the cells. The wall shear stress is a function of the liquid velocity and the friction coefficient, which, at the same time, is a function of the Reynolds number. One additional cause of damage when the culture is subjected to mechanical forces, as those produced by stirrers, paddle wheels, or pumps, is the interaction between the cells and the stirrer, or the damage caused by the passing of the cells through the pump cavity (27). In open systems, implemented by paddle wheels, the shear rate is a function of the number of revolutions per second and the diameter of the impeller. When pumps are used for liquid impulsion, the shear rate is a function of the Reynolds number within the pump cavity.

Finally, power supply gives rise to a certain level of turbulence within the bulk liquid, which determines the length of the small microeddies through which the supplied power is dissipated. Cell damage has been reported when the turbulence is so intense that the fluid microeddy size approaches cellular dimensions (length scale of microeddies < size of the cells) (110). In contrast, if the length scale of the microeddies is greater than the cells, the cells are dragged by the eddies and this turbulence in the bulk liquid does not cause any damage. The energy dissipated per unit mass determines the length scale of the microeddies and the shear rate at which the cells are subjected (99).

The power supply required for flat-panel PBRs is extremely low, with a maximum of 53 W/m^3, and high power input is not suitable for microalgal cultures because of the likelihood of cell damage due to intense turbulence (93,110,111). In bubble columns, the maximum power supply that does not damage the growth of *Dunaliella tertiolecta* is 98 W/m^3 (108), whereas the maximum power supply tolerable for *P. tricornutum* ranges from 230 (99) to 270 W/m^3 (42). The highest power supply in aerated systems ranges from 280 W/m^3 in flat-plate PBRs (57) to 200 W/m^3 in bubble column or internal airlift systems employing split cylinders and draught tube sparger PBRs (26). However, the power supply in tubular PBRs is usually much higher. Thus, in helical PBRs, the power supply ranges from 800 to 3400 W/m^3 (29,49), similar to 2500 W/m^3 in horizontal tubular PBRs (100). In spite of the higher power supply in tubular PBRs, damage to algal cells has never been documented in these types of PBRs (26). This is because the culture velocity in tubular loops usually does not exceed 0.5 m/s, which is less than half the threshold damage value of 1.14 m/s (101). These data point out the different nature of stress in bubble-column flat-plate PBRs and tubular PBRs.

It has been demonstrated that shear rate is the main variable determining the fluid-dynamic stress damage, the value

of shear rate that determines the existence of stress damage varying as a function of strain and culture conditions (99). The shear rate in bubbled cultures, by aeration, is a function of the bubble rise velocity, U_B, and the mean bubble diameter, d_B. The bubble rise velocity can be estimated as 0.24 m/s, while the bubble diameter is a function of fluid properties and fluid-dynamic conditions with the equation proposed by Calderbank (112). These equations are as follows:

$$\gamma_{\text{aeration}} = \frac{2U_B}{d_B} \tag{18.15}$$

$$d_B = 4.15\left(\frac{\sigma^{0.6}}{(\text{Pe/V})^{0.4}\rho_L^{0.2}}\right)\varepsilon^{0.5} + 0.0009 \tag{18.16}$$

The shear rate in peristaltic and diaphragm pumps can be calculated as the shear rate in the cavity pump. Thus, it is a function of the properties of the fluid, the liquid velocity in the cavity pump, and the friction coefficient, C_f. The liquid velocity in the cavity pump is calculated taking into account the acceleration factor and the diameter of the cavity pump. These same terms can be used to calculate the Reynolds number inside these pumps. The equations relating these variables are as follows:

$$\gamma_{\text{pump}} = \frac{1}{2\ \mu_L} C_f \rho_L U_L^2 \tag{18.17}$$

$$C_f = 0.072\left(\frac{\rho_L U_L d}{\mu_L}\right)^{-0.25} \tag{18.18}$$

For the centrifugal pump, the shear rate can be calculated as a function of the impeller velocity and the Reynolds number inside the impeller. The equations relating these variables are (110):

$$\gamma_{\text{pump}} = 6.3N\ Re^{0.5} \tag{18.19}$$

$$\text{Re} = \frac{N\rho_L d^{0.5}}{\mu_L} \tag{18.20}$$

18.4 TUBULAR PHOTOBIOREACTORS DESIGN

Tubular PBRs are the most widely used closed systems for the culture of microalgae. This section proposes a design strategy for them.

18.4.1 Biomass Productivity and Solar Radiation

Biomass productivity is the variable that needs to be optimized in designing a PBR for mass culture of microalgae. As commented in the previous section, production of biomass is governed mainly by the availability of light. This is evaluated using the well-known principles of astronomy (to establish the position of the sun relative to the PBR), solar power engineering (to determine the intensity of the incident radiation), and the Beer–Lambert relationship, as summarized elsewhere (19). For otherwise fixed conditions, the geometric arrangement of the solar collector tubes also determines the irradiance on the surface of the tubes because the mutual shading by tubes is influenced by how they are arranged over a given surface area. From these principles, the average irradiance inside the tube, I_{av}, can be calculated as a function of tube diameter and arrangement of the tubes.

On the other hand, the growth rate, μ, is a function of average irradiance. Various relationships have been developed for this dependence (Eqs 18.4, 18.5). Thus, from the knowledge of the characteristics parameters of the algal strain (i.e. μ_{max}, K_a, I_k, and n), the growth rate may be determined for any combination of external irradiance and the diameter of solar collector tubes. Once the specific growth rate is known, the volumetric productivity of continuous cultures is calculated:

$$P_{bv} = \mu C_b \tag{18.21}$$

where P_{bv} is the volumetric productivity and C_b is the concentration of the biomass in the harvest stream of the continuous flow bioreactor. The areal productivity P_{ba} is related to the volumetric productivity, P_{bv} as follows:

$$P_{ba} = P_{bv}\frac{V}{S} \tag{18.22}$$

where V is the volume of the culture and S is the surface occupied by the reactor.

18.4.2 Power Supply and Liquid Velocity

The design of a tubular PBR must guarantee that the flow in the solar tube is turbulent (i.e. the minimum Reynolds number should exceed 3000) so that the cells do not stagnate in the dark interior of the tube. At the same time, the dimensions of the fluid microeddies should always exceed those of the algal cells so that turbulence-associated damage is prevented. The need to control eddy size places an upper limit on the flow rate through the solar tubing. The length scale of the microeddies may be estimated by applying Kolmogorof's theory of local isotropic turbulence (109).

$$\lambda = \left(\frac{\mu_L}{\rho}\right)^{3/4}\xi^{-1/4} \tag{18.23}$$

where λ is the microeddy length, ξ is the energy dissipation per unit mass, μ_L is the viscosity of the fluid, and ρ is the

fluid density. The specific energy dissipation rate within the tube depends on the pressure drop

$$\xi = \frac{2C_f U_L^3}{d_t} \tag{18.24}$$

where C_f is the Fanning friction factor, which may be estimated using the Blausius equation (Eq. 18.8). Thus, for any selected strain, the cell size is known. Using this value as microeddies length, the maximum energy dissipation rate per unit mass is calculated (Eq. 18.23), and from this the maximum liquid velocity that approaches microeddies length to cell size (Eq. 18.24).

Another restriction on the design of the solar collector is imposed by the acceptable upper limit on the concentration of DO. Thus, the length of the solar collector must be shorter than necessary to achieve an oxygen concentration in the culture that inhibits the photosynthesis. This maximum length, L, is calculated as a function of the liquid velocity, DO concentration, and photosynthesis rate as follows (100):

$$L = \frac{U_L([O_2]_{out} - [O_2]_{in})}{R_{O2}} \tag{18.25}$$

where U_L is the liquid velocity (lower than the maximum velocity imposed by microeddies length), $[O_2]_{in}$ is the oxygen concentration at the entrance of the solar collector (i.e. the saturation value when the fluid is in equilibrium with the atmosphere), $[O_2]_{out}$, is the oxygen concentration at the outlet of the solar collector (i.e. maximum acceptable value that does not inhibit photosynthesis), and R_{O2} is the volumetric rate of oxygen generation by photosynthesis (function of biomass productivity designed). If circulation of the culture is performed by pumps, the type and power of the used pump determines the liquid velocity, whereas if airlift systems are used the liquid velocity is a function of height and aeration rate on it (Eq. 18.7).

18.4.3 Combining Flow and Gas–Liquid Mass Transfer

Design of tubular PBRs must consider gas–liquid mass transfer and hydrodynamics. The carbon dioxide gas injected is transported from the gas phase to the aqueous medium to provide the inorganic carbon and control the pH of the culture. For otherwise fixed conditions, the inorganic carbon supplied is incorporated into cells at a specific rate determined by the rate of photosynthesis. Similarly, the oxygen is produced at a specific rate and transferred from the culture to the gas phase. All these aspects have been treated in a tubular reactor equipped with an airlift system (100). By applying mass balances to the different zones of the reactor for which the fluid-dynamic conditions remained constant, the carbon dioxide and oxygen transfer between the liquid and gas phase was modeled. For the liquid phase, the changes in concentrations of DO and dissolved inorganic carbon along the loop can be related to the gas–liquid mass transfer rates and the generation/consumption rates by mass balances as follows:

$$Q_L d[O_2] = K_l a_{llO_2}([O_2]^* - [O_2])S\mathrm{d}x + R_{O_2}(1 - \varepsilon_l)S\mathrm{d}x \tag{18.26}$$

$$Q_L d[C_T] = K_l a_{llCO_2}([CO_2]^* - [CO_2])S\mathrm{d}x + R_{CO_2}(1 - \varepsilon_l)S\mathrm{d}x \tag{18.27}$$

In these equations, $K_l a_{llO2}$ and $K_l a_{llCO2}$ are the volumetric gas–liquid mass transfer coefficients for oxygen and carbon dioxide respectively; dx is the differential distance along the direction of flow in the solar tube; $[O_2]$, $[C_T]$ and $[CO_2]$ are the liquid phase concentrations of oxygen, inorganic carbon, and carbon dioxide respectively; ε_l is the gas holdup; S is the cross-sectional area of the tube; R_{O_2} and R_{CO_2} are the volumetric generation and consumption rate of oxygen and carbon dioxide respectively; and Q_L is the volumetric flow rate of the liquid. Note that the concentration values marked with asterisks are equilibrium concentrations, i.e., the maximum possible liquid phase concentration of the component in contact with the gas phase of a given composition. The mass balance considers the total inorganic carbon concentration $[C_T]$ and not just that of carbon dioxide. This is because C_T takes into account the dissolved carbon dioxide and the carbonate, CO_3^{2-}, and bicarbonate, HCO_3^-, species generated by it.

As for the liquid phase, a component mass balance can also be established for the gas; hence:

$$\mathrm{d}F_{O_2} = -K_l a_{llO_2}([O_2]^* - [O_2])S\mathrm{d}x \tag{18.28}$$

$$dF_{CO_2} = -K_l a_{llCO_2}([CO_2]^* - [CO_2])S\mathrm{d}x \tag{18.29}$$

Here F_{O_2} and F_{CO_2} are the molar flow rates of the two components in the gas phase. Note that, because of the changes in molar flow rates, the volumetric flow rate of the gas phase may change along the tube. The equilibrium concentrations of the two gases in the liquid can be calculated using Henry's law relationships:

$$[O_2]^* = H_{O_2} P_{O_2} = H_{O_2}(P_T - P_v)\frac{F_{O_2}}{F_{O_2} + F_{CO_2}} \tag{18.30}$$

$$[CO_2]^* = H_{CO_2} P_{CO_2} = H_{CO_2}(P_T - P_v)\frac{F_{CO_2}}{F_{O_2} + F_{CO_2}} \tag{18.31}$$

where H_{O_2} and H_{CO_2} are the Henry's constants for oxygen and carbon dioxide, P_{O_2} and P_{CO_2} are the partial pressures

(or mole fractions) of the components in the gas phase; the partial pressures can be calculated knowing the total pressure (P_T), the vapor pressure (P_v), and the molar flow rates F_{O_2} and F_{CO_2} at any location in the system.

Equations 18.26–18.29 along with the Equations 18.30 and 18.31 for equilibrium concentrations, and the initial conditions, allow numerical integration and, hence, the determination of the CO_2 and O_2 axial profiles in the liquid phase and the molar flow rates of the two components in the gas phase. The accuracy of the proposed equations was verified by Camacho Rubio *et al*., (100) who used these equations for estimating the behavior of a tubular PBR along the day. As shown in Fig. 18.13, through any 24-h period, the simulated data—pH, carbon dioxide losses, and the amount of carbon dioxide injected—closely agreed with the measurements. Although, the degree of correlation differs for different variables, the mean of errors for the entire set of variables is lower than 15%. The predictive capabilities of proposed equations demonstrate its potential as a scale-up tool. The model is simple and can be adapted to any PBR and photoautotrophic strains. Moreover, because the model simulates the system behavior as a function of the tube length and operational variables (superficial gas velocity in the riser, composition of the carbon dioxide injected in the solar receiver, and its injected rate), it allows the rational design and scale-up of PBRs.

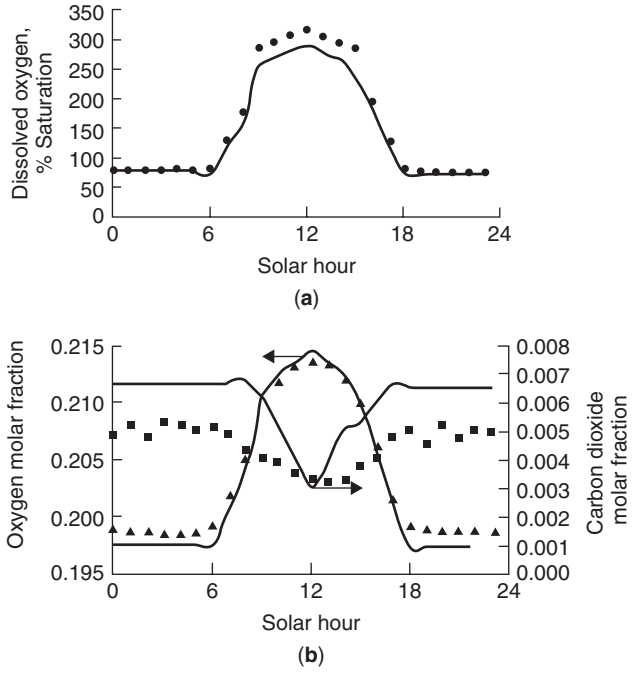


Figure 18.13. Comparison between experimental (symbols) and simulated (lines) data of pH, total inorganic carbon, oxygen, and carbon dioxide in the liquid and gas phase, on an outdoor tubular photobioreactor 0.22 m. [From Ref. 100. With permission.]

18.4.4 Oxygen Removal and Temperature Control

Once the solar collector is designed, it is necessary to design the unit for removal of oxygen and temperature control. This is performed in bubble columns or airlift devices. The use of bubble columns is favorable because these systems are widely used at the industrial scale. The mass transfer coefficient can be calculated as a function of the aeration rate (Eqs 18.10,18.14), then the volume of the bubble column necessary to remove oxygen can be calculated as:

$$V = \frac{Q_L([O_2]_{in} - [O_2]_{out})}{K_L a_L([O_2^*] - [O_2])_{lm}(1 - \varepsilon)} \tag{18.32}$$

where Q_L is the liquid flow rate entering the bubble column, $[O_2]_{in}$ is the oxygen concentration at the inlet of the bubble column, $[O_2]_{out}$ is the oxygen concentration at the outlet of the bubble column, $K_L a_L$ is the volumetric mass transfer coefficient, and ($[O_2^*]$–$[O_2]$) is the driving force for the transport of oxygen from the liquid to the gas phase, calculated as mean logarithmic value from the entrance to the outlet. To avoid recirculation of bubbles from the bubble column to the solar collector, the superficial liquid velocity down must be lower than the bubble rise velocity, U_b. Thus, the minimum diameter of bubble column, d_c, is calculated (Eq. 18.33), along with the minimum height of the column necessary, h_c, (Eq. 18.34).

$$d_c = \sqrt{\frac{4Q_L}{\pi U_b}} \tag{18.33}$$

$$h_c = \frac{4V}{\pi d_c^2} \tag{18.34}$$

Analogous to mass transfer, the heat transfer equipment must be designed. The equipment must be designed to remove the heat absorbed by radiation. This is a function of solar radiation collected by the solar collector, Q_{rad}, and the thermal absorptivity of the culture, a_{rad}. Finally, the area of heat exchanger necessary, $A_{exchanger}$ is calculated as a function of the overall heat transfer coefficient, $U_{exchanger}$, and temperature of cooling water as:

$$A_{exchanger} = \frac{Q_{rad} a_{rad}}{U_{exchanger}(T_{culture} - T_{water})} \tag{18.35}$$

18.4.5 Case Study

Equations 18.21–18.35 were used to design an industrial size PBR operated in a greenhouse in Almería, Spain. First, the light availability inside the greenhouse was calculated according to the solar radiation knowledge, although measurements were performed to validate it. Then, simulations were performed to determine the optimal tube diameter.

Selection was performed on the basis of the microalgae to be produced, *S. almeriensis*, and its characteristic parameters (μ_{max}, I_k, n), the objective being to maximize the size of the reactor that would allow a year-long biomass productivity of roughly 1.0 g/L/day. From this analysis a maximum tube diameter of 0.10 m was selected. According to the target biomass productivity, the photosynthesis rate was calculated, and the maximum length of the solar collector was established accordingly to 400 m. Finally, a bubble column was designed to connect it to the solar collector to remove oxygen generated by photosynthesis as well as to control the temperature of the culture (113). The designed tubular PBR was built (Fig. 18.14) and operated for more than 1 year. Figure 18.15 shows the biomass productivity values measured during the operation of the PBR in an annual cycle. It is observed as the performance of the industrial unit is quite similar to the predicted productivities using the model, Equations 18.21–18.34, with biomass productivities through the year higher and lower than the 1.0 g/L/day average. Now, this design strategy has been applied to build a pilot plant size facility (30 m^3) for the production of the same strain (see Fig. 18.4, bottom).

18.5 PHOTOSYNTHETIC EFFICIENCY IN MICROALGAL MASS CULTURES

As stated earlier, production of microalgae biomass in PBRs face the challenge of improving the efficient use of the enormous high PFDs impinging on the earth's surface. The photosynthetic efficiency (Ψ) of biomass growth is defined as the energy stored in biomass per unit of light energy absorbed (91). This parameter is of fundamental importance in biomass production because the biotechnology for algae production should naturally aim to achieve the maximum attainable photosynthetic efficiency so as to produce the most biomass possible per unit land area (open ponds) or volume (enclosed systems). The explanation accepted for calculating Ψ is as follows (91): Microalgae, as green plants, use only the PAR, which constitutes about 43% of the total solar radiation at the earth's surface and has an energy input equivalent to that of monochromatic light at 575 nm. One Einstein of 575 nm light contains 49.74 kcal of energy, and assuming that free energy stored in photosynthesis is 114 kcal/mol of reduced CO_2, the theoretical maximum energy efficiency for the photosynthetic reduction of CO_2 to glucose with white light is $114/(8 \times 49.74) = 0.286$, or approximately 29% (91). In the previous calculations, it was accepted that the Z-scheme of photosynthesis and thus the light requirement for the transfer of four electrons are eight photons. It should be stressed that, under field conditions, much lower photosynthetic efficiencies have been obtained. The maximum practical photosynthetic efficiency is still a problem to be resolved (114). However, a theoretical photosynthetic yield of 6% to 7% of total solar energy seems possible (115); this represents, depending on the geographic location, a biomass productivity of 35–70 g/m^2/day. A photosynthetic efficiency of 10% during a period of 122 days has been reported (114). These experimental results are in agreement with Richmond (91). Therefore, it is obvious that the challenge to the algal industry may be defined as producing biomass on a large scale under outdoor conditions with efficiency similar to that obtained under controlled laboratory conditions.



Figure 18.14. Photograph of an industrial-size tubular photobioreactor built according to design equations proposed (Eqs 18.21–18.35). [With permission from Ref. 38.] (This figure is available in full color at http://onlinelibrary.wiley.com/book/10.1002/9780470054581.)

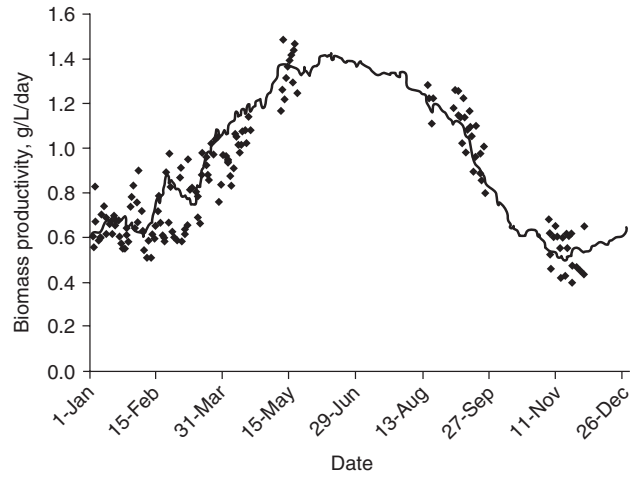


Figure 18.15. Variation in biomass productivity during an annual cycle in the industrial-size tubular PBR built according to proposed strategy design (Eqs 21–35). Data correspond to experimental values, whereas line corresponds to data predicted by the model used in the design.

Goldman (15) summarized the information on algal yields reported for over 30 years. Although the early effort in mass algal culturing resulted in yields no better than 10–15 g dry weight/m^2/day for short periods; currently, it is not uncommon for sustained yields to reach 20–25 g/m^2/day. The maximum growth yields of algae may be represented by models that integrate the factor, limiting production. Goldman presented a thorough study of maximum yield potential of algae based on the thesis that algal production under proper conditions is limited only by light (91). The equation derived was as follows:

$$P_b = 0.28 \cdot I_s \left(\ln \frac{0.45 \cdot I_0}{I_s} + 1 \right) \tag{18.36}$$

in which P_b is the productivity of the system (g/m/^{2}/day), I_0 is the total irradiance at the culture surface, I_s is the saturating light intensity for which the growth rate is the maximum (i.e. at which $\mu = \mu m$). Because the maximum available intensity of sunlight striking the earth's surface is lower than 800 cal/cm^2/min, Equation 18.36 predicts that, for a range of I_s values between 0.02 and 0.06 cal/cm^2/min as is typical for microalgae culture, the upper limit for algal yield is 30–60 g dry weight./m^2/day. According to this model, the factor that most strongly influences algal yield is I_s. These figures, again, are far from those predicted in the carefully conducted indoor cultures work. Why is there a large discrepancy between the outdoor production and those obtained from most laboratory work?

The laboratory work reported above was carried out under conditions of low intensities, at or below saturation for photosynthesis. In practice, when dealing with sunlight, the major problem is not the maximal quantum efficiency but the fraction of absorbed photons that can be actually be used in photosynthesis (97). The problem is that, if algal photosynthesis saturates at low light intensities, but algal cells have a high extinction coefficient (high pigment content), then more light is absorbed than can be used in photosynthesis. Depending on the actual saturation and incident light intensities, the extinction coefficient, K_a, and the biomass concentration, the maximum efficiency (regardless of the minimum quantum requirement) is reduced by a factor of about two- to fivefold from that possible at low light levels.

A new procedure for calculating yields in microalgal mass cultures, at high incident irradiances, was proposed by Molina Grima *et al*. (78). The new approach is based on the averaged irradiance for the assessment of the photon flux absorbed by the biomass. The starting point of Molina Grima and coworker's procedure is the definition of the quantum yield, Ψ_E, in a microalgal culture systems. The quantum yield, Ψ_E, is defined as the amount of biomass generated by the unit of radiation (usually photons or Einstein) absorbed by the culture. Because it represents the ratio of biomass generation to absorbed photon flux, it can be calculated by the expression:

$$\Psi_E = \frac{P_b}{F_{vol}} \tag{18.37}$$

where P_b stands for the volumetric biomass productivity and F_{vol} for the photon flux absorbed in the volume unit. This coefficient can be converted to energy units, commonly noted Ψ_{kJ}, by taking into account the average range of the light used (kJ/E). The photosynthetic efficiency (i.e. the bioenergetic yield), Ψ, quantifies the percent of light energy that is converted to chemical energy and can be calculated as the product of Ψ_{kJ} by the biomass combustion heat, Q_b.

$$\Psi = \Psi_{kJ} \cdot Q_b \tag{18.38}$$

18.5.1 Absorbed Photon Flux

This is a complicated question, especially when it must be evaluated in geometries other than flat reactors. Many factors such as light-scattering effects may lead to a misevaluation of the absorbed flux and, in every case, they need to be evaluated by direct measurement of the light leaving the PBR (96). In this sense, it must be noted that the light absorbed can be evaluated by integrating the local volumetric rate of energy absorption (117) into the total reactor volume. This integral can be readily obtained from the extinction coefficient of biomass, K_a, and the average irradiance I_{av}.

$$F_{vol} = I_{av}\ K_a\ C_b \tag{18.39}$$

The calculation of the photon flux absorbed by the procedure has several advantages. It is independent of the system geometry once I_{av} is known, and can thus be used in any type of PBR as long as I_{av} can be determined by any means. Photon flux losses due to reflection of light off the reactor walls that cannot be neglected (96) are easily obviated by measuring the irradiance inside the culture. Therefore, the irradiance impinging on the reactor surface is taken into account for the determination of I_{av}. The validity of equation 18.39 for assessing the absorbed photon flux has been checked experimentally in a culture of *Isochrysis galbana* (78) and by using data published by Lee and Erickson (118) in a quite different culture of *Chlorella* in a paralellepipedical flat PBR. *I. galbana* showed a maximum efficiency of conversion light into biomass, $\Psi_{E\,max}$ of 0.6 g/E was obtained at $I_0 = 820\ \mu E/m^2/s$ and $D = 0.030/h$; and the maximum capacity of the biomass to metabolize light was found to be 13.1 μE/g/s (78). Above this value, a significant drop

in system efficiency was observed. Moreover, the biomass productivity to be expected in an outdoor tubular PBR growing *I. galbana* was predicted to be in agreement with the actual value (28).

18.6 OPERATIONAL CONSIDERATIONS

For successful maintenance of a microalgal culture facility, the performance of the culture should be continuously assessed in order to prevent the development of conditions that, in turn, could give rise to significant losses. In this sense, the on-line information on DO, temperature, pH as well as the daily microscopic observation make up an excellent source of information for characterizing the physiological state of the culture. Measurement of growth should be accompanied as a rule by detailed microscopic evaluation. Any buildup in the number of other organisms in the culture should be regarded as a warning signal. It might be that the temperature may have deviated too much from the optimal; or it might be a signal that the concentration of a particular nutrient had declined below the optimal. On the other hand, careful monitoring of the nitrogen concentration gives information about the possible depletion in mineral nutrients in the continuous cultures. This information can be used as a guideline for adding, in equivalent amounts, the entire formula of the elements making up the growth medium. Besides, the concentration of DO is a reliable and sensitive indicator of conditions that relate to growth and productivity. There are many indications that early detection of an unexplainable decrease in DO concentration or a decline in the normal rate of the daily increase in DO in outdoor mass culture serve as a reliable warning signal that the culture is stressed and may quickly deteriorate (91).

Cleaning and reliability of the microalgal mass culture are two other important operational considerations from a commercial point of view. Algal cultures grown in closed reactors may have a problem with fouling of the walls of the reactors by the algae. Chamont *et al*. (119) have patented a system using recycling balls for continuous cleaning of the walls of a tubular PBR. Other systems based on small particles that move with the culture have been also developed, although they have not been patented and remain as know-how of the companies. Using such a system, fouling has not been a major problem in the operation of these reactors. Reliability is also an important aspect. Algal cultures grown in tubular PBRs are reasonably stable and several species have been cultured including the marine algae, *P. tricornutum*, *Tetraselmis chuii*, and *Isochrysis* sp. for periods in excess of 3 months (28,120) and *S. almeriensis* for more than 8 months. These systems are particularly suited for continuous or semicontinuous culture, and this permits much better control over the culture conditions and provides a consistent product quality, something that is very difficult to achieve in open systems.

An additional operational advantage of most closed systems is that the cell concentrations reached are much greater than those achieved in open system, thus reducing the harvesting cost. As can be seen in Fig. 18.16, the actual cell density, however, has to be managed carefully in order to maximize productivity. At low cell densities, especially in outdoor systems, the algae may be severely photoinhibited, whereas at very high cell densities self-shading can reduce productivity as individuals algal cells do not receive the optimum level of light.

In short, the aim of management is to achieve and sustain the optimal state of the culture. For maximum biomass productivity, solar irradiance should be the sole limitation.

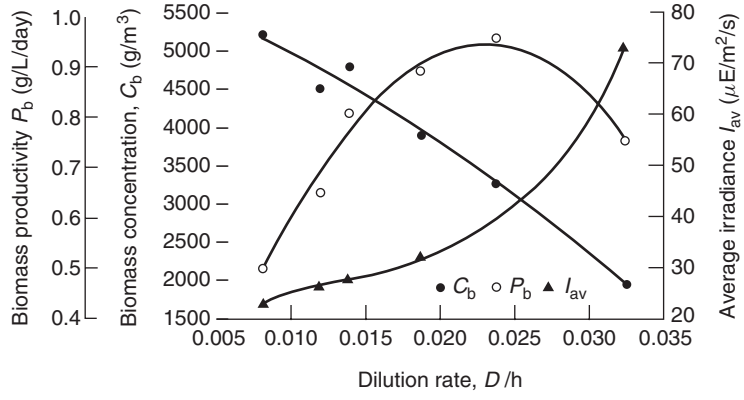


Figure 18.16. Effect of dilution rate, D, on the steady-state biomass concentration, C_b, the biomass productivity, P_b, and the average irradiance inside a PBR, I_{av}. Data were obtained in an outdoor continuous culture of *P. tricornutum*, in a concentric tube airlift bioreactor. [From Ref. 39. With permission.]

TABLE 18.2. Comparison of Properties of Different Large-Scale Algal Cultures Systems

Reactor Type	Mixing	Light Utilization Efficiency	Temperature Control	Gas Transfer	Hydrodynamic Stress	Species Control	Sterility
Unstirred ponds	Very poor	Poor	None	Poor	Very low	Difficult	None
Open raceway	Fair–good	Fair–good	None	Poor	Low	Difficult	None
Airlift	Uniform	Good	Excellent	High	Low	Easy	Easily achievable
Bubble column	Fair	Fair	Excellent	Fair	Low	Easy	Easily achievable
Tubular	Almost uniform	Good	Excellent	High	Low–high	Easy	Achievable
Biocoil	Uniform	Excellent	Excellent	Low–high	Low–high	Easy	Achievable

[From Ref. 41. With permission.]

However, when a metabolite is the desired product, the operational conditions promoting maximal biomass productivities could be different than those for maximizing the productivity of the product.

18.7 CONCLUDING REMARKS

Microalgae represent a large and unknown resource with the genetic potential to produce valuable compounds. The development of algal biotechnology depends, in particular, on the identification of more high value products in algae. However, microalgal biotechnology at present is a limited and small component of the overall field of biotechnology, where advances in industrial fermentation, therapeutic proteins, genetically engineered plants and animals, and diagnostics have attracted major commercial interest and are resulting in many novel products. Currently, there is great interest in the production of biofuels from microalgae. Although the production of microalgal biodiesel is technically feasible, the economy of producing it needs to improve substantially to make it competitive with petrodiesel, but the level of improvement necessary appears to be attainable.

Table 18.2 compares the main algal culture system described in this chapter along with their properties. From this Table, it is clear that open systems are deficient in several aspects. Despite this, open raceway systems are being used on a commercial scale for culturing a few species, and especially for waste treatment applications. The two principal advantages of open culture systems are a small capital investment for production of the biomass and the use of a free source of energy. They are the simplest methods but the productivity obtained is far from the theoretical maximum. Much improvement in photosynthetic activity could be obtained through an increase in the ability of photosynthetic complex to utilize more light before becoming saturated. The goal must be to improve the photosynthetic machinery so that light saturation will take place at a higher light intensity, accompanied by resistance to photoinhibition.

Enclosed PBRs that allow better control of operational conditions may be more suited for reaching this goal. PBRs also have an important role to play in increasing the diversity of algae species for culturing the sensitive and highly valuable strains used in the production of fine chemicals. Enclosed outdoor tubular PBRs have demonstrated the potential of this technology with high biomass productivity of microalgal species such as *Porphyridium*, *Isochrysis*, and *Phaeodactylum*, which, due to the better control of the culture parameters, allow the biochemical composition to be modified by changing the system operating variables and are specially useful for valuable products such as polyunsaturated fatty acids, polysaccharides, antioxidant, and so on. This technology is more capital intensive than the open pond technology but this additional cost can be justified. Temperature and fouling are major problems in such systems. Nonetheless, it should be noted that it is not possible to say that one culture system is better than another. The commercial target, geographic location, and metabolite to be produced determines the choice: axenic or nonaxenic, continuous or batch culture, intensive or extensive culture, opens pond or closed PBRs.

Acknowledgments

The authors wish to acknowledge the contribution of all the colleagues of the Marine Biotechnology Group of the University of Almería that have worked with us on this subject. Special acknowledgement to the financial support of the Plan Andaluz de Investigación (Junta de Andalucía), Dirección General de Investigación (MEC), and European Union for some of the work reported in this manuscript.

NOMENCLATURE

A_d	Cross-sectional area of the downcomer (m^2)
A_r	Cross-sectional area of the riser (m^2)
C_b	Biomass concentration (g/L or g/m^3)
D	Depth channel (m)
f	Fanning friction factor

F_{vol}	Photon flux absorbed in unit volume ($\mu E/m^3/s$)
h_D	Height at which the degasser is situated (m)
I	Hourly incident photosynthetic radiation ($\mu E/m^2/s$)
I_{av}	Photosynthetically active hourly average irradiance inside culture ($\mu E/m^2/s$)
I_0	Solar irradiance impinging on the reactor surface ($\mu E/m^2/s$)
I_s	Saturating light intensity for which the growth rate is maximum ($\mu E/m^2/s$)
K_a	Absorption coefficient (m^2/g)
K_1	First equilibrium constant for bicarbonates buffer (mol/m^3)
K_2	Second equilibrium constant for bicarbonates buffer (mol/m^3)
K_W	Dissociation constant of water
L	Channel length (m)
L_{eq}	Equivalent length of the solar receiver (m)
N	Manning friction factor (s m_1/3), or characteristic parameter of the hyperbolic growth model
n_1	Characteristic parameter of the photolimitation–photoinhibition model
n_2	Characteristic parameter of the photolimitation–photoinhibition model
n_3	Characteristic parameter of the photolimitation–photoinhibition model
P	Power consumption for the culture flow in the channel (kW)
P_b	Biomass productivity ($g/m^3/h$)
Q_b	Heat of combustion of biomass ($\mu E/g$)
S	Cross-section of the tube (m^2) or surface occupied by the photobioreactor
S	Rate of loss of energy in the channel, (dimensionless)
U_L	Superficial liquid velocity in the tube (m/s)
v	Mean culture flow velocity channel (m/s)
w	Width channel (m)
ψ	Bioenergetic yield coefficient (%)
ψ_E	Quantum yield (g/E)
ψ_{kJ}	Energetic yield (g/kJ)
η	Efficiency of the paddle wheel (-)

REFERENCES

1. Oswald WJ. In: Borowitzka MA, Borowitzka LJ, editors. Micro-Algal Biotechnology. Cambridge: Cambridge University Press; 1988. pp 305–328.
2. De Pauw WN, Persoone G. In: Borowitzka MA, Borowitzka LJ, editors. Micro-Algal Biotechnology. Cambridge: Cambridge University Press; 1988. pp 197–221.
3. Benemann JR. J Appl Phycol 1992; 4: 233–245.
4. Metting WB. In: Borowitzka MA, Borowitzka LJ, editors. Micro-Algal Biotechnology, Cambridge: Cambridge University Press; 1988. pp 288–304.
5. Chapman DJ, Gollenbeck KW. In: Cresswell RC, Rees TAV, Shah N, editors. Algal and cyanobacteria biotechnology. New York: Longman; 1989. pp 1–27.
6. Calvin DM, Taylor SE. In: Cresswell RC, Rees TAV, Shah N, editors. Algal and cyanobacteria biotechnology. New York: Longman; 1989. pp 137–160.
7. Glombitza DKW, Koch M. In: Cresswell RC, Rees TAV, Shah N, editors. Algal and cyanobacteria biotechnology. New York: Longman; 1989. pp 161–238.
8. Spolaore P, Joannis-Cassan C, Duran E, Isambert A. J Biosci Bioeng 2006; 101: 87–96.
9. Roessler PG, Brown LM, Dunahay TG, Heacox DA, Jarvis EE, Schneider JC. ACS Symp Ser 1994; 566: 255–270.
10. Ghirardi ML, Zhang JP, Lee JW, Flynn T, Seibert M, Greenbaum E. Trends Biotechnol 2000; 18: 506–511.
11. Gavrilescu M, Chisti Y. Biotechnol Adv 2005; 23: 471–499.
12. Borowitzka MA. Pharmaceuticals and agrochemicals from microalgae. In: Cohen Z, editor. Chemicals from microalgae: Taylor & Francis; 1999. pp 313–352.
13. Pulz O. Appl Microbiol Biotechnol 2001; 57: 287–293.
14. Richmond A, Cheng-Wu Z. J Biotechnol 2001; 85: 259–269.
15. Goldman JC. Water Res 1979; 13: 60–118.
16. Richmond A. Large scale microalgal culture and applications. In: Round FE, Chapman DJ, editors. Volume 7, Progress in psychological research. Bristol: Biopress Ltd.; 1990. pp 269–330.
17. Hu Q, Zarmi Y, Richmond A. Eur J Phycol 1998; 33: 165–171.
18. Molina Grima E, Fernández Sevilla JM, Acién Fernández FG, Chisti Y. J Biotechnol 2001; 92: 113–131.
19. Cohen E, Arad S. Biomass 1989; 18: 59–67.
20. Samon R, Leduy A. Can J Chem Eng 1985; 63: 105–112.
21. Tredici MR, Carlozzi P, Zitelli GC, Materassi R. Bioresour Technol 1991; 38: 153–159.
22. Doucha J, Livansky K. Algol Stud 1995; 76: 129–147.
23. Pohl P, Kohlhase M, Martin M. In: Stadler T, Mollion J, Karamanos MC, Morvan H, Christiaen D, editors. Algal biotechnology. London: Elsevier; 1988. pp 209–217.
24. Hilaly AK, Karim MN, Guyre D. Biotechnol Bioeng 1994; 43: 314–320.
25. James CM, Al-Khars AM. Aquaculture 1987; 87: 381–393.
26. Sánchez Mirón A, Contreras Gómez A, García Camacho F, Molina Grima E, Chisti Y. J Biotechnol 1999; 70: 249–270.
27. Gudin C, Chaumont D. Bioresour Technol 1991; 38: 145–151.
28. Molina Grima E, García Camacho F, Sánchez Pérez JA, Fernández Sevilla JA, Acién Fernández FG, Contreras Gómez A. J Chem Technol Biotechnol 1994; 61: 167–173.
29. Watanabe Y, Hall DO. Appl Microbiol Biotechnol 1996; 44: 693–698.
30. Oswald WJ. In: Gloyna EF, Malina JF, Davis EM, eds. Ponds as wastewater treatment alternative, Water Resources Symposium No. 9. Austin (TX): University of Texas; 1975.

31. Dodd JC. In: Richmond A, editor. Handbook of microalgal mass culture. Boca Raton (FL): CRC Press; 1986. pp 265–283.
32. Oswald WJ. In: Borowitzka MA, Borowitzka LJ, editors. Micro-Algal Biotechnology. Cambridge: Cambridge University Press; 1988. pp 357–394.
33. Borowitzka MA. J Biotechnol 1999; 70:(1): 313–321.
34. Laws EA, Taguchi S, Hirata J, Pang L. Biotechnol Bioeng 1986; 28: 191–197.
35. Heusler P, Castillo J, Morino S, Vasquez V. Arch Hydrobiol 1978; 11: 254–260.
36. Cheng-Wu Z, Zmora O, Kopel R, Richmond A. Aquaculture 2001; 195: 35–49.
37. Tredici MR, Chini G. Scale-up of photobioreactors to commercial size. In: Kretschmer P, *et al*,, editors. Proceedings 2nd European workshop on biotechnology of microalgae; 1995. pp 21–24.
38. Molina Grima E, Fernández Sevilla JM, Acién Fernández FG, Sánchez Pérez JF, García Sánchez JL, Magán Cañadas JJ, Pérez Parra J. In: Proceedings of the 6th European workshop biotechnology of microalgae; Potsdam, Germany; 2005.
39. García Camacho F, Contreras Gómez A, Acién Fernández FG, Fernández Sevilla JM, Molina Grima E. Enzyme Microb Technol 1999; 24: 164–172.
40. Lee YK. Trends Biotechnol 1986; 4: 186–189.
41. Borowitzka MA. J Mar Biotechnol 1996; 4: 185–191.
42. Contreras Gomez A. PhD Thesis. Almeria, Spain: University of Almeria; 1996. p 373.
43. Tamiya H, Hase E, Shibata K, Mituya A, Iwamura T, Nihei T, Sasa T. In: Burlew JS, editor. Algal culture from laboratory to pilot plant. Washington (DC): Carnegie Institution of Washington; 1953. pp 204–232.
44. Chaumont D, Therpenier C, Gudin C. In: Stadler T, Mollion J, Karamanos MC, Morvan H, Christiaen D, editors. Algal biotechnology. London: Elsevier; 1988. pp 199–208.
45. Pirt SJ, Lee YK, Walach MR, Pirt MW, Balyuzi HHM, Bazin MJ. J Chem Technol Biotechnol 1983; 33B: 35–58.
46. Torzillo G, Carlozzi P, Pushparaj B, Montaini E, Materassi R. Biotechnol Bioeng 1993; 42: 891–898.
47. Tredici MR, Zittelli GC. Biotechnol Bioeng 1998; 57: 187–197.
48. Robinson LF, Morrison AW, Bamforth MR. European Pat. 0,239,272. 1988 Mar 6. (to Biotechna Ltd.).
49. Hall DO, Acién FG, Cañizares E, Rao K, Molina E. Outdoor helical tubular photobioreactors for microalgal production: modelling of fluid-dynamics and mass transfer and assessment of biomass productivity. Biotechnol Bioeng 2003; 82(1): 62–73.
50. Lee YK, Low CS. Biotechnol Bioeng 1992; 40: 1119–1122.
51. Borowitzka MA. J Appl Phycol 1992; 4: 267–269.
52. Acién Fernández FG, García Camacho F, Sánchez Pérez JA, Fernández Sevilla JM, Molina Grima E. Biotechnol Bioeng 1998; 58: 505–611.
53. Rebolloso Fuentes MM, García Sánchez JL, Fernández Sevilla JM, Acién Fernández FG, Sánchez Pérez JA, Molina Grima E. J Biotechnol 1999; 70(1–3): 271–288.
54. García-Malea López MC, Del Río Sánchez E, Casas López JL, Acién Fernández FG, Fernández Sevilla JM, Rivas J, Guerrero MG, Molina Grima E. J Biotechnol 2006; 123: 329–342.
55. Little AD. In: Burlew JS, editor. Algal culture from laboratory to pilot plant. Washington (DC): Carnegie Institution of Washington; 1953. pp 235–273.
56. Tredici MR, Materassi R. J Appl Phycol 1992; 4: 221–231.
57. Pulz O, Gerbsch N, Bacholz R. J Appl Phycol 1995; 7: 145–149.
58. Hu Q, Richmond A. J Appl Phycol 1996; 18: 139–145.
59. Hu Q, Gutterman H, Richmond A. Biotechnol Bioeng 1996; 51: 51–60.
60. Zhang K, Miyachi S, Kurano N. Biotechnol Lett 2001; 23: 21–26.
61. Zou N, Richmond A. J Biotechnol 1999; 70: 351–356.
62. Tredici MR, Rodolfi L. Reactor for industrial culture of photosynthetic microorganisms. World patent WO 2004/074423 A2. 2004. (to Università degli Studi di Firenze, Italia).
63. Sierra Alcalde E, Acién Fernández FG, Fernández Sevilla JM, García Sánchez JL, González López C, Molina Grima E. Chem Eng J:2008, 138:(1–3): 136–147.
64. Incropera FP, Thomas JF. Solar Energy 1978; 20: 157–165.
65. Molina Grima E, García Camacho F, Sánchez Pérez JA, Urda Cardona J, Fernández Sevilla J. Biotechnol Appl Biochem 1994; 20: 279–290.
66. Acién Fernández FG, García Camacho F, Sánchez Pérez JA, Fernández Sevilla JM, Molina Grima E. Biotechnol Bioeng 1997; 55: 701–714.
67. Phillips JN, Myer J. Plant Physiol 1954; 29: 152–161.
68. Grobbelaar JU. J Appl Phycol 1994; 6: 331–335.
69. Terry KL. Biotechnol Bioeng 1986; 28: 988–995.
70. Molina Grima E. Mass culture methods. In: Flickinger E, (Eds). Encyclopedia of Bioprocess Technology: Fermentation, Biocatalysis and Bioseparation New York: Wiley; 1999. Volume 3: 1753–1769.
71. Vonshak A. In: 7th International Conference International Association of Applied Algology: opportunities from Microalgae; 1996 Apr 16–19; Knysna; 1996. pp 76–77.
72. Foy RH, Gibson CE. Br Phycol J 1982; 17: 183–193.
73. Foy RH, Gibson CE. Photosynthetic characteristics of planktonic blue-green algae: The response of twenty strains grown under high and low light. Eur J Phycol 1982; 17(2): 169–182.
74. Van Liere L, Mur LR. J Gen Microbiol 1975; 115: 153–160.
75. Lee YK, Tan HM, Hew CS. Biotechnol Bioeng 1985; 27: 555–561.
76. Liu BYH, Jordan RC. Solar Energy 1960; 7: 53–65.
77. Duffie JA, Beckman WA. Solar engineering of thermal processes. New York: Wiley; 1980. p 762.
78. Molina Grima E, García Camacho F, Sánchez Pérez JA, Acién Fernández FG, Fernández Sevilla J. Enzyme Microb Technol 1997; 21: 375–381.
79. Lee YK, Vonshak A. Arch Microbiol 1988; 150: 529–533.
80. Torzillo G, Pushparaj B, Masojidek J, Vonshak A. Biotechnol Bioprocess Eng 2003; 8: 338–348.
81. Björkman O. Low temperature chlorophyll fluorescence in leaves and its relationship to photon yield of photosynthesis in photoinhibition. In: Kyle DJ, Osmond CB, Arntzen CJ, editors. Photoinhibition. Amsterdam: Elsevier Publishers; 1987. pp 123–144.

82. Barber JAA. Trends Biochem Sci 1992; 17: 61–66.
83. Jensen S, Knutsen G. J Appl Phycol 1993; 5: 495–504.
84. Camacho Rubio F, García Camacho F, Fernández Sevilla JM, Chisti Y, Molina Grima E. Biotechnol Bioeng 2003; 81(4): 459–473.
85. Marra J. Mar Biol 1978; 46: 191–202.
86. Sukenik A, Falkowski PG, Bennett J. Biotechnol Bioeng 1986; 30: 970–977.
87. Sukenik A, Levy RS, Levy Y, Falkowski PG, Dubinsky Z. J Appl Phycol 1991; 3: 191–201.
88. Guterman H, Vonshak A, Ben-Yaakov S. Biotechnol Bioeng 1990; 35: 809–819.
89. Pulz O, Scheinbenbogen K. Adv Biochem Eng Biotechnol 1998; 59: 123–152.
90. Molina Grima E, Sánchez Pérez JA, García Camacho F, García Sánchez JL, López Alonso D. Appl Microbiol Biotechnol 1993; 38: 599–605.
91. Richmond A. Crit Rev Microbiol 1986; 4: 369–438.
92. Torzillo G, Vonshak A. Effect of light and temperature on the photosynthetic activity of the cyanobacterium Spirulina platensis. Biomass Bioenergy 1994; 6: 399–403.
93. Silva HJ, Cortinas T, Ertola RJ. J Chem Technol Biotechnol 1987; 40: 41–49.
94. Laws EA, Terry KL, Wickman J, Chalup MS. Biotechnol Bioeng 1983; 25: 2319–2335.
95. Chisti Y. Airlift bioreactors. London: Elsevier; 1989. p 343.
96. Aiba S. Biotechnol Bioeng 1983; 25: 2775–2776.
97. Weisman J, Goebel RP, Benemann J. Biotechnol Bioeng 1988; 31: 336–344.
98. Markl H, Mather M. Arch Hydrobiol 1985; 20: 85–93.
99. Brindley Alías C, García-Malea López MC, Acién Fernández FG, Fernández Sevilla JM, García Sánchez JL, Molina Grima E. Biotechnol Bioeng 2004; 87(6): 723–733.
100. Camacho Rubio F, Acién Fernández FG, García Camacho F, Sánchez Pérez JA, Molina Grima E. Biotechnol Bioeng 1999; 62: 71–86.
101. Acién Fernández FG, Fernández Sevilla JM, Sánchez Pérez JA, Molina Grima E, Chisti Y. Chem Eng Sci 2001; 56: 2721–2732.
102. Livansky K. Algol Stud 1990; 58: 87–97.
103. Lee YK, Hing HK. Appl Microbiol Biotechnol 1989; 31: 298–301.
104. Mazzuca Sobczuk T, García Camacho F, Camacho Rubio F, Acién Fernández FG, Molina Grima E. Biotechnol Bioeng 2000; 67(4): 465–475.
105. García Sánchez JL, Berenguel Soria M, Rodríguez Díaz F, Fernández Sevilla JM, Brindley Alias C, Acién Fernández FG. Biotechnol Bioeng 2003; 84(5): 533–543.
106. Berenguel Soria M, Rodríguez Díaz F, Acién Fernández FG, García Sánchez JL. J Process Control 2004; 14: 377–387.
107. Richmond A. In: Round FE, Chapman DJ, editors. Volume 7, Progress in physiological research. Bristol: Biopress; 1990. pp 269–330.
108. Barbosa MJ, Albrecht M, Wijffels RH. Biotechnol Bioeng 2003; 83(1): 112–120.
109. Kawase Y, Moo-Young M. Chem Eng J 1990; 43: B19–B41.
110. Chisti Y. Shear sensitivity. In: Flickinger MC, Drew SW, editors. Volume 5, Encyclopedia of bioprocess technology: fermentation, biocatalysis and bioseparations. New York: Wiley; 1999. pp 2379–2406.
111. Suzuki T, Matsuo T, Ohtaguchi K, Koide K. J Chem Technol Biotechnol 1995; 62: 351–358.
112. Calderbank PH. Trans Inst Chem Eng 1958; 36: 443–463.
113. FG Acién Fernández, E Molina Grima, J Pérez Parra, JJ Magán Cañadas, MC Cerón García, JM Fernández Sevilla. In: 7th European Workshop in Microalga Biotechnology. Postdam; 2007.
114. Pirt SJ. Biotechnol Bioeng 1983; 25: 1915–1922.
115. Hall DO. In: Richmond A, editor. Handbook of microalgal mass culture. Boca Raton (FL): CRC Press; 1986. pp 1–24.
116. Laws EA, Taguchi S, Hirata J, Pang L. Biomass 1988; 16: 19–32.
117. Alfano OM, Romero RL, Cassano AE. Chem Eng Sci 1986; 41: 421–444.
118. Lee HY, Erickson LE. Biotechnol Bioeng 1987; 29: 476–481.
119. Chaumont D, Dos Santos PF, Gudin C, Assie D, Chaintron G. French Patent 9,115,773. 1991 Jun 25. (to Ussie Inginierie).
120. Chrismadha T, Borowitzka MA. J Appl Phycol 1994; 6: 67–74.

19

MICROBIAL GROWTH MEASUREMENT

ARTHUR L. KOCH
Indiana University, Bloomington, Indiana

19.1 INTRODUCTION

In biotechnology, the denominator is biomass; for example, yield is the desired product per unit of biomass. Biomass concentration is one of the major determinants to identify the stage of the culture cycle. It is necessary to understand the controlling points in the physiology of the bacterial growth. Biotechnologists have extensively talked about growth phase and idiophase as the key measures of fermentation technology. There are a number of approaches for biomass measurement, but they are not very good and have significant limitations. The reader should supplement the treatment presented here with a previous chapter (1) and its revisions, which details a number of procedures and leads back to the earlier literature. Another useful overview is provided by Sonnleitner *et al*. (2). The former paper comes from the approach of a physiologist, and the latter is from the point of view of biotechnologists. For historical interest, the collected source is by Dawson (3).

19.1.1 Principles

Principles of bacterial growth are discussed in microbial physiology texts. I would particularly recommend that by White (4). Although there are many books on bioprocessing, most do little to discuss biomass measurements. The book by Pirt in 1975 (5) was a milestone in the field of microbe growth for product formation; newer publications are now available (6,7), but they do little for the estimation of biomass.

19.1.2 Definitions of Growth

To measure biomass and bacterial growth rate, precise definitions are needed. Although biomass is fundamental to carrying out technology, we have to first consider the growth process that makes the biomass and examine its several definitions. The most basic definition of growth is based on the ability of individual cells to multiply, that is, to repetitively initiate and complete cell and organismal division. This definition implies monitoring the increase in total number of discrete bacterial particles. There are three basic ways to do this: by microscopic enumeration of the particles, by electronic enumeration of the particles passing through an orifice (Coulter counter), and by modern flow cytometry. Assessment of particle number would falsely include dead cells and detritus, which would tend to lower estimations of growth rate. The rate would be artificially raised by the progressive dissolution of aggregates of bacteria and the fragmentation of nongrowing filamentous organisms. An increase in cell number is not exactly correlated with an increase in biomass or useful product. Commonly, at the end of an exponential growth phase, cell division overshoots biomass production and the cells become smaller.

A second definition of growth involves determining the increase in colony-forming units (CFU). Because some cells may be dead or dying, this definition of growth may be different from the one based on the detection of discrete particles as a function of time. Although in the long run, the increase in the number of organisms capable of indefinite growth is the only important consideration for the

Upstream Industrial Biotechnology: Expression Systems and Process Development, Volume 1, First Edition. Edited by Michael C. Flickinger.
© 2013 John Wiley & Sons, Inc. Published 2013 by John Wiley & Sons, Inc.

physiologist, this is not so for the biotechnologist, for several reasons. First, for strain purity, each new production run starts afresh from starter cultures; these cultures would have been specially treated much differently than the cells in the actual production run. This care is to avoid contamination and the buildup of unwanted mutants. Second, dead, dying cells and stationary cells may be the productive members of the culture in terms of product formation. This second definition is the reason that colony counting and most probable number (MPN) methods of measurement are so important. It must be noted that viable counting methods, which seem so natural to a bacteriologist, are really quite special in that cultures are diluted so highly that individual organisms cannot interact. For example, these methods cannot, in principle, be applied to obligate sexually reproducing organisms requiring male–female interaction or to colonial organisms such as myxobacteria that in certain conditions need to be part of a large mass of organisms that produces sufficient exoenzymes to grow. Even when applied to the prokaryote, there are special restrictions and limitations; for example, CO_2 must be available in sufficient concentration, although this need not be supplied if many organisms are present generating CO_2. This and possible detoxification of the medium can lead to a lower count than would have occurred in the more concentrated actual culture. To illustrate, consider a single bacterium and an isolated mammal, both introduced into an environment without any individuals of their own kind. The former would produce a colony, whereas the latter could only produce a viable colony if the founding individual was a pregnant female.

A third definition of growth (and the practical one) is based on an increase in biomass. Macromolecular synthesis and increased capability for the synthesis of cell components are the obvious basis for the measurement of growth by everyone interested in microbes and what they can do. From our point of view, the whole process of chromosome replication and cell division is an essential but minor process that seldom limits growth; what usually limits growth is the ability of enzymatic systems to use available resources to form biomass. Moreover, the restriction of growth of the culture is usually the result of the depletion of resources or degradation of the local environment.

A fourth definition of growth is based on the organisms' action in chemically changing their environments. This category can be simply considered as a different consequence of the increase in biomass. However, it allows the rate of the growth process and the biomass production to be estimated in indirect ways. Most important in industry, the gases coming from the fermentation are analyzed, and the consumption of oxygen and production of carbon dioxide are used as effective and efficient means to follow growth. Especially important is the use of mass spectrometer methods, because of their precision and the ability to automate measurements, and growth of cultures can be followed usefully and effectively.

Biomass is the result of growth; it has various different definitions according to purpose. In most biotechnology, biomass is organic material that is cheap and can be converted into fuel, or heat, or structural materials. It is necessary that such sources be self-generating, cheap, and available. Whether biomass is alive or dead is less relevant; the assumption is that it was, or at least once was, alive. If one has a mixture of coal and fresh plant material, the term biomass is fully ambiguous. For product formation, there is less ambiguity; microbial biomass requires the expenditure of resources, and useful products may be produced by the organisms that may be living or dead according to which of the definitions of growth is used.

19.1.3 Balanced Growth

These four definitions of growth become equivalent under a single circumstance: the state of balanced growth (8). This is certainly an academic concept, but its practicality is clear. An asynchronous culture can be said to be in balanced growth when all intensive properties are constant in time. An intensive property is one that does not matter how big the system is. An extensive property is another term from physical chemistry and refers to those properties of the system that are proportional to the amounts of substances of various kinds in the system. Thus, biomass and cell number are extensive properties of a culture and proportional to the volume of culture considered. These properties increase regularly and exponentially with time during balanced growth. However, temperature or ratios (such as DNA, RNA, or product per cell) are intensive properties that do not change during balanced growth. The application of this physical–chemical principle to bacteriology lies in the assumption that if a culture is grown for a long-enough duration (usually with many subcultures) so that the biomass is sparse enough not to alter the environment significantly, sooner or later the organisms will come to achieve the same growth state for any particular constant environment, no matter what the cell's condition was initially—be it log, lag, or the stationary state. Once this balanced growth state has been achieved, if the conditions remain the same, the culture will remain in balanced growth indefinitely. This would be true of a culture that had grown in a continuous culture or one that was diluted manually at periodical intervals, avoiding entry into either lag or the stationary state. However, if a nutrient is exhausted, or if the culture is altered by mutation and selection, or if the physical nature of the environment is changed, then balanced growth would cease and the culture would be in some nonbalanced state of growth.

The criteria given above are too stringent to be fully met with any practicality, but it is readily possible to study

cultures that are substantially in balanced growth by growing the cultures that are maintained at low density by dilution and using arbitrarily any one measure to follow growth, for example, biomass assayed turbidimetrically. If the doubling time remains constant over an extended period of time, then it is a good assumption that growth is balanced. Studies of these cultures can lead to an understanding of the properties of individual cells in the idealized state of balanced growth. However, they would not bear on the properties of aggregates or clumps of cells or of cells reacting to some calamity or catastrophe in their environment.

Although we may consider any extensive property of a culture in balanced growth, let us first focus on biomass and call it as X for tradition's sake. The rate of formation of biomass will be proportional to the amount of biomass. Call the proportionality constant, μ, then:

$$dX/dt = \mu X$$

Using the laws of calculus, this equation can be integrated and a boundary condition ($X = X_0$ when $t = 0$) is imposed, yielding the well-known equation for exponential growth:

$$X = X_0 e^{\mu t}$$

However, every cellular substance, or even an extracellular product of the cells, could be substituted for our X. Thus, after growth becomes balanced, the increase of any component or group of components will be exponential in time. If the ratio of one substance to every other is to remain constant, the same proportionality constant must apply for every component. This common value of μ is called the *specific growth rate* or *growth rate constant*. Not only any substance but also any combination of substances or the rate of change of any substance will increase exponentially with this same specific growth rate, μ. Practically, this allows the rate of oxygen uptake, heat production, or production of an internal or external metabolite to be used as an index of growth. It will also allow growth to be monitored by the depletion of some medium component or the change in conductivity of the medium.

Intensive properties, such as μ and the ratio of the concentrations of different cell substances, must necessarily remain constant under conditions of balanced growth. In addition, the distribution of cell sizes and the average number of chromosomes will stay constant. An average cell will have a time-independent constant rate of carrying out every cellular process, and newly arisen daughter cells will have a constant probability of being able to form a colony (i.e. the percentage of nonviable cells will remain constant). Therefore, under these special conditions, no matter what measure of growth is used (whether it is particle counting, colony formation, chemical determination of a cell substance, or consumption or excretion of a substance), the same specific growth rate will be obtained and that rate will be constant through time.

19.1.4 Changes in Cell Composition at Different Growth Rates of Balanced Growth

Organisms respond to environmental conditions, both physical and chemical, by altering their own composition. These changes have been well documented for certain enteric bacteria but may occur with all prokaryotes (9). In general, favorable growth conditions mean faster growth, which requires a higher concentration of ribosomes and associated proteins. In terms of gross composition, the most obvious difference in the comparison of a faster culture with a slower culture is the greater RNA content in the former (10). Also, under favorable growth conditions, the cells can lay down reserve materials such as glycogen and poly-β-hydroxybutyric acid. These changes in composition lead to the possible pitfall of the bacteriologist falsely relating one measure of growth to others when comparing growth in different environments.

19.1.5 Unbalanced Growth

Although balanced growth conditions lead to reproducible cultures, much of physiology deals with the responses of organisms to changes in their environment that lead to progressive changes in the organism (i.e. to the study of unbalanced growth). When a stationary culture is inoculated into fresh medium, the properties of organisms drastically change through the course of the batch culture cycle. Though only very well documented for certain enteric bacteria, similar changes probably apply with other prokaryotes. The exact course of changes in composition and morphology depends on the medium and on the age and condition of the inoculum. Culture cycle phenomena have relevance to growth measurements. These phenomena are particularly important in ecological studies, where the conditions under which the organisms grow are critical and, to a large degree, uncontrollable. The changes in characteristics are also involved in response to the fluctuations under natural conditions (11,12). For biotechnology purposes, it is the progression of changes in the so-called idiophase of growth that are paramount.

Noting that a "typical bacterial culture" generally means one of *Escherichia coli* (13), a typical bacterial culture cycle progresses as follows. When a stationary culture is diluted into rich medium, macromolecular synthesis accelerates. The components of the protein-synthesizing system (i.e. ribosomal proteins and ribosomal RNA) are made first. Only after considerable macromolecular growth has ensued, cell division does take place. During this lag phase, the average size of cells significantly increases. When the capacity of the medium to support rapid balanced

exponential growth is exceeded, metabolic processes (both intermediate metabolism and macromolecular synthesis) are slowed down. Different processes slow differentially in a way to make small, RNA-deficient cells. Finally, the cells die and may eventually lyse.

19.1.6 Pitfalls in Measuring Growth

Errors in measuring bacterial growth fall into four classes. The first major pitfall is the general tendency of most organisms toward clumping or a filamentous habit of growth. This can occur even under mildly toxic conditions with bacteria that ordinarily divide regularly. The second pitfall is the differential viability of injured bacteria under different culture conditions. Repair processes may permit the recovery of viable cells under some, but not other, conditions. A third major pitfall is the possible development of resistant stages. Bacteria known to form resistant stages, such as spores, pose no problem because the controls and measurements to correct for such differentiated forms are well known; but when resistant stages are not suspected, error can arise. The fourth pitfall pertains to the way in which the inoculum is exposed to the new environment. Different results may be obtained if the concentration of an agent is raised gradually, if it is raised discontinuously, or if a high concentration is temporarily presented and then removed or lowered, such as when a concentrated solution of a nutrient is added and the mixing is not rapid. The cell concentration at the time of challenge can be critical. Bacteria may have special ways, sometimes inducible mechanisms or sometimes unknown ones, to protect themselves against toxic agents. Finally, the protection may be dependent on the number of organisms cooperating in detoxification.

19.1.7 Mycelial Habit of Growth

The evaluation of mycelial growth (the first pitfall) is both easier and much more difficult than that of well-behaved organisms that engage in binary fission and then promptly separate. The problems and methods for colonial growth have been discussed by Calam (14) and will be briefly dealt with here. Filtering filamentous cells, with or without drying, is easier than with smaller nonfilamentous cells.

The rate of increase in size of the colony in one, two, or three dimensions depends on the rate of elongation of those terminal hyphae that happen to be growing perpendicular to the surface of the colony, but the mobilization of resources into the mycelial mass depends on the surface area of the colony (15,16). Therefore, particularly with shake cultures, the results depend on the nature and size of inoculated fragments; with large fragments, growth becomes limited at an earlier stage by the diffusion of nutrients into the mycelial mass. Thus, the major pitfall with the mycelial habit of growth is that the growth quickly deviates from exponential growth and depends on the geometry of growth and the nature of the inoculum. In shake cultures, the apparent growth may depend on the shape of the vessel and on the shaking speed, its character (circular or reciprocal), and the distance moved, because all of the above can affect the tendency of the mycelia to break into smaller pieces. An important aspect of biotechnology is controlling the filamentous versus pellet conformations.

19.1.8 Cell Differentiation

The change of enteric bacteria from large, RNA-rich forms in the exponential phase to small, RNA-poor forms in the stationary phase has many of the aspects of differentiation. However, bacteriology has much clearer examples of cell differentiation in the cases of transition of rod to coccus, vegetative bacillus to endospore, and in the formation of exospores, cysts, and buds. The tendency to form filaments in certain circumstances can also be considered as a differentiation. These changes and their reversal pose potential pitfalls for all approaches to growth measurement.

19.1.9 Adsorption of Cells to Surfaces

Many bacteria naturally adhere to certain surfaces or can adapt and mutate to achieve a high avidity for solid surfaces, including glass. Many experiments with chemostat culture have failed to achieve their primary goal because the organisms are adhered to the vessel walls. Therefore, plastic or Teflon should be used whenever there is long-term contact of the organism with a culture vessel (16). Other approaches to minimizing the effects of growth on vessel walls include the use of large culture volumes in large containers, the use of violent agitation, and the frequent subculture of the bacteria into fresh glassware. These are the conditions in large biofermenters, but not during the production of the starter cultures. In addition, the use of detergents, vegetable oils, silicone coatings, and a high-ionic-strength medium may, to some degree, alleviate this problem.

This problem is particularly pertinent during dilution of the culture for measurement by highly sensitive means, such as microscopic and plate counts. It is, therefore, given consideration in the discussion of those methods (1,17,18).

19.2 DIRECT PARTICLE COUNTS

For many biotechnology purposes, the counting methods that can be used are limited because the growth medium generally contains particulate matter. This does not preclude their use in the development of strains and other phases of biotechnology.

19.2.1 Microscopic Enumeration

Microscopic enumeration is a commonly used technique that is quick and cheap and uses equipment that is readily available in the bacteriological laboratory. However, the technique is subject to gross errors. These can be overcome to a large degree using improvements suggested by the work of Norris and Powell (19). Precise details are given in my earlier review of this subject that is a further modification of this method (1), and some versatile techniques that have some of the characteristics of viable counts or metabolic measurements are given in the work by Murray *et al*. (20).

Methods and equipment, some linked to computer programs, are now available to record, scan, and view a microscope field. Software and hardware are available that enable a sample to be placed in a counting chamber viewed by a microscope, and then an electronic count can be made from the image. The computer can distinguish between cells adhering side by side and between a long cell and a pair of sister cells that have completed division but have not separated. The capability exists to measure the biomass from the density of the pixels because the phase contrast (see later text) is a measure of the biomass. For filamentous organisms, the computer could output the total length of hyphae and convert that into biomass (21,22). Direct enumeration from charge-coupled device (CCD) images with highly intelligent computer filtering will allow distinguishing the bacteria or fungi from the particulate matter in the brew in many cases.

19.2.2 Electronic Enumeration

The Coulter Counter (Coulter Electronics, Hialeah, Fla.), its commercial competitors, and particularly the laboratory-built versions have been important in the development of bacterial physiology for the past 70 years. Such instruments are used routinely in clinical hematology. They are also very useful in the enumeration of nonfilamentous yeasts and protozoa, but not of mycelial or filamentous organisms.

The principle of electronic enumeration is as follows. A fixed volume of diluted cell suspension is forced to flow through a very small orifice connecting two fluid compartments. Electrodes in each compartment are used to measure the electrical resistance of the system. Even though the medium readily conducts electricity, the orifice is so small that its electrical resistance is very high. Consequently, the electrical resistance of the rest of the electrical path is negligible by comparison. When a cell is carried through the orifice, the resistance further increases because the conductivity of the cell is less than that of the medium. This change in resistance is sensed by a measuring circuit and converted into a voltage or current pulse. The counting rates can be very high, but beware of coincidence errors. The pulses are counted by an electronic circuit similar to that used in counting radioactivity. Very small pulses are eliminated by a discriminator circuit. Very high pulses, which might result from dirt or other irrelevant particles, are eliminated by an upper discriminator. In advanced models, the pulses may be analyzed by size and stored in a multichannel analyzer; later, the data can be recovered and plotted in a histogram, and the numbers, mean size, and standard deviation can be calculated. All the data may be collected, and the discrimination against pulses that are very high or very low can be carried out as the data are analyzed. The instruments have some method of forcing an accurately known volume through the orifice during the counting period. This is usually done by displacing the fluid in contact with a mercury column past triggering electrodes that conduct effectively through the mercury, but not through the diluent medium.

There are three major problem areas in electronic enumeration. The first problem concerns the size and shape of the cells. Some bacterial cells are very small (less than 0.4 μm^3), and the resistance pulses produced as they pass through the orifice are comparable to the noise generated by the turbulence that develops in the fluid flowing through the orifice. One can set the discriminator dial on the instrument to reject the turbulence noise, but one loses sample information, particularly about newly divided cells. One can run blanks and subtract the blank values, but blanks are particularly variable for small cell sizes. In addition, a pattern of turbulence can become established, remain for a while, and then be replaced with another pattern. This can cause major interference. Determining the size of cells has many difficulties, including the effect of the path that the particle takes through the orifice and the resistance of the various layers and compartment of the cell. Therefore, this potential use of the instrument is not discussed in this chapter. Finally, the overall error increases when the blank has large statistical variation. This is not a major problem for biotechnology because currently used microbes are relatively large.

The second major problem for physiological studies in electronic counting results from the failure of cells to separate promptly from each other after cell division. This, and the tendency to form filaments and aggregates, can be minimized by the careful choices of the organism and the conditions. Possibly, it can be reduced by vortexing or sonicating the sample. It was fortuitous for the advancement of microbial physiology that *E. coli* was chosen for physiological and genetic studies in the 1940s and 1950s because only a relatively small number persists in pairs or chains or in the form of aggregates. There is the related problem of coincidence, which is the passage of more than one cell through the orifice in a short enough time so that a single larger cell is registered by the electronic equipment. This problem can be dealt with by increasing the dilution so that the probability of coincidence is reduced.

The third major problem is technical: the clogging of the orifice in electronic counting. The resistance change

is a smaller proportion of the total electrical resistance of the orifice when the orifice diameter is larger. Consequently, for small rod-shaped bacteria such as *E. coli*, orifices with diameters in the range of 12–30 μm must be used. The exact choice is a trade-off between the increased signal strength of small apertures and the increased noise and probability of becoming clogged. Clogging is best prevented by ultrafiltration of all reagents. Alternatively, the diluent can be prepared and allowed to settle for a long time (months) in a siphon bottle so that the particulate-free solution can be withdrawn from above. Additional information about this technique can be found in the works by Drake and Tsuchiya (23) and Kubitschek (24).

19.2.3 Flow Cytometry Technique

Flow cytometry became an extremely powerful method for the study of many aspects of the biology of eukaryotes two decades ago. The instruments are now common in hospitals and in clinical research laboratories. Because prokaryotes are smaller, it is only more recently that the instrumentation and methods have been refined and are coming into their own in the study of bacteria. The instruments operate by forming a small-diameter stream of the sample suspension. This is encased in a stream of particulate-free fluid. The tube through which they flow constrict in such a way that the stream of the sample is made still narrower in diameter. This process is called *hydrodynamic focusing*. The flowing stream is examined with laser light with various frequencies and angles, and the output of the detection circuits is used to detect when a particle passes through and determine its characteristics. The design permits the analysis of biomass by light-scattering methods and by fluorescent staining of chemical components such as DNA. This is discussed in the section Flow Cytometry Methods. The electronic circuits allow cells to be counted very rapidly. Growth can be followed by the increase in counts in samples examined at intervals. The problems for the application to prokaryotes is in sensitivity and background noise.

The original designs were made for the study of problems in immunology. Applications, including microbiology, have been previously described (25–27).

Another quite different instrumental design was developed in Norway (28,29). It depends on flow directly onto a microscope slide on an inverted microscope. This instrument uses an inverted microscope essentially operated in the dark-field mode. It uses a high-intensity mercury arc. Now, with commercially available equipment, it has been utilized to study a variety of problems. Clever applications have been described (30,31).

The instrument of the first type uses a well-collimated laser source and fiberoptics. Great care is needed to maintain the instrument and its calibration. Routinely, polystyrene beads are mixed with the biological sample in a fixed amount. They have a uniform size and serve to quality control the electronics. By relating the biological count to the bead count, the concentration of biological particles can be determined. These kinds of controls can be used with the second type of instrument, which is cheaper and is now in use in many laboratories for many microbiological purposes. It is also capable of counting at very fast rates.

19.3 COLONY COUNTS EQUAL VIABLE COUNTS

Bacteriology really became an experimental science when Herr Dr Robert Koch listened to Frau Fannie Hesse and developed the agar plate. This allowed not only the cloning of pure strains but also the enumeration of colonies arising from individual viable cells. Many variations have been developed and used in the ensuing century: (i) spread plates, (ii) pour plates, (iii) thin-layer plates, (iv) layered plates, and (v) membrane filter methods. Although these techniques are very useful in the development of industrial strains, they consume too much time and cannot be used on-line.

These techniques are described in many places (1). The pour-plate methods have variations in which the cells are grown in roller tubes or microtubes (32) and are examined with low power microscopes when the colonies are small (33). There are many individual variations of techniques, sometimes resulting from historical accidents and sometimes resulting from special bacteriological circumstances. Automation of colony counting has put additional special restrictions on techniques, but allows colonies on the Petri dishes to be counted rapidly without operator error.

It must be further emphasized that mycelial organisms pose special problems. To some degree, they can be overcome by sonication or shearing. A practical approach is to conduct a pilot study to find the amount of ultrasound that produces the maximal count that optimizes the separation of propagules from each other and minimizes their destruction by the physical treatment.

In the future, the development of growth media that is perfectly clear and can be solidified in uniform layers on a new generation of microscope slides will permit the analysis by telometering and computer analysis only after a few hours of incubation. In some cases, observation will be repeated and the difference in the images is used to compute the growth rate as well as the initial CFU and viable biomass. Selectivity and identification of special properties with dyes and chemical reactions could be used as well. Again, particulate matter can be a problem, but less severe as the microcolonies grow to be larger than the detritus in the medium.

19.3.1 Spread Plates

The sample is pipetted onto the surface of solidified agar medium in a Petri dish, and then the cells are distributed with a wire, glass, or Teflon spreader. In the spread-plate technique, the growth forms surface colonies. It is reliable when methods to transfer all of a defined volume of cell suspension to the surface of the agar are used. The method is additionally useful because surface colonies are required to produce the proper color responses with many indicator agars that depend on the redox state of the colonies. In many cases, different colors are given from subsurface colonies because the oxygenation is different, and, therefore, the acid production and reducing potential are different than on the surface, and the selectivity is usually much less. (See Murray *et al*. (20) for recent improvements in technique.)

19.3.2 Pour Plates

An aliquot sample of diluted cells is pipetted into an empty sterile Petri dish; molten, but cool (45°C), agar medium is poured onto the sample; and the contents are mixed by swirling and then allowed to harden. The pour-plate technique is a standard technique. Its main advantage is that most colonies are subsurface. Therefore, they are small, making it possible for a plate to have many colonies and still be countable. This method has a large dynamic range, and automation can be very useful.

19.3.3 Thin-Layer Plates

The use of thin-layer plates came out of virology. The sample is pipetted into a tube containing a small volume (2.5–3.5 mL) of molten but cool (45°C) soft agar (0.6–0.75%) medium. This is then poured onto previously poured and hardened (1.5–2% agar) medium in a Petri dish, and the overlay is allowed to harden. This was the technique developed to measure virus plaques in the 1940s.

19.3.4 Layered Plates

Layered plates are like thin-layer plates except that an additional layer of agar medium is poured onto the newly congealed soft agar medium containing the cells so that all colonies are subsurface, but in the same plane. It is very useful because all colonies are subsurface and, therefore, much smaller and compact. Under the right conditions, they can be intensely colored because they are highly anaerobic. Many more colonies may be present, and yet the coincidence by fusion of colonies is small; this means that several thousand colonies per plate can be used to give meaningful results. This approach is especially recommended because the main difficulty with usual surface colony counting method is its lack of dynamic range. Rules have been issued that between 30 and 300 colonies are required for spread plates. The lower limit is set by statistical accuracy, and the upper limit is set by coincidence limitations. This 10-fold range is inconvenient for many purposes, because in many cases, one cannot predict the number within a factor of 10 when choosing the dilution factor. The extra care needed to prepare the overlay plates is justified because it allows the counting in a larger range of 30–2000 colonies. A second major advantage is flexibility for nutrient supplementation. Minimal agar can be used to pour the basal layer in a large number of Petri plates for indefinite storage. Stock supplies of the minimal soft agar can also be kept on hand. Then, 10- to 50-fold excesses of needed special nutrients can be added to the aliquots that are used for the molten top agar. In some cases, dyes and chromogenic substrates can be added as needed to the soft agar to allow screening of the colonies. Toxic substances can be incorporated to measure frequencies of resistant mutants.

19.3.5 Membrane Filter Methods

The diluted cells are filtered onto an appropriate membrane filter, which is then placed on an agar medium plate or onto blotter pads containing liquid medium. Sometimes, it is necessary to carefully prewash the membranes and the pads with water or medium and then sterilize them. It is also necessary to supply nutrients at a higher level because they must be diffused to where the cells are located.

19.3.6 Automation

Several chapters and books have been devoted to attempts to speed and automate growth measurement (34,35).

19.3.7 Special Situations

Certain organisms are very sensitive to substances present in agar. Meynell and Meynell (36) presented an excellent discussion of these problems. Injured organisms may have additional special requirements, and the entire 26th symposium of the Society for General Microbiology (37) was devoted to these problems. Genetically defective organisms pose individual problems that can be research problems on their own, such as the ability of various repair mutants to form countable colonies (38).

The problem of quantitating the number of organisms in cultures of strict anaerobes is discussed by Holdeman *et al*. (39) and Hungate (40).

19.3.8 Most Probable Number Method

The MPN method consists of making a number of replicate dilutions in a growth medium and recording the fraction

of tubes showing bacterial growth. The tubes exhibiting no growth presumably failed to receive even a single cell that was capable of growth. Because the distribution of such cells must follow a Poisson distribution, the mean number plated at this dilution can be calculated from the formula $P_0 = e{-}m$, where m is the mean number and P_0 is the ratio of the number of tubes with no growth to the total number of tubes. The mean number, estimated by $-\ln P_0$, is then simply multiplied by the dilution factor and by the volume inoculated into the growth tube to yield the viable count of the original sample. The MPN method is a very inefficient method from the point of view of statistics, because each tube corresponds to a small fraction of the surface of a Petri dish in a plate count. Consequently, many tubes or wells in a titer plate must be used, or the worker must be prepared to settle for a very approximate answer.

It is important to understand when the MPN method is of advantage. It can be used if there is no way to culture the bacterium on solidified medium, and it is preferred for mixed cultures if the kinetics of growth of the individual types are markedly different. Suppose some cells grow immediately and rapidly and end up making a large colony on solid agar that spreads over and obscures colonies of the organism of interest that form later. The small colony formers may be numerous but unmeasurable on plates because of the fewer but highly motile or rapidly growing bacteria. Another use of the method is when other organisms that are not of interest are present in the sample, and no selective method is available to prevent their growth. Thus, the method has utility when the bacterium of interest produces some detectable product (e.g. a colored material, specific virus, or antibiotic). Then, even though contaminating organisms may overgrow the culture, the numbers of the bacterium in question can be estimated by the fraction of the tubes that fail to produce the characteristic product. Finally, if agar and other solidifying materials have some factors (such as heavy metals) that may alter the reliability of the count or interfere with the object of the experimental plan, then the MPN method can be used to avoid these difficulties.

Modern developments in currently available laboratory techniques can be used to speed the execution of the MPN method and make it more efficient. Machines are available to fill the wells of plastic trays that have as many as 144 depressions. However, it may be better to use 96-well trays because most apparatus, such as hand-held pipets, currently use them. Scanning devices designed for other purposes can be used to aid in counting the number of wells with no growth. Similarly, automatic and semiautomatic pipets can be used to fill small test tubes. Because these procedures make it possible to examine many more cultures, the classical tables of fixed numbers of tubes and fixed dilution series are obsolete and should be abandoned. A different and more flexible approach and method of calculation has been provided (1). It may easily be optimized for the purpose at hand.

19.4 DIRECT BIOMASS MEASUREMENTS

Some measure of the bacterial cell mass or numbers of a culture is almost always used as the reference basis for the measurements of cellular metabolic activities, the types of morphological characters, or the amount of a chemical constituent; biomass and cell numbers are the two basic independent parameters of bacterial growth. The methods for measuring biomass seem obvious and straightforward, but in fact they are complicated if accuracy if sought. Furthermore, the results may be expressed in different ways and, in some of these ways, the values may be more relative than absolute.

19.4.1 Wet Weight

A nominal wet weight of bacterial cells originally in liquid suspension is obtained by weighing a sample in a tared pan after separation and washing the cells by filtration or centrifugation. However, in either case, diluent is trapped in the interstitial (intercellular) space and contributes to the total weight of the mass. The amount of interstitial diluent may be substantial. A mass of closepacked, rigid spheres contains in its interstices 27% of space. This is independent of sphere size. A mixture of sizes packs more densely, and close-packed bacterial cells may contain an interstitial volume of 5–30%, depending on their shape and amount of deformation. This is a problem that is readily solved if the washing step can be carried out with pure water.

Simple weighing or just measuring the packed volume of cells can be an excellent and rapid method with filamentous organisms or those that grow as pellets. Then filter, wash, and weigh (or centrifuge, and measure the height of the pellet). Both can be very rapid, and the procedures can be calibrated to correct for the exogenous water or shapes of centrifuge tubes. Because the particulate matter in the medium has different physical properties, it can be possible to separate the cells from the particulates and estimate the cell volume directly. This correction could be established with radioactive or fluorescent dextrans or other molecules that are too big to enter the cells.

19.4.2 Dry Weight

A nominal dry weight (solids content) of bacterial cells originally in a liquid suspension is obtained by drying a measured wet weight or volume in an oven at 105°C to constant weight. The cells could be washed with water (possibly extracting cell components), or (better) a correction

could be made for medium or diluent constituents that are dried along with the cells. Separating the cells by filtration poses particular problems. More problems arise if volatile components of the cells can be lost by oven drying, or if some degradation and volatilization occurs, evidenced by discoloration (particularly if a higher temperature is used). Some regain of moisture occurs during the transferring and weighing process in room atmosphere, so this should be done quickly within a fixed time for all replicate samples, especially if the relative humidity is high. It is best, of course, to use tared weighing vessels that can be sealed after drying.

It is possible that more accurate determination can be made by drying the sample to constant weight in a desiccator vessel with P_2O_5 and under oil-pump vacuum at 80°C or by lyophilization. Results with the three methods are indistinguishable within 1% for certain cases (41). An excellent discussion of dry weight procedures and errors is given by Mallette (42).

The dry weight of cells may be reexpressed on a wet weight basis (grams of solids per gram of wet cells) or on a wet volume basis (grams of solids per cubic centimeter of wet cells or per cubic centimeter of cell suspension).

Because the drying can be a time-consuming process, and adequate knowledge about the possibility of volatilization of some cell components is not known, in the future, adequate drying quickly at lower temperature could be done in specially designed vacuum ovens. Such procedures could also be calibrated for the residual water content. Often, a practical method is to dry the cells in a microwave oven.

19.5 BIOMASS BY LIGHT SCATTERING

Light-scattering methods are the techniques most generally used to follow the growth of pure cultures. The major advantages are that they can be performed quickly and nondestructively. However, they may give information about a quantity not of primary interest to the investigator. Although they can be powerful and useful, they can lead to erroneous results. Under a range of conditions, they give information about macromolecular content (dry weight) and not about the number of cells or the state of hydration.

To understand their use in biomass determination, only the basic principle of Huygens is needed. Electromagnetic radiation interacts with the electronic charges in all matter. When the light energy cannot be absorbed (colorless materials), a light quantum of the same energy must be reirradiated. This light photon may emerge in any direction. This means that all atoms in a physical body serve as secondary sources of light. The photons that propagate in the direction of the original wave will stay in phase with the wave arriving directly from the light source, but light reirradiated from different points in the body that propagate in other directions will differ in phase at an observation point. The phase will differ depending on the distance that the photon must travel throughout the object because light going through matter is slowed. (The degree of slowing is measured by the index of refraction.)

It is refraction that controls how light is bent and focused in large bodies such as prisms, lenses, raindrops, or a pane of glass. In the last case, all the light that is scattered in any direction except straight ahead cancels, leaving only a beam of light going in the original direction. However, it is slightly retarded relative to a light ray not going through the pane; this is the basis causing the index of refraction of substances to be greater than 1. For the present purposes, the deflection of the light into different directions is the basis for the three types of useful techniques that are outlined next.

19.5.1 Theoretical Aspects

When the particles are very small, the light scattered is given by the Rayleigh equation:

$$I = \frac{8\pi^4 r^6 \eta_0^4 \left[(\eta/\eta_0)^2 - 1\right]^2}{R^2 \lambda \left[(\eta/\eta_0)^2 + 2\right]^2} v I_0 v \left[1 + \cos^2(\theta)\right] \quad (19.1)$$

In this equation, I is the intensity of the scattered light at a given direction and distance; r is the radius of the spherical equivalent of the actual particle; η_0 is the index of refraction of the suspending medium; η is the index of refraction of the particle; v is the volume illuminated; I_0 is the intensity of the incident light; ν is the concentration of particles; θ is the angle of observation; R is the distance of the observer from the sample; and λ is the wavelength of light in vacuo. The factor depends on the angle of observation, θ, relative to the forward direction of the illuminating beam. The $[1 + \cos^2(\theta)]$ factor takes into account the two mutually perpendicular beams of plane-polarized light that comprise unpolarized light. For a given physical setup, most of these factors can be combined into an empirical constant.

In studies of bacteria, the biomass is commonly measured by turbidity. Turbidity is the amount of light scattered away from the forward direction and is thus a measure of the integral of all the scattered light. Similarly, for the flow cytometer applications, I must be integrated over the directions that are collected by the instrument's optics. This integral will be designated by F. In nephelometry, only light scattered at 90° to the primary beam is recorded. This measure is actually a mixture involving on one hand the size shape and orientation of the particles and on the other the inhomogeneities inside the chapter.

The range of very small particles where Equation 19.1 holds is called the *Rayleigh domain*. For this domain, the actual volume, index of refraction, shape, and orientation

of the particles are irrelevant to the total light scatter. Most viruses are sufficiently small for their total scattered light to belong to this domain. For such small particles, the total light scatter integrated over all angles is proportional to the square of the volume, V^2. This results because the Rayleigh equation contains the radius, r, raised to the sixth power, which is equivalent to the volume squared. From the relative index of refraction, $m = \eta/\eta_0$ of the cells and the refractive index increment, the particle dry mass, q, and the wet weight can be calculated as discussed next, but only if all the parameters in Equation 19.1 are known.

For somewhat larger particles with low index of refraction, such as most bacteria, which typically range from 0.3 to 3 μm in linear measure, light scattered from different parts of the particle can interfere both destructively and constructively as a result of phase differences. This defines the Rayleigh–Gans domain and is the relevant case for most microbes. The shape and orientation of the particles become important for this domain, where the particle's radius is comparable to λ', the wavelength of light in the suspending medium which is equal to $\lambda/\eta o$. For particles in this domain, it is sufficient to take only the constructive and destructive interference into account, whereas phase shifts as the light traverses the particle can be neglected. The light scattering in this domain can be treated relatively simply, and for calculation, Equation 19.1 need only be amended by multiplication with quantities called *P functions*. These functions are specific for shape, size, and orientation. Thus

$$I_{RG} = I(P(\theta)) \tag{19.2}$$

where I_{RG} is the light scattered as corrected by the Rayleigh–Gans method. The P functions are given and discussed in a variety of sources (see Ref. 1).

The mathematics of the third, the Mie, domain applies to particles of any size and index of refraction and are computer intensive. The computations can be carried out much more easily if the particles are spherical. For pigment-bearing cells, such as green and blue-green algae, the computations are very elaborate.

Although the Rayleigh–Gans or Mie mathematics apply as well to the simpler cases, we have defined the Rayleigh–Gans domain as the region in which interference, but not phase, must be taken into account, and the Mie domain is where both interference and phase shifts must be taken into account for accuracy. The choice of the appropriate mathematics depends on both the size and the index of refraction of the particle relative to the medium above that of the medium (i.e. on $\eta/\eta_0 - 1$).

Bacteria (e.g. *E coli* growing in minimal medium) belong to the Rayleigh–Gans domain and not the Rayleigh domain because they are large enough to require correction for interference; however, they do not belong to the Mie domain because they have only a small dry mass, being mostly, water, and have an index of refraction only slightly larger than the aqueous growth medium and thus do not elicit phase shifts. Typically, the index of refraction relative to the growth medium of many bacteria is 1.04. In any case, a relative index of refraction between 1.00 and 1.05 ensures that most bacteria suspended in their growth medium will fall in the Rayleigh–Gans domain (43–46).

Studies (43) show that dilute suspensions of most bacteria, independently of cell size, have nearly the same apparent absorbance per unit of the dry weight concentrations. Measurements at various angles (47) show that light is mainly collimated in the first few degree from the primary beam and at high angles almost purely measures the inhomogeneity within the bacterial cells.

Very different absorbancies (turbidities) are found per particle or per colony-forming unit with different sizes of bacterial cells. An approximate rule commonly assumed is that the dry weight concentration is directly proportional to the absorbance. This rule applies roughly to both cocci and rods and is a first approximation to a more precise rule, that is, the light scattered out of the primary beam is proportional to the four-thirds power of the average volume of cells in the culture. Objects smaller than bacteria, such as suspensions of viruses, will not obey these rules. The rules also fail to apply when the suspensions of very small bacteria have a bluish cast. Larger objects (yeasts and filaments and aggregates of bacteria) may still appear cloudy and not necessarily colored, but may not obey the rule. Where the rule applies, the proportionality constant relating the absorbency measurement to the dry weight concentration is the same for any good, well-collimated photometer.

19.5.2 Turbidimetry

Bacterial suspensions are in between the size limits of atoms and objects such as window panes. Consequently, most of the scattered light is deviated only slightly; it is directed almost but not quite in the same direction as was the incident beam. The light scattered from an atom or a very small particle inversely depends on the fourth power of the wavelength of light. For a pane of glass, there is no light left uncancelled in any but the original direction, so the light retains its original hue and the pane appears transparent. If the glass was powdered to the size of bacteria, a suspension of powdered glass or bacteria (like a cloud) would appear white but not transparent nor colored. Because bacterial suspensions appear cloudy or turbid, instruments to measure the phenomenon are called *turbidimeters* (*turbidus* = confused or disturbed).

The common practice in bacteriology is to use any available colorimeter or spectrophotometer to measure turbidity. Ideally, such instruments measure only the primary beam of light that passes without deviation through the sample and reaches the photocell. Usually, the measurement is made

of the light intensity relative to that which reaches the photocell when a sample of the suspending medium has replaced the cell suspension. From what has been said, an ideal photometer must be designed with a narrow beam and a small detector so that only the light scattered in the forward direction reaches the photocell. That is, the instrument must have well-collimated optics. Such an ideal instrument gives larger apparent absorbance values than simple instruments with poorly collimated optics, because in the latter a large percentage of the light scattered by the suspension is still intercepted by the phototube. Therefore, the measuring system responds as if there were less light scattered than is actually deviated from the forward direction.

If the instrument or the size of organism does not meet these criteria, valid measurements in many cases can be made by establishing a standard curve on either a relative or an absolute basis. Difficulty arises only as physical or biological conditions vary with the samples to be compared, because then the experimenter cannot be sure that the same standard curve applies.

These considerations apply only to dilute suspensions. Deviation from Beer's law must be applied after the absorbance exceeds about 0.3 when light of 500 nm or shorter is used. A good discussion of this question is given by Kavenagh (48). Failure to take this deviation into consideration is the most common difficulty encountered in the microbiological literature that involves turbidimetry. One way to avoid this problem is to restrict culture densities and use only dilute cultures for measurement (i.e. keep the absorbance below 0.3). It is usually better to make measurements at higher densities and correct for deviations from Beer's law. The longer the wavelength of light used, the less important the need for the Beer's law correction.

19.5.3 Nephelometry

Although most of the light scattered by bacteria is nearly in the forward direction, instruments that measure the light scattered at 90° from the primary beam have been used to measure bacterial concentrations. Instruments designed to make right-angle measurements of light scattering are called *nephelometer* (*nephelos* = cloud). Bacterial concentration may be measured with this nephelometric principle in a spectrofluorometer when the dials are set so that the excitation monochromator and the emission monochromator are at the same wavelength.

Nephelometric measurements can be ultrasensitive, so that very small concentrations of bacterial cells can be measured. If it is known which factors are important and whether elongated particles are oriented or randomly distributed in space, then light-scattering measurement over a range of angles can give information about several aspects: the state of aggregation of the protoplasm, such as whether the ribosomes are in polysomes or as monosomes within the living cell; the thickness of the cell envelope (46,47,49,50); and the distribution of cell mass from the center of the cell.

Wyatt (50) (see Wyatt Technology) has developed an apparatus to measure the angular dependency of the light-scattering signal from 30° to 150°. In this range, different organisms, different treatments of a culture, and cultures in different phases of growth give characteristic patterns. These may be of some use as a fingerprint technique for the diagnosis and study of drug action. For the reasons stated above, the light-scattering signals in the high angle range cannot be used reliably for growth measurement because they are sensitive to the details of subcellular structure.

Light-scattering measurements made over a range of angles from 0° to 20° are relatively independent of these three factors, but are more critically dependent on overall size. Measurement in this range could nondestructively yield the biomass concentration, the number concentration, the average axial ratio, and a measure of average biomass distribution around the center of the cells for bacteria in balanced growth.

It may be easily possible to build a device in which an inexpensive neon laser illuminates a flow through a cuvette or a series of cuvettes of different path lengths. It would be so constructed that little stray light from the laser arrives at the detectors. One detector monitors the input beam, and a second detector monitors the light scattered a few degrees from the direction of the primary beam, say at 4°. A third detector measures the light scattered at right angles, and software outputs the dry weight biomass and intracellular heterogeneity that is a measure of the physiological state of the cells. It would avoid problems of the failure of Lambert's law by having multiple path lengths and would usually neglect the signals from the path length cuvettes in which deviations from the Beer–Lambert law were important. A variation would have several laser beams. The appropriate choice would depend on the color of the surrounding medium and the size of the microbes. The farther into the infrared that can be used, the less the Beer's law correction is needed, but there may be more interference from medium constituents.

It is possible to put probes into the fermentation apparatus for light scattering, turbidity, and nephelometry that have light sources and light detectors. These methods usually fail because the organisms grow on the optical surfaces. It is possible to remove, sterilize, and reinsert the probes, but this could lead to contamination. There are some ways around the surface-growth problem that may be effectively implemented in the future to essentially by cleaning the optical surfaces *in situ*.

19.5.4 Flow Cytometry Methods

For the conversion of forward scatter measurements in flow cytometry, the intensity of light pulse from a passing particle must be converted to volume or wet biomass or dry biomass. Our analysis (51) showed that in the Rayleigh region, the biomass is related to the intensity raised to the 0.5 power, and in the Rayleigh–Gans region, the power is approximately 0.75 for the usual bacteria and is somewhere in between for the very small bacteria that we are studying. Rules have been developed to establish the exact power. The results are applicable to bacteria and very small bacteria ($0.02–0.6\ \mu m^3$) that are not usually spherical. The physical limitations and the mathematical basis of the calculations have been justified for the application of the proposed formula for practical use in microbial ecology and physiology of extremely small aquatic bacteria as well as the more well-studied forms. Although the method was developed for the small bacteria present in natural populations that are difficult to size by alternative methods, it will also be useful for industrial cultures of bacteria.

The major problem with both types of instruments discussed earlier is to convert the forward scattered light into a value proportional to the biomass of the particle. Although complicated, this problem has been solved for the first type of instrument (51). Consequently, the number of the channel of the multichannel analyzer can be related to biomass through a power law function. As of yet, a reliable way to do the same for the second class of instrument that uses an inverted microscope is not available. This does not prevent the instrument from being a very valuable instrument, but it will be more valuable when accurate sizes can be developed.

It may not be possible to theoretically analyze the light-scattering pulses from the second type of instrument and to convert them into dry weight biomass, but it is not impossible to imagine that something akin to the polystyrene latex beads that have become so useful in medical technology will be developed that have precisely defined size and an index of refraction in the range that includes most bacteria. Then, the second type of instrument will become useful for biomass determinations. As with light-scattering measurements, aggregation, clumping, and failure of cells to separate will remain problems to be coped with.

19.6 SAMPLING

Attention must be paid to analyzing an appropriate sample. Although this just takes attention to detail, it is so important that it should be emphasized again and again. During bioprocess technology, it is important to sample from a number of parts of the system. Pooling and mixing and then analyzing are appropriate, but in many cases, analysis of each part individually and the body of data analyzed statistically are efficient and useful.

Acknowledgment

I would like to thank George Hegeman and Matt Hilton for help in preparing this chapter.

REFERENCES

1. Koch AL. Growth measurements. In: Reddy CA, Beveridge TJ, Breznak JA, Marzluf G, Schmidt TM, Snyder LR, editors. Methods for general and molecular microbiology. 3rd ed. Washington (DC): American Society of Microbiology; 2007.
2. Sonnleitner B, Locher G, Fiechter A. J Biotechnol 1992; 25: 5–22.
3. Dawson PSS, editor. Microbial growth. New York: Halsted Press; 1974.
4. White D. The physiology and biochemistry of prokaryotes. 3nd ed. New York: Oxford Press; 2005.
5. Pirt SJ. Principles of microbe and cell cultivation. Oxford: Blackwell Scientific Publications; 1975.
6. Pirt SJ. Stoichiometry and kinetics of microbial growth. London: Pirtferm; 1994.
7. Pirt SJ. Bioenergetics of microbial growth and product formation. London: Pirtferm; 1994.
8. Campbell A. Bacteriol Rev 1957; 21: 263–272.
9. Koch AL. The bacteria: their origin, structure, function, and antibiosis. Dordrecht: Springer Academic Publishers; 2006.
10. Schaechter M, Maaløe O, Kjeldgaard NO. J Gen Microbiol 1958; 19: 592–606.
11. Koch AL. Adv Microb Physiol 1971; 6: 147–217.
12. Koch AL. Perspect Biol Med 1976; 20: 44–63.
13. Koch AL, Schaechter M. In: Demain AL, Solomon NA, editors. Volume I, Biology of industrial microorganisms. Reading (MA): Addison-Wesley; 1985. pp. 1–25.
14. Calam CT. In: Norris JR, Ribbons DW, editors. Volume 1, Methods in microbiology. New York: Academic Press; 1969. pp. 567–591.
15. Prosser JI. In: Gow NAR, Gadd GM, editors. The growing fungus. London: Chapman and Hall; 1994. pp. 301–318.
16. Koch AL. Microbiol Mol Biol Rev 1997; 61: 305–318.
17. Kavenagh F, editor. Volume 1, Analytical microbiology. New York: Academic Press; 1963.
18. Kavenagh F, editor. Volume 2, Analytical microbiology. New York: Academic Press; 1972.
19. Norris KP, Powell EO. J R Microsc Soc 1961; 80: 107–119.
20. Murray RGE, Doetch RN, Robinow CF. In: Gerhardt P, editor. Methods for general and molecular bacteriology. Washington (DC): American Society of Microbiology; 1994. pp. 21–41.
21. Reichl U, King R, Gilles ED. Biotechnol Bioeng 1992; 39: 164–170.
22. Paul GC, Kent CA, Thomas CR. Biotechnol Bioeng 1993; 42: 11–23.
23. Drake JF, Tsuchiya HM. Appl Microbiol 1973; 26: 9–13.

24. Kubitschek HE. In: Norris JR, Ribbons DW, editors. Volume 1, Methods in microbiology. New York: Academic Press; 1969. pp. 593–610.
25. Shapiro HM. Practical flow cytometry. 3rd ed. New York: Alan R. Liss; 1995.
26. Melamed MR, Lindmo T, Mendelsohn ML. Flow cytometry and sorting. 2nd ed. New York: Wiley-Liss; 1990. p. 824.
27. Button DK, Robertson BR. Cytometry 1989; 10: 558–563.
28. Steen HB. In: Melamed MR, Lindmo T, Mendelsohn ML, editors. Flow cytometry and sorting. 2nd ed. New York: Wiley-Liss; 1990. pp. 11–25.
29. Lloyd D, editor. Flow cytometry in microbiology. New York: Springer-Verlag; 1993. p. 188.
30. Nir R, Yisraeli Y, Lamed R, Sajar E. Appl Environ Microbiol 1990; 56: 3861–3866.
31. Amann RI, Binder BJ, Olson RJ, Chisholm SW, Devereux R, Stahl DA. Appl Environ Microbiol 1990; 56: 1919–1925.
32. Perfil'ev BV, Gabe DR. Capillary methods of investigation of microorganisms. Toronto: University of Toronto Press; 1969.
33. Postgate JR. Adv Microb Physiol 1967; 1: 2–23.
34. Gall LS, Curby WA. Instrumental systems for microbiological analysis of body fluids. West Palm Beach (FL): CRC Press; 1979.
35. Heden C-G, Illeni T. Automation in microbiology and immunology. New York: Wiley; 1975.
36. Meynell GG, Meynell E. Theory and practice in experimental bacteriology. 2nd ed. Cambridge: Cambridge Press; 1970.
37. Gray TRG. Symp Soc Gen Microbiol 1976; 26: 327–364.
38. Capaldo FN, Barbour SD. In: Hanawalt PC, Setlow RB, editors. Molecular mechanisms for repair of DNA, part A. New York: Plenum Publishing; 1975. pp. 405–418.
39. Holdeman LV, Cato EP, Moore WEC, editors. Anaerobe laboratory manual. 4th ed. Blacksburg (VA): Virginia Polytechnic Institute and State University; 1977.
40. Hungate RE. In: Norris JR, Ribbons DW, editors. Volume 3a, Methods in microbiology. New York: Academic Press; 1971. pp. 117–132.
41. Black SH, Gerhardt P. J Bacteriol 1962; 83: 960–987.
42. Mallette MF. Norris JR, Ribbons DW, editors. Volume 1, Methods in microbiology. New York: Academic Press; 1969. pp. 521–566.
43. Koch AL. Biochim Biophys Acta 1961; 51: 429–441.
44. Koch AL. J Theor Biol 1968; 18: 133–156.
45. Koch AL. Anal Biochem 1970; 38: 252–259.
46. Gunther HH, Berhgter F. Z Allg Mikrobiol 1971; 11: 191–197.
47. Koch AL, Ehrenfeld E. Biochim Biophys Acta 1968; 165: 262–273.
48. Kavenagh F. In: Kavenagh F, editor. Analytical microbiology. New York: Academic Press; 1972. pp. 43–121.
49. Kerker M, Coke DD, Chew H, McNulty PJ. J Opt Soc Am 1978; 68: 592–560.
50. Wyatt PJ. In: Norris JR, Ribbons DW, editors. Volume 8, Methods in microbiology. New York: Academic Press; 1973. pp. 183–263. (See Wyatt Technology).
51. Koch AL, Robertson BR, Button DK. J Microbiol Methods 1996; 27: 49–61.

20

MICROBIAL MEDIA COMPOSITION

ROSALIE J. COTE
Becton Dickinson Microbiology Systems, Sparks, Maryland

20.1 INTRODUCTION

The increased understanding of microbial biochemistry in recent decades, along with major advances in genetic and molecular techniques, has resulted in an expanding diversity of microorganisms entering the biotechnology arena. Be it novel uses for well-studied organisms, such as the commercial production of restriction endonucleases from many common bacteria and yeasts, or the potential for development of new applications from new species such as the unidentified hydrogen-producing bacterium FOX-1 (1), microorganisms, themselves, are integral components in the overall aspects of biotechnology from discovery, through research and development, to production.

For those biotechnologists not formally trained in classical microbial physiology, the too-prevalent assumption is that microorganisms function similarly to the purified reagents used in a well-documented chemical reaction. In reality, microorganisms (even authenticated and characterized strains) are heterogeneous conglomerations of multiple biochemical pathways with the potential for working antagonistically or synergistically, depending upon the environment in which the microorganism resides. For those strains under study in the laboratory or being potentially harnessed for bioprocess use, the microbial environment is the culture medium.

This chapter surveys elements of microbial media and other considerations of microbial nutrition that impact upon the general growth and metabolic activity of microorganisms. Although specific references are given for many useful compendia of microbial media formulations (2–7), the purpose here is not to further cite well-documented media and buffer formulations. The intent of this chapter and its specific examples is to illustrate general principles of controlled media design, formulation, and preparation for the cultivation of microorganisms.

20.2 ESSENTIAL NUTRITIONAL REQUIREMENTS

20.2.1 Water

Depending upon the physiological state of the organism, the chemical composition of bacteria is 70–90% water. As a polar solvent, water dissolves other compounds of similar chemical nature, which also happen to be the biologically important molecules such as amino acids, carbohydrates, and nucleic acids. The polarity of water helps to permit the hydrogen bonding necessary in the formation of the final working configuration of a cell's large macromolecules. As a polar solvent, water chemically forces nonpolar molecules such as lipids into hydrophobic aggregates that are integral in the formation cell membranes. The presence of water is critical to the existence of microorganisms. Under laboratory conditions, microorganisms are cultivated with liquid and solid media. In both situations, the adequacy and purity of water used in media preparation can drastically effect the performance and/or sustained viability of an organism.

Because the availability of high-quality, purified water has become increasingly affordable for even small laboratories, the use of tap water or marginally distilled

Upstream Industrial Biotechnology: Expression Systems and Process Development, Volume 1, First Edition. Edited by Michael C. Flickinger.
© 2013 John Wiley & Sons, Inc. Published 2013 by John Wiley & Sons, Inc.

water for the preparation of media and reagents is not a recommended option. For most municipalities, tap water is seasonably variable with respect to its chemical and microbial content. Hard water ladened with calcium and magnesium will precipitate many media formulations, with deleterious results. The terms *deionized* or *distilled* water with respect to water purity are merely euphemistic unless actual determinations of residual ion and organic levels are known. Water passed through spent deionization beds or boiled and condensed through a scale-clogged distillation system is hardly purified. At minimum, water used in the preparation of microbial media and reagents for general laboratory purposes should meet U.S.P. specifications for purified water; other organizations such as the American Society for Testing and Materials (ASTM) and the National Committee for Clinical Laboratory Standards (NCCLS) have similar criteria with respect to the conductivity, resistivity, and total organic content for Type II water (8). Point of use deionization systems available from many manufacturers (e.g., Barnstead/Thermolyne Corporation, Dubuque, Ia. and Millipore Corporation, Bedford, Mass.) easily produce Type I, 18 MΩ water. Some systems include ultrafiltration to reduce pyrogen levels. Purified water for highly regulated applications and processes (e.g., biopharmaceuticals) must meet U.S.P. specifications for water for injection (9). Water, unless sterilized, should not be held for any length of time in storage containers such as bottles or carboys or allowed to stand in uncirculated piping systems (e.g., dead-legs) because there is a good probability that the water will become populated with bacterial biofilms that grow on container and piping walls. Bacterial contamination will organically pollute water purity in addition to increasing endotoxin and pyrogens to unacceptable levels for certain procedures including product purifications or animal injections. Note that pyrogens are lipopolysaccharides from bacterial membranes. With respect to purified water, they indicate bacterial contamination. Their presence, of course, in bacterial cultures is a mute point. Use of plastics for water storage containers may be a consideration because plasticizer leaching can cause inhibition of sensitive organisms.

20.2.2 Energy

All microorganisms require an exogenous source of energy. The biochemical mechanisms involved with this aspect of metabolism are diverse. *Lithotrophic* organisms obtain energy from inorganic sources. Lithotrophs fall into two metabolic categories with respect to energy procurement. *Photolithotrophic bacteria* and *cyanobacteria* obtain energy from light in conjunction with, respectively, reduced sulfur (e.g., hydrogen sulfide) or water, to release energy for biosynthetic functions. Variations in microbial chlorophyll molecules create adsorption spectra that, in nature, limit a given species to a particular photic zone. Under laboratory conditions, the light requirements necessary for cultivation reflect this consideration. For example, the green and purple sulfur bacteria, such as *Chlorobium* and *Chromatium*, with adsorption peaks above 750 nm, are cultivated under the red wavelengths of tungsten light. Cultures, however, should not be placed too close to an incandescent light source because the heat emitted from the bulbs can quickly raise the temperature of the culture vessel beyond the upper growth limits for an organism. Cyanobacteria (e.g., *Anabaena*) adsorb blue wavelengths of light below 700 nm. This requirement can be satisfied by cultivating the bacteria under fluorescent tubes that emit light at this range of the visible spectrum. *Chemolithotrophic* organisms utilize inorganic compounds for energy. Examples within this second form of energy procurement are *Sulfolobus* spp., which oxidize elemental sulfur to sulfuric acid, and *Nitrobacter* spp., which biochemically exploit the oxidation of nitrites to nitrates. Numerous new genera and species of prokaryotic chemolithotrophs that obtain energy from various inorganic electron donors have been isolated in recent years, including *Archaeoglobus* spp., *Methanococcus* spp., and *Pyrodictium* spp. (10). Many obligate lithotrophs are inhibited by organically rich environments and are best cultivated under chemically defined media conditions.

Organotrophic organisms obtain energy more conventionally from organic compounds. As with the lithotrophs, organotrophs many be either phototrophic or chemotrophic. *Photoorganotrophs* are represented in nature by the anaerobically cultivated purple nonsulfur bacteria (e.g., *Rhodospirillum*), which utilize light in conjunction with organic compounds such as malate, pyruvate, or yeast extract, rather than O_2, as electron acceptors to release energy for growth and nutrition. *Chemoorganotrophs* encompass a vast number of organisms from all the microbial groups including archaea and bacteria, fungi, protozoans, and nonphotosynthesizing eukaryotic cells that obtain energy from the oxidation or other dissimilation of organic compounds.

20.2.3 Major Chemical Elements (C, H, N, O)

Unlike energy-procuring mechanisms, which vary widely between microbial genera and species, the anabolic or biosynthetic requirements of eukaryotic and prokaryotic cells are remarkably similar. Molecular mechanisms for intracellular communication and structural components share much chemistry whether they are bacterial *E. coli* cells or fungal *Aspergillus nidulans* cells. Whereas individual strains may vary in their ability to manufacture basic cell components and metabolites due to specific

mutations at points within biochemical pathways, all known organisms share the same basic cellular needs for carbohydrates, lipids, proteins, and molecular combinations thereof. The elements carbon, hydrogen, nitrogen, and oxygen can be regarded as major essential elements of nutrition because they contribute in significant percentages to the biomass of cells. These major elements may be required in the gaseous form, as organically fixed compounds, or both. Iron, magnesium, phosphorous, potassium, sulfur, and other elements, although critically important to sustained growth and metabolic activity, are often termed minor or trace elements in that they collectively represent less than 2% of cellular dry weight.

20.2.3.1 Carbon. Nutritionally, carbon appears in cellular metabolism in two forms: carbon dioxide gas (CO_2) and organic molecules. CO_2 is required by all organisms for a number of biochemical functions including tricarboxylic acid (TCA) cycling and de novo fatty acid synthesis from acetyl-CoA. Although much of the carbon dioxide is metabolically recycled throughout the cell's biochemical pathways, an initial exogenous source of carbon dioxide is mandatory. Autotrophic organisms readily assimilate atmospheric carbon dioxide; yet, also, all heterotrophic organisms have some ability to fix this compound, although at a much-reduced capacity. Microbial cultures will sometimes experience long lag periods when subcultured at low-volume inoculum into fresh media. This phenomenon is often attributable to suboptimal CO_2 tension, which the culture slowly corrects with cellular respiration before any significant increase in biomass can occur. The term *CO_2 sparking* refers to the sudden increase in bacterial growth observed when a freshly inoculated culture is briefly sparged with the gas. An enriched atmosphere of 5% CO_2 is used for the cultivation of clinical (particularly for fresh isolates) bacterial strains. CO_2 incubators are most efficient for multipurpose cultivations, but the anaerobic gas-pack CO_2-generating systems offered by BBL (Becton Dickinson Microbiology Systems, Cockeysville, Md.) or Difco (Difco Laboratories, Detroit, Mich.) are recommended for small volume or infrequent use. Depending upon the absolute requirement, capnophilic (CO_2-requiring) bacteria can also be cultivated in jars in which inoculated test tubes or agar plates are placed along with a burning candle. The candle jar is then tightly sealed while the candle continues to burn until free oxygen in the jar is consumed. The resulting atmosphere achieves approximately 2% CO_2. Both the anaerobic gas-pack systems and candle jars have draw backs with respect to increased risk of culture contamination. Respiring cultures give off significant amounts of water, which raises the humidity within the sealed jars. As the jars themselves are normally not sterile at time of culture incubation, any environmental bacterial or fungal contaminant within the jar will proliferate in the additional moisture. Capillary action of excess water at the culture vessel openings (particularly petri dishes) can draw contaminating organisms or their spores into the culture vessel.

Autotrophs can use carbon dioxide gas as a sole source of carbon for biosynthesis. Although autotrophy is often regarded by nonbacteriologists as synonymous with photosynthesis, autotrophy and phototrophy are quite independent metabolic functions. For example, methanogenic archaea (e.g., *Methanobacterium* sp.), while nonphotosynthetic, are capable of utilizing carbon dioxide and hydrogen as sole sources of carbon and energy. Yet, as noted elsewhere, purple nonsulfur bacteria are photosynthetic but rely upon organic acids for metabolic reducing power and, ultimately, as the carbon source for biosynthetic functions. Whereas autotrophy is widely represented among prokaryotes, the ability to utilize CO_2 as a sole carbon source is not a general characteristic of fungi. Among filamentous fungi, *Cephalosporium* spp. and *Fusarium* spp. have been documented to be able to do so under long-term cultivation (11).

Heterotrophs obtain carbon principally from organic molecules such as carbohydrates, amino acids, or lipids. For heterotrophs, a compound utilizable for its carbon often also functions as an energy source. Although glucose is widely assimilated by many heterotrophic microorganisms, it is not necessarily the universal carbon source for culture medium supplementation. Many bacteria, whether their characteristics are genuswide or species-specific, show little or no stimulation by glucose and preferentially utilize amino or other organic acids. The marine genus *Oceanospirillum* falls into this category as do many individual species within the diverse genus *Clostridium*. In an extreme example, *C. aminovalericum* (ATCC 13725) appears to be limited to δ-aminovaleric acid as its singular assimilable source of both carbon and energy.

Some organisms can alternate between autotrophy and heterotrophy, depending upon environmental and nutritional conditions. For these cultures, biomass vigor and yield are most often greater with heterotrophic rather than autotrophic conditions; however, secondary metabolites produced can vary considerably between the two conditions.

20.2.3.2 Hydrogen. Certain archaea and bacteria can grow by utilizing atmospheric hydrogen (H_2) as an electron donor and, depending upon the organism, assorted compounds including carbon dioxide, oxygen, nitrate, or sulfate as terminal electron acceptors (10). The hydrogen-oxidizing genus *Hydrogenophaga* (12) is facultative with respect to energy metabolism in that it functions chemoorganotrophically in a nutritionally heterotrophic aerobic environment by metabolizing various amino acids

or sugars for sources of carbon and energy. However, in an atmosphere containing 60% H_2, 10% CO_2, 25% N_2, and 5% O_2, the organisms switch to chemolithoautotrophic pathways. *Methanobacterium thermoautotrophicum*, a strictly anaerobic archeaebacteria, metabolizes hydrogen and carbon dioxide as sole energy and carbon sources to yield methane and water (methanogenesis). For the anaerobic methanogens as well as the aerobic hydrogen bacteria, conditions favoring autotrophy require a high (60–80%) concentration of hydrogen for cultivation. Under all conditions, work with compressed hydrogen gas should be conducted with adherence to pertinent laboratory safety practices. Lower concentrations of H_2 (3–10%) are frequently included in gas mixtures for the cultivation of anaerobic bacteria in gas-generating systems and glove boxes where, in the presence of a palladium catalyst, trace amounts of inhibitory molecular oxygen are chemically reduced to water. The final form of hydrogen required for nutritional purposes is the molecularly combined element required by all organotrophic cells. Combined hydrogen originates from the catabolic metabolism of organic compounds assimilated by a cell as carbon and energy sources.

20.2.3.3 Oxygen. As already noted for combined hydrogen, the bulk of combined oxygen within cells originates from the complex nutritional compounds, including water, assimilated by the cell. If a medium provides enough matter to satisfy the carbon and energy requirements of a culture, then the combined oxygen requirements will also be met. However, molecular oxygen (O_2) is an important, often growth-limiting, variable in microbial nutrition. O_2 is the primary terminal electron acceptor for many aerobic and facultatively anaerobic organisms. In oxygen-depleted or diminished environments, cells with no other biochemical mechanisms for exploiting alternative electron acceptors stop metabolizing and cease multiplying. Facultative organisms switch to fermentative pathways. In either situation, the biochemical activity of the cells, as well as the secondary metabolites produced, is significantly altered by oxygen starvation. Be it large-volume fermentors or small-volume chemostats or Fernbach flasks, the need for O_2 sparging in bulk cultivation vessels is regarded as a basic cultivation requirement for aerobic organisms (13). Be that as it may, one should also be aware that significant O_2 gradients quickly form in liquid test tube cultures, particularly for those cultures that form surface mats or pellicles of growth. Various micrometabolies can occur within the cell population in a standing culture along the O_2 gradients from surface to bottom of the test tube that might, if unrecognized, cause undue problems in scale-up development. Cultures with strong O_2-requirements (even for those that do not form pellicles) may not grow to very high density in a test tube because of the limited liquid–air interface. Better liquid growth of these test tube cultures is effected by incubating the tube at a slant to increase the surface area of the culture, or by shaking.

20.2.3.4 Nitrogen. Cells can assimilate nitrogen by two methods. Nitrogen fixation is the ability to acquire elemental nitrogen from the air and to molecularly combine the element into chemical forms utilizable for biosynthetic processes. The bacterial genera *Azotobacter, Bradyrhizobium*, and *Rhizobium* are most recognized for this characteristic, although some facultative anaerobes as well as anaerobic bacterial species also have the capacity. Fungi are not recognized as competent nitrogen fixers. Nitrogenase activity is induced with cultivation on nitrogen-free media. Growth on chemically defined "nitrogen-free" media might presumptively select for potential nitrogen fixers; however, trace amounts of nitrogen from agars, chemicals, and glassware are present in sufficient concentration to permit effective scavenging and growth (albeit, less than optimal) by many non-nitrogen-fixing organisms. Conclusive nitrogen fixation is best determined by the acetylene reduction assay (14).

The second, and most widely utilized, microbial mechanism for nitrogen procurement is via combined nitrogen assimilation from inorganic or organic molecules. Media formulations satisfy combined nitrogen requirements either with inorganic salts [e.g., NH_4Cl; NH_4NO_3 or KNO_3; $(NH_4)_2SO_4$] or from organic compounds (e.g., amino acids). The ability to utilize inorganic salts as a nitrogen source varies widely even within species. The chemolithotrophs as a group effectively utilize inorganic ammonium or nitrate salts as sole sources for nitrogen. For other organisms, the inability to grow under chemically defined medium conditions with ammonium or nitrate salts as a sole nitrogen source is due not so much to the inability to assimilate the ion directly from the medium or to incorporate it as the glutamine precursor to all subsequent biosynthetic nitrogenous pathways, but to the specific need for additional nitrogenous growth factors such as purines, pyrimidines, amino acids, or small peptides. These kinds of nitrogenous nutritional requirements are discussed in greater detail in the section "Growth Factors".

Nitrate is not a preferentially assimilated or utilized source of nutritional nitrogen for many bacteria or fungi; concentrations as low as 0.2% are inhibitory to the growth of some bacteria. However, the use of nitrate in energy metabolism as a terminal electron acceptor is a widely used mechanism among bacteria and is termed dissimilatory nitrate reduction or denitrification. The biochemical pathways involved with nitrate assimilation for cellular syntheses and for dissimilatory nitrate reduction are different. Nitrate reduction occurs with either aerobic or anaerobic bacteria. Strains of *Clostridium perfringens*, for example, utilize nitrate as an electron sink, which

causes a shift from butyrate to acetate fermentation and an increase in growth yield (15). All recognized species in the extremely halophilic genus *Haloarcula* are capable of using nitrate as a sole nitrogen source and, in addition, are strong denitrifiers with the ability to readily tolerate and reduce 3 M concentrations of KNO_3 under either complex or chemically defined media conditions; aerobic growth of haloarculas with liquid media lacking nitrate supplementation is markedly limited compared to aerobic growth in media supplemented with 0.2% KNO_3 (R. J. Cote, unpublished data, 1995).

20.2.4 Minor and Microelements (Fe, Mg, K, P, S, and Others)

Trace metal function and speciation have been extensively studied in bacteria and fungi (16,17). Nutritionally essential metal ions function metabolically as enzyme cofactors in membrane transport and in structural components. Microbial response to trace metals is detectable at extremely low concentrations (i.e., microgram or nanogram quantities, depending upon the metal). However, the bioavailability of a particular metal is markedly dependent upon proper speciation of the ion as it occurs in the culture medium (18). Depending on interaction with other medium components or methods of sterilization, metal valences can change to nonusable forms, or the ions can irreversibly bind as insoluble precipitates. Although problems with metal-binding phenomena are often directed toward the nutritionally essential metals, the potential for significant and irreversible binding of ions to media components must also be taken into consideration in studies of bacterial resistance to heavy metals. Reports of bacterial resistance to silver and selenium (19,20) could not be verified when the metals were added to culture media in a manner that eliminated their binding to peptones (R. J. Cote and R. L. Gherna, unpublished data, 1994). Similar observations made regarding media influence and metal sensitization of *Enterobacter cloacae* to silver sulfadiazine (AgSu) (21) are explained by heavy-metal binding under complex media conditions. Tilton and Rosenberg (22) discuss the issue of heavy-metal sequestration in a study of the effects of agar on silver inhibition.

Microelement supplementation is not normally required in media formulated with chemically complex components such as yeast extract or protein hydrolysate because the essential metals are naturally present in these materials in sufficient concentration to provide optimum culture growth and performance. Well-designed, chemically defined formulations include calcium, iron, magnesium, manganese, phosphorous (as phosphate), potassium, sodium, and sulfur (as sulfate) in the form of inorganic salts. Other micronutrients may be required in the medium, depending upon the nature of the metal function under study or, in the case of general culture propagation, the purity of the water and cleanliness of the glassware used to prepare the medium. Understanding of cell physiology, as well as any physical interactions within the culture system, is a basic requirement when working with nutritional trace metals. For example, although boric acid is often included in trace metal mixes, a boron deficiency is practically noninducible for cultures grown in borosilicate glass vessels because enough of the element leaches from the glass to satisfy nutritional needs. Table 20.1 lists metal mix formulations that are useful for chemically defined cultivation of numerous microorganisms. As noted elsewhere in this chapter, the use of tap water to satisfy trace element requirements is not recommended because regional and seasonal variability in water purity can introduce considerable ionic variation in a medium, with frequently deleterious results.

The whitish haze or precipitate that develops in some media upon standing or after autoclaving is frequently caused by imbalanced metal compositions. Divalent and trivalent cations (i.e., Ca^{2+}, Fe^{2+}, Fe^{3+}, and Mg^{2+}) will spontaneously bind with OH^- and PO_4^{2-} groups in the medium to form insoluble hydroxides and phosphate complexes. The condition is most evident at neutral to alkaline pH values and is intensified by heat, either boiling or autoclaving. Similarly, precipitation caused by metal binding to proteinaceous material in the medium

TABLE 20.1. Trace Metal Mixes for Bacteriological Media

Metal mix A: Balch's trace element solution

Nitrilotriacetic acid	1.5 g
$MgSO_4 \cdot 7H_2O$	3.0 g
$MnSO_4 \cdot H_2O$	0.5 g
NaCl	1.0 g
$FeSO_4 \cdot 7H_2O$	0.1 g
$CoCl_2 \cdot 6H_2O$	0.1 g
$CaCl_2$	0.1 g
$ZnSO_4 \cdot 7H_2O$	0.1 g
$CuSO_4 \cdot 5H_2O$	10.0 mg
$AlK(SO_4)_2 \cdot 12H_2O$	10.0 mg
H_3BO_3	10.0 mg
$Na_2MoO_4 \cdot 2H_2O$	10.0 mg
Distilled water	to 1.0 L

Suspend nitrilotriacetic acid in about 500 mL water and adjust to pH 6.5 with KOH pellets to dissolve. Add remaining salts one at a time. Bring final volume to 1.0 L with distilled water. Use 10.0 ml trace element solution per 1 L medium.

Metal mix B: modified Balch's trace element solution

To 1.0 L metal mix A add	
$NiSO_4 \cdot 6H_2O$	30.0 mg
Na_2SeO_3	20.0 mg
$Na_2WO_4 \cdot 2H_2O$	20.0 mg

These metals are included for the cultivation of methanogenic bacteria under chemically defined conditions.

Source: From Ref. 23, p. 158.

and darkening of chemically defined agar media are also frequently encountered in poorly designed or manipulated formulations. All of these adverse metal interactions are generally regarded as deleterious and growth limiting. Depending upon the composition of the medium, these kinds of chemical interactions can be eliminated by sterile filtration or separate autoclaving of inorganic salts and any phosphate buffers, and separate autoclaving of agar.

The use of chelating agents can also help to selectively maintain the solubility of polyvalent cations. Care must be taken when using powerful chelators such as ethylenediaminetetraacetic acid (EDTA) or nitrilotriacetic acid (NTA) because overchelation also depletes bioavailability of the metals. For microbial media, 0.5–2.0 mg/L EDTA or 15–150 mg/L NTA are reasonable concentrations. Mild chelation can be achieved with the use of specific amino acids (e.g., glycine, histidine) or carboxylic acids (acetate, citrate, succinate, tartrate). However, their use and concentration must be evaluated with respect to the function of the medium and the physiology of the microbial culture. For example, carboxylic acids are readily utilized carbon and energy sources for many microorganisms, and glycine is inhibitory at 1% concentration to many bacteria.

Under iron-deficient growth conditions, some bacteria produce and secrete chelators called siderophores to improve transport of ionic iron into the cell (24,25). Siderophores have been found in a number of diverse genera including *Aureobacterium (Arthrobacter) flavescens* (26), *E. coli, Klebsiella* (27), *Pseudomonas*, and *Mycobacterium avium* subsp. paratuberculosis (28). Other organisms rely upon the hemin molecule in blood as an easily assimilable iron chelate. A growth factor requirement for hemin is common among medically important bacteria. Hemin requirement (the X-factor) is diagnostic in the identification of *Haemophilus influenzae. Porphyromonas gingivalis* (29) and *Vibrio vulnificus* biotypes 1 and 2 require iron in the form hemin for growth and virulence (29,30). Whereas a number of classical media formulations (e.g., GC Agar) include crude hemoglobin as the source of the iron porphyrin molecule, use of hemin, instead, will produce a medium free of the heavy debris associated with hemoglobin. Hemin is used at a concentration of 0.5 mg/L medium. To improve solubility, initially suspend the compound in 1–2 mL 1 N NaOH, then add the hemin-NaOH solution to the bulk of the medium.

Many of the metals listed here that have been historically categorized as needed by microorganisms only in trace amounts have, in recent years, come to be evaluated on a different metabolic scale. Sulfur serves as an energy source for numerous species of bacteria, and thiosulfate seems to be utilized for energy by some fungi. While the role of sulfate as the terminal metabolic electron acceptor for the many anaerobic sulfate-reducing bacteria has been long recognized, new genera are currently being isolated that possess the ability to utilize one or more biologically important metals [(Fe (III), Mn (IV)], U (VI), and others] as terminal electron acceptors in biochemical dissimilatory metal reduction pathways (31). Because the function of terminal electron acceptor is not recyclable within the cell and bears a heavy metabolic load, the amounts of metal ion needed per liter for efficient energy transfer are orders of magnitude greater than those needed to satisfy trace element nutrition. One to four grams per liter is a guideline, depending upon the specific metabolism of the organism as well as the molecular weight and form of the metal salt selected for use.

20.2.5 Growth Factors

Given less than a dozen essential chemical building blocks and a source of metabolic energy to power the cellular machinery, some organisms, such as the wild-type *E. coli*, can synthesize every molecule needed for cell maintenance, growth, and reproduction. Many other microorganisms (even strains within the same species) are auxotrophic in that they have lost the ability to synthesize one or more key organic compounds essential to their physiology. These missing compounds are called growth factors and must be present in the culture medium if cell growth is to be vigorous, metabolically productive, and sustainable.

20.2.5.1 **L-*Amino Acids.*** L-Amino acids are common growth factor requirements for prokaryotes and eukaryotes. Many bacterial genera (e.g., *Lactobacillus* spp.) have multiple amino acid requirements. The requirement may be absolute or conditional and influenced by the presence and concentration of other amino acids (32–34). Similarly, a phenotypic amino acid requirement may disappear with the addition of an appropriate synthetic pathway intermediate. For example, a tryptophan "requirement" may actually be caused by a metabolic block earlier in the tryptophan pathway and might be satisfied by one of the earlier pathway intermediates (i.e., aspartic acid or indole). Because amino acids may share a common transport system, an excess of one amino acid can result in an increased need for a competing amino acid. Amino acid supplementation is not required in complex media containing peptones or other protein hydrolysates. In chemically defined media, the addition of 20–50 mg/L amino acid stimulates prokaryotic growth (100–200 mg/L for yeast), although adjustment of the concentrations is necessary for media optimization with multiple amino acid-requiring strains to chemically balance the formulation. The most notable exception is the requirement for glutamic acid, which, as precursor to all other amino acid biosyntheses, must be added at 200–500 mg/L to achieve

optimal growth of a bacterial culture. Amino acids, except glutamine, are stable with autoclave sterilization at the working concentrations used in media. Glutamine in aqueous solution will spontaneously break down with time to ammonium and pyrrolidone carboxylic acid residues. This reaction occurs more rapidly at elevated temperatures (37°C and above). The use of glutamine peptides in a medium can eliminate this problem, however, they are expensive for large-scale use. Concentrated stock solutions of amino acids may not be soluble, but neutralization of the stock solution with NaOH or KOH will increase solubility with the formation of amino acid salts for many of these compounds. Stock solutions of cysteine will autooxidize to cystine unless stored anaerobically (e.g., under N_2).

For many years, the perceived need by bacteria for combined amino acids (peptides or proteins) was satisfied by the argument that peptide transport utilized different systems than did amino acids; thus, the need for a specific peptide was actually an alternative cellular method for obtaining a specific amino acid contained within that peptide via a biochemically noncompetitive mechanism. However, increased knowledge of the role of peptides in protein trafficking suggests that peptide auxotrophies can affect cellular physiology and communication (35). Successful laboratory cultivation of *Thermoplasma acidophilum*, having no other known growth factor requirements, is dependent upon specific lots of powdered yeast extract containing a methanol-soluble growth factor, which purification revealed to be a small 1,000-MW peptide (36). Similarly, recent laboratory cultivation of *Treponema maltophilum* also included the requirement for a methanol-soluble growth factor from yeast extract (37). The treponeme requirement has not been further purified. Finally, successful cultivation of the protozoan *Entamoeba histolytica* in complex media enriched with peptone, vitamins, and serum is nevertheless dependent upon an unknown growth factor found only in certain lots of powdered yeast extract (38). Whether the elusive yeast extract growth factor is the same for all these metabolically dissimilar organisms or whether the relatively gentle methods used in the manufacture of yeast extract simply yield a large pool of assorted intact peptides possibly required by some microorganisms poses an interesting question.

20.2.5.2 Whole Proteins. Whole proteins (e.g., albumin, blood, egg, meat, serum) are not known to be essential requirements for microbial growth, although they are an integral medium component for many nutritionally fastidious microorganisms. Clinical isolates of mycobacteria have been historically cultivated with Lowenstein–Jensen medium, containing whole egg and inspissated (coagulated by heating at 80–85°C for 45 min) to form a solid matrix (39). Most mycobacteria, however, can be effectively cultured with Dubos medium or Middlebrook 7H9/or 7H10 media, in which the egg protein is replaced by the more defined components bovine serum albumin, catalase, dextrose, and oleic acid (40). Variations of chopped meat media (2) were for many years the recommended formulations for cultivation of pathogenic clostridia and similar bacteria, yet many of these strains give equal cell yield with the more defined, and more easily prepared, Reinforced Clostridial medium (40), although this basal medium frequently requires the addition of hemin and/or vitamin K_1 to satisfy the growth factor requirements of some strains; additionally, 0.5% cellobiose added to reinforced clostridial medium will enhance the growth of cellulolytic clostridia.

Defibrinated rabbit or sheep blood (5–10% v/v) is a common addition to media used for the cultivation of microorganisms pathogenic to animals. Human blood is not recommended for use for microbial culture work for health safety reasons and also because outdated blood obtained from banks is normally citrated. Citrated blood of any type should not be used in culture media because the anticoagulant may have negative effects on culture growth or hemolytic reactions. Although diagnostic hemolytic reactions differ between rabbit and sheep bloods, the ability to support microbial growth is generally the same. Human or sheep bloods, unless chocolated, are not used for the cultivation of *Haemophilus* spp. or other organisms requiring NAD because these fluids contain enzymes that inactivate the growth factor. Chocolate blood agar is prepared by heating the medium containing blood to 70–80°C for 15 min. Purchase of whole animal blood should be from a reputable supplier and pooled from animals on an antibiotic-free diet. Well-collected and processed defibrinated blood is free from clots and cell lysis. Although commercial blood suppliers carefully collect their products, each lot of blood should be checked for sterility prior to use. Not all types of bacterial contaminants found in blood will grow well in either of the U.S.P.-recommended sterility test media (i.e., Fluid Thioglycollate and Soybean–Casein Digest). To broaden the screening procedure, the battery of media should be enlarged to include Brain Heart Infusion (BBL 11059 or Difco 0037) to enhance the recovery of somewhat fastidious contaminants, as well as HTYE (Trypticase peptone (BBL), 0.5%; yeast extract 0.2%; HEPES, acid, 0.4%; adjust to pH 7.2 ± 0.1 prior to sterilization at 121°C for 15 min), which has wide versatility in the ability to cultivate diverse environmental heterotrophic organisms that do not grow well with conventional, general bacterial growth media. Whole blood should be stored under refrigeration (not frozen) and should be incorporated into media as soon as possible to help stabilize the fluid. Whole blood can not be stored longer than 2–3 weeks without significant deterioration. However, when stored at 4–8°C,

media containing blood can, for most media purposes, have a 4-month shelf life.

Serum (5–10% v/v) is an alternative to blood for the cultivation of pathogens. Horse, fetal, or newborn bovine sera are most frequently used for the cultivation of bacteria, whereas adult bovine serum is specified for the cultivation of many pathogenic protozoans. Sera vary in their intrinsic enzyme activity. For example, horse serum degrades glutamine, a necessary component in many animal cell line media formulations, and as already noted for chocolatizing whole blood, sheep and human blood can inactivate NAD. Preparation instructions for many media formulations call for serum heat inactivation (incubation of the serum at 56°C for 30 min) to inactivate the protein complement. This temperature may not be high enough to eliminate adverse serum enzyme activity. Conversely, heat inactivation may not be a universally advantageous specification for all microbial growth and performance. A researcher should investigate types of sera as well as the effects of heat inactivation upon the performance of a microbial culture.

Whole proteins and their hydrolysates supply an eclectic and undefined mix of nutrients, detoxifiers, and other molecules that slowly release or absorb metabolites that may be required for cell nutrition in small amounts but quickly become toxic at elevated levels (e.g., fatty acids). Proteins hydrolysates supply a myriad of nutritional growth factors and help control physical parameters such as pH and osmolarity.

Be that as it may, the use of proteins and their derivatives in media formulations is becoming problematical with respect to biotechnology for two reasons: (*1*) Because many of the products of interest produced by microorganisms are proteins or substances with chemical affinity to proteins, presence of a complex proteinaceous medium component can significantly complicate a product purification process. (*2*) Biotechnology applications under regulatory compliance are facing increasing scrutiny about the potential presence of unidentified adventitious agents in media components. The international concern with bovine spongiform encephalopathy (BSE) is real and pervasive throughout the field of biotechnology, ranging from final product, to the type and source of medium components used in the preparation of a frozen or lyophilized master cell bank used in the manufacture of a product.

The European Commission decision 97/534/EC bans the importation of specified risk materials (SRM) into the European Union member countries (including Australia, Canada, and New Zealand). U.S. biotechnology companies wishing to deal with the European market must be able to provide a declaration to customs agents that assures their product does not contain, nor is derived from, the specified SRM as defined in 97/534/EC. The specified risk material, in this instance, is defined as "the skull, including the brain and eyes, tonsils and spinal cord of bovine animals over 12 months, ovine and caprine animals which are over 12 months or have a permanent incisor tooth erupted through the gum, and the spleen of ovine and caprine animals" (41).

Many of the peptone hydrolysates used in biotechnology are of animal (bovine) origin and are manufactured from "leftovers" of the slaughterhouse trade. As large-scale animal processing is not a clean operation, SRM contamination of raw material used in the manufacture of peptones is probable, particularly where source material is not directly traceable to government-regulated, clean herds.

The degree of concern with animal peptones with respect to 97/534/EC varies with industry and product. For example, from a regulatory perspective, the manufacture of biopharmaceuticals, especially direct injectables, demands high scrutiny for presence and elimination of any SRM. But the use of an animal peptone in a medium used solely for clinical diagnostic purposes (e.g., a peptone used clinically in MacConkey agar to differentiate *E. coli* from other normal intestinal flora), might be of lesser concern because the peptone never comes in direct contact with animals or humans at risk to BSE or similar prion agents. Acid-hydrolyzed animal peptones are generally of lower risk than enzymatic hydrolysates because the acid and heat associated with acid hydrolysis inactivates viral agents. Ultrafiltration of peptone solutions and sera has been proposed as a mechanism for eliminating possible BSE contaminants as well as reducing endotoxin levels. In any event, the concern with BSE and related animal/human pathogenic agents has caused an escalation of documentation requirements for the tracking of animal-derived media components. Certificates of origin for sera, meat, and milk peptones can, and should, be obtained from reputable vendors of these materials. Although certificates of analysis are now routinely supplied by raw material vendors to the biotechnology industry, certificates of origin are currently customer driven and are generally supplied only as requested.

BSE has fostered much current interest in the development of nonanimal peptones. With yeast, soy, or wheat as the source protein, some of these "veggie peptones" have interesting nutritional attributes but, nevertheless, still suffer the drawback of elevated intrinsic carbohydrate levels characteristic of plant peptones.

Difficulties in medium optimization and performance currently preclude wide use of serum-free or SRM-free media with animal cell lines. However, design of SRM-free media for most bacteria and yeast are feasible and cost-effective.

20.2.5.3 Vitamins. Vitamins are biochemical catalysts and appear in cellular metabolism as coenzymes or as the prosthetic group of enzymes. Vitamins elicit microbial growth response at very low levels, at nanogram concentrations for vitamins such as biotin and cyanocobalamin

(vitamin B_{12}). Although many microorganisms are capable of synthesizing all of the required vitamins, many others are auxotrophic for one or more of these growth factors. The genus *Lactobacillus* characteristically has multiple vitamin requirements, and several strains within the group were widely used for many years in protocols for vitamin assays until replaced by instrumentation-based methodologies. The U.S.P. 23 still retains *Lactobacillus delbrueckii* subsp lactis (*L. leichmannii*) (ATCC 7830) as the assay organism for vitamin B_{12}. Marine bacteria frequently require B_{12}, whereas thiamine and biotin are necessary for the growth of many mycelial fungi. Menadione or its more active form, vitamin K_1, is a supplement for the cultivation of some clinical anaerobic bacteria. As noted with amino acids, a shift in medium composition can spare the need for a specific vitamin. *E. coli* (ATCC 10799; NCIB 8134) requires vitamin B_{12} when cultivated with a chemically defined minimal medium; when grown in the presence of 20 μg/mL methionine, the vitamin requirement is eliminated (42). Vitamin auxotrophies can appear as a need for the vitamin precursor, the intact vitamin, or as conjugates in coenzyme form. Koser noted, many years ago, that vitamin and amino acid auxotrophies in thermophilic bacilli are temperature variable (43). NAD and cocarboxylase (thiamine pyrophosphate) are coenzymes required by many pathogenic bacteria.

All of the vitamins are water soluble and heat stable at working concentrations used in media; coenzymes should be filter sterilized, as should concentrated vitamin stock solutions. Most vitamin stock solutions remain water soluble in significant concentrations, although biotin, folic acid, nicotinic acid, and riboflavin require neutralization with NaOH to retain solubility of the concentrate. Vitamin K and thioctic acid stock solutions are ethanol soluble. Ascorbic acid, used in microbial cultivation as an antioxidant, has a short life (about 3 weeks) in media; use of ascorbate salts rather than the free acid will improve stability. Table 20.2 lists a complete vitamin mix for the cultivation of bacteria and fungi. Yeast extract at a concentration of 0.1–0.5% is used as an undefined vitamin supplement for microbial growth in complex media; however, concentrations of yeast extract as low as 0.05% can elicit growth stimulation by organic growth factors, which may or may not be vitamins.

20.2.5.4 Nucleic Acid Precursors. Nucleic acid precursors are often required by nutritionally fastidious organisms when cultivated in defined or semidefined media. In some instances, the purine or pyrimidine will satisfy the requirement; more commonly, an organism needs preformed nucleosides or nucleotides. Organisms with these types of synthetic deficiencies will show a growth response to 5–50 μg/mL filter-sterilized additive.

20.2.5.5 Lipids. Lipids or their precursors are required by diverse organisms. Some pneumococci have a unique requirement for choline as a lipid precursor. *i*-Inositol is a structural component of some phospholipids. Inositol-deficient strains of *Neurospora crassa* and *Saccharomyces cerevisiae* have been used in studies of phospholipids and cell membrane structure. Fatty acids stimulate the growth of some fungi; certain mutants of *N. crassa* are auxotrophic for fatty acid synthesis (45). Rumen bacteria require short-chain fatty acids for growth. Many mycobacteria have a generalized requirement for exogenously supplied lipid. Various media formulations for nonglycerophobic mycobacteria include 2.0 mL/L glycerol, 0.05 g/L oleic acid, or 0.5 g/L Tween 80 to satisfy this requirement. Most of the bacterial mollicutes (anaeroplasmas, mycoplasmas, and spiroplasmas) require sterols. Cholesterol is a prevalent component in semidefined media formulations for these organisms, whereas fetal calf or horse serum supplies the growth factor in general-use complex mycoplasma media. *Eubacterium coprostanoligenes* (ATCC 51222) and *Eubacterium* sp. (ATCC 21408) represent a novel group of bacteria that use cholesterol and similar sterols as terminal electron acceptors (46,47). The former organism does not require cholesterol but metabolizes and requires phosphatidylcholine for growth, whereas the latter requires cholesterol as well as an alkenyl ether lipid for growth. These bacteria have been used in probiotic studies on decreasing the level of cholesterol in the digestive tract. All the lipids just mentioned are stable to autoclave temperatures. Short-chain fatty acids are water soluble; higher molecular weight lipids are soluble in less polar solvents such as ethanol or chloroform. In the presence of other media components at alkaline pH, some high-weight lipids can form growth-limiting soapy complexes. Separate sterilization of the fatty compounds helps to alleviate the problem.

20.2.5.6 Polyamines. Polyamines (e.g., putrescine, spermidine, spermine) are formed via the arginine pathway

TABLE 20.2. Balch's Vitamin Solution

p-Aminobenzoic acid	5.0 mg
Folic acid	2.0 mg
Biotin	2.0 mg
Nicotinic acid	5.0 mg
Calcium panothenate	5.0 mg
Riboflavin	5.0 mg
Thiamine HCl	5.0 mg
Pyridoxine HCl	10.0 mg
Cyanocobalamin	100.0 mg
Thioctic acid	5.0 mg
Distilled water	1.0 L

Mix all vitamins in distilled water. Adjust to pH 7.0, if necessary, to dissolve. Filter sterilize and store in brown bottle with refrigeration.

Source: From Ref. 44, p. 160.

and have undefined functions in the cell. Research on polyamines has been done principally in vitro where the compounds bind to and neutralize charges on DNA and RNA. Although high concentrations of Mg^{2+} exert the same general ionic neutralization effect, only polyamines have the ability to influence correct tRNA conformation. Much of the cellular polyamine appears bound to ribosomes. In *E. coli*, putrescine and spermidine account for half the total product of the arginine pathway (48). Polyamine supplements as growth stimulants appear in media for the cultivation of *Ureaplasma urealyticum* (2 p. 530), *Haemophtlus parainfluenzae* (49), *Veillonella atypica* (50), and other bacteria. Where complex media are used, there is generally a sufficient polyamine content in yeast extract to satisfy the requirements of deficient strains.

20.2.5.7 Unique Growth Factors. Any organism has the possibility to, either spontaneously or through human intervention, develop mutations in biosynthetic pathways. Thus, unusual or strain-specific growth factors are always a consideration in the development of media for "unculturable" organisms. Deliberate mutation for the inability to synthesize the cell wall component diaminopimelic acid was engineered into early recombinant host strains of *E. coli* as an attenuation factor to reduce the possibility of survival outside of laboratory cultivation. Until recently, *Bacteroides forsythus* had only been culturable in cocultivation with other oral anaerobic bacteria, until its requirement for *N*-acetylmuramic acid was recognized (51). As noted earlier for the L-amino acids, the inability to synthesize functional signal and transport peptides may be limiting factors in the protein chemistry of some organisms.

20.3 PHYSICAL PARAMETERS

20.3.1 pH

pH is a strong selection factor for microorganisms. Although most bacteria have a wide pH range (±3.0 pH units) at which measurable growth occurs, optimum growth is limited to a narrow range. Minimum and maximum pH values can often be distinct and sharply defined. Members of the genus *Bacillus* will grow at pH 6.8 but not at pH 6.5. Extreme halophiles with a biomass yield optimum at pH 7.4 continue to grow slowly at pH 7.0 and exhibit little or no growth below pH 6.7. Eukaryotic and prokaryotic organisms shift their biochemistry according to the pH of their environment and thus change cellular characteristics as well as metabolic by-products. Such changes in cultivation parameters can be consciously directed toward a particular application such as secondary metabolite production. Unfortunately, the effects of pH shifts are too often not critically examined, particularly at the small-scale cultivation stage. For example, in an unbuffered test tube culture of anaerobic carbohydrate-fermenting clostridia, acid production can quickly drop the medium to below pH 4.0, well outside the pH minimum of 6.5 necessary for significant growth. Either the culture will sporulate (if medium conditions are conducive to the process) or viability quickly diminishes as acid concentration increases. Effective media design must be constructed around the pH at which the medium is developed and will be used. Radical adjustment to media naturally posed at a particular pH too often leads to precipitation of components or other problems with performance. Inclusion of buffers, as well as the types of buffers used, are important considerations in media design.

20.3.2 Incubation Temperature

Incubation temperature influences microbial metabolism both with respect to the rates at which cellular processes run and the rates at which nutrients are assimilated. Strains of *Serratia marcesans* produce pink-pigmented colonies at 26°C but are colorless or slow to produce pigment at 37°C. Temperature effects may sometimes be subtle. Bacteria alter the fatty acid compositions of their phospholipids according to temperature. The proportion of low-melting-point fatty acids increases as growth temperature decreases (52,53). Organisms may display fairly broad temperature tolerances within a range, but as with pH, optimum growth range is fairly narrow. Psychrophiles characteristically exhibit efficient metabolic rates at temperatures below 15°C; the obligate psychrophilic bacterial species *Colwellia psychroerythrus* has a temperature optimum around 10°C and lyses above 20°C (54). Mesophiles are active between 20°C and 40°C. Free-living environmental strains are more tolerant of wider temperature ranges than are pathogenic strains that effectively function within only a few degrees of the body temperature of their hosts. Thermophilic microorganisms exist at temperatures above 40°C. Although some fungi (e.g., *Mucor miehet* and *Sporotrichum thermophile*) can grow at temperatures as high as 50°C, extreme thermophily, characterized by the ability to metabolize at temperatures above 70°C, is restricted to members of the archaea and, to a lesser extent, the bacteria.

20.3.3 Oxidation–Reduction Potential

Oxidation–reduction (redox) potential of the culture environment determines the ability of a microorganism to initiate growth. Redox values of media and respiring cultures are measured with a pH meter set to the millivolt (mV) mode and a platinum electrode. Aerobic organisms require positive millivolt conditions. Obligate microaerophiles require 0 to −100 mV; clinical anaerobes

less than −100 mV; obligate and extreme anaerobes less −200 mV. Actively metabolizing anaerobic cultures can drop redox levels below −300 mV. Media for obligate microaerophiles and anaerobes include reducing agents to lower the redox potential to a range optimal for a culture inoculum to be able to initiate metabolic activity. Subsequent cellular growth will maintain an overall redox condition reflecting the varying metabolic activities of the culture. Organic matter such as meat particles, yeast extract, and reducing sugars exert reducing effects in a medium. Filling a culture vessel almost to capacity with medium or adding 0.2% agar to the medium to retard diffusion of O_2 will be adequate to culture less fastidious microaerophiles. Anaerobic organisms with more stringent redox requirements need one or more chemical reducing agents included in the growth medium. Frequently used reducing agents, listed in terms of approximate redox potential in millivolts, include sodium thioglycollate (−100 mV), cysteine hydrochloride (−210 mV), titanium (III) citrate (−480 mV), sodium sulfide (−571 mV), and sodium dithionite (−600 mV). The overall redox level of a medium containing any of these reducing agents will, of course, be dependent upon the chemical interactions of all media components as well as the reducing agent. Media chemically reduced with any of these compounds should not be allowed to reoxidize, because the chemical structure of the reducing agents can be irreversibly altered by oxidation and lose effectiveness; in some instances, the oxidized forms of reducing agents can be toxic to cells (55). For some strict anaerobes cultivated under chemically defined conditions, it is best to add the reducing agent just prior to inoculation because reduced conditions are difficult to maintain under prolonged media storage. Ljungdahl and Wiegel (56), Breznak and Costilow (57), and Balch *et al*. (58) provide excellent detailed instructions for the cultivation of strict anaerobes.

20.3.4 Detoxifiers

Detoxifiers are required for the cultivation of some fastidious microorganisms. In the natural environment, metabolic by-products released by some organisms are enzymatically neutralized or utilized by other organisms for nutritional or other biochemical needs before the compounds accumulate to toxic levels. In vitro, for a pure culture lacking the appropriate enzymatic mechanisms to neutralize its own metabolic wastes, these metabolites can build to inhibitory concentrations before significant culture growth has occurred. The inability to break down hydrogen peroxide by organisms lacking catalase, and strain sensitivity to fatty acid accumulation are two common problems associated with metabolite accumulation in closed culture conditions. To cultivate these types of microorganisms, some media require the addition of detoxifiers, of which most are absorbents. Frequently utilized detoxifiers include blood/serum, bovine serum albumin (BSA, fraction V), catalase, and charcoal. More recently, liposomes have been utilized to slowly release lipid growth factors to deficient organisms, thus eliminating the toxic effects that a full "dose" of a medium lipid supplement would have for these organisms (59). Similarly, cylodextrins have been shown to effectively chelate and then slowly release potentially toxic, yet essential, nutrients for some clinical bacteria under semidefined growth conditions (60,61).

20.4 MEDIA DESIGN AND COMPOSITION

Optimal growth and performance of a microbial culture is most influenced by the design and composition of its growth medium. There is no one "best" medium for a particular application; however, there exist many examples of poorly designed and/or poorly manipulated media, or well-designed media being used for an inappropriate purpose, in which a microorganism manages to survive in spite of the medium and not because of it. Effective media design comes from an understanding of an organism's biochemistry and physiology, as well as the nutritional ecology of the environment from which the organism was isolated. Although isolation media are selective and frequently nutritionally suboptimal to limit the growth of unwanted organisms, general growth or maintenance media should provide conditions to sustain a culture at optimal morphology and physiology through repeated subcultures. Under microscopic examination, bacteria grown under favorable conditions do not have a misshapen or shriveled appearance; cell inclusions are generally minimal or absent; and cell lysis and/or spheroplast development is minimal or absent. At logarithmic phase of growth, motility is detectable for motile strains. Depending upon its application, a medium may be further defined in terms of chemical composition or optimized to increase biomass or cell product yield. An organism exhibiting optimal growth in a nutritionally balanced maintenance medium may not give high yields of a much-wanted metabolic by-product. Thus, medium optimization is a process directed toward a specific application. With so many nutritional and physical variables impacting upon microbial physiology, attempts at media optimization can become unnecessarily expensive, time-consuming, and largely unproductive when blindly tackled one variable at a time. Statistical methods using modified factorial approaches have been developed to aid in systematic media optimization for large-scale development (62), but for general laboratory purposes, knowledge and understanding of an organism's metabolic pathways and physical growth parameters can indicate specific areas in which quick design improvements to an existing formulation can effect significant results.

Media formulations may be chemically defined, in which discrete compound identity and concentration of all components are known, or chemically undefined, in which ingredients include one or more chemically complex substances such as protein hydrolysates and extracts. The choice of defined or undefined medium is dependent upon its application. Chemically defined media are useful in biochemical or metabolic studies of organisms. These types of formulations are also sometimes used in large-scale bacterial or yeast fermentations to produce products which further require stringent purifications such as those from recombinant DNA technology. General laboratory growth media for heterotrophic microorganisms as well as industrial media for large-scale production of metabolites (e.g., antibiotics, alcohols and other solvents) are often chemically complex. Scale-up of any medium formulation must include considerations of availability, cost, performance and lot-to-lot reproducibility of components as balanced against the value of the product. Chemically defined media can be expensive, particularly if the ingredients include a lengthy list of growth factors.

Microorganisms can transport only small molecules across their membranes. Large molecules (e.g., DNA, starch, proteins) can be nutritionally utilized by a microorganism only if it can synthesize and secrete the appropriate extracellular enzymes to digest large molecules into subunits small enough for assimilation into the cell. Because this type of enzymatic activity is absent from many organisms, in vitro microbial cultivation relies upon predigested macromolecules in the form of hydrolysates, peptones, and extracts and simple carbon compounds as nutritional substrates.

20.4.1 Protein Hydrolysates (Peptones)

Protein hydrolysates supply a mixed source of nitrogen and growth factors in the form of amino acids, nucleic acid fractions, peptides, and salts to a complex growth medium. For organisms possessing the metabolic capacity, protein hydrolysates can also serve as complex carbon and energy sources. Industrial large-scale fermentations using bacteria and fungi effectively use by-products from other industrial processes as proteinaceous material for media, including cottonseed, yeast, and soy. Although these substrates are chemically undefined, published analyses of their nutritional content greatly help in determining the appropriateness of a product for inclusion in a medium (63). Manufacturers of refined media and media components offer water-soluble products with more controlled nutritional composition. Table 20.3 lists and briefly describes the extracts and hydrolysates frequently encountered in microbiological laboratory media. Meat, milk, and soy commonly serve as starting material for the manufacture of hydrolysates. Digestion of these proteins can be by acid, alkali, or enzymatic hydrolysis. The source protein and method and degree of hydrolysis determine the nutritional characteristics of a hydrolysate. Prolonged hydrolysis releases free amino acids; more gentle hydrolytic processes yield mixtures of amino acids and peptides. The strong conditions of acid or alkali hydrolysis destroy much intrinsic

TABLE 20.3. Hydrolysates and Extracts

Hydrolysis method	Source	Product/manufacturer[a]	Characteristics
Acid	Casein	Acidicase (BBL) Casamino acids (Difco) Hy-Case (Sheffield)	Free amino acids; deficient in tryptophan and cystine; high intrinsic salt concentration unless designated salt-free
Enzymatic	Casein	Casitone (Difco) NZ-Amine (Sheffield) Trypticase (BBL)	Free amino acids and small peptides; high levels of tryptophan; low in carbohydrates
Enzymatic	Meat	Myosate (BBL) Thiotone (BBL) Primatone (Sheffield) Peptone (Difco) Proteose peptone (Difco)	Mixtures of amino acids and peptides; those designated proteose are hydrolyzed for a high peptide content; Thiotone high in sulfur
Enzymatic	Plant	Phytone (BBL) Soytone (Difco) Hy-Soy (Sheffield)	High in carbohydrates and vitamins
Mixed	Yeast/casein	Biosate (BBL)	Combines amino acids as well as vitamins lost during protein hydrolysis of peptones
	Casein/meat	Polypeptone (BBL)	
Autolysis	Yeast	Yeast extract (BBL; Difco; Sheffield)	High in amino acids, peptides, water-soluble vitamins, and carbohydrates

[a]Items listed are representative of a manufacturer's product line. Consult manufacturers' technical manuals for more information, Refs 39, 40, and 64.

vitamin content of a raw protein, as well as some amino acids such as tryptophan, and reduce the levels of serine and threonine. Acid-hydrolyzed protein hydrolysates are high in salt content formed during the neutralization step; however, some manufacturers feature acid-hydrolyzed peptones with additional processing to reduce the amount of salt [e.g., Casamino Acids (Difco 0230)]. Enzymatic digests contain free amino acids as well as small peptides while maintaining the vitamin content of the original source material. Enzymatic casein digests, reflecting the amino acid composition of the starting material, are high in tryptophan and low in cystine. Peptones from plant proteins [i.e., Soytone (Difco); Phytone (BBL)] contain intrinsic carbohydrate and, while conducive to rapid heterotrophic growth, can cause quick culture decline due to substantial metabolic acid production. Because of the carbohydrate level, plant peptones are also unsuitable in basal media for fermentation or sole carbon source utilization studies. For routine growth, peptones are normally added to media at concentrations of 0.5–1.0%. Growth of microorganisms with diverse and multiple nitrogenous auxotrophies (e.g., the lactobacilli) is enhanced by elevated peptone concentrations as well as nutritional supplementation with peptones of mixed sources and degrees of hydrolysis.

20.4.2 Carbon and Energy Sources

Microorganisms other than autotrophs require organic compounds as a source of carbon and energy. These can include simple sugars, complex carbohydrates, alcohols, amino and other organic acids, and short-chain lipids. Some organisms (e.g., *Aspergillus, Pseudomonas*) possess the complex metabolic machinery that permits numerous classes of organic compounds for carbon/energy substrates. Other taxa exploit specific classes of molecules metabolically ignored by or toxic to general heterotrophs. Methylotrophs (*Methylobacterium* spp., *Methylomonas* spp., *Methylophaga* spp., and others) can extract energy from C_1 compounds such as methanol and formaldehyde, whereas the metabolic diversity of the bacterial genus *Pseudomonas* has allowed selection of strains that can utilize the long-chained hydrocarbons in crude oil or attack the degradation-resistant chemical rings of cresols and phenols as sole carbon/energy sources. Assorted fungal genera (*Cladosporium, Candida*, and others) have been found as actively growing contaminants in aircraft and diesel fuels (65). The type and concentration of a carbon substrate present in a medium will affect overall growth rates, morphology, and metabolites of a culture. Sole carbon utilization profiles are used in identification matrices for prokaryotes and yeasts.

Carbohydrates and related compounds are preferential carbon sources for many genera of microbes. Hexoses are most diversely utilized, followed by the disaccharides, trisaccharides, smaller polysaccharides (starch and glycogen), and pentoses. Glycerol, mannitol, and sorbitol are commonly utilized alcohols. Under laboratory conditions with defined media and mixed sugars at normal substrate levels (e.g., 2–10 g/L), microorganisms often exhibit diauxic growth, in which a culture first utilizes the carbon compound that supports the greatest rate of growth, with concurrent catabolic repression of other substrates (66–68). Enzyme systems then shift accordingly as the organism switches to and consumes each less-preferential carbon compound. This results in a biphasic growth curve. However, under carbon-limited (e.g., microgram to milligram per liter concentrations) chemostat conditions that mimic the low-nutrient conditions of the natural environment, a number of organisms use the components of carbon mixtures simultaneously (69).

Proteolytic organisms have the capacity to utilize L-amino acids and related compounds as sole carbon/energy sources. This metabolic characteristic is more common among bacteria than fungi and varies widely between species; identification keys for the genus *Clostridium* use saccharolytic versus proteolytic metabolisms for species differentiation. As a group, the helical/vibroid Gram-negative bacteria (e.g., *Aquaspirillum, Azospirillum, Camplylobacter, Oceanospirillum*) do not ferment or oxidize carbohydrates but satisfy carbon/energy requirements with amino acid catabolism. *Legionella* spp. also use amino acids as carbon/energy sources. Filamentous fungi vary in their ability to utilize amino acids as effective carbon sources; none, however are limited to nitrogenous sources of carbon. Glutamic acid, alanine, arginine, and proline are frequently utilized by many prokaryotes and yeasts. The aromatic rings of the amino acids tryptophan, phenylalanine, and tyrosine, as well as the purine and pyrimidine rings of the nitrogenous bases, are not readily attacked by many organisms. The ability to do so is used for taxonomic speciation. Degradation of any of these ring compounds, however, is not presumptive of an organism's ability to further use the breakdown products as a sole source of carbon/ energy; in many cases, the compound is not so metabolized. Organisms that catabolize amino acids frequently utilize organic acids in the same fashion (e.g., *Oceanospirillum*). In addition, many carbohydrate-utilizing organisms are also capable of utilizing organic acids. For example, citrate and propionate utilizations are classical tests in the identification of the carbohydrate-metabolizing genus *Bacillus*. When used as sole carbon and energy sources, amino and organic acids may not be soluble at required substrate levels (2–5 g/L); however, neutralization with KOH or NaOH will form soluble salts of these compounds.

Some organisms have the capacity to utilize fatty acids and other nonpolar molecules as carbon and energy sources. In some instances, the requirement is absolute.

The bacterial genus *Leptospira* requires long-chain fatty acids (70), which are supplied in complex growth media by rabbit serum. The anaerobic sulfate-reducing *Desulfovibrio* sp. (DSM 2056) oxidizes the fatty acids butyrate through stearate (71).

Simple sugars and other carbon compounds can undergo chemical changes when autoclaved with other media components. Amino acids and organic acids, though heat stable at growth factor levels, may degrade at substrate concentrations. The characteristic darkening of autoclaved media containing glucose and peptones, called the Maillard reaction, is caused by an interaction of amino acids with the glycosidic hydroxyl group of the sugar. Darkening of autoclaved media can also be caused by the interaction of mono- and disaccharides, particularly glucose, with phosphates; the reaction is more intense at alkaline pH. Carlsson *et al*. (72) demonstrated that the glucose–phosphate reaction produces hydrogen peroxide at levels toxic to catalase-negative organisms. These types of adverse chemical reactions between nutrient components compromise the performance of a medium and are to be avoided either by autoclaving or filter sterilizing the reactive compounds separately from the balance of the medium. Not all commonly used carbon substrates can withstand autoclave sterilization. In particular, arabinose, fructose, lactose, pyruvate, ribose, and xylose should be filter sterilized. Light-weight alcohols and similar solvents are volatile at autoclave temperatures. Autoclaving of heat-stable alcohols can be done in tightly stoppered containers; alternatively, these compounds can be sterilized with appropriate solvent-resistant membrane filters. Long-chain hydrocarbons (e.g., oils and waxes) are hydrophobic and are not sterilizable by autoclaving because the sterilant (steam) cannot adequately penetrate the material. A good chemical reference text, such as the *Merck Index* (73), is invaluable for determining the heat stability, solubility, and other important characteristics of many chemical components used in media formulations.

20.4.3 Extracts

Spray-dried powders derived from infusions of meat, yeast, or other chemically complex proteinaceous materials provide a nutritionally useful but undefined source of water-soluble growth factors and sugars. Because they are not subject to the same harsh conditions as those used in the manufacture of peptones, meat or yeast extracts can supply those nutrients lost during the peptone hydrolysis (e.g., vitamins and certain amino acids). Extracts, in themselves, do not contain sufficient concentrations of essential nitrogen or carbon compounds to effectively function as the sole source of these nutrients in a medium. Meat extracts include appreciable amounts of glycolic and lactic acids, as well as creatine. Yeast extract is high in carbohydrates and, therefore, interferes with fermentation studies. The nutritional properties of the fresh yeast extract solution used in many media formulations for the cultivation of mycoplasmas is not replaceable by powdered yeast extract. Malt extract used in some media for fungi is composed primarily of carbohydrates (glucose, fructose, sucrose, maltose, dextrins) and small amounts of nitrogenous matter. Powdered extracts are generally incorporated in media at a concentration of 0.5–1.0%.

Aqueous extracts and infusions of various materials have historically been used to supply undefined nutritional factors in laboratory media. Concentrated liquid extracts generally are used at 10–20% v/v concentration as a medium supplement, whereas infusions will constitute the entire liquid base of a medium to which additional nutrients are added. As already noted, a filtered, aqueous solution prepared from autolyzed baker's yeast (150 g yeast/L) is a necessary ingredient in media for mycoplasmas and other mollicutes. The fresh yeast extract solution is then filter sterilized and incorporated into the mycoplasma media at 10% v/v concentration. Lactic acid bacteria from milk or milk products have been cultivated with infusions prepared from whole milk, whereas tomato juice or other fruit juice extracts have been used at 10–20% v/v in media for lactic acid bacteria isolated from plants. Potato infusions (200–300 g potatoes/L) serve as a nutritional base in many media for the cultivation of bacterial and fungal plant pathogens. Soil extracts prepared from fertile, chemically uncontaminated soils have been used to induce sporulation in many bacteria. Rumen fluid, containing partially digested nutrients from the first compartment of a cow's stomach, is a supplement in media for the cultivation of rumen microorganisms. Rumen fluid contains an undefined mixture of fatty acids, carbohydrates, peptides, vitamins, and metabolites. As rumen fluid is most commonly added to and autoclaved with basal medium components, any heat-labile nutrients are destroyed. Rumen fluid is obtained from fistulated dairy cows and can often be procured gratis from universities with departments of animal or dairy nutrition. Rumen fluid may or may not contain significant amounts of solid material, depending upon the length of time the material has been in the rumen. Centrifugation will effectively remove the bulk of debris; however, a series of filtrations down through 0.2 μm is necessary to remove dead cells of indigenous microflora that can confuse microscopic examinations of the organism being cultured. A defined mixture of fatty acids (Table 20.4) can effectively replace the need for rumen fluid for many bacteria; however, as with most chemically complex, undefined supplements, cell yield is frequently better when it is included in the medium.

TABLE 20.4. Volatile Fatty Mix for Rumen Bacteria and Fungi

Acetic acid	17.0 mL
Propionic acid	6.0 mL
N-Butyric acid	4.0 mL
N-Valeric acid	1.0 mL
Isovaleric acid	1.0 mL
Isobutyric acid	1.0 mL
DL-α-Methylbutyric acid	1.0 mL

Pipette the given volumes of fatty acids into a container that has a tight-fitting closure and mix well. The objectionable odor of the free fatty acids can be reduced by neutralizing the pH of this solution with the addition of NaOH pellets. Use 3.1 mL of the fatty acid mix per liter of medium.

Source: From Ref. 44, p. 162.

20.4.4 Buffers

pH buffers are molecules that, in solution, resist fluctuations in hydrogen ion concentration. Weak acids, bases, and their corresponding salts in partial dissociation function as pH buffers. Buffering capacity is greatest when the compound is at 50% dissociation. The pH at which this occurs is equal to the pK_a value of the compound, and greatest buffering capacity falls between ± 1 pH unit of the pK_a. Thus, no one buffer can be used across the entire pH range of 1 to 14 (74). Some acids are zwitterions (compounds that can chemically behave as acids or bases) and have more than one pK_a. In an extreme example, glycine when titrated against HCl has pK_a 2.3; titrated against NaOH, pK_a 9.6. Other zwitterions include citric acid (pK_{a1} 3.06, pK_{a2} 4.74, pK_{a3} 5.40), succinic acid (pK_{a1} 4.19, pK_{a2} 5.57), and the Good buffers (see later). The perfect media buffer would be (*1*) completely effective at poising a desired pH throughout the metabolic flux of a culture's growth cycle, as well as any other chemical or environmental changes that may affect pH (e.g., metal ion interaction, temperature), (*2*) resistant to microbial enzymatic activity, (*3*) chemically inert with respect to other medium components, and (*4*) inexpensive. The perfect buffer does not exist.

Lacking perfect buffers, in vitro microbial cultivation relies, for better or worse, upon a standard array of buffering systems. Nevertheless, the choice of buffer must not be made haphazardly. No discussion of buffers could be complete without N. E. Good's comment: "It is impossible even to guess how many exploratory experiments have failed, how many reaction rates have been depressed, and how many processes have been distorted because of imperfections of the buffers employed" (75). The capacity to buffer well at a particular pH is only one of many criteria in the determination of an appropriate buffer for a particular application. Chemical interaction with other media components or culture metabolites will compromise both the buffering capacity as well as the nutritional balance of a medium. The effectiveness of a microbially metabolized buffer diminishes with culture growth. The pH of some buffers can vary, sometimes considerably, with concentration or temperature. Synthetic buffers, while very effective for bench-top laboratory needs, may become prohibitively expensive upon scale-up.

20.4.4.1 Natural Buffering Agents. Natural buffering agents are those compounds most frequently encountered in microbiological media; they are also the buffers subject to the greatest drawbacks in their use. Carboxylic acids (e.g., acetate, citrate, succinate) are effective buffers for the lower ranges (<pH 6) of biological activity. These compounds are metabolically catabolized for carbon and energy by many microorganisms. Also, at the concentrations needed for buffering, carboxylic acids can become cation chelators. The mixtures of amino acids in protein hydrolysates and extracts have significant buffering capacity. Thus, peptone-based complex media frequently do not require additional buffering agents when used at or about the initial pH of the medium. Many peptones are adjusted during manufacture to pH 6.8–7.0. Peptone solutions are stable to sterilization at 121°C; however, they adversely interact at elevated temperatures with other medium components such as glucose, phosphates, and polyvalent cations. In addition, because peptones are nutrients, buffering capacity diminishes or shifts as the amino acids are microbially consumed.

Sodium bicarbonate–carbon dioxide buffers can maintain pH in the range 6.0–8.0. However, when used in conjunction with intrinsically buffered media, bicarbonate buffers have a working range of pH 6.8–7.2. Despite the necessity for closed systems to retain the gaseous CO_2 phase, bicarbonate buffers are widely used in the cultivation of anaerobic bacteria and eukaryotic animal cell lines. Bicarbonate buffers are nutritionally consumed. Also, carbon dioxide has minimal solubility in aqueous solutions, which somewhat limits its buffering capacity. Solid calcium carbonate (powdered) is used in various media for strongly acidifying organisms such as *Acetobacter, Clostridium*, and *Lactobacillus*. Ethanol-tolerant, acid-producing acetobactors can be isolated and differentiated from mixed-culture fermentations using a carbonate-ethanol medium (yeast extract, 3%; calcium carbonate, 2%; agar, 2%; filter-sterilized ethanol, 2%). Strongly acidifying acetobacter isolates able to grow in the presence of ethanol will also dissolve the carbonate and form a zone of clearing around the colony.

Although widely used in media formulations at pH 6–8, phosphate buffers suffer from a great number of drawbacks. Unless a medium is carefully designed and prepared with respect to metal speciation and concentration, phosphates will adversely bind to and precipitate polyvalent cations and proteinaceous material at neutral to alkaline pH.

This chemistry creates two problems: (*1*) buffering capacity is diminished as cations complex with the phosphate anion, and (*2*) cations bound as precipitates are unavailable as nutrients. These unwanted chemical interactions are intensified by heat. The problem can be reduced by autoclaving the phosphate buffer separately from the balance of the medium and then combining both solutions when cooled to room temperature after autoclaving. The addition of a chelator such as EDTA may retard trace metal precipitation; however, overchelation will also restrict the availability of trace metals from the nutrient pool. Above pH 7.2, with poorly designed media formulations, precipitation can become spontaneous even at room temperature; the reaction may be immediate or may slowly develop over time and is often misinterpreted as bacterial contamination. Balanced phosphate-buffered salines (e.g., Dulbecco's, Hank's) containing calcium and magnesium salts are filter sterilized to avoid precipitation of the salts. When autoclaved together, phosphate and glucose will also adversely react at neutral pH and above; trace metals will intensify the reaction. Because soluble phosphates are nutrients, the effectiveness of these buffers can diminish with culture metabolism. Finally, phosphate buffers exhibit a concentration effect characterized by a rise of 0.2–0.3 pH unit with each 10-fold dilution.

20.4.4.2 Synthetic Buffers. Synthetic buffers were developed to alleviate the many problems encountered with the earlier generations of natural buffers. Tris [Tris(hydroymethyl)aminomethane; pK_a 8.3 at 20°C] was the first organic compound widely utilized for its improved buffer characteristics. Tris and Tris HCl can be combined for buffering between pH 7.0 and 9.0, with strongest activity between 7.2 and 8.0. Tris can also be paired with other acids such as acetate, borate, or phosphate for specific buffering applications. Tris does not precipitate calcium ions and helps to maintain the solubility of magnesium salts. Tris is, however, a chemically reactive amine and can penetrate cell membranes; some microorganisms (e.g., *Sporocytophaga myxococcoides* ATCC 10010) have shown growth inhibition by the compound. Tris exhibits marked concentration and temperature effects that can limit its effectiveness for certain biological purposes. Tris buffers fall approximately 0.1 pH unit per 10-fold dilution. At 0.05 M, a Tris buffer at 25°C will be pH 7.20; at 5°C, pH 7.76; at 37°C, pH 6.91. Therefore, when used in culture media, Tris buffers should be constructed with the incubation temperature of the culture in mind and not upon the pH of the buffered medium at room temperature.

During the 1960s Good *et al*. (75) developed a number of zwitterionic compounds for use in biological systems to include as many as possible of the following desired buffer characteristics: (*1*) freely soluble in aqueous solutions to permit preparations of concentrated stock solutions, (*2*) buffering optima within the range of most biological systems, (*3*) biochemically nonreactive and chemically stable, (*4*) inert to microbial or other enzymatic attack, (*5*) minimal temperature and ionic effects upon buffer pH, and to further enhance their versatility to include postculture analytical procedures, (*6*) insoluble in organic solvents and (*7*) transparent to the ultraviolet wavelengths used in many biological spectrophotometric assays. Collectively these compounds have come to be known as the Good buffers, of which, HEPES (pK_a 7.5 at 25°C) is most commonly recognized due to its prevalence in media formulations for the cultivation of animal cell lines. Other Good buffers useful for microbial media formulations include ACES (pK_a 6.8 at 25°C), which is a component in the recommended cultivation medium for *Legionella*; buffered charcoal yeast extract (BCYE) (2p.518); MES (pK_a 6.1 at 25°C), PIPES (Pk$_a$ 6.8 at 25°C), and TES (pK_a 7.5 at 25°C).

HEPES has been implicated in the phototoxicity of RPMI medium for the cultivation of eukaryotic cells; however the effect was eliminated when sodium pyruvate was added to the culture medium (76). Other Good buffers have also shown various types of inhibition in certain cell lines (77). As with any buffering system or other media component, the Good buffers should be evaluated for applicability against the microorganism under study.

Biological buffers for cell growth purposes are commonly used at 0.01–0.05 M; chemical effectiveness of the buffer, initial pH of the medium without the buffer, production of acid or basic metabolites during culture growth, and enzymatic or other reagent optima are considerations in determining appropriate buffer ion concentration. Buffer tables can be found in numerous publications. Lacking a table, buffer solutions can be prepared with either of the two following methods and a calibrated pH meter:

1. Prepare a 2× solution of the buffer compound. Using HCl or NaOH, titrate the solution to the desired pH. Bring the solution to 1× volume with deionized or distilled water.
2. Prepare equimolar solutions of the acidic member and the basic member of the buffer pair. The molarity of these solutions is that of the final concentration needed for the working buffer. Choosing the solution of the buffer pair with a pH closest to that needed for the working buffer, titrate the solution to the desired pH with the equimolar solution prepared with the remaining component of the buffer pair.

20.4.5 Gelling Agents

Many microbial applications, such as strain isolation and purification, necessitate the use of solid media. Growth of aerobic organisms, in addition to specific morphologies, are often enhanced on solid media providing unrestricted gas exchange. The different gelling agents available

to microbiologists each have attributes and drawbacks that one must consider before choosing a particular gelling agent to include in a medium formulation. Although agar is the most frequently encountered gelling agent in microbial culture media, it must be properly used in order to maintain the chemical and nutritional integrity of a formulation. Many chemolithotrophic organisms are inhibited by organics and will not grow on media solidified with agar. Conversely, a number of marine bacteria are agarolytic and can quickly dissolve or soften this support matrix. Other gelling agents, including carrageenan and Gelrite, are alternatives to agar, but each has its own chemical peculiarities that must be understood before they can be effectively used.

20.4.5.1 Agar. Agar is a polysaccharide complex extracted from a number of species of red algae (*Gelidium, Gracilaria*, and others) found in the Pacific and Indian Oceans and the Japan Sea. The agar complex can be separated into (*1*) agarose, a neutral gelling fraction, and (*2*) agaropectin, a sulfated, nongelling fraction. Depending upon the purity and gel strength of the agar, and also upon the chemical composition of the medium in which the agar is used, a molten 1.5% agar solution will set at temperatures between 32 and 39°C. However, agar media with high concentrations of salt (e.g., those for the extreme halophiles, which contain >18% NaCl and 0.5% each of $MgSO_4$ and KCl) gel quickly at temperatures above 55°C. The gelling capacity of agar is thermally reversible, however, repeated remelting of agar-containing media is not recommended because the chemical stability of many nutrients cannot withstand repeated exposure to elevated temperatures. Agar is subject to acid hydrolysis, which destroys the gelling capacity of the polysaccharide; the phenomenon is intensified by heat. Agar-containing media autoclaved at less than pH 5.0 will not gel when cooled. If a low-pH agar is required, it is advisable to prepare and sterilize the medium in two separate solutions: For 1 L of low-pH agar medium, (*1*) heat and dissolve agar, with stirring, in 500 mL water; (*2*) dissolve remaining medium components in 500 mL water; (*3*) sterilize each solution separately at 121°C; (*4*) cool each solution to approximately 50°C; (*5*) aseptically combine both solutions, mix well, and dispense into containers as required.

Agar products vary with respect to nitrogenous and inorganic salt contaminants. A number of manufacturers feature agars purified though repeated water and solvent washes. Some agar products contain significant amounts of metals that can bind to and precipitate with phosphates in the medium, resulting in diminished growth yield with the solid medium as compared with that of the corresponding liquid medium. Similarly, autoclaving any agar in the same solution with the carefully balanced nutrient salts of a chemically defined medium, particularly at neutral to alkaline pH, will frequently give rise to a pronounced darkening or haze that can compromise the effectiveness of the medium. Under chemically defined conditions, component integrity is best preserved by autoclaving a purified agar separately from the autoclaved or filter-sterilized chemical portion of the medium, as already outlined for preparation of a low-pH agar medium. The use of electrophoretic grades of agarose would be more suitable than purified agars for gels in which a minimal level of trace metal contamination is required.

As with all gels, agar exhibits syneresis in that it will squeeze out solute as it contracts. The small puddle of liquid at the bottom of a freshly prepared agar slant is an example of this phenomenon. The amount of syneresis is dependent upon the concentration of the agar in the gel. Agar media can also lose water through desiccation during storage. Once water has been eliminated from the agar gel, it will not reenter the matrix unless the gel is remelted; however, melting of solid media for the purpose of rehydration not recommended because performance of the medium will be markedly reduced.

Agar is normally used at concentration from 1.0 to 2.0% for solid media; at 0.075 to 0.2% to create a viscosity that retards oxygen diffusion in media such as fluid thioglycollate medium U.S.P. and the classical oxidation–fermentation (O-F) medium of Hugh and Leifson (78); and at 0.5 to 0.75% for soft, top-layer agars in media for bacteriophage propagation.

20.4.5.2 Agarose. Agarose, the purified gelling fraction of agar, is used in some formulations for organisms that are inhibited by agar. Purified agarose products, particularly those grades used for electrophoretic work, are low in inorganic and organic contaminant and, therefore, react less with the phosphates present in a medium. Gel clarity is greater than for agar. Low gelling temperature agaroses melt above 65°C and form gels at less than 30°C. Agarose will form solid gels at 0.75–1.0%.

20.4.5.3 Gellan Gum. Gelrite, a gellan gum, is a heteropolysaccharide composed of glucuronic acid, rhamnose, and glucose, produced by bacterial fermentation, and commercialized as a gelling agent by Kelco (Merck & Co., Inc., Kelco Division, San Diego, Calif.). Sigma Chemical Co. (St. Louis, Mo.) distributes the material under the trade name Phytagel. Under either name, this gellan gum is somewhat difficult to work with for routine media solidification purposes, but nevertheless, its unique characteristics make the material the most practical solution to some unusual microbial cultivation requirements. Gelrite/Phytagel is a high-melting-temperature (~70°C) gel, which makes it useful for the cultivation of thermophilic bacteria and fungi at 45–50°C, temperatures at which agar shows considerable syneresis and softening. The gel is generally thermally reversible, although under some conditions,

such as the elevated soluble salt concentrations of marine media, gelling can become permanent. Gelrite/Phytagel is subject to acid hydrolysis when autoclaved at low pH. The gellan is resistant to microbial attack by most organisms and so proves useful in the isolation of organisms such as the marine cytophagas, a group in which many strains characteristically possess the ability to degrade other biopolymer gels including agar, algin, carrageenan, and gelatin. Many chemolithotrophic organisms (e.g., *Nitrobacter*, spp. and *Thiobacillus ferroxidans*), although inhibited by agar and other organic gelling agents, can be grown successfully on a solid medium using the gellan. Full gelling capacity of this polysaccharide is cation dependent, and media formulations may need amending to include at least 0.1% $MgSO_4 \cdot 7H_2O$, or other magnesium salt to permit sufficient gelling. Under chemically defined media conditions, further chemical adjustments to other components may be necessary to retain chemical balance because of a modification in cation level. Recommended concentrations for Gelrite/Phytagel are in the 0.1–0.2% range, however experimentation will probably be needed to select the appropriate concentration for one's own needs. Table 20.5 provides a media formulation that has been successfully used as a solid medium for the cultivation of laboratory strains of *T. ferroxidans* (ATCC 21834 and others); the gel is rigid enough for the isolation and picking of colonies, and growth is rapid (3–5 days) at 20–30°C. Preparation methods for this particular formulation illustrate many of the topics discussed in this chapter with respect to treatment of chemically incompatible salts, acid hydrolysis, and heat instability of media components.

20.4.5.4 Alginic Acid and κ-Carrageenan. Alginic acid (79) and κ-carrageenan (80,81) have been used microbiologically for specialized gelling needs. Gelling efficiency of alginate is Ca^{2+} dependent, whereas κ-carrageenan is K^+ or Na^+ dependent. Since all of these substances are easily degraded by assorted bacteria and fungi, their use as gelling agents is restricted. Microbial degradation of these substances is used for taxonomic purposes.

20.4.5.5 Silica Gel. A final solid substrate for the laboratory cultivation of obligate chemolithotrophic organisms is silica gel, first used by Weintraub and Hanks (82) in 1936 for the isolation of ammonia-oxidizing bacteria. Many authors have since attempted improvements on the tedious method (83–86). Preparation of any quantity of plates is laborious. Briefly, sodium silicate is reacted with strong HCl to produce silicic acid, NaCl and almost immediate gelling. Nutrient salts may be included in the formulation, or the surface of the silica gel may be later flooded with nutrients, with some absorption. Because the amount of NaCl is high (~8–10%), the gel may first need clearing of the salt, with repeated washings with water prior to flooding with a nutrient solution. Silica gels are translucent and rigid with a high degree of syneresis. The gels are autoclavable, with a tendency for cracking, and are not reversible. Table 20.6 provides simplified instructions for silica gel preparation adapted from Ref. 82.

TABLE 20.5. Solid Medium for *Thiobacillus ferroxidans*

Solution A	
$(NH_4)_2SO_4$	0.08 g
$MgSO_4 \cdot 7H_2O$	0.20 g
K_2HPO_4	0.04 g
Trace elements (see Table 20.1, mix A)	0.5 mL
Distilled water	40.0 mL
Adjust Solution A to pH 2.3 with concentrated H_2SO_4. Filter sterilize.	
Solution B	
Phytagel (Sigma P-8169)	0.5 g
Distilled water	40.0 mL
With constant stirring, heat Phytagel to boiling to dissolve. Sterilize at 121°C for 15 min. Cool to no less than 80°C.	
Solution C	
$FeSO_4 \cdot 7H_2O$	2.0 g
Distilled water	20.0 mL
Quickly dissolve ferrous sulfate with constant stirring. Immediately filter sterilize.	
Complete medium	
Warm solution A to about 50°C. Add solution C to solution A and immediately combine with solution B. Mix well and pour plates. As this medium must be poured at a rather high temperature to avoid premature gelling of the Phytagel, it will be necessary to dry the plates before use by leaving the lids ajar in a sterile environment or by incubating them at 37°C overnight to eliminate excess condensation.	

20.5 MEDIA STERILIZATION

With few exceptions, media and buffers used for microbial cultivation must be sterilized as soon as possible after preparation to limit proliferation of environmental contaminants that will alter the nutritional characteristics of the medium either by consumption of nutrients or by production of metabolites. Even nonnutritive buffers or trace metal stock solutions can give rise to unwanted fungal growth if stored unsterilized for any length of time at room or refrigerator temperatures. Sterile media and buffers are necessary for culture propagation; the presence of microbial contaminants, even at a low level, can invalidate any study or production process. The physical stress of sterilization, however, can compromise the nutritional and physiological characteristics of a medium or buffer. Consequently, one must choose a sterilization method that has the least negative impact upon the material being sterilized. Although steam sterilization had historically

TABLE 20.6. Simplified Silica Gel Plates

Stock solutions

Solution 1	
Concentrated HCl (~l37%)	14.5 mL
Distilled water	to 100.0 mL
Solution 2	
$Na_2SiO_3 \cdot 9H_2O$	20.0 g
Distilled water	100.0 mL

Use slight heat and constant stirring to dissolve sodium silicate. Filter out any particulates or colloidal material with Whatman #1 paper.

Preparation of silica gel plate

1. Volumes given are for one 20 × 100 mm petri dish. Gelling will occur within 10–15 s of mixing solutions. Be prepared to work quickly.
2. Add 14.5 mL solution 1 to a 100-mL beaker and stir continuously. (A magnetic stirrer will work best.)
3. Quickly add 19.0 mL solution 2 into the beaker and mix well.
4. As soon as effervescence stops, quickly pour contents of beaker into a 20 × 100 mm petri dish. Use a glass dish if subsequent autoclaving is required.
5. Initial gelling will occur almost immediately. Gel strength will increase slightly over a half-hour period, at which time the gel may be washed to remove excess NaCl and then flooded with nutrient solution.

been the only form of sterilization accessible by many laboratories, the widespread availability and diversity of reasonably priced and reliable disposable filtration units offer more appropriate choices for media sterilization, even for small laboratories.

20.5.1 Steam Sterilization (Autoclaving)

Steam remains the most widely used sterilization method for rugged, heat-stable media and has the advantage of often being the terminal step in media preparation. With no additional manipulation of an uninoculated medium post-sterilization, possibility of inadvertent introduction of contamination is reduced. The term *autoclaving* is often used synonymously for the definitional procedure: "sterilize at 121°C for 15 minutes." This phrase *must* be applied in context to the volume of the medium being sterilized as well as to the efficiency of the autoclave being used. The precise meaning of the phrase infers that the contents of each container within an autoclave cycle must achieve an uninterrupted exposure to 121°C for 15 min; it does not mean that the autoclave itself was set for that temperature and time. From a practical laboratory standpoint, this means that small volumes (e.g., test tubes) will require the minimal amount of autoclaving time, whereas large volumes (e.g., one or two flasks) will require additional autoclaving time. Fully loaded autoclaves may require longer run times. Under laboratory autoclave conditions, a 30–35 min sterilization cycle for 0.5 L liquid medium in a 1-L flask is a practical guideline; agar media that have been allowed to solidify before sterilization may require longer autoclave times. Large-scale fermentation volumes can require hours to sterilize; media processed in poorly maintained autoclaves might never be adequately sterilized. Where mechanical agitation of a medium is not possible during the autoclave cycle, maximum container volumes of media should not exceed the ratio of >1 L media in a 2-L vessel because the prolonged autoclave times required for heat conduction to raise the innermost portions of large volumes of media to 121°C will subject the outer portions of the media to extreme overheating.

Autoclaves and their cycles should be validated for media sterilization. Ideally, this would include replicate autoclave run data from multiple thermocouple probes spaced strategically within the autoclave chamber and load configurations. While this technological expense is beyond the budget of many small research laboratories, quantified preparations of *Bacillus stearothermophilus* sterilization indicators, such as the Verify Biological Indicators (Steris Corporation, Mentor, Ohio), can indicate general "121°C, 15 min" parameters. Chemical indicator strips or labels are not reliable indicators of sterilization and should be used only as visual aids to indicate that a particular item has been run through an autoclave cycle. Under the most elemental quality control conditions, media samples should be held at least 2 weeks at 26°C and 37°C, and also at conditions and temperatures conducive to the growth of the types of environmental bioburden normally encountered during media preparation and sterilization, to ensure that latent contamination does not subsequently proliferate. Unusual media formulations (e.g., extremes in pH, chemolithotrophic conditions, unusual energy sources) that may not allow proliferation of common microorganisms may require inoculation of lot samples into more conventional heterotrophic media (e.g., tryptic soy broth) to encourage the growth of common environmental contaminants.

Steam at pressures below 15 psi (121°C) are used for sterilization of many media components not stable at 121°C. Skim milk (used as a cryoprotectant in lyophilization and as a substrate in phenotypic characterization) is best sterilized at 116°C for 20 min; the lower pressure reduces carmelization of indigenous lactose. Powdered sulfur (S^0) used as an energy source for microorganisms can be treated with Tyndallization (100°C for 30 min for 3 consecutive days) to avoid melting the element into a solid mass that physically limits its availability to organisms. Tyndallization is also used as a method of bioburden reduction (it is *not* a sterilization process) for other extremely heat-labile media. In theory, vegetative cells are killed by the first day's boiling; quickly germinating spores are killed the second day; by the third day, late-germinating spores are killed, leaving a relatively clean preparation.

20.5.2 Filter Sterilization

Heat-labile media components should be filter sterilized. Any chemically balanced liquid buffer or medium can also be filter sterilized to ensure that chemical integrity will not be compromised by the elevated heat and pressure of steam sterilization. Membrane filters, rather than depth filters, are preferred for sterilization purposes because their uniform pore size permits absolute retention of particles down to a specified pore diameter when the membranes are stored, sterilized, and used according to manufacturer's instruction. Depending upon the polymer composition, membrane filters are available in porosities from 10 μm down through nominal molecular weight limit used for ultrafiltration. For general microbiological purposes, 0.2-μm filtration is used for sterilization of media and buffers because this porosity effectively traps many vegetative bacteria and spores. However, in serum-based media, because mycoplasmas are not always held back at 0.2 μm, filtration through a stack of three 0.2-μm membranes rather than a single membrane will increase the probability of retention of these common serum contaminants. In addition, membranes are now available in 0.1-μm porosity that can retain smaller-sized microbial contamination, but flow rates are slower and rate of membrane clogging increases as porosity decreases. In any event, the filtration method selected for sterilization should be challenged against the smallest microbial contaminants known to be present in the working environment and production stream (87). As pore size decreases to submicron diameters, there is the possibility of holding back large molecular weight nutritional components and aggregates.

Water-soluble hydrophilic microbial media, stock solutions, and buffers are most commonly filter sterilized with membranes composed of cellulose acetate or nitrate esters. Fastidious cultures may require initial washing of the membranes with hot water to remove residual organics prior to media filtration; filters and membranes specified for tissue-culture applications are also recommended for sensitive organisms. Nonaqueous media components such as ethanolic concentrates of antibiotics or dimethyl sulfoxide (DMSO) must be filter sterilized with hydrophobic polymer membranes designed to withstand organic solvents. Nylon and Teflon membranes are suitable for many organic-solvent based biological applications. These types of membranes can require initial washing with a weak nonpolar solvent such as methanol to condition them for filtration. Some membranes, such as Nylon, are protein binding; if specific proteins are key media components, choose a membrane specifically identified as low protein binding.

Membrane filters have limited loading capacity and will quickly clog. Consequently, effective membrane filtration with any large volume, especially with particulate-laden preparations, requires sequential filtration from larger through smaller porosities to clarify the medium of debris, as much as possible, prior to the final filtration step. Low-speed centrifugation may also be used to first clarify crude media preparations. Glass fiber depth filters are efficient prefilters for many media applications because they have great loading capacity; however, they do not always eliminate the need for sequential membrane clarification steps prior to sterilization. Sterile filtration can be a slow process. It may be necessary, for critical applications, to perform the entire operation in a cold room to retard environmental microbial or other denaturing activity upon the raw material.

Positive-pressure filtration with an inert gas such as nitrogen is used in most large-scale filtration applications. Positive pressure reduces foaming of the filtrate and possible denaturation of any essential protein components. For critical and regulatory applications, the gas supply must also be sterile filtered before it reaches the medium reservoir. In many laboratories, filter sterilization with vacuum is the only available option. With vacuum, foaming of proteinaceous material will be best reduced with sequential prefiltration through larger membrane porosities as well as with minimal vacuum applied to the process. For most bacterial applications, serum foaming is not a deleterious nutritional problem. However, do note that media foaming can be a serious source of environmental contamination if the foam is not trapped and collected before passing into the laboratory vacuum line.

Disposable, presterilized filtration systems are offered by a number of manufacturers (e.g., Falcon, Corning, Gelman, Millipore, Nalge) in small- to large-volume capacities. Capsule filters are available for small to medium in-line batch processing (20–60 L). Filter/storage systems in the 200-mL to 1-L sizes offer the ease of vacuum-operated membrane sterilization and storage with minimal preparation and clean up. Syringe filters are most used for volumes of less than 50 mL; however some types can sterilize volumes up to 1 L without clogging.

20.5.3 Dry Heat Sterilization

Some materials with microbiological applications require dry heat sterilization. Whereas autoclaving is suitable only for heat-stable aqueous material, and filter sterilization is amenable to those materials capable of passage through membranes, dry heat is used for sterilization of nonaqueous, heat-stable material such as oils and waxes. It is also used for glassware or equipment depyrogenation and enzyme (RNase) elimination in many production as well as research protocols. A minimal standard for dry heat sterilization is 350°C for 30 min, or 121°C for 6 h (88). As with autoclaving, the time can vary considerably with the efficiency of the sterilization oven as well as with the volume and

kind of material being sterilized. Sterilization oven validation is required for many production process. However, for basic laboratory needs, biological dry-heat spore indicators (*Bacillus stearothermophilus* and *B. subtilis*) such as Spore-O-Chex (PyMaH 00190) will give a better indication of actual oven operation than will chemical indicator strips that show only that a particular temperature has been reached, but not for how long, nor if any temperature interruptions occurred. Oils and waxes are best heat sterilized in shallow volumes in large containers to permit rapid and thorough heat penetration of the material because temperature lag is much longer with nonaqueous than with aqueous materials.

20.6 MEDIA STORAGE

Prepared microbial media should stored refrigerated at 4–8°C and in the dark. Containers should be tightly sealed or, in the case of petri dishes, packaged in plastic bags to retard evaporation. Desiccated agar media are characterized by surface cracking and pulling of the agar away from container walls. Water evaporation from liquid or solid media concentrates solutes, which can result in permanent precipitation of some components, alters concentrations of critical nutritional factors or substrates, and increases osmolarity to possibly growth-limiting levels. The ability to freeze media is entirely dependent upon the formulation. As water freezes and concentrates the solutes, poorly soluble chemicals, such as tyrosine, or chemicals, such as phosphates, prone to complexing may not go back into solution when the medium is subsequently thawed. Phototoxicity of media can develop when light activates the glass or plastic containers, as well as media components, and initiates formation of free radicals; aerobic conditions intensify these deleterious reactions as do the blue wavelengths of light emitted by fluorescent tubes (89). The effects of light and free radical formation with respect to tissue culture media have been well studied. In one such mechanism, light at 360 nm and 450 nm activates riboflavin, resulting in a transfer of energy to tryptophan or tyrosine and the formation of cytotoxic free-radical products (90). Similar hydrogen peroxide formation in RPMI medium has been shown to be intensified by the presence of HEPES buffer. With bacteria, an inhibitory effect of light on growth-supporting properties of eosin methylene blue agar has been demonstrated (91). It is recommended that tissue culture media and media for those microorganisms sensitive to the presence of hydrogen peroxide or free radicals (e.g., anaerobic bacteria) be stored and cultured in the dark or in yellow wrappers to reduce the inhibitory effects of light on the media and growth of the organisms.

REFERENCES

1. R.A. Sanford, J.W. Urbance, and J.M. Tiedje, in Abstracts of the Annual Meeting of the American Society for Microbiology, 1996, American Society for Microbiology, Washington, D.C., 1996, abstract O-66, p. 365.
2. P. Pienta, J. Tang, and R. Cote eds., American Type Culture Collection Catalogue of Bacteria and Bacteriophages, 19th ed., American Type Culture Collection, Rockville, Md., 1996.
3. S.C. Jong, F. Dugan, and M.J. Edwards eds., American Type Culture Collection Catalogue of Filamentous Fungi, 19th ed., American Type Culture Collection, Rockville, Md., 1996.
4. DSM Catalogue of Strains 1993, Deutsche Samlung von Microorganismen und Zellkulturen GmbH, Braunscheig, Germany, 1993.
5. E.Y. Bridson, in M. Rechcigl, Jr. ed., CRC Handbook Series in Nutrition and Food, Section G, Diets, Culture Media, Food Supplements, vol. III, CRC Press, Cleveland, Ohio, 1978, pp. 91–281.
6. R.M. Atlas, Handbook of Microbiological Media, CRC Press, Boca Raton, Fla., 1993.
7. P. Gerhardt, R.G.E. Murray, W.A. Wood, and N.R. Krieg eds., Methods for General and Molecular Bacteriology, American Society for Microbiology, Washington, D.C., 1994.
8. C3-A2 Preparation and Testing of Reagent Water in the Clinical Laboratory, 2nd ed., National Committee on Clinical Laboratory Standards, Villanova, Pa., 1991.
9. The U.S. Pharmacopoeia XXIII/The National Formulary XVIII, U.S. Pharmacopoeial Convention, Rockville, Md., 1995, pp. 1635–1636.
10. P. Schönheit and T. Schäfer, World J. Microbiol. Biotechnol. 11: 26–57 (1995).
11. C.J. Microcha and J.E. Devay, Can. J. Microbiol. 17: 1373–1378 (1971).
12. A. Willems, J. Busse, M. Goor, B. Pot, E. Falsen, E. Jantzen, B. Hoste, M. Gillis, K. Kersters, G. Auling, and J. De Ley, Int. J. Syst. Bacteriol. 39: 319–333 (1989).
13. W. Crueger and A. Crueger, in Thomas D. Brock ed., Biotechnology: A Textbook of Industrial Microbiology, English edition, Sinauer Associates, Sunderland, Mass., 1982, pp. 73–80.
14. R.M. Smibert and N.R. Krieg, in P. Gerhardt, R.G.E. Murray, W.A. Wood, and N.R. Krieg eds., Methods for General and Molecular Bacteriology, American Society for Microbiology, Washington, D.C., 1994, pp. 607–654.
15. S.M. Hasan and J.B. Hall, Can. J. Microbiol. 87: 120–128 (1975).
16. S.H. Hutner, L. Provasoli, A. Shatz, and C.P. Haskins, Proc. Am. Philos. Soc. 94: 152–170 (1950).
17. M.O. Garraway and R.C. Evans, Fungal Nutrition and Physiology, Wiley, New York, 1984, pp. 124–170.
18. M.N. Hughes and R.K. Poole, J. Gen. Microbiol. 137: 725–734 (1991).
19. P. Kaur and D.V. Vadehra, Antimicrob. Agents Chemother. 29: 165–167 (1986).
20. C. Lindblow-Kull, A. Schrift, and R.L. Gherna, Appl. Environ. Microbiol. 44: 737–743 (1982).
21. H.S. Rosenbranz, J.E. Coward, T.J. Wjodkowski, and H.S. Carr, Antimicrob. Agents Chemother. 5: 199–201 (1974).

22. R.C. Tilton and B. Rosenberg, Appl. Environ. Microbiol. 35: 1116–1120 (1978).
23. R.J. Cote and R.L. Gherna, in P. Gerhardt, R.G.E. Murray, W.A. Wood and N.R. Krieg eds., Methods for General and Molecular Bacteriology, American Society for Microbiology, Washington, D.C., 1994.
24. J.H. Crosa, Annu. Rev. Microbiol. 38: 69–89 (1984).
25. E. Griffiths, in J.J. Bullen and E. Griffiths eds., Iron and Infection, Molecular and Clinical Aspects, Wiley, Chichester, U.K., 1987, pp. 69–137.
26. M.A.F. Jalal, R. Mocharla, C.L. Barnes, M.B. Hossain, D.R. Powell, D.L. Eng-Wimot, S.L. Grayson, B.A. Benson, and D. Van Der Helm, J. Bacteriol. 158: 683–688 (1984).
27. R.D. Perry and C.L. San Clemente, J. Bacteriol. 140: 129–1132 (1979).
28. M.-F. Thorel, M. Krichevsky, and V.V. Levy-Frebault, Int. J. Syst. Bacteriol. 40: 254–260 (1990).
29. T.E. Bramanti and S.C. Holt, J. Bacteriol. 173: 7330–7339 (1991).
30. B. Fouz, R. Mazoy, M.L. Lemos, M.J. DelOlmo and C. Amaro, Appl. Environ. Microbiol. 62: 2806–2810 (1996).
31. D.R. Lovley, Annu. Rev. Microbiol. 47: 263–290 (1993).
32. M. DeFelice, M. Levinthal, M. Iaccarino, and J. Guardiola, Microbiol. Rev. 43: 42–58 (1979).
33. M.K. Winston and J.K. Bhattacharjee, J. Bacteriol. 152: 874–879 (1982).
34. L.A. Collins and R.L. Thune, Appl. Environ. Microbiol. 62: 848–852 (1996).
35. M.H. Saier, Jr., M.J. Fagan, C. Hoischen, and J. Reizer, in A.L. Sonenshein, J.A. Hoch, and R. Losick eds., Bacillus subtilis and Other Gram-Positive Bacteria: Biochemistry, Physiology, and Molecular Genetics, American Society for Microbiology, Washington, D.C., 1993, pp. 133–156.
36. P.F. Smith, T.A. Langworthy, and M.R. Smith, J. Bacteriol. 124: 884–892 (1975).
37. C. Wyss, B.K. Choi, P. Schüpbach, B. Guggenheim, and U.B. Göbel, Int. J. Syst. Bacteriol. 46: 745–752 (1996).
38. T.A. Nerad, ed., ATCC Catalogue of Protists, 17th ed., 1991, p. 60.
39. D.A. Power ed., and P.J. McCuen, Manual of BBL Products and Laboratory Procedures, 6th ed., Becton Dickinson Microbiology Systems, Cockeyville, Md., 1988, pp. 178–179.
40. Difco Manual, 10th ed., Difco Laboratories, Detroit, Mich., 1984, pp. 567–568.
41. F. Fischer, 97/534/EC, Journal of the European Communities, Brussels, Belgium, 1997.
42. B.D. Davis and E.S. Mingioli, J. Bacteriol. 60: 17–27 (1950).
43. S.A. Koser, in Vitamin Requirements of Bacteria and Yeasts, C. Thomas Publisher, Springfield, Ill. 1968, pp. 379–401.
44. R.J. Cote and R.L. Gherna, in P. Gerhardt, R.G.E. Murray, W.A. Wood, and N.R. Krieg eds., Methods for General and Molecular Microbiology. American Society for Microbiology, Washington, D.C., 1994, pp. 155–178.
45. M.O. Garraway and R.C. Evans, Fungal Nutrition and Physiology, Wiley, New York, 1984, pp. 171–211.
46. T.A. Freier, D.C. Beitz, L. Li, and P.A. Hartman, Int. J. System. Bacteriol. 44: 137–142 (1994).
47. A.W. Brinkley, A.R. Gottesman, and D.E. Mott, Appl. Environ. Microbiol. 40: 1130–1132 (1980).
48. B.D. Davis, R. Dulbecco, H.N. Eisen, H.S. Ginsberg, and W.B. Wood, Jr., Microbiology, 2nd ed., Harper & Row, Hagerstown, Md., 1973, p. 79.
49. E.J. Herbst and E.E. Snell, J. Biol. Chem. 176: 989–990 (1948).
50. M. Rogosa and F.S. Bishop, J. Bacteriol. 87: 574–580 (1964).
51. A.C.R. Tanner, M.A. Listgarten, J.L. Ebersole, and M.N. Strzenko, Int. J. Syst. Bacteriol. 36: 213–221 (1986).
52. J.E. Cronan, Jr., and C.O. Rock, in F.C. Neidhart, J.L. Ingrahan, K.B. Low, B. Magasanik, M. Schaechter, and H.E. Umbarger eds., Escherichia coli and Salmonella typhimurium: Cellular and Molecular Biology, vol. 1, American Society for Microbiology, Washington, D.C., 1987, pp. 474–497.
53. D. DeMendoza, R. Grau, and J.E. Cronan, Jr., in A.L. Sonenshein ed., Bacillus subtilis and Other Gram-Positive Bacteria: Biochemistry, Physiology, and Molecular Genetics, American Society for Microbiology, Washington, D.C., 1993, pp. 411–421.
54. J.W. Deming, J.K. Somers, W.L. Straube, D.F. Swartz, and M.T. MacDonell, System. Appl. Microbiol. 10: 152–160 (1988).
55. G.K. Nyberg, G.P.D. Granberg, and J. Carlsson, Appl. Environ. Microbiol. 38: 29–34 (1979).
56. L.G. Ljungdahl and J. Wiegel, in A.L. Demain and N.A. Solomon eds., Manual of Industrial Microbiology and Biotechnology, American Society for Microbiology, Washington, D.C., 1986, pp. 84–96.
57. J.A. Breznak and R.N. Costilow, in P. Gerhardt, R.G.E. Murray, W.A. Wood, and N.R. Krieg eds., Methods for General and Molecular Bacteriology, American Society for Microbiology, Washington, D.C., 1994, pp. 135–154.
58. W.E. Balch, G.E. Fox, L.J. Magrum, C.R. Woese, and R.S. Wolfe, Microbiol. Rev. 43: 260–296 (1979).
59. R.G. Cluss and N.L. Somerson, Appl. Environ. Microbiol. 51: 281–287 (1986).
60. R. Olivieri, M. Bugnoli, D. Amellini, S. Bianciardi, R. Rappuoli, P.F. Bayeli, L. Abate, E. Esposito, L. DeGregario, J. Asis, C. Basagni, and N. Figura, J. Clin. Microbiol. 31: 160–162 (1993).
61. The Source, 7, Sigma Chemical, St. Louis, Mo., 1992, pp. 1–2.
62. R. Greasham and E. Inamine, in A.L. Demain and N.A. Solomon eds., Manual of Industrial Microbiology and Biotechnology, American Society for Microbiology, Washington, D.C., 1986, pp. 41–48.
63. T.L. Miller and B.W. Churchill, in A.L. Demain and N.A. Solomon eds., Manual of Industrial Microbiology and Biotechnology, American Society for Microbiology, Washington, D.C., 1986, pp. 122–136.
64. Sheffield Series Technical Manual, Quest International, Norwich, N.Y.
65. R.A. Neihof and C.A. Bailey, Appl. Environ. Microbiol. 35: 698–703 (1978).
66. S.E. George, C.J. Costenbader, and T. Melton, J. Bacteriol. 164: 866–871 (1985).
67. R.K. Bajpai and T.K. Ghose, Biotechnol. Bioeng. 20: 927–935 (1978).
68. D.S. Ucker and E.R. Signer, J. Bacteriol. 136: 1197–1200 (1978).

69. P. Loubiere, E. Gros, V. Paquet, and N.D. Lindley, J. Gen. Microbiol. 138: 979–985 (1992).
70. H. Vogel, J. Gen. Microbiol. 26: 223–230 (1961).
71. H.J. Laanbroek and N. Pfenning, Arch. Microbiol. 128: 330–335 (1981).
72. J. Carlsson, G. Nyberg, and J. Wrethen, Appl. Environ. Microbiol. 36: 223–2239 (1978).
73. S. Budavari, M.J. O'Neil, A. Smith, P.E. Heckelman, and J.F. Kinneary eds., The Merck Index. An Encyclopedia of Chemicals, Drugs, and Biologicals, 12th ed., Merck Research Laboratories, Whitehouse Station, N.J., 1996.
74. D.E. Gueffroy ed., Buffers. A Guide for the Preparation and Use of Buffers in Biological Systems, Calbiochem-Behring, La Jolla, Calif., 1983.
75. N.E. Good, G.D. Winget, W. Winter, T.N. Connolly, S. Izawa, and R.M.M. Singh, Biochemistry 5: 467–477 (1966).
76. G.T. Spierenburg, F.T.J.J. Oerlemans, J.P.R.M. can Laarhhoven, and C.H.M.M. deBruyn, Cancer Res. 44: 2253–2254 (1984).
77. Art to Science in Tissue Culture, vol. 6, Hyclone Laboratories, Ogden, Utah, 1987, pp. 4–5.
78. R. Hugh and E. Leifson, J. Bacteriol. 66: 24–26 (1953).
79. E.N. Adaoha Mbanaso and D.H. Roscoe, Plants Sci. Lett. 25: 61–66 (1982).
80. A.D. Lines, Appl. Environ. Microbiol. 34: 637–639 (1977).
81. I.A. Abbott and F.A. Chapman, Arch. Microbiol. 128: 355–359 (1981).
82. J.H. Hanks and R.L. Weintraub, J. Bacteriol. 32: 639–651 (1936).
83. A.S. Dietz and A.A. Yayanos, Appl. Environ. Microbiol. 36: 966–968 (1978).
84. D.A. Bazlinski and F.A. Rosenberg, Appl. Environ. Microbiol. 39: 934 (1980).
85. H.B. Funk and T.A. Krulwich, J. Bacteriol. 88: 1200–1201 (1964).
86. H. Seki, Appl. Microbiol. 26: 318–320 (1973).
87. K.L. Roche and R.V. Levy, Biopharm 5: 22–33 (1992).
88. J.J. Perkins, Principles and Methods of Sterilization in the Health Science, Charles C. Thomas, Publisher, Springfield, Ill., 1976.
89. L.C. Ellis, in Art to Science in Tissue Culture, vol. 10, Hyclone Laboratories, Ogdon, Utah, 1991, pp. 1–5.
90. M.E. Hoffman and R. Meheghini, Photochem. Photobiol. 29: 299–303 (1979).
91. R.L. Girolami and J.M. Stamm, Appl. Environ. Microbiol. 31: 141–142 (1976).

21

MICROSCOPIC CHARACTERIZATION OF CELLS

Erwin Huebner
University of Manitoba, Winnipeg, Manitoba, Canada

21.1 INTRODUCTION AND PERSPECTIVE

The awe and excitement that cell biologists and biotechnologists experience as they probe the inner secrets of cells with the diverse types of microscopy available today are akin to that felt by mankind seeing dramatic images from distant planets and stars from astronomical telescopes and space exploration.

Microscopy opens vistas not possible with the naked eye and allowed early pioneers like Antoine Leuwenhook, Robert Hooke, and the early giants in cell biology to discover that living organisms are composed of cells thus creating the field of cell biology.

For almost 400 years, microscopes have revealed the microcosm of the cellular world. The revealing of this "inner universe" from the 16th century until today has impacted on virtually all facets of humanity as it probes the essence of life itself. Those of us working in cell biology, biotechnology, and developmental biology have the good fortune of sharing and experiencing the incredible wonder past microscopists, like Hooke, Abbe, Zeiss, Zernicke, Nomarski and the many others who developed and used the new advances of their eras, must have felt.

The spectrum of types of light microscopy and electron microscopy that have become available through the genius and creative efforts of the myriad of scientists since Zacharias Jansen made the first two-lens light microscope in 1595 in Holland is astonishing. The renaissance and revolution in light microscopy we are now experiencing has and continues to generate new technologies and new ways of seeing, measuring structures, and characterizing events in living cells. Images now attainable would have been considered science fiction, even 10–20 years ago. So as we enter the new millennium, we can visualize structures in cells with light microscopy and allied methods that were deemed impossible 50–60 years ago when electron microscopes were being brought to bear to resolve the fine structure of cells. The frontiers have been pushed to where we can now see structures like single microtubules, centrioles, pinocytotic vesicles, live organelles; localize gene sequences; observe biochemical processes *in situ* in living cells, see dynamic changes in ions like calcium; and map intracellular pH, to cite a few. Microscopy continues to be a problem-solving tool that is yielding significant benefits in biomedical research, particularly in cell biology. These benefits are being reaped because rapid advances during the past decade have occurred with spectacular advances in optical systems and components, the inclusion of lasers and scanning devices in optical systems, the marriage between microscopes and electronic imaging devices and detectors, the utilization of computers and image processing, as well as the continual introduction of new fluorescent dye molecules to characterize and highlight cellular components and processes.

In view of the enormity of the field of microscopy, past and present, the many excellent research papers, reviews, and books, as well as informative web sites available, it would be presumptuous to do justice to the topic in as short an chapter as this. Thus the aim is to provide a selective perspective, including a cursory coverage of the historic aspects, an overview of some basic information on microscopy in general, and to follow this with highlights of the range of light microscopes from bright-field microscopy to the newest multiphoton microscopy, scanning probe

Upstream Industrial Biotechnology: Expression Systems and Process Development, Volume 1, First Edition. Edited by Michael C. Flickinger.
© 2013 John Wiley & Sons, Inc. Published 2013 by John Wiley & Sons, Inc.

and scanning near-field optic microscopes, electronic imaging and image processing; laser tweezers, and electron microscopy, including TEM, SEM, and freeze-fracture.

21.2 DEVELOPMENTS AND MILESTONES IN MICROSCOPY

The following highlights some of the milestones in microscopy beginning with invention of a two-lens microscope by Jansen in 1595. The term microscope was coined by Giovani Faber in 1625. Subsequently, cells were observed by Robert Hooke in the mid 1660s, and Malpighi visualized blood capillaries. The Dutch draper Leeuwenhoek built many single lens microscopes in the late 1660s and 1670s with which he observed protozoa, bacteria, sperm, and other cells. The eighteenth century yielded advances in mechanical design of compound microscopes and notably the improvement of lenses particularly by the British scientist Lister in 1829 who developed achromatic lenses by using flint glass. Nicol prisms important for polarizing microscopy were introduced in 1829 by Fox-Talbot as was the first use of reflecting microscopy in the 1820s. A watershed in the improvement of microscopy, key to the advances in cell biology from the 1850s to the turn of the century, was the contributions of Abbe in the 1870s–1880s in providing an understanding of image formation and the importance of the collection angle of light received by the objective. The concept of numerical aperture and its relationship to resolution is expressed by the Abbe formula: $d = \lambda/\text{NA}$ where $\text{NA} = n \sin \alpha$. n is the refractive index of the medium between the object and the objective, and α is one-half of the collection angle of the objective. Abbe with Zeiss was instrumental in bringing about major improvements in objectives, so by the 1880s objectives of the highest NA (1.4) were reached and structures 0.2 μM apart could be resolved. Subsequently, there has been a plethora of advances in corrected objectives to this day with computer designed optics. A key advance in the efficient use of microscopes was the consideration of uniform illumination and alignment of the optical components. In 1894 Köhler (1) introduced an illumination alignment system still central to microscopy today, namely, Köhler illumination. For in-depth coverage of resolution, optical pathways, and alignment procedures, the reader is referred to Inoué and Spring (2), Keller (3), Lacey (4), Spencer (5), and Bradbury (6), as well as the various web sites noted at the end of this review.

During the twentieth century there was a blossoming of various types of microscopy including a variety of contrasting approaches (dark-field, phase-contrast, interference-contrast, asymmetrical-illumination, etc.), the application of polarizing microscopy, and the introduction of fluorescence microscopy. More recent advances in light microscopy include confocal and multiphoton microscopy, the use of video and image processing, and allied methods. The 1980s saw the introduction of scanning tunneling microscopy (STM) and atomic force microscopy (AFM), as well as scanning near-field optical microscopy (SNOM). The past few decades are also marked with the imaging of cells using acoustic microscopy, Doppler–shift microscopy, X-ray microscopy, NMR, and others.

The first electron microscope (EM) was built in Germany by Ruska in 1931 (7–10) and rested on the prior findings of de Broglie in 1924, who showed that electrons travel in waves, and those of Busch in 1926 who showed they could be focused with electromagnetic lenses. With the short wavelength attainable in an EM, particularly at higher electron gun accelerating voltages, resolutions of 1–2 Å (10^{-10} m) are possible. Advances in the design and construction of EMs coupled with the advancement of improved fixation, initially due to osmium tetroxide and subsequently glutaraldehyde, made possible the high resolution of cell ultrastructure and descriptions of cell organelles. The 1950s to 1980s are replete with EM studies that characterized hundreds of cell types. Scanning EM (11) made possible three-dimensional viewing of cells, as well as cell interior components when appropriately prepared. The use of ultracryofreezing methods combined with carbon/platinum replica freeze-fracture methods made it possible to visualize the molecular architecture of membranes, cell junctions, and macromolecular arrays such as F-actin filaments and microtubules. Analytical methods have also been incorporated into EMs making possible molecular characterizations using X-ray microanalysis, energy loss spectroscopy, or electron spectroscopic imaging, and other approaches. The combination of immunogold-labeling techniques and the resolving power of EM has impacted significantly on the characterization of cell components, receptor sites, etc. In the 1990s the emphasis has shifted back to light microscopy, in particular with confocal and multiphoton microscopy and the emerging areas of atomic force and scanning near-field optic microscopy. The ability to visualize structures and processes in live cells with fluorescent probes and to utilize digital imaging methods has supplanted electron microscopy in many areas of cell biology. For additional information and perspectives on new developments in microscopy, the reader is referred to Refs 12–19, Ref. 20 (Vol. 3), and the various microscopy web sites.

21.3 LIGHT MICROSCOPY

21.3.1 Basic Concepts, Microscope Components and Principles

A superb up-to-date reference source that is comprehensive in coverage of fundamental principles and practical aspects

of basic microscopy, as well as specialized types, is by Inoué and Spring (2). This is an invaluable resource in any cell biology lab that uses microscopes. Definitions of the terminology used in microscopy are available in the Royal Microscopical Society Dictionary (21).

The essential components of a light microscope are as follows:

21.3.1.1 Illumination Source. A light source which usually is built-in and includes a collector lens, a diaphragm, and has focusing and centering capabilities. The specific type of light source will vary depending on the type of microscope and application. Light sources could be tungsten filament lamps (usually 12 V), quartz-halogen lamps (often 12 V 100 watts), high-pressure arc lamps HB0 100 or 50 mercury or XB0 75 Xenon that are operated with a DC power supply, or various high-intensity laser light sources depending upon which wavelengths are needed. Some setups may have more than one light source fitted for multiple applications.

In most microscopes, the light is introduced directly into the optical path via a collector lens, but increasingly fiber optic light guides are being used to bring the light path to the condenser or other optical components. Where a single fiber optic fiber is being used, improved images are attained if the light field is made uniformly homogeneous with minimal loss of luminance by using a "light scrambler" (2,22). A field diaphragm in the illumination pathway is essential for setting up Köhler illumination and centering the condenser.

21.3.1.2 Condenser. Between the field diaphragm and the condenser lens is a condenser iris diaphragm, and depending upon the specific type of specialized microscopy, there may be other additional components, for example, a polarizing filter in polarizing microscopy, Differential Interference microscopy (DIC), and Hoffman modulation-contrast microscopy, a beam splitter in Nomarski DIC, a center stop in dark-field microscopy, a phase annulus in phase-contrast microscopy, and an off axis aperture in oblique or anaxial illumination, or an excitation filter in fluorescence microscopy.

The quality and numerical aperture of the condenser is important to the overall image quality and resolution. Resolution of the microscope is

$$d = \frac{\lambda}{\text{NA objective} + \text{NA condenser}}$$

where d is the smallest distance between two resolvable points. The best condensers are achromatic-aplanatic condensers. However, Abbe condensers are also common. For condensers with NAs greater than 0.9, optimal results are attained if immersion oil is put between the front lens of the condenser and the specimen. The condenser must also be properly focused as there is a focal length, and the light must be focused at the specimen which will fill the back lens of the objective with even illumination when the iris diaphragm is properly adjusted. High-quality condensers should be free of chromatic and other aberrations. The lens elements should have high transmission properties to minimize light loss.

21.3.1.3 Stage. Next is the specimen which is held on a stage. Most microscopes have mechanical stages for precise positioning, and more sophisticated systems have X-Y computer-controlled positioning stages. Polarizing microscopes usually have circular stages for specimen orientation. Optical factors important in the specimen itself include the glass slide, coverslip, and mounting medium. Slides are usually glass, but in some special applications may be quartz. An especially important factor is coverslip thickness. The thickness of #0 coverslips is 0.1–0.13 mm, #1 is 0.13–0.17 mm, #1.5 is 0.15–1.20 mm, #2 is 0.17–0.25 mm, and #3 is 0.25–0.5 mm. Although some objectives have correction collars to adjust for different coverslip thicknesses, most objectives have a fixed correction factor for a 0.17 mm thickness. Usually, #1.5 coverslips should be used for optimal image quality. The refractive index of the medium that contains the cells and the medium between the coverslip and objective lens also are important factors because reducing the refraction of light as it passes from media of differing refractive indexes reduces light loss and background noise due to random scattering. Because the refractive index of glass is 1.52, the use of immersion oil in place of air between the slide and immersion objective lens allows for higher NAs and higher resolution and image quality. In fluorescence microscopy, the use of media without or minimal fluorescence is essential.

21.3.1.4 Objective Lens. Detailed knowledge of the characteristics, type, and quality of the objective lens is one of the most important aspects in microscopy. Having lenses free of aberrations, with high light-gathering and transmission characteristics and the highest numerical aperture possible are pivotal in attaining high-quality images. Furthermore in various specialized types of microscopy, additional components (e.g., phase plate in phase-contrast microscopy) are positioned in the back focal plane of finite tube length objectives. For in-depth coverage of objectives, refer to Refs 2,3, and 23. The following only skims the highlights and presents some of the terminology. Unfortunately, markings on objectives may vary among manufacturers.

Until recently, the vast majority of microscopes were fixed tube length of 160 or 170 mm (mechanical tube length from objective nosepiece opening to eyepiece opening). In such finite systems, the objective projects a real image in the microscope. The lens focuses convergent light in the interlens space. Most manufacturers have switched over

to infinity-corrected optics (2,3,23). Infinity objectives, marked ∞, are designed to project an image to infinity so that essetially there is parallel light between the objective and eyepiece. The advantage is that one or more optical components such as is needed in polarizing, phase, DIC, or fluorescence microscopy can be inserted without changing the functional tube length. One, two, three or more components can be introduced without affecting microscope performance. So multimode microscopy is easier to design without deleterious effects on image quality. But because the light rays are parallel to make the light convergent and project an image to the eyepiece, a second lens, or so-called tube lens, is needed between the objective and the eyepiece. Finite systems do not have a tube lens. Objectives cannot be interchanged between infinity and finite systems.

Beyond these two fundamental types there are other features important to know for proper selection and use of objectives. Most standard objectives are achromats (sometimes marked Achromat) with chromatic aberration correction for two colors (red and blue) and spherical correction in green. Apochromats are corrected for three spectral colors (blue, green, red). Plan indicates correction for a flat field. Fluorite objectives, often marked FL, fluor, Neofluar, etc., use fluorite glass and are ideal for fluorescence microscopy. Fluorite achromates have better spherical correction than conventional achromates. Etched on the objective could well also be the magnification, coverslip correction (usually 1.7), and numerical aperture (1.4 is highest presently attainable). In terms of final image magnification, a ballpark practical magnification limit should be around 500–1000 times the objective NA, preferably 750 or less. Objectives may also have coverslip thickness correction collars or diaphragms (useful in fluorescence microscopy to adjust image intensity). Some objects are high dry and are to be used in air, and others are designed to have an immersion fluid between the objective and specimen. The immersion medium is most frequently oil (marked oil, oel) but glycerine (gly), water (w), and other immersion objectives are also used. Individual manufacturers often additionally identify these with color-coded rings etched around the objective (see Tables 21.2–21.3 in Ref. 2). As the magnification of objectives increases, the working distance (distance between the objective and specimen when at the focal point) decreases as does the depth of focus. Objectives labeled LD are designed to provide longer working distances (useful for microinjection, manipulation, etc.). For polarizing microscopy, objectives must be strain-free and are often marked POL.

As will be dealt with later in the context of the specialized microscopy types, additional components can be incorporated either in the back focal plane of the objective or between the objective and ocular (depending on the type of system). Examples of such elements are Nicol or Wollaston prisms for Nomarski DIC, analyzer (polarizing filter) and compensator for polarizing microscopy and others, phase plate for phase-contrast microscopy, attenuation filter in single sideband edge-enhancement microscopy, barrier or emission filter in fluorescence microscopy, modulator plate in Hoffman modulation microscopy, etc.

Before moving on to the eyepiece or ocular, it is important to stress that using the highest NA objectives possible is essential for critical excellent microscopic imaging. The light-gathering capability, brightness, and resolving power are dramatically improved in higher NA objectives. The micrographs in Figure 21.1 illustrate that the detail resolved in the diatom test slide is much better with NA 1.4 versus 0.65. This becomes especially important when light intensity is limited (e.g., in polarizing microscopy, certain fluorescence). In addition to the importance of NA in image resolution and spatial frequency, according to Abbe (see Ref. 2), contrast transfer function (CTF) and modulation transfer function (MTF) are also affected. One can determine a specific optical transfer function (OTF) or MTF for any objective under a specific condition of use. The MTF specifies the performance system to image spatial detail. For three-dimensional image reconstruction and deconvolution routines used in image processing (particularly in fluorescence and confocal applications), the determination of the axial intensity distribution above and below the objective's focal point, expressed as a point-spread function, is needed. The axial intensity distribution of a point source above and below focus generates a three-dimensional diffraction pattern. One can calculate a point-spread function from a stack of serial optical sections of a point source (circular aperture or fluorescent bead). Suffice it to say that the quality of the objectives is at the heart and soul of the microscope's performance.

21.3.1.5 Eyepieces and Imaging. The eyepiece projects and magnifies the image formed by the objective lens. The power and diameter of field of view, as well as information on correction of aberrations and special features, are often indicated. CF indicates chromatic aberration free, W or similar markings indicate wide field, C or K indicates compensation, etched glasses are for high focal point, p or pl is for plan, and Kpl indicates a compensating flat field.

Conventionally observations are made by eye. However, increasingly, images are obtained by using a variety of video cameras, detectors, and photomultipliers with linkage to computer-based image processing and display systems. These will be covered in a subsequent section. Particularly useful are test slides to assess the overall imaging quality and spatial and axial resolution of the overall microscope system. Convenient test slides include diatoms with their precise repeat spatial patterns (e.g., *Amphipleura pellucida*—9.24 μM; *Pleurosigma angulatum*—0.62 μM),

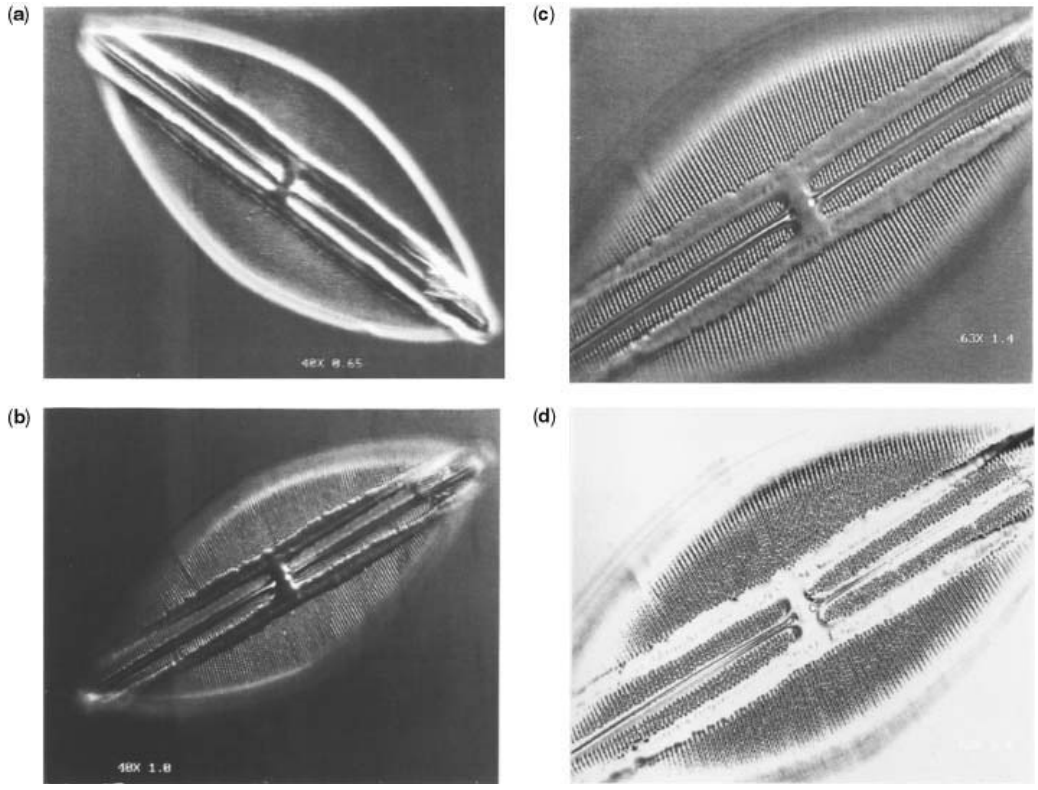


Figure 21.1. These Nomarski differential interference micrographs of a diatom illustrate the improved resolution with increasing objective NA (**a**) 40 × NA 0.65; (**b**) 40 × 1.0 NA; and (**c**) 63 × 1.4 NA; (**d**) this black and white image of a pseudocolored image of (c) reveals the fine structural detail resolvable.

butterfly scales, specially prepared pattern slides [e.g., Richardson slide (24), MBL-NNF slide (2)].

The preceding are the components that comprise a basic light microscope, including the possible variations in optical components and brief reference to concepts and practical aspects. Microscopes can be of the standard upright configuration or can be inverted with the light source in the upper vertical position, as one finds in inverted microscopes often used for examining cells in culture flasks or chambers.

21.3.2 Survey of the Variety of Light Microscopes and Cell Biology Usage

Visualization of structures in cells and tissues requires magnification because cells range from about 10–50 μM in diameter and are not resolvable by the naked eye. Along with magnification, which is achieved by the two magnifying systems (objective and eyepiece) working in tandem, structure can be discerned only by the presence of contrast within cells. The human eye cannot detect phase differences but can discriminate contrast differences in the range of 2–20% (18). Contrast can be achieved in various ways involving absorption, refraction, diffraction, reflection, light scattering, birefringence, and fluorescence. Central is the interaction between matter and light. In instances where this interaction results in phase changes, visualization is achieved only if these can be converted to contrast differences. Most living cells lack sufficient inherent contrast, so that bright-field microscopy reveals little without the use of stains to reduce the amplitude of certain wavelengths and render contrast differences preferentially. A number of different strategies have been developed to generate contrast thereby revealing structures in unstained or live cells and tissues (2,18,20,25–28). The following covers the highlights and uses of the array of light microscope types available for cell technology. A variety of useful contributions can be found in the Royal Microscopical Society Handbook Series (27) and Cell Methods Handbooks [28, also Ref. 20 (Vol. 3)]. A particularly good web site that covers various types of microscopes is the Molecular Expressions-Microscopy Primer (http://micro.magnet.fsu.edu/primer/webresources.html).

21.3.2.1 Bright-Field Microscopy. The fundamental components of the bright-field microscope are as indicated earlier. Live cells and tissues are poorly viewed with a bright field because only opaque or naturally occurring pigment granules absorb or refract sufficient light to

generate discernible contrast. Although there are a few classical vital dyes (e.g., Janus Green B, Evan's Blue) that reveal selected facets of live cells, the primary use of bright-field microscopy is on fixed cells stained with dyes that bind selectively to cell structures. Figure 21.2a shows a typical paraffin section stained for bright-field observation. There is a wide array of selective and semiselective dyes available for cytological, histological, and histochemical uses (20 (Vol. 3), 29). The limitation is that fixed cells are usually used, and the problem of fixation artifacts must be considered.

Contrast visible to the eye in bright-field microscopy is due almost exclusively to the selective absorption of light. Because of differential binding affinities to stains, certain cell components become distinguishable. The classic example is hematoxylin and eosin staining (Fig. 21.2a) which highlights nuclei in shades of blue, and the cytoplasm pink, depending on the protocol used.

21.3.2.2 Dark-Field Microscopy. This is one of the oldest and least costly forms of microscopy that renders contrast to living or unstained cells (30–32). It reveals cells (particularly edges and boundaries) in bright contrast against a dark background (Fig. 21.2b). During the past 20 years, this form of microscopy has received renewed interest because it provides high-contrast viewing of very fine structures below the resolution limit of the microscope (2,3). One can view bacteria, cilia, flagella, single cytoskeletal elements, like F-actin and microtubules, and isolated particles and cell components.

Dark-field microscopes (DF) have special condensers with a center stop which blocks out all of the central rays

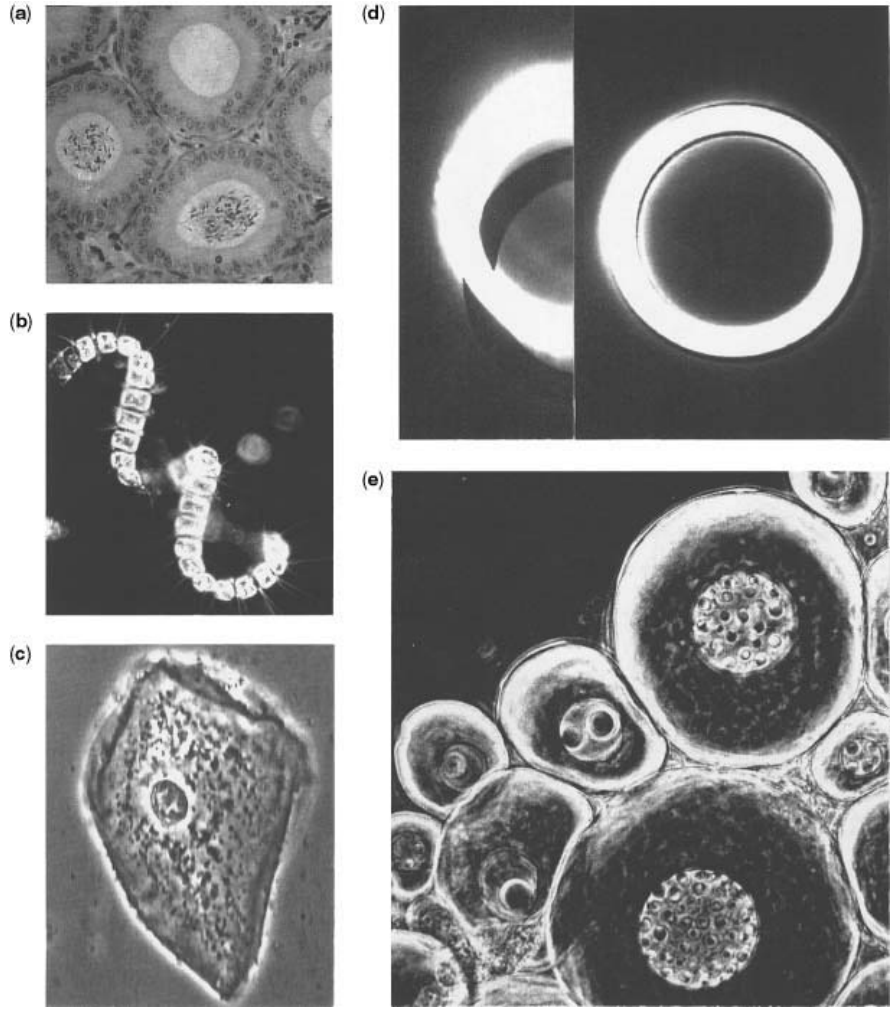


Figure 21.2. These micrographs provide examples of a bright-field and a dark-field on phase-contrast images. (**a**) an H and E stained epidymus section; (**b**) a live marine algal chain viewed in a dark field; (**c**) a live human buccal cell viewed with phase contrast; the two panels of (**d**) show the phase ring and annulus misaligned and aligned; (**e**) a phase view of live multicellular tissue (goldfish ovary) where nuclei and nucleoli are seen.

that create a cone of light. The ray diagrams in Figure 21.3 show dark-field microscopy compared to bright-field. Without a specimen in place and the condenser and objective properly focused, all of the undeviated light of this cone misses the objective. Once a specimen is introduced into the light path, some of this light is diffracted or refracted (deviated light) and enters the objective. So, only light scattered by the cellular components is seen, and the specimen appears as a bright extremely high-contrast structure against a black background. Dry DF condensers are usually used with objectives of NA <0.75. High NA objectives used for DF need a diaphragm to exclude undeviated light, some of which enters the objective. Not only is DF useful for looking at intact cells but has had renewed impact in visualizing exceedingly small structures. It is valuable in studies of cytoskeletal dynamics *in vitro* and cytoskeletal-based transport. In addition to these applications, DF is also very useful in autoradiography because the silver grains are highlighted as bright spots on a dark background making visualization and quantification clearer.

21.3.2.3 Phase-Contrast Microscopy. The absorptive light scattering differences between the variety of components in cells (due to refractive index and thickness differences) generate phase shifts. However, these are not detectable by the human eye or detectors. The interaction between light waves not deviated by cell components and deviated light is insufficient to generate amplitude differences large enough to give contrast. The invention of the phase-contrast microscope by Zernicke in 1935 (33) achieved the goal of producing a sufficient phase shift between undeviated light and specimen-deviated light, so that better interference occurred between the two wave fronts thereby providing sufficient amplitude change to give visible enhanced contrast. The interference between the two wave fronts provides a resultant brightness change (2,3,20,25–28,33). Now structures not visible in bright-field microscopy are easily seen. This provides an easy to use, cost-effective way of viewing live cells in culture and determining general cell features, nuclear shape, size, cell movements, etc. Figure 21.2c and 21.2e show phase-contrast images of both single cells and multicelluar tissue. The impact of phase contrast on cell biology was considered so important that Zernicke was awarded the Nobel prize in 1953.

A phase microscope has a special condenser with a series of phase annuli (each matched for its respective objective) (Fig. 21.4). The phase annulus allows a hollow cone of light (undiffracted zero-order illumination) to enter the objective and fall on a coincident donut-shaped region of a phase plate that is located in the back focal plane of the objective. This circular ring region of the phase plate (often coated by a dielectric) absorbs or attenuates 70–80% of the light and introduces a phase shift of one-quarter of a wavelength. Light scattered and altered by cellular components is deviated and passes through the other transparent regions of the phase plate (Fig. 21.4). The net result is that the introduction of the phase shift allows sufficient interference between the altered and unaltered light to generate visible amplitude differences, that is, contrast (can be negative or positive contrast). This reveals finer cellular detail (Fig. 21.2c, 21.2e). However, an annoying feature is the presence of halos surrounding contrasted structures because some of the diffracted light also passes through the ring area of the phase plate adding to the directly transmitted light. A

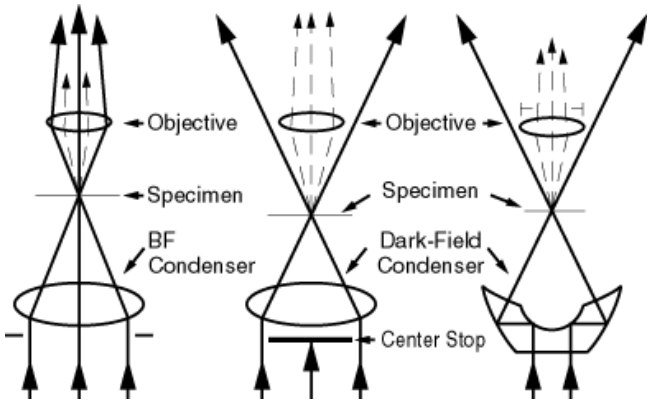


Figure 21.3. These ray diagrams contrast a bright-field microscope (left) with simple center-stop dark-field and dark-field condenser microscopes. A hollow cone of light is created by either the center stop or a dark-field condenser that has a central reflecting surface. This cone of undiffracted or zero-order light (solid line) bypasses the objective, and only the deviated refracted light (dashed line) enters the objective.

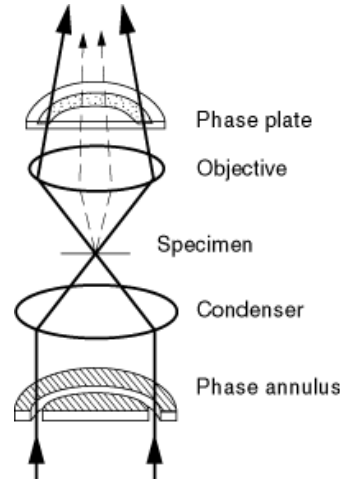


Figure 21.4. The essential components of the phase-contrast microscope. The condenser annulus produces the cone of undiffracted light that passes through the matched-phase ring or phase plate located at the back focal plane of the objective. The dashed lines represent the diffracted light.

second limitation is that one cannot do optical sectioning, so out-of-focus details limit the level of detail discernible.

Phase contrast works best on thinner objects (<5 μM thick), and proper images are obtained only if the correct phase annulus is used for each objective phase plate and if the annulus and ring in the phase plate are precisely aligned. This can be easily done with microscopes having a flip-in Bertrand lens (so the back focal plane of the objective can be seen) or by removing an eyepiece and using a phase-contrast telescope lens (Fig. 21.2d).

The invention of an aperture-scanning phase-contrast system by Ellis in 1988 (described in Ref. 2) uses a small circular fiber optic fiber that scans in a circle at the front focal plane of the condenser. This is conjugate with a phase plate in the back focal plane of the objective where there is a small dot that introduces the 1/4 λ shift instead of the usual ring. The result is improved imaging with less interference of out-of-focus image planes and no high-contrast halos. For detailed coverage of phase-contrast optics, the reader is referred to Ross (34,35), Bennett *et al*. (36), Inoué and Spring (2), Keller (3), and Sanderson (in Ref. 20 (Vol. 3)).

21.3.2.4 Oblique, Anaxial, or Asymmetrical-Illumination Microscopy. The use of oblique or even lateral illumination to yield contrast differences in unstained cells characterizes various modes of microscopy, as well as specially constructed microscope types.

21.3.2.4.1 Oblique or Anaxial (Asymmetrical) Illumination. This is achievable with a bright-field microscope set up for Köhler illumination and then by various means passing only the unaltered (undeviated, zero-order light) through one off-center region of the condenser and objective. Diffracted light passes through other areas of the objective. Oblique illumination can be produced by moving the lamp filament extremely to one side (37), by a variety of asymmetrical stops in front of the condenser or over the field diaphragm (38,39), or simply by offsetting the condenser diaphragm to one side (3) as Abbe did in the 1800s. Asymmetrical illumination due to uneven condenser illumination produces a contrasted differential image that usually has a shadow-cast appearance. This is caused by the components in the cells diffracting the light and creating other orders of diffraction which enhance interference and improve contrast.

21.3.2.4.2 Hoffman Modulation-Contrast Microscopy. This type of microscope developed by Hoffman (40) allows more precise control and refined imaging which is particularly useful for single cells. Shaded images with a three-dimensional appearance, high contrast, optical sectioning, and control of contrast result. The essential optical components are (1) a polarizer over the light source (2), a slit aperture with a rectangular polarizer covering about half of it in the condenser and a special amplitude plate called a modulator in the back focal plane of the objective (Fig. 21.5). The modulator is a trizonal plate with three different transmission regions (3%, 15%, 100%). The condenser slit/pol aperture must be aligned with the modulator. The clear slit is over the 15% zone, and the polarized half of the slit is over the 100% zone. The net result of this off axis illumination is that the small phase-gradient differences within the sample yield deviated or altered light that is converted to intensity variations giving the shadowing and optical sectioning effect.

21.3.2.4.3 Single Sideband Edge-Enhancement Microscopy. This related form of asymmetrical-illumination micrscopy was developed by Ellis (41) and utilizes a half mask (stop) in the condenser and a carrier attenuation filter in the back aperture of the objective. This attenuation or spatial filter is sandwiched between two polarizing filters (see Refs 2,41, for details). The images obtained are much like differential interference-contrast images and are

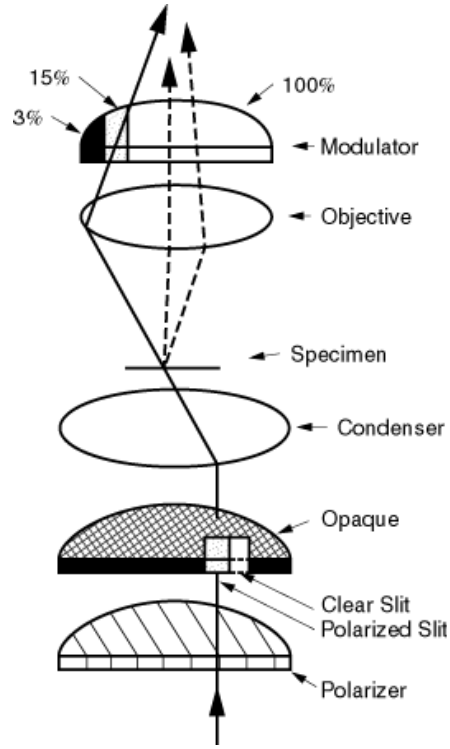


Figure 21.5. A simplified summary of the Hoffman modulation-contrast microscope (HMCM). Located in the front focal plane of the condenser is an opaque plate that contains an asymmetrically located rectangular slit half of which is covered by a polarizer strip. The back focal plane of the objective has a modulator plate with three zones of transmission. The condenser slit is aligned with the 100% and 15% areas. Diffracted light (dashed lines) passes through the rest of the modulator.

extremely rich in fine spatial detail. This is an ideal type of microscopy for viewing thin objects and where high spatial detail is required.

21.3.2.4.4 Multiple Oblique-Illumination 3-D Microscope. Three-dimensional images of cells, tissue slices, and live specimens can be produced by using a 3-D microscope that utilizes multiple (4) oblique fiber optic light polarized sources reflected by a pyramidal mirror. The microscope (3-D edge microscope, Edge Science Institute, Santa Monica) utilizes a field and relay lens to image the objective aperture on top of the optical path where it is split and channeled to the two eyepieces that provide a 3-D stereo image. See Greenberg and Boyde (42) for a general review of the optics and applications of this novel use of oblique illumination.

21.3.2.5 Polarizing Microscopy. Polarizing microscopy is a powerful qualitative and quantitative tool for examining cells and cell components that have structures with high degrees of molecular order. Structures such as filaments, microtubules, crystal arrays, extracellular matrix fibers, DNA, certain lipids, etc., can be viewed with sufficient contrast generated by polarization microscopy. Ordered structures appear as highly birefringent structures when ideally oriented. Anisotropy, the property of matter which has different values when measured in different directions in the same material, is the basis of polarizing microscopy. Polarizing microscopy has a long history dating from the first polarization microscope built by Smith in 1851 (43). Much of our current use of the polarization microscope in cell biology is heavily influenced by the extensive work of Inoué (2,44) and significant new developments introduced by Oldenbourg and Mei in 1995 (45).

A polarization microscope is basically an ordinary bright-field microscope equipped with a polarizer beneath the condenser and a second polarizing filter called the analyzer above the objective (2,46). Figure 21.6 shows a schematic of the components of a polarizing microscope. When light is propagated as a wave, it vibrates in two vectors at right angles to each other. When this passes through a Nicol prism (introduced by Nicol in 1860) or an anistropic structure such as a calcite crystal, the two beams (often called the e and o rays) are split. The polarizer preferentially passes light vibrating in a single plane, so that when the analyzer is crossed, little light is transmitted to the eyepiece. Only the alteration of polarized light by ordered structures in the cells placed in the optical path will generate birefringence (see Fig. 21.8f). The optics should be strain-free, and usually a rotating stage is used for specimen orientation. For analytical work, a compensator is often used between the polarizer and analyzer. This allows one to measure the degree of birefringence. When the polarizer and analyzer are crossed, one has extinction.

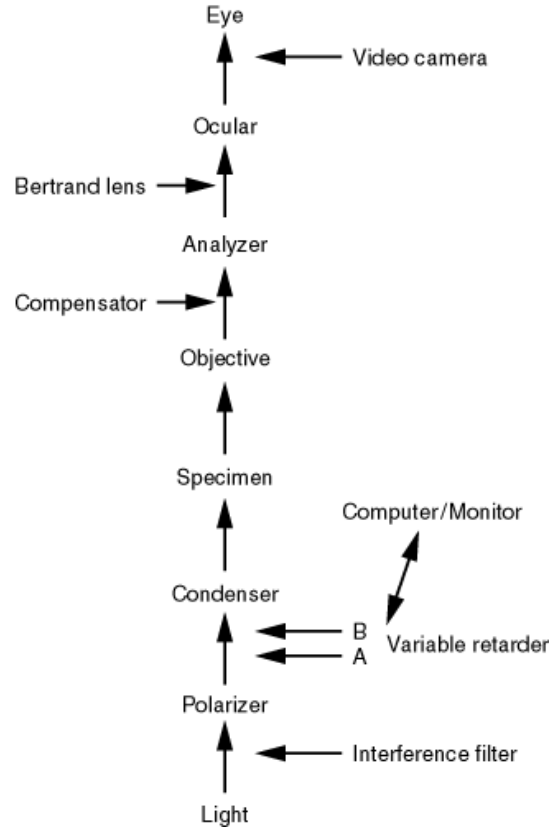


Figure 21.6. In the center is the sequence of components that comprise a basic polarizing microscope. On the left are optional elements (Bertrand lens, compensator frequently present). On the right are the additional components incorporated by Oldenbourg and Mei in their new Pol-Scope. A key component is the electrically controllable variable retarders (A and B). See text for details.

Extinction is a measure of the amount of stray light that is prevented from passing when the filters are crossed. To visualize anisotropic structures in cells and tissues, a high level of extinction is essential. Because the amount of light resulting from birefringent structures (e.g., microtubule arrays, mitotic spindles, DNA, etc.) is small, one needs to use bright light sources to overcome the significant amount lost by extinction. High NA objectives are used, so that maximum light capture is possible. Unfortunately conventional high NA objectives often reduce extinction. This can be corrected by using rectified optics (2).

With a polarizing microscope, anisotropic structures (e.g., microtubules, etc.) with their ordered molecular architecture appear as bright birefringent objects if extinction is high enough to yield a dark background. Birefringence occurs when the refractive index in one axis of the object is different in the orthagonal axis. This birefringence is measured as retardation (birefringence $\times$ thickness) and expressed in nM. Values less than 5 nM are hard to measure. However, this has recently been reduced to 0.02 nM by the introduction of a new innovative approach (45). The

Pol-Scope is a traditional polarizing microscope augmented by electro-optical devices and imaging algorithms to complete specimen birefringences. In a conventional Pol scope, only those anistropic structures in a certain orientation are displayed in a single image. The new Pol-Scope uses a precision universal compensator made of two electrically controllable liquid crystal retardation plates (B $\lambda/2$ 0°; A $\lambda/4$ 45°) that overcome the orientation problem. One can measure dynamically and non-destructively in live cells or isolated cell components with a high degree of sensitivity (as low as 0.02 nM) with excellent spatial resolution (0.2 nM). Recently (1997) Shinya Inoué (47) in conjunction with Hamamatsu and Olympus has added a new centrifuge polarizing microscope to the family of polarizing microscopes. This adds to the possibilities by allowing visualization of live cells and their organelles under centrifugation with high fidelity and resolution.

21.3.2.6 Interference-Contrast Microscopy. Like phase-contrast, interference-contrast microscopy exploits interference differences initially generated by local phase differences in the specimen and converts these to intensity differences. Perhaps the most widely used type of microscopy today to visualize live cells is the differential-interference microscope of which there is the Smith and Nomarski types (see Refs 3,20 (Vol. 3)). Surprisingly, interference microscopy was first introduced in 1893 by Sinks (see Ref. 48). However it was not until after the widespread use of phase-contrast microscopy that interference microscopes were designed and manufactured for general use. As reviewed in Inoué and Spring (2), there are essentially three types of interference microscopes *(1)* the Mach–Zehnder which involves two microscopes for separate reference and modified light paths; *(2)* beam-shearing types where the split beams are displaced laterally as in the Jamin–Lebedeff, Smith, and Nomarski types; and *(3)* the Mirau type where the reference beam is focused to a level differently from the specimen plane. The Jamin–Lebedeff interference microscope initially designed by Piller and built by Zeiss in the 1960s allowed quantitative analysis of live cells making it possible to measure cell volumes, mass of cell components, etc., based on calculations using optical path difference measurements. Such instruments are no longer available. The most widely used modern interference microscopes are the differential-interference microscopes (DIC) (2,18,26,48) developed by Nomarski in 1955 (48–50) and Smith in 1956 (48). In these, the beam splitter at the front focal plane of the condenser is a Wollaston prism that splits the polarized light into two paths displaced laterally relative to each other with shear. These two paths then pass through the specimen and are altered differentially depending on the refractive indexes of the cell components each encounters. At the back focal plane of the objective is another Wollaston prism (which can be adjusted in the Nomarski system) that recombines the two light paths. An analyzer crossed with respect to the polarizer (below the condenser) is next in the optical path. When the two beams are brought together, they interfere (Fig. 21.7). The phase shifts in each result from refractive index differences and thickness gradients in the cells being viewed. This exploitation of local phase differences results in a shadow-cast effect which reveals very fine cell detail and allows optical sectioning because of the very shallow depth of field. Figure 21.8c–21.8d shows DIC views of live cells. For comparison Figure 21.8a provides a HMCM image and Figure 21.8b provides a phase-contrast image.

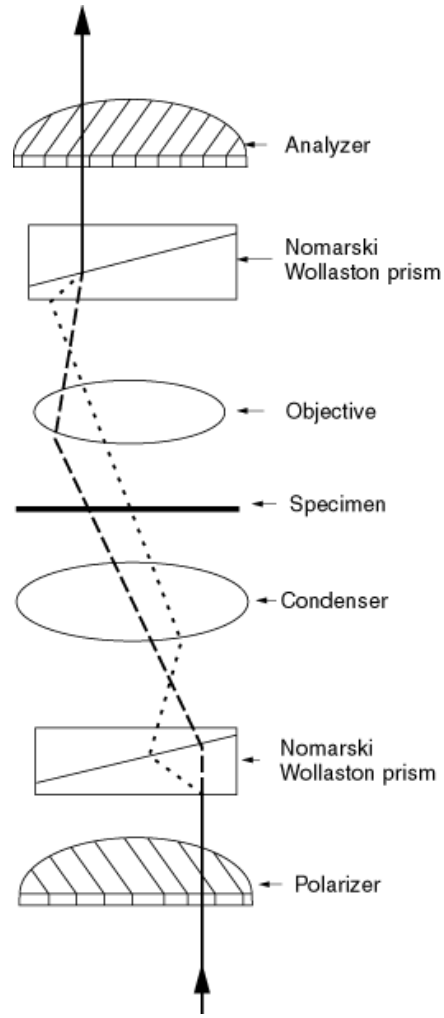


Figure 21.7. An example of one of the types of interference-contrast microscopes shown here is the Nomarski differential interference-contrast system (DIC). Plane-polarized light is split by Wollaston prisms into two paths separated by shear. These are indicated by the dashed and dotted lines. The final recombination of the two paths is via the second Wollaston prism. The interaction produces a differential-interference image with shading and high contrast.

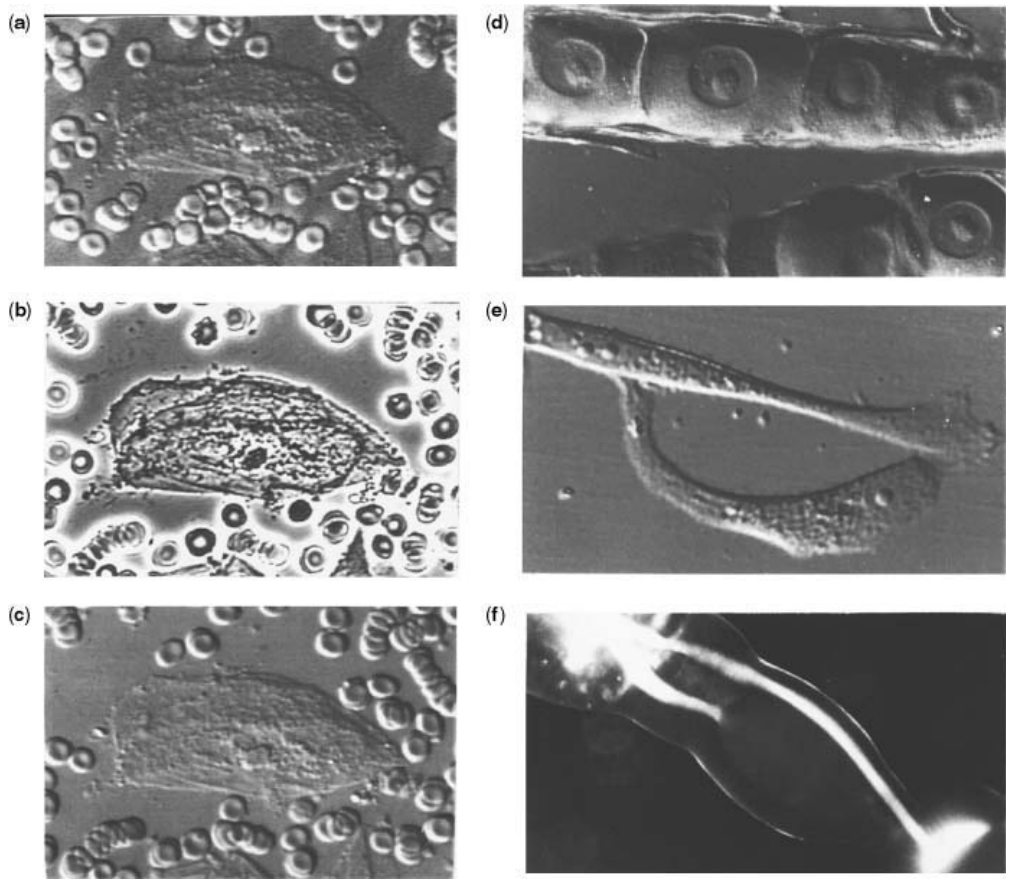


Figure 21.8. (**a–c**) HMCM, phase-contrast, and DIC views of a combined preparation of blood and a buccal cell. Note the graded shading in the DIC (c) and HMCM (a) images, and no halos, as are prevalent in phase image (b). (**d**) The optical sectioning ability of DIC of a praying mantis ovary. The oocyte's large nuclei and prominent nucleoli are delineated. (**e**) A DIC view of HeLa cells. (**f**) A live insect ovariole (of *Rhodnius proxlixus*) as seen in polarizing microscopy. The brilliant birefringent structures are the intercellular bridges or trophic cords that are packed with aligned microtubules.

Organelles and other cell structures appear in relief with variable contrast. For general viewing of cells in culture, this is widely used as the preferred method. However, it cannot be used with plastic culture dishes or plastic coverslips because these are anisotropic materials and affect the polarized light necessary in DIC. A recent improvement in DIC has been introduced by Holzwarth *et al*. (51) which is called polarization-modulated DIC (PM-DIC). This involves using a liquid crystal modulator that can switch the polarization from X to Y rapidly, coupled with a frame grabber and an imaging processing system. The result is a significant improvement in contrast, and with incorporation of background subtraction, one can resolve very fine spatial details of high contrast.

21.3.2.7 Reflection-Contrast Microscopy. Reflection-contrast microscopy (RCM; also sometimes called reflection-interference microscopy, RIM) can be used to study live cells, as well as fixed cells. In its simplest form, it involves passing light (usually polarized via an epi-illumination system with a dichroic mirror down through the objective, and reflected light from the specimen passes through the objective, the dichroic mirror, a polarizer at 90° to the first, and to the eyepiece (52). This was first used by Curtis (53) to investigate cell adhesion and improved by Ploem by placing a quarter λ coating on the front of the objective. Improvements in image quality result if special antiflex objectives are used (54). Izzard and Lochner (55) successfully used RCM (also called interference RCM or IRCM) to look at fibroblast cell substrate adhesion and interactions. Opas and Kalnins (56) also examined cell substrate local adhesion. In RCM, light waves reflected at the sample surface interfere with those reflected from the substrate. The result is an image that highlights contact and adhesion sites in high

contrast. Besides visualizing cell–substrate adhesion sites, RCM is very useful for visualizing nonradioactive *in situ* hybridizations where peroxidase or silver/gold labels are used (57).

Reflection microscopy has also involved using a scanning mode via a spinning Nipkow disk containing 24,000 small holes that produces and detects many points of light. These were first developed independently by Minsky and by Petrán in the 1960s (58–62). They are called tandem-scanning reflecting microscopes and are also used for examining cell–substrate adhesion, as well as cytoskeletal structures. The tandem-scanning reflecting-light microscope developed by Petran was the first use of a confocal microscope approach. For more in-depth information on reflection contrast microscopes, see Verschueren (52); Egger and Petrán (58), Curtis (53), Opas and Kalnins (56), Izzard and Lochner (55), Ploem *et al*. (57), and Bereiter-Hann and Vesely (in Ref. 20 (Vol. 3)).

21.3.2.8 Fluorescence Microscopy. The phenomenon of fluorescence was first discovered in 1833 by Sir David Brewster and named fluorescence by Stokes in 1852. In fluorescence, molecules in specimens absorb light radiation and per Stoke's Law emit light of a higher wavelength. The excitation light of specific wavelengths excites fluorophore molecules such that outershell electrons move to higher orbits. Within 10^{-7} seconds, these drop to lower orbits and lose the energy via emission of light at a higher λ. For a general description, see Refs 3,20 (Vol. 3), 63. A major impetus to use fluorescence in cell biology comes from the immunofluorescence studies of Coons in the 1940s who localized antigens in cells using antibodies conjugated to fluorescent dyes like fluorescein isothiocyanate (FITC). With the tremendous development of immunofluorescent approaches, the fluorescence microscope became a routine instrument in many cell biology and biotechnology labs during the past 40–50 years. Initially, instruments were transmitted fluorescence microscopes. However, these are rarely used today and have been supplanted by epifluorescence microscopes. A schematic of a standard epifluorescence microscope is presented in Figure 21.9.

The essential components of an epifluorescence microscope are a lamp that emits the appropriate range of wavelengths, a filter to select the excitation wavelength, a dichroic mirror to direct that wavelength through the objective to the specimen which will then emit light to be captured by the objective and passed through the dichroic mirror, a barrier or emission filter that blocks wavelengths below the emission λ, and finally imaging by the oculars. Basic information is available from a variety of texts [2,3,20 (Vol. 3), 63,64], as well as a number of web sites, particularly the Molecular Dynamics and Molecular Probes sites.

Various types of lamps are usable in fluorescence, depending upon the intensity and the spectral range needed. Tungsten halogen lamps produce a continuous white light and emit from about 350–1000 nM but of relatively low intensity particularly in the 350–400 nM range. Such lamps are usable for FITC and a number of newer fluorochromes excitable in the visible spectrum. With the advent of low-light and more sensitive CCD cameras, lower intensity is less of a problem. More widely used lamps are xenon arc lamps (e.g., XBO 75) which have high-intensity output over a fairly continuous spectrum from 250–1000 nM. These are preferred where fluorescence ratioing is needed and multiple λs are needed for different probes. Mercury arc lamps (HB050 and 100) are also widely used. They have high intensity but a more varied spectrum with distinct peaks of intensity at certain wavelengths (e.g., 366, 405, 436, 546, 578). Lasers are being increasingly implemented as excitation sources, each with their specific wavelength(s) rather than a broad spectral array. A heat filter is between the collector lens of the lamp housing and the optical path. Initially, excitation filters used were relatively broad (the UG, BG filter) but now most systems have excitation filters with a reasonably narrowly defined transmission window (this varies among manufacturers but, for, example a 450–490 nM range is common for fluorescein). The fluorescence microscope has an epifluorescence condenser. In some systems, the excitation filters may be located in a

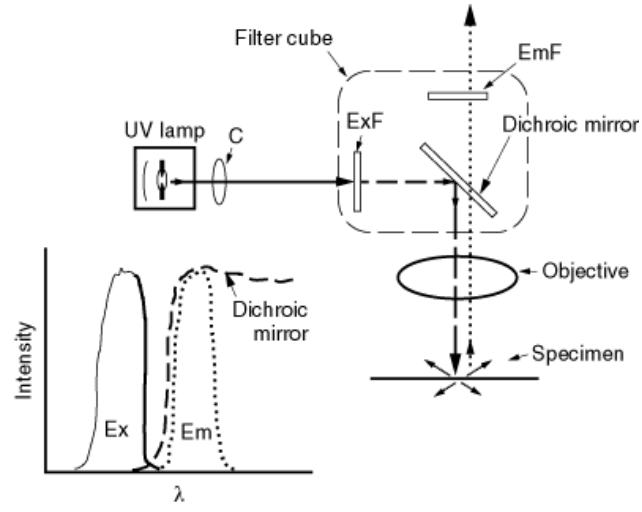


Figure 21.9. A schematic of a typical epifluorescence microscope with a lamp (usually HBO or XBO) that produces a spectrum of λ s. The λ of choice (depending on the stain used) is selected by the excitation filter (ExF). The selected excitation λ is reflected to the specimen by the dichroic mirror (dashed line). Fluorescence (higher λ) enters the objective lens and passes through the mirror with a final selection of the appropriate emission λ by the emission filter (EmF) or barrier filter. The generalized graph shows the spectral pattern for narrow band-pass Ex and Em filters and the dichroic mirror.

computer-controllable filter wheel, and in others the excitation filter along with the dichroic mirror and emission filter is located as a unit (filter cube) in the epifluorescence condenser (Fig. 21.9). The dichroic mirror will reflect the excitation λ into the objective but will transmit only the higher λ of the emitted light, and the higher λ will pass through to the eyepiece. Ideally, the emission filter would be a narrow band-pass filter and would transmit only the λ characteristic of the fluorochrome used. There is a tremendous range of filter combinations available (see the Omega Optical and Molecular Probes web sites, www.sover.net/∼omega and www.probes.com). The inset graph in Figure 21.9 shows a "generic" example of a narrow band-pass filter set. The terminology can be confusing. Dichroic mirrors may also be called chromatic beam splitters.

Because the image and its contrast come from emission of light from the specimen it is important that high NA, high transmission objectives are used, so that a sufficiently bright image results. As covered later, the use of low-light video cameras has opened up new vistas for fluorescence microscopy on live cells without the inherent problems of UV damage from the excitation beam or photobleaching because the intensity of the excitation illumination can be reduced with a neutral density filter or other means (13,14,16,20 (Vol. 3)).

The application of fluorescence microscopy is exceptionally far-reaching. Although there are relatively few endogenous fluorochromes (when present they often pose problems such as autofluorescence), there is an enormous array of fluorescent dyes now available for many applications relevant to cell technology. In-depth coverage of these is beyond the scope of this review, but there is a large and growing literature [3,20 (Vol. 3), 63–68].

The following highlights only a few of the applications of the fluorescence microscope.

A number of fluorescent dyes that selectively stain cell organelles (Fig. 21.10) [20 (Vol. 3), 68] are available. Mitochondria can be visualized in live cells with cell-permeant dyes like Rhodamine 123, Rhodamine 6G, $DiOC_6$, nonylacridine orange, JC-1 (Fig. 21.10a,b), and a range of MitoTracker dyes (Fig. 21.10c) (see Refs 69–71, and the Molecular Probes web site www.probes.com). Endoplasmic reticulum can be visualized (72,73) with labeled conA, $DiOC_6$, ER-Tracker Blue-White DPX (Fig. 21.10d); Golgi (74) with labeled C_5 and C_6 ceramide; DNA in nuclei with DAPI, Hoechst (Fig. 21.11d) or propidium iodide and so on. Fluorescent probes are used for tracking endocytotic uptake, cell to cell coupling, lysosome and lipid inclusions, and cytoskeletal elements, to name a few (75). There are also probes to quickly determine

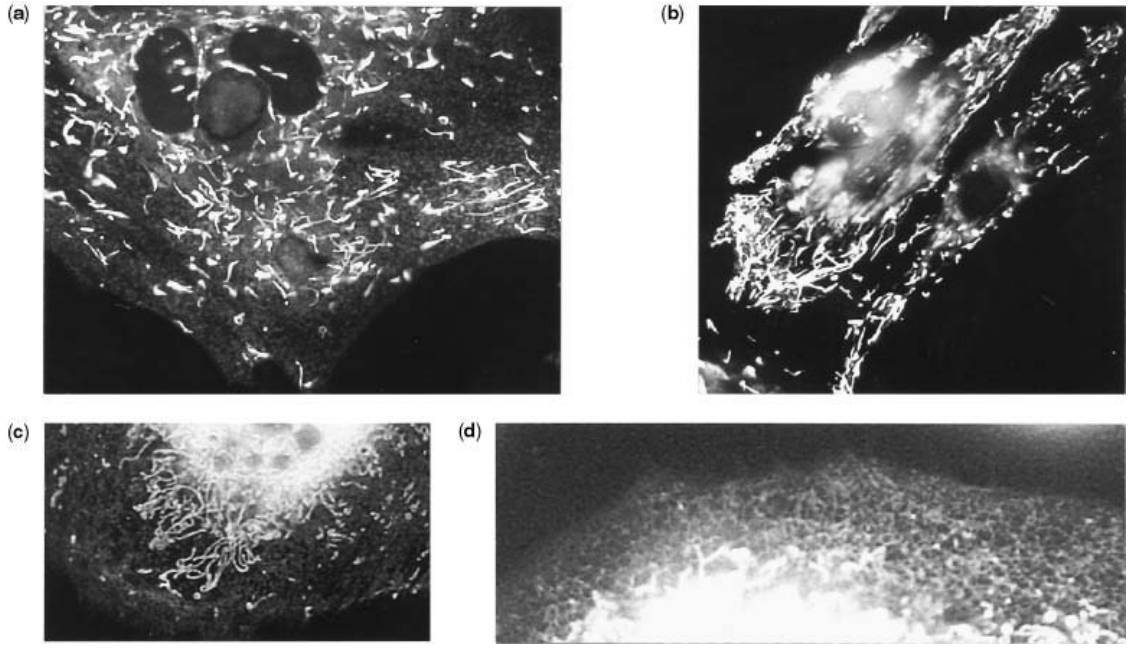


Figure 21.10. These black and white images of the original color fluorescence images show selectively stained organelles in live cells. (**a**) The mitochondria-specific dye JC-1 highlights mitochondria in drug (dexrozoxane)-treated CHO cells. (**b**) In rat fetal cardiac myocytes. (**c**) Long slender mitochondria in dexrozoxane-treated CHO cells stained with MitoTracker Green FM. (**d**) A similar cell stained with the endoplasmic-reticulum-specific stain, ER-Tracker Blue-White DPX. The ER stains as a lacey network seen here in the thinnest peripheral area of a spread cell (E. Huebner and B. Hasinoff, unpublished data, 1999).

live and dead cells in culture and to measure levels of various ions, intracellular pH, and biochemical reactions (75–78). Fluorescently labeled probes are also used in *in situ* hybridization methods commonly known as FISH (fluorescence *in situ* hybridization). Immunofluorescence approaches to visualize cell structures, receptor sites, biosynthetic products, etc. is a major area of application [12–16,20 (Vol. B), 68]. Immunofluorescence has provided a powerful means for visualizing the cytoskeletal organization of cells. Figure 21.10 provides some examples of fluorescence microscopy of the microtubule and F-actin cytoskeleton using IF methods and a specific F-actin probe.

The introduction of new fluorescent probes and stains almost daily has resulted in an explosion of possible ways to study almost all facets of cell morphology and molecular functions of cells with fluorescence microscopy. Improved contrast and brightness is attained with newer dyes that are replacing the classical fluorochromes FITC (Fig. 21.11a) and tetrarhodamine isothiocyanate (RITC). Some of these are Texas Red, the Cy dyes (Fig. 21.11b), Bodipy, and most recently the Alexa dyes. Table 21.1 provides some examples of fluorophores. Some dyes require microinjection (e.g., the calcium-sensing cell, Fura 2) or some alternative physical cell loading method to introduce them into the cytosol. Increasingly dye-permeant forms (e.g., Fura 2 AM) have been produced. Although there are a number of sources of fluorescent dyes, Molecular Probes has become one of the major suppliers of new probes and continues to introduce an impressive array of new dyes.

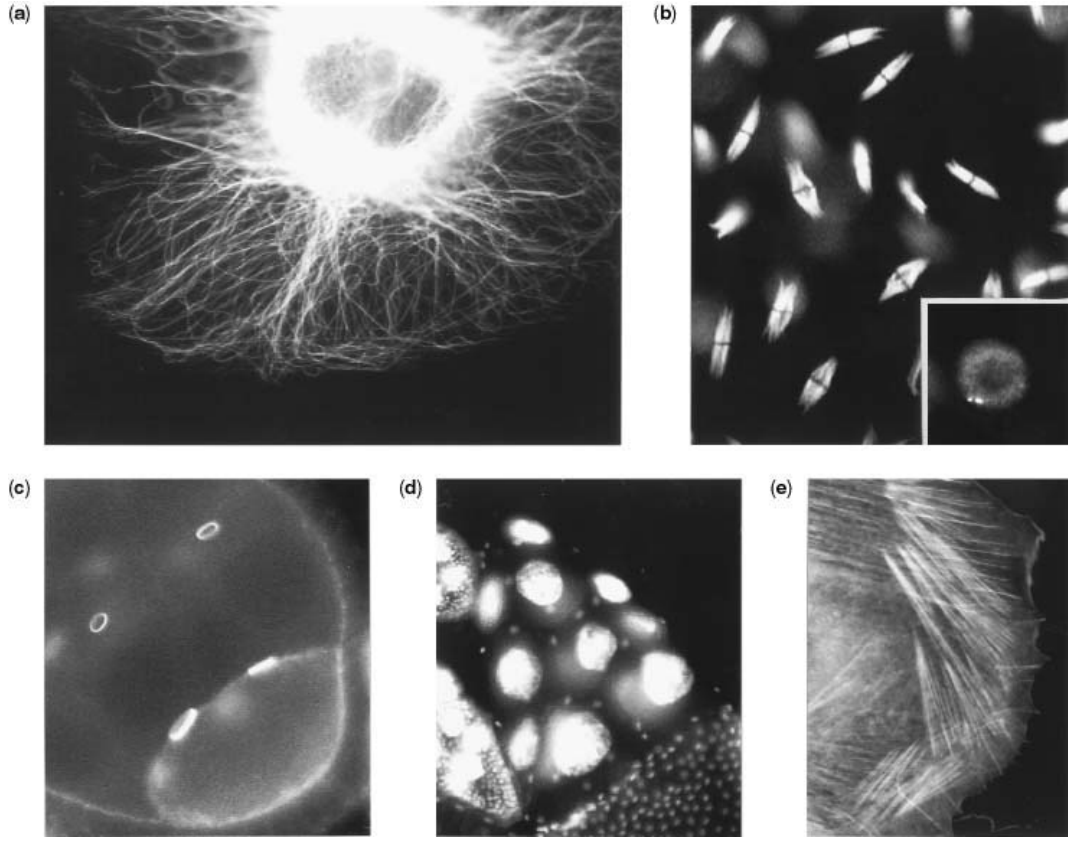


Figure 21.11. These black and white images of the original color fluorescence images illustrate immunofluorescence and other specific probes. (**a**) Dexrozoxane-treated CHO cells greatly enlarge in size. Their dramatic microtubule arrays are stained for acetylated tubulin using a fluorescein-labeled secondary antibody. (**b** and inset) Immunofluorescence of two stages of spermatogenic cells of the insect *Rhodnius*. The inset shows gamma tubulin labeling of the centrioles, and the main figure shows the tubulin of the spindles. The secondary antibody was labeled with Cy3 (E. Byard and E. Huebner, unpublished data, 1999). (**c**) The F-actin-stained ring canals of the *Drosophila* nurse-cell-oocyte cysts of the ovary. The F-actin-specific probe phalloidin is labeled with rhodamine. (**d**) DNA staining of the large polyploid nurse cell and smaller follicle cell nuclei in a *Drosophila* ovariole cyst. The DNA-specific stain is Hoechst 33342. (**e**) The rhodamine-phalloidin staining of F-actin in the stress fibers of an enlarged flattened dexrozoxane-treated CHO cell.

TABLE 21.1. Examples of Fluorophores

Fluorophore	Excitation wavelength	Emission wavelength	Uses
DAPI	358	361	DNA stain
Hoechst 33342	357	461	DNA stain
FITC	495	520	Label
Texas Red[a]	595	615	Label
Cy3[b]	565	590	Label
Bodipy FL[a]	503	513	Label
Alexa 488[a]	495	519	Label
GFP wild-type	396/475	508/503	Expression marker
Lucifer Yellow	428	534	Cell tracer, uptake, gap junctions
MitoTracker[a]	490	517	Mitochondria stain
Green FM	490	517	

[a]Trademarks of Molecular Probes Inc.
[b]Cy3 is trademark of Amersham Intl.

Wild-type green fluorescent protein (GFP) was originally isolated in the 1960s from jellyfish *Aequoria victoria* and cloned in the early 1990s. It absorbs at 395 (brighter) and 475 nM and emits at 508 nM. Chalfie showed that GFP can be linked as a reporter to other genes. This provided the catalyst for methods now routinely used to study gene expression in live cells using GFP fluorescence (79–83). Mutant forms of GFP generally called chameleons provide an array of GFPs as endogenous probes that monitor a variety of changes in pH and other factors (80). pH-sensitive GFP mutants called pHluorins are used to investigate endocytosis, for example (84). Recently, another family of fluorescent proteins, the phyofluors, which are much brighter than GFP, has been introduced (85). Fluorescent reagents can be introduced into cells in bound or caged forms and with appropriate wavelength irradiation are released and participate in reactions generating fluorescent molecules, thereby allowing one to study dynamic reactions at appropriate times [20 (Vol. 3), 86]. Suffice it to say, this is a rapidly advancing field.

A significant drawback in visualizing fluorescently labeled cells with conventional epifluorescence microscopy is the inability to visualize single focal planes. The fluorescence emanating from above and below focus plane levels contributes to the overall image, obscuring fine structural resolution. Image processing can improve visualization, but the introduction of laser scanning confocal microscopy dramatically improved and facilitated fluorescence optical sectioning (see Shotton in Ref. 20 (Vol. 3)).

21.3.2.9 Confocal Microscopy. This form of microscopy is part of the scanning microscopy family. In particular, confocal fluorescence microscopy has become popular as it overcomes the problem of out-of-focus plane fluorescence in fluorescence microscopy. Confocal has its origin in the 1950s and 1960s with its invention by Minsky in 1957 (58–62). Independently, Petran and co-workers in 1968 developed a Nipkow spinning-disc field-scanning or confocal microscope [2,20 (Vol. 3), 87–91].

A specimen can be scanned with the illumination beam by either stage scanning or the more widely used beam-scanning systems. Of these there are basically two common types, the disk-scanning confocals that use a spinning Nipkow or a modified Nipkow disk. In the Petran type the symmetrically placed pinholes alternatively provide the illumination pinhole and the imaging pinhole which are confocal. For current approaches in aperture scanning confocals, see Refs 28 (Vol. 3), 91–93. A newer modification developed by Kino in 1995 (2) uses a beam splitter that makes it possible for each pinhole to act both in illumination and imaging. The incorporation of a second disk with microlenses has further extended the use of the spinning-disk confocal microscope as a significant increase in image brightness was developed (94; also see 2,95). The laser-scanning confocal became the most prevalent confocal in the 1980s and 1990s. Figure 21.12a provides a simplified schematic of a laser-scanning confocal fluorescence microscope. Basically, a focused laser beam is scanned in raster fashion across the specimen. The laser light is directed through the objective via a dichromatic beam splitter, and fluorescence emission light passes through the beam splitter to a pinhole aperture that is confocal with the point source. Because there is fluorescent excitation along the excitation beam path, there is some out-of-focus fluorescence. So the pinhole aperture before the detector is necessary to collect only fluorescence from the in-focus plane. The illumination-focused spot in the sample and the detector pinhole are confocal with each other. The aperture ensures that only light from the confocal plane hits the detector. The net result is that out-of-focus plane fluorescence is minimized, optical sectioning can be done, and by collecting a Z axis series of images, 3-D reconstruction can be done. The advantages of removing obscuring glare, looking at thicker specimens without cutting sections, and the high degree of resolution

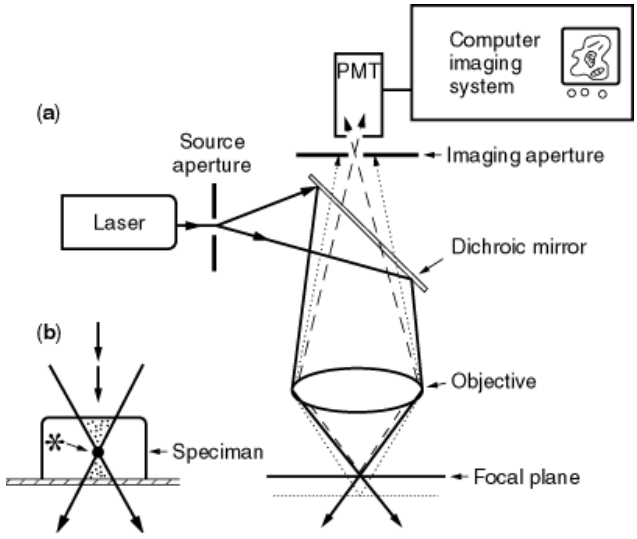


Figure 21.12. (**a**) A simplified schematic of a fluorescence laser-scanning confocal microscope. For simplicity, the excitation and emission filters routinely present in a fluorescence scope have been omitted (see Fig. 21.9 for their normal location). Also omitted is the scanning component. The excitation laser light (solid line) stimulates fluorescence in the sample. The fluorescence from the out-of-focus planes (dotted line) does not reach the detector (photomultiplier—PMT) because of the imaging aperture. Only the fluorescence from the confocal plane (dashed line) is deleted. (**b**) A simplified view of two-photon fluorescence in the specimen where two-femtosecond infrared laser pulses (depicted as two sequential arrows) simultaneously stimulate fluorophores at the focal point. Fluorescence occurs only in the small volume at the focal point (*pointing to solid dot). The stippled area shows, for comparison, the area where fluorophores are stimulated to fluoresce in conventional fluorescence and confocal-fluorescence microscopy.

has had a major impact in the cell biology literature. There are many excellent reference sources on all facets of confocal microscopy [2,3,20, (Vol. 3), 87,89,96–100] and also a number of valuable web sites (see end of chapter).

Figure 21.13 provides two examples of confocal images of an insect ovariole (*Rhodnius*). In normal fluorescence, detailed resolution is difficult (e.g., Fig. 21.13c) due to the fluorescence from multiple levels, but in confocal, as seen in an aqueorin-injected nurse-cell chamber (a) and in an immunofluorescence preparation of a plasma membrane calcium ATPase (PMCA) in the follicle (b), clear focus is acheived.

The significant development and impact of confocal has been aided by the refinement of scanning devices, detectors, varieties of lasers, and the improvements in computers necessary to handle the mass of data essential to 3-D imaging (14,16; Shotton in Ref. 20 (Vol. 3)).

An alternative approach to laser scanning confocals is the so-called digital confocals. These involve using deconvolution algorithms with a stack of serial optical sections obtained with a fluorescence microscope (see Shaw in Ref. 20 (Vol. 3); also see Refs 101–105). Each focal plane is sharpened by eliminating the blur from above and below the focal planes via such algorithms. Excellent optics, calculation of the point-spread functions, high-quality video cameras, and precise Z axis controllers are needed.

Particularly with single cells which are often fairly thin, the potential to resolve fine subcellular detail is now possible with conventional fluorescence microscopy in conjunction with video and image processing, confocal microscopy disk or laser scanning types, or computer deconvolution-based imaging.

21.3.2.10 Two-Photon and Multiphoton Microscopy. Despite all of the positive features of laser confocal fluorescence microscopy, there are some drawbacks (beyond the cost factor). The intense focused laser beam can cause significant photobleaching, and the laser irradiation can cause phototoxicity-generating free radicals and possible cell damage. Fluorescence eminates from all fluorchromes in the excitation pathway, including out-of-focus planes. This puts significant limitations on examining live cells. Two-photon microscopy was invented by Denk, Stickler, and Webb in 1989 (106,107). The suggestion of a two-photon microscope was first proposed in 1978 by Sheppard and Kompfner (108). The principle underlying two-photon and multiphoton absorption is based on the theoretical predictions of Maria Goeppert-Meier in 1931 and used in the field of spectroscopy. Imaging is similar to confocal microscopy except that photobleaching and damage are reduced. The excitation energy is concentrated temporarily and spatially, so that the saturation average power is small. For example, for Rhodamine B this would be 5 mW for a 100-fs pulse of 100 MHz (107). Excitation occurs only at the focal point, so that a pinhole aperture in the imaging path is not necessary because there is no out-of-focus plane fluorescence to remove. Figure 21.12b compares the area of fluorescence in two-photon versus conventional confocal fluorescence. Any damage to the sample that might occur is also restricted to the focal volume itself.

In two-photon microscopy, infrared wavelength high-energy ultrashort (femtasecond) pulsed lasers are used. These can be Ti: sapphire mode-locked lasers pumped by high-power argon ion gas lasers or diode-pumped 532-nM lasers. The excitation of a fluorescent dye molecule by one photon stimulates it to a partially excited short-lived virtual state from which it can be raised to its excited state if a second or more photons hit virtually simultaneously. Subsequently, thermal decay of the molecule yields fluorescence. The net result is that two or more photons of long wavelength create the same excitement normally achieved by short wavelength stimulation (in confocal), as long as they arrive almost simultaneously [for details,

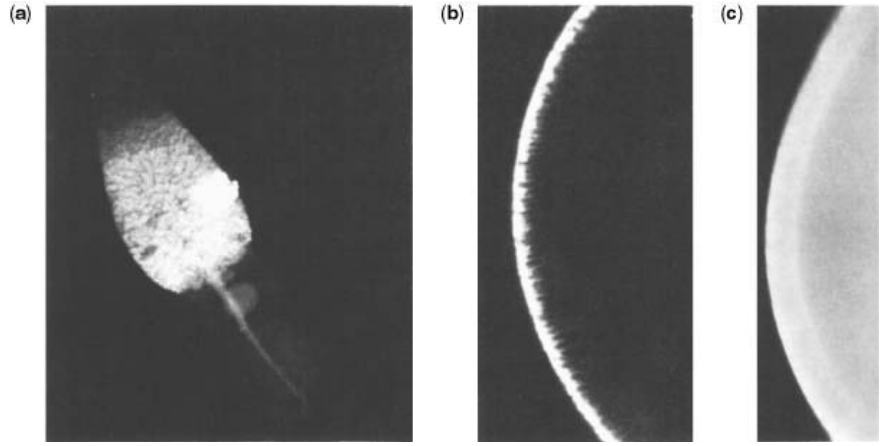


Figure 21.13. Examples of confocal single focal plane views of ovarioles of the insect *Rhodnius*. (**a**) Fluorescence in the nurse chamber and extending intercellular channels (trophic cords) of an ovariole that was injected with fluorescein-labeled aqueorin (Ca^{2+} sensitive photon-emitting protein) (E. Huebner, C. Bjornsson and A. Miller, unpublished data, 1999). (b) and (c) Micrographs of occytes with surrounding follicular epithelium that has been labeled via immunofluorescence for a plasma membrane calcium ATPase. The confocal image (**b**) shows that the label is localized in the outer follicle cell surface and (**c**) a similar preparation with conventional fluorescence microscopy where the out-of-focus plane fluorescence makes definitive localization difficult (Bjornsson and Huebner, unpublished data).

see Refs 28 (Vol. 3), 107,109–113]. Thus, unlike confocal and basic fluorescence microscopy, the excitation wavelength is greater than the emission wavelength. The red wavelengths penetrate deeper than UV so that the imaging range is extended, viability is improved, and there is no out-of-focus photo damage. Unlike confocal microscopy, the range of fluorescent probes that can be visualized is extended and excitation wavelength is not a problem because the excitation spectrum is much wider (113). The impact of two- and multiphoton microscopy is only now being felt with exciting work looking at intracellular pH, Ca^{2+} enzymes like glucose 6-phosphatase, ratio measuring of NAD and NADH, serotonin solutions, GFP, mitochondria, etc., in live cells (83,107,110–112,114,115, and web sites).

A major drawback to photon microscopy is the high cost of the femtosecond lasers and a potential problem of focal heating due to the absorption of infrared light. As manufacturers develop new instruments with improved technology and lower costs, multiphoton microscopy will become more accessible to biologists. The potential to study dynamic events in living cells at the light microscope level has been brought to single-molecule sensitivity levels.

A variety of additional types of microscopy have and are being developed that use not only light but other forms of electromagnetic energy for imaging. These include infrared spectromicroscopy, soft X-ray microscopy, laser Doppler microscopy, scanning acoustic microscopy, nuclear magnetic resonance microscopy, and others (116–119). These are beyond the scope of this chapter.

21.4 LASER TWEEZERS AND SCISSORS

Lasers have had an ancillary impact important in microscopy and cell technology in the form of laser tweezers and scissors that in combination with the light microscope provide a new noninvasive tool to measure forces operating in all processes like molecular motor-based transport and membrane characteristics, to isolate individual cells or cell components, and to do ultrafine microsurgery. Structures can be trapped and held by a laser beam-gradient force, and in essence particles are moved by light. A number of reviews and chapters cover the principles of laser trapping (120–124). A novel tool uses laser capture to isolate single cells from tissue sections thereby opening new frontiers for molecular analysis (125,126).

21.5 SCANNING-PROBE NEAR-FIELD MICROSCOPES

These are the newest microscopy tools impacting cell biology. They have the remarkable potential to resolve structure at the atomic level, thereby revealing structural detail normally seen only with electron microscopy. Involved is scanning of a small probe (1–10 nM) near the surface of structures with images generated as a result of the interaction between the probe and surface. Binnig and Rohrer revolutionized microscopy with the introduction of the scanning-tunneling microscope (STM) in 1981 (127) for which they received the Nobel prize in 1986.

Subsequently in 1986, Binnig, Quate, and Gerber (128) invented a related microscope, the atomic force microscope (AFM). Initially these instruments were primarily used in the physical sciences, but within the past five years they are increasingly being used in cell biology. These instruments represent one of the most important breakthroughs in analytical instrumentation technology in decades. Scanning probe microscopes work in a variety of environments (air, liquid, etc.). They magnify and resolve at the atomic level providing high-resolution, three dimensional morphology by "feeling and sensing" surface structures rather than using a photon or electron beam (129–134).

21.5.1 Scanning Tunnelling Microscopes (STM)

This type of scanning probe microscope requires an electronically conductive sample and is not generally applicable in biological systems. The probe tip scans the sample while being kept at a constant tip-to-sample distance of about 8 Å by an electronic feedback circuit. The tunneling current is kept constant, so that the rigid probe moves up and down indicative of the atomic surface contours being scanned. The probe uses an electron tunnelling current between the sample to activate a piezoelectric ceramide that supports the probe, raising and lowering it. Very sensitive measurements of 0.1 Å can be made.

21.5.2 Atomic Force Microscopes (AFM)

These evolved from STM, were introduced in 1986 (128), and are increasingly being used to study cells and cellular components (135–142).

In AFMs, the probe tip is positioned over the sample and then scans the selected area. The tip is mounted on a flexible cantilever arm. As the tip scans the cantilever, it is deflected, and the force of deflection is measured. A laser beam is usually used to detect cantilever deflection. The degree of deflection relates to the three-dimensional atomic structure of the surface scanned. Probe scans are sensitive to forces on the order of 10^{-12} N. Although care must be taken in interpretations by AFM of soft elastic surfaces that are easily deformed, recent applications to live and fixed cells have given dramatic images. Researchers have obtained images of chromosomes, cytoskeletal elements, whole cells, membrane surfaces, and membrane exocytosis (see web sites for images).

The development of three versions of AFMs and the combination of AFMs with other forms of optical microscopy has made the study of soft material (i.e., cells) and dual imaging more amenable (132,133,140,143). The three forms of AFM are *(1)* contact type, where probe tip friction and adhesion may be factors and bending in the lever is due to van der Waals forces; *(2)* noncontact type, where the probe hovers 1–10 nM above the surface causing less damage to delicate samples but with lower resulting resolution and *(3)* the newer tapping mode, which involves an intermittent contact oscillation providing for high resolution while minimizing mechanical distortion (138; also see the Life Sciences, Digital Instruments, and the merged Park Instruments/Topometrics web sites). These web sites provide examples of images.

Suffice it to say that this new form of microscopy is still in its infancy but growing exponentially as the impact on biological systems is realized. The ability to visualize cellular structures at submicron to atomic resolution is remarkable, particularly because live cells in natural media can be viewed and dynamic events recorded. The full range of applications in cell technology is still to be determined.

21.5.3 Scanning Near-Field Optical Microscopes

In 1928 Synge proposed a microscope without lenses that could circumvent the diffraction limit to resolution. This led to development in the 1990s of near-field aperture-scanning microscopes by Betzig and Trautman that gave super-resolution (144). Such microscopes are scanning near-field optical microscopes (SNOM) (145–148). High resolution is achieved by overcoming the far-field diffraction barrier by making an optical aperture much smaller then the λ of the light used and placing it close to the sample. With such a sub-λ aperture extremely close, the light emanating from the aperture illuminates a small area immediately below the aperture (the near zone), and this is scanned over the sample; the imaging is via a photodetecter multiplier system or, as in new instruments, a high NA objective relays the light to a photodetecter and ultimately, to a computer for image display. The light is carried to the scanning aperture via an optical fiber, and often lasers are used. Resolution depends on the size of the fiber (around 50 nM) and the distance from the sample (within 1 λ). New hybrid instruments that combine SNOM and AFM are becoming available (e.g., Nanomics Instruments) so that both a topographical and an optical image can be obtained. With high NA objectives and appropriate fluorescent dyes, high-resolution fluorescence microscopy is possible with SNOM. Until very recently, SNOM was mainly used on nonbiological material. The potential to use SNOM and continuous-wave two-photon SNOM on cells is in early stages of exploration (147,149–152).

21.6 VIDEO MICROSCOPY AND IMAGE PROCESSING

Along with the growing number of improvements and innovations in optical microscopes and the various scanning probe microscopes, the renaissance in microscopy is also due in large measure to the availability and

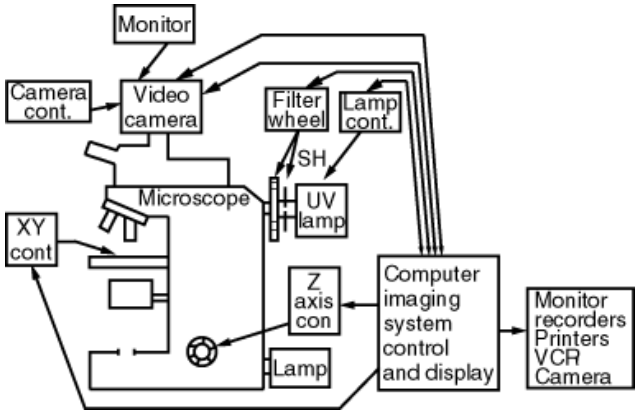


Figure 21.14. A block diagram of a typical system that integrates a computer and image processing with a microscope and peripheral devices. The system depicted has transmitted and epi illumination, X-Y stage and Z axis focus control, fluorescence with shutter and filter wheel, variable HBO lamp control for intensity, multiport head for various possible video cameras, video camera analog control, analog camera, display for video microscopy, computer image processing, computer control of peripherals, and various output options. The complexity of such systems depends on the applications.

improvements in video cameras, the use of computers, and digital processing. Video microscopy and image processing have become essential routine components of most laboratories in cell biology (2,14–16,20 (Vol. 3)). Figure 21.14 provides a block diagram with some of the components one might find in a typical microscope/computer workstation. Peripheral devices include X-Y stages, Z axis focus, filter wheels, shutters, lamps, liquid crystal filters, cameras, and recording devices, to name a few. The variety of cameras range from tube video cameras, CCDs, CMOS, intensified CCDs, cooled CCDs, and digital cameras. Image storage and recording components can also vary considerably.

An invaluable reference source that provides the historic perspective since TV was invented by Zworykin in 1934, the use of various types of video cameras, microscope interfacing and image processing is Inoué and Spring (2, also see 153). Both theoretical and practical aspects are covered. The work of Inoué and Allen in the early 1980s stimulated the widespread use of video microscopy in cell biology (154–157). In its simplest form, using a TV camera (with manual gain and black level control), high NA microscope optics, and a video monitor gives significant analog video enhancement and reveals excellent cell detail in live cells and allows analysis of fast dynamic events. The subsequent introduction of image processing with the use of A/D conversion of the video signal by frame grabbers in computers expanded the capabilities enormously. Image processing software routines made it possible for the cell biologist to do background subtraction, frame averaging, change contrast and brightness digitally, and a variety of other image-enhancement functions. The range of possibilities is broad. Figure 21.15 illustrates some of these using three different cell types (buccal cell, fish hepatocyte, and brain pyramidal neuron). Depicted is image enhancement (a), intensity representation (b,c), various manipulations (d–f), and 3-D integration and merging of stacked images. The cellular detail revealed can be astounding, allowing visualization of structures like microtubules, mitochondria, cytoplasmic movements, etc. [20 (Vol. 3), 157].

The end result is that video-enhanced microscopy is affordable and widely available, and when used on DIC, phase contrast, polarizing, and other forms of light microscopes provides excellent image quality and resolution extending our ability to study cells, live and fixed. Resolution of video systems and printers has improved often achieving photographic film quality. An array of video cameras, including Neuvicon tube cameras, charge-coupled cameras (CCD's), complementary metal oxide semiconductors (CMOS), and digital cameras are used [see 14,16, Shotton and Ladic, in Ref. 20 (Vol. 3), 158–161].

The development of ultrasensitive low-light video cameras has had a major impact in capitalizing on the use of fluorescence microscopy on living cells. Normal fluorescence microscopy uses levels of UV that cause significant cellular damage, making study of living processes difficult or impossible. Reduction of the level of excitation illumination generates a very weak fluorescent signal not detectable by eye or standard cameras. Low-light cameras such as silicon intensified cameras (SIT), intensified SIT (ISITS), intensified CCD (ICCD), cooled CCDs and cameras capable of integration on chip provide output signals of sufficient brightness that fluorescently labeled cellular structures can be studied in live cells without impairing function [14,20 (Vol. 3), 158,160,161]. Furthermore components that are not abundant (e.g., a small number of receptors) can become detectable because the sensitivity of detection is very high.

The combined benefits of video-enhanced contrast and video low-light microscopy makes video microscopy applicable to the full range of light microscope types and a broad spectrum of cell biology problems.

The implications of image processing of digitized images with computers adds an additional dimension in the potential to extract information and also for quantitative and morphometric analysis. Possibilities range from simple measurements such as counting objects, length and surface area measurement, and density profiles to intensity measurements in quantifying fluorescence, staining, etc. The microscope and image processing have become indispensable tools in many cell biology laboratories (14,16,20 (Vol. 3)).

In-depth details of the terminologies and technical aspects of video microscopy imaging is beyond the scope of this chapter. The reader is referred to Inoué and Spring (2), Shotton (in 20 (Vol. 3)), Ladic (in 20 (Vol. 3)), Oshiro (159), CLMIB (158), Lynch (162), Moomaw

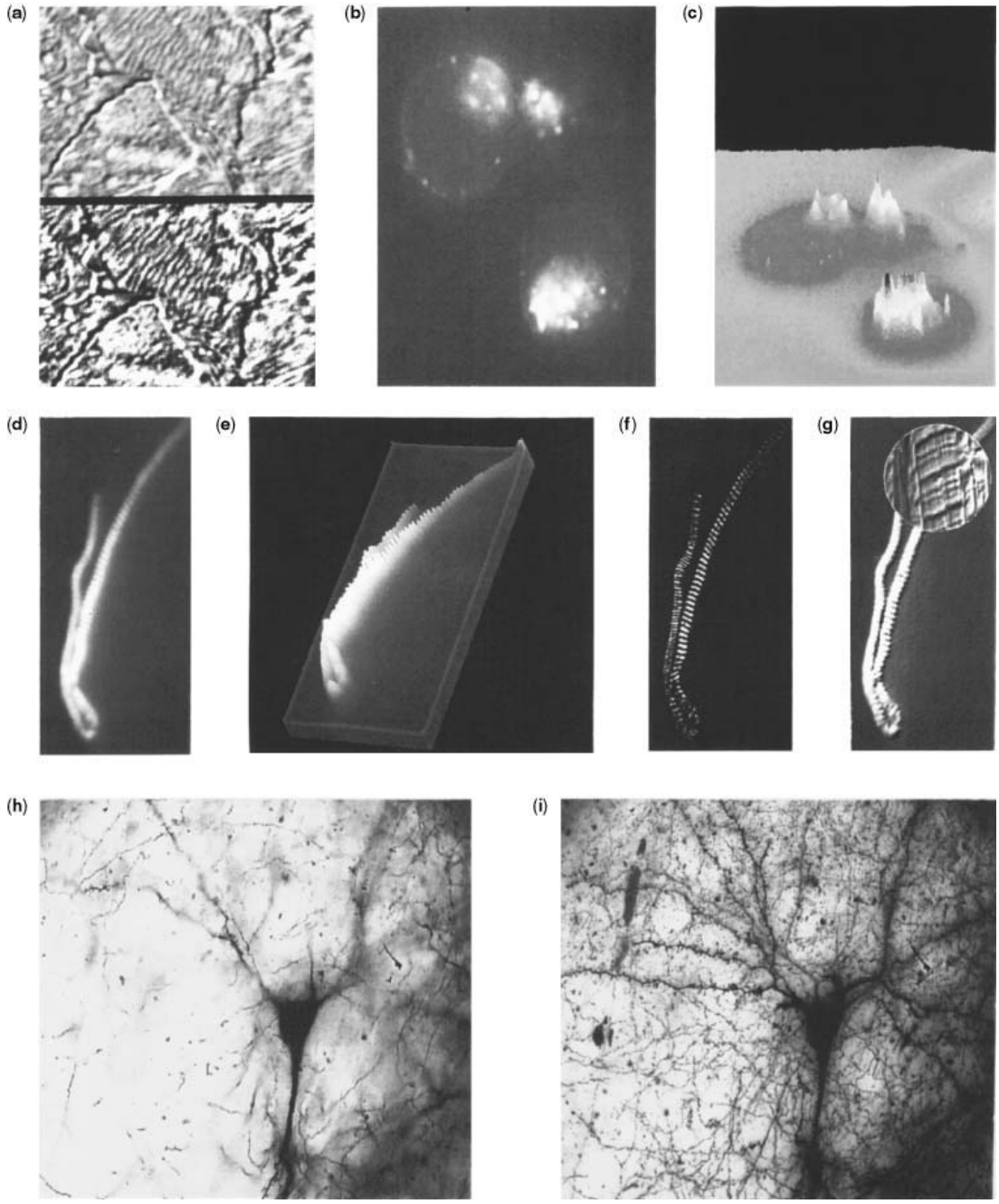


Figure 21.15. Some examples of image processing. (**a**) Contrast enhancement of the surface membrane feature of live buccal cells. (**b**) Trout hepatocytes that have endocytosed the fluorophore lucifer yellow; the relative brightness of the fluorescent areas is illustrated in this black and white image of a pseudocolored 3-D intensity profile in (**c**). (d–g) Various manipulations of a fluorescence image of an isolated insect striated muscle cell stained with rhodamine-labeled phalloidin (**d**). The F-actin of the sarcomeres fluoresces brightly. (**e**) An intensity profile (brightest areas as peaks). (**f**) Contrast enhancement. (**g**) A DIC-like image produced by subtraction of two images with shear. The inset is at higher magnification to show more clearly the DIC-like view of the sarcomeres (the original nonprocessed image was a fluorescence image). (h) and (i) 3-D reconstruction of a stalk of focal planes. (**h**) A single focal plane of a Golgi stained pyramidal neuron cell in a thick section of the cerebrum. Only part of the dendritic structure and the axon are seen. (**i**) Merging of a series of focal planes into a single image. On screen this can be viewed in stereo and rotated.

(161), Lockyer (160), and the web sites of manufacturers. An especially important aspect is the selection of the appropriate camera(s), particularly because new options are becoming available almost daily. There are many manufacturers (e.g., Apogee, Cohu, Cooke, Dage, Dulsa Fairchild, Hamamatsu, Photometrics and Princeton Instruments/Roper Scientific, Kodak, Video Scope, Xybion, RCA, Panasonic, Hitachi, Phillips, and others). Resolution, signal-to-noise ratio improvements, and sensitivity are continually improving, and costs are becoming affordable. The advances in thermoelectric cooling devices or Peltier cooling has allowed for excellent cooled CCD cameras. Digital video cameras are also becoming more commonplace. A broad selection of frame grabbers and imaging software is also available from many manufacturers.

So, on all fronts of video microscopy, this impact on cell biology is strong and growing daily.

21.7 ELECTRON MICROSCOPES

The golden age of electron microscopy was ushered in by the world's first electron microscope built by Knoll and Ruska in 1932 in Berlin (7–9). The first micrographs of biological specimens were produced in Belgium by Marton (163). The first North American EMs were built in Canada by Hall in 1936 and Prebus and Hillier 1983, and other microscopes were developed in the late 1930s in England (Martin, Whelpton, and Parnaim) and Japan (Sugata; Hibi) (see 9,10,164).

The excitement that characterized these early days of EM was based on deBroglie's discovery that electrons travel as a wave and Busch's discovery that they could be focused by electromagnetic lenses. One had the potential to exceed the resolving power of the light microscope. The first commercially available electron microscopes became available in the 1938–1940s first from Siemens in Germany and RCA in North America, and from Phillips, AEI, and various Japanese companies. Improvements in electromagnetic lens aberration correction, use of apertures, and vacuum system advances led to the transmission electron microscopes, that provide unprecedented resolution for cell biologists to determine the ultrastructure of cells and tissues. The first scanning electron microscope was developed in the 1930s by von Ardenne in Germany. The predecessor of the SEM, as we know it, was developed by Oatley in Britain (11) and first commercially produced by Cambridge Instruments. Since then there have been innumerable advances in EM with high voltage EMs, analytical EMs using scanning transmission EM (STEM), imaging based on energy loss spectroscopy, and others. Magnification attainable and routinely used by cell biologists ranges from 1,000 × to 500,000 × with resolving powers as low as to 1 Å or less. Some specialized new EMs in the 300 kV or more range can resolve single atoms. Ease of use has progressed from manual control with manual valves, geiger tubes, etc. to microscopes that are slick, ergonomically designed with microprocessor and digital control, and have sophisticated imaging capabilities. Perusal of the literature and web sites of the major manufacturers of EMs (JEOL, Hitachi, Phillips, Leo, and others) provides some insights into the state of EM technology available today. Many reference texts are available on the theory, principles, and uses of biological electron microscopy and tissue preparation techniques (165–169).

The application of electron microscopes to cell biological research also hinged on the development of specimen preparation methods and cutting sections thin enough for an electron beam to pass through to yield a transmitted image. The selection of fixatives that preserve cell morphology adequately was essential. Osmium tetroxide initially (used in the 1940s–1950s) and glutaraldehyde (introduced in the 1960s) provide excellent cell ultrastructural preservation and are still in use today. The ability to attain ultrathin sections of TEM rested on finding suitable knives and developing microtomes with ultrafine advance capabilities. The implementation of plastic resins (a wide range available today), the utilization of glass and diamond knives, and the design of ultramicrotomes have made biological TEM the widely used tool it is today. The selective enhancement of electron density in cellular components is achieved by using heavy metal stains such as uranyl acetate and lead citrate.

The light microscope was overshadowed from the 1940s to 1960s by an enormous explosion of literature based on electron microscopy that provided incredible resolution and led to new understanding of cell organelles and cell processes. It opened new vistas in cell biology. The electron microscope is still a powerful tool with important applications today, but as covered earlier, the advances in light microscopy and scanning probe microscopy have taken more of a lead role. The exciting prospects for a cell biologist is that there is now an arsenal of instruments available to reveal almost any facet of cell structure and function one wishes to visualize, and the TEM is one these tools.

The transmission EM shares a similar plan with a conventional light microscope. It has electromagnetic lenses in place of glass ones and a filament (either tungsten or lanthanum hexaboride) that emits a stream of electrons by thermionic emission upon heating (to 2700°K) into a vacuum (in the TEM column). In some newer instruments field emission (electrostatic) guns are used. Efficient vacuum is created by various vacuum pumps (e.g., diffusion types, ion getters, turbomolecular pumps). Figure 21.16 shows a simplified diagram (minus the vacuum system and electronic control systems) of a basic TEM, the components added to make it a scanning transmission EM, STEM, or a standard SEM, and compares them with an inverted light microscope ILM. The literature is replete with conventional electron-dense/electron-lucid images

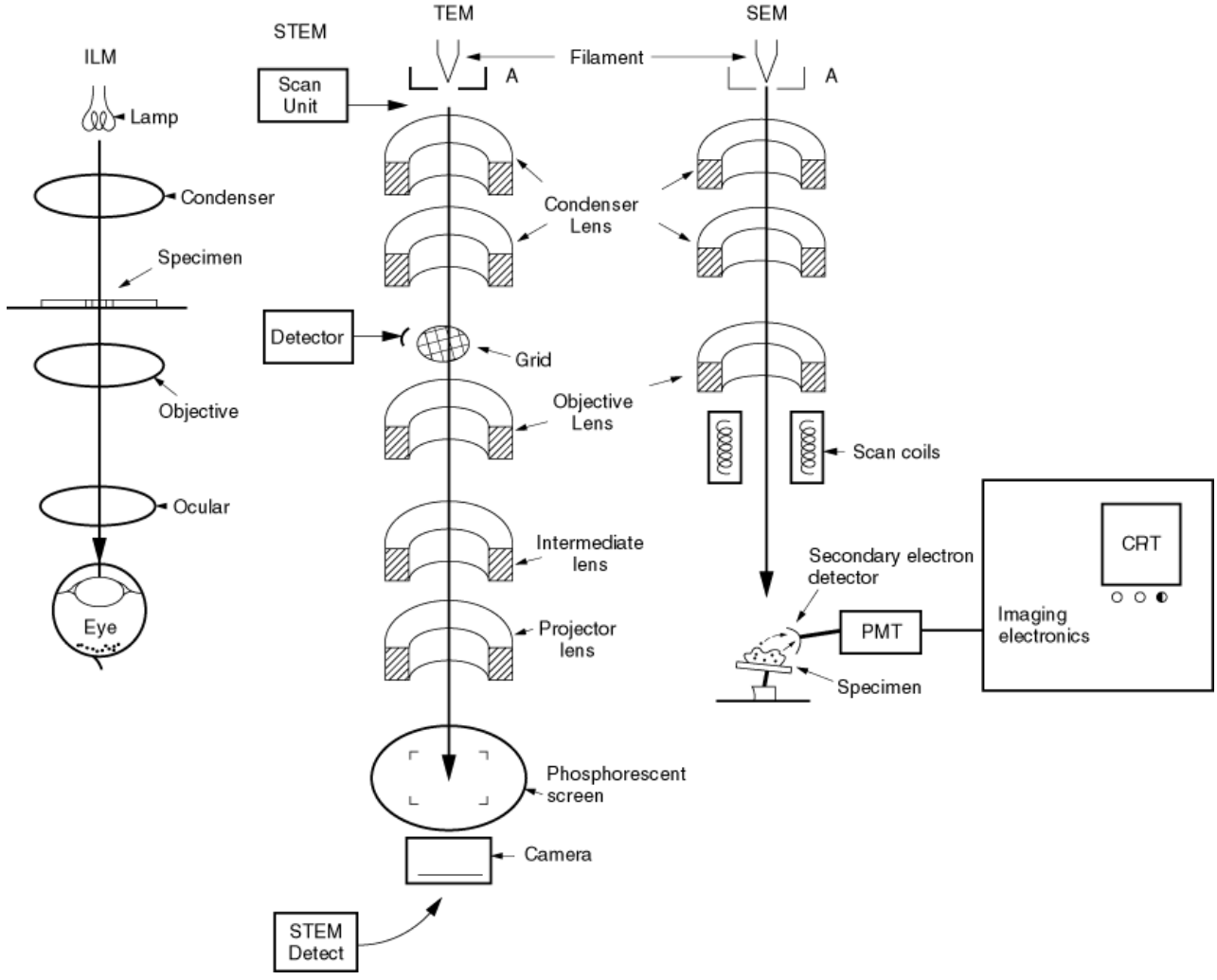


Figure 21.16. This simplified schematic illustrates the key components of electron microscopes (STEM, TEM, and SEM) compared to an inverted light microscope (ILM). The vacuum system and electronic control components are omitted. Presented is the sequence from the electron gun (filament and anode A) through the various electro magnetic lenses and viewing on a phosphorescent screen (TEM) or cathode ray tube (CRT) in SEM. Adding scanning coils and detectors near the sample (e.g., X-ray detector) or a STEM detector below the phosphorescent screen basically converts a TEM to an STEM and greatly expands its range of capabilities. STEM and other detector-generated images are viewed on a CRT via an electronic control unit (not shown).

provided in TEM micrographs that reveal fine cellular detail (membranes, mitochondria, cytoskeletal elements, labeled receptors etc.). The advent of peroxidase, colloidal gold, and other electron-dense labeling methods facilitates immunoelectron microscopy. When fixation interferes with immuno methods, ultracryosectioning and labeling methods can be used. With the addition of scanning coils to a TEM, one can position or raster a beam over a sample or selected area, and combining a host of X-ray microanalysis and other detectors, the TEM becomes a STEM (Fig. 21.16). This extends the EM's capability into the analytical range. Figure 21.17 provides an example of a conventionally stained TEM micrograph. Energy loss spectroscopy has also been used for electron microscopic imaging (170). Using electron spectroscopic imaging with an EM like the Zeiss CEM 902 makes it possible to image unstained sections based on their composition. Figure 21.18a shows microtubules imaged at the carbon edge.

Scanning EM also has major uses in cell biology (171). While utilizing electromagnetic lenses (condenser, objective and field lens), the beam is scanned across a sample, and secondary electrons given off by the surface are collected on a detector nearby converted to photons, which are transmitted to a photomultiplier and are displayed on a screen via the SEM electronics (Fig. 21.16). Usually samples are fixed, dehydrated, dried (critical point drying,

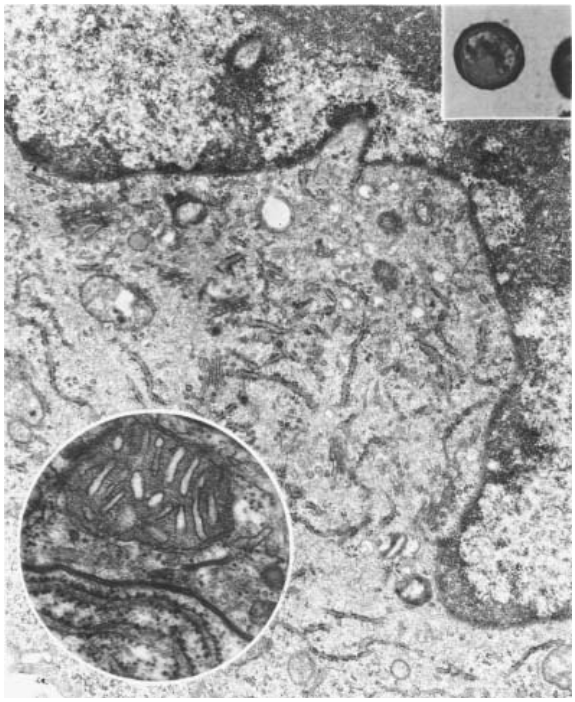


Figure 21.17. A typical TEM micrograph of a thin section of an ascites tumor cell (inset is LM view) depicting the nucleus and array of organelles and filaments stained with uranyl acetate and lead citrate. The circular insets shows a high magnification view of a mitochondrion and the rough endoplasmic reticulum of a gastric epithelial cell from a jellyfish.

freeze-drying, or other means) and have an ultrathin metal coating (gold or gold-palladium) on the surface (by a sputter coater). Now, whole cells (Fig. 21.18c, d), cut surfaces, and isolated organelles can be viewed with resolution at 1 nM or less. Three-dimensional images of high resolution can reveal cell surface specializations, as well as internal cell morphology (e.g., membranous organelles, the cytoskeletal cytoarchitecture, etc.) (172). Figure 21.18e shows an SEM view of a complex microtubular array isolated from an insect ovariole (Huebner, unpublished data).

Improvements in SEMs and innovative approaches have extended the range of the type of sample that can be viewed. Field-emission SEMs with ultravacuums can give magnifications of one million with high resolution. Another new category of SEM, the environmental SEM (ESEM), has removed the constraint of high vacuum. They operate in the range of 1–20 torr. This opens new avenues to examine unfixed hydrated samples without distortion and thus avoids artifacts due to specimen preparation inherent in conventional SEMs (CSEM) or in low-vacuum conventional SEMs (LV-CSEM). Cells and tissues can be imaged in hydrated form with no fixation under nearly natural conditions at EM resolution. The full impact of the ESEM in cell biology is yet to be realized. A variety of analytical probes can also be incorporated into SEMs making them analytical SEMs. Thus the cell biologist also has a variety of high-resolution instruments available under the SEM umbrella that can produce three-dimensional images of cells and cellular components.

A powerful cryomethod used to provide the molecular architecture of structures like membranes, cell junctions, and cytoskeletal elements, is freeze-fracture. Early workers such as Moor, Steere, and others in the 1950s provided the foundations for freezefracture replica methods (167,173–175). In essence, cells are frozen with ultrarapid cryomethods and placed in a freeze-fracture device which has ultralow temperature control, low vacuum, a cracking or fracturing device, and electrodes for carbon and platinum coating. The frozen sample is cracked or fractured leaving randomly cleaved surfaces (interior of membranes and internal cell components). This is followed by a time invacuo when sublimation of water from the frozen sample surface occurs (etching). This is normally a very short period but can be extended in deep etch procedures. Deep etching reveals internal cytoskeletal elements and membranes below the fractured surface. The exposed surface is then coated with carbon and platinum. The sample with its coating is removed from the freeze-fracture unit, thawed, and the tissue washed away leaving only the thin carbon–platinum coating called a replica, which is a cast of the fractured surface. Astonishingly, such replicas faithfully reveal the finest morphology of submembrane architecture (proteins within the bilayer) and molecular subunits of cytoskeletal elements (F-actin and microtubules), for example. Revealing this level of structural detail necessitates using ultrarapid freezing methods. The best molecular architecture is attainable with freeze-slam methods using a copper block cooled with liquid helium, as in the freeze-slam deep etch methods. More commonly in conventional freeze-fracture, immersion freezing with cryogenic liquids is used.

Freeze-fracture replicas are visualized in transmission EMs. The replicas are thin enough for the beam to pass. Due to the shadowing of platinum preferentially on areas due to their three-dimensional contours, one has a range of electron densities reflective of the differential amounts of platinum. Platinum is coated onto the sample from an angle and carbon is coated from above. The net effect is an image that shows high contrast, high resolution and has a shaded, contoured, three-dimensional appearance. Figure 21.18b and insets show a freeze-fracture image of an insect follicle cell. Depicted is the nuclear surface with the inner and outer envelopes and nuclear pores. The rectangular inset shows intramembranous particles of the cell membrane.

21.8 SUMMARY

It is difficult to do justice to the scope of the field of microscopy today in a few pages, but hopefully this

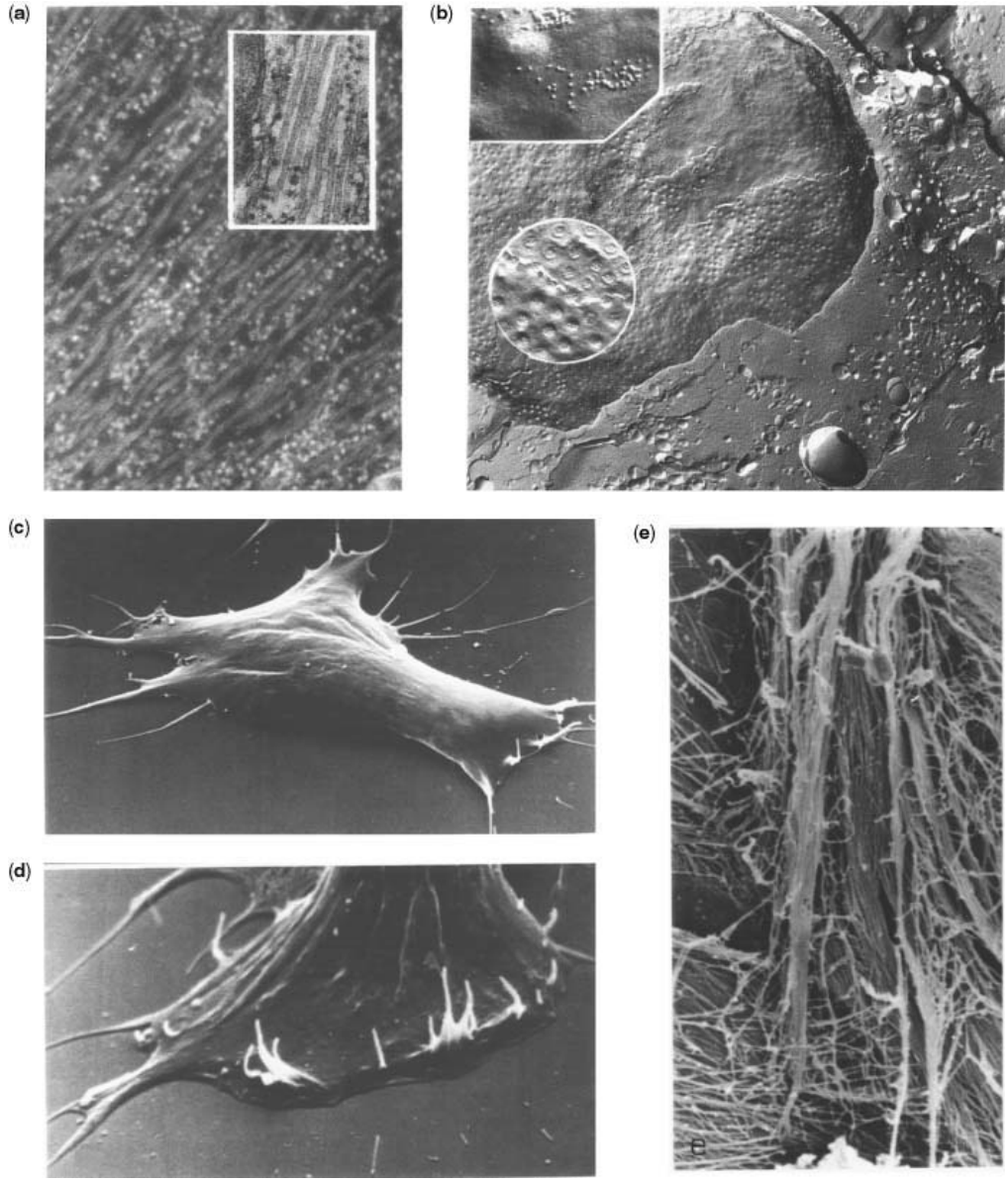


Figure 21.18. (**a**) A TEM view of an unstained section of insect ovary microtubules and ribosomes in the ovarioles of the insect *Rhodnius* imaged on the basis of their carbon content by electron spectroscopic imaging (U. Heinrich and E. Huebner, unpublished data, 1999). The insets show a comparable stained image in conventional TEM. (**b**) A TEM freeze-fracture micrograph of an insect follicle cell in the insect *Rhodnius*. The fracture plane reveals the nucleus with its many nuclear pores, the inner and outer nuclear envelopes, and vesicles and mitochondria in the cytoplasm. The upper inset shows intramembranous particles of the plasma membrane. (c–e) Examples of SEM of whole cell and cell components. (**c, d**) The surface filopodia and ruffles of isolated American lobster hemocytes. (**e**) Isolated microtubular arrays from the ovarioles of the insect *Rhodnius.*

presentation provides the reader with an introduction to the variety of microscopes available today to the cell biologist. The field is growing rapidly, and many exciting prospects undoubtedly await us in the future.

Biology in general and cell biology in particular will be front and center in the science of the next century. It is reassuring to anyone in cell biotechnology, who is exploring the intricacies of cell structure and function to

have such an arsenal of microscopical tools as already exists. The long history of microscopes since Janssen, Hooke, and Leeuwenhoek continues with renewed vigor as we explore the microcosm.

21.9 WEB SITES

The following provides some of the many web sites with microscopy content. Many of these have links to other sites within the list and outside. Included are various educational, personal, and vendor sites. The list is not all inclusive and is not intended to endorse any particular product or manufacturer. Addresses of web sites may change, companies may merge, new sites may appear and others may close, so the list provides some of the vast array of microscopy resources and information available at this time. Due to the nature of the web, it is not possible to predict the future content and details of any site.

21.9.1 Microscopical Societies

- http://www.rms.org.uk (Royal Microscopical Society)
- http://www.MSA.microscopy.com/ (Microscopical Society of America)
- http://www.ualberta.ca/~cherbur.msc (Microscopical Society Canada)

21.9.2 General Microscopy and Variety of Microscopes

- http://micro.magnet.fsu.edu/primer/webresources.html (Molecular Expressions—Microscopy Primer—M. Davidson, M. Abramowitz, Olymus & Florida State University excellent interactive tutorials on LM types)
- http://www.mih.unibas.ch/Booklet/overview.html (LM, EM, and SPM images)
- http://www.pharm.Zrizona.edu/centers/tox_center/swehsc/exp_path/m-i_onw3.html (D. Cromey, University of Arizona, many links)
- http://nsm.fullerton.edu/~skarl/EM/EMLab.html (R. Koch, California State University Fullerton, images, instruction).
- http://members.aol.com/BobCat54/index.links.html (many links to world sites, universities, suppliers)
- http://www.uq.oz.au/nanoworld/nanohome.html/ (University of Queensland, collection of microscopy resources)
- http://www.mwrn.com/ (collection of microscopy web resources, vendors' products)
- http://www.ou.edu/research/electron/www-vl/menu.shtml (University of Oklahoma)
- http://www.ou.edu/research/electron/www-vl/educatio.shtml (University of Oklahoma educational site, many links)
- http://www.ou.edu/research/electron/mirror (C. Jeffries, Bristol, United Kingdom, many links)
- http://www.microscopy-online.com (web magazine with resources, vendors, bulletin board)
- http://www.microrgc.demon.co.uk (microscopy and Analysis Publication, info, links to other sites)
- http://www.MME-Microscopy.com/education/ (national consortium of microscopy experts)
- http://www.yahoo.co.uk/Science/Engineering/optical_Engineering (list of web sites and many links)

21.9.3 Fluorscence Microscopy, Confocal and Multiphoton Microscopy

- http://www.mdyn.com/application_notes/applications.htm# Application Guides
- http://www.probes.com (Molecular Probes, Oregon, many links to journals and microscopy sites via/sites/
- http://www.Fluorescentprobes.com (TEF Labs, Texas)
- http://www.molbio.princeton.edu/facilites/index.html (J. Goodhouse, confocal images and biol. EM)
- http://www.bocklabs.wisc.edu/imr/home2.htm (D. Wokosin, University of Wisconsin. Institute Microscopy Facility, variety of LM, Em, and Imaging)
- http://www.caltech.edu/~pinelab/2photon.html (S. Potter and S. Fraser—excellent two-photon and confocal site)
- http://www.cs.ubc.ca/spider/ladic/confocal.html (Lance Ladic—excellent confocal site)
- http://www.vaytek.com (digital deconvolution, confocal)
- http://www.scanalytics.com (deconvolution, digital confocal)

21.9.4 Scanning Probe, SNOM, and Laser, Tweezers

- http://www.cellrobotics.com/cell (Laser tweezers—Cell Robotics Inc.)
- http://www.thermomicro.com (SPM—Park Instruments and Topometrix merged)
- http://www.di.com (Digital Instruments)

- http://www.molec.com (Molecular Imaging Inc.)
- http://www.omicron-instruments.com/ (Omicron—Twin SNOM)

21.9.5 Electron Microscopy

A number of the general sites listed above also include EM (e.g., University of Wisconsin IMR, Princeton Molbio, University Oklahoma, U.C. Fullerton etc.). The various EM manufacturers also have informative web sites eg. (Hitachi, JEOL, Phillips, Zeiss, etc.) http://www.mos.org/sln/sem/ (This Museum of Science, Boston, site has good SEM info and links to other sites.)

Acknowledgments

I am indebted to Everett Anderson for his mentorship and expertise in revealing the wonders of electron microscopy and to Shinja Inoué for exposing me to the world of analytical light microscopy and the power of light microscopy in his MBL course and since. Research funding from the Canadian Natural Sciences and Engineering Research Council and the University of Manitoba has been invaluable. I thank Madeleine Harris for secretarial help in preparing this chapter.

REFERENCES

1. A. Köhler, Zeitschrift für wissenshaftl. Mikroskopie 10: 433–440 (1893) (reprinted and translated in Royal Microscopical Society Proceedings 28, 181–185 (1993)).
2. S. Inoué and K.R. Spring, Video Microscopy: The Fundamentals, 2nd ed., Plenum, New York, 1997.
3. E. Keller, in D.L. Spector, R.D. Goldman, and L.A. Lein-wand, eds., Cells: A Laboratory Manual, Vol. 2: Cold Spring Harbor Press, Cold Spring Harbor, N.Y., 1997, Chapter 94, pp. 94.1–94.53.
4. A.J. Lacey, ed., Light Microscopy in Biology, IRL Press, Oxford, 1989.
5. M. Spencer, Fundamentals of Light Microscopy, Cambridge University Press, London, 1982.
6. S. Bradbury, An Introduction to the Optical Microscope, Bios Sci. Publ., Oxford, U.K., 1994.
7. E. Ruska, The Early Development of Electron Lenses and Electron Microscopy, Hirzel, Stuttgart, 1980.
8. M. Knoll and E. Ruska, Physik 78: 318–339 (1932).
9. P.W. Hawkes, ed., The Beginning of Electron Microscopy, Adv. Electron. Electron Phys., Suppl. 16, Academic Press, New York, 1985.
10. P. Hawkes, Microsc. Analy. 28: 10–13 (1998).
11. C.W. Oatley, J. Appl. Phys. 53: R1 (1982).
12. D.L. Taylor, M.A. Nederlof, F. Lannia, and A.S. Waggoner, Am. Sci. 80: 322–335 (1992).
13. B. Herman and J.J. Lemasters, eds., Optical Microscopy: Emerging Methods and Applications, Academic Press, San Diego, Calif., 1993.
14. R. Stevenson, Am. Lab. 28: 23–51 (1996).
15. J. Manni, Biophotonics Int. 3: 44–51 (1996).
16. K. Robinson, Biophotonics Int. 4: 46–52 (1997).
17. W.C. McCrone, Am. Lab. 20: 21–28 (1988).
18. J. Plasek and J. Reischig, Proc. R. Microsc. Soc. 33: 196–205 (1998).
19. T. Wilson, Microsc. Microanal. 32: 7–9 (1998).
20. J.E. Cellis, ed., Cell Biology: A Laboratory Handbook, 2nd ed., Vols. 2 and 3: Academic Press, San Diego, Calif., 1998.
21. RMS, RMS Dictionary of Light Microscopy, Bios. Sci. Publ., Oxford, U.K., 1989.
22. G.W. Ellis, J. Cell Biol. 101: 83a (1985).
23. M. Brenner, Am. Lab. 26: 14–19 (1994).
24. T. Richardson, Proc. R. Microsc. Soc. 33: 3–8 (1998).
25. M. Abramowitz, in Basics and Beyond Series, Vol. 2: 1–31. Olympus Corp., New York, 1994.
26. S. Bradbury and P. Everett, Contrast Techniques in Light Microscopy, Bios. Sci. Publ., Oxford, U.K., 1996.
27. S. Bradbury, ed., RMS Microscopy Handbooks, Multivol. Ser, Bios Sci. Publ., Oxford, U.K., 1990–1998.
28. D.L. Spector, R.D. Goldman, and L.A. Leinwand, eds., Cells: A Laboratory Manual, Vol. 2: Cold Spring Harbor Lab. Press, Cold Spring Harbor, N.Y., 1998.
29. J.K. Presnell and M.P. Schreibman, Humason's Animal Tissue Techniques, Johns Hopkins University Press, Baltimore, Md., 1997.
30. F.H. Wenham, Trans. Microsc. Soc. London III: 83–90 (1852).
31. L.V. Martin, Microscopy 36: 124–138 (1988).
32. W. McCrone and R.D. Moss, Microscope 38: 1–8 (1990).
33. F. Zernicke, Physica 9: 686–698, 974–986 (1942).
34. K.F.A. Ross, Phase Contrast and Interference Microscopy for Cell Biologists, Edward Arnold, London, 1967.
35. K.F.A. Ross, Microscopy 36: 97–123 (1998).
36. A.H. Bennett, H. Jupnik, H. Osterberg, and O.W. Richards, Phase Contrast Microscopy: Principles and Applications, Wiley, New York, 1951.
37. B. Kachar, Science 227: 766–768 (1985).
38. A. Strange, Microscope 37: 355–376 (1989).
39. A. Strange, J. Biol. Photogr. Assoc. 62: 91–102 (1994).
40. R. Hoffman, J. Microsc. (Oxford) 110: 205–222 (1977).
41. G.W. Ellis, in E. Dirksen, O. Prescott, and C.F. Fox, eds., Cell Reproduction: In Honor of Daniel Mazia, Academic Press, New York, 1978, pp. 465–476.
42. G.L. Greenberg and A. Boyde, Proc. R. Microsc. Soc. 32, 87–101 (1997).
43. A.A. Hallimond, The Polarizing Microscope, 3rd ed., Vickers Inst. Ltd., York, England, 1970.
44. S. Inoué, in G.L. Clarke, ed., The Encyclopedia of Microscopy, Reinhold, New York, 1961, pp. 480–485.
45. R. Oldenbourg and G. Mei, J. Microsc. (Oxford) 180: 140–147 (1995).
46. P.C. Robinson and S. Bradbury, Qualitative Polarized-Light Microscopy, Bios. Sci. Publ., Oxford, U.K., 1992.
47. S. Inoué *et al*., Am. Soc. Cell Biol. Poster Abstr. No. H-117 (1997).
48. G.A. Dunn, Proc. R. Microsc. Soc. 33: 189–196 (1998).

49. R.D. Allen, G.B. David, and G. Nomarski, Z. Wiss. Mikrosk. Mikrosk. Tech. 69: 193–221 (1969).
50. J. Padawer, J. R. Microsc. Soc. 88: 305–349 (1968).
51. G. Holzwarth, S.C. Webb, D.J. Kubinski, and N.S. Allen, J. Microsc. (Oxford) 188: 249–254 (1997).
52. H. Verschueren, J. Cell Sci. 75: 279–301 (1985).
53. A.S.G. Curtis, J. Cell Biol. 20: 199–215 (1964).
54. H. Piller, J. Microsc. (Oxford) 100: 35–48 (1974).
55. C.S. Izzard and L.R. Lochner, J. Cell Sci. 21: 129–159 (1976).
56. M. Opas and V.I. Kalnins, J. Microsc. (Oxford) 133: 291–306 (1983).
57. J.S. Ploem, I.C.-T. Velde, F.A. Prins, and J. Bonnet, Proc. R. Microsc. Soc. 30: 185–192 (1995).
58. M.D. Egger and M. Petrán, Science 157: 305–308 (1967).
59. M. Petrán, M. Hadravsky, and A. Boyde, Scanning 7: 97–108 (1985).
60. M. Minsky, Scanning 10: 128–138 (1988).
61. A. Boyde, Ann. N.Y. Acad. Sci. 483: 428–439 (1986).
62. R. Harris, Bull.—Microsc. Soc. Can. 26: 15–17 (1998).
63. B. Herman, Fluorescence Microscopy, 2nd ed., Bios Sci. Publ., Oxford, U.K., 1998.
64. F.W.D. Rost, Fluorescence Microscopy, Vol. 1: Cambridge University Press, Cambridge, U.K., 1992.
65. W.T. Mason, ed., Fluorescent and Luminescent Probes for Biological Activity: A Practical Guide to Technology for Quantitative Real-time Analysis, Academic Press, San Diego, Calif., 1993.
66. D.L. Taylor *et al*., ed., Applications of Fluorescence in the Biomedical Sciences, Alan R. Liss, New York, 1986.
67. Y.-L. Wang, in D.L. Spector, R.D. Godman, and L.A. Lein-wand, eds., Cells: A Laboratory Manual, Vol. 2: Cold Spring Harbor Lab. Press, Cold Spring Harbor, N.Y., 1998, Chapter 76, pp. 76.1–76.6.
68. Y.-L. Wang and D.L. Taylor, eds., Methods in Cell Biology, Parts A and B, Vols. 29 and 30: Academic Press, San Diego, Calif., 1989.
69. L.V. Johnson, M.L. Walsh, and L.B. Chen, Proc. Natl. Acad. Sci. U.S.A. 77: 990–994 (1980).
70. L.B. Chen and S.T. Smiley, in W.T. Mason, ed., Fluorescent and Luminescent Probes for Biological Activity, Academic Press, San Diego, Calif., 1993, pp. 124–132.
71. M. Poot, in J.E. Cellis, ed., Cell Biology: A Laboratory Handbook, 2nd ed., Vol. 2: Academic Press, San Diego, Calif., 1998, pp. 513–517.
72. M. Terasaki, in J.E. Cellis, ed., Cell Biology: A Laboratory Handbook, 2nd ed., Vol. 2: Academic Press, San Diego, Calif., 1998, pp. 501–506.
73. C. Lee and L.B. Chen, Cell 54: 37–46 (1988).
74. R.E. Pagano and D.C. Martin, in J.E. Cellis, ed., Cell Biology: A Laboratory Handbook, 2nd ed., Vol. 2: Academic Press, San Diego, Calif., 1998, pp. 507–517.
75. K.A. Giuliano and D.L. Taylor, Curr. Opin. Cell Biol. 7: 4–12 (1995).
76. R.Y. Tsien, Annu. Rev. Neurosci. 12: 227–253 (1989).
77. G. Grynkiewicz, M. Peonie, and R.Y. Tsien, J. Biol. Chem. 260: 3440–3450 (1985).
78. R.B. Silver, Cell Calcium 20: 161–179 (1996).
79. K.F. Sullivan and S.A. Kay, eds., Methods in Cell Biology, Vol. 58: Academic Press, San Diego, Calif., 1998.
80. A.B. Cubitt *et al*., Trends Biochem. Sci. 20: 448–455 (1995).
81. K.A. Giuliano, P.L. Post, K.M. Hahn, and D.L. Taylor, Annu. Rev. Biophy. Biomol. Struct. 24: 405–434 (1995).
82. M. Chalfie *et al*., Science 263: 802–805 (1994).
83. S. Potter, C.-M. Wang, P.A. Garrity, and S.E. Fraser, Gene 173: 25–31 (1996).
84. G. Miesenböck, D.A. DeAngelis, and J.E. Rothman, Nature (London) 394: 192–195 (1998).
85. J.T. Murphy and J.C. Lagarias, Curr. Biol. 7: 870–876 (1997).
86. S.R. Adam and R.Y. Tsien, Annu. Rev. Physiol. 55: 755–784 (1993).
87. J.B. Pawley, ed., Handbook of Biological Confocal Microscopy, 2nd ed., Plenum, New York, 1995.
88. S. Inoué, in J.B. Pawley, ed., Handbook of Biological Confocal Microscopy, 2nd ed., Plenum, New York, 1995, pp. 1–17.
89. A. Hall, M. Browne, and V. Howard, Proc. R. Microsc. Soc. 26: 63–70 (1991).
90. B. Matsumoto, ed., Methods in Cell Biology Vol. 38: Academic Press, San Diego, Calif., 1993.
91. T. Wilson, Proc. R. Microsc. Soc. 33: 259–264 (1998).
92. R. Juskaitis, T. Wilson, M.A.A. Neil, and M. Kozubec, Nature (London) 383: 804–806 (1996).
93. T. Wilson, M.A.A. Neil, and R. Juškaitis, J. Microsc. (Oxford) 191: 116–118 (1998).
94. A. Ichihara *et al*., Bioimages 4: 57–62 (1996).
95. S. Inoué and T.D. Inoué, Biol. Bull. (Woods Hole, Mass.) 191: 269–270 (1996).
96. J.G. White and W.B. Amos, Nature (London) 328: 183–184 (1987).
97. J.G. White, W.B. Amos, and M. Fordham, J. Cell Biol. 105: 41–48 (1977).
98. G.J. Brakenhoff, E.A. Van Spronsen, H.T.M. Van Der Voort, and N. Nanninga, in Y.-L. Wang and D.L. Taylor, eds., Methods in Cell Biology Part B., Vol. 30: Academic Press, Orlando, Fla., 1989, pp. 379–399.
99. C.J.R. Sheppard and D.M. Shotton, Confocal Laser Scanning Microscopy, Bios. Sci. Publ., Oxford, U.K., 1997.
100. P.C. Cheng, T.H. Lin, and W.L. Wu, eds., Multidimensional Microscopy, Springer-Verlag, New York, 1994.
101. D.A. Agard and J.W. Sedat, Nature (London) 302: 676–681 (1983).
102. Y. Hiraoka, D.A. Agard, and J.W. Sedat, J. Cell Biol. 111: 2815–2828 (1991).
103. W.A. Carrington *et al*., Science 268: 1483–1487 (1995).
104. W.A. Carrington, K.E. Fogarty, L. Lifschitz, and F.S. Fay, in J.B. Pawley, ed., Handbook of Biological Confocal Microscopy, Plenum, New York, 1995, pp. 151–161.
105. R. Rizzuto, W. Carrington, and R.A. Tuft, Trends Cell Biol. 8: 288–292 (1998).
106. W. Denk, J.H. Strickler, and W.W. Webb, Science 248: 73–76 (1990).
107. W. Denk, Photonics Spectra 31: 125–130 (1997).
108. C.J.R. Sheppard and R. Kompfner, Appl. Opt. 17: 28, 79–83 (1978).

109. M. Gu and C.J.R. Sheppard, J. Microsc. (Oxford) 177: 128–137 (1995).
110. W. Denk, D.W. Piston, and W.W. Webb, in J.B. Pawley, ed., Handbook of Biological Confocal Microscopy, 2nd ed., Plenum, New York, 1995, pp. 445–458.
111. M.B. Cannell and C. Soeller, Proc. R. Microsc. Soc. 32: 3–8 (1997).
112. M.K. Robinson, Biophotonics Int. 4: 38–45 (1997).
113. J. Mann, Biophotonics Int. 3: 44–52 (1996).
114. W. Denk, M. Sugimori, and R. Llinas, Proc. Natl. Acad. Sci. U.S.A. 18: 8279–8282 (1995).
115. S. Maiti *et al*., Science 275: 530–532 (1997).
116. T.G. Rochow and P.A. Tucker, An introducation to Microscopy by means of Light, Electrons, X-Rays or Acoustics, 2nd ed., Plenum, New York, 1994.
117. A. Briggs, An Introduction to Scanning Acoustic Microscopy, Bios Sci. Publ., Oxford, U.K., 1985.
118. P. Vesely, H. Lüers, M. Riehle, and J. Bereiter-Hahn, Cell Motil. Cytoskel. 29: 231–240 (1994).
119. Y. Wang and C. Jacobsen, J. Microsc. (Oxford) 191: 159–169 (1998).
120. A. Ashkin and J.M. Dziedzic, Science 235: 1517–1520 (1987).
121. S.M. Block, in J.K. Foskett and S. Grinstein, eds., Non-invasive Techniques in Cell Biology, Wiley-Liss, New York, 1990, pp. 375–402.
122. K. Svoboda and S.M. Block, Annu. Rev. Biophys. Biomol. Struct. 23: 247–285 (1994).
123. M. Berns, Sci. Am. 278: 62–67 (1998).
124. M.P. Sheetz, ed., Methods in Cell Biology, Vol. 55: Academic Press, San Diego, Calif., 1998.
125. N.L. Simone *et al*., Trends Genet. 14: 272–276 (1998).
126. R.F. Bonner *et al*., Science 278: 1481–1483 (1997).
127. G. Binnig and H. Röhrer, Science 244: 475–477 (1984).
128. G. Binnig, C.F. Quate, and G. Gerber, Phys. Rev. Lett 56: 930–933 (1986).
129. O. Marti and M.A. Marti, eds., STM and SFM in Biology, Academic Press, San Diego, Calif., 1993.
130. R. Coratger, V. Sivel, F. Ajustron, and J. Beauvillain, Micron 4: 371–385 (1994).
131. H.G. Hansana and J.H. Hoh, Annu. Rev. Biophys. Biomol. Struct. 23: 115–139 (1994).
132. J. Yank and Z. Shao, Micron 26: 35–49 (1995).
133. A. Stemmer, J. Microsc. (Oxford) 178: 28–36 (1995).
134. R. Howland and L. Benatar, A Practical Guide to Scanning Probe Microscopy, Park Sci. Inst. Pub., Sunnyvale, Calif., 1996.
135. M. Radmacher, R.W. Tillman, M. Fritz, and H.E. Gaub, Science 257: 1900–1905 (1992).
136. D. Ricci and M. Grattarola, J. Microsc. (Oxford) 176: 256–261 (1994).
137. J. Vesenka *et al*., BioTechniques 19: 240–249 (1995).
138. C.B. Prater, P.G. Maivald, K.J. Kjoller, and M.G. Heaton, Am. Lab. 27: 50–53 (1995).
139. R. Winn Harden, Biophotonics Int. 4: 46–49 (1997).
140. W.R. Bowen, N. Itilal, R.W. Lovitt, and C. Wright, Microsc. Anal. 33: 7–9 (1998).
141. E. Nagao and J.A. Dvorak, J. Microsc. (Oxford) 191: 8–19 (1998).
142. J.A. Dvorak and E. Nagao, Exp. Cell Res. 1998, 242, 69–74 (1998).
143. M. Hoffman, Am. Sci. 85: 123–124 (1997).
144. E. Betzig and J. Trautman, Science 257: 189–195 (1992).
145. D. Courjon, J. Microsc. (Oxford) 177: 180–185 (1995).
146. G.J. Collins, Bull.—Microsc. Soc. Can. 23: 12–17 (1995).
147. S.P. Marchese-Ragona and P.G. Haydon, Bull.—Microsc. Soc. Can. 24: 10–15 (1996).
148. R. Harris, Bull.—Microsc. Soc. Can. 26: 18–21 (1998).
149. A.K. Kirsch *et al*., Biophysi. J. 75: 1513–1521 (1998).
150. P. Moyer, S.P. Marchese-Ragona, and B. Christie, Am. Lab., April, pp. 30–32 (1994).
151. M.H.P. Moers, J. Microsc. (Oxford) 182: 40–45 (1995).
152. P.G. Haydon *et al*., J. Microsc. (Oxford) 182: 208–216 (1996).
153. G. Sluder and D.E. Wolf, eds., Methods of Cell Biology, Vol. 56: Academic Press, San Diego, Calif., 1998.
154. S. Inoué, J. Cell Biol. 89: 346–356 (1981).
155. R.D. Allen, N.S. Allen, and J.L. Travis, J. Cell Motil. 1: 298–302 (1981).
156. R.D. Allen, Annu. Rev. Biophys. Chem. 14: 265–290 (1985).
157. S. Inoué, in L. Taylor and Y.L. Wang, eds., Methods in Cell Biology, Part B, Vol. 3: Academic Press, Orlando, Fla., 1989, pp. 85–112.
158. CLMIB, Am. Lab. 27: 25–40 (1995).
159. M. Oshiro, in D.L. Spector, R.D. Goldman, and L.A. Leinwand, eds., Cells: A Laboratory Manual, Vol. 2: Cold Spring Harbor Press, Cold Spring Harbor, N. Y., 1997, Chapter 95, pp. 95.1–95.15.
160. E.M. Lockyer, Photonics Spectra 31: 80–90 (1997).
161. B. Moomaw, Biophotonics 5: 48–53 (1998).
162. T.F. Lynch, Am. Lab. 26: 26–32 (1994).
163. L. Marton, Nature (London) 133: 911 (1934).
164. F.W. Doane, G.T. Simon, and J.H.L. Watson, Canadian Contributions to Microscopy, Micros. Soc. Can., Toronto, 1993.
165. M.A. Hayat, Principles and Techniques of Electron Microscopy, Multi vol., Van Nostrand-Reinhold, New York, 1970–1976.
166. A.M. Glauert, Practical Methods in Electron Microscopy, Multi Vol. Ser., North-Holland/Elsevier, New York, 1972–1991.
167. M.J. Dykstra, Biological Electron Microscopy: Theory, Techniques and Troubleshooting, Plenum, New York, 1992.
168. J. Bozzola and L. Russell, Electron Microscopy. Principles and Techniques for Biologists, 2nd ed., Jones & Bartlett, Boston, 1998.
169. A.B. Maunsbach and B.A. Afzelius, Biomedical Electron Microscopy, Academic Press, San Diego, Calif., 1998.

170. R.F. Egerton, Electron Energy-Loss Spectroscopy in the Electron Microscope, 2nd ed., Plenum, New York, 1996.
171. M.A. Hayat, Introduction to Biological Scanning Electron Microscopy, University Park Press, Baltimore, Md., 1978.
172. G.H. Haggis, Microsc. Res. Tech. 22: 151–159 (1992).
173. R.L. Steere, J. Biophys. Biochem. Cytol. 3: 45–60 (1957).
174. H. Moor, Z. Zelforsch. Mikrosk. Anat. 62: 546–580 (1964).
175. C. Stolinski and A.S. Breathnach, Freeze-fracture Replication of Biological Tissues: Techniques, Interpretations and Applications, Academic Press, New York, 1975.

22

MYCOPLASMA CONTAMINATION OF CELL CULTURES

CORD C. UPHOFF AND HANS G. DREXLER
Department of Human and Animal Cell Cultures, DSMZ-German Collection of Microorganisms and Cell Cultures, Braunschweig, Germany

22.1 BIOLOGY AND NOMENCLATURE OF MYCOPLASMAS

22.1.1 Characteristics of Mycoplasmas

Mycoplasmas represent a large group of microorganisms that are characterized by their lack of a rigid cell wall, a standard attribute in all other types of bacteria. Therefore, a distinct class within the prokaryotes, appropriately named *Mollicutes*, was created. For historical and practical reasons, the trivial terms mycoplasmas and mollicutes are often used as synonyms; first, prior to the introduction of the taxonomical term *Mollicutes*, the designation *Mycoplasma* had been generally employed for this class of organisms; secondly, the members of the subsequently established genus *Mycoplasma* are the most common and pathogenically most important organisms of this class with regard to human and animal infections and malignancies. Thus, the trivial term mycoplasmas is still widely used in the broader sense and will be used here as well. The very first term for mycoplasmas was "pleuropneumonia-like organisms" (PPLO), the causative agent of the primary atypical pneumonia. For specific details regarding the biology and taxonomy of mycoplasmas, the reader is referred to specialist textbooks (1–3).

Besides their lack of a cell wall, mycoplasmas are (apart from the controversially discussed nanobacteria) considered to be the smallest self-replicating organisms known at present (Table 22.1). This notion refers not only to the size of these bacteria but also to the size of their genome and their cellular organization, and their physiological capabilities for synthesizing and metabolizing certain compounds. Mycoplasmas contain only the vitally important cell components including membranes, ribosomes, and the bacterial chromosome. The small size of 0.3–0.8 μm in diameter and the flexibility of their cell membrane allow mycoplasmas to pass through commonly used antibacteriological filters with diameters of 0.45 μm. The latter feature and their cohabitation with other organisms, their resistance to antibiotics known at that time as well as the difficulties to culture them without host cells prompted the initial assumption that mycoplasmas were viruses. In fact, the first established mycoplasma pathogen of humans (*Mycoplasma pneumoniae*) was initially believed to be a virus. As a result of their small size and the absence of a cell wall, mycoplasmas are pleiomorphic, varying in shape from spherical or pear-shaped cells, to branched-filamentous or helical cells. Since genome replication is not synchronized with cell division, filamentous forms and chains of beads are frequently observed (4).

The size of the genome ranges from 580 to 1300 kb (*Mycoplasma*) and up to 2200 kb for *Spiroplasma* species, quite in contrast to that of other bacteria with commonly more than 3000 kb (e.g. *Escherichia coli* with 5500 kb). Consequently, mycoplasmas possess only about one fifth of the numbers of genes that are found in other bacteria (about 500 to 1000 in contrast to 5400 in *E. coli*); mycoplasma can be considered to most closely represent the concept of a "minimum cell." This minimal genetic constitution corresponds to their commensalic and parasitic lifestyle, which allows them to minimize the metabolic pathways used. In contrast to other bacteria, the genome has also a rather low G+C content, accounting for only about 25%, which is

Upstream Industrial Biotechnology: Expression Systems and Process Development, Volume 1, First Edition. Edited by Michael C. Flickinger.
© 2013 John Wiley & Sons, Inc. Published 2013 by John Wiley & Sons, Inc.

TABLE 22.1. Synopsis of Salient Characteristics of Mycoplasmas

Physical characteristics
Lack of rigid cell wall
Smallest self-replicating bacteria; size: 0.3–0.8 μm
Filterable through 0.2-μm filter; many mycoplasmas can pass through a 0.45-μm filter
Morphology: polymorph, spherical, pear shaped, branched, helical (*Spiroplasma*)
Biological characteristics
Replication: binary fission (budding forms, chains of spherical cells, branched filaments due to asynchronized genome replication and cell division)
Long generation times: 1–9 h
Genomic features
Genome size: 600 kb (*Mycoplasma* and *Ureaplasma*), 1700 kb (*Acholeplasma, Anaeroplasma*, and *Asteroleplasma*), and 2200 kb (*Spiroplasma*)
G+C content: 23–41%
Use of UGA as tryptophan codon, not as universal termination codon (*Mycoplasma* and *Spiroplasma*)
Number of genes/proteins: <500
DNA polymerase complex consists of one enzyme (*Mycoplasma* and *Ureaplasma*) or three enzymes (*Acholeplasma* and *Spiroplasma*)
Metabolism
Require sterol or cholesterol (except *Acholeplasma* and *Asteroleplasma*)
Require several basic components (e.g. vitamins, nucleic acid precursors, lipids, fatty acids, and amino acids) in species-specific compositions
Generation of energy
Fermentative organisms catabolize carbohydrates with acid production
Most nonfermentative organisms hydrolyze arginine producing ammonia
Ureaplasma hydrolyzes urea
Lifestyle
All mycoplasmas are commensals or parasites; many are pathogens
Extracellular cytadherence to eukaryocytic cells (but *M. penetrans* and others also intracellular)
Infect humans, animals, and plants
Detection
Mycoplasma infections are chronic and difficult to diagnose
Mycoplasmas form typical "fried-egg" colonies on agar (except fastidious "noncultivable" species and strains)

thought to be close to the minimum theoretical value to synthesize proteins with a normal amino acid composition. Only *Anaeroplasma*, *Thermoplasma*, and *M. pneumoniae* exhibit a higher G+C content (~40%) (5).

Another unique characteristic of *Mycoplasma* and *Spiroplasma* species is their use of the codon UGA, commonly representing a stop codon, as a tryptophan codon. They share this feature with mitochondria, which implies a phylogenetic relationship. On the other hand, certain mycoplasmas, for example, *Acholeplasma*, employ the normal codon composition, which suggests that the change in codon usage appeared after the evolutionary separation of the *Mycoplasma/Spiroplasma* from the *Acholeplasma*. Overall, the mycoplasmas display a great genetic diversity; this may be due to either phylogenetic diversity or a rapid evolutionary development of the mycoplasmas caused by their commensalic and parasitic existence, which is supported by the restricted DNA repair system.

Owing to their limited metabolic capabilities, mycoplasmas require a number of nutrients for survival: nucleic acid precursors, amino acids, vitamins, and other basic components. The growth of all mycoplasmas (except *Acholeplasma* and *Asteroleplasma*) depends on the presence of sterol and cholesterol. Moreover, they also need to take up lipids from the environment for the formation of cell membranes. Physiologically, mycoplasmas can be differentiated into two groups, the fermentative and the nonfermentative species. The fermentative strains gain energy and carbon by fermentating carbohydrates (hexoses, starch, and glycogen) mainly to produce lactic acid, pyruvic acid, acetic acid, and acetylmethylcarbinol, leading to a lowering of pH in the culture medium. In contrast, the nonfermentative species do not significantly decrease the pH of their environment, because they oxidize fatty acids and alcohols. But, they cannot metabolize carbohydrates via the glycolysis pathway. The nonfermentative and some of the fermentative species are able to hydrolyze arginine and produce adenosine triphosphate (ATP), CO_2, and ammonia, which is toxic for eukaryotic cells. *Ureaplasma* hydrolyze urea in order to generate ATP. These organisms are sensitive to pH changes which, in fact, they may cause themselves; this observation must be taken into account during attempts to culture them.

The above-described characteristics are presumably the reason for our inability or difficulty to culture many mycoplasma species thus far identified in chemically defined media. Clearly, we have failed to mimick *in vitro* the natural milieu provided by the host; consequently, not all of these fastidious organisms can be cultivated. Most successful culture methods use media that include beef heart infusion, peptone, or tryptone (as sources of proteins and amino acids); glucose, arginine, or urea (as sources of energy); yeast extract (as a source of vitamins and growth factors); and serum (as a source of sterol and cholesterol). Contrary to other bacteria, mycoplasmas grow very slowly, even under optimal conditions. The generation times usually range between 1 and 3 h, but there are also generation times of up to 9 h; in addition, mycoplasmas have a relatively long lag phase. Therefore, it may take more than 1 week to obtain visible colonies on agar. Also, mycoplasmas do not overgrow other organisms.

It has long been assumed that mycoplasmas are extracellularly located on the eukaryocytic cell membrane

(cytadherence). However, studies in recent years have unequivocally demonstrated the intracellular location of certain mollicutes (notably *Mycoplasma fermentans*, *Mycoplasma genitalium*, and *M. pneumoniae*), not only after phagocytosis by granulocytes and monocytes, but also in nonphagocytic epithelial cells. *Mycoplasma penetrans* was shown to be capable of entering a variety of human cells *in vivo* and *in vitro*. Mycoplasma cytadherence and invasion appear to be active, but separable processes. Extensive invasion of cells by *M. penetrans* eventually leads to cell disruption. The total number of mycoplasmas infecting the cells, as well as the percentage of the mycoplasma population able to invade the cells, depends apparently on the mycoplasma species and may be influenced by the eukaryotic cell type and culture conditions. Although the great majority of the infecting mycoplasma population is definitely extracellularly located, the intracellular location, even for only a short period, sequesters mycoplasmas and protects them effectively from mycoplasmacidal therapies. This phenomenon may also explain the difficulty of eradicating mycoplasmas from all infected cell cultures (6).

The dependency on many specific organic compounds force mycoplasmas to live in close relationship with other organisms. They can be found as commensals and parasites in almost all higher organisms including plants, insects, and vertebrates, but are highly host specific in their natural environment. Mycoplasmas are nearly perfectly adapted parasites, rarely killing their hosts. Mycoplasma infections are thus of a more chronic nature and are very frequently difficult to diagnose on the basis of the symptoms alone. In humans, mycoplasmas can be physiologically found on the mucous surface of the respiratory, gastrointestinal and urogenital tract, the eyes, mammary glands, and joints, whereas ureaplasmas occur solely in the urogenital tract. Most species can be regarded as part of the normal microbial flora, a minority, however, may cause diseases in humans and animals. *M. pneumoniae*, for instance, is the causative agent of the primary atypical pneumonia (prevalent particularly in children), while *Mycoplasma arthritidis* appears to be involved in the pathogenesis of arthritis. All farm animals appear to suffer from mycoplasma infections, leading to significant economic losses. For example, *Mycoplasma hyopneumoniae*, in combination with other respiratory bacteria and viruses, causes pneumonia leading to reduced weight gain. Vaccination of the animals is a common treatment to prevent infections. *Anaeroplasma* and *Asteroleplasma* are regularly observed in bovine and ovine rumen. These two genera are obligatory anaerobic. Insects are the hosts of a variety of mycoplasmas, including species from the genera *Mycoplasma*, *Acholeplasma*, and *Spiroplasma*, most of which also can cause diseases in their hosts. But all these species seem to be clearly distinct from those isolated from vertebrates.

Mycoplasmas also cause several hundreds of economically important plant diseases transmitted by insects. *Acholeplasma* and *Spiroplasma* are seen on or in plants. Some *Spiroplasma* species invade the sieve tubes of the plants possibly giving rise to diseases as a result of obstruction. Insects are known to transfer *Spiroplasma* into the plants. The *Acholeplasma* species detected on plants also seem to derive from depositions by insects. Although a large spectrum of various plant and insect infectious agents apparently belongs to the class *Mollicutes*, it is not possible yet to culture them *in vitro*; microscopic observations suggested a certain resemblance to mycoplasmas. These organisms were termed *Phytoplasma* and *Entomoplasma*.

Another most difficult diagnostic problem concerns the detection of mycoplasmas infecting human and animal cell cultures; such contamination is a rather frequent occurrence. Typical for mycoplasma contaminations is that the symptoms are rarely very pronounced as the infection takes a chronic course. Also in this field, the damage occurring in biological research and production owing to the use of contaminated cultures is scientifically and economically substantial.

22.1.2 Taxonomy of Mycoplasmas

Owing to fundamental differences as compared to other bacteria, the *Mollicutes* constitute a class of their own. The class is divided into 14 genera within four orders based on morphological and physiological criteria and on the size of the genome: Acholeplasmatales, Anaeroplasmatales, Entomoplasmatales, Mycoplasmatales (Fig. 22.1). Previously, the order Thermoplasma was assigned to this class on the basis of their lack of a cell wall. However, the members of this order are phylogenetically clearly separated from the other *Mollicutes* and are assigned to the kingdom Archeae. In 2007, more than 200 species within the class *Mollicutes* were recognized. The genus *Mycoplasma* contains the largest number of recognized species (>120); some of the best-studied species are further subdivided into a multitude of strains (2,7). The mollicutes that have already been characterized and taxonomically defined constitute only a part, apparently a minor one, of the mollicutes living in nature. With the advent of new microbiological and molecular biological methods in the field of mycoplasma taxonomy, it is likely that many more species will be detected.

Extensive research was performed in order to clarify the phylogenetic relationship of the mycoplasmas within their class to each other and beyond their class to the other bacteria. For instance, sequence analysis of the highly conserved 16S rRNAs documented that mycoplasmas are not "primitive bacteria" with poorly developed metabolic pathways, but that they apparently intentionally reduced their

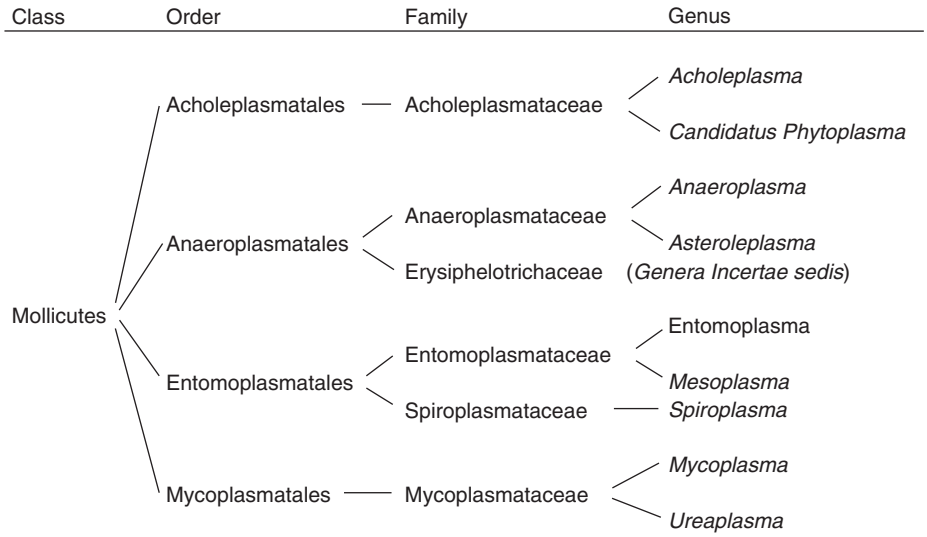


Figure 22.1. Taxonomy of mycoplasmas. For specific details see Refs 2–4.

genome size and their synthesizing properties during their adaptation to cohabitation with other organisms. The molecular investigations employing degrees of similarities in the nucleotide sequences suggested that the closest relatives of the *Mollicutes* are the Gram-positive *Clostridia*, *Bacillus*, and *Lactobacillus*.

22.2 MYCOPLASMA CONTAMINATION OF CELL CULTURES

22.2.1 Incidence of Mycoplasma Contamination

Cell culture of primary cells and continuous cell lines of human or animal origin faces several challenges affecting biological and biotechnological applications. Among these are infections with microorganisms and here in particular with mycoplasmas that may significantly hamper the use of these cells. Mycoplasmas were first isolated in 1956 from a contaminated cell culture. Ironically, during the investigations of the effects of a mycoplasma infection on cell cultures, it was found that the uninoculated negative control cell culture was already contaminated (8). Soon thereafter, it became well established that stable, continuous cell lines are frequently contaminated. Only one mycoplasma cell can grow up to 10^6 CFU/mL within 3–5 days in an infected cell culture. Frequently, there are from 100 to 1000 mycoplasmas attached to each infected cell (cytadsorption) (Fig. 22.2). Contamination may initially go undetected because mycoplasma infections do not produce overt turbid growth as commonly seen with other bacterial or fungal contamination. Often mycoplasmas can achieve very high densities in cell cultures without causing a change in the pH (and therefore without a color change of most culture media). Some mycoplasmas produce very little overt cytopathology, and covert contamination may remain undetected for months. Virtually all reports and research on mycoplasma contamination of cell cultures concern human and animal cells.

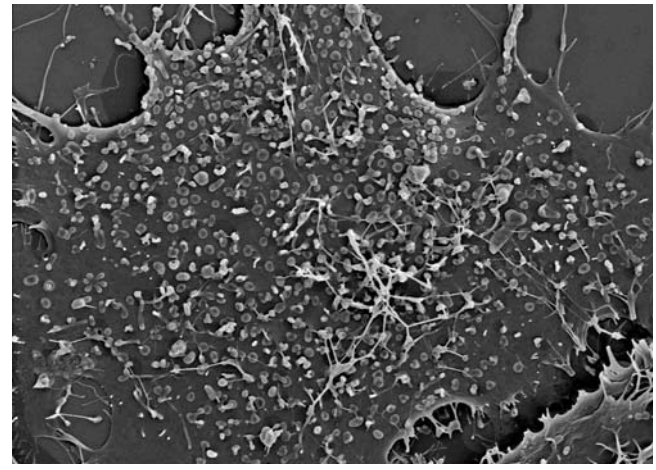


Figure 22.2. Scanning electron micrograph of a critical point-dried HeLa cell culture infected with *M. hyorhinis*. The mycoplasmas adhere to the cellular membrane of the eukaryotic cell; magnification 3000×.

While mycoplasmas have been shown to be present on or in fresh plants (see section titled Characteristics of Mycoplasmas), nothing has been published concerning the occurrence of mycoplasmas in plant cell cultures. It is not known whether mycoplasmas are truly not present in these cultures or whether such a contamination has never been studied in plant cell cultures. It is unlikely that human contact is the source of a possible contamination

as those mycoplasmas found in plants, namely members of the Entomoplasmatales or Candidatus Phytoplasma, do not infect humans. Furthermore, all media used in plant cell cultures are chemically produced and properly processed solutions, and vectors like insects are usually excluded from plant cell cultures. The primary plants from which the callus or suspension cultures are established are theoretically the primary source of mycoplasma contamination. Principally, no type of cell culture, vertebrate, invertebrate, or plant, is safe from mycoplasmal infection. Clearly, specific studies are required to provide some data in this unexplored area.

In general, primary cell cultures and cultures in early passage are less frequently contaminated than continuous cell lines: primary cultures and early passage cultures on the order of 1% and 5%, respectively, and continuous cell lines in the range of 15–35% (Table 22.2). Several large series, mainly in the United States, on tens of thousands of cell cultures analyzed over several decades (1960s–1980s) found an incidence of about 15%. However, more recent studies on smaller series and reports from other countries in South America, Europe, and Asia documented significantly higher infection rates of cell cultures, commonly in the range of 15–35%, but also as high as 65–80% (8–11).

The ever expanding application of cell lines in research and biotechnology (with the resulting exchange of nonauthenticated and mycoplasma-positive lines between scientists) and the increasing use of certain antibiotics (mostly penicillin plus streptomycin, which merely serve to mask but do not remove mycoplasmas) in routine culture have presumably led to this increase in mycoplasma contamination of cell cultures, which has now reached epidemic proportions. It appears that contamination rates are higher for cultures continuously grown with such "cell culture antibiotics."

TABLE 22.2. Incidence, Most Common Species, and Sources of Mycoplasma Contamination

Incidence
Continuous cell lines (15–35%)
Early passage cell cultures (5%)
Primary cell cultures (1%)
Most common species
M. orale (frequency 20–40%; natural host: human)
M. hyorhinis (10–40%; swine)
M. arginini (20–30%; bovine)
M. fermentans (10–50%; human)
M. hominis (10–20%; human)
A. laidlawii (5–20%; bovine)
Sources
Original (primary) tissue isolate (<1%)
Culture reagents (mostly bovine serum)
Laboratory personnel
Cross-contamination from infected cultures (most common source)

22.2.2 Most Common Contaminating Mycoplasma Species

As described in detail above (see section titled Characteristics of Mycoplasmas), mycoplasmas can be found nearly ubiquitously, as long as the given environment offers sufficient amounts of nutrients and the essentials compounds. Commonly, such permissive conditions exist in higher organisms. As the list of mammalian, insect, and plant hosts for mycoplasmas becomes longer, the number of isolated mycoplasma species and strains is also rapidly expanding. Most of the well-known and best-studied mycoplasmas are pathogenic infectants of humans, economically relevant animals (such as cattle or swine), or agriculturally important plants (such as grapevine, fruit trees, rice, and potato). Within the last two decades, mycoplasmas have been recognized as one of the major cell culture problems; consequently, their biology and physiology have become topics of intense research.

Although at least 20 distinct species have been isolated from contaminated cell lines, detailed investigations on the identity of the contaminating species showed that by far the largest portion of infections is caused by a relatively small number of *Mycoplasma* and *Acholeplasma* species: more than 95% of the contaminants identified were *Mycoplasma orale*, *Mycoplasma hyorhinis*, *Mycoplasma arginini*, *M. fermentans*, *Mycoplasma hominis*, or *Acholeplasma laidlawii* (Table 22.2). Depending on the study, the individual percentages of these six species may vary. Although many mycoplasmas are host specific *in vivo*, the various species are not restricted to cell cultures derived from their natural hosts. Species that are rather rarely found in cell cultures (generally <1%), but that are still consistently detected in the reported series, include the following: *Mycoplasma alkalescens* (natural host: bovine), *M. arthritidis* (rodent), *Mycoplasma bovis* (bovine), *Mycoplasma buccale* (human), *Mycoplasma canis* (dog), *Mycoplasma gallisepticum* (avian), *M. genitalium* (human), *Mycoplasma pirum* (bovine), *M. pneumoniae* (human), *Mycoplasma pulmonis* (rodent), and *Mycoplasma salivarium* (human).

Mycoplasmas from human sources are the most prevalent group and account for approximately one third to half of all strains isolated. Generally *M. orale*, which is the most common mycoplasma species in the oral cavity of clinically normal humans, represents the single most common isolate accounting for 20–40% of all mycoplasma infections in cell cultures (Table 22.2); in recent years the infection rate of *M. fermentans* seems to significantly increase. Other nonpathogenic mycoplasma species from the normal human microbial flora of the oropharynx seen in cell cultures are *M. fermentans* and *M. hominis*. *M. salivarium* and *M. buccale*, normally detected in the human oral cavity, have also, albeit rather rarely, been identified as cell culture contaminants.

The bovine group of mycoplasmas accounts for about another third of all strains isolated from cell cultures. Here the most frequent infectious agents are *M. arginini* and *A. laidlawii*. These two species have a relatively wide host range as they are isolated from cattle, sheep, goat, and so on, and from a variety of other mammals, birds, and insects. These cell culture contaminants are thought to be derived from bovine sources as in the early days of cell culture (1950–1970) the bovine sera were not routinely and as strictly screened for mycoplasma contamination as they are today. *M. hyorhinis*, a common inhabitant of the nasal cavity of the swine, accounts also for a high proportion of the infections. Trypsin is usually extracted from porcine pancreas, and via this indispensable reagent, swine mycoplasmas may have found their way into cell cultures. However, it appears that trypsin destroys mycoplasmas; furthermore, no mycoplasmas have been reliably detected in trypsin preparations. On the other hand, because swine and cattle are processed through the same abattoirs, the swine strain of *M. hyorhinis* may have been introduced into bovine sera; *M. hyorhinis* has often been isolated from bovine sera. The finding that mycoplasma infection of cell cultures is clearly limited to a small number of species suggests that specific interactions may exist between the eukaryotic cells and the mycoplasmas. This is supported by the finding that different mycoplasma species behave differently in various cell types.

22.2.3 Sources of Mycoplasma Contamination

Studies of the natural habitat of mycoplasmas implicate human technician, bovine serum and the primary cultures (Table 22.2). Tissue specimens used to initiate cell cultures are not the major sources of mycoplasma infection. The frequency of infection in primary cell cultures is low, on the order of 1% (8,10). Furthermore, murine, avian, and canine species of mycoplasma only account for 0.5–1% within the panel of mycoplasmas isolated from contaminated cultures—despite the wide use of murine cell lines.

The high incidence of bovine mycoplasma species, predominantly *A. laidlawii* and *M. arginini*, implicates the fetal or newborn bovine serum. Studies in the 1960s and 1970s showed that 25–40% of the serum lots provided by commercial suppliers were contaminated (8). In order to prevent contaminations and to eliminate those adventitious agents that are most frequently detected in bovine serum, namely mycoplasmas and bovine viral diarrhea viruses (BVDV), suppliers now apply more sophisticated sterility test procedures, use γ-irradiation and filtration, and have implemented stricter rules and controls at the abattoirs. Although bovine serum contamination has certainly significantly decreased over the last 10–20 years, owing to problems inherent in all sterility test procedures (for instance sample size of large lots), serum lots absolutely free from mycoplasmas cannot be guaranteed. However, the titer in modern serum lots is assumed to be very low and a contamination of all cultures grown with the serum is not likely. As there is no legal requirement for suppliers to provide mycoplasma-free products, bovine serum should still be considered as a possible source of contamination.

Because the largest percentage of mycoplasmas found in cell cultures are of human origin, it is logical to assume that the laboratory personnel is one of the major sources of contamination. If the human cell culturist, the bovine serum or the primary culture were the only sources of infection, then there should be random mycoplasmal contaminations in culture laboratories and only some cultures within a laboratory unit should be mycoplasma-positive. However, this is not the pattern of contamination that has been observed. Clearly, in laboratories with contaminated cells, most or all cultures are positive containing the same mycoplasma species (10). Thus, mycoplasma-infected cell lines are themselves the single most important source for further spreading of the contamination. This is due to the ease of droplet generation during handling of cell cultures, the high concentration of mycoplasmas in infected cultures (10^6 to 10^8 CFU/ml of supernatant), and the prolonged survival of dried mycoplasmas. Although mycoplasma-positive cell cultures account for more mycoplasma infections now than bovine sera and laboratory personnel together (4,8,10), the cell culture technician is of course involved in the propagation of the infection, as the mycoplasmas themselves do not "jump from culture to culture" on their own. Operator-induced contamination is a multifaceted problem (see section titled Routine Working Protocol for Prevention). Suffice it to mention here that mycoplasmas are spread by using laboratory equipment, media, or reagents that have been contaminated by previous use in processing mycoplasma-infected cells. One more finding argues for the operator-induced contamination of cell cultures with mycoplasmas: the high rate of cross-contaminations of cell cultures. At present, the rate of cross-contaminations is as high as 15% of all cell cultures (11).

22.2.4 Effects of Mycoplasma Contamination

The *in vitro* culture of cells has opened many doors in research; unfortunately, it has also brought new problems for the researcher. One of the biggest problems, mycoplasma contamination, resembles the opening of Pandora's box as mycoplasma infections can have a myriad of different effects on the contaminated cell cultures. However, this multitude of different effects does not affect the various cells in the same manner and to the same degree (Table 22.3). Many mycoplasma species produce severe cytopathic effects in some cell lines while

TABLE 22.3. Effects of Mycoplasma Contamination on Cell Cultures

General effects on eukaryotic cells
Altered levels of protein, RNA, and DNA synthesis
Alteration of cellular metabolism
Induction of chromosomal aberrations (numerical and structural alterations)
Change in cell membrane composition (surface antigen and receptor expression)
Alteration of cellular morphology
Induction (or inhibition) of lymphocyte activation
Induction (or suppression) of cytokine expression
Increase (or decrease) of virus propagation
Interference with various biochemical and biological assays
Influence on signal transduction
Promotion of cellular transformation
Alteration of proliferation characteristics (growth and viability)
Total culture degeneration and loss
Specific effects on hybridomas
Inhibition of cell fusion
Influence on selection of fusion products
Interference in screening of monoclonal antibody reactivity
Monoclonal antibody against mycoplasma instead of target antigen
Reduced yield of monoclonal antibody
Conservation of hybridoma

others may cause very little overt cytopathology. There can be qualitative and quantitative differences in the same parameter depending on the infecting mycoplasma species, the culture conditions, the type of the infected cell culture, the intensity and duration of the infection, an additional infection with viruses, and other parameters. Thus, contaminations can interfere with virtually every parameter measured in cell cultures during routine cultivation or in experimental investigations. Consequently, the mycoplasmas in these cultures cannot simply be ignored or regarded as harmless bystander organisms. Besides the loss of an important culture, in the worst case all experiments might be influenced by the infections and artefacts are produced. Because of the virtually unlimited number of reported mycoplasmal effects on cultured cells, only some of the most important parameters will be described here in order to highlight the diversity of possible effects. Clearly, the term mycoplasma infection is a rather general term similar to virus infection (12).

Mycoplasmas have an enormous spectrum of cytopathogenic effects on cells, ranging from no noticeable change in morphology to minimal alterations characterized by an increase in cytoplasmic granularity to a frank cytopathic effect with occasional cell lysis. A characteristic change in nuclear morphology often associated with mycoplasmal contamination is the appearance of condensed chromatin, nucleolar aggregation, and other signs of imminent apoptosis. These morphological effects can be reversed by changing the medium or by replenishing with fresh nutrients. As with morphology, the effects of mycoplasmal contamination upon cell growth are extremely variable, ranging from none to complete cessation of proliferation depending on the cell type, mycoplasmal species, and concentration of mycoplasmas. Even enhancement of cell growth has been reported. Strongly infected cultures are characterized by stunted, abnormal growth and rounded, degenerated cells with a macroscopically "moth-eaten" appearance at the edge of monolayers. Detachment of monolayers due to mycoplasma contamination has also been observed (4).

One of the most obvious reasons for these effects is that mycoplasmas consume the nutrients in the culture medium depleting glucose, arginine, nucleic acid precursors, amino acids, vitamins, and so on, thereby being direct competitors of the cultured eukaryotic cells. Often the concentration of the mycoplasmas in the medium or on the cells exceeds the number of eukaryotic cells by more than a thousand times. The depletion of medium nutrients results in profound effects on cell metabolism and function. The mycoplasmas usually metabolize the nutritional elements significantly faster than their hosts. They further induce the host cells to produce nucleotides, as has been demonstrated for infections with *M. orale* in which deoxyadenosine is highly increased and converted to ribonucleotides and these nucleotides are incorporated into mycoplasmal RNA.

Moreover, the metabolites can be harmful for the eukaryotic cells, for example, by acidifying the medium (fermentative mycoplasmas producing acidic metabolites) or by producing ammonia (arginine-hydrolyzing mycoplasmas). Ammonia is known to be a highly toxic agent and has been shown to inhibit cell growth in a variety of cell lines. In addition to this effect, the depletion of the basic amino acids, arginine and glutamine, may result in alterations in protein synthesis and inhibition of proliferation; they may also lead to chromosomal aberrations because these amino acids are used in high amounts in the histones of the eukaryotic nuclei. Depletion and alterations of nucleic acid precursors can produce mutations in the eukaryotic DNA; host cell DNA can be degraded by mycoplasmal nucleases and endonucleases. *In vitro* induction of chromosomal aberrations such as chromosome breakage, multiple translocation events, and numerical chromosome changes were seen in various cell cultures infected with different mycoplasma species (13).

A biotechnologically important effect of the nucleotide-transforming mycoplasmal enzymes is the activity of the uridine phosphorylase, which can inactivate the artificial bromodeoxyuridine (BrdU). This reagent is universally applied as a thymidine analog for the selection of cells with a thymidine kinase defect; the presence of this defect is exploited in cell fusion techniques. Thymidine kinase phosphorylates BrdU which is then incorporated

into eukaryotic DNA causing cell death. As the BrdU is metabolized by mycoplasmas, it may appear that cells growing in the presence of BrdU carry this enzyme defect (14). In hematopoietic cell cultures, several mycoplasma species are known to stimulate (or inhibit) activation, proliferation, and differentiation, enhance immunoglobulin secretion by B cells, and induce expression and elaboration of cytokines and growth factors, for instance interleukin-1β (IL-1β), IL-2, and IL-6, tumor necrosis factor, and various colony stimulating activities (12).

A final example of the detrimental effects of mycoplasma contamination concerns work with viruses. Some mycoplasmas have no detectable effect on viral growth while others may decrease, or even increase, virus yields in infected cultures. For example, the titer of the arginine-dependent DNA viruses is significantly reduced by mycoplasma contamination. In some cell lines, mycoplasmas can either enhance or block expression of interferon-γ, which inhibits propagation of viruses in cells. Certain virus-like cytopathic effects caused by mycoplasmas may be falsely ascribed to the presence of viruses. Like viruses, mycoplasmas are filterable, hemabsorbant, hemagglutinant, resistant to certain antibiotics, inhibited by antisera, able to induce chromosomal aberrations, and sensitive to detergents, ether, and chloroform (4).

TABLE 22.4. Various Mycoplasma Detection Methods

Histological staining
Histochemical stains and light microscopy
Electron microscopy
Transmission electron microscopy
Scanning electron microscopy
Biochemical methods
Enzyme assays
Gradient/electrophoresis separation of labeled RNA
Protein analysis
Determination of carbamate and acetate kinase activity (MycoAlert)
Immunological procedures
Fluorescence/enzymatic staining with antibodies
ELISA
Autoradiography
DNA fluorochrome staining
DAPI stain
Hoechst 33258 stain
Microbiological culture
Colony formation on agar
RNA hybridization
Filter hybridization
Liquid hybridization
Fluorescence *in situ* hybridization
Polymerase chain reaction
Species-/genus-specific PCR primers
Universal PCR primers

22.3 DETECTION OF MYCOPLASMA CONTAMINATION

22.3.1 Various Detection Methods

Over the last four decades, a vast array of techniques has been developed to detect mycoplasma contamination of cell cultures (Table 22.4). Most of these methods are relatively lengthy, involve subjective assessments, and use measurements that are often quite complex in nature. The two classical detection methods DNA fluorochrome staining and microbiological colony assay together with the recently introduced and highly specific and sensitive methods RNA hybridization and polymerase chain reaction (PCR) are described in greater detail from section titled DNA Fluorochrome Staining to Polymerase Chain Reaction. Ideal detection methods should be highly sensitive and specific, but also simple, rapid, efficient, and cost effective. The evaluation of tests comprises the components' validity and reproducibility pertaining to the statistical parameters (operating characteristics): sensitivity (detection of true positives), specificity (detection of true negatives), accuracy (detection of true positives and true negatives—combination of sensitivity and specificity), and predictive value (probability of correct result). Further aspects of the evaluation of a test are technical reproducibility and interobserver reproducibility (concordance of interpretation of the results). Many detection methods rely on subjective reading and interpretation of the results, which obviously requires training, experience, and consensus (15).

Traditionally, mycoplasmologists discerned direct and indirect detection methods. While the term direct method referred to the classical microbiological colony growth of mycoplasmas on agar, indirect detection techniques included procedures that measure a gene product that is associated with mycoplasmas rather than with the mammalian cells in culture. Furthermore, tests may be performed directly on the specimen taken from a given cell culture or indirectly using the so-called indicator cell culture procedure whereby the specimen is inoculated into another cell culture known to be free of mycoplasmas (monkey cell line Vero and murine cell lines NIH 3T3 or 3T6 have been used with equal success). Use of an indicator cell culture promotes better standardization and allows appropriate positive and negative controls to be included in each assay (8,15). Mycoplasmologists advise identifying every cell culture mycoplasma isolate as identification presents a clearer picture of the nature of the infection and may be helpful in determining its source. Identification can be achieved with various immunological techniques [e.g. using species-specific antibodies in immunostaining or enzyme-linked immunosorbent assay (ELISA)] or nowadays' species-specific PCR primers. However, to the cell culturist, the chief concern appears to

be whether the culture is free from contamination rather than specific identification of the contaminant.

The first detection methods involved histological staining and light microscopy, applying the classical histological stains, hematoxylin-eosin, May-Grünwald-Giemsa, and acridine orange. Some of the larger cytadsorbing mycoplasmas, for example, *M. hyorhinis*, are observable as small pleomorphic bodies lining the infected cell membrane. Smaller organisms and mycoplasmas that do not readily cytadsorb to cultured cells, for example, *M. orale*, are more difficult to detect with histochemical techniques. Cell debris, organelles, surface structures, and so on, may mimic mycoplasmal bodies. An alternative method for the visual demonstration of mycoplasmas uses hypotonic treatment of infected cells, fixation, and orcein staining followed by phase contrast microscopy. The major limitation is the probable insensitivity of histological staining when small numbers of mycoplasmas are present.

Mycoplasmas have been studied extensively by electron microscopic techniques, both scanning and transmission electron microscopy. Mycoplasmas can usually be distinguished from viruses, yeast, rickettsiae, chlamydiae and other bacteria. Although these techniques are quite useful for mycoplasma basic research and certainly provide extremely interesting and beautiful pictures, the diagnostic value of electron microscopy for mycoplasma detection is, however, limited by the complex technology and the need for expensive equipment and trained staff. Mycoplasmas can often be confused with cytoplasmic blebs and a large number of possible artefacts; low-level contamination is essentially not detectable with electron microscopy; large numbers of cultures cannot be assayed. Clearly, electron microscopy cannot be regarded as a routine mycoplasma detection test.

A variety of biochemical detection methods have been developed, including colorimetric, chromatographic, and biological enzyme assays; separation of radioactively labeled DNA or RNA by density gradient or gel electrophoresis; and protein analysis (two-dimensional electrophoresis and isoenzyme analysis). The enzyme assays are based on the detection of an enzymatic activity present in mycoplasmas, but minimal or absent in tissue cells. The enzymatic activities exploited include arginine deiminase; thymidine, uridine, adenosine, or pyrimidine nucleoside phosphorylase; and hypoxanthine or uracil phosphoribosyl transferase. Arginine deiminase catalyzes the conversion of arginine to citrulline, which can be measured colorimetrically. Unfortunately, this enzyme activity is a property of nonfermentative mycoplasmas, and consequently most fermentative species that include common culture contaminants cannot be detected by this method. Nucleoside phosphorylase is responsible for the cleavage of thymidine to thymine with subsequent release of deoxyribose, which is measured colorimetrically. However, certain mycoplasma species gave negative results. A chromatographic technique measures uridine phosphorylase activity: cells to be tested are lysed and incubated with [^{14}C]-uridine; the lysate is chromatographed; the conversion of [^{14}C]-uridine to [^{14}C]-uracil is determined. Cleavage of other nucleosides (e.g. thymidine and adenosine) by mycoplasmal phosphorylases but not by mammalian cells has also been reported, taking advantage of the avid uptake of exogenous nucleosides by mollicutes. However, the difficulty with these approaches is that mycoplasmas vary widely in their ability to incorporate nucleic acid precursors (10,16).

A biological enzyme assay utilizes a purine analog, 6-methylpurine deoxyriboside (6-MPDR). This nontoxic analog of adenosine is converted by adenosine phosphorylase into 6-methyl purine and 6-methyl purine riboside, both of which are toxic to mammalian cells. Mycoplasmas generally have much higher levels of adenosine phosphorylase than do cultured eukaryotic cells and, accordingly, hydrolyze 6-MPDR more rapidly. The release of toxic products from 6-MPDR in the presence of mycoplasma is detected by including a sensitive indicator cell line (for instance murine cell line 3T6). However, the interpretation of the results is highly subjective. False-negative results can be explained by mycoplasma species and strains having either no adenosine phosphorylase activity or activities below the sensitivity level of the assay and further by differences between the cell lines regarding sensitivity to the metabolites (15).

Mycoplasmal RNA can be distinguished from mammalian RNA. One technique relies on the identification of [^{3}H]-uridine-labeled mycoplasmas after sucrose density gradient centrifugation, whereby mycoplasma-positive cultures give a distinguishable peak that is not observed in mycoplasma-free cultures. Another method measures uridine and uracil uptake by mycoplasmas. After polyacrylamide gel electrophoresis, results are expressed as the ratio of uridine to uracil incorporated. Several species were difficult to detect and a number of false negatives were reported. Taken together, positive biochemical results are based on arbitrary values making low orders of mycoplasma contamination difficult to detect. Not all mycoplasma contaminants possess higher distinguishing levels of enzymatic activity. Overall, the above-described biochemical detection methods give inconsistent results when comparing different cell lines and have lower sensitivities than, for instance, microbiological cultivation and DNA fluorochrome staining methods, making their use problematic (15,17). Recently, a new biochemically based assay was invented, which takes advantage of two enzymes from principal energy producing pathways of mycoplasmas: carbamate kinase used in arginine hydrolyzation and acetate kinase used in fermentation

of carbohydrates. The activity of these enzymes can be measured in a luminometric assay, which is very fast and is further described below.

Immunological methods use mainly species-specific polyclonal antisera and monoclonal antibodies to detect and identify mycoplasmas, applying immunofluorescence, immunoenzymatic, or radioimmuno-precipitation techniques, immunobinding onto nitrocellulose paper, or ELISAs. These specific immuno-assays are used primarily for mycoplasma speciation. Several ELISAs have been shown to produce false-negative results in mycoplasma detection as only certain species are addressed. Although ELISAs are easy to perform, their use is hampered by the relatively weak sensitivity of this technique (lowest detection level of 10^7 CFU/mL). A monoclonal antibody has been produced that recognizes a common antigen (elongation factor TU) shared by most mycoplasmas; this protein, essential for all prokaryotes, mediates the transport of aminoacyl-tRNA to the ribosomes. In theory, the approach using a "pan-mycoplasma" antibody with fluorescence staining has considerable potential, as it might be possible to detect single cells harboring few mycoplasmas. However, the interpretation of the stainings are very subjective and difficult to reproduce between observers (17). Autoradiography of infected cells previously labeled with [^{3}H]-thymidine or uridine reveals extranuclear localization (throughout the cytoplasm and cell periphery) of silver grains. This method suffers from a lack of sensitivity; another limitation of autoradiography is the exposure time needed. Finally, one method exploits the growth-inhibitory effects of mycoplasma contamination on eukaryotic cells: supernatant from the culture to be tested is added to an indicator cell line; the eventually resulting growth modulation is quantitated by [^{3}H]-thymidine β-scintillation counting. This method is certainly not very sensitive regarding low-level infections, very subjective, and time consuming.

22.3.2 Most Reliable Detection Methods

Until the arrival of RNA hybridization and PCR, DNA fluorochrome staining and microbiological culture had been regarded as the "gold standards" for detection of mycoplasma contamination (8,10). Although the classical methods certainly have kept their eminent place in the armamentarium of mycoplasma detection methods, the new approach to a highly sensitive, specific and rapid diagnosis of mycoplasmal infection is based on the development of gene or DNA probes, which were first introduced in the 1980s. The principle is simple as genes or genomic sequences, that are specific for a single species or a particular group of mycoplasma or universally for nearly all mycoplasmas, are identified and synthesized; these probes are used for DNA or RNA hybridization. The development of PCR enables the amplification of the target DNA in the specimen using specific synthetic oligonucleotides complementary to conserved rRNA sequences and increases the sensitivity by several orders of magnitude (18). Positive hybridization signals as dots on filters or scintillation counts and visual demonstration of the PCR amplicon in gels indicate the presence of the infectious agent. Another technique applying specific probes was adopted from cytogenetic methods. Mycoplasma-specific fluorescently labeled oligonucleotides are hybridized to ribosomal RNA and can be detected with a fluorescent microscope. The technique is more sensitive and specific than the DNA fluorochrome staining method. In the following sections, all six procedures, the classical and the modern molecular biological, biochemical, PCR, and fluorescence *in situ* hybridization (FISH) techniques, are presented in greater detail.

22.3.2.1 DNA Fluorochrome Staining. Fluorescent dyes binding to DNA were first used to detect mycoplasmal infection in the 1970s. The two primary DNA-binding stains are 4′-6-diamidino-2-phenylindole (DAPI) and bisbenzimide (Hoechst 33258); further, but rather rarely employed stains are the olivomycin fluorescent dye and a conjugated benzoxazinone kanamycin fluorescent probe. The fluorescent dyes rapidly and selectively bind to eu- and prokaryotic DNA, forming strongly fluorescent DNA–DAPI/Hoechst complexes with high specificity. Under fluorescence microscopy, an uncontaminated cell culture shows only nuclear fluorescence against a dark background. Mitochondrial DNA does bind the fluorochrome, but at levels imperceptible by routine microscopy. Mycoplasmas, however, that have approximately 10 times the DNA content of mitochondria are readily detected as bright foci over the cytoplasm, lining the cell membrane or in intercellular spaces (Fig. 22.3). This procedure is not diagnostic for mycoplasmas as other prokaryotic nonmycoplasma contaminants will also be detected. To overcome problems associated with the analysis of many different cells, to detect low-level contaminations, and to screen potentially infected sera, the use of an indicator cell line such as murine cell line 3T6 or monkey cell line Vero is recommended (the so-called indirect DAPI/Hoechst staining). Specimens to be analyzed are inoculated into the indicator cell culture known to be mycoplasma negative, and after an appropriate incubation period, the indicator cell line is examined under ultraviolet (UV) light.

DNA fluorochrome staining will detect titers of 10^5 organisms or greater per milliliter. False-positive results can be caused by staining artefacts or cell detritus. Particularly, apoptotic cells distribute their DNA fragments over a broad avenue in the intercellular region and might mimic infected cell cultures. Thus, the condition of the cell culture is crucial for the quality of the assay. This

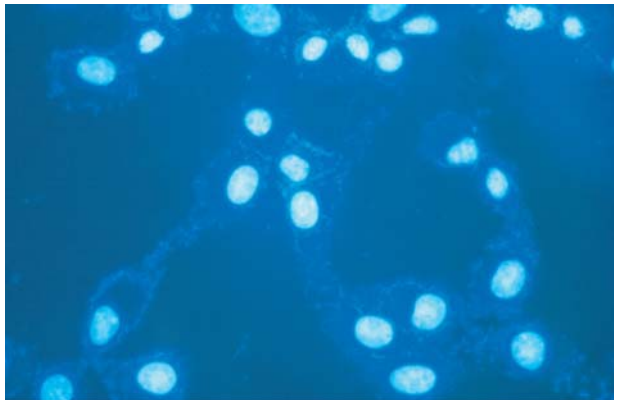


Figure 22.3. Detection of mycoplasma contamination by DAPI–DNA fluorescence staining. Fluorescent micrograph of the adherently growing cell line VERO-B4, which was inoculated with supernatant of a mycoplasma-contaminated cell culture and cultured for 5 days. The fluorochrome DAPI binds to any DNA present on the slide. The large fluorescent (blue) bodies are eukaryotic cell nuclei. The mycoplasmas are seen as dense clouds on the cells. For technical details see Ref. 17. Photographs were taken with a Nikon Labophot photomicroscope using a 60× objective. (This figure is available in full color at http://onlinelibrary.wiley.com/book/10.1002/9780470054581.)



Figure 22.4. Detection of mycoplasma contamination by colony growth on agar. Mycoplasmas (*M. arginini*) from the human suspension cell line U-937 were first enriched in a liquid broth medium and then plated on agar to allow for formation of characteristic colonies. A typical field of an agar plate incubated for 1 week is shown. Note the characteristic "fried-egg"-type mycoplasma colonies. For technical details see Ref. 17. Photograph was taken with a Nikon Diaphot inverted microscope using a 3.2 × objective. (This figure is available in full color at http://onlinelibrary.wiley.com/book/10.1002/9780470054581.)

test is dependent on the intensity of the infection since only massively contaminated cultures can be identified, thus easily leading to false negatives. The majority of false-positive and false-negative readings are due to equivocal stainings with the ensuing difficulties in the (subjective) interpretation of the results and borderline decisions. Use of an indicator cell line significantly enhanced sensitivity, specificity, accuracy, and predictive value of the DNA fluorochrome assays (15). Here, the main disadvantage appears to be the necessity to carry permanently an adherent cell line (however, the cell lines Vero and 3T6 are relatively easy to maintain and have no or few background artifacts) and the extended incubation period. Advantages of the fluorochrome tests are that they are inexpensive, simple, and rapid, and can be applied for regular screening and long-term monitoring.

22.3.2.2 Microbiological Culture. For decades, the mainstay of mycoplasma detection was based on standard microbiological culture procedures. Specimens are inoculated into mycoplasma broth and subsequently onto agar both containing thallous acetate that inhibits the growth of conventional bacteria, but does not affect the growth of mycoplasmas. Broths are transferred to agar plates after 4–7 days of incubation. Most mycoplasmas produce microscopic colonies (100–400 μm in diameter) with a "fried-egg" appearance growing embedded beneath the surface of the agar (Fig. 22.4). Because the contaminants grow embedded, they maintain their morphological shape. Consequently, they are easily distinguishable from bacterial colonies. Certain mycoplasmas may produce a more diffuse, granular type of colony (8,10).

This procedure has the advantage of ease of manipulation and visual recognition of colonies. Some artifacts are occasionally seen on agar after inoculation of cell culture specimens: colonies must be distinguished from cell clumps by their eventual increase in size; pseudocolonies (e.g. calcium- and magnesium precipitates and air bubbles) can be a problem for the inexperienced observer since they can increase in size and can actually be transferred. There are wide variations in size, morphology, and speed of growth of the mycoplasma colonies isolated from different cell cultures. Colonies become usually detectable after an average of 3–6 days, but also later sometimes. In 1973, the existence of "noncultivable" mycoplasmas were reported and were recognized as *M. hyorhinis* (8). These contaminants grow poorly or not at all on well-standardized broth and agar media. A large percentage of *M. hyorhinis* strains does not propagate at all on cell-free medium. On the other hand, colonies of other bacteria can be distinguished by their different morphology or a PCR might be performed to confirm identity of the colonies and to exclude a bacterial contamination of the broth or agar plates.

Although the microbiological culture has the advantages of being inexpensive, highly sensitive with a high detection rate, and an established and important reference method, the

disadvantages are the long incubation time, the need for a subjective and experienced interpretation, and the fact that not all mycoplasmas can be successfully cultured.

22.3.2.3 Molecular RNA Hybridization. The assays of this category of mycoplasma detection are based on the principle of nucleic acid hybridization: complementary nucleic acid strands come together to form stable double-stranded complexes. The highest sensitivity is achieved in DNA–RNA hybridization that is commonly used, but also DNA–DNA hybridization would work satisfactorily. The availability of rRNA sequences in databases allows for the construction of species-specific, group-specific, or universal oligonucleotide probes to cover all mycoplasmas commonly isolated from cell cultures. Two unique features make rRNA the most suitable target for probes: the general organization of the molecule with conserved, semiconserved, and variable regions; and the high copy number of rRNA present in each mycoplasma cell (about 1×10^4). The probes represent sequences of the 16S or 23S rRNA genes. Some other bacterial species may also be detected by these tests. Importantly, RNA from eukaryotic cells will not hybridize with the probes.

The liquid solution hybridization (best exemplified by the commercially available kit "Gen-Probe", Mycoplasma Tissue Culture NI Rapid Detection System) uses an acridinium ester-labeled single-stranded DNA probe homologous to 16S and 23S rRNA sequences. After the rRNA is released from the organism, the chemiluminescently labeled DNA probe combines with the target rRNA to form a stable DNA–RNA hybrid. The acridinium ester of the single-stranded nonhybridized probe is then destroyed by addition of a hydrolysis buffer; positive signals are measured in a luminometer. The assay can be completed within approximately 1 h. The second method uses filter hybridization, whereby cell culture samples are simply heat fixed on the membranes, hybridized with the [^{32}P]deoxycytidine triphosphate (dCTP) labeled probe derived from 16S or 23S rRNA sequences, and incubated for autoradiography. The detection limits are in the range of 10^3 to 10^4 organisms; the filter method is reportedly more sensitive than the liquid hybridization.

The advantages of these assays are broad specificity, high sensitivity, convenient sample preparation, processing of large sample numbers, and rapid results. Validity and reproducibility of the Gen-Probe test are very high (15).

22.3.2.4 Polymerase Chain Reaction. The first reports on the application of PCR in the diagnosis of mycoplasma infections appeared in 1989. The PCR technique is based on repeated cycles of high temperature template denaturation, oligonucleotide primer annealing, and thermostable polymerase-mediated extension; the number of DNA molecules theoretically doubles after each cycle. Nearly all mycoplasmic 16S rRNA sequences have been determined and form the basis for a systematic phylogenetic analysis of mollicutes (see section titled Taxonomy of Mycoplasmas). Computer alignment studies of mollicute 16S rRNA sequences reveal regions with sequence variability or conservation at the species, genus, or class level allowing for the selection of appropriate oligonucleotides (primers) for detection and identification of mycoplasmas. The highly conserved regions of the genes enable the selection of primers of wide specificity ("universal primers"), which will react with DNA of any mycoplasma and even with the DNA of other prokaryotes; this is satisfactory for detection of mycoplasma cell culture infection where the goal is just to screen the cultures for contamination. Besides the conserved regions of mycoplasmal 16S rRNA genes, the 16S–23S intergenic regions are quite useful for mycoplasma detection (18,19). It is important that no cross-reactions with the DNA of cell lines occur.

As PCR can be performed with frozen and lyophilized material, this offers a means for a retrospective analysis and facilitates the transport, collection, and storage of samples. The amplification may be performed as a single-step PCR (Fig. 22.5) or as a two-step (nested) PCR; the latter approach not only considerably increases the sensitivity and specificity, but also increases the risk of contamination by DNA carryover. Southern blotting of PCR products and hybridization with a specific radio-labeled internal probe is another possibility to improve sensitivity. However, a very high sensitivity level may not usually be required in routine diagnosis as acute and particularly chronic cell culture mycoplasma infections involve a large number of organisms (commonly 10^6 per milliliter or higher). The very high sensitivity may be an advantage at a very early phase of infection or under conditions where mycoplasma growth is suppressed (e.g. in the testing and monitoring of cell cultures post treatment with antibiotics for elimination of the contaminants).

The detection limit using a set of nested universal primers was determined to be 1 fg mycoplasmal DNA which is equivalent to 1–2 genome copies of the 16S mRNA coding region (mollicute genomes carry only one or two rRNA gene sets). The ability to detect a single mycoplasma cell makes PCR the most sensitive detection method available, clearly more so than microbiological culture. In theory, a positive cell culture may be derived from a single mycoplasma cell (18).

The high sensitivity of PCR may cause problems in producing false-positive results due to contamination with target DNA. Another possible problem is false-negative data caused by the inhibition of the *Taq* polymerase by components in the samples. This problem can be overcome by performing a DNA preparation of the sample and by spiking an internal control DNA into the sample. Using a limiting dilution of the internal control DNA, the PCR reaction can

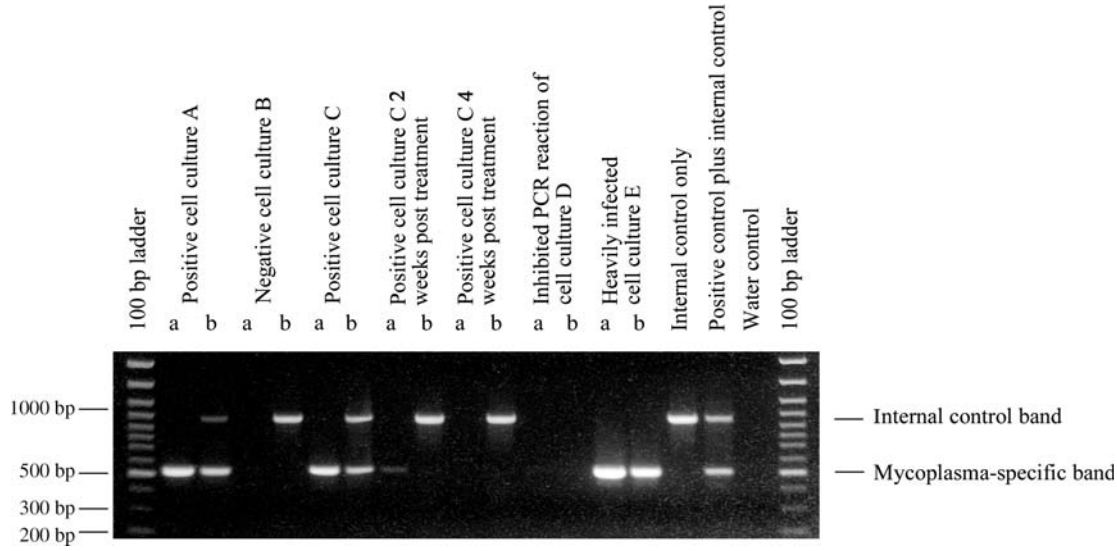


Figure 22.5. Detection of mycoplasma contamination by PCR. An ethidium bromide-stained gel containing the reaction products following PCR amplification is shown. Products of about 510 bp represent the contamination of the cell culture and the products of about 1000 bp derived from the internal control DNA added to the reaction b. For technical details see Ref. 20.

easily be standardized. Ideally, the internal control is amplified with the same primers as the wild-type mycoplasma DNA fragment. In this case, the control DNA should contain an insertion or a deletion to be distinguished from the wild-type PCR product. However, once all PCR-related problems are properly addressed, single-step or two-step PCR are clearly superior to other mycoplasma detection methods in many respects as this method combines simplicity and speed with high specificity and extreme sensitivity, in addition to objectivity, accuracy, and reproducibility (21). In particular, PCR is not limited by the ability of an organism to grow in culture; in certain areas, this molecular nucleic acid amplification may eventually replace biological amplification (i.e. growth in artificial media), a feature of paramount importance considering the fastidious nature of mycoplasmas (18).

Additionally, some PCR assays allow a simplified determination of the infecting mycoplasma species, provided only the limited number of usual cell culture contaminating mycoplasma species are present.

A further development of the conventional PCR method is the real-time PCR. This technique utilizes either SYBR green, which fluoresces when intercalated into double-stranded DNA. The fluorescence can be determined during each cycle of the PCR and the amount of newly amplified DNA can be continuously observed. This method does not discriminate between a mycoplasma-specific and a nonspecific PCR product. The identification of a mycoplasma-specific product requires a melting point determination of the PCR product. On the other hand, the reaction can be performed with a third quenched fluorescently labeled oligonucleotide, which can hybridize specifically to the amplified product emanating from mycoplasmal DNA. Hybridization abolishes the quench and the fluorescence can be determined during each cycle.

Real-time PCR offers the ability to quantify the amount of the target DNA when known standards are used in parallel reactions. But this is usually not necessary for the detection of mycoplasma contaminations. While the conventional PCR assay can be performed within approximately 2 h including sample preparation, PCR run and visualization of the PCR product on an ethidium bromide-stained gel, real-time PCR takes longer to be completed (4 h). Thus, PCR should prove to be a reliable technique of choice for mycoplasma detection in cell cultures. PCR protocols for the establishment of the tests in any laboratory (20) as well as several PCR kits are commercially available.

22.3.2.5 Fluorescence In Situ Hybridization. Another sensitive and rapid method to detect mycoplasma in cell cultures is the FISH. The advantage of the assay is the visualization of the mycoplasmas under the microscope. This allows to determine the intensity of the infection. A fluorescently labeled oligonucleotide is applied to cells fixed on microscope slides. The oligonucleotide hybridizes to a conserved region of the 16S rRNA. The high amount of ribosomes in the mycoplasmas leads to a multiplication of signals per cell. Owing to the specificity of the probe, only the mycoplasmas show fluorescence after hybridization and stringent washes. In contrast to the fluorochrome assays, the fluorescence is restricted to the mycoplasmas and no eukaryotic DNA or RNA influences

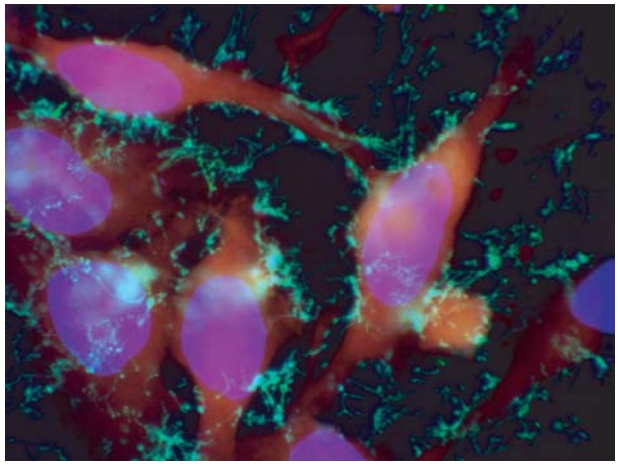


Figure 22.6. Detection of mycoplasma contamination by FISH fluorescent micrograph of an adherently growing HeLa cell line infected with *M. fermentans*. Cells were grown on slides, fixed with 4% paraformaldehyde, and exposed to fluorescein isothiocyanate (FITC) labeled oligonucleotides specific for mycoplasma (green). The cells were counterstained with tetramethylrhodamine isothiocyanate (TRITC) phalloidin to show the cytoplasma (red) and with DAPI to stain the nuclei of the eukaryotic cells (blue). (This figure is available in full color at http://onlinelibrary.wiley.com/book/10.1002/9780470054581.)

the result (Fig. 22.6). The assay can be performed within 2–3 h including hybridization step.

22.3.2.6 MycoAlert. A recently launched assay for the detection of mycoplasmas is the MycoAlert test (distributed by Lonza). The method is based on the luminometric determination of two enzymes specific for certain microorganisms, presumably including all mycoplasma strains occurring in cell cultures. The enzymes are involved in two vital energy gaining processes: arginine metabolization and fermentation of carbohydrates. The carbamate kinases are specific for mycoplasmas hydrolyzing arginine. Arginine is metabolized into L-citrulline and ammonia, L-citrulline is cleaved with participation of inorganic phosphate into L-ornithin and carbamoyl phosphate, which is then used for the generation of ATP in the presence of carbamate kinase resulting in carbonate and ammonia. Acetate kinase is involved in the metabolization of glucose into acetate: acetyl phosphate and adenosine diphosphate (ADP) are converted into acetate and ATP. By adding the substrates of the enzymes to the mycoplasma-infected cultures, the generation of ATP can be measured luminometrically. Luciferin, luciferase, ADP, adenosine monophosphate (AMP), and inorganic phosphate are added to the cell culture supernatant in a cell lysing buffer and the background of ATP concentration is determined. Carbamoyl phosphate and acetyl phosphate are then added to the solution and the additional production of ATP is indicative for the contamination with mycoplasma.

The test can be performed within 30 min and is very reliable when applied in routine cell culture, although the background concentration of ATP is occasionally very high.

22.4 ELIMINATION OF MYCOPLASMA CONTAMINATION

22.4.1 Various Elimination Methods

Ever since mycoplasma contamination of cell cultures was first reported, attempts to develop methods for elimination of the mycoplasma have been made. It has been suggested that efforts to eradicate mycoplasmas from contaminated cells should be considered as a last resort (in order to prevent spread of the contaminant) and that it would be often far better to eliminate the problem completely by autoclaving the infected cultures and replacing them with fresh stocks known to be mycoplasma free (11). However, all, too often, cell lines are not replaceable with a mycoplasma-free aliquot, and purging of mycoplasmas from such cultures is a necessity.

Four general types of procedures have been used to eliminate mycoplasmas from infected cell cultures: physical, chemical, immunological, and chemotherapeutic treatment (Table 22.5). Many of the methods were shown to be unreliable. Some techniques may apply to some, but not all mycoplasma species; some of them are too laborious or simply impractical. Elimination is typically time consuming, often unsuccessful, and poses risks of secondary infection to other cell cultures. Methods of elimination should ideally be simple and easy, rapid and efficient, reliable and inexpensive, have minimal effect on the eukaryotic cell, and result in no loss of specialized characteristics; accidental cloning selection of treated cells also should not occur. However, there is clearly not a single method available that is both 100% effective and fulfills all the ideal requirements.

The effectiveness of some elimination methods has been investigated only in experimentally contaminated cell cultures, yet experimentally infected cultures may not realistically reflect the laboratory situation since chronic infections certainly result in complex interactions between mycoplasmas and cells. If a cleanup is attempted, it is imperative to closely monitor the effectiveness of treatment relative to mycoplasma elimination and eukaryotic cytotoxicity. A variety of procedures have been described and utilized. Administration of antibiotics is by far the most common and efficient approach and is discussed in greater detail in section titled Antibiotic Treatment as the Most Effective Method.

The physical elimination methods include prolonged heat treatment at 40–42°C and filtration through microfilters (100–200 nm). For obvious reasons, both approaches

TABLE 22.5. Various Mycoplasma Elimination Methods

Procedures	Applicable To
Physical procedures	
Heat treatment	Hardware and heat-resistant cell culture reagents or products
Filtration through microfilters	Heat-sensitive cell culture reagents and products
Induction of chromosomal or cell membrane damage with photosensitizing	Insensitive cell cultures and cell cultures reagents and products
Chemical procedures	
Exposure to detergents	Surfaces, hardware
Washings with ether–chloroform	Hardware
Treatment with methyl glycine buffer	Surfaces, hardware
Incubation with sodium polyanethol sulfonate	Surfaces, hardware
Culture in 6-methylpurine deoxyriboside	Hardware
Immunological procedures	
Cocultivation with macrophages	Cell cultures
In vivo passage through nude mice	Cell cultures
Culture with specific antimycoplasma antisera	Cell cultures, cell culture reagents, products
Exposure to complement	Cell cultures, cell culture reagents, products
Cell cloning	Cell cultures
Chemotherapeutic procedures	
Antibiotic treatment in standard culture	Cell cultures
Antibiotic treatment plus hyperimmune sera or cocultivation with macrophages	Cell cultures
Soft-agar cultivation with antibiotics	Cell cultures

do not seem to be very promising. Another procedure takes advantage of the nutritional requirements of mycoplasmas offering them 5-bromouracil (or 5-BrdU), which is then selectively incorporated into the mycoplasmal genome. Exposure to visible light induces chromosomal breaks leading to cell death; this photosensitivity was greatly enhanced by the binding of the fluorochrome Hoechst 33258 to the DNA (8). The method is labor intensive and time consuming (requiring several rounds of treatments and subsequent cloning), can be highly cytotoxic to the eukaryotic cells, may produce cellular mutants, and was reported to activate endogenous C-type retroviruses in murine cells. A variation of the latter method is the use of the lipophilic fluorescent probe Merocyanine 540 that is incorporated into the cell membrane of mycoplasmas. Again illumination with visible light of cultures incubated with Merocyanine 540 together with Hoechst 33258 leads to a significant degree of mycoplasma eradication. The relative merit of this technique is not yet established and the use for cell lines derived from leukemia, lymphoma, neuroblastoma, and some other solid tumors might be limited, because these cell types are also sensitive against photosensitization.

The more recently developed membrane-active peptides, for example, alamethicin, dermaseptin B2, gramicidin S, and surfactin, are highly efficient in pure mycoplasma cultures, but in the presence of serum their activities are decreased. Thus, the concentrations and treatment times required for the elimination of mycoplasmas from cell cultures are toxic to the eukaryotic cells (22).

The chemical procedures involve the exposure of the cultures to various reagents for a given period, once or repeatedly. Described are treatments with methyl glycine buffer, sodium polyanethol sulfonate, and 6-MPDR. Treatment with detergents such as Triton-X 100 were reported to be effective. Another method uses washings with 2:1 parts ether and chloroform overnight in the cold. Overall, these chemicals will hardly be selective in harming only the mycoplasmas without untoward sequelae for the eukaryotic cells.

Immunological elimination methods exploit the physiological mechanisms of the normal immune responses, using either cellular components of the immune system with their intrinsic abilities of phagocytosis (*in vitro* in culture dishes or *in vivo* in mice) or the soluble mediators of immunity, namely, complement and antibodies (immunoglobulins). Mycoplasma-infected cells were cocultivated with primary and purified human or murine macrophages extracted from the peripheral blood, bone marrow, or peritoneum; some protocols suggested the addition of antibiotics, others used pooled human immunoglobulin. Nude mice, which still possess macrophages, but cannot mount a full immunological response due to the lack of T lymphocytes, were used for the *in vivo* passage of mycoplasma-contaminated cell lines in the form of an ascites tumor. This method requires animal facilities. Culture with macrophages, *in vivo* or *ex vivo*, will reduce the mycoplasma content, although it does not appear to be sufficient to eliminate mycoplasma completely; furthermore, it carries the risk of introducing murine viruses (e.g. C-type viruses) from the murine host and the procedure will not eliminate intracellular mycoplasma.

Considerable efforts have been spent in producing high titer neutralizing antimycoplasma antisera in rabbits, guinea pigs, and cows. They clearly do not work in every instance and simply reduce the mycoplasma load temporarily; thus, their elimination efficacy is rather low. Incubation with complement contained in fresh human serum was suggested as a rapid and efficient procedure building on the destructive

interaction between components of the classical complement pathway and mycoplasmas.

Concerning the efficiency of immunological mycoplasma purging methods, it is of note that the mycoplasma membrane, being exposed to the external environment, is the cell organelle that comes into contact with components of the host immune system (in the mammalian organism). Lacking the protection of a rigid cell wall, mycoplasmas should be particularly sensitive to growth inhibition and lysis by antibodies and complement. Yet, despite this apparent exposure to a possible immunological attack, mycoplasma infections are usually chronic in nature, indicating the frequent failure of the host defense mechanisms to eradicate the parasites. Mycoplasmas may have certain mechanisms at their disposal for rapid adaptation to the microenvironment and thus can escape any immunological actions (5). These *in vivo* observations may explain the lack of success in using immunological approaches for mycoplasma decontamination of cell cultures. Finally, cell cloning of an infected culture in 96-well plates may lead to a mycoplasma-free culture, in the hope of selecting cells without any cytadsorbed contaminants. The success rate is generally very low while the amount of work involved is clearly very high.

The physical, chemical, and immunological methods are usually of restricted value since the mycoplasmas, although not detected for sometime afterwards, commonly reappear (low efficiency); some methods are time consuming or have detrimental effects on the eukaryotic cells and other techniques are complex or impractical as they require extensive resources or special equipment and knowledge. Considering the various advantages and disadvantages of any elimination procedure, chemotherapeutic treatment appears to be superior compared to the other mycoplasma eradication techniques and thus the method of choice. The simple addition of another reagent to a cell culture is within the technical and financial capabilities of every cell culture laboratory.

22.4.2 Antibiotic Treatment as the Most Effective Method

Mycoplasmas, which lack a cell wall and are incapable of peptidoglycan synthesis, are theoretically not susceptible to antibiotics such as penicillin and its analogs, which are effective against most other bacterial contaminants of cell cultures. However, it has been reported that several bacteriostatic antimicrobial agents inhibit the growth of mycoplasmas; thus, they may not eradicate the contaminants, but simply suppress the full-blown picture of an infection and tend to mask the presence of mycoplasmas. A number of different antibiotics have been explicitly used for mycoplasma control (Table 22.6). The contaminant strains, however, often developed resistance to certain antibiotics, which were thus completely ineffective. Other antibiotics (for instance some aminoglycosides and lincosamides) were moderately to highly effective in

TABLE 22.6. Various Antimicrobial Agents against Mycoplasma Contamination in Cell Cultures

Antibiotic Category: Specific Antibiotic	Mode of Action	Effect on Bacteria	Effectiveness against Mycoplasmas[a]	Cytotoxicity for Eukaryotic Cells[b]
Aminoglycosides	Protein synthesis inhibitor	Bacteriocidal		
Gentamicin			+	–
Kanamycin			+	+
Spectinomycin			+	+
Tetracyclines	Protein synthesis inhibitor	Bacteriostatic		
Chlortetracyline			+	(+)
Doxycycline			+	(+)
Minocycline			++	(+)
Lincosamides	Protein synthesis inhibitor	Bacteriostatic		
Clindamycin			+	+
Lincomicin			+	+
Macrolides	Protein synthesis inhibitor	Bacteriostatic		
Erythromycin			(+)	–
Roxitromycin			–	–
Tiamulin (pleuromutilin)			++	–
Tylosin			+	+
Quinolones	Nucleic acid synthesis inhibitor	Bacteriocidal		
Ciprofloxacin			++	–
Enrofloxacin			++	–
Sparfloxacin			–	–
Novobiocin	Cell wall inhibitor	Bacteriostatic	–	–

[a] ++ = highly effective; + = moderately effective; (+) = rarely or weakly effective; – = ineffective.

[b] Cytotoxicity at effective mycoplasmacidal antibiotic doses: + = cytotoxic; (+) = mildly cytotoxic or cytostatic; – = not cytotoxic.

eliminating mycoplasmas, but only at concentrations that had detrimental effects on the eukaryotic cells, such as marked cytotoxicity and genotoxicity.

Ideally, a basic procedure should involve isolating, speciating, and determining the antibiotic susceptibility of the contaminants to the arsenal of possible reagents to maximize success; then the cultures should be exposed to the effective antibiotics. However, this approach is extremely time consuming, labor intensive, and requires certain expertise. It might be fair to say that few scientists (for whom a cell culture is normally only a means to an end) would use this complex approach and would prefer a quicker solution.

The pharmacological and clinical testing and application of mycoplasmacidal antibiotics has shown that tetracyclines are generally effective antimycoplasmal agents; also quinolones were found to be highly effective against mycoplasmas. Recently, these antibiotics have been introduced for purging of mycoplasmas from cell cultures and are commercially marketed. Of note are, in particular, the fluoroquinolones ciprofloxacin (distributed as Ciprobay by Bayer), enrofloxacin (Baytril; Bayer), sparfloxacin (distributed by Sanofi-Aventis Pharma), and an unpublished reagent available as mycoplasma removal agent (MRA; Flow Laboratories ICN); the product BM-Cyclin (Roche) combines the macrolide tiamulin (a pleuromutilin derivative) and the tetracycline minocycline (Fig. 22.7); Plasmocin (InvivoGen) is a combination of a macrolide and a fluoroquinolone.

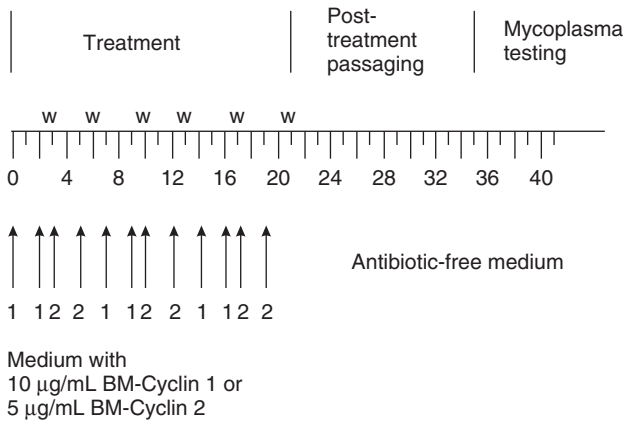


Figure 22.7. Treatment protocol for elimination of mycoplasma contamination using BM-Cyclin. BM-Cyclin containing the macrolide tiamulin (1) and the tetracycline minocycline (2) (Table 22.6) is added to the cell culture for 3 weeks in three alternating cycles (as indicated in this example by the arrows). Cells are thoroughly washed (W) prior to switching to the other reagent, at the beginning, and at the end of treatment. Post therapy, it is important to grow the culture in antibiotic-free medium. After a minimum of 2 weeks, mycoplasma testing is performed. Thereafter, cells are regularly monitored for reemergence of the contamination or for new infection. For technical details see Refs 23–25.

Tetracyclines inhibit protein synthesis by binding to subunits of ribosomes, thereby blocking peptide chain elongation. Tetracyclines inhibit both prokaryotic and eukaryotic ribosomal protein synthesis. Nalidixic acid is the prototype of a class of synthetic antibacterial agents, the fluoroquinolones, a subset of the quinolones. The mode of action of the quinolones involves the binding to and inhibition of the bacterial DNA gyrase that is essential for DNA replication, transcription, repair, and recombination. Despite their documented selectivity for prokaryotic enzymes, the quinolones may also exert an inhibitory effect on eukaryotic DNA polymerase α, topoisomerases, and DNA deoxynucleotidyl transferases; the activity of these enzymes is especially high in rapidly dividing cells. Indeed, high doses of quinolones induced double-stranded DNA breaks in human cells. Selectivity of the quinolones for the bacterial cell is at least partly due to the far greater sensitivity of the bacterial enzymes compared to the mammalian enzymes.

Antibiotic treatment of mycoplasma contamination in cell cultures has a high degree of efficiency as illustrated by the percentages of successful outcomes in various studies: 65–74% of the mycoplasma-positive cultures were cured with MRA, 74–100% with Ciprobay, 76–91% with Baytril, and 82–100% with BM-Cyclin (23); data on the treatment with Plasmocin are not yet available, but presumably they are similar to the ones found for the other antibiotics. Thus, two-thirds to three-quarters of all cultures treated can be cleansed by one of these antimycoplasma chemotherapeutic regimens. Besides cure, two other possible outcomes are loss of the culture and resistance. Culture death, occurring in 5–15% of the cases, is presumably caused by cytotoxic effects of the reagents. Not unexpectedly, BM-Cyclin (containing a tetracycline) shows the greatest growth-inhibiting effect, which may be either cytostatic or cytotoxic. Generally, 1 week after cessation of treatment, cell growth will return to normal. Cytostatic and cytotoxic effects of the antibiotics may be enhanced by the poor condition of cell cultures commonly found in chronically infected cells. This situation is clearly different from that of experimentally contaminated cell cultures. It was found that increasing the serum concentration and incubating the cells at higher densities (at or near clonal densities) were advantageous for the cell cultures.

With regard to resistance, the fluoroquinolones showed cross-resistance. This is not surprising given their basic structural similarity. Fortunately, sequential administration of BM-Cyclin to the same cells that were first exposed to a fluoroquinolone can still result in eradication of the resistant infectant. Higher concentrations of the antibiotics may be more effective in purging mycoplasma-contaminated cultures decreasing the rate of resistance, but this success would be counterbalanced by significantly higher cytotoxicity. It is not known whether the resistance of cell culture

mycoplasmas to antibiotics is acquired during treatment or exists already prior to exposure to these reagents. In any event, antimycoplasma antibiotics should be reserved for the specific situation of mycoplasma eradication in an infected cell culture and should not be routinely added as a common panacea to the culture medium as this would run a substantial risk of selecting resistant mycoplasma strains. The discovery of intracytoplasmatic mycoplasmas may explain the resistance of some cases where prior testing documented susceptibility of the particular contaminant to antibiotics. In these instances, the antibiotics mentioned above do not have physical access to the mycoplasmas. On the other hand, some antibiotics, for example, ciprofloxacin, were shown to be accumulated in the eukaryotic cells.

Antimycoplasma treatment conditions are certainly stressful to the eukaryotic cells. Thus, cells might no longer express the desired properties as a result of antibiotic administration. Outgrowth of a selected clone is another possibility. Some data suggest that cured cells generally preserve their characteristics. Still, any alterations to the cell lines induced by antibiotic treatment are obviously a matter of concern and require further detailed studies.

Taken together, the technically simplest alternative for mycoplasma decontamination with the most promising results is antibiotic treatment. The convenience of use and general availability of the reagents render it a reliable routine laboratory procedure. However, antibiotic mycoplasma elimination is laborious and time consuming as the duration of the treatment plus the minimum antibiotic-free posttreatment period ranges from 3 to 5 weeks depending on the protocol used. Furthermore, special attention must be placed on possible cytotoxic effects or effects that alter the characteristics of the cell line. Nevertheless, the effect of mycoplasma infection is in all probability greater than the effects of antibiotic treatment.

Finally, variations of the antibiotic eradication procedure involve the pretreatment or simultaneous exposure to surfactin, hyperimmune antimycoplasma serum, and coculture with macrophages (Table 22.5). The idea behind these techniques is to eliminate the bulk of the contaminants prior to the addition of the antibiotics or to combine different approaches that may complement one another in the efficacy with which they eliminate residual infectants. Another treatment model demonstrated improvement in the cure rate achieved with the use of soft agar and antibiotics over that obtained with antibiotics alone. The soft-agar technique consists of suspending infected cultures in soft agar containing appropriate antibiotics. The method is based on the survival of cells in soft agar and on the fact that the cells remain in suspension, thus facilitating exposure of mycoplasmas to the antibiotics. The advantage of the method lies in its speed and simplicity as only one cycle of treatment (indicated as 1–3 days) is adequate.

22.5 WORKING PROTOCOLS FOR DETECTION, ELIMINATION, AND PREVENTION OF MYCOPLASMA CONTAMINATION

There are three main components to be considered when regarding the problem of mycoplasma contamination of cell cultures: detection, elimination, and above all prevention of mycoplasma infection. In the following, several routine protocols are presented with regard to these three fundamental issues. Mycoplasmal contamination is now and will always be a potential threat to cell cultures. Overall, detection methods have dramatically improved in recent years and the availability of testing kits has also increased. Instead of discarding mycoplasma-infected cultures (without any possible clean replacement), elimination of the contaminants has become a realistic and practical possibility. Critical to maintaining cell cultures free of mycoplasma (and other adventitious organisms) is the establishment of routine operating and testing procedures by the cell culturist. The primary difficulty in controlling the epidemic mycoplasma contamination lies in convincing the culture operator of the necessity for validating the absence of these covert organisms and in creating a certain level of awareness for the dangers that lurk.

22.5.1 Routine Working Protocol for Detection

The high frequency of mycoplasma-contaminated cell cultures and the rapid spread of the infection within the laboratory impose a requirement for rigorous mycoplasma testing of any new incoming cell culture and also for regular screening of every permanently cultured cell line. The best test will fail if the sample submitted for testing is not representative or is not properly treated. Antibiotics can mask mycoplasma infection resulting in false-negative test results. Therefore, although it is highly desirable that cell lines always be cultured without any antibiotics, for mycoplasma testing purposes it is essential that cell cultures be maintained antibiotic free for several passages. Furthermore, cultures should be assayed a sufficient time after the last passage or exchange of medium; this allows organisms, if present, to grow to high titers. Although PCR is definitely the test of choice (see section titled Most Reliable Detection Methods), this method can also produce false-positive or false-negative results. Thus, conduction of at least two (better three) different techniques on the same sample is suggested to obtain a reliable diagnosis.

A routine working protocol for detection of mycoplasma contamination in the form of a flow chart is shown in Fig. 22.8. Newly arriving cell lines should be quarantined in a separate cell culture laboratory. The initial mycoplasma testing determines the mycoplasma contamination status of the cells. If the culture is contaminated and no clean replacement is available, decontamination might be

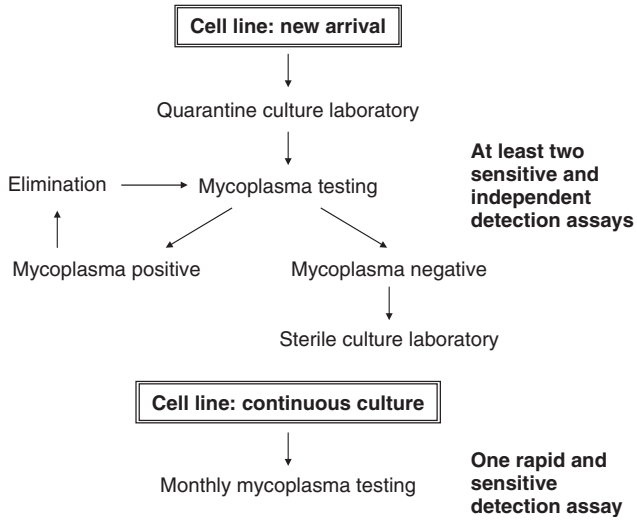


Figure 22.8. Routine working protocol for detection of mycoplasma contamination. A flow chart for mycoplasma testing of newly arriving and continuously cultured cell lines is shown. Use of at least two (better three or even four) different mycoplasma detection assays is suggested; best suited for determining the initial mycoplasma contamination status are PCR, RNA hybridization (Gen-Probe), FISH, biochemical assay (MycoAlert), and DAPI/Hoechst staining while for routine screening and continuous monitoring PCR, RNA hybridization (Gen-Probe), FISH, and biochemical assay (MycoAlert) are recommended; it is useful to check continuous cell cultures at monthly intervals. For technical details see Refs 15,17, and 19–21.

attempted followed by strict retesting post treatment (see section titled Routine Working Protocol for Elimination). It is absolutely mandatory that clean cultures also be regularly assayed for mycoplasma contamination, for instance, at monthly intervals. PCR with its extreme sensitivity, MycoAlert as very rapid and effortless assay, and DNA fluorochrome staining (DAPI/Hoechst stains) or FISH as inexpensive, simple and rapid methods can be applied for regular screening.

22.5.2 Routine Working Protocol for Elimination

If a cell culture is found to be infected with mycoplasmas, the advised procedure is to replace it whenever possible; frozen stocks can be examined or cell culture repositories can be contacted. An invaluable or irreplaceable cell line can be cured as decontamination with various methods has become a practical and highly successful endeavor. However, a number of factors should be weighed carefully. The treatment protocol plus the obligatory intensive monitoring thereafter is a laborious and time-consuming task. The possibility exists that upon exposure to potentially toxic conditions, the cell line will be subjected to selective pressure and the cured population might differ from the original. Also, the procedure entails extensive work with mycoplasma-positive cultures, thus carrying the risk of further spread of the contamination. We have had success with chemotherapeutic purging of cultures applying various antimycoplasma antibiotics. A flow diagram of the antibiotic treatment protocol is shown in Fig. 22.9.

As a general rule, if cell cultures are diagnosed as being positive for mycoplasma, as quickly as possible they should be either discarded, frozen, and stored in liquid nitrogen or treated with antimycoplasma procedures in order to prevent spread of the contaminant. The whole decontamination process should be undertaken in a quarantined culture laboratory until sterility is attained. It is advisable to freeze some cells for further elimination attempts in case the first treatment fails to achieve freedom from mycoplasma contamination. The basic principle of antibiotic treatment involves exposure of the positive culture to a recommended antibiotic concentration for a given number of days, followed by maintenance of the cells for at least 2 weeks in antibiotic-free medium, and then the close monitoring of the mycoplasma status by adequate tests to detect residual or new contaminants. Resistant cell lines may be rescued by subsequent incubation with a noncrossresistant antibiotic (for instance quinolone-resistant cells can be cured with BM-Cyclin). An alternative would be a second attempt with an untreated, mycoplasma-positive aliquot of the same culture using different antibiotics or higher concentrations. The application of elimination methods other than antibiotics remains a further possibility.

The recommendation that mycoplasmacidal antibiotics should be used as a permanently preventive measure to avoid contamination must be strongly rejected. Antibiotics, in general, and antimycoplasma reagents, in particular, should not be used as a substitute for good cell culture technique.

22.5.3 Routine Working Protocol for Prevention

Of primary importance in preventing mycoplasma contamination of cell cultures is an awareness of sources of infection combined with a program of cell maintenance, regular quality, and identity checks, and repeated characterization of the cells (27). The protocol for prevention of mycoplasma contamination should be designed to minimize risk of exposure of cells to mycoplasmas. As pointed out above (see section titled Sources of Mycoplasma Contamination), human sources and bovine serum constitute two of the main infectant reservoirs; undoubtedly, lateral spread from one cell line to another accounts for the majority of infections. A variety of specific steps can be adopted to prevent cell culture contamination with mycoplasmas (Table 22.7) (9–11).

Any sterile cell culture work should be performed in a vertical laminar flow biohazard hood. It is critical to

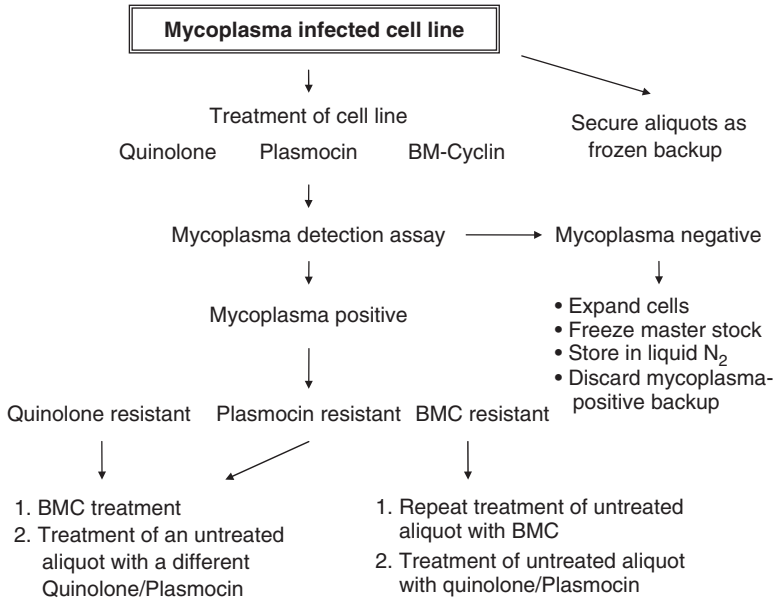


Figure 22.9. Routine working protocol for elimination of mycoplasma contamination. A suggested flow chart for planning antibiotic treatment of mycoplasma-positive cell lines is shown. It is proposed that aliquots of the contaminated cultures be frozen; these serve as a backup in case the initial antibiotic administration fails to achieve freedom from mycoplasma contamination. Cells may be treated with one, several, or all of the five regimens indicated, but in separate culture vessels as single agent treatment (the antibiotics should not be mixed). After an antibiotic-free phase of at least 2 weeks post treatment, cells must undergo several rigorous mycoplasma testings with at least two methods and must be examined afterwards at periodic short intervals (for instance monthly). In the case of antibiotic resistance, resistant cultures may be treated a second time with an effective, noncrossresistant reagent or backup (still contaminated) cultures may be treated in another attempt, or other purging methods may be used. For technical details see Refs 23 and 24–26.

disinfect all work surfaces before and after culture manipulations, including the various devices entering the laminar flow hood. Mycoplasmas are extremely sensitive to most disinfectants, but can show prolonged survival in a dried state. Thus, the main point is simply to keep the laboratory and its inventory as clean as possible. Clearly, nothing replaces good house keeping and good aseptic techniques in the control of mycoplasmal contamination. It is important that cell culture laboratories establish effective and scheduled mycoplasma testing procedures in the form of a routine screening program for all forms of microbial contamination, including mycoplasmas. Sera, media, and supplements (and also cell lines whenever possible) should be purchased from reputable suppliers that adequately test for mycoplasmal contamination.

All incoming cell lines should be quarantined until the contamination status is verified. Mycoplasma-free cultures should be separated in time and space from infected cultures. Reagents for the two sets of cultures should be separate. The general use of antibiotics is not recommended except in special applications and then only for short durations. Use of antibiotics may lead to lapses in aseptic technique, to selection of drug-resistant organisms, and to delayed detection of low-level infection by either mycoplasmas or other bacteria. Master stocks of mycoplasma-free cell lines should be frozen and stored to provide a continuous supply of cells should working stocks become contaminated. Mycoplasma-infected cell lines should be discarded or treated with mycoplasmacidal measures as quickly as possible in order to prevent lateral spread.

Strict adherence of the cell culturist to aseptic culture techniques is another fundamental aspect in mycoplasma control. Cell culturists should continually be aware of the danger of contaminating clean cultures with aerosols from mycoplasma-containing cultures manipulated in the same area. For example, the following procedures with liquid media generate droplets: pipetting, decanting, centrifuging, sonicating. These relatively large droplets do not remain airborne but settle within seconds into the immediate environment where they remain viable for days. Furthermore, mouth pipetting and unnecessary talking are not acceptable.

TABLE 22.7. Routine Working Protocol for Prevention of Mycoplasma Contamination

Cell culture facility
Facility should be designed and equipped for aseptic culture procedures
Certified laminar flow biological safety cabinets should be used and their function should be regularly examined
Work surfaces should be chemically disinfected prior to and following work, and thoroughly cleaned at regular intervals (monthly)
Incubators should be regularly controlled and cleaned (monthly)
Discarded glass and plastic ware and spent media should be carefully disinfected
Cell culture materials should be properly disposed of by central sterilization
Effective house keeping procedures should be followed to minimize contamination of the environment (e.g. floor, sinks, faucets, and water baths)
Unauthorized persons should not be allowed entry
Animals should not be kept in the cell culture room
Laboratory should be kept clean
Quality control
A defined quality and identity and characterization program should be established
Mycoplasma testing should be performed at the time of arrival of the culture and at regular intervals (monthly)
Reliable mycoplasma detection methods should be established and performed
Medium components (especially serum) should be tested for sterility before use
Strict aseptic techniques and good laboratory procedures should be followed
Cell cultures
Cell cultures should be obtained from reputable cell repositories
Incoming cell cultures should be held in quarantine until proof of sterility (or at least separated in time and space from sterile cultures)
Aliquots free of mycoplasma (and other adventitious agents) should be stored in a master and working stock system in liquid nitrogen
Antibiotic-free media should be used whenever possible
Periodic standardization checks of the cell culture (quality and identity program, characterization) should be made
Mycoplasma-positive cultures should be immediately discarded or treated with mycoplasmacidal measures
Cell culturist
Handwashing prior to and following work should be required
Mouth pipetting should be prohibited
There should be no unnecessary talking or traffic at the clean bench or in the immediate work area
Protective clothing should be used to protect both the culture and the culturist
Jewelry (rings, bracelets, and wristwatches) should be taken off
Written laboratory records for every cell culture should be made
The same medium aliquot should not be used for different cell lines
Medium should not be poured from bottles or flasks, but pipetted
Only one cell line should be handled at a given time

The prohibition of eating, drinking, smoking, or application of makeup in the laboratory is obvious. The recommendation to thoroughly wash and disinfect the hands, to take off jewelry (rings, bracelets, wristwatches), to wear protective clothing, and to tie back long hair (or use of head covering) are further precautions that are necessary to minimize the risk of contamination.

REFERENCES

1. Razin S, Freundt EA. In: Holt JG, editor. Volume 1, Bergey's manual of systematic bacteriology. New York: Williams & Wilkins; 1984. pp. 740–794.
2. Razin S. In: Dworkin M, Falkow S, Rosenberg E, Schleifer KH, Stackebrandt E, editors. Volume 4, The prokaryotes. 3rd ed. New York: Springer; 2006. pp. 836–904.
3. Tully JG. In: Lederberg J, editor. Encyclopedia of microbiology. San Diego: Academic Press; 2000.
4. Rottem S, Barile M. TIBTECH 1993; 11: 143–151.
5. Razin S. In: Razin S, Tully JG, editors. Volume 1, Molecular and diagnostic procedures in mycoplasmology. San Diego: Academic Press; 1995. pp. 1–25.
6. Razin S, Yogev D, Naot Y. Microbiol Mol Biol Rev 1998; 62: 1094–1156.
7. National Center for Biotechnology Information (NCBI) 2007. Available at http://www.ncbi.nlm.nih.gov/Taxonomy/. Accessed 2007 Apr 17.
8. Barile MF, Rottem S. In: Kahane I, Adoni A, editors. Rapid diagnosis of mycoplasmas. New York: Plenum Press; 1993. pp. 155–193.
9. Del Guidice RA, Gardella RS. In: Stevenson RE, editor. Uses and standardization of vertebrate cell cultures—in vitro monograph no. 5. Gaithersburg, Maryland: Tissue Culture Association; 1984. pp. 104–115.
10. McGarrity GJ, Vanaman V, Sarama J. Am Soc Microbiol News 1985; 51: 170–183.
11. Uphoff CC, Drexler HG. Hum Cell 2001; 14: 244–247.
12. McGarrity GJ, Kotani H, Butler GH. In: Maniloff J, McElhaney RN, Finch LR, Baseman JB, editors. Mycoplasmas—molecular biology and pathogenesis. Washington, DC: American Society for Microbiology; 1992. pp. 445–454.
13. McGarrity GJ, Vanaman V, Sarama J. In Vitro 1984; 20: 1–18.
14. Boyle JM, Hopkins J, Fox M, Allen TD, Leach RH. Exp Cell Res 1981; 132: 67–72.
15. Uphoff CC, Brauer S, Grunicke D, Gignac SM, MacLeod RAF, Quentmeier H, Steube K, Tümmler M, Voges M, Wagner B, Drexler HG. Leukemia 1992; 6: 335–341.
16. Schneider EL, Stanbridge EJ. In Vitro 1975; 11: 20–34.
17. Uphoff CC, Gignac SM, Drexler HG. J Immunol Methods 1992; 149: 43–53.
18. Uphoff CC, Drexler HG. Hum Cell 1999; 12: 229–236.
19. Rawadi G, Dussurget O. PCR Methods Appl 1995; 4: 199–208.
20. Uphoff CC, Drexler HG. In: Helgason CD, Miller CL, editors. Basic cell culture protocols. 3rd ed. Totowa, NJ: Humana Press; 2005. pp. 13–24.
21. Uphoff CC, Drexler HG. In Vitro Cell Dev Biol Anim 2002; 38: 79–85.

22. Nir-Paz R, Prévost M-C, Nicolas P, Blanchard A, Wróblewski H. Antimicrobial Agents Chemother 2002; 46: 1218–1225.
23. Drexler HG, Gignac SM, Hu ZB, Hopert A, Fleckenstein E, Voges M, Uphoff CC. In Vitro Cell Dev Biol 1994; 30A: 344–347.
24. Uphoff CC, Drexler HG. In Vitro Cell Dev Biol Anim 2002; 38: 86–89.
25. Uphoff CC, Drexler HG: Eradication of mycoplasma contaminations. In: Helgason CD, Miller CL, editors. Basic cell culture protocols. 3rd ed.. Totowa, NJ: Humana Press; 2005. pp. 25–34.
26. Fleckenstein E, Uphoff CC, Drexler HG. Leukemia 1994; 8: 1424–1434.
27. Drexler HG, Dirks W, Quentmeier H, MacLeod RAF, Steube K, Uphoff CC, editors. DSMZ catalogue of human and animal cell lines. 8th ed.. Braunschweig, Germany: DSMZ—German Collection of Microorganisms and Cell Cultures; 2001. pp. 8–13.

23

PROTEIN GLYCOSYLATION: ANALYSIS, CHARACTERIZATION, AND ENGINEERING

Mikael R. Andersen
Technical University of Denmark, Department of Systems Biology, Lyngby, Denmark
Jong Hyun Nam
Rensselaer Polytechnic Institute, Department of Chemical and Biological Engineering, Troy, New York
Susan T. Sharfstein
University at Albany, College of Nanoscale Science and Engineering, Albany, New York

23.1 INTRODUCTION

With increasing numbers of glycoproteins entering the biotechnology pipeline as potential therapeutics, there is a growing need to understand what role glycosylation plays in the therapeutic effectiveness of glycoproteins and how best to select the host, culture environment, and possible modifications of the host for production of recombinant proteins. Therapeutic glycoproteins include thromobolytics, cytokines, blood-clotting factors, growth factors, and immunoglobulins. In 1993, four of the approved recombinant protein therapeutics were in the top 25 selling pharmaceutical products (1). Since 1996, more than 20 additional recombinant enzymatic glycoproteins and antibodies have been approved as therapeutics and diagnostics. Many of the recombinant glycoproteins (e.g., erythropoietin, colony-stimulating factors, and glucocerebrosidase) represent therapeutic breakthroughs, treating conditions that were previously untreatable (2). Still others are recombinant versions of proteins (e.g., clotting factors) that were previously purified from blood or tissues with the associated disease risks.

While the field of protein glycosylation has been reviewed extensively both from the perspective of the basic biology (3–7) and with a focus on the glycosylation of recombinant proteins (8–14), our knowledge of the field is evolving rapidly. In particular, there have been advances in the use of insect cells and fungi, efforts to modify rodent cell lines to present more human-like glycoforms, studies of *in vitro* glycosylation, and a deeper understanding of the effects of culture conditions on protein glycosylation.

The tools available for separation and characterization have also advanced dramatically. Routine use of mass spectrometry and LC–MS techniques in the biotechnology industry has made detailed glycan characterization possible as part of a routine quality analysis of recombinant glycoproteins. This chapter provides an overview of protein glycosylation, a discussion of the effects of glycosylation on the stability, activity, and clearance of glycoproteins, and then discusses techniques and strategies for separating and analyzing glycoproteins.

23.2 OVERVIEW OF PROTEIN GLYCOSYLATION

Protein glycosylation is the most common posttranslational modification. Among the proteins in the SWISS-PROT database, more than two-thirds of the proteins contain consensus sequences for N-linked glycosylation. On the

Upstream Industrial Biotechnology: Expression Systems and Process Development, Volume 1, First Edition. Edited by Michael C. Flickinger.
© 2013 John Wiley & Sons, Inc. Published 2013 by John Wiley & Sons, Inc.

basis of the characterization of site occupancy of known glycoproteins, Apweiler and coworkers (15) estimate that more than half of the proteins in the database are glycosylated. Moreover, the mass of the carbohydrate added to proteins is substantial, between 10% and 60% of the molecular weight of a glycoprotein. All integral membrane proteins in higher organisms are glycosylated as are many secreted proteins. In addition, glycoproteins also exist in the cytoplasm and nucleus (3).

Carbohydrate modification falls into three general categories. N-linked glycans involve the amide nitrogen in the asparagine side chain; O-linked glycans involve the oxygen in the side chains of serine, threonine, hydroxylysine, or hydroxyproline; and glycosylphosphatidyl inositol (GPI) derivatization occurs on the carboxy-terminal carboxyl group. In addition, there are some unusual forms of glycosylation that have been recently discovered. A glycoprotein may have one or more glycosylation sites. Each putative glycosylation site may be always occupied, variably occupied (referred to as *macroheterogeneity*), or never occupied. In addition, the glycan attached to each site may vary from molecule to molecule (referred to as *microheterogeneity*) leading to a highly variable population of glycoproteins from a single polypeptide backbone.

The glycan diversity results from the large number of different sugars and linkages available to synthesize an oligosaccharide. A large number of hexose and some pentose sugars that can be incorporated into polysaccharides are available. The most common sugars, their structures, abbreviations, and symbols are given in Table 23.1. Each monosaccharide has a number of hydroxyl groups that can be linked to other sugars. Multiple linkages are possible, yielding a variety of branches. In addition, there are two anomeric forms available for each linkage, α- and β-forms.

23.2.1 N-Linked Glycosylation

In the case of N-linked glycans, the consensus sequence Asn-X-Ser/Thr where X is any amino acid except proline is necessary, but not sufficient, for glycosylation. It is estimated that between 10% and 30% of potential glycosylation sites are not occupied (16). N-Linked glycans can be grouped into three main categories all of which contain a common core structure ($Man_3GlcNAc_2$): complex, which contain no mannose residues other than in the core; high mannose; and hybrid, in which some of the branches are of the complex type and some are of the high-mannose type (Fig. 23.1). In each case, the GlcNAc is linked in a β-linkage to the amide nitrogen of the asparagine side chain. In the complex structures, each branch frequently terminates in a sialic acid although sulfated lactosamine is also seen, particularly in glycoprotein hormones such as LH, FSH, and TSH. Site analysis has shown that the distribution of different classes of N-linked structures is frequently specific for each site on a protein. For example, in the rat brain protein Thy1, site 23 has only high-mannose structures, site 74 has only complex and hybrid structures, and site 98 contains all three types (17,18).

Proteins targeted for secretion or membrane insertion are translocated to the endoplasmic reticulum by means of a 15–30 amino acid signal sequence comprising primarily hydrophobic amino acids during translation. The newly synthesized protein enters the lumen of the endoplasmic reticulum where it is subject to co-translational folding and N-linked glycosylation. N-Linked glycosylation occurs by the transfer of a lipid-linked oligosaccharide species ($Glc_3Man_9GlcNAc_2$–PP–dolichol) to an asparagine residue on the newly synthesized polypeptide chain. The oligosaccharide is trimmed by two glycosidases and one or more mannosidases in the endoplasmic reticulum and the protein is then translocated to the Golgi apparatus where it undergoes further modification of oligosaccharide chains and O-glycosylation, followed by packing and processing for secretion (Fig. 23.2).

N-Linked glycosylation and trimming also serves a quality control function and helps ensure proper folding. Monoglucosylated proteins (i.e., proteins with one terminal glucose remaining on the mannose core) are selectively bound by calnexin or calreticulin. This binding allows ERp57, a thiol-disulfide oxidoreductase, to bind to the glycoprotein and facilitate disulfide bond formation (19). Glycoproteins are released from calnexin and calreticulin by the action of glucosidase II which removes the terminal glucose from the glycan structure. If the glycoprotein is incorrectly folded, it is recognized by UDP-glucose:glycoprotein glucosyltransferase which adds a glucose back onto the glycan, allowing for another cycle of binding to calnexin/calreticulin to prevent misfolded proteins from leaving the ER.

23.2.2 O-Linked Glycosylation

The most common form of O-linked glycosylation is the mucin type which contains an α-glycosidic linkage between GalNAc (and sometimes GlcNAc) and the hydroxyl group of serine or threonine (Fig. 23.3). There is no clear consensus sequence for O-linked glycosylation; however, the serine or threonine acceptor amino acid appears to be preferentially surrounded by Ser, Thr, Pro, Ala, and Gly residues (7). O-Linked glycosylation of secreted proteins occurs in the Golgi apparatus, and hence is limited to residues present on the protein surface after the protein is completely folded in the ER. Currently, there are eight different core structures known to occur beyond the Ser/Thr-GlcNAc linkage (Fig. 23.3). There are a limited number of monosaccharides present in mucin-type glycans, namely GalNAc, Gal, GlcNAc, Fuc,

TABLE 23.1. Monosaccharide Nomenclature and Structures

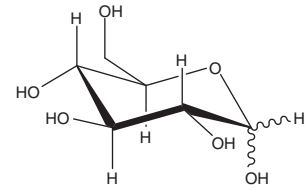
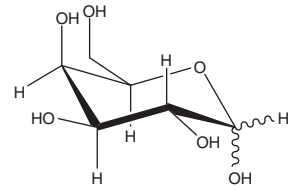
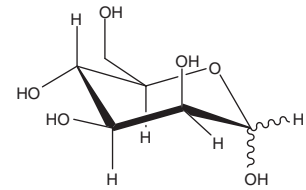
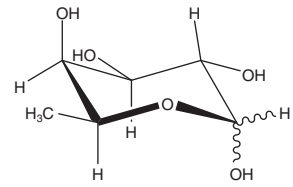
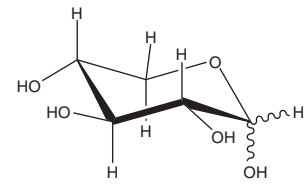
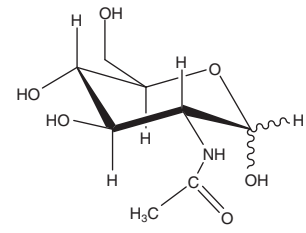
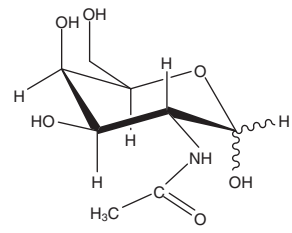
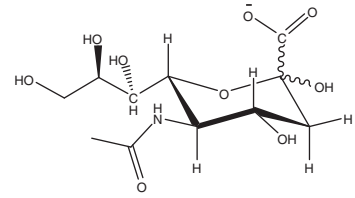
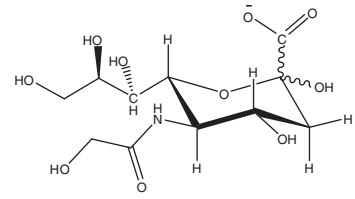
Family	Sugar	Abbreviation	Symbol[a]	Structure
Hexose	Glucose	Glu		
	Galactose	Gal		
	Mannose	Man		
Deoxyhexose	Fucose	Fuc		
Pentose	Xylose	Xyl		
N-acetyl hexosamine	*N*-Acetylglucosamine	GlcNAc		
	N-acetylgalactosamine	GalNAc		

TABLE 23.1. (*Continued*)

Family	Sugar	Abbreviation	Symbol[a]	Structure
Sialic acid	*N*-acetylneuraminic acid	Neu5Ac or Sia		
	N-glycolylneuraminic acid	Neu5Gc		

[a]This symbol set represents the newly agreed upon symbols as established by the Consortium for Functional Glycomics and NLM/NCBI. See http://grtc.ucsd.edu/Essentials_Materials/EssentialsSymbols2ndEd.pdf for more information.

and sialic acid. Sulfation is also a frequent modification. In general, Glc and Man are not found in these structures. Biosynthesis occurs in a stepwise manner with individual nucleotide-activated monosaccharides added by site-specific glycosyltransferases. While the O-linked mucin structures are much more compact and generally smaller than the N-linked structures, they are also much more diverse. For example, human lung mucin contains more than 100 different glycans (7). A fairly common structure, particularly for cell surface glycoproteins, is the presence of many O-linked glycan in close proximity. These structures appear to serve both as passive and active barriers preventing proteolytic and infectious attacks.

23.2.3 Glucosylphosphatidylinositol (GPI) Anchors

GPI anchors are used to anchor surface membrane proteins to the cells in eukaryotes. They are particularly prevalent in mammalian cells and some parasitic protozoa, and are also found in other lower eukaryotes. Eisenhaber et al. (21) estimated by sequence analysis that ~0.5% of all eukaryotic proteins are GPI anchored. It is hypothesized that they allow the protein greater mobility than maintaining a transmembrane domain, but this has not been established. Proteins slated for GPI anchor attachment contain the usual amino-terminal signal sequence that directs them to the ER during synthesis. In addition, they contain a 15–30 amino acid signal sequence at the carboxy terminus. Like the amino terminal signal sequence, the amino acids are primarily hydrophobic. This signal sequence is cleaved when the GPI anchor is attached to the carboxy terminus of the resulting peptide. Three critical amino acids exist at the cleavage site, generally referred to as ω, $\omega+1$, and $\omega+2$. Cleavage occurs between the ω and $\omega+1$ amino acids and the ω amino acid becomes the carboxy terminus to which the GPI anchor is attached. The amino acid preference for the ω site is serine $\approx$ asparagine $>$ alanine $\approx$ glycine $\approx$ aspartate $>$ cysteine valine $\approx$ leucine. In the $\omega+1$ site, all amino acids are permitted except proline. At the $\omega+2$ site, the preference is alanine $\approx$ glycine $>$ serine $>$ threonine$>$ aspartate $>$ valine. (See Ref. 22 for a detailed review.)

The GPI moiety is synthesized on the cytoplasmic face of the ER and then translocated into the lumen. All GPI anchors appear to have a conserved core consisting of ethanolamine-phospho-6Manα 1-2Manα 1-6Manα 1-4GlnNα 1-6-myo-inositol-1-phospholipid. The lipid portion is very diverse and varies from species to species and within species (23). The GPI anchor is attached by the action of a GPI transamidase. This enzyme cleaves the peptide bond at the GPI anchor attachment site and creates an amide linkage between the ethanolamine of the GPI and the newly generated carboxyl group at the end of the cleaved precursor protein (24). The GPI-anchored protein is then sorted and transported to the cell membrane by a mechanism that is still unclear.

23.2.4 Other Less Common Forms of Glycosylation

In addition to the mucin form of O-glycosylation, a variety of other linkages exist between sugars and the hydroxyl groups of serine, threonine, hydroxylysine, and hydroxyproline. Xyl is β-linked to either Ser or Thr to link glycosaminoglycans (GAGs) to peptides to form proteoglycans. Epidermal growth factor (EGF)-like

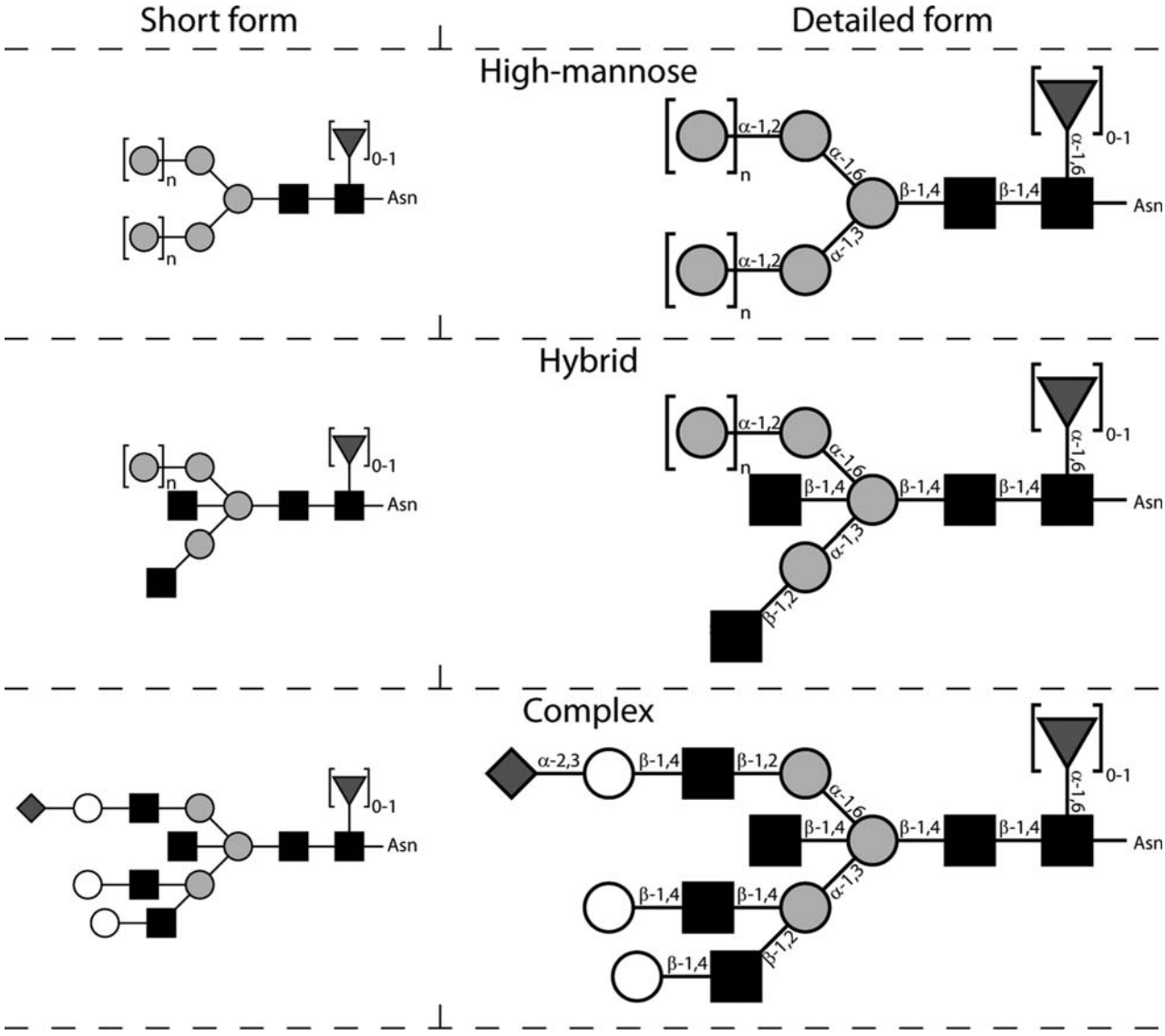


Figure 23.1. Overview of the three main types of *N*-glycans. The short form is an example of the notation described in Table 23.1.

domains of several proteins (including clotting factors) are modified by the addition of Glc or Fuc. Of particular interest is the addition of a single GlcNAc in a β-linkage to a variety of cytoplasmic and nuclear proteins. This modification is reversible and appears to serve a function similar to that of phosphorylation. Gal is bound in a β-linkage to hydroxylysine in collagen; yeast and other fungi exhibit Man α-linked to Ser/Thr, and a variety of other linkages are also seen (7,12). Some surprising linkages recently observed include a C–C bond between Man and Trp in human RNase 2 (7) and the discovery of phosphoglycosylation in which the oligosaccharides are linked to the peptide chain via a phosphodiester linkage (25).

23.3 EFFECTS OF GLYCOSYLATION ON PROTEINS

Protein glycosylation affects the structure, activity, immunogenicity, protease sensitivity, stability, and biological clearance of the glycoprotein. It also plays a role in protein trafficking and cell signaling. Our current understanding of these functions with specific examples, particularly for recombinant proteins produced in heterologous hosts, is described below.

23.3.1 Structure and Stability

Protein glycosylation affects protein structure in two ways. As the protein is glycosylated co-translationally,

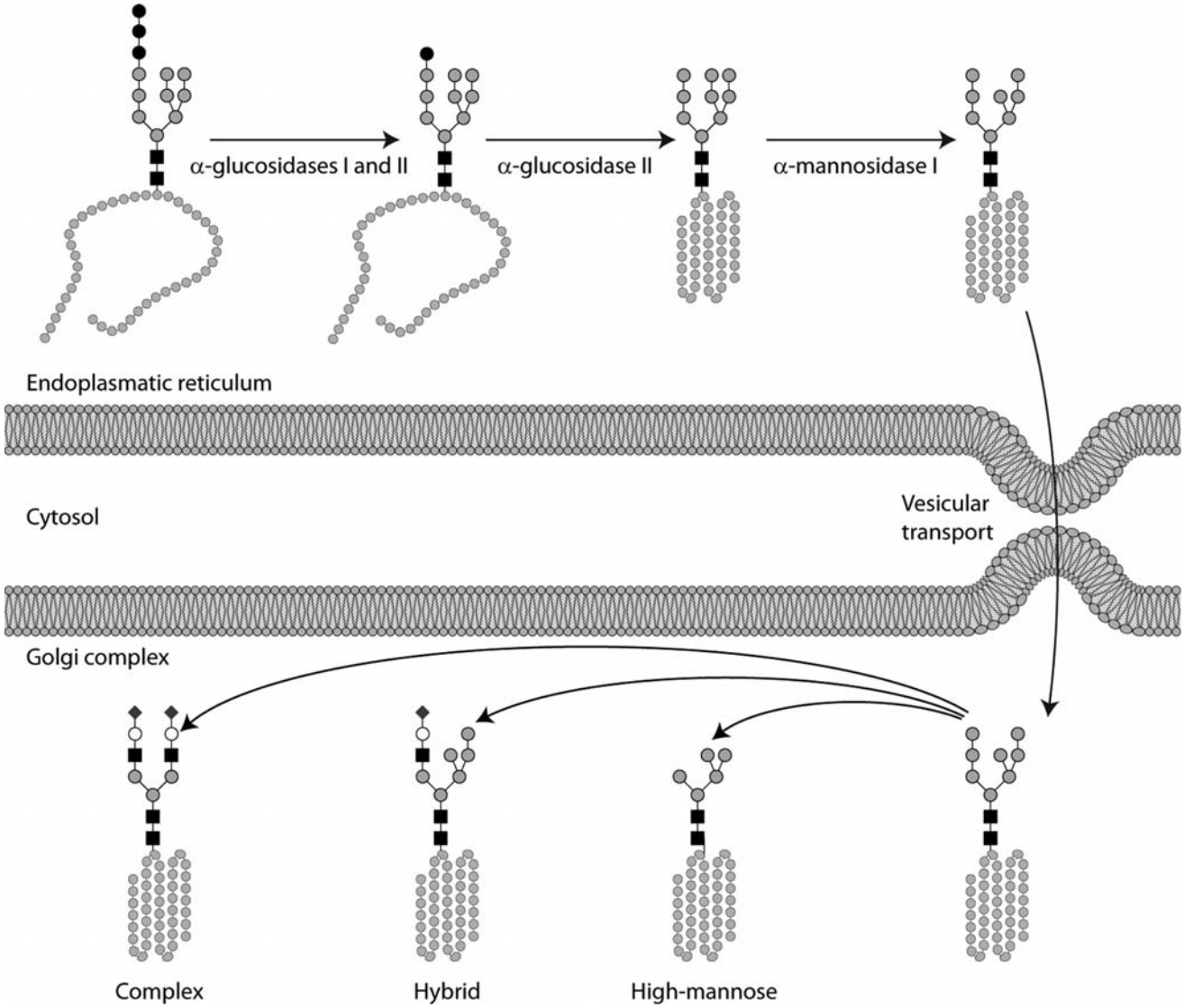


Figure 23.2. Schematic and simplified overview of the modification of *N*-glycans in the endoplasmatic reticulum and the Golgi complex, resulting in the three main types of N-glycosylation: high mannose (>3 mannose residues), hybrid (one antennae and >3 mannose residues), and complex (multiple antennae).

the presence or absence of the correct glycans can affect the nascent peptide's ability to fold correctly. When glycosylation is inhibited using tunicamycin or by removal of consensus sequences by mutagenesis, many proteins fail to fold correctly (26). The unfolded proteins aggregate soon after synthesis and are frequently bound noncovalently by BiP/GRP78, an ER chaperone. Frequently, the misfolded proteins are cross-linked by interchain disulfide bonds. The need for glycosylation varies dramatically with some proteins being unaffected and others very sensitive. In addition, it is sometimes possible to move the glycosylation site by site-directed mutagenesis and obtain correct folding, suggesting that oligosaccharides play a more global than local role in folding. In addition, as discussed above, the trimming of the N-linked glycans serves a quality control function in the ER. Incorrectly glycosylated and folded proteins are recycled for further processing. Ultimately, proteins that are incorrectly folded or glycosylated are targeted for degradation by the unfolded protein response (UPR).

Glycosylation enhances protein stability by a variety of mechanism. Wang and coworkers (27) examined five different glycoproteins, both in their native and deglycosylated forms. Deglycosylated proteins were less thermally stable and their thermal denaturation showed less reversibility than the native proteins. They found that the effect depended

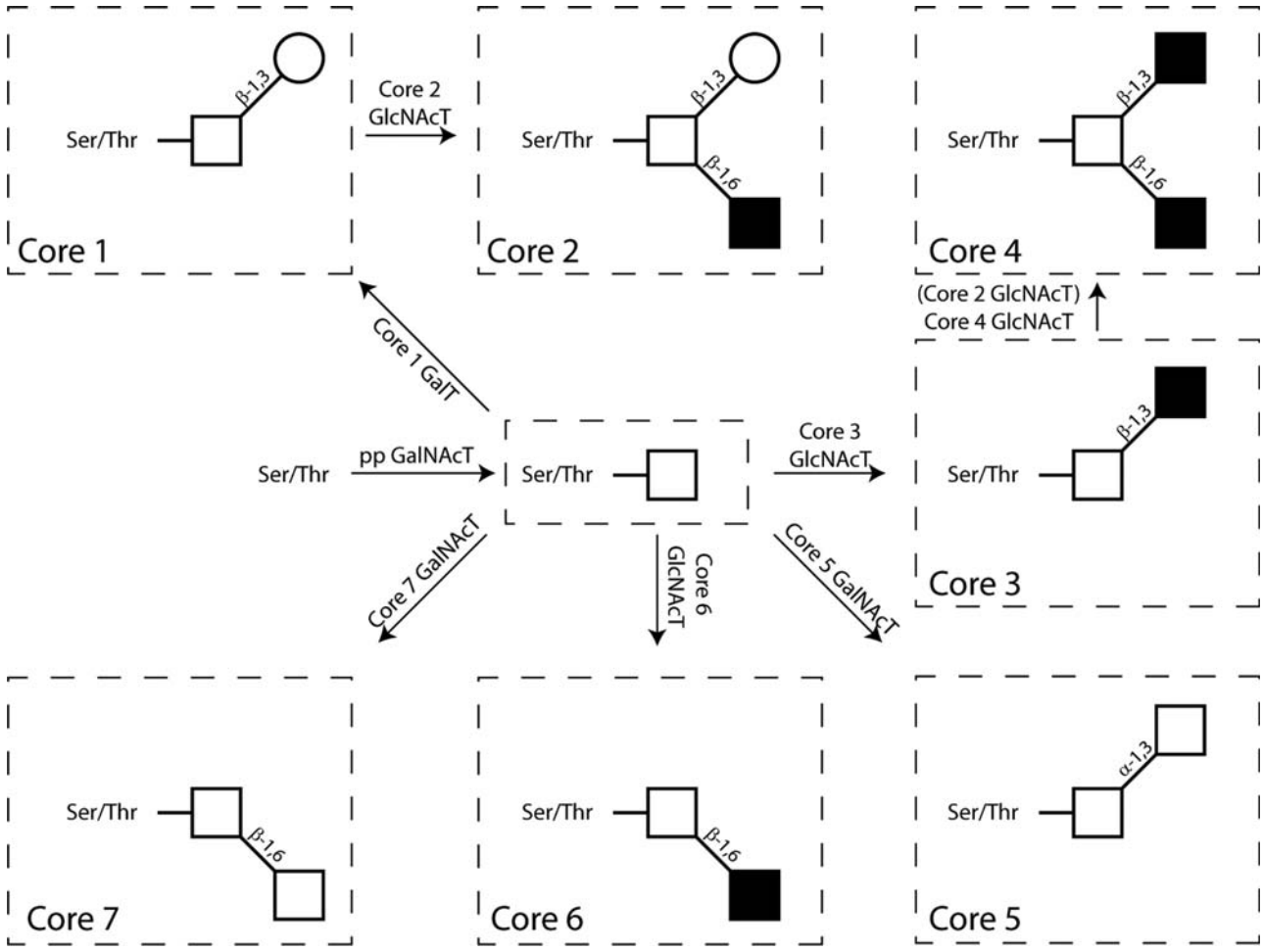


Figure 23.3. The seven core structures of mucin-like O-glycosylation found in humans. *Source:* Reproduced from information found in (20). GalNAc, *N*-acetylgalactosamine; GalNAcT, GalNAc transferase; GalT, Galactose transferase; GlcNAc, *N*-acetylglucosamine; GlcNAcT, GlcNAc transferase.

primarily on the amount of carbohydrate bound to the protein rather than the type of linkage. O'Connor and Imperiali (28) examined N-linked oligosaccharides attached to small peptides using NMR spectroscopy. They found that glycosylation causes the peptides to adopt more compact, folded conformations, particularly β-turns. Several investigators observed that glycosylated proteins had significantly less dynamic fluctuation, which appears to lead to increased stability (29).

23.3.2 Activity

Glycosylation can affect the activity of proteins using a variety of different mechanisms. The first mechanism is to alter the physiochemical properties including solubility and proper folding as described above (3). Alterations in glycosylation that affect protein folding are implicated in a number of diseases, including carbohydrate-deficient glycoprotein syndrome, cystic fibrosis, amyloid diseases such as Alzheimers, and lysosomal storage diseases such as Tay-Sachs (12). In addition, in a small, but significant number of cases, glycosylation can directly affect the biological activity of a correctly folded protein. Tissue plasminogen activator (t-PA), a serine protease produced recombinantly as an anti-thromobolytic, is one of the best known examples. t-PA contains four putative glycosylation sites, three of which are occupied (Asn-117, Asn-184, and Asn-448). It naturally occurs in two major molecular species, type I (glycosylated at all three sites) and type 2 (glycosylated only at Asn-117 and Asn-448). It is synthesized in a one-chain form and subsequently undergoes proteolytic cleavage by plasmin to a two-chain form. The occupancy of the Asn-184 site has been shown to affect the glycan structure at the Asn-448 site, the rate of conversion to the two-chain (more active) form, the affinity of t-PA for fibrin, and the fibrinolytic activity (16).

Similar effects were observed for both plasminogen and ribonuclease.

Hormone and receptor activities are also affected by their glycosylation. A number of glycoprotein hormones which activate adenylate cyclase exhibited drastically reduced activity on deglycosylation. In the case of hCG, the ability of the hormone to bind to its receptor was not inhibited; however, its ability to activate the signal transduction cascade was significantly impaired (3). Glycosylated receptors exhibited a variety of responses to changes in glycosylation. Leutenizing hormone receptor has six potential glycosylation sites; site-directed mutagenesis of three of them substantially decreased binding, while mutation of the other three sites had no effect.

23.3.3 Immunogenicity and Biological Clearance

Glycosylation plays a significant role in both immunogenicity and the rate of biological clearance both by the immune system and by the liver. Carbohydrate epitopes are responsible for blood-type determinants, indicating that even between humans, there is significant immune recognition based on carbohydrates. Moreover, close to half of the monoclonal antibodies (mAbs) generated against animal cells or cell membranes are directed against glycan groups. Plant glycoproteins are highly immunogenic, particularly because of the presence of xylose or an α-1,3-linked fucose (3). Many mammalian species, but not humans, contain a nonreducing terminal Galα 1-3Gal linkage. Antibodies against this epitope are present in all human sera and are the major reason for rejection of xenotransplants (30). Patients with rheumatoid arthritis, an autoimmune disease, exhibit a significant increase in serum IgG (immunoglobulin G) that is deficient in galactose and terminal *N*-acetylglucosamine. It is hypothesized that this alteration in glycosylation could lead to conformational changes in the Fc region of the immunoglobulin, creating new antigenic sites, leading to the autoimmune response (3). Of particular concern in the production of recombinant glycoproteins is the possible introduction of antigenic domains that could lead to severe allergic or immune responses.

Many recombinant glycoproteins exhibit rapid clearance, requiring frequent dosing to maintain biological activity. Desialylated glycoproteins are rapidly cleared by the liver via the hepatic asialoglycoprotein receptor, indicating that it is critical to maintain proper sialylation for recombinant proteins. Weikert et al. at Genetech demonstrated that overexpression of galactosyltransferase and sialyltransferase in Chinese hamster ovary (CHO) cells producing recombinant glycoproteins led to an increase in terminal sialylation with a resulting increase in mean residence time in a rabbit model (31). Insect cells have also been engineered to improve sialylation of recombinant proteins produced in insect cells, although the levels are still relatively low (32). Recently, significant efforts have been employed to glycoengineer recombinant proteins to improve their biological half-lives. Elliot et al. at Amgen demonstrated that recombinant human erythropoietin could be engineered to contain additional N-glycosylation consensus sequences. The engineered proteins were shown to contain an increase in N-linked glycans and molecules could be selected which maintained *in vitro* activity and receptor binding and showed increased *in vivo* activity because of decreased clearance rates (33).

23.4 TECHNIQUES FOR ANALYZING GLYCOPROTEINS, GLYCOPEPTIDES, AND THEIR ATTACHED GLYCANS

There are two major issues in characterizing the glycan structures on glycoproteins. One is referred to as *macroheterogeneity*, in which some glycosylation sites on glycoproteins are variably occupied and the other is referred to as *microheterogeneity*, in which glycan structures at each glycosylation site vary even with the same backbone peptide sequence. There are two possible approaches to characterization of glycans, analysis of the glycans while still attached to the peptide or hydrolysis and analysis of the released glycans. Since the amount of glycan and glycoprotein samples available is often limited, characterization of the glycan structures and the site occupancy simultaneously with the same sample (site-specific glycan analysis) conserves material and provides information about macroheterogeneity (i.e., variable site occupancy). While liquid chromatography/mass spectrometry (LC–MS) is well equipped to perform this characterization and is currently widely used to analyze glycan structures with the improved detection limits of MS technology (34,35), it is still unable to identify isomers that have identical masses. In this section, we first discuss techniques for analysis of intact glycoproteins and glycopeptides, and then discuss techniques for analysis of glycans that have been chemically or enzymatically removed from the peptide backbone. In the last several years, substantial advances have been made in both chromatography and mass spectrometry and, more importantly, in combining the two techniques that have permitted better assignments of glycan structures and assignments of structures at particular glycosylation sites (36–45).

23.4.1 Techniques for Characterizing Intact Glycoproteins and Glycopeptides

23.4.1.1 Lectin Affinity Capture. Lectins are plant proteins that specifically recognize a variety of glycan

structures. Lectins can have fairly narrow or very broad specificities, allowing them to be used for different applications. For example, concanavalin A (con A) has a broad specificity for high-mannose N-linked oligosaccharides and will also bind hybrid-type *N*-glycans and to a lesser extent bi-antennary complex glycans. It will not bind complex glycans with additional branches. In contrast, Sambucus Nigra lectin (SNA) binds specifically to glycans with terminal sialic acids, preferentially those attached to a terminal galactose in (α-2,6) linkage although to a lesser degree those attached with an (α-2,3), linkage. SNA lectin does not appear to bind sialic acid linked to *N*-acetylgalactosamine. Lectins with broad specificity can be used to chromatographically select a wide variety of glycosylated proteins or peptides from mixture of non-glycosylated and glycosylated proteins or peptides in a method termed *glyco-catch* (46). Alternatively, a lectin or a series of lectins with narrow specificity can be used to selectively capture glycoproteins with a particular glycan form, termed *serial lectin affinity chromatography* (47). More recently, these tools have been employed in conjunction with proteomic studies (e.g., mass spectrometry) to characterize glycans and glycoproteins (48,49).

23.4.1.2 LC–MS of Glycopeptides. The most common enzyme for generating glycopeptides for LC–MS analysis is trypsin. Trypsin is a serine endopeptidase, which specifically cleaves peptide bonds C-terminal to arginine or lysine. Depending on the glycoproteins that are to be characterized, other proteolytic enzymes such as chymotrypsin, Lysine C, and Glu-C can also be used. Sometimes, a combination of two or more enzymes is used to generate the appropriate size or sequence of peptides to facilitate the chromatographic separation of peptides.

In LC–MS analysis of tryptic peptides, there are three main steps. First, glycopeptides are generated with trypsin (usually modified trypsin to minimize autolysis of trypsin) after reduction and carboxymethylation of disulfide bonds (50). The peptide/glycopeptide mixtures generated with trypsin are then separated by HPLC on a hydrophobic column (often C_{18}). Usually, glycopeptides elute earlier than peptides because of the hydrophilic effect of the sugar moiety. In 2005, Wuhrer and coworkers reported using a hydrophilic column for separating and site-specifically characterizing glycopeptides (51), and this method has been increasingly used for analysis of both glycopeptides (37,42) and glycans (36,39). Finally, the glycopeptides in the peptide/glycopeptide mixtures are detected and the glycans are site-specifically characterized using mass spectrometry. Glycopeptides can be identified from among the peptide/glycopeptide mixtures by monitoring glycopeptide precursor ions such as *m*/*z* 204 ($HexNAc^+$), 274 ($[NeuAc-H_2O]^+$), 292 ($NeuAc^+$), and 366 ($Hex\text{-}Hex\text{-}NAc^+$) (52–56). Alternatively, chromatography can be used to enrich the sample for glycopeptides before mass spectrometry analysis (37,40). Depending on the properties of the samples, different types of mass spectrometry (nano-electrospray ionization MS, MALDI-TOF MS (matrix-assisted laser desorption/ionization time-of-flight mass spectrometry), etc.) can be used. With state-of-the-art LC–MS equipment, mass spectrometry can usually provide data-dependent multistage MS (MS^n), which can generate the fragments of oligosaccharides and peptides. This fragment information can be used to confirm the glycosylation site (peptide sequences) and the glycan structures and glycosidic linkages. This feature can be more powerful if combined with a method such as nano-electrospray ionization MS which consumes a very small fraction of samples (57). This significantly reduces the labor-intensive work and costs for characterizing glycans by eliminating extensive purification and other laborious tasks such as exoglycosidase digestion used in the conventional methods. As an example, Ivancic and coworkers recently used LC–MS to characterize α_1-acid glycoprotein (AAG). AAG has five N-linked glycosylation sites, each varying in its glycan structure. By using a high-low cone voltage switch during the analysis of the tryptic peptides, they were able to alternate between carbohydrate fragmentation for structural analysis (high voltage) and maintaining an intact oligosaccharide on the glycopeptide (low voltage) to determine the mass of each glycan structure (41). A similar approach was used to characterize a biosimilar mAb and compare the biosimilar with the innovator molecule (58).

One of the limitations of trypsin is that it is often unable to effectively cleave near a glycosylation site, presumably because of steric hinderance. To address this issue, several new approaches have been proposed. Segu and coworkers (59) explored the use of microwave-assisted digestion and found that the rate of tryptic cleavage (and, in general, the efficiency) could be substantially improved by microwave heating. Zauner and colleagues (42) reported the use of proteinase K, which leads to much smaller fragments improving mass spectral analysis.

23.4.1.3 Identification of Glycosylation Sites. Identification of glycosylation sites generally depends on enzymatic or chemical cleavage of the protein chain, separation of the resulting peptides and glycopeptides by reversed-phase HPLC, and detection by mass spectrometry (60).

The peptide fragments must be separated to identify the potential glycosylation sites because the analysis of unseparated enzymatic digests, commonly used for protein identification, cannot be used reliably since the glycopeptides may be discriminated against both because of their size and charge; sialic acid, phosphorylation and sulfation

may all introduce partial negative charges. In addition, glycopeptides are usually present in substoichiometric quantities because of the carbohydrate heterogeneity at any given site (61).

Glycopeptides are usually separated by HPLC on a hydrophobic column (C_{18}-reversed-phase HPLC), but either hydrophilic columns or capillary electrophoresis (CE) can also be used. Glycopeptides on the chromatogram can be identified by running the (partially) deglycosylated peptide mixtures and identifying the peak shifts (34,62). Enzymatic release of *N*-glycans using the endoglycosidase peptide *N*-glycanase (PNGase) F from the glycopeptides increases the mass by 1 Da by converting the asparagine residues at the glycosylation sites to aspartic acid residues. This 1 Da mass increase can be detected using MALDI-TOF MS, leading to the identification of glycosylation sites. If the incubation is performed in water containing $H_2^{18}O$, the labeled oxygen is incorporated into the aspartic acid resulting in doublet peaks separated by two mass units in mass spectra, further improving the detection (60). PNGase A can be used to release oligosaccharides containing α1,3-linked core fucose that is resistant to PNGase F digestion. *endo*-β-*N*-Acetylglucosaminidases D, F1, F2, F3, and H that cleave between the core GlcNAc residues can also be employed. Since the resulting peptides still bear an GlcNAc unit, the molecular mass observed after digestion should be higher than the predicted mass by 203 Da per glycosylation site for any given sequence stretch.

Site-specific information (site occupancy) can be characterized using glycopeptide mixtures. Proteolysis of glycoproteins is usually achieved with trypsin following reduction and alkylation of the proteins. The common method for the analysis of site occupancy is separating the glycopeptide mixtures on reversed-phase HPLC and analyzing the separated peptide masses on-line or off-line using mass spectrometry (LC–ESI MS, ESI-QqTOF MS, hybrid Q linear ion trap (LIT) MS, ESI-Q-TOF MS, and MALDI-TOF MS, etc.) This method can generate enough information to confirm the glycosylation sites (peptide sequence) and glycan structures (glycan fragments). In on-line LC–MS, glycopeptides eluting from HPLC can be identified by the appearance of oxonium ions such as *m*/*z* 204 ($HexNAc^+$), 274 ($[NeuAc\text{-}H_2O]^+$), 163 (hexose), 292 ($NeuAc^+$ sialic acid) or 366 ($Hex\text{-}Hex\text{-}NAc^+$) that appear at high source-orifice potential (selected ion monitoring method) (55). In the case of triple quadrupole MS (QqTOF, hybrid-Q-LIT LC–MS etc.), the oxonium marker ions can be more efficiently identified through collision induced dissociation cells (precursor ion scanning method) (53). In the precursor ion scanning method, the second quadrupole is set to pass the oxonium ion of interest and the first is scanned. Only compounds that fragment to produce the selected oxonium ion can be identified. Collision induced dissociation (CID) fragments reveal the identity of glycopeptides, as well as yield information on the carbohydrate structure (63). In MS^2 (MS/MS) of CID, fragments are rich in b-type oxonium ions of the nonreducing end of oligosaccharides (64) or y-type ions with peptides. These fragment information can be reconstructed to infer the oligosaccharide sequences. MS^3 of CID produces the extensive peptide bond cleavages that confirm the amino acid sequence of the peptides and thereby the glycosylation sites (65). The use of alternative fragmentation technologies such as electron capture dissociation (ECD) (66–68) and electron transfer dissociation (ETD) (69) provides for fragmentation of the peptide backbone, giving additional information about the sites of modification.

O-Linked glycans are not as amenable to these techniques because they are often grouped on adjacent or closely spaced amino acids, and it is not possible to acquire glycopeptides containing a single glycan from a known position of the protein chain. However, MS/MS spectrometry can provide some information as the masses of the b and y ions from the protein chain sometimes yield information on the location of glycosylation, but usually only when one site is occupied (70). The alternative fragmentation strategies, ECD and ETD, described above have also been employed to improve analysis of O-linked glycans (71,72).

23.4.2 Techniques for Deglycosylation

Among major protein glycosylation forms, N-linked and O-linked glycans have major impact on the proteins and have been extensively studied. In this section, the major techniques for releasing N- and O-linked glycans from glycoproteins are discussed. There are broadly two methods to release the glycans from the glycoproteins.

23.4.2.1 Chemical Methods. In order to release glycans, a general method is required that is independent of the protein to which the glycan is attached. For this reason a chemical method is used, which usually involves the use of hydrazine to cleave both N- and O-glycosidic bonds (73) (Fig. 23.4). Hydrazine releases both N- and O-linked glycans by cleavage of all peptide bonds in the glycoprotein. O-Linked glycans are released at 60°C, whereas incubation at 95°C is needed to release the N-linked sugars. The major advantages of the chemical method are that it releases glycans that are intact and with a free reducing terminus, it is nonselective (with respect to the glycans), and the process is amenable to automation (74). However, because all peptide bonds are destroyed in this method, all information related to the glycosylation sites on the proteins is lost. The acyl groups are cleaved from the *N*-acetylamino sugars and sialic acids and are normally

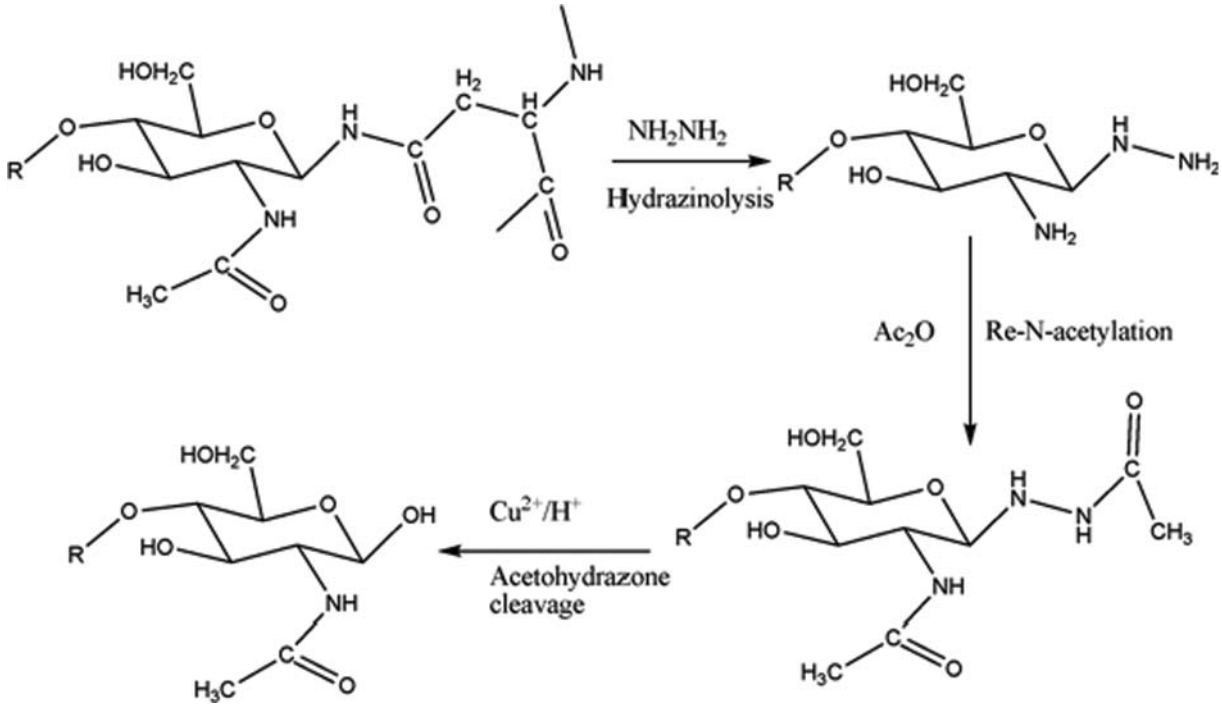


Figure 23.4. Hydrazine-based cleavage of glycosidic bonds.

replaced chemically (Fig. 23.4), with the assumption that they were originally acetylated, which is not always true, as with *N*-glycolylneuraminic acids (60). If the hydrazinolysis conditions are too harsh, some *N*-acetylamino groups or terminal GlcNAc residues can be removed (75).

O-Linked glycans are traditionally detached from the protein by β-elimination using strong bases such as sodium hydroxide or hydrazine (73). Recently, Yamada and colleagues have developed an automated method for releasing *O*-glycans coupled with MALDI-TOF MS to improve the speed and efficiency of *O*-glycan analysis (76).

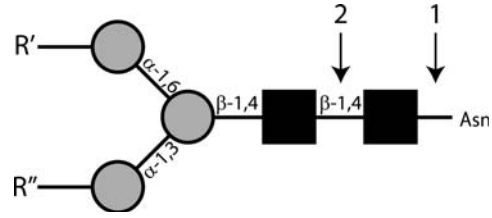


Figure 23.5. Common *N*-glycan cleavage sites on enzymatic treatment for glycan sequencing. Peptide *N*-glycanase (PNGase) F cleaves the glycan at the arrow marked with 1, whereas Endo D and H cleave at 2.

23.4.2.2 Enzymatic Methods. The most common enzyme for releasing N-linked glycans from glycoproteins is the peptide PNGase F, which is an amidase that cleaves between the innermost GlcNAc and the asparagine residue (Fig. 23.5, arrow 1). PNGase F hydrolyzes nearly all types of N-glycan chains except the ones containing fucose α-1-3-linked to the reducing-terminal GlcNAc from glycopeptides/proteins. In this case, PNGase A can cleave N-linked glycans containing α-1-3-linked core fucose.

Other useful enzymes are Endo D and H, which cleave between the two acetylglucosamine residues within the chitobiose (Fig. 23.5, arrow 2). Endo D releases all kinds of N-linked glycans while Endo H is limited to high-mannose- or hybrid-type N-linked glycans. Endo-β-*N*-acetylglucosaminidases F1, F2, and F3 are also often used. All three enzymes cleave within the chitobiose core (Fig. 23.5, arrow 2). While Endo F1 cleaves only oligomannose and hybrid glycans, Endo F2 cleaves oligomannose and bioantennary glycans, and Endo F3 is specific for bi- and triantennary *N*-glycans (77). Recently, Segu et al. (78) used PNGase F, Endo M, and a combination of Endo M and exoglycosidases on tryptic digests of fetuin in conjunction with LC–MS/MS to identify glycosylation sites and core fucosylation of bovine fetuin.

In contrast to the release of N-linked glycans, there are no universal *O*-glycans due to the lack of universal consensus sequence for O-linked glycans. Thus, enzymatic release of *O*-glycans from glycoproteins is limited by the high substrate specificity of *O*-glycosidases available (20,79). For example, the *endo*-GalNAcase D from *Diplococcus*

TABLE 23.2. Glycoprotein Oligosaccharide-Releasing Enzymes[a]

Enzyme	Source	Susceptible *N*-glycans
Endo D	*Diplococcus pneumoniae*	Some high mannose Some (few) hybrids
Endo H	*Streptomyces plicatus*	High mannose Most hybrids
Endo C_I	*Clostridium perfringens*	Similar to endo D
Endo C_{II}	*Clostridium perfringens*	Similar to endo H (narrower)
Endo F_1	*Flavobacterium meningosepticum*	Similar to endo H (narrower)
Endo F_2	*Flavobacterium meningosepticum*	High mannose Biantennary complex
Endo F_3	*Flavobacterium meningosepticum*	Biantennary complex Triantennary complex
Endoglycosidase	*Arthrobacter protophormiae*	Similar to endo C_{II}
Endoglycosidase	*Bacillus circulans*	High mannose
Endoglycosidase	*Bacillus alvei*	Similar to endo C_{II}
Endo S	*Dictyostelium discoideum*	Similar to endo C_{II}
Endo M	*Mucor hiemalis*	Similar to endo F_2
Endo B	*Sporotrichum dimorphosporum*	Similar to endo F_2
Endoglycosidase	*Aspergillus oryzae*	Similar to endo H
Endoglycosidase	Jack bean	Similar to endo C_{II}
Endoglycosidase	Human kidney (enzyme 1)	Mostly high mannose
Endoglycosidase	Human kidney (enzyme 2)	High mannose and complex (free oligosaccharides only)
Endoglycosidase	Rat liver	Similar to endo F_2
Glycoamidase A	Almond	Similar to Glycoamidase F
Glycoamidase F	*Flavobacterium meningosepticum*	All N-linked (except 1,3-core Fuc)
Glycoamidase	Jack bean	Similar to glycoamidase F
EndoGalNAcase D	*Diplococcus*	Gal-β-1,3-GalNAc only
EndoGalNAcase A	*Alcaligenes*	Gal-β-1,3-GalNAc only
EndoGalNAcase S	*Streptomyces*	Gal-β-1,3-GalNAc (plus larger structures)

[a] *Source:* Adapted from O'Neill (80).

pneumoniae cleaves only the disaccharide Gal β1-3GalNAc (20). Major glycan-releasing enzymes, their sources, and usages are summarized in Table 23.2 (80).

23.4.3 Strategies for Analysis and Characterization of Glycans

There are many strategies available for the analysis and characterization of released glycans from glycoproteins. The choice of methods or strategies depends on the properties of samples that are analyzed and information that is needed. A combination of the methods described below is often used to fully characterize the glycan structures on the glycoproteins.

23.4.3.1 Mass Spectrometry. Mass spectrometry has played a critical role in characterizing the glycan structures from glycoproteins. The most common mass spectrometry sources for ionization of oligosaccharides are either matrix-assisted laser desorption/ionization (MALDI) or electrospray ionization (ESI). A variety of detectors are combined with these ion sources. Popular combinations of ion sources and detectors for characterization of oligosaccharides are MALDI-time of flight (TOF), ESI-quadrupole ion trap (QIT), hybrid-Q-LIT MS, and ESI-Q-TOF MS, often connected to an HPLC on-line.

MALDI-TOF MS is the most commonly used mass spectrometry technique for characterizing sugar structures. The analysis of N-linked glycans and, to a lesser extent, O-linked glycans from glycoproteins is the area in which MALDI MS has had the most impact on carbohydrate analysis (60). The advantages of MALDI-TOF MS in characterization of glycans are that the mass spectra are relatively easy to interpret because most peaks represent singly charged species; hence, there is no need to deconvolute the mass spectra. In addition, to a certain extent, MALDI-TOF tolerates contaminants in the sugar samples, and it requires a very small amount of sample, unlike ESI MS. However, the automation is difficult; thus, it is most often used off-line.

The most critical part in MALDI-TOF MS for the study of glycans is to choose the right matrix for the samples. 2,5-DHB (dihydroxybenzoic acid) is the most popular matrix for the analysis of free carbohydrates (81). $[M + Na]^+$ ions are the dominant products in the positive ion mode. $[M\text{-}H]^-$ ions are the dominant form in the negative ion mode. When a 2,5-DHB sample solution evaporates, DHB tends to crystallize from the periphery of the target spot in the form of long needles that point toward the centre of the target. To overcome this problem, Super-DHB matrix (10% 2-hydroxy-5-methoxybenzoic acid added to DHB) was introduced (82). This matrix crystallizes more evenly than DHB and has been reported to enhance signal strength and resolution (48). 2,4,6-THAP (trihydroxyacetophenone) has been reported to effectively ionize sialylated glycans in negative ion mode (83) with

less loss of sialic acid during fragmentation than when DHB is used as the matrix. In addition to these matrices, 4-HCCA (α-cyano-4-hydroxy-cinnamic acid) and HABA (2-(*p*-hydroxyphenylazo)-benzoic acid) are also often used (60).

Derivatization of free oligosaccharides can increase the detection sensitivity and stability, simplifying the fragments in MALDI-TOF MS analysis. Thus, in certain cases, it can be advantageous to analyze derivatized sugars. Depending on the sample size, permethylation (>5μg) with methyl iodide or methyl esterification (<5μg) can be performed (84), and they can improve the sensitivity by about an order of magnitude. Reducing sugars are also often derivatized at their reducing end with chromophores or fluorophores, usually by reductive amination.

The composition of oligosaccharides can be inferred on the basis of the masses on the mass spectra. One of the popular web-based software tools for inferring the composition of glycans is GlycoMod. GlycoMod (http://www.expasy.ch/tools/glycomod/) is a software tool designed to find all possible compositions of glycan structures from their experimentally determined masses. The program can be used to predict the composition of any glycoprotein-derived oligosaccharide comprising either underivatized, methylated, or acetylated monosaccharides, or oligosaccharides with a derivatized reducing terminus (85). A typical mass spectrum of N-linked glycans isolated from secreted alkaline phosphatase (SEAP) produced by CHO cells is shown in Fig. 23.6; the glycan assignments made by GlycoMod are given in Table 23.3.

LC–MS/MS techniques with ESI have been increasingly employed in the analysis of glycans (36); the use of CID allows for identification of structures that cannot be elucidated with MALDI-TOF.

23.4.3.2 Chromatographic Profiling. A variety of chromatographic techniques can be used to separate and characterize glycans after release from the protein or peptide backbones. While individual techniques are useful, they are particularly powerful when combined in series as described in the section titled "Multidimensional Liquid Chromatography." With the exception of pulsed amperometric detection (PAD) which is generally applied with anion exchange chromatography, glycans separated chromatographically are most commonly detected by fluorescence labeling as described in the section titled "Detection Methods for Chromatography and Capillary Electrophoresis."

23.4.3.2.1 Anion Exchange Chromatography. High pH-weak anion exchange chromatography (HPAEC) is employed to separate glycans based on the number of

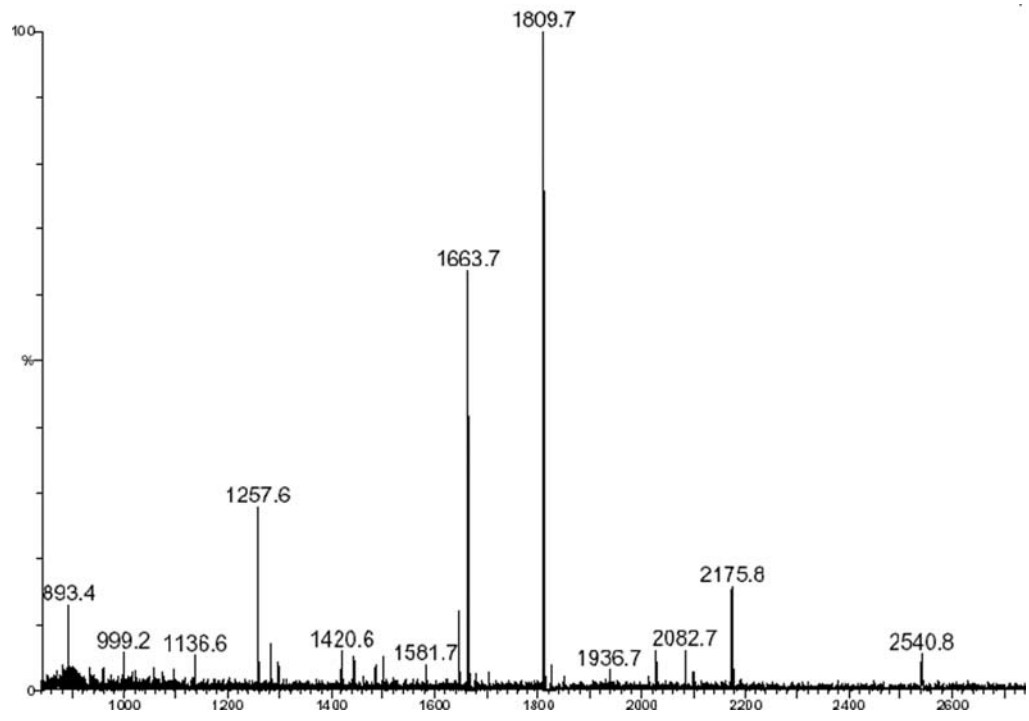


Figure 23.6. A typical mass spectrum of N-linked glycans isolated from secreted alkaline phosphatase (SEAP) produced by Chinese hamster ovary (CHO) cells. See Table 23.3 for the assignment of glycans to masses.

TABLE 23.3. GlycoMod Analysis of *N*-Glycan Compositions for Secreted Alkaline Phosphatase Produced in CHO Cells

			Positive Ion Mode
No.	Observed $m/z^{ab}[M + Na]^+$	Calculated $m/z^{a}[M + Na]^+$	Composition/Sequence
1	1257.6	1257.4	(Hex)2+(Man)3(GlcNAc)2
2	1282.6	1282.5	(HexNAc)1(Deoxyhexose)1+(Man)3(GlcNAc)2
3	1298.6	1298.4	(Hex)1(HexNAc)1+(Man)3(GlcNAc)2
4	1420.6	1419.5	(Hex)3+(Man)3(GlcNAc)2
5	1444.6	1444.5	(Hex)1(HexNAc)1(Deoxyhexose)1+(Man)3(GlcNAc)2
6	1460.7	1460.5	(Hex)2(HexNAc)1+(Man)3(GlcNAc)2
7	1485.6	1485.5	(HexNAc)2(Deoxyhexose)1+(Man)3(GlcNAc)2
8	1501.7	1501.5	(Hex)1(HexNAc)2+(Man)3(GlcNAc)2
9	1581.7	1581.5	(Hex)4+(Man)3(GlcNAc)2
10	1647.7	1647.6	(Hex)1(HexNAc)2(Deoxyhexose)1+(Man)3(GlcNAc)2
11	1663.7	1663.6	(Hex)2(HexNAc)2+(Man)3(GlcNAc)2
12	1809.7	1809.6	(Hex)2(HexNAc)2(Deoxyhexose)1+(Man)3(GlcNAc)2
13	1825.7	1825.6	(Hex)3(HexNAc)2+(Man)3(GlcNAc)2
14	2028.8	2028.7	(Hex)3(HexNAc)3+(Man)3(GlcNAc)2
15	2175.8	2174.8	(Hex)3(HexNAc)3(Deoxyhexose)1+(Man)3(GlcNAc)2
16	2540.8	2539.9	(Hex)4(HexNAc)4(Deoxyhexose)1+(Man)3(GlcNAc)2

[a] Mass (m/z) is monoisotopic.
[b] Some low-intensity peaks are not labeled in the mass spectrum (Fig. 23.6)

charged groups such as sialic acid, sulfate, phosphate, or uronic acid present on the glycan. Within the same charge group, large structures elute before small ones. In HPAEC, the column resin is a MicroBead pellicular resin in which small anion-exchange resin spheres are ionically attached to a larger cation-exchange resin sphere (86). The mobile phase is highly alkaline (e.g., 100 mM sodium hydroxide) often coupled with a gradient of sodium acetate. Anion exchange chromatography is frequently coupled with PAD which gives picomole (or lower) sensitivity without the need for derivatization. One limitation of PAD is that it gives a different response for each compound, making it difficult to compare quantities of different glycans within a sample. Recently, HPAEC has been employed with a capillary-scale column and both on-line PAD and on-line electrospray ion trap mass spectrometry (IT-MS), providing subpicomole sensitivity and the ability to characterize complex samples (87).

23.4.3.2.2 Reversed-Phase Chromatography. In addition to its application for separating glycopeptides, reversed-phase chromatography can also be applied to the separation of glycans. C-18 silica resins are most commonly employed (88); more recently, graphitized carbon has also been used (89). Underivatized oligosaccharides are generally separated with pure water in the mobile phase while gradient separations with increasing concentrations of organic solvents in the eluent are typically performed for derivatized glycans. The most common derivatization is reductive amination with fluorophores or chromophores as described in the section titled "Detection Methods for Chromatography and Capillary Electrophoresis."

23.4.3.2.3 Hydrophilic-Interaction Liquid Chromatography. Hydrophillic-interaction liquid chromatography (also known as *normal-phase chromatography*) is used to separate highly polar compounds and has been increasingly used to separate both glycopeptides and released glycans (39). In general, the retention of the glycans increases with increasing numbers of sugar residues. One of its main advantages is the ability to separate different structural isomers (38). Amide functional groups, using aminopropyl silica, are commonly employed as the stationary phase. The mobile phase usually consists of acetonitrile and water, although buffer salts are sometimes added. A recent modification, using zwitterionic sulfobetaine (ZIC-HILIC) functionality, has been used to separate sialylated glycans and glycopeptides as well as non-sialylated glycans from mAbs. This separation has been combined with ESI MS to characterize the glycans removed from mAbs (36).

23.4.3.2.4 Multidimensional Liquid Chromatography. Takahashi (90) have used sequential chromatographic steps to perform 2D and 3D mapping of neutral and charged oligosaccharides, respectively. In both cases, the glycans are derivatized with 2-aminopyridine (2-PA) before separation. Neutral glycans are separated initially by normal-phase chromatography on an amide column. As described in the section titled "Chromatographic Profiling," this separation is based primarily on glycan size. Each fraction is then subjected to reverse-phase chromatography on an octadecylsilica (ODS, C-18) column. The C-18 column provides separation based on the fine structure of the glycan. Each column can be calibrated with isomaltooligosaccharide mixtures to give a retention time in glucose units. The retention times of each

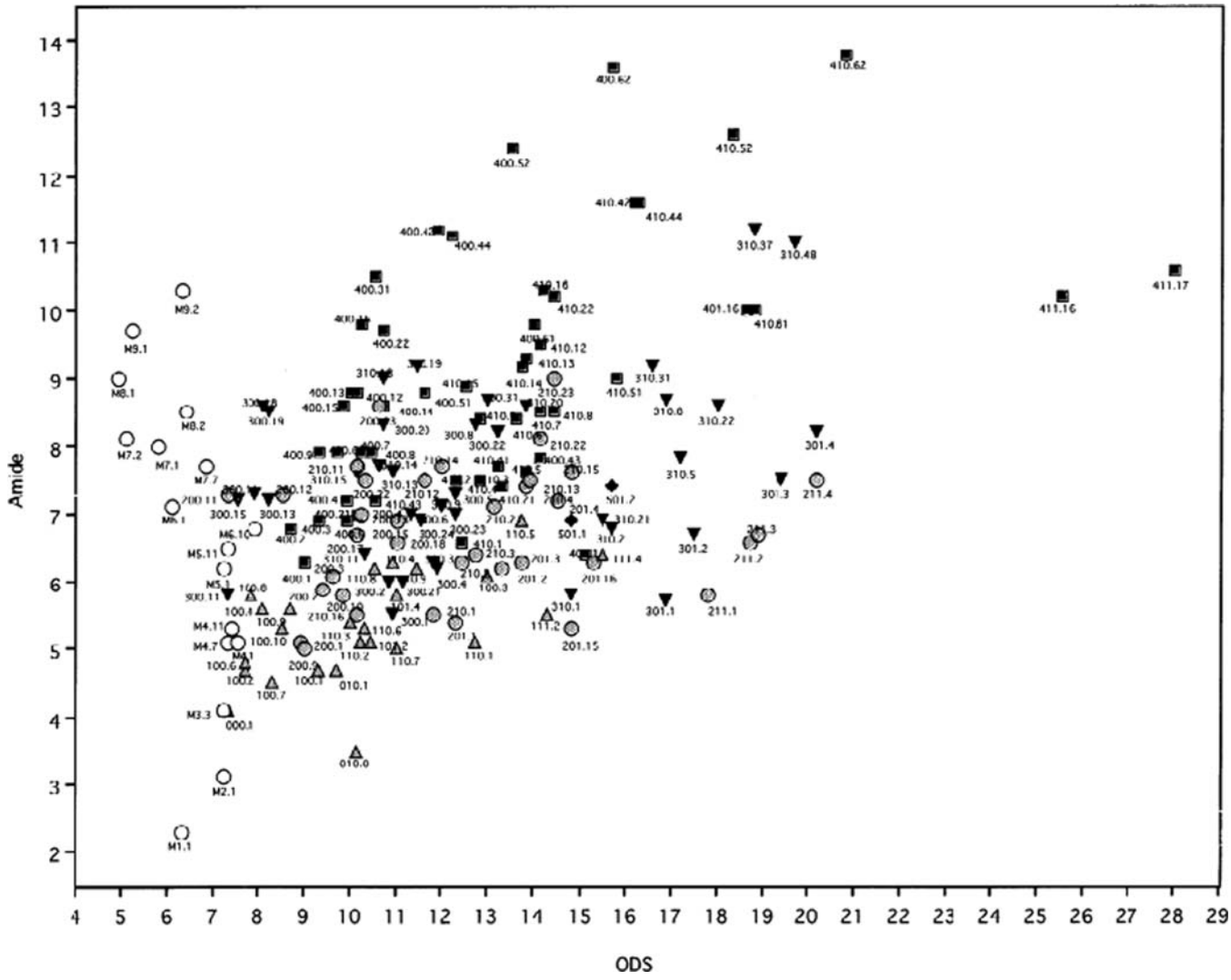


Figure 23.7. 2D plot of glycan liquid chromatography retention times. Retention time on a C-18 column versus retention time on an amide column. ***Source:*** Data originally from http://www.gak.co.jp/ECD/Hpg_eng/hpg_eng.htm. Symbols represent different types of *N*-glycans: (◯) high-mannose type, ( ) core and monoantennary, (◯) biantennary, ( ) triantennary, ( ) tetraantennary, and ( ) pentaantennary. For details on glycan structures and numbering system see the website mentioned above. *Source:* Reprinted from Hirabayashi and Kasai (46) with permission from Elsevier.

glycan on both columns can then be represented in a 2D plot as shown in Fig. 23.7. For charged oligosaccharides, an initial separation is performed on a diethylamino-ethyl (DEAE) ion exchange resin to separate the neutral, mono, di-, tri-, and tetrasialyated sugars. Each charge group is then applied to the C-18 column, followed by the amide column, generating a series of 2D plots. By mapping known glycans, reference plots can be obtained and applied to identify mixtures of unknown glycans. In the case of glycans that do not correspond to a known position on the retention map, sequential digestion with glycosidases as described in the section titled "Sequential Enzymatic Digestion" can be applied to reduce the unknown structure to a common core structure. Gillmeister and coworkers have developed a modification of these 2D chromatographic analyses combined with automated sample spotting onto plates for conventional MALDI MS analysis that allows them to process a large number of very small samples ($<100\mu g$) rapidly. They have applied this approach to characterize the effects of culture conditions on the glycan profile of a recombinant therapeutic protein produced in CHO cells (91).

23.4.3.2.5 Frontal Affinity Chromatography. Frontal affinity chromatography (FAC) is a quantitative affinity method developed by Kasai and Ishii, which can accurately determine affinity constants between various biomolecules. To apply this method, an excess volume of an analyte (e.g., a glycan) is applied to a column on which an affinity ligand (e.g., a lectin) is immobilized. By comparing the volume of the elution front of an analyte that has no affinity for the ligand with the elution front of an analyte that binds to the ligand, the dissociation constant can be determined. Hirabayashi and Kasai have suggested that this method could be used for glycomics (i.e., the study of glycan structures from an organism or cell line) using a large number of lectins to probe various elements of glycan structures (46).

23.4.3.3 Capillary Electrophoresis. CE is a high-resolution analytical technique that has been widely used for the separation of oligosaccharides. It consumes an extremely small amount of sample and is capable of rapid, high-resolution separation, characterization, and quantitation of analyses. CE separates analytes under the influence of an applied electrical field as they migrate in a narrow capillary column spanning two buffer reservoirs and filled with a conducting buffer solution (92). The capillary column is made of fused silica, and invariably carries a negative charge on its inner surface because of the presence of silanol groups. At high voltage, the positive buffer ions migrate toward the cathode, and a narrow capillary provides a flat flow profile due to electro-osmotic flow. The electro-osmotic flow affects the mobility of analytes through the capillary. Separation is optimized by manipulating this flow, for example, by changing the pH of the operating buffer (93).

Normal-polarity mode is the most common mode of separation by CE. In normal polarity, the sample is injected at the anode and detected at the cathode and basic or neutral buffer is required. The normal polarity separation in basic borate buffer containing sodium dodecyl sulfate gives the best separation of mixtures of higher oligosaccharides (93). In reversed-polarity mode, the sample is applied at the cathode and detected at the anode, and an acidic buffer is required. This mode was successfully used for analysis of a variety of GAG-derived oligosaccharides (94). The resolution achieved by CE under a given set of conditions is dependent mainly on the charge, mass, and molecular mobility of the analytes present (93).

23.4.3.4 Detection Methods for Chromatography and Capillary Electrophoresis. Detection is typically performed by ultraviolet absorbance or fluorescence emission, although mass spectrometry is sometimes employed.

23.4.3.4.1 Derivatization and Fluorescent/UV Detection. Derivatization not only provides a useful method for sensitive detection by fluorescence and/or UV but also improves resolution of separation, through the introduction of charge and the alteration of the analyte. The most frequently used method for the derivatization of carbohydrates is reductive amination. The reductive amination reaction takes place between the aldehyde group at the reducing end of the sugar and the amino group of a labeling reagent employing sodium cyanoborohydride as a reductant. A number of labeling reagents have been used including 2-AP, 4-aminobenzoic acid (4-AB), 7-amino-1,3-naphthalenedisulfonic acid (AGA), 8-amino-naphthalene-1,3,6-trisulfonic acid (ANTS), and 1-phenyl-3-methyl-5-pyrazolone (PMP) (93). The various labeling agents and their detection wavelengths are summarized in Table 23.4.

23.4.3.4.2 Direct UV Detection Following Capillary Electrophoresis. On-column complexation of native carbohydrates with borate allows direct UV detection at 195 nm. Nanogram amounts of nonderivatized carbohydrates can be detected in this way. UV detection of glycopeptides is straightforward since the peptide bond gives rise to sufficient absorbance at 200 nm (95).

23.4.3.4.3 Indirect UV Detection Following Capillary Electrophoresis. Indirect detection methods are a viable alternative for compounds lacking a chromophore. The detection principle is based on the displacement of the chromophore in the background electrolyte by the analyte molecule, resulting in negative peaks (95). Buffers of benzene-1,2,4-tricarboxylic acid and of 5-sulfosalicylic acid are generally used (96).

23.4.3.4.4 MS Detection. On-line CE–MS has been performed using ESI MS, continuous-low fast atom bombardment ionization sources, and a time-of-flight mass spectrometer (97). Although ESI MS is the most convenient and promising method, MALDI-TOF MS has been evaluated as a fast detector that can provide excellent detection range from a low femtomole range to attomole range (97). The additional structural data obtained by MS reduces reliance

TABLE 23.4. Labeling Agents and Detection Wavelengths

	Fluorescent detection		UV detection
Agent	λ_{ex} (nm)	λ_{em} (nm)	λ_{max} (nm)
2-AP	320	380	237
4-AB	—	—	285
AGA	325	425	—
ANTS	325	520	—
PMP	—	—	245

on precise retention migration time measurements required by other methods that involve separations based solely on electrophoresis or chromatography (98).

23.4.3.5 Electrophoresis. Both isoelectric focusing (IEF) and fluorophore-assisted carbohydrate electrophoresis (FACE®) can be used to characterize glycans. In IEF, samples are applied to a gel with an intrinsic pH gradient. In the presence of an electric field, samples migrate until the pH equals the pK_a of the sample at which point they cannot migrate any further. IEF is very effective in characterizing the charge heterogeneity, particularly because of the degree of sialylation of the glycan.

Uncharged glycans will not migrate in an electric field; hence, they need to be derivatized before separation. Labeling with a negatively charged fluorophore (usually ANTS) at the reducing terminus by reductive amination permits electrophoretic separation as well as high sensitivity detection. FACE uses a polyacrylamide gel to perform the separation of glycans based on size; however, most glycans are relatively small (~1000 Da for oligosaccharides and ~180–300 Da for monosaccharides) requiring gels with a very high concentration of acrylamide (20–40% T acrylamide). These high percentage gels have limited stability and must be used as early as possible after casting or purchase. It is also important to cool the gel during electrophoresis as significant amount of heat is generated. FACE is often combined with sequential enzymatic digestion (described in the section titled "Sequential Enzymatic Digestion") to characterize both the glycan size and linkages.

FACE can also be used to characterize the monosaccharide composition of an oligosaccharide or of a glycoprotein. For monosaccharide characterization, the intact glycan (or glycoprotein) must be hydrolyzed to its component monosaccharides. Hydrolysis is generally performed at 100°C for 3–5 h in 2N trifluoroacetic acid (TFA) or 4N HCl for neutral or amino sugars, respectively. After hydrolysis, amino sugars require reacetylation before labeling. The monosaccharides are then labeled with 2-aminoacridone (AMAC) to permit visualization by fluorescence and to maximize the differential migration rates between the differential monosaccharides. After electrophoresis, the labeled monosaccharides can be visualized and quantitated using a long-wave (368 nm) UV light box as shown in Fig. 23.8.

23.4.3.6 Sequential Enzymatic Digestion. Exoglycosidase sequential digestion can be used to identify sugar structures, as well as glycosidic linkages, because exoglycosidases have specificity for cleaving only one kind of sugar and only in a single linkage position (61). A popular approach for glycan sequencing is the use of exoglycosidases in conjunction with the detection of respective reaction products by MS or HPLC. The underlying idea of this approach is that the substrate specificity of the employed enzyme defines the structural feature of susceptible glycans. Glycans can be treated either sequentially with single enzymes in order to establish their structure or the glycan pool can be divided into several portion and then treated with arrays of enzymes in parallel (99). The commonly used exoglycosidases for oligosaccharide sequencing are summarized in Table 23.5.

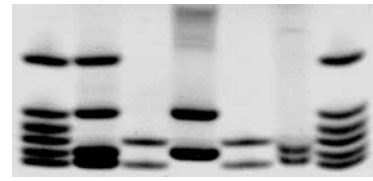


Figure 23.8. Monosaccharide composition analysis (using FACE® monosaccharide composition kit, ProZyme product code GK90100): AMAC (2-aminoacridone)-labeled monosaccharides released by two hydrolysis methods and analyzed on a monosaccharide composition gel against purified monosaccharide standards. FACE® is a registered trademark of ProZyme, Inc. (www.prozyme.com).

23.4.3.7 Sialic Acid and Monosaccharide Composition.

23.4.3.7.1 Sialic Acid Analysis. Terminal sialic acid residues on glycans play diverse biological roles in many glycoproteins. Sialic acids are key mediators in a plethora of cellular events, including cell–cell recognition and cell–matrix interactions. Incomplete sialylation of glycans that are normally sialylated leads to more rapid clearance *in vivo* through asialoglycoprotein receptors in the liver. Thus, the amount of terminal sialic acid is critical on the effectiveness of therapeutic proteins *in vivo*. On purified proteins, sialic acids are liberated either by hydrolytic procedures or by treatment with specific enzymes. Acidic hydrolysis with 2 M TFA at 80°C ensures the hydrolytic cleavage of all sialic acid linkages, deacylation, and decarboxylation of these residues. Many sialidases are commercially available and their specificity depends on O-acetylation, the occurrence of *N*-glycolyl groups, and the type of the glycosidic linkage (100). Sialic acids are typically quantitated using either a colormetetric or a fluorometric assay. In the colorimetric assay, the products of periodate oxidation of the sialic acid are coupled with thiobarbituric acid to form a red chromophore (λ_{max} 549 nm) (101). A modified thiobarbituric acid assay provides fluorometric detection of sialic acid with picomolar sensitivity. The fluorescence of the thiobarbituric acid

TABLE 23.5. Commonly Used Glycosidases for Oligosaccharide Sequencing[a]

Enzyme	Source	Susceptible Linkage
Sialidase	*Arthrobacter ureafaciens*	α 2–3,6,8,9
	Clostridium perfringens	α 2–3,6,8
	Vibrio cholerae	α 2–3,6,8
	Salmonella typhimurium	α 2–3,6,8,9
	Newcastle disease virus	α 2–3,8
	Streptococcus pneumoniae	α 2–3
Galactosidase	Coffee bean	α 1–3,4,6
	Jack bean	β 1–4,6
	Streptococcus pneumoniae	β 1–4
	Bovine testes	β 1–3,4,6
	Chicken liver	β 1–4
Endo β-galactosidase	*Bacteroides fragilis*	β 1–4
β-Hexosaminidase	Jack bean	β 1–2,3,4,6
	Streptococcus pneumoniae	β 1–2,3,4,6
	Chicken liver	β 1–3,4
Mannosidase	Jack bean	α 1–2,3,6
	Aspergillus satoi	α 1–2
	Helix pomatia	β 1–4
α-Fucosidase	Chicken liver	α 1–2,3,4,6
	Bovine kidney	α 1-2,3,4,6
	Almond meal	α 1-3,4
	Xanthomonas manihotis	α 1–2
α-Glucosidase I	Porcine liver	α 1–2
α-Glucosidase II	Porcine liver	α 1–3

[a] *Source:* Adapted from Kuster et al. (99). See also http://glycotools.qa-bio.com/ and http://prozyme.com/product_family_index.html?key=glyko_enzymes.

reaction product of periodate-cleaved sialic acid is readily detected by excitation at 550 nm and analysis of emitted light at 570 nm (102).

23.4.3.7.2 Monosaccharide Composition Analysis. Prior to monosaccharide analysis, monosaccharides must be released from the oligosaccharide chain by acidic hydrolysis. The choice of analysis method of monosaccharides depends mainly on the amount of material available. The most frequently used techniques are HPLC, CE, and FACE, all of which allow both quantitative and qualitative analysis of monosaccharide mixtures. More detailed information can be obtained by physicochemical method such as mass spectrometry and nuclear magnetic resonance (NMR) spectrometry (103). A mass spectrometer is often connected to the HPLC or CE apparatus which makes automated high-throughput analysis possible.

TABLE 23.6. Major Carbohydrate Structure Databases[a]

Database	URL
GlycomeDB	http://www.glycome-db.org/
EUROCarbDB	http://www.ebi.ac.uk/eurocarb/
CarbBank	http://www.boc.chem.uu.nl/sugabase/carbbank.html
KEGG	http://www.genome.jp/kegg/glycan/
GLYCOSCIENCES.de	http://www.glycosciences.de/
CFG	http://www.functionalglycomics.org/
BCSDB	http://www.glyco.ac.ru/bcsdb3/
GlycoSuiteDB	http://glycosuitedb.expasy.org/
GlycoBase (Dublin)	http://glycobase.ucd.ie/
GlycoBase (Lille)	http://glycobase.univ-lille1.fr/base/
JCGGDB	http://jcggdb.jp/

[a] *Source:* Adapted from Frank and Schloissnig (104).

23.4.4 Bioinformatics Resources for Analysis and Assignment of Glycans

As the field of glycobiology has expanded, the bioinformatic and computational resources for the analysis of glycans have also expanded. These resources have been reviewed recently by Frank and Schloissnig (104). These resources include carbohydrate structure databases (Table 23.6), tools for glycan analysis (Table 23.7), and tools for prediction and analysis of glycosylation sites (Table 23.8). These tools are particularly useful for identifying carbohydrate structures from HPLC chromatograms and MS and NMR spectra. In addition, there are a variety of tools for molecular dynamics calculations and for determining carbohydrate–protein interactions. These are described in much greater detail by Frank and Schloissnig.

23.5 GLYCOSYLATION OF RECOMBINANT PROTEIN THERAPEUTICS

As of 2009, more than 165 recombinant protein pharmaceuticals have been approved for human use, with another 500 in preclinical and clinical trials. Of these, approximately 70% are glycosylated proteins (105,106), which correlates well with the estimate that more than 50% of the proteins in the human body are glycosylated (15). The glycans are well established determinants for the protein function, folding, serum half-life, and immunogenicity. As evermore complex recombinant therapeutic proteins are ectopically expressed in nonhuman host organisms, it will become increasingly important to produce products with more human-like glycosylation and to enhance their phamacokinetic properties through glycoengineering.

The structural information of the peptide chain of the recombinant protein is an important factor in directing glycosylation, but the glycan structures are also affected by

TABLE 23.7. Free Software Tools for Glycan Analysis[a]

Name	Content	URL
GlycoWorkbench	Glycan MS spectra annotation	http://www.eurocarbdb.org/applications/ms-tools http://www.ebi.ac.uk/eurocarb/gwb/home.action
Glyco-Peakfinder	Determination of glycan compositions from their mass signals	http://www.eurocarbdb.org/applications/ms-tools http://www.glyco-peakfinder.org/
GlycoPep ID	Identifying the peptide moiety of glycopeptides generated using a nonspecific enzyme	http://hexose.chem.ku.edu/predictiontable.php
GlycoMiner	Glycopeptide composition analysis	http://www.chemres.hu/ms/glycominer/index.php
AutoGU	HPLC analysis	
ProspectND	NMR spectra processing	http://www.eurocarbdb.org/applications/nmr-tools
CCPN Tools	Annotation of NMR spectra	http://www.ccpn.ac.uk/
CASPER	Structure determination of oligosaccharides and regular polysaccharides	http://www.eurocarbdb.org/applications/nmr-tools http://relax.organ.su.se:8123/eurocarb/casper.action

[a] *Source:* Adapted from Frank and Schloissnig (104).

TABLE 23.8. Tools for Prediction and Analysis of Glycosylation Sites[a]

Name	Description	URL
Big-Pi	GPI anchors	http://mendel.imp.ac.at/sat/gpi/gpi_server.html
GPI-SOM	GPI anchors	http://gpi.unibe.ch/
NetCGlyc	C-Mannosylation	http://www.cbs.dtu.dk/services/NetCGlyc/
NetNGlyc	N-Glycosylation	http://www.cbs.dtu.dk/services/NetNGlyc/
NetOGlyc	O-Glycosylation	http://www.cbs.dtu.dk/services/NetOGlyc/
YinOYang	O-β-GlcNAc-ylation	http://www.cbs.dtu.dk/services/YinOYang/
EnsembleGly	O-, N-, and C-glycosylation	http://turing.cs.iastate.edu/EnsembleGly/
CKSAAP_OGlySite	Mucin-type O-glycosylation	http://bioinformatics.cau.edu.cn/zzd_lab/CKSAAP_OGlySite/
GPP	O- and N-glycosylation	http://comp.chem.nottingham.ac.uk/glyco/
GlySeq	Statistical analysis of glycosylation sites based on sequence	http://www.dkfz.de/spec/glycosciences.de/tools/glyseq/
GlyVicinity	Statistical analysis of glycosylation sites based on 3D structures	http://www.dkfz.de/spec/glycosciences.de/tools/glyvicinity

[a] *Source:* Adapted from Frank and Schloissnig (104).

other factors, including the type of the host cell and the culture conditions. In this section, we, therefore, first present an overview of the native glycans for various potential hosts. This is followed by reviews of efforts to genetically modify the organisms to alter the glycans and modeling studies to address how specific glycans structures are produced for recombinant proteins. Finally, the effects of culture conditions on glycan structures, thus summarizing current knowledge of the effect of these factors, as well as an overview of the efforts in cellular and metabolic engineer targeted toward optimizing protein glycosylation, are discussed.

23.5.1 Effects of Host Cell Selection

The production of pharmaceutically active heterologous proteins is currently based on relatively few production platforms; mainly, hamster-derived cells (CHO and BHK) and mouse cells (SP2/0 and NS0). However, with the recent emergence of a number of new cell systems, for example, human PER.C6 cells, the bioreactor-grown moss *Physcomitrella patens*, and the glycoengineered yeast *Pichia pastoris* which all have reached the development and/or production phase (107–109), the scope of cell factories has been increased. The following sections present the typical glycosylation structures of the human system, and describe the glycosylation structures found in mammalian and nonmammalian cell-culture-based expression systems. In this context, we are also giving attention to the discussion on how non-human glycosylation patterns found in specific expression systems may affect the pharmacokinetics and, potentially, the immunogenicity of the recombinant protein. The sections titled "Insect Cells," "Plants," "Yeast and Filamentous Fungi," and "Bacteria" describe how these features have been engineered to facilitate the production of biopharmaceuticals with human-like glycosylation.

23.5.1.1 Mammalian Expression Systems. Within mammalian expression systems, the main types of cell lines employed are derived from human, hamster, and mouse cells.

23.5.1.1.1 Human Cell Lines. The glycosylation chemistry of the human cell can generally be seen as the ultimate goal of recombinant production of glycoproteins. It is desirable to obtain a glycosylation profile similar to the native protein in terms of pharmacokinetics, patient safety, and regulatory approval. However, human glycoproteins may contain quite a number of different glycosylation structures; a feature that other mammalian-derived cell cultures cannot fully emulate.

Human *N*-glycans generally have a core mannose structure, which in many cases will include a proximal α-1,6-bound fucose (10,110–112). Up to four antennae (110,113) and a bisecting GlcNAc (10,106,111,114) may be attached to the core structure. These antennae may be of type 1 (Gal-β-1,3-GlcNAc repeats) or type 2 (Gal-β-1,4-GlcNAc repeats) (111,113,115). The antennae may be capped in the nonreducing end with NeuAc-α-2,3-Gal (10,115) or NeuAc-α-2,6-Gal (10,110,114,116). The sialic acid residues may have further sialic acid residues added to them to form polysialic acid, [NeuAc-α-2,8-]$_n$NeuAc, where n may be greater than 55 (117). The antennae may also have fucose residues added as side groups to form the Lewis antigens; Lewis X (Le^X) (Gal-β-1,3/4-[Fuc-α-1,3/4-]GlcNAc) and sialylated Lewis X (sLe^X) (NeuAc-α-2,3/6-Gal-β-1,3/4-[Fuc-α-1,3/4-]Glc NAc) type structures (10,106,110,113). Finally, sulfonation of the antennae has been shown to occur, for example, in the form of sulfonated GalNAc residues (SO4-GalNAc-β-1,4-GlcNAc) (118) and keratan (SO4-Gal-β-1,4-GlcNAc) (119,120). For an overview, see Figure 23.9.

Human O-glycosylation is dominated by mucin-like-type *O*-glycans, especially in the context of heterologous proteins. This glycan type is initiated by the addition of GalNAc to a serine or threonine residue, which may then be extended in seven standard types, of roughly decreasingly abundance with core 1 being the most abundant (Fig. 23.3). Type 1 and 2 antennae, Lewis antigens, sialylation (121), or glycans of the ABH blood group type may then be added to additionally elongate these seven structures (122).

Owing to the potential complexity of the glycosylation structures described above, cell lines derived from human (cancer) tissue thus have the innate advantage of having the genetic basis for human-like O- and N-glycosylation. This said, a cancer cell line may display other glycans, simply due to genetic mutations, or the changed metabolism of the cell, making the glycosylation—to some extent—cell line and protein dependent. For instance, avian IgY expressed in HEK-293 cells has glycosylation similar to the native protein (123), but IgG from HEK-293 has an overly high content of proximal fucose (124). While widely used for research, the HEK-293 cell line is not widely applied in the production of biopharmaceuticals, although there is increasing interest in its use as a host for transient expression, both for preclinical materials as well as in the area of personalized medicine. Xigris® (activated protein C) has for a while been the only recombinant pharmaceutical protein produced in HEK-293 cells (106). Most recombinant protein pharmaceuticals from human cell lines are produced in the human fibrosarcoma cell line HT-1080, such as Elaprase® for the

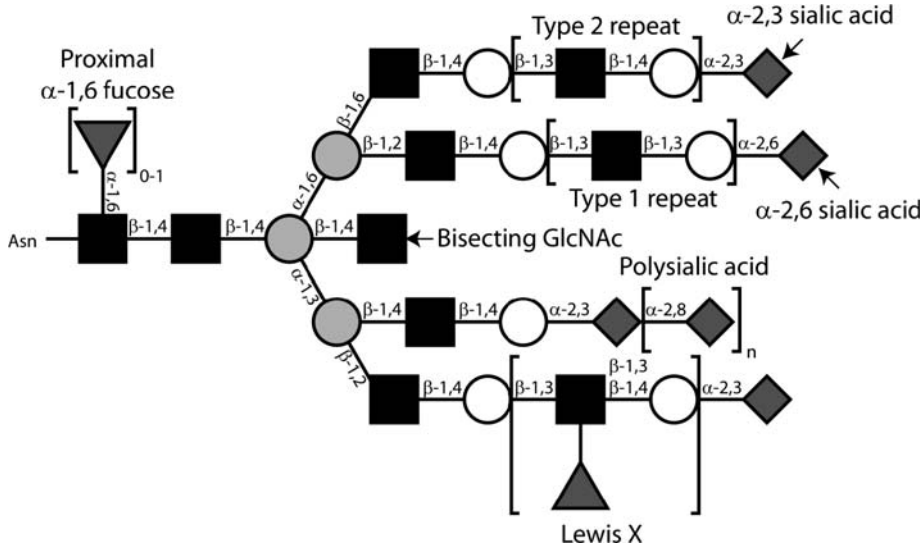


Figure 23.9. Examples of typical N-glycosylation features in human cell lines. The amount and extent of all the shown features may vary, including the number of antennae (horizontal branches). Sulfonation may also occur as sulfonated GalNAc residues (SO4-GalNAc-β-1,4-GlcNAc) and keratan (SO4-Gal-β-1,4-GlcNAc), but has not been represented here.

treatment of Hunters syndrome, and Dynepo (erythropoietin) (105,106). Some are also purified from cultures of cell lines naturally expressing the protein of interest, for example, interferons (106). The PER.C6 cell line, a cell line derived from retinal cells, has received increasing interest, partially because of its ability to provide correct glycosylation (125). Efficient protein production vectors have been presented for the system (126), and, in 2009, 14 products based on the PER.C6 cell line were in Phase I/II clinical trials (106).

23.5.1.1.2 Hamster Cell Lines. The varieties of N-glycosylation in the predominantly used hamster cell lines CHO and BHK-21 (Fig. 23.10) are generally viewed as being less complex than those found in human cells (Fig. 23.9). Owing to the broad variety of recombinant proteins expressed in these cell lines, the N-glycosylation potential is well known (Table 23.9). Both cell lines may generate up to tetraantennary structures (115,127–140), with proximal α-1,6-Fuc (10,128,130,132–135,138,141,142), NeuAc-α-2,3-Gal (10,129,130,132,134,136,138,139,141–144), and type 2 antennae (115,128,134,136,139,141,142,145). In addition to this, high-mannose-, hybrid-, and complex-type N-glycans as shown in Fig. 23.1 can be found (128,135,145). BHK-21 cell lines are also known to have at least two extra transferase activities not found in CHO cells, namely those resulting in the structures GalNAc-β-1,4-GlcNAc (138,140) and the immunogenic Gal-α-1,3-Gal-β-1,4-GlcNAc epitope. The α-1,3-Gal transferase creating this structure was shown to be inactive in CHO-K1 and DUKX-B11 (10,115,129,133).

A number of human N-glycosylation structures have been found absent in hamster cells, such as α-2,6-NeuAc (10,11,132), NeuAc-α-2,8-NeuAc, bisecting GlcNAc (162,166,169,178), and Le^X and sLe^X. However, in these cases, the genes have been found, but are only active in mutants (44,179,180). Finally, CHO and BHK cell lines may incorporate minor amounts of the immunogenic sialic acid Neu5Gc in the sialylation (10,106,152,157).

Studies of O-glycosylated recombinant proteins in hamster cells are mostly limited to erythropoietin and interleukins. *O*-Glycans on these are predominately of the core 1 mucin type with one or two sialic acid residues (136,138,139,141,170,172) as the core 2 transferase is normally not active in CHO cells (133,172,181).

Recombinant protein pharmaceuticals from CHO cells have a long history of regulatory approval, and the glycosylation structures produced by CHO cells are not known to elicit any serious immunogenic responses (106). Even so, the potential immunogenicity of the non-human structures is worth examining. Especially noteworthy is that the Gal-α-1,3-Gal-β-1,4-GlcNAc epitope is found in some BHK-21 lines. The epitope is not found in humans, apes, and Old world monkeys and is known to be immunogenic. More than 1% of human serum IgG recognizes this epitope (10,105). Another issue is the presence of Neu5Ac residues. A diverse antibody response to Neu5Ac residues in glycans is known to exist in humans (182). There seems to be a critical limit of Neu5Ac content needed to elicit a response, as fetuin with 7% Neu5Gc did give a significant response (152), but EPO with 1% Neu5Gc did not. The levels produced in CHO cells have been shown to vary between 1% and 15% (129), which makes it, in some cases, a possible point of concern.

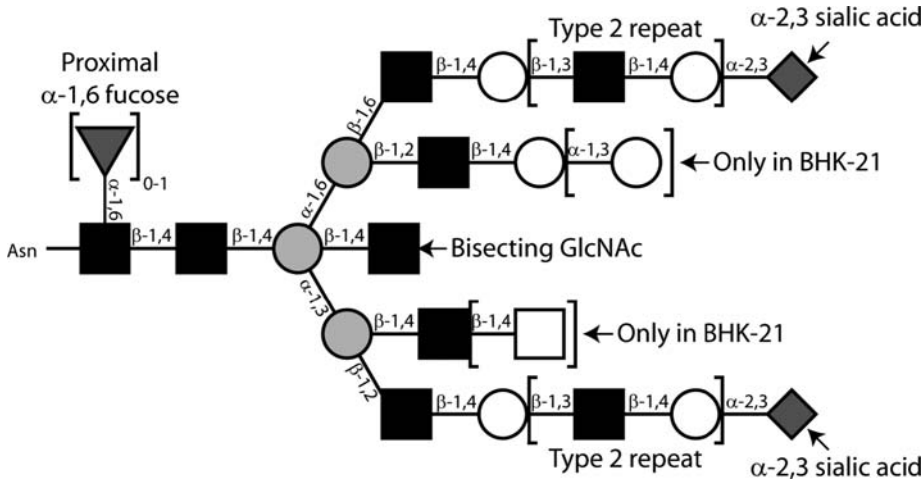


Figure 23.10. Examples of typical N-glycosylation features in hamster cell lines. The amount and extent of all the shown features may vary, including the number of antennae (horizontal branches). Note that two of the structures, GalNAc-β-1,4-GlcNAc and Gal-α-1,3-Gal-β-1,4-GlcNAc (on the center antennae), are only found in BHK-21.

TABLE 23.9. Studies of Glycan Structures of Recombinant Protein Expressed in Hamster Cells

Cell Line	Protein	References
BHK-21	AT-III	(146)
CHO	CD4	(145)
CHO	FSH	(143)
BHK-21	FVII	(140)
CHO	FVII	(140)
CHO	FVIII	(147,148)
CHO	GlialCAM	(149)
BHK-21	hEPO	(136,138)
CHO	hEPO	(134,139,144, 150–154)
CHO	HGF	(155)
CHO	HIV-gp120	(135,156)
CHO	IFN-β 1	(115)
CHO	IFN-γ	(157–161)
CHO	IgG	(31,112,144, 162–169)
BHK-21	IgG-IL2	(141)
BHK-21	IL2	(170)
CHO	IL2	(170)
CHO	IL-CT	(171)
CHO	K2tu-PA	(130)
CHO	Leukosialin	(172)
CHO	mEPO	(173)
CHO	mPL-I	(174,175)
CHO	SEAP	(137)
CHO	TIMP-1	(129)
BHK-21	Total	(128)
CHO	t-PA	(31,145,176)
CHO	TSH	(132,177)

[a] AT-III, antithrombin III; FSH, follicle-stimulating hormone; FVII, blood coagulation factor VII; FVIII, blood coagulation factor VIII; hEPO, human erythropoietin; HGF, hepatocyte growth factor; HIV-gp120, human-immunodeficiency virus envelope glycoprotein gp120; IFN, interferon; IgG, immunoglobulin G; IgG-IL2, IgG-IL2-fusion protein; IL-2, interleukin 2; IL-CT, IL-4/13 cytokine trap fusion protein; K2tu-PA, human plasminogen activator hybrid variant; mEPO, murine erythropoietin; mPL-I, mouse placental lactogen-I; SEAP, secreted human placental alkaline phosphatase; TIMP-1, tissue inhibitor of metalloproteinases 1; t-PA, tissue plasminogen activator; TSH, thyroid stimulating hormone.

While not strictly immunogenic, both the α-1,6-Fuc and the absence of bisecting GlcNAc have been shown to be problematic in terms of antibody production. It has been shown that the presence of α-1,6-Fuc on the core structure decreases Antibody Dependent Cell-mediated Cytotoxicity (ADCC) up to 50-fold (112). CHO cell lines add α-1,6-Fuc to a high percentage of the *N*-glycans in IgG (112). It has also been demonstrated several times that the absence of the bisecting GlcNAc decreases ADCC up to 10-fold (165,166). Furthermore, low *N*-glycan sialylation has been observed on IgG (see Table 23.9 and for example Ref. 169). This might decrease mAb effectivity as glycoproteins without sialic acids are cleared from the blood by the asialoglycoprotein receptor in the liver (183,184). Several engineering efforts have thus been targeted toward increasing the extent of sialylation (see the section titled "Mammalian Cells").

23.5.1.1.3 Mouse Cell Lines. Murine cell lines generally have some N-glycosylation features similar to human cells, but their glycans resemble those on human glycoproteins less than those of hamster-derived proteins. Typical cell lines used for the production of recombinant protein, such as C127 (10,11,185), ltk- (11), myeloma cell lines (NS0 and Sp2/0) (10), and hybridoma (10) cell lines, can all produce tetraantennary structures, with a proximal α-1,6-Fuc, type 2 antennae, and terminal α-2,3-NeuAc (10,11,129). This process is in many cases protein dependent. However, murine cell lines also have *N*-glycan structures not found in human cells, particularly Neu5Gc-α-2,3-Gal (11) and Gal-α-1,3-Gal (11,115,129,164,186). There are also a number of *N*-glycan structures that have not been reported in mouse cell lines, including Le^X (10,11), sLe^X (10,11), Fuc-α-1,2-Gal (10), Gal-β-1,3-GlcNAc (11), and GalNAc-β-1,4-GlcNAc (11). Finally, the choice of cell line, even within the same species, has a strong effect on the glycosylation. α-2,6-Sia is found in myeloma cells and C127 (11,115). Sulfonation has been seen in C127 (10), and a bisecting GlcNAc has been reported in C127 and ltk- lines (11). Polysialylation has been reported in ltk- cells (11). Hybrid or high-mannose structures are seen in myeloma and hybridoma cells (187,188). In summation, NS0 and Sp2/0 have quite similar N-glycosylation (10) as do different varieties of hybridoma cells (10,189), whereas C127 and ltk- cell lines have more disparate profiles (10,11,115). See Figure 23.11 for a summary.

In general, most of the detailed glycosylation studies in mouse cell lines have been performed on mAbs (162,164,189–193), possibly because of the production of the recombinant antibody Cetuximab in murine cell lines. This gives a bias on the reported murine N-glycosylation. Recombinant IgG produced in murine cell lines has *N*-glycans that are fairly independent of the cell line. The *N*-glycans are typically asialylated biantennary *N*-glycans with a proximal fucose and low galactose content as reported for NS0 (188,192), NS1 (191), and hybridoma cell lines (189–191). Slight variations are seen, such as no proximal fucose in *N*-glycans on IgG derived from NS0 (162), partial sialylation on IgG from a hybridoma line (193), and *N*-glycans of the Man_{5-9} type have also been found (188). One very significant observation is that some hybridoma cells glycosylate the light chain, often with α-1,3-Gal (10). α-1,3-Gal has also been found in recombinant IgG1 and IgG4 produced in NS0 cells (164).

While O-glycosylation in murine cell lines has been studied less than the N-glycosylation, possibly because of the absence of O-glycosylation on antibodies, it is reportedly largely similar to human *O*-glycans. The *O*-glycans of human IL-2 (interleukin 2) produced in mouse ltk- cells are the same as those added by the human T lymphocytes, namely core 1 glycans with one or two sialic acid residues (170). A study of recombinant human interferon

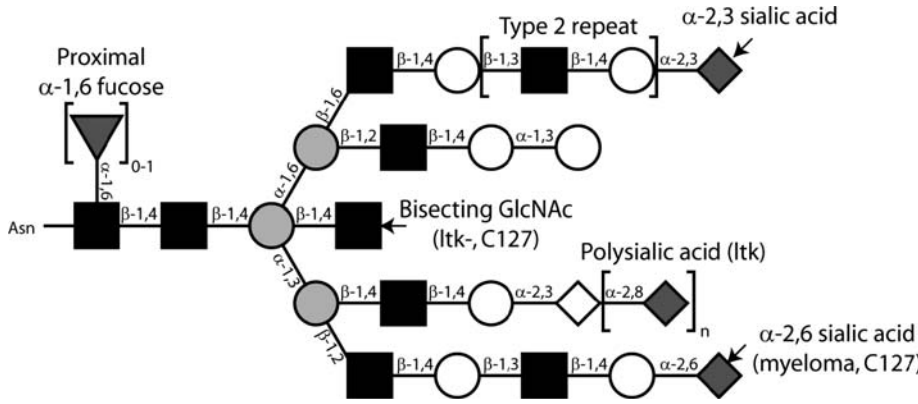


Figure 23.11. Examples of typical N-glycosylation features in mouse cell lines. The amount and extent of all of the shown features may vary, including the number of antennae (horizontal branches). Note that some of the structural features are only found in specific cell lines. Where nothing is marked, the structure may be found in all of the cell lines above and hybridoma cells.

α-2b expressed in NS0 also reported O-glycosylation at the same site as the human version (194).

The non-human epitopes found in murine cells have some potential effects on the pharmacokinetics and immunogenicity of heterologous protein produced in these cell lines. As described in section on hamster cell cultures (see section titled Hamster Cell Lines), the Gal-α-1,3-Gal-epitope is known to be immunogenic as more than 1% of human serum IgG recognizes this epitope (10,105). More specifically, up to 22% of patients have had a reaction toward the recombinant antibody Cetuximab due to the presence of this epitope (195). Additionally, the non-human sialic acid Neu5Gc is the most abundant sialic acid in murine myeloma cells (196) and in mouse cells (197). While the Neu5Gc-epitope is discussed in more detail above with the hamster cell lines, it is important to note that owing to the abundance of this epitope, the problem is more pronounced for murine lines. Other non-human glycans such as hybrid, or high-mannose structures (188), may also induce higher clearance through the mannose-specific receptors on the dendritic cells (198,199). In contrast to these reports, researchers from Novartis did, however, not find a significant negative effect of free mannose structures in IgG (200).

23.5.1.2 Nonmammalian Expression Systems. The use of expression systems, which are not based on mammalian cell cultures, has been historically limited for production of heterologous protein where N- or O-glycosylation effectively influences the protein function. Other eukaryotes, specifically yeast, insect cells, and plant cells, are often used for heterologous expression of proteins, but these all have (in their un-engineered states) limited capabilities in terms of protein glycosylation. Furthermore, the effect of the added glycans of the nonmammalian expression systems is often an immune response in the patient, as is described in the following sections.

23.5.1.2.1 Invertebrate Cells. Glycosylation in invertebrate cell lines has been reported to vary between cell lines for addition of both *N*- and *O*-glycans (11,201). A relatively large number of insect cell lines are used for the expression of recombinant protein. The most commonly used cell lines are/include *Spodoptera frugiperda* (*Sf9* or *Sf21*), and *Trichoplusia ni* BTI-Tn-5B14 (High Five™), but *Bombyx mori* SPC-Bm36 (11), *B. mori* BmN (202), *Mamestra brassicae* (11), *Estigmene acrea* (BTI-EaA) (11) are also used. The greater variety of insect cell lines utilization, compared to mammalian cell line usage, diversifies the picture somewhat. For N-glycosylation, the difference lies mainly in glycan size, extent of fucosylation, and absence of sialylation.

Generally, *N*-glycans are smaller in insect cells than in mammalian cell lines (Fig. 23.12). Insect cell lines have low activity of GnT I (203) and only trace levels of GnT II (203) and GalT (204–206) have been reported. Furthermore, insect cells posess an *N*-acetyl-*β*-glucosaminidase, which removes the GlcNAc transferred by GnT I after the

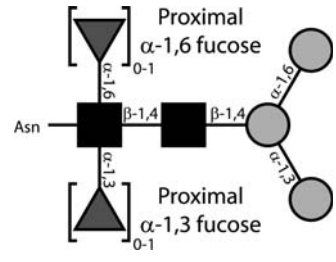


Figure 23.12. Example of typical N-glycosylation features in insect cell lines. Variations with 0 or 1 proximal fucoses and only 2 mannose residues are also seen.

action of mannosidases (207,208). Consequently, insect *N*-glycans are generally paucimannosidic with only 2–3 mannose residues and without antennae (11,209–213). However, BTI-EaA cells have been reported to produce Man_3 structures with up to three antennae (11).

N-Glycans from insect cell lines (11,202,214) and *Drosophila melanogaster* (215) may also have both a proximal α-1,6-Fuc and α-1,3-Fuc (di-fucosylation). The High Five cell line has a particular high percentage of di-fucosylation when compared to *Sf9*/*Sf21* (11).

The presence of sialylation has been discussed (213), but seems to be absent in insect cell lines (202,211,216,217). This is due to the almost complete absence of sialyltransferase activity (206,218), and the low activity of vital components of the biosynthetic pathway of the donor molecule in the sialylation reaction, and sialylation (CMP-Sia). Consequently, neither *Sf9, M. brassicae* SPCMb-92-C6, nor High Five show sialylation of *N*-glycans (201).

O-Glycosylation in invertebrates has mostly been studied in the model organisms *Caenorhabditis elegans* and *D. melanogaster* (209), but some reports have been made in invertebrate cell lines. Core 1 O-glycosylation is the predominant form and has been found in *D. melanogaster*, with a typical size of 1–3 sugar residues (219) as well as in *C. elegans* (220). In studies of *Sf9, M. brassicae* SPCMb-92-C6, and High Five, Gal-β-1,3-GalNAc-O-Ser/Thr (core 1) was found in all three cell lines (201,221). SPCMb-92-C6 and High Five also express an additional galactosyltransferase giving a Gal-α-1,4-Gal-β-1,3-GalNAc-O-Ser/Thr glycan (201,222). No sialyltransferase activity was detected in any of the cell lines (201), which seems to be a general feature (211,217).

The effect of the short insect glycosylation pathway is apparent on heterologous proteins. Kim et al. expressed human EPO in *D. melanogaster* cells, which resulted in significantly smaller *N*-glycans compared to those on EPO expressed in CHO cells. In the study, $Man_3GlcNAc_2Fuc_{0-1}$-Asn accounted for 60% of the glycans (212). This was also reported in another study for hepatocyte growth factor (155). As for the immunogenic effect of the insect epitopes, proximal α-1,3-Fuc is known to be immunogenic in rodents (223,224). Additionally, there may also be cross-reactivity with plants as serum from pollen-allergic patients has antibodies against α-1,3-fucose (224). The absence of sialylation also has a negative effect on serum half-life due to the increased clearance by the liver asialoglycoprotein receptor (183,184). Finally, the Gal-α-1,4-Gal-β-1,3-GalNAc-O-Ser/Thr has been speculated to be immunogenic in humans (201,222). Although efforts have been made to remedy these problems (see the section titled "Insect Cells"), no therapeutic proteins are currently produced in insect cells (106).

23.5.1.2.2 Plants. For plants, the N-glycosylation pathway is more or less similar to the mammalian up to and including the action of GnT I, which catalyzes the final step(s) in the formation of $GlcNAc_1Man_5GlcNAc_2Asn$. At this point, an α-1,3-fucose may be linked to the proximal GlcNAc as well as β-1,2-xylose may be linked to the innermost of the core mannose residues. These two sugar residues are widely found, and are also found on recombinant proteins expressed in plants (106,223–229). An advantage of utilizing plant hosts for IgG production is that the mammalian proximal α-1,6-fucose is absent from the product (202,230). Furthermore, the addition of a second terminal GlcNAc after the action of ManII has been demonstrated in several plants (202,230), for example, alfalfa (*Medicago sativa*) (225) and tomato (227), and is present in recombinant antibodies produced in tobacco (231), but no further GlcNAc transferases are known, thus allowing a maximum of two antennae (202,230).

As a result of the presence of *N*-acetylglucosaminidases, which remove GlcNAc residues from the nonreducing end after the action of ManII (208), many glycans are paucimannosidic (1–3 mannose residues). The paucimannosidic glycans may therefore have a core structure of $Man_{1-3}(Xyl)GlcNAc_2(Fuc)$-Asn (228). This structure with a proximal α-1,3-fucose and a core β-1,2-xylose is a consequence of the addition of the two sugars prior to the actions of ManII and the *N*-acetylglucosaminidase. All paucimannosidic, hybrid-type *N*-glycans, and complex-type glycans may be found, depending on the plant species, organ, and cellular organelle (202,232).

The elongation of the *N*-glycans is also limited. No β-1,4-galactose transferase activity or β-1,4-Gal residues have been found in plant *N*-glycans, and thus no type 2 elongation of the antennae is seen (233). The presence of sialic acids in *N*-glycans from plants has been discussed (234), but has now seemingly been disproved by the work of Zeleny et al. (235), who found that the levels found in plants were indistinguishable from the levels found in buffer blanks. The one type of elongation that has been shown to be present in a number of plants (236), including *Arabidopsis thaliana* (237), maize (226), cell suspension cultures (238), and alfalfa (225), is the Lewis a antigen (Le^a) (Gal-β-1,3-[Fuc-α-1,4-]GlcNAc). A summary may be found in Fig. 23.13.

The O-glycosylation pathways of plants are less studied than N-glycosylation, and are still partially in the dark (209). However, it is clear that it varies significantly from that of humans. A thorough review of *O*-glycan structures on plant allergens (239) shows a high *O*-glycan diversity. *O*-glycan backbones of GalNAc, similar to those typically found in humans, are seen, but also backbones of GlcNAc, mannose, arabinose, galactose and glucose are found with varying sugars attached as side chains. Some details are known on O-linked arabinogalactans commonly found on

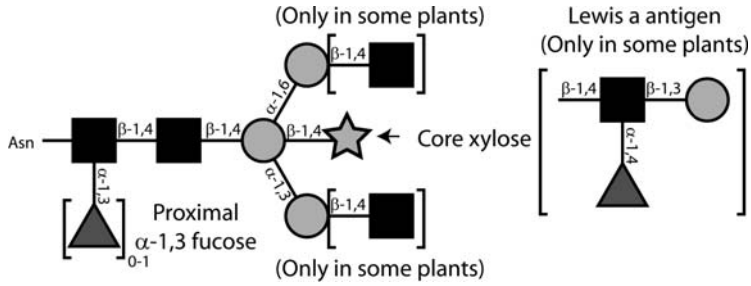


Figure 23.13. Example of typical N-glycosylation features in plants. Variations with 0 or 1 proximal fucoses and only 2 mannose residues are also seen.

plant cell surfaces. One example of this is the O-linked polysaccharide characterised by Tan et al. It has a galactose backbone, with side chains consisting of arabinose, glucuronic acid, galactose, and rhamnose residues (240). Another significant characteristic of plant *O*-glycans is that, in addition to serine and threonine linkages, plant proteins may also have O−glycans attached to a hydroxyproline residue (240,241).

What the effect of the plant-specific glycosylation is on the immune system, and what the clinical significance is, has been the subject of much debate. Especially the effects of proximal α-1,3-fucose and core β-1,2-xylose have received much attention as they are potentially immunogenic (239). Both epitopes are involved in pollen allergy (230,242,243). Even so, the reported effect varies. While mouse antibody expressed in tobacco plants have both α-1,3-fucose and core β-1,2-xylose attached (244), reports showed no immune response in mice to injection with antibody produced in plant cells (245). In contrast to this, Jin et al. (231) showed an immune response in rabbits to antibodies produced in *Nicotiana bethamiana*. An immune response was also seen when immunizing mice and rats with horseradish peroxidase (HRP) with these glycoforms (223). Injection of plant proteins into humans also elicits an antibody production targeted toward the glycans. However, the authors did not find it likely that this would have a significant clinical effect (246).

Even so, plant *N*-glycans can be allergenic. A study among blood donors showed that 50% of non-allergenic donors have antibodies for core β-1,2-xylose and 25% have antibodies for core α-1,3-fucose (223). 29% of pollen allergenic patients react positively to bromelian with *N*-glycans with both core β-1,2-xylose and core α-1,3-fucose, whereas 12.5% of the same patients reacted to defucosylated bromelian (239). A study by Bencúrová et al. (224) used a recombinant *P. pastoris* to test the effect of the fucose and xylose separately, and was unable to find a significant separate effect of the β-1,2-xylose, but did show a significant effect of α-1,3-fucose on its own. A de-fucosylation of bromelain also decreased the IgE reactivity in allergenic patients, but not to the levels of fibrin with neither fucose nor xylose in the *N*-glycans (239). Thus, it seems that both epitopes may elicit an immune response - especially in pollen-allergic patients - with a more significant response caused by α-1,3-fucose.

Effects are also seen in the absence of galactosylation and sialylation of the antennae also has detrimental effects, as glycoproteins without sialic acids are cleared from the blood by the asialoglycoprotein receptor in the liver (183,184).

The dicersity of *O*-glycan structures makes a generalization of the effects difficult. While some plant *O*-glycans have also been known to be immunogenic (239), the serum half-life of hGH has been increased by the addition of a hydroxyproline-O-glycosylation domain (241).

Despite the variations in glycosylation, recombinant glycoproteins produced in plants have not been known to elicit an immune response when applied topically, which makes the production of therapeutics and edible vaccines interesting (106,228,247).

A few plant derived therapeutics have been approved in the European Union, such as glucocerebrosidase, for the treatment of Gauchers disease, from carrot cells (106,248), interferon α (Locteron®) from duckweed (*Lemna minor)* (106), human intrinsic factor from *Arabidopsis* (228) and an anti-caries IgA (228).

23.5.1.2.3 Yeast. The main difference between N-glycosylation in yeast and mammalian cells lies in the processing of the *N*-glycans in the Golgi complex. In both cases, the predominant *N*-glycan entering the Golgi is $Man_8GlcNAc_2$. However, in mammalian cells; this structure is subject to trimming by mannosidases, leaving ultimately as few as three mannose residues (See Ref. 249 and the beginning of the section on "Mammalian Expression Systems"). In *Saccharomyces cerevisiae*, mannose residues are added to form a mannan core structure of 9−14 α-1,6-linked mannose residues (250). For some proteins, such as a yeast invertase, even larger structures of 30−54 mannose residues have been found (251,252). Additions to this high-mannose structure include α-1,2-Man sidechains as well as phosphomannose

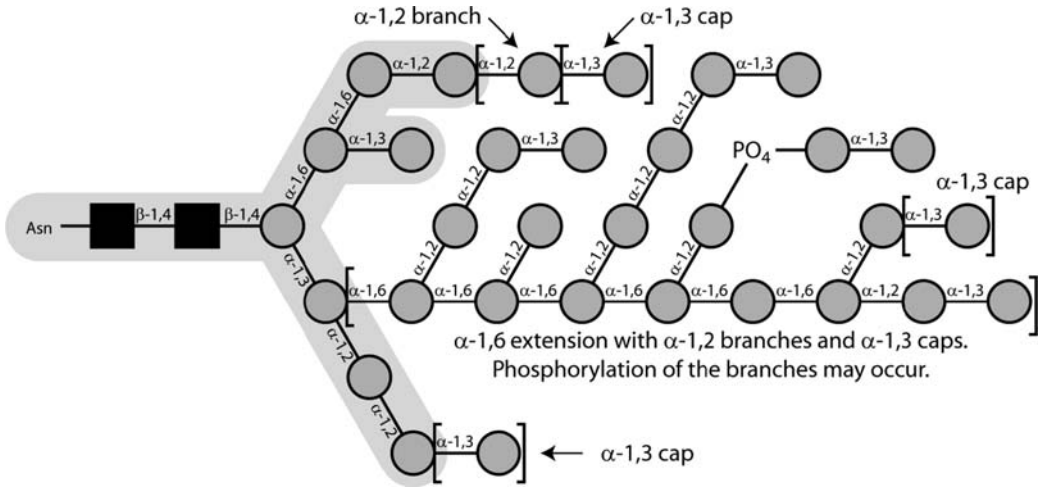


Figure 23.14. Example of typical N-glycosylation features in yeast. The length and branching of the chains may vary greatly, up to more than 50 mannose units (251,252). Pichia pastoris mannosylation is generally less extensive than that of *S. cerevisiae*.

groups, which both can be capped with α-1,3-Man residues (202,253). For a summary, see Figure 23.14.

The α-1,6-linked mannose chains of glycoproteins in the yeast *P. pastoris* are generally shorter (254) than in other yeasts (254). On one heterologous secreted protein, 85% of the *N*-glycans had 14 or less mannose residues in *P. pastoris*, while for *S. cerevisiae* this was only true for 20% of the *N*-glycans. This makes the *N*-glycans of *P. pastoris* more similar to those of mammals than those produced by *S. cerevisiae* (254,255).

There also seem to be differences in the occupancy of N-glycosylation sites with the common motif Asn-X-Thr/Ser. Human interleukin-1b has one possible N-glycosylation site, which is unoccupied when the protein is secreted from human monocytes, but the recombinant protein is N-glycosylated by S. cerevisiae (256).

Protein O-glycosylation in yeast seems to be restricted to protein O-mannosylation, which has also been reported in mammalian cells in a few cases (257). O-mannosylation differs from standard human O-glycosylation in that it is initiated in the ER with the attachment of one or two mannoses to a Ser or a Thr residue, followed by the addition of 1–3 mannosyl residues in the Golgi complex. The specificity of the O-mannosylation machinery also seems to be different. In one example, human insulin-like growth factor I is O-mannosylated when expressed in *S. cerevisiae*, while only the unglycosylated form is found in human serum (258). Furthermore, *S. cerevisiae* may have mannosylphosphate as a part of the O-mannosylation chain (257). *P. pastoris* does not seem to have this, and similar to what is seen for N-glycosylation, proteins expressed in *P. pastoris* generally have shorter O-mannosylation chains compared to those produced in *S. cerevisiae* (254,257).

Most interesting in the context of pharmaceutical proteins is the observation that O- and N-mannosylation of proteins increases the clearance rate of the protein. Even with the shorter mannosylation chains typically found in *P. pastoris*, mannose-sensitive receptors on the surface of dendritic cells initiate an immune response to the mannosylated proteins (198,199). This decreases serum half-life as well as the ADCC (259).

Due to the systemic differences in protein glycosylation, heterologous expression of pharmaceutically active proteins has been limited to unglycosylated proteins such as insulin, and growth hormone (106,260).

23.5.1.2.4 Bacterial strains. Bacterial N-glycosylation has been reported in some cases, but normally consists of only short chains. While some examples of N-linked GlcNAc residues have been reported - see below - the N-linked residue can be quite exotic with e.g. rhamnose or glucose bound directly to the peptide chain (10,261–264). A special case is the human-like N-glycosylation such as bi- and triantennary *N*-glycans found in some pathogenic bacterial species such as *Chlamydia trachomatis*, and *Campylobacter jejuni* (265,266).

Bacterial O-glycosylation has also been reported in several species. O-mannosylation occurs in pathogenic species such as *Mycobacterium tuberculosis* and *Chlamydia trachomatis* (257,267,268). and O-glycosylation in *Pseudomonas aeruginosa* (pili) and *Campylobacter jejuni* (flagellae) that differs significantly from human *O*-glycans by containing exotic residues such as 2,4-diacetamido-2,4,6-trideoxyhexose, N-acetylfucosamine, and pseudaminic acid (267,269). While a heptose residue has been identified in two *E. coli* proteins (267), no other

significant N- or O-glycosylation have been reported in industrial workhorses such as *E. coli* or *Bacillus subtilis*.

Due to the these reasons, the production of heterologous proteins in bacterial species have so far been limited to proteins without glycosylation, or proteins where the absence of the native glycosylation does not seem to have a noteworthy negative effect on the pharmacokinetics, such as the recombinant human insulin or human growth hormone produced by Eli Lilly in *E. coli* cells (260).

23.5.2 Genetic Engineering of Glycosylation Pathways

Genetic engineering of the glycosylation pathways has been applied both to the glycosylation machinery of mammalian cells as well as nonmammalian expression systems. The ultimate goal of metabolic engineering in the context of glycosylation is the construction of a host organism that which provides a consistent, "optimal" glycosylation of the heterologous protein it produces. For mammalian cells (see the section titled "Mammalian Cells"), approaching this is relatively uncomplicated focusing predominately on single-gene studies directed towards adding activities which improve pharmacokinetics (PK), and removing epitopes which cause immune responses and/or rapid blood clearance rates.

While mammalian cell culture provides a starting point where the glycosylation is closer to the native protein than any other expression systems, the relative complexity and cost of cultivating mammalian cells with high yields and titer are less attractive than systems featuring lower eukaryotes and bacteria. For this reason, genetic engineering has permitted significant advances towards using simpler organisms for production of human-like glycoproteins, with the promise of further improvements.

In this section we will describe the metabolic engineering efforts that have been applied to improve the glycosylation potential of mammalian cell cultures, plants and plant cells, insect cells, yeast and bacteria.

23.5.2.1 Mammalian cells. As described above, the glycosylation patterns of mammalian cell culture are quite close to those of the native human proteins. Most biosimilar are proteins produced in the human cell lines Per.C6, HT-1080 and HEK-293. The mouse cell lines (C127, ltk-, NS0, Sp2/0, and hybridoma cells) may all produce the immunogenic Gal-α-1,3-Gal-β-1,4-GlcNAc epitope, an epitope which may also be found in BHK-21-based hamster cell line. In this regard, the relatively smaller protein glycosylation repertoire of the CHO cell lines is an advantage, giving products a more uniform safety profile relative to mouse cells.

A literature survey of glycosylation engineering efforts in mammalian cells (Table 23.10) also confirms that the CHO based cell systems have received a special interest, as most of the studies that have been conducted in CHO cells with a small number in BHK-21 cells or/and human cells. In general, this may be explained by the rough generalization that human cell lines do not require glycosylation engineering, mouse cells do not present enough of an advantage over the hamster cell lines to attract the effort, and CHO cells, while making relatively harmless glycosylation, can benefit from having certain activities added or removed.

These glycosylation engineering efforts can be divided into two main sections, namely fucosylation engineering, and enhanced sialylation.

Fucosylation engineering is concerned with two main avenues: 1) expression of the α-1,3-Fuc transferase to form the Le^X and sLe^X structures in hamster or mouse cells and 2) removal of the core α-1,6-Fuc, which is found on almost all recombinant glycoprotein from CHO cells (See Figure 23.10). The core α-1,6-Fuc has been shown to have a detrimental effect on the ADCC of IgG (274,275), and removal of this residue has been shown to increase ADCC up to 100-fold (298), while having no visible phenotype (291). Due to the commercial interest in recombinant antibodies for therapeutics, de-fucosylation of antibodies is covered quite heavily by patents, e.g. WO00/61739, the first patent on defucosylated therapeutic antibodies (299).

Most approaches targeting the fucosylation pathway are based on the knock-out or RNA interference (RNAi) of CHO α-1,6-FucT (FUT8), or the knock-out or silencing of GDP-D-mannose-4,6-dehydratase (GMD) (Table 23.10). The latter approach is derived from the fucosylation-deficient Lec13 CHO-mutant which was shown to be deficient in this activity (300). A more indirect approach, which however, does not completely remove core fucose residues, is the expression of GnT III, the enzyme responsible for adding the bisecting GlcNAc in *N*-glycans. This residue blocks the addition of the core fucose and thus increases ADCC (165). An improvement on this strategy is re-localizing GnT III to earlier stages in the glycosylation pathway, which more efficiently blocks fucosylation (293). Another approach is the co-overexpression of GnT III and ManII to increase the competition for the substrate on which Fut8 is active (293).

A poor degree of sialylation is a relatively large issue for recombinant proteins produced in hamster cells. As mentioned in the section on "Immunogenicity and Biological Clearance", sialylation increases the residence time in serum (183,184). More than 20 studies exist where the α-2,3- or α-2,6-sialyltransferase has been overexpressed or expressed in CHO, BHK-21, or HEK 293 cells (Table 23.10). Mostly, the increase in sialylation gained from this strategy is modest (10-20%), but an increase in PK properties has been reported (285). It has also been attempted to improve sialylation by modifications up-stream of the sialyltransferase. A one-gene approach

TABLE 23.10. Overview of Glycosylation Engineering Efforts in Mammalian Cell Cultures.

Target gene(s)	Type	Method	Reported effect	Cell line	Protein	References
α-1,3-FucT	N	Expression	Synthesis of the sLe^X epitope in CHO DHFR-. No effect was seen in CHO Pro^-	CHO DHFR-	Surface protein	(270)
α- (1,3)-FucT	N	Expression	Introduction of the sLe^X epitope in BHK cells	BHK-21	β-TP	(11)
α- (1,3)-FucT	N/O	Expression	Addition of α-1,3-bound fucose, but not a fully active Lewisx antigen.	C127	PTA	(271)
α-1,6-FucT	N	siRNA	Decreased proximal fucosylation and increased ADCC	CHO DG44	IgG	(272)
α-1,6-FucT	N	siRNA	Decreased α-1,6-fucosylation to 28%	CHO DG44	IgG	(273)
α-1,6-FucT	N	Knock-out	Fucose removed. ADCC increased two orders of magnitude.	CHO DG44	IgG1	(274)
α-1,6-FucT	N	siRNA	Increase in de-fucosylation from 10 to 60%. More than 100-fold increase in ADCC.	CHO DG44	IgG	(275)
α-1,6-FucT	N	Mutant	Expression of IgG in this cell line gave a up to 50 fold increase in ADCC.	CHO Lec13	IgG1	(112)
α-1,6-FucT	N	Knock-out	Removed α-1,6-fucosylation. 100-fold increase in ADCC.	CHO DG44	IgG1	(276)
α-1,6-FucT+GMD	N	siRNA	Removed α-1,6-fucosylation.	CHO DG44	IgG	(273)
α-2,3-SiaT	N	Expression	Increase in sialylation from 6.7 to 7.5%. Increase in triantennary glycans.	CHO EC1	EPO	(277)
α-2,3-SiaT	N/O	Overexpression	Increased sialylation.	CHO	EPO	(278)
α-2,3-SiaT	N	Overexpression	Increased sialylation to >90%.	CHO	TNK-tPA	(31)
α-2,3-SiaT	N	Overexpression	33% increase in molar content of sialic acid, sialylation increased to >90%.	CHO	TNFR-IgG	(31)
α-2,3-SiaT	N/O	Overexpression	Increase in sialylation from 61 to 80%.	CHO	IFN-γ	(279)
α-2,3-SiaT + β-1,4-GalT	N/O	Co-expression	Increase in sialylation from 6.7 to 8.2%. Increase in triantennary glycans.	CHO EC1	EPO	(277)
α-2,3-SiaT+CMP-SAS+CMP-SAT	N/O	Co-overexpression	Synergetically increased sialylation.	CHO	EPO	(278)
α-2,6-SiaT	N/O	Expression	Added α-2,6-sialylation. 4% increase in sialylation. Improved the PK of the HP.	CHO DUKX-B11	IFN-γ	(280)
α-2,6-SiaT	N	Addition	39% α-2,6-sialic acid introduced	CHO UH	hTSH	(132)
α-2,6-SiaT	N	Expression	Introduction of α-2,6-bound Sia in BHK cells	BHK-21B	β-TP	(11)
α-2,6-SiaT	N/O	Expression	A-2,6-sialylation on 60% of the RP	CHO DHFR-	IFN-γ	(281)
α-2,6-SiaT	N	Expression	Added ability of α-2,6-sialylation	CHO	-	(282)
α-2,6-SiaT	N	Expression	Up to 60% Increase in sialylation	CHO DUKX-B11	IFN-γ	(283)
α-2,6-SiaT	N/O	Expression	Added ability of α-2,6-sialylation	BHK-21A	EPO	(284)
α-2,6-SiaT	N/O	Expression	Added α-2,6-sialylation. Improved PK.	CHO Pro-	EPO	(153)
α-2,6-SiaT	N	Expression	Added α-2,6-sialylation. 7% increase in sialylation.	CHO K1	IgG3	(285)
α-2,6-SiaT	N/O	Overexpression	Increase in sialylation from 61 to 80%.	CHO	IFN-γ	(279)
α-2,6-SiaT	N/O	Overexpression	Increased sialylation and serum half-life	HEK-293	rHuAChE	(286)
α-2,6-SiaT	N/O	Overexpression	Serum half-life increases with sialylation	HEK-293	rHuAChE	(287)
β-1,4-GalT	N	Overexpression	Decreased GlcNAc-termination from 6 to <1%.	CHO	TNFR-IgG	(31)
β-1,4-GalT	N	Knock-out	Increased bisecting GlcNAc	human B cell	IgM	(288)
β-1,4-GalT	N	Overexpression	Decreased bisecting GlcNAc	human B cell	IgM	(288)

TABLE 23.10. (*Continued*)

Target gene(s)	Type	Method	Reported effect	Cell line	Protein	References
CMP-Neu5Ac-hydroxylase	N	Anti-sense RNA	Neu5Ac content decreased from 3.7 to 0.6%	CHO DUKX-B11	total protein	(289)
CMP-SAT	N/O	Overexpression	4-16% increase in sialylation	CHO	IFN-γ	(290)
Core 2 GnT	O	Expression	Allows the addition of a core 2 *O*-glycan	CHO DG44	PLTA	(172)
Core 2 GnT + α-2,3-SiaT	O	Expression+anti-sense RNA	Decreased core 1 galactosylation, increased core 2 formation	CHO K1	-	(181)
GFT	N	siRNA	Decreased α-1,6-fucosylation to 58%	CHO DG44	IgG	(273)
GMD	N	siRNA	Decreased α-1,6-fucosylation to 22%	CHO DG44	IgG	(273)
GMD	N/O	Knock-out	Complete absence of N- and O-fucosylation.	CHO DG44	IgG	(291)
GnT III	N	Addition	48-71% bisecting GlcNAc introduced and improved ADCC 10-20-fold	CHO DG44	IgG	(292)
GnT III	N	Relocalization	Decreased fucosylation, increased hybrid glycans and improved ADCC	HEK-293	IgG	(293)
GnT III	N	Expression	Detrimental to growth	CHO DUKX	-	(294)
GnT III	N	Expression	Addition of bisecting GlcNAc to IgG increased ADCC 3-fold.	CHO DUKX	IgG1	(165)
GnT III	N	Overexpression	Increased bisecting GlcNAc	human B cell	IgM	(288)
GnT III+ManII	N	Co-overexpression	Decreased fucosylation, increased hybrid glycans and improved ADCC	HEK-293	IgG	(293)
GnT IV	N	Overexpression	Increase in triantennary structures	CHO	IFN-γ	(295)
GnT V	N	Overexpression	Detrimental to growth	CHO DUKX	.	(294)
GnT V	N	Overexpression	Increase in triantennary structures	CHO	IFN-γ	(279)
GnT V	N	Overexpression	Increase in triantennary structures	CHO	IFN-γ	(295)
GnT V+GnT III	N	Overexpression	Increase in tri- and tetraantennary structures	CHO	IFN-γ	(295)
Sialidase	N/O	Anti-sense RNA	20-37% increase in sialic acid content	CHO DHFR-	DNAse	(296)
α-2,6-SiaT	N	Expression	Increased sialylation	CHO	t-PA	(297)

[a] AT-III, Antithrombin III; CMP-SAS, CMP-sialic acid synthase; CMP-SAT, CMP-sialic acid transporter; FSH, Follicle-stimulating hormone; GFT, GDP-fucose transporter; GMD, GDP-mannose 4,6-dehydratase; HP, Heterologously expressed protein; hTSH, Human thyroid stimulating hormone; IFN, Interferon; IgG, Immunoglobulin G; PDI, protein disulfide isomerase; PK, Pharmacokinetics; PLTA, polyoma large tumor antigen; PTA, Polyoma T antigen; rHuAChE, Recombinant human acetylcholinesterase; siRNA, Small interfering RNA; TIMP-1, tissue inhibitor of metalloproteinases 1; TNFR-IgG Tumor necrosis factor receptor–IgG1 fusion protein; TNK-tPA, Amino acid-modified tissue plasminogen activator; β-TP, β-trace protein.

has been the overexpression of the CMP-sialic acid transporter (CMP-SAT) which increased sialylation of IFN-γ. Jeong et al. (278) co-overexpressed α-2,3-SiaT, CMP-sialic acid synthase and CMP-SAT, and showed this to have a cumulative and even synergistic effect on sialylation of EPO.

As seen in Table 23.10, genetic knock-out studies are rare, mainly due to the previous lack of efficient gene targeting tools in mammalian cells as well as the lack of a genome sequence for hamster cells. However, fairly recently, zinc-finger-endonuclease-mediated gene knock-outs have been made commercially available through the CompoZr™ technology (301,302). We anticipate that this will have a large impact on metabolic engineering in mammalian cells in general, and specifically in glycoengineering.

23.5.2.2 Insect cells. As discussed in the section on "Non-Mammalian Expression Systems", the protein N-glycosylation pathway of insect cell lines is stunted compared to mammalian cells and produces primarily paucimannosidic structures with the possible addition of two fucose residues to the proximal GlcNAc. The main reasons for these truncated (relative to human glycoforms) structures are low activities of the GnT I, almost absent GnT II and β-1,4-Gal-T, and a dysfunctional sialic acid biosynthesis pathway. The native structure of insect cell N-glycosylation can be seen in Figure 23.15, along with the target enzymatic activities of N-glycosylation engineering.

Generally, the glycoengineering of insect cells attempts humanization by two main avenues:

1. Addition of mammalian glycosyltransferases to form antennae and elongate these.
2. Reconstruction of sialic acid biosynthesis and glycoform sialylation.

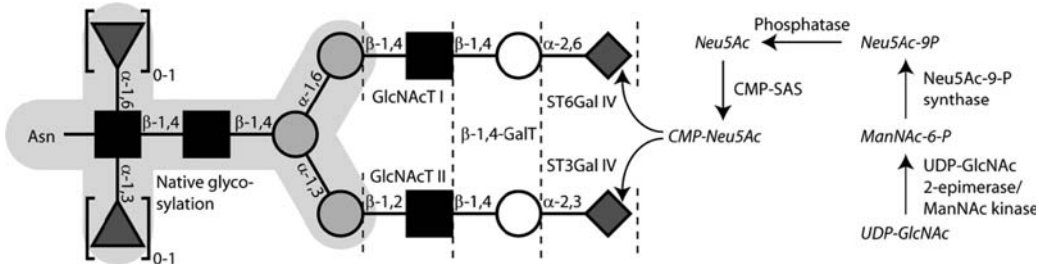


Figure 23.15. Enzyme activites targeted for glycoengineering of insect cells lines. The structure in light grey on the left shows the typical extent of N-glycosylation in insect cell lines; however the number of attached fucose residues may vary. On the right of the core structure are shown residues that have been added by genetic engineering. On the far right is the mammalian biosynthetic pathway for CMP-neuraminic acid, the precursor for sialic acid residues on N-glycosylation. Several of the enzymes of this pathway have been the target of engineering. See Table 23.10 for an overview of studies targeting each of the represented enzymes. Abbreviations: GalT: Galactose transferase. GlcNAc: N-Acetylglucose. GlcNAcT: GlcNAc transferase. Neu5Ac: Neuraminic acid. SAS: Sialic acid synthase. ST3Gal: α-2,3-(N)-sialyltransferase. ST6Gal: α-2,6-(N)-sialyltransferase.

TABLE 23.11. Overview of Insect Cell N-Glycosylation Genetic Engineering Studies. Unless Otherwise Noted, the Engineering Resulted in the Corresponding Extended Glycosylation. (X): Modification Present in the Cell Line, but Constructed in a Previous Study. X: Modification Performed in the Present Study. See Figure 23.15

References	Cell line	GlcNAcT I	GlcNAcT II	β-1,4 GalT	ST6Gal I	ST3Gal IV	CMP-SAS	SAS	UDP-GlcNAc 2-epimerase/ ManNAc kinase
(303)	Sf9	X							
(304)	Sf9			X					
(205)	Sf9			X					
(214)	*Trichoplusia ni*			X					
(218)	Sf9			(X)	X				
(305)	HighFive			X	X				
(206)	Sf9			X	X				
(306)	Sf9			X	X				
(216)	Sf9						X	X	
(307)	Sf9	X	X	X	X	X			
(217)	Sf9	(X)	(X)	(X)	(X)	(X)	X	X	
(308)	Sf9							(X)	X
(309)	*Trichoplusia ni*		X	(X)					

Table 23.11 presents an overview of the studies employing these strategies. In general, the field has progressed from early pioneering work inserting single genes from the mammalian N-glycosylation pathway (303,304) to the concerted expression of seven mammalian genes (217). While the furthest advances were achieved in Sf9 cells, *Trichopulsia ni* has also shown to be a possible host for developing an insect cell-based alternative to mammalian cell culture for heterologous protein production.

23.5.2.3 Plants. By far the majority of glycan engineering efforts in plants in the context of heterologous protein expression have been targeted towards removal of the immunogenic core β-1,2-Xyl and α-1,3-Fuc (See Section on "Non-mammalian Expression Systems" and Figure 23.13). However, several strategies have been applied to achieve this.

One strategy to avoid the core β-1,2-Xyl and α-1,3-Fuc epitopes is the retention of the recombinant protein in the ER by the addition of the C-terminal amino acid motif KDEL or HDEL. This retention theoretically limits the glycosylation to high-mannose types ($Man_8GlcNAc_2$-Asn). Applications of this strategy include α 1-antichymotrypsinin produced in tobacco (BY-2) cells (310) and mAb in tobacco plants (311–314). All of these studies report high-mannose structures on the recombinant protein. Rademacher et al. applied the technique to mAb produced in maize endosperm, but reported the addition of GlcNAc addition (315). This has later been suggested to be an artifact (228). A minor disadvantage of this technique

is the increased clearance rates resulting from the mannose structures as described above for yeast systems. However, for some products, such as the glucocerebrosidase (GCD) produced by Protalix, which requires uptake through the macrophage mannose receptors, this may be advantageous (248). In the case of Protalix, the technique was modified to target GCD to the vesicles of the macrophages.

Another strategy to produce less immunogenic glycans in plants is to delete or silence the genes encoding the enzymes, core-XylT and core-FucT, which catalyze the formation of the core β-1,2-Xyl and α-1,3-Fuc epitopes. One such study in *A. thaliana* has produced a double-knockout line by crossing two single-knockout lines (316), which has been used for the expression of a mAb (317). Core-XylT and core-FucT have been knocked down in *M. sativa* (alfalfa) (318), *Nicotiana benthamiana* (319) and *L. minor* (320) using RNAi. A resulting antibody from one of the studies was demonstrated to have a 20–30 times higher ADCC than a reference mAb expressed in a CHO cell line (320).

Due to the presence of homologous recombination in the moss *P. patens*, the genetic knock-out of the core-XylT and core-FucT genes is possible in this organism. Cell lines with the double knock-out have been used to produce human vascular endothelial growth factor VEGF (321), EPO (322) and IgG (323). As a result of this modification, the IgG showed up to a 40-fold improvement in ADCC. With a similar objective, Huether et al. (324) rather elegantly disrupted the genes for core-XylT and core-FucT in *P. patens* by replacing it with a human β-1,4-Gal transferase. This removes the plant-specific residues from *N*-glycans, while adding the human β-1,4-Gal residue.

Yet another strategy to achieve a more human-like glycosylation and eliminate xylose and fucose from the core structures is based on the addition of glycosyltransferases. For this, the addition of bisecting GlcNAc to *N*-glycans by GnT III is favorable, as it enhances the pharmacokinetic properties of the protein and blocks the addition of Fuc or Xyl to the core of the *N*-glycan (228,325,326). Human GnT III has been expressed in tobacco plants by Rouwendal et al. (327), which added bisecting GlcNAc to more than half of the plant *N*-glycans. Frey et al. (328) expressed rat GnT III with and without a relocalization signal to the Golgi. Without the relocalization signal, results similar to those generated by Rouwendal et al. were obtained. The relocalization of rat GnT III to the Golgi improved the addition of the bisecting GlcNAc further and removed xylose and fucose from the *N*-glycans in app 60% of the glycans due, to out-competition for the core glycan substrate.

Another humanization strategy is to ectopically express GalT I. The terminal β-1,4-Gal (added by GalT I) blocks for the addition of both core β-1,2-Xyl and α-1,3-Fuc and gives a more human-like *N*-glycan. One example is the genetic transfer of human GalT I to tobacco BY2 cultures (329). This resulted in galactose being added to approximately half the total *N*-glycans as well as giving a virtual absence of both core β-1,2-Xyl and α-1,3-Fuc. A similar result was seen for the expression of HRP in the same cell line (330). At the same time, however, expression of mAb in this cell line seemed to be less effective in terms of both galactosylation, and the reduction of both core β-1,2-Xyl and α-1,3-Fuc (331). An application of this strategy in tobacco plants for mAb production has also been reported (233). An improvement of this technique has been an insertion of the GalT I earlier in the glycosylation pathway by adding targeting domains for the medial Golgi-cisternae to the transferase. Expression of a human GalT I fused with the targeting domain of *A. thaliana* core-XylT (332) in tobacco plants allowed the production of a mAb having *N*-glycans with undetectable xylose, very litte fucose and added galactose (333). A similar approach has been used in *T. benthamiana* (334).

A final target to be mentioned for engineering plant glycosylation is the recreation of the human sialylation pathway in plants. The insertion of the genes for the four biosynthetic enzymes and the transporter for the CMP-NeuAc precursor molecule has not yet been fully accomplished. References (335–337) all describe the insertion of two or more of the five steps in either plants or plant cells, but the full functional combination of all biosynthetic steps with a functional sialyltransferase has yet to be seen.

23.5.2.4 Yeast and filamentous fungi. This section will describe the immensely successful glycosylation engineering conducted in the yeast *P. pastoris*. However, minor efforts have also been undertaken in *S. cerevisiae* and filamentous fungi, for which we will also provide an overview here.

The methylotrophic yeast *P. pastoris* is a commonly used platform for heterologous protein expression due to its native ability to secrete properly folded proteins in high yields. The native *P. pastoris* generally adds a large number of mannose residues to *N*-glycans, producing *N*-glycans with a typical structure of $Man_{9-14}GlcNAc_2$, making it ill-suited for production of pharmaceutical glycoproteins (See Figure 23.14). However, a very successful series of genetic engineering studies by the company GlycoFi Inc. (now acquired by Merck & Co. Inc.) have reformed this to allow engineered *P. pastoris* to produce secreted human-like glycoproteins.

The first effort in glycoengineering was the deletion of the *och1* gene. Och1p is an a-1,6-mannosyltransferase, which initiates hypermannosylation. The *och1* deletion reduces yeast mannosylation to $Man_5GlcNAc_2$ sugar chains, which are compatible with the human immune system (First shown in S. cerevisiae (338,339)). A *P. pastoris och1* deletion strain formed the basis for the first

work of GlycoFi which, by the application of combinatorial genetics with a library of targeting sequences (340), achieved correct targeting of N-glycosylation enzymes to the organelles of *P. pastoris*. Applying this techology allowed for correct targeting of five eukaryotic proteins, namely mannosidases I and II, GlcNAcT I and II, and the UDP-GlcNAc transporter to achieve the production of proteins with a $GlcNAc_2Man_3Man_2$ structure (341).

Further improvement of the core *N*-glycan was attempted by the elimination of the Alg3p α-1,3-mannosyltransferase (342). This was shown to prevent the α-1,3- and α-1,6- mannose additions to the 1,6 arm of the dolichol-bound precursor, although with a slightly leaky phenotype, as some highly mannosylated glycoforms are still formed.

The strain of Ref. 341 was improved with the deletion more genes (Δoch1, Δpno1, Δmnn4B, Δbmt2, Δhis1), and the insertion of three more genes allowing for galactosylation of the *N*-glycans, namely galactose epimerase, a UDP-Gal transporter, and β-1,4-galactosyltransferase, giving $Gal_2GlcNAc_2Man_3GlcNAc_2$ $N-$glycans on mAbs (343).

The final step was the insertion of UDP-N-GlcNAc-2-epimerase/ManNAc kinase, N-acetylneuraminate-9-phos phate synthase, CMP−sialic acid synthase, a CMP−sialic acid transporter, and a library of chimeric sialyltransferases linked to yeast type-II transmembrane localization peptides to reconstruct the entire mammalian sialylation pathway in *P. pastoris*. The strain was validated by the production of recombinant human EPO with more than 90% terminal sialylation (108).

After the acquisition of GlycoFi Inc. by Merck & Co. Inc, the GlycoFi technology has been shown to give stable production of antibodies with human-like N-glycosylation under a range of cultivation process parameters (344), thus making it a very promising system for production of recombinant biopharmaceuticals.

The use of *S. cerevisiae* in glycosylation engineering has been limited, mostly due to the advantages of the *P. pastoris* system for heterologous protein production. However, a few successful attempts of engineering are to be found. Most notable is the *och1* deletion studies mentioned above as the basis for the further development of the GlycoFi technology (338,339). Another technique, which is complementary to the GlycoFi, is the reconstruction of the O-fucosylation pathway, including biosynthesis of the GDP-fucose precursor (345). This allowed the production of secreted recombinant epidermal growth factor domains with O-fucosylation.

Minor efforts have also been carried out in filamentous fungi. While filamentous fungi normally only produce mannosylated *N*-glycan, complex *N*-glycans have been achieved by the insertion of GlcNAcT I in *Aspergillus nidulans* (346) and *Trichoderma reesei* (347).

23.5.2.5 Bacteria. Mammalian glycosyltransferases are typically required to be glycosylated in order to be functional, which complicates the expression of the functional enzymes in bacteria. However, as discussed in above, a number of pathogenic bacteria mimic human glycosylation to support evasion of the human immune system. This allows for the transfer of glycosylation pathways into industrial workhorses such as *E. coli* or *B. subtilis* (262). The best example of this is the transfer of N-glycosylation steps from *C. jejuni* to *E. coli* (266,348). Zhang et al. (349) used an interesting strategy of tRNA-synthase evolution to introduce a first step of O-glycosylation to *E. coli* from *Methanococcus jannaschii*. Unfortunately, the authors could not reproduce the experiments, and the chapter was later retracted (350).

23.5.3 Modeling of glycosylation control

While some of the theoretical framework and quantitation required of modeling posttranslational modifications of proteins was established in the 1980's (351,352), and early 1990's (353−355), the actual modeling of N-glycosylation of proteins was not achieved until 1997 by the complementary studies of Monica et al. (356) and Umana and Bailey (357). Monica et al. focus on reactions occurring in the trans-Golgi network, and establishes and discusses the key assumptions for modeling a single compartment. Applying these assumptions within a mathematical framework based on ordinary differential equations allowed the authors to accurately model the extent of sialylation of secreted protein from Chinese hamster cells. Umana and Bailey published a multi-compartmental model accounting for 33 different glycoforms, which however does not account for sialylation. Here, assumptions for modeling multiple compartments were established. This more sophisticated model allowed the prediction of the effect of overexpressing of GlcNAc-transferase III.

Extending the principles of Monica et al and Umana and Bailey mentioned above, the most extensive model for an industrially relevant cell line was published by Krambeck and Betenbaugh (358), where the glycosylation modeling was extended to 7565 glycoforms generated by 22,871 enzymatic reactions. This model, together with an advanced model for human cells by the same authors (359) is currently the state of the art.

23.5.4 Effects of process conditions

It has long been known that protein glycosylation may be affected through the modification of culture conditions, both in terms of overall process parameters such as temperature, pH, dissolved oxygen, culture duration and mode of cultivation, and by the addition of small molecules to the cultivation medium. Typically, the changes made by

overall process parameters are not a part of a glycosylation design strategy (but not necessarily undesirable), while studies made with the addition of compounds are often seeking to directly improve glycosylation by shifting the chemical equilibrium of the glycosyltransferase reactions in the ER and Golgi. Overall, these effects are often both cell line and protein dependent.

In this section, we have compiled an overview of studies (Table 23.12). The overview is limited to mammalian cell cultures, both due to the abundance of work performed in this field, and due to the maturity of mammalian cells as production vessels of recombinant proteins. In the following, we discuss the effect of the most studied pertubations. For the effects of lesser studied manipulations, we direct the reader to Table 23.12.

23.5.4.1 Ammonium. Ammonium is typically formed from the degradation of glutamine, an essential medium component in most mammalian cell cultivations. However, even low concentrations of ammonium (2 mM), may disrupt the intracellular pH levels and inhibit cell growth and protein productivity (364,416). In studies of the effect on protein glycosylation (Table 23.12), it is clear that this detrimental effect of ammonium extends to both N- and O-glycosylation. Again, as little as 2 mM ammonium has been shown to decrease site occupancy, *N*-glycan branching, sialylation, and glycan size in general.

23.5.4.2 Butyrate. While the addition of sodium butyrate (NaBu), has been shown to cause growth arrest and induce apoptosis in mammalian cell cultures (417,418), it often improves the productivity (q_p) of cell cultures (386,402,404). However, the effects of NaBu on glycosylation are quite diverse. In some studies, the site occupancy, *N*-glycan extension and sialic acid content was increased, whereas in others, NaBu had a strongly detrimental effect on glycosylation (Table 23.12). This may be explained by the de-condensating effect NaBu has been described to have on chromatin (419), which one can assume will be very dependent on the genetic content of the individual cell lines.

23.5.4.3 Cell viability. It has been established in several studies that low viability of the cells may have a large effect on the glycosylation of the produced protein. Intracellular carbohydrate-active enzymes and sialylases may leak into the medium when cells die and decrease the value of the product (373,374,399).

23.5.4.4 Glucosamine and N-acetylglucosamine. The addition of glucosamine (GlcN) to the cell culture media is of special interest in protein glycosylation, as it is a precursor for UDP-GlcNAc, which is required in the Golgi as a precursor for *N*-glycan branching as well as for Type 1 and 2 extensions of the *N*-glycans. The intracellular level of UDP-GlcNAc may be increased by adding GlcN to the media, and more so by co-adding uridine (129). The effect of this has been shown in some cases to increase antennarity (Table 23.12). However, adding GlcN alone may decrease branching, galactosylation and sialylation. Substituting glucose for GlcN has been shown in one case to increase the biological affinity of the produced recombinant antibody ten-fold due to modification of the mAb light-chain *N*-glycans (388).

23.5.4.5 Glucose. Glucose is (along with glutamine) the main carbon source in mammalian cell cultures and thus the main source of carbon for protein glycosylation. While smaller changes in the concentration of glucose do not affect glycosylation notably (141), low concentrations decreased site occupancy. Furthermore, galactosylation and sialylation were also decreased (Table 23.12).

23.5.4.6 Oxygen. The level of dissolved oxygen (DO) in the culture is of great importance to the overall cellular metabolism and affects cell growth and overall metabolism directly. This sensitivity is also known to be cell line-dependent (420). Increasing DO has been reported to both increase (143,381,382), and decrease (385) protein glycosylation across a broad range of cell lines and proteins (Table 23.12). While these studies were limited mainly to investigation of sialylation or galactosylation, a study with a broader focus (384) found oscillation of DO to increase sialylation, branching, and galactosylation.

23.5.4.7 pH. The level of pH in the culture affects cellular metabolism greatly, even with small (0.1 pH units) variations (385). In the studies of the effect of pH on protein glycosylation, the effects are mostly determined for one specific level of pH, which makes generalization difficult. However, the observation of Borys et al. (408) that a pH below 6.9 and above 8.2 decreases glycosylation seems to be generally valid. Within this area, some variation in the results is seen.

23.5.4.8 Serum. While the addition of bovine serum traditionally has been an essential component of mammalian cell culture, concerns of contamination from the bovine source spreading to humans such as the Creutzfeldt–Jakobs disease, has decreased the use of serum to an absolute minimum. The effect of this change to serum-free growth medium is quite dependent on the cell line. In nearly all of the studies in Table 23.12, removal of serum increased the level of glycosylation, both in terms of site occupancy (396), and especially sialylation. One exception is for BHK-21 cells, where site occupancy dropped with the removal of serum.

TABLE 23.12. Effect of manipulation with process parameters and medium components on protein glycosylation. For the cell line, information is shown on the immediate progenitor (before transformation with the recombinant protein) if known.

Parameter	Reported effect	Cell line	Protein	Reference(s)
Amino acid supplementation	Adding glycine, threonine and proline increased α-2,3- and α-2,6-sialylation and galactosylation	CHO DUKX-B11	t-PA	(360)
Amino acid supplementation	Addition of depleted amino acids decreased glycosylation due to a bottleneck in β-galactosylation	CHO DHFR-	hEPO	(361)
Ammonium conc.	Adding >2 mM ammonium decreases α-2,6-sialylation of *O*-glycans	CHO	G-CSF	(362,363)
Ammonium conc.	Adding ammonium decreases glycosylation. The effect increases with pH.	CHO DHFR-	mPL-I	(174)
Ammonium conc.	Increasing ammonium concentrations decreases the expression of CMP-SiaT and α-2,3-sialyltransferase	CHO DUKX-B11	t-PA	(364)
Ammonium conc.	Sialylation is inhibited by ammonium.	Plasma cells	IgM	(365)
Ammonium conc.	Addition of ammonia decreases O-glycosylation and reduces sialylation in both O- and *N*-glycans	CHO-K1	hEPO	(366)
Ammonium conc.	Increased ammonium decreases tetraantennary structures and sialylation.	CHO-K1	hEPO	(367)
Ammonium conc.	The branching of the *N*-glycans decreased with increasing ammonium concentration	CHO	hEPO	(368)
Ammonium conc.	Increased ammonium concentrations may give increased branching due to an indirect effect of UDP-HexNAc pool size	BHL-21	IL-2	(369)
Ammonium conc.	Polysialylation decreases with higher concentrations	CHO MT2-1-8	NCAM	(370)
Ammonium conc.	20 mM NH_4Cl decreased polysialylation	SCLC N417	NCAM	(371)
Ammonium conc.	20 mM NH_4Cl decreased polysialylation	CHO MT2-1-8	NCAM	(371)
BSA addition	Decreases percentage of glycosylated protein	CHO DHFR-	IFN-γ	(157)
Calcimycin addition	Inhibits N- and O-glycosylation	CHO DHFR-	EPO, M-CSF	(372)
Cell viability	Sialidase, β-galactosidase, β-hexosaminidase, and fucosidase activities were found in cell lysates, potentially leading to degradation in the medium	CHO DHFR- (WB1), NS0, HEK-293, human-mouse hybridoma	-	(373,374)
Cell viability	Low viability correlates with lower sialylation and shorter glycans, possibly due to degradation	CHO DUKX	IFN-γ	(375)
Chloroquine addition	Sialylation is inhibited	Plasma cells	IgM	(365)
Cultivation mode	Sialylation may decline in the course of a batch cultivation relative to perfusion	CHO-K1	IFN-γ	(376)
Cultivation mode	Glycan content and sialylation was higher in perfusion than in fed-batch	CHO-DG44	SEAP	(377)
Cultivation mode	Galactosylation is decreased by: Lower chemostat dilution rate, hollow fibre cultivation (rel. to chemostat or batch), and low oxygen levels.	NS1	IgG	(191)
Cultivation mode	Fed-batch improved protein yields relative to batch cultivation	CHO DUKX	IFN-γ	(375)
Cultivation mode	Medium feeding increased glycosylation site occupancy	CHO	IFN-γ	(159)
Culture duration	Glycan truncation was shown to increase up to 52% of the RP after 240h	CHO	IFN-γ	(378)
Culture duration	The extent of glycosylation decreased with the cultivation period	CHO	IFN-γ	(379)

TABLE 23.12. (*Continued*)

Parameter	Reported effect	Cell line	Protein	Reference(s)
Cycloheximide addition	Increased the percentage of glycosylation protein from 20 to 80%	C127	Prolactin	(380)
Cytidine addition	Decreased polysialylation	CHO MT2-1-8, SCLC N417	NCAM	(371)
Dissolved oxygen (DO)	Sialylation increases with% DO.	CHO	hFSH	(143)
Dissolved oxygen (DO)	Reducing DO reduces galactosylation	Sp2/0	IgG1	(381)
Dissolved oxygen (DO)	No detectable effect of hypoxia, protein activity is decreased by anoxia	CHO DUKX-B11	t-PA	(382)
Dissolved oxygen (DO)	Glycosylation was similar from 3-200% air saturation with the exception of fucosylation which decreases below 50% and above 100%	CHO-K1	hEPO	(383)
Dissolved oxygen (DO)	Oscillating oxygen tension increases sialylation, branching and galactosylation	murine hybridoma	IgG1	(384)
Dissolved oxygen (DO)	Decreased sialylation with 100% DOT	CHO DUKX-B11	EPO-Fc	(385)
DMSO addition	Decreased sialylation	CHO	hIFN-β	(386)
Fructose addition	Glycosylation was lower than on a glucose-medium	human hybridoma	IgG	(387)
Galactose addition	Insignificant increase in *N*-glycan galactosylation	GS-NS0	IgG1	(188)
Galactose addition	Glycosylation was lower than on a glucose-medium	human hybridoma	IgG	(387)
Galactose addition	Did not increase sialylation	CHO	IL-CT	(171)
GlcN+Uridine addition	Increased antennarity	GS-NS0	TIMP-1	(129)
GlcN+Uridine addition	Increases the percentage of tetraantennary *N*-glycans	BHK-21	IL-2	(369)
GlcN+Uridine addition	Large decrease in polysialylation	CHO MT2-1-8, SCLC N417	NCAM	(371)
GlcN addition	No effect on glycosylation	CHO DHFR-	IFN-γ	(157)
GlcN addition	57% reduction in *N*-glycan galactosylation	GS-NS0	IgG1	(188)
GlcN addition	Decreases *N*-glycan site occupancy	CHO-K1	hEPO	(127)
GlcN addition	Decreases *N*-glycan branching	CHO	hEPO	(368)
GlcN addition	Decreased polysialylation	CHO MT2-1-8	NCAM	(371)
GlcNAc addition	Substitution of 20 mM glucose for 20 mM GlcNAc increased the biological affinity of the antibody 10x by modification of light-chain *N*-glycans	human hybridoma	IgG	(388)
Glucose concentration	N- and O-glycosylation is stable with changing concentrations	BHK-21	IgG-IL2	(141)
Glucose concentration	Glucose limitation led to decreased glycosylation site occupancy	CHO-K1 DHFR-	IFN-γ	(389)
Glucose concentration	Glucose limitation led to decreased glycosylation site occupancy	CHO	IFN-γ	(161)
Glucose concentration	Glycosylation was higher on glucose than on fructose, mannose or galactose	human hybridoma	IgG	(387)
Glucose concentration	Galactosylation decreases under low glucose concentrations	CHO DXB-11	IgG	(167)
Glucose concentration	Low concentration leads to decreased sialylation and increased presence of hybrid and high-mannose glycans	CHO DUKX	IFN-γ	(375)
Glucose concentration	Very low concentrations of glucose decreased glycosylation site occupancy	CHO	IFN-γ	(159)
Glutamine addition	Reduces degradation of the *N*-glycans	CHO-K1	hEPO	(127)
Glutamine concentration	N- and O-glycosylation is stable with changing concentrations	BHK-21	IgG-IL2	(141)
Glutamine concentration	Glutamine limitation led to decreased glycosylation site occupancy	CHO	IFN-γ	(161)

(*continued*)

TABLE 23.12. (*Continued*)

Parameter	Reported effect	Cell line	Protein	Reference(s)
Glutamine concentration	Low concentration leads to decreased sialylation and increased presence of hybrid and high-mannose glycans	CHO DUXK	IFN-γ	(375)
Glycerol addition	Improves the time-dependent de-sialylation	CHO	hIFN-β	(386)
Glycine betaine addition	Beneficial for polysialylation at high osmolality (>435 mOsm/kg), but decreases polysialylation decreases with higher concentrations at lower osmolality.	CHO MT2-1-8	NCAM	(370)
Growth phase	Sialylation was higher during the stationary phase (compared to exponential and death phase). This effect increases with temperature.	CHO DUKX-B11	EPO	(390)
Growth rate	Glycosylation site occupancy decreases at growth rates <0.014 h-1	CHO DHFR-	IFN-γ	(391)
Lipid supplements	BSA with a mixture of lipids increased glycosylation	CHO DHFR-	IFN-γ	(392)
Lipid+BSA supplements	Decreases percentage of glycosylated protein	CHO DHFR-	IFN-γ	(157)
ManNAc addition	Decreased sialylation	GS-CHO, GS-NS0	TIMP-1	(129)
ManNAc addition	Feeding 20 mM increased complete sialylation of bi-antennary *N*-glycans with 15%	CHO	IFN-γ	(393)
ManNAc addition	No effect on sialylation	GS-NS0	IgG1	(188)
ManNAc addition	Sialylation is decreased	Rat hepatocytes	total protein	(394)
ManNAc addition	Increased polysialylation	CHO MT2-1-8	NCAM	(371)
ManNAc addition	Slight increase in polysialylation	SCLC N417	NCAM	(371)
Mannose addition	Glycosylation was lower than on a glucose-medium	human hybridoma	IgG	(387)
Medium selection	Glycosylation was more complete on a protein-free medium than on a serum-free in batch cultures	CHO K1	IFN-γ	(395)
Microcarrier culture	Higher degree of branching in a suspension culture than in microcarrier culture	BHK-21	IL-Mu6	(396)
Microcarrier culture	Microcarrier culture had increased sialylation and decreased fucosylation relative to suspension	CHO-K1	SEAP	(137)
Microcarrier culture	No significant difference between microcarrier and suspension culture	CHO	β-IFN	(397)
Microcarrier culture	Glycosylation is unaffected by scale-up	CHO	EPO	(154)
Microcarrier culture	No significant difference between microcarrier and suspension culture	CHO	IFN-γ	(398)
Miscellaneous additives	Addition of 2,3-dehydro-2-deoxy-N-acetylneuraminic acid to the culture supernatant inhibits extracellular sialidases	CHO DUXB11	gp120	(399)
Mn^{2+} concentration	Increased galactosylation, site occupancy, and decreased branching		hEPO	(361)
Mn^{2+} concentration	Increased site occupancy with increased Mn2+ concentration	CHO DUKX	t-PA	(400)
Mn^{2+} concentration	Manganese addition partially counteracts the negative effects of calcimycin and Thapsigargin addition	CHO DHFR-	EPO, M-CSF	(372)
Mn^{2+} concentration	Manganese is essential for O-glycosylation	CHO DHFR-	EPO, M-CSF	(372)
NaBu addition	Increases *N*-glycan site occupancy	CHO DUKX	t-PA	(176)
NaBu addition	Sialic acid content increased	CHO	hFSH	(143)

TABLE 23.12. (*Continued*)

Parameter	Reported effect	Cell line	Protein	Reference(s)
NaBu addition	Increased extension of the *N*-glycan antennae with polylactosamine units. No effect on sialylation	HT1080	hEPO	(401)
NaBu addition	Increases *N*-glycan site occupancy	CHO DUKX	t-PA/GP2	(400)
NaBu addition	No change in glycosylation while production increased	CHO K1	IgG3	(402)
NaBu addition	Decreased sialylation	CHO	hIFN-β	(386)
NaBu addition	Dramatic decrease in sialylation	CHO DUKX	IACM	(403)
NaBu addition	Decreased sialylation, decreased biological activity	CHO DUKX-B11	hTPO	(404)
NaBu addition	Decreased fully sialylated biantennary *N*-glycans and increased branching	CHO	IFN-γ	(398)
NaCl addition	Polysialylation decreases with higher concentrations	CHO MT2-1-8	NCAM	(370)
NaCl addition	40 mM NaCl did not affect glycosylation significantly	CHO	IFN-γ	(398)
Osmolality	Galactose content decreased with increased osmolality	Sp2/0	IgG2a	(405)
Osmolality	Polysialic acid content decreases with higher osmolality	CHO MT2-1-8	NCAM	(370)
Osmolality	Increase only affects sialylation slightly	CHO MT2-1-8	t-PA	(370)
pCO_2	Neu5Gc proportion of total sialic acid content decreased under elevated pCO2. No other difference in glycosylation was seen	CHO MT2-1-8	t-PA	(406)
pCO_2	Elevated pCO2 increased glycan galactose content	Sp2/0	IgG2a	(405)
pCO_2	Glycosylation was not found to be dependent on pCO2	CHO DXB-11	IgG	(167)
pCO_2	Polysialylation decreases with increasing pCO2 and pH	CHO MT2-1-8	NCAM	(407)
pH	Glycosylation decreases outside the range of 6.9–8.2	CHO K1	mPL-I	(408)
pH	In the presence of 9 mM ammonium, increasing pH decreases glycosylation.	CHO	mPL-I	(174)
pH	Increasing pH decreases *N*-glycan site occupancy	CHO DUKX	GP2	(400)
pH	pH 7.4 increases the NeuAc/Neu5Gc ratio and increases galactosylation. Sialylation is higher at pH 7.2.	mouse hybridoma	IgG	(190)
pH	Reducing pH at decreased temperature (30 or 33 °C) counteracted decreased sialylation	CHO DUKX-B11	EPO-Fc	(409)
pH	No significant effect on sialylation	CHO DUKX-B11	EPO-Fc	(385)
pH	Sialylation decreased with increasing pH	CHO DUKX-B11	EPO	(390)
pH	Polysialylation decreases with increasing pH and pCO2	CHO MT2-1-8	NCAM	(407)
Serum addition/removal	Serum decreases terminal sialylation and proximal fucose as well as site occupancy.	BHK-21	IL-Mu6	(396)
Serum addition/removal	Serum addition decreases glycosylation	CHO DHFR-	IFN-γ	(157)
Serum addition/removal	Sialylation is higher in serum-free medium	CHO	EPO	(173)
Serum addition/removal	Sialylation is higher in serum-free medium	murine hybridoma	IgG1	(193)
Serum addition/removal	An osmolality-dependent decrease in polysialylation was lower on serum-free medium	CHO MT2-1-8	NCAM	(370)
Serum addition/removal	Removal of serum decreases glycosylation site occupancy	BHK-21	AT-III	(146)
Serum substitution	Addition of animal tissue hydrolysate decreased sialylation	CHO	IFN-γ	(131)

(*continued*)

TABLE 23.12. (*Continued*)

Parameter	Reported effect	Cell line	Protein	Reference(s)
Shear stress	*N*-glycan site occupancy decreases with shear stress	CHO DUKX-B11	t-PA	(410)
Temperature	32 °C was shown to be the optimal in terms of glycosylation complexity	CHO DUKX-B11	hEPO	(411)
Temperature	Decreased temperature (33 °C) increases *N*-glycan site occupancy.	CHO DUKX	t-PA	(176)
Temperature	Decreased temperature (33 °C) did not affect glycosylation	CHO-K1	hGM-CSF	(412)
Temperature	Sialidase activity was not affected by decreased temperature	CHO DUKX-B11	t-PA	(413)
Temperature	Decreased temperature (33 °C) increases *N*-glycan site occupancy.	CHO DUKX	t-PA	(400)
Temperature	Decreased temperature (33 °C) increased sialylation and decreased fucosylation	CHO-K1	SEAP	(137)
Temperature	Decreased temperature (30 or 33 °C) decreased sialylation	CHO DUKX-B11	EPO-Fc	(385,409)
Temperature	Decreased temperature had no effect on sialylation	CHO DUKX-B11	hEPO	(414)
Temperature	Decreased temperature had no effect on glycosylation	CHO	IFN-γ	(398)
Temperature	Cultivation at 21 degrees increases Golgi residence time and increases glycosylation	HL.-60	LAMP	(415)
Thapsigargin addition	Inhibits O-glycosylation	CHO DHFR-	M-CSF	(372)
Thyroxine	Increases *N*-glycan site occupancy	CHO DUKX	t-PA	(400)
Triiodothyronine addition	Increases *N*-glycan site occupancy	CHO DUKX	t-PA	(400)
Uridine addition	Decreased polysialylation	CHO MT2-1-8	NCAM	(371)

[a] ASB, human arylsulfatase B; AT-III, Antithrombin III; BSA, Bovine serum albumin; CSP, Cell surface protein; G-CSF, Granulocyte colony-stimulating factor; GlcN, Glucosamine; hGM-CSF, human granulocyte macrophage colony-stimulating factor; hEPO, Human erythropoietin; IACM, An immunoadhesion chimeric molecule; IFN, Interferon; IgG, Immunoglobulin G; IgG-IL2, IgG-IL2 fusion protein; IL2, Interleukin-2; IL2-GP, Interleukin-2 Mu6; IL-CT, IL-4/13 cytokine trap fusion protein; LAMP, lysosomal membrane glycoprotein; M-CSF, Macrophage colony-stimulating factor; mPL-I, mouse placental lactogen-I; NCAM, neural cell adhesion molecule; SCLC, Small Cell Lung Cancer; SEAP, secreted human placental alkaline phosphatase; TIMP-1, tissue inhibitor of metalloproteinases 1.

23.5.4.9 Temperature. Decreasing temperature from 37°C (typically to 33°C) during the production phase of the cultivation is often employed to increase q_p and arrest growth (106). In general, the hypothermic effect may increase protein glycosylation in terms of *N*-glycan site occupancy as well as glycan complexity, elongation and sialylation. Additionally, it has been reported that decreased core fucosylation may improve the PK of the heterologous protein (Table C). The increased glycan processing has been hypothesized to be due to a temperature-induced residence time in the cisternae of the Golgi complex (415).

23.6 CONCLUSIONS

As the number of glycoprotein therapeutics entering the biopharmaceutical market increases over the coming decades, there will be a commensurate need to identify the effects of glycosylation on the biological activity of the protein therapeutics and to characterize the glycosylation state of the recombinant protein products. We have described here a variety of techniques that can be used for that analysis. However, the bioseparations field is changing rapidly, and it is likely that new techniques will evolve which will allow higher-throughput, on-line characterization which will allow feedback to modify process conditions to improve glycosylation during biosynthesis or to improve purification by selecting more desirable glycoforms.

ACKNOWLEDGMENTS

The authors would like to thank Dr. Dmitri Zagorevski of the Mass Spectrometry facility at RPI for assistance with mass spectrometry and Bo Larsen for constructive feedback on parts of the manuscript.

REFERENCES

1. Gosse ME, DiMasi JA, Nelson TF. Recombinant protein and therapeutic monoclonal antibody drug development in the United States from 1980 to 1994. Clin Pharmacol Ther 1996; 60(6):608–618.
2. Bienz-Tadmor B, Dicerbo PA, Tadmor G, Lasagna L. Biopharmaceuticals and conventional drugs: clinical success rates. Biotechnology (N Y) 1992; 10(5):521–525.
3. Lis H, Sharon N. Protein glycosylation. Structural and functional aspects. Eur J Biochem 1993; 218(1):1–27.
4. Furukawa K, Kobata A. Protein glycosylation. Curr Opin Biotechnol 1992; 3(5):554–559.
5. Warren CE. Glycosylation. Curr Opin Biotechnol 1993; 4(5):596–602.
6. Roth J. Protein N-glycosylation along the secretory pathway: relationship to organelle topography and function, protein quality control, and cell interactions. Chem Rev 2002; 102(2):285–303.
7. Reuter G, Gabius HJ. Eukaryotic glycosylation: whim of nature or multipurpose tool? Cell Mol Life Sci 1999; 55(3):368–422.
8. Jenkins N, Curling EM. Glycosylation of recombinant proteins: problems and prospects. Enzyme Microb Technol 1994; 16(5):354–364.
9. Jenkins N. Monitoring and control of recombinant glycoprotein heterogeneity in animal cell cultures. Biochem Soc Trans 1995; 23(1):171–175.
10. Jenkins N, Parekh RB, James DC. Getting the glycosylation right: implications for the biotechnology industry. Nat Biotechnol 1996; 14(8):975–981.
11. Grabenhorst E, Schlenke P, Pohl S, Nimtz M, Conradt HS. Genetic engineering of recombinant glycoproteins and the glycosylation pathway in mammalian host cells. Glycoconj J 1999; 16(2):81–97.
12. Bhatia PK, Mukhopadhyay A. Protein glycosylation: implications for in vivo functions and therapeutic applications. Adv Biochem Eng Biotechnol 1999; 64:155–201.
13. Goochee CF, Monica T. Environmental effects on protein glycosylation. Biotechnology (N Y) 1990; 8(5):421–427.
14. Goochee CF, Gramer MJ, Andersen DC, Bahr JB, Rasmussen JR. The oligosaccharides of glycoproteins: bioprocess factors affecting oligosaccharide structure and their effect on glycoprotein properties. Biotechnology (N Y) 1991; 9(12):1347–1355.
15. Apweiler R, Hermjakob H, Sharon N. On the frequency of protein glycosylation, as deduced from analysis of the SWISS-PROT database. Biochim Biophys Acta 1999; 1473(1):4–8.
16. Rudd PM, Woods RJ, Wormald MR, Opdenakker G, Downing AK, Campbell ID, Dwek RA. The effects of variable glycosylation on the functional activities of ribonuclease, plasminogen and tissue plasminogen activator. Biochim Biophys Acta 1995; 1248(1):1–10.
17. Parekh RB, Tse AG, Dwek RA, Williams AF, Rademacher TW. Tissue-specific N-glycosylation, site-specific oligosaccharide patterns and lentil lectin recognition of rat Thy-1. EMBO J 1987; 6(5):1233–1244.
18. Williams AF, Parekh RB, Wing DR, Willis AC, Barclay AN, Dalchau R, Fabre JW, Dwek RA, Rademacher TW. Comparative analysis of the N-glycans of rat, mouse and human Thy-1. Site-specific oligosaccharide patterns of neural Thy-1, a member of the immunoglobulin superfamily. Glycobiology 1993; 3(4):339–348.
19. Ellgaard L, Frickel E-M. Calnexin, calreticulin, and ERp57: teammates in glycoprotein folding. Cell Biochem Biophys 2003; 39(3):223–247.
20. Ravanat C, Gachet C, Herbert JM, Schuhler S, Guillemot JC, Uzabiaga F, Picard C, Ferrara P, Freund M, Cazenave JP. Rat platelets contain glycosylated and non-glycosylated forms of platelet factor 4. Identification and characterization by mass spectrometry. Eur J Biochem 1994; 223(1):203–210.
21. Eisenhaber B, Bork P, Eisenhaber F. Post-translational GPI lipid anchor modification of proteins in kingdoms of life: analysis of protein sequence data from complete genomes. Protein Eng 2001; 14(1):17–25.
22. Udenfriend S, Kodukula K. How glycosylphosphatidylinositol-anchored membrane proteins are made. Annu Rev Biochem 1995; 64:563–591.
23. Englund PT. The structure and biosynthesis of glycosyl phosphatidylinositol protein anchors. Annu Rev Biochem 1993; 62:121–138.
24. Mayor S, Riezman H. Sorting GPI-anchored proteins. Nat Rev Mol Cell Biol 2004; 5(2):110–120.
25. Haynes PA. Phosphoglycosylation: a new structural class of glycosylation? Glycobiology 1998; 8(1):1–5.
26. Helenius A. How N-linked oligosaccharides affect glycoprotein folding in the endoplasmic reticulum. Mol Biol Cell 1994; 5(3):253–265.
27. Wang C, Eufemi M, Turano C, Giartosio A. Influence of the carbohydrate moiety on the stability of glycoproteins. Biochemistry 1996; 35(23):7299–7307.
28. O'Connor SE, Imperiali B. Modulation of protein structure and function by asparagine-linked glycosylation. Chem Biol 1996; 3(10):803–812.
29. Wyss DF, Wagner G. The structural role of sugars in glycoproteins. Curr Opin Biotechnol 1996; 7(4):409–416.
30. Lisowska E. The role of glycosylation in protein antigenic properties. Cell Mol Life Sci 2002; 59(3):445–455.
31. Weikert S, Papac D, Briggs J, Cowfer D, Tom S, Gawlitzek M, Lofgren J, Mehta S, Chisholm V, Modi N, Eppler S, Carroll K, Chamow S, Peers D, Berman P, Krummen L. Engineering Chinese hamster ovary cells to maximize sialic acid content of recombinant glycoproteins. Nat Biotechnol 1999; 17(11):1116–1121.
32. Chang G-D, Chen C-J, Lin C-Y, Chen H-C, Chen H. Improvement of glycosylation in insect cells with mammalian glycosyltransferases. J Biotechnol 2003; 102(1):61–71.
33. Elliott S, Lorenzini T, Asher S, Aoki K, Brankow D, Buck L, Busse L, Chang D, Fuller J, Grant J, Hernday N, Hokum M, Hu S, Knudten A, Levin N, Komorowski R, Martin F, Navarro R, Osslund T, Rogers G, Rogers N, Trail G, Egrie J. Enhancement of therapeutic protein in vivo activities through glycoengineering. Nat Biotechnol 2003; 21(4):414–421.
34. Bloom JW, Madanat MS, Ray MK. Cell line and site specific comparative analysis of the N-linked oligosaccharides

on human ICAM-1des454-532 by electrospray ionization mass spectrometry. Biochemistry 1996; 35(6):1856–1864.

35. Dage JL, Ackermann BL, Halsall HB. Site localization of sialyl Lewis(x) antigen on alpha1-acid glycoprotein by high performance liquid chromatography-electrospray mass spectrometry. Glycobiology 1998; 8(8):755–760.
36. Mauko L, Nordborg A, Hutchinson JP, Lacher NA, Hilder EF, Haddad PR. Glycan profiling of monoclonal antibodies using zwitterionic-type hydrophilic interaction chromatography coupled with electrospray ionization mass spectrometry detection. Anal Biochem 2011; 408(2):235–241.
37. Palmisano G, Lendal SE, Engholm-Keller K, Leth-Larsen R, Parker BL, Larsen MR. Selective enrichment of sialic *acid*–containing glycopeptides using titanium dioxide chromatography with analysis by HILIC and mass spectrometry. Nat Protoc 2010; 5(12):1974–1982.
38. Mariño K, Bones J, Kattla JJ, Rudd PM. A systematic approach to protein glycosylation analysis: a path through the maze. Nat Chem Biol 2010; 6(10):713–723.
39. Melmer M, Stangler T, Schiefermeier M, Brunner W, Toll H, Rupprechter A, Lindner W, Premstaller A. HILIC analysis of fluorescence-labeled N-glycans from recombinant biopharmaceuticals. Anal Bioanal Chem 2010; 398(2):905–14.
40. Snovida SI, Bodnar ED, Viner R, Saba J, Perreault H. A simple cellulose column procedure for selective enrichment of glycopeptides and characterization by nano LC coupled with electron-transfer and high-energy collisional-dissociation tandem mass spectrometry. Carbohydr Res 2010; 345(6):792–801.
41. Ivancic MM, Gadgil HS, Halsall HB, Treuheit MJ. LC/MS analysis of complex multiglycosylated human alpha(1)-acid glycoprotein as a model for developing identification and quantitation methods for intact glycopeptide analysis. Anal Biochem 2010; 400(1):25–32.
42. Zauner G, Koeleman CAM, Deelder AM, Wuhrer M. Protein glycosylation analysis by HILIC-LC-MS of Proteinase K-generated N- and O-glycopeptides. J Sep Sci 2010; 33(6–7):903–910.
43. Wu Y, Mechref Y, Klouckova I, Mayampurath A, Novotny MV, Tang H. Mapping site-specific protein N-glycosylations through liquid chromatography/mass spectrometry and targeted tandem mass spectrometry. Rapid Commun Mass Spectrom 2010; 24(7):965–972.
44. North SJ, Huang HH, Sundaram S, Jang-Lee J, Etienne AT, Trollope A, Al-Chalabi S, Dell A, Stanley P, Haslam SM. Glycomics profiling of Chinese hamster ovary (CHO) cell glycosylation mutants reveals N-glycans of a novel size and complexity. J Biol Chem 2010; 285(8):5759–5775.
45. Damen CWN, Chen W, Chakraborty AB, Oosterhout M, Mazzeo JR, Gebler JC, Schellens JHM, Rosing H, Beijnen JH. Electrospray ionization quadrupole ion-mobility time-of-flight mass spectrometry as a tool to distinguish the lot-to-lot heterogeneity in N-glycosylation profile of the therapeutic monoclonal antibody trastuzumab. J Am Soc Mass Spectrom 2009; 20(11):2021–2033.
46. Hirabayashi J, Kasai K. Separation technologies for glycomics. J Chromatogr B Analyt Technol Biomed Life Sci 2002; 771(1–2):67–87.
47. Cummings RD, Kornfeld S. The distribution of repeating [Gal beta 1,4GlcNAc beta 1,3] sequences in asparagine-linked oligosaccharides of the mouse lymphoma cell lines BW5147 and PHAR 2.1. J Biol Chem 1984; 259(10):6253–6260.
48. Ji J, Chakraborty A, Geng M, Zhang X, Amini A, Bina M, Regnier F. Strategy for qualitative and quantitative analysis in proteomics based on signature peptides. J Chromatogr B Biomed Sci Appl 2000; 745(1):197–210.
49. Qiu R, Regnier FE. Use of multidimensional lectin affinity chromatography in differential glycoproteomics. Anal Chem 2005; 77(9):2802–2809.
50. Harazono A, Kawasaki N, Kawanishi T, Hayakawa T. Site-specific glycosylation analysis of human apolipoprotein B100 using LC/ESI MS/MS. Glycobiology 2005; 15(5):447–462.
51. Wuhrer M, Koeleman CA, Hokke CH, Deelder AM. Protein glycosylation analyzed by normal-phase nano-liquid chromatography–mass spectrometry of glycopeptides. Anal Chem 2005; 77(3):886–894.
52. Medzihradszky KF, Maltby DA, Hall SC, Settineri CA, Burlingame AL. Characterization of protein N-glycosylation by reversed-phase microbore liquid-chromatography electrospray mass-spectrometry, complementary mobile phases, and sequential exoglycosidase digestion. J Am Soc Mass Spectrom 1994; 5(5):350–358.
53. Ritchie MA, Gill AC, Deery MJ, Lilley K. Precursor ion scanning for detection and structural characterization of heterogeneous glycopeptide mixtures. J Am Soc Mass Spectrom 2002; 13(9):1065–1077.
54. Wang F, Nakouzi A, Angeletti RH, Casadevall A. Site-specific characterization of the N-linked oligosaccharides of a murine immunoglobulin M by high-performance liquid chromatography/electrospray mass spectrometry. Anal Biochem 2003; 314(2):266–280.
55. Sullivan B, Addona TA, Carr SA. Selective detection of glycopeptides on ion trap mass spectrometers. Anal Chem 2004; 76(11):3112–3118.
56. Huddleston MJ, Bean MF, Carr SA. Collisional fragmentation of glycopeptides by electrospray ionization LC/MS and LC/MS/MS: methods for selective detection of glycopeptides in protein digests. Anal Chem 1993; 65(7):877–884.
57. Satomi Y, Shimonishi Y, Hase T, Takao T. Site-specific carbohydrate profiling of human transferrin by nano-flow liquid chromatography/electrospray ionization mass spectrometry. Rapid Commun Mass Spectrom 2004; 18(24):2983–2988.
58. Xie H, Chakraborty A, Ahn J, Yu YQ, Dakshinamoorthy DP, Gilar M, Chen W, Skilton SJ, Mazzeo JR. Rapid comparison of a candidate biosimilar to an innovator monoclonal antibody with advanced liquid chromatography and mass spectrometry technologies. MAbs 2010; 379–394 2(4).
59. Segu ZM, Hammad LA, Mechref Y. Rapid and efficient glycoprotein identification through microwave-assisted enzymatic digestion. Rapid Commun Mass Spectrom 2010; 24(23):3461–3468.
60. Harvey DJ. Matrix-assisted laser desorption/ionization mass spectrometry of carbohydrates and glycoconjugates. Int J Mass Spectrom 2003; 226(1):1–35.
61. Medzihradszky KF. Characterization of protein N-glycosylation. Methods Enzymol 2005; 405:116–138.
62. Papac DI, Briggs JB, Chin ET, Jones AJ. A high-throughput microscale method to release N-linked oligosaccharides from glycoproteins for matrix-assisted laser desorption/ionization time-of-flight mass spectrometric analysis. Glycobiology 1998; 8(5):445–454.

63. Stimson E, Hope J, Chong A, Burlingame AL. Site-specific characterization of the N-linked glycans of murine prion protein by high-performance liquid chromatography/electrospray mass spectrometry and exoglycosidase digestions. Biochemistry 1999; 38(15):4885–4895.
64. Domon B, Costello CE. A systematic nomenclature for carbohydrate fragmentations in FAB-MS/MS spectra of glycoconjugates. Glycoconj J 1988; 5(4):397–409.
65. Demelbauer UM, Zehl M, Plematl A, Allmaier G, Rizzi A. Determination of glycopeptide structures by multistage mass spectrometry with low-energy collision-induced dissociation: comparison of electrospray ionization quadrupole ion trap and matrix-assisted laser desorption/ionization quadrupole ion trap reflectron time-of-flight approaches. Rapid Commun Mass Spectrom 2004; 18(14):1575–1582.
66. HÅkansson K, Chalmers MJ, Quinn JP, McFarland MA, Hendrickson CL, Marshall AG. Combined electron capture and infrared multiphoton dissociation for multistage MS/MS in a fourier transform ion cyclotron resonance mass spectrometer. Anal Chem 2003; 75(13):3256–3262.
67. HÅkansson K, Cooper HJ, Emmett MR, Costello CE, Marshall AG, Nilsson CL. Electron capture dissociation and infrared multiphoton dissociation MS/MS of an N-glycosylated tryptic peptide to yield complementary sequence information. Anal Chem 2001; 73(18):4530–4536.
68. Mirgorodskaya E, Roepstorff P, Zubarev RA. Localization of O-glycosylation sites in peptides by electron capture dissociation in a fourier transform mass spectrometer. Anal Chem 1999; 71(20):4431–4436.
69. Alley WR, Mechref Y, Novotny MV. Characterization of glycopeptides by combining collision-induced dissociation and electron-transfer dissociation mass spectrometry data. Rapid Commun Mass Spectrom 2009; 23(1):161–170.
70. Harvey DJ. Identification of protein-bound carbohydrates by mass spectrometry. Proteomics 2001; 1(2):311–328.
71. Perdivara I, Petrovich R, Allinquant B, Alliquant B, Deterding LJ, Tomer KB, Przybylski M. Elucidation of O-glycosylation structures of the beta-amyloid precursor protein by liquid chromatography-mass spectrometry using electron transfer dissociation and collision induced dissociation. J Proteome Res 2009; 8(2):631–642.
72. Seipert RR, Dodds ED, Lebrilla CB. Exploiting differential dissociation chemistries of O-linked glycopeptide ions for the localization of mucin-type protein glycosylation. J Proteome Res 2009; 8(2):493–501.
73. Patel T, Bruce J, Merry A, Bigge C, Wormald M, Jaques A, Parekh R. Use of hydrazine to release in intact and unreduced form both N- and O-linked oligosaccharides from glycoproteins. Biochemistry 1993; 32(2):679–693.
74. Dwek RA. Glycobiology: toward understanding the function of sugars. Chem Rev 1996; 96(2):683–720.
75. Costa J, Ashford DA, Nimtz M, Bento I, Frazäo C, Esteves CL, Faro CJ, Kervinen J, Pires E, Veríssimo P, Wlodawer A, Carrondo MA. The glycosylation of the aspartic proteinases from barley (Hordeum vulgare L.) and cardoon (Cynara cardunculus L.). Eur J Biochem 1997; 243(3):695–700.
76. Yamada K, Hyodo S, Kinoshita M, Hayakawa T, Kakehi K. Hyphenated technique for releasing and MALDI MS analysis of O-glycans in mucin-type glycoprotein samples. Anal Chem 2010; 82(17):7436–7443.
77. Rudd PM, Dwek RA. Rapid, sensitive sequencing of oligosaccharides from glycoproteins. Curr Opin Biotechnol 1997; 8(4):488–497.
78. Segu ZM, Hussein A, Novotny MV, Mechref Y. Assigning N-glycosylation sites of glycoproteins using LC/MSMS in conjunction with endo-M/exoglycosidase mixture. J Proteome Res 2010; 9(7):3598–3607.
79. Peter-Katalinić J. Methods in enzymology: O-glycosylation of proteins. Methods Enzymol 2005; 405:139–171.
80. O'Neill RA. Enzymatic release of oligosaccharides from glycoproteins for chromatographic and electrophoretic analysis. J Chromatogr A 1996; 720(1–2):201–215.
81. Strupat K, Karas M, Hillenkamp F. 2,5-dihydroxybenzoic acid - a new matrix for laser desorption ionization mass-spectrometry. Int J Mass Spectrom Ion Process 1991; 111:89–102.
82. Karas M, Ehring H, Nordhoff E, Stahl B, Strupat K, Hillenkamp F, Grehl M, Krebs B. Matrix-assisted laser-desorption ionization mass-spectrometry with additives to 2,5-dihydroxybenzoic acid. Org Mass Spectrom 1993; 28(12):1476–1481.
83. Papac DI, Wong A, Jones AJ. Analysis of acidic oligosaccharides and glycopeptides by matrix-assisted laser desorption/ionization time-of-flight mass spectrometry. Anal Chem 1996; 68(18):3215–3223.
84. Zaia J. Mass spectrometry of oligosaccharides. Mass Spectrom Rev 2004; 23(3):161–227.
85. Cooper CA, Gasteiger E, Packer NH. GlycoMod–a software tool for determining glycosylation compositions from mass spectrometric data. Proteomics 2001; 1(2):340–349.
86. Lee YC. Carbohydrate analyses with high-performance anion-exchange chromatography. J Chromatogr A 1996; 720(1–2):137–149.
87. Bruggink C, Wuhrer M, Koeleman CAM, Barreto V, Liu Y, Pohl C, Ingendoh A, Hokke CH, Deelder AM. Oligosaccharide analysis by capillary-scale high-pH anion-exchange chromatography with on-line ion-trap mass spectrometry. J Chromatogr B Analyt Technol Biomed Life Sci 2005; 829(1–2):136–143.
88. Rassi ZEL. Recent progress in reversed-phase and hydrophobic interaction chromatography of carbohydrate species. J Chromatogr A 1996; 720(1–2):93–118.
89. Koizumi K. High-performance liquid chromatographic separation of carbohydrates on graphitized carbon columns. J Chromatogr A 1996; 720(1–2):119–126.
90. Takahashi N. Three-dimensional mapping of N-linked oligosaccharides using anion-exchange, hydrophobic and hydrophilic interaction modes of high-performance liquid chromatography. J Chromatogr A 1996; 720(1–2):217–225.
91. Gillmeister MP, Tomiya N, Jacobia SJ, Lee YC, Gorfien SF, Betenbaugh MJ. An HPLC-MALDI MS method for N-glycan analyses using smaller size samples: application to monitor glycan modulation by medium conditions. Glycoconj J 2009; 26(9):1135–1149.
92. Linhardt RJ, Pervin A. Separation of negatively charged carbohydrates by capillary electrophoresis. J Chromatogr A 1996; 720(1–2):323–335.
93. Mao W, Thanawiroon C, Linhardt RJ. Capillary electrophoresis for the analysis of glycosaminoglycans and glycosaminoglycan-derived oligosaccharides. Biomed Chromatogr 2002; 16(2):77–94.

94. Pervin A, al-Hakim A, Linhardt RJ. Separation of glycosaminoglycan-derived oligosaccharides by capillary electrophoresis using reverse polarity. Anal Biochem 1994; 221(1):182–188.
95. Paulus A, Klockow A. Detection of carbohydrates in capillary electrophoresis. J Chromatogr A 1996; 720(1–2):353–376.
96. Damm JB, Overklift GT. Indirect UV detection as a non-selective detection method in the qualitative and quantitative analysis of heparin fragments by high-performance capillary electrophoresis. J Chromatogr A 1994; 678(1):151–165.
97. Lazar IM, Xin BM, Lee ML, Lee ED, Rockwood AL, Fabbi JC, Lee HG. Design of a time-of-flight mass spectrometer as a detector for capillary electrophoresis. Anal Chem 1997; 69(16):3205–3211.
98. Bazin HG, Wolff MW, Linhardt RJ. Exoglycosidase based analysis of fluorescently labeled oligosaccharides by electrospray ionization mass spectrometry and capillary electrophoresis. Biotechnol Tech 1999; 13:797–801.
99. Küster B, Krogh TN, Mørtz E, Harvey DJ. Glycosylation analysis of gel-separated proteins. Proteomics 2001; 1(2):350–361.
100. Lamari FN, Karamanos NK. Separation methods for sialic acids and critical evaluation of their biologic relevance. J Chromatogr B Analyt Technol Biomed Life Sci 2002; 781(1–2):3–19.
101. Warren L. The thiobarbituric acid assay of sialic acids. J Biol Chem 1959; 234(8):1971–1975.
102. Hammond KS, Papermaster DS. Fluorometric assay of sialic acid in the picomole range: a modification of the thiobarbituric acid assay. Anal Biochem 1976; 74(2):292–297.
103. Jiménez-Barbero J, Asensio JL, Cañada FJ, Poveda A. Free and protein-bound carbohydrate structures. Curr Opin Struct Biol 1999; 9(5):549–555.
104. Frank M, Schloissnig S. Bioinformatics and molecular modeling in glycobiology. Cell Mol Life Sci 2010; 67(16):2749–2772.
105. Hossler P, Khattak SF, Li ZJ. Optimal and consistent protein glycosylation in mammalian cell culture. Glycobiology 2009; 19(9):936–949.
106. Durocher Y, Butler M. Expression systems for therapeutic glycoprotein production. Curr Opin Biotechnol 2009; 20(6):700–707.
107. Sethuraman N, Stadheim TA. Challenges in therapeutic glycoprotein production. Curr Opin Biotechnol 2006; 17(4):341–346.
108. Hamilton SR, Davidson RC, Sethuraman N, Nett JH, Jiang Y, Rios S, Bobrowicz P, Stadheim TA, Li H, Choi B-K, Hopkins D, Wischnewski H, Roser J, Mitchell T, Strawbridge RR, Hoopes J, Wildt S, Gerngross TU. Humanization of yeast to produce complex terminally sialylated glycoproteins. Science 2006; 313(5792):1441–1443.
109. Decker EL, Reski Rf. Current achievements in the production of complex biopharmaceuticals with moss bioreactors. Bioprocess Biosyst Eng 2008; 31(1):3–9.
110. Yamashita K, Tachibana Y, Nakayama T, Kitamura M, Endo Y, Kobata A. Structural studies of the sugar chains of human parotid alpha-amylase. J Biol Chem 1980; 255(12):5635–5642.
111. Tsuji T, Irimura T, Osawa T. The carbohydrate moiety of band 3 glycoprotein of human erythrocyte membranes: structures of lower molecular weight oligosaccharides. J Biol Chem 1981; 256(20):10497–10502.
112. Shields RL, Lai J, Keck R, O'Connell LY, Hong K, Meng YG, Weikert SHA, Presta LG. Lack of fucose on human IgG1N-linked oligosaccharide improves binding to human Fcgamma RIII and antibody-dependent cellular toxicity. J Biol Chem 2002; 277(30):26733–26740.
113. Schmid K, Binette JP, Dorland L, Vliegenthart JF, Fournet B, Montreuil J. The primary structure of the asialo-carbohydrate units of the first glycosylation site of human plasma alpha 1-acid glycoprotein. Biochim Biophys Acta 1979; 581(2):356–359.
114. Takasaki S, Yamashita K, Suzuki K, Kobata A. Structural studies of the sugar chains of cold-insoluble globulin isolated from human plasma. J Biochem 1980; 88(6):1587–1594.
115. Kagawa Y, Takasaki S, Utsumi J, Hosoi K, Shimizu H, Kochibe N, Kobata A. Comparative study of the asparagine-linked sugar chains of natural human interferon-beta 1 and recombinant human interferon-beta 1 produced by three different mammalian cells. J Biol Chem 1988; 263(33):17508–17515.
116. Alhadeff JA, Holzinger RT. Solubilization and stabilization of human liver glycoprotein sialyltransferase. Biochim Biophys Acta 1979; 570(1):56–64.
117. Livingston BD, Jacobs JL, Glick MC, Troy FA. Extended polysialic acid chains (n greater than 55) in glycoproteins from human neuroblastoma cells. J Biol Chem 1988; 263(19):9443–9448.
118. Okuda T, Mita S, Yamauchi S, Fukuta M, Nakano H, Sawada T, Habuchi O. Molecular cloning and characterization of GalNAc 4-sulfotransferase expressed in human pituitary gland. J Biol Chem 2000; 275:40605–40613.
119. Fukuta M, Inazawa J, Torii T, Tsuzuki K, Shimada E, Habuchi O. Molecular cloning and characterization of human keratan sulfate Gal-6-sulfotransferase. J Biol Chem 1997; 272(51):32321–32328.
120. Fukuta M, Kobayashi Y, Uchimura K, Kimata K, Habuchi O. Molecular cloning and expression of human chondroitin 6-sulfotransferase. Biochim Biophys Acta 1998; 1399(1):57–61.
121. Loignon M, Perret S, Kelly J, Boulais D, Cass B, Bisson L, Afkhamizarreh F, Durocher Y. Stable high volumetric production of glycosylated human recombinant IFNalpha2b in HEK293 cells. BMC Biotechnol 2008; 8:65.
122. Varki A, Cummings R, Esko J, Freeze H, Hart G, Marth J. Essentials of glycobiology. New York: Cold Spring Harbor Laboratory Press; 1999.
123. Greunke K, Spillner E, Braren I, Seismann H, Kainz S, Hahn U, Grunwald T, Bredehorst R. Bivalent monoclonal IgY antibody formats by conversion of recombinant antibody fragments. J Biotechnol 2006; 124(2):446–456.
124. Arnold JN, Wormald MR, Sim RB, Rudd PM, Dwek RA. The impact of glycosylation on the biological function and structure of human immunoglobulins. Annu Rev Immunol 2007; 25:21–50.
125. Jones D, Kroos N, Anema R, van Montfort B, Vooys A, Kraats S, Helm E, Smits S, Schouten J, Brouwer K, Lagerwerf F, Berkel P, Opstelten D-J, Logtenberg T, Bout A.

High-level expression of recombinant IgG in the human cell line PER.C6. Biotechnol Prog 2003; 19(1):163–168.

126. Havenga MJE, Holterman L, Melis I, Smits S, Kaspers J, Heemskerk E, Vlugt Rvander, Koldijk M, Schouten GJ, Hateboer G, Brouwer K, Vogels R, Goudsmit J. Serum-free transient protein production system based on adenoviral vector and PER.C6 technology: high yield and preserved bioactivity. Biotechnol Bioeng 2008; 100(2):273–283.
127. Yang M, Butler M. Enhanced erythropoietin heterogeneity in a CHO culture is caused by proteolytic degradation and can be eliminated by a high glutamine level. Cytotechnology 2000; 34(1–2):83–99.
128. Yamashita K, Ohkura T, Tachibana Y, Takasaki S, Kobata A. Comparative study of the oligosaccharides released from baby hamster kidney cells and their polyoma transformant by hydrazinolysis. J Biol Chem 1984; 259(17):10834–10840.
129. Baker KN, Rendall MH, Hills AE, Hoare M, Freedman RB, James DC. Metabolic control of recombinant protein N-glycan processing in NS0 and CHO cells. Biotechnol Bioeng 2001; 73(3):188–202.
130. Bergwerff AA, Oostrum J, Asselbergs FA, Bürgi R, Hokke CH, Kamerling JP, Vliegenthart JF. Primary structure of N-linked carbohydrate chains of a human chimeric plasminogen activator K2tu-PA expressed in Chinese hamster ovary cells. Eur J Biochem 1993; 212(3):639–656.
131. Gu X, Xie L, Harmon BJ, Wang DI. Influence of Primatone RL supplementation on sialylation of recombinant human interferon-gamma produced by Chinese hamster ovary cell culture using serum-free media. Biotechnol Bioeng 1997; 56(4):353–360.
132. Damiani R, Oliveira JE, Vorauer-Uhl K, Peroni CN, Vianna EG, Bartolini P, Ribela MTCP. Stable expression of a human-like sialylated recombinant thyrotropin in a Chinese hamster ovary cell line expressing alpha2,6-sialyltransferase. Protein Expr Purif 2009; 67(1):7–14.
133. Butler M. Optimisation of the cellular metabolism of glycosylation for recombinant proteins produced by Mammalian cell systems. Cytotechnology 2006; 50(1–3):57–76.
134. Hokke CH, Bergwerff AA, Dedem GWV, Kamerling JP, Vliegenthart JF. Structural analysis of the sialylated N- and O-linked carbohydrate chains of recombinant human erythropoietin expressed in Chinese hamster ovary cells. Sialylation patterns and branch location of dimeric N-acetyllactosamine units. Eur J Biochem 1995; 228(3):981–1008.
135. Mizuochi T, Spellman MW, Larkin M, Solomon J, Basa LJ, Feizi T. Carbohydrate structures of the human-immunodeficiency-virus (HIV) recombinant envelope glycoprotein gp120 produced in Chinese-hamster ovary cells. Biochem J 1988; 254(2):599–603.
136. Mueller PP, Schlenke P, Nimtz M, Conradt HS, Hauser H. Recombinant glycoprotein product quality in proliferation-controlled BHK-21 cells. Biotechnol Bioeng 1999; 65(5):529–536.
137. Nam JH, Zhang F, Ermonval M, Linhardt RJ, Sharfstein ST. The effects of culture conditions on the glycosylation of secreted human placental alkaline phosphatase produced in Chinese hamster ovary cells. Biotechnol Bioeng 2008; 100(6):1178–1192.
138. Nimtz M, Martin W, Wray V, Klöppel KD, Augustin J, Conradt HS. Structures of sialylated oligosaccharides of human erythropoietin expressed in recombinant BHK-21 cells. Eur J Biochem 1993; 213(1):39–56.
139. Sasaki H, Bothner B, Dell A, Fukuda M. Carbohydrate structure of erythropoietin expressed in Chinese hamster ovary cells by a human erythropoietin cDNA. J Biol Chem 1987; 262(25):12059–12076.
140. Sutkeviciute I, Mistiniene E, Sereikaite J, Bumelis VA. The influence of different glycosylation patterns on factor VII biological activity. Biochimie 2009; 91(9):1123–1130.
141. Cruz HJ, Peixoto CM, Nimtz M, Alves PM, Dias EM, Moreira JL, Carrondo MJ. Metabolic shifts do not influence the glycosylation patterns of a recombinant fusion protein expressed in BHK cells. Biotechnol Bioeng 2000; 69(2):129–139.
142. Spellman MW, Basa LJ, Leonard CK, Chakel JA, O'Connor JV, Wilson S, Halbeek H. Carbohydrate structures of human tissue plasminogen activator expressed in Chinese hamster ovary cells. J Biol Chem 1989; 264(24):14100–14111.
143. Chotigeat W, Watanapokasin Y, Mahler S, Gray PP. Role of environmental conditions on the expression levels, glycoform pattern and levels of sialyltransferase for hFSH produced by recombinant CHO cells. Cytotechnology 1994; 15(1–3):217–221.
144. Kawasaki N, Ohta M, Hyuga S, Hyuga M, Hayakawa T. Application of liquid chromatography/mass spectrometry and liquid chromatography with tandem mass spectrometry to the analysis of the site-specific carbohydrate heterogeneity in erythropoietin. Anal Biochem 2000; 285(1):82–91.
145. Spellman MW, Leonard CK, Basa LJ, Gelineo I, Halbeek Hvan. Carbohydrate structures of recombinant soluble human CD4 expressed in Chinese hamster ovary cells. Biochemistry 1991; 30(9):2395–2406.
146. Teige M, Weidemann R, Kretzmer G. Problems with serum-free production of antithrombin III regarding proteolytic activity and product quality. J Biotechnol 1994; 34(1):101–105.
147. Kaufman RJ, Wasley LC, Dorner AJ. Synthesis, processing, and secretion of recombinant human factor VIII expressed in mammalian cells. J Biol Chem 1988; 263(13):6352–6362.
148. Thim L, Vandahl B, Karlsson J, Klausen NK, Pedersen J, Krogh TN, Kjalke M, Petersen JM, Johnsen LB, Bolt G, Nørby PL, Steenstrup TD. Purification and characterization of a new recombinant factor VIII (N8). Haemophilia 2010; 16(2):349–359.
149. Gaudry J-P, Arod C, Sauvage C, Busso S, Dupraz P, Pankiewicz R, Antonsson B. Purification of the extracellular domain of the membrane protein GlialCAM expressed in HEK and CHO cells and comparison of the glycosylation. Protein Expr Purif 2008; 58(1):94–102.
150. Takeuchi M, Inoue N, Strickland TW, Kubota M, Wada M, Shimizu R, Hoshi S, Kozutsumi H, Takasaki S, Kobata A. Relationship between sugar chain structure and biological activity of recombinant human erythropoietin produced in Chinese hamster ovary cells. Proc Natl Acad Sci USA 1989; 86(20):7819–7822.
151. Delorme E, Lorenzini T, Giffin J, Martin F, Jacobsen F, Boone T, Elliott S. Role of glycosylation on the secretion and biological activity of erythropoietin. Biochemistry 1992; 31(41):9871–9876.

152. Noguchi A, Mukuria CJ, Suzuki E, Naiki M. Immunogenicity of N-glycolylneuraminic acid-containing carbohydrate chains of recombinant human erythropoietin expressed in Chinese hamster ovary cells. J Biochem 1995; 117(1):59–62.

153. Zhang X, Lok SH, Kon OL. Stable expression of human alpha-2,6-sialyltransferase in Chinese hamster ovary cells: functional consequences for human erythropoietin expression and bioactivity. Biochim Biophys Acta 1998; 1425(3):441–452.

154. Wang M-D, Yang M, Huzel N, Butler M. Erythropoietin production from CHO cells grown by continuous culture in a fluidized-bed bioreactor. Biotechnol Bioeng 2002; 77(2):194–203.

155. Park JS, Kim H, Park J, Yu S, Kim D, Lee J, Oh H, Baek K, Yoon J. Overproduction of recombinant human hepatocyte growth factor in Chinese hamster ovary cells. Protein Expr Purif 2010; 70(2):231–235.

156. Zhu X, Borchers C, Bienstock RJ, Tomer KB. Mass spectrometric characterization of the glycosylation pattern of HIV-gp120 expressed in CHO cells. Biochemistry 2000; 39(37):11194–11204.

157. Castro PM, Ison AP, Hayter PM, Bull AT. The macroheterogeneity of recombinant human interferon-gamma produced by Chinese-hamster ovary cells is affected by the protein and lipid content of the culture medium. Biotechnol Appl Biochem 1995; 21(Pt 1): 87–100.

158. Gu X, Harmon BJ, Wang DI. Site- and branch-specific sialylation of recombinant human interferon-gamma in Chinese hamster ovary cell culture. Biotechnol Bioeng 1997; 55(2):390–398.

159. Xie L, Nyberg G, Gu X, Li H, Möllborn F, Wang DI. Gamma-interferon production and quality in stoichiometric fed-batch cultures of Chinese hamster ovary (CHO) cells under serum-free conditions. Biotechnol Bioeng 1997; 56(5):577–582.

160. Zhang J, Wang DI. Quantitative analysis and process monitoring of site-specific glycosylation microheterogeneity in recombinant human interferon-gamma from Chinese hamster ovary cell culture by hydrophilic interaction chromatography. J Chromatogr B Biomed Sci Appl 1998; 712(1–2):73–82.

161. Nyberg GB, Balcarcel RR, Follstad BD, Stephanopoulos G, Wang DI. Metabolic effects on recombinant interferon-gamma glycosylation in continuous culture of Chinese hamster ovary cells. Biotechnol Bioeng 1999; 62(3):336–347.

162. Lifely MR, Hale C, Boyce S, Keen MJ, Phillips J. Glycosylation and biological activity of CAMPATH-1H expressed in different cell lines and grown under different culture conditions. Glycobiology 1995; 5(8):813–822.

163. Routier FH, Davies MJ, Bergemann K, Hounsell EF. The glycosylation pattern of humanized IgGI antibody (D1.3) expressed in CHO cells. Glycoconj J 1997; 14(2):201–207.

164. Sheeley DM, Merrill BM, Taylor LC. Characterization of monoclonal antibody glycosylation: comparison of expression systems and identification of terminal alpha-linked galactose. Anal Biochem 1997; 247(1):102–110.

165. Umaña P, Jean-Mairet J, Moudry R, Amstutz H, Bailey JE. Engineered glycoforms of an antineuroblastoma IgG1 with optimized antibody-dependent cellular cytotoxic activity. Nat Biotechnol 1999; 17(2):176–180.

166. Hodoniczky J, Zheng YZ, James DC. Control of recombinant monoclonal antibody effector functions by Fc N-glycan remodeling in vitro. Biotechnol Prog 2005; 21(6):1644–1652.

167. Takuma S, Hirashima C, Piret JM. Dependence on glucose limitation of the pCO2 influences on CHO cell growth, metabolism and IgG production. Biotechnol Bioeng 2007; 97(6):1479–1488.

168. Ye J, Kober V, Tellers M, Naji Z, Salmon P, Markusen JF. High-level protein expression in scalable CHO transient transfection. Biotechnol Bioeng 2009; 103(3):542–551.

169. Kim W-D, Tokunaga M, Ozaki H, Ishibashi T, Honda K, Kajiura H, Fujiyama K, Asano R, Kumagai I, Omasa T, Ohtake H. Glycosylation pattern of humanized IgG-like bispecific antibody produced by recombinant CHO cells. Appl Microbiol Biotechnol 2010; 85(3):535–542.

170. Conradt HS, Nimtz M, Dittmar KE, Lindenmaier W, Hoppe J, Hauser H. Expression of human interleukin-2 in recombinant baby hamster kidney, Ltk-, and Chinese hamster ovary cells: structure of O-linked carbohydrate chains and their location within the polypeptide. J Biol Chem 1989; 264(29):17368–17373.

171. Clark KJ-R, Griffiths J, Bailey KM, Harcum SW. Gene-expression profiles for five key glycosylation genes for galactose-fed CHO cells expressing recombinant IL-4/13 cytokine trap. Biotechnol Bioeng 2005; 90(5):568–577.

172. Bierhuizen MF, Fukuda M. Expression cloning of a cDNA encoding UDP-GlcNAc:Gal beta 1-3-GalNAc-R (GlcNAc to GalNAc) beta 1-6GlcNAc transferase by gene transfer into CHO cells expressing polyoma large tumor antigen. Proc Natl Acad Sci USA 1992; 89(19):9326–9330.

173. Le Floch F, Tessier B, Chenuet S, Guillaume J-M, Cans P, Marc A, Goergen J-L. HPCE monitoring of the N-glycosylation pattern and sialylation of murine erythropoietin produced by CHO cells in batch processes. Biotechnol Prog 2004; 20(3):864–871.

174. Borys MC, Linzer DI, Papoutsakis ET. Ammonia affects the glycosylation patterns of recombinant mouse placental lactogen-I by chinese hamster ovary cells in a pH-dependent manner. Biotechnol Bioeng 1994; 43(6):505–514.

175. Colosi P, Ogren L, Southard JN, Thordarson G, Linzer DI, Talamantes F. Biological, immunological, and binding properties of recombinant mouse placental lactogen-I. Endocrinology 1988; 123(6):2662–2667.

176. Andersen DC, Bridges T, Gawlitzek M, Hoy C. Multiple cell culture factors can affect the glycosylation of Asn-184 in CHO-produced tissue-type plasminogen activator. Biotechnol Bioeng 2000; 70(1):25–31.

177. Cole ES, Lee K, Lauziere K, Kelton C, Chappel S, Weintraub B, Ferrara D, Peterson P, Bernasconi R, Edmunds T. Recombinant human thyroid stimulating hormone: development of a biotechnology product for detection of metastatic lesions of thyroid carcinoma. Biotechnology (N Y) 1993; 11(9):1014–1024.

178. Yamashita K, Tachibana Y, Ohkura T, Kobata A. Enzymatic basis for the structural changes of asparagine-linked sugar chains of membrane glycoproteins of baby hamster kidney cells induced by polyoma transformation. J Biol Chem 1985; 260(7):3963–3969.

179. Howard DR, Fukuda M, Fukuda MN, Stanley P. The GDP-fucose:N-acetylglucosaminide 3-alpha-L-fucosyltransferases of LEC11 and LEC12 Chinese hamster ovary

mutants exhibit novel specificities for glycolipid substrates. J Biol Chem 1987; 262(35):16830–16837.

180. Prati EG, Scheidegger P, Sburlati AR, Bailey JE. Antisense strategies for glycosylation engineering of Chinese hamster ovary (CHO) cells. Biotechnol Bioeng 1998; 59(4):445–450.
181. Prati EG, Matasci M, Suter TB, Dinter A, Sburlati AR, Bailey JE. Engineering of coordinated up- and down-regulation of two glycosyltransferases of the O-glycosylation pathway in Chinese hamster ovary (CHO) cells. Biotechnol Bioeng 2000; 68(3):239–244.
182. Padler-Karavani V, Yu H, Cao H, Chokhawala H, Karp F, Varki N, Chen X, Varki A. Diversity in specificity, abundance, and composition of anti-Neu5Gc antibodies in normal humans: potential implications for disease. Glycobiology 2008; 18(10):818–830.
183. Fukuda MN, Sasaki H, Lopez L, Fukuda M. Survival of recombinant erythropoietin in the circulation: the role of carbohydrates. Blood 1989; 73(1):84–89.
184. Stockert RJ. The asialoglycoprotein receptor: relationships between structure, function, and expression. Physiol Rev 1995; 75(3):591–609.
185. Birch JR, Froud SJ. Mammalian cell culture systems for recombinant protein production. Biologicals 1994; 22(2):127–133.
186. Smith DF, Larsen RD, Mattox S, Lowe JB, Cummings RD. Transfer and expression of a murine UDP-Gal:beta-D-Gal-alpha 1,3-galactosyltransferase gene in transfected Chinese hamster ovary cells. Competition reactions between the alpha 1,3-galactosyltransferase and the endogenous alpha 2,3-sialyltransferase. J Biol Chem 1990; 265(11):6225–6234.
187. Leibiger H, Hansen A, Schoenherr G, Seifert M, Wüstner D, Stigler R, Marx U. Glycosylation analysis of a polyreactive human monoclonal IgG antibody derived from a human-mouse heterohybridoma. Mol Immunol 1995; 32(8):595–602.
188. Hills AE, Patel A, Boyd P, James DC. Metabolic control of recombinant monoclonal antibody N-glycosylation in GS-NS0 cells. Biotechnol Bioeng 2001; 75(2):239–251.
189. Rothman RJ, Warren L, Vliegenthart JF, Härd KJ. Clonal analysis of the glycosylation of immunoglobulin G secreted by murine hybridomas. Biochemistry 1989; 28(3):1377–1384.
190. Müthing J, Kemminer SE, Conradt HS, Sagi D, Nimtz M, Kärst U, Peter-Katalinić J. Effects of buffering conditions and culture pH on production rates and glycosylation of clinical phase I anti-melanoma mouse IgG3 monoclonal antibody R24. Biotechnol Bioeng 2003; 83(3):321–334.
191. Majid FAA, Butler M, Al-Rubeai M. Glycosylation of an immunoglobulin produced from a murine hybridoma cell line: the effect of culture mode and the anti-apoptotic gene, bcl-2. Biotechnol Bioeng 2007; 97(1):156–169.
192. Robinson DK, Chan CP, Yu lp C, Tsai PK, Tung J, Seamans TC, Lenny AB, Lee DK, Irwin J, Silberklang M. Characterization of a recombinant antibody produced in the course of a high yield fed-batch process. Biotechnol Bioeng 1994; 44(6):727–735.
193. Patel TP, Parekh RB, Moellering BJ, Prior CP. Different culture methods lead to differences in glycosylation of a murine IgG monoclonal antibody. Biochem J 1992; 285(Pt 3): 839–845.
194. Rossmann C, Sharp N, Allen G, Gewert D. Expression and purification of recombinant, glycosylated human interferon alpha 2b in murine myeloma NS0 cells. Protein Expr Purif 1996; 7(4):335–342.
195. Chung CH, Mirakhur B, Chan E, Quynh-Thu L, Berlin J, Morse M, Murphy BA, Satinover SM, Hosen J, Mauro D, Slebos RJ, Zhou Q, Gold D, Hatley T, Hicklin DJ, Platts-Mills TAE. Cetuximab-induced anaphylaxis and IgE specific for galactose-alpha-1,3-galactose. N Engl J Med 2008; 358(11):1109–1117.
196. Muchmore EA, Milewski M, Varki A, Diaz S. Biosynthesis of N-glycolyneuraminic acid: the primary site of hydroxylation of N-acetylneuraminic acid is the cytosolic sugar nucleotide pool. J Biol Chem 1989; 264(34):20216–20223.
197. Raju TS, Briggs JB, Borge SM, Jones AJ. Species-specific variation in glycosylation of IgG: evidence for the species-specific sialylation and branch-specific galactosylation and importance for engineering recombinant glycoprotein therapeutics. Glycobiology 2000; 10(5):477–486.
198. Dasgupta S, Navarrete A-M, Bayry J, Delignat S, Wootla B, André S, Christophe O, Nascimbeni M, Jacquemin M, Martinez-Pomares L, Geijtenbeek TBH, Moris A, Saint-Remy J-M, Kazatchkine MD, Kaveri SV, Lacroix-Desmazes S. A role for exposed mannosylations in presentation of human therapeutic self-proteins to CD4+ T lymphocytes. Proc Natl Acad Sci USA 2007; 104(21):8965–8970.
199. Lam JS, Huang H, Levitz SM. Effect of differential N-linked and O-linked mannosylation on recognition of fungal antigens by dendritic cells. PLoS One 2007; 2(10):e1009.
200. Millward TA, Heitzmann M, Bill K, Längle U, Schumacher P, Forrer K. Effect of constant and variable domain glycosylation on pharmacokinetics of therapeutic antibodies in mice. Biologicals 2008; 36(1):41–47.
201. Lopez M, Tetaert D, Juliant S, Gazon M, Cerutti M, Verbert A, Delannoy P. O-glycosylation potential of lepidopteran insect cell lines. Biochim Biophys Acta 1999; 1427(1):49–61.
202. Betenbaugh MJ, Tomiya N, Narang S, Hsu JT, Lee YC. Biosynthesis of human-type N-glycans in heterologous systems. Curr Opin Struct Biol 2004; 14(5):601–606.
203. Altmann F, Kornfeld G, Dalik T, Staudacher E, Glössl J. Processing of asparagine-linked oligosaccharides in insect cells. N-acetylglucosaminyltransferase I and II activities in cultured lepidopteran cells. Glycobiology 1993; 3(6):619–625.
204. Die I, Tetering A, Bakker H, Eijnden DH, Joziasse DH. Glycosylation in lepidopteran insect cells: identification of a beta 1–>4-N-acetylgalactosaminyltransferase involved in the synthesis of complex-type oligosaccharide chains. Glycobiology 1996; 6(2):157–164.
205. Hollister JR, Shaper JH, Jarvis DL. Stable expression of mammalian beta 1,4-galactosyltransferase extends the N-glycosylation pathway in insect cells. Glycobiology 1998; 8(5):473–480.
206. Hollister JR, Jarvis DL. Engineering lepidopteran insect cells for sialoglycoprotein production by genetic transformation with mammalian beta 1,4-galactosyltransferase and alpha 2,6-sialyltransferase genes. Glycobiology 2001; 11(1):1–9.

207. Wagner R, Geyer H, Geyer R, Klenk HD. N-acetyl-beta-glucosaminidase accounts for differences in glycosylation of influenza virus hemagglutinin expressed in insect cells from a baculovirus vector. J Virol 1996; 70(6):4103–4109.

208. Gutternigg M, Kretschmer-Lubich D, Paschinger K, Rendić D, Hader J, Geier P, Ranftl R, Jantsch V, Lochnit G, Wilson IBH. Biosynthesis of truncated N-linked oligosaccharides results from non-orthologous hexosaminidase-mediated mechanisms in nematodes, plants, and insects. J Biol Chem 2007; 282(38):27825–27840.

209. Wilson IBH. Glycosylation of proteins in plants and invertebrates. Curr Opin Struct Biol 2002; 12(5):569–577.

210. Seppo A, Tiemeyer M. Function and structure of Drosophila glycans. Glycobiology 2000; 10(8):751–760.

211. Harrison RL, Jarvis DL. Protein N-glycosylation in the baculovirus-insect cell expression system and engineering of insect cells to produce "mammalianized" recombinant glycoproteins. Adv Virus Res 2006; 68:159–191.

212. Kim YKyu, Shin HS, Tomiya N, Lee YC, Betenbaugh MJ, Cha HJ. Production and N-glycan analysis of secreted human erythropoietin glycoprotein in stably transfected Drosophila S2 cells. Biotechnol Bioeng 2005; 92(4):452–461.

213. Marchal I, Jarvis DL, Cacan R, Verbert A. Glycoproteins from insect cells: sialylated or not? Biol Chem 2001; 382(2):151–159.

214. Ailor E, Takahashi N, Tsukamoto Y, Masuda K, Rahman BA, Jarvis DL, Lee YC, Betenbaugh MJ. N-glycan patterns of human transferrin produced in Trichoplusia ni insect cells: effects of mammalian galactosyltransferase. Glycobiology 2000; 10(8):837–847.

215. Fabini G, Freilinger A, Altmann F, Wilson IB. Identification of core alpha 1,3-fucosylated glycans and cloning of the requisite fucosyltransferase cDNA from Drosophila melanogaster. Potential basis of the neural anti-horseadish peroxidase epitope. J Biol Chem 2001; 276(30):28058–28067.

216. Lawrence SM, Huddleston KA, Tomiya N, Nguyen N, Lee YC, Vann WF, Coleman TA, Betenbaugh MJ. Cloning and expression of human sialic acid pathway genes to generate CMP-sialic acids in insect cells. Glycoconj J 2001; 18(3):205–213.

217. Aumiller JJ, Hollister JR, Jarvis DL. A transgenic insect cell line engineered to produce CMP-sialic acid and sialylated glycoproteins. Glycobiology 2003; 13(6):497–507.

218. Seo NS, Hollister JR, Jarvis DL. Mammalian glycosyltransferase expression allows sialoglycoprotein production by baculovirus-infected insect cells. Protein Expr Purif 2001; 22(2):234–241.

219. Kramerov AA, Arbatsky NP, Rozovsky YM, Mikhaleva EA, Polesskaya OO, Gvozdev VA, Shibaev VN. Mucin-type glycoprotein from Drosophila melanogaster embryonic cells: characterization of carbohydrate component. FEBS Lett 1996; 378(3):213–218.

220. Guérardel Y, Balanzino L, Maes E, Leroy Y, Coddeville B, Oriol R, Strecker G. The nematode Caenorhabditis elegans synthesizes unusual O-linked glycans: identification of glucose-substituted mucin-type O-glycans and short chondroitin-like oligosaccharides. Biochem J 2001; 357(Pt 1): 167–182.

221. Thomsen DR, Post LE, Elhammer AP. Structure of O-glycosidically linked oligosaccharides synthesized by the insect cell line Sf9. J Cell Biochem 1990; 43(1):67–79.

222. Lopez M, Gazon M, Juliant S, Plancke Y, Leroy Y, Strecker G, Cartron JP, Bailly P, Cerutti M, Verbert A, Delannoy P. Characterization of a UDP-Gal:Galbeta1-3GalNAc alpha1, 4-galactosyltransferase activity in a Mamestra brassicae cell line. J Biol Chem 1998; 273(50):33644–33651.

223. Bardor M, Faveeuw C, Fitchette A-C, Gilbert D, Galas L, Trottein F, Faye L, Lerouge P. Immunoreactivity in mammals of two typical plant glyco-epitopes, core alpha(1,3)-fucose and core xylose. Glycobiology 2003; 13(6):427–434.

224. Bencúrová M, Hemmer W, Focke-Tejkl M, Wilson IBH, Altmann F. Specificity of IgG and IgE antibodies against plant and insect glycoprotein glycans determined with artificial glycoforms of human transferrin. Glycobiology 2004; 14(5):457–466.

225. Bardor M, Loutelier-Bourhis C, Paccalet T, Cosette P, Fitchette A-C, Vézina L-P, Trépanier S, Dargis M, Lemieux R, Lange C, Faye L, Lerouge P. Monoclonal C5-1 antibody produced in transgenic alfalfa plants exhibits a N-glycosylation that is homogenous and suitable for glyco-engineering into human-compatible structures. Plant Biotechnol J 2003; 1(6):451–462.

226. Samyn-Petit B, Dubos J-PW, Chirat F, Coddeville B, Demaizieres G, Farrer S, Slomianny M-C, Theisen M, Delannoy P. Comparative analysis of the site-specific N-glycosylation of human lactoferrin produced in maize and tobacco plants. Eur J Biochem 2003; 270(15):3235–3242.

227. Zeleny R, Altmann F, Praznik W. Structural characterization of the N-linked oligosaccharides from tomato fruit. Phytochemistry 1999; 51(2):199–210.

228. Karg SR, Kallio PT. The production of biopharmaceuticals in plant systems. Biotechnol Adv 2009; 27(6):879–894.

229. Strasser R, Mucha J, Mach L, Altmann F, Wilson IB, Glössl J, Steinkellner H. Molecular cloning and functional expression of beta1, 2-xylosyltransferase cDNA from Arabidopsis thaliana. FEBS Lett 2000; 472(1):105–108.

230. Lerouge P, Cabanes-Macheteau M, Rayon C, Fischette-Lainé AC, Gomord V, Faye L. N-glycoprotein biosynthesis in plants: recent developments and future trends. Plant Mol Biol 1998; 38(1–2):31–48.

231. Jin C, Altmann F, Strasser R, Mach L, Schähs M, Kunert R, Rademacher T, Glössl J, Steinkellner H. A plant-derived human monoclonal antibody induces an anti-carbohydrate immune response in rabbits. Glycobiology 2008; 18(3):235–241.

232. Gomord V, Chamberlain P, Jefferis R, Faye L. Biopharmaceutical production in plants: problems, solutions and opportunities. Trends Biotechnol 2005; 23(11):559–565.

233. Bakker H, Bardor M, Molthoff JW, Gomord V, Elbers I, Stevens LH, Jordi W, Lommen A, Faye L, Lerouge P, Bosch D. Galactose-extended glycans of antibodies produced by transgenic plants. Proc Natl Acad Sci USA 2001; 98(5):2899–2904.

234. Séveno M, Bardor M, Paccalet T, Gomord V, Lerouge P, Faye L. Glycoprotein sialylation in plants? Nat Biotechnol 2004; 22(11):1351–1352; author reply; 1352–1353.

235. Zeleny R, Kolarich D, Strasser R, Altmann F. Sialic acid concentrations in plants are in the range of inadvertent contamination. Planta 2006; 224(1):222–227.

236. Fitchette-Lainé AC, Gomord V, Cabanes M, Michalski JC, Macary MSaint, Foucher B, Cavelier B, Hawes C, Lerouge P, Faye L. N-glycans harboring the Lewis a epitope are expressed at the surface of plant cells. Plant J 1997; 12(6):1411–1417.

237. Léonard R, Costa G, Darrambide E, Lhernould S, Fleurat-Lessard P, Carlué M, Gomord V, Faye L, Maftah A. The presence of Lewis a epitopes in Arabidopsis thaliana glycoconjugates depends on an active alpha4-fucosyltransferase gene. Glycobiology 2002; 12(5):299–306.

238. Melo NS, Nimtz M, Conradt HS, Fevereiro PS, Costa J. Identification of the human Lewis(a) carbohydrate motif in a secretory peroxidase from a plant cell suspension culture (Vaccinium myrtillus L.). FEBS Lett 1997; 415(2):186–191.

239. Fötisch K, Vieths S. N- and O-linked oligosaccharides of allergenic glycoproteins. Glycoconj J 2001; 18(5):373–390.

240. Tan L, Qiu F, Lamport DTA, Kieliszewski MJ. Structure of a hydroxyproline (Hyp)-arabinogalactan polysaccharide from repetitive Ala-Hyp expressed in transgenic Nicotiana tabacum. J Biol Chem 2004; 279(13):13156–13165.

241. Xu J, Okada S, Tan L, Goodrum KJ, Kopchick JJ, Kieliszewski MJ. Human growth hormone expressed in tobacco cells as an arabinogalactan-protein fusion glycoprotein has a prolonged serum life. Transgenic Res 2010; 19(5):849–867.

242. Ree R, Aalberse RC. Demonstration of carbohydrate-specific immunoglobulin G4 antibodies in sera of patients receiving grass pollen immunotherapy. Int Arch Allergy Immunol 1995; 106(2):146–148.

243. Wilson IB, Harthill JE, Mullin NP, Ashford DA, Altmann F. Core alpha1,3-fucose is a key part of the epitope recognized by antibodies reacting against plant N-linked oligosaccharides and is present in a wide variety of plant extracts. Glycobiology 1998; 8(7):651–661.

244. Cabanes-Macheteau M, Fitchette-Lainé AC, Loutelier-Bourhis C, Lange C, Vine ND, Ma JK, Lerouge P, Faye L. N-Glycosylation of a mouse IgG expressed in transgenic tobacco plants. Glycobiology 1999; 9(4):365–372.

245. Chargelegue D, Vine ND, van Dolleweerd CJ, Drake PM, Ma JK. A murine monoclonal antibody produced in transgenic plants with plant-specific glycans is not immunogenic in mice. Transgenic Res 2000; 9(3):187–194.

246. Aalberse RC, Koshte V, Clemens JG. Immunoglobulin E antibodies that crossreact with vegetable foods, pollen, and Hymenoptera venom. J Allergy Clin Immunol 1981; 68(5):356–364.

247. Davoodi-Semiromi A, Samson N, Daniell H. The green vaccine: a global strategy to combat infectious and autoimmune diseases. Hum Vaccin 2009; 5(7):488–493.

248. Shaaltiel Y, Bartfeld D, Hashmueli S, Baum G, Brill-Almon E, Galili G, Dym O, Boldin-Adamsky SA, Silman I, Sussman JL, Futerman AH, Aviezer D. Production of glucocerebrosidase with terminal mannose glycans for enzyme replacement therapy of Gaucher's disease using a plant cell system. Plant Biotechnol J 2007; 5(5):579–590.

249. Kornfeld R, Kornfeld S. Assembly of asparagine-linked oligosaccharides. Annu Rev Biochem 1985; 54:631–664.

250. Trimble RB, Atkinson PH. Structure of yeast external invertase Man8-14GlcNAc processing intermediates by 500-megahertz 1H NMR spectroscopy. J Biol Chem 1986; 261(21):9815–9824.

251. Tarentino AL, Plummer TH, Maley F. The release of intact oligosaccharides from specific glycoproteins by endo-beta-N-acetylglucosaminidase H. J Biol Chem 1974; 249(3):818–824.

252. Verostek MF, Atkinson PH, Trimble RB. Glycoprotein biosynthesis in the alg3 Saccharomyces cerevisiae mutant. II. Structure of novel Man6-10GlcNAc2 processing intermediates on secreted invertase. J Biol Chem 1993; 268(16):12104–12115.

253. Ballou CE. Isolation, characterization, and properties of Saccharomyces cerevisiae mnn mutants with nonconditional protein glycosylation defects. Methods Enzymol 1990; 185:440–470.

254. Bretthauer RK, Castellino FJ. Glycosylation of Pichia pastoris-derived proteins. Biotechnol Appl Biochem 1999; 30(Pt 3): 193–200.

255. Grinna LS, Tschopp JF. Size distribution and general structural features of N-linked oligosaccharides from the methylotrophic yeast, Pichia pastoris. Yeast 1989; 5(2):107–115.

256. Livi GP, Ferrara AA, Roskin R, Simon PL, Young PR. Secretion of N-glycosylated human recombinant interleukin-1 alpha in Saccharomyces cerevisiae. Gene 1990; 88(2):297–301.

257. Lommel M, Strahl S. Protein O-mannosylation: conserved from bacteria to humans. Glycobiology 2009; 19(8):816–828.

258. HÅrd K, Bitter W, Kamerling JP, Vliegenthart JF. O-mannosylation of recombinant human insulin-like growth factor I (IGF-I) produced in Saccharomyces cerevisiae. FEBS Lett 1989; 248(1–2):111–114.

259. Wright A, Morrison SL. Effect of altered CH2-associated carbohydrate structure on the functional properties and in vivo fate of chimeric mouse-human immunoglobulin G1. J Exp Med 1994; 180(3):1087–1096.

260. Walsh G. Biopharmaceutical benchmarks 2006. Nat Biotechnol 2006; 24(7):769–776.

261. Schäffer C, Graninger M, Messner P. Prokaryotic glycosylation. Proteomics 2001; 1(2):248–261.

262. Brooks SA. Appropriate glycosylation of recombinant proteins for human use: implications of choice of expression system. Mol Biotechnol 2004; 28(3):241–255.

263. Abu-Qarn M, Eichler J, Sharon N. Not just for Eukarya anymore: protein glycosylation in Bacteria and Archaea. Curr Opin Struct Biol 2008; 18(5):544–550.

264. Jones MB, Rosenberg JN, Betenbaugh MJ, Krag SS. Structure and synthesis of polyisoprenoids used in N-glycosylation across the three domains of life. Biochim Biophys Acta 2009; 1790(6):485–494.

265. Kuo C, Takahashi N, Swanson AF, Ozeki Y, Hakomori S. An N-linked high-mannose type oligosaccharide, expressed at the major outer membrane protein of Chlamydia trachomatis, mediates attachment and infectivity of the microorganism to HeLa cells. J Clin Invest 1996; 98(12):2813–2818.

266. Wacker M, Linton D, Hitchen PG, Nita-Lazar M, Haslam SM, North SJ, Panico M, Morris HR, Dell A, Wren BW, Aebi M. N-linked glycosylation in Campylobacter jejuni and its functional transfer into E. coli. Science 2002; 298(5599):1790–1793.

267. Benz I, Schmidt MA. Never say never again: protein glycosylation in pathogenic bacteria. Mol Microbiol 2002; 45(2):267–276.

268. Sartain MJ, Belisle JT. N-Terminal clustering of the O-glycosylation sites in the Mycobacterium tuberculosis lipoprotein SodC. Glycobiology 2009; 19(1):38–51.

269. Castric P, Cassels FJ, Carlson RW. Structural characterization of the Pseudomonas aeruginosa 1244 pilin glycan. J Biol Chem 2001; 276(28):26479–26485.

270. Goelz S, Kumar R, Potvin B, Sundaram S, Brickelmaier M, Stanley P. Differential expression of an E-selectin ligand (SLex) by two Chinese hamster ovary cell lines transfected with the same alpha (1,3)-fucosyltransferase gene (ELFT). J Biol Chem 1994; 269(2):1033–1040.

271. Valli M, Bardoni A, Trinchera M. Mouse C127 cells transfected with fucosyltransferase fuc-TIII express masked Lewisx but not Lewisx antigen. Glycobiology 1999; 9(1):83–91.

272. Beuger V, Künkele K-P, Koll H, Gärtner A, Bähner M, Burtscher H, Klein C. Short-hairpin-RNA-mediated silencing of fucosyltransferase 8 in Chinese-hamster ovary cells for the production of antibodies with enhanced antibody immune effector function. Biotechnol Appl Biochem 2009; 53(Pt 1): 31–37.

273. Imai-Nishiya H, Mori K, Inoue M, Wakitani M, Iida S, Shitara K, Satoh M. Double knockdown of alpha1,6-fucosyltransferase (FUT8) and GDP-mannose 4,6-dehydratase (GMD) in antibody-producing cells: a new strategy for generating fully non-fucosylated therapeutic antibodies with enhanced ADCC. BMC Biotechnol 2007; 7:84.

274. Kanda Y, Yamane-Ohnuki N, Sakai N, Yamano K, Nakano R, Inoue M, Misaka H, Iida S, Wakitani M, Konno Y, Yano K, Shitara K, Hosoi S, Satoh M. Comparison of cell lines for stable production of fucose-negative antibodies with enhanced ADCC. Biotechnol Bioeng 2006; 94(4):680–688.

275. Mori K, Kuni-Kamochi R, Yamane-Ohnuki N, Wakitani M, Yamano K, Imai H, Kanda Y, Niwa R, Iida S, Uchida K, Shitara K, Satoh M. Engineering Chinese hamster ovary cells to maximize effector function of produced antibodies using FUT8 siRNA. Biotechnol Bioeng 2004; 88(7):901–908.

276. Yamane-Ohnuki N, Kinoshita S, Inoue-Urakubo M, Kusunoki M, Iida S, Nakano R, Wakitani M, Niwa R, Sakurada M, Uchida K, Shitara K, Satoh M. Establishment of FUT8 knockout Chinese hamster ovary cells: an ideal host cell line for producing completely defucosylated antibodies with enhanced antibody-dependent cellular cytotoxicity. Biotechnol Bioeng 2004; 87(5):614–622.

277. Jeong YT, Choi O, Lim HR, Son YD, Kim HJ, Kim JH. Enhanced sialylation of recombinant erythropoietin in CHO cells by human glycosyltransferase expression. J Microbiol Biotechnol 2008; 18(12):1945–1952.

278. Jeong YT, Choi O, Son YD, Park SY, Kim JH. Enhanced sialylation of recombinant erythropoietin in genetically engineered Chinese-hamster ovary cells. Biotechnol Appl Biochem 2009; 52(Pt 4): 283–291.

279. Fukuta K, Yokomatsu T, Abe R, Asanagi M, Makino T. Genetic engineering of CHO cells producing human interferon-gamma by transfection of sialyltransferases. Glycoconj J 2000; 17(12):895–904.

280. Bragonzi A, Distefano G, Buckberry LD, Acerbis G, Foglieni C, Lamotte D, Campi G, Marc A, Soria MR, Jenkins N, Monaco L. A new Chinese hamster ovary cell line expressing alpha2,6-sialyltransferase used as universal host for the production of human-like sialylated recombinant glycoproteins. Biochim Biophys Acta 2000; 1474(3):273–282.

281. Jenkins N, Buckberry L, Marc A, Monaco L. Genetic engineering of alpha 2,6-sialyltransferase in recombinant CHO cells. Biochem Soc Trans 1998; 26(2):S115.

282. Lee EU, Roth J, Paulson JC. Alteration of terminal glycosylation sequences on N-linked oligosaccharides of Chinese hamster ovary cells by expression of beta-galactoside alpha 2,6-sialyltransferase. J Biol Chem 1989; 264(23):13848–13855.

283. Monaco L, Marc A, Eon-Duval A, Acerbis G, Distefano G, Lamotte D, Engasser J-M, Soria M, Jenkins N. Genetic engineering of α-2,6-sialyltransferase in recombinant CHO cells and its effects on the sialylation of recombinant interferon-gamma. Cytotechnology 1996; 22:197–203.

284. Schlenke P, Grabenhorst E, Nimtz M, Conradt HS. Construction and characterization of stably transfected BHK-21 cells with human-type sialylation characteristic. Cytotechnology 1999; 30(1–3):17–25.

285. Jassal R, Jenkins N, Charlwood J, Camilleri P, Jefferis R, Lund J. Sialylation of human IgG-Fc carbohydrate by transfected rat alpha2,6-sialyltransferase. Biochem Biophys Res Commun 2001; 286(2):243–249.

286. Chitlaru T, Kronman C, Zeevi M, Kam M, Harel A, Ordentlich A, Velan B, Shafferman A. Modulation of circulatory residence of recombinant acetylcholinesterase through biochemical or genetic manipulation of sialylation levels. Biochem J 1998; 336(Pt 3): 647–658.

287. Chitlaru T, Kronman C, Velan B, Shafferman A. Overloading and removal of N-glycosylation targets on human acetylcholinesterase: effects on glycan composition and circulatory residence time. Biochem J 2002; 363(Pt 3): 619–631.

288. Fukuta K, Abe R, Yokomatsu T, Omae F, Asanagi M, Makino T. Control of bisecting GlcNAc addition to N-linked sugar chains. J Biol Chem 2000; 275(31):23456–23461.

289. Chenu S, Grégoire A, Malykh Y, Visvikis A, Monaco L, Shaw L, Schauer R, Marc A, Goergen J-L. Reduction of CMP-N-acetylneuraminic acid hydroxylase activity in engineered Chinese hamster ovary cells using an antisense-RNA strategy. Biochim Biophys Acta 2003; 1622(2):133–144.

290. Wong NSC, Yap MGS, Wang DIC. Enhancing recombinant glycoprotein sialylation through CMP-sialic acid transporter over expression in Chinese hamster ovary cells. Biotechnol Bioeng 2006; 93(5):1005–1016.

291. Kanda Y, Imai-Nishiya H, Kuni-Kamochi R, Mori K, Inoue M, Kitajima-Miyama K, Okazaki A, Iida S, Shitara K, Satoh M. Establishment of a GDP-mannose 4,6-dehydratase (GMD) knockout host cell line: a new strategy for generating completely non-fucosylated recombinant therapeutics. J Biotechnol 2007; 130(3):300–310.

292. Davies J, Jiang L, Pan LZ, LaBarre MJ, Anderson D, Reff M. Expression of GnTIII in a recombinant anti-CD20 CHO production cell line: Expression of antibodies with altered glycoforms leads to an increase in ADCC through higher affinity for FC gamma RIII. Biotechnol Bioeng 2001; 74(4):288–294.

293. Ferrara C, Brünker P, Suter T, Moser S, Püntener U, Umaàna P. Modulation of therapeutic antibody effector functions by glycosylation engineering: influence of Golgi enzyme localization domain and co-expression of heterologous beta1, 4-N-acetylglucosaminyltransferase III and Golgi alpha-mannosidase II. Biotechnol Bioeng 2006; 93(5):851–861.

294. Umaàna P, Jean-Mairet J, Bailey JE. Tetracycline-regulated overexpression of glycosyltransferases in Chinese hamster ovary cells. Biotechnol Bioeng 1999; 65(5):542–549.

295. Fukuta K, Abe R, Yokomatsu T, Kono N, Asanagi M, Omae F, Minowa MT, Takeuchi M, Makino T. Remodeling of sugar chain structures of human interferon-gamma. Glycobiology 2000; 10(4):421–430.

296. Ferrari J, Gunson J, Lofgren J, Krummen L, Warner TG. Chinese hamster ovary cells with constitutively expressed sialidase antisense RNA produce recombinant DNase in batch culture with increased sialic acid. Biotechnol Bioeng 1998; 60(5):589–595.

297. Minch SL, Kallio PT, Bailey JE. Tissue plasminogen activator coexpressed in Chinese hamster ovary cells with alpha(2,6)-sialyltransferase contains NeuAc alpha(2,6)Gal beta(1,4)Glc-N-AcR linkages. Biotechnol Prog 1995; 11(3):348–351.

298. Iida S, Misaka H, Inoue M, Shibata M, Nakano R, Yamane-Ohnuki N, Wakitani M, Yano K, Shitara K, Satoh M. Nonfucosylated therapeutic IgG1 antibody can evade the inhibitory effect of serum immunoglobulin G on antibody-dependent cellular cytotoxicity through its high binding to FcgammaRIIIa. Clin Cancer Res 2006; 12(9):2879–2887.

299. Satoh M, Iida S, Shitara K. Non-fucosylated therapeutic antibodies as next-generation therapeutic antibodies. Expert Opin Biol Ther 2006; 6(11):1161–1173.

300. Ohyama C, Smith PL, Angata K, Fukuda MN, Lowe JB, Fukuda M. Molecular cloning and expression of GDP-D-mannose-4,6-dehydratase, a key enzyme for fucose metabolism defective in Lec13 cells. J Biol Chem 1998; 273(23):14582–14587.

301. Reik A, Zhou Y, Collingwood TN, Warfe L, Bartsevich V, Kong Y, Henning KA, Fallentine BK, Zhang L, Zhong X, Jouvenot Y, Jamieson AC, Rebar EJ, Case CC, Korman A, Xiao-Yong L, Black A, King DJ, Gregory PD. Enhanced protein production by engineered zinc finger proteins. Biotechnol Bioeng 2007; 97(5):1180–1189.

302. Santiago Y, Chan E, Liu P-Q, Orlando S, Zhang L, Urnov FD, Holmes MC, Guschin D, Waite A, Miller JC, Rebar EJ, Gregory PD, Klug A, Collingwood TN. Targeted gene knockout in mammalian cells by using engineered zinc-finger nucleases. Proc Natl Acad Sci USA 2008; 105(15):5809–5814.

303. Wagner R, Liedtke S, Kretzschmar E, Geyer H, Geyer R, Klenk HD. Elongation of the N-glycans of fowl plague virus hemagglutinin expressed in Spodoptera frugiperda (Sf9) cells by coexpression of human beta 1,2-N-acetylglucosaminyltransferase I. Glycobiology 1996; 6(2):165–175.

304. Jarvis DL, Finn EE. Modifying the insect cell N-glycosylation pathway with immediate early baculovirus expression vectors. Nat Biotechnol 1996; 14(10):1288–1292.

305. Breitbach K, Jarvis DL. Improved glycosylation of a foreign protein by Tn-5B1-4 cells engineered to express mammalian glycosyltransferases. Biotechnol Bioeng 2001; 74(3):230–239.

306. Jarvis DL, Howe D, Aumiller JJ. Novel baculovirus expression vectors that provide sialylation of recombinant glycoproteins in lepidopteran insect cells. J Virol 2001; 75(13):6223–6227.

307. Hollister J, Grabenhorst E, Nimtz M, Conradt H, Jarvis DL. Engineering the protein N-glycosylation pathway in insect cells for production of biantennary, complex N-glycans. Biochemistry 2002; 41(50):15093–15104.

308. Viswanathan K, Lawrence S, Hinderlich S, Yarema KJ, Lee YC, Betenbaugh MJ. Engineering sialic acid synthetic ability into insect cells: identifying metabolic bottlenecks and devising strategies to overcome them. Biochemistry 2003; 42(51):15215–15225.

309. Tomiya N, Howe D, Aumiller JJ, Pathak M, Park J, Palter KB, Jarvis DL, Betenbaugh MJ, Lee YC. Complex-type biantennary N-glycans of recombinant human transferrin from Trichoplusia ni insect cells expressing mammalian [beta]-1,4-galactosyltransferase and [beta]-1,2-N-acetylglucosaminyltransferase II. Glycobiology 2003; 13(1):23–34.

310. Benchabane M, Saint-Jore-Dupas C, Bardor M, Faye L, Michaud D, Gomord V. Targeting and post-translational processing of human alpha1-antichymotrypsin in BY-2 tobacco cultured cells. Plant Biotechnol J 2009; 7(2):146–160.

311. Ko K, Tekoah Y, Rudd PM, Harvey DJ, Dwek RA, Spitsin S, Hanlon CA, Rupprecht C, Dietzschold B, Golovkin M, Koprowski H. Function and glycosylation of plant-derived antiviral monoclonal antibody. Proc Natl Acad Sci USA 2003; 100(13):8013–8018.

312. Tekoah Y, Ko K, Koprowski H, Harvey DJ, Wormald MR, Dwek RA, Rudd PM. Controlled glycosylation of therapeutic antibodies in plants. Arch Biochem Biophys 2004; 426(2):266–278.

313. Triguero A, Cabrera G, Cremata JA, Yuen C-T, Wheeler J, Ramírez NI. Plant-derived mouse IgG monoclonal antibody fused to KDEL endoplasmic reticulum-retention signal is N-glycosylated homogeneously throughout the plant with mostly high-mannose-type N-glycans. Plant Biotechnol J 2005; 3(4):449–457.

314. Triguero A, Cabrera G, Royle L, Harvey DJ, Rudd PM, Dwek RA, Bardor M, Lerouge P, Cremata JA. Chemical and enzymatic N-glycan release comparison for N-glycan profiling of monoclonal antibodies expressed in plants. Anal Biochem 2010; 400(2):173–183.

315. Rademacher T, Sack M, Arcalis E, Stadlmann J, Balzer S, Altmann F, Quendler H, Stiegler G, Kunert R, Fischer R, Stoger E. Recombinant antibody 2G12 produced in maize endosperm efficiently neutralizes HIV-1 and contains predominantly single-GlcNAc N-glycans. Plant Biotechnol J 2008; 6(2):189–201.

316. Strasser R, Altmann F, Mach L, Glössl J, Steinkellner H. Generation of Arabidopsis thaliana plants with complex N-glycans lacking beta1,2-linked xylose and core alpha1,3-linked fucose. FEBS Lett 2004; 561(1–3):132–136.

317. Schähs M, Strasser R, Stadlmann J, Kunert R, Rademacher T, Steinkellner H. Production of a monoclonal antibody in plants with a humanized N-glycosylation pattern. Plant Biotechnol J 2007; 5(5):657–663.

318. Sourrouille C, Marquet-Blouin E, D'Aoust M-A, Kiefer-Meyer M-C, Seveno M, Pagny-Salehabadi S, Bardor M, Durambur G, Lerouge P, Vezina L, Gomord V. Down-regulated expression of plant-specific glycoepitopes in alfalfa. Plant Biotechnol J 2008; 6(7):702–721.

319. Strasser R, Stadlmann J, Schähs M, Stiegler G, Quendler H, Mach L, Glössl J, Weterings K, Pabst M, Steinkellner H. Generation of glyco-engineered Nicotiana benthamiana for the production of monoclonal antibodies with a homogeneous human-like N-glycan structure. Plant Biotechnol J 2008; 6(4):392–402.

320. Cox KM, Sterling JD, Regan JT, Gasdaska JR, Frantz KK, Peele CG, Black A, Passmore D, Moldovan-Loomis C, Srinivasan M, Cuison S, Cardarelli PM, Dickey LF. Glycan optimization of a human monoclonal antibody in the aquatic plant Lemna minor. Nat Biotechnol 2006; 24(12):1591–1597.

321. Koprivova A, Stemmer C, Altmann F, Hoffmann A, Kopriva S, Gorr G, Reski R, Decker EL. Targeted knockouts of Physcomitrella lacking plant-specific immunogenic N-glycans. Plant Biotechnol J 2004; 2(6):517–523.

322. Weise A, Altmann F, Rodriguez-Franco M, Sjoberg ER, Bäumer W, Launhardt H, Kietzmann M, Gorr G. High-level expression of secreted complex glycosylated recombinant human erythropoietin in the Physcomitrella Delta-fuc-t Delta-xyl-t mutant. Plant Biotechnol J 2007; 5(3):389–401.

323. Schuster M, Jost W, Mudde GC, Wiederkum S, Schwager C, Janzek E, Altmann F, Stadlmann J, Stemmer C, Gorr G. In vivo glyco-engineered antibody with improved lytic potential produced by an innovative non-mammalian expression system. Biotechnol J 2007; 2(6):700–708.

324. Huether CM, Lienhart O, Baur A, Stemmer C, Gorr G, Reski R, Decker EL. Glyco-engineering of moss lacking plant-specific sugar residues. Plant Biol (Stuttg) 2005; 7(3):292–299.

325. Ikeda Y, Taniguchi N. Enzymatic Properties and Biological Functions of beta 1,4-N-Acetylglucosaminyltransferase III. Trends Glycosci Glycotechnol 2001; 13(70):167–176.

326. Narasimhan S. Control of glycoprotein synthesis. UDP-GlcNAc:glycopeptide beta 4-N-acetylglucosaminyltransferase III, an enzyme in hen oviduct which adds GlcNAc in beta 1–4 linkage to the beta-linked mannose of the trimannosyl core of N-glycosyl oligosaccharides. J Biol Chem 1982; 257(17):10235–10242.

327. Rouwendal GJA, Wuhrer M, Florack DEA, Koeleman CAM, Deelder AM, Bakker H, Stoopen GM, Die I, Helsper JPFG, Hokke CH, Bosch D. Efficient introduction of a bisecting GlcNAc residue in tobacco N-glycans by expression of the gene encoding human N-acetylglucosaminyltransferase III. Glycobiology 2007; 17(3):334–344.

328. Frey AD, Karg SR, Kallio PT. Expression of rat beta(1,4)-N-acetylglucosaminyltransferase III in Nicotiana tabacum remodels the plant-specific N-glycosylation. Plant Biotechnol J 2009; 7(1):33–48.

329. Palacpac NQ, Yoshida S, Sakai H, Kimura Y, Fujiyama K, Yoshida T, Seki T. Stable expression of human beta1,4-galactosyltransferase in plant cells modifies N-linked glycosylation patterns. Proc Natl Acad Sci USA 1999; 96(8):4692–4697.

330. Fujiyama K, Palacpac NQ, Sakai H, Kimura Y, Shinmyo A, Yoshida T, Seki T. In vivo conversion of a glycan to human compatible type by transformed tobacco cells. Biochem Biophys Res Commun 2001; 289(2):553–557.

331. Fujiyama K, Furukawa A, Katsura A, Misaki R, Omasa T, Seki T. Production of mouse monoclonal antibody with galactose-extended sugar chain by suspension cultured tobacco BY2 cells expressing human beta(1,4)-galactosyltransferase. Biochem Biophys Res Commun 2007; 358(1):85–91.

332. Pagny S, Bouissonnie F, Sarkar M, Follet-Gueye ML, Driouich A, Schachter H, Faye L, Gomord V. Structural requirements for Arabidopsis beta1,2-xylosyltransferase activity and targeting to the Golgi. Plant J 2003; 33(1):189–203.

333. Bakker H, Rouwendal GJA, Karnoup AS, Florack DEA, Stoopen GM, Helsper JPFG, Ree R, Die I, Bosch D. An antibody produced in tobacco expressing a hybrid beta-1,4-galactosyltransferase is essentially devoid of plant carbohydrate epitopes. Proc Natl Acad Sci USA 2006; 103(20):7577–7582.

334. Vézina L-P, Faye L, Lerouge P, D'Aoust M-A, Marquet-Blouin E, Burel C, Lavoie P-O, Bardor M, Gomord V. Transient co-expression for fast and high-yield production of antibodies with human-like N-glycans in plants. Plant Biotechnol J 2009; 7(5):442–455.

335. Misaki R, Fujiyama K, Seki T. Expression of human CMP-N-acetylneuraminic acid synthetase and CMP-sialic acid transporter in tobacco suspension-cultured cell. Biochem Biophys Res Commun 2006; 339(4):1184–1189.

336. Paccalet T, Bardor M, Rihouey C, Delmas F, Chevalier C, D'Aoust M-A, Faye L, Vézina L, Gomord V, Lerouge P. Engineering of a sialic acid synthesis pathway in transgenic plants by expression of bacterial Neu5Ac-synthesizing enzymes. Plant Biotechnol J 2007; 5(1):16–25.

337. Castilho A, Pabst M, Leonard R, Veit C, Altmann F, Mach L, Glössl J, Strasser R, Steinkellner H. Construction of a functional CMP-sialic acid biosynthesis pathway in Arabidopsis. Plant Physiol 2008; 147(1):331–339.

338. Nakanishi-Shindo Y, Nakayama K, Tanaka A, Toda Y, Jigami Y. Structure of the N-linked oligosaccharides that show the complete loss of alpha-1,6-polymannose outer chain from och1, och1 mnn1, and och1 mnn1 alg3 mutants of Saccharomyces cerevisiae. J Biol Chem 1993; 268(35):26338–26345.

339. Chiba Y, Suzuki M, Yoshida S, Yoshida A, Ikenaga H, Takeuchi M, Jigami Y, Ichishima E. Production of human compatible high mannose-type (Man5GlcNAc2) sugar chains in Saccharomyces cerevisiae. J Biol Chem 1998; 273(41):26298–26304.

340. Byung-Kwon C, Bobrowicz P, Davidson RC, Hamilton SR, Kung DH, Li H, Miele RG, Nett JH, Wildt S, Gerngross TU. Use of combinatorial genetic libraries to humanize N-linked glycosylation in the yeast Pichia pastoris. Proc Natl Acad Sci USA 2003; 100(9):5022–5027.

341. Hamilton SR, Bobrowicz P, Bobrowicz B, Davidson RC, Li H, Mitchell T, Nett JH, Rausch S, Stadheim TA, Wischnewski H, Wildt S, Gerngross TU. Production of complex human glycoproteins in yeast. Science 2003; 301(5637):1244–1246.

342. Bobrowicz P, Davidson RC, Li H, Potgieter TI, Nett JH, Hamilton SR, Stadheim TA, Miele RG, Bobrowicz B, Mitchell T, Rausch S, Renfer E, Wildt S. Engineering of an artificial glycosylation pathway blocked in core oligosaccharide assembly in the yeast Pichia pastoris: production of

complex humanized glycoproteins with terminal galactose. Glycobiology 2004; 14(9):757–766.

343. Li H, Sethuraman N, Stadheim TA, Zha D, Prinz B, Ballew N, Bobrowicz P, Choi B-K, Cook WJ, Cukan M, Houston-Cummings NR, Davidson R, Gong B, Hamilton SR, Hoopes JP, Jiang Y, Kim N, Mansfield R, Nett JH, Rios S, Strawbridge R, Wildt S, Gerngross TU. Optimization of humanized IgGs in glycoengineered Pichia pastoris. Nat Biotechnol 2006; 24(2):210–215.
344. Potgieter TI, Cukan M, Drummond JE, Houston-Cummings NR, Jiang Y, Li F, Lynaugh H, Mallem M, McKelvey TW, Mitchell T, Nylen A, Rittenhour A, Stadheim TA, Zha D, d'Anjou M. Production of monoclonal antibodies by glycoengineered Pichia pastoris. J Biotechnol 2009; 139(4):318–325.
345. Chigira Y, Oka T, Okajima T, Jigami Y. Engineering of a mammalian O-glycosylation pathway in the yeast Saccharomyces cerevisiae: production of O-fucosylated epidermal growth factor domains. Glycobiology 2008; 18(4):303–314.
346. Kalsner I, W Hintz, LS Reid, Schachter H. Insertion into *Aspergillus nidulans* of functional UDP-GlcNAc: alpha 3-D- mannoside beta-1,2-N-acetylglucosaminyl-transferase I, the enzyme catalysing the first committed step from oligomannose to hybrid and complex N-glycans. Glycoconj J 1995; 12:360–370.
347. Maras M, De Bruyn A, Vervecken W, Uusitalo J, Penttilä M, Busson R, Herdewijn P, Contreras R. In vivo synthesis of complex N-glycans by expression of human N-acetylglucosaminyltransferase I in the filamentous fungus Trichoderma reesei. FEBS Lett 1999; 452(3):365–370.
348. Wacker M, Feldman MF, Callewaert N, Kowarik M, Clarke BR, Pohl NL, Hernandez M, Vines ED, Valvano MA, Whitfield C, Aebi M. Substrate specificity of bacterial oligosaccharyltransferase suggests a common transfer mechanism for the bacterial and eukaryotic systems. Proc Natl Acad Sci USA 2006; 103(18):7088–7093.
349. Zhang Z, Gildersleeve J, Yang Y-Y, Xu R, Loo JA, Uryu S, Wong C-H, Schultz PG. A new strategy for the synthesis of glycoproteins. Science 2004; 303(5656):371–373.
350. Zhang Z, Gildersleeve J, Yang Y-Y, Xu R, Loo JA, Uryu S, Wong C-H, Schultz PG. Retraction. Science 2009; 326(5957):1187.
351. Mosteller RD, Goldstein BE. A mathematical model that applies to protein degradation and post-translational processing of proteins and to analogous processes for other molecules in non-growing and exponentially growing cells. J Theor Biol 1984; 108(4):597–621.
352. Noe DA, Delenick JC. Quantitative analysis of membrane and secretory protein processing and intracellular transport. J Cell Sci 1989; 92(Pt 3): 449–459.
353. Bibila TA, Flickinger MC. A model of interorganelle monoclonal antibody transport and secretion in mouse hybridoma cells. Biotechnol Bioeng 1991; 38(7):767–780.
354. Bibila TA, Flickinger MC. Use of a structured kinetic model of antibody synthesis and secretion for optimization of antibody production systems: II. Transient analysis. Biotechnol Bioeng 1992; 39(3):262–272.
355. Bibila TA, Flickinger MC. Use of a structured kinetic model of antibody synthesis and secretion for optimization of antibody production systems: I. Steady-state analysis. Biotechnol Bioeng 1992; 39(3):251–261.
356. Monica TJ, Andersen DC, Goochee CF. A mathematical model of sialylation of N-linked oligosaccharides in the trans-Golgi network. Glycobiology 1997; 7(4):515–521.
357. Umaña P, Bailey JE. A mathematical model of N-linked glycoform biosynthesis. Biotechnol Bioeng 1997; 55(6):890–908.
358. Krambeck FJ, Betenbaugh MJ. A mathematical model of N-linked glycosylation. Biotechnol Bioeng 2005; 92(6):711–728.
359. Krambeck FJ, Bennun SV, Narang S, Choi S, Yarema KJ, Betenbaugh MJ. A mathematical model to derive N-glycan structures and cellular enzyme activities from mass spectrometric data. Glycobiology 2009; 19:1163–1175.
360. Chen P, Harcum SW. Effects of amino acid additions on ammonium stressed CHO cells. J Biotechnol 2005; 117(3):277–286.
361. Crowell CK, Grampp GE, Rogers GN, Miller J, Scheinman RI. Amino acid and manganese supplementation modulates the glycosylation state of erythropoietin in a CHO culture system. Biotechnol Bioeng 2007; 96(3):538–549.
362. Andersen DC, Goochee CF, Cooper G, Weitzhandler M. Monosaccharide and oligosaccharide analysis of isoelectric focusing-separated and blotted granulocyte colony-stimulating factor glycoforms using high-pH anion-exchange chromatography with pulsed amperometric detection. Glycobiology 1994; 4(4):459–467.
363. Andersen DC, Goochee CF. The effect of ammonia on the O-linked glycosylation of granulocyte colony-stimulating factor produced by chinese hamster ovary cells. Biotechnol Bioeng 1995; 47(1):96–105.
364. Chen P, Harcum SW. Effects of elevated ammonium on glycosylation gene expression in CHO cells. Metab Eng 2006; 8(2):123–132.
365. Thorens B, Vassalli P. Chloroquine and ammonium chloride prevent terminal glycosylation of immunoglobulins in plasma cells without affecting secretion. Nature 1986; 321(6070):618–620.
366. Yang M, Butler M. Effects of ammonia on CHO cell growth, erythropoietin production, and glycosylation. Biotechnol Bioeng 2000; 68(4):370–380.
367. Yang M, Butler M. Effect of ammonia on the glycosylation of human recombinant erythropoietin in culture. Biotechnol Prog 2000; 16(5):751–759.
368. Yang M, Butler M. Effects of ammonia and glucosamine on the heterogeneity of erythropoietin glycoforms. Biotechnol Prog 2002; 18(1):129–138.
369. Grammatikos SI, Valley U, Nimtz M, Conradt HS, Wagner R. Intracellular UDP-N-acetylhexosamine pool affects N-glycan complexity: a mechanism of ammonium action on protein glycosylation. Biotechnol Prog 1998; 14(3):410–419.
370. Schmelzer AE, Miller WM. Effects of osmoprotectant compounds on NCAM polysialylation under hyperosmotic stress and elevated pCO(2). Biotechnol Bioeng 2002; 77(4):359–368.
371. Zanghi JA, Mendoza TP, Schmelzer AE, Knop RH, Miller WM. Role of nucleotide sugar pools in the inhibition of NCAM polysialylation by ammonia. Biotechnol Prog 1998; 14(6):834–844.
372. Kaufman RJ, Swaroop M, Murtha-Riel P. Depletion of manganese within the secretory pathway inhibits O-linked

glycosylation in mammalian cells. Biochemistry 1994; 33(33):9813–9819.

373. Gramer MJ, Goochee CF. Glycosidase activities in Chinese hamster ovary cell lysate and cell culture supernatant. Biotechnol Prog 1993; 9(4):366–373.
374. Gramer MJ, Goochee CF. Glycosidase activities of the 293 and NS0 cell lines, and of an antibody-producing hybridoma cell line. Biotechnol Bioeng 1994; 43(5):423–428.
375. Wong DCF, Wong KTK, Goh LT, Heng CK, Yap MGS. Impact of dynamic online fed-batch strategies on metabolism, productivity and N-glycosylation quality in CHO cell cultures. Biotechnol Bioeng 2005; 89(2):164–177.
376. Goldman MH, James DC, Rendall M, Ison AP, Hoare M, Bull AT. Monitoring recombinant human interferon-gamma N-glycosylation during perfused fluidized-bed and stirred-tank batch culture of CHO cells. Biotechnol Bioeng 1998; 60(5):596–607.
377. Lipscomb ML, Palomares LA, Hernández V, Ramírez OT, Kompala DS. Effect of production method and gene amplification on the glycosylation pattern of a secreted reporter protein in CHO cells. Biotechnol Prog 2005; 21(1):40–49.
378. Hooker AD, Goldman MH, Markham NH, James DC, Ison AP, Bull AT, Strange PG, Salmon I, Baines AJ, Jenkins N. N-glycans of recombinant human interferon-gamma change during batch culture of chinese hamster ovary cells. Biotechnol Bioeng 1995; 48(6):639–648.
379. Curling EM, Hayter PM, Baines AJ, Bull AT, Gull K, Strange PG, Jenkins N. Recombinant human interferon-gamma. Differences in glycosylation and proteolytic processing lead to heterogeneity in batch culture. Biochem J 1990; 272(2):333–337.
380. Shelikoff M, Sinskey AJ, Stephanopoulos G. The effect of protein synthesis inhibitors on the glycosylation site occupancy of recombinant human prolactin. Cytotechnology 1994; 15(1–3):195–208.
381. Kunkel JP, Jan DC, Jamieson JC, Butler M. Dissolved oxygen concentration in serum-free continuous culture affects N-linked glycosylation of a monoclonal antibody. J Biotechnol 1998; 62(1):55–71.
382. Lin AA, Kimura R, Miller WM. Production of tPA in recombinant CHO cells under oxygen-limited conditions. Biotechnol Bioeng 1993; 42(3):339–350. JulR.
383. Restelli V, Wang M-D, Huzel N, Ethier M, Perreault H, Butler M. The effect of dissolved oxygen on the production and the glycosylation profile of recombinant human erythropoietin produced from CHO cells. Biotechnol Bioeng 2006; 94(3):481–494.
384. Serrato JA, Palomares LA, Meneses-Acosta A, Ramírez OT. Heterogeneous conditions in dissolved oxygen affect N-glycosylation but not productivity of a monoclonal antibody in hybridoma cultures. Biotechnol Bioeng 2004; 88(2):176–188.
385. Trummer E, Fauland K, Seidinger S, Schriebl K, Lattenmayer C, Kunert R, Vorauer-Uhl K, Weik R, Borth N, Katinger H, Müller D. Process parameter shifting: Part I. Effect of DOT, pH, and temperature on the performance of Epo-Fc expressing CHO cells cultivated in controlled batch bioreactors. Biotechnol Bioeng 2006; 94(6):1033–1044.
386. Rodriguez J, Spearman M, Huzel N, Butler M. Enhanced production of monomeric interferon-beta by CHO cells through the control of culture conditions. Biotechnol Prog 2005; 21(1):22–30.
387. Tachibana H, Taniguchi K, Ushio Y, Teruya K, Osada K, Murakami H. Changes of monosaccharide availability of human hybridoma lead to alteration of biological properties of human monoclonal antibody. Cytotechnology 1994; 16(3):151–157.
388. Tachibana H, Kim J, Shirahat S. Building high affinity human antibodies by altering the glycosylation on the light chain variable region in N-acetylglucosamine-supplemented hybridoma cultures. Cytotechnology 1997; 23:151–159.
389. Hayter PM, Curling EM, Baines AJ, Jenkins N, Salmon I, Strange PG, Tong JM, Bull AT. Glucose-limited chemostat culture of chinese hamster ovary cells producing recombinant human interferon-gamma. Biotechnol Bioeng 1992; 39(3):327–335.
390. Yoon SK, Choi SL, Song JY, Lee GM. Effect of culture pH on erythropoietin production by Chinese hamster ovary cells grown in suspension at 32.5 and 37.0 degrees C. Biotechnol Bioeng 2005; 89(3):345–356.
391. Hayter PM, Curling EM, Gould ML, Baines AJ, Jenkins N, Salmon I, Strange PG, Bull AT. The effect of the dilution rate on CHO cell physiology and recombinant interferon-gamma production in glucose-limited chemostat culture. Biotechnol Bioeng 1993; 42(9):1077–1085.
392. Jenkins N, Castro P, Menon S, Ison A, Bull A. Effect of lipid supplements on the production and glycosylation of recombinant interferon-gamma expressed in CHO cells. Cytotechnology 1994; 15(1–3):209–215.
393. Gu X, Wang DI. Improvement of interferon-gamma sialylation in Chinese hamster ovary cell culture by feeding of N-acetylmannosamine. Biotechnol Bioeng 1998; 58(6):642–648.
394. Rijcken WRP, Overdijk B, Van den Eijnden DH, Ferwerda W. The effect of increasing nucleotide-sugar concentrations on the incorporation of sugars into glycoconjugates in rat hepatocytes. Biochem J 1995; 305(Pt 3): 865–870.
395. Kochanowski N, Blanchard F, Cacan R, Chirat F, Guedon E, Marc A, Goergen J-L. Influence of intracellular nucleotide and nucleotide sugar contents on recombinant interferon-gamma glycosylation during batch and fed-batch cultures of CHO cells. Biotechnol Bioeng 2008; 100(4):721–733.
396. Gawlitzek M, Valley U, Nimtz M, Wagner R, Conradt HS. Characterization of changes in the glycosylation pattern of recombinant proteins from BHK-21 cells due to different culture conditions. J Biotechnol 1995; 42(2):117–131.
397. Spearman M, Rodriguez J, Huzel N, Butler M. Production and glycosylation of recombinant beta-interferon in suspension and cytopore microcarrier cultures of CHO cells. Biotechnol Prog 2005; 21(1):31–39.
398. Spearman M, Rodriguez J, Huzel N, Sunley K, Butler M. Effect of culture conditions on glycosylation of recombinant beta-interferon in CHO cells. Cell technology for cell products. Springer Netherlands: Springer; 2007. pp. 71–85.
399. Gramer MJ, Goochee CF, Chock VY, Brousseau DT, Sliwkowski MB. Removal of sialic acid from a glycoprotein in CHO cell culture supernatant by action of an extracellular CHO cell sialidase. Biotechnology (N Y) 1995; 13(7):692–698.
400. Gawlitzek M, Estacio M, Fürch T, Kiss R. Identification of cell culture conditions to control N-glycosylation

site-occupancy of recombinant glycoproteins expressed in CHO cells. Biotechnol Bioeng 2009; 103(6):1164–1175.

401. Crowell CK, Qin Q, Grampp GE, Radcliffe RA, Rogers GN, Scheinman RI. Sodium butyrate alters erythropoietin glycosylation via multiple mechanisms. Biotechnol Bioeng 2008; 99(1):201–213.
402. Mimura Y, Lund J, Church S, Dong S, Li J, Goodall M, Jefferis R. Butyrate increases production of human chimeric IgG in CHO-K1 cells whilst maintaining function and glycoform profile. J Immunol Methods 2001; 247(1–2):205–216.
403. Santell L, Ryll T, Etcheverry T, Santoris M, Dutina G, Wang A, Gunson J, Warner TG. Aberrant metabolic sialylation of recombinant proteins expressed in Chinese hamster ovary cells in high productivity cultures. Biochem Biophys Res Commun 1999; 258(1):132–137.
404. Sung YH, Song YJ, Lim SW, Chung JY, Lee GM. Effect of sodium butyrate on the production, heterogeneity and biological activity of human thrombopoietin by recombinant Chinese hamster ovary cells. J Biotechnol 2004; 112(3):323–335.
405. Schmelzer AE, Miller WM. Hyperosmotic stress and elevated pCO2 alter monoclonal antibody charge distribution and monosaccharide content. Biotechnol Prog 2002; 18(2):346–353.
406. Kimura R, Miller WM. Glycosylation of CHO-derived recombinant tPA produced under elevated pCO2. Biotechnol Prog 1997; 13(3):311–317.
407. Zanghi JA, Schmelzer AE, Mendoza TP, Knop RH, Miller WM. Bicarbonate concentration and osmolality are key determinants in the inhibition of CHO cell polysialylation under elevated pCO(2) or pH. Biotechnol Bioeng 1999; 65(2):182–191.
408. Borys MC, Linzer DI, Papoutsakis ET. Culture pH affects expression rates and glycosylation of recombinant mouse placental lactogen proteins by Chinese hamster ovary (CHO) cells. Biotechnology (N Y) 1993; 11(6): 720–724.
409. Trummer E, Fauland K, Seidinger S, Schriebl K, Lattenmayer C, Kunert R, Vorauer-Uhl K, Weik R, Borth N, Katinger H, Müller D. Process parameter shifting: Part II. Biphasic cultivation-A tool for enhancing the volumetric productivity of batch processes using Epo-Fc expressing CHO cells. Biotechnol Bioeng 2006; 94(6):1045–1052.
410. Senger RS, Karim MN. Effect of shear stress on intrinsic CHO culture state and glycosylation of recombinant tissue-type plasminogen activator protein. Biotechnol Prog 2003; 19(4):1199–1209.
411. Ahn WS, Jeon J-J, Jeong Y-R, Lee SJ, Yoon SK. Effect of culture temperature on erythropoietin production and glycosylation in a perfusion culture of recombinant CHO cells. Biotechnol Bioeng 2008; 101(6):1234–1244.
412. Bollati-Fogolín M, Forno G, Nimtz M, Conradt HS, Etcheverrigaray M, Kratje R. Temperature reduction in cultures of hGM-CSF-expressing CHO cells: effect on productivity and product quality. Biotechnol Prog 2005; 21(1):17–21.
413. Clark KJ, Chaplin FW, Harcum SW. Temperature effects on product-quality-related enzymes in batch CHO cell cultures producing recombinant tPA. Biotechnol Prog 2004; 20(6):1888–1892.
414. Yoon SK, Kim SH, Lee GM. Effect of low culture temperature on specific productivity, transcription level, and heterogeneity of erythropoietin in Chinese hamster ovary cells. Biotechnol Bioeng 2003; 82(3):289–298.
415. Wang WC, Lee N, Aoki D, Fukuda MN, Fukuda M. The poly-N-acetyllactosamines attached to lysosomal membrane glycoproteins are increased by the prolonged association with the Golgi complex. J Biol Chem 1991; 266(34):23185–23190.
416. Schneider M, Marison IW, Stockar U. The importance of ammonia in mammalian cell culture. J Biotechnol 1996; 46(3):161–185.
417. Kim NS, Lee GM. Inhibition of sodium butyrate-induced apoptosis in recombinant Chinese hamster ovary cells by constitutively expressing antisense RNA of caspase-3. Biotechnol Bioeng 2002; 78(2):217–228.
418. Arden N, Betenbaugh MJ. Regulating apoptosis in mammalian cell cultures. Cytotechnology 2006; 50(1–3):77–92.
419. Vidali G, Boffa LC, Mann RS, Allfrey VG. Reversible effects of Na-butyrate on histone acetylation. Biochem Biophys Res Commun 1978; 82(1):223–227.
420. Nienow AW. Reactor engineering in large scale animal cell culture. Cytotechnology 2006; 50(1–3):9–33.

24

SECRETION OF HETEROLOGOUS PROTEINS, GRAM POSITIVE BACTERIA

ERIC MORELLO
Unité Biologie Moléculaire du Gène chez les Extrêmophiles, Institut Pasteur, Paris, France
ISABELLE POQUET
Unité des Bactéries Lactiques et pathogènes Opportunistes (UR888), Jouy-en-Josas, France
PHILIPPE LANGELLA
Unité d'Ecologie et Physiologie du Système Digestif (UR910), INRA, Jouy-en-Josas, France

24.1 PROTEIN SECRETION VIA THE GENERAL EXPORT PATHWAY IN GRAM-POSITIVE BACTERIA

Positioning newly synthesized proteins at their site of action is a vital function for all cells. Secretion allows certain proteins to cross the various structures that give integrity to the cell, and to be subsequently released into the extracellular medium. There exist specialized cases of protein export where in addition to secretion, integration, and/or anchoring of the protein to the different cell envelopes occurs. These special cases will not be discussed in this review.

A multitude of studies focusing on protein secretion have highlighted that similar mechanisms exist among very divergent organisms. Generally, the secreted protein crosses a membrane barrier formed by a phospholipid bilayer: that of the endoplasmic reticulum in eukaryotes and the plasma membrane of gram-positive and gram-negative bacteria.

This review will focus on the secretion of proteins in the bacterium *Lactococcus lactis*, a model organism for the lactic acid bacteria (LAB). *L. lactis* is a gram-positive bacterium with distinct cellular compartments: (i) the cytosol, (ii) the plasma membrane, and (iii) the cell wall which forms a rigid exoskeleton protecting the cell against external aggression. This final structure represents, for secreted proteins, an additional barrier to overcome.

In gram-positive bacteria, several secretion pathways have been reported: (i) the general export pathway (GEP) or "Sec" pathway represents the primary pathway used for the majority of proteins, and on which this review will focus. More specific and rare systems, which will not be covered here, included (ii) the "Tat" pathway (Twin Arginine Translocation), targeted toward transporting proteins that have adopted their tertiary conformation along with their associated cofactors; (iii) ABC transporters (ATP-Binding Cassette); and (iv) the type IV prepilin system.

The secretion of proteins via the "Sec" or "Sec-dependent" pathway can be divided into three major steps (Fig. 24.1):

1. The synthesized protein is a cytoplasmic precursor (or preprotein) containing a secretion signal or signal peptide (SP) that is cleaved leading to the mature secreted protein. Comparative studies of SP primary sequences in prokaryotic and eukaryotic organisms have revealed a common overall structure (1–3): (i) an N-terminal region (N) carrying positive charges; (ii) a hydrophobic region with a helical fold (H); and (iii) a C-terminal region (C) carrying the cleavage site recognized by the signal peptidase (SPase) that releases the mature protein (Fig. 24.2). Compared

Upstream Industrial Biotechnology: Expression Systems and Process Development, Volume 1, First Edition. Edited by Michael C. Flickinger.
© 2013 John Wiley & Sons, Inc. Published 2013 by John Wiley & Sons, Inc.

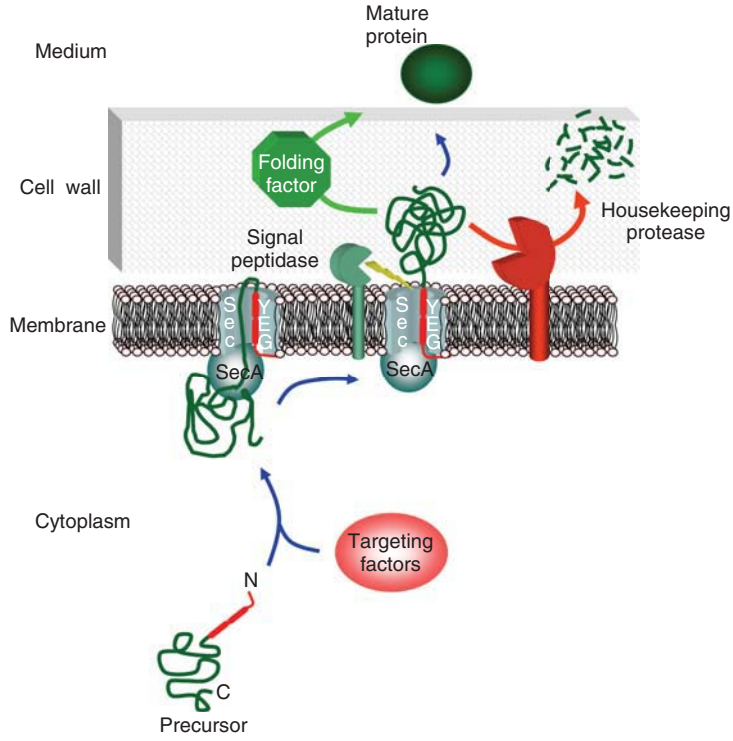


Figure 24.1. Protein secretion in gram-positive bacteria. The secreted proteins are synthesized as a precursor bearing a signal peptide at its N-terminal end. The precursor is recognized by dedicated factors which transport it to the secretion machinery. This machinery is composed of a motor protein, SecA, along with additional subunits, SecY, SecE, and SecG, which form a transmembrane channel permitting the precursor to translocate across membrane (Sec translocon). During or after translocation, the cleavage of the signal peptide by the signal peptidases releases the mature protein into the extracellular medium. (This figure is available in full color at http://onlinelibrary.wiley.com/book/10.1002/9780470054581.)

with SPs of secreted proteins in *Escherichia coli*, the SPs of the gram-positive bacteria are generally longer in all three domains N, H, and C (1). During the synthesis of the precursor, the SP is recognized by cytosolic transport factors that can be general (chaperons) or dedicated to secretion. Their role is to maintain the precursor in an unfolded state which is able to be translocated and to direct it toward the membrane Sec proteins involved in translocation. In gram-positive bacteria, gene conservation and experimental data show that the addressing process via the complex signal recognition particle (SRP) and its receptor FtsY play a major role in the secretion of proteins.

2. Translocation of the precursor across the membrane involves several components. In most bacteria, SecA is the motor of protein translocation and SecY, SecE, and SecG form a hydrophilic transmembrane channel (Sec translocon) through which the precursor crosses the lipid membrane in an unfolded form (4–6). In some microorganisms, other proteins termed *accessory proteins* (some of them seem to be dispensable or not conserved, and their function is not as well established as that of SecA-SecYEG) can be associated with the Sec translocon and improve the secretion. Examples in *E. coli* include the SecDSecFYajC complex that has been shown to stimulate translocation (7) and YidC (8) that is mainly involved in the insertion of transmembrane proteins.
3. After crossing the plasma membrane, precursors undergo a maturation step in which (i) the SP is cleaved and (ii) proteins adopt their stable and active conformation. The cleavage of the SP involves the type I SPase that allows release of the secreted mature protein into the extracytoplasmic environment (periplasmic compartment of gram-negative bacteria, and extracellular medium in the case of gram-positive bacteria). The adoption of the active and stable conformation is subject to rigorous quality control in the cell envelope. This step may involve

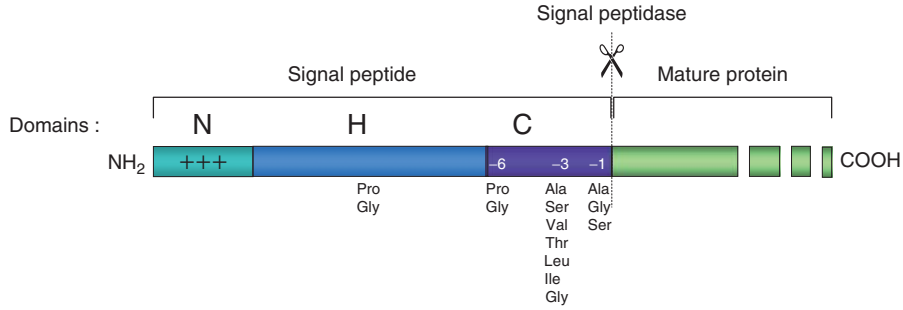


Figure 24.2. The three-part structure of the signal peptide (SP). The SP, fused to the mature protein, is composed of three domains: N, positively charged (+) N-terminal; H, hydrophobic; and C, C-terminal, containing the cleavage site of the SP recognized by the signal peptidases. Proline and Glycine residues are usually found in the middle of the H domain and between the H and C domains at position −6 with respect to the cleavage site: they allow for the disruption of the helix structure of the H domain. The signal-peptidase recognition site is composed of aliphatic residues, most commonly Alanine, at the −1 and −3 positions (3). (This figure is available in full color at http://onlinelibrary.wiley.com/book/10.1002/9780470054581.)

exported folding factors (chaperons and folding catalysts) its role is to assist the secreted protein in the adoption of its functional conformation. Under stress conditions, in particular environmental (thermal) stress or biotechnological stress (secretion of heterologous overexpressed proteins), folding may be compromised leading to an accumulation of unfolded or misfolded proteins that are not functional and might be toxic. In response to such stresses, bacteria induced the expression of exported factors involved in protein quality control: folding factors to repair the damaged proteins and exported proteases to degrade them (9,10). Among these proteases, the HtrA family that is widely conserved in eukaryotes and prokaryotes (and in particular in gram-positive bacteria) (11), is the most studied, but other exported proteases are also involved in a similar housekeeping function (furthermore, in gram-positive bacteria, secreted proteases of broad specificity are known to degrade secreted heterologous proteins).

24.2 SECRETION OF HETEROLOGOUS PROTEINS IN *L. LACTIS*

An understanding of the secretion mechanism in *Bacillus subtilis* has allowed the development of effective strategies to construct and improve optimized expression strains (9–12). Currently, the genus *Bacillus* is widely used for the production of high yields of naturally secreted proteins (60% of enzymes commercially available) (9,12,13). However, secretion yields of heterologous proteins in this system are generally much lower (9,12,13). As a consequence, other gram-positive bacteria are proving competitive for the secretion of heterologous proteins. Among them, LAB possesses several natural advantages, such as their status of food component and optimized recombinant strains, which represent a particularly interesting alternative especially for the production of therapeutic proteins and peptides that are destined to human. To date, the optimized recombinant LAB are the subject of two major areas of advanced research (i) for the production of proteins in a fermenter and (ii) for the *in situ* delivery of therapeutic proteins such as interleukins, bacterial, and viral antigens (14).

Among the LAB, *L. lactis* is the most well studied and is considered as a model organism. It is a homofermenting mesophilic bacterium, which is divided into two subspecies, *L. lactis* subsp. *lactis* and *L. lactis* subsp. *cremoris* (15,16). A number of genetic tools have been developed for this species, and the genomes of three strains have been sequenced (17–19).

In terms of heterologous protein production, *L. lactis* has several interesting characteristics that make it the species of choice when compared with other common bacterial systems, such as *E. coli* (20) and *B. subtilis* (12). Importantly, as *L. lactis* has safely been used in the dairy industry for years, and does not produce endotoxins, proteins produced in this bacterium should be GRAS (generally recognized as safe) according to FDA (Food and Drug Administration, USA) as in many other LAB. *L. lactis* is efficient for heterologous secretion and it naturally secretes a single protein, Usp45 (in significant amounts in the supernatant) (21,22), thereby limiting the downstream purification steps necessary to recover the heterologous secreted protein. Moreover, the strains used in the laboratory have only a single extracellular housekeeping protease, HtrA, and in *htrA* mutants, extracellular proteolysis of heterologous proteins is completely abolished (32–73). As extracellular protease-free strains, *htrA* mutants are very efficient hosts to improve protein

yield (23,26). In *B. subtilis* whose extracellular proteolytic system is much more complex, extracellular protease-free strains are not available: although nine extracellular proteases have been inactivated, four active surface proteases, including the three members of the HtrA family, are remaining (27,28). Finally, in *L. lactis*, the relatively simple fermentative metabolism ensures that optimized culture conditions, as defined in the laboratory, are easily transferable to an industrial scale (29,30).

Because of its advantages, many studies have used *L. lactis* to produce secreted recombinant proteins (Table 24.1) (31). The various strategies that have been used to improve the production yields of secreted proteins

TABLE 24.1. Heterologous Proteins Produced and Secreted by *L. lactis*[a]

Proteins	Gene	Species	References
Reporter			
Nuc	*nuc*	*Staphylococcus aureus*	Dieye *et al*, (33) Le Loir *et al*, (34)
β-lactamase	*bla*	*E. coli*	Sibakov *et al*, (35)
α-amylase	*amyS*	*Geobacillus stearothermophilus*	Van Asseldonk *et al*, 1993 (21–22) Le Loir *et al*, (36)
Bacterial antigens			
L7/L12	*L7/L12*	*Brucella abortus*	Ribeiro *et al*, (37)
Urease		*Helicobacter pilori*	Lee *et al*, (38)
TTFC	*ttfc*	*Clostridium tetani*	Wells *et al*, (39)
Eucaryotic antigens			
Fusion GLURP-MSP3		*Plasmodium falciparum*	Theisen *et al*, (40)
Viral antigens			
E7	E7	Type-16 human papillomavirus	Cortes-Perez *et al*, (41) Bermudez-Humaran *et al*, (42)
Epitope BCV	BCV	Coronavirus bovin	Langella et Le Loir, (43)
VP8*	VP8*	Rotavirus	Gil *et al*, (44)
Interleukines			
IL-2	IL-2	Mouse	Steidler *et al*, (45)
IL-6	IL-6	Mouse	Steidler *et al*, (46)
IL-10	IL-10	Mouse	Steidler *et al*, (47)
IL-12	IL-12	Mouse	Bermudez-Humaran *et al*, (48)
IFN-ω	IFN-ω	Ovin	Bermudez-Humaran *et al*, (49)
Allergens			
Betalactoglobulin	Blg	Bovin	Bernasconi E, *et al*, (50) Chatel *et al*, (51) Chatel *et al*, (52)
Virulence factors			
Enterotoxine A	*sea*	*Staphylococcus aureus*	Charlier, unpublished
Bacteriocins			
ABP-118	*abp118*	*Lactobacillus salivarius sp. salivarius*	Flynn *et al*, (53)
Enterocin A	*ent*	*Enterococcus faecium*	Martinez *et al*, (54)
Pediocin PA-1	*ped*	*Pediococcus acidilactici*	Martinez *et al*, (54)
Colicin V		*E. coli*	Van Belkum *et al*, (55)
Enzymes			
Bacteriophage lytic enzyme	*ply118*	*Listeria monocytogenes* bacteriophage	Gaeng *et al*, (56)
Protéase neutre	*npr*	*B. subtilis*	Van de Guchte *et al*, (57)
Aminopeptidase N	*pepN*	*Lactobacillus helveticus*	Kahala et Palva, 1999 (58)
Dextrane sucrase	*dsrD*	*Leuconostoc mesenteroïdes*	Neubauer *et al*, (59)
Streptodornase	*sdc*	*Streptococcus equisimilis*	Wolinowska *et al*, (60)
Prochymosine	PC	Bovin	Simons *et al*, (61)
Lipase	*lip*	*Staphylococcus hyicus*	Drouault *et al*, (62)
plasmine		bovin	Arnau *et al*, 1997 (63)
Others			
F18 fimbrial adhesin	*fedF*	*E. coli*	Lindholm *et al*, (64)

[a]From Ref. 31

are described in *L. lactis*. Most strategies involve developing effective expression systems (32) and optimized strains (31).

24.3 EXPRESSION SYSTEMS

In bacteria, expression systems for recombinant proteins typically use plasmids, which are easily manipulated. These plasmids carry the signals of expression and all the information necessary for the synthesis of the protein of interest. Most of expression systems available in LAB generally derived from those that have been developed in *L. lactis*. In other commonly used LAB, such as those belonging to the *Lactobacillus* genus, very few alternative expression systems have been developed (65).

24.3.1 Vectors

In lactococci, plasmids have been implicated in contributing to the plasticity of the genome by promoting the exchange of DNA between and within species. This plasticity allows the cell to adapt to a sometimes hostile environment, and can play a vital role in cell physiology by providing new properties. Some of these new properties have proven of technological interest (66). The natural plasmids of these bacteria present several advantages toward the development of genetic tools: (i) they are of limited size, facilitating extraction, and manipulation and (ii) many of them are easily selectable and transformable in large host range. Several types of vectors have been developed and characterized for protein production in *L. lactis*. The stability of expression vectors, related to their replication and selection, affects the efficiency of expression of the genes they carry (67).

24.3.2 Expression of the Target Gene

In prokaryotes, an understanding of the molecular mechanisms implicated in protein synthesis allowed for the characterization of signals. These signals are encoded in the gene sequence and modulate its expression through the transcription and translation steps. The optimization of these signals on expression vectors can thus enhance expression of heterologous proteins, particularly in *E. coli* (20,68–71).

24.3.2.1 Promoters. The transcription of a gene is a critical step in the synthesis of a protein. It defines, when factoring in degradation, the level of mRNA present in a cell. This process includes several steps: initiation followed by elongation and termination.

In *L. lactis*, the molecular mechanism of transcriptional initiation is considered identical to that which has been elucidated for *E. coli*, *B. subtilis*, and most other prokaryotes. This step involves two key elements: the promoter sequence or gene promoter and the RNA polymerase subunit which binds to the promoter sequence in order to initiate transcription (32,72). RNA polymerase is a protein complex comprising a main factor, encoded by the *rpoD* gene, which is homologous to the ρ^{70} factor of *E. coli* and ρ^{43} of *B. subtilis*. This main factor binds to the promoter, and to additional subunits 2 $\alpha\beta\beta'$, ω and $\tilde{\delta}$. The binding affinity of the ρ factor for the promoter regulates the strength of the promoter and thus influences the frequency with which transcription initiates. The model of the promoter region upstream of the +1 of transcriptional initiation includes two consensus hexanucleotide sequences, TATAAT (−10 box) and TTGACA (−35 box), with an optimal spacing of 17 nucleotides, although some promoters only include one extended −10 sequence: TGNTATAAT. In *L. lactis*, the promoters that are functional *in vivo* are consensual (32,73).

Most studies to identify or characterize promoters are based on the use of screening vectors carrying a reporter gene without a promoter. Many reporter genes have been described. They generally encode enzymes carrying an easily detectable and/or measurable activity such β-galactosidase (74,75), luciferase (76) or nuclease (Nuc) from *Staphylococcus aureus* (Nuc) (77). They may also confer a selective advantage such as antibiotic resistance (78–83) der van Rooijen *et al*., 1992.

In random screens, chromosomal DNA libraries are cloned upstream of the reporter ORF to create either transcriptional or translational fusions on an appropriate plasmid vectors. Alternatively, the reporter ORF is cloned into a transposon which is randomly inserted into the genome. In the second method, integration into the chromosome can be stimulated by inserting a transposon into the screening vector (74). Additionally, a large library of synthetic promoters has been generated by the cloning of degenerate oligonucleotides in which consensus sequences were conserved (84). In *L. lactis*, many promoters have been identified by targeted analysis of genes whose expression profile is linked to cellular metabolism (80,83,85–87).

Taken together, the results of these studies have identified two types of promoters: constitutive promoters and regulated or inducible promoters. Constitutive promoters, for which no regulation is described, allow for continuous and stable transcription under standard culture conditions. By contrast, regulated promoters modify the level of transcription of genes they control to allow the cell to adapt to environmental variables. These promoters involve regulators that interact with the promoter sequence and modulate the capacity binding of the RNA polymerase. In this section, we mainly describe the promoters used for recombinant protein production in *L. lactis*.

24.3.2.1.1 Constitutive Promoters. In *L. lactis*, a wide range of constitutive promoters of varying strength are

present. The most common of these have been isolated and characterized by Vander Vossen *et al*. (79). In this study, a genomic DNA library of strain *L. lactis* sp. *cremoris* WG2 was cloned into a screening vector carrying the reporter gene *cat-86* which confers resistance to chloramphenicol. This library allowed for the random selection and isolation of five genomic DNA fragments (P21, P23, P32, P44, and P59) which gave chloramphenicol resistance in *L. lactis* and *B. subtilis*. The differences in levels of measured CAT activity (from 0.2 to 5.1 U/mg) suggested the isolation of promoters of varying strengths: P59> P23> P21> P32> P44 where P59 is the strongest promoter. As has been observed in other bacteria, analysis of the nucleotide sequence showed that sequences driving the highest level of activity were those with −35 and −10 hexanucleotides which most closely resembled the consensus.

These promoters have been widely used and integrated into systems for the expression of food-related recombinant proteins (Table 24.2). Some of this work was used to compare the effectiveness of these promoters and yielded results that were sometimes in disagree with previously reported values (88). However, these studies directly compared the production of proteins whose genes had been placed under the control of these promoters, thus eliminating the bias introduced by differences in translation efficiency. No study has yet compared of the strength of these promoters by direct measurement of the amount of transcripts.

24.3.2.1.2 Inducible Promoters. In contrast to constitutive promoters, the level of mRNA for a gene of interest can be controlled using regulated/inducible promoters. These promoters are generally derived from genes whose regulated transcription allows the cell to adapt to its environment. Integrated into expression systems, these promoters allow fine tuning of transcription for the gene of interest in accordance with growth conditions. Regulators, positive or negative, bind to specific sequences on these promoters, influencing the efficiency of RNA polymerase binding and the frequency of transcriptional initiation. Inducible promoters are particularly interesting in instances where a protein toxic to the cell as higher yields can be achieved by allowing an increase in biomass prior to induction of the protein. A wide range of inducible promoters is described in *L. lactis* where induction can be induced (i) by exposure to different stresses such as changes in temperature, pH or phage attack and (ii) a change in cellular metabolism related to the chemical composition of the medium (32,98,99). However, the use of some promoters such as the heat-inducible promoter (100) or that induced by phage φ 31 attack (101) can be problematic during the processes fermentation and large scale production. Only well-defined systems will be of significant interest in these types of processes in *L. lactis*.

24.3.2.1.2.1 Nisin Promoter/NICE system. Nisin Inducible Controlled Expression (NICE) system was developed using the regulatory elements of the *nis* operon that is involved in the biosynthesis of nisin, an antimicrobial peptide naturally secreted by certain strains of *L. lactis* (102). The NICE system is based on the nisin promoter P_{nisA} and the two-component system *nisRK* that naturally regulates *nis* operon (103). NisK is a membrane sensor with kinase activity which activates the transcription factor NisR of the promoter P_{nisA} in the presence of nisin in the medium (Fig. 24.3). NICE system is widely used for the expression of heterologous proteins in *L. lactis* (31,104,105). A wide variety of expression vectors in which expression of a gene of interest is placed under the control of the P_{nisA} promoter have been developed

TABLE 24.2. Heterologous Proteins Expressed in *L. lactis* under the Control of Constitutive Promoters

Proteins	Species	Promoter	References
Chitinase	*Serratia marcescens*	P32, P59	89
M6	*Streptococcus pyogenes*	P23, P59	90
SlpH	*Lactobacillus helveticus*	P32	91
Phenylalanine ammonia-lyase	*Petroselinum crispum*	P32	92
Carnobacteriocin A	*Carnobacterium piscicola*	P32	93
Ply118, Ply511	*Listeria monocytogenes*	P21, P32, P59	56
ClfA	*Staphylococcus aureus*	P23, P59	88
FnBPA	*S. aureus*	P23	94
Nuclease	*S. aureus*	P59	33
VP2, VP3	Infectious bursal disease virus (IBDV)	P59	95
Cu/Zn Superoxide dismutase	*Homo sapiens*	P32	96
Enterocin A	*Enterococcus faecium*	P32	54
Pediocin PA-1	*Pediococcus acidilactici*		
Neutral protease	*Bacillus subtilis*	P32	97
Lipase	*Staphylococcus hyicus*	P44	62

[a] From the library isolated by van der Vossen *et al*. (79)

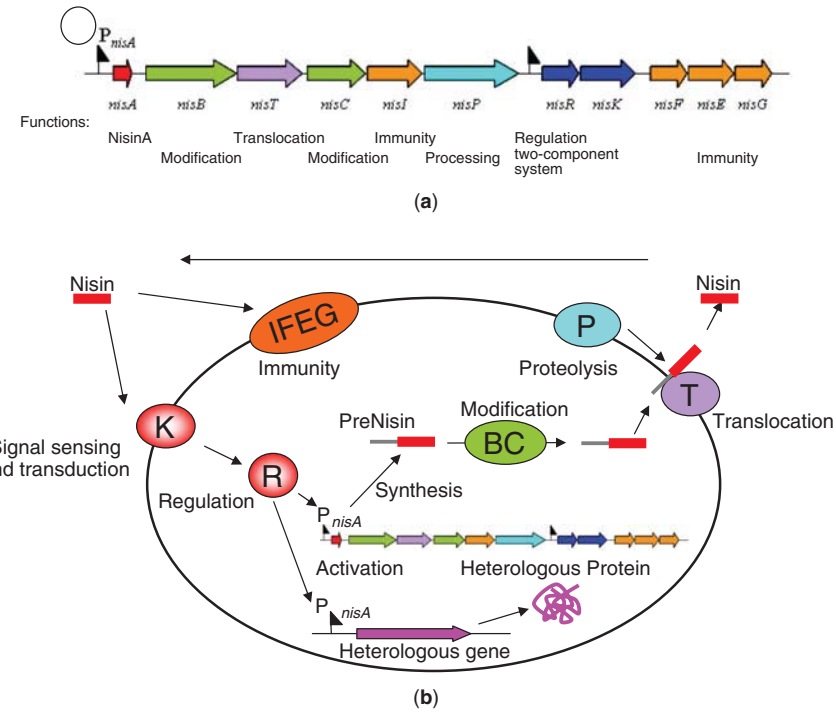


Figure 24.3. The NICE system. (a) Genetic organization of the nisin biosynthetic operon: *nisA* is the structural gene coding for nisin and *nisRK* genes are regulating the transcription of the whole *nis* operon. The products of the genes *nisBC* are implicated in the modification of the nisin precursor while *nisTP* translocates and cleaves it. The products of the genes *nisIFEG* play a role in nisin immunity. (b) Model of biosynthesis and regulation: The sensor, NisK, is autophosphorylated in the presence of nisin in the medium. The phosphate group is transferred to NisR, a transcriptional activator. The nisin precursor is modified by NisBC before being translocated by NisT and activated by NisP cleavage. The active nisin is then released into the medium. NisIFEG protects the cell against the bactericidal effect of nisin. At subinhibitory concentrations of nisin in the medium, only the presence of NisRK is required for activation of the promoter P_{nisA}. A protein of interest can be expressed and regulated if placed under the control of P_{nisA} in the presence of *nisRK* genes (106). (This figure is available in full color at http://onlinelibrary.wiley.com/book/10.1002/9780470054581.)

and they are generally used in recombinant strains where *nisRK* genes have been integrated into the chromosome. The nisin inducible system and derivatives are the most widely used in LAB.

This system has many advantages including ease of use, tight regulation, and high expression levels. Furthermore, recent studies have described the use of this system in the industrial scale production of a cytoplasmic recombinant form of lysostaphin from *Staphylococcus simulans* biovar staphylolyticus. Optimized growth conditions and media composition during fermentation, including the amount of nisin added, can triple production yields of this protein (100–300 mg/L) (29). A follow-up study revealed that this production level is linear along production scales from 1–3000 L (30) demonstrating the strong potential of this system for industrial scale production. However, the use of nisin as inducer agent may be pose both technical and economic constraints due to high cost and the need for downstream purification and disposal.

24.3.2.1.2.2 P170 Promoter. The pH-inducible P170 system is another expression system compatible with large scale production. In *L. lactis*, P170 promoter controls transcription of or*fX*, a gene of unknown function, and it is induced by a decrease in pH at the stationary phase of growth (107). The growth of *L. lactis*, under classical culture conditions, in which glucose is the carbon source, causes the accumulation of lactic acid in the medium. This accumulation of lactic acid causes a decrease in pH (pH <6), activating the promoter during the transition from exponential growth to stationary phase (107). The P170 promoter is regulated by RcfB (108).

This system was also improved by defining (i) an optimal promoter sequence for the P170gx which permitted more efficient binding, and (ii) an optimized synthetic medium used to achieve high levels of expression (300 mg/L) while using Nuc as the protein model. Compared with other inducible systems, the P170 has the advantage of being autoinducible, limiting most intervention by the researcher.

Reproducibility is improved under this promoter as expression is induced for all cultured cells at the same time. Moreover, production tests carried out at scales of 200 L and 1 L showed comparable production yields, purity, and stability.

24.3.2.1.2.3 P_{Zn} PROMOTER. A new expression system has recently been identified and developed in *L. lactis*. It is based on the use of the ZitR-regulated P_{Zn} promoter, which naturally controls the expression of the *zit* operon *(zitRSQP)*. By homology with *adc* operons in streptococci, the *zitRSQP* is involved both in zinc uptake by the ABC transporter ZitSQP, and in the control of its own expression by ZitR, a repressor of the MarR family (99,109). An expression vector, pVE8062 was constructed, carrying the P_{Zn} promoter and its regulator *zitR* (99). Using two reporter proteins, a form of the secreted Nuc from *S. aureus* and a cytoplasmic galactosidase (LacLM) from *Leuconostoc mesenteroides*, it has been shown that heterologous expression controlled by ZitR-regulated P_{Zn} varies in response to the concentration of zinc cations in the culture medium (99,109,110): it is totally repressed by Zn^{2+} in a wide range of concentrations (from profusion to toxicity), and highly induced by severe Zn^{2+} starvation (after addition of a chelator of metals for example) [Fig. 24.4; (99,109,110)].

The addition of zinc to the growth medium could be useful to tightly repress heterologous expression during growth and allow for an increase in biomass before induction by addition of EDTA (a chelator of divalent cations) on exponentially growing cells. Moreover, if a low level of expression can be tolerated throughout culturing, a zinc-limited medium, such as the chemically defined SA medium (111) can be used. This allows for progressive spontaneous induction and requires no modification of culture conditions (99,112). This system is particularly interesting because the implementation of various culture conditions is simple, inexpensive, and totally compatible with large-scale fermentation and production of injectable therapeutic compounds.

24.4 PROTEIN SECRETION IN *L. LACTIS*

Of the 2597 putative proteins detected in the genome of *L. lactis* IL1403 (4107 for *B. subtilis)*, 188 proteins have a unique N-terminal TM segment that might correspond to an SP (284 for *B. subtilis)*. Among them are 39 lipoproteins (114 for *B. subtilis)* and 146 secreted proteins (166 for *B. subtilis)*. When comparing the size of their genomes, *L. lactis* secretes more proteins (handled by SPase I) than *B. subtilis* through Sec (5% against 4.3%, respectively) (Poster, G. (113), 7th Symposium on Lactic Acid Bacteria).

In *L. lactis* most components involved in secretion have been identified through homologies to those described in both the *E. coli* and *B. subtilis* models (Table 24.3). This sequence conservation allows us postulate that their roles in protein secretion are identical to those described in these model bacteria. Comparisons of the different systems do reveal some differences that will be identified by us. Work to improve secretion in *L. lactis* focuses on the modification of the precursor protein and the expression of genes involved in protein quality control. Based on numerous complete genomes of LAB that are currently available, it appears that most of LAB displays secretion machinery comparable to the *L. lactis* one (KEGG Encyclopedia website: http://www.genome.jp/kegg/catalog/org_list.html).

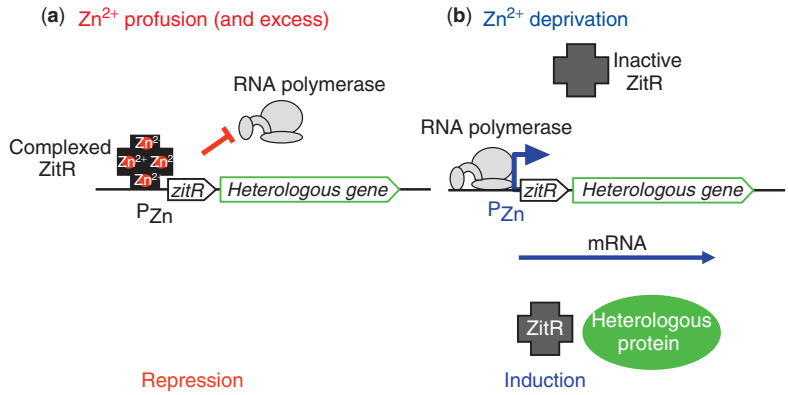


Figure 24.4. Model of regulation and expression of a gene under the control of ZitR-regulated P_{Zn} promoter. (a) Under conditions where zinc is present in sufficient amounts (profusion) or even in excess (toxicity), ZitR repressor is complexed to Zn and active as a DNA-binding protein: its binding on P_{Zn} promoter prevents the initiation of transcription by RNA polymerase. (b) When zinc is scarce in the medium, through use of a zinc-poor medium or by addition of a chelator, ZitR becomes inactive and is unable to bind to the promoter, allowing RNA polymerase to initiate transcription. (This figure is available in full color at http://onlinelibrary.wiley.com/book/10.1002/9780470054581.)

TABLE 24.3. Comparison of Protein Secretion and Quality Control Machineries in *L. lactis* and *B. subtilis*

Components	*L. lactis*	*B. subtilis*
Secretion		
Intracellular chaperonnes and general targeting factors	GroEL, GroES	GroEL, GroES
	DnaK, DnaJ, GrpE	DnaK, DnaJ, GrpE
	Trigger factor	Trigger factor
Specialized targeting factors	Ffh, FtsY, scRNA	Ffh, FtsY, scRNA
		CsaA?
Translocon	SecA	SecA
	SecY, SecE, SecG	SecY, SecE, SecG
Accessory proteins	—, YwaB	SecDF, YrbF
	YbdC/YfgG	SpoIIIJ/YqjG
Type I SPases	SipL	SipS, SipT, SipU, SipV, SipP
		SipW
SPPases	—	SppA
		TepA
Extra-cellular Quality control		
Extracellular folding factors	PmpA	PrsA
	—	BdbA/B/C
Housekeeping surface proteases	HtrA	HtrA, HtrB, HtrC (YyxA)
	—	WprA
	—	CtpA
Secreted Proteases	—	AprE, AprX, Bpr, Epr, Mpr, NprB, NprE, Vpr

24.4.1 Optimization of Precursor

24.4.1.1 The SP. Among the numerous expression systems described for *L. lactis*, many have been designed to allow secretion of a protein of interest into the extracellular medium through GEP by fusing the protein of interest to an SP.

In bacteria, the conservation of the SP structure (described earlier) allows the export of heterologous proteins via their natural SP. Thus, the native form of Nuc of *S. aureus* is secreted in *L. lactis* (34,36). However, it is often assumed that the secretion of a heterologous protein will be more efficient if it is fused to an SP from the production host. To explain this difference, the implication of species-specific factors involved in the recognition of SP is possible.

As was the case for promoter identification, the identification and characterization of the SP is the result of both the study of specific genes encoding a secreted protein and of random strategies. The resulting SP used for the production of heterologous proteins in *L. lactis* comes from the gene *usp45* (21). Its function is unknown, but sequence homology suggests that it might be involved in cell segregation in the hydrolysis of the cell wall (114). SP_{Usp45} has been used in many expression systems combined with constitutive promoters such as P59 (33) or inducible promoters such as the nisin promoter (29–31,115). Moreover, the SP_{Usp45} has been successfully used in other LAB such as in *Lactobacillus plantarum* in which it allows to efficiently drive the export of the human papillomavirus type-16 E7 antigen (116). Furthermore, strategies employing random fusions in order to induce the secretion of a reporter protein have resulted in the generation of several collections of efficient SPs as AL1 (117) and cassettes for expression/secretion as ssx collections (35), PS_{Exp} (77) or SP310 (118,119).

In *L. lactis*, while the fusion of a protein to an SP does not necessarily ensure its efficient secretion into the extracellular environment, it may still confer protection against intracellular degradation (31). Production of the protein NSP4 (nonstructural protein 4) of bovine rotavirus (120), of BLG $\tilde{\beta}$-Lactoglobuline bovine) (51) and GroEL of *Brucella abortus* (121), where little or no secretion is observed, is nonetheless stabilized by their fusion to $SP_{Usp45.}$ The stabilization of these proteins by fusion to the SP could result from a conformational change induced either by interaction with accessory factors and/or intracellular chaperons (31) or by an intramolecular chaperon effect of the SP (122).

24.4.1.2 Propeptide Leisstcda. In *L. lactis*, the fusion of a synthetic propeptide, consisting of the nine residues, LEISSTCDA, between the SP and the mature part of the protein improves the efficiency of secretion of several heterologous

proteins. The protein Nuc (36), the L7/L12 antigen of *B. abortus* (37) and the α- amylase of *Geobacillus stearothermophilus* (31,36,123) are some examples. The effect of the peptide LEISSTCDA has been observed in various expression contexts using different promoters such as that for nisin (48,49,123) or the zinc promoter (GTP-Technology, unpublished) and various SPs such as SP_{Nuc} (123), and SP_{Usp45} (37,48,49) or SP_{Exp4} [(48,49), GTP-Technology, Labège, France, unpublished]. The positive effect of the fusion to this propeptide on translocation could be explained by the introduction of negative charges on the N-terminus of the mature protein, which would restore a balance of charges associated with SP-membrane interaction (31,36,123). Moreover, this positive effect on secretion is generally accompanied by an increase in the amount of protein, suggesting an indirect effect on intracellular proteolysis of the precursor (31). The use of the LEISSTCDA propeptide has also been shown to improve the secretion of Nuc and BLG heterologous proteins in *Lactobacillus casei* BL23 (124).

24.4.1.3 Carrier Proteins. In *L. lactis*, the fusion of a protein of interest to a protein known to be produced and secreted well by the cell can also help in stabilize production and improve secretion. The fusion of the protein L7/L12 to the secreted form of the Nuc from *S. aureus*, induced by SP_{Usp45}, improves the production rate by a factor of 2.5. This fusion also increases the amount of L7/L12 present in the supernatant in the form Nuc-L7/L12 (37). However, this stabilizing effect on protein production does not always lead to an increase in the amount of protein found in the supernatant. In the case of a Nuc-E7 fusion, the efficiency of secretion decreased from 95% to 5% despite increased expression (42). Secretion can be subsequently improved by factor 3 by inserting the LEISSTCDA synthetic propeptide (125).

In *L. lactis*, the different tools used to modify the precursor can also increase the level of total production (resulting from an improved synthesis and/or stability) and/or efficiency of secretion. The contribution of each effect toward improving the amount of protein found in the media varies and is difficult to predict.

24.4.2 Mechanism of Protein Secretion in *L. lactis*

24.4.2.1 Protein Targeting and Translocation. In *L. lactis*, no experimental data is yet available concerning factors involved in the targeting of the precursor to the membrane. *L. lactis* has the genes encoding for the ubiquitous intracellular chaperon systems GroEL/GroES (126) and Dna K/DnaJ/GrpE (127,128). The expression of GroES/GroEL is increased in response to various stresses such as temperature, acidity, ultraviolet irradiation, or concentrated salts (129–131). In response to heat stress, it was shown that expression is increased by a factor of 10 for *dnaJ* and *groEL* genes and of 100-fold for *dnaK* (132). Moreover, their overexpression increases the resistance of bacteria to stress (133). A homolog of *hrcA* from *B. subtilis* along with the CIRCE sequences was also detected in the genome of *L. lactis* (21,22,134). These proteins likely play a role similar to those described for *B. subtilis* and *E. coli* in protein folding. In contrast, in *L. lactis*, the effect of modulating the overexpression of these chaperons on the intracellular production of heterologous secreted proteins has not been the subject of any published studies.

Genomic analysis of *L. lactis* has detected genes encoding homologs of Ffh (*ffh*), HBsu (*hslA*), FtsY, and scRNA from the SRP system (17,135). Models of secondary structures of RNAs from *L. lactis, E. coli* and *B. subtilis* that associate with the SRP were constructed and compared. They show that the structure of the *L. lactis* RNAsc is closer to that of the 4.5 S RNA of *E. coli* than to that of *B. subtilis* (135). No homologs of *E. coli* SecB or *B. subtilis* CsaA have been identified in the genome of *L. lactis* IL1403. In this organism, it is thought that secretion is mainly cotranslational.

With regard to its mechanism of translocation and maturation of precursor proteins, SecA and SecYEG of *L. lactis* are highly homologous to the prototypes in *E. coli* or *B. subtilis*. Among the putative accessory proteins associated with this translocon, YbdC and YfgG, are homologous to SpoIIIJ and YqjG, respectively, of *B. subtilis* (17), and they all belong to the same protein family: Oxa1/YidC. In contrast, no protein homolog of SecDF protein from *B. subtilis* or both SecD and SecF proteins from *E. coli* can be identified by genomic analysis. Finally, *L. lactis* has only one type I SPase, SipL, and no SP peptidase has been identified (17).

The analysis of the genome sequence of the strain IL1403 of *L. lactis* shows that most proteins involved in secretion are present and may play an identical role to those described above. The influence of these different components on the secretion of proteins in this organism has not been reported in the literature.

A strategy of random mutagenesis was used to identify accessory genes directly or indirectly influencing the rate of secretion and/or production of a form of Nuc (136). A collection of mutants called *hypo- and hyper-secretors* were isolated. One of these, carrying a mutation in the gene *dltA* was identified as a hyper-secretor mutant. This study reported that the decrease in D-alanylation of the cell wall affects the release of Nuc into the media resulting in its retention in the cell (136).

On the other hand, the absence of certain factors such as SecDF, which can be regarded as accessory proteins associated with the translocon, and the simplicity of the mechanism of maturation, suggest that the capacity of translocation and precursor maturation in *L. lactis* is limited compared with that of the gram-positive model bacterium

B. subtilis which has a high capacity secretion. Complementation of the *L. lactis* translocation machinery by SecDF from *B. subtilis* allowed to improve the production of both *S. aureus* Nuc protein and *B. abortus* L7/L12 antigen (136).

24.4.2.2 Quality Control of Exported Proteins. As we have seen in this second part, the folding of proteins has a major influence on the process of secretion. It involves many factors, intra- and extracellular, for protein quality control. *In L. lactis*, such a network exists and functions on both sides of the membrane.

24.4.2.2.1 Folding. A network of proteins involved in quality control of the surface is also present in *L. lactis*. The lipoprotein PmpA, homologous to PrsA of *B. subtilis*, belongs to the parvuline family of PPIases, although it lacks the PPIase motif. Depending on conditions, its expression is induced by exposure to salt stress (62). Its overexpression influences the rate of production of a heterologous secreted protein, the lipase of *Staphylococcus hyicus*, suggesting that PmpA could be a chaperon protein (62). The overproduction of the PrsA factor from *B. subtilis* in *L. lactis* can also improve the amount of secreted heterologous proteins such as AmyL when they are overproduced (138).

L. lactis has no homologous counterpart to *B. subtilis* disulfide-bond-oxydo-reductases that are involved in the formation of disulfide bonds, although the formation of disulfide bonds in a secreted heterologous protein (murine interleukin 12) has been described (48,49). However, the low proportion of proteins in which bridges are formed between the two subunits p35 and p40 suggests that they may form spontaneously.

24.4.2.2.2 Degradation of Exported Proteins. For protein quality control at the cell surface, *L. lactis* has the advantage of possessing a single extracellular housekeeping protease, HtrA (23,26). Its inactivation confers a thermosensitive phenotype, probably resulting from the toxic accumulation of misfolded proteins at the cell surface (23). *htrA* expression is induced by exposure to different stresses (heat, salt, and ethanol) (25). The mechanism of *htrA* regulation is not yet known: one of *L. lactis* two-component systems could be involved in this regulation, as in *B. subtilis*, CssRS two-component system is responsible for *htrA* and *htrB* induction in response to thermal or secretion stress. HtrA was also shown to process AcmA, the major autolysin in the cell wall (23).

As part of the production of heterologous secreted proteins, inactivation of the protease is of interest as demonstrated for the lipase of *S. hyicus*. The production of this lipase, which is normally degraded by HtrA, is increased fourfold in the *htrA* mutant (23,24,26,110). This drastic stabilization effect makes *htrA* mutant strain a very attractive host for the production and secretion of stable heterologous proteins (23,26).

24.5 CONCLUSION

Among the broad host range available to produce heterologous protein in bacteria, LAB emerged as very interesting host cell factories. These bacteria naturally offer several advantages compared to other bacterial expression system, their food-grade property being one of the major one. This is of a major concern in the case of therapeutic proteins or peptides especially for human applications. Limited production yields led to many studies aiming to improve yield productions. Numerous tools including expression and secretion systems as well as engineered strains have then been successfully developed in the model LAB *L. lactis* making it an attractive and efficient cell factory to produce heterologous proteins. Based on this knowledge, efficient expression system could be provided in many other LAB such as lactobacilli. It has to be noticed that compared to *L. lactis*, some lactobacilli may offer additional natural advantages such as probiotic activity, better production yield and in some cases, mucosal persistance and/or immune system stimulation (14,116,139). Together, all these studies enlarged LAB scope mostly in production of heterologous proteins and mucosal delivery of therapeutic and prophylactic molecules. Depending on the application, LAB should be now considered as important host production candidates.

REFERENCES

1. von Heijne G, Abrahmsen L. FEBS Lett 1989; 244: 439–446.
2. Tjalsma H, Bolhuis A, Jongbloed JD, Bron S, van Dijl JM. Microbiol Mol Biol Rev 2000; 64: 515–547.
3. van Roosmalen ML, Geukens N, Jongbloed JD, Tjalsma H, Dubois JY, Bron S, van Dijl JM, Anne J. Biochim Biophys Acta 2004; 1694: 279–297.
4. Driessen AJ, Manting EH, and van der Does C. Nat Struct Biol 2001; 8: 492–498.
5. Economou A. FEBS Lett 2000 2000; 476: 18–21.
6. Veenendaal AK, van der Does C and Driessen AJ. Biochim Biophys Acta 2004; 1694: 81–95.
7. Duong F and Wickner W. The SecDFyajC domain of preprotein translocase controls preprotein movement by regulating SecA membrane cycling. Embo J 1997; 16: 4871–4879.
8. Samuelson JC, Wickner W, Chen M, Jiang F, Moller I, Wiedmann M, Kuhn A, Phillips GJ, and Dalbey RE. YidC mediates membrane protein insertion in bacteria. Nature 2000; 406: 637–641.
9. Westers H, Darmon E, Zanen G, Veening JW, Kuipers OP, Bron S, Quax WJ., and van Dijl JM. The Bacillus secretion stress response is an indicator for alpha-amylase production levels. Lett Appl Microbiol 2004; 65: 65–73.

10. van Wely KH, Swaving J, Freudl R and Driessen AJ Translocation of proteins across the cell envelope of Gram-positive bacteria. FEMS Microbiol Rev 2001; 25: 437–454.
11. Clausen T, Southan C and Ehrmann M and Driessen AJ. The HtrA family of proteases: implications for protein composition and cell fate. Mol Cell 2002; 10: 443–455.
12. Westers L, Westers H, Quax WJ. Biochim Biophys Acta 2004; 1694: 299–310.
13. Simonen M, Palva I. Microbiol Rev 1993; 57: 109–137.
14. Wells JM, Mercenier A. Nat Rev Microbiol 2008; 6: 349–362.
15. Garvie E, Farrow J. Int J Syst Bacteriol 1982; 32: 453–455.
16. Schleifer KH, R, Kilpper-Balz. 1987. Syst Appl Microbiol: 1–19.
17. Bolotin A, Wincker P, Mauger S, Jaillon O, Malarme K, Weissenbach J, Ehrlich SD, Sorokin A. Genome Res 2001; 11: 731–753.
18. Makarova K, Slesarev A, Wolf Y, Sorokin A, Mirkin B, Koonin E, Pavlov A, Pavlova N, Karamychev V, Polouchine N, Shakhova V, Grigoriev I, Lou Y, Rohksar D, Lucas S, Huang K, Goodstein DM, Hawkins T, Plengvidhya V, Welker D, Hughes J, Goh Y, Benson A, Baldwin K, Lee JH, Diaz-Muniz I, Dosti B, Smeianov V, Wechter W, Barabote R, Lorca G, Altermann E, Barrangou R, Ganesan B, Xie Y, Rawsthorne H, Tamir D, Parker C, Breidt F, Broadbent J, Hutkins R, O'Sullivan D, Steele J, Unlu G, Saier M, Klaenhammer T, Richardson P, Kozyavkin S, Weimer B, Mills D. Proc Natl Acad Sci U S A 2006; 103:(42): 15611–15616.
19. Wegmann U, O'Connell-Motherway M, Zomer A, Buist G, Shearman C, Canchaya C, Ventura M, Goesmann A, Gasson MJ, Kuipers OP, van Sinderen D, Kok J. J Bacteriol 2007; 189:(8): 3256–3270.
20. Jana S, Deb JK. Appl Microbiol Biotechnol 2005; 67: 289–298.
21. van Asseldonk M, de Vos WM, Simons G. Mol Gen Genet 1993; 240: 428–434.
22. van Asseldonk M, Simons A, Visser H, de Vos WM, Simons G. J Bacteriol 1993; 175: 1637–1644.
23. Poquet I, Saint V, Seznec E, Simoes N, Bolotin A, Gruss A. Mol Microbiol 2000; 35: 1042–1051.
24. Miyoshi A, Poquet I, Azevedo V, Commissaire J, Bermudez-Humaran L, Domakova E, Le Loir Y, Oliveira SC, Gruss A, Langella P. Appl Environ Microbiol 2002; 68: 3141–3146.
25. Foucaud-Scheunemann C, Poquet I. FEMS Microbiol Lett 2003; 224: 53–59.
26. Poquet I, Bolotin A, Sorokin A and Gruss A. 2006. INRA Patent in USA (US 6∼994∼997). Also in 2002 in France (FR 98 16462).
27. Kodama T, Endo K, Sawada K, Ara K, Ozaki K, Kakeshita H, Yamane K, Sekiguchi J. J Biosci Bioeng 2007; 104:(2): 135–143.
28. Murashima K, Chen CL, Kosugi A, Tamaru Y, Doi RH, Wong SL. J Bacteriol 2002; 184:(1): 76–81.
29. Mierau I, Leij P, van Swam I, Blommestein B, Floris E, Mond J, Smid EJ. Microb Cell Fact 2005; 4: 15.
30. Mierau I, Olieman K, Mond J, Smid EJ. Microb Cell Fact 2005; 4: 16.
31. Le Loir Y, Azevedo V, Oliveira SC, Freitas DA, Miyoshi A, Bermudez-Humaran LG, Nouaille S, Ribeiro LA, Leclercq S, Gabriel JE, Guimaraes VD, Oliveira MN, Charlier C, Gautier M, Langella P. Microb Cell Fact 2005; 4: 2.
32. de Vos WM. Curr Opin Microbiol 1999; 2: 289–295.
33. Dieye Y, Usai S, Clier F, Gruss A, Piard JC. J Bacteriol 2001; 183: 4157–4166.
34. Le Loir Y, Gruss A, Ehrlich SD, Langella P. J Bacteriol 1994; 176: 5135–5139.
35. Sibakov M, Koivula T, von Wright A, Palva I. Appl Environ Microbiol 1991; 57: 341–348.
36. Le Loir Y, Gruss A, Ehrlich SD, Langella P. J Bacteriol 1998; 180: 1895–1903.
37. Miyoshi A, Bermudez-Humaran LG, Ribeiro LA, Le Loir Y, Oliveira SC, Langella P, Azevedo V. Microb Cell Fact 2006; 5: 14.
38. Lee MH, Roussel Y, Wilks M, Tabaqchali S.. Vaccine 2001; 19: 3927–3935.
39. Wells JM, Wilson PW, Norton PM, Gasson MJ, Le Page RW. 1993. Mol Microbiol 8: (1155–1162).
40. Theisen M, Soe S, Brunstedt K, Follmann F, Bredmose L, Israelsen H, Madsen SM, Druilhe P. Vaccine 2004; 22: 1188–1198.
41. Cortes-Perez NG, Bermudez-Humaran LG, Le Loir Y, Rodriguez-Padilla C, Gruss A, Saucedo-Cardenas O, Langella P, Montes-de-Oca-Luna R. FEMS Microbiol Lett 2003; 229: 37–42
42. Jensen PR, Hammer K. Appl Environ Microbiol 1998; 64: 82–87.
43. Langella P, Le Loir Y. Braz J Med Biol Res 1999; 32: 191–198.
44. Gil MT, Perez-Arellano I, Buesa J, Perez-Martinez G. FEMS Microbiol Lett 2001; 203: 269–274.
45. Steidler L, Wells JM, Raeymaekers A, Vandekerckhove J, Fiers W, Remaut E. Appl Environ Microbiol 1995; 61: 1627–1629.
46. Steidler L, Robinson K, Chamberlain L, Schofield KM, Remaut E, Le Page RW, Wells JM. Infect Immun 1998; 66: 3183–3189.
47. Steidler L, Hans W, Schotte L, Neirynck S, Obermeier F, Falk W, Fiers W, Remaut E. Science 2000; 289: 1352–1355.
48. Bermudez-Humaran LG, Langella P, Commissaire J, Gilbert S, Le Loir Y, L'Haridon R, Corthier G. FEMS Microbiol Lett 2003; 224: 307–313.
49. Bermudez-Humaran LG, Langella P, Cortes-Perez NG, Gruss A, Tamez-Guerra RS, Oliveira SC, Saucedo-Cardenas O, Montes de Oca-Luna R, Le Loir Y. Infect Immun 2003; 71: 1887–1896.
50. Bernasconi E, Germond JE, Delley M, Fritsche R, Corthesy B. Appl Environ Microbiol 2002; 68: 2917–2923.
51. Chatel JM, Langella P, Adel-Patient K, Commissaire J, Wal JM, Corthier G. Clin Diagn Lab Immunol 2001; 8: 545–551.
52. Chatel JM, Nouaille S, Adel-Patient K, Le Loir Y, Boe H, Gruss A, Wal JM, Langella P. Appl Environ Microbiol 2003; 69: 6620–6627.
53. Flynn S, van Sinderen D, Thornton GM, Holo H, Nes IF, Collins JK. Microbiology 2002; 148: 973–984.

54. Martinez JM, Kok J, Sanders JW, Hernandez PE. Appl Environ Microbiol 2000; 66: 3543–3549.
55. van Belkum MJ, Worobo RW, Stiles ME. Mol Microbiol 1997; 23: 1293–1301.
56. van Belku MJ, Worobo RW, Stiles ME. Mol Microbiol 1997; 23: 1293–1301.
57. van de Guchte M, van der Vossen JM, Kok J, Venema G. Appl Environ Microbiol 1989; 55: 224–228.
58. Kahala M, Palva A. Appl Microbiol Biotechnol 1999; 51: 71–78.
59. Neubauer H, Bauche A, Mollet B. Microbiology 2003; 149: 973–982.
60. Wolinowska R, Ceglowski P, Kok J, Venema G. 1991. Gene 106: (115–119).
61. Simons G, Rutten G, Hornes M, Nijhuis M, van Asseldonk M. Adv Exp Med Biol 1991; 306: 115–119.
62. Drouault S, Corthier G, Ehrlich SD, Renault P. Appl Environ Microbiol 2000; 66: 588–598.
63. Arnau J, Hjerl-Hansen E, Israelsen H. Appl Microbiol Biotechnol 1997; 48: 331–338.
64. Lindholm A, Smeds A, Palva A. Appl Environ Microbiol 2004; 70: 2061–2071.
65. Zhu Y, Zhang Y, Li Y. Appl Microbiol Biotechnol 2009; 83: 597–610.
66. Mills S, McAuliffe OG, Fitzgerald GF, Ross RP. FEMS Microbiol Rev 2006; 30: 243–273.
67. de Vos WM, Simons G. Biochimie 1988; 70: 461–473.
68. Sorensen HP, Mortensen KK. J Biotechnol 2005; 115: 113–128.
69. Choi JH, Lee SY. Appl Microbiol Biotechnol 2004; 64: 625–635.
70. Baneyx F. Curr Opin Biotechnol 1999; 10: 411–421.
71. Makrides SC. Microbiol Rev 1996; 60: 512–538.
72. Mooney RA, Artsimovitch I, Landick R. J Bacteriol 1998; 180: 3265–3275.
73. de Vos WM, Kleerebezem M, Kuipers OP. Curr Opin Biotechnol 1997; 8: 547–553.
74. Israelsen H, Madsen SM, Vrang A, Hansen EB, Johansen E. Appl Environ Microbiol 1995; 61: 2540–2547.
75. Nauta A, van Sinderen D, Karsens H, Smit E, Venema G, Kok J. Mol Microbiol 1996; 19: 1331–1341.
76. Waterfield NR, Le Page RW, Wilson PW, Wells JM. Gene 1995; 165: 9–15.
77. Poquet I, Ehrlich SD, Gruss A. J Bacteriol 1998; 180: 1904–1912.
78. van der Vossen JM, Kok J, Venema G. Appl Environ Microbiol 1985; 50: 540–542.
79. van der Vossen JM, van der Lelie D, Venema G Isolation and characterization of *Streptococcus cremoris* Wg2-specific promoters. Appl Environ Microbiol 1987; 53: 2452–2457.
80. van Rooijen RJ, Gasson MJ, de Vos WM. J Bacteriol 1992; 174: 2273–2280.
81. Koivula T, Sibakov M, Palva I. Appl Environ Microbiol 1991; 57: 333–340.
82. Djordjevic G, Bojovic B, Banina A, Topisirovic L. Can J Microbiol 1994; 40: 1043–1050.
83. Khunajakr N, Liu CQ, Charoenchai P, Dunn NW. Gene 1999; 229: 229–235.
84. Jensen PR, Hammer K. Appl Environ Microbiol 1998; 64: 82–87.
85. Kuipers OP, Beerthuyzen MM, de Ruyter PG, Luesink EJ, de Vos WM. J Biol Chem 1995; 270: 27299–27304.
86. Kilstrup M, Jessing SG, Wichmand-Jorgensen SB, Madsen M, Nilsson D. J Bacteriol 1998; 180: 3900–3906.
87. Martin MG, Sender PD, Peiru S, de Mendoza D, Magni C. J Bacteriol 2004; 186: 5649–5660.
88. Que YA, Haefliger JA, Francioli P, Moreillon P. Infect Immun 2000; 68: 3516–3522.
89. Brurberg MB, Haandrikman AJ, Leenhouts KJ, Venema G, Nes IF. Appl Microbiol Biotechnol 1994; 42: 108–115.
90. Piard JC, Jimenez-Diaz R, Fischetti VA, Ehrlich SD, Gruss A. Adv Exp Med Biol 1997; 418: 545–550.
91. Callegari ML, Riboli B, Sanders JW, Cocconcelli PS, Kok J, Venema G, Morelli L. Microbiology 144 1998;.(Pt 3): 719–726
92. Xiang H, Liu J, Hu W, Zhu J, Zhu Z. 1999. Wei Sheng Wu Xue Bao 39: (196–204).
93. Franz CM, van Belkum MJ, Worobo RW, Vederas JC, Stiles ME. Microbiology 2000; 146 (Pt 3): 621–631.
94. Que YA, Francois P, Haefliger JA, Entenza JM, Vaudaux P, Moreillon P. 2001. Infect Immun 69: (6296–6302).
95. Dieye Y, Hoekman AJ, Clier F, Juillard V, Boot HJ, Piard JC. Appl Environ Microbiol 2003; 69: 7281–7288.
96. Wei W, Xiang H, Tan H. 2003. Wei Sheng Wu Xue Bao 43: (347–353).
97. van de Guchte M, Kodde J, van der Vossen JM, Kok J, Venema G. 1990. Appl Environ Microbiol 56: (2606–2611).
98. Miyoshi A, Jamet E, Commissaire J, Renault P, Langella P, Azevedo V. FEMS Microbiol Lett 2004; 239: 205–212.
99. Llull D, Poquet I. Appl Environ Microbiol 2004; 70: 5398–5406.
100. Nauta A, van den Burg B, Karsens H, Venema G, Kok J. Nat Biotechnol 1997; 15: 980–983.
101. Walker SA, Klaenhammer TR. J Bacteriol 1998; 180: 921–931.
102. de Vos WM, Beerthuyzen MM, Luesink EL, Kuipers OP. Dev Biol Stand 1995; 85: 617–625.
103. de Ruyter PG, Kuipers OP, Beerthuyzen MM, van Alen-Boerrigter I, de Vos WM. J Bacteriol 1996; 178: 3434–3439.
104. Mierau I, Kleerebezem M. Appl Microbiol Biotechnol 2005; 68: 705–717.
105. Kunji ER, Slotboom DJ, Poolman B. Biochim Biophys Acta 2003; 1610: 97–108.
106. Kuipers OP, Rollema HS, Siezen RJ, de Vos WM. Dev Biol Stand 1995; 85: 605–613.
107. Madsen SM, Arnau J, Vrang A, Givskov M, Israelsen H. Mol Microbiol 1999; 32: 75–87.
108. Madsen SM, Hindre T, Le Pennec JP, Israelsen H, Dufour A. Mol Microbiol 2005; 56:(3): 735–746.
109. Llull D, Son O, Trémillon N, Blanié S, Briffotaux J, Blugeon S, Morello E, Rogniaux H, Danot O, Poquet I In press.
110. Morello E, Bermudez-Humaran LG, Llull D, Sole V, Miraglio N, Langella P, Poquet I. J Mol Microbiol Biotechnol 2008; 14: 48–58.

111. Jensen PR, Hammer K. Appl Environ Microbiol 1993; 59: 4363–4366.
112. Poquet I and Llull D 2006. INRA Patent in Europe (EP 1 537∼215) and in France (FR 2 843∼973).
113. Buist 2002. In 7th Symposium on Lactic Acid Bacteria.
114. Borges F, Layec S, Thibessard A, Fernandez A, Gintz B, Hols P, Decaris B, Leblond-Bourget N. J Bacteriol 2005; 187: 2737–2746.
115. Novotny R, Scheberl A, Giry-Laterriere M, Messner P, Schaffer C. FEMS Microbiol Lett 2005; 242: 27–35.
116. Cortes-Perez NG, Lefevre F, Corthier G, Adel-Patient K, Langella P, Bermudez-Humaran LG. Vaccine 2007; 25: 6581–6588.
117. Perez-Martinez G, Kok J, Venema G, van Dijl JM, Smith H, Bron S. Mol Gen Genet 1992; 234: 401–411.
118. Ravn P, Arnau J, Madsen SM, Vrang A, Israelsen H. Gene 2000; 242: 347–356.
119. Ravn P, Arnau J, Madsen SM, Vrang A, Israelsen H. Microbiology 2003; 149: 2193–2201.
120. Enouf V, Langella P, Commissaire J, Cohen J, Corthier G. Appl Environ Microbiol 2001; 67: 1423–1428.
121. Miyoshi A, Bermudez-Humaran LG, Ribeiro LA, Le Loir Y, Oliveira SC, Langella P, Azevedo V. Microb Cell Fact 2006; 5: 14.
122. Sarvas M, Harwood CR, Bron S, van Dijl JM. Biochim Biophys Acta 2004; 1694: 311–327.
123. Le Loir Y, Nouaille S, Commissaire J, Bretigny L, Gruss A, Langella P. Appl Environ Microbiol 2001; 67: 4119–4127.
124. Hazebrouck S, Pothelune L, Azevedo V, Corthier G, Wal JM, Langella P. Microb Cell Fact 2007; 6: 12.
125. Bermudez-Humaran LG, Cortes-Perez NG, Le Loir Y, Gruss A, Rodriguez-Padilla C, Saucedo-Cardenas O, Langella P, Montes de Oca-Luna R. Biotechnol Prog 2003; 19: 1101–1104.
126. Kim SG, Batt CA. Gene 1993; 127: 121–126.
127. Eaton T, Shearman C, Gasson M. J Gen Microbiol 1993; 139: 3253–3264.
128. Barril JS, Kim SG, Batt CA. Gene 1994; 142: 91–96.
129. Hartke A, Frere J, Boutibonnes P, Auffray Y. Curr Microbiol 1997; 34: 23–26.
130. Kilstrup M, Jacobsen S, Hammer K, Vogensen FK. Appl Environ Microbiol 1997; 63: 1826–1837.
131. Koch B, Kilstrup M, Vogensen FK, Hammer K. J Bacteriol 1998; 180: 3873–3881.
132. Arnau J, Sorensen KI, Appel KF, Vogensen FK, Hammer K. Microbiology 1996; 142:(Pt 7)): 1685–1691.
133. Desmond C, Fitzgerald GF, Stanton C, Ross RP. Appl Environ Microbiol 2004; 70: 5929–5936.
134. Wiegert T, Hagmaier K, Schumann W Analysis. FEMS Microbiol Lett 2004; 234: 9–17.
135. Regalia M, Rosenblad MA, Samuelsson T. Nucleic Acids Res 2002; 30: 3368–3377.
136. Nouaille S, Commissaire J, Gratadoux JJ, Ravn P, Bolotin A, Gruss A, Le Loir Y, Langella P. Appl Environ Microbiol 2004; 70: 1600–1607.
137. Nouaille S, Morello E, Cortez-Peres N, Le Loir Y, Commissaire J, Gratadoux JJ, Poumerol E, Gruss A, Langella P. Appl Environ Microbiol 2006; 72: 2272–2279.
138. Lindholm A, Ellmen U, Tolonen-Martikainen M, Palva A. 2006. Appl Microbiol Biotechnol.
139. Oliveira ML, Areas AP, Campos IB, Monedero V, Perez-Martinez G, Miyaji EN, Leite LC, Aires KA, Lee Ho P. Microbes Infect 2006; 8: 1016–1024.

25

SOLUBLE PROTEIN EXPRESSION IN BACTERIA

Catherine H. Schein

Departments of Biochemistry & Molecular Biology/Microbiology & Immunology,
Sealy Center for Structural Biology and Molecular Biophysics, Member, Sealy Center for Vaccine Development,
University of Texas Medical Branch, Galveston, Texas

25.1 INTRODUCTION

My first publications on techniques to avoid the formation of inclusion bodies (IBs) in *Escherichia coli* (1,2) were met with a stream of positive responses from workers in the field. Many others had experienced the problems summarized in the second column of Table 25.1 and were tired of dealing with "solutions of renatured proteins" that contained particulate microdispersions of inactive protein. They also shared my concern that proteins treated with strong denaturants were not the best starting point for biophysical studies, especially in cases where the specific activity had not been determined previously. Spectral techniques such as Fourier transform infrared spectroscopy (FTIR) (1,2,16) and nuclear magnetic resonance (NMR) (3) revealed different folded forms in preparations from IBs. This indicates that there are differences in structure of proteins isolated from IBs compared to those expressed solubly (4). While correctly folded protein is present in IBs (5,6), purification procedures require complete unfolding. The great recent challenge, the structural genomics initiative, further emphasized the need for better methods for soluble expression (7,8). As renaturation from IBs has to be optimized for each protein, one of the first criteria used for targets for structural characterization was whether it could be expressed solubly in *E. coli* (9). However, even after lowering the growth temperature, many proteins are not expressed properly, or aggregate, requiring additional modification of the expression methods. Cell free growth (in lysates), or expression in yeast, insect cells or transfected mammalian cells are all possible alternatives. While expression systems in yeast (10,11) such as *Pichia pastoris* (12–15) and the baker's yeast *Saccharomyces cerevisiae* (16) are inexpensive and well developed, eukaryotic or insect cell culture methods are significantly more expensive than bacterial. Stably transformed higher eukaryotic cell lines are given to variability, tests for expression tests are time consuming, and the scale-up can be quite difficult.

There are numerous illustrations of how difficult it is to prepare proteins from IBs (17). Obtaining an apparently pure protein in solution after renaturing is no guarantee of activity. For example, human tyrosine kinase Lck was completely inactive if expressed insolubly in *E. coli* and renatured from IBs. The protein was active, however, as measured by autophosphorylation, if solubly expressed by coproduction with either gro ESL or TRX (18).

Further, even for proteins that renature well from IBs, point mutations can differ in their solubility as well as their specific activity. Ribonuclease A is probably the most common model for protein refolding experiments. However, a graduate student with experience in expressing RNase A mutants in *E. coli* and isolating them from IBs was unable to obtain an active form of a mutant that represented the ancestral protein of the hooved animals (the gene contains 16 amino acid changes chosen by evolutionary considerations) (19). Undergraduate students in a lab course recloned the gene into an *E. coli* secretion system (20), expressed the mutant protein in a soluble form, and were able to

Upstream Industrial Biotechnology: Expression Systems and Process Development, Volume 1, First Edition. Edited by Michael C. Flickinger.
© 2013 John Wiley & Sons, Inc. Published 2013 by John Wiley & Sons, Inc.

TABLE 25.1. A List of Perceived Advantages and Actual Disadvantages of Expressing Recombinant Proteins as Inclusion Bodies in *E. coli*

Advantages of IBs	Disadvantages
Many mutants of a single protein can be tested by using an individual shaker flask (or wells of a multiplate) for expression.	Mutants of proteins can differ greatly in their specific activity and ability to refold.
	Shaker flasks do not allow good control of growth conditions.
High expression level means reduced fermentation costs.	Refolding shifts problems and costs downstream.
Production can be monitored with PAGE or immunoblotting.	Production cannot be monitored directly by activity.
Cytoplasmic proteins are washed away, simplifying purification. "95%" purity can be quickly achieved.	The other "5%" contaminants are hydrophobic, insoluble membrane proteins and cell wall fragments.
Removal of cytoplasmic proteins early means less proteolysis.	Significant proteolysis accompanies refolding in dilute solution.
The major contaminants are oligomers and misfolded or proteolyzed forms of the desired protein.	Separation of multiple forms of the same protein is the most difficult purification step.
Protein in inclusion bodies is often the only way to get problem proteins or those toxic to bacteria	If the protein does not refold well, another expression system will still be needed.

determine its specific activity with respect to that of the modern protein (unpublished results).

Most researchers wish to obtain their protein in a soluble form with a minimum amount of work. I thus begin by suggesting alterations in growth conditions which can be tested with most expression systems. The section titled "**Altering the Host Strain and Vector to Direct Soluble Expression"** then discusses alternative host strains and plasmids that are better for directing soluble protein expression. The section titled **"Altering the Protein Sequence for Solubility**" is devoted to discussing ways of altering the protein itself to avoid IB formation. One can try many of the suggestions for expressing a given protein by using robotics (21).

Today, bacterial culture and cloning techniques are used by many whose specialties are far from the area of microbiology. For this reason, the section titled "**Growth Conditions and Variables that Affect Yields of Soluble Protein**" contains detailed suggestions for preparing and maintaining stock cultures and inocula as well as a phage-free environment. One must stress the importance of good sterile technique, a topic that is never presented in other areas of the physical sciences. The last section includes tips on maintaining solubility during harvesting and the preliminary washing/lysis steps. Co-solvents for retaining solubility of proteins in solution are discussed in more detail in the accompanying review ("Protein Aggregation, Denaturation").

25.2 ALTERING GROWTH CONDITIONS TO INCREASE SOLUBLE EXPRESSION

25.2.1 Lowering Growth Temperature

For intracellular production, simply lowering the growth temperature (T) (22,23) can greatly increase the soluble fraction of protein. This result has been generalized now to many different recombinant proteins, eukaryotic to bacterial in origin, all of which are more soluble when expressed at a lower growth T in bacteria (Table 25.2 gives a partial list). Others have found a similar temperature effect in two strains of yeast, *Pichia*, and *Saccaromyces* (i.e. higher protein production if the induction temperature was reduced from 28°C to 19°C) (24).

Although most of the examples in Table 25.2 used 25−30°C for production, there is evidence that one can go much lower in T to increase the yield of soluble protein (see e.g. section **titled "Choice of Promotor"** on cold shock expression vectors). The vaccinia virus large subunit of ribonucleotide reductase (vvR1, 87-kDa) was completely insoluble in *E. coli* when expressed at 37°C (0.4 m*M* isopropyl β-D-thiogalactopyranoside) but was partly soluble if induction was at 15°C (51). The quantity of soluble and insoluble human androgen receptor (AR) fusion protein occurring at different times following induction at 12°C, 22°C, and 37°C, suggested there are numerous steps in the folding of the AR hormone-binding domain to a conformation that is both soluble and able to bind hormone (67). Six different areas of the protein were converted to insoluble protein at the higher temperature. Cold shock vectors (see below) can also be induced by low T in the range of 12−18°C.

There is a lower limit of about 8−10°C below which *E. coli* will not grow at all. In general, K12 strains grow very slowly below 23°C; at 10°C only a few dozen proteins are produced (68). There are additional problems with induction at very low temperatures. While one can move a shaker into the cold room to reach lower temperatures in the lab, industrial scale fermentors require special (and expensive) cooling to maintain temperatures below 25°C while agitating.

TABLE 25.2. A Few of the Proteins Listed in the Literature that are More Soluble When Produced in *E. coli* Grown at 30°C or Less. Where no Reference is Cited, the Data are from (23). This List only includes Proteins that are Produced in a Soluble Form at 30°C or lower for which Comparative Data is given in the Reference on Solubility at a Higher Growth T

Proteins more soluble at growth temperatures <30°C
Animal/Mammalian
Apurinic endonuclease (25)
Aplysia Attractin and related Pheromones (26–29)
Bovine heart mitochondrial ubiquinol-cytochrome-C reductase (fusion protein) (30)
Bovine pancreatic procarboxypeptidase A (31)
Chick brain ß-tubulins, 33kD (32)
Chicken riboflavin carrier protein (21)
Cystic fibrosis transmembrane conductance regulator (fused to glutathione-S-transferase) (33)
Apoglobin (34) and hemoglobin (34)
Human androgen receptor (AR) fusion protein 12
Human initiation factor-4E (35)
Human Interferon-α2
Human Interferon-β(36)
Human Interferon-γ
Human indoleamine 2,3-dioxygenase (37)
Human transforming growth factor-β(38)
Human testes antigen (39)
Human triose phosphate isomerase double mutant(M14Q/R98Q) (40)
Mouse DNA polymerase delta (41)
Murine cAMP-dependent protein kinase (catalytic subunit) (42)
Murine Mx
Rabbit muscle glycogen phosphorylase (43)
Rat phosphatidylinositol transfer protein (44)
Regulator of chromosome condensation (RCC1) (45)
Xenopus Cu,Zn Superoxide dismutase (46)
Fish
Herring antifreeze protein 13
Plant
Amylase (47)
Radish 3-OH-3-methyl glutarylcoenzyme A reductase (48)
Rice lipoxygenase L-2 (49)
Viral
Herpes simplex thymidine kinase fusion protein (50)
Vaccinia virus large subunit of ribonucleotide reductase (vvR1, 87-kDa) (51)
Yeast/Fungal
Cephalosporin-C acylase from Pseudomonas N176 (52)
Isopenicillin-N-synthases (53)
Streptomyces pro-transglutaminase (54)
Streptomyces jumonjinensis isopenicillin N synthase (56)
yeast α-glucosidase P1 (56)
Bacterial
β-galactosidase, (of Thermus thermophilus!) (57)
Carbamoylase and hydantoinase (58)
Diphtheria toxin and fusion proteins thereof (59)
Heparinase II and III from *Flavobacterium heparium* (60)
Lycopene cyclase from *Erwinia uredovora* (61)
P22 tailspike (62)
Propionibacterium acnes lipase (63)
Ricin A-chain (64)
Salmonella typhimurium CheY mutant gene (65)
T4 DNA polymerase (66)

TABLE 25.3. Useful Expression Partners for Recombinant Proteins

DSB-A
DNA-k and DNA-J
E. coli gro ESL
Phospholipids
Thioredoxin
Antibodies to the protein
Vitreoscilla hemoglobin

Point mutations may make a protein more or less prone to temperature induced aggregation. For example, human triose phosphate isomerase is soluble at 37°C during production in *E. coli*. Two mutants of this enzyme, Met14Gln and RArg98Gln, are partially and completely inactive, respectively. A double mutant with both alterations was inactive, T-sensitive, and could only be produced in a soluble form at a growth T of 28°C (40).

While in some cases the production of soluble protein may appear to be the same at both growth temperatures (69), lowering the growth temperature has two additional great advantages. The first is that at lower temperature, the O_2 solubility in the growth medium is much higher. Thus the cell density can be increased as the culture is not forced to grow anaerobically as quickly. Anaerobic growth and particularly the production of acetate has been shown to limit cell growth and the production of protein (70).

The second advantage is that several plasmid expression systems have been shown to be more stable when bacteria are grown at lower temperatures. This may be due to the fact that the half-life of the antibiotics used to select plasmid bearing bacteria during the cultivation also have a longer half-life at the lower temperature.

Higher growth temperature can also inhibit processing. When chicken riboflavin carrier protein, a phosphoglycoprotein, was expressed in the T7 system at 37°C, two products were seen in whole cell lysates for protein with and without the pelB leader sequence encoded in the pET20b vector. The signal sequence was correctly cleaved in soluble protein expressed at 22°C, and that isolated from IBs (!) (71). This brings up yet a further point: even the aggregated protein formed at lower temperatures may be in a more active conformation (16).

Low growth temperature can also be combined with other modifications to achieve more soluble protein. For example, coexpression of certain proteins and foldases may be of use (section titled "Coexpressing other Proteins"; Table 25.3). Many of the proteins in Table 25.2 are fusions with common linkers that facilitate purification and may promote solubility, as discussed in the section titled "**Selecting Signal Sequences or Fusion Partners**" and Table 25.4.

There is one area where higher growth temperature may be an advantage. Secretion of RNases from *E. coli* was improved by growing the bacteria at 37°C (20). However, this phenomenon might better be referred to as *periplasmic shedding*, rather than true secretion, as indicated by the increase in total medium protein. Production of antibodies in secretion systems, for example is still done at lower growth temperature to maintain the product as much as possible within the bacteria. This avoids having to use ultrafiltration to concentrate the medium as well as the deleterious effects on the protein itself from aeration (as discussed later in this chapter).

25.2.1.1 Possible Reasons for the Effect of Temperature.

The reasons for the effect of lowering growth temperature are hard to pinpoint. The effect is not simply due to slowing the production rate of the protein or to a decreased growth rate. The protein Mx was sequestered into IBs at 37°C, regardless of the absolute production rate (which was controlled by varying the distance between the Shine Dalgarno and the initial ATG in otherwise similar expression plasmids) (23). The rate of synthesis of a particular protein does not necessarily increase with temperature. Further, decreasing the growth rate in other ways does not increase soluble expression; on the contrary, substrate limitations lower recombinant protein expression. A direct effect between protein folding and temperature has been detected in several studies, for example, the viability of phage produced at temperatures above 37°C decreases sharply (80). Others have found correct folding within IBs formed at the lower, but not higher temperatures, using FTIR (16,81).

It is possible that compartmentalization of protein production is more efficient at the lower growth temperature. For example, RNase A was insoluble at 37°C when produced cytoplasmically, but soluble at this temperature when directed to the periplasm/medium in a secretion system (20). In mammalian cells, proteins expressed in the nucleus were more susceptible to thermal denaturation *in situ* compared to those expressed in the cytoplasm (82).

Another possibility is the presence or lack of some proteins important for folding or aggregation at different temperatures. Postranslational modifications also affect solubility. Phosphorylation may occur at the higher temperature, thus altering the characteristics of the protein, as has been shown for GroEL (83). Proteolysis increases at higher temperatures, as does the catabolism of amino acids in central metabolic pathways such as serine (84). Studies of the expression of various heat shock proteins, which are induced by growth at higher temperatures, has indicated that their presence alone cannot mimic the effects on cell growth of increasing temperature. Indeed, as we will see in the section titled "**Altering the Host Strain and Vector to Direct Soluble Expression"**, coexpression of some of these proteins can selectively increase the amounts of

TABLE 25.4. Linkers that Improve the Solubility of Fusion Proteins or Allow More Specific Purification

Linker	Comments
Calmodulin (72)	Calmodulin binds to phenol sepharose tightly.
E. coli maltose binding protein (MBP)	Purify fusion protein by binding to amylose beads and eluting with maltose. The linker may be cloned at either end. Reported to be quite effective at rendering problem proteins soluble (73–75).
Glutathione-S-transferase	Purify fusion protein by binding to glutathione beads.
Hexa- (or more) poly histidine linker	Allows purification with metal chelate columns; may render proteins more soluble as well (32); usually does not interfere with activity although there are exceptions reported (76).
Thioredoxin (TRX)	Very commonly used linker system 78 useful for many proteins (33,57,58). Antibodies to thioredoxin may be useful in purifying the fusion proteins (78).
Ubiquitin (79)	Easily cleavable fusion protein.

soluble recombinant protein. Possible explanations for the effect of primary sequence on IB formation is discussed in the section titled "**Altering the Protein Sequence for Solubility**".

25.2.2 Medium Composition

Generally a defined medium that will allow high density growth is preferred for purification purposes (85). Batch feeding during induction has been shown to increase yield considerably. Glycerol may be a better carbon source than glucose as less acetate is produced when it is metabolized (86). In general, growth limitations should be avoided, with the exception of expression with negatively regulated induction systems, such as those based on the tryptophan promotor. Mathematical models have also been developed to aid in increasing cell density (87).

Adding compatible co-solvents during the culture may help maintain solubility, whereby in some cases their effect may actually be during harvesting (section titled "**Growth Conditions and Variables that Affect Yields of Soluble Protein**"). Increasing medium osmolarity by the addition of nonmetabolizable sugars may also increase protein solubility at higher temperatures: 0.4 M sucrose added to the growth medium increased the production of soluble ß-lactamase protein (88). There are relatively few examples, however, where compatible co-solvents have been tried, perhaps because of the large amount of solutes that must be added to the culture, that becomes especially prohibitive on scale-up. Solubility of bovine heart mitochondrial ubiquinol-cytochrome-C reductase, expressed as a fusion protein with glutathione, was greatly improved by adding 2.5 m*M* betaine and 440 m*M* sorbitol to the growth medium. Presumably, the increased osmolarity of the growth medium forced the uptake of betaine and a corresponding increase within the cells of glycyl betaine (31). Addition of detergents such as the Tween series to the growth medium may increase yields in secretion systems (however, these may simply change lower the amount of secreted protein associated with the cell membrane; so, addition of detergent should not be used by those who prefer to harvest the cells with the protein rather than directly from the medium) (20). Adjusting the growth medium may also compensate for the effects of higher growth temperatures (89).

Before eliminating casein hydrolysates from the growth medium, one should insure that their presence is not essential for controlling protease activity. Addition of protease inhibitors to the growth medium, in the form of an ill-defined extract of potato, was essential for production of interferon in *Bacillus subtilis* (90) and addition of 0.2 m*M* EDTA inhibited *Vibrio* exoproteases (91). Specific inhibitors of toxic enzymes may also be added to the growth medium. Yields of vvR1, for example, were improved by adding the ribonucleotide reductase inhibitor hydroxyurea (51).

Proteins induced under stress conditions may serve to control the production of acetate. The universal stress protein (USPA), a 13.2 kDa protein, is induced by a variety of stress conditions. This protein's role during stress may be to control the pathways of glycoslysis, as mutants in its gene secrete large amounts of acetate (92).

25.2.3 Induction Conditions

The timing of addition and amount of inducer should be strictly controlled. Many have found it advantageous to induce at low cell density in shaker flask culture to avoid growth limitation by the medium. The concentration of inducer may also be important; several authors have reported better yields of soluble protein if the isopropyl-D-thiogalactopyranoside (IPTG) inducer concentration was reduced from the usual 1 m*M* (44,45,93).

Yields of vvR1, for example, were improved by inducing at a low cell density, and using a low concentration (0.05 m*M*) of the inducer IPTG (51). A higher cell density

TABLE 25.5. Several Common *E. coli* Host Strains and Their Genotypes. See Tables in Sambrook *et al*. (94) For More Strains and An Explanation of The Abbreviations

C600 (96)	*sup*E44,*thi*-1,*hsd*R,*thr*-1,*leu*B6,*lac*Y1,*ton*A21, *mcr*A.
HB101 (97)	*sup*E44,hsdS20(r-Bm-B)recA13*ara*-14proA2*lac*Y1*gal*K2*rps*L20*xyl*-5mtl-1
JM101 (98)	F', tra D36, proAB,*lac*Z,ΔM15/Δ(lac,pro), *sup*E44,*thi*-1
JM109(DE3) 19	[F', tra D36, proAB, lac I^q, *lac*Z,ΔM15] λ(DE3),Δ(lac,pro), *end*A1,*hsd*R17(Rk^{-mk+}) *sup*E44,*thi*-1, *rec*A1, *gyr*A96, *rel*A1
RV308 (99)	lac74-galISII::OP308-strA
XL1-Blue (100)	*end*A1,*hsd*R17(Rk^-Mk^+)*sup*E44, *thi*-1,λ-, *rec*A1, *gyr*A96, *rel*A1, *lac*[F',proAB, *lac*I^qΔM15, TN10(tet^R)]

may be preferable with induction at very low temperatures, as for example, when using a cold shock promotor, as the cells will grow quite slowly after that point.

25.3 ALTERING THE HOST STRAIN AND VECTOR TO DIRECT SOLUBLE EXPRESSION

25.3.1 Choice of Host Strain

25.3.1.1 Strain Choice for Expression versus Transformation. Correct host strain selection is also essential. Table 25.5 lists the phenotypes of a few commonly used *E. coli* strains. Although some of their markers may determine how well a strain produces protein, several of them are potentially undesirable leftovers added for the use for which the strain was originally designed. For example, *sup*E is an amber suppressor that inserts a glutamine at UAG codons. This was incorporated into strains of *E. coli* for replication of M13 vectors that were required, according to NIH guidelines that no longer apply, to contain amber mutations (94). As the effects of these additions on overall expression levels are not clear, strains with fewer markers may be preferable for production purposes (95).

Careful cultivation and preservation of host strains is essential for optimal production. As host strains for protein production often do not transform well, strains such as JM101 or HB101 are used for transformations after ligation or for vector propagation. Choose a host strain that is suitable for the problem at hand. Many commercial vector systems come with a recommended host strain that should be optimal.

25.3.1.2 Low Protease Strains and those with Better Redox Characteristics. Protease minus strains of *E. coli* are particularly valuable for production of soluble proteins and those expressed from secretion vectors (101). For example, *E. coli* BL21(DE3), a protease-deficient strain, was used to express bacterial glutamyl-tRNA reductase (102) and is often used for expression of other proteins. A lon-htpr-strain (lacking the lon protease of *E. coli* (103)) significantly increased the production of RNases in a secretion system (20) and the strain SG21173 (lon-, htpR-, clp) was used to express the human T cell receptor V β 5.3 under the control of the hybrid trc promoter containing the *E. coli* heat-stable enterotoxin II (STII) signal sequence for protein secretion (104).There are also strains that facilitate the formation of disulfide bonds in the reducing environment of the cytoplasm (105). These should be considered for expression of proteins with multiple cysteine cross-links.

25.3.1.3 Coexpressing other Proteins. Co-cloning of molecular chaperones, can include such diverse molecules as thioredoxin reductase (106); for membrane proteins, phospholipids (107) can be of help, but they must be selectively chosen. Coexpression of *E. coli* heat shock proteins gro ESL has solubilizing effect only on certain mammalian proteins. For example, coexpression of gro ESL increased the solubility of four of eight eukaryotic proteins (mammalian c-myb, CRE-BP1, p53 and the *Xenopus* protooncogene Mos), while coexpression of thioredoxin increased the solubility of these and the other four tested (SnoN, c-Myc, adenovirus E1A, and the human tyrosine kinase Lck) (108). Thioredoxin also increased the production of antibodies (109).

There is also a report that association with GroEL decreased the solubility of the cystic fibrosis transmembrane conductance regulator (expressed as a glutathione-S-transferase fusion protein). A 60 kD protein co-eluted from affinity columns with the protein and was shown by sequencing to be GroEL. The authors were able to break up the complex and purify the protein (which was induced at $25-28^\circ$C) by adding 5 m*M* MgATP to the bacterial extract and incubating at 37°C (110).

Other reports indicate that Gro ESL may only have a solubilizing effect at certain temperatures. The aggregation of Pre-S2-S′-β-galactosidase, a three-domain fusion protein in the cytoplasm of *E. coli*, was reduced three- to sixfold by co-overexpression of the DnaK and DnaJ molecular chaperones over a wide range of growth temperatures ($30-42^\circ$C), while an increase in the concentration of the GroEL and GroES chaperonins had a significant effect only at 30°C. Co-immunoprecipitation experiments

confirmed that pre-S2-S′-β-galactosidase formed a stable complex with DnaK, but not with GroEL, at 42°C. When the intracellular concentration of chromosomal heat shock proteins was increased by overproduction of the heat shock transcription factor sigma, or by addition of 3% ethanol (v/v) to the growth medium, a two- to threefold higher recovery of active enzyme was observed at 30 and 42°C, but not at 37°C. The overexpression of all heat shock proteins or specific chaperone operons did not significantly affect the synthesis rates or stability of pre-S2-S′-β-galactosidase and did not lead to the disaggregation of preformed IBs. Rather, the improvements in the recovery of soluble and active fusion protein resulted primarily from facilitated folding and assembly. Titration of the DnaK–DnaJ early folding factors may trigger the formation of pre-S2-S′-β-galactosidase IBs (111).

Coexpression of proteins that improve solubility or the overall growth of the bacteria can also be useful. For example, coexpression of *Vitreoscilla* hemoglobin can increase the total cell protein of various common *E. coli* cloning strains (JM101, pRed2, and W3110) and *B. subtilis* (112). Their production characteristics should also be improved as the point of oxygen limitation is delayed (113). There are now several versions of these vectors to choose from, allowing expression of different hemoglobin forms (114). The role of another regulator of iron homeostasis, in *E. coli*, the small noncoding RNA RyhB, in bacterial growth and protein expression, is also being investigated (115). Cocloning demonstrated that the function of at least one of the six homologous insulin-like growth factor binding proteins is to assist in the formation and maintenance of the native disulfides of IGF-I (116).

Cocloning of specific antibodies to the protein may increase yields. For example, the heat induced aggregation of carboxypeptidase A could be greatly reduced *in vitro* in the presence of monoclonal antibodies that did not inhibit its activity (117). In addition, coexpression of tRNA genes for the preferred mammalian codons may increase the expression of mammalian genes in *E. coli*. For example, the expression of argU tRNA enhances expression of interferon (coded from the mammalian sequence) in *E. coli* (118).

25.3.1.4 Alternative Hosts to E. coli. There are millions of different bacteria yet very few are used currently as hosts for protein production. *E. coli* itself, isolated originally from infant diarrhea, was chosen as an experimental strain by Monod soon after World War II as it was relatively non pathogenic and grew quickly. In general, alternative bacteria tested for recombinant enzyme production were selected because they had some previous industrial application, and usually were approved for use in foods. Lactobacillus, found in cheese cultures, is a possible expression host.

B. subtilis is one of the earliest alternate hosts for recombinant proteins, as there was a history of successful industrial level expression of enzymes, and the bacterium was known to secrete proteins into the growth medium. Early strains were mostly suitable for the production of stable, protease resistant proteins (119). If the basic problems of protease degradation, and processing problems that may lead to insoluble product (120,121) can be avoided, there are several possible expression vectors (122), including one based on the α-amylase signal sequence and promoter (90) and, more recently, a cold shock expression system (123). The physical properties of the protein itself greatly affect expression in *B. subtilis*, however. IFN-γ, which has a stretch of positively charged amino acids at the *C*-terminus, accumulated as an uncleaved precursor in the cells and was hardly secreted, while we managed to obtain a few milligram per litre of soluble IFN-α, which is more negatively charged (124). Other Bacilli may also be useful; the vaccine strain *Bacillus Calmette–Guerin* has been used to produce a *Schistosoma mansoni* antigen (125).

As *E. coli* does not grow well at low T, an alternative bacteria has been suggested: *Rhodococcus erythropolis*, which can grow from 4 to 35°C. Successful expression in this bacterium was reported for several proteins that could not be expressed in *E. coli* (126). Other suggested hosts include *Staphylococcus carnosus*, used for surface display of a malaria antigen (127) and a secretion/expression system in *Salmonella* has been suggested for vaccine production (128). There are "shuttle vectors" available that can function in both *E. coli* and various alternative host bacteria.

Various *Vibrio* species were used to express the nontoxic B subunit of *E. coli* heat-labile enterotoxin linked to a 27-residue C-terminal fragment of Pol, the catalytic subunit of DNA polymerase of herpes simplex virus type 1. The highest yields were reported to be 3.5 mg/l. 0.3 m*M* EDTA added to the growth medium blocked proteolysis of the secreted protein (91).

25.3.2 Altering the Vector

25.3.2.1 Choice of Promotor. Having accepted that one should induce recombinant production at a lower culture temperature, there are a variety of promoter systems that can be used. Another factor, particularly important for potentially toxic recombinant proteins, is that transcriptional control should be tight, so that the protein is first produced in the cell after induction. Expression levels in the T7 system can be increased by tighter transcriptional control before induction (129). The most commonly used vectors for protein expression in *E. coli*, such as the pET series (130,131) have promoters that can be induced below 30°C (there are now many versions of the pET vectors that can be purchased from various vendors, that

allow one to select the linkers and other characteristics). After induction, expression temperatures as low as 18°C (over a 24 h period) have been used to enhance soluble production.

25.3.2.2 Cold shock vectors. The effect of temperature on solubility, as discussed above, is still a puzzle. The simplest explanation, that lowering the temperature slowed the absolute production rate of the protein, was proven to be incorrect by our initial experiments. Matthieu Noteborn cloned protein genes behind a weak (low producing) and strong (production levels 10–100 times better) promoter. Both the high and low expressing plasmid produced IBs at 37°C and soluble protein at 28 – 30°C (23). Our results indicated that the folding state of the protein or some other function of the bacterial metabolism must change at higher temperature.

Other authors explored the effects of cold shock on the bacterium. They found that while most bacterial proteins cease to be produced when the culture temperature is lowered to below 20°C, a whole group of *E. coli* proteins are *induced*. The promotor for one of these genes, cold shock promotor CspA (132), became the basis for a recombinant protein expression vector that could be induced by lowering the growth temperature (133). The cspA protein, when expressed, represses the synthesis of other proteins (an effect referred to as Low temperature-dependent Antibiotic effect of cspA Expression (LACE) (134). Normally, cspA expression reaches its peak about 1 h after cold shock, and then is reduced to basal level. Most of the increase in cspA can be attributed to enhanced stability of the mRNA at the lower growth temperature (136). Other members of the cspA family aid in transcription antitermination by "melting" the secondary structure of RNAs, thus permitting translation at the lower temperature (18). Initial tests of the cspA promoter indicated that it would direct the overproduction of recombinant protein upon cold shock and was a promising way to express toxic proteins (135). However, similar to cspA protein expression, there was pronounced repression of the synthesis of the recombinant proteins after a few hours at the lower temperature. Although production time could be enhanced by temperature cycling (33), the production levels for most test proteins were not better than those using the pET vectors.

Inouye's group discovered nonsense mutants of cspA that, when induced, would inhibit cellular protein synthesis, leading to cell death by LACE. This effect, which requires the 5′-untranslated region (UTR) of the cspA gene, is due to sequestration of ribosomes at the initiation site of the cspA mRNAs, thereby enhancing their stability. A new series of cold shock expression vectors were designed based on this data. These contain the cspA promoter, modified 5′UTR and 3′ transcription termination site, a translation enhancing element, and a lac operator after the promoter to maintain tight transcriptional control during bacterial growth (136,137). Synthesis of the recombinant protein, induced by adding IPTG and downshifting the temperature, continues for at least 48 h. We have successfully used these commercially available vectors to express several proteins in the soluble fraction of *E. coli*, including pheromones from Aplysia (26–29), and viral proteins (unpublished), and generally found that 24 h expression at 12 – 15°C gives substantial amounts of soluble protein that is relatively easy to purify. An additional advantage may be that, if production is induced after the bacteria are transferred to suitable labeling medium, the whole cell lysate can be used to do NMR analysis of the recombinant protein.

Many other common promotors, such as those based on the tryptophan operon, are useful for low temperature expression, as is a modified tryptophanase promotor (138). Secretion of specific proteins from *E. coli* is already possible using a variety of vectors (20,139). Secretion expression systems are particularly suited to mutant analysis (146), as the culture supernatant can be directly analyzed. *Pichia* systems are also useful for secretion at lower T (11,141). Further study of the factors affecting protein transport is needed for more general secretion systems.

25.3.2.3 Selecting Signal Sequences or Fusion Partners. The sequence of the protein itself can be altered by adding linkers, or stretches of amino acids with distinct properties. Many of the commonly used linkers (Table 25.4) were initially added to improve the purification of proteins, but later proved to improve protein folding, solubility, protease resistance, and/or overall yield. Adding signal sequences can be used to achieve secretion into the culture medium. Individual domains of the same protein, such as the carboxyl-terminal region of α hemolysin, may be required to achieve correct folding and soluble expression (142). In the same fashion, expressing a protein in series with a specific linker, or adding stretches of positively charged residues (143), may be a general way to achieve better folding. For example, DNA polymerase delta could be expressed as a glutathione-S-transferase conjugate (41). Indeed, expression of small proteins or fragments of a larger protein may only be possible if the desired sequence is expressed as a fusion protein (144). For example, domains of the rotavirus VP4 protein could be produced to 27%–35% of the soluble protein in *E. coli*, if they were fused to the Hepatitis B core antigen (145). Interleukin-2 was expressed in a nonaggregating fashion by expression as a fusion protein on a phage (146). Thioredoxin fusions of many proteins are soluble, especially if produced at lower growth T. These are, in some cases, active even before removal of the thioredoxin portion, and may be purified by heating lysates to 80°C. A DDDDK linker, the recognition site for mammalian intestinal protease

enteropeptidase, allows removal of the thioredoxin moiety (147). IGF-1 was >100 times more soluble when fused to one or two *Z*-domains from *Staphylococcus* protein A, and the solubilizing effect could also be seen during *in vitro* refolding (148). Although several linkers have been reported, the choice should be optimized depending on the protein (149).

Several linkers, such as hexa-histidine (His6), can aid in the detection and purification of recombinant proteins. Indeed, a recent survey of researchers involved in the structural genomics initiatives showed that these groups overwhelmingly use a T7 RNA polymerase based expression system and a 6-His affinity tag, because this allows the use of immobilized metal affinity chromatography (IMAC) to purify the recombinant proteins (131). Many vectors also include a protease site between the linker and the protein, to permit isolation of the natural protein [as there are reports of negative effects on activity if the histidine tag is left on the protein (150)]. This expression system has the advantage that the protein can often be expressed without an *N*-terminal methionine, but the disadvantage that yields are reduced due to the additional processing step and that the protease may cleave the protein itself. Yields may be low but sufficient for characterization. The 54-kDa subunit of the canine signal recognition particle (SRP) was expressed in *E. coli* using a T7 expression system with an amino-terminal extension encoding an initiating methionine and 10 histidine residues followed by an enterokinase cleavage site; 0.3 mg of HIS-SRP 54-kDa was purified to give a single band on SDS-PAGE in 20% yield from 500 mL of cultured *E. coli* (151). The hexokinase of *S. mansoni* has been expressed in *E. coli* as a fusion protein including an *N*-terminal polyhistidine tag and enterokinase cleavage site. The enzyme was purified by metal chelate chromatography to >95% homogeneity, based on analysis by SDS-gel electrophoresis and isoelectric focusing (152). Recombinant vvR1 was purified from a high salt extract of the *E. coli* lysate in four steps, the last utilizing an affinity column consisting of the carboxyl-terminal seven amino acids of the vvR2 protein linked to an insoluble resin (57).

The *E. coli* maltose-binding protein (MBP) is a handy fusion partner that allows simple purification and secretion of the chimeric proteins. Pollen major allergen Bet v 1 from *Betula verrucosa* (White Birch) has been cloned and expressed in *E. coli* as a fusion with MBP and a Factor Xa proteolytic cleavage site. A generally applicable cloning strategy based on polymerase chain reaction was designed to position the Factor Xa proteolytic site so that the authentic amino terminus of Bet v 1 was generated after cleavage. The fusion protein was isolated by amylose affinity chromatography and enzymatically cleaved by incubation with Factor Xa (153). The kringle V domain of the lipoprotein apolipoprotein (a) from human liver was solubly expressed in *E. coli* as a MalE fusion protein and purified by amylose–agarose affinity chromatography by eluting with 10 m*M* maltose (154). Human osteocalcin (hOC), a 49-amino acid peptide produced mainly by bone osteoblasts could be expressed as a glutathione-S-transferase (GST) fusion. The protein was soluble, and could be affinity-purified and then cleaved with activated protease factor X releasing the rhOC portion (155).

25.3.2.4 Altering the Gene Sequence of the Protein. Bacterial codon usage is often significantly different from mammalian. Genes for several proteins have been synthesized to reflect the bacterially preferred codons for degenerate amino acids and eliminate elements in the noncoding region of genes that lower productivity. One of the first examples was RNase A, where much more recombinant protein was obtained; the protein was synthesized from a synthetic gene that reflected bacterial codon usage than was produced from its murine counterpart expressed from the natural mammalian gene (20). Several companies now offer custom gene synthesis for such recloning purposes. There may also be specific mammalian codons in the cDNA that may inhibit translation in bacteria. For example, 4.9% of the adult isoform of human cardiac troponin (288 amino acids) is arginine, and in the native gene is encoded by AGG and AGA, codons rarely used in *E. coli*. Changing two areas where these codons occurred consecutively [AGG(165) AGG(166) and AGG(215) AGG(216)] to the bacterially preferred codon CGT increased expression 10-fold when one pair of the rare arginine codons was replaced and a 40-fold increase when both pairs were replaced (156). One can also use strains that express tRNAs for the mammalian preferred codons, as discussed above. Another study has indicated that AT rich regions in the cDNA should be avoided in *Pichia* expression (157).

A combination of methods may be necessary, especially for proteins that interact with hydrophobic substrates (63,158) or membranes (159). For example, the aggregation of the vaccinia virus large subunit of ribonucleotide reductase (vvR1, 87-kDa) (51) was prevented by lowering the induction temperature (to 15°C), lowering the cell density during induction, and the concentration of the inducer (to 0.05 m*M* IPTG). Addition of hydroxyurea, an inhibitor of ribonucleotide reductase, further increased production of soluble vvR1 in a dose-dependent manner.

25.3.3 Cell Free Expression Systems

Although often considered too expensive for large scale production of proteins, the need to express large amounts of protein in a quality good enough for characterization by the structural genomics initiative (160) has stimulated many groups to develop efficient cell free systems to produce soluble proteins. The least expensive but potentially

most versatile is an extract of wheat germ (161,162), which can be made in the lab or purchased commercially. As a eukaryotic system, wheat germ offers the potential for correct protein glycosylation, and often contains factors that can aid in the correct folding of multidomain proteins. Correct disulfide bond formation can also be favored in such systems (163) and special systems have been designed to express membrane proteins (159).

25.4 ALTERING THE PROTEIN SEQUENCE FOR SOLUBILITY

25.4.1 Why Do Inclusion Bodies Form?

This has been the subject of much debate since the phenomenon was first observed. Lowering growth temperature to achieve more soluble protein does not work for all proteins; further, we do not understand the physical characteristics that account for why some proteins are perfectly soluble even at 42°C while point mutations thereof can render them insoluble at all temperatures. Even very large proteins (e.g. heparinases II and III, Table 25.2, are over 700 amino acids long) can be expressed in soluble form.

Although even point mutations can render proteins more or less soluble (164), specific effects cannot be directly related to hydrophobicity (Gravy scores (53)) and effects of individual point mutations cannot be easily explained (55). While one multifactorial analysis (165) could not relate sequence to solubility, some correlations have been found in other studies (166). For example, the content of the individual amino acids Asn, Thr, and Tyr, and certain tripeptides correlated well with its solubility (167); another systematic study suggested replacing Asn, Gln, and Thr with Asp, Glu, and Ser to enhance solubility (168). The context is also important, however. In carbonic anhydrase, a Glu117Gln mutation caused aggregation, while Glu106Gln gave a soluble but inactive protein (169). There may also be a correlation between thermostability and *in vivo* half life of the protein (167), and secondary structure tendency may also be important (170). Another analysis related fibril formation to the isoelectric point (IP) of the protein, as of course the protein is least soluble at its IP (171). Please see the accompanying review of aggregation phenomena *in vitro* for more details on this point ("Protein Aggregation, Denaturation").

The sequence may also affect which system one should use to produce a protein. As noted above, positively charged proteins probably will not be secreted well in *Bacillus*. Analysis of 78 human proteins produced in *P. pastoris* revealed a correlation with only three factors: the presence of AT rich regions in the cDNA and a high IP of the expressed protein were both negative indicators for expression, while the existence of a native protein in yeast that was similar usually indicated that the protein could be produced there (157).

The effects of mutations throughout a protein on aggregation have been explored, for example, for Aβ1−42. This protein fragment, the protein accumulates as "amyloid plaques" in the brain of Alzheimer's disease patients. Here, the effect of mutating each residue in Aβ to Pro or Ala on fibril formation and peptide denaturation curves (172,173) and found that many proline mutations enhances solubility and destabilized fibril formation. On the other hand, mutating Asp23, which, in the solid state NMR structure of the fibril is in a salt bridge with Lys28 (174), to alanine rendered the protein completely insoluble.

25.4.1.1 Role of Proteolysis. Protein preparations from IBs often contain misfolded protein and proteolytic fragments. IB formation in *E. coli* was probably first observed when cells were treated with amino acid analogues (175); this relationship between abnormal protein and aggregation has been born out by other studies. In general, proteolysis accompanies IB formation (23); indeed, several authors attributed the effects on solubility of a lower growth temperature to reduced proteolytic cleavage of their protein (36,93,176). Further, the proteins seem to assume certain intermediate states that are difficult to define but can be identified by some techniques (177).

Two observations may shed some light on the process of aggregation. The first is that protein aggregates, as viewed by PAGE, appeared identical in the presence or absence of another protein. Thus the protein appeared to aggregate only with itself and not to co-aggregate with a potential partner (178). Of course, the authors could not analyze the more insoluble, larger molecular weight aggregates which did not penetrate into the gel, but the results strongly suggest that aggregation follows a very specific pathway.

The second observation is that the oligomers seen in many crystal structures are not due to the monomers aligning themselves at surface exposed hydrophobic sites. Rather, the monomers exchange a whole section of the protein to form a compact structure. Requirements for the swapped domain are that it have both a hydrophilic and hydrophobic face and that it be joined to the rest of the protein by a flexible linker. "Domain swapping" is one possible mechanism for aggregation that accounts for many of the observations about IB formation (179), in particular:

- *Specificity.* The swapped domain is connected to the oligomeric partner in much the same way as to the original monomer.
- *Speed.* Thermodynamically speaking, the major barrier to overcome during the initial formation of the dimer molecule is the barrier toward opening two monomers simultaneously that lie within a permissible distance

of one another. Once a dimer has formed, however, addition of another monomer requires only the opening up of one more molecule at a time. Thus aggregation will proceed quite quickly once the initial template has formed.

- *Proteolysis.* If one assumes that a long flexible linker joins the swapped domains, this essentially unstructured area would present a good site for the attack of proteases. The domains liberated by hydrolysis might serve as fragments to participate further in aggregate formation.
- *Association with synthesis.* Pulse labeling studies with *E. coli* overexpressing the *Salmonella typhimurium* gene CheY have shown that newly formed protein aggregates more quickly than existing protein (65). However, preexisting protein can also become involved in IBs if incubation is continued for a sufficiently long time (23). This makes sense if one assumes that protein immediately after synthesis is not yet completely folded. Possibly the stable domains fold first, followed by folding of the whole protein. A protein in solution exhibits a certain amount of folding out (so-called "breathing") that can be observed by techniques such as hydrogen exchange. Presumably, new protein whose secondary structure is formed but is still unfolded at the tertiary level can exchange domains easily, while existing protein can only join the aggregate at the appropriate stage in its breathing state. As the breathing rate increases with temperature, this can also account for the observed temperature dependence of aggregation. Aggregation would thus be one aspect of the protein solution half-life, which can be related to temperature by an Arrhenius plot (lnk vs 1/T, where k is an intrinsic instability constant and T is the temperature in $^{\circ}$K.) (180)
- *Irreversibility.* As the area of the domain that is swapped is substantial, the energy required to form (and hence to separate) oligomers is very large. Presumably the energy to form the aggregate is kinetic in nature. It has been calculated that the ΔG_0 for domain swapping is as high as 40 kcal/mol, an impressive barrier to overcome spontaneously.
- *Other miscellaneous observations.* These observations include the presence of active protein in IBs (16,181), the ability of some IBs to be separated by ion exchange, and the lack of a general relationship between protein sequence and aggregation. To some extent, the influence of heat shock proteins and chaperonins on solubility can also be explained by this mechanism, as they may bind to the partially unfolded protein and prevent proteolysis or reduce its ability to join the aggregate.

Domain swapping accounts quite neatly for the effects of specific point mutations (182) and their corresponding suppressors on the solubility of proteins (183). If one accepts that domain swapping is involved in oligomer formation, designing peptides to prevent aggregation may be a greatly simplified process, especially if a crystal structure is available or one has knowledge of interacting faces within the protein. One can direct changes in the protein itself to inhibit its aggregation or design peptides that will bind reversibly to these sites and prevent the initiation of aggregation (176).

These peptides need not be very large; for example, a simple tetramer, Arg-Gly-Asp-Ser, from fibrinogen, was sufficient to inhibit the aggregation of platelets (184). A change in a few discrete amino acids at the end of the B-chain of insulin considerably reduced the oligomerization state (185). Several different peptides have been designed to inhibit the aggregation of amyloid proteins, including that of the Aβ protein implicated in Alzheimer's disease (186–188). One can also internally encode a binding sequence. A monomeric λ-cro protein was made from the homo-dimer by duplicating the dimer interface region (six amino acids) at the *C*-terminus of the molecule. The monomeric mutant was more thermostable and appeared from NMR studies to have a solution structure similar to that of the dimer (189).

25.4.2 Mutation to Increase Solubility

Single point mutations may greatly improve solubility, whereby the mutations may also affect stability to proteolysis or improved interaction with a chaperone (190). A double mutation (Gly32Asp/Ile33Pro) in a turn/loop region between two helices rendered *E. coli* MBP insoluble (191). The solubility and stability to proteolysis during production in *E. coli* of a 101-amino acid fragment from the human respiratory syncytial virus (RSV) major glycoprotein (G protein) was significantly improved by altering several phenylalanine residues. Two Cys to Ser changes did not affect the solubility or stability of the gene product. The mutant G-proteins appeared antigenically similar to the parent and had similar secondary structures (192).

Destruction due to proteases can be minimized by identifying degradation "hot spots" in proteins (193). Some of these sites have been discussed elsewhere (2,165). It should be noted that such sites in mammalian proteins may be one mechanism for controlling the activities of enzymes and even cytokines. For example, proteolytic cleavage of the *C*-terminal of human interferon-γ, which also occurs in blood, can increase activity several fold. Efficient production of this cytokine in *E. coli* was only possible if the *N*-terminal residues Cys-Tyr-Cys, which are also not found in serum isolates, was removed from the coding sequence (194).

25.5 GROWTH CONDITIONS AND VARIABLES THAT AFFECT YIELDS OF SOLUBLE PROTEIN

The following is a brief accounting of more general growth conditions that can affect the amount and quality of recombinant protein.

25.5.1 Inoculum Preparation and Storage

One of the greatest causes of variation in the production of proteins in bacteria is plasmid and host strain instability. The plasmid should be checked periodically during large-scale cultivation. Loss of plasmid or alterations (including changes in the sequence of the desired protein or even deletion of the whole segment and insertion of unrelated DNA into the plasmid) can occur. Several different "insertion sequences" are known in *E. coli*. Correct preparation of inocula to minimize variation is essential.

Most strain stability problems are not discussed openly in papers dedicated to studying the proteins themselves (with notable exceptions (195))

The following general recommendations are made for the start of culture:(i) larger inocula are preferred; and (ii) glycerol cultures should be made from the first culture after a transformation, be stored at temperatures below -70°C and should not be reused. Study the restriction digest carefully after preparing stock cultures. Remember that 1 μl of a commercial EcoRI or BamHI preparation will cut an entire miniprep of plasmid completely in a matter of minutes. Unexplainable high molecular weight bands are probably not residual host DNA and may indicate either latent bacteriophage contamination or insertion sequences in the plasmid. When in doubt, throw it out (i. e. the culture) and do another transformation. For consistency, cultures should be stored in numbered boxes and a file kept of their location in the -70°C or liquid nitrogen storage. Excess glycerol cultures of strains no longer in use should be weeded at regular intervals (usually done when the compressor needs replacing or the contents of the freezer must be moved) (196).

A good plasmid library of minipreps of vectors is the ultimate backup. Some short cuts may be taken if using a reliable kit; for example, if one is sure that a sufficient number of bacteria will be transformed, it may be possible to prepare glycerols directly from the initial transformation mix.

25.5.2 Trouble Shooting Protein Producing Recombinant Bacteria

Most host *E. coli* strains carry a portfolio of mutations that may or may not be essential to their success in producing protein. Some of several cloning and expression strains and their genotypes are listed in Table 25.5. The requirements for a cloning strain (basically high efficiency of transformation) are different from those for a good expression host. The latter should grow vigorously on minimal media and be low in proteases, while the former, such as HB101, should have few host restriction systems and high sensitivity to the selection marker. Do not store host strains on agar plates in the cold room; the best method to preserve the phenotype is to lyophilize the cells or prepare glycerol cultures and store at -70°C or liquid N_2 temperature.

It is vital to continuously monitor the quality of these host strains, especially when several researchers share stock cultures. When performing a transformation, a control plate of competent cells with no DNA added should be used to test for unwanted development of antibiotic resistance. Look for differences in the characteristic color, size, and odor of host strain colonies plated out on nonselective agar.

If necessary, one can test the host strain for the presence of markers. Reversion to a protease producing phenotype can be detected by plating on casein agar. A complete listing of the meaning of various markers for *E. coli*, with alternate notation possibilities, can be found on the Internet (197) (http://www.uni-giessen.de/~g×1052/ECDC/ecdc.htm).

25.5.2.1 Protecting Your Cultures from Contamination. Most labs limit work with phages to discrete areas as they are recognized to be invasive. A widespread M13 phage contamination can be caused from one shaker accident that is not adequately cleaned up after, and months and even years of subsequent work can be wasted if the problem is ignored. The best method is to prevent the original contamination.

Frequent hand washing with antiseptic hand soap and wearing disposable gloves is essential to avoid cross contamination of cultures when handling plasmids and other replication competent nucleic acids. Surfaces should be covered with absorbent paper and changed regularly, preferably at the end of every experiment. Isolation precautions such as those used throughout the medical field and the food preparation industry should be automatic during work with recombinant organisms. One should avoid touching hair or face during work; long hair should be tied back. Protective coats should be removed at the door to the lab and never worn in public areas, especially lunchrooms.

On shakers, all cultures must be stoppered properly and the stopper should be properly fixed so it will not fly off during culture. Flasks should be removed from the shaker area or room to make additions. The shaker should be cleaned often with an antiseptic solution. The shaker room can be periodically sterilized by using a UV-light (one with a time switch can be installed in any area for very little money). Do not use a light for >300 h operation and/or leave it on for more than 15 min at a time. Note

however, that improperly used UV irradiation is worse than no sterilization at all, as a weak light can select for mutant bacteria that will be resistant to most killing methods. An easy way to determine if the lamp is still in order is to inoculate a plate with 1 mL of a dense culture of bacteria (preferably a spore former such as *Bacillus* or *Clostridia*) and leave it open under the lamp for 15 sec (time accurately!). If any colonies grow on the plate after 24 h incubation at 30−37°C, install a new fluorescent bulb.

25.5.3 Shaker Flask versus Fermentor Cultivation; Effect of Aeration

Expressing recombinant proteins solubly does not necessarily require great expertise. However, unlike expression in IBs, which can be done under relatively uncontrolled growth conditions, high level expression of proteins in a soluble form requires control over many variables during growth and induction. These include temperature, medium pH, oxygenation, and concentration of essential nutrients such as glucose (or glycerol) and toxic by-products of the bacteria, including acetate and carbon dioxide. Several industrial biotechnology groups have developed elegant solutions for all the problems encountered in soluble expression (95,198). In general, fermentor cultivation is to be preferred, as one can easily control all of the growth variables. Presumably because of stability problems with respect to both the host strain and plasmid, continuous culture methods are generally not used. The highest yielding processes to date are based on fed-batch technology, which is also standard for antibiotic production.

The medium during growth in shaker flasks, especially at higher temperature, rapidly becomes anaerobic and acidic, meaning that the bacteria are struggling to grow and are not able to produce optimal levels of product. Under these conditions, significant production requires completely subverting the bacterial metabolism into recombinant protein production, which usually means the use of induction methods such as temperature shock that favor IB production.

Good aeration, even beyond the O_2 uptake requirements of the culture, can increase production of proteins in *E. coli*. Rapid aeration reduces the concentration of CO_2 and acetate, both of which can be toxic. High acetate production has been implicated in reducing yields, especially in shaker flasks, even when the pH is controlled by using highly buffered media. Strains that produce less acetate have been created by metabolic pathway engineering; however, these may grow too slowly to be useful. Controlling the growth conditions of a prototrophic strain so that it did not experience anaerobiosis or stress has been shown to be a more useful way to reduce acetate production in large scale, high density culture (6).

Heavy aeration can, however, lower the yields of secreted proteins. For example, surface aeration with supplemental O_2 was used to produce interferon-α in *B. subtilis* as large activity losses were found when nitrogen was bubbled through a solution of medium and the purified protein (120). Antifoam can also seriously lower yields, especially for secreted proteins, and should be used sparingly.

To determine plasmid stability as a function of culture time, one can compare the specific plasmid content of the bacteria at the end of a large-scale fermentation to that of the inoculum. The easiest way to do this is to prepare plasmid minipreps and determine the colony forming units (CFUs) of a transformation into HB101, or some other high frequency of transformation strain, at various culture points. Alternatively, comparing the amount of DNA and its restriction map on an agarose gel can be done in a semiquantitative fashion.

25.5.3.1 Stability of Selection Stress. Most antibiotics, in particular, penicillin derivatives, should not be stored in frozen aqueous solution, nor should antibiotic containing agar plates be stored before use. The half-life of the closed ß-lactam ring is extremely short in aqueous solution, particularly at neutral pH. Ampicillin should be dissolved in sterile water, filter sterilized, and added to the growth medium as close to time of inoculation as humanly or mechanically possible.

Before ignoring this caveat, note that frozen ampicillin solutions have lost their ability to lyse bacteria but may inhibit growth of nontransformed bacteria. Week old refrigerated antibiotic containing plates used for transformation selection will show no colonies for the control Ca^{2+} cells. As the transformed bacteria grow, they secrete ß-lactamase that, coupled with the instability of the antibiotic itself at 37°C, will rapidly eliminate any selective pressure in that area of the plate (or in the vessel during a large-scale cultivation). Colonies picked from the transformation plates will contain nontransformed but viable bacteria. The initially inhibited nonproducers will be able to grow, diluting the plasmid bearers and lowering yield. If the plasmid confers any negative growth characteristics, the plasmid containing bacteria will rapidly become the minority in the vessel. Additional proteins from all those nonproducing bacteria will render the purification even more difficult.

25.5.4 Maintaining Solubility during Harvesting and Cell Lysis

If one is fortunate, the protein to be isolated has distinct characteristics that separate it from most of the host proteins in the lysate. Unfortunately, the majority of naturally occurring proteins are moderately hydrophobic, with a pK_a of between 6 and 7. This means they will elute from hydrophobic interaction columns at salt concentrations between 0.1

and 0.5 N, and from ion exchange resins with the vast majority of bacterial proteins. Thus a typical protein, if expressed at low concentration in the bacterial cytoplasm, will be difficult to separate by general methods of purification, and may be destroyed by proteases before ever being seen on a gel. This problem can be alleviated by using linkers that aid in purification (Table 25.4).

IB formation would appear to confer an enormous advantage in these initial stages, as the protein is clearly visible on a polyacrylamide gel and an apparently purified preparation can be quickly obtained. The denaturants used at the early stages of preparation inhibit most proteases and the overall yield, estimated visually, would seem to be very high. However, the protease problem returns when the protein is dialyzed in dilute solution to remove the denaturants (199). Thus a variety of methods have been used to modify the solution conditions during refolding (73,200–203).

The ability to wash away contaminants from IBs is often a Trojan horse. Membrane fragments and proteins that are equally insoluble persist through many detergent washes (indeed, there is a report that protein is rendered insoluble by these agents, particularly Triton X-100 (204)). These proteins are not always visible on gel electrophoresis as they "stick in the slot" or do not stain with silver stain reagents or Coomassie blue. An even greater problem arises: the protein is contaminated with proteolytic fragments, alternate folded forms and oligomers of itself. If solubly expressed protein required isolation from bacterial proteins with similar characteristics, the problem in IB schemes comes down to isolating the protein from what is essentially the same protein. This is the hardest of all purification steps.

Even proteins that are initially soluble in bacteria may be induced to aggregate, sometimes irreversibly, during cell breakage and washing. Aggregation and proteolysis can be minimized by adding a proteolysis inhibitor to the cell culture at the end of growth and maintaining a low temperature during centrifugation. Especially on the large scale, this may require special cooling equipment for centrifuges, and small batch processing using machines such as Manton/Gaulin or French presses.

In addition, it has been reported that detergents such as Triton X-100 and Nonidet P-40 can render proteins insoluble when added during cell washing/breakage steps. In one example, the solubility of two different forms of tubulin was increased by addition of 1 M NaCl to the extraction buffer (204). However, others have noted that extraction with 1% Triton X-100 was necessary for obtaining high yields of bovine heart mitochondrial ubiquinol-cytochrome-C reductase (fusion protein with glutathione). They solved later aggregation problems by resolubilizing the protein in the detergent dodecyl maltoside in 300 m*M* NaCl; the resultant protein appeared active as it gave a blue shift in the visible spectrum when incubated with ubiquinone (31). The preliminary breakage steps to maintain the solubility of T7 RNA polymerase had to be done in buffer containing large amounts of glycerol and detergent to prevent the protein precipitating. Once its extremely narrow salt range for solubility was determined (205), the purification was straightforward.

Even the pH of the extraction buffer can have a profound effect on solubility. For example, UMP-kinase from *E. coli* was insoluble if extracted from cells with a pH 7.4 Tris buffer, but was soluble if 1 m*M* UTP was added to this buffer or if 100 m*M* borate buffer pH 9 was used for the extraction. Reversible aggregation could be induced by adding Mg^{2+} to the UTP containing solutions or lowering the pH. A point mutant, D159N, was soluble at up to 5 mg/mL at pH 7.4 (206).

25.6 CONCLUSIONS AND OUTLOOK

As described above, there are a wide variety of choices available to enhance the production of soluble protein, ranging from vectors to bacterial strains to new methods for growing and inducing the bacteria. All aspects of the process must be considered to optimize protein quality, as well as quantity. For the first steps, a recent review, with many authors, also contains suggestions for "what to try first" (131). The tables here suggest a variety of ways that can be tried, if the first attempts at expression in bacteria yield too little protein, or if most of the protein is found in the insoluble pellet. Changing the bacterial strain and growth conditions can be first attempted. Many times it may be necessary to alter the sequence of the expressed protein, either by direct mutations in the primary sequence or adding linkers to enhance the solubility. Optimizing and controlling the growth and induction conditions are central to insuring a high yield of recombinant protein.

Finally, many of the problems of expression and solubility are also encountered if an inclusion body purification scheme is chosen. As outlined above, producing soluble proteins in *E. coli* requires no more work than producing insoluble proteins, and the researcher will be rewarded with a protein preparation that is considerably easier to work with than the product of most refolding methods.

REFERENCES

1. Schein CH. Production of soluble recombinant proteins in bacteria. Bio/Technology 1989; 7: 1141–1149.
2. Schein CH. Optimizing protein folding to the native state in bacteria. Curr Opin Biotechnol 1991; 2: 746–750.
3. Bertone P, Kluger Y, Lan N, Zheng D, Christendat D, Yee A, Edwards AM, Arrowsmith CH, Montelione GT, Gerstein M. SPINE: an integrated tracking database and data mining approach for identifying feasible targets in

high-throughput structural proteomics. Nucl Acids Res 2001; 29(13): 2884–2898.

4. Vera A, González-Montalbán N, Arís A, Villaverde A. The conformational quality of insoluble recombinant proteins is enhanced at low growth temperatures. Biotechnol Bioeng 2007; 96(6): 1101–1106.
5. Burda MR, Miller S. Folding of coliphage T4 short tail fiber in vitro - analysing the role of a bacteriophage-encoded chaperone. Eur J Biochem 1999; 265(2): 771–778.
6. Rumlova-Klikova M, Pichova I, Hunter E, Ruml T. Conditions resulting in formation of properly assembled retroviral capsids within inclusion bodies of *Escherichia coli*. Collect Czech Chem Commun 1999; 64(8): 1348–1356.
7. Wunderlich Z, Acton TB, Liu JF, Kornhaber G, Everett J, Carter P, Lan N, Echols N, Gerstein M, Rost B, Montelione GT. The protein target list of the northeast structural genomics consortium. Prot-Struct Func Bioinform 2004; 56(2): 181–187.
8. Bhattacharya A, Tejero R, Montelione GT. Evaluating protein structures determined by structural genomics consortia. Prot-Struct Func Bioinform 2007; 66(4): 778–795.
9. Goh CS, Lan N, Douglas SM, Wu BL, Echols N, Smith A, Milburn D, Montelione GT, Zhao HY, Gerstein M. Mining the structural genomics pipeline: identification of protein properties that affect high-throughput experimental analysis. J Mol Biol 2004; 336(1): 115–130.
10. Hensing MC, Rouwenhorst RJ, Heijnen JJ, van Dijken JP, Pronk JT. Physiological and technological aspects of large-scale heterologous-protein production with yeasts. Antonie van Leeuwenhoek 1995; 67: 261–279.
11. Guo M, Lu FP, Pu J, Bai DQ, Du LX. Molecular cloning of the cDNA encoding laccase from Trametes versicolor and heterologous expression in Pichia methanolica. Appl Microbiol Biotechnol 2005; 69(2): 178–183.
12. Mistry AR, Falciola L, Monaco L, Tagliabue R, Acerbis G, Knight A, Harbottle RP, Soria M, Bianchi ME, Coutelle C, Hart SL. Recombinant HMG1 protein produced in Pichia pastoris: a nonviral gene delivery agent. BioTechniques 1997; 22: 718–729.
13. Li ZJ, Xiong F, Lin QS, d'Anjou M, Daugulis AJ, Yang DSC, Hew CL. Low-temperature increases the yield of biologically active herring antifreeze protein in Pichia pastoris. Protein Expr Purif 2001; 21(3): 438–445.
14. Hasslacher M, Schall M, Hayn M, Bona R, Rumbold K, Luckl J, Griengl H, Kohlwein SD, Schwab H. High-level intracellular expression of hydroxynitrile lyase from the tropical rubber tree Hevea brasiliensis in microbial hosts. Protein Expr Purif 1997; 11(1): 61–71.
15. Yokoyama S. Protein expression systems for structural genomics and proteomics. Curr Opin Chem Biol 2003; 7(1): 39–43.
16. Doglia S, Ami D, Natalello A, Gatti-Lafranconi P, Lotti M. Fourier transform infrared spectroscopy analysis of the conformational quality of recombinant proteins within inclusion bodies. Biotechnol J 2008; 3(2): 193–201.
17. Harper JW, Logsdon NJ. Refolded HIV-1 tat protein protects both bulge and loop nucleotides in TAR RNA from ribonucleolytic cleavage. Biochemistry 1991; 30: 8060–8066. &
18. Phadtare S, Inouye M, Severinov K. The mechanism of nucleic acid melting by a cspA family protein. J Mol Biol 2004; 337(1): 147–155.
19. Opitz JG, Ciglic MI, Haugg M, Trautwein-Fritz K, Raillard SA, Jermann TM, Benner SA. Origin of the catalytic activity of bovine seminal ribonuclease against double-stranded RNA. Biochemistry 1998; 37(12): 4023–4033.
20. Schein CH, Boix E, Haugg M, Holliger KP, Hemmi S, Frank G, Schwalbe H. Secretion of mammalian ribonucleases from *E. coli* using the signal sequence of murine spleen ribonuclease. Biochem J 1992; 283: 137–144.
21. Ahn WS, Ahn JY, Jung CH, Hwang KY, Kim EE, Kim J, Im H, Kim JO, Yu MH, Lee C. Optimization of expression conditions for soluble protein by using a robotic system of multi-culture vessels. J Microbiol Biotechnol 2007; 17(11): 1868–1874.
22. Schein CH. Production of Soluble Recombinant Proteins in Bacteria. Bio-Technology 1989; 7(11): 1141–1147.
23. Schein CH, Noteborn MHM. Formation of Soluble Recombinant Proteins in Escherichia-Coli Is Favored by Lower Growth Temperature. Bio-Technology 1988; 6(3): 291–294.
24. Cassland P, Jonsson LJ. Characterization of a gene encoding Trametes versicolor laccase A and improved heterologous expression in Saccharomyces cerevisiae by decreased cultivation temperature. Appl Microbiol Biotechnol 1999; 52(3): 393–400.
25. Izumi T, Schein CH, Oezguen N, Feng Y, Braun W. Effects of backbone contacts 3' to the abasic site on the cleavage and the product binding by human apurinic/apyrimidinic endonuclease (APE1). Biochemistry 2004; 43: 684–689.
26. Cummins SF, Xie F, de Vries MR, Annangudi SP, Misra M, Degnan BM, Sweedler JV, Nagle GT, Schein CH. Aplysia temptin - the ' glue ' in the water-borne attractin pheromone complex. FEBS J 2007; 274(20): 5425–5437.
27. Cummins SF, Xie F, Misra M, Amare A, Jakubowski JA, de Vries MR, Sweedler JV, Nagle GT, Schein CH. Recombinant production and structural studies of the Aplysia water-borne protein pheromone enticin indicates it has a novel disulfide stabilized fold. Peptides 2007; 28(1): 94–102.
28. Garimella R, Xu Y, Schein CH, Rajarathnam K, Nagle GT, Painter SD, Braun W. NMR solution structure of attractin, a water-borne protein pheromone from the mollusk Aplysia californica. Biochemistry 2003; 42(33): 9970–9979.
29. Painter SD, Cummins SF, Nichols AE, Akalal DBG, Schein CH, Braun W, Smith JS, Susswein AJ, Levy M, de Boer P, ter Maat A, Miller MW, Scanlan C, Milberg RM, Sweedler JV, Nagle GT. Structural and functional analysis of Aplysia attractins, a family of water-borne protein pheromones with interspecific attractiveness. Proc Natl Acad Sci U S A 2004; 101(18): 6929–6933.
30. Yu L, Deng KP, Yu CA. Cloning, gene sequencing, and expression of small molecular mass ubiquinone binding protein of mitochondrial ubiquinol cytochrome-C reductase. J Biol Chem 1995; 270: 25634–25638.
31. Seddi R, Chaix JC, Puigserver A, Guo XJ. Expression of a soluble and activatable form of bovine procarboxypeptidase A in *Escherichia coli*. Protein Expr Purif 2003; 27(2): 220–228.
32. Rajan SS, Lackland H, Stein S, Denhardt DT. Presence of an N-terminal polyhistidine tag facilitates stable expression of an otherwise unstable N-terminal domain of mouse tissue inhibitor of metalloproteinase-1 in *Escherichia coli*. Protein Expr Purif 1998; 13(1): 67–72.

33. Vasina JA, Marvin S, Peterson Baneyx F. Scale-up and optimization of the low-temperature inducible cspA promoter system. Biotechnol Prog 1998; 14: 714–721.
34. Weickert MJ, Pagratis M, Curry SR, Blackmore R. Stabilization of apoglobin by low temperature increases yield of soluble recombinant hemoglobin in *Escherichia coli*. Appl Environ Microbiol 1997; 63(11): 4313–4320.
35. Morino S, Hazama H, Ozaki M, Teraoka Y, Shibaata S, Doi M, Ueda H, Ishida T, Uesugi S. Analysis of the messenger-RNA Cap-binding ability of human eukaryotic initiation factor-4E by use of recombinant and mutant forms. Eur J Biochem 1996; 239: 597–601.
36. Mizukami T, Komatsu Y, Hosoi N, Itoh S, Oka T. Production of active human interferon-ß in *E. coli* I. Preferential production by lower culture temperature. Biotechnol Lett 1986; 8: 605–610.
37. Austin CJD, Mizdrak J, Matin A, Sirijovski N, Kosim-Satyaputra P, Willows RD, Roberts TH, Truscott RJW, Polekhina G, Parker MW, Jamie JF. Optimised expression and purification of recombinant human indoleamine 2,3-dioxygenase. Protein Expr Purif 2004; 37(2): 392–398.
38. Seow HF, Goh CR, Porter AG, Krischnan L. Bacterial expression, facile purification and properties of recombinant human lymphotoxin (tumor necrosis factor- ß). Gene 1989; 83: 117–129.
39. Mburu DN, Roberts TK, Boettcher B. Overexpression of human testis antigens in *Escherichia coli* host cells is influenced by site of expression and the induction temperature. Biochem Mol Biol Int 1999; 47(6): 1009–1018.
40. Mainfroid V, Terpstra P, Beauregard M, Frere JM, Mande SC, Hol WGJ, Martial JA, Goraj K. 3 HTIM mutants that provide new insights on why Tim is a dimer. J Mol Biol 1996; 257: 441–456.
41. Hindges R, Hubscher U. Production of active mouse DNA polymerase delta in bacteria. Gene 1995; 158: 241–246.
42. Slice LW, Taylor SS. Expression of the catalytic subunit of cAMP-dependent protein-kinase in *Escherichia coli*. J Biol Chem 1989; 264: 20940–20946.
43. Browner MF, Rasor P, Tugendreich S, Fletterick RJ. Temperature sensitive production of rabbit muscle glycogen phosphorylase in *E. coli*. Protein Eng 1991; 4: 351–357.
44. Tremblay JM, Helmkamp GM, Yarbrough LR. Limited proteolysis of rat phosphatidylinositol transfer proteinby trypsin cleaves the C-terminus, enhances binding to lipid vesicles, and reduces phospholipid transfer activity. J Biol Chem 1996; 271: 16139–16143.
45. Tsai AM, Betenbaugh MJ, Shiloach J. The kinetics of RCC1 inclusion body formation in *Escherichia coli*. Biotechnol Bioeng 1995; 48: 715–718.
46. Battistoni A, Carri MT, Mazzetti AP, Rotilo G. Temperature dependent protein folding in vivo- lower growth temperature increases yield of two genetic variants of *Xenopus* laevis Cu, Zn superoxide dismutase in *Escherichia coli*. Biochem Biophys Res Commun 1992; 186: 1339–1342.
47. Abe R, Yoshida K, Aoyagi M, Kasahara S, Ichishima E, Nakajima T. Characterization of chimeric enzymes constructed between two distinct alpha-amylase cDNAs from cultured rice cells. Biosci Biotechnol Biochem 1999; 63(8): 1329–1335.
48. Ferrer A, Aparicia C, Nogués N, Wettstein A, Bach TJ, Boronat A. Expression of catalytically active radish 3-hydroxy-3-methylglutaryl coenzyme A reductase in *Escherichia coli*. FEBS Lett 1990; 266: 67–71.
49. Shirano Y, Shibata D. Low temperature cultivation of *Escherichia coli* carrying a rice lipoxygenase L-2 cDNA produces a soluble and active enzyme at a high level. FEBS Lett 1990; 271: 128–130.
50. Fetzer J, Folkers G. Temperature dependent formation of inclusion bodies during the expression of recombinant viral thymidine kinase. Pharm Pharmacol Lett 1992; 2: 112–114.
51. Slabaugh MB, Davis RE, Roseman NA, Mathews CK. Vaccinia virus ribonucleotide reductase expression and isolation of the recombinant large subunit. J Biol Chem 1993; 268: 17803–17810.
52. Saito Y, Ishii Y, Fijimura T, Sasaki H, Noguchi Y, Yamada H, Niwa M, Shiomura K. Protein engineering of a cephalosporin-C acylase from Pseudomonas strain N176. Ann NY Acad Sci 1996; 782: 79–86.
53. Tiow-suan S, Tan DSH. Biophysical factors affecting the expression of isopenicillin-N synthase isozymes in *Escherichia coli*. Biochem Mol Biol Int 1995; 35: 1069–1078.
54. Marx CK, Hertel TC, Pietzsch M. Soluble expression of a pro-transglutaminase from Streptomyces mobaraensis in *Escherichia coli*. Enzyme Microb Technol 2007; 40(6): 1543–1550.
55. Wong E, Sim J, Sim TS. Construction of Streptomyces jumonjinensis isopenicillin N synthase double mutants, Ser119Ala/Glu120Gly and Thr308Ala/Thr309Val, overcomes insoluble expression in *Escherichia coli*. J Mol Catal B-Enzym 2001; 13(1-3): 17–25.
56. Kopetzki E, Schumacher G, Buckel P. Control of formation of active soluble or inactive soluble baker's yeast α-glucosidase P1 in *Escherichia coli* by induction and growth conditions. Mol Gen Genet 1989; 216: 149–155.
57. Nam ES, Jung HJ, Ahn JK. Improving soluble expression of beta-galactosidase in *Escherichia coli* by fusion with thioredoxin. Asian-Australas J Anim Sci 2004; 17(12): 1751–1757.
58. Chao YP, Chiang CJ, Lo TE, Fu H. Overproduction of D-hydantoinase and carbamoylase in a soluble form in *Escherichia coli*. Appl Microbiol Biotechnol 2000; 54(3): 348–353.
59. Bishai WR, Rappuoli R, Murphy JR. High-level expression of a proteolytically sensitive diphtheria toxin fragment in *Escherichia coli*. J Bacteriol 1987; 169: 5140–5151.
60. Su HS, Blain F, Musil RA, Zimmermann JJF, Gu KF, Bennett DC. Isolation and expression of *Escherichia coli* of HepB and HepC, genes coding for the glycosaminoglycan degrading enzymes Heparinase II and Heparinase-III respectively from Flavobacterium heparinum. Appl Environ Microbiol 1996; 62: 2723–2734.
61. Schnurr G, Misawa N, Sandmann G. Expression, purification, and properties of lycopene cyclase from Erwinia uredovora. Biochem J 1996; 315: 869–874.
62. Mitraki A, King J. Amino acid substitutions influencing protein folding pathways. FEBS Lett 1992; 307: 20–25.
63. Miskin JE, Farrell AM, Cunliffe WJ, Holland KT. Propionibacterium acnes, a resident of lipid-rich human skin, produces a 33 kDa extracellular lipase encoded by gehA. Microbiology-UK 1997; 143: 1745–1755.
64. Piatak M, Lane JA, Laird W, Bjorn MJ, Wang A, Williams M. Expression of soluble and fully functional ricin A chain

in *Escherichia coli* is temperature-sensitive. J Biol Chem 1988; 263: 4837–4843.

65. Klein J, Dhurjati P. Protein aggregation kinetics in an *Escherichia coli* strain overexpressing a Salmonella typhimurium CheY mutant gene. Appl Environ Microbiol 1995; 61: 1220–1225.
66. Lin TC, Rush J, Spicer EK, Konigsberg WH. Cloning and expression of T4 DNA polymerase. Proc Natl Acad Sci 1987; 84: 7000–7004.
67. Cooper B, Gruber JA, McPhaul MJ. Hormone-binding and solubility properties of fusion proteins containing the ligand-binding domain of the human androgen receptor. J Steroid Biochem Mol Biol 1996; 57: 251–257.
68. Jones PG, VanBogelen RA, Neidhardt FC. Induction of proteins in response to low temperature in *Escherichia coli*. J Bacteriol 1987; 169(5): 2092–2095.
69. McKenna M-C, Muchardt C, Gaynor R, Eisenberg D. Preparative scale culture of *Escherichia coli* cells expressing the human immunodeficiency virus Type 1 Tat protein. Protein Expr Purif 1994; 5: 105–111.
70. Sakamoto S, Terada I, Lee YC, Uehara K, Matsuzara H, Iijima M. Efficient production of Thermus protease aqualysin I in *Escherichia coli*: effects of cloned gene structure and two stage culture. 1996.
71. Sooryanarayana. Adiga PR. Visweswariah SS. Hyperexpression of chicken riboflavin carrier protein: antibodies to the recombinant protein curtail pregnancy in rodents. Protein Expr Purif 1996; 7(2): 147–154.
72. Ishii Y *et al*. Preparation of soluble recombinant T-cell receptor-alpha chain by using a calmodulin fusion expression system. J Immunol Methods 1995; 186: 27–36.
73. Sachdev D, Chirgwin JM. Solubility of proteins isolated from inclusion bodies is enhanced by fusion to maltose-binding protein or thioredoxin. Protein Expr Purif 1998; 12(1): 122–132.
74. Kapust RB, Waugh DS. *Escherichia coli* maltose-binding protein is uncommonly effective at promoting the solubility of polypeptides to which it is fused. Protein Sci 1999; 8(8): 1668–1674.
75. Goh LL, Loke P, Singh M, Sim TS. Soluble expression of a functionally active Plasmodium falciparum falcipain-2 fused to maltose-binding protein in *Escherichia coli*. Protein Expr Purif 2003; 32(2): 194–201.
76. Araujo APU, Oliva G, Henrique-Silva F, Garratt RC, Caceres O, Beltramini LM. Influence of the histidine tail on the structure and activity of recombinant chlorocalechol 1,2-dioxygenase. Biochem Biophys Res Commun 2000; 272(2): 480–484.
77. LaVallie ER, Lu ZJ, Diblasio-Smith EA, Collins-Racie LA, McCoy JM. Thioredoxin as a fusion partner for production of soluble recombinant proteins in *Escherichia coli*. In: Applications of chimeric genes and hybrid proteins, Pt A. Volume 326, Methods in enzymology; 2000. p 322–340.
78. Dickason RR, Edwards RA, Bryan J, Huston DP. Versatile *Escherichia coli* thioredoxin specific monoclonal antibodies afford convenient analysis and purification of prokaryote expressed soluble fusion protein. J Immunol Methods 1995; 185: 237–244.
79. Koken MHM *et al*. Biochem Biophys Res Commun 1993; 195: 643–653.
80. Pope WH, Haase-Pettingell C, King J. Protein folding failure sets high-temperature limit on growth of phage p22 in Salmonella enterica serovar typhimurium. Appl Environ Microbiol 2004; 70(8): 4840–4847.
81. Ami D, Natalello A, Gatti-Lafranconi P, Lotti M, Doglia SM. Kinetics of inclusion body formation studied in intact cells by FT-IR spectroscopy. FEBS Lett 2005; 579(16): 3433–3436.
82. Michels AA, Nguyen VT, Konings AW, Kampinga HH, Bensaude O. Thermostability of a nuclear-targeted luciferase expressed in mammalian cells. Destabilizing influence of the intranuclear microenvironment. Eur J Biochem 1995; 234: 382–389.
83. Sherman MY, Goldberg AL. Heat shock in *Escherichia coli* alters the protein-binding site of the chaperonin groEL by inducing its phosphorylation. Nature 1992; 357: 167–169.
84. Matthews RG, Neidhardt FC. Elevated serine catabolism is associated with the heat shock response in *Escherichia coli*. J Bacteriol 1989; 171(5): 2619–2625.
85. Riesenberg D. High-cell density cultivation of *Escherichia coli*. Curr Opin Biotechnol 1991; 2: 380–384.
86. Luo SQ, Huang CYF, McClelland JF, Graves DJ. A study of protein secondary structure by Fourier transform infrared/photoacoustic spectroscopy and its application for recombinant proteins. Anal Biochem 1994; 216(1): 67–76.
87. Andersson L, Strandberg L, Haggstrom L, Enfors SO. Modeling of high cell density fed batch cultivation. FEMS Microbiol Rev 1994; 14(1): 39–44.
88. Bowden GA, Paredes AM, Georgiou G. Structure and morphology of protein inclusion bodies in *Escherichia coli*. Bio/Technology 1991; 9: 725–730.
89. Van Derlinden E, Bernaerts K, Van Impe JF. Dynamics of *Escherichia coli* at elevated temperatures: effect of temperature history and medium. J Appl Microbiol 2008; 104(2): 438–453.
90. Palva I, Lehtovaara P, Kèèrièinen L, Sibakov M, Cantell K, Schein CH, Kashiwagi K, Weissmann C. Secretion of interferon by *Bacillus subtilis*. Gene 1983; 22: 229–235.
91. Loregian A, Hirst TR, Marsden HS, Palu G. Use of *Vibrio* spp. for expression of *Escherichia coli* enterotoxin B subunit fusion proteins: purification and characterization of a chimera containing a C-terminal fragment of DNA polymerase from herpes simplex virus type 1. Protein Expr Purif 1996; 8: 381–389.
92. Nystrom T, Neidhardt FC. Isolation and properties of a mutant of *Escherichia coli* with an insertional inactivation of the uspA gene, which encodes a universal stress protein. J Bacteriol 1993; 175(13): 3949–3956.
93. Smith GR, Ford R, Bryant JD, Gambley RL, Meghia TK, Harding RM, Dale JL. Expression, purification and use as an antigen of recombinant surgarcane mosaic virus coat protein. Arch Virol 1995; 140: 1817–1831.
94. Sambrook J, Fritsch EF, Maniatis T. Molecular cloning: a laboratory manual, Cold Spring Harbor New York: Cold Spring Harbor Laboratory Press; 1989.
95. Horn U, Strittmayer W, Krebber A, Knupfer U, Kujau M, Wenderoth R, Muller K, Matzku S, Pluckthun A, Riesenberg D. High volume yields of functional dimeric miniantibodies in *E. coli*, using an optimized expression vector and high-cell-density fermentation under non-limited conditions. Appl Microbiol Biotechnol 1996; 46: 524–532.
96. Huynh TV, Young RA, Davis RA. Construction and screening cDNA libraries in lambdagt10 and lambdagt11. In:

Glover D, editor. DNA cloning, Oxford: Oxford University Press; 1985. p 56–110.

97. Bolivar F, Backman K. Plasmids of *Escherichia coli* as cloning vectors. Meth Enzymol 1979; 68: 245.
98. Yanish Perron C, Viera J, Messing J. Improved M13 phage cloning vectors and host strains:nucleotide sequence of the M13mp18 and pUC19 vectors. Gene 1985; 33: 103–199.
99. Maurer R, Meyer BJ, Ptashne M. Gene regulation at the right operator (O_R) of bacteriophage L-OR3 and autogenous negative control by repressor. J Mol Biol 1980; 139: 147–161.
100. Bullock WO, Fernandez JM, Short JM. XL1-Blue: a high efficiency plasmid transforming recA *E. coli* strain with B-galactosidase selection. Biotechniques 1987; 5: 376–379.
101. Yarranton GT, Mountain A. Expression of proteins in procaryotic systems-principles and case studies. In: Rees RR, Sternberg MJE, Wetzel R. editors. Protein engineering a practical approach. New York: IRL Press; 1992. p 303–325.
102. Chen W, Wright L, Lee S, Cosloy SD, Russell CS. Expression of glutamyl-tRNA reductase in *Escherichia coli*. Biochim Biophys Acta 1996; 1309: 109–121.
103. Goff SA *et al*. Proc Natl Acad Sci 1984; 81: 6647–6651.
104. Andrews B, Adari H, Hannig G, Lahue E, Gosselin M, Martin S, Ahmed A, Ford PJ, Hayman EG, Makrides SC. A tightly regulated high level expression vector that utilizes a thermosensitive lac repressor: production of the human T cell receptor V beta 5.3 in *Escherichia coli*. Gene 1996; 182: 101–109.
105. Derman AJ, Prinz WA, Belin D, Beckwith J. Mutations that allow disulfide bond formation in the cytoplasm of *Escherichia coli*. Science 1993; 262: 1744–1747.
106. Proba K, Ge L, Pluckthun A. Functional antibody single chain fragments from the cytoplasm of *E. coli*: influence of thioredoxin reductase (TrxB). Gene 1995; 159: 203–207.
107. Bogdanov M, Sun J, Kaback HR, Dowhan W. A phospholipid acts as a chaperone in assembly of a membrane transport protein. J Biol Chem 1996; 271: 11615–11618.
108. Yasukawa T, Kanei-ishii C, Maekawa T, Fujimoto J, Yamamoto T, Ishii S. Increase of solubility of foreign proteins in *Escherichia coli* by coproduction of the bacterial thioredoxin. J Biol Chem 1995; 270: 25328–25331.
109. Proba K, Ge L, Plueckthun A. Functional antibody single chain fragments for the cytoplasm of *Escherichia coli*: influence of thioredoxin reductase (TrxB). Gene 1995; 459: 203–207.
110. Randak C, Roscher AA, Hadorn B, Aaafalgmachleidt I, Auerswald EA, Machleidt W. Expression and functional properties of the 2nd predicted nucleotide binding fold of the cystic fibrosis transmembrane conductance regulator fused to glutathione-S-transferase. FEBS Lett 1995; 363: 189–194.
111. Thomas JG, Baneyx F. Protein misfolding and inclusion body formation in recombinant *Escherichia coli* cells overexpressing heat-shock proteins. J Biol Chem 1996; 271: 11141–11147.
112. Lallio PT, Bailey JE. Intracellular expression of Vitreoscilla Hemoglobin (Vhb) enhances total protein secretion and improves the production of alpha-amylase and neutral protease in *Bacillus subtilis*. Biotechnol Prog 1996; 12: 31–39.
113. Bailey JE, Sburlati A, Hatzimanikatis V, Lee K, Renner WA, Tsai PS. Inverse metabolic engineering: a strategy for directed genetic engineering of useful phenotypes. Biotechnol Bioeng 1996; 52: 109–121.
114. Koskenkorva T, Frey AD, Kallio PT. Characterization of heterologous hemoglobin and flavohemoglobin promoter regulation in *Escherichia coli*. J Biotechnol 2006; 122(2): 161–175.
115. Bollinger CJT, Kallio PT. Impact of the small RNA RyhB on growth, physiology and heterologous protein expression in *Escherichia coli*. FEMS Microbiol Lett 2007; 275(2): 221–228.
116. Hober S, Hansson A, Uhlen M, Nilsson B. Folding of insulin-like growth factor I is thermodynamically controlled by insulin-like growth factor binding protein. Biochemistry 1994; 33: 6758–6761.
117. Katzav-Gozansky T, Hanan E, Solomon B. Effect of monoclonal antibodies in preventing carboxypeptidase A aggregation. Biotechnol Appl Biochem 1996; 23: 227–230.
118. Garcia OL, Gonzalez B, Menendez A, Sosa AE, Fernandez JR, Santana H, Meneses N. The Argu gene product enhances expression of the recombinant human interferon-alpha-2 in *Escherichia coli*. Ann N Y Acad Sci 1996; 782: 79–86.
119. Takagi M, Lee SP, Imanaka T. Diversity in size and alkaliphily of thermostable alpha-amylase-pullulaneses (Aapt) produced by recombinant *Escherichia coli*, *Bacillus subtilis* and the wild-type Bacillus Sp. J Ferment Bioeng 1996; 81: 557–559.
120. Schein CH, Kashiwagi K, Fujisawa A, Weissmann C. Secretion of mature IFN-α2 and accumulation of uncleaved precursor by *Bacillus subtilis* transformed with a hybrid gene encoding the α-amylase signal sequence fused to the mature IFN-α2 gene. Bio/Technology 1986; 4: 719–725.
121. Dahan D, Srikumar R, Laprade R, Coulton JW. Purification and refolding of recombinant Haemophilus influenzae Type B porin produced in *Bacillus subtilis*. FEBS Lett 1996; 392: 304–308.
122. Schumann W Production of recombinant proteins in *Bacillus subtilis*. In: Advances in applied microbiology, Volume 62, Advances in applied microbiology; 2007. p 137–189.
123. Le ATT, Schumann W. A novel cold-inducible expression system for *Bacillus subtilis*. Protein Expr Purif 2007; 53(2): 264–269.
124. Schein CH, Kashiwagi K, Fujisawa A, Weissmann C. Secretion of mature Ifn-Alpha-2 and accumulation of uncleaved precursor by Bacillus-Subtilis transformed with a hybrid Alpha-Amylase signal Sequence-Ifn-Alpha-2 Gene. Bio-Technology 1986; 4(8): 719–725.
125. Kremer L, Riveau G, Baulard A, Capron A, Locht C. Neutralizing antibody-responses elicited in mice immunized with recombinant *Bacillus-Calmette-Guerin* producing the Schistosoma-Mansoni Glutathione-S-transferase. J Immunol 1996; 156: 4309–4317.
126. Nakashima N, Tamura T. A novel system for expressing recombinant proteins over a wide temperature range from 4 to 35 degrees C. Biotechnol Bioeng 2004; 86(2): 136–148.
127. Samuelson P, Hansson M, Ahlborg N, Andreoni C, Gotz F, Bachi T, Nguyen TN, Binz H, Uhlen M, Stahl S. Cell surface display of recombinant proteins on Staphylococcus carnosus. J Bacteriol 1995; 177: 1470–1476.
128. Liljeqvist S, Haddad D, Berzins K, Uhlen M, Stahl S. A novel expression system for Salmonella typhimurium allowing high production levels, product secretion and efficient recovery. Biochem Biophys Res Commun 1996; 218: 356–359.

129. Mertens N, Remaut E, Fiers W. Tight transcriptional control mechanism ensures stable, high-level expression from T7-promotor based expression plasmids. Biotechnology 1995; 13: 175–179.

130. Studier F, Moffatt B. Use of bacteriophage T7 RNA polymerase to direct selective high-level expression of cloned genes. J Mol Biol 1986; 189: 113–130.

131. Graslund S, Nordlund P, Weigelt J, Bray J, Gileadi O, Knapp S, Oppermann U, Arrowsmith C, Hui R, Ming J, Dhe-Paganon S, Park HW, Savchenko A, Yee A, Edwards A, Vincentelli R, Cambillau C, Kim R, Kim SH, Rao Z, Shi Y, Terwilliger TC, Kim CY, Hung LW, Waldo GS, Peleg Y, Albeck S, Unger T, Dym O, Prilusky J, Sussman JL, Stevens RC, Lesley SA, Wilson IA, Joachimiak A, Collart F, Dementieva I, Donnelly MI, Eschenfeldt WH, Kim Y, Stols L, Wu R, Zhou M, Burley SK, Emtage JS, Sauder JM, Thompson D, Bain K, Luz J, Gheyi T, Zhang F, Atwell S, Almo SC, Bonanno JB, Fiser A, Swaminathan S, Studier FW, Chance MR, Sali A, Acton TB, Xiao R, Zhao L, Ma LC, Hunt JF, Tong L, Cunningham K, Inouye M, Anderson S, Janjua H, Shastry R, Ho CK, Wang DY, Wang H, Jiang M, Montelione GT, Stuart DI, Owens RJ, Daenke S, Schutz A, Heinemann U, Yokoyama S, Bussow K, Gunsalus KC. Protein production and purification. Nat Methods 2008; 5(2): 135–146.

132. Vasina JA, Baneyx F. Recombinant protein expression at low-temperature under the transcriptional control of the major *Escherichia coli* cold shock promotor. Appl Environ Microbiol 1996; 62: 1444–1447.

133. Vasina JA, Baneyx F. Expression of aggregation-prone recombinant proteins at low temperatures - a comparative study of the *Escherichia coli* cspa and tac promoter systems. Protein Expr Purif 1997; 9: 211–218.

134. Xia B, Etchegaray J-P, Inouye M. Nonsense mutations in cspA cause ribosome trapping leading to complete growth inhibition and cell death at low temperature in *Escherichia coli*. J Biol Chem 2001; 276: 35581–35588.

135. Mujacic M, Cooper KWC, Baneyx F. Cold-inducible cloning vectors for low-temperature protein expression in *Escherichia coli*: application to the production of a toxic and proteolytically sensitive fusion protein. Gene 1999; 238: 325–332.

136. Qing GL, Ma LC, Khorchid A, Swapna GVT, Mal TK, Takayama MM, Xia B, Phadtare S, Ke HP, Acton T, Montelione GT, Ikura M, Inouye M. Cold-shock induced high-yield protein production in *Escherichia coli*. Nat Biotechnol 2004; 22(7): 877–882.

137. Schein CH. A cool way to make proteins. Nat Biotechnol 2004; 22(7): 826–827.

138. Sitney KC, Mann MB, Stearns GW, Menjares AD, Stevenson JL, Snavely MD, Fieschko JC, Curless C, Tsai LB. Use of a modified tryptophanase promoter to direct high-level expression of foreign proteins in *Escherichia coli*. Ann N Y Acad Sci 1996; 782: 297–310.

139. Schein CH. Solubility and secretability. Curr Opin Biotechnol 1993; 4: 456–461.

140. Boix E, Nogués MV, Schein CH, Benner SA, Cuchillo CM. Reverse transphosphorylation by ribonuclease A needs an intact p2 binding site. Point mutations at Lys-7 and Arg-10 alter the catalytic properties of the enzyme. J Biol Chem 1994; 269: 2529–2534.

141. Li PZ, Anumanthan A, Gao XG, Ilangovan K, Suzara VV, Duzgunes N, Renugopalakrishnan V. Expression of recombinant proteins in Pichia pastoris. Appl Biochem Biotechnol 2007; 142(2): 105–124.

142. Sangha N, Kaur S, Sharma V, Krishnasastry MV. Importance of the carboxyl terminus in the folding and function of alpha-hemolysin of Staphylococcus aureus. J Biol Chem 1999; 274(14): 9193–9199.

143. Kato A, Maki K, Ebina T, Kuwajima K, Soda K, Kuroda Y. Mutational analysis of protein solubility enhancement using short peptide tags. Biopolymers 2007; 85(1): 12–18.

144. Larsson M, Brundell E, Nordfors L, Hoog C, Uhlen M, Stahl S. A general bacterial expression system for functional analysis of cDNA-encoded proteins. Protein Expr Purif 1996; 7: 447–457.

145. Ibrahim N, McCrae MA. High-level expression of bovine rotavirus VP4 protein in *Escherichia coli* using a hepatitis B core antigen vector. Biotechnol Lett 2001; 23(8): 643–646.

146. Vispo NS, Callejo M, Ojalvo AG, Santos A, Chinea G, Gavilondo JV, Arana MJ. Displaying human interleukin-2 on the surface of bacteriophage. Immunotechnology 1997; 3(3): 185–193.

147. LaVallie ER, DiBlasio EA, Kovacic S, Grant KL, Schendal PF, McCoy JM. A thioredoxin gene fusion expression system that circumvents inclusion body formation in the *E. coli* cytoplasm. Bio/Technology 1993; 11: 187–193.

148. Samuelsson E, Uhlen M. Chaperone-like effect during in vitro refolding of insulin-like growth factor I using a solubilizing fusion partner. Ann N Y Acad Sci 1996; 782: 486–494.

149. Dyson MR, Shadbolt SP, Vincent KJ, Perera RL, McCafferty J. Production of soluble mammalian proteins in *Escherichia coli*: identification of protein features that correlate with successful expression. BMC Biotechnol 2004; 4: 32.

150. Goela A, Colcherb D, Kooc JS, Boothd BJM, Pavlinkovad G, Batraa SK. Relative position of the hexahistidine tag effects binding properties of a tumor-associated single-chain Fv construct. Biochim Biophys Acta (BBA)/General Subjects 2000; 1523: 13–20.

151. Patel S, Austen BM. Expression and purification of the canine 54-kDa subunit of signal recognition particle as a his-tagged protein from *Escherichia coli*. Protein Expr Purif 1996; 8(3): 283–294.

152. Armstrong RL, Wilson JE, Shoemaker CB. Purification and characterization of the hexokinase from Schistosoma mansoni, expressed in *Escherichia coli*. Protein Expr Purif 1996; 8(3): 374–380.

153. Spangfort MD, Ipsen H, Sparholt SH, Aasmul-Olsen S, Larsen MR, Mortz E, Roepstorff P, Larsen JN. Characterization of purified recombinant Bet v 1 with authentic N-terminus, cloned in fusion with maltose-binding protein. Protein Expr Purif 1996; 8(3): 365–373.

154. Chenivesse X, Huby T, Chapman J, Franco D, Thillet J. Expression of a recombinant kringle V of human apolipoprotein(a): antibodycharacterization and species specificity. Protein Expr Purif 1996; 8(2): 145–150.

155. Kakonen SM, Hellman J, Pettersson K, Lovgren T, Karp M. Purification and characterization of recombinant osteocalcin fusion protein expressed in *Escherichia coli*. Protein Expr Purif 1996; 8(2): 137–144.

156. Hu X, Shi Q, Yang T, Jackowski G. Specific replacement of consecutive AGG codons results in high-level expression of human cardiac troponin T in *Escherichia coli*. Protein Expr Purif 1996; 7(3): 289–293.

157. Boettner M, Steffens C, von Mering C, Bork P, Stahl U, Lang C. Sequence-based factors influencing the expression of heterologous genes in the yeast Pichia pastoris - a comparative view on 79 human genes. J Biotechnol 2007; 130(1): 1–10.

158. SchmidtDannert C, Rua ML, Schmid RD. Two novel lipases from thermophile Bacillus thermocatenulatus: screening, purification, cloning, overexpression, and properties. Lipases, Part A. Volume 284, Methods in enzymology; 1997. p 194–220.

159. Klammt C, Lohr F, Schafer B, Haase W, Dotsch V, Ruterjans H, Glaubitz C, Bernhard F. High level cell-free expression and specific labeling of integral membrane proteins. Eur J Biochem 2004; 271(3): 568–580.

160. Hughes RC, Ng JD. Can small laboratories do structural genomics? Cryst Growth Des 2007; 7(11): 2226–2238.

161. Endo Y, Sawasaki T. Cell-free expression systems for eukaryotic protein production. Curr Opin Biotechnol 2006; 17(4): 373–380.

162. Sawasaki T, Hasegawa Y, Morishita R, Seki M, Shinozaki K, Endo Y. Genome-scale, biochemical annotation method based on the wheat germ cell-free protein synthesis system. Phytochemistry 2004; 65(11): 1549–1555.

163. Yin G, Swartz JR. Enhancing multiple disulfide bonded protein folding in a cell-free system. Biotechnol Bioeng 2004; 86(2): 188–195.

164. Schein CH. Controlling oligomerization of pharmaceutical proteins. Pharm Acta Helv 1994; 69: 119–126.

165. Wilkinson DL, Harrison RG. Predicting the solubility of recombinant proteins in *Escherichia coli*. Bio/Technology 1991; 9: 443–448.

166. Swalley SE, Fulghum JR, Chambers SP. Screening factors effecting a response in soluble protein expression: formalized approach using design of experiments. Anal Biochem 2006; 351(1): 122–127.

167. Idicula-Thomas S, Balaji PV. Understanding the relationship between the primary structure of proteins and its propensity to be soluble on overexpression in *Escherichia coli*. Protein Sci 2005; 14(3): 582–592.

168. Trevino SR, Scholtz JM, Pace CN. Amino acid contribution to protein solubility: Asp, Glu, and Ser contribute more favorably than the other hydrophilic amino acids in RNase Sa. J Mol Biol 2007; 366(2): 449–460.

169. Mohanty AK, Kannan KK, Mahajan SK. Human carbonic anhydrase I: effect of specific site mutations on its function. J Biosci 1998; 23(3): 235–246.

170. Sim J, Sim TS. Amino acid substitutions affecting protein solubility: high level expression of Streptomyces clavuligerus isopenicillin N synthase in *Escherichia coli*. J Mol Catal B-Enzym 1999; 6(3): 133–143.

171. Schmittschmitt JP, Scholtz JM. The role of protein stability, solubility, and net charge in amyloid fibril formation. Protein Sci 2003; 12(10): 2374–2378.

172. Williams AD, Wetzel R. Alanine scanning mutagenesis of Abeta(1-40) amyloid fibril stability. J Mol Biol 2006; 357: 1283–1294.

173. Williams AD, Kheterpal I, Guo JT, Cook KD, Xu Y, Wetzel R. Mapping abeta amyloid fibril secondary structure using scanning proline mutagenesis. J Mol Biol 2004; 335: 833–842.

174. Petkova AT, Yau WM, Tycko R. Experimental constraints on quaternary structure in Alzheimer's beta-amyloid fibrils. Biochemistry 2006; 45(2): 498–512.

175. Prouty WF, Karnovsky MJ, Goldberg AL. Degradation of abnormal proteins in *Escherichia coli*. Formation of protein inclusions in cells exposed to amino acid analogs. J Biol Chem 1975; 250: 1112–1122.

176. Weickert MJ, Curry SR. Turnover of recombinant human hemoglobin in *Escherichia coli* occurs rapidly for insoluble and slowly for soluble globin. Arch Biochem Biophys 1997; 348(2): 337–346.

177. King J, Hassepettingell C, Robinson AG, Speed M, Mitraki A. Thermolabile folding intermediates - inclusion body precursors and chaperonin substrates. FASEB J 1996; 10: 57–66.

178. Speed MA, Wang DIC, King J. Specific aggregation of partially folded polypeptide chains: the molecular basis of inclusion body composition. Nat Biotechnol 1996; 14: 1283–1287.

179. Bennett MJ, Schlunegger MP, Eisenberg D. 3D domain swapping: a mechanism for oligomer assembly. Protein Sci 1995; 4: 2455–2468.

180. Fágáin CÓ. Understanding and increasing protein stability. Biochim Biophys Acta 1995; 1252: 1–14.

181. Tokatlidis K, Dhurjati P, Millet J, Béguin P, Aubert J-P. High activity of inclusion bodies formed in *Escherichia coli* overproducing Clostridium thermocellum endoglucanase D. FEBS Lett 1991; 282: 205–208.

182. Wetzel R, Perry JL, Veilleux C. Mutations in human interferon gamma affecting inclusion body formation identified by a general immunochemical screen. Bio/technology 1991; 9: 731–737.

183. Mitraki A, Fane B, Haase-Pettingell C, Sturtevant J, King J. Global suppression of protein folding defects and inclusion body formation. Science 1991; 253: 54–58.

184. Krishnamurthi S *et al*. 1989. Biochem Biophys Res Commun 163: 1256–1264.

185. Brems DN, Alter LA, Beckage MJ, Chance RE, DiMarchi RD, Green LK, Long HB, Pekar AH, Shields JE, Frank BH. Altering the association properties of insulin by amino acid replacement. Protein Eng 1992; 5: 527–533.

186. Kim JR, Gibson TJ, Murphy RM. Predicting solvent and aggregation effects of peptides using group contribution calculations. Biotechnol Prog 2006; 22(2): 605–608.

187. Kim JR, Gibson TJ, Murphy RM. Targeted control of kinetics of {beta}-Amyloid self-association by surface tension-modifying peptides. J Biol Chem 2003; 278(42): 40730–40735.

188. Adessi C, Frossard MJ, Boissard C, Fraga S, Bieler S, Ruckle T, Vilbois F, Robinson S, Mutter M, Banks WA, Soto C. Pharmacological profiles of peptide drug candidates for the treatment of Alzheimer's disease. J Biol Chem 2003; 278(16): 13905–13911.

189. Mossing MC, Sauer RT. Stable, monomeric variants of l Cro obtained by insertion of a designed b-Hairpin sequence. Science 1990; 250: 1712–1715.

190. Nygren PA, Stahl S, Uhlen M. Engineering proteins to facilitate bioprocessing. Trends Biotechnol 1994; 12: 184–188.
191. Betton JM, Hofnung M. Folding of a mutant maltose binding protein of *Escherichia coli* which forms inclusion bodies. J Biol Chem 1996; 271: 8046–8052.
192. Murby M, Samuelsson E, Nguyen TN, Mignard L, Power U, Binz H, Uhlen M, Stahl S. Hydrophobicity engineering to increase solubility and stability of a recombinant protein from respiratory syncytial virus. Eur J Biochem 1995; 230(1): 38–44.
193. Murby M, Uhlen M, Stahl S. Upstream strategies to minimize proteolytic degradation upon recombinant production in *Escherichia coli*. Protein Expr Purif 1996; 7: 129–136.
194. Schein CH, Haugg M. The role of the C-terminus of human interferon-γ in RNA binding and activation of the cleavage of ds-RNA by bovine seminal ribonuclease. Biochem J 1995; 307: 123–127.
195. McKenna M-C, Muchardt C, Gaynor R, Eisenberg D. Preparative scale culture of *Escherichia coli* cells expressing the human immunodeficiency virus type 1 Tat protein. Protein Expr Purif 1994; 5: 105–111.
196. Schein CH. Producing soluble recombinant RNases and assays for measuring their interaction with interferon-g in vitro. In: Schein CH, editor. Nuclease methods and protocols. Volume 160, Methods in molecular biology. Totowa, NJ: Humana Press; 2001. p 113–137.
197. Kroger M, Wahl R. Compilation of DNA sequences of *Escherichia coli* K12: description of the interactive databases ECD and ECDC (update 1996). Nucleic Acids Res 1997; 25(1): 39–42.
198. Carter P, Kelley RF, Rodrigues ML, Snedecor B, Cavarrubias M, Velligan MD, Wong WLT, Rowland AM, Kotts CE, Carver ME, Yang M, Bourell JH, Shepard HM, Henner D. High level *Escherichia coli* expression and production of a bivalent humanized antibody fragment. Bio/technology 1992; 10: 163–167.
199. Jungbauer A, Kaar W. Current status of technical protein refolding. J Biotechnol 2007; 128(3): 587–596.
200. Ramon-Luing LA, Cruz-Migoni A, Ruiz-Medrano R, Xoconostle-Cazares B, Ortega-Lopez J. One-step purification and immobilization in cellulose of the GroEL apical domain fused to a carbohydrate-binding module and its use in protein refolding. Biotechnol Lett 2006; 28(5): 301–307.
201. Guo CY, Li ZY, Shi YW, Xu MQ, Wise JG, Trommer WE, Yuan JM. Intein-mediated fusion expression, high efficient refolding, and one-step purification of gelonin toxin. Protein Expr Purif 2004; 37(2): 361–367.
202. Tsumoto K, Umetsu M, Yamada H, Ito T, Misawa S, Kumagai I. Immobilized oxidoreductase as an additive for refolding inclusion bodies: application to antibody fragments. Protein Eng 2003; 16(7): 535–541.
203. Lilie H, Schwarz E, Rudolph R. Advances in refolding of proteins produced in *E-coli*. Curr Opin Biotechnol 1998; 9(5): 497–501.
204. Gonzalez C, Lagos R, Monasterio O. Recovery of soluble proteins after expression in *Escherichia coli* depends on cellular disruption conditions. Microbios 1996; 85: 205–212.
205. Schein CH. Solubility as a function of protein structure and solvent components. Bio/Technology 1990; 8: 308–317.
206. Serina L, Bucurenci N, Gilles AM, Surewicz WK, Fabian H, Mantsch HH, Takahashi M, Petrescu I, Batelier G, Bârzu O. Structural properties of UMP-kinase from *Escherichia coli*-modulation of protein solubility by pH and UTP. Biochemistry 1996; 35: 7003–7011.

FURTHER READING

Hansen R, Eriksen NT. Activity of recombinant GST in *Escherichia coli* grown on glucose and glycerol. Proc Biochem 2007; 42(8): 1259–1263.

PART III

MEDIA, CELL LINES AND PROCESS DEVELOPMENT

26

ANIMAL CELL CULTURE MEDIA

Natarajan Vijayasankaran*
Late Stage Cell Culture, Genentech, Inc., San Francisco, California
Jincai Li*
Oceanside Process Research & Development, Genentech. Inc, Oceanside, California
Robert Shawley
Late Stage Cell Culture, Genentech, Inc., San Francisco, California
Aaron Chen
Oceanside Process Research & Development, Genentech. Inc, Oceanside, California
Masaru Shiratori and Martin Gawlitzek
Late Stage Cell Culture, Genentech, Inc., San Francisco, California
Feng Li
Oceanside Process Research & Development, Genentech. Inc, Oceanside, California
Robert Kiss
Late Stage Cell Culture, Genentech, Inc., San Francisco, California
Ashraf Amanullah
Oceanside Process Research & Development, Genentech. Inc, Oceanside, California

26.1 INTRODUCTION

Animal cell culture technology has advanced significantly since the preliminary investigations on nutritional requirements for cell growth (1). Since the approval of Tissue Plasminogen Activator (tPA) in 1987, the majority of biopharmaceuticals, including monoclonal antibodies, vaccines, growth factors, and hormones, have been produced using mammalian cell culture (2). While Chinese hamster ovary (CHO) cells are the primary workhorse of cell culture technology, hybridoma, mouse myeloma (NS0 and Sp2/0), Madin–Darby canine kidney (MDCK), human (PER.C6®), baby hamster kidney (BHK), and human embryonic kidney (HEK) cells may also be used (3–7).

Challenges facing the industry today include the optimization of volumetric productivity to minimize capital investment and to increase plant throughput, the rapid development of "platform" processes especially for molecules in early stages of development and the greater understanding of cell culture processes and their effects on the quality of the biopharmaceutical products produced (8,9). In addition to significant advances in cell line engineering to develop highly productive cell lines, development and optimization of cell culture media and feeding strategies continue to be a requirement for accomplishing these challenges.

Designing cell culture media requires a good understanding of cell metabolism as well as knowledge

*equal contributor

Upstream Industrial Biotechnology: Expression Systems and Process Development, Volume 1, First Edition. Edited by Michael C. Flickinger.
© 2013 John Wiley & Sons, Inc. Published 2013 by John Wiley & Sons, Inc.

gained from empirical experimentation. While earlier formulations benefitted from the presence of serum and protein hydrolysates, there is a growing trend toward removing these undefined components to mitigate safety concerns, increase reproducibility, and to gain greater fundamental knowledge about the process. Well-developed cell culture media should be capable of supporting good growth and productivity and should be applicable across clones expressing different recombinant proteins for implementation in a platform process. Media should be robust, especially during preparation and storage, and support consistent performance across multiple scales of operation in manufacturing facilities. To meet the demands of fast timelines for early stage process development, the cell culture medium is often standardized as part of a robust platform technology applicable to multiple cell lines. However, both culture media and feeding strategies need to be customized for specific cell lines when there is a need to achieve high titers (for example for high commercial product demand). Since accomplishing these objectives with serum-free and peptone-free media continues to be a major challenge, this chapter will focus primarily on development strategies for chemically defined media.

While animal cell cultures may be operated in batch and perfusion modes, fed-batch cell culture processes in which depleted nutrients are supplemented periodically through the course of the process have emerged as the standard platform technology (10–12). Recent advances in cell line development and in the design of culture media have significantly increased both the volumetric and specific productivity of fed-batch processes (13–16). While design of the basal media is important for achieving high growth and productivity, design of the feed media is essential for sustaining performance over the course of the production culture. Designing media requires an understanding of practical and business-related constraints. The developed media should not only work in the lab environment at small-scales, but also not pose any problems during scale-up to clinical or commercial scales. The liquid media should not have any solubility concerns, should have a relatively long shelf life and be stable under any heat treatment that may be required for reducing the risk of viral contamination (17). This chapter will briefly discuss the common nutrients found in cell culture media and focus on approaches to the optimization of the chemically defined basal and feed media, as well as the practical considerations during experimentation and industrial implementation of the developed media.

26.2 NUTRIENTS IN CELL CULTURE MEDIA

In this section we draw upon published literature and our own experiences to discuss the role of the various components included in the typical culture medium used for industrial-scale production of biopharmaceutical proteins. While this applies specifically to CHO cell culture processes, it should be applicable across many animal-derived cell lines used for protein production.

26.2.1 Carbohydrates

Glucose is generally used as the primary carbohydrate source. Glucose metabolism in CHO cultures is generally very inefficient resulting in significant by-product formation in the form of lactate. In an effort to constrain the conversion of glucose to lactate and to influence product quality attributes, other carbohydrates such as galactose and fructose are frequently added to the culture medium (18,19). While growth rates of CHO cells are significantly reduced when galactose or fructose is used as the sole carbon source, cells will proliferate freely given some amount of initial glucose. CHO cells are also able to metabolize and grow on mannose as the sole carbon source (20). Pyruvate, which is the key branch point of glycolysis and the citric acid cycle, is also often present in cell culture media formulations (21,22).

26.2.2 Amino Acids

Amino acids not only provide the building blocks for protein synthesis but may also serve as a source of energy through amino acid catabolism (23,24). Depletion of essential amino acids may lead to immediate cessation of growth and loss of viability via apoptosis (25). The required amino acids for growth of cells *in vitro* include the physiologically essential amino acids arginine, histidine, isoleucine, leucine, lysine, methionine, phenylalanine, threonine, tryptophan, and valine. For most CHO cell lines which are proline auxotrophic, proline supplementation is also required. Even though glutamine is considered a nonessential amino acid, it becomes essential to CHO cells in culture if asparagine is depleted, since asparagine can only be synthesized from aspartate and glutamine through transamination. Similarly, asparagine becomes essential under glutamine depletion. Careful experimentation is required for determining the levels of amino acids since we have observed inhibitory effects at high levels of serine, tryptophan, tyrosine, cysteine, glutamine, glutamate, asparagine, and aspartate (unpublished results).

Since the enzymatic reactions for the synthesis of cysteine and tyrosine occur only in the liver, these two physiologically "nonessential" amino acids become essential for the culture of most animal cells. Many cell culture formulations contain either cysteine or its dimer cystine or a combination of both, and media derived from the popular DMEM/F12 medium contain both forms (26). Cystine is widely used due to the fact that, in this form, the amino acid is more readily transported into the cell where it is

rapidly reduced to cysteine (27). Since cystine has low solubility at neutral pH, it may have to be predissolved in acidic stock solutions prior to addition to the final culture medium. Alternately, salt versions of cystine could be substituted to improve solubility. Because of its superior solubility, cysteine is often used in place of, or in addition to, cystine. However, media formulations containing only cysteine invariably contain a proportion of cystine since cysteine is readily oxidized into cystine in the presence of copper and/or iron (28).

26.2.3 Vitamins

Eagle showed in 1955 that choline, folic acid, nicotinamide, pantothenate, pyridoxal, riboflavin, and thiamine are essential for cell growth (1). Care should be taken while choosing storage conditions for media containing these vitamins since high concentrations of riboflavin could lead to the formation of cytotoxic photodegradation products (29). The fat soluble vitamins A, D, E, and K do not seem to confer any advantage. It appears that ascorbic acid is not essential for growth or productivity, even though it may be added in some cell culture media for its potential antioxidant properties (30,31). Biotin is often added to cell culture medium in small quantities, but may also be present as a contaminant. Biotin is a cofactor in the metabolism of fatty acids and enhances cell growth and protein synthesis (32). Assays for many of the vitamins are readily available and can provide useful information about vitamin limitation. In some instances, since these vitamins are recycled within the cells and often not readily excreted, intracellular accumulation may occur even while supernatant concentrations appear limiting.

26.2.4 Other Inorganic Salts, Metals, and Trace Elements

Cell culture medium is often supplemented with Na^+ and K^+ ions, supplied as chloride salts (33). These are primarily present to supply an appropriate osmotic balance for the cells, but all three (Na^+, K^+, and Cl^-) regulate membrane transport of many nutrients and macromolecules into and out of the cells, as well as maintain the appropriate ionic strength for the functionality of many enzymes or directly participate in enzymatic reactions. The normal physiological Na^+/K^+ ratio of blood is of the order of 25–40, whereas in our experience, production media with this ratio between 1 to 5 seem to work well (22). For both sodium and potassium, there seems to be a lower limit below which cell growth is not supported to any major degree (below 40 m*M* Na^+ in our experience) though this may be cell line–specific and dependent on other factors of the medium composition.

Iron can be provided in various forms, typically as ferrous or ferric salts and as chelated ferric iron combined with citrate or EDTA (34,35). In most cases, no additional benefit of ferric forms or chelated iron over sufficient ferrous iron has been observed. The other inorganic salts and metals that are required such as calcium, copper, magnesium, and zinc are often provided as their sulfate salt. They play crucial roles in energy metabolism and as enzyme components, cofactors or catalysts, as well as regulators of membrane transport. Other components required in trace amounts, hence their moniker of "trace elements", include selenium, manganese, molybdenum, and vanadium (36). A number of trace elements, 19 in all, were added to the commercially available Ham's MCDB 301 (37). Even though 15 of these were subsequently removed from MCBD 302, a medium devised specifically for the growth of CHO cells, fibroblasts, and cell lines with less stringent nutritional requirements, they are often included in many commercially available and other production media. Their concentration needs to be carefully optimized since they could be toxic above certain concentrations (38–40).

26.2.5 Other Cofactors or Substrates

Putrescine, the polyamine precursor of spermidine and spermine, acts as a cofactor for DNA elongation, and is crucial for cell division in CHO cells and a number of other cell types (41,42). Spermine and spermidine derivatives are important in stabilizing the helical structure of DNA. Some media contain either spermidine or spermine or both, rather than putrescine, although the presence of putrescine alone seems to suffice.

Reduced glutathione (GSH), which is a tripeptide synthesized from the amino acids L-cysteine, L-glutamic acid, and glycine, is often added to cell culture media. In most instances, the amount of GSH present in the medium formulation is greatly surpassed by that produced by the cells. GSH participates as a coenzyme in cellular oxidation–reduction reactions and protects the cells from the oxidative damage related to those reactions and other free radical damage (43). The requirement for selenium as a medium component is tied to the activity of GSH, as selenium acts as a catalyst in many of these reactions (44,45). It has recently been reported that selenium could also function as an iron carrier (46).

26.2.6 Lipids and Lipid Precursors

Choline chloride and inositol, which primarily function as substrates, are usually added to cell culture media (36). While supplementing choline appears to be imperative, we do not find much evidence for the supplementation of inositol, although it may be beneficial in an osmo-protective

capacity. Lipoic acid is an eight-carbon, sulfur-containing fatty acid that is synthesized by eukaryotic cells like inositol, but it is often incorporated into many cell culture media for the numerous functions it performs. It is required for pyruvate metabolism as a cofactor in the pyruvate dehydrogenase complex along with thiamine, and possesses antioxidant properties (47,48). Linoleic and oleic acids are sometimes included in the formulation (22), even though substantial growth can be achieved in the absence of these lipids provided that the medium is rich enough in precursors. Many media employ lipid mixtures, often of soy origin and provided as emulsions or complexed with cyclodextran, to supply a raw source of lipids (36,49,50). Most are dominated in composition by cholesterol. These, along with ethanolamine may be useful, even essential, in some instances, especially in hybridoma/NS0 cell lines, but appear not to be necessary for CHO cells.

26.2.7 Nucleosides

The purine nucleoside hypoxanthine, the pyrimidine nucleoside thymidine, and potentially glycine are required for the survival and growth of cell lines suffering from folic acid deficiency. This is particularly true of mutants with defective dihydrofolate reductase (dhfr) activity (51). Satisfactory growth of such parental cell lines often requires supplementation with folinic acid (a synthetic version of active tetrahydrofolate) to facilitate DNA synthesis and, thus, adequate growth in the absence of serum. None of these precursors or other nucleosides appear necessary for the growth and productivity of cell lines reconstituted with a fully functional *dhfr* gene, though they may provide some benefit in lessening any metabolic burden coincident to their production by the cells. Many nucleosides may have either desired or unwanted impacts on product quality by influencing nucleotide pools within the cell.

26.2.8 Growth Factors and Carrier Proteins

Many medium formulations used for commercial production do contain some amount of insulin or insulin-like growth factor (IGF-1) (52). Both facilitate glucose uptake and lipid metabolism. In the case of CHO cells, while their benefit to growth is obvious at low cell density, it appears that they can often be dispensed at higher cell densities. It is observed that for certain cell lines, removal of insulin from the production medium significantly reduces cell growth in the production culture and the resultant titer in the culture media. In such instances, adaptation over a few passages may alleviate this dependence. Transferrin was traditionally used to facilitate iron uptake and serum albumen was often used as a safe transport mechanism for lipid supplementation (53). In the absence of recombinant versions of these carrier proteins, many cell culture media have forgone them and instead, have significantly higher concentrations of iron and free fatty acids or their salts. The current availability of recombinant versions of these growth factors may see a resurgence of their use in production-scale cell culture media should their benefit be cost-effective.

26.2.9 Other Media Additives

Even though a variety of pH control strategies have been tested, sodium bicarbonate is usually still added to the culture for its buffering capacity (54). The culture pH is controlled at a value close to neutral pH using a combination of CO_2 sparging to lower pH and the addition of sodium hydroxide or sodium carbonate to increase pH. Phosphate, along with some amino acids, can provide additional buffering to the medium. Bicarbonate could be used with other buffers such as HEPES, when additional buffering capacity is required in smaller culture scales where there is no active pH control. In sparged cultures, Pluronic F68, methylcellulose or polyvinylalcohol are usually added to reduce cell death associated with bursting bubbles (55–60). Due to ease of use, Pluronic F68 (Lutrol®) is most typically used (61–63).

26.2.10 Osmolality

In general, cell growth is most rapid at osmolalities around 280 mOsm/kg. The osmolality of the basal media in which the production cultures are initiated, is initially set around this value while the feed media usually have much higher osmolalities since they are prepared in concentrated formulations and then diluted when added to the culture. Osmolality outside of physiological ranges has often been exploited to enhance or retard cell growth and control loss of viability due to apoptosis. This can often lead to significant increases in volumetric productivity (64,65). The upper limit that cells seem to tolerate appears quite variable, since there seems to be a threshold upper osmolality at which there is a detrimental impact on culture viability.

26.3 BASAL MEDIUM DEVELOPMENT

The term "basal medium" refers to the medium that is used at the beginning of a culture, as opposed to the "feed medium" which is added to the culture after the initial growth phase. Basal media should contain all essential nutrients that are required to support and promote culture growth, whereas feed media mainly serve to support high cell density and prolonged culture viability, as well as maintaining good productivity. A robust and productive basal medium is a prerequisite of any medium development effort and essential for successful feed

medium development and overall cell culture process development.

The history of systematic basal medium development dates back to the 1950s, where Harry Eagle pioneered the concept of minimally required nutrient categories for mammalian cells and introduced the "Minimal Essential Medium (MEM)" (1,23). The MEM medium contains 29 components, including 13 amino acids, 8 vitamins, 6 ionic species, glucose, and serum protein with appropriate pH, buffering capability, and osmolality. Serum protein was an essential element of the basal medium developed at that time. Evolution of the basal medium formulation started soon after the MEM medium was published. The various efforts can be grouped to two categories: one for removing serum and replacing it with defined, specific nutrients; and the other for achieving higher cell density in the presence of serum (66). Among the well-known formulations derived from the MEM formulation are Dulbecco's Modified Minimal Essential Medium, or DMEM (67), which has higher levels of many of the MEM components like vitamins, glucose, and choline chloride; Iscove's modified DMEM or IMDM (68), which has supplemental buffering capacity and supports even higher cell densities. Additionally, the RPMI (Roswell Park Memorial Institute) media series was developed to achieve high density lymphocyte proliferation (69). In contrast, Ham's Nutrient Mixtures (F−12 and F−10) (70) offered substantially different formulations than that of MEM and support the low density growth and maintenance of many cultured cell types. An exhaustive list of media formulations is given in Burgener and Butler (22). A break-through was achieved when Sato and his coworkers reported on the DMEM/F12 formulation by mixing the two formulations at a 1:1 ratio (26). The resulting formulation combined favorable properties of both formulations and quickly became very popular.

Most of the earlier formulations were supplemented with serum. Development of serum-free basal media dates back to the 1960s. Although effective, the complex chemical compositions of serum limited the ability to improve the understanding of cellular needs. In addition, issues related to cost, source availability, lot-to-lot variability, and potential adventitious contaminants have fueled the desire to develop serum-free media (71,72). However, despite substantial development efforts, serum-free media often suffered decreased growth and reduced recombinant protein production. To compensate for the lack of serum, animal- or plant-derived hydrolysates (peptones) were successfully introduced as an alternative nutrient source and are widely used for commercial manufacturing processes (73). Peptones are generally acid hydrolyzed or enzymatically digested, boiled, and dried preparations derived from various protein sources, and are primarily used by the food and cosmetics industry. In recent years there has been widespread abandonment of animal-derived peptones for bioproduction use, especially those of bovine origin or containing animal-derived enzymes in their production, due to the risk of transmissible spongiform encephalopathy (TSE) contamination. Replacement with commercially available peptones from soy, wheat, rice, cottonseed, or others of plant origin has been a first step in many instances, but this has drawbacks due to the risk of plant mycoplasma in some preparations (74). Animal-derived peptones, which are a potential source of viral contamination in cell culture, will require either heat treatment (Code of Federal Regulations, 9CFR, for use in human products) (75) or extensive adventitious agents testing to reduce any potential viral introduction. Hydrosylates are also a significant source of endotoxin in the medium as well as the toxic Maillard reaction products (caramelization of sugars and amino acids such as lysine) due to the heat used in their processing. They can, however, provide a source of salts, metals, trace elements and act as a reserve amino acid supply, both through the free amino acid content and that bound in peptides (76). This offers an additional benefit due to the reduced osmotic contribution offered by adding amino acids sequestered in peptides rather than entirely as free amino acids, along with improved solubility due to the nature of the preparation of the hydrosylates. Numerous efforts have been taken over the years to elucidate what factors seem to contribute the beneficial effects attributed to peptones. In addition to their nutritional benefit, certain peptone fractions have also been identified to have growth-promoting effects (77,78). Because they contain a milieu of both growth-promoting and inhibitory components, individual peptones demonstrate an optimum concentration, beyond which they become inhibitory. This may be both media and cell line–dependent and requires empirical determination. Due to their undefined nature and potential lot-to-lot variability, they are often scrutinized when growth, titer or product quality issues arise; hence the drive to replace them with defined components. More importantly, use of peptones or serum greatly limits the evaluation of cellular nutrient needs, and therefore can become a bottleneck for further improvement of growth and productivity. Due to these concerns, a number of biopharmaceutical companies are in the process of transitioning from peptone-containing media to chemically defined media (13,15,16).

26.3.1 Chemically Defined Basal Medium Development Strategies

Medium development is historically referred to as both art and science. However, advances are rooted in sound scientific study. It usually requires a synergy of approaches that combine understanding of cellular nutritional needs and metabolism with trial and error experimental approaches.

Given the complexities of cell metabolism and phenotypic variations observed between cell lines, a universal procedure for media optimization probably does not exist. Rather, the presented techniques should be viewed as a tool-kit with specific experimental details and strategies that need to be developed based on the specific needs and the stage of medium and process development.

The first challenge in basal medium optimization is to choose the starting formulation. The starting formulation should ideally be chosen after a thorough evaluation of available candidates, which might include formulations derived from literature, in-house formulations and their blended derivatives (22). Most likely, a peptone(s) supplemented basal medium already exists, as is the case for many established companies. In such cases, the existing basal medium after removing peptone(s) should be considered as one of the leading candidates. The main advantages of using the existing peptone-free medium is the familiarity and experience with various aspects of the existing medium, such as medium powder manufacturing, medium preparation, heat treatment, and scale-up. Because of the undefined nature of peptones, replacing them with chemically defined components and achieving satisfactory performance is not a trivial task. This may include addition of many new components that are present in peptones, and reoptimization of concentrations for some of the existing components (76). The in-house peptone-free formulation should be evaluated with other formulations derived from literature or their derivatives in an appropriate scale-down model using representative cell lines. The results of one such study conducted with CHO cell lines derived from dhfr-DUKX CHO host (51) is presented in Fig. 26.1. The formulations screened included several in-house chemically defined media, various commercially available media, and differing concentrations of these formulations. The screenings were conducted in batch mode shake flask cultures and used glucose feeds to prevent the depletion of glucose. After the superior growth and volumetric productivity of the best formulation from these studies was confirmed in well-controlled small-scale bioreactor experiments, it was designated as the prototype basal medium. It was used as the starting point to design subsequent optimization studies for the basal and feed medium.

In general, subsequent experiments for optimizing basal medium should use design of experiment (DoE) principles. DoE has gained increasing popularity in many disciplines, as a way to maximize knowledge gained from the experimental studies conducted with limited resources

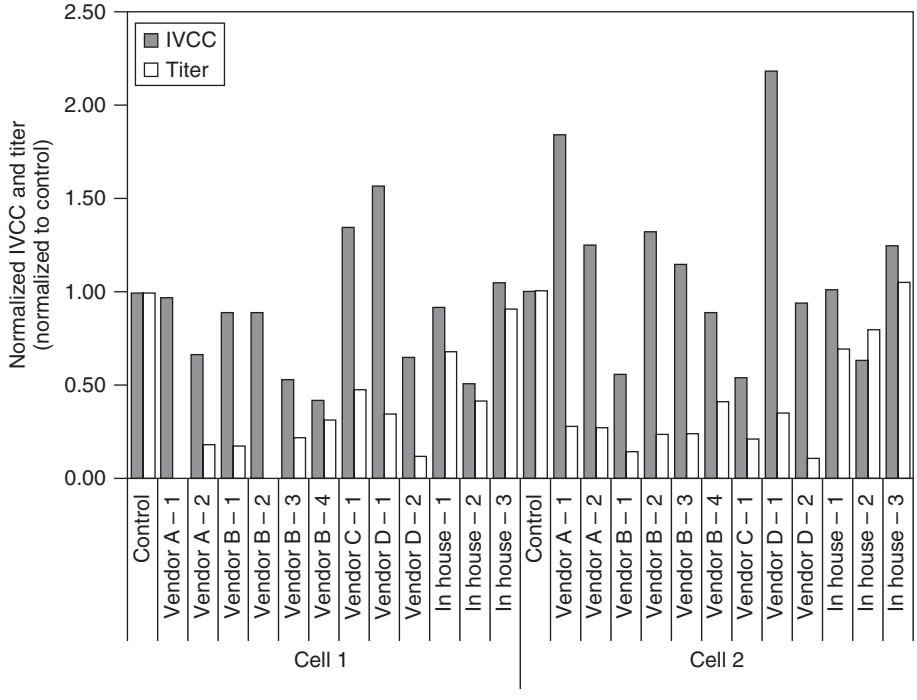


Figure 26.1. Normalized integral viable cell concentration (IVCC) and titer results for the various vendor media and in-house media. IVCC, which is a measure of cell growth, is the integrated, viable cell concentration (VCC) over time, $\int_0^t VCCdt$, and it is an indicator of the total product synthesizing capacity of the culture. Results were normalized against the peptone-containing medium, as the goal was to replace it with a chemically defined medium. Note that several of the vendor media supported better growth than the control, but titers were far lower.

(79–81). Due to the complex nature of mammalian cell metabolism and nutrient requirement, which can be further complicated by cell line and host specific needs, it is impractical to design a basal medium that has each of the 60–80 components optimized. Furthermore, many of the components have interactions with each other, and therefore experimental efficiency may improve by employing statistical design and analysis.

There are several well-documented approaches for basal medium development (22,71,82). Although many of the approaches were initially described for development of serum-free medium from serum-containing medium, they are still relevant for development of chemically defined medium. In general, these strategies can be classified as the "top–down" or "bottom–up" approaches. The bottom–up approach evaluates the concentration effect of individual components on culture performance. A classic example of the bottom–up approach is component titration, where one aims to establish dose responses for the components and appropriately adjust media composition. This approach may be very time-consuming and labor-intensive and might not be feasible if tight timelines are required for process development. The top–down approach focuses less on individual components and their roles in the formulation, and relies more on screening various formulations or component subgroups to find the best combination for culture performance. For example, media blending is an approach that has been proven to be very effective in combining synergistic effects of different formulations. The popular DMEM/F12 medium (26) is the best example of such an approach. An example of such an approach conducted at Genentech, Inc. is illustrated in Fig. 26.2. In this instance, the existing basal medium was subdivided into component subgroups and various medium formulations were derived from these subgroups based on fractional factorial screening design principles. However, all the derived basal media were evaluated in fed-batch mode using the same platform feed medium. These experiments identified that the trace element subgroup in the basal medium was limiting. When the concentration of the trace elements was increased five-fold based on the results of a response surface design study, the volumetric productivity of the process is improved more than three-fold from 0.6 g/L to 2.2 g/L.

Another decision that needs to be made during the optimization of the basal medium is whether to evaluate the test basal media in batch or fed-batch mode. Experimentation with batch mode cultures for basal media optimization enables the evaluation of the relative merits of the basal media in isolation and has the advantage of simplicity of experimentation. However, if a standard feed medium is available, it might be useful to evaluate test basal media in fed-batch mode with the feed medium included. Since batch cultures would invariably lead to depletion of amino acids or vitamins during the course of the culture, they would not be representative of a typical fed-batch process. Furthermore, use of the fed-batch mode could lead to immediate optimization of the existing process without further confirmation experiments. Generally, in early stages of medium development, when the medium is being developed *de novo*, no viable feed medium is available. In these instances, the batch mode experimentation with glucose feeding alone is appropriate. However, when a viable process with both batch and feed media is available, it might be appropriate to conduct basal medium optimization experiments in fed-batch mode with the feed media included, except when a complete overhaul of the existing process is desired.

26.4 FEED MEDIUM DEVELOPMENT

The aim of bioprocess development is the maximization of volumetric productivity without compromising the quality of the product. Cell growth is often limited in batch culture due to the depletion of essential nutrients such as glucose and amino acids. Excessive initial addition of these nutrients in the batch medium can increase osmolality to inhibitory levels and/or cause the accumulation of metabolic by-products such as lactate or ammonia. To overcome such limitations, industrial mammalian cell cultures generally use a fed-batch culture strategy for maximizing culture growth and productivity. The culture is initiated in the batch medium by inoculation with a seed culture and after a certain number of days, feeding is initiated using a feed medium that supplies depleted nutrients at appropriate levels. The constituents of feed media are usually glucose, amino acids, vitamins, and phosphate while trace elements and salts are usually not included. The feed medium is more concentrated than the basal medium to prevent loss of volumetric productivity due to dilution during feeding. The feed medium and the feeding strategy need to be optimized such that essential nutrients are supplied without overfeeding which might increase osmolality and have detrimental effects on cell growth. Feed medium optimization significantly affects the overall volumetric productivity of the process since the majority of the product is synthesized during the latter half of the culture when feed medium is likely to have the most impact. As with basal media, the demands imposed on process development due to rapid timelines require that two different approaches are used for the development of feed media. There is an industry-wide emphasis on the development of platform approaches for feed composition and feeding strategy development that would be applicable to multiple cell lines and easily transferred among multiple facilities and equipment. Intensive optimization of this platform is usually required for enhancing productivity for specific cell lines (83).

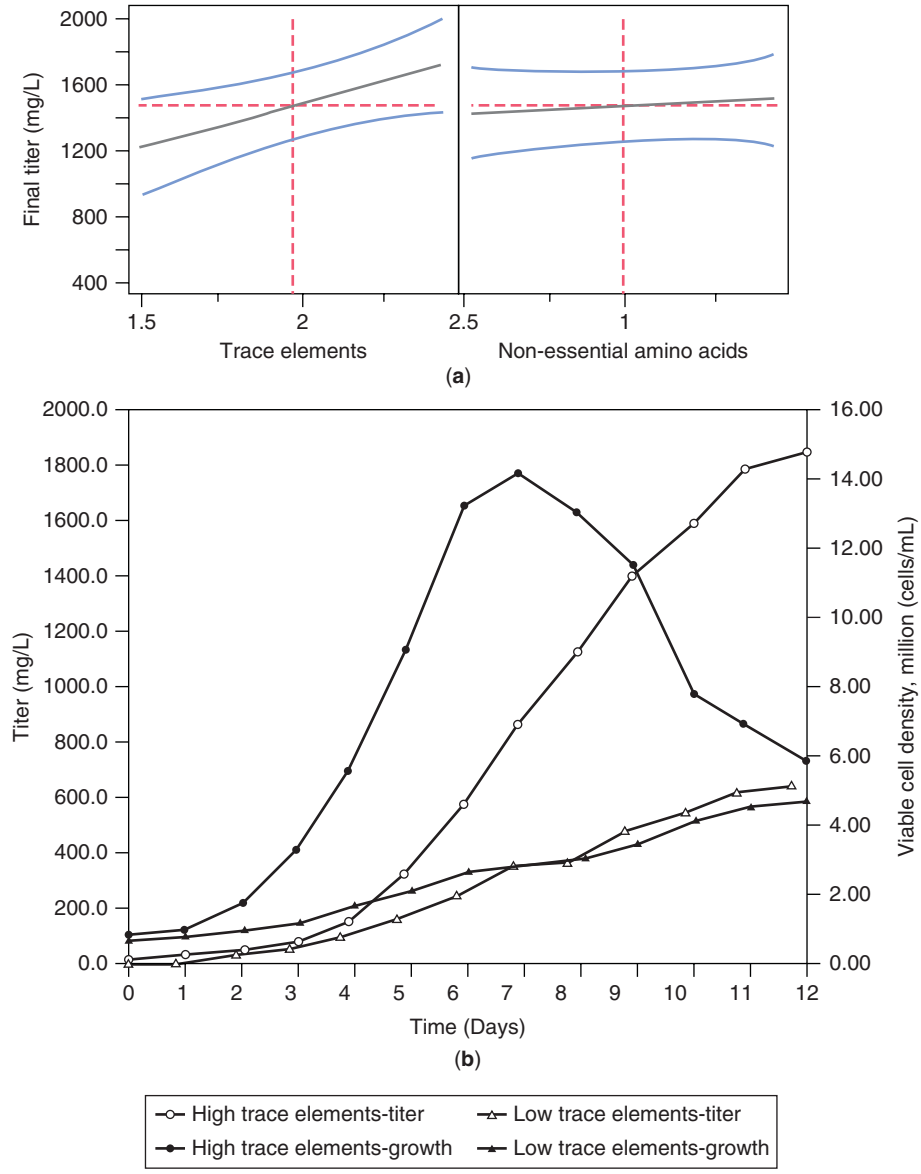


Figure 26.2. These experiments were conducted to optimize the basal medium. The basal medium was divided into subgroups and the concentration of the subgroups were varied using successive DoE experiments. The initial experiment was a fractional factorial design to screen the effects of the various nutrient subgroups (data not shown). The results from this experiment were used to design the subsequent experiment, which tested various concentrations of the trace elements and nonessential amino acid subgroups using a response surface design. (a) The results of the regression model between factor values and final titer for the response surface experiment is plotted. (b) Confirmation experiments conducted in controlled 2-L bioreactors confirmed that the final titer increased from 0.6 g/L to 2.2 g/L. (This figure is available in full color at http://onlinelibrary.wiley.com/book/10.1002/9780470054581.)

26.4.1 Feed Medium and Feeding Strategy Development

The primary purpose of feed medium is to increase cell growth, extend viability, and enhance the volumetric productivity. It is well-known that depletion of nutrients could induce apoptosis and this is avoided by appropriate supply of nutrients in the feed medium (25,84). Feed medium composition and feeding strategy need to be optimized such that the nutritional demands of the cells are met without the synthesis of harmful metabolic by-products, namely lactate

and ammonia. Lactate metabolism in industrially cultured animal cells is similar to the "Warburg effect" observed in cancer cells (85). In growing cells, the majority of the energy demand is met by the generation of ATP in glycolysis. Regeneration of NAD^+ from NADH, which is critical for the continued use of glycolysis for the synthesis of energy, is accomplished by the conversion of pyruvate to lactate. In contrast, when cells stop growing, ATP is primarily synthesized through oxidative phosphorylation in the mitochondria. Except in specific lactogenic cell lines, the stationary phase is characterized either by the cessation of lactate synthesis or by lactate consumption. In addition to glucose, mammalian cells utilize glutamine as an energy source and while majority of the lactate is generated from glucose through glycolysis, it is also known that lactate is generated from glutamine (86–88). Ammonia is primarily produced during the catabolism of glutamine (88). While there are reports that lactate itself could cause both growth and productivity to decrease, its effects are magnified due to the increase in osmolality that accompany lactate accumulation in pH-controlled bioreactors (89). It is believed that ammonia detrimentally affects the culture by impacting the metabolism of UDP-*N*-acetylgalactosamine and UDP-*N*-acetylglucosamine (90). While there are varying reports about the extent of growth and productivity inhibition caused due to the accumulation of lactate and ammonia (91–93), there is a general consensus about the desirability of limiting their accumulation. Accordingly, limiting their accumulation has been the focus of feed medium and feeding strategy development.

Early studies reported that culture viability and productivity can be extended by simply feeding glucose to prevent its depletion and limiting the supply of glutamine. Since ammonia is a by-product of glutamine catabolism, limitation of glutamine supply was suggested as a strategy to limit ammonia (88). It was shown that the constant feeding of glutamine at a rate that was lower than the culture's maximum consumption rate led to reduced accumulation of ammonia (94). In addition, biomass yield on glucose, glutamine, and other essential amino acids was increased. Bushell *et al*. (95) designed their feed media based on measured uptake rates of various amino acids to show that both, the final titer and the culture viability can be improved. However, designing a feed medium based on measured uptake rates of nutrients can be difficult since these rates change during different phases of the culture. Recognizing that uptake rates can vary during the course of the culture, they formulated their feeds based on rates measured at different phases of the culture and showed that productivity is maximized when they designed the feed based on uptake rates measured in the growth phase. Zhou *et al*. (96) used on-line oxygen uptake rate measurement as a proxy to estimate the nutritional demands of the culture and designed their feed based on measured amino acid uptake rates. The feeding strategy was coupled to on-line measurements of the oxygen uptake rates to achieve enhanced cell growth (97). Xie and Wang took a more rigorous approach and proposed a stoichiometric model that related the consumption of glucose, amino acids, and vitamins to cell growth and product formation.

$$\theta_{glc}[glu\ \cos\ e] + \sum_i \theta_{a,i}[\text{amino acid}]_i + \sum_i \theta_{v,i}[\text{vitamin}]_i = [\text{cell mass}] + \theta_p[\text{product}] + \theta_{ATP}[\text{ATP}]$$

They estimated the stoichiometric coefficients based on the known roles of these nutrients in metabolism and measured cell composition and used them to rationally design feed medium composition and feeding strategy (98). They showed that such a strategy reduced the specific synthesis rate of lactate and ammonia as well as increased both cell growth and productivity. It was further shown that the supplementation of the above feed medium with serum and trace metals further enhanced growth, indicating that factors other than carbon source, amino acids or vitamins might be limiting (99).

Another strategy commonly used for reducing the accumulation of toxic by-products is the substitution of glucose and glutamine with alternative energy sources. Substitution of glucose and glutamine by galactose and glutamate was shown to decrease the levels of lactate and ammonia (19,20). Since galactose is transported more slowly than glucose, it was observed that substitution of glucose by galactose led to net consumption of lactate. Similarly, substitution of glutamine by glutamate had the effect of reducing the levels of ammonia since glutamate has only one amino group and it is metabolized slower than glutamine. It has also been established that the substitution of glutamine with pyruvate could have the same effect of reducing ammonia accumulation (21). Similarly, stable expression of the GLUT5 fructose transporter in CHO cells enabled the replacement of glucose by fructose (18). Since fructose is transported slower than glucose, lactate was also synthesized at a lower rate.

26.5 PRODUCT QUALITY

While culture media are commonly optimized for the purposes of increased productivity of the process, it is essential to ensure that such changes do not affect the efficacy and safety of the product. After any major changes to the culture media, it is necessary to ensure that the product quality has not changed significantly and if it has, that the changes do not adversely affect the safety or efficacy of the product (9). Factors that are considered to be part of the product quality profile include integrity of amino acid sequence, glycosylation (100), aggregation, deamidation of asparagine or

glutamine (101), methionine oxidation (102), and removal of C-terminal lysine (103). The quality profile of the therapeutic product could influence efficacy, immunogenicity, and *in vivo* clearance (104–107). Product quality is usually characterized using methods including peptide mapping (sequence integrity), ion exchange chromatography and capillary isoelectric focusing (acidic, basic variants), capillary electrophoresis (glycosylation), size exclusion chromatography (aggregation), and other techniques based on specific needs (e.g., HPLC or high performance liquid chromatography for sialic acid analysis).

Glycosylation is typically a product quality attribute that may be most dependent on culture media. Glycosylation is a posttranslational modification that involves the covalent attachment of oligosaccharide chains to the protein. The pattern of glycosylation can vary depending on the expression host. Bacterial cells generally cannot glycosylate proteins, and the primary reason many therapeutic proteins are produced in mammalian cells is that they need posttranslational modifications that microbial cells are unable to perform. Glycosylation is classified as one of two main varieties, *N*-linked and *O*-linked. In *N*-linked glycosylation, the oligosaccharide is linked to the asparagine residue with the consensus sequence Asn-X-Ser/Thr, and in *O*-linked glycosylation, the oligosaccharide is attached to serine or threonine through an *O*-glycosidic bond. No consensus sequence has been identified for *O*-linked glycosylation. The IgG class of antibodies is *N*-glycosylated at an asparagine residue in the CH_2 domain. This is typically a complex biantennary type with the core composed of two *N*-acetylglucosamine residues and three mannose residues. The oligosaccharide is composed of further additions of mannose, fucose, galactose, sialic acid, and *N*-acetylglucosamine to the core glycoform. Figure 26.3 shows some commonly observed *N*-linked glycoforms in CHO cells. This oligosaccharide is essential for the antibody to display functionality beyond antigen binding and the pattern of glycosylation can affect antibody function (108).

Heterogeneity in glycosylation can result from "Macroheterogeneity" or "Microheterogeneity". Macroheterogeneity can result from the presence or absence of the oligosaccharide at a specific site in the protein. Iron, manganese, butyrate, triiodothyronine, and thyroxine had the effect of increasing site-occupancy for tPA (109). It was shown that site-occupancy in tPA was inversely correlated with growth rate (110). In contrast, nucleoside precursor molecules uridine and guanosine decreased site-occupancy by 2%, while mannose and dolichol phosphate did not have an effect. Microheterogeneity can result due to variable additions of sugars to the core glycoform since the synthesis of the oligosaccharide is not template-driven, but through a series of enzyme-catalyzed addition and trimming reactions (100). Controlling the

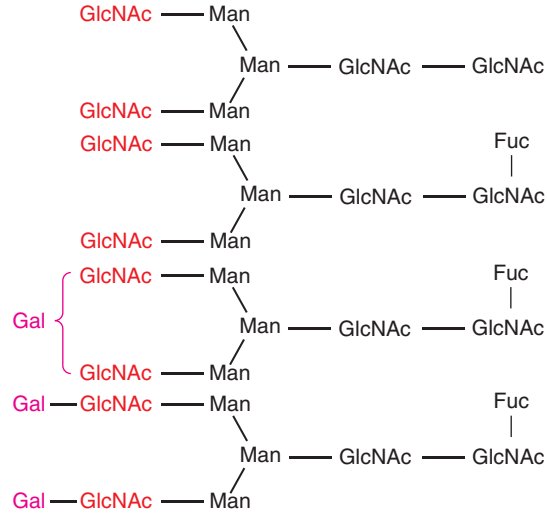


Figure 26.3. *N*-linked oligosaccharides commonly observed in monoclonal antibodies produced in CHO cells. GlcNAc: *N*-acetylglucosamine, Man: Mannose, Gal: Galactose, Fuc: Fucose. (This figure is available in full color at http://onlinelibrary.wiley.com/book/10.1002/9780470054581.)

concentration of glucose and glutamine at low levels, which is a strategy used to reduce metabolic by-products, was found to decrease sialylation and increase the level of high mannose glycan species (111). Increasing culture time, which is commonly used to enhance volumetric productivity, led to increase in truncated and oligo-mannose structures, potentially in response to glucose starvation (112,113). Truncated and high mannose glycans were also observed in fed-batch cultures with culture time exceeding three weeks even though metabolite depletion was not a factor (114). Increased levels of sialylation and core fucosylation were observed in the absence of serum for cultures of BHK-21 cells producing a human interleukin-2 variant (115). Inclusion of glucosamine and *N*-acetylmannosamine increased the antennarity of glycans by increasing the pools of UDP-*N*-acetylhexosamine and CMP-sialic acid (116). Glucosamine addition in the media also had the effect of decreasing galactosylation by increasing UDP-*N*-acetylhexosamine levels and decreasing UDP-galactose levels (117). Decrease in UDP-galactose was believed to be due to the entrapment of cellular uridine in UDP-*N*-acetylhexosamine. Supplementation of *N*-acetylmannosamine, a precursor of sialic acid, was found to enhance sialylation of interferon-γ in CHO cells (118).

Culture media are often enriched with amino acids with the aim of enhancing volumetric productivity. Enhanced levels of amino acids could lead to the formation of ammonia, which could affect product quality. Ammonia is incorporated into UDP-*N*-acetylglucosamine, which is a precursor of oligosaccharides linked to proteins (119). Ammonia and glucosamine increased the intracellular

levels of UDP-*N*-acetylhexosamines which increased the antennarity of glycans and reduced sialylation (120). Increasing concentration of ammonium chloride also decreased the *N*-linked glycosylation of mouse placental lactogen-I produced in CHO cells (121). The effect of ammonium chloride was exacerbated by increasing pH, indicating that glycosylation was affected by the level of ammonia (NH_3) species. Increasing concentrations of ammonium chloride were also implicated in the decrease in galactosylation and sialylation (122).

Even though there is a significant amount of information in the literature about the general effect of certain medium components on product quality profile, the qualitative and quantitative impact on specific molecules and cell lines may vary. Hence, the product quality profile should be separately evaluated for each cell line after any changes, especially if they involve the transition from hydrolysate containing to chemically defined medium. The product quality assessment is also based on the then current stage of clinical development for a specific molecule (9). Culture medium changes are generally of less concern if they are proposed at an early stage of development before clinical and nonclinical studies. In fact, major modifications to the platform culture media, applicable to multiple cell lines in early stages of development, could be proposed based on new knowledge about productivity gains. In such a scenario, the impact of the change on product quality should be elucidated in small-scale bioreactor experiments based on its effect on multiple cell lines with different characteristics of growth and productivity. If the change is proposed for commercial products or for products in stages of development when no additional clinical studies are planned, a thorough comparability assessment should be performed. The product quality profile before and after the change should be elucidated. If the product quality profile is not adequately comparable, additional nonclinical or clinical studies might be required depending on data available about the product or its product class. Hence, major changes in culture media that affect product quality are usually avoided for commercial therapeutic products.

26.6 USE OF APPROPRIATE SMALL-SCALE MODEL AND HIGH THROUGHPUT SYSTEMS

An area that is often overlooked is the use of appropriate small-scale models during experimentation to optimize cell culture media. The media are usually developed for use in large-scale bioreactor cultures with working volumes ranging from 100–25,000 L. Since it is impractical to develop cell culture processes at this scale, small-scale models are used to mimic large-scale cell culture performance. The most commonly used models are small-scale bioreactors with working volumes ranging from 1–5 L. Even though the cellular microenvironment in these bioreactors do not exactly mimic the conditions at the large scale, the appropriate design and operation of these reactors can generate data comparable to larger scales. However, due to the large number of experimental conditions that need to be tested especially at early stages of media development, higher throughput than those offered by liter-scale bioreactors is required. To accomplish this objective, 96-well plates, microbioreactors (123), shake flasks (124–126) and Tubespins™ (50 mL conical bottom tubes with vented caps) (127) can all be effective smaller scale models.

Use of these smaller scale models also enables the construction of high throughput cell culture systems that can screen a large number of culture conditions simultaneously. Two common high throughput systems that have been developed are (i) reduced working volume "bioreactors" (hundreds of microliters to a few milliliters working volumes) and (ii) shaken container systems using flasks, tubes, and plates (hundreds of microliters to hundreds of milliliters working volumes). The reduction in working volume provides the potential to increase the throughput of the experiments particularly if the reactor vessels lend themselves to easy automation of unit operations required for the inoculation, sampling, control, and harvest of the reactors. Small volume reactors in hundreds of microliters to a few milliliters capacity have been developed with some form of control systems in place. A 24-well system using working volumes of 4–6 mL was developed by MicroReactor Technologies, Inc. (Mountain View, CA) for microbial applications (128). This system was then adapted for cell culture work but required modifications for foaming and pH control that resulted in the need for manual base addition (129). This system allows the control of temperature, dissolved oxygen, and pH at the individual well level but still needs to be inoculated, sampled, and harvested manually. Using their proprietary robotics technologies, Hudson Control Group (Springfield, NJ), have developed a system that automatically loads, samples, and feeds cells growing under 24 independent reaction conditions simultaneously. The entire unit is placed in a standard biosafety cabinet to allow aseptic feeding and sampling. The samples can be transferred to chilled microtiter plates for further analysis and users can input triggered automated feeding using multiple feeds and/or sampling of the wells based on measured events and/or time. This system is relatively "low" high throughput since consumers would have to purchase multiple 24-well plate systems to compete with shaken systems offering more vessels and greater automation. Another promising high throughput system is the SimCell™ microbioreactor platform from Seahorse Bioscience Inc. (North Billerica, MA). This is a cassette-like system with biocompatible, gas-permeable materials containing six reactors per cassette. The handling

of the reactors is highly automated and includes functions such as set-up, culture control, monitoring, and sampling (130). This system is capable of running ~1000 cultures simultaneously (131,132). A potential drawback of these systems is the cost, which may range from tens of thousands to millions for set-up and implementation in addition to the cost of consumables. For a potentially low cost solution, shaken container systems can be used for screening cell culture conditions including conditions for medium development. Automated systems for the shaken tubes have been developed as an alternative between shake flasks and automated shaken plate systems (133). Finally, shaken deep well–plate cell culture systems that are also easily automated have been described and are capable of executing 1500 cell culture runs per month (130).

For medium development, it should be noted that many of the smaller scale model systems do not offer a pH-controlled cell culture environment and hence, are not ideal scale-down models. It has been postulated that the qualitative effects of different medium components could be accurately investigated in these noncontrolled small-scale shaken systems (134). To test this, we performed studies comparing productivity and growth characteristics for a specific cell line in shaken TubeSpins™ (133), shaken flasks, and pH-controlled stirred tank 2 L bioreactors with three different media formulations. Figure 26.4, which shows the final titer from each of these cases, indicates that all these systems give similar qualitative results even though they differ quantitatively. This indicates that screening for qualitative performance deviations from appropriate control conditions could be representative even in systems that are not ideal scale-down models. We observe that this conclusion is true for medium components that have large effects across the majority of cell lines tested. Since cell lines display varying levels of sensitivity to pH changes, care should be taken to not interpret reduced growth or productivity of pH-sensitive cell lines in smaller scale shaken models as due to nutrient limitation or other medium effects. It is unavoidable that early stages of medium development are usually conducted in these smaller scales due to the large number of screening experiments required. It is recommended that bioreactor studies be conducted for verifying major conclusions drawn from such smaller scale screening studies. We believe that automated shaken systems could offer a viable high throughput methodology for medium formulation screening if the data is carefully interpreted.

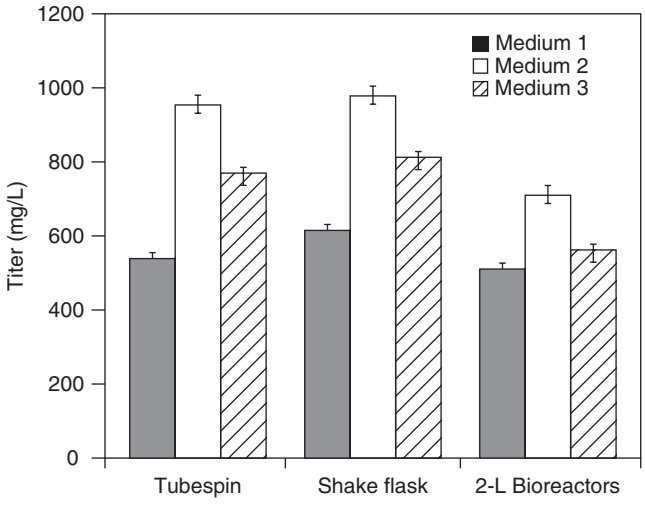


Figure 26.4. Three formulations designated as medium 1, 2, and 3 were evaluated in shaken tubes, shake flasks, and 2-L stirred tank bioreactors. The end-of-run secreted antibody titer data for cultures are plotted.

26.7 INDUSTRIAL CONSIDERATIONS FOR THE OPTIMIZATION AND IMPLEMENTATION OF BASAL AND FEED MEDIA

26.7.1 Platform and Customized Processes

While the focus of the literature has been primarily on the reduction of toxic waste products and enhancement of growth and productivity, several other considerations arise in the industrial setting for optimizing and implementing fed-batch cell culture processes. A "platform" process that is applicable across multiple cell lines expressing different products is highly desirable, especially for early stages of clinical development. Process development for new molecular entities in early stages of clinical trials when there is a high likelihood of failure, tends to be rapid. During such early development, the process platform is implemented with minimal changes; changes to the composition of the media are rarely made. In early development, the only changes made to the media are usually the concentrations of glucose, glutamine, and peptone. Optimization of volumetric productivity is more critical for molecules that are more likely to be commercialized. Since molecules in the later stage of clinical development have a greater probability of being approved, late stage process development tends to be more extensive with greater emphasis on process optimization and robustness. However, even in later stages of process development, a major overhaul of medium composition is not recommended because it is desirable to maintain consistency between processes developed at the same company and to facilitate scale-up and technology transfers across multiple clinical/commercial sites. Thus, the basal and feed media developed as part of this platform need to be appropriately optimized such that minimal modifications are required.

The platform feed media should be applicable to many cell lines with different growth characteristics. Different

cell lines expressing the same or different molecules, even when derived from the same parental cell line, could have different growth and metabolite profiles. For example, feed medium composition that is determined based on nutritional demands for a high growth/productivity cell line might overfeed another cell line with lower nutritional requirements due to slower growth. Hence media developed for the platform process are usually tested with multiple representative cell lines, which display different profiles of growth, metabolism, and productivity. A set of three to four model cell lines can generally satisfy this need for platform medium development. Two "typical" cell lines, which display growth and productivity characteristics typically observed in the existing process, could be used along with two "outliers", spanning high and low growth and productivity characteristics. The two typical cell lines could be used for most of the studies with the outliers included for studies that aim to confirm significant conclusions. The high growth outlier cell lines are also a good test on potential nutrient limitations since greater growth could lead to faster depletion while the low outlier cell line could indicate potential inhibitory effects and ensure that the selected media do not cause significant negative responses. In addition to growth and productivity, the performance indicators should also include lactate and ammonia profiles, since excessive lactate or ammonia synthesis could indicate deficient or excessive concentrations of certain nutrients in the media. Furthermore, these waste products can potentially affect culture performance and/or product quality, particularly when a scale-up exercise results in differences in the culture environment and influence metabolic behavior.

The feeding strategy that is developed as part of the platform should be relatively simple, manufacture-friendly, and easily transferred across multiple sites either within the company or to a contract manufacturing organization. On-line or continuous feeding strategies that are widely used in academia have not yet gained favor in industrial cell culture processes due to these constraints as well as the cost and complexity of automation and validation efforts. Usually, a predefined volume of the feed media is fed at one or more times during the course of the fed-batch culture. The feed volume can be determined based on the nutritional demands of the cell as well as the concentration of the feed media. The feed volume in the platform process is also determined based on investigations with multiple representative cell lines. Feeding is usually initiated approximately three days after batch inoculation. Feed initiation should occur after a significant fraction of nutrients initially present in the batch media are near depletion. Since the concentrations of amino acids and vitamins are not routinely measured during manufacturing, a proxy variable such as glucose or glutamine concentration could be used to initiate the first feed. Alternately, the feed initiation could also be defined by culture time. It is essential that such a process be extremely robust in order to operate with such a simplified criterion.

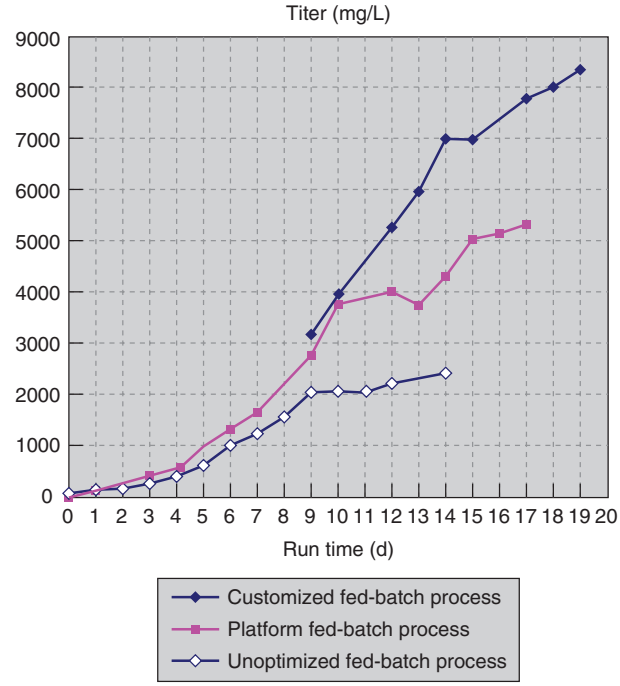


Figure 26.5. Experiments were conducted in 2-L controlled bioreactors. Titer profiles are shown for fed-batch cultures of a specific cell line, which used the same basal medium but different feed media (unoptimized, platform, and customized feed). While the platform feed led to significant improvement over the unoptimized feed, customization of the process to this specific cell line led to even higher titers. (This figure is available in full color at http://onlinelibrary.wiley.com/book/10.1002/9780470054581.)

Due to increased market demand or manufacturing capacity constraints, processes for specific therapeutic products might require extensive optimization. Under these conditions, the specific characteristics of the cell line need to be considered to customize the feed medium to achieve high titers. Figure 26.5 shows the product titer profiles for the same cell line in the unoptimized fed-batch process, the developed platform fed-batch process, and in the fed-batch process customized for this specific cell line. While unoptimized process led to a titer of 2.4 g/L, use of the platform process led to a titer of approximately 4 g/L. Intensive optimization of the platform process led to a final titer of approximately 8 g/L. It is to be noted that such high volumetric productivity was achieved in serum and peptone-free chemically defined media. Among the strategies that might be considered for such customized optimization are feed composition optimization based on nutritional demands of the specific cell line, sophisticated feeding strategies, and the option of using multiple feeds to deliver different nutrients or to account

for varying nutritional demands during different phases of cell culture. Recently, titers higher than 10 g/L have been reported (135).

26.7.2 Liquid Media Stability and Scalability

Other important considerations that need to be tested are the stability of the liquid medium formulation and scalability of the process developed using the medium. The shelf life of developed liquid formulations may be limited to as little as two weeks due to precipitation of specific amino acids such as cystine and tyrosine. While short shelf life is less of a concern in manufacturing where the medium is used immediately after preparation, longer shelf of at least a month at 4°C is usually desired in process development to allow for experiment schedule flexibility. The most problematic medium components with regard to solubility include cysteine and/or cystine, tyrosine and iron (if added in the chelated forms). Forms of cysteine or cystine are more soluble in acid, whereas tyrosine is most soluble at high pH (above pH 10.5). It is often difficult to supply both in adequate concentrations, even in the basal medium. Combining them together in a single, concentrated nutrient feed is particularly more challenging. In most media formulations, tyrosine is the limiting factor due to its low solubility (2.5 m*M*). For this reason, tyrosine is typically added as a separate component late in the feed preparation, and it is added as the free base dissolved in sodium hydroxide or as the disodium salt. At very high concentrations, the disodium salt dissolves readily in water. Cystine, being less soluble, may be added from an acidic stock solution. Alternatively, the cystine–disodium–monohydrate form is more soluble and may be dissolved directly in the medium. Since cysteine is more soluble, it is usually preferred over cystine. However, cysteine in the media readily converts mostly to cystine during medium preparation and could eventually precipitate. The media need to be formulated such that these components do not precipitate over the required shelf life. Various strategies to extend shelf life could include testing lower concentrations or alternate forms of the amino acids in question, changing the final pH of the media or changing storage conditions.

Even though media are developed for eventual use in large-scale bioreactors, it might not be cost-effective or necessary to test prototype media in early stages of development in such large scales. However, the developed media should at least be tested in pilot scale to ensure that the newly developed media can be solubilized and sterilely filtered without problems in the larger scale equipment and to ensure comparability of data to lab-scale. When a medium is used in manufacturing scale reactors, it may be subjected to high temperature treatment for short times (HTST) to ensure viral inactivation (17). Newly formulated media should be subjected to such treatment at pilot scale to ensure that there is no loss of productivity after such treatment. If such heat treatment leads to adverse effects on productivity, the specific medium constituent(s) that are susceptible to this treatment should be identified. These constituent(s) should either be supplied at increased concentrations or added to the medium after the heat treatment step.

26.8 CONCLUDING REMARKS

In just over two decades recombinant protein titers have increased from about 50 mg/L to over 10 g/L. Today cell culture is a mature technology capable of synthesizing tons of recombinant biopharmaceutical products, in the process meeting market demand for life saving drugs. Alongside advances in cell line engineering, medium optimization provides the greatest tool in cell culture technology to optimize productivity, modulate product quality, and improve robustness of the cell culture process. Development of robust and productive cell culture media is at the crossroads of fundamental understanding of animal cell metabolism, empirical experimentation, and business needs. We have shown that through systematic and rational media development, it is possible to achieve high volumetric productivities, using peptone-free, serum-free chemically defined media in fed-batch cell culture processes. The focus for future research areas could include greater fundamental understanding of the cell culture process, specifically on factors in the media that affect metabolite and product quality profiles. While considerable progress has been made in achieving high titers with specific cell lines, clonal variations in productivity and metabolite profiles continue to exist, even for clones derived from the same parental host. Future research could also focus on influencing the behavior of these cell lines that display inherently undesirable phenotypic behavior, namely high lactate or ammonia synthesis rates and inherently low productivity.

Acknowledgment

We are grateful to thank Steven Meier (Late Stage Cell Culture, Genentech, Inc.) for critical review of this manuscript and David Chang (Global MSAT, Genentech, Inc.) for technical discussions.

REFERENCES

1. Eage H. Science 1955; 122(3168): 501–504.
2. Ozturk SS. In: Hu WS, Ozturk SS, editors. Cell culture technology for pharmaceutical and cell based therapies. Boca Raton (FL): CRC Press; 2006.
3. Spens E, Häggström L. Biotechnol Bioeng 2007; 98(6): 1183–1194.
4. Cruz HJ, Moreira JL, Carrondo MJT. Biotechnol Bioeng 1999; 66(2): 104–113.

5. Seifert DB, Phillips JA. Biotechnol Prog 1999; 15(4): 655–666.
6. Pau MG, Ophorst C, Koldijk MH, Schouten G, Mehtali M, Uytdehaag F. Vaccine 2001; 19(17–19): 2716–2721.
7. Yang J-D, Lu C, Stasny B, Henley J, Guinto W, Gonzalez C, Gleason J, Fung M, Collopy B, Benjamino M, Gangi J, Hanson M, Ille E. Biotechnol Bioeng 2007; 98(1): 141–154.
8. Guidance for Industry PAT—A Framework for Innovative Pharmaceutical Development. Manufacturing, and Quality Assurance, Food and Drug Administration (FDA). 2004.
9. Comparability of biotechnological/biological products subject to changes in their manufacturing process. Food and Drug Administration (FDA), 2005.
10. Chu L, Robinson DK. Curr Opin Biotechnol 2001; 12: 180–187.
11. Farid SS. J Chromatogr B 2007; 848(1): 8–18.
12. Whitford WG. Bioprocess Int 2006; 4: 30–40.
13. Zhang J, Robinson D. Cytotechnology 2005; 48: 59–74.
14. Zhou W, Chen C-C, Buckland B, Aunins J. Biotechnol Bioeng 1997; 55(5): 783–792.
15. Burky JE, Wesson MC, Young A, Farnsworth S, Dionne B, Zhu Y, Hartman TE, Qu L, Zhou W, Sauer PW, Burky JE, Wesson MC, Young A, Farnsworth S, Dionne B, Zhu Y, Hartman TE, Qu L, Zhou W, Sauer PW. Biotechnol Bioeng 2007; 96(2): 281–293.
16. Ma M, Ellet J, Okediadi C, Hermes P, McCormick E, Casnocha S. Biotechnol Prog Early View 2009; 25: 1353–1363.
17. Sofer G. Biopharm Int 2003; 16: 50–57.
18. Wlaschin KF, Hu W-S. J Biotechnol 2007; 131(2): 168–176.
19. Altamirano C, Paredes C, Illanes A, Cairo JJ, Godia F. J Biotechnol 2004; 110(2): 171–179.
20. Altamirano C, Paredes C, Cairo JJ, Godia F. Biotechnol Prog 2000; 16(1): 69–75.
21. Genzel Y, Ritter JB, König S, Alt R, Reichl U. Biotechnol Prog 2005; 21(1): 58–69.
22. Burgener A, Butler M. In: Ozturk SS, Hu W-S, editors. Cell culture technology for pharmaceutical and cell-based therapies. Boca Raton (FL): CRC Press; 2006. pp. 41–80.
23. Eagle H. Science 1959; 130(3373): 432–437.
24. Franek F, Biotechnol Bioeng 1995; 45(1): 86–90.
25. Franek F, Chládková-Šrámková K. Cytotechnology 1995; 18(1): 113–117.
26. Barnes D, Sato G. Anal Biochem 1980; 102: 255–270.
27. Bannai S, Ishii T. J Cell Physiol 1988; 137(2): 360–366.
28. Neville RG. J Am Chem Soc 2002; 79(10): 2456–2457.
29. de La Rochette A, Silva E, Birlouez-Aragon I, Mancini M, Edwards A-M, Morliere P. Photochem Photobiol 2009; 72(6): 815–820.
30. Englard S, Seifter S. Annu Rev Nutr 1986; 6(1): 365–406.
31. Padayatty SJ, Katz A, Wang Y, Eck P, Kwon O, Lee J-H, Chen S, Corpe C, Dutta A, Dutta SK, Levine M. J Am Coll Nutr 2003; 22(1): 18–35.
32. Bhullar RP, Dakshinamurti K. J Cell Physiol 1985; 123(3): 425–430.
33. Tsao YS, Gould SL, Robinson DK. In: Spier RE, editor. Encyclopedia of cell technology New York: John Wiley & Sons Inc.: 2003.
34. Trinder D, Morgan E. Am J Physiol Gastrointest Liver Physiol 1998; 275(2):G279–G286.
35. Crichton RR, Charloteaux-Wauters M. Eur J Biochem 1987; 164(3): 485–506.
36. Ham RG, McKeehan WL. Method Enzymol 1979; 58: 44–93.
37. Hamilton WG, Ham RG. In Vitro Cell Dev Biol Plant 1977; 13(9): 537–547.
38. Yamamoto A, Honma R, Tanaka A, Sumita M. J Biomed Mater Res A 1999; 47(3): 396–403.
39. Reinhardt CA, Pelli DA, Sandvold M. Cell Biol Toxicol 1985; 1(2): 33–43.
40. Yamamoto A, Honma R, Sumita M. J Biomed Mater Res A 1998; 39(2): 331–340.
41. Olle H. Differentiation 1981; 19(1–3): 1–20.
42. Pegg AE, McCann PP. Am J Physiol Cell Physiol 1982; 243(5):C212–C221.
43. Mullineaux PM, Creissen GP. In: Scandalios JG, editor. Oxidative stress and the molecular biology of antioxidant defenses. New York: Cold Springs Harbor Laboratory Press; 1997. pp. 667–713.
44. Ursini F, Maiorino M, Sevanian A. In: Sies H, editor. Oxidative stress: oxidants and antioxidants. San Diego (CA): Academic Press Inc.; 1991. pp. 319–336.
45. MatÉs JM, Pérez-Gómez C, De Castro IN. Clin Biochem 1999; 32(8): 595–603.
46. Zhang F, Robinson D, Salmon P. Biotechnol Bioeng 2006; 95(6): 1188–1197.
47. Biewenga GP, Haenen GRMM, Bast A. Gen Pharmacol 1997; 29(3): 315–331.
48. Navari-Izzo F, Quartacci MF, Sgherri C. Plant Physiol Biochem 2002; 40(6–8): 463–470.
49. Jenkins N, Castro P, Menon S, Ison A, Bull A. Cytotechnology 1994; 15(1): 209–215.
50. Castro PML, Ison AP, Hayter PM, Bull AT. Cytotechnology 1995; 19(1): 27–36.
51. Urlaub G, Chasin LA. Proc Natl Acad Sci U S A 1980; 77(7): 4216–4220.
52. Butler M. In: Thilly WG, editor. Mammalian cell technology. Stoneham (MA): Butterworth Publishers; 1986.
53. Sunstrom N-AS, Gay RD, Wong DC, Kitchen NA, DeBoer L, Gray PP. Biotechnol Prog 2000; 16: 698–702.
54. Eagle H. Science 1971; 174(4008): 500–503.
55. Orton DR. PhD thesis. Cambridge (MA): Massachusetts Institute of Technology; 1992.
56. Meier SJ, Hatton TA, Wang DIC. Biotechnol Bioeng 1999; 62(4): 468–478.
57. Cherry RS, Hulle CT. Biotechnol Prog 2002; 8(1): 11–18.
58. Garcia-Briones M, Chalmers JJ. Biochemical engineering VII: cellular and reactor engineering. Ann N Y Acad Sci 1992; 665: 219–229.
59. Handa A, Emery AN, Spier RE. Dev Biol Stand 1987; 66: 241–253.
60. Oh SKW, Nienow AW, Al-Rubeai M, Emery AN. J Biotechnol 1992; 22(3): 245–270.

61. Tharmalingam T, Ghebeh H, Wuerz T, Butler M. Mol Biotechnol 2008; 39(2): 167–177.
62. Gigout A, Buschmann MD, Jolicoeur M. Biotechnol Bioeng 2008; 100(5): 975–987.
63. Kilburn DG, Webb FC. Biotechnol Bioeng 1968; 67(6): 657–670.
64. Hu W-S, Aunins JG. Curr Opin Biotechnol 1997; 8(2): 148–153.
65. Oh SKW, Vig P, Chua F, Teo WK, Yap MGS. Biotechnol Bioeng 1993; 42(5): 601–610.
66. Jayme D, Watanabe T, Shimada T. Cytotechnology 1997; 23(1): 95–101.
67. Dulbecco R, Freeman G. Virology 1959; 8(3): 396–397.
68. Iscove NN. In: Barnes DW, Sirbasku DA, Sato F, editors. Volume 1, Methods for preparation of media, supplements, and substrata for serum-free animal cell culture, cell culture methods for molecular and cell biology. New York: Liss; 1984. pp. 169–185.
69. Moore GE, Gerner RE, Franklin HA. JAMA 1967; 199(8): 519–524.
70. Ham RG. Proc Natl Acad Sci U S A 1965; 53: 288–293.
71. Jayme DW, Greenwald DJ. Biotechnology 1991; 9: 716–721.
72. Jayme DW, Epstein DA, Conrad DR. Nature 1988; 334(6182): 547–548.
73. Jan DCH, Jones SJ, Emery AN, Al-Rubeai M. Cytotechnology 1994; 16(1): 17–26.
74. Jornitz MW, Meltzer TH. Genet Eng Biotechnol Rev 2009; 29: 6.
75. Note for guidance on production and quality control of animal immunoglobulins and immunosera for human use, EMEA. 2002.
76. Heidemann R, Zhang C, Qi H, Larrick Rule J, Rozales C, Park S, Chuppa S, Ray M, Michaels J, Konstantinov K, Naveh D. Cytotechnology 2000; 32(2): 157–167.
77. Franek F, Hohenwarter O, Katinger H. Biotechnol Prog 2000; 16(5): 688–692.
78. Shen C, Kiyota T, Jardin B, Konishi Y, Kamen A. Cytotechnology 2007; 54(1): 25–34.
79. Hammett K, Kuchibhatla J, Hunt C, Holdread S, Brooks J. In: Smith R, editor. Cell technology for cell products. Dordrecht: Springer Netherlands; 2007. pp. 683–691.
80. Chun C, Heineken K, Szeto D, Ryll T, Chamow S, Chung JD. Biotechnol Prog 2003; 19: 52–57.
81. Kennedy M, Krouse D. J Ind Microbiol Biotechnol 1999; 23(6): 456–475.
82. Fletcher T. Bioprocess Int 2005; 3(1): 30–36.
83. Bibila TA, Robinson DK. Biotechnol Prog 1995; 11(1): 1–13.
84. DiStefano DJ, Mark GE, Robinson DK. Biotechnol Lett 1996; 18(9): 1067–1072.
85. DeBerardinis RJ, Lum JJ, Hatzivassiliou G, Thompson CB. Cell Metab 2008; 7: 11–20.
86. Zielke HR, Zielke CL, Ozand PT. Fed Proc 1984; 43(1): 121–125.
87. Glacken MW, Fleischaker RJ, Sinskey AJ. Biotechnol Bioeng 1986; 28(9): 1376–1389.
88. Glacken MW. Biotechnology 1988; 6: 1041–1050.
89. Lao MS, Toth D. Biotechnol Prog 1997; 13(5): 688–691.
90. Ryll T, Valley U, Wagner R. Biotechnol Bioeng 1994; 44: 184–193.
91. Omasa T, Ishimoto M, Higashiyama K-I, Shioya S, Suga K-I. Cytotechnology 1992; 8(1): 75–84.
92. Hassell T, Gleave S, Butler M. Appl Biochem Biotechnol 1991; 30(1): 29–41.
93. Chen P, Harcum S. Appl Biochem Biotechnol 2007; 141(2): 349–359.
94. Ljunggren J, Häggström L. Cytotechnology 1992; 8(1): 45–56.
95. Bushell BE, Bell SL, Scott MF, Spier RE, Wardell JN, Sanders PG. Biotechnol Bioeng 1994; 44(9): 1099–1106.
96. Zhou W, Rehm J, Europa A, Hu W-S. Cytotechnology 1997; 24(2): 99–108.
97. Zhou W, Rehm J, Hu WS. Biotechnol Bioeng 1995; 46(6): 579–587.
98. Xie L, Wang DIC. Biotechnol Bioeng 1994; 43(11): 1175–1189.
99. Xie L, Wang DIC. Biotechnol Bioeng 1996; 51(6): 725–729.
100. Harcum S. In: Ozturk SS, Hu WS, editors. Cell culture technology for pharaceutical and cell-based therapies. Boca Raton (FL): CRC Press; 2006. pp. 113–153.
101. Huang L, Lu J, Wroblewski VJ, Beals JM, Riggin RM. Anal Chem 2005; 77(5): 1432–1439.
102. Liu H, Gaza-Bulseco G, Xiang T, Chumsae C. Mol Immunol 2008; 45(3): 701–708.
103. Harris RJ. J Chromatogr A 1995; 705(1): 129–134.
104. Varki A. Glycobiology 1993; 3(2): 97–130.
105. Chirino AJ, Mire-Sluis A. Nat Biotechnol 2004; 22(11): 1383–1391.
106. Walsh G, Jefferis R. Nat Biotechnol 2006; 24(10): 1241–1252.
107. Delorme E, Lorenzini T, Giffin J, Martin F, Jacobsen F, Boone T, Elliott S. Biochemistry 1992; 31(41): 9871–9876.
108. Wright A, Morrison SL. Trends Biotechnol 1997; 15(1): 26–32.
109. Gawlitzek M, Estacio M, Furch T, Kiss R. Biotechnol Bioeng 2009; 103: 1164–1175.
110. Andersen DC, Bridges T, Gawlitzek M, Hoy C. Biotechnol Bioeng 2000; 70(1): 25–31.
111. Wong DCF, Wong KTKW, Goh LT, Heng CK, Yap MGS. Biotechnol Bioeng 2005; 89(2): 164–177.
112. Hooker AD, Goldman MH, Markham NH, James DC, Ison AP, Bull AT, Strange PG, Salmon I, Baines AJ, Jenkins N. Biotechnol Bioeng 1995; 48(6): 639–648.
113. Hayter PM, Curling EMA, Baines AJ, Jenkins N, Salmon I, Strange PG, Tong JM, Bull AT. Biotechnol Bioeng 1992; 39(3): 327–335.
114. Robinson DK, Chan CP, Lp CY, Tsai PK, Tung J, Seamans TC, Lenny AB, Lee DK, Irwin J, Silberklang M. Biotechnol Bioeng 1994; 44(6): 727–735.
115. Gawlitzek M, Valley U, Nimtz M, Wagner R, Conradt HS. J Biotechnol 1995; 42(2): 117–131.
116. Baker KN, Rendall MH, Hills AE, Hoare M, Freedman RB, James DC. Biotechnol Bioeng 2001; 73(3): 188–202.
117. Hills AE, Patel A, Boyd P, James DC. Biotechnol Bioeng 2001; 75(2): 239–251.

118. Gu X, Wang DIC. Biotechnol Bioeng 1998; 58(6): 642–648.
119. Valley U, Nimtz M, Conradt HS, Wagner R. Biotechnol Bioeng 1999; 64(4): 401–417.
120. Gawlitzek M, Valley U, Wagner R. Biotechnol Bioeng 1998; 57(5): 518–528.
121. Borys MC, Linzer DIH, Papoutsakis ET. Biotechnol Bioeng 1994; 43(6): 505–514.
122. Gawlitzek M, Ryll T, Lofgren J, Sliwkowski MB. Biotechnol Bioeng 2000; 68(6): 637–646.
123. Buchenauer A, Hofmann MC, Funke M, Büchs J, Mokwa W, Schnakenberg U. Biosens Bioelectron 2009; 24(5): 1411–1416.
124. Büchs J, Maier U, Lotter S, Peter CP. Biochem Eng J 2007; 34(3): 200–208.
125. Maier U, Losen M, Büchs J. Biochem Eng J 2004; 17(3): 155–167.
126. Seletzky JM, Otten K, Lotter S, Fricke J, Peter CP, Maier HR, Buchs J. Biotech Histochem 2006; 81: 133–138.
127. De Jesus MJ, Girard P, Bourgeois M, Baumgartner G, Jacko B, Amstutz H, Wurm FM. Biochem Eng J 2004; 17(3): 217–223.
128. Isett K, George H, Herber W, Amanullah A. Biotechnol Bioeng 2007; 98(5): 1017–1028.
129. Chen A, Chitta R, Chang D, Amanullah A. Biotechnol Bioeng 2009; 102(1): 148–160.
130. Heath C, Kiss R. Biotechnol Prog 2007; 23(1): 46–51.
131. Schreyer HB, Miller SE, Rodgers S. Genet Eng Biotechnol Rev 2007; 27(17):44–4–.
132. Legmann R, Schreyer HB, Combs RG, McCormick EL, Russo AP, Rodgers ST. Biotechnol and Bioeng 2009; 104(6): 1107–1120.
133. Luo S, Cheung L, Bevilacqua C, Gawlitzek M. In: LabAutomation 2008 Conference; 2008; Palm Spings (CA).
134. Kennedy MJ, Reader SL, Davies RJ, Rhoades DA, Silby HW. J Ind Microbiol 1994; 13: 212–216.
135. Huang Y-M, Hu W, Rustani E, Yusuf-Makagiansar H, Ryll T. 236th ACS National Meeting; 2008; Philadelphia (PA).

27

ANIMAL CELL CULTURE, EFFECTS OF OSMOLALITY AND TEMPERATURE

JAMES C. WARREN AND SHYAMSUNDAR SUBRAMANIAN
Department of Fermentation and Cell Culture, Merck & Co. Inc., West Point, Pennsylvania

27.1 EFFECT OF OSMOLALITY OF THE CELLULAR MICROENVIRONMENT

27.1.1 Introduction

The osmolality of the extracellular environment is critical to the maintenance of cellular hydration and biovolumes at levels which promote optimal cellular functions (1,2). Most tissues in the human body are protected from fluctuations in osmotic pressures due to the essential functions of the kidney, and as a result these cells are primarily exposed to the osmolality levels of serum, of which the normal range is 285–295 mOsm. In order to simulate physiologically optimal conditions, animal cells in culture are typically propagated under isotonic conditions defined by culture media osmolalities between 280 and 320 mOsm (3). Exposure of cells to anisotonic (4) conditions results in a variety of physiological responses, including volume-regulatory responses, cytoskeletal reorganization, cellular signaling responses, regulation of gene expression, and metabolic changes. This chapter will proceed to describe the various physiological responses of cells to anisotonic conditions and focus on the impact and applications to industrial bioprocess systems.

27.1.2 Cellular Responses to Osmolality Perturbations

27.1.2.1 Volume-Regulatory Responses. Depending on the osmolality of the extracellular environment, animal cells are subject to regular exchanges of water in either direction due to the high water permeability of their membranes. Exposure of cells to hyperosmotic conditions drives water out, resulting in cell shrinkage, while exposure to hypoosmotic conditions causes cells to swell due to water influx. These changes in cellular volume are usually transient and can be corrected by various volume-regulatory responses which are triggered by cell shrinking or swelling. Regulatory volume decrease (RVD) mechanisms are triggered by exposure to hypoosmotic conditions, while regulatory volume increase (RVI) mechanisms are triggered under hyperosmotic conditions (2). Both RVI and RVD are primarily mediated by various ion channels, cotransporters, exchangers, and symporters, which actively and passively regulate the intracellular concentrations of ions (Na^+, Ca^{2+}, K^+, Cl^-, others) or organic osmolytes in order to return the osmosis-driven cellular hydration level to optimum levels. Osmolytes are organic molecules synthesized by the cell which serve little metabolic function other than maintaining intracellular osmolality (5). Some common cellular osmolytes include sorbitol, glycerophosphorylcholine (GPC), inositol, taurine, and betaine. Specific cellular responses vary among cell types and species.

Under hypoosmotic conditions, RVD is mediated by the activity of at least three main classes of channels: voltage-gated Cl^- channels (CLC2, sCLC3), voltage sensitive organic osmolyte and anion channels [volume-sensitive osmolyte and anion channel (VSOAC)], and "maxi" volume-sensitive anion channels (6). These channels are all triggered by cell swelling and mediate the efflux of Cl^- (and other anions), organic osmolytes,

Upstream Industrial Biotechnology: Expression Systems and Process Development, Volume 1, First Edition. Edited by Michael C. Flickinger.
© 2013 John Wiley & Sons, Inc. Published 2013 by John Wiley & Sons, Inc.

acetate, and bicarbonate, respectively. Under hypoosmotic conditions, cells excrete organic osmolytes which are at relatively high concentrations relative to their metabolic activity (7). Incubation at 230 mOsm stimulated the release of the organic osmolyte taurine from human neuroblastoma cells and this release was regulated by VSOAC (7).

Whereas low osmolality conditions stimulate cell swelling and subsequent RVD via anion and osmolyte efflux, high osmolality stimulates cell shrinking and subsequent RVI via ion and osmolyte influx. RVI is mediated primarily by the uptake of ions and osmolytes by the activity of the following systems: $K^+/Na^+/2Cl^-$ symport, Na^+/H^+ and Cl^-/HCO_3^- antiports, Na^+ and K^+ channels, Cl^- channel inhibition, and various osmolyte transport systems (8). The ability of a cell to increase volume through RVI mechanisms may mean the difference between life and death, as cell volume increase is necessary for mitosis, while reduction in cell volume is often the hallmark of apoptosis (9).

27.1.2.2 Cytoskeletal Reorganization. In addition to cell volume changes, exposure of cells to hyperosmotic or hypoosmotic conditions lead to specific rearrangements of the actin cytoskeleton which accompanies both RVD and RVI (10). Cell swelling in response to hypoosmotic conditions causes a breakdown in actin stress fibers, disruption of filamentous actin at the cell periphery, and formation of peripheral F-actin patches (11–15). Efficient RVD requires an intact actin cytoskeleton, as actin depolymerization agents inhibit the activation of ion or osmolyte channels which typically mediate the RVD response (11,15,16). Recent evidence has demonstrated direct interactions between filamentous actin and the voltage-gated Cl^- channel sCLC3, which are necessary for efficient RVD response (17).

Alterations in the actin cytoskeleton has also been associated with cell shrinking and RVI following exposure of cells to hyperosmotic conditions, although the results are more subtle than those associated with RVD (18). In contrast to the distinct swelling-induced actin depolymerization which is associated with RVD, hyperosmotic conditions induce rearrangement of the actin cytoskeleton, such as depolymerization of cortical networks and redistribution and polymerization to dense peripheral actin networks (19). The RVI response is tightly linked to the organization of the actin cytoskeleton, as actin polymer stabilization agents inhibit RVI, whereas actin depolymerization agents enhance the RVI response (19,20).

27.1.2.3 Cellular Signaling. Exposure to changes in osmotic pressure induces a variety of cellular signaling responses which allow cells to appropriately compensate to changing environments through coordinated networks of molecular regulation. Volume-regulatory responses and the associated cytoskeletal reorganization responses are dependent upon specific osmosensory signaling molecules which are activated in response to sudden changes in osmolality and/or cell size. Among other signaling molecules, the functional relationship between osmotic regulatory responses and activation of the mitogen-activated protein (MAP) kinases has been extensively reported (19,21–25).

All three groups of signaling molecules within the MAP kinase family, ERKs, and p38 have been connected with RVD and/or RVI responses. Hypoosmotic stress and cell swelling activates ERK1, ERK2, p38, and JNK and the inhibition of these signaling molecules perturbs the RVD response (21,24,26,27). The swelling-activated MAP kinase responses are dependent upon upstream activation of MEK, protein tyrosine kinase, or protein kinase C (PKC) (28). Raf-1 has recently been identified as a stretch-induced signaling molecule (29), confirming the essential role of the Raf/MEK/ERK pathway in the RVD response.

The MAP kinase p38, and to a lesser extent ERK and JNK are also associated with the cell shrinking response to hyperosmotic conditions (19,30,31). Hyperosmotic stress-induced cell shrinkage increases intracellular levels of the signaling molecule PIP2, which is dependent upon a specific PIP kinase PIP5Kiβ and acts upstream of the cell shrinkage response (32). Hyperosmotic stress also stimulates the expression of serum- and glucocorticoid-inducible protein kinase (Sgk) by a p38-dependent mechanism (33).

27.1.3 Effect of Osmotic Stress on Cultured Mammalian Cells: Bioprocess Applications

As the demand for mammalian cell culture-derived monoclonal antibodies and therapeutic proteins continues to increase (34), there is continued interest in enhancing the volumetric productivity of cell culture systems while preserving the product quality profile. Traditional approaches to enhancing productivity of cell culture systems have focused on optimizing feeding strategies to replace depleted nutrient levels and/or remove inhibitory metabolic by-products, resulting in increased maximum cell density, maintenance of high cell viability and prolonged periods of high antibody production (35). As a result of the extensive research that has been performed over the last 20 years toward these fundamental goals, the biotechnology industry has successfully implemented various batch-feed, fed-batch, and perfusion-based methodologies to supply the market with what is now a long list of cell culture-based therapeutic proteins and antibodies (34,36).

27.1.3.1 Effect of Culture Media Osmolality on Protein Productivity. Besides increasing cell density and prolonging culture longevity, various approaches to increasing cell-specific productivity have been employed.

Specifically, the positive effect on cell-specific protein production following exposure to hyperosmolar culture conditions (350–425 mOsm) has been demonstrated repeatedly (37–42). In general, hyperosmolar culture conditions enhance specific protein productivity in a variety of host cell systems, in some cases by twofold or more, but high osmolarity typically has negative impact on cell health and growth rates. As a result of the negative impact of hyperosmolar conditions on cell viability and diminished cell growth, the osmolarity-induced increase in specific protein productivity does not always result in substantial volumetric increases in antibody productivity (43,44). This section addresses the degree to which changes in culture osmolality affects cell-specific and volumetric protein productivity, what mitigating factors have been applied to address negative impacts of hyperosmolar conditions, and how this varies among the most commonly utilized cell types.

Ozturk and Palsson (37) reported the observation that specific protein productivity of a murine hybridoma cell line increased proportionally with culture osmolality between 290 and 435 mOsm (37). In these studies, exposure of cells to 435 mOsm resulted in greater than twofold increase in cell-specific antibody production, although this was coupled with approximately threefold increase in cell death rate in hyperosmolar relative to isotonic conditions. Although the increase in osmolality in this case was generated by increasing levels of NaCl in the culture medium, similar increased antibody productivity was reported with hybridoma cells grown in hyperosmolar conditions generated by elevated sugar levels (45). As suboptimal pH conditions had also been associated with reports of enhanced specific antibody production (46), a causality developed linking stressful culture environmental factors and subsequent suppression of cell growth to increased cell-specific protein production.

The effects of growth-suppressing conditions on specific antibody production were further exploited in studies where hyperosmolar conditions (350 mOsm) and treatment with 0.1 m*M* sodium butyrate were combined (47). Butyrate is a known suppressor of cell growth, although it has recently shown to have more specific impacts to cellular protein processing, including histone modification, chaperone activity, and lipid metabolism (48). The combination of exposures to high osmolarity and moderate levels of butyrate resulted in greater than twofold increase in volumetric antibody production relative to control conditions. In these experiments, hyperosmolar/butyrate conditions reduced maximum cell concentrations by approximately 30% relative to controls, but the combination of enhanced specific productivity and prolonged culture duration in the high osmolarity/butyrate conditions ultimately resulted in increased volumetric protein production.

Although the positive effect of hyperosmotic conditions on specific protein or antibody production has been observed across multiple cell lines, this effect has been cell line specific and variable (49). For example, whereas S3H5/γ2bA2 hybridomas exhibit greater than 200% increase in specific antibody production at ~400 mOsm relative to the specific production observed at 280 mOsm, DB9G8 hybridomas exhibit only a 10% increase in specific antibody production under the same hyperosmolar conditions relative to control.

27.1.3.2 Use of Osmoprotective Compounds to Mitigate Inhibitory Effects. Within 2–3 years following the first report of enhanced specific productivity resulting from exposure to hyperosmolar conditions (45), it became clear that for most cell lines the enhanced antibody productivity was coupled with a substantial suppression in cell growth. The inhibitory effect on cell growth occurred in a dose-dependent fashion with increasing osmolality levels above 330 mOsm, and the effect was independent of the raw material used to induce the hyperosmolar conditions (50). Hybridoma cell growth ceased when media osmolality levels reached approximately 435 mOsm through the addition of either NaCl, KCl, or sucrose (50). Subsequent research was directed toward identifying ways to maintain high cell concentration and longevity under hyperosmolar conditions.

As previously described, mammalian cell membranes are unable to selectively maintain substantial differentials in osmotic pressure relative to their surroundings, so intercellular osmolality is usually equivalent to that of the extracellular environment. The function of mammalian kidneys maintains isosmotic balance, and as a result most tissues are protected from exposure to extreme osmolality levels. Exception to this rule includes tissues such as those in mammalian excretory systems which are regularly exposed to high salt conditions. Renal cells are able to avoid the damaging effects of cell volume fluctuations by synthesizing organic osmolytes which help to maintain cellular water balance during exposure to high or fluctuating osmolality conditions (51). Examples of osmolytes typically synthesized in renal tissues to counteract the damaging effects of high osmolality include betaine, myoinositol, amino acids, sorbitol and GPC. In response to exposure to high osmolality, these osmolytes accumulate in the cell by either enhancing the transfer rate from the extracellular space, increased intracellular synthesis, or decreased intracellular breakdown (51). Previously, these osmolytes were also found to accumulate in the brains of salt-loaded rats (52).

With the knowledge that the protective effects of organic osmolytes could be achieved by cellular uptake of these compounds from the extracellular environment, a variety of osmoprotective osmolytes were added to culture media and evaluated for their ability to counteract the

inhibitory effect of hyperosmolar conditions in bioprocess systems. A variety of amino acids and methyl amines were identified as having a positive effect on cell growth when coupled with addition of high salt or sucrose (50). Among these, asparagine, proline, glycine, sarcosine, dimethylglycine, and glycine betaine were found to have the highest osmoprotective activity on hybridoma cells propagated under hyperosmolar conditions. Interestingly, with glycine compounds the degree of osmoprotection increased with increasing *N*-linked methlyation (50). Glycine betaine (trimethylglycine) provided the highest osmoprotection, followed by dimethylglycine, with glycine and sarcosine (methylglycine) providing comparatively moderate osmoprotection.

It is now known that glycine betaine provides superior protection against the inhibitory effects of hyperosmolar conditions on cells in bioprocess systems (41,50,53). In hybridoma cells exposed to extreme osmolality levels (465, 525 mOsm/kg), glycine betaine addition (15 m*M*) restored cell growth rates to a level at or near that observed with isosmotic conditions (50). As expected, cell-specific antibody production doubled under high osmolality conditions relative to isosmotic conditions. The net effect of culturing hybridoma cells at high osmolality (465–525 mOsm) in the presence of 15 m*M* glycine betaine was approximately twofold increase in volumetric antibody production (50).

The positive effect of incorporating glycine betaine in culture media under conditions of high osmolality has also been confirmed with CHO cells for the production of therapeutic proteins (53). A two to threefold increase in volumetric production of erythropoietin (EPO) from CHO cells was observed by combining hyperosmotic shock with supplementation of 15 m*M* glycine betaine (53). In a follow-up study, CHO cells grown in hyperosmolar conditions (435 mOsm) grew at half the rate relative to cells grown under isosmotic conditions, and glycine betaine (25 m*M*) mitigated this inhibition, restoring cell growth to control levels (41). In this case, however, high osmolality resulted in decreased cell-specific protein production. It is not clear whether this negative effect is related to the fact that, in this case, high osmolality was coupled with extreme carbon dioxide saturation in the liquid phase (195 mmHg).

27.1.3.3 Effect of Culture Medium Osmolality on Hybridoma Cell Size. As discussed previously, the typical cellular volume-regulatory response to a hyperosmolar shock is a transient shrinking event due to water loss, followed by a recovery phase in which intracellular ion and osmolyte levels accumulate, water is regained, and cell size is recovered. Ion and osmolyte accumulation results in increased water influx, which over time may result in an overall increase in cell size. Consistent with this principle, hybridoma cells exposed to hyperosmotic stress are up to 50% larger than cells grown in isosmotic conditions (37,39,47,54). The mechanisms responsible for this osmolality-induced increase in cellular volume have not been characterized, although increased intracellular ion, amino acid, protein, or nucleic acid concentrations have been implicated (47). Cell size increases with progression through the cell cycle, from smallest to largest in G0/G1, S, and G2/M, respectively (54). As exposure of cells to environmentally unfavorable conditions is known to decrease cell growth rate and presumably decrease the mitotic index, these conditions may lead to an overall increase in the relative proportions of cells locked in S- or G2-phase, resulting in an increase in average cell size.

27.1.3.4 Effect of Culture Medium Osmolality on Protein Posttranslational Modification. Although cell-specific and volumetric protein productivity is of utmost concern in a bioprocess production system, the maintenance of proper posttranslational modifications for these proteins is of utmost concern to the product quality profile. Among other posttranslational modifications, the addition of glycans to polypeptide chains, or glycosylation, has received a great deal of attention due to the link between glycosylation patterns and bioactivity. Most therapeutic glycoproteins undergo a complex series of oligosaccharide linking and processing in the endoplasmic reticulum and golgi (55) which have a substantial impact on protein stability, immunogenicity, biological activity, and binding specificity. Due to the critical need to maintain and promote proper glycosylation in therapeutic protein and antibody production processes, the effects of metabolic biproducts and stressful culture conditions on protein glycosylation has been studied extensively (56–58). These studies have shown overall that increased environmental stress on cells in culture leads to an increase in the variability of glycosylation patterns.

The composition and charge of glycan structures are critical to the potency and pharmacokinetics of therapeutic proteins. Addition of multiple sialic acid residues increase the net negative charge of glycoproteins which has a significant impact on the activity and efficacy of some therapeutic proteins (59,60). The polysialylation (PSA) of neural cell adhesion molecule (NCAM) is particularly sensitive to stressful culture conditions (56) and was used as a model system to understand how hyperosmotic conditions effects glycoprotein production profile. CHO cells were exposed to a series of increasingly high osmolality levels, and levels of NCAM PSA decreased as a function of increased osmolality. At approximately 500 mOsm/kg, NCAM PSA levels were 75%–80% lower than levels observed when cells were grown under isosmotic conditions (61). Addition of the osmoprotectant glycine betaine only marginally mitigated

this dramatic decrease in protein sialylation induced by hyperosmotic conditions.

Another way of characterizing general changes in posttranslational modification is to track the generation of degradation products, under the assumption that deficiencies in modifications such as *N*-linked glycosylation will generate degraded or misfolded protein products. *N*-linked glycosylation is necessary to mediate interactions with chaperones in the ER and ensure proper protein folding (62). When hybridoma cell growth and IgG production were compared in control conditions (290 mOsm/kg) and hyperosmotic conditions (400 mOsm/kg), the cell-specific antibody production rate increased by 60%, while the cell growth rate decreased accordingly (54). To determine whether posttranslational modifications were rate-limiting to the specific antibody production rate, pulse-chase labeling experiments were performed to quantify degradation in immunoglobulin light chain (LC) and heavy chain (HC) (54). No change in degradation profiles were observed between cultures propagated under control and hyperosmotic conditions, indicating that rates of posttranslational modifications increased with enhanced rates of antibody production.

27.1.3.5 Effect of Hypoosmotic Conditions on Specific Protein Productivity. Although particular attention has been devoted to understanding the positive effects of hyperosmotic conditions on specific protein or antibody productivity, a much fewer number of cases have been reported describing the positive effects of hypoosmotic conditions on specific protein productivity. CHO cells exposed to hypoosmotic conditions (150 mOsm/kg) exhibited approximately 70% lower cell growth rates relative to cells cultured under control conditions (300 mOsm/kg) (63). Exposure to these hypoosmotic conditions resulted in a dramatic increase in specific antibody production rate, greater than twofold relative to control conditions (63). This trend was confirmed in another CHO cell line, engineered for the production of EPO. Cells propagated under conditions of low osmolality (210 mOsm/kg) exhibited a twofold increase in specific protein production rates relative to control (310 mOsm/kg) conditions (64). When multiple stressful conditions were applied to this cell line, including low osmolality (210 mOsm/kg), low temperature (32°C), and sodium butyrate addition (1 m*M*), specific protein production rate increased by fivefold relative to control conditions. These observations put into question the precise mechanism responsible for osmolality-induced enhancements to cellular-specific protein productivity. In particular, these observations suggest an overall nonspecific mechanism by which the exposure of cells to environmentally unfavorable conditions may result in enhanced product production or secretion. This topic is explored in greater detail in the following section.

27.1.4 Potential Mechanisms Responsible for Osmotic Stress-Induced Enhancement of Recombinant Protein Production

In order to understand the mechanisms responsible for osmolality-induced increases in cell-specific protein production which have been observed as previously described herein, it is necessary to understand how changes in extracellular osmolality affects rates of gene expression (i.e. levels of immunoglobulin (Ig) mRNA), translation (i.e. Ig synthesis rates), and protein secretion.

27.1.4.1 Effect of Hypermolar Stress on Immunoglobulin mRNA Levels and Transcription Rates. Exposure of cells to hyperosmolar conditions results in a substantial increase in total cytoplasmic RNA, including preferentially higher levels of Ig mRNA (39,42,65). Hybridoma cells propagated at elevated osmolality levels (425 mOsm/kg) exhibited greater than 50% more total RNA per cell relative to cells grown under isosmotic conditions (285 mOsm/kg) (39). When this analysis was extended to quantify the levels of Ig heavy chain (HC) and light chain (LC) mRNA, it was found that cells exposed to high osmolality conditions produced greater than threefold higher Ig (both HC and LC) mRNA levels relative to cells maintained under control conditions. Overall, this data reflects that hyperosmolar conditions result in nearly a fivefold increase in Ig HC and LC transcription rates (39). In a subsequent study, approximately 10–60 h after shifting the osmolality from 290 to 400 mOsm/kg, an enhancement (~30%) of Ig-specific fractions of total RNA levels (both LC and HC) were observed relative to control conditions (54).

These results were confirmed in another commonly used antibody-producing cell line, GS-NS0 (42). Out of approximately 7000 GS-NS0 genes analyzed, approximately 550 genes were upregulated by twofold or more when cells were cultured under hyperosmolar conditions (450 mOsm/kg) relative to cells grown at isosmotic conditions (290 mOsm/kg). The hyperosmolality-induced upregulation was observed among all classes of NS0 genes, including those genes associated with cell proliferation, physiology, signaling, transport, and metabolism. Most notably, the category in which the highest number of upregulated genes were observed was transcriptional regulation. In this category, 41 individual genes were upregulated in response to hyperosmotic stress (42). Most recent data has confirmed that hyperosmotic stress induces the upregulation of approximately 20 genes involved in regulation of transcription in hybridoma cells (65). Within 4 h post hyperosmotic shock, these genes are present in two to fourfold higher levels relative to those seen in

control cells, and the enhanced levels are maintained for greater than 12 h (65).

It is possible that exposure of mammalian cells to hyperosmotic shock induces chromatin remodeling, thereby stimulating the engagement of osmoresponsive promoter elements and enhancing gene expression. In yeast, hyperosmotic conditions trigger the HOG1 pathway (analogous to mammalian cell mitogen-activated protein kinases [MAPK]) which recruits a histone deacetylase to remodel chromatin structure, thereby facilitating the expression of osmoresponsive genes (66).

Despite multiple observations of higher total RNA and Ig mRNA levels in hyperosmotic stressed cells, it is unlikely that mRNA levels are rate limiting, and there does not seem to be a direct relationship between increased mRNA production and increased antibody production. Because the kinetics of mRNA production is distinct from antibody production kinetics, there is yet no clear correlation between elevated levels of Ig mRNA levels and increased mAb production (54,67).

27.1.4.2 Effect of Hyperosmolar Stress on Immunoglobulin mRNA Translation Rates. In further support of the claim that Ig mRNA levels do not represent rate-limiting steps toward increasing protein productivity, studies have shown that >fourfold increases in Ig mRNA transcription rates lead to only approximately twofold increase in Ig mRNA specific translation rates (39). In these experiments, a biosynthetic labeling approach was used to quantify the amount of LC and HC polypeptides synthesized over a 30 minute pulse time. Hybridoma cells exposed to hyperosmolar stress exhibited increases in levels of HC and LC polypeptide levels of 1.7- and 2.4-fold (respectively) when compared to the same measurements in cells maintained at isosmotic conditions (39). Sun *et al*. observed similar levels of protein synthesis increase in response to hyperosmotic stress, with an approximately 1.6-fold increase in total protein synthesis relative to controls (54). In these experiments, there was no preferential increase in Ig-specific protein synthesis above the 1.6-fold increase which was attributed to the nonspecific enhancement in total protein levels.

In contrast to observations in transcription-specific genes, hyperosmotic stress does not induce upregulation of a large number translation-specific genes. Whereas two genes associated with regulation of translation were found to be upregulated (approximately 1.5–2.5-fold) following exposure of cells to hyperosmotic conditions, two others in this category were significantly downregulated (65). At least one hyperosmotic stress-regulated promoter element has been identified, a GC-rich sequence which binds a p38-responsive transcription factor, resulting in stimulation of Sgk production through a well-characterized stress-response pathway (33).

Overall, the existing data suggests that Ig mRNA translation and protein synthesis rates, not Ig mRNA transcription rates, are rate-limiting with respect to cell-specific antibody production. While hyperosmotic stress may induce four to fivefold increases in Ig-specific transcription rates, the subsequent increase in Ig-specific translation rates of approximately twofold relative to control are consistent with the expected increases in specific antibody productivity. This trend is supported by recent findings that NS0 cells which exhibit higher specific antibody productivity have significantly higher levels of ER chaperone, non–ER chaperone, cytoskeletal, cell signaling, metabolic, and mitochondrial protein levels per cell relative to those with lower specific antibody productivity (68). In short, increased antibody productivity requires increases in the protein machinery required for the modulation of cell physiology, signaling, and protein synthesis.

27.1.4.3 Effect of Hyperosmolar Stress on Antibody Secretion Rates. Antibody transport from the ER through the Golgi Apparatus and secretion into the extracellular space has been modeled to account for the nongrowth associated kinetics displayed by hybridoma cells in batch culture (69). Nongrowth associated antibody secretion kinetics predicts that antibody secretion rates are inversely proportional to cell growth rates, and as such maximum secretion rates are obtained when cell growth rate approaches zero, as in batch culture stationary phase (70). To date, most experimental evidence supports the claim that factors which enhance Ig-specific translation and protein synthesis result in corresponding increases in antibody secretion rates (39,54). In other words, once the Ig LC and HC peptides are synthesized, assembled, and processed, the extracellular transport of antibodies is not a rate-limiting step. In hybridoma cells, antibody secretion rates were maintained at high levels throughout the batch culture when cells were exposed to hyperosmotic conditions (54). These antibody secretion rates were approximately 50%–60% higher than those observed under control conditions, where levels steadily declined throughout the course of the batch. This increase in antibody secretion was in direct accord with the percentage increase in LC and HC protein synthesis described previously (54). In this way, antibody secretion rates are responsive to increased protein synthesis, not specifically to changes in extracellular osmolality.

27.1.5 Effect of Hyperosmolality on Virus Expression Systems

Virus expression systems are frequently used in industry in the production of recombinant proteins, gene therapy vectors, and vaccines. The effect of culture medium osmolality on virus expression systems have been described by two

distinct observations: (i) enhancement of recombinant protein synthesis, or (ii) the enhancement in virus productivity and infectivity.

27.1.5.1 Baculovirus Expression Vector System. The baculovirus expression vector system (BEVS) is widely used in industry as a platform for the production of recombinant proteins in insect cells (71). In contrast to mammalian cell lines, insect cells have a relatively high tolerance for hyperosmolar conditions (72,73). After a 24 h adaptation period, the growth rate of Tn-5 cells was not inhibited when exposed to a range of osmolality (350–500 mOsm/kg) which would clearly be inhibitory in mammalian cells (73). In these studies, exposure to hyperosmolar conditions resulted in enhanced cellular metabolism as indicated by almost threefold increase in specific glucose uptake rate at 500 mOsm/kg compared to those propagated at 350 mOsm/kg. Only moderate increase in recombinant protein production has been associated with baculovirus-infected insect cell exposure to hyperosmolar conditions. When nutrient limitations were mitigated by feeding or media replacement, cells exposed to 500 mOsm/kg exhibited 30%–40% higher recombinant protein production relative to the production in cells exposed to lower osmolality (350 mOsm/kg) (73).

27.1.5.2 Sensitivity of Animal Virus Replication to Osmotic Conditions. Consistent with observations previously described of enhanced protein production under hyperosmolar conditions, hyperosmolar conditions have also been described to result in enhanced virus production in cultured animal cells. Bovine rotavirus production and infectivity was enhanced by 2 logs when 100 m*M* NaCl was added to the MEM virus maintenance media (74). Productivity of duck hepatitis B virus (DHBV) in primary cultured duck hepatocytes was inhibited by 50% under hypoosmotic conditions (277 mOsm/kg) and enhanced by fourfold when cultured under hyperosmotic conditions (addition of 46 m*M* NaCl, 421 mOsm/kg) (4).

Cell-specific production of a retroviral gene therapy vector has been enhanced by exposure of a continuous human cell line (TE Fly A7) to hyperosmolar conditions (75), although this effect was not observed with salt addition alone. While NaCl had an inhibitory effect on Moloney murine leukemia virus (MoMLV) production, increased osmolality up to 500 mOsm/kg by the addition of sorbitol or sugars enhanced the cell-specific production of retroviral vectors by three- to fourfold (75). Hyperosmolar conditions also resulted in approximately twofold increases in cell volume, consistent with results described for hybridoma cells previously cited in this chapter.

A thorough investigation of the effect of medium osmolality on adenovirus production in 293 human embryonic kidney cells has revealed that exposure of cells to hyperosmolar conditions did not impact cell-specific virus productivity (76). Adenovirus productivity remained relatively unchanged relative to control throughout a range of 300–430 mOsm/kg. Previous studies have shown that exposure of 293 cells to hyperosmolar conditions result in enhanced production of recombinant proteins (77). This highlights the likelihood that mechanisms responsible for osmotic shock-induced enhancements to protein production may not directly apply to virus production systems.

27.2 EFFECTS OF TEMPERATURE PERTURBATIONS ON CELLULAR PHYSIOLOGY AND PERFORMANCE IN BIOPROCESS SYSTEMS

27.2.1 Introduction

Temperature is a critical process variable to be controlled for animal/mammalian cell culture. Mammalian cells are typically cultured at a temperature slightly (0.5°C) below the optimum physiological temperature of 37°C (3). This is due to the fact that deviations below set point are tolerated better than deviations above. Temperature variations may occur due to tolerance in control schemes or failures in these control schemes. Overall impact of temperature excursions above 37°C is quite different from the impact of excursions below 37°C, and highly variable effects on cell growth, physiology, and protein productivity have been observed. While the effects of temperature on mammalian cell growth (78,79) and protein production (80) have been demonstrated previously, this section will mainly focus on current understanding of temperature effects in industrially relevant cell culture systems on the production of therapeutic proteins, viral vaccines, and gene therapy vectors.

27.2.2 Cell Culture Responses to Temperature Perturbations: Hyperthermia

27.2.2.1 Heat-Shock Response. Exposure of animal cells to temperature greater than 37°C induces a cascade of events termed *the heat-shock response*, characterized by the expression a family of proteins called heat-shock proteins (HSPs) (81,82). The response does vary based on the temperature, time of exposure, and, perhaps, the rate at which the temperature changes. Exposure to temperature greater than 39°C results in a mild heat-shock response, while exposure to temperature greater than 42°C leads to a full blown response with induction of cell death (83). Changes in membrane fluidity, permeability, DNA, RNA, and protein synthesis, and cytoskeletal rearrangements have been reported (83,84). Broad changes in signaling, specifically with MAP kinases (MAPK) and protein kinase B (PKB/Akt), have also been documented (85). These changes were observed to precede the induction of HSPs

and contributed either to counteracting the effects of heat or directing the cell to programmed cell death.

27.2.2.2 Cell Growth, Metabolism, and Physiology. The optimal temperature for mammalian cell growth (specific growth rate) is typically close to mammalian 37°C, if not precisely at that temperature. Increase in temperature up to 39°C resulted in specific growth rates similar to (86) or lower than (87) the specific growth rate observed at 37°C. However, cell growth has been observed to cease with increased cell death rates at temperatures greater than 39°C. In some cases cell growth ceases even at 39°C (88), but even if this does not occur maximum cell density obtained in batch culture at ≥39°C was always lower than that obtained at 37°C (86,87), presumably due to activation of cell death pathways. The specific glucose consumption has been reported to increase up to 39°C (86,87,89), with concomitant increase in specific lactate production. While many of these observations are from hybridomas, this effect is also generalizable to other cell types such as CHO.

27.2.2.3 Recombinant Protein Production: Quantity and Quality. With hybridomas, specific productivity of antibodies was maintained (86,88) or increased (87) with higher temperature of cultivation (upto 38–39°C), but final yield is at best comparable (88) and typically lower than at 37°C due to lower cell density (86,87). Specific productivity of EPO-Fc in CHO cells was maintained up to 38°C and then decreased (specific productivity decreases by 20%) when temperature was increased to 39°C (90). Heat-shocking CHO cells (91) or hybridomas (92) at temperatures ≥42°C did not demonstrate a negative impact on cellular health and protein productivity (EPO from CHO cells), but this data is limited and only explores brief exposure to these high temperatures. EPO glycosylation patterns were not apparently affected after a 1-hr heat-shock at 42°C (91). The only positive data reported for the use of temperature greater than 37°C comes from Jenkins and Hovey (93,94), who generated a temperature sensitive (ts) CHO cell line and demonstrated that alternating between 39°C (nonpremissive for the ts mutant) and 34°C resulted in a 35% improvement in volumetric productivity of tissue inhibitor of metalloproteinases (TIMP), compared to control cultures maintained constant at 34°C. Cultures were arrested at the G0/G1 cell cycle phase and also showed reduced metabolism under this mode of cultivation. The use of a heat-responsive promoter and altered heat-shock profiles led to even better improvements in TIMP production with this ts cell line (94).

27.2.2.4 Viral Vector Production: Quantity and Quality. Viruses also do not show higher production at temperatures beyond the optimum temperature for the cells they are adapted to grow in, since they rely heavily on the cell machinery for their replication. It is well known that enveloped viruses such as retroviruses are heat-labile (95–97), but it is interesting to note that even stable nonenveloped viruses such as adenovirus replicated efficiently with highest virus titers at a cultivation temperature of 35°C postinfection, especially when cells were cultured at 37°C preinfection in HEK293 cells (98,99) and PER.C6 cells (100). Interestingly, if PER.C6 cells were cultured at lower temperatures prior to infection (33°C), the optimal temperature for infection changed to 37°C (100) with peak titer obtained faster. Information of changes to quality of viruses upon production at temperatures ≥37°C is not available.

27.2.3 Effect of High Temperature: Potential Mechanisms

The mechanism behind changes in protein and virus productivity is less clear than the effects on cell growth and metabolism. At least in a small range around the optimal temperature, the kinetics of enzymatic and other cellular processes can be expected to respond to changes in temperature as per Arrhenius models. Therefore, slight increases in temperature resulting in increases in growth rate and metabolism can be rationalized. When these temperature excursions from optimal are sustained or if the excursions are large, other processes induced as part of the heat-shock response (protein aggregation, induction of apoptosis) can be expected to play a bigger role (101–103). Heat-shock for short duration and cultivation at lower temperature both curtail growth and could lead to synchronization of mammalian cells with respect to the cell cycle. Therefore we can speculate that certain effects seen, as with PER.C6 cells grown at 33°C producing adenovirus at 37°C, may be as a result of infection under synchronized conditions. Higher adenovirus productivity with culture synchronized with respect to the cell cycle has indeed been reported (104). However, cell cycle synchronization was not reported and so other mechanisms cannot be ruled out.

27.2.4 Cell Culture Responses to Temperature Perturbations: Hypothermia

27.2.4.1 Cold-Shock Response. Recent work has revealed that mammalian cells have an orchestrated response to hypothermia with the induction of ~20 proteins (105). Notable among the induced proteins were cold-inducible Ribonucleic acid-binding protein (CIRP) (106,107) and RNA binding motif 3 (RBM3) (108,109). Enhancement of protein synthesis could be due to increases in cap-independent translation via internal ribosome entry sites (110) or mediated through interaction with microRNA (111). These hypotheses have been demonstrated in at least one system, but await further studies to generalize.

27.2.4.2 Cell Growth, Metabolism, and Physiology. A reduction in temperature from 37°C generally leads to a reduction in the growth rate of mammalian cells, with cell cycle arrest observed at ~30°C incubation temperature, while viability was maintained for longer periods (88,90,101,112–117). Apoptosis was also generally reduced in mammalian cell cultures at reduced cultivation temperature (101,102,118,119), while exceptions to this rule have been reported (120). Oxygen consumption rates decreased with cultivation at lower temperatures (101,121) and were described using a simple Arrhenius model within the 6–37°C range (122). The decreased oxygen consumption rate is an important factor to consider when growing cells at high cell concentrations such as in perfusion cultures (123). The specific uptake rate for nutrients such as glucose, glutamine, and amino acids and the specific production rate for metabolites such as lactate decreased in general, while the lactate production to glucose utilization ratios remained constant (87,89,124), increased (90) or decreased (123). The changes in metabolism are more substantial at temperatures much lower than 37°C (<35°C). Downregulation of CIRP increased mammalian cell growth rate in mouse fibroblasts (107) but the manipulation of CIRP levels in CHO cells did not alter growth rates (125,126). In the temperature range of 28–39°C, shear sensitivity of BHK-21 cells increased with temperature (127). While shear sensitivity to temperature variation has not been reported in other cell lines, this finding may be important to consider.

27.2.4.3 Recombinant Protein Production: Quantity and Quality. Hybridomas were the first cell lines subjected to temperature optimization studies for industrial production of antibodies. None of the hybridomas studied showed significant improvements in specific productivity upon cultivation at temperatures lower than 37°C (86–88,116,128).

Research has demonstrated that there is some benefit to cultivating NS0 myeloma cells engineered for antibody production at temperatures below 37°C. In one study, slightly higher antibody yields were obtained with continuous cultivation at lower temperature (34°C) due to a combination of comparable specific productivity and higher average viable cell density (119). In another study, lower antibody yields were obtained when cells were initially grown at 37°C before switching to 37°C or 32°C (117). In the latter case, the viable cell density was lower at 32°C in comparison to 37°C, while specific productivity was similar despite increases in levels of heavy chain and light chain mRNA at the lower temperature. Reduction of temperature to 27°C resulted in poor antibody yields (117), as did continuous cultivation at 22°C (119), due to negative effects on both cell growth and specific productivity.

BHK-21 production of human antithrombin III (AT III) was not affected with a reduction in temperature to 30–33°C (129), while growth rate and metabolism (glucose consumption and lactate production) decreased, the peak cell densities obtained were similar at 33°C and 37°C. The volumetric productivity was similar with an increase in cycle time at 33°C. Chuppa *et al*. (123) used hamster cells (presumably BHK-21 or CHO) and demonstrated that reduced temperature cultivation (34, 35.5°C) in perfusion culture enabled a higher cell density to be supported (due to reduced specific oxygen/nutrient consumption). In addition, an increase in specific productivity was realized under these conditions, resulting in higher recombinant protein yield with comparable glycosylation and increased product stability.

CHO cell-based expression of recombinant proteins for therapeutic use is by far the predominant method used industrially, and accordingly has the most number of published studies (a subset is captured in Table 27.1). Production of several recombinant proteins such as EPO (64,130–132), interferon-γ (133,134,134), GM-CSF (124), antibodies and fragments (116,135–138) utilized a temperature shift down (to 30–34°C) and observed improved process productivity since the production phase could be extended (due to reduction in cell death, etc.) with similar or higher specific productivity. Even lower temperatures are used for the production of certain complex proteins such as Factor VIII, where cultivation at a temperature of 27°C and a reduced residence time in perfusion mode bioreactors increases productivity tremendously (up to sixfold) in COS-7 or CHO cells (139). Decreased aggregation and potential reduction in proteolysis were hypothesized to be partially responsible.

The improvement in recombinant protein production at low temperature is not universal, and in one study clonal variation of response to temperature shift was observed in CHO cells expressing an antibody during different stages of dihydrofolate reductase (DHFR) amplification (136). Adaptation of cell lines to enhance growth at lower temperature did not result in anticipated productivity improvements with a negative correlation observed between growth rate and specific productivity for EPO and FSH (146). Since volumetric productivity and product yield depend on both the viable cell density and specific productivity, a temperature shift strategy where cells are grown up to a desired high cell density at around 37°C following which the temperature is reduced to the desired temperature set point for production has worked effectively (112,132,133). This was also borne in direct comparisons where both single temperature (89,124) and dual temperature (141,144) strategies for growth/production have been applied. The optimal temperature shift down in single temperature cultivation (35°C) (89) may not be the same as the optimal temperature shift down for dual temperature cultivation (37°C/32°C) (141). Transient expression of proteins in CHO cells also show

TABLE 27.1. Summary of Temperature-Induced Changes to Protein Productivity Observed in Mammalian Cell Culture Bioprocess Systems

Cell Line	Protein	Temperature (°C) Growth	Temperature (°C) Production	Fold-change Specific Productivity	Fold-change Volumetric Productivity	Fold-change Yield*	Quality Comments	Quality	References
CHO	SEAP	37°C	30°C	1.7	2.3	3.4	T-flask Batch; Serum present	Sialylation ↑	112,113
CHO	IFN-γ	32°C	32°C	2.0	1.37	2.2	Shaker flasks; Serum-free; Batch	Negative impact on sialylation	133
CHO	ATIII	37°C	33°C	~1	1.2	1.3	Serum-free; Fed-Batch in bioreactors	N/A	140
		33°C	33°C	~1	0.81	1.5			
CHO	C-terminal α-amidating enzyme	35°C	35°C	1.71	1.8	1.8	Serum-free; Batch in bioreactors	No effects on glycosylation or activity	89
		32°C	32°C	2.42	1.14	1.14			
CHO	C-terminal α-amidating enzyme	37°C	32°C	3.5	1.6	2.9	Serum-free; Batch/Perfusion in bioreactors		141
		37°C	34°C	2.2	1.6	1.64			
CHO	EPO-Fc	30/33°C	30/33°C	1.4/1.7	0.35/0.62	0.74/1.14	Serum-free; Batch in bioreactors	Sialylation 0.6/0.8× ↓	90
	EPO-Fc	37°C	30/33°C	1–1.93/2.0	1.2–1.4/1.4–1.7	1.7–3.2/2.3		Sialylation 0.6× ↓ @30°C	90
CHO	*t*-PA	37°C	32°C	—	—	1.7	*T*-flask/Spinner; Serum-free; batch	No effect on glycosylation or activity	142
CHO	IFN-β	30°C	30°C	—	—	2.2	Spinner, Batch, Serum-free	Reduced aggregation	103
		37°C	30°C	—	—	5.3			
CHO	Not disclosed	37°C	33.5°C	2.5–4.5	—	—	Packed bed bioreactor; Serum-free; Continuous Culture	Not reported	121
		37°C	32°C	3.3–6.6	—	—			
CHO	*t*-PA	37°C	34°C	~1	~1	~1.0	Batch; Spinner, Serum+	No effect on activity	143
CHO	GM-CSF	33°C	33°C	2.1	—	2.3	Batch; Spinner; Serum +	No effects on glycosylation or activity	124,144
		37°C	33°C	2.5	—	6			
CHO	Fab	37°C	28°C	21 (w/ serum), 47 (w/o serum	—	14 (w/ serum), 38 (w/o serum)	*T*-flask; Batch; Serum +	Not reported	135
CHO	Anti-4-1BB	33°C	33°C	~1.2	—	~1	*T*-flask batch, serum + for growth	Not reported	114
		30°C	30°C	~1	—	~0.3			

CHO	EPO	33°C	33°C	4	—	2.6	*T*-flask, Batch, Serum	degree of sialylation maintained and activity slightly increased	130
		30°C	30°C	5.4	—	0.85			
CHO	EPO	32°C	32°C	1.5	0.72	1.7	Batch, SFM, spinners	—	145
CHO	EPO	32.5°C	32.5°C	1.4–1.6	~1.4	2.7	Batch, SFM, bioreactors	% acidic forms lower at 37°C during death phase	131
CHO	FSH	32°C	32°C	2.6	2.7#	4.3	Batch, SFM, spinners	Not reported	146
CHO	*t*-PA	37°C	33°C	~1	—	—	Bioreactors/ spinners, batch/fed-batch, SFM,	Site occupancy increased	147
CHO	EPO	37°C	32°C	~1.8	—	—	*T*-flasks, batch, serum	% acidic forms decreased	64
CHO	FSH	37°C	28°C	13	—	28	Bioreactor, batch/ perfusion, SFM	Not reported	145
CHO	cB72.3 antibody	37°C	32°C	~1	0.91	1.0	Shake flasks with serum-free media; batch	Not reported	117
			27°C	~1	0.7	0.7			
CHO	EPO	37°C	32°C	4.1	—	8.1	Bioreactor, perfusion, SFM	<32°C % acidic and tetra-antennary, tetra-sialylated forms decreases	148
			30°C	4.8	—	7.8			

- *Increased cycle time to obtain increase in yield
- Note that older references may not have used methods to detect fine quality differences
- # cell growth was similar at temperatures

enhanced productivity when low cultivation temperatures are used (149–151).

The effect of temperature on specific productivity also depends on other operating conditions such as pH, osmolality, presence of sodium butyrate and or serum in the media (64,131,135). For instance at pH 7.0, incubation at 32.5°C resulted in 1.5 fold improvement in specific productivity of EPO, while at pH <7.0 or >7.4, the specific productivity was lower at 32.5°C than at 37°C (131). The use of serum-free media instead of serum containing media resulted in greater enhancement of maximal Fab fragment yields (135). So, optimization of temperature should be considered along with other process variables using design of experiments (DOE) methodology, rather than individually.

Glycosylation is a critical quality attribute for therapeutic proteins (152–154) that affects protein function and pharmacokinetics and it has been clearly established that process conditions can have significant impact on glycosylation (147,155,156). In terms of product quality, the effects are mixed with depression in production temperature leading to detrimental (148), beneficial (112,113), or no (123,124,144) observable effects on glycosylation. Reduced temperature (<30°C) decreased fraction of protein with tetra-antennary structures and the degree of sialylation of EPO (148), while increased sialylation was seen with secreted alkaline phosphatase (112,113). Other process conditions can alleviate or exacerbate the changes to product quality attributes like glycosylation. For instance, lower pH increased the degree of sialylation when the cultivation temperature is low (90). Combining osmolality, sodium butyrate and low temperature treatments resulted in detrimental effects on quality of EPO (64).

27.2.4.4 Viral Vector Production: Quantity and Quality. The dual temperature mode of operation with physiological temperature for cell growth and a lower temperature during virus propagation is very common in virus production systems (157). This is mainly due to the fact that viruses used as vaccines are typically passaged at low temperature for attenuation and so cultivation at physiological temperature is considered risky in terms of reversing attenuation (157). The other reason is the labile nature of enveloped viruses such as retroviruses where stability at physiological temperature (37°C) is a concern (95). Increased productivity of several enveloped viruses (retrovirus, lentivirus, rabies virus, herpesviruses and reovirus) are reported at cultivation temperatures lower than 37°C (96,97,158–163). In most cases, increased stability of synthesized virus may be the reason, but improved cell physiology at lower temperature may also contribute. There are recent studies that point out that retrovirus prepared at low temperature were less stable than retrovirus prepared at 37°C (164), which was related to the presence of higher levels of cholesterol. These authors also did not see improvements in productivity at lower temperature. There are many other studies that do demonstrate higher titers at lower cultivation temperatures (96,97,158,160–162).

27.2.5 Effect of Low Temperature: Potential Mechanisms

Induction of a few proteins such as CIRP and RBM3 have been reported under hypothermic conditions (107,108). It is plausible that altered regulation at low temperature may happen at the mRNA level and there is some support from literature. Increases in mRNA levels for interferon γ were observed for instance, when temperature was reduced to 32°C from 37°C during cultivation of CHO cells (134) and similar increases in EPO mRNA levels were seen at 30–33°C (130). Increased levels for HC and/or LC mRNA does not guarantee higher antibody productivity in CHO or NS0 cells (117). It is also conceivable that product stability improvements contribute to increased productivity at low temperature for entities that are unstable such as Factor VIII (139) or retrovirus (95,96). There is less cell lysis and reduced levels of proteases released at lower cultivation temperatures (89,123). However, there are other publications that argue this is not always true (143).

Shotgun approaches to measure changes in mRNA, protein, and miRNA are being applied to determine if there are other hypothermia markers (119,165–169). These studies are in a preliminary stage and have not resulted in new hypotheses. However, it is not clear that these proteins alone are the effectors for any benefit seen in protein/virus production.

It is interesting to note that new data is revealing growth at low temperature (134,149) rather than the lack of growth (i.e. cell cycle arrest) (88) is more associated with increased productivity. However, as previously mentioned, cell-type and product differences probably play a role in these apparently contradictory observations.

27.3 CONCLUSIONS

Temperature reduction (30–34°C) has an overall positive effect on recombinant protein and virus production, especially when applied to the production phase for CHO and other cell types. While the mechanism is not completely understood, a combination of extended culture viability, reduced proteolysis/increased stability of product, increased mRNA expression seem to be responsible for these effects. However, the reader should view these results in the context of culture systems (batch vs fed-batch vs perfusion), operation set points for environmental variables (pH, DO) and media used (for e.g. presence of serum) and their potential interactions with temperature. Furthermore, these effects are variable between cell lines and even within clones of

the same cell line and therefore not necessarily predictable. Temperature greater than 37°C is generally not beneficial for cell growth and/or production of recombinant proteins or viruses.

REFERENCES

1. Lang F, Ritter M, *et al*. The biological significance of cell volume. Ren Physiol Biochem 1993; 16(1–2): 48–65.
2. Haussinger D. The role of cellular hydration in the regulation of cell function. Biochem J 1996; 313(3): 697–710.
3. Freshney RI. Culture of animal cells: a manual of basic technique. New York: John Wiley & Sons; 1994.
4. Offensperger WB, Offensperger S, *et al*. Effects of anisotonic exposure on duck hepatitis B virus replication. Hepatology 1994; 20(1 Pt 1): 1–7.
5. Lang F, Busch G, Völkl H. The diversity of volume regulatory mechanisms. Cell Physiol Biochem 1998; 8: 1–45.
6. Strange K, Emma F, *et al*. Cellular and molecular physiology of volume-sensitive anion channels. Am J Physiol 1996; 270(3 Pt 1): C711–C730.
7. Heacock AM, Dodd MS, *et al*. Regulation of volume-sensitive osmolyte efflux from human SH-SY5Y neuroblastoma cells following activation of lysophospholipid receptors. J Pharmacol Exp Ther 2006; 317(2): 685–693.
8. Wehner F, Olsen H, *et al*. Cell volume regulation: osmolytes, osmolyte transport, and signal transduction. Rev Physiol Biochem Pharmacol 2003; 148: 1–80.
9. Lang F, Foller M, *et al*. Cell volume regulatory ion channels in cell proliferation and cell death. Methods Enzymol 2007; 428: 209–225.
10. Pedersen SF, Hoffmann EK, *et al*. The cytoskeleton and cell volume regulation. Comp Biochem Physiol A Mol Integr Physiol 2001; 130(3): 385–399.
11. Calloe K, Nielsen MS, *et al*. KCNQ channels are involved in the regulatory volume decrease response in primary neonatal rat cardiomyocytes. Biochim Biophys Acta 2007; 1773(6): 764–773.
12. Tamma G, Procino G, *et al*. Hypotonicity causes actin reorganization and recruitment of the actin-binding ERM protein moesin in membrane protrusions in collecting duct principal cells. Am J Physiol Cell Physiol 2007; 292(4): C1476–C1484.
13. Kerrigan MJ, Hall AC. Stimulation of regulatory volume decrease (RVD) by isolated bovine articular chondrocytes following F-actin disruption using latrunculin B. Biorheology 2005; 42(4): 283–293.
14. Pritchard S, Guilak F. The role of F-actin in hypo-osmotically induced cell volume change and calcium signaling in anulus fibrosus cells. Ann Biomed Eng 2004; 32(1): 103–111.
15. Jorgensen NK, Pedersen SF, *et al*. Cell swelling activates cloned Ca(2+)-activated K(+) channels: a role for the F-actin cytoskeleton. Biochim Biophys Acta 2003; 1615(1–2): 115–125.
16. Liu X, Bandyopadhyay BC, *et al*. A role for AQP5 in activation of TRPV4 by hypotonicity: concerted involvement of AQP5 and TRPV4 in regulation of cell volume recovery. J Biol Chem 2006; 281(22): 15485–15495.
17. McCloskey DT, Doherty L, *et al*. Hypotonic activation of short ClC3 isoform is modulated by direct interaction between its cytosolic C-terminal tail and subcortical actin filaments. J Biol Chem 2007; 282(23): 16871–16877.
18. Lionetto MG, Pedersen SF, *et al*. Roles of the cytoskeleton and of protein phosphorylation events in the osmotic stress response in eel intestinal epithelium. Cell Physiol Biochem 2002; 12(4): 163–178.
19. Bustamante M, Roger F, *et al*. Regulatory volume increase is associated with p38 kinase-dependent actin cytoskeleton remodeling in rat kidney MTAL. Am J Physiol Renal Physiol 2003; 285(2): F336–F347.
20. Kerrigan MJ, Hook CS, *et al*. Regulatory volume increase (RVI) by in situ and isolated bovine articular chondrocytes. J Cell Physiol 2006; 209(2): 481–492.
21. Schliess F, Sinning R, *et al*. Calcium-dependent activation of Erk-1 and Erk-2 after hypo-osmotic astrocyte swelling. Biochem J 1996; 320(Pt 1): 167–171.
22. Tilly BC, Gaestel M, *et al*. Hypo-osmotic cell swelling activates the p38 MAP kinase signalling cascade. FEBS Lett 1996; 395(2–3): 133–136.
23. Niisato N, Post M, *et al*. Cell swelling activates stress-activated protein kinases, p38 MAP kinase and JNK, in renal epithelial A6 cells. Biochem Biophys Res Commun 1999; 266(2): 547–550.
24. Shen MR, Chou CY, *et al*. Human cervical cancer cells use Ca2+ signalling, protein tyrosine phosphorylation and MAP kinase in regulatory volume decrease. J Physiol 2001; 537(Pt 2): 347–362.
25. Kultz D, Burg M. Evolution of osmotic stress signaling via MAP kinase cascades. J Exp Biol 1998; 201(Pt 22): 3015–3021.
26. Kim RD, Darling CE, *et al*. Hypoosmotic stress activates p38, ERK 1 and 2, and SAPK/JNK in rat hepatocytes. J Surg Res 2000; 90(1): 58–66.
27. Belsey MJ, Davies AR, *et al*. Inhibition of ERK and JNK decreases both osmosensitive taurine release and cell proliferation in glioma cells. Neurochem Res 2007; 32(11): 1940–1949.
28. Pan Z, Capo-Aponte JE, *et al*. Differential dependence of regulatory volume decrease behavior in rabbit corneal epithelial cells on MAPK superfamily activation. Exp Eye Res 2007; 84(5): 978–990.
29. Krepinsky JC, Li Y, *et al*. Stretch-induced Raf-1 activation in mesangial cells requires actin cytoskeletal integrity. Cell Signal 2005; 17(3): 311–320.
30. Bildin VN, Wang Z, *et al*. Hypertonicity-induced p38MAPK activation elicits recovery of corneal epithelial cell volume and layer integrity. J Membr Biol 2003; 193(1): 1–13.
31. Roger F, Martin PY, *et al*. Cell shrinkage triggers the activation of mitogen-activated protein kinases by hypertonicity in the rat kidney medullary thick ascending limb of the Henle's loop. Requirement of p38 kinase for the regulatory volume increase response. J Biol Chem 1999; 274(48): 34103–34110.
32. Yamamoto M, Chen MZ, *et al*. Hypertonic stress increases phosphatidylinositol 4,5-bisphosphate levels by activating PIP5KI beta. J Biol Chem 2006; 281(43): 32630–32638.
33. Bell LM, Leong ML, *et al*. Hyperosmotic stress stimulates promoter activity and regulates cellular utilization of the serum- and glucocorticoid-inducible protein kinase (Sgk)

by a p38 MAPK-dependent pathway. J Biol Chem 2000; 275(33): 25262–25272.

34. Reichert JM, Rosensweig CJ, *et al*. Monoclonal antibody successes in the clinic. Nat Biotechnol 2005; 23(9): 1073–1078.
35. Jain E, Kumar A. Upstream processes in antibody production: evaluation of critical parameters. Biotechnol Adv 2008; 26(1): 46–72.
36. Chu L, Robinson DK. Industrial choices for protein production by large-scale cell culture. Curr Opin Biotechnol 2001; 12(2): 180–187.
37. Ozturk SS, Palsson BO. Effect of Medium Osmolarity and Hybridoma Growth, Metabolism, and A. 1991.
38. Reddy S, Miller WM. Effects of abrupt and gradual osmotic stress on antibody production and content in hybridoma cells that differ in production kinetics. Biotechnol Prog 1994; 10(2): 165–173.
39. Lee MS, Lee GM. Hyperosmotic pressure enhances immunoglobulin transcription rates and secretion rates of KR12H-2 transfectoma. Biotechnol Bioeng 2000; 68(3): 260–268.
40. Kim NS, Lee GM. Response of recombinant Chinese hamster ovary cells to hyperosmotic pressure: effect of Bcl-2 overexpression. J Biotechnol 2002; 95(3): 237–248.
41. deZengotita VM, Schmelzer AE, *et al*. Characterization of hybridoma cell responses to elevated pCO2 and osmolality: Intracellular pH, cell size, apoptosis, and metabolism. Biotechnol Bioeng 2002; 77(4): 369–380.
42. Wu M-H, Dimopoulos G, *et al*. The effect of hyperosmotic pressure on antibody production and gene expression in the GS-NS0 cell line. Biotechnol Appl Biochem 2004; 40: 41–46.
43. Lin J, Takagi M, *et al*. Metabolic flux change in hybridoma cells under high osmotic pressure. J Biosci Bioeng 1999; 87(2): 255–257.
44. Zhu MM, Goyal A, *et al*. Effects of elevated pCO2 and osmolality on growth of CHO cells and production of antibody-fusion protein b1: a case study. Biotechnol Prog 2005; 21(1): 70–77.
45. Øyaas K, Berg TM, *et al*. Hybridoma growth and antibody production under conditions of hyperosmotic stress. In: Spier RE, Griffiths JB, Stephenne J, Crooy PJ, editors. Advances in animal cell biology and technology for bioprocesses. London: Butterworth; 1989. pp. 212–220.
46. Miller WM, Blanch HW, *et al*. A kinetic analysis of hybridoma growth and metabolism in batch and continuous suspension culture: effect of nutrient concentration, dilution rate, and pH. Biotechnol Bioeng 1988; 32(8): 947–965.
47. Oh SKW, Vig P, *et al*. Substantial overproduction of antibodies by applying osmotic pressure and sodium butyrate. Biotechnol Bioeng 1993; 42(5): 601–610.
48. De Leon Gatti M, Wlaschin KF, Nissom PM, Yap M, Hu WS. Comparative transcriptional analysis of mouse hybridoma and recombinant Chinese hamster ovary cells undergoing butyrate treatment. J Biosci Bioeng 2007; 103(1): 82–91.
49. Lee GM, Park SY. Enhanced specific antibody productivity of hybridomas resulting from hyperosmotic stress is cell line-specific. Biotechnol Lettt 1995; 17(2): 145–150.
50. Øyaas K, Ellingsen TE, *et al*. Hyperosmotic hbridoma cell cultures: Increased monoclonal antibody production with addition of glycine betaine. Biotechnol Bioeng 1994; 44(8): 991–998.
51. Beck FX, Neuhofer W. Response of renal medullary cells to osmotic stress. Contrib Nephrol 2005; 148: 21–34.
52. Heilig CW, Stromski ME, *et al*. Characterization of the major brain osmolytes that accumulate in salt-loaded rats. Am J Physiol 1989; 257(6 Pt 2): F1108–F1116.
53. Ahn YH, Han K, *et al*. Effect of glycine betaine as osmoprotectant on the production of erythropoietin by CHO cells in hyperosmotic serum free media culture. Animal Cell Technology: Basic and Applied Aspects. Nagoya: Springer Netherlands; 1997.
54. Sun Z, Zhou R, *et al*. Hyperosmotic stress in murine hybridoma cells: effects on antibody transcription, translation, posttranslational processing, and the cell cycle. Biotechnol Prog 2004; 20(2): 576–589.
55. Goochee CF, Monica T. Environmental effects on protein glycosylation. Biotechnology (N Y) 1990; 8(5): 421–427.
56. Zanghi JA, Mendoza TP, *et al*. Role of nucleotide sugar pools in the inhibition of NCAM polysialylation by ammonia. Biotechnol Prog 1998; 14(6): 834–844.
57. Gawlitzek M, Ryll T, *et al*. Ammonium alters N-glycan structures of recombinant TNFR-IgG: degradative versus biosynthetic mechanisms. Biotechnol Bioeng 2000; 68(6): 637–646.
58. Schmelzer AE, Miller WM. Effects of osmoprotectant compounds on NCAM polysialylation under hyperosmotic stress and elevated pCO(2). Biotechnol Bioeng 2002; 77(4): 359–368.
59. Macdougall IC. Optimizing the use of erythropoietic agents-- pharmacokinetic and pharmacodynamic considerations. Nephrol Dial Transplant 2002; 17 Suppl 5: 66–70.
60. Yuen CT, Carr SA, *et al*. The spectrum of N-linked oligosaccharide structures detected by enzymic microsequencing on a recombinant soluble CD4 glycoprotein from Chinese hamster ovary cells. Eur J Biochem 1990; 192(2): 523–528.
61. Schmelzer AE, Miller WM. Hyperosmotic stress and elevated pCO2 alter monoclonal antibody charge distribution and monosaccharide content. Biotechnol Prog 2002; 18(2): 346–353.
62. Paulsson K, Wang P. Chaperones and folding of MHC class I molecules in the endoplasmic reticulum. Biochimica et Biophysica Acta (BBA) - Mol Cell Res 2003; 1641(1): 1–12.
63. Lee MS, Lee GM. Effect of hypoosmotic pressure on cell growth and antibody production in recombinant Chinese hamster ovary cell culture. Cytotechnology 2001; 36(1–3): 61–69.
64. Yoon SK, Hong JK, *et al*. Effect of simultaneous application of stressful culture conditions on specific productivity and heterogeneity of erythropoietin in chinese hamster ovary cells. Biotechnol Prog 2004; 20(4): 1293–1296.
65. Shen D, Sharfstein ST. Genome-wide analysis of the transcriptional response of murine hybridomas to osmotic shock. Biotechnol Bioeng 2006; 93(1): 132–145.
66. De Nadal E, Zapater M, *et al*. The MAPK Hog1 recruits Rpd3 histone deacetylase to activate osmoresponsive genes. Nature 2004; 427(6972): 370–374.
67. Leno M, Merten OW, *et al*. Kinetic studies of cellular metabolic activity, specific IgG production rate, IgG mRNA

stability and accumulation during hybridoma batch culture. Enzyme Microb Technol 1992; 14(2): 135–140.

68. Dinnis DM, Stansfield SH, *et al*. Functional proteomic analysis of GS-NS0 murine myeloma cell lines with varying recombinant monoclonal antibody production rate. Biotechnol Bioeng 2006; 94(5): 830–841.
69. Bibila TA, Flickinger MC. A model of interorganelle monoclonal antibody transport and secretion in mouse hybridoma cells. Biotechnol Bioeng 1991; 38(7): 767–780.
70. Kromenaker SJ, Srienc F. Stability of producer hybridoma cell lines after cell sorting: a case study. Biotechnol Prog 1994; 10(3): 299–307.
71. Ikonomou L, Schneider YJ, *et al*. Insect cell culture for industrial production of recombinant proteins. Appl Microbiol Biotechnol 2003; 62(1): 1–20.
72. Rosinski M, Reid S, *et al*. Osmolarity effects on observed insect cell size after baculovirus infection are avoided using growth medium for sample dilution. Biotechnol Prog 2000; 16(5): 782–785.
73. Olejnik A, Grajek W, *et al*. Effect of hyperosmolarity on recombinant protein productivity in baculovirus expression system. J Biotechnol 2003; 102(3): 291–300.
74. Begin ME. Enhanced production of infectious rotavirus in BSC-1 cell cultures by various factors in the presence of absence of trypsin. J Gen Virol 1980; 51(Pt 2): 263–270.
75. Coroadinha AS, Silva AC, *et al*. Effect of osmotic pressure on the production of retroviral vectors: Enhancement in vector stability. Biotechnol Bioeng 2006; 94(2): 322–329.
76. Ferreira TB, Ferreira AL, *et al*. Two different serum-free media and osmolality effect upon human 293 cell growth and adenovirus production. Biotechnol Lett 2005; 27(22): 1809–1813.
77. Nadeau I, Garnier A, *et al*. Improvement of recombinant protein production with the human adenovirus/293S expression system using fed-batch strategies. Biotechnol Bioeng 1996; 51(6): 613–623.
78. Rao PN, Engelberg J. Hela cells: effects of temperature on the life cycle. Science 1965; 148: 1092–1094.
79. Watanabe I, Okada S. Effects of temperature on growth rate of cultured mammalian cells (L5178Y). J Cell Biol 1967; 32(2): 309–323.
80. Giard DJ, Fleischaker RJ, *et al*. Kinetics of human beta interferon production under different temperature conditions. J Interferon Res 1982; 2(4): 471–477.
81. Lindquist S. The heat-shock response. Annu Rev Biochem 1986; 55: 1151–1191.
82. Lindquist S, Craig EA. The heat-shock proteins. Annu Rev Genet 1988; 22: 631–677.
83. Laszlo A. The effects of hyperthermia on mammalian cell structure and function. Cell Prolif 1992; 25(2): 59–87.
84. Coss RA, Linnemans WA. The effects of hyperthermia on the cytoskeleton: a review. Int J Hyperthermia 1996; 12(2): 173–196.
85. Nadeau SI, Landry J. Mechanisms of activation and regulation of the heat shock-sensitive signaling pathways. Adv Exp Med Biol 2007; 594: 100–113.
86. Sureshkumar GK. The influence of temperature on a mouse mouse hybridoma growth and monoclonal-antibody production. Biotechnol Bioeng 1991; 37(3): 292–295.
87. Barnabe N, Butler M. Effect of temperature on nucleotide pools and monoclonal-antibody production in a mouse hybridoma. Biotechnol Bioeng 1994; 44(10): 1235–1245.
88. Bloemkolk JW, Gray MR, *et al*. Effect of temperature on hybridoma cell-cycle and mab production. Biotechnol Bioeng 1992; 40(3): 427–431.
89. Furukawa K, Ohsuye K. Effect of culture temperature on a recombinant CHO cell line producing a C-terminal alpha-amidating enzyme. Cytotechnology 1998; 26(2): 153–164.
90. Trummer E, Fauland K, *et al*. Process parameter shifting: Part I. Effect of DOT, pH, and temperature on the performance of Epo-Fc expressing CHO cells cultivated in controlled batch bioreactors. Biotechnol Bioeng 2006; 94(6): 1033–1044.
91. Tsao EI, Bohn MA, *et al*. Effects of heat-shock on the production of human erythropoietin from recombinant CHO cells. Biotechnol Bioeng 1992; 40(10): 1190–1196.
92. Passini CA, Goochee CF. Response of a mouse hybridoma cell line to heat shock, agitation, and sparging. Biotechnol Prog 1988; 5(4): 175–188.
93. Jenkins N, Hovey A. Temperature control of growth and productivity in mutant chinese-hamster ovary cells synthesizing a recombinant protein. Biotechnol Bioeng 1993; 42(9): 1029–1036.
94. Hovey A, Bebbington CR, *et al*. Control of growth and recombinant protein-synthesis by heat-shock - in a mutant mammalian-cell line. Biotechnol Lett 1994; 16(3): 215–220.
95. Andreadis ST, Brott D, *et al*. Moloney murine leukemia virus-derived retroviral vectors decay intracellularly with a half-life in the range of 5.5 to 7.5 hours. J Virol 1997; 71(10): 7541–7548.
96. Le Doux JM, Davis HE, *et al*. Kinetics of retrovirus production and decay. Biotechnol Bioeng 1999; 63(6): 654–662.
97. McTaggart S, Al-Rubeai M. Effects of culture parameters on the production of retroviral vectors by a human packaging cell line. Biotechnol Prog 2000; 16(5): 859–865.
98. Jardon M, Garnier A. pH, pCO(2), and temperature effect on R-adenovirus production. Biotechnol Prog 2003; 19(1): 202–208.
99. Cortin V, Thibault J, *et al*. High-titer adenovirus vector production in 293S cell perfusion culture. Biotechnol Prog 2004; 20(3): 858–863.
100. Xie L, Goochee CF. Methods of virus production: W. I. P. Organization, Publication Number WO/2003/085138; 2003.
101. Moore A, Mercer J. Effects of temperature shift on cell cycle, apoptosis and nucleotide pools in CHO cell batch cultures. Cytotechnology 1997; 23(1–3): 47–54.
102. Nagarathnamma M, Rajan M, *et al*. Apoptosis extent increases in hybridoma cultures with temperature. Biotechnol Lett 1997; 19(7): 669–673.
103. Rodriguez J, Spearman M, *et al*. Enhanced production of monomeric interferon-ss by CHO cells through the control of culture conditions. Biotechnol Prog 2005; 21(1): 22–30.
104. Nadeau I, Kamen A. Production of adenovirus vector for gene therapy. Biotechnol Adv 2003; 20(7–8): 475–489.
105. Fujita J. Cold shock response in mammalian cells. J Mol Microbiol Biotechnol 1999; 1(2): 243–255.

106. Nishiyama H, Higashitsuji H, *et al*. Cloning and characterization of human CIRP (cold-inducible RNA-binding protein) cDNA and chromosomal assignment of the gene. Gene 1997; 204(1–2): 115–120.

107. Nishiyama H, Itoh K, *et al*. A glycine-rich RNA-binding protein mediating cold-inducible suppression of mammalian cell growth. J Cell Biol 1997; 137(4): 899–908.

108. Danno S, Nishiyama H, *et al*. Increased transcript level of RBM3, a member of the glycine-rich RNA-binding protein family, in human cells in response to cold stress. Biochem Biophys Res Commun 1997; 236(3): 804–807.

109. Danno S, Itoh K, *et al*. Decreased expression of mouse Rbm3, a cold-shock protein, in Sertoli cells of cryptorchid testis. Am J Pathol 2000; 156(5): 1685–1692.

110. Chappell SA, Owens GC, *et al*. A 5' leader of Rbm3, a cold stress-induced mRNA, mediates internal initiation of translation with increased efficiency under conditions of mild hypothermia. J Biol Chem 2001; 276(40): 36917–36922.

111. Dresios J, Aschrafi A, *et al*. Cold stress-induced protein Rbm3 binds 60S ribosomal subunits, alters microRNA levels, and enhances global protein synthesis. Proc Natl Acad Sci U S A 2005; 102(6): 1865–1870.

112. Kaufmann H, Mazur X, *et al*. Influence of low temperature on productivity, proteome and protein phosphorylation of CHO cells. Biotechnol Bioeng 1999; 63(5): 573–582.

113. Kaufmann H, Mazur X, *et al*. Comparative analysis of two controlled proliferation strategies regarding product quality, influence on tetracycline-regulated gene expression, and productivity. Biotechnol Bioeng 2001; 72(6): 592–602.

114. Yoon SK, Kim SH, *et al*. Effect of low culture temperature on specific productivity and transcription level of anti-4-1BB antibody in recombinant Chinese hamster ovary cells. Biotechnol Prog 2003; 19(4): 1383–1386.

115. Hunt L, Hacker DL, *et al*. Low-temperature pausing of cultivated mammalian cells. Biotechnol Bioeng 2005; 89(2): 157–163.

116. Chong SL, Mou DG, *et al*. Cell growth, cell-cycle progress, and antibody production in hybridoma cells cultivated under mild hypothermic conditions. Hybridoma 2008; 27(2): 107–111.

117. Marchant RJ, Al-Fageeh MB, *et al*. Metabolic rates, growth phase, and mRNA levels influence cell-specific antibody production levels from in vitro-cultured mammalian cells at sub-physiological temperatures. Mol Biotechnol 2008; 39(1): 69–77.

118. Sakurai T, Itoh K, *et al*. Low temperature protects mammalian cells from apoptosis initiated by various stimuli in vitro. Exp Cell Res 2005; 309(2): 264–272.

119. Swiderek H, Al-Rubeai M. Functional genome-wide analysis of antibody producing NS0 cell line cultivated at different temperatures. Biotechnol Bioeng 2007; 98(3): 616–630.

120. Chen ZL, Wu BC, *et al*. Temperature shift as a process optimization step for the production of pro-urokinase by a recombinant chinese hamster ovary cell line in high-density perfusion culture. J Biosci Bioeng 2004; 97(4): 239–243.

121. Ducommun P, Ruffieux PA, *et al*. Monitoring of temperature effects on animal cell metabolism in a packed bed process. Biotechnol Bioeng 2002; 77(7): 838–842.

122. Jorjani P, Ozturk SS. Effects of cell density and temperature on oxygen consumption rate for different mammalian cell lines. Biotechnol Bioeng 1999; 64(3): 349–356.

123. Chuppa S, Tsai YS, *et al*. Fermenter temperature as a tool for control of high-density perfusion cultures of mammalian cells. Biotechnol Bioeng 1997; 55(2): 328–338.

124. Fogolin MB, Wagner R, *et al*. Impact of temperature reduction and expression of yeast pyruvate carboxylase on hGM-CSF-producing CHO cells. J Biotechnol 2004; 109(1–2): 179–191.

125. Hong JK, Kim YG, *et al*. Down-regulation of cold-inducible RNA-binding protein does not improve hypothermic growth of Chinese hamster ovary cells producing erythropoietin. Metab Eng 2007; 9(2): 208–216.

126. Tan HK, Lee MM, *et al*. Overexpression of cold-inducible RNA-binding protein increases interferon-gamma production in Chinese-hamster ovary cells. Biotechnol Appl Biochem 2008; 49(Pt 4): 247–257.

127. Ludwig A, Tomeczkowski J, *et al*. Influence of the temperature on the shear stress sensitivity of adherent BHK 21 cells. Appl Microbiol Biotechnol 1992; 38: 323–327.

128. Reuveny S, Velez D, *et al*. Factors affecting cell growth and monoclonal antibody production in stirred reactors. J Immunol Methods 1986; 86(1): 53–59.

129. Weidemann R, Ludwig A, *et al*. Low-temperature cultivation - a step towards process optimization. Cytotechnology 1994; 15(1–3): 111–116.

130. Yoon SK, Song JY, *et al*. Effect of low culture temperature on specific productivity, transcription level, and heterogeneity of erythropoietin in chinese hamster ovary cells. Biotechnol Bioeng 2003; 82(3): 289–298.

131. Yoon SK, Choi SL, *et al*. Effect of culture pH on erythropoietin production by chinese hamster ovary cells grown in suspension at 32.5 and 37.0 degrees C. Biotechnol Bioeng 2005; 89(3): 345–356.

132. Yoon SK, Kim SH, *et al*. Biphasic culture strategy for enhancing volumetric erythropoietin productivity of Chinese hamster ovary cells. Enzyme Microb Technol 2006; 39(3): 362–365.

133. Fox SR, Patel UA, *et al*. Maximizing interferon-gamma production by Chinese hamster ovary cells through temperature shift optimization: experimental and modeling. Biotechnol Bioeng 2004; 85(2): 177–184.

134. Fox SR, Tan HK, *et al*. A detailed understanding of the enhanced hypothermic productivity of interferon-gamma by Chinese-hamster ovary cells. Biotechnol Appl Biochem 2005; 41: 255–264.

135. Schatz SM, Kerschbaumer RJ, *et al*. Higher expression of Fab antibody fragments in a CHU cell line at reduced temperature. Biotechnol Bioeng 2003; 84(4): 433–438.

136. Yoon SK, Hwang SO, *et al*. Enhancing effect of low culture temperature on specific antibody productivity of recombinant Chinese hamster ovary cells: clonal variation. Biotechnol Prog 2004; 20(6): 1683–1688.

137. Shi M, Xie ZG, *et al*. Controlled growth of Chinese hamster ovary cells and high expression of antibody-IL-2 fusion proteins by temperature manipulation. Biotechnol Lett 2005; 27(23–24): 1879–1884.

138. Oguchi S, Saito H, *et al*. pH Condition in temperature shift cultivation enhances cell longevity and specific hMab productivity in CHO culture. Cytotechnology 2006; 52(3): 199–207.

139. Rasmussen P. Methods of producing proteins with FVIII activity and/or FVIII derivatives, 1991.

140. Rossler B, Lubben H, *et al*. Temperature: a simple parameter for process optimization in fed-batch cultures of recombinant Chinese hamster ovary cells. Enzyme Microb Technol 1996; 18: 423–427.
141. Furukawa K, Ohsuye K. Enhancement of productivity of recombinant alpha-amidating enzyme by low temperature culture. Cytotechnology 1999; 31(1–2): 85–94.
142. Hendrick V, Winnepenninck P, *et al*. Increased productivity of recombinant tissular plasminogen activator (t-PA) by butyrate and shift of temperature: a cell cycle phased analysis. Cytotechnology 2001; 36: 71–83.
143. Clark KJR, Chaplin FWR, *et al*. Temperature effects on product-quality-related enzymes in batch CHO cell cultures producing recombinant tPA. Biotechnol Prog 2004; 20(6): 1888–1892.
144. Bollati-Fogolin M, Forno G, *et al*. Temperature reduction in cultures of hGM-CSF-expressing CHO cells: effect on productivity and product quality. Biotechnol Prog 2005; 21(1): 17–21.
145. Yoon SK, Ahn YH, *et al*. Effect of culture temperature on follicle-stimulating hormone production by Chinese hamster ovary cells in a perfusion bioreactor. Appl Microbiol Biotechnol 2007; 76(1): 83–89.
146. Yoon SK, Hong JK, *et al*. Adaptation of Chinese hamster ovary cells to low culture temperature: cell growth and recombinant protein production. J Biotechnol 2006; 122(4): 463–472.
147. Andersen DC, Bridges T, *et al*. Multiple cell culture factors can affect the glycosylation of Asn-184 in CHO-produced tissue-type plasminogen activator. Biotechnol Bioeng 2000; 70(1): 25–31.
148. Ahn WS, Jeon J-J, *et al*. Effect of culture temperature on erythropoietin production and glycosylation in a perfusion culture of recombinant CHO cells. Biotechnol Bioeng 2008. DOI: 10.1002/bit.22006.
149. Galbraith DJ, Tait AS, *et al*. Control of culture environment for improved polyethylenimine-mediated transient production of recombinant monoclonal antibodies by CHO cells. Biotechnol Prog 2006; 22(3): 753–762.
150. Underhill MF, Marchant RJ, *et al*. On the effect of transient expression of mutated eIF2 alpha and eIF4E eukaryotic translation initiation factors on reporter gene expression in mammalian cells upon cold-shock. Mol Biotechnol 2006; 34(2): 141–149.
151. Wulhfard S, Tissot S, *et al*. Mild hypothermia improves transient gene expression yields several fold in chinese hamster ovary cells. Biotechnol Prog 2008; 24(2): 458–465.
152. Elliott S, Egrie J, *et al*. Control of rHuEPO biological activity: the role of carbohydrate. Exp Hematol 2004; 32(12): 1146–1155.
153. Jefferis R. Glycosylation of recombinant antibody therapeutics. Biotechnol Prog 2005; 21(1): 11–16.
154. Jefferis R. Antibody therapeutics: isotype and glycoform selection. Expert Opin Biol Ther 2007; 7(9): 1401–1413.
155. Yang M, Butler M. Effects of ammonia on CHO cell growth, erythropoietin production, and glycosylation. Biotechnol Bioeng 2000; 68(4): 370–380.
156. Restelli V, Wang MD, *et al*. The effect of dissolved oxygen on the production and the glycosylation profile of recombinant human erythropoietin produced from CHO cells. Biotechnol Bioeng 2006; 94(3): 481–494.
157. Aunins JG. Viral vaccine production in cell culture; 2000. pp. 1182–1217.
158. Palsson B, Andreadis S. The physico-chemical factors that govern retrovirus-mediated gene transfer. Exp Hematol 1997; 25(2): 94–102.
159. Wechuck JB, Ozuer A, *et al*. Effect of temperature, medium composition, and cell passage on production of herpes-based viral vectors. Biotechnol Bioeng 2002; 79(1): 112–119.
160. Kwon YJ, Peng CA. High-yield retroviral production using a temperature-modulated two-stage operation. Biotechnol Bioeng 2005; 90(3): 365–372.
161. Kotani H, Newton PB, *et al*. Improved methods of retroviral vector transduction and production for gene-therapy. Hum Gene Ther 1994; 5(1): 19–28.
162. Kaptein LCM, Greijer AE, *et al*. Optimized conditions for the production of recombinant amphotropic retroviral vector preparations. Gene Ther 1997; 4(2): 172–176.
163. Jung S, Behie LA, *et al*. Optimization of reovirus production from mouse L-929 cells in suspension culture. Biotechnol Bioeng 2004; 85(7): 750–760.
164. Beer C, Meyer A, *et al*. The temperature stability of mouse retroviruses depends on the cholesterol levels of viral lipid shell and cellular plasma membrane. Virology 2003; 308(1): 137–146.
165. Baik JY, Lee MS, *et al*. Initial transcriptome and proteome analyses of low culture temperature-induced expression in CHO cells producing erythropoietin. Biotechnol Bioeng 2006; 93(2): 361–371.
166. Sonna LA, Kuhlmeier MM, *et al*. Effect of moderate hypothermia on gene expression by THP-1 cells: a DNA microarray study. Physiol Genomics 2006; 26(1): 91–98.
167. Gammell P, Barron N, *et al*. Initial identification of low temperature and culture stage induction of miRNA expression in suspension CHO-K1 cells. J Biotechnol 2007; 130(3): 213–218.
168. Underhill MF, Smales CM. The cold-shock response in mammalian cells: investigating the HeLa cell cold-shock proteome. Cytotechnology 2007; 53(1–3): 47–53.
169. Kumar N, Gammell P, *et al*. Differential protein expression following low temperature culture of suspension CHO-K1 cells. BMC Biotechnol 2008; 8.
170. Trummer E, Fauland K, *et al*. Process parameter shifting: Part II. Biphasic cultivation—A tool for enhancing the volumetric productivity of batch processes using Epo-Fc expressing CHO cells. Biotechnol Bioeng 2006; 94(6): 1045–1052.

28

ANIMAL CELL STABILITY

Martin S. Sinacore, Timothy S. Charlebois, Denis Drapeau, Mark Leonard, Scott Harrison, and S. Robert Adamson
Genetics Institute, Andover, Massachusetts

The genotypic and phenotypic stability of animal cells in culture are of great interest to cell and molecular biologists conducting basic biological investigations and to those in the biopharmaceutical sector engaged in the applied aspects of cell-culture-based process development. The genotypic and phenotypic status of animal cells is under constant assault by both intrinsic and extrinsic factors that conspire to invoke change in the nature of animal cell in culture. Since change is one of few certainties in nature, it is the context in which changes manifest that define their impact. The cell transformation process profoundly changes the genotype and phenotype of animal cells. In the context of a living organism, this can have significant negative effects while, in another context, it can enable cells to grow perpetually *in vitro* to the benefit of basic biological investigations. The focus of this chapter will be to review and discuss the mechanisms by which the genotypes and phenotypes of transformed animal cells change and, once established, the means by which genotypes and phenotypes can be stably maintained in continuous culture.

The starting place for the discussion of animal cell stability is to review factors that affect genomic stability of endogenous genes at the molecular level. This discussion is centered on the incompletely understood mechanisms and manifestations of genetic and phenotypic instability associated with oncogenic transformation of cells in culture. This is by no means a comprehensive review of the field of cell transformation but rather is focused on several key aspects of the transformation process that have been shown to directly impact genetic and phenotypic stability of animal cells during continuous culture.

Cell transformation is a profound alteration in the genotypic and phenotypic attributes of animal cells and represents a critical turning point in the molecular decision making process that signals continued proliferation of cells, cellular senescence, or activation of apoptotic pathways. The balance between the activation of proto-oncogenes and the inactivation of tumor suppressor genes is at the center of the transformation process. Just as important are processes by which the genetic integrity of animal cells is protected and preserved through the action of DNA repair systems activated by errors generated during DNA replication or in response to DNA damage inflicted by radiation or chemical assaults to cells.

With some understanding of the molecular processes that preserve the stability of endogenous genes, we then move on to consider the factors that affect the stability of heterologous genes in recombinant cells and factors that influence maintenance of stable phenotypes during continuous culture. These subjects are of particular interest to scientists focused on the development of biological systems that rely upon the stable expression of heterologous genes in continuously cultured animal cells. Frequently in these systems, the level of foreign protein expression is maximized through gene amplification strategies that create additional challenges with respect to genetic stability that arises from the dispersion of gene integrants throughout the cell genome. Flexibility or adaptability of animal cell phenotypes within the context of cell biology and biopharmaceutical process development offers the opportunity to shape animal cells to fit a particular experimental system or cell-culture process paradigm.

Upstream Industrial Biotechnology: Expression Systems and Process Development, Volume 1, First Edition. Edited by Michael C. Flickinger.
© 2013 John Wiley & Sons, Inc. Published 2013 by John Wiley & Sons, Inc.

However, once the appropriate genotypes and phenotypes are established through cell line adaptation strategies or by direct genetic manipulation, further change (instability) of those attributes is not welcome. Herein lies the paradox of animal cell technologists—practitioners depend and rely on the pliability of cell genotypes and phenotypes in developing for instance, large-scale cell culture processes to produce recombinant proteins, yet once established, strive to make those attributes stable to provide assurance of process and recombinant product consistency.

For the cell and molecular biologists set upon the task of developing cell-culture-based manufacturing processes, the possible linkage between genetic (and phenotypic) stability and recombinant product quality has historically been the subject of discussion and investigation. The consequence of genotypic and phenotypic instability on recombinant protein quality is discussed by way of specific examples derived from experience in cell-line and cell-culture process development at Genetics Institute. These case studies provide a basis for arguments against a linkage between cell stability and recombinant protein quality and exemplify the nature of the challenges that are faced in developing robust cell-culture-based processes used in the manufacture of biotherapeutic proteins. Finally, approaches taken at Genetics Institute to characterize genotypes of recombinant cell lines for evaluating the genetic stability of recombinant cell lines and cell culture processes are discussed.

28.1 FACTORS THAT AFFECT GENETIC STABILITY OF ENDOGENOUS GENES

28.1.1 Oncogenic Transformation, Aneuploidy, and Genetic Stability

Genetic instability, manifested as various chromosomal aberrations such as aneuploidy, gene amplification, translocation, deletions and point mutations, is frequently observed during oncogenic transformation of cells. The cause and effect relationship between genetic instability and cell transformation has been a subject of much discussion, particularly with respect to the role of aneuploidy in these processes. Aneuploidy (an abnormal complement of chromosomes) is a massive genetic abnormality observed in nearly all of the many thousands of solid human cancers examined. This fundamental observation has led to the "aneuploidy-genetic instability" hypothesis which holds that the degree of aneuploidy is proportional to the degree of genetic instability associated with oncogenic transformation.

The aneuploidy-genetic instability hypothesis gained support over the years through the tight association between aneuploidy, genetic instability, and carcinogenesis. Recently, investigations using clones of chemically and spontaneously transformed Chinese hamster embryo cells indicated that clones were 50–100% aneuploid. Furthermore, colonies of transformed cells were highly heterogeneous with respect to chromosomal number, suggesting that aneuploidy can perpetually destabilize the karyotypes of these cells (1). Likewise, it was found that karyotypic instability was proportional to the degree of aneuploidy in cultures of continuously passaged clonal Chinese hamster embryo transformants (2). Furthermore, the quasidiploid karyotype of wild-type and a variety of mutant Chinese hamster ovary (CHO) cells were shown to be relatively stable after being cultured for extended periods of time. In contrast, quasitetraploid cells, derived spontaneously or by Sendai virus-induced fusion, were more prone to losses and gains in whole chromosomes, rearrangements of chromosomes, and the appearance of new and distinctive chromosomes (3). A model has emerged from these observations in which the loss of genes (or sets of genes in chromosomes) involved in mitosis perpetuates unequal segregation of chromosomes in subsequent cell divisions. Clearly, under such a model, stable maintenance of a genotype that contains an abnormal number of chromosomes would be improbable.

The notion that aneuploidy is a cause of genetic instability was challenged by data suggesting that an abnormal number of chromosomes in a cell, in and of itself, could not account for the high level of chromosomal instability found in aneuploid colorectal cancer cells (4). The authors proposed that dominant genetic defects in chromosomal segregation result in chromosomal instability, which drives aneuploidy. The basis for this assertion came from experiments in which the genetic stability of cells was not disturbed by the introduction of a single extra chromosome or by gross aneuploidy created by cell fusion techniques. Similarly, using gene amplification as an index for genetic instability, results from another study indicated that the propensity of methotrexate-resistant CHO cells to amplify endogenous dihydrofolate reductase genes was comparable in quasidiploid and quasitetraploid subclones (5). However, it was noted that genetic instability of aneuploid cells created spontaneously or by cell fusions was more pronounced when the resultant chromosomal number was nonmodal (4). Although a cause and effect relationship between aneuploidy and genetic instability has not been firmly established, it seems clear that once an aneuploid karyotype has been established in transformed animal cells, maintaining a stable karyotype in successive culture passages becomes more difficult.

28.1.2 Molecular Regulation of Genetic Stablity

28.1.2.1 Tumor Suppressor Genes and Proto-Oncogenes. A hypothesis opposing the aneuploid-genetic instability hypothesis, termed the "somatic gene mutation" hypothesis, holds that activation of proto-oncogenes and inactivation of tumor suppressor genes trigger transformation and

genetic instability. Under the somatic gene mutation hypothesis, animal cell transformation is the result of a multistage process starting with the activation of cellular proto-oncogenes and inactivation of tumor suppressor genes. These and other events arise from (or lead to) an enhanced state of genetic instability in which the genotypic (and phenotypic) diversity among clones increases. Most notably, this diversification manifests itself in changes in cell morphology and karyology among clones in a transformed cell population. The molecular mechanisms that underlie the genotypic and phenotypic instabilities associated with cell transformation are incompletely understood. However, some key molecules have been identified and their roles in regulating and maintaining genetic stability have become clearer. The following discussions focus on these key molecular factors and the mechanisms by which they influence the stability of cell genomes.

28.1.2.1.1 The p53 Tumor Suppressor Gene. Genetic alterations that involve inactivation of tumor suppressor genes are among the most thoroughly documented changes associated with animal cell transformation. In particular, mutation in the p53 tumor suppressor gene is frequently observed in human cancers.

The p53 tumor suppressor gene has been associated with critical cellular events involved in cell immortalization, growth arrest at the G1/S boundary in the cell cycle (i.e., cellular senescence), and activation of cell death by apoptosis (6,7). In these capacities, p53 has been considered a central factor of a genomic protection system in which, it has been hypothesized, accumulation of excess somatic mutations is prevented by growth arrest (presumably to facilitate DNA repair) or by the prevention of the further propagation of such DNA defects via apoptotic cell death. Because of the pivotal role of p53 in protecting cells and tissues from the generation and proliferation of genetic defects, it has been called the "guardian of the genome" (8).

Consistent with its role in maintaining genomic stability, the loss of p53 tumor suppressor functions results in genetic instability manifested by changes in chromosomal ploidy (9–14) and gene amplifications and deletions (12,13,15,16). Furthermore, in contrast to normal mouse fibroblast cells, mouse fibroblast cells that lack p53 protein display abnormal centrosomal amplification that causes unequal segregation of chromosomes (17).

The role of the p53 tumor suppressor function in genetic stability may have its basis in its proposed role in DNA repair. The human p53 protein contains both specific and non-specific DNA-binding domains that are hot spots for mutations that inactivate p53 function (6). Wild-type p53 protein can bind to damaged DNA and it has been shown that it plays a role in nucleotide excision repair in response to ionizing radiation (18–22) and bridge-breakage fusion of DNA (23), which has been implicated in gene amplification processes.

28.1.2.1.2 The Retinoblastoma Tumor Suppressor Gene. The possible role of tumor suppressor genes in genomic stability was also exemplified in studies involving the retinoblastoma tumor suppressor gene (pRb). Like p53, pRb is central in regulating cell-cycle progression and can act alone or in concert with p53 to arrest cell growth in response to DNA damage induced by gamma or UV irradiation or treatment with chemotherapeutic drugs (24,25). Linkage between pRb- and p53-mediated arrest pathways appears to come about via inhibition of pRb phosphorylation by cyclin-dependent kinases. Hypophosphorylated pRb promotes a growth-suppressive state via E2F transcription-factor-mediated repression of genes required for cell cycle progression (26). Similar to the model proposed for p53, pRb-mediated growth arrest and activation of DNA repair systems prevent replication of damaged DNA.

28.1.2.1.3 Proto-Oncogenes and Genomic Instability. The proto-oncogene *c-myc* is a key regulator of both cell growth and apoptosis and has been associated with cell immortalization and transformation (27). Gene amplification, a marker for genetic instability in mammalian cells, is often associated with *c-myc*-mediated transformation. Targets of *c-myc*-induced gene amplification include dihydrofolate reductase (28,29). Amplification of the dihydrofolate reductase gene may be associated with ongoing gene rearrangements and further genomic instabilities that lead to neoplastic transformation (30). Furthermore, it has been shown that *c-myc* has a direct role in activating telomerase by inducing the catalytic subunit, telomerase reverse transcriptase (31). As discussed in a section later in this chapter, it has been shown that telomerase is critical in maintaining genomic stability.

Likewise, expression of the human H-ras oncogene in mammalian cells results in cell transformation and DHFR gene amplification within a single cell cycle (32–34). H-ras tranformation is also associated with loss of contact inhibition of growth and the ability to form colonies in soft agar. Furthermore coexpression of the Ras-related tumor suppressor gene, *Rap1*, suppressed H-ras-induced amplification of the DHFR gene (35). Coexpression of the *Rap1* gene also caused H-ras-transformed cells to revert to a flat morphology and reestablished contact inhibition of growth and loss of the capacity to grow in soft agar. These studies demonstrated the profound influence of proto-oncogenes on cell phenotypes and genotypes.

28.1.2.1.4 Phenotypic Change Due to DNA Methylation and Gene Silencing. Enzymatic methylation of the C-5 position of cytosine residues in DNA motifs termed CpG islands may lead to inactivation of genes in a heritable

fashion (36). Hypermethylation of promoter sequences may lead to silencing of genes by inhibiting DNA transcription as a result of interference with transcription factor binding. Several tumor-suppressor genes contain CpG islands in their promoters and show evidence of methylation-based gene silencing. In addition, the majority of colorectal carcinomas with microsatellite DNA instability have hypermethylation of the promoter CpG island of the DNA mismatch repair gene MLH1 (37). Hypermethylation-induced attenuation of the DNA mismatch-repair system may, in turn, render the genome susceptible to additional genetic hits that lead to further genomic instability and oncogenic transformation. However, whether hypermethylation of DNA sequences is a cause or consequence of gene inactivation is highly disputed.

28.1.2.2 Poly(ADP-Ribose) Polymerase. Interruptions of DNA strands brought about by DNA-damaging agents (e.g., γ irradiation, alkylating reagents) elicit a rapid response that involves the mobilization of several DNA repair systems. Components of these DNA repair systems have been implicated in DNA gap repair and religation, DNA integration and recombination efficiency, and genomic stability. One such rapid response to DNA damage involves attachment of poly(ADP-ribose) polymerase (PARP) to DNA strand breaks (38,39). PARP is found in abundance tightly associated with chromatin in the nuclear compartment of eukaryotic cells. The PARP protein contains three functional domains: a DNA-binding domain, an automodification domain, and a catalytic domain. The DNA-binding domain rapidly binds to DNA strand breaks which in turn stimulates the catalytic domain. Using NAD as substrate, the catalytic domain carries out extensive ADP-ribosylation of PARP in the automodification site, as well as in a variety of nuclear target proteins, including topoisomerase and histones. PARP and other ADP-ribosylated proteins are recycled to their active state by the action of poly(ADP-ribose) glycohydrolase.

ADP-ribosylated PARP has a reduced affinity for DNA because of electrostatic repulsion, and the complex falls off the DNA strand and allows other DNA repair enzymes to dock and carry out DNA repair. Therefore, PARP functions as a "molecular nick sensor" in eukaryotes and, by way of direct interaction with nicked DNA, protects the site from the action of nucleases and other DNA-binding proteins. Furthermore PARP may be acting to home in other proteins at the damaged site, such as XRCC1, DNA ligase III, DNA polymerase β, p53 and DNA-dependent protein kinase and, in so doing, primes damaged DNA for repair.

The temporary protection of nicked DNA by PARP and the rapidity of the response have been considered indicative of the critical role of PARP in maintaining DNA integrity. Several lines of investigation have implicated its role in genomic stability (40–42) gene amplification (43), efficient retroviral infection (44), DNA transfection (45,46), and DNA base excision repair (47). Compelling evidence of the critical role of PARP in maintaining genomic stability comes from work done with PARP (−/−) knockouts. Mice that lack the gene that encodes PARP display no phenotypic abnormalities but are sensitive to γ irradiation and treatment with genotoxic agents like *N*-methyl-*N*-nitrosourea (48–50). In addition, primary cultures of PARP (−/−) cells are more prone to sister chromatid exchange that indicates a higher rate of rejoining of chromosomal breaks (41,43,48,49). Cells from PARP (−/−) animals also tend to display an increased number of micronuclei (a marker for genomic stability) after γ irradiation or treatment with mitomycin C (41,48) and exhibit a larger number of chromatid breaks and chromatid exchanges (49).

The potential interplay between PARP and other DNA-binding proteins like p53 and DNA-dependent protein kinase (discussed in the section following) has also been a subject of investigation. Agarwall *et al*. (49) observed a twofold lower basal level of p53 in PARP (−/−) cells and diminished induction of p53 in response to DNA damage that combine to reduce the induced level of p53 protein by four- to fivefold compared to normal cells. However, a decrease in the induction of p53 activity in PARP-deficient cells was not noted in these cells. In contrast, splenocytes from PARP knock-out mice exhibit normal or even elevated p53 (50). These results indicated that p53 protein induction may be regulated by a combination of PARP-dependent and-independent pathways. Finally, using PARP-specific antibody, it was shown that PARP and p53 coimmunoprecipitate in HeLa cell extracts after induction of apoptosis (51). This suggests that PARP and p53 may directly interact under these conditions.

28.1.2.3 DNA-Dependent Protein Kinase. It is thought that DNA-dependent protein kinase (DNA-PK) is critical in T-cell receptor V(D)J recombination in lymphoid cells and DNA double-strand break repair (52). The recombination process involves site-specific cleavage by recombination activating gene (RAG)1 and RAG2, that generates double-strand breaks that are specifically joined and repaired. DNA-PK binds to DNA double-strand breaks leading to activation of the protein kinase catalytic subunit. Phosphorylation of DNA-binding proteins such as transcription factors Sp1, c-Jun, and p53 takes place along with autophosphorylation of DNA-PK subunits. Localized phosphorylation of transcription factors may arrest transcription in the vicinity of the double-strand break that allows docking and assembly of DNA repair machinery.

Cells derived from animals that bear the spontaneous severe combined immunodeficiency (SCID) mutation lack DNA-PK activity and are defective in V(D)J recombination and DNA repair (53–55). The role of DNA-PK in DNA

recombination and repair has been definitively confirmed in murine DNA-PK null knockouts (56,57) and in a variety of murine and CHO cell mutants that lack DNA-PK activity (58–62).

Both DNA-PK and PARP are nuclear proteins that bind to DNA at strand breaks and may, in fact, compete for binding to DNA strand breaks induced by genotoxic agents or by normal recombination. These similarities have led some to suggest that PARP and DNA-PK can substitute for one another under different physiological circumstances (38). Because PARP mutant cells have elevated levels of spontaneous sister chromatid exchange, indicative of a higher rate of rejoining of chromosomal breaks, some have hypothesized that a PARP deficiency might permit processing and ligation of V(D)J recombination intermediates. Indeed, Morrison *et al*. (63) tested this hypothesis directly by creating SCID/PARP (−/−) double knock-out mice. These mice have a reduced survival rate, and double knock-out survivors appear to have regained, to a limited extent, the ability to carry out V(D)J recombination. These results suggest that PARP deficiency partially rescues animals from the SCID phenotype and may play a direct role in the V(D)J recombination process. In this context, PARP appears to be acting as an "antirecombinogenic molecule" suggesting that PARP and DNA-dependent protein kinase act cooperatively to minimize genomic damage caused by DNA strand breaks. These observations confirm the critical roles of both PARP and DNA-PK in maintaining genomic stability.

28.1.2.4 Telomeres and Telomerase. Cultures of primary human and other mammalian cells undergo a limited number of cell divisions, cease to divide thereafter, and often go on to die. This phenomenon, termed replicative senescence, has been a model for cellular aging (64). As cells age, the specialized nucleoprotein structures located at the ends of chromosome, called telomeres, become progressively shorter. Telomeres protect chromosomes from DNA degradation, end-to-end fusions, rearrangements, and chromosomal loss.

Telomeres are composed of tandem $(TTAGGG)_n$ nucleotide repeats bound to a unique family of telomere-binding proteins, including telomerase, which maintains telomeric length by synthesizing telomeric repeats (65,66). Telomerase is an enzyme that consists of an RNA-protein complex containing a reverse transcriptase component and an RNA template. The small proportion of cells that become immortalized and emerge from a growth crisis associated with cellular senescence were correlated with the presence of telomerase activity whereas precrisis cells were not (67,68). Therefore, continued maintenance of telomeres by the action of telomerase is considered a critical event responsible for preventing cellular senescence and for continued growth of transformed cells. Indeed, direct demonstration of the role of telomerase activity in overcoming senescence was obtained by overexpressing telomerase in cells (68–70) and the observation that immortal HeLa cells can be forced to crisis when telomerase activity is inhibited by expression of the antisense transcript to the RNA component of telomerase (71).

A critical role of telomerase function in maintaining genomic stability was observed in mice in which the gene that encodes the telomerase RNA component was knocked out (72). As these telomerase-deficient mice aged, an increased frequency of chromosomal fusions and a twofold increase in aneuploidy were observed. A model emerged from these studies in which chromosomal aberrations associated with crisis may be brought about by shortening telomeric structures into subtelomeric regions that lead to the formation of dicentric chromosomes via end-to-end fusion (73). In addition, the observed genomic instability was coincident with an increased frequency of spontaneous cancer in aged animals. All of these observations were correlated with shortening of telomeric length.

Activation of telomerase and cell immortalization has been associated with inactivation of p53 and pRb (73–75), and the telomerase gene is a direct target for activation by *c-myc* (76). The potential interplay between p53 and telomerase functions was also suggested by the observation that inhibition of telomerase activity triggered cell death (77).

28.2 GENOTYPIC AND PHENOTYPIC STABILITY OF RECOMBINANT CELL LINES

28.2.1 Stable Integration of Heterologous Genes in Animal Cell Genomes

Animal cells have been used as hosts for expressing a wide variety of heterologous proteins. Introduction of foreign DNA into animal cells by using any one of a number of transfection techniques (e.g., electroporation, lipofection and calcium phosphate coprecipitation) leads to transient expression of genes for up to several days. Stable expression of heterologous genes, however, is associated with integration into the host-cell genome. The mechanism by which foreign DNA integrates into the genome of host cells is not fully understood. Presumably, the integration process involves the normal DNA excision-repair systems, DNA ligase, and possibly eukaryotic analogs of prokaryotic integrase activities (78,79). Consistent with this model are observations in which perturbations of the eukaryotic DNA replicative and repair systems have been shown to affect the frequency of cell transformation, indicating that integration of foreign DNA (via heterologous recombination) may arise from normal DNA replication and/or double-strand break repair mechanisms (80), including PARP (81).

Isolation of transfected cells that have stably integrated and express heterologous genes can be achieved by

coexpressing selectable (and often amplifiable) marker genes that confer resistance to cytotoxic agents on recipient cells. The use of the selectable and amplifiable marker genes dihydrofolate reductase (DHFR) and glutamine synthetase (GS) has been extensively studied (82). In the former, coexpression of DHFR and another gene of interest renders recipient cells resistant to the cytotoxic folate analog, methotrexate (MTX). Further selection of drug-resistant transfected cell populations with increased concentrations of MTX results in coamplifying DHFR and the gene of interest. Drug-resistant cells cultured in the absence of the selective agent are vulnerable to the loss of amplified genes, whereas it has been shown that extended cultivation of cells under selective pressure increases the stability of amplified genes (83,84).

Once integrated, the genomic localization of amplified genes, it has been shown, influences their stability. Unstable amplified genes tend to be found in acentric double minute chromosomes that do not segregate properly during mitosis and are rapidly lost with each cell division. In contrast, stably amplified genes are usually found integrated into the chromosome associated with homogeneously staining regions that replicate in the early part of the S phase (85–87). Furthermore, amplified plasmid DNA was found associated at or near the ends of chromosomes or on unstable dicentric chromosomes. These observations suggested that integration and/or amplification of DNA may disrupt telomeres and facilitate formation of unstable dicentric chromosomes. Instability of amplified genes in the absence of selective pressure may also be related to the tendency of integrated genes to be arranged in a "head-to-tail" mode, that increases the frequency of homologous recombination between the integrated plasmids (87).

The distribution of amplified genes in a recombinant CHO cell line was elucidated using flourescent *in situ* hybridization (88,89). In highly amplified cells cultured under selective pressure, integrated amplification units were widely dispersed throughout the genome. Upon removing drug selection, subpopulations of recombinant CHO cells displayed genotypic instability marked by the loss of amplified genes in multiple and heterogeneous integrations dispersed throughout the genome. Continued cultivation of unstable cell lines under nonselective conditions resulted in the appearance of a dominant integration, termed the "master integration," which remained stable for up to 100 days in the absence of selective pressure.

Other examples of genomic positional effects come from work done to optimize expression of heterologous genes in cultured cells and transgenic animals. In one example of positional effects, Wurm *et al*. (90) showed that incorporation of retroviral sequences, endogenous to CHO cells, within expression plasmids significantly improved the efficiency with which high-expressing clones were obtained. The authors speculated that homologous recombination of the retroviral sequences in the expression plasmid with endogenous sequences in the CHO genome targeted the integration of foreign DNA into transcriptionally active regions of the CHO genome. In another example, the targeted insertion of a hypoxanthine phosphoribosyl transferase (HPRT) marker gene at different loci in embryonic stem cells resulted in heterogeneity in expressing stability phenotypes (91). Interestingly, loci displaying expression instability were associated with hypermethylation of the promoter which could be corrected by inserting a different promoter that contains a CpG island.

28.2.2 Phenotypic Heterogeneity and Population Dynamics

Recombinant CHO cells, in which amplified coexpression of DHFR and a heterologous gene of interest has been achieved, generally display good correlation between gene copy number, RNA transcription levels, and heterologous protein expression (92–94). Although this relationship is generally true, there are examples in which divergence in these parameters has been noted. Gene silencing by hypermethylation may play a role in creating phenotypic divergences within cell populations. However, phenotypic divergences can come about through alternate mechanisms as well. For example, it has been shown that expression levels of recombinant hepatitis B surface antigen in CHO cells became uncoupled from gene copy number because of decreased secretion efficiencies and increased intracellular degradation of recombinant protein (92). In another study, population analysis of recombinant CHO cells after extended culture in the presence of methotrexate indicated an increase in heterogeneity among subclones with respect to their cellular productivity phenotypes. In contrast, the recombinant CHO cell population became more homogeneous with respect to expression of DHFR (95). These results indicate that coexpression of DHFR and heterologous proteins can diverge post-transcriptionally at the level of protein translation, post-translational modifications, or protein secretion.

Instability of amplified genes in recombinant CHO cell populations may result from phenotypic changes caused by the amplification process itself or by the large increase in heterologous gene copy number in the host-cell genome. Results from several investigations have suggested that increased gene copy number may impose a metabolic burden on recombinant cells that manifests in a decrease in cellular growth rates (92,96). The model emerging from these observations would be one in which the population is overcome by faster growing, low-producing subpopulations. This model also has precedent in populations of hybridoma cells in which increased monoclonal antibody secretion rates can be associated with decreased growth rates (97,98) and expression instability associated with the

appearance of fast-growing, nonproducing subpopulations (99,100). However, other investigations point to a mechanism of population instability in which no increase in nonproducers was noted, but rather a general decline in heterologous protein secretion rates was observed (95,101). Furthermore, the growth rates of clones isolated from a population of recombinant CHO cells went unchanged despite a decrease in cellular productivity after extended culture in the absence of selective pressure (94).

In general, a positive correlation between cell growth rates and cellular productivity of heterologous proteins has been observed in triphasic batch cultures that experience an initial lag phase followed by a logarithmic growth phase and a plateau phase in which cell growth ceases (102–105). However, it has been shown that an increase in cellular productivity was obtained in growth-arrested recombinant CHO cells (106–108) and hybridoma cells (97). The promoter/enhancer systems used to drive expression of heterologous genes (109) and possibly the chromosomal location/environment into which the genes are integrated, are likely to play roles in the degree to which cellular growth rates and cellular productivity phenotypes are coupled.

28.2.3 Genetic and Epigenetic Manipulation of Cell Phenotypes

Cell phenotypes can, and have been, altered, by genetic modifications in which, for example, cells can be made resistant to cytotoxic drugs by introducing the appropriate drug-resistance marker genes. Furthermore, fundamental phenotypic attributes of animal cells such as the proliferative requirement for attachment strata (anchorage-dependency) and dependence on serum or exogenous growth factors, can be genetically manipulated. Renner *et al*. (110) showed that the anchorage-dependence of Chinese hamster ovary cells was eliminated by expression of cyclin E. Similarly, a loss in the anchorage-dependency of fibroblasts was associated with overexpression of cyclin A (111). In another series of experiments, the robust growth of hybridoma and CHO cells under a variety of culture stresses was enhanced by overexpression of antiapoptotic genes such as *bcl*-2 (112).

Cellular phenotypes can also be shaped in response to environmental conditions imposed upon them during cell culture. Examples of this phenomenon come from successful laboratory attempts to alter a variety of phenotypes through strategies that involve cell line adaptation. Much of the impetus for intentionally reshaping cellular phenotypes comes from the desire to eliminate the serum- and anchorage-dependency of animal cells used in producing protein biopharmaceuticals (113).

Without the use of adaptation procedures, the growth of CHO and BHK cells tends to be both anchorage-dependent and serum-dependent. In addition, once a serum-free suspension-adapted lineage is established, the volumetric productivity of the cell culture process can be optimized by adaptation strategies that lead to significant improvements in the final cell densities of cultures (113). Although the mechanism by which animal cells adapt to high cell-density conditions is unclear, one means is by developing tolerance to growth-inhibiting substances released by the cells, such as lactic acid and ammonia (114–118).

The adaptation to serum-free suspension or high cell-density conditions is generally performed using cell lineages that have already been engineered to express the desired protein biotherapeutic through recombinant technologies or methods based on cell fusion (102,119–124). However, reports have been made of CHO (125–127), murine myeloma (128,129), and Namalwa (130) cell lineages that were adapted to growth in serum-free suspension culture before serving as host cells. This approach greatly reduces or eliminates the need for further adaptation once expression of the desired protein is achieved in these preadapted mammalian-cell host lineages.

The transition to high cell-density, serum-free suspension culture can lead to changes in the growth performance phenotypes of cells and the structural characteristics of secreted proteins. Some decline in growth performance (i.e., decreased growth rate or cell viability) following serum withdrawal and/or removal of cell attachment substrata was reported (126,131). This response to changes in culture conditions is potentially due to a perturbation of events associated with cell-cycle progression and entry into the S phase (132). In the most severe case, recovery from such perturbations may be prevented by activating apoptotic pathways (133,134). Furthermore, significant differences in the carbohydrate structures of secreted proteins were documented (135–140). Finally, cell populations that undergo a "growth crisis" (i.e., a significant decline in growth rate and cell viability) during the adaptation process may be vulnerable to outgrowth of nonrepresentative or undesirable subpopulations of cells that may not have optimum performance characteristics (126,141).

Cell growth and expression phenotypes can also be significantly influenced by cell-culture parameters such as temperature, medium pH, and dissolved oxygen levels. For instance, lowering the temperature of cell cultures can decrease cell growth rates, increase protein expression rates, and alter nutrient metabolism (106,142). These results suggest that culture temperature is a variable with the potential for improving the performance of cell-culture processes, such as fed-batch and perfusion-based processes, in which static growth and prolongation of relatively high protein-expression rates are desired outcomes.

In addition to the effects of temperature, cell phenotypes can be reshaped by the action of agents that alter gene expression patterns. The most widely studied of these agents is sodium butyrate. Butyrate inhibits cell growth

and alters gene expression of butyrate-responsive elements (positively or negatively) by increasing acetylation of nucleosomal histone proteins via inhibition of histone deacetylase (143). Sodium butyrate administration alone or in combination with a temperature shift has been shown to improve the expression of recombinant proteins (143,144).

28.3 CONSEQUENCES OF GENETIC INSTABILITY ON RECOMBINANT PROTEIN QUALITY

The genetic stability of recombinant cell lines and its impact on the quality and consistency of protein biopharmaceuticals continues to be a topic of great interest to process scientists and regulatory agencies. Many different technologies have been used in constructing expression vectors and expression systems, as well as manufacturing processes. The genetic stability of recombinant cells, defined within the limits of a particular cell-culture manufacturing process, has historically been a surrogate marker for biopharmaceutical protein consistency. However, the link between genetic stability and recombinant protein quality and consistency has not been absolutely established or may be of reduced importance in view of improved analytical methods for protein product characterization.

Two key phenotypic markers thought to be relevant to protein synthesis have been emphasized when assessing the stability of recombinant cell lines and cell-culture processes: specific growth rate (hours^{-1}) and cellular productivity (units of product produced per cell per unit time). To date, where possible, cell lines have generally been selected and manufacturing processes designed so that the product was made during a period when growth rate and cellular productivity are essentially constant. This approach can be restrictive at times, adds significant time and resources to the development process (e.g., when a number of candidate cell lines need to be evaluated to select a stable production cell line), or disallows flexibility in a manufacturing process (e.g., when a process has to be limited in duration to ensure that the product is made during a period of stable growth rate and cellular productivity).

The challenges of establishing the stable performance of cell-culture processes used in manufacturing recombinant biotherapeutic proteins are complex because of the variations inherent in biological systems and the metrics used to monitor their performance. An example of this can be seen when one examines cellular productivity data from a recombinant CHO (rCHO)-cell-based process developed and used by Genetics Institute to manufacture recombinant human antihemophiliac factor (rAHF, Recombinate). rAHF is a highly complex glycoprotein used therapeutically in treating hemophilia A (145). Efficient expression of rAHF by CHO cells is greatly facilitated by coexpressing von Willebrand factor (vWF) which binds to and stabilizes the rAHF molecule. In constructing the rCHO cell line used in the commercial production of rAHF, amplified coexpression of rAHF and vWF was driven by separate selectable/amplifiable markers: DHFR and adenosine deaminase, respectively (82). Therefore, complete evaluation of the expression phenotype of rAHF-producing rCHO cells required evaluating both rAHF and vWF cellular productivities. Based on this analysis, a rCHO cell line was identified and used to develop a rAHF commercial manufacturing process.

A conventional two-tiered cell banking system was used in which a Master Cell Bank (MCB) and Working Cell Bank (WCB) were prepared. The batch-refeed cell-culture process developed and used in the large-scale manufacturing of rAHF starts when cells are inoculated into a production bioreactor (2500 L) after expansion from the frozen WCB. After inoculation, WCB cells are grown for three days (which constitutes a single batch), by which time they have reached maximum cell density (just before the onset of the stationary phase). At this point, approximately 80% of the cell suspension is removed from the bioreactor for cell separation and purification and is replaced with an equivalent volume of fresh medium. The remaining 20% of the cell suspension acts as the inoculum for the next cycle. This process continues up to a maximum number of batches which is established for an individual cell line based on cell-culture performance characteristics and product characterization. Throughout this process, cells are cultured in the absence of selective pressure.

The perspective that genetic stability served as a surrogate marker for recombinant protein quality and consistency led to establishing operational limits for the rAHF cell-culture process within which rAHF expression was relatively stable. To establish process limits, the rAHF cell-culture process was operated at full scale for an extended period in which the number of cumulative population doublings (CPD) allowed for the WCB cell population was extended to more than 120. The rAHF and vWF cellular productivity data were acquired and analyzed for trends. Figure 28.1a shows the rAHF and vWF cellular productivity data obtained during the operation of the extended process. Upon extended culture of the WCB cell line to greater than 70 CPD, both rAHF and vWF productivity gradually declined. Southern blot and Northern blot analysis of in-process samples indicated that qualitative changes in the genes or RNA transcripts that encode either protein could not be detected (data not shown). The results also indicated that a significant change in rAHF gene copy number or RNA transcript level was not observed over the course of the extended cell culture (approximately 127 CPD from the WCB). However, a reduction in vWF gene copy number and transcript level was observed after 110 CPD of continuous culture (data not shown). Consistent

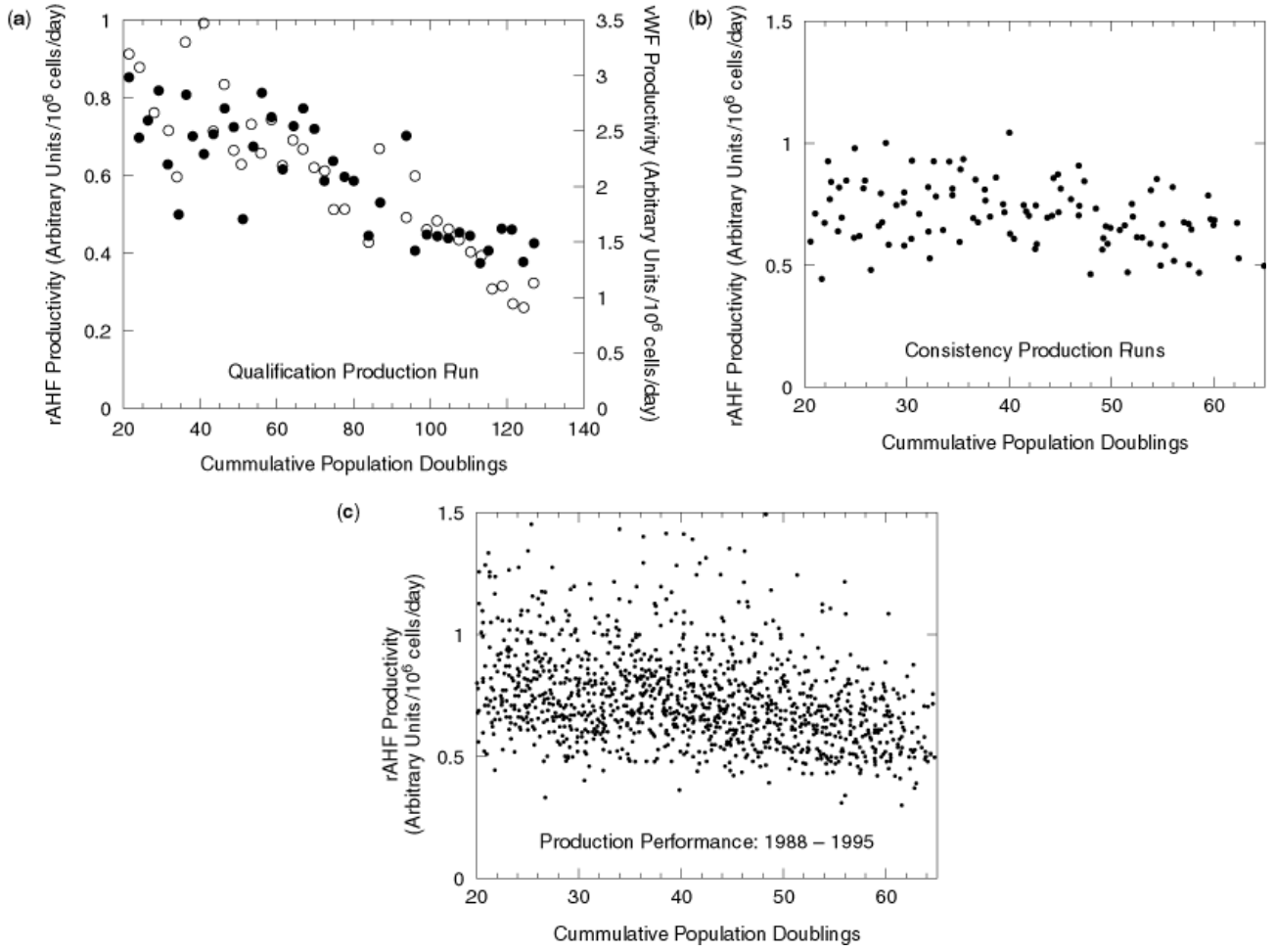


Figure 28.1. Performance of the rAHF cell-culture manufacturing process. The rAHF cell-culture process was operated, as described in the text, for an extended period of time or for periods restricted to 65 total CPD. Expression of rAHF (closed circles) and vWF protein (panel A, open circles) in conditioned medium was determined by using an activity assay and by ELISA, respectively, and the cellular productivities were calculated.

with the physiological role of vWF in stabilizing rAHF protein and because a detectable change in rAHF gene copy number or transcript level was not found, we interpreted these results to mean that the decline in rAHF productivity was driven by vWF expression instability after 70 CPD of continuous culture. With this information in hand, the duration of the cell-culture process was restricted to 65 CPD to ensure consistent process performance.

To validate the consistency of the manufacturing process operationally restricted to 65 CPD, two additional production runs were performed to establish a database for process consistency. The results obtained from the process consistency runs indicated that the cellular productivity phenotype of WCB cells was relatively stable when operationally restricted to 65 CPD (Fig. 28.1b). However, when cellular productivity data obtained from commercial production runs carried out from 1989 through 1995 are plotted, a slight negative trend (representing a decline of approximately 30%) was observed in the data (Fig. 28.1c). Therefore, the phenotypic stability of the production cell line and cell-culture process may be difficult to evaluate fully in the absence of a suitably large performance database. Thorough biochemical characterization of the rAHF produced during this period indicated that a detectable qualitative change in the product did not occur, challenging the notion that cellular productivity is an appropriate surrogate marker for recombinant protein quality.

To further investigate whether a correlation exists between changes in the cellular productivity (and growth rate) phenotypes of rCHO cells and recombinant product quality, a series of studies was performed at both bench and production scale, and the effect of variations in both phenotypic markers on product characteristics, with emphasis on N-linked glycan, were examined. The focus on

protein glycosylation was based on an expectation that this complex, energy-requiring post-translational modification might well be influenced by changes in global phenotypic markers such as growth rate and cellular productivity. In all cases, a host/expression vector system was employed which uses CHO cells genetically engineered to contain multiple genomic copies of the product gene by using DHFR as the selectable/amplifiable marker.

In one such study, a rCHO cell line that produced a thrombolytic protein was cultured using a generic serum-free, suspension-culture-based, batch-refeed cell-culture process. Figure 28.2 shows the cellular productivity of a rCHO cell line as a function of generations from the WCB in a 2500-L batch-refeed process. Cellular productivity dropped by approximately 50% from the beginning to the end of the process. It was of interest to establish whether the progressive drop in cellular productivity caused a progressive change in the product profile. Accordingly, product derived from sequential batches was characterized by using a number of biochemical and biophysical analyses, including peptide mapping and specific activity (potency) determination. A significant change in product characteristics was not evident from batch to batch. This qualitative similarity is illustrated in Figure 28.3, which shows that high pH anion-exchange chromatographic (HPAEC) carbohydrate fingerprints (147,148) of complex type, N-linked glycan released from product produced from batches early (26 generations) and late in the process (76 generations) are indistinguishable. This case again illustrates that a substantial change in cellular productivity can take place within a population of continuously cultured cells without causing detectable changes in product characteristics.

Another study involved a large-scale production process employing a rCHO cell line that produced a glycosylated lymphokine. Figure 28.4 shows a profile of cell growth during a serum-free, suspension-culture-based, batch-refeed process similar to that described before. Population doubling time (inversely proportional to growth rate), calculated as an average over each three-day growth period, increased from an initial value of approximately 22 h in the first batch to approximately 32 h in batch 3 (B3) and then declined in batches 4, 5, and 6. The improved growth rate resulted in significantly higher cell densities in batches 5 and 6. Subsequent product characterization revealed that the observed fluctuations in growth rate and maximum cell density did not cause any detectable change in the product (characterization included peptide mapping and specific activity determination, among others). Consistent with this conclusion, HPAEC-carbohydrate fingerprints of complex type, N-linked glycan from batches 2 to 6 were indistinguishable (Fig. 28.5). This study illustrates that substantial changes in growth rate can take place under the production conditions described without causing significant changes in product characteristics.

The final study involved a large-scale production process employing a rCHO cell line that produced a glycosylated cytokine in a serum-free, suspension-culture-based, batch-refeed system similar to that described before. Figure 28.6 shows the growth rate and cellular productivity (in arbitrary units) of the production cell line as a function of generations from the WCB. The growth rate increased as a function of generations from the WCB from approximately 0.025 h^{-1} (28 hour doubling time) at around 20 generations to approximately 0.033 h^{-1} (21 hour doubling time) at around 70 generations. In the same time frame, the cellular productivity declined by approximately 40%. It was of interest to establish whether this coordinate change in growth rate and cellular productivity caused any change in the product profile.

Subsequent product characterization, which included peptide mapping and specific activity determination, showed that the observed concurrent increase in growth rate and decline in cellular productivity had no effect on the product profile from batch to batch. HPAEC-carbohydrate

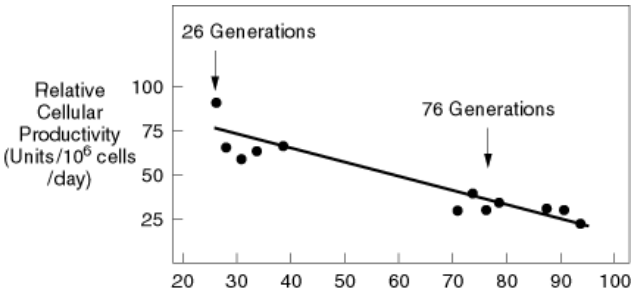


Figure 28.2. Relative cellular productivity of a rCHO cell line in a 2500-L batch-refeed process. Reprinted from Ref. 146 with permission.

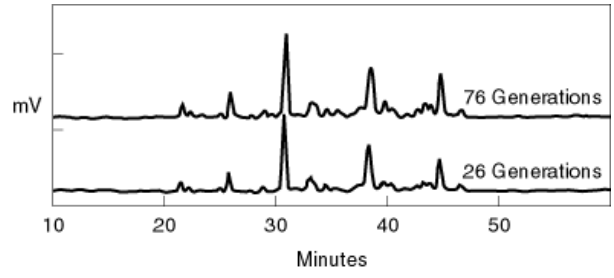


Figure 28.3. HPAEC carbohydrate fingerprint analysis of N-linked glycans. HPAEC carbohydrate fingerprints analysis was performed on complex type, N-linked glycans released from product produced from batches at the beginning (26 generations) and toward the end (76 generations) of a 2500-L batch-refeed process. Reprinted from Ref. 146 with permission.

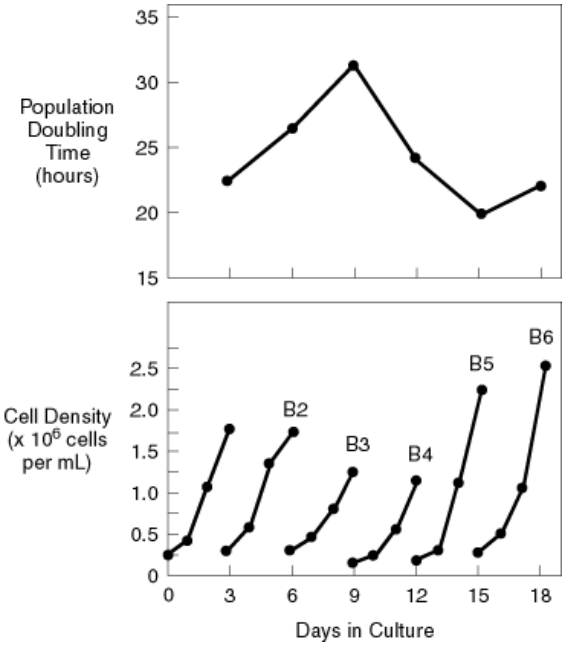


Figure 28.4. Population doubling time (t_d) and cell density of six batches of a large-scale rCHO production process. Reprinted from Ref. 146 with permission.

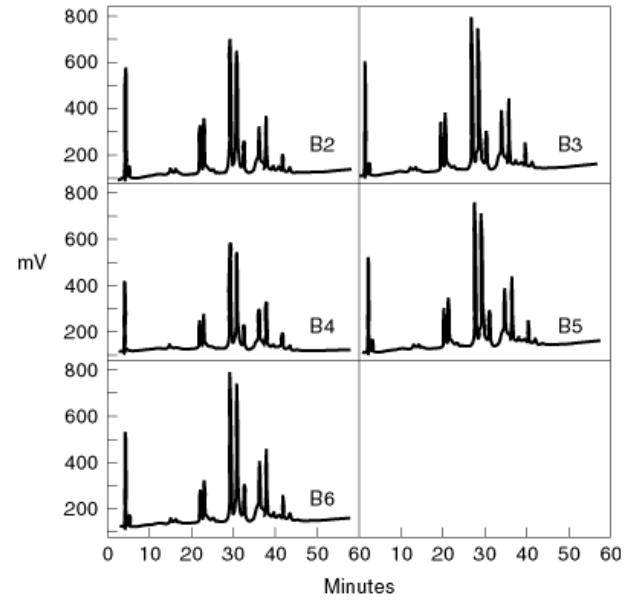


Figure 28.5. HPAEC carbohydrate fingerprint analysis of complex type, N-linked glycans. HPAEC carbohydrate fingerprint analysis was performed on samples obtained from five consecutive batches of a large-scale rCHO production process in which significant batch-to-batch changes in growth rate were observed. Reprinted from Ref. 146 with permission.

fingerprint analysis was carried out in this case on the high-mannose glycan released from product that was purified at five different points in the production process. Figure 28.7 shows that glycan fingerprints were comparable from generation 28 to 66. This case study illustrates that significant changes can take place simultaneously in growth rate and cellular productivity without causing significant changes in product characteristics. The results from these studies clearly demonstrate that significant changes in growth rate and cellular productivity, under the conditions described, do not necessarily predict changes in product quality. Similar observations (with respect to cellular productivity) were made by others working with rCHO production systems (149).

These studies, at both small scale and manufacturing scale, illustrate a key principle pertaining to the development, implementation, and long-term success of a cell-culture-based biopharmaceutical manufacturing process. Manufacturers should not assume that absolute consistency of process performance is necessary to ensure that qualitatively consistent product is produced. In particular, for biopharmaceutical products whose active substance can be characterized in great detail using modern analytical methods, it is possible to determine with a high degree of confidence that variations in process parameters such as growth rate and cellular productivity do not lead to significant variations in the quality of the active substance produced. Therefore the emerging paradigm for "well-characterized" (150) or specified biotechnology products (151) is one that makes it possible for a manufacturer to rely on analytical characterization of an active substance to determine which measures of process performance are important for ensuring consistent product quality.

28.4 GENOTYPIC CHARACTERIZATION AND VALIDATION OF GENETIC STABILITY

Genotypic instability has the potential to impact the quality of heterologous proteins expressed by a recombinant cell line. Obviously, changes in the DNA sequence via point mutations (which can occur spontaneously at a frequency of $\geq 10^{-6}$), deletions, or gene rearrangements can alter the structure of the gene product. Accordingly, extensive genotypic characterization of recombinant cell lines needs to be carried out as part of a package that provides assurance of recombinant protein quality. A general practice for characterizing the expression construct is outlined here. Emphasis is placed on characterizing the MCB cells and the transcripts derived from them, so that a comprehensive understanding of the structure of integrated and amplified genes is established at the starting point of the manufacturing process. Once the manufacturing process has been established, end-of-production (EOP) cells taken from a representative run are analyzed in a manner similar to

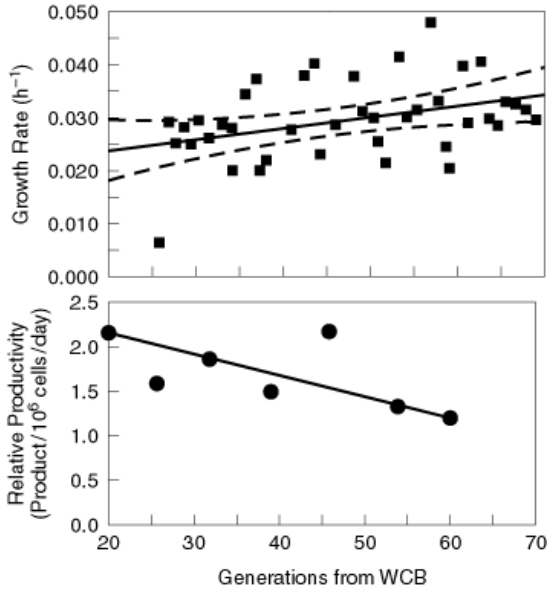


Figure 28.6. Characteristics of a large-scale rCHO production process in which changes in growth rate and cellular productivity were observed. Growth rate and relative productivity are indicated as a function of increasing generations. Reprinted from Ref. 146 with permission.

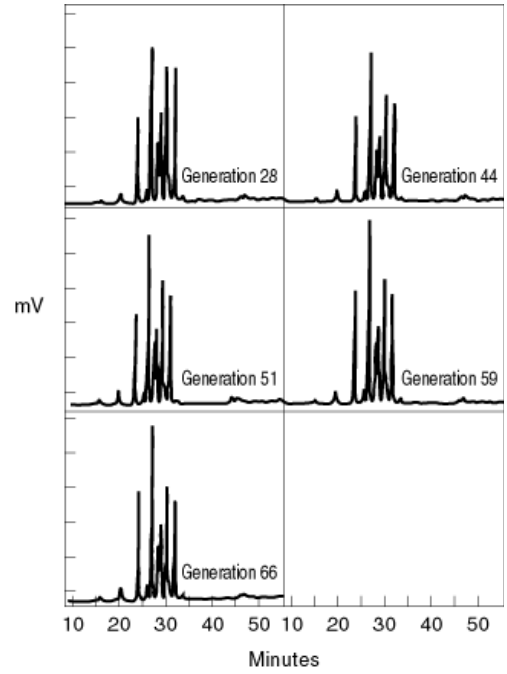


Figure 28.7. HPAEC carbohydrate fingerprint analysis of high-mannose glycan. HPAEC carbohydrate fingerprint analysis was performed on samples released from product produced at five different points in a large-scale rCHO production process. Reprinted from Ref. 146 with permission.

the MCB, to ensure that significant changes in the product genes or closely flanking sequences do not occur during the production process.

28.4.1 Gross Structural Evaluation of Genes and Transcripts

The evaluation of the expression construct includes an analysis of the integrity of the RNA transcripts that encode the protein(s) representing the active substance. This analysis employs standard molecular techniques (such as Northern blot hybridization) to establish that the predicted transcript(s) is produced by the production cell line and that significant qualitative changes in transcript structure do not occur over the course of production.

Similarly, the copy number of the expression construct is evaluated by using standard techniques. This analysis is undertaken not because the exact number of integrated and amplified copies is considered critical (it requires a very substantial effort to credibly obtain even a reasonably precise estimate of gene copy number). Rather, this estimate is useful as part of the general description of the way the cell line was established and how suitable expression levels were achieved. What is much more relevant to establish is that the correct coding sequence of the product has been incorporated into the host-cell genome and is maintained during culture to the end of production. Methods which can be employed to provide this assurance are illustrated here with several examples.

The gross structural integrity of integrated and amplified genes is evaluated by digesting genomic DNA at restriction sites that immediately flank the coding regions, followed by Southern blot analysis to establish the presence of the appropriately sized fragment in genomic DNA (usually compared directly to expression plasmid digested with the same restriction enzymes). Detection of fragments other than those predicted indicate the presence of rearranged or aberrant copies of these genes. By loading various amounts of control (expression plasmid) DNA in adjacent lanes, it is possible to estimate the sensitivity of this method for detecting variant sequences. In our experience, if aberrant fragments are electrophoretically distinguishable, they are detectable at a level of 1–5% of the intact genes.

The second level of characterization is directed toward a more detailed understanding of the initial expression plasmid integrants that are represented in the amplified DNA of the cell line. In particular, we seek to determine if one or more plasmid molecule is integrated into host CHO cell DNA (often in tandem at a single chromosomal site). This question is approached by using genomic Southern blot analysis, taking advantage of the known restriction map of the expression plasmid to permit identifying restriction fragments in which one site is contributed by host-cell genomic DNA flanking the expression plasmid. Such chimeric fragments are generally distinct in size for each of the original integrations. Thus, the number of

distinct fragments identified can be used to determine the number of unique sites of integration and potentially, the number of plasmid molecules that were integrated upon transfection and before amplification. This information is valuable in planning a rational DNA cloning and sequencing strategy (discussed in more detail following).

Our approach to integration unit characterization is illustrated by considering the example of a rCHO cell line that produces recombinant human interleukin-12 (IL-12), a novel immunomodulator (152). The IL-12 molecule is a heterodimer of molecular weight 75 kDa, consisting of 35-kDa (p35) and 40-kDa (p40) subunits. IL-12-producing rCHO cells were generated by introducing p35 and p40 cDNAs into independent DHFR expression plasmids and subsequently amplifying DHFR/IL-12 genes with increasing levels of methotrexate. The approach by which we characterized the integration units of both p35 and p40 genes is illustrated in Figure 28.8, which depicts the integrated linearized expression plasmids for both genes flanked by host-cell genomic DNA.

DNA derived from the MCB was digested with restriction enzymes for which recognition sites are present in the expression plasmid on only one side of the gene of interest. This is illustrated for the p40 gene in Figure 28.8 (right-hand panel), where a single *Bgl* II site is present within the p40 expression plasmid, just 5′ of the p40 cDNA (indicated by the dotted arrow below the expression plasmid). The next downstream *Bgl* II recognition site cannot come from this same expression plasmid, but instead must derive from DNA that flanks the integrated plasmid. Therefore, visualization of a single p40-positive *Bgl* II fragment on genomic Southern analysis argues that the 3′ DNA segment that flanks all copies of the integrated p40 plasmid is the same (i.e., contains a *Bgl* II site at the same position relative to the 3′ end of the integrated plasmid). This suggests that a single p40 expression plasmid integrated into the host-cell genome (with a *Bgl* II site just

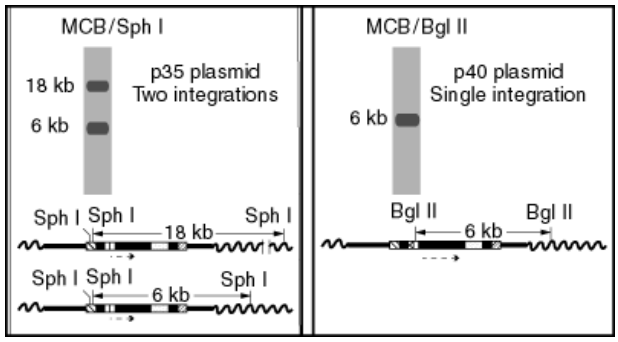


Figure 28.8. Evaluation of plasmid integration units in a recombinant human IL-12 cell line. The position and orientation of the p35 and p45 cDNA inserts are indicated by dotted arrows. Genomic Southern blots are shown from a representative digest for both p35 and p40. Reprinted from Ref. 146 with permission.

downstream) and that the configuration of the gene and local flanking DNA was maintained upon gene amplification. In contrast, the presence of two fragments in the p35 (*Sph* I-digested) Southern blot (Fig. 28.8, left-hand panel) argues that at least two distinct copies of the p35 plasmid (with *Sph* I sites at unique distances from the 3′ ends of the integrated plasmids) were integrated and amplified in the cell line. In each case, the results shown are representative of a number of experiments using different restriction enzymes which, taken together, allow conclusions to be drawn regarding the number of initial plasmid integrations that are represented in the amplified DNA of the cell line.

The insertion sites described before should not be confused with chromosomal sites that contain multiple copies of amplified genes, observed on cytogenetic analysis and designated as homogeneously staining regions (84–86), or smaller chromosomally amplified sequences detected by fluorescent *in situ* hybridization (88). The insertion sites described before are likely to reflect integrations which took place on transfection of the cells. As discussed previously, subsequent gene amplification and extended serial propagation of the cell line under methotrexate selection is normally accompanied by translocation of the original plasmid inserts and flanking DNA to different sites in the genome. The average size of such amplicons (including flanking host-cell DNA) has been observed to be on the order of 1 megabase, significantly larger than the fragments evaluated by the Southern blot method. Nevertheless, the value of establishing the number of original sites of integration for a particular gene is that this information directs our strategy in the next step in the genotypic characterization process, gene cloning, and DNA sequence analysis.

28.4.2 Sequence Analysis of Genes and Transcripts Encoding the Product

In the IL-12 p40 gene, cloning and DNA sequence were analyed on genomic DNA prepared from the MCB. Subsequent DNA sequence analysis of the cloned p40 gene was used to establish that the sequence completely agreed with that present in the expression plasmid. This indicated that the initial plasmid integrant represented in all the amplified copies of the p40 gene contained a completely intact coding region at the DNA sequence level. However, because we detected two independent plasmid integrants represented in the amplified p35 genes, it was necessary to carry out an additional investigation to demonstrate that both copies integrated with complete fidelity. Accordingly, the two Sph I fragments shown in Figure 28.8 (p35 plasmid) were isolated, cloned, and sequenced. DNA sequences from both fragments completely agreed with the p35 coding sequence in the original expression plasmid. Thus the DNA sequencing approach described allowed us to conclude that both p40 and p35 expression plasmids were integrated into

the CHO genome with complete fidelity. However, this DNA sequencing strategy does not allow us to ascertain the fidelity of all, or even the majority of multicopy amplified genes or the RNA transcripts derived from these originally integrated plasmid molecules. For this reason, a complementary approach needs to be applied to address the bulk population of transcripts present in the cell line.

Recent regulatory guidance (153) has called for DNA sequencing approaches such as DNA sequence analysis of bulk cDNA derived from reverse transcriptase polymerase chain reaction (RT-PCR) treatment of total RNA. Althought it does not set a required sensitivity limit for such methods, the guidance document requested that the sensitivity of methods employed to detect variant sequences be estimated. Accordingly, DNA sequencing was performed on cDNA clones derived from product genes expressed in a rCHO MCB and end-of-production (EOP) cells (see also Genetic Stability discussion following). Emphasis in these experiments was placed on establishing limits of detection of aberrant sequences.

Total RNA was isolated from the MCB or EOP cells, reverse transcribed into cDNA, and the entire coding region of the recombinant protein was amplified by high-fidelity PCR. The expression plasmid used in constructing the MCB lineage was subjected to the same PCR procedure as a control. Pairs of PCR primers were designed to permit amplification of the coding region in four overlapping fragments. Only fragments of the predicted size were observed upon agarose gel analysis of the RT-PCR products, and these were indistinguishable from the expression plasmid control PCR fragments, further confirming the integrity of the coding region of expressed genes in MCB cells.

The products of each PCR reaction were cloned and sequenced. Similarly, PCR-products from expression plasmids that encode defined structure-function mutants of the product gene were cloned. The cloned mutant PCR-products were used to evaluate the ability of the DNA sequencing methodology to detect sequence variants by spiking the wild-type DNA preparations with known quantities of the mutant DNA preparations. The DNA sequencing of these samples indicated that mutations could be quantitatively detected to a level of about 20% (Table 28.1).

Population sequencing provides a convenient and sensitive method for evaluating the protein coding sequence in a large and statistically significant number of independently derived cDNA clones. The results confirm that the predominant sequence at each position is correct, but the method cannot demonstrate that the actual sequence of any one clone is correct in its entirety. For this reason, these data are complemented by sequencing individual product genes cloned from MCB genomic DNA, as described before. In conjunction with Northern and Southern blot data (not shown), the sequencing results confirm that expression plasmids with the expected product coding sequence are stably maintained in the genome of these cells during inoculum buildup and full-scale production.

28.4.3 Genetic Stability

The purpose of analyzing the expression construct is to establish that the correct coding sequence for the product has been incorporated into the host cell and is maintained over the course of production. Our approach, which is consistent with current regulatory guidance (150), is to comprehensively analyze the expression construct at least

TABLE 28.1. Evaluation of the Ability to Detect DNA Sequence Variants

Sample	Mutation 1[a]	Mutation 2[a]	Mutation 3[a]	Mutation 4[a]
Mix 1: actual %[b]	0	0	0	0
% by seq.[c]	0	0	0	0
Mix 2: actual %	30	30	30	30
% by seq.	20–25	30–35	30–35	30–35
Mix 3: actual %	30	0	0	0
% by Seq.	25–30	0	0	0
Mix 4: actual %	0	30	30	30
% by seq.	0	30–40	30–40	30–40
Mix 5: actual %	20	40	40	40
% by seq.	20 or less	40–50	40–50	40–50
Mix 6: actual %	30	20	20	20
% by seq.	25–30	20 or less	20 or less	20 or less
Mix 7: actual %	15	15	15	15
% by seq.	NQ[d]	NQ	NQ	NQ

Notes:

[a] Mutation 1: Arg (AGG) to Lys (AAG) at amino acid position −1; mutation 2: Glu (GAA) to Asp (GAT) at amino acid position 33; mutation 3: Glu (GAA) to Asp (GAT) at amino acid position 36; mutation 4: Glu (GAA) to Asp (GAT) at amino acid position 40.

[b] Known starting proportion, % of wild type (w/t) at indicated position.

[c] Proportion of mutant estimated by blinded DNA sequencing (both strands), % of w/t at indicated position.

[d] Mutation was detected but not quantifiable.

once at the end of production. The analysis of EOP cells covers all of the major characteristics of the expression construct that are also analyzed in MCB cells: gross structural integrity of genes and transcripts that encode the product, gene organization and copy number, and DNA sequencing. For this analysis, EOP cells at the "limit of *in vitro* age used for production" are characterized, so that the data can be used to establish that no significant change occurs in the product-encoding genes during production. Over the course of several years of commercial production at Genetics Institute, analysis of EOP cells has not revealed any detectable genetic instability in rCHO cells.

REFERENCES

1. R. Li *et al*., Proc. Natl. Acad. Sci. U.S.A. 94: 14506–14511 (1997).
2. P. Duesberg, C. Rausch Rasnick, and R. Hehlmann, Proc. Natl. Acad. Sci. U.S.A. 95: 13692–13697 (1998).
3. R.G. Worton, C.C. Ho, and C. Duff, Somatic Cell Genet. 3: 27–45 (1977).
4. C. Lengauer, K.W. Kinzler, and B. Vogelstein, Nature (London) 386: 623–627 (1997).
5. M.W. Hashimoto *et al*., Carcinogenesis 17: 389–394 (1996).
6. L.J. Ko and C. Prives, Genes Dev. 10: 1054–1072 (1996).
7. K.W. Kinzler and B. Vogelstein, Nature (London) 379: 19–20 (1996).
8. R.R. Reddel, Ann. N.Y. Acad. Sci. 854: 8–19 (1998).
9. S.M. Cross *et al*., Science 267: 1353–1356 (1995).
10. C.A. Reznikoff *et al*., Genes Dev. 8: 2227–2240 (1994).
11. J.E. Hundley *et al*., Mol. Cell. Biol. 17: 723–731 (1997).
12. L.A. Donehower *et al*., Genes Dev. 9: 882–895 (1995).
13. K. Fukasawa, F. Wiener, G.F. Vande Woude, and S. Mai, Oncogene 15: 1295–1302 (1997).
14. M. Harvey *et al*., Oncogene 8: 2457–2467 (1993).
15. L.R. Livingstone *et al*., Cell 70: 923–935 (1992).
16. Y. Yin *et al*., Cell 70: 937–948 (1992).
17. K. Fukasawa *et al*., Science 271: 1744–1747 (1996).
18. X.W. Wang *et al*., Nat. Genet. 10: 188–195 (1995).
19. J.M. Ford and P.C. Hanawalt, Proc. Natl. Acad. Sci. U.S.A. 92: 8876–8880 (1995).
20. M.B. Kastan *et al*., Cancer Res. 51: 6304–6311 (1991).
21. M.L. Smith *et al*., Oncogene 10: 1053–1059 (1995).
22. P.A. Havre *et al*., Cancer Res. 55: 4420–4424 (1995).
23. Y. Ishizaka, M.V. Chernov, C.M. Burns, and G.R. Stark, Proc. Natl. Acad. Sci. U.S.A. 92: 3224–3228 (1995).
24. E.A. Harrington, J.L. Bruse, E. Harlow, and N. Dyson, Proc. Natl. Acad. Sci. U.S.A. 95: 11945–11950 (1998).
25. M.L. Smith, Q. Zhan, I. Bae, and A.J. Fornace, Exp. Cell Res. 215: 386–389 (1994).
26. D. Cobrink, Curr. Top. Microbiol. Immunol. 208: 31–61 (1996).
27. C. Taylor, A. Jalava, and S. Mai, Curr. Opin. Microbiol. Immunol. 224: 210–207 (1977).
28. C. Taylor and S. Mai, Cancer Detect. Prev. 22: 350–356 (1998).
29. S. Mai, J. Hanley-Hyde, and M. Fluri, Oncogene 12: 277–288 (1996).
30. S. Mai, M. Fluri, D. Siwarski, and K. Huppi, Chromosome Res. 4: 365–371 (1996).
31. K.-J. Wu *et al*., Nat. Genet. 21: 220–224 (1999).
32. M.A. Wani, X. Xu, and P.J. Stambrook, Cancer Res. 54: 2504–2508 (1994).
33. N.C. Denko, A.J. Giaccia, J.R. Stringer, and P.J. Stambrook, Proc. Natl. Acad. Sci. U.S.A. 91: 5124–5128 (1994).
34. N. Denko, J. Stringer, M. Wani, and P.J. Stambrook, Somatic Cell Mol. Genet. 21: 241–253 (1995).
35. M.A. Wani, N.C. Denko, and P.J. Stambrook, Somatic Cell Mol. Genet. 23: 123–133 (1997).
36. P.A. Jones and P.W. Laird, Nat. Genet. 21: 163–167 (1999).
37. C.C. Gurin, M.G. Federici, L. Kang, and J. Boyd, Cancer Res. 59: 462–466 (1999).
38. T. Lindahl, Satoh, G.G. Pirier, and A. Klungland, Trends Biochem. Sci. 20: 405–411 (1995).
39. Y.L. Rhun, J.B. Kirkland, and G.M. Shah, Biochem. Biophys. Res. Commun. 245: 1–10 (1998).
40. V. Schreiber *et al*., Proc. Natl. Acad. Science U.S.A. 92: 4753–4757 (1995).
41. I. D'Agano *et al*., Environ, Mol. Mutagen. 32: 56–63 (1998).
42. R. Ding and M. Smulson, Cancer Res. 54: 4627–4634 (1994).
43. J.-H. Kupper, M. Muller, and A. Burkle, Cancer Res. 56: 2715–2717 (1996).
44. J.A. Gaken *et al*., J. Virol. 70: 3992–4000 (1996).
45. B.C. Waldman, J.R. O'Quinn, and A.S. Waldman, Biochem. Biophys. Acta 1308: 241–250 (1996).
46. F. Farzaneh *et al*., Nucleic Acids Res. 16: 11319–11326 (1988).
47. C. Trucco, F.J. Oliver, G. de Murcia, and J. Menissier-de Murcia, Nucleic Acids Res. 26: 2644–2649 (1998).
48. Z.-Q. Wang *et al*., Genes Dev. 11: 2347–2358 (1997).
49. M.L. Agarwall *et al*., Oncogene 15: 1035–1041 (1997).
50. J.M. de Murcia *et al*., Proc. Natl. Acad. Sci. U.S.A. 94: 7303–7307 (1997).
51. S.R. Kumari, H. Mendoza-Alvarez, and R. Alvarez-Gonzalez, Cancer Res. 58: 5075–5078 (1998).
52. P.A. Jeggo, G.E. Taccioli, and S.P. Jackson, BioEssays 17: 949–957 (1995).
53. T. Blunt *et al*., Cell 80: 813–823 (1995).
54. N. Nicolas *et al*., J. Exp. Med. 188: 627–634 (1998).
55. E.K. Shin, L.E. Perryman, and K. Meek, J. Immnol. 158: 3565–3569 (1997).
56. G. Taccioli *et al*., Immunity 9: 355–366 (1998).
57. C. Jhappan *et al*., Nat. Genet. 17: 483–486 (1977).
58. S.R. Peterson *et al*., Proc. Natl. Acad. Sci. U.S.A. 92: 3171–3174 (1995).
59. R. Fukumura *et al*., J. Biol. Chem. 273: 13058–13064 (1998).
60. S.R. Peterson *et al*., J. Biol. Chem. 272: 10227–10231 (1997).

61. A. Errami *et al*., Nucleic Acids Res. 26: 3146–3153 (1998).
62. G.E. Taccioli *et al*., J. Biol. Chem. 269: 7439–7442 (1994).
63. C. Morrison *et al*., Nat. Genet. 17: 479–482 (1997).
64. L. Halflick, Exp. Gerontol. 33: 639–653 (1998).
65. J.W. Shay and E.W. Woodring, Curr. Opin. Oncol. 8: 66–71 (1996).
66. D.E. Shippen, Curr. Opin. Genet. Dev. 3: 759–763 (1993).
67. T.L. Halvorsen, G. Leibowitz, and F. Levine, Mol. Cell. Biol. 19: 1864–1870 (1999).
68. C.M. Counter *et al*., EMBO J. 11: 1921–1929 (1992).
69. A.G.M. Bodnar *et al*., Science 277: 349–352 (1998).
70. H. Vaziri and S. Benchimol, Curr. Biol. 8: 279–282 (1998).
71. J.W. Feng *et al*., Science 269: 1236–1241 (1995).
72. K.L. Rudolph *et al*., Cell 96: 701–712 (1999).
73. B. Van Steensel, A. Smororzewska, and T. de Lange, Cell 92: 401–413 (1998).
74. H. Vaziri *et al*., Mol. Cell. Biol. 19: 2372–2379 (1999).
75. J.D. Coursen *et al*., Exp. Cell Res. 235: 245–253 (1997).
76. R.A. Greenberg *et al*., Oncogene 18: 1219–1226 (1999).
77. J. Karlseder *et al*., Science 283: 1321–1325 (1999).
78. F.M. Wurm and Petropoulos, Biologicals 22: 95–102 (1994).
79. Y. Voziyanov, S. Pathania, and M. Jayaran, Nucleic Acids Res. 27: 930–941 (1999).
80. R.T. Schimke, S.W. Sherwood, A. Hill, and R.N. Johnston, Proc. Natl. Acad. Sci. U.S.A. 83: 2157–2161 (1986).
81. A.J. Strain, Dev. Biol. Stand. 68: 27–32 (1986).
82. R.J. Kaufman, Methods Enzymol. 185: 537–566 (1990).
83. R.J. Kaufman and R.T. Schimke, Mol. Cell. Biol. 1: 1069–1076 (1981).
84. R.J. Kaufman, P.C. Brown, and R.T. Schimke, 1979. Proc. Natl. Acad. Sci. U.S.A. 76: 5669–5673 (1979).
85. J.H. Nunberg *et al*., Proc. Natl. Acad. Sci. U.S.A. 75: 5553–5556 (1978).
86. R.J. Kaufman, P.A. Sharp, and S.A. Latt, Mol. Cell. Biol. 3: 699–711 (1983).
87. U.H. Weidle, P. Buckel, and J. Weinberg, Gene 66: 193–203 (1988).
88. M.G. Pallavicini *et al*., Mol. Cell. Biol. 10: 401–404 (1990).
89. F.M. Wurm *et al*., in R.A. Spier, J.B. Griffiths, and B. Meig- nier, eds., Production of Biologicals from Animal Cells in Culture, 1991, pp. 316–323.
90. F.M. Wurm *et al*., Ann. N.Y. Acad. Sci. 782: 70–78 (1996).
91. D.W. Melton, A.-M. Ketchen, and J. Selfridge, Nucleic Acids Res. 25: 3939–3943 (1997).
92. G.J. Pendse, S. Karkare, and J.E. Bailey, Biotechnol. Bioeng. 40: 119–129 (1992).
93. S.J. Kim *et al*., Biotechnol. Bioeng. 58: 73–84 (1998).
94. N.S. Kim, S.J. Kim, and G.M. Lee, Biotechnol. Bioeng. 60: 679–688 (1998).
95. M.S. Sinacore *et al*., in E.C. Beuvery, Griffiths, and Zeijlemaker, eds., Animal Cell Technology, 1995, pp. 63–67.
96. M.B. Gu, J.A. Kern, P. Todd, and D.S. Kompala, Cytotechnology 9: 237–254 (1992).
97. P.M. Hayter, N.F. Kirkby, and R.E. Spier, Enzyme Microb. Technol. 14: 454–461 (1992).
98. E. Suzuki and D.F. Ollis, Biotechnol. Bioeng. 34: 1398–1402 (1989).
99. A.S. Chuck and B.O. Palsson, Biotechnol. Bioeng. 39: 354–360 (1992).
100. J.M. Coco-Martin *et al*., Hybridoma 11: 653–665 (1992).
101. S.W. Bae, H.J. Hong, and G.M. Lee, Biotechnol. Bioeng. 47: 243–251 (1995).
102. P.M. Hayter *et al*., Appl. Microbiol. Biotechnol. 34: 559–564 (1991).
103. M.I. Cocket, C.G. Bebbington, and G.T. Yarranton, Bio/Technology 8: 662–667 (1990).
104. D.K. Robinson and K.W. Memmert, Biotechnol. Bioeng. 38: 972–976 (1991).
105. A.L. Smiley, W.-S. Hu, and D.I.C. Wang, Biotechnol. Bioeng. 33: 1182–1190 (1989).
106. K. Furukawa and K. Ohsuye, Cytotechnology 26: 153–164 (1998).
107. X. Mazur, M. Fussenegger, W.A. Renner, and J.E. Bailey, Biotechnol. Prog. 14: 705–713 (1998).
108. M. Fussenegger *et al*., Nat. Biotechnol. 16: 468–472 (1998).
109. R.G. Werner, W. Noe, K. Kopp, and M. Schluter, Arzneim.-Forsch. 48: 870–880 (1998).
110. W.A. Renner *et al*., Biotechnol. Bioeng. 47: 476–482 (1995).
111. T.M. Guadagno, M. Ohtsubo, K.M. Roberts, and R.K. Assosian, Science 262: 1572–1575 (1993).
112. R.P. Singh and M. Al-Rubeai, Adv. Biochem. Eng. Biotechnol. 62: 167–184 (1998).
113. M.S. Sinacore, D. Drapeau, and S.R. Adamson, Methods Biotechnol. 8: 11–22 (1999).
114. W.M. Miller, C.R. Wilke, and H.W. Blanch, Bioprocess Eng. 3: 113–122 (1988).
115. M. Matsumura, M. Shimoda, T. Arii, and H. Kataoka, Cytotechnology 7: 103–112 (1991).
116. B. Schumpp and E.-J. Schlaeger, Cytotechnology 8: 39–44 (1992).
117. U.S. Pat. 5,156,964 (1992). D. Inlow, B. Maiorella, and A.E. Shauger.
118. U.S. Statutory Invention Registration H1532 (1996). S.R. Adamson, D. Drapeau, Y.-T. Luan, and D.A. Miller.
119. M. Murata, Y. Eto, and H. Shibai, J. Ferment. Technol. 66: 501–507 (1988).
120. D.T. Berg, D.B. McClure, and B.W. Grinnell, Bio Techniques 14: 972–978 (1993).
121. D. Broad, R. Boraston, and M. Rhodes, Cytotechnology 5: 47–55 (1991).
122. J.P. Mather, Methods Enzymol. 185: 567–577 (1990).
123. M.J. Keen and T.R. Nicholas, Cytotechnology 17: 153–163 (1995).
124. P. Perrin *et al*., Vaccine 13: 1244–1250 (1995).
125. M.S. Sinacore *et al*., Biotechnol. Bioeng. 52: 518–528 (1996).
126. M. Zang *et al*., Bio/Technology 13: 389–392 (1995).
127. C. Gandor, C. Leist, A. Feichter, and F. Asselbergs, FEBS Lett. 377: 290–294 (1995).
128. T. Kawamoto *et al*., Anal. Biochem. 130: 445–453 (1983).
129. J. Kovar and F. Franek, Immunol. Lett. 7: 339–345 (1984).

130. H. Miyaji *et al*., Cytotechnology 3: 133–140 (1990).
131. J.B. Griffiths and A.J. Racher, Cytotechnology 15: 3–9 (1994).
132. R.K. Assoian, J. Cell Biol. 136: 1–4 (1977).
133. E. Rouslahti and J.C. Reed, Cell 77: 477–478 (1994).
134. B.D. Jeso *et al*., Biochem Biophys. Res. Commun. 214: 819–824 (1995).
135. E.M. Curling *et al*., Biochem. J. 272: 333–337 (1990).
136. E. Watson *et al*., Biotechnol. Prog. 10: 39–44 (1994).
137. W. Chotigeat, Y. Watanapokasin, S. Mahler, and P.P. Gray, Cytotechnology 15: 217–221 (1994).
138. M.R. Lifely *et al*., Glycobiology 5: 813–822 (1995).
139. N. Jenkins, R.B. Parekh, and D.C. James, Nat. Biotechnol. 14: 975–981 (1996).
140. M. Gawlitzek *et al*., J. Biotechnol. 42: 117–131 (1995).
141. S.S. Ozturk and B.O. Palsson, Biotechnol. Bioeng. 37: 35–46 (1991).
142. S. Chuppa *et al*., Biotechnol. Bioeng. 55: 328–338 (1997).
143. J. Kruh, Mol. Cell. Biochem. 42: 65–82 (1982).
144. U.S. Pat. 5,705,364 (1998), T. Etcheverry and T. Rhyll.
145. R.J. Kaufman, Trends Biotechnol. 9: 353–359 (1991).
146. S.R. Adamson and T.S. Charlebois, Dev. Biol. Stand. 83: 31–44 (1994).
147. R.R. Townsend *et al*., Anal. Biochem. 182: 1–8 (1989).
148. D.A. Cumming, Glycobiology 1: 115–130 (1991).
149. A.S. Lubiniecki *et al*., Dev. Biol. Stand. 76: 105–115 (1992).
150. A.S. Lubiniecki, Dev. Biol. Stand. 96: 173–175 (1998).
151. Guidance for Industry: Changes to an Approved Application for Specified Biotechnology and Specified Synthetic Biological Products, U.S. Food and Drug Administration, Washington, D.C., 1997.
152. S.F. Wolf *et al*., J. Immunolo. 146: 3074–3081 (1991).
153. Final Guideline on Quality of Biotechnological Products: Analysis of the Expression Construct in Cells Used for Production of r-DNA Derived Protein Products, Int. Conf. Harmonization (endorsed), U.S. Food and Drug Administration, Washington, D.C., 1995.

29

ANIMAL CELL TYPES, HYBRIDOMAS

K. Heilmann and B. Micheel
Institute of Biochemistry and Biology, University of Potsdam, Germany

29.1 INTRODUCTION

29.1.1 Biotechnological Production of Proteins for Biomedical Use

Large-scale production methods offer new possibilities for the diagnostic and therapeutic application of many proteins which were identified in basic biomedical sciences as regulators of important metabolic processes. Several of these proteins are now established as medical drugs for the treatment of different diseases. The overall requirements, for example, of insulin for the treatment of diabetes mellitus in the industrial countries are now estimated to come to 5 to 6 tons per year. These amounts cannot be realized without recombinant techniques (1). Further examples are several growth factor proteins, such as granulocyte colony stimulating factor (G-CSF) which is applied after chemotherapy for the treatment of cancer (2) or nerve growth factor (NGF) with application in Parkinson's or Alzheimer's disease (3). Other proteins widely used in biomedicine and therefore produced in very vast amounts are antibodies. Antibodies are applied for diagnostic purposes in pregnancy tests, for blood typing, or for the detection of inflammatory markers or tumor markers (4). More than 10 monoclonal antibodies (in most cases modified by recombinant methods) are already approved in many countries for the treatment of cancer, infectious diseases, and immunological disorders, and many more antibodies are in the progress of clinical testing (5) (Table 29.1). To provide the extremely large quantities of antibodies for therapeutic application is a great challenge for the biotechnological industry.

29.1.2 Animal Cell Types Used for Industrial Protein Expression (Insect Cells, Mammalian Cells)

Relatively simple proteins can easily be produced by recombinant methods in bacteria. But for the production of more complicated molecules other cell types have to be employed. Unfortunately, antibodies belong to a structurally complicated family of proteins. For the production of antibodies or antibody fragments several expression systems were used, including bacteria, yeast, plants, insect cells, or mammalian cells in addition to hybridoma cells. Since bacteria and yeasts can so far only be used exclusively (or almost exclusively) for the production of antibody fragments and plant cell, cultures do not directly offer an alternative for the production of intact antibody molecules (which is possible in plants growing in the fields which might be some day a real alternative); only hybridoma cells and other animal cells will be dealt with here. The expression of proteins in insect cells is characterized by simple handling and minor costs in cultivation. The expressed proteins get folded correctly and many modifications like disulfide bond formation or acetylation are performed as good as in mammalian cells (7). Moreover the proteins are able to form tertiary and quaternary structures. The infection of insect cells with recombinant baculoviruses is carried out with commercially available shuttle vectors. These vectors have a promoter for virus proteins, mostly the polyhedrin- or p10-promoter, which induces a strong transcription of DNA sequences behind. The coding DNA sequence is the desired one for the recombinant protein. Vectors with both

Upstream Industrial Biotechnology: Expression Systems and Process Development, Volume 1, First Edition. Edited by Michael C. Flickinger.
© 2013 John Wiley & Sons, Inc. Published 2013 by John Wiley & Sons, Inc.

TABLE 29.1. Monoclonal Antibody-Based Therapeutics

Substance Name	Therapeutic Use	Molecule	Registered	Company
Muromomab	Reversal of acute kidney transplant rejection	Murine mAb	1986	Ortho Biotech
Abciximab	Prevention of blood clots	Fab derived from chimeric mAb	1994	Centocor
Edrecolomab	Treatment of Duke's C stage colorectal cancer	Murine mAb	1995	Centocor/Glaxo SmithKline
Rituximab	Treatment of non-Hodgkin's lymphoma	Chimeric mAb	1997 1998	Genentech Hoffmann-La-Roche
Daclizumab	Prevention of acute kidney transplant rejection	Humanized mAb	1997 1999	Hoffmann-La-Roche
Trastuzumab	Treatment of metastatic breast cancer overexpressing HER-2 protein	Humanized mAb	1998	Genentech
Palivizumab	Prophylaxis of lower respiratory tract disease caused by respiratory syncytical virus in children	Humanized mAb	1998 1999	MedImmune/Abbott
Basiliximab	Prophylaxis of acute organ rejection in allogenic renal transplantation	Chimeric mAb	1998	Novartis
Infliximab	Treatment of Crohn's disease and rheumatoid arthritis	Chimeric mAb	1998 2000	Centocor
Gemtuzumab	Treatment of acute myeloid leukemia	Humanized mAb conjugated to calichaemicin	2000	Celltech group
Alemtuzumab	Treatment of B cell chronic lymphocytic leukemia	Humanized mAb	2001	Millenium Pharmaceuticals Inc.ILEX Oncology Inc.

[Modified after Van Dijk et al. 2001] (6).

promoters are used to express protein complexes from two subunits. The selection of positive viruses is performed by plaque assays with a combined blue-white screening. These viruses will be used to infect insect cells. The maximum protein expression is normally achieved after 30 to 60 h of infection and a high expression rate of nearly 50% can be obtained. But for every virus the expression conditions have to be tested to reach the optimum. Disadvantages could be a possible aggregation of proteins and a different glycosylation pattern. For protein expression in stable cell clones, blasticidin or hygromycin resistant vectors are used to infect Sf, High Five®, or S2 cells. Sf cells are ovary cells from *Spodoptera frugiperda* and High Five cells are alternative derivative ovary cells from *Trichoplusia ni* and S2 cells are originated from *Drosophila melanogaster*. The vectors are generated with an ampicillin resistence and a pUC-origin for selection and replication in *E.coli*. But the yield of recombinant proteins with this method is diminished if compared to the baculovirus system (7). Insect cells have also been used to produce recombinant antibodies, but so far mammalian cells are preferred which might be because of higher concentrations of the recombinant protein.

Protein expression in mammalian cells is common and several vector systems are offered for this purpose. Mostly, immortal cells with high transfection efficiencies are used; for example, Chinese hamster ovary (CHO) cells, human embryonic kidney cells-293 (HEK-293) or CV-1 cells transformed by origin-defective mutant of SV40 cells (COS 1/7). For better yields of recombinant proteins cells growing in suspension are favored. Mostly, lipofectamine, electroporation, or $CaCl_2$ methods are used for transfection. The vectors often have a hygromycin or geneticin resistence. Viral associated vector systems are applied if the transfection efficiency is too low, but actually these vector systems are out of biological safety and have very stringent safety conditions (8).

29.1.3 Cultivation Methods

For efficient protein expression in mammalian cells the used cultivation conditions or supplementals are extremely important for high yields. There exist several favorite strategies for different cell lines. Hybridoma cells are often cultivated in complete media with fetal bovine serum, glutamine, and mercaptoethanol. But recent data has shown that the supplemental coating of tissue culture polystyrene with components of the extracellular matrix such as fibronectin, laminin, or collagen I is inducing a significant higher synthesis of antibodies (9). These results are different for every hybridoma because of the malignant properties, but in summary the yield of monoclonal antibodies can be increased by nearly 20% to 50%. Other

strategies are the cultivation under serum-free conditions in order to minimize the interactions with animal proteins and to avoid contaminations of the antibody products. The disadvantage of serum-free conditions is an extremely long adaptation phase for mammalian cells, especially for fresh transfected cells, but if the recombinant proteins are needed for therapeutic approaches this step is absolutely necessary to avoid strong side effects. For large-scale production of recombinant proteins, different strategies for cell cultivation are pursued to increase the yields and the lifetime of the cells. The cultivation takes place in bioreactors, mainly hollow fiber reactors or huge stirring bioreactors, in which the cells are grown within macroporous carriers to reduce the extent of toxic metabolites in long-term culture. Additionally, different feeding procedures based on mathematical equations related to the kinetics of cell metabolism were adapted to the cell culture process. Mostly, these strategies are not published because of the competitiveness of the related pharma companies.

29.2 ANTIBODY PRODUCTION BY ANIMAL CELLS *IN VITRO*

29.2.1 Introduction

The mammalian immune system is principally characterized by two ways of immune defense (10) (Fig. 29.1). The first step in eliminating pathogens is known as *innate host defense*. This means a rather common immune response characterized by physical barriers such as skin, the acidic environment in the stomach, or different proteins, for example, lysozyme in tear fluid or saliva. Moreover, a very important function in the first line of defense is the complement system, which causes the degradation of infected or exogenous cells by induction of terminal cytolytic complexes in the cell membrane. The cellular response to pathogens is performed by phagocytes. These cells are specialized to eliminate infected or exogenous cells by endocytotic mechanisms. The recognition is principally initiated by toll-like receptors, which bind exogenous surface markers like lipopolysaccharides or virus-related peptides like CpG. There are different cell populations such as monocytes, macrophages, neutrophilic granulocytes, and dendritic cells, which are able to phagocytose. But, moreover, macrophages and dendritic cells are antigen-presenting cells (APC), which process exogenous proteins and present them at the cell surface to B and T lymphocytes. Therefore, these cell populations are defined as mediators between innate and adaptive immune response (11). Dendritic cells represent the most potent and efficient APC in mammalians (10). It is known that very small numbers of dendritic cells are able to induce strong T cell responses. Only one dendritic cell may stimulate 100 to 3000 T cells, so that the amplification accomplished by dendritic cells leads to very potent immune responses (12). The presentation of antigens is carried out by major histocompatibility complexes (MHC) on the cell surface of APC. The peptides are recognized by T-cell receptor complexes and this leads to an activation and differentiation in T helper cells or cytotoxic T cells. T helper cells are necessary to activate B lymphocytes and to induce antibody responses. B lymphocytes indeed are able to recognize antigens by themselves but need further cytokine signals to start the secretion of antibodies. The

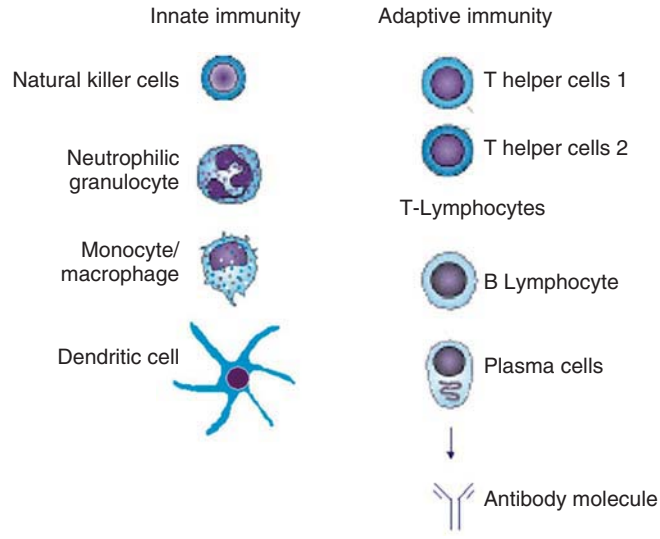


Figure 29.1. Cell Types of the immune system. (This figure is available in full color at http://onlinelibrary.wiley.com/book/10.1002/9780470054581.)

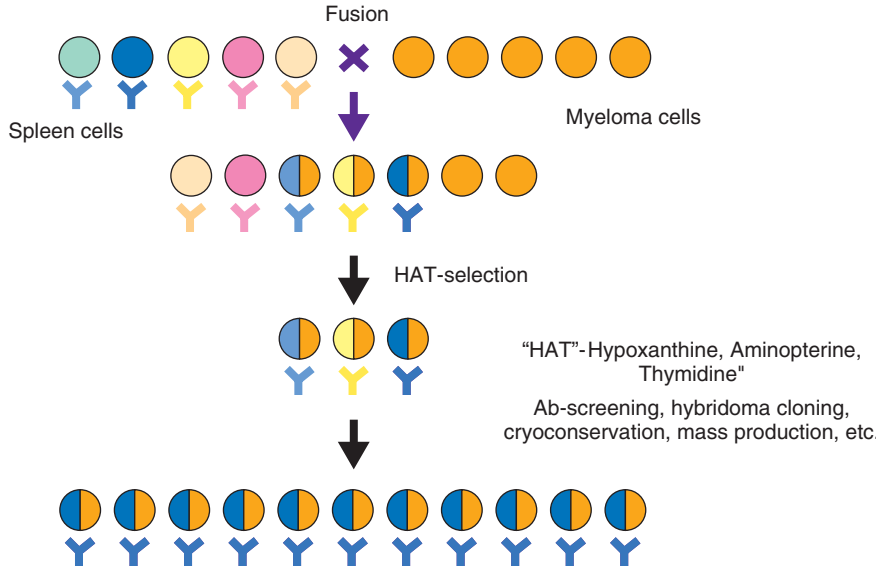


Figure 29.2. Schematic description of the hybridoma technology. (This figure is available in full color at http://onlinelibrary.wiley.com/book/10.1002/9780470054581.)

adaptive immune response is highly specific and directed to single types of pathogens. Furthermore, this response leads to the establishment of an immunological memory for faster and more effective immune responses by later infections with the same pathogen. The antibody response is called *humoral immune response* because antibodies are secreted into the surrounding body fluid and are therefore able to find the pathogen also if the induction takes place far away from the site of infection (11).

29.2.2 Antibody Production by Hybridoma Technique

29.2.2.1 Induction of Antibody Responses. To initiate an immune reaction by artificial immunization, an intraperitoneal injection with purified antigen and adjuvant is performed. Only after this step the generation of antibodies takes place and antibody molecules can be detected in the serum. The generation of monoclonal antibodies is based on the hybridoma technology developed by Köhler and Milstein in 1975 (13) (Fig. 29.2). The basic principle is the fusion of antibody-producing B lymphocytes with immortal myeloma cells to get immortal antibody-producing cells (14). The lifetime of B lymphocytes in vivo is restricted to approximately 7 days, so that gaining immortality constitutes the most important feature of the technique. The used myeloma cell lines are modified and are not able to generate immunoglobulins by themselves. Therefore, fused cells have the two attributes from the parental cells: immortality from the myeloma cells and antibody secretion from the B lymphocytes. So, it is possible to generate biochemically defined and uniform antibody molecules in huge amounts. The selection of hybridomas is performed by utilization of a hypoxanthin-guanin-phosphoribosyl-transferase (HGPRT)-deficiency of myeloma cells (15). This enzyme is necessary for using the alternative way (salvage pathway) for purine synthesis. The culture media additionally contains azaserine or aminopterine, which is blocking the main pathway (the *de novo* pathway) for purine synthesis. Myeloma cells do not survive the selection process because they are unable to use one of the pathways for nucleotide synthesis and B lymphocytes are restricted because of their shortened lifetime in culture. That means, only hybridomas are able to survive and grow under these conditions. At regular intervals hybridoma cells are expanded by limited dilution to obtain a homogeneous cell clone tested for the wanted antibody secretion. Making them immortal the hybrid cells can be stored in liquid nitrogen. The screening processes are extremely time consuming and could not be automated till now because of the necessity of sterile conditions. The hybridoma technique is a scientific standard for over 20 years now and there are several established fusion protocols and myeloma cell lines used for this purpose. In the following sections these strategies are described in more detail.

29.2.2.2 Cell Fusion Strategies to Produce Hybridoma. In the last decades a few myeloma cell lines were established as fusion cell lines, the most common ones till now are X63-Ag 8.653 (16) and Sp2/0-Ag 14 (17) from a Balb/c mouse strain. Table 29.2 shows the most important myeloma cell lines used to generate hybridomas. In the beginning of hybridoma technique myeloma tumor cells were used which synthesized or secreted immunoglobulin chains by themselves. This was a much undesired fact and

TABLE 29.2. Mouse Myeloma Cell Lines Used for Hybridoma Generation

Mouse Strain	Cell Line	Ig Chains Produced/ Expressed	References
Balb/c	X63-Ag 8.653	—	16
Balb/c	Sp2/0-Ag 14	—	17
Balb/c	P3X63-Ag 8 (P3)	$\gamma 1 + \kappa$ chain	13
Balb/c	P3/NS-1/1-Ag4-1	κ chain	13
Balb/c	F0	—	17
C57BL6	EL4BU	NA	Salk Institute

by now these cell lines are replaced by sublines which do not produce any heavy or light chains. Moreover, these myeloma cells are very stable, so that emerging hybridomas survive the selection process.

Cell fusion is mostly facilitated by polyethylene glycol (PEG), a polywax that promotes cell adherence and the exchange of nuclei. PEG has become the agent of choice because it is relatively nontoxic and highly effective. For successful fusions the optimal concentration, molecular weight, and exposure time seem to be crucial (18). In our laboratory, we prefer PEG with a molecular weight of 8000. Myeloma cells and splenocytes are mixed in a ratio of 1:4 and fused by electroporation according to a modified protocol of Stoicheva and Hui (19). The mixed cell population is aligned by exposure to a low-level nonuniform electric field and because of emerging dipoles the cells are oriented. Through a brief pulse of high voltage, microscopic pores are created in the membrane that allow a physical fusion of both cell types after cultivation under normal conditions without any stress. Other fusion strategies are related to virus induced cell fusions. But this approach is not really useful for hybridoma technique. Therefore, fusion with PEG and electroporation has established a technical standard (19).

There are other strategies to fuse human B lymphocytes with Epstein-Barr virus (EBV) to get immortal antibody-producing cells (20). The fused cells are termed *lymphoblastoid cell lines* (LCL) and were provided as a source of human monoclonal antibodies, but they also have serious deficiencies. They possess a poor stability and a low Ig secretion rate, which is limiting the properties of the approach. Further, the application of EBV immortalized cells needs a higher protection stage than working with myeloma cells alone and for therapeutic approaches it is difficult to get an approval for the treatment of human diseases by applying antibodies which are originated from an EBV-induced cell culture.

29.2.2.3 Large-Scale Production of Hybridoma Antibodies. The generation of monoclonal antibodies is one of the most important discoveries in the biomedical field because these molecules are highly specific for their target and show a long-term stability. Hence, it is not surprising that monoclonal antibodies are produced in large amounts in industry. The material mostly applied to cultivate hybridoma cells *in vitro* is tissue culture polystyrene (21). Bioreactor technology for mass production of monoclonal antibodies is based on large-scale stirring bioreactors, and hollow fibers or flat-sheet membranes to cultivate hybridoma cells (22) (Fig. 29.3). The most frequently used membranes in these systems are hydrophilic ones, such as cellulose acetate or polymethylmethacrylate (23). The specific cutoffs of these membranes between 10

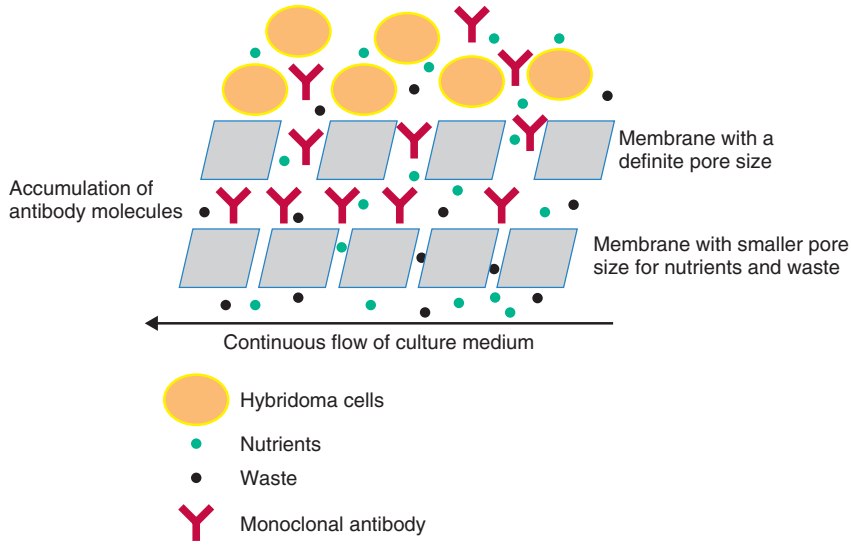


Figure 29.3. Bioreactor technology for mass scale production of monoclonal antibodies. (This figure is available in full color at http://onlinelibrary.wiley.com/book/10.1002/9780470054581.)

and 15 kDa allow a continuous influx of essential components, for example, amino acids, vitamins, and so on and an effective removal of toxic metabolites like ammonia or lactate (24). Secreted antibodies cannot pass the membrane because of their higher molecular weight. They are enriched in the "cellular" compartment of the bioreactor and large quantities of monoclonal antibodies can be accumulated. The quantities achieved in these systems vary between 1 and 4 mg/mL, while the yield of monoclonal antibodies is limited to 10–100 μg/mL in the conventional tissue culture technology (24,25). Bioreactor technology has been optimized so far for supply of nutrients and oxygen and removal of waste materials. Advantages of these systems are a warranted purity and a product, generally free of contaminants or fragmented or denatured antibodies in high concentrations. Big pharma companies dispose of huge 2000 L fermenters in which the production of recombinant proteins is performed. With a protein concentration of approximately 4 mg/mL, it means, a yield of up to 8 kg recombinant protein is produced by one fermenter.

29.2.3 Production of Human Antibodies

An overview is shown in Fig. 29.4.

29.2.3.1 Chimeric and Humanized Antibodies. For therapeutic purposes, human or human-like antibodies have to be applied to avoid an immune reaction against the injected protein. One aspect in this area is the chimerization and humanization of mouse-generated antibodies (26). The murine variable parts of the antibody molecule are fused to human originated constant domains, which reduce the murine part to approximately 35% (chimeric antibodies). A second possibility was established in which only the complimentarity-determined regions (CDRs) are of murine origin and that is reducing the murine part to 5%–10% (humanized antibodies) (27). For these purposes, the mRNA of the antibody-producing hybridoma has to be isolated, translated into cDNA, and cloned in vectors for chimerization or humanization, based on genomic sequences for the human constant domains and cloning cassettes for the insertion of murine cDNA. The expression is performed by transformation of mammalian cells, cultivation under serum-free conditions, and secreted chimerized or humanized antibodies are purified from the culture supernatant via protein A or affinity chromatography. The experimental design is extensive, cost-intensive, and associated with current problems regarding molecular cloning and transformation

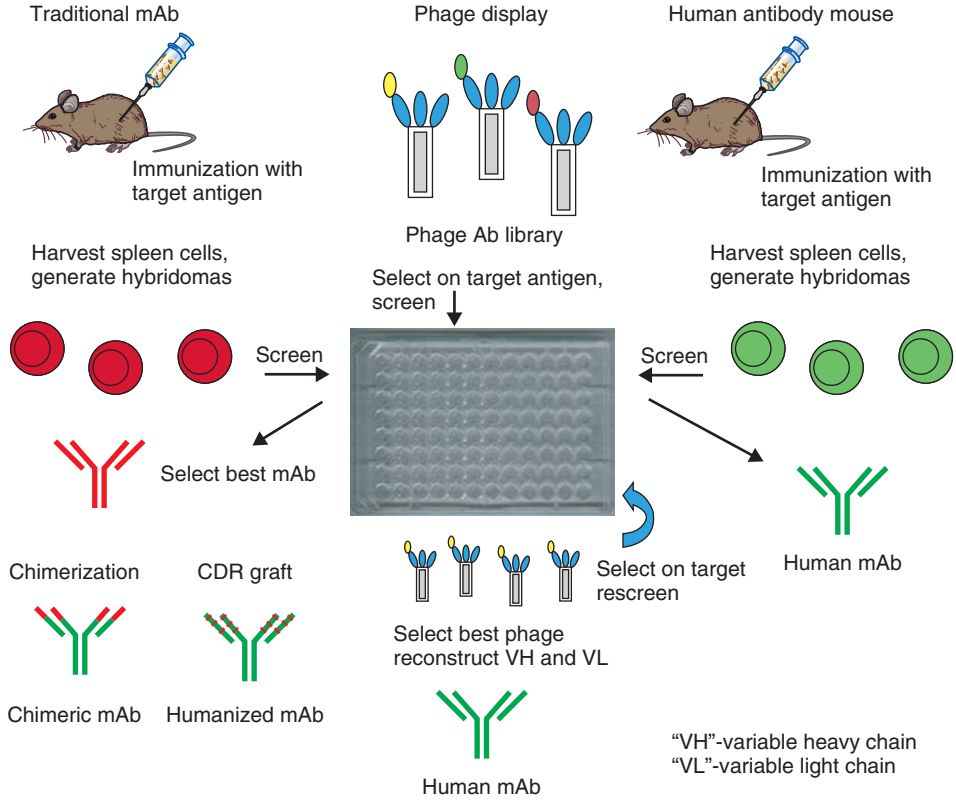


Figure 29.4. Overview of antibody technologies for chimerization and humanization of murine antibodies. (This figure is available in full color at http://onlinelibrary.wiley.com/book/10.1002/9780470054581.)

of mammalian cells. Frequently, the substitution of amino acid residues by back-mutations or affinity maturation leads to drops in affinity relative to the original mouse antibody.

29.2.3.2 Human Antibodies Obtained From Phage Antibody Libraries. Another promising technique in generating immunmodulating molecules is the creation of single chain antibodies of human origin (28). These very small molecules are joined variable segments consisting of the variable light and heavy chains of an antibody. The linker between the variable segments allows the flexible orientation of antigen-binding sites toward the target as in natural antibodies. These single chain fragments are usually expressed on bacteriophage outer coat proteins. Hence, the generation takes place by a technique called *phage display*. For this purpose, DNA from nonimmunized donors is used to generate large antibody libraries of variable light and heavy chains. The target cDNA is cloned into phagemid-vectors containing the major coat protein pIII of the bacteriophage M13. The major coat protein is responsible for the introduction of the single chain molecule into the envelope of the phage. After cotransfection with a M13 helper phage the genetic information for heavy and light chain is incorporated into a phage particle containing the phagemid. Thereby, recombinant phages are designed with single chain fragments in their envelopes and the genetic information inside comparable to B lymphocytes in mammalian organisms. The screening for target structures is called *biopanning* in which relevant antibody genes can be isolated and used to reconstruct a fully humanized antibody. This method is very useful to generate antibodies against self-antigens and allow the successful production of therapeutic antibodies. Continuative strategies combine single chain molecules against tumor markers with toxic ligands to eliminate the target cell. In cases where complete intact antibodies are needed the human single chain antibody fragments can be combined by DNA technology with human constant antibody parts as in antibody chimerization. Such fully human antibodies can then be propagated by large-scale techniques such as phage display as *in vitro* selection system (29). By now recombinant antibodies represent nearly 30% of all biopharmaceuticals being in clinical trials. That, in fact shows the great potential in biotechnology and biomedicine as useful strategy in controlling human diseases more effectively.

29.2.3.3 Human Antibodies From Human Hybridomas and Hybridomas From Humanized Mice. The technique to create human hybridomas is not as well developed as the production of murine hybridomas. Therefore, only very few human antibodies are available going back to B cells of human origin. To generate completely human originated antibody molecules, immunodeficient mice (30) or xenomice (31) are used currently. Human stem cells were transferred into severe combined immunodeficient (SCID) mice (SCID mice) which then develop a temporary human immune system. After challenging these mice with antigen the antibody-producing cells can be isolated by standardized hybridoma technology but for fusion a human immortal cell line is required. For this purpose, heterohybridomas from mouse and human origin as HF2x653 (human WI-L2-729-FF2, mouse P3X63/Ag.8.653) or K6H6/B5 (human nodular lymphoma cells from a patient with non-Hodgkin's lymphoma, mouse NS-1-Ag4) were used. The animal husbandry for immunodeficient mice is strongly regulated. The mice need a completely sterile environment because of their established immune deficiency. Further limitation for this system is the dependence of appropriate donors and the generation of antibodies against unknown targets is not possible because of the immunological tolerance. This makes it very difficult and not common to produce human antibodies in higher amounts.

The next "evolutionary" step in creating fully human antibodies is a genetically engineered mouse, a so-called *xenomouse*. These mice have inactivated murine antibody genes, and therefore, cannot produce murine antibodies (32). But by gene transfer, human gene segments for heavy and light chains were introduced successfully into the mouse genome. The segments were incorporated completely and fully functional so that these mice can produce human antibodies against every target, also of human origin, and are able to initiate affinity maturation and isotype switching. Difficulties can appear regarding compatible glycosylation patterns of antibody molecules generated with mouse hybridomas but this should be avoided by using heterohybridomas or fully human-related fusion cell lines. Another recently presented technology is the transgenic rabbit technology which implies the use of transgenic rabbits for the production of human antibodies after immunization with therapeutic targets (33). The advantage of using transgenic rabbits is the higher immune competence (compared to mice) to create antibodies against different targets which could not be achieved by common technologies as described earlier.

29.3 NEW METHODS FOR HUMAN ANTIBODY PRODUCTION (*IN VITRO* IMMUNIZATION, ARTIFICIAL LYMPH NODE SYSTEMS)

By now the development of promising alternatives and new tools for generating human antibodies are unfortunately in its infancy. There are some interesting experimental designs like *in vitro* immunization or the development of artificial lymph node systems. Several approaches have been tried to achieve an *in vitro* immunization but the definition of the term is interpreted differently by different authors.

Borrebaeck *et al*. (34) described the production of human monoclonal antibodies by an *in vitro* immunization of peripheral blood lymphocytes. In other studies, the activation of dendritic cells with selected antigens was carried out to generate cytotoxic T lymphocytes and this procedure was also named as *in vitro immunization* (35). In spite of some positive results there is no established routine method, currently, combining the most important *in vivo* components for an *in vitro* immunization. For long-term studies the accomplishment of an immune response *in vitro* requires the cooperation of the important populations of immune cells involved normally *in vivo* together with a lymph node–like surface as biomimetic support. This would result in an experimental design with possibilities to generate human antibodies and could be a basis to obtain a defined activation status to nearly every antigen so that the production of specific antibodies against these antigens could be accomplished. Problems which need to be solved in this technology is first the shortened lifetime of B and T-lymphocytes and second the constant requisition of new cell populations which can be activated against specific antigen. These problems could be prevented by fusion with adequate cell lines or by special biomimetic cultivation supports related to an extracellular matrix as seen in the paracortical area of lymph nodes. By now, several bioreactor systems are in progress in which the permanent cultivation and activation of dendritic cells is possible. These systems are supported by an alginate layer that allows the self-assembly of human lymphatic tissue due to proper emulation of human architecture and homeostasis (36). The development of extracorporeal human lymphatic organs would be a highly specific application to study matrix organization, cell-matrix interactions, and immunological tolerance processes which could broaden the knowledge of human immune responses in a superior manner. But all these new and advanced experimental tools are possible only due to one brilliant invention in 1975—the hybridoma technology from Köhler and Milstein—and there could be no better proof that the nobel prize was awarded right for this part of scientific history.

29.4 ALTERNATIVES TO ANTIBODIES FOR USE IN HUMAN BEINGS

Antibodies are the most successful binding molecules in science since nearly 20 years, but for all that there are disadvantages based on their complicated molecular composition. Immunoglobulins show a large and multidomain structure with specific glycosylation patterns and disulfide bonds, both essential for assembly and function. Hence, the manufacturing process is very expensive and some of the immune effector functions of the constant domains seem to be undesirably in many therapeutic approaches. The generation of antibody fragments like Fab fragments or single chain antibodies was the next step to avoid effector functions but this resulted in a lack of stability. Further, it was difficult to tag them for detection. For this reason, alternative binding proteins other than antibody molecules were needed to handle with the upcoming problems. Such alternative binding molecules were invented in nonvertebrate animal groups as defense molecules and so it was logical to try the usefulness of such protein molecules as universal binding molecules, too. Alternative binding molecules are entering the field of classical antibody application stepwise and are currently being evaluated. Examples for alternatives are affibodies, lipocalins, designed ankyrin repeat protein (DARPins), and nanobodies (37,38). Affibodies are small protein domains that are derived from a bacterial surface receptor like the immunoglobulin-binding domain from *Staphylococcus aureus* protein A (39). The selected protein domains are folded individually, no disulfide bonds are necessary, and they show a high proteolytic and thermic stability. Affibodies were selected by phage display technology from a protein library and some have entered the diagnostic and therapeutic market, for example, affibody-alexa fluor conjugates for the semiquantitative imaging of HER2 expressing cells *in vivo* (40). Lipocalins are a broadly distributed protein family consisting of β-barrel structures with an internal ligand binding site that are present in nearly all organisms (41). The natural function of these proteins is the transport of small hydrophobic proteins such as retinoids, lipids, or steroids. These properties are currently used for genetic engineering to modify the binding sites. The generated molecules are then called *anticalins*. The application of recombinant neutrophil gelatinase-associated lipocalin (NGAL) to mice with acute kidney injury has recently attracted great attention as this resulted in marked preservation of kidney function and structure (42). DARPins are designed ankyrin-repeat proteins with consecutive copies of small structural units (20–40 amino acid residues) that stack together to form elongated repeat domains displaying variable and modular target-binding surfaces (43). Because of the repeat domains the molecule can be adapted to every target size and they are characterized by a high affinity, high thermodynamic stability, and reverse folding behavior. Further, the generation seems to be beneficial because the expression in *E. coli* is extremely high and accompanied by low aggregation tendencies. Recent data showed that ankyrin-repeat domains are also useful for therapeutic approaches. Schweizer *et al*. (44) designed a novel type HIV entry inhibitor based on the DARPin technology. The proteins were highly specific for CD4 and potently inhibit infection of genetically divergent HIV isolates. They seem to be therefore promising candidates for the use in human beings. Nanobodies or single domain antibodies are derived from camelids and are functional antibodies

devoid of light chains but fully capable of antigen binding (38). These properties cause some interesting features like an improved solubility and stability. Further the molecules are characterized by a more simple expression in microorganisms comparing to the expression of complex antibody molecules in mammalian cells and the suitability to construct larger molecules and selection techniques such as phage, yeast, and ribosome display. Nanobodies are offering new therapeutic strategies, especially for an oral immunization because of the resistance in the extremes of pH and the property to bind their target. so in high concentration of chaotropic agents. Till now, several therapeutic approaches could be realized with nanobodies like the treatment of diarrhea, sepsis, or rheumatoid arthritis.

29.5 OUTLOOK

The hybridoma technology developed from Köhler and Milstein over 20 years ago is currently the scientific standard in generating monoclonal antibodies and demonstrates a hallmark in biotechnology and biomedicine. This basic method and all arising technologies opened up a new field for experimental designs and innovative results in understanding and clarifying courses in diseases. The possible application of antibodies in research leads to well-defined characterizations of cell types, cell–cell and cell–matrix interactions, and correlation of signaling cascades. An outstanding example is the identification of nearly over 300 cluster of differentiation (CD) antigens (14). With this knowledge it is possible to understand intracellular processes and last but not least, to develop new and highly effective strategies in controlling diseases. The hybridoma technology has provided scientists and clinicians with invaluable tools for research and diagnostic. Several genome projects with mammalian genomes identified thousands of functional genes, which have to be identified, characterized, and investigated regarding protein expression and regulation processes. These perspectives indicate a continuous requirement and therefore have a huge global demand for antibody molecules, related detection markers, and biomedical tools. In the course of this development, a multitude of new techniques is necessary and will be designed in future to simplify the generation of human therapeutic antibodies, which, in fact, seems to be a highly effective tool in the treatment of malignant or autoimmune diseases.

REFERENCES

1. American Diabetes Association. Diabetes Care 2002; 25: S5–S20.
2. Hill CP, Osslund TD, Eisenberg D. Proc Natl Acad Sci U S A 1993; 90: 5167–5171.
3. Levi-Montalcini R. Science 1987; 237: 1154–1162.
4. Breitling F, Dübel S. Rekombinante antikörper. Berlin: Spektrum Akademischer Verlag GmbH; 1997.
5. Dübel S. Handbook of therapeutic antibodies. Weinheim: Wiley-VCH Verlag; 2007.
6. van Dijk M.A. and van de Winkel J.G.J., Curr Opin Chem Biol 2001; 5: 368–374.
7. Wink M. Molekulare biotechnologie. Weinheim: Wiley-VCH Verlag; 2004.
8. Yazaki PJ, Wu AM. Antibody engineering: methods and protocols: Springer Verlag; 2003. pp. 255–268.
9. Heilmann K, Groth Th, Behrsing O, Albrecht W, Schossig M, Lendlein A, Micheel B. J Biotechnol 2005; 115: 291–301.
10. Banchereau J, Steinman RM. Nature 1998; 392: 245–252.
11. Murphy K, Travers P, Walport M. Janeway's immunobiology. New York: Garland Science; 2008.
12. Dilioglu S, Cruse JM, Lewis RE. Exp Mol Pathol 2003; 75: 217–227.
13. Köhler G, Milstein C. Nature 1975; 256: 495–497.
14. Mason D. Leukocyte typing VII: white cell differentiation antigens: Oxford University Press; 2002.
15. Nelson PN, Reynolds GM, Waldron EE, Ward E, Giannopoulos K, Murray PG. J Clin Pathol-Mol Pathol 2000; 53: 111–117.
16. Kearney JF, Radbruch A, Liesegang B, Rajewski K. J Immunol 1979; 123: 1548–1550.
17. Shulman M, Wilde CD, Köhler G. Nature 1978; 16: 269–270.
18. Osterhaus AD, UyteHaag AG. Tijdschr Diergeneeskd 1985; 110: 835–839.
19. Stoicheva NG, Hui SW. J Membr Biol 1994; 141: 177–182.
20. Steinitz M, Klein G, Koskimies S, Mäkelä O. Nature 1977; 269: 420–422.
21. Amstein CF, Hartman PA. J Clin Microbiol 1975: 46–54.
22. Bruce MP, Boyd V, Duch C, White JR. J Immunol Methods 2002; 264: 59–68.
23. Lowrey D, Murphy S, Goffe RA. J Biotechnol 1994; 36: 35–38.
24. Nagel A, Koch S, Valley U, Emmrich F, Marx U. Report Integra Biosciences. 2003.
25. Falkenberg FW, Weichert H, Krane M, Bartels I, Palme M, Nagels HO, Fiebig H. J Immunol Methods 1995; 179: 13–29.
26. Morrison SL, Oi VT. Immunglobulin genes. London: Academic Press; 1989. p. 260.
27. Riechmann L, Clark M, Waldmann H, Winter G. Nature 1988; 332: 323–327.
28. Thie H, Meyer T, Schirrmann T, Hust M, Dübel S. Curr Pharm Biotechnol 2008; 9: 439–446.
29. Konthur Z, Hust M, Dübel S. Gene 2005; 30: 19–29.
30. Dick JE. Mol Genet Med 1991; 1: 77–115.
31. Green LL. J Immunol Methods 1999; 231: 11–23.
32. Lonberg N. Nat Biotechnol 2005; 23: 1117–1125.
33. Eur Biotechnol News 2007; 6: 28–32.
34. Borrebaeck CAK, Danielsson L, Möller SA. Proc Natl Acad Sci U S A 1988; 85: 3995–3999.
35. Zietvogel L, Mayordomo JI, Tjandrawan T, DeLeo AB, Clarke MR, Lotze MT, Storkus WJ. J Exp Med 1996; 183: 87–97.

36. Giese C, Demmler CD, Ammer R, Hartmann S, Lubitz A, Miller L, Müller R, Marx U. Artif Organs 2006; 30: 803–808.
37. Binz HK, Amstutz P, Plückthun A. Nat Biotechnol 2005; 23: 1257–1268.
38. Harmsen MM, de Haard HJ. Appl Microbiol Biotechnol 2007; 77: 13–22.
39. Nord K, Gunneriusson E, Ringdahl J, Stahl S, Uhlen M, Nygren P. Nat Biotechnol 1997; 15: 772–777.
40. Lee SB, Hassan M, Fisher R, Chertov O, Chernomordik V, Kramer-Marek G, Gandjbakhche A, Capala J. Clin Cancer Res 2008; 15: 3840–3849.
41. Flower DR, Altwood TK, North AC. Protein Sci 1993; 2: 753–761.
42. Devarajan P. Cancer Ther 2007; 5: 463–470.
43. Forrer P, Stumpp MT, Binz HK, Plückthun A. FEBS Lett 2003; 27: 2–6.
44. Schweizer A, Rusert P, Berlinger L, Ruprecht CR, Mann A, Corthesy S, Turville SG, Aravantinou M, Fischer M, Robbiani M, Amstutz P, Trkola A. PLoS Pathog 2008; 4: e1000109.

FURTHER READING

Pegram MD, Lopez A, Konecny G, Slamon DJ. Semin Oncol 2000; 27: 21–25.
Stefanova I, Dorfman JR, Germain RN. Nature 2002; 420: 429–434.
Stephen SB. N Engl J Med 1996; 334: 841–848.
Rosati G. Neurol Sci 2001; 22: 117–139.
Majithia V, Geraci SA. Am J Med 2007; 120: 936–939.

30

ANTIBODY PRODUCTION, HUMAN RECOMBINANT

STEFAN DÜBEL

Technische Universität Braunschweig, Institute of Biochemistry and Biotechnology, Spielmannstr, Braunschweig, Germany

30.1 INTRODUCTION

The main function of antibodies in nature is the specific labeling of pathogen determinants for their subsequent recognition by the immune system. A very large collection of antibodies with different binding specificities can be produced by our body for this purpose. However, it would be far too inefficient to store individual genes for each of the approximated $>10^8$ different antibodies present in the human organism, and the amount of DNA required would exceed the size of the entire human genome itself. The solution to this problem depends instead on the principle of genetic recombination. The final antibody gene is individually assembled in every B cell from a limited number of different gene fragments. In addition to the recombination of gene fragments, further coincidental mechanisms introduce new, short sequences at one of the fusion points of the different gene fragments. The diversity of possible structures is further increased through the combination of two different protein chains (*light* and *heavy* antibody chains).

The generation of binding diversities, while maintaining constant functions of the effector mechanisms of the immune system is made possible through the modular construction of the antibody. A typical immunoglobulin polypeptide chain is constituted from two or more very similar protein units (“regions”)having the same folding structure (“immunglobulin superfamily fold”). Two or more of these polypeptide chains are then assembled to the complete immunglobulin. Antigen binding is achieved by the aminoterminal folded units, named the variable regions, which contain the *hypervariable regions*. Structurally, these form the complementary determining regions (CDRs) because they form a structure which is complementary to the antigen. Six of these hypervariable regions in total (three in the light chains and three in the heavy chains) are organized throughout the rest of the sequence (the so-called framework regions) so that they come together with the top end of the T or Y forming structure of the molecule (Fig. 30.1 and Fig. 30.2). This structure, made up of the CDRs and the framework regions, forms the V domain (variable domain) of the antibody.

The constant domains mediate the effector function; different constant domains can therefore mediate a large range of different biological effects. Among these effects are the activation of complement, a protease cascade finally leading to the lysis of target cells, or antibody dependent cellular cytotoxicity (ADCC), where the antibody targets effector cells to the antigen. Further, the type of constant domains determine the strength of these effects as well as the half-life in the blood plasma. Immediately evident when looking at an immunoglobulin is its modular structure, as the individual domains are all of the same fold, and many variations can be achieved by adding more or less domains. For example, the number of constant domains varies, and immunoglobulin forms with 2–10 binding sites are made in our body, based on combination of a variable number of IgG-like modules.

The selection of the B lymphocyte (B cell) which produces a corresponding antigen-binding antibody occurs after contact with the antigen through selective reproduction of this B cell (a process called *clonal selection*). This selection was previously achieved using the immune system of animals (mainly mice or rabbits).

Upstream Industrial Biotechnology: Expression Systems and Process Development, Volume 1, First Edition. Edited by Michael C. Flickinger.
© 2013 John Wiley & Sons, Inc. Published 2013 by John Wiley & Sons, Inc.

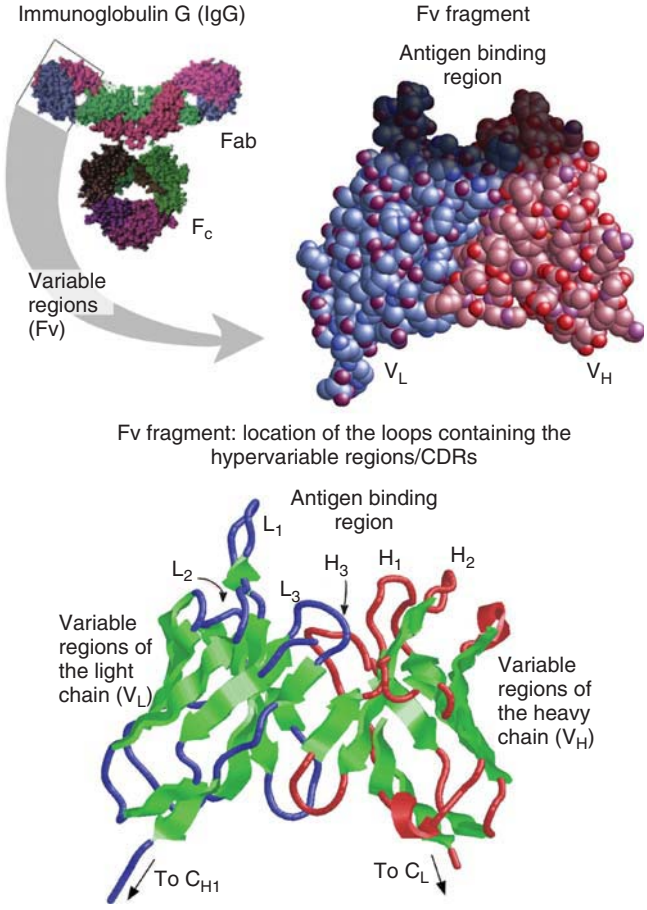


Figure 30.1. Structure of immunoglobin and the antigen-binding fragment (Fv). Below: The structure of the immunoglobin domains are defined by the sheet region (green) of the framework, whereas the antigen-binding sites are formed from six loops (H1–H3, L1–L3). The carboxyl-terminal of both variable polypeptide chains of an Fv fragment (C) lies on the antigen-binding site at opposite ends of the molecules, therefore it is the preferred site for protein fusion. (This figure is available in full color at http://onlinelibrary.wiley.com/book/10.1002/9780470054581.)

In this way either antisera (polyclonal antibodies) or B lymphocytes, which after immortalization produce monoclonal antibodies, were obtained (refer to section on *hybridoma technology monoclonal antibodies*). In each case, however, it was necessary to first immunize an animal. In the late 1980s, a third method of manufacturing antibody fragments, based on gene technology, became available. Using this method, the antibodies are no longer made in research animals (or in humans) but instead they are produced *in vitro* in bacteria or cultured cells. Further, it was realized at the beginning of the 1990s that the selection of specific antigen-binding sequences could be carried out completely *in vitro*. The methods that were developed in this way are explained in the following sections.

30.2 WHY RECOMBINANT ANTIBODY SELECTION AND PRODUCTION?

30.2.1 Human Monospecific Antibodies

In the late nineteenth century, the German army doctor Emil von Behring (1854–1917), later first Nobel laureate for medicine, pioneered the therapeutic application of antibodies. It took an entire century, however, to develop methods allowing the development of monospecific antibodies for the therapy of human diseases. Why? Behring used blood serum for the treatment of tetanus and diphtheria ("Blutserumtherapie"). Following the underlying principle of this approach, today there is still a significant number of blood products based on the effect of naturally occurring immunoglobulins. These agents are used mainly for passive vaccination. If they are made in animals, an immune response against the foreign protein can be expected, prohibiting repeated use of these agents. Human blood products are used as well, but bear the risks of virus contamination arising from any pool of donor blood preparation. Further, a continuous quality is difficult to achieve, since it depends on a mixture of individual and quite limited sources of donor blood. So, there is no way to utilize these blood derived antibodies for the treatment of chronic diseases, like cancer or autoimmune diseases. Also, human monoclonal antibodies are rarely used for two main reasons. First, an immunization for the production of antibodies in humans is only possible in exceptional cases. Second, the hybridoma generation with human cells has proven to be very difficult, and many of the few existing human monoclonal antibodies are derived from cells immortalized by other methods, for example, Epstein–Barr Virus (EBV) infection—a method not really preferable for the generation of drugs for human use due to the inherent risk of EBV contamination.

These restrictions explain why the clinical use of monoclonal antibodies only flourished starting a 100 years after the first human serum therapy by Behring. It was necessary to develop novel methods for the generation and production of human antibodies.

Nowadays, human antibodies for *in vivo* use (such as therapy and diagnosis) can be obtained from recombinant methods such that the antibodies are not recognized as *foreign* by the human immune system, resulting in a lower immune response by the patient against the antibody. This minimizes the risk of a patient's response which neutralizes the therapeutic antibody. Even further, human antibodies can be generated completely *outside* of a vertebrate organism. Some methods even allow the adjustment of antibody features since the biochemical properties for the binding can be precisely controlled during *in vitro* selection. For this reason antibodies are available that could never be produced in animals, for example, antibodies against transient conformation of a molecule

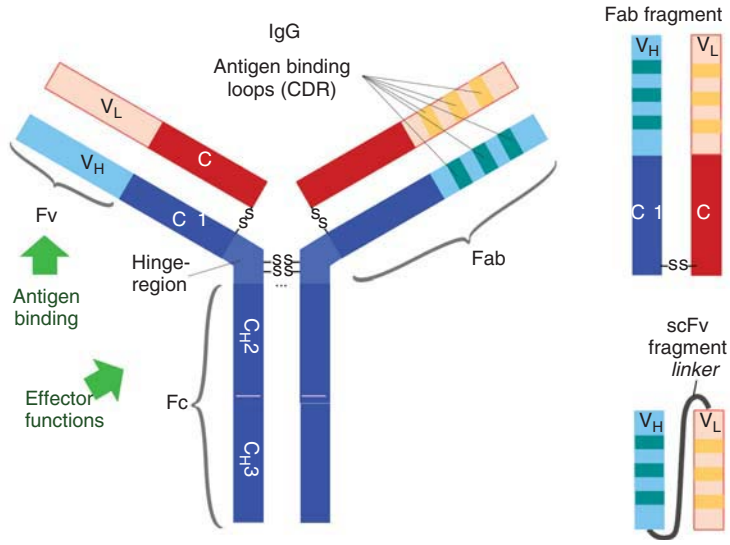


Figure 30.2. Schematic diagram of IgG and recombinant antibody fragments derived from it which can be produced in bacteria. (This figure is available in full color at http://onlinelibrary.wiley.com/book/10.1002/9780470054581.)

after cofactor binding. Cross reactivities can be suppressed by the addition of a respective competitor during selection. Antibodies against antigens with which an immunization is not possible can also be obtained, for example, antibodies against highly toxic substances, lethal pathogens, or evolutionary conserved molecules. Thus, only recombinant antibody technology made the manufacture of *human* antibody therapeutics possible in a systematic manner (Fig. 30.3).

30.2.2 Antibodies with Improved Functions and Properties can be Created

Once a recombinant antibody clone is obtained, it can be manipulated using the entire arsenal of modern genetic engineering. By strategies ranging from employing *in vitro* evolution (mutation and reselection) to computer aided molecular design, almost all biochemical properties of an antibody nowadays can be adjusted, from net surface charge, molecular mass and valency to affinity, stability, serum half-life, and immunogenicity.

This is perfectly illustrated by the antibody variants made to block the Tumor Necrosis Factor (TNF)/Tumor Necrosis Factor Receptor (TNFR) interaction to down-regulate overshooting inflammations (Fig. 30.4). Starting with a clinically failed mouse hybridoma antibody, the next steps were chimeric and then humanized antibodies. A completely human antibody and a human soluble receptor-Fc fusion were the next clinically tested and approved iterations of the idea. Recently, a humanised Fab fragment fused to polyethylene glycol (PEG) to improve pharmacokinetics marks the sixth generation of TNF antagonist antibody constructs. Already, the list includes two examples of novel designs based on antibody fragments, but not anymore resembling a molecule present in nature. Recombinant antibody technology may even reach its limits here, and a seventh generation TNF antagonist could well be a novel synthetic binder of nonantibody structure ("alternative scaffold").

Many promising new concepts for the treatment of a huge variety of different diseases could now be envisaged. For example, the antibody genes can be coupled to a gene of interest, so that both genes are fused together and produced as a single protein. The antigen-binding site and the carboxyl-terminal of the V domain are on opposite sides of the molecule. Therefore, through the introduction of heterologous proteins to the carboxyl-terminal of a V domain it is possible to provide the antigen-binding site of the antibody with new biochemical functions, which would not occur naturally. For example, an enzyme can be specifically directed to a tumor with the help of an antibody fragment—such *bifunctional antibodies* can lead to new cancer therapies.

The connection of two different antigen binding sites to form a *bispecific antibody* is also possible. Recombinantly produced genetic fusions offer the advantage, that the coupling product and the stoichiometry of both partners are exactly defined.

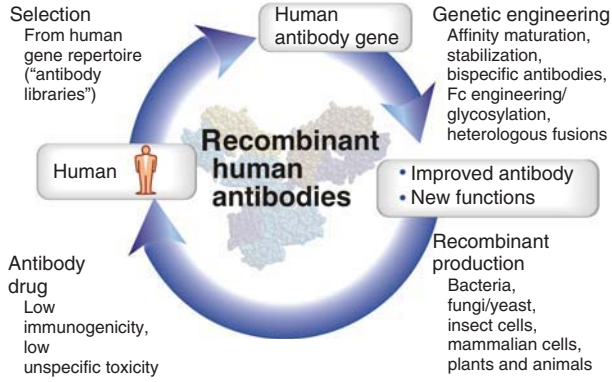


Figure 30.3. The idealized production cycle of human recombinant antibodies. (This figure is available in full color at http://onlinelibrary.wiley.com/book/10.1002/9780470054581.)

30.3 MAKING HYBRIDOMA-DERIVED ANTIBODIES MORE HUMAN

After the discovery of human anti-mouse antibody (HAMA) responses in patients treated with hybridoma-derived monoclonals, various attempts have been followed to make animal derived immunoglobulin molecules looking more human. Two of these strategies led to success in form of several approved therapeutics. In the late 1980s, the molecular details of epitope specificities in T-lymphocyte responses to foreign proteins were barely known. The transformation from mouse to human-like protein sequences was therefore attempted by exchanging parts of the immunoglobulin polypeptide with homologous human sequences. So, this strategy was based on the assumption that human sequences, when given as a drug, may cause less adverse reactions due to the lack of specific T-cells in the patients. When looking on the immune responses observed in clinical application of these antibodies, it is evident that this concept not only worked, but was the

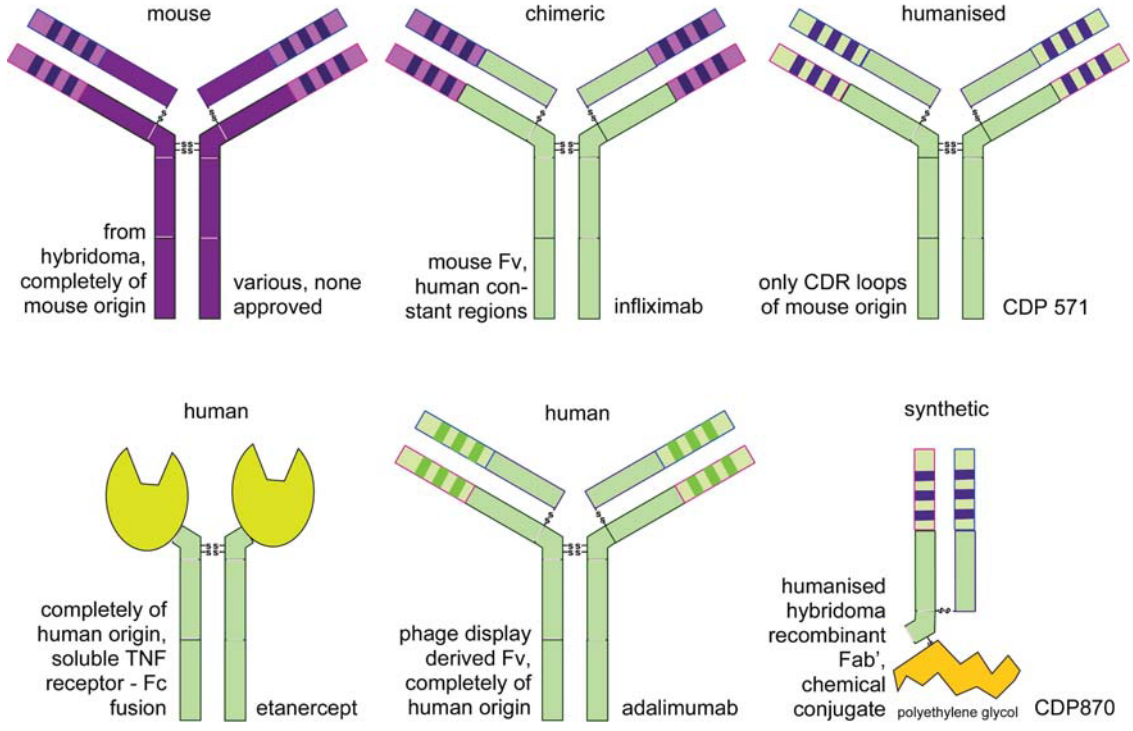


Figure 30.4. Development steps of antibody-derived TNF antagonists for the therapy of overshooting immune responses. Approval dates given in Table 30.2. (This figure is available in full color at http://onlinelibrary.wiley.com/book/10.1002/9780470054581.)

spark to ignite an entirely new industry for the generation of these recombinant antibodies (see approved antibody therapeutics in Table 30.1). However, it became evident finally with the approval of completely human antibody sequences (like in Humira) that the absence on nonhuman polypeptide sequences does not guarantee a complete lack of immune response against the therapeutic protein. This can be explained by three factors: first allelic variations are not studied yet to an extent allowing broad conclusions on the differences between individual patients. Second, the fact that the antigen-binding domains of every antibody contain randomly rearranged amino acid compositions, even with newly synthesized sequences in CDR3H, suggest that individual patients will have different tolerance patterns to these parts of the antibody molecule. No humanization strategy known so far, however, can completely eliminate this potential source of immunogenicity since it would effect antigen specificity and affinity as well. Third, most approved antibodies are produced in hamster cell cultures, which may lead to different post-translational modifications when compared to human plasma cells, where immunoglobulins are naturally made. These modifications, in particular those of the glycosylation pattern, may effect immunogenicity as well. In addition, carefully adjusted galenics can lower immunogenicity, for example, by avoiding aggregation.

30.3.1 Chimerization

The first approach to lower the fraction of animal derived protein sequence from hybridoma antibodies was the genetic fusion of the original mouse antigenic binding domain to human constant domains. The resulting *chimeric antibody* (Fig. 30.4) gene was then introduced to CHO (Chinese hamster ovary) cells for recombinant production. The advantage of this method is that the structural integrity of the variable domains of heavy and light chain remains untouched, thus increasing the chances that a chimerized antibody retains the antigen-binding properties of the original hybridoma antibody. However, two domains out of the 12 forming an IgG molecule are encoded by mouse sequences, and consequently HAMA antibodies can be found in patients treated with chimeric antibodies.

30.3.2 Humanization

A large number of different approaches has been conceived to eliminate as much as possible the mouse-derived sequences from the IgG molecule. Based on the structural knowledge of the antigen-binding site, many of these strategies aim to transfer the six peptide loops contacting the antigen to a human framework ("CDR grafting"). When following this approach, it soon became evident that in almost all cases where a one-to-one transfer of mouse CDRs to even highly homologous human framework parts led to a dramatical loss in affinity or even specificity. Other variants created this way were difficult to being produced in cell culture. So, the approved antibodies required several "back"-mutations, reintroducing mouse-specific amino acid side chains into the human framework, to cure these deficiencies. Consequently, the nomenclature "humanized" does not mean that the resulting antibody is consisting only of human sequences.

Other humanization strategies rely on changing just the outside of the antibody which is exposed to the blood, but leaving the structural core of the antibodies V regions in their original mouse-derived organization. A more radical method uses the successive exchange of the two V domains by human domains, either in *guided selection* or *chain shuffling* approaches.

In many cases, the primary sequence of different mouse antibodies, when analyzed, shows individual differences forcing to combine two different humanization methods. So, every humanization approach should start with a thorough analysis of the real differences between the mouse gene and its nearest human homolog. It has been proposed that the use of genomic sequences instead of sequences of somatically mutated IgG lowers the risk for immunogenicity, but despite all these attempts, also humanized antibodies induce responses in patients, because of the reasons mentioned above.

30.3.3 *In silico* Humanization

The experimental assessment of the immunogenicity of a protein in man is still not satisfactory. *In vitro* studies relying on activation of T-lymphocyte preparations can give a hint, but a negative result in these assays does not allow the conclusion that this will be mirrored in a living human body. With the advent of increasing knowledge on the molecular mechanisms of antigenic peptide processing and presentation on the major histocompatibility complex (MHC) molecules, methods were developed to predict the "immunogenicity" of polypeptide sequences by bioinformatic algorithms (*"in silico"*). Various approaches were followed here and it developed into an industry standard to check potential immunogenicity of antibodies before the start of a clinical study. Unfortunately, it is very difficult to judge the success rate of the various algorithms, since negative controls (without *in silico* humanization/deimmunization) are usually not available.

30.4 OBTAINING HUMAN RECOMBINANT ANTIBODIES

The lengthy procedures and limited success of humanization strategies inspired the development of completely new methods to obtain human antibody sequences from the start.

TABLE 30.1. Production Systems for Recombinant Antibodies[a]

Host Prokaryotes	Antibody Format	Production System	Maximal Yield
Gram-negative bacteria			
Escherichia coli	$F(ab')_2$	Fermentor	2.5 g/L
	V_{HH}	100 L shake flask	10 mg/L
	Fab	10 L fermentor	1–2 g/L
	VL single domain	1.5 L fermentor	35–65 mg/L
	scFv	3 L fermentor	1.2 g/L
	IgG	10 L fermentor	130–150 mg/L
	Fv	Fermentor	450 mg/L
Proteus mirabilis	scFv	50 mL shake flask	~12 mg/L
Gram-positive bacteria			
Bacillus brevis	Fab	2 L shake flask	100 mg/L
Bacillus megaterium	scFv	400 mL shake flask	0.41 mg/L
Bacillus subtilis	scFv	N.d	12 mg/L
Lactobacillus paracasei	V_{HH}	N.d.	~1 mg/L
Streptomyces lividans	Fv	N.d.	~1 mg/L
Eukaryotes			
Yeast			
Pichia pastoris	V_{HH}	Baffle flask	10–15 mg/L
	scFv	Baffle flask	60–250 mg/L
	Fab	5 L fermentor	458 mg/L
	scFv-Fc	5 L fermentor	10–30 mg/L
	scFv-$(G_2S_2)_2$-GS-C_{1-3}	4 L fermentor	60 mg/L
	Tetravalent scFvs	20–30% tetramers	15–20 mg/L
Saccharomyces cerevisiae	V_{HH}	100 mL shake flask	Up to 100 mg/L
	Fab	N.d.	100–200 μg/L
	IgG	N.d.	50–80 μg/L/
Filamentous fungi			
Aspergillus niger var. *awamori*	IgG1	50 mL shake flask	0.9 g/L
	Fab	50 mL shake flask	1.2 g/L
	scFv	N.d.	10 mg/L[b]
	V_{HH}	Shake flask	7.5 mg/L
Trichoderma reesei	Fab	15 L fermentor	1 mg/L
Insect cells			
Drosophila melanogaster, DS2	scFv	25-cm^2 flasks	25 mg/L
Spodoptera frugiperda, Sf9	scFv	6 L bioreactor	32 mg/L
	Several IgGs	T75 flasks	6–18 mg/L
	IgG1	N.d.	10 mg/L
Trichoplusia ni	IgG2a	150 mL shake flasks	N.d.
Mammalian cells			
Transient			
HEK293T	IgG and scFv-Fc	lipofectamine (LP), HEKfectin, tissue culture plates	1–20 mg/L
HEK293E	IgG	Polyethylenimine (PEI), 10 L shake bottle	80 mg/L
CHO-K1	IgG	LF, 1 L spinner flask	20 mg/L
CHO-K1-S	IgG4	PEI, 10 L, shake flask	39 mg/L
Stable			
CHO	Fv	Roller bottle	4 mg/L
GS-NS0	cIgG4	Fermentor, fed-batch, airlift	560 mg/L
NS0	scFv-CH3	N.d.	60 mg/L
SP2/0	IgG	Serum free	300 mg/L
GS-NS0	IgG	Fermentor, fed-batch	2.7 g/L
CHO-S	IgG	Fermentor	4.7 g/L
Transgenic plants			
Arabidopsis thaliana	Fab	Leaves	1.3, 3–6% total soluble protein
Medicago sativa	IgG	Leaves	0.1–1% total soluble protein
Nicotiana tabacum	V_{HH}	Leaves	28–136 mg/kg
	scFv	Leaves	1% soluble protein
	Fab	Leaves	0.044% total soluble protein

TABLE 30.1. *(Continued)*

Host Prokaryotes	Antibody Format	Production System	Maximal Yield
	IgG	Leaves	1.3% total protein
	IgG	Leaves	0.04–0.16% total protein, 1.56 mg/kg
	IgG	Suspension culture	37.6 mg/kg
Oryza sativa	scFv	Leaves	1.5–29 mg/kg
Petunia hybrida	scFv	Leaves	1% total soluble protein
Triticium aestivum	scFv	Leaves	50–900 μg/kg
Transgenic animals			
Mouse	IgA	Milk	5–6 g/L
	IgG-RNase	Milk	0.8 g/L
	IgG	Milk	0.5 g/L

[a]Based on data collected by Schirrmann T, *et al*. Production systems for recombinant antibodies. Front Biosci 2008;13:4576–4594.
[b]Five times higher yield was obtained after fusion to glucoamylase.

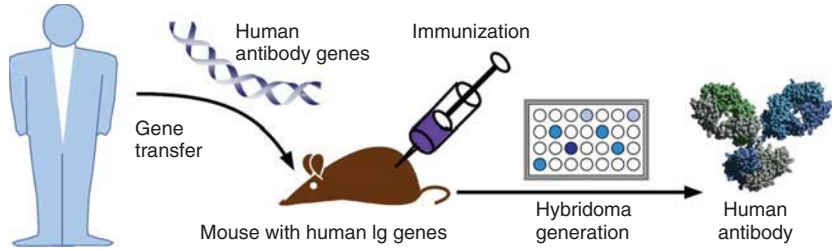


Figure 30.5. Human antibodies can be generated by obtaining hybridoma cell lines from immunized mice carrying the human Ig gene locus. (This figure is available in full color at http://onlinelibrary.wiley.com/book/10.1002/9780470054581.)

Two major methods were conceived. First, transgenic mice have been made to yield hybridomas secreting antibodies with human sequence. Second, a couple of methods allows the selection of antibodies completely *in vitro*, that is, outside of any immune system.

30.4.1 Transgenic Mice

With the help of genetic methods, individual genes can be specifically inactivated (*knockout*) and foreign genes can be introduced in mice (*knockin*). Therefore mice are bred whose immunoglobin gene locus has been inactivated and replaced by homologous stretches of the human immunoglobin genes. Human antibody genes rearrange in the same way as mouse genes; they can undergo class switching and somatic hypermutation. After immunization, these transgenic mice produce human antibodies in mouse cells, which (as apposed to human hybridoma cells) can easily be used to generate mouse hybridomas (Fig. 30.5). This serves as a system for the production of human antibodies, which methodically resorts to the large experience with mouse hybridoma technology avoiding the problems with the generation of human hybridomas. However, this system is based on the conventional method of immunization. This prevents the production of antibodies against substances with low immunogenicity, toxins, or lethal pathogens. Affinity maturation occurs analogous to the human immune system, so that high affinity antibodies can also be obtained. These methods have already been introduced successfully for the production of a few therapeutically relevant human antibodies.

30.4.2 Selection of Human Antibodies *In Vitro*

There are three major elements needed to select a specific antibody. For the *in vitro* generation, these three basic elements have to be realized independent of the mammalian immune response:

1. the construction of the gene collection encoding the multitude of antibody genes (in the form of recombinant gene libraries);
2. the effective selection of the correct gene from this initial repertoire (typically with the help of a surface expression vector);
3. the improvement of affinity and specificity of a selected antibody fragment (through *in vitro* mutagenesis and re-selection using (2)).

For the ease of genetic manipulation and their fast growth, microorganisms are the most convenient hosts

to perform *in vitro* antibody selections. However, it is not too simple since antibody folding requires a complex molecular helper apparatus and an oxidative biochemical environment for the production of the disulfide bonds. Consequently, in bacteria, a production of functional antibody domains is first of all acquired through a fusion of the antibodies to a bacteria signal sequence, which leads to the secretion into the periplasmatic space (PS). This PS lies between the two cell membranes of gram-negative bacteria and contains a biochemical environment that, unlike the cytoplasm, allows the correct folding of the antibody and the correct formation of disulfide bonds.

30.4.2.1 Recombinant Antibody Gene Repertoires ("Antibody Libraries"). In transgenic mice used for making human antibodies, the human recombinant gene repertoire is present within the B lymphocyte population of the mouse (Fig. 30.5). In contrast, for all *in vitro* methods, this antibody gene repertoire has first to be generated. It is estimated that in humans more than 10^8 different antibody genes are available through the random combination of gene fragments. This genetic diversity can be extracted from B lymphocyte mRNA through polymerase chain reaction (PCR) with the help of oligonucleotide primer sets which bind to conserved sequences at the ends of the antibody gene. These PCR primers contain restriction sites, so that the antibody genes can be assembled in expression vectors. The PCR has to be performed for both the variable fragment of the heavy and the light chain to provide both the polypeptides of a functional antigen-binding site. A typical flow chart for the generation of an antibody library is given in Fig. 30.6. Antibody libraries can also be assembled from the complete set of human genomic sequences taken from our respective gene locus. Here, the native combinatorial assembly of V, D, and J domains could be repeated *in vitro*.

There is also a plethora of methods for the generation of an additional variety through the introduction of synthetic sequences. These mostly include randomized sequences, which largely increase the diversity in the region of the antigen contact site. Completely synthetic gene libraries have been generated using randomized CDR regions, but much care has to be taken to avoid that the possible sequence space (i.e. the total number of possible sequence combinations) does exceed the maximum number of clones which can physically be generated. This limitation results from the observation that many random sequences impede antibody production or folding, or do not provide sufficient rigidity to structurally maintain a high affinity binding site. Even when avoiding cysteins while creating randomized CDR variants, the 19 remaining amino acids provide about 10^9 different sequences if only seven positions are randomized. When randomizing more positions, it is obvious that the transformation efficiency of microorganisms becomes a limiting factor. Consequently, after initial failures, libraries using careful and limited randomization have proven to be useful.

30.4.2.2 Selection Systems for Recombinant Antibodies. After a recombinant repertoire of antibody genes has been created, the next step requires the selection of a single antibody out of these huge gene libraries. Conventional selection systems, requiring individual characterization of every clone to identify a hit, are not anymore applicable for the library sizes of "universal" antibody gene repertoires. Despite selection from blots obtained from arrays of gridded clones have been used to select binders from smaller repertoires (with less than a million members), all larger libraries require another selection principle. They are done in *Escherichia coli* or completely *in vitro*, and rely on physical linkage of the protein to its encoding gene. The *in vitro* selection systems, in contrast to transgenic mice, do not require a complete immunoglobin, but instead use the antigen-binding fragment, generally either in the form of a single chain Fv fragment (scFv) or in the form of a Fab fragment (given below and in Fig. 30.2).

30.4.2.2.1 Cellular Display. The underlying principle of the *in vitro* selection systems is to imitate our immune system by physically coupling function (antigen-binding domain) and genetic information (antibody coding nucleic acids) into one particle (Fig. 30.7)—very much like the immune system does with the IgM-presenting B cells. For *in vitro* selections, such particles can be bacteria or yeast cells, with the antibody fragments anchored to the cell surface, while the encoding gene is carried on a plasmid inside. Selection can be achieved by affinity enrichment of the cells on antigen, or in a Fluorescence Activated Cell Sorter (FACS), after labeling with fluorescently labeled antigen.

30.4.2.2.2 Ribosomal/Molecular Display. The most complex libraries, however, to date use the expression of antibody fragments on much smaller particles: either the surface of filamentous phage (M13) or directly linked to their mRNA.

Ribosomal/molecular display utilizes *in vitro* transcription/translation systems for the generation of antibody fragments from PCR amplified gene fragments. These antibody fragments, after completing their synthesis, keep being linked to their encoding mRNA. This is achieved by either the lack of a stop codon preventing the ribosome from leaving the mRNA/antibody complex and thus keeping them together, or a chemical linker (puromycin) between the mRNA and the freshly synthesized polypeptide chain of the antibody fragment. The advantage that library size is not limited by transfection efficiency of bacteria is however, countered by the low efficiency of antibody folding in the cytoplasmic extracts

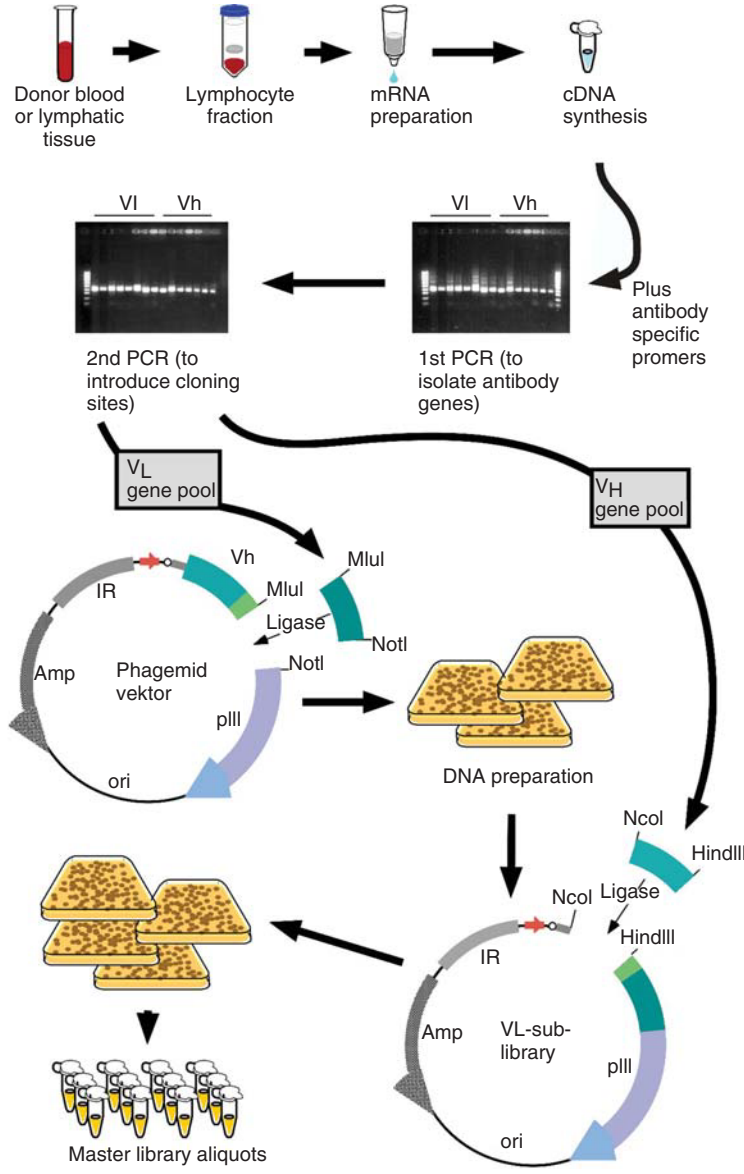


Figure 30.6. Experimental flowchart for the production of an antibody genetic library for phage display. (This figure is available in full color at http://onlinelibrary.wiley.com/book/10.1002/9780470054581.)

used for *in vitro* transcription/translation. For this reason, antibody selections from large "universal" libraries by ribosomal/molecular display remain difficult.

30.4.2.2.3 Phage Display. Phage display has developed into the most robust and thus most widely employed *in vitro* antibody selection system in the past 18 years. Through the combination of the peptide display principle demonstrated by George P. Smith in 1985 with the possibility of production of antibody fragments in the PS of *E. coli*, a method was created for the *in vitro* selection of antibody fragments by their binding characteristics (Fig. 30.8).

Phage display is based on the fusion of scFv or Fab fragments with a surface protein, normally pIII (minor coat protein, gene III product, g3p) of the filamentous phage M13. Fusions with pVIII have not really proven to be practical. As a result of this fusion, the antibody fragment is exposed on the outside of the virion. In a step similar to affinity chromatography, called "*panning*," specific antibody gene-containing particles are selected from a mixture of more than 10^9 different phages by their binding capability under biochemical conditions that can be completely controlled. After elution from the antigen, the enriched

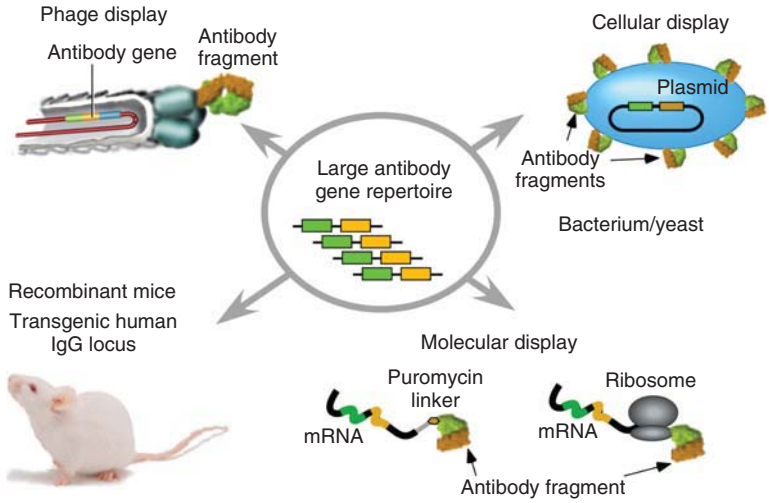


Figure 30.7. Recombinant selection systems for antibodies from gene repertoires. (This figure is available in full color at http://onlinelibrary.wiley.com/book/10.1002/9780470054581.)

phage is used to re-infect *E. coli* cells and thus can be multiplied and propagated, leading to an immortal monoclonal cell line producing the encoded antibody fragment. It is important to the understanding of the potential, but also the possible experimental problems of phage display, to realize that here the molecular interactions of single, individual protein molecules are utilized for selection. Therefore, it is of paramount importance to decrease the unspecific binding to avoid unspecific enrichment. Further, it has been observed that the affinity of the best isolated antibody is proportional to the diversity of the initial library. Phage display has matured to a method nowadays that allows us to obtain human antibody fragments for virtually any antigen.

Furthermore, phage display can be employed for humanizing monoclonal mouse antibodies. For this purpose the genes of a Fv or Fab fragment to be humanized are cloned in a phage selection vector and expressed as a fusion protein on the phage surface. The gene fragment of the light and heavy chains, respectively, are then sequentially substituted by a library of human antibody genes (chain shuffling, see above), followed by re-selection on the antigen. Through the introduction of mutations into CDRs or the entire variable regions, followed by reselection using phage display, the affinity of an antibody fragment for an antigen can be increased by orders of magnitude (affinity maturation).

30.5 PRODUCTION OF RECOMBINANT ANTIBODIES

Recombinant antibodies, mainly in the form of antigen-binding fragments are usually initially selected and characterized in *E. coli* (see above). *E. coli*, however, only has a limited suitability for the production of recombinant antibodies. Small functional fragments of immunoglobins can easily be produced in *E. coli*, whereas production of complete IgG molecules has only been achieved in rare cases. The reason for this is the complexity of the molecule (four chains, many intra-/ intermolecular disulfide bridges) and the folding pathway involved, which is available in mammalian cells, but not in *E. coli*. A secretion into the periplasm is therefore essential for domain folding. This limits the overall yield to only a small fraction of the cytoplasmic synthesis capacity of the bacterium. *In vitro* re-folding methods have been tried, but they suffer from low yields of functional molecules.

Due to the presence of an outer membrane, the production of antibodies in gram-negative bacteria requires a laborious processing by partial lysis, in order to obtain the periplasmatic extracts.

The optimal conditions for folding and glycosylation are only provided by the cells of the mammalian immune system, which are responsible for antibody production in our bodies. For example, in order for the antibody to bind the complementary component C1q or the cell surface receptor Fc receptor (FcR), a correct glycosylation of Asn297 of the CH2 region is necessary. If however only the antigen binding without Fc effector functions is required, it is easier to produce the scFv, dsFv (disulphide-stabilized Fv), or Fab fragments in yeast or bacteria. The production in transgenic animals is only then recommended if a large number of correctly glycosylated antibodies are required. Table 30.1 describes production systems for recombinant antibodies and their fragments.

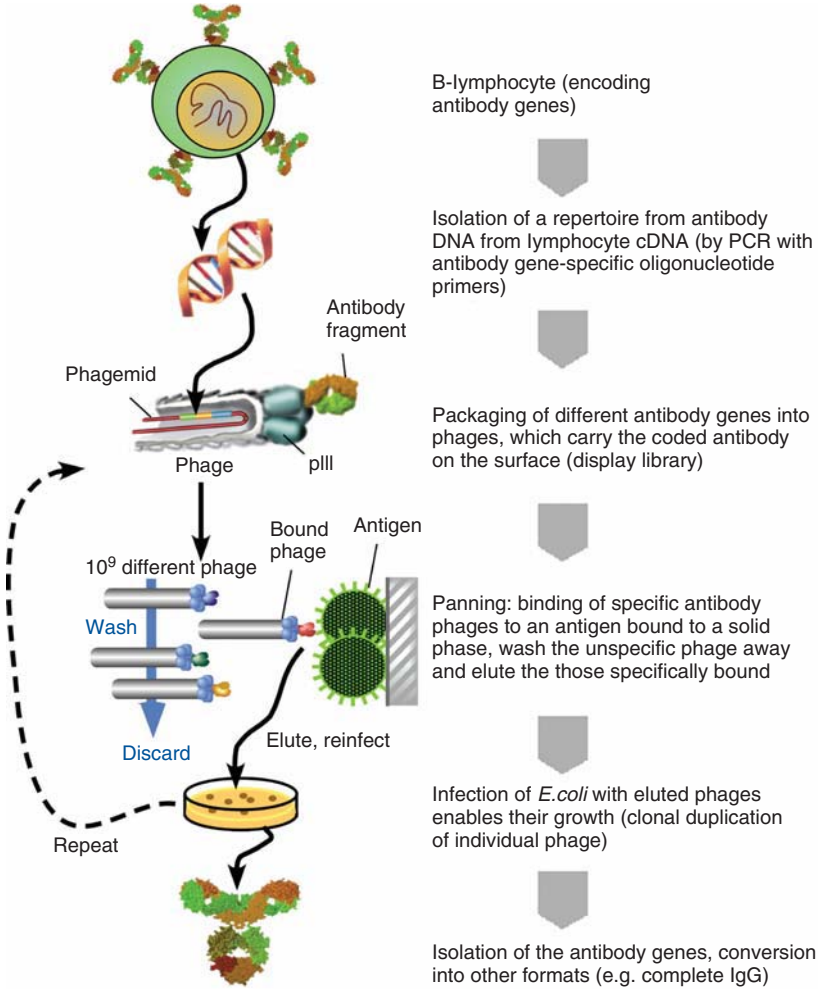


Figure 30.8. Experimental flowchart of the selection of an antibody fragment using phage display. (This figure is available in full color at http://onlinelibrary.wiley.com/book/10.1002/9780470054581.)

30.6 RECOMBINANT ANTIBODY VARIANTS

Numerous modifications of the constant domains of complete IgG molecules have been carried out. By changing the isotype (exchange of the C domains) the type of interaction with the immune system is affected. After identification of binding sites on the Fc fragment cellular receptors, it is possible to modulate the binding characteristics of IgG antibodies via specific mutations of amino acids that code for different receptors. This can lead to improved pharmacokinetic characteristics. Particular influence on therapeutic efficacy is attributed to the glycosylation pattern of the antibodies. Here, by using either selected cell lines with improved glycosylation or recombinant cells carrying a genetically changed repertoire of sugar processing enzymes, glycosylation can be optimized upon production, and nowadays even achieved in non-mammalian cells, like yeast.

Many modifications, however, are done on the antigen-binding site, leading to a multitude of different variants with very different biochemical and pharmacokinetic properties, which are described in the following section.

Even if the antigen-binding characteristics of a monoclonal antibody in relation to its specificity and affinity appear ideal, its therapeutic use can be limited by its isotype. The different isotypes are defined through the structure of the constant domain and affect the type of the effector molecule, which is activated after antigen binding. Many stem cells exhibit receptors for the Fc fraction of an immunoglobin and therefore induce an antigen-independent background binding.

In applications which require the infiltration of an antibody in specific cells or the localization of an antigen, for example, tumor imaging, it can be an advantage to reduce the size of an antibody through removing domains from or even completely deleting the Fc fragment, respectively.

Antibodies too small to be retained by the filtration limit of the kidney (approximately 60 kDa), suffer a very rapid clearance from the plasma. This only may be of advantage if rapid clearance is beneficial, for example, in case of some radionuclide labeled antibodies used for imaging.

30.6.1 Fab Fragments

In contrast to the normal (bivalent) IgG, Fab fragments are monovalent molecules. This results in a reduction in their apparent binding affinity compared with the complete antibody if the antigen is present in several copies close to each other. Fab fragments no longer have the ability to form a precipitate with antigens. In solution they are as stable as the complete IgG molecule, since their protein chains are linked via a disulphide bridge. When produced in *E. coli*, the necessity for the synthesis of two different chains and their association in the periplasm means that the yield is decreased in comparison to single proteins.

30.6.2 Single Chain Antibody Fragments (scFv)

The Fv fragment of an antibody consists of the variable domains of the heavy (V_H) and light (V_L) chain. It constitutes the smallest entity of a human immunoglobin, which includes a complete antigen-binding site. Due to the often relatively low affinities of their variable domains to each other, Fv fragments are rarely successfully produced in *E. coli*. Additional stabilization elements are necessary in order to prevent the dissociation of both subunits of the Fv fragment.

One possibility to kinetically stabilize Fv fragments is to attach their V_H and V_L domains with the help of a short peptide to create so-called scFv or sFv (Figs 30.2 and 30.6). The peptide linker has to bridge the distance from 3.2–4.3 nm in order to allow the correct steric arrangement of both domains. Therefore flexible, hydrophilic 15–20 amino acid long spacer peptides are used, typically linking the carboxyl-terminal end of V_H with the amino-terminal end of the V_L domain. The frequently used $(G_4S)_3$ linker has been especially proved through its protease resistance and its large conformational flexibility.

ScFv fragments (26 kDa) usually have an antigen-binding activity comparable to the Fab fragment (50 kDa) of the same antibody. Compared to Fv or Fab fragments, the construction of a single scFv gene strongly simplifies the production and phage display of recombinant antibodies. If the expressed protein domains exist on a polypeptide chain, the association of the V_H and V_L domains requires no further biomolecular reaction, but just an intramolecular rearrangement. Here the concentration of both domains in the previous reaction space is high, their association to the Fv module is favored, so the scFv fragments are kinetically stabilized. A disadvantage of this format, however, is that labile scFv molecules at high concentrations tend to form aggregates. A low affinity of the variable domains of a scFv module for each other leads to their temporary dissociation, after which the variable domains of a scFv fragment can associate with one of the others. This results in the formation of dimers, oligomers, and aggregates. The rate of dissociation depends on the length of the linkers as well as other external factors and the germ line origin of the V region sequence.

30.6.3 Single Chain Fab Fragments (scFab)

Recently it has been shown that the introduction of a polypeptide linker between the Fd and LC chains of an antibody can have beneficial effects for production of Fab fragments. This strategy combines the advantages of Fab (additional constant domains improve stability and provide detection by routine secondary antibody reagents in research) and scFv (better *E. coli* production). Particularly helpful to improve the yields was the elimination of the disulfide bond between Fd and V_L.

30.6.4 Disulfide-Stabilized Fv Fragments (dsFv)

An alternative approach to the stabilization of Fv fragments lies in the introduction of mutations in the scaffolding regions of both variable domains, which lead to the formation of a covalent linkage between the two contact surfaces. Structural analysis has identified pairs of amino acids in the complementary framework regions of the V_H and V_L domains, which, when mutated to cysteine, are positioned at exactly the right distance from each other for the formation of disulfide bridges. These dsFv fragments usually exhibit similar, antigen-binding activity than their homologous scFv fragments. They show improved stability against heat, denaturing agents and proteases. Due to the direct covalent linkage between the contact surfaces of their variable regions they also tend not to aggregate at high concentrations. Some dsFv fragments have been reported to more stable in blood serum than their homologous scFv fragments, which seems however not to be a general advantage, since other scFv fragments with already extremely good stability have been described as well.

30.6.5 V_H and Camel Antibodies

Many experiments have been carried out to minimize further the antigen-binding region of an immunoglobin. It has been attempted to separately express the V_H domains as the smallest functional entity of an antibody. However, this caused a lack of interaction with the corresponding V_L domain and therefore the exposure of the hydrophobic contact surfaces, which in turn lead to reduced solubility and stability. A loophole appeared here for the expression of

V_H domains of immunoglobins from camels and their relatives, since a fraction of their immunoglobulins are naturally formed from the heavy chains only. The improved solubility of these antibodies arise from substitution of amino acids on the surfaces which would normally be masked by the variable region of a light chain. Through the absence of the V_L domains, the complexity of this antibody repertoire is reduced. This is compensated with a CDR3 region longer and more heterologous than in human antibodies. So-called *single domain* V_H antibodies are typically isolated from immunized camels and llamas. S*ingle domain* V_H antibody gene libraries derived from human genes are successfully used as well, utilizing the lessons learned from camels.

30.6.6 Antibodies with New Functions

For many therapeutic *in vivo* applications, especially, for example, against tumor associated antigens, the antibody binding alone is often not sufficient to achieve a therapeutic effect. After the antigen binding, further steps are necessary for a successful destruction of the tumor tissue. For this reason, many hopes are aimed at the development of antibodies carrying an additional effector element. The antibody fragment mediates the specific binding to the target cell, whereas the heterologous part assumes the desired effector function. For example, for immune scintigraphy, antibody-bound radio nuclides are used. Through their decay, nuclides reveal the exact position of the tumor-bound antibody. The fusion of an antibody fragment with a toxin results in a specifically binding cell toxin. Cytokines, growth factors such as interleukin-2 (IL-2), interleukin-12(IL-12), and granulocyte/macrophage colony-stimulating factor (GM-CSF) as well as liposomes, viruses, or finally entire effector cells (T bodies) have been implemented as further fusion partners. Alternatively, an enzyme fused to the antibody can turn a nontoxic precursor molecule into a toxic substance, thus killing the adjacent tumor cell. This concept is named antibody-directed enzyme prodrug therapy (ADEPT).

30.6.7 Oligovalent and Bispecific Antibodies

Natural immunoglobins, especially the *ten-armed* IgM antibody have a significantly higher apparent affinity to antigens available in several copies close to each other comparison to the respective monovalent Fab fragments. This is essentially a result of reduced dissociation of the antibody, where multiple interactions with two or more antigens, for example, from the cell surface, allow the re-binding of an initially dissociated Fv module, without the entire molecule leaving the surface. This effect is called *avidity*. For recombinant antibody variants, an analogous increase of avidity can be achieved when Fab or scFv fragments are combined to form dimers, trimers, or large complexes.

The production of bivalent recombinant $F(ab')_2$ fragments was initially done by oxidation of the reduced cysteine of their *hinge* region. In addition, monovalent Fab fragments were expressed in *E. coli*, purified and subsequently combined to homodimers by oxidation. Meanwhile, the direct production of functional bivalent $F(ab')_2$ fragments in bacteria was also successful. Unpaired cysteine residues were found to be useful for the dimerization of Fv or scFv fragments *in vitro* or *in vivo*.

An elegant method for the production of multivalent antibody fragments is the reduction of the linker length between the variable domains of a scFv fragment, which significantly influences the molecular architecture of the resulting construct. If this peptide bond is reduced to less than 8–12 amino acids, for sterical reasons both of the variable domains of a scFc polypeptide chain are no longer able to associate to an Fv fragment. Instead, the complementary domains of two scFv molecules come together and form a homodimer, a so-called *diabody* (50 kDa) with two antigen-binding sites. If the peptide linker is decreased even further in length, to less than three amino acids, or if the variable regions are fused directly together, the scFv fragments usually associate as *triabodies* (75 kDa) or also *tetrabodies* (100 kDa). As well as the length and the composition of the linker, the primary structure and orientation of the variable domains of the scFv molecule influence the exact molecular architecture of the scFv construct.

A second antibody with a different specificity can also serve as an antibody fusion partner. In the last few years such bispecific antibodies have gained particular importance in the diagnostics and therapy of malignant tumors, as they have the ability to effectively bring two molecules or cells together. This concept is now proven by the recent approval of the first bispecific antibody for clinical use (catumaxomab for the treatment ascites). Here, cells from the immune system are introduced into the tumor, compensating the lack of recognition of a tumor cell by the immune system.

Typically, tumor-specific antibodies are bound to a second antibody fragment, which can activate the immune system. At the same time, surface molecules such as CD3 or CD28 are used as target molecules for cytotoxic T cells, CD16 for natural killer (NK) cells, or CD64 for macrophage. In addition, bispecific antibodies have been described which can introduce viruses into tumor cells for gene therapy; here, one of the antibodies binds to the virus and the other to a receptor on the surface of the target cell. An alternative use of bispecific antibodies is the simultaneous binding of two different, but adjacent, surface epitopes of the same target molecule. These constructs have a significant advantage of avidity and specificity over monospecific antibodies.

In order to produce bispecific antibodies, two IgG molecules were initially joined together via a simple chemical coupling. However, such complexes, at around 300 kDa, are too large to ensure effective tumor penetration. Their connected Fc parts can also bind to other somatic cells with the corresponding receptors and induce a relatively high background effect. The production of bispecific immunoglobins via the fusion, two different hybridomal cell lines that leads to hybrid–hybridoma (or quadroma) cells has also been attempted. However, through the random combination of different heavy and light immunoglobin chains, 90% of the immunoglobin variants are wrongly assembled immunoglobins, which are difficult to remove in subsequent purification. To avoid this, different bispecific recombinant antibody constructs with molecular masses of between 60 and 120 kDa have been developed, that on the one hand are small enough to enable the rapid penetration of a tumor, and on the other hand they are large enough to prevent their filtration through the kidneys, and finally they accumulate effectively and specifically in the target tissue. In contrast to immunoglobins produced with hybridoma technology, recombinant antibodies can be modified and combined with other genes or gene fragments with little effort. The recombinant production of bispecific antibodies also avoids the non-functional by-products of quadromas.

A large range of recombinant coupling strategies have been developed, that are usually either based on the introduction of a dimerizing domain at the end of the C-terminal of two antibody fragments or on the direct fusion of the genes of both partners. One of these such methods for the production of bispecific antibodies is the direct fusion of two scFv fragments forming so-called tandem antibodies.

The diabody design was also employed for the construction of bispecific antibody fragments. The genetic fusion of the variable domains of two antibodies A and B via the formation of two crossover polypeptide chains (V_HA-V_LB and V_HB-V_LA) results in a significant number of the desired bispecific molecules in addition to homodimers. The fraction of functional heterodimers compared to the inactive homodimers is increased significantly via the introduction of *knob-into-hole* mutations at the V_H/V_L contact surfaces. Diabodies have already been described, which couple colon carcinoma cells to serum immunoglobins, whereby inducing phagocytosis, the complement cascade as well as a T-cell response to tumor cells.

As a further example, C1q targeted bispecific diabodies activate the complement cascade against the target cell. In addition, bispecific antibodies have been produced against surface proteins of immune effector cells, such as CD3 for T cells, and different surface molecules, which are overexpressed in specific tumor cells, such as CEA, Ep-CAM, Her-2, or CD19.

A constructional dependent disadvantage of the diabody format is that the contact surfaces of the variable domains are not covalently linked. The lack of constant domains can result in the typical dissociation of scFv fragments' variable domains with subsequent formation of aggregates. This problem of stability has been partially solved through the expression of single chain diabodies (sc diabodies), tetravalent tandem diabodies, knob-into-hole diabodies, and also through the formation of disulfide stabilized diabodies (ds diabodies).

In an alternative approach to the production of bivalent and bispecific molecules, the interaction of constant domains of the immunoglobins is exploited. For example, bivalent *minibodies* are generated by the fusion of a scFv fragment with the C_H3 domain of an IgG, which serves as a dimerization domain. The production of bivalent antibodies is also achieved through the fusion of a scFv fragment with the constant domains of an IgG heavy chain. These strategies are admittedly not very suitable for producing bispecific heterodimers due to the symmetrical formation of the product. Nevertheless, the dimerization of bispecific single chain diabodies through their fusion with the C_H3 domain or the entire Fc part of an antibody has been successful. Bispecific minibodies have been produced through the fusion of a scFv fragment with the constant domain of the light chain, as well as the fusion of the other scFv fragment with the constant C_H1 domain of the heavy chain. The association of both of the different constant domains then resulted in the *in vivo* formation of bispecific heterodimers. In the previously described cases, the antigen bound Fv fragments, analogous to native IgGs, were always fused with the N-terminal of the constant domains. Alternatively, scFv fragments can also be fused with the C-terminal of C_H1-, C_L-, C_H3-domains or with hinge regions, to generate such Fab scFv or Fab $(scFv)_2$ constructs with two or three antigen-binding sites. Fusion with bispecific $(scFv)_4-IgG$ molecules, $(Fab\ scFv)_2$ or $IgG-(scFv)_2$ fusion proteins generate constructs with four antigen-binding sites.

Another set of designs rely on the use of heterologous peptides or proteins as oligomerization domains. The short leucine zipper motif of the two transcription factors *fos* and *jun* are useful here. These oligopeptide motifs from transcription factors form secondary structures which tend to dimerize by the formation of *coiled coils*. This type of peptide could be used for the production of bivalent and bispecific antibodies. Other helical structures have been used as tetramerization domains for the formation of tetravalent antibody molecules according to the same principle. Following formation of four-helix bundles, they dimerize and are used for the production of bivalent and bispecific scFv antibody constructs with two or four antibody-binding sites, respectively. Larger multivalent multimer scFv fusion proteins have been obtained through the use of protein domains such as Streptavidin, the tetramerization domain of the p53

protein, or the octamerization domain of the C4 binding protein.

30.7 APPLICATIONS OF RECOMBINANT ANTIBODIES

At present, about 24 antibodies are approved for clinical use, on a fast growing list. Over 500 antibody-based products are presently being developed. Because about a decade is needed to develop and approve therapeutics, the antibodies approved today reflect the state of the art of *antibody engineering* from 10 years ago. From 1988 until the middle of the 1990s, recombinant humanization or chimerization was used as the method of choice, while by now, recombinantly produced complete human antibodies from transgenic mice and phage display enter development in increasing numbers. An overview of approved antibody products is given in Table 30.2.

The next generation of antibody therapeutics will include more examples using the possibilities of the bifunctionality/bispecificity approach or fusion proteins when compared to the currently approved therapeutics, most of which consist of IgG molecules made in CHO cells.

The methods developed for the *in vitro* generation of human antibodies have also opened up new opportunities for areas where a human origin is not essential, but which benefit from the advantage of the recombinant process. Despite commercial contractors of recombinant antibody production are usually focused on obtaining therapeutic antibodies, a growing number of academic initiatives now employ *in vitro* antibody selection to create the large numbers of antibodies needed for future proteomic and systems biology approaches. Three cases where these recombinant technologies are of particular advantage, or even offer the only way to succeed, are described below.

30.7.1 Recombinant Antibodies can be Selected to Avoid Cross Reactivity

The advantage of recombinant production of antibodies is that it allows to select binders to toxic substances or with specificities, which cannot be achieved with immunization. For example, highly specific antibodies against the heroin metabolite 6-mono-acetyl-morphine (6-MAM) could be obtained from a phage display library, which in contrast to the previously available mouse antibodies, can distinguish between this indicator of drug abuse and other morphines (e.g. those contained in cough syrup). This was achieved by adding the unwanted antigens as competitors during panning. The use of very complex mixtures (even whole cell extracts) as competitors has been successfully demonstrated, for example, to avoid the selection of antibodies to host cell proteins on the surface of membranous virus particles.

TABLE 30.2. Clinically Approved Antibody Products (In Chronological Order of Approval as of 2009)

Name (Product/Antibody)	Origin/Type	Indication	Year of Approval
Orthoclone®(Muromonab-CD3)	Mouse hybridoma	Graft rejection	1986
ReoPro® (Abciximab)	Chimeric, Fab	Platelet aggregation	1994/-1997
Humaspect® (Votumumab)	Human, radiolabelled	Colon cancer *in vivo* diagnostics	1996
Rituxan® (Rituximab)	Chimeric	Non-Hodgkin's lymphoma	1997
Zenapax® (Daclizumab)	Humanized	Graft rejection	1997
Simulect® (Basiliximab)	Chimeric	Graft rejection	1998
Synagis® (Palivizumab)	Humanized	Respiratory syncytial virus	1998
Remicade® (Infliximab)	Chimeric	Rheumatoid Arthritis, Morbus Crohn	1998/–1999
Herceptin® (Trastuzumab)	Humanized	Breast cancer	1998
Mylotarg™(Gemtuzumab ozogamicin)	Humanized immunotoxin	Leukemia	2000
Campath® (Alemtuzumab)	Humanized	Leukemia	2001
Humira® (Adalimumab)	Human	Rheumatoide arthritis	2002
Xolair® (Omalizumab)	Humanized	Asthma	2003
Bexxar®(Tositumomab-I131)	Maus, radioactives conjugate	Non-Hodgkin lymphoma	2003
Raptiva® (Efalizumab)	Humanized	Psoriasis	2003
Erbitux® (Cetuximab)	Chimeric	Colon cancer	2004
Avastin® (Bevacizumab)	Humanized	Colon cancer	2004
Tysabri® (Natalizumab)	Humanized	Multiple sclerosis	2004
Lucentis® (Ranibizumab)	Humanized, fab	Macular degeneration	2006
Vectibix® (Panitumumab)	Human	Colon cancer	2006
Soliris® (Eculizumab)	Humanized	Paroxysmal nocturnal hämoglobinurie (PNH)	2007
Cimzia® (Certolizumab pegol)	PEGylated humanized fab	Morbus Crohn, Rheumatoid Arthritis	2008
Simponi® (Golimumab)	Human	Rheumatoid arthritis	2009
Removab® (Catumaxomab)	Mouse/rat bispecific	Ascites	2009

30.7.2 Intracellular Antibodies

In many cases, the deactivation of the antigens inside the cell has been attempted by the expression of antibody fragments in the cytoplasm. This has frequently failed due to the inadequate folding of the antibody (intracellular antibody, intrabody) in the reduced environment of the cytoplasm. Success could be achieved if the natural intracellular IgG production pathway was used. Antibodies with signal sequences as well as retention signals for the endoplasmic reticulum (peptide sequence: KDEL) have been shown to knock down molecules form the secretory/membrane pathway. This offers a novel approach for functional genomics, in particular, since potentially useful antibodies are provided by research initiatives in increasing numbers. Here, a knock down phenotype of an unknown open reading frame can be observed requiring just one subcloning of the selected scFv into a respective eukaryotic vector and transfection to a suitable system.

30.7.3 Recombinant Antibodies for Proteomics and Interactomics

After sequencing of the human genome, there is an enormous demand for binding molecules for the further functional analysis of the new genes. Here, antibodies are the tools of choice for the biochemical and cell biological characterization of the gene products and their functions (immunoblots, immunohistology, FACS, purification, pull-downs, etc.). The use of hundreds of different antibodies in a *protein microarray* (proteome chip) is already being intensively evaluated. Many proteins have splice form polymers or complexes. The availability of binders able to discriminate between these different forms is essential for the understanding of gene function, and can only be assessed on the post-translational/protein level. To systematically study the interactions of proteins (*interactomics*), antibodies are the agents of choice for the enrichment of complexes from various cells and tissues prior to the proteomic analysis by 2D-gels or mass spectrometry. Therefore, the demand for antibodies is rapidly increasing beyond the supposed number of human 22,000 genes. Without recombinant technology the production of these antibodies would require around one million animals! The effort of producing an antibody against every gene product and their relevant variants can therefore be best accomplished with a highly parallel *in vitro* selection approach, such as phage display.

30.8 OUTLOOK

Despite all of the recent success stories of recombinant human antibodies, they do not mark the end of the development, but just the start. As we understand more and more of the complex molecular interactions between immune cells or in cancer tissues, and in expectation of a significant speed-up of knowledge gain from the "-omics" and systems biology approaches, we can endeavor to expand the design limits of a future antibody drug. Fascinating concepts are under evaluation in hundreds of labs. There are so many ideas—and so many parameters affecting therapeutic efficiency to be learned about—that the development of recombinant human antibody therapeutics will not reach saturation for any foreseeable time. Further, major technology patents which blocked some developments in the past are expired or close to do so. Given that only the first generation of antibody drugs just has been approved in significant numbers, given the availability of recombinant human antibodies and the vast number of targets in the developer's pipelines plus the advent of completely novel therapeutic strategies using antibody fusion proteins, therapeutic antibodies look forward to a golden future.

FURTHER READING

Benny KC, editor. Antibody engineering: methods and protocols (Methods in molecular biology). Totowa, NJ: Humana Press; 2003. ISBN: 1588290921. (collection of relevant protocols)

Breitling F, Dübel S. Recombinant antibodies. New York: John Wiley & Sons, Inc.; 1999. ISBN: 0471178470 (introduction to basic principles and applications)

Dübel S, editor. Handbook of therapeutic antibodies. Weinheim: Wiley-VCH; 2007. ISBN-10: 3-527-31453-9. (comprehensive three volume resource for the entire topic)

Kontermann R, Dübel S, editors. Volume 2, Antibody engineering. Heidelberg, New York: Springer; 2010. ISBN: 3540413545,. (collection of relevant protocols)

Monoclonal Antibody Index (MAI), Barcelona 2005ff. (collection of data on therapeutic antibodies, updated regularily)

Subramanian G, editor. Antibodies: Volume 2, Novel technologies and therapeutic use. Heidelberg, New York: Springer; 2004. ISBN: 0306483157.

Urch CE, George AJT, editors. Diagnostic and therapeutic antibodies (Methods in Molecular Medicine). Totowa, NJ: Humana Press; 2000. ISBN: 0896037983.

REVIEWS

Brekke OH, Sandlie I. Therapeutic antibodies for human diseases at the dawn of the twenty-first century. Nat Rev Drug Discov 2003; 2: 52–62.

Carter PJ. Potent antibody therapeutics by design. Nat Rev Immunol 2006; 6: 343–357.

Chowdhury PS, Wu H. Tailor-made antibody therapeutics. Methods 2005; 36: 11–24.

Dübel S. Recombinant therapeutic antibodies. Appl Microbiol Biotechnol 2007; 74: 723–729.

Gavilondo JV, Larrick JW. Antibody engineering at the millennium. Biotechniques 2000; 29: 128–132.

Groner B, Hartmann C, Wels W. Therapeutic antibodies. Curr Mol Med 2004; 4: 539–547.

Haurum J, Bregenholt S. Recombinant polyclonal antibodies: therapeutic antibody technologies come full circle. IDrugs 2005; 8: 404–409.

Hudson P, Souriau C. Engineered antibodies. Nat Med 2003; 9: 129–134.

Hust M, Thie H, Schirrmann T, Dübel S. Antibody phage display. In: An Z, Strohl W, editor. Handbook of therapeutic monoclonal antibodies: Wiley-VCH; 2009. ISBN-10: 0-470-11791-5.

Huston JS, George AJ. Engineered antibodies take center stage. Hum Antibodies 2001; 10: 127–142.

Krauss J, Arndt M, Dübel S, Rybak SM. Antibody-targeted RNase-fusion proteins (ImmunoRNases) for cancer therapy. Curr Pharm Biotechnol 2008; 9: 231–234.

Monoclonal Antibodies and Therapies. Supplement of Nature Biotech. 2004 (collection of reviews)

Presta LG. Engineering antibodies for therapy. Curr Pharm Biotechnol 2002; 3: 237–256.

Reichert JM. Probabilities of success for antibody therapeutics mAbs. 2009; 1: 387–389.

Reichert JM, Rosenzweig CJ, Faben LB, Dewitz MC. Monoclonal antibody successes in the clinic. Nat Biotechnol 2005; 23: 1073–1078.

REMARK: THIS CHAPTER IS BASED ON AND/OR CONTAINS MATERIALS DERIVED FROM OF OTHER CHAPTERS WRITTEN BY THE SAME AUTHOR IN DETAIL:

Dübel S. Recombinant antibodies and phage display. In: Wink M, editor. An introduction to molecular biotechnology. Weinheim: Wiley-VCH; 2006. pp. 479–509. ISBN 3-527-31412-1.

Dübel S. Therapeutic antibodies - from past to future. In: Dübel S, editor. Handbook of therapeutic antibodies. Weinheim: Wiley-VCH; 2007. pp. 3–16. ISBN-10: 3-527-31453-9.

31

ANTIFOAMS AND PLURONIC POLYOLS, CELL PROTECTION

David W. Murhammer
University of Iowa, Iowa City, Iowa

31.1 INTRODUCTION

Animal cell cultures are widely used in the production of some products (e.g. complex recombinant DNA proteins) because of the inability of other expression systems (e.g. bacteria) to properly perform posttranslational modifications (e.g. glycosylation and proper folding). Unfortunately, animal cells lack a protective cell wall and thus are subject to damage from sparging and other environmental stresses. In large-scale bioreactors, however, aerating the cultures through direct sparging is the most practical method of supplying oxygen to the culture medium. Therefore, in order to realize the full potential of using animal cells to produce recombinant DNA proteins on an industrial scale, there is a critical need for large-scale sparged bioreactors capable of supporting animal cell growth. Currently, the generally accepted approach to solving this problem is to supplement the medium with a protective agent, such as the commercially available surfactant Pluronic F-68.

31.2 PROPERTIES OF PLURONIC POLYOLS

A wide range of Pluronic polyols are available that are capable of protecting animal cells in suspension cultures from the adverse effects of sparging. Of these, Pluronic F-68 is by far the most widely used. Properties of Pluronic polyols that are relevant to the selection of a protective agent are discussed in this section.

31.2.1 Synthesis and Structure

Pluronic polyols, commercially available from the BASF Corporation (Wyandotte, Mich.), are block copolymer nonionic surfactants consisting of a center block of poly(oxypropylene) (hydrophobe) and end blocks of poly(oxyethylene) (hydrophile). They are synthesized by the two-step process shown in Fig. 31.1 (1). In the first step, a poly(oxypropylene) block is synthesized by the addition of propylene oxide to propylene glycol. The poly(oxyethylene) blocks are then added to both ends by reacting the resulting poly(oxypropylene) with ethylene oxide. The oxyalkylation steps are carried out in the presence of an alkaline catalyst (e.g. potassium hydroxide) that is subsequently neutralized and removed from the final product. The properties of the Pluronic polyols are altered by varying the relative sizes of the poly(oxypropylene) and poly(oxyethylene) blocks (note that the sizes of the two poly(oxyethylene) blocks are statistically identical). The properties of a variety of Pluronic polyols are given in Table 31.1.

31.2.2 Nomenclature

The letters L, P, and F in the Pluronic polyol nomenclauture represent liquid, paste, and flake, respectively (Table 31.1) (1). The first two digits of the three-digit polyol number or the first digit of a two-digit polyol number are indicative of the hydrophobe [poly(oxypropylene)] molecular weight; for example, 6, 8, and 12 represent average hydrophobe

Upstream Industrial Biotechnology: Expression Systems and Process Development, Volume 1, First Edition. Edited by Michael C. Flickinger.
© 2013 John Wiley & Sons, Inc. Published 2013 by John Wiley & Sons, Inc.

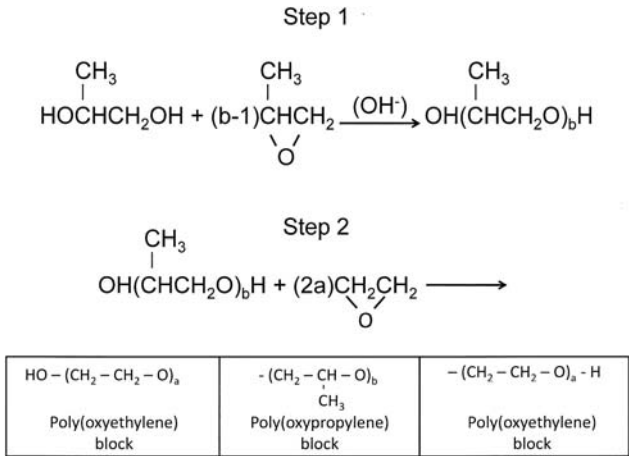


Figure 31.1. Pluronic polyol synthesis.

molecular weights of 1750, 2250, and 4000, respectively. The last digit in the polyol number represents approximately 1/10th the percentage of hydrophile [poly(oxyethylene)] in the molecule. For example, Pluronic F-68, a flake (i.e. a white powder), has a hydrophobe molecular weight of approximately 1750, and contains approximately 80% hydrophile.

31.2.3 Impurities

Commercial-grade Pluronic polyols have been demonstrated to contain low molecular weight impurities, including aldehydes, formic acid, and acetic acid (3,4). In addition, peroxide derivatives of the Pluronic polyols can be formed during steam sterilization. The formation of the peroxide derivatives can be prevented by filter sterilizing the Pluronic polyol solutions instead of using steam sterilization. The low molecular weight impurities can be removed from aqueous solutions of Pluronic polyols by silicagel column absorption (3).

31.2.4 Hydrophilic–Lipophilic Balance

The hydrophilic–lipophilic balance (HLB) is an empirical measure of the emulsifying capabilities of surfactant molecules (5). Lower values of the HLB are representative of molecules with a higher degree of hydrophobicity. In general, molecules with high HLBs tend to be water soluble, and those with low HLBs tend to be oil soluble. The HLBs given in Table 31.1 are given in terms of ranges to indicate that the effective HLB of the Pluronic polyols varies with the emulsion system (6). From the results given in Table 31.1, it is clear that Pluronic polyols with low HLBs are unsuitable for use as protective agents because medium supplemented with 0.2% (w/v) of these Pluronic polyols either lysed *Spodoptera frugiperda* Sf-9 cells or significantly inhibited their growth in the absence of sparging, specifically in 50-mL spinner flasks oxygenation by surface diffusion (2). It was further demonstrated that at higher HLB values, Sf-9 cell growth was not inhibited in the absence of sparging and that protection from the adverse effects of sparging was provided in airlift bioreactor studies. Thus, the key to finding a Pluronic polyol that served as a protective agent for the Sf-9 cells in a sparged environment corresponded to finding one that did not inhibit cell growth in the absence of sparging. It should be noted that the results may be different with other cell lines.

31.2.5 Foaming Characteristics

Excessive foaming is generally undesirable in animal cell cultures. Therefore, if Pluronic polyols that exhibit

TABLE 31.1. Pluronic Polyols Tested for Their Effect on *Spodoptera Frugiperda* Sf-9 Insect Cell Growth in the Absence and Presence of Sparging

Pluronic polyol	Average MW	wt% of Hydrophobe	HLB Range	Effect on Cell Growth in the Absence of Sparging	Protects From Sparging?
L-61	2,000	90	1–7	Cell lysis	N/A
L-121	4,400	90	1–7	Cell lysis	N/A
P-103	4,950	70	7–12	Cell lysis	N/A
P-123	5,750	70	7–12	Cell lysis	N/A
P-84	4,200	60	12–18	Cell lysis	N/A
P-104	5,900	60	12–18	Cell lysis	N/A
P-65	1,900	50	12–18	Inhibition	N/A
P-105	6,600	50	12–18	Inhibition	N/A
L-35	1,900	50	18–23	None	Yes
F-127	12,600	30	18–23	None	Yes
F-38	4,700	20	>24	None	Yes
F-68	8,400	20	>24	None	Yes
F-108	14,600	20	>24	None	Yes

MW, molecular weight.
Source: Adapted from Murhammer and Goochee (2)

unacceptable levels of foaming are used, either an antifoam should be added to the medium (2) or an alternative Pluronic polyol should be used (6). Of the Pluronic polyols given in Table 31.1, F-68, P-105, and P-65 are the most active foam generators (6) and other Pluronic polyols could be used if foaming is problematic (e.g. L-35 or F-127).

31.2.6 Surface Tension

Because the Pluronic polyols are surfactants, it would be expected that they would reduce the air–water static surface tension. Indeed, according to BASF literature (6), the addition of 0.1% (w/v) Pluronic polyols to aqueous solutions reduces the static surface tension from 72 dyne/cm for pure water to a range of 22 (L-121) to 52 dyne/cm (F-38). In addition, the static surface tension of a 0.1% (w/v) aqueous solution of Pluronic F-68 is 50 dyne/cm. Michaels *et al*. (7), however, have given a convincing argument that the dynamic surface tension is a more suitable measure for sparged systems since interfacial properties are sensitive to the physical state of the interface. They found that the reduced dynamic surface tension afforded by Pluronic F-68 addition correlated well with reduced cell–bubble interactions and thereby provided cell protection.

31.2.7 Oxygen Transport

Zhang *et al*. (8) found that the addition of Pluronic F-68 to growth medium had minimal effect on K_La values for large bubbles (~5 mm diameter), but significantly enhanced K_La for intermediate (~1 mm diameter) and micron-sized (~100 μm diameter) bubbles. It is generally accepted that surfactants can affect oxygen transport from bubbles in two different ways: affecting the diffusional resistance and affecting the interfacial area, K_L and a, respectively. The addition of surfactants usually results in decreased K_L (9) and in increased a (10). Consistent with this expected behavior, Zhang *et al*. (8) found that there was a significant reduction in the Sauter mean bubble size for the intermediate and micron-sized bubbles, thereby resulting in an increased a. Pluronic F-68 addition, however, had minimal effect on the size of the large bubbles. No measurements directly related to the K_L term were taken in this study, although the results clearly demonstrate that the presence of the Pluronic F-68 resulted in a greater increase in a than decrease in K_L. Recently, Lee and Kim (11) found that K_La increased with increasing Pluronic F-68 concentration up to 0.1% (w/v) and then remained essentially constant as the Pluronic F-68 concentration was increased from 0.1% to 1.0% (w/v). Although no data were provided regarding the effect of Pluronic F-68 concentration on bubble size, previous results from other researchers suggest that a increased (due to decreased bubble size) faster than K_L, with decreasing Pluronic F-68 concentration up to 0.1% (w/v), and that the effect on a and K_L were balanced at higher Pluronic F-68 concentrations.

31.3 PROTECTIVE EFFECTS OF PLURONIC POLYOLS

It has been clearly demonstrated that Pluronic polyols can protect insect and mammalian cells from the adverse effects of sparging. Evidence supporting this protective effect, as well as protection (or lack thereof) from shear and agitation damage, is discussed in this section. Furthermore, the corresponding mechanisms are discussed.

31.3.1 Sparging Damage

In 1968, Kilburn and Webb (12) were the first to report the use of Pluronic polyols to protect animal cells from sparging. Specifically, they found that supplementing the medium with 0.02% (w/v) Pluronic F-68 protected mouse LS cells from the adverse effects of sparging in short-term studies. They did not, however, show any results from long-term tests, such as an entire bioreactor run. No comprehensive studies regarding the use of Pluronic polyols to protect animal cells from the adverse effects of sparging were conducted until the late 1980s, when Handa-Corrigan *et al*. (13,14) and Murhammer and Goochee (2,15,16) demonstrated the ability of Pluronic F-68 to protect mammalian and insect cells. Handa-Corrigan *et al*. (13,14) demonstrated that the survival of a variety of mammalian cells (hybridomas, mouse myeloma [NS1] cells, baby hamster kidney [BHK-21] cells, and human lymphoblastoid [RAJI]) cells in the presence of sparging depends on cell type and bubble size and frequency (i.e. small bubbles and high flow rates are more detrimental). They further demonstrated that the protective effect of Pluronic F-68 was concentration dependent, with 0.1% (w/v) being sufficient to protect cells under the most severe conditions reported. Murhammer and Goochee (15) investigated the protective effect of Pluronic F-68 in both airlift and sparged agitated bioreactors. It was found that supplementing the medium with 0.1% (w/v) Pluronic F-68 resulted in a major protective effect and that 0.2% (w/v) provided full protection for Sf-9 cells grown in both types of bioreactors. It was also demonstrated that recombinant protein synthesis (produced after infection of the cells with a recombinant baculovirus) in the airlift bioreactor significantly decreased compared to the unsparged control even after increasing the Pluronic F-68 concentration to 0.5% (w/v). This was hypothesized to result from the increased susceptibility of virally infected cells to lysis in a sparged environment. This decrease in productivity was not due to an inhibitory effect of Pluronic

F-68 since it was found that recombinant protein production was not affected by Pluronic F-68 in the absence of sparging (15). This is in contrast to the results of Palomares *et al*. (17), who found that Pluronic F-68 significantly affects the recombinant protein and baculovirus production of baculovirus-infected insect cells in the absence of sparging.

After the development of conclusive evidence regarding the ability of Pluronic F-68 to protect mammalian and insect cell cultures from the adverse effects of sparging, the research focus in this field shifted to the mechanisms of this protective effect and of cell damage in the absence of protective agents. In regard to bubbles in sparged bioreactors, there are three regions in which cell damage could potentially occur: (i) the bubble formation region at the gas distributor; (ii) the rising bubble region between the gas distributor and medium surface; and (iii) the bursting bubble region at the medium surface. The results of Handa-Corrigan *et al*. (14) and Tramper *et al*. (18) clearly demonstrated that the primary source of cell damage is not in the region of rising bubbles in their bioreactor systems. Specifically, they demonstrated that cell damage decreased as the height of the bioreactors increased. In addition, Michaels *et al*. (19) demonstrated that cell-to-bubble interactions in the bulk of the bioreactor are not responsible for cell damage in studies, in which the headspace above the medium where bubbles can burst was eliminated. Murhammer and Goochee (16) demonstrated that it is possible to have cell damage in the sparger region and that this damage correlates with a high pressure drop across the sparger. In most practical applications (i.e. when the sparger is properly designed), however, significant cell damage occurs only at the medium surface in the bursting bubble region, as first proposed by Handa *et al*. (13). It has also been demonstrated that cells tend to adhere to air–medium interfaces and that fatal damage occurs to these attached cells as the bubbles burst at the medium surface; that is, the energy released by the bursting bubbles results in extensive cell lysis (20–23). Additional details of the mechanisms involved with cell damage in sparged bioreactors are discussed in a review chapter by Wu (24).

Michaels *et al*. (25) suggested that the protective effect of Pluronic polyols could result either from a biological mechanism (i.e. through changes in the cells' ability to resist shear) or from a physical mechanism (i.e. through changes in the medium properties that affect the level of frequency of forces experienced by cells). They concluded that the protective effect of Pluronic F-68 in sparged bioreactors is caused by a physical effect. Consistent with this hypothesis, it was later demonstrated that the protective effect of Pluronic F-68 resulted from its ability to cover the medium–bubble surface and thereby prevent cell adhesion to the bubbles (23,26). Thus, cells are not in the immediate vicinity of bursting bubbles at the medium surface.

It has also been demonstrated that Vero cells grown on microcarriers are damaged in sparged bioreactors (27). It was suggested that the addition of Pluronic F-68 to the medium may be able to protect cells grown on microcarriers from the adverse effects of sparging. It has subsequently been demonstrated, however, that the addition of Pluronic F-68 does not protect animal cells from spaaging damage in microcarrier cultures (28).

Although Pluronic F-68 has become the predominantly used additive to protect insect and mammalian cells from sparging damage, other additives have also demonstrated effectiveness. For example, Murhammer and Goochee (2) demonstrated that many other Pluronic polyols could serve as protective agents (Table 31.1). Furthermore, Chattopadhyay *et al*. (23) and Wu *et al*. (29) have shown that other substances that lower liquid–vapor interfacial tension at a sufficiently rapid rate can protect cells from sparging.

31.3.2 Agitation Damage

Although a few studies have reported that supplementing the medium with Pluronic F-68 can protect attachment-independent cells growing in suspension from agitation damage (30), this is generally not a relevant issue because insect (16) and mammalian (19) cells are commonly tolerant to relatively high agitation rates. For example, it was found that Sf-9 cell damage did not occur unless the agitation rate was high enough to induce bubble incorporation via cavitation or vortexing (16). Furthermore, supplementing the medium with Pluronic F-68 protected the cells from damage caused by bubble incorporation by either of these mechanisms. It is assumed that the corresponding mechanisms of cell damage without Pluronic F-68 and protection by Pluronic F-68 are similar to those reported above for sparged bioreactors.

In spite of the lack of evidence demonstrating that Pluronic F-68 can protect cells from agitation damage, there is some evidence that Pluronic F-68 can make cells more resistant to shear damage. For example, Goldblum *et al*. (31) demonstrated that the addition of Pluronic F-68 (0.2% and 0.3% [w/v]) to the medium protected Sf-9 and *Trichoplusia ni* Tn-368 insect cells from shear damage in viscometer studies in a concentration-dependent manner. In contrast to these results, Michaels *et al*. (25) found that Pluronic F-68 did not make hybridoma (CRL-8018) cells more shear tolerant. These results suggest that the ability of Pluronic F-68 to increase a cell's shear tolerance may be cell line dependent. Direct interaction with the cell (e.g. incorporation of the hydrophobic portion of Pluronic F-68 with the cell membrane) is a possible mechanism through which Pluronic F-68 may increase the shear tolerance of cells. Several lines of evidence are consistent with an interaction of Pluronic F-68 with the cell membrane. First, Pluronic polyols of low HLB values

lyse cells (Table 31.1). Secondly, Pluronic F-68 inhibits the uptake of trypan blue dye that would normally be taken up in the absence of Pluronic F-68 (15). Thirdly, treating sickled erythrocytes with Pluronic F-68 decreases their rigidity (32). Finally, Pluronic F-68 increases the fluidity of hybridoma membranes, which correlates with increased resistance to shear (33).

31.4 APPLICATION

If attachment-independent insect or mammalian cells are to be grown in sparged bioreactors, then it is recommended that the medium be supplemented with a Pluronic polyol. Many commercially available serum-free media already contain Pluronic F-68; therefore, additional supplementation may not be necessary. If supplementation is necessary, then a 10% (w/v) aqueous solution of Pluronic F-68 (obtained from BASF Corp.) can be prepared and filter sterilized. This solution can then be used to supplement the medium at 0.1–0.2% (w/v) Pluronic F-68. Ready-made solutions of Pluronic F-68 are also commercially available (e.g. Invitrogen, Carlsbad, CA; Mediatech, Inc., Herndon, VA; Sigma–Aldrich Company, St. Louis, MO). The resulting medium should first be tested in the absence of sparging (e.g. in spinner or shaker flasks) to detect any potential inhibitory effects. Note that purification of the Pluronic F-68 (as mentioned above) may be necessary to remove inhibitory impurities. The next step is to test the ability of the medium to protect cells in small-scale sparged bioreactors. Success in protecting the cells at this scale is a good indicator of similar success in large-scale sparged bioreactors. The use of Pluronic F-68 allows sparging with micron-sized bubbles that significantly enhance culture oxygenation. If Pluronic F-68 is not successful, then many other Pluronic polyols are available for testing (Table 31.1). Another concern is that Pluronic polyols may interact with the protein of interest and interfere with downstream purification (34). Winzerling *et al*. (35) have demonstrated, however, that recombinant insect transferrin can be purified from Sf-9 cell supernatant containing 0.1% (w/v) Pluronic F-68 by using high metal ion capacity gel chromatography. Finally, it should be noted that surfactants (e.g. Pluronic F-68) in the medium may clog chromatography columns and thus it may be desirable to remove the Pluronic F-68 from the medium, which can be accomplished through dialysis, prior to introducing to the column (36).

REFERENCES

1. Schmolka IR. J Am Oil Chem Soc 1977; 54: 110–116.
2. Murhammer DW, Goochee CF. Biotechnol Prog 1990; 6: 142–148.
3. Bentley PK, Lowe KC, Johnson OL, Sharma SK, Washington C, Davis SS. J Pharm Pharmacol 1988; 40(Suppl):143P.
4. Bentley PK, Gates RMC, Lowe KC, de Pomerai DI, Walker JAL. Biotechnol Lett 1989; 11: 111–114.
5. Becher P, Birkmeier RL. J Am Oil Chem Soc 1964; 41: 169–172.
6. BASF Publication, Pluronic and tetronic surfactants, Ludwigschafen, Germany: BASF; 1987.
7. Michaels JD, Nowak JE, Mallik AK, Koczo K, Wasan DT, Papoutsakis ET. Biotechnol Bioeng 1995; 47: 420–430.
8. Zhang S, Handa-Corrigan A, Spier RE. Biotechnol Bioeng 1992; 40: 252–259.
9. Sheppard JD, Cooper DG. J Chem Technol Biotechnol 1990; 48: 325–336.
10. Heijnen JJ, Van't Riet K. Chem Eng J 1984; 28:B21–B42.
11. Lee S-Y, Kim D-I. J Microbiol Biotechnol 2004; 14: 1129–1133.
12. Kilburn DG, Webb FC. Biotechnol Bioeng 1968; 10: 801–814.
13. Handa A, Emery AN, Spier RE. Dev Biol Stand 1987; 66: 241–253.
14. Handa-Corrigan A, Emery AN, Spier RE. Enzyme Microb Technol 1989; 11: 230–235.
15. Murhammer DW, Goochee CF. Biotechnology (NY) 1988; 6: 1411–1418.
16. Murhammer DW, Goochee CF. Biotechnol Prog 1990; 6: 391–387.
17. Palomares LA, Gonzalez M, Ramirez OT. Enzyme Microb Technol 2000; 26: 324–331.
18. Tramper J, Joustra D, Vlak JM. In: Webb C, Mavituna F, editors. Plant and animal cells. Chichester, England: Ellis Horwood Ltd.; 1987. pp. 125–136.
19. Michaels D, Mallik AK, Papoutsakis ET. Biotechnol Bioeng 1996; 51: 399–409.
20. Bavarian F, Fan LS, Chalmers JJ. Biotechnol Prog 1991; 7: 140–150.
21. Chamlers JJ, Bavarian F. Biotechnol Prog 1991; 7: 151–158.
22. Garcia-Briones M, Chalmers JJ. Ann NY Acad Sci 1992; 665: 219–229.
23. Chattopadhyay D, Rathman JF, Chalmers JJ. Biotechnol Bioeng 1995; 45: 473–480.
24. Wu J. J Biotechnol 1995; 43: 81–94.
25. Michaels JD, Petersen JF, McIntire LV, Papoutsakis ET. Biotechnol Bioeng 1991; 38: 169–180.
26. Jordan M, Sucker H, WIdmer F, Eppenberger HM. In: Spier RE, Griffiths JB, Berthold JB, editors. Animal cell technology: products of today, prospects for tomorrow, Oxford, UK: Butterworth-Heinemann; 1994. pp. 302–304.
27. Martens DE, Nollen EAA, Hardeveld M, van der Velden-de Groot CAM, de Grooijer CD, Beuvery EC, Tramper J. Cytotechnology 1996; 21: 45–59.
28. Bauer P, Hancock L, Rathman J, Chalmers JJ. Biotechnol Prog 2000; 16: 125–132.
29. Wu J, Daugulis AJ, Faulkner P, Goosen MFA. Biotechnol Prog 1995; 11: 127–132.
30. Mizrahi A. J Clin Microbiol 1975; 2: 11–13.
31. Goldblum S, Bae Y-K, Hink WF, Chalmers J. Biotechnol Prog 1990; 6: 383–390.

32. Smith CM, Hebbel RP, Tukey DP, Clawson CC, White JG, Vercellotti GM. Blood 1987; 69: 1631–1636.
33. Ramirez OT, Mutharasan R. Biotechnol Bioeng 1990; 36: 911–920.
34. Kioukia N, Nienow AW, Al-Rubeai M, Emery AN. Biotechnol Prog 1996; 12: 779–785.
35. Winzerling JJ, Pham DQ-D, Kunz S, Samaraweera P, Law JH, Porath J. Protein Expr Purif 1996; 7: 137–142.
36. SafcBiosciences Technical Bulletin. Removing surfactants from serum-free suspension media. http://www.sigmaaldrich.com/sigma/bulletin/t012.pdf. Accessed 2007 Jun 21.

32

BIOMINIATURIZATION OF BIOREACTORS

Michael A. Hanson
Bio-Manufacturing Sciences Group, Pfizer, New York
Govind Rao
Center for Advanced Sensor Technology, University of Maryland Baltimore County, Baltimore, Maryland

32.1 INTRODUCTION

For centuries, microorganisms have played an essential role in producing everyday commodities, such as alcoholic beverages and bread, as well as specialty items like medicines and enzymes. Throughout this time, submerged culturing of cells has emerged as the primary mode of cultivation. As demand for products has increased, so has the size of the vessels in which cells are grown, up to hundreds of thousands of liters (1). It is extremely expensive to execute these large-scale reactions due to the cost of supplies, energy, and equipment. Total costs can be minimized, in part, by making processes as efficient as possible. This is done by carrying out developmental experiments with the following objectives: (i) selection and genetic engineering of production strains, (ii) formulation of appropriate growth media, and (iii) optimization of bioreactor parameters and cultivation strategy (i.e. fed-batch vs perfusion). To achieve these goals, hundreds of development experiments must be carried out. Due to the reasons stated above, it is fairly obvious that experiments cannot be carried out at production scale. Also, since the length of the development timeline is inversely proportional to the number of experiments that can be carried out simultaneously, it is common practice to carry them out at a small scale in a high throughput and highly parallel manner.

Traditionally, strain selection and media development have taken place in flasks on the scale of 50–6000 mL (2). There are several related drawbacks to using standard shake flasks for these purposes. The first is the inability to monitor environmental conditions, most importantly pH and dissolved oxygen (DO) concentration, within flasks. Favorable behavior exhibited by production strains in flasks may not be displayed at production scale because of differences in environmental conditions, resulting in a process hampered by an inefficient, poorly chosen strain (3). Environmental monitoring would ensure strain selection under conditions comparable to the production scale. Similarly, during media development the importance of a specific media component may not be discernable if the productivity of the culture is being impeded by an unsuitable environmental condition, such as oxygen limitation. Without knowing the environmental state in the flask, these outcomes cannot be avoided. Related to these, is that without the ability to monitor environmental conditions, it is impossible to accurately control them. In addition to these monitoring-related shortcomings of flasks, higher throughput can be achieved with the reduced culture volumes afforded by other platforms, such as multiwell plates.

As mentioned previously, the third objective in upstream bioprocess development is to choose a cultivation strategy and optimize bioreactor parameters. Historically, this has occurred in lab scale bioreactors with volumes of up to tens of liters as opposed to smaller scale vessels. This is due to, again, the inability to monitor and control important process parameters in the latter. Lab-scale bioreactors are relatively low throughput in comparison to plates and flasks due to space requirements and various tasks that accompany their

Upstream Industrial Biotechnology: Expression Systems and Process Development, Volume 1, First Edition. Edited by Michael C. Flickinger.
© 2013 John Wiley & Sons, Inc. Published 2013 by John Wiley & Sons, Inc.

use, such as reactor sterilization, calibration of electrodes, and aseptic processing of fluids. Low throughput results in slow process develop-breakment. Ultimately, regardless of the platform used for bioreactor development, it must be able to provide a process solution that can be implemented at production scale.

Based on the proceeding discussion on shortcomings in traditional upstream development, it follows that the ideal culturing platform is one where (i) culture volume is small, (ii) the necessary information to compare scales is accessible, (iii) samples should be large enough to enable off-line assaying where needed, and (iv) development scale is able to provide a culture solution that is applicable at the production scale. These industrial needs have resulted in a sudden increase of research in the field of bioreactor miniaturization. Here it must be qualified as to what is meant by *bioreactor*: a culturing vessel that is equipped with sensors to monitor any number of critical process parameters. By definition, standard shake flasks and multiwell plates are excluded unless they have been equipped with monitoring capabilities.

Two key reviews of this field have been carried out recently by Betts and Baganz (4) and Kumar *et al*. (5). The previous review gave an overview of many small-scale technologies and some examples of their usage. The latter emphasized the engineering design and characterization of small-scale bioreactors and the future directions of the field. The current review will describe in detail the practical usage of many small-scale systems. In many situations, data will be presented where small-scale systems were compared to larger traditional systems. The reviewed systems were chosen based on the capabilities to monitor at the small scale or if they were particularly innovative and had at least some engineering characterization carried out. As in the other reviews, a method of mixing was used to organize the miniature bioreactor systems. Here we have used the following groups: static, shaken, stirred, bubble column, and convective flow.

32.2 BIOREACTOR MONITORING TOOLS

Over the years bioreactors have been equipped with a variety of tools for the on-line monitoring of environmental conditions and assessing the physiological state of cells. For industrial processes electrochemical probes are the standard means to observe culture broth conditions, while off-gas analyzers are used for gas exiting the reactor headspace. In general, these technologies have not been utilized at a small scale due to the size constraints imposed by such small volumes. Although microelectrodes have been developed and are commercially available (6), other problems still exist. For example, electrodes have stability issues due to the strain shaking imposes on wire-based connections.

For decades culture fluorescence has been used to assess the physiological state of cells, for instance, by determining their internal redox potential (7). More recently, the need for small-scale process monitoring has been a driving force for the development of optical sensors utilizing analyte specific fluorophores. In general, optical sensing in this way requires the following three steps: the fluorophores are (i) brought into physical contact with the material which contains their analyte; (ii) excited by light sources of characteristic wavelengths; and (iii) properties of the resulting emission are measured (8). Application of this technology has varied by changing the way in which fluorophores are exposed to analytes and how excitation and fluorescence detection is carried out. Different approaches will be described for many of the miniature bioreactor platforms presented here. For a more detailed look into fluorescence spectroscopy and its application, see *Principles of Fluorescence Spectroscopy* (8).

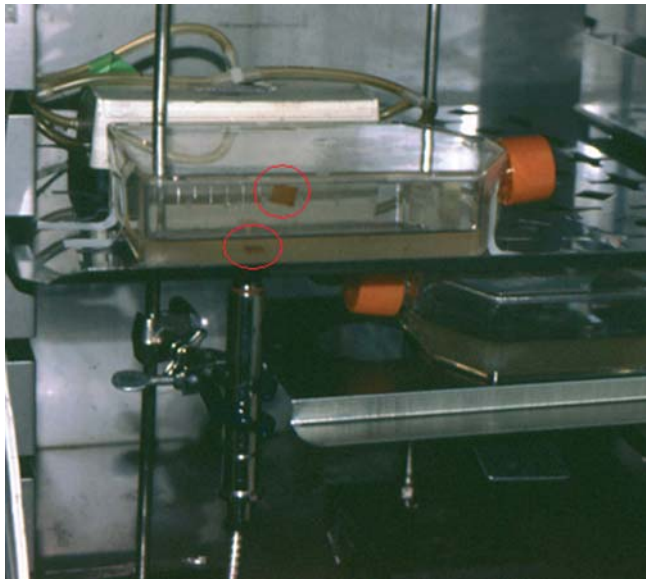
32.3 STATIC BIOREACTOR SYSTEMS

32.3.1 Tissue Culture Flasks (T Flasks)

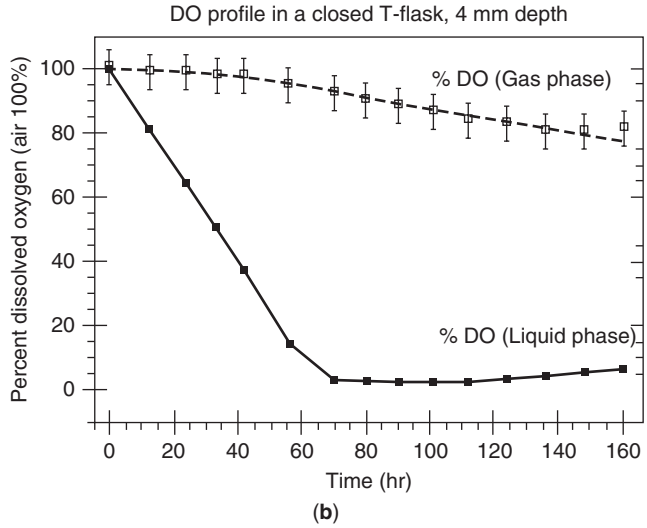
T-flasks are a common platform for small-scale mammalian cell culture. They are generally used for the expansion of selected clones, in industrial seed trains to generate inocula for spinner flasks and bioreactors, or just as simple vessels for which to carry out cell culture related experiments in. They are often coated with proteins, such as collagen or fibronectin, which make them ideal for the growth of adherent cells. Their skinny boxlike shape results in a large headspace aeration area to liquid volume ratio (A_S/V), enhances the diffusional mass transfer of gaseous species in and out of the media. Without convective mixing, diffusion is the sole mode of transport. Therefore, during culture a DO concentration gradient forms from saturation at the air-liquid interface to some lower percentage at the flask bottom.

The Clark-type electrode has been the standard method for measuring DO tension in bioreactors. However, based on several factors, it is not a feasible option for measuring DO concentration in T-flasks. First, the Clark-type electrode consumes oxygen to make its measurement. At low DO concentrations this is undesirable and can impact the accuracy of the reading. Also, based on its design and that of the T-flask's opening, the electrode is not suitable for making measurements in culture broth that is only several millimeters in height. Lastly, also based on design, the maintenance of sterility would be difficult.

Randers-Eichhorn *et al*. characterized the mass transfer of oxygen during the culture of mouse hybridoma cells by



(a)



(b)

Figure 32.1. (a) T-flask with DO sensor patches on the wall in the gas phase and on the bottom in the liquid phase. Located below the flask is the fiber optic used for fluorophore excitation and emission detection of the liquid-phase patch. (b) Liquid and gas-phase DO profiles obtained using optical sensors during the culture of hybridoma mouse cells (9). (This figure is available in full color at http://onlinelibrary.wiley.com/book/10.1002/9780470054581.)

fitting a standard T-flask with optical sensors in both the gas and liquid phases (9). Here an oxygen sensitive fluorophore was immobilized in sensor patches that were affixed to the inside sidewall and bottom of the T-flask (Fig. 32.1a). An external fiber-optic optrode was used to both excite the fluorophore and detect its emission. The DO profiles in Fig. 32.1b show DO concentrations near 0% air saturation at the bottom of the flask, and a gas-phase concentration of greater than 80% throughout the experiment justifies closing the T-flask lids completely.

32.4 MICROFABRICATED REACTORS

Since 2004, researchers at MIT have developed several versions of microfabricated microbioreactors with working volumes as low as 5 μL (10). A membrane aerated version, shown in Fig. 32.2, constructed out of poly(dimethylsiloxane) (PDMS) and glass was equipped with optical sensors for pH, DO, and optical density (OD). The top layer of PDMS served as the aeration membrane through which oxygen diffused into the reactor. Zanzotto *et al*. compared 5–50 μL *E. coli* fermentations carried out in this reactor and in 500 ml SixFors bioreactors (SixFors to be discussed in the Stirred Bioreactor Systems section). Run conditions in the larger reactors were configured to match the k_La of the smaller vessels. Fig. 32.3 shows the pH, DO, and OD profiles for this comparison. Samples for high performance liquid chromatography (HPLC) analysis of organic acids (data not shown) were obtained by sacrificing entire microbioreactors. In another experiment, the same bioreactor system and DNA microarrays were used to determine how gene expression changes upon switching from the complex to defined media (11).

The scale of bioreactors has been decreased even further to the realm of nanoliters using two-level soft lithography (12). The 4 cm^2 64-unit array and a 3-nL individual reactor are shown in Fig. 32.4. The C-shaped reactors were designed so that the opening was smaller than the cell size, trapping the cells within, and microfluidic controlled media flows in the rings surrounding the reactors, allowing the nutrients to diffuse through the opening. The array is not equipped with any sensors, but its transparency allowed for visualization after fluorescent staining. Lee *et*

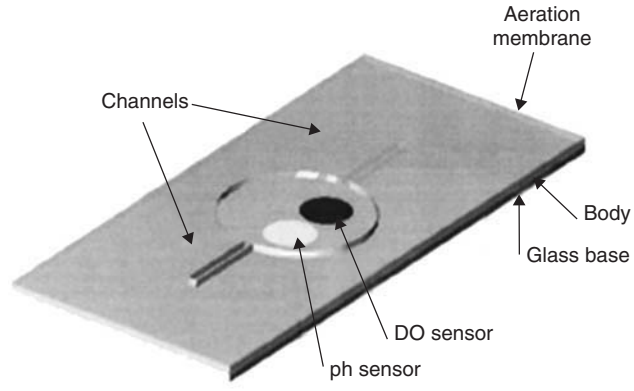


Figure 32.2. An optical sensor equipped microfabricated 50 μL bioreactor made of PDMS and glass (10).

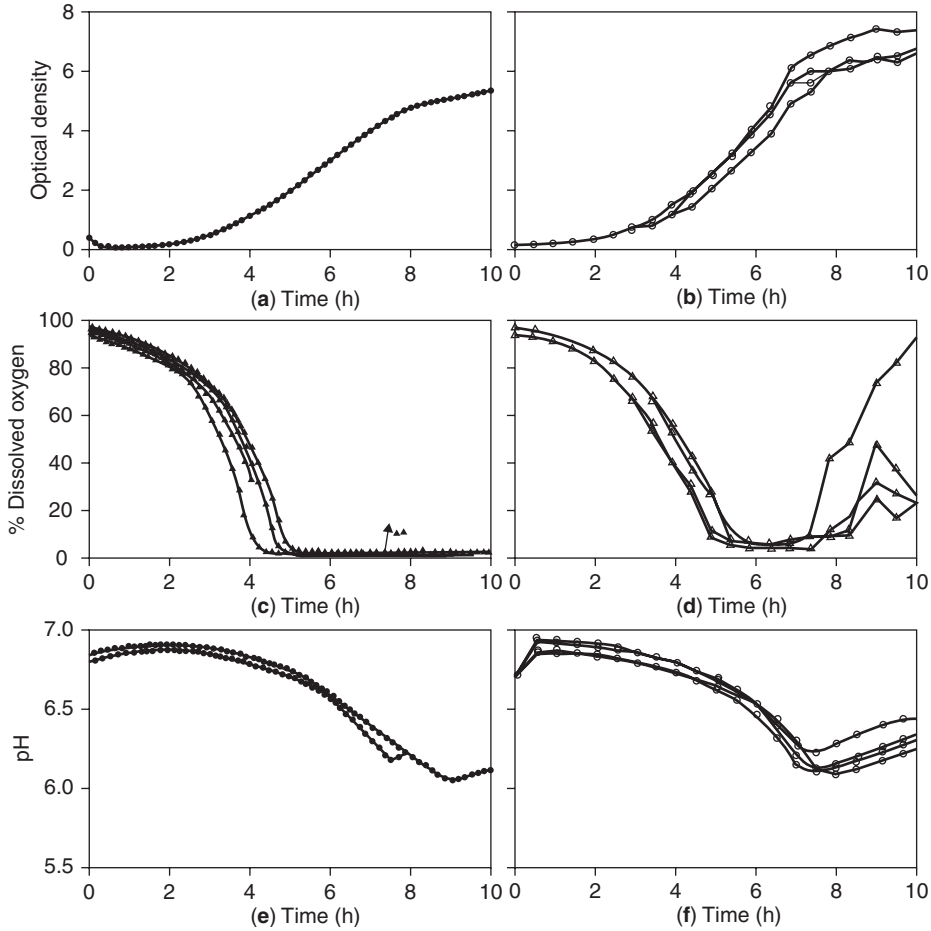


Figure 32.3. Replicate fermentations with *E. coli* in defined medium in the microbioreactor (shown in Fig. 32.2) and a bench-scale bioreactor: (a) OD in microbioreactor; (b) OD in bench-scale bioreactor; (c) DO in microbioreactor; (d) DO in bench-scale bioreactor; (e) pH in microbioreactor; (f) pH in bench-scale bioreactor (10).

al. demonstrated the utility of the system by observing the serum response of HeLa human cancer cells.

32.5 SHAKEN BIOREACTOR SYSTEMS

The goal during development is to expose cultures to a variety of conditions with the objective of finding ones where productivity (or some end goal) is maximized. Shaken systems are still the most high throughput approach we have for process development, enabling many conditions to be tested simultaneously. However, control over conditions is fairly limited in traditional shaken systems given the restricted number of variables we have to alter, and whether changing them affects individual bioreactors or groups. For instance, to investigate the impact of increased DO tension, the rotational rate of the shaker can be increased to raise the k_La. However, no differences would be observed amongst units on a single shaking platform since mass transfer in all the bioreactors would improve. In order to influence only a subset of reactors, their culture volume must be reduced, thus improving the transfer area to volume ratio. The flask closures could also be changed to ones with less transfer resistance.

Instead of only qualitatively controlling the reactor environment as described above, it is more empowering to have a quantitative measurement of to what extent conditions are changing. Sensors allow for this. This following section will describe how various sensors and apparatus have enabled the characterization and monitoring of cultures in shaken bioreactor systems.

32.5.1 Shake Flasks

The design of shake flasks is slightly more conducive to measurements with electrochemical probes as they can be fixed in a stopper at the top or inserted into specially made ports on the flask wall as shown in Fig. 32.5a (13). Hodson

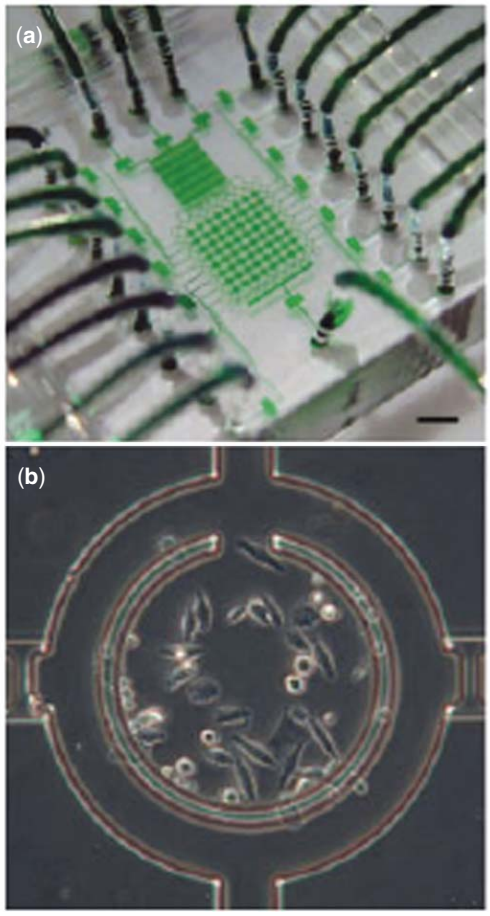


Figure 32.4. Nanoliter scale bioreactor for quantitative cell biology: (a) the 4 cm^2 64-unit array; (b) an individual 3-nL reactor (12). (This figure is available in full color at http://onlinelibrary.wiley.com/book/10.1002/9780470054581.)

used that system to monitor gas and liquid-phase oxygen concentrations (Fig. 32.5b) during the cultivation of *Bacillus subtillis*. An air purge device ensured that there was air saturation in the gas phase which was confirmed with the gas-phase sensor. Even in the early days of industrial biotechnology, the prevalence of oxygen limitation during microbial cultivation in large-scale fermentors was well know. As shake flasks were (and are) the primary tool for development, pioneering engineers wanted to know how much DO flasks could provide to growing cultures under defined (agitation speed, culture volume, liquid viscosity, etc.) conditions. There are various techniques to characterize the mass transfer in bioreactors, such as the gassing out, water evaporation, and sulfite oxidation methods. Change in flask mass due to water evaporation can be used to analyze gas transfer through shake flask enclosures (14). The sulfite oxidation method has drawbacks,for instance sampling at regular intervals (15). This technique and improvements of it will be described in the next section on *Multiwell Plates*.

The gassing-out method requires carrying out a mass balance over the liquid and/or gas phases within the flask. This requires one or more oxygen sensors depending on the analysis being carried out and the associated assumptions. For instance by tracking the oxygen concentration in a liquid-less flask during the gassing-out method, the resistance being measured is only that of the plug. Schultz carried this out finding that the density and dimensions of the plug impact its resistance to the oxygen flow (16). Tribe *et al*. warned of the large errors that are introduced into the mass transfer coefficient by the gassing-out method if the response time of the electrode is not taken into consideration (17). This caution was observed by Nikakhtari and Hill who developed and incorporated models for mass transfer into the growth and substrate utilization models of *Pseudomonas putida* fermentation in shake flasks while taking both the air-liquid interface and a variety of flask closures into consideration (18).

However, during the shake flask development many experiments are carried out simultaneously. Thus it becomes cumbersome to calibrate and sterilize each Clark-type electrode beforehand and maintain sterility during sampling throughout the experiment. All the wires running from the flasks to the data acquisition system could pose a logistical problem as well. Recently Vasala *et al*. developed a shake flask (Fig. 32.6) equipped with steam sterilizable "wireless" DO and pH electrochemical sensors (19). The flask has ports for the probes, which are connected to a small transmitter that is strapped to the flask. The transmitter broadcasts a signal to the receiver which is connected to the computer responsible for logging the data.

Another problem of using a liquid-phase DO electrode is that it becomes a baffle, confounding the mass transfer characteristics it is measuring. Anderlei *et al*. developed an oxygen transfer rate (OTR) measuring device, where OTR is defined as the rate at which a species is moving from gas to liquid phase (20). The specially made flask instead uses a gas-phase oxygen sensor in cooperation with computer controlled gas in- and out-let valves where the inlet was hooked up to a gas mixing system. By introducing defined concentrations of gas, and opening and closing the valves in a time defined manner, the phases shown in Fig. 32.7 are carried out, OTR can be determined during fermentation. This device is the basis for an advanced instrument, named the respiration activity monitoring system (RAMOS), capable of also measuring the carbon dioxide transfer rate (CTR) and thus the respiratory quotient (RQ) of cultures. The instrument is commercially available through AC Biotec GmbH (Jülich, Germany) (21). Freyer *et al*. used a prototype of the system to demonstrate the utility of using OTR as a scaling factor between scales (22) while Losen *et al*. used OTR via RAMOS to identify critical growth parameters, such as deficiencies in media components and

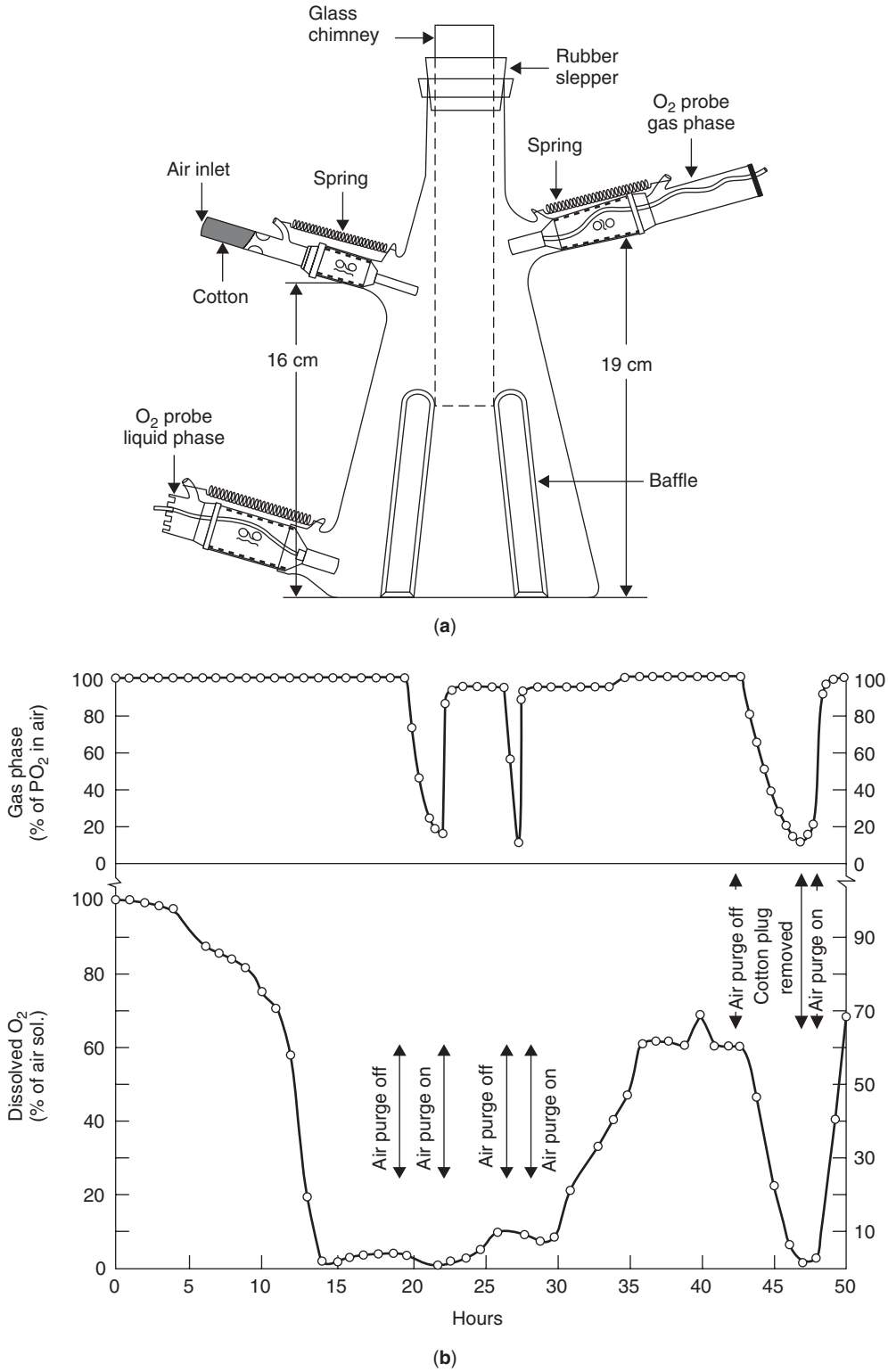


Figure 32.5. (a) A specially made shake flask with ports for gas and liquid-phase electrochemical oxygen probes and an air purge system to supply fresh air; (b) gas and liquid-phase oxygen concentrations during a 2-L shake flask cultivation of the *Bacillus subtilis* (13).



Figure 32.6. A wireless system for measuring pH and DO in shake flasks. The system is composed of a specially designed flask, electrochemical pH and DO electrodes, a transmitter (shown strapped to the flask and in the picture to the right), and a receiver which interfaces to a computer for data storage and analysis (19). (This figure is available in full color at http://onlinelibrary.wiley.com/book/10.1002/9780470054581.)

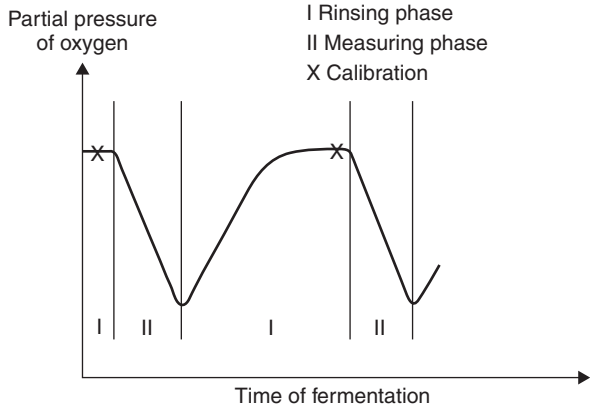


Figure 32.7. The sequence of phases during OTR determination using a sterile on-line device (20).

oxygen limitation (23). Short of actual culture broth DO data, OTR is a great solution to understanding the oxygen consumption during culture.

Optical sensors have provided a more manageable solution to monitoring in DO tension in shake flasks. Tolosa *et al*. demonstrated their first use in shake flask fermentations of *E. coli* and *S. cerevisiae* (24). The optical sensing setup is shown in Fig. 32.8. The oxygen sensing patch was affixed to the inside bottom of the shake flask. Both the flask and the coaster, which housed the optical instrumentation, were shaken. The system is designed to be modular enabling easy hookup to laptops or any available computer. Gupta and Rao used the same setup to characterize the combined resistance across the flask enclosure and the air-liquid interface (25). Fig. 32.9 shows the impact of enclosure type and addition of baffles on DO profiles during *E. coli* fermentation. The results comparing a shake flask fermentation to one carried out in a 1-L fermentor are shown in Fig. 32.10. The similarities in on-line DO, and offline OD and product expression via green fluorescent protein (GFP) fluorescence support scaling is based on k_La where enclosure is accounted for.

A complementary study of mass transfer in shake flasks with optical DO sensors manufactured by a different supplier was performed by Wittmann *et al*. (26). There k_La was quantified over several liquid volumes and agitation speeds and utilized in the fermentation of *Corynebacterium glutamicum*. A 45-s pause in shaking was necessary for the offline sampling of the culture. During this time a 20% drop in DO tension occurred which, if extrapolated on, would predict that all residual oxygen in the media would be consumed in about 2 min if the nonshaking persisted. This type of information is incredibly valuable when designing protocols to carry out screening experiments, and would not be available without monitoring on a small scale.

The pH monitoring in shake flasks has less attention than that of DO. This may be due to the fact that growth media is often buffered, leading researchers to believe that pH is not changing significantly. Also, in the case of cell culture media, a pH indicator, such as phenol red, is sometimes included in the media, enabling a rough estimate of culture pH. However, this is surprising given the pH sensitivity of microbial (27) and especially mammalian (28) cells. For use in shake flasks, electrochemical pH probes have many of the disadvantages already described for DO electrodes.

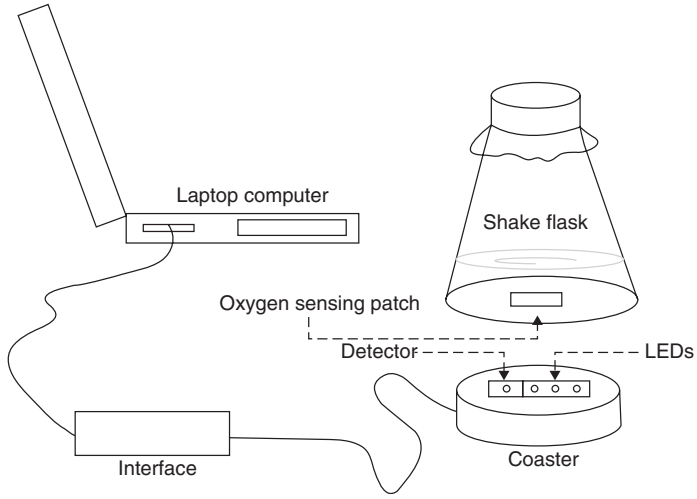


Figure 32.8. The setup for optical DO sensing in shake flasks. The system consists of a flask with an immobilized sensor patch on the bottom, a coaster that houses the optical instrumentation, and an interface which converts the data for storage and analysis in the laptop (24).

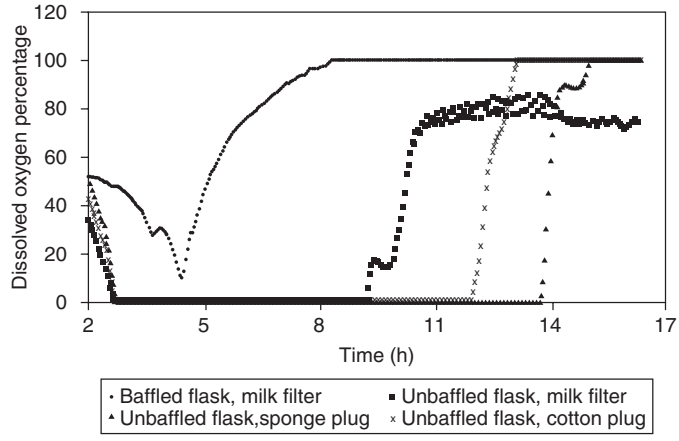


Figure 32.9. Use of the optical DO sensing platform is shown in Fig. 32.8 to measure the impact of flask baffling and various enclosures on DO profiles during *E. coli* fermentations (25).

For the same reasons, optical pH sensors have been developed. Optical monitoring of pH was first demonstrated in a shake flask by Kermis *et al*. during fermentation of *E. coli* (29). A setup similar to that for DO in Fig. 32.8 was employed where the pH sensing patch used here is shown in Fig. 32.11a. A comparison of the on- and off-line pH values are shown in Fig. 32.11b.

The pH monitoring and control was demonstrated by Weuster-Botz *et al*. in the fed-batch parallel shake flask system pictured in Fig. 32.12 that is commercially available from DASGIP AG (Jülich, Germany) (30,31). The pH was monitored during *E*. coli cultivation using pH electrodes inserted in ports of flasks made specially for the system and controlled starting at 4.5 h into the experiment (Fig. 32.12b). Differences between on- and off-line pH measurements were not accounted for.

Another parallel flask shaking system, shown in Fig. 32.13a, developed by Akgun *et al*. was designed for continuous culture (32). The specially made flasks used in their system were fully characterized based on filling volume, substrate feed rate, outlet height, shaking diameter, aeration rate, and shaking frequency. Fig. 32.13b shows that the same dilution rate in a continuous culture comparison between this system and a 1-L bioreactor resulted in the same steady-state biomass and substrate concentrations, as well as ethanol produced.

In designing a screening system, the goal is to make as many parameters as similar to the production scale as possible. Thus far, tools for quantifying transport and process monitoring have been discussed. However, there are other parameters of interest. Buchs *et al*. designed a device to measure power consumption (per unit volume) in culture

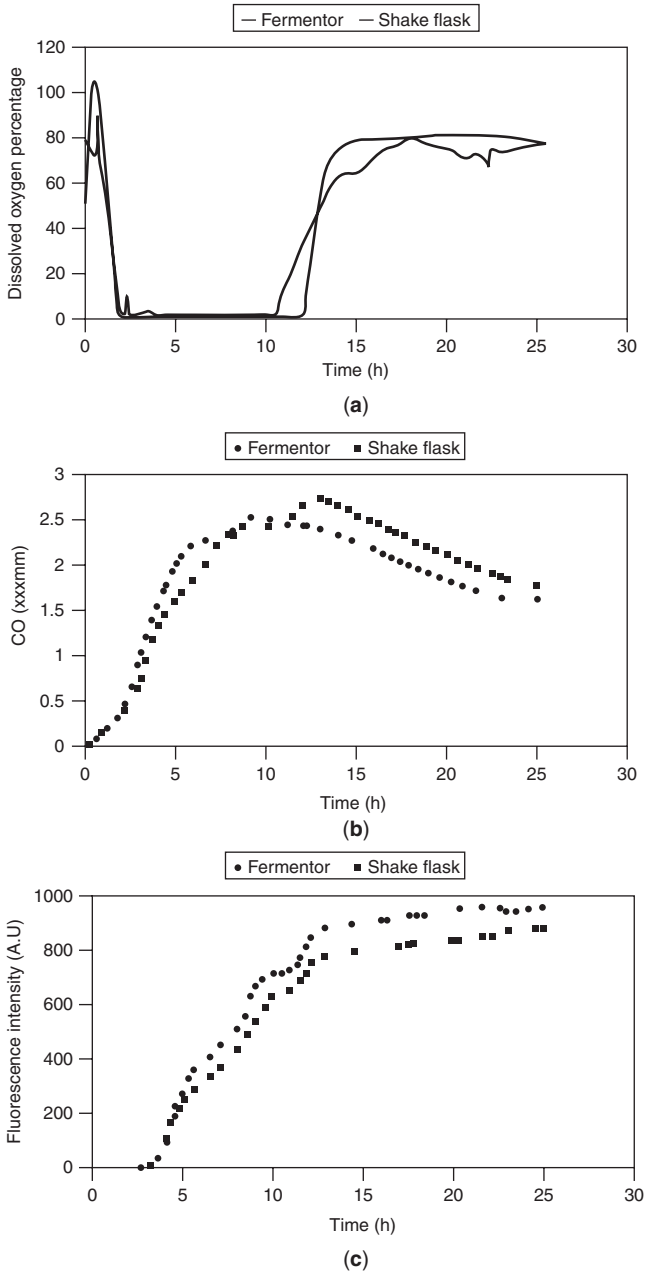


Figure 32.10. A comparison of *E. coli* fermentations carried out in a shake flask and a 1-L fermentor. (a) On-line DO, (b) offline OD, and (c) GFP expression are shown for the two systems (25).

broth, which plays an essential role in the fermentation of microbes and is regarded as one of the critical values for characterizing and upscaling cultures (33). Another parameter of importance is the extent of hydromechanical stress imposed on cells. Peter *et al*. measured this via energy dissipation rate (EDR) (34). EDR was correlated with a maximum stable drop size in a coalescence inhibited liquid/liquid dispersion.

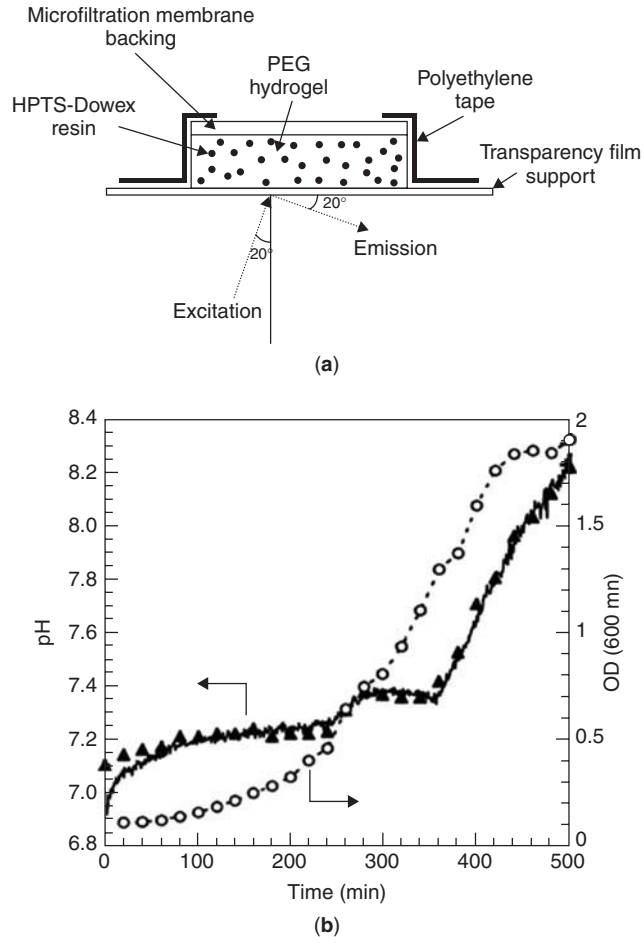
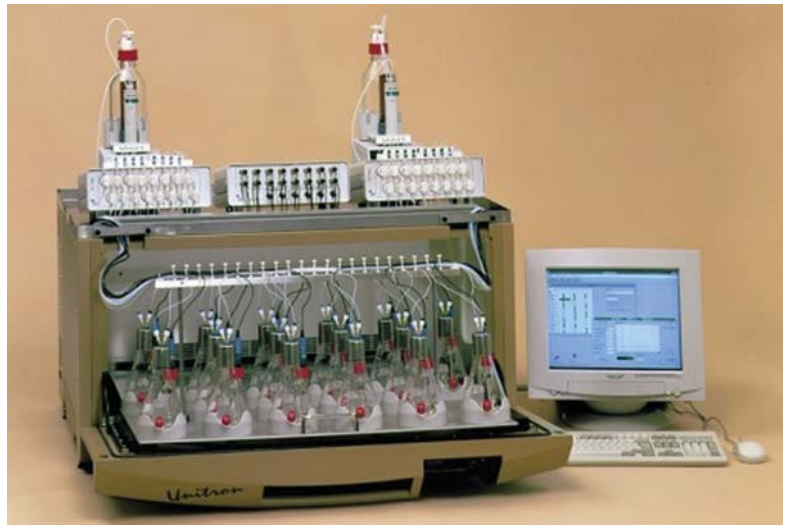


Figure 32.11. (a) An optical sensing patch for pH. The fluorophore encapsulated patch is affixed to the inside of a transparent reaction vessel. (b) Comparison of on-line optical (–) pH measurements with those made off-line (▲) during cultivation of *E. coli* in a shake flask (29).

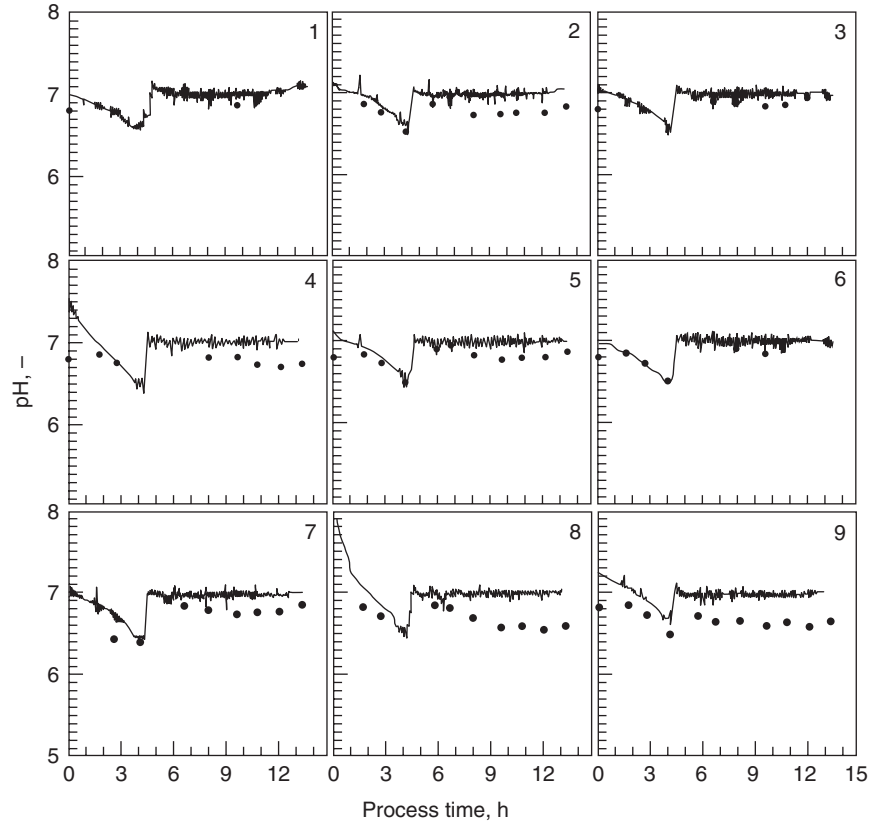
32.5.2 Multi-Well Plates

Since very little culture volume is needed for small-scale operations in upstream bioprocessing, such as screening and cloning, multiwell plates are well-suited to perform these functions. However, at such small volumes, fluid handling and well-to-well reproducibility are often difficult to control. Duetz *et al*. developed a system capable of reproducibly accessing 96 different frozen glycerol stocks, a plate each on agar, and ultimately inoculate 96 wells in a new plate with the agar cultures (35). The 40-mm deep well plate system was also able to shake and rotate at a variety of speeds and angles (Fig. 32.14), respectively, in order to maximize OTR as determined by the sulfite oxidation method utilizing a gas-phase electrode.

Two methods for measuring OTR were improved upon for use in multiwell plates by Hermann *et al*. as a result of incorporating a gas-phase oxygen sensor and an LCD

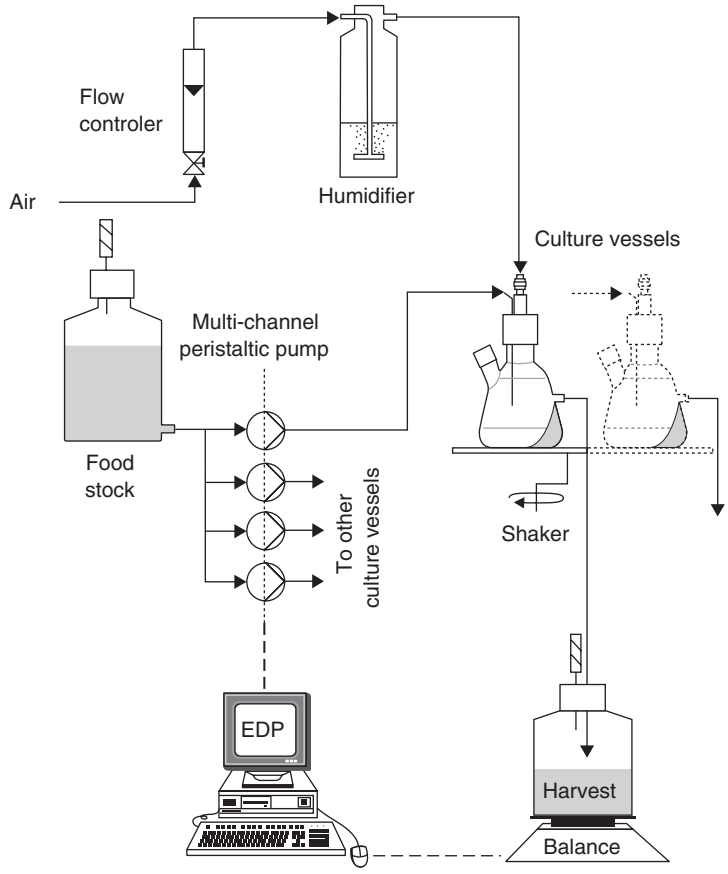


(a)



(b)

Figure 32.12. (a) A Fed-batch parallel shake flask system manufactured by DASGIP AG that is capable of monitoring and controlling pH. (b) On- (–) and off-line (□) pH measurements made during parallel cultures of *E. coli* in DASGIP AG's fed-batch parallel shake flask system (30). (This figure is available in full color at http://onlinelibrary.wiley.com/book/10.1002/9780470054581.)



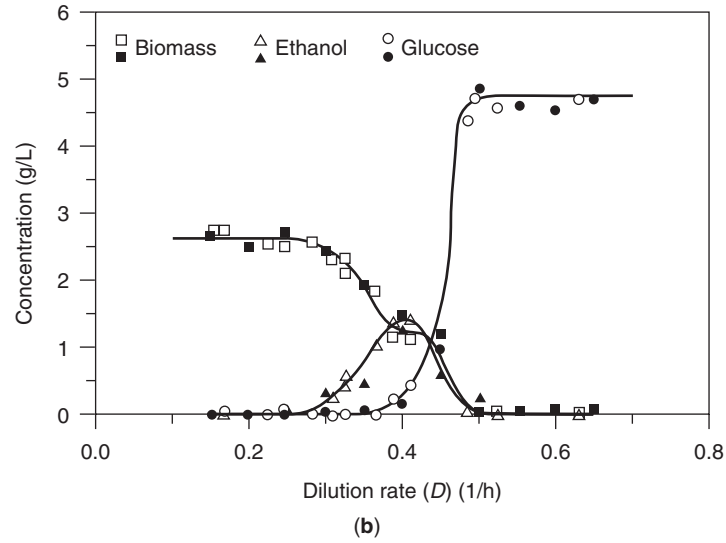


Figure 32.13. (a) A multiflask continuous culture shaking system. Flask liquid volumes, and thus the dilution rate, are controlled by measuring harvest mass and controlling media addition rates with computer controlled pumps for each flask. Humidified air is also supplied to each reactor. (b) The continuous culture of *S. cereveisiae* in the continuous culture shake flask system (open symbols) and in a 1-L stirred-tank fermentor (closed symbols). Steady-state biomass, product (ethanol), and substrate (glucose) concentrations are shown as a function of dilution rate (32).

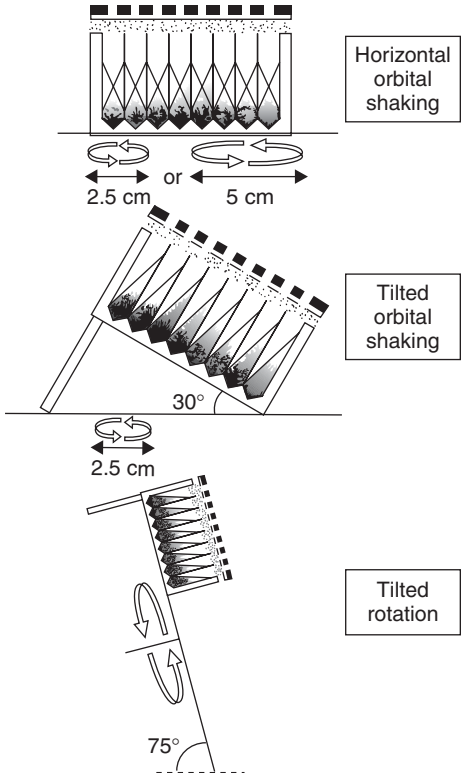


Figure 32.14. A 96 deep-well system capable of shaking and rotating at a variety of speeds and angles in order to increase the OTR (35).

camera (36). The gas-phase sensor was sealed to the top of a single well in a plate and used to monitor the parti al pressure of oxygen over time. This accepted technique was used to validate the proposed sulfite oxidation LCD camera-based method. When using the sulfite oxidation method to measure OTR, a characteristic drop in pH occurs upon completion of the sulfite oxidation reaction, signaling oxygen depletion. By adding bromophenol blue, the change in pH was accompanied by a solution color change. The camera was used to visualize the time taken to achieve the color change, thus a reaction rate could be calculated based on the amount of oxygen necessary to stoichiometrically react with the starting quantity of sulfite. Hermann *et al*. went on to use the camera-based method for characterizing 96-well plates, for example by correlating OTR_{max} and shaking frequency at different shaking diameters, as shown in Fig. 32.15 (37). The 48-well plates were characterized in three different ways by Kensy *et al*. by utilizing the camera-based method above, replacing the gas-phase sensor with a modified RAMOS device, and verifying both biologically using a *Hansenula polymorpha* cultivation (38).

Optical sensing for bioprocessing was first demonstrated in multiwell plates by Li *et al*. who used GFP to study the galactose-inducible *GAL1* promoter in *Saccharomyces cerevisiae* (39). Comparable *GAL1*-controlled GFP profiles were observed in shake flasks and in the 96-well plate format. Girard *et al*. used fluorescence from a GFP-expressing Chinese hamster ovary (CHO) cell line as a surrogate indicator of cell density in 12-well plates (40). The culture pH was quantitatively monitored as well by phenol red absorbance. DO concentration was first monitored optically in multiwell plates by John *et al*. during the culture of *Corynebacterium glutamicum* in 96-well plates (41). DO sensor spots were immobilized and optical instrumentation was positioned as shown in Fig. 32.16a. DO profiles are shown in Fig. 32.16b.

Optical fluorescent sensing of pH was first used in multiwell plates to study mixing (42). Weiss *et al*. utilized two different pH sensitive fluorophores: 8-hydroxypyrene-1,3,6-trisulfonic acid (HPTS) dissolved in buffer solution and fluorescein immobilized in a sensor

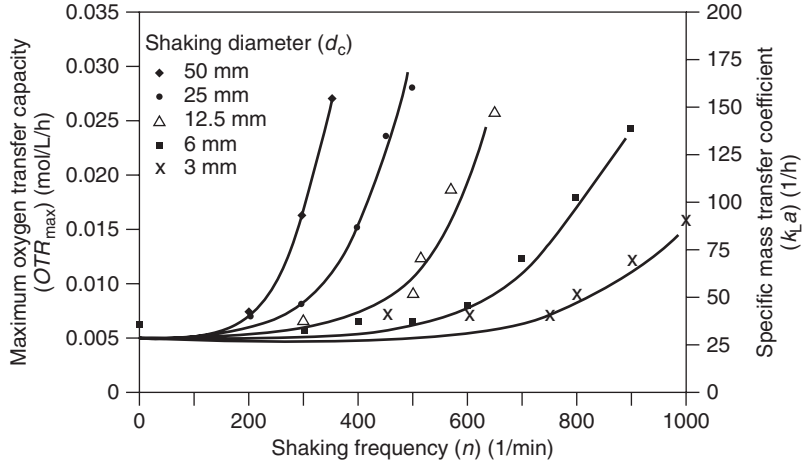


Figure 32.15. The OTR and k_La as a function of shaking diameter and frequency in 48-well multiwell plates (37).

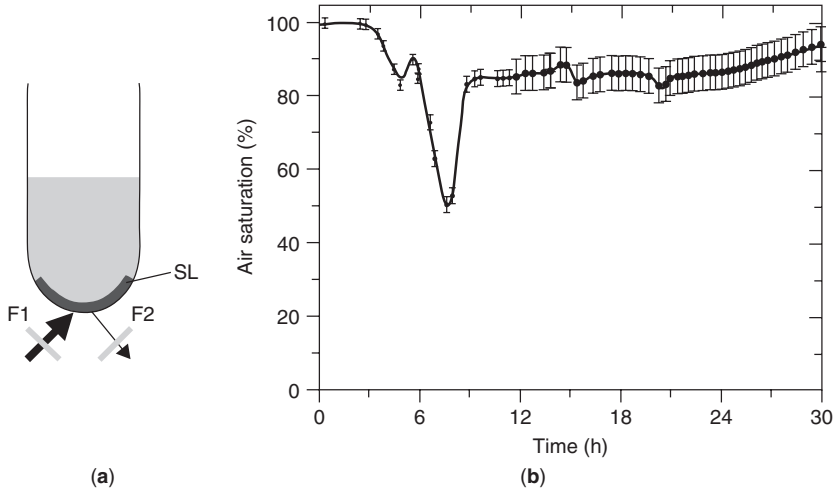


Figure 32.16. (a) A schematic of a single well of a multiwell plate with optical monitoring of DO. A DO-sensitive fluorophore encapsulated sensor spot is affixed to the inside bottom of the well with an excitation source (F1) and detector (F2) located underneath.(b) The DO profile obtained with optical sensing during fermentation of *Corynebacterium glutamicum* in 96-well plates (41).

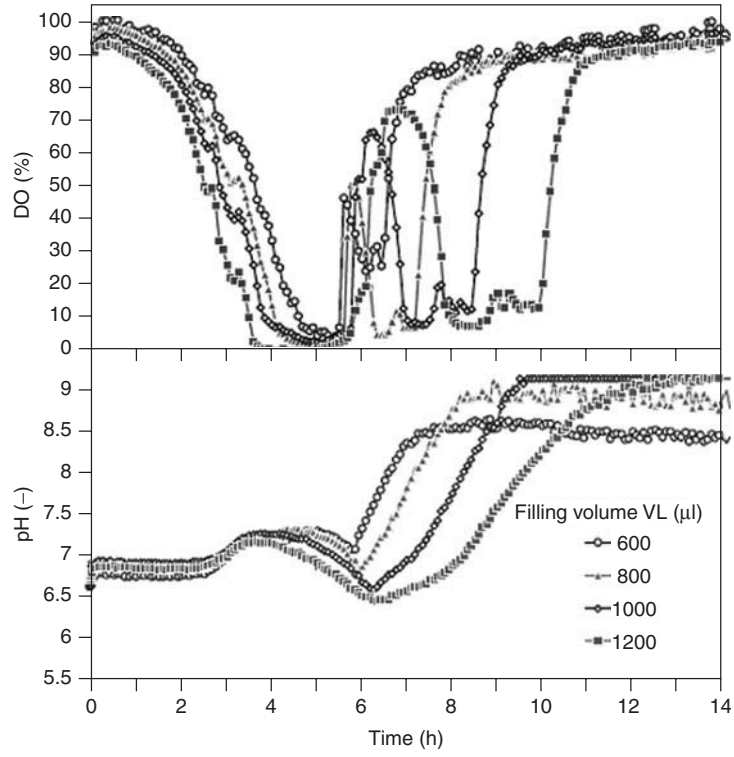


Figure 32.17. Optical pH and DO profiles during the fermentation of *E. coli* in 24-well plates. Only one of the parameters per culture could be monitored in the plates, therefore the other parameter was observed in a second, replicate culture (43).

spot that was affixed to the inside bottom of the well. Results from the fluorescent experiments were compared to visualization experiments where a camera recorded the color change of a pH indicator, thymolphthalein. Controlled drops of alkali addition were responsible for pH changes.

The DO concentration and pH were both optically monitored by Kensy *et al*. in experiments carried out in 24-well

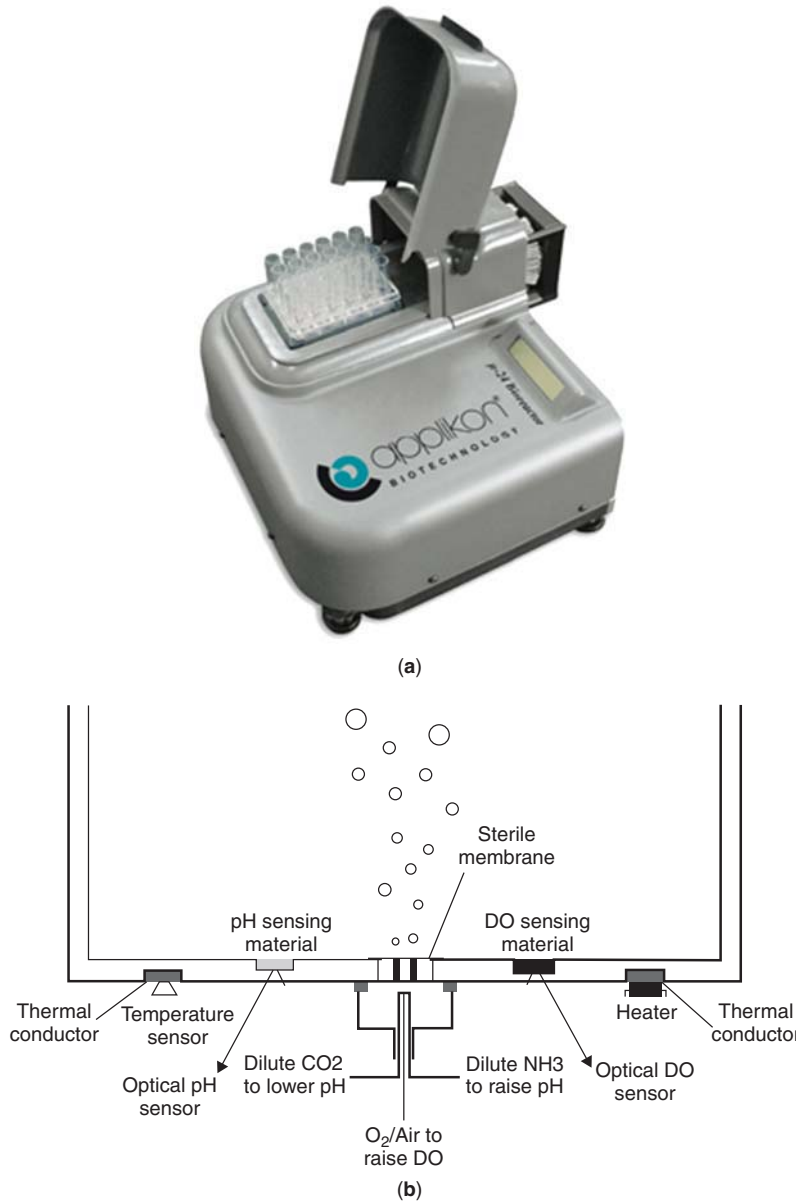


Figure 32.18. (a) The Applikon μ-24 bioreactor: a 24 deep-well plate with sensors and control for temperature, DO, and pH. (b) A schematic of a single well in the μ-24 system. Located underneath each well in the plate are a temperature sensor, a heater, optical DO and pH sensors, a sterile membrane for aeration, and a mixing chamber for CO_2, O_2, air, and NH_3 gases (45). (This figure is available in full color at http://onlinelibrary.wiley.com/book/10.1002/9780470054581.)

plates (43). Similar to Weiss *et al*., sensor spots were immobilized on well bottoms. Although pH and DO were both monitored, they weren't done in the same experiment. The experimental setup only allowed for one of the two parameters to be measured per plate. Therefore, the other parameter was monitored in a subsequent replicate plate. Figure 32.17 shows how changes in culture volume affect the pH and DO profiles of the *E. coli* cultures.

The simultaneous monitoring of DO and pH in shaken multiwell plates was first achieved by Tang *et al*. using a prototype of a commercially available system, Fig. 32.18a, from Applikon (Shiedam, Netherlands) (44,45). Each individual reactor, shown in Fig. 32.18b, consists of a deep well that is equipped with optical sensors for DO and pH, a temperature sensor, a heater, gas lines for aeration and pH control, and a sterile gas membrane. On-line temperature,

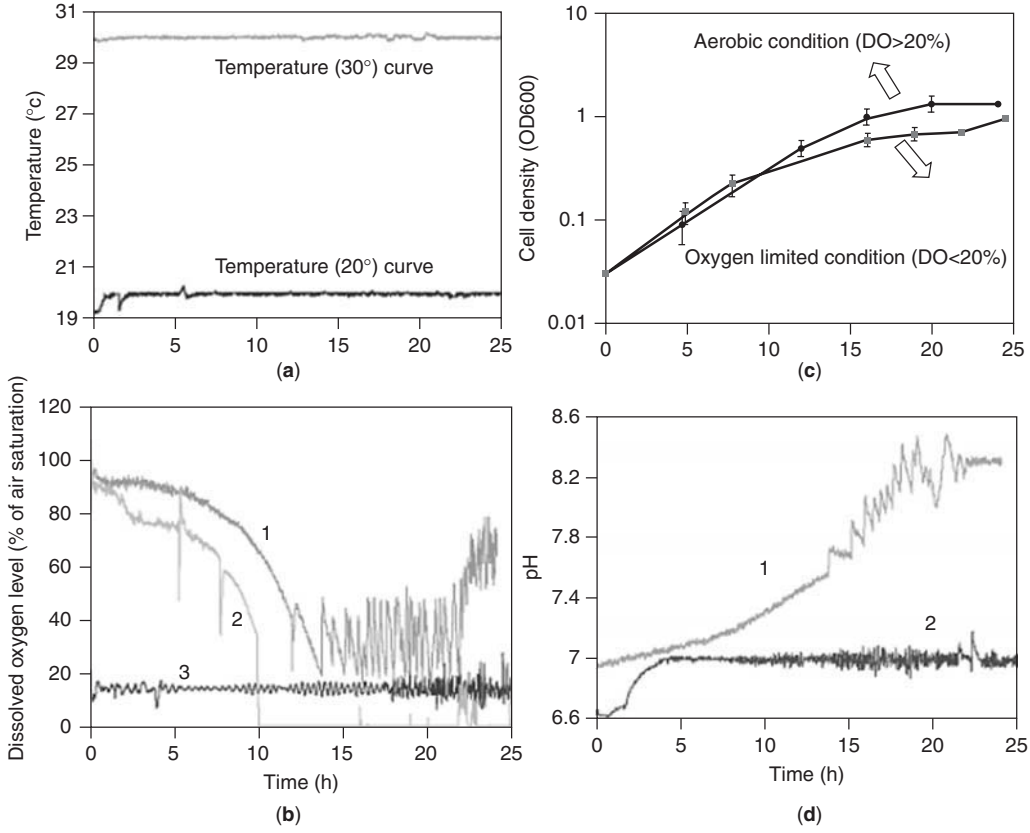


Figure 32.19. The demonstration of control of MR-1 growth conditions in individual wells. (a) Controlling and monitoring temperature at 30 and 20°C. (b) Dissolved oxygen control. (1) Dissolved oxygen was controlled above 20%; (2) dissolved oxygen control was off; (3) dissolved oxygen was controlled at 15%.; (c) MR-1 growth curves under aerobic (◇) and oxygen-limited (■) conditions at 30°C; (d) Control of pH (at 7.0) during growth on 60 m*M* sodium lactate using CO_2: (1) no pH control, incubation at 30°C; (2) pH control (45).

DO, and pH profiles, as well as offline OD are shown for the fermentation of *Shewanella oneidensis* in Fig. 32.19. The same system has also been used to cultivate *S. cerevisiae*, *E. coli*, *Pichia pastoris* and CHO cell lines (46,47). However, in the latter, the standard pH and DO control strategies had to be modified to resolve foaming and pH control issues, thus more work is needed for cell culture applications.

For many shaken plate systems, a pause in shaking is necessary in order to perform the optical measurement. This pause can disrupt the culture in terms of OTR, cell settling, and so on Samorski *et al*. developed a system which enabled the optical monitoring with uninterrupted shaking (48). The plate-optics configuration, shown in Fig. 32.20a, is capable of monitoring scattered light and culture fluorescence. Comparisons were made between this 96-well system and 250 ml shake flasks equipped with the RAMOS device discussed previously. An increase in OTR and offline OD correlated with on-line scattered light and NADH fluorescence (Fig. 32.20b and c).

Maharbiz *et al*. constructed a parallel microbioreactor array from two 8-well strips (49). Each of the 250 μL wells continuously reports OD, temperature, and oxygen input. Oxygen is individually controlled and supplied to each reactor by electrolytic generation in the lower strip. Temperature is individually monitored and controlled by film thermistors and heaters under each well. The impact of different oxygen input rates on OD profiles is shown in Fig. 32.21a. Because of the printed circuit board framework, additional sensors can be added. To demonstrate this modularity, a solid-state pH sensor chip was added to the 8th well of the strip for an *E. coli* fermentation. A pH profile from this additional sensor and the corresponding OD profile are shown in Fig. 32.21b.

32.5.3 Tubes

In an effort to make cell culture simultaneously high-throughput and simple, De Jesus *et al*. developed the TubeSpin cell culture centrifuge tubes (50). The tubes,

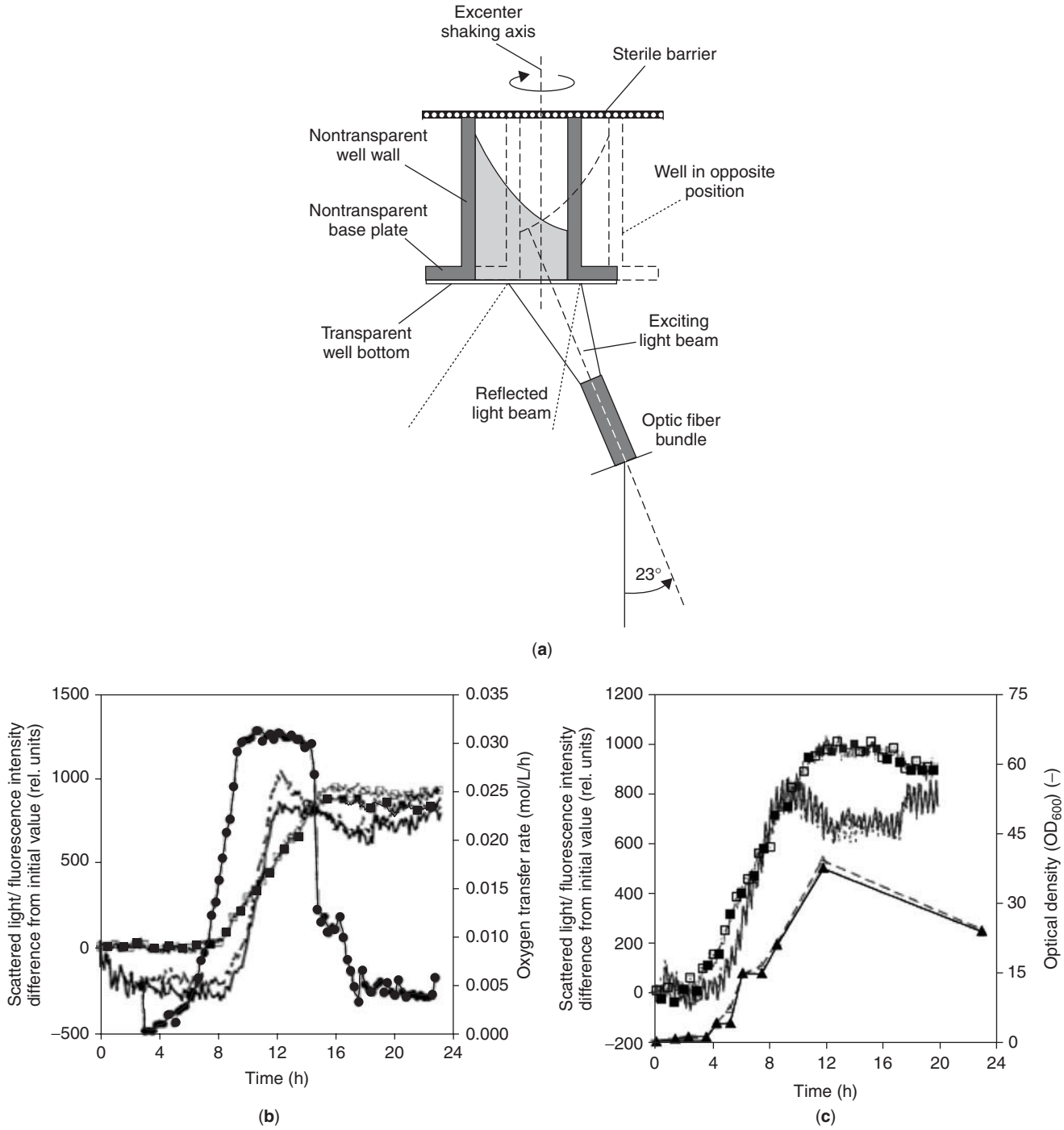


Figure 32.20. (a) A 96-well plate system capable of monitoring scattered light and fluorescence without stopping shaking. (b) Scattered light (—, –) and NADH fluorescence (■, □) intensities of two wells of a microtiter plate in comparison to the oxygen transfer rate of a simultaneously shaken Erlenmeyer flasks culture (•) all during fermentation of *E. coli* JM 109. Scattered light and NADH fluorescence are shown in duplicates. (c) Scattered light (—, –) and NADH fluorescence (■, □) intensities of two wells of a microtiter plate in comparison to off-line measured optical density at 600 nm of simultaneously conducted normal shaken 250 mL Erlenmeyer flasks cultures (▲, Δ) of *E. coli* JM 109. All measurements are shown in duplicates (48).

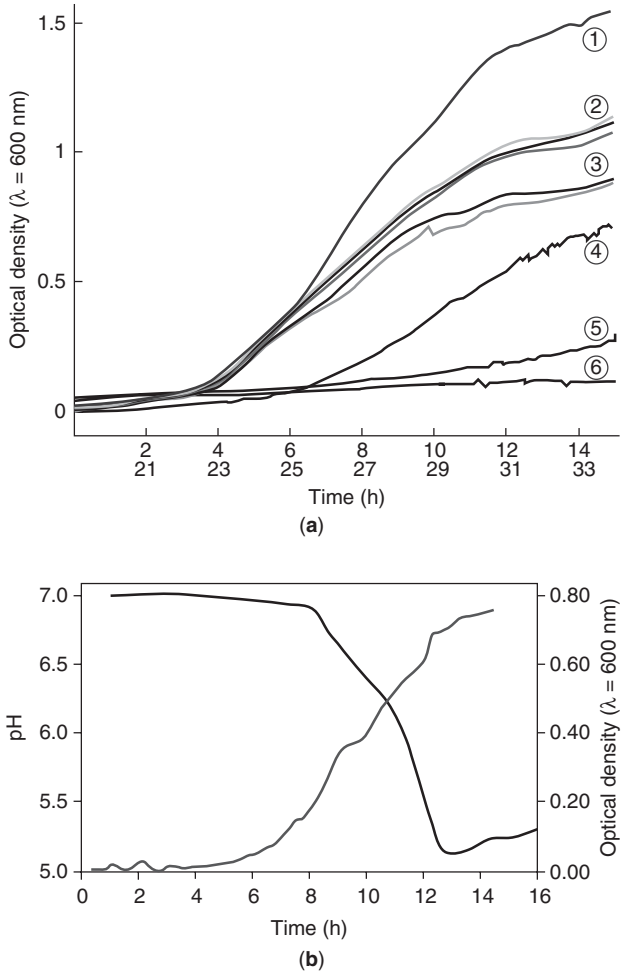


Figure 32.21. (a) *E. coli* growth as a function of oxygen generation. Oxygen supplied: (1) 10 mmol O_2/h, (2) 6 mmol O_2/h, (3) 3 mmol O_2/h, (4) 0 mmol O_2/h, (5) 6 mmol O_2/h (lower time axis), (6) 0 mmol O_2/h. Multiple curves are shown for curves (2) and (3) to illustrate reproducibility. Cultures 1–4 were grown in LB medium. Cultures 5–6 were grown in M9 minimal medium with 1% glycerol (lower time axis). (b) An ISFET chip from Sentron Europe (E2310000, 0.5–1.5 mm) and reference electrode were assembled into the eighth well of a microreactor array. Using the ISFET, pH was monitored during the course of a 16-h *E. coli* fermentation. OD600 is also plotted (49).

commercially available through Techno Plastic Products (Trasadingen, Switzerland), have specially made caps with holes allowing for aeration. Racks and large incubators allow for many experiments to be carried out concurrently. Other than incubator temperature and shaker speed, no sensors or controls exist for the platform.

32.5.4 Roller Bottles

Roller bottles are used for both small-scale culture and commercial manufacturing of therapeutic proteins, primarily for adherent cells. The cylindrical vessels rotate around their axis allowing cells to attach over the entire inner surface area. A thin layer of liquid results when rolling, allowing for an adequate oxygen mass transfer to the cells. Although, no on-line monitoring or control exists beyond rotational speed and temperature, in depth characterization of flow patterns and particle settling has been carried out (51,52). The addition of a recirculation loop by Berson *et al*. enabled a threefold increase in cell density over standard roller bottles due to enhanced liquid mixing and oxygen transfer (53).

32.6 STIRRED BIOREACTOR SYSTEMS

The majority of upstream commercial bioprocesses, regardless of size, utilize bioreactors of the stirred-tank variety. This fact is the biggest motivation to carry out small-scale developmental studies in stirred bioreactor systems. Similarity in the reactor geometry and a means of agitation can aid in scale-up, allowing for comparable behavior across all scales of production.

32.6.1 Spinner Flasks

Spinner flasks are most commonly used for the culturing of mammalian cells in volumes greater than can be achieved in T-flasks but less than in bench-top bioreactors. Incubator temperature and gaseous CO_2 concentration are generally controlled along with a magnetically controlled impeller agitation speed.

Optical monitoring in spinner flasks was first carried out by Bambot *et al*. during the fermentation of *E. coli* (54). The spinner flask was equipped with both an optical DO sensor and a Clark-type electrode. The offline OD and on-line DO concentrations from both sensors are shown in Fig. 32.22. Chang *et al*. optically monitored dissolved

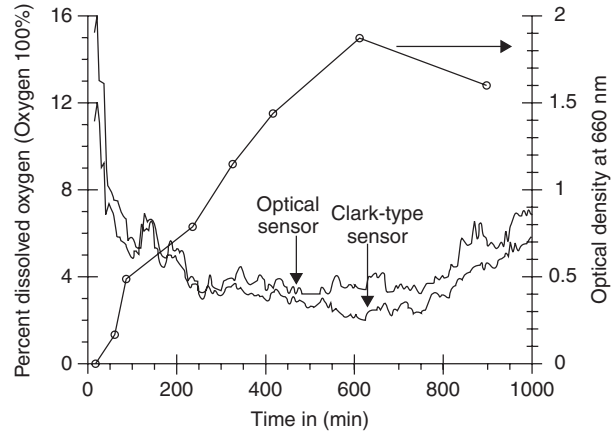


Figure 32.22. The monitoring of DO simultaneously with an optical sensor and an electrochemical probe during spinner flask culture of *E. coli*. OD is also plotted (54).

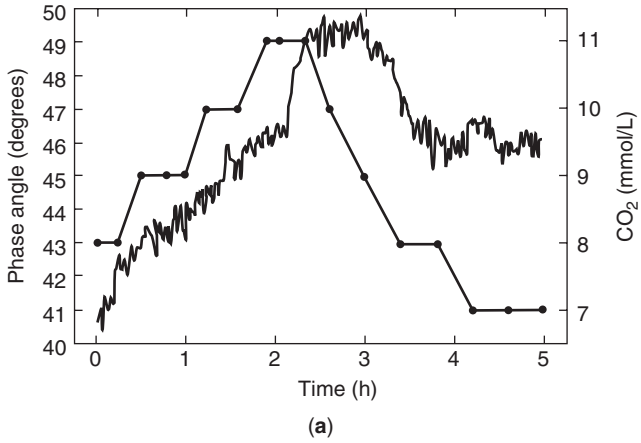


Figure 32.23. On- (–) and off-line (·) measurements of dissolved CO_2 during spinner flask fermentation of *E. coli* (55).

the CO_2 in spinner flask fermentations of *E. coli* by circulating culture broth from a spinner flask through a sensor equipped cuvette and back (55). In Fig. 32.23 the on- and off-line measurements are compared.

32.6.2 Cuvette

A proof-of-concept 2-mL bioreactor was constructed by Kostov *et al*. out of a standard cuvette (56). A schematic of the reactor, shown in Fig. 32.24, was capable of optical on-line monitoring of OD, pH, and DO concentration, stirred with a magnetic stir bar, and was aerated by sparging. Using k_La as a scaling factor, fermentations of *E. coli* in the cuvette reactor and a 1-L fermentor were compared (Fig. 32.25). The Gaden Award-winning publication was the first to demonstrate simultaneous on-line monitoring of OD, pH, and DO at such a small scale.

32.6.3 Plate Type

Based on the simple design of standard plates, their typical means of agitation is by shaking, as was highlighted above. However, plate-type platforms have also been equipped with stirring mechanisms, enabling increases in the mass transfer over shaking. Puskeiler *et al*. developed a parallel bioreactor system, shown in Fig. 32.26, capable of carrying out 48 fermentations of less than 20 ml (57). On-line DO and at-line pH monitoring was carried out optically. The pH was controlled via a liquid handling system. At-line sampling involved the automatic pipetting of culture broth from the reaction block and transferring it to a microtiter plate (MTP). The MTP was automatically transferred to a plate reader and the OD and pH were determined.

On-line optical sensing of pH and DO during *E. coli* fermentation in a 24-well plate was demonstrated by Harms *et al*. (58). The system is capable of monitoring OD, pH, DO, and GFP on-line, as the schematic shows in Fig. 32.27a. The sensing board, on which the plate sits, housing all the optical instrumentation and the sensor patch orientation in several wells are shown in Fig. 32.27b and c. Figures 32.28a and b show the DO and pH data from the *E. coli* cultivations. DO was controlled at 20% air saturation by automatically changing agitation speed, but significant oscillations resulting from the controller were present.

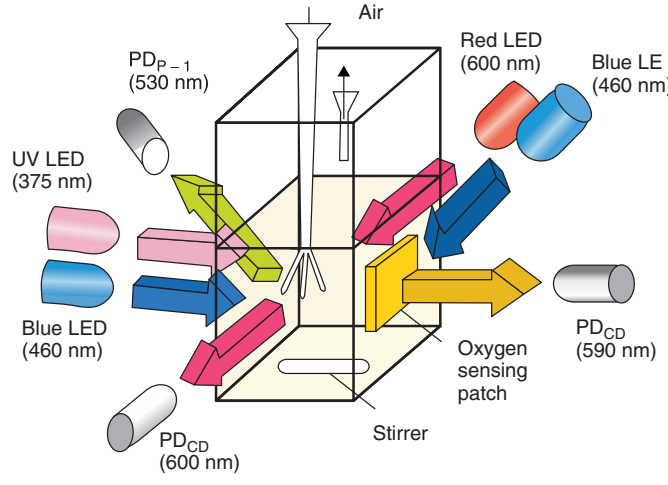


Figure 32.24. A schematic of the cuvette bioreactor equipped with optical sensing of OD, pH and DO. The pH and DO sensors consisted of sensor patches, LEDs for excitiation (blue for DO, pink and blue for pH), and photo detectors (590 nm for DO, 530 nm for pH). The optical density was measured using a 600-nm LED and a 600-nm detector. A 100-μL pipette tip was used as a sparger for aeration and a magnetic stir bar was used for stirring (56). (This figure is available in full color at http://onlinelibrary.wiley.com/book/10.1002/9780470054581.)

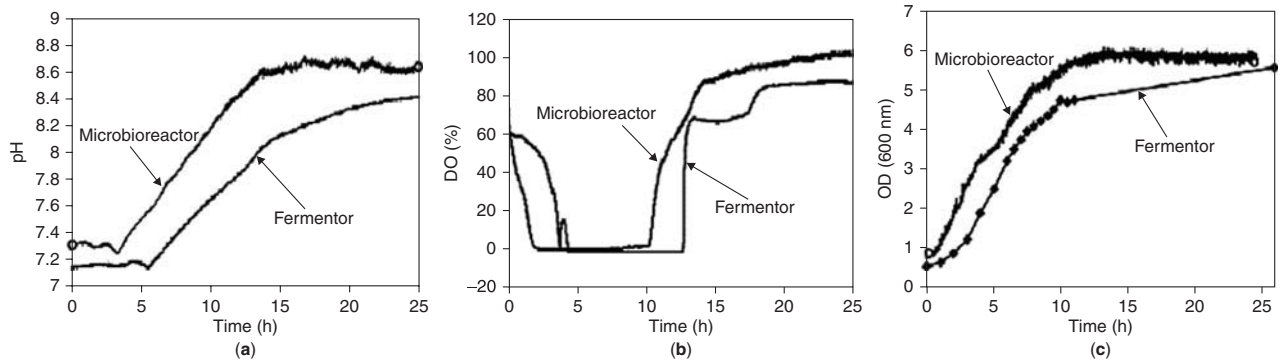


Figure 32.25. pH, DO, and OD profiles during *E. coli* fermentations carried out in the cuvette bioreactor and a 1-L fermentor. Conditions in the two reactor systems were scaled on the basis of $k_L a$ (56).

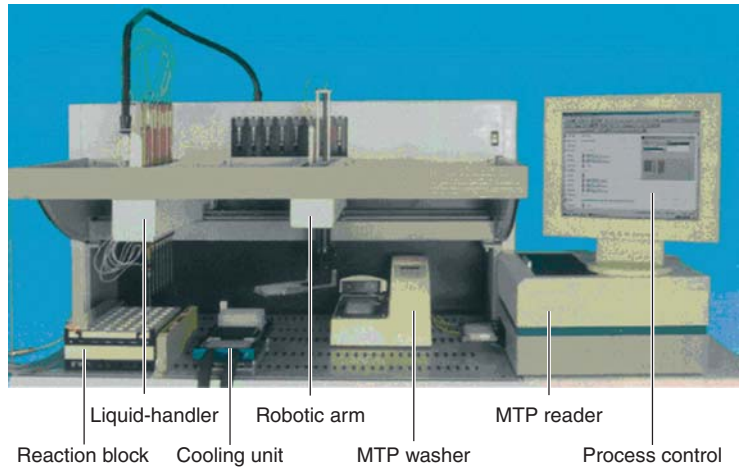
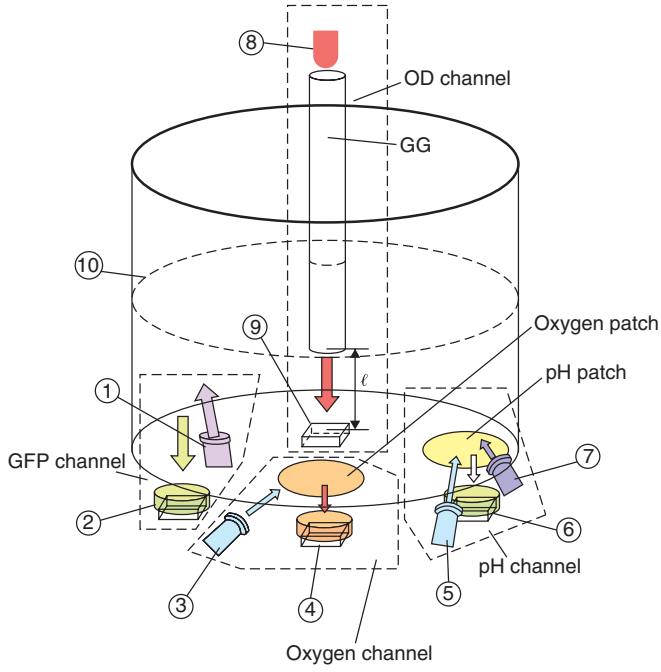


Figure 32.26. The automation concept consisting of the reaction block with 48 parallel bioreactors integrated in a liquid-handling system. The robotic arm enables independent microtiter plate (MTP) movements to an MTP reader and MTP washer. All devices are controlled by a process control program (57). (This figure is available in full color at http://onlinelibrary.wiley.com/book/10.1002/9780470054581.)

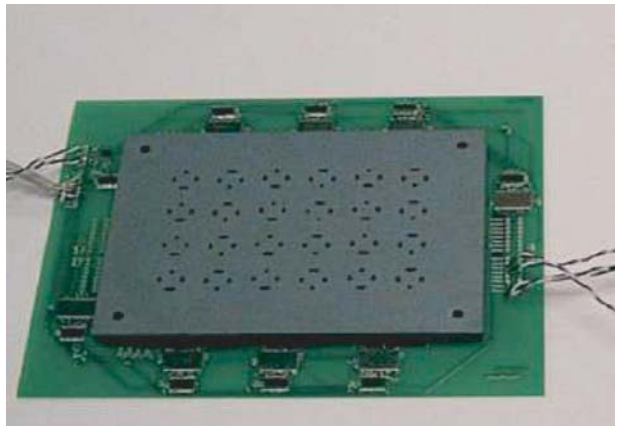
32.7 BIOREACTORS

In the early 1990s, Infors HT (Bottmingen, Switzerland) developed the first generation Sixfors parallel bioreactor system, of which a recent model is shown in Fig. 32.29 (59). The system consists of six stirred-tank bioreactors of 300–500 mL, working volume, each equipped with pH and DO monitoring using traditional electrochemical probes. The control of pH is carried out by acid or base additions while impeller speed is modulated to control DO concentration. The system was used as a basis for comparison by smaller platforms already presented in this review. Trummer *et al*. used the system for an in-depth study of the impact of pH, DO, and culture temperature on CHO growth and EPO-FC production (60). Three system runs were carried out to compare 16 different reactor conditions, the results of which are shown in Fig. 32.30. The Sixfors system enables highly parallel cultures to be carried out, however, the reactor volumes are not small enough to significantly improve throughput.

Lamping *et al*. designed a 6-mL bioreactor made of Plexiglass with the same diameter as a well in a standard 24-well plate and a height of 4.8 cm (61). The reactor, shown in Fig. 32.31 (4), has optical sensors for DO, pH, and OD, a three blade impeller, and a sparger for gas delivery. This reactor was compared to a 15-L (working volume) reactor for performance in *E. coli* fermentation (Fig. 32.32). Run conditions were not scaled to achieve comparable results. Also, the immobilized pH sensitive dye behaved erratically, therefore pH readings shown are a result of dissolving the pH sensitive dye (HPTS) directly into the culture broth. This reactor was used by Betts *et al*.



(a)



(b)



(c)

Figure 32.27. (a) Schematic of the positioning of the optical sensors around a single well in a 24-well microplate. The light source and the detectors are not drawn to scale. Interference filters are positioned in front of the LEDs and photodiodes (represented here by small disks). A pinhole is installed in front of every detector for better collection of the light (not shown). The spatial positioning is selected in such a way that the excitation light from one channel creates minimum interference to the other channels. The glass optical guide GG extends below the liquid level to achieve a constant light path length l for OD measurements. (1) excitation UV LED for the GFP channel; (2) detection photodiode for the GFP channel; (3) excitation blue LED for the oxygen channel; (4) detection photodiode for the oxygen channel; (5, 7) excitation blue and UV LEDs for the pH channel; (6) detection photodiode for the pH channel; (8) red LED for the OD channel; (9) detection photodiode for the OD channel; (10) the liquid level.(b) A measurement board which the 24-well plate sits on. All LEDs and detectors decribed in (a) are precisely positioned within the board (58). (c) 24-well plate with optical sensing patches for dissolved oxygen and pH. (This figure is available in full color at http://onlinelibrary.wiley.com/book/10.1002/9780470054581.)

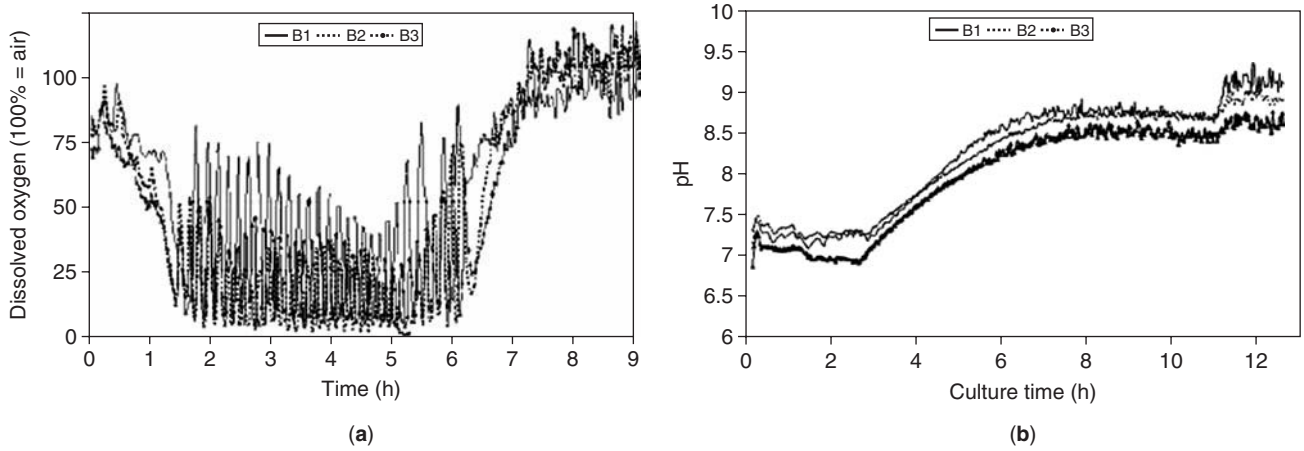


Figure 32.28. (a) The DO profiles of triplicate *E. coli* fermentations where the concentration was controlled using an on-off algorithm. (b) The pH profiles of triplicate *E. coli* fermentations (58).



Figure 32.29. The Infors HT Sixfors parallel bioreactor system. Each of the six bioreactors has a working volume of 300–500 mL, and monitoring (via electrochemical probes) and control of DO and pH (59). (This figure is available in full color at http://onlinelibrary.wiley.com/book/10.1002/9780470054581.)

to demonstrate scale-down utilizing power input per unit volume, k_La, and mixing time as scaling parameters (62). Results from the scale-down of a 7-L bioreactor based on power input per unit volume during the oxygen-limited fermentation of *E. coli* are shown in Fig. 32.33.

The static bioreactor of Zanzotto *et al*. discussed previously suffered from an oxygen gradient from the membrane surface to the bottom of the reaction well (10). This gradient becomes more pronounced if the reactor volume is enlarged by increasing the vessel depth. Zhang *et al*. counteracted this phenomenon by adding a magnetic stirrer to a deeper welled (150 μL) version of the Zanzotto *et al*. reactor (63). When the enhanced reactor was compared to the SixFors system, test tubes, and shake flasks, comparable OD, DO (microbioreactor and SixFors only), and pH profiles were obtained as shown in Fig. 32.34. These reactors have been multiplexed to form a parallel reactor system (64).

A schematic of a 12-unit high throughput bioreactor (HTBR) system developed by Ge *et al*. is shown in Fig. 32.35a (65). The system is capable of monitoring GFP, OD, pH, and DO. The carousel, which also serves as a water bath for temperature control, holds the individual glass reactor vessels and positions them above the detector arm when optical sensing is to commence. The system's performance was evaluated during the culture of murine hybridoma cells. Offline viable cell density and viability, and on-line pH and DO profiles are shown in Fig. 32.35b and Fig. 32.35c. The DNA microarray analysis showed that light exposure for optical monitoring had no impact on the global gene expression. A similar system, shown in Fig. 32.36, with smaller, 6 ml volumes was presented by Harms *et al*. where each reactor had its own set of instrumentation for optical monitoring (58). Data from an experiment where all 24 units were utilized in fermentation of *E. coli* are shown in Fig. 32.37. These vessels were characterized by Vallejos *et al*. using a fluorescence optical mixing sensor (66). This sensor functions by measuring the size of dissipating droplet via its fluorescence as illustrated in Fig. 32.38.

32.7.1 Bubble Column Bioreactors

Bubble column reactors consist of a cylindrical vessel with a gas distributor at the bottom. Aeration is carried out by gas sparging in the form of bubbles into liquid or a liquid–solid suspension (67). Miniaturization of bubble columns faces the same hurdle as other bioreactor platforms in terms of the need for a small sensing instrumentation. Weuster-Botz *et al*. characterized bubble columns 200 ml in volume; large

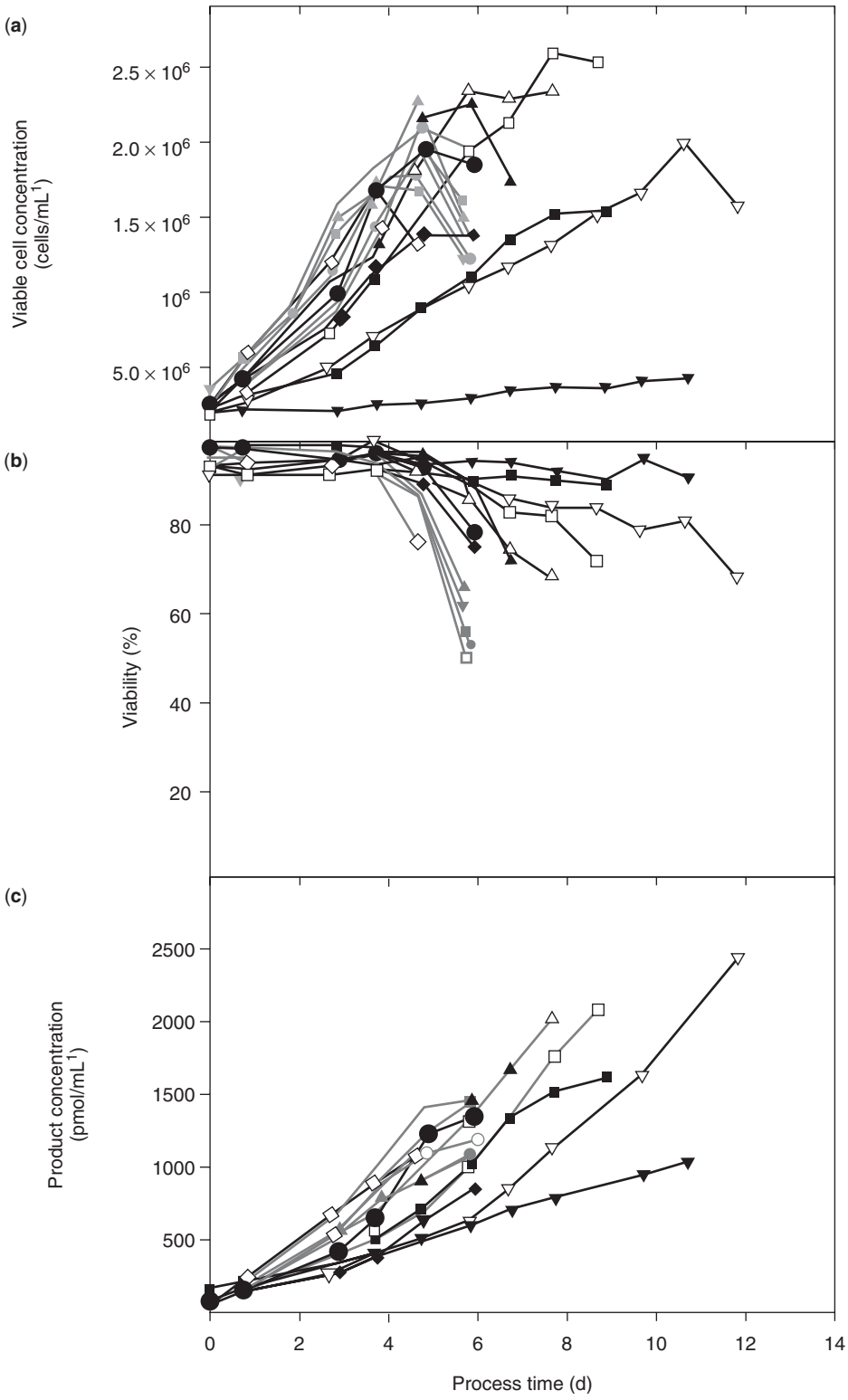


Figure 32.30. Progression of viable cell concentration, viability and product concentration at tested process parameters. (a) Viable cell concentration; (b) cell viability; (c) product concentration. (•, control culture; ∇, pH 6.80; □, pH6.90; Δ, pH7.00; ◇, pH7.30; ▼, 30°C; ■, 33°C; ▲, 35°C; ◇, 39°C; gray symbols and lines represent unaffected cultures (•, pH 7.20; ▼, dissolved oxygen tension DOT 10%; ▲, DOT 50%; ◇, DOT 70%; ■, DOT 90%; —, DOT 100%; O, 38°C).

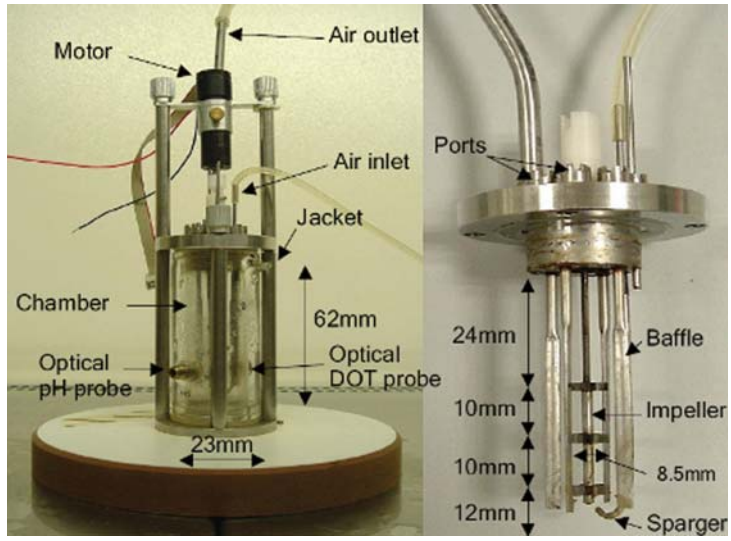


Figure 32.31. A miniature 6-mL (working volume) bioreactor made of Plexiglas. The reactor has three six-blade impellers, baffles, a sparging tube with a perforated end, and optical monitoring of OD, pH, and DO (4). (This figure is available in full color at http://onlinelibrary.wiley.com/book/10.1002/9780470054581.)

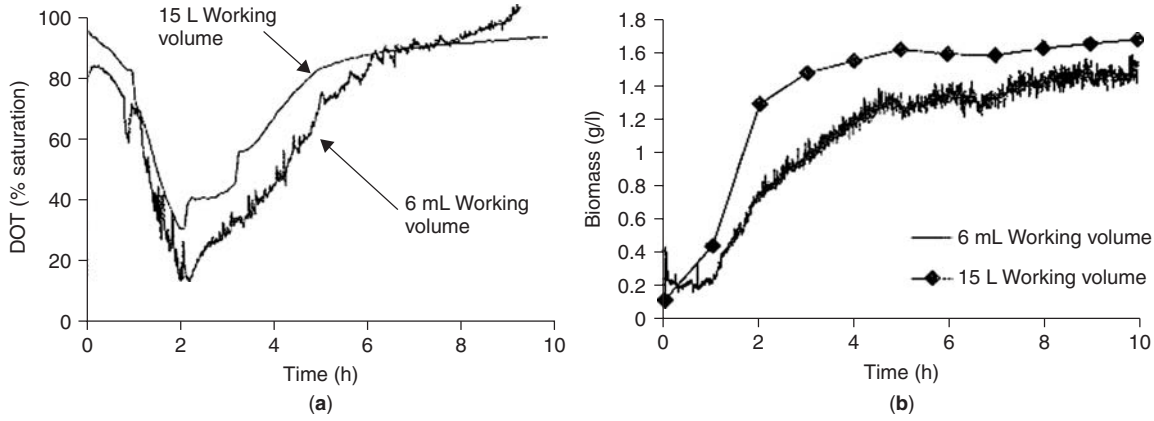


Figure 32.32. (a) DO tension in the miniature bioreactor and a 15-L (working volume) fermentor during *E. coli* fermentation. (b) Biomasses during the two fermentations: OD in the miniature bioreactor and the 15-L fermentor were measured on-line and offline, respectively (61).

enough to use standard polarographic electrodes for measuring oxygen (68). Bubble diameter, gas holdup percentage, k_La, liquid evaporation rate, and power input were correlated to distributor pore diameter, superficial gas velocity, and liquid height. It was concluded that power input per unit volume for bubble columns is an order of magnitude less than for shaking flasks and stirred bioreactors. Changes in energy dissipation into the broth can result in changes in culture biology, for instance in the expression of particular genes (69). Therefore, if power input changes significantly, so will the behavior of cells.

Significantly smaller bubble columns with volumes of 2-mL were characterized and used for fermentation of *E. coli* by Doig *et al*. (70). Rules for scale-up were determined based on volumetric power input and bubble formation characteristics. Based on two gas flow rates in the bubble column and two impeller speeds in a conventional stirred-tank reactor, two corresponding k_Las were determined and utilized for *E. coli* fermentations. Comparable cell density profiles are shown Fig. 32.39. Frachon *et al*. designed a battery of microfermentor bubble columns, shown in Fig. 32.40a, each 80 ml in working volume (71). Production of several model proteins in the microfermentor battery was compared to that in a traditional fermentor where in both cultures DO was automatically maintained at greater than 80% air saturation by mixing in pure oxygen

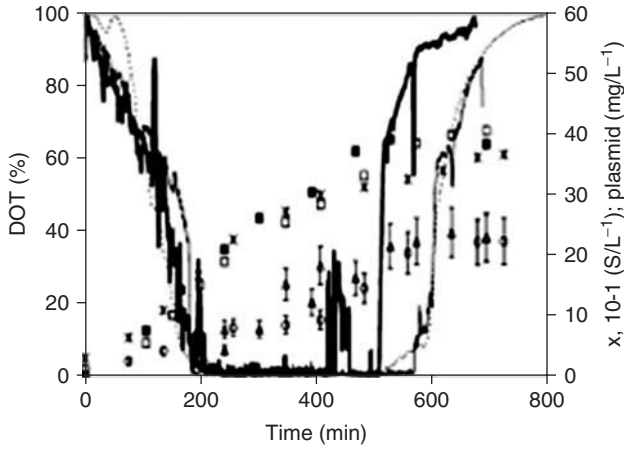


Figure 32.33. *E. coli* DH5α pSVβ fermentation profiles in the 7-L bioreactor and 10-mL MBR under oxygen limiting conditions. Key to symbols: (-) DOT 10 mL 1; (—) DOT 10 mL 2; (- - -) DOT 7 L; (■) (biomass) 10 mL 1; (□) (biomass) 10 mL 2; (∗) (biomass) 7 L; (▲) (plasmid) 10 mL 1; (Δ) (plasmid) 10 mL 2; (O) (plasmid) 7 L. Error bars for the plasmid DNA concentration data represent standard deviations from the mean of a quadruple assayed sample (62).

in the former and by increasing the agitation speed in the latter. The amount of protein recovered per ml of culture was comparable in both fermentors for all proteins tested.

A novel 4.5 mL bubble column with smooth periodic constrictions in the tube, shown in Fig. 32.41, was described by Reis *et al*. and utilized in a proof-of-concept fermentation of *S. cerevisiae* (72). No in-depth characterization of the reactor was carried out; however, data from when the system was compared to a stirred-tank bioreactor is shown in Fig. 32.42.

32.8 OTHER METHODS OF CONVECTIVE MIXING

Other reactors exist which cause the convective mixing of fluid by different means. Another microfabricated bioreactor from MIT described by Lee *et al*. used peristaltic mixing to circulate liquid within a bioreactor (73). The 100 μL (working volume) reactors were complexed to have four vessels per chip. Each reactor had optical sensing of pH, DO, and OD. This bioreactor system is set apart from others of its scale by the ability to automatically control the pH and DO by the injection of acid or base and by changing the oxygen concentration in the peristaltic mixing system.

A commercially successful system manufactured by bioprocessors called *SimCell* (Fig. 32.43) rotates bioreactors, utilizing gravity to circulate a bubble through the 1-mL reactor vessel, thus mixing the culture (74). The SimCell

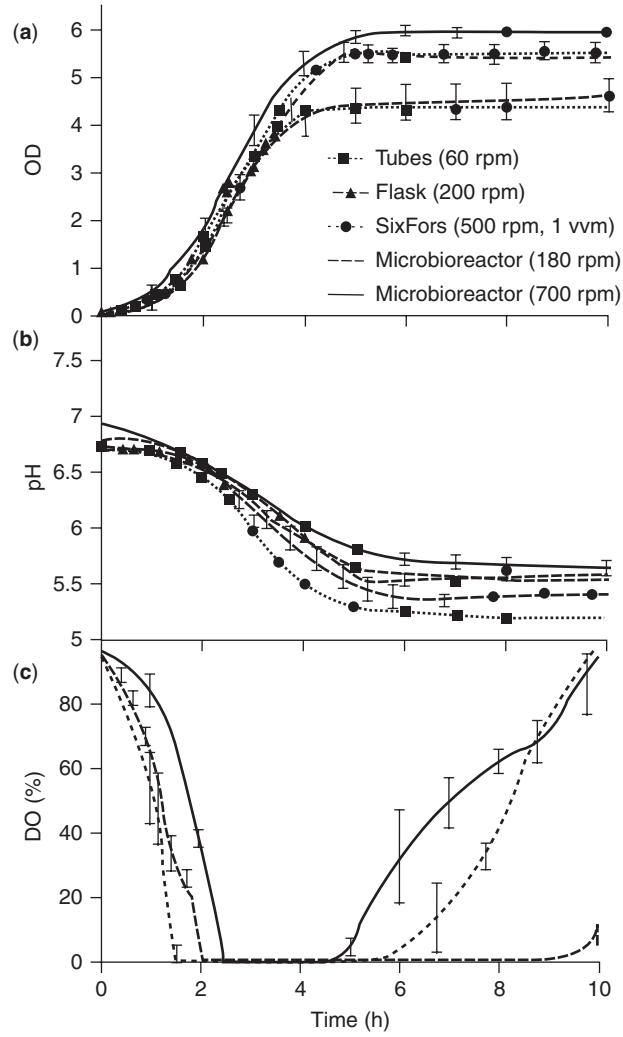


Figure 32.34. The comparison of *E. coli* FB21591 growth kinetics in an LB medium in the microbioreactor (n = 3, stirring speed at 180 and 700 rpm, respectively) with conventional bioreactors including test tubes (n = 4), shake flasks (n = 4), and Sixfors (n = 3). Each growth curve represents the average value with standard deviation from *n* replicate experiments carried out in separate bioreactors. (a) OD, (b) pH, (c) DO.

system can simultaneously carry out thousands of experiments where the pH and DO are optically monitored and controlled.

32.9 CONCLUSION

Clearly, advances in biominiaturization have moved what was once an exotic laboratory technology into the mainstream. Importantly, the technology has proven to be scalable, so data generated at a small scale is representative of larger scale operations. The consistent use of process monitoring across scales should also

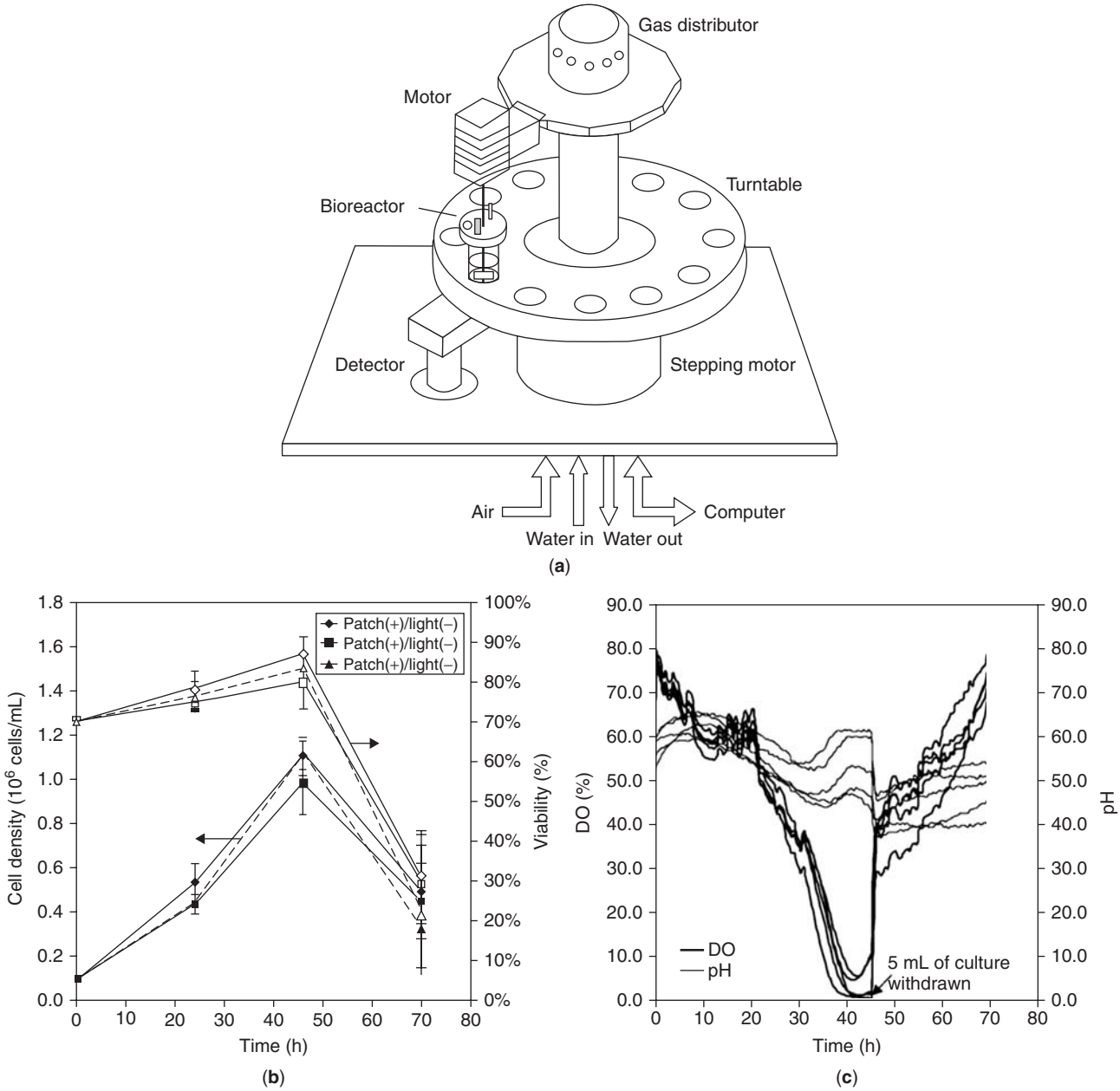


Figure 32.35. (a) The HTBR system capable of simultaneously carrying out 12 cell cultures: The reactor vessels are housed in the turntable which also serves as a water-jacket for temperature control. For DO, pH, GFP, or OD measurements, the turntable rotates placing the vessels directly above the detector arm, which houses the optical instrumentation. Each reactor also has a motor for independent control of agitation speed. (b) Viable cell densities and viabilities of hybridoma cell cultures carried out under three different optical sensing configurations: patches (+) and light (+), patches (−) and light (−), and patches (−) and light (+). (c) The pH and DO profiles obtained using optical monitoring for five replicate hybridoma cell cultures carried out in the HTBR (65).

facilitate the adoption of Process Analytical Technologies (PAT). It is now possible to conduct High Throughput bioprocess development as a statistically driven experimental paradigm. There is almost no limit to the combinatorial number of experimental conditions that can be examined. These advances should allow for much more efficient process development as well as impact other areas such as bioprospecting, where hitherto "uncultivable" species now may be grown by screening samples for growth under matrices of conditions that were previously impractical.

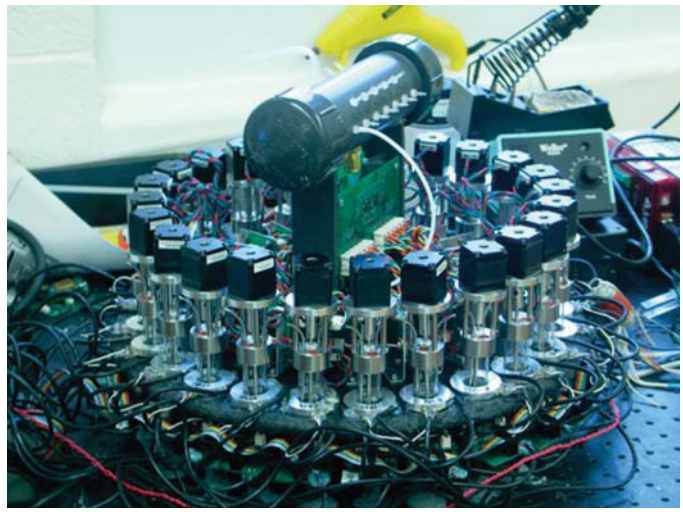


Figure 32.36. The HTBR system capable of simultaneously carrying out 24 experiments. The system is able to monitor DO, GFP, pH, and OD in each reactor (58). (This figure is available in full color at http://onlinelibrary.wiley.com/book/10.1002/9780470054581.)

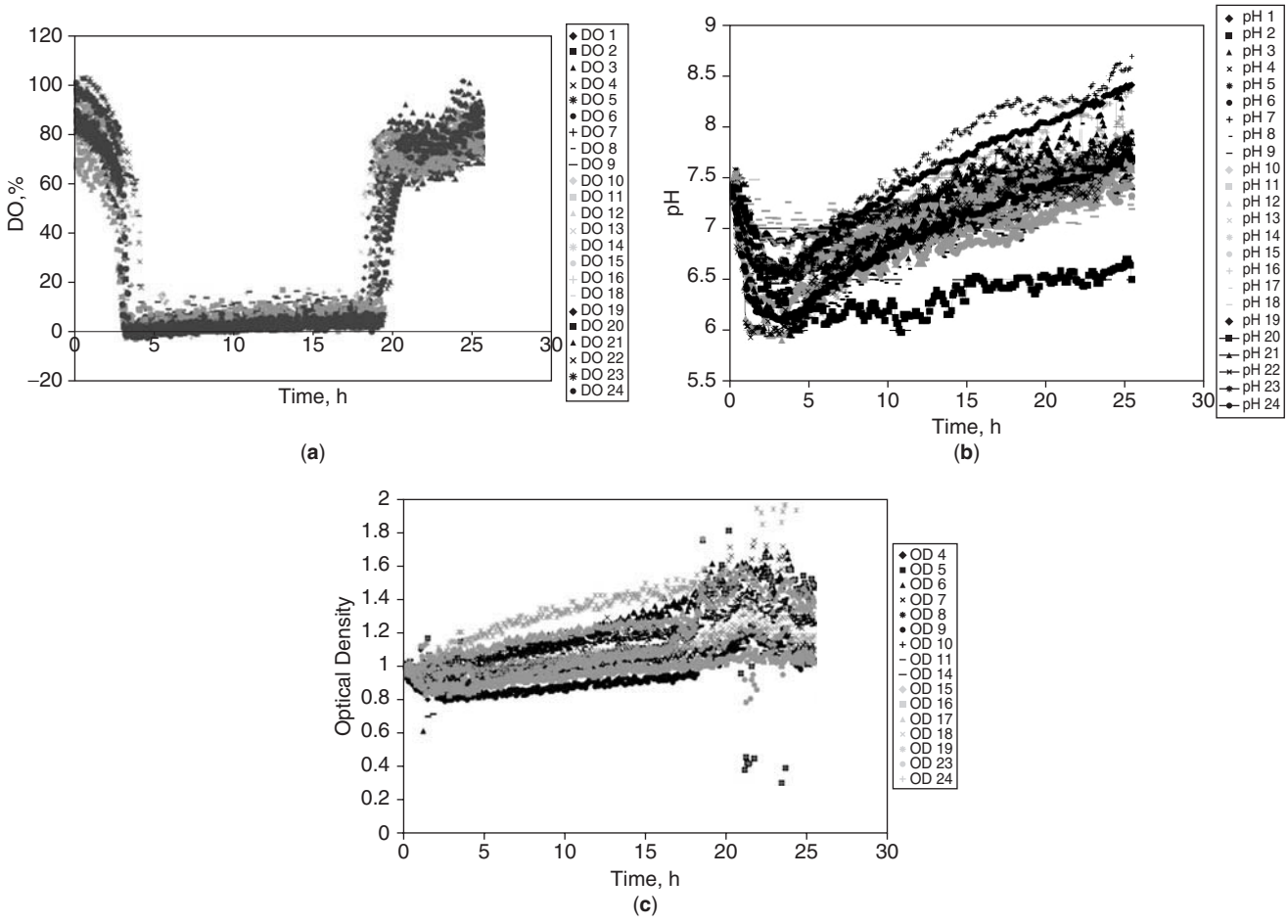
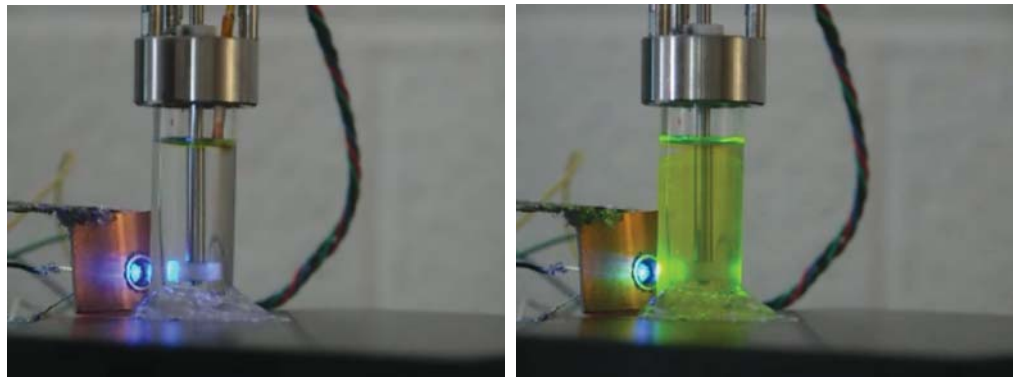
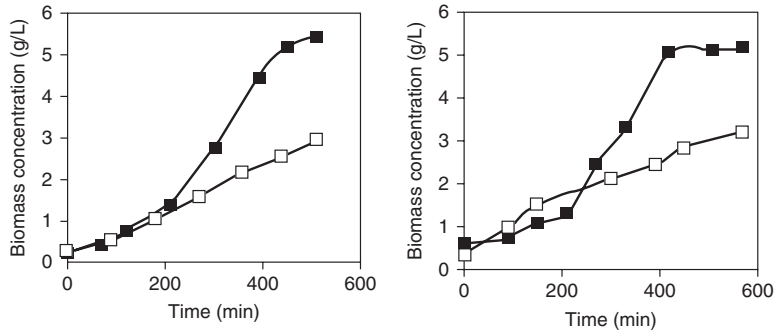


Figure 32.37. (a) The DO profiles for 23 replicate *E. coli* fermentations; (b) the pH profiles for 24 replicate *E. coli* fermentations; (c) the OD profiles for 16 replicate *E. coli* fermentations (58).



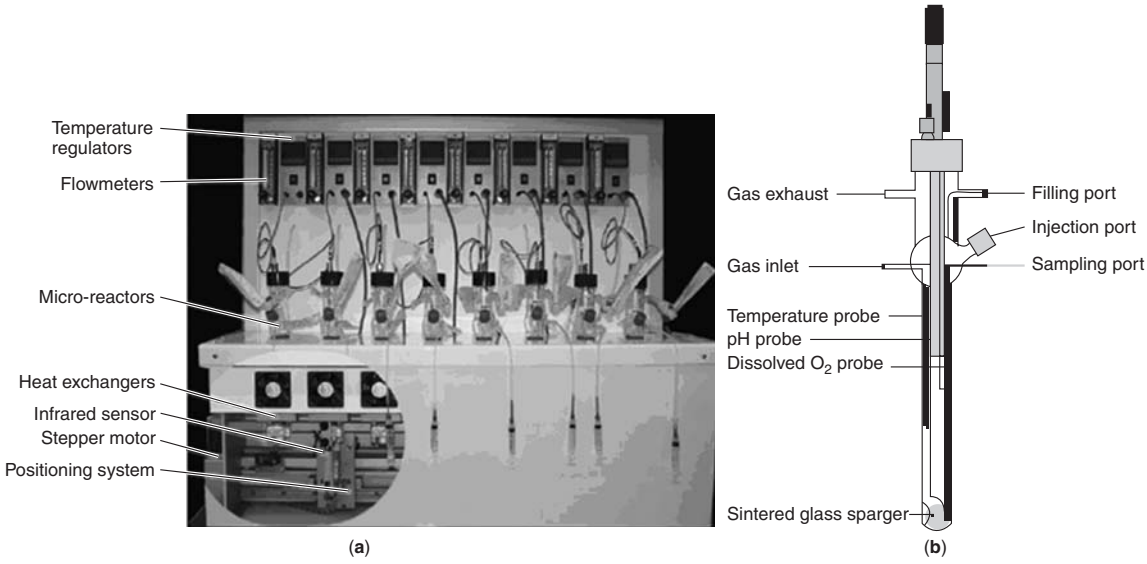
(a) (b)

Figure 32.38. An optical sensor used to measure mixing-time in bioreactors. The sensor measures the presence or dissipation of a fluorescent indicator under different mixing conditions (66). (This movie clipping is available at http://onlinelibrary.wiley.com/book/10.1002/9780470054581.)



(a) (b)

Figure 32.39. The *E. coli* biomass concentrations in (A) a 2-L stirred-tank fermentor at 700 (□) and 1200 (■) rpm, and in (B) a 2-mL miniature bubble column at 0.0015 (□) and 0.004 (■) m/s superficial gas velocities. High and low oxygen transfer conditions scaled in the two systems according to k_La values (70).



(a) (b)

Figure 32.40. (a) A microfermentor battery consisting of eight bubble column reactors. Heat exchangers, infrared sensor, stepper motor, and positioning system are shown with the metal casing removed for clarity. (b) The design of the bubble column bioreactor vessels. The gas inlet is fitted with 0.22 μm filters. The injection port is plugged by a septum through which an inducer can be injected by means of a syringe needle. Miniaturized temperature and electrochemical DO and pH probes monitor reactor conditions (71).

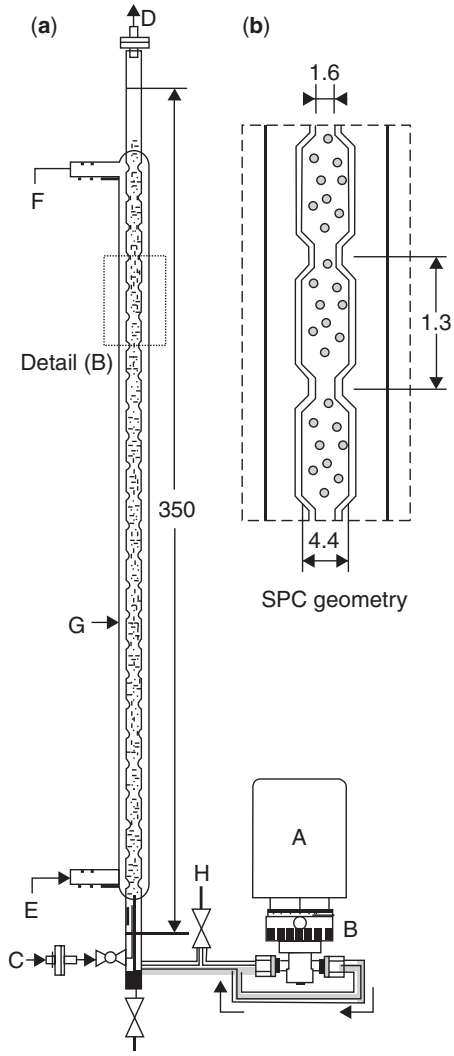


Figure 32.41. A novel bubble column bioreactor with constricted walls. (a) An experimental setup used in batch fermentations of *S. cerevisiae*: A, rotary motor; B, piston pump; C, gas inlet; D, gas outlet; E, fluid heating inlet; F, fluid heating outlet; G, smooth periodic constricted (SPC) tube; H, purging port; I, sampling port. (b) Details of SPC tube geometry, which composes the novel, designed oscillatory flow microbioreactor. All dimensions are in mm (72).

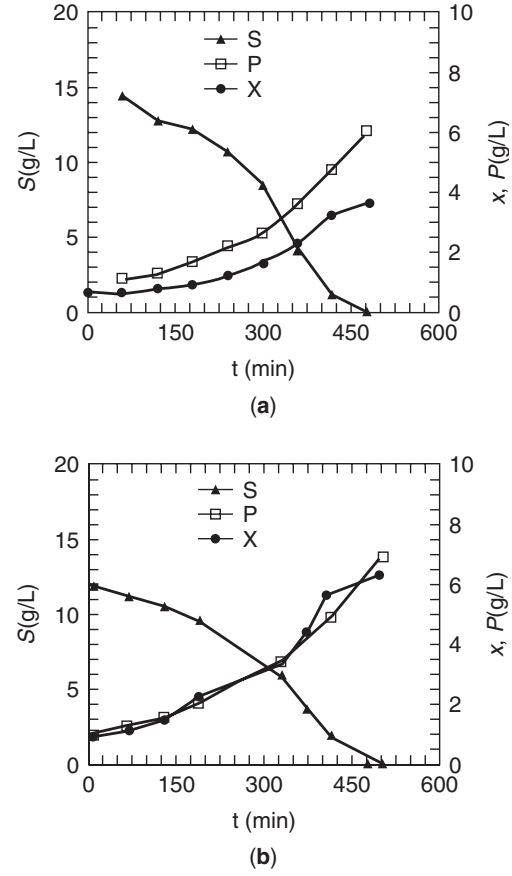


Figure 32.42. The comparison of a stirred tank and a novel bubble column bioreactor. Time coure of glucose concentration (S), cell dry weight (X), and ethanol concentration (P) in batch aerobic-growth on glucose of *S. cerevisiae*. Fermentations in a 5-L stirred-tank bioreactor (a) with an aeration rate of 1.1 vvm and in the microbioreactor (b) with an aeration rate of 0.064 vvm (72).

However, along with the developments in this technology, new challenges will be presented. Two obvious ones are the need for efficient mining of the large amounts of data that will be generated. The other will be the need to interface High Throughput analytical techniques with the miniature bioreactor systems. Fortunately, great strides have been made in both these areas and their careful integration will ultimately provide systems of the greatest value to the experimentalist.

Optical sensors that have been extensively used in the miniature systems described here are now finding their way into larger scale systems. Fluorometrix, Ocean Optics, Presense, and Polestar are some of the companies that market optical sensors that can be used in fermentation and cell culture applications at larger scales. Sartorius has just introduced its Cultibag line of disposable bag reactors that include noninvasive optical sensors, as shown in Fig. 32.44 (75). Clearly, process integration is currently under way.

Acknowledgments

We thank all of the authors who have spent years generating the advances presented here and the publishers who have allowed the use of copyrighted figures. Our own work has been generously supported by NSF, NIH, Maryland TEDCO, Dupont, Fluorometrix, Genentech, Merck, Pfizer and Sartorius over the years.

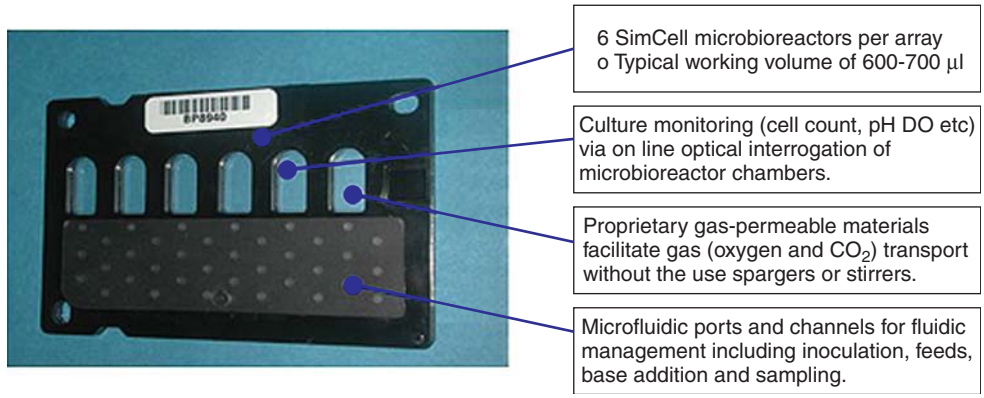


Figure 32.43. The Simcell microbioreactor array from bioprocessors (74). (This figure is available in full color at http://onlinelibrary.wiley.com/book/10.1002/9780470054581.)

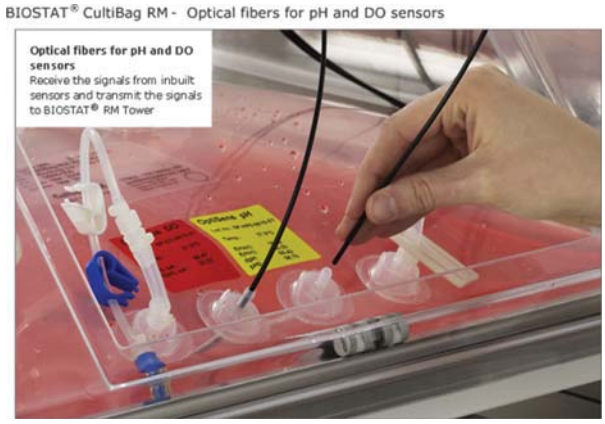


Figure 32.44. A Sartorius CultiBag disposable bioreactor. Fiber optics responsible for optical sensor excitation and emission detection are being inserted into an exterior sensing part (75). (This figure is available in full color at http://onlinelibrary.wiley.com/book/10.1002/9780470054581.)

REFERENCES

1. Humphrey A. Biotechnol Prog 1998; 14: 3–7. DOI: 10.1021/bp970130k.
2. Buchs J. Biochem Eng J 2001; 7: 91–98. DOI: 10.1016/S1369-703X(00)00106-6.
3. Zimmermann HF, Anderlei T, Buchs J, Binder M. Appl Microbiol Biotechnol 2006; 72: 1157–1160. DOI: 10.1007/s00253-006-0414-6.
4. Betts JI, Baganz F. Microb Cell Fact 2006; 21 DOI: 10.1186/1475-2859-5-21.
5. Kumar S, Wittmann C, Heinzle E. Biotechnol Lett 2004; 26: 1–10.
6. Lazar Research Laboratories, Inc. Web Information. Available at http://www.shelfscientific.com. Accessed 2007 Feb 27.
7. Zabriskie DW, Humphrey AE. Appl Environ Microbiol 1978; 35: 337–343.
8. Lakowicz JR. Principles of fluorescence spectroscopy. New York: Kluwer Academic/Plenum Publishers; 1999.
9. Randers-Eichhorn L, Bartlett RA, Frey DD, Rao G. Biotechnol Bioeng 1996; 51: 466–478. DOI: 10.1002/(SICI)1097-0290(19960820)51:4<466::AID-BIT10>3.0.CO;2-G.
10. Zanzotto A, Szita N, Boccazzi P, Lessard P, Sinskey AJ, Jensen KF. Biotechnol Bioeng 2004; 87: 243–254.
11. Boccazzi P, Zanzotto A, Szita N, Bhattacharya S, Jensen KF, Sinskey AJ. Appl Microbiol Biotechnol 2005; 68: 518–532. DOI: 10.1007/s00253-005-1966-6.
12. Lee PJ, Hung PJ, Rao VM, Lee LP. Biotechnol Bioeng 2006; 94: 5–14. DOI: 10.1002/bit.20745.
13. Hodson PH. Appl Microbiol 1970; 19: 551–554.
14. Mrotzek C, Anderlei T, Henzler H, Buchs J. Biochem Eng J 2001; 7: 107–112. DOI: 10.1016/S1369-703X(00)00108-X.
15. Cooper CM, Fernstrom GA, Miller SA. Ind Eng Chem 1944; 36: 504–509.
16. Schultz JS. Appl Microbiol 1964; 12: 305–310.
17. Tribe LA, Briens CL, Margaritis A. Biotechnol Bioeng 1995; 46: 388–392.
18. Nikakhtari H, Hill GA. Biotechnol Bioeng 2006; 95: 15–21. DOI: 10.1002/bit.20930.
19. Vasala A, Panula J, Bollok M, Illmann L, Halsig C, Neubauer P. Microb Cell Fact 2006; 5: 8. DOI: 10.1186/1475-2859-5-8.
20. Anderlei T, Buchs J. Biochem Eng J 2001; 7: 157–162. DOI: 10.1016/S1369-703X(00)00116-9.
21. AC Biotec GmbH Web Information. Available at http://www.acbiotec.com/english/1_home.htm. Accessed 2007 Mar 1.
22. Freyer SA, Konig M, Kunkel A. Biochem Eng J 2004; 17: 169–173. DOI: 10.1016/S1369-703X(03)00175-X.
23. Losen M, Frolich B, Pohl M, Buchs J. Biotechnol Prog 2004; 20: 1062–1068.
24. Tolosa L, Kostov Y, Harms P, Rao G. Biotechnol Bioeng 2002; 80: 594–597. DOI: 10.1002/bit.10409.
25. Gupta A, Rao G. Biotechnol Bioeng 2003; 84: 351–358.
26. Wittmann C, Kim HM, John G, Heinzle E. Biotechnol Lett 2003; 25: 377–380. DOI: 10.1023/A:1022402212537.
27. Luedeking R, Piret EL. J Biochem Microbiol Technol Eng 1959; 1: 393–412.
28. Ozturk SS, Palsson BO. Biotechnol Prog 1991; 7: 481–494.
29. Kermis HR, Kostov Y, Harms P, Rao G. Biotechnol Prog 2002; 18: 1047–1053. DOI: 10.1021/bp0255560.

30. Weuster-Botz D, Altenbach-Rehm J, Arnold M. Biochem Eng J 2001; 7: 163–170. DOI: 10.1016/S1369-703X(00)00117-0.
31. DASGIP AG Web Information. Available at http://www.dasgip.com/home_engl.php3. Accessed 2007 Mar 2.
32. Akgun A, Maier B, Preis D, Roth B, Klingelhofer R, Buchs J. Biotechnol Prog 2004; 20: 1718–1724. DOI: 10.1021/bp034289a.
33. Buchs J, Maier U, Milbradt C, Zoels B. Biotechnol Bioeng 2000; 68: 589–593. DOI: 10.1002/(SICI)1097-0290(20000620)68:6.
34. Peter CP, Suzuki Y, Buchs J. Biotechnol Bioeng 2006; 93: 1164–1176. DOI: 10.1002/bit.20827.
35. Duetz WA, Ruedi L, Hermann R, O'Connor K, Buchs J, Witholt B. Appl Environ Microbiol 2000; 66: 2641–2646. DOI: 10.1128/AEM.66.6.2641-2646.2000.
36. Hermann R, Walther N, Maier U, Buchs J. Biotechnol Bioeng 2001; 74: 355–363. DOI: 10.1002/bit.1126.
37. Hermann R, Lehmann M, Buchs J. Biotechnol Bioeng 2003; 81: 178–186. DOI: 10.1002/bit.10456.
38. Kensy F, Zimmermann HF, Knabben I, Anderlei T, Trauthwein H, Dingerdissen U, Buchs J. Biotechnol Bioeng 2005; 89: 698–708. DOI: 10.1002/bit.20373.
39. Li J, Wang S, VanDusen WJ, Schultz LD, George HA, Herber WK, Chae HJ, Bentley WE, Rao G. Biotechnol Bioeng 2000; 70: 187–196. DOI: 10.1002/1097-0290(20001020)70:2<187::AID-BIT8>3.0.CO;2-H.
40. Girard P, Jordan M, Tsao M, Wurm FM. Biochem Eng J 2001; 7: 117–119. DOI: 10.1016/S1369-703X(00)00110-8.
41. John GT, Klimant I, Wittmann C, Heinzle E. Biotechnol Bioeng 2003; 81: 829–836. DOI: 10.1002/bit.10534.
42. Weiss S, John GT, Klimant I, Heinzle E. Biotechnol Prog 2002; 18: 821–830. DOI: 10.1021/bp0200649.
43. Kensy F, John GT, Hoffman B, Buchs J. Bioprocess Biosyst Eng 2005; 75: 75–81. DOI: 10.1007/s00449-005-0010-7.
44. Applikon Web Information. Available at http://www.applikon-bio.com/cgi-bin/applikonbio/menu-micro-bioreactor-u24.html. Accessed 2007 Mar 6.
45. Tang YJ, Laidlaw D, Gani K, Keasling JD. Biotechnol Bioeng 2006; 95: 176–184. DOI: 10.1002/bit.21002.
46. Isett K, George H, Herber W, Amanullah A. Biotechnol Bioeng 2007; 98: 1017–1028.
47. Chen A, Chitta R, Chang D, Amanullah A. Biotechnol Bioeng 2008.
48. Samorski M, Muller-Newen G, Buchs J. Biotechnol Bioeng 2005; 92: 61–68. DOI: 10.1002/bit.20573.
49. Maharbiz MM, Holtz WJ, Howe RT, Keasling JD. Biotechnol Bioeng 2004; 86: 485–490.
50. De Jesus MJ, Girard P, Bourgeois M, Baumgartner G, Jacko B, Amstutz H, Wurm FM. Biochem Eng J 2004; 17: 217–223. DOI: 10.1016/S1369-703X(03)00180-3.
51. Muzzio FJ, Unger DR, Liu M, Bramble J, Searles J, Fahnestock P. Biotechnol Bioeng 1999; 63: 185–196. DOI: 10.1002/(SICI)1097-0290(19990420)63:2<185::AID-BIT7>3.0.CO;2-C.
52. Unger DR, Muzzio FJ, Aunins JG, Singhvi R. Biotechnol Bioeng 2000; 70: 117–130. DOI: 10.1002/1097-0290(20001020)70:2<117::AID-BIT1>3.0.CO;2-8.
53. Berson RE, Pieczynski WJ, Svihla CK, Hanley TR. Biotechnol Prog 2002; 18: 72–77. DOI: 10.1021/bp0101482.
54. Bambot SB, Holavanahali R, Lakowicz JR, Carter GM, Rao G. Biotechnol Bioeng 1994; 43: 1139–1145.
55. Chang Q, Randers-Eichhorn L, Lakowicz JR, Rao G. Biotechnol Prog 1998; 14: 326–331.
56. Kostov Y, Harms P, Randers-Eichhorn L, Rao G. Biotechnol Bioeng 2001; 72: 346–352. DOI: 10.1002/1097-0290(20010205)72:3<346::AID-BIT12>3.0.CO;2-X.
57. Puskeiler R, Kaufmann K, Weuster-Botz D. Biotechnol Bioeng 2005; 89: 512–523. DOI: 10.1002/bit.20352.
58. Harms P, Kostov Y, French JA, Soliman M, Anjanappa M, Ram A, Rao G. Biotechnol Bioeng 2006; 93: 6–13. DOI: 10.1002/bit.20742.
59. Infors HT Web Information. Available at http://www.infors-ht.com/images/stories/gallery/Sixfors/Sixfors%20with%20O2%20Option.jpg. Accessed 2007 Mar 1.
60. Trummer E, Fauland K, Seidinger S, Schriebl K, Lattenmayer C, Kunert R, Vorauer-Uhl K, Weik R, Borth N, Katinger H, Muller D. Biotechnol Bioeng 2006; 94: 1033–1044. DOI: 10.1002/bit.21013.
61. Lamping SR, Zhang H, Allen B, Ayazi Shamlou P. Chem Eng Sci 2003; 58: 747–758. DOI: 10.1016/S0009-2509(02)00604-8.
62. Betts JI, Doig SD, Baganz F. Biotechnol Prog 2006; 22: 681–688. DOI: 10.1021/bp050369y.
63. Zhang Z, Szita N, Boccazzi P, Sinskey AJ, Jensen KF. Biotechnol Bioeng 2006; 93: 286–296. DOI: 10.1002/bit.20678.
64. Szita N, Boccazzi P, Zhang Z, Boyle P, Sinskey AJ, Jensen KF. Lab Chip 2005; 5: 819–826. DOI: 10.1039/b504243g.
65. Ge X, Hanson M, Shen H, Kostov Y, Brorson KA, Frey DD, Moreira AR, Rao G. J Biotechnol 2006; 122: 293–306. DOI: 10.1016/j.jbiotec.2005.12.009.
66. Vallejos JR, Kostov Y, Ram A, French JA, Marten MR, Rao G. Biotechnol Bioeng 2006; 93: 906–911. DOI: 10.1002/bit.20785.
67. Kantarci N, Borak F, Ulgen KO. Process Biochem 2005; 40: 2263–2283.
68. Weuster-Botz D, Altenbach-Rehm J, Hawrylenko A. Bioprocess Biosyst Eng 2001; 24: 3–11. DOI: 10.1007/s004490100222.
69. Lakhotia S, Bauer KD, Papoutsakis ET. Biotechnol Bioeng 1993; 41: 868–877.
70. Doig SD, Ortiz-Ochoa K, Ward JM, Baganz F. Biotechnol Prog 2005; 21: 1175–1182. DOI: 10.1021/bp050064j.
71. Frachon E, Bondet V, Munier-Lehmann H, Bellalou J. Appl Environ Microbiol 2006; 72: 5225–5231. DOI: 10.1128/AEM.00239-06.
72. Reis N, Goncalves CN, Vicente AA, Teixeira JA. Biotechnol Bioeng 2006; 95: 744–753. DOI: 10.1002/bit.21035.
73. Lee HL, Boccazzi P, Ram RJ, Sinskey AJ. Lab Chip 2006; 6: 1229–1235. DOI: 10.1039/b608014f.
74. Bioprocessors Web Information. Available at http://www.bioprocessors.com/imgs/overviewpop.jpg Accessed 2007 Mar 10.
75. Sartorius BBI Web Information. Available at http://www.sartorius.com/index.php?id=3976. Accessed 2007 Apr 30.

33

INOCULUM PREPARATION

Craig J.L. Gershater
S.B. Pharmaceuticals, Harlow, Essex, England

33.1 INTRODUCTION

Inoculum preparation is the part of the fermentation development process that secures the microbial genotype for experimental and/or production purposes by providing a viable biomass capable of high productivity. Microbial processes generally consist of two distinct elements: a biotic factor the biomass and an abiotic factor (the growth environment). Hence, in applied microbiology terms

$$\text{pheotype} = \text{genotype} + \text{environment}$$

where the phenotype represents the desired attribute (accumulation of biomass or a valuable product of that biomass), the genotype represents the collection of metabolically useful genes and associated gene products, and the environment provides a system (principally a fermenter) of control over gene expression, that is, growth and product formation. At some point in the fermentation development program, the biotic and abiotic elements must be linked; this will be defined as the supply of consistent biomass to the fermenter plus growth medium. The growth and productive phases of fermentation are, of course, the subject of intense investigatory work; much has been written about the strict control requirements of the fermenter system, including the response of the microorganism to the nutritional and environmental factors. However, the requirements for the inoculum and the influence the inoculum can have on the outcome of the fermentation has received only scant attention (in terms of literature citations). A detailed assessment of the effect of the inoculum on microbial productivity can be justified, particularly in the case of nonrecombinant microorganisms, on the basis that commercially useful microbes will be isolated directly or indirectly from an ecosystem very remote from the fermentation laboratory, where the influences on growth are unknown.

33.1.1 Microbial Ecology

The microbial metabolic attribute to be exploited has evolved as a result of environmental influences unknown to the fermentation scientist. There is a case to be made for the basic ecology of the microorganism to be understood prior to culture preservation and inoculum preparation. A simple classification of organisms isolated from soil provides a loose context against which culture maintenance and development may be defined; soil organisms may be divided into two basic categories (1,2), the attributes of which are summarized in the following:

1. Indigenous, or autochthonous species, which have lower reproductive rates and are specialized for a particular habitat or more complex/intractable substrate. These are known as K strategists and include ascomycetes, basidiomycetes, and some actinomycetes.
2. Invaders, or allochthonous species, which have high reproductive rates and tend to function as pioneer species utilizing simple soluble substrates. The zymogenous fungi within this group include the sugar-fungi *Mucor, Rhizopus, Trichoderma, Penicillium*, and *Aspergillus*; organisms such as

Upstream Industrial Biotechnology: Expression Systems and Process Development, Volume 1, First Edition. Edited by Michael C. Flickinger.
© 2013 John Wiley & Sons, Inc. Published 2013 by John Wiley & Sons, Inc.

these may be activated by the presence of fresh substrate (breaking spore dormancy). These types of organisms, sometimes termed r strategists, possess good competitive abilities, which (along with some K strategists) include the ability to produce toxins (antibiotics), which is of obvious commercial interest.

Cognizance of the background ecology of the microorganism may permit a more appropriate culture storage and recovery method to be devised to maximize the chances of the organism successfully colonizing the next stage in the fermentation process.

33.1.2 Inoculum Development Conundrum

Process optimization must endeavor to replicate those factors responsible for the expression of the desired attribute in the totally artificial environment of monoculture; nutrient sufficiency (feast); and relatively stable physical parameters, such as temperature, pH, and oxygen availability. Although relatively few studies on the influence of inoculum on final stage fermentations have been made, it is certain that the inoculum preparation stage of most fermentations will affect the expression of the desired phenotype, whether qualitatively, quantitatively, or temporally. Hence, inoculum development is faced with a fundamental problem; the factors tested in seed stage or inoculum preparation investigations can only be assessed retrospectively in various high-productivity, final stage fermentations, remote from the seed stage influence. The conclusions drawn from inoculum development studies must deconvolute effects due to seed from those due to final stage fermentations. This chapter therefore seeks to explore how inoculum preparation can be incorporated into standard fermentation development programs.

33.1.3 Factors Critical to Inoculum Preparation

To adequately define the essential requirements for inoculum preparation, it is necessary to identify the elements that make up the process:

- Culture storage
- Stock culture
- Culture assessment
- Inoculum development
- Inoculation criteria

These elements will now be discussed and placed in the context of an overall inoculum strategy for fermentation development.

33.2 CULTURE STORAGE

Culture storage is only successful if the subsequent growth and productivity of the microorganism is consistent with expectations. Culture storage methodologies have been described in several authoritative texts (3–7) and are reviewed only briefly here.

33.2.1 Subculture

Depending on how cultures are received for fermentation development, some growth stage on agar will generally be required. The method of subculture relies on transferring colonies from one solid (depleted) medium to a fresh medium. This method is only suitable for short-term storage. Each transfer to fresh medium provides a comparatively nutrient replete environment, adaptation to which may select for an altered phenotypic expression. To minimize this possibility, minimal media are selected and the numbers of subcultures carried out are kept to a minimum. Minimal media agars are prepared in test tubes or screw-top Universal bottles, with the agars slanted to maximize surface area. Colonies from a master plate can be streaked onto the agar slants, allowed to grow for a minimum period, and then stored for a few weeks.

33.2.2 Desiccation

Removal or immobilization of water from the culture prevents metabolic activity, which is the key requirement of preservation. Drying methods are suitable for spore-forming fungi and streptomycetes; the principle is based on providing a solid, inert surface onto which spore suspensions can be dried. The methods differ in terms of the solid support that is used, which can include sterile soil, silica gel, dry sand, filter-paper disks, and various types of inert beads (glass, plastic, or porcelain). A suspension of spores (or possibly vegetative culture) is added to the sterile inert support, and after aseptic stoppering of the tube or vessel the mixture is allowed to dry at 25°C. This method provides a mechanism to store, typically, spore suspensions for perhaps months, but it is generally not recommended for long-term storage of process critical stock cultures.

33.2.3 Freeze-Drying (Lyophilization)

Freeze-drying removes water from a frozen culture by sublimation under a vacuum. It is suitable for the long-term preservation of many types of culture and is particularly suitable for the preservation of vegetatively grown cells. Bacteria, while frequently stored by lyophilization, may be susceptible to damage by random mutation (7,8). The benefits of freeze-drying cultures is that the lyophials are relatively easy to store, transport, and identify. The cultures

may be stable for up to 10 years. The disadvantages include the need to purchase a relatively expensive freeze-drier and the risk of mutation occurring in stored bacteria, which may be minimized by storing the lyophials in the dark at 5°C.

33.2.4 Freezing

Freezing the culture effectively deprives the cell of water and slows all metabolic and chemical activity. Intracellular water deprivation arises as a result of osmotic pressure induced at temperatures between −5°C and −15°C, the temperature at which ice forms in extracellular fluid but the intracellular space remains unfrozen (9). Under these circumstances there is solute enrichment of the extracellular fluid, and water leaves the cell by osmosis, freezes outside, and the volume fraction of the cell is thus reduced. The rate of freezing will affect the size distribution of the ice crystals and with slow cooling will tend to result in considerable water loss from the cell and large extracellular crystals; rapid freezing (−200°C/min, obtained by plunging the sample in liquid nitrogen) will result in smaller extracellular ice crystals and some intracellular ice crystal formation. It is necessary to determine the correct freezing rate for the particular cell under investigation. The properties and composition of the growth medium qualitatively affect the success of cryopreservation. Recovery from cryopreservation may also be critical due to an effect known as recrystallization, which refers to small crystals rearranging themselves into potentially more damaging larger crystals, leading to cell rupture. This may typically happen at temperatures between −100°C and −20°C. The potentially damaging effects are minimized by rapid thawing.

To minimize the general effect of ice crystal damage, high-viscosity cryopreservants are often added to the cell suspension (in the case of vegetative culture storage); these may be of two basic types, intracellular (membrane penetrating) or extracellular (nonmembrane penetrating). The intracellular agents used include dimethylsulfoxide (DMSO) and glycerol. Glycerol (added at 5–10% v/v to the final culture dispensing fluid) has the effect of reducing lesions due to osmotic shock by reducing the size of ice crystals. Extracellular cryopreservants include various carbohydrates, such as sucrose, mannitol, dextrin, and starch; 20% powdered skim milk and 12% sucrose are widely used.

The principal advantage of freezing as a method of culture storage is the relatively long duration of culture stability. The lower the temperature, the longer the duration. At −20°C it is reasonable to consider that microbial cultures will remain stable for 1 to 2 years; at −80°C, cultures should remain stable for 5 years or more, indefinite storage is obtained at temperatures of less than −80°C using liquid nitrogen. The vapor phase of liquid nitrogen is −156°C, and the liquid phase is −196°C; extreme care must be exercised when recovering culture vials from the liquid phase, because leakage of liquid nitrogen into vials may result in explosion of the sealed ampoules due to gas expansion at elevated temperatures. The main disadvantages of freezing for culture storage are the relatively high capital costs for compressor freezers (particularly those for less than −80°C) and secure purchasing and management procedures for maintaining liquid nitrogen stocks and reliability of electrical supplies. In addition, frozen ampoules are not easily transported.

Fungal culture storage may require a combination of all the methods described earlier for long-term storage, dependent on the morphological characteristics of the strain in question; for example, aconidial strains may be impossible to preserve by lyophilization (10), but may be stored on silica gel under liquid nitrogen. Methods appropriate to bacterial culture storage using both drying and liquid nitrogen have been reviewed (11).

33.3 STOCK CULTURE

A fermentation development or production process involving the culturing of commercially significant microorganisms demands that a robust system be in place for stock culture generation and maintenance. Variability of stock culture performance cannot be tolerated because culture variation masks the influence of nutritional or environmental factors within a development program.

33.3.1 What Is a Stock Culture?

The stock culture represents the current microbial investment in a fermentation program, which is manifested in both qualitative and quantitative terms. Qualitatively, the stock culture defines the current genotypic status of a commercially significant microorganism (i.e., its product formation capacity in a defined environment). Quantitatively, the stock culture is represented by a carefully controlled holding of cultivar, which will be drawn on for development and production purposes. At some critical point this holding must be replenished with equivalent stock culture or be replaced by an improved stock. Awareness of the microbial ecology of the culture may be important given that the cultivar will be required to propagate within a new environment (the ecological niche represented by fresh fermentation medium) by rapid colonization. If, for example, the culture of interest is considered to be an allochthonous species (r strategist) capable of colonizing fresh medium from spore inoculum, then the stock culture should be evaluated as a spore-based stock culture.

Management of the microbial culture resources is the most important facet of a microbiological bioprocess enterprise. Each bioprocess organization defines its own

protocols to secure the microbial investment; however, the principal objective must be to ensure that the bioprocess enterprise is never placed at risk due to stock culture mismanagement.

33.3.2 Stock Culture Generation

At various stages in a microbial development program it will be necessary to generate stock culture. The method chosen is dictated in part by the preservation protocol appropriate for the fermentation program. In my laboratory, with a relatively high turnover in new cultures for fermentation development, vegetative stock cultures are often generated and stored at −80°C. The stock generation model for cryopreservation is shown in Figure 33.1.

The model in Figure 33.1 assumes that the culture to be laid down to stock has been evaluated or in some other way nominated for long-term storage. Hence, prior to long-term culture storage, working stocks of the same culture will have been available. Working stock cultures may similarly be prepared using the model described earlier, but perhaps with far fewer vials, or they may be preserved using one of the other methods described previously.

The generation of fresh stocks may be dictated by several factors that may or may not be interrelated. As the stock culture holding is depleted, it must be replenished with fresh stocks with performance criteria as close to the existing stocks as possible. Stock culture management protocols determine at what point this should be; for critical bioprocesses (main line production) this may be initiated when 60% to 70% of the existing stock has been utilized. With less critical bioprocesses, stock culture replenishment may commence when 70% to 80% of the existing stock is depleted. Fresh stocks are also required when there is qualitative change in the culture component of the bioprocess. This may result from a deliberate attempt to improve the culture by strain improvement or culture reselection; alternatively, it may result from an inexplicable, irreversible deterioration in culture performance. If fresh stocks are to be generated from an improved strain, then the working stocks evaluated as part of the strain improvement process serve as the progenitor to the stock culture generation model previously described. If, however, the need to generate new stocks arises from severe culture deterioration, then a previous generation stock must be used for current stock culture generation. This deterioration may be accounted for by a reduction in culture viability, culture productivity performance, or microbial or viral contamination.

As new stock cultures are prepared, a family tree of related strains will be generated. To replenish stocks from an existing stock culture, a vial of the parental working stock can be used to generate a new daughter stock. Within the stock culture model each time a new generation stock culture is prepared after testing, a portion of that stock holding must be set aside for permanent retention. In my laboratory, at each stage in the stock maintenance program a portion of the existing stock is nominated as the master or "crown–jewel" stock and is held inviolable for process operations but represents a temporal marker in the history of a culture development program. To keep track of culture usage and family history, a suitable nomenclature must be devised. We use a simple decimal notation system in which the integer before the decimal point represents the current generation number and the figure after the decimal point represents the sibling stock number for the current generation.

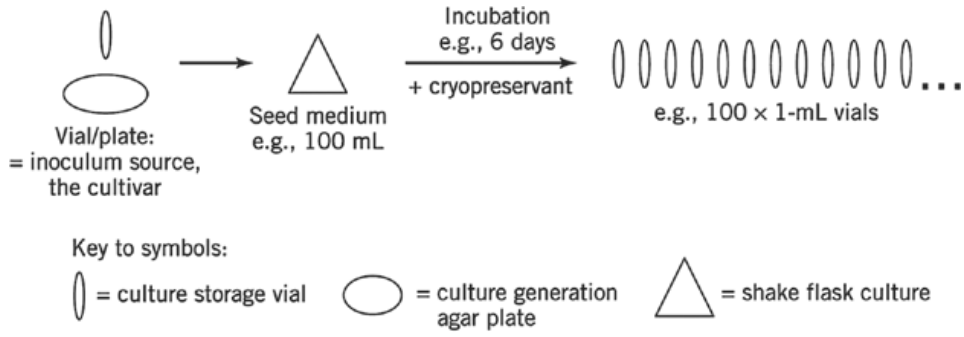


Figure 33.1. Stock culture generation models. Inoculum source for the first-stock generation is usually culture grown on agar plates; this is typically a plug (agar plugs are aseptically cut through the colony center) inoculated to liquid seed medium. The seed medium provenance, selected for vegetative growth, resides within relevant literature or, in the case of screening derived cultures, from original cultivation protocols. The incubation conditions for the culture are determined from the literature or from preexisting protocols. Dispensing of adequately grown vegetative culture to long-term culture vials is carried out under strict aseptic techniques; the number of vials dispensed to must be restricted to prevent the heterogeneous distribution of culture between first and last vials in the series.

Eventually even master or crown-jewel stocks may become depleted or obsolete, but within the active lifetime of a bioprocess, the master stock can only be drawn on in the event of a catastrophic failure of the main working stocks due to either an inexplicable loss of viability or performance or mechanical failure of the entire culture preservation system. To provide additional protection to the culture storage facility, a decision may be made to preserve split stocks not just in separate freezers but also on different sites, if possible. This type of stock culture management can be determined within an organization's disaster planning protocols.

33.4 CULTURE ASSESSMENT

The generation of new stocks imposes a profound influence on the bioprocess, and performance criteria must be reestablished at each stage in the culture maintenance program. As with any biological system, the inherent variability of the culture must be assessed prior to any development or production processes being committed to the new stock culture. The elements of culture maintenance that must be in place before an assessment of culture variability can be carried out include the following:

- Adequate numbers of culture vials (previously found to be monoculture)
- A suitable seed culture fermentation protocol
- A final or production phase fermentation protocol
- Suitable response variables to the final stage fermentation
- Validated assays for quantitatively determining the levels of the response variables
- Full supporting documentation to all of the elements mentioned

Culture variability must be addressed directly by the use of suitable statistical evaluation procedures. These procedures are largely based on a system of replication at each stage of the evaluation so as to obtain sufficient data describing the spread of variability and the contribution to total variation by each critical stage in the evaluation protocol. If the culture is being generated and evaluated as part of a good management practice (GMP) process, the stringency of these requirements may be greater. Figure 33.2 broadly defines the type of testing that may be carried out using a newly generated or existing stock.

This model permits replication sufficient to explore the contribution to the total variation of each of the stages capable of being a source of variation. This is sometimes known as a nested design, and data arising are analyzed using standard analysis of variance (ANOVA) procedures. Not only are data generated that capture the inherent variation associated with vial-to-vial variation, but the relative robustness of the remaining system can also be evaluated. Data from this kind of trial may be summarized in the form of statistical tables, but perhaps of more use would be data summarized using graphical plots. Figure 33.3 represents the actual data obtained for a reproducibility trial exploring the vial-to-vial variability of a fungal culture producing an antibiotic.

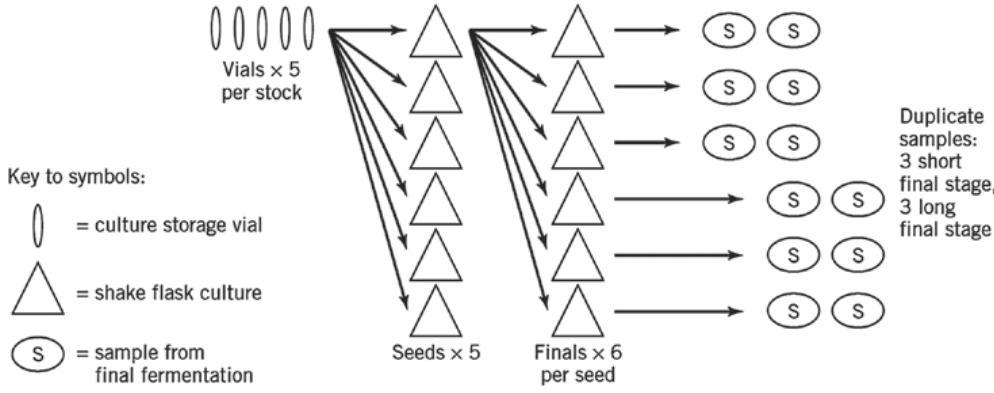


Figure 33.2. Culture variability testing model. To ensure adequate data is generated for a statistical analysis of variance to be undertaken, appropriate numbers of elements at each stage in the procedure must be selected. In this (model) case, five vials of stock culture are each used to inoculate each of five seed-media shake flasks. Each seed culture, after incubation to generate adequate biomass, is used to inoculate each of six final stage fermentations and will be assessed for reproducibility of growth. Half of the final stage shake flasks (three fermentation flasks) are incubated for a relatively short time and then duplicate sampled; the remaining half are incubated for a relatively longer time and then duplicate sampled. Each sample can be the source of duplicate or triplicate assays to enhance the analysis of variance (not shown in the model).

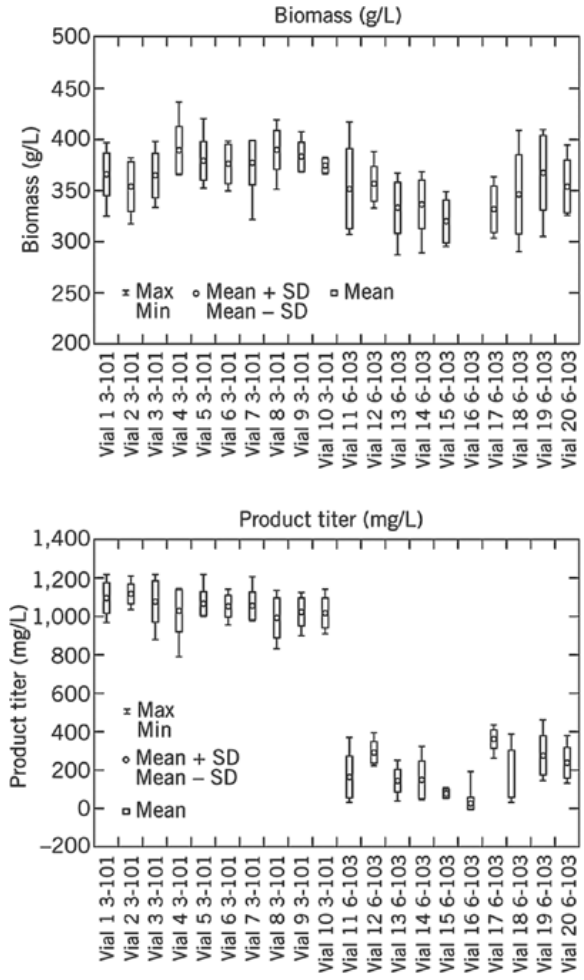


Figure 33.3. Reproducibility data from an antibiotic-producing culture. A fungal culture subject to a fermentation development program generated a number of reisolates that were tested in a reproducibility trial similar to one described in the model (Fig. 33.2). The two reisolates were called 3-101 and 6-103. Preliminary testing in single shake-flask experiments had indicated that although 3-101 was superior to 6-103, the difference was not great, therefore, working stocks of both cultures were prepared. In terms of biomass the two cultures appear very similar, although the variability of culture 6-103 was greater than that of 3–101. Biomass data was unavailable for vial 16, but this did not prevent an ANOVA of the data. In terms of product titer, 3-101 was clearly far superior to 6-103, both in terms of overall titre as well as vial-to-vial variation. The ANOVA for these experiments revealed that vial-to-vial variation was the greatest contributor to variation of 6-103 performance, and that factor tended to mask the true culture productivity.

33.5 INOCULUM DEVELOPMENT

As stated earlier, the key to successful inoculum preparation lies in the outcome in the final stage of the fermentation, hence, evaluation of seed protocols is always retrospective. The factors that can influence the inoculum and therefore the final-stage productivity are multifarious. This chapter has already identified certain key functions that may or may not influence the development of a successful seed culture, such as, microbial ecology, culture storage, and variability. In addition, some of the factors that may need to be considered in developing a inoculum preparation strategy include:

- Seed medium
- Seed incubation conditions
- Microbial growth dynamics
- Optimum transfer criteria (qualitative inoculum variable)
- Volume of inoculum on transfer (biomass concentration, quantitative inoculum variable)
- Number of seed-stage passages
- Assessing inoculum development

Several of these influences have been investigated in the past, but often in isolation from one another. The recognition that inoculum development can play a key role in fermentation development programs was recognized over 20 years ago; in a remark attributed to Hockenhull but reported by Calam (12), he stated that “once a fermentation had started it can be made worse but not better.” Despite this recognition, the bioprocess industry (high-added-value products), appears to have been very relaxed about setting resources aside to investigate the influence of inoculum on final stage fermentation productivities. This is perhaps somewhat in contrast to the fermentation food industries, where starter culture methods have been developed to provide high quality and consistent product.

In the dairy industry, factors such as correct carbon and nitrogen sources, vitamin and mineral supplements, and the addition of phage inhibitory agents, antioxidants, and neutralizers have all been considered important in defining the correct formulation for bulk starter media for lactic acid bacteria (13) in cheese production.

In the case of alcohol fermentation, relatively little work appears to have been done to investigate the influence of inoculum on alcohol yields. When reported, the studies are often limited to just one aspect of the inoculum process, for example, that inoculum levels may vary greatly with *Saccharomyces cerevisiae*, at between 0.05 and 60% (14). More recent studies with yeast fermentations have attempted to define the effect of inoculum on growth and ethanol production (15), including investigating at which point in the microbial growth curve inoculation should take place—in this case exponentially growing cells were favored. In addition, these studies were carried out while keeping factors such as medium formulation, medium sterilization, and culture growth conditions all constant, while varying inoculum size, under these circumstances inoculum levels of

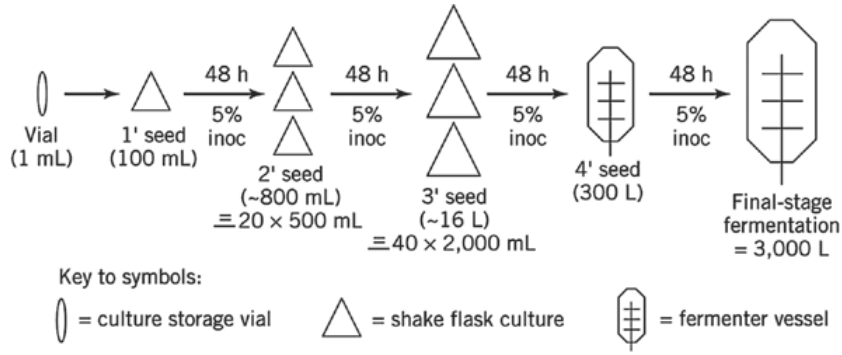


Figure 33.4. Typical multiple growth cycle fermentation seed train. The illustration indicates the logistics in preparing the inoculum for a 3,000-L final stage fermentation. In the example given, the seed train is defined by having a quaternary seed-stage inoculate the final-stage fermentation. The incubation times defined for each stage of the fermentation are designed to yield optimal inoculum to the next stage in the process. Throughout the seed train, the shock of culture transfer to nutrient feast is minimized by maintaining a relatively short residence in each seed fermentation, thus minimizing the risk of transferring from famine to feast at each stage. Inoculum transfer volumes impose logistic constraints on the seed train such that at the tertiary seed stage 40 2-L shake flasks must be inoculated. This represents a risk to the system in terms of contamination and culture heterogeneity, but small-scale fermenters can be used to overcome these problems.

10% were found to generate maximum biomass and, hence, ethanol.

Fermentations devoted to solvent formation have also been investigated to determine the influence of inoculum. The production of acetone, butanol, and ethanol by anaerobic fermentation using *Clostridium butylicum* was found to be adversely affected by repeated subculturing. This can be partly ameliorated by incorporating heat shocking and subculturing into an inoculum development program wherein the effect of heat shocking the culture to 75°C for 1.5 min may reduce the degenerative effects of subculturing (16). Again, more recent studies have confirmed the deleterious effect of repeated subculture with saccharolytic clostridia (17). Using *Clostridium acetobutylicum* it was recognized that there would be an abrupt decrease in solventogenesis after 10–12 successive transfers incorporating heat shock; further, after 25 transfers, the culture failed to form spores, and after heat shock failed to grow at all. The dramatic decrease in solventogenesis on subculture was found to be associated with deficiencies in acetate/butyrate CoA transferase and acetoacetate decarboxylase activity. The addition of exogenous acetic and butyric acids maintained solventogenesis to at least the 40th transfer.

The influence of inoculum development for fungal cultures has been investigated. The production of γ-linolenic acid (GLA) by shake flask culture of the sporulation-deficient strain of *Cunninghamella echinulta* was found to be profoundly affected by the use of fragmented mycelia, increasing biomass and GLA titre (18).

Most investigations into the influence of inoculum involving fungal and filamentous bacterial cultures have been carried out for the production of various bioactive metabolites at the high-value-added end of the bioprocess industry, some of the issues of inoculum preparation here will be now considered in more detail.

33.5.1 Multiple Growth Cycles

The generation of inoculum for large-scale bioactive metabolite production by fermentation generally necessitates a buildup of active biomass through multiple growth cycles. This is illustrated in Figure 33.4 for a typical 3,000-L pilot-plant fermentation.

In developing the multiple-growth cycle seed train, several experimental objectives must be met. The first of these is the seed medium for culture growth. There are virtually no references to seed stage medium development in the literature (19,20), however, some general principles do apply. The seed medium formulation should seek to minimize nutrient shift effects while supporting good vegetative growth over a short time scale. The overriding proviso for seed medium formulation is that high productivity is supported in the final stage medium. In the case of bioactive metabolite fermentations, the seed stage fermentation should not result in production of the metabolite of interest. Bioactive metabolites may be growth inhibitory to the producing strain (and hence are secondary metabolites), and their presence in the seed stage broth may complicate or inhibit the final stage product accretion. Sterilization control profiles for the seed stage medium, just as for the final stage medium, should ensure that Maillard reactions (browning) adversely affecting protein and glucose availability are minimized. Sterilization cycles should also be

designed such that vitamin destruction is minimized and so the formulation of the seed medium will seek to prevent trace element precipitation (e.g., phosphate and magnesium combinations and iron complexes formed on heating or pH shifts).

The overall inoculation protocol seeks to define a quality standard for the inoculum. Earlier studies had identified that larger volumes of inocula of *Trichoderma reesei* (in the range 0.5 to 5.0% v/v) ended to reduce subsequent lag phases (21). These sorts of studies were extended (22) using *Penicillium chrysogenum* for penicillin production; it had been established that the spore concentration in shake-flask seed culture was critical to growth and antibiotic production. Above 10^4–10^5 spores/mL, growth of the production cultures was good, critical enzyme levels were high, and penicillin production was good. Below 10^3 spores/mL, the fermentations were suboptimal in every respect. In further studies (23), *Penicillium* spores were seeded at different concentrations into seed medium, and samples were removed at regular intervals and examined for growth on agar for numbers of viable centers. At some critical point in the fermentation, the number of viable growth centers fell by up to 85%, presumably due to aggregation and increased branching frequency in the hyphae. These observations have been confirmed by image-analysis work (24), which demonstrates a morphology shift from dense pellet formations to more dispersed forms with inocula above 10^5 spores/mL. These data tend to confirm the notion of a quality curve for inoculum development, as illustrated in Figure 33.5.

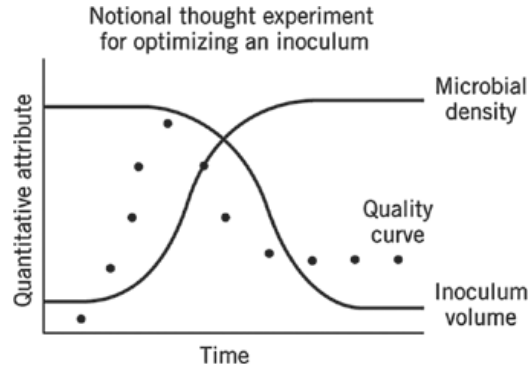


Figure 33.5. Notional quality curve for a seed stage fermentation. The thought experiment described suggests that there may be a compromise between inoculum volume and the qualitative attributes associated with the inoculum. Determining the notional quality curve requires an investigation into the optimization of the desired response variable in the subsequent fermentation stage. This may be achieved by carrying out timed transfers and measuring the physiological status of the organism at each time point.

33.6 INOCULATION/SEED TRANSFER CRITERIA

Multistage inoculum transfers and the success criteria associated with those transfers must be determined experimentally. Each stage in the process can be examined individually, but at some point the seed train protocol must be established. As already indicated, seed stage assays may be expensive in terms of numbers and time required for full analysis, and care must exercised to ensure that seed stage data correlate with final stage fermentation productivity. The use of complex media may impose additional variation on a multistage process, and wherever additional variation is suspected, greater replication in the data-gathering phase will be required.

The principal physiological markers that can be used for seed transfer criteria include:

- Biomass density or an analyte reflecting that variable (ATP)
- Gross morphology attributes (particularly for filamentous bacteria and fungi)
- Respiratory gas analysis from aerated fermenters (carbon dioxide evolution rate)
- Macromolecular titre (DNA, RNA)
- Final stage productivity

Final stage productivity can only be determined by inoculating final-stage fermentations from each seed stage and analyzing for productivity at each stage. The format for this type of experiment is shown in Figure 33.6.

33.7 INOCULUM PREPARATION STUDIES

There are very few studies reported in the literature examining the complete inoculum preparation process from initial inoculation to final stage productivity. *Streptosporangium* cultures that are capable of producing useful secondary metabolites, including chloramphenicol (25), dihydrosinefungin (26), and endothelin-converting enzyme inhibitors (27), have been investigated for various inoculum stage conditions (28). The factors examined with respect to the inoculum stage of *Streptosporangium* cultures include inoculum storage, media sources, and inoculum size on two antibiotic fermentations. Three culture preservation methods were examined: spores, slant tubes, and frozen agar plugs. When each of these sources were tested in different media and analyzed for growth, slant transfer tubes were found to be the most effective for maintaining high growth concentrations in the final stage. Examining incubation conditions with various *Streptosporangium* cultures indicated that aeration and growth phase of the inoculum may affect the time course

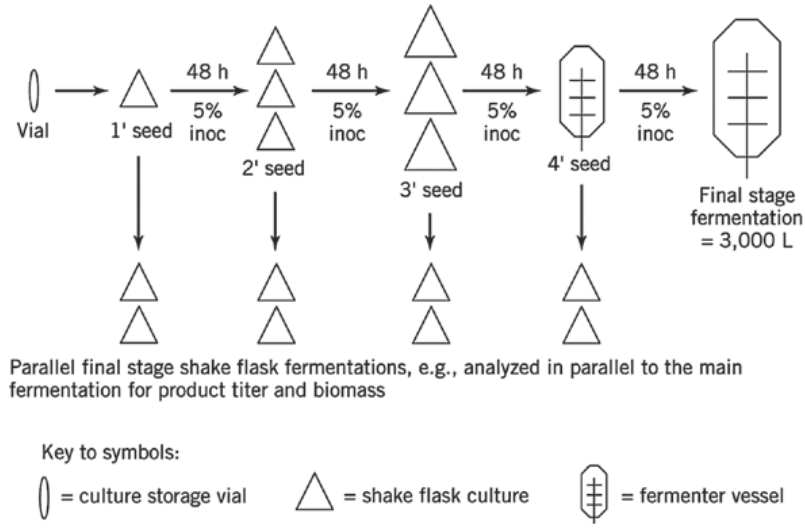


Figure 33.6. Inoculation–seed transfer experimental design. Final stage shake flask fermentations running in parallel to the main seed train, inoculated from seed stage broth generated in the inoculum train. Principal objective with this type of design is to compare productivity between each final stage fermentation to help determine if there are effects due to passage or some other seed incubation condition.

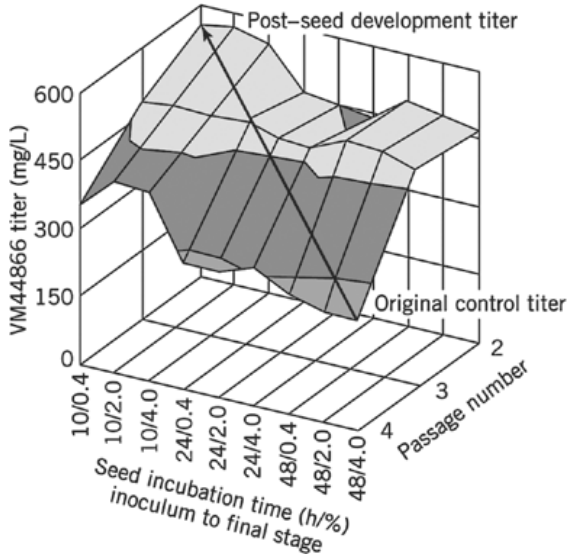


Figure 33.7. Response surface plot for milbemycin production under the influence of seed stage development factors. The response surface plot shows the final stage titers of milbemycin obtained under the seed inoculum conditions indicated by the three-dimensional plots. These data show that percentage inoculum levels into the final stages were not a key factor. However, passage number was significant, with quaternary seed stages giving rise to the lowest final stage titers. Similarly, juvenile seed was optimal for all conditions tested.

of the final stage fermentation, particularly if that fermentation stage is relatively short. These influences may be less pronounced if longer final stage fermentations are required.

The improved production of milbemycin (a macrolide with anthelminthic properties) from *Streptomyces hygroscopicus* as a result of intensive seed stage development has been reported (29). In this work an attempt was made to examine several interacting factors affecting seed stage development and subsequent final stage production of milbemycin. Time-course fermentation profiles of the seed stage revealed that a major component of the seed medium, dextrin, was not utilized, and the other major carbohydrate component, glucose, could be reduced fourfold without affecting the productivity of the final stage fermentation. Aside from medium composition, the other seed development factors investigated included:

- Age of culture at transfer
- Temperature of seed-stage incubation
- Inoculum level
- Passage number of seed stages

Inoculum age was found to have a profound influence on final stage titers, with more juvenile seeds (10 h as compared to 48 h for the control) proving beneficial to milbemycin production. Inoculum levels could be halved from 4% v/v without loss of productivity. Passage number was found to be critical in seed media containing dextrin, as these seed fermentations showed a marked decrease in final stage titers in the tertiary and quaternary seed stages. Studies investigating the combined effects of seed incubation times, percentage inoculum into each seed stage or the final stage fermentations, and passage number were undertaken. Figure 33.7 shows the response surface plot summary

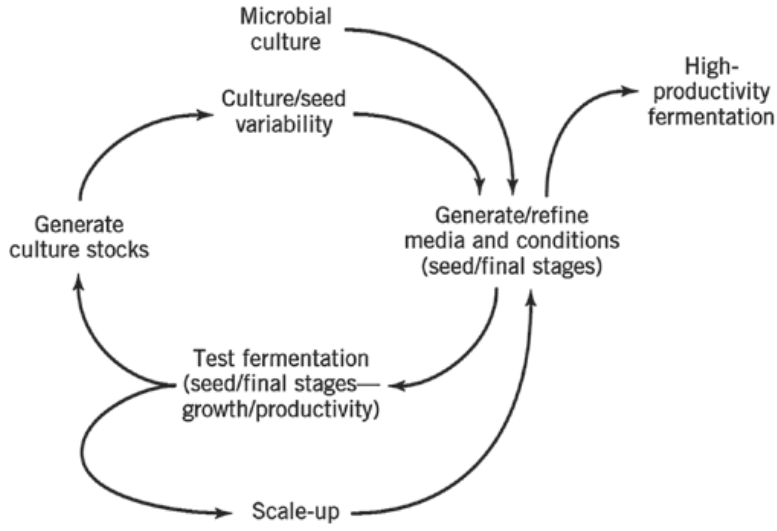


Figure 33.8. Fermentation development model incorporating seed stage investigations. The model shown assumes the process starts with receipt of the microbial culture. Seed and final stage media are identified initially. Fermentations are carried out to assess growth, and if adequate to the purpose, then culture stocks may be generated. These stocks must be tested for variability before further studies can commence. Seed and final stage fermentation conditions can then be refined with the newly generated and tested stock culture. The fermentation development process continues until performance criteria for the system are met, the process is scaled up, and if necessary further refined. Finally a high-productivity fermentation can be defined using a well-characterized and genotypically secure process.

of that work, where by examining the various seed stage factors, overall the titer of the final stage fermentation was increased fourfold.

33.8 INOCULUM DEVELOPMENT SUMMARY

This chapter has attempted to describe the various influences that may be examined when trying to define the optimal inoculum-development protocols. As indicated from the literature, this part of the fermentation process has been largely neglected, and yet the evidence indicates (from the relatively few studies undertaken) that inoculum preparation may have a profound effect on the outcome of a fermentation development process. Figure 33.8 describes how inoculum development may be incorporated into the overall fermentation development strategy for a bioprocess enterprise.

REFERENCES

1. R. Campbell, Microbial Ecology, 2nd ed., Blackwell Scientific Publications 1983, pp. 82, 90.
2. M. Alexander, Introduction to Soil Microbiology, 2nd ed., Wiley, New York, 1977, pp. 16–17.
3. L.T. Chang and R.P. Elander, in A.L. Demain and N.A. Solomon eds., Manual of Industrial Microbiology and Biotechnology, American Society of Microbiology, Washington, D.C., 1986, pp. 49–55.
4. J.J.S. Snell, in B.E. Kirsop and J.J.S. Snell eds., Maintenance of Microorganisms: A Manual of Laboratory Methods, Academic Press, Inc, London, 1984, pp. 11–21.
5. D. Smith and A.H.S. Onions, The Preservation and Maintenance of Living Fungi, Commonwealth Mycological Institute, Kew, U.K., 1983, pp. 5–30.
6. A. Dietz and B.W. Churchill, in M. Moo-Young ed., Comprehensive Biotechnology: The Principles, Applications, and Regulations of Biotechnology in Industry, Agriculture, and Medicine, vol. 1, Pergamon Press, Oxford, 1985, pp. 37–49.
7. A. Dietz, in H.-J. Rehm and G. Reed eds., Biotechnology: A Comprehensive Treatise in 8 Volumes, vol. 1, Verlag Chemie, Weinheim, 1981, pp. 411–434.
8. M.J. Ashwood-Smith and E. Grant, Cryobiology 13: 206–213 (1976).
9. C. Herbert, P. Roux-Salembien, and J.-M. Egly, Biofutur 128: 3–11 (1993).
10. C. Wilson, Fungal Genet. Newsletter 33: 47–48 (1986).
11. I.J. Bousfield, in B.E. Kirsop, and J.J.S. Snell eds., Maintenance of Microorganisms: A Manual of Laboratory Methods, Academic Press, Inc, London, 1984, pp. 63–68.
12. C.T. Calam, Process Biochem. 7–12 (April 1976).
13. W.E. Whitehead, J.W. Ayers, and W.E. Sandine, J. Dairy Sci. 76: 2344–2353 (1993).
14. P. Strehaino, M. Mota, and G. Goma, Biotechnol. Lett., 5: 135–140 (1983).

15. G. Birol and K. Ozergin-Ulgen, Turk. J. Chem. 19: 250–257 (1995).
16. J.R. Gapes, V.F. Larsen, and I.S. Maddox, J. Appl. Bact. 55: 363–265 (1983).
17. O. Assobhei, A. El Kanouni, M. Ismaili, M. Loutfi, and H. Petitdemange, J. Ferment. Bioeng. 85: 209–212 (1998).
18. H.-C. Chen and T.-M. Liu, Enz. Microbiol. Technol. 21: 137–142 (1997).
19. G.R. Hunt and R.W. Stieber, in A.L. Demain and N.A. Solomon eds., Manual of Industrial Microbiology and Biotechnology, American Society of Microbiology, Washington, D.C., 1986, pp. 32–40.
20. S. John Pirt, Principles of Microbial and Cell Cultivation, Blackwell Scientific, Oxford, 1975, pp. 118, 196–198.
21. D.E. Brown and M.A. ZainudeEn, Biotechnol. Bioeng. 20: 1045–1061 (1978).
22. G.M. Smith and C.T. Calam, Biotechnol. Lett. 2: 261–266 (1980).
23. C.T. Calam and G.M. Smith, FEMS Microbiol. Lett., 10: 231–234 (1981).
24. K.T. Tucker and C.R. Thomas, Biotechnol. Lett., 14: 1071–1074 (1992).
25. A. Tamura, I. Takeda, S. Naruto, and Y. Yoshimura, J. Antibiot. 24: 270 (1971).
26. R. Cooper, P. Das, C. Federbush, R. Mierzwa, M. Patel, P. Birendra, and I. Truumees, J. Indust. Microbiol. 5: 1–8 (1990).
27. Y. Tsurumi, N. Ohata, T. Iwamoto, S. Kyoto, and S. Okuhara, J. Antibiot. 47: 619–630 (1994).
28. G. Platas, J. Collado, H. Martinez, M. Arrese, P. Pelaez, and M.T. Diez, Microbiologia SEM 13: 193–200 (1997).
29. S.R.C. Warr, C.J.L. Gershater, and S.J. Box, J. Indust. Microbiol. 16: 295–300 (1996).

34

MICROCARRIER CULTURE

SUSAN T. SHARFSTEIN
Department of Chemical and Biological Engineering and Center for Biotechnology and Interdisciplinary Studies, Rensselaer Polytechnic Institute, Troy, New York

CHRISTIAN KAISERMAYER
Project Manager Cell Culture Applications & Support, GE Healthcare, Vienna, Austria

34.1 HISTORY AND DEVELOPMENT

Microcarrier development began in the 1960s when Antonius L. van Wezel first cultivated human fibroblast cells on DEAE Sephadex™ beads (1). The beads were at that time already in use as an anion exchanger in chromatography. van Wezel achieved a homogenous unit process and was thus the first to cultivate adherent cells without attachment to the vessel surface. The cultivation technique was further developed under his direction at the Laboratory for Inactivated Virus Vaccines (Bilthoven, The Netherlands). van Wezel also recognized the potential of microcarriers for large-scale culture of adherent cells and performed extensive research in the field of vaccine production (2–4). According to van Wezel, a microcarrier must have the following properties.

- The surface must allow cell adhesion.
- The diameter should be between 150 and 250 μm. This is a compromise between achieving maximum surface area and reducing adherence of the cells due to excessive curvature.
- The variation in bead size must be small to ensure that cells on all microcarriers reach confluence at the same time.
- The density of the microcarriers should be between 1.05 and 1.15 g/cm^3 to keep the carriers in suspension by relatively low stirrer speeds, thereby reducing shear forces that could hinder cell attachment and proliferation. However, the carriers should settle rapidly in the absence of stirring to allow cell separation and media change.
- The carriers should be transparent to allow microscopic observation of the cells.

For large-scale applications, handling is much easier if the carriers are autoclavable. In addition, they should be available in large batch sizes, have a good long-term stability, and have a suitable documentation (i.e. a drug master file or a regulatory support file from the manufacturer) to permit the carriers to be used for industrial purposes.

Subsequent work in the 1970s showed that the technique was scaleable for a variety of production processes (2,5). Since the yield of adherent cells depends on the surface area available for growth, it was believed that the maximum cell concentration in microcarrier cultures would increase linearly with microcarrier concentration. However, when the quantity of DEAE Sephadex A-50 exceeded 1–2 g/L, no proportional increase in cell yield was achieved, which was attributed to the toxicity of high microcarrier concentrations (2,6). This toxicity was manifested by the failure of many cell types to survive the early stages of culture, long lag phases, and limited cell concentrations at the plateau stage of culture. Explanations for this phenomenon have varied, but it was widely believed that the degree of substitution of DEAE Sephadex

Upstream Industrial Biotechnology: Expression Systems and Process Development, Volume 1, First Edition. Edited by Michael C. Flickinger.
© 2013 John Wiley & Sons, Inc. Published 2013 by John Wiley & Sons, Inc.

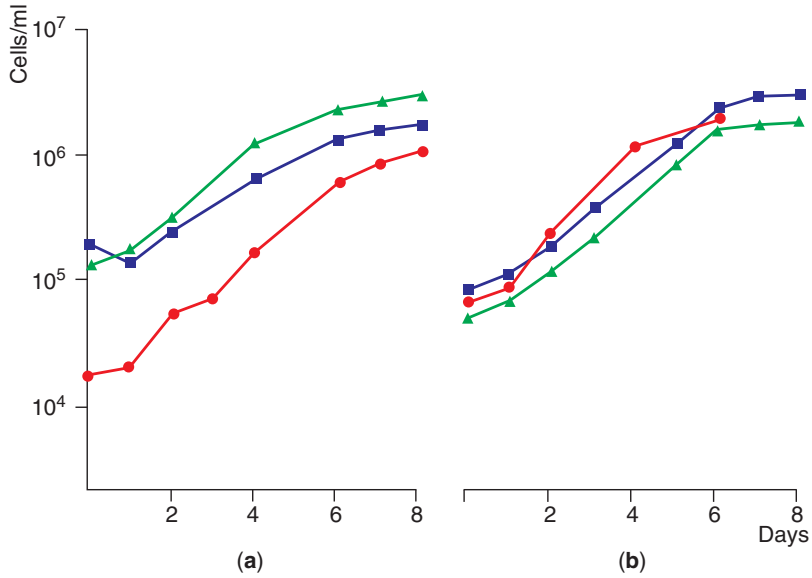


Figure 34.1. Growth of various cell types on Cytodex microcarriers in stirred cultures. (a) Blue squares—human fibroblasts MRC 5, red triangles—chicken fibroblasts, red dots—human nasopharangal carcinoma cells KB. (b) Blue squares—mouse fibroblasts J129, red triangles—normal rat kidney cells NRK, red dots—Rhesus monkey kidney cells LLC-MK2. (Data reproduced by kind permission of S. Toyama, Inst. Virus Res., Kyoto University, Kyoto, Japan.) (This figure is available in full color at http://onlinelibrary.wiley.com/book/10.1002/9780470054581.)

A-50 was not optimal for cell growth (7–9). Horng and McLimans (8), Inooka (10), and Kuchler *et al*. (11) suggested that alterations in the ion-exchange capacity of DEAE Sephadex A-50 could lead to improvements in cell attachment and growth. The problem was overcome by the development of microcarriers with a much lower degree of substitution, yet that still fulfilled van Wezel's requirements for an optimal microcarrier. These microcarriers were the result of collaboration between van Wezel and Pharmacia Biotech AB. Instead of DEAE Sephadex A-50, a different matrix, namely, Sephadex G-50, was substituted with varying DEAE concentrations.

Cytodex™ 1 was launched in 1981. Due to the different matrix and the lower degree of DEAE substitution, the charge concentration on this carrier was only 1.5 meq/g compared to the 3.5 meq/g in the original DEAE Sephadex A-50 carrier. This new carrier avoided the toxic effects associated with the high charge concentration and was suitable for growing a wide variety of cells (12–14). Cytodex 1 was thus the first commercial product to allow the full potential of microcarrier culture to be exploited at volumes up to several hundred liters (15–17). The carrier did not show toxic effects at concentrations well above 2 g/L and cell yields increased with carrier concentration. The recommended concentration for Cytodex 1 is 3 g/L (18); however, for high cell density fermentations, it has been increased to 5 g/L and even 10 g/L (19–21) without negative effect on cell growth. Opportunities for microcarrier culture of animal cells have been further increased by the development of Cytodex 3, which consists of a dextran matrix coated with denatured porcine collagen. The collagen-coated surface of the carrier thus creates an environment similar to that encountered by the cells *in vivo*, which is important for maximizing the plating efficiency and function of cell types such as hepatocytes, fibroblasts, chondrocytes, myoblasts, and epidermal cells (22,23). Growth curves of different cell lines on Cytodex carriers are shown in Fig. 34.1.

van Wezel's requirements for microcarriers apply only to smooth or microporous carriers where cell growth takes place on the surface of the beads. Significant improvements have been made to develop microcarriers suitable for various cell types and also for different cultivation methods. Table 34.1 gives an overview of commercially available microcarriers. In addition to dextran, polystyrene, polyethylene, glass, and collagen have also been used as matrices. Carrier surfaces were modified with extracellular matrix (ECM) proteins such as collagen or fibronectin as well as with synthetic coatings like poly lactic acid, poly L-lysine, or trimethyl ammonium. A further important development was the introduction of macroporous carriers that allow cell growth inside the pores, thereby protecting

TABLE 34.1. Commercially Available Microcarriers

Name	Material	Surface Modification	Manufacturer	Diameter (μm)
Cytodex 1	Dextran	DEAE	GE Healthcare	180
Cytodex 3	Dextran	Gelatin-coated	GE Healthcare	175
Cytoline 1, 2	Polyethylene, silica		GE Healthcare	Length 1700–2500, thickness 400–1100
Cytopore 1, 2	Cellulose	DEAE	GE Healthcare	200–270
Hillex	Polystyrene	Cationic trimethyl ammonium	SoloHill Engineering Inc.	90–212
ProNectin F	Polystyrene	Recombinant fibronectin	SoloHill Engineering Inc.	90–212
Biosil	Polystyrene	Glass coated	SoloHill Engineering Inc.	90–212
Carboseed S	Carbon	Cationic modification	Blue Membranes GmbH	800
Carboseed P	Carbon	Cationic modification	Blue Membranes GmbH	1000
Biosilon	Polystyrene		Nunc	160–300
Microhex	Polystyrene		Nunc	Length 125, thickness 25
Cellagen	Collagen		MP Biomedicals	100–400
Cultisphere G	Collagen		Percell Biolitica	170–270
Cultisphere S	Collagen		Percell Biolitica	170–270
Siran	Glass		Schott Glaswerke	3000–5000
Fibracell	Polyester		New Brunswick	Disc 6000 × 2000

the cells from shear forces introduced by stirring or aeration, particularly rising gas bubbles, while at the same time increasing the available surface area to achieve higher cell concentrations (24–26).

34.2 CELL CULTIVATION

34.2.1 Cellular Adhesion Mechanisms

Cell attachment to microcarriers is influenced by a number of factors. In the beginning of microcarrier development in the 1960s, it was proposed that the charge density of positively charged surfaces was the main factor for cell attachment. Indeed, Mukopadhyay *et al*. (27) showed that adsorbed serum proteins on microcarrier surfaces, which masked the carrier charge, resulted in a lower cell-attachment rate. On Cytodex 1, cell attachment was shown to follow first-order kinetics and to rely on the electrostatic interaction between the negatively charged cell surface and positively charged amino groups on the microcarrier (18). The negative charge on the cell surface is conveyed by the glycocalyx, the carbohydrate part of glycoproteins and glycolipids embedded in the cell surface (28).

Collagen-coated surfaces are used frequently for establishing primary cultures and for growing cells that are difficult to handle or have low plating efficiency, such as hepatocytes, fibroblasts, chondrocytes, myoblasts, or epidermal cells (22,23). Collagen is almost neutrally charged and promotes cell attachment via receptor-mediated interactions (29). Cells in tissues *in vivo* are surrounded by a complex network of macromolecules to which they attach using a number of heterodimeric cell-surface adhesion receptors known as integrins (30). Integrins are noncovalently linked heterodimeric proteins that recognize proteins of the ECM or counterreceptors on adjacent cells in a cation-dependent manner. The RGD (arginine-glycine-aspartic acid) sequence is known to be the key adhesion site (31) found in many proteins of the ECM, including fibronectin, type 1 collagen, vitronectin, and laminin. Antibodies against integrin subunits block cell adhesion to vitronectin-coated surfaces (32). As cell adhesion to surfaces coated with ECM-like proteins occurs via receptor-mediated interactions, the process is slower than attachment to charged surfaces.

34.2.2 Cell Types Cultured

As Table 34.1 shows, a wide selection of microcarriers is available. Selecting the appropriate carrier for a specific cell line depends on the attachment characteristics of the cells, the process design, and whether the cultivation medium contains serum or recombinant attachment factors. In general, microporous or surface carriers will be more applicable for the cultivation of adherent cells, while the sponge-like structure of macroporous carriers is suitable for all cell types. Macroporous carriers will also facilitate the immobilization of cells that can grow in suspension. Table 34.2 shows a selection of cells that have been cultivated on microporous carriers. Examples of cells grown on macroporous carriers are given in Table 34.3. Figures 34.2–34.4 show microphotographs of cells grown on microporous and macroporous carriers.

TABLE 34.2. Cell Types Cultured on Cytodex Microcarriers

Tissue	Cell Line
Adrenal	Mouse cortex tumor—Y-1
Amnion	Human—WISH
Amniotic cells	Human amniotic fluid
Bone Marrow	Human—Detroit 6
	Human—Detroit 38
Carcinoma	Human nasal—RPMI 2650
	Human larynx—HEp 2
	Human oral—KB
	Human cervical—HeLa
	Human colon
	Human thyroid
Conjunctiva	Human—Chang "D"
Cornea	Rabbit—SIRC
Endothelium	Rabbit coronary endothelium
	Human coronary endothelium
	Mouse brain capillary endothelium
	Bovine pulmonary artery endothelium
Epithelium	Human—NITC 2544
Fibroblast	Human foreskin—FS-4
	Human foreskin—Detroit 532
	Mouse—SC-1, 3T3, 3T6, L-cells, L-929, A9
	Mouse—transformed
	Mouse—embryo
	Chicken—embryo
	Human—embryo
	Rat—embryo
	Rabbit—embryo
	Human—*Xeroderma pigmentosum*
	Muntjac—adult skin
Fibrosarcoma	Human—HT 1080
	Mouse
Fish	Rainbow trout gonad—RTG
	Fat head minnow—FHM
	Carp eptihelioma—EPC
Glial	Rat
Glial tumor	Rat—C6
Glioma	Human
Heart	Human atrial appendage—Girardi heart
Hepatoma	Rat—HTC, Morris MH1C1
Insect	Drosophila
	Spodoptera
	Trichoplusia
Kidney	Human embryo
	Human embryo—Flow 4000, L-132
	Bovine embryo—MDBK
	Monkey—primary
	Dog—primary, MDCK, transformed
	Rabbit—primary, NZ white, LLC-RK
	RK-13
	Rat—NRK, transformed
	Pig—PK-15, IBR
	Syrian hamster—HaK, BHK, transformed
	Potroo—Pt-k-1
	Rhesus monkey—LLC-MK2
	African Green monkey—Vero, CV-1
	BSC-1, BGM, GL-V3
Liver	Human primary hepatocytes
	Rat primary hepatocytes
	Chimpanzee
	Human—Chang liver
	Human embryo—L-132, MRC-5, MRC-9,
Lung	Chinese hamster—Don
	Chimpanzee embryo—CR-1
	WI-38, IMR-90, Flow 2002, HEL 299
	Cat embryo
	Bat—Tb 1 Lu
	Mink—Mv 1 Lu
Lymphoid	Human—lymphoblastoid
	Human—lymphocytes
Macrophage	Mouse—peritoneal, peripheral blood
	Rat—peritoneal
	Human—peripheral blood
	Mouse—P388D1
Melanoma	Human
	Mouse
Muscle	Chicken myoblasts
	Rat muscle-derived fibroblasts
Neuroblastoma	Mouse—Neuro-2a
Osteosarcoma	Human
Ovary	Chinese hamster—CHO
Pancreas	Rat
Pituitary	Rat
	Bovine
Rhabdomyosarcoma	Human—RD
Synovial fluid	Human—McCoy
Thyroid	Pig

TABLE 34.3. Cells Cultured on Cytoline and Cytopore Microcarriers

Cells	Media
CHO-K1	2% FCS; 5% FCS, protein-free
r-CHO based on DHFR-	2% FCS; 5% FCS, protein-free
r-CHO based on CHOK1	2% FCS; 5% FCS, protein-free
Murine hybridoma	2% FCS; protein-free
Human hybridoma	2% FCS; protein-free
SP2/0	
NSO	
m-Fibroblasts	10% FCS
BHK-21	2% FCS; protein-free
Melanoma	Protein-free
Vero	5% FCS, protein-free
Ea.hy.926	
C127	
TE-fly	
Dog kidney	

34.2.3 Practical Aspects

The bexst results from microcarrier cultures are obtained with equipment that gives even suspension of the microcarriers with gentle stirring. Static culture can be used for initial experiments. Whenever microcarriers based on a dextran or glass matrix come into contact with glassware, the



Figure 34.2. Chicken embryo myoblasts 2 days after inoculation on Cytodex. Original photographs by R. Przybylski, R. Pawlowski, R. Loyd, Department of Anatomy, School of Medicine, Case Western Reserve University, Cleveland, OH 44106, USA; work supported by the Muscular Dystrophy Association and National Institutes of Health. Reproduced with permission. (This figure is available in full color at http://onlinelibrary.wiley.com/book/10.1002/9780470054581.)

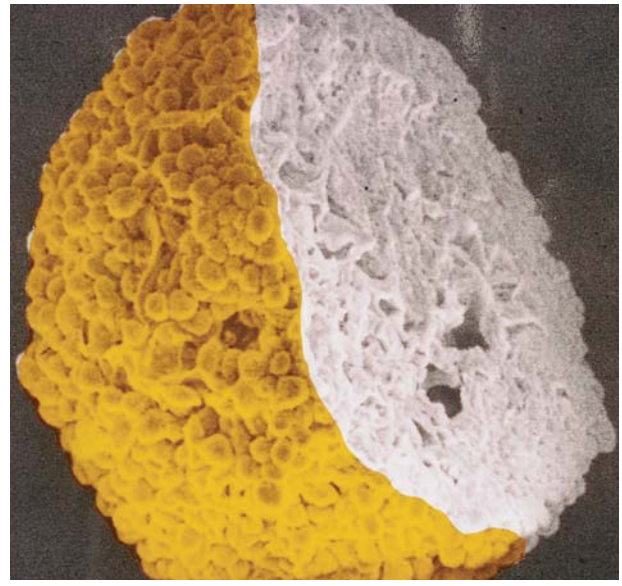


Figure 34.3. Cross-section through a Cytopore carrier fully colonized with CHO cells (magnification = 500X). (This figure is available in full color at http://onlinelibrary.wiley.com/book/10.1002/9780470054581.)

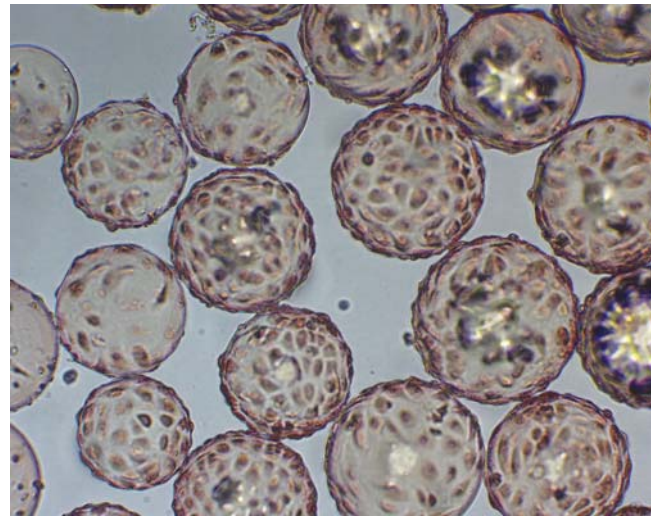


Figure 34.4. Vero cells grown on Cytodex (magnification = 100X). (This figure is available in full color at http://onlinelibrary.wiley.com/book/10.1002/9780470054581.)

inside of the glass vessels should be siliconized to prevent the microcarriers from sticking to the surface.

For small-scale culture, plastic bacterial petri dishes are often used for stationary cultures, while roller bottles or shake flasks are used for mixed cultures and spinner flasks for stirred cultures. Addition of microcarriers to culture bottles (tissue culture flasks or roller bottles) dramatically increases the surface area available for cell growth, thereby increasing cell yield several fold. When using shake flasks for cell cultivation on microcarriers, an orbital shaker is preferred over a reciprocal shaker as its mixing is gentler. The rate of rocking should be just sufficient to prevent sedimentation of the microcarriers. If necessary, 5–10% (w/v) Ficoll™ 400 can be added to the cultivation medium to increase its density, which facilitates microcarrier suspension.

The most suitable vessels for general purpose laboratory scale microcarrier culture are those with a stirring rod or impeller driven by a magnetic base unit. These vessels have been used for many years to cultivate suspension cells. The stirring rod or bar should never come into contact with the inside surface of the vessel since this may damage the microcarriers. Spinner vessels used under closed culture conditions are suitable for cultures ranging from about 50 mL to 5 L. The capacity of the closed culture system is limited by the gas exchange capabilities (i.e. headspace aeration) that require a minimum surface area-to-volume ratio to ensure oxygenation of the culture. For larger-scale culture, bioreactors are necessary to effectively control culture conditions. Bioreactor microcarrier cultures can be operated at very high cell densities (up to 2×10^8 cells/mL carrier in fluidized and packed beds) as well as scaled up to several thousand liters. Microcarrier cultivation can be done in very different reactor types. In addition to classical stirred-tank

reactors (STRs), microcarriers have also been used successfully in disposable bioreactors such as the Wave bioreactor (33–35). Cells can also be grown in fluidized-bed reactors using Cytoline™ carriers or packed-bed reactors with Fibracel™, Carboseed™, Cytoline, or Siran™ carriers. Cultivation in fluidized- or packed-bed mode can increase cell concentrations 15–25-fold compared to classic fed-batch culture of suspension cells, with cell concentrations of up to 2×10^8 cells/mL carrier volume. In packed beds, the cage compartment of the reactor is filled with beads or discs. In fluidized beds, microcarriers make up 10–50% of the reactor volume. Carrier concentration in homogenous stirred tanks is normally 2–3 g/L. However, especially for surface carriers, the carrier concentration can be increased to obtain higher cell concentrations. Carrier concentrations of up to 10 g/L have been reported (20,21), providing a surface area of up to 45,000 cm^2/L.

34.2.3.1 Inoculation and Attachment. It is essential to equilibrate and stabilize all culture parameters before adding the inoculum. Temperature and pH are especially important. Depending on the type of carrier, there may be an optimum pH for cell attachment. For collagen-coated surfaces, pH had no significant effect on cell attachment over a range of 7.1–8.0, while on Cytodex 1, the attachment rate varied considerably, with an optimum at pH 7.1 (36). At the time of inoculation, the cells should be in exponential growth phase to avoid lag phases in the microcarrier culture. It is also important to use single-cell suspensions for the inoculum as aggregates cause heterogeneity.

Cell attachment to microcarriers is influenced by a number of factors. For optimum attachment, the cells used for inoculation should be in a good nutritional state, preferably in late exponential phase. The harvesting procedure should result in a single-cell suspension with minimal damage to the cell-surface receptors to facilitate quick reattachment. Cell and microcarrier concentrations as well as agitation speed also play important roles. For cells with low plating efficiency, intermittent stirring (e.g. 3–5 min stirring out of every 30 min) has been reported to be beneficial (36,37). However, for large-scale culture, intermittent stirring should be avoided as the carrier settling time increases with increasing vessel height. Furthermore, microcarriers at the bottom are subject to oxygen limitation. Higher seeding densities or carrier concentrations increase the cell attachment rate because the frequency of cell-bead contacts is increased. For a given cell number, a higher carrier concentration can be simulated by reducing the vessel volume during the inoculation phase and adding more cultivation medium after the cells have attached. The initial cell concentration is not only important in terms of the attachment rate but also to ensure that every microcarrier is populated. Adherent cells can cover a surface only by growth, not by detachment and reattachment. Therefore, carriers that are unpopulated at the start of the culture remain in this state during cultivation. Mendonca *et al*. (38) showed that for Cytodex 1, a minimum initial ratio of eight cells per bead is necessary to ensure that all carriers are populated. At carrier concentrations recommended by the manufacturer (typically 2–5 g/L), surface carriers are normally inoculated with 0.5 to 2×10^5 cells/mL, which is equivalent to 0.5 to 2×10^4 cells/cm^2. Macroporous carriers are normally inoculated with a similar cell concentration. Fluidized beds are inoculated with 1 to 2×10^6 cells/mL of carrier volume. Beyond these general heuristics, the optimal inoculation density is highly dependent on cell line characteristics and media composition.

34.2.4 Optimizing Culture Conditions

34.2.4.1 Cultivation Medium. The requirements for cell growth in microcarrier culture are similar to those in other monolayer methods. The growth medium used during routine culture can therefore be used for initial experiments with microcarriers. However, several media components need to be considered if culture conditions are to be optimized. Compared to static flask or roller-bottle culture, much higher cell concentrations are reached in microcarrier culture; hence, it is important to closely follow the consumption rate of nutrients. Additionally, cell physiology often changes upon reaching confluence (39). Medium requirements during growth and maintenance phases may therefore be different. To prevent depletion, it will often be necessary to increase the concentration of glucose, amino acids, vitamins, or choline. Nutrients that are often consumed quickly include glutamine, arginine, aspartic acid, asparagine, and, when growing human, diploid cell lines, cysteine. Glucose is essential for continued cell attachment; if its concentration falls to nonphysiological levels, cells may detach from the microcarriers (40). Adding retinoids can promote the adhesion of cells (41). Choline is incorporated into membrane phospholipids and decreasing levels may result in perturbation of membrane composition, thus causing rounding of cells and decreased adhesion (42). Besides optimizing the medium for batch cultivation, the use of feeding strategies, especially for glucose and glutamine, may also be considered. Starting at a relatively low glucose concentration of 2–3 g/L and adding more after the initial cultivation phase will also help to reduce lactate formation. Alternatively, other carbon sources, for example, fructose or galactose, can be used to decrease lactate production (21).

During long-term cultivation, it is not sufficient to prevent nutrient depletion; waste products must be removed as well. This can be done by continuous or discontinuous perfusion where spent medium is removed from the reactor and fresh medium added. As microcarriers not only provide

a growth surface for the cells, but are at the same time a means of cell immobilization, they lend themselves well to perfusion culture.

34.2.4.2 Gas Supply. Supplying the correct amounts of O_2 and CO_2 is important for achieving high yields with microcarrier culture. Both gases have metabolic functions and CO_2 is also involved in controlling culture pH when using conventional bicarbonate buffers. The gas requirements for individual cells are the same whether grown in microcarrier culture or other systems; however, due to the higher cell concentrations in microcarrier cultures, special attention should be given to ensuring sufficient oxygen supply. Stirred microcarrier cultures with volumes of approximately 500 mL to 1 L are usually kept as closed systems. Provided that the liquid volume is not more than 50% of the total vessel volume, oxygen transfer should be sufficient. The gas in the headspace is renewed when taking samples or replenishing the medium. At high cell concentrations, the headspace can briefly be flushed with gas (15–20 s of 95% air and 5% CO_2) forced through a sterile filter to ensure removal of excess CO_2 generated by the culture.

For large-scale cultures in bioreactors, three aeration methods are in principal, available: surface aeration, direct sparging of gas, and bubble-free aeration through membranes. Surface aeration only works for small reactor volumes that have a sufficient liquid surface area-to-volume ratio. Bubble-free aeration using silicon or Teflon tubing has been used successfully in bioreactors (43). However, due to the large membrane area required, this approach is also limited in scale. The standard method therefore is still direct sparging of air or pure oxygen into the culture. This technique is widely used for suspension cells and can also be applied to microcarrier cultures, especially for macroporous carriers where the cells grow inside the pores and are protected from shear forces introduced by the gas bubbles. When using microcarriers in STRs, it is important to select a sparger that does not create excessively small bubbles. Small bubbles rise more slowly than large bubbles and may attach to microcarriers, transporting them into a foam layer at the surface and thereby removing carriers and cells from the fluid phase. In general, ring spargers with hole diameters of 0.5–1 mm will provide sufficient oxygenation capacity without creating a stable foam layer. For microporous carriers, the same oxygen tension can be used as for suspension cultures, usually 15–30% of air saturation. When using macroporous carriers for high cell density cultures, the oxygen tension should be raised to 40–60% of air saturation to increase the concentration gradient and facilitate diffusion into the pores. Cultures should not be excessively aerated since high oxygen tensions (above ambient) can be toxic and reduce growth rate (44). Due to the high cell concentration that is reached in macroporous carriers, several studies have been conducted to evaluate whether sufficient oxygen concentrations are maintained inside the pores. The low solubility of oxygen (6–7 mg/L) combined with a consumption rate of 2–3 $\mu g/(10^6$ cells h) for Vero cells (45) and about 9 $\mu g/$ (10^6 cells*h) for fibroblasts (46) makes it clear that oxygen is the most critical nutrient in terms of diffusional limitation. Fortunately, optimal culture performance can be obtained for a wide range of oxygen concentrations. Meuwly *et al*. (47) found that cell growth was unaffected in a concentration range of 10–80% of air saturation.

Three major effects influence oxygen concentration in a macroporous carrier: the boundary layer at the carrier surface, the diffusional limitation within the carrier, and the intraparticle convection. The thickness of the boundary layer decreases with the turbulence of the surrounding fluid. The diffusion of oxygen into pores is influenced by the shape of the pores and the presence or absence of cells. A convective flux through parts of the carrier can occur if large pore carriers are used. Fassnacht and Pörtner (48) evaluated oxygen supply in a packed-bed reactor with Siran microcarriers. The diameter of the carriers was 3–5 mm and the pore size 60–300 μm. They found that cell growth was limited due to restricted oxygen supply at 100% of air saturation. By increasing the oxygen concentration to 300% of air saturation, the nutrient consumption increased and they achieved a threefold increase in product formation. A further increase of oxygen concentration had no effect. While Taylor *et al*. (44) found a toxic effect of hyperoxic conditions on cells cultivated in a packed-bed reactor, Pörtner and Fassnacht found no such effect. They also calculated the maximum penetration depth of oxygen into the microcarrier pores. This parameter is dependent on the cell concentration and on the dissolved oxygen concentration. At a cell concentration of 2×10^8 cells/mL carrier and a dissolved oxygen concentration of 400% of air saturation, they found a maximum penetration depth of 1 mm. When the dissolved oxygen concentration was lowered to 100% of air saturation, the maximum penetration depth was reduced to 500 μm. This is in good agreement with the results of Preissmann *et al*. (46) who found a maximum penetration depth of 300 μm at 40% air saturation.

To ensure a sufficient oxygen supply, three parameters can be varied. First, the turbulence at the carrier surface should be kept high to reduce the thickness of the boundary layer. Second, the carrier diameter should be constrained to stay within the maximum oxygen penetration depth. Finally, large pore sizes facilitate a convective flow and thereby improve oxygen supply.

34.2.4.3 Culture pH. Since pH influences cell survival, attachment, growth, and function, maintaining the correct pH is vital to achieving optimal cell growth and high yields. Cell attachment to carriers with a charged surface is highly

dependent on the correct pH and has been shown to be optimal at pH 7.1 for Vero cells and Cytodex 1 (36). When initiating small-scale cultures, the cultivation medium is often exposed to the atmosphere for prolonged periods. This causes the pH to rise if bicarbonate buffer systems are used. To achieve high plating efficiency, it is important to equilibrate the cultivation vessel before inoculation to achieve a pH that is near neutral. Most cultivation media use a bicarbonate buffer system, but its capacity is often not sufficient to prevent a pH decrease toward the end of the culture cycle. HEPES (10–20 m*M*) can be used as an alternative if the buffering capacity needs to be increased (49).

34.2.4.4 Mixing and Shear. Mixing is used to provide a homogenous concentration of nutrients, to keep carriers in suspension, and to prevent the formation of pH or pO_2 gradients. The type of impeller and the stirring speed influence mixing time and oxygen transfer capacity. For cultivating animal cells, only stirrers creating low shear forces, mainly marine impellers, are used. Minimizing shear forces is especially important when cultivating cells on microporous carriers. Gregoriades *et al*. (50) have shown that cells attached to such carriers are much more susceptible than suspension cells to damage by shear forces. In similar experiments, Venkat *et al*. (51) estimated the dissipation of local energy in a turbulent spinner vessel and reported cell damage above 150 rpm. It is thus important to select a stirring rate that ensures suspension of the microcarriers but still creates low shear forces. Depending on the stirrer configuration, normal stirring speeds are 50–100 rpm. While mixing time is usually not a problem in small-scale vessels and bioreactors, mixing time at equivalent tip speeds can increase by an order of magnitude when comparing a 10- and a 10,000-L bioreactor (52). An important consequence of long mixing times is that the concentration of sodium hydroxide used for pH control must be lowered to minimize cell damage caused by elevated local concentrations of extended duration.

All animal cells are susceptible to damage from shear forces in any type of agitated culture. A number of studies have suggested that cells grown on microcarriers may be particularly sensitive due to increased energy dissipation at the microcarrier–liquid interface, adherence of microcarrier beads to gas–liquid interfaces, and the inability of the cells to rotate freely in the culture medium. In particular, Croughan *et al*. evaluated the effects of different agitation rates on FS-4 human fibroblasts grown on Cytodex 1 microcarriers in spinner flasks (53). They observed an optimum agitation rate of 60 rpm, with significantly decreased growth at higher rates. The extent of growth showed a sigmoidal dependence on integrated shear factor as shown in Fig. 34.5, with 20 s^{-1} being the transition to reduction

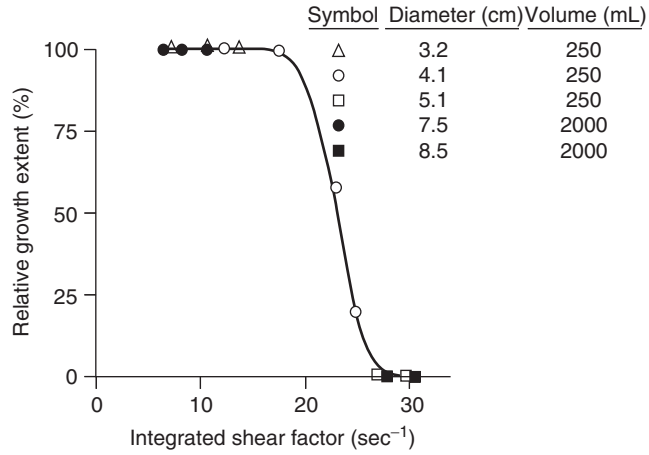


Figure 34.5. Relative growth extent of FS-4 human fibroblasts grown on Cytodex 1 microcarriers as a function of integrated shear factor. Reprinted with permission of Wiley-Liss, Inc, a subsidiary of John Wiley & Sons, Inc, from Croughan *et al*. Biotechnol Bioeng 29:132, Copyright © 1987, John Wiley & Sons.

in growth. The relative growth extent depends on Kolmogorov eddy length with no growth seen at length scales less than 100 μm and full growth seen at length scales greater than 150 μm. Results from Jeff Chalmers laboratory (50,54) confirmed that cell damage occurred at much lower energy dissipation levels for cells grown on microcarriers than cells grown in suspension [10^4 vs 10^8 ergs/(cm^3 s)]. However, their experiments, which were conducted in a novel extensional flow device with no turbulence, showed that the eddy-length explanation was apparently incorrect. Other studies from this group examined the attachment of microcarriers to gas–liquid interfaces (55). They found that microcarriers, with or without cells, tended to attach much more readily to rising bubbles than cells in suspension, and to become entrapped in a foam layer. Cell death was caused not by bubble rupture, but rather by cells being stripped off the microcarriers. In a more biological study, Mufti and Shuler observed that HepG2 human hepatoma cells cultured on microcarriers exhibited increased cytochrome P-4501A1 (CYP1A1, a marker for cellular stress) activity in an agitation rate-dependent manner (Fig. 34.6) (56).

34.2.5 Sampling

34.2.5.1 Visualization of Cells. If cells are grown on transparent microporous carriers, microscopic observation can be used routinely to obtain information about cell morphology, distribution of the cells on the microcarriers, degree of confluence, and the formation of aggregates. The microcarriers can be viewed without further preparation in an inverted microscope. For microphotography, it may be desirable to stain the cells for improved contrast. The most suitable routine procedures for staining microcarrier

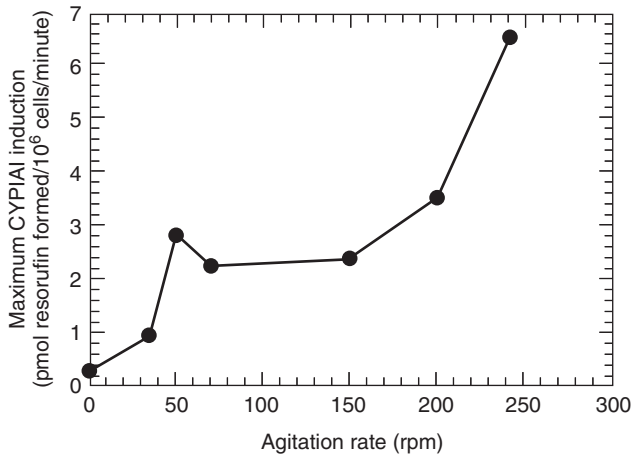


Figure 34.6. Effect of agitation intensity on the maximum induction of CYPlAl in Hep G2 cells in a 50-mL spinner flask. Reprinted with permission from Mufti, NA, Shuler, ML. Biotechnology Progress 11 : 551, Copyright © 1995, American Chemical Society and American Institute of Chemical Engineers.

cultures are Giemsa stain or Harris' hematoxylin. The latter can be used when better nuclear detail is required. Both staining methods are described in Ref. 18. Many other, more specific, staining procedures are also possible. However, it should be noted that some carbohydrate or protein-specific staining procedures may give high backgrounds due to interaction with the carrier matrix. Cells on macroporous carriers are best viewed using laser confocal microscopy after staining with acridine orange.

34.2.5.2 Cell Quantification. Cell concentration in microcarrier cultures can be determined by several direct and indirect methods. Direct methods include cell enumeration by counting whole cells after trypsinization from the carrier or determining the concentration of released nuclei. In the latter method, modified by van Wezel (6), cells growing on microcarriers are incubated in a hypotonic solution. The released nuclei are then counted using a Coulter counter or counted manually after staining with crystal violet (57). Counting released nuclei is also the preferred method for cultures grown on macroporous carriers since trypsinization will not result in complete cell release.

Cell viability is more difficult to quantify. This parameter is often determined by trypan blue or erythrosin staining after detaching the cells with trypsin. However, depending on the cell line, trypsinization may influence the result. An alternative is the MTT colorimetric method (58) that is also a good choice for cultures on macroporous carriers. Cell viability can also be assessed by staining methods. Two fluorescent dyes (fluorescein diacetate for living cells and ethidium bromide for dead cells) can be used to estimate cell viability in three-dimensional structures (59,60).

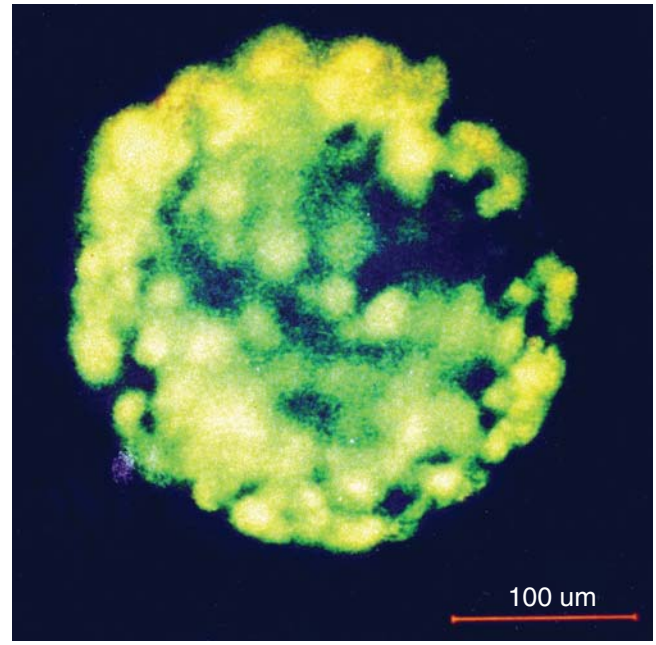


Figure 34.7. Confocal laser-scanning microscope photograph of fluorescein diacetate-stained CHO cells covering a Cytopore bead. (This figure is available in full color at http://onlinelibrary.wiley.com/book/10.1002/9780470054581.)

Fluorescein diacetate-stained Chinese hamster ovary (CHO) cells on a Cytopore™ carrier can be seen in Fig. 34.7.

Indirect methods often measure metabolic activities such as glucose or oxygen consumption, lactic or pyruvic acid production, or CO_2 production. All these methods must be calibrated using direct cell counting methods. The resulting cell-specific consumption and production rates are unique for every cell line and cultivation medium. In addition, metabolic rates will be different during the exponential growth and plateau phases of the culture. However, when a standardized process is run, these methods often provide a good estimation of the viable cell number.

In large-scale culture, it is often desirable to have on-line measurement of cell concentration. One possibility to achieving this is to continuously measure the oxygen consumption. This method is highly dependent on cell line and culture conditions, so it is only useful if the monitored process is run in exactly the same way each time. A relatively new technique is to measure capacitance and thereby determine the viable cell volume (61). Capacitance measurement has been used for cells grown in suspension, on microporous and macroporous carriers, in stirred tanks, as well as fluidized and packed beds (62,63). Sterilizable and GMP-compliant probes for this application are available from Aber Instruments (http://www.aber-instruments.co.uk/).

The main source of error for direct cell quantification of suspension cultures is aggregate formation. This can

often be circumvented by using image analysis that can distinguish the single cells up to a certain aggregate size, for example, Cedex automated cell culture analyzers (http://www.innovatis.com). Alternatively, the total cell number can be easily determined by counting the nuclei after cell lysis. This is also the recommended analysis method for microcarrier cultures. However, depending on the type of bioreactor and microcarrier used, obtaining a homogenous sample might be more difficult than in suspension culture. In packed-bed reactors, normally no removal of microcarriers is possible. The cell number in such cultures must be determined by indirect methods as described above. Fluidized-bed reactors are by definition an inhomogeneous cultivation system as the carrier compartment is separated from the rest of the vessel. However, carrier removal during the cultivation process is possible. Cell quantification can therefore be done using direct methods, for example, nuclei counting, correlating the measured cell concentration to the number of microcarriers and then calculating the cell number per milliliter of microcarriers. If digital image analysis is used for cell enumeration on macroporous carriers, staining procedures are usually necessary. However, cell loss may occur during the accompanying washing steps.

34.2.6 Cell Harvesting and Scale-Up

Culture scale-up is a key task when growing adherent cells on microcarriers. Adherent cells are unable to detach and reattach to fresh microcarriers during continuous stirring. The simple addition of fresh microcarriers will not alone achieve scale-up as the cells are in general unable to populate them. In the case of microporous carriers, there is limited data available on scale-up by adding of microcarriers and the use of special stirring regimes. Wang and Ouyang (37) expanded a culture of Vero cells on Cytodex 3 carriers without actively detaching the cells. In the study, the cells did not migrate between the carriers during continuous stirring, but this problem was solved by intermittent stirring. Microscopic observation showed that cell transfer occurred by bridging when bare beads came into contact with confluent ones. A similar approach was used by Pohlscheidt *et al*. (64). They describe the direct cell expansion of adherent bovine kidney cells by migration between Cytodex 3 microcarriers during a period of alternated stirring. To shorten the time for cell transfer and adapt the procedure to large-scale requirements, cells are usually actively detached from the beads so that they can subsequently reattach to freshly added microcarriers. Various methods can be used for cell removal, and it is important to choose procedures that minimize damage.

The optimal harvesting procedure can usually be deduced from that normally used to detach a particular cell type in monolayer culture. The aim of this step should be to have an inoculum consisting of a suspension of highly viable, single cells that were in exponential growth phase prior to harvesting. The main task is to break the cell–surface and cell–cell interactions. If the cells secrete copious amounts of ECM, it will be easier to harvest them before they are fully confluent. As cell binding is dependent on divalent ions, the carriers must be washed with citric acid or EDTA (0.2% w/v) containing buffers to help detach the cells. The methods for cell harvesting are primarily enzymatic ones using trypsin, collagenase, Pronase™ (Calbiochem), Dispase™ (Worthington Biochemical Corp.), or Accutase™ (PAA laboratories). Trypsin is the most commonly used general protease, although Pronase has advantages when harvesting cells from primary cultures. Dispase as well as Accutase can be used for cells that are sensitive to trypsin.

If the medium contains serum, alpha-1-anti-trypsin, a trypsin-blocking protein abundant in serum must also be washed out. Porous carriers require more extensive washing than solid ones, normally two washings with 10–20% of the original suspension volume. The substrate concentration for proteolytic enzymes increases drastically when they are applied to sedimented beads as compared to ordinary monolayer cultures. Normally, this means increasing trypsin concentration (e.g. to 0.25%) to perform cell detachment in a suitable volume, typically about 10% of the original volume of the culture. Cell detachment from the microcarriers is greatly enhanced if some shear force is applied by gentle stirring. However, the stirring must be brief as the carrier concentration is very high, and the cells may be damaged by bead-to-bead collisions.

After detachment, the cells can be separated from the microcarriers by a variety of methods. The simplest way is differential sedimentation, which can be used for routine harvesting, or subcultivation when maximum recovery is not required. After harvesting, the culture medium is added and the microcarriers are allowed to settle for about 5 min. The supernatant, which contains the majority of the cells and is essentially microcarrier-free, can then be removed. Better recovery can be achieved if the microcarriers are washed a second time. Pooled supernatants can then be used directly to inoculate the next culture. Filtration devices can be used when it is important to obtain very high recoveries of the harvested cells without contamination by microcarriers. Any sterilizable filter with a mesh size of approximately 100 μm is suitable. A convenient filter for small-scale work is the "Cellector" supplied by Bellco Glass Inc. (Vineland, New Jersey, USA). Alternatively, a suitable stainless steel mesh can be obtained from Spörl KG (Sigmaringendorf, Germany).

For large-scale applications, fluidized-bed separation systems have also been developed. The best reactor design in this case is a conical shape (Fig. 34.8). The fluid stream comes from the bottom and harvest occurs at the top. A



Figure 34.8. A fluidized bed for carrier/cell separation. (This figure is available in full color at http://onlinelibrary.wiley.com/book/10.1002/9780470054581.)

top filter with a mesh size of around 100 μm reduces the risk of losing microcarriers from the system. It is also possible to detach the cells and then transfer the whole mixture of used beads and cells to the new reactor. In this case, the split ratio should be as high as possible because the cells tend to preferentially reattach to the used beads, which can lead to inhomogeneous culture conditions.

When the cells have been harvested using enzymatic methods, the detachment reagents need to be inactivated or sufficiently diluted to allow reattachment. In chemically defined, protein-free media, trypsin can be inactivated with soybean trypsin inhibitor; Pronase is inhibited by EDTA. For other enzymes a specific cell culture compatible inhibitor is not always available. In that case, sufficient dilution, that is, a high split ratio, can help.

In addition to proteolytic enzymes, other methods can also be applied to detach cells from microcarriers. Incubation in hypotonic solution can be used for harvesting cells that do not have strong adhesion properties. Lai *et al*. (65) used this method to harvest CHO cells from Cytodex 1. Chelating agents such as EDTA can be used to remove certain epithelial and transformed cells. In general, these chemicals are not very efficient in cell detachment, but they have the advantage that they leave the cells part of their ECM, and they do not harm cell-surface receptors. Some cells are extremely difficult to remove from culture surfaces, for example, macrophages. To improve recovery rate, Lignocaine (30 m*M* in PBS, pH 6.7) at 22°C can be used for detachment (66).

Once the detached cells have been transferred to the new cultivation vessel and the detachment reagent is inactivated, it is important to find a suitable stirring regimen and cultivation medium to support efficient reattachment and rapid cell spreading. During the initial time after transfer, the cells are rounded and therefore only have a limited contact area with the carrier surface. It is important to select a cultivation medium that minimizes this time period and facilitates cell spreading, as rounded cells are more sensitive to shear forces.

Scale-up generally involves a substantial amount of process development. Simulation of the vessel's fluid dynamics must be performed to ensure that the larger vessel is similar to the small-scale reactor and that it will not negatively influence growth behavior or productivity. It is also important to test cell line stability beyond the planned duration of the production process. An essential part of scale-up is the cellular multiplication at each step. It is important to work with a split ratio as high as possible to minimize the number of subcultivation steps and thereby bioreactors and other equipment. If it is possible to inoculate at a low cell density, for example, 2 to 5×10^4 cells/mL, and the process then reaches high yields of about 5×10^6 cells/mL, the multiplication factor is 100-fold. Such a scale-up factor has been reported for Vero cells by Lindner *et al*. (67). It would thus be possible to inoculate a 100-L fermentor from a 1-L spinner flask. Scaling up microcarrier cultures can be done by increasing the size of the vessel or by increasing the microcarrier concentration. Production units up to 6000 L (Fig. 34.9) have been achieved by increasing the size. Important factors that influence this strategy are the reactor configuration and the power input of mixing. Larger impellers at lower speeds generate less shear force, and marine impellers are usually preferred over pitched blade impellers. Desirable features of a stirred microcarrier reactor include the absence of baffles, curved bottom for better mixing, double jacket for heating and cooling, top driven stirrer, and a smooth surface finish (electropolished).

Scale-up by increasing microcarrier concentration requires perfusion to ensure nutrient supply at the resulting high cell concentrations. It is necessary to retain carriers in the reactor, which can be achieved by settling zones or filtration devices. The limiting factor for higher cell concentrations is usually oxygen supply. It is difficult to use microspargers in carrier cultures grown in conventional stirred tanks as the carriers may accumulate and float in the foam created. The easiest solution is to use spargers that create larger bubbles and do not cause the formation of a stable foam layer. If a higher oxygen transfer rate is required, pure oxygen can be used. The problem of



Figure 34.9. Influenza production plant (6000-L vessels for cultivating Vero cells on Cytodex). Courtesy of Baxter Biosciences. (This figure is available in full color at http://onlinelibrary.wiley.com/book/10.1002/9780470054581.)

microcarrier entrapment in the foam can be circumvented by oxygenation via an external loop and oxygenation devices/vessels (68). It is easier to increase oxygen supply via sparging in packed or fluidized beds as the cells are protected inside the macroporous carriers and the density of the microcarriers is usually high enough to prevent entrapment in a foam layer.

34.2.7 Trouble-Shooting

The following list contains points of occasional difficulty, frequently asked questions, and the most likely solutions. It can also serve as a checklist when culturing a new cell type on microcarriers.

Medium turns acidic upon addition of the microcarriers:

Check that the microcarriers have been properly hydrated and washed.

Medium is alkaline at inoculation stage:

Gas the culture vessel and equilibrate with 95% air, 5% CO_2.

Loss of microcarriers on surface of culture vessel:

Check that the culture vessel has been properly siliconized.

Poor attachment of cells and slow initial growth:

Ensure that the culture vessel is nontoxic and well washed after siliconization.

Dilution of culture by PBS remaining after sterilization; rinse microcarriers in growth medium.

Modify initial culture conditions; increase length of static attachment period; reduce initial culture volume, or increase inoculum concentration.

Check that the inoculum consists of a viable single-cell suspension.

Eliminate vibration transmitted from stirring unit.

Change to a more enriched medium for the initial culture phase.

Check the quality of the serum supplement.

Check for contamination by mycoplasma.

Microcarriers with no cells attached:

Modify initial culture conditions; increase length of static attachment period; reduce culture volume during inoculation phase.

Check that the inoculum concentration is correct.

Ensure that all microcarriers are suspended during the stirring phase if intermittent stirring is used.

Aggregation of cells and microcarriers:

Modify initial culture conditions; reduce length of static attachment period.

Increase stirring speed during growth phase.

Reduce concentration of serum supplement as culture reaches confluence.

Reduce concentration of Ca^{2+}, Mg^{2+} in the medium..

Rounded morphology of cells and poor flattening during growth phase:

Replenish medium.

Check osmolarity and pH of culture medium.

Reduce concentration of antibiotics.

Check for contamination by mycoplasma

Rounding of cells when medium is changed:

Check temperature, pH, and osmolarity of replacement medium.

Cessation of growth during culture cycle:
- Replenish medium.
- Check that pH is optimal for cell growth.
- Re-gas culture vessel.
- Reduce stirring speed.

Difficulties controlling pH:
- Check that the buffer system is appropriate.
- Improve the supply of gas to culture vessel; lower concentration of CO_2 in headspace or increase supply of oxygen.
- Improve the supply of glutamine, supplement the medium with biotin, or use an alternative carbon source (galactose, fructose) to reduce lactate formation.

Difficulties maintaining confluent monolayers:
- Check that pH and osmolarity are optimal.
- Reduce the concentration of serum supplement.
- Improve the schedule for medium replenishment.
- Reduce the concentration of antibiotics.

Broken microcarriers:
- Ensure that dry microcarriers are handled carefully.
- Check the design of culture vessel/impeller; ensure that the mechanical seal is designed properly, that is, no gaps where microcarriers can be sheared.

Difficulty in harvesting cells:
- Ensure that the carriers have been washed extensively.
- Switch to enzymatic methods; use trypsin as a more nonspecific protease.
- Check that approximately the same amount of protease (U/cell) is used as when harvesting from T-flasks.
- Ensure that sufficient agitation is used in addition to the detachment reagent.

Microcarriers float in foam due to sparging:
- Reduce serum/protein concentration as much as possible.
- Aerate with sparger that creates larger bubbles.
- Sparge with pure oxygen to reduce gas flow rate.
- Aerate via external loop.

34.3 MICROCARRIERS IN VACCINE PRODUCTION

The majority of viral vaccines are produced in adherent cells. Table 34.4 gives an overview of the viruses that have been grown in microcarrier culture. The most important vaccines produced by this method are influenza, polio, rotavirus, Japanese encephalitis, hepatitis A, hoof, and mouth disease (69–72). Cell lines used include Vero (monkey kidney epithelial cells), human embryonic kidney (HEK) 293 cells, baby hamster kidney (BHK) cells, and Madin Darby canine kidney (MDCK) cells.

TABLE 34.4. Viruses Grown in Microcarrier Culture

Adenovirus	Marek's	Rous sarcoma
Bovine rhinotrachteritis	Papovavirus	Rubella
Endogenous C type	Parapoxvirus	Sendai
Equine rhinopneumonitis	Polio	SV40
Foot and mouth	Polyoma	Sindbis
Group B arboviruses	Pseudorabies	Small pox
HAV	Rabies	Vaccinia
Influenza	Herpes	Vesicular stomatitis
Japanese encephalitis	RSV	

Proliferation of anchorage-dependent cells occurs only after adhesion to a suitable surface. In large-scale cultivation, the microcarrier technique has proven to be more effective than cell culture on flat substrates such as culture dishes, multiple trays, or roller bottles. Microcarriers provide a suitable growth surface and at the same time allow treatment of the process as suspension culture. This enables the use of bioprocess technologies that are not feasible when cultivating cells on vessel surfaces. Large-scale production in roller bottles is possible but requires multiplication of vessels during scale-up. The drawbacks associated with cultivation in multiple vessels are a substantially higher risk of contamination and a rather poor control of process parameters in the individual vessels. Moreover, scale-up of roller-bottle processes can only be done using automatic roller stations. Such stations can handle up to 40,000 roller bottles (TTP Labtech, Cambridge, UK). The same surface area as in 40,000 roller bottles (850 cm^2) can be obtained in a 2500-L tank with a Cytodex 1 concentration of 3 g/L. Cultivation in a single vessel allows incomparably better process control and reduces the contamination risk. Due to the high cell concentration, growth on microcarriers also creates an environment that more closely mimics the *in vivo* environment.

The cost advantage of virus production in microcarrier culture has been demonstrated in a study by Isayeva *et al*. (73). Adenovirus was grown on HEK 293 cells that were cultivated on microporous microcarriers, roller bottles, and in a hollow-fiber reactor. At the same virus yield, microcarrier cultivation was 30% cheaper than the two other systems. Moreover, monitoring cell density in the hollow-fiber system could only be done by indirect methods as the cells growing in the extracapillary space were inaccessible during the process. The savings in the microcarrier process were attributed to a reduction in labor costs as well as lower expenses for disposables. In a presentation by E. Malhaise, GSK, at the National Academy of Engineering/Institute of Medicine (NAE/IOM) topical conference 2006 (Cleveland, Ohio), the consequences of

microcarrier cultivation on facility design were evaluated. In this example, microcarrier application allowed a fivefold reduction of fermentation volume due to increased cell concentration. The smaller vessel size shortened hardware engineering lead times and also resulted in an overall reduced facility footprint. The feasibility of industrial production of vaccines derived from Vero and MDCK cell lines has already been demonstrated. Kemble and Greenberg reported a production volume of 1200 L (74). Werthenstein Chemie AG, Sachen, Switzerland use a 2000-L vessel to produce recombinant adenovirus in a microcarrier-based process. Baxter AG, Orth/Donau, Austria has recently started production for clinical trials using 6000-L vessels for the cultivation of Vero cells on Cytodex carriers.

BHK cells can be in grown adherent as well as in suspension culture. For the production of rabies virus, the cells are grown on microcarriers (75,76). Geserick *et al*. (76) used microcarriers to retain BHK cells in perfusion culture. An important application for BHK cultivation in suspension is the large-scale production of vaccines against foot-and-mouth disease (FMD). Amadori *et al*. (77) have compared virus progeny from anchorage-dependent and suspension cells. They found a lower stability of FMD virus from suspension cells during the standard inactivation method. This was attributed to an altered integrin expression in suspension-adapted BHK cells compared to adherent cells. Expression of these cell-surface receptors affects the distribution of actin microfilaments, which plays a crucial role in the replication of FMD virus.

Usually, microporous carriers are used in vaccine production because the cells usually grow as a monolayer on them and are therefore easily accessible for virus infection. However, macroporous carriers have also been used successfully for virus propagation. The advantages of macroporous carriers are higher cell/bead loadings due to the increased surface area and the ability to protect cells against detrimental hydrodynamic forces generated by high agitation rates or direct sparging. Yokomizo *et al*. (78) compared the growth of rabies virus on a microporous (Cytodex 1, DEAE-dextran) and two macroporous carriers (Cytopore 1, cellulose; Cultispher™ G, gelatin). All microcarriers gave similar maximum volumetric cell densities; however, the maximum viral titers were 25% and nearly 50% higher on the Cultispher G and Cytopore carriers, respectively, than on the Cytodex microcarrier. Successful propagation on macroporous carriers was also reported for vesicular stomatitis virus (79) and hepatitis A virus (80).

The standard cultivation method in vaccine production is batch culture as the cells are usually infected with lytic viruses. However, there is also the possibility to run perfusion cultures if the cells are used to propagate nonlytic viruses that are shed into the supernatant. In this case, the microcarriers can be used for cell retention while the nutrient supply is ensured by a constant influx of cultivation medium and a removal of harvest from which the virus particles are then purified. Yokomizo *et al*. (78) performed cell cultures in semicontinuous perfusion mode with medium replacement every 48 h, while Meyer *et al*. (80) claim patent protection for the continuous production of hepatitis A virus for at least 60 days.

A number of production processes still rely on the use of serum. In these cases, the medium has to be exchanged to serum free before infection (81). As the cells are immobilized on the microcarriers, the cultivation method offers a quick possibility for medium replacement by leaving the carriers to settle.

A microcarrier application that has seen substantial growth in the last few years is the production of influenza vaccine. The worldwide production capacity in 2006 was about 350 million doses (82). The majority of these doses are still produced in embryonated hen's eggs (81). However, production in eggs is hampered by the cumbersome procedures required for egg inoculation and harvesting, as well as the extensive downstream processing to remove the egg protein that can cause allergic reactions. Additionally, virus propagation in eggs allows only limited process control, and the procurement of SPF eggs requires long lead times for production. In recent years, several continuous cell lines such as MDCK, Vero (83), the human cell line Per.C6 (84), and St. Jude porcine lung epithelial cell line (85) have been tested for the cultivation of influenza virus. Tree *et al*. (86) compared virus yields from MDCK cell cultures and hen's eggs. Although the titer from embryonated eggs was the highest (3.9×10^9 pfu/mL), MDCK cultures on microcarriers (1.3×10^9) and in roller bottles (1×10^9) produced sufficient amounts of virus. When comparing the yield from microporous and macroporous carriers, the study found that the optimum virus yield was achieved using a solid microcarrier composed of dextran with a positive charge. From the experimental results, it was concluded that the virus yield from a 1000-L bioreactor using solid microcarriers was equivalent to that from 12,000 roller bottles or 30,800 eggs. Influenza production in cell culture can be done in serum-free medium, which practically eliminates the risk of contamination with transmissible spongiform encephalitis or other viruses.

34.4 MICROCARRIERS IN RECOMBINANT PROTEIN PRODUCTION

34.4.1 Academic and Industrial Use of Microcarriers for Recombinant Protein Production

While vaccine production is the most common industrial use of microcarriers, a number of cell lines producing

recombinant therapeutic proteins have been grown on microcarriers, with approximately 10 industrial processes currently in use for therapeutic proteins. The primary interest is in the production of therapeutics other than monoclonal antibodies, particularly proteins with complex glycosylation as these often show much lower specific productivities than recombinant monoclonal antibodies. These lower productivities lead to lower titers, necessitating higher cell densities and/or perfusion processes to obtain the desired product concentrations. Both microporous and macroporous carriers have been explored using stirred tanks and fluidized-bed bioreactors with and without perfusion. Cell lines investigated include CHO, BHK, murine hybridoma cells (87,88), HeLa (cervical carcinoma) cells (89,90), COS-7 cells (91), and insect cell lines (92). Publicly available information on commercial processes using microcarriers includes the production of Aldurazyme™ on Cytopore carriers by Biomarin, recombinant human follicle-stimulating hormone (r-hFSH; INN: follitropin alfa) and recombinant human-luteinizing hormone (r-hLH; INN: lutropin alfa) on Cytodex 3 microcarriers by Seorono, Feron™ (recombinant interferon-beta) on Cytodex 1 microcarriers by Toray, and Cerezyme™, Myozyme™, and Fabrazyme™ on Cytopore microcarriers by Genzyme.

Kong *et al*. at Human Genome Sciences compared the production of recombinant human osteoblast-derived antiviral protein (OAP) for CHO cells grown on Cytoline 1 (macroporous) carriers in a fluidized-bed bioreactor and cells grown on Cytodex 1 (microporous) carriers in a STR (93). They found much higher cell densities on the macroporous carriers in the fluidized bed (3.3×10^7 cells/mL vs 2.6×10^6 cells/mL) as well as a sixfold increase in specific productivity in the fluidized-bed bioreactor. However, as the available surface area for cell growth was much higher for the macroporous carriers, the coverage was much lower (2.4×10^8 cells/m^2 on the Cytoline carriers vs 1.2×10^9 cells/m^2 on the Cytopore carriers). In a separate study, they analyzed the growth and productivity of a CHO cell line producing monocyte-colony inhibition factor (M-CIF) using 13 different microcarriers in spinner flasks and the ability of the cells to transfer autonomously between carriers (94). As shown in Table 34.5, Cytodex and Cytopore microcarriers showed the highest initial attachment, leading to the highest maximum viable cell densities. These carriers all possess a positive charge, and the more highly charged Cytodex 1 and Cytopore 2 carriers showed a faster attachment rate. Interestingly, in this study, the product titers in batch culture were similar for most of the microcarriers, indicating an inverse relationship between cell density and specific productivity.

Other proteins produced in CHO cells grown on microcarriers include prourokinase (88), urokinase-type plasminogen activator (95), and arylsulfatase B (96,97). We recently compared growth and productivity for CHO cells producing tissue plasminogen activator (t-PA) and secreted alkaline phosphatase (SEAP) for cells grown in suspension and attached to Cytodex 3 (microporous) and Cytopore 1 (macroporous) carriers (98). In static batch culture for CHO cells producing SEAP, Cytodex 3 microcarriers showed higher cell densities and product titers than suspension cells. However, in controlled, agitated, fed-batch bioreactors, suspension cultures showed higher cell densities than either Cytodex 3 or Cytopore 1 cultures for CHO cells producing either t-PA or SEAP.

TABLE 34.5. Comparison of Attachment, Growth Rate, and Productivity for a CHO Cell Line Producing Monocyte-Colony Inhibition Factor (M-CIF) using 13 Different Microcarriers in Spinner Flasks

	Attachment		Cell Growth			Batch		Media Exchanges		
Microcarrier	1 h	1 day	Maximal 10^6/mL	Batch folds	Floating Cells	HPLC mg/L	ELISA mg/L	mg/L	mg/L/day	mg/billion cells/day
Biosilicon	19.9	22.2	0.829	2.69	6.1	11.72	13.43	14.88	5.08	7.02
Cytodex 1	86.5	99.0	1.73	4.15	0.82	13.64	14.36	15.35	5.21	3.31
Cytodex 3	43.9	97.2	2.32	4.08	1.88	14.19	16.01	16.39	5.54	2.87
Collagen	30.9	27.2	0.469	1.22	20.2	11.19	10.98	11.96	3.38	7.93
Plastic	26.9	17.2	0.386	1.60	90.0	11.70	12.02	9.443	2.34	12.60
FACT	12.6	69.1	0.815	2.93	14.1	11.32	14.35	13.54	3.89	5.76
ProNectin	37.6	15.2	0.385	2.01	32.6	10.54	11.80	9.04	2.31	8.88
Plastic Plus	18.1	51.5	0.346	1.77	13.6	10.65	11.69	7.57	2.18	6.99
Cultispher-G	4.5	13.9	0.698	1.59	37.4	n/a	8.12	5.80	2.50	6.03
Cultispher-GL	0	39.1	0.475	1.22	51.0	n/a	6.81	3.11	1.02	3.21
Cultispher-S	35.6	47.3	1.16	1.83	15.3	n/a	10.23	14.74	6.74	7.73
Cytopore 1	73.5	100.0	2.00	2.31	0	9.87	n/a	10.99	4.22	2.27
Cytopore 2	84.0	99.4	2.08	2.57	0.32	10.26	14.03	13.56	5.40	3.60

Reprinted with kind permission from Springer Science and Business Media from Kong *et al*. Cytotechnology 2:151–158, Copyright © 1999, Springer Science and Business Media. Reprinted with permission from Springer Science from Kong *et al*. Cytotechnology 29:151–158.

The effects of culture conditions on specific productivity were cell line and/or protein product dependent as microcarrier cultures producing SEAP showed lower specific productivities than the comparable suspension cultures, while microcarrier cultures producing t-PA showed higher specific productivities than the comparable suspension cultures.

Viral infection has been used extensively for producing recombinant proteins in insect cells and more recently using vaccinia virus in HeLa cells (89,90). Viral infection provides the ability to rapidly generate recombinant proteins without the time-consuming selection and screening of other transfection methods. As HeLa cells are generally anchorage dependent and viral transfer requires cell–cell contact, a solid support was required for this system. Bleckwenn and coworkers evaluated 12 different microcarriers and found that Cytodex 3 microcarriers showed the best growth without forming multiple cell layers that might inhibit viral infection (99). They subsequently used this system to produce recombinant enhanced green fluorescent protein (EGFP) and HIV envelope coat protein, gp120 (89,90).

34.4.2 Cultivation Modes

While microcarriers can be used in batch or fed-batch modes in STRs, the greatest advantages of microcarrier use for recombinant protein production occur in perfusion or fluidized-bed cultures. Perfusion can be performed using a packed-bed reactor or a variety of separating devices, including spin filters and settlers. Voisard and coworkers have recently reviewed cell retention devices and techniques for suspension mammalian cell cultures (100). The two primary characteristics by which cells can be separated from culture media are based on differences in size or density.

For size separations, a variety of filtration modes can be used, including hollow-fiber filters and spin filters. The key challenge when using filters is preventing clogging. Microcarriers present significant advantages for filter-based retention systems as they are much larger than cells. Large pores or mesh can thus be used, thereby reducing clogging. Hu *et al*. produced urokinase-type plasminogen activator on Cytopore carriers using a spin filter to retain the cells (95). They were able to maintain perfusion for approximately 21 days before the filter clogged. They subsequently changed to batch perfusion by permitting the carriers to settle every 12 h before removing half of the culture medium. Using this technique, they were able to maintain the culture for over 100 days. Bleckwenn *et al*. used an alternating tangential flow hollow-fiber system (ATF™, Refine Technology Inc.) for production of recombinant proteins from vaccinia virus-infected HeLa cells grown on Cytodex 3 microcarriers (90). Alternating tangential flow helps prevent clogging of the hollow-fiber filter. Perfusion extended the culture duration by at least 50 h (as compared with batch culture) and increased the maximum viable cell density by nearly a factor of three, from 1.5×10^6 cells/mL to 4.4×10^6 cells /mL.

Microcarrier cultures are also advantageous for density-based separations. The specific density of a mammalian cell is only slightly greater than the density of the medium, yielding a sedimentation velocity of 0.04 cm/min. In contrast, microcarriers typically have specific densities from 1.02 to 1.04, yielding sedimentation velocities of 12–19 cm/min. Microcarriers specifically designed for fluidized-bed culture generally have significantly higher specific densities (∼1.3), resulting in sedimentation velocities of up to 220 cm/min.

As most cell lines used for recombinant protein production can be readily grown in suspension (e.g. CHO, BHK, hybridoma, and myeloma), microcarrier cultures are most commonly employed in systems that would benefit from perfusion or media exchange or require higher cell densities than can be obtained in fed-batch systems. Packed and fluidized beds are the most widely reported culture modes using microcarriers for recombinant proteins. In packed beds, carriers are either placed into a basket in an STR such as the CelliGen™ bioreactor available from New Brunswick Scientific (www.nbsc.com) or placed into a column. Packed columns provide a significant advantage of very low shear forces. However, they tend to suffer from nutrient limitations, particularly oxygen. Park and Stephanopoulos were to some extent able to overcome these limitations by inducing intraparticle convective flow (101), and McTaggart and Al-Rubeai reported retroviral vectors for gene therapy produced by the human packaging cell line LYRD18/LNChB7 grown on ImmobaSil™ G porous silicone carriers in a packed bed (102). However, unlike fluidized beds, packed beds are inherently limited in scale due to the oxygen gradients (103). Even with the convective flow described by Park and Stephanopoulos (101), a taller bed requires a faster recirculation rate to maintain adequate convection. Pressure drop, however, increases with increasing bed length and increasing fluid velocity. Additionally, packed beds have the problem of preferred flow-path formation, and it is very difficult, if not impossible, to sample carriers or cells during the run.

Fluidized beds are the most widely used culture system for porous microcarriers. In a fluidized bed, the microcarrier beads are suspended by the upward flow of medium. Recirculation can either be external as shown in Fig. 34.10 or internal as shown in Fig. 34.11. Very good mixing and oxygen mass transfer can be achieved in fluidized beds with very low shear forces. Dürrschmid and coworkers reported a comparison of fluidized-bed culture for CHO cells grown

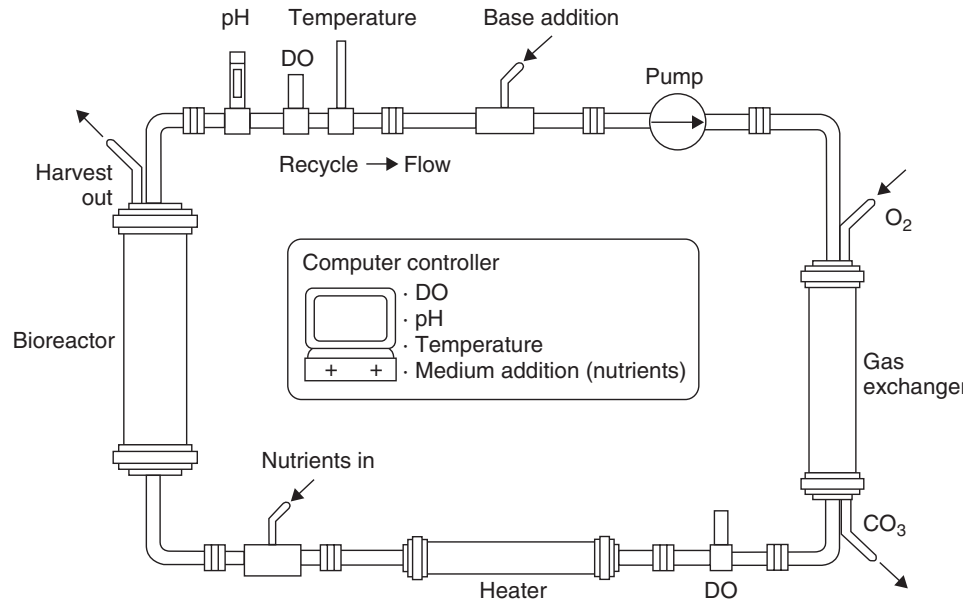


Figure 34.10. Fluidized bed with external recirculation.

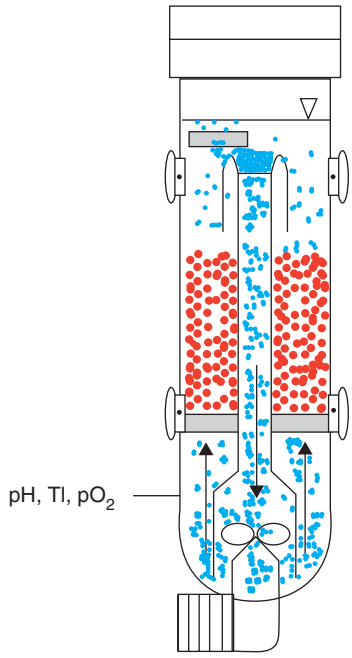


Figure 34.11. Fluidized bed with internal recirculation. (This figure is available in full color at http://onlinelibrary.wiley.com/book/10.1002/9780470054581.)

on microcarriers and ultrasonic cell retention for suspension cultures (104). Both systems showed similar growth and productivity.

Production of a number of recombinant products in fluidized beds has been reported in research studies, including erythropoietin (105), interferon-gamma (106), and arylsulfatase B (96). In their study of CHO cells producing arylsulfatase B, Dürrschmid *et al*. found that additional non-inoculated microcarriers could be added to the fluidized bed and that these carriers would subsequently be colonized by the cells on the existing microcarriers (96).

34.4.3 Effects of Microcarrier Culture on Protein Glycosylation

A critical issue in the use of microcarrier cultures for production of recombinant proteins is the effect of microcarrier culture on glycosylation. Protein glycosylation plays critical roles in protein folding, activity, immunogenicity, and protease sensitivity *in vivo* (107). A number of studies have examined variations in glycosylation of recombinant proteins for CHO cells grown in suspension and in an adherent manner. Watson and coworkers compared the distribution of N-linked oligosaccharides in kallikrein (a serine proteinase with pharmacological potential) for CHO cells grown in suspension or attached to microcarriers (108). They noted a change in the glycosylation pattern between the kallikreins produced under the two conditions, both in the amount of branching and in the amount of sialic acid present in the oligosaccharides. Unfortunately, the culture medium used for the two sets of conditions differed slightly, adding an additional complication in the interpretation of the data.

Two studies looked specifically at fluidized beds containing microcarriers. Goldman and coworkers compared a perfused fluidized bed containing cells grown on Cytoline microcarriers with a stirred-tank, batch suspension

culture for CHO cells producing recombinant human interferon-gamma (106). They found that the perfused culture maintained a more stable glycoform distribution and a higher fraction of glycosylation than did the batch cultures. However, it is difficult to separate the effects of perfusion from the effects of microcarrier culture. Wang and coworkers investigated erythropoietin produced by CHO cells grown on microcarriers in a perfused fluidized-bed reactor, as well as suspension cultures in continuous and batch STRs and spinner and T-flasks (105). They found substantial differences in specific productivity, with the highest specific productivities occurring in spinner and T-flasks. Glycoform analysis of the fluidized-bed cultures did not show any new glycoforms, but the authors did not report whether the distribution of glycoforms was the same as observed under other culture conditions.

Spearman and coworkers recently evaluated the yield and glycosylation patterns of recombinant β-interferon produced in suspension and on Cytopore microcarriers (109). As we observed previously, there was a significant decrease in cell growth in the microcarrier cultures compared with the suspension cultures. However, they found a substantial increase in specific productivity (approximately fivefold) for the microcarrier cultures leading to a threefold increase in yield. They observed no difference in the glycosylation profile. However, they did not evaluate glycan occupancy. They also observed that microcarrier culture significantly reduced aggregation of the β-interferon, leading to a larger fraction of useful product.

A limited number of similar studies have also been performed for recombinant proteins produced in BHK cells. Gawlitzek and colleagues evaluated the changes in glycosylation for a mutant version of interleukin-2 genetically engineered to include an N-linked glycosylation site in addition to the native O-linked site (110). They compared cells grown in suspension and on Cytodex 3 microcarriers in perfusion culture in medium containing 2% fetal bovine serum and serum-free medium. In suspension culture, serum-free medium significantly increased the N-linked glycosylation and reduced the fraction of nonglycosylated protein compared to serum-containing medium. In addition, when serum-free cultures in suspension and on microcarriers were compared, the suspension cultures had a lower fraction of nonglycosylated proteins. The glycan structures were also compared for the four culture conditions. Sialylation was increased significantly in serum-free cultures both in suspension and on microcarriers. The degree of fucosylation and antennary distribution was also affected by culture conditions, with an increase in fucosylation in serum-free medium for both microcarrier and suspension cultures, and a decrease in branching in microcarrier cultures on changing from serum-containing to serum-free medium.

More recently, we evaluated the effects of two different microcarriers and suspension culture on the glycosylation of recombinant SEAP (111). As shown in Table 34.6, the net effect of growth on microcarriers was to increase the sialylation of the SEAP and decrease the fucosylation. While increased sialylation of recombinant proteins is usually beneficial (due to reduced biological clearance), the role of fucosylation is less well understood. Human IgG_1 produced in a fucosylation-deficient mutant CHO cell line (112) or produced in rat hybridoma cells and fractionated by lectin affinity chromatography for reduced fucosylation (113) exhibited up to 50-fold increased affinity to human FcγRIIIA and increased antibody-dependent cellular cytotoxicity (ADCC). Core fucosylation affects the flexibility of the antennary structures, which may be the key to lectin recognition of fucosylated glycans (114). Alterations in fucosylation also play a role in human diseases, including cancer and cystic fibrosis (115). However, beyond the effects of defucosylation of IgG, there have been no studies on the effects of fucosylation on the biological activity of recombinant proteins. Nonetheless, understanding the modulation of fucosylation by culture conditions may prove important for other recombinant proteins.

34.5 FUTURE DIRECTIONS IN MICROCARRIER CULTURE

Microcarriers are increasingly employed for more biomedically oriented applications, including tissue engineering, stem-cell culture, and *in vitro* toxicology (116). This has resulted in new culture modalities, new microcarrier chemistries, and new cell lines. While a comprehensive review of this area is beyond the scope of this chapter, a few key references and reviews are discussed below.

King and Miller recently reviewed bioreactor development for stem-cell expansion and differentiation (117). They note that greater expansion of stem cells is observed in agitated cultures than in static culture for both aggregates and cells cultured on microcarriers. However, they pointed out that, as has been observed for cells producing recombinant proteins, shear must also be considered for cells on microcarrier beads. Microcarriers have also been employed in tissue-engineering studies of liver (118,119) and bone and cartilage (120), for extracorporeal devices, cell expansion, and cell transplantation. New chemistries include chitosan (121), poly(3-hydroxybutyrate-co-3-hydroxyvalerate) (122), and polyethylene glycol (123). New culture modalities include rotating-wall-vessel bioreactors (124) and single-use bioreactors (33–35).

TABLE 34.6. The Relative Percentage of N-Linked Glycans of SEAP under Different Culture Conditions

	Neutral N-Linked Glycans (%)		Sialylated N-Linked Glycans (%)							
			Monosialylated		DiSialylated		TriSialylated			
Culture Condition	Fucosylated	Nonfucosylated	Fucosylated	Nonfucosylated	Fucosylated	Nonfucosylated	Fucosylated	Nonfucosylated	Total Sialylated	Total Fucosylated
Suspension	35.1	20.0	11.3	30.1	0	3.5	0	0	44.9	46.4
Cytodex 3	11.3	14.4	2.2	55.1	6.7	6.1	0	4.2	74.3	20.2
Cytopore 1	27.0	13.1	3.3	42.2	0	10.4	0	4.1	59.9	30.3

34.6 CONCLUSIONS

Microcarriers play an important role in the culture of mammalian cells, particularly for industrial applications such as viral vaccine and recombinant protein production. A wide variety of chemistries exist, permitting cultivation of a myriad of cell types. Advantages of microcarrier culture include high surface area-to-volume ratios for adherent cultures, good scalability, and ease of perfusion in packed or fluidized beds as well as stirred tanks. These advantages must be weighed against mass-transfer limitations, particularly for macroporous carriers and fixed beds, and the possibility of increased shear sensitivity. Novel applications of microcarrier technology, such as tissue engineering, stem-cell cultivation, and *in vitro* toxicology, have renewed interest in microcarrier development, leading to new microcarrier compositions and culture modes. As new vaccines and therapeutics, particularly enzymatic compounds, enter the biopharmaceutical pipeline, microcarriers will remain an important technology in the bioprocessing arena.

REFERENCES

1. van Wezel AL. Nature 1967; 216: 64–65.
2. van Hemert PA, Kilburn DG, van Wezel AL. Biotechnol Bioeng 1969; 11: 875–885.
3. van Wezel AL, Herwaarden JAM, van de Henvel-de Rijk EW. Dev Biol Stand 1978; 42: 65–69.
4. van Wezel AL, van Steenis G, Hannik ACh, Cohen H. Dev Biol Stand 1978; 41: 159–168.
5. van Wezel AL, van der Velden-de Groot CAM. Process Biochem 1979; 13: 6–8.
6. van Wezel AL. In: Kruse PF, Patterson MK, editors. Tissue culture: methods and applications. New York: Academic Press; 1973. pp. 372–377.
7. Horng C-BC. [PhD thesis]. Buffalo (NY): State University of New York; 1975.
8. Horng C-BC, McLimans W. Biotechnol Bioeng 1975; 17: 713–732.
9. Levine DW, Wang DIC, Thilly WG. Biotechnol Bioeng 1979; 21: 821–845.
10. Inooka S, Tohoku J. Agric Res 1969; 20: 19–26.
11. Kuchler RJ, Marlowe ML, Merchant DJ. Exp Cell Res 1960; 20: 428–437.
12. Hirtenstein M, Clark J, Lindgren G, Vretblad P. Dev Biol Stand 1980; 46: 109–116.
13. Hirtenstein M, Clark J. In: Richards RJ, Rajan, KT, editors. Tissue culture in medical research. Oxford: Pergamon Press; 1980. pp. 97–104.
14. Clark J, Hirtenstein M. Ann N Y Acad Sci 81; 369: 33–46.
15. Meignier B, Meugot H, Favre H. Dev Biol Stand 1980; 46: 249–256.
16. van Wezel AL, van der Velden-de Groot CA, van Herwaarden JA. Dev Biol Stand 1980; 46: 151–158.
17. Montagnon BJ, Fanget B, Nicolas AJ. Dev Biol Stand 1981; 47: 55–64.
18. Microcarrier cell culture—principles and methods, GE healthcare, technical booklet series. Uppsala, Sweden; 2006.
19. Chun B-H, Chung S-I. Cytotechnology 2001; 37: 1–12.
20. Forestell SP, Kalogerakis N, Behie LA. Biotechnol Bioeng 1992; 39: 305–313.
21. Mendonca RZ, Pereira CA. Bioprocess Eng 1998; 18: 213–218.
22. Nikolovski J, Moony DJ. Biomaterials 2000; 20: 2025–2032.
23. Wang Y, Ouyang F. Bioprocess Eng 1999; 21: 207–210.
24. Nilsson K, Mosbach K. FEBS Lett 1980; 118: 145–150.
25. Young MW, Dean RC. Biotechnology 1987; 5: 835–837.
26. Reiter M, Blüml G, Zach N. In: Spier RE, Griffiths JB, MacDonald C, editors. Animal cell technology: developments, processes and products. Oxford: Butterworth-Heinemann Ltd.; 1992. pp. 501–504.
27. Mukopadhyay A, Mukopadhyay S, Talwar GP. J Chem Technol Biotechnol 1993; 56: 369–374.
28. Koller M, Papoutsakis E. In: Hjortso M, Roos J, editors. Cell adhesion: fundamentals and biotechnological applications. New York: Marcel Dekker; 1994.
29. Bhadriraju K, Hansen L. Biomaterials 2000; 21: 267–272.
30. Hynes RO. Cell 2002; 110: 673–687.
31. Humphries JD, Askari JA, Zhang XP, Takada Y, Humphries MJ, Mould AP. J Biol Chem 2000; 275: 20337–20345.
32. Rosalba S, Patarroyo M. Cell Immunol 1995; 160: 165–172.
33. Hundt B, Best C, Schlawin N, Kassner H, Genzel Y, Reichl U. Vaccine 2007; 25: 3987–3995.
34. Genzel Y, Olmer RM, Schäfer B, Reichl U. Vaccine 2006; 24: 6070–6087.
35. Genzel Y, Reichl U. In: Pörtner R, editor. Animal cell biotechnology –methods and protocols. Totowa (NJ): Humana Press Inc.; 2007. pp. 457–473.
36. Ng Y-C, Berry JM, ButlerM. Biotechnol Bioeng 1996; 50: 627–635.
37. Wang Y, Ouyang F. Bioprocess Eng 1999; 21: 211–213.
38. Mendonca RZ, Prado JC, Pereira CA. Bioprocess Eng 1999; 20: 365–371.
39. Möhler L, Bock A, Reichl U. Biotechnol Prog 2008; 24: 110–119.
40. Zielke HR, Ozand PT, Tildon JT. J Cell Physiol 1978; 95: 41–48.
41. Adamo S, De Luca LM, Akalovsky I, Bhat PV. J Natl Cancer Inst 1979; 62: 1473–1477.
42. Lynch RD, Schneeberger EF, Geyer RP. Exp Cell Res 1979; 122: 103–113.
43. Schneider M, Reymond F, Marison IW, von Stockar U. Enzyme Microb Technol 1995; 17: 839–847.
44. Taylor WG, Camalier RF, Sanford KK. J Cell Physiol 1978; 95: 33–40.
45. Reiter M, Weigang F, Ernst W, Katinger HWD. Cytotechnology 1990; 3: 39–42.
46. Preissmann A, Wiesmann R, Buchholz R, Werner RG, Noe W. Cytotechnology 1997; 24: 121–134.
47. Meuwly F, Loviat F, Ruffieux PA, Bernard AR, Kadouri A, von Stockar U. Biotechnol Bioeng 2005; 93: 791–800.
48. Fassnacht D, Pörtner R. J Biotechnol 1999; 72: 169–184.

49. Good NE, Wingate GD, Winter W. Biochemistry 1963; 5: 467.
50. Gregoriades N, Clay J, Ma N, Koelling K, Chalmers JJ. Biotechnol Bioeng 2000; 69: 171–182.
51. Venkat RV, Chalmers JJ. Cytotechnology 1996; 22: 95–102.
52. Tramper J. Cytotechnology 1995; 18: 27–34.
53. Croughan MS, Hamel JF, Wang DIC. Biotechnol Bioeng 1987; 29: 130–141.
54. Mollet M, Ma NN, Zhao Y, Brodkey R, Taticek R, Chalmers JJ. Biotechnol Prog 2004; 20: 1437–1448.
55. Bauer P, Hancock L, Rathman J, Chalmers JJ. Biotechnol Prog 2000; 16: 125–132.
56. Mufti NA, Shuler ML. Biotechnol Prog 1995; 11: 659–663.
57. van Wezel AL. In: Spier RE, Griffiths JB, editors. Animal cell biotechnology. London: Academic Press Inc.; 1985. pp. 266–281.
58. Mosmann T. J Immunol Methods 1983; 65: 55–63.
59. Nikolai TJ, Peshwa MV, Goetghebeur S, Hu WS. Cytotechnology 1991; 5: 141–146.
60. Peshwa MV, Kyung YS, McClure DB, Hu WS. Biotechnol Bioeng 1993; 41: 179–187.
61. Carvell JP, Dowd JE. Cytotechnology 2006; 50: 35–48.
62. Cerkel I, Garcia A, Degouys V, Dubois D, Fabry L, Miller AOA. Cytotechnology 1993; 13: 185–193.
63. Guan Y, Kemp R. In: Merten OW, Perrin P, Griffiths B, editors. New developments and new applications in animal cell technology. Dordrecht: Kluwer Academic Publishers; 1997. pp. 321–328.
64. Pohlscheidt M, Langer U, Minuth T, Böderker B, Apeler H, Hörlein H-D, Paulsen D, Rübsamen-Waigmann H, Henzler H-J, Reichl U. Vaccine 2008; 26: 1552–1565.
65. Lai CS, Hopwood LE, Swartz HM. Exp Cell Res 1980; 130: 437–442.
66. Reiter M. Cell Culture and Upstream Processing Conference; 2004; Sep 13–14, Berlin; Germany.
67. Lindner E, Arvidsson AC, Wergeland I, Billig D. Dev Biol Stand 1987; 66: 299–305.
68. Prokop A, Rosenberg MZ. Adv Biochem Eng 1989; 39: 29–71.
69. Widell A, Hansson GB, Nordenfeldt E. J Virol 1984; 8: 63–71.
70. Wu S, Huang GY. Biotechnol Prog 2002; 18: 124–128.
71. El-Karamany RM. Acta Virol 1987; 31: 321–328.
72. Montagnon BJ. Dev Biol Stand 1989; 70: 27–47.
73. Isayeva T, Kotova O, Krashnyk V, Kotov A. Bioprocess J 2003; 2: 75–81.
74. Kemble G, Greenberg H. Vaccine 2003; 21: 1789–1795.
75. Kallel H, Rouru S, Majoul S, Loukil H. Appl Microbiol Biotechnol 2003; 61: 441–446.
76. Geserick C, Bonarius HPJ, Kongerslev L, Hauser H, Mueller PP. Biotechnol Bioeng 2000; 69: 266–274.
77. Amadori M, Volpe G, Defillippi P, Berneri C. Biologicals 1997; 25: 65–73.
78. Yokomizo AY, Antonazzi MM, Galdino PL, Azambuja N, Jorge SAC, Pereira CA. Biotechnol Bioeng 2004; 85: 506–515.
79. Nikolai TJ, Hu WS. Enzyme Microb Technol 1992; 14: 203–208.
80. Meyer H, Reiter M, Mundt W, Barett N, Dorner F, inventors; to Baxter Healthcare SA. World patent WO03049767. 2003.
81. Bardiya N, Bae JH. Appl Microbiol Biotechnol 2005; 67: 299–305.
82. WHO working paper 1 on increasing production capacity for influenza vaccines. Available at www.who.int/vaccine_research/diseases/influenza/Working_Paper_1.pdf. Accessed 2006.
83. Kistner O, Barett PN, Mundt W, Reiter M, Schober-Bendixen S, Dorner F. Vaccine 1998; 16: 960–968.
84. Pau MG, Ophorst C, Klodijk MH, Schouten G, Methali M, Uytdehaag F. Vaccine 2001; 19: 2716–2721.
85. Seo SH, Goloubeva O, Webby R, Webster RG. J Virol 2001; 75: 9517–9525.
86. Tree JA, Richardson C, Fooks RF, Clegg JC, Lobby D. Vaccine 2001; 19: 3444–3450.
87. Voigt A, Zintl F. J Biotechnol 1999; 68: 213–226.
88. Xiao CZ, Huang ZC, Li WQ, Hu XW, Qu WL, Gao LH, Liu GY. Cytotechnology 1999; 30: 143–147.
89. Bleckwenn NA, Bentley WE, Shiloach J. Biotechnol Prog 2005; 21: 554–561.
90. Bleckwenn NA, Golding H, Bentley WE, Shiloach J. Biotechnol Bioeng 2005; 90: 663–674.
91. Knibbs RN, Dame M, Allen MR, Ding Y, Hillegas WJ, Varani J, Stoolman LM. Biotechnol Prog 2003; 19: 9–13.
92. Ikonomou L, Drugmand JC, Bastin G, Schneider YJ, Agathos SN. Biotechnol Prog 2002; 18: 1345–1355.
93. Kong D, Cardak S, Chen M, Gentz R, Zhang J. Cytotechnology 1999; 29: 215–220.
94. Kong D, Chen M, Gentz R, Zhang J. Cytotechnology 1999; 29: 149–156.
95. Hu XW, Xiao CZ, Huang ZC, Guo ZX, Zhang ZG, Li ZH. Cytotechnology 2000; 33: 13–19.
96. Dürrschmid M, Landauer K, Simic G, Blüml G, Doblhoff-Dier O. Biotechnol Bioeng 2003; 83: 681–686.
97. Landauer K, Wiederkum S, Dürrschmid M, Klug H, Simic G, Blüml G, Doblhoff-Dier O. Biotechnol Prog 2003; 19: 21–29.
98. Nam JH, Ermonval M, Sharfstein ST. Biotechnol Prog 2007; 23: 652–660.
99. Bleckwenn NA, Bentley WE, Shiloach J. Biotechnol Prog 2003; 19: 130–136.
100. Voisard D, Meuwly F, Ruffieux PA, Baer G, Kadouri A. Biotechnol Bioeng 2003; 82: 751–765.
101. Park S, Stephanopoulos G. Biotechnol Bioeng 1993; 41: 25–34.
102. McTaggart S, Al-Rubeai M. Biotechnol Prog 2000' 16: 859–865.
103. Meuwly F, Ruffieux PA, Kadouri A, von Stockar U. Biotechnol Adv 2007; 25: 45–56.
104. Dürrschmid MP, Landauer K, Simic G, Klug H, Keijzer T, Trampler F, Oudshoorn A, Gröschl M, Müller D, Doblhoff-Dier O. Biotechnol Prog 2003; 19: 1045–1048.
105. Wang MD, Yang M, Huzel N, Butler M. Biotechnol Bioeng 2002; 77: 194–203.
106. Goldman MH, James DC, Rendall M, Ison AP, Hoare M, Bull AT. Biotechnol Bioeng 1998; 60: 596–607.

107. Jenkins N, Curling EM. Enzyme Microb Technol 1994; 16: 354–364.
108. Watson E, Shah B, Leiderman L, Hsu Y-R, Karkare S, Lu HS, Lin F-K. Biotechnol Prog 1994; 10: 39–44.
109. Spearman M, Rodriguez J, Huzel N, Butler M. Biotechnol Prog 2005; 21: 31–39.
110. Gawlitzek M, Valley U, Nimtz M, Wagner R, Conradt HS. J Biotechnol 1995; 42: 117–131.
111. Nam JH, Zhang F, Ermonval M, Linhardt RJ, Sharfstein ST. Biotechnol Bioeng 2008; 100: 1178–1192.
112. Shields RL, Lai J, Keck R, O'Connell LY, Hong K, Meng YG, Weikert SHA, Presta LG. J Biol Chem 2002; 277: 26733–26740.
113. Shinkawa T, Nakamura K, Yamane N, Shoji-Hosaka E, Kanda Y, Sakurada M, Uchida K, Anazawa H, Satoh M, Yamasaki M, Hanai N, Shitara K. J Biol Chem 2003; 278: 3466–3473.
114. Stubbs HJ, Lih JJ, Gustafson TL, Rice KG. Biochemistry 1996; 35: 937–947.
115. Butler M. Cytotechnology 2006; 50: 57–76.
116. Ghanem A, Shuler ML. Biotechnol Prog 2000; 16: 471–479.
117. King JA, Miller WM. Curr Opin Chem Biol 2007; 11: 394–398.
118. Wu YM, Kumaran V, Benten D, Gupta S. Biotechnol Bioprocess Eng 2007; 12: 1–8.
119. Hammond JS, Beckingham IJ, Shakesheff KM. Expert Rev Med Devices 2006; 3: 21–27.
120. Malda J, Frondoza CG. Trends Biotechnol 2006; 24: 299–304.
121. Wu C, Pan JL, Bao ZM, Yu YT. J Mater Sci Mater Med 2007; 18: 2211–2214.
122. Zhu XH, Wang CH, Tong YW. J Biomed Mater Res Part B-Appl Biomater 2007; 82B: 7–16.
123. Underhill GH, Chen AA, Albrecht DR, Bhatia SN. Biomaterials 2007; 28: 256–270.
124. Song KD, Liu TQ, Li XQ, Cui ZF, Sun XY, Ma XH. Biomed Environ Sci 2007; 20: 91–98.

35

MONOCLONAL ANTIBODY PRODUCTION, CELL LINES

JULIA F. MARKUSEN AND DAVID K. ROBINSON
Bioprocess Research & Development, Merck Research Laboratories, Rahway, New Jersey

35.1 INTRODUCTION

Production of recombinant antibodies begins with construction of the cell line that will be used for expression of the final MAb product (Fig. 35.1). There are many steps downstream of cell line construction for ensuring safety, efficacy, quality, productivity, and regulatory acceptability of the cell culture process. Consideration of these attributes at the initial point of cell line selection is critical. This chapter outlines how the cell line can influence each of these key attributes and, in this context, reviews the host cell lines and expression systems that are commonly used to produce MAb products.

35.2 ROLE OF THE CELL LINE

MAbs are produced in biological systems, because their structural complexity prohibits their construction by chemical synthesis. Production occurs in ascites fluids of immunized animals, in hybridomas that result from the fusion of a B cell with a mouse myeloma cell or in a recombinant system as a heterologous gene product.

Due to the high therapeutic dosage requirements, production of MAbs occurs at scales ranging from kilograms to hundreds of kilograms per year which makes productivity and high reproducibility of product quality important selection criteria. Additionally, the limitations of using potentially immunogenic murine MAbs (1) have resulted in a trend toward using humanized or human MAbs. These MAbs are most often expressed as recombinant gene products that can be produced in a wide array of biological systems including animal cell lines, fungi, bacteria, and transgenic plants and animals. All currently licensed therapeutic MAbs in the United States are produced in animal cells, and all but two are produced as recombinant gene products (2).

35.2.1 Most Important Features of a Cell Line

The cell line chosen for production can heavily impact the MAb being expressed. It ultimately influences the productivity of the process and the drug product quality, safety, and regulatory acceptability. The role of each of these features is highlighted in the subsections that follow. Other factors that should be considered are economics and rapid development. Increased pressure on the pricing of pharmaceuticals (3) forces manufacturers to pay careful attention to the cost of production and purification as well as all royalties that may be associated with licensing the host cell line and expression system. Rapid development of gene into purified protein is a vital component of the overall drug development timeline, as it dictates the speed in which preclinical candidates can move into clinical studies.

35.2.1.1 Regulatory Acceptability. It is instructive to look at the cell lines that produce MAbs that are currently licensed for use as human therapeutics, since it is safe to assume that these cell lines were deemed acceptable by the regulatory agency that granted the license. Looking at the 20 therapeutic antibodies licensed in the United States up to December 2007, one sees that they are all mammalian cell lines including Chinese hamster ovary (CHO), murine myeloma (NS0 and SP2/0), or hybridoma

Upstream Industrial Biotechnology: Expression Systems and Process Development, Volume 1, First Edition. Edited by Michael C. Flickinger.
© 2013 John Wiley & Sons, Inc. Published 2013 by John Wiley & Sons, Inc.

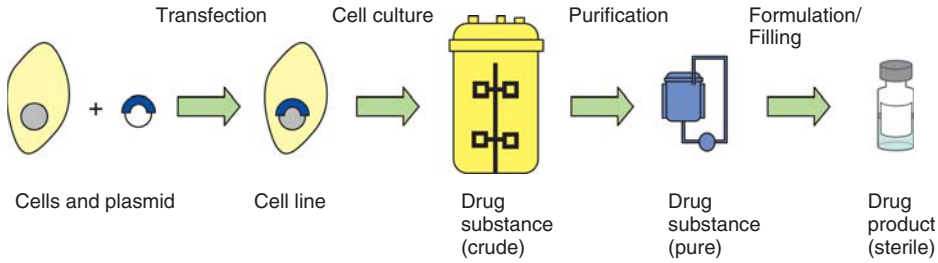


Figure 35.1. Schematic overview of a process for the production of therapeutic recombinant antibodies. (This figure is available in full color at http://onlinelibrary.wiley.com/book/10.1002/9780470054581.)

(Table 35.1). To date, there are no approved therapeutic MAbs in the United States that are produced in human, fungal, bacterial, or transgenic systems. However, one therapeutic protein that is produced in a human cell line has been approved in the United States which suggests that such cell systems may also receive regulatory approval for MAbs (see section titled "Human Cell Lines"). The reader should refer to the relevant regulatory guidance documents with the ICH guidelines on viral safety Q5A (4), the analysis of expression constructs Q5B (5), and the derivation of cell substrates Q5D (6) being of particular interest.

35.2.1.2 Safety. The safety of an antibody drug product can be greatly impacted by the quality and the handling of the cell line used to produce it. Two primary safety concerns are adventitious agents (e.g. viruses) and host cell impurities [e.g. Deoxyribonucleic acid (DNA)].

Cell lines can become contaminated with adventitious agents and could potentially serve as a source for the propagation and potential transmission of these agents to patients. There are three major routes by which contamination with adventitious agents might occur: (i) carryover of residual viruses that are harbored within the host cell line, (ii) introduction through contaminated raw materials (e.g. serum, screening antibodies) used to propagate or isolate the cell line, and (iii) through contact with contaminated personnel, equipment, or facilities. Though patient risk remains hypothetical, since a host cell line has not as of yet been implicated as the cause of any known transmission, special care

TABLE 35.1. FDA-approved MAbs (Therapeutic Full length, Unconjugated IgGs), Hamster (CHO) and Murine Cell Lines (SP2/0 and NS0) Predominate the Industry (as of 2007)

Product	Manufacturer	Launch	Indication	Production Host
Orthoclone OKT3	J&J	1986	Transplant rejection	Hybridoma
ReoPro	Centocor	1994	Cardiovascular disease	SP2/0
Rituxan	IDEC/Genentech	1997	Non-Hodgkin's lymphoma	CHO
Zenapax	Roche	1997	Organ rejection	NS0
Simulect	Novartis	1998	Organ rejection	SP2/0
Remicade	Centocor	1998	Rheumatoid arthritis	SP2/0
Herceptin	Genentech	1998	Breast cancer	CHO
Synagis	MedImmune	1998	Respiratory syncytial virus	NS0
Mylotarg	Wyeth	2000	Acute myelogenous leukemia	NS0
Campath	Millennium	2001	Lymphocytic leukaemia	CHO
Zevalin	IDEC	2002	Non-Hodgkin's lymphoma	CHO
Humira	Abbott	2002	Rheumatoid arthritis	CHO
Xolair	Genentech	2003	Asthma	CHO
Bexxar	Corixa/GSK	2003	Non-Hodgkin's lymphoma	Hybridoma
Raptiva	Xoma/Genen	2003	Plaque psoriasis	CHO
Avastin	Genentech	2004	Colorectal cancer	CHO
Erbitux	Imclone/ Bristol–Myers Squibb	2004	Colon, head and neck cancer	SP2/0
Tysabri[a]	Biogen/IDEC	2004	Multiple sclerosis	Murine myeloma
Vectibix	Amgen	2006	Colorectal cancer	CHO
Soliris	Alexion	2007	Paroxysmal nocturnal hemoglobinuria	Murine myeloma

[a]Tysabri was withdrawn from market in 2005; then reintroduced in 2006 under restricted distribution.

must still be taken to minimize this risk by appropriately documenting, handling, and testing the cell substrate (ICH Q5A) (4). Likewise, a detailed history of the host (ICH Q5D) (6), the raw materials, and the propagation techniques are helpful for devising procedures for clearing and testing for these agents. Detailed guidance is available in the regulatory documents (ICH Q5B) (5).

Contaminating residuals like DNA pose a similar hypothetical risk. However, since the process for the production of antibodies typically clears these to very low levels and ensures the absence of any live cells in the final product, additional testing such as tumorigenicity testing is rarely required for most cell lines of animal origin that are generally assumed to be tumorigenic.

35.2.1.3 Product Quality

35.2.1.3.1 Glycosylation. The basic structure of IgG antibodies consists of two heavy chains and two light chains that form two Fab regions that provide the specific antigen binding site. The Fab regions connect through a hinge region to the Fc region that interacts with receptors that activate clearance mechanisms of the target (see Jefferis (7), Fig. 35.1, p. 12). IgG antibodies have a conserved glycosylation site on the constant region of the heavy chain in the hinge region. The nature of the glycans subtly influences the three-dimensional orientation of the hinge region and can alter the binding of a variety of Fc receptors to the antibody (7,8). This change in binding can affect the half-life of the antibody as well as its ability to evoke effector functions like complement-dependent cytotoxicity (CDC) and antibody-dependent cellular cytotoxicity (ADCC). These properties depend on the interactions that occur between the antibody and the Fc receptor, for example, FcRn mediates half-life and FcγRIII mediates ADCC (9). The extent of these interactions is controlled by the antibody isotype, that is, whether the antibody is of isotype IgG1, IgG2, IgG3 or IgG4, and if the interaction involves receptor binding to the hinge region (10).

The product quality attribute most likely to be influenced by the cell line chosen for manufacture of an antibody is glycosylation. The extent to which an antibody is glycosylated and the structure and heterogeneity of those glycans is controlled by properties of the host cell line and, to an important but lesser extent, by the culture and purification conditions. For example, *E. coli* and other prokaryotes typically do not produce any posttranslational modification, whereas animal or yeast cell lines can provide species-specific glycosylation. The NS0 (mouse) cell line produces unique glycans such as the nonhuman galactose-α1,3-galactose glycan structure (7). The CHO (hamster) cell line produces the α2,3-linked sialic acid, but not the α2,6-linked sialic acid commonly found in human glycoproteins (11). Yeast cells produce nonhuman, *N*-linked glycans with high mannose structures (12). These nonhuman, host cell-dictated glycans can have a detrimental effect by increasing the immunogenicity of the antibody when administered in a clinical setting to a human. They also have the ability to evoke different levels of Fc effector function (reviewed in Jefferis (7)). Barbin *et al*. (13) demonstrated this with an anti-CD19 IgG1 for which the oligosaccharide structure and ADCC activity varied greatly depending upon whether the antibody was expressed in insect cells, human 293T cells, or modified 293T cells that over expressed a glycosylation enzyme GnTIII.

Rather than producing a highly homogeneous oligosaccharide structure, most host cell lines produce antibodies with an array of different oligosaccharide structures. The extent and degree of this microheterogeneity is greatly influenced by the culture conditions. Factors including the pH of the medium, the nutritional environment (14), the osmolarity, and the buildup of certain metabolites such as ammonia combine to impact upon the decoration of the antibody with oligosaccharides (15). Since it is important to reproducibly control both the type of oligosaccharide present and the extent of micro-heterogeneity, careful control of these factors is essential to ensure a reproducible product.

Lately, a number of efforts have started to bear fruit with regard to genetic manipulation of host cell systems for controlling both the type and homogeneity of glycosylation. This includes recent efforts to alter the expression of fucosyltransferase: an enzyme responsible for addition of a core fucose unit. Antibodies with fucose-deficient glycans confer higher ADCC activity as a result of higher binding affinity of the Fc region to FcγRIII (16). For certain MAbs, ADCC may be a very important therapeutic mechanism such that increasing ADCC by targeting methods to obtain fucose-deficient glycans may enhance the therapeutic activity of the antibody. In one report, a knock out CHO cell line was used to produce afucosylyated anti-CD19 antibodies that had significantly higher ADCC (17). In another report, a RNA interference construct was used during expression of an anti-CD30 antibody to favor production of afucosylated glycans in the plant *Lemna minor*. The resulting antibody had higher ADCC activity (18). It is interesting to note that removing glycosylation eliminates FcγRIII binding (10) which may be a desirable property when ADCC activity is not desired. There is no evidence currently that shows removing glycosylation affects binding to FcRn; and therefore, it presumably does not affect the antibody's circulating half-life (7).

Yeast cells are able to carry out *N*-linked glycosylation but typically attach complex high mannose structures that are rapidly cleared from the body (19). Scientists recently demonstrated that they could knock out selected yeast glycosylation pathways. In addition, they cloned five human glycosidases into the *Pichia pastoris* yeast strain enabling

the expression of antibodies with human oligosaccharide structures (12).

35.2.1.3.2 Proteolytic and Glycolytic Activity. A common posttranslational modification observed in recombinant protein production is the removal of the C-terminal lysine or arginine residue that is expected based on the gene sequence. This modification has been reported in a number of host cell lines (see Harris (20), Table 35.1, p. 131). Cleavage of the C-terminal lysine or arginine seems to occur to a variable extent (0, 1, or 2 residues cleaved) and may be due to activity of a carboxypeptidase (20). However, this posttranslational modification does not appear to negatively impact product quality or pose a regulatory concern (20).

Another subtle effect of the host cell line is the extent to which the cell line secretes glycosidases that might be active in culture conditions. For example, extracellular CHO cell sialidase was shown to trim terminal sialic acid from the recombinant glycoprotein gp120 (21). Mammalian cell lines can also express other proteases that can have a negative impact on product quality (22), but given that the glycans on the heavy chain are relatively inaccessible and that antibodies usually have greater resistance to proteolytic activity, the effect of endogenous sialidases and proteases is typically not severe.

35.2.1.3.3 Antibody Dissociation. Most of the recombinant antibodies used as therapeutics are of the immunoglobulin class IgG1. For some applications, isotypes such as IgG4 that are much less active in invoking effector functions may be preferable. However, this isotype is known to have a propensity to dissociate into "half-molecules" consisting of a heavy and light chain (reviewed by Aalberse and Schuurman (23)). The extent of dissociation can be influenced by both the choice of the host cell line and the choice of the clone itself (24).

35.2.1.3.4 Clonal Variability. Recombinant cell lines show great variability in properties such as cell growth and productivity. Although rare, genetic variations can occur during transfection, selection, and amplification of the gene transcripts that can lead to subpopulations of cells that express altered protein sequences (25). Therefore, selected cells are typically isolated from transfections under conditions that increase the probability of starting growth from a single cell. These methods include selection by multiple rounds of limiting-dilution cloning and/or selection of single cells by flow cytometry. Given the potential for each cell clone to exert different influences on the product, the selection criteria for a clone should include measures of cell growth and productivity, and analyses of the resultant antibody for appropriate mass, integrity, and glycosylation patterns.

"Clonal" recombinant cell lines can show a high degree of variation in growth and productivity in the presence or absence of selective pressure (26,27). Further, variability in growth has also been reported after three rounds of cloning of the untransfected host NS0 cell lines (28). Therefore, regulatory guidelines suggest passaging cells beyond the planned level of use for routine manufacturing and analyzing the product to verify that critical properties remain unchanged (ICH Q5D) (6).

35.2.1.4 Productivity. The cell line has a large impact on the overall productivity of a process through two different attributes, antibody production and cell density. The amount of antibody produced by each individual cell is often expressed as the specific productivity in units of picograms per cell per day (pcd). Typically, cell lines can be isolated that produce antibody at specific productivities ranging from 10 to 50 pcd (29) that is usually sufficient to generate amounts necessary to support clinical or commercial needs.

Other key attributes are the ability of the cell line to grow to high cell densities, typically 2–10 million cells per mL, and to maintain their viability for extended periods of time while continuing to secrete high levels of antibody (30) (Fig. 35.2). Although many methods are available for the propagation of cells, industry has largely settled into growing these cell lines in stirred tank reactors and fed-batch cultures, where nutrients are periodically added in a concentrated form to maintain high cell density and viability (2). Improvements in the selection of high producing, recombinant cell lines and in the optimization of fed-batch processes have allowed the typical titer of antibodies produced in a fully developed industrial process to increase almost 10-fold each decade since the first production of monoclonal antibodies (Fig. 35.3). See Wurm (31) and Birch and Racher (32) for reviews on MAb production improvements.

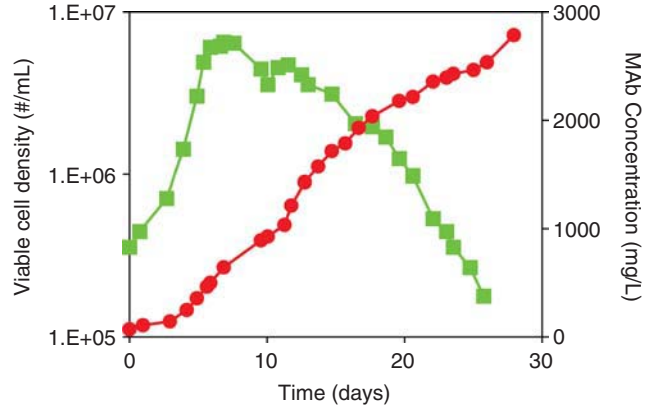


Figure 35.2. Example of the productivity (●) and viable cell concentration (■) as a function of culture time from an optimized fed-batch process. (This figure is available in full color at http://onlinelibrary.wiley.com/book/10.1002/9780470054581.)

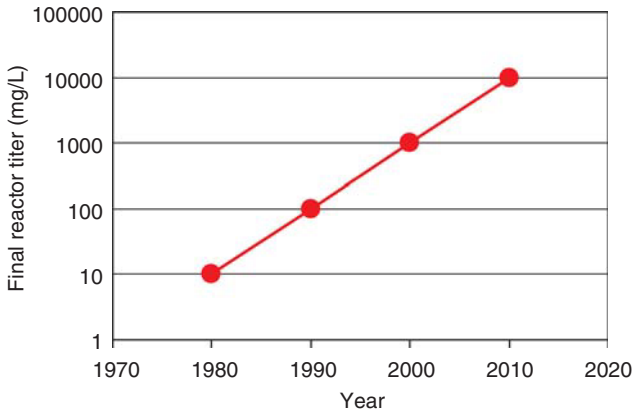


Figure 35.3. Final fed-batch process titers as a function of the year in which the process was developed. References for the range of titers reported include: Bibilia and Robinson (30) (Table 35.1, p. 3), Wurm (31) (Figure 35.2, p.1395), Birch and Racher (32) (Table 35.2, p. 680), Birch *et al*. (35) (Figure 4.6.b., p. 827), and Luan (36). (This figure is available in full color at http://onlinelibrary.wiley.com/book/10.1002/9780470054581.)

Scientists have tried to clarify the connection between phenotypic and genetic parameters that determine the productivity and stability of recombinant protein production in mammalian cells. Overall, the level of mRNA expression tends to correlate with the protein productivity, whereas the number of copies of genes integrated into the host cells does not (33,34). These two parameters are related to the general attributes of the cell line and expression system used; these properties are discussed next.

35.3 PROPERTIES OF MOST-COMMONLY USED MAMMALIAN CELL LINES AND VECTOR SYSTEMS

Productive recombinant protein expression systems used in the biopharmaceutical industry are achieved by obtaining high levels of gene transcription using appropriately designed expression vectors in concert with the intended host cell line. For MAbs, the host cell lines must be capable of efficient translation of heavy and light chain mRNAs into correctly assembled MAbs and effective secretion of the product with reproducible quality attributes that are aligned with the intended therapeutic effect. Since all of the currently licensed MAbs are expressed in mammalian host cells, this section focuses on the important genetic elements of the expression vector and methods that are used to improve protein expression by overcoming transgene silencing or by cell line engineering. A review of the methods currently used for transfection, selection, and screening for the most established mammalian cell lines is also included.

35.3.1 Mammalian Cell Expression Vectors

Expression vectors are used to deliver the genes coding for the therapeutic protein of interest to the host cell line. Therapeutic protein expression, in mammalian cell lines, relies on integration of the transgene into the host cell chromosome. The vector contains genetic elements that control transcription and translation. These elements typically include a 5' (upstream) promoter, a multiple cloning site (MCS) where the genes of interest are inserted, and a 3' (downstream) transcription terminator (polyadenylation) sequence. A mammalian selectable marker is required for selection of stable integrants in the host cell line. The most frequently used selectable markers include glutamine synthetase (GS) (37), dihydrofolate reductase (38–40) and hypoxanthine–guanine phosphoribosyl transferase (41,42). Alternatively, a resistance marker to an antibiotic like geneticin (G418, also known as *neomycin*) (43) or hygromycin (44) can be used. The most common promoters are human cytomegalovirus (hCMV) and simian virus 40 (SV40). The relative strength of the promoter is used to alternatively drive the heavy and light chain transcription rate higher than the selectable marker, or an internal ribosome entry site (IRES) can be inserted between the gene of interest and the selectable marker to drive the expression off a single promoter (45). The final essential components that are included in the mammalian expression vector are elements for bacterial cell propagation. These elements include a bacterial replication origin and a resistance marker to the antibiotic kanamycin or ampicillin. A generic example of a mammalian cell expression vector is shown in Fig. 35.4. The use and position of these elements within the vector can greatly affect gene expression (38,46,47).

Expression vectors also include translation control elements (e.g. Kozak sequence) and 5' and 3' untranslated regions (UTR) that increase efficiency of translation for improved mRNA stability. For MAbs, a leader (signal) sequence is needed for efficient intracellular transport and secretion. Intron (noncoding) sequences can affect promoter performance as well as transcription efficiency of the genes of interest and the selectable marker (45,46). Further, codon usage can be optimized to improve translational efficiency as a means to increase protein expression, because the frequency of different codons varies significantly between different organisms. In one series of experiments, optimized codon usage for CHO cell lines was shown to improve product yields, whereas removal of introns in heavy chain sequence did not affect productivity (48).

A frequent challenge with mammalian cell line selection is low and unstable recombinant protein expression that is caused by position effect, which is gene silencing at the level of chromatin due to the random nature of the transgene integration into the cell line chromosome. If the site of integration of the transgene is within or near

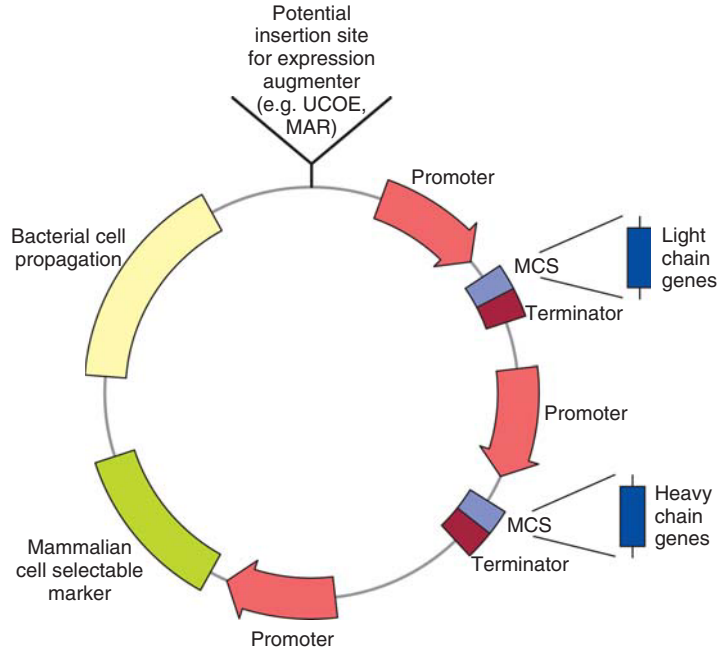


Figure 35.4. Generic schematic of a mammalian cell expression vector (MCS = multiple cloning site). (This figure is available in full color at http://onlinelibrary.wiley.com/book/10.1002/9780470054581.)

heterochromatin (i.e. highly condensed regions), transcription is repressed, whereas integration of the transgene into euchromatin (i.e. open regions) generally results in active transcription. A number of approaches have been developed to overcome epigenetic gene silencing that include: (i) incorporating specific DNA elements into the expression vector, (ii) interfering with posttranslational modifications to the histones, proteins that are directly associated with DNA structure, and (iii) targeting specific integration sites of high gene expression (reviewed in Kwaks and Otte (49)). These approaches are outlined briefly below.

Incorporating specific DNA elements into mammalian expression vectors (Fig. 35.4) can reduce the effect of integration into heterochromatin. Some examples of these elements are scaffold attachment sequences (SARs) or matrix attachment sequences (MARs) (40,50), ubiquitous opening elements (UCOEs) (44), and expression augmenting sequence elements (EASEs) (51). Other DNA elements will block chromatin-associated repressors which are also known as stabilizing and anti-repressor (STAR) elements (52). Effectiveness of these elements for increasing protein expression and stability is largely dependent on the design of the expression vector, the host cell line, the selection system, and the experimental conditions (40,45,53,54).

Another alternative used to overcome epigenetic gene silencing is interfering with posttranslational modifications to the histones. The basic building block of chromatin consists of double-stranded DNA wrapped around proteins called *histones*. Acetylation, methylation, phosphorylation, and ubiquitination of lysine and serine residues located in the *N*-termini of histones have an impact on gene activity (55). Active transcription of DNA in the euchromatin is associated with histone acetylation and demethylation. One method commonly used to block deacetylation of histones is the addition of sodium butyrate to the culture medium (56) which has been shown to improve MAb productivity (57,58). In another example, the demethylating drug 5-azacytidine was used to overcome cholesterol auxotrophy that was associated with gene silencing while establishing cholesterol-independent NS0 cell lines (59).

The third approach for overcoming epigenetic gene silencing is to target site-specific integration. In this approach, enzymes are used to exchange the transfected DNA into the donor "hot spots" in the preestablished host cell line. Three examples include the Cre recombinase-mediated recombination at a loxP site (60), Flp recombinase-mediated recombination at a Flp recombination target (FRT) site (61), and zinc finger nuclease-mediated recombination (62).

35.3.2 Transfection, Selection, and Screening Methods

Recombinant proteins can be expressed as transient or stable gene products in mammalian cells. Transfection is used to shuttle the genes encoding for the protein of interest into the host cell nucleus. Transient transfections are generally

performed to generate microgram to milligram quantities of protein within a short amount of time (e.g. 3–14 days). No selection agent is applied after transfection; therefore, the plasmid DNA is not retained after cell division and protein production decreases rapidly. Stable transfections, that are the focus of this chapter, are performed to generate gram to kilogram quantities of protein and generally take a couple of months to screen the cell population for the rare high producing cells. A selection agent is applied after transfection; therefore, surviving cells have the plasmid DNA integrated into their genome, and protein expression is maintained with cell division.

Prior to transfection, the expression vector, which is in the form of plasmid DNA as described in section titled "Mammalian Cell Expression Vectors", is propagated in *E. coli* cells and then purified. A number of transfection methods can be successfully used to deliver DNA into a mammalian cell's nucleus including the use of electroporation or transfection reagents such as calcium phosphate, cationic polymers or cationic lipids (63). The DNA is linearized before transfection to improve the efficiency of stable integration into the chromosome of the host cell line. After transfection, the cells are diluted in culture medium and plated into petri dishes or microwell plates at a suitable concentration to obtain single colony outgrowth (i.e. limiting-dilution cloning). The selection agent is applied a day or two after transfection so that only cells expressing the selectable marker survive. A large numbers of cells are usually transfected to obtain an array of transfectants that can be expanded and measured for productivity. At each expansion stage, the cultures are evaluated and strategically reduced so that only the most productive cultures are carried forward. The cell line and expression system, as well as the methods used to screen, can affect the amount of time required to identify a high producing cell line. Examples of screening methods are shown in Fig. 35.5 as well as in Birch *et al*. (35) (Fig. 4.3, p. 817), Wurm (31) (Fig. 35.1, p. 1394), and Charlebois (64).

It typically takes 3–6 months to produce a relatively small number of high producers (Fig. 35.5), but transfection and selection conditions such as electroporator settings, concentration of selection agent, and seeding density can be optimized to increase the number of colonies that grow out of selection as well as the range of productivity (35,47,65). Flow cytometry can be used to identify highly productive cells earlier in the screening process using fluorescent-activated cell sorting (FACS). This approach permits analysis of attributes like protein expression to be performed on a single cell basis. Some reported examples include direct measurement of protein secretion by cell encapsulation in gel microdrops (66,67), membrane trapping of secreted proteins (68), and binding to a cellular affinity matrix (69,70). Other FACS screening methods measure surrogate markers for protein expression such as RNA expression levels using fluorgenic epitope tags (71) or selectable marker expression using fluorescent analogs like fluorescein-conjugated methotrexate (F-MTX) (39,72). These flow cytometry sorting methods have the potential to identify high producer cell lines much more rapidly than the traditional limiting-dilution cloning approach.

35.3.3 Cell Line Engineering

Cell lines can be further engineered to improve protein expression. Considerable effort has been placed in development of anti-apoptotic cell lines, reviewed by Vives (73). During production, cells are exposed to adverse conditions including nutrient depletion, buildup of toxic by-products, oxygen limitation, and shear stress that leads to programmed cell death, or apoptosis. This effect can be mitigated by over-expressing the anti-apoptosis genes involved in different phases of the apoptotic cascade, including those belonging to the protective Bcl-2 family and those involved in caspase inhibition. Over-expression of the Bcl-2 gene is the most extensively studied approach (35,73). Cell lines expressing this anti-apoptosis gene generally can be sustained for longer culture periods, primarily due to improved cell viability. However, the overall results vary particularly when evaluated under commercially relevant conditions. A successful case was reported using another Bcl-2 family member, Bcl-X_L, using chemically defined medium at 2000-L scale (74). More recently, expression of a combination of inducible anti-apoptosis genes Aven and EIB-19K was found to significantly improve cell viability and MAb expression in extended CHO cultures (75).

Finally, proteomics is being used to elucidate further bottlenecks in recombinant MAb production. Chaperone proteins, such as BiP and PDI that are present in the endoplasmic reticulum that affect immunoglobin folding and assembly, have been shown to increase in abundance with increasing recombinant protein production in murine myeloma cells (76). Incorporation of discrete chaperones into genetically engineered mammalian cell lines have not as of yet increased their capacity for protein production. However, this approach has successfully enhanced production of mammalian recombinant proteins in yeast and insect cells (77).

35.3.4 Mammalian Cell Lines

CHO and mouse myelomas are the most frequently used mammalian cell lines for production of MAbs (Table 35.1). These cell lines originated in the 1950–80s after selection for nutritional mutant cells that are deficient in an essential amino acid and/or enzyme required for survival. These cell lines are ideal for recombinant gene transfection, because their amino acid or enzyme deficiencies can be exploited

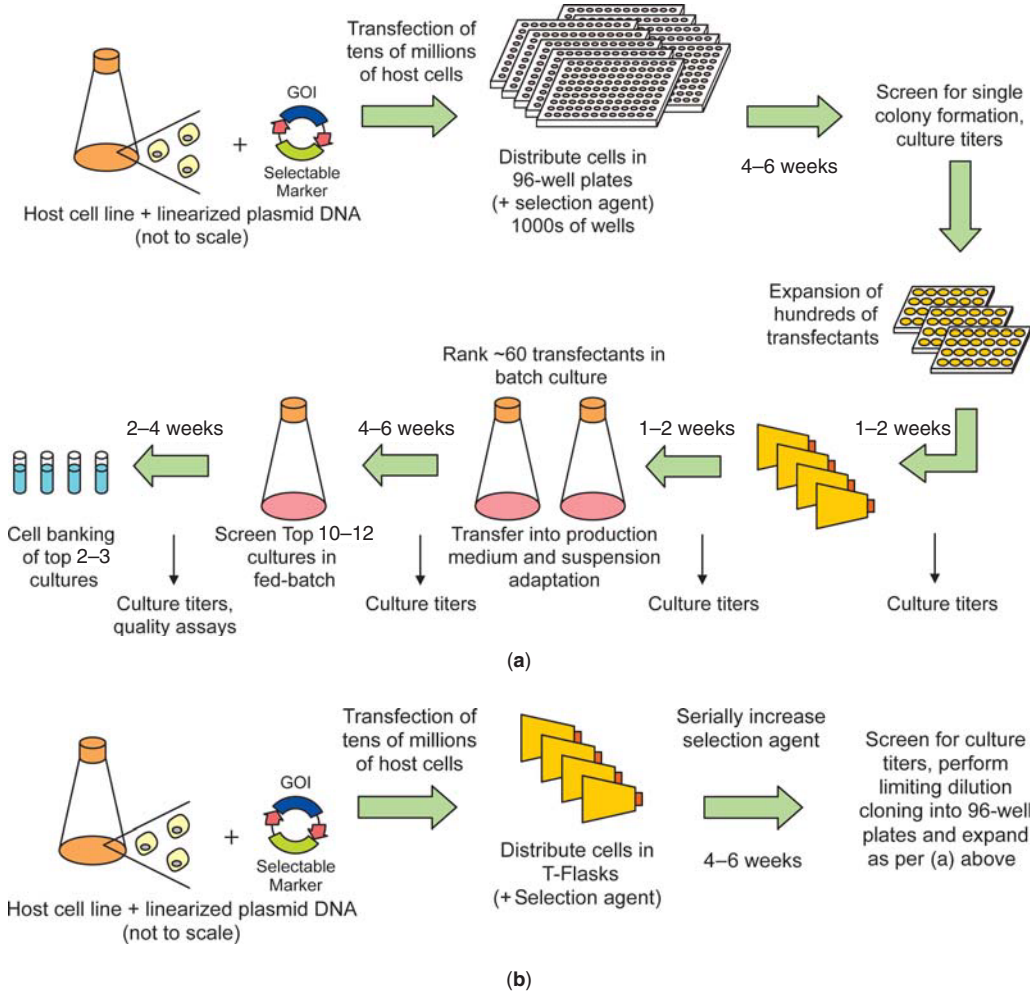


Figure 35.5. Example time lines for mammalian cell line screening (a) starting with limiting-dilution cloning immediately after transfections, and (b) starting with pools and including amplification. (This figure is available in full color at http://onlinelibrary.wiley.com/book/10.1002/9780470054581.)

during the selection process through the use of a strategically designed expression vector and deficient selection medium.

35.3.4.1 Chinese Hamster Ovary. CHO cells used for commercial manufacture of MAbs were originally isolated by Puck *et al*. (78) from outbred hamsters from G. Yerganian's lab. Multiple lineages of proline deficient (pro-) mutants were subsequently derived (79,80) including CHO/pro-K1 (81), also known as *CHO-K1*, and *CHOpro-3* (82), also known as *CHO Toronto*, as it was used extensively by L. Siminivitch and his colleagues in that city (communication from L. Chasin).

Cell lines originating from CHO-K1 and CHOpro-3 were subjected to chemical mutagenesis and exposed to γ irradiation to generate cell lines deficient in dihydrofolate reductase (dhfr-), an enzyme required for nucleotide metabolism. Two resulting cell lines known as *DXB11* (83) and DG44 (84) are used in biopharmaceutical industry for the production of MAbs. Cell line DXB11 is also sometimes referred to as *DUK-XB11*, *DUK-B11* or *DUKX* (communication from L. Chasin). When these cell lines are used as part of a selection system, cells transfected with an expression vector containing the dhfr gene can grow in medium lacking glycine, hypoxanthine, and thymidine (GHT). Methotrexate (MTX), a cytotoxic folate analog specific for the DHFR enzyme, can be added to the GHT-free medium to increase selection pressure or to amplify gene transcripts for increased productivity (38,39), but some cases of instability have been observed (34,85) as well as appearance of genetic variants (25). An antibiotic resistance gene can often be used in conjunction with DHFR expression vectors (38–40) to permit rapid selection using antibiotic resistance and MTX to amplify

the dhfr transcript co-localized with the gene of interest. Reff and colleagues demonstrated that DHFR selection combined with an impaired neomycin gene as a dominant selectable marker can further facilitate selection of cell lines that only have transgenes integrated into hot spots within the genome (86).

Another common selection system used with cell lines derived from CHO-K1 is the GS system (35). GS is an enzyme involved in glutamine synthesis from glutamate and ammonia. Since glutamine is an essential amino acid, cell lines that lack endogenous GS must be fed glutamine for survival. When used as a selection system, cells transfected with the GS gene can grow in glutamine-free medium (37). Methionine sulfoximine (MSX), an inhibitor of GS, can be added to the medium to increase selection pressure if the cells such as CHO-K1 have endogenous GS, or to amplify gene expression (37,87).

35.3.4.2 Mouse Myeloma. Mouse myeloma cells were isolated originally from a mineral oil induced plasmacytoma by peritoneal injection in a BALB/c female mouse (88). The original mutant P3K (MOPC) was selected to be deficient in hypoxanthine-guanine phosphoribosyl transferase (hgprt-), an enzyme required for purine metabolism; however, the cells still expressed endogenous immunoglobin. Many rounds of selection and subcloning were performed to identify cells that no longer expressed the endogenous heavy and light chains. Three cell lines from slightly different lineages were derived from P3K, and represent the mouse myeloma cell lines frequently used today.

The first subclone, X63/Ag8.653, was derived from P3-X63/Ag8 (89). Another subclone, Sp2/0-Ag14 (also called Sp2/0), was derived from the fusion of P3-X63/Ag8 with the spleen of a BALB/c mouse immunized with sheep red cells and subsequently identified for its lack of immunoglobin expression (90). The third non-immunoglobin secreting subclone, NS0 (also called NS0/1), was a subline identified from NSI/1-Ag4-1, a light chain synthesizing subclone of P3K lineage (91). Table I, p.12 in Galfre and Milstein (91) has a clear summary of these lineages.

Due to their lineage as immunoglobin secretors, myeloma cells are a natural choice for recombinant gene transfection (reviewed in Yoo (92)). The GS expression system works particularly well for NS0 cell line, since they do not express endogenous GS. Cell line selection can be achieved in glutamine-free medium (35). MSX can be added to increase selection pressure (37). As compared to NS0, Sp2/0 cells were found to have a higher frequency of glutamine-independent variants (37).

Alternatively, myeloma cells can be transfected with selection vectors containing the xanthine–guanine phosphoribosyl transferase (gpt) gene or in combination with the neomycin gene (93). Mycophenolic acid is added for selection and MTX can be used to further inhibit the purine biosynthesis pathway to increase the stringency of this expression system. Myeloma cell line expression systems with gpt and/or neomycin genes have been used to express MAbs of commercial significance (41,42,94,95).

35.3.4.3 Hybridomas. The earliest antibodies created with predefined specificity were produced by hybridomas that were generated by fusing MAb-producing murine B cells with a tumor cell line (96). This procedure involves immunizing mice with a complex antigen mixture that gives rise to murine B cells expressing diverse antibodies directed against different antigens and epitopes. The B cells are isolated from the spleen or peripheral lymph nodes from the mice and fused with myeloma cells such as SP2/0-Ag14 or X63-Ag8.653. Supernatants from the resulting hybridomas are either screened by ELISA using plates coated with the antigen of interest or are analyzed by FACS for recognition of the native protein expressed on the surface of target cells. The origin of hybridomas and their impact on the field were reviewed by Milstein, one of the founding scientists (97).

Unfortunately, MAbs produced by hybridomas isolated from murine B cells were found to be immunogenic to humans (1). This issue was improved by creating recombinant chimeric or humanized MAbs in which portions of the mouse DNA sequence were replaced with the human sequence (10). However, now B cells can be taken from transgenic mice that possess an immune system in which the mouse antibody-producing genes were inactivated and functionally replaced by human antibody-producing genes. When immunized with human antigens, the mouse immune system recognizes the antigen as foreign, yet the transgenic mouse produces fully human antibodies rather than murine antibodies (98,99). This approach has been successfully used to generate investigational MAbs for human clinical studies.

35.3.4.4 Human Cell Lines. To date, no human cell lines have been licensed for the production of MAbs, and only one therapeutic protein has been approved by the FDA that is produced in human embryonic kidney (HEK293) cells (100,101). The HEK293 cell line was originally isolated after transfection with adenovirus-5 DNA (102). HEK293 is one of the most widely used cell line for large-scale transient transfection because it is highly susceptible to gene transfer (reviewed in Pham (103)). Two variants of this cell line were engineered for transient transfection: HEK293E which stably expresses the nuclear antigen of the Epstein–Barr virus (EBNA-1) and HEK293T which stably expresses the T-antigen of Simian virus 40. These cell lines can be transiently transfected with expression vectors containing either the EBV or SV40 origin of replication to produce large quantities of MAbs within a short

time (103,104) as compared to stable transfections. This approach is frequently used to produce MAbs for preclinical evaluation.

Another human cell line, PER.C6®, was derived by immortalizing human embryonic retina cells with the E1 gene of adenovirus (105). PER.C6® cells were originally generated for production of viral vectors, but recently MAbs have been produced from this cell line using G418 (neomycin) as the selection agent (43). Several vaccines and one MAb are reported to be in clinical trials (106).

35.3.4.5 Baby Hamster Kidney. One additional mammalian cell line that has been used to produce therapeutic proteins is the baby hamster kidney cell line, BHK-21. The BHK-21 cell line was derived from the polyoma-virus-induced transformation of kidney cells from one day old hamsters (107). The FDA has approved several recombinant blood factors produced as recombinant gene products in BHK cells. Thus far BHK cells have not been widely adopted for commercial MAb production which is probably because higher productivity can be achieved with CHO and murine myeloma cell lines. But, there are a few reports of MAbs expressed in BHK cells (108,109) including efforts to improve productivity using an inducible promoter for labile or toxic proteins (110).

35.4 OTHER HOST PLATFORMS

Despite the continued advancement of mammalian cell culture productivity (Fig. 35.3), there are several other host platforms that have some technical and economic advantages over mammalian cells. They have faster growth rates and can be grown to higher cell densities; and therefore, they usually have shorter production cycle times. Their growth media are less complex and can be well-defined resulting in less expense (111). However, as previously reviewed in "Product Quality", glycosylation plays an essential role in the function of many therapeutic products. Robust industrial fermentation organisms such as *E. coli* and fungi have been used successfully to produce simple nonglycosylated recombinant proteins. Prokaryotic organisms like *E. coli* do not glycosylate proteins. Lower eukaryotic hosts like yeast, insect, and plant cells produce glycan structures distinct from mammalian cells. The native *N*-glycan structures of these host cells are potentially immunogenic to humans and can adversely affect the safety and pharmacokinetic properties of the product. But, the availability of the genomic sequences for these organisms has enabled substantial headway to be made in the genetic modification of the *N*-glycan processing pathways for generation of mammalian-like *N*-glycans (review by Betenbaugh *et al*. (112) and Sethuraman and Stadheim (113)). Some of these advances are mentioned in the following sections.

35.4.1 Fungi

All yeast-based therapeutic proteins (e.g. anticoagulants, growth factors) and vaccines currently on the market are produced in *Saccharomyces cerevisiae* (111). Yeasts are capable of glycosylating proteins, but the resulting high mannose structures are nonhuman forms that are highly immunogenic (114) and result in rapid clearance (19,115). For this reason, yeast systems were not considered for MAb production. Recently, however, human glycosylation pathways were genetically engineered into *Pichia pastoris* that resulted in the production of MAbs with human *N*-glycosylation (116). There are at least seven therapeutic proteins under development using *P. pastoris* (12). Although yet to be approved for production of MAbs for human clinical trials, success of this technology will likely have a great impact on the future landscape of host cell lines used for MAb production.

35.4.2 Bacteria

E. coli is a very effective host system for production of simple recombinant proteins (e.g. insulin, human growth hormone, growth factors, interferons, and interleukins) and antibody fragments (111). Because antibody fragments lack the Fc domain, they do not bind to the FcRn receptor and are cleared *in vivo* rapidly. This attribute limits their therapeutic effectiveness (117). Initial attempts to express full length MAbs in *E. coli* resulted in the formation of insoluble aggregates called *inclusion bodies* that were biologically inactive. Efforts were made, with limited success, to solubilize and refold MAbs *in vitro* from denatured conditions (118). Recent improvements were made to the expression cassettes by Simmons and colleagues (119), in which a two promoter system with optimized translation initiation regions was used to control heavy chain and light chain distribution, resulting in the correct assembly of full length MAbs. The *E. coli*-expressed antibodies were active, and as expected for aglycosylated antibodies, they did not bind to C1q or FcγRI receptors. In addition, the *E. coli* antibodies showed similar circulating half-life in chimpanzees as those produced in mammalian cells (119). This approach appears promising, as there are appropriate therapeutic indications for which effector function leading to target cell depletion is undesirable (120,121).

35.4.3 Insect Cells

The insect cell–baculovirus expression system has been widely used to produce recombinant proteins and glycoproteins, see reviews by Kost *et al*. (122) and Jarvis (123). Despite its extensive use in research, only one vaccine comprised of recombinant viral proteins has been successfully licensed in the European Union for human use (124).

This host system has been limited from gaining traction for therapeutic use, particularly for MAb production, because insect cells are unable to produce human *N*-glycan structures (123), and mammalian cells have served as more predominant and suitable host for these products (111). Recently, the lepidopteran insect cell line has been engineered to express multiple enzymes for the expression of humanized glycoproteins, including glycosyltransferase, sialyltransferase, *N*-acetylglucosamininyltransferase, sialic acid synthase, and CMP-sialic acid synthetase (125). These cells produce sialylated recombinant glycoproteins in serum-free medium and represent the most extensively processed structures produced by any transgenic insect line described to date.

35.4.4 Plants

The first generation of recombinant proteins produced in plants is approaching commercial status for vaccines, human hormones or growth regulators, and antibodies (reviewed in Schillberg *et al*. (126)). A MAb against EGFR has been expressed in corn. In this example, the aglycosylated MAb possessed similar *in vivo* pharmacokinetics in primate studies compared to the mammalian cell culture derived MAb, whereas the glycosylated MAb had poor pharmacokinetics due to its rapid clearance (127). A number of plants have been genetically engineered to eliminate nonhuman glycan structures. Human antibody production has been optimized in a small green aquatic plant, *Lemna minor*, by co-expressing the antibody with an RNA interference construct that targets expression of β1,2-xylosyltransferase and core α1,3-linked fucosyltransferase genes (18). Tobacco plants have been genetically modified to produce mouse antibodies devoid of plant carbohydrate epitopes (128). And knockout *Arabidopsis thaliana* plants have been created that are free of immunogenic *N*-glycan structures like β1,2-linked xylose and core α1,3-linked fucose residues found in endogenous oligosaccharides (129). The economic implications for this type of production will certainly drive further progress in modifying plant *N*-glycan pathways for the production of humanized oligosaccharides.

35.4.5 Transgenic Animals

The production of recombinant proteins in milk or other body fluids using transgenic animals is another potential method that has been extensively investigated (reviewed by Houdebine (130)). For mammary gland expression, the genes coding for the protein of interest are introduced into the animal germ line using an expression vector fused to milk-specific regulatory elements (reviewed in Pollock *et al*. (131)). As with all other host systems, expression level varies with the expression vector and regulatory sequence. A humanized IgG1 MAb has been expressed in transgenic goat milk in multiple grams per liter quantities (131). Chimera chickens have been bred that express a MAb in the tubular gland cells of the oviduct that is secreted into the egg white to yield eggs that contain milligram quantities of the MAb (132). The oligosaccharide profile of this MAb was different from those produced in CHO cultures, in that the chicken-produced MAb contained high mannose type *N*-glycans, very low levels of galactose residues, and no α1,6-fucose residues (132). Progress in improving and simplifying therapeutic MAb expression in transgenic animals continues to make it a compelling process for future large-scale production.

35.5 CLOSING COMMENTS

Mammalian cell lines, in particular, CHO and mouse myeloma, are currently established as the dominant host cell platform for commercial production of recombinant MAbs because of their regulatory acceptance and ability to effectively and efficiently produce MAbs with consistent human-like glycan structures. Mammalian cell culture productivity has improved significantly over the past 20 years, due in part to enhanced vector design and optimized transfection, selection, and screening techniques for identification of the most highly productive cell lines. Progress in cell line engineering indicates further opportunity for improvement. Recent advances made in genetically engineering human *N*-glycan pathways into yeast and plants have the potential to alter the mammalian cell line dominance in the field. The impact of this paradigm shift in MAb production is yet to be realized; however, the establishment of high producing host cell lines that are used to develop robust manufacturing processes and demonstrate safe and consistent product quality attributes is one of the paramount requirements for gaining regulatory acceptance.

Acknowledgments

The authors thank Tracy M. Janus for reviewing and editing this manuscript, and Sheri L. Nidositko and Venkata R. Mangalampalli for their suggestions about the content.

REFERENCES

1. Shawler DL, Bartholomew RM, Smith LM, Dillman RO. J Immunol 1985; 135: 1530–1535.
2. Chu L, Robinson DK. Curr Opin Biotechnol 2001; 12: 180–187.
3. DiMasi JA, Hansen RW, Grabowski HG. Journal of Health Economics 2003; 22: 151–185.

4. ICH quality guidelines. Q5A(R1)-viral safety evaluation of biotechnology products derived from cell lines of human or animal origin. Available at http://www.ich.org/cache/compo/276-254-1.html. Accessed 2008 Jan 25.
5. ICH quality guidelines. Q5B-quality of biotechnological products: analysis of the expression construct in cells used for production of r-DNA derived protein products. Available at http://www.ich.org/cache/compo/276-254-1.html. Accessed 2008 Jan 25.
6. ICH quality guidelines. Q5D-derivation and characterisation of cell substrates used for production of biotechnological/biological products. Accessed 2008 Jan 25.
7. Jefferis R. Biotechnol Prog 2005; 21: 11–16.
8. Gurbaxani BM, Morrision SL. Mol Immunol 2006; 43: 1379–1389.
9. Wright A, Morrison SL. Trends Biotechnol 1997; 15: 26–32.
10. Jefferis R. Expert Opin Biol Ther 2007; 7: 1401–1413.
11. Lee EU, Roth J, Paulson JC. J Biol Chem 1989; 264: 13848–13855.
12. Gerngross TU. Nat Biotechnol 2004; 22: 1409–1414.
13. Barbin K, Stieglmaier J, Saul D, Stieglmaier K, Stockmeyer B, Pfeiffer M, Lang P, Fey GH. J Immunother 2006; 29: 122–133.
14. Butler M. Cytotechnology 2006; 50: 57–76.
15. Andersen DC, Goochee CF. Curr Opin Biotechnol 1994; 5: 546–549.
16. Shields RL, Lai J, Keck R, O'Connell LY, Hong K, Meng YG, Weikert SH, Presta LG. J Biol Chem 2002; 277: 26733–26740.
17. Yamane-Ohnuki N, Kinoshita S, Inoue-Urakubo M, Kusunoki M, Iida S, Nakano R, Wakitani M, Niwa R, Sakurada M, Uchida K, Shitara K, Satoh M. Biotechnol Bioeng 2004; 87: 614–622.
18. Cox KM, Sterling JD, Regan JT, Gasdaska JR, Frantz KK, Peele CG, Black A, Passmore D, Moldovan-Loomis C, Srinivasan M, Cuison S, Cardarelli PM, Dickey LF. Nat Biotechnol 2006; 24: 1591–1597.
19. Lee SJ, Evers S, Roeder D, Parlow AF, Risteli J, Risteli L, Lee YC, Feizi T, Langen H, Nussenzweig MC. Science 2002; 295: 1898–1901.
20. Harris RJ. J Chromatogr A 1995; 705: 129–134.
21. Gramer MJ, Goochee CF, Chock VY, Brousseau DT, Sliwkowski MB. Biotechnology 1995; 13: 693–698.
22. Clark KJR, Chaplin FWR, Harcum SW. Biotechnol Prog 2004; 20: 1888–1892.
23. Aalberse RC, Schuurman. Immunology 2002; 105: 9–19.
24. Chan CP. CHI 3rd Annual Optimizing Cell Culture Development Conference; Abst 2007, Boston, MA.
25. Harris RJ, Murnane AA, Utter SL, Wagner KL, Cox ET, Polastri GD, Helder JC, Sliwkowski MB. Biotechnology 1993; 11: 1293–1297.
26. Kim NS, Kim SJ, Lee GM. Biotechnol Bioeng 1998; 60: 679–688.
27. Barnes LM, Bentley CM, Dickson AJ. Biotechnol Bioeng 2001; 73: 261–270.
28. Barnes LM, Moy N, Dickson AJ. Biotechnol Bioeng 2006; 94: 530–537.
29. Robinson DK, DiStefano D, Gould SL, Cuca G, Seamans TC, Benincasa D, Munshi S, Chan CP, Stafford-Hollis J, Hollis GF, Jain D, Ramasubramanyan K, Mark GE, Silberklang M. In: Wang H, Imanaka T, editors. Antibody expression and engineering. Worthington (OH): ACS; 1995. pp. 1–14.
30. Bibila TA, Robinson DK. Biotechnol Prog 1995; 11: 1–13.
31. Wurm FM. Nat Biotechnol 2004; 22: 1393–1398.
32. Birch JR, Racher AJ. Adv Drug Deliv Rev 2006; 58: 671–685.
33. Lonza web information. Available at http://www.lonza.com/group/en/company/news/publications_of_lonza.-ParSys-0002-ParSysdownloadlist-0034-DownloadFile.pdf/final%20poster%20APorter%20CCE%20X.pdf. Accessed 2008 Jan 25.
34. Derouazi M, Martinet D, Besuchet Schmutz N, Flaction R, Wicht M, Bertschinger M, Hacker DL, Beckmann JS, Wurm FM. Biochem Biophys Res Commun 2006; 340: 1069–1077.
35. Birch JR, Mainwaring DO, Racher AJ. In: Knäblein J, editor. Modern biopharmaceuticals. Weinheim: Wiley-VCH Verlag GmbH & Co. KGaA; 2005. pp. 809–832.
36. Luan YT. IBC BioProcess International Cell Culture & Upstream Processing Conference; Abst 2006, San Francisco, CA.
37. Bebbington CR, Renner G, Tomson S, King D, Abrams D, Yarranton GT. Biotechnology 1992; 10: 169–175.
38. Lucas BK, Giere LM, DeMarco RA, Shen A, Chisholm V, Crowley CW. Nucleic Acids Res 1996; 24: 1774–1779.
39. Bianchi AA, McGrew JT. Biotechnol Bioeng 2003; 84: 439–444.
40. Girod PA, Zahn-Zabal M, Mermod N. Biotechnol Bioeng 2005; 91: 1–10.
41. Shearman CW, Pollock D, White G, Hehir K, Moore GP, Kanzy EJ, Kurrle R. J Immunol 1991; 147: 4366–4373.
42. Knight DM, Trinh H, Le J, Siegel S, Shealy D, McDonough M, Scallon B, Moore MA, Vilcek J, Daddona P, Ghrayeb J. Mol Immunol 1993; 30: 1443–1453.
43. Jones D, Kroos N, Anema R, van Montfort B, Vooys A, van der Kraats S, van der Helm E, Smits S, Schouten J, Brouwer K, Lagerwerf F, van Berkel P, Opstelten DJ, Logtenberg T, Bout A. Biotechnol Prog 2003; 19: 163–168.
44. Benton T, Chen T, McEntee M, Fox B, King D, Crombie R, Thomas TC, Bebbington C. Cytotechnology 2002; 38: 43–46.
45. Ludwig DL. Bioprocess Int 2006; 4 Suppl 3: 14–23.
46. Lonza web information. Available at http://www.lonza.com/group/en/company/news/tradefairs/biologics_2004_presentations_posters.-ParSys-0017-DownloadFile.tmp/060705_Towards%20stronger%20gene%20expression.pdf. Accessed 2008 Jan 25.
47. Page MJ, Sydenham MA. Biotechnology 1991; 9: 64–68.
48. Kalwy S, Rance J, Young R. Mol Biotechnol 2006; 34: 151–156.
49. Kwaks THJ, Otte AP. Trends Biotechnol 2006; 24: 137–142.
50. Kim JM, Kim JS, Park DH, Kang HS, Yoon J, Baek K, Yoon Y. J Biotechnol 2004; 107: 95–105.
51. Aldrich TL, Vaije A, Morris AE. Biotechnol Prog 2003; 19: 1433–1438.
52. Kwaks THJ, Barnett P, Hemrika W, Siersma T, Sewalt RGAB, Satijn DPE, Brons JF, van Blokland R, Kwakman P, Kruckeberg AL, Kelder A, Otte AP. Nat Biotechnol 2003; 21: 553–558.

53. Kayser K, Lin N, Allison D, Dohahue L, Caple M. Bioprocess Int 2006; 4 Suppl 3: 6–13.
54. Kim HY. Bioprocess Int 2006; 4 Suppl 3: 24–31.
55. Peterson CL, Laniel MA. Curr Biol 2004; 14: R546–R551.
56. Cuisset L, Tichonicky L, Delpech MA. Biochem Biophys Res Commun 1998; 246: 170–173.
57. Oh SKW, Vig P, Chua F, Teo WK, Yap MGS. Biotechnol Bioeng 1993; 42: 601–610.
58. Cherlet M, Marc A. Cytotechnology 2000; 32: 17–29.
59. Seth G, Ozturk M, Hu WS. Biotechnol Bioeng 2005; 93: 820–827.
60. Kito M, Itami S, Fukano Y, Yamana K, Shuibui T. Appl Microbiol Biotechnol 2002; 60: 442–448.
61. O'Gorman S, Fox DT, Wahl GM. Science 1991; 251: 1351–1355.
62. Porteus MH. Mol Ther 2006; 13: 438–446.
63. Colosimo A, Goncz KK, Holmes AR, Kunzelmann K, Novelli G, Malone RW, Bennett MJ, Gruenert DC. Biotechniques 2000; 29: 314–324.
64. Charlebois TS. Cell Culture Engineering X Conference. Abst 2006, Whistler, BC.
65. Edmonds MC, Tellers M, Chan C, Salmon P, Robinson DK, Markusen J. Mol Biotechnol 2006, 34: 179–190.
66. Powell KT, Weaver JC. Biotechnology 1990; 8: 333–337.
67. Gray F, Kenney JS, Dunne JF. J Immunol Methods 1995; 182: 155–163.
68. Brezinsky SCG, Chaing GG, Szilvasi A, Mohan S, Shapiro RI, MacLean A, Sisk W, Thill G. J Immunol Methods 2003; 277: 141–155.
69. Holmes P, Al-Rubeai M. J Immunol Methods 1999; 230: 141–147.
70. Borth N, Zeyda M, Katinger H. Biotechnol Bioeng 2000; 71: 266–273.
71. Shekdar K, Blobel G. US patent 6,692,965. 2004 (to Chromocell Corp.).
72. Yoshikawa T, Nakanishi F, Ogura Y, Oi D, Omasa T, Katakura Y, Kishimoto M, Suga K. Biotechnol Bioeng 2001; 74: 435–442.
73. Vives J, Juanola S, Cairo JJ, Godia F. Metab Eng 2003; 5: 124–132.
74. Chiang GG, Sisk WP. Biotechnol Bioeng 2005; 91: 779–792.
75. Figueroa B, Ailor E, Osborne D, Hardwick JM, Reff M, Betenbaugh MJ. Biotechnol Bioeng 2007; 97: 877–892.
76. Alete DE, Racher AJ, Birch JR, Stansfield SH, James DC, Smales CM. Proteomics 2005; 5: 4689–4704.
77. Dinnis DM, James DC. Biotechnol Bioeng 2005; 91: 180–189.
78. Puck TT, Cieciura SJ, Robinson A. J Exp Med 1958; 108: 945–955.
79. Puck TT. In: Gottesmann MM, editor. Molecular cell genetics. New York: Wiley-Interscience; 1985. pp. 37–64.
80. Chasin L. In: Gottesmann MM, editor. Molecular cell genetics. New York: Wiley-Interscience; 1985. pp. 449–488.
81. Kao FT, Puck TT. Proc Natl Acad Sci U S A 1968; 60: 1275–1281.
82. Stanley P, Caillibot V, Siminovitch L. Somatic Cell Genet 1975; 1: 3–26.
83. Graf LH, Chasin LA. Mol Cell Biol 1982; 2: 93–96.
84. Urlaub G, Mitchell PJ, Kas E, Chasin LA, Funanage VL, Myoda TT, Hamlin JL. Somat Cell Mol Genet 1986; 12: 555–566.
85. Pallavicini MG, DeTeresa PS, Rosette C, Gray JW, Wurm FM. Mol Cell Biol 1990; 10: 401–404.
86. Barnett RS, Limoli KL, Huyuh TB, Ople EA, Reff ME. In: Wang HY, Imanaka T, editors. Antibody expression and engineering, ACS symposium series 604: Oxford University Press; 1995. pp. 27–40.
87. Cockett MI, Bebbington CR, Yarranton GT. Biotechnology 1990; 8: 662–667.
88. Potter M. Physiol Rev 1972; 52: 631–719.
89. Kearney JF, Radbruch A, Liesegang B, Rajewsky K. J Immunol 1979; 123: 1548–1550.
90. Shulman M, Wilde CD, Kohler G. Nature 1978; 276: 269–270.
91. Galfre G, Milstein C. In: Langone JJ, Van Vunakis H, editors. Volume 73B, Methods in enzymology. New York: Academic Press; 1981. pp. 3–75.
92. Yoo EM, Chintalacharuvu KR, Penichet ML, Morrison SL. J Immunol Methods 2002; 261: 1–20.
93. Mulligan RC, Berg P. Proc Natl Acad Sci U S A 1981; 75: 2072–2076.
94. Schlapfer BS, Scheibler M, Holtorf AP, Nguyen HV, Pluschke G. Biotechnol Bioeng 1995; 45: 310–319.
95. Hartman TE, Sar N, Genereux K, Barritt DS, He Y, Burky JE, Wesson MC, Tso JY, Tsurushita N, Zhou W, Sauer PW. Biotechnol Bioeng 2007; 96: 294–306.
96. Köhler G, Milstein C. Eur J Immunol 1976; 6: 511–519.
97. Milstein C. Bioessays 1999; 21: 966–973.
98. Green LL, Hardy MC, Maynard-Currie CE, Tsuda H, Louie DM, Mendez MJ, Abderrahim H, Noguchi M, Smith DH, Zeng Y, David NE, Sasai H, Garza D, Brenner DG, Hales JF, McGuinness RP, Capon DJ, Klapholz S, Jakobovits A. Nat Genet 1994; 7: 13–21.
99. Mendez MJ, Green LL, Corvalan JRF, Jia X-C, Maynard-Currie CE, Yang X-D, Gallo ML, Louie DM, Lee DV, Erickson KL, Luna J, Roy CM-N, Abderrahim H, Kirschenbaum F, Noguchi M, Smith DH, Fukushima A, Hales JF, Finer MH, Davis CG, Zsebo KM, Jakobovits A. Nat Genet 1997; 15: 146–156.
100. McCoy C, Matthews SJ. Clin Ther 2003; 25: 396–421.
101. Yan SB, Chao YB, Vanhalbeek H. Glycobiology 1993; 3: 597–608.
102. Graham FL, Smiley J, Russell WC, Nairn R. J Gen Virol 1977; 36: 59–74.
103. Pham PL, Kamen A, Durocher Y. Mol Biotechnol 2006; 34: 225–237.
104. Girard P, Derouazi M, Baumgartner G, Bourgeois M, Jordan M, Jacko B, Wurm FM. Cytotechnology 2002; 38: 15–21.
105. Fallaux FJ, Bout A, van der Velde I, van der Wollenberg DJ, Hehir KM, Keegan J, Auger C, Cramer SJ, van Ormondt H, van der Eb AJ, Valerio D, Hoeben RC. Hum Gene Ther 1998; 9: 1909–1917.
106. Crucell web information. Available at http://www.crucell.com/Partners%20-%20General%20Overview. Accessed 2007 Feb 3.
107. Macpherson I, Stoker M. Virology 1962; 16: 147–151.

108. Cruz HJ, Conradt HS, Dunker R, Peixoto CM, Cunha AE, Thomaz M, Burger C, Dias EM, Clemente J, Moreira JL, Rieke E, Carrondo MJT. J Biotechnol 2002; 96: 169–183.
109. Inoue Y, Kawamoto S, Shoji M, Hashizume S, Teruya K, Katakura Y, Shirahata S. Cytotechnology 2000; 33: 21–26.
110. Geserick C, Bonarius HPJ, Kongerslev L, Hauser H, Mueller PP. Biotechnol Bioeng 2000; 69: 266–274.
111. Walsh G. Nat Biotechnol 2006; 24: 769–776.
112. Betenbaugh MJ, Tomiya N, Narang S, Hsu JTA, Lee YC. Curr Opin Struct Biol 2004; 14: 601–606.
113. Sethuraman N, Stadheim TA. Curr Opin Biotechnol 2006; 17: 341–346.
114. Ballou CE. Methods Enzymol 1990; 185: 440–470.
115. Mistry PK, Wraight EP, Cox TM. Lancet 1996; 348: 1555–1559.
116. Hamilton SR, Bobrowicz P, Bobrowicz B, Davidson RC, Li H, Mitchell T, Nett JH, Rausch S, Stadheim TA, Wischnewski H, Wildt S, Gerngross TU. Science 2003; 301: 1244–1246.
117. Reff ME, Heard C. Crit Rev Oncol Hematol 2001; 40: 25–35.
118. Cabilly S, Riggs AD, Pande H, Shively JE, Holmes WE, Rey M, Perry LJ, Wetzel R, Heyneker HL. Proc Natl Acad Sci U S A 1984; 81: 3273–3277.
119. Simmons LC, Reilly D, Klimowski L, Raju TS, Meng G, Sims P, Hong K, Shields RL, Damico LA, Rancatore P, Yansura DG. J Immunol Methods 2002; 263: 133–147.
120. Reddy MP, Kinney CAS, Chaikin MA, Payne A, Fishman-Lobell J, Tsui P, Dal Monte PR, Doyle ML, Brigham-Burke MR, Anderson D, Reff M, Newman R, Hanna N, Sweet RW, Truneh A. J Immunol 2000; 164: 1925–1933.
121. Armour KL, Clark MR, Hadley AG, Williamson LM. Eur J Immunol 1999; 29: 2613–2624.
122. Kost TA, Condreay JP, Jarvis DL. Nat Biotechnol 2005; 23: 567–575.
123. Jarvis DL. Virology 2003; 310: 1–7.
124. Harper DM, Franco EL, Wheeler CM, Moscicki AB, Romonowski B, Roteli-Martins CM, Jenkins D, Schuind A, Clemens SAC, Dubin G. Lancet 2006; 367: 1247–1255.
125. Aumiller JJ, Hollister JR, Jarvis DL. Glycobiology 2003; 13: 497–507.
126. Schillberg S, Fischer R, Emans N. Cell Mol Life Sci 2003; 60: 433–445.
127. Ludwig DL, Witte L, Hicklin DJ, Prewett M, Bassi R, Burtrum D, Pereira DS, Jimenez X, Fox F, Saxena B, Zhou Q, Ma Y, Kang X, Patel D, Barry M, Kussie P, Zhu Z, Russell DA, Petersen WL, Jury TP, Gaitan-Gaitan F, Moran DL, Delannay X, Storrs BS, Tou J, Zupec ME, Gustafson KS, McIntyre J, Tarnowski SJ, Bohlen P. Hum Antibodies 2004; 13: 81–90.
128. Bakker H, Rouwendal GJA, Karnoup AS, Florack DEA, Stoopen GM, Helsper JPFG, van Ree R, van Die I, Bosch D. Proc Natl Acad Sci U S A 2006; 103: 7577–7582.
129. Strasser R, Altmann F, Mach L, Glössl J, Steinkellner H. FEBS Lett 2004; 561: 132–136.
130. Houdebine LM. Transgenic Res 2000; 9: 305–320.
131. Pollock DP, Kutzko JP, Birck-Wilson E, Williams JL, Echelard Y, Meade HM. J Immunol Methods 1999; 231: 147–157.
132. Zhu L, van de Lavoir MC, Albanese J, Beenhouwer DO, Cardarelli PM, Cuison S, Deng DF, Deshpande S, Diamond JH, Green L, Halk EL, Heyer BS, Kay RM, Kerchner A, Leighton PA, Mather CM, Morrison SL, Nikolov ZL, Passmore DB, Pradas-Monne A, Preston BT, Rangan VS, Shi MX, Srinivasan M, White SG, Winters-Digiacinto P, Wong S, Zhou W, Etches RJ. Nat Biotechnol 2005; 23: 1159–1169.

36

PLANT CELL CULTURE, LABORATORY TECHNIQUES

MARK RICHARD FOWLER
Leicester School of Pharmacy, De Montfort University, Leicester, United Kingdom

36.1 INTRODUCTION

Plant cell cultures are proving to be extremely useful model systems in a wide variety of investigations. They have several advantages over the use of whole plants, conceptually the most important being the ability to precisely control and manipulate the growth environment of a homogeneous population of cells. The effects of specific treatments on metabolism, growth, and division can be investigated without the complicating factors present when working with whole plants. Cell cultures therefore, find widespread use as systems to study gene expression (particularly during the cell division cycle and in studies of plant growth regulator function), the degradation or biotransformation of xenobiotics, and the production of secondary metabolites.

As with any model system, results obtained using plant cell cultures must be interpreted with some caution. The formation of cell cultures involves a degree of dedifferentiation and reprogramming of gene expression. Cell cultures may not therefore, be a true representation of the situation in plants. However, for fundamental studies and applied research, they often remain the system of choice.

This chapter will cover the basic techniques (and facilities) required to establish, maintain, and monitor plant cell cultures. Where possible, the theoretical background will be given to help the reader fully appreciate the advantages and limitations of plant cell cultures.

36.2 LABORATORY FACILITIES

The growth of plant cell cultures places some novel technical and infrastructural problems on the laboratory (1,2). In order to successfully grow plant cell cultures, certain facilities must be available. The equipment required must not only include items needed for the maintenance of the cell cultures themselves, but also facilities for the growth of donor material if cell cultures are to be established routinely. The laboratory should therefore provide areas suitable for:

1. growth media production, sterilization, and storage;
2. the manipulation of plant material under aseptic conditions;
3. the growth of both donor plant material and the cell cultures themselves under controlled conditions.

A media room suitable for producing plant cell culture media need not be very complicated, as it requires little equipment that would not be present in any laboratory. Required items include both a top pan balance and a fine analytical balance, stirrer plates (heated ones can be useful), a source of high-purity water, pH meters, an autoclave (a large pressure cooker can be used, but only if small volumes of media are to be used), and refrigerators and freezers. Useful additions to this list would include a steamer or microwave oven (for melting agar-gelled media) and an automatic pipetter unit.

Growth rooms or growth chambers should be used to provide areas where plant cell cultures and donor plant material can be grown in controlled conditions. Growth rooms are ideal if a large volume of plant cell culture work is to be undertaken, and with cultures that grow in the same conditions. Growth chambers provide smaller areas for the growth of plants or cell cultures, but are self-contained

Upstream Industrial Biotechnology: Expression Systems and Process Development, Volume 1, First Edition. Edited by Michael C. Flickinger.
© 2013 John Wiley & Sons, Inc. Published 2013 by John Wiley & Sons, Inc.

and can therefore provide facilities dedicated to a particular plant or cell culture type. The growth rooms or growth chambers should be equipped with time-controllable lights, a temperature control system (capable of dealing with the large amount of heat given out by any lighting), and some way of controlling humidity. Plant cell cultures are usually grown at about 25°C, and the humidity should not be lower than 50% or culture media will dry out very quickly (3). There should also be areas where cultures can be grown in complete darkness. Conditions in growth rooms used for growing donor plants should match as closely as possible the natural conditions for that particular plant (although this may be less important for plants that are to be used eventually to establish cell cultures, as they are not normally required to flower or set seed unless specialized cell types such as endosperm or pollen are required), as the condition of the donor material may prove to be critical in being able to establish a cell culture.

Cell suspension cultures require constant agitation and therefore a shaker bed must be available in a controlled environment room. Shaker beds are gyratory (orbital) with platforms, and with clips of various sizes to hold conical flasks. They should have variable speed settings.

Areas for the manipulation of plant material under aseptic conditions should ideally be self-contained rooms in which laminar-flow transfer cabinets can be placed. Laminar-flow transfer cabinets should be used for all manipulations that require an aseptic environment. Transfer cabinets are available in a variety of sizes, and consist basically of a high-efficiency filter to remove airborne contaminants and a fan to produce a laminar flow of air, from the back of the cabinet toward the user (or from the top to the bottom of the cabinet). They are made of a variety of materials, stainless steel probably being the best as it is robust, and easy to keep clean and surface-sterilize. The cabinets can also be supplied with a gas source for a burner, although self-contained gas burners can be used. Items within the cabinet should ideally be kept to a minimum, as anything that interferes with the laminar flow of the filtered air can compromise performance. Laminar-flow cabinets should be serviced regularly to ensure that the filter is working correctly. The performance of transfer cabinets can also be checked by placing unlidded petri dishes of media in the cabinet and checking for the growth of any microorganisms. If genetically manipulated plant material that may still be harboring microorganisms is to be used, a transfer cabinet specially designed to prevent contamination of the environment should be used. Laminar-flow cabinets may be provided with a UV light source to maintain a sterile environment, although the use of such devices is of questionable efficiency and can present some health risks (4).

Additional equipment that should be present in a plant cell culture laboratory includes both binocular (dissecting) and high-magnification microscopes, the latter preferably with a UV light source. The binocular microscopes should be portable so as to allow their use in a laminar-flow transfer cabinet. Both types of microscope should have attachments to allow photography.

36.3 PLANT CELL CULTURE MEDIA

The culture media must provide all the essential elements and nutrients necessary for the growth of the cell culture. As such, plant culture media are composed of three basic components:

1. a supply of essential elements, which are supplied in the form of a complex mixture of salts;
2. an organic supplement that supplies essential vitamins and other organic supplements (although plants are capable of synthesizing vitamins and amino acids, the biosynthetic capability of plant cell cultures often differs from that of whole plants, necessitating the supply of these in the culture medium);
3. a fixed carbon source (again, although whole plants are capable of fixing carbon from atmospheric carbon dioxide, plant cell cultures are, except in specialized cases, not autotrophic; this necessitates a supply of carbon in the medium), usually sucrose (which is cheap and readily available).

The three basic components of plant cell culture media can be further divided into categories that become apparent if the formulations of particular media are examined (Tables 36.1–36.3). The supply of essential elements falls into three groups:

1. macroelements (or macronutrients),
2. microelements (or micronutrients),
3. iron source.

Plant cell culture medium is therefore usually made by combining several different components to give a complete medium. Concentrated stock solutions of macroelements, microelements, iron source, and organic supplement are commonly made, while the carbon source is usually added as a solid.

36.3.1 Stock Solution Components

Macroelements. As the name suggests, this stock solution contains the elements required in large amounts for plant growth (these are elements that generally comprise at least

TABLE 36.1. Formulations of Gamborg's B5 Medium

Essential Element	Concentration in Stock (mg/L)	Concentration in Medium (mg/L)
	Macronutrients (50 mL)	
KNO_3	50,000	2,500
$CaCl_2 \cdot 2H_2O$	3,000	150
$(NH_4)_2SO_4$	2,680	134
$MgSO_4 \cdot 7H_2O$	5,000	250
$NaH_2PO_4 \cdot H_2O$	3,000	150
	Micronutrients (25 mL)	
KI	30	0.75
H_3BO_3	120	3
$MnSO_4 \cdot 4H_2O$	400	10
$ZnSO_4 \cdot 7H_2O$	80	2
$Na_2MoO_4 \cdot 2H_2O$	10	0.25
$CuSO_4 \cdot 5H_2O$	1	0.025
$CoCl_2 \cdot 6H_2O$	1	0.025
	Iron source (10 mL)	
FeNaEDTA	3,670	36.7
	Vitamins (1 mL)	
Myo-inositol	Add as solid	100
Pyridoxine–HCl	1,000	1
Phiamine–HCl	10,000	10
Nicotinic acid	1,000	1
	Carbon source	
Sucrose	Add as solid	20,000
pH 5.5		

Note: Formulations of plant cell culture media have been adapted from Refs 5 and 6. The composition of the various stock solutions is given, as is the amount of each stock solution needed for 1 L of medium. It should be noted that the composition of plant cell culture media varies to some degree from source to source. A full list of media formulations can be found in Ref. 7.

TABLE 36.2. Formulations of Murashige and Skoog Medium

Essential Element	Concentration in Stock (mg/L)	Concentration in Medium (mg/L)
	Macronutrients (50 mL)	
NH_4NO_3	33,000	1,650
KNO_3	38,000	1,900
$CaCl_2 \cdot 2H_2O$	8,800	440
$MgSO_4 \cdot 7H_2O$	7,400	370
KH_2PO_4	3,400	170
	Micronutrients (5 mL)	
KI	166	0.83
H_3BO_3	1,240	6.2
$MnSO_4 \cdot 4H_2O$	4,460	22.3
$ZnSO_4 \cdot 7H_2O$	1,720	8.6
$Na_2MoO_4 \cdot 2H_2O$	50	0.25
$CuSO_4 \cdot 5H_2O$	5	0.025
$CoCl_2 \cdot 6H_2O$	5	0.025
	Iron source (5 mL)	
$FeSO_4 \cdot 7H_2O$	5,560	27.8
$Na_2EDTA \cdot 2H_2O$	7,460	37.3
	Vitamins (5 mL)	
Myo-inositol	20,000	100
Nicotinic acid	100	0.5
Pyridoxine–HCl	100	0.5
Thiamine–HCl	100	0.5
Glycine	400	2
	Carbon source	
Sucrose	Add as solid	30000
pH 5.7–5.8		

Note: Linsmaier and Skoog (LS) medium is basically the same except for the small variations in the vitamins.

0.1% by dry weight of plants) (5). The macronutrients are usually considered to be carbon (which is supplied as a separate component and is considered later), nitrogen, phosphorus, potassium, magnesium, calcium, and sulfur.

Nitrogen is usually supplied as nitrate and/or ammonium salts. To be incorporated into biological macromolecules, nitrogen must be in the reduced form (such as ammonium ions). Nitrate ions present in the media must be reduced in order to be incorporated into molecules, an energetic process. Therefore, there is a theoretical advantage in supplying nitrogen solely as ammonium ions. Ammonium ions, however, can be toxic in high concentrations (although plant cell cultures are generally less susceptible to ammonium toxicity than are animal cell cultures, for example) and uptake of ammonium ions causes acidification of the medium. Hence, the use of ammonium ions as the sole nitrogen source requires that the culture medium be buffered. Most plant cell culture media supply nitrogen as a mix of nitrate and ammonium salts which also has the advantage of weakly buffering the media. Uptake of ammonium ions causes H^+ ions to be excreted into the culture medium, whereas nitrate uptake causes OH^- ion excretion. The buffering depends on both nitrate and ammonium ions being present in the medium, and the fact that ammonium ion uptake is reduced at acidic pH while the uptake of nitrate ions is reduced at alkaline pH (5).

Phosphorus (involved in energy transfer and a component of RNA and DNA), is usually supplied as the phosphate ion and is present at lower concentrations than nitrate/ammonium ions. High concentrations of phosphorus in media can lead to precipitation of other elements as insoluble phosphates.

Potassium is usually supplied as the chloride, nitrate, or orthophosphate salt, and is an important cellular cation involved in many processes.

TABLE 36.3. Formulations of Schenk and Hildebrandt Medium

Essential Element	Concentration in Stock (mg/L)	Concentration in Medium (mg/L)
	Macroelements	
KNO_3 (25 mL)	101,000	2525
$MgSO_4 \cdot 7H_2O$ (15 mL)	24,640	36.6
$NH_4H_2PO_4$ (25 mL)	11,500	287.5
$CaCl_2 \cdot 2H_2O$ (15 mL)	14,680	220.2
	Microelements (10 mL)	
$MnSO_4$	1,320	13.2
H_3BO_3	500	5
$ZnSO_4 \cdot 7H_2O$	100	1
KI	100	1
$CuSO_4 \cdot 4H_2O$	20	0.2
Na_2MoO_4	10	0.1
$CoCl_2 \cdot 6H_2O$	10	0.1
	Iron source (10 mL)	
$FeSO_4 \cdot 7H_2O$	1,500	15
Na_2EDTA	2,000	20
	Vitamins (10 mL)	
Thiamine–HCl	500	5
Nicotinic acid	500	5
Pyridoxine–HCl	50	0.5
Myo-inositol	Add as solid	1,000
	Carbon source	
Sucrose	Add as solid	30,000

Magnesium is usually supplied as magnesium sulfate. Like potassium, it is an important cellular cation, and can, in some cases, substitute for potassium.

Calcium is usually supplied as the chloride salt (although calcium nitrate is used in some medium formulations). Calcium has important structural and regulatory roles.

Sulfur is usually supplied as magnesium sulfate or occasionally as ammonium sulfate (many micronutrients are also supplied as sulfates). Sulfur is an important component of some amino acids and as such, helps to determine protein structure.

A 10× or 20× stock solution of macroelements is usually made in deionized water and can be stored at 4°C for several months.

Microelements. These are elements required in trace amounts for plant growth and development and have diverse roles. Microelements comprise manganese, copper, cobalt, boron, molybdenum, and zinc, which are usually considered to be essential (5,8). Nickel is included in the microelement formulations of some media (such as Heller's medium) and as a component of urease (5), may be necessary for the growth of some cell cultures (9). Other elements (such as aluminum and iodine) are also often present in microelement formulations, but whether these are strictly necessary is doubtful.

A more concentrated (100x or 200x) stock solution can be made, as these elements are present at much lower levels than the macroelements. Store the stock solution at 4°C, where it should be stable for several months.

Iron source. Iron is usually supplied as iron sulfate (iron citrate can also be used) and is generally considered to be the most important micronutrient. EDTA (ethylene diamine tetra-acetic acid; the disodium salt) is usually used in conjunction with the iron sulfate to chelate the iron, so as to allow a slow and continuous release into the medium (the commercially obtainable ferric-sodium salt of EDTA can also be used as the iron is already complexed). Uncomplexed iron can undergo rearrangement and precipitate out of the medium as ferric oxide (5). The iron source should be specially prepared so as to ensure chelation of the iron. The Na_2EDTA should be dissolved in almost boiling water, after which the iron sulfate should be added, the solution allowed to cool, and then made up to volume (7). The Fe/EDTA stock solution (100x) should be protected from light (10) and stored at 4°C. It has been observed that EDTA, which chelates other divalent cations, can have inhibitory effects on some plant cultures (11).

It has been reported that Fe/EDTA produced by this method can lead to precipitation of iron from media (such as Murashige and Skoog), if used at standard concentrations. One-third of the original amount of iron (with the same amount of EDTA) can be used in order to avoid this problem (7).

Vitamins/organic supplements. These are included in plant cell culture media, often for historical reasons. Only two vitamins are considered to be essential, thiamine (vitamin B_1) and myo-inositol, although this may vary from culture to culture (5,9,12). Other vitamins, although not essential, may improve the growth of certain cell cultures (13).

Reduced nitrogen can also be supplied to plant cell cultures in the form of amino acids (usually arginine, glutamic acid, glutamine, and glycine). The uptake of amino acids, like the uptake of ammonium ions, causes acidification of the medium (5). Glycine is a standard component of many media, but in most cases is not required. Casein hydrolysate can be used as a source of amino acids (and therefore reduced nitrogen) and is also rich in calcium and phosphate (5).

Stock solutions of organic supplements (100x–1000x) should be stored in the freezer (in suitable aliquots). Generally, the vitamin or organic supplement stock is added before the media is autoclaved; however, if specific studies on vitamins are being conducted, they should be filter-sterilized and added after the medium has been autoclaved (7).

Carbon source. For several reasons, sucrose is by far the most used carbon source. It is cheap, readily available, relatively stable under autoclaving, and readily assimilated by plant cells. Other carbohydrates can be used, such as glucose (glucose is easily caramelized though), maltose, and galactose, as can the sugar-alcohols glycerol and sorbitol. Many of the latter are used only in specialized circumstances though. The carbon source is added to the medium as a solid.

These then, are the basic components of most plant cell culture media formulations. However, other components are commonly added for specific purposes.

Gelling agents. These are used to "solidify" the plant culture medium so plant cells can be grown on the surface of the medium. Agar is the most common agent used for gelling (incorrectly called solidifying) media. A natural product from seaweed, it is relatively cheap. Agar is insoluble in cold water, but produces relatively inert gels at about 100°C and "solidifies" at around 45°C. Agar is used at concentrations of 0.6–0.8% (w/v). Low pH inhibits gelling. Agar is relatively impure, and the use of special "Plant Cell Culture" grade agar is recommended. Being a natural product, its quality can vary from batch to batch and manufacturer to manufacturer; so it is best to stick to one supplier. Some agar preparations also contain significant amounts of some salts which can alter the composition of the medium (14). Purified agar or agarose can be used for more demanding procedures (such as protoplast culture) but the routine, large-scale use of agarose is expensive.

Alternative gelling agents such as the gellan (a bacterial product) gums Gelrite or Phytogel are becoming more popular as they may be more suited to the growth of some cells. These gellan gums are more expensive (per unit weight) than agar, but can be used at concentrations as low as 0.2% (w/v). Gellan gums are used in the same way as agar. A variety of other gelling agents are also available commercially. All gelling agents have effects on the water potential of the medium and affect the rate of diffusion of nutrients (and toxic by-products).

For plant cell cultures to proliferate, further additions to the medium may be required. Plant growth regulators are often required by plant cell cultures for cell division and expansion (and other developmental pathways). These plant growth regulators are most commonly plant hormones or their synthetic analogues, and thus give the cells the correct signals for proliferation. These are supplied in the medium because the biosynthetic capability may not be present in plant cell cultures. Plant growth regulators can be divided into several groups (Table 36.4).

1. Auxins
2. Cytokinins
3. Gibberellins
4. Abscisic acid (ABA)
5. Ethylene
6. Others

TABLE 36.4. Plant Growth Regulators Commonly Used in Plant Cell Culture Medium

Regulator	Molecular Weight
Auxins[a,b]	
IAA (indole-3-acetic acid)	175.2
IBA (3-indolebutyric acid)	203.2
2,4-D (2,4-dichlorophenoxyacetic acid)	221
2,4,5-T (2,4,5-trichlorophenoxyacetic acid)	255.5
NAA (1-naphthylacetic acid)	186.2
NOA (2-naphthyloxyacetic acid)	202.2
Picloram (4-amino-3,5,6-trichloropicolinic acid)	241.5
Dicamba (2-methoxy-3,6-dichlorobenzoic acid)	221
MCPA (2-methyl-4-chlorophenoxyacetic acid)	200.6
Cytokinins[b,c]	
Zeatin (4-hydroxy-3-methyl-trans-z2-butenylaminopurine)	219.2
IPA [N^6-(2-isopentyl)adenine]	203.3
BAP (6-benzylaminopurine)	225.2
Kinetin (6-furfurylaminopurine)	215.2
Thidiazuron (N-phenyl-N′-1,2,3-thiadiazol-5-ylurea)	220.25
Gibberellic acid (GA_3)[d]	346.4
Abscisic acid[d]	264.3

[a] Auxins are usually titrated into solution with NaOH (0.1 ***M***). DMSO can also be used, as can 95% ethanol.
[b] If auxins and cytokinins are dissolved in alkali and acid, the pH of the stock solutions should be brought to the pH of the medium before use.
[c] Cytokinins are usually dissolved in a small volume of HCl. Cytokinins can also be dissolved in DMSO.
[d] Gibberellic acid (GA) and ABA are soluble in water.

Auxins. Indole-3-acetic acid (IAA) is the only (or predominant) natural auxin, but its use in *in vitro* cell cultures is complicated. IAA is not very stable to heat and is also photolyzed (stock solutions are degraded within a few days) (15). IAA can also be rapidly inactivated in plant cells by conjugation, which makes the internal concentration of IAA uncertain. In order to partially alleviate this problem, relatively stable amino acid conjugates of IAA (such as indole-acetyl-L-alanine and indole-acetyl-L-glycine) can be used, although their use is not widespread (5). Stable chemical analogues of IAA are therefore, usually used in plant cell culture media. 2,4-Dichlorophenoxyacetic acid (2,4-D) is perhaps the most commonly used auxin and is very effective. Others, such as indole-3-butyric acid (IBA), 1-napthylacetic acid (NAA), 2-napthyloxyacetic

acid (NOA), 2,4,5-trichlorophenoxyacetic acid (2,4,5-T), 2-methyl-4-chlorophenoxyacetic acid (MCPA), 2-methoxy-3,6-dichlorobenzoic acid (dicamba), and 4-amino-3,5,6-trichloropicolinic acid (piclorom) are also available. Not all are equally efficient at promoting growth and cell division, and there may be species-to-species variation in efficacy. Synthetic auxins should be handled with care as many (or contaminants present in the preparation) are mammalian carcinogens. Synthetic auxins are also known to promote somaclonal variation (5).

There also exists a class of compounds that are known to antagonize auxin action, the so-called anti-auxins. Anti-auxins act either by inhibiting auxin transport or the correct recognition of auxin molecules by cells and can prove useful in studies of auxin action. Commonly used anti-auxins include 2,3,5-triiodobenzoic acid (TIBA), *p*-chlorophenoxyisobutyric acid (PCIB), and 2,4,6-trichlorophenoxyacetic acid (2,4,6-T).

Auxins are usually included in plant cell culture media in order to promote cell division and cell growth.

Cytokinins. The natural cytokinins are a wide variety of related (purine derivative) compounds. Some naturally occurring cytokinins used in cell culture media are 4-hydroxy-3-methyl-trans-2-butenylaminopurine (zeatin) and -(2-isopentyl) adenine (2iP or IPA). These naturally occurring compounds are very expensive (especially zeatin) and relatively unstable. The synthetic analogues 6-furfurylaminopurine (kinetin) and 6-benzylaminopurine (BA or BAP) therefore find widespread use in plant cell culture media. Other, non-purine-based chemicals (such as substituted phenylureas) also find use as cytokinins (9). Cytokinins are often included in plant cell culture media along with auxins, in order to promote cell division.

Combinations of auxins and cytokinins can be used to initiate specific forms of organogenesis in plant tissue cultures. Generally, high levels of cytokinin coupled with low levels of auxins promote shoot formation, while high levels of auxin in conjunction with low levels of cytokinins promote root formation.

Gibberellins or GAs. There are many variations on the gibbane carbon skeleton that, in plantae, are involved in regulating cell elongation. Commercially, only a few of the possible gibberellins are available. Anti-gibberellins, which act by preventing synthesis (such as ancymidol), are available.

ABA. ABA is generally regarded as inhibiting cell growth. It is most commonly used in media to promote specialized developmental pathways such as somatic embryogenesis.

Ethylene. Ethylene is a naturally occurring gaseous plant growth regulator, most commonly associated with controlling fruit ripening in climacteric fruits. It is not often used in plant cell tissue cultures, but can be supplied to cultures as a gas or by ethephon (2-chloroethylphosphoric acid). Ethylene action can be antagonized by silver ions, and aminoethoxyvinylglycine (AVG) which inhibits ethylene biosynthesis.

Others. A bewildering array of other compounds (polyamines, phenolic compounds, and jasmonic acid, among others) have been postulated to have growth regulatory properties. In general, it is the auxins and cytokinins that find the most widespread use in plant cell culture.

Stock solutions (10 mg/mL or 10 m*M*) of plant growth regulators are usually prepared. If the plant growth regulators are to be added after the culture medium has been sterilized, the pH of the stock solutions should be brought to the pH of the medium.

Plant cell culture media can be bought from a variety of commercial suppliers, and may offer some advantages for routine cell culture work. But, buying pre-made media is relatively expensive, and does not allow the easy manipulation of individual media components. It has also been observed that some commercial plant cell culture media have a tendency to precipitate out during autoclaving.

36.3.2 Preparation of Media

Stock solutions of the basic medium components (such as macronutrients) can be prepared and stored as indicated. They are then added to deionized water (about half the final volume) in the indicated proportions, along with the sucrose. Any other heat-stable components can also be added. When the sucrose has dissolved, the volume is brought to about 90% of the final, and the pH of the medium adjusted to the desired value. The medium is then brought to the correct final volume (with thorough mixing) and dispensed into suitable containers for autoclaving. After autoclaving, the media should be clear with a slight yellow color from the iron source. Any browning of the medium indicates that the carbon source has caramelized and it should be discarded.

It is important to remember that while most components of plant cell culture medium are considered to be thermostable, some are not and there are conflicting data on others. Gibberellins are rapidly degraded by autoclaving, and therefore should be filter sterilized and added to the medium after autoclaving (16). Auxins are generally considered to be thermostable (although there is some disagreement, and for some applications better results have been achieved using filter-sterilized auxins) (7,15,17). Cytokinins (except zeatin) are also considered to be thermostable (although some substituted phenylureas are not), as are most vitamins (calcium pantothenate excepted and thiamine is destroyed if the medium pH is too high) (7,9). Some plant growth regulators are soluble in ethanol, which results in a stock solution that is inherently sterile and can therefore be added after sterilization; the final concentration of alcohol in the

medium is negligible. Sucrose is also added to the medium before autoclaving, although this results in a degree of hydrolysis (approximately 5%, depending on the duration of autoclaving) to a mixture of D-glucose and D-fructose (18).

36.3.3 Media Sterilization

In most cases, plant cell culture media are sterilized by steam in an autoclave. This is usually done for 20–30 min at 121°C (103 kPa). These criteria are set on the general rule that 121°C must be maintained for at least 15 min in order to kill thermophilic indicator microorganisms such as *Bacillus steriothermophilus*. It should be remembered that this standard autoclave regime will be insufficient to ensure sterilization of large volumes of media (5). However, thermophilic organisms are rarely a problem in plant cell cultures, and standard autoclave cycles of 20–30 min at 121°C are widely used regardless of culture vessel size. Excessively long autoclave cycles should be avoided, as they result in caramelization of the carbon source and may well result in the breakdown of other medium components.

The efficacy of steam sterilization can be checked by the use of special indicator tubes that change color when they have been exposed to a certain temperature, for a set length of time (various combinations can be obtained). Ideally, they should be placed in a vessel containing a liquid of similar volume if media are being sterilized, to ensure that the medium is sterile. A cheaper alternative is to use special tape having indicator strips that change color when autoclaved. However, this tape only indicates that the vessel has been autoclaved, not whether the contents are sterile.

The heat-labile components of media can be sterilized by filtration through a sterile fine-pore membrane (0.45 or 0.22 μm). These are available commercially, either as presterilized sealed units or as self-assembly units that are autoclaved before use. They are simple to use, as either the liquid is forced through the membrane into a sterile receptacle from a syringe or on larger units, a vacuum source is used. These filter units will remove bacteria and fungi, but not viruses, viroids, and mycoplasma.

36.3.4 Aseptic Technique

It is obviously important to ensure that any plant cell cultures are sterile, in order to avoid loss of the culture and invalidating any experimental results. It is vital then that all possible precautions against contamination are taken. We have already seen that plant cell culture media can be sterilized by autoclaving and that any heat-labile components can be filter-sterilized. However, when manipulating plant material and/or plant cell cultures, the whole environment should be as free from contamination as is possible.

Hands should thoroughly washed before any work is commenced, and latex gloves can be worn. These gloves can be occasionally swabbed with 70% ethanol to ensure that they are sterile. Face masks can also be worn to prevent airborne contaminants spreading, and long hair should be tied back (or a hair net used).

Any surfaces where aseptic techniques are to be used, should be surface sterilized before and after use. This is usually done by swabbing the area with a 70% (v/v) solution of ethanol or isopropanol, although industrial methylated spirit can be used and is much cheaper. Acidified alcohol (70%, pH 2) or a solution of phenolic disinfectant can also be used. As a further precaution, any manipulation can be carried out on autoclaved ceramic tiles that can be changed regularly to ensure asepsis.

Any vessels, surfaces and so on that are going to be used within the aseptic environment, should be sterile. This can be achieved by autoclaving or by dry heat. If items are autoclaved, the openings should not be sealed so tightly so as to prevent the steam from penetrating into them. This is because steam sterilizes by transfer of its thermal energy to any surface in contact with it. Simply heating to 121°C will not ensure sterility. Dry heat can also be used to sterilize items (check if they will withstand the temperature), but it is less efficient and therefore requires longer times. Any small items to be sterilized by dry heat can be wrapped in aluminum foil. The total time taken for dry heat sterilization is considered to be well over 3 h (5) at about 180°C (1 h for the load to reach the sterilization temperature, 2 h at the sterilization temperature and a cooling-down period). Prior to sterilization, glassware used for plant tissue culture can be rinsed in water with any commonly used detergent. Traces of detergent, which can be detrimental to plant tissue culture growth, can be removed by rinsing in dilute acetic acid.

Instruments used for the manipulation of plant material should initially be sterilized by autoclaving or dry heat (dry heat will blunt scalpels). They can be kept sterile during use by placing them in a container of 80% (v/v) ethanol which is quickly flamed off. There is no need to heat instruments in a flame for a long period; this will blunt scalpel blades and cause delays while instruments are allowed to cool down. Obviously, precautions need to be taken to ensure that the ethanol does not ignite (this is particularly so with transfer cabinets, where the flow of air will blow the fire toward the user); so it should be kept capped whenever possible and kept in a container that will not smash or tip over (a boiling tube with cotton wool in the end, which is then placed in a weighted beaker to prevent tipping over, works well).

Any plant material that is going to be used to establish a cell culture needs to be surface-sterilized. This is usually achieved by treating the plant material with chemicals such as bleach. The conditions needed to ensure sterility have to be determined on a case-by-case basis. It will depend on many factors such as the initial degree of contamination, the type of contaminating microorganism, the morphology

of the material to be sterilized, and the susceptibility of the plant material itself to damage from the bleach. It is important that the plant material is not exposed to the sterilizing agent for too long a period, as this will have detrimental effects. If explants can be taken from seedling tissue, a good way of producing sterile donor material is to sterilize seeds and produce sterile plants *in vitro*; otherwise, the explant source must be surface-sterilized.

Most workers use a commercial bleach (such as Domestos), which contains approximately 5% sodium hypochlorate. The commercial bleach is usually diluted before use with water, but the precise dilution needs to be determined. The addition of surfactants (0.1–1% v/v) such as Tween or Triton (or Teepol, which is cheaper, though less pure) can improve sterilization, presumably by improving contact with the bleach solution. A 70% solution of ethanol is also commonly used in conjunction with bleach to sterilize explants. If treatment with bleach proves ineffective at ridding contamination, the tissue can also be treated with Virkon (a commercial disinfectant that has a pH different from than that of bleach). In cases where this proves ineffective, alternative chemical sterilization agents include hydrogen peroxide (about 10%), bromine water (about 1–2%), and mercuric chloride (0.1–1%), although some of these are extremely dangerous (such as mercuric chloride). After treatment with chemical sterilizing agents, the plant tissue must be washed thoroughly with copious amounts of sterile distilled water to ensure removal of the chemical. Some surface sterilization methods are given:

Tobacco or Arabidopsis seeds (or other small, smooth seeds)

1. Submerge in 70% ethanol for 10 s.
2. Submerge in 10% household bleach for 20 min.
3. Wash three times in sterile distilled water.

1. *Sugar beet seeds (seeds with a rough seed coat).* Submerge in 70% ethanol for 10 s.
2. Submerge in 50% household bleach or 0.1% Teepol for 30 min.
3. Wash three times in sterile distilled water.

Tobacco leaves

1. Submerge in 10% household bleach for 15 min.
2. Wash three times in sterile distilled water.

36.3.5 Vessels for Cell Culture *In Vitro*

A wide variety of vessels for cell cultures can be obtained commercially, and so long as they are capable of fulfilling the basic needs of containing the cell culture and its medium and excluding contaminants, all are acceptable. Unless they are disposable and purchased presterilized, the culture vessels must be capable of being sterilized.

Petri dishes are widely used vessels for plant cell cultures. They are cheap, can be stacked (and therefore occupy little space), and can be bought presterilized. Originally designed for work with microorganisms, their main drawback is the lack of space for vertical growth. They are, however, ideal for the initiation of callus cultures. Petri dishes must be sealed with a plastic film such as "cling-film" (plastic food wrap), Nescofilm, or Parafilm to prevent the medium from drying out and the entry of contaminants.

A variety of plastic containers for the growth of plants *in vitro* can be obtained commercially. These are either disposable or made from autoclaveable plastic. They have the advantage of offering more height than Petri dishes. Glass "jam" or "powder" jars can be used in the same way. These vessels have tighter-fitting lids than Petri dishes, but it may still be necessary to seal them with a plastic film.

Cell suspension cultures are usually grown in glass conical flasks (Erlenmyer), which are stoppered with foam, paper, or cotton wool bungs and aluminum foil.

36.4 CELL CULTURE SYSTEMS

36.4.1 Callus Cultures and Cell Suspensions

Cell suspension cultures are usually initiated by producing a callus culture (an unorganized mass of cells) from a suitable explant (a piece of plant tissue such as leaf, root, or cotyledon) or from a specific cell type (such as endosperm). The size of the explant used to initiate the callus is not usually considered to be critical (although explants of a very small size may not be viable). Callus is usually produced by placing explants on a suitable medium gelled with agar which contains an auxin and/or a cytokinin. No hard-and-fast rule indicates which medium will prove successful, but general-purpose media such as Murashige and Skoog (19), Gamborg's B (5,12), or Schenk and Hildebrandt (20) are good starting points. Again, no hard-and-fast rules indicate the precise nature or concentration of the plant growth regulators that will be needed in order for the callus to form. A grid of various concentrations (0 to 10 μM) of an auxin (often 2,4-D) and a cytokinin (often BAP or kinetin) is usually set up in order to establish the levels of plant growth regulators needed (6). The plant growth regulator regime necessary to induce callus formation must be determined empirically because of the difference in biosynthetic capability of different plant cell types, and its composition will depend, at least partly, on the plant hormone composition and levels in the donor material. Therefore, the age of the explant material, its position on the plant, and the cell type that forms the callus, will all have an effect on the conditions needed for callus initiation. Sterile explants are gently pressed on to the surface of the medium to ensure

good contact and left (often in the dark). Callus, which is observed as a lump of unorganized cell growth usually at the cut surface (wounding the explant may be beneficial for callus formation), will then form on media of the correct composition, usually within 2 months.

Then, cell suspension cultures are usually initiated by transferring lumps of callus into a liquid medium of the same composition, which is then shaken to encourage the formation of a cell suspension culture. The callus transferred into the liquid medium should be friable (easily broken up into smaller cell clumps), and a relatively large inoculum should be used so that cell density builds up quickly. However, if the inoculum is too large, toxic products (presumably from the stress of transfer to liquid medium) can quickly build up to lethal levels. Callus established from some plants or from some particular cell types may not be friable, and will not easily form a good cell suspension, instead growing as large cell clumps. The friability of the callus may be improved by changes to the composition of the medium or by repeated subculturing (21). Alternatively, the formation of cell suspensions can sometimes be encouraged by culturing the callus on lower concentrations of agar before transferring to the liquid medium, or by placing a small amount of liquid on the surface of the solid medium. After the initial cell suspension culture has formed, any remaining large cell clumps can be removed by filtering the suspension, allowing large clumps to settle out, or by transferring the suspension with a small-bore pipette.

Cell suspensions are most easily grown as batch cultures, usually in conical flasks. The cell suspension culture occupies 20–33% of the total graduated volume of the conical flask. If the culture volume occupies a greater proportion of the culture vessel, then problems can be encountered with gaseous exchange across the surface of the media, leading to anoxia. Cell suspension cultures are continually propagated by transferring a small volume of the culture into fresh medium, a process called subculture. This subculturing results in the dilution of the cell suspension culture (the amount of culture added to fresh medium during subculture; therefore, the degree of dilution depends on the individual culture and must be determined empirically), after which the biomass of the culture increases in a characteristic fashion until the nutrients present are used up and/or toxic by-products accumulate to inhibitory levels (22). This is called the stationary phase, where no further increase in biomass or cell number is evident. Cells left in the stationary phase of the batch growth cycle for extended periods usually lose viability and die, leading to loss of the cell suspension or an extension of the subsequent lag phase upon subculturing. It is therefore important that the growth of the culture is monitored to determine the optimum batch culture cycle length. The degree of dilution of the culture at subculture also has to be determined (one part in five is a good starting point), as too great a dilution will result in an extension of the lag phase, the death of the culture, or the need for the use of culture medium with special supplements (23,24). Cells can be transferred by using a simple plugged pipette (the ends may be removed if large cell aggregates are present), or a "Howell" syringe equipped with a large-diameter cannula.

Although termed cell suspension cultures, plant cell suspension cultures very rarely consist of separated single cells. Usually small clumps of cells are formed. These clumps can cause problems in some experiments as the metabolism of individual cells in these clumps may vary (25–27). Cell suspensions can be filtered in an attempt to reduce the size of these cell clusters; however, it is often observed that this filtering has an inhibitory effect on the growth of the culture, often until cell clumps are formed again. Alternatively, low concentrations of macerozyme and cellulase can be added to the culture medium to reduce cell clumping (25). Cell suspension cultures need to be aerated; this is usually achieved by placing the cultures on a gyratory (orbital) shaker. Speeds are usually around 30–150 rpm, with displacements of 2–4 cm. Again the precise speed needs to be determined for each cell suspension culture, as it will depend on the size of the cell clusters and cell density. However, speeds much above the higher limit quoted are likely to cause excessive cell damage, and speeds below 30 rpm will almost certainly result in the cells settling out and not being properly aerated.

Like many plant cultures, cell suspension cultures are prone to contamination due to the rich nature of the medium and the relatively slow growth rate of plant cells. Sometimes this contamination will be obvious, the culture may take on a cloudy appearance, a "slime" may be visible on the sides of the culture vessel, or small balls of fungi may be found floating in the medium. Surprisingly, a strange smell noticed at subculture or during experimental sampling can also be a good indicator of contamination problems that are not yet evident. Experience will indicate the strange smell! It is, therefore, worth testing the cell suspension culture for latent contamination at regular intervals. This can be done by plating out small aliquots of the cell suspension culture on microbiological media designed for the growth of fungi and bacteria (such as nutrient agar, malt extract, potato dextrose, and corn meal agars). Incubation of the plates in suitable conditions will reveal the presence of any contamination. See Contamination Detection and Elimination.

One source of contamination that is altogether more difficult to detect and deal with, is mycoplasma infection. Mycoplasma infection will not usually be fatal to the cell suspension culture, but can have deleterious effects on growth and may distort experimental data. Some antimycoplasma agents are now available, as are some

detection kits. These are often designed to treat and detect mycoplasma contamination in mammalian cell cultures and should be used with due caution.

In batch culture systems, the culture environment never stabilizes (as they are closed systems). Thus efforts to couple cellular metabolism to cell growth over a long culture period cannot succeed (24,25,28). This is a major drawback of batch culture systems and means that any investigation should be conducted over as short a time period as possible.

Cell suspensions can also be grown as continuous cultures, either in a chemostat or a turbidostat, which to some extent overcomes the problems of batch cultures. Continuous cultures are used when investigations are conducted that require the cells to be kept in a constant, steady state of growth. The setup of continuous cultures is technically much more demanding than the growth of batch cultures, and therefore, the use of continuous cultures is limited.

The plant growth regulator requirements of cell suspension cultures should be periodically checked to see whether such additions are still required. This is because cell suspensions (and indeed callus cultures,) can develop the ability to grow in the absence of an external supply of plant growth regulators, a process referred to as habituation. This phenomenon is not noted with all cell cultures, but is prevalent in, for instance, cell cultures of *Beta vulgaris* (29,30). The mechanism by which habituation occurs has not been clearly established, although factors such as the plant growth regulators used to establish the culture and changes in cellular biochemistry have all been implicated (31,32).

Plant growth regulator autonomy, or habituation, may be of value in specific circumstances. Synthetic auxins such as 2,4-D can interfere with the assembly of the mitotic spindle and increase the duration of the cell cycle (33–35).

36.4.2 Assessing Cell Growth

It is vital that the growth of the cell suspension is monitored in order to establish a batch growth cycle. The growth of cell suspension cultures can be assessed in several ways.

1. Packed cell volume (PCV)
2. Cell number
3. Fresh (or wet weight)
4. Dry weight
5. Medium conductivity
6. Macromolecule content.

PCV. The determination of PCV is a quick and simple way of assessing the growth of cell suspension cultures, although it will not help to determine between cell division and cell expansion (without further examination of cell size). A known volume of cell suspension culture is centrifuged at low speed (approximately 500*g*) in a graduated centrifuge tube. The results are expressed as the percentage of the total volume occupied by the cell pellet.

Cell number. As its name suggests, this is a fairly simple (though time-consuming) technique where the number of cells per unit volume are counted using a microscope and a suitable graticule-etched slide. In cell suspensions that grow as very finely divided small cell clumps or as single cells, a hemocytometer can be used. A Sedgewick–Rafter counting slide or a "home-made" counting cell with a receptacle of known volume can also be used. However, as cell suspensions usually grow as cell clumps, which makes counting individual cells impossible, the accuracy of this technique can be improved by treating the cell suspension culture to remove or reduce these cell clumps. This can be done in two ways, by either treating the cell suspension culture with enzymes (such as pectinase at 0.25%) or more commonly, by treatment with chromium trioxide at 70°C. The exact treatment needed will have to be determined empirically, as it will depend on the degree of cell clumping (two volumes of 10% (w/v) chromium trioxide for 15 min is a good starting point, but if the cell clumps are large, a longer incubation time may be required). After the mixture has cooled, vortex mixing can be used to aid the breakup of the clumps into single cells. Care must be taken that the cells are not overtreated, as single cells or small cell clumps may be destroyed by harsh treatments.

Fresh weight. It can be determined fairly simply by filtering under reduced pressure, a known volume of cell suspension culture onto a glass or nylon fiber filter paper (weighed in the wet condition), which can then be reweighed and the weight of the cells calculated by difference.

Dry weight. It can be determined after wet weight, by drying the filter papers and cells to a constant mass in an oven (at 60–80°C).

Medium conductivity. Combinations of these techniques allow average cell volume and cell mass to be calculated and to determine increases in biomass. Cell division and cell expansion can also be distinguished.

Macromolecule content. Other techniques are also used, although less often. In some cell suspensions the conductivity of the medium has been found to be related to the fresh weight of the cells in suspension culture. The protein and DNA content of a known aliquot of cell suspension culture can also be used to assess growth, although this is a relatively time-consuming approach.

36.4.3 Assessing Cell Viability

These techniques (with the exception of identifying obviously dead cells while counting) do not, however, directly indicate whether cells are alive or dead. Not all the cells in a culture will be viable, and some measure of viability

gives useful insights into the health of the cell suspension culture. A simple method to determine cell viability is to use a dilute solution (0.025% w/v) of Evan's blue. Healthy cells will exclude this dye, whereas damaged or dead cells will stain blue. These can be scored under a microscope and the results expressed as a percentage of total cell number. Fluorescein diacetate can also be used to assess viability. This method relies on functioning esterases being present in healthy cells; these produce fluorescein which can be observed with the aid of a UV microscope. A simple method is given (6):

1. Add fluorescein diacetate to a concentration of approximately 0.01% (make a 0.5% stock solution in acetone and store at 4°C).
2. Leave for 5 min.
3. Examine the cells under a UV microscope; living cells fluoresce green; score as a percentage of total cell number.

Other methods rely on the reduction of tetrazolium salts such as 2,3,5-triphenyltetrazolium chloride (TTC); respiratory efficiency is monitored by spectrophotometric measurement of the red dye formazan. The TTC method is more labor-intensive, and it should be optimized with respect to pH, time, and % TTC (6).

36.4.4 Synchronization of Cell Suspension Cultures

One area where plant cell suspension cultures find widespread use, is in studies of gene expression during the cell division cycle. Cell suspensions are particularly suited to this type of investigation, as a homogeneous population of cycling cells can be produced.

Early attempts at synchronizing the cell division cycle of suspension cultured plant cells relied either on the withdrawal and subsequent re-supply of a nutrient (36–38) or a plant growth regulator (39,40). These treatments caused the cells to arrest at a particular point in the cell division cycle and, following addition of the substance back to the medium, resume cell division in a synchronous fashion. However, these techniques may not be universally applicable or result in arrest at more than one point in the cell cycle (35,41). More recent work has focused on the use of chemicals that prevent either DNA replication, such as aphidicolin and hydroxyurea (42,43), or mitosis, such as colchicine, oryzalin, or other antimicrotubule drugs (44).

36.5 SUMMARY

Plant cell cultures provide excellent experimental model systems. Unfortunately, due to the wide variation in the requirements of individual plant cell cultures, there is no real substitute for experience in plant cell culture. However, with knowledge from this chapter it should be possible to initiate, maintain, and monitor the growth of cell cultures from most plant species. These provide the basic steps necessary for any investigations involving the use of cell cultures.

REFERENCES

1. Gamborg OL, Phillips GC, editors. Plant cell, tissue and organ culture. Berlin: Springer-Verlag; 1995. pp. 3–20.
2. Street HE, editor. Plant tissue and cell culture. Oxford: Blackwell; 1973. pp. 11–30.
3. Bhojwani SS, Razdan MK. Plant cell culture: theory and practice. Amsterdam: Elsevier; 1983. pp. 11–24.
4. Dodds JH, Roberts LW. Experiments in plant cell culture. Cambridge: Cambridge University Press; 1995. pp. 25–41.
5. Hunter CF. *In Vitro* cultivation of plant cells. Oxford: Butterworth-Heinemann; 1993. pp. 43–64.
6. Dixon RA, Gonzales RA, editors. Plant cell culture a practical approach. Oxford: IRL Press, Oxford University Press; 1994. pp. 1–25.
7. George EF, Puttock DJM, George HJ. Volume 2, Plant culture media. England: Exegetics Ltd; 1988. pp. 398–405.
8. Marschner H. Mineral nutrition of higher plants. Orlando (FL): Academic Press; 1986.
9. Dodds JH, Roberts LW. Experiments in plant cell culture. Cambridge: Cambridge University Press; 1995. pp. 42–66.
10. Hangarter RP, Stasinopoulos TC. Plant Physiol 1996; 96: 843–847.
11. Bonga JM, Durzan DJ, editors. Tissue culture in forestry. The Hague: Martinus Nijhoff; 1982. pp. 4–35.
12. Gamborg OL, Miller RA, Ojima K. Exp Cell Res 1968; 50: 151–158.
13. Gamborg OL, Phillips GC, editors. Plant cell, tissue and organ culture. Berlin: Springer-Verlag; 1995. pp. 21–34.
14. van Bragt J, Mossel DA, Pierik RLM, Veldstra H, editors. Effects of sterilization on components in nutrient media. Wageningen: Veenman and Zonen; 1971. pp. 3–13.
15. Nissen SJ, Sutter EG. HortScience 1990; 25: 800–802.
16. van Bragt J, Mossel DA, Pierik RLM, Veldstra H, editors. Effects of sterilization on components in nutrient media. Wageningen: Veenman and Zonen; 1971. pp. 133–137.
17. Dunlap JR, Kresovich S, McGee RE. Plant Physiol 1986; 81: 934–936.
18. Hagen SR, Muneta P, Augustin J, LeTourneau D. Plant Cell Tissue Organ Cult 1991; 25: 45–48.
19. Murashige T, Skoog F. Physiol Plant 1962; 15: 312–313.
20. Schenk RU, Hilderbrandt AC. Can J Bot 1972; 50: 199–204.
21. Wilson HM, Street HE. Ann Bot 1975; 39: 671–682.
22. George EF, Sherington PD. Plant propagation by tissue culture. England: Exegetics Ltd.; 1984.
23. Stuart R, Street HE. J Exp Bot 1969; 64: 556–571.
24. Street HE, editor. Plant tissue and cell culture. Oxford: Blackwell; 1973. pp. 59–99.
25. King PJ, Mansfield KJ, Street HE. Can J Bot 1973; 51: 1807–1823.

26. deJong DE, Jansen E, Olsen A. Exp Cell Res 1967; 47: 139–156.
27. Verma D, Van Hustee R. Can J Bot 1970; 48: 429–431.
28. Barz W, editor. Plant tissue culture and its bio-technological application. Berlin: Springer-Verlag; 1977. pp. 253–265.
29. Masuda H, Nakagawa R, Sugawara S. Plant Cell Physiol 1988; 29: 75–78.
30. Doley WP, Saunders JK. Plant Cell Rep 1989; 8: 222–225.
31. deGreef W, Jacobs M. Plant Sci Lett 1979; 17: 55–61.
32. Kevers C, *et al*. Physiol Plant 1981; 51: 281–286.
33. Bayliss MW. Plant Sci Lett 1977; 8: 99–103.
34. Bryant JA, editor. The cell division cycle in plants. Cambridge: Cambridge University Press; pp. 157–177.
35. Dolezal J, Lucretti S, Novak F-J. Biol Plant 1988; 29: 253–257.
36. Bayliss MW, Gould AR. J Exp Bot 1974; 25: 772–783.
37. Gould AR, Everett NP, Wang TL, Street HE. Protoplasma 1981; 106: 1–13.
38. Amino S, Fujimura T, Komamime A. Physiol Plant 1983; 59: 393–396.
39. Jouanneau JP. Exp Cell Res 1971; 77: 167–174.
40. Nishi A, Kato K, Takahashi M, Yoshida R. Physiol Plant 1977; 39: 9–12.
41. Wareing PF, editor. Plant growth substances. London: Academic Press; 1982. pp. 59–67.
42. Qin LX, *et al*. Plant Mol Biol 1996; 32: 1093–1101.
43. Soni R, Carmichael JP, Shah ZH, Murray JAH. Plant Cell 1995; 7: 85–103.
44. Shaul O, *et al*. Proc Natl Acad Sci U S A 1996; 93: 4868–4872.

FURTHER READING

Gamborg OL. *In Vitro* Cell Dev Biol Plant 2002; 38: 84–92.

Ramage CM, Williams RR. *In Vitro* Cell Dev Biol Plant 2002; 38: 116–124.

Slater A, Scott NW, Fowler MR. Plant biotechnology-the genetic manipulation of plants. Oxford: Oxford University Press; 2003.

37

SCALE-UP OF BIOTECHNOLOGICAL PROCESSES

MARKO ZLOKARNIK
Chemical Process Engineering, University of Köln, Cologne, Germany

37.1 INTRODUCTION

A chemical engineer is generally concerned with industrial implementation of processes in which chemical or microbiological conversion of material takes place in conjunction with transfer of mass, heat, and momentum. These processes are scale-dependent; that is, they behave differently on a small scale (in laboratories or pilot plants) and a large scale (in production). They include heterogeneous chemical reactions and most unit operations. Understandably, chemical engineers have always wanted to find ways of simulating these processes in models to gain insights that will assist them in designing new industrial plants. Occasionally, they face the same problem for another reason. An industrial facility already exists but will not function properly, if at all, and suitable measurements have to be carried out to discover the cause of difficulties and provide a solution.

Irrespective of whether the model involved represents a "scale-up" or a "scale-down", certain important questions always apply:

1. How small can a model be? Is one model sufficient or should tests be carried out in models of different sizes?
2. When must or when can physical properties differ? When must measurements be carried out on a model with an original system of materials?
3. Which rules govern the adaptation of process parameters in model measurements to those of a full-scale plant?
4. Is it possible to achieve complete similarity between the processes in the model and those in its full-scale counterpart? If not: how should one proceed?

These questions touch on the fundamentals of the theory of models, which are based on dimensional analysis. Although they have been used in the field of fluid dynamics and heat transfer for more than a century—cars, aircraft, vessels, and heat exchangers were scaled up according to these principles—these methods have gained only a modest acceptance in chemical engineering. University graduates are usually not skilled enough to deal with such problems at all. On the other hand, there is no motivation for this type of research at universities since, as a rule, they are not confronted with scale-up tasks and are not equipped with the necessary devices on the bench-scale. This gives a totally wrong impression that these methods are, at most, of marginal importance in practical chemical engineering, otherwise they would have been taught and dealt with in greater depth.

37.2 DIMENSIONAL ANALYSIS

37.2.1 Fundamental Principle

Dimensional analysis is based on the recognition that the mathematical formulation of a physicotechnological problem can be of general validity only when the process equation is dimensionally homogenous.

Upstream Industrial Biotechnology: Expression Systems and Process Development, Volume 1, First Edition. Edited by Michael C. Flickinger.
© 2013 John Wiley & Sons, Inc. Published 2013 by John Wiley & Sons, Inc.

37.2.2 What is a Dimension?

A dimension is a purely qualitative description of a perception of a physical entity or a natural appearance. Length can be experienced as height, depth or breadth. Mass presents itself as a light or a heavy body, time as a short moment or a long period. The dimension of length is Length *L*, the dimension of mass is Mass *M*, and so on.

37.2.3 What is a Physical Quantity?

Unlike a dimension, a physical quantity represents a quantitative description of a physical quality (e.g. mass of 5 kg). It consists of a measuring unit and a numerical value. The measuring unit of length can be a meter, a foot, a cubit, a yardstick, a nautical mile, a light year, etc. The measuring unit of temperature can be °C (Centigrade), R (Rankine), F (Fahrenheit) or K (Kelvin). (It is therefore necessary to establish measuring units in an appropriate measuring system.)

From these definitions, we conclude that a measuring unit is the counterpart of a dimension.

37.2.4 Basic and Derived Quantities, Dimensional Constants

We distinguish between basic and secondary quantities, the latter often being referred to as *derived quantities*. The basic quantities are defined. They are based on standards and are quantified by comparison with them. The secondary units are derived from the primary ones according to physical laws (e.g. velocity = length/time). The borderline separating both types of quantities is largely arbitrary: 50 years ago a measuring system was used in which force was a primary dimension instead of mass!

All secondary units must be coherent with the basic units (Table 37.1). For example, the measuring unit of velocity must not be miles per hour or kilometres per hour, but meters per second!

A secondary unit that has been established by a physical law may sometimes contradict another one. For example, according to the Newton's second law of motion, the force F is expressed as a product of mass m and acceleration a: $F = ma$, having the measuring unit of kilogram meter per second square or N. According to Newton's law of gravitation, the force is defined by $F \propto m_1 m_2 / r^2$, which leads to a completely different measuring unit (kg^2/m^2). To remedy this, the gravitational constant G—a dimensional constant—had to be introduced to ensure the dimensional homogeneity of this equation: $F = G m_1 m_2 / r^2$.

Another example entails the universal gas constant R, the introduction of which ensures that in the perfect gas equation of state $p\,V = n\,R\,T$ the secondary unit for work $W = pV[\mathrm{M\,L^2/T^2}]$ is not offended.

Another class of derived quantities is represented by coefficients in diverse physical equations (e.g. transfer equations). They are established by respective equations and determined by measuring their constituents (e.g. mass and heat transfer coefficients).

TABLE 37.1. Base Quantities, their Dimensions and Units According to SI

Base Quantity	Base Dimension	Base Unit
Mass	M	kg
Length	L	m
Time	T	s
Thermodynamic, temperature	Θ	K
Amount of substance	N	mol
Electric current	I	A
Luminous intensity	J	cd

37.2.5 Dimensional Systems

A dimensional system consists of all primary and secondary dimensions and corresponding measuring units. The currently used International System of Dimensions (*Système International d'Unités*; SI) is based on seven base dimensions. They are presented in Table 37.1, together with their corresponding base units. For some of them, a few explanatory remarks may be necessary.

Temperature expresses the thermal level of a system and not its energetic contents. (A five-fold mass of matter has a five-fold thermal energy at the same temperature!). Thermal energy of a system can indeed be converted into mechanical energy (base unit Joule).

Moles are a certain amount of matter and must not be confused with the quantity of mass. Molecules react as individual entities regardless of their mass: 1 mole of hydrogen (2 g/mol) reacts with 1 mole of chlorine (71 g/mol) to produce 2 moles (73 g) of hydrochloric acid, HCl.

Table 37.2 shows the most important secondary dimensions. Table 37.3 refers to some very frequently used secondary units that are named after famous researchers.

TABLE 37.2. Important Secondary Measuring Units in Mechanical Engineering, Named after Famous Researchers

Secondary Quantity	Dimensions	Measuring Unit	Name
Force	$\mathrm{M\,L\,T^{-2}}$	$\mathrm{kg\ m\ s^{-2} \equiv N}$	Newton
Pressure	$\mathrm{M\,L^{-1}T^{-2}}$	$\mathrm{kg\ m^{-1}\ s^{-2} \equiv Pa}$	Pascal
Energy	$\mathrm{M\,L^{-2}T^{-2}}$	$\mathrm{kg\ m^{-2}\ s^{-2} \equiv J}$	Joule
Power	$\mathrm{M\,L^{2}T^{-3}}$	$\mathrm{kg\ m^{2}\ s^{-3} \equiv W}$	Watt

TABLE 37.3. Often Used Physical Quantities and their Dimensions According to the Currently Used SI and the Dimensional System in which the Amount of Heat was a Basic Quantity with the Dimension of H

Physical Quantity	SI [MLT Θ]	[MLT ΘH]
Mass	M	
Length	L	
Time	T	
Temperature	Θ	
Amount of heat		H
Volume	L^3	
Angular velocity		
Frequency, shear rate	T^{-1}	
Velocity	$L\,T^{-1}$	
Acceleration	$L\,T^{-2}$	
Kinematic viscosity		
Diffusion coefficient thermal diffusivity	L^2T^{-1}	
Density	$M\,L^{-3}$	
Moment of inertia	$M\,L^2$	
Surface tension	$M\,T^{-2}$	
Dynamic viscosity	$M\,L^{-1}T^{-1}$	
Momentum	$M\,L\,T^{-1}$	
Force	$M\,L\,T^{-2}$	
Pressure, stress	$M\,L^{-1}T^{-2}$	
Angular momentum	$M\,L^2T^{-1}$	
Energy, work, torque	$M\,L^2T^{-2}$	
Power	$M\,L^2T^{-3}$	
Mechanical equivalent of heat J	1	$M\,L^2T^{-2}H^{-1}$
Specific heat capacity	$L^2T^{-2}\Theta^{-1}$	$M^{-1}\Theta^{-1}H$
Thermal conductivity	$M\,L\,T^{-3}\Theta^{-1}$	$L^{-1}T^{-1}\Theta^{-1}H$
Heat transfer coefficient	$M\,T^{-3}\Theta^{-1}$	$L^{-2}T^{-1}\Theta^{-1}H$
Stefan–Boltzmann constant	$M\,T^{-3}\Theta^{-4}$	$L^{-2}T^{-1}\Theta^{-4}$

37.2.6 Dimensional Homogeneity of a Physical Content

The aim of dimensional analysis is to check whether physical content of the case under consideration can be formulated in a dimensionally homogeneous manner or not. The procedure necessary to accomplish this consists of two parts:

1. All physical parameters necessary to describe the problem are listed. This "relevance list" of the problem consists of the quantity in question and of all the parameters which influence it. In each case, only *one* target quantity must be considered. It is the only dependent variable. On the other hand, all the influencing parameters must be primarily independent of one another.
2. Dimensional homogeneity of physical content is examined by transferring it into a dimensionless form. (Note: A physical content which can be transformed into dimensionless expressions is dimensionally homogeneous.)

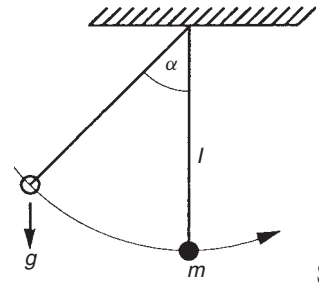
The information given thus far will be made clear by a well-known example (1):

37.2.7 Example 1

37.2.7.1 What Determines the Period of Oscillation of a Pendulum? First, a pendulum will be sketched and all the quantities that could be involved written down. It may be assumed that the period of oscillation of a pendulum depends on the length and mass of the pendulum, gravitational acceleration, and the amplitude of swing.

(In the case of a real pendulum, density and the viscosity of air, which both cause friction resistance, should also be included in the relevance list. However, this would unnecessarily complicate the problem at this stage. Therefore, we will consider a physical pendulum with a point mass in vacuum.)

Physical Quantity	Symbol	Dimension
Period of oscillation	θ	T
Length of pendulum	l	L
Mass of pendulum	m	M
Gravitational acceleration	g	LT^{-2}
Amplitude (angle)	α	—



Sketch of the pendulum

Our aim is to express θ as a function of l, m, g, and α:

$$\theta = f(l, m, g, \alpha).$$

Can this dependence be dimensionally homogeneous? No! The first thing that now becomes clear is that the base unit of the mass M occurs only in the mass m itself. Changing this base unit (e.g. from kilograms to pounds) would change the numerical value of the function. This is unacceptable. Either our list should include a further variable containing M, or mass is not a relevant variable. If we assume the latter, the above relationship is reduced to:

$$\theta = f(l, g, \alpha).$$

Both l and g incorporate the base unit of length. When combined as a ratio (l/g) they become dimensionless with regard to L and thus independent of changes in the basic unit of length:

$$\theta = f(l/g, \alpha)$$

Because the angle α has no dimension, we are left with the dimension T on the left-hand side of the equation and T^2 on the right. To remedy this, we will have to write

$$\sqrt{l/g}$$

This expression will keep its dimension T only if it remains unchanged, so we have to take it out of the function f and we finally obtain:

$$\theta = \sqrt{l/g} \quad f(a) \quad \text{or} \quad \theta\sqrt{g/l} = f(\alpha)$$

The dependence between four dimensional quantities, containing two basic dimensions (L and T) is reduced to a $4 - 2 = 2$ parametric relationship between dimensionless expressions ("numbers")!

This equation is the only statement that dimensional analysis can offer in this case. It is not capable of producing information as to the form of f. The integration of Newton's equation of motion for small amplitudes leads to $f = 2\pi$ and is independent of α. The relationship can now be expressed as:

$$\theta\sqrt{g/l} = 2\pi$$

The elegant solution of this first example should not tempt the reader to believe that dimensional analysis can be used to solve any problem at his desk. To treat this example by dimensional analysis, the law of free fall had to be known. This knowledge was gained empirically by Galilei in 1604 through his *experiments* with the inclined plane. Bridgman's (1) comment on this situation is particularly appropriate:

> "The problem cannot be solved by the philosopher in his armchair, but the knowledge involved was gathered only by someone at some time soiling his hands with direct contact."

This transparent and easy example clearly shows how dimensional analysis deals with specific problems and what conclusions it allows. It should now be easier to understand the sarcastic comment with which Lord Rayleigh began his short essay on "The Principle of Similitude" (2):

> "I have often been impressed by the scanty attention paid even by original workers in physics to the great principle of similitude. It happens not infrequently that results in the form of "laws" are put forward as novelties on the basis of elaborate experiments, which might have been predicted *a priori* after a few minutes' consideration."

From Example 1, we also learn that a transformation of a physical dependence from a dimensional into a dimensionless form is automatically accompanied by an essential *compression* of the statement: the set of dimensionless numbers is smaller than the set of quantities contained in them, but it describes the problem equally comprehensively. In the above example, the dependence between four dimensional parameters is reduced to a dependence between only two dimensionless numbers! This is the proof of the so-called pi theorem (pi after Π, the sign used for products), which is given below.

37.3 THE PI THEOREM

Every physical relationship between $\boldsymbol{n}$ *physical quantities can be reduced to a relationship between* $\boldsymbol{m} = \boldsymbol{n} - \boldsymbol{r}$ *mutually independent dimensionless groups, whereby* $\boldsymbol{r}$ *stands for the rank of dimensional matrix, made up of the physical quantities in question and generally equal to the number of the base quantities contained in them*.

(The pi theorem is often associated with Buckingham, who introduced this term in 1914, but the proof of it was already accomplished in 1911 in the course of a mathematical analysis of partial differential equations by Federmann (3).

37.4 DETERMINATION OF A PI SET BY MATRIX CALCULATION

37.4.1 Establishment of a Relevance List for a Problem

As a rule, more than two dimensionless numbers will be necessary to describe a physicotechnological problem and therefore, they cannot be derived by the method described above. In this case, the easy and transparent matrix calculation introduced by Pawlowski (4) is increasingly used. It will be demonstrated by the following example, which treats an important problem in industrial chemistry and biotechnology because the mixing vessel is an important production equipment.

37.4.2 Example 2

37.4.2.1 Which is the Pi Set for the Mixing Power of a Stirrer? In this case, too, first a sketch of the device is drawn. Then we facilitate our work by proceeding systematically.

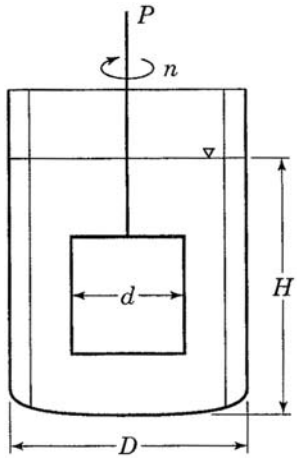
Target quantity: mixing power P

Parameters:

(a) geometrical: stirrer diameter d

(b) physical properties: fluid density ρ and kinematic viscosity ν

(c) process-related: stirrer speed n



Sketch of the mixing vessel.

We obtain the following relevance list:

$$\{P; d; \rho, \nu; n\} \tag{37.1}$$

We interrupt the procedure by asking an important question concerning the determination of the characteristic geometric parameter.

37.4.3 Determination of the Characteristic Geometric Parameter

Obviously, we could name all the geometric parameters indicated in the sketch. They were all the geometric parameters of the stirrer and the vessel, especially its diameter D and the liquid height H. In case of complex geometry, such a procedure would deflect from the problem. It is therefore advisable to introduce only one (or a few) characteristic geometric parameters, knowing that all the others can be transformed into dimensionless geometric numbers by division with this one or a few of them.

In the case of Example 2, we introduced the stirrer diameter as the characteristic geometric parameter. This is reasonable. One can only think of how the mixing power would react to an increase in the vessel diameter D. It is obvious that above a certain size, D would have no influence, but a small change in the stirrer diameter d would always have an impact.

We now set forth a procedure for solving Example 2.

37.4.4 Constructing and Solving the Dimensional Matrix

In transforming the relevance list (Eq. 37.1) of the five physical quantities into a dimensional matrix, we can minimize calculations required by keeping to the following points:

1. The dimensional matrix consists of a square core matrix and a residual matrix.
2. The rows of the matrix are formed of basic dimensions, contained in dimensions of the quantities, and they will determine the rank r of the matrix. The columns of the matrix are presented by the physical quantities or parameters.
3. Quantities of the square core matrix may appear later on in all dimensionless numbers as "fillers", whereas each element of the residual matrix will appear only in one dimensionless number. For this reason, the residual matrix should be loaded with essential variables like the target quantity and the most important physical properties and process-related parameters.
4. By the (extremely easy) matrix calculation (linear transformations), the core matrix is transformed into a matrix of unity. The main diagonal consists only of ones and the remaining elements are all zero. One should therefore arrange the quantities in the core matrix in such a way as to facilitate this procedure.
5. After the matrix of unity has been generated, dimensionless numbers are created as follows. Each element of the residual matrix forms the numerator of a fraction, while the denominator consists of the fillers from the matrix of unity with exponents indicated in the residual matrix.

Let us return to Example 2. The dimensional matrix reads as follows:

	ρ	d	n	P	ν
Mass M	1	0	0	1	0
Length L	−3	1	0	2	2
Time T	0	0	−1	−3	−1
	Core matrix			Residual matrix	

Only one linear transformation is necessary to transform −3 in the cell formed by the L-row and the ρ-column into zero. The subsequent multiplication of the T-row by −1 transfers −1 to 1:

	ρ	d	n	P	ν
M	**1**	0	0	1	0
$3M + L$	0	**1**	0	5	2
$-T$	0	0	**1**	3	1
	Unity matrix			Residual matrix	

The residual matrix contains only two parameters, therefore only two Π numbers result:

$$\Pi_1 \equiv \frac{P}{\rho^1 n^3 d^5} = \frac{P}{\rho n^3 d^5} \equiv \text{Ne (Newton number)}$$

$$\Pi_2 \equiv \frac{\nu}{\rho^0 n^1 d^2} = \frac{\nu}{n d^2} \equiv \text{Re}^{-1} \text{ (Reynolds number)}$$

The interdependence of five dimensional quantities of the relevance list (Eq. 37.1), is reduced to a set of only $5 - 3 = 2$ dimensionless numbers:

$$\{\text{Ne, Re}\} \text{ or } f(\text{Ne, Re}) = 0 \qquad (37.2)$$

thus again confirming the pi theorem.

37.4.5 Determination of the Process Characteristics

The functional dependence (Eq. 37.2), is the maximum that dimensional analysis can offer here. It cannot provide any information about the form of the function f. *This can be accomplished solely by experiments*. But these experiments can now be conducted in a far easier manner, because it is the Reynolds number which has to be varied. This can be accomplished by altering the characteristic stirrer speed n, or the characteristic length d, or the kinematic viscosity ν. By choosing appropriate model fluids, the viscosity can be very easily altered by several orders of magnitude. In this way, measurements were conducted to determine the *power characteristic* Ne (Re) of a blade stirrer of fixed geometry in a vessel. From Fig. 37.1 it follows that

1. In the range $\text{Re} < 20$ the proportionality $\text{Ne} \propto \text{Re}^{-1}$ is found, which results in the expression $\text{Ne}\,\text{Re} \equiv P/(\eta\ n^2 d^3) = a$ constant. Density is irrelevant here since we are dealing with the *creeping* flow region.
2. In the range $\text{Re} > 50$ (vessel with baffles) or $\text{Re} > 5 \times 10^4$ (unbaffled vessel) a constant Newton number $\text{Ne} \equiv P/(\rho n^3 d^5)$ is found. In this case, viscosity is irrelevant because we are dealing with a *turbulent* flow region.
3. Understandably, the baffles do not influence the power characteristics in the creeping flow region. However, their influence is extremely strong at $\text{Re} > 5 \times 10^4$. Here, the installation of baffles under otherwise unchanged operating conditions increases the power consumption of the stirrer by a factor of 20.
4. When liquid is stirred in an unbaffled vessel, it begins to rotate and a vortex is formed. Gravitational acceleration g, and hence the Froude number $\text{Fr} \equiv n^2\ d/g$, plays no role under these circumstances as determined experimentally (Fig. 37.1). For confirmation, one needs only to look at the points on the lower Ne (Re) curve, where the *same* Re value was set for fluids with *different* viscosities. This was possible only with a proportional alteration of the stirrer speed. Where Re = idem (= identical value), Fr was clearly not idem, but this has no influence on Ne. g is therefore irrelevant!

37.5 FUNDAMENTALS OF THE THEORY OF MODELS AND OF SCALE-UP

37.5.1 Theory of Models

The results in Fig. 37.1 could also have been acquired by changing the stirrer diameter. It does not matter, how a relevant number is changed. This is a clear evidence that the representation of a physicotechnological problem in a dimensionless form is independent of scale, it is *scale-invariant*. This aspect is of special importance with respect to changes in linear dimension because it is the foundation of a reliable scale-up:

Two processes may be considered completely similar if they take place in similar geometrical space and if all the dimensionless numbers necessary to describe them have the same numerical value (Π_i = identical or idem).

Clearly, the scale-up of a desired process condition from a model to industrial scale can be accomplished reliably only if the problem was formulated and dealt with according to dimensional analysis.

37.5.2 Model Experiments and Scale-Up in the Process Point

In Example 2, we evaluated process characteristics that presented a comprehensive description of the process. This is often an expensive and time consuming method, which is superfluous, if one has only to scale-up a given process condition from a model to an industrial plant (or vice versa). With Example 2, and assuming that the Ne (Re) characteristics like those in Fig. 37.1 are unknown, the task is to predict the power consumption of a leaf stirrer of $d = 2$ m, installed in a baffled vessel of $D = 4$ m ($D/d = 2$) and rotating with $n = 10\ \text{min}^{-1}$. The kinematic viscosity of the liquid is $\nu = 1 \times 10^{-4}\ \text{m}^2/\text{s}$.

One only needs to know—and this is *essential*—that the hydrodynamics in this case are governed solely by the Reynolds number and that the process is described by an unknown dependence Ne (Re). Then the Re number of the industrial plant can be calculated:

$$\text{Re} \equiv n\ d^2/\nu = 6.7 \times 10^3$$

Let us assume that we have a geometrically similar laboratory device of $D = 0.2$ m and $d = 0.1$ m and that the stirrer speed can be arbitrarily chosen. What stirrer

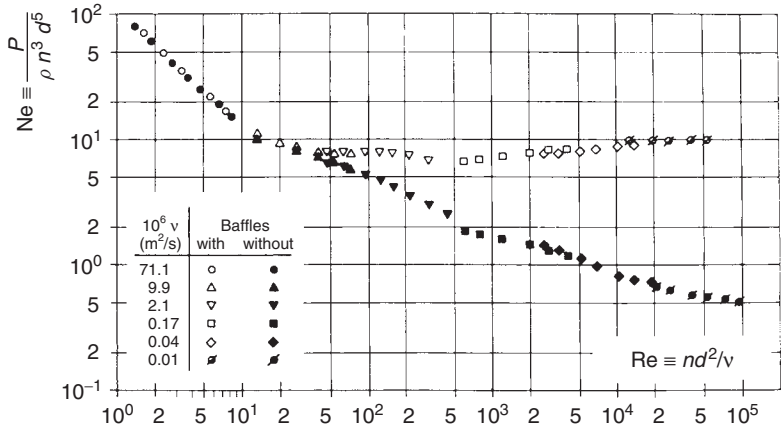


Figure 37.1. Power characteristics of a leaf stirrer of a given geometry and given installation conditions. [From Ref. 5.]

speed should be used to obtain Re = idem using water ($\nu = 1 \times 10^{-6}$ m^2/s) as a model liquid? The answer is

$$n\ d^2/\nu = 6.7 \times 10^3 \rightarrow \text{n} = 40\ \text{min}^{-1}$$

Under these conditions, the stirrer power must be measured and the power number $\text{Ne} \equiv P/(\rho n^3 d^5)$ calculated. We find Ne = 8.0. Due to the fact that Re = idem results in Ne = idem, the power consumption P_T *of the industrial stirrer can be obtained:*

$$Ne = idem \rightarrow Ne_\text{T} = Ne_\text{M} \rightarrow \left(\frac{P}{\rho n^3 d^5}\right)_\text{T} = \left(\frac{P}{\rho n^3 d^5}\right)_\text{M}$$

From Ne = 8.0 found in a laboratory measurement, it follows for the leaf stirrer having $d = 2$ m and a stirrer speed of $n = 10\ \text{min}^{-1}$

$$P = \text{Ne}\ \rho n^3 d^5 = 8.0 \times 1 \times 10^3 \times (10/60)^3 \times 2^5 = 1,185\ \text{W} \simeq 1.2\ \text{kW}$$

We realize that in scale-up, knowledge of functional dependence $f(\Pi_\text{i}) = 0$ (Fig. 37.1) is unnecessary. All we need to know is which pi space describes the process.

37.6 FURTHER PROCEDURES TO ESTABLISH A RELEVANCE LIST

37.6.1 Consideration of Acceleration due to Gravity g

If a natural or universal physical constant has an impact on the process, it has to be incorporated into the relevant list, regardless of whether it will be altered. In this context a major mistake is made with regard to gravitational constant g. Lord Rayleigh (2) complained bitterly, saying:

> "I refer to the manner in which gravity is treated. When the question under consideration depends essentially upon gravity, the symbol of gravity (g) makes no appearance, but when gravity does not enter the question at all, g obtrudes itself conspicuously."

This is all the more surprising in view of the fact that the relevance of this quantity is easy enough to recognize if one asks the following question:

> "Would the process function differently if it took place on the moon instead of Earth?"

If the answer to this question is affirmative, g is a relevant variable.

Gravitational acceleration g can be effective solely in connection with the density as gravity $g\rho$. When inertial forces play a role, the density ρ has to be listed additionally. Thus, it follows that

1. in cases involving the ballistic movement of bodies, the formation of vortices in stirring, the bow wave of a ship, the movement of a pendulum and other processes affected by the Earth's gravity, the relevance list comprises $g\rho$ *and* ρ;
2. creeping flow in a gravitational field is governed by the gravity $g\rho$ alone;
3. in heterogeneous physical systems with density differences (sedimentation or buoyancy), the difference in gravity $g\Delta\rho$ *and* ρ play a decisive role.

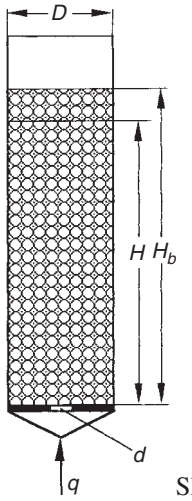
In the next example, we shall treat a problem where gravitational constant is of prime importance, due to extreme differences in the density in the gas–liquid system. Dealing with this example, we will have the opportunity to improve our skills in solving dimensional matrices and to

gain deeper insights into possibilities offered by dimensional analysis.

37.6.2 Example 3

37.6.2.1 Gas HoldUp in Bubble Columns. Bubble columns are important appliances for the absorption of gases in liquids and, consequently, for the execution of chemical and biotechnological reactions in a gas–liquid system. In this context, the attainable interface ($\hat{=}$ sum of the surfaces of all gas bubbles) is of considerable interest because it affects mass transfer in a directly proportional manner. If a gas throughput q is introduced into a bubble column with diameter D and liquid height H, the liquid height rises by the amount occupied by the gas bubbles in the liquid. The gas fraction in the liquid, the so-called gas holdup H^* can be determined from the liquid height H_b of the gassed and the non-gassed liquid H (see sketch).

$$H^* \equiv \frac{V_G}{V_L} = \frac{H_b - H}{H} \tag{37.3}$$



Sketch of the bubble column.

In the course of extensive measurements (6) on bubble columns of different dimensions, the gas holdup H^* proved to be directly proportional to the volume-related mass transfer coefficient $k_L a$. For this reason, H^* will be the *target number* in the following considerations. Bubble columns with a single-hole plate as gas distributor (see sketch) were used in these investigations. D, H, and d (= hole diameter) therefore describe their *geometry* in full.

The densities (ρ and ρ') and the viscosities (ν and ν') of both phases (gas) and the surface tension, σ, must be taken into account as *physical properties*.

The *process parameters* are the gas throughput q and, on account of extreme differences in density, the gravity difference $g\Delta\rho = g(\rho - \rho')$.

The complete relevance list is therefore

$$\{H^*; D, H, d; \rho, \rho', \nu, \nu', \sigma; q, g\Delta\rho\}. \tag{37.4}$$

If we exclude the (dimensionless) target number H^* and the trivial numbers H/D, d/D, ρ'/ρ and ν'/ν, the remaining relevance list is

$$\{D; \rho, \nu, \sigma; q, g\Delta\rho\}$$

from which, via the dimensional matrix, the following three dimensionless numbers result:

$$\Pi_1 \equiv \frac{\sigma D}{\rho\nu^2} \equiv \frac{\mathrm{Re}^2}{\mathrm{We}} \quad \Pi_2 \equiv \frac{q}{D\nu} \equiv \mathrm{Re}$$

$$\Pi_3 \equiv \frac{g\Delta\rho D^3}{\rho\nu^2} \equiv \mathrm{Ar} \equiv \frac{\mathrm{Re}^2}{\mathrm{Fr}}$$

	ρ	D	ν	σ	q	$g\Delta\rho$
M	1	0	0	1	0	1
L	−3	1	2	0	3	−2
T	0	0	−1	−2	−1	−2
M	**1**	0	0	1	0	1
$3M \equiv L \equiv 2T$	0	**1**	0	−1	1	−3
$-T$	0	0	**1**	2	1	2

This dimensional analysis produces two dimensionless numbers, Π_1 and Π_3, which, apart from the column diameter, contain only physical properties, and the Reynolds number Π_2 as the process number (because it contains q).

However, this is unsatisfactory because we must expect the hydrodynamics of a bubble column to be substantially governed by $g\Delta\rho$. Consequently, the process number must contain $g\Delta\rho$. We must therefore combine Π_2 and Π_3 in order to obtain the modified Froude number Fr*, which is probably the *true process number*:

$$\Pi_2^2\ \Pi_3^{-1} \equiv \frac{q^2\rho}{D^5 g\Delta\rho} \equiv \mathrm{Fr}^*$$

The complete pi set now becomes:

$$\{H^*; H/D, d/D; \rho'/\rho, \nu'/\nu, \mathrm{Fr}^*, \mathrm{Re}, \mathrm{We}\}$$

Comprehensive measurements (6) were performed to verify this pi space and to evaluate the following process characteristics:

1. The relationship $H^* = f(\mathrm{Fr}^*)$ was examined using a bubble column of given geometry. Water was used

as the liquid and the physical properties of the gas were varied over a wide range. Air, nitrogen, and nitrogen–hydrogen mixtures were used. The result in Fig. 37.2 demonstrates that Fr* takes full account of the influence of both densities and that ν'/ν is obviously irrelevant. The process equation is

$$H^* = 15.0\mathrm{Fr}^{*0.35} \tag{37.5}$$

2. Further measurements were carried out with one single material system (water/air) in bubble columns of different geometries (Fig. 37.3). The extended process relationship now reads

$$H^* = 16.7\mathrm{Fr}^{*0.35}(H/D)^{-0.25}(d/D)^{-0.125}$$

As far as the scale-up of a bubble column from a laboratory to an industrial scale is concerned, one will have to keep in mind that the scale-up rule is not $v =$ idem, as is often stated in the chemical engineering literature, but $\mathrm{Fr} \equiv v^2/(D\ g) =$ idem. This means

$$v_\mathrm{T} = v_\mathrm{M}\sqrt{D_T/D_M} = v_\mathrm{M}\ \mu^{0.5} \tag{37.6}$$

μ being the scale factor $\mu \equiv D_\mathrm{T}/D_\mathrm{M}$.

3. The influence of physical properties of the liquid phase was also investigated in one single model bubble column using water and, in addition, 12 different pure organic liquids, the physical characteristics of which varied substantially [given in Table 37.2 in (6)]. The result of these measurements is presented in Fig. 37.4. The dimensionless numbers had to be combined as follows in order to correlate the measured values:

$$B \equiv \frac{\rho/\rho'\ \mathrm{Fr}^*}{\mathrm{Re}\ \mathrm{We}^{0.5}} \equiv \frac{\nu(\sigma\rho)^{0.5}}{D^{2.5}g\Delta\rho}$$

The disadvantage of the number combination B is that it is not a pure material number, but it still contains the column diameter, D. For safe scale-up, the validity of this correlation will therefore have to be examined on columns of different diameters and with simultaneous alteration of the material system.

The presented example, in which the column diameter D was varied by a scale factor of $\mu = 1{:}2$ and the extended Froude number was enlarged—by employing air and mixtures of N_2/H_2 —by a factor of 4, shows that the extended Froude number clearly represents the pertinent scale-up criterion for bubble columns. This means that using the same material system in a four-fold bubble diameter ($\mu = 4$) entails a double superficial velocity v.

37.6.3 Introduction of Intermediate Quantities

Many engineering problems involve several parameters, a condition that impedes the elaboration of the pi space. Fortunately, in some cases a closer look at a problem (or previous experience) facilitates reduction of the number of physical quantities in the relevance list. This is the case when some relevant variables affect the process by way of a so-called intermediate quantity. Assuming that this intermediate variable can be measured experimentally, it should be included in the problem relevance list if this facilitated the removal of more than one variable from the list.

Example 3 shows that the so-called superficial velocity $v = q/S$ (q the gas throughput, $S = \pi D^2/4$ –superfice of the device) is by no means an intermediate quantity; it replaces the fluid throughput q but not the diameter D of the device. The fluid motion in pipes, mixing vessels, and bubble columns is described with kinematic dimensionless numbers such as Re and Fr, which all contain a characteristic linear dimension; the fluid motion is an extremely scale-dependent process.

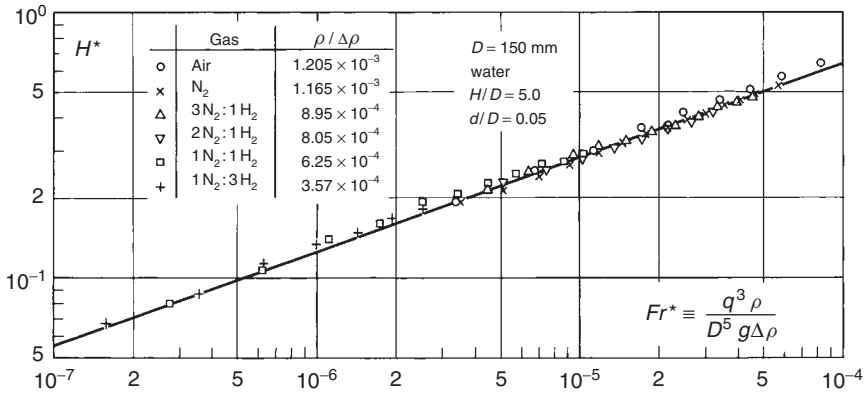


Figure 37.2. The relationship $H^*(\mathrm{Fr}^*)$ confirms the expectation that the gas holdup H^* in a bubble column is dependent on the process number Fr*. [From Ref. 6.]

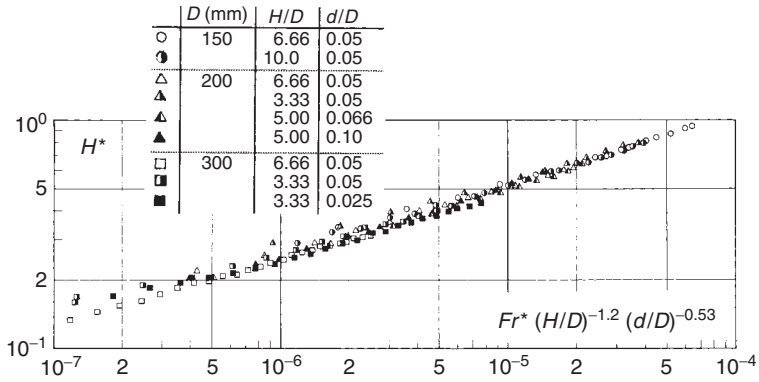


Figure 37.3. Dependence of the gas holdup H^* on the geometry of the column. [From Ref. 6.]

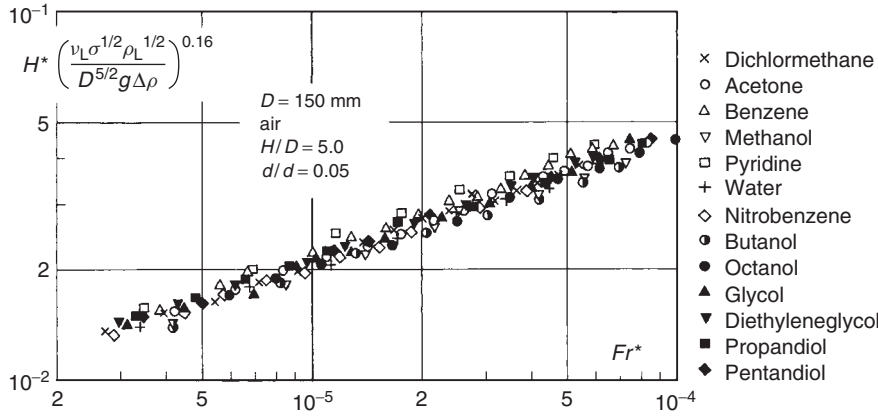


Figure 37.4. Influence of the physical properties of the liquid phase on the gas holdup H^* in a bubble column of a given geometry. [From Ref. 6.]

There are a lot of important processes where a set of material and physical parameters can be replaced by an intermediary quantity:

1. A settling process (sedimentation) depends on the parameters of the dispersed phase. They can be substituted by the sedimentation velocity v_s:

$$v_s = f(d_p, g\Delta\rho, \varphi_p, \mu)$$

(d_p is mean particle diameter, $g\Delta\rho$ the weight difference, φ_p the volume portion of the solid phase, μ is the dynamic viscosity of the liquid.)

2. In a flotation process, it is possible to replace a great many influencing parameters with only one or two intermediate quantities. Then it is legitimate to speak of intermediate quantities as "lumped parameters" (Example 4).
3. A tablet-making process depends on the physical parameters such as mean particle diameter d_p, bulk density (porosity), and flow behavior (lubricating ability) of the powder which also depends on humidity. These physical properties can be replaced by the lumped parameter powder compressibility κ [Example 36 in (3)].

The importance of introducing intermediate quantities will now be demonstrated by the following example.

37.6.4 Example 4

37.6.4.1 Description of the Dissolved Air Flotation Process. In a flotation process tiny gas bubbles adhere to the naturally or artificially hydrophobic surface of solid particles, making them float to the liquid surface from where they can be removed as foam. For the removal and concentration of activated sludge in the biological wastewater purification process, both dissolved air and degasifying flotation (7) can be used. In both cases, a gas mixture (air and $CO_2 + N_2$, respectively) is first dissolved in the respective liquid under higher pressure and is

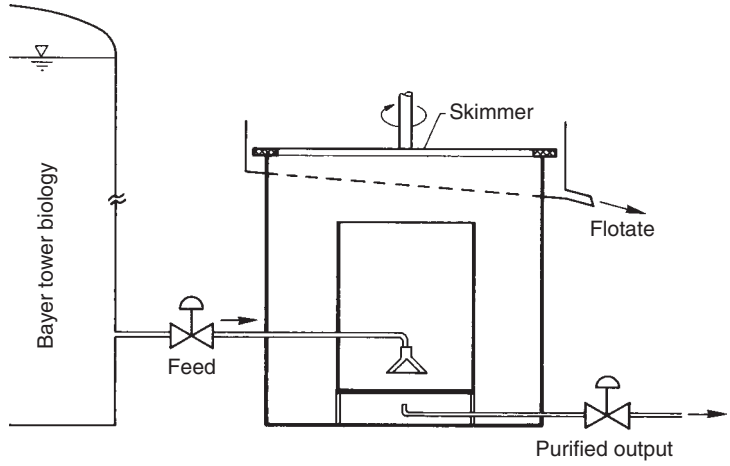


Figure 37.5. Sketch of a flotation cell with spatially separated aeration and separation zones for dissolved air flotation [from Ref. 7].

released after decompression, in the form of tiny gas bubbles. The devices for this procedure consist of either longitudinally streamed-through basins or of flotation cells (Fig. 37.5). To enable a vertical flow through the flotation cell, the cell is spatially separated into a flotation chamber and an annular space. In the latter, the liquid flows slowly downward and the residual flocks rise upward. In this way, a complete removal of the particles is achieved.

Flotation is a depletion process, hence it obeys a time law of the first order and is described by the flotation rate constant, k_F. The target quantity, "solids discharge A", corresponds to the chemical conversion, X, in first order reactions:

$$A \equiv X \equiv (c_0 - c)/c_0 = 1 - c/c_0 = 1 - \exp(-k_F t)$$

Now, we will examine a flotation process taking place in the described flotation cell of a given geometry (characteristic linear dimension of length being the cell diameter D).

The problem here consists in listing the material parameters because, in activated sludge, they fluctuate strongly (in contrast to ore flotation for example). Surely, the degree of hydrophobicity (wettability) of the particle surface (contact angle, Θ) will be of importance. Furthermore, the pH value, the flocculant (polyelectrolyte) concentration c_F, the portion of solids in the system φ, and the weight difference between the bacteria and the liquid $g\Delta\rho$—just to mention a few—will play an important role.

In contrast, it is easy to list all of the process parameters involved: liquid input q_{in}, which leaves the cell divided into the flotate discharge q_F and the processed liquid output q_{out}; releasable gas content of the liquid feed $q_G/q_{in} = H_y \Delta p/\rho_G$. ($H_y$ is the Henry's law constant).

The relevance list now reads

$$\{A;\ D;\ \Theta,\ pH,\ c_F,\ \varphi;\ q_{in},\ q_{out};\ q_G/q_{in},\ g\Delta\rho\} \qquad (37.7)$$

This relevance list, which is certainly incomplete with respect to physical properties, can be streamlined significantly by introducing two intermediate quantities:

1. the *superficial velocity*, v, in the annulus of the flotation cell (Fig. 37.5):

$$v = f_1(q_{in},\ D)$$

and

2. the *rising velocity*, w, of the flocks:

$$w = f_2(\Theta,\ pH,\ c_F,\ \varphi,\ q_G/q_{in},\ g\Delta\rho)$$

[w has to be separately determined with an appropriate measuring device, refer (7)].

The 10-parametric relevance list in Equation 37.7, which has been assumed to be fairly complete, is now reduced to a 5-parametric one:

$$\{A,\ v,\ w,\ q_{in},\ q_{out}\} \qquad (37.8)$$

This relevance list delivers the following simple three-parametric pi set:

$$\{A,\ v/w,\ q_{in}/q_{out}\} \qquad (37.9)$$

In this pi space, measurements performed in a bench-scale flotation cell (Fig. 37.5) of $D = 0.6$ m were evaluated. The flotation cell input consisted of biologically purified wastewater, containing ≈ 3 g TS/L activated sludge (TS being total solids), which was processed in the 30-m high bubble columns, the so-called "Tower Biology" of BAYER AG/Leverkusen, Germany.

The result in Fig. 37.6 cannot be considered satisfying. This is certainly not surprising because the processed

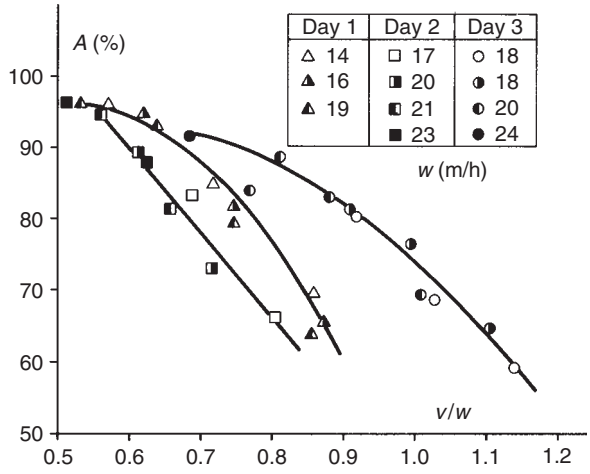


Figure 37.6. Correlation between the activated sludge discharge A and the ratio v/w of the superficial velocity, v, to the rising velocity of flocks, w [from Ref. 7].

wastewaters of this chemical giant originated from about 150 production sites and constantly changed their composition. Nevertheless, it can be seen that at least the process parameters are correctly taken into account with the ratio v/w. (The rising velocity w, was varied to a small extent each day by the addition of different amounts of polyelectrolitic flocculants.)

The results of this examination show that biologically purified wastewater can be completely freed from activated sludge under the precondition that the superficial velocity of the input v, amounted to the half value of the rising velocity of the flocks w. (The fact that $A = 100\%$ was never achieved is understandable because in the determination of the solid content by drying, the dissolved inorganic salts were also measured, which, of course, cannot be removed by flotation.)

In the preceding example, one only needs to compare the tentative relevance list (Eq. 37.7) with the final five-parametric relevance list (Eq. 37.8) to fully realize the advantage of introducing intermediate quantities in complex interrelations.

37.6.5 Material Systems of Unknown Physical Properties

With foams, sludges, and slimes often encountered in biotechnology, we are confronted with the problem of not being able to list the physical properties because they are still unknown and therefore cannot be quantified. This situation often leads to the opinion that dimensional analysis would fail in such cases.

It is obvious that this is the wrong conclusion. Dimensional analysis is a *method* based on logical and mathematical fundamentals (1,3,4). If relevant parameters cannot be listed because they are unknown, one could hardly blame the method! The only solution is to perform model measurements with the same material system and to change the scale of the model .

37.6.6 Example 5

37.6.6.1 Scale-Up of a Mechanical Foam Breaker. The question posed is about the mode of performing and evaluating model measurements with a given type of mechanical foam breaker (foam centrifuge, sketch in Fig. 37.7) to obtain reliable information on dimensioning and scale-up of these devices. Preliminary experiments have shown that for each foam emergence—proportional to the gas throughput q_G—for each foam breaker of diameter d, a minimum rotational speed n_{min} exists which is necessary to control it (8). The dynamic properties of the foam (e.g. density and viscosity, elasticity of the foam lamella etc.) can neither be fully named nor measured. We will have to content ourselves by listing them wholesale as material properties S_i. In our model experiments we will of course be able to replace S_i by the known type of surfactant (foamer) and its concentration c_f (in ppm).

In discerning the process parameters, we realize that the gravitational acceleration g has no impact on the foam breaking *within* the foam centrifuge. The centrifugal acceleration n^2d exceeds the gravitational one (g) by far! However, we have to recognize that water content of the foam entering the centrifuge depends very much on gravitational acceleration. On the moon, the water drainage would be by far less effective! In contrast to the dimensional analysis presented elsewhere (8), we are well-advised to add g to the relevance list:

$$\{n_{min};\, d;\ \text{type of foamer},\, c_f;\, q_G,\, g\}. \tag{37.10}$$

For the sake of simplicity, in the following n_{min} will be replaced by n and q_G by q. For each type of foamer we obtain the following pi space:

$$\left\{\frac{nd^3}{q}, \frac{n^2d}{g}, c_f\right\} \text{ or abbreviated } \{Y, \mathrm{Fr}, c_f\} \tag{37.11}$$

To prove this pi space, measurements in different-sized model equipment are necessary to produce reliable process characteristics. For a particular foamer (Mersolat H of Bayer AG, Germany) the results are given in Fig. 37.7. They fully satisfy the pi space of Equation 37.11.

The straight line in Fig. 37.7 corresponds to the analytical expression

$$Y = \mathrm{Fr}^{-0.4} c_f^{0.32}$$

which can be put down to

$$n\, d = \text{constant}\, q^{0.2} f(c_f)$$

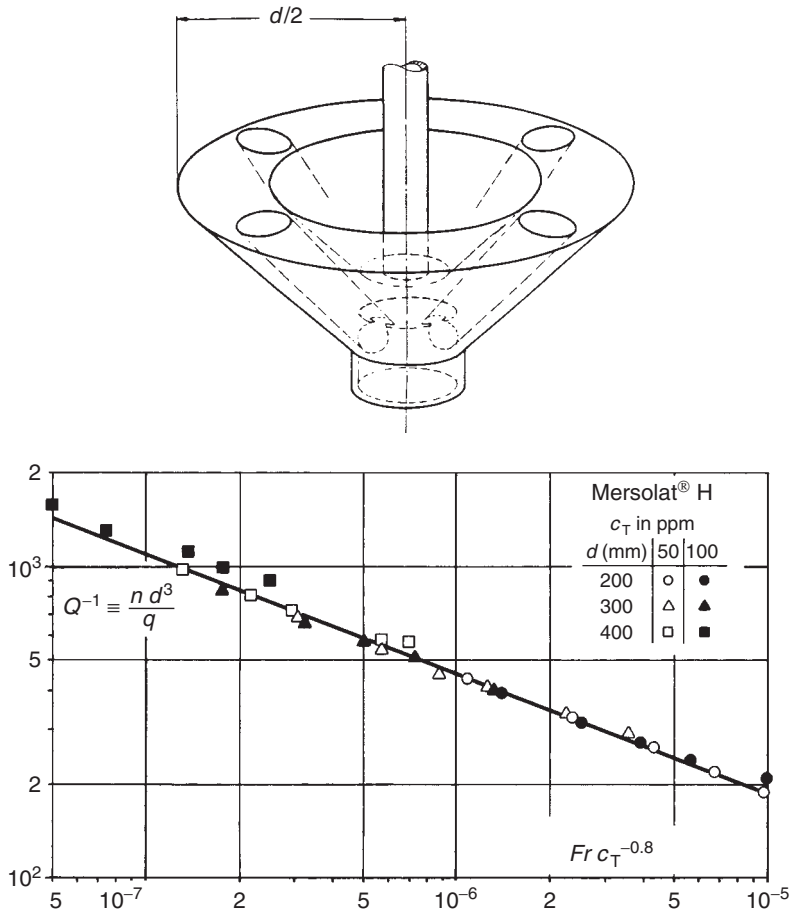


Figure 37.7. Process characteristics of the foam centrifuge (insert) for a particular foamer (Mersolat H, Bayer AG, Germany). [From Ref. 8.]

Here, the foam breaker will be scaled up according to its tip speed $u = \pi nd$ in model experiments, which will also moderately depend on the foam yield (q).

In all the other foamers examined in (8), the correspondence $Y \propto \mathrm{Fr}^{-0.45}$ was found. If the correlation

$$Y \propto \mathrm{Fr}^{-0.5} f(c_\mathrm{f})$$

proves to be true, then it can be deduced to

$$n^2\, d/g = \text{constant } (c_\mathrm{f}).$$

In this case, the centrifugal acceleration ($n^2\ d$) would present the scale-up criterion and would depend only on foamer concentration and not on foam yield (q).

Since the exponent of Fr in the process (Eq. 37.11) exhibits a numerical value of $a = 0.45$ for four foaming agents and $a = 0.40$ for Mersolat $H^{®}$ (8), the numerical value of the constant at Fr = constant can be plotted for all five foaming agents as a function of the foaming agent concentration. In this way, the mechanical stability of foams produced by individual surfactants can be quantified. [It is shown in (8) that the effect of the type of foaming agent on the foam stability is surprisingly low.]

In order to design and scale-up a foam centrifuge of the type presented, measurements with the material system in question would have to be performed by means of an appropriate model appliance. In this manner, the design of the full-scale foam centrifuge presents no problem. Apart from that, these tests and their representation in the sense of Fig. 37.7 give manufacturers of foaming agents a quantifiable assessment of the mechanical stability of the foams produced.

In addition to the information given so far, this example also indicates the following. If material properties of the systems in question are not known, one is compelled (i) to perform the measurements with the given system in differently sized models, that is under change of scale, and (ii) to indicate the chemical or trade name of the product and its concentration instead of its unknown (nor measurable) physical properties.

37.7 SHORT SUMMARY OF THE ESSENTIALS OF THE DIMENSIONAL ANALYSIS AND SCALE-UP

37.7.1 Advantages Gained by Proper Use of Dimensional Analysis

The advantages made possible by correct and timely use of dimensional analysis are as follows:

1. *Reduction of the number of parameters required to define the problem*. The Π theorem states that a physical problem can always be described in dimensionless terms. This has the advantage that the number of dimensionless groups which fully describe it is much smaller than the number of dimensional physical quantities. It is generally equal to the number of physical quantities minus the number of base units contained in them.
2. *Reliable scale-up of the desired operating conditions from the model to the full-scale plant*. Due to the fact that a dimensionless pi space is scale-invariant, two processes may be considered similar to one another if they take place under geometrically similar conditions and all dimensionless numbers which describe the process have the same numerical value.
3. *A deeper insight into the physical nature of the process*. By presenting experimental data in a dimensionless form, one distinct physical state can be isolated from the other (e.g. turbulent or laminar flow region) and the effect of individual physical variables can be identified.
4. *Flexibility in the choice of parameters and their reliable extrapolation within the range covered by dimensionless numbers*. These advantages become clear if one considers the well-known Reynolds number, $\mathrm{Re} = vL/\nu$, which can be varied by altering the characteristic velocity v, or the characteristic length L, or the kinematic viscosity ν. By choosing appropriate model fluids, the viscosity can very easily be altered by several orders of magnitude. Once the effect of the Reynolds number is known, extrapolation of both v and L is allowed within the examined range of Re.

37.7.2 Area of Applicability of Dimensional Analysis

The application of dimensional analysis is indeed heavily dependent on the available knowledge. The following five steps (Fig. 37.8) can be outlined as follows:

1. The physics of the basic phenomenon is unknown. Dimensional analysis cannot be applied.
2. Enough is known about the physics of the basic phenomenon to compile the first, tentative relevance list. The resultant pi set is unreliable.
3. All the relevant physical variables describing the problem are known. The application of dimensional analysis is not problematic.
4. The problem can be expressed in terms of a mathematical equation. A closer insight into the pi relationship is feasible and may facilitate a reduction of the set of dimensionless numbers.
5. A mathematical solution of the problem exists. The application of dimensional analysis is superfluous.

It must, of course, be said that approaching a problem from the point of view of dimensional analysis also remains useful even if all the variables relevant to the problem are not yet known. The timely application of dimensional analysis may often lead to the discovery of forgotten variables or the exclusion of artifacts.

37.7.3 Experimental Methods for Scale-Up

In the introduction a number of questions were posed which are often asked in connection with model experiments.

How small can a model be? The size of a model depends on the scale factor L_T/L_M, and on experimental precision of measurement. Where $L_T/L_M = 10$, a ± 10% margin of error may already be excessive. A larger scale for the model will therefore be chosen to reduce the error.

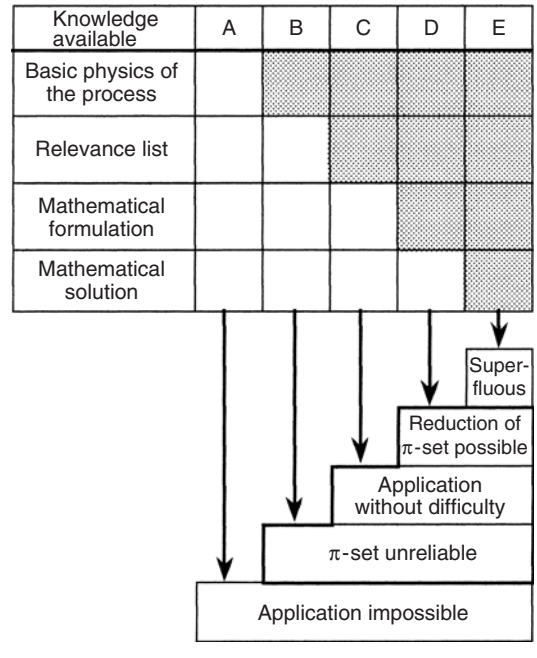


Figure 37.8. Graphical representation of the four levels of knowledge and their impact on the treatment of the problem by dimensional analysis. [After J. Pawlowski. Taken from Ref. 3.]

Is one model scale sufficient or should tests be carried out in models of different sizes? One model scale is sufficient if relevant numerical values of dimensionless numbers necessary to describe the problem (the so-called "process point" in the pi space describing the operational condition of the technical plant) can be adjusted by choosing appropriate process parameters or physical properties of the model material system. If this is not possible, process characteristics must be determined in models of different sizes, or the process point must be extrapolated from experiments in technical plants of different sizes.

When must model experiments be carried out exclusively with the original material system? If a material model system is unavailable (e.g. in the case of non-Newtonian fluids) or relevant physical properties are unknown (e.g. foams, sludges, slimes) model experiments must be carried out with the original material system. In this case, measurements must be performed in models of various sizes (Example 5).

37.7.4 Carrying Out Experiments by Changing the Scale

As a rule, model experiments are carried out in the laboratory in one and the same apparatus. There are certain reasons why this is often inadequate:

1. If you assume that the process in question essentially depends on acceleration due to gravity, g—which cannot be changed on Earth—experiments have to be performed by changing the scale. Relevant examples are scale-up rules for bubble columns as well as for surface aerators in wastewater treatment.
2. If physical properties cannot be varied, one is compelled to perform experiments by a change in the scale in order to vary the operational (process) number. A pertinent example is elaboration of the scale-up rules for a mechanical foam breaker.
3. If laboratory measurements are performed in a single vessel (d = constant) filled with water or a liquid of similar viscosity ($\nu \approx$ constant), one cannot differentiate whether the Reynolds or the Froude number represents the process number. In mixing experiments in which d, ν, and g remained practically constant it follows:

$$\mathrm{Re} \equiv nd^2/\nu \rightarrow \text{constant} \times n$$
$$\mathrm{Fr} \equiv n^2 d/g \rightarrow \text{constant} \times n^2$$

   To find out if the process depends on Re or Fr number or on both of them, one must perform the experiments in differently scaled models.

4. In mass transfer in G/L system in volume aeration, the target number $k_L a$ is an intensively formulated (volume-related) quantity. This implies that process parameters (mixing power P and the gas throughput q) also have to be formulated as intensive quantities. The question occurs whether the gas throughput q has to be related to the liquid volume V as q/V, or to the cross-sectional area S of the vessel as the superficial velocity $v \propto q/S$. To determine this, laboratory measurements have to be performed by a change in the scale.

37.8 TREATMENT OF VARIABLE PHYSICAL PROPERTIES BY DIMENSIONAL ANALYSIS

A complete similarity between a model and its technical realization implies geometric, material, and process-related similarity. The geometric similarity can be realized without a problem in most cases. The same is true of process-related similarity, as could be seen from the examples presented so far. Material similarity can cause difficulties if in model experiments, materials used must be different from those in the technical plant.

The scale invariance of the pi space allows working with different material systems in the model as compared to the industrial scale. This presents one of the essential advantages offered by the scale invariance of the pi space. A lot of conditions of flow in the technical plant can only be scaled down to the model scale when an appropriate model material system has been chosen. This will be clearly shown by the following example:

The Reynolds number for a mixing vessel is given by $\mathrm{Re} \equiv n\, d^2/\nu$. Due to the fact that the scale of length (stirrer diameter d) enters Re with its square, in an essential scale-down, it will also be necessary to diminish essentially, the kinematic viscosity of the liquid in order to work with a reasonable stirrer speed.

The process point of the technical plant is given by

$$d = 1 \text{ m}; n = 1 \text{ s}^{-1} (= 60 \text{ min}^{-1});$$
$$\nu = 1 \times 10^{-4} \rightarrow \mathrm{Re} = 10^4.$$

In a laboratory device which is scaled down by a relatively big scale factor of $\mu = 10{:}1$ and which applies the same fluid ($\nu = 1 \times 10^{-4}$), stirrer speed must have an extreme value of $n = 100 \text{ s}^{-1} (= 6000 \text{ min}^{-1})$ in order to sustain the same flow condition ($\mathrm{Re} = 10^4$). If on the other hand, the measurements are performed with water ($\nu = 1 \times 10^{-6}$), the experiment can be carried out with a reasonable stirrer speed of $n = 1 \text{ s}^{-1} (= 60 \text{ min}^{-1})$.

In this example it is assumed that the liquid is a Newtonian one and the temperature is constant. So physical

properties of the fluid (viscosity μ and density ρ) remain constant.

However, constancy of physical properties cannot be assumed in every physical process. A temperature *field* may generate a viscosity *field* or even a density *field* in the material system treated. In non-Newtonian (pseudoplastic and/or viscoelastic) liquids, a shear rate will also produce a viscosity *field*.

The variability of viscosity is of essential importance in biotechnology in view of the fact that this discipline deals with heterogeneous material systems exhibiting mostly non-Newtonian viscosity behaviors, which often change their properties under shear stress. This is an additional reason for treating this topic more comprehensively here.

37.8.1 Dimensionless Representation of the Material Function

Similar behavior of a certain physical property common to different material systems can only be visualized by dimensionless representation of the material function of that property. This can be achieved by its dimensionless "standard representation".

Figure 37.9 presents the dependence of the dynamic viscosity μ on the temperature T for eight different fluids,

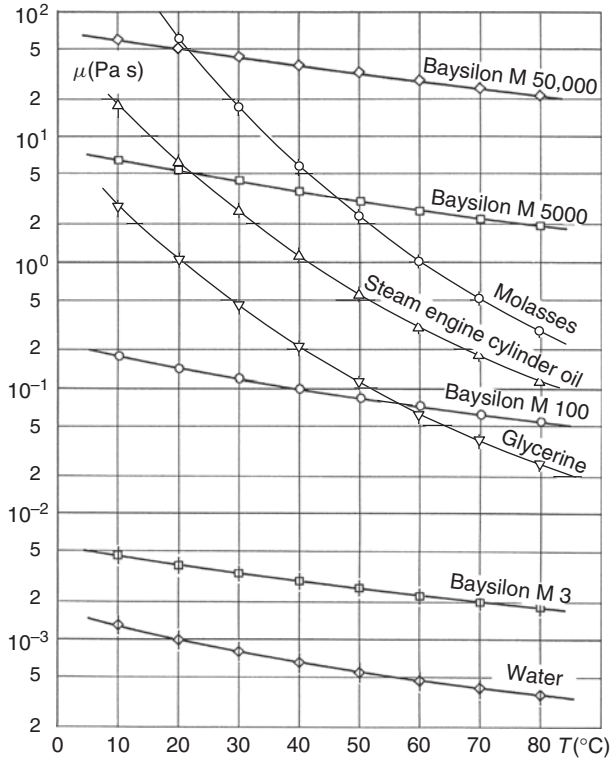


Figure 37.9. The dependence $\mu(T)$ for eight different fluids, which differ strongly in their temperature coefficient of the viscosity [from Ref. 9].

which differ in the viscosity at room temperature for five decades. Five of them show a relatively small temperature dependence of the viscosity (water and 4 Baysilone, the silicone oils of the Bayer AG), the remaining three (glycerin, steam engine cylinder oil, molasses) a pronounced one.

From the representation $\mu(T)$ a similarity between the eight fluids cannot be concluded. To determine this, the dimensional space $\mu(T)$ must be transformed into a dimensionless one. This is possible through a standardization (normalization) of this dependence.

For the purpose, we choose a reference temperature T_0 (preferably the mean temperature of the measuring range), to which a reference viscosity is related. Further on, we determine in the point T_0 the gradient $\Delta\mu/\Delta T$, with which the temperature coefficient of the viscosity

$$\gamma_0 \equiv \left(\frac{1}{\mu}\frac{\partial\mu}{\partial T}\right)_{T_0} < 0$$

is calculated.

By doing this, the dimensional space $\mu(T)$ is widened by three parameters. Now the relevance list

$$\{\mu, \mu_0, T, T_0, \gamma_0\} \tag{37.12}$$

delivers without a problem three dimensionless numbers

$$\{\mu/\mu_0, T/T_0, \gamma_0\Delta T\} \tag{37.13}$$

The following can be realized (Fig. 37.10):

1. With respect to the temperature dependence $\mu(T)$ all investigated fluids behave similarly to each other; they correspond to the same standard representation $\mu/\mu_0 = f(\gamma_0\Delta T)$.
2. The standard representation proves invariant to the reference temperature T_0: The parameter T/T_0 in the equation (Eq. 37.13) has no influence.
3. The fitting curve corresponds to the reference invariant χ function after Pawlowski (10). Water values are described with $\mu = -1.2$ and a logarithmic variance of 5.25×10^{-3}. For all remaining materials $\mu = -0.167$ and the log variance amounts to 1.51×10^{-2}.
4. Water is obviously a special stuff. Its μ/μ_0 values coincide with the other values only in the range near to the reference point (i.e. at $\gamma_0\Delta T \approx 0\pm 1$). Outside this range they deviate stronger.
5. The thinly plotted straight line is a very good approximation of this dependence in the range near the reference point (at $\gamma_0\Delta T \approx 0 \pm 1$). This is the engineering representation of the temperature dependence of the viscosity of a liquid $\ln(\mu/\mu_0) = \exp(\gamma_0\Delta T)$.

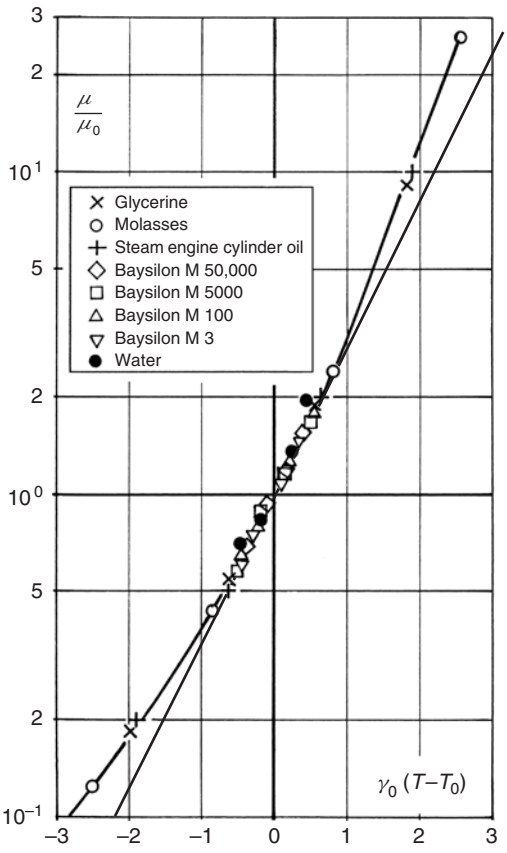


Figure 37.10. Standard representation $\mu/\mu_0 = f(\gamma_0 \Delta T)$ for fluids from Fig. 37.9. Reference temperature $T_0 = 50^\circ$C. The fitting curve corresponds to reference invariant χ-function [details in (10)].

Due to the equivalence between μ/μ_0 and $\gamma_0 \Delta T$ the quotient μ/μ_0 is preferably used in the engineering literature as the viscosity number $Vis \equiv \mu_w/\mu$ (μ_w is wall viscosity, μ is bulk viscosity); see the heat transfer characteristics given in Fig. 37.17.

In this way, variable physical properties are treated. In (3) the dependence of the density on temperature, the dependence of the particle strength on the particle diameter, the dependence of the diffusion coefficient of a polymer mass on temperature and on moisture content are presented and discussed.

37.8.2 Rheological Standardization Functions

In Newtonian liquids, it is the dynamic viscosity μ (Pa s), which combines the shear stress τ (Pa) with the shear rate $\dot{\gamma}(s^{-1})$ in the rheological equation of state

$$\tau = \mu \, \dot{\gamma} \tag{37.14}$$

μ is a constant, depending only on material and temperature.

In non-Newtonian fluids μ depends on the actually effective shear rate $\dot{\gamma}$ and occasionally also on history. Such fluids are subdivided into classes according to their flow behavior, only two of which—pseudoplastic and viscoelastic ones—are treated in the following.

37.8.3 Flow Behaviour of Non-Newtonian Fluids of the Type Pseudoplastic Fluids

Pseudoplastic ("shear-thinning") fluids are those in which stress viscosity is *decreased* due to shear. Under shear stress solid aggregates of a dispersion L/S (e.g. dye pigments) or L/L decompose into single particles, which then orientate themselves toward flow direction. Intermingled chains of macromolecules of a polymer solution or melt are stretched to the flow direction; spheres of erythrocytes of blood are elongated. In all these cases, the viscosity is decreased due to shear.

The rheological material function $\mu(\dot{\gamma})$ is formulated in a dimensionless way with material standardization parameters μ_0 or μ_∞ (or similar) and $\dot{\gamma}_0$ or $\dot{\gamma}_\infty$ (or similar) and transformed into a rheological standardization function:

$$\mu/\mu_0 = f(\dot{\gamma}/\dot{\gamma}_0) \tag{37.15}$$

Liquids whose rheological equation of state coincide in this dimensionless frame—whose standardization functions are identical—are rheologically similar to one another.

An important subclass of pseudoplastic fluids consists of those fluids whose material function is represented in the whole measured range in a log–log scale by a straight line with a negative slope. In this case, one speaks of an *Ostwald–de Waele* Fluid, whose viscosity curve obeys the so-called *"power law"* (K being consistency index, m the flow index):

$$\mu_0 \, \dot{\gamma}_0^{1-m} = K \;\rightarrow \tau = K \, \dot{\gamma}^m \rightarrow \mu_0 = K \, \dot{\gamma}^{m-1} \tag{37.16}$$

To demonstrate this flow behavior in the form of a standardization function, $\dot{\gamma}_0$ is arbitrarily chosen and μ_0 assigned to it. This degree of freedom facilitates the choice of reference points for the standardization of the material function.

Pawlowski (4) has already pointed out that Equation 37.16 is against the principle of consistency of physical quantities because the dimension of $[K] = ML^{-1}T^{m-2}$ depends on the numerical value of exponents. This brings about that in the case of a temperature-dependent viscosity in a temperature field, the quantity K changes its dimension from point to point and therefore neither *grad* K nor K/K_0 can be built.

Physical consistency of Equation 37.16 remains preserved if it is transformed by Equation 37.15 to the relationship

$$\mu/\mu_0 = f(\dot{\gamma}/\dot{\gamma}_0)^{m-1} \tag{37.17}$$

whereas K is eliminated.

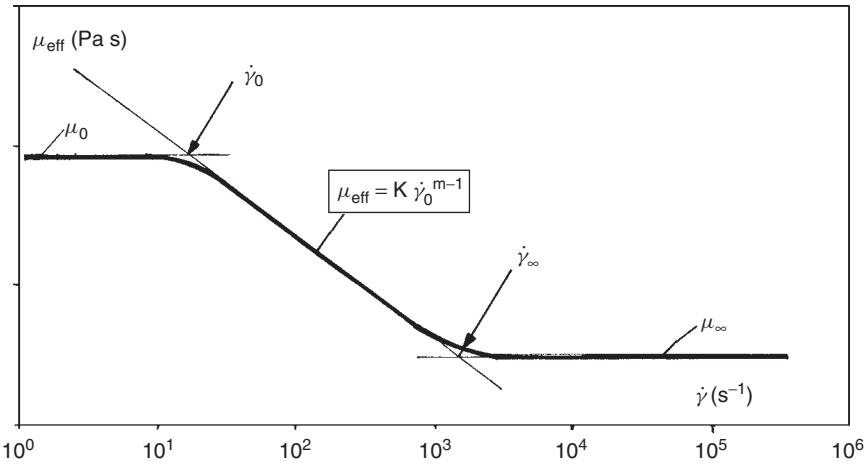
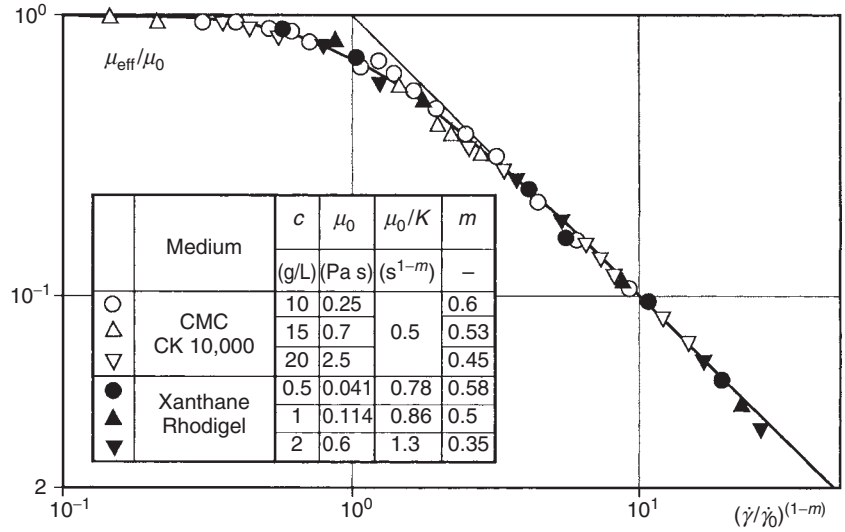


Figure 37.11. Principal course of viscosity of a pseudoplastic fluid which in a certain $\dot{\gamma}$ range behaves like an *Ostwald–de Waele* Fluid.



	Medium	c (g/L)	μ_0 (Pa s)	μ_0/K (s^{1-m})	m –
○	CMC CK 10,000	10	0.25	0.5	0.6
△		15	0.7		0.53
▽		20	2.5		0.45
●	Xanthane Rhodigel	0.5	0.041	0.78	0.58
▲		1	0.114	0.86	0.5
▼		2	0.6	1.3	0.35

Figure 37.12. Dimensionless standardization functions of some pseudoplastic fluids (11). For the meaning of $\dot{\gamma}$ refer Fig. 37.11.

In most pseudoplastic fluids at sufficiently low and sufficiently high shear rates $\dot{\gamma}$ Newtonian flow behavior can be observed (Fig. 37.11). Viscosity approaching a constant value with low shear rates is called zero-shear viscosity, μ_0, and its constant value at very high shear rates is called the infinite shear viscosity, μ_∞. Classic model fluids of this type are aqueous solutions of macromolecular organic compounds as for example carboxy-methyl-cellulose (CMC), poly-acryl-amide (PAA), Carbopol (very sour acrylic acid polymerisates of Goodrich Co.), but also of biopolymers such as Xanthane.

In mixing vessels, shear rates usually appear in the range of $\dot{\gamma} = 50\text{–}500\ s^{-1}$ in which many pseudoplastic fluids behave like *Ostwald–de Waele* Fluids. This explains why the "power law" is often used to describe the rheological behavior.

In these pseudoplastic fluids, the rheological standardization function can be presented in the pi space

$$\{\mu/\mu_0,\ \dot{\gamma}/\dot{\gamma}_0, \Pi_{rheol}\} \text{ or } \{\mu/\mu_\infty,\ \dot{\gamma}/\dot{\gamma}_\infty, \Pi_{rheol}\}$$

In the publication of Henzler (11), $\dot{\gamma}_0/\dot{\gamma}_\infty$ is represented by the exponent m of the straight line, which stands for an upsetting/stretching of the course of the curve belonging to the power law. In Fig. 37.12, CMC and Xanthane solutions of various concentrations are correlated in this pi space.

These materials are obviously not thoroughly similar to one another. They would be, if the exponent m were

constant and the dependences could be correlated in the space $\mu/\mu_0 = f(\dot{\gamma}/\dot{\gamma}_0)$. Here, the exponent varies by factor two: $m = 0.35–0.6$.

In the introduction to this chapter it was pointed out that the importance of the rheological standardization function consists in recognizing materials which are similar to one another and thus build a class of material belonging to a common master curve, and are therefore suitable as model substances. Figure 37.13 presents a class of aqueous PAA solutions of different concentrations which correlate excellently with one another in the space

$$\mu/\mu_0 = f(\dot{\gamma}/\dot{\gamma}_0).$$

The finding and working out of model substances of a family of those building a master curve is a task of prime importance when model measurements are necessary for dimensioning a process in which non-Newtonian fluids take place.

37.8.4 Flow Behaviour of Non-Newtonian Fluids of the Type Viscoelastic Fluids

In viscoelastic fluids, the distortion work performed by shear stress is not completely, immediately, and irreversibly transformed into friction heat but partially elastically stored in order to relax with delay. In this respect they are similar to solids. The liquid strains give way to the mechanical shear stress as do elastic bonds by contracting. This is shown in shear experiments as a restoring force acting against the shear force which, at the sudden ending of the effect of force, moves back the plate to a certain extent. In mixing a viscoelastic fluid it climbs up the stirrer shaft, in order to evade the shear stress which the rotating stirrer shaft exerts on the liquid on its surface ("Weissenberg phenomenon") [Example 17 in (3)].

For dimensionless presentation of viscoelastic behavior of a fluid normally the ratio of normal stress N_1 to shear stress τ is used. The so-called Weissenberg number Wi is defined as

$$\mathrm{Wi} \equiv N_1/\tau \tag{37.18}$$

The material function of a viscoelastic fluid is presented in space $\mathrm{Wi}(\dot{\gamma})$ the standardization function here is $\mathrm{Wi}/Wi_0 = f(\dot{\gamma}/\dot{\gamma}_0)$.

On the right side of Fig. 37.12 the correspondence $(\psi_1 \equiv 2\ \psi_2)\dot{\gamma}_0/\mu_0 = f(\dot{\gamma}/\dot{\gamma}_0)$ is shown. This figure does not represent a standardization function. The proof of similarity for two material functions (congruence separately for each kind of function as well as for its relative position to each other) can only be obtained if these functions refer to quantities of equal dimension. Material functions $(\psi_1 \equiv 2\ \psi_2) = f(\dot{\gamma})$ do not fulfill the condition of congruence of the relative position to the corresponding material functions. Only after the transformation to $(\varphi_1 \equiv 2\ \varphi_2) = f(\dot{\gamma})$ with $\varphi \equiv \psi/\dot{\gamma}$, it follows that the fluids in Fig. 37.13 can really be used as model substances to one another [details in (13)].

37.8.5 Process Equations for Non-Newtonian Fluids

In the introduction to this chapter it was already pointed out that certain parameters of the rheological normalization functions have to be included into the relevance list of a given process in order to be assured that the process equation is also valid for the treatment of non-Newtonian

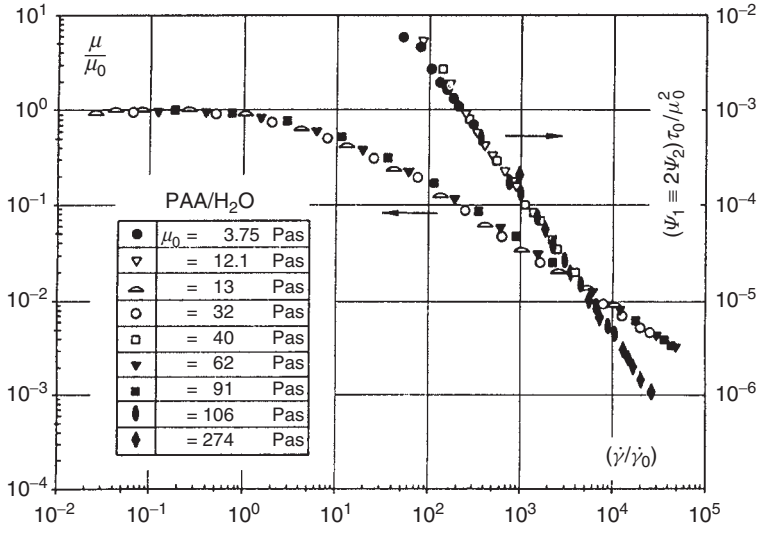


Figure 37.13. Master curves μ/μ_0 and $(\psi_1 \equiv 2\psi_2)\dot{\gamma}_0/\mu_0 = f(\dot{\gamma}/\dot{\gamma}_0)$, respectively, for a class of aqueous PAA solutions of different concentrations and viscosities [from Ref. 12].

liquids. This will be shown here with some examples from mechanical and thermal process engineering in connection with pseudoplastic and viscoelastic fluids.

Unfortunately, it is still current engineering practice to formulate the process number Re according to the Metzner–Otto concept (14) with a so-called effective viscosity μ_{eff} as $\text{Re}_{\text{eff}} \equiv v\ l\rho/\mu_{\text{eff}}$. and to ignore clear dimensional analytical rules for non-Newtonian fluids (3,4). This fact makes it necessary to discuss this quantity first. [A detailed critical argument with this concept is given in 12,15).]

37.8.6 Concept of the Effective Viscosity μ_{eff} According to Metzner–Otto

This concept has been developed in association with the determination of the stirrer power in a non-Newtonian liquid (14). It is assumed that in the immediate surroundings of the stirrer, a representative shear rate $\dot{\gamma}_{\text{MO}}$ exists, which is proportional to the stirrer speed, n:

$$\dot{\gamma}_{\text{MO}} = k_{\text{MO}} n \tag{37.19}$$

k_{MO} is a constant, depending only on the type of stirrer and on geometric conditions in the stirring vessel. The determination of $\dot{\gamma}_{\text{MO}}$ proceeds as follows:

1. A stirrer arrangement is used for which the power characteristics Ne (Re) for Newtonian liquids is known.
2. Using the non-Newtonian fluid, the stirrer power is determined for some stirrer speeds and the Ne numbers are calculated.
3. With these Ne values the corresponding Re values are taken from the Ne (Re) correlation for Newtonian liquids.
4. With these Re values the effective viscosity μ_{eff} is determined.
5. From the flow curve $\mu = f(\dot{\gamma})$ of the used liquid the representative shear rate $\dot{\gamma}_{\text{MO}}$ is found.

The concept of "effective viscosity" is well-known in rheology. For the "viscosimetric flow" in a capillary viscosimeter it is theoretically justified, but it is valid only for creeping flow and fluids without viscoelastic properties. In case of a mixing vessel, we deal with a *field quantity* which cannot even describe the flow behavior in the immediate surroundings of the stirrer where the power is dissipated (Fig. 37.14).

37.8.7 Process Equations for Mechanical Processes with Non-Newtonian Fluids

In a relevance list of a process, there is no place for field variables such as μ_{eff}, because these are results and not arguments known in advance. These can only be the rheological normalization parameters μ_0, $\dot{\gamma}_0$, $N_{1,0}$ etc.

As it has already been pointed out with regard to the pi space, the transition from a Newtonian to a non-Newtonian fluid requires the following consequences:

1. All pi numbers of the Newtonian case also appear in the non-Newtonian case, whereby instead of μ the normalization parameter of the same dimension, mostly μ_0, appears.

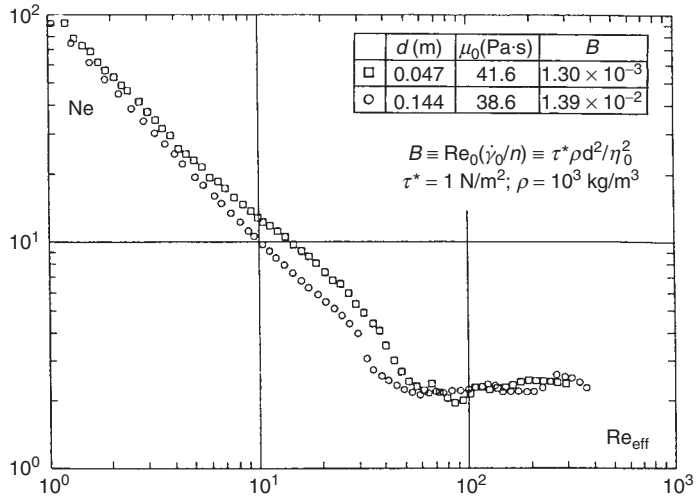


Figure 37.14. Power characteristics of a turbine stirrer ($D/d = 2$, $h/d = 1$) under geometrically similar conditions in two mixing vessels of different size, $\mu \approx 1{:}3$. The employed aqueous PAA solutions have practically the same viscosity. [From Ref. 12]. Re_{eff}, is built with μ_{eff} according to Metzner–Otto. $\tau* = 1$ Pa.

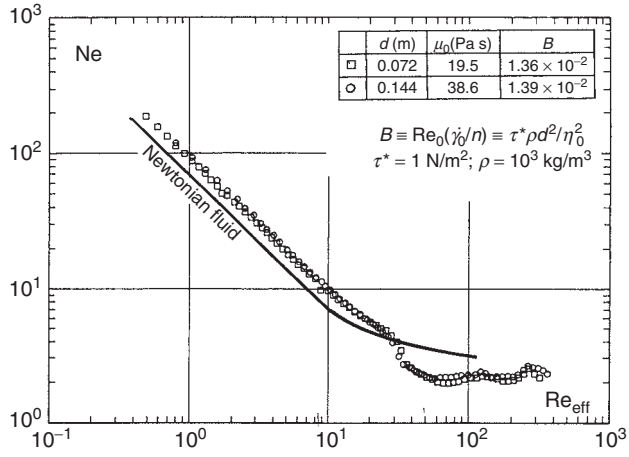


Figure 37.15. Power characteristics $Ne(Re_{eff})$ of a turbine stirrer as in Fig. 21 determined in two geometrically similar mixing vessels of different shape (scale-up factor $\mu = 2.0$) with two aqueous PAA solutions of adopted viscosity (B = idem). [From 12.]

2. An additional pi number appears which contains the normalization parameter, mostly $\dot{\gamma}_0$.
3. Pure material numbers are increased by $\Pi_{rheol} = m, Wi_0$ etc.

The power characteristics of a stirrer in a Newtonian liquid was produced from the relevance list

$$\{P; d, \rho, \mu, n\}$$

and leads to the dimensionless dependence

$$\mathrm{Ne} = f(\mathrm{Re}) \text{ with } \mathrm{Ne} \equiv P/(\rho\, n^3 d^5) \text{ and } \mathrm{Re} \equiv n\, d^2\rho/\mu$$

In a pseudoplastic liquid, both normalization parameters $\dot{\gamma}_0$ und μ_0 have to be introduced. This means that the relevance list is enlarged by $\dot{\gamma}_0$ and μ is replaced by μ_0:

$$f(P; d, \rho, \mu_0, \dot{\gamma}_0, n) = 0 \tag{37.20}$$

Therefore, the pi set is enlarged with regard to Equation 37.2 by one pi number

$$\mathrm{Ne} = f(R_0, Q) \text{ with } \mathrm{Re}_0 \equiv n\, d^2\rho/\mu_0 \text{ and } Q \equiv \dot{\gamma}_0/n \tag{37.21}$$

Because both process numbers Re_0 and $Q \equiv n/\dot{\gamma}_0$ contain stirrer speed, it is advisable to combine them in a way that the stirrer speed is eliminated. The number consequently produced, B, is identical to the Hedström number He, where μ_0 is related to the liquids exhibiting the yield stress, τ_0:

$$B \equiv \frac{\mathrm{Re}_0}{n/\dot{\gamma}_0} \equiv \frac{d^2\rho\dot{\gamma}_0}{\mu_0} \equiv \frac{d^2\rho\tau_0}{\mu_{0^2}} \tag{37.22}$$

Thus it follows:

$$\mathrm{Ne} = f(R_0, B) \tag{37.23}$$

Due to the correspondence $d^2 \propto \mu_0^2$ in Equation 37.22, in doubling the scale (here the stirrer diameter d) the viscosity also has to be doubled. Fig. 37.15 documents that at B = idem the function $\mathrm{Ne} = f(\mathrm{Re}_{eff})$ has an identical course in differently shaped vessels.

37.9 DIMENSIONAL ANALYTICAL TREATMENT OF HEAT TRANSFER PROCESSES

37.9.1 Driving Force and the Target Quantity of the Process

At first, it is to be pointed out that heat transfer is normally an indirect process. In the case of cooling, for example, the part which receives heat is divided by a wall from the part where heat is produced. We deal with three different heat transfer steps, two of which belong to heat transfer by convection (under obviously different conditions) and the third one is heat conduction through a solid wall.

In the following, we will investigate only that part of the mixing vessel where a reaction takes place and the reaction heat produced has to be removed through the wall. The driving force of the process is the temperature difference ΔT between both spaces separated by the wall because the temperature stands for energy levels of the systems which are to be equalized.

The target quantity of this process is heat transfer coefficient at the inner wall, h. It can be regarded as the heat conductivity, k, in the boundary layer, divided by its thickness, δ that is, $h = k/\delta$. Because of the unknown δ, h is not measurable. It can only be calculated from the general heat transfer equation by using it as the determining equation for h:

$$h \equiv Q/A\Delta T.$$

(Q is heat flow through the heat exchanger area, A)

37.9.2 Steady-State Heat Transfer in Mixing Vessels

The pi space of the heat transfer characteristics of a mixing vessel is obtained by the following relevance list:

Target quantity: heat transfer coefficient at the inner wall, h

Geometric parameters: vessel and stirrer diameters: D, d

Material parameters: density ρ; viscosity of liquid bulk, μ, and at the inner wall, μ_w; heat capacity, C_p; heat conductivity, k

Process parameter: stirrer speed, n.

The complete nine-parametric relevance list reads as follows:

$$\{h; D, d; \rho, \mu, \mu_w, C_p, k; n\} \tag{37.24}$$

Here two characteristic lengths were introduced. D stands for that geometric part of the device where the heat is transferred (in the case of cooling coils, coil diameter D_c had to be introduced instead), whereas d is the stirrer diameter which together with n governs the hydrodynamics of the vessel.

This nine-parametric relevance list leads to $9-4 = 5$ dimensionless numbers, the fourth base dimension being the temperature Θ:

$$\{\text{Nu, Pr, Re, Vis}, D/d\} \tag{37.25}$$

where:

$\text{Nu} \equiv hD/k$–Nusselt number, the target number
$\text{Pr} \equiv C_p\mu/k$–Prandtl number, pure material number
$\text{Re} \equiv nd^2\rho/\mu$–Reynolds number, the process number
$\text{Vis} \equiv \mu_w/\mu$–Viscosity ratio
D/d–Wall clearance, the geometric number

Figure 37.16 shows the dependence (Eq. 37.25) for an anchor stirrer with two arms and a close wall clearance ($D/d = 1.02$). The figure consists of two parts representing the same measuring results in two different pi spaces: above as $\text{Nu} = f$ (Re), below as $\text{Nu} = f$ (Re, Pr).

A comparison of both representations verifies that the consideration of the Prandtl number by $Pr^{1/3}$ starts gaining weight increasingly from about $\text{Re} > 200$; in the range $\text{Re} < 200$ its contemplation is rather negative. [For the heat transfer from tube wall to the fluid flowing under laminar conditions, Levêque (16) found that the heat transfer coefficient h is proportional to the third root of the shear rate at the wall.]

The scattering of the measuring data in the range of $\text{Re} < 200$ is well-founded by the measuring technique applied here. The mean bulk temperature in the vessel in the laminar flow region could not be measured with a thermometer because an insulating border layer was formed round its wall. In this range, the average temperature of the bulk liquid had to be calculated from the heat balance. In the range $Re > 200$ the correspondence between the calculated and measured values was approximately 10% (9).

The fitting lines in the lower figure verify the following dependences:

$$\text{Re} > 200 : \text{Nu} = 0.28\ \text{Re}^{2/3}\ \text{Pr}^{1/3} \tag{37.26}$$

$$\text{Re} < 200 : \text{Nu} = 0.8\ \text{Re}^{1/3}\ \text{Pr}^{1/3} = 0.8\ \text{Pe}^{1/3} \tag{37.27}$$

This is compulsory. If in the creeping flow range ($\text{Re} < 200$) the influence of the Prandtl number is considered by $\text{Pr}^{1/3}$, then the Reynolds number must also have the same exponent. Only then the result is a number (Peclet number Pe) which does not contain the liquid viscosity and the liquid density ρ is combined with the *mass* related

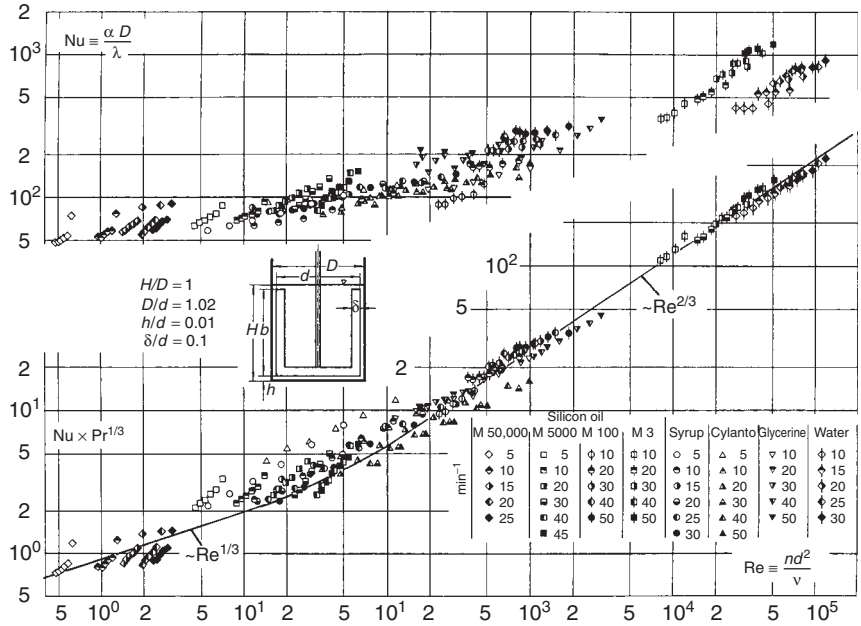


Figure 37.16. Heat transfer characteristics of a mixing vessel with an anchor stirrer with two arms and $D/d = 1.02$ [from Ref. 9].

heat capacity C_p to produce the *volume*-related one. In the creeping flow range liquids behave like solids and then neither viscosity nor density affect heat transfer:

$$\mathrm{Pe} \equiv \mathrm{Re} \cdot \mathrm{Pr} \equiv n\, d^2 \rho C_p / k \equiv n\, d^2 / a$$

$a \equiv k/(\rho C_p)$ means thermal conductivity.

Judat, in (5), investigated heat transfer in a mixing vessel with an anchor stirrer with four arms equipped with wipers ($D/d = 1$). With the wipers, the liquid border layer at the wall is completely removed. As a result, the Nu values ($\hat{=}$ α_i values) in the creeping flow area are increased by a full decade and, in addition, the creeping flow range expands up to $\mathrm{Re} = 2 \times 10^3$ because the stirrer beams dip into the laminar border layer. Here, too, $Nu \propto Pe^{1/3}$ holds.

Delaplace *et al*. (17) studied heat transfer in a vessel ($D = 0.346$ m) equipped with an Ekato-PARAVISC stirrer ($d = 0.32$ m, $D/d = 1.08$) and found for Newtonian as well as for non-Newtonian liquids the same heat transfer equations (Fig. 37.17):

$$\mathrm{Re} > 200 : \mathrm{Nu} = 0.27\ \mathrm{Re}^{2/3}\mathrm{Pr}^{1/3}\ \mathrm{Vis}^{-0.14} \qquad (37.28)$$

$$\mathrm{Re} < 200 : \mathrm{Nu} = 1.59\ \mathrm{Pe}^{1/3}\ \mathrm{Vis}^{-0.14} \qquad (37.29)$$

The fact that no difference was found between heat transfer in Newtonian and in non-Newtonian liquids (fluids of the pseudoplastic and yield stress type were investigated and their viscosity considered according to the Metzner–Otto concept), verifies that non-Newtonian fluid behavior affects only the turbulent flow region. A comparison of process equations between the Paravisc stirrer and the old-fashioned anchor stirrer (at $D/d \simeq$ similar) shows that the Paravisc stirrer delivers better heat transfer values only in the creeping flow area ($\mathrm{Re} < 200$) by a factor of 2. But in the turbulent region every stirrer delivers the same results!

In the optimization of stirrers to achieve the optimum heat removal in a cooling process, it should not be forgotten that the removable heat flow, Q [kW], increases in the range of $\mathrm{Re} > 200$ (in technical mixing vessels $\mathrm{Re} < 100$ is seldom achieved) according to the heat transfer characteristic with $\mathrm{Re}^{2/3} \propto n^{2/3}$, whereas the thereby associated stirrer power ($\hat{=}$ stirring heat) increases substantially over-proportionally according to the power characteristic of the stirrer with P [kW] $\propto n^3$. Thus it follows that there is an optimum stirrer speed at which the maximum process heat such as chemical reaction heat, R, can be removed:

$$R + Q - P$$

Figure 37.18 illustrates this situation with a concrete example. It shows that the optimum range with respect to the stirrer speed is very flat, 90% of the maximum value being removed in the range $n_{opt} = 20\ \mathrm{min}^{-1} \pm 60\%$.

To compare an anchor stirrer (at $D/d = 1.02$) with Ekato-PARAVISC stirrer (at $D/d = 1.08$), their power characteristics have to be taken into account. In the range of $\mathrm{Re} < 100$ they read:

Anchor stirrer: $\mathrm{Ne} \times \mathrm{Re} = 420$

Ekato-PARAVISC stirrer: $\mathrm{Ne} \times \mathrm{Re} = 250$

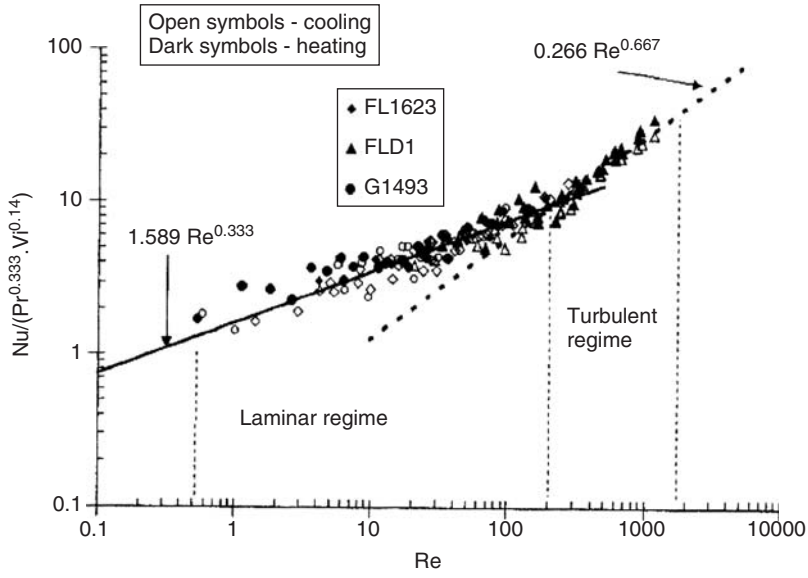


Figure 37.17. Heat transfer characteristics of a mixing vessel equipped with an Ekato-PARAVISC stirrer ($D/d = 1.06$) and measured with three different Newtonian fluids. Open signs stand for cooling, dark ones for heating [from Ref. 17].

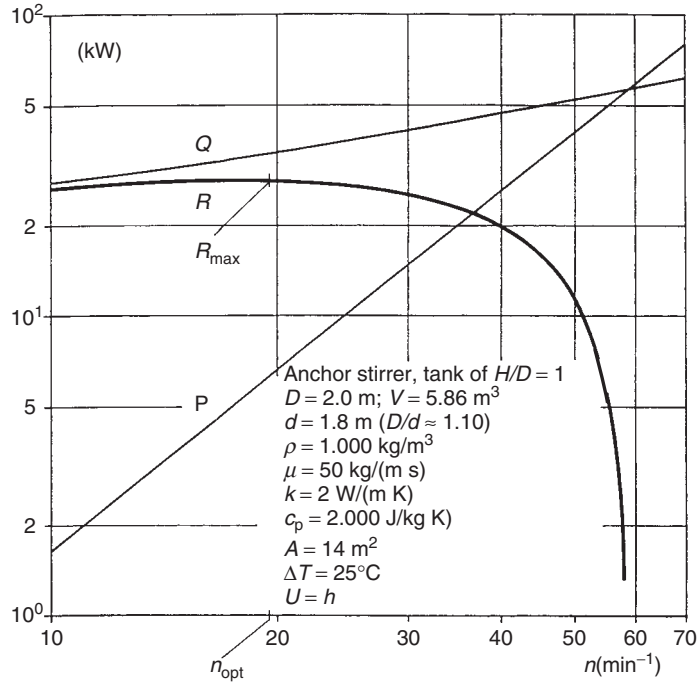


Figure 37.18. Graphical representation of the course of $R \equiv Q - P$ as a function of the stirrer speed n for the example given in the plot [from Ref. 18].

For Re > 100 see (5) and (17). Obviously, the Paravisc stirrer is more suitable than the anchor stirrer for heat removal. The reason for this advantage lies possibly in the pumping action of the stirrer, with which the liquid is more effectively removed from the wall.

37.10 DIMENSIONAL ANALYTICAL TREATMENT OF MASS TRANSFER PROCESSES

37.10.1 Driving Force and Target Quantities of the Process

In mass transfer processes, mass is transferred from one phase to the other through an interface. This can be either solid (dissolution in the systems S/L) or a fluid one: L/L, G/L (absorption and desorption processes). In the first case, the interface is known, in the second case the fluid interface is neither known nor measurable. This distinction has a big impact on dimensional analytical treatment of the process.

In mass transfer, the driving force consists of the removal of an equilibrium disturbance and concerns a thermodynamic quantity; namely, the chemical potential μ.

It is often presumed that the leveling out of concentration differences between two phases is the cause for mass transfer. That is not the case. This fact can easily be demonstrated with a number of examples. It should suffice to remark that a material system consisting of granular cooking salt in saturated aqueous solution is in equilibrium. The chemical potential in both phases is equal, but the concentration of NaCl in granular cooking salt is 100%, whereas in the saturated aqueous solution it is only 26.4% (at 20°C).

The bridge between the chemical potential, which is very difficult to determine, and the concentration difference, which is easily determined, was erected by Lewis and Whiteman in 1923/24, who postulated in their "Two Film Theory" (with regard to the system G/L) the following:

1. On both sides of the interface, laminar boundary layers exist which the gas can pass only by *diffusion*.
2. In the interface, the thermodynamic equilibrium immediately occurs.

In the material system G/L, the transfer from the gas phase to the interface can be neglected because it is by at least 50% faster than the transfer from the interface through the laminar liquid boundary layer to the bulk of a liquid. If, as postulated, a thermodynamic equilibrium always exists in the interface then also the saturation concentration c_s of the gas is always present. Under these conditions the driving force of mass transfer is in fact given by concentration difference:

$$\Delta c = c_s - c \tag{37.30}$$

Thus the general mass transfer equation is given by the following relationship:

$$G = k_L\ A\ \Delta c \tag{37.31}$$

where:

G [kg gas/s] –	mass transfer rate through the interface
A [m^2] –	interfacial area (e.g. the sum of the surfaces of all gas bubbles)
k_L [m s^{-1}] –	liquid-side mass transfer coefficient
Δc [kg m^{-3}] –	characteristic concentration difference of the dissolved gas between the interface and the liquid bulk

k_L can physically be comprehended as $k_L \propto D/x_L$, where D is the diffusion coefficient of the gas in the liquid-side laminar boundary layer of thickness x_L. Thus k_L represents a definition quantity, which is as little measurable as the interfacial area A. Both of them are influenced by the kinematics of the process and by material conditions. In surface aeration, they are combined into only one quantity, which can easily be determined by constituents of the overall mass transfer (Eq. 37.31):

$$k_L A \equiv G/\Delta c \tag{37.32}$$

$k_L A$ represents the target quantity of mass transfer in *surface aeration*.

In volume (bulk) aeration it is assumed that the process takes place in a liquid which is turbulently mixed and thus an equal number of gas bubbles of an equal size exist in each volume element. Under these circumstances, it is advisable to formulate the general mass transfer equation (Eq. 37.31) as a volume-related one:

$$G/V = k_L(A/V)\Delta c \tag{37.33}$$

(This contains an additional advantage because Δc, too, is a volume-related quantity per definition.) A/V is abbreviated to $a \equiv A/V$ and since it is not measurable, combined with k_L to the "overall liquid-side mass transfer coefficient" $k_L a$:

$$k_L a \equiv G/(V\,\Delta c) \tag{37.34}$$

$k_L a$ is easily measured by Equation 34 and represents the target quantity of mass transfer in *bulk aeration*.

From the point of view of dimensional analysis, there is a considerable distinction between the two target quantities $k_L A$ and $k_L a$.

$k_L A$ is an extensively defined quantity, which therefore must compulsorily depend on extensive parameters like the stirrer diameter d and the stirrer speed n.

$k_L a$, in contrast, is a volume-related, intensive quantity, which therefore must compulsorily depend on intensively formulated process parameters like power per liquid volume P/V and gas throughput q per aerated cross-sectional area S, the so-called superficial velocity, $v \propto q/S$.

37.10.2 Mass Transfer G/L in Surface Aeration

The supply of atmospheric oxygen to municipal sewage purification plants has been performed for decades by turbine surface aerators installed in the liquid surface of shallow wastewater treatment ponds (H $\leq$ 4 m). The stirrers work as water pumps: they suck in waste water, spray it over the liquid surface and, in addition, they whirl it up. In this way the mass transfer G/L is effected.

Target quantity: mass transfer coefficient in surface aeration, $k_L A$

Geometric parameter: diameter of the turbine stirrer, d

Material parameters: density and kinetic viscosity of the liquid, ρ, ν

Process parameters: stirrer speed of the turbine, n acceleration due to density, g

The acceleration due to gravity, g, is essential in this process because it influences the parabolic throw of the ejected liquid. Two further possible parameters, the diffusion coefficient D and the surface tension σ, will be renounced, because in wastewater treatment the only liquid of interest is water. Thus the constricted relevance list reads:

$$\{k_L A;\, d;\, \rho,\, \nu, n,\, g\} \tag{37.35}$$

This six-parametric set delivers the following three dimensionless numbers:

$(k_L A)^* \equiv \dfrac{G}{d^3\ \Delta c}\left(\dfrac{\nu}{g^3}\right)^{1/3}$ sorption number

$\mathrm{Re} \equiv nd^2/\nu$ Reynolds number

$\mathrm{Fr} \equiv n^2 d/g$ Froude number

To ensure that the only variable process parameter, n, does not appear in both process numbers (Fr and Re), we first determine which of the two process numbers is essential, and then we free the other one by combining it with the first one from n.

The process takes place in water, and the state of flow will be a turbulent one. Hence, Re cannot play an important role. The process will be governed essentially by the Froude number. We will combine Re with Fr and obtain

$$\mathrm{Ga} \equiv \frac{\mathrm{Re}^2}{\mathrm{Fr}} \equiv \frac{d^3 g}{\nu^2} \quad \text{Galilei number}$$

Thus, the pi space reads:

$$\{(k_L A^*, \mathrm{Fr}, \mathrm{Ga}\} \tag{37.36}$$

Due to the circumstance that the second essential parameter, acceleration due to gravity, g, cannot be varied on Earth, measurements must be performed with measuring devices of different scale. (This is the only way to decouple Fr and Re.)

The process equation for a turbine stirrer ("Rushton turbine"), the disk of which was installed in the water surface, reads:

$$(k_L A)^* = 1.41 \times 10^{-4}\mathrm{Fr}^{1.205}\mathrm{Ga}^{0:115}$$
$$\mathrm{Fr} = 0.02 - 0.34;\ \mathrm{Ga} = 1.5 \times 10^9 - 2 \times 10^{11}$$

The investigated range of the scale-up factor was $\mu = 1{:}5$; details in (19).

37.10.3 Mass Transfer G/L in Bulk Aeration in Mixing Vessels

There are a number of chemical and biotechnological reactions between gas (G) and liquid (L) which take place in mixing vessels: hydrogenation, oxydation, chlorination, phosgenization, aerobic bioconversion. The relevance list for this operation reads as follows:

- Target quantity: volume-related mass transfer coefficient, $k_L a$
- Geometric parameters: none
- Material parameters: density and kinetic viscosity of the liquid, ρ, ν diffusivity of the gas in the liquid, D bubble coalescence behaviour of the liquid, S_i
- Process parameters: volume-related mixing power, *P/V* superficial velocity of the gas, v gravitational acceleration, g

Here, some remarks are to be made: first, despite extensive research, bubble coalescence phenomena have still not been clarified to such an extent as to permit explicit formulation of the coalescence parameters (5). In the following, they will be taken into consideration in a lump as S_i. Second, the decision in favor of *P/V* and v instead of *P/V* and *q/V* is based on extensive research results (Fig. 37.19).

We start from the relevance list:

$$\{k_L a, \rho, \mu, D, S_i, P/V, v, g\} \tag{37.37}$$

and obtain the pi space

$$\{(k_L a^*, (P/V)^*, v^*, \mathrm{Sc}, S_i^*\} \tag{37.38}$$

where:

$(k_L a)^* \equiv k_L a \left(\frac{v}{g^2}\right)^{1/3}$ – sorption number

$(P/V)^* \equiv \frac{P/V}{\rho(\nu g^4)^{1/3}}$ – dimensionless *P/V* number

$v^* \equiv \frac{v}{(\nu g)^{1/3}}$ – dimensionless superficial velocity number

$\mathrm{Sc} \equiv D/\nu$ – Schmidt number

S_i^* – unknown numbers describing the bubble coalescence

Figure 37.19 shows a correlation of mass transfer measurements in this pi space. The measurements were performed under unsteady-state conditions by several authors in a water–air system, which is bubble coalescent, using a turbine stirrer as a mixing device. The measurements cover an extreme experimental scale of $\mu \approx 1$–80. The geometric parameters were broadly varied: $d = 0.05$–3.1 m; $D = 0.15$–12.2 m; $H = 0.15$–6.1 m, $V = 1.5$ l –906 m^3. Between B and v^* the following correlation exists: $B = (\pi/4)v^*$.

The process equation reads:

$$(k_L a^* = 9.8 \times 10^{-5}(P/V)^{*0.40}/$$
$$(B^{-0.60} \equiv 0.81 \times 10^{-0.65/B})$$

Ignoring the additive term in this equation, we find $(k_L a)^* \propto (P/V)^{*0.40}\ B^{0.60}$.

In contrast, Fig. 37.20 shows the results of mass transfer in the system: aqueous 1 N sodium sulphite solution–air. These measurements were carried out under steady-state conditions in vessels with hollow stirrers on the scale $\mu = 1{:}5$ (21,22). In this material system, the high salt concentration (70 g Na_2SO_3/L) fully suppresses bubble coalescence. In the case of the self-aspirating hollow stirrer, the stirrer power and gas throughput were coupled via the stirrer speed and were therefore dependent on each other. Consequently, v^* does not occur explicitly in the representation in Fig. 37.18, because it is a function of $(P/V)^*$.

Here, the process equation reads:

$$(k_L a)^* + 1.1 \times 10^{-4}(P/V)^{*0.80} \tag{37.39}$$

These results can be summarized as follows: in the case of a coalescent material system, for example in pure liquids of low viscosity (e.g. water), the absorption rate depends to an equal extent on *P/V* and on $v \propto q/D^2$:

$$(k_L a)^* \propto (P/V)^{*0.4} v^{*0.5} \tag{37.40}$$

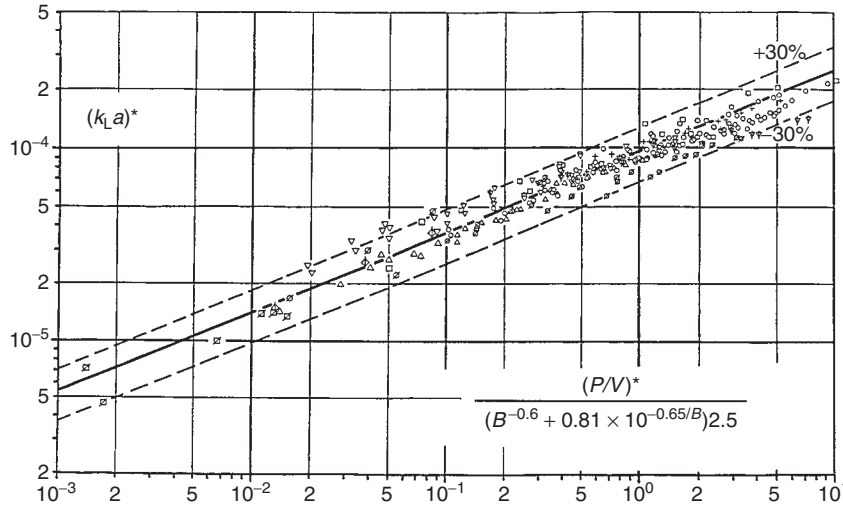


Figure 37.19. Sorption characteristic of a mixing vessel with a turbine stirrer for a coalescing material system (water/air) [from 20].

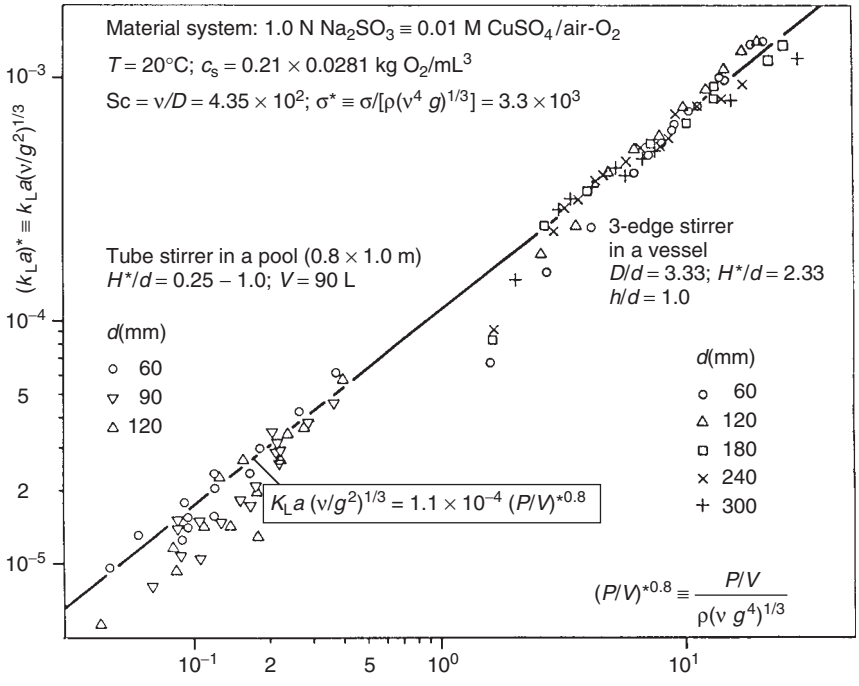


Figure 37.20. Sorption characteristic of a mixing vessel with a self-aspirating hollow stirrer in a material system with fully suppressed coalescence [taken from Ref. 19].

In completely coalescence suppressed systems, for example in many highly concentrated aqueous salt solutions (5), in contrast to the above, the following applies:

$$(k_La)^* \propto (P/V)^{*0.7} v^{*0.2} \tag{37.41}$$

Only with self-aspirating hollow stirrers, where v^* is not an independent process parameter, the correlation (Eq. 37.39) was found.

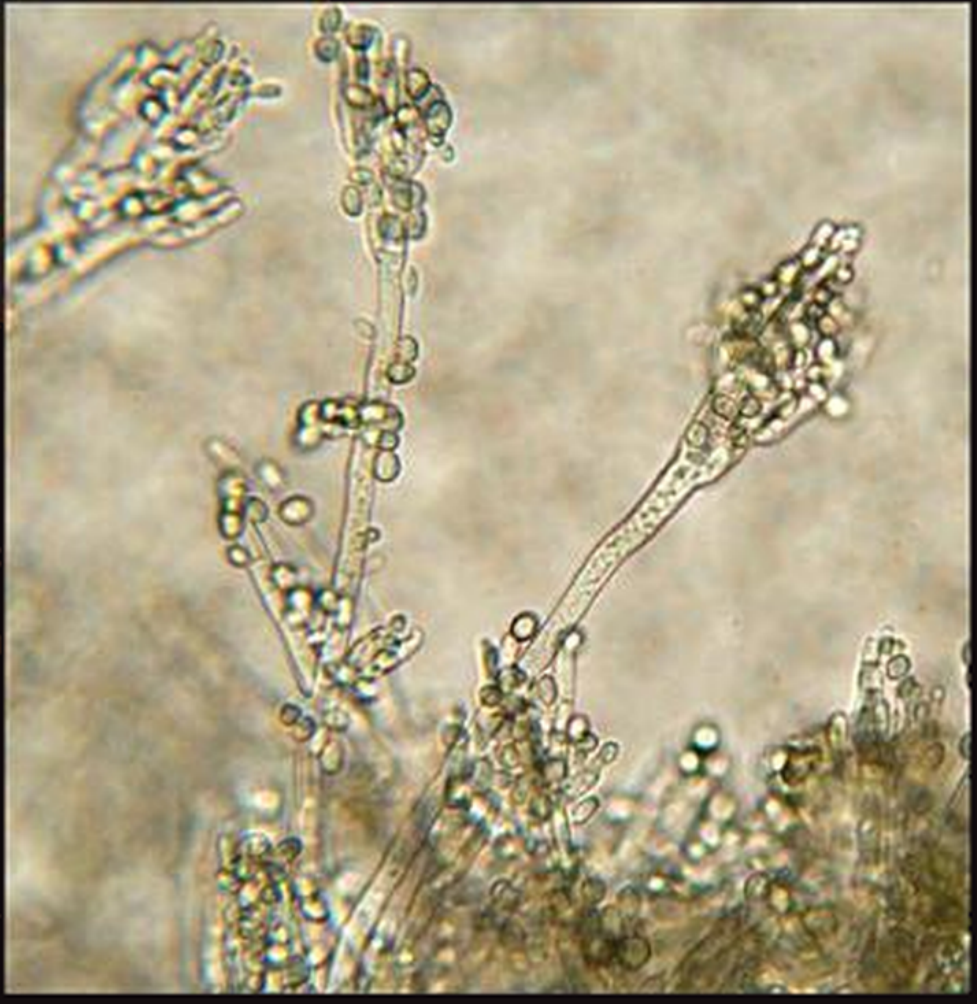
From the above, the following conclusion can be made. High power inputs (P/V) are justified only in coalescence-inhibited material systems. In other words, the generation of very fine primary gas bubbles in coalescent-prone systems is not economically justified.

Dimensional analysis and scale-up rules for two component nozzles ("injectors") for mass transfer in the G/L system in bubble columns are given in (24).

REFERENCES

1. Bridgman PW. Dimensional analysis. New Haven: Yale University Press; 1922, 1931, 1951; Reprint by AMS Press, New York; 1978.
2. Rayleigh L. Nature 1915; 95(2368): 66–68.
3. Zlokarnik M. Scale-up in chemical engineering. Weinheim: Wiley-VCH Verlag; 2006. ISBN-13: 978-3-527-31421-8.
4. Pawlowski J. Die Ähnlichkeitstheorie in der physikalisch-technischen Forschung. (Theory of Similarity in the physicotechnological research; in German). Heidelberg, New York: Springer-Verlag Berlin; 1971.
5. Zlokarnik M. Stirring–theory and practice. Weinheim: Wiley-VCH Verlag; 2001. ISBN 978-3-527-29996-3.
6. Zlokarnik M. Chem-Ing-Tech 1971; 43: 329–335.
7. Zlokarnik M. Korresp Abwasser 1985; 32: 598–603.
8. Zlokarnik M. Ger Chem Eng 1986; 9: 314–320.
9. Zlokarnik M. Chem-Ing-Tech 1969; 41: 1995–1202.
10. Pawlowski J. Veränderliche Stoffgrößen in der Ähnlichkeitstheorie. (Variable physical properties in the theory of similarity; in German). Aarau and Frankfurt/M.: Salle–Sauerländer; 1991.
11. Henzler H-J. Chem-Ing-Tech 1988; 60: 1–8.
12. Böhme G, Stenger M. Chem Eng Technol 1988; 11: 199–905.
13. Pawlowski J. Chem-Ing-Tech 2005; 77: 1910–1914.
14. Metzner AB, Otto RE. AIChE J 1957; 3: 3–10.
15. Pawlowski J. Chem Eng Technol 2005; 28: 37–41.
16. Levêque MA. Ann Mines 1928; 12:201, 305, 381.
17. Delaplace G, Torrez C, Leuliet J-C, Belaubre N, Andre C. Trans IChemE 2001; 79A: 927–937.
18. Pawlowski J, Zlokarnik M. Chem-Ing-Tech 1972; 44: 982–986.
19. Zlokarnik M. Adv Biochem Eng 1979; 11: 158–180.
20. Judat H. Ger Chem Eng 1982; 5: 357–363.
21. Zlokarnik M. Chem-Ing-Tech 1966; 38: 717–723.
22. Zlokarnik M. Adv Biochem Eng 1978; 8: 133–151.
23. Zlokarnik M. Korresp Abwasser 1980; 27: 14–21.
24. Zlokarnik M. Chem Eng Sci 1979; 34: 1265–1271.

VOLUME 2





UPSTREAM INDUSTRIAL BIOTECHNOLOGY

Equipment, Process Design, Sensing, Control, and cGMP Operations

MICHAEL C. FLICKINGER, EDITOR

WILEY

Volume 2

Equipment, Process Design, Sensing, Control, and cGMP Operations

PART IV

BIOREACTOR DESIGN, ENGINEERING, PROCESS SENSING AND CONTROL

38

AERATION, MIXING, AND HYDRODYNAMICS IN ANIMAL CELL BIOREACTORS

RUBEN GODOY-SILVA
Department of Chemical and Biomolecular Engineering, The Ohio State University, Columbus, Ohio
Department of Chemical and Environmental Engineering, Universidad Nacional de Colombia, Bogotá, Colombia
CLAUDIA BERDUGO AND JEFFREY J. CHALMERS
Department of Chemical and Biomolecular Engineering, The Ohio State University, Columbus, Ohio

38.1 INTRODUCTION

Animal cells have an innate ability for proper folding, posttranslational processing, and secretion of proteins, which makes them preferable as hosts for producing biological components of therapeutic and diagnostic interest; as a result, culture of mammalian cells has been used extensively for the production of biologics, including virus vaccines, monoclonal antibodies (MAbs), hormones, enzymes, growth, and blood factors. Although the industrial exploitation of animal cell cultures started over five decades ago with the production of Salk polio virus vaccine in primary monkey kidney cells (1), it has been during the last 21 years that there has been a rapid increase in the number of Food and Drug Administration (FDA)-approved products produced in mammalian cell culture, starting in 1986 with the production of recombinant tissue plasminogen activator (tPA) with genetically engineered Chinese hamster ovary (CHO) cells and the simultaneous introduction of the first MAb, ORTOCLONE OKT3 (muromonab-CD3), as a treatment for solid transplant rejection. Since then, 29 MAbs and many other therapeutic agents have been approved for marketing in the United States for the diagnosis or treatment of diverse diseases, a majority of which are produced in animal cell cultures (2,3). By 2005, one estimate of the world market for antibodies produced in animal cell culture was $14 billion, and this number was expected to grow to more than $16 billion by 2006 (4). While the specific and/or volumetric productivity continues to improve, that is, greater than 5 g/L of product is now considered the norm, this rapid growth in the number and demand of biologics has driven the industry to expand the size and the number of production facilities, and has led to statements that shortfalls in manufacturing capacity exist (5). All of this positive growth puts significant pressure to continually improve the size and productivity of commercial animal cell culture systems.

Despite the fact that reports exist showing that animal cell culture has been conducted for over a 100 years (6,7), no universally accepted method of design or scale-up of animal cell culture has been developed. Diverse culture methodologies including static cultures (T-flask), roller bottles, cultures on microcarriers and freely suspended cells in batch, fed-batch or perfusion systems, among others, have evolved. While freely suspended, fed-batch processes have emerged as the predominant methodology, much of this evolution has been guided by the particularities of the process, the cell line and, most importantly, the in-house expertise of the researchers, specific to each organization. Although there are reports of large-scale (1000–2000 L) airlift bioreactors for protein/antibody production (8–10), at least 70% of the licensed processes for recombinant proteins, antibodies, and vaccines using microcarriers or freely

Upstream Industrial Biotechnology: Equipment, Process Design, Sensing, Control, and cGMP Operations, Volume 2, First Edition. Edited by Michael C. Flickinger.
© 2013 John Wiley & Sons, Inc. Published 2013 by John Wiley & Sons, Inc.

suspended cultures use traditional stirred tank bioreactors with reported capacities up to 20,000 L (11–13). Several reasons account for this preference including the vast empirical knowledge accumulated for the design, scale-up, and operation of this type of reactor in the chemical and biochemical industries over the last century, the versatility of this reactor type allowing its adaptation to several different processes with minor or no modifications and, finally, the relative simplicity. As a result, most guidelines for bioprocess design and scale-up are based on stirred tank reactors and as such will be the primary focus for the remainder of this review.

All animal cell processes are aerobic; oxygen is a crucial nutrient involved in growth and energy production in such cells. Unfortunately, because of its low solubility in water-based media, dissolved oxygen (DO) is consumed quickly, requiring a continuous supply in order to keep cells alive. The easiest way of providing oxygen to a stirred culture is through surface aeration; however, surface aeration is not generally sufficient for cultures beyond ~100 L. Other aeration methods [i.e. perfluorocarbons (PFCs), membrane aeration, oxygen carriers] have been used successfully at scales of up to 500 L, but their use is limited by high cost and downstream concerns (PFCs) or by limited design data and difficulties in maintenance (membrane aeration). These limitations have placed air and oxygen-enriched air sparging as the most common and the simplest method for continuously providing oxygen in bioreactors.

Agitation, on the other hand, is essential for satisfactory mass transfer and homogeneity in a bioreactor with or without sparging; this homogeneity is crucial for process control. Although sparging provides some degree of agitation by itself, most animal cell cultures rely on some sort of mechanical device to impart enough kinetic energy to the fluid.

Both agitation and sparging are essential for the success of industrial cultures of animal cells; yet, both are associated with cell damage as a result of cell–bubble, liquid–cell, and/or solid–cell interactions. Significant progress has been made over the last two decades in the understanding of cell damage mechanisms, and in this chapter, we will attempt to present an overview of the current practices and protocols for aeration and mixing in the bioreactor design and operation, as well as their connection to hydrodynamic damage in animal cell processes.

38.2 AERATION

Oxygen is a key substrate in animal cell cultures; unfortunately, its sparing solubility in water-based media (7.8 mg/L when bubbling air in water at 760 mmHg and 25°C) requires a continuous supply throughout the culture for most larger-scale situations. At high cell concentrations, the rate of oxygen consumption may exceed the rate of oxygen supply; in those conditions, the DO concentration falls to a point (the critical oxygen concentration) where it becomes limiting. Reported critical oxygen concentration for animal cells ranges typically between 1% and 10% of air saturation (14,15). Below this range, the oxygen consumption rate as well as the mitochondrial activity typically decreases, while the specific glucose and glutamine consumption rates increase (to compensate for ATP production) with a corresponding increase in the lactate and ammonium formation rates (16–18). Together with a reduced mitochondrial activity, there is a reduction in the specific secretion rate of proteins and volumetric accumulation of product, which translates into higher cell viability, delayed death, and lower chromosomal damage, but lower product yield (17,19).

Conversely, elevated oxygen concentration (~100% of air saturation) may stimulate the generation of reactive oxygen species (ROS) that can alter cellular macromolecules such as DNA, proteins, and lipids, impairing cell growth or even causing death (15).

As a result, cell cultures should be constrained within an optimal range of DO that must be determined experimentally, taking into account that optimal DO values for cell growth may be different than optimal values for protein production. Oh *et al*. (20) reported satisfactory cultivation of mammalian cells from approximately 5–100% of air saturation. Jan *et al*. (21) studied the effect of DO from 10% to 150% of air saturation on the growth of a murine hybridoma cells at steady state in serum-free continuous culture; while no significant effect on cell viability, growth rate, or specific antibody production rate was reported, an increase in the amount of glucose utilized at higher oxygen concentrations was detected. It was speculated that this increased glucose consumption rate was associated with an increased activity of antioxidant enzymes needed to reduce the cytotoxic effect of ROS. Using the same system, Kunkel *et al*. (22) described an increase in the level of galactosylation of the MAb chains with increased DO.

For common animal cell lines under favorable oxygen supply, reported specific oxygen uptake rates (q_{O2}) range between 6.4×10^{-18} and 4.5×10^{-16} mol oxygen/cell/s (Table 38.1). Given that, currently, cell densities of up to 10^7 cells/mL are common place at the commercial scale (23–25), the actual oxygen uptake rate in a typical culture may range from $6.4 \times 10^{-5} - 4.5 \times 10^{-3}$ mol oxygen/m^3/s; this value is at least one or two orders of magnitude lower compared to yeast [i.e. 2.2×10^{-2} mol oxygen/m^3/s for *Candida guilliermondii* (26)] and bacteria [i.e. 3.3×10^{-1} mol oxygen/m^3/s for *E. coli*, corresponding to q_{O2}= 12–21 mmol/gDW/h (27) and up to 190 gDW/L (28)]. This relatively low oxygen requirement may help explain why even with an agitation intensity for animal cell cultures about 100-fold lower than for

TABLE 38.1. Specific Oxygen Uptake Rates (q_{O2}) Reported for Animal Cell Lines

q_{O2}(mol oxygen·cell/s)	Cell Line	References
5.8×10^{-17}–6.9×10^{-17}	Hybridoma NB1	Boraston *et al*. (31)
5.3×10^{-17}–1.1×10^{-16}	Hybridoma AB20143.2	Miller *et al*. (16); Miller *et al*. (32)
4.2×10^{-17}–1.0×10^{-16}	Hybridoma KS1/4	Backer *et al*. (33)
9.2×10^{-17}–1.0×10^{-16}	Hybridoma HB-32	Ramirez and Mutharasan (34)
6.4×10^{-18}–2.4×10^{-17}	Hybridoma 167.4G5.3	Ozturk.and Palsson (17)
6.4×10^{-17}–1.2×10^{-16}	Hybridoma X-D	Hiller *et al*. (35)
1.67×10^{-16}	Sf-9	Hensler and Agathos (36)
8.6×10^{-17}–1.0×10^{-16}	Sf-9	Wong *et al*. (37)
1.28×10^{-16}	Hybridoma MAK	Zhou and Hu (38)
6.08×10^{-17}–1.13×10^{-16}	NS0	Yoon and Konstantinov (39)
6.5×10^{-17}	Hybridoma C1a	Dorresteijn *et al*. (40)
5.6×10^{-17}	Hybridoma HFN7.1	Eyer *et al*. (41)
5.53×10^{-17}	CHO	Gray *et al*. (42)
8.0×10^{-17}–1.6×10^{-16}	*Trichoplusia ni* BTI-Tn-5B1-4	Rhiel *et al*. (43)
2.5×10^{-17}–4.5×10^{-16}	Sf-9	Rhiel *et al*. (43)
3.3×10^{-17}–5.3×10^{-17}	Sp2/0-Ag14 derived cells (ATCC CRL-1581)	Sauer *et al*. (44)
3.3×10^{-17}–1.2×10^{-16}	B-lymphocyte hybridoma (CC9C10)	Barnabé and Buttler (45)
2.3×10^{-17}–1.7×10^{-16}	GS-NS0	deZengotita *et al*. (23)
9.0×10^{-17}	CHO SSF3	Ducommun *et al*. (46)
5.6×10^{-17}–2.2×10^{-16}	CHO K1 (ATCC CCL 61)	Carvalhal *et al*. (47)
5.3×10^{-17}–8.9×10^{-17}	T-CHO ATIII	Deshpande and Heinzle (48)
1.1×10^{-16}–2.6×10^{-16}	Sf9 (ATCC 1711)	Palomares *et al*. (49)

microbial or fungi cultures (average power drawn per unit volume ~10 W/m^3 vs ~1000 W/m^3 respectively), current bioreactors are still able to provide enough oxygen to meet animal cell needs (9,29). However, with the advent of perfusion cultures, fortified media, and improved fed-batch culture strategies, it is expected that cell concentrations will increase by an order of magnitude (30). Therefore, an equivalent increase in oxygen transfer rate (OTR) must be achieved to supply enough oxygen to the culture.

The OTR is determined from the product of the mass transfer coefficient, k_La (s^{-1}), and the driving force, which is the difference between the saturated DO concentration in the medium, $C^*_{O_2}$, and the actual DO concentration in the broth, C_{O_2}:

$$OTR = k_La \cdot \left(C^*_{O_2} - C_{O_2}\right) \tag{38.1}$$

The saturating DO concentration in the medium in equilibrium with the gas phase, is determined by

$$C^*_{O_2} = \frac{y_{O_2} \cdot P_T}{\mathcal{H}} \tag{38.2}$$

where y_{O_2} is the molar fraction of oxygen in the gas (0.21 for air), P_T is the total pressure of the gas, and $\mathcal{H}$ is the Henry's constant, which is a function of the temperature and the composition of the medium. A simple inspection of Equation 38.1 reveals that in order to increase OTR, it is necessary to increase either k_La or $C^*_{O_2}$, since C_{O_2}can only be reduced to a minimum threshold to avoid productivity issues as explained above. An increase of $C^*_{O_2}$can be achieved by an increase in the pressure of the gas (Eq. 38.2); but this action also results in an increase in the concentration of dissolved carbon dioxide (CO_2), and this may result in inhibitory effects. OTR also may be increased up to five times by increasing the molar fraction of oxygen in the gas using oxygen-enriched air or even a separate stream of pure oxygen into the broth. While this strategy is commonly used in bench bioreactors, it can lead to increased levels of dissolved CO_2, which can have a negative effect on pH control and osmolality (25).

Although, k_La can be affected by several different factors, most proposed correlations in the literature (some of them presented in Table 38.2) adopt the form of an equation dependent on two parameters that are independent of the impeller type, the media composition, and the scale:

$$k_La = A \cdot \left[(\overline{\varepsilon}_T)_g\right]^{\alpha} \cdot [V_S]^{\beta} \tag{38.3}$$

where α and β are approximately 0.5 ± 0.1, respectively (25). In Equation 38.3, the coefficient A is associated with the influence of the chemical composition on interface characteristics, V_s is the superficial velocity of the gas, and $(\overline{\varepsilon}_T)_g$ is the average total energy dissipation rate (EDR) drawn into the liquid by both the impeller $(\overline{\varepsilon}_T)_{Ig}$ and the gas sparging $(\overline{\varepsilon}_T)_S$:

$$(\overline{\varepsilon}_T)_g = (\overline{\varepsilon}_T)_{Ig} + (\overline{\varepsilon}_T)_S \tag{38.4}$$

The energy delivered to the system from air sparging can be calculated from

$$(\overline{\varepsilon}_T)_S \approx V_S \cdot g \cdot \rho \tag{38.5}$$

TABLE 38.2. Examples of Empirically Derived Equations Found in Literature for k_La Estimation

Correlation	Units	System Information	References
$k_La = 93.6 \cdot \left((\overline{\varepsilon}_T)_{Ig}\right)^{0.4} (V_s)^{0.5}$	$[k_La]$: h^{-1}	Water	Van't Riet (50)
	$[(\overline{\varepsilon}_T)_{Ig}]$: W/m^3	$2 < V_R < 4400$	
	$[V_s]$: m/s	$5.0 \times 10^2 < \varepsilon_{Ig} < 1.0 \times 10^4$	
	$[V_R]$: L	$0.5 \times 10^{-2} < V_S < 4 \times 10^{-2}$	
$k_La = 7.2 \cdot \left((\overline{\varepsilon}_T)_{Ig}\right)^{0.7} (V_s)^{0.2}$	$[k_La]$: h^{-1}	Water plus ions	Van't Riet (50)
	$[(\overline{\varepsilon}_T)_{Ig}]$: W/m^3	$2 < V_R < 4400$	
	$[V_s]$: m/s	$5.0 \times 10^2 < \varepsilon_{Ig} < 1.0 \times 10^4$	
	$[V_R]$: liter	$0.5 \times 10^{-2} < V_S < 4 \times 10^{-2}$	
$k_La = 0.255 \cdot (T)^{0.2} (H_L)^{-1.3} (N)^{1.5} (D)^{2.3} (V_S)^{0.6}$	$[k_La]$: h^{-1}		Asay and Kono (51)
	$[T]$: m		
	$[D]$: m	Water plus ions	
	$[H_L]$: m	100 L $< V_R <$ 100 000 L	
	$[N]$: rpm		
	$[V_s]$: m/h		
	$[k_La]$: h^{-1}	$2000 < V_R < 8000$	Langheinrich *et al*. (52)
	$[V_R]$: liter	$0.3 < H_L < 1.3$	
$k_La = 125 \cdot \left((\overline{\varepsilon}_T)_g\right)^{0.72} (V_s)^{0.7}$(see note)	[T]: m	$T = 2$ m	
	$[H_L]$: m	$D = 0.45$ m	
	$[(\overline{\varepsilon}_T)_g]$: W/ m^3	$1 \times 10^{-4} < V_s < 5 \times 10^{-4}$	
		$5.0 \times 10^2 < (\overline{\varepsilon}_T) < 1.0 \times 10^4$	
		Culture of CHO 320 cells in	
	$[V_s$: m/s]	serum free medium	

The correlation was derived by the authors of this chapter exclusively from data in Figures 38.3 and 38.5 of Langheinrich *et al*. (52).

where g is the acceleration due to gravity (9.81 m/s^2), ρ is the liquid density, and V_s is the superficial velocity, given by

$$V_S = \frac{Q}{A} = \frac{4 \cdot Q}{\pi \cdot T^2} = \frac{4 \cdot \left[\frac{\varphi \cdot V_R}{60}\right]}{\pi \cdot T^2} \qquad (38.6)$$

where Q is the air flow rate (cubic meter per second), T is the vessel diameter (meter), V_R is the volume of the medium in the reactor (cubic meter), and ϕ is the air flow rate expressed as vvm. Since cell damage as a result of bubble bursting (see section titled "Detrimental Effects of Sparging") is typically minimized at low air flow rates, $(\overline{\varepsilon}_T)_S$ can often be neglected for stirred tank reactors used for animal cells.

The energy drawn into the liquid by one impeller under the gassed conditions, $(\overline{\varepsilon}_T)_{Ig}$, can be estimated as

$$(\overline{\varepsilon}_T)_{Ig} = P_{0_g} \frac{\rho \cdot N^3 \cdot D^5}{V_R} \qquad (38.7)$$

where N is the impeller speed (s^{-1}), D is the impeller diameter (meter) and P_{0g} is the power number under aerated conditions, which depends on the Reynolds number, the impeller type, and the gas flow rate. For typical culture conditions, the properties of the fluid are quite similar to those of water, so the flow is essentially turbulent ($Re = \rho_L \cdot N \cdot D^2/\mu \sim 10^5$). When turbulent, P_{0g} becomes independent of the Reynolds number; additionally, as the gas flow rate (ϕ) is low, typically ranging from 0.005 to 0.01 vvm (53), P_{0g} is essentially equal to the power number of the impeller under nongassed conditions (P_0). In spite of that, the relationship between P_{0g} and P_0 is typically important in impeller selection. Values for P_0 are presented in Table 38.3 for impellers typically used in animal cell bioreactors (25). Further details about P_0 and P_{0g} are presented in the section titled "Mixing".

The term A in Equation 38.3, and therefore, k_La, are very sensitive to composition. For example, by introducing ions in water up to a limiting concentration of ~10 g/L NaCl, Van't Riet (50) showed that k_La can easily increase by a factor of 100% with respect to the value for distilled or tap water at the same conditions of $(\overline{\varepsilon}_T)_{Ig}$ and V_S; the presence of ions strongly changes the coalescent characteristic of pure water, drastically increasing the interfacial area. In contrast, Metz *et al*. (58) showed that in a stirred bioreactor with otherwise constant conditions (400 rpm, $V_S = 30.6$ m/h), the addition of 0.5 ppm of a surfactant reduced the k_La from ~180 to ~115 h^{-1}. Similar results were presented by Morão *et al*. (59) for three different types of antifoaming substances. Addition of Pluronic F-68 also lowers k_La (60); therefore, caution should be exercised when choosing a particular correlation for designing purposes.

TABLE 38.3. Power Number for Selected Impellers for Turbulent Regime

Impeller	Po_t	References
45° pitched blade turbine (4 blades, $wD = 0.1$, baffled tank)	0.88	Tatterson (54)
45° pitched blade turbine (4 blades, $w/D = 0.3$, baffled tank)	1.69	Tatterson (54)
Marine Propeller (square pitch, 3-bladed)	0.32	Chisti (55)
Lightnin A310 hydrofoil	0.31	Chisti (55)
Rushton (6 blades, central disk, 10% baffled tank)	5.0	Tatterson (54)
Paddle (2 blades)	1.70	Chisti (55)
Scaba 6SRGT ($D/T = 0.44$)	1.6	Amanullah *et al*. (56)
"Elephant ear" impeller (3 blades, unbaffled)	0.006	Menisher *et al*. (57) (calculated)
Prochem Maxflo T. (6 blades, $D/T = 0.44$)	1.3	Amanullah *et al*. (56)

38.2.1 Surface Aeration

Oxygen transfer through the headspace is, obviously, the most common and easy method of gas exchange used for small vessels at the laboratory scale, including T-flasks, spinners, roller bottles, and small bench-scale reactors. The maximum volume at which surface aeration can be used alone depends on a series of factors such as cell concentration, whether or not the headspace gas is enriched with oxygen, and whether or not bubble entrainment is allowed (if the system is agitated). However, a general principle, which holds for scale-ups, is that the area per unit volume for mass transfer decreases with the reciprocal of the diameter of the vessel. To alleviate this problem at moderate scale, the use of surface impellers (an impeller close to the liquid–gas interface) can significantly increase the OTR as a result of an increased renewal of the liquid directly in contact with the gas. If bubble entrainment occurs, a further increase in OTR can be achieved as a result of the significant increase in the interfacial surface. Working with a 500-mL spinner vessel, Aunis *et al*. (61) reported a 50% increase in the OTR by moving the impeller within 0.13 times of the impeller diameter from the liquid surface. Hu *et al*. (62) reported an increase in the oxygen supply up to four times in their reactor by using an additional surface impeller. Another approach for high values of surface OTR involves the use of special impeller types inducing bubble entrainment such as helical and double helical ribbons together with surface baffles (63).

A variation in the surface aeration approach is the disposable bag reactor (i.e. the Wave® bioreactor), which can range in size from 100 mL to 300 L. This system achieves sufficient OTR by means of a rocking motion that induces a wave within the bag, which is sufficient to suspend the cells, mix the medium, and provides a virtually bubble-free oxygen transfer through the rapid turnover of the medium surface. Singh (64) presents data for Wave reactors from 100 mL up to 100 L, with corresponding k_La values ranging from 1.6 to 4 h^{-1}. While for a small scale, these values of k_La are in the same range as for other surface aerated reactors, it is in the lower end of the range for sparged, mechanically stirred reactors (60). However, for volumes larger than 10 L, the k_La in a wave reactor can still be up to one order of magnitude larger than for a spinner or reactor of comparable size; consequently, it is reported to be able to support cell growth up to concentrations of 7×10^6 cells/mL (64).

38.2.2 Perfluorocarbons

PFCs are hydrocarbons whose hydrogen atoms are partly or totally replaced by fluorine. They are hydrophobic and immiscible in water-based media; therefore, the addition of PFCs yields a four-phase (two liquid, one solid, and one gas phase) mixture in sparged bioreactors. Because of the much higher solubility of oxygen in PFCs than in water (see Table 38.4), there has been an active interest in using them as gas vectors to improve oxygen transfer and CO_2 removal in bioreactors. The benefits of using PFCs are summarized by Lowe *et al*. (65) and presented in Table 38.5, together with their main disadvantages.

Several studies have been conducted with animal cell cultures in which the medium was supplemented with PFC emulsions. Cho and Wang (67) employed perfluoromethyldecalin to oxygenate mouse-hybridoma cells, resulting in increased cell density and rate of MAb

TABLE 38.4. Relative Oxygen-Carrying Capacities (k) of Water, Perfluorochemicals and Gas Vesicles (Modified from Sundararajan and Ju (66))

Substance	k (at 37°C) (mol $O_2/m^{3/}$ Mpa)	k/k_{water}
Water	9.7	1.0
Perfluoro-decaline	164	16.9
Perfluoro-tripropylamine	176	18.1
Perfluoro-tributylamine	156	16.1
Gas vesicles	388	40

TABLE 38.5. Benefits and Drawbacks of PFCs [modified from Lowe *et al*. (65)]

Benefits	Drawbacks
High oxygen carrying capacity	Dispersion is unstable requiring high amounts of surfactants and energy
Ease of sterilization (e.g. by autoclave)	Surfactants may become toxic to cells
Provide a two-phase (perfluorocarbon–liquid and aqueous medium) interface and physical support for cell division (in stationary cell culture)	Once suspension is formed it is difficult to separate PFCs for reoxygenation
Chemically and biologically inert scavengers of gaseous cellular products (e.g. ethylene)	Downstream concerns
Recoverable and recyclable	Expensive

synthesis. Using the PFC FC40™, Ju and Armiger (68) found that the exponential growth phase of mouse hybridoma cells was prolonged, along with a more than sixfold increase in viable cell concentration, which was consistent with theoretical predictions based on the enhanced oxygen transfer. Although the high concentration of surfactants needed to keep PFCs in suspension might be deleterious for cells or for downstream operations, such effects have not been reported. It has also been suggested that the formation of emulsions itself might be problematic for recycling and reoxygenation. Gotoh *et al*. (14,69) proposed two interesting alternatives to solve this potential problem with emulsions: they developed a loop column reactor having a wetted-wall of PFCs to culture insect cells (Sf9). With this arrangement, the oxygen was transferred by direct contact of the broth with the liquid film created on the annular wall of the column. They reported a twofold increase in the viable cell density and specific growth rate of the cells, as well as a fivefold reduction in the specific lactate yield. In the second permutation, the same authors grew cell suspensions using a planar layer of PFC at the medium–PFC interface in a spinner flask, and the PFC was recirculated and reoxygenated in an outer aeration unit. With this arrangement, the maximum cell density attained in the PFC-mediated aeration culture was higher than that in a surface aeration control culture; also, the recombinant protein production by virus-infected insect cells was significantly increased. The PFC itself did not seem to cause any negative effects on insect cell growth, viral infection, or recombinant protein production. However, in spite of all the previous advantages, PFCs introduce additional costs and the potential problems in downstream processing have kept PFCs in the research laboratory (9).

38.2.3 Oxygen Carriers

At least two other oxygen carriers, in addition to PFC, have been suggested for use to enhance oxygen supply in cell culture: cyanobacterial gas vesicles (GVs) and hemoglobin (66). While the use of hemoglobin as an oxygen carrier has only been tried in microbial cultures and it has been limited by its high cost and by its high affinity for oxygen (i.e. it requires long residence times in the reactor to effectively release the bound oxygen), GVs have actually been tested in animal cell culture. GVs in cultures of Vero cells on microcarriers have been reported to increase by 30%, the glucose uptake rate, although no effect on cell concentration was described. GVs can be produced at a relatively low cost from simple cyanobacterial cultures; they do not require any suspension stabilizing agent (unlike PFCs), and they have more than twice the oxygen carrying capacity as PFCs (Table 38.4). However, they can not be autoclaved; consequently, sterilization is cumbersome and time-consuming (66). It remains to be seen if a commercial application will be found for GVs.

38.2.4 Membrane Aeration

In membrane aeration, the membrane provides enough interfacial area for oxygen diffusion, while it acts as a physical barrier that keeps cells away from gas–liquid interfaces, eliminating any cell damage related to bubble-bursting phenomena or cell entrapment in foam. This methodology has been reported to give high OTRs (i.e. $\sim$0.5 g O_2/L/h) that are comparable to sparging, although they require higher gas pressure and flow rates (70,71). Ma *et al*. (29) categorize the different types of membranes into two groups: a microporous type and a diffusional type. The microporous type typically is a thin membrane made up of nylon, polyvinylidene fluoride, polyester, and so on, with pore sizes ranging from 0.01 μm to about 20 μm, and where the medium is in direct contact with the air in the micropores of the membrane. The liquid–gas interface is held stationary via both hydrophobic forces and gas pressure. In the diffusional type of membrane, the oxygen diffuses through the actual membrane material. Some of the most common examples are silicon tubing and silicon hollow-fiber membrane oxygenators.

There are reports of the use of membranes for oxygen transfer up to 150 L (72,73); however, their use at larger scales is problematic. While there is always the risk of rupture, clogging, and fouling of the membranes, these risks significantly increase during scale-up, since one is faced with classical surface-to-volume ratio problems; that is, as the volume of the vessel increases, one needs to increase the surface area of the membranes, typically tubing, even faster. At some point, the amount of tubing required becomes

unmanageable, especially when one considers the challenge of cleaning and sterilizing large vessels (29,74).

38.2.5 Sparging

Despite all of the alternatives reviewed above, the most commonly used way to introduce and remove gaseous nutrients and by-products from animal cell culture, after simple head space mass transfer, is by sparging the gas directly into the medium. While potentially catastrophic effects can occur (i.e. cell death of the whole culture in a few hours), the use of specific additives can prevent a majority of the cell destruction. More on both the mechanism(s) of death and prevention will be presented later.

38.2.6 Sparger Design

Proper selection of a gas sparger involves a compromise between maximizing gas transfer (O_2 and CO_2), minimizing cell damage and foam formation, and complying with good manufacturing practices (GMP) considerations (easily cleanable, steam sterilizable, and free draining). Ideally, spargers should be designed to disperse bubbles sufficiently to avoid coalescence into larger bubbles as they rise within the vessel (75); however, excessive pressure drop across the orifice may create sufficient hydrodynamic forces to inhibit net cell growth (76) and therefore, should be avoided.

There are three commonly used designs in cell culture: the point sparger, ring sparger, and frit sparger (75). Point sparger is the simplest design consisting of a pipe ending in a nozzle through which air is introduced into the vessel; its simplicity makes it ideal for cleaning and sterilization. However, the moderate control of the bubble size that can be achieved by changing the nozzle diameter, gas flow rates, and position (depth) of the nozzle results in the formation of large bubbles (77). Although Orton and Wang (78) suggested the use of macrospargers producing large bubbles (diameter in the range of 6–8 mm) to minimize foaming and bubble-related cell death, the low surface per unit volume created with these spargers results in the use of higher flow rates in order to provide enough oxygen to the culture.

To address the high flow rates needed when a single point sparger is used, and yet allow easy cleaning and sterilization, a common approach is to add a number of air nozzles drilled at the bottom of a ring, allowing for free drainage from the tube. While it is an improvement with respect to a reduction in air flow through a single hole, it has been argued that this enhancement is not sufficient to justify the added expense and cleaning difficulties (75). Recently, Harris *et al*. (79) presented a new approach for a multipoint sparger design called the *multiple slot disperser*, which consists of an assembly of flat, parallel arrays of slot nozzles. In water, it produced a dense, three-dimensional plume of air bubbles with a consistently narrow bubble size distribution and a relatively sharply defined median bubble diameter. Most importantly, the plume attributes may be modified within wide limits by changing the slot width, plate, and array dimensions, as well as the gas flow rate. Additionally, the method of construction is highly adaptable, avoiding the need for pores or drilled holes and it is relatively easy to clean and autoclave.

A significant alternative to the single or multiple hole disperser, is the well-known and well-used frit sparger that utilizes porous materials (ceramic, sintered stainless steel, or Teflon) to create an almost unmeasureable amount of very small bubbles within the bioreactor. These bubbles are nearly ideal for gas transfer because of the large interfacial gas–liquid area they provide and the extended time of contact as a result of lower rising velocities of the smaller bubbles. However, disadvantages of these spargers include cleaning difficulty, more stable foam, and reduced CO_2 stripping capability, forcing in some cases the use of both a frit and a large bubble sparger, and the use of antifoaming chemicals (75). The cleaning challenge can be so significant that the authors know of at least one commercial process in which the frit sparger is replaced after every batch. Documenting some of these reported advantages and disadvantages, Nehring *et al*. (80) tested both a stainless steel porous sparger and a porous ceramic (TiO_2) microsparging system for the cultivation of Madin–Darby canine kidney (MDCK) cells from a 2- to 100-L scale. The ceramic system produced bubble diameters of 100–500 μm, and values of $k_L a$ up to 50 h^{-1}, three times higher than those produced by the stainless steel sparger at the same gas flow rate; however, formation of compact, stable foam, and pH problems were observed. Similarly, Chisti (81), found the use of a multihole sparger to be preferable over a porous metal sparger for scale-up of a bioreactor as a result of foaming problems caused by the smaller bubble size generated by the fritted sparger.

38.2.7 CO_2 Accumulation and Removal

Somewhat ironically, as animal cell culture progressed from a research scale to a relatively large-scale commercial process, the addition of oxygen became less of a concern and the removal, and in some cases the initial addition, of CO_2 became more problematic. This results from a number of issues as a consequence of the complex role CO_2 plays in cell culture. Carbon dioxide is a nutrient needed for synthesis of nucleic acid components such as purines and pyrimidines (82); therefore, low levels of this component may inhibit cell growth. Alternatively, CO_2 is also a by-product of aerobic metabolism and high levels of dissolved CO_2 are inhibitory for cells and have been reported to strongly affect cell growth and metabolism (83–85). To further complicate the situation, carbon dioxide forms part

of a complex buffer system given by the next set of equilibrium reactions:

$$CO_{2(g)} \leftrightarrow CO_{2(\text{dissolved})};\ [CO_2]_{\text{dissolved}} = \frac{pCO_2}{\mathcal{H}} \tag{38.8}$$

$$CO_{2(\text{dissolved})} + H_2O \leftrightarrow H_2CO_3;$$

$$K_h = \frac{[H_2CO_3]}{[CO_2]_{\text{dissolved}}} = 1.70 \times 10^{-3} \text{ at } 25^\circ\text{C} \tag{38.9}$$

$$H_2CO_3 \leftrightarrow H^+ + HCO_3^-;$$

$$K_{a1} = \frac{\left[HCO_3^-\right] \cdot \left[H^+\right]}{[H_2CO_3]} = 2.5 \times 10^{-4} \text{ mol/L at } 25^\circ\text{C} \tag{38.10}$$

$$HCO_3^- \leftrightarrow H^+ + CO_3^{2-};$$

$$K_{a2} = \frac{\left[CO_3^{2-}\right] \cdot \left[H^+\right]}{\left[HCO_3^-\right]} = 5.61 \times 10^{-11} \text{ mol/L at } 25^\circ\text{C} \tag{38.11}$$

Since sodium bicarbonate is typically used as a pH buffer in the culture medium, from the previous set of reactions it is easy to deduce that a change in the dissolved CO_2 concentration could lead to a change in the pH through the following relationship

$$\left[H^+\right] = \frac{10^{-14}}{\left[H^+\right]} + \frac{K_h \cdot K_{a1} \cdot pCO_2}{\left[H^+\right] \cdot \mathcal{H}} + 2\frac{\cdot K_{a1} \cdot K_{a2} \cdot pCO_2}{\left[H^+\right]^2 \cdot \mathcal{H}} \approx \sqrt{10^{-14} + \frac{K_h \cdot K_{a1} \cdot pCO_2}{\cdot \mathcal{H}}} \tag{38.12}$$

where pCO_2 is the partial pressure of CO_2 in the exit gas in equilibrium with the medium. A rise of pCO_2 at a controlled pH typically leads to an associated increase in the medium osmolality as a result of both an increased dissolved CO_2 concentration and the addition of a base, such as sodium hydroxide, to maintain a constant pH. The combined influence of high osmolality and pCO_2 might lead to an even more significant change in the metabolism of the cell. Finally, to add a final level of complexity to the situation, CO_2 is much more soluble than O_2, and this CO_2 solubility is sufficiently sensitive to pressure, such that a significant gradient in CO_2 can exist between the top and bottom of a 1000-L, weakly mixed, animal cell culture bioreactor.

Several published examples of the effect of the concentration of dissolved CO_2 on a cell culture exist. Drapeau *et al*. (86) studied the effect of increasing dissolved CO_2 concentration from 53 to 165 mmHg on recombinant CHO cells for the production of human macrophage colony stimulating factor (hM-CSF) in a 2500-L reactor. At the highest pCO_2, the specific cell growth rate decreased by 52% and the specific production rate of hM-CSF dropped by 56% relative to the culture with the lower pCO_2. While the DO and pH were constant and equal in both cultures, it is unclear if the osmolality was kept constant. Gray *et al*. (42) also described an inhibitory effect in CHO cell density and specific production rate with reported reductions of 33% and 44%, respectively, in a system in which pure oxygen microbubbles using a fritted sparger or silicone diffusion aerators were used to transfer oxygen to the culture. Mostafa and Gu (84) also reported a 40% drop in the specific production rate of a therapeutical glycoprotein produced by CHO cells when pCO_2 increased from 68 mmHg in bench-scale (1.5 L) reactors to 179 mmHg in pilot-plant (1000 L) bioreactors. In the last two cases, osmolality was not controlled, so the real cause of the dramatic effects observed is potentially a combination of the effects of increased pCO_2 and osmolality.

To isolate the impact of pCO_2 and osmolality on CHO cell growth, Zhu *et al*. (85) performed experiments in bench-scale bioreactors where they changed only one variable at a time. Raising pCO_2, from 50 to 150 mmHg, under a controlled osmolality of approximately 350 mOsm/kg, resulted in a 9% reduction in specific cell growth rate. Increasing osmolality from 316 to 450 mOsm/kg, resulted in a linear reduction in specific cell growth rate (0.008 h^{-1} per 100 mOsm/kg) of up to 60%. The combined effects of high pCO_2 (140–160 mmHg) and osmolality (400–450 mOsm/kg) caused a 20% drop in viable cell density.

In contrast to CO_2 buildup as a result of low levels of gas-medium exchange, the high rates of aeration in bubble columns or airlift reactors may lead to excessive CO_2 stripping, which can have equally inhibitory effects (87). To solve this problem, the gas for aeration usually includes a certain amount of CO_2 to both keep the pH in a proper value and avoid a reduction of pCO_2 below 40–50 mmHg range, usually considered optimal for animal cell culture (88).

38.3 MIXING

Mixing can be defined as "the operation in which two or more materials (gas, liquid and/or solid) are distributed throughout a mass in varying degrees of uniformity dependent upon the change and state to be accomplished" (89). In animal cell bioreactors, this mixing is typically accomplished by the addition of energy to the broth in the form of mechanical agitation and gas sparging. Ideally, this energy should be delivered to the culture broth in a completely homogenous manner such that any fluid element, or in this case any cell, will experience a similar distribution of

energy in a similar period of time. Also ideally, this energy delivery should be sufficient to distribute both the cells, and molecularly sized nutrients and by-products, in such a manner that no "process effecting concentration gradients" exist in the vessel. The term, *process effecting concentrations*, is used since a concentration gradient is also a time-dependent phenomenon in a dynamic environment such as a bioreactor, and the characteristic time scales need to also be considered. As it will be discussed below, far from ideal situations exist in most animal cell bioreactors.

In general, the hydrodynamic environment experienced by a particular cell in a culture is a function of its spatial position in the interior of the bioreactor, the characteristics of the mixing system, and time. With the exception of fungal and some microbial cultures, the rheological characteristics of the broth do not change dramatically with time, remaining essentially Newtonian and very similar to water. Depending on the final cell concentration and the potential release of nucleic acids into the culture, a slight increase of the viscosity at the end of the culture may become apparent, but typically this is not considered important. However, in spite of the low viscosity, a poor design of the mixing system may lead to catastrophic consequences. If the mixing is not intense enough, cells will settle at the bottom of the reactor creating zones with limitations of mass and energy transfer and unsatisfactory homogeneity, rendering the control systems of the reactor inefficient and ending up with low viability and productivity. Even if the agitation is sufficient to maintain a suspended culture, a number of reports exist of an undermixed commercial animal cell culture process in which significant dissolved CO_2 concentrations exist between the top and the bottom of the bioreactor, and "zones" of relatively unmixed, high-pH "clouds" exist in the vessel after base addition for considerable periods of time. Langheinrich and Nienow (90) measured pH in three different zones of an 8 m^3 bioreactor equipped with a 0.225T Rushton turbine intended for the culture of mammalian cells; they found pH gradients close to one unit between the alkali addition zone and the impeller discharge when addition of the Na_2CO_3 was done on the liquid surface. Ozturk (91) observed "snow-ball" aggregation of mammalian cells, corresponding to alkaline cell lysis, close to the headspace addition point of base in a poorly agitated bioreactor: the concept of an animal cell suspended in a "pool" of pH 9 or 10 is not a desirable thought!

On the other hand, a common concern that is substantiated with little data is that if suspended animal cell cultures are mixed too aggressively in typically designed bioreactors, the hydrodynamic forces experienced by the cells may inhibit cell growth, productivity, or have other undesirable effects. Unfortunately, historically, no universally accepted algorithm or protocol allowing for a fundamentals-based design of mixing systems for animal cell cultures has existed; consequently, an empirical, case-by-case process has typically been conducted at each organization (company) as an animal cell process was scaled up. Also, many of these established processes might be undermixed. While this approach has resulted in a number of organizations having significant "in-house" expertise, well-documented, fundamentally based, peer reviewed scale-up protocols are still lacking. However, a sufficient amount of experimental data is beginning to accumulate, which allows for the development of such scale-up algorithms.

The importance of mixing to animal cell culture is far from unique; in fact, specific professional societies, such as the North American Mixing Forum, are dedicated solely to understanding and optimizing mixing in the chemical process industry. Taken in a proper perspective, the challenge of mixing in animal cell culture is not nearly as complex as mixing in many other industries. Consequently, much can be learned from this community.

38.3.1 Stirred Tank Reactors

As mentioned before, for a number of reasons, not the least of which is the relative simplicity and considerable knowledge/database, the classical stirred tank reactor is the predominate method to culture animal cells from bench-scale up through large-scale, commercial systems. While a complete review of stirred tank bioreactors is beyond the scope of this chapter, a quick summary will be presented. The interested practitioner is encouraged to read more complete discussions on the topic (54,92,93).

38.3.2 Geometry

A typical, stirred tank, animal cell bioreactor is a mixing vessel with an aspect ratio of tank height (H) to tank diameter (T) of approximately (H/T) 2–3 (see Fig. 38.1). This tank is penetrated by a shaft that extends down the center line of the tank; the outside end of this shaft is attached to a motor, while the other end is attached to one or more impellers, which are suspended in the culture broth. Typically, the impeller diameter (D) is about one-third to one-half of the tank diameter. The tank is filled with broth up to a height (H_L) of $\sim 0.7\ H$. The off-bottom clearance (C), is usually around $\sim 0.1–0.3\ T$. In the case of multiple-impeller systems, the separation between impellers (ΔC) is highly variable as it will be discussed next, but normally is set around one impeller diameter.

38.3.3 Impeller

A number of different impeller designs exist and are used (see Fig. 38.2), ranging from radial-flow impellers such as the traditional Rushton turbine (RT) used extensively in the

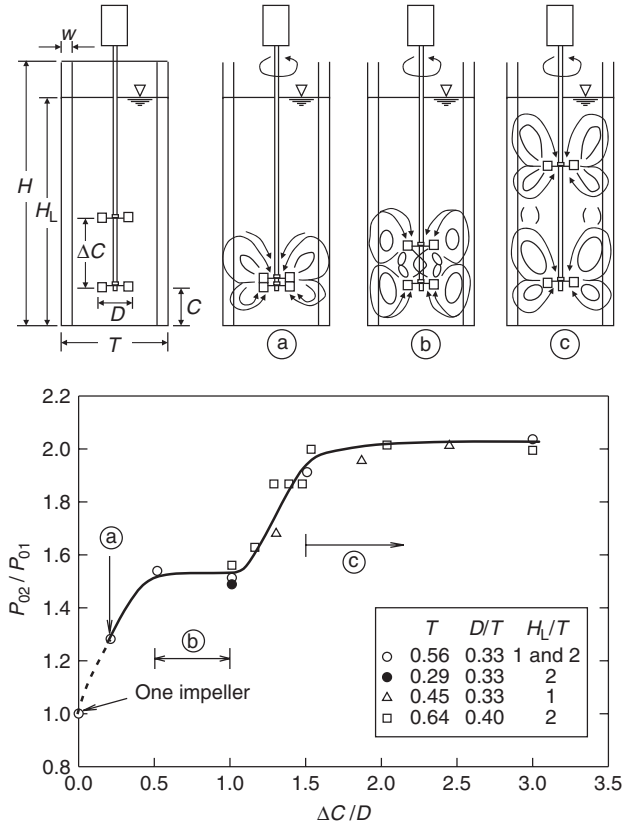


Figure 38.1. Geometrical configuration, flow patterns, and total nongassed power drawn into the liquid as a function of impeller spacing for a mixing system with multiple Rushton turbines. [Adapted from Hudcova *et al*. (94).]

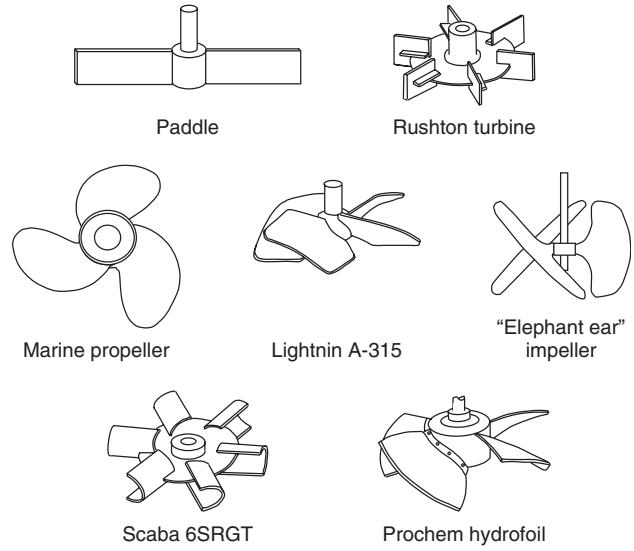


Figure 38.2. Impeller configurations commonly employed in animal cell culture.

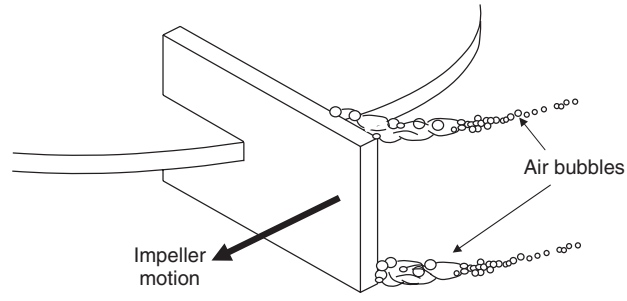


Figure 38.3. Regions of highest shear rate and highest energy dissipation rate; behind the blades of a Rushton turbine.

mixing community to provide a high level of intense mixing by way of a high local shear rates, to axial-flow impellers like the marine propeller, which provide better bulk movement of the broth, relative to the Rushton. Impeller selection is based on a series of considerations including its power number (P_0) and its pumping number (Nq). Impellers with larger ratio Nq/P_0 are superior in producing better bulk mixing at lower shear rates. At the same average energy per unit volume drawn into the liquid, $(\overline{\varepsilon}_T)_{Ig}$, impellers with a larger diameter have a higher pumping capacity, and therefore, may have a better mixing performance. Impeller designs generating lower shear rates are thought to be superior in reducing alleged cell damage as a result of hydrodynamic forces. In this sense, hydrofoils are superior to pitched blade turbines (PBTs) and PBTs are superior to Rushton turbines (29). Chen *et al*. (95) presented a novel methodology to evaluate impellers based on dinoflagellates: when stimulated by hydrodynamic forces, these organisms generate light. At speeds corresponding to the same oxygen transfer coefficient, a Rushton turbine (150 rpm) generated a much higher luminescence (~20,000 counts in 10 ms) compared to marine propellers (170 rpm; ~2000 counts in 10 ms) indicating that much higher forces are created in the bioreactor with the former impeller.

In nongassed conditions, the power drawn by an impeller is a function of Reynolds number, impeller type, and its geometry. For impeller Reynolds numbers over 10^4 (normal conditions in culture), the power number becomes independent of Reynolds and depends only on variables such as blade angle, number and width, baffle number and width, and clearance ratio (C/D).

Equation 38.7 governs the power drawn by a single impeller under gassed conditions. In such circumstances, the gas reaching the impeller is driven to the back of the blades (see Fig. 38.3) of the impeller, generating air cavities that are stabilized by the lower pressure in such zones and reduce the amount of power the liquid is able to transmit to the broth; depending on the amount of gas, the size of such cavities may grow to a point where they surround the whole impeller; this phenomena is known as *flooding*, and reduces drastically the amount of power the impeller is able to draw

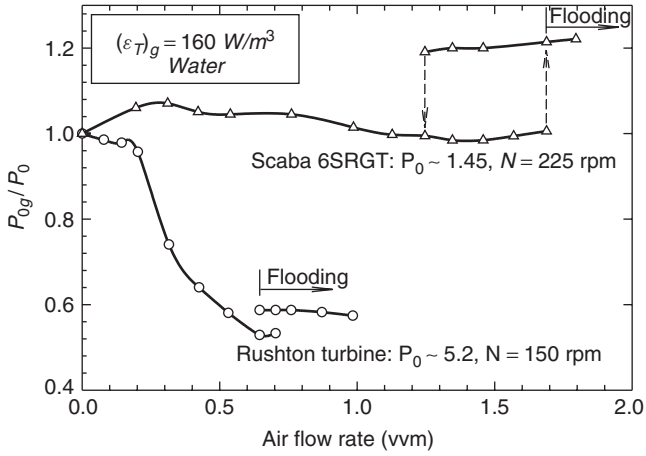


Figure 38.4. Effect of the gas flow rate on the power drop under gassed conditions for two impeller geometries in Newtonian, water-like fluids. [Adapted from Galindo and Nienow (96).]

into the liquid, because now the impeller is practically rotating in air. Characteristic curves of P_{0g}/P_0 are presented in Fig. 38.4; observe that impellers like the Scaba, are much less prone to flooding than the Rushton turbine and the reduction in power drawn is limited or nonexistent as a result of their design.

When the tank is sufficiently large, multiple impellers can be attached to a single shaft, with the potential to use a combination of impellers (i.e. both a Rushton and a marine type) to improve the mixing performance. Under nonsparged conditions, the power drawn into the liquid by the different impellers depends on the distance between them. Hudcova *et al*. (94) established that in the case of Newtonian, low-viscosity media, the power drawn in nongassed conditions by two Rushton turbines is maximized when the impellers are placed apart by a minimum ~1.8 times the impeller diameter. At this distance, the flow patterns generated by each impeller do not significantly interfere with each other (see Fig. 38.1); consequently, the total power drawn into the system is simply the sum of the power drawn by each impeller. Similar results were obtained by Machon *et al*. (97) for a diversity of combinations of impellers. Under gassed conditions, however, there is an uneven distribution of the gas between the impellers: the lower impeller draws less power than the upper one and usually works as a gas disperser. A similar behavior (uneven power drawn) is observed when the separation of the impellers is increased until a maximum is reached when the impellers are apart by a distance greater than $2D$; in this situation, the prediction of the total power drawn into the liquid is much more complex. Correlations proposed by Cui *et al*. (98) to calculate the power drawn by individual impellers in gassed systems with multiple (one to three) Rushton turbines are presented in Table 38.6. Linek *et al*. (99) also developed gassed power correlations for a system with four Rushton turbines; the interested reader is advised to consult their work.

38.3.4 Baffles

To further improve the effectiveness of the impeller, baffles are used, typically up to four, in which case they are placed perpendicular to the tank wall at 90° increments around the vessel. The width of the baffles influences the power drawn into the liquid, and therefore, the mixing performance (Fig. 38.5). A typical width of the baffle is on the order of 10% of the tank diameter.

38.3.5 Mixing Times and Energy Dissipation Rates

Many bioreactors have been designed assuming that cells have a high "shear sensitivity," which translates into suboptimum mixing performance and a corresponding lack of homogeneity. In turbulent systems under nongassed conditions, the time required for mixing the content of a bioreactor up to a certain degree of homogeneity (usually 95% of the final response), which is referred to as the *mixing time*, θ_m, is independent of the impeller type, and can be related to design and operational parameters by the next set of equations (29):

$$\theta_m = 5.3 \cdot \left[N^{-1} \cdot P_0^{-(1/3)} \cdot (T/D)^2 \right] \quad \text{for } H_L/T = 1 \tag{38.13}$$

$$\theta_m = 3.3 \cdot \left[N^{-1} \cdot P_0^{-(1/3)} \cdot (T/D)^{2.43} \right] \quad \text{for } H_L/T > 1 \tag{38.14}$$

TABLE 38.6. Correlations Derived by Cui *et al*. (98) for Power Drawn in Systems with Multiple Rushton Impellers

Condition	Impeller	Equation	Mean Deviation
$Q \cdot N^{0.25} \cdot D^{-2} \leq 0.055$	Bottom	$1 - P_{0g}/P_0 = 9.9 \cdot \left(Q \cdot N^{0.25} \cdot D^{-2}\right)$	<6%
$Q \cdot N^{0.25} \cdot D^{-2} > 0.055$	Bottom	$1 - P_{0g}/P_0 = 0.52 + 0.62 \cdot \left(Q \cdot N^{0.25} \cdot D^{-2}\right)$	<6%
$Q \cdot N \leq 0.013$	Middle and Top	$1 - P_{0g}/P_0 = 37.6 \cdot (Q \cdot N)$	2.3%
$Q \cdot N > 0.013$	Middle and Top	$1 - P_{0g}/P_0 = 0.375 + 8 \cdot (Q \cdot N)$	1.4%

Q: gas flow rate (cubic meters per second); N: impeller rotational speed (s^{-1}). Conditions for correlated data: $0.238 < T < 1.83$ m; 1–3 impellers; $0.92 < N < 10\ s^{-1}$; $D/T = 1/3$–$1/2$; $Fl = 0$–0.26

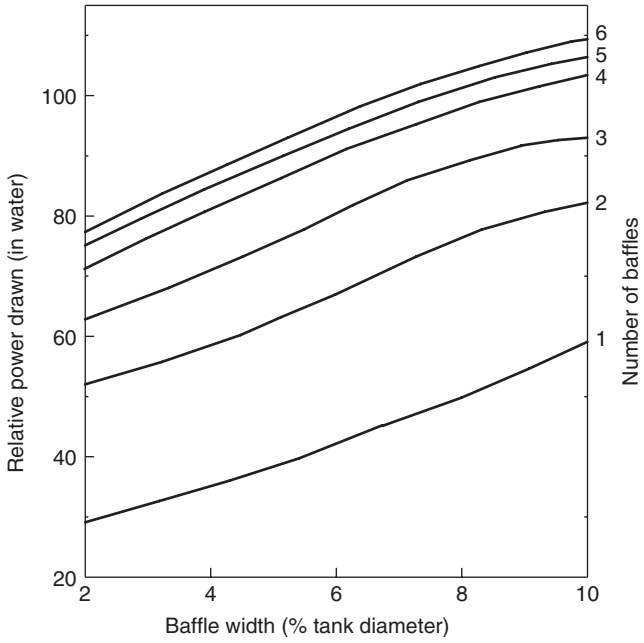


Figure 38.5. Effect of the number and size of the baffles on the power drawn by an impeller in a cylindrical stirred tank reactor. [Adapted from Oldshue (92).]

where θ_m will be in the units of the inverse of the impeller rotational speed. Equation 38.13 correlates very closely for a wide variety of impellers with an almost identical equation derived by Kresta *et al*. (100), except the coefficient changes from 5.3 to 5.8. For clarity purposes, Equation 38.13 can be rearranged by assuming a cylindrical tank $\left(V_R = (\pi/4) \cdot T^2 \cdot H_L\right)$ and using Equation 38.7 to give

$$\theta_m = 57.4 \cdot (T/D)^{(1/3)} \cdot \left[(\overline{\varepsilon}_T)_g\right]^{-(1/3)} \cdot T^{2/3} \text{ for } H_L/T = 1 \tag{38.15}$$

where θ_m will be in seconds and the remaining variables are in SI units. For the derivation of Equation 38.15, it was assumed that the density of the fluid is very close to that of water (1000 kg/m^3), and that usual gas flow rates are so low in animal cell culture that $P_{0g} \approx P_0$ and $(\overline{\varepsilon}_T)_g \approx (\overline{\varepsilon}_T)_{Ig}$. Equation 38.15 is identical to that obtained by Nienow (101) and indicates that during scale-up (increase of T) for geometrically similar tanks (*T/D* constant), the mixing time can be kept constant only if the power input per unit volume is increased. In contrast, the concern of potential hydrodynamic cell damage has resulted in many (a majority?) of large-scale animal cell bioreactors designed with power per unit volume significantly decreased relative to laboratory-scale vessels.

One concept commonly used in the mixing industry is the EDR, which has units of power per unit volume (i.e. watts per cubic meter). On a bulk or average basis, this is a very appealing parameter, since the average total EDR, $(\overline{\varepsilon}_T)_g$, is just the rate of energy added to the system divided by the volume where the energy is delivered. From a fundamental point of view, the *EDR*, ε, can be determined using the following first principle equation (102,103):

$$\varepsilon \equiv \tau : \nabla U \tag{38.16}$$

where τ is the stress tensor and ∇U is the velocity gradient tensor. For an incompressible Newtonian fluid, Equation 38.16 becomes (103)

$$\varepsilon \equiv \tau : \nabla U = \mu \left[\nabla U + (\nabla U)^T\right] : \nabla \mathrm{U} = \mu \sum_i \sum_{\mathrm{j}} \left[\nabla U + (\nabla U)^T\right]_{ij} \nabla U_{ji} \tag{38.17}$$

In Equation 38.17, μ is the viscosity of the medium, ∇U^{T} is the transpose of ∇U, and ∇U is the gradient of the velocity vector given by:

$$\nabla U = \begin{bmatrix} \frac{\partial U_x}{\partial x} & \frac{\partial U_y}{\partial x} & \frac{\partial U_z}{\partial x} \\ \frac{\partial U_x}{\partial y} & \frac{\partial U_y}{\partial y} & \frac{\partial U_z}{\partial y} \\ \frac{\partial U_x}{\partial z} & \frac{\partial U_y}{\partial z} & \frac{\partial U_z}{\partial z} \end{bmatrix} \tag{38.18}$$

Equation 38.16 can be derived from first principles using the second law of thermodynamics. More specifically, Equation 38.16 emerges from the loss term in the energy balance equation. Much like the Navier–Stokes equation, Equation 38.16 is valid for any flow regime, be it laminar, transitional, or fully turbulent.

It is this dual nature, a pragmatic value (the power of the mixing motor turning the impeller shaft going into the bioreactor divided by the number of liters in the vessel) and the fundamental, first principle definition, that has lead to the use of EDR to characterize the flow conditions acting on cells for over 30 years (104), and has been extensively used in the fluid mechanical/mixing community for even longer (105).

As it might be imagined, but not typically fully appreciated, the flow in a stirred tank reactor is highly inhomogeneous. Qualitatively, this was demonstrated in the 1970s, visually, by demonstrating that very strong vortices emanate from the tips of the impeller blades; such vortices are responsible, for example, for gas dispersion in the impeller blades (Fig. 38.3). These qualitative observations have been quantified by experimental studies, using a variety of experimental techniques to demonstrate that the local EDR in the impeller region, and specifically in these vortices, has been reported to be over 103 times

higher than the local EDR in the bulk fluid away from the impeller (106–109).

Given the importance that high, local EDR levels have on rapid, molecular mixing, Zhou and Kresta (108,110) conducted a significant number of quantitative studies on the maximum and distribution of EDR as a function of a number of variables in stirred tank vessels, including tank volume, impeller type, and impeller rotational speed (rpm). These studies were, in general, consistent with other published studies. Several important conclusions that are relevant to animal cell bioreactors can be made:

1. The EDR is always high in the *impeller discharge stream*. Specifically, 43.5% of mechanical energy added to the vessels is dissipated in the impeller discharge region of a Rushton turbine, which represents only about 10% of the volume of the tank. In contrast, for the PBT, 70.5% of the energy is dissipated in the larger impeller discharge region. In addition, the "average" EDR is over an order of magnitude higher in the impeller region when compared to bulk average for the whole vessel.
2. For a given impeller type, the *maximum*, *local EDR* in the impeller region can be approximated using a nondimensional constant and to a specific, nondimensional location relative to the impeller. This nondimensional constant, ψ, is given by:

$$\psi = \varepsilon_{max}/\rho \cdot N^3 \cdot D^2 \qquad (38.19)$$

3. where D is the impeller diameter and N is the impeller speed with units of s^{-1}. If specific geometric ratios are held constant (including the type of impeller), it has been shown that ψ did not vary significantly over a large range of impeller speeds (108,110). If the *D/T* (impeller diameter/vessel diameter) or *C/T* (off-bottom clearance/vessel diameter) ratio changed, within certain limits, up to a 46% increase in the value of ψ was observed when working with an RT. These observations also held for the PBT impeller.

Using this relationship for the maximum EDR in a stirred tank vessel, along with the classical P_0 and P_{0g}, one can approximate the mean and the maximum local EDR as one scales the stirred tank mixing, keeping the H_L/T, D/T, and *C/T* ratios nearly the same and using the same type of impeller. Figures 38.6–38.8 present predictions of vessel size and dimensions, maximum local EDR, and average EDR. Specifically, Fig. 38.6 presents the change in the tank diameter and impeller diameter as the volume of the vessel increases from 0.5 to 10,000 L, keeping geometrical ratios constant. Figure 38.7 presents lines of constant, maximum EDR as a function of RPM and impeller diameter, and

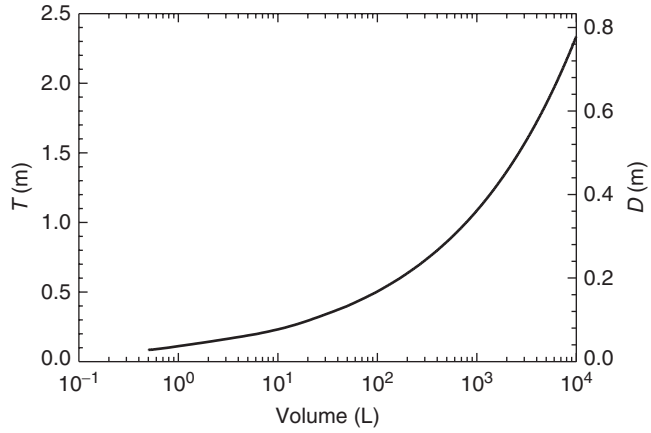


Figure 38.6. Change in the tank diameter and impeller diameter as the volume of the vessel increases from 0.5 to 10,000 L keeping constant the geometrical ratios $H/T = 1$ and $T/D = 3$.

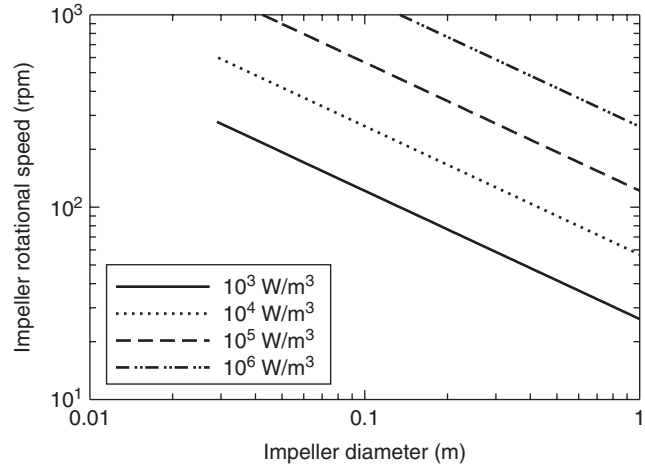


Figure 38.7. Lines of constant, maximum EDR in a vessel as a function of impeller rotational speed and diameter for Rushton turbine in water. $H/T = 1$ and $T/D = 3$.

Fig. 38.8 presents the average EDR for the whole vessel as a function of impeller diameter and RPM.

Alternatively, Fig. 38.9 presents the mean and the maximum EDR, calculated respectively with the power number (Eq. 38.7) and the maximum EDR relationship (Eq. 38.19, using a value of $\psi = 13.7$), as a function of impeller rotational speed. This plot corresponds specifically to a 2-L Applikon® bioreactor, which was mixed with a standard Rushton turbine impeller. The circle and square data points correspond to specific values of EDR measured with a particle tracking technology (109).

While all of this discussion on EDR is helpful, a significant question should be raised with respect to how EDR relates to cells. This will be addressed in the next section.

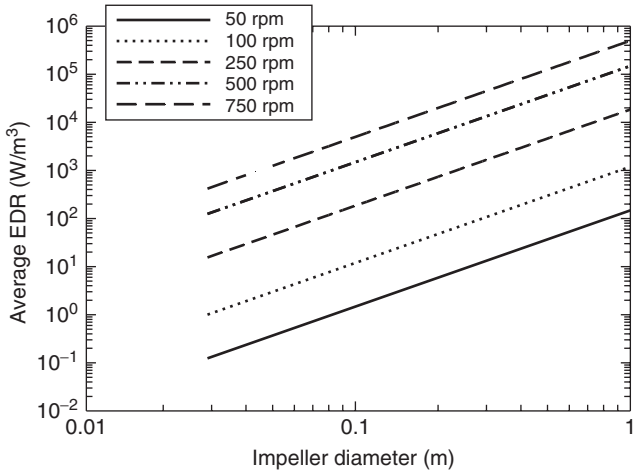


Figure 38.8. Average EDR for the whole vessel as a function of impeller diameter and RPM using a Rushton turbine in water. $H/T = 1$ and $T/D = 3$.

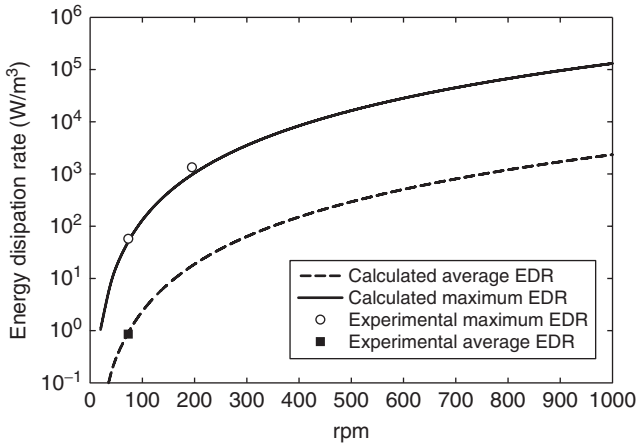


Figure 38.9. Calculated maximum and average energy dissipation rate as a function of RPM for an Applikon bioreactor containing four baffles. The single points correspond to experimental measurements without baffles. [Adapted from Mollet *et al*. (109).]

38.4 THE RELATIONSHIP OF ANIMAL CELLS TO HYDRODYNAMIC FORCES

Historically, there is probably no subject in animal cell culture cultivation that is more misunderstood and misquoted as being a "major limitation" to large-scale animal cell culture than the "shear sensitivity" of the cells. This misunderstanding, at least partially, arose from early reports (111,112), whose significance will be discussed later on. It also seems logical to think that a sufficiently intense force could disrupt the integrity of the cell membrane, causing cell death, especially, when animal cells lack a "cell wall" compared to robust bacteria. To further reinforce this perception, there are clear, well-established studies, which demonstrate almost complete cell destruction as a result of purely hydrodynamic forces and forces associated with gas sparging.

This misunderstanding has had a negative impact on the field in the past, and its legacy continues to this day in both the perception of many cell culturists, as well as in the under mixed, large-scale animal cell culture bioreactors that are currently in operation in many facilities. To begin establishing some structure to the notion of the "shear sensitivity" of animal cells, a number of concepts need to be further defined and/or refined:

1. The term *shear stress* is misleading. In reality, except for specific studies in specifically designed vessels, at the most fundamental level, cells are subjected to time varying shear and elongational forces in typical bioprocessing equipment. In addition, it has been argued that elongational forces might be more damaging to cells than shear forces (113).
2. There is a big difference between the hydrodynamic forces needed to create lethal or nonlethal effects on a cell attached to a surface relative to a cell in free suspension. This difference will be quantified below.
3. There is a big difference in the potential to damage cells when gas–medium interfaces are present relative to their absence, and this is especially true when protective surfactants are not present. This also will be discussed later on.
4. The sensitivity of animal cells to hydrodynamic forces can vary from one cell line to another and even within different clones of the same cell line; however, these differences have not been documented to prevent most cells of commercial interest to be cultured in bioreactors.
5. Because of the complexity of hydrodynamics, and especially under turbulent conditions, fundamental, first principle, mathematical models describing the hydrodynamic forces operating on cells in most bioprocessing equipment do not exist and probably never will. Consequently, we are left with continually improving empirical models and experimental studies that allow us to develop reasonable scale-up methodologies.

With this introduction, what is known on the effect of hydrodynamic forces on cells, both attached and in free suspension, as well as a scale-up methodology will be presented next.

38.4.1 Molecular Mechanism Involved in the Response of Animal Cells to Mechanical Forces

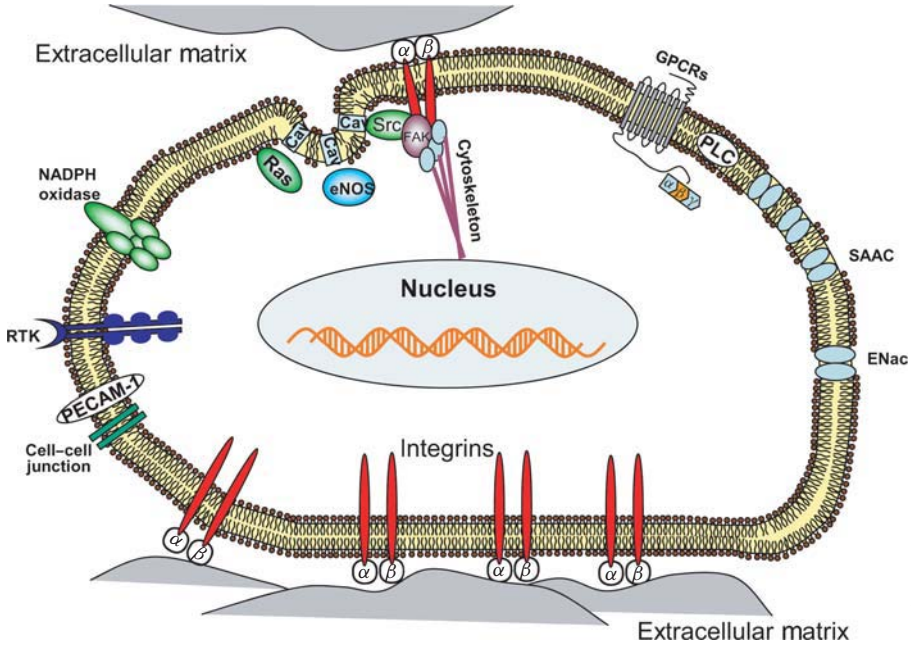
Liquid–cell interactions resulting from fluid flow have been extensively studied, predominately with cells that normally experience fluid flow, such as endothelial cells (ECs). Particularly interesting are models of the interactions of fluid forces with EC and their subsequent response to small changes of shear stress in laminar flow. Related to the EC response is that of smooth muscle cells (SMCs) to cyclic stretch resulting from the pulsatile nature of blood flow. These studies provide models to begin understanding the physiological responses to mechanical forces inside the human and animal circulatory and respiratory systems. While it is challenging to extrapolate the results from experiments with EC/SMC cells in laminar flow chambers to non-EC/SMC cells in the much more complex nature of turbulent flow in bioreactors, the significant, nonlethal effects of hydrodynamic forces provide insight into potential mechanisms and responses to investigate.

Several excellent reviews, including those of Malek and Izumo (114), Li *et al*. (115), Lehoux *et al*. (116), Tzima (117), Li and Xu (118), Chien (119) and Haga *et al*. (120), document what is known about the response of vascular endothelial and SMCs to sublethal hydrodynamic forces. One of the hallmarks of the EC response appears to be the rearrangement of the cell's cytoskeleton under the influence of fluid flow (121). The cytoskeleton is a three-dimensional intracellular network of several different types of protein filaments (i.e. actin) that determines the shape, mechanical properties, and movements of the cell. The filaments interplay closely with the cellular and nuclear membranes by anchoring to specific membrane proteins. When the cell is exposed to mechanical forces, the cytoskeleton attempts to resist them and undergoes deformation, especially if the cell is attached to a solid surface. Such deformation implies spatial reorganization of the cytoskeletal lattice; it is presumed that this reorganization is able to transmit the mechanical force along the whole cytoplasm to the nucleus. This mechanism suggests that the deformation of the cell brings together different cell components (i.e. proteins, enzymes, transcription factors and nucleic acids) in both the cytoplasm and the nucleus, originating a cascade of reactions that may lead to a wide diversity of cell responses.

A second proposed mechanism that allows cells to respond to fluid flow involves molecules at the luminal cell surface since they are in direct contact with the fluid. These molecules can be activated by direct conformational change as a result of flow (i.e. rupture or formation of disulfide bonds or bending/stretching of protein domains) or indirectly through mass transfer gradients. Such molecules include the following (115):

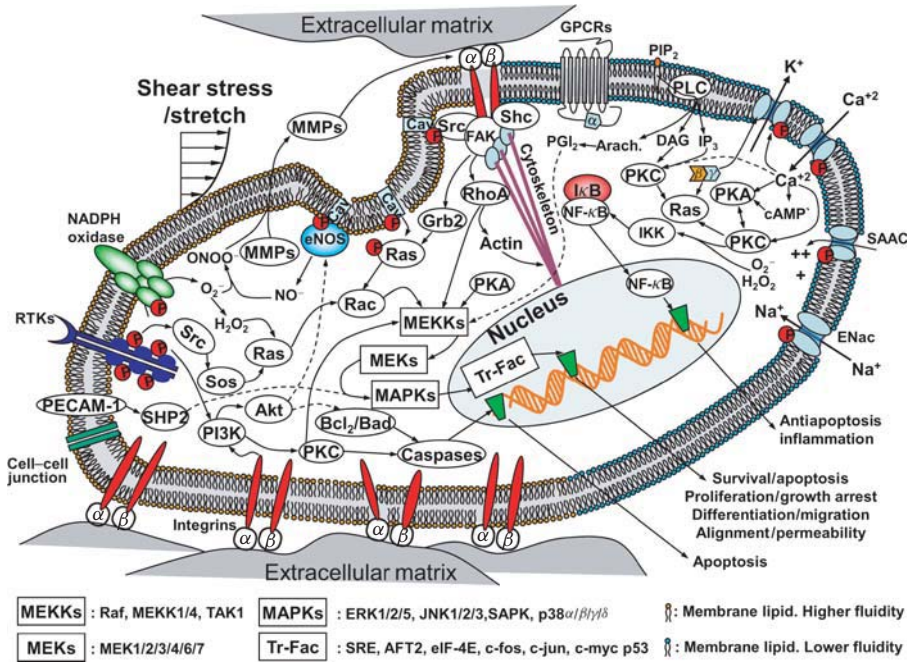
1. *Integrins.* These are a family of more than 20 transmembrane heterodimers normally connected to specific extracellular ligands such as fibronectin, vitronectin, and collagen. After the onset of flow, the integrin activation starts within 1 min and lasts for more than 6 h, originating an intracellular cascade involving kinases and cytoskeletal proteins.
2. *Ion channels.* Shear stress increases Ca^{+2} influx; higher Ca^{+2} concentration can lead to multiple Ca^{2+}-dependent cellular responses, including regulation of other channels (Cl^- and K^+). The response of this receptor is fast (within a minute) but subsides ~5 min after the beginning of the stress.
3. *Receptor Tyrosine Kinases.* These are a series of surface proteins (like Flk-1) transiently activated by shear stress, resulting in their oligomerization, tyrosine phosphorylation, association with other proteins (i.e. Shc), and a series of consequent gene transcription events.
4. *GPCRs and G Proteins.* G proteins are activated within 1 s after the onset of shear stress and they are involved in shear-induced Ras-GTPase activity that serves as molecular switches for a variety of cellular signaling events.
5. *PECAM-1.* Shear stress causes the transient phosphorylation of PECAM-1 within 1 min, a glycoprotein expressed in EC, platelets, and leucocytes that plays an important role in leucocyte aggregation and EC–leukocyte interaction.
6. *Membrane Lipid Bilayer.* Application of shear stress to EC cells causes an immediate (<10 s) increase in the fluidity of their membrane lipid bilayer in the upstream direction followed by a secondary, larger increase reaching a peak at 7 min. Alternatively, the fluidity of the membrane is reduced on the downstream side of the cell, indicating that the EC membrane lipid bilayer can sense the applied shear stress with spatial discrimination.

After sensing mechanical forces, the transduction of shear stress to the interior of the cell ends up in a series of fast signaling cascades that include opening of K^+ and Ca^{+2} channels, activation of heterotrimeric G proteins, production of NO^-, tyrosine phosphorylation of proteins such as Shc, c-src, and focal adhesion kinase (FAK), activation of mitogen-activated protein kinase (MAPK), protein kinase C (PKC), and C-Jun-*N*-terminal kinase (JNK), release of ROS, and activation of transcriptional regulators such as c-fos, c-jun, c-myc, and nuclear factor (NF)-κB. Slower responses include increased expression of genes for intercellular cell adhesion molecule (ICAM)-1, nitric oxide synthetase (NOS), platelet-derived growth factor (PDGF), tissue factor, transforming growth factor



(a)

PLC: Phospholipase c
SAAC: Single amino acid chelates
ENac: Epithelial Na channel
eNOS: endothelial Nitric oxide synthetase
RTK: Receptor Tyrosine Kinases



(b)

PIP: Phosphatidylinositol phosphate
PIP2: Phosphatidylinositol 4,5-biphosphate
FAK: Focal adhesion kinase
MMP: Metalloprotease
DAG: Diacylglycerol
PKC: Protein kinase C
PKA: Protein kinase A
cAMP: Cyclic adenosine monophosphate
IKK: Ikappa Kinase complex
MAPK: Mitogen activated protein kinase
MEKK: Serine/threonine-specific protein kinase (acts upon MAP kinase kinase)
SHP: Protein tyrosine phosphatase
ERK: Extracellular signal-regulated kinase
SAPK: Stress-activated protein kinase

Figure 38.10. Molecular signaling and response cascade in endothelial and smooth muscle cells (a) before and (b) after stimulation by hydrodynamic forces. (This figure is available in full color at http://onlinelibrary.wiley.com/book/10.1002/9780470054581.)

(TGF)-β, and monocyte chemoattractant protein (MCP)-1 and decreased expression of the vasoconstrictor endothelin 1 (Et-1) (117). Figure 38.10a and b describe the signaling cascade in EC/SMC that ends up in effects such as increased gene expression, proliferation or apoptosis, cell migration and alignment, increased cell membrane permeability, and changes in the mechanical properties of the cell.

While these results are interesting from a molecular biology point of view, few of these observations have been confirmed in suspended cells of biotechnological interest.

However, they do provide potential responses and mechanisms to investigate.

38.4.2 Cell Damage Mechanisms

The ambiguity in defining the concept of cell damage may arise owing to the fact that conditions that generate biological responses in cells may not be the same that generate negative effects on the process from the point of view of yield or productivity. Consider, for example, the culture of murine neural stem cells (NSCs) in 125-mL spinner flasks (122). Obviously, NSCs are not selected in nature to stand hydrodynamical forces as they grow in still environments and we might anticipate that increased hydrodynamical forces could affect cells' behavior. However, Fig. 38.11 shows that increasing agitation rate (starting from static culture in T-flask) increases significantly the number of viable cells, probably as a result of improved mass transfer and control of environmental variables inside the spinner; at the same time, viability is notoriously increased at higher stirring speeds and the mean diameter of aggregates is reduced, which translates into avoiding limiting conditions (specially oxygen) in the core of aggregates that could conduce to apoptosis or necrosis. The combined effect of an improved mass transfer and a decreased resistance to the transport of nutrients to every cell overcomes any negative effect of cellular damage that may exist, resulting in an increment of cell productivity. Quite similar results were obtained by Moreira *et al*. (70) for BHK cells grown as suspended natural aggregates, where again the maximum stirrer speed evaluated was 100 rpm.

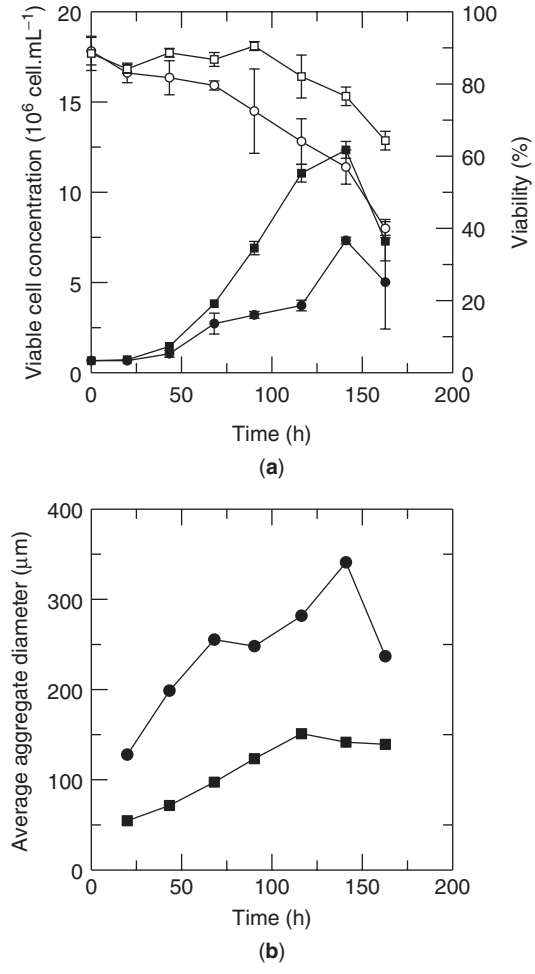


Figure 38.11. Effect of agitation rate on cell concentration, viability, and aggregate diameter of murine NSC, in batch suspension in a 125-mL spinner flask. Data points are average of duplicate runs. (a) Cell concentration: (●) 60 rpm; (■) 100 rpm. Viability: (○) 60 rpm; (□) 100 rpm. (b) Average aggregate diameter:(●) 60 rpm; (■) 100 rpm. [Adapted from Sen *et al*. (122).]

On the other hand, several reports indicate that highly stirred environments can *per se* affect viability of suspended mammalian cell cultures. As an example, Hirtenstein and Clark (123) showed that while agitation has a beneficial effect in the growth of Vero cells on microcarriers in spinner vessels, a further increase in stirrer speed after the optimum level dramatically affects the cell concentration in the system (see Fig. 38.12). Similarly, Kunas and Papoutsakis (124) reported that stirrer speeds above 700 rpm reduced the cells' viability on cultures of suspended hybridoma CRL-8018 when no bubbles are present, while not damage was seen at speeds less than 600 rpm. To further add complexity to the observations, Venkat *et al*. (125) and Croughan *et al*. (126) reported that 150–210 rpm in spinner vessels can result in significant damage to CHO cells attached to microcarriers.

From the two previous paragraphs the obvious conclusion is the existence of a maximum threshold of stirring speed beyond which stresses from hydrodynamic

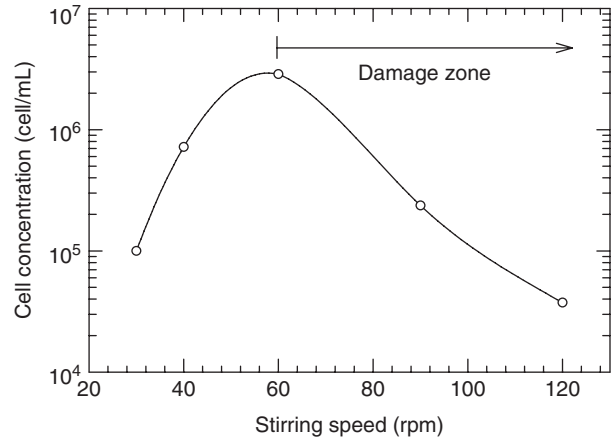


Figure 38.12. Effect of stirring speed on cell concentration after 7 days of culture of Vero cells on Cytodex microcarriers on 250-mL spinner vessels. [Data from Hirtenstein and Clark (123).]

forces can cause detrimental effects. However, how stirring speed relates to more fundamental properties of the fluid, the flow, and the cells remains more of an experimental exercise than a theoretically one. For practical purposes, detrimental effects can extend beyond conditions causing cell death (reduced viability, increased necrosis or apoptosis) to poorer product quality or lower productivity as compared with an appropriate control.

Reports detailing cell hydrodynamical damage or death are abundant; the first reports appeared simultaneously with early attempts to scale-up cultures of mammalian cells (111,112). Augenstein *et al*. (127) passed cultures of HeLa S3 and mouse L929 through capillary tubes of different diameters. Cell death occurred during the residence time of cells in the capillary and it could be correlated to average wall shear stress (10–200 N/m^2) as well as the power dissipated. Midler and Finn (128) reported that damage to shear-sensitive protozoa cells in a uniform shear device showed a two-phase behavior: a rapid primary damage followed by a slow decline of viable cells. This indicates that not only the magnitude of the hydrodynamic force, but also the exposure time should be taken into account when considering cell damage.

A diversity of methodologies has been used in the literature to assess the effects of mechanical forces on cells; the most representative are presented in the Table 38.7. Rheometers and parallel-plates laminar flow chambers have been often used to study cell sensitivity to shear stress, as the stress tensor can be defined with great precision and can be kept constant for long periods in those devices; Joshi *et al*. (129) present an extensive review of the use of rheometers on animal cells and outline a number of limitations of these devices, including

- Limited or null oxygenation capacity restricts experiments to short periods.
- Settling of cells forces continuous mixing and also restricts experiments to short intervals.
- Normal stresses (i.e. extensional flow) can not be applied to cells, even though it has been suggested that they can be as harmful or even more damaging to cells than shear (113,144,152).
- Hydrodynamic stress fluctuations, normally found in turbulent flows, may be even more damaging that steady shear stresses. Although laminar flow chambers are suitable to apply such fluctuations, the ability of rheometers to exert them is limited.
- It is difficult to apply the results obtained within these devices to figure out proper conditions for the cells inside bioreactors, given the much greater complexity of the turbulent flow and the wide range of hydrodynamic forces that a single cell may experience along the culture time.

TABLE 38.7. Methodologies Reported in Literature for Measurement of Properties of Animal Cells and/or Determination Effect of Hydrodynamical Forces on Animal Cells

Method	References
Laminar flow in capillary tubes	Thomas *et al*. (130)
Turbulent flow in capillary tubes	Augenstein *et al*. (127)
Magnetic twisters	Wang *et al*. (131)
Optical deformation	Guck *et al*. (132)
Micromanipulation (poking) devices	Zhang *et al*. (133); Goldman (134)
Stretching devices	Graf *et al*. (135)
Aspiration devices	Discher *et al*. (136); Jones *et al*. (137)
Cone and plate rheometers	Graf *et al*. (135); Goldblum *et al*. (138) Born *et al*. (139)
Concentric cylinder rheometers	Joshi *et al*. (129); Schürch *et al*. (140); Mardikar and Niranjan (141)
Laminar flow between parallel plates	Motobu *et al*. (142); Keane *et al*. (143)
Contracting flow devices	Gregoriades *et al*. (144); Ma *et al*. (145)
Stirred tanks	Telling and Elsworth (112); Hirtenstein and Clark (123); Croughan *et al*. (126); Oh *et al*. (20); Kunas and Papoutsakis (124,146); Oh *et al*. (147); Thomas *et al*. (130); Sen *et al*. (122)
Free jets	McQueen *et al*. (148)
Bioluminescence	Chen *et al*. (95)
Atomic force microscopy	Hoh and Schoenenberger (149); Mahaffy *et al*. (150)
Pressure probe	Tomos (151)

Because of the previous limitations, studies performed in stirred tanks are often preferred from a design point of view (see Table 38.7). Unfortunately, the wide diversity of geometrical configuration of bioreactors and bioprocess equipment, and the corresponding conditions used for such studies makes it difficult to also translate the results from these studies to other systems. For that reason, authors normally resort to try to explain their results based on a series of parameters, some of them based on fluid-dynamics theory, some of them strictly empiric. Some of those parameters are presented in Table 38.8 and a rationalization for their use will be presented in the next section.

Harmful effects other than cell lysis or death caused by hydrodynamic forces are often referred to as *sublethal*;

TABLE 38.8. Some Parameters Reported in Literature to Correlate the Effect of Hydrodynamical Forces on Cells

Parameter	Definition	References
Agitation rate	N	Kunas and Papoutsakis (124); Moreira *et al*. (70)
Impeller tip speed	$\pi N D$	Middler and Finn (128); Croughan *et al*. (126)
Mean power input	$\overline{\varepsilon} = \frac{P}{V} = \frac{N_p \rho N^3 D^5}{V}$	Ujcová *et al*. (153)
Integrated shear factor	$\mathrm{ISF} = \frac{2\pi N D}{T - D}$	Sinskey *et al*. (154); Croughan *et al*. (126); Chen *et al*. (95)
Volumetric integrated shear factor	$\mathrm{VISF} = \frac{2\pi N D}{T - D}\left(\frac{V_s}{V}\right)$	Chen *et al*. (95)
Kolmogorov eddy size	$\eta = \left(\frac{\nu^3}{\varepsilon}\right)^{1/4}$	Croughan *et al*. (126); Croughan *et al*. (155); Cherry and Papoutsakis (156); Oh *et al*. (20)
Local energy dissipation rate	$\varepsilon = \tau : \nabla U$	Bluestein and Mockros (104); Ma *et al*. (145); Mollet *et al*. (109)
Shear stress tensor	τ	Keane *et al*. (143)
Turbulent collision severity	$\mathrm{TCS} = (\varepsilon\nu)^{3/4}\left(\frac{\pi^2 \cdot \rho_b \cdot \alpha \cdot d_b}{72}\right)$	Cherry and Papoutsakis (156)
Impeller collision severity	$\mathrm{ICS} = \left(\frac{9\pi^4 \cdot \rho_b \cdot n_b \cdot n^3 \alpha \cdot D \cdot d_b^4}{512 \cdot V}\right)$	Cherry and Papoutsakis (156)
Energy dissipation-circulation function	$EDCF = \frac{\varepsilon}{t_c}$	Jüsten *et al*. (157); Rocha-Valadez *et al*. (158)

studies focusing on sublethal effects in bioprocessing equipment have been limited and sometimes contradictory. Al-Rubeai *et al*. (159) found increased glucose consumption and mitochondrial activity under intense agitation and in the absence of air bubbles. Al-Rubeai *et al*. (160) also reported that in addition to cell death under conditions of intensive agitation (1500 rpm), sublethal effects included lost of microvilli on the cell's surface and changes in cycle distribution of the cell population. Al-Rubeai *et al*. (161) and Lakhotia *et al*. (162) reported changes in DNA synthesis rate at sublethal conditions; in contrast, Passini and Goochee (163) did not find any effect. Mufti and Shuler (164) observed that human hepatoma cells attached to microcarriers and grown in 50 mL spinners responded to moderate levels of agitation by inducing a cytochrome P450 monooxygenase (CYP1A1) activity; CYP1A1 is involved in the oxidation of arachidonic acid, a substance whose metabolism has been observed to be altered by hydrodynamic stress in ECs cultured in parallel-plate flow chambers (165).

38.4.3 Quantification of Cell Damage

The often contradictory nature of sublethal hydrodynamic effects may be the result of the combination of mechanism classified within the same category. As an example, cells growing attached to a surface (surface culture or microcarriers) could experience similar nonlethal effects as those described for ECs; however, cells growing freely in suspended culture are less likely to exhibit these effects since the cells now are free to rotate, reducing considerably the deformation of the cytoskeleton and varying continuously the surface exposed to the hydrodynamic forces. Consistent with this concept, Ma *et al*. (145) experimentally demonstrated that CHO cells in suspension are four to five orders of magnitude less sensitive to rupture as result of the same level of EDR, than CHO cells attached to 200 μm microcarriers. Cherry and Papoutsakis (156,166) invoked collision between microcarriers and solid parts of the bioreactor (impeller and walls) as the main factors behind the increased sensitivity of cells growing in microcarriers; as a logical consequence, new parameters (turbulence collision

severity and impeller collision severity) were proposed by the authors to correlate cell damage, parameters that can not be used properly in freely suspended cells as the inertia of free cells is much lower than that of microcarriers.

The core of the challenge to develop methodologies and parameters to assess cell damage is threefold. First, the difficulty to relate results obtained with laminar flow devices with those results obtained at the turbulent conditions prevalent in industrial bioreactors as a result of our inability to properly characterize and quantify the bulk and local hydrodynamic in the vessel; second, the lack of a biological model explaining how the cells are affected by hydrodynamic forces and how that effect changes depending on characteristics such as cell type, age, and mode of growth (i.e. anchorage dependent or suspended). Third, the lack of a relationship or mathematical model relating the first two points; such relationship should link the lethal and sublethal effects of hydrodynamic forces to both a hydrodynamic descriptor or parameter and to the time of exposure to it.

Having a single parameter (or at least a reduced set of them) that can be related to overall yield, productivity, cell growth, and so on, is highly desirable from an engineering point of view to facilitate design and scale-up of new processes. Garcia and Chalmers (113) suggested that "ideal" parameters should be independent of the geometric characteristics of the culture system as cells do not "sense" the average conditions of the bioreactor but the characteristics of the microenvironment surrounding each one of them at each time. Consequently, criteria as mean power input, agitation rate, impeller tip speed, impeller-based Reynolds number or integrated shear factor should not be used as they represent average values derived from the particular geometric configuration of every system and because it has been shown that it is not possible to hold constant more than one of these parameters at the same time during scale-up (167).

While the idea proposed by Garcia and Chalmers (113) is theoretically appealing, its real implementation is currently an impossible task; first, the microenvironment surrounding every cell is not only dependent on the position (three-dimensional) but also is time-dependent as most industrial cultures are batch or fed-batch and therefore their properties change constantly; second, the turbulent nature of the fluid dynamics inside an stirred bioreactor further complicates the parameter, as its description will require a second-order stress tensor consisting of nine distinct stress vectors. Third, the behavior of every cell is likely to be history-dependent: two cells obtained from the same culture and placed in *exactly* identical conditions will probably respond differently as their previous history is expected not have been the same. Finally, a precise characterization of turbulent phenomena is out of reach: from a theoretical point of view, the number of unknown variables is greater than the number of equations, so turbulent flow can not be solved mathematically from first principles; from a practical point of view, available techniques are limited to a very few points at a time (laser Doppler anemometry, constant temperature wire anemometry); increasing the number of points evaluated makes the cost prohibitive or imposes limitations in the resolution of the velocity profiles (particle tracking velocimetry). Therefore, in the end it is necessary to rely on some kind of *average* (time-average, spatial-average) or on a *very gross distribution* of some factor to describe hydrodynamic phenomena inside a bioreactor.

A commonly cited parameter for analysis of mixing phenomena is the Kolmogorov's mixing microscale, η, which is a function of the ratio between the turbulence intensity (represented by the local EDR, ε, and the kinematic viscosity of the liquid, ν:

$$\eta = \left(\frac{\nu^3}{\varepsilon}\right)^{1/4} \tag{38.20}$$

Kolmogorov's mixing microscale (also referred to as *Kolmogorov eddy size*) was derived from classic dimensional analysis of turbulence by Andrey Kolmogorov in 1941; this theory of isotropic turbulence proposed that energy introduced into the liquid by the impeller undergoes a cascade from large, energy-containing scales to small, energy-dissipative scales. In the smallest scale, the fluid forms eddies where kinetic energy is ultimately converted into heat dissipation. As the Kolmogorov microscale depends only on fluid's and flow's properties and not on the system's geometry or large-scale flow patterns, it is a good candidate for a general parameter to correlate hydrodynamic conditions to cell damage. In fact, it has been proposed that cell damage occurs whenever the eddy-length η, reaches the size of a freely suspended cell or the size of a microcarrier. Good agreement was reported for small-scale vessels (126,156); however, this parameter suffers from several weaknesses: it requires turbulent flow (so it can not be properly applied to laminar flow); additionally, it has been shown experimentally that turbulence is not really isotropic although one can always assume "local" isotropy. Finally, the volume in which the energy is dissipated can not be determined from first principles. Suggested volumes used by some authors include the volume around the impeller or the small volumes associated with the trailing vortices emanating from the impellers (168).

In contrast to the Kolmogorov's mixing microscale, the EDR is a scalar parameter that is independent of the flow regime (turbulent/laminar) and accounts for both shear and extensional components of three-dimensional flow. EDR represents the rate at which work is done on a fluid element or, for the purpose of this review, a cell (169). The

EDR has been widely used to quantify local mixing performance in stirred tanks (105) as well as laminar flow devices (109,170); even Kolmogorov's mixing microscale is based on the local EDR. Therefore, it seems quite appealing to use this parameter to correlate the hydrodynamic cell damage in diverse devices. Although EDR can not be measured directly, it can be calculated in a relatively straightforward manner from Equations 38.17 and 38.18 provided that the broth behaves like an incompressible, Newtonian fluid (common situation in animal cell culture where the medium has water-like properties) and that the velocity vector has been accurately determined. This last requirement, however, limits the application of EDR to systems where the determination of the velocity vector U has been done experimentally or it can be determined analytically (laminar flow).

Ma *et al*. (145), designed and manufactured a microfluidic device in which suspended cells could be exposed to acute, high levels of EDR in a laminar flow environment; the advantages of this device include very well defined hydrodynamical characteristics and the possibility of emphasize the potentially more damaging extensional flow, although some degree of shear is present. Using such device, they subjected an insect cell line (Sf-9), a CHO cell line, a mouse-hybridoma cell line (HB-24) and a human breast cancer cell line (MCF-7) to single exposures of EDR and measured the release of the cytoplasmic enzyme lactate dehydrogenase (LDH) as an indication of cell membrane rupture. Every one of the cell lines studied showed significant cell lysis beginning around an EDR of 10^7 W/m^3 as observed in Fig. 38.13. This is in agreement with previous results from Zhang and Thomas (171), who demonstrated that an average EDR in the range of 10^8–10^9 W/m^3 in capillary tubes would completely disrupt TB/C3 hybridoma and NS1 myeloma cells.

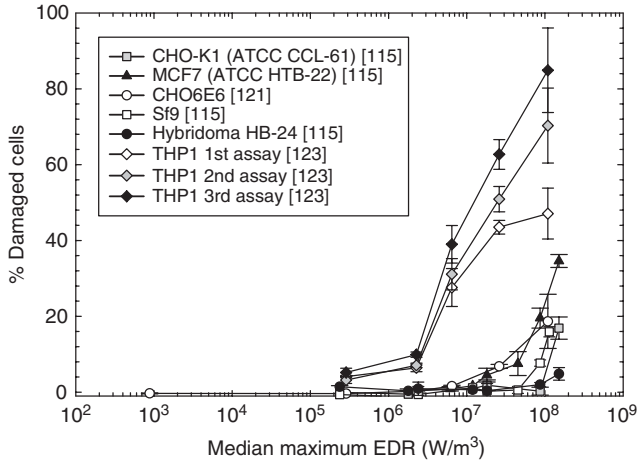


Figure 38.13. Experimental curves for the percentage of damage experienced by cells in a custom-design microfluidic device for single abuse experiments. [Adapted from Ma *et al*. (145) and Mollet *et al*. (172).]

To better express their results, Ma *et al*. (145) developed a one-dimensional plot whose improved version is presented in Fig. 38.14. As it can be appreciated, the values of EDR required to cause significant lysis in industrial cells are at least two orders of magnitude higher than the maximum EDR measured under normal conditions in bioreactors. Mollet *et al*. (170) developed an improved, autoclavable second-generation microfluidic device to further investigate if besides the evident levels of necrosis already reported, the effect of single exposures to high levels of EDR could lead to apoptosis. In addition to being consistent with the previous work by Ma *et al*. (145) in the levels of necrosis obtained after passing the cells once through the microdevice, Mollet *et al*. (170) observed that only a small fraction of CHO cells (CHO-K1) became apoptotic when exposed to sublethal levels of EDR.

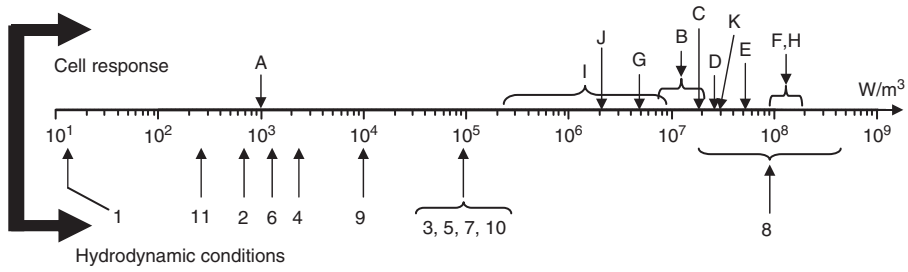
In a related subject, Mollet *et al*. (172) used the improved microfluidic device as well as computer fluid dynamics (CFD) commercial software to simulate the single passage of cells through the nozzle of a commercial fluorescence activated flow sorter (FACS). In the FACS, the cells experience high levels of EDR as a result of hydrodynamic focusing in the nozzle, with levels of cell necrosis on the order of 20–35% using CHO cells under typical operating conditions. They also found that nonadapted cells (THP1) may be much more sensitive to hydrodynamic stress than adapted, industrial cell lines (see Fig. 38.13).

38.4.4 Detrimental Effects of Sparging

It is a well reported observation that a dramatic reduction in cell number and viability of animal cells can be caused by sparging of gas into bioreactors (20,124,178,179). Even under conditions of unusually high stirring speeds, Oh *et al*. (20) and Kunas and Papoutsakis (124,146) showed that as long as there is no air introduction into the culture medium (i.e. sparging or bubble entrainment from the central vortex), hybridomas could withstand stirring speeds as high as 600 rpm without detectable cell damage.

The specific cause responsible for cell damage as a result of cell–bubble interactions may be attributed to four different events: bubble formation and detachment at the sparger, bubble break-up and coalescence in the impeller trailing vortices, bubble rising through the fluid or bubble disengagement at the surface of the culture. In the next lines, we present a brief summary of the results of research on each of these potential events.

Significant cell damage occurring near the sparger was suggested by Tramper *et al*. (180) who estimated that shear stress produced as a result of bubble formation and detachment could be up to one order of magnitude higher than that



Cell response

Symbol	Cell	Mode of Growth	References
A	CHO-K1, necrosis	Anchoraged	Gregoriades *et al.* [107]
B	Hybridoma, necrosis	Suspended	Thomas *et al.* [152]; Zhang *et al.* [153]
C	MCF-7, necrosis	Suspended	Ma *et al.* [115]
D	Mouse myeloma, necrosis	Suspended	McQueen and Bailey [154]
E	HeLa S3, mouse L929, necrosis	Suspended	Augenstein *et al.* [103]
F	CHO-K1, SF-9, HB-24, necrosis	Suspended	Ma et al. [115]
G	Uninfected and viral infected PERC6 cells, necrosis	Suspended	Submitted
H	Enthomopathogenic nematodes, necrosis	Suspended	Fife *et al.*[155]
I	CHO-K1, apoptosis	Anchorage	Mollet *et al.* [121]
J	THP-1, necrosis	Anchorage	Mollet *et al.* [123]
K	Algae, loss of flagella	Suspension	Hu *et al.* [156]

Hydrodynamic Conditions

Symbol	Process	Description	References
1	Agitation	Volume average in typical animal cell bioreactors.	Varley and Birch [9]
2	Agitation	Volume average in a 10 L mixing vessel (RT, 700 rpm)	Zhou and Kresta [84]
3	Agitation	Maximum in the 10 L mixing vessel (RT, 700 rpm)	
4	Agitation	Maximum in spinner vessel (200 rpm)	Wernersson and Trägårdh [157]
5	Agitation	Maximum in the 22,000 L mixing vessel	
6	Agitation	Volume average in a 22,000 L mixing vessel (RT, 240 rpm)	Venkat et al. [101]
7	Bubble rupture	Pure water, bubble diameter: 6.32 mm	Garcia-Briones *et al.* [137]
8	Bubble rupture	Pure water, bubble diameter: 1.7 mm	Boulton-Stone and Blake [136] Garcia-Briones *et al.* [137]
9	Flow through a pipe	Pure water, 100 mL/min, 1 mm diameter	Mollet *et al.* [85]
10	Flow through a micropipette tip	Flow through a 200 μL micropipette tip in 0.2 s	Mollet *et al.* [85]
11	Agitation	Volume average in a highly agitated animal cell bioreactor	Oh *et al.* [128]

Figure 38.14. Summary of the reported energy dissipation rate at which cells are affected as well as the reported levels of energy dissipation rate in various bioprocess environments. [Adapted from Ma *et al*. (145) and Mollet *et al*. (109).]

of bursting bubbles. Murhammer and Goochee (76) noticed an inverse correlation between the pressure drop across the sparger and the net growth of insect cells in airlift reactors, and suggested that the damage could be concentrated in the sparger zone as a result of the turbulent oscillation of the detaching bubbles or the fast liquid movement to fill in the space vacated by them.

In a series of insightful experiments under identical aeration and agitation conditions, Oh *et al*. (147) showed that bubble break-up as a result of the interaction of sparged air with the impeller is significant for cell damage. By comparing the results of placing the sparger in several positions, the authors showed that sparging air directly under the impeller led to an increase in the number of smaller bubbles and also to an increment in cell death, although it is difficult to say if it was caused by damage in the impeller region or was because of the increased bubble bursting in the medium-air interface.

Kioukia *et al*. (181) grew hybridoma cells in a 2.5-L reactor stirred with a Rushton turbine and oxygenated

only by surface aeration. In experiments with baffles in the reactor, successful growth and similar kinetic results were obtained at all speeds up to 400 rpm. In contrast, in experiments without baffles the peak cell density and growth rate decreased with increased speeds and cell death occurred from the start of the batch culture even though the average EDR was only 20% of that for baffled conditions. The authors argued that the cause for this behavior was the entrainment of air bubbles into the bulk of the liquid, and the further disengagement of these entrained bubbles at the top interface. This entrainment was the result of a vortex formed from the mixing; furthermore, since the bubbles never reached the impeller region, the damage could not be related to bubble break-up/coalescence in the impeller and only was associated with the bubbles bursting at the medium-air interface.

Tramper *et al*. (180) and Glasgow *et al*. (182) showed that values of shear stress derived from rising bubbles are extremely low (~0.1 Pa) and should, therefore, be neglected. To confirm these results, Handa-Corrigan *et al*. (183) and Jöbses *et al*. (184) introduced air in bubble columns of different sizes. With all other variables being constant, increasing column height, and thereby increasing the distance a bubble had to travel to rise to the top of the column, did not result in a reduction of viability for several cell types tested (hybridoma, BHK-21, myeloma, and lymphoblastoid cell lines).

Several researchers suggest that bubble-induced cell damage takes place only when a bubble, at the gas–liquid interface, ruptures (178,185,186). Phenomenologically, a bubble at a gas–liquid interface rises to a particular height above the flat liquid surface while the remaining part is submerged; the extent of the submerged part depends on the diameter. During rupture, the liquid drains by gravity from the film covering the raised part of the bubble up to a point where the film is so thin that a hole develops on the top and the bubble bursts; then, the liquid rapidly moves down the walls of the bubble cavity until the liquid reaches the bottom of the cavity; the resulting impact creates simultaneous upward and downward jets. Several studies indicate that this process creates a very high EDR over the very short period of time in which the rupture occurs. This bursting process was qualitatively presented by MacIntyre (187), in a series of cinephotography-derived profiles of the liquid–gas interface during the bubble break-up event. Subsequently, Boulton-Stone and Blake (188) and Garcia-Briones *et al*. (189) reported the results of computer simulations of bubble break-up with simulated profiles very close to those photographed by MacIntyre (187); their model indicates that the film at the top of the bubble retreats at speeds as high as ~8 m/s. Of more significance, the calculated maximum EDR is many orders of magnitude higher than those typically generated by an impeller. Additionally, such maximum EDRs are a function of the bubble radius being larger for smaller bubbles, indicating that smaller bubbles are potentially more damaging to cells. Interestingly, this result has been observed experimentally in several different studies (183,184).

The maximum EDRs (watts per cubic meter) calculated by García-Briones *et al*. (189) during bubble break-up ranged from 9.52×10^7 and 1.66×10^7 for bubbles with diameters of 0.77 and 1.70 mm, respectively. In contrast, for a 6.32 mm bubble, the EDR is only 9.4×10^4 W/m^3. Inspection of Fig. 38.14 indicates that these higher EDR values are well within the range of EDR values that were able to kill cells in the flow contraction device. This consistency between the simulated values of EDR during a bubble rupture, the values of EDR shown to kill cells in the flow contraction device, and the significantly lower EDR values in the impeller region provide an overall consistent picture that cell damage occurs because of bubble rupture at the liquid surface and the foam layer. The question that remains is whether enough cells are killed because of bubble bursting to account for all the cell death one can observe in a sparged culture.

To address this question, a study showed that on average $\sim 10^3$ cells are killed per 2 mm bubble burst (186) and the cell concentration collected from the upward jet is twice the bulk concentration in the culture. This result is in agreement with observations by Chalmers and Bavarian (190) and García-Briones and Chalmers (191), who, using video microscopy, detected cell attachment and accumulation on gas–liquid interfaces, especially in rising bubbles and the foam layer in the surface of the liquid in the reactor.

Parker and Barsom (192) reported that the chemical composition of the film surrounding air–liquid interfaces contained more hydrophobic materials compared to the bulk water; therefore, the phenomena of cell attachment to such film (microlayer) could potentially be explained as a result of the hydrophobic characteristics of the cell membrane. Chattopadhyay *et al*. (193,194) attempted to explain thermodynamically the cell adhesion to the gas–liquid interface and suggested a model for the variation of free energy as a function of the surface tension of the interfaces involved (gas–liquid–cells). According to their model, modifying the gas–liquid surface tension via chemical additives (such as Pluronic F-68) may create a condition where the change in free energy becomes positive and so the adherence stops being spontaneous. While a number of different surface active agents have been studied, including serum, dextran, hydroxyethyl starch, polyethylene glycol, or polyvinyl alcohol, Pluronic F-68 continues to be the additive of choice. Pluronic F-68 is a block copolymer of poly(oxyethylene) and poly(oxypropylene) and it is typically added to the culture medium in concentrations of 0.5–3 kg/m^3 (195).

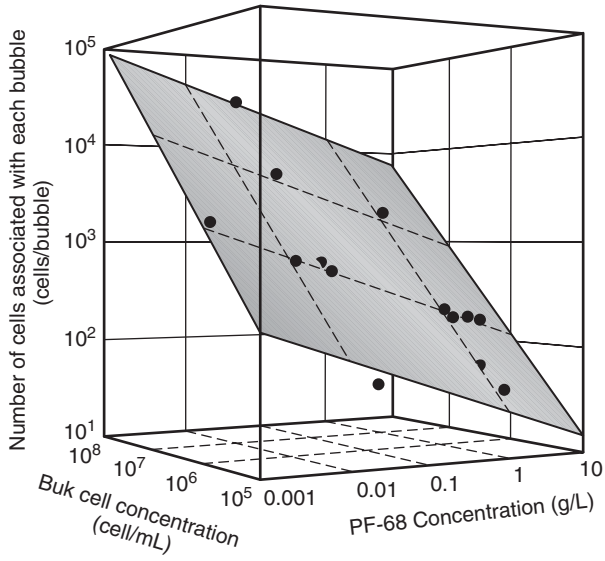


Figure 38.15. A three-dimensional plot of the number of cells associated with each bubble as a function of cell concentration (cells per milliliter) and Pluronic F-68 concentration. The dots indicated experimental data and the surface is the plot of a multiple variable regression. [Adapted from Ma *et al*. (202).]

In addition to reducing or inhibiting cell adhesion to the microlayer (190,191) by changing either the bubble film (196,197) or the cell membrane properties (198,199), other mechanisms have been proposed to explain the reduction or virtual elimination by surfactant agents of cell death as a result of bubbling; they include the following:

1. Interaction of the surfactant with the cell membrane, reducing its fluidity and rendering it stronger to mechanical stresses (200,201).
2. Nutritive effects of the surfactant on the cells. As mentioned by Ma *et al*. (29), the short time needed for detection of protective effects after addition of most chemical substances suggests that this mechanism of protection is not important.

In spite of the success of Pluronic F-68, a word of caution is in order: as the cell densities increase, the effectiveness of surfactants, even at high concentration, diminishes. A recent study by Ma *et al*. (202) demonstrated that even at high concentrations of F-68, a significant number of cells can be retained in the foam layer. Figure 38.15 is a figure from that report and as it can be observed, at cell concentrations greater than 10^7 cells/mL (which can be routinely obtained in industrial cultures) and relatively high F-68 concentration, more than 200 cells/bubble are removed into the foam layer.

38.5 SUMMARY

Animal cell culture has been used extensively for the production of a wide variety of proteins with biological and therapeutic activity. In spite of being a mature area of development, no universally accepted method of design or scale-up, based on purely fundamental principles, exists; however, the success of commercial processes, and published, peered review studies provide sufficient information to allow rational scale-up principles to be followed.

REFERENCES

1. Griffiths JB. Animal cell products, overview. In: Spier RE, editor. Volume 1, Encyclopedia of cell technology. New York: Wiley; 2000. pp 71–76.
2. Ozturk SS. Cell culture technology – an overview. In: Ozturk SS, Hu W-S, editors. Cell culture technology for pharmaceutical and cell-based therapies. Boca Raton (FL): CRC Press; 2006. pp 1–13.
3. Thomson Centerwatch. Drugs approved by the FDA. Available at http://www.centerwatch.com/patient/drugs/druglist.html. 2007.
4. Research and Market. Monoclonal antibodies 2007: competitive landscape & pipeline insight. Available at http://www.researchandmarkets.com/reportinfo.asp?report_id=367599. 2007.
5. Molowa DT, Mazanet R. The state of biopharmaceutical manufacturing. Biotechnol Annu Rev 2003; 9: 285–302.
6. Harrison RG. Observations on the living developing nerve fiber. Proc Soc Exp Biol Med 1907; 4: 140–143.
7. Carrel A. On the permanent life of tissues outside the organism. J Exp Med 1912; 15(5): 516–528.
8. Birch JR, Boraston R, Wood L. Bulk production of monoclonal antibodies in fermenters. Trends Biotechnol 1985; 3: 162–166.
9. Varley J, Birch J. Reactor design for large scale suspension animal cell culture. Cytotechnology 1999; 29: 177–205.
10. Hesse F, Ebel M, Konisch N, Sterlinski R, Kessler W, Wagner R. Comparison of a production process in a membrane-aerated stirred tank and up to 1000-L airlift bioreactors using BHK-21 cells and chemically defined protein-free medium.
11. Chu L, Robinson DK. Industrial choices for protein production by large-scale cell culture. Curr Opin Biotechnol 2001; 12: 180–187.
12. Butler M. Animal cell cultures: recent achievements and perspectives in the production of biopharmaceuticals. Appl Microbiol Biotechnol 2005; 68: 283–291.
13. Meier SJ. Cell culture scale-up: mixing, mass transfer, and use of appropriate scale-down models. Biochemical engineering XIV. Canada : Harrison Hot Springs; 2005.
14. Gotoh T, Mochizuki G, Kikuchi K-I. Perfluorocarbon-mediated aeration applied to recombinant protein production by virus-infected insect cells. Biochem Eng J 2001; 7(1): 69–78.
15. Zeng A-P, Bi J-X. Cell culture kinetics and modeling. In: Ozturk SS, Hu W-S, editors. Cell culture technology for

pharmaceutical and cell-based therapies. Boca Raton (FL): CRC Press; 2006. pp 299–348.

16. Miller WM, Wilke CR, Blanch HW. Effect of dissolved oxygen concentration on hybridoma growth and metabolism in continuous culture. J Cell Physiol 1987; 132: 524–530.
17. Ozturk SS, Palsson BO. Effects of dissolved oxygen on hybridoma cell growth, metabolism and antibody production kinetics in continuous culture. Biotechnol Prog 1990; 6: 437–446.
18. Lin AA, Miller WM. Modulation of glutathione level in CHO cells. Effects of oxygen concentration and previous exposure to hypoxia. Ann N Y Acad Sci 1992; 665: 117–126.
19. Packer L, Fuehr K. Low oxygen concentration extends the lifespan of cultured human diploid cells. Nature 1977; 267: 423–425.
20. Oh SKW, Nienow AW, Al-Rubeai M, Emery AN. The effect of agitation intensity with and without continuous sparging on the growth and antibody production of hybridoma cells. J Biotechnol 1989; 12: 45–62.
21. Jan DCH, Petch DA, Huzel N, Butler M. The effect of dissolved oxygen on the metabolic profile of a murine hybridoma grown in serum-free medium in continuous culture. Biotechnol Bioeng 1997; 54: 153–164.
22. Kunkel JP, Jan DCH, Jamieson JC, Butler M. Dissolved oxygen concentration in serum-free continuous culture affects N-linked glycosylation of a monoclonal antibody. J Biotechnol 1998; 62: 55–71.
23. deZengotita VM, Miller WM, Aunins JG, Zhou W. Phosphate feeding improves high-cell-concentration NS0 myeloma culture performance for monoclonal antibody production. Biotechnol Bioeng 2000; 69(5): 566–576.
24. Wurm FM. Production of recombinant protein therapeutics in cultivated mammalian cells. Nat Biotechnol 2004; 22(11): 1393–1398.
25. Nienow AW. Reactor engineering in large scale animal cell culture. Cytotechnology 2006; 50: 9–33.
26. Gimenes MAP, Carlos LCS, Faria LFF, Pereira N Jr. Oxygen uptake rate in production of xylitol by *Candida guilliermondii* with different aeration rates and initial xylose concentrations. Appl Biochem Biotechnol 2002; 98–100(1–9): 1049–1059.
27. Fong SS, Joyce AR, Palsson BØ. Parallel adaptive evolution cultures of Escherichia coli lead to convergent growth phenotypes with different gene expression states. Genome Res 2005; 15: 1365–1372.
28. Shiloach J, Fass R. Growing E. coli to high cell density – a historical perspective on method development. Biotechnol Adv 2005; 23: 345–357.
29. Ma N, Mollet M, Chalmers JJ. Aeration, mixing and hydrodynamics in bioreactors. In: Ozturk SS, Hu W-S, editors. Cell culture technology for pharmaceutical and cell-based therapies. Boca Raton (FL): CRC Press; 2006. pp 225–248.
30. Kompala DS, Ozturk, SS. Optimization of high cell density perfusion reactors. In: Ozturk SS, Hu W-S, editors. Cell culture technology for pharmaceutical and cell-based therapies. Boca Raton (FL): CRC Press; 2006. pp 387–416.
31. Boraston R, Thompson PW, Garland S, Birch JR. Growth and oxygen requirement of antibody-producing mouse hybridoma cells in suspension culture. Dev Biol Stand 1983; 55: 103–111.
32. Miller WM, Wilke CR, Blanch HW. Transient responses of hybridoma metabolism to changes in the oxygen supply rate in continuous culture. Bioprocess Eng 1988; 3: 103–113.
33. Backer MP, Metzger LS, Slaber PL, Nevitt KL, Boder GB. Large scale production of monoclonal antibodies in suspension culture. Biotechnol Bioeng 1988; 32: 993–1000.
34. Ramirez OT, Mutharasan R. Cell cycle- and growth phase-dependent variations in size distribution, antibody productivity and oxygen demand in hybridoma cultures. Biotechnol Bioeng 1990; 36(8): 839–848.
35. Hiller GW, Aeschlimann AD, Clark DS, Blanch HW. A kinetic analysis of hybridoma growth and metabolism in continuous suspension culture on serum-free medium. Biotechnol Bioeng 1991; 38: 733–741.
36. Hensler WT, Agathos SN. Evaluation of monitoring approaches and effects of culture conditions on recombinant protein production in baculovirus-infected insect cells. Cytotechnology 1994; 15: 177–186.
37. Wong TKK, Nielsen LK, Greenfield PF, Reid S. Relationship between oxygen uptake rate and time of infection of Sf9 insect cells infected with a recombinant baculovirus. Cytotechnology 1994; 15: 157–167.
38. Zhou W, Hu W-S. On line characterization of a hybridoma cell culture process. Biotechnol Bioeng 1994; 44: 170–177.
39. Yoon S, Konstantinov KB. Continuous, real-time monitoring of the oxygen-uptake rate (OUR) in animal-cell bioreactors. Biotechnol Bioeng 1994; 44: 983–990.
40. Dorresteijn RC, Degooijer CD, Tramper J, Beuvery EC. A method for simultaneous determination of solubility and transfer coefficient of oxygen in aqueous media using off-gas mass spectrometry. Biotechnol Bioeng 1994; 43: 149–154.
41. Eyer K, Oeggerli A, Heinzle E. On-line gas analysis in animal cell cultivation: II. Methods for oxygen uptake rate estimation and its application to controlled feeding of glutamine. Biotechnol Bioeng 1995; 45: 54–62.
42. Gray DR, Chen S, Howarth W, Inlow D, Maiorella L. CO_2 in large-scale and high-density CHO cell perfusion culture. Cytotechnology 1996; 22: 65–78.
43. Rhiel M, Mitchell-Logean CM, Murhammer DW. Comparison of *Trichoplusia* ni BTI-Tn-5B1-4 (High Five™) and *Spodoptera frugiperda* Sf-9 insect cell line metabolism in suspension cultures. Biotechnol Bioeng 1997; 55: 909–920.
44. Sauer PW, Burky JE, Wesson MC, Sternard HD, Qu L. A high-yielding, generic fed-batch cell culture process for production of recombinant antibodies. Biotechnol Bioeng 2000; 67(5): 585–597.
45. Barnabé N, Butler M. The effect of glucose and glutamine on the intracellular nucleotide pool and oxygen uptake rate of a murine hybridoma. Cytotechnology 2000; 34: 47–57.
46. Ducommun P, Bolzonella I, Rhiel M, Pugeaud P, von Stockar U, Marison IW. On-line determination of animal cell concentration. Biotechnol Bioeng 2001; 72(5): 515–522.
47. Carvalhal AV, Marcelino I, Carrondo MJT. Metabolic changes during cell growth inhibition by p27 overexpression. Appl Microbiol Biotechnol 2003; 63: 164–173.
48. Deshpande RR, Heinzle E. On-line oxygen uptake rate and culture viability measurement of animal cell culture using microplates with integrated oxygen sensors. Biotechnol Lett 2004; 26: 763–767.
49. Palomares LA, Lopez S, Ramirez OT. Utilization of oxygen uptake rate to assess the role of glucose and glutamine in the

metabolism of infected insect cell cultures. Biochem Eng J 2004; 19(1): 87–93.

50. Van't Riet K. Review of measuring methods and results in non-viscous gas liquid mass transfer in stirred vessels. Ind Eng Chem Process Des Dev 1979; 18(3): 357–363.
51. Asay T, Kono T. Estimation of oxygen absorption coefficient and power consumption in a stirred-tank fermentor. J Ferment Technol 1982; 60(3): 265–268.
52. Langheinrich C, Nienow AW, Eddleston T, Stevenson NC, Emery AN, Clayton TM, Slater NKH. Oxygen transfer in stirred bioreactors under animal cell culture conditions. Food Bioprod Process 2002; 80(1): 39–44.
53. Nienow AW, Langheinrich C, Stevenson NC, Emery AN, Clayton TM, Slater NKH. Homogenization and oxygen transfer rates in large agitated and sparged animal cell bioreactors: some implications for growth and production. Cytotechnology 1996; 22: 87–94.
54. Tatterson GB. Fluid mixing and gas dispersion in agitated tanks. New York: Mc-Graw Hill; 1991.
55. Chisti Y. Hydrodynamic damage to animal cells. Crit Rev Biotechnol 2001; 21(2): 67–110.
56. Amanullah A, Serrano-Carreon L, Castro B, Galindo E, Nienow AW. The influence of impeller type in pilot scale xanthan fermentations. Biotechnol Bioeng 1998; 57(1): 95–108.
57. Menisher T, Metghalchi M, Gutoff EB. Mixing studies in bioreactors. Bioprocess Eng 2000; 22(2): 115–120.
58. Metz B, Kossen NWP, van Suijdam JC. The rheology of mold suspensions. Adv Biochem Eng 1979; 11: 103–156.
59. Morão A, Maia CI, Fonseca MMR, Vasconcelos JMT, Alves SS. Effect of antifoam addition on gas-liquid mass transfer in stirred fermenters. Bioprocess Biosyst Eng 1999; 20(2): 165–172.
60. Lavery M, Nienow AW. Oxygen transfer in animal cell culture medium. Biotechnol Bioeng 1987; 30(3): 368–373.
61. Aunins JG, Woodson BA Jr., Hale TK, Wang DIC. Effects of paddle impeller geometry on power input and mass transfer in small-scale animal cell culture vessels. Biotechnol Bioeng 1989; 34(9): 1127–1132.
62. Hu WS, Meier J, Wang DIC. Use of surface aerator to improve oxygen transfer in cell culture. Biotechnol Bioeng 1986; 28: 122–125.
63. Kamen AA, Chavarie C, Andre G, Archambault J. Design parameters and performance of a surface baffled helical ribbon impeller bioreactor for the culture of shear sensitive cells. Chem Eng Sci 1992; 27: 2375–2380.
64. Singh V. Disposable bioreactor for cell culture using wave-induced agitation. Cytotechnology 1999; 30: 149–158.
65. Lowe KC, Davey MR, Power JB. Perfluorochemicals: their applications and benefits to cell culture. Trends Biotechnol 1998; 16: 272–277.
66. Sundararajan A, Ju L-K. Use of cyanobacterial gas vesicles as oxygen carriers in cell culture. Cytotechnology 2006; 52: 139–149.
67. Cho MH, Wang SS. Enhancement of oxygen-transfer in hybridoma cell-culture by using a perfluorocarbon as an oxygen carrier. Biotechnol Lett 1988; 10: 855–860.
68. Ju L-K, Armiger WB. Use of perfluorocarbon emulsion in cell-culture. Biotechniques 1992; 12: 258–263.
69. Gotoh T, Mochizuki G, Kikuchi K-I. A novel column fermentor having a wetted-wall of perfluorocarbon as an oxygen carrier. Biochem Eng J 2001; 8(2): 165–169.
70. Moreira JL, Cruz PE, Santana PC, Feliciano AS. Influence of power input and aeration method on mass transfer in a laboratory animal cell culture vessel. J Chem Technol Biotechnol 1995; 62: 118–131.
71. Lütz S, Rao NN, Wandrey C. Membranes in biotechnology. Chem Eng Technol 2006; 29(12): 1404–1415.
72. Lehmann J, Vorlop J, Buntemayer H. Bubble-free reactors and their development for continuous culture with cell recycle. In: Spier RE, Griffiths JB, editors. Volume 3, Animal cell biotechnology. London: Academic Press; 1988. pp 221–237.
73. Vorlop J, Lehmann J. Oxygen transfer and carrier mixing in large scale membrane stirred cell culture reactors. In: Spier RE, Griffiths JB, Stephenne J, Crooy PJ, editors. Advances in animal cell biology and technology for bioprocesses. Svenoaks: Butterworths; 1989. pp 366–369.
74. Kretzmer G. Industrial processes with animal cells. Appl Microbiol Biotechnol 2002; 59: 135–142.
75. Marks DM. Equipment design considerations for large scale cell culture. Cytotechnology 2003; 42: 21–33.
76. Murhammer DW, Goochee CF. Sparged animal cell bioreactors: mechanism of cell damage and Pluronic F-68 protection. Biotechnol Prog 1990; 6: 391–397.
77. Kulkarni AA, Joshi JB. Bubble formation and bubble rise velocity in gas-liquid systems: a review. Ind Eng Chem Res 2005; 44: 5873–5931.
78. Orton D, Wang DIC. Fluorescent visualization of cell death in bubble aerated bioreactors. Cell culture engineering III: United Engineering Foundation; 1991.
79. Harris R, Ng KW, Wraith AE. Spargers for controlled bubble size by means of the multiple slot disperser (MSD). Chem Eng Sci 2005; 60: 3111–3115.
80. Nehring D, Czermak P, Vorlop J, Lübben H. Experimental study of a ceramic microsparging aeration system in a pilot-scale animal cell culture. Biotechnol Prog 2004; 20: 1710–1717.
81. Chisti Y. Animal cell culture in stirred bioreactors: observations in scale-up. Bioprocess Eng 1993; 9: 191–196.
82. Smith CM, Marks AD, Lieberman MA. Marks' basic medical biochemistry: a clinical approach. 2nd ed. Philadelphia (PA): Lippincott Williams & Wilkins; 2005.
83. deZengotita VM, Kimura R, Miller WM. Effects of CO_2 and osmolality on hybridoma cells: growth, metabolism and monoclonal antibody production. Cytotechnology 1998; 28: 213–227.
84. Mostafa SS, Gu X. Strategies for improved dCO2 removal in large-scale fed-batch cultures. Biotechnol Prog 2003; 19(1): 45–51.
85. Zhu MM, Goyal A, Rank DL, Gupta SK, VandenBoom T, Lee SS. Effects of elevated pCO_2 and osmolality on growth of CHO cells and production of antibody-fusion protein B1: a case study. Biotechnol Prog 2005; 21(1): 70–77.
86. Drapeau D, Luan, YT, Whiteford, JC, Lavin, DP, Adamson, SR. Cell culture scale-up in stirred tank reactors. Presented at the Annual Meeting of Society of Industrial Microbiology; Orlando (FL); 1990.
87. Birch JR, Thompson PW, Boraston R, Oliver S, Lambert, K. The large scale production of monoclonal antibodies in airlift

fermenters. In: Webb C, Mavituna F, editors. Plant and animal cells: process possibilities. Chichester: Ellis Horwood; 1987.

88. Gódia F, Cairó JJ. Cell metabolism. In: Ozturk SS, Hu W-S, editors. Cell culture technology for pharmaceutical and cell-based therapies. Boca Raton (FL): CRC Press; 2006. pp 81–112.
89. Uhl VW, Gray JB. Volume II, Mixing: theory and practice. San Diego (CA): Academic Press; 1967. p 254.
90. Langheinrich C, Nienow AW. Control of pH in large-scale, free suspension animal cell bioreactors: alkali addition and pH excursions. Biotechnol Bioeng 1999; 66: 171–179.
91. Ozturk SS. Engineering challenges in high cell density cell culture systems. Cytotechnology 1996; 22: 3–16.
92. Oldshue JY. Fluid mixing technology. New York: McGraw-Hill; 1983.
93. Hempel DC. Fundamentals of scale-up for biotechnological processes in stirred fermentors. In: Finn RK, Präve P, Schlingmann M, Crueger W, Esser K, Thaver R, Wagner F, editors. Biotechnology focus 1: fundamentals, applications, information. Munich: Hanser Publishers; 1988. pp 51–94.
94. Hudcova V, Machon V, Nienow AW. Gas liquid dispersion with dual Rushton turbine impellers. Biotechnol Bioeng 1989; 34: 617–628.
95. Chen AK, Latz MI, Frangos JA. The use of dinoflagellate bioluminescence to characterize cell stimulation in bioreactors. Biotechnol Bioeng 2003; 83(1): 93–103.
96. Galindo E, Nienow AW. Performance of the Scaba 6SRGT agitator in mixing of simulated xanthan gum broths. Chem Eng Technol 1993; 16(2): 102–108.
97. Machon V, Vlcek J, Skrivanek J. Dual impeller systems for aeration of liquids: an experimental study. Proceedings of the 5th European Conference on Mixing; Würzburg, Germany; 1985. pp 155–169.
98. Cui YQ, van der Lans RGJM, Luyben KCAM. Local power uptakes in gas liquid systems with single and multiple Rushton turbines. Chem Eng Sci 1996; 51(11): 2631–2636.
99. Linek V, Moucha T, Sinkule J. Gas–liquid mass transfer in vessel stirred with multiple-impellers I: gas–liquid mass transfer characteristics in individual stages. Chem Eng Sci 1996; 51(12): 3203–3212.
100. Kresta SM, Mao D, Roussinova V. Batch blend time in square stirred tanks. Chem Eng Sci 2006; 61(9): 2823–2825.
101. Nienow AW. On impeller circulation and mixing effectiveness in the turbulent flow regime. Chem Eng Sci 1997; 52(15): 2557–2565.
102. Bird RB, Stewart WE, Lightfoot EN. Transport phenomena. 2nd ed. New York: John Wiley & Sons; 2006.
103. Brodkey RS. The phenomena of fluid motions. New York: Dover Publishing; 1995.
104. Bluestein M, Mockros LF. Hemolysis effects of energy dissipation in flowing blood. Med Biol Eng Comput 1969; 7(1): 1–6.
105. Kresta S. Turbulence in stirred tanks: anisotropic, approximate and applied. Can J Chem Eng 1998; 76: 563–575.
106. Cutter LA. Flow and turbulence in a stirred tank. AIChE J 1966; 12: 35–45.
107. Costes J, Couderc JP. Study by laser Doppler anemometry of the turbulent flow induced by a Rushton turbine in a stirred tank: Influence of the size of the units – II. Spectral analysis and scales of turbulence. Chem Eng Sci 1988; 43(10): 2765–2772.
108. Zhou G, Kresta SM. Distribution of energy dissipation between convective and turbulent flow for three frequently used impellers. Chem Eng Res Des Trans Inst Chem Eng Part A 1996; 74: 379–389.
109. Mollet M, Ma N, Zhao Y, Brodkey R, Taticek R, Chalmers JJ. Bioprocess equipment: characterization of energy dissipation rate and its potential to damage cells. Biotechnol Prog 2004; 20: 1437–1448.
110. Zhou G, Kresta SM. Impact of tank geometry on the maximum turbulence energy dissipation rate for impellers. AIChE J 1996; 42: 2476–2490.
111. Bryant JC, Schilling EL, Earle WR, Evans VJ. Massive fluid suspension cultures of certain mammalian tissue cells. III. Exploratory supplementation experiments with chemically defined medium NCTC 109. J Natl Cancer Inst 1960; 24: 859–871.
112. Telling RC, Elsworth R. Submerged culture of hamster kidney cells in a stainless steel vessel. Biotechnol Bioeng 1965; 7(3): 417–434.
113. Garcia-Briones MA, Chalmers JJ. Flow parameters associated with hydrodynamic cell injury. Biotechnol Bioeng 1994; 44: 1089–1098.
114. Malek AM, Izumo S. Molecular aspects of signal transduction of shear stress in the endothelial cell. J Hypertens 1994; 12(9): 989–999.
115. Li Y-SJ, Haga JH, Chien S. Molecular basis of the effects of shear stress on vascular endothelial cells. J Biomech 2005; 38: 1949–1971.
116. Lehoux S, Castier Y, Tedgui A. Molecular mechanisms of the vascular responses to haemodynamic forces. J Intern Med 2006; 259: 381–392.
117. Tzima E. Role of small GTPases in endothelial cytoskeletal dynamics and the shear stress response. Circ Res 2006; 98: 176–185.
118. Li C, Xu Q. Mechanical stress-initiated signal transduction in vascular smooth muscle cells *in vitro* and *in vivo*. Cell Signal 2007; 19: 881–891.
119. Chien S. Mechanotransduction and endothelial cell homeostasis: the wisdom of the cell. Am J Physiol Heart Circ Physiol 2007; 292: 1209–1224.
120. Haga JH, Li Y-SJ, Chien S. Molecular basis of the effects of mechanical stretch on vascular smooth muscle cells. J Biomech 2007; 40: 947–960.
121. Papadaki M, Eskin SG. Effects of fluid shear stress on gene regulation of vascular cells. Biotechnol Prog 1997; 13(3): 209–221.
122. Sen A, Kallos MS, Behie LA. Effects of hydrodynamics on cultures of mammalian neural stem cell aggregates in suspension bioreactors: novel reactor engineering for the new millennium. Ind Eng Chem Prod Res Dev 2001; 40(23): 5350–5357.
123. Hirtenstein MD, Clark JM. Critical parameters in the microcarrier culture of animal cells. In: Richards R, Rajan K, editors. Volume 2, Tissue culture in medical research. Oxford: Pergamon Press; 1980.
124. Kunas KT, Papoutsakis ET. Damage mechanisms of suspended animal cells in agitated bioreactors with and without bubble entrainment. Biotechnol Bioeng 1990; 36: 476–483.

125. Venkat R, Stock R, Chalmers JJ. Study of hydrodynamics in microcarrier culture spinner vessels: a particle tracking velocimetry approach. Biotechnol Bioeng 1996; 49: 456–466.
126. Croughan MS, Hamel JF, Wang DIC. Hydrodynamic effect on animal cells grown in microcarrier cultures. Biotechnol Bioeng 1987; 29: 130–141.
127. Augenstein DC, Sinskey AJ, Wang DIC. Effect of shear on the death of two strains of mammalian tissue cells. Biotechnol Bioeng 1971; 13: 409–418.
128. Midler J Jr., Finn RK. A model system for evaluating shear in the design of stirred fermentors. Biotechnol Bioeng 1966; 8: 71–84.
129. Joshi JB, Elias CB, Patole MS. Role of hydrodynamic shear in the cultivation of animal, plant and microbial cells. Chem Eng J 1996; 62: 121–141.
130. Thomas CR, Al-Rubeai M, Zhang Z. Prediction of mechanical damage to animal cells in turbulence. Cytotechnology 1994; 15: 329–335.
131. Wang N, Butler JP, Ingber DE. Mechanotransduction across the cell surface and through the cytoskeleton. Science 1993; 260(5111): 1124–1127.
132. Guck J, Ananthakrishnan R, Mahmood H, Moon TJ, Cunningham CC, Käs J. The optical stretcher: a novel laser tool to micromanipulate cells. Biophys J 2001; 81: 767–784.
133. Zhang Z, Ferenczi MA, Thomas CR. A micromanipulation technique with a theoretical cell model for determining mechanical properties of single mammalian cells. Chem Eng Sci 1992; 47(6): 1347–1354.
134. Goldman WH. Mechanical manipulation of animal cells: cell indentation. Biotechnol Lett 2000; 22: 431–435.
135. Graf R, Apenberg S, Freyberg M, Friedl P. A common mechanism for the mechanosensitive regulation of apoptosis in different cell types and for different mechanical stimuli. Apoptosis 2003; 8: 531–538.
136. Discher DE, Mohandas N, Evans EA. Molecular maps of red cell deformation: hidden elasticity and *in situ* connectivity. Science 1994; 266(5187): 1032–1035.
137. Jones WR, Ting-Beall HP, Lee GM, Kelley SS, Hochmuth RM, Guilak F. Alterations in the Young's modulus and volumetric properties of chondrocytes isolated from normal and osteoarthritic human cartilage. J Biomech 1999; 32: 119–127.
138. Goldblum S, Bae YK, Hink WF, Chalmers JJ. Protective effect of methylcellulose and other polymers on insect cells subjected to laminar shear stress. Biotechnol Prog 1990; 6: 383–390.
139. Born C, Zhang Z, Al-Rubeai M, Thomas CR. Estimation of disruption of animal cells by laminar shear stress. Biotechnol Bioeng 1992; 40(9): 1004–1010.
140. Schürch U, Kramer H, Einsele A, Widmer F, Eppenberger HM. Experimental evaluation of laminar shear stress on the behaviour of hybridoma mass cell cultures, producing monoclonal antibodies against mitochondrial creatine kinase. J Biotechnol 1988; 7(3): 179–184.
141. Mardikar SH, Niranjan K. Observations of the shear damage to different animal cells in a concentric cylinder viscometer. Biotechnol Bioeng 2000; 68(6): 697–704.
142. Motobu M, Wang PC, Matsumura M. Effect of shear stress on recombinant Chinese hamster ovary cells. J Ferment Bioeng 1998; 85(2): 190–195.
143. Keane JT, Ryan D, Gray PP. Effect of shear stress on expression of a recombinant protein by Chinese hamster ovary cells. Biotechnol Bioeng 2003; 81(2): 211–220.
144. Gregoriades N, Clay J, Ma N, Koelling K, Chalmers JJ. Cell damage of microcarrier cultures as a function of local energy dissipation created by a rapid extensional flow. Biotechnol Bioeng 2000; 69: 171–182.
145. Ma N, Koelling K, Chalmers JJ. The fabrication and use of a transient contraction flow device to quantify the sensitivity of mammalian and insect cells to hydrodynamic forces. Biotechnol Bioeng 2002; 80: 428–437.
146. Kunas KT, Papoutsakis ET. The protective effect of serum against hydrodynamic damage of hybridoma cells in agitated and surface aerated bioreactors. Biotechnology 1990; 15: 57–70.
147. Oh SKW, Nienow AW, Al-Rubeai M, Emery AN. Further studies of the culture of mouse hybridoma in an agitated bioreactor with and without continuous sparging. J Biotechnol 1992; 22: 245–270.
148. McQueen A, Meilhoc E, Bailey JE. Flow effects on the viability and lysis of suspended mammalian cells. Biotechnol Lett 1987; 9(12): 831–836.
149. Hoh JH, Schoenenberger CA. Surface morphology and mechanical properties of MDCK monolayers by atomic force microscopy. J Cell Sci 1994; 107(5): 1105–1114.
150. Mahaffy RE, Shih CK, MacKintosh FC, Kas J. Scanning probe-based frequency-dependent microrheology of polymer gels and biological cells. Phys Rev Lett 2000; 85: 880–883.
151. Tomos D. The plant cell pressure probe. Biotechnol Lett 2000; 22: 437–442.
152. Taylor GI. The formation of emulsions in definable fields of flow. Proc R Soc Lond Ser A 1934; 146: 501–523.
153. Ujcová E, Fencl Z, Musílková M, Seichert L. Dependence of release of nucleotides from fungi on fermentor turbine speed. Biotechnol Bioeng 1980; 22: 237–241.
154. Sinskey AJ, Fleischaker RJ, Tyo MA, Giard DJ, Wang DIC. Production of cell-derived products: virus and interferon. Ann N Y Acad Sci 1981; 369: 47–59.
155. Croughan MS, Sayre ES, Wang DIC. Viscous reduction of turbulent damage in animal cell cultures. Biotechnol Bioeng 1989; 33: 862–872.
156. Cherry RS, Papoutsakis ET. Physical mechanisms of cell damage in microcarrier bioreactors. Biotechnol Bioeng 1988; 32: 1001–1014.
157. Jüsten P, Paul GC, Nienow AW, Thomas CR. Dependence of *Penicillium chrysogenum* growth, morphology, vacuolation and productivity in fed-batch fermentations on impeller type and agitation intensity. Biotechnol Bioeng 1998; 59(6): 762–775.
158. Rocha-Valadez JA, Hassan M, Corkidi G, Flores C, Galindo E, Serrano-Carreon L. 6-pentyl-α-pyrone production by *Trichoderma harzianum*: the influence of energy dissipation rate and its implications on fungal physiology. Biotechnol Bioeng 2005; 91(1): 54–61.
159. Al-Rubeai M, Oh SKW, Musaheb R, Emery AN. Modified cellular metabolism in hybridomas subjected to hydrodynamic and other stresses. Biotechnol Lett 1990; 12: 323–328.

160. Al-Rubeai M, Singh RP, Goldman MH, Emery AN. Death mechanisms of animal cells in conditions of intense agitation. Biotechnol Bioeng 1995; 45: 463–472.
161. Al-Rubeai M, Emery AN, Chalder S, Goldman MH. A flow cytometric study of hydrodynamic damage to mammalian cells. J Biotechnol 1993; 31(2): 161–177.
162. Lakhotia SK, Bauer KD, Papoutsakis ET. Damaging agitation intensities increase DNA synthesis rate and alter cell-cycle phase distributions of CHO cells. Biotechnol Bioeng 1992; 40: 978–990.
163. Passini CA, Goochee CF. Response of a mouse hybridoma cell line to heat shock, agitation and sparging. Biotechnol Prog 1989; 5: 175–188.
164. Mufti NA, Shuler ML. Induction of cytochrome P-450IA1 activity in response to sublethal stresses in microcarrier-attached Hep G2 cells. Biotechnol Prog 1995; 11(6): 659–663.
165. McIntire LV, Frangos JA, Rhee BG, Eskin SG, Hall ER. The effect of fluid mechanical stress on cellular arachidonic acid metabolism. Ann N Y Acad Sci 1987; 516: 513–524.
166. Cherry RS, Papoutsakis ET. Hydrodynamic effects on cells in agitated tissue culture reactors. Bioprocess Eng 1989; 1: 29–41.
167. Kossen NWF. Scale-up. In: Galindo E, Ramirez OT, editors. Advances in bioprocess engineering. Dordrecht: Kluwer Academic Publishers; 1994. pp 53–65.
168. Aloi LE, Cherry RS. Cellular response to agitation characterized by energy dissipation at the impeller tip. Chem Eng Sci 1996; 51: 1523–1529.
169. Clay JD. Molecular degradation of polymer solutions in fast transient extensional flow [PhD Thesis]: Chemical Engineering Department, The Ohio State University; 1997.
170. Mollet M, Godoy-Silva R, Berdugo C, Chalmers JJ. Acute hydrodynamic forces and apoptosis: a complex question. Biotechnol Bioeng 2007; 98(4): 772–788.
171. Zhang Z, Thomas CR. Modeling of animal cell damage in turbulent flows. In: Nienow AW, editor. Proceedings of the 3rd International conference on bioreactor and bioprocess fluid dynamics. London: Mechanical Engineering Publications Ltd; 1993. pp. 475–482.
172. Mollet M, Godoy-Silva R, Berdugo C, Chalmers JJ. Computer simulations of the energy dissipation rate in a fluorescence activated cell sorter: implications to cells. Biotechnol Bioeng 2008; 100: 260–272.
173. Zhang Z, Al-Rubeai M, Thomas CR. Estimation of disruption of animal cells by turbulent capillary flow. Biotechnol Bioeng 1993; 42: 987–993.
174. McQueen A, Bailey JE. Influence of serum level, cell line, flow type and viscosity on flow-induced lysis of suspended mammalian cells. Biotechnol Lett 1989; 11: 531–536.
175. Fife JP, Derksen RC, Ozkan HE, Grewal PS, Chalmers JJ, Krause CR. Evaluation of a contraction flow field on hydrodynamic damage to enthomopathogenic nematodes – a biological pest control agent. Biotechnol Bioeng 2004; 86(1): 96–107.
176. Hu W, Gladue R, Hansen J, Wojnar C, Chalmers JJ. The sensitivity of the dinoflagellate *Crypthecodinium cohnii* to transient hydrodynamic forces and cell-bubble interactions. Biotechnol Prog 2007; 23: 1355–1362.
177. Wernersson ES, Trägårdh C. Scale-up of Rushton turbine-agitated tanks. Chem Eng Sci 1999; 54(19): 4245–4256.
178. Handa A, Emery AN, Spier PE. On the evaluation of gas-liquid interfacial effects on hybridoma viability in bubble column bioreactors. Dev Biol Stand 1987; 66: 241–253.
179. Kioukia N, Nienow AW, Al-Rubeai M, Emery AN. The influence of agitation and sparging on the growth rate and infection of insect cells in bioreactors and a comparison with hybridoma culture. Biotechnol Prog 1996; 12: 779–785.
180. Tramper JJ, Joustra D, Vlak JM. Bioreactor design for growth of shear sensitive insect cells. In: Webb C, Mavituna F, editors. Plant and animal cell cultures: process possibilities. Chichester: Ellis Horwood; 1987. pp 125–136.
181. Kioukia N, Nienow AW, Al-Rubeai M, Emery AN. The impact of fluid dynamics on the biological performance of free suspension animal cell culture: further studies. Food Bioprod Process Trans Inst Chem Eng Part C 1992; 70: 143–148.
182. Glasgow LA, Hua J, Yiin, T-Y, Erickson, LE. Experiment studies of interfacial phenomena in sparged reactors. In: Tatterson GB, Calabrese, RV, editors. Volume 88, Process mixing: chemical and biological applications, AIChE symposium series No. 286. New York: American Institute of Chemical Engineers; 1992. pp 103–108.
183. Handa-Corrigan A, Emery AN, Spier RE. Effects of gas-liquid interfaces on the growth of suspended mammalian cells: mechanisms of cell damage by bubbles. Enzyme Microb Technol 1989; 11: 230–235.
184. Jöbses I, Martens D, Tramper JJ. Lethal events during gas sparging in animal cell culture. Biotechnol Bioeng 1991; 37: 484–490.
185. Bavarian F, Fan LS, Chalmers JJ. Microscopic visualization of insect cell-bubble interactions. I: rising bubbles, air-medium interface and the foam layer. Biotechnol Prog 1991; 7: 140–150.
186. Trinh K, García-Briones MA, Hink FH, Chalmers JJ. Quantification of damage to suspend insect cells as a result of bubble rupture. Biotechnol Bioeng 1994; 43: 37–45.
187. MacIntyre F. Flow patterns in breaking bubbles. J Fluid Mech 1972; 77: 5211–5228.
188. Boulton-Stone JM, Blake JR. Gas bubbles bursting at a free surface. J Fluid Mech 1993; 254: 103–111.
189. Garcia-Briones MA, Brodkey RS, Chalmers JJ. Computer simulations of the rupture of a gas bubble at a gas-liquid interface and its implications in animal cell damage. Chem Eng Sci 1994; 49(14): 2301–2320.
190. Chalmers JJ, Bavarian F. Microscopic visualization of insect cell-bubble interactions II: the bubble film and bubble rupture. Biotechnol Prog 1991; 7: 151–158.
191. García-Briones MA, Chalmers JJ. Cell-bubble interactions: mechanisms of suspended cell damage. Ann N Y Acad Sci 1992; 665: 219–229.
192. Parker B, Barsom G. Biological and chemical significance of surface microlayers in aquatic ecosystems. BioScience 1970; 20: 87–93.
193. Chattopadhyay D, Rathman J, Chalmers JJ. The protective effect of specific medium additives with respect to bubble rupture. Biotechnol Bioeng 1995; 45: 473–480.
194. Chattopadhyay D, Rathman J, Chalmers JJ. Thermodynamic approach to explain cell adhesion to gas-liquid interfaces. Biotechnol Bioeng 1995; 48: 649–658.

195. Chisti Y. Shear sensitivity. In: Flickinger MC, Drew SW, editors. Volume 5, Encyclopedia of bioprocess technology: fermentation, biocatalysis, and bioseparations. New York: John Wiley & Sons; 1999. pp 2379–2406.

196. Jordan M, Sucker H, Einsele A, Widmer F, Eppenberger HM. Interactions between animal cells and gas bubbles: the influence of serum and Pluronic F-68 on the physical properties of the bubble surface. Biotechnol Bioeng 1994; 43(6): 446–454.

197. Michaels JD, Nowak JE, Mallik AK, Koczo K, Wasan DT, Papoutsakis ET. Interfacial properties of cell culture media with cell-protecting additives. Biotechnol Bioeng 1995; 47(4): 420–430.

198. Wu J. Insights into protective effects of medium additives on animal cells under fluid stresses: the hydrophobic interactions. Cytotechnology 1996; 22(1–3): 103–109.

199. Wu J, Ruan Q, Lam HYP. Effect of surface-active medium additives on insect cell surface hydrophobicity relating to cell protection against bubble damage. Enzyme Microb Technol 1997; 21(5): 341–348.

200. Ramirez OT, Mutharasan R. The role of the plasma membrane fluidity on the shear sensitivity of hybridomas grown under hydrodynamic stress. Biotechnol Bioeng 1990; 36(9): 911–920.

201. Zhang Z, Handa-Corrigan A, Spier RE. Oxygen transfer properties of bubbles in animal cell culture media. Biotechnol Bioeng 1992; 40(2): 252–259.

202. Ma N, Chalmers JJ, Aunins JG, Zhou W, Xie L. Quantitative studies of cell damage in sparged bioreactors using a bubble collector to segregate bubble rupture events. Biotechnol Prog 2004; 20(4): 1183–1191.

39

BIOCATALYTIC MEMBRANE REACTORS

Lidietta Giorno and Enrico Drioli
Institute on Membrane Technology, ITM-CNR, At University of Calabria, Rende, Italy

39.1 INTRODUCTION

Membrane reactors using catalysts of biological origin represent a suitable technology for production, processing, and manufacturing operations.

Nowadays, a growing need for environmentally friendly and low energy input technologies is generally recognised, along with waste minimization and recycling that are consistent with the strategy of process intensification to guarantee sustainable development.

The process intensification strategy consists of the development of novel apparatuses and techniques that, compared to those commonly used today, are expected to bring improvements in manufacturing and processing; substantially decreasing equipment-size/production capacity ratio, energy consumption and waste production, thus resulting in sustainable technologies.

Governmental bodies formalize directives that strongly require industries to advance their processes with the best available technologies. Membrane technologies are listed among the best available technologies in EC directives (e.g. the Integrated Pollution Prevention and Control, IPPC—Directive, 1996). In this scenario, biocatalytic membrane reactors are well located, as they are able to work under mild conditions of temperature and pressure, do not require additives, reduce the formation of by-products, and can be highly selective, efficient and flexible systems.

The catalytic action of catalysts of biological origin is extremely efficient and selective when compared to ordinary chemical catalysts; they require milder reaction conditions, show higher reaction rates, and greater stereospecificity. The huge interest toward biocatalysts application has promoted research activities both at academic and industrial levels. This led to developments in various technological sectors including bioengineering techniques and membrane technology for their immobilization and related process design, respectively.

Since 1950, after protease was immobilized on diazotized polystyrene, many enzymes, microorganisms and cells have been used in membrane reactors to catalyze bioconversions of productive interest. The possibility of using biotransformation in productive cycles improves biocatalyst life-times. This makes possible the use of biocatalysts for production at large scales.

Artificial membranes are among the most suitable supports and devices to engineer biocatalysts which can be used suspended in solution and compartmentalised by a membrane in a reaction vessel, or immobilized within the membrane matrix itself. In the first case, the system might consist of a traditional stirred tank reactor combined with a membrane separation unit. In the latter one, the membrane simultaneously acts as a support for the catalyst and as a separation unit.

Reaction yield and selectivity may strongly depend on membrane characteristics. In fact, in addition to the effects of membrane selectivity on reactions (such as removal of product-poisoning components and/or supplying substrates at controlled rates), the physicochemical properties of membranes may influence catalyst structure (and therefore catalyst selectivity). Biocatalytic reactors more commonly use polymeric membranes as compared to inorganic ones since they work under mild conditions of temperature and pressure. The membrane can be flat-sheet shaped and assembled

Upstream Industrial Biotechnology: Equipment, Process Design, Sensing, Control, and cGMP Operations, Volume 2, First Edition. Edited by Michael C. Flickinger.
© 2013 John Wiley & Sons, Inc. Published 2013 by John Wiley & Sons, Inc.

in plate-and-frame or spiral-wound modules, or tubular and assembled in tube-and-shell modules; it can have symmetric or asymmetric structure. (Specific information on membranes and membrane processes can be found in Ref. 1.)

The biocatalyst can be flushed along a membrane module; segregated within a membrane module; immobilized in/on the membrane by entrapment, gelification, physical adsorption, ionic binding, covalent binding or cross-linking.

The choice of the reactor configuration depends on the properties of the reaction system. For example, bioconversions for which a homogeneous catalyst distribution is particularly important, are better performed in a reactor with the biocatalyst compartmentalised by the membrane in the reaction vessel. The membrane is used to retain large components (i.e enzyme and substrate) while permeating small molecules (i.e. the product).

The reactor with the biocatalyst segregated in the membrane module is suitable for those cell cultures and enzymes that can be deactivated by shear stress. Reactors with segregated cells are studied for therapeutic applications, for example, as bioartificial pancreas, bioartificial liver, and extracorporeal detoxification device.

As stated previously, besides functioning as a selective separation barrier, the membrane can also exhibit catalytic properties. In fact, the biocatalyst can be loaded within the porous structure or on the surface of the membrane. The objectives of immobilizing enzymes are to increase reactor stability and productivity, improve purity and quality of products, and minimize wastes.

The enzymes or cells can be entrapped within the polymeric matrix during the preparation of the membrane by phase inversion technique, or can be entrapped by filtration within the porous layer of asymmetric hydrophilic membrane, symmetric hydrophobic membrane and so on. When the biocatalyst is within the membrane, in order for the reaction to occur, the substrate has to be transported across the membrane to the catalyst and the product recovered as permeate from the other side of the membrane. In general, mass transport resistance is the parameter that most influences the performance of these reaction systems.

Actual gelation of enzyme proteins on the membrane surface is possible when the protein concentration at the membrane–liquid interface reaches the gel concentration value. When the biocatalyst is immobilized on the surface, flushing the substrate solution along the enzymatic gel causes conversion of substrate into product in the retentate stream also. If the enzyme is product inhibited, performance of the reactor at steady state is decreased.

Attachment of the enzyme can be obtained by ionic binding to ion exchanger supports; by adsorption through van der Waals interactions to hydrophobic supports; and covalent binding between amino or carboxyl groups of amino acids and the support.

In addition to the type of immobilization, membrane bioreactors are also named on the basis of type of solvents and/or separation process used. For example, "ultrafiltration (UF) membrane reactors", "affinity membrane reactors" where a chemical reaction is coupled to a separation by ultrafiltration or affinity membrane, respectively; "extractive membrane bioreactors" where organic molecules permeate across a membrane into the biological active reactor; "ion exchange membrane bioreactor" where ionic compounds are transported through nonporous ion exchange membrane into a biological active compartment; "biphasic membrane reactors" (or two-separate phase membrane reactors), where the membrane is placed between two different phases which are kept separated and in contact at the same time; and "enantioselective membrane reactors" where the membrane-assisted reaction system is able to distinguish between chiral molecules. Sometimes they are named on the basis of the type of membrane used: "flat-sheet membrane reactor," "hollow fiber membrane reactor" and so on. When hollow fibers are used, a membrane reactor is just a plug-flow reactor that contains an additional porous cylinder within it.

Biocatalytic membrane reactors can also be distinguished on the basis of membrane module location in the plant, that is there is a sidestream configuration and an immersed one. In the sidestream configuration the module is externally positioned with respect to the fluid to treat, and the fluid is recirculated along the membrane module by a pump. In the immersed configuration, the module is immersed in the fluid to treat and a suction pump is used to remove the permeate from the module.

The UF membrane reactor is used when the substrate has a higher molecular weight with respect to the product and both are soluble in the same solvents. In this way, by choosing a membrane with the appropriate pore size, the substrate is transported to the enzyme immobilized in or on the membrane but it cannot pass through the membrane, while the obtained product can freely permeate through it and can be recovered from the other side of the membrane.

If the substrate has a different solubility with respect to the product (as in the case of an ester and its hydrolysis product), then a biphasic membrane reactor can be used. In this type of system, the enzyme-loaded membrane is located between two immiscible liquid phases, in general an organic and an aqueous phase. The organic phase contains the substrate and it is flushed along one side of the membrane; the substrate is transported (by diffusion) to the enzyme, where the reaction takes place, and the product is extracted into the aqueous phase and flushed along the other side of the membrane. When the biocatalyst is selective for only one of the two enantiomers present in a racemic mixture, the system is useful for producing pure enantiomers. This field is receiving growing attention due to the importance of using bioactive molecules as pure isomers when they have

TABLE 39.1. General Properties of Biocatalytic Membrane Reactors

Technological Benefits	Needs for Further Technological Innovation
Enzymes are heterogenized by immobilization	—
Large surface per unit volume	—
Easy to separate enzyme from the other reagents	—
Increase of enzyme stability	Sometimes decrease of catalytic activity and selectivity
Combining of selective reactions with selective separation	Mass transfers through the membrane
Independent control of kinetic and separation parameters	—
Mild temperature and pressure conditions	—
Optimal substrate administration rate	—
Removal of inhibiting components	—
Increased reaction yield	—
Control of sequential reactions	—
Removal of reaction intermediates (e.g. achieve new molecules not available in nature)	—
Increase catalytic activity of enzymes used in organic solvents	—
Avoid side reactions (e.g. hydrolysis or isomerization)	—
Minimize microbial contamination[a]	—
Redesign of innovative production lines	—
Continuous operation	—
Conceptual simplicity	—
Easy in scaling up	Reproducibility at large scales
Remote control and automatization	—
Easy in scaling down (preparation of microreactors, i.e. optimal biocatalytic microstructured organized systems)	—

[a] Biocatalytic membrane reactors used in organic solvents or nonaqueous media.

to be administered to human beings, animals, environment, and so on.

Traditionally, membrane reactors were applied in equilibrium limited reactions. Nowadays, new applications are growing, for example, in biocatalytic reactors, the membrane can be used to remove some intermediate or side product that might deactivate the biocatalyst. The membrane can assist the extraction of different intermediates into proper solvents that better preserve their stability. It can also allow controlling of complex multistep reaction systems.

Additional general properties of biocatalytic membrane reactors are summarised in Table 39.1.

Further insight can be found in Refs 1–6.

39.2 FUNDAMENTALS

Enzyme specificity is thought to be a consequence of its elaborate three-dimensional conformation which allows formation of the "active site" which is a hydrophobic cavity responsible for the catalytic ability of the enzyme. In general, binding to create the substrate-enzyme complex is due to weak attractive forces. Although a little controversial, the notions of active sites and the enzyme-substrate complex are universally accepted and form the starting point for most theories of enzyme action.

The relative chemical equation is as follows

$$E + S \underset{k_{-1}}{\overset{k_1}{\rightleftharpoons}} ES \underset{k_{-2}}{\overset{k_2}{\rightleftharpoons}} E + P \tag{39.1}$$

The mathematical expression of the kinetic behavior of enzymes is commonly known as *Michaelis–Menten equation*:

$$V_0 = \frac{V_{\max}[S]}{K_m[S]} \tag{39.2}$$

The Lineweaver–Burk equation is obtained by rearranging the M–M equation in linear form:

$$\left[\frac{1}{V_0}\right] = \frac{K_m}{V_{\max}}\left[\frac{1}{[S]}\right] + \frac{1}{V_{\max}} \tag{39.3}$$

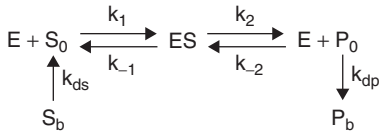
By plotting $\frac{1}{V_0}$ versus $\frac{1}{[S]}$ data, a straight line is obtained, where the intercept to y axis is $1/V_{\max}$ and the slope is $K_m/V_{\max}$.

From this graph it is easy to estimate K_m and V_{max}. Here, V_0 is the initial reaction rate, K_m is the Michaelis–Menten constant, S is the substrate, and V_{max} is the maximum reaction rate.

The modeling of biochemical membrane reactors mainly depends on the function of the membrane. For example, if the membrane works as a separation unit independent from the reaction, then the reactor is modeled according to traditional systems (e.g. continuous stirred tank reactors and plug-flow reactors) combined to a membrane separation; if the membrane is catalytic, then the intrinsic kinetic and mass transport at the membrane level must be considered.

When the enzyme is immobilized in a matrix such as a polymeric membrane, the observed reaction rate depends upon the reagent transport and intrinsic catalytic activity of the enzyme.

Under these conditions the Michaelis–Menten equation can no longer account for the intrinsic kinetics and a new reaction model that takes into account mass transfer is needed. In some cases the reaction mechanism of immobilized catalysts may also change and completely new approaches are needed. In general, when the Michaelis–Menten reaction model is considered valid, the kinetic mechanism for an immobilized enzyme can be simply represented as follows:



(39.4)

where, S_0 and P_0 are the concentrations next to the immobilised enzymes, while S_b and P_b are the concentrations in the bulk phase. The constant k_{ds} is related to the diffusion of substrate from the bulk to the enzyme and k_{dp} is related to the diffusion of product from the immobilized enzyme to the bulk phase. In Fig. 39.1 the concentration gradients for substrate and product through porous supports containing immobilized catalysts are schematized. The gradients in region A–B are due to diffusion in the outer diffusion liquid film. The gradients in region B–C are due to the joint effects of diffusion and reaction.

The use of Lineweaver–Burk plots with immobilized enzymes to determine apparent values for V_{max} and K_m is very common. For a kinetically controlled reaction system, a straight line is obtained. A linear extrapolation to the axes allows the apparent values of these parameters to be accurately determined.

In the presence of diffusional limitations, the Michaelis constant's apparent value obtained by extrapolation of the Lineweaver–Burk plot is usually larger than the intrinsic value obtained for the enzyme in soluble form.

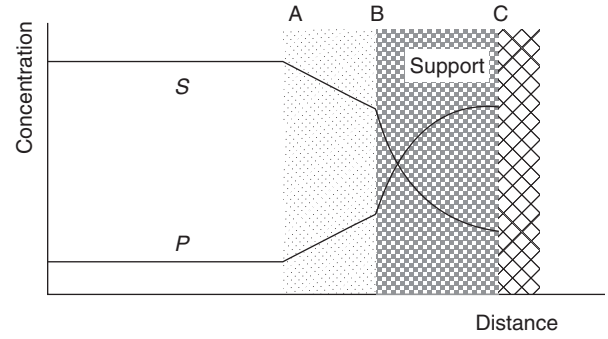


Figure 39.1. Concentration gradients through immobilized enzyme matrix.

39.2.1 Enzymes Immobilized on the Surface

For enzymes immobilized on the surface, a stagnant film (as called by chemical engineers) or Nernst diffusion layer(as called by biochemists) forms around the particle, through which the substrate molecules must diffuse to reach the surface. Thus, the surface concentration is less than the bulk concentration; the reaction proceeds less rapidly than the bulk substrate concentration would suggest (Fig. 39.2).

The Michaelis–Menten equation shows that an increase of k_m also corresponds to a decreased reaction rate. The flux of substrate from bulk to immobilized interfaces is given by $J_s = k_s(S - S_0)$, where J_s is the flux (moles per unit time per unit area); S and S_0 are the substrate concentration in the bulk phase and at immobilized enzyme interface; k_s is the mass transfer coefficient.

At steady state, at the interface, the mass transfer of substrate must be counterbalanced by the consumption rate of the substrate. Then, assuming that the Michaelis–Menten equation applies to systems immobilized on the surface

$$k_s(S - S_0) = \frac{V_{max}[S]}{k_m + [S]} \tag{39.5}$$

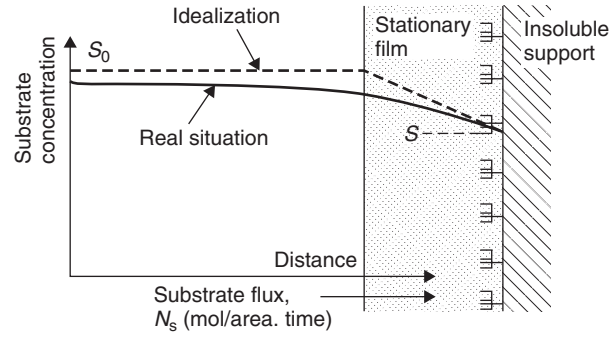


Figure 39.2. Schematic representation of transport for catalyst immobilized on the surface of insoluble support.

The following dimensionless variable

$$Da = \frac{V_{mx}}{k_s S_0} \tag{39.6}$$

known as the Damköhler number is the ratio between the maximum reaction rate and maximum mass transfer rate.

When $Da \ll 1$, the maximum transfer rate is much larger than the maximum reaction rate, which means that the system works at low mass transfer resistance. This is the case known as *reaction-limited regime*, where the system is kinetically controlled and the equation

$$V_{kin} = \frac{V_{max}\,[S]_b}{k_m + [S]_b} \tag{39.7}$$

can be assumed. Here, $[S]_b$ is the bulk substrate concentration.

When $Da \gg 1$, the reaction rate is larger than the mass transfer, which means that the mass transfer resistance is large and it is the limiting process. This is the case known as *diffusion-limited regime* and $V_{diff} = k_s[S]_b$.

The Damköhler number can be interpreted as the ratio of the slope of $V_{kin}(= V_{max}/k_m)$ to that of $V_{diff}(= k_s)$. If the slope of V_{diff} is less than that of V_{kin}, then $Da[= (V_{max}/K_M)/(k_s)] > 1$ and the reaction is diffusion controlled; while, in the opposite case, the reaction is kinetically controlled.

The influence of mass transfer on the overall reaction is usually represented using the effectiveness factor, η defined as

$$\eta = \frac{\text{Observed reaction rate}}{\text{Rate that would be observed in absence of mass transfer resistance}}$$

When $\eta \leq 1$ it means that the mass transfer resistance is large and the effect is a reduction of the observed activity of the catalyst.

For *Da* approaching zero (very slow reaction relative to maximum mass transfer rate), η approaches 1. This means that for the reaction-limited regime, the observed reaction kinetics can be approximate to the intrinsic reaction kinetics.

39.2.2 Enzyme Within the Porous Matrix

When enzymes are immobilized within the internal surface of porous supports (Fig. 39.3), calculation of the observed substrate conversion rate needs evaluation of the concentration profile of the substrate within the diffusion layer.

For these cases, it should be considered that the effective diffusion coefficient (D_{eff}) and the local rate of substrate conversion (V) differ conceptually from their counterpart in solution, and important quantitative difference can also arise.

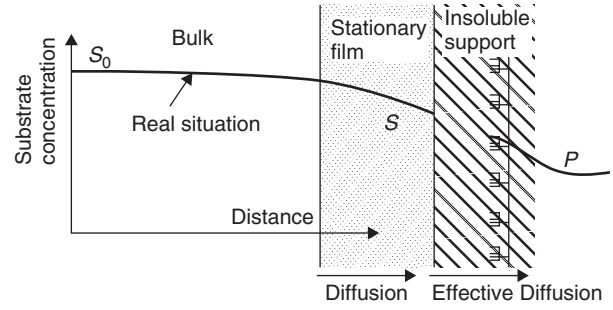


Figure 39.3. Concentration profiles through catalytic porous matrix.

Besides substrate diffusivity (D_{S_0}) in the bulk phase, diffusion rate through a porous support is influenced by porosity ($\varepsilon_{p,}$ = area of pores/area of support, only part of the support is void and available for diffusive transport, while most part is occupied by solids. The porosity value is less than 1); tortuosity (τ, the pore network is complex and not straight, diffusion occurs by changing direction continuously. The tortuosity factor is assumed to be in the range of 1.4–7); pores can have a very small diameter, similar to substrate molecular dimensions and lead to a situation of restricted diffusion (expressed as K_p/K_r roughly estimated as $[1 - r_{substrate}/r_{pore}]^4$).

Taking into account these considerations, the effective diffusion coefficient can be written as:

$$D_{eff} = D_{S_0}\frac{\varepsilon_p}{\tau}\frac{K_p}{K_r} \tag{39.8}$$

In the 1930s, Thiele, Damköhler, and Zeldovitch studied the influence of *diffusion within porous catalysts* upon reaction kinetics. They considered the example of a planar surface containing an enzyme distributed uniformlythroughout. The result of combining the steady-state diffusion equation with the applicable kinetics rate expression, the Michaelis–Menten equation, is:

$$D_{eff}\frac{d^2[S]}{dx^2} - \frac{V_{max}\,[S]}{K_m + [S]} = 0 \tag{39.9}$$

where D_{eff} is the effective diffusivity; $[S]$ is the substrate concentration; V_{max} is the maximum velocity of the reaction; K_m is the Michaelis constant, which means that, at steady state, the substrate diffusion rate through the porous support containing the enzyme is equal to the conversion rate.

The values V_{max} and K_m are those, which characterize the kinetic expression for the microenvironment within the porous structure.

A useful parameter to evaluate if an immobilized reaction system is limited by kinetics or mass transport, is the Thiele modulus, ϕ, given by

$$\phi = L\left(\frac{V_{\max}}{D_{\text{eff}}K_{\text{m}}}\right)^{1/2} \tag{39.10}$$

which has the physical meaning of a *reaction rate/diffusion rate*.

Finally, it should be noted that, as for the enzyme in solution, immobilized enzyme kinetics may differ from the irreversible single substrate Michaelis–Menten model. In the case where the intrinsic kinetics is inhibited by the substrate, if the substrate at the external phase is higher than the substrate concentration giving the maximum reaction rate, it happens that the local reaction rate inside the support is larger than that at the external phase. In this specific situation it is possible to observe an effectiveness factor higher than unity. Other frequent cases are heterogeneous systems, such as when the substrate reaches solubility limit or at the liquid–liquid interface.

Additional readings on immobilized catalyst kinetics and membrane bioreactors modeling can be found in Refs 1, 5, (7–11).

39.2.3 Process Design and Operation

General concepts in reactor design can be applied to the membrane reactor too. The information needed for reactor development are summarized in Fig. 39.4.

The building of models and their comparison with experimental data are useful and reasonable approaches to investigate and understand reactor performance.

Both kinetic and transport properties are needed.

The general procedure to formulate the mass balance is as follows:

- Choose the balance region so that the variables are constant or change little within the system, and draw boundaries around the balance region.

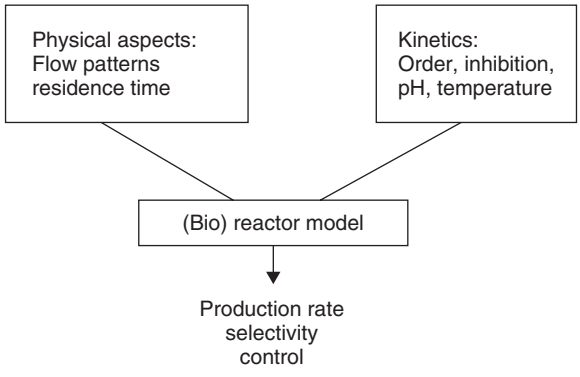


Figure 39.4. Data needed for reactor design.

- Identify the transport streams which flow across the system boundaries (e.g. convective in, convective out; diffusive in, diffusive out).
- Write the balance (e.g. rate of accumulation of mass of i = rate of i in by flow–rate of i out by flow + rate of production of i by reaction).
- Express each balance term by measurable variables in mathematical form. Pressure (P), volume (V), concentration (C), flow rate (F), are usually the measured variables (total mass = ρV; mass of $i = C_i V$).
- Introduce other relationships and balances so that the number of equations equals the number of dependent variables.
- Express the total mass balance:

$$\frac{\mathrm{d}VC}{\mathrm{d}t} = (FC_i)_{\text{IN}} - (FC_i)_{\text{OUT}} + (r_i V)_{\text{system}} \tag{39.11}$$

The steady-state balance equation for a membrane reactor working in reaction-limited regime can be written as

$$FC_{\text{f}} - FC_{\text{p}} + v_{\text{r}}V = 0 \tag{39.12}$$

where C_{f} and C_{p} are the feed and permeate concentration, respectively, v_{r} is the reaction rate, and V the reactor volume.

From this, the reaction rate can be derived:

$$V_{\text{r}} = \frac{F(C_{\text{f}} - C_{\text{p}})}{V} \tag{39.13}$$

Table 39.2 summarizes the component balances for various (membrane) reactor systems.

39.3 MEMBRANE REACTOR CONFIGURATIONS

Depending on various parameters (enzyme kinetics, membrane configuration, fluid dynamics, etc.), different reactors are used to optimize system yield. The most common types of reactors are summarized in Fig. 39.5 and the most common membrane processes combined with reactions are listed in Table 39.3.

Concentration polarization phenomena severely affect the performance of reactors where the membrane is used as a separation medium under pressure-driven processes. Then it is necessary to control the polarization layer on the membrane-pressurized side by means of reactor fluid dynamics or appropriate design. Membrane fouling is also a phenomenon to control and govern, in order to maintain good steady-state performances (1)

TABLE 39.2. Component Balances for Various Reactor Systems

Reactor type[a]	Terms in equation	Final form
Batch reactor	Flow term = 0	Acc = Production
Fed batch or Semicontinuous reactor	Flow term out = 0	Acc = In + Production
Steady-state CSTR	Accumulation = 0	In−Out + Prod = 0
Component Ci does not react	Production = 0	Acc = In−Out
Constant volume CSTR	simplifies to $V(ds/dt) = F(S_0 - S_1) + rsV$	Acc = In−Out + Prod

[a]The general term also includes membrane reactors.

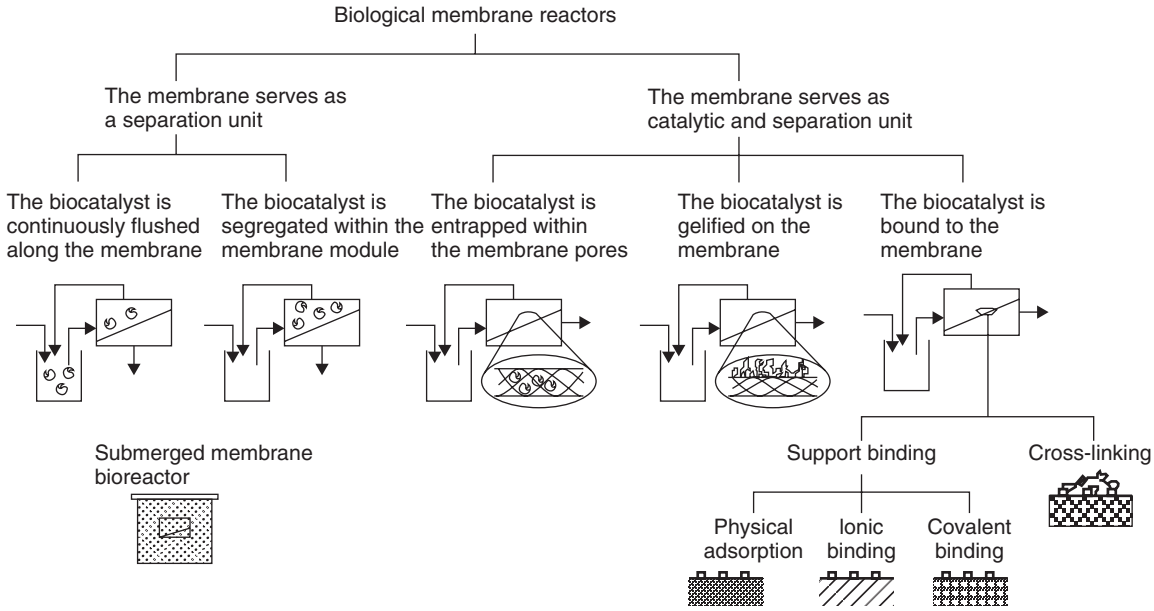


Figure 39.5. Common types of membrane reactors.

39.3.1 External Sidestream Membrane Bioreactors

39.3.1.1 Membrane Bioreactors with Membrane Used as a Separative Unit. This type of membrane reactor is based on the combination of a continuously stirred tank reactor (CSTR) with a membrane separation process. The membrane simply acts as a separation unit and does not directly take part in the reaction. The reactor works as a CSTR, but the product (or substrate) passes through the membrane unit where the enzyme is either retained and recycled back into the reactor or remains confined in the membrane module.

An appropriate membrane separation is used to keep larger components in the reaction vessel (i.e. cells, enzyme, and macromolecular substrates) and remove low molecular weight molecules (i.e. product, intermediates, and inhibitor). The biocatalyst is immobilized by the fact that it is compartmentalised by the membrane in the reaction vessel. This allows continuous processing with the biocatalyst suspended in a homogeneous solution. Direct contact between the substrate and biocatalyst limits diffusional resistance. Typical reactions that require a biocatalyst suspended in a solution are those that need cellular growth, high biomass density, and direct contact between substrate and biocatalyst. Examples of this kind of reaction systems include fermentation processes; plant cell culture (e.g. for secondary metabolite production); the hydrolysis of starch and cellulose; the hydrolysis of pectins; the hydrolysis of casein; the hydrolysis of collagen; and cofactor-dependent dehydrogenation reactions.

The most common separation process used in this kind of setup is ultrafiltration. Dead-end and continuous stirred ultrafiltration cells with flat membranes have been widely used; furthermore, cross-flow ultrafiltration through tubular membrane modules has also been investigated.

Additional applications include the use of hydrophobic microporous membranes for cell culture aeration; hydrophilic microporous membranes for nutrient supply to cultured cells and removal of catabolites from them; dense membranes and/or ion exchange membranes for organic and ionic contaminants separation; and supply of contaminants to biomass compartment for biodegradation.

Biocatalyst activity is usually not constant with time. Physicochemical changes in enzyme structure; thermal

TABLE 39.3. Most Common Membrane Processes Combined with Reactions

Process	Driving Force	Mode of Transport	Species Passed	Species Retained
Microfiltration (MF)	Pressure difference 100–500 kPa	Size exclusion convection	Solvent (water) and dissolved solutes	Suspended solids, fine particulars, some colloids
Ultrafiltration (UF)	Pressure difference 100–800 kPa	Size exclusion convection	Solvent (water) and low molecular weight solutes (< 1000 Da)	Macrosolutes and colloids
Nanofiltration (NF)	Pressure difference 0.3–3 MPa	Size exclusion, solution diffusion, Donnan exclusion	Solvent (water), low molecular, weight solutes, monovalent ions	Molecular weight compounds > 200 Da multivalent ions
Membrane-based solvent extraction (MBSX)	Chemical potential or concentration difference	Diffusion partition	Compounds soluble in the extraction solvent	Compounds insoluble in the extraction solvent
Gas separation (GS)	Pressure difference 0.1–10 MPa	Solution diffusion mechanism	Gas molecules having low molecular weight or high solubility-diffusivity	Gas molecules having high molecular weight or low solubility-diffusivity
Pervaporation (PV)	Chemical potential or concentration difference	Solution diffusion mechanism	High permeable solute or solvents	Less permeable solute or solvents
Membrane emulsifier (ME)	Pressure difference	Convection	Dispersed phase	—

denaturation, and microbial contamination cause enzyme activity to continuously decrease with time. When enzymes or cells are compartmentalised in UF cells, biocatalyst losses can occur even due to the wrong choice of chemical properties and morphology of the membrane. It is conventional to measure the biocatalyst stability in terms of its half-life time ($t_{1/2}$), that is the time at which the enzyme biocatalyst's activity is reduced to half its initial value. It can be calculated from the following equations:

$$K_{\mathrm{d}} = \frac{2.303}{\vartheta} \log \frac{A_{E_0}}{A_{E_\vartheta}} \qquad t_{1/2} = \frac{0.693}{K_{\mathrm{d}}} \tag{39.14}$$

K_{d} is the enzyme deactivation constant; ϑ is the operation time; A_{E_0} is the initial biocatalyst activity; A_{E_ϑ} is the enzyme activity at time ϑ.

Biotransformations by means of enzymes are continuous processes, as long as the reactor working life is longer than the native enzyme biocatalyst half-life. In these systems biocatalyst activity decay with time must be taken into account in order to correctly assess reactor performance.

The CSTR/UF reactor (Fig. 39.6) is useful for several types of reactions where a typical immobilized biocatalyst would not be effective.

A particular case of membrane reactors, with the biocatalyst flushed along the membrane, are the continuous membrane fermentors (or cell-recycle membrane fermentor), where microporous membranes are used to separate the fermentation broth from the product stream, thus retaining viable cells in the fermentor.

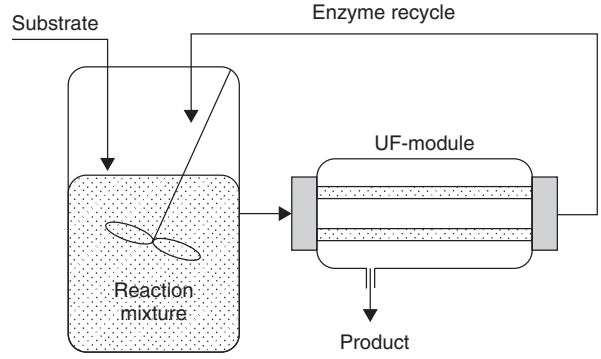


Figure 39.6. CSTR coupled with UF-module.

Membrane bioreactors coupling biological treatment to membrane separation processes, are effective and very promising for wastewater treatment. Mainly, two different configurations have been investigated: membrane bioreactors with the membrane module outside the activated sludge tank, and membrane bioreactors with the membrane submerged in the biological reactors. Due to lower energy requirements, the submerged membrane bioreactors (SMBRs) have been found to be more successful than the external ones, especially at the industrial level. They will be discussed in detail in a subsequent section.

Regarding the sidestream configuration, the most common function of the membrane is to remove the treated water while retaining cells and contaminants and recycling them back to the bioreactor.

Alternative uses have also been successfully explored, such as the use of membranes to selectively separate organic or ionic microcontaminants from water, and supply them to bioreactors for their metabolization to non-harmful components. This option has the advantage of wastewater pH and composition not affecting the biomass performance, as well as of not releasing biomass catabolites into the treated water. Examples of this kind of application can be found in Refs 12 and 13, where extractive membrane bioreactors employing silicon rubber membranes are used to selectively extract hydrophobic organic compounds from industrial water into a bioreactor; and in Refs 14 and 15, where ion exchange membrane bioreactor employing nonporous ion exchange membranes are used to remove ionic micropollutants from water into the microbial culture compartment.

39.3.1.1.1 Membrane Bioreactors with Biocatalyst Segregated in the Membrane Module. In these reactors, enzymes or cells are not linked but only confined in a defined region of membrane module space. The segregation of the biocatalyst is achieved by means of membranes with a suitable molecular weight cutoff. In this way, enzymes, as well as bacterial, plant, animal cells are not lost in the effluent stream, and low molecular weight products and inhibitors can be removed through the membrane (Fig. 39.7). The development of hollow fibers with diameters down to about 100 microns makes possible tube-and-shell reactors with a high surface-to-volume ratio.

Biocatalytic reactors can segregate enzymes or cells either within the hollow fiber lumen, within the shell surrounding the outer surface of the fibers, or within the porous membrane support. There is growing interest in therapeutic applications of compartmentalised cells or microsomes functioning as a bioartificial pancreas or extracorporeal detoxification device. Evaluation of stability and catalytic properties of the immobilized system must take into account possible pH differences between the site of the fiber, where the reaction takes place, and the bulk of the feed solution.

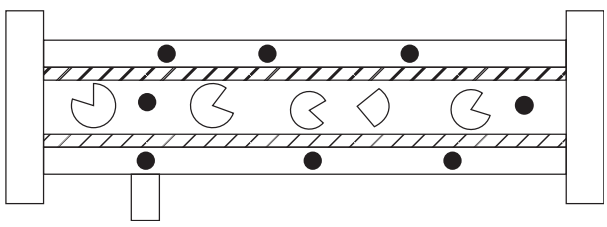


Figure 39.7. Membrane segregated enzyme reactor.

In order to avoid membrane plugging when using microorganisms or plant cells in this type of membrane reactor, cell growth must be appropriately controlled and if possible, kept in a "vegetative" stage. On the other hand, if cell growth is needed, then a different reactor configuration must be considered, such as a cell-recycle membrane bioreactor or a biofilm membrane bioreactor, depending on whether cells need to be suspended or attached to a support.

39.3.1.2 Biocatalytic Membrane Reactors. In these type of reactors, the membrane acts as a catalytic and separation unit. Biocatalysts are represented by enzymes or nongrowing cells. As shown in Fig. 39.5, reactors with biocatalyst-loaded membranes can be prepared in various ways. Important parameters which must be considered in immobilized enzyme reactors are: immobilization procedure; microenvironment conditions; optimal balance between molecular rigidity and flexibility (to guarantee both enzyme stability and catalytic activity and selectivity); enzyme activity; half-life time and activity decay profile; optimal substrate concentration; optimal residence time; pH and temperature; by-product formation; inhibitors; pressure drop; flow regime; particle size, shape and distribution; and mass transfer of reagents through the catalytic membrane. In the following paragraphs, the different types of reactors and their relative applications will be discussed.

39.3.1.2.1 Biocatalytic Membrane Reactors with Catalysts Entrapped within the Pores of Asymmetric Membranes. A number of microorganisms can withstand high temperatures and organic solvents and have been processed with polymeric solutions. Polysulfone and cellulose acetate membranes have been cast with microbial cells in the casting solution using the phase inversion technique. Microbial enzymes maintain their activity presumably because of cellular membrane protection. Cell-loaded membranes appear to be kinetically active and stable over a long period of time. It is noteworthy that cell entrapment can enhance microbial activity as compared to cell behavior in a homogeneous solution, an effect probably due to cellular membrane permeabilization as a consequence of the entrapment procedure.

Asymmetric hollow fibers can provide an interesting support for immobilizing enzymes. If the pores in the dense layer are small enough to retain enzyme molecules but large enough to allow the free passage of substrates and products, the enzymes are effectively immobilized or segregated within the spongy annular section (Fig. 39.8). Enzymes can be entrapped within the outer sponge layer of the fibers by cross-flow filtration of an enzyme solution and the amount of immobilized protein can be determined by the mass balance between initial and final solutions.

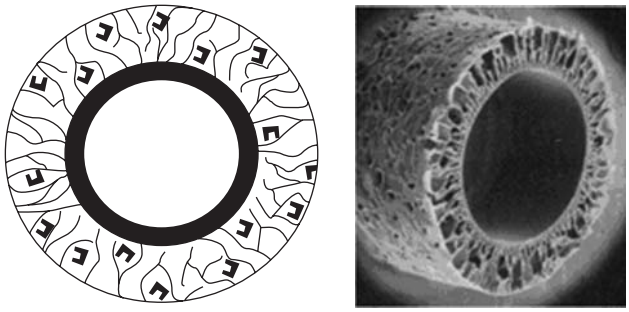


Figure 39.8. (a) Cross-section of CMBR with enzyme entrapped within the porous support. (b) Asymmetric hollow fiber membrane.

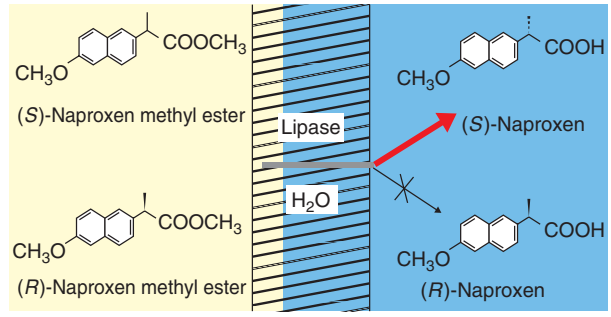


Figure 39.9. Biphasic membrane reactor for phase transfer catalysis. (This figure is available in full color at http://onlinelibrary.wiley.com/book/10.1002/9780470054581.)

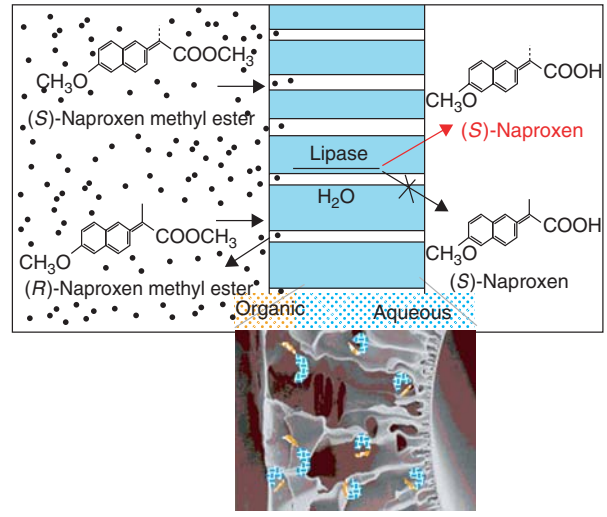


Figure 39.10. Schematic representation of an emulsion enzyme membrane reactor. (This figure is available in full color at http://onlinelibrary.wiley.com/book/10.1002/9780470054581.)

The dynamics of substrate conversion depends on enzyme kinetics as well as on mass transport conditions. Enzymes are not able to work at high concentrations, hence the amount of immobilized catalyst strongly affects reactor performance. Usually, the reactor performance may strongly decrease at high enzyme loading because of both, deactivation effects due to macromolecular aggregation and additional barrier to mass transport. When the substrate is transported by convection through the enzyme-loaded membrane, the residence time is an important parameter to optimise.

For systems where the substrate is transported by diffusion, quick graphical procedures are available in literature for evaluating the extent to which external and internal diffusion affect immobilized enzyme kinetics (16). Suggested models can be used to predict reactor performances in the case of enzymes with relatively simple kinetics (such as α-galactosidase, invertase, glucose isomerase, and urease) and when the kinetic and transport parameters are known.

A widely reported case of reactor using enzymes entrapped within the pores is the biphasic organic/aqueous membrane reactor (or two-separate phase enzyme membrane reactor). A schematic representation of a biphasic membrane is reported in Fig. 39.9. The system is suitable for bioconversions of low water-soluble substrates. The enzyme-loaded membrane separates two immiscible phases: the substrate is present in the organic phase while the product is extracted in the aqueous phase. Particularly interesting is the case where the biocatalyst is enantiospecific and converts only one of the substrate isomers, giving in one step, the production and separation of enantiomers in the optically pure form.

The multiphase extractive membrane reactor targeted at the enzymatic resolution of chiral drug intermediates was developed in the early 1990s (17,18).

A further improvement on multiphase reactor systems (emulsion enzyme membrane reactors) has been reported recently where the organic–water interface within the pores at the enzyme level is achieved by stable oil-in-water emulsion prepared by membrane emulsification, so that each pore can work as a microreactor containing immobilized enzyme (Fig. 39.10) (19,20). In this way, the enzyme works in the membrane pores under the same conditions as in the stirred tank reactor, but with no shear stress due to stirring.

This configuration improved the selectivity and productivity of the biocatalytic system as well as its catalytic stability, confirming that the observed inversion relationship between activity and stability of immobilized enzymes is not a general rule.

A comparison between performances of different reactor configurations is reported in Table 39.4.

39.3.1.2.2 Catalytic Membrane Bioreactors with Biocatalysts Gelified on the Membrane. Concentration polarization phenomena, which are the main drawbacks of membrane processes, can be used to form a gel layer of enzyme proteins on a membrane. It is even possible to establish more

TABLE 39.4. Performance of Biphasic Membrane Reactors with Different Enzyme Immobilization Sites

Lipase	Membrane	Reactor	Immobilization Site	Lipase Amount (mg)	eep	*E*	Activity (mmol/h g)
Crude	PA 10 kDa	B-EMR	Thin	2.3	77	7.8	1.9
Crude	PA 50 kDa	B-EMR	Thin	5.5	90	20	6.36
Crude	PA 50 kDa	B-EMR	Sponge	8.2	76	6.2	–
Crude	PA 50 kDa	E-EMR (emulsion by membrane)	Sponge	2.6 < 1	9496	3050	14.5

Note: eep, enantiomeric excess of the product.

than one enzyme layer and no coupling agent is needed to carry out the immobilisation. Reduced catalytic efficiency due to mass transport limitations and the possibility of preferential pathways in the enzyme gel layer can be typical systemic disadvantages.

Actual gelation of enzyme proteins, and hence their dynamic immobilisation, depends strictly on enzyme concentration at the membrane–liquid interface. When the maximum enzyme concentration is lower than the gel concentration value, enzymes are not immobilized. Although they are confined near the membrane surface at fairly high concentration levels, they are still in soluble form.

39.3.1.2.3 Catalytic Membrane Bioreactors with Biocatalyst Bound to the Membrane. Attachments of biocatalysts to membranes can result from ionic binding, cross-linking and covalent linking. In this section enzymes bound to synthetic polymeric membranes via covalent binding will be mainly discussed. Protease was the first covalently bound enzyme. This was achieved in 1950s. Since then, enzyme immobilisation via covalent bonds has been an established immobilisation technique, usually carried out by means of bi- or multifunctional reagents, such as glutaraldehyde. When the extent of initial denaturation is acceptable in the economics of the process, enzymes bound to membranes can be used in continuous flow reactors.

Applications of covalently immobilized systems are: membrane electrodes for analytical purposes; reactions of substrates whose molecular weight is low as compared to membrane molecular weight cut-off; and enzymatic conversion of macromolecules to lower molecular weight species able to permeate the supporting membrane.

39.3.2 Submerged Membrane Bioreactors

Submerged membrane Bioreactors are among the membrane operations that have received a huge amount of attention all over the world in the last few decades. They are mainly used for the treatment of wastewater at the industrial level.

This was also the result of the increase in demand for potable water and the increase in domestic and industrial wastewater discharges linked to population growth. In addition, more stringent legislation targeting environmental protection forces industries to minimize the input of energy and water.

The potentiality of the technology rests on low energy input, long-term operation without cleaning, and lower dependence on variation of rheology behavior with concentration. The main limitation is in the requirement for high membrane area which is due to the low fluxes linked to the low transmembrane pressure.

The combination of bioreactors and membrane technology enables an innovative and effective cleaning process. Conventional wastewater technology is characterized by large wastewater volumes. It usually uses open basins and needs high surface and long hydraulic retention time of wastewater flows. In conventional activated sludge processes, the purification stage (aeration tank) and the separation of the biomass from the purified wastewater (settling tank) are carried out separately and independently of each other. Large basin volumes are necessary for the aeration tank and the final clarifier. The biomass concentration in the aeration tank usually tends to be in the range of $3 - 5\ g_{dry\ weight}/L$.

The membrane bioreactor combines biological treatment with membrane separation. The treated water is separated from the purifying bacteria (active sludge) by a process of membrane filtration, rather than in a settling tank. Only the treated effluent passes through the membrane which is then pumped out, while the sludge is recovered. The sedimentation in the final clarifier is then replaced by the implementation of membrane filtration which allows separation of the biomass from the water, the quality of the purified water is also considerably improved. The use of microfiltration membranes with pore sizes usually between 0.1 and 0.4 μm ensures the complete retention of suspended matter and leads to a considerable reduction in the amount of bacteria in the outflow of the sewage plant.

Compared with conventional wastewater technology, membrane bioreactors have a short hydraulic retention time and high biomass concentrations of up to 20 $g_{dry\ weight}/L$. Additionally, because of the compact way in which they are constructed, membrane bioreactors have a relatively low surface area requirement.

SMBRs employ membrane module cassettes made of bundles of hollow fibers or flat-sheet membrane panels. The cassettes are vertically immersed within a tank containing wastewater and activated sludge and are aerated by a bubble system from the bottom of the units (Fig. 39.11). The

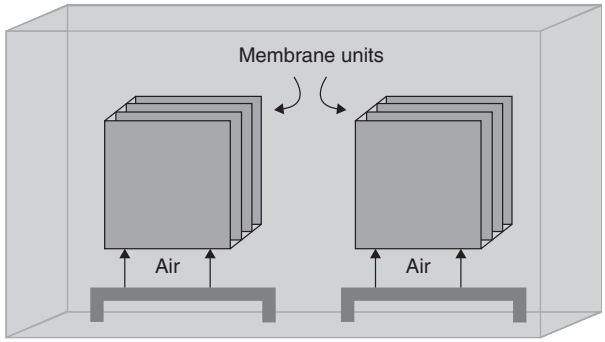


Figure 39.11. Submerged membrane cassettes with aeration by a bubble system from the bottom of the unit.

aeration serves to activate the sludge and to control concentration polarization and fouling at the membrane level as it generates an upward cross-flow over the membrane. In addition, it ensures effective tank mixing and even distribution of the biomass. The biomass can work at a very high level of concentration which enables a low tank volume and a long sludge age to be utilised; this substantially reduces sludge production. Treated effluent is removed from the membrane units using gravity head (typically 1–1.2 m), or a pumped suction operation can be utilised.

Similar to the bioreactors with the external module, the membrane in submerged bioreactors can also contain biocatalytic systems, which in principle can be obtained with the same approaches previously discussed. However, at the moment only few examples have been tested, mainly using biofilms growing on the membrane surface, to optimize the treatment process.

Membrane aerated biofilm reactors, where the biomass is immobilized on the membrane through which gas is supplied, seem the most promising configuration (21). The dissolved oxygen gradient across the membrane and the biofilm, offers an ideal environment for aerobic strains. However, biofilm growth should be controlled in order to avoid excessive biofilm thickness or density. In fact, this contributes to an increased resistance to mass transfer and may lead to decrease of gas fluxes (22).

An alternative biofilm membrane reactor configuration has been developed by integrating separate steps consisting of a moving-bed biofilm reactor followed by a submerged membrane module placed externally to the biomass compartment (23). This permits working with a very high biomass density with no or very limited effect on fouling of the submerged membranes.

39.4 APPLICATIONS

The use of biocatalysts is of particular interest for certain applications, specifically in terms of energy consumption, safety, pollution prevention, and the high quality of obtained products. Although the use of biocatalysts on an industrial level is not yet fully established, bioreactors running at large scale are increasing. A few examples are summarized here: (i) production of L-aspartic acid with *Escherichia coli* cells entrapped in polyacrylamides; (ii) lactase (β-galactosidase) entrapped into the fibers of cellulose acetate and used for the hydrolysis of milk and whey lactose; (iii) synthesis of the dipeptide Aspartame™ using thermolysin; (iv) production of L-alanine using *Pseudomonas dacunahe* immobilized with glutaraldehyde; (v) glucose isomerase reticulate with glutaraldehyde used in the production of fructose-concentrated syrups; (vi) L-amino acids produced from racemic mixtures by means of an amino acylase immobilized on DEAE-Sephadex; (vii) production of L-malic acid by *Brevibacterium ammoniagenes* entrapped in polyacrylamide; (viii) production of (2*R*,3*S*)-*trans* isomer of methyl ester of 4-methoxyphenylglycidic acid (a chiral intermediate of diltiazem, an important calcium-channel blocker used in the treatment of hypertension and angina, produced at 75 tons/year); (ix) production of phenylalanine.

The major technological difficulties of using biological immobilized systems on an industrial level include (i) the availability of pure enzymes at an acceptable cost (often the commercial enzymes are mixtures of several proteins); (ii) difficulties in immobilizing enzymes that often need expensive cofactors; (iii) the necessity for biocatalysts to operate at low substrate concentrations; (iv) microbial contaminations; and (v) the opposing requirements of crucial conditions (for example, treatment of solutions requires the use of microporous supports for creating high surface area per unit volume–thus equipment requirements are small–but by contrast, solutions with high turbidity cause fouling of pores thus reducing the advantages).

Currently, the development of catalytic systems specifically devoted to meeting the requirements of biomanufacturing and bioprocessing are likely to overcome these difficulties.

Examples of the most common membrane bioreactor applications are discussed in the following sections.

39.4.1 Biocatalytic Membrane Reactors in Food and Beverage Processing

Consumer demand for different food products has significantly changed in developed countries due to lifestyle changes, increasing incomes, demographic shifts, and so on. These countries share a rising trend toward higher consumption of meat, cheese, fruits, vegetables, and bottled drinks. And, the demand is for food products that are convenient to use and yet have all the qualities of a fresh product.

Simultaneously, significant structural changes in food production and processing sectors have been promoted

because of technological innovations, public policy and private attitudes to food safety, nutritional labeling, environmental concerns, farm policy and programmes, and competition in the international food market.

The most significant aspects in food manufacturing include the following:

Quality	maintenance or improvement of flavor, color, and texture
Safety	microbiologically and chemically, materials and methodologies used during processing and preservation do not introduce hazardous compounds
Stability	"fresh food" with medium to long-term shelf-life
Convenience	food is made into forms that are convenient (ease to use)
Wastes	prevention, minimization, valorization and recycling but prevention is better cleaning it up
Formulation	New products obtained from engineered raw materials and enabling processes
Sustainability	to meet today's needs without compromising the ability of future generations to meet their own needs

To achieve these challenges, all steps in food manufacturing have to be considered (e.g. where and how the food is produced, processed, packaged, preserved, distributed, prepared, consumed and disposed of).

To afford sustainable growth it is necessary to maximize mass and energy utilization as well as maximize recover and recycling. The technologies to be used need to be clean, safe, consume less energy, be able to preserve properties of products and coproducts, and allow new product formulations.

Membrane operations are among the most suitable technologies for food processing due to the peculiar properties mentioned earlier (Table 39.1). In the food and beverage industries, membrane filtration is state-of-the-art technology for clarification, concentration, fractionation, desalting, recycling, recovery and purification. The use of membrane technology in this field was dominated by its application in the treatment of whey and milk, whey protein concentration, followed by beverages, wine, beer, and juices. The integrated use of biocatalytic reactors and membrane processes is particularly suitable both for improving efficiency of more traditional membrane operations and for developing innovative production and processing systems. In the first case, for example, the combination of bioconversion with separation processes can be used as an initial or simultaneous treatment to reduce fluid viscosity, control membrane fouling, improve product quality and stability, govern coproduct formation, and minimize waste production. In the second case, the concept of biocatalytic membrane reactors is used to implement the formulation of new food products and functional food ingredients with improved texture and shelf-life.

The main applications are reported in Table 39.5 and are discussed in the following sections.

39.4.2 Milk and Dairy Products

The production of hydrolyzed milk, including dairy products, is of crucial importance for people who are lactose-intolerant. The use of membrane reactors to hydrolyze lactose in whole milk or cheese whey in continuous systems is a technique used on a large scale. Both lactose conversion and recovery of high molecular weight proteins can be accomplished in a single step. The hydrolysis of lactose is carried out using immobilized β-galactosidase.

An innovative process using hollow fiber membrane reactors to produce lactose-reduced skimmed milk without any ultrafiltration step before the enzymatic conversion was recently proposed (24). The system is composed by an UF unit that consists of a bundle of hollow fibers. The outside (shell side) compartment has closed circulation and is filled with the enzyme solution. A continuous flow of the substrate (skim milk) is applied to the inside (tube side) of the hollow fiber membranes. In this way, continuous, enzymatic lactose hydrolysis is possible without inherent problems of immobilized enzymes. The driving force for this system is the lactose diffusion, which mainly depends on the concentration gradient, the temperature and the flow rates of the substrate and the enzyme solution. In comparison to a batch process, enzyme activity could be used for a longer duration and enzyme release into the product does not occur. The system resulted in high conversion rates at high flow rates and consequently, high productivity.

Intolerance to milk is not only caused by lactose, but also by high molecular weight proteins. In fact, some children and old people have difficulty hydrolyzing proteins with molecular weight higher than 5 kDa; in other words they cannot digest such proteins, which causes them pain, stomachache, and can also lead to allergy. The hydrolysis of high molecular weight proteins into polypeptides lower than 5 kDa in biocatalytic membrane reactors is a new approach to producing low allergenic fresh milk with improved properties as compared to the reconstituted powdered milk that was traditionally used. The biocatalytic membrane reactor can be designed so that a membrane of appropriate cutoff can remove hydrolyzed fragments lower than 5 kDa while retaining the nonhydrolyzed proteins. In order to achieve high efficiency, the hydrolytic step should be part of an

TABLE 39.5. Applications of Biocatalytic Membrane Reactors in Food Processing

Reaction	Biocatalyst	Membrane Bioreactor	Application
Conversion of D-glucose to D-fructose	Glucose isomerase	Cross-linked enzyme	Sweetner industry
Hydrolysis of lactose to glucose and β-galactose	β-Galactosidase	Axial-annular flow reactor	Delactosization of milk or whey for human consumption
Hydrolysis of high molecular weight protein in milk	Trypsin and chymotrypsin	Asymmetric hollow fiber with enzyme	Production of low allergenic milk, and milk-based functional beverages
Hydrolysis of raffinose	α-Galactosidase and invertase	Hollow fiber reactor with segregated enzyme	Production of monomeric sugars
Hydrolysis of starch to maltose	α-, β-Amylase, pullulanase	CSTR with UF membrane	Production of syrups
Fermentation of sugars	Yeast	CSTR with UF membrane	Brewing industry
Anaerobic fermentation	Yeast	CSTR with UF membrane	Production of alcohol
Hydrolysis of pectins	Pectinase	CSTR with UF membrane	Production of bitterness and clarification of fruit juice and wine
Aerobic fermentation	*Lactobacillus bulgaricus*	CSTR with UF membrane	Production of carboxylic acids
Removal of limonene and naringin	β-Cyclodextrin	CSTR with UF membrane	Production of bitterness and clarification of fruit juice
Hydrolysis of K-casein	Endopeptidase	CSTR with UF membrane	Milk coagulation for dairy products
Hydrolysis of collagen and muscle proteins	Protease, papain	CSTR with UF membrane	Meat tenderization
Conversion of glucose to gluconic acid	Glucose oxidase and catalase	Packed bed reactor	Prevention of discoloration and off-flavour of egg products during storage
Hydrolysis of cellulose to cellobiose and glucose	Cellulase and β-glucosidase	Asymmetric hollow fiber reactor	Production of ethanol and protein
Hydrolysis of malic acid to lactic acid	*Lactobacillus oenos*	MF capillary membranes with entrapped cells	Improve taste in white wine
Hydrolysis of fumaric acid to L-malic acid	Fumarase	UF capillary membrane reactor	Production of food additives
Hydrolysis of oleuropein	β-Glucosidase	Hollow fiber reactor with entrapped enzyme	Production of antioxidants and bactericides
Hydrolysis of triglycerides to fatty acids and glycerol	Lipases	UF capillary membrane reactor	Production of foods, cosmetics and emulsifiers, treatment of fats and oils
		Hydrophobic plate-and-frame membrane reactor	
		Spiral-wound polypropylene membrane reactor	
Synthesis of dipeptide aspartame	Thermolysin®	—	Production of sweetner
Conversion of bitter naringin into no-bitter naringinin + glucose	Rhamnosidase and β-glucosidase	—	Improvement of fruit juice quality and stability
Conversion of bitter limonin to deoxylimonin acid	*Acinobacter* sp., *Corynebacterium* sp.	—	

CSTR, continuous stirred tank reactor; UF, ultrafiltration; MF, microfiltration.

integrated system where up- and downstream processing of milk is properly considered.

Biocatalytic membrane reactors can also be used to valorize coproducts of cheese-making processes. Cheese whey is a highly polluting product, containing protein (~0.7%), lactose (~5%), salts and water (~93%). The recovery and reuse of these valuable compounds allows increased cost-effectiveness and reduced wastes production. The whey proteins, having excellent functional properties (such as α-lactalbumin and β-lactoglobulin), can be recovered and concentrated by ultrafiltration and nanofiltration and hydrolyzed to polypeptides useful as pharmaceutical intermediates. In addition, permeates from the ultrafiltered milk and whey contain lactose that can be recovered and used in the production of glucose and galactose syrup.

39.4.3 Treatments of Oils

Biocatalytic membrane reactors using immobilized lipases and esterases represent a sustainable alternative for the treatment of oils and fats by replacing traditional chemical processes with biotechnological ones. The performance of different membrane reactors depends on the physicochemical properties of membrane and reaction components. The most advanced systems are represented by two-separate phase enzyme membrane reactors. In these systems, the mass transfer of triglycerides through the enzyme-loaded membrane can be improved by the presence of stable emulsion droplets within the internal liquid phase of the porous polymeric matrix. The optimized mass transfer properties allow working in a reaction-limited regime to maximize reaction efficiency. Immobilized enzymes increase their half-life time; in addition, if they are immobilized under proper conditions they can also maintain native catalytic activity. Biocatalytic systems using immobilized lipase on membranes have been used for hydrolysis of triglycerides in olive oil, palm oil and various other vegetable oils, for improving oil quality and producing foods, home and health-care ingredients. Recently, they have also been investigated for the production of energy-related components.

In addition to hydrolysis of triglycerides, an innovative strategy for oil processing is the use of β-glucosidase to hydrolyze oleuropein into dialdehydes with better taste and higher nutriaceutical and bactericidal properties.

39.4.4 Hydrolysis of Pectins in Fruit Juices

The interactions between pectins and sugars (e.g. galactose, arabinose, and rhamnose) are predominantly responsible for the high turbidity and viscosity of fruit juices. Pectinases (able to hydrolyze the polygalacturonic chain) and pectinesterases (able to hydrolyze the ester bonds of pectins to produce pectic acids) are largely used to reduce the viscosity of fruit juices. The use of pectinases immobilized in membrane reactors may allow reusing the enzymes and controlling membrane fouling during the clarification process by cross-flow ultrafiltration. Using the enzyme immobilized on the membrane (polysulfone spiral-wound module), the permeate flux can be increased by approximately 30% with respect to that obtained when the enzyme is freely suspended in solution. Nevertheless, the steady-state permeate flux needs further improvements for large-scale applications. Other important parameters affecting the permeate flux are (i) amount of immobilized biocatalyst; (ii) transmembrane pressure; (iii) axial velocity; and (iv) operation mode. High performance is obtained with low concentrations of immobilized enzyme, low transmembrane pressure, and high axial flow rate.

39.4.5 The Treatment of Wine

The characteristic organoleptic taste and color of wine depends on the polyphenolic compounds present in must. In order to stabilize musts, white and rosée wines, laccase is used to oxidize polyphenols in solution, as well as anthocianase immobilized on synthetic and natural polymers used in hydrolyzing anthocianes.

During the maturation process of white wine, a secondary fermentation occurs that converts malic acid into lactic acid. In order to obtain a wine with very good organoleptic properties the control of this reaction is of crucial importance. Cells of *Leuconostic oenos* immobilized in a microporous membrane can be used to carry out the malolactic fermentation in white wine. Cells are immobilized by cross-flow filtration through polypropylene capillary membranes and the wine is recycled along the membrane module and permeate is collected aside. Using the appropriate cell density on the membrane, it is possible to control the conversion to the desired degree. The conversion of malic acid to lactic acid allows increasing the pH of wine from 3.4 to 4.2 or higher desired values. This gives a better taste to the wine because the slightly higher pH prevents precipitation of proteins in the mouth.

39.4.6 Biocatalytic Membrane Reactors in Pharmaceutical Productions

Biocatalytic membrane reactors are used for the production of amino acids, antibiotics, anti-inflammatories, anticancer drugs, vitamins, and so on. Reaction systems are mainly constituted of enzyme or cells immobilized on membranes or by cells cultured in membrane-assisted devices. Some of the most common applications in pharmaceutical production are summarized in Table 39.6.

Most of the studies in this field concern the production of optically pure enantiomers. This is due to the fact that at the molecular level, asymmetry dominates biological processes as regulatory principles and biochemical reactions are based on chiral recognition phenomena. In view of this, it is clear that it is important for bioactive compounds having pharmacological activities to have the proper enantiomeric shape. In fact, this allows improvement of efficiency and reduction in the amount of pharmaceuticals to be administered.

Membrane technological strategies are widely exploited in the production of optically pure isomers. Many studies focus on the production of amino acids, arylpropionic acids, amines and carboxylic acids. The technological problems associated with the production of these compounds at a large scale are connected to the need for enzymes of expensive cofactors, low water solubility of substrates, and presence of products in complex solutions from which they have to be separated and purified.

TABLE 39.6. Biocatalytic Membrane Reactors in Pharmaceutical Applications

Reaction	Biocatalyst	Membrane Reactor	Purpose
Production of ampicillin and amoxycillin	Penicillin amidase	Entrapment in cellulose triacetate fibers	Production of antibiotics
Hydrolysis of a diltiazem precursor	Lipase	Entrapment in biphasic hollow fiber reactor	Production of calcium-channel blocker in optically pure form
Hydrolysis of a cyano-ester to (*S*)-ibuprofen; naproxen esters to (*S*)-naproxen, etc.	Lipase	Entrapment in biphasic hollow fiber reactor	Production of optically pure nonsteroidal anti-inflammatory drugs
Conversion of cortexolone to hydrocortisone and prednisolone	*C. lunata*/*C. simplex*	Entrapment in polyacrylamide gel	Production of steroids
Conversion of fumaric acid to L-aspartic acid	*E. coli* with aspartase	Entrapment in polyacrylamide gel	Pharmaceuticals and feed additives
Conversion of L-aspartic acid to L-alanine	*P. dacunhae*	Entrapment in polyacrylamide gel	Pharmaceuticals
Conversion of acetyl-D,L-amino acid to L-amino acid	Aminoacylase	Ionic binding to DEAE-sephadex	Production of L-amino acids for pharmaceutical use
Synthesis of tyrosine from phenol, pyruvate, and ammonia	Tyrosinase	Entrapment in cellulose triacetate membrane	Production of L-amino acids for pharmaceutical use
Hydrolysis of 5-p-HP-hydantoine to D-p-HP-glycine	Hydantoinase and carbamilase	Entrapment in UF polysulfone membrane	Intermediate for the production of cephalosporin
Dehydrogenation reactions	(NAD(P)H-dependent enzyme systems	Confination with UF-charged membrane	Production of enantiomeric amino acids
Hydrolysis of DNA to olygonucleotides	DNase	Gelification on UF capillary membrane	Production of pharmaceutical substances
Hydrolysis of hydrogen peroxide	Bovine liver catalase	Entrapment in cellulose tryacetate membrane	Treatment in liver failure
Hydrolysis of whey proteins	Trypsin, chymotrypsin	Polysulfone UF membrane	Production of peptides for medical use
Hydrolysis of arginine and asparagine	Arginase and asparaginase	Entrapment in polyuretane membrane	Care and prevention of leukemia and cancer
Complex biotransformation cycles	Cell cultures	UF CSTR	Production of pharmaceuticals

In reactor systems using coenzyme-dependent reactions, negatively charged membranes are used to retain the cofactor in the reaction vessel. The retention is obtained by electrostatic repulsion between both, the negatively charged cofactor and the membrane. In other cases, the cofactor can be attached chemically to water-soluble polymers in order to increase its size and be retained by an ultrafiltration or nanofiltration membrane. Degussa has developed such a system for ton-scale production of L-*tert*-leucine by means of leucine dehydrogenase (LEUDH), which converts α-chetoacid into L-leucine reducing the $NADH_2$ to NAD; the NAD is then regenerated into $NADH_2$ by formate dehydrogenase (Fig. 39.12) (25,26).

When substrates have low water solubility, the heterogeneous reaction is carried out in multiphase membrane reactors in two-separate phase configurations (see description in previous sections). In general, enzyme activity and enantioselectivity of immobilized enzymes are preserved, provided the mass transport of reagents through the enzyme-loaded membrane is not limiting and the oil/water interface is realised at the level where the catalyst is immobilized. Many studies have been carried out with enzymes in biphasic systems. Lopez *et al*. (27) reported an example of this process at a large scale. The reactor is used to produce the (2*R*,3*S*)-methylmethoxyphenylglycidate ester, a chiral intermediate for the preparation of diltiazem (Fig. 39.13).

The full-scale facility comprises two banks of 12 60-m^2 modules for a total effective membrane reactor area of 1440 m^2. The annualized plant production rate is 53 kg/ m^2/year of 99% enantiomeric excess ester. Tanabe Seyaku (Japan), which selected the lipase specific for the reaction of interest, and Sepracor Inc. (USA), which studied the membrane device, developed this reactor. Sepracor Inc. commercialized other membrane reactors, such as a full-scale enzyme membrane reactor plant used in the production of the angina and hypertension drug

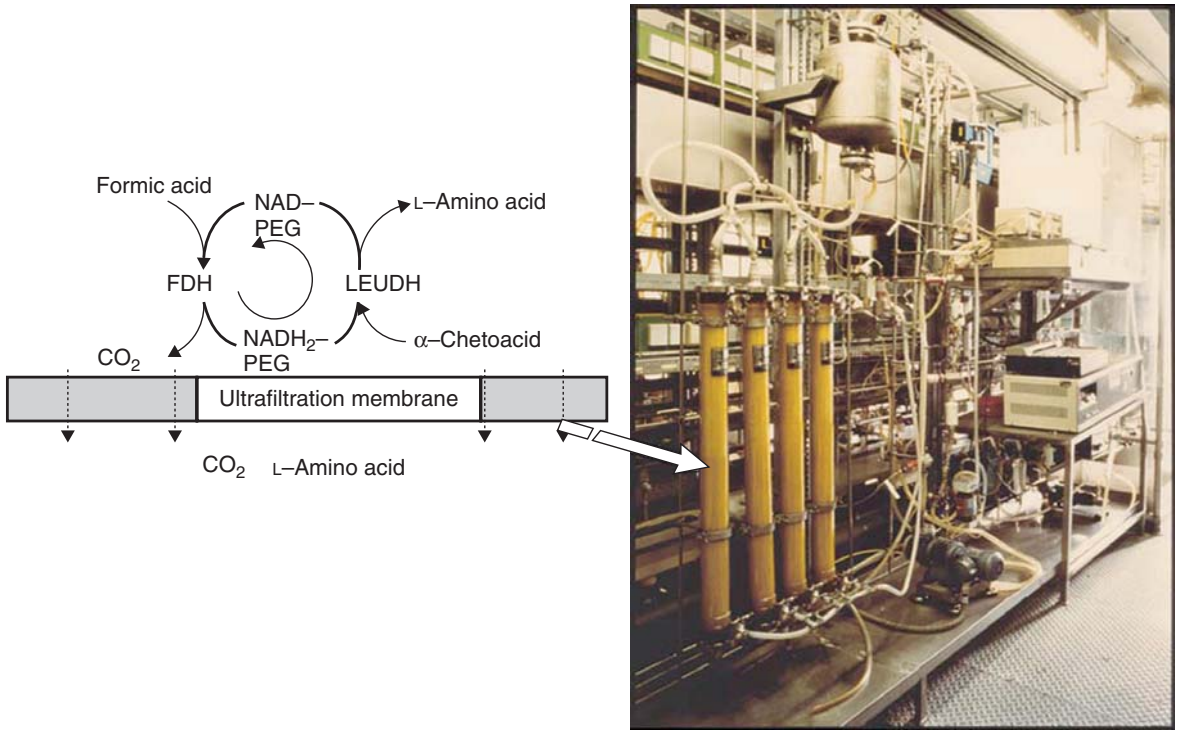


Figure 39.12. Large-scale membrane filtration for separation of L-amino acids. (This figure is available in full color at http://onlinelibrary.wiley.com/book/10.1002/9780470054581.)

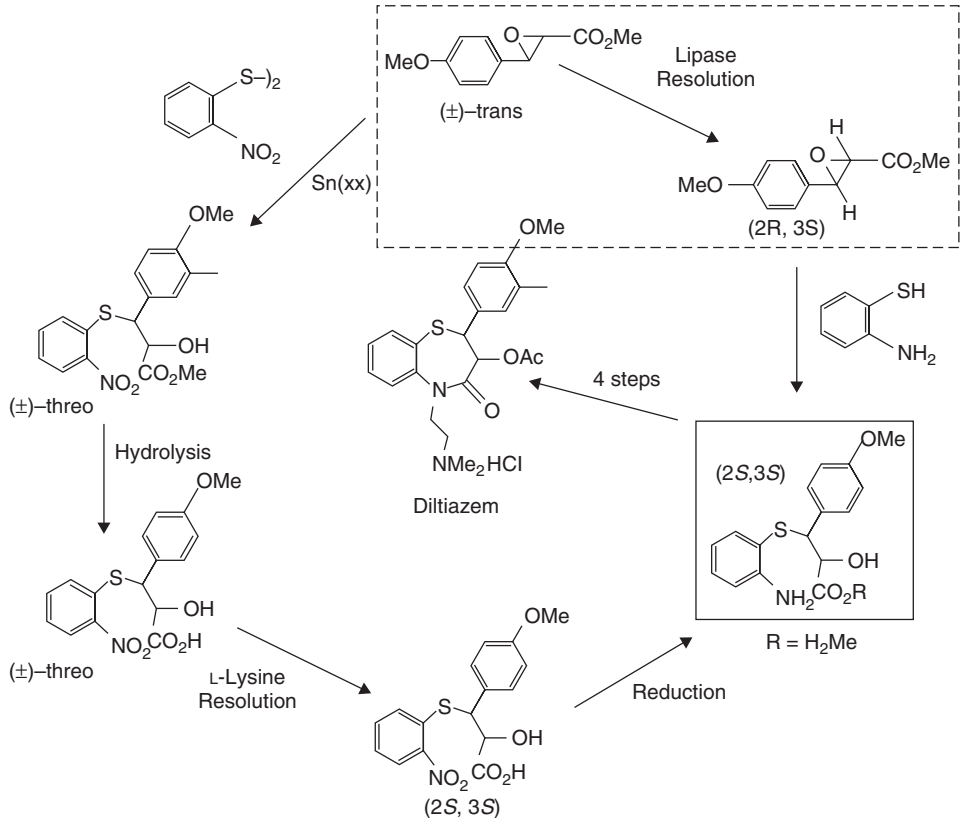


Figure 39.13. Schematic diagram of the classical chemical route and the new alternative reaction steps to obtain the chiral intermediate by means of lipase (18).

Cardizem®. The company focused on developing improved single-isomer and active-metabolite versions of existing drugs, and markets or out-licenses a number of respiratory drugs including Allegra®, Clarinex®, and Xopenex®.

When the compound of interest is obtained by fermentation, it is present in complex solutions from which it needs to be separated and purified. In these cases, integrated membrane systems can be used for continuous production and downstream separation. For example, the production of L-amino acids is obtained by continuous fermentation in a cell-recycle membrane fermentor. During operation, the bioreactor volume is kept constant by adding fresh medium at the same rate at which it permeates through the ultrafiltration membrane. The solution recovered as permeate contains the product, L-amino acid, together with other small molecules not retained by the membrane, while the cells and macromolecules are recycled back to the bioreactor. The product is then in a clarified solution from which it needs to be purified and concentrated. The purification can be obtained by membrane-based solvent reactive extraction carried out through two membrane modules. This operation is based on the transport of the solute from an aqueous solution (feed) to another at different pH (stripping) via an organic phase (extracting) containing a reactive carrier. The two phases are kept in contact at the pore entrance of the membrane interposed between them. When specific carriers are used at the extracting phase, the separation can be very selective.

An integrated process based on membrane operations is used to produce L-phenylalanine from glucose fermentation by *E. coli* (Fig. 39.14) (26,28).

The L-phenylalanine is produced in a 40 L fermentor, clarified through a first membrane filtration step, and then selectively extracted through a kerosene solution containing 10% D_2EHPA as carrier. The L-phenylalanine is then lyophilized from the extracted solution. Degussa developed the enzyme membrane reactor process on a productive scale, in cooperation with the Research Center Julich in 1981.

Electrodialysis with bipolar membranes can be used for the recovery of organic acids from fermentation processes. There are many acids that can be produced by this technique (29). A commercially operated industrial plant has been installed for the production of lactic acid (30). The simplified flow diagram of the conventional lactic acid production and the production with integrated electrodialysis is given in Fig. 39.15a and b. In the conventional lactic acid production process which is shown in Fig. 39.15a, the separation and purification of lactic acid is achieved mainly by ion exchange and requires different ion exchange steps resulting in a large volume of wastewater from regeneration salts. In the production process with integrated electrodialysis, which is shown in Fig. 39.15b, a minimum of ion exchange resin is needed in a final purification step. The concentration of the lactate salt is achieved by conventional electrodialysis and the conversion of the lactate into lactic

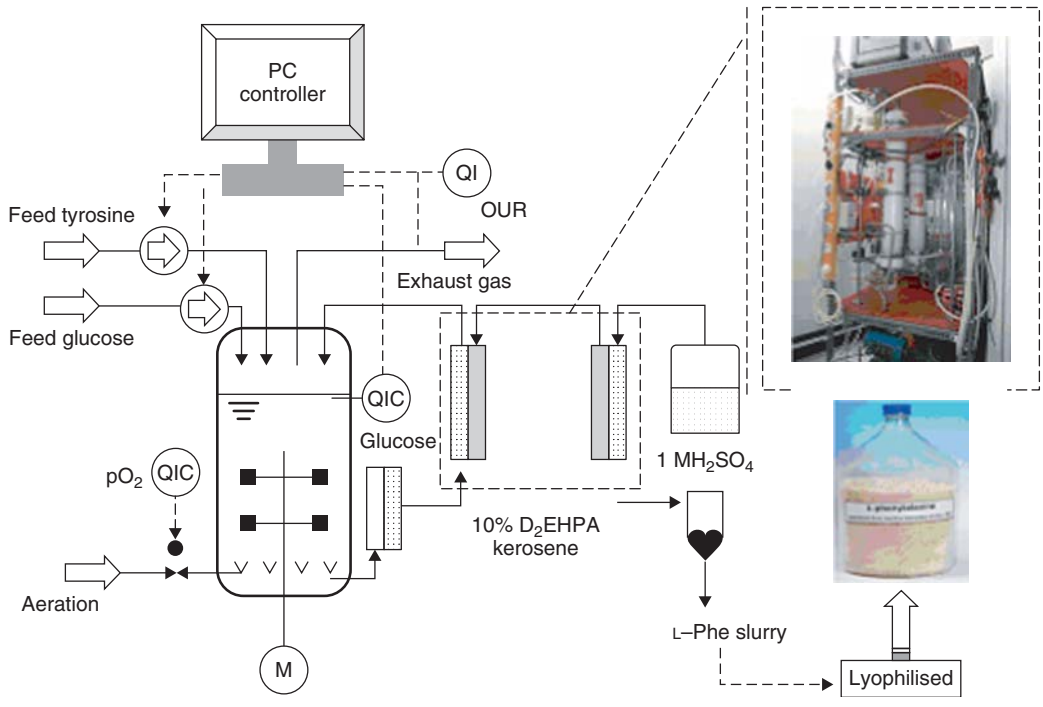


Figure 39.14. Integrated system for the production of L-phenylalanine (adapted from Refs 2, 17). (This figure is available in full color at http://onlinelibrary.wiley.com/book/10.1002/9780470054581.)

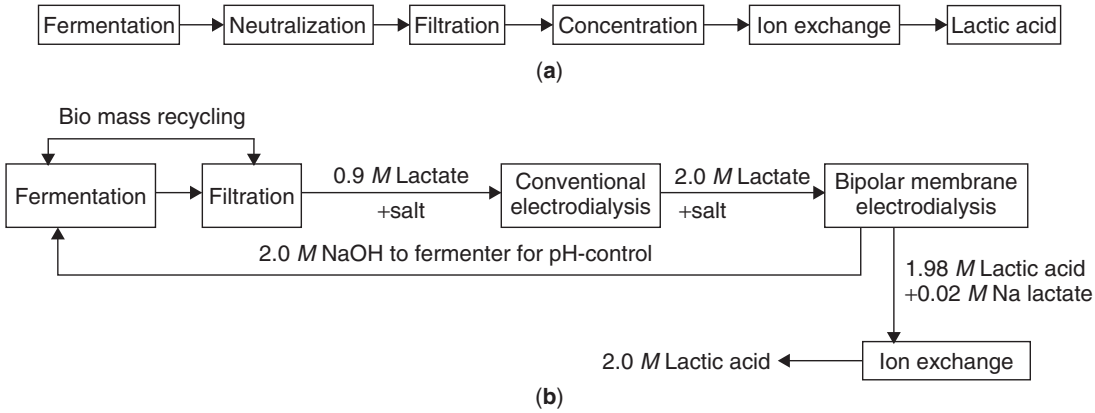


Figure 39.15. Simplified flow diagram illustrating (a) the conventional lactic acid production process and (b) the production process with integrated electrodialysis (2).

acid by bipolar membrane electrodialysis. The simultaneously produced base is recycled to the fermenter to control the pH-value.

Further readings for biocatalytic membrane reactors for enantiomers production are found in Refs 1, 4, 27, 31–34.

Producing pharmaceuticals from cell cultures is a complex and costly process which requires equipment and systems capable of handling fragile living cells without damaging them. Sterilization, cleanliness and quality control requirements are also extremely important. The bioreactor plays a central role in a cell culture facility. In the bioreactor, recombinant (genetically engineered) cells are grown and induced to produce the active pharmaceutical molecule which is then separated from the harvested cell culture and purified. Bioreactor systems for mammalian cell cultures and bacterial fermentation are available for pilot-scale as well as industrial-scale operations in sizes from 20 to 25,000 L (e.g. Alfa Laval Biokinetics. http://here.alfalaval.com/). Membrane filtration is already widely accepted for recovery of the active principles from mammalian cell cultures and fermentation. It is believed that the big challenge is combining the separation technology available with membrane filtration, to get the optimal solution. Cell separation is usually the first step after cell cultivation in the sequence of downstream processing. Cross-flow microfiltration has been used in separations involving different cell types. Membrane filtration also offers the possibility of washing and recycling the cells, for example by diafiltration. Cell washing is necessary to remove impurities in the culture medium if the cells themselves are products or the cells need to be disintegrated to release intracellular proteins. Recycling of cells is used to increase productivity in some fermentation processes.

The advantages of membrane filtration compared to conventional techniques such as centrifugation for the purification of biopharmaceuticals has largely been documented. Most of the information on process-scale membrane operations used in biotechnology is proprietary; numerous reports have appeared on laboratory or pilot-scale experiments; they deal primarily with separations of bacteria and yeast, and less with mammalian cells (35–40).

39.4.7 Biocatalytic Membrane Reactors in Biomedical Applications

Membrane processes play a key role in modern therapy for treating acute and chronic organ failure and in the management of immunologic diseases. In fact, membrane devices are employed in most extracorporeal blood purification methods, and the next generation of artificial organs and tissue engineering therapies are likely to be grounded on membrane technology. Intracorporeal uses of membrane devices include contact lens, biosensors, drug delivery systems, and artificial grafts.

The use of membrane reactors in the development of new artificial organs is currently attracting significant attention. Over 20 million patients are sustained by functional organ replacement. Most of recent research activity has been focused on organ replacement and extracorporeal treatment. Two main strategies are as follows: (i) the use of membranes as toxin separators and (ii) the use of cells combined with membranes to both remove toxins and supply metabolic organ functions. Membrane bioartificial pancreases, using isolated islets of Langerhans segregated by membranes, represent an alternative approach to the transplantation of whole pancreas in patients with insulin-dependent diabetes. Various investigations are directed to protect cells from immunorejection, maintain the cell viability and functions, reduce diffusion resistance of nutrients and metabolites, and study the kinetics of transformation of glucose into insulin.

39.4.7.1 Bioartificial Kidney. The limitation of dialysis, filtration, or adsorption to detoxify blood of patients with acute renal failure is that the artificial devices are not able to endow the readsorptive and endocrine functions expressed by the real kidney, thereby causing an accumulation of components or lack of metabolites that alter the physiological equilibrium.

To replace not only the filtration, but also the numerous other functions of the kidney, the combination of filtration with living cells seems a promising solution.

In 2001, Fissel reported a bioreactor system called the "renal assist device" (41). The multiple hollow fiber bioreactor contains renal tubule cells. After completion of animal experiments, the first clinical trials involving patients with acute renal failure have been executed successfully.

The kidney is the first organ whose function has been substituted by an artificial device; it is also the first successfully transplanted organ.

39.4.7.2 Bioartificial Liver. Isolated hepatocytes supported on membranes can work as a bioartificial liver for the temporary treatment of patients with acute liver failure. They are mainly used as extracorporeal devices where the membrane acts as a support for cell adhesion, as an immunological barrier between the patient's blood and the isolated hepatocytes, and as a selective mass transfer system allowing a sufficient exchange of small-molecular-weight solutes such as toxins and smaller proteins.

The extracorporeal biohybrid systems are suitable for short-term treatments to sustain the patient for the period they need to wait for an available organ or after transplantation, to give sufficient time for the transplanted organ to get grafted. In addition to acting as a "bridge" for transplants, the bioartificial liver gives damaged livers time to recuperate and enables as many as 20% of the patients to recover without transplants. Since the liver is an extremely complex organ and it performs a variety of functions, many of which are still poorly understood, artificial liver support is one of medicine's longest-standing challenges, with nearly 40 years of basic and clinical research. For a long time, it seemed impossible to develop an artificial liver by trying to design devices to perform each of the liver's functions. A breakthrough occurred when Kenneth Matsumura took a completely different approach and designed a device that used liver cells obtained from animals. The device contained both biological and manufactured components so it is called a bioartificial liver. Matsumura (42) published the first clinical report of a bioartificial membrane liver in 1987. The equipment used is reported in Fig. 39.16.

In the system, a patient's blood circulates through this bioartificial liver, where a synthetic membrane separates it from the animal cells. The membrane prevents immunologic rejection of the cells, but allows the cells to detoxify

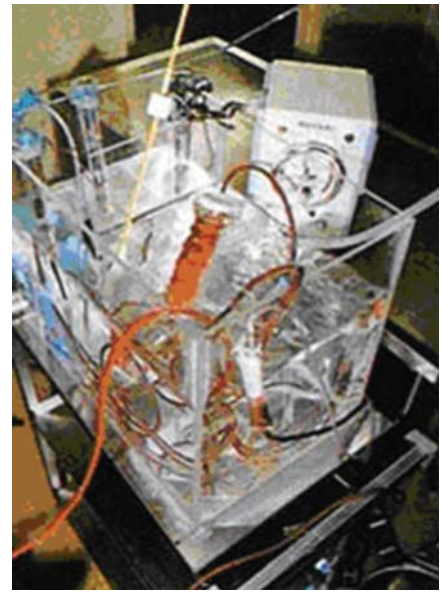


Figure 39.16. Equipment representing Matsumura bioartificial liver device (http://www.alinfoundation.com/Medical%20Research/Liver.htm). (This figure is available in full color at http://onlinelibrary.wiley.com/book/10.1002/9780470054581.)

the blood in the same way as a natural liver. Disposable units can be used for a series of brief treatments, as with kidney dialysis.

Since then, following the same strategy, this area of research made great progress and although there are no bioartificial devices yet that are able to replace the organ, they are able to to keep the patient alive during the wait for an organ to be transplanted. Scientists at Berlin University's surgery and transplant unit developed a bioreactor containing a concentrated culture of metabolically-active pig liver cells, which are able to work as an "emergency liver" (43). The patient's plasma and blood cells are separated in an external circuit, with the plasma being directed to the bioreactor, which performs the normal liver functions in general and detoxification in particular. The plasma and blood cells are then recombined and reinjected into the patient. The main technological innovation of such bioartificial livers is in the organisation of the culture medium of pig liver cells in a three-dimensional structure (Fig. 39.17). This configuration allows cells to survive for several weeks by efficient oxygenation, properly supplying nutrients, and eliminating toxic waste.

By the end of January 1999, the system was used to support patients awaiting a transplant.

Bioartificial livers are exploited at clinical levels. Among other companies, Circe Biomedical Inc. developed a hollow fibre-based model with porcine hepatocytes–the HepatAssist™ liver support system. The Hybrid Organ GmbH Company, located in Germany, also developed a biohybrid liver system based on a hollow fiber design

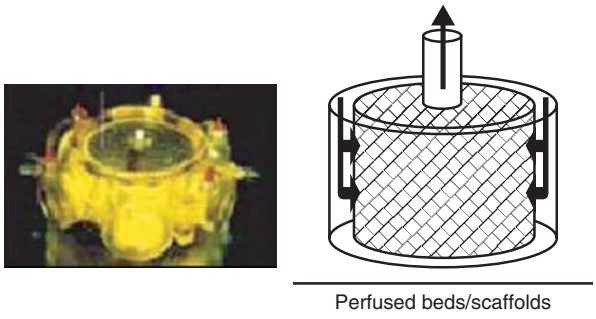


Figure 39.17. Three-dimensional structure of the bioartificial liver (picture from website: http://europa.eu.int/comm/research/rtdinf23/en/biotech.html). (This figure is available in full color at http://onlinelibrary.wiley.com/book/10.1002/9780470054581.)

with porcine hepatocytes. In general, artifical liver devices containing pig cells can be used for about six to eight hours each day.

There has been much concern about exposing patients to animal cells, which may function slightly differently and harbor infectious agents. Devices that incorporate human rather than pig liver cells might be preferable as these may reduce risks and eventually function more like a normal human organ.

VitaGen Inc. of La Jolla, Califonia developed the first human-cell based bioartificial liver system designed to increase the liver's ability to regenerate and recover, the so-called Extracorporeal Liver Assist Device (ELAD®). The ELAD liver device is based on a hollow fiber bioreactor that uses human C3A hepatoblastoma cells. The device is designed to be used continuously for up to 10 days.

Cell-Loaded Membranes in Regenerative Medicine. There is currently great expectation over the possibility of replacing damaged body parts, through the new field of regenerative medicine. Potential strategies of regenerative medicine include stem cell transplantation, implantation of bioartificial tissues synthesized in the laboratory, and the induction of regeneration from the body's own cells by rendering the injury environment and/or the responding cells regeneration-competent.

The engineering aspects of regenerative medicine, such as membrane technology, scaffolds, and biointerface engineering, will play a key role in smart biomaterials, tailor-made surfaces, *in vitro* lymph nodes, bioreactors as assist devices, polymers for extracellular matrices, and biomimetic material development.

Currently, the only way to compensate for diseased or injured tissues is through bionic implants and organ transplants. Attempts to establish regenerative medicine have been ongoing for over two decades. The vast majority of work has been done with experimental animals, although human clinical trials to restore several types of tissues, such as islet cells of the pancreas to cure diabetes and dopaminergic neurons of the *substantia nigra* to cure Parkinson's disease have been conducted.

Three strategies have been used:

- cell transplants;
- the construction *in vitro* of implantable bioartificial tissues ("tissue engineering");
- the chemical induction of regeneration *in vivo* by controlled-release.

Cell transplants involve replacing the cells of a damaged tissue by transplanting aggregates of donor cells into the lesion. The transplanted cells can be differentiated cells, embryonic stem cells (ESCs) derivatives, or adult stem cells (ASCs).

The concept of bioartificial tissue construction (tissue engineering) is to seed cells into a biomaterial support (e.g. membranes and scaffold), then implant this construct into the body. The constructs can be open (biomimetic support moulded in the shape of the tissue, open to vascularization by the host) or closed (cells encapsulated in biomaterials and dependent on diffusion for survival). Ideally, substrates for tissue engineering should be highly biomimetic, not only providing the proper geometry and adhesive qualities to maximize cell migration, but also incorporating the biological cues and signals essential for proliferation and differentiation, as well as any factors for neutralization of molecules inhibitory to regeneration. They should also be biodegradable on a schedule that matches the growth and differentiation of the regenerating tissue. Widely used biomaterial supports are collagen I, alginate, ceramics, polylactic and polyglycolic acid meshes, and pig small intestine submucosa (SIS). No existing biomaterial meets all the criteria deemed necessary for good tissue regeneration, however, and research on new materials is of high priority.

39.5 OTHER MEMBRANE BIOREACTOR APPLICATIONS

39.5.1 Submerged Membrane Bioreactors in Wastewater Treatment

In the last decade membrane bioreactors have increasingly gained attention in the field of wastewater technology. The combination of bioreactors and membrane technology enables an innovative and effective cleaning process both in municipal and industrial wastewater technology. This is particularly important in view of the reduced inflows of drinking and rain water expected in the future.

A submerged membrane bioreactor combines biological treatment with membrane separation. The treated water is separated from the purifying bacteria (active sludge) by a

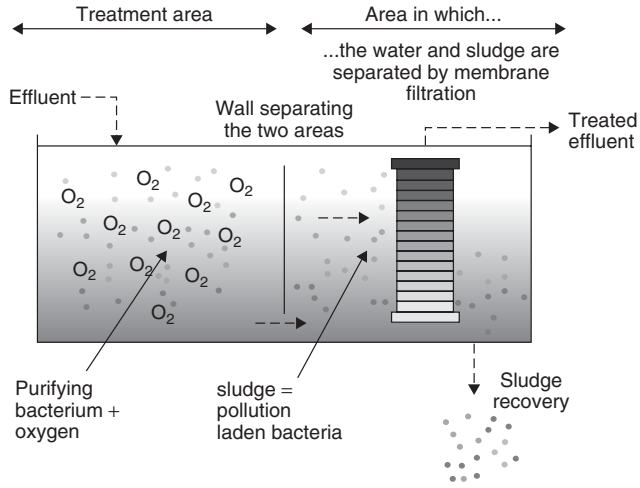


Figure 39.18. Schematic of a membrane bioreactor for wastewater.

process of membrane filtration rather than in a settling tank as in conventional systems. Only the treated effluent passes through the membrane. It is then pumped out. The sludge is recovered and dewatered (Fig. 39.18).

Large wastewater volumes characterize conventional wastewater technology. That means that municipal wastewater treatment plants have to treat high volume flows with relatively low contaminated dirty water. In order to ensure the purification performance of the plant even on days with more wastewater, caused for example by rainfall, large basin volumes are necessary in the area of the aeration tank and the final clarifier. These basins, which are usually open, are characterized by a large surface requirement and a long hydraulic retention time of the wastewater flows on dry days.

Compared with conventional wastewater technology, membrane bioreactors have a short hydraulic retention time and high biomass concentrations. Additionally, because of the compact way in which they are constructed, membrane bioreactors have a relatively low surface area requirement.

The sedimentation in the final clarifier is generally replaced by the implementation of membrane filtration. Using membrane technology, not only the biomass is separated from the water but also the quality of the purified wastewater is considerably improved. The use of microfiltration membranes with pore sizes usually between 0.1 and 0.4 μm ensures the complete retention of suspended matter and leads to a considerable reduction of the amount of bacteria in the outflow of the sewage plant.

The major benefits of the technology are: final effluent quality suitable for reuse; small ecological footprint <50% of a conventional plant; easy to control, can be monitored remotely; less sludge production, (generally 40% less).

In 1998, the US Environmental Protection Agency (EPA) promulgated final effluent limitation guidelines and standards in the Clean Water Act (CWA) for four subcategories of the pharmaceutical industry: (A) Fermentation; (B) Extraction; (C) Chemical Synthesis; (D) Mixing, Compounding, and Formulating. The regulations specifically identify "advanced biological treatment" as the basic technology for Best Practicable Control Technology (BPT) for Subcategory A, B, C, and D facilities; Best Available Control Technology (BAT) for Subcategory A, B, C, and D facilities; and New Source Performance Standard (NSPS) for Subcategory A, B, C, and D facilities. Membrane bioreactors fit as advanced biotreatment, and have been field-tested to provide reliable, cost-effective removal of chemicals from wastewater. The technology can treat many of the compounds listed in the regulations, including alcohols, aldehydes, alkanes, amides, amines, aromatics, chlorinated alkanes, esters, ethers, ketones, and miscellaneous compound groups.

Various companies are active in developing membrane bioreactors for wastewater treatment. Some of the most active ones are summarized in Table 39.7, while the membrane properties of some of the commercial modules are reported in Table 39.8.

Zenon, one of the leaders in membrane bioreactor technology worldwide, began by specializing in wastewater treatment over 20 years ago. The company has been selected to supply King County in the state of Washington with the largest membrane bioreactor in the world. The ZeeWeed MBR will treat an average day-flow of approximately 144,000 m^3 of municipal sewage or 38 million gallons per day (MGD) with peak flows up to 204,000 m^3 or 54 MGD, serving over 100,000 households [http://www.ecologicinvestor.com/news/printready.asp?ID=643].

Kubota process dominates the Japanese membrane wastewater treatment market. It provides the largest

TABLE 39.7. Examples of Companies and Immersed Modules Present Worldwide

Company Name	Membrane Module Configuration
Zenon Environmental Inc. (Canada) (acquired by General Electrics)	Immersed hollow fiber modules
Kubota (Japan)	Immersed flat-sheet modules
Toray Industries (Japan)	Immersed flat-sheet modules
Asahi Kasei (Japan)	Immersed hollow fiber modules
Mitsubishi Rayon (Japan)	Immersed hollow fiber modules
Korea Membrane Separation (Korea)	Immersed hollow fiber modules
USFilter (USA)	—
Koch Membrane Systems Inc. (USA)	Immersed hollow fiber modules
Biosep (Europe)	—
Brightwater Engineering	Immersed flat-sheet modules
Colloide Engineering Systems	Immersed flat-sheet modules
Huber Technology	Immersed flat-sheet modules
Memcor	Immersed hollow fiber modules
ITT Industries	Immersed hollow fiber modules
Kolon Membrane Systems (Korea)	Immersed hollow fiber modules
Tianjin Motimo Membrane Technology (China) (acquired by Dow Chemicals)	Immersed hollow fiber modules

TABLE 39.8. Membrane Properties Used in Commercial Submerged Membrane Bioreactors

Commercial Supplier	Membrane Configuration	Membrane Material	Membrane Pore Size (mm)
Zenon	Hollow fiber	PVDF	0.04
Asahi Kasei	Hollow fiber	PVDF	0.1
Koch-Puron	Hollow fiber	PES	0.05
Mitsubishi Rayon	Hollow fiber	PE	0.4
Brightwater	Flat sheet	PES	0.08
Toray	Flat sheet	PVDF	0.08
Kubota	Flat Sheet	PEZ	0.4

number of membrane bioreactors, with more than 2140 plants installed worldwide. Most of them are of small or medium size, with flows of less than 200 m^3 perday with a membrane operation time of more than 11 years. Large plants are also installed, for example, a plant with an area of 97,320 m^2 allowing a flow of 75,000 m^3 per day was installed in Oman, in June 2006.

Most of the submerged membrane bioreactor applications are used in Asia (Japan, Korea and China), Europe (United Kingdom, Germany and Spain), and USA. Their overall geographical distribution for wastewater applications is illustrated in Fig. 39.19.

Major drivers for SMBRs implementation include more stringent legislation; local water scarcity; state incentives to encourage improvements in wastewater technology; decreasing investment costs; increasing confidence in and acceptance of SMBRs technology; and public concern.

The cost of membranes has decreased in the last 15 years from about US \$400 m^{-2} to about \$50 m^{-2}. Representative costs for life cycle for a membrane system are illustrated in Fig. 39.20. They only represent about 8% of the overall costs.

Drivers for membrane cost decrease include improvements in process design; improved operation and

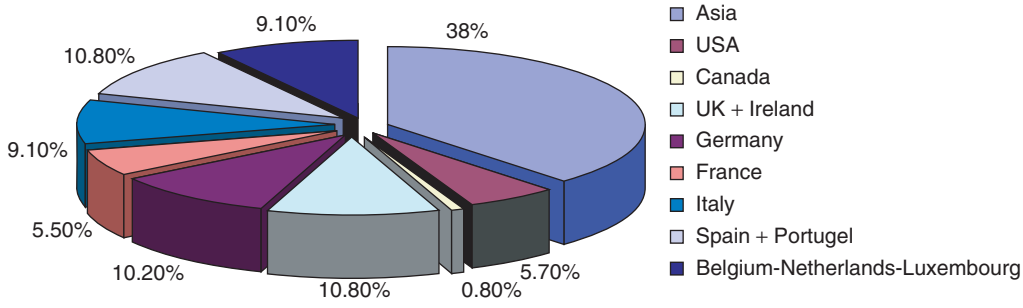


Figure 39.19. Geographical distribution of submerged membrane bioreactors. (This figure is available in full color at http://onlinelibrary.wiley.com/book/10.1002/9780470054581.)

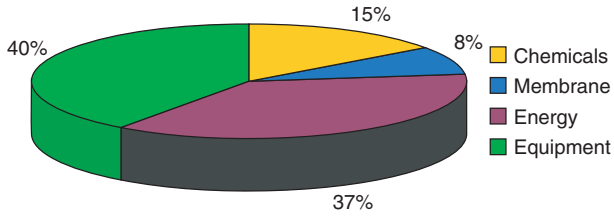


Figure 39.20. Representative costs for life cycle for a submerged membrane bioreactor in wastewater treatment (data referred to a Zenon membrane system). [After (34).] (This figure is available in full color at http://onlinelibrary.wiley.com/book/10.1002/9780470054581.)

maintenance schedules, and greater membrane life. Additional cost reductions can be expected upon standardization of element dimensions.

In conclusion, SMBRs are regarded by the water industry as "new" technology, although they are over 15 years old now. They provide lower ecological footprint, higher product quality, lower waste discharge, and meet more stringent regulation requirements.

SMBRs are expected to become more and more easily available due to the increasing number of investors (particularly from Asia), stakeholders, decision makers, technological innovation, and improved knowledge-base, for example with reference to membrane life, module design, operation mode.

Further reading on SMBRs can be found in Refs 1, 44–48.

39.6 CONCLUSIONS

In the last few years, biocatalytic membrane reactors have increased their potentiality in the rationalization of productive systems. Their intrinsic characteristics of efficiency, operational simplicity and flexibility, relatively high selectivity and permeability for the bioconversion and transport of specific components, low energy requirements, good stability, environmental compatibility, easy control and scale-up has been confirmed in various applications. As shown in Fig. 39.21, membrane bioreactors are already at a developing-maturing stage with respect to submerged membrane bioreactor configurations for wastewater treatment, and at an emerging-exploratory stage when considering the sidestream configurations for production systems. In the latter case, the real potentiality of the technology is still underestimated. Further demonstration over a long-term operation time is needed to prove the robustness of the technology in order to increase investor confidence and stakeholder acceptance.

Moreover, this new membrane bioreactor technology is very consistent with the strategy of process intensification, which today represents the most realistic answer to the demands of sustainable industrial growth.

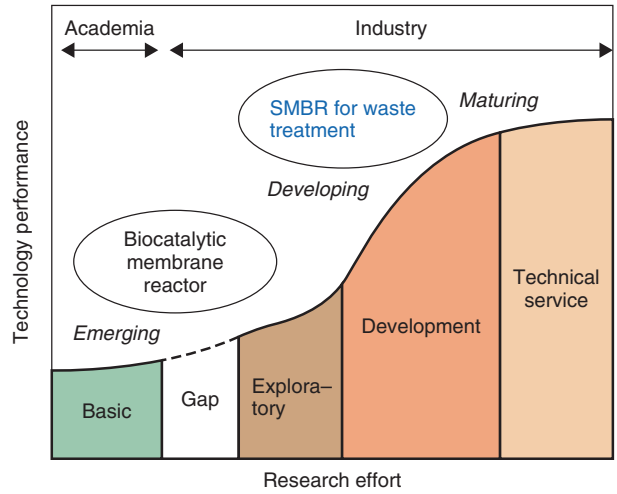


Figure 39.21. Membrane bioreactors' technology performance as a function of research effort. (This figure is available in full color at http://onlinelibrary.wiley.com/book/10.1002/9780470054581.)

Developments in membrane engineering, reactor design and control, genetically engineered biocatalysts and biomass, consumer demand of natural-like products, public concern and governmental regulations about environment, will fuel a renaissance of biocatalytic membrane reactors, and in particular their use in integrated systems. The field is expected to progress and contribute to innovative production, processing, and treatment strategies beyond the current technological solutions in various sectors including the fields of biotechnology, pharmaceutical, biomedical, agro-food, fine chemicals, water, fuel, and energy. To move from incremental progress to breakthrough advances, a holistic and interdisciplinary approach is mandatory considering that "the whole is more than the sum of its parts". It is therefore necessary to take into the account the sustainability of the entire life cycle of integrated systems, from development to operation, to disposal. There is no doubt that biocatalytic membrane reactors are among the best available technologies and they can certainly play a major role in facing the challenges of promoting sustainable processes.

REFERENCES

1. Strathmann H, Giorno L, Drioli E. An introduction to membrane science and technology. Rome: CNR; 2006.
2. Drioli E, Giorno L. In: Drioli E, Giorno L, editors. Biocatalytic Membrane Reactors: applications in biotechnology and the pharmaceutical industry. London: Taylor & Francis; 1999.
3. Baker RW. Membrane technology and applications. Chichester: John Wiley & Sons; 2004.
4. Crosby J. Synthesis of optically active compounds: a large scale perspective. Tetrahedron 1991; 47: 4789–4846.

5. Drioli E, Iorio G, Catapano G. In: Mark CP, editor. Handbook of industrial membrane technology. Park Ridge (NJ): Noyes Publications; 1989. pp. 401–481.
6. Giorno L, Drioli E. Biocatalytic membrane reactors: applications and perspectives. Trends Biotechnol 2000; 18: 339–348.
7. Bailey JE, Ollis DF. Biochemical engineering fundamentals. 2nd ed. New York: McGraw- Hill; 1986. pp. 202–227.
8. Rony PR. Biotechnol Bioeng 1971; 13: 431.
9. Waterland LR, Michaels AS, Robertson CR. AIChE J 1974; 20: 50.
10. Lewis W, Middleman S. AIChE J 1974; 20: 1012.
11. Davis JC. Biotechnol Bioeng 1974; 16: 1113.
12. Livingston AG, Arcangeli J-P, Boam AT, Zhang S, Maragon M, Freita dos Santos LM. J Memb Sci 1998; 151: 29–44.
13. Splendiani A, Nicolella C, Livingston AG. Biotechnol Bioeng 2003; 83(1): 8–19.
14. Velizarov S, Crespo JG, Reis MA. Biotechnol Prog 2002; 18: 296–302.
15. Crespo JG, Velizarov S, Reis MA. Curr Opin Biotechnol 2004; 15: 463–468.
16. Giorno L, Zhang J, Drioli E. Study of mass transfer performance of naproxen acid and ester through multiphase enzyme-loaded membrane system. J Memb Sci 2006; 276(1–2): 59–67.
17. Matson SL. Patent No. US4800162. 1989.
18. Lopez JL, Wald SA, Matson SL, Quinn JA. Ann N Y Acad Sci 1990; 613: 155–167.
19. Giorno L, Li N, Drioli E. Membrane emulsification and its application to emulsion enzyme membrane reactor for production of (S)-naproxen enantiomer. Biotechnol Bioeng 2003; 84: 677.
20. Giorno L, D'Amore E, Mazzei R, Piacentini E, Zhang J, Drioli E, Cassano R, Picci N. An innovative approach to improve the performance of a two separate phase enzyme membrane reactor by immobilizing lipase in presence of emulsion. J Memb Sci 2007; 295: 95–101.
21. Williamson KJ, Woods S, Strand SE. Patent No. US5116506. 1992.
22. Shanahan JW, Semmens MJ. J Memb Sci 2006; 277: 65–74.
23. Leiknes T, Ødegaard H. Desalination 2007; 202: 135–143.
24. Novalin S, Neuhaus W, Kulbe K. A new innovative process to produce lactose-reduced skim milk. J Biotechnol 2005; 119: 212–218.
25. Koch C-J, Simonyova S, Pabel J, Kartner A, Polborn K, Wanner KT. Eur J Org Chem 2003; 7: 1244.
26. Wandrey C. Biochemical reaction engineering for redox reactions. Chem Rec 2004; 4: 254–265.
27. Lopez JL, Matson S. A multiphase/extractive enzyme membrane reactor for production of diltiazem chiral intermediate. J Memb Sci 1997; 125: 189–211.
28. Wandrey C, Flaschel E. Volume 12, Advances in biochemical engineering. Berlin: Springer Verlag; 1979. p. 147.
29. Berglund KA, Elankovan P, Glassner DA. Carboxylic acid purification and crystallization process. US patent 5034105. 1991.
30. Pourcelly G. Conductivity and selectivity of ion exchange membranes: structure-correlations. Desalination 2002; 147: 359–361.
31. Sheldon RA. Chirality and biological activity. Chirotechnology. New York: Marce Dekker; 1993. pp. 39–72.
32. Pirkle HW, Bowen WE. Preparative separation of enantiomers using hollow-fibre membrane technology. Tetrahedron: Asymmetry 1994; 5(5): 773–776.
33. Celgene Corporation. US patent 5,346,828. 1994.
34. Creagh AL, Hasenack BBE, van der Paad A, Sudhlter EJR, van't Riet K. Separation of amino-acid enantiomers using micellar-enhanced ultrafiltration. Biotechnol Bioeng 1994; 44: 690–698.
35. Reid DE, Adlam C. Large-scale harvesting and concentration of bacteria by tangential flow filtration. J Appl Microbiol 1974; 29: 464.
36. Goto S, Kuwajima T, Okamoto R, Inui T. Separation of biomass by membrane filtration and continuous culture with filtrate recycling. J Ferment Technol (1979); 57: 47.
37. Giorno L, Chojnacka K, Donato L, Drioli E. Study of a cell-recycle membrane fermentor for the production of lactic acid by L. Bulgaricus. Ind Eng Chem Res 2002; 41(3): 433–440.
38. Blanc P, Goma G. Propionic acid and biomass production using continuous ultrafiltration fermentation of whey. Biotechnol Lett 1989; 11: 189–194.
39. Xavier AMRB, Crespo JPSG, Carrondo MJT. Effect of cell purge on the stability of microfiltration cell recycle fermentation systems. J Chem Technol Biotechnol 1999; 69(2): 203–208.
40. van Reis R, Zydney AL. In: Flickinger MC, Drew SW, editors. Encyclopedia of bioprocess technology: fermentation, biocatalysis, and bioseparation: John Wiley & Sons; 1999.
41. Fissel WH, Kimball J, Mackay SM, Funke A, Humes D. Ann N Y Acad Sci 2001; 944: 284–295.
42. Matsumura KN, Guevara GR, Huston H, *et al.* Hybrid bioartificial liver in hepatic failure: preliminary clinical report. Surgery. 1987; 101: 99–103.
43. Gerlach JC, Schnoy N, Encke J, Smith MD, Muller C, Neuhaus P. Improved hepatocyte in vitro maintenance in a culture model with woven multicompartment capillary systems—electron microscopy studies. Hepatology 1995; 22: 546–552.
44. Judd S. The MBR book, principles and applications of membrane bioreactors in water and wastewater treatment. Amsterdam: Elsevier; 2006.
45. Zhang J, Chua HC, Zhou J, Fane AG. Factors affecting the membrane performance in submerged membrane bioreactors. J Memb Sci 2006; 284: 54–66.
46. Melin E, Leiknes T, Helness H, Rasmussen V, Ødegaard H. Effect of organic loading rate on a wastewater treatment process combining moving bed biofilm and membrane reactors. Water Sci Technol 2006; 51(6–7): 421–430.
47. Park J-S, Lee C-H. Removal of soluble COD by a biofilm formed on a membrane in a jet loop type membrane bioreactor. Water Res 2005; 39: 4609–4622.
48. Le Clech P, Jefferson B, Chang IS, Judd SJ. Critical flux determination by the flux-step method in a submerged membrane bioreactor. J Memb Sci 2003; 227: 81–93.

40

BIOREACTOR SCALE-DOWN

Laura A. Palomares
Departamento de Medicina Molecular y Bioprocesos, Instituto de Biotecnología, Universidad Nacional Autónoma de México, Cuernavaca, México

Alvaro R. Lara
Departamento de Procesos y Tecnología, Universidad Autónoma Metropolitana-Cuajimalpa, Cuernavaca, México

Octavio T. Ramírez
Departamento de Medicina Molecular y Bioprocesos, Instituto de Biotecnología, Universidad Nacional Autónoma de México, Cuernavaca, México

Ideally, a bioreactor should operate under controlled and homogeneous conditions. However, concentration gradients due to deficient mixing can develop in inhomogeneous systems, such as hollow fibers, packed beds and microcarrier reactors, and also in the so-called homogeneous systems such as stirred-tanks, airlifts and bubble columns. Environmental heterogeneities are the result of bioreactor design and operating conditions, and in general, lead to poor process performance. Diverse environmental heterogeneities have been documented for suspended cultures of animal and plant cells, including gradients in carbon dioxide, pH, microcarrier concentration, and culture segregation due to formation of cell aggregates and clumps. Gradients in pH, dissolved oxygen or substrate concentration can also occur in large-scale animal and plant cell culture as predicted from analysis of the characteristic times of a particular process/bioreactor combination. In turn, gradients and heterogeneities occur in a variety of conditions during microbial cultures, such as pellet formation in mycelial fermentation, development of biofilms in chemostats and waste water systems, in culture broths with complex rheology, in solid-state fermentation, or during fermentations at very high cell densities. Here, scale-down is described as a method of approaching the problem of heterogeneity in large-scale cultures.

The classical approach for scaling-up a fermentation process on the basis of geometrical similarity basis has the long recognized drawback that only one fundamental variable can be maintained constant, whereas the rest will vary as the process is translated to the larger scale. Constant power input per unit volume, constant volumetric oxygen transfer coefficient, or constant speed at the impeller tip are among the most commonly used scale-up criteria. However, as seen in Table 40.1 (1), using any of these criteria will result in a lower agitation rate in the large-scale vessel compared to the small-scale bioreactor. Lower agitation rates will, in turn, favor the development of a nonuniform environment for fast bioreaction rates. If the desired scale-up goal is to maintain the same homogeneity as in the small-scale bioreactor, then the mixing time should be maintained constant. Nonetheless, this would require a substantial increase in agitation rate on the larger scale, a task that is usually not possible due to equipment limitations and/or the fragile nature of most animal cell, filamentous fungi, and other shear sensitive cultures. Increasing agitation speed also poses economical considerations due to elevated power

Upstream Industrial Biotechnology: Equipment, Process Design, Sensing, Control, and cGMP Operations, Volume 2, First Edition. Edited by Michael C. Flickinger.
© 2013 John Wiley & Sons, Inc. Published 2013 by John Wiley & Sons, Inc.

TABLE 40.1. Comparison of Scale-Up Methods. Scaling-Up of a 10 L Vessel at 500 rpm and 1 VVM to a Geometrically Similar 10,000 L Vessel Operated at the Same Volumetric Aeration Rate

Method	N for the 10,000 L Vessel
Constant power/unit volume, P/V	
Nongassed power	107
Gassed power	85
Constant volumetric O_2 transfer rate, k_La	79
Constant shear, ND	50
Constant mixing time	1260
Constant momentum factor	5

Reprinted From (1).

consumption in the large scale. Accordingly, the well-mixed condition obtained in laboratory-scale vessels cannot be maintained on larger scales. This is evidenced in Fig. 40.1 (2), where it can be seen that the mean circulation time (t_c) of Newtonian and pseudoplastic fluids increases with reactor volume.

Circulation time is defined as the time necessary for a fluid element to return to a fixed reference position after circulating through a stirred tank. As a rule of thumb, circulation time (t_c) is (3):

$$t_c = t_M/4 \tag{40.1}$$

where t_M is mixing time.

Several correlations exist to estimate t_c, some of which are listed here. However, correct estimation of t_c demands a case by case analysis. Circulation time is considered to be the total tank volume divided by the impeller pumping capacity (Q_p) (4,5). The impeller pumping capacity is defined as:

$$Q_p = KND^3 \tag{40.2}$$

where K is the discharge coefficient, N is the impeller speed and D is the impeller diameter. The discharge coefficient is a function of tank and impeller geometries. Some discharge coefficients for baffled tanks with standard configuration are listed in Table 40.2. Accordingly, the general form of t_c is:

$$t_c = \frac{V}{KND^3} \tag{40.3}$$

Tank geometry is explicitly included in other correlations for calculating t_c for example, (3):

$$t_c = \frac{V}{2HN\pi^2 T_v^2} \tag{40.4}$$

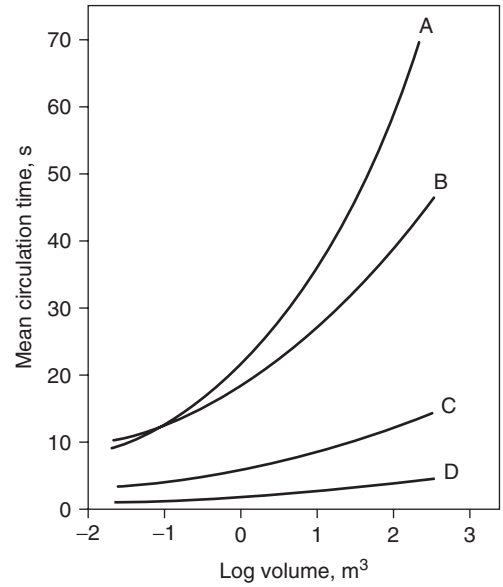


Figure 40.1. Variation of mean circulation time with vessel volume. Tank configuration $H/t_v = 1$, single disc turbine $D/t_v = 0.33$, power 1.67 kW/m^3. A, pseudoplastic fluid. B, Newtonian fluid (1 Pa s). C, Newtonian fluid (0.1 Pa s). D, Newtonian fluid (0.01 Pa s). (Reprinted from Ref. 2).

TABLE 40.2. Typical Discharge Coefficients for Standard Baffled Tanks (5)

Impeller	Discharge Coefficient
Disk style	0.95 ± 0.28
Propeller	0.55 ± 0.1
Pitched blade turbine, six-blade 45°	0.92
Pitched blade turbine, three-blade 45°	0.76
Reciprocating impellers	0.15–0.30[a]

[a] Various D/T_v ratios.

where H is liquid height and T_v is tank diameter.

In a culture where concentration gradients are present, a cell will be exposed to a fluctuating environment during its circulation through the bioreactor. If severe gradients develop, then localized zones differing from bulk conditions will exist in the bioreactor that can adversely affect the culture. For instance, dissolved oxygen (DO) or substrate can be limiting in stagnant zones, whereas in point-of-addition zones, the cells can be inhibited by high substrate or acid/base concentrations, resulting in pH gradients. Special attention should also be placed on shear stress gradients, particularly with fragile cells that will be exposed to deleterious shear stresses on a frequency determined by the circulation time.

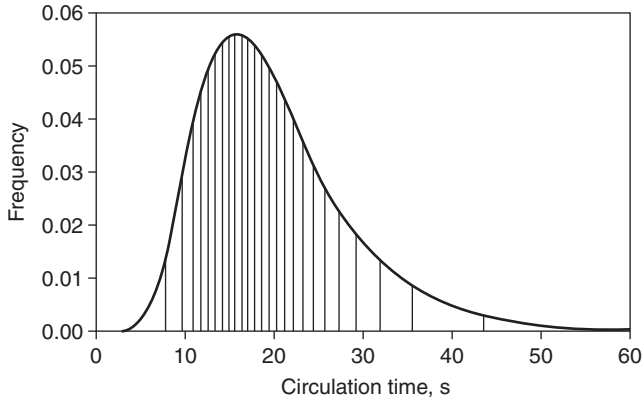


Figure 40.2. Frequency of circulation times for a lognormal distribution. (Reprinted from Ref. 6).

Circulation time is a fundamental parameter in scale-down studies because it determines the time spent by a cell in the various bioreactor regions and provides the framework for scaling the fluctuations in a large-scale fermenter into a test system (6). As indicated by Yegneswaran *et al*. (6), actual circulation times in large fermenters are distributed over a range of values, which can be described by a lognormal probability distribution (Fig. 40.2). Therefore, using a circulation time distribution rather than a mean circulation time should better mimic the real situation. As seen in Fig. 40.1, mean circulation times for typical microbial pilot and small-scale fermenters (less than 100 L) do not exceeded 10 s. In 10,000 L fermenters, t_c can range from 5 to 30 s for Newtonian fluids, and can be as high as 40 s for pseudoplastic fluids. In comparison, t_c for animal and plant-cell cultures are several-fold higher than those for microbial fermentations at equivalent scales. As reviewed in detail by Lara *et al*. (7), mixing times for typical large-scale stirred-tank cell culture vessels can range between 40 to 360 s, whereas for airlift and bubble column bioreactors for cell culture, t_M can range between 200 to 1000 s. Accordingly, circulation times for large animal and plant cell cultures will be between 10 to 250 s. In the case of industrial microbial fermentations, the reported t_M for stirred-tank reactors are in the range of 10–110 s (7), and as high as 1000 s for a 150-m^3 bubble column.

40.1 THE SCALE-DOWN APPROACH

Scale-down is a semiempirical method, based on regime analysis, which consists of reproducing on a small scale the conditions prevailing (or those that will be possible to attain) on the large scale (3,8). Scaling-down can be applied to two general situations. It can be used as a method for scaling a new process or operation to new larger scale equipment or installation. Alternatively, scale-down can be used for diagnosing problems (poor yields, cell death, etc.) and predicting the outcome of modifications to existing large-scale processes or equipment (changes in cell line, media composition, operation conditions or bioreactor fittings). In practice, the second general situation is most commonly encountered (3). In both cases, small-scale experiments are designed from knowledge of the fundamental parameters limiting the process at the large scale. The experimental results can then be used to optimize and predict the performance of the new (or modified) process or operation on the large scale. An underlying value of down scaling experiments is generating data under conditions resembling real conditions but without actual experimentation on the real scale, a task that is impractical and economically unfeasible. A schematic representation of the scale-down method is presented in Fig. 40.3, which shows that it consists of four main steps (9,10): regime analysis, simulation, optimization, and application. A more detailed review of the scale-down method can be found in Ref. 10.

40.2 REGIME ANALYSIS

Regime analysis is based on identifying the limiting mechanisms that determine the bioprocess on a large scale (11). This is achieved by obtaining the characteristic times (also called *relaxation times* or *time constants*) of the subprocesses conforming the system (3). Characteristic time is defined as capacity divided by flow of the particular subprocess (10,11). Three types of information are needed for determining characteristic times: the bioreactor configuration, physical models (for instance, models that describe mixing, heat, and mass transfer), and bioreaction models (for instance, models that describe the relationship between production rate and growth rate or between growth rate and substrate concentration or pH) (12). Any model has inherent limitations and thus, must be used with caution. Accordingly, analysis of subprocesses should be based only on comparison of the order of magnitude of the various characteristic times (12). When characteristic times of intracellular mechanism are of the same order of magnitude as those of changes in the extracellular microenvironment

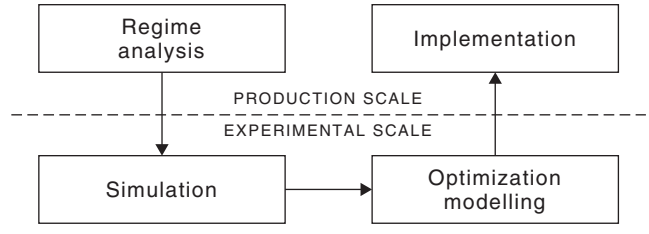


Figure 40.3. Scale-down procedure. Adapted from Refs 9,10.

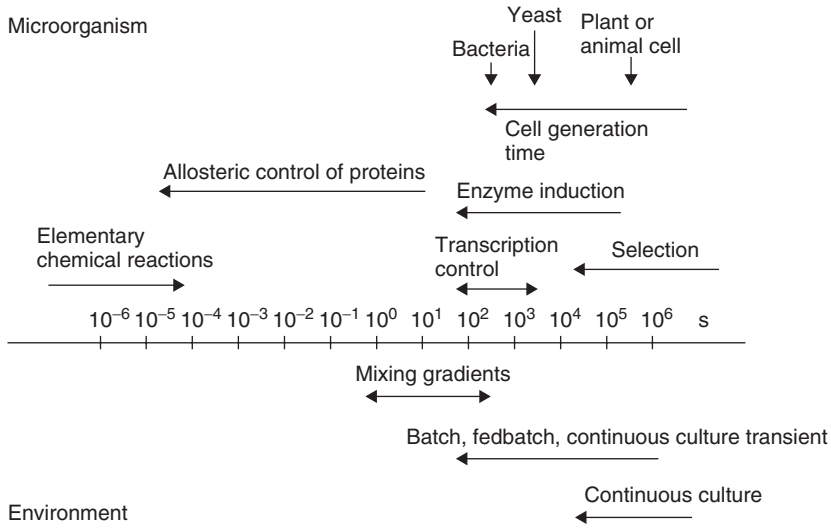


Figure 40.4. Characteristic times of important cellular and environmental processes. (Adapted from Refs 3,13).

(such as mixing and mass transfer), then both subprocesses will interact and will affect the behavior of the cell (3). In Fig. 40.4 (13), the relative magnitudes of characteristic times of important cellular and environmental processes are compared. Characteristic times of various subprocesses relevant to cell culture and microbial fermentations are summarized in Table 40.3. A more detailed discussion of characteristic times, including some examples and their derivation, as well as indications for selecting significant subprocesses can be found in Refs 3,8 and 10.

Small characteristic times are indicative of a fast process. In contrast, a slow process is distinguished by a large characteristic time and will be the potentially limiting step (14). For instance, Nienow *et al*. (14) reported oxygen uptake, mass transfer, and mixing characteristic times for recombinant CHO cells and NS0 cells in an 8-m^3 agitated bioreactor (Fig. 40.5). As seen in Fig. 40.5, oxygen uptake characteristic time for CHO cells is larger than the mass transfer and mixing characteristic times at all energy dissipation rates studied. Thus, it can be anticipated that no oxygen limitation or dissolved oxygen gradients will form under these conditions. In contrast, for higher cell concentrations and/or specific oxygen uptake rates, as is the case for the NS0

TABLE 40.3. Characteristic Times

Process	Formula
Mixing	t_M (experimentally determined)
Oxygen mass transfer	$t_{mt} = \frac{1}{k_L a}$
Circulation	$t_c = \frac{t_M}{4}$
Growth	$t_\mu = \frac{1}{\mu}$
Heat transfer	$t_{ht} = \frac{V\rho Cp}{UA}$
Difussion	$t_{\text{diff}} = \frac{\lambda_k^2}{D_{o/w}}$
Oxygen uptake	$t_{rxn} = \frac{c}{q_{O_2} X}$

Adapted From (12).

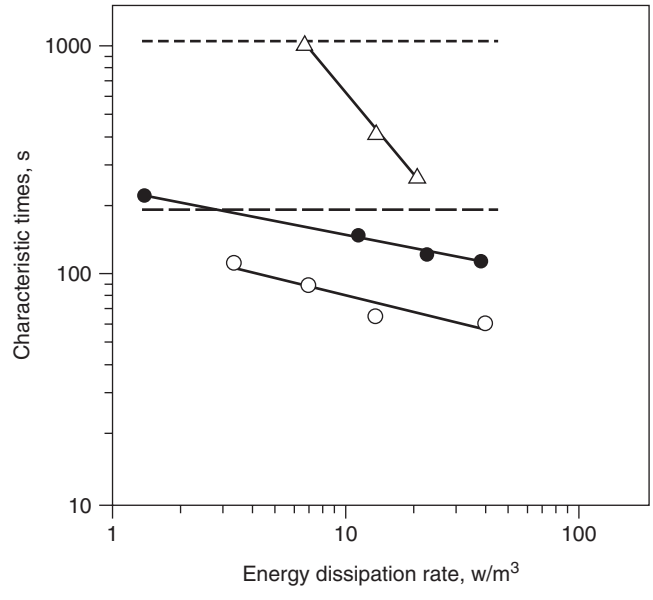


Figure 40.5. Characteristic times in an agitated tank at the 8-m^3 scale with 2/9 t_v Rushton turbine. Mass transfer time (open triangle) and t_M (open circle) at a superficial gas velocity of 2×10^{-4} m/s. t_M (closed circle) without aeration. Short dashed line indicates reaction time for 4×10^5 CHO 320 cells/mL. Long dashed line indicates reaction time for 2×10^6 NS0 cells/mL. (Reprinted from Ref. 14).

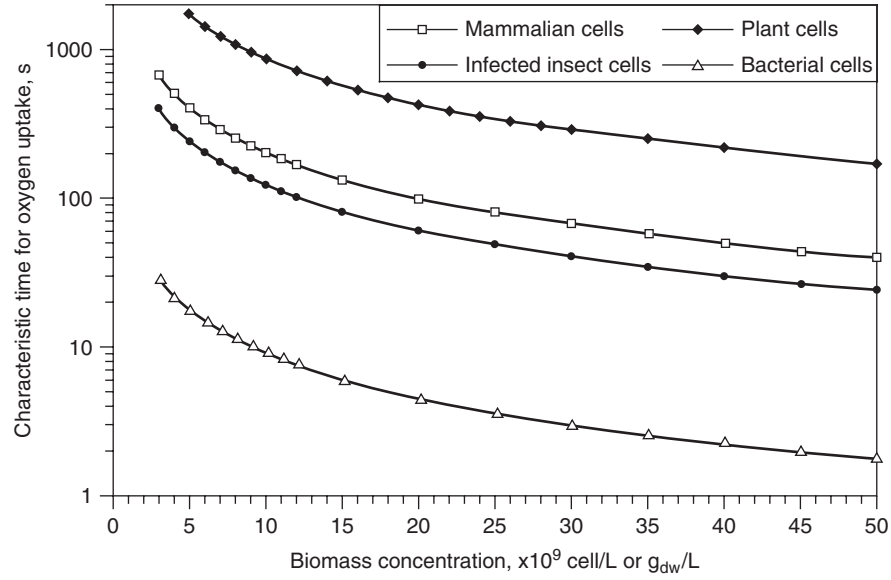


Figure 40.6. Characteristic time for oxygen uptake t_{rxn} (calculated after Table 40.3) of bacterial, animal, and plant cell cultures at different biomass concentrations. The q_{O2} utilized for calculations were 2.8 μmol/g_{dcw}/s, 0.031 μmol/g_{dcw}/s for plant cells, 0.111 μmol/10^9 s for mammalian cells, and 0.225 μmol/10^9 s for infected insect cells. Concentration of bacterial and plant cells in g_{dcw}/L, of mammalian and insect cells in 10^9 cell/L. The initial value for dissolved oxygen concentration (DO) was 50% of air saturation. (Reprinted by permission from Ref. 7).

cells, characteristic time for mass transfer will be longer than for oxygen uptake. Accordingly, it can be predicted that oxygen supply will be insufficient. Figure 40.6 shows the t_{rxn} (or oxygen consumption time) for plant, animal, and microbial cells as function of the cell concentration of a culture (7). A simple comparison of t_{rxn}, illustrated in Fig. 40.6, with the previously mentioned t_M for large-scale bioreactors reveals that there will be a variety of conditions where t_{rxn} is shorter than t_M. Therefore, dissolved oxygen gradients can easily occur in large-scale bioreactors.

40.3 SIMULATION

In this step, the rate limiting mechanism (or mechanisms), identified from regime analysis of the production scale, is simulated on a laboratory scale. It is not necessary to maintain geometric similarity during scaling-down in order to have conditions representative of the full scale. What is important is to maintain constant the relevant characteristic times between both scales (8). A fundamental difference between large and laboratory-scale bioreactors is that the latter are inherently well mixed. Because phenomena resulting from mixing deficiencies at large-scale are among the most common problems analyzed during scaling-down, ingenious experimental setups have to be designed for creating a nonuniform environment during laboratory-scale simulations. Furthermore, spatial gradients (i.e. those that are a function of the location in the reactor and that originate from mixing deficiencies) can result in fluctuating phenomena of low characteristic times (in the order of seconds to minutes). Therefore, spatial gradients can be difficult to simulate since very fast fluctuations will be usually required in the downscaled experiments (15). In contrast, temporal gradients (those that depend on process time) are associated to high characteristic time (in the order of minutes to hours) and are relatively simple to simulate (15). The commonly employed experimental configurations for scale-down studies are described in detail later.

40.4 OPTIMIZATION AND MODELING

After the limiting mechanisms on the large scale have been identified and reliable methods have been established to simulate them in a laboratory bioreactor, then an optimization study can be pursued. A broad range of conditions can be readily tested in scale-down experiments, including the effect of period, amplitude, and axis of oscillations of a particular culture variable on cell physiology and metabolism. The period, amplitude, and oscillation axis will correspond to circulation time, magnitude of gradients, and mean bulk condition, respectively, present on the full scale. In this way, the influence of changes in physical subprocesses on cellular subprocesses can be assessed. Unfortunately, very little information exists on bioprocess

optimization with respect to gradients (15). Furthermore, equipment, economic or operation constraints at the large scale can prevent the implementation of some possible optimization results (3). For instance, an optimization result can dictate the best configuration for distributing an ideal number of base addition or substrate feeding ports in a fed-batch or perfusion operation, as well as the best concentration of the corresponding feeding solutions. However, on the full scale, it may be impractical to implement the exact results of such optimization exercise due to concerns of contamination risks and/or increased operating and equipment complexity. In any case, the optimization results should consider only the attainable regimes in the full scale. An alternative approach is the modification of the cellular metabolism to develop cells with a reduced sensitivity to environmental fluctuations. This will be described later in this chapter.

The results of the optimization step can be used to generate improved microbiological models. This is important because the vast majority of microbiological models are based on balanced growth (pseudo), steady-state phenomena, or temporal gradients. Although there have been significant advances in modeling, the metabolic response of microbial cells to environmental perturbations (16,17), almost no models exist describing cell metabolism and physiology under transient oscillatory conditions resulting from spatial gradients (3,15). Furthermore, computational fluid dynamics (CFD) can be a powerful tool for complementing the simulation and optimization studies through estimations of concentration, fluid velocity, and shear rate profiles. In particular, CFD can yield important information on the maximum and minimum values of relevant variables such as pH, shear stress, temperature, and concentration of substrate, dissolved oxygen, carbon dioxide, and by-products. In addition, the fraction of culture volume exposed to a particular detrimental condition (information that is necessary for representative downscaling experiments) can be derived from CFD. Progress in CFD studies, including bioreaction, mass transfer, and fluid mixing in fungal fermentation, has been reported (18,19). A recent study by Lapin *et al*. (20) described the behavior of a heterogeneous population in a 900-L fed-batch culture of *Escherichia coli*. This study coupled the effects of nonideal mixing with previous knowledge on changes of metabolite concentrations as a result of environmental perturbations. The numerical simulation showed oscillations of key glycolytic metabolites as a function of the exposure to glucose gradients. Also, differences in intracellular concentration of pyruvate and phosphoenol pyruvate of the cells as function of the spatial position in the bioreactor were described. In contrast to these relatively advanced studies for microbial fermentations, only limited studies of CFD for plant or animal-cell cultures exist (21). However, the scarce knowledge of the impact of fluid dynamics and environmental gradients in biological systems makes difficult to verify the results of CFD predictions, especially in the case of cyclic exposures to environmental gradients.

40.5 APPLICATION

The final step in the downscaling method is translating the laboratory experimental results to the production scale (Fig. 40.3). The traditional scale-down approach considers the implementation of process or equipment modification based on the laboratory-scale experiments. Here again, quantitative published information is very scarce for the general area of microbial fermentations and is almost nonexistent for the area of animal and plant cell culture. An interesting case study is reported by Geraats (22) for the production of a lipase by *Pseudomonas alcaligenes*. In such study, a 65% reduction in maximum lipase concentration occurred when the process was scaled-up from 10 L to an existing 100-m^3 fermenter. To investigate the possible causes of the production loss, downscaling experiments at 10 L and 100 L were performed. The aspects studied included gradients of soy oil, pH, and oxygen, raw materials, medium preparation, and sterilization and inoculation procedures, dissolved carbon dioxide concentration, and shear and air-broth interfaces. Through such an approach, dissolved carbon dioxide was identified as the main cause of scaling-up problems. By increasing the ventilation rate and decreasing the head pressure combined with a lower pH, lipase production at full scale finally reached the values obtained on the 10-L scale.

A different strategy for improving process performance through scale-down studies has been reported by Lara *et al*. (23,24). These authors performed studies to investigate the physiological responses of a recombinant *E. coli* strain, expressing green fluorescence protein (GFP), to DO gradients simulated in a two-compartment scaled-down system, at a mean t_c of 50 s. Within the experimental setup used, the cells spent about 33 s under anaerobiosis, followed by about 17 s under aerobic conditions on a cyclic fashion (23). The production of GFP was 19% lower in the scaled-down cultures in comparison to fully aerobic cultures. The DO gradients also reduced the specific growth rate, and resulted in accumulation of all the metabolites from mixed-acid fermentation pathways. Transcriptional response to DO gradients was also analyzed. A generalized increase of up to sixfold on the transcriptional level of anaerobic genes, relative to transcription level of cultures at constant DO concentration was observed. Also, differential transcriptional level of genes from the tricarboxilic acids cycle and cytochromes in downscaled cultures was reported. This is an important observation because, as

illustrated in Fig. 40.4, the characteristic time for mixing gradients, transcription control, and enzyme induction can be of the same order of magnitude. Consequently, data of fermentation metabolites accumulation during the downscaled cultures is not enough to elucidate if the activation of fermentation pathways occurs at the level of enzymatic induction or gene expression. Based on the transcriptional and kinetic data, Lara *et al*. (24) inactivated genes involved in the production of acetate, formate, and lactate, which were the most importantly accumulated by-products in the downscaled cultures. Compared to the parental strain, a triple mutant *E. coli* strain only produced low amounts of acetate and did not produce formate or lactate when cultured under simulated DO gradients. More importantly, the specific growth rate and GFP production of the mutant strain was only slightly affected by DO gradients. This approach represents a valuable tool for process improvement because, as explained before, it is not always possible to implement in the larger scale equipment the results of scale-down studies.

It should be noted that culture parameters on a larger scale will not necessarily be inferior to those on a smaller scale. For instance, although antibody production by CHO cells was worst in a 1000 L production tank compared to a 2-L bioreactor, cell growth in the larger vessel was almost doubled (25). In this case, analysis of the hydrodynamic parameters for the two vessels revealed that cell damage due to disengagement of small bubbles was more important than mechanical stresses. Therefore, cell death was higher in the smaller bioreactor because superficial gas velocity was also higher compared to the larger vessel. Furthermore, if scale-down studies reveal an absence of detrimental effects caused by environmental gradients, there could be situations where an oscillatory operation could be beneficial on the large scale. For instance, when a cell culture is insensitive to particular dissolved oxygen gradients, then energy savings and reduction of deleterious shear stresses could be achieved by an intermittent mixing and/or gassing operation. Examples of the beneficial effects of an oscillatory environment can be found for various microbial fermentations (26–28).

A different approach for the scaling-down of industrial cultures has been recently applied to microbial and animal-cell processes. This approach is not necessarily based on regime analysis, but relies on matching the same performance in the large and small-scales, using the same power input values, superficial gas velocities, and oxygen transfer characteristics among others. This approach emerged from the need for faster screening of strains or cell lines, development, and optimization of culture processes. During recent years, the design and evaluation of bioreactors at mL and even at μL-scale have been under intense research. For instance, Bocazzi *et al*. (29), reported the design of a multiplexed bioreactor with a working volume of 50 μL. Global gene expression profiles of *E. coli* cultures carried out in the micro-bioreactor and cultures at 500 mL-scale were similar, which demonstrate the potential of the miniaturized systems for process development. The application of miniaturized bioreactors has allowed reproducing the performance of microbial fed-batch cultures (30). The utility of miniaturized bioreactors for the scale-up of microbial and cell culture has also been tested. For example, shaken microtiter cultures of *E. coli* and hybridoma cells have been scaled-up to 1.4 L- and 100 mL-scale cultures. In the case of *E. coli* cultures, a constant k_La allowed matching the results at both scales, whereas for hybridoma cells, keeping the mean energy dissipation rate constant yielded reproducibility at both scales (31). Islam *et al*. (32), scaled-up an *E. coli* culture from microwell plates scale to a 7.5 L STR by matching a constant k_La, with good results. The success of miniaturized bioreactors in the near future will rely on effective pH and DO control, and the capacity to emulate typical production conditions, like fed-batch mode.

40.5.1 Scale-Down Studies in Cell Culture

The development of improved operating strategies, aimed at attaining higher cell concentrations than in conventional cultures, will result in increased oxygen consumption and heat and carbon dioxide evolution. Moreover, a move toward the use of highly concentrated feeding solutions should be expected in improved fed-batch and perfusion strategies. Undoubtedly, all of this will worsen the problems of bioreactor heterogeneity observed until now. Diverse culture heterogeneities and problems due to scale-up or transient environmental changes have been reported for plant- and animal-cell culture (described in Refs 25 and 33). For instance, culture segregation due to cell clumping is common in plant cell culture, changes in protein glycosylation patterns can be caused by transient periods of glucose excess, heat shock proteins are induced by transient changes in temperature, and protein structural changes can occur during scale-up. A detailed description of other environmental heterogeneities and their adverse effects in cell culture is presented by Lara *et al*. (7). Nonetheless, scale-down has scarcely been used as a tool for simulating gradients or predicting their effect in cell culture. The reports by Slater (25), discussed previously, and by Nienow *et al*. (14), are among the very few available studies of scale-down in cell culture. In the latter study, Nienow *et al*. (14) used scaled-down vessels to simulate the mixing times of an 8-m^3 animal-cell bioreactor, and concluded that severe pH gradients are likely to develop in the full-scale system. Rhiel and Murhammer (34) assessed the effect of oxygen oscillations in animal-cell culture, specifically on the physiology of

insect cells. They reported an adverse effect of dissolved oxygen oscillations between 0 and 15% in cell growth and recombinant protein production. In their study, the cultures remained at each DO concentration for 30 min, and it took from 6 to 7 min to shift between both DO set-points. Serrato *et al*. (35) reported the effects of DO oscillations in the production and glycosylation pattern of a monoclonal antibody (MAb) produced in hybridoma cultures. By manipulating the composition of the inlet gas, sinusoidal DO oscillations were simulated in a one-compartment scale-down system at oscillation periods ranging from 800, 1600, 6400, and 12,800 s. As shown in Fig. 40.7, DO oscillations reduced the viable cell concentration and the specific growth rate in about 38 and 35% respectively. In contrast, the amount of MAb produced was only slightly affected. Despite this, the glycosylation pattern of the MAb produced under the highest DO oscillating period presented a higher amount of trigalactosylated and sialylated glycans, which can have a strong influence on the therapeutic function of the antibody. In the previous two studies, the oscillation frequencies tested were well above the t_c reported for large-scale bioreactors for cell culture. However, the reported results are very relevant due to the limited information available of scale-down studies for cell culture processes.

The impact of pH gradients is also a relevant problem in cell culture. The pH value in the medium usually tends to decrease during a culture, often as a result of metabolic activity. The addition of a base concentrated solution in a given point of the bioreactor, and the large t_c of the large-scale bioreactor operated for cell cultures can potentially lead to important pH gradients. For instance, it has been reported the existence of pH gradients of up to 1 unit between the alkali addition zone and the bulk liquid in an 8-m^3 stirred-tank bioreactor designed for mammalian-cell culture (36). Culture aggregation, nutrient gradients, and the use of inherently inhomogeneous bioreactors like packed beds or other systems with immobilized cells can also cause pH gradients (37). Exposure of cells to pH gradients may result in reduction of viability or cell lysis. Ozturk (38) reported cell lysis as a consequence of high pH values in the point of base addition. In another study (39), it was shown that although NS0 cells were robust with respect to a single pH perturbation (a transient step increase from 7.2 to 8), submitting the cell to cyclic perturbation of different frequency and duration (by adding 2 M NaOH pulses), importantly decreased their viability.

The scarcity of scaling-down studies can be a consequence of the relatively small scale at which plant- and animal-cell cultures have been commonly performed, as well as their high metabolic characteristic times, compared

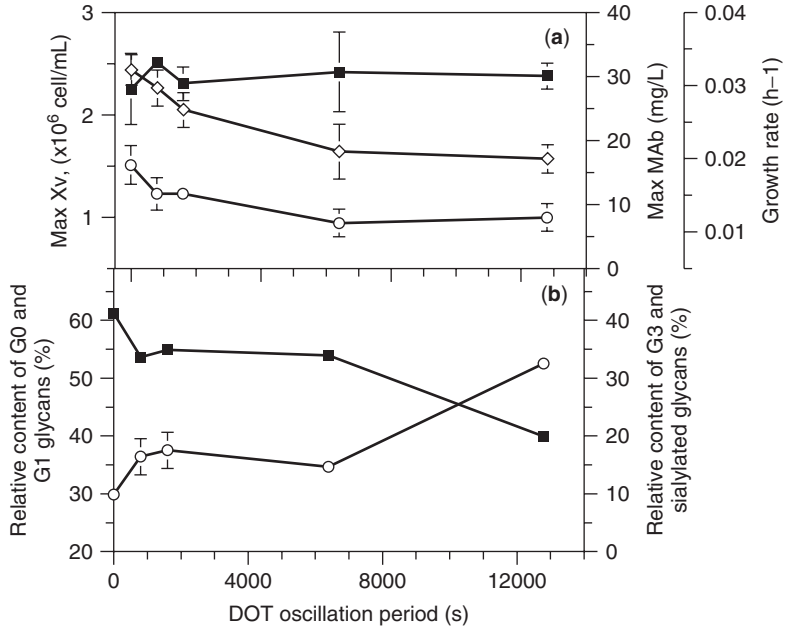


Figure 40.7. Dissolved oxygen tension (DOT) oscillations change the glycosylation profile of a monoclonal antibody produced by hybridoma cells. (a) Maximum viable cell concentration (open circles), maximum monoclonal antibody concentration (closed squares) and specific growth rate (open diamonds). (b) Relative content of glycans *N*-linked to the monoclonal antibody. Ungalactosylated and monogalactosylated glycans (closed squares), trigalactosylated and sialylated glycans (open circles). (Adapted from Serrato *et al*. Ref. 35).

to microbial cultures. However, it can be expected that, as operation of high cell density large-scale cultures increases, the application of downscaling experiments will increase. The characteristics of animal and plant cells and their culture systems will demand the design of novel experimental configurations to adequately simulate large-scale conditions in laboratories. However, there is a lack of published information of systems expressly designed for cell cultures. Accordingly, the description of experimental configurations for scale-down studies, presented in the next sections, is based on information generated from the microbial fermentations area. Most of the experimental configurations described in the next sections can be readily applied to animal and plant cells, and only particular attention must be placed on the fact that circulation times and shear sensitivity of cell cultures are several-fold higher than those of microbial fermentation.

40.6 SCALE-DOWN STUDIES IN MICROBIAL FERMENTATIONS

The vast majority of published scale-down studies have dealt with microbial fermentations. Several biological models have been the subject of study, such as the bacteria *E. coli*, *Bacillus subtilis*, and *Corynebacterium glutamicum*, the yeasts *Saccharomyces cerevisiae* and *Kluyveromyces marxianus*, and the fungi *Penicillium chrysogenum*, *Streptomyces clavuligerus*, and *Aspergillus niger*. Different environmental fluctuations have been studied, such as pH, DO, and substrate oscillations. Also, most of the different scale-down systems have been developed for the purpose of studying microbial fermentations. For instance, Sandoval *et al*. (40) reported the effect of DO gradients, simulated in a two-compartment scale-down system, on the production of recombinant human proinsulin (Fig. 40.8). Such study is relevant as it assessed the direct effect of DO gradients, independent from other environmental parameters variations, in a t_c range (20–180 s) similar to that present on large-scale bioreactors. Lara *et al*. (7) recently published a detailed review of available scale-down studies.

Scale-down studies of microbial fermentations have generally focused only on macrokinetic effects, whereas only two studies have characterized the expression of several genes of *E. coli* as a result of fluctuating environments (23,41). Such reports are valuable for establishing rational scale-up criteria and developing improved bioprocess monitoring. Furthermore, validation of industrial processes through scale-down studies is an important activity when producing therapeutic molecules, as it is necessary to ensure the consistency of product quality. For instance, Bylund *et al*. (42) analyzed the effect of scaling-up an *E. coli* culture on the degradation pattern of recombinant human growth

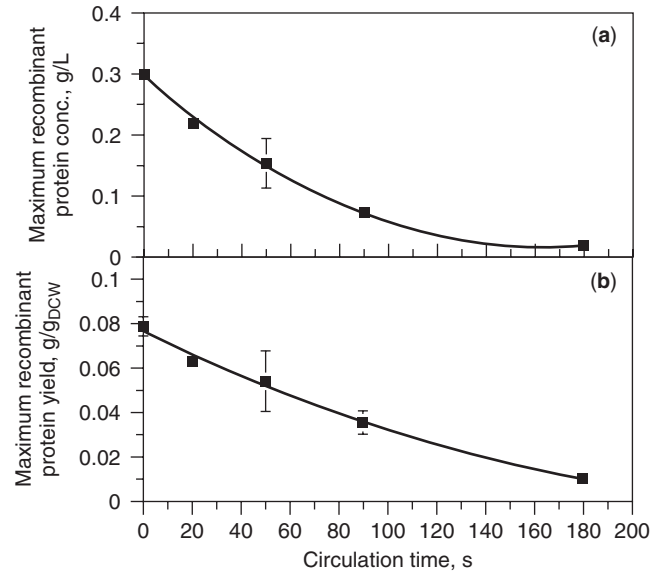


Figure 40.8. Effect of circulation time on: (a) maximum recombinant protein concentration; (b) recombinant protein yield on biomass, in cultures of *E. coli* producing recombinant human proinuslin under DO gradients simulated in a two-compartment scale-down system. Data points at t_c of 0 sec represent values obtained from control cultures maintained at constant 10% DO. (Reprinted by permission from Ref. 34).

hormone. Although the recombinant protein produced at the industrial-scale (3-m^3 fermenter) was 35% lower than at laboratory-scale (15-L fermenter), the fraction of degraded human growth hormone was similar on both scales. Despite the relatively large number of scale-down studies involving microorganisms, it is evident that more information is needed to understand the molecular mechanisms involved in the complex responses of microbial cells to fluctuating environments. Besides, the effects of temperature, pH and dissolved CO_2 oscillations on microbial cultures have been scarcely studied. Moreover, the available information on the effect of gradients on the production of recombinant proteins or plasmid DNA for therapeutic purposes is still very limited (7) and of crucial importance for developing commercial processes for such products.

40.7 EXPERIMENTAL CONFIGURATIONS FOR SCALE-DOWN STUDIES

Special experimental configurations are needed for simulating in laboratory the oscillatory environment to which a cell is exposed when spatial gradients are formed in a large-scale vessel. Scale-down systems can be classified in two general groups depending on the component studied: those for simulating gradients in dissolved oxygen or carbon

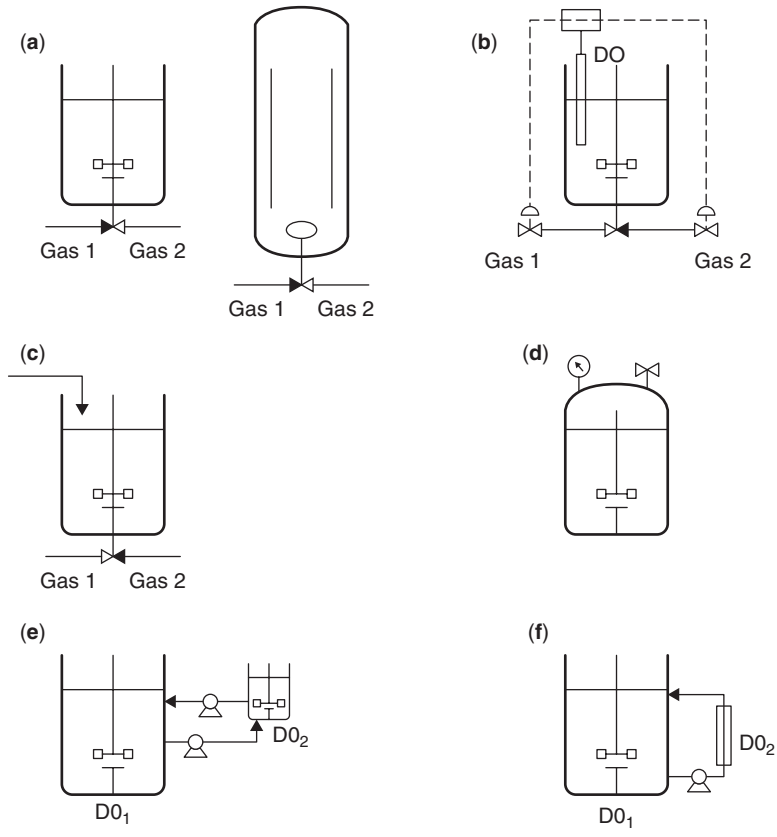


Figure 40.9. Experimental configurations for simulating dissolved oxygen or carbon dioxide gradients. One-compartment systems: (a) batch stirred and airlift bioreactors with open-loop gas control; (b) with closed-loop gas control; (c) chemostat; (d) pressure manipulated reactor. Two-compartment systems: (e) combination of STR with different oxygen concentrations; (f) STR and plug-flow reactor (PFR) combination. DO_1 and DO_2 refer to different dissolved oxygen or carbon dioxide concentrations, DO refers to a dissolved oxygen electrode.

dioxide, and those for simulating substrate or pH gradients. A detailed description of these two general scale-down systems and comparison of advantages and disadvantages of the various configurations in cell culture and microbial fermentation applications follow. Design of novel experimental configurations, not discussed here, will be necessary for simulating gradients of other variables such as temperature and shear stress, as well as gradients in inhomogeneous systems. Recent developments on miniaturized bioreactors (43) can help design multicompartment scale-down systems where each compartment can be independently controlled and interact with others by circulating culture broth between them. Such systems should be able to better represent the excursion of cells through the various regions that present different environmental conditions in a large-scale bioreactor. Important advances have also been achieved on the monitoring of miniaturized bioreactors (44,45), which will help to precisely monitor the physiological response of cell to environmental perturbation in very short time exposures to changing environments.

40.7.1 Simulation of Dissolved Oxygen or Carbon Dioxide Gradients

The most commonly used experimental arrangements for oscillating the concentration of a dissolved gas are schematically summarized in Fig. 40.9. Such general designs have been applied to oscillating DO but can also be readily applied for oscillating dissolved carbon dioxide concentration, which is of particular importance in cell culture. These designs can be divided into two general groups: one- (Fig. 40.9: a, b, c, and d) and two-compartment (Fig. 40.9: e and f) systems.

In one-compartment systems, the cells are maintained in a single vessel and the dissolved gas concentration is oscillated by various means (6,28,34,46,47). In the simplest arrangement (Fig. 40.9a), two different gas streams are intermittently sparged (or alternatively transferred through a membrane or liquid surface) to a stirred-tank, airlift or bubble column bioreactor. Various combinations of gas streams can be used, such as carbon dioxide and air, air and nitrogen, oxygen-enriched air and air, or on/off

aeration. Cyclic shifts between the two gases are generated by following a predetermined pattern that is independent of the actual DO of the culture (i.e. open-loop control). By assigning unequal sparging times to each gas, it is possible to simulate different culture volume fractions subjected to different conditions (for instance, the volumes of stagnant and well-mixed zones). In this way, the time spent by a cell in each condition can be simulated. Likewise, switching frequency can also be manipulated to simulate the circulation time. A mean constant circulation time can be manipulated by choosing a constant switching frequency. However, as described before, a real situation is better represented by a circulation time distribution (Fig. 40.2), which can also be simulated by establishing a random switching frequency. For instance, in a laboratory-scale reactor Yegneswaran *et al*. (6) utilized the Monte Carlo method to control random on/off cycles of aeration to reproduce the lognormal distribution of circulation times shown in Fig. 40.2. A simulation of the expected DO profile using such random method, compared to a constant switching frequency, is shown in Fig. 40.10. It can be seen that the Monte Carlo strategy, compared to constant oscillations, resulted in occasional longer periods of low DO which could have caused the reported reduction in antibiotic productivity. These results clearly indicate that the strategy chosen for simulating spatial gradients can strongly affect the experimental outcome.

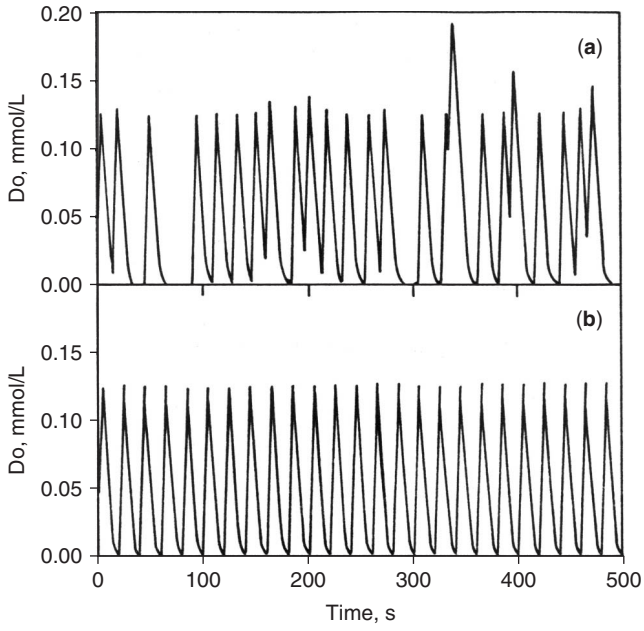


Figure 40.10. Simulated dissolved oxygen profiles for Monte Carlo and periodic aeration experiments in bacterial cultures. Aeration was on for 5 s and off for 15 s on average. (Reprinted from Ref. 6).

Single-compartment systems with open-loop control, as those described previously (Fig. 40.9a), have the advantages of simple operation and reduced equipment and instrumentation requirements. However, actual control of DO (or dissolved carbon dioxide) cannot be attained in such systems. In the case of DO, this problem can be overcome if the flows of the various gases used are controlled through a closed-loop algorithm based on the signal of a DO electrode (Fig. 40.9b). For instance, a closed-loop proportional-integral-derivative (PID) control, where oxygen partial pressure was varied according to the difference between DO measurements and a square-type oscillating DO set point, is shown in Fig. 40.11 (26). In this case, it was possible to obtain periodic sinusoidal DO profiles of predetermined periods, amplitudes, and oscillation axes, in actual fermentations (26). Only other few closed-loop algorithms for oscillating DO have been reported (23,28,35,40,46). A disadvantage of the closed-loop systems, besides their complexity, is the need for fast response electrodes when short oscillation periods are required.

Many experimental scale-down systems are based on batch operation, and thus, spatial gradients are simulated along with temporal gradients. In some instances, it is desirable to discriminate between the effects of both types of gradients and/or assess the effect of gradients under steady-state conditions. This can be achieved in experimental arrangements similar to those described above, but where a continuous or perfusion operation mode is established (Fig. 40.9c). An example of this configuration was reported by Buse *et al*.(47). A fluctuating dissolved gas concentration can also be attained in one-compartment configurations simply by oscillating the total pressure of the system (Fig. 40.9d). This system was used by Serrato *et al*. (48) for simultaneously simulating dissolved

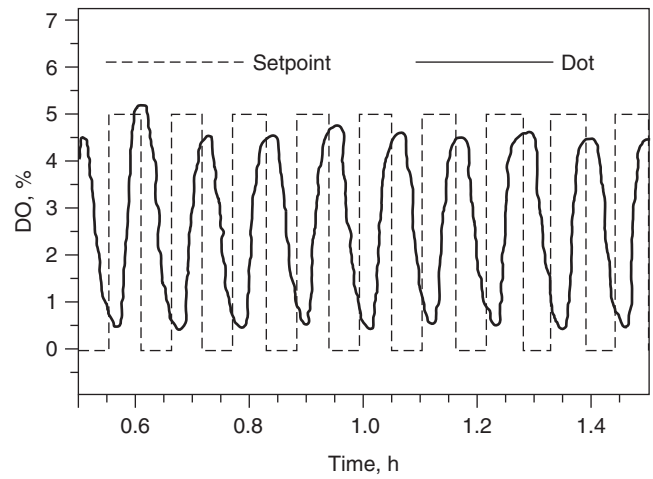


Figure 40.11. Closed-loop control strategy for oscillating dissolved oxygen at a predetermined frequency, amplitude, and oscillation axis. (Reprinted from Ref. 26).

CO_2 and pH oscillations on the production of a MAb by hybridoma. An advantage of these configurations is that pressure gradients, which can occur in large-scale vessels, can also be simulated (46). Nonetheless, special pressure-proof vessels are required and foaming problems can originate during decompression.

A general disadvantage of single-compartment (open-loop and closed-loop) systems is their slow dynamic response. This is a drawback when short oscillation periods are desired, but can be partially solved by increasing agitation and gassing rates, if shear sensitive cultures are not damaged. A questionable aspect of single-compartment systems is that all cells are simultaneously exposed to the same condition, potentially inducing a synchronization phenomenon, especially on yeast and animal-cell cultures, something that is unlikely to occur in a real large-scale culture. Some limitations of the experimental arrangements described above can be overcome by two-compartment systems.

The most commonly used two-compartment configurations are composed of two interconnected stirred-tank bioreactors, each maintained at a different dissolved gas concentration, and where culture broth is circulated between them via a pump system (Fig. 40.9e) (23,24,40,49,50). In this case, mean circulation time will be equal to the total volume of the two vessels divided by the circulation flow rate (49). A large-scale vessel can be considered to be composed of two main zones, a small well-mixed zone at the impeller vicinity, and a poorly mixed region in the rest of the tank. Thus, vessels of different sizes are commonly used to simulate these two different culture volume fractions (49). Accordingly, for the case of DO, the large vessel maintained at a low DO will simulate the large poorly mixed zone, whereas the small vessel maintained at a high DO will represent the well-mixed zone. The residence time distribution in each compartment will simulate the circulation time distribution in the large scale by manipulating the pumping rates in the scale-down system. An advantage of these systems is that the residence time distribution in each vessel will naturally simulate the circulation time distribution present in a large-scale culture. In addition, algorithms for controlling dissolved gas concentration in each vessel will be simpler than for one-vessel configurations, because complex dynamic behavior of mass transfer and electrode response is not involved. Furthermore, short oscillation periods can be attained in these systems simply by increasing the flow rate between the two vessels, as reported by Sandoval *et al*. (40). Nonetheless, shear stresses at the pumps will limit their use for fragile cells. Disadvantages of two-vessel configurations also include the need for duplicate equipment, increased contamination risk and operation failure at the circulation loops/pumps. It could also be questionable that cells in the two stirred-tank configuration will experience a step change between two different dissolved gas concentrations, contrary to what happens in a real situation where cells gradually move between both conditions. This sudden step change can be prevented if a two-compartment configuration, as shown in Fig. 40.9f, is used. In this case, cells are circulated from a stirred vessel to a PFR, where a gradual change in dissolved gas concentration due to cell metabolism occurs (51). Such types of systems have been successfully used for microbial cultures with high metabolic demands (23,24,40), but might result inadequate for animal and plant cells with relatively lower metabolic demands. Finally, it is interesting to note that for cultures where pH is controlled by a carbonate buffer system, as in most mammalian-cell cultures, the configuration shown in Fig. 40.9e can also be used to simulate pH gradients simply by maintaining a different dissolved carbon dioxide concentration in each vessel.

40.8 SIMULATION OF SUBSTRATE OR pH GRADIENTS

Substrate gradients can occur in large-scale cultures at feeding points during fed-batch and perfusion operation modes, and pH gradients can occur at acid/base addition zones. In both cases, cells will be transiently exposed to potentially deleterious high substrate or acid/base concentrations. Simulating gradients in a small-scale bioreactor can be a challenge because, in contrast to the experimental designs discussed in the previous section, recovery of the basal condition after pH or substrate pulses will strongly depend on metabolic activity. A notable exception is the case mentioned before for generating pH oscillations by fluctuations of dissolved carbon dioxide concentration. Various experimental configurations for simulating substrate concentration or pH gradients are schematically summarized in Fig. 40.12. It should be noted that only very few reports exist describing these experimental arrangements, even for microbial fermentation systems (52,53). Accordingly, their utility in animal- and plant-cell culture, which present much lower metabolic demands than microbial fermentations, remains to be proven.

The simplest experimental design for simulating substrate or pH gradients consists of a chemostat with pulsed additions of substrate or acid/base solutions (Fig. 40.12a) (54). In this case, the circulation time is simulated by the frequency of the pulses, whereas the magnitude of the gradient is simulated by the concentration of the pulse. Alternatively, two-compartment systems have also been proposed for simulating nutrient (55,56) and pH gradients (52,53). These usually consist of a stirred tank and a PFR connected in parallel in which medium is circulated between the two compartments via a pump system (Fig. 40.12b, c). The stirred-tank reactor represents the well-mixed zone of a large bioreactor, whereas the PFR represents the stagnant

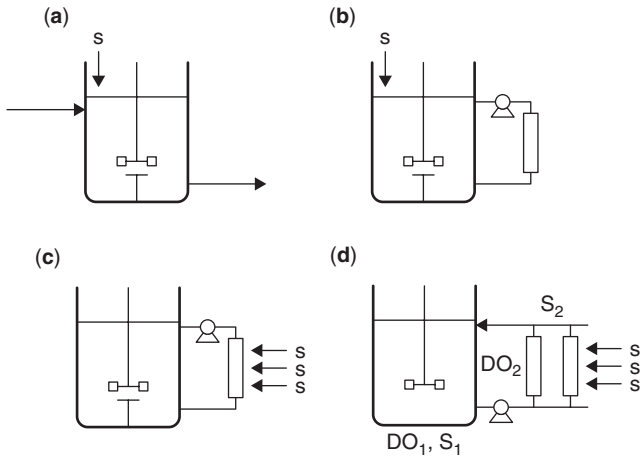


Figure 40.12. Experimental configurations for simulating substrate or pH gradients. (a) chemostat. (b) STR and PFR. Substrate added to the STR to simulate substrate limited regions. (c) STR and PFR. Substrate added to the PFR to simulate high substrate concentration zones. (d) Combination of a stirred-tank with two PFR for simultaneous simulation of substrate and oxygen gradients. S, S_1, and S_2 refer to substrate, acid, or base feeding solutions.

or feed injection zone (57). Depending on where substrate is added, zones of low or high nutrient concentration or pH can be simulated. If substrate is added in the stirred-tank reactor, as shown in Fig. 40.12b, then zones of low substrate concentration will develop in the PFR. Likewise, zones of high substrate concentration will develop in the PFR if the addition is performed directly into it. In this case, t_c will be represented by the residence time in each reactor, as already discussed in the previous section. The addition of substrate in the PFR often leads to oxygen depletion. Although it is commonly accepted that this occurs in the PFR, no direct measurement of dissolved oxygen profiles in the PFR have been reported. Finally, experimental arrangements shown in Fig. 40.12d can be designed for simulating simultaneously gradients of dissolved gas concentration and pH or substrate concentration (27). It should be stressed that the practical feasibility of applying such experimental designs in animal- and plant-cell culture still needs to be demonstrated. In particular, it should be tested if simulation of real cell culture circulation times can be attained under practical operation conditions.

40.9 SIMULATION OF SIMULTANEOUS ENVIRONMENTAL GRADIENTS

Although most scale-down studies have addressed the simulation of environmental gradients of one parameter, the existence of gradients on several physical parameters simultaneously is the most probable situation. This can be exemplified in the case of glucose-limited fed-batch cultures. The addition of glucose causes a gradient in substrate concentration, as usually the bulk of the reactor is kept at concentrations close to zero, whereas the zone close to the addition point will have a higher concentration. When cells transit from a glucose-depleted to a glucose-rich region, glucose uptake and hence the respiratory activity will be triggered. This may in turn lead to the production of acidic by-products and local depletion of the DO. The accumulation of acidic by-products can cause an acid region in the bioreactor. The combined effect of glucose gradients and DO depletion in *E. coli* cultures has been simulated using a STR–PFR configuration [for instance, see (53,58,59). Accumulation and reassimilation of lactate and formate in addition to acetate, showed the existence of dissolved oxygen gradients additionally to glucose gradients in the scale-down system. The STR-PFR system has been extensively used to simulate combined gradients. Recent work has included the evaluation of pH gradients by adding alkali to the PFR and combining this with the glucose and (potentially) DO gradients. Using such experimental design, the effect of pH, DO, and glucose heterogeneities was evaluated in *E. coli* cultures (60). Cultures at 5-L and 20-m^3 scale were compared to the cultures in the scale-down model. Although the biomass concentration reached in the 5-L fermentation was around 64% higher than in the 20-m^3 culture, the viability was about 18% higher in the large-scale than in the laboratory-scale culture. These results at large scale were better mimicked when pH, glucose, and DO (this latter not shown) gradients in the *E. coli* cultures were simulated and the cells spent 50 s in the PFR.

One limitation of the previously mentioned experiments is that no dissolved oxygen profiles in the zone of glucose addition (usually the PFR) have been shown. Consequently, the direct effect of glucose gradients from the DO depletion has not been completely dissected, which makes difficult the interpretation of the effects of combined gradients. More refined scale-down models can help to evaluate these conditions. For instance, a mini PFR has been connected to a STR to simulate a glucose gradient under both, fully aerobic or fully anaerobic conditions (61,62). The design of the mini-PFR (63) allowed controlling and monitoring of the DO levels during the glucose pulse, and sampling 11 different exposure times to the environmental gradients. It was found that *E. coli* accumulated acetate and formate as early as 5 s after the exposure to the glucose gradient even during fully aerobic conditions (62). Also, fully anaerobic conditions were generated during exposure to a glucose gradient, which triggered the mixed-acid fermentation metabolism in less than 5 s. The information generated in this short time frame, under properly controlled environmental conditions can help to improve the scale-down studies and to perform metabolic modifications in the cells that can lead to a better performance under industrially relevant conditions.

Acknowledgments

Financial support by grant CONACYT Salud 44126 and 2007-c01-69911 is acknowledged.

NOMENCLATURE

A	Area
C_p	Heat capacity
D	Impeller diameter
$D_{O/W}$	Diffusion coefficient of oxygen in water
DO	Dissolved oxygen concentration
DOT	Dissolved oxygen tension
H	Liquid height
K	Discharge coefficient
N	Impeller speed
P	Power
Q	Specific production rate
Q_p	Pumping capacity
STR	Stirred-tank reactor
t_c	Circulation time
t_M	Mixing time
t_{mt}	Time constant for mass transfer
t_{rxn}	Time constant for oxygen consumption
t_v	Vessel diameter
U	Overall heat transfer coefficient
V	Liquid volume
VVM	Volume of air per volume of liquid per minute
λ_k	Size of the smallest turbulence generated eddy
μ	Specific growth rate
ρ	Liquid density

REFERENCES

1. Wang DIC, Cooney CL, Demain AL, Dunnill P, Humprey AE, Lilly MD. Fermentation and enzyme technology. New York: Wiley Interscience; 1979. p. 208.
2. Anderson C, LeGrys GA, Solomons GL. Chem Eng February 1982: 43–49.
3. Luyben KCAM. Regime analysis for the scale–down of biotechnological processes. In: Mortensen U, Noorman HJ, editors. Proceedings international symposium on bioreactor performance. Denmark: Nordic Programme on Bioprocess Engineering; 1993. pp. 159–169.
4. Dunn IJ, Heinzle E. Types of understanding in scaling down and up, as illustrated with and oxygen-sensitive culture. In: Mortensen U, Noorman HJ, editors. Proceedings international symposium on bioreactor performance. Denmark: Nordic Programme on Bioprocess Engineering; 1993. pp. 189–206.
5. Tatterson GB. Fluid mixing and gas dispersion in agitated tanks. New York: Mc Graw Hill; 1991. pp. 121–323.
6. Yegneswaran PK, Gray MR, Thompson BG. Biotechnol Bioeng 1991; 38: 1203–1209.
7. Lara AR, Galindo E, Ramírez OT, Palomares LA. Mol Biotechnol 2006; 34: 355–381.
8. Kossen NWF. Scale-up. In: Galindo E, Ramírez OT, editors. Advances in bioprocess engineering. The Netherlands: Kluwer Academic Publishers; 1994. pp. 53–65.
9. Oosterhuis NMG. Scale up of bioreactors: a scale down approach [PhD thesis]. Delft, The Netherlands: Delft University of Technology; 1984.
10. Sweere APJ, Luyben KCHAM, Kossen NWF. Enzyme Microb Technol 1987; 9: 386–398.
11. Frandsen S, Nielsen J, Villadsen J. Application of regime analysis of yeast fermentation for down-scaling. In: Mortensen U, Noorman HJ, editors. Proceedings international symposium on bioreactor performance. Denmark: Nordic Programme on Bioprocess Engineering; 1993. pp. 171–179.
12. Feijen J, Homeester JJ. Gradients in production scale bioreactors. In: Berovic M, Koloini T, editors. Bioreactor engineering course workshop notes. Ljubljana: Boris Kidric Institute of Chemistry; 1991. pp. 93–116.
13. Bailey JE, Ollis DF. Biochemical engineering fundamentals. 2nd ed. New York: Mc Graw-Hill; 1986. pp. 208–214.
14. Nienow AW, Langheinrich C, Stevenson NC, Emery AN, Clayton TM, Slater NKH. Cytotechnology 1996; 22: 87–94.
15. Feijen J, Hofmeester JJM, Groen D. Scale up of heterogeneous bioprocess. In: Alberghina L, Frontali L, Sensi P, editors. ECB6: proceedings of the 6th european congress on biotechnology. London: Elsevier Science; 1994. pp. 919–926.
16. Chassagnole C, Noissomit-Rizzi N, Schmid JW, Mauch K, Reuss M. Biotechnol Bioeng 2002; 79(1): 53–73.
17. Visser D, Heijnen JJ. Metab Eng 2003; 5(3): 164–176.
18. Vlaev D, Mann R, Lossev V, Vlaev SD, Zahradnik J, Seichter P. Trans IChemE 2000; 78(Part A): 354–362.
19. Hristov H, Mann R, Lossev V, Vlaev SD, Seichter P. Trans IChemE 2001; 79(Part C): 232–241.
20. Lapin A, Schmid J, Reuss M. Chem Eng Sci 2006; 61: 4783–4797.
21. Boysan F, Cliffe KR, Leckie F, Scragg AS. The growth of *Catharanthus roseus* in stirred tank reactors. In: King R, editor. Bioreactor fluid dynamics. London: Elsevier Applied Science; 1988. pp. 245–258.
22. Geraats SMG. Scaling-up of a lipase fermentation process: a practical approach. In: Galindo E, Ramírez OT, editors. Advances in bioprocess engineering. The Netherlands: Kluwer Academic Publishers; 1994. pp. 41–46.
23. Lara AR, Leal LI, Flores N, Gosset G, Bolívar F, Ramírez OT. Biotechnol Bioeng 2006; 93: 372–385.
24. Lara AR, Vázquez-Limón C, Gosset G, Bolívar F, López-Munguía A, Ramírez OT. Biotechnol Bioeng 2006; 94: 1164–1175.
25. Slater NKH. Scale-up problems. In: Mortensen U, Noorman HJ, editors. Proceedings international symposium on bioreactor performance. Denmark: Nordic Programme on Bioprocess Engineering; 1993. pp. 15–22.
26. De León A, Galindo E, Ramírez OT. In: Schmid RD, editor. Biochemical engineering 3. Germany: Universität Stuttgart; 1995. pp. 200–2002.
27. Larsson G, George S, Törnkvist M, Enfors SO. Methodology for scale-down of bioprocess. In: Mortensen U, Noorman HJ, editors. Proceedings international symposium on bioreactor

performance. Denmark: Nordic Programme on Bioprocess Engineering; 1993. pp. 15–22.
28. Träger M, Qazi GN, Buse R, Onken U. J Ferment Bioeng 1992; 74: 282–287.
29. Boccazzi P, Zanzotto A, Szita N, Bhattacharya S, Jensen KF, Sinskey AJ. Appl Microbiol Biotechnol 2005; 68: 518–532.
30. Knorr B, Schlieker H, Hohmann HP, Weuster-Botz D. Biochem Eng J 2007; 33: 263–274.
31. Micheletti M, Barret T, Doig SD, Baganz F, Levy MS, Woodley JM, Lye GJ. Chem Eng Sci 2006; 61: 2939–2949.
32. Islam RS, Tisi D, Levy MS, Lye GJ. Biotechnol Bioeng 2008; 99: 1128–1139.
33. Taticek RA, Moo-Young M, Legge RL. Plant Cell Tissue Organ Cult 1991; 24: 139–158.
34. Rhiel M, Murhammer DW. Biotechnol Bioeng 1995; 47: 640–650.
35. Serrato JA, Palomares LA, Meneses-Acosta A, Ramírez OT. Biotechnol Bioeng 2004; 88: 176–188.
36. Langheinrich C, Nienow AW. Biotechnol Bioeng 1999; 66: 171–179.
37. McDowell C, Papoutsakis ET, Borys MC. Animal cell culture, physicochemical effects of pH. In: Spier RE, editor. Volume 1, The encyclopedia of cell technology. New York (NY): John Wiley & Sons; 2000. pp. 63–70.
38. Ozturk SS. Cytotechnology 1996; 22: 3–16.
39. Osman JJ, Birch J, Varley J. Biotechnol Bioeng 2002; 79: 398–407.
40. Sandoval–Basurto E, Gosset G, Bolívar F, Ramírez OT. Biotechnol Bioeng 2005; 89: 453–463.
41. Schweder T, Krüger E, Xu B, Jürgen B, Blomsten G, Enfors S-O, Hecker M. Biotechnol Bioeng 1999; 65: 151–159.
42. Bylund F, Castan A, Mikkola R, Veide A, Larsson G. Biotechnol Bioeng 2000; 69: 119–128.
43. Harms P, Kostov Y, French JA, Soliman M, Anjanappa M, Ram A, Rao G. Biotechnol Bioeng 2006; 93: 6–13.
44. Aboka FO, Yang H, de Jonge LP, Kerste R, van Winden WA, van Gulik WM, Hoogendijk R, Oudshoorn A, Heijnen JJ. Biotechnol Bioeng 2006; 95: 1033–1042.
45. Samorski M, Muller-Newen G, Büchs J. Biotechnol Bioeng 2005; 92: 61–68.
46. Takebe H, Takane N, Hiruta O, Satoh A, Kataoka H, Tanaka H. J Ferment Bioeng 1994; 78: 93–99.
47. Buse R, Qazi GN, Onken U. J Biotechnol 1992; 26: 231–244.
48. Serrato JA, Palomares LA, Hernández V, Ramírez OT. Heterogeneous conditions in pH and dissolved CO_2 concentration on hybridoma cultures: implications on growth and monoclonal antibody glycosylation. Poster Presented at the "Cell culture Engineering X" Conference; Whistler, Canada; 2006.
49. Osterhuis NMG, Kossen NWF, Olivier APC, Schenk ES. Biotechnol Bioeng 1985; 27: 711–720.
50. Larsson G, Enfors SO. Bioprocess Eng 1988; 3: 123–127.
51. Abel C, Hübner U, Schügerl K. J Biotechnol 1994; 32: 45–57.
52. Amanullah A, McFarlane CM, Emery AN, Nienow AW. Biotechnol Bioeng 2001; 73: 390–399.
53. Hewitt CJ, von Caron GN, Axxelsson B, McFarlane CM, Nienow AW. Biotechnol Bioeng 2000; 70: 381–390.
54. Heinzle E, Moes J, Dunn IJ. Biotechnol Lett 1985; 7: 235–240.
55. Neubauer P, Häggström L, Enfors SO. Biotechnol Bioeng 1995; 47: 139–146.
56. Bylund F, Guillard F, Enfors SO, Trägardh C, Larsson G. Bioprocess Eng 1999; 20: 377–389.
57. George S, Larsson G, Enfors SO. Bioprocess Eng 1993; 9: 249–257.
58. Xu B, Jahic M, Blomsten G, Enfors S-O. Appl Microbiol Biotechnol 1999; 51: 564–571.
59. Lin HY, Neubauer P. J Biotechnol 2000; 79: 27–37.
60. Onyeaka H, Nienow AW, Hewitt CJ. Biotechnol Bioeng 2003; 84: 474–484.
61. Mashego MR, van Gulik WM, Heijnen JJ. FEMS Yeast Res 2007; 7: 48–66.
62. Lara AR, Taymaz-Nikerel H, Mashego MR, van Gulik WM, Heijnen JJ, Ramirez OT, van Widen WA. Biotechnol Bioeng 2009; 104: 1153–1161.
63. Mashego MR, van Gulik WM, Vinke JL, Visser D, Heijnen JJ. Metab Eng 2006; 8: 370–383.

41

BIOREACTOR SCALE-UP*

Laura A. Palomares and Octavio T. Ramírez
Departamento de Medicina Molecular y Bioprocesos, Instituto de Biotecnología, Universidad Nacional Autónoma de México, Cuernavaca, México

41.1 INTRODUCTION

Bioprocess and bioreactor scale-up are clearly activities that strictly depend on the substance being produced. For many biotechnology products, such as antibiotics, alcohols, organic acids, amino acids, and enzymes, a commercially viable process is attained only if a final fermenter scale on the order of hundreds of thousands of liters is reached. Such large volumes are needed to satisfy markets requiring very large amounts (10^2 to 10^7 t/year) of products with very low added value (10^{-1} to 10^3 \$/kg). In contrast, products derived from animal and plant cell culture are, in general, costly therapeutics or fine chemicals whose price can be as high as 10^4 to 10^9 \$/kg, but their worldwide demand is only 10^{-1} to 10^3 kg/year. Such a behavior is depicted in Fig. 41.1 where an inverse logarithmic relationship between product costs and market size exists (1). Accordingly, for the production of many substances derived from tissue or cell culture, at most only hundreds to thousands of liters per year are required to satisfy the demand, and, thus, the largest bioreactors needed hardly come close to the scales of other biotechnology products. This can be exemplified by two extreme cases, human erythropoietin (EPO) and taxol. EPO has the largest market for any therapeutic recombinant protein produced by mammalian cell culture. At an EPO selling price of \$0.013/U (130,000 U/mg), the total 2006 demand (\$11,500 $\times$ 10^6/yr) could be satisfied with only ca 7 kg/yr. Such production could be generated through a modest hypothetical bioprocess (batch operation, overall yield 500 U/mL cycle, 10-day cycles) in six bioreactors of less than 10,000 L. Similarly, the estimated world requirements of taxol (200 kg/yr at a bulk price of \$500,000/kg) could be satisfied by a single 70,000 L plant cell bioreactor yielding 0.25 g/L of product and operated in 15-day cycles (assuming a 50% purification yield) (1,2). These examples assume that a single manufacturer using a single vessel, which is a very improbable scenario, satisfies the market. Furthermore, the development of improved cell lines and bioreactor operation modes, such as perfusion culture, has resulted in substantial increases in cell and product concentrations, which would further reduce the bioreactor volumes calculated above.

In general, while the largest homogeneous cultures of suspended animal cells range between 4000 and 20,000 L, heterogeneous systems (microcarrier, packed beds, etc.) for anchorage-dependent animal cells usually do not exceed the 1000 L scale. Problems such as mass transfer limitations and concentration gradients, inherent to heterogenous systems, can explain their lower scales. Published data on the industrial production of products derived from cell culture is limited. Nonetheless, some of the largest cultures reported in the literature are summarized in Table 41.1. For example, the foot-and-mouth disease vaccine, obtained from baby hamster kidney (BHK-21) cells, has been produced by Wellcome for almost 30 years in a 1000 L reactor, and more recently at a 10,000 L scale (3). Cells from human origin (lymphoblastoid Namalwa cells) have

*This contribution is an update of the following chapter: L. A. Palomares, O. T. Ramírez; "Bioreactor Scale-Up"; The Encyclopedia of Cell Technology; Spier, R.E. (ed) The Wiley Biotechnology Series, John Wiley and Sons; Vol 1, 183–201 (2000). ISBN 0-471-16643-x.

Upstream Industrial Biotechnology: Equipment, Process Design, Sensing, Control, and cGMP Operations, Volume 2, First Edition. Edited by Michael C. Flickinger.
© 2013 John Wiley & Sons, Inc. Published 2013 by John Wiley & Sons, Inc.

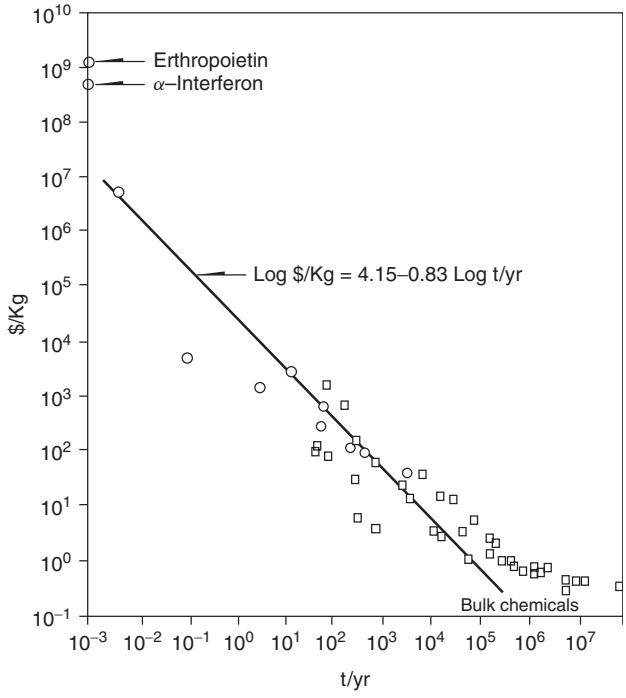


Figure 41.1. Relationship of chemical prices to annual production. Cell culture-derived products (open circles). [Adapted and reprinted with permission from Ref. 1.]

been cultured for interferon production up to 8000 L (4), and hybridomas for Mab production have been cultured in 2000-L airlift bioreactors (5). Recombinant antibodies are nowadays routinely produced in bioreactors of 10,000 L. Some of the largest reported scales for microcarrier cultures, packed beds, and ceramic cartridges are 7000, 100 and 240 L, respectively (6,7). Compared to animal cells, the scales of plant cell cultures tend to be larger. For instance, tobacco plant cells have been cultured in 20,000-L reactors (3), while a 75,000-L bioreactor is in operation for taxol production (2). Nevertheless, despite these successful experiences, large-scale culture of higher eukaryotic cellsis still a challenge, particularly for anchorage-dependent cell lines or very fragile cells, such as insect cells.

The first step to translate a cell culture process to a commercial scale is to define the product requirements and the overall production and downstream processing economics. A decision has to be taken whether a single large-scale batch reactor or smaller multiple continuous reactors are used. This decision can only be made after considering the whole process, operation and capital costs, available facilities, and even assessment of the consequences of a possible contamination during the culture. From a technical standpoint, one of the major issues for scaling up a cell culture bioreactor is the oxygen transfer problem. In general, the fragile nature of most higher eukaryotic cells and foaming associated problems due to the proteinaceous composition of many medium formulations limit the use of high power inputs and intense submerged aeration. As a process is scaled up, bioreactors must be more reliable, safe, cheap, and comply with regulations. In particular, the tight regulation imposed on the production of cell culture-derived therapeutics has significantly constrained the free development of improved and novel bioprocesses at a commercial scale. The dogma that the "process determines the product," mostly hatched from our analytical limitations to fully characterize cell culture products, has resulted in a costly and treacherous path for any company trying to modify its approved process. Thus, many therapeutics are produced by suboptimal processes and scales; however, this should change as regulation moves toward placing its attention on the characterization of products rather than on the bioprocess.

TABLE 41.1. Some of the Largest Scale Cultures Reported

Cell Line	Scale (L)	Reactor	Product	Reference
Taxus sp.	75, 000	Agitated tank	Taxol	2
Tobacco cells	20, 000	Agitated tank	Nicotine	3
BHK-21[a]	10, 000	Agitated tank	Foot-and-mouth disease vaccine	8
CHO[b]	10, 000	Agitated tank	tPA	6
Namalwa cells	8, 000	Agitated tank	Lymphoblastoid interferon	4
Bowes melanoma	7, 000	Agitated tank/microcarriers	tPA	6
Murine hybridomas	2, 000	Airlift	Mab	5
Vero cells	1, 000	Agitated tank/microcarriers	Killed polio virus vaccine	7
Murine hybridomas	1, 000	Stirred tank	Mab vs cell surface antigens of adenocarcinomas	9
BHK cells	500	Agitated tank/perfusion	Factor VIII	10
Microorganisms	400, 000	Bubble column	—	11
Microorganisms	400, 000	Airlift	—	11
Yeast	1, 500, 000	Bubble column	Baker's yeast	12

[a] Baby Hamster Kidney.
[b] Chinese Hamster Ovary.

41.2 ASPECT RATIO, HOMOGENEITY, AND GRADIENTS

41.2.1 Stirred Tanks

The purpose of a bioreactor is to provide proper environmental conditions required for optimal growth and/or product production under a contained system. Ideally, the culture environment should also be homogeneous and controlled. These conditions can be better accomplished in agitated tanks, which are the preferred design for scaling up anchorage-independent cells. Stirred-tank bioreactors for cell culture are cylindrical vessels with an aspect ratio (liquid height-to-diameter ratio) usually in the range of 1:1–3:1 (3,8). Nonetheless, the aspect ratio should be kept under 2:1 and impellers should be spaced properly (1.0–1.5 impeller diameters apart) to avoid top-to-bottom heterogeneity (13). Furthermore, oxygen transfer from the liquid surface, which is particularly important for animal cell culture, can be improved by keeping the aspect ratio close to unity. Special attention should be placed to the headspace dimensions if foaming problems are anticipated. In general, foam and liquid height increase from gas holdup are handled by leaving 20–30% of the vessel empty (13). A common feature of stirred-tank bioreactors is a hemispherical bottom, which prevents stagnant zones even under mild agitation rates. Nonetheless, as pointed out by Charles and Wilson (13), the cost of a hemispherical bottom vessel can increase by as much as 50%; yet, no clear evidence of its superior performance over a standard dished-bottom vessel exists. Probably the most distinguishing feature between different stirred-tank bioreactor designs is the impeller configuration. Many different types of impellers have been used for the culture of animal and plant cells in stirred tanks, including marine propellers, sails, pitched blades, Vibromixers (perforated discs placed on a vertically reciprocating shaft), anchors, paddles, helical screws, cell lift, and centrifugal impellers. Typical geometric characteristics of commonly used impellers are shown in Fig. 41.2. Many of such impellers have been designed with the objective of preventing mechanical damage to the fragile cells, but still maintaining a homogeneous environment and high oxygen transfer rates (OTR). Likewise, excluding baffles, and minimizing other inserts, while placing the impeller shaft eccentrically to avoid vortex formation, can reduce mechanical damage to the cells. Finally, vessel design should optimize the use of available materials; however, excessive costs are usually reduced by simply selecting a vessel among reactors already available from specialized vendors.

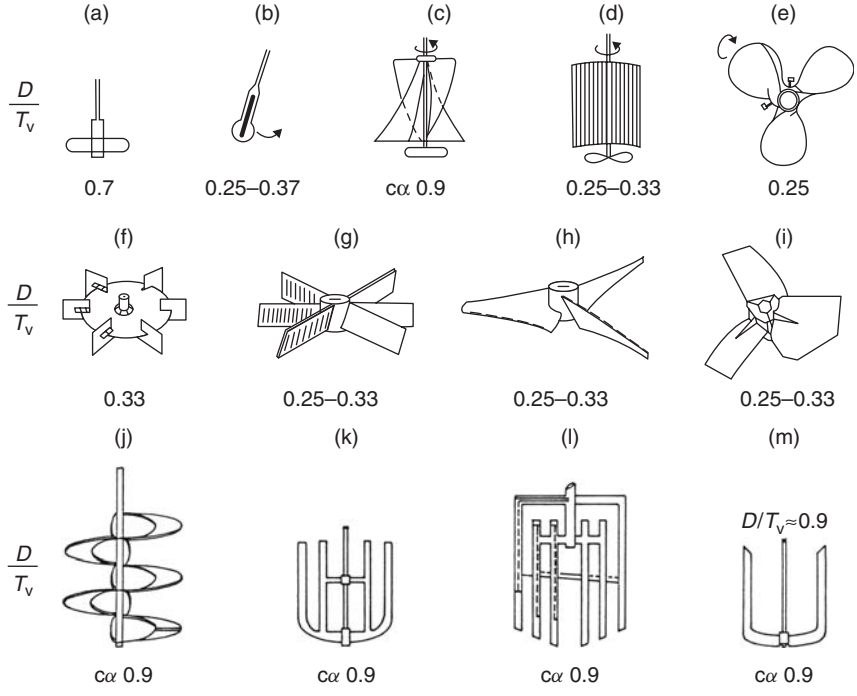


Figure 41.2. Commonly used impellers, and their geometric characteristics, used in animal and plant cell culture. D = impeller diameter, T_v = vessel diameter. (a) Suspended magnetic bar, (b) spherical rotating flex stirrer, (c) sail impeller, (d) membrane basket agitator, (e) marine propeller, (f) disc turbine, (g) angled blade, (h) and (i) profiled impellers, (j) helical ribbon impeller, (k) gate-anchor impeller, (l) gate impeller, and (m) anchor impeller. [Adapted from Refs. 14–16.]

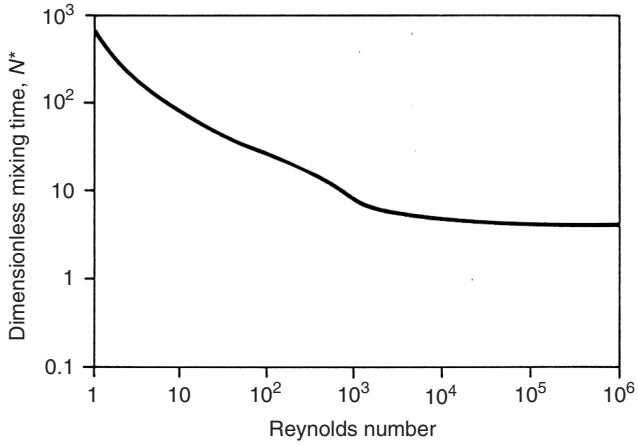


Figure 41.3. Dimensionless mixing time as a function of Reynolds number for turbine impellers in baffled vessels as determined from pH tracer experiments. [Reprinted with permission from Ref. 18.]

Tank geometry must be carefully selected as it influences the homogeneity of the bioreactor, especially as scale increases. Furthermore, heat and mass transfer are directly influenced by mixing, which in turn depends on operating variables and geometric characteristics of the bioreactor. For instance, the mixing time (time required for the system to reach a specified degree of uniformity) for a nonaerated Newtonian fluid in a baffled stirred tank with a flat-blade turbine impeller can be obtained from Fig. 41.3 and Equation 41.1 (15,17,18).

$$N^* = N t_M \left(\frac{g}{N^2 D}\right)^{1/6} \frac{D^2}{T_v^{1.5} H^{0.5}} \qquad (41.1)$$

where N^* is dimensionless mixing time, N is impeller speed, t_M is mixing time, g is gravitational acceleration, D is impeller diameter, T_v is vessel diameter, and H is liquid height.

Mixing times of different culture systems have been summarized elsewhere (19). Only very scarce information exists of homogenization and concentration gradients in large-scale animal or plant cell bioreactors. Among such studies, Langheinrich *et al*. (20) obtained mixing time data for typical operation conditions (maximum agitation speed of 1 s^{-1}, maximum air sparging rate of 0.005 VVM (volume of air per volume of liquid per minute), superficial air velocity of 2×10^{-4} m/s) of an 8000-L stirred-tank bioreactor (Rushton turbine $D = 2/9T_v$) used for animal cell culture at Glaxo Wellcome Research and Development. As a draw-and-fill operation is employed during production, aspect ratios of 0.3, 1.0, and 1.3 were studied. It was shown that mixing time, obtained from pH tracer and decolorization experiments, could be correlated with the total energy dissipation rate, ε_T (Figs 41.4 and 41.5), defined by Equation 41.2:

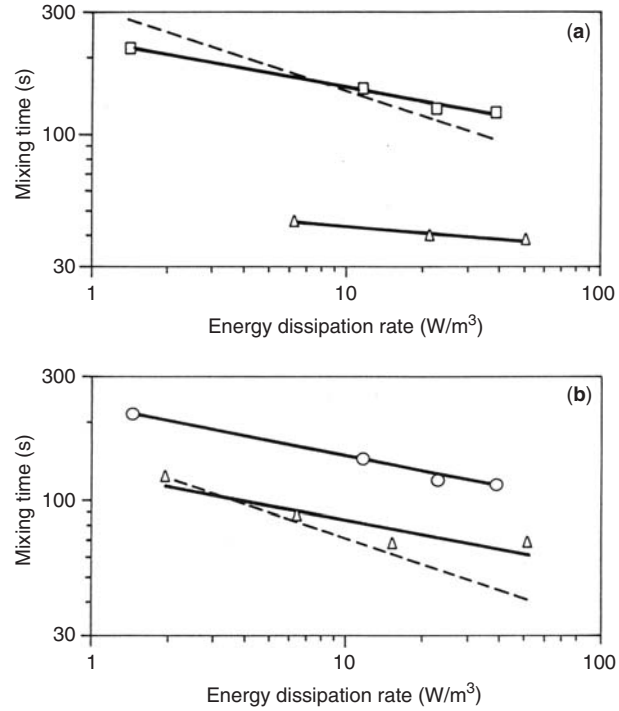


Figure 41.4. Effect of specific energy dissipation rate from agitation on mixing time. Determinations based on pH tracer experiments for various aspect ratios in an unaerated large-scale bioreactor. (a) $H = 0.3\ T_v$ (open triangle), $H = 1.3\ T_v$ (open square), dashed line = prediction by Cooke *et al*. (22) and (b) $H = T_v$ (open triangle), $H = 1.3\ T_v$ (open circle), dashed line—prediction by Ruszkowski *et al*. (21). [Reprinted with permission from Ref. 20.]

$$\varepsilon_T = \frac{P_0 \rho N^3 D^5}{V} + u_G g \rho \qquad (41.2)$$

where P_o is power number (Eq. 41.27), ρ is liquid density, V is liquid volume, and u_G is superficial gas velocity. The first term on the right hand side of Equation 41.2 is the contribution from agitation, whereas the second term is from aeration. Interestingly, experimental data of Langheinrich *et al*. (20) fitted well literature correlations (Eqs 41.3 and 41.4) obtained under agitation and aeration conditions two orders of magnitude above those studied in the animal cell culture bioreactor.

$$t_M N P_0^{1/3} = 5.3 \left(\frac{T_v}{D}\right)^2 \qquad (41.3)$$

for aspect ratios of 1 (21), and

$$t_M N P_0^{1/3} = 3.3 \left(\frac{H}{D}\right)^{2.43} \qquad (41.4)$$

for aspect ratios of 1–3 (22).

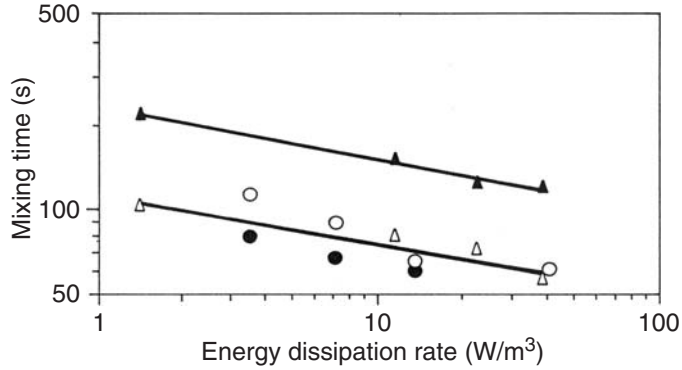


Figure 41.5. Effect of specific energy dissipation rate from agitation and aeration on mixing time. Determinations based on pH tracer experiments for various aspect ratios in a large-scale bioreactor. Closed symbols, determinations at the liquid surface and open symbols, determinations at the end of impeller discharge stream. Unaerated (triangles) and aerated (circles) at $u_G = 2 \times 10^{-4}$ m/s. [Adapted and reprinted with permission from Ref. 20.]

Several important conclusions, for the particular system used, are drawn from the study of Langheinrich *et al*. (20). First, gradients in pH and dissolved oxygen can potentially occur in large-scale animal cell culture since high mixing times, in the range of 40–200 s, were obtained under typical operation conditions. Computational fluid dynamics (CFD) has been used to predict gradients in microbial cultures (23,24). Secondly, homogenization is dramatically affected by geometric characteristics, as a fourfold increase in mixing times can occur as aspect ratios increase from 0.3 to 1.3 (Fig. 41.4). And finally, sparging substantially enhances mixing, particularly in the upper parts of the vessel and at aspect ratios greater than 1 (Fig. 41.5).

Poor mixing in stirred-tank reactors has been reported to cause significant problems in *Escherichia coli*, other microbial cultures, myeloma, hybridoma, Chinese hamster ovary (CHO), and insect cell cultures at high cell density (25–30). Undesirable carbon dioxide accumulation has been found to occur in 110–1000-L reactors as a result of low mass transfer characteristics of the systems (31,32). Furthermore, heterogeneities in microcarrier concentration and pH gradients have been found in large-scale stirred vessels (33–35). For instance, severe localized cell lysis problems at the point of base addition, allegedly caused by high mixing times, were observed in a 15-L reactor with cell retention (30). Another problem aggravated by deficient mixing is culture segregation, which originates from the formation of cell aggregates and clumps during high cell density cultures (30). Problems related to mixing can negatively affect overall culture performance. However, due to the fragile nature of animal cells, increasing agitation intensity cannot solve such problems. Therefore, other solutions must be found. For instance, pH gradients can be eliminated by adding base through multiple points properly localized in the reactor (30), while carbon dioxide removal can be enhanced by manipulation of air bubble size through proper design of the sparging system (29).

41.2.2 Disposable Bioreactors

Disposable bioreactors represent a novel development that is increasingly employed (36,37), particularly within the pharmaceutical area. This new paradigm in bioprocess technology has been motivated by several advantages that disposable bioreactors have over traditional stainless steel systems. Regulatory aspects impose important constraints in the pharmaceutical industry; among them, the most important is the need to guarantee that all bioprocess equipment in contact with the product has been perfectly cleaned between operation runs. This requirement substantially increases capital investment in a stainless steel-based facility since costly and sophisticated equipment such as steam-in-place and clean-in-place systems, as well as those needed for associated services such as clean steam generators, must be considered in the manufacturing plant. In addition, the initial cost of a stainless steel bioreactor can be several-fold higher than that of a disposable system of equivalent volume. Altogether, capital costs for a plant based on stainless steel bioreactors can be between three- and fourfold higher than an equivalent one based on disposable systems (38). In addition, operating costs for disposables are lower than for stainless steel bioreactors, as the former systems do not require labor-intensive procedures such as cleaning and sterilization validation, and shorter turnaround times between lots can be attained. Furthermore, stainless steel bioreactors require laborious specification and purchasing procedures, long times for design, construction and delivery, long times and

high costs of installation and qualification, and precious facility space is occupied by hard pipe installations and ancillary equipment. Accordingly, in addition to the higher capital and operating costs, a facility based on stainless steel bioreactors has limited flexibility, and compared to disposables, has higher risks of contamination and longer start-up times. Such issues are important for multipurpose plants and new start-up companies, as well as for rapid development, scale-up, and manufacture of new drug substances or drug candidates. Criteria and analysis tools for aiding in the decision process for selecting between disposable and stainless steel systems can be found elsewhere (39).

Disposable bioreactors consist of γ-irradiated presterilized multilayered bags formed by films of polyester, polyethylene, ethylene vinyl alcohol polymer, and other US Pharmacopoeia (USP) class VI materials with low or negligible leaching of extractable compounds. Bags are placed in various types of containers for conferring them structural rigidity. Various types of ports and accessories are attached to the bags, such as exhaust gas filters and aseptic rapid-type connectors. Different designs exist to attain homogeneity and to transfer gases to the liquid medium, the most common being those consisting of bags placed on rocking platforms that create a wave-like liquid movement (40), reciprocating bellows, and bags integrated to various types of molded polyethylene impellers and impeller shafts that are then placed into cylindrical containers (38,41). The latter systems allow the design of bioreactors with conventional geometric ratios, although unlike traditional stainless steel equipment, the bottom of the vessels is flat. Different design challenges exist; in particular, the need for mechanically agitated shafts and impellers contained within a closed presterilized bag. This has been solved by different means, including bottom-driven magnetically levitated impellers or impellers connected to sheaths for inserting an external top-driven shaft. Another challenge is placement of sensors, such as pH and dissolved oxygen, which has been solved using disposable probes based on optical sensor technology or alternatively using traditional probes sterilized in disposable bellows that are inserted through quick-connectors to the sterile bag. Liquid transfer, inoculation, and sampling from and to the bags are usually performed through sterile tubing welding equipment, and in some systems aeration is performed through porous patch membranes, open-end tubing, or jet nozzle diffusers. Disposable bioreactor systems are available in volumes ranging form 100 mL to 1000 L. Some companies are developing bioreactors of 2000 L, which could be the highest volume attainable for disposable technology.

In addition to bioreactors, there is a growing trend for designing and developing other disposable process equipment for extending the advantages of disposable bioreactors to other bioprocess operations. At present, there is a widespread use of disposable bags for buffer preparation and media containers. Likewise, disposable cartridges for microfiltration and ultrafiltration are commonly employed in manufacturing facilities. Also, there is a growing interest for developing disposable downstream processing equipment, such as chromatography media and columns (36). In particular, disposable bags have been designed for use in special continuous centrifuges. Such equipment, placed in series to disposable bioreactors, offer important advantages for separating cells during perfusion culture mode in a complete sterile and disposable operation.

In spite of the convenient features of disposable bioreactors, there still exist important disadvantages that limit their application in fields other than production of certain pharmaceuticals. In general, operation is limited to low agitation rates (<200 rpm), low aeration rates (<0.02 VVM), and low total pressure (<0.5 psig). Accordingly, the maximum volumetric oxygen transfer coefficients and OTR that can be attained are below 18 h^{-1} and 15 mmol/L h, respectively. Such constraints usually restrict the application of disposable bioreactors to animal and plant cell cultures operated at low or medium cell concentrations, although applications in microbial cultures are starting to appear (42). In addition, the maximum bioreactor volume available to date (1000 L) implies that multiple systems operated simultaneously will be required for manufacturing products requiring production outputs above 100 kg/yr. Finally, disposable bags are expensive and disposing the used bags and accessories must be considered under environmentally sustainable practices. Risk of puncture during operation must also be considered. Qualification of extractables and leachables must be necessary for particular processes that have not been previously validated by the bag vendors.

41.2.3 Airlift and Bubble Column Bioreactors

Airlift and bubble columns are also commonly used bioreactor configurations for the culture of suspended cells (typical geometric characteristics are shown in Fig. 41.6). These bioreactors are useful for culture broths with Newtonian behavior. They have higher energy efficiency than stirred tanks. Also, they have no moving parts, which can decrease maintenance time and costs, and in general they provide low shear. However, foaming can be a major problem, while bubble coalescence can reduce their performance (43). The height-to-diameter ratio of these reactors can range between 6:1 and as high as 12:1, but is typically 10:1. Nonetheless, airlift reactors with aspect ratios even below 2 have been reported for animal and plant cell cultures. As in stirred-tank vessels, geometric characteristic directly influence homogeneity, mass, and heat transfer in airlift and bubble column bioreactors. For instance, the relationship

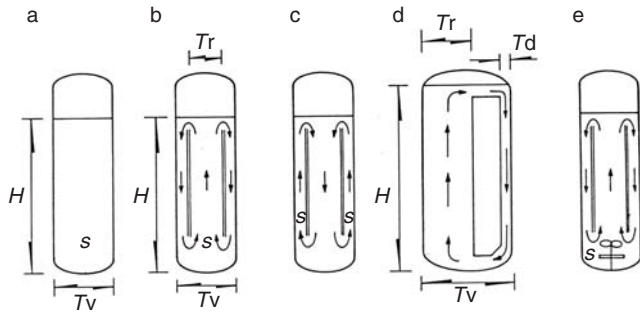


Figure 41.6. Typical geometric characteristics of common airlift and bubble column bioreactors used for cell culture. For all vessels shown, $H/T_v > 2$. For internal-loop airlifts, $T_r/T_v > 0.6$. For external-loop airlifts, $T_r/T_d \approx 2$. (a) bubble column, (b) and (c) internal-loop airlifts, (d) external-loop airlift, and (e) airlift with impeller. Arrows indicate direction of liquid flow and "s" indicates sparger position. [Adapted from Ref. 14.]

between geometric characteristics and mixing time is shown in Equations 41.5 and 41.6 (15,44):

$$t_M = Bt_c \left(\frac{A_d}{A_r}\right)^{0.5} \tag{41.5}$$

where B is a constant equal to 3.5 and 5.2 for internal- and external-loop airlift reactors, respectively, A_d and A_r are the downcomer and riser cross-sectional areas, respectively, and t_c is the circulation time or time taken for a liquid element to complete a circulation cycle in the reactor. Circulation time of airlift reactors (either internal loop or external loop with short horizontal top and bottom sections) can be determined from the superficial liquid velocity and geometric parameters according to

$$t_c = \frac{H_r}{u_{Lr}} + \frac{H_d A_d}{u_{Lr} A_r} \tag{41.6}$$

where H_r and H_d are the riser and downcomer heights, respectively, and u_{Lr} is the superficial liquid velocity in the riser. u_{Lr} is affected, among other variables, by liquid density, gas holdups, frictional loss coefficients, and frictional pressure drops, in riser and downcomer, through complex relationships usually solved by iterative algorithms. However, simplified correlations between u_{Lr} and geometric characteristics and operation parameters have been developed for particular conditions. For instance, Popovic and Robinson (45) proposed the following equation for a pseudoplastic fluid in an external-loop airlift ($u_{Gr} \geq 0.04$ m/s, $H = 1.88$ m, and A_d/A_r of 0.111, 0.25 and 0.44):

$$u_{Lr} = 0.23 u_{Gr}^{0.32} \left(\frac{A_d}{A_r}\right)^{0.97} \mu_{app}^{-0.39} \tag{41.7}$$

where u_{Gr} is superficial gas velocity in the riser and μ_{app} is the apparent viscosity (Pa s), this last variable being important only in some plant cell cultures.

Using Equations 41.1, 41.5, 41.6, and 7, Doran (15) compared the time constants of hypothetical 10,000-L stirred tank and external-loop airlift plant cell reactors of typical dimensions [details of geometric characteristics given in Doran (15)]. From the results of such simulation, shown in Fig. 41.7, several conclusions can be drawn. First, under typical operation conditions, the mixing time for a large-scale airlift can be substantially longer than that for a stirred vessel of the same volume. For instance, while mixing times from 200 to as high as 1000 s were predicted for the airlift, the range of mixing times for the stirred vessel was only between 20 and 200 s. A similar conclusion was reported by Bello *et al*. (44) where the mixing time per unit volume of stirred tanks was three to five times shorter than that of airlifts (either internal- or external loop) at the same total power input per unit volume. It is interesting to note that the calculations shown in Fig. 41.7 are in close agreement with experimental determinations by Langheinrich *et al*. (20), discussed in the previous section, for an animal cell stirred-tank reactor of similar size. Doran (15) also calculated the time constants for oxygen consumption, t_{rxn} (ratio of equilibrium oxygen concentration in the culture liquid to the volumetric oxygen consumption rate), and for mass transfer, t_{mt} (inverse of the volumetric mass transfer coefficient), while Lara *et al*. (19) calculated the time constants for oxygen consumption of different organisms and compared them with reported t_{mt}. Mixing problems will be encountered if $t_M > t_{rxn}$, while oxygen limitation will occur if $t_{mt} > t_{rxn}$. Accordingly, it was concluded that even for the long mixing times of the airlift, neither oxygen limitation nor dissolved oxygen gradients will occur at low plant cell concentrations (5 kg/m^3, Fig. 41.7a). Nonetheless, as cell concentration increases to 30 kg/m^3, mixing becomes limiting in the airlift reactor at gas velocities below 0.5 m/s and, thus, oxygen gradients will develop (Fig. 41.7c). Furthermore, for the high cell concentration case, oxygen limitation will occur in the airlift below gas velocities of 0.1 m/s and in the stirred tank below an agitation rate of 6 s^{-1} (Fig. 41.7c and d). Note that, due to cell fragility, most bioreactors are operated at a gas velocity and agitation rates well below 0.5 m/s and 6 s^{-1}, respectively.

Mixing problems in airlift vessels have been documented experimentally (46). As for stirred-tank vessels, the fragile nature of most higher eukaryotic cells limits the options for improving homogeneity in airlift and bubble column reactors. Accordingly, some solutions to mixing problems, such as addition of impellers to the draft tube of airlifts, have not been widely applied and appear to contradict the design essence of an airlift. Proper design of reactor geometry can be an efficient alternative to

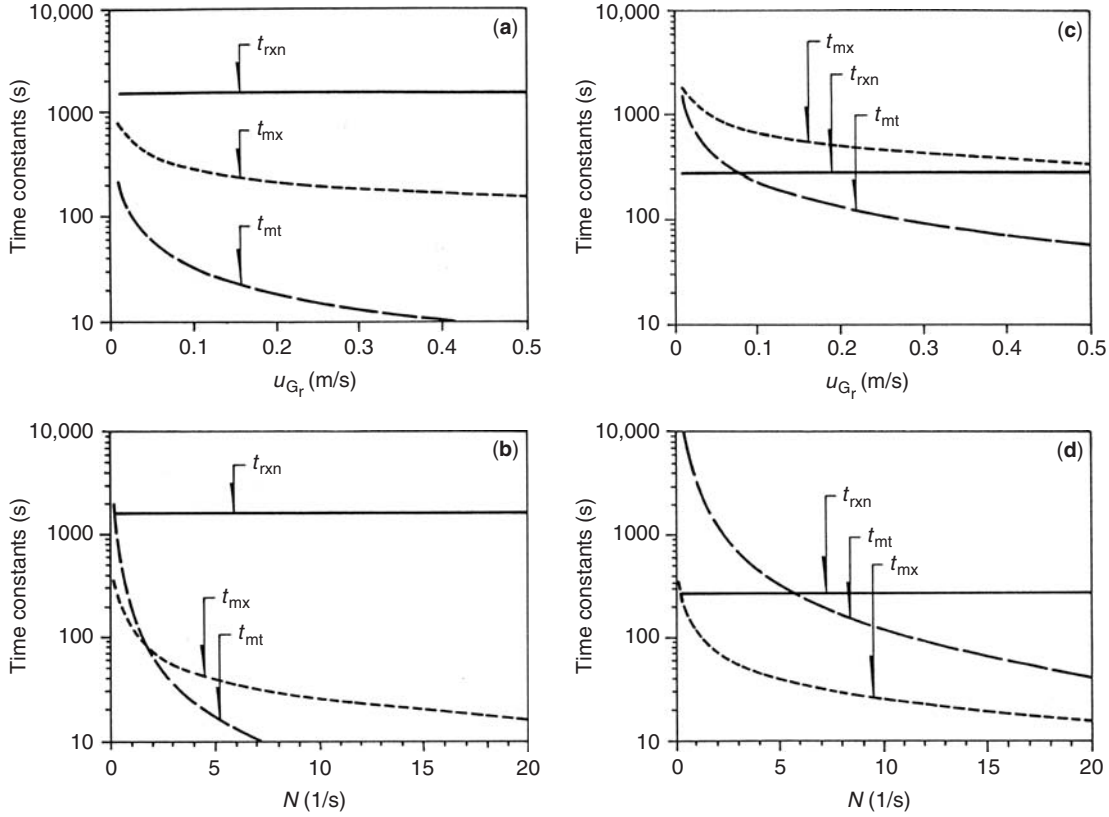


Figure 41.7. Comparison of time constants for 10,000-L hypothetical plant cell bioreactors. (a) External-loop airlift reactor: cell concentration 5 kg/m^3 dry weight. (b) Stirred-tank reactor: cell concentration 5 kg/m^3 dry weight. (c) External-loop airlift reactor: cell concentration 30 kg/m^3 dry weight. (d) Stirred-tank reactor: cell concentration 30 kg/m^3 dry weight. [Reprinted with permission from Ref. 15.]

improve homogeneity. For instance, minimal mixing times of internal-loop airlift reactors have been observed for riser-to-column diameter ratios (T_r/T_v) above 0.6 (15). Accordingly, a riser-to-downcomer cross-sectional area equal to unity ($T_r/T_v = 0.71$) has been proposed as a good design criterion (47). Other geometric characteristics that can considerably affect homogeneity of airlift reactors are the draft tube and sparger positions, the draft tube to liquid height ratio, and the curvature of the bottom sections.

In the case of bubble columns, two types of flow regimes have been described, homogeneous and heterogeneous (48). Homogeneous flow regime, characterized by the absence of a circulatory flow, occurs at low gas superficial velocities (<0.04 m/s) and when the sparger holes are uniformly distributed on the bottom of the vessel. In typical conditions, mostly all bubble columns operate under heterogeneous flow regimen where circulatory flow is present as a result of uneven distribution of sparger holes or high superficial gas velocities. Mixing time has been correlated with geometric characteristics and operation parameters for bubble columns under heterogeneous flow regime according to (48):

$$t_M = 11\frac{H}{T_v} + \left(g u_{Gs} T_v^{-2}\right)^{-0.33} \tag{41.8}$$

where u_{Gs} is the superficial gas velocity corrected for local pressure.

A comparison of calculated mixing times for airlift and bubble column bioreactors has been presented by van't Riet and Tramper (48). Such comparison revealed that for low superficial gas velocities (0.001 m/s), mixing times of bubble columns were shorter than that for airlifts, and the opposite occurs for gas velocities above 0.001 m/s. Nonetheless, for all conditions calculated and an aspect ratio of 10, differences in mixing times between both reactors were small and never exceeded 30%. Furthermore, such differences were even smaller as the reactor volume increased. Accordingly, the behavior of large-scale airlift and bubble column reactors in terms of homogeneity and presence of concentration gradients should be relatively similar.

Although high superficial velocities improve homogeneity and prevent formation of concentration gradients in airlift and bubble column reactors, foaming problems and bubble-associated cell damage limit the use of high aeration rates. Tramper *et al*. (49) have proposed a killing volume hypothesis, where cells are killed within a hypothetical volume associated with each air bubble. The specific death rate constant, k_d, was then correlated with operation and geometric characteristics of bubble columns according to

$$k_d = \frac{24 F_g V_k}{\pi^2 d_b^3 T_v^2 H} \tag{41.9}$$

where F_g is gas flow rate, d_b is bubble diameter, and V_k is killing volume, which is constant for a particular system and can be experimentally determined. Equation 41.9 shows that the aspect ratio of bubble column bioreactors can have important consequences on animal cell survival. For instance, a decrease in aspect ratio will result in an increase in the death rate constant for a given reactor volume and superficial gas velocity. Thus, a high aspect ratio should be the design criterion. However, Meier *et al*. (50) showed that cell damage increases with liquid height. As liquid height is increased, a higher number of cells attach to bubbles, due to their longer ascension time. Cell attachment to bubbles is reduced by the addition of Pluronic F68 or other shear protectants to culture medium.

41.2.4 Heterogeneous Bioreactors

Heterogeneous systems can be defined as those where cells grow either attached to or entrapped by a solid substratum arranged within a particular device or bioreactor configuration. Many different types of substrata and geometric configurations exist; however, heterogeneous systems can be simply classified according to Table 41.2 (51). In almost all heterogeneous systems, oxygen transfer will be the limiting factor, and, thus, as discussed below, dissolved oxygen concentration gradients will be present. Accordingly, predicting dissolved oxygen profiles constitutes the basis for a rational design of many heterogeneous systems. The simplest designs include static units, such as dishes, flasks, and trays, where oxygen is transferred through the liquid surface only by diffusional mechanisms. As described by Murdin *et al*. (52), the dissolved oxygen profile can then be predicted from a steady state mass balance according to:

$$c = \frac{\mathrm{OUR}}{2D_{o/w}} \left[\left(\frac{2D_{o/w} c_m}{\mathrm{OUR}} \right)^{0.5} - y \right]^2 \tag{41.10}$$

where c and c_m are dissolved oxygen concentration in the liquid and at saturation, respectively, OUR is oxygen uptake rate, y is liquid depth, and $D_{o/w}$ is the diffusion coefficient of oxygen in water (2.6×10^{-5} cm^2/s). For a typical maximum cell concentration (3×10^6 cell/mL) and typical specific oxygen consumption rate (4×10^{-10} mmol/cell h), Equation 41.10 predicts that medium height must be maintained below 2 mm in order to avoid oxygen limitation. This result indicates that very high superficial area to culture volume ratios (A/V), usually in the range of 2.5–5 cm^{-1}, are required. That is, two to three orders of magnitude higher than that of large-scale homogeneous bioreactors. A modest increase (two- to threefold) in substratum area, without a corresponding increase in A/V ratios, can be achieved by circulating medium through multistacked static units or by rotating vessels and flasks containing multiple internal surfaces. Scalability of high A/V culture units is limited, since their cumbersome configurations require labor-intensive operations; yet, volumes as large as 200 L have been reported (51). Very high substratum areas to culture volume ratios, and concomitantly very high cell concentrations ($>1 \times 10^8$ cell/mL), can be attained in some heterogeneous bioreactors, such as packed beds (4–100 cm^{-1}) and hollow fiber (HF) (30–200 cm^{-1}). High gas/liquid areas needed for oxygen transfer are eliminated by perfusing oxygen-saturated medium. This results in very compact bioreactor designs, as well as in the possibility of culturing anchorage-independent cells in perfusion mode, at very low shear stresses, and close to *in vivo* cell concentrations.

In spite of the fact that heterogeneous systems are extensively used in lab-scale applications and commercial size operations, a strictly controlled and uniform environment cannot be maintained. Thus, undesirable heterogeneities and existence of concentration gradients will inevitably occur during scale-up. Accordingly, heterogeneous systems are usually scaled up by increasing the number of small-scale units, rather than increasing the size of the equipment. Many disadvantages exist for such an approach, including higher capital and operation costs, poorly controlled and monitored operation, and unit-to-unit variability. Therefore, the challenge is to design heterogeneous bioreactors that approach a more uniform environment. This can be

TABLE 41.2. Classification of Heterogeneous Systems

Plate devices	
Static	T-flasks, plate units, trays, multiwell plates, petri dishes
Dynamic	Plate units, roller bottles
Films	Bags, spiral wound
Tubes	Macroforms, hollow fibers
Packed beds	Ceramic, glass spheres, helixes, springs, diatomeceous earth, polystyrene jacks, sponges
Monolithic	Ceramic matrix
Microcarriers	Simple solid, collagen coated, porous
Microencapsulation	Alginate, agarose, polylysine

Adapted from Ref. 51.

achieved through proper design of geometric characteristics and operation conditions. Since many different types of heterogeneous systems exist, each case deserves a unique analysis. Nonetheless, geometric and homogeneity considerations of microcarrier systems, HF, and packed-bed reactors are analyzed below, since these are among the most important systems for a commercial scale operation.

41.2.4.1 Hollow Fiber Reactors. Conventional HF reactors are composed by a bundle of HF sealed into an outer casing, forming a shell and tube configuration of 3.2–9 cm in diameter and 6–30 cm in length. HF are anisotropic structures composed of a thin (0.1–2.0 μm) inner or "active" skin and a thick (50–85 μm) spongy support layer. The internal fiber diameter commonly ranges from 40 to 200 μm and the molecular weight (MW) cutoffs (MW of species retained) vary from 300 to 300,000 Da. Medium is perfused from the lumen side and transported through the porous membrane to the shell side, where the cells are immobilized. As illustrated in Fig. 41.8, there are three common operation modes (open shell, closed shell, and crossflow), each resulting in a different pressure distribution throughout the HF cartridge (53). The axial pressure drop inside the fibers can be expressed, to a good approximation, by Equation 41.11, obtained from the Hagen–Poiseuille equation for flow in a pipe (54):

$$\frac{dp_c}{dz} = -\frac{8\mu_b}{r_c^2}\overline{u_c} \tag{41.11}$$

where p_c, and $\overline{u_c}$ are pressure and average axial velocity inside the capillary, respectively, z is axial position, and r_c is the inside capillary radius. The transmembrane flux depends on the pressure difference between the shell and lumen sides of the fiber. For the open and closed shell operation modes, the pressure gradient, and thus medium flux, decreases along the axial direction, causing undesirable concentration gradients. The result is a higher cell concentration at the inlet section and only negligible growth after a certain cartridge length. Most commercial HF devices operate on the closed mode, resulting in a reversed flux at the downstream section of the reactor. Thus, while fresh medium is supplied to the cells in the inlet section, exhausted medium and toxic wastes are removed in the outlet segment, creating severe environmental heterogeneities. Accordingly, scale-up of HF reactors in the axial direction is limited and explains the short length of commercially available devices. In conventional HF reactors, only diffusional transport exists on the shell side. Thus, fibers must be tightly packed to avoid nutrient limitation and/or by-products accumulation at the interstitial zones. Even so, necrosis usually occurs since distance from the interstices to the inner capillary skin is, at best, 150 μm. Necrotic zones will still occur even if convective transport is forced through the shell side, as the tissue-like cell concentrations prevent a uniform flow distribution. Accordingly, severe radial gradients are also present in many HF reactors. Concentration polarization and fouling of the inner lumen surface are additional problems that can lead to reactor heterogeneities. Experimental determinations of axial and radial heterogeneities are well documented (53,55–57).

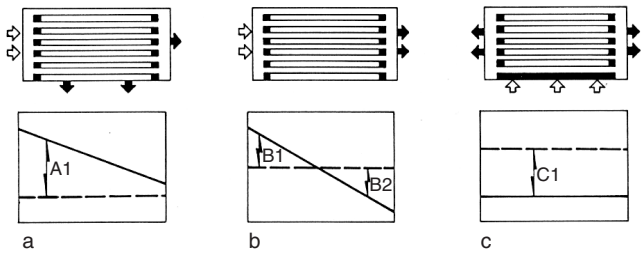


Figure 41.8. Schematic representation of common operation modes and pressure distribution in hollow fiber reactors. Open arrows indicate feed inlet and closed arrows indicate effluent streams. The tube-side pressure is represented by a solid line and shell-side pressure by a dashed line. (a) Open shell ultrafiltration and transmembrane pressure difference, A1. (b) Closed shell ultrafiltration and transmembrane pressure difference, B1 and B2. (c) Crossflow ultrafiltration and transmembrane pressure difference, C1. [Reprinted with permission from Ref. 53.]

Many solutions have been proposed for improving homogeneity and preventing nutrient limitation and by-products buildup in HF reactors, most of them on the basis of modifying geometric characteristics and operation conditions (55–57). For instance, combination of fibers and membranes in flat-bed HF arrangements; introduction of porous distribution tubes to perfuse either fresh medium or oxygen; mixing aeration and medium supply fibers; combination of different fiber types; selection of MW cutoffs; flow alternation between shell and lumen sides; and flow reversal at different interval times. Still, scale-up of HF reactors is primarily performed by increasing the number of devices in a modular fashion. Predicting dissolved oxygen profiles in the radial direction can help design more efficient HF reactors (fiber size, distance between fibers, etc.). A simplified approach is to perform a steady state mass balance around a cylindrical capillary where only diffusion is considered. Dissolved oxygen profiles can then be obtained, as detailed by Murdin *et al*. (52), from the following equation:

$$c = c_m + \frac{\mathrm{OUR}}{4D_{o/w}}\left[r^2 - r_c^2 - 2r_0^2 \log\frac{r}{r_c}\right] \tag{41.12}$$

where r is radius and r_0 is radius at which oxygen concentration falls to zero.

41.2.4.2 Packed-Bed Reactors. Packed-bed reactors are also widely used for the culture of anchorage-dependent and independent cells (58). In general, an aspect ratio of 3 is suitable for packed beds. As shown in Table 41.2, many different materials have been used as packing matrix. The diameter of the various matrix particles commonly range from 0.1 to 5 mm, resulting in typical void fractions of 0.3–0.6. Depending on the packing material used, very high substratum area to culture volume ratios can be reached (see above), which approximate those of HF reactors. However, in contrast to HF, properly designed packed-bed reactors should not present radial gradients, and, thus, a straightforward scale-up in this direction is possible. Still, axial concentration gradients are inherently present and will limit reactor length. Again, dissolved oxygen is almost always the limiting substrate and its concentration profile along the axial direction can be determined using a macroscopic mass balance (59):

$$c = c_0 - \left(\frac{\text{OUR}}{u_\text{L}}\right) z \tag{41.13}$$

where c_0 is inlet dissolved oxygen concentration and u_L is superficial liquid velocity based on empty bed. Concentration gradients will decrease as u_L increases (Eq. 41.13). Nonetheless, maximum u_L will be limited by permissible maximum pressure drop, which can be determined from the Ergun equation (60):

$$\Delta_\text{p} = \frac{150 z \mu_\text{b} (1-\varepsilon)^2 u_\text{L}}{T_\text{p}^2 \varepsilon^3} + \frac{1.75 z \rho u_\text{L}^2 (1-\varepsilon)}{T_\text{p} \varepsilon^3} \tag{41.14}$$

where ε is void fraction, T_p is particle diameter, and μ_b is culture medium viscosity. Maximum shear stresses in the bed must also be considered for determining the maximum allowable u_L.

41.2.4.3 Microcarriers. Stirred vessels and airlifts are the reactor configurations used for cultivation of cells attached to microcarriers. Furthermore, the density of microcarriers is only slightly above that of culture medium (1.03–1.05 g/mL). Thus, geometric considerations and homogeneity characteristics of the bulk liquid phase will be the same as for homogeneous systems. Nonetheless, concentration gradients within porous microcarriers (typical diameter range between 100 and 500 μm) can still exist. Dissolved oxygen profiles within porous microcarriers can be modeled from a steady state mass balance of oxygen diffusion into a sphere, as has been described by Murdin *et al*. (52). Alternatively, mass transfer limitations, and, thus, formation of undesirable gradients within a porous microcarrier can be determined from plots of the observable module (obtained from the Thiele modulus), Φ, versus the effectiveness factor, η, shown in Fig. 41.9 (61). For spherical particles and OUR being the rate of interest, Φ and η are defined as

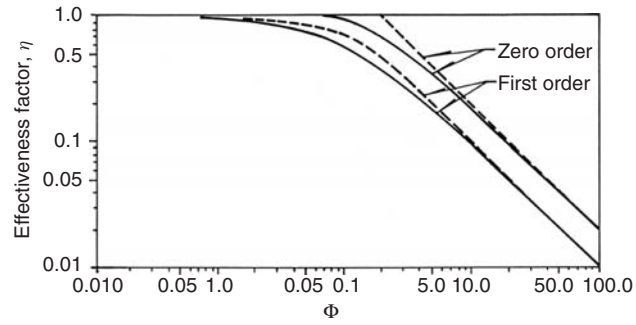


Figure 41.9. Effectiveness factor as a function of the observable modulus. Michaelis–Menten kinetics. Continuous line, spherical geometry and dashed line, slab geometry. [Reprinted with permission from Ref. 61.]

$$\eta = \frac{\text{Observed OUR}}{\text{OUR without diffusional limitation}} \tag{41.15}$$

$$\Phi = \frac{\text{OUR}_\text{o}}{D_\text{e} c_\text{m}} \left(\frac{V_\text{p}}{A_\text{p}}\right)^2 \tag{41.16}$$

where A_p and V_p are the external surface area and volume of a microcarrier, respectively, and OUR_o is the observed OUR. D_e is effective diffusion coefficient, which in turn is a function of the microcarrier porosity and tortuosity factor. From Fig. 41.9 and Equations 41.15 and 41.16, it can be seen that oxygen limitation will occur at an observable module above 0.3. Accordingly, oxygen limitation can be avoided ($\Phi < 0.3$) through proper design of microcarrier geometry (Fig. 41.9 and Eqs 41.15 and 41.16). This approach can also be applied to other immobilized systems such as HF and microencapsulation.

41.3 HEATING AND COOLING

Maintenance of a constant and homogeneous temperature is an essential requirement in cell culture. Temperature variations of 1°C can reduce cell growth, viability, and/or product production (62). Temperature has also been reported to affect cell cycle phases, metabolism, and cell resistance to shear (63), while its control is particularly relevant when temperature inducible genes are used for recombinant protein production (64). High temperatures may also increase proteolytic activity and alter protein posttranslational modifications (63). Moreover, culture susceptibility to viral infection can be modified by temperature (65). Although for some processes, viral infection is an undesirable event, in others, such as virus

TABLE 41.3. Optimum Temperatures for Cell Culture

Cell line	Optimum Temperature (°C)	Parameter (Maximum Value)	Reference
Murine hybridoma HB-32	33	Viability index	66
Murine hybridoma HB-32	39	qMab	66
Rat–mouse–mouse trioma	37	Xt and qMab	68
CHO cells	37	Growth rate	62
Insect cells	27–29	Xt	69
Insect cell—baculovirus expression system	22–29	Recombinant protein production[a]	69
Catharantus roseus plant cells	30	Xt	70
	21.5	Product synthesis	70
Perilla frutescens plant cells	28	Xt	71
	25	Anthocyanin productivity	71
Chlorella vulgaris SO-26 green alga cells	20	Specific growth rate	72
	14	Cellular sugar content	72
Salmonid fish cell lines	15–20	Xt	73
Non-salmonid fish cell lines	20–30	Xt	73

[a]Optimum temperature should be determined for each recombinant protein produced.

production for vaccines or bioinsecticides, viral progeny is the desired product. As shown in Table 41.3, there exists a wide range of optimum temperatures for tissue culture. Mammalian cell lines are usually cultured at or near 37°C, while cells from other origins, such as insect, amphibian, fish, or plant, require lower temperatures, usually between 10 and 30°C. Optimum temperature for growth is not always the best for product production. In an attempt to provide the most favorable conditions for growth and product production, several groups have proposed production strategies that demand a fine control of temperature (63,66). Moreover, temperature monitoring has been proposed as a tool for designing control strategies (63,67). Altogether, it is clear that optimum temperature control and monitoring are imperative, especially when applications of cell culture are scaled up to a commercial level.

For fermentations of lower eukaryotes or prokaryotes, heat transfer becomes increasingly problematic as the fermenter is scaled up. This is due to the high cell concentrations reached, the high heat generated from metabolic activity, and the very large volumes of fermenters employed. The importance of heat transfer in such processes can be illustrated by the production of single-cell protein, where operating costs from heat removal can be higher, or at least equal, than that from oxygen transfer (14). A particular problem that occurs at very large scales is that heat transfer from the vessel walls is severely limited since reactor volume increases to the cube while reactor area increases only to the square. A contrasting situation exists for cell culture, where heat transfer is not considered an important problem and has been widely overlooked, while other aspects such as oxygen transfer have received much more attention. The reasons for this are the lower cell concentrations, smaller power inputs, lower size of commercial reactors, and lower generation of metabolic heat of animal and plant cell culture compared to microbial fermentations. Nonetheless, careful attention must still be placed on the design of the heat transfer and temperature control systems of large-scale cell cultures, particularly if temperatures near ambient are required. Heat transfer can become an important issue as higher cell density cultures are developed and larger reactor volumes are needed. Also, particular operation strategies can result in temperature gradients. Druoin *et al*. (74) observed transient temperature increases when CHO cells were circulated through a sonic separator in perfusion cultures. Temperature increases in animal and microbial cell cultures trigger heat shock responses, which have various effects on metabolism and productivity (75,76). Moreover, the fragile nature of most animal cells limits the use of highly turbulent mixing, necessary if high heat transfer rates are needed. Accordingly, heat transfer phenomena must be considered during the design of a large-scale cell culture and microbial process.

Effective heat transfer is required not only for maintaining a constant temperature in the bioreactor, but also for sterilizing and cooling the vessel, the latter being important for assuring product stability at the end of the culture. In this section, a general introduction to heat transfer in bioreactors is given, with special emphasis to cell culture. Only the maintenance of a desired temperature during the culture phase is discussed, as sterilization and product recovery are discussed elsewhere. Finally, the relevance of heat transfer is evaluated from calculations for hypothetical large-scale cultures.

41.3.1 Heat Transfer in Bioreactors: The Basics

The main heat flows in a stirred-tank bioreactor are shown in Fig. 41.10. The heat accumulation rate in such a reactor,

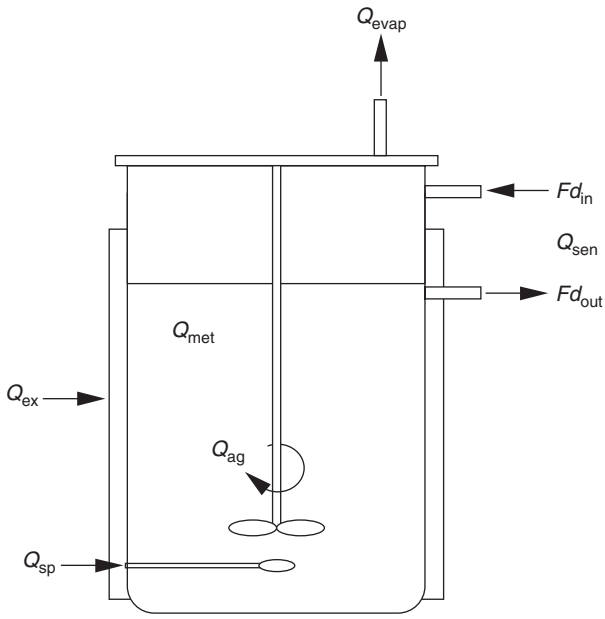


Figure 41.10. Main heat flows in a stirred-tank bioreactor.

for constant pressure, is given as follows:

$$Q_{acc} = Q_{met} - Q_{sen} + Q_{sp} + Q_{ag} - Q_{evap} + Q_{ex} \tag{41.17}$$

where Q_{met} is heat produced by metabolism of the cells, Q_{sen} is sensible enthalpy gain by flow streams (outlet–inlet), Q_{ag} is heat generated by power input from agitation, Q_{sp} is heat generated by sparging, Q_{evap} is heat removed by evaporation, and Q_{ex} is heat transferred by the heat exchanger. Heat transferred between the environment and the reactor can be important for small-scale vessels, but becomes negligible as volume increases. Heat transferred from the environment can be included in Q_{ex}. If temperature of the reactor is maintained constant, then

$$Q_{acc} = 0 \tag{41.18}$$

Each of the terms in Equation 41.17 is individually analyzed below.

41.3.1.1 Metabolic Activity. Heat generated by metabolic activity depends, among other things, on the type of cell, growth phase, type and concentration of substrates, concentration of by-products, shear and osmotic stresses, and physicochemical properties of the culture medium (77). This has been extensively analyzed for cultures of prokaryotes or lower eukaryotes, but only very scarce information exists for animal and plant cell cultures. Heat generated from aerobic growth can be calculated from the oxygen consumption using the oxycaloric equivalent, which is defined as the heat yield from oxygen consumed. For any cell type, fully aerobic metabolism, and all biologically useful organic substrates, the oxycaloric equivalent has been determined to be −450 (±5%) kJ/mol O_2 (77). However, compared to *in vivo*, the oxycaloric equivalent is always more negative for cells grown *in vitro*. This is caused by nutritional deficiencies present in the *in vitro* environment, which must be fulfilled by rapidly growing cells through anaerobic processes (77). Under such conditions, use of the oxycaloric equivalent to calculate the heat produced from cell metabolism can lead to an underestimation of almost 40%. Heat flow rates for several biological models have been determined under controlled pH and dissolved oxygen using microcalorimeters or bench-scale calorimeters (67,77,78). Heat fluxes (heat flow rate per cell) for some mammalian cell lines are shown in Table 41.4. However, caution should be taken when using such values, as the heat generated by metabolism is affected by the various parameters mentioned above.

If metabolic pathways are lumped into one global reaction, then heat produced by cellular metabolism can also be calculated from the standard enthalpies of substrates, biomass, and products. Again, caution should be taken as metabolic reactions are very variable, and depend on the particular system studied, including substrate availability, physicochemical conditions, and toxicity of by-products.

TABLE 41.4. Specific Heat Flux for Some Cell Types

Cell Type	Heat flux (pW/cell)
Human erythrocytes	0.01
Human platelets	0.06
Bovine sperm	1.3 ± 0.1
Human neutrophils	2.5 ± 0.3
Human lymphocytes	5
Horse lymphocytes	8
Human T-lymphoma	8 ± 1
3T3 mouse fibroblasts	17
Chinese hamster ovary 320 (recombinant)	~23
kB	25
Vero	27 ± 2
Mouse lymphocyte hybridoma	30–50
HeLa-53G	31.2
Mouse macrophage hybridoma, 2C11-12	32 ± 2
Chinese hamster ovary K1	38
Human foreskin fibroblast	40 ± 10
Rat white adipocytes	40
Human white adipocytes	49 ± 15
Human melanoma, H1477	80
Human keratinocytes	83 ± 12
Hamster brown adipocytes	110
SV-K14 (transformed) keratinocytes	134 ± 35
Rat hepatocytes	329 ± 13
Kluyveromyces fragilis	1.2[a]

Reprinted with permission from Ref. 77.

[a] In grams per liter, calculated from data of Ref. 78.

Even when catabolism of higher eukaryotic cells is very complex, Kemp and Guan (77) have concluded that, for heat balance considerations, the metabolic processes of animal cells can be described essentially by glycolysis, oxidative phosphorylation, the pentose phosphate pathway, and glutaminolysis. Accordingly, they summarized animal cell growth and product production as follows:

$$\text{Glucose} + \text{Glutamine} + O_2 \rightarrow \text{Biomass} + \text{Product} + \text{Lactate} + CO_2 + NH_3 + H_2O \quad (41.19)$$

Q_{met} can then be calculated from the standard enthalpies of formation of each compound, if reaction stoichiometry is known, according to (14)

$$Q_{\text{met}} = \sum_{i=1}^{m} b_i H_{\text{p},i} - \sum_{j=1}^{n} a_j H_{\text{s}j} \quad (41.20)$$

where m and n are the number of products and substrates, respectively; b_i and a_j are the stoichiometric coefficients of product i and substrate j, respectively; and $H_{\text{p},i}$ and $H_{\text{s},j}$ are the enthalpies of product i and substrate j, respectively. It should be noted that the contribution of anabolism to heat generation is generally negligible (67). Some standard enthalpies of formation for common cell culture substrates and by-products are shown in Table 41.5. von Stockar and Marison (78) have determined that neither temperature nor the thermodynamic state of compounds is significant for energy balance calculations of aerobic (or mainly aerobic) cell growth. Therefore, values shown in Table 41.5 can be utilized for energy balances for culture temperatures different at 25°C without any further corrections.

TABLE 41.5. Standard Formation Enthalpies of Various Compounds (25°C, 1 atm)

Compound	Formula	$\Delta H^0{}_f$ (kcal/mol)
Acetic acid	$C_2H_4O_2$(aq)	−94.5
Acetate ion	$C_2H_3O_2{}^-$ (aq)	−116.1
Alanine	$C_3H_7O_2N$(s)	−88.9
Ammonia	NH_3(g)	−41.4
	NH_3(aq)	−19.4
Ammonium chloride	NH_4Cl(s)	−75.4
Ammonium ion	$NH_4{}^+$(aq)	−31.8
Bicarbonate ion	$HCO_3{}^+$(aq)	−165.5
Biomass	$CH_{1.8}O_{0.5}N_{0.2}$(aq)	−21.9
Carbon dioxide	CO_2(g)	−94.0
	CO_2(l)	−98.9
Carbonic acid	H_2CO_3	−167.2
Ethanol	C_2H_5OH(l)	−66.3
Formic acid	CH_2O_2(aq)	−85.1
$\alpha - \beta$-D-Glucose	$C_6H_{12}O_6$(aq)	−302.0
Glutamic acid	$C_5H_8O_4N$(s)	−170.4
Hydrochloric acid	HCl(g)	−22.1
	HCl(aq)	−18.0
Hydrogen ion	H^+(aq)	0
Lactic acid	$C_3H_6O_3$(l)	−124
Methane	CH_4(g)	−17.9
Methanol	CH_3OH(l)	−57.0
Oxygen	O_2(g)	0
	O_2(aq)	−2.9
Potassium chloride	KCl(s)	−104.2
Pyruvic acid	$C_3H_3O_3$(s)	−114.1
Sodium chloride	NaCl(s)	−98.2
Sodium hidroxide	NaOH(s)	−102.0
Succinic acid	$C_4H_6O_4$(l)	−178.8
Sucrose	$C_{12}H24O_{12}$(s)	−371.6
Sulfuric acid	H_2SO_4(l)	−193.9
Water	H_2O(g)	−57.8
	H_2O(l)	−68.3

Adapted from Refs 14,79,80. (s), (l), (g), and (aq) refer to the thermodynamic state of compounds.

41.3.1.2 Inlet and Outlet Flows. The heat flow contributed by substances fed to or eliminated from the reactor, Q_{sen}, if no phase change occurs and if inlet and outlet flows are equal, is given as follows:

$$Q_{\text{sen}} = F_{\text{fd}} C_{\text{p}} (T_{\text{out}} - T_{\text{in}}) \quad (41.21)$$

where F_{fd} is flow rate, C_{p} the heat capacity of the stream, and T_{out} and T_{in} are the temperature of the outlet and inlet flows, respectively. Heat generation can also originate from the temperature difference between the gas and the culture broth. For instance, if gases are compressed adiabatically, their temperature can be higher than the liquid, particularly for cultures controlled at low temperatures (48). Accordingly, the sensible enthalpy gain by the gaseous stream is given as

$$Q_{\text{sen}_{\text{g}}} = F_{\text{g}} C_{\text{p}_{\text{g}}} \rho_{\text{g}} \left(T_{\text{g}} - T_{\text{b}}\right) \quad (41.22)$$

where T_{b} is the temperature of the culture broth, ρ_{g} is gas density, and the subindex g refers to the gas phase.

Other reactions occurring in the system simultaneously to cell growth, such as neutralization of buffers in culture media, also contribute to the energy balance (80). The enthalpies of neutralization of physiological buffers are shown in Table 41.6, which are usually exothermic in culture conditions (80).

41.3.1.3 Power Input by Agitation and Sparging. An important source of heat in a bioreactor is the power input from agitation and sparging. The power transferred to the reactor from sparging, P_g, can be calculated from the following equation (14,81):

$$P_{\text{g}} = \rho_{\text{g}} F_{\text{g}} \left[\frac{R T_{\text{b}}}{\text{MW}} \ln \frac{p_1}{p_2} + \alpha \frac{u_{\text{G}_{\text{o}}}^2}{2} \right] \quad (41.23)$$

TABLE 41.6. Enthalpies of Neutralization of Physiological Buffer Systems for the Reaction $A^- + H^+ \rightarrow AH$

Buffer System	T(°C)	$\Delta\ _bH_H+$ (kcal/mol) H^+	pk_a
Bicarbonate	25	−2 to −1.8	6.4
HCO_3/CO_2(aq)	37	−1.2	6.3
Carboxyl groups			
Succinate	25	−0.07	5.6
Citrate	25	+0.8	6.4
Phosphate	25	−1	6.9
$HPO_4^{2-}/H_2PO_4^-$	37	−0.86	pH 6.6

Adapted from Ref. 80.

where R is the gas constant, MW is the gas molecular weight, p_1 is pressure at the sparger, p_2 is pressure at the top of the vessel, α is the fraction of gas kinetic energy transferred to the liquid (typically 0.06) and u_{G_o} is the gas velocity at the sparger orifice. For well-designed spargers, the term $\alpha\frac{u_{G_o}^2}{2}$, which represents the jet kinetic energy developed at the sparger holes, is small and can be neglected (14). Equation 41.23 can be used to calculate power dissipation due to sparging into stirred tanks, bubble columns, and airlift bioreactors. Notice that, Equation 41.23, neglecting the jet kinetic energy at the sparger holes, corresponds to the term of energy dissipation rate from aeration of Equation 41.2. This is obtained by substituting in Equation 41.23 the molar gas flow rate and pressure difference between the sparger and top of the vessel, given by Equations 41.24 and 41.25, respectively:

$$\dot{n} = \frac{F_g\,(p_1 - p_2)}{\ln\left(\frac{p_1}{p_2}\right) RT_b} \tag{41.24}$$

$$(p_1 - p_2) = \rho_g H \tag{41.25}$$

where $\dot{n}$ is the molar gas flow rate.

The power, P, transferred to a Newtonian fluid by agitation depends on the fluid density, viscosity, agitation speed, impeller type, impeller diameter, vessel diameter, liquid height, and other geometric characteristics and parameters of the system (18). Then, using dimensional analysis, the energy dissipated to the liquid by agitation is a function of

$$\frac{P}{\rho N^3 D^5} = fn\left\{\frac{\rho N D^2}{\mu_b}, \frac{N^2 D}{g}, \frac{T}{D}, \frac{W}{D}, \frac{H}{D}, \text{etc.}\right\} \tag{41.26}$$

where W is impeller width. P_0, Re, and Fr are the power, Reynolds, and Froude numbers, respectively, defined as

$$P_0 = \frac{P}{\rho N^3 D^5} \tag{41.27}$$

$$Re = \frac{\rho N D^2}{\mu_b} \tag{41.28}$$

$$Fr = \frac{N^2 D}{g} \tag{41.29}$$

Fr is important only if gross vortexing exists in the reactor. If vortexing is prevented by baffling or off-center stirring, then the power number will be only a function of Re and geometrical ratios (18). As shown in Fig. 41.11, this is true for the laminar flow regime ($Re < 3 \times 10^5$), where P_0 is related to Re through the proportionality constant, K_p, which only depends on the system geometry:

$$P_o = \frac{K_p}{Re} \tag{41.30}$$

In turbulent flow regime the power input is independent of Re. Figure 41.11 can be used to predict P_0 for various system geometries. For other geometries, P_0 must be determined experimentally. For vessels equipped with multiple

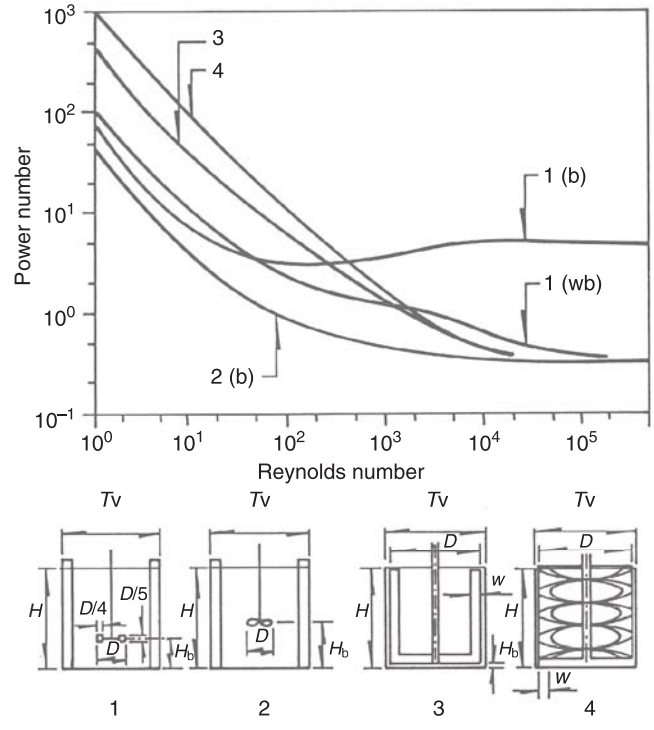


Figure 41.11. Power number as a function of Reynolds number. (1) Turbine stirrer, $T_v/D = 3.33$, $H_b/D = 1$, wb = without baffles, b = with baffles. (2) Marine propeller, angle 25°, $T_v/D = 3.33$, $H_b/D = 1.5$. (3) Anchor impeller, $T_v/D = 1.02$, $H_b/D = 0.01$, $W/D = 0.1$. (4) Helical ribbon impeller, $T_v/D = 1.02$, $H_b/D = 0.1$, $W/D = 0.1$. [Reprinted with permission from Ref. 48.]

impellers, the interaction between them is not significant if the distance between impellers exceeds their diameter (48). Power consumed will then be the addition of the power consumed by each impeller. Furthermore, if an agitated vessel is also aerated, then power input from agitation will decrease with respect to the unaerated case. van't Riet and Tramper (48) recommend the correlation by Hughmark for turbine stirrers in water for calculating aerated power inputs P_a:

$$\frac{P_a}{P} = 0.10\left(\frac{F_g}{NV}\right)^{-0.25}\left(\frac{N^2D^4}{gWV^{2/3}}\right)^{-0.20} \tag{41.31}$$

41.3.1.4 Evaporation. If the inlet gas is at a lower temperature than the bioreactor, heat loss due to evaporation can be significant. Furthermore, evaporation can contribute to substantial water loss in the fermenter, which has to be replaced or avoided through the use of effective condensers. As the gas temperature increases, the water content of saturated air increases. The latent heat of evaporation for water, λ, is 41 kJ/mol, and the heat loss due to evaporation can be calculated as (14)

$$Q_{evap} \approx \lambda F'_g(w_{out} - w_{in}) \tag{41.32}$$

where F'_g is dry air flow and w_{out} and w_{in} are the water contents of the inlet and outlet flows, respectively. Water contents can be calculated from psychrometric charts.

41.3.1.5 Heat Exchangers. Heat exchangers have to be included in vessels for controlling the culture temperature. Vessels can be jacketed, have internal or external coils, and even an external heat exchanger can be used. Jacketed vessels are used in low-scale reactors, but as scale increases, the heat transfer area per unit volume decreases, and internal or external coils may be required for efficient control of temperatures. As illustrated in the practical cases shown below, a jacket is more than enough for transferring the necessary heat in typical large-scale cell cultures. Furthermore, shear damage of cells in pumps and risk of contamination limit the use of external heat exchangers.

In order to maintain a constant culture temperature, the heat generated (or removed) by all the processes analyzed previously must equal the heat transferred by the exchanger. Heat transfer depends on the overall heat flow resistance, R', and the temperature gradient, ΔT, between the exchanger and the culture broth:

$$Q_{ex} = \frac{\Delta T}{R\prime} \tag{41.33}$$

Calculation of ΔT depends on the system geometry and on the direction of motion of the fluids. For heat transfer from jackets in agitated-tank reactors, ΔT is given by the log-mean temperature difference (LMTD):

$$\text{LMTD} = \frac{(T_i - T_o)}{\ln\left(\frac{T_b - T_o}{T_b - T_i}\right)} \tag{41.34}$$

where T_i and T_o are the temperatures of the coolant entering and leaving the reactor, respectively. T_b is constant if a perfectly mixed vessel is assumed. In turn, R' is defined as

$$R\prime = \frac{1}{UA} \tag{41.35}$$

where A is the area for heat transfer and U is the overall heat transfer coefficient. U depends on the nature of the material across which heat is transferred, the system geometry, and the nature of the fluid flows involved. As a rule of thumb, U for a clean vessel usually ranges between 280 and 1137 W/m^2 °C (13). However, a wider range exists for various practical situations (82). Lower values correspond to very viscous non-Newtonian fluids, while larger values correspond to nonviscous Newtonian fluids. The overall heat transfer resistance is the sum of the individual resistances in series in the path of heat transfer. Therefore, for the jacket of thin-walled vessels, where the area normal to the direction of heat transfer can be considered constant, U is given by the following expression:

$$\frac{1}{U} = \frac{1}{h_i} + \frac{t}{k_m} + \frac{1}{h_o} + \frac{1}{h_{f_i}} + \frac{1}{h_{f_o}} \tag{41.36}$$

where h_i and h_o are the broth and coolant side heat transfer coefficients, respectively; t is vessel wall thickness; k_m is the metal thermal conductivity; and h_{f_i} and h_{f_o} are the inside and outside fouling heat transfer coefficients, respectively. Fouling factors are caused by deposits (microbial film, scale, dirt, etc.), which depend on operating conditions and should be kept to a minimum by maintaining vessels and jackets or coils clean. Fouling resistances for various systems can be found elsewhere (82). Individual heat transfer coefficients depend on the fluid properties, geometric characteristics, and operation conditions of the system through complex relations. Thus, from a practical standpoint, individual heat transfer coefficients are obtained from empirical correlations, some provided by vessel vendors, relating the Nusselt number, Nu, with the Reynolds and Prandtl, Pr, numbers. For instance, h_i for stirred vessels can be determined as:

$$Nu = aRe^b Pr^c \left(\frac{\mu_b}{\mu_w}\right)^d \tag{41.37}$$

TABLE 41.7. Values of Constants in Equation 37 for Jacketed Vessels

Impeller	*a*	*b*	*c*	*d*	*Re*
Jacketed vessels					
Paddle	0.36	0.66	0.33	0.21	300 to 3×10^5
Pitched-blade turbine	0.53	0.66	0.33	0.24	80–200
Disk flat-blade turbine	0.54	0.66	0.33	0.14	40 to 3×10^5
Propeller	0.54	0.66	0.33	0.14	2×10^3
Anchor	1	0.5	0.33	0.18	10–300
Anchor	0.36	0.66	0.33	0.18	300–40,000
Helical ribbon	0.63	0.5	0.33	0.18	$8–10^5$
Helical coils					
Paddle	0.87	0.62	0.33	0.14	300 to 4×10^5

Adapted from Ref. 82.

where a, b, c, and d are constants (listed in Table 41.7 for various reactor configuration), μ_w is broth viscosity at the wall temperature, and Nu and Pr are defined as

$$Nu = \frac{h_i T_v}{k} \tag{41.38}$$

$$Pr = \frac{C_p \mu_b}{k} \tag{41.39}$$

where k is broth thermal conductivity. Equation 41.37 is acceptable for unaerated fluids; however, no correlations have been published for aerated conditions (13). Depending on stirring speed and flooding phenomena, aeration can improve or deteriorate h_i. Nonetheless, the influence of gassing is minor in relation to other variables (48).

Liquid circulation in bubble columns is determined by the gas flow rate, and, thus, h_i can be determined as (48)

$$h_i = 9391 \left(u_{G_s}\right)^{0.25} \left(\frac{\mu_{wt}}{\mu_b}\right)^{0.35} \tag{41.40}$$

where μ_{wt} is the water viscosity and μ_b is broth viscosity. Equation 41.40 is applicable for vessels with diameters ranging from 0.1 to 1 m and for broths viscosities between 10^{-3} and 5×10^{-2} N s/m^2.

The liquid velocity has to be known in order to perform heat transfer calculations in airlift bioreactors. This is rather complex and, as exemplified by van't Riet and Tramper (48), an average liquid velocity can be estimated only from numerical simulations. Alternatively, simplified correlations, such as the one shown in Equation 41.7, exist. However, liquid velocity gradients are present, and, thus, a single value for heat transfer cannot be given. Flow in the downcomer can be considered as a single phase. Thus, h_i can be determined from correlations of turbulent flow in pipes (48):

$$\frac{h_i T_d}{k} = 0.027 \left(\frac{\rho \overline{u_{L_d}} T_d}{\mu_b}\right)^{0.8} Pr^{0.33} \tag{41.41}$$

where $\overline{u_{L_d}}$ is average superficial liquid velocity in the downcomer and T_d is diameter of the downcomer. The flow regime in the riser can be described in the same manner as in a bubble column; that is, either homogeneous or heterogeneous flow (see previous section) (48). The flow regime is determined mainly by the total hydrodynamic resistance of the bioreactor. If the riser acts as a bubble column in the heterogeneous flow regime, Equation 41.40 can be used for calculating the heat transfer coefficient. For a "true" airlift flow (homogeneous flow), Equation 41.41 can be used.

For packed-bed reactors, the heat transfer coefficient between the inner container surface and the fluid stream can be calculated from the following correlation (82):

$$Nu = b_1 b T_v^{0.17} \left(\frac{T_p G}{\mu_b}\right)^{0.83} Pr \tag{41.42}$$

where T_p is particle diameter, G is superficial mass velocity, k and C_p are used to calculate Pr (refer to the liquid phase), b is a coefficient dependent on T_p/T_v (Fig. 41.12), and b_1 is equal to 1.22 (SI) or 1 (US customary).

Heat transfer coefficients for other heterogeneous systems, such as HFs and fluidized beds, have to be evaluated for each individual case, as the packing, liquid velocity, and the aspect ratio have to be considered. Various correlations for such systems can be found elsewhere (82). Finally, once all the terms of Equation 41.36 are known, the heat transferred by the exchanger can be calculated by combining

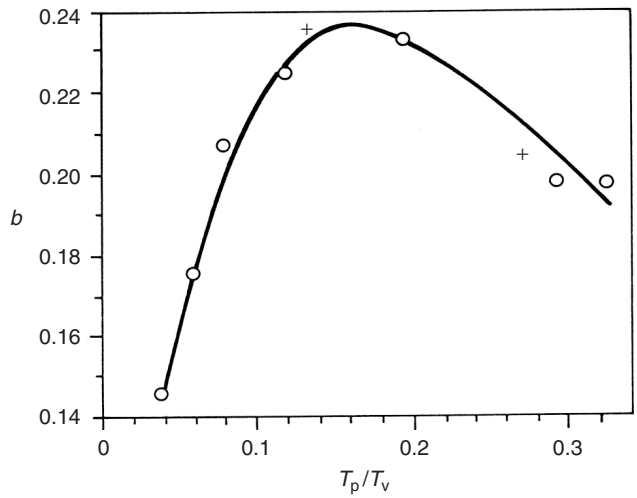


Figure 41.12. Coefficient b of Equation 41.42, T_p/T_v in inches per foot. [Reprinted with permission from Ref. 82.]

Equations 33, 34, and 35:

$$Q_{ex} = UA\left(\frac{T_i - T_o}{\ln\left[\frac{T_b - T_o}{T_b - T_i}\right]}\right) \tag{41.43}$$

and the cooling water flow rate, F_w, can be calculated from

$$F_w = \frac{Q_{ex}}{C_p\,(T_o - T_i)} \tag{41.44}$$

Many industrial operations still rely on simply multiplying the number of small-scale units (such as T-flasks or roller bottles) and placing them in contained suites. For such cases, a very different approach for solving heat transfer problems must be taken. These are usually solved through proper design of the HVAC (heating, ventilation, and air conditioning) systems. A "mega roll" industrial unit has been described by Panina (83). This unit has a capacity of 7200 roller bottles of 1 L in cylindrical wire racks. Racks are positioned in an incubator of 269.8 m^3 heated with electric heaters that generate 14 kW. Heat is uniformly distributed by forced air circulation and temperature is controlled by a heat exchanger fed with cold water.

41.3.2 Practical Cases

In order to assess the magnitude of the various heat flows, and thereby the importance of heat transfer in a cell culture process, heat balances for a hybridoma culture in a hypothetical 10,000-L water-jacketed stirred-tank reactor are presented. Comparison is made with a hypothetical baculovirus-infected insect cell culture in the same vessel. The behavior of the large-scale hybridoma culture is assumed to follow real kinetic data obtained from a 1-L agitated batch reactor under the experimental conditions described by Higareda *et al*. (84). Such an assumption is valid since the data at the 1-L scale, shown in Fig. 41.13, are very similar to data reported by Backer *et al*. (9) at the 1000-L scale. The calculations are performed for a hypothetical vessel, detailed in Table 41.8, which closely resembles the reactor used for CHO cell culture at Glaxo Wellcome and described by Nienow *et al*. (85).

Viable cell concentration and OUR are shown in Fig. 41.13a. The horizontal line represents the time of glutamine depletion that corresponds to the onset of respiration cessation and the end of exponential growth. A similar behavior has been described by Higareda *et al*. (84). Heat flow during the lag and exponential growth phases was calculated using 50 pW/cell, which corresponds to the highest heat flux reported for a mouse hybridoma (Table 41.4). By choosing such a high value, the calculated results should yield the worst case scenario in terms of heat generation. Guan *et al*. (67) showed

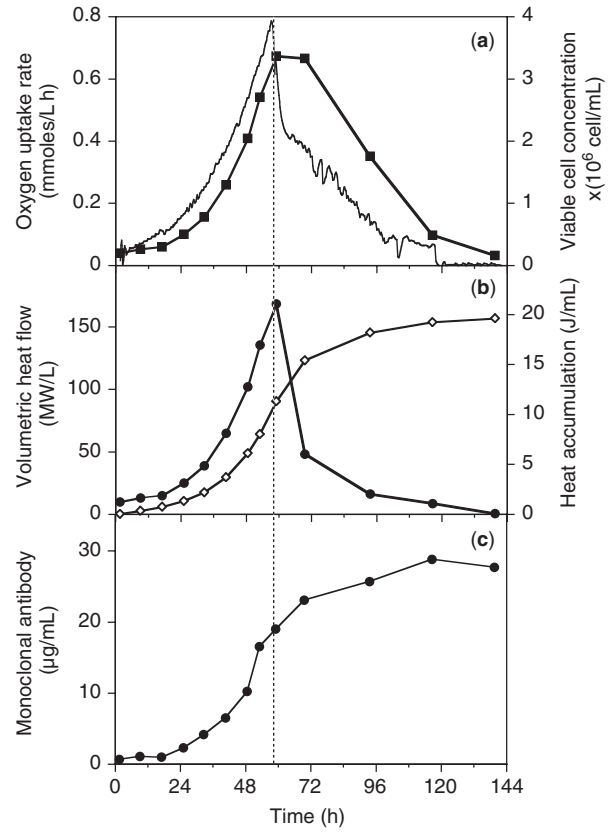


Figure 41.13. Kinetic data of a hybridoma batch culture in a 1-L stirred-tank reactor. (a) Oxygen uptake rate (–) and viable cell concentration (closed squares). (b) Heat flow (closed circles) and heat accumulation (open diamonds). (c) Monoclonal antibody. Dotted-line represents the time of Gln depletion.

that as metabolic activity of a culture decreases, the heat generated approaches the oxycaloric equivalent. Accordingly, during the stationary and death phases, the heat flow was calculated using the oxycaloric equivalent, 450 J/mmol O_2. The calculated profiles of volumetric heat flow and accumulated heat (integral of heat flow with time) are shown in Fig. 41.13b. It can be seen that volumetric heat flow and accumulated heat will have a maximum of 0.17 W/L and 20 J/mL. Thus, for the 10,000-L reactor (8000 L working volume), a maximum heat flow of 1.36 kW will be expected. In comparison, maximum heat flows of 7.4 W/L and 26 W/L have been reported for typical aerobic growth of yeast (at a relatively low maximum biomass concentration of 6.2 g/L) and unicellular protein production in a 2.3×10^6-L reactor, respectively (78). That is, heat generated from metabolism of the hypothetical hybridoma culture will be between 1 and 2 orders of magnitude lower than that for other microbial fermentations.

To satisfy the oxygen requirements of the culture shown in Fig. 41.13, OTR must equal OUR. In this example,

TABLE 41.8. Details of the Hypothetical 10,000-L Bioreactor

Working volume	8000 L
Aspect ratio	1.3
Liquid height	2.54 m
Tank diameter	2 m
Vessel wall thickness	6×10^{-3} m
Baffles	4
Turbine	1 Rushton
Turbine diameter	0.44 m
Distance of turbine from vessel bottom	2/9 T_v
Heat exchanger	Water jacket
Area of water jacket	12 m^2
Aeration	Superficial and submerged
Superficial gas velocity	2×10^{-4} m/s
Temperature	37°C
Dissolved oxygen concentration	20% wrt air saturation
Metal conductivity	80 W/m^2°C

Some values are based on Ref. 85.

maximum OUR was 0.8 mmol/L h. Thus, an oxygen transfer coefficient, k_La, of at least 5.47 h^{-1} is required. As determined by Nienow *et al*. (85), such a k_La can be obtained if 50 W/m^3 are supplied to the reactor by agitation and sparging. Total heat dissipated by the reactor would then be 1.76 kW. Interestingly, under such situations, 80% of the heat flux will originate from cellular metabolism, whereas only 23% from aeration and agitation. For a superficial gas velocity of 2×10^{-4} m/s (Table 41.8) and using Equations 41.23 or 41.2, the power supplied by sparging will be 1.96 W/m^3. Thus, 48.04 W/m^3 is needed for agitation. An impeller speed of 1.67 s^{-1} can be calculated from Equation 41.27 if a power number of 5 is assumed for the reactor (85). This results in a fully turbulent flow regime with a Reynolds number of 323,312 (assuming that culture broth behaves like water), but where shear damage is not expected. A broth side heat transfer coefficient of 1694 W/m^2°C can then be calculated using Equation 41.37. Finally, if no fouling layers in the tank or jacket are formed, and if the heat transfer coefficient on the coolant side is negligible, an overall heat transfer coefficient of 1503 W/m^2°C results from Equation 41.36 and data from Table 41.8 (vessel wall thickness and metal thermal conductivity). This value agrees with overall heat transfer coefficients of jacketed vessels using brine as coolant and water as fluid in vessel, which range from 230 to 2625 W/m^2°C (82).

In order to maintain the temperature of the reactor constant, heat generated from cellular metabolism, agitation, and sparging has to be removed by the water jacket, dissipating to the environment, and evaporation. Again, for the worst case scenario, maximum heat removal from the exchanger can be determined if heat losses to the environment and from evaporation are neglected. This is possible if the reactor is well insulated and a water saturated gas stream at the culture temperature is used for aeration. Accordingly, solving Equation 41.43 for a jacket area of 12 m^2 yields an LMTD of 0.09°C. Multiple combinations of inlet and outlet water temperatures below 37°C, but above 36°C, can satisfy the calculated LMTD. For instance, water entering the jacket at a temperature of 36°C and a flow rate of 22 L/min (Eq. 41.44) would be necessary for maintaining the culture temperature at 37°C. Interestingly, such a result indicates that for the hypothetical hybridoma culture, the heat transfer problem actually becomes a heating task, as jacket inlet water is required at a temperature above ambient.

A different situation will result for another model culture, for instance, protein production by the insect cell baculovirus expression vector system (69,86,87). An insect cell culture, typically maintained at 27°C, can reach a concentration of 8×10^6 cell/mL and an OUR of 17 mmol/L h during infection with a baculovirus. Using the oxycaloric equivalent, a heat flow from metabolic activity of 17.2 kW will result for the same hypothetical vessel described above, that is, about 13 times higher than that for the hybridoma culture. For comparison purposes, the same agitation and aeration rates used for the hybridoma culture are also used in this case. Since OUR is several-fold higher, it is assumed that OTR can be increased by oxygen enrichment, additional membrane aeration and/or pressure increase, or other means. It should be cautioned that for a real situation, the practical utility of such alternatives must be carefully evaluated. The fragile nature of insect cells also rules out the use of higher agitation and aeration rates. Accordingly, the total heat generated will be 17.6 kW. Following the same procedure as before, an LMTD of 0.98°C can be calculated. Such an LMTD could be satisfied, at least theoretically, for inlet water temperatures ranging from 6 to 26°C. Thus, more options exist than that for the hybridoma culture, for designing the heat transfer system. In conclusion, the cases illustrated show that jacketed vessels are more than enough to satisfy heat transfer requirements for cell culture at the typical largest scales performed to date. Moreover, compared to microbial systems or oxygen transfer requirements in cell culture, the heat transfer problem is not a major challenge, but cannot be overlooked.

41.3.3 Acknowledgment

Financial support by grant CONACYT 46408-Z and Conacyt-Salud 69911 is acknowledged. Technical assistance by R. Pastor.

NOMENCLATURE

A	area
A_d	downcomer cross-sectional area
a_j	stoichiometric coefficient of substrate j

A_p	area of microcarrier
A_r	riser cross-sectional area
b_i	stoichiometric coefficient of product i
c	dissolved oxygen concentration
c_m	dissolved oxygen concentration at saturation
c_0	inlet dissolved oxygen concentration
C_p	heat capacity
D	impeller diameter
d_b	bubble diameter
D_e	effective diffusion coefficient
$D_{o/w}$	diffusion coefficient of oxygen in water
F_g	gas flow rate
F'_g	dry gas flow rate
F_{fd}	flow rate (feed)
Fr	Froude number
F_w	cooling water flow rate
g	gravitational acceleration
G	superficial mass velocity
H	liquid height
H_b	height of stirrer above vessel bottom
H_d	downcomer height
h_{f_i}	inside fouling heat transfer coefficient
h_{f_o}	outside fouling heat transfer coefficient
h_i	broth side heat transfer coefficient
h_o	coolant side heat transfer coefficient
$H_{p,i}$	enthalpy of product i
H_r	riser height
$H_{s,j}$	enthalpy of substrate j
k	thermal conductivity
k_d	specific death rate constant
k_m	metal thermal conductivity
K_p	proportionality constant
LMTD	log-mean temperature difference
m	number of products
Mab	monoclonal antibody
MW	molecular weight
n	number of substrates
$\dot{n}$	molar gas flow rate
N	impeller speed
N^*	dimensionless mixing time
Nu	Nusselt number
OUR	oxygen uptake rate
P	power
p_1	pressure at the sparger
p_2	pressure at top of vessel
P_a	aerated power input
p_c	pressure in capillary
P_g	power transferred to liquid from sparging
P_o	power number
Pr	Prandtl number
q	specific production rate
Q_{acc}	heat accumulation rate
Q_{ag}	heat produced by agitation
Q_{evap}	heat removed by evaporation
Q_{ex}	heat transferred by the heat exchangers
Q_{met}	heat produced by metabolism
Q_{sen}	sensible enthalpy gain by flow streams
Q_{seng}	sensible enthalpy gain by gas stream
Q_{sp}	heat produced by sparging
R	gas constant
R'	resistance to heat flow
R	radius
r_0	radius at which oxygen concentration falls to zero
r_c	capillary radius
Re	Reynolds number
t	vessel wall thickness or time
T	temperature
T_b	broth temperature
t_c	circulation time
T_d	downcomer diameter
T_g	temperature of gas
T_i	jacket fluid inlet temperature
T_{in}	temperature of the inlet flow
t_M	mixing time
t_{mt}	time constant for mass transfer
T_o	jacket fluid outlet temperature
T_{out}	temperature of the outlet flow
T_p	diameter of particle
T_r	riser diameter
t_{rxn}	time constant for oxygen consumption
T_v	vessel diameter
U	overall heat transfer coefficient
$\overline{u_c}$	average axial velocity inside capillary
u_G	superficial gas velocity
u_{G_o}	gas velocity at the sparger orifice
u_{G_r}	superficial gas velocity in the riser
u_{G_s}	pressure corrected gas velocity
u_L	superficial liquid velocity
u_{Lr}	superficial liquid velocity in the riser
$\overline{u_{L_d}}$	average superficial liquid velocity in downcomer
V	liquid volume
V_k	killing volume

V_p	volume of a microcarrier
VVM	volume of air per volume of liquid per minute
W	width of impeller
w_{in}	water content of inlet gas stream
w_{out}	water content of outlet gas stream
X_t	total cell concentration
y	liquid depth
z	axial position
α	fraction of gas kinetic energy transferred to the liquid
Δp	pressure drop
ε	void fraction
ε_T	total energy dissipation rate
Φ	observable module
η	effectiveness factor
λ	latent heat of evaporation of water
μ	viscosity
μ_{app}	apparent viscosity
μ_b	broth viscosity
μ_w	broth viscosity at the wall temperature
μ_{wt}	water viscosity
ρ	liquid density
ρ_g	gas density

REFERENCES

1. Humphrey AE. Plant cells as chemical factories: control and recovery of valuable products. In: Galindo E, Ramírez OT, editors. Advances in bioprocess engineering. The Netherlands: Kluwer Academic Publishers; 1994. pp. 103–107.
2. Venkat K. Seeing and harnessing opportunities in natural products. International course on medicinal plants. Mexico, DF: Instituto Mexicano del Seguro Social; 1997.
3. Arathoon WR, Birch JR. Science 1986; 232: 1390–1395.
4. Handa-Corrigan A. Oxygenating animal cell cultures: the remaining problems. In: Spier RE, Griffiths JB, editors. Volume 4, Animal cell biotechnology. San Diego, CA: Academic Press; 1990. pp. 123–132.
5. Finter NB, Garland AJM, Telling RC. Large scale mammalian cell culture: a perspective. In: Lubiniecki AS, editor. Large scale mammalian cell culture technology. New York, NY: Marcel Dekker Inc; 1990. pp. 1–14.
6. Cartwright T. Production of tPA from animal cell culture. In: Spier RE, Griffiths JB, editors. Volume 5, Animal cell biotechnology. San Diego, CA: Academic Press; 1992. pp. 217–245.
7. Spier RE. Animal cell biotechnology in the 1990s: from models to morals. In: Spier RE, Griffiths JB, editors. Volume 5, Animal cell biotechnology. San Diego, CA: Academic Press; 1992. pp. 1–46.
8. Smith GL. Large-scale animal cell culture. In: Lydersen BK, D'Elia NA, Nelson KL, editors. Bioprocess engineering: systems, equipment and facilities. New York, NY: John Wiley and sons; 1994. pp. 69–84.
9. Backer MP, Metzger LS, Slaber PL, Nevitt KL, Boder GB. Biotechnol Bioeng 1988; 32: 993–1000.
10. Bödeker BGD, Newcomb R, Yuan P, Baufman A, Kesley W. Production of recombinant factor VIII from perfusion culture: I large scale fermentation. In: Spier RE, Griffiths JB, Berthold W, editors. Animal cell technology: products of today, prospects for tomorrow. Oxford, UK: Butterworth-Heinemann; 1994. pp. 580–583.
11. Schügerl K. Bioprocess Eng 1993; 9: 215.
12. Sweere APJ, Luyben KCAM, Kossen NWF. Enzyme Microb Technol 1987; 9: 386.
13. Charles M, Wilson J. Fermentor design. In: Lydersen BK, D'Elia NA, Nelson KL, editors. Bioprocess engineering: systems, equipment and facilities. New York, NY: John Wiley and Sons; 1994. pp. 3–68.
14. Atkinson B, Mavituna F. Biochemical engineering and biotechnology handbook. 2nd ed. New York, NY: Stockton Press; 1991. p 476–485.
15. Doran PM. Design of reactors for plant cells and organs. In: Fietcher A, ed. Volume 48, Advances in biochemical engineering/biotechnology. Berlin, Germany: Springer-Verlag; 1993. pp. 115–168.
16. Griffiths JB. Overview of cell culture systems and their scale-up. In: Spier RE, Griffiths JB, editors. Volume 3, Animal cell biotechnology. San Diego, CA: Academic Press; 1988. pp. 179–220.
17. Norwood KW, Metzner AB. AIChE J 1960; 6: 432.
18. Edwards MF. Mixing of low viscosity liquids in stirred tanks. In: Harnby N, Edwards MF, Nienow AW, editors. Mixing in the process industries. London, UK: Butherwoths; 1985. pp. 131–144.
19. Lara AR, Galindo E, Ramírez OT, Palomares LA. Mol Biotechnol 2006; 34: 355.
20. Langheinrich C, Nienow AW, Eddleston T, Stevenson NC, Emery AN, Clayton TM, Slater NKH. Trans IChemE 1998; 76: 107–116.
21. Ruszkowski S. A rational method for measuring blending performance and comparison of different impeller types. 8th European Conference of Mixing, IChemE Symposium Series 136; 1994. 283–292.
22. Cooke M, Middleton JC, Bush J. Mixing and mass transfer in filamentous fermentations. In: King R, editor. 2nd International conference on bioreactor fluid dynamics. New York, NY: Elsevier Applied Science; 1988. pp. 37–64.
23. Hristov H, Mann R, Lossev V, Vlaev SD, Seichter P. Trans IChemE part C 2001; 79: 232.
24. Amanullah A, Buckland BC, Nienow AW. Mixing in the fermentation and cell culture industries. In: Paul EL, Atiemo-Obeng VA, Kresta SM, editors. Handbook of industrial mixing: science and practice. Hoboken, NJ: John Wiley and Sons; 2004. pp. 1071–1170.
25. Amanullah A, McFarlene CM, Emery AN, Nienow AW. Biotechnol Bioeng 2001; 73: 390.
26. Onyeaka H, Nienow AW, Hewitt CJ. Biotechnol Bioeng 2003; 84: 474.
27. McDowell C, Papoutsakis ET, Borys MC. Animal cell culture: physiochemical effects of pH. In: Spier RE, editor. Volume

1, The encyclopedia of cell technology. New York, NY: John Wiley and Sons; 2000. pp. 63–70.
28. Garnier A, Voyer R, Tom R, Perret S, Jardin B. Cytotechnology 1996; 22: 53–63.
29. Gray DR, Chen S, Howarth W, Inlow D, Maiorella BL. Cytotechnology 1996; 22: 65–78.
30. Ozturk S. Cytotechnology 1996; 22: 3–6.
31. Castan A, Näsman A, Enfors SO. Enzyme Microb Technol 2002; 30: 847.
32. Mostafa SS, Gu X. Biotechnol Prog 2003; 19: 45–51.
33. Aunins JG, Bibila T, Buckland BC, Glazomitsky K, Gould S, Ranucci C, Robinson D, Seamans TC, Silberklang M. Fluid mechanical issues in industrial cell culture. Presented in Cell Culture Engineering IV; San Diego, CA; 1994 March 7–12.
34. Brown ME, Birch JR. The effect of ph on growth and productivity of cell lines producing monoclonal antibodies at large scale. Presented in Cell Culture Engineering V; San Diego, CA; 1996 January 28-February 2.
35. Nyberg G, Green K, Hashimura Y, Rathore AS. Biopharm Int 2008; 21: 56.
36. Morrow KJ. Biotechnol Annu Rev 2007; 13: 95.
37. Jain E, Kumar A. Biotechnol Adv 2008; 26: 46.
38. Ozturk SS. From concept to GMP implementation: large-scale stirred-tank disposable bioreactor. Presented at: Cell Culture Engineering XI; Australia; 2008.
39. Farid SS, Washbrook J, Titchener-Hooker NJ. Biotechnol Prog 2005; 21: 486.
40. Singh V. Cytotechnology 1999; 30: 149.
41. Fisher M. Bioproc Int 2006; 4:S28.
42. Mikola M, Seto J, Amanullah A. Bioprocess Biosyst Eng 2008. 30: 231–241.
43. Shuler ML, Kargi F. Bioprocess engineering. 2nd ed. Upper Saddle River, NJ: Prentice Hall; 2001.
44. Bello RA, Robinson CW, Moo-Young M. Can J Chem Eng 1984; 62: 573–577.
45. Popovic M, Robinson CW. Biotechnol Bioeng 1988; 32: 301–312.
46. Tanaka H. Process Biochem 1987; 22: 106–113.
47. Rousseau I, Bu'Lock JD. Biotechnol Lett 1980; 2: 475–480.
48. van't Riet K, Tramper, J. Basic bioreactor design. New York: Marcel Dekker; 1991.
49. Tramper J, Smit D, Straatman J, Vlak JM. Bioprocess Eng 1988; 3: 37–41.
50. Meier SJ, Hatton TA, Wang DIC. Biotechnol Bioeng 1999; 62: 468.
51. Spier RE. Monolayer growth systems: heterogeneous unit processes. In: Spier RE, Griffiths JB, editors. Volume 1, Animal cell biotechnology. London, UK: Academic Press; 1985. pp. 243–263.
52. Murdin AD, Kirkby NF, Wilson R, Spier RE. Immobilized hybridomas: oxygen diffusion. In: Speir RE, Griffiths JB, editors. Volume 3, Animal cell biotechnology. San Diego, CA: Academic Press; 1988. pp. 55–74.
53. Tharakan JP, Chau PC. Biotechnol Bioeng 1986; 28: 1064–1071.
54. Dandavati MS, Doshi MR, Gill WN. Chem Eng Sci 1975; 30: 877–886.
55. Griffiths B. Perfusion systems for cell cultivation. In: Lubiniecki AS, editor. Large-scale mammalian cell culture technology. New York, NY: Marcel Dekker; 1990. pp. 217–250.
56. Schonherr OT, Van Gelder PJTA. Culture of animal cells in hollow-fibre dialysis systems. In: Speir RE, Griffiths JB, editors. Volume 3, Animal Cell Biotechnology. San Diego, CA: Academic Press; 1988. pp. 337–355.
57. Hammer BE, Heath CA, Mirer SD, Belfort G. Bio/Technol 1990; 8: 327.
58. Griffiths B. Advances in animal cell immobilization technology. In: Speir RE, Griffiths JB, editors. Volume 4, Animal cell biotechnology. San Diego, CA: Academic Press; 1990. pp. 149–166.
59. Smith JM. Chemical engineering kinetics. 3rd ed. New York, NY: McGraw-Hill; 1981.
60. Bird RB, Stewart WE, Lightfoot EN. Transport phenomena. New York, NY: John Wiley and Sons; 1960. pp. 180–207.
61. Bailey JE, Ollis DF. Biochemical engineering fundamental. 2nd ed. New York, NY: Mc Graw-Hill; 1986. pp. 208–214.
62. Kurano N, Leist C, Messi F, Kurano S, Fietcher A. J Biotechnol 1990; 15: 101–112.
63. Chuppa S, Tsai Y, Yoon S, Shacklefor S, Rozales C, Bhat R, Tsay G, Matanguihan C, Konstantinov K, Naveh D. Biotechnol Bioeng 1997; 55: 328–338.
64. Fiorino AS, Diehl AM, Lin HZ, Lemishchka IR, Reid LM. In Vitro Cell Dev Biol Anim 1998; 34: 247–258.
65. David-Pfeuty T, Nouvian-Dooghe Y. Oncogene 1992; 7: 1611–1623.
66. Sureshkumar GK, Mutharasan R. Biotechnol Bioeng 1992; 37: 292–295.
67. Guan Y, Evans PT, Kemp RB. Biotechnol Bioeng 1998; 58: 464–477.
68. Bloemkolk JW, Gray MR, Merchant F, Mosmann TR. Biotechnol Bioeng 1992; 40: 427–431.
69. Palomares LA, Ramírez OT. Insect cell culture: recent advances, bioengineering challenges and implications in protein production. In: Galindo E, Ramírez OT, editors. Advances in bioprocess engineering II. The Netherlands: Kluwer Academic Publishers; 1998. pp. 25–52.
70. Bailey CM, Nicholson H. Biotechnol Bioeng 1990; 35: 252–259.
71. Zhong JJ, Yoshida T. J Ferment Bioeng 1993; 76: 530–531.
72. Hosono H, Uemura I, Takumi T, Nagamune T, Yasuda T, Kishimoto M, Nagashima H, Shimomura N, Natori M, Endo I. J Ferment Bioeng 1994; 78: 235–240.
73. Fernandez RD, Yoshimizu M, Kimura T, Ezura Y. J Aquat Anim Health 1993; 5: 137–147.
74. Druoin H, Ritter JB, Gorenflo VM, Bowen BD, Piret JM. Biotechnol Prog 2007; 23: 1473.
75. Caspeta L, Flores N, Pérez NO, Bolívar F, OT Ramírez. Biotechnol Bioeng 2009; 102: 468–482.
76. Yamamori T, Yura T. J Bacteriol 1980; 142: 843.
77. Kemp RB, Guan Y. Thermochim Acta 1997; 300: 199–211.
78. von Stockar U, Marison IW. Thermochim Acta 1991; 193: 215–242.
79. Castellan GW. Physical chemistry. Reading, MA: Adison-Wesley; 1971.

80. von Stockar U, Gustafsson L, Larsson C, Marison I, Tissot P, Gnaiger E. Biochim Biophys Acta 1993; 1183: 221–240.
81. Tatterson GB. Fluid mixing and gas dispersion in agitated tanks. New York, NY: Mc Graw Hill; 1991. pp. 302–304.
82. Knudsen JG, Bell KJ, Holt AD, Hottel HC, Sarofim AF, Standiford FC, Stuhlbarg D, Uhl VW. Heat transmission. In: Perry RH, Green D, editors. Perry's chemical engineer's handbook. Volume 184, New York, NY: McGraw Hill; 1984. pp. 10-1–10-68.
83. Panina GF. Monolayer growth systems: multiple processes. In: Spier RE, Griffiths JB, editors. Volume 1, Animal cell biotechnology. San Diego, CA: Academic Press; 1985. pp. 211–242.
84. Higareda AE, Possani LD, Ramírez OT. Biotechnol Bioeng 1997; 56: 555–563.
85. Nienow AW, Langheinrich C, Stevenson NC, Emery AN, Clayton TM, Slater NKH. Cytotechnology 1996; 22: 87–94.
86. Palomares LA, Ramírez OT. Cytotechnology 1996; 22: 225–237.
87. Palomares LA, Estrada-Mondaca S, Ramírez OT. Principles and applications of the insect-cell-baculovirus expression vector system. In: Ozturk S, Hu WS, editors. Cell culture technology for pharmaceutical and cellular applications. New York, NY: Taylor and Francis; 2006. pp. 627–692.

42

BIOREACTORS: AIRLIFT REACTORS

J.C. Merchuk
Ben-Gurion University of the Negev, Beer-Sheva, Israel
F. Garcia Camacho
Universidad de Almeria, Almeria, Spain

42.1 INTRODUCTION

42.1.1 Airlift Reactors

An airlift reactor (ALR) is a gas–liquid or gas–liquid–solid pneumatic contacting device that is characterized by fluid circulation in a defined cyclic pattern through channels built specifically for this purpose. In ALRs, the content is pneumatically agitated by a stream of air or by other gases. In these cases, the name *gas lift reactors* has been used. In addition to agitation, the gas stream has the important function of facilitating exchange of material between the gas phase and the medium; oxygen is usually transferred to the liquid, and in some cases, reaction products are removed through exchange with the gas phase.

The main difference between ALRs and bubble columns (BCs, also pneumatically agitated) lies in the type of fluid flow, which depends not only on the gas input but also on the geometry of the system. The BC is a simple vessel into which gas is injected, usually at the bottom, and random mixing is produced by the ascending bubbles. In the ALR, the major patterns of fluid circulation are determined by the design of the reactor, which has a channel for gas–liquid upflow—*the riser*—and a separate channel for the downflow (Fig. 42.1). The two channels are linked at the bottom and at the top to form a closed loop. The gas is usually injected near the bottom of the riser. The extent to which the gas disengages at the top, in the section termed the *gas separator*, is determined by the design of this section and by the operating conditions. The fraction of the gas that does not disengage, but is instead entrapped by the descending liquid and taken into the downcomer, has a significant influence on the fluid dynamics in the reactor and hence on the overall reactor performance.

42.1.2 Reactor Morphology

ALRs can be divided into two main types on the basis of their structure (Fig. 42.1): (i) external loop vessels, in which circulation takes place through separate and distinct conduits, and (ii) baffled (or internal loop) vessels, in which baffles placed strategically in a single vessel create the channels required for the circulation. All ALRs comprise four distinct sections with different flow characteristics:

1. *Riser:* The gas is injected at the bottom of this section, and the flow of gas and liquid is predominantly upward.
2. *Downcomer:* This section, which is parallel to the riser, is connected to the riser at the bottom and at the top. The flow of gas and liquid is predominantly downward. The driving force for recirculation is the difference in mean fluid density between the downcomer and the riser; this difference generates the pressure gradient necessary for liquid recirculation.
3. *Gas separator:* This section at the top of the reactor connects the riser to the downcomer, facilitating liquid recirculation and gas disengagement. Designs that allow for a gas residence time in the separator

Upstream Industrial Biotechnology: Equipment, Process Design, Sensing, Control, and cGMP Operations, Volume 2, First Edition. Edited by Michael C. Flickinger.
© 2013 John Wiley & Sons, Inc. Published 2013 by John Wiley & Sons, Inc.

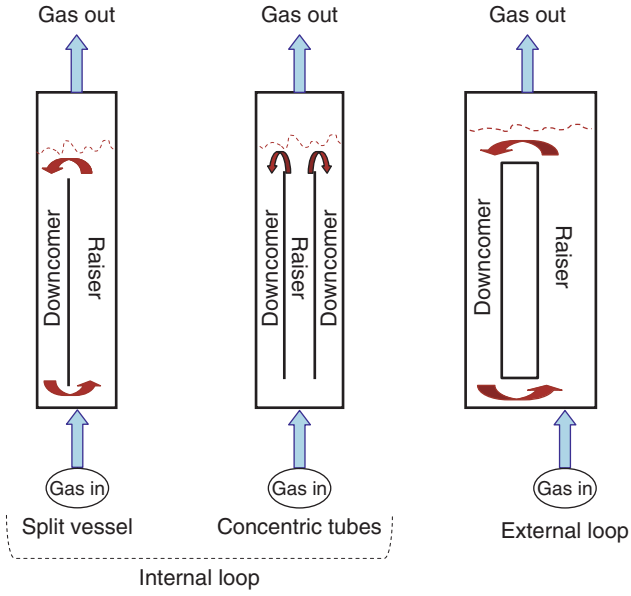


Figure 42.1. Different configurations of ALRs. In all cases clearly directional circulation of the liquid results from the gas input to the system.

that is substantially longer than the time required for the bubbles to disengage will minimize the fraction of gas recirculating through the downcomer (1,2).

4. *Base:* In the vast majority of airlift designs, the bottom connection zone between the riser and downcomer is very simple. The design of this section may sometimes influence gas holdup, liquid velocity, and solid phase flow (3,4).

Momentum, mass transfer, and heat transfer will be different in each section, but the design of each section may influence the performance and characteristics of each of the other sections, because the four regions are interconnected.

42.1.3 Advantages

ALRs are superior to traditional stirred-tank fermenters (STRs) for many processes based on biomass growth, despite the fact that the conventional fermenters provide the major requirements for culturing microorganisms: large gas–medium interface for the supply of oxygen and the removal of waste gases; good agitation to ensure proper nutrient distribution and to minimize damage, resulting from local addition of concentrated acid or base (for pH control); means of heat transfer (for temperature control); and a contamination-free environment. The reason for the more successful growth reported in ALRs (5–14) appears to lie in the difference in the fluid dynamics of ALRs and STRs. In conventional STRs, the energy required for the movement of the fluids is introduced focally at a single point in the reactor, via a stirrer. Energy dissipation is very high in the immediate surroundings of the stirrer and decreases away from it toward the walls. Similarly, shear will be greatest near the stirrer (15,16), because the momentum is transferred directly to the fluid in that region (17), which, in turn, transfers this energy to the slower moving, more distant elements of the fluid. This results in a wide variation of shear forces; for example, the maximum shear gradient in a STR with a flat-blade turbine has been reported to be approximately 14 times the mean shear gradient (18). An even more dramatic difference is found following the calculation methods recommended by Henzler (19), leading to a ratio of the maximum and mean energy dissipation rate in a stirred reactor of the order of 30 for standard operation conditions.

Cells in culture may thus be exposed to very different environments in a mechanically stirred vessel, either to minimal shear forces that may generate potentially undesirable gradients in temperature and in substrate, metabolite, and electrolyte concentrations. Alternatively, cells will be exposed to highly turbulent zones, with no problems of heat or mass transfer, but with very high shear gradients that may endanger cell integrity or exert some influence on cell morphology and metabolism (17). Changes in the morphology of microorganisms associated with high shear forces in the medium have frequently been observed (20–22). In the case of plant cell cultures, it has been shown that high shear conditions may also lead to changes in the production rate and yield of secondary metabolites (23,24). The nature of the relationship between such morphological changes and the rates of growth and metabolite production is still not properly understood, although it may be of great importance in the design and scale-up of bioreactors.

In ALRs, as in BCs, the gas is injected at a single point, but in ALRs, the direct contribution of gas injection to the dynamics of the system is small; circulation of liquid and gas is facilitated by the difference in gas holdup between the riser and the downcomer, which creates a pressure difference at the bottom of the equipment.

$$\Delta P_b = \rho_L g h(\varphi_r - \varphi_d) \tag{42.1}$$

where ΔP_b is the pressure difference, ρ_L is the density of the liquid (the density of the gas being considered negligible), g is the gravitation constant, and ϕ_r and ϕ_d are the fractional gas holdup of the riser and downcomer, respectively. This pressure difference forces the fluid from the bottom of the downcomer toward the riser, generating the circulation in the ALR. As ϕ_r and ϕ_d are both average values, integrated along the height of the reactor, it follows that no focal points of energy input exist and shear distribution is homogeneous throughout the ALR. This creates a relatively constant environment, minimizing sharp changes in the mechanical forces acting on suspended cells. One of

the most critical points is the bottom, where a sharp 180° turn takes place (3,25).

It has been reported (26) that the driving force in Equation 42.1 is important only for lower values of gas flow rate, because at higher values, the circulation velocity is governed by friction in the reactor vessel. While this is essentially true, and frictional loss control that may be found in small ALRs used in laboratory trials and especially in draught tubes devices with small gaps in the annulus, the usual range of operation of medium and large-scale ALR in bioprocesses assures that ΔP_b indeed controls the circulation in the system.

Shear-sensitive mammalian and plant cells in culture should benefit from ALRs as bioreactors for these cells need to minimize shear-related damage (17–19,24–39). Mammalian and plant cells in culture are more susceptible than microorganisms to the flow conditions in the reactor. Dinoflagellata are another example of cells extremely sensitive to shear damage (27–29). Mammalian cells, which lack the rigid cell wall of microorganisms, have a larger size than microorganisms and are very sensitive to mechanical stress. Plant cells have a rigid cellulose wall, but they are also much larger than microorganisms (usually by about an order of magnitude) and are therefore also sensitive to reactor conditions. Kolmogoroff's model of isotropic turbulence (30) indicates that serious damage may occur at relatively large values of the length scale. The last length is a parameter of the model and indicates the size of the eddy where energy starts to be dissipated by viscous resistance. It has been observed that plant cells, in spite of their rigid wall, are shear sensitive, and growth problems have been found in stirred-tank cultures, especially in large-scale systems. Although high agitation rates may be detrimental to cell growth, low agitation rates lead to an increase in the number and size of cell aggregates—also an undesirable phenomenon. The aggregates are formed as a result of daughter cells failing to separate after division and as a consequence of the stickiness of the polysaccharides excreted by the cells, especially at the end of the growth phase. An optimal shear rate between these two extremes must be found for each culture.

It has been shown experimentally that velocity fluctuations related to turbulent shear are relatively homogeneously distributed in an ALR (31–34). Measurements of fluctuating velocity made show that the liquid turbulence in ALRs is homogeneously distributed in both the riser and the downcomer (31). It thus seems reasonable to assume that the homogeneity of the stress forces is the main advantage offered by ALRs and that this homogeneity is responsible for the success of shear-sensitive cultures in the ALR type of fermenter (5,14,35–40). Another advantage of the ALR is the mechanical simplicity of the device. The absence of a shaft and of the associated sealing, which is always a weak element from the point of view of sterility, confers on the ALR an obvious advantage over agitated tanks. This consideration is especially important in processes involving slow-growing cultures, such as animal and plant cells, for which the risk of contamination is large.

ALRs may also be used for processes involving low value products, in which case efficiency of energy use may well become the key point for design, as in wastewater treatment (41). The superiority of ALRs over mechanically agitated contactors in terms of mass transfer rates for a given energy input has been demonstrated (42). Comparison of the efficiency of oxygen transfer, that is, the mass of oxygen absorbed per unit energy invested and unit time, showed that the efficiency of the ALR is among the highest in agitated systems (41). The ALRs are particularly suited to processes with changing oxygen requirements because aeration efficiency and performance are relatively insensitive to changes in operating conditions. Performance decreases markedly in mechanically stirred systems as the energy input [or oxygen transfer rate (OTR)] increases, but it is quite constant in ALRs (43). The introduction of mechanical agitation in an ALR increases, as expected, the rate of oxygen absorption from the gas, but leads to a decrease in the efficiency of mass transfer (44,45).

The efficiency of ALRs decreases only slowly as the energy input per unit volume of reactor is increased as shown in Fig. 42.2, for a split vessel airlift reactor (SV-ALR) of rectangular section with different configurations in the gas separation section. In contrast, the mass transfer rate can be easily enhanced in STR by increasing the power input, but this improvement is achieved at the expense of a considerable decrease in the efficiency of oxygen transfer. This decrease may constitute a crucial disadvantage in a bioprocess such as wastewater treatment, where the energy input is an important element in the cost, and flexibility of operating conditions is required because of changing feed composition and flow rate.

Energy economy in the ALR may be improved by placing a second sparger in the upper part of the downcomer (1,41). If the liquid velocity is greater than the free-rising velocity of the bubbles generated, the gas is carried down, resulting in a longer contact time between the bubble and the liquid. This diminishes the energy requirements, because part of the gas is injected against a lower hydrostatic pressure This principle has been used in processes developed for CO_2 removal from flue gas (46,47).

The advantages described earlier counterbalance the obvious disadvantage of ALRs, which is the requirement for a minimum liquid volume for proper operation. Indeed, the changes in liquid volume in these reactors are limited to the region of the gas separator, because the liquid height must always be sufficient to allow liquid recirculation in

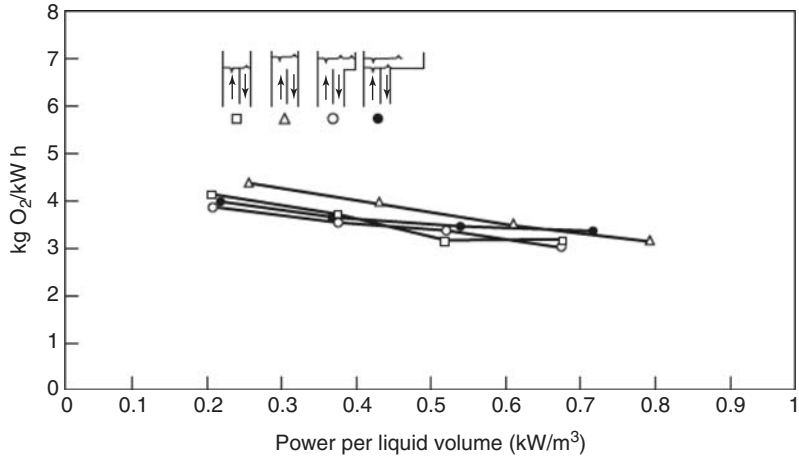


Figure 42.2. Aeration efficiency as a function of pneumatic power of gas input per unit volume in a straight baffle ALR. The level indicated corresponds to no-aeration conditions. Adapted from Ref. 41.

the reactor and must therefore be above the separation between the riser and the downcomer.

42.2 FLUID DYNAMICS

The interconnections between the design variables, the operating variables, and the observable hydrodynamic variables in an ALR are presented diagrammatically in Fig. 42.3 (48). The design variables are the reactor height, the riser-to-downcomer area ratio, the geometrical design of the gas separator, and the bottom clearance [in draft tube airlift reactor (DT-ALR) C_b is the distance between the bottom of the reactor and the lower end of the draft tube. In general, it is the free area for flow in the bottom, and accounts for the resistance to flow in this part of the reactor]. The main operating variables are primarily the gas input rate and the top clearance (C_t, the distance between the upper part of the draft tube and the surface of the nonaerated liquid). These two independent variables set the conditions that determine the liquid velocity in the ALR via the mutual influences of pressure drops and holdups (Fig. 42.3) (48). Viscosity is not shown in the figure as an independent variable because in the case of gas–liquid mixtures, it is a function of the gas holdup (and of liquid velocity in the case of non-Newtonian liquids), and because in a real process, it will change with time due the changes in the composition of the liquid.

42.2.1 Flow Configuration

42.2.1.1 Riser. In the riser, the gas and the liquid flow upward, and the gas velocity is usually larger than that of the liquid. The only exception is homogeneous flow, in which case both phases rise at the same velocity. This can happen only with very small bubbles, in which case the free-rising velocity of the bubbles is negligible with respect to the liquid velocity. Although about a dozen different gas–liquid flow configurations have been described (49), only two of them are of interest in ALRs (50):

1. homogeneous bubbly flow regime, in which the bubbles are relatively small and uniform in diameter and turbulence is low
2. churn-turbulent regime, in which a wide range of bubble sizes coexist within a very turbulent liquid.

The churn-turbulent regime can be reached from homogeneous bubbly flow by increasing the gas flow rate or by starting from slug-flow and increasing the liquid turbulence, by increasing either the flow rate or the diameter of the reactor (Fig. 42.4) (51). The slug-flow is to be avoided because large bubbles offer very poor capacity for mass transfer. In small diameter tubes (<0.1-m diameter) slugs may bridge the entire cross section.

Comparison of flow configurations described for BCs to those appearing in ALR shows that the transitions due to increases in the gas superficial velocity are delayed in the ALR till higher gas flow rates, due to the high circulation velocity and its directionality (53,54). Figure 42.5 shows graphically such a comparison of the flow configuration transitions in a stirred tank, an ALR, and a BC. In the case of the ALR, the configurations in the downcomer are indicated (55).

42.2.1.2 Downcomer. In the downcomer, the liquid flows downward and may carry bubbles down with it. For bubbles to be entrapped and flow downward, the liquid velocity must be greater than the free-rise velocity of the bubbles.

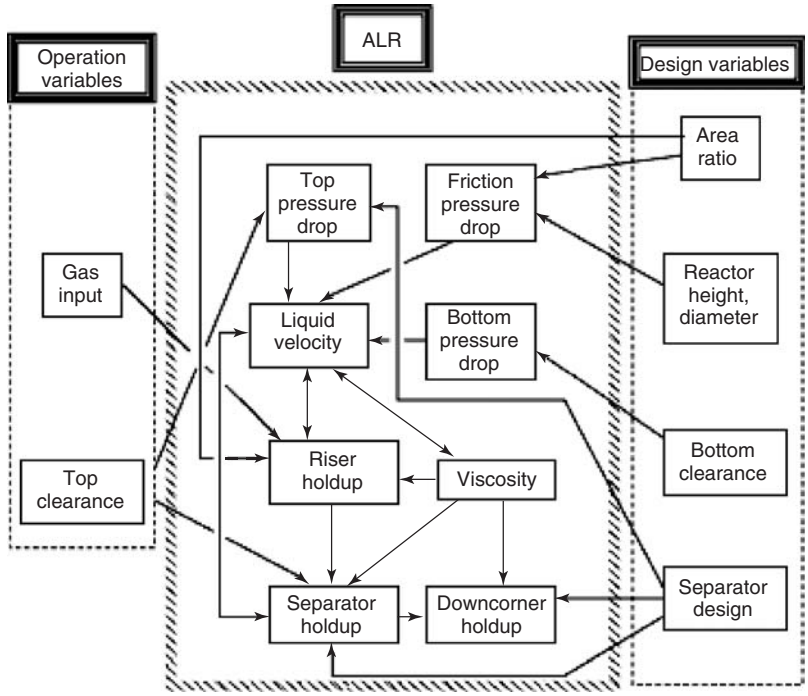


Figure 42.3. Interaction between design and operation variables in an ALR. Adapted from Ref. 48.

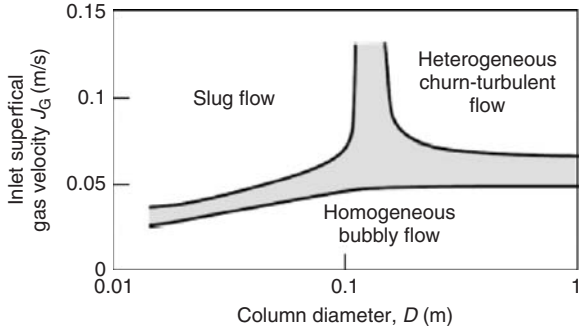


Figure 42.4. Map of flow configurations for gas–liquid concurrent flow in a vertical tube, as a function of the superficial gas velocity, J_G and the diameter of the tube D adapted from Ref. 52, with permission.

At very low gas flow input, the liquid superficial velocity is low, practically all the bubbles disengage, and clear liquid circulates in the downcomer. As the gas input and concomitantly the gas holdup in the riser increase, the liquid velocity becomes sufficiently high to entrap the smallest bubbles. On further increase in liquid velocity, larger bubbles are also entrapped. Under these conditions, the presence of bubbles reduces the cross section available for liquid flow, and the liquid velocity increases in this section. Bubbles are thus entrapped and carried downward, until the number of bubbles in the cross section decreases, the liquid velocity diminishes, and the drag forces are not sufficient to overcome the buoyancy. This feedback loop in the downcomer causes stratification of the bubbles, which is evident as a front of static bubbles, from which smaller bubbles occasionally escape downward and larger bubbles, produced by coalescence, escape upward. The bubble front descends, as the gas input to the system is increased, until the bubbles eventually reach the bottom and recirculate to the riser. When this point is reached, the bubble distribution in the downcomer becomes much more uniform. This is the most desirable flow configuration in the downcomer, unless a single pass of gas is required. The correct choice of cross-sectional area ratio of the riser to the downcomer will determine the type of flow.

The operation of a reactor under the condition of stratified static bubbles in the downcomer described earlier has attracted the attention of researchers (55–57), because it allows the detailed observation of a rising (and, nevertheless, static to the observer's eye) bubble or swarm of bubbles. The practical use of this flow configuration in an actual industrial setting is, however, doubtful. The static bubbles become very soon depleted of, or saturated with, the component that is being transferred and become an inert volume. In general, the only interest in this flow configuration are the limits of operation conditions (55,58) that lead to a situation that is to be avoided.

42.2.1.3 Gas Separator. The gas separator is often overlooked in descriptions of experimental ALR devices, although it has considerable influence on the fluid dynamics of the reactors. The geometric design of the gas separator will determine the extent of disengagement

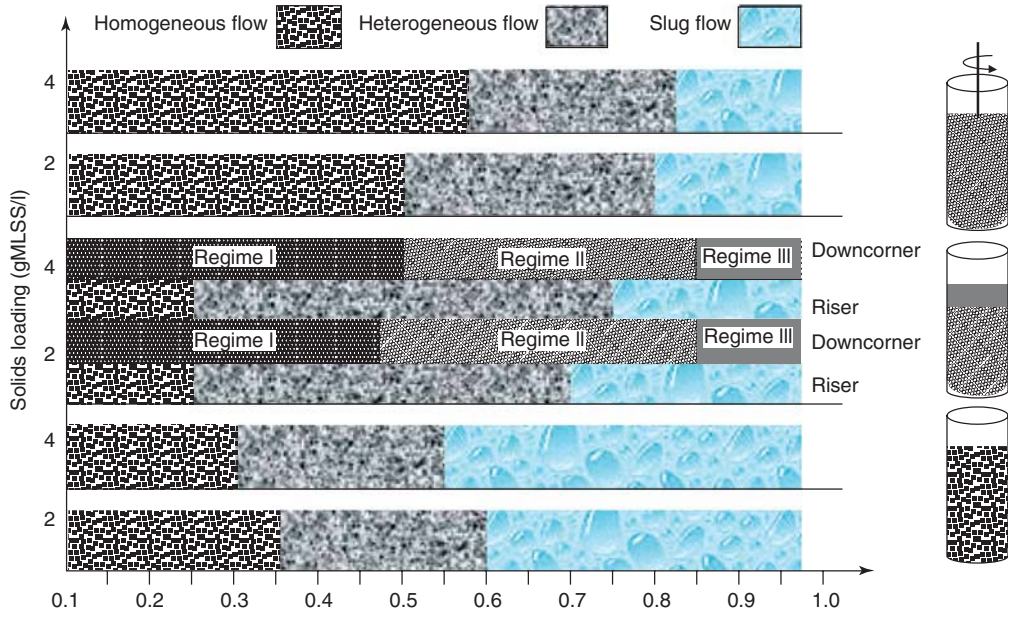


Figure 42.5. Comparison of flow configuration transitions in a stirred vessel, an ALR, and a BC. From Ref. 54, with permission.

of the bubbles entering from the riser (17,59,60). In the case of complete disengagement, clear liquid will be the only phase entering the downcomer. In the general case, a certain fraction of the gas will be entrapped and recirculated. It is quite common to enlarge the separator section to reduce the liquid velocity and to facilitate better disengagement of spent bubbles. Experiments have been reported in which the liquid level in the gas separator was high enough to be represented as two mixed vessels in series (51,61). Fresh gas may also be entrapped from the headspace if the fluid is very turbulent near the interface. This entrapment may influence gas holdup and liquid velocity in the whole reactor.

42.2.2 Gas Holdup

Gas holdup is the volumetric fraction of the gas in the total volume of a gas–liquid–solid dispersion:

$$\varphi_i = \left(\frac{V_G}{V_G + V_L + V_S} \right)_i \qquad (42.2)$$

where the subindexes L, G, and S indicate liquid, gas, and solid, and i indicates the region in which the holdup is considered, that is, the gas separator (s) the riser (r), the downcomer (d), or the total reactor (T).

The importance of the holdup is twofold: (i) the value of the holdup gives an indication of the potential for mass transfer, because for a given system, a larger gas holdup indicates a larger gas–liquid interfacial area, and (ii) the difference in holdup between the riser and the downcomer generates the driving force for liquid circulation (strictly true for gas–liquid systems: if other dispersed phases are present as well their holdup differences will count as well, but the gas will always be the main factor). It should be stressed, however, that when referring to gas holdup as the driving force for liquid circulation, only the total volume of the gas is relevant. This is not the case for mass transfer phenomena. In this case, the interfacial area is of paramount importance, and therefore, some information on bubble size distribution is required for a complete understanding of the process.

Gas holdup values will vary within a reactor. Average values, referring to the whole volume of the reactor, and more frequently to one of its zones (defined in Fig. 42.1) such as the riser or the downcomer are usually reported. These types of data are most valuable because they provide a basis for determining liquid velocity and mixing. While total holdup in a reactor is measured quite accurately from the change in height of the gas–liquid dispersion with and without gas injection, the measurement of local gas holdups requires more sophisticated methods. The measurement of pressures along the tube is the most common technique and assumes that the hydrostatic pressure is dominant. If the frictional losses are considerable, they should be taken into account (62), or more sophisticated methods should be used, as electrodes that measure the gas content in a small volume of the liquid (63–67).

The geometric design of the ALR has a significant influence on the gas holdup. Changes in the ratio A_d/A_r, the cross-sectional areas of the downcomer and the riser, respectively, and in the bottom clearance will change the

liquid and gas residence time in each part of the reactor and hence their contributions to the overall holdup.

42.2.2.1 Internal Loop ALRs. The factors that influence the performance of ALRs (Fig. 42.3) would be expected to be present in any expression representing or correlating gas holdup, liquid velocity, or mass transfer data. However, usually only some of those variables are considered in the form:

$$\varphi_r = a(J_G)^{\alpha}\left(\frac{A_d}{A_r}\right)^{\beta}(\mu_{ap})^{\gamma} \qquad (42.3)$$

where J_G is the superficial gas velocity (gas volumetric flow rate per unit of cross-sectional area), μ_{ap} is the effective viscosity of the liquid, and $\alpha\beta\gamma$ and a are constants that depend on the geometry of the reactor and the properties of the liquid. This expression has been justified by fundamental fluid dynamic considerations (68) and can be used to predict the holdup in a system that is being designed or simulated as a function of the operating variables, the geometry of the system, or the liquid properties. Such correlations are effective for fitting data for the same type of reactor (e.g. a SV reactor) with different area ratios or even different liquid viscosities, but they are mostly reactor-type specific (69–76). For example, Equation 42.3 does not consider any effects of changes in variation of the diameter or of the height of the reactor.

Some of the most published correlations are shown in Table 42.1. Only in few cases, the correlations show the influence of all the variables, both those of design and those of operation. As shown in Koide's correlations, variations in

TABLE 42.1. Gas Holdup in IL-ALRs

Source	Correlation	J_G
79	$\varphi_r = \left[(\mu_L - \mu_w)^{2.75} + 161\left(\frac{73.3-\sigma}{73.3-\sigma}\right)\right]10^{-4}(100J_{Gr})^{0.88}$	R^a
69	$\varphi_r = 0.16\left(1+\frac{A_d}{A_r}\right)\left(\frac{J_{Gr}}{J_{Lr}}\right)^{0.56}$	C^b
80	$\varphi_r = 0.465J_{Gr}^{0.65}\left(1+\frac{A_d}{A_r}\right)^{-1.06}\mu_{ap}^{-0.103}$	R
70	$\varphi_r = \frac{0.4Fr}{1+0.4Fr\left(1+\frac{J_{Lr}}{J_{Gr}}\right)}$	R
81	$\varphi_r = 44.1J_{Gr}^{0.841}\mu_{ap}^{-0.135}$	
	$\varphi_d = 29.7J_{Gr}^{0.935}\mu_{ap}^{-0.107}$	R
82	$\frac{\varphi_T}{(1-\varphi_T)^4} = \frac{0.124(Ca)^{0.966}Mo^{-0.294}\left(\frac{d_{dr}}{d}\right)^{0.114}}{1-0.276[1-\exp(-0.0386Ma)]}$	C, gas into draft tube
4	$\frac{\varphi_T}{(1-\varphi_T)^4} = \frac{0.160(Ca)^{0.964}Mo^{-0.283}\left(\frac{d_{dr}}{d}\right)^{-0.222}\left(\frac{d_{sp}}{d}\right)^{-0.0237\exp(-0.00185Ma)}}{1-1.61[1-\exp(-0.00565Ma)]}$	C, gas into annulus
83	$\varphi_T = (1.49-0.496C_s)J_G^{0.892}$	R
	$\varphi_r = 1.5Fr^{0.87}M^{-0.4}C_b^{-0.19}C_t^{-0.2}$	
84	$\varphi_d = 14.76Fr^{1.3}M^{-3.8}Ga^{-0.09}$	C
	$\varphi_T = 0.29Fr^{1.05}M^{-2.5}C_b^{-0.1}C_t^{-0.07}$	
85	$\varphi_T = 0.473J_G^{0.691}$	R

[a] Refers to A_r.
[b] Refers to A_r.

the performance of an internal loop airlift reactor (IL-ALR) are expected weather the gas is introduced in the annulus or in the draught tube (which is the most usual design). Some of the correlations have been formulated using usual dimensionless groups. Koide's correlation in Table 42.1 considers the frothing characteristics of the liquid, using the Marrucci's group (77). Coalescence is a very important property in ALRs, because it affects by means of bubble diameter, the gas holdup, liquid dynamics, and mass transfer rate. Zahradnik et al. (78) studied the influence of addition of electrolytes and alcohols and gave a correlation for their data on the transition concentrations, which indicate a sudden increase in coalescence inhibition. In most cases, the experimental data are not wide enough to justify the use of dimensional groups. Figure 42.6 shows the gas holdup following some of the correlations shown in Table 42.1. The figure was drawn taking the ratio of areas $A_d/A_r = 1$, the bottom clearance $C_b = 0.4$, the top clearance $C_t = 1$, a diameter of the separator equal to that of the reactor, and the physical properties of pure water. Another point that is extremely important to the user of those correlations is that special care should be taken inspecting how the gas superficial velocity was defined by the authors. This may be clear in the case of external loop airlift reactors (EL-ALRs), where the following definition is followed:

$$J_{Gr} = \frac{Q_{Gr}}{A_r} \tag{42.4}$$

where Q_{Gr} is the gas flow rate in the riser. In the case of IL-ALRs, this is not so clear. Many researchers have used the following definition

$$J_{Gr} = \frac{Q_{Gr}}{A_T} \tag{42.5}$$

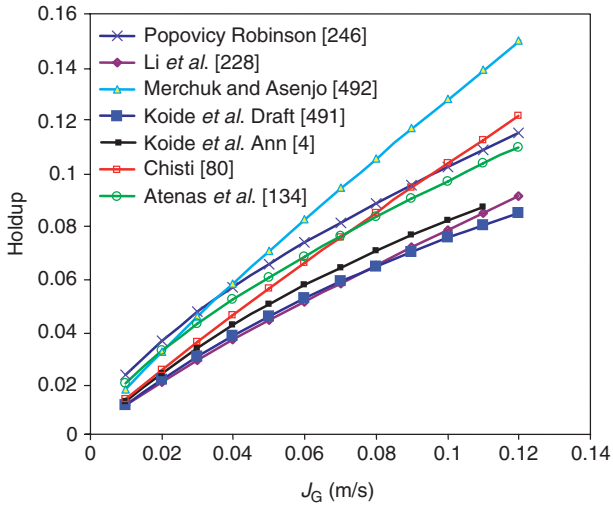


Figure 42.6. Gas holdup in IL-ALRs. Correlations are shown in Table 42.1.

probably because of their intention of comparing the performance of the ALR to a BC, where definition (42.5) applies. In Table 42.1, the definition used for J_G is indicated either with an R (riser) or with a C (column), indicating which cross-sectional area was used by the authors of the correlation. As the influence of only one variable is shown, the main point in this figure is the consensus respect the general form of the dependency of ϕ_i >on the $J_{Gi,Li}$.

The cyclic flow in the ALR complicates the analysis of the system. The riser gas holdup depends strongly on the geometric configuration of the gas–liquid separator and the water level in the gas separator. This has been shown experimentally in a rectangular SV-ALR (17), but the premise can essentially be extended to any IL-ALR. Analysis of the system revealed that these factors influence the gas disengagement and hence the gas recirculation in the downcomer. When this influence is taken into account and the holdup is plotted against the true gas superficial velocity, $J_{Gr,true}$, which is defined as the sum of the gas superficial velocity of the freshly injected gas, Q_{in}, and the recirculated gas, Q_{out}, that is,

$$J_{Gr,true} = \left(\frac{Q_{in} + Q_{out}}{A_r}\right) \tag{42.6}$$

then all the data for the different gas separators may be represented by a single relationship. In other words, if the actual gas flow is known, the influence of gas recirculation (which depends on A_d/A_r and the design of the gas separator) is taken into account and does not need to be considered again. Nevertheless, this simple approach has a drawback in that the true gas superficial velocity is difficult to measure because the gas recirculation rate is usually not known. A method for evaluation of the extent of the maximum gas recirculation has been proposed (78).

The safest procedure for the prediction of the gas holdup in an ALR under design is to take data provided by researchers who have made the measurements in that particular type of reactor with similar physicochemical properties of the system. Using a correlation from the literature without studying in depth the equipment used and the experimental conditions may be a very dangerous exercise for the designer. Only if such type of data is not available, correlations in Table 42.1 are recommended for prediction of the gas holdup in the riser. More sophisticated models, including those using computational fluid dynamics (CFD) methods, will be mentioned latter on.

Gas holdup in the downcomer is lower than that in the riser. The extent of this difference depends mainly on the design of the gas separator (86). The simplification proposed by Chisti and Moo-Young (68), which assumes that the ratio of the gas holdups in downcomer and riser is constant, has been widely used. This is an approximation that

seems to be close to reality in two-phase systems. In the case of three-phase flow, the point becomes more complicated. A liquid balance at the top results in

$$\varphi_d = \left(\frac{U_{Lr}A_r}{U_{Ld}A_d}\right)\varphi_r - \left(\frac{U_{Lr}A_r}{U_{Ld}A_d}\right)(1-\varphi_{sr}) + (1-\varphi_{sd}) = \alpha\varphi_r + \beta \quad (42.7)$$

and the range over which α and β can be considered constants is still an open question (87).

Many empirical expressions showing linearity, or almost linear relationship between gas holdup in the riser and the downcomer have been published (83,87,88). At low liquid flow rates, ϕ_d is usually negligible, because most of the bubbles have enough time to disengage from the liquid in the gas separator. This usually happens at the low gas flow rates frequently used for animal cell cultures.

The gas holdup in the separator is very close to the mean gas holdup in the whole reactor (61), as long as the top clearance C_t is relatively small (one or two diameters). For larger top clearances, the behavior of the gas separator begins to resemble that of a BC, and the overall performance of the reactor is influenced by this change.

42.2.2.2 External Loop ALRs. From the point of view of fluid dynamics, neither the external configuration (shape and architecture) nor the fact that both riser and downcomer are easily accessible is the most important difference between external and internal loop reactors. The most important point is that the gas separator of the EL-ALR is buil t in such a way that gas disengagement is usually much more effective in this type of reactor. In DT-ALRs or SV-ALRs, the shortest path that a bubble has to cover from the riser to the downcomer is a straight line across the baffle that separates the two sections. In the case of EL-ALRs, there is usually a minimum horizontal distance to be covered, which increases the chances of disengagement of the bubbles. In this case, it is worth pointing out that if gas does appear in the downcomer, then most of it will be fresh air entrained in the reactor because of interfacial turbulence or vortices that appear in the gas separator above the entrance to the downcomer. In many of the studies reported in the literature on holdup in EL-ALRs, total disengagement is attained. No such data are available for the concentric tubes of SV-ALRs, because total disengagement is possible only at very low gas flow rates.

Several authors (48,88–106) have presented their results of gas holdup as the gas velocity versus the superficial mixture velocity, based on the drift flux model of Zuber and Findlay (89). These authors derived general expressions for prediction of the gas holdup and for interpretation of experimental data applicable to nonuniform radial distributions of liquid velocity and gas fraction. The drift velocity is defined as the difference between the velocity of the particular phase (U) and the volumetric flux density of the mixture (J), where

$$J = J_G + J_L \quad (42.8)$$

The drift velocities of the gas and liquid phases may thus be expressed as

$$J_G = U_G - J \quad (42.9)$$

$$J_L = U_L - J \quad (42.10)$$

Zuber and Findlay (89) derived the relationship (9), which has been shown to be adequate to provide a correlation of gas holdup measurements in tower reactors with high liquid velocities, such as ALRs (90):

$$U_G = \frac{J_G}{\varphi} = C_o J + \frac{\frac{1}{A}\int_A \varphi(U_G - J)dA}{\frac{1}{A}\int_A \varphi dA} \quad (42.11)$$

The value of C_o depends mainly on the radial profile of the gas holdup. Zuber and Findlay (89) calculated $C_o = 1$ for a flat profile and $C_o = 1.5$ for a parabolic profile. Experimental values have been reported in the range of 1.03–1.2 for upflow (90–96) and 1.0–1.16 for downflow (92,94,97) and others reported higher values, approaching 2, for transition regime, that is, between homogeneous to heterogeneous bubbling (97,98). This is consistent with the physical meaning of C_o, because it is known that the transition zone is characterized by the existence of macrocirculation patterns that disappear as a fully heterogeneous regime is established (Fig. 42.7) (97). The opening percentage shown indicates the position of a valve located in the downcomer to control the liquid velocity. The authors report that in spite of the changes in the value of J at which the flow regime transition occurs, the J_G was approximately the same in all cases, indicating that the transition depends mainly on the gas superficial velocity. Guet et al. (96) studied the effects of bubble size on the parameters of the drift flux model and presented models that allow the consideration of bubble size in the calculations; however, for biological reactors, the gas flow rates used will be modest, and the transition and heterogeneous regimes are not relevant. For a bioreactor that is being designed in absence of specific data, $C_o = 1$ would be a solid choice.

The last term in the right-hand side of Equation 42.11 is the weighted mean value of the drift velocity. Zuber and Findlay (89) recommend the following expression:

$$U_{GJ} = 1.53\left(\frac{\sigma g \Delta\rho}{\rho_L}\right)^{1/4}(1-\varphi)^{3/2} \quad (42.12)$$

It has been shown (93) that a plot of U_G versus J gives a straight line, suggesting that a constant value of the drift

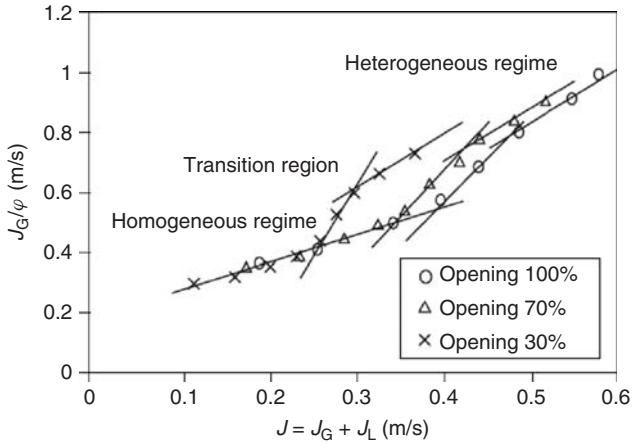


Figure 42.7. Experimental determination of C_o in the draft tube of an external tube ALR. The opening percentage shown indicates the position of a valve located in the downcomer, which controlled the liquid velocity. From Ref. 97, with permission.

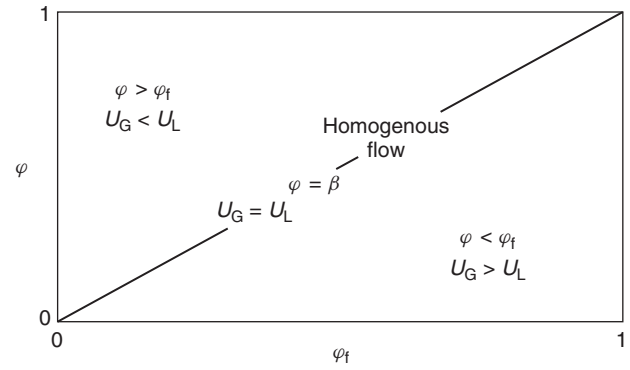


Figure 42.8. Gas holdup φ versus flowing volumetric concentration φ_f. The different zones in the plane $\varphi - \varphi_f$ correspond to different flow configurations. Adapted from Ref. 107.

velocity satisfactorily represents the two-phase flow in the riser of an EL-ALR. The distribution parameter was $C_o = 1.03$, and U_{GS}, the value of the slip velocity of a bubble, was taken as the mean drift velocity. Siegel et al. (1) applied the same model for the study of gas recirculation in a SV-ALR and obtained the values of $C_o = 1.11$. The slip velocity that they obtained fitting their data to Equation 42.11 was 0.238 m/s. It has been suggested (90) that this simplification holds as long as coalescence is not a predominant factor in the process.

It is very important to stress the difference between holdup, ϕ, and the flowing volumetric concentration, ϕ_f, which is defined as

$$\varphi_f = \frac{Q_G}{Q_G + Q_L} = \frac{J_G}{J} \tag{42.13}$$

Zuber–Findlay's drift flux model allows us to derive the following equation, which establishes a connection between the gas holdup and ϕ_f:

$$\frac{\varphi_f}{\varphi} = C_o + \frac{U_{b\infty}}{J} \tag{42.14}$$

where $U_{b\infty}$ is the terminal bubble velocity. Figure 42.8 gives a representation of the $\phi - \phi_f$ plane. The 45° line indicates that $\phi = \phi_f$, an equality that is true only for non-slip flow, where the velocity of the gas is equal to the velocity of the liquid. Such a situation can be visualized for the case of very small bubbles in a relatively fast liquid. In this case, there is no influence of one phase on the motion of the other. As indicated in Fig. 42.8, all the points below the 45° line indicate operation situations in which the liquid is driven by the gas:

$$U_G > U; \varphi < \varphi_f \tag{42.15}$$

This happens in the riser of ALRs. For all points above the line, the opposite is true:

$$U_G < U; \varphi > \varphi_f \tag{42.16}$$

This latter condition reflects the operation of the downcomer.

A number of authors (90,95,99–102) have measured the local holdup profile along the riser of an EL-ALR. In general, it was found that the holdup increases with height. This finding concurs with the expected expansion of gas bubbles as regions of lower pressure are reached. This situation must be limited to a certain range; an increase in bubble size will enhance turbulence and result in an increase in bubble encounters, leading eventually to bubble coalescence. The larger bubbles will rise much faster, resulting in a decrease in holdup. Such a scenario was indeed observed (90) who reported the tendency to a maximum in the holdup profile for the case of a single-orifice gas distributor. For a multiple-orifice sparger, producing a more homogeneous bubble size distribution, straight lines were observed within the studied length of the riser, which was 4 m. Similar holdup distributions have been observed by others (97,101).

Literature data from different sources for gas holdup in the riser under conditions of little or no carryover of gas from the separator into the downcomer for different A_d/A_r and top clearance C_t may be represented by the simple exponential:

$$\varphi_r = \alpha J_G^{\beta} \tag{42.17}$$

where the constant α depends on the friction losses in the loop, and β is usually a value between 0.6 and 0.7 (Fig. 42.9) (103). The data correspond to various A_d/A_r. The fact that neither the area ratio (within certain limits) nor the top clearance affects the gas holdup demonstrates the role of the gas–liquid separator in determining the performance of the reactor in general. In the absence of gas

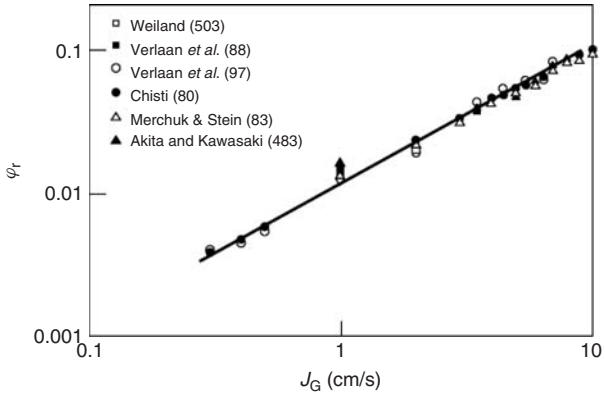


Figure 42.9. Gas holdup reported for the gas holdup φ_r under conditions of little or no gas recirculation.

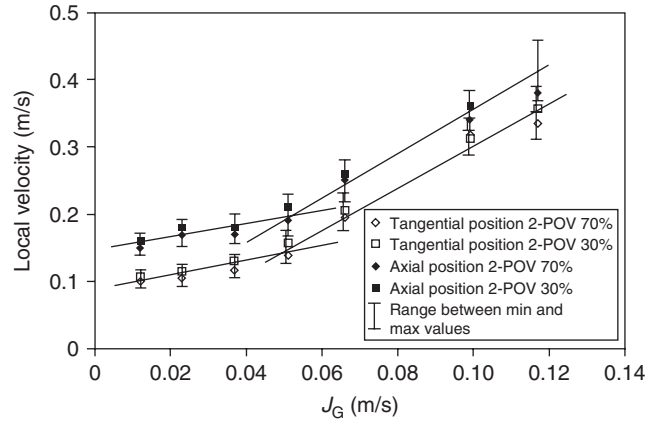


Figure 42.10. Local values of the axial and tangential velocity in the riser, with two different valve positions, 70% and 30% of aperture of a valve controlling the liquid recirculating velocity. From Ref. 97, with permission.

recirculation, there is no effect on these variables. Moreover, this means that under conditions of no gas entrainment from the separator to the downcomer, it is possible to predict the riser gas holdup as a function of the riser superficial gas velocity alone, which is of great importance for design purposes (79).

It is accepted that liquid velocity has a mild negative effect on gas holdup in the riser. This effect is usually studied by reducing the liquid flow; this is achieved by adding resistance to the liquid loop by means of a valve or other controlled obstruction (74,90,97,99,100,104,105) under conditions of low or nil gas recirculation. Such experiments, which are relatively simple in EL-ALRs, indicate that the holdup decreases as the liquid velocity is increased from zero (BC) to 0.3 m/s (which is close to the bubble free-rise velocity). For higher velocities, the effect of U_L is small. These findings add to our understanding of the fluid dynamics in the column. At liquid velocities that are smaller than the bubble free-rising velocity, the liquid transported in the wake of the bubbles, which must return downward to balance the mass flux, is the cause of the meandering and loops that typically appear in BC operation (53). As the overall liquid flux increases, the patterns straighten out, the bubbles begin to ascend in a straight pattern, and the holdup goes down. This is because the main component of bubble velocity is axial, and the decrease in holdup for further increases in liquid velocity is due solely to the change in the ratio of gas–liquid volumetric flow rates. Vial et al. (97) reported a very detailed study of the fluid dynamics in the riser of an external tube ALR, analyzing the influence of the liquid circulation rate by the method of generating a controlled pressure drop in the downcomer mentioned earlier, under conditions of complete gas disengagement. An important conclusion they arrive to is that while holdup and liquid mean velocity are mainly influenced by the geometric design variables, bubble-scale phenomena are almost independent of the geometry. The measurements shown in Fig. 42.10 display local values of the axial and tangential velocity in the riser, with two different valve positions, 70% and 30% of aperture. It can be seen that even in heterogeneous regime (the higher range of J_{Gr}), the axial velocity that depends on the gas holdup is predominant and higher than the tangential velocity, driven by bubble-scale phenomena. This is in fact the most important difference between flow characteristics of ALRs and BCs.

When there is gas recirculation, the area ratio A_d/A_r becomes an important variable affecting gas holdup. This effect starts in the region in which gas entrainment from the separator to the downcomer occurs. If it is assumed that the riser cross-sectional area A_r remains unchanged and the downcomer cross-sectional area A_d is increased, then it can be expected that the liquid velocity in the riser will increase as a result of the smaller resistance to flow in the loop, which in turn leads to a decrease in the riser gas holdup. An increase in A_d/A_r will result in a decrease in the liquid velocity in the downcomer, which leads to a decrease in the gas recirculation, because fewer bubbles are entrapped in the downcomer. The final outcome of increasing A_d/A_r is thus a decrease in the riser gas holdup. A similar argument can be applied in the discussion of the effect of reactor height on the riser gas holdup, that is, an increase in the height of the downcomer will result in a higher liquid velocity, which will in turn lead to a decrease in the holdup in the riser. In contrast, an increase in A_d/A_r will lead to an increase in the extent of bubble entrapment in the downcomer, which will serve to inject some additional gas into the riser. On the other hand, an increase in gas holdup in the downcomer diminishes the driving force for recirculation, as shown in Equation 42.1, and simultaneously reduces the free area for liquid circulation, and this will moderate the increase in liquid velocity generated.

TABLE 42.2. Some of the Published Correlations for Gas Holdup in EL-ALRs

Source	Correlation	
69	$\varphi_r = 0.76\left(1-\frac{A_d}{A_r}\right)^{-2} J_{Gr}^{0.8}$	
80	$\varphi_r = 0.02\left(1-\frac{A_d}{A_r}\right)^{-1.06} J_{Gr}^{0.65}\mu_{eff}^{-1.03}$	
108	$\varphi_r = 0.65\left(1-\frac{A_d}{A_r}\right)^{-0.258} J_{Gr}^{0.603+0.78C_s}$	
109	$\frac{\varphi_r}{1-\phi_r} = 2^{\frac{(3n+5)}{(n+1)}} n^{-\frac{(n+2)}{2(n+1)}}\left(1-\frac{A_d}{A_r}\right)^{-\frac{3(n+2)}{4(n+1)}} J_{Gr}^{\frac{(n+2)}{4(n+1)}}\left(\frac{\kappa}{\rho}\right)^{-\frac{1}{2(n+1)}} g^{-\frac{n}{2(n+1)}}$	
110	$\varphi_r = 0.203\frac{Fr^{0.31}}{Mo^{0.012}}\left(\frac{J_{Gr}A}{J_{Lr}A_d}\right)^{0.74}$	
111	$\varphi_r = 8.7^{*}10^{-4}\left(\frac{\rho J_{Gr}h}{\mu}\right)^{0.74}\left(1+\frac{A_d}{A_r}\right)^{1.32} F_f^{1.7}$	
112	$\varphi_r = \frac{J_{Gr}}{0.24+1.35(J_{Gr}+J_{Lr})^{0.93}}$	
113	$\varphi_r = a J_G^b\left(\frac{\mu}{\mu_w}\right)^c$	
Regime	Homogeneous	Heterogeneous
a	1.59	0.45
b	0.9	0.46
c	−0.05	−0.08

This feedback control of the liquid velocity is one of the characteristics particular to ALRs.

Table 42.2 shows several of the expressions published for the correlation of experimental data of ϕ_r obtained in EL-ALRs. Some of these expressions are presented in Fig. 42.11. The differences between the predictions obtained with the different correlations are probably due to the design of the gas separator. The equation given by Popovic and Robinson (106) seems to give an average of the proposed correlations. More general, simultaneous evaluations of several of the fluid dynamic parameters (gas holdups and velocities) can be obtained using mathematical models.

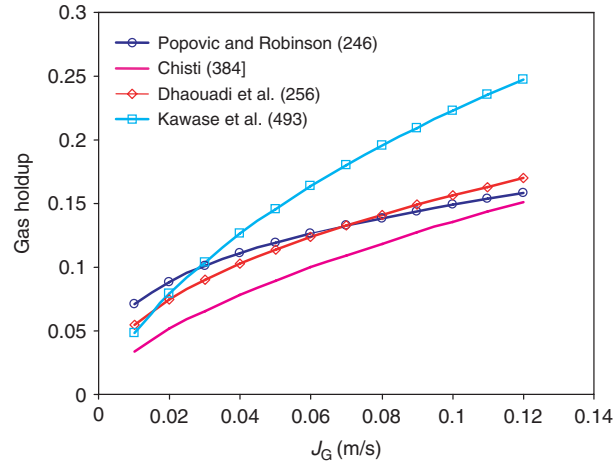


Figure 42.11. Correlations proposed for the gas holdup in the riser, φ_{Gr}, in EL-ALRs. The gas holdup in presented as a function of J_G only, for physical properties of water and $A_d/A_r = 1$.

42.2.2.3 Effects of Liquid Rheology. The effect of rheology on the reactor behavior and performance is of great interest because in most biotechnological processes, an increase in biomass provokes changes in the rheology of the fluid, especially in the case of mycelial growth. This effect is enhanced when in addition to the biomass growth, a product of the process is released into the medium in appreciable amounts (114), particularly the biosynthesis of polysaccharides, which cause an increase in the liquid viscosity (115,116). Klein et al. (117) reported measurements of liquid circulation velocity in an ALR with high cell density of an highly flocculating recombinant

strain of *Sacharomyces cerevisiae*. Their work showed the existence of a critical value of biomass concentration at which a dramatic deceleration of net liquid flow appeared with increasing biomass quantity. Rheological analysis revealed exponential increase in viscosity of the yeast flock suspension at the same biomass concentration. Thus, rheology changes during bioprocesses may influence the fluid dynamics in many aspects and should be considered.

The effect of viscosity on gas holdup in BCs has been studied and the main problem is non-Newtonian flow. If the viscosity changes with the shear rate (non-Newtonian systems), then the evaluation of shear rates becomes particularly relevant for the definition of the system. Nishikawa et al. (118) and Nakanoh and Yoshida (119) analyzed the problem of heat transfer in a BC with non-Newtonian liquids. They found a direct proportionality between the superficial gas velocity and the global shear rate:

$$\gamma = 5000 J_G,\ J_G > 0.04 \text{ m/s} \tag{42.18}$$

Moo-Young et al. (120) extended the expression to low the range of J_G, most common in bioprocesses, as follows:

$$\gamma = 1000 J_G^{0.5},\ J_G < 0.04/ \text{ ms} \tag{42.19}$$

This global shear rate can be used to calculate an effective or apparent viscosity:

$$\begin{aligned} \mu_{\text{eff}} &= \kappa (5000 J_{Gr})^{n-1} \\ \tau &= \kappa \gamma^n \end{aligned} \tag{42.20}$$

In shear-sensitive cultures, the global shear rate a is of great importance, because it predicts viability and productivity. Henzler (121), Kawase and Moo-Young (122), and Schumpe and Deckwer (123) have followed the approach of Nishikawa et al. (118) but have suggested different proportionality constants relating the global shear rate to the superficial gas velocity. This approach is, however, questionable from the rheological point of view because it will predict the same shear rate for a certain superficial gas velocity, no matter which liquid is used. El-Tamtamy et al. (124) introduced an improvement by calculating the shear rate from the bubble velocity divided by the bubble diameter. However, accurate evaluation of the latter two parameters is difficult. Henzler and Kauling (125) suggested relating the shear rate to power input based on dimensional analysis by expressing the shear rate as a function of the power input per unit volume, $[P/(V\rho\mu)]^{1/2}$. Their analysis gives different shear rates for liquids with different rheology. The above-described relationships predict different shear rates that vary up to three orders of magnitude.

In contrast to the influence of rheology on gas holdup in BCs, the data available for ALRs clearly show that the effect of liquid viscosity is less dramatic. Figure 42.12 shows the effects of the addition of carboxymethyl cellulose (CMC) (103). The change in CMC concentration had only a slight effect on the gas holdup for additions in the range 0.01–0.05% CMC. Only for solutions with concentrations higher than 0.5% CMC was an appreciable decrease in holdup seen (103). The viscosities corresponding to these solutions ranged from 4 to 14 mPa s. The addition of glycerol to water, that is, the change in viscosity keeping a Newtonian behavior of the liquid gave similar effects on the gas holdup. At low additions of the viscous fluid, a moderate increase in the gas holdup is evident, particularly in the downcomer and also in the riser. These increases are caused by the lower free-rise velocity of the bubbles, which increase the gas residence time. In addition, the entrapment of the bubbles into the downcomer is increased, and this is manifested mainly in ϕ_d. Further increases in viscosity, however, have a much smaller effect.

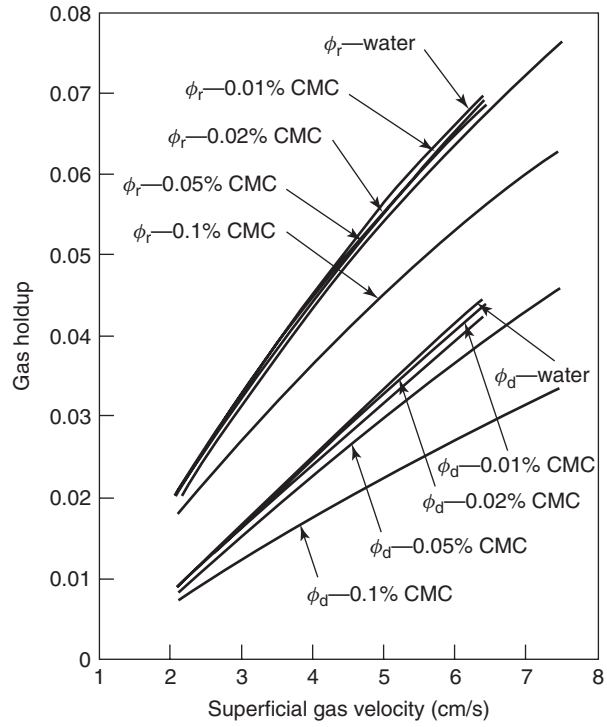


Figure 42.12. Effect of liquid rheology on the gas holdup of the riser and the downcomer of an IL-ALR. The apparent viscosity corresponding to the solutions used varied from 5 to 56 (mPa s). Adapted from Ref. 103, with permission.

42.2.2.4 Effect of Liquid Level. The influence of the liquid level C_t on the gas holdup is manifested as changes in the extent of disengagement of the bubbles in the gas separator. This influence is therefore dependent on the geometric design of this section. Whether a bubble will disengage or will be entrapped into the downcomer depends on the interrelationship of several parameters—the free-rising velocity

of the bubble $U_{b\infty}$ (a function of size and viscosity), the liquid velocity in the downcomer U_{Ld} (a function of the difference in gas holdup between the riser and the downcomer and frictional losses), and the residence time of the bubble in the gas separator (a function of geometric design and liquid height). For a given bubble size, if U_{Ld} is smaller than the $U_{b\infty}$ corresponding to the smallest bubble, there is no carryover. For smaller bubbles, the balance between the time required to cover the path from the end of the riser to the zone near the entrance of the downcomer and the time needed for disengagement will give the fraction of bubbles recirculated. It should, nevertheless, be kept in mind that this is a feedback process. A higher bubble disengagement rate leads to a lower gas holdup in the downcomer, which in turn increases the liquid velocity, enabling larger bubbles to be trapped, until the system eventually reaches a balance.

Due to the above-explained mechanism of control exerted by the geometric design, the influence of the liquid height is completely different in internal and EL-ALRs. In IL-ALRs, an increase in C_t increases the zone of the separator in which the gas holdup is higher, and as a result, the gas holdup increases. The extent of this increase depends, as said earlier, on the free-rise velocity of the bubbles. Figure 42.13 shows the gas holdup in the riser and downcomer of a 30-L ALR for two values of the top clearance, $C_t = 0.178$ m and $C_t = 0.308$ m, for two different liquids, water and a 0.5% CMC solution. It can be seen that although for water C_t has a small effect, this is not so for the more viscous solution. In the latter, the lower rising velocity of the bubbles causes a greater number of bubbles to be entrained and carried down by the liquid. Thus, the residence time in the disengagement section becomes very important in determining the fraction of bubbles that recirculate. A lower C_t will give

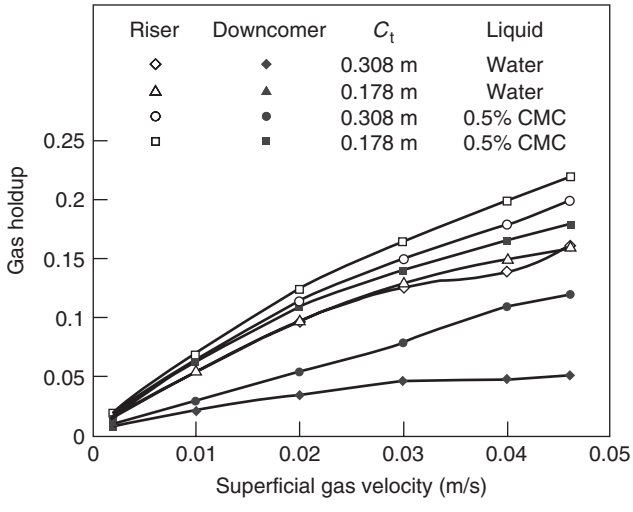


Figure 42.13. Riser and downcomer gas holdup in an IL-ALR for two different top clearances and two liquids. Adapted from Ref. 3.

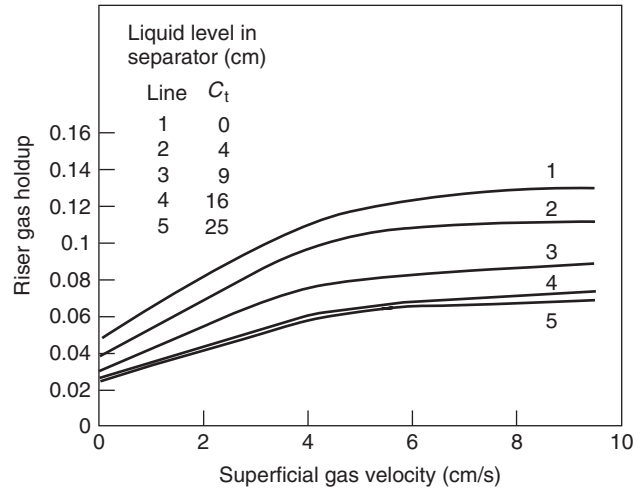


Figure 42.14. Gas holdup in the riser of an EL-ALR for several top clearances. Adapted from Ref. 103, with permission.

a shorter residence time in the separator, a larger bubble recirculation, and, hence, a larger gas holdup.

In EL-ALRs, the opposite effect is obtained, as may be seen in Fig. 42.14 (103). The data in Fig. 42.14, obtained for a 4-m high EL-ALR, show that the holdup in the riser decreases as C_t increases. This is due to the construction of these reactors, in which much of the gas that enters into the downcomer is trapped from the headspace due to the turbulence in this zone. An increase in the liquid height serves to reduce the amount of gas trapped, so that less gas circulates in the downcomer and the liquid velocity increases. The final result is a reduction in the gas holdup, both in the riser and the downcomer (103).

Although in general C_t is a fixed design characteristic, it may be used as an operation variable as well. Galindez-Meyer et al. (126) presented SV design with perforated baffle that allowed a variable-volume operation of the system. The behavior of ϕ and k_La observed were in essence similar to that described earlier.

The gas separation section also has a leading influence on the overall mixing in the reactor. Mehrnia et al. (2) studied the mixing and mass transfer characteristics of DT-ALRs for a water-in-kerosene microemulsion. Among the design variables studied, they included the gas separator design. They expressed the height of the liquid not as C_t, top clearance ratio, but as the ratio of volumes of separator to the rest of the reactor, defined as a "filling factor," F_f (127).

The top section of the airlift bioreactors is usually considered the best-mixed part of these bioreactors (61,86,128–131). Merchuk and Yunger (86) presented a model for airlift bioreactors in which the top section was considered to be perfectly mixed, while the riser and the downcomer were considered as two plug-flow sections.

Surprisingly, this simple model adequately represents quite adequately the effect of geometrical design factors on the mixing performance of an ALR.

42.2.3 Gas Recirculation

The degree to which gas flowing in the riser is entrapped and recirculated through the downcomer is an important variable, because it influences not only the flow configuration in the downcomer but also the performance of the ALR as a whole. The liquid velocity depends mainly on the difference in holdup between the riser and the downcomer, and it in turn influences the gas holdup in the riser. Despite the importance of recirculation, very little quantitative data are available on this phenomenon. Siegel et al. (1) evaluated the gas recirculation in a SV-ALR by an indirect method based on holdup measurements. From their results (Fig. 42.15), it may be seen that the recirculation rate is determined largely by the geometric configuration of the gas–liquid separator and the liquid level in the separator.

Three zones are evident in Fig. 42.15; they represent operating conditions giving oscillating, borderline, and straight bubble flow in the downcomer. Oscillating flow patterns produce much larger fractions of gas retained in the downcomer, but they are much more sensitive to J_G. At low superficial gas velocity, the recirculation increases very sharply with J_G. The bubbles exhibit an oscillating swirling flow pattern, with some larger bubbles escaping toward the top. The borderline condition is defined as oscillatory bubble flow at a low gas flow rate that shifts to straight bubble flow with increasing input gas flow rate. The straight flow operation zone is distinguished by bubble flow in a straight, well-defined flow pattern for all the input gas flow rates studied. If a straight bubble flow pattern is desired, the reactor should be operated at high riser gas flow rates, at which the reactor will shift toward stable operation.

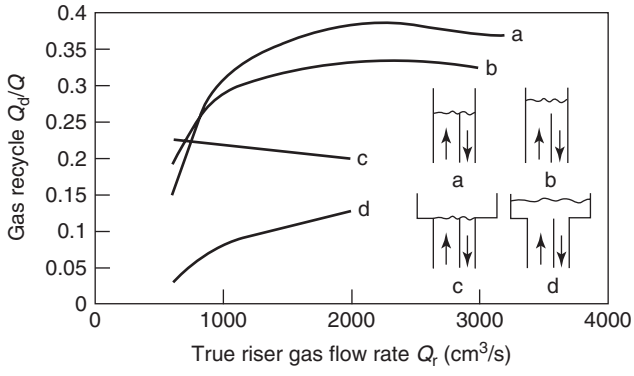


Figure 42.15. Gas recirculation in a SV-ALR. The liquid level in the separator schematically indicated corresponds to no-aeration conditions. Adapted from Ref. 1, with permission.

Lubbert et al. (132) attempted to evaluate the recirculation of gas during the cultivation of yeast (*S. cerevisiae*) on waste from a starch factory in a 4-m^3 pilot plant. They used microprocessor-aided pseudostochastic tracer input and cross-correlation techniques, which made possible the use of very reduced tracer feeds due to a high signal-to-noise ratio. The response to a pulse of helium was measured directly at the surface of the liquid in the separator by a quadruple mass spectrometer. The peak obtained showed pronounced shoulders, which could be interpreted as superimposition of a second peak that represents the helium tracer one loop after. The fitting of such a model to the experimental data suggested recirculation of 25% of the gas. This figure is in the range of the recirculation rates presented by Siegel et al. (1), considering the differences in the coalescing properties of the liquids used in these two works and the corresponding differences in the downcomer holdup. Burris et al. (133) evaluated the recirculation of bubbles in a full-scale ALR, and concluded that the recirculation varied from 0% to 50% of the gas, depending on the operation conditions.

Merchuk and Berzin (107) developed a mathematical model based on the application of the first law of the thermodynamics to each of the regions of an ALR. This model facilitates the evaluation of the maximum liquid recirculation possible in the system. The calculation is based on the premise that the gas recirculated must be compressed from the pressure at the top of the downcomer to the pressure at its bottom. The mathematical expression that gives this maximal gas recirculation is

$$Q_{Gd} = \frac{Q_L(P_2 - P_3) + Q_L \rho_L g h - \frac{1}{2} r_L C_d A_d (1 - \varphi_d) U_L^2}{P_4 \ln\left(\frac{P_3}{P_2}\right)} \tag{42.21}$$

where Q_{Gd} is the gas flow rate in the downcomer, Q_L is the liquid circulation flow rate, P_i is pressure at point i of the reactor (1 is top of the riser, 2 is top of the downcomer, 3 is bottom of the downcomer, and 4 is bottom of the riser), h is dispersion height, and C_d is the hydraulic resistance coefficient. The calculation of Q_d thus requires knowledge of the liquid flow rate, the pressures, and the geometry of the reactor. This equation represents the maximum recycling of gas in the downcomer, which will take place only if all the energy dissipated in the downcomer is invested in gas compression.

42.2.4 Liquid Velocity

The liquid velocity is one of the most important parameters in the design of ALRs. It affects the gas holdup in the riser and downcomer, the mixing time, the mean residence time of the gas phase, the interfacial area, and the mass and heat transfer coefficients.

Circulation in ALRs is induced by the difference in hydrostatic pressure between the riser and the downcomer as a consequence of a difference in gas holdup. Liquid velocity—like gas holdup—is not an independent variable, because (Fig. 42.3) the gas flow rate is the only variable that can be manipulated. As shown in Fig. 42.3, the geometric design of the reactor will also influence the liquid velocity, but it will usually remain constant during operation. Experiments have been carried out in devices specially designed to artificially change the resistance to flow, with the aim of studying the effect of the velocity at a fixed rate of aeration (90,95,97,100,105). The information from these experiments indicates that an increase in the liquid velocity leads to a decrease in the mean residence time of bubbles in the riser and hence of the gas holdup in the riser. In practice, when the gas flow rate is increased, the higher liquid velocity increases the carryover of bubbles from the gas separator into the downcomer; the carryover dampens the liquid flow by reducing the hydrostatic driving force. As a result, the overall change in liquid velocity is tempered.

42.2.4.1 Liquid Velocity Measurement. Several different methods can be used for measuring the liquid velocity. The most reliable ones are based on the use of tracers in the liquid. If a tracer is injected and two probes are installed in a section of the tube, the velocity of the liquid traveling the distance between probes can be taken directly from the recorded peaks, as the quotient of the distance between the two electrodes and the time required by the tracer to travel from one to the other. The latter is obtained as the difference between the first moments of the two peaks. The tracer may be an electrolyte that can be followed by conductometry (57,97) or with a pH meter (57). The tracer may also be a particle with high magnetic permeability followed with a magnetic metal locator (60) or, in special cases, with image analysis (134). Those tracer methods can also be used to calculate the mean liquid velocity (U_L), from the circulation time (t_c) and holdup (ϕ) as

$$\overline{U}_L = \frac{V_L}{t_c \overline{A}(1-\varphi_T)} \tag{42.22}$$

where $\overline{A}$ is the mean cross-sectional area. In this case, only one electrode is necessary, and the circulation time is obtained from two successive peaks recorded by the electrode. This is a velocity that is representative of the flow in a general way and does not necessarily correspond to the actual velocity in any of the regions of the ALR.

A more sophisticated method that has also been used is laser Doppler velocimetry (LDV) (97,135–137). Operation in the backscatter mode allows liquid-phase analysis, while forward mode gives access to gas-phase properties (138,139). LDV makes possible to obtain multiple local velocity readings, and its limits of applicability have been studied (136).

42.2.4.2 Liquid Flow from Energy Balances. Two main methods have been used for the modeling of two-phase flow in ALRs—energy balances and momentum balances. Chakrabarty et al. (79) used the energy balance approach to obtain a relationship between superficial gas velocity, holdup, and liquid velocity. Lee et al. (140) calculated U_L by a similar type of model for a series of data for DT-ALRs and EL-ALRs and from their own results for SV-ALR. In both the above-mentioned models, constants accounting for friction losses were obtained by adjusting the models to the experimental data. Jones (141), on the other hand, managed to express the results of his energy balance [based on previous work of Nicklin (142) and Freedman and Davidson (94)] in a relationship free of empirical constants. His results, however, fit the experimental data only qualitatively, and the fit is satisfactory only for very small diameters. An improvement of this method was suggested by Clark and Jones (143), who took into account the radial distribution of the gas holdup through the drift flux model. However, the values of the distribution coefficient C_o needed for satisfactory fitting of the experimental data for lager diameters is far from the range usual in this type of flow.

Chisti and Moo-Young (144) extended a model originally proposed by Bello (145), based on an energy balance over the airlift loop. Their expression for the average superficial liquid velocity in the riser is

$$U_{Lr} = \frac{2gh_D(\varphi_r - \varphi_d)}{\frac{K_t}{(1-\varphi_r)^2} + K_b\left(\frac{A_r}{A_d}\right)^2 \frac{1}{(1-\varphi_d)^2}} \tag{42.23}$$

where h_d is the downcomer height and K_b and K_t are the hydraulic pressure loss coefficients.

By choosing suitable values for the friction coefficients in each case, the authors showed that much of the published data on liquid velocity for the different types of ALRs could be satisfactorily correlated by Equation 42.23. Only one coefficient has to be adjusted, because the authors assume that K_t, the friction coefficient at the top of the loop, is negligible in DT-ALRs and that in EL-ALRs K_t can be taken as equal to K_b, the friction coefficient for the bottom of the loop. Equation 42.21 has thus been adopted by many scientists (85). Wachi et al. (146) claimed that their derivation of the same equation gives a clearer physical meaning to the adjustable parameters. Equation 42.22 can also be derived from a simple momentum balance (107). Chisti et al. (147) presented an empirical correlation for K_b obtained by comparison of results obtained from several sources:

$$K_b = 11.402\left(\frac{A_d}{A_b}\right)^{0.789} \tag{42.24}$$

where A_b is the minimal cross section at the bottom of the ALR. Equation 42.21, as most of the expressions derived

from energy balances, has the particularity that the gas flow rate, which is the main, and often the only manipulable variable in the operation, is not present directly but exerts its influence through the gas holdup. Therefore, either experimental data or a valid mathematical expression for the gas holdup in both the riser and the downcomer are required, in contrast with the empirical correlations where the arguments are known.

Chisti and Moo-Young (144) extended this model (Eq. 42.23) further to facilitate the prediction of liquid circulation in ALRs operating with pseudoplastic fluids, such as mould suspensions. This improvement is very important, because many commercial fermentation processes involve such non-Newtonian liquids. Kemblowski et al. (110) presented a method for the prediction of gas holdup and liquid circulation in EL-ALRs. In their experiments, there was almost no gas recirculation, because of the large size of the gas separators used.

García-Calvo (148) presented an ingenious model based on energy balances and on an idea originally proposed by Richardson and Higson (149), and García-Calvo and Leton (150) extended the model to BCs. The model is based on the assumption that the superficial gas velocity (J_G) in any region can be considered to be the sum of two streams (J' and J'') as follows. The J' stream has a velocity equal to that of the liquid and can therefore be treated by the laws of homogeneous two-phase flow (no slip between the bubbles and the liquid). The second stream (J'') is considered to be responsible for all the energy losses at the gas–liquid interface. The concept in itself is simple and elegant, and it is possible to envisage its application even to the flow in the downcomer, where $U_G < U_L$. In such a case, they would divide the gas flow rate into two parts as follows: One part would be larger than the actual flow rate, that is, it would have the same velocity as the liquid. To arrive at the actual gas flow rate, the second flow rate must have the reverse direction. This type of gas flow can actually be seen under certain conditions, such as when there is coalescence of bubbles and larger bubbles ascend along the walls of the downcomer.

An alternative technique used by several researchers to predict liquid velocity is the momentum balance of the ALR. This method has been used by Blenke (151) in jet-loop reactors and by Hsu and Dudukovic (152), Kubota et al. (153), Bello (145), Koide et al. (154), and Merchuk and Stein (90). Merchuk and Stein presented a simple model for the prediction of the liquid velocity as a function of the gas input in an ALR. They assumed that the pressure drop between the bottom and the top of their external loop reactor return (top, downcomer, and bottom) could be expressed as a continuation of the downcomer, using an equivalent length L_{eq}. This length was set as an adjustable parameter describing the pressure loss in the loop. Kubota et al. (153) used a similar approach for the analysis of Imperial Chemical Industries' deep-shaft reactor. They were able to simulate the operation of the reactor and to predict the minimum air supply required to prevent flow reversal.

Verlaan et al. (95) used a similar model, in combination with the expression of Zuber and Findlay (89), to calculate the friction coefficients from experimental data reported by several authors for a wide range of reactor volumes. Koide et al. (154) presented an analysis of the liquid flow in a concentric tube ALR that was also based on a momentum balance. The main difference between this model and that used by Merchuk and Stein (90) was that Koide et al. (154) used a convergence–divergence flow model for the bottom and the top of the loop. At the bottom, the effect of flow reversal on the pressure drop was included in the effective width of the gas–liquid flow path under the lower end of the draft tube, which was smaller than the actual gap. Miyahara et al. (155), who studied both the bubble size distribution in an IL-ALR and the pressure drop at the top and the bottom of the draft tube, also presented a model facilitating the prediction of the liquid velocity.

Other models use the drift flux model (122) presented in Equations 42.5–42.7, as

$$U_{Lr} = \frac{J_{Gr}(\frac{1}{\varphi_r} - C_o) - U_{GJ}}{(1 - \varphi_r)C_o} \tag{42.25}$$

For the range of flow rates usual in bioreactors, U_{GJ} can be taken from Equation 42.12. The range of variation of C_o is rather narrow, as shown in the previous section, and therefore, it is not difficult to make a judicious guess as to the value of C_o in an unknown system. The drift flux model has also been used together with energy balances (156) or with the momentum balance (157).

Some studies on liquid flow present the results in the form of empirical correlations (61,69,158). The usefulness of these correlations (Table 42.3 and Fig. 42.16) depends on the amount of data and the number of parameters taken into account. In general, the superficial liquid velocity increases with an increase in the superficial gas velocity, but its rate of increase is much lower at high superficial gas velocities. The A_d/A_r area ratio and the reactor height are the main parameters that affect the superficial liquid velocity at constant superficial gas velocity. The superficial liquid velocity increases with an increase in A_d/A_r.

The effects of the properties of the liquid, such as viscosity, surface tension, and ionic strength, on the superficial liquid velocity are much milder in ALR than in BC (162). Increasing the liquid viscosity will decrease the liquid velocity because of frictional losses, but this will increase the gas holdup in the riser and consequently increase the driving force for liquid recirculation. These two effects balance each other partially and result in a milder effect on the superficial liquid velocity. The effects

TABLE 42.3. Gas Correlations of Liquid Velocity in ALRs

Source	Correlation	Type of ALR
69	$J_{Lr} = 1.55\left(\frac{A_d}{A_r}\right)^{0.74} J_{Gr}^{0.333}$	EL
159	$J_{Lr} = 2.058\left(\frac{A_d}{A_r}\right)^{0.416} J_{Gr}^{0.482}\mu_{eff}^{0.0105}$	
106	$J_{Lr} = 0.052\left(\frac{A_d}{A_r}\right)^{0.794} J_{Gr}^{0.322}\mu_{eff}^{-0.395}$	EL
147	$U_{Lr} = \frac{2gh(\varphi_r - \varphi_d)}{\frac{K_t}{(1-\varphi_r)^2} + K_b\left(\frac{A_r}{A_d}\right)^2 \frac{1}{(1-\varphi_d)^2}}$	High viscosity EL, IL
110	$J_{Lr} = \sqrt{\frac{2gh_d(\varphi_r - \varphi_d)}{\frac{K_t}{(1-\varphi_r)^2} + K_b\left(\frac{A_r}{A_d}\right)^2 + 4h_d\left[\frac{f_r}{d_r} + \frac{f_d}{d_d}\left(\frac{A_r}{A_d}\right)^2\right]}}$	EL
160	$J_{Lr} = 0.11h_d J_{Gr}^{0.32}\left(\frac{A_d}{A_r}\right)^{0.97}\mu^{-0.39}$	EL
61	$J_{Lr} = 0.9J_{Gr}^{0.44}h^{0.47}$	IL
111	$J_{Lr} = 0.95\left(\frac{\rho J_{Gr} h}{\mu}\right)^{0.165}\left(1 + \frac{a_d}{A_r}\right)^{-1.84} F_f^{1.38}$	EL
161	$R_{eL} = 0.065R_{eG}^{1.33}Fr^{0.93}J_{Gr}^{0.322}\mu_{eff}^{-0.395}\frac{A_d}{A_r}^{0.81}\ R_{eL} < 2000$	EL
	$R_{eL} = 0.662R_{eG}^{1.03}Fr^{-0.63}Ct^{0.318}\mu_{eff}^{-0.395}\left(\frac{A_d}{A_r}\right)^{0.58}\ R_{eL} < 2000$	
113	$\varphi_r = aJ_G^b\left(\frac{\mu}{\mu_w}\right)^c$	EL
Regime	Homogeneous	Heterogeneous
a	0.71	0.42
b	0.44	0.26
c	−0.12	−0.12

of the surface tension and the ionic strength are also exerted via their influence on the gas holdup, as analyzed earlier.

As a rule, it can be recommended that the Zuber–Findlay expression (Eq. 42.25) be used when the holdup is known and the liquid circulation velocity is high. For low liquid velocity, a correlation obtained in a piece of equipment as similar as possible to the one under design should be used.

42.2.5 Liquid Mixing

A thorough knowledge of mixing behavior is necessary for the design, modeling, and operation of ALRs. This is of particular importance during the process of scale-up from laboratory- to industrial-scale reactors. The optimum growth rate of a microorganism or the optimum production rate of a specific secondary metabolite usually relates to well-defined environmental conditions, such as pH range, temperature, substrate level, limiting factors, dissolved oxygen, and inhibitor concentration in a specific well-mixed laboratory-scale vessel. Because of the compromises made during scale-up, it is difficult to keep the same hydrodynamic conditions established in the laboratory; mixing on an industrial scale may not be as good as mixing on a laboratory scale (16). In smaller scale reactors, it is easier to maintain the optimal conditions of pH, temperature, and

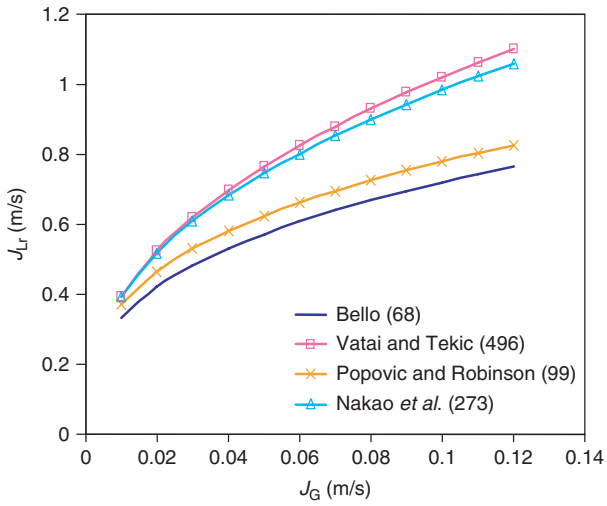


Figure 42.16. Liquid velocity predicted by some of the proposed correlations.

substrate concentration required for maximum productivity of metabolites in a fermenter.

Furthermore, in fermentation systems, efficient mixing is required to keep the pH within the limited range, giving maximum growth rates or maximum production of the microorganism during addition of acid or alkali for pH control. Mixing time—or the degree of homogeneity—is also very important in fed-batch fermentation, where a required component, supplied either continuously or intermittently, inhibits the microorganisms or must be kept within a particular concentration range (163,164). A large number of commercially important biological systems are operated in batch or fed-batch mode. In this operation mode, fast distribution of the incoming fluid is required, and the necessity for understanding the dynamics of mixing behavior in these vessels is obvious. Even for batch systems, good control of the operating conditions, such as pH, temperature, and dissolved oxygen, require prior estimation of mixing so that the addition rates can be suitably adjusted. Deviation of the pH or temperature from the permitted range may cause damage to the microorganism, in addition to its effect on the growth and production rates. Moreover, a knowledge of the mixing characteristics is required for modeling and interpreting mass and heat transfer data.

A parameter used frequently to represent mixing in reactors is the mixing time (t_m). It has the disadvantage that it is specific to the reactor design and scale, but it is easy to measure and understand. Mixing time is defined as the time required to achieve the desired degree of homogeneity (usually 90–95%) after the injection of an inert tracer pulse into the reactor. The so-called degree of homogeneity (I) is given by

$$I = \frac{C - C_m}{C_m} \tag{42.26}$$

where C is the maximum local concentration and C_m is the mean concentration of tracer at complete mixing.

A more comprehensive way of analyzing mixing, applicable to continuous systems, is a study of the residence time distribution (RTD). Although ALRs are usually operated in a batchwise manner, at least in the laboratory, advantage is taken of the fact that the liquid circulates on a definite path to characterize the mixing in the reactor. Hence, a single-pass RTD through the whole reactor or through a specific section is usually measured. On the basis of the observed RTD, several models have been proposed. These models have the advantage of reducing the information of the RTD to a small number of parameters, which can later be used in design and scale-up.

The axial dispersion model, which has the advantage of having a single parameter, is widely accepted for the representation of tower reactors. This model is based on visualization of the mixing process in the tower reactor as a random, diffusion-like eddy movement superimposed on a plug-flow. The axial dispersion coefficient D_z is the only parameter in the formulation:

$$\frac{\partial C}{\partial t} = D_z \frac{\partial^2 C}{\partial z^2} + U_L \frac{\partial C}{\partial z} \tag{42.27}$$

where C is the concentration of a tracer. The boundary conditions depend on the specific type of tower reactor. This model is attractive, because it has a single parameter, the Bodenstein number (Bo), which is used to describe the mixing in the reactor:

$$Bo = \frac{U_L L}{D_z} \tag{42.28}$$

where L is the characteristic length (distance between tracer injection and detection points). When the Bo number tends to infinity, the mixing conditions are similar to those of a plug-flow reactor, and the reactor can be considered as well mixed for low Bo numbers.

The alternative approach of Buffham and Mason (165) states that the mixing characteristics of a piece of equipment should be expressed as the variance σ^2 of the distribution obtained by injection of a pulse of tracer without adopting any mechanistic model (165). The relationship between Bo and σ^2 depends on the reactor configuration (166). The approach of Buffham and Mason facilitates the presentation of mixing characteristics free of any modeling assumptions. The variance σ^2 is the second moment of the distribution and carries information on the spread of the distribution around the mean value (first moment). Nevertheless, most of the data on mixing in bioreactors have been presented either as t_m or as overall Bo numbers, which can be obtained by relatively simple experiments of pulse injection.

Single-pass mixing in the ALR is due to mixing in the individual and interrelated sections of the reactor riser, separator, downcomer, and bottom. Repeated passage mixing is the sum of the mixing in the subsequent passages. The latter is usually reported as the mixing time (t_m), the former as *Bo* or σ^2. Indeed, these parameters are interrelated, and knowledge of *Bo* or t_m is sufficient for calculating, theoretically, the mixing time (122,132) based on the deviation of the envelope of the maxima in the response curve to a pulse, which is a measure of the degree of in homogeneity. Verlaan et al. (104) and Lin et al. (167) correlated their results as follows:

$$t_m = M Bo \tag{42.29}$$

where M is a constant equal to 0.093 (104) or 0.089 (167). The coefficient M given by Verlaan et al. (104) is in exact agreement with the theoretical relationship derived by Murakami et al. (168) for $Bo > 50$ and a degree of inhomogeneity, $I = 0.05$. The results obtained lately by Sánchez Mirón et al. (169) confirm this form of the dependency of t_m on *Bo*.

Equation 42.28 shows that the circulation path, which enters in the definition of *Bo*, has a linear effect on the mixing time. If the mean circulation time and the axial dispersion coefficients are known, it is possible to estimate theoretically the mixing time using Equation 42.27. Experimental details must, however, be carefully planned to avoid complications. Note that to simplify data processing, it is important to inject the signal and to measure the response at exactly the same point (170) (in some reports, the position of the injection point is not specified despite its effect on the mixing time). In a study of the effect of the injection point on the dynamics of the mixing time, Schügerl (171) concluded that the gas–liquid separator is the best choice for tracer injection for short mixing times. Fields and Slater (163) reported a marked dependence of the respiratory quotients on the injection point of methanol during unlimited fed-batch growth of *Methylophilus methylotropus* in a DT-ALR. Assuming that this is due to poor mixing of the substrate, this would be an indication of the importance of the injection point for the mixing process.

Figure 42.17 shows experimental data for *Bo* reported for different types of ALR in which the reactor is considered as a single unit. Because of the definition of the overall *Bo*, the values are specific to the reactor for which they were obtained and can be used only as indication of trends and orders of magnitude. The sources are provided in Table 42.4.

An alternative way of correlating mixing in ALRs was proposed by Sánchez Mirón et al. (169), using the velocity of the gas phase instead of that of the liquid:

$$Bo_{LG} = \frac{J_G D}{D_z} \tag{42.30}$$

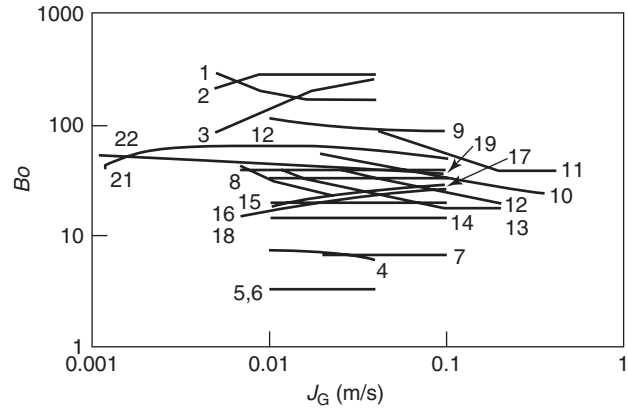


Figure 42.17. Global Bodenstein numbers reported for ALRs. See references in Table 42.4.

and managed to correlate successfully the experimental data of overall mixing obtained in both DT-ALRs and SV-ALRs with expressions of the following form:

$$Bo_{LG} = \beta \left(Fr^{\frac{1}{3}} \right)^{\lambda} \tag{42.31}$$

As explained earlier, the ALR is, in fact, a combination of several regions having quite different fluid dynamic characteristics. The overall mixing is the result of the contributions of each of them, and the overall *Bo* represents this combination for a particular reactor. This value thus has some limitations for extrapolation to other configurations or scales. Because each section has different mixing characteristics (it may have a different cross section, flow configuration, etc.), from a strictly engineering point of view, the mixing in each of the sections of the ALR should be defined and considered separately.

One way of obtaining information on the mixing characteristics of each of the regions of the ALR is the simultaneous measurement of the response in the ALR at several points, so that after one single pulse injection, the response of each section in the loop can be obtained (48,104,176). This method of measurement has the advantage that multiple measurements are made for the same tracer injection experiment. This enables us to check the consistency of the liquid velocity results obtained, because independent measurements can be obtained in the same run, as can be seen in Fig. 42.18.

The results for *Bo* obtained by Verlaan et al. (104) in an EL-ALR are shown in Fig. 42.19 (the much higher *Bo* in the downcomer was explained by the fact that the data were obtained under conditions of complete gas disengagement). The results indicated that most of the mixing took place in the gas separator, and both riser and downcomer could be considered as plug-flow conduits. The same conclusions were drawn for IL-ALRs by Merchuk et al. (48)

TABLE 42.4. Bodenstein Number—Key for Fig. 42.17

Line	Source	Type	A_d/A_r	H/D	Liquid
1	99	EL	0.25	85.0	Water
2	99	EL	0.25	85.0	2-Propalol 1.65%
3	99	EL	0.25	85.0	CMC 50%
4	172	EL	0.11	20.0	Water
5	172	EL-baffled	0.11	20.0	Water
6	172	EL	0.11	40.0	Water
7	145	EL	0.69	12.0	Water
8	145	EL	0.69	12.0	Water
9	145	EL	0.11	20.0	Water
10	173	EL	1.00	30.0	Water
11	163	IL	1.56	10.5	Water
12	163	IL	1.56	21.0	Water
13	163	IL	1.56	10.5	Ethanol 1%
14	163	IL	1.56	10.5	Water, antifoam
15	69	IL	0.13	39.6	Water
16	69	IL	0.56	55.6	Water
17	174	EL, Bo_T	0.25	16.5	50 mM KCl
18	174	EL, Bo_r	0.25	16.5	50 mM KCl
19	174	EL, Bo_d	0.25	16.5	50 mM KCl
20	175	IL		20.0	Sea water
21	169	IL	1.00	0.8	Sea water

by analysis of mixing times: the shift in results for mixing times obtained with different probes in response to the same impulse perturbation indicated that the riser and the downcomer were introducing a pure delay in the response, that is, they behaved as plug-flow sections.

The simplest model of an ALR, from the point of view of fluid dynamics, is a combination of two plug-flow reactors, representing the riser and the downcomer, and a perfectly stirred tank, representing the gas (86,177). The validity of using this simple model as a first approximation is supported by experimental evidence that shows that the mixing time decreases when the separator volume increases (38,129). When the volume of the separator is increased substantially without changing the reactor diameter, the gas separator becomes tall and slender and may depart from total mixing behavior. It has been reported that under such conditions the circulation time measured from two successive peaks of a probe is not influenced by changes in the top clearance (61,178). This indicates that the gas separator acts as two interconnected well-mixed regions, one of them being the link between riser and downcomer.

The extent of mixing in the gas separator of IL-ALRs can probably be compared with that in a BC of the same dimensions. In the case of EL-ALRs, the extent of mixing depends on the geometric design. In designs such as the channel-loop reactor (179), a different approach must be taken. However, in general, consider that all the mixing takes place in the gas separator, and calculate the degree of mixing in it using data for BCs. Godboole and Shah (180) recommend the use of the correlation proposed by Deckwer et al. (181):

$$D_z = 0.678 d^{1.4} J_G^{0.3} \tag{42.32}$$

where d is the column diameter, or the relationship proposed by Joshi et al. (182):

$$D_z = 0.33(U_c + J_L)d \tag{42.33}$$

where J_L is the superficial liquid velocity and U_c is the cell circulation velocity given by

$$U_c = 1.31\left[gd\left(J_G - \frac{\varphi_s}{1-\varphi}J_L - \varphi U_{b\infty}\right)\right] \tag{42.34}$$

where $U_{b\infty}$ is the terminal bubble velocity. The liquid superficial velocity (J_L) can be easily calculated for EL-ALRs, and for IL-ALRs, J_L may be taken as half the liquid velocity in the riser. The viscosity may also play a role in the rate of mixing. An increase in liquid viscosity will increase the energy dissipation in the loop and result in an increase in mixing time and Bo. In non-Newtonian fluids, however, the behavior may be different (Fig. 42.20). In the case of the addition of polymers that confer pseudoplastic behavior to the liquid, low concentrations produce a decrease in the mixing time (183,184). This can be explained in terms of the drag reduction due to the presence of polymers in the boundary layer near the walls. Fields and Slater (184) found that the mixing time increased for xanthan gum, above the critical concentration. (The critical concentration is a theoretically

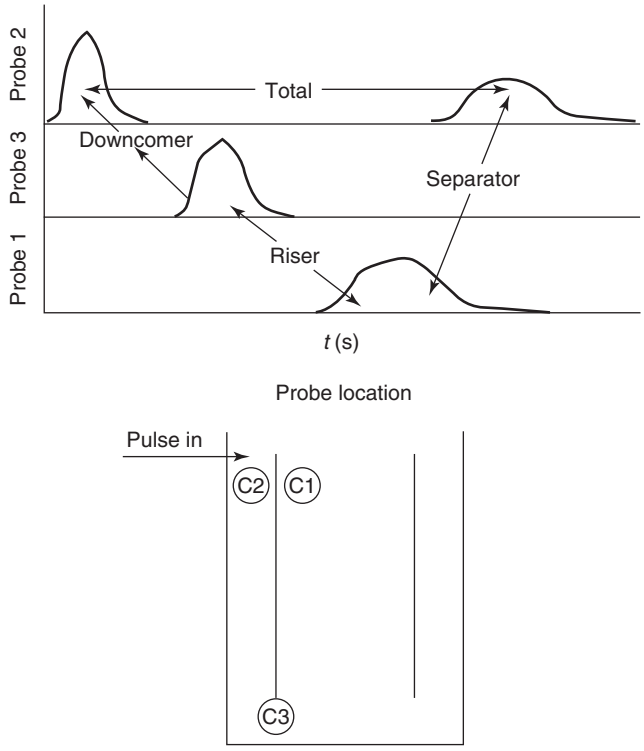


Figure 42.18. Response of three electrodes in the riser, separator, and downcomer to a pulse of electrolyte. The information that can be obtained from a single experiment is indicated by the arrows. From Ref. 48, with permission.

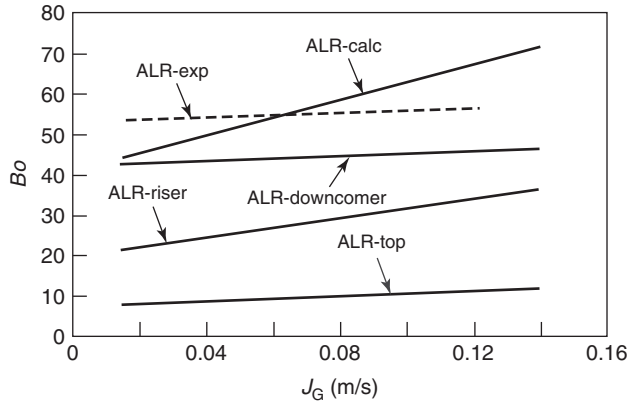


Figure 42.19. Bodenstein numbers as a function of the superficial gas velocity in an EL-ALR. ALR-exp, experimental values for the whole reactor; ALR-calc, calculated values for the whole reactor. Adapted from Ref. 104, with permission.

calculated value at which appreciable overlapping of polymer molecules occurs and which marks the onset of a rapid increase in the apparent viscosity).

Gavrilescu et al. (185) presented a model based on two-phase theory and takes into account all the basic

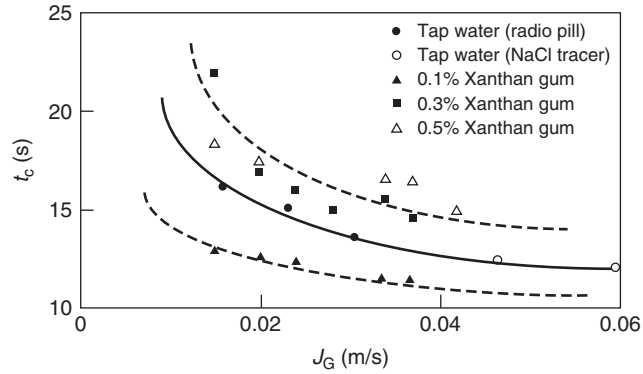


Figure 42.20. Variation of mean circulation times with J_G for several solutions. Adapted with permission from Ref. 184.

parameters that characterize an ALR, as area ratio, gas and liquid superficial velocities, and holdup. Hari and Tan (186) present an alternative way of analyzing the cyclic flow in ALRs. Their approach is based on concepts rooted in the dynamical system theory, not very usual in chemical engineering practice, and claim good prediction of mixing time.

The use of CFD for the calculation of mixing characteristics in ALRs has also been extremely successful.

42.2.6 Mixing in the Gas Phase

For all practical purposes, the gas in the riser of an ALR exhibits plug-flow behavior. Only for extremely high J_G or hindered liquid circulation will the axial dispersion of the bubbles have some effect on the gas RTD. In the downcomer, the gas flow is almost plug-flow when the bubble recirculation is fully developed. But at the stage at which a stationary phase of suspended bubbles appears at the top of the downcomer, appreciable dispersion will occur. This zone has a large degree of mixing due to coalescence and consequent rise of larger bubbles amid smaller ones, with repeated events of breakup and coalescence. However, this type of operation has no relevance to practical applications as it is an operation mode to be avoided. No data on mixing under these conditions have been reported. The main question related to the mixing of the gas phase is related to gas recirculation. When a particular gas flow has developed in the downcomer, part of the gas is being recirculated. A pulse of gas tracer at the inlet would produce, as a response, a series of pulses, separated one from the other by the gas circulation time. In practice, not many of these pulses would be detected, due to dilution and disengagement of the tracer in each pass through the separator.

Fröhlich et al. (187) reported on gas-phase mixing in an ALR. The distribution of the gas residence times in two reactors, one of $0.08\,m^3$ and the other of $4\,m^3$, was measured using pseudostochastic tracer signals and a mass

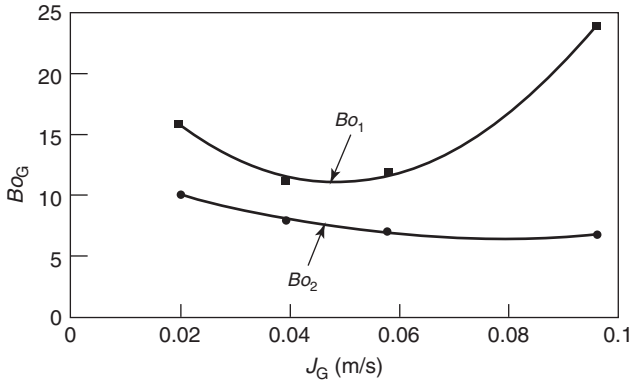


Figure 42.21. Bodenstein numbers for the gas-phase dispersion calculated from first (Bo_1) and second peak (Bo_2) of the RTD after pulse injection in a 80-L IL-ALR. From Ref. 187, with permission.

spectrometer. The values of Bo_G were calculated from the first and second peaks, indicating the main gas stream and the recirculation. Figure 42.21 shows the Bo_G obtained for a laboratory-scale ALR. The values obtained in a pilot plant were of the same order.

An interesting method for the study of the dynamics of the gas phase in pneumatically agitated reactors (ARs) is the "dynamic gas disengagement" (188), which consists in studying the rate of bubble disengagement following the height of the dispersion, or the concomitant changes in pressure. The interpretation of this type of data considering the effect of the internal liquid circulation was presented by Deshpande et al. (189). Thus, the dynamic gas holdup during gas disengagement can be used to provide new insights into the fundamentals of BC behavior. In this way, it becomes possible in principle to interrelate macroscopic properties such surface area, gas-phase residence tune distribution, and intensity of mixing in the liquid phase, even in opaque industrial reactor systems (190,191). Toye et al. (191) used this method coupling pressure probes to electric resistance tomography (ERT), producing images that show the difference between Newtonian and non-Newtonian liquids. In the latter, the range of existence of homogeneous bubbling is reduced, probably because of increased coalescence (Fig. 42.22).

42.2.7 Energy Dissipation and Shear Rate

ALRs are being increasingly used in processes involving shear-sensitive cells (mammalian, insect, plant cell, and microalgae) (5,17,22,39,192–201). This has created the need for considering shear stress as one of the relevant parameters in reactor design. Although the evaluation of shear rates is a matter that has been studied for many years in STRs, information on this subject is scanty for pneumatically stirred reactors. The first approach made in this direction in pneumatically agitated vessels was that of Clark et al. (92), who were interested in the problem of heat transfer to a non-Newtonian liquid in a BC. This study was extended to mass transfer by Nishikawa et al. (118), who proposed the expression (17).

This expression has been widely accepted despite the criticism sometimes leveled at it (86,177,202–204). Some modifications have thus been proposed (123,125,205), which, like the original approach, were based on data for BC performance and therefore have limited application for ALRs. A method facilitating the prediction of the distribution of the energy dissipated in an ALR, based on a simple thermodynamic approach, has been developed (107). Energy dissipation was considered to occur in the ALR by two main mechanisms: wall friction and bubble-associated dissipation (ideal gas behavior was assumed). The work done by the gas on the liquid (and vice versa) was expressed assuming isothermal expansion of the bubbles. The energy dissipation inside the gas phase was considered negligible. The general energy balance (206) was written as

$$\Delta(PQ) + \Delta E_p + E_D = W_s \tag{42.35}$$

In this equation, the first term represents the flow work lost by the system under consideration, E_D is the energy dissipated per unit of time, and W_s is the shaft work done by the surroundings on the system under consideration. The schematic representation of the DT-ALR in Fig. 42.23 indicates the different points in the reactor considered in the mathematical expressions. The expressions found for the energy dissipated in each zone were the following: *Riser:*

$$(E_D)_r = Q_L(P_4 - P) - Q_L\rho gh - Q_{Gr}P_4 \ln\left(\frac{P_5}{P_4}\right) \tag{42.36}$$

Gas separator:

$$(E_D)_s = Q_L(P_5 - P_2) - Q_{Gin}P_4 \ln\left(\frac{P_1}{P_5}\right) - Q_{Gd}P_4 \ln\left(\frac{P_{21}}{P_5}\right) \tag{42.37}$$

Downcomer:

$$(E_D)_d = Q_L(P_2 - P_3) - Q_L\rho gh - Q_{Gd}P_4 \ln\left(\frac{P_3}{P_2}\right) \tag{42.38}$$

Bottom:

$$(E_D)_b = Q_L(P_2 - P_4) - Q_{Gd}P_4 \ln\left(\frac{P_4}{P_3}\right) \tag{42.39}$$

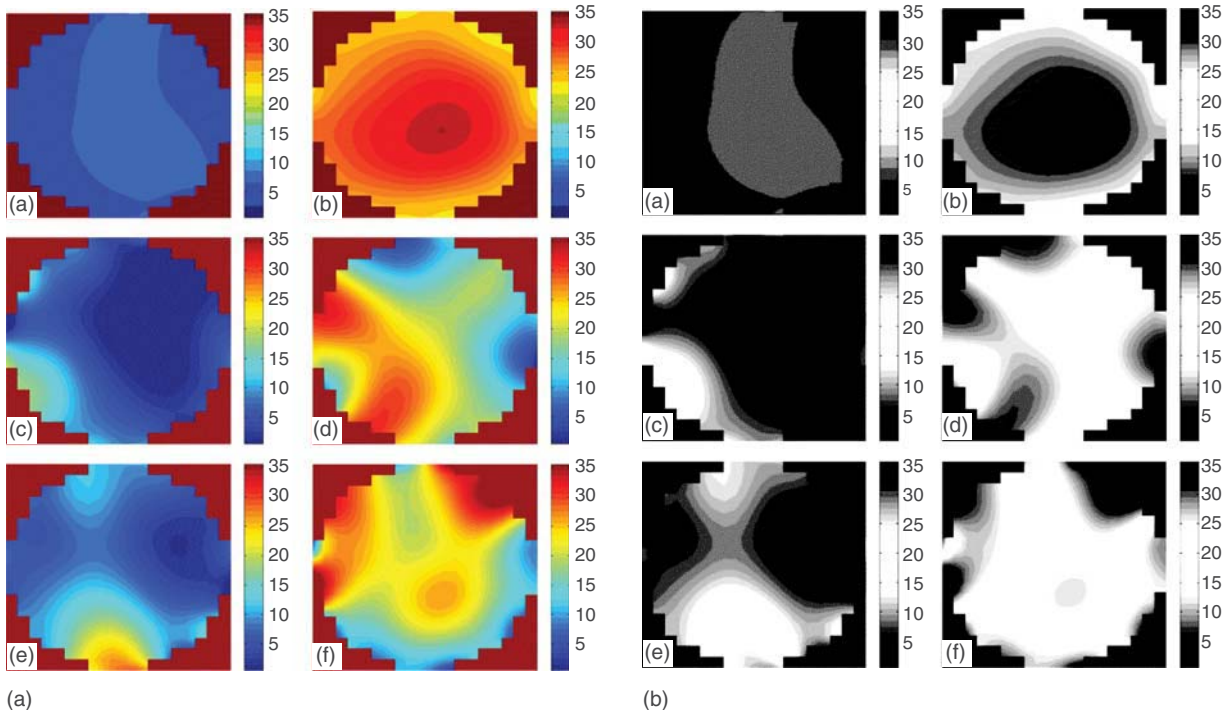


Figure 42.22. Reconstructed images of the gas holdup distribution obtained by ERT: (a) water, $J_G = 0.02$ m/s; (b) water, $J_G = 0.11$ m/s; (c) 3 g/L xanthan, $J_G = 0.02$ m/s; (d) 3 g/L xanthan, $J_G = 0.11$ m/s; (e) 5 g/L xanthan, $J_G = 0.02$ m/s; (f) in 5 g/L xanthan, $J_G = 0.11$ m/s. From Ref. 191, with permission.

Results of this model of an ALR can also be used to estimate the energy dissipation in each region of the reactor. Some approaches have been published on the relationship between dissipation and shear rate have been proposed.

42.2.7.1 Cell Damages due to Bubbles in ALRs. While shear rate in reactors is usually related to macroscopic flow, in the case of suspensions of cells and of some enzymes, the gas bubbles themselves are associated to shear damages that are independent of the bulk flow of the liquid. This damage may become a limitation that must be considered in reactor design for production of therapeutic proteins, vaccines, and antibodies in animal cells (207–209) and in plant cell cultures (210–212), because bubbling is an essential element in ALR operation. The effects of bubbles may range from changes in metabolite production to cell lyses and depend strongly on cell type and bubble size. Models have been offered describing a microenvironment in the surroundings of a bubble, associated with the turbulent wake generated. The "killing volume" defined by Tramper et al. (192,213) allows the mechanistic formulation of a cell death kinetic that is first order on biomass concentration, which agrees with the common knowledge on cellular lyses. The kinetic constant in this model is inversely proportional to bubble volume or the cube of bubble diameter. Wang (214) proposed a model where the damage rate would be inversely proportional rather to the interfacial area or the square of bubble diameter. These models agree in principle with the recognized fact (192,215–218) that small bubbles (<2-mm diameter) are much more damaging than larger ones (>10-mm diameter). Several researchers found, however, that the source of damage is not the mere presence of bubbles, but the fluid dynamic events happening during their disengagement of the liquid (219–222). When a bubble emerges through a free surface, its upper part remains enclosed by a thin liquid film that eventually ruptures, starting at the highest point where the film is thinner. The rupture of the thin liquid film liberates an amount of energy that is relatively larger for smaller bubbles. As the film retracts, a "crown" is generated and small jets of liquid are ejected at very high velocities. In addition, a central jet is also generated. This process is highly damaging for the cells caught in the liquid jets, and also for those in the immediate surrounding, because of the rapid velocity fluctuations in the liquid, which follow the jet ejection.

The indications that the main source of damage is the burst of the bubble rather than its passage through the reactor led to a corresponding design strategy in column reactors for fragile cells. It seems practical to maximize the mass transferred by each bubble before bursting, using a longer residence time that is obtained using higher columns

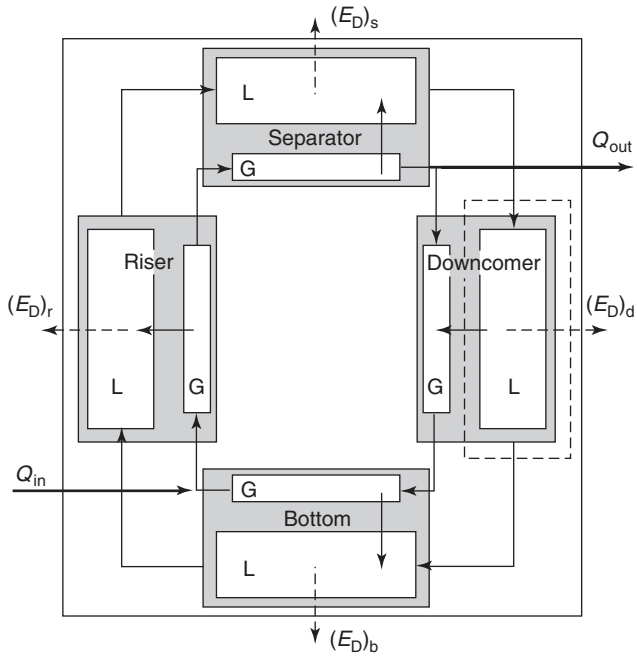


Figure 42.23. Schematic description of the energy fluxes in the thermodynamic model of an ALR, from Ref. 107, with permission.

(192,201,213,216,223–225). This mechanism of the cell damages also indicates the convenience of minimizing the amount of cells in the surroundings of the bubble at bursting time. This may be achieved by a stable foam layer maintained at the top of the reactor. The relatively long time spent by each bubble queuing before bursting increases the draining of the liquid and the thinning of the film where cells are usually in a higher concentration than in the bulk.

On the other hand, this mechanism of cell damage explains the effects of many of the additives used for cell protection, as serum and Pluronic F68. Those molecules change the surface properties of the liquid, as surface tension, diminishing the crown and jet effects, and therefore the intensity of the microscopic fluctuations at bubble burst. A review of the use of those additives for animal cell bioreactors can be found in Ref. 209.

The bubble-burst central position in the cell-damaging phenomena in bioreactors is, however, still a polemic subject. Ma et al. (226) have recently reported that indeed the number of cells attached to bubbles decreases as the concentration of Pluronic F68 increases. At low PF-68 concentrations (0.001 g/L), cells had a very high affinity for bubbles in those experiments, indicating a more than 10-fold increase in cell concentration in the foam layer liquid versus the bulk liquid. At high PF-68 concentrations (<3 g/L), however, the cell concentration in the foam layer liquid was only $< 40\%$ of that in the bulk cell suspension. On the other hand, they reported that most of the cell damage took place in processes other than cell burst. In any case, the number of cells damaged by each bubble increased with decreasing PF-68 concentration and increasing bulk cell concentration. It can be concluded that bubble damage to suspended cells is an open question. There are no doubts on its great relevance to bioreactor design, but the quantitative aspects of the mechanistic explanations and the solutions proposed to solve it should be carefully studied for each particular case.

42.3 MASS TRANSFER

The volumetric mass transfer coefficient k_La is the rate of transfer across the gas–liquid interface, per unit of driving force (the driving force is the gradient of concentration between the liquid and gas phases). The mass transfer coefficient k_La can be seen as the product of two terms: the mass transfer coefficient k_L and the specific interfacial area, a. They both depend on variables that can be grouped into three categories: (i) static properties of the liquid such a density, diffusivity, and surface tension; (ii) dynamic properties of the liquid (related to liquid flow), such as the rheologic parameters; and (iii) parameters that depend on liquid dynamics. In general, the variables in group 1 do not change very drastically. The variables in groups 2 and 3 span over quite wide ranges.

42.3.1 Mass Transfer Rate Measurement

The methods for determination of k_La in a reactor can be classified as steady- and unsteady-state methods. In the steady-state methods, the rates of oxygen uptake in steady-state operation are evaluated, be it by measurement of inlet and outlet rates of oxygen or from known consumption rates. One of the problems of measuring inlet and outlet gas amounts is that the changes in oxygen concentration in the gas streams are usually small, and the errors of measurement are important. An example of the direct analysis of a compound that reacts with the oxygen is the case of the sulfite method. In this case, the experiment can be run for enough time to obtain a reliable reading of the concentration of sulfite, which reacts catalytically with the oxygen. However, when a chemical is added to the system as part of the k_La evaluation procedure, the question arises of whether the addition has not provoked changes in the physicochemical properties of the liquid, changing the bubble size distribution of the original system.

Transient methods follow the response of the dissolved oxygen concentration in the system after a step change in oxygen concentration in the inlet stream of gas. They have the advantage that no addition of any alien material is required and that a single concentration is followed. The correct use of this method has been analyzed in depth by Linek et al. (227).

One important point to take into account is the dynamics of the oxygen electrode. The lag in the response of the oxygen electrode makes it necessary to discern between the electrode response and the real oxygen concentration, especially when close to a sharp change in concentration. A correct analysis should also include the model of the dynamic behavior of the electrode. To simplify the procedures, approximations based on the truncation of parts of the response curve have been proposed (204,228). These methods are based on truncating the first part of the electrode response obtained in a transient experiment. Once the error admitted in the value of k_La is set, the extent of truncation is fixed, allowing simplification in the analysis of the remainder of the recorded concentration curve. It should be kept in mind that this simplification implies the loss of part of the information, and due care should be given to statistical analysis of the results.

The dynamic gassing out technique (229) is a very simple and ingenious method for studying bubble dispersions (8,230–239). Variations of the dynamic method have been proposed to minimize disturbances in the system, by introduction of step variations of agitation or pressure (227,240). In this way, the method can be applied bioreactors during real operation of the system.

One problem in the measurement of mass transfer rates, especially when viscous liquids are used, is related to the presence of very small bubbles that are depleted from oxygen very rapidly, but do not disengage in the gas separator, becoming an inert volume of gas in the reactor (205). Kawase and Moo-Young (241) analyzed the use of transient absorption of CO_2 for the determination of k_La and concluded that the error due to small bubble retention was much smaller than that in the case of using O_2.

Whatever the method used for the determination of k_La, the process of data elaboration is basically the same as that shown in Fig. 42.24 (242). The measured variable (usually oxygen concentration) is compared with the value that a mathematical model of the process predicts. The model includes k_La as a parameter. The value of k_La that minimizes the difference between the two outputs is chosen.

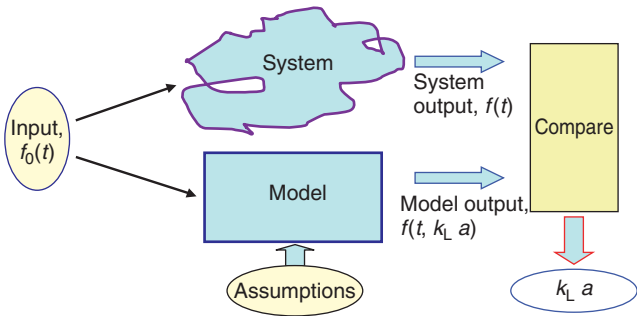


Figure 42.24. Steps in the determination of the mass transfer coefficient k_La.

This stresses that the choice of the model is very important and poor assumptions on flow characteristics of the gas or the liquid phases may lead to errors and deviations from the true values (243). All models are a simplified (to make them amenable to mathematical treatment) description of the system. It should be kept in mind, therefore, that k_La is not a property of the system, but a parameter of the model adopted. If, for example, total mixing is assumed in the model adopted, the mass transfer coefficient obtained will be limited consequently. Regrettably, assumption of complete mixing is so common in practice that many reports do not even specify explicitly that this was done, and in many texts, it can be found that the equation

$$\text{OTR} = k_La(C^* - C) \tag{42.40}$$

is taken as the definition of the mass transfer coefficient k_La, forgetting to state that this equation is valid only for perfectly mixed systems. The question that naturally emerges here is whether the liquid in an ALR can be considered as perfectly mixed.

Strictly, in ALRs, the different sections (riser, downcomer, and gas separator) have different flow characteristics, and the mass transfer coefficient may thus be expected to differ from one region to another. Some (69) have assumed that the contribution of the downcomer to the overall mass transfer is negligible and have reported values of k_La that are, in fact, the whole of the mass transfer divided by the fractional volume of the riser. The fact that the values of the mass transfer coefficient are calculated and reported in different ways introduces some ambiguity into the data; special care should therefore be taken when comparing data or using published mass transfer coefficients for design purposes.

The assumption of perfect mixing in the liquid phase may be questionable in the case of tall reactors. One very simple method to verify this assumption is the simultaneous measurement of the response of the concentration in different points of the reactor to a step change in the inlet. In a perfectly mixed system, the location of the probe should be irrelevant. It was shown (179) that the criterion originally proposed by Andre et al. (244) may be used for ALRs. This criterion compares the circulation time in the reactor with the characteristic time for mass transfer, which is the inverse of the mass transfer coefficient:

$$t_c k_L a < 0.5 \tag{42.41}$$

If this condition is not fulfilled, the bioreactor cannot be considered as a perfectly mixed volume, and more sophisticated ways of analysis are required. The mathematical model and consequently the analysis of the experimental data become much more complicated in this case. Nevertheless, this approach has been used (81,129,245,246), and

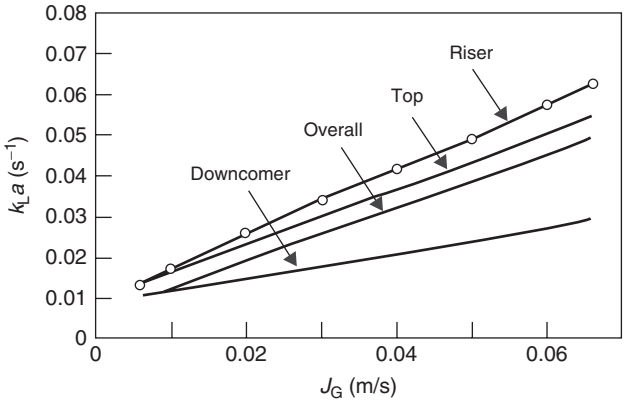


Figure 42.25. Local values of k_La in the different regions of an ALR. Adapted from Ref. 246, with permission.

the mass transfer experiments render in this case the k_La for each of the regions of the ALR. Figure 42.25 shows the results reported by Hwang and Lu (246) in an IL-ALR. The graph shows that the mass transfer takes place at the highest rate in the riser. The downcomer shows 50% lower values, and the gas separator is between them. The overall mass transfer rate is the result of the balance of the respective volumes and rates in the three sections.

The gas composition should also be carefully considered. While in a short equipment the oxygen concentration may change very little, and many times can be considered as constant, this is not so in taller columns, especially at low J_G, when the gas stream depletion is greater. Distributions of gas composition have been modeled and presented and can be of use to the designer (247–249).

In addition, the value of the volumetric OTR determined for a microbial system can differ substantially from that obtained for oxygen absorption in nonreacting solutions with an invariable composition of the liquid media with time. Hence, it is preferable that k_La be determined in bioreactors, which involve the actual media and microbial population (250,251). Figure 42.26a shows the k_La variation with the superficial gas velocity in the riser for absorption in water. Figure 42.26b shows the evolution of k_La through an actual fermentation course employing two different nitrogen sources, at $J_G = 0.05$ (m/s). The k_La decreases and reaches a minimum value at about 24 h. After this time, the k_La starts to increase, and after 48 h of fermentation, it reaches a more or less constant value, which remains until the end of the process. This behavior is similar irrespective of the nitrogen source and is related to changes in rheology.

Various design modifications proposed for ALRs imply changes in mass transfer characteristics. The addition of plates or other internals that reduce the liquid velocity, and in some cases, produce a redistribution of the gas phase as it ascends in the riser, also affects the mass transfer rate.

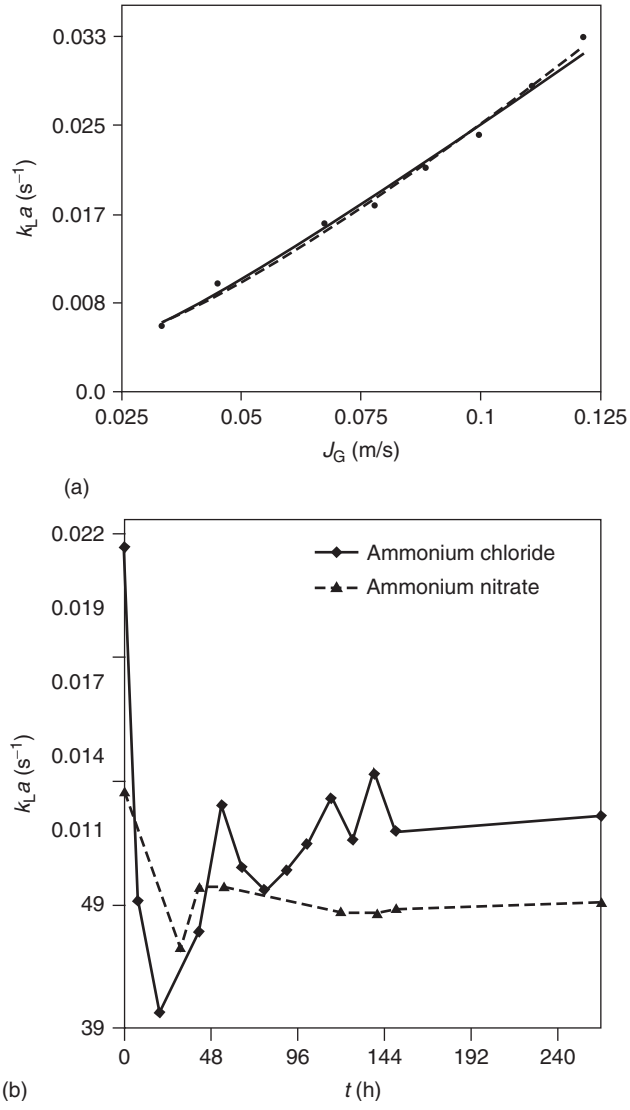


Figure 42.26. Oxygen absorption during growth of *Gibberella fujikuroi* in an airlift bioreactor. (a) k_La variation with the superficial gas velocity in the riser in water. (b) Evolution of k_La through an actual fermentation with two different nitrogen sources (producing different viscosities), at $J_G = 0.05$ m/s. From Ref. 251, with permission.

Nikakhtari and Hill (252) reported an increase in the absorption of volatile organic chemical (VOC) in an EL-ALR due to the addition of internals. The same was observed using a wire mesh made using a draught tube (253). The addition of a stirrer to the ALR to increase liquid circulation, as reported by Chisti et al. (44), improved mixing and mass transfer rate, but strongly reduced the efficiency of oxygen transfer. While the mass transfer rate, as well as other characteristics of the reactors, are expected to have trends similar to those described for ALRs in general, the actual value of the coefficients must be carefully evaluated in each case.

Another point of interest is the question of the enhancement of the mass transfer rate due to the biochemical reaction. This old controversial issue (254) has been lately revived by García-Ochoa et al. (232,255,256), claiming there is a measurable enhancement in the absorption of oxygen during the growth of aerobic cultures.

42.3.2 Bubble Size and Interfacial Area

The interfacial area per unit volume is an important component of the volumetric mass transfer coefficient. In fact, it is the part of $k_L a$ that is more susceptible to changes. The mass transfer coefficient k_L varies only within a limited range (257). The interfacial area is mainly responsible for the changes in mass transfer rate due to variations in turbulence, initial bubble size, and liquid properties:

$$a = \frac{6\varphi}{d_{32}} \tag{42.42}$$

where the Sauter mean diameter (d_{32}) is given by

$$d_{32} = \frac{\sum n_i d_i^3}{\sum n_i d_i^2} \tag{42.43}$$

where n_i is the number of bubbles with diameter d_i. For the riser, the correlation presented by Miyahara et al. (155) for the volumetric mean diameter of the bubbles in the riser of a concentric tube ALR can be used. They proposed

$$\overline{d}^{=} f(N_W) \tag{42.44}$$

where d_o is the diameter of the sparger orifice and ρ the surface tension,

$$N_W = \frac{We}{Fr^{0.5}} \tag{42.45}$$

and the function $f(N_W)$ is different for each range of N_W:

$$\begin{aligned} f(N_W) &= 2.9 N_W < 1 \\ f(N_W) &= 2.9 N_W^{-0.188}, \quad 1 < N_W < 2 \\ f(N_W) &= 2.9 N_W^{-0.188}, \quad 2 < N_W < 4 \\ f(N_W) &= 3.64 < N_W \end{aligned} \tag{42.46}$$

Data on bubble size in the downcomer of an ALR were published by Popovic and Robinson (106).

Bubble size results from an equilibrium between bubble beak up and bubble coalescence. Bubble break up phenomenon was shown by Bhavaraju et al. (258) to be related to liquid turbulence in the vessel rather than gas turbulence in the orifice. Procedures were developed by the authors through a simple liquid circulation model to obtain a criterion for the onset of bubble breakup. The optimal design of a sparger for sparging air into a liquid of given properties (ρ, σ, μ) was studied. They correlated the bubble size for the equilibrium between physicochemical and hydrodynamic forces in a gas–liquid dispersion under a certain energy input.

Bubble coalescence may happen on bubble collision in the core of a liquid. Collision phenomenon implies that the liquid between the two bubbles is reduced to a thin film, which may break producing a larger single bubble or may not withstand the process leaving the two bubbles as they were. Marrucci (259) studied this point and presented criteria that allow to predict the breaking of the film, presenting the group (Crk^2/σ) This group has been used to correlate bubble dispersion properties, as holdup (4), and it is called the *Marrucci group* (Ma).

42.3.3 Data Correlation for Mass Transfer Rate

There are two ways of correlating experimental data from ALRs. First, a hydrodynamic point of view suggests that the movement of the fluid in the reactor determines its overall behavior, and the gas superficial velocity is therefore the more appropriate independent variable. Second, a thermodynamic point of view would suggest considering energy balance—a more global approach to the system. This will lead to correlation of the phenomena in the system as a function of the energy input. Indeed, it is easier to compare mass transfer coefficients in ALRs with those in conventional reactors where the data are presented as a function of the total power input (both mechanical and pneumatic) per unit volume of the medium (43,44). Figure 42.27 shows data of mass transfer coefficients as a function of specific power input (177,260).

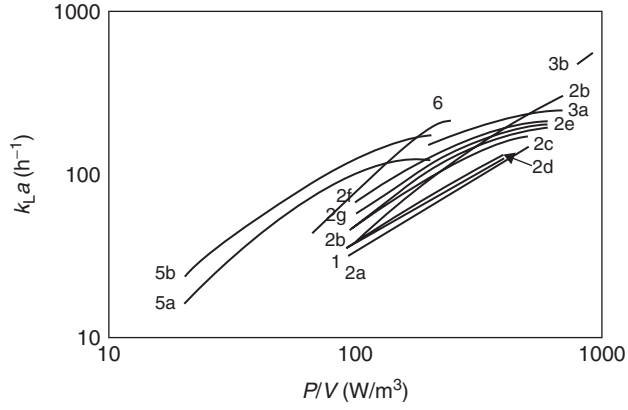


Figure 42.27. Mass transfer coefficient in ALRs as a function of power input per unit volume. See Table 42.5 for sources. From the study by Siegel et al. (177), with permission.

TABLE 42.5. Mass Transfer in ALRs as a Function of Power Input—Key for Fig. 42.27

Line	ALR Type	h (m)	D_r (m)	A_d/A_r	Source
1	DT	1.43	0.21	1.04	261
2a	EL	1.80	0.152	0.69	69
2b	EL	1.80	0.152	0.25	69
2c	EL	1.80	0.152	0.11	69
2d	DT	1.80	0.089	0.56	69
2e	DT	1.80	0.076	0.35	69
2f	DT	1.80	0.051	0.13	69
2g	BC	1.80	0.152	—	69
3a	RSV	4.50	0.09×0.25	0.78	41
3b	RSV	4.50	0.09×0.25	0.78	41
4	EL	8.50	0.100	0.25	99
5a	DT	1.70	0.117	0.19	262
5b	DT	1.70	0.176	0.26	262
6	EL	1.80	0.15	0.69	263
7	DT	3.21	0.755	1.27	44

Selected correlations proposed for the prediction of mass transfer coefficients are shown in Tables 42.6 and 42.7, for internal and EL-ALRs, respectively (the warning on the applicability of correlations obtained in different experimental setups must be kept in mind). Among the internal loop reactors, two correlations presented for reactors with rectangular cross section are shown (41,264). For EL-ALRs, the correlation by Popovic and Robinson (80) is recommended. In the case of IL-ALRs, most of the correlations predict similar values. The correlation by Merchuk et al. (48) can be recommended on the basis that more geometrical parameters have been taken into account, and this gives more generality.

42.4 HEAT TRANSFER

Because of the relatively low reaction rates of processes involving microorganisms and cells, heat effect problems related to local variations of temperature are not common in bioreactors. Even in the case when polymeric products are released to the medium and a very high viscosity is attained, heat transfer is not the controlling step, because such viscous media will also hinder the mass transfer and the heat generation will consequently be limited. The case of reactions catalyzed by immobilized enzymes, on the other hand, may require another sort of considerations, because of the higher reaction rates.

Data on heat transfer in BCs are much more frequent than that in ALRs, and some of the basic observations are valid for both. The heat transfer rate in BCs is much larger than the one expected from single-phase flow (270). This is caused by the bubble-driven turbulence and liquid recirculation, which are characteristic of the flow in BCs.

Several correlations have been proposed for the prediction of the heat transfer coefficient in bioreactors (271) based on the surface renewal model and Kolmogorov's theory of isotropic turbulence:

$$St = 0.1(\mathrm{Re}FrPr^2)^{-0.25} \tag{42.47}$$

Kawase and Moo-Young (202) presented an expression that fits satisfactorily most of the published data for non-Newtonian systems. The model is based on Levich's (272) three-zone concept and Kolmogoroff's (273) isotropic turbulence theory and has no empirical adjustable parameters. For Newtonian systems, the resulting equation is

$$Nu = 0.134^{1/3}(Pr)^{1/3}Fr^{-1/4}(\mathrm{Re})^{3/4} \tag{42.48}$$

Roy et al. (274) reviewed data of heat transfer and concluded that the correlation proposed by Joshi et al.(182) fits all of them within 8% error:

$$Nu = 0.087\left(\frac{d^{1.33}g^{1.33}(U_G - \phi_T U_{b\infty})^{0.33}\rho_L}{\mu}\right)^{0.8} Pr^{0.33}\left(\frac{\mu_E}{\mu_w}\right)^{0.14} \tag{42.49}$$

This expression is therefore quite general, but requires knowledge on actual gas holdup in the system, which can be calculated from the corresponding correlations or models.

Because, as noted by Roy et al. (274), the heat transfer process is governed by the flow pattern and thermal diffusivity, the use of CFD with correct velocity and holdup profiles and correct eddy diffusivity should lead to correct predictions of the heat transfer coefficients (274,275).

An interesting question is the effect of suspended microorganisms on the rate of heat transfer. Blakebrough et al. (276,277) studied the heat transfer rates in an external loop airlift fermenter. They reported an enhancement of this rate due to the presence of microorganisms in the case of laminar flow. In their studies, carried out with mycelial suspensions of *Aspergillus niger*, they conclude that this enhancement can be explained by two mechanisms: disturbances of the liquid layer near the surface at low microbial concentrations and a "scraped surface" type of heat transfer at high concentrations or when the microorganism grows in the form of pellets. While this interpretation may be questioned on the grounds that most of the researchers have agreed that boundary layers are irrelevant in BC liquid flow, which is mainly controlled by bubble-scale dynamics, the reported enhancement possibility should be considered.

For the case of denser solids, Dhaouadi et al. (113) have used glass beads in their experiments and found opposite

TABLE 42.6. Mass Transfer in IL-ALRsGas Holdup in IL-ALRs

Source	Correlation	Notes
69	$k_L a = 0.76 J_G^{0.8} \left(1 + \frac{A_d}{A_r}\right)^{-2}$	
83	$k_L = 5.63 \times 10^{-5} \left(\frac{g\rho^2 D\sigma}{\mu_L^3}\right)^{0.5} d_B e^{-0.131 C_s^2}$	d_B, bubble diameter
80	$k_L a = 0.00153 J_G^{0.52} \mu_{app}^{-0.89}$	
71	$Sh = 0.68 n^{-6.72} Re_G^{(0.38n+0.52)} Sc^{(0.38n-0.14)}$	
4	$Sh = 0.477 Sc^{0.50} Ga^{0.257} Bo^{0.873} \left(\frac{d_d}{d}\right)^{-0.542} \varphi_T^{1.36}$	Gas in draft tube
82	$\left(\frac{k_L a\sigma}{Dg\rho}\right) = 2.25 Sc^{0.50} Mo^{-0.136} \left(\frac{d\text{no}}{d}\right)^{-0.0905} \varphi_T^{1.26}$	Gas in annulus
77	$Sh = 4.04 Sc^{0.50} Ga^{0.26} Bo^{0.67} \left(\frac{d_d}{d}\right)^{-0.047} \varphi_T^{1.34}$	Gas in draft tube, solids
129	$k_L a = 4.490 J_{Gr}^{0.384} C_s^{0.595} \left(1 - \frac{\rho}{\rho_s}\right)^{0.337}$	
265	$k_L a = 0.0343 J_{Gr}^{0.524} \mu_{app}^{-0.255}$	
3	$Sh = 6.82 \times 10^4 Fr^{0.9} M^{-3.4} Ga^{0.13} Cb^{-0.07} Ct^{-0.18} \left(1 + \frac{A_d}{Ar}\right)^{-1}$	
266	$k_L a = 0.1919 J_{Gr}^{0.8252} \left(\frac{A_s}{A_r}\right)^{-0.505} \left(\frac{h}{D}\right)^{0.015} Ct^{-0.011}$	

TABLE 42.7. Mass Transfer Correlations in EL-ALRs

Source	Correlation	Notes
69	$k_L a = 0.76 J_G^{0.8} \left(1 + \frac{A_d}{A_r}\right)^{-2}$	
267	$k_L a = \left(1 - \frac{A_d}{A_r}\right)^{-1} (0.349 - 0.102 C_s) J_{Gr}^{0.837}$	
80	$k_L a = 1.911 \times 10^{-4} \left(1 - \frac{A_d}{A_r}\right)^{-0.853} J_{Gr}^{0.525} \mu_{app}^{-0.89}$	
268	$k_L a = 4.49 J_{Gr}^{0.384} \varphi_T^{0.595} \left(1 - \frac{\rho}{\rho_s}\right)^{0.337}$	Fluidized bed
269	$k_L a = 0.484 \left(\frac{\rho J_{Gr} h^{0.76}}{\mu}\right) \left(1 + \frac{A_d}{A_r}\right)^{2.41} F_f^{1.9}$	
112	$k_L a = 1.53 \times 10^{-2} \varphi_r^{1.3} J_{Gr}^{0.52} \mu_{app}^{-0.73} h^{0.3}$	Partitioning plates

results (Fig. 42.28). An addition of solids up to 3% in volume produced a reduction in the heat transfer coefficient (Fig. 42.29). This effect may be associated with the difference introduced by the presence of the solids on the bubble size distribution, indicated by the change in the frequency spectra reported. This concurs with the fact that in bubbly flow, the heat transfer to the walls is related to bubble-scale phenomena.

While the most common heat exchange surface is the wall of the reactor, some processes require the presence of heat exchangers in the bulk, bringing into question the nonhomogeneity of heat transfer. Special probes for measurement of heat transfer coefficients have been developed and used (278–280). In general, and as expected from the radial distribution of bubbles and of liquid velocities, the values of the heat transfer coefficient at the center are of the

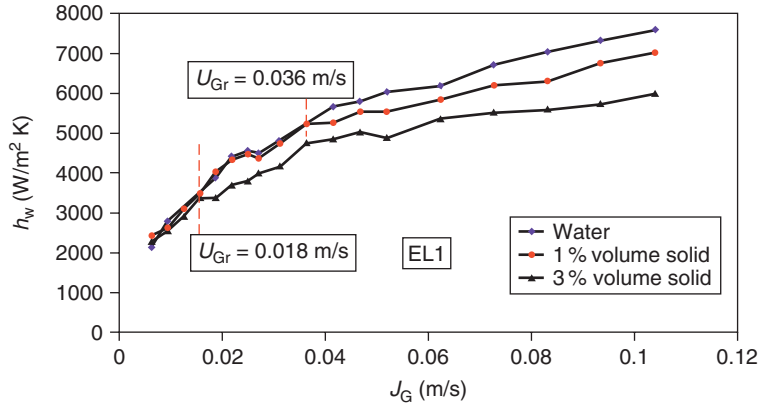


Figure 42.28. . Heat transfer coefficient to the wall of an EL-ALR, with three concentrations of 90-μm diameter glass beads. From Ref. 113, with permission

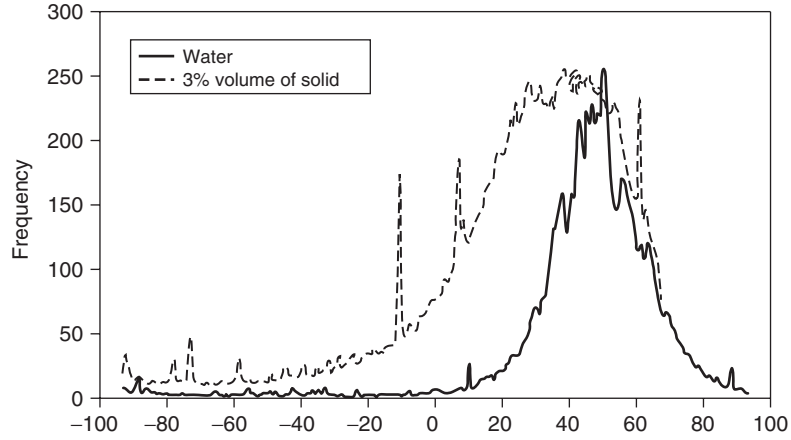


Figure 42.29. Effect of solids concentration (90-mm glass beads) on the measured frequency spectra. The wider spectra indicate a larger bubble size distribution. From Ref. 113, with permission.

order of 10% higher than that at the walls. High pressure produces a decrease in these coefficients (281).

42.5 MULTIPHASE AIRLIFT BIOREACTORS

The special qualities of the ALR stem, as stated before, from its fluid dynamic characteristics. One such characteristic is the directionality of the liquid flow. Independently of superimposed fluctuations, a clear net flow is present in the reactor, with exception of the gas separator in internal loop designs. Therefore, it is to be expected that the fluidization capacity of the ALR will be markedly superior to that of a BC.

42.5.1 Three-Phase ALRs

The most used combinations of phases in ALR have been gas–liquid–solid, but more complex systems have as well been used. Many studies have been conducted on the suspension of solids in ALRs, particularly on the use of this type of device for catalytic processes in the chemical industry (282–287). A very important point is the minimum gas superficial velocity that leads to complete solid fluidization (161,282,285,287–293). Hysteresis has been observed in some cases (294,295); once total fluidization has been attained, the superficial velocity can be reduced to values lower than that required to reach this state. This is due to the high pressure drop related to passage of liquid through a bed of solids, before fluidization, as compared with the drag forces required to maintain the solid in suspension after all the solids are suspended.

Contradictory data on the effect of the suspended solids on the reactor performance have been reported. Fan et al. (296) claimed that the overall gas holdup increased due to the presence of the solids, whereas Koide et al. (77,297) showed the opposite effect on the gas holdup and reported

a small decrease in $k_L a$ as well. It is possible that these discrepancies are due to the use of different solids. One of the properties of solids that is often overlooked is wettability (298). Small bubbles may adhere on wettable solids, leading to a change in the apparent density of the particle and thus changing their solid circulation velocity. Some authors use activators or dispersants to increase the wettability to distribute them evenly and stabilize the solids (299), but the contribution of these additives to the hydrodynamics and mass transfer properties has not been studied.

In the case of suspended solids that take an active part in the process, the mass transfer rate from the liquid to the solid may become the limiting step. The dependence of particle size on the mass transfer to the suspended solids has been studied (35,300,301).

All the comments made above relate to heavy solids. This situation is not very frequent in biological processes, with the exception of biolixiviation (302) or the special case of microbial desulfuration of coal (303). In most of the biological processes that may take place in an ALR, the solids are either cells, clumps of cells, or supports that are not much denser than the medium. Therefore, neither fluidization nor the distribution of solids in the reactor constitutes a problem. Assa and Bar (304) found very small variations in the axial distribution of animal and plant cells suspended in an IL-ALR. This is due to the small free-falling velocity of the solids, which is the reason for the difference in loading between the riser and the downcomer when heavy particles are used (284,285,305). Because of the small difference between solid and medium density, the movement of the particles usually present in biological processes is not as dependent on gravity forces as on liquid and bubble movement. In this case, the transport of liquid in the wake of the bubbles may be considered to be the prevailing transport mechanism (306). Snape and Thomas (307) proposed a Monte Carlo algorithm for modeling particle movement by this mechanism in bubbly flow to predict distribution of circulation times in the reactor. Koide et al. (77) conducted a broad study of gas holdup and mass transfer rates in an IL-ALR containing Ca-alginate beads, which are often used for cell immobilization. The authors found that solid loading had a negative effect on both parameters, but the particle diameter had no influence in the range studied ($1.8\,\text{mm} < d_p < 3.98\,\text{mm}$). Chang et al. (38) studied the influence of suspended pellets (cylindrical pellets of immobilized penicillin acylase) on the mixing time in an IL-ALR. They found that mixing time increased when the solid volumetric concentration was raised up to 15%. For higher concentrations, the trend inverted, and the mixing time decreased. No such effects were observed with heavier solids. Increases in gas superficial velocity and in top clearance both led to decreases in mixing time in all cases.

The use of light particles whose density is smaller than that of water is more and more frequent. The energy necessary to maintain them suspended and in motion is lower than with heavier particles. Their roughness and porosity is also an important parameter in the growth of attached microorganisms. Couvert et al. (308) characterized the hydrodynamic behavior and the oxygen mass transfer characteristics of a three-phase ALR, under the influence of two types of plastic materials less dense than water, a regular smooth one (P1) and a rough one (P4), both used in bioprocesses. The addition of solid at the assayed percentages (10–40% of P1 particles and 10–70% of P4 particles) had little impact on the mixing parameters. Neither did the solids affect the hydrodynamic parameters, except for the gas holdup if the solid concentration is below 16% and high gas velocities are used. The material P4 distribution and hydrodynamic parameters were more homogeneous in the reactor than for P1. The quantity of solid not only had influence on the mass transfer, but also the nature of the solid particles (shape, size, porosity, etc.). Although P1 seemed to increase $k_L a$, the presence of P4 caused a decrease in $k_L a$. Nevertheless, below a solid holdup of 16%, both types of solids did not alter the volumetric mass transfer coefficient in the reactor.

A special type of gas–liquid–solid three-phase bioreactors are the particle-based biofilm reactors (PPBRs). In them, cell aggregates are formed spontaneously as large dense granules or attached to suspended carriers to improve gravity separation. PPBRs are extensively used in environmental biotechnology because they can be operated at high biomass concentrations to treat the large volumes of dilute aqueous solutions that are typical of industrial and municipal wastewaters without the need for separating the biomass and the treated effluent.

Lately, an extensive review of the latest generation of PPBRs was presented (309). Two of them based on gas lift pumps outstand: biofilm airlift suspension reactors (BASRs) and internal circulation reactors (ICRs) (Fig. 42.30a and 42.30b). The main difference of BASR with the conventional ALR is the three-phase separator on the top. The ICR is a more novel and original adaptation of airlift pumping system. In essence, it consists of two reactor compartments situated on top of each other, one highly loaded and the other scarcely loaded. The biogas produced in the first compartment is collected by the lower level phase separator and is used to generate a gas lift pumping system. Several full-scale IC and BAS systems are presently in operation in Europe.

42.5.2 Four-Phase ALRs

Secondary metabolites from cell cultures are either stored within the cells and/or excreted into the medium (they may also appear in the medium due to cell lysis). In cases where the yield of bioproduct of interest is low due to

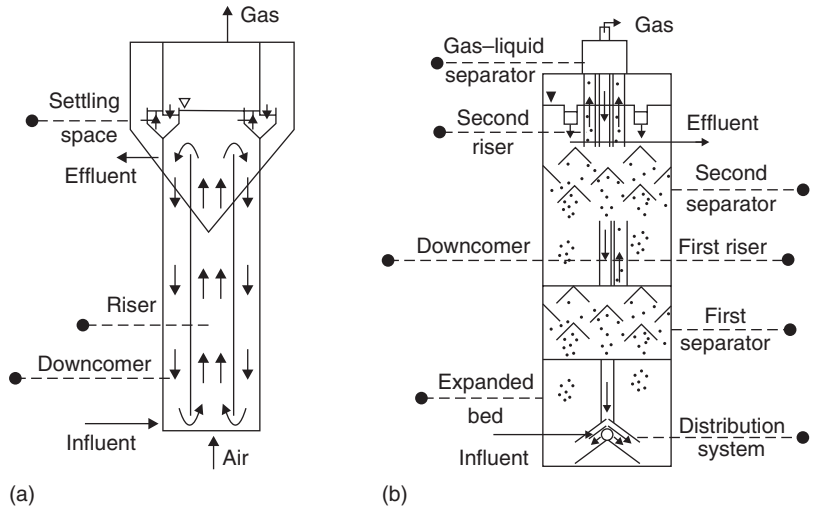


Figure 42.30. Particle-based biofilm reactors (PPBRs) based on gas lift pumps. (a) Biofilm airlift suspension reactor (BASR) and (b) internal circulation reactors (ICRs). Reprinted with permission from Nicolella et al. (309).

cellular-mediated regulation of the ratio between intracellular and extracellular bioproduct concentrations, extractive fermentation seems to provide excellent results, particularly for metabolites produced by plant cell cultures (310). This process increases the net production by reducing the concentration of the secondary metabolites in the culture medium. The same approach can be used for removing substances from culture broth either to avoid their degradation or to increase the biosynthetic rates by reducing feedback inhibition of biosynthesis.

In extractive fermentations, the addition of the solvent directly to the bioreactor is the simplest operation way, but it can lead to the formation of stable emulsions of organic phase in the aqueous medium due to high shear rates required for solvent dispersion. Therefore, the bioreactor design is extremely important. In this sense, ALRs are serious candidates because shear is lower and they are more uniform, eliminating the formation of very small solvent drops. Sajć and Vunjak-Novakovic (311) presented a very interesting extractive bioconversion in a four-phase external loop airlift bioreactor. The aim was the extractive bioconversion of anthroquinones by plant cells. The cells were immobilized in alginate beads suspended in an aqueous medium. In the riser, a gas and a solvent (silicone oil or *n*-hexadecane) were injected. The gas bubbles provided the energy for the circulation of the system and the solvent drops extracted the anthroquinones produced. Both gas and solvent were completely separated at the top and only the aqueous medium and the suspended alginate beads circulated (Fig. 42.31).

Previously, Sajc et al. (312) performed a exhaustive study in which the influence of gas, solvent, calcium alginate particles, and culture medium composition on gas and

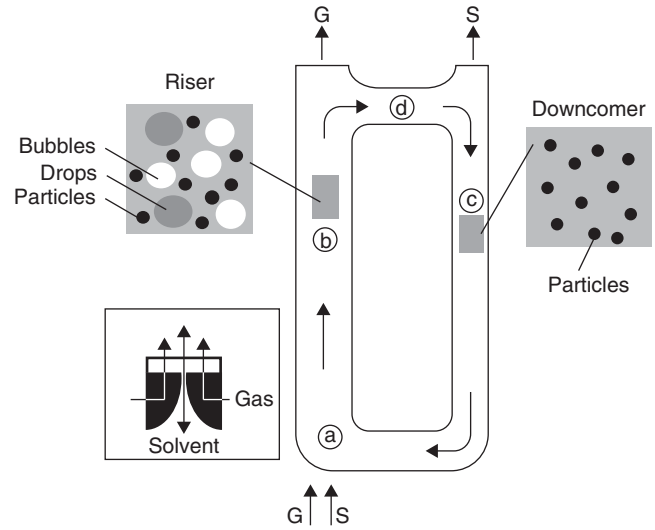


Figure 42.31. Extractive bioconversion in a four-phase external loop airlift bioreactor. In the riser, gas and a solvent are injected. Both gas and solvent are completely separated at the top and only the aqueous medium and the suspended alginate beads circulate. From Ref. 311, with permission.

solvent holdup, liquid circulation velocity, mixing in aqueous liquid phase, and mass transfer coefficients of oxygen and plant cell product was analyzed. They showed that the gas holdup is the principal variable determining the properties of the four-phase system, and a unified correlation for the gas holdup, derived from drift flux flow in a three-phase system (313), was proposed to the four-phase system. No differences under bubbly flow regime were observed in the bubble size and size distribution when water or culture

medium was used as aqueous phase. Consequently, hydrodynamic parameters for the four-phase system such as gas holdup, liquid circulation velocity, oxygen mass transfer coefficient, and axial liquid dispersion were similar for both aqueous phases tested.

In spite of interest of this four-phase EL-ALR, the authors did not study the impact of dispersed solvent liquid phase on fluid dynamics compared with the same system without it. Although with a different purpose, Mehrnia et al. (2,266,314) studied hydrodynamics and mass transfer in airlift bioreactors containing water-in-oil microemulsions as models of the biocatalytic desulfurization of petroleum. Several configurations of gas separator and draft tube heights were tested. The rate of gas recirculation and consequently the rate of liquid circulation were influenced by the small bubble sizes generated with the microemulsion. In general, gas holdup and volumetric gas–liquid oxygen transfer coefficient for water-in-oil systems were significantly higher than those for the distilled water system. For all assayed microemulsions with kinematic viscosities up to about 8×10^{-6} m^2/s, the bubbly flow regime prevailed. However, an increase in kinematic viscosity up to around 32×10^{-6} m^2/s, either through changing the oil base or the water-to-oil phase volume ratio of the microemulsion, resulted in the onset of churn-turbulent regime at most of the air rates employed. A concomitant decrease in the gas holdup and k_La values was also observed.

42.6 SELECTION AND DESIGN

42.6.1 Scale-Up

The methods available for scale-up of bioreactors have been reviewed by Oosterhuis (315), Kossen and Oosterhuis (316), Sweere et al. (317), Sola and Godia (318), and Zlokarnik (319), among others. Unfortunately, there are still no exact and well-established rules ensuring an accurate transition from one scale to another, particularly for scale-up of ALRs.

42.6.1.1 Integrated Kinetics and Fluid Dynamics. In general, design from first principles cannot be undertaken because of the lack of basic knowledge on the hydrodynamics of the bioreactors. One possible solution is the semifundamental method, which comprises simple approximate models for fluid dynamics integrating them with basic known kinetics and heat and mass transfer rates. For example, Sikula et al. (320) have modeled the biotransformation of glucose to gluconic acid by *A. niger*, performed in IL-ALRs of different scale (12, 40, and 200 L), using a tank in series model. Kinetic parameters were estimated from data obtained in the smallest reactor. Hydrodynamic parameters (i.e. gas holdups, circulation velocities of the liquid and the gas, and the volumetric mass transfer coefficient of oxygen) were predicted from semiempirical correlations reported in the literature. The end of the fermentation process was reasonably predicted with an error of about 10%; this error was mainly associated to the strong dependence of the results on the initial concentration of the biomass in the reactor. An improved simulation may have been achieved incorporating the physiological state of inoculum to the model (e.g. morphology, internal nutrient pool, and growth phase).

Recently, Boyadjiev (321) also used integrated modeling to tackle the problem of scale effect associated to the radial nonuniformity of the velocity distribution in column reactors (the scale effect has been erroneously regarded as an increase in the longitudinal dispersion in many works). He developed an elegant model based on velocities and concentrations averaged over a cross section of an airlift three-phase catalytic reactor. The model includes radius-dependent parameters determined using average concentrations, which is easier than parameter determination involving measurement of local concentration.

42.6.1.2 Rules of Thumb. It does not happen very often that all the information relative to integrated modeling is available with a degree of certainty that allows safe design of a large system. Thus, the designer must usually resort to dimensional analysis. The method implies the description of the problem by a complete set of pi-numbers, and knowing initially all relevant physical quantities that describe the problem. As prerequisite, a thorough and critical knowledge of the process in question is needed. In fact, Zlokarnik (319) established degrees of applicability of dimensional analysis, depending on the knowledge available.

A simplified version of this method is to limit the number of variables to one or two and to follow rules of thumb (322), which, depending on the specific case, may be kept constant alone or combined with each other (P/V, k_La, N, Re, t_m, etc.). Figure 42.32 shows some typical examples carried out in STRs.

More recently, Liu et al. (324) have successfully scaled-up L-lactic acid production by *Rhizopus* sp. MK-1196-96 from 0.003 to 5 m^3 ALR using OTR as the scale-up criterion. The correlation between OTR and L-lactic acid production in the 0.003, 0.1, and 5 m^3 ALRs is plotted in Fig. 42.33, suggesting that OTR can be used as a scale-up criterion for this fermentation process.

The literature shows, however, many cases of inconsistency for this method. For example, design of a scaled-up bioreactor in which the OTR is kept constant can lead to a better performance than expected (325) or worse than expected (326).

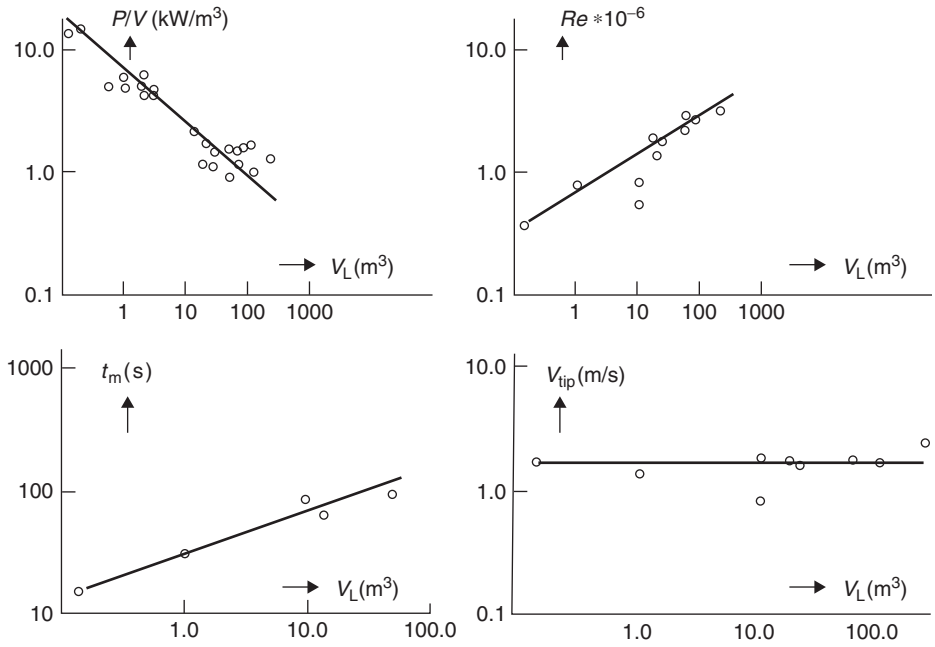


Figure 42.32. Specific power input, Reynold number, mixing time, and impeller tip speed versus for different volumes in STRs. Adapted from Ref. 323.

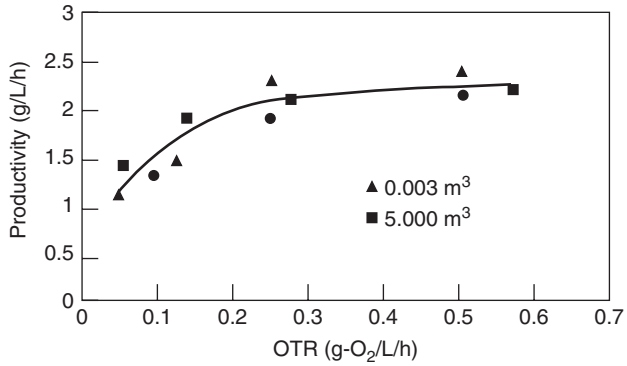


Figure 42.33. Correlations between OTR and L-lactic acid production in ALRs. Adapted from Ref. 324.

42.6.1.3 Regime Analysis and Scale-Down. The method of regime analysis and scale-down (315,316,327) combines two tools to overcome the problem posed by the complexity of biochemical reactors. Their method is based on considering the regime of the full-scale process as the objective and planning the strategy of process development from this point on. This method is therefore applicable only to conventional and well-studied bioreactors that are to be used in a new bioprocess.

Regime analysis is based on the consideration that, generally, biochemical processes involve a series of steps, some being mass or heat transfer by convection, some being diffusive mechanisms (activated or not), and others being chemical reaction steps. In the latter case, a mass transfer mechanism is superimposed, because molecules must encounter one another to react, and usually a heat effect will accompany the reaction. Therefore, regime analysis involves the identification of the time and length scales for the phenomena of particular interest (Figs. 42.34 and 42.35).

Depending on whether these steps take place in parallel or in series and on the relaxation time for each step (328), the rate of the total process is often given as the rate of one single step. But the equilibrium between all the individual rates can be (and usually is) upset by a change in scale. This is to be expected, because a change in scale will not bring a change in the physicochemical or kinetic parameters (scale-insensitive variables) but will affect the overall convective mass and heat rates (scale-sensitive variables). A new equilibrium will be established, and the interplay of all the parameters of the system may lead to a regime in which a different step becomes the step controlling the process rate.

The method of Kossen and Oosterhuis (316) starts with an analysis of the operation of the large-scale system. Once the regime is clarified, a small-scale system is designed in such a way that it simulates the operation regime of the larger one. Optimization studies can be done on the smaller model, and conclusions will then be extrapolated to the full-scale process (Fig. 42.36). An example is given by Oosterhuis (315), in which a large-scale STR is simulated on a laboratory scale by two interconnected vessels; one

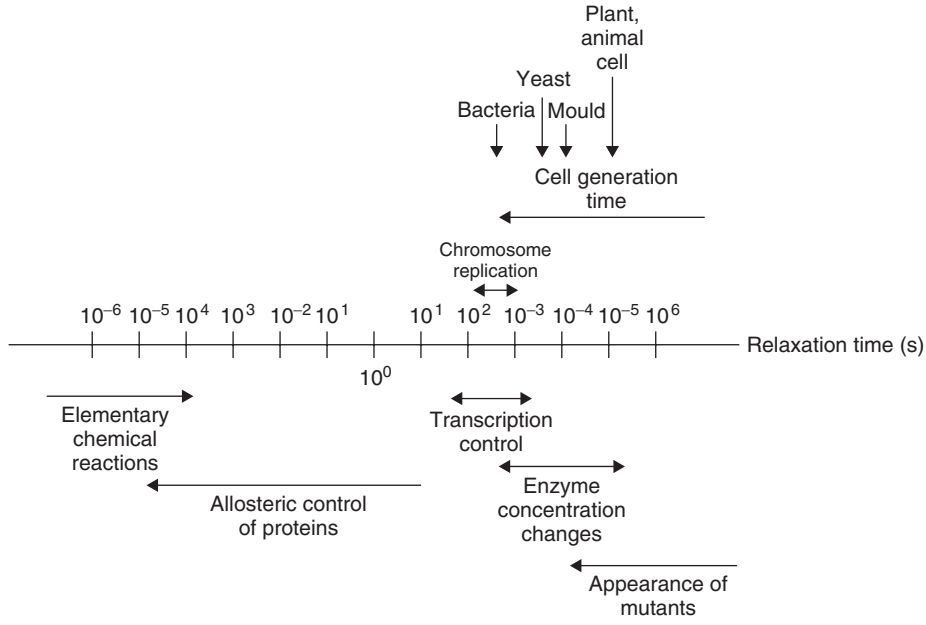


Figure 42.34. Characteristic times for biological responses important in bioreactor engineering. From Ref. 229, with permission.

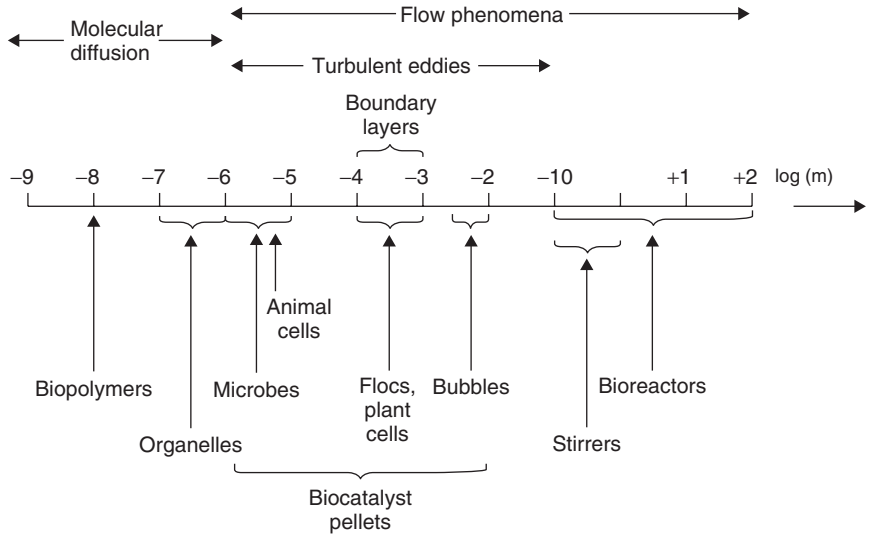


Figure 42.35. Characteristic length scales encountered in bioreactor design and analysis. From Ref. 229, with permission.

with a small liquid volume, high agitation rate, and high rate of oxygen supply (representing the zone near the impeller sparger in the reactor), and a second vessel with a much larger liquid volume, oxygen consumption (simulated by nitrogen sparging), and gentle agitation. The success of this model suggests that large vessels must be carefully analyzed and their internal structure studied for proper modeling and design to be performed. The analysis starts with the definition of the characteristic time constants of the system.

An analysis of the time constants required for the design of an ALR for plant cell culture was presented by Doran (40). Figure 42.37 shows the reported values of the time constants calculated for an EL-ALR for mixing, mass transfer, and oxygen consumption at two different cell concentrations: 5 and 30 kg/m^3. These graphs exemplify the changes in the controlling mechanism that may take place as the physical properties of the broth change in the course of the bioprocess.

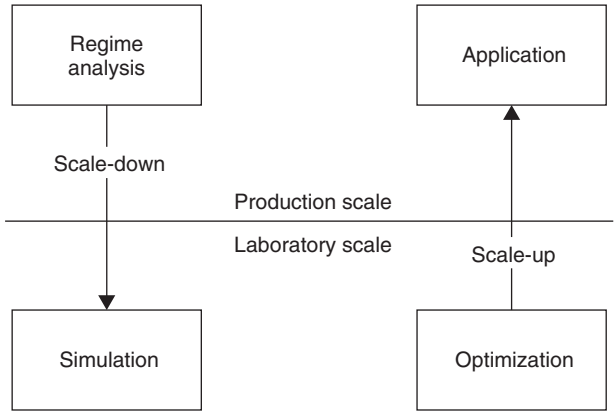


Figure 42.36. Schematic representation of the scale-down method. Adapted from Ref. 315.

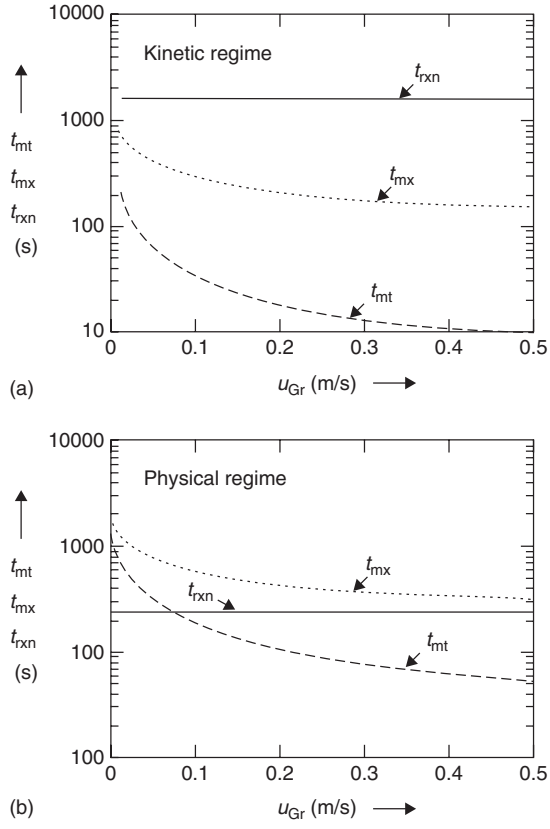


Figure 42.37. Time constants calculated in an EL-ALR as a function of the superficial gas velocity. (a) CS = 5kg/^{3}; (b) CS = 30 kg/^{3} (t_{mx}, mixing time; t_{rxn}, time constant for oxygen consumption; t_{mt}, mass transfer time constant). From Ref. 40, with permission.

A complete example of how to use this methodology of regime analysis and scale-down for scaling-up the continuous production of isopropanol–butanol mixtures by immobilized *Clostridium* sp. was presented by Schoutens et al. (329). Two reactor types were studied: a fluidized bed reactor (FBR) with liquid recycling and an EL-ALR. Initially, a regime analysis, by evaluating time constants associated to flow, mixing, and conversion, was conducted in 50–65 m^3 large-scale bioreactors to identify the reigning regime. Next, two representative model reactors were developed using scale-down approach: a 10-L FBR and a 15-L EL-ALR. For both reactors, the hydrodynamic behavior and the total reactor performance were exhaustively studied.

In an innovative work, Papagianni et al. (330) designed a bioreactor as a tool for scale-up/scale-down studies. It consisted of an EL-ALR that simulated circulation loops experienced in conventional STRs; the circulation time was a measure of reactor size. The ALR was tested using the citric acid fermentation by *A. niger* as a model system. Citric acid production and fungal morphology were used successfully as the response variables for evaluation. The relationship between product concentration and circulation time is given in Fig. 42.38. High circulation times in the EL-ALR correspond to inadequate mixing in larger STRs. Because other parameters such as number of impellers, baffles, and power input may also influence the above-mentioned relationship, a correlation for each parameter should be obtained.

42.6.1.4 Computational Fluid Dynamics. CFD tools have been published showing the capability of handling the complex problem of multiphase flow in ALRs (97,133,274,331–344). CFD gives much more detailed information, reaching the level of local velocities and local holdup (Fig. 42.39) (339). Local gas holdup and axial liquid velocity along the radius of a column (345)

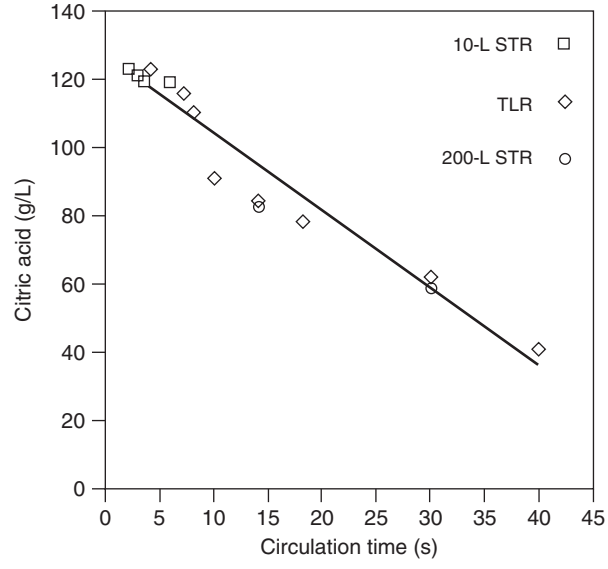


Figure 42.38. Comparative effect of circulation time on the production of citric acid by *A. niger* in an EL-ALR and stirred-tank reactors of different size. Adapted from Ref. 330.

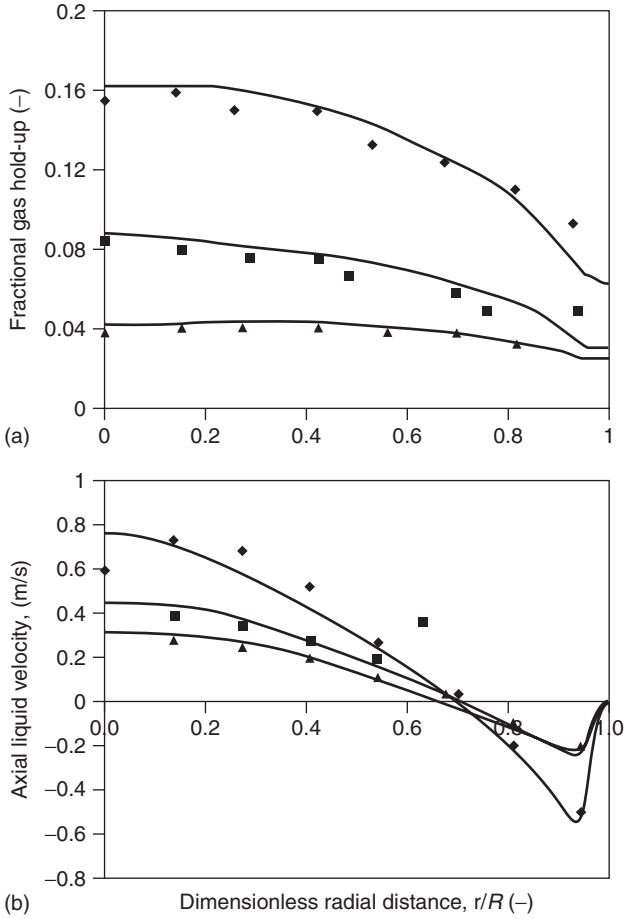


Figure 42.39. Gas holdup and liquid velocity radial distribution as calculated using CDF. Comparison with experimental data of Menzel et al. (345). Liquid velocity: ▲$J_G = 0.012$ m/s; ■$J_G = 0.024$ m/s; ♦$J_G = 0.048$ m/s. From Ref. 339, with permission.

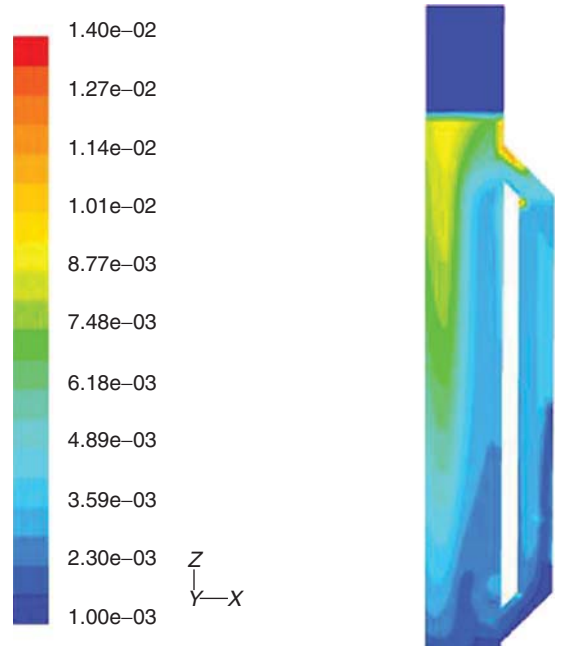


Figure 42.40. Contours of the Sauter mean diameter in millimeters along symmetry plane for superficial velocity of 0.03 m/s. With permission from Ref. 346.

can be predicted with a remarkable precision, and CFD results were validated. This tool also allows the prediction of mixing times and axial dispersion coefficients (339). One of the most difficult obstacles in the simulation of a multiphase system as those that we are analyzing is the behavior of the gas dispersion (346), most of the literature does not account for the dynamic breakage and coalescence of bubbles. These phenomena affect the bubble size distribution, a key factor that influences OTR in aerobic fermentation systems, because it modifies the interfacial area. Dhanasekharan et al. (346) proposed a modeling approach in which these effects are included by solving a population balance model with bubble breakage and coalescence. The population balance model was coupled to multiphase flow equations and solved using a commercial computational fluid mechanics code, FLUENT 6. Predicted values of gas holdup and volumetric mass transfer coefficients for different superficial velocities were validated with experimental data from Kawase and Hashimoto (347). Figure 42.40 shows a contour plot of the Sauter mean bubble diameter in an ALR. In Fig. 42.41, examples of CFD predictions are displayed. The results of modeling showed good agreement with the experiments. In this case, the use of CFD seems to overcome the need for correlations whose application is restricted to certain geometric configurations and flow conditions.

Feng et al. (348) have recently developed a coupled CFD model to simulate the phenol biodegradation by yeast *Candida tropicalis* in an IL-ALR. The model combines hydrodynamics with biochemical reactions, without accounting for the dynamic breakage and coalescence of bubbles. The local instantaneous flow and phenol biodegradation features, gas holdup, gas velocity, liquid velocity, cell concentration, and phenol concentration inside the ALR were successfully predicted by the proposed model (Fig. 42.42). In a previous work conducted with BCs, Feng et al. (349) reported similar results. The predictions of the hydrodynamic characteristics and phenol biodegradation behavior were accomplished in a virtual BC bioreactor, but the results were not validated experimentally.

It therefore seems that in the near future, with the improvement of CFD, this technique will progressively replace the use of empirical correlations for the prediction of gas and liquid velocity, gas and solids holdup, and mixing parameters and will also provide evaluations of shear rate and energy dissipation. It should be kept in mind that CFD should always be validated with experimental data.

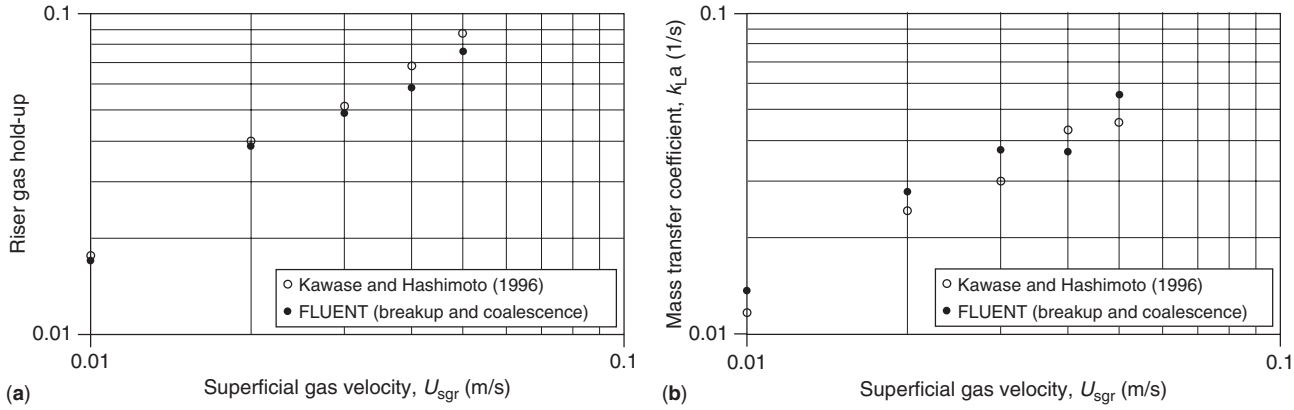


Figure 42.41. Comparison of CFD predictions of (a) gas holdup and (b) volumetric mass transfer coefficient with experimental results of (347). Adapted from Ref. 346.

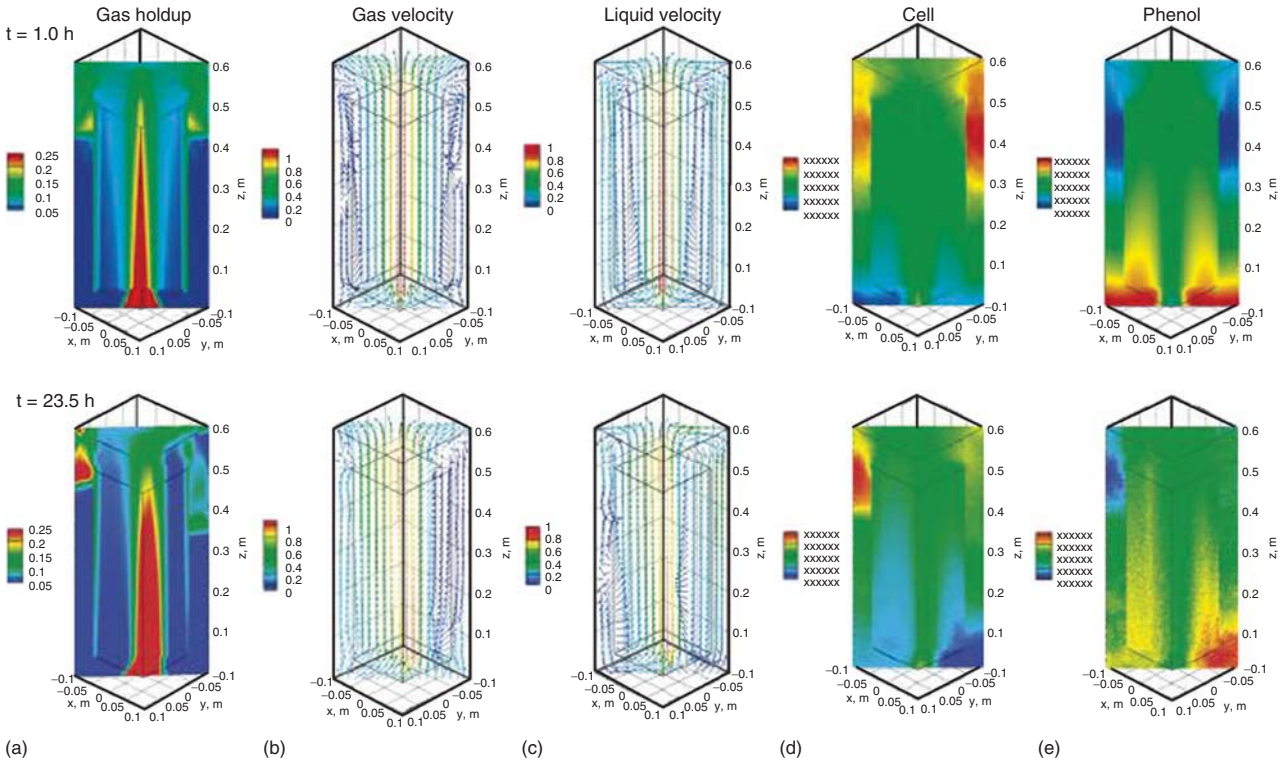


Figure 42.42. Transient model predictions of (a) gas holdup, (b) gas velocity, (c) liquid velocity, (d) cell concentration, and (e) phenol concentration at the time of culture. From Ref. 349, with permission.

42.6.1.5 Artificial Neural Networks. It is clear that there is a great need of correlations for predicting the hydrodynamics and mass transfer parameters in ALRs, which should be system-independent and could further be used for proper design and scale-up of industrial bioprocesses. In general, the available literature correlations for predicting hydrodynamics and mass transfer in ALRs are based on dimensionless numbers and specific mixing power input, supposedly independent of the gas–liquid system. However, they often provide large deviations when compared with experimental data. Artificial neural networks (ANNs) are emerging as a powerful tool for predicting the hydrodynamic parameters in aerated and ARs (350).

Al-Masry (351) applied basic principles of ANNs to analyze the effects of changing the volume of the liquid in the gas–liquid separators on the hydrodynamics of EL-ALRs.

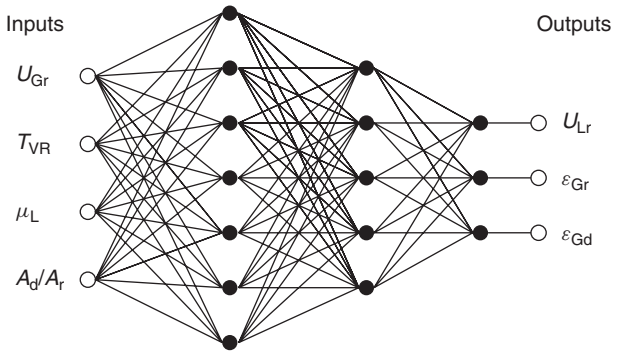


Figure 42.43. Three-layer feed-forward neural network with four inputs and three outputs. Adapted from Ref. 351.

The used neural network was very simple and consisted of four inputs and three outputs with two hidden layers. The inputs were superficial gas velocity J_{Gr}, volume ratio T_{VR}, liquid viscosity μ_L, and scale-up factor A_d/A_r, while the outputs were liquid circulation velocity J_{Lr}, riser gas holdup ε_{Gr} and downcomer gas holdup ϕ_{Gd} (Fig. 42.43). The network was trained on 60% of the data and then used to predict 40% of the data that had never been seen by the network. The training was successfully accomplished because the neural network noticeably improved the predictions of the hydrodynamics variables in relation to those calculated from correlations reported by Al-Masry (98).

The correlations for gas holdup usually have a validity over a limited range of J_G. Shaikh and Al-Dahhan (352) developed a unified correlation for gas holdup using a combination of dimensional analysis and ANN modeling. A databank of around 3500 measurements was collected from 60 sources (Table 42.8). Authors identified four relevant dimensionless groups (Re_g, Fr_g, Eo/Mo, and ρ_g/ρ_L) to predict overall gas holdup. A comparison with selected correlations in the literature showed that the developed ANN correlation noticeably improved prediction of overall gas holdup. The developed correlation also shows better prediction over a wide range of operating conditions, physical properties, and column diameters, and it predicts properly the trend of the effect of the operating and design parameters on overall gas holdup. The developed ANN correlation should be useful in the scale-up of BC reactors.

Lemoine and Morsi (238) developed empirical and back-propagation neural network (BPNN) correlations to predict the hydrodynamic and mass transfer parameters in gas–liquid ARs. They also used a large number of experimental data points (7374) obtained from their laboratory, as well as from the literature, covering wide ranges of reactor geometry, impeller diameter, physicochemical properties, and operating variables. One of the reactors included in this study was a DT-ALR. Correlations were employed to construct a simple algorithm for predicting the gas holdup (ϕ_G), volumetric mass transfer coefficients (k_La), Sauter mean bubble diameter (d_{32}), gas–liquid interfacial area (a), and liquid-side mass transfer coefficient (k_L) in different ARs under industrial conditions. The developed algorithm based on the BPNN correlations was used to predict the effects of liquid-phase viscosity and composition of the gaseous feed to the reactor on the hydrodynamic and mass transfer parameters in a soybean oil hydrogenation carried out in a large-scale gas-sparging AR (2.5-m inside diameter and 5-m height).

TABLE 42.8. Range of the Key Variables and Physical Properties, and Type of Spargers Included in the Collected Databank

Variable	Range
Column diameter	0.045–5.5 m
Liquid density	684–2965 kg/m^3
Liquid viscosity	0.41–2.95 cP
Surface tension	20–72 m N/m
Gas density	0.083–1.2 MPa
Superficial gas velocity	0.005–0.75 m/s
Superficial liquid velocity	0 (bath liquid)
Overall gas holdup	0.05–0.685

Source: Adapted from Ref. 352.
Gases: Air, N_2, CO_2, He, Ar, mixture of N_2, and H_2. Liquids: water, tetradecane, paraffin oil (A, B), soltrol-130, isopropanol, monoethylene glycol, *n*-heptane, isopar-G, and so on. Sparger types: perforated plates with different number of holes, geometry and hole sizes, single nozzle sparger, cross-sparger, sintered plate, and so on. Number of sources: 60 (1965–2000). Number of data points: 3500.

42.6.1.6 Global Strategy. Each case of scale-up has particularities that should be considered. For example, average shear rate is one of the more important parameters used in the design of bioreactors for culture shear-sensitive microorganisms. But, shear rates are unevenly distributed in the different zones of ALRs (353,354). Al-Masry (355) found that the wall shear rates developed in EL-ALRs with aerated non-Newtonian liquids can be significant: the ratio of wall shear rates to bulk shear rates ranged from 5% to 40%. More recently, Al-Masry (356) observed that wall shear rates could be strongly influenced by the scale and proposed a new empirical correlation for estimating them given by

$$\gamma_w = 4800 U_{Gr}^{1.86} \left(1 + \frac{A_d}{A_r}\right)^{-0.14} h^{0.48} \qquad (42.50)$$

The used working volume, A_d/A_r ratio, and height of dispersion (H_D) ranged from 40 to 700 L, from 0.1 to 1.0, and 1.2 to 6.2 m, respectively. Polymer solutions of xanthan gum and CMC were used to simulate non-Newtonian behavior of biological systems. Therefore, because frequency of passage of sensitive cells through these high shear regions may be determinant, wall shear rates should be kept in mind in any strategy of scale-up.

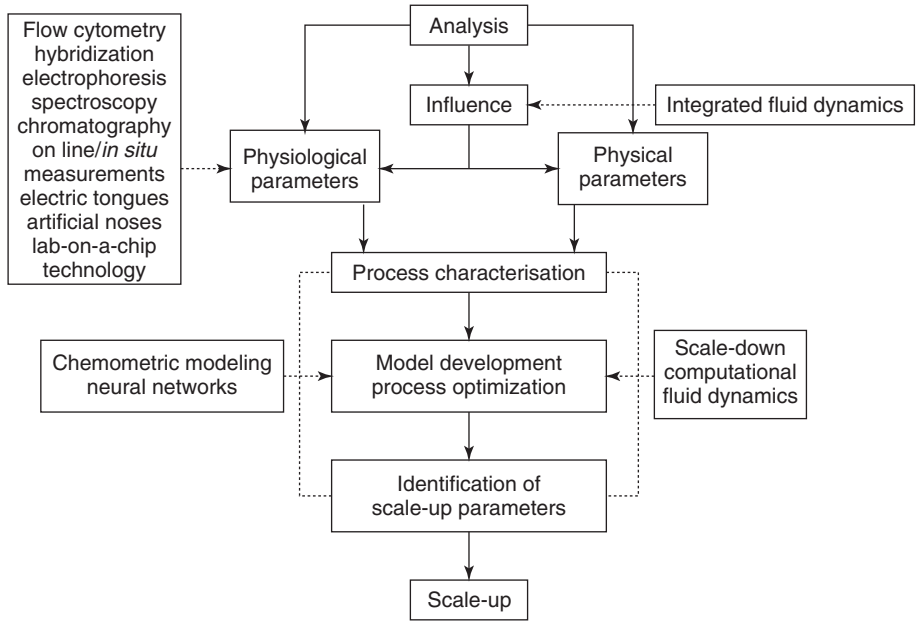


Figure 42.44. Conceptualization of a global strategy for scale-up of ALRs. Adapted from Ref. 357.

Unfortunately, despite the central role of the scale-up issue in bioprocess engineering, there is not a clear generally applicable strategy of scale-up in ALRs. For each individual bioproduct, microorganism, and type of ALR, a suitable strategy has to be elaborated. Schmidt (357), in a comprehensive review about optimization and scale-up of industrial fermentation processes, proposed a holistic scale-up strategy that may be adopted for ALRs. It consisted of a complete and detailed process characterization to identify key factors and parameters influencing product yield and quality, and of an appropriate process control and process design ensuring optimum mixing and bioreaction conditions, supported by appropriate knowledge and models as well as computational tools (Fig. 42.44).

Nonetheless, any approach and any model will always be based on approximations and will not completely reflect the highly complex interactions and relationships of the physical conditions governing the fermentation process. Successful scale-up will not be the result of a conclusive and straight-lined experimental strategy, but rather of an independent optimization on each scale, which highly depends on the experience, skill, and the intuition of the researcher (357).

42.6.2 Design Improvements

Several modifications to the classic ALR morphologies (Fig. 42.1) have been proposed. Figure 42.45 collects some of these designs aimed at the improvement of some of the characteristics of the equipment.

42.6.2.1 Multistage ALRs. One of the earliest modifications was the two-staged ALR (43). This design was inspired by the improvement observed in the performance obtained with multistage sieve trays over single-stage BCs. A substantially higher mass transfer coefficient and a better performance in terms of oxygen transferred per unit of energy invested were obtained.

A more complex version of multistage ALR was recently presented (358,359). Authors devised a novel multistage EL-ALR operating in three stages to remove trace pollutants from wastewater. The staging effect was achieved through hydrodynamically induced continuous bubble generation, breakup through rupture and coalescence (Fig. 42.46). The ALR was constructed with three vertical stages operating in a series. Bubbles were generated at the lowest part of the column below the first stage. At the beginning of the first stage, bubbles were ruptured and coalesced by imposing a flow disturbance using a disk with single central orifice (contraction disk). The G/L dispersion passing through the orifice was subjected to dynamic instabilities in the form of flow expansion followed by flow contraction. The flow expansion was achieved by positioning a mesh (expansion disk). Both types of disks were alternatively arranged along the riser. A screen positioned between two contraction disks was defined as one stage. At the end of each stage, bubbles lost their individual identity and new bubbles were generated at the beginning of each stage. The gas holdup achieved was higher than that in the single-stage system for the same superficial gas and liquid velocities. The values of a and $k_L a$ obtained at low power consumption were significantly higher than in other gas–liquid contactors. Maximum

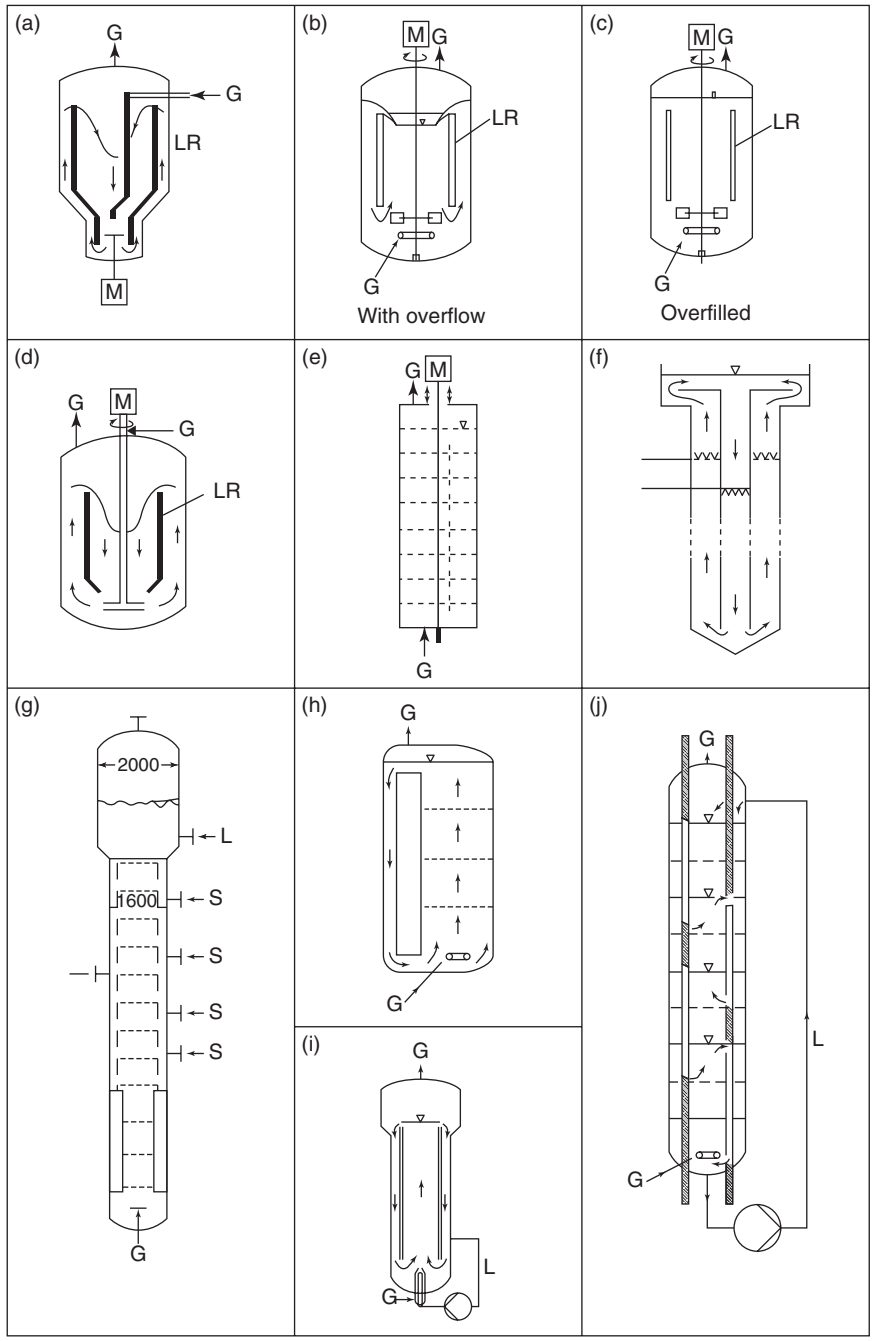


Figure 42.45. Some modifications from classic ALR morphologies. (a–e) configurations using mechanically moved internals for energy input, (f) downstream air ALR, (g) ALR with static mixer, (h) multistage EL-ALR, (i) nozzle loop ALR, and (j) multistage ALR. From Ref. 229, with permission.

mass transfer rate was found out through modifications in the riser-to-downcomer ratio.

42.6.2.2 ALRs Using Mechanically Moved Internals. The combination of a DT-ALR with a marine propeller (1000 rpm) was studied and compared with other column reactors (360) (Fig. 42.47). In this modification, the stirrer located near the bottom of the draft tube served to increase the circulation rate, which may be low for viscous liquids. This configuration showed enhanced oxygen transfer and more uniform distribution of the dissolved oxygen concentration throughout the reactor in comparison with

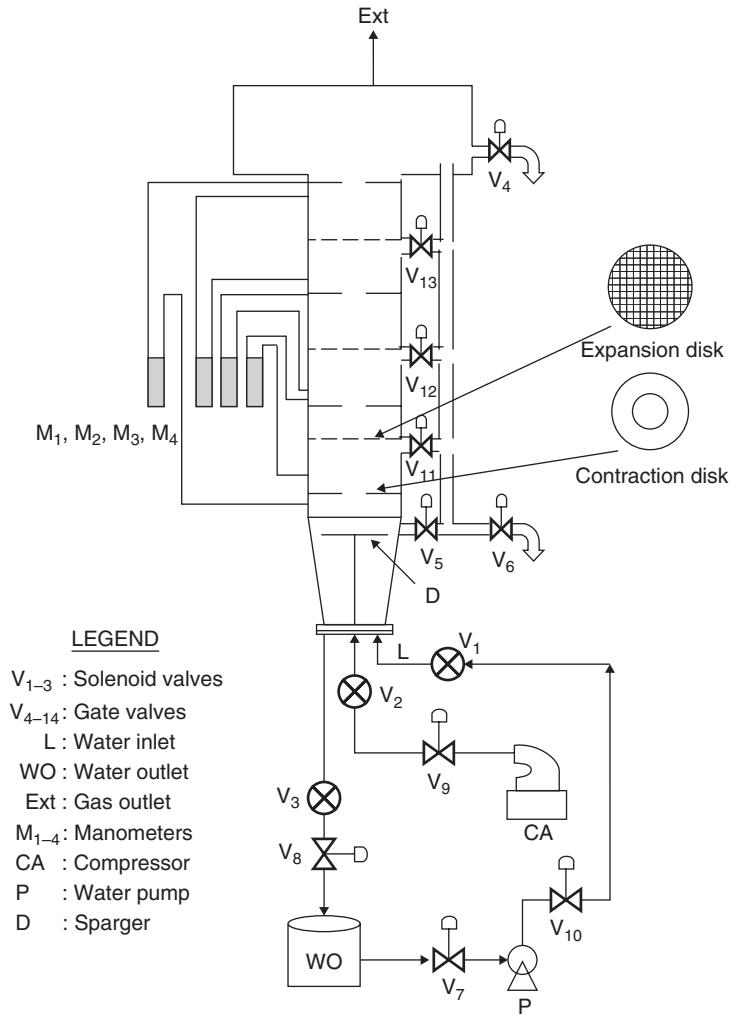


Figure 42.46. Schematic diagram of an experimental multistage EL-ALR. Disks of contraction and expansion were alternatively arranged along the riser. From Ref. 358, with permission.

that of the unmodified ALR. The liquid circulation was also intensified. However, the improvement was achieved at the cost of the introduction of a focus of energy input. As mentioned before, the absence of such a high shear region is one of the advantages of the ALR. It is interesting to note that a bakers' yeast culture (360) grown in the same type of modified reactor did not reveal any improvement. This may be related to the strong shear rate in the vicinity of the propeller.

42.6.2.3 ALRs with Static Mixers. Different types of static mixers, usually located in the riser, have also been used for enhancing the performance of ALRs. Potucek (361) studied the influence of static mixers on the gas holdup and interfacial gas–liquid area in a DT-ALR and found an improvement in interfacial area. Enhancement of $k_L a$ has also been obtained, especially in viscous liquids, as reported by Gaspillo and Goto (362) and Chisti et al. (363). Zhou et al. (364) showed better growth of *Cephalosporum acremonium* in an ALR with static mixers.

One of the advantages of the directionality of flow in ALRs is the improved fluidization capacity. The strengthening of this advantage was the aim of another modification, the helical flow promoter (HFP), proposed by Gluz and Merchuk (300). The HFP causes the fluid to flow down in the downcomer in a helical pattern (Fig. 42.48). The device comprises several fins or baffles, which have the effect of modifying the flow paths; instead of going in straight lines along the axis, the flow paths move along a helix. The baffles may be installed in a small section at almost any place along the riser or the downcomer, and the effect is perceived throughout the reactor. One of the best positions for the HFP is the top of the riser. A helical flow is then generated in the downcomer to produce a swirl at the bottom and a corkscrew-like path in the riser. This has a strong potential for the culture of photosynthetic microorganisms. The

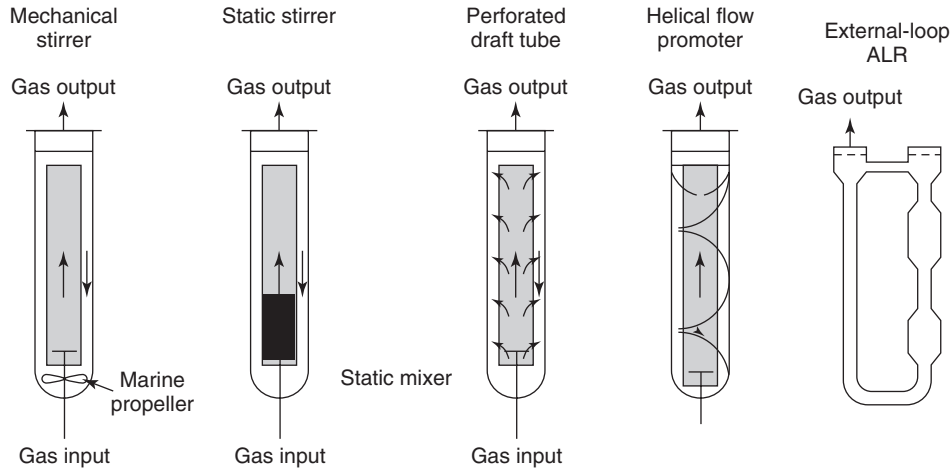


Figure 42.47. Modifications proposed in ALRs.

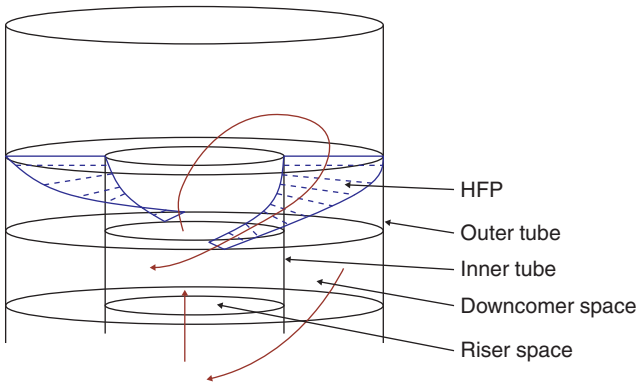


Figure 42.48. The helical flow promoters (HFPs) proposed for modification of the flow pattern in ALRs. From Refs (308) and (365).

helical movement causes secondary flow, which leads to enhanced radial mixing, and therefore more homogeneous distribution of light and heat among liquid elements and suspended particles. With the HFP, it is thus more likely that all the elements of the fluid get the same exposure to light and heat exchange.

One of the most important characteristics of the HFP is the enhanced capacity for fluidizing solid particles. This is due to the swirls that develop at the bottom of the reactor. Thus, this modification is especially suited to processes operating with cells immobilized on a solid. The minimal gas flow rate for complete fluidization of solids in an ALR may be reduced drastically by the use of a HFP (187). In addition, the mass transfer rate to suspended solids may be enhanced up to 50%, because of the higher relative velocity between the particles and solids.

Another interesting aspect of the performance of HFPs was highlighted by Schlotelburg et al. (366). Mass transfer coefficients obtained in a BC, an ALR, and an ALR with HFP were compared for water and two solutions of CMC: 0.2% and 0.04%. The corresponding effective viscosities for $\gamma = 50/\text{s}$ are 16 and 38 mPa s, respectively. It is clearly shown that although with water there is a consistent difference in favor of the BC, the differences diminish as the CMC concentration increases, and for the highest concentration tested, the difference is negligible. This implies that under these conditions, the disadvantage of the HFP in mass transfer vanishes, whereas all the advantages mentioned before subsist.

Vorapongsathorn et al. (367) studied the effect of cross-sectional baffles located in the riser of an ALR on hydrodynamics and mass transfer. Baffles reduced liquid circulation velocity (U_L) compared with the unbaffled configuration and significantly enhanced the gas holdup in the riser zone. However, because U_L was diminished, baffles caused a reduction in the gas holdup of the downcomer. Thus, the baffles had scarcely any influence on the overall gas holdup and on k_La. The authors highlighted as disadvantage the development of the stagnant regions beneath the baffles (Fig. 42.49). These regions could become contamination niches. This phenomenon and the risk of fouling are common among ALRs carrying static mixers.

42.6.2.4 External Loop and Draft Tube. As mentioned earlier, it has been shown repeatedly that the mass transfer rate in a BC is usually higher than that in the conventional ALR. It therefore makes sense to try to bring into the ALR some of the characteristics of BCs in a controlled fashion. This was done by several authors (368–375), who tested different perforated draft tubes in a DT-ALR. The perforations in the draft tube facilitated communication between the less-well aerated liquid in the downcomer and the better aerated riser. The reported improvements in mass transfer rates were undoubtedly obtained at the cost of a reduction

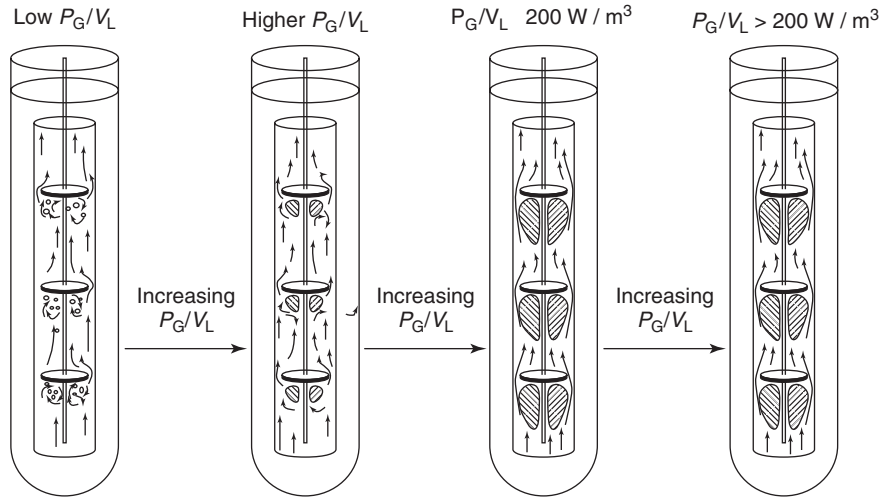


Figure 42.49. Development of stagnant regions in baffled ALRs as a function of specific power input. From Ref. 367, with permission.

in circulation velocity. Similar results were observed (253) in a modified ALR with rectangular wire mesh draft tubes. The draft tubes improved the liquid mixing and decreased the bubble coalescence in the ALR. The ALRs, in both the small and large scales, had the highest capabilities of liquid mixing and mass transfer in comparison with those of the conventional BC. By using the proposed reactor, the mixing time was reduced up to 30%, volumetric mass transfer coefficient and gas holdup increased up to 50% and 90%, respectively.

Another variant tested is the converging–diverging EL-ALR (376). The authors reported that the changes in cross section in the riser produced an increase in the gas holdup. An analogous study was accomplished by Wei et al. (377,378), but in an IL-ALR in which different convergence–divergence draft tubes were employed. The coalescence and distribution of bubbles were considerably affected and the gas holdup was much higher than that in a conventional draft tube ALR. The tested variation of structural parameters has scarce effect on gas holdup. At the same superficial gas velocity, the liquid circulation rate for ALR with different convergence–divergence draft tubes was lower than that for a conventional DT-ALR. However, the volumetric mass transfer coefficient was at least 10% higher than that of the conventional ALR.

A novel modified ALR with divided draft tubes was designed by Liu and Tay (379) for aerobic granulation. This configuration guaranteed the even discharging of the mixture of liquid and solids from the draft tube and from the downcomer compared with conventional DT-ALR, allowing the successful cultivation of aerobic granules and the stable operation of aerobic granular sludge in 5 months.

Futselaar et al. (380) have recently tested a new side-stream system for municipal wastewater treatment [NORIT Airlift membrane bioreactor (MBR) system]. It consists of an EL-ALR with filtration membranes positioned in the loop outside the bioreaction section. The membrane modules were arranged vertically and were aerated continuously at the bottom. This continuous aeration was the main driving force for the circulation of the activated sludge, while the feed pump was used to compensate the hydraulic losses. Permeation was controlled by a suction pump. A combination of forward flushing and periodic backflushing and/or relaxation intervals was used to control the cake layer formation inside the membrane tubes and to extend the intervals between maintenance cleanings. In industrial applications, this way of applying membranes in separation of water from sludge has lead to very compact units.

42.6.2.5 Split Baffle. Jajuee et al. (231) conceived a three-phase ALR in which a semipermeable membrane was used as split baffle between riser and downcomer (Fig. 42.50). The bioreactor was used for biodegradation of hydrocarbon compounds (381). The dividing membrane consisted of a rectangular sheet of nonwoven polyester textile that was supported by stainless steel mesh. The structure of textile membrane allowed the entrapment and immobilization of a wide range of solid particle sizes and microorganisms attached. The horizontal bulk motion due to hydrostatic pressure differences between the riser and downcomer was responsible for entrapment of suspended particles. This ALR provided higher mass transfer efficiency for lower superficial gas velocities where lower liquid circulation velocity and mixing rate could be compensated by horizontal flows through the porous membrane. In fact, higher biological degradation

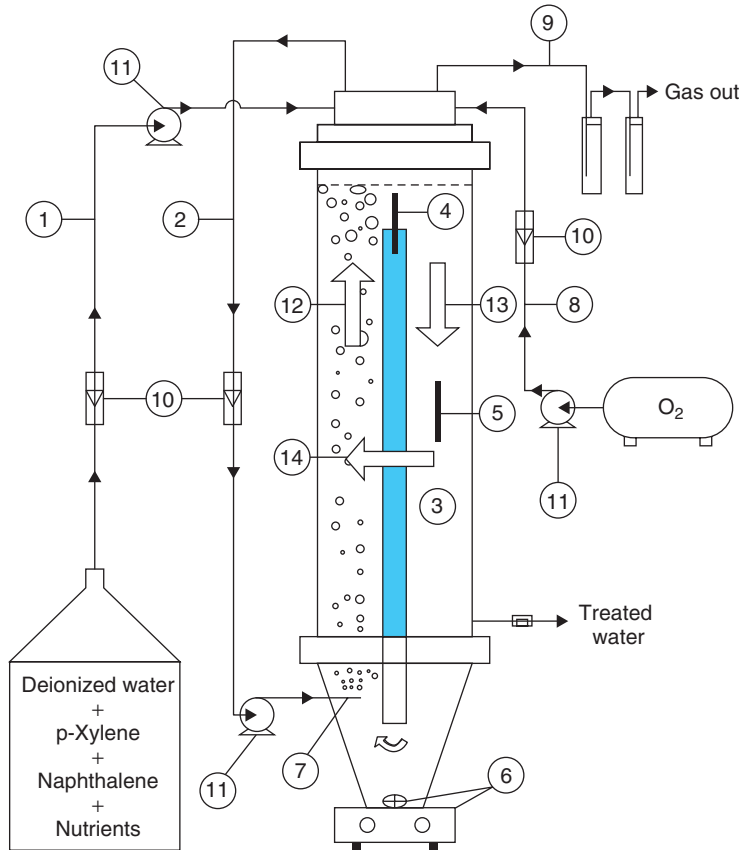


Figure 42.50. Experimental setup: 1—feed stream, 2—gas circulation system, 3—polyester nonwoven textile membrane, 4—dissolved oxygen probe inside the membrane, 5—dissolved oxygen probe and thermometer in downcomer, 6—magnet and stirrer, 7—sparger, 8—pure oxygen in, 9—vent system, 10—rotameters, 11—peristaltic pumps. From Ref. 231.

rates compared with similar bioreactor systems reported in the literature were obtained.

42.6.2.6 Inverse Fluidization. Garnier et al. (382) proposed the internal loop inverse fluidized bed airlift reactor (IL-IALR). In essence, it consisted of DT-ALR where light particles, such as expanded polystyrene beads, were placed in the annulus, and the bed was expanded toward the bottom of the reactor by the resultant downward liquid flow, creating an inverse fluidized bed. The advantage of the setup is the decoupling of gas contact with the solid phase, thereby limiting shear damage to the microorganisms. However, this configuration still allowed gas entrainment in the downcomer and the adherence of the light particles to the bubbles and subsequent disengagement and bursting of the bubbles could result in some cellular damage.

This problem was circumvented by Guo et al. (268), who proposed the use of an external loop inverse fluidized airlift reactor (EL-IALR). The sparger was located in the middle of the riser, so that heavy particles were fluidized in the lower section of the riser. In this device, gas–liquid and solid–liquid contacts were also decoupled. Flow reversal occurred between the bottom bend and the injection point of gas. However, it was necessary to lengthen the riser to increase gas holdup and favor the fluidization. The downcomer had scarce functionality, except as part of the liquid circulation path.

In both IL-IALR and EL-IALR, the gas holdup was fixed for a given gas superficial velocity and a solids loading. Due to the importance of maintaining high dissolved oxygen concentration in the treatment of wastewater containing high phenol concentrations, Loh et al. (383,384) proposed a simple modification of an external loop fluidized bed airlift bioreactor (EIFBAB). The main characteristic of this ALR was the installation of a globe valve between the riser and the downcomer at the bottom. By varying the extent of the valve opening, gas holdup could be increased at a fixed gas velocity without the need to increase the solids loading. Under high phenol concentrations, where the degradation rate is oxygen limited, EIFBAB provided the advantage of increasing dissolved oxygen tension by adjusting the valve opening when operating at high gas velocities.

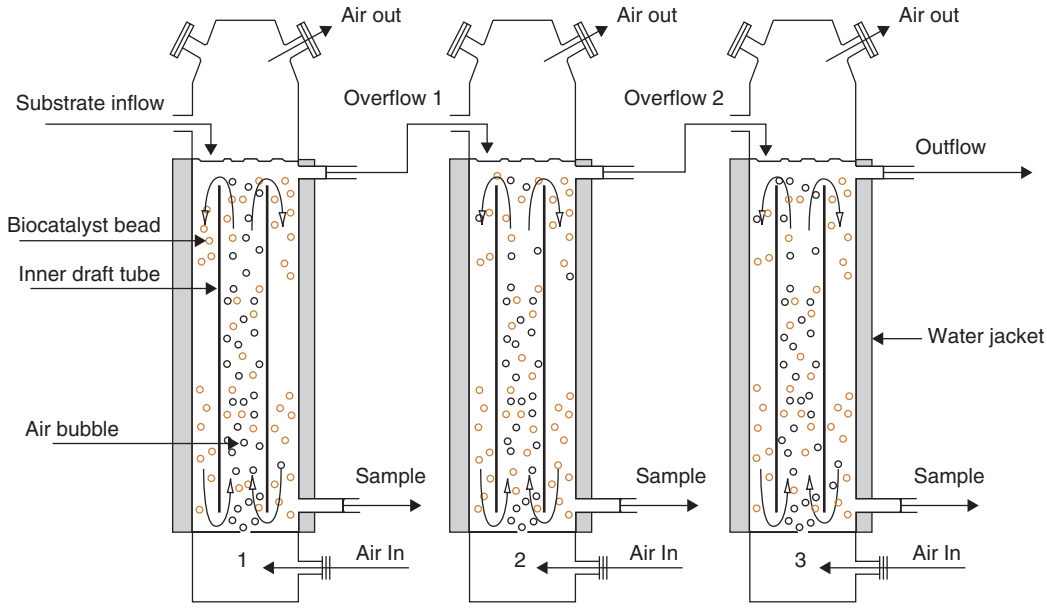


Figure 42.51. Cascade of three ALRs for producing a glycopeptide antibiotic from immobilized *A. teichomyceticus* cells. From Ref. 386, with permission.

42.6.2.7 Type of Contact. A novel integrated bioreaction–crystallization process bioprocess for the continuous production of calcium gluconate crystals has been proposed (385). The system consists of two EL-ALRs in a series, one being bioreactor and the other crystallizer. The concentrated calcium gluconate solution produced in the bioreactor is fed into the crystallizer in which the product is crystallized for its recovery. The mother liquid of the crystallizer is recycled to the bioreactor. Hence, the feed of solid glucose and calcium hydroxide to the bioreactor with simultaneous removal of calcium gluconate crystals from the crystallizer led to a continuous production of the crystals. The overall productivity in the proposed process was comparable to that of the batch fermentation process. However, the process advantages, reduced waste streams and simplicity, make it more attractive than the batch process.

Jovetic et al. (386) have recently proposed the culture of immobilized *Actinoplanes teichomyceticus* cells in three ALRs connected in a serial flow arrangement for continuous biotransformation of a glycopeptide antibiotic (Fig. 42.51). Distinct operational regimes were examined in independent laboratory-scale experimental trials. Very high final conversions of 95–99% combined with an extensive continuous operation time were achieved representing an advantage over the batch process.

42.6.2.8 Arrangement and Shape Modifications. The vast majority of ALRs reported in the literature have cylindrical geometry. However, many of them are being versioned in rectangular geometry because it provides good mixing and betters mass transfer performance (80,88,253,387–390). One of the interesting applications of rectangular shape is the microalgal mass culture because it could improve the efficiency of light utilization (391–395). For example, the new flat panel airlift bioreactor with a defined circulation path developed by Degen et al. (396) for culturing photosynthetic microalgae. The bioreactor exposes the cells to intermittent light to improve the efficiency of light utilization through the flashing light effect. A small downcomer zone was located on one side of the reactor (Fig. 42.52). The riser was

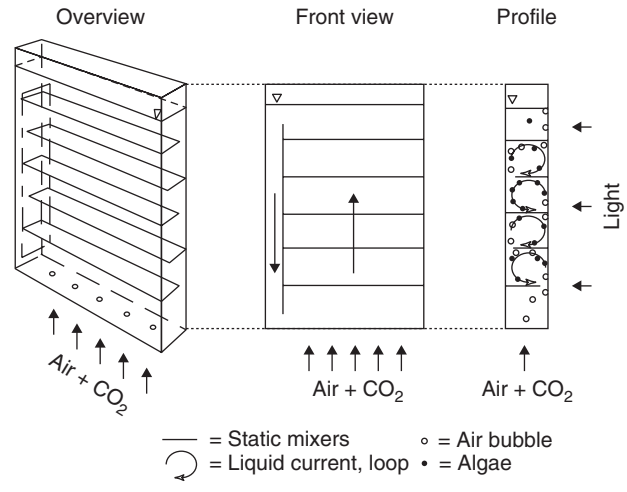


Figure 42.52. Flat panel airlift bioreactor to culture photosynthetic microorganisms. From Ref. 396, with permission.

subdivided into interconnected chambers by means of horizontal baffles. The baffles were attached alternately to the front and the back of the larger flat faces of the reactor. The fluid in the chambers circulated so that the cells regularly moved between the narrow illuminated zone and the deeper dark zone.

Chen et al. (397) compared a rectangular mesh baffle-plates ALR with conventional ALR and BC. Mesh baffle-plates improved mass transfer and mixing with the mass transfer coefficient of the proposed reactor being up to 12% higher than that in a conventional ALR under the same operating condition. The mixing time of the proposed reactor was 95% lower than that of the conventional ALR.

The effect of the bioreactor position in relation to a vertical plane has been barely studied. Lu et al. (398) observed a drastic change in hydrodynamic behavior of a rectangular BC when it was inclined up to 10° from the vertical. The liquid velocities in the inclined column were from 10- to 50-fold the superficial gas velocity. Further inclination of the column in the range of 10–45° had little effect on liquid velocity and mixing time. This observation was exploit by the same authors to efficiently culture murine hybridoma cells in a BC inclined 45° from vertical (399). This inclination allowed to separate the rising bubbles at the column upper surface, leaving the bulk of the liquid bubble-free. Liquid circulated due to the airlift effect. The adherence of cells to rising bubbles and the exposure of the cells to bursting bubbles on surface were minimized. This arrangement may be interesting to avoid cell damage by shear stresses associated to bubbling.

However, the more evident positive effects of tilting bioreactors have been observed in the field of microalgal biotechnology. The appropriate inclination of culture system facing the sun increases the irradiance level on photobioreactor surface and consequently improves the cell photosynthetic activity. Merchuk et al. (400) have recently presented a novel inclined tube ALR, which integrates the excellent hydrodynamic characteristics of ALRs and the benefices of a enhanced irradiance with inclination. The reactor consists of a tube with a flat baffle inserted in its bore, so as to generate two volumes that communicate at both ends of the tube, as shown in Fig. 42.53. Two gas streams are injected, one above the baffle (Q air top) and one below it (Q air bottom). The latter has the role of generating a cyclic, airlift-type flow in the device, while the gas injected above the baffle has the role of modifying the flow of the liquid going down to enhance radial mixing generating light/dark cycles, which are of fundamental importance in algal optimal growth. Those cycles can be seen in three experimentally measured trajectories (Fig. 42.54). The upper part of the tube acts as a downcomer and the lower part as a riser. There are no previous reports on this type of reactors. The feasibility of the algal culture in this type of reactor with actual flue gas was demonstrated

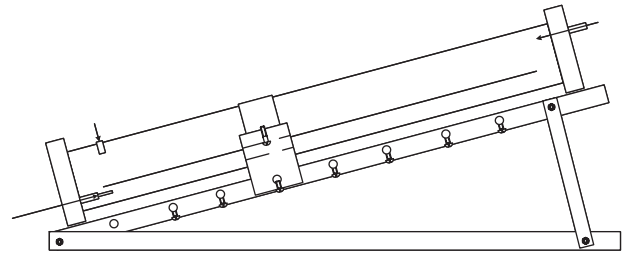


Figure 42.53. Scheme of the two-dimensional inclined tube bioreactor. The figure shows gas and liquid inlet and outlet and the series of anchoring positions for the camera along the duct. From Refs (400) and (401), with permission.

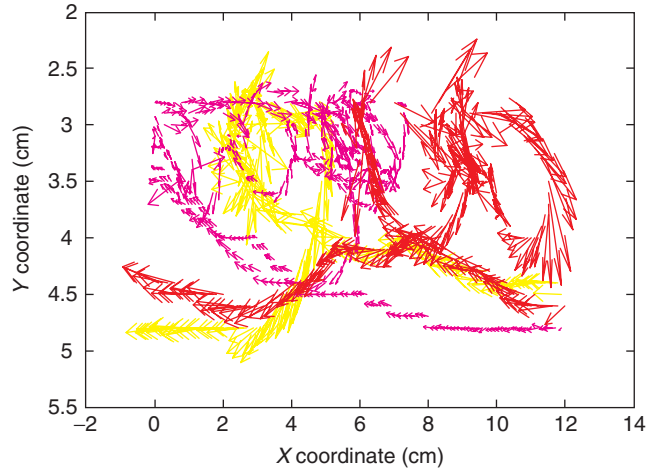


Figure 42.54. Liquid flow in the downcomer (upper region of the inclined tube) in presence of gas injection in this zone. Three successive passages of the tracer are shown. The x-axis is parallel to the tube. From Ref. 401, with permission.

in a 4-week culture of *Dunaliella parva*. The experiments were carried out in a medium size device connected directly to the flue gas in a power plant.

42.6.2.9 Special Designs Based on Airlift Pump. The gas lift advanced dissolution (GLAD) is a method for sequestration of low purity CO_2 emitted by thermal power plants (402). The dissolution tube is approximately 200-m long, and the drainpipe reaches more than 1000 m in depth. In fact, this is not a gas lift reactor, because this is a once-through system, and recirculation, a basic characteristic of ALRs, does not exist. It is, therefore, a gas lift pump in which gas dissolution is especially important (Fig. 42.55).

Low dissolved oxygen concentrations in the hypolimnia of lakes or reservoirs can have a negative effect on environment and on water treatment processes. Hypolimnetic

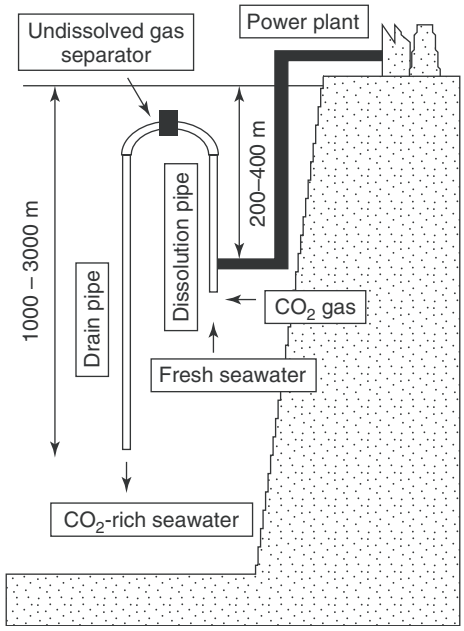


Figure 42.55. The gas lift advanced dissolution (GLAD), a method for sequestration of low purity $J_G = 0.024$ emitted by thermal power plants. From Ref. 402, with permission.



Figure 42.56. Photograph of full-lift aerator before installation (photo from Bob Kortmann of Ecosystem Consulting Service, Inc.), with permission (403).

aeration and oxygenation are commonly used to add dissolved oxygen to water bodies while preserving stratification. Airlift devices have also been used for hypolimnetic aeration. They typically consist of a vertical riser tube, a diffuser inside the bottom of the riser tube, an air–water separation chamber at the top of the riser, and one or two return pipes (downcomers). Figure 42.56 displays a photograph of full-lift aerator. Compressed air is delivered to the aerator and bubbles freely from the diffuser. This creates a positively buoyant gas–water mixture that ascends the riser. At the top of the riser, bubbles are released to the atmosphere, and some may be entrained in the water that enters the downcomers. The oxygenated water descends the downcomers and is returned to the hypolimnion (403).

42.7 MODELS

A considerable number of researchers have tackled the task of describing the flow of liquids, gases, and solids in ALR and the mass transfer between those phases. Early models were mainly aimed at the description of liquid velocity as a function of the easily measured gas holdups and were based on energy balances (79,108) (Table 42.9). Some of them model gas/liquid systems, and eight attempt the representation of three-phase, gas/liquid/solid systems. Some overlapping exists, because several models are presented in a general form that fits both G/L and G/L/S systems.

The table shows that the liquid velocity and the gas holdup in the riser are seen as the main variables studied and appear in all the proposed models. Indeed, those variables are closely related, because the difference in gas holdup between riser and downcomer is the only driving force for liquid circulation in the system. This has been clearly stated by Heijnen et al. (420), who expressed the pressure difference per unit height required as

$$\frac{\Delta P}{gH} = (\varepsilon_{Gr} - \varepsilon_{Gd}) - (\varepsilon_{Sr} - \varepsilon_{Sd})(\rho_S - \rho_L) \qquad (42.51)$$

In closed reactors, or as long as the overall solid amount does not change, the last term is the product of two differences that always have the same sign, because if the density of the solid is larger than that of the liquid, its rising velocity will be smaller and the holdup of solids in the riser will be larger than that in the downcomer and vice versa. The presence of solids, therefore, will always diminish the driving force for circulation, independently of their density. The hydrodynamic model presented by Heijnen et al. (420) is one of the most interesting and offers a complete representation of the fluid dynamics in an ALR from a macroscopic point of view. The model is able to describe both two- and three-phase flow. The ingenuity of the model

TABLE 42.9. Models Presented for ALRs

Source	Two-Phase	Three-Phase	Gas Recirculation	$k_La = 4.49J_G^{0.384}\varphi_T^{0.595}$ $\left(1-\frac{\rho}{\rho}\right)^{0.337}$	$k_La = 0.484\left(\frac{\rho J_{Gr}h}{\mu}\right)^{0.76}$ $\left(\frac{1+A_d}{A_r}\right)^{2.41}F_f^{1.9}$	$k_La = 1.53^{*}10^{-2}\varphi_r^{1.3}$ $J_{Gr}^{0.52}\mu_{app}^{-0.73}h^{0.3}$	[3]	N_2, CO_2	N_2	CFD
79	×			×	×	×			×	
404	×		×	×	×	×			×	
144	×		×	×	×	×				
405	×		×	×	×	×			×	
247	×		×	×	×	×				
406	×			×	×	×				×
56	×	×	×	×					×	
407	×			×	×	×	×			
408		×	×							
409		×	×	×						
410	×	×	×	×	×	×	×	×		
411	×	×	×	×						
412		×		×	×		×	×		
413				×		×				
412		×		×	×					
414	×			×	×	×				
415	×		×	×	×	×				×
416	×		×	×	×	×				
75	×			×	×	×				
249	×		×	×	×	×				
337	×			×	×					×
417	×			×	×					
418	×			×	×					
97	×			×	×	×				×
419	×			×	×					×
342	×		×	×	×	×			×	×
57	×		×	×	×	×	×	×	×	
274	×		×	×	×	×			×	×

consists in avoiding the need of dealing with four different variables (the holdups of gas and liquid in both riser and downcomer) by writing the difference in gas holdups $\phi_r - \phi_d$ as a function of the overall gas holdup ε_G, the gas superficial velocity, and the circulation liquid velocity. A similar procedure is followed with respect to solids holdup. The simplification proposed by Chisti (83) assumes that the ratio of the gas holdups in downcomer and riser is constant. This is an approximation that seems to be close to reality in two-phase systems, but strictly, it contradicts simple liquid mass balance.

Several of the models listed in Table 42.9 consider gas recirculation. As Heijnen et al.'s (420) model circumvents the need of knowing the gas holdup in riser and downcomer, in spite of handling the regime of gas recirculation, it does not provide an evaluation of the fraction of gas recirculated. The model presented by Freitas et al. (410) uses a pseudohomogeneous liquid approach and assumes that the concentration of solids is homogeneous all over the reactor. This is strictly valid only for solid density that is very close to the density of the liquid, $\rho_{sol} < \rho_L$. Indeed, they use alginate beads as solid carriers, with density close to that of water. Friction coefficients are calculated from one-phase correlations. The model confirms that an increase in solids produces a decrease in holdup. The gas holdup in the downcomer is calculated as in the model by Heijnen et al. (420), assuming a linear relationship between riser and downcomer holdups. For the external loop, they assume no gas recirculation. They optimize their parameters (four parameters) and get excellent fitting of their data.

Tall ALRs constitute a special type because of the high liquid velocities that can be reached. Not only can gas be entrapped into the downcomer, but it can also be directly injected in this section, with a considerable gain in gas-phase residence time and in energy required for gas injection. One of the most promising applications is the disposal of carbon dioxide from flue gas by injection into deep waters (402). Sanders et al. (416) have presented a model for the prediction of liquid velocity in such reactors. A basic analysis based on the Zuber and Findlay (89) two-phase flow approach seems to represent satisfactorily the trends of pressure drops and liquid velocities in a high recirculation ALR.

García-Calvo et al. (421) presented a thermodynamic model (based on the first principle), which is simply an extension of a previous two-phase model (148) to the three-phase airlift reactor (TPAL). The model requires knowledge of the bubble slip velocity. They show that it is possible to predict the transition from packed bed to fluidized bed and to circulating bed, as well as the hysteresis phenomenon that has been observed in these flow configurations (422), and good concurrence with experimentally observed transitions is reported. These transitions between flow configurations, classified taking the solid phase as reference, are different from the transitions between configurations based on the gas behavior (58).

Mousseau et al. (409) present a model for a rectangular section ALR with suspended solids of lower density than water, used for wastewater treatment: The model allowed the prediction of the changes in ammonia, dissolved oxygen, and biomass. They use the penetration model and the isotropic turbulence model for the description of the gas–liquid mass transfer.

In some of the papers in Table 42.9, the problem of gas/liquid mass transfer is addressed and is given more attention than fluid dynamics: Hwang and Lu (246), Tobajas et al. (412), and Camacho-Rubio et al. (423). Hwang and Lu (246) present an analysis of "gassing out" experiments, where a different value of the mass transfer coefficient k_La is considered in each of the three distinct regions: riser, downcomer, and separator. This is in fact an improved version of the original paper by Merchuk et al. (245), where this structured analysis of an ALR was first presented, structured means the zones of different fluid dynamic characteristics are recognized. This work was successfully extended to three-phase reactors by Wen et al. (57)

The model by Tobajas et al. (412) refers to a three-phase system, because it deals specifically with the biotreatment of marine sediment. A simple model is proposed combining Higbie's penetration model and Kolmogoroff's theory of isotropic turbulence and is used for prediction of mass transfer rates. No parameters are adjusted, and slip velocity, friction coefficients, equivalent length, and so on are taken from independent sources. Excellent match of experimental and predicted values was found for gas holdup in the riser, liquid velocity, and mass transfer rate.

Rubio et al. (423) deal with the axial profiles of oxygen in tall ALRs, which are frequently ignored. They show that, as a consequence of the hydrostatic pressure variation, steady-state axial dissolved oxygen concentration profiles exist even if no oxygen consumption exists. These axial inhomogeneties increase as the gas flow rate increases. It is obvious, therefore, that the conventional method of k_La determination, which is based on the assumption of perfect mixing in the reactor, is not valid in a tall bioreactor. The problem of inhomogeneity in dissolved oxygen concentration was also touched by Dhaouadi et al. (424) and Korpijarvi et al. (415), starting from the dynamic response of an ALR to sudden changes in inlet gas concentration. In all those cases, the main point of interest is the recognition that the so common assumption of perfect mixing may not hold in the case of tall reactors.

The fundamental and solid model presented by Young et al. (405) for an external ALR was upgraded (407), adding to the initial model the effect of gas buoyancy forces in the gas. Based only on the physical properties of the gas and liquid phases, the reactor dimensions, and the gas input,

the model predicts gas and liquid velocity and gas holdup along the riser for bubbly flow. Total disengagement of the gas at the top is assumed.

The seminal model by Ho et al. (404) has been an inspiration and a basis for much improved models that represent the ALR as a sequence of perfectly mixed cells (413,417,425). Those models are convenient for handling biological or chemical reactions. The simplification of the mathematical treatment may sometimes outweigh the unrealistic stepwise change in the variables along the reactor that is obtained. Steiff et al. (425) produced a considerable amount of experimental data that can be used to calibrate the model parameters. Of special interest, because these data are scarce in the literature, are the data of gas recirculation, measured following the technique proposed by Siegel et al. (1).

Shechter and Merchuk (426) presented a three-phase model for the fluid dynamic description of an airlift unit. The model is based on a momentum balance over riser and downcomer, and a series of macroscopic equations that describe the continuity of liquid and solid as it passes from the riser to the downcomer. Figure 42.57 shows the effect of solid density on the behavior of the system: while the gas holdup in the riser and the velocity of the solids in the riser remain almost constant when the density of the solid changes by 5% under and over the density of water, the solids holdup in the riser and downcomer are affected in opposite ways: while ε_{Sr} increases, ε_{Sd} decreases. The lines cross at a particle density equal to that of water. The difference between riser and downcomer solids holdup thus changes from negative to positive as ρ_s increases. The difference in absolute terms is smaller (approximately 0.03 vs 0.074) at higher particle density, and the predicted increase in liquid velocity, therefore, concurs with the general conclusions from Equation 42.1. This simulation refers to solids with density close to that of the liquid. When the density of the particle is substantially higher, the additional problem of complete fluidization appears. This is especially critical in systems with short draft tubes (427).

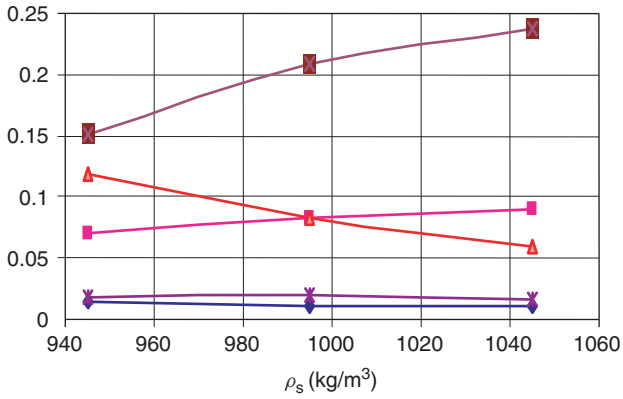


Figure 42.57. Influence of suspended solid density on the gas and solid holdup in an ALR for wastewater treatment. The legends for the vertical axis are: ♦, φ_{Gr}; ■, φ_{Sr}; ▲, φ_{Sd}; ×, U_{Lr}; *, U_{Sr} from Ref. 426, with permission.

Table 42.9 also lists models that deal with the application of CFD codes to the description of the flow in ALRs. Cockx et al. (406) presents a simulation based on one-dimensional two-fluid mass and momentum balances. Their results produce axial profiles of gas holdup in both riser and downcomer and a flow map of the liquid that includes radial profiles of velocity. Mudde and Van Den Akker (337) carried out two- and three-dimensional simulation of an airlift, trying to minimize the use of *ad hoc* closure terms. Surprisingly, they do not find clear advantage in the three-dimensional model, because both approaches coincide with experimental measurements of gas holdup. The two-dimensional model predicts a strong influence of the sparger geometry and seems to be better at low gas superficial velocities. Of special relevance is the model presented by Roy et al. (274). The model presented stems from an exhaustive analysis of the two-phase flow in an ALR. The input parameters are those related to energy dissipation in a three-dimensional two-phase flow, including the distribution parameter C_o because the Zuber and Findlay drift flux model is adopted for the description of the interaction between phases. With this input, a remarkable fit of previously published data was obtained. The calculated results of local values of fluid velocity, radial and axial distribution of gas holdup, and global parameters as mixing time and axial dispersion coefficient concurred with experimental results of other researchers. This excellent fit indicates that models making use of CFD are an alternative to the empirical correlations that are used today.

42.8 BIOPROCESSES

42.8.1 Drugs

ALRs may find successful applications in plant cell and roots suspension cultures (428–436). Airlift bioreactors are also used for the production of recombinant proteins and monoclonal antibodies from large-scale mammalian cell cultures (14,437–439) or to produce penicillin G from immobilized *Penicillium chrysogenum* in a DT-ALR, utilizing a magnetic field.

42.8.2 Biopolymers

The microbial exopolysaccharides (EPSs) are a class of highly valuable biopolymers with diverse biological activities. ALRs have been tested for production of biopolymers from fungi *Ganoderma applanatum* (440),

Tremella fuciformis (441), *Paecilomyces tenuipes* (442), *Grifola frondosa* (443), and *Sclerotium glucanicum* (444). κ-Carrageenan for the phycocolloid industry may also be obtained from *Kappaphycus alvarezii* calluses in a DT-ALR (445). The production of biodegradable thermoplastics from bacterial polyhydroxyalkanoates synthesized by *Ralstonia eutropha* in a membrane ALR (446) and a DT-ALR (447) has been examined. Obtaining of bacterial cellulose from cultures of *Acetobacter xylinum* in a DT-ALR has also been documented (448,449).

42.8.3 Exploitation of Lignocellulosic Wastes

Lignocellulosic biomass is a very important waste worldwide. The microbial biomass production from the hydrolysate of rice straw by yeast *Candida arborea* using a laboratory-scale EL-ALR has been recently evaluated (450). The influences of gas flow rate, initial liquid volume, hole diameter of gas sparger, and numbers of sieve plates on microbial biomass production were examined. The culture system was proved to be better than the conventional STR, opening the possibility of reducing the cost for microbial biomass production from this type of waste. Approximately 70% of municipal solid waste in industrialized countries consists of waste cellulosics, waste paper being the major component. A means of recycling is the conversion of cellulose to soluble sugars via enzymatic processes have been carried using an ultrasonic EL-ALR (293,451). In these works, the effects of paper size, sparging gas, humidity, and ultrasonic irradiation on the process kinetics and rate were studied.

42.8.4 Hydrocarbons in Groundwater

An immobilized cell ALR by Karamanev et al. (452,453) for the biodegradation of recalcitrant compounds has also been proposed for the aerobic bioremediation of simulated diesel fuel contaminated groundwater. It was tested with *p*-xylene and naphthalene in batch and continuous regimes. The culture system consists of two stages: an immobilized soil bioreactor where an efficient microbial consortium is developed from the indigenous microorganisms (which exists in diesel fuel contaminated soil) serves for inoculating another immobilized cell ALR in which microorganisms were immobilized on the fibers of a membrane (454).

42.8.5 Treatment of Waste Gas

Bioremediation rates of VOCs as air pollutants are limited by the mass transfer rates of oxygen and the low solubility of VOCs into the water phase. The EL-ALRs may provide a well-mixed environment appropriate for this purpose without the need for an impeller. Thus, it has been demonstrated that the use of a stainless steel mesh packing in the riser section of an EL-ALR can improve VOC mass transfer rates compared with an unpacked reactor and provide a large surface area for cell immobilization (252,455). In a recent work, the transient behavior of a DT-ALR for degradation of toluene in a waste gas stream was examined (456). The gas pollutant flowed into the ALR from the bottom, and it was then degraded by microorganisms suspended in the liquid phase. A mathematical integrated model was proposed to describe the dynamic behavior of toluene degradation. The biological removal of ethyl acetate in air streams was also feasible in a DT-ALR using microorganisms immobilized on activated charcoal particles (457,458).

42.8.6 Removing of Heavy Metals

The accumulation of heavy metals in the environment has received special attention because they carry a serious risk to public health and to the environment. The effectiveness of commonly used methods for the treatment of heavy metal-polluted wastes, such as chemical precipitation and ion exchange, remains limited because the large volumes of wastewater do not always meet regulatory standards. This limitation has encouraged the development of technologies to replace or complement conventional techniques. The utilization of microorganisms as biosorbents in ALRs to remove heavy metal ions from wastewaters offers a potential alternative for their detoxification and the recovery and reuse of toxic/precious metals [e.g. Cd(II)] removal from aqueous solution by immobilized waste brewery yeast (459), and hexavalent chromium (460), especially in dealing with large volumes of effluents with low concentrations of pollutants (Zn, Cu, Co, Fe, Al, Ag, Cr, As, and Se) (461).

42.8.7 Food Additives

Sotolone, a flavor widely used in the food and tobacco industries, and precursors may be produce in a meshed DT-ALR from *Trigonella foenum-graecum* root cultures (462). Production of betacyanins, red-violet pigments commercially important as natural dyes, was examined from roots of *Beta vulgaris* L. grown in different types of ALR (463). Vegetative cells of *Haematococcus pluviales* were cultured in a DT-ALR; this microalgal strain produces astaxanthin, a pigment with high antioxidant activity and extensively employed as a pigmentation inducer (464). It has also been demonstrated that ALRs of different configurations can be suitable to culture microalgae and fungi producers of highly valuable polyunsaturated fatty acids (392,465,466).

Commercial preparations of lipases produced from fungi and bacteria grown in ALRs have been proved to be feasible (467,468). Other microbial enzymes of great interest to food industry (e.g. proteinases, proteases, amylases, glucanases) may also be produced in ALRs (469–472).

42.8.8 Wastewater Treatment

As one of the recognized characteristics of ALRs is the potential for scaling-up and the relatively low power consumption for agitation and oxygenation, it is natural that many processes related to wastewater treatment use this type of reactor. Some applications of ALR included below have been reported in processes where the point of interest was simply that the process can be run using an ALR with savings in energy requirements.

42.8.8.1 Starch Processing Wastewater. Starch is a major rough material for the food industry, and starch processing wastewater (SPW) must be treated. Jin et al. (473) used an ALR in a pilot plant system for SPW reclamation by *Aspergilius orizae* and *Rhizopus oligosporus*. The efficient removal of COD, BOD, nitrogen, phosphorus, and suspended solids makes possible the use of reclaimed SPW for farm irrigation with production of α-amylase (<50 EU/mL), a value-added bioproduct. Fungal morphology was a function of ALR fluid dynamics. Free mycelial growth increases the viscosity, limiting the OTR from the gas to the culture. The solution that has been almost universally adopted for this problem—for production of citric and other organic acids and antibiotics—is to find the conditions under which the biomass forms pellets. The advantage in gas–liquid transfer rate, because of the decrease in viscosity, usually outweighs the added transfer resistance stemming from the intraparticle diffusion of oxygen. But the formation of pellets in optimal size and compactness is a very complex matter. Metz and Kossen (474) pointed out the multiplicity of variables and the difficulties of a priori prediction of the operation conditions required. Jin et al. (475) found empirically the optimal gas flow rate in a 4.5-L ALR and was able to scale-up these conditions to a pilot plant 160-L ALR.

42.8.8.2 Domestic Wastewater. The use of suspended solids as a support for a biofilm is gaining popularity in wastewater treatment. Lazarova et al. (476) studied experimentally the fluid dynamics and the performance of a SV-ALR with a rectangular section for wastewater treatment. They carefully studied the influence of suspended solids on gas holdup both in the riser and the downcomer, as well as the influence of the ratio of riser-to-downcomer cross-sectional areas on liquid velocity. Their measurements of mass transfer rate did not reveal important changes with respect to those obtained in water once the biofilm was developed. The main aspect stressed by the researchers was the capacity for nitrification observed in various stages. Bakker et al. (477) immobilized *Nitrobacter agilis* inside κ-carrageenan gel beads and used a cascade of two small-scale ALRs to study the oxidation of nitrite to nitrate. This is an important step in the nitrification process (i.e. the oxidation of ammonia to nitrate via nitrite, usually followed by a denitrification stage with reduction of nitrate to N_2). The use of two bioreactors in series presented some advantages that were attributed to the kinetics of the process (noncompetitive substrate and product inhibition). Because the density of the beads was close to unity, there was no problem in fluidizing of the beads in spite of the small scale. While the basic characteristics of an ALR indicate its advantages for aeration of large volumes of wastewater, the problem of ammonia removal calls for special handling. Two approaches have been presented incorporating the nitrification denitrification element into a basic airlift arrangement. The first one is the already mentioned BASR (58,478) (Fig. 42.30). The conventional airlift with its three phases is enclosed into an additional vessel (extension) that becomes the anaerobic volume. Part of the liquid and suspended biofilm-coated solids overflow the aerobic airlift core and enter the top of the extension, reentering at the bottom. The design allows the control of aerobic/anaerobic times for the biofilm-coated particles suspended in the system to improve the nitrification/denitrification of wastewater. The flow of liquid and suspended solids in the extension, which is the anaerobic volume, can be controlled manipulating the overpressure in the headspace of the reactor. A mathematical model was developed and used for the design of a pilot plant. The experimental results of gas and solid holdups concur satisfactorily with the model. Garrido et al. (479) showed that in the BASE (56) they could manipulate the system to obtain higher nitrite than nitrate, in the presence of both *Nitrosomonas* ($\rightarrow$nitrite) and *Nitrobacter* strains ($\rightarrow$nitrate). They presented a simple model based on diffusion in the biomass film, with homogeneous distribution of microorganisms. At low O_2 tensions, nitrification was improved. The model assumes zero-order reaction for *Nitrosomonas* and Blackman kinetics for *Nitrobacter*.

Zhou et al. and de Kreuk et al. (480,481) evaluated a BASR filled with ceramic materials as biocarriers with different diameters for treatment of domestic wastewater. A mathematical model was proposed to describe the internal liquid circulation. Froude number and superficial gas velocity at different biocarrier concentrations were correlated. The internal liquid circulation velocity was function on the square root of the reactor height and the superficial gas velocity. Because the internal liquid circulation flow rate was much higher than influent flow rate, the BASR showed a great resistance to significant changes in influent organic matter concentration. Resistance increased with the height of a BASR. In comparison with the conventional activated sludge process, the BASR is a promising wastewater treatment process with high efficiency and low operation cost.

Granular growth of sludge is an important matter in aerobic and anaerobic processes of wastewater treatment systems (482). Adequate granulation of sludge implies high settling velocities leading to good solid–liquid separation, high biomass retention, high activity, and an ability to withstand high loading rates. Beun et al. (483) demonstrated that aerobic granular sludge from both heterotrophic and nitrifying bacteria could easily be cultivated in a sequencing batch airlift reactor (SBAR), under stable operation for months. The difference in settling velocity between the granules (fast settling biomass) and the filaments and flocs (slow settling biomass) seemed to be the key factor to obtain granular sludge. The density of the granules in the SBAR was much higher than the density of comparable biofilms in a BASR. Authors attributed this difference to the different operation modes between both ALRs. Probably, selection of granules had been improved by increasing H/D ratio (column height/column diameter), taking advantage of the differences in settling velocity.

Additional advantages of SBARs have been demonstrated in similar applications. Ivanov et al. (484) observed that microbial granules with a diameter from 0.4 to 3.0 mm produced in SBAR, used for model wastewater treatment, were able not only to degrade organic matter but also to remove nano- and microparticles from wastewater due to microchannels and pores in the matrix of the granules. Granulation has also been used for many other processes: Kim and Seo (485) selectively enriched and granulated ammonia oxidizers from wastewater nitrification. Wang et al. (486) studied the effects of operation cycle time on properties of aerobic granules in SBARs using synthetic wastewater. Wang et al. (487) also demonstrated the efficacy of SBAR to treat brewery wastewater.

The composition of the microbial population may also be manipulated. Kim and Kim (488) used a continuous biofilm ALR and a SBAR for demonstrating the hypothesis that species of genus *Nitrospira* are K-strategists (it can exploit low amounts of nitrite more efficiently than *Nitrobacter*) and *Nitrobacter* species are r-strategists that can grow faster than *Nitrospira*. Genus *Nitrospira* and *Nitrobacter* species are the key nitrite-oxidizing bacteria in nitrifying wastewater treatment plants.

A different approach to the integration of nitrification–denitrification in a wastewater treatment process is the one presented by Merchuk and Shechter (489). They present an approach aiming at the upgrade of existing wastewater treatment plants rather than de novo design. The experiments presented were obtained in a 230-m^3 aeration basin that was divided into nine sections. Seven of these were converted to airlift operation, with two anaerobic sections. In this case, therefore, the system is a once-through aerobic/anoxic/aerobic/anoxic/aerobic sequence, with options of recirculation for improved denitrification. The conceptual difference between this approach and the BASE system is that the biomass is not recirculated and remains stationary in each of the nine stages, because solids circulate in each airlift stage, but only liquid passes from one stage to the other. In the BASE approach, all the biofilm-coated particles transit cyclically both aerobic and anaerobic sections.

42.8.8.3 Xenobiotics. Many organic sulfonates considered xenobiotic compounds (e.g. benzene and naphthalene sulfonates) that are used as intermediates or obtained as byproducts in the manufacture of several chemical products (e.g. dispersants, detergents, and azo-dyes) may appear in wastewater streams from these industrial processes. They are in general scarcely biodegradable (490). Their biological oxidation is carried out by slow-growing microorganisms, requiring a long retention time inside the reactor, resulting in large volumes required to complete the degradation and large areas to be occupied by the treatment device.

ALRs have provided satisfactory results (12,309). These reactors allow biomass retention at high dilution rates, thus enabling high reactor biomass concentrations to be achieved without the need of biomass separation and recirculation as in the activated sludge process. Wagner and Hempel (491) used a biofilm EL-ALR to study the biodegradation of naphthalene-2-sulfonate with *Pseudomonas* sp. Recently, Nicolella et al. (492,493) used an IL-ALR to degrade a mixture of aromatic sulfonates with biofilms generated from industrial sewage sludges. The degradation rate observed in the ALR was higher than that in the activated sludge process installed at the industrial site producing the leachate.

The biodegradation of an azo dye typical of textile, paper-making, and cosmetic industries by means of *Pseudomonas* sp. OX1 was studied by Lodato et al. (494). The culture system was a conventional internal ALR operated in batch and fed-batch modes with respect to the liquid phase, continuously with respect to the gas phase, and batchwise with respect to the biomass phase. Assadi et al. (495,496) used *A. niger* and *Phanerochaete chrysosporium* for textile wastewater treatment (biological decoloration) in an ALR.

42.8.8.4 Metal Refinery Wastewater. Metal refinery wastewater (MRWW) contains high amounts of metal-bound nitrogen species. Biological treatment methods routinely adopted for municipal wastewater nitrification/denitrification are hardly applicable to treatment of MRWWs. Metal complexes in MRWW alter or occupy the active sites of nitrification and denitrification enzymes, complicating its treatment (497). Manipura et al. (498) compared a CSTR, an DT-ALR, and a packed bed reactor (PBR) for removing ammonium from MRWW. The efficiencies were $>85\%$ in all cases.

42.8.8.5 Toilet Wastewater. As most of the ammonia or phosphorus, and a significant part of organic pollutants in domestic wastewater, come from toilet wastewater, mainly in big cities, this is becoming a problem of special interest. Fan et al. (499,500) have developed a novel full-scale MBR named airlift external circulation membrane bioreactor (AECMBR) to treat toilet wastewater for reuse. AECMBR has the advantages of the conventional cross-flow MBRs and the submerged MBRs. As there is no recycling pump in AECMBR, the energy consumption and operation cost are lower. The membrane cleaning or maintaining can be done online or only in the membrane tank without interfering with the aeration tank.

42.8.8.6 Phenol Biodegradation. Phenol and their derivatives are one of the most highly toxic water pollutants (501). Many attempts are being devoted to explore the efficiency of bioreactors in the treatment of wastewater-containing phenol. IL-ALR has been used with success. Rao et al. (502) found that the biodegradation of phenol under the application of a superimposed magnetic field was faster in airlift bioreactor than that in BC. Quan et al. (503) developed a packed DT-ALR, with honeycomb-like ceramic as the carrier to immobilize *Achromobacter* sp., for simultaneous phenol and 2,4-dichlorophenol biodegradation under fed-batch and continuous operations. Viggiani et al. (504) addressed phenol biodegradation with *Psudomonas stutzeri* OX1 by continuous operation of a bench-scale biofilm three-phase reactor operated in the IL-ALR mode.

Jia et al. (505) have recently proposed a mathematical model for simulating the dynamic behavior of batch phenol biodegradation processes in a DT-ALR using *C. tropicalis* freely suspended cells. Fluid dynamics, mass balances, and kinetics were satisfactorily coupled in the model. Loh and Liu (383) used an EIFBAB for treatment of high strength phenolic wastewater. To control the oxygen transfer, they used the increase in gas holdup that they got by closing a valve in the downcomer and restricting liquid circulation. The range of variation in their device goes in fact from holdup in an airlift with unrestricted circulation to the holdup in a BC, for similar diameters and gas superficial velocity. Obviously, the case of a completely closed valve implies that the downcomer volume will not contribute to the process. Later, Loh and Ranganath (384) integrated a fluidized bed of granular activated carbon into the EIFBAB for the enhanced cometabolic biotransformation of 4-chlorophenol (4-cp) in the presence of phenol as a growth substrate.

42.8.8.7 Wastewater from Fertilizer Production. The chemical fertilizer industry generates effluents with enormous loads of NH_4-N and COD. Its environmental impact on aquatic environments has been clearly established. Removal of NH_4-N by biological nitrification is a widely used process in wastewater treatment. Appropriate bioreaction conditions need to be handled to obtain a full conversion of NH_4-N to nitrate. Airlift bioreactors appear to meet these requirements. Wen et al. (506,507) used a 80-m^3 pilot-scale three-phase ALR consisting of several internal draught tubes and a low ratio of height-to-diameter, in which a biological membrane (bacteria attached onto the carriers) replaced the activated sludge, for nitrifying treatment of a real effluent from a fertilizer plant. The influences of the ratio of bed (settled) volume to bioreactor volume, superficial air velocity, hydraulic residence time, and pH value on ammonia nitrogen and COD reduction were analyzed. Under the optimum operating conditions, the COD and NH_4-N in the effluent were far below the primary discharge standards for the chemical fertilizer industry in the People's Republic of China. The sludge waste generated by this biotreatment system was significantly inferior to that from traditional activated sludge process. The same authors previously experimented with a laboratory-scale ALR of an only draught tube and similar results were obtained (508). Liu et al. (13) have also used satisfactorily a 170-m^3 pilot-scale three-phase ALR for aerobic biotreatment of the refinery wastewater. The bioreactor produced only one third of the sludge waste generated in the traditional activated sludge process.

42.9 SUMMARY

ALRs are suitable for the particular characteristics of biological processes where high mass transfer rate is required, but excessive power input may lead to damage of the cells due to shear effects. ALRs also have very appealing characteristics for bioprocesses for low value products in which efficiency of energy utilization is essential for design. Such is the case for ALRs for wastewater treatment. The ALR is particularly effective for solid fluidization, which is important in many biological processes in which the biocatalyst is in the form of pellets or immobilized on a solid support.

The distinctive characteristics of ALRs are conferred by the fluid dynamics of the liquid–gas or liquid–gas–solid mixtures in it. These characteristics are expressed as gas holdup, liquid velocity, and mixing in each of the zones of the ALR. It is important to recognize the differences in the fluid dynamic characteristics of these zones: the riser, the gas separator, and the downcomer. Only a correct understanding of behavior and interconnection of these regions can make possible the correct design of a new reactor or the scale-up of a laboratory device up to pilot or industrial size.

The purpose of scale-up is to conserve and repeat on a larger scale the fluid dynamics of the reactor. Therefore, one of the most important factors in the design and scale-up of reactors is the influence of the geometric characteristics of the system on the flow of the different phases present. The variables affecting the performance of the reactor are geometric design, operation variables, and fluid properties. Several correlations are available for predicting the fluid dynamic characteristics of the reactor (gas holdup, liquid velocity, and mixing time of axial dispersion coefficient) and the mass and heat transfer coefficients. Significant progress has been done in the application of computational tools to the simulation and design of ALRs. In parallel, innovative and sophisticate methods have been applied to obtain a deeper insight into the mechanisms of fluid motion and the flow patterns in the reactor. Although attempts have been made to study all the aspects described, no single research group has managed to cover all the variables over a wide range. It is therefore extremely important that the engineer confronting scale-up or de novo design of an ALR analyzes in depth the range of validity of the correlations and computation methods used for the calculations.

Acknowledgments

The authors acknowledge the support of the Ministerio de Educación y Ciencia de Espa na (Programa de ayudas para estancias de profesores e investigadores en Espa na SAB-2005-0064 and Project AGL2005-07924-C04-04) and of the Department of Chemical Engineering, Universidad de Almería.

LIST OF ABBREVIATIONS

AECMBR	airlift external circulation membrane bioreactor
ALR	airlift reactor
ANN	artificial neural network
BASR	biofilm airlift suspension reactor
BC	bubble column
BPNN	back-propagation neural networks
CFD	computational fluid dynamics
CMC	carboxymethyl cellulose
DT	draft, draught, or concentric tube in ALR
SV	split vessel
EL	external loop
EL-IALR	external loop inverse fluidized ALR
ERT	electric resistance tomography
GLAD	gas lift advanced dissolution
ICR	internal circulation reactor
IL	internal loop
IL-IALR	internal loop inverse fluidized bed ALR
LDV	laser Doppler velocimetry
MRWW	metal refinery wastewater
PPBR	particle-based biofilm reactors
RTD	residence time distribution
RSV	rectangular split vessel
SBAR	sequencing batch ALR
STR	stirred-tank bioreactor, fermenter, or reactor
VOC	volatile organic chemical

NOMENCLATURE

a	interfacial area ($m - 1$) or constant in Equation 42.8
A	cross-sectional area ($m - 2$)
B	heat transfer area (m^2)
Bo	bond number or Bodenstein number
C	concentration (mg/L), fiction losses coefficient
Ca	capillary number
C_b	bottom clearance (m)
C_t	top clearance (m)
C_d	hydraulic resistance coefficient
C_o	distribution parameter
C_p	heat capacity of liquid (J/K/K)
C^*	equilibrium concentration (mg/L)
d	diameter (mm)
d_0	diameter of the sparger orifice (m)
d_{32}	Sauter mean diameter (m)
D_L	diffusivity (m^2/s)
D_z	axial dispersion coefficient (m^2/s)
E	energy (J)
f	friction factor
F_f	filling factor
F_r	Froude number
g	gravitational constant (m/s^2)
Ga	Galileo number
h	height (m)
h_w	overall heat transfer coefficient ($W/m^2/s/K$)
I	degree of homogeneity
J	superficial velocity, volumetric flow density (cm/s)
K_b	hydraulic coefficient bottom
k	thermal conductivity of liquid (W/K/m) (Eq. 42.49)
k_La	volumetric mass transfer coefficient ($h - 1$)
K_t	hydraulic coefficient top
L	loop length, characteristic length (m)
M	wetted surface parameter, constant in Equation 42.29
Ma	bubble coalescence parameter
Mo	Morton number
n	flow index
n_i	number of bubbles with diameter d_i
N	agitation speed ($s - 1$)
Nu	Nusselt number
N_W	power consumption function
OTR	oxygen transfer rate ($mol/m^3/s$)

P pressure (Pa), power input (W)
Pe Peclet number
Pr Prandtl number
Q volumetric flow rate (m^3/s)
Re Reynolds number
S surface area (m^2)
Sc Schmidt number
Sh Sherwood number
t time (s)
U velocity (m/s)
U_b bubble terminal rise velocity (m/s)
$U_{b\infty}$ single bubble rise velocity (m/s)
U_c cell circulation velocity
U_{GS} gas slip velocity
U_L overall liquid circulation velocity (m/s)
U_{GJ} weighted mean drift velocity (m/s)
V volume (m^3)
We Weber number
Wi Weissenberg number
W_s shaft work done by the surroundings on the system

Greek Letters

α coefficient, constant in Equations 42.3 and 42.17
β constant in Equations 42.3 and 42.17
γ shear rate $(s-1)$
Δ difference
ε_e solvent holdup
ε_L liquid holdup
ε_S particles holdup
κ behavior coefficient (Pa s, $n+2$)
λ relaxation time (s)
μ dynamic viscosity of the liquid (Pa s), specific growth coefficient $(h-1)$
ν kinematic viscosity (m^2/s)
ρ density of liquid (unless index indicates otherwise) (kg/m^3)
ρ surface tension (N/m)
τ shear stress (Pa)
ϕ holdup of gas (unless index indicates otherwise)
ϕ_f flowing volumetric concentration (m^3/m^3)

Subscripts

ab all bubbles
ap apparent
b bottom
b∞ terminal
c circulation
d downcomer, dissipation
dr draft tube
D dissipation, dispersion
eff effective
g growth
G gas
ht heat transfer
hm heat production by the microorganisms
hs heat production by stirring
i region of reactor
in Input
L liquid
m mixing
max maximal
mt mass transfer
o orifice
oc oxygen consumption
out output
p potential
r riser
s gas separator, solid, shaft
sc sugar consumption
sh shaft
sol solid
sp separator
T top
T total
W water

Dimensionless Groups

$Bo = \frac{U_L L}{D_z}$	Bodenstein refers to U_L
$BoLG = \frac{J_G D}{D_L}$	Bodenstein refers to J_G
$Ca = \frac{J_G \mu}{\sigma}$	capillary number
$Eo = \frac{\Delta \rho g D^2}{\sigma}$	Eotvos
$Fr = \frac{J_{Gr}}{\sqrt{gD}}$	Froude
$Ga = \frac{g\rho^2 Ds^3}{\mu^2}$	Galileo
$Ma = \left(\frac{Crk^2}{\sigma}\right)$	Marucci
$Mo = \frac{g\mu^4}{\rho\sigma^3}$	Morton
$Nu = \frac{h_w D}{k}$	Nusselt
$Pr = \frac{Cp\mu}{k}$	Prandtl
$\Re = \frac{U_L D\rho}{\mu}$	Reynolds
$We = \frac{\rho U o^2 d_o}{\sigma}$	Weber number
$Wi = \frac{\lambda}{\gamma}$	Weissenberg number

REFERENCES

1. Siegel MH, Merchuk JC, Schügerl K. AIChE J 1986; 32(10): 1585–1596.

2. Mehrnia MR, Towfighi J, Bonakdarpour B, Akbarnegad MM. J Chem Technol Biotechnol 2004; 79(3): 260–267.
3. Merchuk JC, Ladwa N, Cameron A, Bulmer M, Pickett A. AIChE J 1994; 40(11): 1900–1900.
4. Koide K, Kurematsu K, Iwamoto S, Iwata Y, Horibe K. J Chem Eng Jpn 1983; 16(5): 413–418.
5. Tanaka H. Process Biochem 1987; 22: 106–112.
6. Wase DAJ, McManamey WJ, Raymahasay S, Vaid AK. Biotechnol Bioeng 1985; 27(8): 1166–1172.
7. Kessler WR, Popovic MK, Robinson CW. Can J Chem Eng 1993; 71(1): 101–106.
8. Srinivasulu B, Prakasham RS, Jetty A, Srinivas S, Ellaiah P, Ramakrishna SV. Process Biochem 2002; 38(4): 593–598.
9. Sun SL, Liu CJ, Wei WS, Bao XJ. Powder Technol 2006; 162(3): 201–207.
10. Mousavi SM, Yaghmaei S, Vossoughi M, Jafari A, Hoseini SA. Hydrometallurgy 2005; 80(1–2): 139–144.
11. Fang D, Zhou LX. Chemosphere 2007; 69(2): 303–310.
12. Nicolella C, van Loosdrecht MCM, Heijnen JJ. J Biotechnol 2000; 80(1): 1–33.
13. Liu XL, Wen JP, Yuan Q, Zhao XM. Biochem Eng J 2005; 27(1): 40–44.
14. Hesse F, Ebel M, Konisch N, Sterlinski R, Kessler W, Wagner R. Biotechnol Prog 2003; 19(3): 833–843.
15. Oldshue JY. Chem Eng (New York) 1983; 90(12): 82–108.
16. Oldshue JY. Fluid mixing technology. New York: McGraw-Hill; 1983.
17. Siegel M, Merchuk JC. Can J Chem Eng 1991; 69(2): 465–473.
18. Weetman RJ, Oldshue JY. Papers Presented at Sixth European Conference on Mixing; 1988 May 24–26; Pavia, Italy; Milan, Italy: Aidic-Association Italiana (69); 1988. pp 43–50.
19. Henzler HJ. Adv Biochem Eng Biotechnol 2000; 67: 25–81.
20. Markl H, Bronnenmeier R, Wittek B. Int Chem Eng 1991; 31(2): 185–197.
21. Wase DAJ, Patel YR. J Gen Microbiol 1985; 131(4): 725–736.
22. Edwards N, Beeton S, Bull AT, Merchuk JC. Appl Microbiol Biotechnol 1989; 30(2): 190–195.
23. Kieran PM, Malone DM, MacLoughlin PF. Adv Biochem Eng Biotechnol 2000; 67: 139–177.
24. Trejo-Tapia G, Cerda-García-Rojas CM, Rodríguez-Monroy M, Ramos-Valdivia AC. Biotechnol Prog 2005; 21(3): 786–792.
25. Kilonzo PM, Margaritis A, Bergougnou MA, Yu JT, Qin Y. Chem Eng J 2006; 121(1): 17–26.
26. Blazej M, Kisa M, Markos J. Chem Eng Process 2004; 43(12): 1519–1527.
27. García Camacho F, Gallardo Rodríguez JJ, Sánchez Mirón A, Cerón García MC, Belarbi EH, Molina Grima E. Process Biochem 2007; 42(11): 1506–1515.
28. Camacho FG, Rodríguez JG, Mirón AS, García MCC, Belarbi EH, Chisti Y, Grima EM. Biotechnol Adv 2007; 25(2): 176–194.
29. Gallardo-Rodríguez JJ, Cerón García MC, García-Camacho F, Sánchez-Mirón A, Belarbi EH, Molina-Grima E. Biotechnol Prog 2007; 23(2): 339–350.
30. Landau LD, Lifshitz EM. Fluid mechanics. New York: Pergamon Press; 1975.
31. Tan WS, Dai GC, Ye W, Shen JP. Chem Eng J Biochem Eng J 1995; 57(3): B31–B36.
32. Svendsen HF, Jakobsen HA, Torvik R. Chem Eng Sci 1992; 47(13–14): 3299–3304.
33. Barbosa MJ, Janssen M, Ham N, Tramper J, Wijffels RH. Biotechnol Bioeng 2003; 82(2): 170–179.
34. Blazej M, Annus J, Markos J. Chem Eng Res Des 2004; 82(A10): 1375–1382.
35. Tanaka H, Semba H, Jitsufuchi T, Harada H. Biotechnol Lett 1988; 10(7): 485–490.
36. Rodríguez-Mendiola MA, Stafford A, Cresswell R, Arias-Castro C. Enzyme Microb Technol 1991; 13(9): 697–702.
37. Gebauer A, Scheper T, Schügerl K. Bioprocess Eng 1987; 2(1): 13–23.
38. Chang CM, Lu WJ, Own KS, Hwang SJ. Biotechnol Tech 1993; 7(4): 317–322.
39. Sánchez-Mirón A, Cerón-García MC, Contreras-Gómez A, García-Camacho F, Molina-Grima E, Chisti Y. Biochem Eng J 2003; 16(3): 287–297.
40. Doran P. Adv Biochem Eng Biotechnol 1993; 48: 115–168.
41. Siegel MH, Merchuk JC. Biotechnol Bioeng 1988; 32(9): 1128–1137.
42. Legrys GA. Chem Eng Sci 1978; 33(1): 83–86.
43. Orazem ME, Erickson LE. Biotechnol Bioeng 1979; 21(1): 69–88.
44. Chisti Y, Jauregui-Haza UJ. Biochem Eng J 2002; 10(2): 143–153.
45. Fadavi A, Chisti Y. Chem Eng J 2005; 112(1–3): 73–80.
46. Saito T, Kosugi S, Kajishima T, Tsuchiya K. Energy Fuels 2001; 15(2): 285–292.
47. Niwa K, Kosugi S, Saito T, Kajishima T, Hamaogi K. Energy 2005; 30(11–12): 2308–2317.
48. Merchuk JC, Ladwa N, Cameron A, Bulmer M, Berzin I, Pickett AM. J Chem Technol Biotechnol 1996; 66(2): 174–182.
49. Barnea D, Taitel Y. In: Cheremisinoff NP, editor. Encyclopedia of fluid mechanics. Houston (TX): Gulf Publishing Company; 1986. pp 403–491.
50. Wallis GB. J Appl Mech Trans ASME 1973; 40(4): 1150–1151.
51. Merchuk JC. In: Schügerl K, editor. Biotechnology. New York: Springer; 1990. pp 349–382.
52. Wiswanathan K. In: Cheremisinoff NP, editor. Volume 3, Encyclopedia of fluid mechanics. Houston (TX): Gulf Publishing Co; 1986. pp 291–308.
53. Merchuk JC. Chem Eng Sci 1986; 41(1): 11–16.
54. Jin B, Lant P. Chem Eng Sci 2004; 59(12): 2379–2388.
55. Van Benthum WAJ, Van Der Lans RGJM, Van Loosdrecht MCM, Heijnen JJ. Chem Eng Sci 1999; 54(18): 3995–4006.
56. Heijnen JJ, Hols J, Van Der Lans RGJM, VanLeeuwen HLJM, Mulder A, Weltevrede R. Chem Eng Sci 1997; 52(15): 2527–2540.
57. Wen JP, Jia XQ, Cheng XR, Yang P. Bioprocess Biosyst Eng 2005; 27(3): 193–205.

58. Van Benthum WAJ, Van Den Hoogen JHA, Van Der Lans RGJM, Van Loosdrecht MCM, Heijnen JJ. Chem Eng Sci 1999; 54(12): 1909–1924.
59. Klein J, Godo S, Dolgos O, Markos J. J Chem Technol Biotechnol 2001; 76(5): 516–524.
60. Klein J, Vicente AA, Teixeira JA. Can J Chem Eng 2003; 81(3–4): 433–443.
61. Russell AB, Thomas CR, Lilly MD. Biotechnol Bioeng 1994; 43(1): 69–76.
62. Meng AX, Hill GA, Dalai AK. Can J Chem Eng 2002; 80(2): 194–199.
63. Jin H, Yang S, Wang M, Williams RA. AIP Conference Proceedings; 2007. pp 869–876.
64. Du JX, Cao NJ, Gong CS, Tsao GT, Yuan NJ. Appl Biochem Biotechnol 1997; 63–65: 541–556.
65. Wang F, Liang GW, Xie DL. Chin J Sens Actuators 2007; 20(3): 628–631.
66. Widyanto MR, Utomo MB, Kawamoto K, Kusumoputro B, Hirota K. Sens Actuators A Phys 2006; 126(2): 447–454.
67. Jin H, Yang S, Guo Z, He G, Tong Z. Chem Eng J 2005; 115(1–2): 45–50.
68. Chisti MY, Moo-Young M. Chem Eng J 1988; 38(3): 149–152.
69. Bello RA, Robinson CW, Mooyoung M. Biotechnol Bioeng 1985; 27(3): 369–381.
70. Miyahara T, Hamanaka H, Takino T, Akagi Y, Okada K. J Chem Eng Jpn 1997; 30(5): 958–961.
71. Kawase Y, Mooyoung M. J Chem Technol Biotechnol 1986; 36(11): 527–538.
72. Cai JA, Nieuwstad TJ. Environ Technol 1992; 13(2): 101–113.
73. Al-Masry WA. J Chem Technol Biotechnol 1999; 74(10): 931–936.
74. Al-Masry W. Int J Chem React Eng 2006; 4: 1–11.
75. Couvert A, Bastoul D, Roustan M, Line A, Chatellier P. Chem Eng Process 2001; 40(2): 113–119.
76. See KH, Roberts GW, Saez EA. AIChE J 1999; 45(11): 2467–2471.
77. Koide K, Shibata K, Ito H, Kim SY, Ohtaguciii K. J Chem Eng Jpn 1992; 25(1): 11–16.
78. Zahradnik J, Fialova M, Linek V. Chem Eng Sci 1999; 54(21): 4757–4766.
79. Chakrabarty M, Singh HD, Baruah JN, Lyengar MS. Indian Chem Eng 1974; 16: 17–22.
80. Popovic MK, Robinson CW. AIChE J 1989; 35(3): 393–405.
81. Li GQ, Yang SZ, Cai ZL, Chen JY. Chem Eng J Biochem Eng J 1995; 56(2): B101–B107.
82. Koide K, Sato H, Iwamoto S. J Chem Eng Jpn 1983; 16(5): 407–413.
83. Chisti MY. Airlift bioreactors. New York: Elsevier; 1989. p 345.
84. Merchuk JC, Asenjo JA. In: Merchuk JC, Asenjo JA, editors. Bioreactor system design. New York: Marcel Dekker; 1994. pp 139–206.
85. Atenas M, Clark M, Lazarova V. Ind Eng Chem Res 1999; 38(3): 944–949.
86. Merchuk JC, Yunger R. Chem Eng Sci 1990; 45(9): 2973–2975.
87. Contreras A, Chisti Y, Molina E. Chem Eng Sci 1998; 53(24): 4151–4154.
88. Kilonzo PM, Margaritis A, Bergougnou MA, Yu JT, Ye Q. Biochem Eng J 2007; 34(3): 279–288.
89. Zuber N, Findlay JA. J Heat Transf Trans ASME 1965; 87(4): 453–468.
90. Merchuk JC, Stein Y. AIChE J 1981; 27(3): 377–388.
91. Hills JH. Trans Inst Chem Eng 1974; 52(1): 1–9.
92. Clark NN, Atkinson CM, Flemmer RLC. AIChE J 1987; 33(3): 515–518.
93. Glennon B, Almasry W, Macloughlin PF, Malone DM. Chem Eng Commun 1993; 121: 181–192.
94. Freedman W, Davidson JF. Trans Inst Chem Eng 1969; 47(8): 251–262.
95. Verlaan P, Tramper J, Vantriet K, Luyben K. Chem Eng J Biochem Eng 1986; 33(2): B43–B53.
96. Guet S, Ooms G, Oliemans RVA, Mudde RF. Chem Eng Sci 2004; 59(16): 3315–3329.
97. Vial C, Poncin S, Wild G, Midoux N. Chem Eng Sci 2002; 57(22–23): 4745–4762.
98. Al-Masry WA. Chem Eng Res Des 2004; 82(A3): 381–389.
99. Weiland P, Bieker A. Chem-Ing-Tech 1981; 53(11): 869–870.
100. Bendjaballah N, Dhaouadi H, Poncin S, Midoux N, Hornut JM, Wild G. Chem Eng Sci 1999; 54(21): 5211–5221.
101. Vial C, Camarasa E, Poncin S, Wild G, Midoux N, Bouillard J. Chem Eng Sci 2000; 55(15): 2957–2973.
102. Freitas C, Fialova M, Zahradnik J, Teixeira JA. Chem Eng Sci 2000; 55(21): 4961–4972.
103. Hallaile M. External loop airlift reactors. Beer-Sheva: Ben Gurion University of the Negev; 1993.
104. Verlaan P, Vaneijs AMM, Tramper J, Vantriet K, Luyben K. Chem Eng Sci 1989; 44(5): 1139–1146.
105. Yun JX, Shen ZQ. Chem Eng Sci 2003; 58(2): 377–385.
106. Popovic M, Robinson CW. Biotechnol Bioeng 1988; 32(3): 301–312.
107. Merchuk JC, Berzin I. Chem Eng Sci 1995; 50(14): 2225–2233.
108. Chisti Y. Appl Mech Rev 1998; 51(1): 33–112.
109. Kawase Y, Tsujimura M, Yamaguchi T. Bioprocess Eng 1995; 12(1–2): 21–27.
110. Kemblowski Z, Przywarski J, Diab A. Chem Eng Sci 1993; 48(23): 4023–4035.
111. Al-Masry WA, Abasaeed AE. Chem Eng Sci 1998; 53(24): 4085–4094.
112. Tsuge H, Otatsume S, Kobayashi K, Terasaka K, Hayasaki M, Kobayashi H. J Chem Eng Jpn 2004; 37(8): 941–946.
113. Dhaouadi H, Poncin S, Hornut JM, Wild G. Chem Eng Sci 2006; 61(4): 1300–1311.
114. Sánchez MJ, Jiménez-Aparicio A, Gutiérrez López G, Trejo Tapia G, Rodríguez-Monroy M. Biochem Eng J 2002; 12(1): 37–41.
115. Merchuk JC, Ronen M, Giris S, Arad S. Biotechnol Bioeng 1998; 59(6): 705–713.
116. Rotem A, Merchuk JC, Arad Malis S. J Chem Technol Biotechnol 1992; 55(3): 263–267.
117. Klein J, Maia J, Vicente AA, Domingues L, Teixeira JA, Jurascik M. Biotechnol Bioeng 2005; 89(4): 393–399.

118. Nishikawa M, Kato H, Hashimoto K. Ind Eng Chem Process Des Dev 1977; 16(1): 133–137.
119. Nakanoh M, Yoshida F. Ind Eng Chem Process Des Dev 1980; 19(1): 190–195.
120. Moo-Young M, Halard B, Allen DG, Burrell R, Kawase Y. Biotechnol Bioeng 1987; 30(6): 746–753.
121. Henzler HJ. Chem-Ing-Tech 1980; 52(8): 643–652.
122. Kawase Y, Moo-Young M. Chem Eng Commun 1986; 40: 67–83.
123. Schumpe A, Deckwer WD. Bioprocess Eng 1987; 2(2): 79–94.
124. El-Tamtamy SA, Khalil SA, Nour-El-Din AA, Gaber A. Appl Microbiol Biotechnol 1984; 19: 376–381.
125. Henzler HJ, Kauling J. Proceedings of the 5th European Conference on Mixing; Würzburg, BHRA, Cranfield; 1985. pp 303–313.
126. Galindez-Mayer J, Sánchez-Teja O, Cristiani-Urbina E, Ruiz-Ordaz N. Bioprocess Biosyst Eng 2001; 24(3): 171–177.
127. Chirardini M, Donati G, Rivetti F. Chem Eng Sci 1992; 47(9–11): 2209–2214.
128. Choi KH, Chisti Y, Mooyoung M. J Chem Technol Biotechnol 1995; 62(4): 327–332.
129. Lu WJ, Hwang SJ, Chang CM. Ind Eng Chem Res 1994; 33(9): 2180–2186.
130. Merchuk JC. In: Cheremisinoff NP, editor. Encyclopedia of fluid mechanics. Houston (TX): Gulf Publishing Company; 1986. pp 1485–1511.
131. Petrovic DL, Posarac D, Dudukovic A. Chem Eng Commun 1995; 133: 1–9.
132. Lubbert A, Fröhlich S, Larson B, Schugerl K, King R, editors. Bioreactor fluid dynamics. Cranfield, England: BHRA; 1988. pp 379–393.
133. Burris VL, McGinnis DF, Little JC. Water Res 2002; 36(18): 4605–4615.
134. Wu XX, Merchuk JC. Chem Eng Sci 2003; 58(8): 1599–1614.
135. Mudde RF, Groen JS, Van Den Akker HEA. Chem Eng Sci 1997; 52(21–22): 4217–4224.
136. Vial C, Bendjaballah-Lalaoui N, Poncin S, Wild G, Midoux N. Can J Chem Eng 2003; 81(3–4): 749–755.
137. Vial C, Poncin S, Wild G, Midoux N. Chem Eng Process 2001; 40(2): 135–151.
138. Kulkarni AA, Joshi JB, Kumar VR, Kulkarni BD. Chem Eng Sci 2001; 56(21–22): 6437–6445.
139. Kulkarni AA, Joshi JB, Ravi Kumar V, Kulkarni BD. Chem Eng Sci 2001; 56(20): 5739–5747.
140. Lee CH, Glasgow LA, Erickson LE, Patel SA. Liquid circulation in airlift fermentors. New York: American Institute of Chemical Engineers; 1987.
141. Jones AG. Chem Eng Sci 1985; 40(3): 449–462.
142. Nicklin DJ. Chem Eng Sci 1962; 17: 693–702.
143. Clark NN, Jones AG. Chem Eng Sci 1987; 42(2): 378.
144. Chisti Y, Moo-Young M. J Chem Technol Biotechnol 1988; 42(3): 211–219.
145. Bello RA. PhD thesis. Ontario, Canada: University of Waterloo; 1981.
146. Wachi S, Jones AG, Elson TP. Chem Eng Sci 1991; 46(2): 657–663.
147. Chisti MY, Halard B, Mooyoung M. Chem Eng Sci 1988; 43(3): 451–457.
148. García-Calvo E. Chem Eng Sci 1989; 44(2): 321–323.
149. Richardson JF, Higson DJ. Trans Inst Chem Eng 1962; 40: 169–182.
150. García-Calvo E, Leton P. Chem Eng Sci 1991; 46(11): 2947–2951.
151. Blenke H. Adv Biochem Eng 1979; 13: 121–214.
152. Hsu YC, Dudukovic MP. Chem Eng Sci 1980; 35(1/2): 135–141.
153. Kubota H, Hosono Y, Fujie K. J Chem Eng Jpn 1978; 11(4): 319–325.
154. Koide K, Iwamoto S, Takasaka Y, Matsuura S, Takahashi E, Kimura M, Kubota H. J Chem Eng Jpn 1984; 17(6): 611–618.
155. Miyahara T, Hamaguchi M, Sukeda Y, Takahashi T. Can J Chem Eng 1986; 64: 718–725.
156. Shamlou PA, Pollard DJ, Ison AP, Lilly MD. Chem Eng Sci 1994; 49(3): 303–312.
157. Lu WJ, Hwang SJ, Chang CM. Chem Eng Sci 1995; 50(8): 1301–1310.
158. Vatai G, Tekis MN. Effect of pseudoplasticity on hydrodynamic characteristics of airlift loop contactors. Prague; 1986.
159. Vatai G, Tekic MN. Chem Eng Sci 1987; 42(1): 166–169.
160. Popovic MK, Robinson CW. Chem Eng Sci 1993; 48(8): 1405–1413.
161. Nakao K, Azakami F, Furumoto K, Yoshimoto M, Fukunaga K. Can J Chem Eng 2003; 81(3–4): 444–450.
162. Zahradnik J, Fialova M, Kastanek F, Green KD, Thomas NH. Chem Eng Res Des 1995; 73(A3): 341–346.
163. Fields PR, Slater NKH. Chem Eng Sci 1983; 38(4): 647–653.
164. Yamane T. In: Asenjo JA, Merchuk JC, editors. Bioreactor system design. New York: Dekker; 1994. pp 479–510.
165. Buffham BA, Mason G. Chem Eng Sci 1993; 48(23): 3879–3887.
166. Levenspiel O, Bishoff KB. Adv Chem Eng 1963; 4: 95–198.
167. Lin CH, Fang BS, Wu CS, Fang HY, Kuo TF, Hu CY. Biotechnol Bioeng 1976; 18: 1557–1572.
168. Murakami Y, Hirose T, Ono S, Nishijima T. J Chem Eng Jpn 1982; 15: 121–125.
169. Sánchez Mirón A, Cerón García MC, García Camacho F, Molina Grima E, Chisti Y. Chem Eng Res Des 2004; 82(10): 1367–1374.
170. Merchuk JC, Slatter NKH. Chem Eng Sci 1985; 40: 539.
171. Schügerl K. Adv Biochem Eng 1981; 19: 71–94.
172. Lin WC, Mao ZS, Chen JY. Chin J Chem Eng 1997; 5(1): 11–22.
173. Nagar M. Mixing in a split vessel airlift reactor. Graduation report in chemical engineering. Beer-Sheva: Ben-Gurion University of the Negev; 1992.
174. Verlaan P, Vos JC, Vantriet K. J Chem Technol Biotechnol 1989; 45(2): 109–121.
175. Merchuk JC, Contreras A, García F, Molina E. Chem Eng Sci 1998; 53(4): 709–719.
176. Sánchez O, Michaud S, Escudie R, Delgenes JP, Bernet N. Chem Eng J 2005; 114(1–3): 1–7.

177. Siegel MH, Hallaile M, Merchuk JC. In: Mizrahi A, editor. Advances in biotechnological processes. New York: Liss; 1988. pp 79–124.
178. Gómez AC. PhD thesis. Almería, Spain: University of Almeria; 1996.
179. Siegel M, Merchuk JC. Influence of the gas–liquid separator on air-lift reactor design and operation 1990.
180. Godboole SP, Shah YT. Design and operation of bubble column reactors. Houston (TX): Gulf; 1986.
181. Deckwer WD, Burckhart R, Zoll G. Chem Eng Sci 1974; 29(11): 2177–2188.
182. Joshi JB, Sharma MM, Shah YT, Singh CPP, Ally M, Klinzing GE. Chem Eng Commun 1980; 6(4–5): 257–271.
183. Hallaile M. PhD thesis. Beer-Sheva, Israel: Ben Gurion University of the Negev; 1993.
184. Fields PR, Slater NKH. Biotechnol Bioeng 1984; 26(7): 719–726.
185. Gavrilescu M, Muntean O, Tudose RZ. Bioprocess Eng 2000; 23(6): 543–549.
186. Hari M, Tan RBH. Chem Eng J 1999; 73(1): 29–35.
187. Fröhlich S, Lotz M, Korte T, Lubbert A, Schügerl K, Seekamp M. Biotechnol Bioeng 1991; 38(1): 43–55.
188. Sriram K, Mann R. Chem Eng Sci 1977; 32(6): 571–580.
189. Deshpande NS, Dinkar M, Joshi JB. Int J Multiphase Flow 1995; 21(6): 1191–1201.
190. Jordan DG. Volume 6, Chemical process development. New York: Wiley; 1968.
191. Toye D, Fransolet E, Simon D, Crine M, L'Homme G, Marchot P. Can J Chem Eng 2005; 83(1): 4–10.
192. Tramper J, Smit D, Straatman J, Vlak JM. Bioprocess Eng 1988; 3(1): 37–41.
193. Martens DE, Degooijer CD, Vanderveldendegroot CAM, Beuvery EC, Tramper J. Biotechnol Bioeng 1993; 41(4): 429–439.
194. Silva HJ, Cortinas T, Ertola RJ. J Chem Technol Biotechnol 1987; 40(1): 41–49.
195. Zhang ZG, Chisti Y, Mooyoung M. J Biotechnol 1995; 43(1): 33–40.
196. Stannard B, Zahir S, Rosenbloom ES. Asia Pac J Oper Res 2006; 23(1): 61–76.
197. Wilkinson PJ. In: Moody GW, Baker PB, editors. Biotransformations. London: Elsevier; 1992.
198. Sanchez-Mirón A, Garcia-Camacho F, Gómez AC, Molina-Grima E, Chisti Y. AIChE J 2000; 46(9): 1872–1887.
199. Contreras A, García F, Molina E, Merchuk JC. Biotechnol Bioeng 1998; 60(3): 317–325.
200. Tramper J, Vlak JM, deGooijer CD. Cytotechnology 1996; 20(1–3): 221–229.
201. Visnovsky G, Claus JD, Merchuk JC. Lat Am Appl Res 2003; 33(3): 207–211.
202. Kawase Y, Moo-Young M. Chem Eng Res Des 1987; 65(2): 121–126.
203. Chisti Y, Mooyoung M. Biotechnol Bioeng 1989; 34(11): 1391–1392.
204. Merchuk JC, Yona S, Siegel MH, Ben Ziv A. Biotechnol Bioeng 1990; 35(11): 1161–1163.
205. Godbole SP, Schumpe A, Shah YT, Carr NL. AIChE J 1984; 30(2): 213–220.
206. Bird RB. Chem Eng 1993; 27: 102–109.
207. Lubiniecki AS. Large-scale mammalian cell culture technology. New York: Marcel Dekker; 1990.
208. Tokashiki M, Yokoyama S. In: Hauser H, Wagner R, editors. Mammalian cell biotechnology in protein production. Berlin: de Gruyter; 1997. pp 279–317.
209. Chisti Y. Trends Biotechnol 2000; 18(10): 420–432.
210. Doran PM. Curr Opin Biotechnol 2000; 11(2): 199–204.
211. Hellwig S, Drossard J, Twyman RM, Fischer R. Nat Biotechnol 2004; 22(11): 1415–1422.
212. Marks DM. Cytotechnology 2003; 42(1): 21–33.
213. Tramper J, Joustra D, Vlak JM. In: Webb C, Mavituna F, editors. Plant and animal cells: process possibilities. Chichester: Ellis Horwood; 1987. pp 125–136.
214. Wang NS. J Biotechnol 1994; 33(2): 107–122.
215. Chisti Y. Bioprocess Eng 1993; 9(5): 191–196.
216. Handa A, Emery AN, Spier RE. Dev Biol Stand 1987; 66: 241–253.
217. Kioukia N, Nienow AW, Al-Rubeai M, Emery AN. Biotechnol Prog 1996; 12(6): 779–785.
218. Oh SKW, Nienow AW, Al-Rubeai M, Emery AN. J Biotechnol 1992; 22(3): 245–270.
219. Boulton-Stone JM, Blake JR. J Fluid Mech 1993; 254: 437–466.
220. García-Briones MA, Brodkey RS, Chalmers JJ. Chem Eng Sci 1994; 49(14): 2301–2320.
221. Chalmers JJ, Bavarian F. Biotechnol Prog 1991; 7(2): 151–158.
222. Cherry RS. Biotechnol Prog 1992; 8(1): 11–18.
223. Handa-Corrigan A, Emery AN, Spier RE. Enzyme Microb Technol 1989; 11(4): 230–235.
224. Emery AN, Lavery M, Williams B, Handa A. In: Webb C, Mavituna F, editors. Plant and animal cells: process possibilities. Chichester: Ellis Horwood; 1987. pp 137–146.
225. Van Der Pol L, Bakker WAM, Tramper J. Biotechnol Bioeng 1992; 40(1): 179–182.
226. Ma N, Chalmers JJ, Aunins JG, Zhou W, Xie L. Biotechnol Prog 2004; 20(4): 1183–1191.
227. Linek V, Vacek V, Benes P. Chem Eng J 1987; 34(1): 11–34.
228. Philichi TL, Stenstrom MK. J Water Pollut Control Fed 1989; 61(1): 83–86.
229. Atkinson B, Mavituna F. Biochemical engineering and biotechnology handbook. 2nd ed. Hampshire, England: MacMillan Publishers; 1991.
230. Deshpande RR, Heinzle E. Biotechnol Lett 2004; 26(9): 763–767.
231. Jajuee B, Margaritis A, Karamanev D, Bergougnou MA. Chem Eng J 2006; 125(2): 119–126.
232. Santos VE, Galdeano C, Gómez E, Alcón A, García-Ochoa F. Biochem Eng J 2006; 32(3): 198–204.
233. García-Ochoa F, Castro EG, Santos VE. Enzyme Microb Technol 2000; 27(9): 680–690.
234. Behkish A, Lemoine R, Sehabiague L, Oukaci R, Morsi BI. Chem Eng J 2007; 128(2–3): 69–84.
235. Lu G, Zheng P, Jin RC, Qaisar M. J Environ Sci 2006; 18(1): 58–61.

236. Sehabiague L, Lemoine RO, Behkish A, Heintz YJ, Morsi BI. AIChE Annual Meeting, San Francisco Conference Proceedings; 2005.
237. Jin H, Yang S, Zhang T, Tong Z. Chem Eng Technol 2004; 27(9): 1007–1013.
238. Lemoine R, Morsi BI. Chem Eng J 2005; 114(1–3): 9–31.
239. Zhang T, Jin H, He G, Yang S, Tong Z. Huagong Xuebao/J Chem Ind Eng (China) 2004; 55(3): 476–480.
240. Mignone CF, Ertola RJ. J Chem Technol Biotechnol 1984; 34B(2): 121–126.
241. Kawase Y, Moo-Young M. Biotechnol Bioeng 1987; 30(3): 345–347.
242. Merchuk JC, Ben-Zvi S, Niranjan K. Trends Biotechnol 1994; 12(12): 501–511.
243. Deckwer WD. Bubble column reactors. Chichester, GB: Wiley; 1991.
244. Andre G, Robinson CW, Young-Moo M. Chem Eng Sci 1983; 38(11): 1845–1854.
245. Merchuk JC, Osemberg G, Siegel M, Shacham M. Chem Eng Sci 1992; 47(9–11): 2221–2226.
246. Hwang SJ, Lu WJ. Chem Eng Sci 1997; 52(5): 853–857.
247. Merchuk JC, Stein Y, Mateles RI. Biotechnol Bioeng 1980; 22(6): 1189–1211.
248. Znad H, Tokumura M, Kawase Y. Chem Eng Technol 2006; 29(9): 1042–1047.
249. Camacho Rubio F, Acién Fernández FG, Sánchez Pérez JA, García Camacho F, Molina Grima E. Biotechnol Bioeng 1999; 62(1): 71–86.
250. Tobajas M, García-Calvo E. Heat Mass Transf 2000; 36(3): 201–207.
251. Chavez-Parga MC, Gonzalez-Ortega O, Negrete-Rodríguez MLX, Medina-Torres L, Silva EME. World J Microbiol Biotechnol 2007; 23(5): 615–623.
252. Nikakhtari H, Hill GA. J Chem Technol Biotechnol 2006; 81(6): 1029–1038.
253. Wang PM, Huang TK, Cheng HP, Chien YH, Wu WT. J Chem Eng Jpn 2002; 35(4): 354–359.
254. Merchuk JC. Biotechnol Bioeng 1977; 19: 1885–1889.
255. Gómez E, Santos VE, Alcon A, García-Ochoa F. Chem Eng Sci 2006; 61(14): 4595–4604.
256. Gómez E, Santos VE, Alcon A, Martin AB, García-Ochoa F. Energy Fuels 2006; 20(4): 1565–1571.
257. Merchuk JC. Trends Biotechnol 1990; 8(3): 66–70.
258. Bhavaraju SM, Russell TWF, Blanch HW. AIChE J 1978; 24(3): 454–466.
259. Marrucci G. Chem Eng Sci 1969; 24: 975–985.
260. Siegel MH. PhD thesis. Israel: Ben-Gurion University; 1991.
261. Malfait JL, Wilcox DJ, Mercer DG, Barker LD. Biotechnol Bioeng 1981; 23(4): 863–877.
262. Weiland P. Ger Chem Eng 1984; 7(6): 374–385.
263. Kawagoe M, Otake T, Robinson CW. J Chem Eng Jpn 1989; 22(2): 136–142.
264. Chisti MY, Moo-Young M. Biotechnol Bioeng 1988; 31(5): 487–494.
265. Li Guo Q, Yang Shou Z, Cai Zhao L, Chen Jia Y. Chem Eng J Biochem Eng 1995; 56(2): 101–107.
266. Mehrnia MR, Towfighi J, Bonakdarpour B, Akbarnejad MM. Biochem Eng J 2005; 22(2): 105–110.
267. Chisti MY, Fujimoto K, Moo-Young M. In: Ho CS, Oldshue JY, editors. Biotechnology processes: scale-up and mixing. New York: American Institute of Chemical Engineers; 1987. pp 72–81.
268. Guo YX, Rathor MN, Ti HC. Chem Eng J 1997; 67(3): 205–214.
269. Al-Masry WA, Dukkan AR. Ind Eng Chem Res 1998; 37(1): 41–48.
270. Shah YT, Kelkar BG, Godbole SP, Deckwer WD. AIChE J 1982; 28(3): 353–379.
271. Deckwer WD. Chem Eng Sci 1980; 35(6): 1341–1346.
272. Levich VG. Physicochemical hydrodynamics. Englewood Cliffs (NY): Prentice Hall; 1962.
273. Kolmogoroff AN. Dokl Akad Nauk SSSR 1949; 66: 825–828.
274. Roy S, Dhotre MT, Joshi JB. Chem Eng Res Des 2006; 84(8A): 677–690.
275. Joshi JB. Chem Eng Sci 2001; 56(21–22): 5893–5933.
276. Blakebrough N, Fatile IA, McManamey WJ, Walker G. Chem Eng Res Des 1983; 61(6): 383–387.
277. Blakebrough N, McManamey WJ, Waler G. Chem Eng Res Des 1983; 61(4): 264–266.
278. Luo X, Jiang P, Fan LS. AIChE J 1997; 43(10): 2432–2445.
279. He SM, An WH, Luo FQ, Huang Z, Fan XL. Nat Gas Ind 2007; 27(4): 53–55.
280. Yang GQ, Luo X, Lau R, Fan LS. Ind Eng Chem Res 2000; 39(7): 2568–2577.
281. Wu C, Al-Dahhan MH, Prakash A. Chem Eng Sci 2007; 62(1–2): 140–147.
282. Koide K, Horibe K, Kawabata H, Ito S. J Chem Eng Jpn 1984; 17(4): 368–374.
283. Douek RS, Hewitt GE, Livingston AG. Chem Eng Res Des 1995; 73(A3): 336–340.
284. Livingston AG, Zhang SF. Chem Eng Sci 1993; 48(9): 1641–1654.
285. Herskowitz M, Merchuk JC. Can J Chem Eng 1986; 64(1): 57–61.
286. Fan L-S, Hwang SJ, Matsuura A. Chem Eng Sci 1984; 39(12): 1677–1688.
287. Koide K, Terasawa M, Takekawa H. J Chem Eng Jpn 1986; 19(4): 341–344.
288. Posarac D, Petrovic D, Dudukovic A, Skala D. J Serb Chem Soc 1991; 56: 227–240.
289. Petrovic D, Posarac D, Skala D. Chem Eng Sci 1989; 44(4): 996–998.
290. Petrovic DLJ, Posarac D, Dudukovic A, Skala D. Chem Eng Sci 1990; 45(9): 2967–2970.
291. Immich M, Onken U. Chem Eng Sci 1992; 47(13–14): 3379–3386.
292. Muthukumar K, Prasad BN, Velan M. J Chem Technol Biotechnol 2004; 79(12): 1376–1380.
293. Li C, Matsunaga T, Seki K, Yoshimoto M, Furumoto K, Fukunaga K, Nakao K. Chem Eng Technol 2006; 29(9): 1090–1096.
294. Heck J, Onken U. Chem-Ing-Tech 1986; 58(2): 131–133.
295. Zhu C, Yu Q, Dave RN, Pfeffer R. AIChE J 2005; 51(2): 426–439.

296. Fan L-S, Fujie K, Long TR. AIChE Symposium Series; 1984. pp 102–109.
297. Koide K, Horibe K, Kawabata H, Ito S. J Chem Eng Jpn 1985; 18(3): 248–254.
298. Heck IJ, Onken U. Chem Eng Technol 1988; 11(1): 335–340.
299. Wen JP, Jia XQ, Feng W. Chem Eng Technol 2005; 28(1): 53–60.
300. Gluz MD, Merchuk JC. Chem Eng Sci 1996; 51(11): 2915–2920.
301. Kushalkar KB, Pangarkar VG. Chem Eng Sci 1994; 49(1): 139–144.
302. Rossi G. Biohydrometallurgy. Hamburg, Germany: McGraw-Hill; 1990.
303. Smith BC, Skidmore DR. Biotechnol Bioeng 1990; 35(5): 483–491.
304. Assa A, Bar R. Biotechnol Bioeng 1991; 38(11): 1325–1330.
305. Douek RS, Hewitt GF, Livingston AG. Chem Eng Res Des 1995; 73(A3): 336–340.
306. Schmidt J, Nassar R, Lubbert A. Chem Eng Sci 1992; 47(9–11): 2295–2300.
307. Snape JB, Thomas NH. Biotechnol Bioeng 1992; 40(3): 337–345.
308. Couvert A, Bastoul D, Roustan M, Chatellier P. Chem Eng Process 2004; 43(11): 1381–1387.
309. Nicolella C, Van Loosdrecht MCM, Heijnen SJ. Trends Biotechnol 2000; 18(7): 312–320.
310. Choi JW, Cho GH, Byun SY, Kim DI. Adv Biochem Eng Biotechnol 2001; 72: 63–102.
311. Sajć L, Vunjak-Novakovic G. AIChE J 2000; 46(7): 1368–1375.
312. Sajc L, Obradovic B, Vukovic D, Bugarski B, Grubisic D, Vunjak-Novakovic G. Biotechnol Prog 1995; 11(4): 420–428.
313. Chen Y-M, Fan L-S. Chem Eng Sci 1990; 45(4): 935–945.
314. Mehrnia MR, Bonakdarpour B, Towfighi J, Akamejad MM. Environ Prog 2004; 23(3): 206–214.
315. Oosterhuis NMG. PhD thesis. Delft, The Netherlands: Department of Chemical Technology, University of Technology; 1984.
316. Kossen NWF, Oosterhuis NMG. In: Rhem NJ, Reed J, editors. Biotechnology. Weinheim, Germany: VCH; 1985.
317. Sweere APJ, Luyben KCAM, Kossen NWF. Enzyme Microb Technol 1987; 9(7): 386–398.
318. Sola C, Godia F. In: Asenjo JA, Merchuk JC, editors. Bioreactor system design. New York: Dekker; 1994. pp 511–552.
319. Zlokarnik M. Scale-up in chemical engineering. 2nd ed. Weinheim, Germany: Wiley-VCH Verlag GmbH & Co. KGaA; 2006.
320. Sikula I, Jurascik M, Markos J. Chem Eng Sci 2007; 62(18–20): 5216–5221.
321. Boyadjiev C. Theor Found Chem Eng 2006; 40(6): 633–638.
322. Jordan DG. Volume 15, Kirk-Othmer encyclopedia of chemical technology. 2nd ed. New York: Wiley; 1968. pp 605–637.
323. Einsele A. Process Biochem 1978; 13(7): 13–14.
324. Liu TJ, Miura S, Yaguchi M, Arimura T, Park EY, Okabe M. J Biosci Bioeng 2006; 101(1): 9–12.
325. Taguchi TIH, Teramoto S, Takatsu M, Sato M. J Ferment Technol 1986; 46: 823–830.
326. Takei KMH, Yoshida F. Ferment Technol 1975; 53: 151–156.
327. Oosterhuis NMG, Groesbeek NM, Olivier APC, Kossen NWF. Biotechnol Lett 1983; 5(3): 141–146.
328. Roels JA. Energetics and kinetics in biotechnology. Amsterdam, Holland: Elsevier Biomedical Press; 1983.
329. Schoutens GH, Guit RP, Zieleman GJ, Luyben KCAM, Kossen NWF. J Chem Technol Biotechnol 1986; 36(7): 335–343.
330. Papagianni M, Mattey M, Kristiansen B. Biotechnol Prog 2003; 19(5): 1498–1504.
331. Bezzo F, Macchietto S, Pantelides CC. AIChE J 2003; 49(8): 2133–2148.
332. Buwa VV, Deo DS, Ranade VV. Int J Multiphase Flow 2006; 32(7): 864–885.
333. Buwa VV, Ranade VV. Can J Chem Eng 2003; 81(3–4): 402–411.
334. Monahan SM, Fox RO. AIChE Annual Meeting, Conference Proceedings, San Francisco; 2005.
335. Monahan SM, Fox RO. Chem Eng Sci 2007; 62(12): 3159–3177.
336. Monahan SM, Vitankar VS, Fox RO. AIChE J 2005; 51(7): 1897–1923.
337. Mudde RF, Van Den Akker HEA. Chem Eng Sci 2001; 56(21–22): 6351–6358.
338. Rampure MR, Buwa VV, Ranade VV. Can J Chem Eng 2003; 81(3–4): 692–706.
339. Roy S, Joshi JB. Chem Eng Technol 2006; 29(9): 1034–1041.
340. Scargiali F, Salvaggio S, Grisafi F, Brucato A. CHISA 2006—17th International Congress of Chemical and Process Engineering. Prague, Czechoslovakia; 2006.
341. Van Baten JM, Ellenberger J, Krishna R. Chem Eng Process 2003; 42(10): 733–742.
342. Van Baten JM, Ellenberger J, Krishna R. Can J Chem Eng 2003; 81(3–4): 660–668.
343. Vial C, Poncin S, Wild G, Midoux N. Chem Eng Sci 2005; 60(22): 5945–5954.
344. Wang TF, Wang JF, Zhao B, Ren F, Jin Y. Chem Eng Commun 2004; 191(8): 1024–1042.
345. Menzel T, In Der Weide T, Staudacher O, Wein O, Onken U. Ind Eng Chem Res 1990; 29(6): 988–994.
346. Dhanasekharan KM, Sanyal J, Jain A, Haidari A. Chem Eng Sci 2005; 60(1): 213–218.
347. Kawase Y, Hashimoto N. J Chem Technol Biotechnol 1996; 65(4): 325–334.
348. Feng W, Wen JP, Liu CY, Yuan Q, Jia XQ, Sun Y. Biotechnol Bioeng 2007; 97(2): 251–264.
349. Feng W, Wen J, Liu C, Yuan Q, Jia X, Sun Y. Biotechnol Bioeng 2007; 97(2): 251–264.
350. Simon H. Neural networks: a comprehensive foundation. Upper Saddle River (NJ): Prentice Hall; 1999.
351. Al-Masry WA. Chem Eng Res Des 2006; 84(A6): 483–486.
352. Shaikh A, Al-Dahhan M. Chem Eng Process 2003; 42(8–9): 599–610.

353. Contreras A, García F, Molina E, Merchuk JC. Enzyme Microb Technol 1999; 25(10): 820–830.
354. Chisti Y. In: Flickinger MC, Drew SW, editors. Volume 5, Encyclopedia of bioprocess technology: fermentation, biocatalysis and bioseparation. New York: Wiley; 1999. pp 2379–2406.
355. Al-Masry WA. Biotechnol Bioeng 1999; 62(4): 494–498.
356. Al-Masry WA, Al-Ahmed MI. J Chem Technol Biotechnol 2005; 80(11): 1230–1235.
357. Schmidt FR. Appl Microbiol Biotechnol 2005; 68(4): 425–435.
358. Mohanty K, Das D, Biswas MN. Chem Eng Sci 2006; 61(14): 4617–4624.
359. Mohanty K, Das D, Biswas MN. Chem Eng J 2007; 133(1–3): 257–264.
360. Pollard DJ, Shamlou PA, Lilly MD, Ison AP. Bioprocess Eng 1996; 15(5): 279–288.
361. Potucek F. Collect Czech Chem Commun 1990; 55(4): 981–986.
362. Gaspillo P-AD, Goto S. J Chem Eng Jpn 1991; 24(5): 680–682.
363. Chisti Y, Kasper M, Mooyoung M. Can J Chem Eng 1990; 68(1): 45–50.
364. Zhou WC, Holzhauerrieger K, Bayer T, Schügerl K. J Biotechnol 1993; 28(2–3): 165–177.
365. Merchuk J, Gluz M. In: Flickinger MC, Drew SW, editors. Volume 5, Encyclopedia of bioprocess technology: fermentation, biocatalysis and bioseparation. New York: Wiley; 1999. pp 320–353.
366. Schlotelburg C, Gluz M, Popovic M, Merchuk JC. Can J Chem Eng 1999; 77: 804–810.
367. Vorapongsathorn T, Wongsuchoto P, Pavasant P. Chem Eng J 2001; 84(3): 551–556.
368. Bando Y, Nishimura M, Sota H, Suzuki S, Kawase N. Chem Eng Sci 1992; 47(13–14): 3371–3378.
369. Bando Y, Nishimura M, Hayashi A, Hiura S, Ido S, Idota A. J Chem Eng Jpn 1995; 28(2): 225–227.
370. Fu CC, Wu WT, Lu SY. Enzyme Microb Technol 2003; 33(4): 332–342.
371. Fu CC, Lu SY, Hsu YJ, Chen GC, Lin YR, Wu WT. Chem Eng Sci 2004; 59(14): 3021–3028.
372. Tung HL, Tu CC, Chang YY, Wu WT. Bioprocess Eng 1998; 18(5): 323–328.
373. Wu WT, Wu JY. J Ferment Bioeng 1990; 70(5): 359–361.
374. Wu WT, Wu JY, Jong JZ. Biotechnol Prog 1992; 8(5): 465–468.
375. Wu WT, Hsiun DY. Bioprocess Eng 1996; 15(2): 59–62.
376. Ghosh TK, Maiti BR, Bhattacharyya BC. Biotechnol Tech 1993; 7(4): 301–307.
377. Wei CH, Xie B, Xiao HL. Chem Eng Technol 2000; 23(1): 38–45.
378. Wei CH, Xie B, Xiao HL, Wang DS. Chem Eng Technol 2000; 23(7): 597–603.
379. Liu YQ, Tay JH. Biochem Eng J 2007; 34(1): 1–7.
380. Futselaar H, Schonewille H, de Vente D, Broens L. Desalination 2007; 204(1–3): 1–7.
381. Jajuee B, Margaritis A, Karamanev D, Bergougnou MA. Biotechnol Bioeng 2007; 96(2): 232–243.
382. Garnier A, Chavarie C, Andre G, Klvana D. Chem Eng Commun 1990; 98: 31–45.
383. Loh KC, Liu J. Chem Eng Sci 2001; 56(21–22): 6171–6176.
384. Loh KC, Ranganath S. Chem Eng Sci 2005; 60(22): 6313–6319.
385. Bao J, Koumatsu K, Furumoto K, Yoshimoto M, Fukunaga K, Nakao K. Chem Eng Sci 2001; 56(21–22): 6165–6170.
386. Jovetic S, Marinelli F, Tramper J. Enzyme Microb Technol 2006; 38(1–2): 34–39.
387. Lu XP, Ding J, Wang YR, Shi J. Chem Eng Sci 2000; 55(12): 2257–2263.
388. Kilonzo PA, Margaritis A. Biochem Eng J 2004; 17(1): 27–40.
389. Petersen EE, Margaritis A. Crit Rev Biotechnol 2001; 21(4): 233–294.
390. Gourich B, El Azher N, Bellhaj MS, Delmas H, Bouzidi A, Ziyad M. Chem Eng Process 2005; 44(10): 1047–1053.
391. You WL, Chen BL, Wang J. J Plant Resour Environ 2006; 15(1): 30–33.
392. Meiser A, Schmid-Staiger U, Trosch W. J Appl Phycol 2004; 16(3): 215–225.
393. Richmond A, Cheng-Wu Z. J Biotechnol 2001; 85(3): 259–269.
394. Zhang K, Kurano N, Miyachi S. Appl Microbiol Biotechnol 1999; 52(6): 781–786.
395. Hu Q, Guterman H, Richmond A. Biotechnol Bioeng 1996; 51(1): 51–60.
396. Degen J, Uebele A, Retze A, Schmid-Staiger U, Trosch W. J Biotechnol 2001; 92(2): 89–94.
397. Chen CP, Yang SJ, Wu WT. Biotechnol Tech 1997; 11(6): 439–441.
398. Lu GZ, Bittorf K, Thompson BG, Gray MR. Can J Chem Eng 1997; 75(2): 290–298.
399. Lu GZ, Thompson BG, Suresh MR, Gray MR. Biotechnol Bioeng 1995; 45(2): 176–186.
400. Vunjak-Novakovic G, Kim Y, Wu XX, Berzin I, Merchuk JC. Ind Eng Chem Res 2005; 44(16): 6154–6163.
401. Merchuk JC, Rosenblat Y, Berzin I. Chem Eng Sci 2007; 62(24): 7414–7425.
402. Kosugi S, Niwa K, Saito T, Kajishima T, Hamaogi K. Chem Eng Sci 2001; 56(21–22): 6205–6210.
403. Singleton VL, Little JC. Environ Sci Technol 2006; 40(24): 7512–7520.
404. Ho CS, Erickson LE, Fan LT. Biotechnol Bioeng 1977; 19(10): 1503–1522.
405. Young MA, Carbonell RG, Ollis DF. AIChE J 1991; 37(3): 403–428.
406. Cockx A, Line A, Roustan M, Do-Quang Z, Lazarova V. Chem Eng Sci 1997; 52(21–22): 3787–3793.
407. Sáez AE, Márquez MA, Roberts GW, Carbonell RG. AIChE J 1998; 44(6): 1413–1423.
408. Hwang SJ, Cheng YL. Chem Eng Sci 1997; 52(21–22): 3949–3960.
409. Mousseau F, Liu SX, Hermanowicz SW, Lazarova V, Manem J. Water Sci Technol 1998; 37(4–5): 177–181.
410. Freitas C, Fialova M, Zahradnik J, Teixeira JA. Chem Eng Sci 1999; 54(21): 5253–5258.

411. Van Benthum WAJ, van den Hoogen JHA, Van Der Lans R, Van Loosdrecht MCM, Heijnen JJ. Chem Eng Sci 1999; 54(12): 1909–1924.
412. Tobajas M, García-Calvo E, Siegel MH, Apitz SE. Chem Eng Sci 1999; 54(21): 5347–5354.
413. Orejas JA. Chem Eng Sci 1999; 54(21): 5299–5309.
414. Márquez MA, Amend RJ, Carbonell RG, Sáez AE, Roberts GW. Chem Eng Sci 1999; 54(13–14): 2263–2271.
415. Korpijarvi J, Oinas P, Reunanen J. Chem Eng Sci 1999; 54(13–14): 2255–2262.
416. Sanders DA, Cawte H, Hudson AD. Int J Energy Res 2001; 25(6): 487–500.
417. Camarasa E, Carvalho E, Meleiro LAC, Maciel R, Domingues A, Wild G, Poncin S, Midoux N, Bouillard J. Chem Eng Sci 2001; 56(2): 493–502.
418. Camarasa E, Carvalho E, Meleiro LAC, Maciel R, Domingues A, Wild G, Poncin S, Midoux N, Bouillard J. Chem Eng Process 2001; 40(2): 121–128.
419. Sotiriadis AA, Thorpe RB, Smith JM. Chem Eng Sci 2005; 60(22): 5917–5929.
420. Heijnen JJ, Hols J, vanderLans R, vanLeeuwen H, Mulder A, Weltevrede R. Chem Eng Sci 1997; 52(15): 2527–2540.
421. García-Calvo E, Rodríguez A, Prados A, Klein J. Chem Eng Sci 1999; 54(13–14): 2359–2370.
422. Heck J, Onken U. Chem Eng Sci 1988; 44: 1743–1745.
423. Camacho-Rubio F, García JL, Molina-Grima E, Chisti Y. Chem Eng J 2001; 84(1): 43–55.
424. Dhaouadi H, Poncin S, Midoux N, Wild G. Chem Eng Process 2001; 40(2): 129–133.
425. Steiff A, Gran-Heedfeld S, Schlüter S, Weinspach PM. Presented at the Preprints of the 4th Japanese/German Symposium Bubble Columns'97; Kyoto, Japan; 1997. Unpublished.
426. Shechter R, Merchuk JC. Can J Chem Eng 2003; 81(3–4): 900–905.
427. Kojima H, Sawai J, Uchino H, Ichige T. Chem Eng Sci 1999; 54: 5181–5185.
428. Yu F, Zhang DY, Bai FW, An LJ. Plant Cell Tissue Organ Cult 2005; 81(2): 159–163.
429. Kintzios S, Makri O, Pistola E, Matakiadis T, Shi HP, Economou A. Biotechnol Lett 2004; 26(13): 1057–1059.
430. Kintzios S, Kollias H, Straitouris E, Makri O. Biotechnol Lett 2004; 26(6): 521–523.
431. Navia-Osorio A, Garden H, Cusido RM, Palazon J, Alfermann AW, Pinol MT. J Plant Physiol 2002; 159(1): 97–102.
432. Zhao JA, Zhu WH, Hu Q. Biotechnol Lett 2000; 22(6): 509–514.
433. Ouyang J, Wang XD, Zhao B, Wang YC. Enzyme Microb Technol 2005; 36(7): 982–988.
434. Hu WW, Yao H, Zhong JJ. Biotechnol Prog 2001; 17(5): 838–846.
435. Polzin JP, Rorrer GL. Biotechnol Bioeng 2003; 82(4): 415–428.
436. Caspeta L, Quintero R, Villarreal ML. Biotechnol Prog 2005; 21(3): 735–740.
437. Birch JR, Arathoon R. Bioprocess Technol 1990; 10: 251–270.
438. Pickett AM. World Biotech Rep 1987; 1: 153–162.
439. Wang DL, Liu WS, Han BQ, Xu RA. Curr Pharm Biotechnol 2005; 6(5): 397–403.
440. Lee WY, Park Y, Ahn JK, Ka KH, Park SY. Enzyme Microb Technol 2007; 40(2): 249–254.
441. Cho EJ, Oh JY, Chang HY, Yun JW. J Biotechnol 2006; 127(1): 129–140.
442. Xu CP, Kim SW, Hwang HJ, Yun JW. Bioresour Technol 2006; 97(5): 770–777.
443. Lee BC, Bae JT, Pyo HB, Choe TB, Kim SW, Hwang HJ, Yun JW. Enzyme Microb Technol 2004; 35(5): 369–376.
444. Kang X, Wang H, Wang Y, Harvey LM, McNeil B. J Ind Microbiol Biotechnol 2001; 27(4): 208–214.
445. Munoz J, Cahue-Lopez AC, Patino R, Robledo D. J Appl Phycol 2006; 18(2): 209–218.
446. Du GC, Chen LXL, Yu J. J Polym Environ 2004; 12(2): 89–94.
447. Tavares LZ, da Silva ES, Pradella JGD. Biochem Eng J 2004; 18(1): 21–31.
448. Ishida T, Mitarai M, Sugano Y, Shoda M. Biotechnol Bioeng 2003; 83(4): 474–478.
449. Chao YP, Mitarai M, Sugano Y, Shoda M. Biotechnol Prog 2001; 17(4): 781–785.
450. Zheng YG, Chen XL, Wang Z. J Biotechnol 2005; 118(4): 413–420.
451. Li CZ, Seki K, Matsunaga T, Yoshimoto M, Fukunaga K, Nakao K. J Chem Eng Jpn 2004; 37(8): 1041–1049.
452. Karamanev DG, Samson R. Environ Sci Technol 1998; 32(7): 994–999.
453. Karamanev DG, Chavarie C, Samson R. Biotechnol Bioeng 1998; 57(4): 471–476.
454. Kermanshahi Pour A, Karamanev D, Margaritis A. Water Res 2005; 39(15): 3704–3714.
455. Nikakhtari H, Hill GA. Ind Eng Chem Res 2005; 44(24): 9299–9306.
456. Lo CS, Hwang SJ. Chem Eng Sci 2004; 59(21): 4517–4530.
457. Wen JP, Chen Y, Chen DY, Jia XQ. Biochem Eng J 2005; 24(2): 135–139.
458. Wen JP, Chen Y, Jia XQ, Mao GZ. J Chem Technol Biotechnol 2006; 81(1): 17–22.
459. Marques P, Pinheiro HM, Rosa MF. Desalination 2007; 214(1–3): 343–351.
460. Morales-Barrera L, Cristiani-Urbina E. Enzyme Microb Technol 2006; 40(1): 107–113.
461. Diels L, Spaans PH, Van Roy S, Hooyberghs L, Ryngaert A, Wouters H, Walter E, Winters J, Macaskie L, Finlay J, Pernfuss B, Woebking H, Pumpel T, Tsezos M. Hydrometallurgy 2003; 71(1–2): 235–241.
462. Peraza-Luna F, Rodríguez-Mendiola M, Arias-Castro C, Bessiere JM, Calva-Calva G. J Agric Food Chem 2001; 49(12): 6012–6019.
463. Shin KS, Murthy HN, Ko JY, Paek KY. Biotechnol Lett 2002; 24(24): 2067–2069.
464. Kaewpintong K, Shotipruk A, Powtongsook S, Pavasant P. Bioresour Technol 2007; 98(2): 288–295.
465. Yu LJ, Qin WM, Lan WZ, Zhou PP, Zhu M. Bioresour Technol 2003; 88(3): 265–268.
466. Sevilla JMF, García MCC, Mirón AS, Belarbi E, Camacho FG, Grima EM. Biotechnol Prog 2004; 20(3): 728–736.

467. Millitzer M, Wenzig E, Peukert W. Biotechnol Bioeng 2005; 92(6): 789–801.
468. Burkert JFD, Maldonado RR, Maugeri F, Rodrigues MI. J Chem Technol Biotechnol 2005; 80(1): 61–67.
469. Aleksieva P, Peeva L. Enzyme Microb Technol 2000; 26(5–6): 402–405.
470. Zheng YG, Wang Z, Chen XL. Biochem Eng J 2000; 5(2): 115–121.
471. Zheng YG, Wang Z, Chen XL, Zhang CH. Biotechnol Prog 2001; 17(2): 273–277.
472. Jayus BM, McDougall and Seviour RJ. Enzyme Microb Technol 2002; 31(3): 289–299.
473. Jin B, Yan XQ, Yu Q, Van Leeuwen JH. Adv Environ Res 2002; 6(2): 179–189.
474. Metz B, Kossen NWF. Biotechnol Bioeng 1977; 19: 781–799.
475. Jin B, Van Leeuwen JH, Doelle HW, Yu QM. World J Microbiol Biotechnol 1999; 15(1): 83–90.
476. Lazarova V, Meyniel J, Duval L, Manem J. Chem Eng Sci 1997; 52(21–22): 3919–3927.
477. Bakker WAM, Kers P, Beeftink HH, Tramper J, De Gooijer CD. J Ferment Bioeng 1996; 81(5): 390–393.
478. Van Benthum WAJ, Van Der Lans R, Van Loosdrecht MCM, Heijnen JJ. Chem Eng Sci 2000; 55(3): 699–711.
479. Garrido JM, Campos JL, Mendez R, Lema JM. Water Sci Technol 1997; 36(1): 157–163.
480. Zhou P, He JH, Qian Y. Water Air Soil Pollut 2003; 144(1): 81–100.
481. Zhou P, He JH, Qian Y. J Environ Eng ASCE 2005; 131(6): 874–882.
482. de Kreuk MK, Kishida N, Van Loosdrecht MCM. Water Sci Technol 2007; 55: 75–81.
483. Beun JJ, Van Loosdrecht MCM, Heijnen JJ. Water Res 2002; 36(3): 702–712.
484. Ivanov V, Tay JH, Tay STL, Jiang HL. Water Sci Technol 2004; 50(12): 147–154.
485. Kim DJ, Seo D. Process Biochem 2006; 41(5): 1055–1062.
486. Wang F, Yang FL, Zhang XW, Liu YH, Zhang HM, Zhou J. World J Microbiol Biotechnol 2005; 21(8–9): 1379–1384.
487. Wang SG, Lu XW, Gong WX, Gao BY, Zhang DH, Yu HQ. Bioresour Technol 2007; 98(11): 2142–2147.
488. Kim DJ, Kim SH. Water Res 2006; 40(5): 887–894.
489. Merchuk JC, Shechter R. Can J Chem Eng 2003; 81: 900–905.
490. Cook AM, Laue H, Junker F. FEMS Microbiol Rev 1998; 22(5): 399–419.
491. Wagner K, Hempel DC. Biotechnol Bioeng 1988; 31(6): 559–566.
492. Nicolella C, Zoezzi M, Rabino M, Furfaro M, Rovatti M. Water Res 2005; 39(12): 2495–2504.
493. Nicolella C, Zolezzi M, Furfaro M, Cattaneo C, Rovatti M. Ind Eng Chem Res 2007; 46(21): 6674–6680.
494. Lodato A, Alfieri F, Olivieri G, Di Donato A, Marzocchella A, Salatino P. Enzyme Microb Technol 2007; 41(5): 646–652.
495. Assadi MM, Jahangiri MR. Desalination 2001; 141(1): 1–6.
496. Assadi MM, Rostami K, Shahvali M, Azin M. Desalination 2001; 141(3): 331–336.
497. Principi P, Villa F, Bernasconi M, Zanardini E. Water Res 2006; 40(1): 99–106.
498. Manipura A, Barbosa VL, Burgess JE. Miner Eng 2007; 20(6): 617–620.
499. Li G, Wu LL, Dong CS, Wu GX, Fan YB. J Environ Sci 2007; 19(1): 12–17.
500. Fan YB, Li G, Wu LL, Yang WB, Dong CS, Xu HF, Fan W. Process Biochem 2006; 41(6): 1364–1370.
501. Muthukumar K, Velan M. J Chem Eng Jpn 2005; 38(4): 253–263.
502. Rao T, Sonolikar RL, Saheb SP. Chem Eng Sci 1997; 52(21–22): 4155–4160.
503. Quan XC, Shi HC, Zhang YM, Wang HL, Qian Y. Sep Purif Technol 2004; 34(1–3): 97–103.
504. Viggiani A, Olivieri G, Siani L, Di Donato A, Marzocchella A, Salatino P, Barbieri P, Galli E. J Biotechnol 2006; 123(4): 464–477.
505. Jia XQ, Wen JP, Jiang Y, Liu XL, Feng W. Chem Eng Sci 2006; 61(11): 3463–3475.
506. Wen JP, Liu XL, Yuan Q, Zhao XM. J Chem Technol Biotechnol 2006; 81(5): 817–822.
507. Wen JP, Jia XQ, Pan L, Wang CL, Mao GZ. Biochem Eng J 2005; 25(1): 33–37.
508. Wen J, Pan L, Xu X, Zhu Z. Chem Eng Technol 2003; 26(6): 271–275.

43

BIOREACTORS, CONTINUOUS CULTURE OF PLANT CELLS

H.J.G. Ten Hoopen
Delft University for Technology, Delft, The Netherlands

43.1 INTRODUCTION

The first suspension culture of plant cells in a nutrient solution was reported in 1954 by Muir (1). Only two years later cultures of plant cells in bioreactors were carried out by Melchers and Engelmann (2). Bioreactors can be employed in batch, fed batch, or continuous mode. In a continuous culture, the nutrients consumed by the organisms are continuously replenished by an inflow of fresh medium. In most cases the culture volume is kept constant by an equal outflow of the cell suspension (Fig. 43.1). Stable steady states can be achieved at dilution rates (flow rate/volume) smaller than the maximum specific growth rate of the organism, as predicted by mathematical derivation. Intuitively, it is understandable that steady states occur, because the limiting nutrient concentration and the biomass growth are coupled in a stable control cycle: Increasing nutrient concentration stimulates growth resulting in increased biomass concentration, but increased biomass concentration decreases the limiting nutrient concentration. In a steady state, all concentrations (biomass, biomass composition, and nutrients) are constant. The biomass concentration in the culture is controlled by the concentration of the growth-limiting nutrient in the medium; the average specific growth rate in the culture is identical with the dilution rate. This "balanced growth" in the chemostat is a very attractive tool in physiological studies or in research on growth and production kinetics. It provides an experimental system with completely controlled conditions. In fact, it is opposite to batch culture, where all conditions are continuously changing. (In specific cases this may be advantageous; for example, nongrowing cells in the stationary stage can only be studied in a batch culture.) Furthermore, in continuous culture it is possible to study a cell culture under various limitations (carbon, nitrogen, or phosphate source). Continuous culture could be attractive for industrial fermentations too because of the relatively long run times compared to short down times in the production process. However, the number of current applications in the fermentation industry is rather small. The most common type of continuous culture, controlled by the influent flow, is more specifically called a *chemostat.*

A different approach of running a continuous culture is by monitoring the biomass concentration and controlling the influent/effluent rate by this parameter. The monitoring device used is a turbidimeter, and the system is called *turbidostat*. A disadvantage of this system is that the tubidimetric biomass determination is not very reliable, because of its sensitivity for changes in cell or aggregate size. Phototrophic biomass uses light as an energy source. Therefore, phototrophic cultures can be grown in continuous culture with light as the limiting "nutrient." The concept of this photostat has several specific features, such as the correlation between cell density and light absorbance. In a low-density culture part of the "nutrient" light is lost through the glass wall or absorbed by the wall of the vessel. This makes the theoretical and practical basis considerably different from the chemostat. Phototrophic plant cell cultures are not very common. Therefore, only the chemostat will be discussed in detail. Some publications refer

Upstream Industrial Biotechnology: Equipment, Process Design, Sensing, Control, and cGMP Operations, Volume 2, First Edition. Edited by Michael C. Flickinger.
© 2013 John Wiley & Sons, Inc. Published 2013 by John Wiley & Sons, Inc.

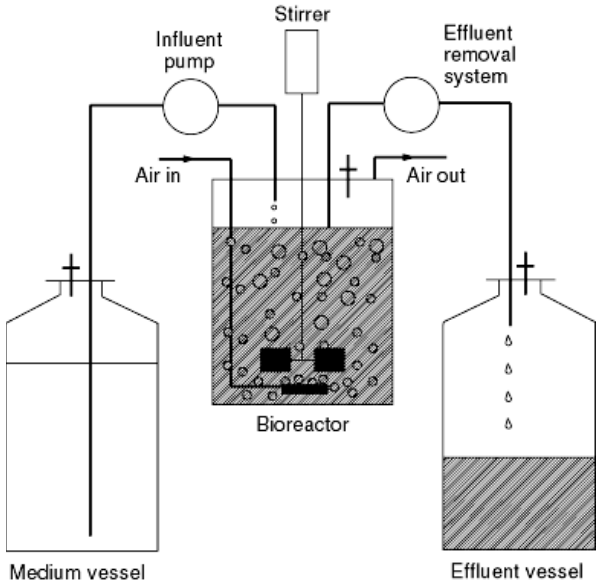


Figure 43.1. Basic setup of continuous culture.

to continuous culture systems, if the medium flow is continuous but the biomass is retained in the culture vessel (perfusion cultures, hairy root cultures, immobilized cells). These systems are not discussed here.

The number of applications of continuous culture of plant cells is small compared to continuous cultures of bacteria and yeasts. There are several reasons for this difference. Plant cells in suspension culture have some characteristics that complicate the performance of a continuous culture. The low specific growth rate of plant cells (generation times usually between 20 and 60 h) means that it takes a long time to reach a steady state; the total duration of an experiment can extend from some weeks up to more than a year. The risk of calamities (contamination, equipment failure) is then, of course, considerable. On a volume basis, plant cells are up to 200,000 times larger than bacteria and may have a relatively high specific density because of the formation of intracellular starch. Furthermore, in a plant cell culture there will be always some aggregate formation. The size of these aggregates can vary widely with the cell line and the environmental conditions, but it can be up to several millimeters in diameter. The large and "heavy" cells and aggregates tend to settle in the reactor. Another problem is the sticky character of several cell lines and the excretion of sticky and viscosity-increasing polysaccharides. This makes it difficult to maintain an ideally mixed suspension, a prerequisite for continuous culture.

In subsequent sections, practical problems and pitfalls in the setup of the continuous culture, the design of continuous culture equipment, the mathematical description of the continuous culture, and a literature survey will be discussed, all with an emphasis on plant cells in suspension culture.

TABLE 43.1. Assumptions in the Operation of Continuous Culture

Assumption	Points of concern
Continuous feed	Addition by drops
All biomass in suspension and ideally mixed	Wall growth, settling, buoyancy
Biomass in reactor and effluent equal (100% efficiency)	Effluent removal device
Biomass in steady state	Intracellular adaptation
Limiting factor defined	Defined media, validation

43.2 ASSUMPTIONS IN CONTINUOUS CULTURE THEORY AND THEIR PITFALLS

Continuous culture theory is built on a set of assumptions (Table 43.1). The inflow of fresh medium into the well-mixed culture should be continuous. All cells in the culture should face the same environmental conditions, particularly the concentration of the growth-limiting component. However, in most cases influent is added dropwise at one place in the culture, hence discontinuously in time and place. After addition to the culture, nutrients are diluted by mixing, taken up by the cells, and metabolized. The problem of the discontinuous addition can be analyzed by a comparison of the characteristic times of the involved mechanisms: addition, mixing, uptake, and metabolic conversion. When the characteristic time for uptake is short compared to the mixing time, a drop of medium serves only a part of the culture. This effect is smoothed if the mixing time is short compared to the metabolic conversion time: All cells will pass through a relatively nutrient-rich zone before starvation will occur. However, a fast uptake of the limiting nutrient and a slow metabolic conversion causes a relatively high nutrient concentration in the cell; this could trigger alternative metabolic pathways like formation of storage products or production of secondary metabolites, especially in the case of plant cells.

Another assumption in continuous culture theory is that the biomass suspension is ideally mixed. Then the biomass concentration in the vessel and in the effluent are equal. As already mentioned in the introduction, this is a critical point with plant cells. This assumption can be checked by estimating the *effluent efficiency*. This efficiency is 100% if the biomass concentration in the vessel and in the effluent are equal. Inadequate mixing in the culture vessel is caused by three phenomena: wall growth, settling, and buoyancy. The effect (decrease) on the effluent efficiency is increased by the use of an inadequate effluent removal system. It is more common than realized, not only in plant cell cultures. Noorman *et al*. (3) analyzed the kinetic consequences of nonideal mixing.

The biomass in a continuous culture is assumed to be in steady state. However, multicompartment plant cells

may require a relatively long intracellular adaptation time to reach balanced growth and steady-state biomass composition compared to bacteria. After a change in conditions it takes roughly 5 residence times [= 5/dilution rate, where dilution rate = flow (m^3/s)/volume (m^3)] to reach a steady state if hydrodynamics is the ruling mechanism. In plant cell cultures, where the intracellular adaptation might be controlling, there are examples known where as many as 12 residence times were needed to attain a constant biomass composition in a phosphate-limited continuous culture.

The growth-limiting factor in continuous culture studies is always assumed to be known, but analysis of such experiments may reveal scepticism about this. A completely defined medium is advantageous, and medium components such as coconut milk should be avoided. A distinct test of the limiting factor is to decrease the concentration of the apparent limiting component; if this results in a proportional change in the biomass concentration, the assumption is correct.

43.3 THE PRACTICAL SETUP OF A CONTINUOUS CULTURE

The concept of the continuous culture as described in the introduction can be translated into the basic design (Fig. 43.1): a culture vessel with an ideally mixed cell culture, a medium vessel for the addition of fresh medium through the influent pump, and an effluent system (a pump or an overflow device) connected to a waste vessel. The influent pump controls the dilution rate; the effluent system is designed in such a way that the volume remains constant for example through the level of the outlet tube. Many additions to and modifications of this setup are possible, dependent on the particular application. A culture of aerobic organisms needs an aeration system. Probes for online measurements of volume, temperature, pH, redox potential, and foam development can be attached. Control systems based on the sensor signals to control volume, temperature, pH, and foam level may be installed. Online analysis equipment to determine the influent and effluent gas composition and essential medium components are very useful. A sampling device for off-line analysis of the broth is in fact essential. A condenser to avoid loss of water from the culture vessel by evaporation is especially recommended for slow-growing organisms, such as plant cells. In these cultures the evaporation can be considerable in comparison with the medium flow through the system. Several modifications have been reported on the aeration and stirring systems. In the case of plant cells the objective is to achieve sufficient mixing of the culture without damaging the cells. Aeration and stirring generate hydrodynamic (shear) stress in the reactor. Therefore, the applicability of stirred tank reactors have been disputed for several years. However, Scragg *et al*. (4) and Meijer *et al*. (5,6) demonstrated that cells from various plant species are relatively shear tolerant. They concluded that large differences in shear sensitivity exist among plant cell lines, and that stirred tank reactors in most cases are the best choice for plant cell cultures. An option to reduce the negative effects of shear stress imposed by the impeller in a stirred tank can be achieved by modifying the design of the routinely used Rushton turbine impeller. Among those modified impellers are the hollow paddle (7,8), the marine (9), the cell lift (9,10), the large flat blade (11), and the helical-ribbon (12) impeller.

The effluent system needs special attention in continuous cultures of plant cells. As mentioned before, plant cells settle and stick to themselves and the culture vessel relatively easy. In combination with the low flow rates in a continuous culture of plant cells (because of the low growth rate), this makes the common effluent systems fail. These systems remove effluent from the surface of the culture, either by an overflow device, or an effluent pump through a level tube. Application of this system in a plant cell culture causes a low effluent efficiency, because the surface of the culture shows a difference in composition with the average of the culture due to settling or buoyancy. Furthermore, the cells will stick and eventually block the effluent tubing, especially because of the low flow rates in continuous culture of plant cells. Van Gulik *et al*. (13) developed an outflow device avoiding these problems (Fig. 43.2). The objective was to design a system that removes effluent from an optimally mixed section of the reactor (close to the stirrer) and at a high flow rate to avoid sticking or settling in the tubes. To achieve this the outflow device operates discontinuously. At regular time intervals a pneumatic valve system forces the effluent under air pressure into the waste vessel at a high flow rate. The timing is such that the culture volume stays within 1% of the set point. The effluent efficiency of this system was tested and approached the theoretical maximum of 100%.

The sticky and foamy character of some cell cultures makes it difficult to keep the cells inside the broth: They tend to form a layer above the suspension. Bertola and Klis (14) attacked this problem by the use of short periods of increased stirrer speed at regular intervals. Cells were taken up in the suspension again, and no cell damage was observed. Another way to avoid this problem is to leave out as much as possible objects protruding through the culture surface, such as baffles and probes. A double-wall bioreactor with sensor ports on the bottom is advantageous from this viewpoint. The wall can be cleaned either by shaking the culture vessel daily, or with a magnetically activated cleaner. Foam can be controlled by addition of antifoam substances, either at regular time intervals based on observation of the foam development, or controlled by a foam sensor. Bond *et al*. (15) published a study on the effect

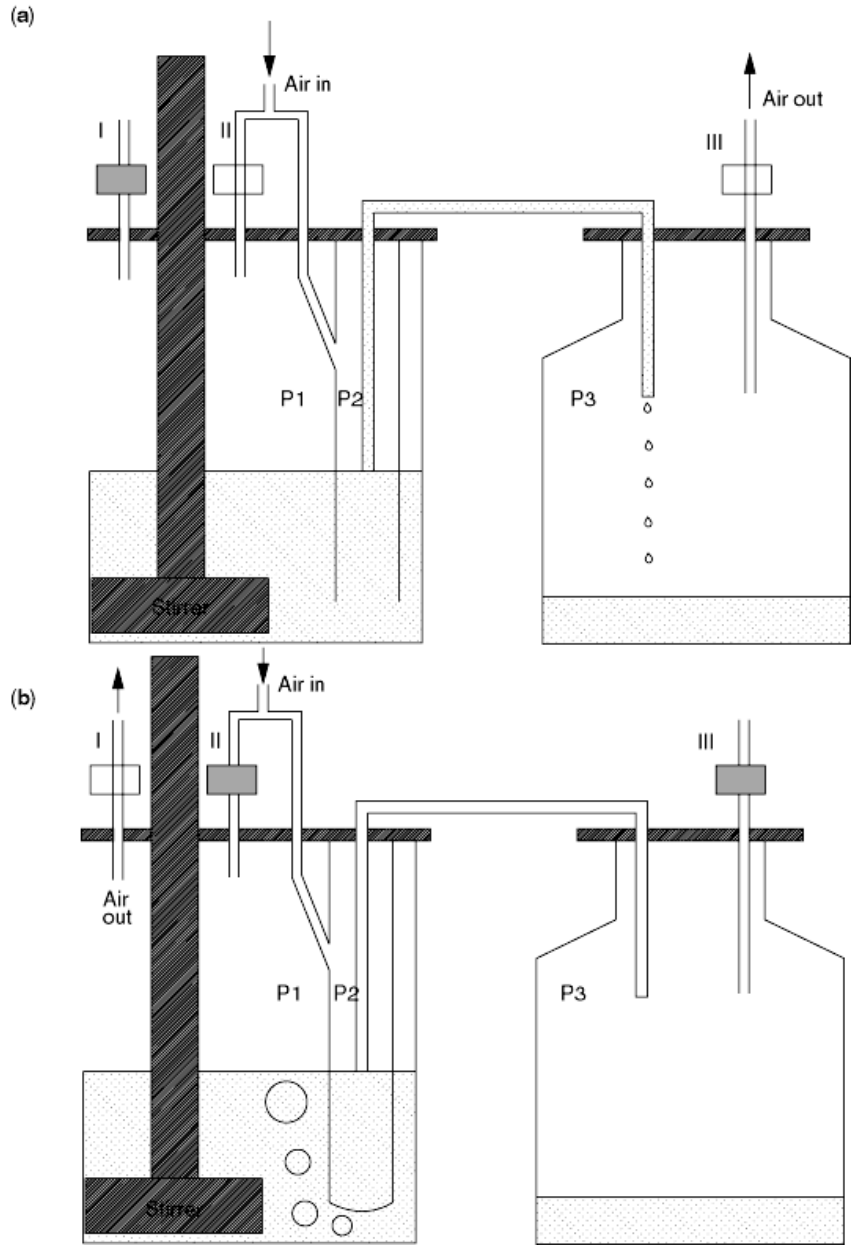


Figure 43.2. Principle of the effluent removal system. P1 = pressure inside the headspace of the reactor, P2 = pressure inside the effluent removal tube, and P3 = pressure inside the headspace of the effluent vessel. (**a**) When valve I is closed while at the same time valves II and III are opened, this will cause pressure P2 being equilibrated with pressure P1, resulting in a rise of the culture fluid in the effluent removal tube. Because of the aeration of the reactor, P1 (=P2) will exceed P3, resulting in withdrawal of all culture fluid above the inner tube. (**b**) If valve I is open and valves II and III are closed, a small stream of air keeps the effluent removal tube empty to avoid wall growth and clogging. In this case pressure P2 (=P3) exceeds P1 (13).

of antifoam on plant cells. The tested antifoam substances appeared not to harm the plant cells under normal experimental conditions. A point of general concern in continuous culture is of course the maintenance of aseptic conditions. High-quality equipment is a first prerequisite, particularly with the long run times of the continuous culture. A thorough leak test before sterilization is essential. In general, membrane filters are excellent to prevent contamination. However, it should be realized that the amount of aeration gas passing through the bioreactor during the culture period

is huge. Therefore, it is advisable to extend the contamination prevention in the air inlet with a large cottonwool depth filter. Membrane filters may be clogged by moisture. To avoid blowing up the equipment in such a case, because of the pressure of the air inlet line, it is essential to build in some safety device. An inexpensive safety measure is to provide a relatively loosely connected tube in the setup.

43.4 MATHEMATICAL DESCRIPTION OF CONTINUOUS CULTURE

The formulation of unstructured models of fermentation processes is comprehensively treated in textbooks on biotechnology (16,17). Here, only a few very general aspects are presented. The basis of these models is a set of balance equations for extensive properties. The general form of the balance equation is:

$$\begin{aligned}\text{rate of accumulation} = {} & \text{rate of inflow} - \text{rate of outflow} \\ & + \text{formation rate} \\ & - \text{consumption rate}\end{aligned}$$

The extensive properties considered to be important in the case of continuous culture of plant cells will be viable biomass X, nonviable biomass, limiting substrate S, and product. Nonviable biomass and product can be left out if the concentrations are negligible. This set of equations is completed with kinetic rate equations for biomass growth, biomass decay, substrate consumption, and product formation. As an example the general balance for biomass read (See end of chapter for nomenclature):

$$d\frac{VX}{dt} = F_i X_i - F_o X_o + V r_X - V r_d \tag{43.1}$$

In a standard chemostat the biomass concentration in the influent is zero. With the assumption that the death rate of the biomass may be neglected, and realizing that the accumulation term in a steady-state situation is zero, Eq. (43.1) becomes:

$$0 = -F_o X_o + V r_x \tag{43.2}$$

Introduction of the dilution rate D and the specific growth rate μ in Eq. (43.2):

$$D = \frac{F}{V} \tag{43.3}$$

$$\mu = \frac{r_x}{X} \tag{43.4}$$

gives the important correlation:

$$\mu = D \tag{43.5}$$

This illustrates the characteristic of the chemostat that the average specific growth rate can be controlled by setting the dilution rate.

By introduction of relations for r_X and r_s, the system is completely described. The commonly used growth expression is the Monod equation:

$$r_X = \mu X = \mu_{\max}\frac{S}{S + K_s}X \tag{43.6}$$

where $\mu_{\max}$ is the maximum specific growth rate and K_s the saturation constant. Substrate is assumed to be used for growth and for maintenance purposes of the biomass according to the expression:

$$r_s = q_s X = \left(\frac{\mu}{Y_{SX}} + m_s\right)X \tag{43.7}$$

Y_{sx} is the true yield of biomass on substrate and m_s gives the substrate consumption for maintenance processes. Worked examples of Eqs. (43.6) and (43.7) are depicted in Figure 43.3. The parameters used are typical of plant cells. On the curve of r_x it is shown that at a substrate concentration equal to the saturation constant K_s the growth rate has half the value of the maximum growth rate. The curve of r_s shows a shortcoming of the model used at substrate concentration 0; there is still substrate consumption although there is no substrate available. This situation is better described by a different concept, where the maintenance energy is provided by endogenous respiration of biomass. With the introduction of the Eqs. (43.6) and (43.7) the set of equations describing the growth of an organism

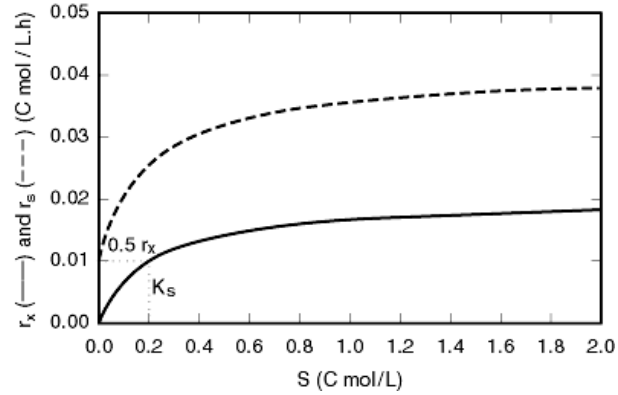


Figure 43.3. Growh rate r_x (—) and consumption rate r_s (- - -) versus limiting substrate concentration S [Eqs. (43.6) and (43.7)]. Parameters used $\mu_{\max} = 0.02\ h^{-1}$, $K_s = 0.2$ C mol/L, $Y_{sx} = 0.65$ C mol/C mol, $m_s = 0.01\ h^{-1}$, $X = 1$ C mol/L.

in continuous culture is complete. The biomass and the substrate concentration can be solved as a function of the dilution rate D, resulting in:

$$X = \frac{D(S_i - S_o)}{D/Y_{SX} + m_s} \tag{43.8}$$

$$S = \frac{k_s D}{\mu_{\max} - D} \tag{43.9}$$

These solutions still contain the organism-dependent parameters Y_{sx}, m_s, and K_s.

The yield Y_{sx} and the maintenance coefficient m_s can be determined from a series of continuous culture experiments at various dilution rates. An example of Eqs. (43.8) and (9) is plotted in Figure 43.4. At low dilution rates (= specific growth rates), the substrate consumption for maintenance is relatively important, resulting in a low apparent yield of biomass on substrate. At high dilution rates near the maximum specific growth rate, the culture starts to wash out, resulting in biomass concentration zero and maximal unconsumed substrate concentration. Van Gulik *et al*. (18,19) used this model extended with balance and rate equation for product formation and validated this model in a comprehensive continuous culture study. They could fit their experimental data roughly with this model and could estimate the organism-specific parameters. However, statistical analysis revealed that this model was certainly not a perfect description of a plant cell culture in continuous culture. Important observations were that although the carbon source was presumed to be the limiting nutrient, the phosphate concentration was always almost zero in the broth, and that the cells formed internal storage polysaccharides ("starch") in a dilution-rate-dependent quantity. On the basis of these observations van Gulik *et al*. (19) developed a structured

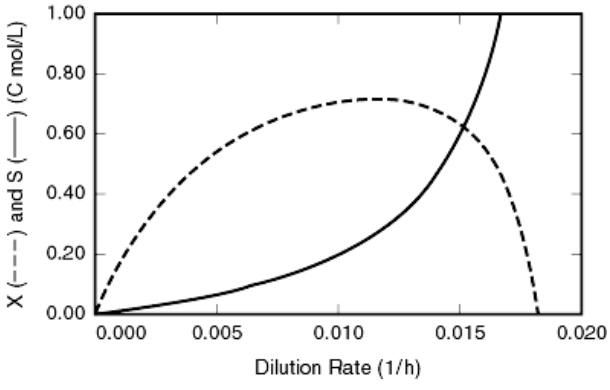


Figure 43.4. Biomass concentration X (- - -) and limiting substrate concentration S (—) versus dilution rate D in a chemostat [Eqs. (43.8) and (9)]. Parameters used S_i = 2 C mol/L; for other parameters see Figure 43.3.

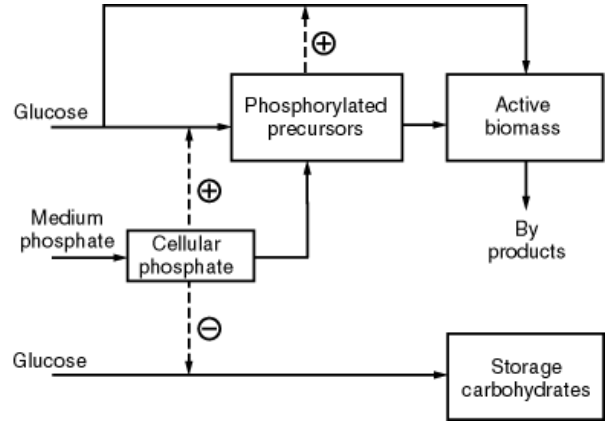


Figure 43.5. Schematic representation of the structured growth model (19).

model as depicted in Figure 43.5. The biomass was divided into two compartments: the active biomass part where all the biochemical activities take place, and the storage compartment containing the storage polysaccharides. The flow of material between medium and active biomass compartment, and between active biomass and the storage compartment, was controlled by the external carbon source and the internal phosphate concentration. This model is considerably more complex than the basic model mentioned previously. It includes 7 balance equations, 9 rate equations, and 15 unknown parameters. The number and structure of the equations is not a problem; it can be simulated by a computer. However, for a validation of the model it is necessary to have estimates of the real values of the parameters. A sensitivity analysis of the parameters revealed that only 7 of them were important. These parameters were either determined or obtained from the literature. Three parameters were optimized by fitting the experimental data with the model equations. The results of continuous culture and batch experiments were used to validate the model. It presented a satisfactory description of both type of experiments.

43.5 APPLICATIONS OF THE CONTINUOUS CULTIVATION OF PLANT CELLS

The earliest attempts to set up a continuous culture of plant cells were published by Tulecke (20) in 1966 and by Miller *et al*. (21) in 1968. These studies have only historical value, because the authors could not achieve any steady states. The systems developed by Wilson *et al*. in 1971 (22), Kurz (23), and Wilson (24) are more important, because these designs have been used in several other studies. The chemostat system of Wilson (22) consisted of a round-bottomed Pyrex flask with a volume of 4 L. The culture was aerated through a sintered glass sparger, and mixing of the

culture broth was accomplished by means of a magnetic stirrer. Effluent was withdrawn using a specially designed system consisting of a valve, controlled by an constant-level device. They achieved steady-state growth of *Acer pseudoplatanus* cells at several dilution rates. Kurz (23) designed a chemostat that was rather unique in its mixing and aeration system. A small and long cylindrical vessel is mixed and aerated by large air bubbles filling up the diameter of the tube rising at regular intervals from the bottom of the cylinder. Influent was introduced at the bottom, and effluent was removed through an overflow device at the top. A different air-mixed chemostat culture system was used by Wilson (24). This relatively simple chemostat was made of an inverted erlenmeyer flask. Mixing and oxygenation of the culture were accomplished by forced aeration. Also in this design the effluent was withdrawn by means of an overflow tube. Unfortunately, Sahai and Shuler (25) concluded in a detailed study that the outflow efficiency of these systems is below 100%. This makes the quantitative results of these investigations relatively useless. However, several studies using these setups showed at least that continuous cultures of plant cells could be carried out under carbon, nitrogen, and phosphate limitation. The work done by de Gucht and van der Plas (26) is an exception. They used the Kurz chemostat, but were aware of the problem of the outflow efficiency and took it into account in their calculations. They achieved six steady states with a culture of *Petunia hybrida* cells. From their experimental data they estimated the maintenance and true yield of biomass on glucose and ATP.

Bertola and Klis (14) reported the use of a continuous culture system that was based on a 2-L standard turbine-stirred fermenter and the outflow system designed by Wilson (22). These authors published glucose-limited chemostat cultures of *Phaseolus vulgaris* cells. They determined the outflow efficiency to be 53%. After some modifications the outflow efficiency was improved to 80% (27). Their results were corrected for the outflow efficiency of the chemostat system. Van Gulik *et al*. (18,19) used a comparable system, but with a more sophisticated outflow device and coupled gas analysis equipment. Combination with off-line analysis of the spent medium and the biomass provided the opportunity to check their experimental data with elemental balances. Results of these investigations have been mentioned.

The aim of these studies was mainly the formulation and validation of models describing growth kinetics. The application of continuous culture for production of secondary metabolites has not been investigated extensively. In most cases secondary product formation is considerably depressed under growth conditions. Sahai and Shuler (28) proposed a multistage continuous culture system with variation in growth rates to create optimal conditions for both growth of the biomass and product formation. Lima Costa (29) investigated the production of an extracellular protease by a cell culture of *Cynara cardunculus* in continuous culture. The production of this protease was growth coupled, and continuous culture appeared superior to batch culture in this particular case.

NOMENCLATURE

D	dilution rate (1/s)
F	flow (m^3/s)
S	substrate concentration (kg/m^3)
X	biomass concentration (kg/m^3)
V	volume (m^3)
K_s	saturation coefficient (kg/m^3)
Y_{sx}	true yield (−)
m_s	maintenance coefficient (1/s)
r_d	death rate (kg/m^3/s)
r_s	substrate consumption rate (kg/m^3/s)
r_x	growth rate (kg/m^3/s)
q_s	specific substrate consumption rate (1/s)
μ	specific growth rate (1/s)
μ_{max}	maximum specific growth rate (1/s)

Subscripts

i	inflow
o	outflow

REFERENCES

1. W.H. Muir, A.C. Hildebrandt, and A.J. Riker, Science 119: 877–878 (1954).
2. G. Melchers and U. Engelmann, Naturwissenschaften 20: 564–565 (1955).
3. H.J. Noorman, J. Baksteen, and J.J. Heijnen, J. Gen. Microbiol. 137: 2171–2177 (1991).
4. A.H. Scragg, E.J. Allan, and F. Leckie, Enzyme Microb. Technol. 10: 361–367 (1988).
5. J.J. Meijer *et al*., Enzyme Microb. Technol. 16: 467–477 (1994).
6. J.J. Meijer, H.J.G. ten Hoopen, K.Ch.A.M. Luyben, and K.R. Libbenga, Enzyme Microb. Technol. 15: 234–238 (1993).
7. K. Matsubara *et al*., J. Chem. Technol. Biotechnol. 46: 61–69, (1989).
8. H. Tanaka, Process Biochem. 22: 106–113 (1987).
9. W.J. Treat, C.R. Engler, and E.J. Soltes, Biotechnol. Bioeng. 34: 1191–1202 (1989).
10. D.I. Kim, G.H. Cho, H. Pedersen, and C.K. Chin, Appl. Microbiol. Biotechnol. 34: 726–729 (1991).
11. B.S. Hooker, J.M. Lee, and G. An, Biotechnol. Bioeng. 35: 296–304 (1990).
12. M. Jolicoeur, C. Chavarie, P.J. Carreau, and J. Archambault, Biotechnol. Bioeng. 39: 511–521 (1992).

13. W.M. van Gulik *et al*., Appl. Microbiol. Biotechnol. 30: 270–275 (1989).
14. M.A. Bertola and F.M. Klis, J. Exp. Bot. 30: 1223–1231 (1979).
15. P.A. Bond, P. Hegarty, and A.H. Scragg, in O.M. Neijssel, R.R. van der Meer, and K.Ch.A.M. Luyben, eds., Proceedings of the 4th European Congress on Biotechnology 1987, Vol. 2: Elsevier, Amsterdam, 1987, pp. 440–443.
16. J.A. Roels, Energetics and Kinetics in Biotechnology, Elsevier, New York, 1983, pp. 223–237.
17. J. Bu'lock and B. Kristiansen, Basic Biotechnology, Academic Press, London, 1987, pp. 75–131.
18. W.M. van Gulik, H.J.G. ten Hoopen, and J.J. Heijnen, Biotechnol. Bioeng. 40: 863–874 (1992).
19. W.M. van Gulik, H.J.G. ten Hoopen, and J.J. Heijnen, Biotechnol. Bioeng. 41: 771–780 (1993).
20. W. Tulecke, Ann. N.Y. Acad. Sci. 139: 162–175 (1966).
21. R.A. Miller, J.P. Shyluk, O.L. Gamborg, and J.W. Kirkpatrick Science 159: 540 (1968).
22. S.B. Wilson, P.J. King, and H.E. Street, J. Exp. Bot. 22: 177–207 (1971).
23. W.G.W. Kurz, Exp. Cell Res. 64: 476–479 (1971).
24. G. Wilson, Ann. Bot. (London) [N.S.] 40: 919–932 (1976).
25. O.P. Sahai, and M.L. Shuler, Can. J. Bot. 60: 692–700 (1982).
26. L.P.E. de Gucht, and L.H.W. van der Plas, Biotechnol. Bioeng. 47: 42–52 (1995).
27. M.A. Bertola, Ph.D. thesis, University of Amsterdam, 1980, pp. 45–60.
28. O.P. Sahai and M.L. Shuler, Biotechnol. Bioeng. 26: 27–36 (1984).
29. M.E. Lima Costa *et al*., Enzyme Microb. Technol. 19: 493–500 (1996).

44

BIOREACTORS, FLUIDIZED-BED

WINFRIED STORHAS
Department of Technical Microbiology and Biochemical Engineering, Mannheim University of Applied Sciences, Mannheim, Germany

44.1 HISTORY AND INTRODUCTION

44.1.1 Background and Development

Nearly 90 years ago, on September 28 1922, the first patent for a fluidized-bed reactor (FBR) was applied. The applier was, BASF, the Chemical Company. The purpose was for coal gasification, a long way from any biotechnological purpose (1). Nevertheless, this technology has classic applications in the modern mammalian cell biotechnology as well (2).

Solid–liquid FBRs are also very widely distributed in ion-exchange technology and drinking water preparation as well as in wastewater treatment.

Coming from the very simple concept of a fixed bed, the fluidized bed should help to eliminate all the disadvantages such as channel-forming, resulting in a nonhomogeneous bed, reduced efficiency, reduced heat transfer, a tendency to block, and reduced replacement of dead cells.

Fluidized-bed technology presents several advantages, with the only disadvantages being a larger volume and abrasion of cells from the surface of beads. In some cases, this abrasion can be an advantage when the thickness of the biofilm has to be controlled.

It has to be remembered that high-tech development and application started before biotechnology became important in modern industry. There was a time before this!

A lot of historical papers (publications) dealing with FBRs, which are still up-to-date have been cited in this chapter. Nevertheless, this traditional and well-tried technology is validated by current research and publications (papers). This chapter deals only with homogeneous particulate liquid fluidization.

44.1.2 Introduction

Biotechnological processes use any kind of enzyme available as catalysts for biotransformation. Most are available only in living, complete, and active cells, but if it is possible to isolate the only enzyme responsible, it could be a step toward becoming an economically viable process. Since enzymes are soluble in water and other solvents, they are used in homogeneous catalysis. There are different ways to fix enzymes. One uses physical and chemical properties (forces) such as physical adsorption, covalent chemical binding, cross-linking, or complete encapsulation in a gel (Fig. 44.1). A very common technique is the chemical reaction using covalent binding as shown in Fig. 44.2. Usually after an immobilization procedure, some activity gets lost but greater temperature, pH and other media concentration stability can be achieved as well longer duration. There are a lot of biotransformations of industrial importance, which use immobilized enzymes as catalysts (3).

Using immobilized enzymes in a bioreactor offers the possibility to retain the enzymes inside the reactor. Immobilized enzymes (fixed onto carriers) bring not only easier reusability (recycling) but also more stabile enzymes (Table 44.1 and Fig. 44.2) for longer process operation.

A suitable concept to handle economic carrier systems is FBR. These types involve a lot of processes which can be very advantageous regarding mass and heat transfer. The obvious advantages in such a system are:

- higher active surface of the particle,
- good conditions for heat and mass transfer,

Upstream Industrial Biotechnology: Equipment, Process Design, Sensing, Control, and cGMP Operations, Volume 2, First Edition. Edited by Michael C. Flickinger.
© 2013 John Wiley & Sons, Inc. Published 2013 by John Wiley & Sons, Inc.

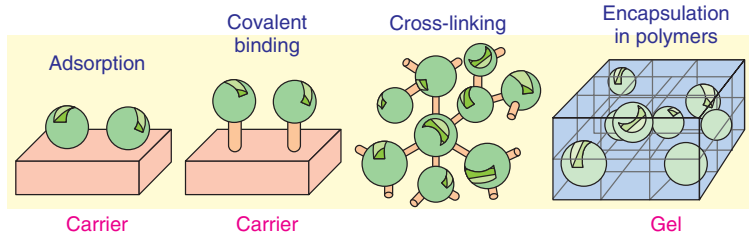


Figure 44.1. Different opportunities for immobilization of enzyme cells (4). (This figure is available in full color at http://onlinelibrary.wiley.com/book/10.1002/9780470054581.)

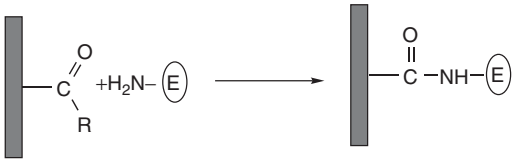


Figure 44.2. The acylic reaction as an example of a covalent binding of an enzyme (E) at a carrier.

- the pressure drop stays constant, and
- low temperature and concentration gradients.

A necessary condition for these advantages is good homogeneity. Without this, heat and mass transfer are inhibited.

Because of better mass transfer, a high cell density is possible. An increase of the catalyst concentration (cells or enzymes) brings a higher reaction rate space time yield (STY), and if there is no transfer limitation, a reduction of the reaction volume is possible (lower investment for better economy).

When using mammalian cells in biotechnological processes, most of the time, it is necessary to offer carriers on which the cells can grow because of the adherent behavior of these cells. These beads can be compact solids or porous particles. In the case of compact particles, the available surface to grow on is small compared to porous beads with their large inner surface (Fig. 44.3), and the cells are more mechanically stressed. If mass and heat transfer by diffusion inside the beads is too slow, this can cause substrate limitation and/or product and heat inhibition of cellular activity (2,5).

For bioreactions, a lot of bioreactors are available. In the case of handling carriers, bed reactors as already shown, are the best choice (2,5,6).

44.1.2.1 Using Fluidized Bed in Biotechnology. There are two ways to run an FBR, the gas–solid system (GSS) (5), and the liquid–solid system (LSS) (2). In the field of biotechnology, GSSs are used for cleaning pollution from exhaust gas streams. Here, microorganisms are immobilized on a microcarrier, and the exhaust gas stream expands (fluidized) the carrier bed in an FBR. The gas components are transported by convection and diffusion to the enzyme-loaded carrier. There follows a chain of operations: adsorption, reaction, desorption, transport back, and the metabolites are transported out of the FBR via the exhaust gas stream.

Generally, it is necessary to moisten the inlet gas to keep the water activity at a necessary level. In a GSS, bubble formation makes the system very complicated for modeling. However, in a LSS, such phenomena do not appear (1).

For biotechnological purposes, an LSS is usually chosen (2,5). This system is described below.

The fluidized bed is not only used directly as a bioreactor, but is also suitable in downstream processing. It has been shown that lactic acid can be purified directly from fermentation utilizing a fluidized-bed column refilled with a

TABLE 44.1. Characterization of Carrier Fixed Enzymes

Advantages	Procedures	Group	Bindings	Materials
Retention of the enzymes in the process	Cross-linking	Amino groups	Acrylic, acylic, arylic, and carbamyl reaction	Porous glass
Stabilization (temperature, pH, time, concentrations, against organic solvents)	+ Adsorption	Carboxyl groups	Amide forming	Polydextran
	Enclosement	Mercapto groups	Bromcyanic coupling	Cellulose (polysulfone)
	Covalent binding		Azo coupling	Agarose
			Disulfite coupling	Nylon
			Anorg. bridge building	Polyvinyl alcohol
				Vinyl copolymer



(a)



(b)

Figure 44.3. (a) A bead collective with mammalian cell fouling. (b) One bead with mammalian cell fouling. (This figure is available in full color at http://onlinelibrary.wiley.com/book/10.1002/9780470054581.)

strong anionic exchange resin. By changing the settling bed height, it is possible to obtain a 50% increase in the binding capacity (7). This technology is also known as expanded bed adsorption (EBA).

More for analytical purposes, a fluidized-bed cell culture reactor with on-line radioactivity detection was developed for the *in vitro* evaluation of radio pharmaceuticals. The technique was applied to measure the dependency of the lumped constant (LC) of FDG (2-[^{18}F]luoro-2-deoxyglucose) on the glucose concentration in the culture medium in a human glioma cell line (8).

There is a variety of applications of fluidized-bed systems, often technically or industrially useful, for instance, in producing erythropoietin (EPO) from CHO cells in a continuous FBR (9). It was possible to run this process in a 2-L scale in serum-free and protein-free medium for 48 days. The cell density increased to a maximum of 2.3×10^7 cell/mL. The product concentration (EPO) was significantly higher at least twice that in a controlled stirred-tank bioreactor, in a spinner flask or in a stationary T-flask culture.

FBR is also used for environmental purposes. A liquid–solid FBR was used to carry out sulfate reduction with a mixed culture of sulfate-reducing bacteria. The bacteria were immobilized on porous glass beads where stable fluidized-bed operation with these biofilm-coated beads was possible. The low specific gravity of the hydrated beads allowed operation at low liquid circulation rates, meaning at low superficial velocity (10). Sulfate reduction rates of up to 6.33 g of sulfate/L/day were attained in the reactor at a hydraulic retention time of 5.1 h. The efficiency of sulfate reduction increases considerably as the hydraulic retention increases until the bacteria became very strongly substrate-limited at a hydraulic retention time (HRT) of 55 h.

A model for the reactor was developed. Simulation of the continuous flow experiments indicate that the model can describe the system well, and can therefore be used in the design/scale-up of such reactors (10).

Another way to apply fluidized bed is in combination with downstream processing as an integrated purification step. As an example, a dual-particle liquid–solid circulating fluidized bed (DP-LSCFB) bioreactor was constructed and used in the investigation of the simultaneous production and extraction of lactic acid using immobilized *Lactobacillus bulgaricus* and ion-exchange resins. The studies in a lab-scale reactor system of approximately 70 L volume showed 93% lactic acid removal and 46% recovery. Such results prove the functionality of using the newly developed bioreactor design for the continuous production and recovery of products of biotechnological significance (11).

Recent investigations in production of biotechnological products prove the applicability of fluidized-bed technology (12). A continuous production of oxytetracycline in a fluidized-bed bioreactor by immobilized cells was investigated under the special effects of dilution and glucose load rates. The *Streptomyces varsoviensis* cells were immobilized on cross-linked calcium alginate beads (Fig. 44.1) and it seems to be a technology with a future.

Since one of the smaller disadvantages for an FBR is oxygen supply, anaerobic processes can be prioritized. One such application is the treatment of high strength corn steep liquor using cultivated polyvinyl alcohol (PVA) gel beads (13). The wastewater treatment process achieved a chemical oxygen demand (COD) removal efficiency in excess of 96% at an organic load rate (OLR) of 27.5 g/L/h with an HRT of only 6 h.

44.2 PLANT CONCEPTION AND OPERATION

44.2.1 Design of a Fluidized-Bed Reactor

An FBR consists of a cylindrical reaction tube frequently with a widening at the top. The widening leads to a reduction of the superficial fluid velocity of the fluid and prevents entrainment velocity of (smaller) particles (Figs 44.4 and 44.5).

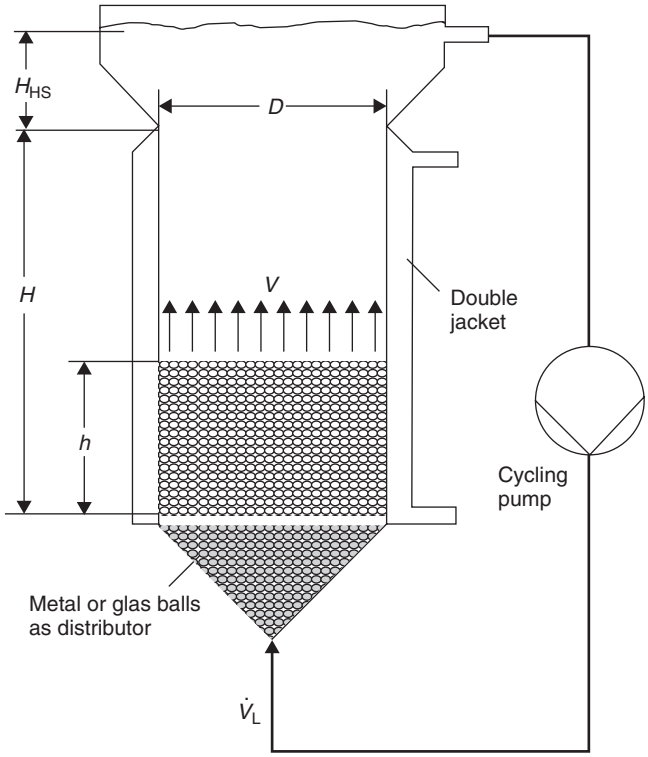


Figure 44.4. Principle sketch of a fluidized-bed reactor (FBR) with the main dimensions.

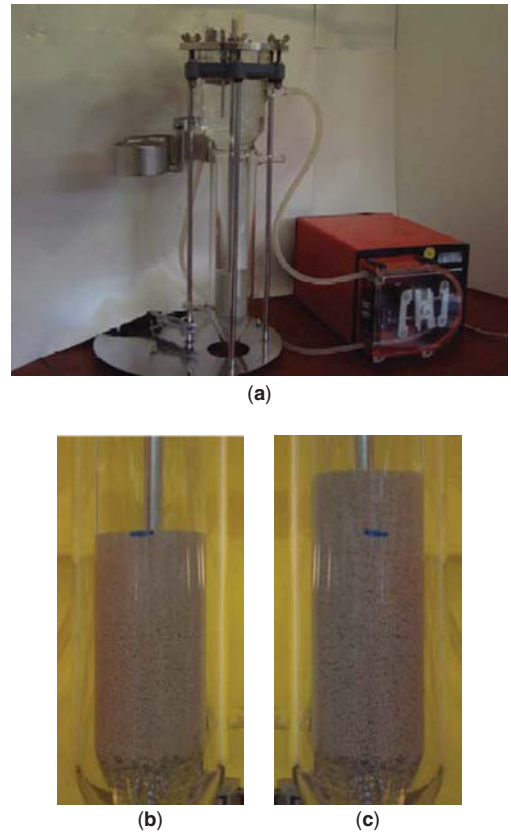


Figure 44.5. (a) Laboratory-scale FBR ($V_{B,max} = 1.0$ L): $D = 50$ mm; $H = 300$ mm; $h = 115$ mm (Fig. 44.4) [Bioengineering AG, Wald CH]; (b) before starting, fixed bed; (c) expanded bed with superficial velocity $v = 0.0089$ m/s. (This figure is available in full color at http://onlinelibrary.wiley.com/book/10.1002/9780470054581.)

Since a fluidized bed is only fed from the bottom, a distributor system should be installed in front of the bed. The role of this distributor is to provide a higher axial pressure drop compared to the radial one so that it is possible to distribute the flow evenly. For the purposes of heat transfer and temperature control, the reactor tube is coated with a jacket as a heat exchange area. The next piece of equipment is a pump to provide the flow and the necessary power input.

As the probe positioning is not so easy in an incomplete mixed reactor, it is advisable to use a control vessel where all the parameters (temperature, pH, and concentrations of components) are checked (Fig. 44.6).

44.2.2 Operation of a Fluidized-Bed Reactor

If the immobilized cells or enzymes, which are fixed on the carrier are filled into a bed reactor, then the particle will settle down to the bottom of the column and build a fixed-bed reactor as long as the density of the particles is higher than the surrounding fluid (liquid, Figs 44.7 and 44.8). Packing is achieved when the distance between the particles is fixed and stable (immobilized) (6).

In fixed-bed reactors the pressure drop can be calculated by Carman (14):

$$\Delta p = \frac{3}{4} \frac{\rho_L \times v^2 \times h}{\varphi_S \times d_{PS}} \frac{1 - \varepsilon_L}{\varepsilon_L^3} c_W \qquad (44.1)$$

A fixed-bed reactor can be driven from the bottom as well as from the top (Fig. 44.8). From the point of view of a fluidized bed, the fixed bed is only a special case when the superficial velocity is below the minimal velocity at the incipient fluidization point.

There are some advantages in the fixed bed. First, the catalysts are more densely packed and this increases the specific reaction rate and reduces abrasion.

The disadvantages are mass and heat transfer limitations, channel-forming, and problems with loose material (with bad packing) to remove or blocking.

In a fixed bed, no or negligible back mixing appears, which leads to a concentration gradient.

As an example for substrate consumption:

$$r = \frac{dc}{dt} = -k(T) \times c^n \qquad (44.2)$$

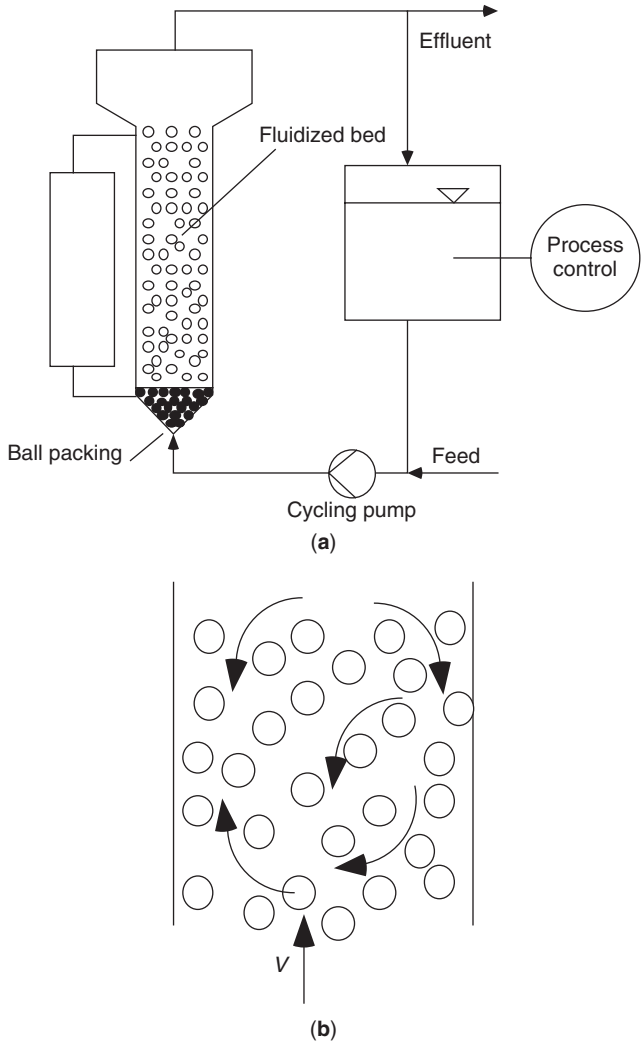


Figure 44.6. (a) Principles of a fluidized-bed reactor plant. (b) Details of a fluidized bed: the flow direction for a fluidized-bed reactor is from the bottom. A minimum fluid velocity is necessary to keep the particles in motion (movement, incipient fluidization). Compared to the empty reactor, the liquid velocity v is the superficial liquid velocity. The maximum velocity is the wash out point (entrainment velocity). Beyond this point, a single particle will sink down. Only a group of particle will rise again.

with n = reaction order (0 order, reaction rate $\neq f$(substrate concentration) (Fig 44.8).

Fluid (gas or liquid) now passes upwards through a fixed bed. On increasing the flow rate, a point is reached when the solid bed hovers. The next small step in increasing the velocity leads to fluidization of the bed. The velocity in this state is the minimal or minimum fluidizing velocity v_L (incipient fluidization) (Fig. 44.9a).

A further increase of fluid velocity brings the expansion of the bed and some channels appear (channelling and aggregative fluidization, see Fig. 44.9b). Since a collection

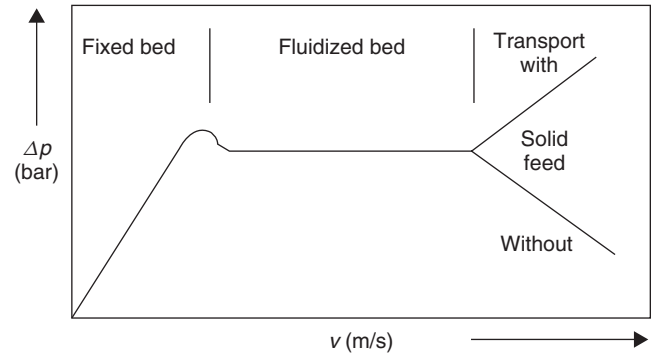


Figure 44.7. Fixed-bed reactor.

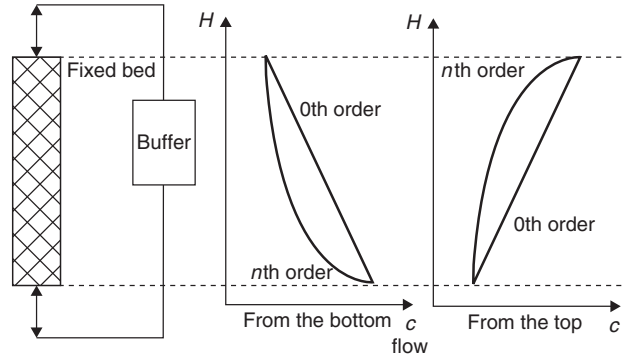


Figure 44.8. Concentration gradient in the fixed-bed reactor is given, and is a function of the reaction order because there is a minimum of back mixing.

of particles act like a larger particle for the flow, it is lifted up until the particle escapes from this compound and then sinks as a single particle, refinds neighbors, forms a new compound and rises again, and so on, a dynamic behavior in a steady state.

By increasing the velocity further, the next state in a fluidized-bed operation is a particulate fluidization. A further slight increase in velocity leads to the entrainment velocity of the particles. The velocity a little below this point is the entrainment velocity w_f (Fig. 44.9c). So, the stationary fluidized bed has a well-defined existing range (space).

In this state of the fluidized bed, the pressure drop is equal to the remaining weight gravity per cross section (gravity force −lift force) in pascal.

The pressure drop in the incipient fluidization can be calculated as:

$$\Delta p = (1 - \varepsilon_L) \times h \times \Delta\rho \times g + \rho_L \times g \times h \qquad (44.3)$$

In Equation 44.3, the first term represents the flow resistance and the second term shows the overcoming of the hydraulic pressure in the start position of the fluidized bed (packing in pending, see Figs 44.4 and 44.7).

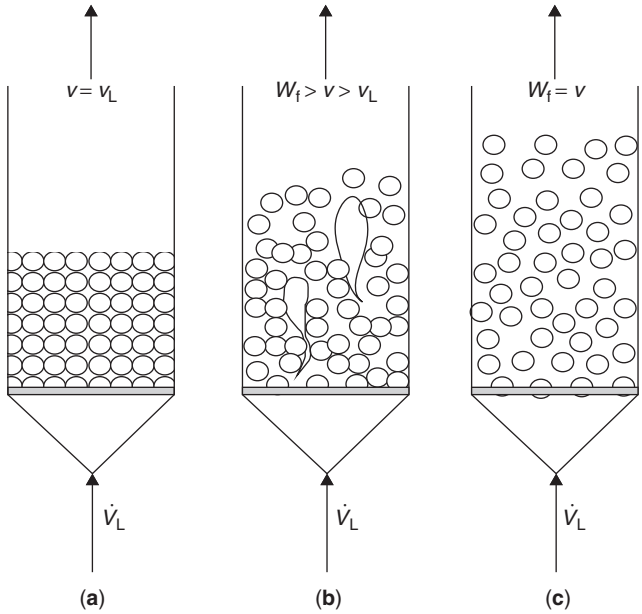


Figure 44.9. Three states of a fluidized bed. (a) The whole tower packing is in the incipient fluidization. (b) Some particles start fluidizing and leave the packing. The packing starts to fluidize. (c) Expanded fluidized bed just before the entrainment velocity (wash out).

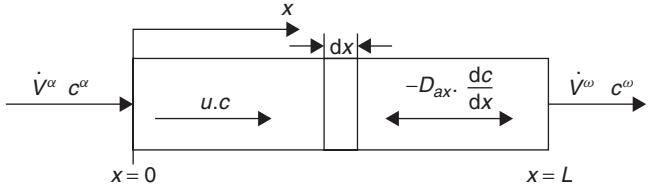


Figure 44.10. Model for describing retention time distribution in a tube reactor (15,16).

44.2.3 Design of a Fluidized-Bed Reactor

44.2.3.1 Hydrodynamic Conditions. In engineering, suitable dimensionless numbers are often used, and some important ones are used to describe a fluidized bed (Figs 44.11 and 44.12) (17).

One of them is the Archimedes number, which is defined by Equation 44.4. The Archimedes number only represents system parameters and no process parameter. Archimedes number:

$$Ar = Re^2 \times Fr^{-1} \frac{\Delta\rho}{\rho_L} = \frac{g \times d_{PS}^3}{\nu^2} \frac{\Delta\rho}{\rho_L} \tag{44.4}$$

The second number is the omega number. In this number, only the left process parameter, the superficial (relative) velocity v, is involved. In classical stationary fluidized bed, the superficial velocity is

$$v = \frac{\dot{V}_L}{A_R} \tag{44.5a}$$

Omega number:

$$\Omega = Re \times Fr \frac{\rho_L}{\Delta\rho} = \frac{v^3}{\nu \times g} \frac{\rho_L}{\Delta\rho} \tag{44.5b}$$

with

$$Fr = \frac{v^2}{g \times d_{PS}} \tag{44.6a}$$

and

$$Re = \frac{v \times d_{PS}}{\nu} \tag{44.6b}$$

$$\text{Archimedes number} = f(\text{system parameter particle, diameter}) \neq f(\text{velocity})$$

$$\Omega \text{ number} = f(\text{process parameter, superficial velocity}), \neq f(\text{particle diameter})$$

$$\text{Froude number} = \frac{\text{inertia} \times \text{force}}{\text{gravity}} \times \left(\frac{\rho_L}{\Delta\rho}\right).$$

The correction $\frac{\rho_L}{\Delta\rho}$ considers the lift force. A very important tool for working with fluidized beds is the fluidized-bed state diagram. In Figs 44.11–44.13 the working sector, the working conditions, and the drag resistance coefficient can be found (17). This is a great help.

In designing a fluidized bed, the following series of steps is helpful:

- Archimedes number via system parameters.
- For the Ω number, the superficial velocity has to be chosen (it is between v_L and w_f).
- With Ar and Ω, we can obtain the working point in the diagram (Fig. 44.11, Fig. 44.7) and this has to be in the fluidized-bed section.
- Additional boundary conditions come from heat and mass transfer, shear stress $= f$(velocity), and looking for the optimum working point.

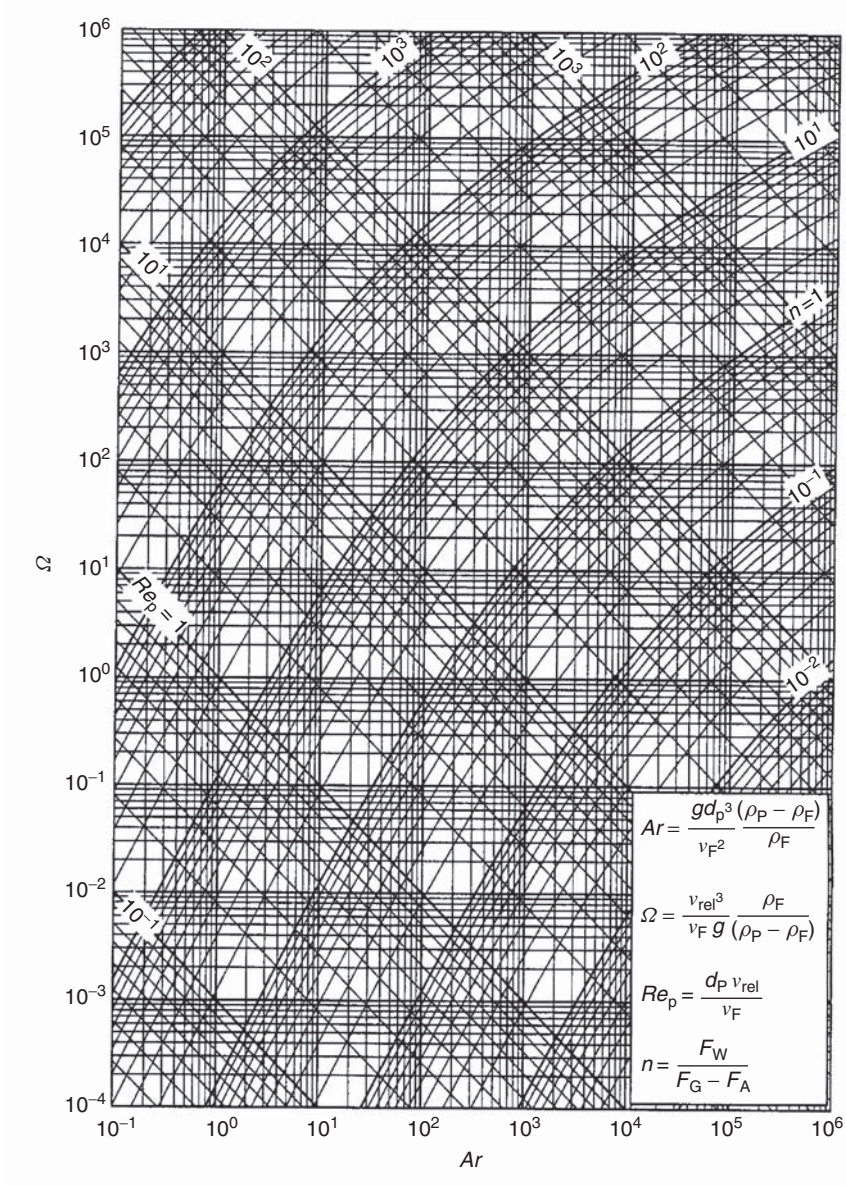


Figure 44.11. Ar-Ω diagram for a single stiff spherical particle. Principles of the fluidized-bed state diagram (17). From this diagram one can get the Ar number to find the section of fluidized bed. The Ar number can be calculated with system parameters (Eq. 44.4) and for Ω number (Eq. 5) the average superficial velocity is necessary.

- Pressure drop inside the fluidized bed is calculated by Equation 44.3. The pressure drop before, for the fixed bed, is calculated by Equation 44.1.
- The pressure drop in the fluidized bed is (nearly) constant, because the losses through resistance on the column wall is negligible.
- In practice, there is a rough value: the expansion of the bed should be of a factor of 1.3–2.5 above fixed bed (packing).

44.2.3.2 Basic Design Details

44.2.3.2.1 Range of Operation Velocities. Because of the immobilization of the cells or the enzymes on FBRs, FBRs have a high cell and enzyme concentration through the help of carriers, which the cells or the enzymes are immobilized on (Fig. 44.1).

In the FBR, the particles are fluidized by lift forces and resistance (friction) forces, which are at least equal to the gravity force.

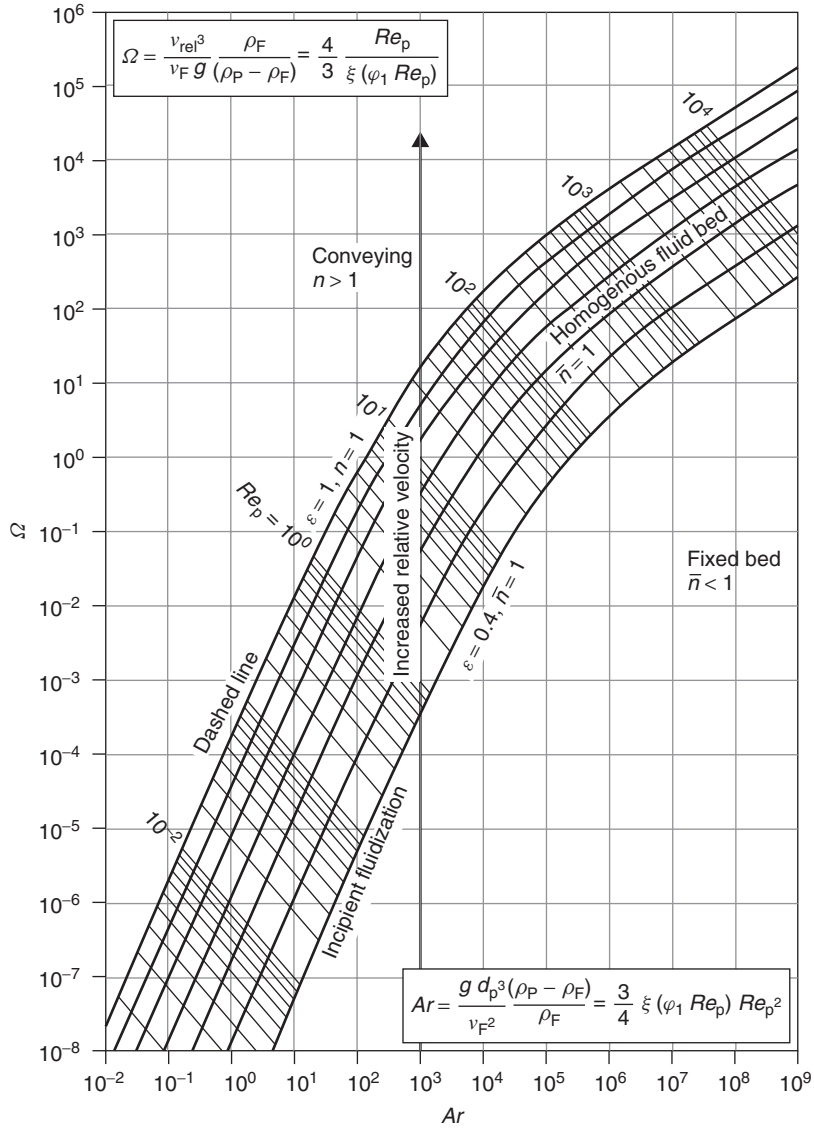


Figure 44.12. Diagram of situation for monodispersed, spherical particles at even flow input.

Flow should be evenly distributed. This is done by spherical particle packing—the axial pressure drop is much higher than the radial (Figs 44.4–44.6).

The velocity has to overcome the minimum velocity v_L = incipient fluidization. The drag force can be calculated as:

$$F_R = c_W \times \rho_L \times A_C \times \frac{v^2}{2} \tag{44.7}$$

The resistance factor c_W can be found from Fig. 44.14. The other parameters, density ρ_L, projected area of the particle, and the velocity v are system parameters.

The first thing which has to be considered when designing an FBR is the calculation of the existence range of a fluidized bed in the velocity between the minimal fluidizing velocity (incipient fluidization) v_L and the entrainment velocity w_f.

The necessary parameters are the average particle diameter, the density of both solid and liquid, and the viscosity. The velocity in the lowest working point (incipient fluidization) can be calculated as
laminar,

$$Re_L = \frac{v \times d_{PS}}{\nu} \leq 1,0: \tag{44.8}$$

$$v = v_L = \frac{1}{150} \frac{\varphi_S^2 \times \varepsilon_L^3}{1 - \varepsilon_L} \frac{g \times d_{PS}^2}{\nu} \times \left(\frac{\rho_S}{\rho_L} - 1 \right) \tag{44.9}$$

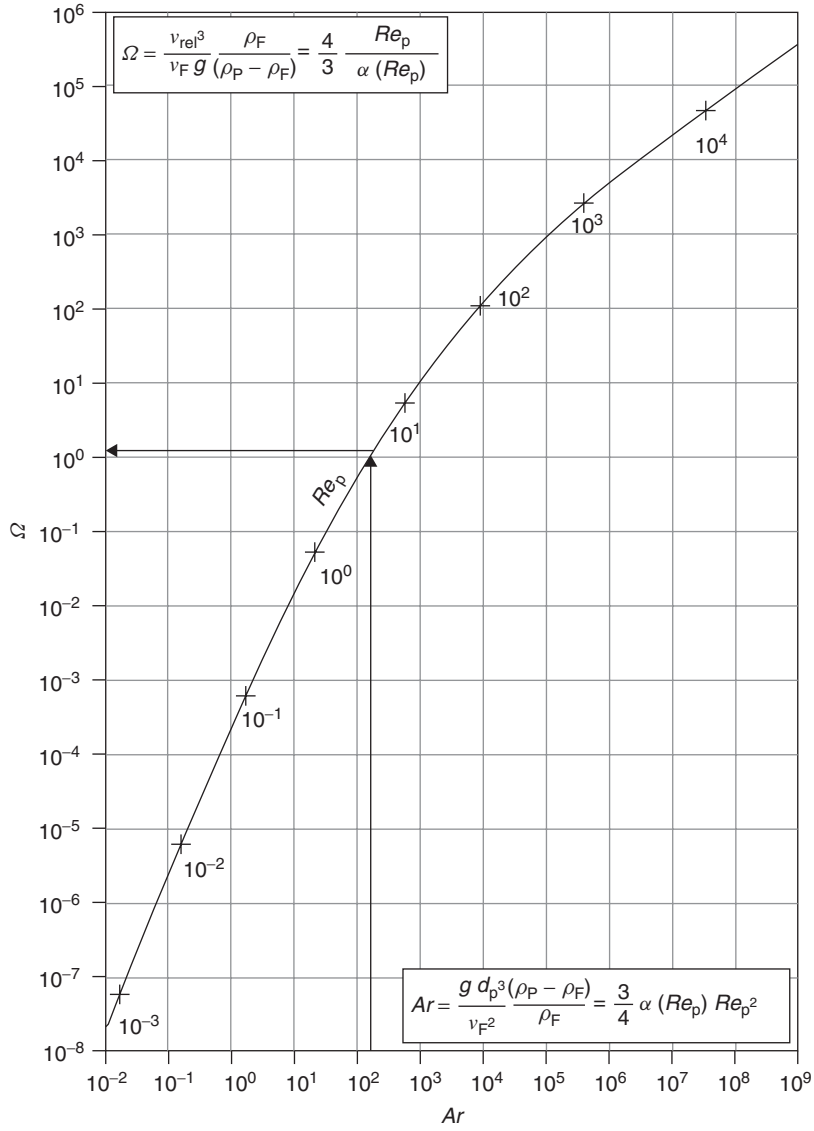


Figure 44.13. Ar-Ω diagram for a stationary, sinking, stiff spherical particle (the arrows show the way to the sink velocity).

turbulent,

$$Re_L > 500 : v = v_L = \left(\frac{1}{1.75} \times \varphi_S \times \varepsilon_L^3 \times g \times d_{PS} \times \frac{\Delta\rho}{\rho_L} \right)^{0,5} \quad (44.10)$$

First we start with either a laminar or turbulent assumption, and then follow the calculation with a control check. If the assumption is wrong, the opposite situation has to be considered.

The next step is to calculate the sink velocity, which is roughly equal to the entrainment velocity w_f. Again, it is necessary to make the assumption laminar or turbulent flow and in the case of a wrong assumption, again the opposite route has to be taken.

The equation for the velocity in the incipient fluidization is given as:
laminar, $Re \leq 1.0$ (Eq. 44.8):

$$v = w_f = \frac{1}{18} \frac{g \times \varphi_S \times d_{PS}^2}{\nu} \times \left(\frac{\rho_S}{\rho_L} - 1 \right) \quad (44.11)$$

turbulent, $Re > 500$:

$$v = w_f = \left(\frac{4}{3} \frac{g \times \varphi_S \times d_{PS}}{c_W} \frac{\Delta\rho}{\rho_L} \right)^{0,5} \quad (44.12)$$

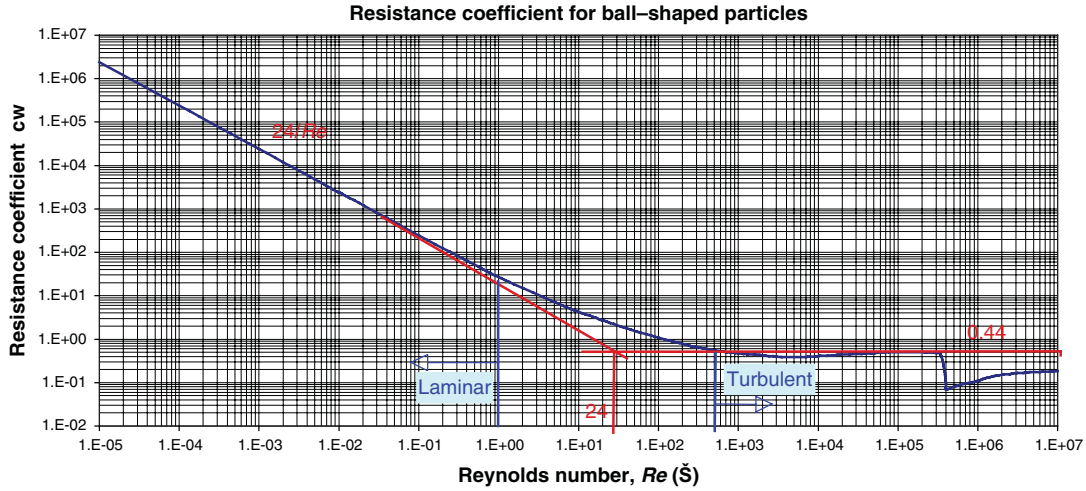


Figure 44.14. Flow resistance coefficient of a ball-shaped particle as a function of the Reynolds number. Below $Re = 1.0$ conditions are laminar conditions, and above $Re = 500$, turbulent. At $Re > 500$ the resistance coefficient is constant ($c_W = 0.44$). In the laminar section, $c_W = 24/Re$. (This figure is available in full color at http://onlinelibrary.wiley.com/book/10.1002/9780470054581.)

For a spherical particle, Equation 6 can be easily determined using a force balance.

In this situation, a force equilibrium is given:

$$F_L + F_R = F_W \tag{44.13}$$

$$\text{lift} + \text{resistance} = \text{weight}$$

For the different forces, the following calculations are useful:

$$F_R = c_W \times \rho_L \times A_C \times \frac{w_f^2}{2} \tag{44.14}$$

$$F_L = V_P \times \rho_L \times g \tag{44.15}$$

$$F_W = V_P \times \rho_P \times g \tag{44.16}$$

In Equations (14–16) the particle volume is

$$V_P = \frac{d_{PS}^3 \times \pi}{6} \tag{44.17}$$

and the projected area is

$$A_C = \frac{d_{PS}^2 \times \pi}{4} \tag{44.18}$$

By transforming Equation 44.13 with Equations 14–16 we get:

$$w_f = \left(\frac{4}{3}\frac{g \times d_{PS}}{c_W}\frac{\Delta\rho}{\rho_L}\right)^{0,5} \tag{44.19}$$

Equation 44.19 is very similar to Equation 44.12. The only difference is the spherical factor ϕ_S (Eq. 44.24), which is a correction factor for the deviation of the particle shape from a spherical particle.

Using Stoke's law (Fig. 44.14) for the laminar regime:

$$c_W = \frac{24}{Re} \tag{44.20}$$

we get:

$$w_f = \frac{1}{18}\frac{g \times d_{PS}^2}{\nu}\frac{\Delta\rho}{\rho_L} \tag{44.21}$$

and this equation is similar to Equation 44.11, except again, for the parameter ϕS.

The expansion behavior of a fluidized bed can be calculated by Richardson and Zaki (18)

$$\varepsilon = \sqrt[n]{\frac{v}{w_f}} \tag{44.22}$$

With:

$$n = 4.65 \text{ for } Re < 0.2$$

$$n = 4.35 \times Re^{-0.03} \text{ for } 0.2 < Re < 1.0$$

$$n = 4.45 \times Re^{-0.10} \text{ for } 1.0 \leq Re < 500$$

$$n = 2.39 \text{ for } Re > 500$$

This allows us to calculate the column height:

$$H = h\frac{1 - \varepsilon_L}{1 - \varepsilon} \tag{44.23}$$

All models assume spherical particle and uniform diameters. A representative particle in the case of shape and diameter has to be found. For another shape we correct with the sphericity factor ϕ_S and the diameter with the Sauter mean diameter.

The spherical factor is defined as ratio of the surface of a spherical particle with the same volume as the original particle to the surface of the particle:

$$\phi_S = \frac{A_B(V_P)}{A_P} \tag{44.24}$$

Since the surface of a spherical particle with a given volume has the smallest available surface, the spherical factor is always lesser than 1, that is, $\phi S \leq 1.0$.

To define a mean diameter $d_{P32,}$ using the Sauter mean diameter d_{PS} is advisable. This diameter is a common measure in fluid dynamics as a way to estimate the average particle size. It is defined as the diameter of a sphere that has the same volume/surface area ratio as a particle of interest and is defined as (23,20)

$$d_{PS} = d_{P32} = 6 \times \frac{V_P}{A_P} = \frac{\sum_{i=1}^{m} n_i \times d_i^3}{\sum_{i=1}^{m} n_i \times d_i^2} \tag{44.25}$$

44.2.3.2.2 Oxygen Supply. When using living cells, adequate oxygen supply is necessary. Mammalian cells are sensitive to high levels of dissolved oxygen as well to rising bubbles because of shear stress (2). Therefore, the aim is to both avoid and provide bubble-free oxygen externally, outside the cell-containing reactor (6). An aeration vessel with different equipment is used in combination with an FBR. A bubble-free membrane aeration or submersed aeration (considering foam situation) is possible.

44.2.3.2.3 Energy Dissipation. Each event required the energy to be managed and should be conducted in a closed time frame; so, it is necessary to provide the required power. In technical operations, we use the specific power input or the mass related power density ε (watt per kilogram). This value can be calculated from the absolute power input, the system volume (reaction volume), and the system density (medium) (6)

$$\varepsilon \equiv \left(\frac{P_i}{V_R \times \rho_M} \right) \tag{44.26}$$

Generally, the volume in a reactor is the reaction medium (gas or liquid) and the density of the medium, M. For power input into a reactor, three types are available: power input by gas prepressure and expansion, by pumps and hydraulic stream, and by mechanical equipment such as agitators (stirrers).

FBRs belong to type two; they are hydraulically driven reactors. The pump causes a medium flow $\dot{V}_L$ (L–liquid) against a drag resistance, causing a pressure drop Δp. These two parameters allow us to calculate the necessary power input generated by the pump:

$$P_L = \dot{V}_L \times \Delta p \tag{44.27}$$

With the reaction liquid volume $V_{R,L}$ and the liquid density Δ_L, we get the specific power input:

$$\varepsilon_L = \frac{P_L}{V_{R,L} \times \rho_L} \tag{44.28}$$

There are several ways to get this required power input. In the volume stream, the desired capacity of production is C_P representing what has to be produced in, for example, 1 year. With the available hours per year HPA (e.g. 7000 h/a), the product concentration P (gram per liter) in the effluent of the reactor, and the overall downstream efficiency α we get:

$$\dot{V}_L = \frac{C_P}{HPA \times P \times \alpha} (m^3/h) \tag{44.29}$$

Using Equation 44.29 combined with Equation 44.1 in the case of fixed bed, and Equation 44.3 for a fluidized bed, we can calculate the power input with Equations 44.27 and 44.28.

44.2.4 Heat Exchange

In a fixed bed, the heat transfer is influenced by three factors:

- convection through fluid;
- transport from solid, conductivity in solid, transfer of heat from solid to fluid;
- conductivity through solid.

It is conceivable that a lot of transport resistance inhibits the overall transfer a great deal as the predominate part is the convective transport.

A better situation is given in the fluidized bed (Fig. 44.4). As expected, the bed to wall heat transfer coefficient increases with increased velocity.

In contrast to fixed beds, in a fluidized bed, heat transfer is caused not only by fluid but also by moving solids. The solids act as a heat transfer medium (transporter). In zones of lower temperatures, they lose heat and vice versa.

An improvement of heat transport is reached by:

- increasing the turbulent mixing movement of the fluid and
- additional nonstationary heat transfer of the solids.

The laminar border layer between reactor wall and fluidized bed, in contrast to a fixed bed, is continuously destroyed and therefore thinner.

Within equal conditions, with the same fluidization, the same density, the same particle size, and the same surface shape and configuration, the heat transfer increases by 35% or more in a fluidized bed.

With the assumption that:

- no temperature gradient in the particle;
- the heat exchange surface corresponds to the projected area of the particle on the wall

the following calculation for an individual particle results:

$$\begin{aligned} \mathrm{d}q \times \mathrm{d}t &= \frac{\lambda_\mathrm{f}}{\delta}\frac{d_\mathrm{P}^2 \times \pi}{4} \times (T_\mathrm{wall} - T_\mathrm{P}) \\ &= c_\mathrm{P} \times \gamma_\mathrm{P}\frac{d_\mathrm{P}^3 \times \pi}{6}\Delta T \end{aligned} \tag{44.30}$$

which means transported heat in a moving particle = transfer to wall = lost heat (watt second).

The more particles which arrive at the wall over time and area, the more heat can be exchanged. Heat transfer is influenced by:

- heat conductivity in the laminar boundary layer while the thickness of the laminar layer is influenced by the flow conditions and the impulse forces of the particles;
- the time of contact of the particle at the wall. The smaller the contact time, the better the heat transfer(!).

As it is seen in Fig. 44.15, the heat transfer coefficient has a maximum. For this situation, a relationship to calculate the maximal heat transfer coefficient (19) is given as:

$$\frac{Nu_\mathrm{max}}{1-\varepsilon_0} = 1.8 \times Ar^{0.18} \times \left(\frac{c_\mathrm{P}}{c_\mathrm{L}}\right)^{0.36} \tag{44.31}$$

In reality, there is an approximate range of $0.5 < Nu_\mathrm{max} < 8$. The following characteristic numbers are often very useful:

Reynolds:

$$Re \equiv \frac{v \times x}{\nu} \text{with } x = \text{characteristic length (m)} \tag{44.32}$$

Nusselt:

$$Nu \equiv \frac{k_\mathrm{q} \times x}{\lambda} = \frac{\text{heat} \times \text{transfer}}{\text{heat} \times \text{conductivity}} \tag{44.33}$$

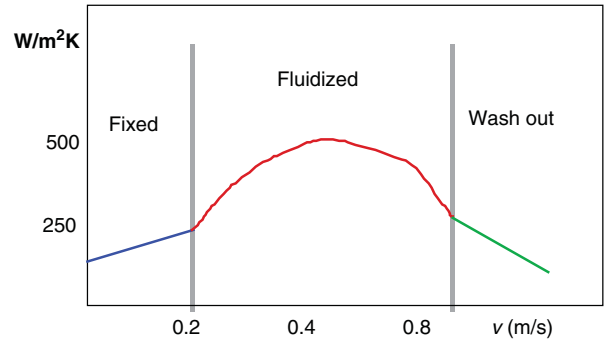


Figure 44.15. Heat transfer coefficient in a fluidized bed (qualitative manner). (This figure is available in full color at http://onlinelibrary.wiley.com/book/10.1002/9780470054581.)

Prandtl:

$$Pr \equiv \frac{\nu}{\frac{\lambda}{\rho \times c_\mathrm{p}}} = \frac{\nu}{a} = \frac{\text{impulse} \times \text{transport}}{\text{heat} \times \text{transport}} \tag{44.34}$$

For mass transfer:

Schmidt:

$$Sc \equiv \frac{\nu}{D} = \frac{\text{impulse} \times \text{transport}}{\text{mass} \times \text{diffusion}} \tag{44.35}$$

Sherwood:

$$Sh \equiv \frac{k_i \times x}{D_i} = \frac{\text{mass} \times \text{transfer}}{\text{mass} \times \text{diffusion}} \tag{44.36}$$

There are numerous relationships between several characteristic numbers in literature. For the Nusselt number we find (15)

$$Nu \equiv \frac{k_\mathrm{q} \times x}{\lambda} = 0.664 \times \sqrt{Re_x} \times \sqrt[3]{Pr} \tag{44.37}$$

The Prandtl and the Schmidt number combine mass and heat transfer:

$$Sh = Nu \times \sqrt[3]{\frac{Sc}{Pr}} \tag{44.38}$$

All these relationships are very helpful in designing an FBR.

44.3 SCALE-UP CONSIDERATIONS

44.3.1 Heat Exchange Situation

Heat transfer needs a suitable heat exchange area but heat production comes from the reaction volume. One pattern is related with a length square and the other to power to length cube. In scale-up, this involves the available heat exchange area decreasing with increased volume.

In terms of formula we get:
for input,

$$\dot{Q}_{\text{in}} = \Delta H \times STY \times V_{\text{R,L}} \propto V \propto \text{L}^3 \tag{44.39}$$

for output,

$$\dot{Q}_{\text{out}} = k \times A \times \Delta T \propto A \propto \text{L}^2 \tag{44.40}$$

So the ratio is

$$\frac{\dot{Q}_{\text{in}}}{\dot{Q}_{\text{out}}} \propto \text{L} \tag{44.41}$$

which means with rising volume, the removal of the heat becomes more and more difficult and can only be achieved with additional heat transfer area.

44.3.2 Scale-Up of Fluidized Bed

Scale-up considerations look into the results from the model scale to laboratory scale or pilot scale to production scale for the conditions for transfer. Because it is not possible to keep all parameters constant, it is very important to find the most sensitive one and test whether these are transferable. For instance, the mixing time is a parameter, which is often not possible to be transferred because of the necessary increase of the power input.

To analyze the parameter responsible for scaling up in an FBR system, it is very helpful to draw up a relevance list. The first law for scale-up is geometric similarity, which means all length ratios in each scale are equal.

It seems to be necessary to keep the local microdynamic situation constant to achieve the same conditions for the reaction rate to fulfill the desired capacity rate. Therefore, for the superficial velocity, all medium parameters (densities, diffusion coefficients, particle shape and size, and so the bed porosities in fixed as well in expanded position) and geometric factors as well as the feed concentrations should be kept constant.

The value necessary for the flow rate leads directly through the superficial velocity v to the main dimension parameters H and D. The condition for H is a very good distribution of the inlet flow at the bottom. If this is realizable, then the height has to be increased by about 10%.

There are a few parameters that will inevitably change during scale-up. Of course, for the capacity, these are the flow rate, all geometric nonspecific parameter, pressure and pressure drop, as well as temperature gradient to the heat exchange area and the heat exchange area itself.

All these considerations lead to the following relevance list:

Scale independent parameters or to be kept constant: $\{v, \epsilon, \epsilon_{\text{L}}, d_{\text{PS}}, \phi_{\text{S}}, \rho_{\text{L}}, \rho_{\text{P}}, \upsilon, D_{\text{i}}, c^{\alpha}, f_{\text{S}}, f_{\text{B}}\}$

Scale-dependent parameters to be adapted: $\dot{V}_{\text{L}}, V_{\text{R}}, H, \text{h}, \text{p}, \Delta p, A_{\text{J}}, \Delta T_{\text{wall}})$.

To successfully transfer the process from model to the production scale, a few further investigations are necessary to clear up the pressure and the temperature situation. The solubility of gases is directly connected with changing pressure and if there are still problems with the heat exchange, it is not possible to have the best conditions for the reaction.

To avoid problems with too small bed diameter D because of the wall influenced flow behavior, it may sometimes be advisable in model (laboratory) scale to use diameters above 50 mm.

44.4 MODELING AND SIMULATION

Generally, the FBR is a hydraulically driven tube-type reactor. If there is no carrier inside, the reactor is a simple tube reactor with more or less back-mixing behavior. Under the assumption of plug flow and an overlapped dispersing flow to describe the back mixing, the balance for a compound "i" with the concentration c_i in a small element $dV = A \times dx$ at the position "x" reads as follows (15,16) under steady-state conditions (Fig. 44.10):

$$\begin{aligned} \text{d}V \times \frac{\text{d}c_i}{\text{d}t} &= 0 \\ &= -\frac{\text{d}}{\text{d}x}\left(u \times c_i + D_{\text{ax}} \times \frac{\text{d}c_i}{\text{d}x}\right)\text{d}\,x \times A - \dot{n}_{\text{diff}} \end{aligned} \tag{44.42}$$

In this small element, convection ($u \times c_i$), back mixing ($D_{\text{ax}} \times dc_i/dx$), and the supply for the consumption inside the beads (n_{diff}) determine the result.

The assumed average plug flow velocity has to be corrected because of the solids present: $u = \frac{F}{A \times \varepsilon_{\text{L}}}$

With dimensionless length

$$\chi \equiv \frac{x}{\text{L}} \tag{44.43}$$

and concentration

$$C \equiv \frac{c}{c^{\alpha}}, \tag{44.44}$$

we get

$$\frac{\text{d}^2\text{C}}{\text{d}\chi^2} = -Bo \times \left(\frac{\text{dC}}{\text{d}\chi} + \dot{n}_{\text{diff}}\right) \tag{44.45}$$

The diffusion terms in Equation 44.45 look for the path along z (coordinate inside the particle from the center to

$z = r_{PS} = d_{PS}/2$) inside the porous particle. Again for steady-state conditions, we get

$$\frac{dn_i}{dt} = D_i^e \times 4 \times \pi \times (z + dz)^2 \times \frac{dc_i}{dz} - D_i^e \times 4 \times \pi \times z^2 \times \left(\frac{dc_i}{dz} - \frac{d^2 c_i}{dz^2} dz \right) - k_S \times S_V \times c_i \times \left(4 \times \pi \times z^2 \times dz\right) = 0 \quad (44.46)$$

transferred by neglecting all dz^2 terms as they can be assumed as zero, we get

$$k_S \times S_V \times c_i^n = \frac{2}{z} \times D_i^e \times \frac{dc_i}{dz} + D_i^e \times \frac{d^2 c_i}{dz^2} \quad (44.47)$$

Again with dimensionless length and concentration (Eqs 44.43 and 44.44), we get

$$r_{PS}^2 \frac{k_S \times S_V}{D_i^e} \frac{c_i}{c_{i,S}} = \frac{2}{z/r_{PS}} \frac{d\left(c_i/c_{i,S}\right)}{d\left(z/r_{PS}\right)} + \frac{d^2\left(c_i/c_{i,S}\right)}{d\left(z/r_{PS}\right)^2} \quad (44.48)$$

with the solution

$$\frac{c_i}{c_{i,S}} = \frac{\sinh\left[\Phi \frac{z}{r_{PS}}\right]}{\frac{z}{r_{PS}} \sinh \Phi} \quad (44.49)$$

Last, but not least, we get the effective reaction rate, which is equal to $\dot{n}_{diff}$:

$$r_{eff} = \frac{3}{\phi} \times k_S \times S_V \times c_{i,S} \times \left(\frac{1}{\tanh \phi} - \frac{1}{\phi} \right) \quad (44.50)$$

where $c_{i,S}$ is the concentration of the considered component in front of the particle (carrier, bead) at position x.

In the mathematical model, Equation 44.50 replaces the diffusion term in Equation 44.42.

In a solid containing tube reactor, the diffusion (dispersion) coefficient is inhibited because of the obstacles (beads, carriers, and solids) and became smaller. This change diffusion coefficient is called *effective diffusion coefficient* D^e. In practise, the effective diffusion coefficient is approximately 10% compared to the original, uninhibited coefficient.

In the Equations 44.49 and 44.50, the Thiele modulus Φ appears. This dimensionless number is defined as follows:

$$\Phi = \frac{d_{PS}}{2} \sqrt{\frac{k_S \times S_V}{D_i^e}} = \frac{r_S \text{without pore diffusion inhibition}}{\text{diffusion inside pore}} \quad (44.51)$$

All the equations discussed above are available for modeling and simulation to optimize the fluidized bed process. Further aspects for a mathematical model for use in the design and optimization of fluidized-bed reactors can be found in literature (21,22).

44.5 PRAXIS EXAMPLES

Let us calculate the situation shown in Figs 44.4 and 44.5. The laboratory plant has the following dimensions:

$H_{max} = 300$ mm; $D = 50$ mm; $h = 115$ mm; pump rate $F = 63.5$ L/h; $d_{PS} = 8 \times 10^{-4} m$; $\rho_P = 1.25$ kg/L; $\rho_L = 0.98$ kg/L; $v = 0.95 \times 10^{-6}$ m^2/s; $\phi_S = 0.95$.

First we calculate the superficial velocity v.

The cross section is:

$$A = \frac{0.05^2 \times \pi}{4} = 2 \times 10^{-3} \text{m}^2$$

$$v = \frac{1.06}{2 \times 10^{-3} \times 10^3 \times 60} = 0.0089 \text{ m/s}$$

The entrainment velocity, assuming turbulent conditions is

$$w_f = \left[\frac{4}{3} \frac{g \times 0.9 \times \left(8 \times 10^{-4}\right) \times 0.27}{0.44} \right]^{0.5} = 0.076 \text{ m/s}$$

Control is

$$Re = \frac{0.076 \times 8 \times 10^{-4}}{0.95 \times 10^{-6}} = 64 < 500 \rightarrow \text{not turbulent!}$$

Next laminar assumption is

$$w_f = \frac{1}{18} \frac{g \times 0.9^2 \times \left(8 \times 10^{-4}\right)^2}{0.95 \times 10^{-6}} \times 0.27 = 0.08 \text{ m/s}$$

New Reynolds number is

$$Re = \frac{0.08 \times 8 \times 10^{-4}}{0.95 \times 10^{-6}} = 67.4$$

This is in the same range, but still above $Re = 1.0$ but much nearer to 1.0 than to 500, and so we decide to calculate the next steps with this value.

Next, we calculate the expansion with (18) $n = 4.45 \times Re^{-0.1}$. Thus we need Re for the running conditions

$$Re = \frac{0.0089 \times 5 \times 10^{-4}}{0.95 \times 10^{-6}} = 4.7 \rightarrow n$$
$$= 4.45 \times 4.7^{-0.1} = 3.81.$$

We get for the liquid fraction in bed, Equation 44.22

$$\varepsilon = \sqrt[3.81]{\frac{0.0089}{0.08}} = 0.56$$

With this porosity, we can calculate the height of the expanded bed:

$$H = 115 \cdot \frac{1-0.4}{1-0.56} = 156.4\,\text{mm}$$

The reaction volume is now:

$$V_{R,L} = 2 \times 10^{-3} \times 0.1564 \times 10^3 = 0.31\,\text{L}$$

Power input Equations 44.1 and 44.27:

$$\Delta p = g \times 0.115 \times [(1-0.4) \times 0.27 + 0.98] \times 10^3$$
$$= 1288.35\,\text{Pa}$$

$$P_L = \frac{63.5 \times 1288.35}{3600 \times 10^3} = 0.0227\,\text{W}$$

$$\varepsilon_L = \frac{0.0227}{0.31} = 0.073\,\text{W/L}$$

Just to compare the pressure drop via the tube flow, this amounts to only 0.03%!!

This specific hydraulic power input is low for bacteria or yeast fermentation processes, but rather high for mammalian cell cultivation.

44.5.1 Using the Reh Diagram for Homogeneous Fluidization

With the system parameter, we first calculate the Archimedes number:

$$Ar = Re^2 \times Fr^{-1} \frac{\Delta\rho}{\rho_L} = \frac{g \times d_{PS}^3}{\nu^2} \frac{\Delta\rho}{\rho_L}$$
$$= 4.7^2 \times 61.9 \frac{0.27}{0.98} = 375 \qquad (44.52)$$

Then the Ω-number:

$$\Omega = Re \times Fr \frac{\rho_L}{\Delta\rho} = \frac{v^3}{g \times \nu} \frac{\rho_L}{\Delta\rho}$$
$$= \frac{(0.0089)^3}{g \times 0.95 \times 10^{-6}} \frac{0.98}{0.27} = 0.28 \qquad (44.53)$$

Now in the Reh diagrams (Figs 44.11–44.13), we find a value for the force ratio $n = 0.35$, which enables us to calculate the resistance coefficient under these conditions:

$$c_W = \frac{4}{3} \frac{n \times g \times d_{PS}}{\nu^2} \frac{\Delta\rho}{\rho_L}$$
$$= \frac{4 \times 0.33 \times g \times \left(510^{-4}\right) \times 0.27}{3 \times (0.0089)^2 \times 0.98} = 7.5 \qquad (44.54)$$

Compared with Fig. 44.14 this value fits.

NOMENCLATURE

A	heat exchange area (m^2)
A_B	surface of a spherical particle (m^2)
A_C	projected area (m^2)
A_P	surface of a particle (m^2)
A_R	cross section of the reactor (m^2)
Ar	Archimedes number (Eq. 44.4)
Bo	Bodenstein number (Eq. 44.47)
c	concentration (mol/L)
C	dimensionless concentration (Eq. 44.44)
C_P	capacity of product (kg/a)
c_P, c_L	heat capacity of particle, liquid (J/kg/K)
c_W	resistance factor
D_{ax}	dispersion coefficient, back-mixing factor (m^2/s)
D^e	effective diffusion coefficient (m^2/s)
d_{P32}	Sauter LNCS diameter (m)
d_{PS}	Sauter mean particle diameter (m) (Eq. 44.25)
F	flow rate (L/min)
f_B	bed to reactor height ratio
f_S	slenderness factor; H/D
F_L, F_R, F_W	forces for lift, resistance, weight (N)
g	gravity = 9.81 (m/s^2)
h	bed height (m)
H	height of reactor, expanded bed (m)
h	height of the bed (m)
HPA	available working hours per year (h/a)
k	heat transfer coefficient ($W/m^2/K$)
k_S	surface related reaction rate constant (m/s)
$k(T)$	reaction rate constant $\left[\frac{m^{3\cdot(n-1)}}{s\times mol^{(n-1)}}\right]$
L	characteristic length of a system (m)
n	reaction order
n	exponent in Equation 44.22
n	force ratio $= \frac{F_R}{F_W - F_L}$, Fig. 44.11
$\dot{n}_{diff}$	diffusion stream ($mol/s/m^3$)
Nu	Nusselt number (Eq. 44.33)
P	product concentration (g/L)
P_i	general power input (W)
Pr	Prandtl number (Eq. 44.34)
Q	heat flow (W)
dq	differential heat (J)
r	reaction rate (mol/s/L)
Re	Reynolds number (Eq. 44.32)
Sc	Schmidt number (Eq. 44.35)
Sh	Sherwood number (Eq. 44.36)
STY	space time yield ($kg/h/m^3$)
S_V	specific active catalyst surface (m^{-1})
t	time (s; min; h)
T	temperature (K)
ΔT	temperature difference (K)

dV	volume element (m^3)
$\dot{V}_L$	flow rate, volume stream, liquid (m^3/s)
V_P	particle volume (m^3)
$V_{R,L}$	volume (m^3)
w_f	sink velocity, to the entrainment velocity (m/s)
x	coordinate (m)
z	coordinate (m)
α	downstream efficiency
Δp	pressure drop (Pa)
ε	porosity of the expanded bed
ε	specific power, power density (W/kg)
ρ_L	bed porosity $= V_L/V_B$
F	Thiele modulus (Eq. 44.51)
v	kinematic viscosity (m^2/s)
ρ_L	density of liquid (kg/L)
ρ_L	liquid density (kg/m^3)
ρ_P	particle density (kg/m^3)
ϕ_S-	sphericity coefficient (Eq. 44.24)
X	dimensionless coordinate

REFERENCES

1. Werther J, Molerus O. 50 jahre wirbelschichttechnik, Chemie-Technik 1976; 5. Jhg., (4).
2. Eibl R, Eibl D, Pörtner R, Catapano G, Czermak P. Cell and tissue reaction engineering: Springer Verlag; 2008. ISBN 978-3-540-68175-5.
3. Liese A, Seelbock K, Wandrey C. Industrial biotransformation. Weinheim: Wiley-VCH; 2000. ISBN 3-527-30094-5.
4. Fond der Chemischen Industrie. Biotechnologie/Gentechnik, Folienserie des Fond der Chemischen Industrie. 1996. ISSN 0174-366X.
5. Werther J. Fluidized-bed biorectors. Ullmann's encyclopedia of industrial chemistry. Weinheim: Wiley-VCH Verlag GmbH & Co. FGaA; 2007.
6. Storhas W. Bioreaktoren und periphere einrichtungen. Heidelberg: Springer-Verlag; 1994. ISBN 3-528-06510-9.
7. Sosa AV, Cordoba RP, Peritti IN. Fluidized bed design parameters affecting novel lactic acid downstream processing. Biotechnol Prog 2001; 17(6), 1079–1083.
8. Noll T, Mühlensiepen H, Engels R, Hamacher K, Papaspyrou M, Langen K-J, Biselli M. A cell-culture reactor for the on-line evaluation of radiopharmaceutical: evaluation of the lumped constant of FDG in human glioma cells. J Nucl Med 2000; 41(3) 556–564.
9. Wang MD, Yang N, Huzel N, Butler M. Erythropoietin production from CHO cells grown by continuous culture in a fluidized-bed bioreactor. Biotechnol Bioeng 2002; 77(2), 194–203.
10. Nagpal S, Chuichuicherm S, Peeva L, Livingston A. Microbial sulfate reduction in a liquid-solid fluidized reactor. Biotechnol Bioeng 2000; 70(4), 370–380.
11. Patel M, Bassi AS, Zhu JJ-X, Gomaa H. Investigation of a dual-particle liquid-solid circulating fluidized bed bioreactor for extractive fermentation of lactic acid. Biotechnol Prog 2008; 24(4), 821–831.
12. Jetty AS, Ramakrishna R, Rao AG, Rao BS, Ramakrishna RV. Continuous production of oxytetracycline in fluidized bed bioreactor by immobilized cells of *Streptomyces varsoviensis* MTCC-1537: Effect of Dilution and Glucose Loading Rates, Applied Chemistry and Biotechnology 2009; 159(2): 579–588.
13. Zhang W, Xie Q, Rouse JD, Qiao SA, Furukawa K. Treatment of high-strength corn steep liquor using cultivated Polyvinyl alcohol gel beads in an anaerobic fluidized-bed reactor. Biosci Bioeng 2009; 107, 50–53.
14. Carman PC. Fluid flow through granular beds. Trans Inst Chem Eng 1937; 190, p. 15.
15. Storhas W. Bioverfahrensentwicklung. Weinheim: Wiley-VCH; 2003. ISBN 3-527-28866-X.
16. Levenspiel O. Chemical reaction engineering: John Wiley & Sons, Inc.; 1976. ISBN 0-471-53019-0.
17. Reh L. Fluidized bed processing. Chem Eng Prog 1971; 67(21).
18. Richardson JF, Zaki WN. Sedimentation and fluidisation: Part 1. Trans Inst Chem Eng 1954; 32: 35.
19. Mersmann: CIT 39 5/6. 1967. pp. 349/353.
20. Mößner G, Ramspeck W, Sittig W. Chemische Technik. 8. Jhg, nr. 7, 1979. pp. 329–336.
21. Andrews GF. Fluidized-bed fermenters: a steady state analysis. Biotechnol Eng 1982; XXIV: 2013–2030.
22. Andrews GF, Przezdziecki J. Design of fluidized-bed fermenters. Biotechnol Bioeng 1985; XXVIII: 802–810.
23. Werther J. Strömungsmechanische grundlagen der wirbelschichttechnik. Chem Ing Tech 1977; 49(3): 193–202.

45

BIOREACTORS, GAS-TREATMENT

Graham Andrews
MMBD Consulting, Gresham, Oregon,
William Apel
Idaho National Engineering and Environmental Laboratory, Idaho Falls, Idaho

45.1 INTRODUCTION

The most common type of bioprocess, at least in the United States, is the aerobic treatment of wastewater, in which contaminants in the aqueous phase are biodegraded with the help of oxygen transferred from the gas phase (air) to generate a metabolic product (carbon dioxide) that, being volatile, is then stripped out of the aqueous phase into the gas. The familiarity of this arrangement should not be allowed to limit our imaginations about the possibilities of bioprocessing. It is perfectly possible to construct a process in which a gas-phase contaminant (hydrogen sulfide) is biodegraded with the help of a nonvolatile oxidant (nitrate), generating a product (sulfuric acid) that remains dissolved in the aqueous phase. The bioreactor for such a process must share many of the features found in aerobic wastewater treatment, such as efficient gas–liquid contacting, cell recycling or immobilization to create a high concentration of biomass, control of temperature and pH, and addition of nutrients in order to create a comfortable environment for microbial metabolism. However, the different objective, the treatment of a gas rather than a liquid, must dictate differences in the details. This point can be illustrated by thinking of a conventional trickling filter not as a device for treating sewage, but as one for removing oxygen from the air that flows through it. It would work, but terribly inefficiently, with a fractional removal on the order of 1%.

This chapter presents a three-step study of the use of bioprocesses for the removal of undesirable components from gas streams. The existing and potential applications are described first, followed by the types of bioreactors that may be employed. A simple process analysis is then presented to illustrate how the choice and design of the bioreactor is dictated by the particular application, the type of microbial metabolism involved, the concentration and solubility of the contaminant, and so on. It should be noted that there are also a number of potential bioprocesses in which the objective is not the removal of a contaminant from a gas stream, but the bioconversion of gaseous substrates into useful products. They include the partial oxidation of methane to methanol, and the production of ethanol and acetic acid from mixtures of carbon monoxide and hydrogen. Work on these processes is not described in detail, except when doing so illustrates the common problems of bioreactors with gaseous substrates.

45.2 MICROORGANISMS AND APPLICATIONS

Due to inherent difficulties in achieving the sterile conditions necessary for prolonged maintenance of pure cultures in field-scale bioreactors, most gas treatment bioreactors contain a mixed culture or consortium of microorganisms. These consortia may be derived from a number of different inocula, from common sources such as sewage-treatment facilities, biofilms from established bioreactors used for similar applications, or soils and waters from areas contaminated with the substrate of interest. In some instances, it is possible to enrich for the desired microbial consortium directly from the bioreactor bed medium, particularly

Upstream Industrial Biotechnology: Equipment, Process Design, Sensing, Control, and cGMP Operations, Volume 2, First Edition. Edited by Michael C. Flickinger.
© 2013 John Wiley & Sons, Inc. Published 2013 by John Wiley & Sons, Inc.

when media components such as soil, compost, peat, or bark chips are used, because these materials naturally contain a mixture of microbes with wide-ranging physiological capacities. Regardless of the inoculum source, the bioreactor must be operated under conditions that select for and maintain, over the life of the bioreactor, microorganisms with the physiological capabilities necessary to catalyze the desired bioconversion. Typical selective factors include the electron donor (i.e., the metabolizable energy source), available terminal electron acceptors, supplemental nutrients, pH, Eh, and temperature.

Regardless of the selection strategy used to achieve a microbial consortium with the desired physiological properties, the use of a consortium versus the attempted use of a pure culture of microbes has a number of practical advantages. As mentioned above, it is difficult to achieve the sterility standards necessary to maintain a pure culture of microbes in a gas treatment bioreactor under field conditions. In addition, a pure culture of microbes is often metabolically incapable of fully degrading a contaminant, so hazardous intermediates may be created and build up within the bioreactor or in effluent streams from the bioreactor. Because mixed consortia inherently tend to be composed of a number of different microbial species with a gamut of physiological capabilities, undesired intermediates that may be created by pure cultures are often fully degraded by consortia. Similarly, in many applications, the concentrations and chemical compositions of gas streams to be treated may be transient. Consortia generally have a higher probability than pure cultures of adapting to this transience. The contaminant gases and vapors that can be successfully biodegraded can be classified by their role in microbial metabolism.

45.2.1 Electron Donors

Microorganisms require a constant supply of metabolic energy, which is normally derived from the oxidation of either organic or inorganic compounds, with these compounds serving as electron donors to the microorganisms. Many environmentally or industrially significant gases and vapors are metabolically oxidizable by microorganisms and can serve as electron donors. Thus, many different types of gas and vapor streams can be and have been, treated microbiologically (1). Microbially oxidizable gases and vapors that have been treated in bioreactors include hydrocarbons, ketones, ammonia, xylene, alcohol, terpene, and carbon disulfide vapors, as well as gases such as methane and hydrogen sulfide (2–10). In the case of carbon-containing substrates (hydrocarbons, carbon monoxide, etc.), the metabolism of these compounds provides heterotrophic microbes not only with an electron source, but also with a source of cellular carbon. Non-carbon-containing substrates such as ammonium, while providing a metabolic electron source, must be metabolized by autotrophic microorganisms capable of obtaining their cellular carbon via the fixation of atmospheric carbon dioxide.

45.2.2 Cometabolism

Some substrates cannot serve as sole energy sources for microorganisms, but are nevertheless potentially bioconvertable. Their biodegradation is achieved in the presence of another compound that serves as the microorganism metabolic electron donor, a process that is termed cometabolism. Trichloroethylene (TCE) provides a well-documented example of a substrate that is oxidized cometabolically by microorganisms. Typical of cometabolic TCE degraders are the methanotrophic bacteria, aerobes that oxidize methane as their sole carbon and energy source (11). This oxidation takes place in a sequential manner, with methane first being converted to methanol, which is in turn oxidized to formaldehyde, formate, and finally, carbon dioxide. Along this oxidative pathway, the methanotrophs generate cellular energy as well as fixing methane-derived carbon into additional biomass. The first step, in which methanol is formed from methane, is catalyzed by the enzyme methane monooxygenase (MMO) (12,13). Although MMO is selective for its natural substrate, it can, under certain conditions, catalyze the oxidation of a variety of other compounds (12–14), including partially chlorinated aliphatic solvents such as TCE. Two distinct forms of MMO have been identified, membrane MMO (mMMO) and soluble (sMMO) (15,16). sMMO, expressed by methanotrophs growing under copper-limited conditions, supports much higher rates of TCE oxidation than does mMMO, which is expressed under conditions of copper sufficiency (17).

Air streams contaminated with TCE and similar chlorinated solvents are generated by industrial operations and the remediation of contaminated ground and water by air stripping. They can be treated in a bioreactor that is started up with methane as the sole carbon and energy source, while supplying the necessary oxygen and supplemental nutrients under copper-limiting conditions (6). After the methanotrophic consortium is established, the methane load to the reactor can be decreased or fed on an intermittent basis concurrently with TCE vapors. The methanotrophic microbes then will be maintained by the lessened methane feed, while catalyzing the oxidation of the TCE via their sMMO. The reduced or intermittent methane feed not only reduces the amount of methane that must be supplied, but is essential in achieving optimal TCE removal rates since methane itself is an effective competitive inhibitor of TCE oxidation. An alternate, but more expensive, strategy used to avoid this type of

competitive inhibition is to supply a catabolic intermediate such as formate in order to provide energy to the methanotrophs, because formate does not compete with TCE for access to the sMMO. It should be noted that a number of other microbial oxygenases have been shown to be capable of catalyzing cometabolic TCE oxidation. These include toluene oxygenases from a number of *Pseudomonas* spp., propane monooxygenases from propanotrophs, and ammonia monooxygenase from *Nitrosomonas europea* (18–21).

45.2.3 Electron Acceptors

Most gas treatment bioreactors remove contaminants from air streams and oxidize them to innocuous end products (CO_2, Cl^-, etc.), using the oxygen in the air as the electron acceptor. However, there are also gas streams containing little or no oxygen where the objective is to remove a compound that can act as an alternative physiological terminal electron acceptor. This approach has been shown to work for compounds like sulfur oxides (SO_x) and nitrogen oxides (NO_x) (8,24,25). NO_x biofilters have been developed using a consortia of denitrifying microbes that have the physiological capacity, as a part of their normal metabolism, to use a variety of NO_x compounds as terminal electron acceptors, reducing them to innocuous nitrogen gas (N_2). This process generally requires low-oxygen conditions because denitrifiers preferentially use oxygen, if present, as their terminal electron acceptor. As a result, selective conditions for denitrifying microbes include a suitable carbon and energy source with a NO_x compound as a terminal electron acceptor, a lack of oxygen, and the presence of supplemental nutrients necessary for microbial growth. The potential application to stack gases raises the question of the maximum temperature at which the microbes will function. Research (25) has shown that naturally occurring thermophilic microbes selected for from compost are capable of reducing nitric oxide (NO) to nitrogen gas (N_2) at temperatures up to 60°C.

Other processes are far more sensitive than denitrification to trace amounts of oxygen. The sulfite-reducing bacteria responsible for the removal of SO_2 are obligate anaerobes, although they may be active in anoxic microniches, for example, deep in a biofilm. Chlorinated aliphatic solvents will also accept electrons under anaerobic conditions, a degradative mechanism that works best on the completely chlorinated compounds that are not touched by the oxidative enzymes already discussed (22,23). Carbon tetrachloride, for example, will be progressively reduced to chloroform, dichloromethane, and methyl chloride. This mechanism is often categorized as cometabolism, implying that the microbes derive no metabolic benefit from it, but this remains uncertain.

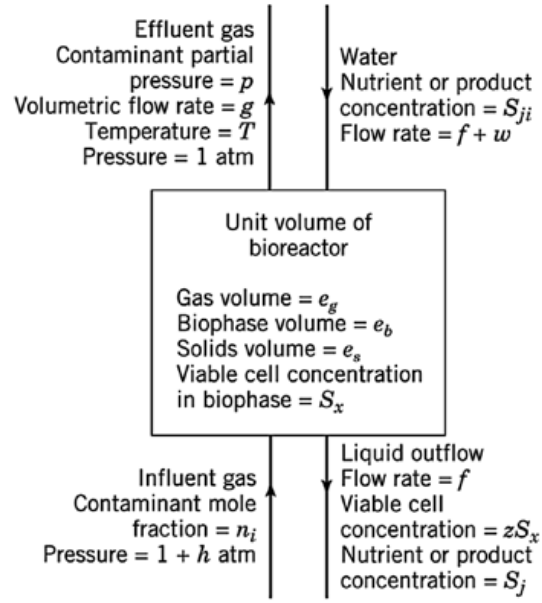


Figure 45.1. The generic gas-treatment bioreactor.

45.3 BIOREACTOR TYPES

Figure 45.1 shows a generic gas treatment bioprocess along with the nomenclature to be used in the subsequent analysis. Gas treatment bioreactors are sometimes described as *gas-phase bioreactors*, but this term is inexact in the sense that the actual reactions happen inside a microbial cell, which is necessarily an aqueous phase. Some reactions carried out in immobilized enzyme reactors do seem to involve direct interaction between the gas and the enzyme (33), although even here the humidity remains a critical variable and the enzyme may be covered with a layer of water a few molecules thick. For our purposes, the bioreactor is divided into a gas phase, a solid phase consisting of any solid packing or biofilm support particles, and a biophase, which contains the water and the microorganisms. The fraction of the bioreactor volume occupied by each phase is called its holdup, and the three values, e_g, e_s, and e_b, must add up to 1.

For convenience, we think in terms of a bioreactor of unit volume and express the gas flow rate as the volume per volume per minute (VVM) flow rate, g, at the effluent gas conditions, taken as temperature T and atmospheric pressure. Others choose to work in terms of the molar outlet gas flow rate (g/RT, where R is the gas constant) or a gas residence time, either the empty bed residence time, $1/g$, or the average time an element of gas actually spends in the reactor, e_g/g. The flow rate of the influent gas is not the same as g because its temperature may not be T, it is at a higher pressure, ($1 + h$ atmospheres, where h is

the pressure drop through the reactor), and because various components (contaminant, oxygen, metabolic products, water vapor) are added to, or removed from, the gas stream as it flows through the reactor. When these effects are significant, it is essential to specify exactly what is meant by "gas flow rate."

The objective of some processes is to remove a gaseous contaminant by converting it into a soluble, nonvolatile metabolic product. Some such products, H^+ for example, can be neutralized in the bioreactor, but others, such as the Cl^- from the degradation of chlorinated organics, must be removed in the liquid if they are not to accumulate to concentrations that inhibit the microorganisms. There may therefore be a liquid outflow, f per unit bioreactor volume, and an inflow that must be greater than f to allow for the evaporation rate, w. This outflow tends to wash microorganisms out of the bioreactor, and it is usually beneficial to retain them either by cell recycle or immobilization, making the parameter z in Figure 45.1 less than 1.

The question is what type of bioreactor should be put in the "black box" in Figure 45.1. Almost every possible configuration by which a gas can be contacted with a biofilm or a suspension of microorganisms has been employed in some application, and these can be roughly divided into four categories.

45.3.1 Biofilters

The earliest gas-treatment bioreactors were used to control odors in air coming from slaughterhouses and rendering plants and consisted of porous pipes buried in the ground, the noxious compounds being removed by a combination of adsorption and biodegradation as the air flowed up through the soil (26). Applications of the idea have since expanded to include the removal of hazardous, volatile compounds from chemical plants, paint shops, foundries, and a variety of agricultural and food-processing operations. Although often effective, the operation of these simple soil beds depends critically on the local soil and weather conditions. Unless they are covered and/or periodically sprayed with water, they may stop working, either due to becoming waterlogged or to drying out. They have largely been replaced by custom-made biofilters, which are essentially boxes made of plastic, wood, sheet metal, concrete, or even stainless steel, containing a bed of media and a gas distribution system to ensure uniform flow of the gas through the bed.

In terms of the variables defined in Figure 45.1, biofilters are the small e_b, small f, and small z approach. The biophase consists of individual microorganisms attached to the media, perhaps enough to constitute a thin biofilm. The amount of moisture in this layer is critical, and is controlled by humidification of the inlet gas and/or by spraying water directly over the bed. Little or no water drips out of the bed, making it difficult to provide soluble nutrients and pH control chemicals, or to wash out nonvolatile metabolic products. Biofilters are thus best suited to applications that generate no such products and involve no pH swings, the treatment of air streams containing low levels of volatile organics being the obvious example.

The great advantage of biofilters over the early soil beds is that they allow the choice of the nature and particle size of the bed media. This media must support a high density of attached microorganisms suited to the particular application, perhaps even providing some of the nutrients needed for their growth. The ability to adsorb the contaminant is an advantage because adsorption can provide some contaminant removal during the start-up period, before a large population of well-acclimated microorganisms has developed (sometimes called "the bed-ripening period"), and during any sudden slugs of concentrated contaminant in the influent gas. Also, although the interactions between such adsorption and biodegradation are complex and poorly understood, they are generally favorable to biofilter performance. Finally, the media must be mechanically strong and resistant to disintegration, compacting, and the resulting channeling of gas flow. Soil, compost, peat, and wood-chip mixtures are all inexpensive media that have been used successfully. Materials such as activated carbon and limestone, although more expensive, may be mixed in to provide extra adsorption and pH buffering.

The particle size of the media is critical. Small particles give a huge gas–biophase interfacial area per unit bed volume (a quantity subsequently called "a"), thus eliminating concerns about mass-transfer limitations between the two phases. But beds of small particles have a higher resistance to gas flow, are more prone to waterlogging and plugging by excess biofilm, and if too light, may get blown out of the reactor altogether. A general guideline is to choose the smallest available particles that avoid the latter problems, and then ensure that the shape of the bed is optimized to give the desired contaminant removal with a reasonable pressure drop (see "Scale-Up").

If the life of the bed is found to be finite due to compaction, loss of pH buffering capacity, accumulation of salts from the evaporation of added water and so on, one solution is to employ two beds in series. Bed 1 can provide most of the contaminant removal, while bed 2 polishes the effluent, mainly by adsorption, while developing its own population of well-acclimated microorganisms. When bed 1 is exhausted it can be replaced by bed 2, which is itself replaced by a bed of fresh media. The arrangement of the media on a series of trays in the bioreactor facilitates this mode of operation.

45.3.2 Bubble-Gasified Reactors

Conventional bubble-aerated fermenters make poor gas treatment bioreactors because they are designed for a high rate of transfer of gaseous nutrients and products (O_2 in and CO_2 out), rather than a high fractional removal of a component from the air stream. This latter objective requires taller bioreactors with longer gas residence times, but tall reactors mean higher pressure drops due to the hydrostatic head. Nevertheless, tall, mechanically agitated bioreactors with multiple impellers have been proposed for removing H_2S from industrial gas streams (29), and bubble columns with no mechanical agitation have been demonstrated for the removal of TCE from air using a toluene-oxidizing organism (30).

These bioreactors are in many ways at the opposite extreme from biofilters. The biophase occupies most of the reactor ($e_b \rightarrow 1$ in Fig. 45.1), and it is dilute and well-mixed rather than dense and immobilized. The large volume of water makes it easy to add soluble nutrients, control the pH, and remove water containing nonvolatile products. However, care must be taken to not wash out the biomass, because $z = 1$ (Fig. 45.1) unless there are extra surfaces in the bioreactor for the attachment of a biofilm, or if a cell separation and recycle loop is added. Another major difference is that the gas–biophase interfacial area, a, is not only much smaller than in a biofilter, but is not even a constant, varying with the gas flow rate. Bubble gasified bioreactors are therefore best suited to contaminants like NO_x that are very soluble in water (thus reducing concerns about the gas–liquid mass-transfer rate), whose dissolution in water cause pH swings, and whose metabolism requires large amounts of dissolved nutrients.

45.3.3 Biotrickling Filters

Trickling filters for gas treatment are similar to, but usually taller than, those in use for decades for the secondary treatment of municipal and industrial wastewaters. Like biofilters, they consist of a bed of media through which the gas flows either upward or downward, but unlike biofilters, the microbial culture is recirculated continuously over the bed from a reservoir beneath it. Stone aggregate or wood chips are the traditional media, but even seashells have been used (27). Most modern filters employ ceramic or plastic media, Pall rings, Raschig rings, and so on specifically designed to make a bed with a high surface area to maximize gas transfer, and a high porosity to minimize the pressure drop and the chance of clogging or flooding (28).

These bioreactors can be thought of as intermediate between biofilters and bubble-gasified systems and are best suited to applications between those already described. If the characteristics of the media and the microorganisms are such that most of the biomass stays attached, then a trickling filter is essentially a biofilter with a higher liquid flow and a smaller gas–biophase interfacial area, a, due to the larger media. If on the other hand, most of the biomass stays suspended and the recycle ratio (RR = flow of recycled liquid/f) is high enough to keep the biophase well mixed, then it is functionally similar to a bubble-gasified bioreactor. The main differences are that the pressure drop, h, is usually much smaller, and the interfacial area, a, is a constant that is independent of the gas flow rate.

45.3.4 Bioscrubbers

The systems just described essentially combine two functions, stripping the contaminant from the gas into the aqueous biophase and then subjecting it to biodegradation. But what if the physicochemical conditions in the biophase resulting from the stripping are not suitable for the microbial metabolism? The removal of sulfur dioxide from stack gas is a good example because stack gases contain a small percentage of oxygen that although relatively insoluble, inhibits the bacteria responsible for the reduction of the sulfite formed by the dissolution of SO_2. One solution is the bioscrubber, which consists of an aqueous stripper in which the contaminant is transferred from the gas to water, and a separate bioreactor, in which the liquid effluent from the stripper is essentially treated as wastewater. The bioreactor should be a completely mixed, immobilized-cell type so that a large population can grow up in a well-controlled environment without continuously being recirculated through the potentially toxic environment in the stripper. Several configurations are possible, the simplest being that in which the liquid reservoir at the bottom of a packed-bed stripper is used as the bioreactor. Bioscrubbers are not considered further here because building a separate bioreactor and stripper is necessarily more expensive than combining them in a single unit, and when it is necessary, the two unit operations can be designed by conventional methods.

45.4 BIOREACTOR DESIGN

A process variable is any quantity that is under the direct control of the designer or operator of the process. For gas treatment bioreactors, the variables to be fixed by the designer include the bioreactor type, shape, and size, whereas those fixed by the operator include the addition of water, nutrients, and chemicals for pH control. The objective in fixing these variables is to satisfy a set of process requirements that specify the flow rate and composition of the gas stream, the nature and concentration of the contaminant, and the fractional removal required. The difficulty is that many designs, that is, many combinations of the process variables, will meet the process requirements for a particular case. The proper

goal of engineering design is not simply to pick one of these designs at random, but to find the single design that meets the requirements at the lowest possible cost. The design of gas treatment bioreactors, like that of any other process, is an economic optimization problem, but one that is so complex that the exact solution cannot be found within the constraints of time and money normally imposed on the design process. The best solution for a particular case will certainly depend on the scale of the problem, the solubility and possible inhibitory effects of the contaminant, the type of microbial metabolism (aerobic or anaerobic, growth associated or cometabolic, etc.) needed to degrade it, and the temperature and pressure of the gas stream. Even coming close to the best solution requires a careful scale-up program in which the insights available from education and experience are used to integrate experiments at different scales with mathematical models that can extrapolate the results from one scale to the design of the equipment at the next scale. The bioreactor analysis presented in this section is intended as a guide to this program, suggesting which bioreactor types be chosen for experimental evaluation in each case, specifying the operating conditions around which the experiments should be designed, and showing how performance may be expected to vary with scale.

Because the design goals are essentially economic, the relationship of the variables shown in Figure 45.1 to the process costs must be kept in mind. The volume of the commercial-scale bioreactor equals the actual gas flow to be treated (a process requirement) divided by g; a large value for g translates directly into a smaller and, all other things being equal, cheaper bioreactor. The liquid flow, f should be kept as small as possible because providing clean water and disposing of any process wastewater both cost money, as do any nutrients and chemicals that must be added. The pressure drop, h, through the bioreactor may be significant, particularly on a large scale, and it determines the capital cost of the gas compressors and the energy costs for running them. Compressing the feed gas is not only expensive in itself, it heats the feed such that heat exchangers may be needed to cool it to the desired temperature.

45.4.1 Process Analysis

It will be assumed that the biophase is completely mixed and that the gas approximates plug flow through the bioreactor. This provides a realistic description of some bioreactors (bubble columns, some biotrickling filters), and a reasonable starting point for quantitative thinking about the others. More detailed mathematical models are available in the literature for specific types of bioreactors and metabolism (31,32). The equilibrium solubility of the contaminant in the biophase, S^*, will be described by Henry's law, $S^* = p/H$, where p=partial pressure of the contaminant in the gas and H=Henry's law constant. Although this is adequate for relatively insoluble and dilute contaminants, it is a considerable oversimplification for others. For example, the dissolution of oxides of nitrogen (NO_x: a mixture of NO and NO_2) from stack gases into water is an extremely complex process (34,35) that involves the gas-phase chemical oxidation of NO to NO_2 and a dissociation reaction that generates H^+, NO_3^-, and NO_2^- when the gas dissolves. In such cases, Henry's law can only be interpreted in the purely qualitative sense that low H means a soluble gas.

Any complete bioprocess model combines the mass conservation equations that describe the bioreactor with equations that try to approximate the complexities of microbial metabolism. Because the objective here is to compare different bioreactor configurations, it is essential to have consistent descriptions of the metabolism. In most gas treatment applications the contaminant is a major microbial nutrient, either the electron donor or the electron acceptor. Its consumption provides metabolic energy for growth and cell maintenance, so its specific consumption rate, q is given by the yield equation

$$q = \frac{\mu}{Y} + k \tag{45.1}$$

where μ is the specific growth rate of cells, Y is the cell-yield coefficient, and k is the cell-maintenance coefficient.

In a well-operated bioreactor, the pH and temperature are carefully controlled and all required nutrients are provided in adequate amounts, making the specific consumption rate a function only of the concentrations of contaminant, S, and any inhibitory product, S_m, dissolved in the biophase. The exact form of this function, written $q(S, S_m)$, will not be specified because it varies among cases, but it must describe the effects on the metabolic rate of substrate limitation, product inhibition, and possibly (when n_i/H is large) substrate inhibition. It is more common to describe the specific cell growth rate, μ, by a Monod-type function of the concentration S, but this is clearly incorrect at the low concentrations found in gas treatment bioreactors, because it predicts that growth stops and substrate uptake continues when no substrate is available ($\mu = 0$ and $q = k$ when $S = 0$). In fact, when a major nutrient is exhausted, its consumption must stop, and the microorganisms go into an endogenous state in which the viable biomass declines, a phenomenon correctly approximated by requiring that $q(S, S_m) = 0$, and thus $\mu = kY$ (equation 45.1) when $S = 0$. Cell growth now stops at a nonzero "stationary phase" concentration, S_s, corresponding to the point where substrate uptake is just sufficient to satisfy the maintenance requirement, and defined by $q(S_s, 0) = k$.

For cometabolic processes, the contaminant is neither the main electron donor nor the acceptor; two rate equations are needed, and equation 45.1 contains an extra parameter whose value may be found from knowledge of the degradative pathway. See, for example, the analysis by Andrews of chloroform degradation by methanotrophic bacteria (36). The design of cometabolic bioreactors follows many of the principles described here but is too complex and case specific to be analyzed in detail.

At steady state the conservation of mass requires that the rate of growth of microorganisms in the bioreactor, $\mu e_b S_x$, equals the rate at which they flow out, fzS_x (see Fig. 45.1 for nomenclature). The loss of microorganisms in mist suspended in the effluent gas may be significant in some bioreactors without demisting devices but is not included explicitly in the analysis. The specific growth rate, μ, a measure of the physiological state of the microorganisms, thus equals zf/e_b, the reciprocal of the mean cell-residence time (the number of cells in the bioreactor divided by the cell outflow rate), which is a quantity under our direct control. This remarkable result, although well known for chemostats, has not been fully appreciated for gas treatment. It follows from equation 45.1 that the concentrations in the biophase, S and S_m, are constrained by

$$q(S, S_m) = k(1 + D) \tag{45.2}$$

where $D = zf/Yke_b$ is the dimensionless dilution rate or reciprocal mean cell-residence time.

The steady-state conservation of mass for the contaminant requires that whatever is removed from the gas phase be transferred to the biophase, where it is either consumed by the microorganisms or flows out in the liquid. For a bioreactor, as opposed to a gas stripper, the latter term should be negligible, but the flows of dissolved nutrients and nonvolatile metabolic products must be included

$$\frac{g}{RT}(n_i - p) = \frac{k_1 a(n_i - p)}{H\ ln\dfrac{(n_i - HS)}{(p - HS)}}$$

$$= e_b q S_x = \pm\frac{(fS_j - (f + w)S_{ji})}{y_j} \tag{45.3}$$

where y_j is the amount of component j produced (+ sign) or consumed (− sign) per unit of contaminant consumed (see "Nutrient Addition and Start-Up").

The description of the driving force for mass transfer in terms of the log–mean concentration difference in the second term of this equation follows from the assumption of plug flow of the gas. The expression is not strictly correct when the pressure drop through the bioreactor is large, as in a tall bubble column, because the contaminant partial pressure in the influent is then $(1 + h)n_i$; but this complication is rarely included in practice. The essential points here are that the mass-transfer factor, k_1a, is an empirically determined parameter, that it can be based on different forms of the driving force, and that the best choice depends on the reactor type and must be clearly understood by everyone involved in a project.

Equation 45.3 can be rearranged to give the fractional removal of the contaminant from the gas, only the product (subscript m) being considered in the last term:

$$x = 1 - \frac{p}{n_i} = (1 - e^{-G})\left(1 - \frac{HS}{n_i}\right)$$

$$= \frac{S_x}{X}(1 + D) = FD\frac{S_m}{S'_m} \tag{45.4}$$

where $G = k_1 aRT/gH$ is the dimensionless mass transfer coefficient; $F = YS'_m/zXy_m$ is the dimensionless product inhibition factor; $X = gn_i/ke_bRT$ is the maximum possible viable cell concentration in the biophase; and S'_m is the product concentration that completely inhibits cell growth.

Rather than solving equations 45.2 and 45.4 exactly, which would require the form of the inherent kinetic function $q(S, S_m)$, consider some limiting cases in order of decreasing liquid outflow rate. These cases are used to summarize the bioreactor performance in Figure 45.2, a graph that can be universal, at least within the limitations of the assumptions, because the parameters describing the contaminant (H, n_i), the reactor (f, k_1a), and the metabolism (k, S'_m) in individual cases have been incorporated into the dimensionless numbers x, D, F, and G.

- *Washout*. $D > (q(n_i/H, 0)/k) - 1$: Because the dissolved concentration, S, must obviously be less than that in equilibrium with the feed gas, n_i/H, equation 45.2 now has no solution, meaning that all of the biomass is washed out of the reactor and there can be no contaminant removal.

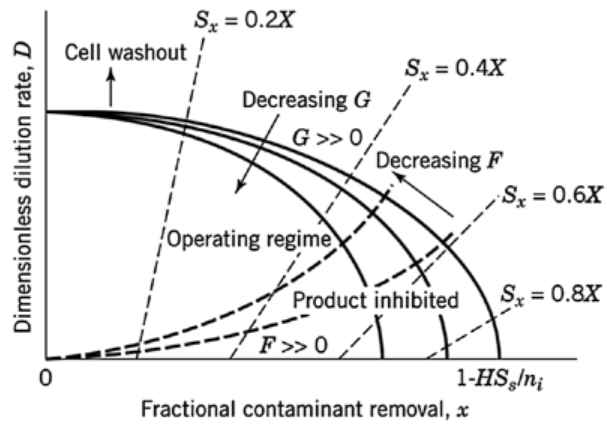


Figure 45.2. Operating regime for a completely mixed bioreactor.

- *Substrate limitation*. $D > (1 - e^{-G})/F$: Equation 45.4 shows that under this condition, $S \to 0$, while $S_m < S'_m$, meaning that microbial kinetics are limited by the availability of substrate rather than product inhibition and the exact value of the inhibition number, F, is irrelevant. If gas-biophase mass transfer is very rapid, the dissolved contaminant is in equilibrium with the outlet gas, giving the best possible bioreactor performance. The shape of this $G = \infty$ line in Figure 45.2 is simply a reflection of the relationship between $\mu(= zf/e_b)$ and $S(= p/H)$ from the inherent microbial kinetics. Mass-transfer limitation ($G < \infty$) leads to a progressive reduction in the contaminant removal, x.
- *Product inhibition*. $D < (1 - e^{-G})/F$: Now the concentration of metabolic products, S_m reaches inhibitory levels, S'_m, while dissolved contaminant is still available, meaning that metabolism is limited by product inhibition rather than substrate limitation, and the exact value of G is irrelevant. Increasingly stronger inhibition (smaller F) produces a series of curves in Figure 45.2 whose exact shape depends on the details of the inherent inhibition kinetics. All of these curves pass through the origin because, with no liquid outflow ($D = 0$), any soluble, nonvolatile metabolic products must eventually accumulate to inhibitory levels.

45.4.2 Consequences for Process Design

Any pair of values of F and G define a regime in Figure 45.2 within which the bioreactor can operate. The most important result is that for any such pair of values there exists a value of D that maximizes the contaminant removal, x. If the form of the rate equation $q(S, S_m)$ were known, the pointed maximum seen in Figure 45.2 would be replaced by a smooth curve that defined this optimum design more accurately. In the absence of such detailed modeling the optimum must be found experimentally, the analysis providing a starting point and overall guidance. Because the gas flow rate, g, appears in the denominator of both F and G, the first step is to establish the maximum g for which the desired contaminant removal, x, falls safely within the operating regime. It is clear from equation 45.4 that a high removal rate (e.g., $x = 0.95$) with reasonable values of $S(\gg Hn_i)$ and $S_m(< 0.5\ S'_m)$ requires both $G \sim 3$ and $FD \sim 2$, and such values are reasonable, if approximate, general design goals. Much larger values represent inefficient design because they imply excessive consumption of energy and water.

For processes that produce large amounts of very inhibitory, nonvolatile, soluble metabolic products, the problem is to wash the products out of the bioreactor without washing out the biomass. Mathematically, $y_m/S'_m \to \infty$, making it difficult to keep $FD > 2$ without D exceeding the washout criterion. These are the processes that require cell retention ($z \to 0$), either by cell recycle or by immobilization as a biofilm. For processes with more moderate values of y_m/S'_m, the analysis shows that there exists an optimum set of values of the process variables g, f, and z. Some processes, the aerobic mineralization of hydrocarbons for example, generate only innocuous (H_2O) or gaseous (CO_2) products, so $y_m/S'_m \to 0$, and the analysis suggests operating with no liquid outflow. This not only gives the best effluent-gas quality (Fig. 45.2 with $F = \infty$) but, because the biomass is in a maintenance condition ($\mu = 0$ when $D = 0$), it also avoids the cost of adding nutrients, such as phosphates, that are needed for microbial growth (see "Nutrient Addition and Start-Up"). In practice there are reasons to avoid this condition. Even if y_m/S'_m is too small to be observed in short-term laboratory experiments, any nonvolatile product must eventually accumulate to inhibitory levels in a continuous bioreactor with no liquid outflow. Salts in the water added to compensate for evaporation or for pH control will also accumulate in the biophase. Also, it must not be forgotten that complete mixing of the biophase is an abstraction never achieved in practice and sometimes, as in the biofilter, not even attempted. The discussion prior to equation 45.2 shows that any bioreactor with $D = 0$ must have a cell growth rate $\mu = 0$ as an average, but it will contain microniches where cells are dying because conditions are worse than average, and others where conditions are slightly better and cells are growing. Although the growing cells may assimilate some of the material released by the lysis of the dying cells, there must be some long-term accumulation of dead biomass, with consequent reduction in bioreactor performance. Keeping D on the of order of 1, a very low flow rate in most cases can wash out the dead biomass and ensure stable operation for the cost of a few growth nutrients.

The analysis assumed the usual case in which the cell concentration in the bioreactor is kept as high as possible, with sufficient amounts of other nutrients provided to ensure that the contaminant is the limiting nutrient. The quantity X, defined under equation 45.4, is then the maximum possible viable-cell concentration in the biophase, corresponding to the situation where all of the contaminant flowing into the bioreactor, gn_i/RT, is being used to satisfy the cell maintenance requirement, ke_bX. The actual concentration at any given operating condition, S_x, can be calculated from the fourth term of the equation and is shown in Figure 45.2 as a function of D and x. There is, however, no guarantee that this concentration corresponds to a dilute, easily mixed cell suspension. If the maintenance requirement, k, is small, and the contaminant loading gn_i is large, it may be a paste of cells too dense to be, for example, pumped around a biotrickling filter. Although it is possible

to reduce S_x by restricting the amounts of growth nutrients provided, such artificial reductions in the microbial "catalyst" concentration are generally poor bioprocess design. The alternative is to choose the right type of bioreactor, recognizing that, although the mass of microorganisms in the bioreactor is fixed by the process requirements and the microbial metabolism, the amount of water is a process variable that can be controlled. The concentration, X, is an order of magnitude higher in a trickle-bed type bioreactor where $e_b \approx 0.1$, than in a bubble column where $e_b \approx 1$.

45.4.3 Nutrient Addition and Start-Up

In some processes, the aerobic mineralization of organics in beds of compost for example, the air provides the electron acceptor and the media provides what little growth nutrients are needed. In other processes these substances, and sometimes the electron donor, must be provided in the liquid inflow. The amounts can be estimated from the "stoichiometry" of metabolism, a procedure best illustrated by example. Ongcharit et al. (37) have shown that hydrogen sulfide can be removed from industrial gas streams by the acidophilic, autotrophic, sulfur-oxidizing, denitrifying bacterium *Thiobacillus denitrificans*. Even such esoteric metabolism can be approximated by a pseudo-chemical reaction in which all of the main nutrients and products are written in the ionic form in which they enter or leave the reactor. After performing all of the element and charge balances the result is

$$\begin{aligned} H_2S + (1.6 - 0.2y\gamma)NO_3^- + yCO_2 + ypH_2PO_4^- \\ \rightarrow\!\!\!\!\rightarrow\ yCH_hN_nO_oS_sP_p + (0.8 - 0.1y(\gamma + 5n))N_2 \\ + (1 + ys)SO_4^{2-} + (0.4 + y(0.2\gamma - p - 2s))H^+ \\ + wH_2O \end{aligned} \tag{45.5}$$

The first term on the right-hand side represents the dry weight of the biomass produced. $\gamma = 4 + h - 2o + 6s + 5p$ is a measure of its oxidation/reduction state and is remarkably consistent between species (36) (note that the base oxidation state for nitrogen here is N_2). The actual cell yield is y, the ratio of cells produced to H_2S consumed. For a completely mixed biophase this equals μ/q or, from equations 45.1 and 45.2,

$$y = \frac{DY}{(1 + D)} \tag{45.6}$$

The "stoichiometric coefficients" on the other components in equation 45.5 then provide the y_j values needed to calculate the concentrations of nutrients and products from the last term in equation 45.3. These simple calculations can provide a surprising amount of approximate information about process design and development. A feature of the example in equation 45.5 is the large amount of acid (H^+) produced by the metabolism. Even with the high liquid flow rate allowed by cell immobilization or recycle (29,37) its neutralization requires a high pH in the liquid inflow, so the biophase must be very well mixed if metabolism is not to be inhibited by pH gradients, suggesting some type of bubble-gasified bioreactor. If all of the NO_3^- and OH^- are provided by their sodium salts, then the salinity in the biophase would be high, suggesting a need for halophilic strains of bacteria. A reasonable alternative would be to explore the use of calcium salts, which would precipitate some of the product sulfate as gypsum, reducing inhibitory effects.

Like all the previous analyses, equation 45.6 applies only to steady-state operation. Gas treatment bioreactors, like any other bioprocess, are generally started with a relatively small inoculum of acclimated microorganisms, the objective of the start-up period being to increase the population to the steady-state value, S_x. This requires additional growth nutrients, and the initial feed concentration, S_{ji}, can be calculated as above, but with setting the observed cell yield, y, equal to the growth yield coefficient, Y. These concentrations can then be decreased slowly as steady state is approached. Start-up of biofilters is sometimes called ripening of the bed, and it is not always necessary to add growth nutrients, because the microorganisms capable of growth on the contaminant may obtain nutrients from the support material (compost, soil, etc.), or may grow at the expense of cells that die and lyse under conditions in the biofilter. If these sources are not sufficient to produce the biofilm thickness needed for maximum contaminant removal, some nutrient addition after steady-state contaminant removal has been reached will further improve performance. However, excessive nutrient addition must be avoided because modeling (38) suggests that, under contaminant limited conditions, a biofilm will grow much thicker than is needed. The inlet end of the biofilter may plug with useless biofilm.

Just because a steady state exists in theory, it does not follow that it can be reached by any start-up procedure. Of particular concern are those contaminants that are so concentrated (high n_i) and soluble (low H) that they will cause substrate inhibition of the microbial metabolism if their dissolved concentration in the biophase ever reaches equilibrium with the feed (n_i/H). The steady state analyzed above still exists, but $S \ll n_i/H$ only as a consequence of the metabolism of the large numbers of microorganisms present. Starting with a small inoculum, the dissolved concentration in the biophase will be much higher, metabolism will be inhibited, and the biomass may wash out. For similar reasons, batch experiments may produce the erroneous conclusion that the gas cannot be treated biologically. A proper start-up procedure may involve dilution of the feed gas and careful control of the dilution rate and nutrient

addition, until a dense, well-acclimated microbial culture has developed.

45.4.4 Gas-Biophase Mass Transfer

Figure 45.2 shows that high levels of contaminant removal require high values of the dimensionless mass-transfer factor, G, which is actually the product of two dimensionless numbers: H/RT, an inverse measure of the contaminant solubility, and k_1a/g, a measure of the efficiency with which the gas flow generates mass transfer. This is not usually a difficulty for biofilters with their thin biophase and very large a but how can it be achieved for other bioreactor types? Measurements of gas–liquid mass transfer factors (28) are often given as correlations of the form

$$k_1a = AU_g^c \tag{45.7}$$

The superficial gas velocity U_g is related to the flow rate g by $U_g = gL$, where L is the bioreactor height. Consider first an idealized bubble column, a hypothetical device in which all the bubbles are the same size, and doubling U_g simply doubles their number. The exponent c must then be 1, making $k_1a/g = AL$, a constant dependent upon scale but independent of gas-flow rate. In real bubble columns, with their imperfect bubble dispersion, c is closer to 0.7, but this still implies that G varies only slightly with g. The copious data available for oxygen transfer from air (28) shows that, at normal gas flows (g on the order of 1 VVM), k_1a/g is on the order of 1 at the laboratory scale, rising toward 10 in commercial-scale equipment. Assuming for the purposes of illustration that k_1 for a gas is proportional to its diffusivity in water raised to the 2/3 power (strictly valid only for relatively insoluble gases, for which most of the mass-transfer resistance is on the liquid side of the gas–biophase interface), this can be used to estimate G and the maximum possible fractional removal, $1 - e^{-G}$, (equation 45.4 with $S \to 0$) for contaminant gases of low, medium, and high solubility. The results shown in Table 45.1 suggest that bubble columns would be useless for insoluble contaminants like carbon monoxide, but worth consideration for moderately soluble contaminants like hydrogen sulfide. Most hydrocarbon vapors fall into the former category, but many alcohols and chlorinated aliphatic solvents are in the latter (30). For very soluble contaminants, such as sulfur dioxide, G tends to be unnecessarily large in bubble columns, and while acceptable removal with a moderate pressure drop could be achieved in very short, wide columns, this configuration has not been explored in practice.

The addition of a mechanical agitator can increase k_1a by roughly one order of magnitude, mainly by breaking up the gas flow into many small bubbles with a large interfacial area. Equation 45.7 still applies, but the A parameter becomes a function of the mechanical power input per unit reactor volume. Unfortunately, agitation also undermines the assumption that the gas moves though the reactor in plug flow. In a mechanically agitated tank, the gas bubbles are assumed to recirculate several times so that the gas phase is completely mixed; a sample of gas containing many bubbles taken from anywhere in the tank would have the same composition as the outlet gas. The effect on the driving force for mass transfer can be seen by comparing the concentration profiles shown in Figure 45.3a and b. Mathematically, the long-mean concentration difference used in equation 45.3 must be replaced by the more familiar effluent partial pressure driving force ($p/H - S$), which makes the maximum possible removal not $(1 - e^{-G})$, but $G/(1 + G)$. These two functions are virtually identical at small G, which explains why the exact definition of the driving force is not an issue for aeration (oxygen is an insoluble gas, $H/RT = 30$ at 20°C, and its small fractional removal from the air stream in conventional fermenters is unimportant). However, a goal of 95% contaminant removal now requires not $G > 3$, but $G > 19$, which gives some idea of the lower effectiveness of a completely mixed gas phase. The numbers in Table 45.1 show that this lower effectiveness cancels out the increased k_1a leading to conclusions similar to those for bubble columns. The extra expense of mechanical agitation is rarely justified in gas treatment bioreactors, although reactors designed for a high k_1a/g with large aspect (height:diameter) ratios and multiple impellers to prevent bubble coalescence (29) have been proposed for removing hydrogen sulfide. Stirred tanks have been used successfully (39) for the microbial production of ethanol and acetic acid from carbon monoxide and hydrogen (another insoluble gas; $H/RT = 51$ at 20°C), but the objective there was high volumetric productivity, rather

TABLE 45.1. Performance of Bioreactors for which $k_1a/g = 1 - 10$ for O_2

			Maximum possible removal	
Contaminant gas	H/RT at 20°C	G	Mixed gas phase $G/(1 + G)$	Plug flow gas $1 - \exp(-G)$
CO	37	0.023–0.23	0.022–0.19	0.023–0.20
H_2S	0.41	1.8–18	0.65–0.95	0.84–1
SO_2	0.0088	88–880	0.99–0.999	1

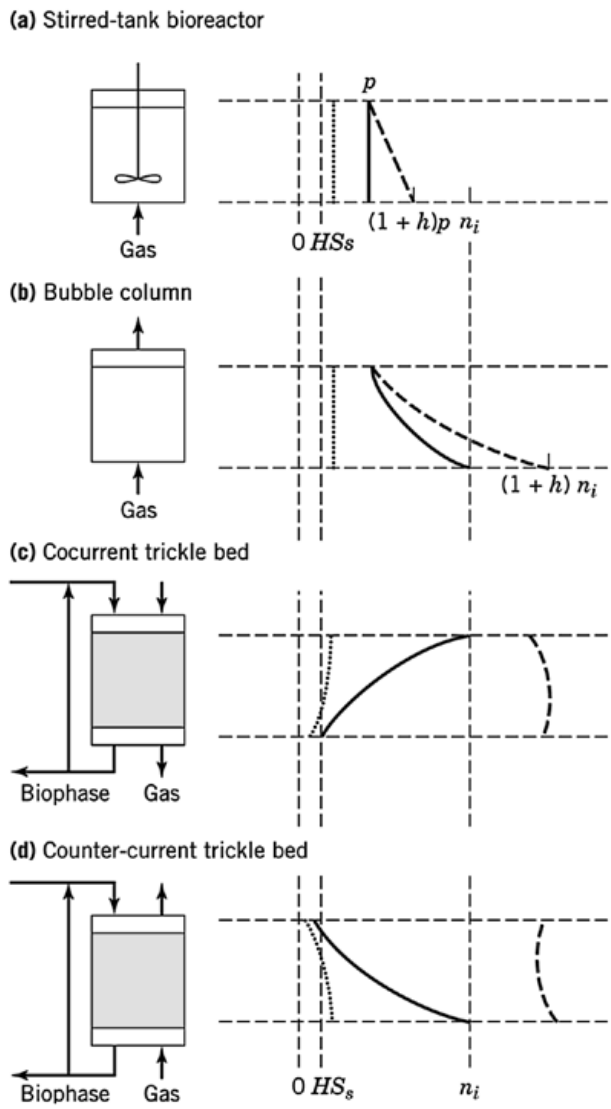


Figure 45.3. Concentration Profiles in Different Bioreactors. (**a**), (**b**) Partial pressure in gas phase, dot-dash line (**c**), (**d**) Viable biomass concentration, dot-dash line. Dotted line, partial pressure in biophase $= HS$; solid line, mole fraction in gas phase.

than complete gas consumption. Several tanks were used in series, and they were pressurized to several atmospheres to improve gas transfer.

In contrast to bubble-gasified reactors, the gas–biophase interfacial area in biotrickling filters is almost constant, fixed by the choice of packing media and only slightly influenced by U_g and the superficial velocity at which the liquid is pumped over the bed U_1. This makes it possible to achieve the necessary value of G for contaminants of almost any solubility by appropriate choice of the packing media and the gas flow per unit volume, g. Many types of packing are available and the best choice in a particular situation is a complex trade-off between the following considerations:

- Less soluble contaminants will need the large a provided by smaller media and the small g implied by the lower permeability of such media to gas flow. For these contaminants, most of the gas–biophase mass-transfer resistance is on the biophase side of the interface, so in correlations of the form of equation 45.7, $c \to 0$, but A is a fairly strong function of U_1.
- More soluble contaminants can achieve the same G with the smaller a and larger g given by larger media. In this case most of the mass-transfer resistance is on the gas side of the interface, so $c \rangle 0$ and A is less dependent on U_1.
- The conservation of mass shows that the change in concentration of a nonvolatile metabolic product in the biophase as it moves down the bed is $U_g x n_i y_m / U_1 RT$. If this number is small then the biophase approximates complete mixing. If it is large, then the concentration gradients, including that of pH, may be large enough to inhibit metabolism.
- Although a high liquid flow improves mixing and mass transfer, there is a definite upper limit of U_1 at which the bed floods. This limit is predictable (28) and is much smaller for small media.
- It is difficult to generalize about the attachment of the microorganisms to the media because this depends on both the nature of the media and the type of biomass involved. However, it is clear that a bed of small media with attached biomass may quickly become plugged if the contaminant is sufficiently concentrated and the biofilm is allowed to grow. It is reasonable to suppose that the larger the media and the higher the liquid velocity, the more cells will be suspended in the liquid rather than being attached. The z parameter in Figure 45.1 will be correspondingly larger.
- A biophase containing suspended and attached biomass may, if too thick or too dense, have its own mass-transfer resistance (38). While such resistance is usually to be avoided, it may be beneficial. For example, in trying to separate one electron acceptor, NO_x, from stack gases that contain another, O_2, which is preferred by the microorganisms, it should be possible to take advantage of the much higher solubility of the NO_x to create locally anaerobic environments in the biophase.

Somewhere among all of these considerations is a best choice of media for any situation. For dilute, less-soluble contaminants whose metabolism does not produce any nonvolatile metabolic products, the biotrickling filter will

look more like a biofilter, with small media, little liquid flow, and attached biomass. For more soluble contaminants which do generate such products, it will tend toward the other extreme of high liquid flows and a completely mixed biophase. If there seems to be no sensible solution, the answer may be to adopt a bioscrubber. Although more expensive, it greatly simplifies the design problem by separating gas–liquid mass transfer from the microbiological considerations. It is certainly preferable to think in terms of this continuum of possibilities and to choose the one best suited to a particular application, rather than considering the different types of gas treatment bioreactors as completely separate technologies, each of which can be forced to fit any job.

45.4.5 Biophase Mixing and the Minimum Effluent Concentration

The single bioreactors with a completely mixed biophase analyzed here have an obvious drawback: all of the microorganisms are exposed to the same physicochemical environment, it is the worst possible environment for metabolism, with the lowest nutrient concentrations and the highest concentrations of metabolic products. One consequence appears in Figure 45.2. Even with no mass transfer resistance ($G = \infty$), no product inhibition ($F = \infty$), and no wastage of biomass ($D = 0$), the analysis suggests that complete contaminant removal is still impossible. With no biomass outflow there is no net cell growth, and all of the contaminant is used for maintenance metabolism (equation 45.2 with $\mu = D = 0$ gives $q = k$). Under these conditions, the dissolved contaminant concentration is not zero, but the stationary phase concentration, S_s, so the partial pressure in the effluent gas cannot be less than HS_s, and the fractional removal, x, can never exceed $(1 - HS_s/n_i)$, even with perfect mass transfer (equation 45.4 with $G = \infty$). This maximum removal also exists for completely mixed biological wastewater treatment systems, but in that case it does not matter because S_s is much less than common effluent standards. It may matter for some insoluble gas-phase contaminants because the corresponding minimum-achievable partial pressure, HS_s, may be significant, even when S_s is small. Bioreactors with a completely mixed biophase are a poor choice for such contaminants.

The simplest improvement would be two bioreactors through which the gas flows in series and between which the microbial culture is continuously recirculated. Reactor 1 would have a relatively high effluent partial pressure and dissolved contaminant concentration, providing a good environment for metabolism and cell growth. If the process variables are fixed correctly (a complete analysis is beyond the scope of this chapter) reactor 2 could run with a dissolved concentration $S < S_s$. The biomass in reactor 2 would then be in an endogenous state, but this would no longer matter because fresh, viable cells would be continuously supplied from reactor 1, and the dying cells would either flow back there to recover or be lost in the liquid effluent. The liquid inflow would go to reactor 1, where the growth nutrients are needed, and where it would dilute the concentrations of any metabolic products.

The more bioreactors in series, the better the average physicochemical environment for metabolism. Columns containing many sieve trays or bubble-cap trays have long been used for gas–liquid contacting in the chemical process industry and should be considered for the biological treatment of gases in cases where the biomass grows best in suspension and the contaminant is relatively dilute, insoluble, and a poor microbial substrate (i.e., HS_s/n_i is large). These columns are inherently countercurrent contacting devices with the gas flowing upward while the microbial culture falls down from tray to tray. An individual microorganism experiences a series of environments with ever-increasing dissolved contaminant concentration, S, until it is suddenly pumped back to the top tray where conditions are endogenous ($S < S_s$), but where it can continue metabolizing contaminant and survive long enough to start through the cycle again. Nutrient addition and pH control can be done on each tray as needed, and the liquid effluent can be taken from near the top of the column where cell viability is lowest.

A similar effect, with the gas closer to the theoretical optimum of plug flow, can be achieved in an upflow biotrickling filter with a small liquid recycle ratio. The only drawbacks are that pH control and nutrient addition can now only be done at the top of the bed, and the liquid can only be removed from the bottom, which is not necessarily the best arrangement. If all the microbial cells are suspended, the concentration profiles of viable biomass and contaminant will be as shown in Figure 45.3d. In real trickle beds some of the biomass remains attached, which is a great advantage over tray columns when a nonvolatile metabolic product is generated, because it allows a large liquid outflow to remove the product without the danger of washing out the biomass. (Mathematically, D is small because z is small, even though f is large.) Biotrickling filters can also be operated in the gas-downflow, cocurrent mode, which gives concentration profiles (again assuming suspended biomass) more like those shown in Figure 45.3c. Now, the microorganisms moving down the bed experience an ever-worsening environment for metabolism, with lower S and higher product concentration S_m. They leave the bottom of the bed in an endogenous, low-viability state, which is very suitable for the liquid outflow stream, but which may cause a significant lag phase when cells are recycled to the better environment at the top of the bed. The question of whether the cocurrent mode works better can only

be answered definitively by experiments on a particular gas stream.

In biofilters the biophase is far from being completely mixed. It consists of an immobilized mass of up to xXe_b viable cells per unit bioreactor volume (less if cell growth has been limited by some nutrient other than the contaminant), and one of the goals of media selection is to provide sufficient surface area so that these cells can be distributed as a biofilm thin enough to avoid mass transfer limitation due to diffusion through the film. However, simple models (38) suggest that biofilters should share the minimum effluent partial pressure, HS_s, predicted earlier for bioreactors with a completely mixed biophase, because biofilms exposed to any lower partial pressures near the biofilter effluent would be in an endogenous state and eventually die. Experience suggests otherwise, probably because the adsorption of the contaminants on the media increases their effective concentration in the microorganisms' immediate environment. It follows that highly adsorptive support particles, such as compost or activated carbon, will work best, and that biofilters can treat very insoluble, hydrophobic contaminants if they adsorb well.

45.4.6 Scale-Up

First-stage scale-up experiments can be done in a reactor of any size that is convenient or available, as long as it is large enough so that the flows of gas and liquid are not significantly altered by entrance effects, channeling, or wall effects. Ideally, several different bioreactor types or packing materials are studied, but this is not always possible. The objective is to vary the gas flow, g, the liquid flow, f, nutrient addition, S_{ji}, and so on, to determine how the specified contaminant removal can be achieved most economically. The scale-up problem is then to extrapolate the results in order to calculate the necessary volume (volume = gas flow to be treated/g) and shape (specifically the height, L) of the commercial-scale bioreactor, which must satisfy the process requirements without further experimentation immediately after start up. The best combination of process variables found in the experiments must be close to the optimum identified by the point at the right end of the operating region in Figure 45.2. To preserve this solution at the commercial scale, the dimensionless numbers D, F, and G that define this point must be kept the same between scales. Scaling up a gas treatment bioreactor is thus an example of Reynold's similarity principle, which states that two physical situations are similar only if the all of the relevant dimensionless numbers are identical.

Consider first the case where there is no inhibitory metabolic product and the process needs little or no liquid outflow. $F(\rightarrow \infty)$ and $D(\rightarrow 0)$ both drop from the list of relevant dimensionless numbers, and the scale-up problem reduces to finding combinations of gas flow, g, and bioreactor height, L, that keep G constant between scales. Given a mass-transfer correlation of the form of equation 45.7, G can be written $ARTL^c/Hg^{(1-c)}$. The problem is illustrated graphically in Figure 45.4, where lines of constant G are drawn on a log–log plot of g versus L. If the small-scale experiments have found different combinations of g and L that produce the specified contaminant removal, x, then this data should fall on such a line, labeled *empirical* in Figure 45.4, because the theory suggests that "constant x" implies "constant G." Also shown in Figure 45.4 is an upper limit on the gas superficial velocity, $U_g = gL$, caused by physical phenomena such as slugging of bubble columns, fluidization of the media in upflow biofilters, or flooding of the impeller in stirred tanks. This limit may be slightly different at different scales. Two extreme cases of the scale-up problem can be identified.

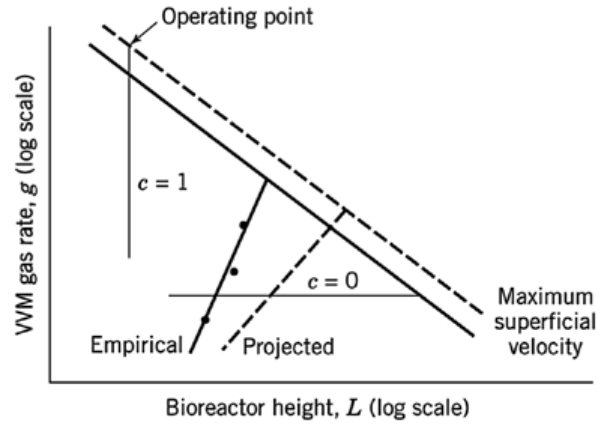


Figure 45.4. Dotted line, large scale; solid line, small scale.

For a biofilter or a biotrickling filter treating sparingly soluble contaminants, the mass-transfer factor is little affected by the gas velocity, implying that $c = 0$ and making the empirical line horizontal. Several important phenomena are lumped into the parameter A, but there is no reason to expect them to vary with scale because microorganisms cannot "know" if they are in a small or large bioreactor. Consequently, performance on the large scale is defined by the same horizontal line, meaning that scale-up is done at constant g, or equivalently at constant gas-residence time ($= 1/g$). Because $g = U_g/L$, constant g can be achieved either with a deep bed and a high gas velocity, the right end of the $c = 0$ line in Figure 45.4, or with a shallow bed and a low velocity, the left end of the line. Although the former are easier and cheaper to build, they have a much higher pressure drop though the bed, meaning higher costs for gas compression and possibly subsequent cooling to return the gas to a temperature tolerable to the microorganisms. The latter are much cheaper to operate and work well as long as the beds are deep

enough (at least several hundred times the particle size) to avoid problems of channeling and short-circuiting of the gas flow. Many biofilters consist of shallow beds of media on trays arranged in various configurations in a reactor designed to ensure an even flow of gas into the beds.

At the other extreme is the ideal bubble column described in the section "Gas Biophase Mass Transfer" for which $c = 1$. The value of G, and thus the contaminant removal, is now independent of gas flow but proportional to bioreactor height. Scale-up must therefore be done by keeping L constant but increasing the reactor width, the large-scale bioreactor operating at maximum g in order to minimize its volume (the *operating point* in Figure 45.4). Although this ideal bubble column is an abstraction, it illustrates a paradox that can arise in scaling up practical bubble columns (for which $c \cong 0.7$); if the desired removal can be achieved in a small-scale column, then a bubble column is probably not the best solution at the commercial scale. For very soluble contaminants, the L needed to obtain the desired fractional removal may be in the range of laboratory reactors, around 1 m. Scale-up would produce a very unusually shaped large-scale bioreactor, a similar height but several meters wide. There would be no point in making it any deeper, except to provide a safety factor in the design, and it could not be made any narrower and still meet the process requirements. For insoluble contaminants the necessary L may be several meters. The conclusion from laboratory experiments would then be that a bubble column is not a feasible bioreactor, even though the desired contaminant removal may be achievable (albeit with a high pressure drop) with the reactor heights used at the commercial scale.

All practical situations fall between these two extremes, so neither simple scale-up rule, constant g or constant L, is necessarily appropriate. The empirical line will have a positive slope, and a similar line for the same G at the larger scale can be projected from it if any variations of the parameters A and c with scale can be estimated from the published literature, experience, consultations with equipment manufacturers, and so on. The design of the large-scale bioreactor can be anywhere along this projected line in Figure 45.4, the exact design point again being constrained by the maximum U_g line, but essentially an economic trade-off between the large bioreactors demanded by a small g and the large pressure drops associated with a large L. The essential point is that the shape, and the size of the large-scale bioreactor are fixed by this procedure and should not be chosen based simply on guesswork or convenience.

Some bioreactor types allow design flexibility because they have variables that can be adjusted when drawing the projected line. Both A and c tend to decrease with scale in any bubble-gasified reactor due to poorer gas dispersion, but in mechanically agitated tanks, A is a function of the power input per unit volume, which can be varied to some extent. For trickle beds and biofilters, both A and the bed permeability are predictably related to packing size, allowing the packing to be chosen to give the large-scale reactor both a convenient shape and a reasonable pressure drop. Note that, whether or not such changes are made between scales, the estimates on which the projected line in Figure 45.4 is based should always be conservative in order to provide a factor of safety in the large-scale design.

When product inhibition is significant, the liquid outflow, f, becomes a critical variable, and all three dimensionless numbers D, F, and G must be kept constant if the physicochemical environment of the biomass (S, S_m) and the optimum bioreactor performance established in the small-scale experiments are to be extrapolated to the large scale. An exact solution is possible only when the retention of the biomass by cell immobilization or recycle (the z parameter) can be controlled, although when retention is almost complete ($z \to 0$) only the product DF (from which z cancels) is important, implying that the liquid flow, f, must be kept proportional to the gas flow, g. Biotrickling filters have an extra dimensionless number, the liquid recycle ratio, RR, which introduces the extra difficulty that increasing the bed height, while keeping f and RR constant increases the liquid superficial velocity [$U_l = Lf(1 + RR)$], thus changing the mass-transfer situation and possibly flooding the bed. The procedure just described will not work in these more complex situations (constant x no longer implies constant G), but the general considerations still apply, including the physical limits on the gas superficial velocity, the desirability of tall small-scale bioreactors to reduce uncertainties, the need for compromise between capital and energy costs, and the possibility of predicting a very inconvenient aspect ratio for the large-scale bioreactor. Judgment and calculation are needed in each case because the trivial solution to the scale-up problem—"build a bigger bioreactor with the same shape, f, and g as the small one"—is unlikely to be the best. Gas treatment bioreactors are one of the few devices whose performance tends to improve with scale, but taking advantage of this tendency in practice is not straightforward.

NOMENCLATURE

a	Gas–biophase interfacial area per unit bioreactor volume
A, c	Constants in mass-transfer correlation
D	$zf/e_b Yk$ = dimensionless liquid flow rate
e	Hold-up
f	Liquid outflow rate per unit bioreactor volume
F	$YS'_m/zy_m X$ = dimensionless product-inhibition number
g	Volumetric gas outflow rate per unit bioreactor volume (the VVM gas rate)

G	k_1aRT/Hg = dimensionless mass-transfer-effectiveness number
h	Gauge pressure (atm) at gas inlet
H	Henry's law constant
k	Cell maintenance coefficient
k_1	Gas-to-biophase mass-transfer coefficient
L	Bioreactor height
n_i	Mole fraction of contaminant in feed gas
p	Partial pressure (atm) of contaminant in effluent
q	Specific consumption rate of contaminant
R	Gas constant
S	Dissolved concentration in biophase
S_s	Stationary phase contaminant concentration (concentration at which $\mu = 0$)
S'_m	Product concentration that totally inhibits metabolism
T	Outlet gas temperature
U_g	Superficial gas velocity at bioreactor outlet
U_1	Superficial liquid velocity in a trickle bed
X	gn_i/ke_bRT = maximum possible cell concentration in biophase
x	$1 - p/n_i$ = fractional removal of contaminant
w	Evaporation rate per unit bioreactor volume
y	Mole of nutrient consumed or product formed per unit of contaminant metabolized
Y	Cell-yield coefficient
z	Cell concentration in liquid effluent/cell concentration in biophase
γ	Available electrons per carbon equivalent of biomass
μ	Specific growth rate of biomass

Subscripts

i	Inlet conditions
j	Any nutrient or product
m	Metabolic product
x	Biomass

REFERENCES

1. G. Leson and A.M. Winer, J. Air & Waste Management Assoc. 41: 1045–1053 (1991).
2. D.S. Hodge, V.F. Medina, R.L. Islander, and J.S. Devinny, Environ Technol. 12: 655–662 (1991).
3. W.A. Apel, W.D. Kant, F.S. Colwell, B. Singleton, B.D. Lee, G.F. Andrews, A.M. Espinosa, and E.G. Johnson, Emerging Technologies in Hazardous Waste Management IV, American Chemical Society, Washington, D.C., 1994, pp. 142–159.
4. S. Dharmavaram, J. Casey, and C. van Lith, Proc. Air Waste Management Association, 93-WP-52C.01, Denver, Colo., June 13–18, 1993.
5. I. Togashi, M. Suzuki, M. Hirai, M. Shoda, and H. Kubota, J. Ferment. Technol., 64: 425–432 (1986).
6. W.A. Apel, P.R. Dugan, M.R. Wiebe, E.G. Johnson, J.H. Wolfram, and R.D. Rogers, Emerging Technologies in Hazardous Waste Management, vol. 3, American Chemical Society, Washington, D.C., 1993, pp. 411–428.
7. W.A. Apel, B.D. Lee, M.R. Walton, L.L. Cook, and K.B. Dinerstein, Proceedings of the Air & Waste Management Association, 95-TP9C.07, San Antonio, Tex., June 18–23, 1995.
8. P. Plumb, K.H. Lee, and K.L. Sublette, Appl. Biochem. Biotechnol. 24/25: 785–797 (1990).
9. J. Croonenberghs, F. Varani, and P. Le Fevre, Proceedings of the Air & Waste Management Association, 94-RP115B.06., Cincinnati, Ohio, June 19–24, 1994.
10. Y. Yang, A.P. Tongas, and J.R. Blunk, Proceedings of the Air & Waste Management Association, 94-RA115A.04., 1994.
11. R. Whittenbury, K.C. Phillips, and J.E. Wilkinson, J. Gen. Microbiol. 61: 205–218 (1970).
12. C.L. Haber, L.N. Allen, S. Zhao, and R.S. Hanson, Science. 221: 1147–1153 (1983).
13. J. Pilkington, and H. Dalton, Methods in Enzymology, vol. 88, Academic, New York, 1990, pp. 4181–190.
14. J. Colby, D.I. Stirling, and H. Dalton, Biochem. J. 165: 395–402 (1977).
15. D. Scott, J. Brannan, and I. Higgins, J. Gen. Microbiol. 125: 63–72 (1981).
16. Stanley, S. Prior, D.J. Leak, and H. Dalton, Biotechnol. Lett. 5: 487–492 (1983).
17. R. Oldenhuis, R.L.J.M. Vink, D.B. Janssen, and B. Witholt, Appl. Environ. Microbiol. 55: 2819–2826 (1989).
18. V. Hecht, D. Brebbermann, P. Bremer, and W.D. Deckwer, Biotechnol. Bioeng. 47: 461–469 (1995).
19. B.R. Folsom, P.J. Chapman, and P.H. Pritchard, Appl. Environ. Microbiol. 56: 1279–1285 (1990).
20. D. Arciero, T. Vannelli, M. Logan, and A.B. Hooper, Biochem. Biophys. Res. Commun. 159: 640–643 (1989).
21. L.P. Wackett, G.A. Brusseau, S.R. Householder, and R.S. Hansen, Appl. Environ. Microbiol. 55: 2960–2964 (1989).
22. M. Kastner, Appl. Environ. Microbiol. 57: 2039–2046 (1991).
23. J.N. Petersen, R.S. Skeen, K.M. Amos, and B.S. Hooker, Biotechnol. Bioeng. 43: 521–528 (1994).
24. J.M. Barnes, W.A. Apel, and K.B. Barrett, J. Hazard. Mat. 41: 315–326 (1995).
25. W.A. Apel, J.M. Barnes, and K.B. Barrett. Proceedings of the Air & Waste Management Association, San Antonio, Tex., June 18–23, 1995.
26. H.L. Bohn, J. Air Pollut. Control Assoc. 25: 953–95 (1975).
27. M. Shields, M. Reagin, R. Gerger, C. Somerville, R. Schaubhaut, R. Campbell, and J. Hu-Primmer, in R.E. Hinchee, A. Leeson, L. Senprini, and S.K. Ong, eds., Bioremediation of Chlorinated and Polycyclic Aromatic Compounds, Lewis, Ann Arbor Mich. 1994, pp. 50–65.
28. R.H. Perry and C.H. Chilton, Chemical Engineers Handbook, 6th ed., McGraw Hill, New York, 1988.
29. H.M. Lizama and E.N. Kaufmann, in D.S. Holmes and R.W. Smith eds., Minerals Bioprocessing II, TMS, Warrendale, Penn, 1995, pp. 241–253.
30. B.D. Ensley, Dept. of Energy Report DOE/CH-9207, 1992.
31. Z. Shareefden and B.C. Baltzis, Chem. Eng. Sci. 49: 4347–4360 (1994).

32. R.M. Diks and S.P. Ottengraf, Bioprocess Eng. 6: 93–99 (1991).
33. S. Lamare and M. Legoy, Trends in Biotechnology 11: 413–419 (1993).
34. R.M. Counce and J.J. Perona, in N. Cheremisenoff ed., Handbook of Heat and Mass Transfer, vol. 2, Gulf, Houston, Tex., 1986, pp. 953–966.
35. Y.N. Lee and S.E. Schwartz, J. Phys. Chem. 85: 840–848 (1981).
36. G.F. Andrews, Appl. Biochem. Biotechnol. 51/52: 329–338 (1994).
37. C. Oncharit, Y.T. Shah, and K.L. Sublette. Chem. Eng. Sci. 45: 2383–2389 (1990).
38. G.F. Andrews and K.S. Noah, Biotechnol. Prog. 11: 498–509 (1995).
39. K.T. Klasson, M.D. Ackerson, E.C. Classen, and J.L. Gaddy, Fuel 72: 1673–1678 (1993).

46

BIOREACTORS, PERFUSION

Wei Wen Su
Department of Molecular Biosciences and Bioengineering, University of Hawaii, Honolulu, Hawaii

46.1 INTRODUCTION

Mass cultures of higher eukaryotic cells derived from mammalian, insect, and plant systems represent important sources of high value therapeutic products. While mammalian cell culture has progressed to a state that allows reliable process development and operation at large scales, the use of mammalian cell expression system remains very costly compared with some alternative expression systems such as insect and plant cell cultures (1). These latter systems are not as widely used in the industrial settings, but do offer certain merits and have continued to attract interest as alternatives to mammalian cell culture (1–3). Advocates for insect cell cultures point to advantages such as ease of culture, higher tolerance to osmolarity and by-product concentration, and higher expression levels when infected with a recombinant baculovirus (3). As for plant cells, they are easier and less expensive to culture compared to their mammalian counterparts, requiring only simple, chemically defined media (4). For now, mammalian cell culture remains the production system of choice in the biotechnology and pharmaceutical industries for large-scale production of complex recombinant proteins, monoclonal antibodies, recombinant viral vectors, and vaccines (1,5). This is due, in part, to the fact that mammalian cell expression systems produce proteins with *N*-glycans similar to those in human proteins (1). A survey of biological products (protein drugs, vaccines, and cells) approved by the US Food and Drug Administration (FDA) from 1996 to 2000 indicated that 21 approved therapeutic and diagnostic biological products were produced by mammalian cell cultures (5). As shown in a more recent survey, over 20 new therapeutic biological products had been approved by FDA between mid 2000 till early 2004, with over 60% being produced using mammalian cell cultures (6). This trend of mammalian cell culture dominance on producing therapeutic biological products continues as evidenced in the latest information on biological license approvals (BLAs) issued by FDA (Center for Drug Evaluation & Research; visit Drugs@FDA).

Various systems have been used to culture higher eukaryotic cells in bioreactors. These include free cell suspension, suspension of immobilized or entrapped cells, as well as immobilized cell culture in packed bed or hollow fiber reactors. Among these systems, free cell suspension culture is most amenable to large-scale operation. Suspension cultures, as opposed to immobilized cultures, provide a more homogeneous culture environment that is easier to operate, monitor, and control. Although growth of most mammalian cells requires surface attachment, for example via growth on microcarriers, hollow fibers, or beads, some can grow or be adapted to grow as suspension without surface attachment. Hydrodynamic shear problem associated with free suspension of mammalian cells can be minimized by appropriate design of agitation and aeration systems in the bioreactor, and by including protective polymeric additives such as Pluronic F68 in the media (5). Surveys of FDA BLAs indicated that the biotech industry has converged on using suspension culture of mammalian cells in large-scale stirred-tank bioreactors for producing therapeutic biological products (5,6). Currently, three suspension cell lines have been most widely used. They are suspension-adapted Chinese hamster ovary

Upstream Industrial Biotechnology: Equipment, Process Design, Sensing, Control, and cGMP Operations, Volume 2, First Edition. Edited by Michael C. Flickinger.
© 2013 John Wiley & Sons, Inc. Published 2013 by John Wiley & Sons, Inc.

(CHO) cells, and murine myeloma lines SP2/0 and NS0 (5).

Suspension culture can be operated in a batch, fed-batch, semi-continuous (repeated batch), continuous, or perfusion mode, or even a hybrid fed-batch/perfusion mode (7). In general, a relatively simple process with low up-front investment requirement that is readily scalable and capable of providing high and stable volumetric productivity with low nutrient input is preferred. In addition, the operating strategy is selected based on the kinetic pattern of product formation and the way the product is translocated following its synthesis (i.e. whether the product is excreted into the medium or retained in the cell). It is most common to relate the pattern of product synthesis to cell growth. That is, product synthesis is frequently characterized as growth associated or non-growth associated.

Industrial mammalian cell culture processes for production of recombinant proteins and monoclonal antibodies are currently dominated by fed-batch and perfusion processes (8,9). In fed-batch processes, concentrated nutrient solution is supplied to the culture via an appropriate, typically computer-controlled feeding strategy. Perfusion culture entails a continuous or semi-continuous flow of a nutrient solution through a cell population while the cells are retained in bioreactor (Fig. 46.1). Oftentimes, a cell bleed stream is implemented in perfusion cultures. Fed-batch processes are popular since they are relatively simple and flexible, with reduced quantities of product at risk because it is limited to a single batch if a process failure occurs, and they oftentimes yield much higher product titers than their batch-culture counterparts. On the other hand, perfusion culture offers the following advantages over batch and fed-batch cultures:

1. Longer operation with reduced plant downtime
2. Reduced unproductive growth phase as a proportion of the total process time
3. Potentially more consistent product quality as a result of constant nutrient supply and removal of toxic extracellular metabolic byproducts
4. Requiring a smaller bioreactor [and lower up-front start-up cost (10)]
5. Higher cell density and productivity
6. Reduced product residence time (via product recovery and hence reduced product degradation).

As a result of the above advantages, under optimal operating conditions, perfusion culture generally gives similar or higher productivity compared with fed-batch operations (11,12). According to Kompala and Ozturk (9), at least eight marketed pharmaceutical products have been produced using perfusion mammalian cell culture systems. A notable disadvantage of perfusion culture, however, is its added complexity from incorporating a cell-retention device. For long-term perfusion cultivation, a major concern is the steady-state instability and process variability. To this end, it is also important to determine the long-term genetic stability of the cells employed in such a process.

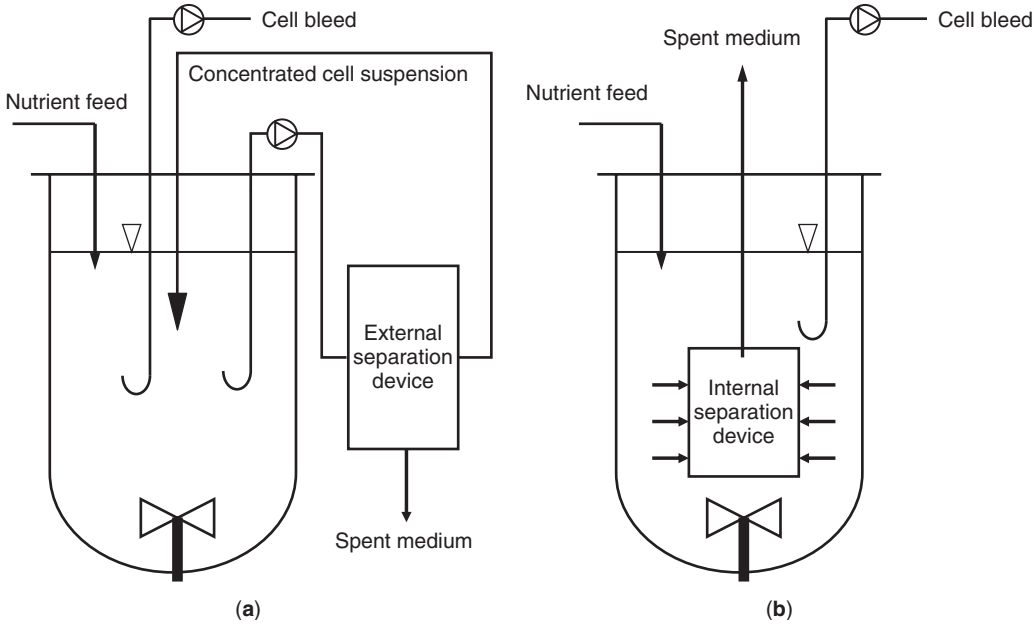


Figure 46.1. In a perfusion bioreactor a cell-retention device installed external (a) or internal (b) to the bioreactor is used to retain the cells within the bioreactor while allowing exchange of the culture medium. Sometimes, a cell bleed stream is used to stabilize the culture.

Since culture perfusion typically leads to high cell densities, oxygen transfer often becomes a limiting factor and introduces additional constraints on the process. Lim *et al*. used a computer-aided decision-support tool to compare the cost effectiveness of large-scale production of monoclonal antibodies by fed-batch and perfusion culture modes (10). In that study, Monte Carlo simulation technique was used to account for uncertainties in titer and yield, as well as the risks of contamination and malfunctioning of the perfusion device so as to imitate the randomness inherent in biopharmaceutical manufacture. The study by Lim *et al*. stressed the importance of minimizing probabilities of contamination and malfunctioning of the cell-retention device to achieve the high productivity promised by the perfusion option.

Generally, the most suitable type of products to be produced using perfusion bioreactors is the non-growth-associated, secreted products. In this case, the reactor is operated at a high cell density without rapid cell division for a long period. The product can be continuously harvested from the spent medium. For growth-associated, secreted products, a cell bleed stream may be incorporated in the perfusion operation. A high perfusion rate with the bleed stream adjusted to give a high specific cell growth rate could be used to increase the product output. For growth-associated, intracellular products, a culture strategy that gives a high biomass output rate with high product content is most desirable. Perfusion culture with a bleed stream may be considered for the production of this type of products. In this case, a much higher cell density can be obtained in perfusion cultures compared to continuous or semi-continuous cultures, because cells are retained within the reactor via a cell-retention device. By incorporating a bleed stream, the perfusion reactor can in principle be operated under a steady state at a very high cell concentration. For a culture system that follows simple Monod kinetics, the maximum biomass output rate in a perfusion reactor with a bleed stream is higher than that in a chemostat by a factor of $1/\zeta$, where ζ is the bleed ratio (the ratio between flow rates of the bleed stream and the feed stream) (13).

In this chapter, perfusion bioreactor development is reviewed, with emphasis on the design of the cell-retention system. In a perfusion culture, a means for cell–medium separation, or a cell-retention device, needs to be incorporated into the perfusion bioreactor (Fig. 46.1). Practical cell–medium separation in large-scale perfusion bioreactors is most commonly achieved on the basis of cell size or a combination of size and density differences between the cells and surrounding media, whereas other properties such as cell electrical charges, surface properties, and dielectric properties may be considered in small-scale operations (14). Thus far, two major classes of techniques have been employed to separate cells from the medium in perfusion reactors, namely, filtration and gravitational or centrifugal sedimentation. A summary of cell-retention systems used in perfusion bioreactors is summarized in Table 46.1. In this review, emphasis is placed on those systems that have been identified as capable of operating at a scale greater than 250 L per day [Table 46.1; (14)]. A more detailed discussion on other retention systems can be found in several extensive reviews published within the last decade (9,12,14–16).

46.2 CELL RETENTION BASED ON FILTRATION

Cell retention by filtration is based mainly on the size difference between the cell particles and the pore opening of the filter. It is also affected by a number of additional factors. These include cell morphology, cell concentration, viscosity of the cell suspension culture, and compositions of the spent media (e.g. presence of cell debris and bio-macromolecules such as nucleic acids, proteins, and polysaccharides that might clog the filter). As far as the filter is concerned, size of pore opening and porosity, filter/membrane material, filter geometric properties and configuration, and hydrodynamics in the filter systems are of primary importance. Since a physical barrier is used to retain the cells in the perfusion bioreactor, a major consideration in using filtration for cell retention is to minimize filter/membrane fouling. As summarized in Table 46.1, several notable culture perfusion systems are based on filtration. These include spin filters, membrane stirrers, circulating cross-flow filters with hollow fiber, plate-and-frame, or spiral-wound modules, controlled shear filtration, vortex flow filtration (VFF), and alternating tangential flow (ATF) filters. Some of these devices can be used externally or internally, and involve stationary or moving filters/membranes. It is easier to retrofit an existing reactor with an external separator than with an internal separation device. The major drawback of external separators, however, involves potential problems associated with prolonged continuous circulation of the culture suspension through an external loop that may cause shear damage or oxygen deprivation. To alleviate oxygen deprivation, the external separators are commonly operated under reduced temperature so as to slow the metabolism of the cells while outside the bioreactor. Among filtration-based perfusion systems, spin filter and the ATF systems have been considered most attractive for large-scale operations to produce perfusion rates in the range of 250–1000 L per day (14). Spin filter has been scaled up to produce a perfusion rate of 500 L per day (36); although the manufacturer of the ATF filters claims a scale-up capacity up to 1200 L per day (37), data in refereed literature to confirm this claim are not yet available. The following discussion focuses on these two systems; information for other filtration-based

TABLE 46.1. Cell-Retention Systems for Perfusion Bioreactors

	Schematics	Perfusion Rate > 250 L/d[a]	Representative References
Filtration			
Spin filter	Figure 46.2	Yes	17,18
Hollow-fiber membrane stirrer	—	No	19,20
Vortex flow filtration	Figure 46.4	No	21–23
Recirculating cross-flow filter (using hollow fiber, plate-and-frame, or spiral-wound modules)	Figure 46.5a	No	14
Alternating tangential flow (ATF) filter	Figure 46.5b	Yes	24,25
Controlled shear filtration	—	No	26
Sedimentation			
Vertical settler	Figure 46.7	No	27
Inclined/lamella settler	Figure 46.8	Yes	28,29
Acoustic resonator	Figure 46.9	Yes	30,31
External centrifuge	Figure 46.12[b]	Yes	32–34
Centrifugal bioreactor	—	No	35

[a] According to Voisard *et al*. (14) and Kampala and Ozturk (9).
[b] Only Centritech centrifuge (Pneumatic Scale, Akron, OH; (34)) is shown.

cell-retention systems can be found in recent reviews on perfusion bioreactors published elsewhere (9,12,14).

Spin filter is among the first filtration devices used in perfusion culture of mammalian cells, and the one that is most widely used in industrial-scale operations. It is a rotating cylindrical filter cage housed internal or external to the bioreactor. Various spin filter designs have been reported and are depicted schematically in Fig. 46.2. Having separate motor drives for the spin filter and the bioreactor stirrer is preferred but it adds additional mechanical complexity to the bioreactor construction. Placing baffles within the spin filter has been reported to improve medium homogeneity and reduce cell accumulation within the spin filter (6). During the culture perfusion process, cell particles are subject to gravity force, axial force from bioreactor agitation, centrifugal force generated by the spin-filter rotation, radial force (drag) resulting from the perfusion flux, as well as a hydrodynamic lift force produced by the rotation of the filter cage that counteracts the drag force generated by the perfusion flux (12). The balance of these forces determines the migration of the cell particles around the spin-filter surface and hence the cell-retention efficiency. Beyond certain filter rotation speeds, centrifugal and lift forces are sufficiently high as to exceed perfusion flow and result

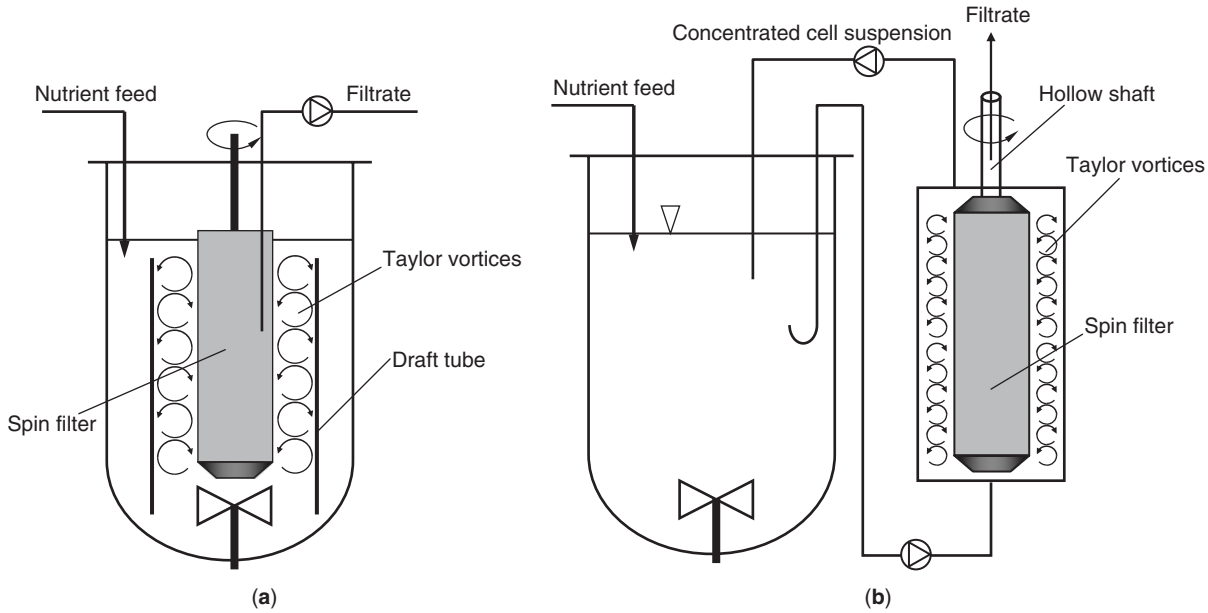


Figure 46.2. Spin-filter bioreactor: (a) internal spin filter with a draft tube; (b) external spin filter.

in the movement of cell particles away from the filter to enable effective particle retention. By considering only the lift force and the permeation drag (assuming centrifugal force is nil compared with the lift force), Yabannavar *et al*. (17,18) proposed to use the ratio of permeation drag to lift drag, φ, as the basis for designing and scaling up spin-filter systems, using the following equation:

$$\varphi \propto J_p/u_f^2 \tag{46.1}$$

where J_p is the perfusion flux and u_f is the tangential rotation velocity at the spin-filter surface. Since $J_p = D \cdot V/\varepsilon A$, where D is the specific perfusion rate (i.e. volumetric perfusion rate divided by the reactor volume), V is the reactor volume, ε is the filter porosity, and A is the filter surface area, Equation (46.1) can be rewritten as

$$\varphi \propto \frac{D \cdot V}{A \cdot u_f^2} \tag{46.2}$$

assuming constant screen porosity. By keeping φ constant at a value less than 1, Yabannavar *et al*. (18) demonstrated that efficient spin-filter operation could be scaled up without filter fouling. The same authors also showed that by keeping geometric similarity during scale-up, the filter rotation speed or angular velocity ω_f is proportional to $(V)^{-1/6}$. Furthermore, they suggested that the rotation speed of the agitator should be proportional to $V^{-2/9}$ to maintain a constant power per unit volume during scale-up. Under these conditions, fluid exchange per unit volume decreases slightly during scale up ($\propto V^{-1/18}$). According to Yabannavar *et al*. (18), increased fluid exchange may lead to more serious cell leakage through the perfusate, especially if the screen pore size is much greater than the cell size (e.g. 50 μm screen for 10–15 μm mammalian cells). A strategy similar to that of Yabannavar *et al*. (18) was adopted by Deo *et al*. (36) to scale up spin-filter perfusion cultures. Deo *et al*. (36) found that the perfusion flux at which the actual perfusion rate drops below the expected perfusion rate (indicating filter fouling) is proportional to u_f^2/X and derived the following equation for the maximum specific perfusion rate D_{max}:

$$D_{\max} \propto \frac{A \cdot u_f^2}{V \cdot X} \quad \text{and} \quad A \cdot u_f^2 \propto h_f \cdot r_f^3 \cdot \omega_f^2 \tag{46.3}$$

where X is the cell concentration, and h_f and r_f are, respectively, the height and radius of the spin filter. It should be noted that although the effect of cell concentration was included in the above equation, changes in cell morphology/aggregation and culture rheology during long-term perfusion cultivation were not considered. Therefore, if these changes are substantial in particular perfusion culture systems, the above approach should be examined further and applied with caution. Guided by Equation (46.3), Deo and coworkers (36) successfully scaled up a perfusion culture of a recombinant myeloma cell line to 500 L based on 5-L results. By keeping the same *A/V* ratio during scale up, both scale-up strategies of Yabannavar *et al*. (18) and Deo *et al*. (36) are based on maintaining a constant filter tangential velocity (i.e. perfusion capacity increases with square of the screen tangential velocity) (14). Spin-filter tangential velocities in the range of 28–60 cm/s have been reported to give satisfactory performance without serious filter fouling (14). Keeping constant *A/V* ratio during scale up implies that as the size of the bioreactor increases, the spin filter will occupy proportionally a larger volume of the reactor vessel. Also in these analyses, the centrifugal force due to spin-filter rotation was considered negligible, which might need to be evaluated more closely for a given operating condition. As an alternative to filter rotation, filter vibration using a piezo actuator installed inside a stationary filter cage has been shown recently to slightly prolong the operation of the filter (compared to the stationary filter without vibration) (38).

In some designs a draft tube is installed around the spin filter (Fig. 46.2a) or in the case of an external spin filter, the rotating filter is housed in a cylindrical vessel with a narrow annular gap (Fig. 46.2b). This is done in a way to produce axial and rotational shear and Taylor vortices in the gap between the spin filter and the draft tube (or the vessel wall in external spin filters) to clean the filter surface, thus preventing the plugging of pores of the filter medium. Taylor vortices are pairs of counter-rotating, toroidal vortices stacked in the annulus between a rotating inner cylinder and a concentric, stationary outer cylinder (Fig. 46.2). The transition from the stable circular Couette flow to Taylor vortex flow and hence generation of the Taylor vortices occurs when the Taylor number ($\mathrm{Ta} = \omega_i r_i d/\nu$, where ω_i is the angular rotation velocity of the inner cylinder, *i.e*. the spin filter, r_i the radius of the inner cylinder, d the gap between the cylinders, and the kinematic fluid viscosity) exceeds a critical value Ta_c. The value of Ta_c for a spin filter in a draft tube can be estimated based on the flow between rotating porous cylinders with radial and axial flow that has been reported by Johnson and Lueptow (39). In Fig. 46.3 (taken from Johnson and Lueptow (39)), the critical Taylor number is shown as a function of the radial Reynolds number α, at two representative axial Reynolds numbers β (0 and 10) and three radius ratios η ($= r_i/r_o$ where r_o is the radius of the outer cylinder, i.e. the draft tube). Note that $\alpha = u_i r_i/\nu$and $\beta = \overline{w}d/\nu$, where u_i is the radial velocity through the wall of the inner porous cylinder, i.e. the perfusion flux, with a positive value when outward from the axis of rotation, and $\overline{w}$ is the average axial velocity. In a spin filter system with solid draft tube, α is typically between -10 and -0.1, while β is between 1 and 50 (39). Since Ta_c is not very sensitive to axial flow, and hence to β, Fig, 46.3 could be used as a guideline to aid the design and

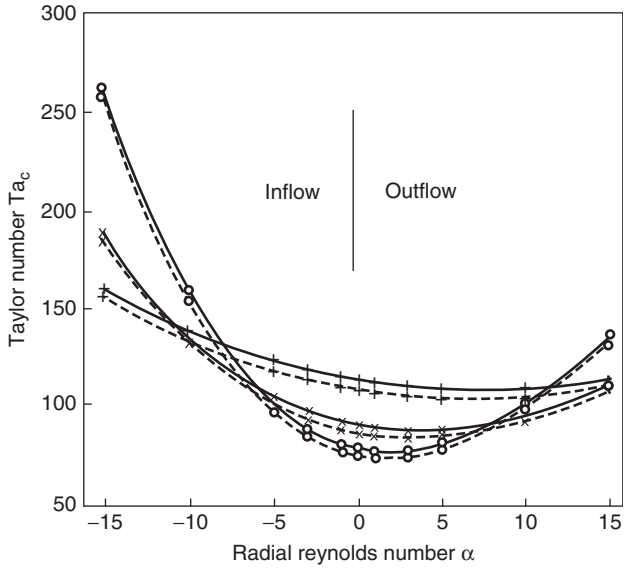


Figure 46.3. Estimation of the critical Taylor number based on the radial Reynolds number α, at two axial Reynolds numbers β (0 and 10) and three radius ratios η (see text for details; taken with permission from Johnson and Lueptow (39)).

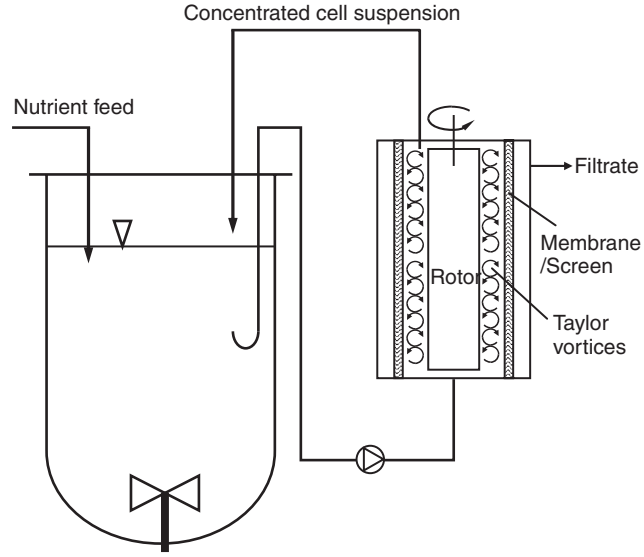


Figure 46.4. Perfusion bioreactor using an external vortex flow filtration device for cell retention.

operation of a draft-tube/spin-filter system for perfusion cultures. According to Fig. 46.3, Ta_c for systems with smaller η (i.e. bigger gap between the spin filter and the draft tube) is more sensitive to changes in the radial Reynolds number, and hence the perfusion flux. At a high perfusion flux, a higher filter rotation rate is required to achieve Taylor vortex flow (i.e. higher Ta_c) in systems having a bigger gap between the filter and draft tube (i.e. lower values of η), yet at low or zero perfusion rates, the phenomenon is reversed. According to Schwille *et al*. (40), rotational shear resulting from the circular Couette flow is as important or more so than the Taylor vortices in assuring high permeation fluxes in rotating filter systems. Since the induction of rotational shear is favored with small constant annular gaps between the rotor and the filter screen, Voisard *et al*. (14) warned that such condition might be difficult to realize at a very large scale. Another filtration system that takes advantage of the Taylor vortices to reduce filter fouling is the VFF (21–23). Hydrophilized microporous polysulfone membranes (22,23) and 10-μm stainless steel wire screens (21) have been used in VFF for perfusion culture and the latter was reported to allow operation up to 100 L/day for 30–60 days without clogging (21). Unlike spin filters, in VFF systems, the cylindrical filter membrane/screen is kept stationary whereas Taylor vortices are generated through the rotation of a concentric cylindrical rotor (Fig. 46.4). VFF is typically used as an external filtration system in perfusion culture. Again, Fig. 46.3 should provide a reasonable estimate of the Ta_c necessary to have vortical flow, except in this case the flow is outward, corresponding to the positive values of α.

In addition to the above-mentioned operating and geometric parameters, the spin filter performance is greatly affected by the properties of the filter screen (pore size, screen structure, and material). Most commonly, stainless steel mesh screens with pore sizes larger than the average cell size are used to make spin filters for mammalian cell cultures. For instance, Varecka and Scheirer (41) used wire cages with 53-μm mesh opening and cells of approximately 20 μm size, and observed no sign of fouling for more than 2 months of continuous operation. Esclade *et al*. (42) compared fouling of spin filters made out of stainless steel versus polyamide mesh (both having about 10 μm pore size). Using scanning electron microscopy, Esclade *et al*. (42) revealed that nearly all the pores in the stainless steel screen were fouled with DNA and cell debris, whereas the polyamide screen was relatively clean. To combat fouling by DNA, addition of nuclease such as deoxyribonuclease I may help, as demonstrated by Favre and Thaler (43). The difference in the extent of fouling seen with steel versus polymeric screens was believed to be owing to the different surface charge densities on the two materials. Since metal is highly positively charged, although polyamide is more neutral, more cells and cell debris (which are rather negatively charged) were attracted to the metal screen. Avgerinos *et al*. (44) carried out perfusion cultivations up to 54 days using a spin filter made out of a polymeric ethylene-tetrafluoroethylene (ETFE) screen (120 μm pore size) without filter fouling. The hydrophobic nature of the ETFE screen apparently minimized the cell attachment of cells to the screen and thus extended the life of the spin filter. In the commercial Sartorius (Goettingen, Germany) external spin filters, a multilayer stainless steel woven wire cloth with a mean pore opening up to 20 μm was used

for bioreactors up to 50 L in scale. Sartorius also offers an internal spin filter made out of precision-woven, open mesh polyethylene terephthalate polyester (PETP) fabric with pore sizes up to 40 μm.

Microporous membranes configured as hollow fibers, spiral-wound membrane cartridges, or plate-and-frame modules in tangential-flow filtration systems have been widely used in small-scale culture perfusion (14). Although hydrophilic microporous polypropylene membrane fibers can be installed inside a bioreactor as a microfilter/membrane stirrer to retain and mix animal cells (20), most membrane filtration systems have been used externally and involve continuous unidirectional recirculation of the culture suspension through the filter (Fig. 46.5a). The fluid flow in the circulating loop has to be optimized to minimize shear damage yet at the same time provide sufficient tangential flow to reduce premature membrane fouling. Oftentimes, membrane back flushing is necessary to prolong the operation, yet membrane fouling was frequently reported to be inevitable, in part, owing

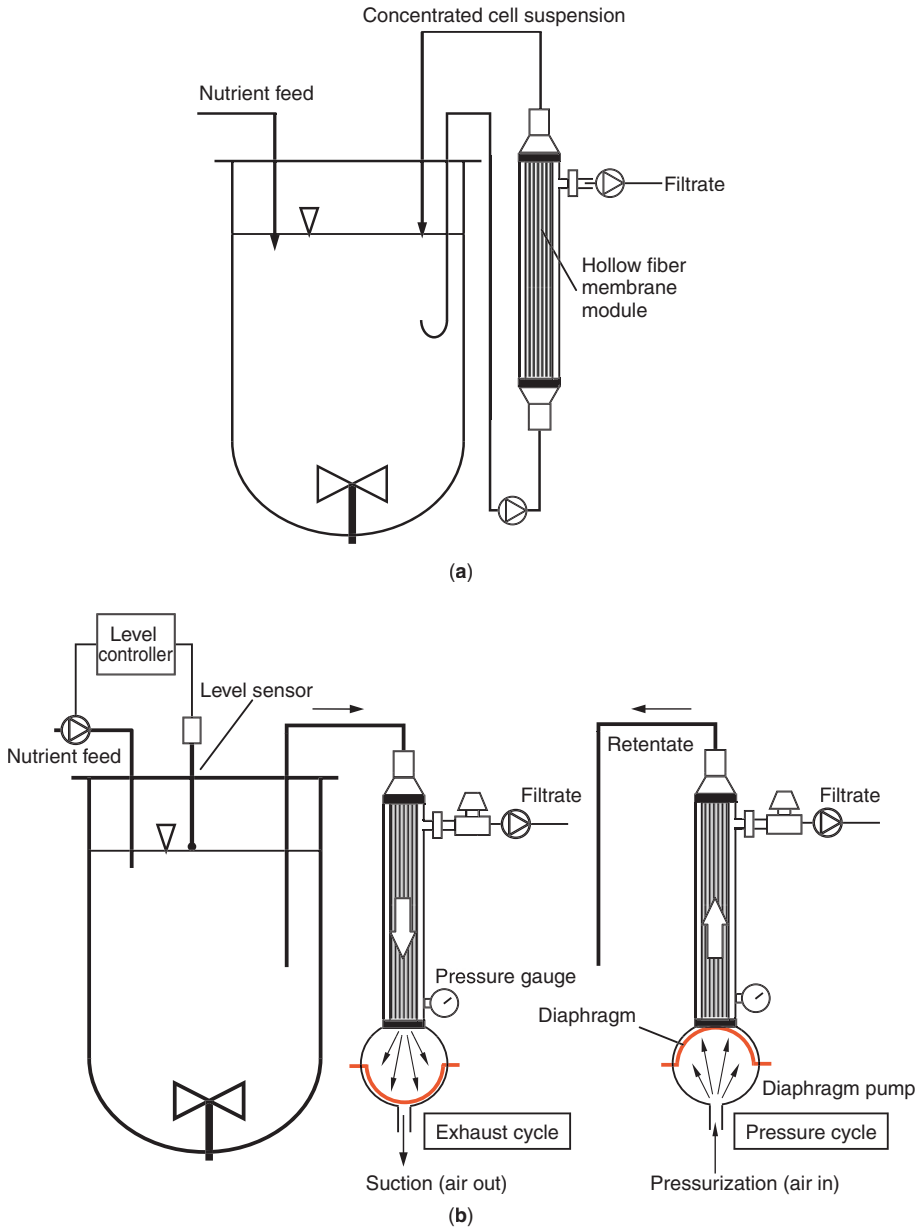


Figure 46.5. Cell retention via (a) unidirectional recirculation of culture fluid through an external cross-flow microporous membrane module; or (b) an alternating tangential flow (ATF) filtration system. (This figure is available in full color at http://onlinelibrary.wiley.com/book/10.1002/9780470054581.)

to the small pore size used in these membrane filtration systems. In the ATF filtration system developed by Refine Technology (Edison, NJ), culture suspension is circulated back and forth between the bioreactor and an external filter via a single port. A diaphragm pump is used to draw culture suspension into a filter module and to push concentrated culture back to the perfusion bioreactor while removing filtrate in the process (37). By reversing the culture flow directions in the filter module during each pump cycle, the pressure gradient across the filter wall is reversed, resulting in a momentary back flush during each pump cycle, and thus prevent filter fouling under low shear. The ATF system uses a 0.22-μm hollow fiber module for perfusion of suspension cell culture and a mesh screen module for microcarrier cultures. Using a hollow fiber membrane module with a surface area of 16.8 m^2, the ATF in principle can operate at over 1000 L/day, and thus representing a promising system for large-scale perfusion culture. Bleckwenn *et al*. (25) applied the ATF system containing a polyester 200-mesh screen module with 75 μm pores for perfusing microcarrier culture of HeLa cells in a 1.5-L bioreactor at up to 1 reactor volume per day. The system cycled about four times per minute for a slow pull up of the culture into the mesh filter module followed by a fast push of the culture back into the reactor to clean the mesh surface and allowed sufficient mixing with the contents of the reactor (25). The ATF diaphragm pump displaced approximately 80–100 mL bioreactor culture per cycle. In another study, Yuk *et al*. (24) reported perfusion culture of the HeLaS3 human tumor cell line using ATF at the bench (15 L) and pilot (70 L) scales for propagating a recombinant oncolytic adenoviral vector. The hollow fiber module used by Yuk *et al*. (24) had a 0.46 m^2 filter area, a 1-mm lumen, and a 0.2-μm pore rating. The cell-free spent media withdrawn by a peristaltic pump on the filtrate side of the hollow fiber module was automatically replenished with fresh medium using a medium supply pump actuated via a level sensor. Volumetric perfusion rates up to 3.5 culture volumes per day were used. The average shear rate in the filter module due to culture circulation was estimated to be about 750/s which was low enough not to create shear damage to the cells (24). According to the original ATF patent (45), it is desirable to install a pressure dampener for damping the pressure in the overall system to facilitate passage of the filtrate across the membrane and to improve membrane back flushing.

46.3 CELL RETENTION BASED ON SEDIMENTATION

The simplest type of sedimentation is driven by gravitational force, while enhanced sedimentation by centrifugal force or by promoting temporary cell aggregation via acoustic standing waves has also been reported for cell retention in perfusion bioreactors. Gravitational sedimentation provides a gentle process for cell separation. It is mechanically simple, exploiting the inertial properties of the cells instead of using physical barriers as in the case of filtration, to perform the separation. Sedimentation devices, however, do have a large holdup volume with potentially suboptimal culture conditions. To begin an analysis of cell sedimentation, one may consider the simple process of a particle freely falling in a liquid. For a dilute suspension of spherical cell particles, the terminal cell settling velocity (v_{so}) in the laminar region under the influence of a gravitational or centrifugal field can be estimated using the Stokes' law:

$$v_{so} = \frac{d_p^2}{18\mu}(\rho_s - \rho)\psi \tag{46.4}$$

where d_p is the cell particle diameter, μ is the suspension viscosity, ψ is the acceleration, ρ_s and ρ are the density of the cell and media, respectively. In a gravitational field, ψ is equal to gravitational acceleration, g, while in the centrifugal field, ψ is equal to $r\omega^2$ where r is the radial distance from the center of the centrifuge to the cell particle and ω is the angular rotation velocity. In concentrated suspensions, hindered sedimentation occurs as a result of interactions between neighboring particles. The settling rate in this case is greatly affected by the solids concentration. The hindered settling during gravitational sedimentation could be accounted for in calculating the particle settling rate using, for instance, Equation (46.5):

$$v_s = v_{so} \cdot e^{-KC} \tag{46.5}$$

where K is an empirical constant related to cell suspension's surface properties, size distribution, morphology, and viscosity (46), which can be determined from batch sedimentation data. To size a conventional continuous gravitational settler, the following analysis, based on the design of settling tanks, for wastewater treatment can be employed (29). Based on batch sedimentation experiments, the ascending height of the solid–suspension liquid interface (h) is recorded over time (t), and from which Equation (46.6) can be used to estimate the particle sedimentation velocity (v_s) as a function of particle concentration (C) for a given initial solids concentration (C_o) and initial interface height (h_o) (29).

$$h = \frac{C_o h_o}{C} - v_s \cdot t \tag{46.6}$$

For a continuous settler shown schematically in Fig. 46.6, and by assuming no solids in the clarified effluent, the settler area, A_S, can be estimated as

$$A_S = \frac{Q_o C_o}{G} \tag{46.7}$$

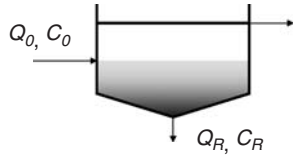


Figure 46.6. Flow diagram of a continuous vertical gravitational settler.

and

$$G = \frac{v_s}{\left(\frac{1}{C} - \frac{1}{C_R}\right)} \tag{46.8}$$

for a given volumetric feed rate to the settler (Q_o) and desired C_R value (the solids concentration in the concentrated suspension withdrawn from the bottom of the settler). Here G is known as the sedimentation capacity and A_S is typically calculated based on the minimum G value (29). Total volume of the settler is divided into two compartments: the volume occupied by the clarified liquid that contains no solids, and the volume occupied by the solids suspension. The latter (V_S) can be estimated using the following equation:

$$V_S = \frac{\tau \cdot Q_o \cdot h_\tau}{h_o} \tag{46.9}$$

where τ is the desired cell residence time in the settler and h_τ is the interface height at time τ, which is determined from the batch sedimentation tests. The desired cell residence time needs to be evaluated for each cell lines to avoid metabolic deterioration as a result of prolonged retention in the settler. The total settler volume is then estimated by adding the clarification zone volume, which has no influence on the sedimentation and hence can be freely adjusted within a large margin (29). For internal settling devices, most commonly countercurrent sedimentation occurs at the bottom entrance of the settler, the settling zone may be sized by equating the upward superficial liquid velocity and the terminal sedimentation rate of the cell particles. Here the hindered settling effect should be considered in determining the particle settling rate.

Vertical settlers were among the first tested for retaining mammalian cells in perfusion bioreactors. Conical-shaped vertical settlers, installed internal or external to the bioreactor, are commonly used. The conical designs take advantage of the reduced culture fluid superficial upward velocity in a settling zone with enlarged cross section area. Conical settlers have usually been placed external to the bioreactor as, for example, in the work of Hulscher *et al*. (Fig. 46.7a) (27). Sato *et al*. (47) described an internal conical cell separator consisting of a tapered conical sedimentation chamber affixed to the head plate of a stirred bioreactor. Spent medium was removed through the top of the cone and cells settle and slide down the steep wall of the cone to the bioreactor (Fig. 46.7b). Hamamoto (48) incorporated an annular settling zone with a stirred-tank bioreactor for continuous perfusion culture of mammalian cells. In this case, a cylindrical baffle was inserted into a stirred-tank reactor to create an annular settling zone (Fig. 46.7c). A similar design was adapted for continuous perfusion culture of plant cell suspension (49). Pressure equilibration between the settler and the reactor is crucial for the proper operation of the system. Internal settlers in the form of internal settling zones have also been incorporated into the downcomer section of an external-loop air-lift bioreactor to enable continuous culture perfusion of plant cells (50) and fungal pellets (51). The very design concept was adopted by Wen *et al*. (52) for perfusion culture of mammalian cells. In its simplest form, the internal settling zone in the external-loop air-lift perfusion bioreactor is created by inserting a baffle plate into the upper portion of the downcomer (Fig. 46.7d). Clarified spent medium containing secreted metabolic products is continuously removed via the overflow from the settling zone, while fresh medium is fed into the well-mixed riser to replenish nutrients. By incorporating the settling zone into an external-loop, instead of an internal-loop air-lift reactor, improvement on cell-retention efficiency was noted with plant cell suspension culture, which resulted from the much lower downcomer gas holdup in the external-loop air-lift reactor due to its more efficient gas disengagement at the reactor headspace (50). By taking advantage of the well-defined flow pattern in the air-lift reactor, the downward bulk liquid flow in the downcomer can guide the cell particles away from the settling region so that only few cell particles are present in the settler. However, it should be pointed out that there were noticeable eddies that provoked some degrees of mixing at the entrance of the settling region. The eddies carried some of the cells into the inlet region of the settler. These cells nonetheless were carried back to the bulk of the culture by the downward liquid flow, and hence there was a constant turnover of cells at the settler entrance. With increased gas velocity and thus faster culture circulation, mixing at the settler entrance was augmented. The effect of aeration on cell-retention efficiency, however, was minor compared with perfusion rate and cell loading (50). This was due to the fact that the settling zone for the most part was not stirred by the localized mixing at its entrance. To improve the sedimentation capacity, a conical settling zone can be incorporated into the upper portion of the downcomer (16). To enhance oxygen supply in the settler, membrane aeration tubing or surface aerator may be installed to provide bubble-free aeration without disturbing cell sedimentation (16).

Gravitational sedimentation can be enhanced in a shallow tilted settling chamber via inclined sedimentation. This

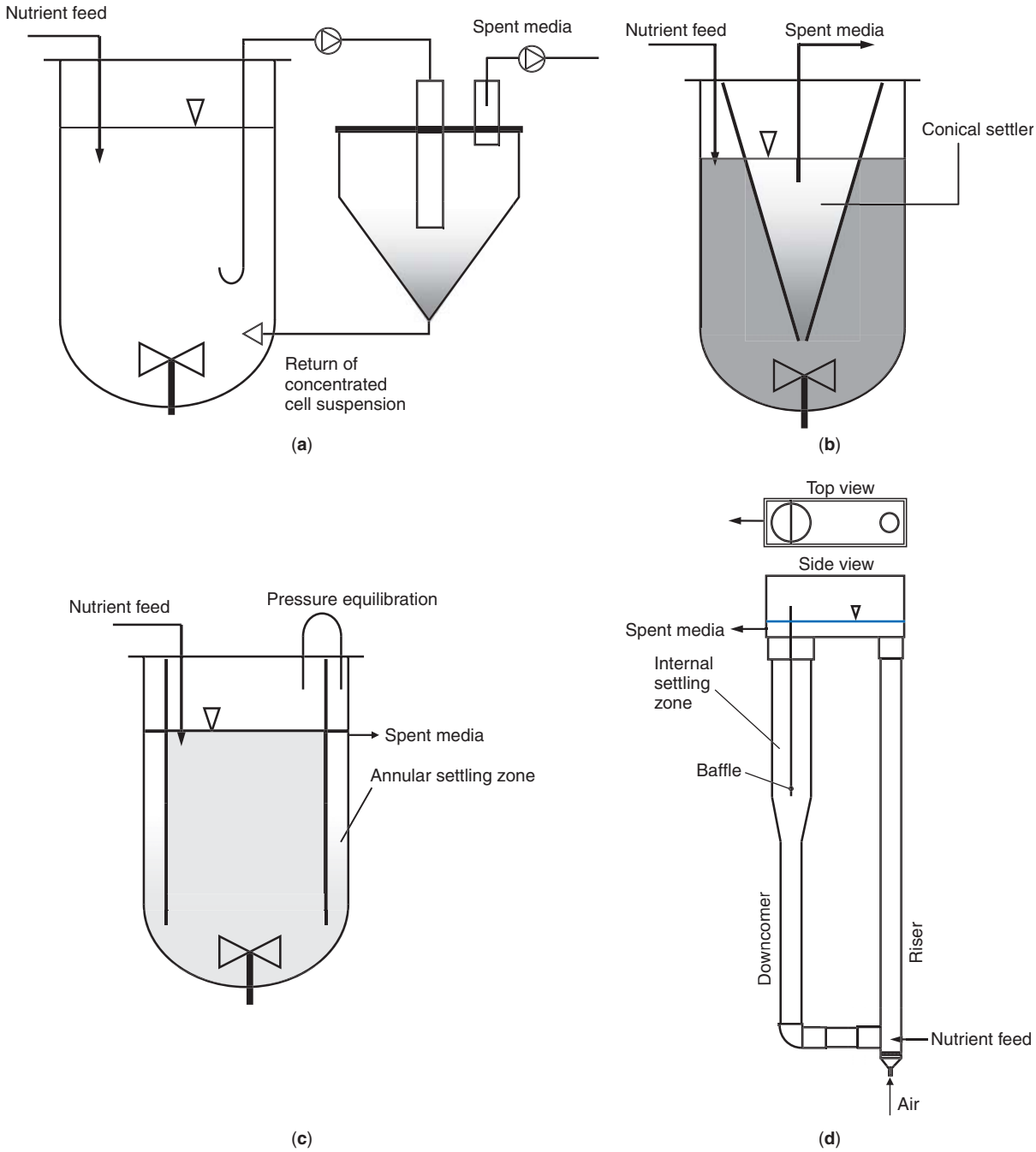


Figure 46.7. Perfusion bioreactors with vertical settlers: (a) external conical settler; (b) internal conical settler; (c) internal annular settler; (d) air-lift bioreactor with an internal settling zone. (This figure is available in full color at http://onlinelibrary.wiley.com/book/10.1002/9780470054581.)

phenomenon was first observed by Boycott (53), and analyzed, among others, by Acrivos and Herbolzheimer (54). For a dilute, monodisperse particle suspension, the particle sedimentation rate can be expressed as

$$v_{si} = v_{sv}\left(1 + \frac{h_s}{H}\sin\theta\right) \tag{46.10}$$

where v_{si} is the settling rate in inclined sedimentation, v_{sv} is the settling rate in vertical sedimentation, h_s is the vertical height of the solid suspension, H is the plate distance of the settler, and θ is the angle of inclination from the vertical axis. Note that in order to take full advantage of inclined sedimentation, a shallow settler (small H) with a large angle of inclination should be used. The large inclination angle,

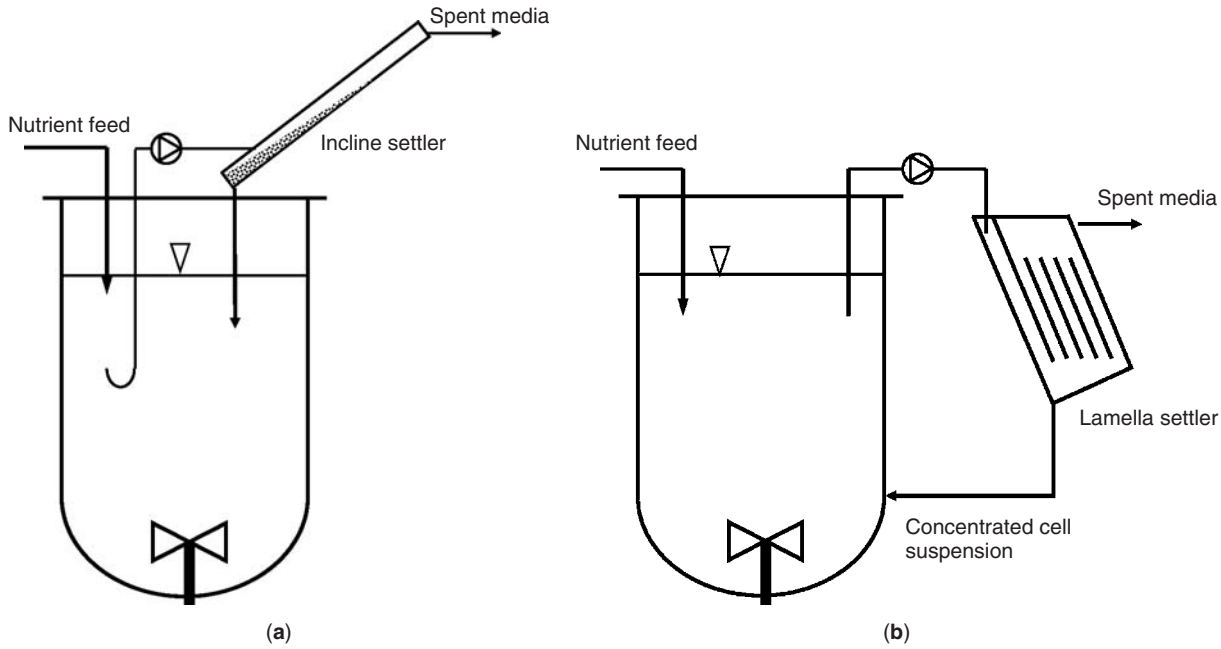


Figure 46.8. Perfusion bioreactor with (a) inclined settler; (b) lamella settler.

however, needs to be counter-balanced by the ease of cells to slide back to the bioreactor. Typically, inclination angle from 30 to 60° and plate distance from 0.5 to 2 cm is used (9). In the reactor of Davison *et al*. (55), a large inclined shallow settling chamber is integrated into a stirred fermenter as a side arm. As the culture is withdrawn through the settling chamber, cells undergo countercurrent inclined sedimentation, settle, and slide down the lower surface of the settler to the fermenter. Searls *et al*. (28) modified the inclined settler of Davison *et al*. by placing it on the top of the bioreactor and therefore allow cells to undergo cross-current sedimentation (Fig. 46.8a). To alleviate cell attachment to the settler wall, Searls *et al*. also tried bubbling and vibrating to periodically clean the settler. According to Kompala and Ozturk (9), an inclined plate settler has been scaled up to industrial operation by Biotechnology Solution (Orinda, CA). Incline sedimentation in the form of lamella settlers contain a large number of closely packed, parallel inclined plates, and hence analogous to multiple inclined plate settlers stacked together (Fig. 46.8b). This type of settler has been used by a number of researchers for perfusion culture of mammalian cells. Tyo and Thilly (56) described an interesting internal lamella settler system consisting of a series of nested truncated cones with an innermost solid cone. In this reactor, cells and medium are pumped up through the cones while cells are collected on the lower face of the cones, thereby resulting in a virtually cell-free fluid. For the same settler volume, the lamella settler offers much more sedimentation area than a conventional vertical settler. The total effective sedimentation area in a lamella settler is about half of the sum of the horizontally projected areas of all plates (12). One common problem with inclined settlers is that the cells tend to adhere to the plates and hence are not able to slide back to the bioreactor. Surface coating of the plates and vibration of the lamella pack have been suggested to alleviate this problem (12). Even though lamella settlers are more compact than conventional vertical settlers for the same sedimentation area, they are still associated with a relatively large holdup volume and long cell residence time that may be especially problematic as the settler is scaled up.

A relatively new approach to enhance cell sedimentation and thus improve cell retention involves the use of ultrasonic field forces to promote cell aggregation (Fig. 46.9a). When an ultrasonic wave is reflected in the direction opposite to the propagation of the wave, resonant standing waves are formed (Fig. 46.9b). As cells are exposed to this ultrasonic field, they are initially trapped in the pressure node planes of the standing wave, and then coalesce to form aggregates that sediment from the fluid by gravity. There are three major forces responsible for the aggregation of cells in the resonance field. They are the primary radiation force, the secondary radiation force, and the Bernoulli force. The primary radiation force drives cells toward the velocity antinodes of the resonance field, bringing the cells close together. When the cells become very close to each other, there also exists the secondary radiation force that results from the interaction between the cells. The magnitude of the primary radiation force is generally much greater than that of the secondary radiation force. The magnitudes of both primary and secondary radiation forces are proportional to the cell

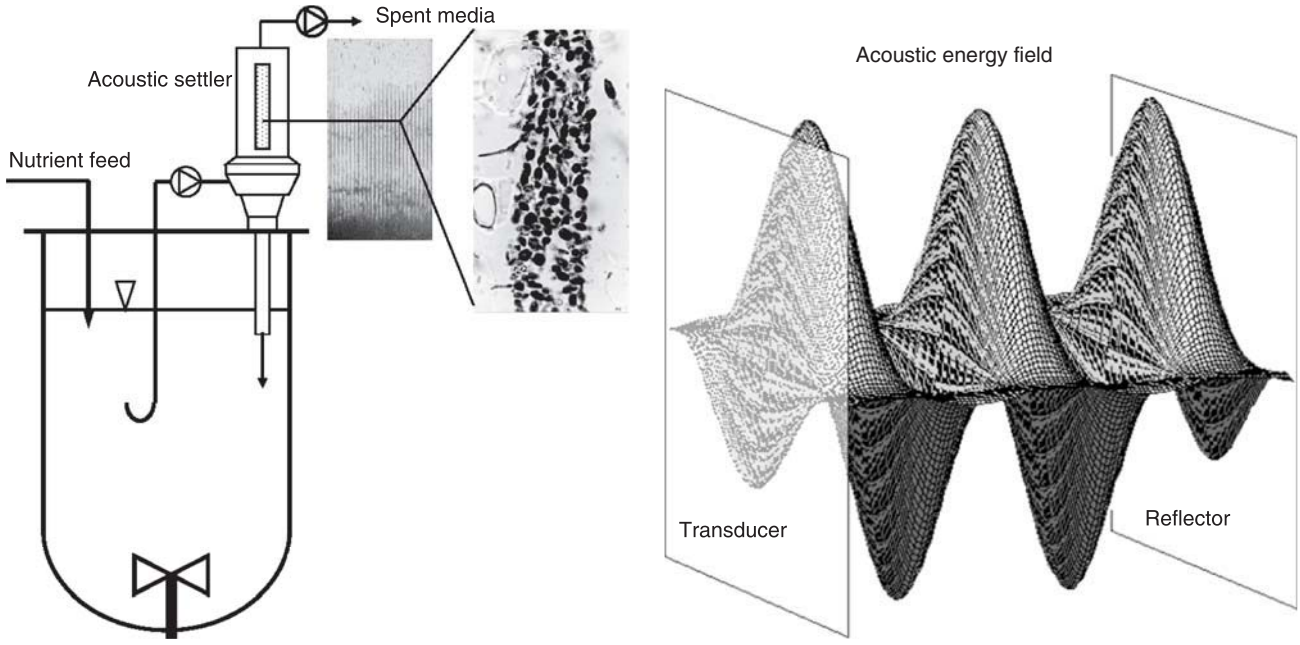


Figure 46.9. (a) Perfusion using an acoustic settler; note that cells within the velocity antinode planes are driven to form striated columns of cell aggregates oriented perpendicular to the antinode planes. (b) When an ultrasonic wave is reflected in the direction opposite to the propagation of the wave, resonant standing waves are formed.

volume, and hence increase with the size of the aggregates. The Bernoulli force results from the nonuniform acoustic field that drives the cells within the velocity antinode planes to form striated columns of cell aggregates oriented perpendicular to the antinode planes (Fig. 46.9a). The performance of acoustic cell-retention devices depends on the magnitude of the acoustic forces that are a function of the acoustic energy density distribution in the liquid. This distribution is a function of the dimensions, imposed boundary conditions, and physical properties of the reflector and transducer. Factors affecting the separation efficiency of acoustic cell-retention devices include (i) acoustic frequency, (ii) power input, (iii) duty cycle, (iv) culture recirculation rate, (v) perfusion/harvest rate, and (vi) back-flush frequency. Among these factors, power input and perfusion/harvest rate are considered most important (31). Most of the acoustic cell-retention devices operate at a fixed frequency (ranges between 2 and 3 MHz) but with adjustable power input. Power input requirement increases with increasing perfusion capacity and hence scale of the acoustic retention device. For a 10-L separator, 5–7 W power input is required, whereas for a 200-L separator, it requires 60–90 W to achieve similar retention efficiency (31). Acoustic cell settler is capable of operating in the pulse mode with on/off duty cycles. Duty cycle facilitates the removal of the aggregated cells in the chamber and, hence, to minimize the residence time of the cells in the acoustic settler. However, according to Shirgaonkar *et al*. (31), duty cycle has little influence on the performance of the acoustic settler. Standard operation of the acoustic settler involves pumping the cell suspension from the reactor to the acoustic settler below the separation chamber at a recirculation rate higher than the harvest rate (Fig. 46.9a). Gorenflo *et al*. (30) suggested an optimum recirculation rate that is twice that of the perfusion rate. Shirgaonkar *et al*. (31) recommended not to increase the recirculation rate above three times the harvest rate at high cell density to avoid shear damage and excess turbulence in the bottom portion of the settler that may disturb the sedimented cells in the acoustic chamber. For shear sensitive cell lines, constant recirculating of the cell suspension using a peristaltic pump may lead to shear damage. Merten (57) therefore recommended an alternative operation strategy of the acoustic settler by eliminating the recirculating stream. To do so, the settler is basically operated under countercurrent, as opposed to crosscurrent, sedimentation. A portion of the spent medium leaving the acoustic settler can be used to periodically back flush the settler (Fig. 46.10). In this case, however, the recirculation rate and perfusion rate become a single parameter, and hence reduces the process flexibility and complicates dynamic adjustment of culture perfusion. Perfusion rate or the harvest rate of clarified spent media affects the settler performance greatly. At high perfusion

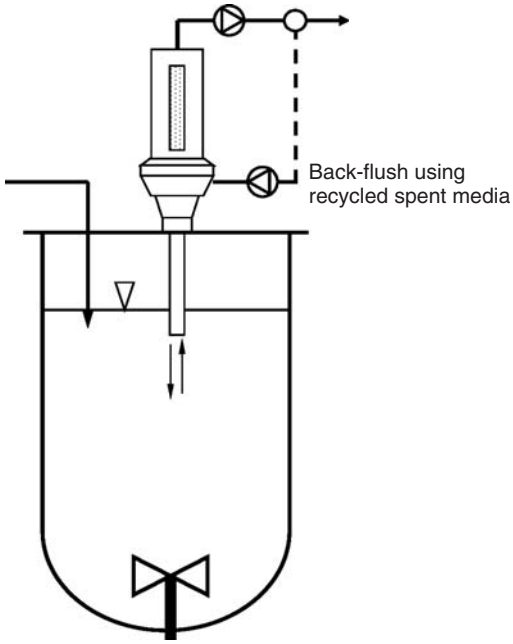


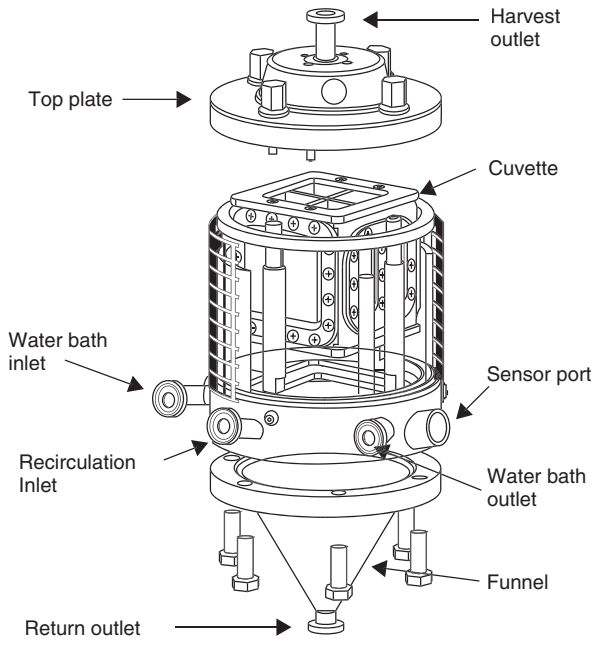
Figure 46.10. An alternative operating strategy of the acoustic settler (cf. Fig. 46.9a).

rates, cell washout may occur, which may be alleviated by increasing the acoustic power input. However, acoustic power cannot be increased indefinitely as excess power results in heating the transducer and raising medium temperature in the acoustic chamber to generate slow but free convective flow (58). Pui *et al*. (59) reported temperature increase at a rate of 1.3°C/min in a 75-mL static batch acoustic chamber operated at 0.7 L/h and 13.5 W. This temperature rise resulted from attenuation of the acoustic energy in the transducer, reflector, and cell suspension. To overcome this drawback a good cooling system is necessary to maintain the temperature of the transducer. A two-chamber acoustic device was proposed by Doblhoff-Dier *et al*. (60) to cool the transducer by passing water through one chamber while introducing cell suspension into the other, leading to substantially improved separation efficiency. In the commercial BioSep 200 L system (AppliSens), the chamber's temperature is controlled by means of a refrigerated water bath circulator (30). At high cell densities, the acoustic chamber may be filled with entrained cells, which could reduce the separation efficiency due to attenuation of the intensity of the standing waves. This also increases the residence time of the cells in the acoustic chamber. It is therefore necessary to transport the cells back to the bioreactor via back flushing. Gorenflo *et al*. (58) suggested an air back-flushing approach in which an injection of bioreactor air downstream of the separator periodically returned the trapped cell aggregates back to the reactor. During air back flushing, the acoustic power and the harvest pump are turned off while the fresh media feed pump remains on. Afterwards, the back-flush pump is reversed to refill the acoustic chamber with fresh cell suspension from the bioreactor. Gorenflo *et al*. (58) reported that the separation efficiency increased from 73% at a back-flush frequency of 6/h to a maximum of 91% at frequencies between 12 and 20/h. A further increase in back-flush frequencies requires an increase in the harvest flow rate to the point that separation efficiency starts to decrease. Acoustic cell settlers have been used quite extensively for mammalian and insect cell cultures (31) up to 200 L/d perfusion rate, using a BioSep-200 system that contains a sectioned resonator made out of four 500-mL 1.4-MHz BioSep resonator chambers (Fig. 46.11a, b). A large 1000 L/d capacity acoustic settler (BioSep 1000) has been developed by AppliSens which is believed to be the largest possible scale of this technique (14) mainly because of the technical challenge in keeping the temperature down in the acoustic chamber to prevent liquid convection that reduces the separation efficiency. In the BioSep 1000 system, five BioSep 200 resonators are bundled in a single housing (Fig. 46.11c). It is worthy of pointing out that by proper tuning of the acoustic settler, one may achieve selective retention of viable cells in the bioreactor (31), which is a major advantage of this type of separator over membrane-based systems.

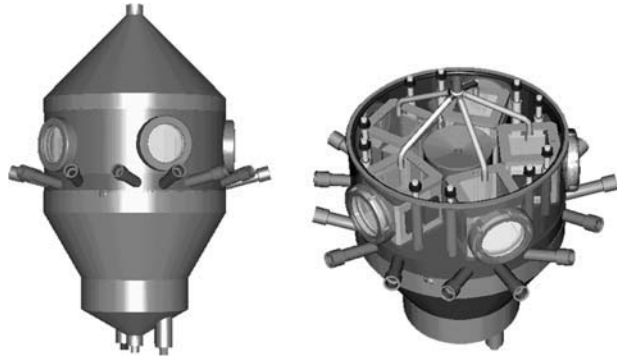
Another way to enhance sedimentation is by virtue of centrifugal forces, typically via the use of external centrifuges operated under continuous or semi-continuous modes (14,15). Conventional centrifugal separators involve rotary seals and are constructed to provide a good clarification of the supernatant, but usually generate too much mechanical stress to the cells and it is difficult to operate under sterile conditions for prolonged periods. An interesting centrifuge design (Centritech centrifuge, Pneumatic Scale, Akron, OH) was used by Johnson *et al*. for hybridoma perfusion cultures (34). In this study, an average perfusion rate of 0.5 culture volume per day, with over 98% viable cell retention was reported. More recently, Cruz *et al*. used the Centritech centrifuge in perfusion culture of (BHK) cells at a volumetric perfusion rate up to two culture volumes per day (61). The centrifuge (Fig. 46.12a) utilizes an "inverted question mark" anti-twist mechanism that makes it possible to rotate one end of a flexible tube while the other is standing still, thus eliminating the need for rotating seals (Fig. 46.12b). A key to the anti-twist design is to rotate the conical rotor at a velocity equal to twice the velocity of the rotating platform (Fig. 46.12a, b). This mechanism was first disclosed in a patent by Adams (62) and later modified in a number of other patents, among others, US patent 4778444 of Westberg and Ehnstrom (63). In the Centritech system, separation takes place in a disposable insert (Fig. 46.12c), where the suspension enters at an



(a)



(b)



(c)

Figure 46.11. (a) BioSep acoustic settlers with three different perfusion capacities; (b) mechanical drawing of the BioSep 200 L system; (c) BioSep 1000-L acoustic settler (courtesy of Applikon/AppliSens).

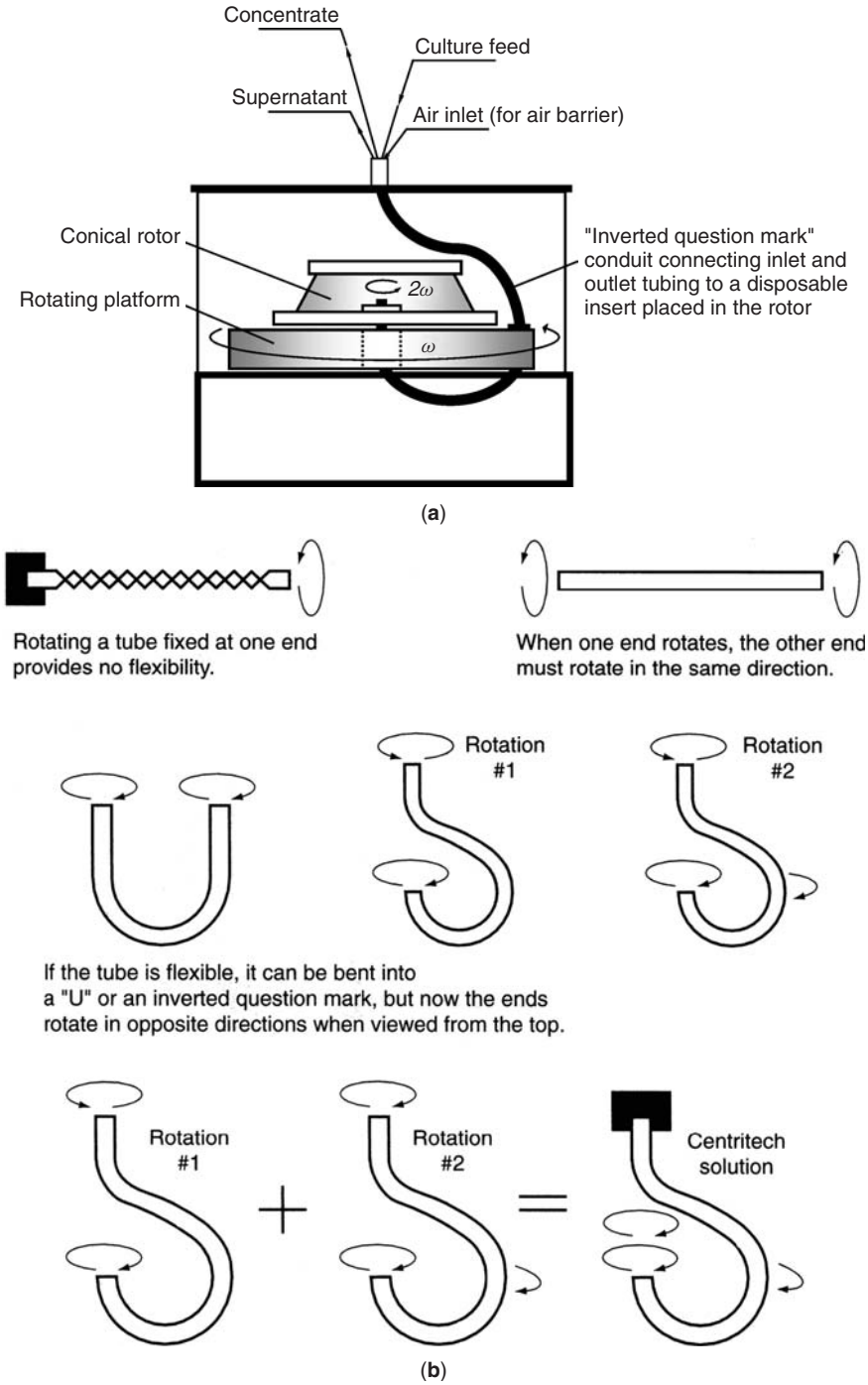
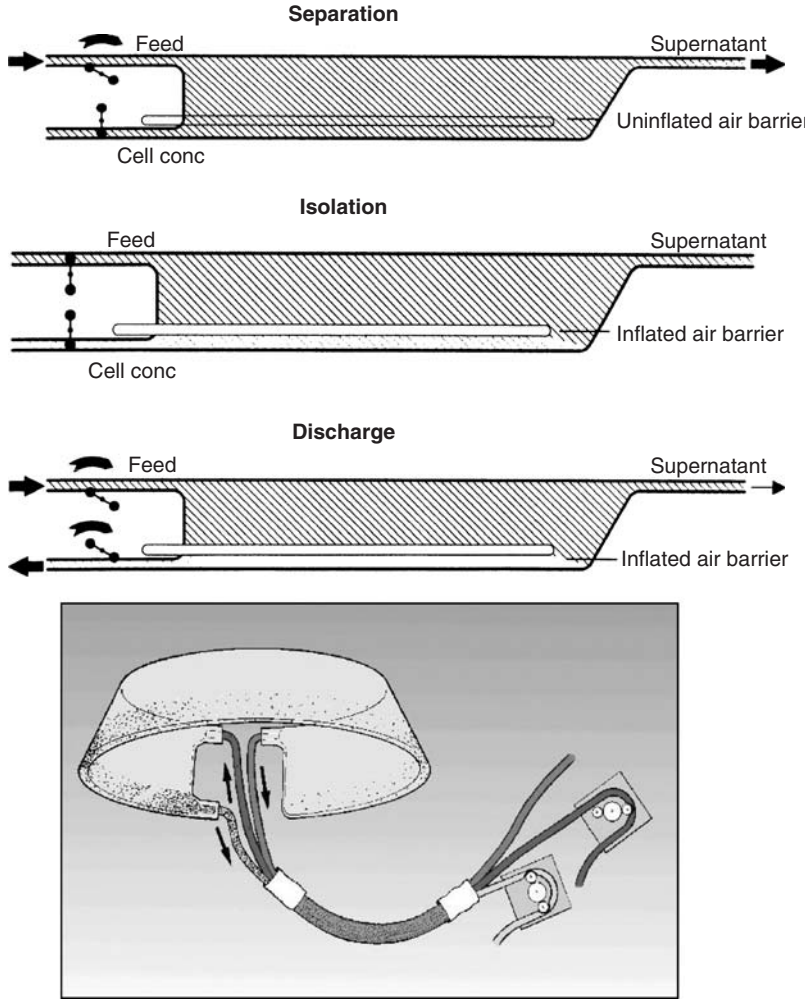


Figure 46.12. The Centritech centrifuge for culture perfusion: (a) Schematic of the centrifuge (note the relative rotation speeds of the conical rotor and the rotating platform); (b) the "inverted question mark" anti-twist mechanism; (c) the disposable insert (courtesy of Pneumatic Scale).

inner radius through a tube at one end of the rotor, flows around the circumference, and exits through the tube at the other end. Since cells are slightly heavier than the liquid, they move outward and are discharged using a pneumatic system through a tube connected to the separation chamber at its outer radius. As the suspension flows around the rotor's circumference, it is subject to low centrifugal forces for enough time for separation to occur. Utilization of the centrifuge in an intermittent fashion decreased the daily cell residence time outside the bioreactor, the



(**c**)

Figure 46.12. (Continued)

daily pelleted-cell residence time in the centrifuge, and the frequency of cell passage to the centrifuge (34). It was suggested by Johnson *et al*. (34) that having cells periodically packed at the bottom of the centrifuge insert is deleterious to the culture by exposing the pelleted cells to prolonged nutrient limitations. In general, centrifugal separators, although more suitable for large-scale perfusion operations, are complex and more prone to mechanical failure than simple gravitational sedimentation devices. These devices are also associated with the drawbacks inherent to external separators. For continuous centrifugal separators, the Sigma factor concept ($\Sigma = Q'/v_{so}$, where Q' is the volumetric throughput of the centrifuge) (13) may be applied to determine the size of the centrifuge. The Sigma factor for certain newer centrifuge types, such as the Centritech centrifuge, has yet to be derived. The residence time in the centrifuge, frequency of cell passage to the centrifuge (during intermittent operations), the magnitude of centrifugal force applied, and the rate of external culture circulation (which may lead to shear and anoxic stresses), will need to be optimized.

46.4 CONCLUSION

Culture perfusion is a proven approach to achieving high productivity in mammalian cell cultures. As reviewed in this chapter, although several cell-retention systems have been demonstrated to enable culture perfusion at a capacity over 200 L/day, a key technical challenge to continuing success and more widespread usage of culture perfusion in industrial-scale operations remains on developing systems that can handle even higher perfusion rates (over 1000 L/day) with improved robustness but

without compromising their mechanical simplicity, to allow stable long-term operations with minimum operator attendance.

Acknowledgments

The author is grateful to National Science Foundation (NSF) (BES97-12916 and BES01-26191), United States Department of Agriculture (USDA) Tropical and Subtropical Agriculture Research (TSTAR) Program (01-34135-11295), and the USDA Scientific Cooperative Research Program (58-3148-9-080) for support of his research on plant cell perfusion cultures. Professor Richard Lueptow of the Northwestern University is acknowledged for his helpful inputs and review of the section on the Taylor vortex flow.

REFERENCES

1. Sethuraman N, Stadheim TA. Challenges in therapeutic glycoprotein production. Curr Opin Biotechnol 2006; 17(4): 341–346.
2. Hellwig S, Drossard J, Twyman RM, Fischer R. Plant cell cultures for the production of recombinant proteins. Nat Biotechnol 2004; 22(11): 1415–1422.
3. Ikonomou L, Schneider YJ, Agathos SN. Insect cell culture for industrial production of recombinant proteins. Appl Microbiol Biotechnol 2003; 62(1): 1–20.
4. James E, Lee JM. The production of foreign proteins from genetically modified plant cells. Adv Biochem Eng Biotechnol 2001; 72: 127–156.
5. Chu L, Robinson DK. Industrial choices for protein production by large-scale cell culture. Curr Opin Biotechnol 2001; 12(2): 180–187.
6. Vallez-Chetreanu F. PhD Chemical Engineering. dissertation. Lausanne: École Polytechnique Fédérale de Lausanne; 2006. p. 188.
7. Yang JD, Angelillo Y, Chaudhry M, Goldenberg C, Goldenberg DM. Achievement of high cell density and high antibody productivity by a controlled-fed perfusion bioreactor process. Biotechnol Bioeng 2000; 69(1): 74–82.
8. Heath C, Kiss R. Cell culture process development: advances in process engineering. Biotechnol Prog 2007; 23(1): 46–51.
9. Kompala D, Ozturk S. Optimization of high density perfusion bioreactors, in cell culture technology for pharmaceutical and cellular therapies. In: Ozturk S, Hu W-S, editors. Cell culture technology for pharmaceutical and cellular therapies. New York: Taylor & Francis; 2006.
10. Lim AC, Washbrook J, Titchener-Hooker NJ, Farid SS. A computer-aided approach to compare the production economics of fed-batch and perfusion culture under uncertainty. Biotechnol Bioeng 2006; 93(4): 687–697.
11. Hu WS, Aunins JG. Large-scale mammalian cell culture. Curr Opin Biotechnol 1997; 8(2): 148–153.
12. Castilho LR, Medronho RA. Cell retention devices for suspended-cell perfusion cultures. Adv Biochem Eng Biotechnol 2002; 74: 129–169.
13. Bailey JE, Ollis DE. Biochemical engineering fundamentals. Biochemical engineering fundamentals, 2nd ed. New York:McGraw Hill; 1986.
14. Voisard D, Meuwly F, Ruffieux PA, Baer G, Kadouri A. Potential of cell retention techniques for large-scale high-density perfusion culture of suspended mammalian cells. Biotechnol Bioeng 2003; 82(7): 751–765.
15. Woodside S, Bowen B, Piret J. Mammalian cell retention devices for stirred perfusion bioreactors. Cytotechnology 1998; 28: 163–175.
16. Su W. Perfusion bioreactors. In: Spier R, editor. Encyclopedia of cell technology. New York: Wiley; 2000. pp. 230–242.
17. Yabannavar VM, Singh V, Connelly NV. Mammalian cell retention in a spinfilter perfusion bioreactor. Biotechnol Bioeng 1992; 40: 925–933.
18. Yabannavar VM, Singh V, Connelly NV. Scaleup of spinfilter perfusion bioreactor for mammalian-cell retention. Biotechnol Bioeng 1994; 43: 159–164.
19. Büntemeyer H, Bohme C, Lehmann J. Cytotechnology 1994; 15: 243–251.
20. Heidemann R, Riese U, Lutkemeyer D, Büntemeyer H, Lehmann J. The Super-Spinner: a low cost animal cell culture bioreactor for the CO_2 incubator. Cytotechnology 1994; 14(1): 1–9.
21. Roth G. Using an external vortex flow filtration device for perfusion cell culture. Biopharm 1997; 10: 30–35.
22. Mercille S, Johnson M, Lemieux R, Massie B. Filtration-based perfusion of hybridoma cultures in protein-free medium—reduction of membrane fouling by medium supplementation with DNAse-I. Biotechnol Bioeng 1994; 43: 833–846.
23. Mercille S, Johnson M, Lanthier S, Kamen A, Massie B. Understanding factors that limit the productivity of suspension-based perfusion cultures operated at high medium renewal rates. Biotechnol Bioeng 2000; 67: 435–450.
24. Yuk IH, Olsen MM, Geyer S, Forestell SP. Perfusion cultures of human tumor cells: a scalable production platform for oncolytic adenoviral vectors. Biotechnol Bioeng 2004; 86(6): 637–642.
25. Bleckwenn NA, Golding H, Bentley WE, Shiloach J. Production of recombinant proteins by vaccinia virus in a microcarrier based mammalian cell perfusion bioreactor. Biotechnol Bioeng 2005; 90(6): 663–674.
26. Vogel J, Kroner K. Biotechnol Bioeng 1999; 63:663-674.
27. Hulscher M, Scheibler U, Onken U. Selective recycle of viable animal cells by coupling of airlift reactor and cell settler. Biotechnol Bioeng 1992; 39: 442–446.
28. Searls J, Todd P, Kompala D. Biotechnol Prog 1994; 10: 198–206.
29. Tabera J, Iznaola M. Design of a lamella settler for biomass recycling in continuous ethanol fermentation process. Biotechnol Bioeng 1989; 33: 1296–1305.
30. Gorenflo VM, Smith L, Dedinsky B, Persson B, Piret JM. Scale-up and optimization of an acoustic filter for 200 L/day perfusion of a CHO cell culture. Biotechnol Bioeng 2002; 80(4): 438–444.
31. Shirgaonkar IZ, Lanthier S, Kamen A. Acoustic cell filter: a proven cell retention technology for perfusion of animal cell cultures. Biotechnol Adv 2004; 22(6): 433–444.

32. Tokashiki M, Takamatsu H. Perfusion culture apparatus for suspended mammalian cells. Cytotechnology 1993; 13(3): 149–159.
33. Takamatsu H et al. Large-scale perfusion culture process for suspended mammalian cells that uses a centrifuge with multiple settling zones. Appl Microbiol Biotechnol 1996; 45(4): 454–457.
34. Johnson M, Lanthier S, Massie B, Lefebvre G, Kamen A. Biotechnol Prog 1996; 12: 855–864.
35. van Wie B et al. Biotechnol Bioeng 1991; 38: 1190–1202.
36. Deo YM, Mahadevan MD, Fuchs R. Practical considerations in operation and scale-up of spin-filter based bioreactors for monoclonal antibody production. Biotechnol Prog 1996; 12(1): 57–64.
37. Furey J. Scale up of a cell culture perfusion process. Gen Eng News 2002; 22: 62–63.
38. Vallez-Chetreanu F, Fraisse Ferreira LG, Rabe R, von Stockar U, Marison IW. An on-line method for the reduction of fouling of spin-filters for animal cell perfusion cultures. J Biotechnol 2007; 130(3): 265–273.
39. Johnson E, Lueptow R. Hydrodynamic stability of flow between rotating porous cylinders with radial and axial flow. Phys Fluids 1997; 9: 3687–3696.
40. Schwille JA, Mitra D, Lueptow RM. Design parameters for rotating cylindrical filtration. J Memb Sci 2002; 204(1–2): 53–65.
41. Varecka R, Scheirer W. Use of a rotating wire cage for retention of animal cell in a perfusion fermentor. Dev Biol Stand 1987; 66: 269–272.
42. Esclade L, Carrel S, Peringer P. Influence of the screen material on the fouling of spin filters. Biotechnol Bioeng 1991; 38: 159–168.
43. Favre E, Thaler T. An engineering analysis of rotating sieves for hybridoma cell retention in stirred tank bioreactors. Cytotechnology 1992; 9(1–3): 11–19.
44. Avgerinos G, Drapeau D, Socolow J, Mao J, Hsiao K, Broeze R. Spin filter perfusion system for high density cell culture: production of recombinant urinary type plasminogen activator in CHO cells. Biotechnology 1990; 8: 54–58.
45. Shevitz J, inventor; Refined Technology Company. US patent 6,544,424. 2003.
46. Klei H, Baena R, Anderson T, Sundstrom D, Bertucco A. In: Ho C, Oldshue J, editors. Biotechnology processes - scale-up and mixing. New York: AIChE; 1987. pp. 185–199.
47. Sato S, Kawamura K, Fujiyoshi N. J Tissue Cult Methods 1983; 8: 167–172.
48. Hamamoto K, inventor; Teijin Limited. US patent 4,814,278. 1989.
49. Su W, Arias R. Continuous perfusion plant cell culture: Bioreactor characterization and secreted enzyme production. J Biosci Bioeng 2003; 95: 13–20.
50. Su W, He B, Liang H, Sun S. A perfusion air-lift bioreactor for high density plant cell cultivation and secreted protein production. J Biotechnol 1996; 50: 225–233.
51. Su W, He B. Secreted enzyme production by fungal pellets in a perfusion bioreactor. J Biotechnol 1997; 54: 43–52.
52. Wen ZY, Teng XW, Chen F. A novel perfusion system for animal cell cultures by two step sequential sedimentation. J Biotechnol 2000; 79(1): 1–11.
53. Boycott A. Nature 1920; 104: 532.
54. Acrivos A, Herbolzheimer E. Enhanced sedimentation in settling tanks with inclined walls. J Fluid Mech 1979; 92: 435.
55. Davison B, San K, Stephanopoulos G. Biotechnol Prog 1985; 1: 260–268.
56. Tyo M, Thilly W. Paper 30G. AIChE Annual Meeting, San Francisco, CA. 1989.
57. Merten O-W. Cytotechnology 2000; 34: 175–179.
58. Gorenflo VM, Angepat S, Bowen BD, Piret JM. Optimization of an acoustic cell filter with a novel air-backflush system. Biotechnol Prog 2003; 19(1): 30–36.
59. Pui PW, Trampler F, Sonderhoff SA, Groeschl M, Kilburn DG, Piret JM. Batch and semicontinuous aggregation and sedimentation of hybridoma cells by acoustic resonance fields. Biotechnol Prog 1995; 11(2): 146–152.
60. Doblhoff-Dier O, Gaida T, Katinger H, Burger W, Groschl M, Benes E. A novel ultrasonic resonance field device for the retention of animal cells. Biotechnol Prog 1994; 10(4): 428–432.
61. Cruz HJ, Conradt HS, Dunker R, Peixoto CM, Cunha AE, Thomaz M, Burger C, Dias EM, Clemente J, Moreira JL, Rieke E, Carrondo MJ. Process development of a recombinant antibody/interleukin-2 fusion protein expressed in protein-free medium by BHK cells. J Biotechnol 2002; 96(2): 169–183.
62. Adams D, inventor; to undisclosed. US patent 3,586,413. 1971.
63. Westberg E, Ehnstrom L, inventor; Alfa-Laval, Sweden. US patent 4,778,444. 1988.

47

BIOREACTORS: ROTATING BIOLOGICAL CONTACTORS

Susana Cortez, Pilar Teixeira, Rosário Oliveira, and Manuel Mota
Institute for Biotechnology and Bioengineering, Centre of Biological Engineering, University of Minho, Braga, Portugal

47.1 INTRODUCTION

At present, there are a wide variety of bioreactors in wastewater treatment, which may be broadly categorized as suspended or attached growth processes. During the 1970s and 1980s, due to its advantages, the rotating biological contactor (RBC), an efficient attached biofilm system, became very popular and thousands of RBC units were installed all around the world. Many of these facilities did not perform as predicted and experienced mechanical failures well before their expected lifetime. As a consequence, the process has fallen into disfavor with many consulting engineers. However, experience with existing installations, over the past 40 years, has established the appropriate range of applications for the RBC process, as well as the range of operating conditions resulting in acceptable performance. Furthermore, RBC manufacturers have reexamined the basic process to identify shortcomings and deficiencies and while many design parameters have remained unaltered, significant changes have been made in other areas to produce a low cost, robust process where unnecessary costs are eliminated. For these reasons, we believe that the RBC system should deserve greater consideration than what is currently paid during process selection.

Existing RBC facilities can now be reliably upgraded and expanded. Plant owners and operators can also properly evaluate RBCs as an alternative for new applications. This has resulted in an increase in interest from both academic and industrial sources. Indeed, there are recent publications detailing the development of RBC technology to accomplish higher levels of treatment and documenting its appropriate range (1–5).

This chapter provides an overview of RBCs, focusing on their main characteristics, advantages and drawbacks, hydrodynamics, factors affecting performance, biofilm characteristics, and some aspects about design and scale-up. The main operational problems and their resolution as well as the general application areas of this reactor are also presented.

47.2 BACKGROUND

47.2.1 Description of the RBC

Different terms are used in the literature to describe the RBC, namely, rotating biological disks, biodisks, rotating disk bioreactor, rotating biological surfaces, and rotating biological filters.

An RBC unit typically consists of a set of closely spaced large flat or corrugated disks that are mounted on a common horizontal shaft and are partially or completely submerged in the effluent to be treated (Fig. 47.1).

A drum filled with packed supports can also be used instead of conventional disks. The shaft continually rotates by a mechanical motor or a compressed air drive and a biofilm is built-up onto the entire surface area of the supporting media, metabolizing the organic materials contained in the wastewater. In aerobic processes, rotation of the media promotes oxygen transfer and maintains the biomass in aerobic conditions. Rotation also provides turbulence in the mixed liquor surface and originates shearing forces,

Upstream Industrial Biotechnology: Equipment, Process Design, Sensing, Control, and cGMP Operations, Volume 2, First Edition. Edited by Michael C. Flickinger.
© 2013 John Wiley & Sons, Inc. Published 2013 by John Wiley & Sons, Inc.

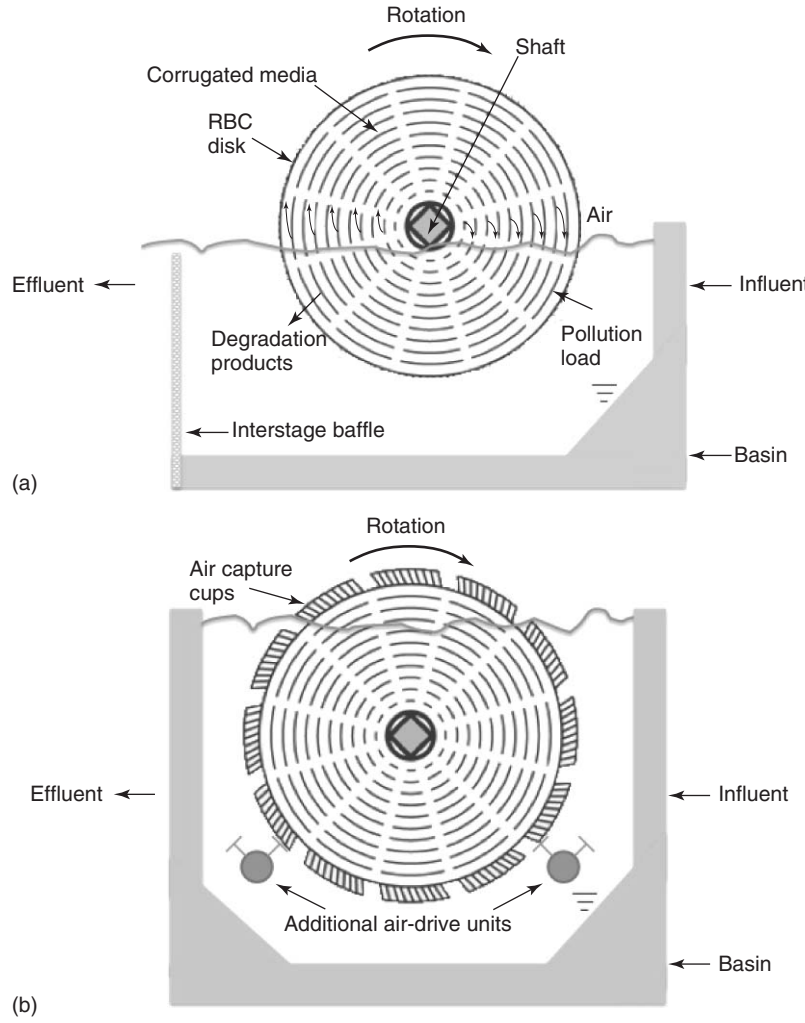


Figure 47.1. Schematic representation of (a) a rotating biological contactor, with approximately 40% submergence, and (b) a deeper submerged rotating biological contactor.

enabling the removal of the surplus microorganisms from the media (6,7). This excess of biomass is carried out along with the flow of effluent to a clarifier where it is separated from the treated effluent. The reactor may comprise a single compartment (one stage) or several compartments, with a group of disks or a random packed medium in each stage. Stages are accomplished by using baffles fixed to the tank or using a series of tanks.

The main equipment items of RBCs include a basin, baffles, shafts, supporting media, drive systems, and a cover. It must be noted that the designation for individual equipment components may differ slightly, depending on the manufacturer. The reactor basin is the physical tank that holds the media, shaft, and drive assembly through which the wastewater flows. Internal baffling or weir structures separate the stages of the RBC reactors, preventing short-circuiting of wastewater. Removable baffles are often used to allow process changes after the facility is constructed. The shaft is the central structure of an RBC unit. RBC shafts are used to support and rotate the media (disks or filled drums) and expose the media to alternate cycles of wastewater and air. The shafts are usually fabricated from steel and are covered with a heavy protective coating suitable for water and high humidity. RBC drive shafts are mounted perpendicular or parallel to the direction of flow. The media provide the support for organisms to attach and to develop a biofilm. Various media configurations with different thickness, shape, or corrugation patterns have been available from manufacturers, each with its own claimed advantages. The drive assembly rotates the media. There are two types of drive assemblies: mechanical drives and air drives. A mechanical drive is attached directly to the shaft providing constant speed capability only. This type of



(a)



(b)

Figure 47.2. Examples of commercial-scale rotating biological contactors. (a) Detail of a rotating biological contactor with biofilm in the support media. (b) Rotating biological contactors covered. Photographs courtesy: Seprotech Systems Inc.

drive is used most often. An air drive consists of deep plastic cups attached to the perimeter of the media, an air header located beneath the media, and an air compressor. The release of air into the cups tends to aid in shearing excess biomass from the media, thereby reducing film thickness and corresponding loads on the shafts. Both types of drives have bearings to support the RBC shafts. Covers or enclosures are often made of fiberglass or other reinforced resin plastics. Another approach involves housing a number of shafts in a building. In either case, the RBC enclosure must have ventilation, humidity and condensation control, and heat loss provisions. RBCs are covered to protect the media from UV radiation, which can weaken them, to protect biological slimes from freezing, to prevent intensive rain from washing off biofilm growth, and to control media exposure to sunlight, which results in algae growth. Examples of commercial RBC units are presented in Fig. 47.2.

47.2.2 Advantages and Disadvantages

Due to their advantages, RBCs are widely used for secondary and/or advanced treatment in municipal and industrial wastewater applications. In fact, these reactors have more advantages than disadvantages (Table 47.1).

47.2.3 Typical Applications

RBCs have been successfully used to provide secondary treatment (the removal of organic carbon) of municipal wastewater in small to medium size wastewater treatment plants. They have also been applied to the oxidation of ammonium (NH_4^+) to nitrate (NO_3^-), either in combined carbon oxidation and nitrification applications or in separate stage nitrification applications, denitrification (reduction of NO_3^- to N_2), and phosphorus removal (9–11). In addition, they have also been used in bioremediation of landfill leachate (12–14), refinery and petrochemical effluents (1,15), pulp and paper mills effluents (16,17), leather tanneries effluents (18), mining, nuclear and electronics industries effluents (19,20), effluents from food and beverage industries, including wineries (22,21), bakeries (23), or food processors (24,25), as well as for decolorization of wastewaters such as textile dyes (26,27), colored sugar refinery (28), or paper mill effluents (29).

TABLE 47.1. Advantages and Disadvantages of Rotating Biological Contactors

Advantages	Disadvantages
Mechanically simple	Performance susceptible to wastewater characteristics
Simple process control and monitoring	Limited process flexibility
Easy to operate	Limited ability to scale-up
Low energy requirements	Adequate primary treatment and secondary clarifier required
Modular configuration allows easy construction and expansion	Slow process start-up
Low land requirement	Sensitivity to industrial wastes
Compact design with separate compartments	Must be protected against sunlight, rain and snow
Low operating and maintenance cost	Requires permanent skilled technical labor for operation and maintenance (but less than the required by a conventional activated sludge plant)
Short hydraulic retention times	Mechanical failures
High oxygen transfer efficiency	
High biomass concentration per volume reactor	
Low solids generation	
No requirement of sludge recirculation	
High process stability	
Process relatively silent	

Source: Adapted from Ref. 8.

47.2.4 Hydrodynamics

The efficiency of wastewater treatment in an RBC depends on the active biofilm developed on disk surface and at the contact area between the biofilm and the effluent to be treated. Therefore, an efficient mixing regime in the reactor is needed. In this type of reactor, the mixture depends on the media rotational speed, the degree of media submergence, the hydraulic retention time (HRT), and the biomass present. The existence of corners in the reactor, for example, may give rise to stagnant areas, which disturb mixing conditions and must be avoided. Regarding the mixing conditions within the RBCs, no common agreement exists on whether RBC behaves like a plug-flow or a completely mixed reactor. Experimental results of Banerjee (30) justify the use of staging in an RBC reactor, because mixing decreases gradually along the reactor, approximating the system to a plug-flow regime. Patwardhan (6) reported that as a first approximation, one could assume that each unit of an overall RBC system behaves as a continuous stirred-tank reactor (CSTR). It must be noted that most studies have been performed without biomass in the reactor, which does not reflect a real situation and may lead to erroneous results on the hydraulics of the reactor. Teixeira *et al.* (31) studied the effect of biofilm in the nonideal behavior of a laboratory anoxic RBC through the determination of residence time distribution using the stimulus–response technique. These authors observed that when the disks were covered by biofilm and with biogas production, the existence of hydraulic dead volumes decreased significantly. In practice, the hydrodynamic behavior of any biofilm reactor lies somewhere between these two ideal flow patterns and is always affected by the existence of bypass, short-circuiting, recycling, and dead zones. Another point to be considered is that most RBC hydrodynamic studies were performed in RBC systems with plain disks. Detailed experimental investigations with other media need to be carried out to assess the axial mixing.

47.2.5 Factors Affecting Performance

Although the parameters that determine the efficiency of the reactor will depend on the wastewater to be treated, there are always factors that are common to all processes and that affect the performance of the RBCs. Particularly significant are rotational speed, organic and hydraulic loading rates (HLRs), HRT, RBC media, staging, temperature, dissolved oxygen (DO) levels, effluent and solids recirculation, step-feeding, and medium submergence. There is no consensus on which parameter is more important.

47.2.5.1 Rotational Speed. The rotational speed of the RBC media is crucial for the RBC efficiency because it affects the mixing regime in the reactor, biofilm thickness, and nutrient and oxygen mass transfer inside the biofilm and consequently substrate removal. Many authors have investigated the effect of rotational speed in the performance of RBC systems (1,3,9,32,33). Usually, an increase in the rotational speed increases the DO concentration available to the microorganisms and as a result they are able to degrade the substrate at a higher rate (1). For instance, Najafpour *et al.* (32) observed that the soluble chemical oxygen demand (SCOD) increased from 62.7% to 93.7% relative to a disk rotational speed increase from 3 to 11 rpm. However, the removal efficiency of any substrate increases with the medium speed of rotation

up to a limit. High rotational speed leads to high shear stress, causing the detachment of biomass, deteriorating the effluent quality and reducing the biodegradation rate in the reactor. Besides, an increase in the rotational speed leads to higher power consumption, which may not be economical for wastewater treatment applications (29). Packed supports will provide considerably more oxygenation than disk RBCs at the same rotational speed, but they will require greater power consumption (34). Thus, the guiding principle is to adopt the minimum speed commensurate with acceptable treatment. According to Mathure and Patwardhan (35), typically, rotational speeds are 1–10 rpm for RBC media in disk form with disks of 1- to 4-m diameter mounted on shafts around 5- to 10-m long.

The use of variable rotational rates or the ability to reverse shaft rotation have been suggested to enhance the sloughing of biofilm, in RBC units (36).

47.2.5.2 Organic Loading. The organic loading of an RBC reactor must be accurately defined during planning and designing, but is often overlooked. This parameter allows direct comparison of the RBC system performance when operated under various circumstances and with different kinds of wastewater. The variation of the organic loading rate (OLR) is generally accomplished by changing the inlet flow rate or the HRT, which also results in a change in the hydraulic loading (32). Table 47.2 summarizes the experimental details and performance results of different studies on the effect of organic load on the performance of some RBC systems.

Available data show that, for a given system, as the applied OLR increases, removal efficiency decreases and the substrate removal rate increases. This substrate removal rate rises up to a limit, after which the loading rate has no or limited impact on the removal rate (33,41).

Under normal operating conditions and for low organic loadings, the carbonaceous substrate is mainly removed in the first stage of the RBC. To avoid oxygen transfer limitations, the first-stage design load must be limited to a 5-day biochemical oxygen demand (BOD_5) load 30 g BOD_5/m^2 day or to a soluble BOD_5 load of 12–20 g BOD_5/m^2 day according to Water Environment Federation (WEF) and American Society of Civil Engineers (ASCE) (42). The use of higher first-stage organic loadings will increase the probability of developing problems such as excessive biofilm thickness, depletion of DO, deterioration of process performance, appearance of H_2S odors, and excessive growth of nuisance organisms such as *Beggiatoa* (8,36). Overloading problems can be overcome by removing baffles between the first and second stages to reduce surface loading and increase oxygen transfer. Other approaches include supplemental air systems, step-feed, or recycle from the last stage (40).

The organic loading strongly affects nitrification in an RBC unit. In the initial stages, where the organic load is high, heterotrophic bacteria offer strong competition to nitrifiers displacing them within the bioreactor (43). Therefore, the maximum nitrification rate occurs when the soluble BOD load reduces sufficiently, which always takes place in the latter stages of the RBC. In the case of full-scale RBCs for nitrification of municipal wastewater, Griffin and Findlay (44) found that the OLR imposed to the RBC system should not exceed 4 or 2.5 g BOD_5/m^2 day to achieve an effluent quality of 15 or 10 mg $N–NH_4^+/L$. Nowak (45) proposed that an OLR of 2.5 g BOD_5/m^2 day is desirable to keep the effluent ammonium concentration below 5 mg $N–NH_4^+/L$, at temperatures above 12°C.

47.2.5.3 Hydraulic Loading. As in any other reactor, the performance of RBC units is highly correlated with hydraulic loading, defined as the flow of wastewater introduced into an RBC per surface area unit. In general, increasing the flow rate through the bioreactor reduces the liquid retention time in the system and results in a reduction in removal efficiency (Table 47.2). In defined conditions, increasing HLR also leads to an increase in the attached biomass on RBC media surface (46).

HLR values vary widely depending on the design, the substrate being removed, and the effluent concentration desired (34). Some RBC manufacturers developed design relationships for municipal wastewater in which effluent quality is plotted as a function of hydraulic loading, at a specified temperature. These relationships are very useful to predict the unit performance, although they do not take into account the intrinsic biodegradation constants and hydrodynamics of the system. Moreover, equipment manufacturers often provide optimistic estimates, thus attention should be paid to the selection and application of such empirical relationships (8). Typical HLR range recommended by RBC manufacturers is 1.292–6.833 $dm^3/m^2/h$ (36).

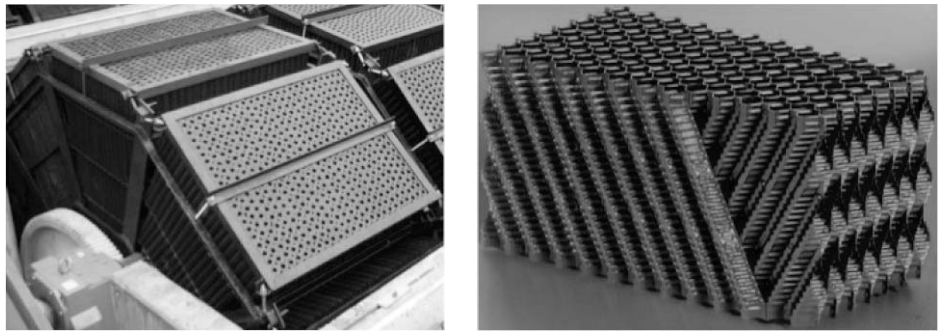
Due to the large amount of biological mass present (low operating feed/microorganisms), RBCs offer good stability under high or toxic hydraulic and organic loadings (38).

47.2.5.4 Hydraulic Retention Time. The HRT depends directly on the volume of liquid in the tank, and the effluent flow studies with RBC systems have shown that longer contact times improve the diffusion of the substrate into the biofilm and its consequent removal from the influent (9,32). This trend is also verified with toxic and heavy metal substrates (17,47,48).

A too short HRT will result in low removal rates, whereas a too long HRT will not be economically feasible. For a biological system to compete successfully with conventional physicochemical methods of treatment, the shortest possible HRT associated with the most efficient

TABLE 47.2. Experimental Details and Summary of Results of Different Studies on the Effect of Organic and Hydraulic Loading in the Performance of RBC Systems

Types of operation and scale	Reactor Specifications: Type of Material and Media	Reactor Specifications: Media Dimensions	Reactor Specifications: No. of Stages/No. of Disks or Filling Ratio	Reactor Specifications: Sub-mergence (%)	Reactor Specifications: Rotational Speed (rpm)	Type of Wastewater	Modified Parameters: Hydraulic Loading/ Influent Flow Rate	Modified Parameters: Inlet Organic Loading/ Substrate Concentration	Modified Parameters: HRT (h)	Performance	Reference
Aerobic lab-scale	Polyvinyl chloride disks	Diameter: 0.2 m	1/10	50	3–10	Synthetic municipal wastewater	17–113 dm^3/m^2d	5–35 g TOC/m^2d	—	At 3 rpm, for HLR = 17 dm^3/m^2d and 5 mg TOC/m^2d: 93.2% TOC removal; for HLR = 113 dm^3/m^2d and 35 mg TOC/m^2d: 22.8% TOC removal	(33)
	Acrylic disks	Diameter: 0.25 m	3/42	32	5	High strength municipal wastewater	20–32 dm^3/m^2d	10–32 g COD/m^2d 1.1–3.3 g N/m^2d	24–15	For HRT = 24 h and HLR = 20 dm^3/m^2d, at 20 g COD/m^2d and 2.2 g N/m^2d: 19.4 g COD/m^2d removed in the first stage and 99.45% $N–NH_4^+$ overall removed; 10 g COD/m^2d and 1.1 g N/m^2d: 8.7 g COD/m^2d removed in the first stage and 90.50% $N–NH_4^+$ overall removed	(37)
	Propylene square rings	Diameter: 68 mm	1/–	40	3	Synthetic food industrial wastewater	0.6–1.2 g $BOD_5/dm^3/d$	2.04–4.07 g BOD_5/m^2d	16–8	At 2.04 g BOD_5/m^2d and 0.6 g $BOD_5/dm^3/d$: 91.7%, 92.5%, and 47.4% for COD, BOD_5, and TKN removal, respectively; at 4.07 g BOD_5/m^2d and 1.2 g $BOD_5/dm^3/d$: 87.4%, 90.0%, and 44.1% for COD, BOD_5, and TKN removal, respectively	(38)
Aerobic pilot-scale	Hard polyethylene disks	Diameter: 0.5 m	6/16	37	8	Industrial wastewater	0.013 m^3/m^2d	5.3–17.8 mg $SBOD_5/m^2d$	16	At 5.3 mg $SBOD_5/m^2d$: 76%, 75%, and 85% for COD, BOD_5, and $SBOD_5$ removal, respectively; 17.8 mg $SBOD_5/m^2d$: 59%, 65%, and 74% for COD, BOD_5, and $SBOD_5$ removal, respectively	(39)
Aerobic full-scale	Disks	—	4/–	—	—	Municipal wastewater	3785 m^3/d	18–42 mg $N–NH_4^+/dm^3$ 164.4–430 mg $SCOD/dm^3$	—	At 164.4 mg $SCOD/dm^3$: 72.7% and 20.2% for SCOD and $N–NH_4^+$ removal, respectively; 430 mg $SCOD/dm^3$: 67.4% and 25.6% for SCOD and $N–NH_4^+$ removal, respectively	(40)



(a) (b)

Figure 47.3. Examples of commercial RBC packing media: (a) BIO-NET packing consists of grid tubes, which together form blocks; the media is made of HDPE, UV-stabilized with carbon filling. Photograph courtesy: NSW. (b) KFP319 cross-fluted fill: the media is made of PP/PVC, measures 600 × 300 × 300 mm (length × width × height) and presents a void ratio superior to 97%. Photograph courtesy: GEA 2H Water Technologies.

removal rates is required (47). A significant advantage offered by full-scale RBCs is to require short hydraulic retention periods (generally <1 h) (49).

47.2.5.5 Media. The main functions of the RBC media are to provide surface area for biological growth, to promote the contact between the wastewater and the microorganisms, and to achieve oxygen transfer from air into the film of wastewater and biofilm. Over the years, RBC systems have evolved considerably from the original design of rotating disks made from wood. With the introduction of plastic (polyvinyl chloride, polymethylmethacrylate, polycarbonate, polystyrene, polyethylene, etc.), the media fabrication costs reduced and many variations now exist, ranging from simple flat disks through corrugations to cellular meshes.

It has been shown that the adhesion of bacteria to scratched or corrugated media is stronger than adhesion to flat surfaces (3). Furthermore, biofilm build-up is slower on flat surfaces. Rough surfaces ensure zones of low shear stress where attached bacteria are protected from the forces that could remove them. Corrugations enhance structural stability, improve mass transfer, and increase the available surface area (8). High density polyethylene (HDPE) is the material most used in RBC media and is commercialized in different configurations or corrugation patterns commonly termed *low (or standard) density, medium density*, and *high density* according to the basis of surface area provided (7). Standard-density media are defined as having $115\,m^2m^3$ of reactor, with larger spaces between media layers, and are normally used in the former stages of an RBC process train. Medium and high density media have $135-200\,m^2m^3$ of reactor and are used typically in the middle and final stages of an RBC system where thinner biological growth occurs (36).

Some modifications of conventional RBC media have been explored at laboratory-scale with positive results concerning substrate removal. To increase the area and volume for filamentous organisms, one has to solve the problem of slow start-up, improve turbulence near the bulk liquid interface, facilitate efficient mass transfer, and enhance the capacity of handling high OLR; Guimar aes *et al.* (28) attached a layer of polyurethane foam on plastic disks. More recently, Tawfik and Klapwijk (50) compared the efficiency between polyurethane foam and polystyrene rotating disk units, at the same operational conditions, and even though both reactors achieved almost the same chemical oxygen demand (COD) removal, the unit with polyurethane disks performed significantly better for ammonium and *Escherichia coli* removal. These authors concluded that channels and pores of the polyurethane material make substrate transfer efficient, which increased the performance of the simultaneous nitrification and denitrification (SND) processes. Chen *et al.* (51) modified the RBC disks covering them with a net-like structural rubber material with 97% porosity and also verified the occurrence of SND.

During the past two decades, random packed media were successfully used as substitutes for disks at the laboratory and pilot-scale. Such media provide more area for attachment of the biofilm within the same reactor size, contributing to higher mass transfer efficiency due to increased turbulence. In addition, the fabrication cost is nearly one third of that of disks (35). Different types of packing such as Pall rings, saddles, and cylindrical plastic elements with distinctive sizes have been applied in random packed RBC systems presenting attractive results (23,35,38) (Fig. 47.3).

While the use of random packed media is not new, few manufacturers are commercially exploiting it. At large-scale, such as with conventional disks, some

operational problems can occur, leading to a lot or variable biofilm growth. With careful design and further research, it may be possible to develop packing media with the appropriate orientation and movement, allowing the development of a suitable biofilm in a full-scale packed cage.

As recommendation, at the design stage of a particular RBC system, it is necessary to evaluate the characteristics of the wastewater to be treated and the treatment objectives and to compare the various types of biofilm-supporting media reported in the literature in terms of costs, the interfacial area offered, mass transfer coefficients, and power consumption. This will enable the consulting engineer to choose the most appropriate type of medium (6). However, it must be noted that as the supporting medium gets more complex, its cost increases accordingly.

47.2.5.6 Staging. Radwan and Ramanujam (52) referred that staging in the design of RBC systems is especially important at higher organic loadings and also if high effluent treatment quality is required. According to Tawfik *et al.* (53), staging of RBC decreases the detrimental effect of shock load on the performance of the system.

As the wastewater flows through an RBC system, each subsequent stage receives an influent with an organic concentration lower than the previous stage. Because heterotrophic bacteria usually grow faster than nitrifiers, the first stage of an RBC tends to be primarily a BOD or COD removal device, unless the wastewater organic content is very low. As the wastewater moves to the second and subsequent stages, the RBC tends to first remove ammonium and then nitrite with the final product being nitrate, assuming the RBC is sized and operated correctly (34). These facts are corroborated, for instance, by Tawfik *et al.* (53), who studied two RBC units connected in series and observed that the two-stage RBC system provide a better effluent quality over a single-stage RBC. Most of the COD reduction was observed in the first stage, while in second-stage nitrification was performed efficiently. Therefore, staging promotes a variety of conditions where different kinds of microorganisms can flourish.

In secondary treatment applications, RBCs shall be designed and operated in a series of three stages per flow. For combined BOD_5 and $N–NH_4^+$ removal, a minimum of four stages is recommended per effluent flow. When there is recycling of wastewater from the last stage to the first one, denitrification may be achieved in the first stage, where there is high organic loading and low DO content.

For small plants, multiple stages are acceptable on a single shaft oriented in parallel to the direction of flow. In larger installations, shafts are mounted perpendicular to the flow with several stages in series (36). Typical RBC staging arrangements are illustrated in Fig. 47.4.

Different numbers of stages have been used in several applications (Table 47.2). Staging calculations, based on COD and $N–NH_4^+$ effluent concentrations, can be assessed using literature tables, with the appropriate adaptations.

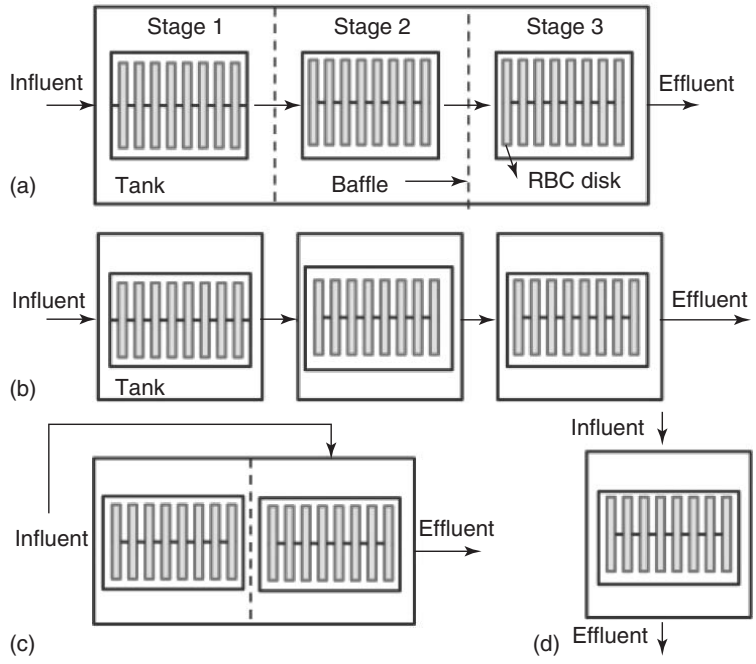


Figure 47.4. (a) One flow parallel to shaft, one RBC unit, three stages; (b) one flow parallel to shaft, three RBC units; (c) step-feed flow, one RBC unit, two stages; (d) one flow perpendicular to shaft, one RBC unit.

47.2.5.7 Temperature. The performance of the RBC system is temperature dependent because temperature is one of the most important parameters that affect the rate of biological processes. At limited conditions, an increase in the influent temperature leads to an increase in the microbial activity and a higher substrate removal can be observed in all RBC stages (1,30). Low influent temperatures can adversely affect biofilm establishment and consequently the reactor performance, particularly in its early stages (47). However, water will hold more DO at colder temperatures as compared with warmer temperatures. Water in the winter can hold almost twice as much DO as in the summer.

Temperature correction factors need to be taken into account in design criteria and can be obtained from the equipment manufacturers or from pilot studies. Generally, when the temperature drops from 13 to 5°C, nearly 2.5 times more media surface area is required for achieving the same performance (7). In biofilms, the nitrification process is less temperature dependent than in activated sludge (AS). The nitrification rate increases by about 4.5%/°C (45). Year-round operation requires that rotating contactors be covered to protect the biological growth from freezing temperatures or excessive heat gain, which accelerates media deterioration. The highest removal efficiencies occur in warmer weather.

47.2.5.8 Dissolved Oxygen Levels. The importance of DO in aerobic wastewater treatment is well known. An inadequate DO concentration may be a major cause of process failure. In an aerobic RBC system, the biofilm gradually forms on the disk surface. The constant rotation of the disk causes mixing of the liquid. Also, the rotating disk surface alternately comes into contact between air and wastewater and thus acts as an aeration device for wastewater treatment. Oxygen transfers from the air to the RBC unit in three ways: by oxygen absorption at the liquid film over the biofilm surface when the biofilm is in the air, by direct oxygen transfer at the air–water interface, and by direct oxygen absorption by the microorganisms during the air exposures (54).

Occasionally, as a consequence of an active respiration in the initial stages, the oxygen concentration reaches minimal levels, increasing along the reactor where substrate concentration is low. In these conditions, in the former compartments, denitrification might take place.

An increase in the speed of rotation, at a given level of submergence, leads to an increase in the oxygen transfer capacity of an RBC, in terms of the overall oxygen transfer coefficient, $K_L a$ (7). At a particular rotational speed, as submergence increases, the $K_L a$ decreases (35). Some researchers (33,55) have improved empirical/mathematical models for the estimation of $K_L a$ in RBC reactors (Table 47.3).

It is very difficult to model the oxygen transfer because these systems are very complex and include biofilm growth and detachment, the participation of suspended biomass,

TABLE 47.3. Proposed $K_L a$ Models for RBC Reactors

model	RBC Media	Predicted $K_L a$ Model	Nomenclature	Reference
Kim and Molof	Disks	$K_L a = 0.011\left(\frac{w^{1.5}D^{0.5}}{d}\right)^{0.732}$	ω - rotational speed [T]$^{-1}$ D - disk diameter [L] d - distance between the discs [T]	(56)
Kubsad et al.	Disks	$K_L a = 0.01315\left(\frac{1.697Anw^{1.5}D^{0.5}}{V}\right)^{0.73778}$	A - exposed surface area to air of one disc [L]2 n - number of discs ω - rotational speed [T]$^{-1}$ D - disc diameter [L] V - working volume of the reactor [L]3	(57)
Chavan and Mukherji	Disks	$K_L a = \left(\frac{D}{A_d^{0.5}}\right)^{\psi}\left(\frac{\rho A_d \omega}{\mu}\right)^{\varepsilon}\left(\frac{A_d}{A_t}\right)^{\theta}\left(\frac{\delta}{V^{1/3}}\right)^{\lambda}\left(\frac{\mu}{\rho A_d}\right)$	D - disc diameter [L] A_d - disc area [L]2 ρ - liquid density [M] [L]$^{-3}$ ω - rotational speed [T]$^{-1}$ μ - liquid viscosity [M] [L]$^{-1}$ [T]$^{-1}$ A_t - cross-sectional tank area [L]2 δ - liquid film thickness [L] V - working volume of the reactor [L]3 $\psi\varepsilon\theta\lambda$ - fitting parameter	(55)
Palma and Verdone	Disks	$K_L a = 134.07\omega^{1.5}C^{0.5}\left(\frac{2.15}{\omega} + 0.006\right)$	ω - rotational speed [T]$^{-1}$ C - carbon removal rate reduction in oxygen limiting conditions (%)	(33)

and so on. However, the proposed empirical models will facilitate the scale-up of RBC units.

During operation oxygen levels must be properly controlled and to prevent oxygen concentration from becoming a limiting factor, initial stages should have at least 2 mg DO/L (45). If the rotating motion does not supply sufficient oxygen, a supplemental aeration system should be installed (7,40). Usually this promotes a remarkable performance of the RBC, with an established thinner and active aerobic biomass, allowing considerable cost savings in design and construction of RBC units.

47.2.5.9 Effluent and Solids Recirculation. Recirculation of the RBC-treated effluent (either before or after the secondary clarifier) does not significantly improve the treatment efficiency (5). Nevertheless, under certain conditions (e.g. during the start-up or in the treatment of high strength effluents), recirculation may avoid overloading and thus lead to more reliable RBC performance. Therefore, in spite of being optional, recirculation should be considered in the RBC design for adverse conditions. The rate of recirculation recommended is approximately 25% of the average design flow (58).

Improved ammonium removal efficiencies have been occasionally reported when recirculation is applied, increasing with recirculation ratios (59,60). Improved nitrification with recirculation is attributed to the dilution of influent biodegradable organic carbon.

47.2.5.10 Step-Feeding. To reduce or prevent overloads and increase the process capacity, a step-feeding of the RBC stage(s) should be provided. Lv *et al.* (61) and Saikaly and Ayoub (62) indicated that working in a step-feed mode improved the removal rates of both total nitrogen (TN) and $N–NH_4^+$. The latter authors also found higher DO values in RBCs with step-feeding. The combined effect of step-feed and effluent recirculation in increasing RBC activity was reported by Ayoub and Saikaly (63), but for a simple soluble substrate.

47.2.5.11 RBC Medium Submergence. Typically, in aerobic processes of municipal wastewater treatment, the RBC media submergence is about 40%, although in nutrients removal it can attain 60%. Considering industrial effluents, due to their diversity, there is no standard value for media submergence. Submergence to 70–90% might be an alternative option, providing the advantages of less loading on the shafts and bearings, larger media volume available, and fewer RBC units required (64). However, if the deeper submerged RBC is used to treat wastewater aerobically, DO in the liquid will be lower and as a consequence, additional air drive units must be used to provide oxygen and rotation (7). The increased submergence combined with the air drive rotation of the deeper submerged RBC has dramatic economic and operating benefits (64).

The deeper submerged RBC units can also be applied as anaerobic RBCs (65,66) or used for denitrification (9,14,67,68). In these applications, the reactors are completely closed to avoid air entrance.

According to Laquidara *et al.* (69), anaerobic RBC systems combine advantages of the aerobic RBC reactor with the anaerobic process (no oxygen transfer limitations, low quantities of waste biological solids, and recovery of the usable energy in the form of methane). Due to these advantages, the anaerobic RBC process appears to be well suited for treating both medium and high strength organic wastewater (66). Lu *et al.* (66) studied the effect of increasing disk submergence (40%, 70%, and 100%) in an anaerobic RBC and verified that the degree of mixing increased with the decrease in disk submergence. On the contrary, COD removal efficiency increased with the increase in submergence. There is a great scope of application for anaerobic RBCs in industrial wastewater treatment, which are at present considered suitable for treatment by other anaerobic processes. It is in anaerobic degradation that RBCs could prove to be even more successful than they have been in aerobic treatment (70).

Teixeira and Oliveira (67) investigated the effect of disk submergence on the performance of lab-scale RBCs, in terms of the denitrification process. For an influent $N–NO_3^-$ concentration of 50 mg/dm^3, the removal efficiencies obtained were 37 and 17 g $N–NO_3^-$/m^3·m^2 for, respectively, 100% and 64.5% disk submergence. Using a pilot-scale RBC with a completely submerged plastic tubular medium, Mohseni-Bandpi and Elliot (68) achieved a maximum nitrate removal rate of 168 mg $N–NO_3^-$/m^{2}h for an influent of 130 mg $N–NO_3^-$/dm^3.

Cortez *et al.* (14) observed that the completely immersed disks of the anoxic RBC achieved $N–NO_3^-$ removal efficiencies above 95% for concentrations up to 100 mg $N–NO_3^-$/dm^3. The highest observed denitrification rate was 55 mg $N–NO_3^-$/dm^3/h (15 g $N–NO_3^-$/m^2 day) at a nitrate concentration of 560 mg $N–NO_3^-$/dm^3.

Recently, a three-stage, fully submerged anaerobic/anoxic/aerobic RBC hybridized with a suspended sludge system was found to be an efficient and controllable process for carbon, nitrogen, and phosphorus removal (71).

47.2.5.12 Biofilm Characteristics. A layer of biological growth, also known as a *biofilm*, develops on the surface of the RBC media. This layer constitutes a biocatalyst and the degradation of the substrate depends on the rate of metabolism of the microorganisms present. The microorganisms grow by degrading the substrate and, in turn, promote biofilm growth. A biofilm consists of a complex structured community of bacterial cells enclosed

in a self-produced polymeric matrix and adherent to an inert or living surface (72).

Observations of full-scale RBC biofilms treating municipal wastewater report that a biofilm from the initial stages has a gelatinous aspect, being usually grayish and may present some white zones probably due to filamentous bacteria-like *Beggiatoa*. In addition, in this part of the reactor, biofilm is almost entirely constituted by species of ciliates. Biofilm of the last stages is always thinner than in the first stages, has a brown-like color or sometimes reddish, and shows more diversified communities, not only in species of ciliates but also in flagellates, amoebae, and metazoa (rotifers, nematodes, and annelids). The main limiting factor of microfauna growth is the degree of pollution in the influent expressed in terms of COD or BOD_5. As long as this parameter decreases along the RBC, its effect as a limiting factor decreases too, resulting in an increase in the majority of existing species (73).

The outer biofilm layer of a full-scale RBC disk is very heterogeneous and complex, while the inner layer is more uniform and compact with a reduced microbial density and a larger percentage of nonviable bacteria (7). According to Okabe *et al.* (74), the active metabolic cell fraction decreases from $35 \pm 13\%$ in the outermost to $15 \pm 4\%$ in the innermost biofilm.

When the depth of the biofilm is large and the concentration of DO in air is low, the outer layer acts aerobically and the inner side acts anoxic or anaerobically (23). For example, Chen *et al.* (51) verified SND in a net-like RBC. Biofilm DO gradients adequately supplied growth conditions for nitrifying bacteria in the surface layers and for denitrifying bacteria in the deeper layers.

Biofilms ranging from 0.5 to 4.5 mm in thickness have been found in full-scale disk RBCs treating municipal wastewater. Biofilm thickness control is very important to avoid clogging or material fatigue stresses (44) and it is achieved through the hydrodynamic shear experienced by the biofilm.

The development of *Beggiatoa* is always taken as a warning for the performance of RBC units because its blooming prevents the sloughing of thick biofilm from the disks, which can lead to overload on the media supports (7).

The characterization of a biofilm in terms of thickness, density, total dry weight, humidity, chemical and biological composition, and activity is very useful when analyzing the performance of an RBC.

47.2.6 Process Design Aspects and RBC Scale-Up

To achieve the optimal degree of treatment, the RBC process design must consider the type and dimensions of the medium, the degree of submergence, the rotational speed, as well as the number of stages, among other parameters. The physical facilities, including the motor, gear system, and so on, have to be designed accordingly. Moreover, the selected RBC configuration must be such that the overall operation becomes economically viable and competitive (6).

During the 1970s and 1980s, the design of RBC units for the treatment of domestic and common industrial effluents relied on empirical design relationships. RBC manufacturers have developed their own empirical design curves, equations, and guidelines based on treatment data collected using their equipment. However, empirical models cannot be relied on to predict the concentration profile of a substrate through an RBC for conditions other than those studied experimentally. In addition, available RBC design curves and equations are not useful for the treatment of distinctive effluents that differ in composition from the well-characterized municipal or industrial effluents for which they were developed. Thus, the relatively slow acceptance and use of RBCs has been attributed, in part, to the lack of standardized design procedures (75).

For the rational design of an RBC system, it is important to consider the underlying hydrodynamics, biodegradation kinetics, oxygen transfer, development, and detachment of the biological film. Thus, the first step in the overall design process should be to carry out laboratory or pilot-scale experiments over a wide range of operating conditions with the particular wastewater. A step-wise process design algorithm is presented in Fig. 47.5.

From the data collected at laboratory or pilot-scale, it will be possible to scale-up the RBC system with confidence. Some RBC design recommendations, such as not to use high density media in the first stage or to prevent the biofilm from cold weather with an enclosure, along with many others, were referred along this chapter and should be respected. The performance of a RBC will be favored if it is designed to withstand both normal and unusual operation conditions. The possibility of applying supplemental aeration, step-feed, recirculation, or removable baffles (between stages) significantly improve operational flexibility of RBCs.

47.2.7 Operation and Maintenance

As any treatment process, the RBC system demands routine supervision provided by professional operators to avoid operating problems. This supervision will be different among plants but typical routine maintenance should include the inspection and maintenance of chain drives, belts, sprockets, rotating shafts, replacement of broken air cups, or media that might otherwise jam or interfere with shaft rotation and inspection of other moving parts according to the manufacturers' instructions or with guidance from the design engineer. Lubrication of all these moving parts and cleaning the attached growth media by

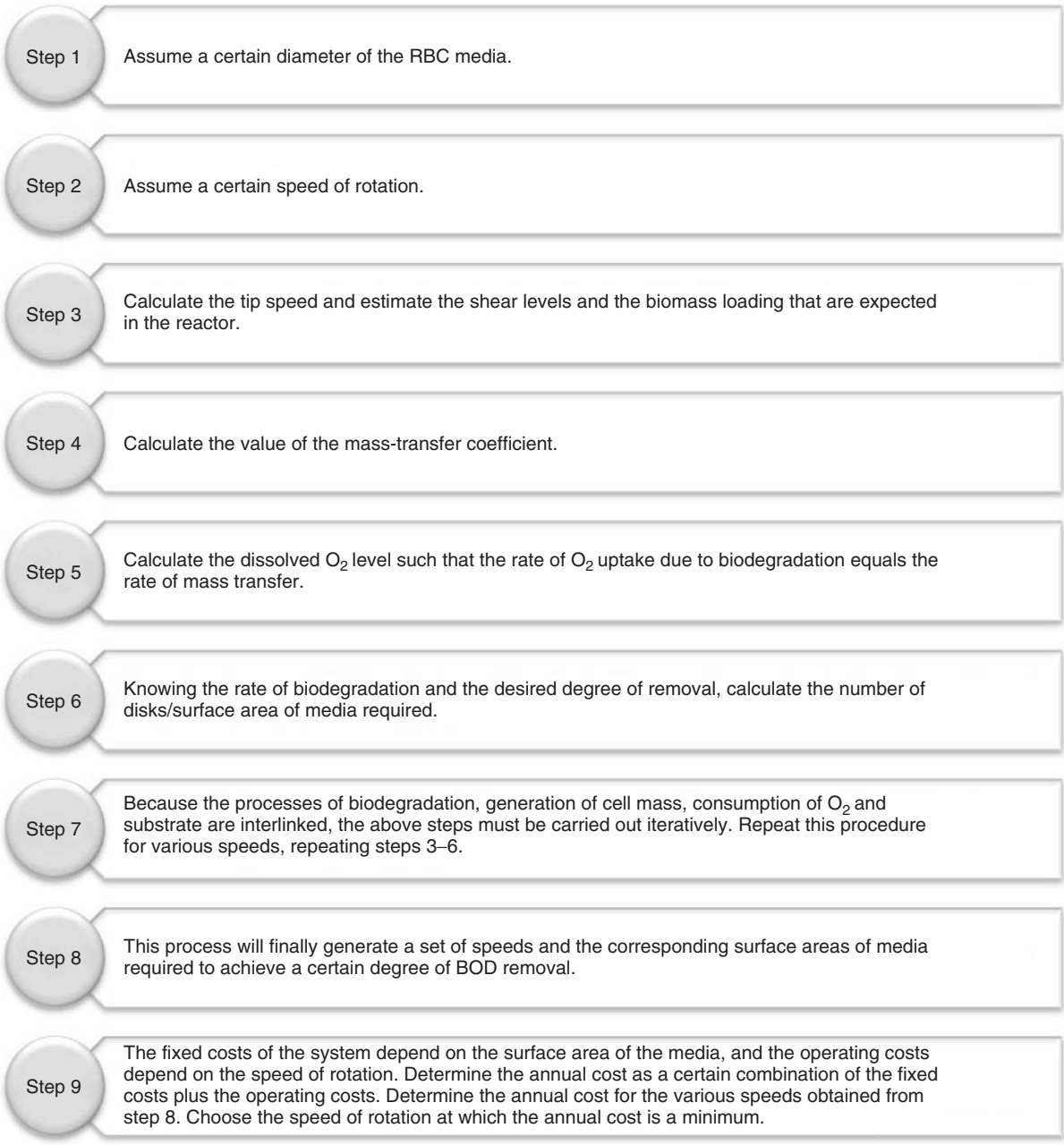


Figure 47.5. Scheme of a step-wise RBC process design algorithm (adapted from Ref. 6).

spray-washing of disks and purging of settled sludge are needed. Other metal parts should be periodically painted for protection.

In spite of all the mentioned advantages, RBC systems have some operating problems. Table 47.4 presents a troubleshooting guide for some problems associated with the design, operation, and maintenance of these reactors.

Considering mechanical failures, the most common are shaft breakage, stub shaft damage bearing failure, and media support structure fracture and degradation. These may arise due to overloading conditions, excess of biofilm growth, microbiologically influenced corrosion, low frequency corrosion fatigue, improper greasing and inadequate locking of nuts and bolts, or poor engineering design (77). Any one, or combinations, of these faults will require prompt replacement of the failed component. The most severe form of mechanical breakdown due to total replacement costs is the shaft fracture that results in complete collapse of the unit.

TABLE 47.4. Problems and Solutions for RBC Operation

Observation	Probable Cause	Monitor	Solution
Decreased treatment efficiency	Low wastewater temperature	Influent temperature	Cover RBC unit
	Organic overload	Influent BOD, TSS, pH, temperature, DO	Install equalization tanks before RBC to dilute high strength load and provide preaeration; add extra treatment units, if available; install supplemental aeration equipment to handle higher DO demands; recirculate secondary clarifier effluent to dilute influent flow
	Hydraulic overload	Influent flow	Flow equalization; eliminate source of excessive flow; balance flow between reactors
	Toxic influent	Influent COD, pH, temperature, DO	Sample the collection system to identify the source of toxicity; implement sewer ordinances to establish prohibitions and limitations of substance discharge and criminal fines if discharges occur; install equalization tanks before RBC to dilute high strength load and provide preaeration; install supplemental aeration equipment to handle higher DO demands; recirculate secondary clarifier effluent to dilute influent flow
	Short-circuiting	Check basin surface for visibly stagnant sections or dead zones	Install manifolds or diffusers on inlets and outlets; provide multiple inlets and outlets for more equal hydraulic distribution; change location of inlets and outlets; keep inlets and outlets as far apart as possible; eliminate dead zones
	pH too high or too low	Influent pH. Desired range is 6.5–8.5 for secondary treatment; 8–8.5 for nitrification	Eliminate source of undesirable pH or add an acid or base to adjust pH; when nitrifying, maintain alkalinity at seven times the influent ammonia concentrations
Excessive sloughing of biomass from disks	Toxic influent	Determine material and its source	Eliminate toxicmaterial if possible; use flow equalization tanks to reduce variations in concentration so biomass can acclimate
	Excessive pH variations	Influent pH	Eliminate source of pH variations or maintain control of influent pH
Development of white biofilm	High H_2S concentration	Influent odor	Preaerate wastewater or add $NaNO_3$, H_2O_2, or $FeSO_4$; apply supplemental aeration in the first stages
	First stage is overloaded	Organic load on first stage	Adjust baffles between first and second stages to increase fraction of total surface area in first stage
Solids accumulation	Inadequate pretreatment	Determine if solids are grit or organic	Remove solids from reactors and provide better grit removal or primary settling
Shaft bearings or motors running hot	Inadequate maintenance	Maintenance schedules, oil level, alignment	Lubricate per manufacturer's instructions

Source: Adapted from Ref. 81.

With a thorough understanding of the mechanisms involved in mechanical failure and with the development of improved RBC biofilm supports and bearings and stronger shafts, among others, a new approach to RBC design has resulted in reliable units with an expected operational life of 20 years. Furthermore, the improved design could revolutionize applicability of RBCs to high flow/highly populated regions (43,77).

47.2.8 RBC Versus Other Wastewater Treatment Systems

Although it is not possible to find easily comparable values in the literature between RBCs and other biological processes, Table 47.5 presents the characteristics and performance of several RBCs and other aerobic biofilm and AS processes.

TABLE 47.5. Performance of Different Aerobic Wastewater Treatment Systems

Type of Reactor	Type of Material and Media	Type of Wastewater	pH	HRT (h)	Hydraulic Loading/ Influent Flow Rate	Inlet Organic Loading/ Substrate Concentration	Other Related Data	Performance	Reference
Lab-scale									
Attached growth reactors									
Rotating biological contactor									
	PVC disks	Food industry wastewater	5.2	—	0.03 kg COD/m^3/d		Four-stage RBC	95%, 94%, 78%, 94%, and 87% for COD, BOD_5, TON, TSS, and oil and grease removal, respectively	(24)
	Polypropylene square-packed rings	Synthetic food industrial wastewater	6.8	12	—	2.72 g BOD_5/m^2d	One-stage RBC	89.4%, 92.0%, and 45.2% for COD, BOD_5, and TKN removal, respectively	(38)
Packed-bed reactor									
	Plastic corrugated cylindrical tubes with 2-cm length and 1.5-cm diameter	Food industry wastewater	4.6–5.0	—	0.31 m^3/m^2d 0.45 kg BOD/m^3/d 0.03 kg N/m^3/d			87%, 93%, 65%, 78%, and 73% for COD, BOD_5, TKN, TSS and oil and grease removal, respectively	(78)
Moving-bed biofilm reactor									
	Kaldnes carrier elements with 7-mm length and 10-mm diameter	Thermomechanic pulping whitewater	7.0	17.9	2.7 kg SCOD/m^3/d		Reactor temperature: 55°C	44% and 64% for COD and BOD_7 removal, respectively	(79)
Suspended growth reactors									
Activated sludge									
		Chemical industry wastewater	7.2	24			3 g MLSS/dm^3	93%, 95%, 92%, 98%, and 89% for COD, BOD_5, TON, TSS, and oil and grease removal, respectively	(80)
		Food industry wastewater	5.2	3 (SRT)			3 g MLSS/dm^3	96%, 98%, 41%, 94%, and 74% for COD, BOD_5, TON, TSS, and oil and grease removal, respectively	(24)

Large-scale									
Attached growth reactors									
Rotating biological contactor									
Pilot-scale	Polystyrene foam disks	Municipal wastewater	6.7–7.1	5	—	22 g COD/m^2d	Two-stage RBC	77%, 20%, and 31% for COD, $N–NH_4^+$, and TKN removal, respectively	(81)
Full-scale	Disks	Leather wastewater	9.0	—	—	15–20 g BOD/m^2d 50–65 g COD/m^2d	Four-stage RBCs	52.69% and 76.36% for COD and BOD_5 removal, respectively	(18)
Full-scale	Plastic packed rings	Food industry wastewater	5.2	—	0.02 m^3/m^2d		Four-stage RBC	86%, 88%, 71%, 73%, and 77% for COD, BOD_5, TON, TSS, and oil and grease removal, respectively	(24)
Moving-bed biofilm reactor									
Pilot-scale	Polypropylene corrugated cylinders with 20- to 30-mm length and 15- to 20-mm diameter	Municipal wastewater	—	—	0.61 kg COD/m^3/d	5.5 g COD/m^2d	Filling ratio: 70% Two reactors in series	76% and 92% for COD and $N–NH_4^+$ removal, respectively	(82)
Full-scale (upgrade)	Polypropylene corrugated cylinders with 20- to 30-mm length and 15- to 20-mm diameter	Municipal wastewater	—			7.9 g COD/m^2d	Filling ratio: 53%	73%, 83%, and 72% for COD, BOD_5, and $N–NH_4^+$ removal, respectively	(83)
Suspended growth reactors									
Activated sludge									
Pilot-scale		Municipal wastewater	—	—	0.61 kg COD/m^3/d	5.5 g COD/m^2d	Sludge recirculation	84% and 98% for COD and $N–NH_4^+$ removal, respectively	(82)

The efficiency of an RBC with a high rate packed-bed reactor for the treatment of an upflow anaerobic sludge blanket (UASB) reactor effluent was compared by van Buuren (84). At an HRT of 3.3 h, the packed-bed reactor removed 50% of COD, while the RBC removed 70%, indicating a better performance of the RBC. Moreover, at a much shorter HRT of 0.24 h, the RBC still achieved 40–80% COD removal.

Specifically, comparing the most common suspended growth process, the AS process, with the RBC shows that both the processes can produce high levels of treatment. However, the RBC process is easier to operate, occupies slightly less area, requires less than half of the energy, and reduces the cost of other plant processes by the nature of the excess biosolids that are generated when compared with those created in the AS process. Nasr *et al.* (80) compared, at laboratory-scale, these two biological processes for the treatment of chemical industrial wastewater (5239 mg COD/L and 2615 mg BOD_5/L). As both proved to be effective, producing effluents within the permissible limits, the engineering design of each treatment system (full-scale) was developed and the cost estimate indicated that the construction cost was similar for both the systems, while the running cost of AS was almost twice as that of the RBC. Thus, the use of the RBC system was recommended.

47.2.9 Costs Considerations

RBC units are variable with climate and location. Generally, these reactors involve high capital costs as not all materials may be locally available and motor and special material for rotation is required. Another cost factor may be the implementation, which requires skilled experts. According to a published article in 2009 (85), for the studied process, the construction cost of an RBC is US$624/inhab., while for a packed-bed filter is US$882/inhab. and for a wetland system is US$311/inhab. However, usually, maintenance and operating costs are lower for RBC units. In another research, cost estimate for the AS indicated that the construction system is US$54,912/year, while the running cost is US$19,912/year. The construction cost of the RBC is US$54,035/year, while the running cost is US$10,614/year. Therefore, an RBC system is recommended because of the management and operation of the system that will be easier and technically feasible by low skilled personnel (80).

47.3 CONCLUSIONS AND PROSPECTS

RBCs have been widely used as an efficient method of treating wastewater due to its simple process control and monitoring, ease of operation, low energy and land requirements, ability to withstand shocks or toxic loads, freedom from odors, and good sludge settling properties. These reactors offer an alternative treatment technology to the conventional AS process.

RBC units have been mainly used in aerobic processes because they provide high oxygen transfer efficiency. In this field, RBC media evolved considerably from the original design of several rotating disks into a unit filled with packed supports. There are not many studies on the influence of physical characteristics in these reactors' performance. Furthermore, studies on power consumption, hydrodynamics, mass transfer, and biofilm properties also need to be investigated for each type of packing material. Such studies should have an important bearing on scale-up and are encouraged.

Deeper submerged and covered RBCs are being used successfully at full-scale in denitrification and for the treatment of high strength industrial wastewater, constituting a promising technology. Thus, it is expected that the application of anoxic, anaerobic, or anammox RBC systems, at full-scale, with conventional or packing media, will increase. More studies with modified and improved RBC media, through utilization of new porous materials and/or application of biocoatings (86), and hybridized RBC units are likely to appear in the coming years.

Few mathematical models and with many limitations have been proposed to describe the performance of RBC reactors. For the appropriate design of an RBC system and to achieve the highest degree of treatment in an economical and suitable way, with low power input, it is important to consider the underlying hydrodynamics, biodegradation kinetics, oxygen transfer, and development and detachment of the biological film. Thus, further studies on this subject should continue to be carried out, together with laboratory or pilot-scale experiments.

To conclude, application of RBCs in new fields, such as the production of metabolites (e.g. antibiotics and vitamins) or the treatment of contaminants in different physical phases (e.g. pollutant gases), taking advantage from intense mass transfer at low power input, presents a great potential.

Acknowledgment

Susana Cortez fully acknowledges the financial support provided from Fundação para a Ciência e Tecnologia (FCT) through Grant SFRH/BPD/73720/2010.

LIST OF ABBREVIATIONS

AS	Activated sludge
BOD	Biochemical oxygen demand
BOD_5	5-day biochemical oxygen demand
BOD_7	7-day biochemical oxygen demand

COD	Chemical oxygen demand
CSTR	Continuous stirred-tank reactor
DO	Dissolved oxygen
HDPE	High density polyethylene
HLR	Hydraulic loading rate
HRT	Hydraulic retention time
$N–NH_4^+$	Nitrogen-ammonium
$N–NO_2^-$	Nitrogen-nitrite
$N–NO_3^-$	Nitrogen-nitrate
OLR	Organic loading rate
RBC	Rotating biological contactor
$SBOD_5$	Soluble 5-day biochemical oxygen demand
SCOD	Soluble chemical oxygen demand
SND	Simultaneous nitrification and denitrification
TKN	Total Kjeldahl nitrogen
TN	Total nitrogen
TOC	Total organic carbon
TON	Total organic nitrogen
TSS	Total suspended solids
UASB	Upflow anaerobic sludge blanket

REFERENCES

1. Israni SHI, Koli SS, Patwardhan AW, Melo JS, D'souza SF. J Chem Technol Biotechnol 2002; 77: 1050–1057.
2. Liu S, Yang F, Xue Y, Gong Z, Chen H, Wang T, Su Z. Bioresour Technol 2008; 99: 8273–8279.
3. Alnnasouri M, Lemaitre C, Gentric C, Dagot C, Pons MN. Biochem Eng J 2011; 57: 38–45.
4. García-Mesa JJ, Poyatos JM, Delgado-Ramos F, Muñio MM, Osorio F, Hontoria E. Bioresour Technol 2010; 101: 8038–8045.
5. Dutta S, Hoffman E, Hahn HH. Water Sci Technol 2007; 55: 345–353.
6. Patwardhan AW. Ind Eng Chem Res 2003; 42: 2035–2051.
7. Rodgers M, Zhan XM. Rev Environ Sci Biotechnol 2003; 2: 213–224.
8. Grady CPLJ, Daigger GT, Lim HC, editors. Biological wastewater treatment. New York; Mercel Dekker Inc.; 1999. p 907–947.
9. Hanhan O, Orhon D, Krauth K, Gunder B. Water Sci Technol 2005; 51: 131–139.
10. Gabet-Giraud V, Miège C, Choubert JM, Ruel SM, Coquery M. Bioresour Technol 2010; 408: 4257–4269.
11. Martin-Cereceda M, Perez-Uz B, Serrano S, Guinea A. Water Sci Technol 2002; 46: 199–206.
12. Castillo E, Vergara M, Moreno Y. Waste Manage 2007; 27: 720–726.
13. Kulikowska D, Józwiak T, Kowal P, Ciesielski S. Bioresour Technol 2010; 101: 3400–3405.
14. Cortez S, Teixeira P, Oliveira R, Mota M. Biodegradation 2010; 22: 661–671.
15. Chavan A, Mukherji S. J Hazard Mater 2008; 154: 63–72.
16. Brar SK, Gupta SK. Water Res 2000; 34: 4207–4214.
17. Majumder PS, Gupta SK. Bioresour Technol 2007; 98: 118–129.
18. Zao-yan Y, Zhen-san F. Water Sci Technol 1990; 22: 119–126.
19. Costley SC, Wallis FM. Water Res 2001; 35: 3715–3723.
20. Nikolov L, Karamanev D, Dakov L, Popova V. Environ Prog 2001; 20: 247–250.
21. Malandra L, Wolfaardt G, Zietsman A, Viljoen-Bloom M. Water Res 2003; 37: 4125–4134.
22. Coetzee G, Malandra L, Wolfaardt GM, Viljoen-Bloom M. Water SA 2004; 30: 407–412.
23. Nahid P, Vossoughi M, Alemzadeh I. Process Biochem 2001; 37: 447–451.
24. Nasr FA, Badr NM, Doma HS. Environmentalist 2006; 26: 31–39.
25. Chowdhury P, Viraraghavan T, Srinivasan A. Bioresour Technol 2010; 101: 439–449.
26. Axelsson J, Nilsson U, Terrazas E, Aliaga TA, Welander U. Enzyme Microb Technol 2006; 39: 32–37.
27. Abraham TE, Senan RC, Shaffiqu TS, Roy JJ, Poulose TP, Thomas PP. Biotechnol Progr 2003; 19: 1372–1376.
28. Guimarães C, Porto P, Oliveira R, Mota M. Process Biochem 2005; 40: 535–540.
29. Ramsay J, Shin M, Wong S, Goode C. J Ind Microbiol Biotechnol 2006; 33: 791–795.
30. Banerjee G. Water Res 1997; 31: 2500–2510.
31. Teixeira P, Alves M, Oliveira R. Environ Technol 2001; 22: 1169–1175.
32. Najafpour GD, Zinatizadeh AAL, Lee LK. Biochem Eng J 2006; 30: 297–302.
33. Di Palma L, Verdone N. Bioresour Technol 2009; 100: 1467–1470.
34. Hoccheimer JN, Wheaton F. 12th International Conference on Recirculation Aquaculture, VA, USA; 1998. p 291–318.
35. Mathure P, Patwardhan AW. J Chem Technol Biotechnol 2005; 80: 413–419.
36. Tchobanoglous G, Burton FL. *Wastewater engineering: treatment, disposal and reuse*. New York: Metcalf and Eddy Inc.; 1991.
37. Gupta AB, Gupta SK. Water Res 2001; 35: 1714–1722.
38. Sirianuntapiboon S. Bioresour Technol 2006; 97: 1735–1744.
39. Torkian A, Hashemian SJ, Alinejad K. Wat Environ Res 2003; 75: 232–237.
40. Surampalli RY, Baumann ER. Water Air Soil Poll 1997; 98: 1–15.
41. Al-Ahmady KK. Int J Environ Res Publ Health 2005; 2: 469–477.
42. WEF and ASCE. WEF manual of practice no. 8, ASCE manual and report on engineering practice no. 76. Alexandria and Reston, VA; 1998.
43. Brazil BL. Aquacult Eng 2006; 34: 261–274.
44. Griffin P, Findlay GE. Water Sci Technol 2000; 41: 137–144.
45. Nowak O. Water Sci Technol 2000; 41: 145–153.
46. Alemzadeh I, Vossoughi M. Process Biochem 2001; 36: 707–711.

47. Costley SC, Wallis FM. J Ind Microbiol Biotechnol 2000; 24: 244–250.
48. Sirianuntapiboon S, Chuamkaew C. Bioresour Technol 2007; 98: 266–272.
49. Benefield LD, Randall CW. Biological process design for wastewater treatment. Englewood Cliffs (NJ): Prentice-Hall Inc.; 1980.
50. Tawfik A, Klapwijk A. J Environ Manage 2010; 91: 1183–1192.
51. Chen Z, Wen Q, Wang J, Li F. Process Biochem 2006; 41: 2468–2472.
52. Radwan KH, Ramanujam TK. Bioproc Biosyst Eng 1997; 16: 77–81.
53. Tawfik A, Klapwijk B, el-Gohary F, Lettinga G. Water Res 2002; 36: 147–155.
54. Grady CPLJ. First International Conference on Fixed-Film Biological Processes. Pittsburgh: University of Pittsburgh; 1982. p 344–403.
55. Chavan A, Mukherji S. Bioresour Technol 2008; 99: 3721–3728.
56. Kim BJ, Molof AH. Water Sci Technol 1982; 14: 569–579.
57. Kubsad V, Chaudhari S, Gupta SK. Water Res 2004; 38: 4297–4304.
58. Le Group Teknika. Les disques biologiques pour le traitement des eaux usées des petites et moyennes municipalités, Rapport final, Projet de développement technologique n° DT87.001; 1988.
59. Klees R, Silverstein J. Water Sci Technol 1992; 26: 545–553.
60. Neu KE. Water Sci Technol 1994; 29: 197–206.
61. Lv Y, Wang L, Wang X, Yang Y, Wang Z, Li J. J Environ Sci 2011; 23: 1679–1683.
62. Saikaly P, Ayoub GM. Water Air Soil Poll 2003; 150: 177–191.
63. Ayoub GM, Saikaly P. Water Res 2004; 38: 3009–3016.
64. Schwingle TA, Lepak AJ, Wenta RJ. Hydrocarbon Eng 2005; 10: 97–98.
65. Lu C, Yeh AC. Environ Int 1995; 21: 313–323.
66. Lu C, Li HC, Lee LY. Environ Int 1997; 23: 253–263.
67. Teixeira P, Oliveira R. Process Biochem 2001; 37: 345–349.
68. Mohseni-Bandpi A, Elliott DJ. Water Sci Technol 1996; 34: 323–330.
69. Laquidara MJ, Blanc FC, O'Shaughnessy JC. J Water Pollut Control Fed 1986; 58: 107–114.
70. Ware AJ, Pescod MB, Storch B. Water Sci Technol 1990; 22: 113–117.
71. Akhbari A, Zinatizadeh AAL, Mohammadi P, Irandoust M, Mansouri Y. Chem Eng J 2011; 168: 269–279.
72. Costerton JW. Int J Antimicrob Ag 1999; 11: 217–221.
73. Martin-Cereceda M, Serrano S, Guinea A. Water Air Soil Poll 2001; 126: 193–206.
74. Okabe S, Hiratia K, Ozawa Y, Watanabe Y. Biotechnol Bioeng 1996; 50: 24–35.
75. Spengel DB, Dzombak DA. Water Environ Res 1992; 64: 223–235.
76. Culp GL, Heim NF. Operations. In: Field manual for performance evaluation and troubleshooting at Municipal Wastewater Treatment Facilities. Washington (DC): Environmental Protection Agency, Office of Water Program Operations; 1978.
77. Mba D, Bannister RH, Findlay GE. Water Res 1999; 33: 3679–3688.
78. Abou-Elela SI, Nasr FA, El-Shafai SA. Environmentalist 2008; 28: 289–296.
79. Jahren SJ, Rintala JA, Ødegaard H. Water Res 2002; 36: 1067–1075.
80. Nasr FA, Doma HS, Abdel-Halim HS, El-Shafai SA. Environmentalist 2007; 27: 275–286.
81. Tawfik A, Temmink H, Zeeman G, Klapwijk B. Water Air Soil Poll 2006; 175: 275–289.
82. Andreottola G, Foladori P, Ragazzi M, Tatàno F. Water Sci Technol 2000; 41: 375–382.
83. Andreottola G, Foladori P, Ragazzi M. Water Sci Technol 2000; 41: 177–185.
84. van Buuren. JCL Post-treatment methods for effluent of UASB reactors treating domestic sewage. The Netherlands: Wageningen University, Department of Environmental Technology; 1991.
85. Fountoulakis MS, Terzakis S, Chatzinotas A, Brix H, Kalogerakis N, Manios T. Sci Total Environ 2009; 407: 2996–3003.
86. Flickinger MC, Schottel JL, Bond DR, Aksan A, Scriven LE. Biotechnol Progr 2007; 23: 2–17.

48

BIOREACTORS, STIRRED TANK FOR CULTURE OF PLANT CELLS

PAULINE M. DORAN

School of Biological Sciences, Department of Chemical Engineering, Monash University, Victoria, Australia

48.1 PRODUCTS FROM SUSPENDED PLANT CELL CULTURES

Plants produce a diverse range of natural products used as active ingredients in pharmaceuticals, fragrances, flavors, dyes, and insecticides. Most of these chemicals are small but complex molecules that are difficult to synthesize chemically using economically viable methods. Most valuable phytochemicals are produced by plants as secondary metabolites by means of highly branched and regulated pathways that cannot be genetically engineered readily into microorganisms.

Plant tissue culture is an alternative to whole plants for production of plant compounds, offering important advantages such as better control over product quality and quantity. Of the many different forms of plant tissue culture available, such as callus, cell suspensions, immobilized cells, embryos, roots, and shoots, suspended plant cells have been most frequently applied for bioreactor-scale production of plant compounds. Table 48.1 illustrates the wide range of natural phytochemicals synthesized using plant suspensions.

As well as natural products, plant cells are also applied for production of heterologous proteins. The advantages of using recombinant plant systems for foreign protein production include the ability to correctly assemble and fold multimeric proteins and carry out posttranslational modifications, and the low risk of contamination by animal-borne pathogens. In principle, any protein can now be expressed in plant cells. Examples of foreign proteins that have been produced using plant cell suspensions are listed in Table 48.1.

48.2 PROPERTIES OF SUSPENDED PLANT CELL CULTURES: IMPLICATIONS FOR BIOREACTOR ENGINEERING

For commercial production of natural or foreign compounds using plant cells, scale-up of the cultures into bioreactors is essential. Various conventional and novel bioreactors, including stirred tanks, bubble columns, airlift vessels, fluidized beds, bubble-free systems, spin filter devices, and cell-lift configurations, have been applied for suspended plant cell cultures. In many cases, the performance of cultures measured in terms of cell growth and/or product accumulation declines with scale-up. This reflects the difficulty of optimizing all the conditions necessary for culture activity within the bioreactor environment.

The principal functions of a bioreactor used for aerobic cell culture are to provide adequate mixing, oxygen transfer, and heat transfer without the deleterious effects of excessive hydrodynamic shear. The properties of the biomass and culture fluid can impose significant technical constraints on the design and operation of appropriate bioreactors, and this is particularly true for suspended plant cells. Unfortunately, it is difficult to generalize about several of the important engineering characteristics of plant suspensions. For example, some cultures produce viscous non-Newtonian broths (1–5), while others exhibit essentially Newtonian behavior (6) and only moderate viscosities (7,8). The tendency of plant cells to clump together as aggregates varies considerably depending on the species and culture conditions (3,5,9–14), and there are differing reports about the extent to which plant

Upstream Industrial Biotechnology: Equipment, Process Design, Sensing, Control, and cGMP Operations, Volume 2, First Edition. Edited by Michael C. Flickinger.
© 2013 John Wiley & Sons, Inc. Published 2013 by John Wiley & Sons, Inc.

TABLE 48.1. Examples of Natural Products and Foreign Proteins Produced Using Plant Cell Suspensions

Natural phytochemicals	Ajmalicine, anthocyanins, anthraquinones, artemisinin, azadirachtin, berberine, betalains, codeine, digoxin, ginsenoside saponins, hyoscyamine, morphine, paclitaxel, podophyllotoxin, polysaccharides, rosmarinic acid, scopolamine, serpentine, shikonin, steroidal alkaloids, thiophenes
Foreign proteins	Albumin, antibodies (IgA, IgG1, IgG2b/κ), antibody fragments (scFv, IgG heavy chain), α_1-antitrypsin, bryodin 1, erythropoietin, β-glucuronidase, granulocyte-macrophage colony-stimulating factor, hepatitis B surface antigen, interleukins (2 and 4), invertase, lysozyme, ricin

TABLE 48.2. Properties of Suspended Plant Cell Cultures and Implications for Bioreactor Engineering

Property	Engineering implication
Slow growth	Cultures prone to contamination; batch cultures prolonged and therefore expensive
Shear sensitivity	Input of mechanical forces restricted, resulting in poor mixing and solids suspension and inadequate oxygen transfer
Sensitivity to gas-phase components such as CO_2 and ethylene	Gas throughputs restricted to avoid stripping of gaseous components; greater reliance on mechanical stirring for mixing and oxygen transfer
Non-Newtonian rheology	Poor mixing and solids suspension; inadequate oxygen transfer
Tendency to clump	Complex broth rheology; wall growth; conditions experienced by cells in clumps and wall growth are difficult to control
Tendency to foam	Reduced bioreactor working volumes, resulting in low volumetric productivity; conditions experienced by cells in foams and meringues are difficult to control; use of chemical antifoams reduces oxygen transfer
Low product yield	High biomass densities needed for economic feasibility, exacerbating problems with mixing and oxygen transfer

cells are shear sensitive (4,14–18). Another property affecting many suspended plant cell cultures is low product yield. This applies to natural phytochemicals, as low yields of secondary metabolites are often associated with dedifferentiated plant cells, but also to foreign proteins, as protein yields are affected by low levels of heterologous expression as well as subsequent protein degradation (19). As a consequence, high biomass densities are required for economic feasibility for many plant cell culture systems.

Whereas the properties of suspended plant cells, such as morphology, aggregate size, and rheology, affect the performance of bioreactors and have important engineering implications, they are not always independent of the bioreactor. As an added complexity, the properties of plant cell cultures can change depending on bioreactor operating conditions. For example, cell aggregates may be smaller (5,20) and individual cells either larger (21) or smaller (22) in stirred bioreactors compared with shake flasks. The rheology of the plant cell broth may also change as a result of protein and polysaccharide secretion into the medium in response to hydrodynamic shear levels in stirred vessels (4).

Typically, plant cell cultures offer a highly challenging combination of features that distinguishes them from microbial and animal cell systems. These properties and their implications for bioreactor engineering are summarized in Table 48.2. When complex broth rheology and cell shear sensitivity are coupled together, providing adequate mixing, solids suspension, and oxygen transfer can be difficult. Although plant cultures also possess some ameliorating characteristics such as relatively low oxygen demand and, consequently, low cooling requirements, mixing and oxygen transfer are still of major concern, particularly in the presence of high biomass densities. Developing technology to meet these challenges is critical for the success of plant cell culture applications.

48.3 SUITABILITY OF STIRRED BIOREACTORS FOR SUSPENDED PLANT CELL CULTURE

Stirred tank bioreactors offer several advantages for culturing suspended plant cells. Although stirred, airlift, and bubble-column reactors achieve similarly adequate rates of mixing and mass transfer in low-viscosity fluids, air-driven reactors do not perform well with high-density cultures of viscosity greater than about 100 mPa s (23). Stirred vessels are more suitable for viscous broths because greater power can be input by mechanical agitation. Experimental (7,24,25) and theoretical (26) studies have demonstrated that mixing becomes limiting in airlift reactors when plant cell densities reach 20–30 kg/m^3

dry weight. At these concentrations, airlift performance deteriorates markedly due to poor gas disengagement, impeded liquid circulation, development of unmixed zones, and gravity settling of the cells. Increasing the aeration rate is the only operating response available to improve the hydrodynamic functioning of air-driven reactors; however, overventilation of plant cell cultures has been shown to reduce growth and product formation because carbon dioxide and other necessary volatile components such as ethylene are stripped from the broth at high gas throughputs (20,27,28). The tendency of plant cell cultures to develop dense foam layers and cell flotation is more pronounced at high aeration rates (29). Foaming should be avoided because its treatment ultimately requires the addition of chemical antifoam agents to the culture; these agents are known to significantly reduce $k_L a$ values for oxygen transfer (29,30). Mechanical agitation and the ability to increase the power input independent of gas flow rate helps ameliorate these problems in stirred tank reactors.

The engineering advantages of stirred bioreactors relative to airlift vessels for plant cell culture can be demonstrated using theoretical regime analysis (26). In regime analysis, characteristic times for different bioreactor functions such as mixing and mass transfer are used to assess the rates of these processes relative to the demand of the cells for a critical metabolic component such as oxygen (23,31). The characteristic time or time constant is defined as the ratio of capacity to flow: a small time constant represents a fast process and vice versa. Ideally, the characteristic times for mixing and mass transfer should be smaller than that for biological uptake of oxygen to ensure that cell metabolism is not limited by bioreactor function.

Characteristic times for mixing and mass transfer in airlift and stirred vessels can be estimated from equations, available in the literature, as a function of bioreactor operating conditions and the properties of the culture broth (26). The results shown in Fig. 48.1 were calculated for an external-loop airlift vessel and a baffled stirred tank, both of working volume 10 m^3. Characteristic times in the stirred tank were calculated for a single Rushton turbine and aeration at a constant superficial velocity of 0.05 m/s. The culture broth contained a moderate-to-high plant cell density of 30 kg/m^3 dry weight, yielding a non-Newtonian pseudoplastic culture fluid with flow behavior index $n = 0.71$ and consistency index $K = 0.99$ Pa s^n. The specific rate of oxygen consumption by the cells was taken to be 10^{-6} kg/(kg dry weight)/s. As indicated in Fig. 48.1a, the airlift reactor performs poorly at this biomass density: the characteristic time for mixing is greater than the characteristic time for oxygen consumption even at very high gas flow rates. Mixing is therefore likely to be inadequate, resulting in dead zones within the vessel. This prediction is consistent with laboratory findings of cell settling and poor mixing in airlift reactors containing moderate-to-high plant cell densities (7,24,25). Figure 48.1a shows that the rate of oxygen transfer in the model airlift reactor becomes adequate when the superficial gas velocity in the riser increases above a certain value (around 0.1 m/s); at this aeration rate, the characteristic time for mass transfer becomes less than that for oxygen consumption. Results for the stirred tank reactor (Fig. 48.1b) show much better mixing performance than for the airlift: the mixing time is significantly lower than the characteristic time for oxygen consumption. The characteristic time for oxygen transfer becomes smaller than that for oxygen consumption above a certain stirrer speed (shown as about 5 s^{-1}). From this theoretical analysis, stirred vessels can be considered to have greater potential for accommodating the requirements of dense suspended plant cell cultures than airlift devices.

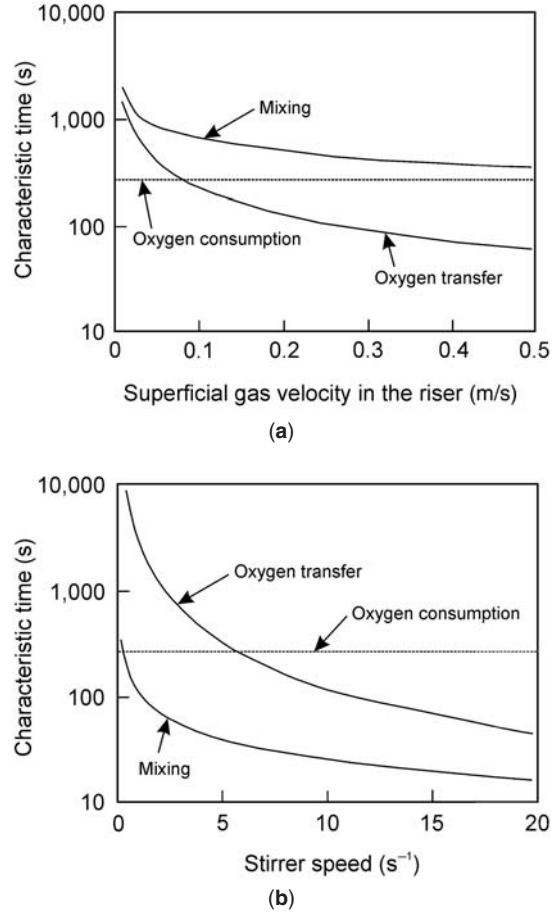


Figure 48.1. Results from theoretical analysis of characteristic times for mixing, oxygen transfer, and oxygen consumption for a suspended plant cell culture with cell concentration 30 kg/m^3 dry weight: (a) 10-m^3 external-loop airlift reactor, and (b) 10-m^3 baffled stirred tank reactor with single Rushton turbine. (Data from Ref. 26.)

A critical question in the application of stirred bioreactors for plant cell culture is whether the stirrer can be operated at the speeds required for adequate oxygen transfer without causing shear damage to the cells. Although application of stirred reactors is standard fermentation technology, conventional high shear agitation is inappropriate for plant cell culture. Modification of equipment and/or operating practice is usually required to avoid mechanical damage of the cells or other detrimental metabolic effects associated with high levels of hydrodynamic shear. The main parameters that affect shear levels in stirred vessels are the impeller geometry and stirrer speed; however, although many different styles of impeller have been tested experimentally, there are few general guidelines for optimizing this aspect of stirred reactor design for suspended plant cell culture (32). Because the generation of shear forces is intimately related to the effectiveness of mixing and mass transfer in bioreactors, development of systems for low-shear agitation that still provide adequate circulation and gas dispersion remains a key challenge. The trade-off between shear damage effects and the requirements for adequate mixing, mass transfer, and gas–liquid–solid hydrodynamics in stirred bioreactors is discussed in more detail below in the section titled "Plant Cell Culture in Stirred Bioreactors: Theoretical Analysis."

As well as providing important technical benefits for high-density plant cell culture, stirred bioreactors have a proven record of performance and reliability in the fermentation industry and have been well studied and characterized in large-scale operations. These features account for stirred tanks being the bioreactor configuration of choice for commercial scale-up of suspended plant cell processes, as indicated in Table 48.3.

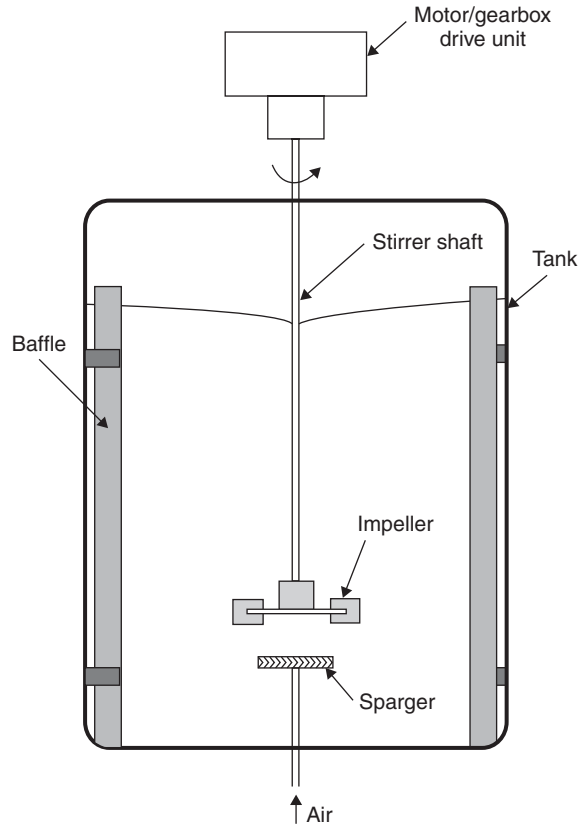


Figure 48.2. Typical equipment configuration for a stirred tank bioreactor with single impeller used for aerobic cell culture.

48.4 STIRRED TANK EQUIPMENT AND OPERATING CHARACTERISTICS

The functions of stirring in a bioreactor used for aerobic cell culture are: (i) to eliminate concentration and temperature gradients by homogenizing the vessel contents, (ii) to disperse gas in the broth to aerate the culture, (iii) to promote heat transfer between the broth and heat exchange surfaces, and (iv) to suspend the cells. The equipment chosen for stirring has a significant influence on how well these functions can be performed. The principal mechanical features and operating details of a range of mixing hardware are outlined briefly in the following paragraphs. This description provides a background for the more detailed discussion of plant cell applications in subsequent sections.

48.4.1 Stirred Vessels

Figure 48.2 shows a typical arrangement of equipment in a stirred tank (43). Not shown is the equipment for heat transfer: in large vessels this may be a helical cooling coil immersed in the broth; for small bioreactors an external water jacket is often sufficient. Standard stirred tank reactors are cylindrical in cross-section. The base profile of the tank may vary as illustrated in Fig. 48.3; rounded rather than angled corners discourage the formation of stagnant pockets into which fluid currents cannot penetrate. The energy dissipation rate required to suspend solids in stirred tanks is very sensitive to the shape of the vessel base: the modified geometries shown in Fig. 48.3b–e can all significantly enhance the suspension of particles compared with flat-bottom tanks (44,45). Because the solubility of oxygen in aqueous liquids is limited to only about 8 ppm under typical cell culture conditions, the oxygen content of the culture broth must be continuously replenished as oxygen is consumed by the cells. In stirred vessels, this is most commonly achieved using a sparger that releases air bubbles into the culture below the impeller (Fig. 48.2). When headplate access is at a premium or when mechanical stresses on the stirrer can be alleviated by using a shorter shaft, for example, in viscous fluids, the stirrer shaft may enter through the base of the vessel rather than the top, as shown in Fig. 48.4. For either top-entering or bottom-entering stirrers, the point at which the stirrer shaft enters the tank is

TABLE 48.3. Stirred Tank Bioreactors for Scale-Up of Suspended Plant Cell Cultures

Bioreactor Volume (L)	Equipment and Operating Conditions	Plant Species	Company	References
75, 750, 7500, 15,000, and 75,000	Cascade of five stirred tanks; semicontinuous operation	*Echinacea purpurea*, *Panax ginseng*, *Rauwolfia serpentine*, *Chenopodium* sp. tobacco	DIVERSA Gesellschaft für Bio- und Verfahrenstechnik mbH, Germany	33
		Taxus spp.	Phyton, Inc. and Bristol-Meyers Squibb Co., USA	B. Bringi (personal communication)
20,000 and 25,000	Two-stage operation; culture period of 4 weeks	*Panax ginseng*	Nitto Denko Corp., Japan	34,35
20,000	Batch, semicontinuous and continuous operation; dual four-blade paddles, 45° blade angle	*Nicotiana tabacum*	Japan Tobacco Inc., Japan	36
10,000	Semicontinuous operation; axial flow impeller	Various, for polysaccharide production	Cooperative Research Centre for Industrial Plant Biopolymers, Australia	D. McManus (personal communication)
6000	High density fed-batch culture	*Coptis japonica*	Mitsui Petrochemical Industries Ltd, Japan	37
5000	Batch operation; triple six-flat-blade turbines	*Catharanthus roseus*	Gesellschaft für Biotechnologische Forschung mbH, Germany	38
4000	Axial flow turbine with draft tube	*Polianthes tuberosa*	KAO Corp., Japan	H. Sawada (personal communication)
200 and 2000	Batch operation; dual disk turbines	*Nicotiana tabacum*	Japan Tobacco Inc., Japan	36
800	Batch operation; dual six-flat-blade turbines	*Solanum demissum*	Gesellschaft für Biotechnologische Forschung mbH, Germany	39
200 and 750	Two-stage culture	*Lithospermum erythrorhizon*	Mitsui Petrochemical Industries Ltd, Japan	40,41
100 and 630	Culture cycle of 14 days	Ginseng	Omutninsk Chemical Plant, Russia	42

a potential contamination site, and several types of stirrer seal have been developed to combat this problem. Large fermenters are usually equipped with mechanical seals; for smaller vessels, magnetically coupled drives may be used so that the stirrer shaft does not actually pass through the fermenter body. In this case, a magnet attached to the end of the shaft inside the fermenter is driven by a rotating magnet in a housing outside. Use of magnetic coupling is limited to relatively small fermenters ($\leq \sim$800 L) and low-viscosity broths. In vessels with a single impeller of diameter 1/4–1/2 the tank diameter, the depth of liquid is usually limited to 1.0–1.25 times the tank diameter to facilitate good mixing. In tall fermenters with large aspect ratios, multiple impellers mounted on the stirrer shaft are commonly used to improve oxygen transfer conditions; an example is shown in Fig. 48.5. In multiple impeller systems, the distance between the agitators is an important consideration. If the impellers are too far apart, unagitated zones develop between them; conversely, impellers located too close together produce flow streams that interfere with each other and disrupt circulation to the far reaches of the vessel.

48.4.2 Baffles

Baffles are vertical strips of metal mounted against the walls of stirred vessels (Fig. 48.2) to prevent gross vortexing of

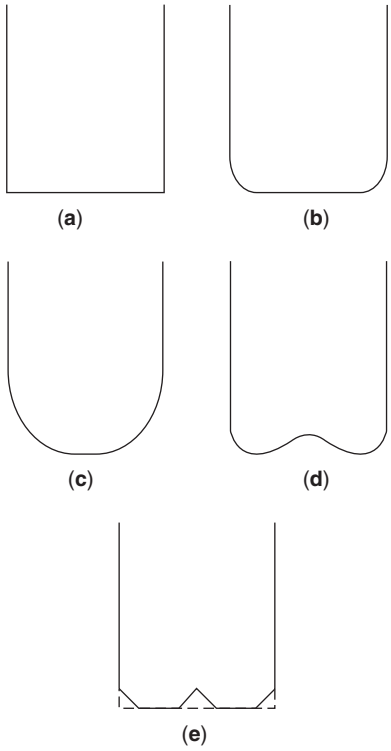


Figure 48.3. Bottom variations in stirred tank bioreactors: (a) flat, (b) dished, (c) round, (d) contoured, and (e) cone-and-fillet.

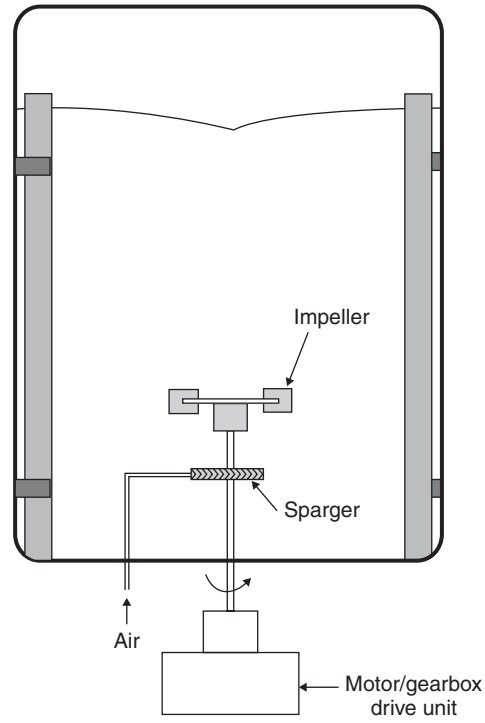


Figure 48.4. Stirred tank bioreactor with bottom-entry stirrer.

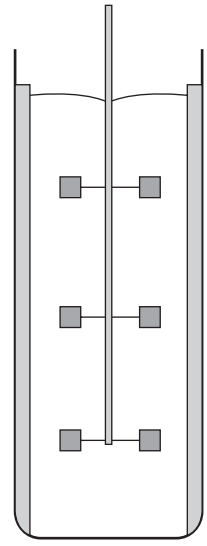


Figure 48.5. Stirred tank bioreactor with multiple impellers.

the liquid. Typically, four baffles of width 1/10–1/12 the tank diameter are installed with equal spacing around the tank circumference. Baffles may be attached to the vessel wall (Fig. 48.5), or mounted slightly away from the wall (Fig. 48.2) to prevent sedimentation of solids or development of stagnant zones at the inner edge. Baffles generate turbulence in the fluid by breaking up the circular flow produced by rotation of the stirrer. Circular flow is relatively ineffective for mixing, which is better facilitated by axial and radial currents. Circular flow can also lead to vortex development down the stirrer shaft and gas entrainment. If allowed to reach down to the impeller, deep vortices impose extraordinarily high mechanical stresses on the stirrer shaft, bearings, and seals, which must be avoided to prevent equipment damage.

48.4.3 Impellers

Impellers can be classified broadly depending on whether they generate high local shear rates or have strong pumping capacity for development of large-scale flow currents. Both functions are required for good mixing, but they do not usually work together. The relative prominence of shear- and flow-generating functions for a wide range of impellers is shown in Fig. 48.6.

Propellers, paddles, and turbines are remote-clearance impellers with typical diameters of 1/4–2/3 the tank diameter. These devices are operated at high speeds to generate tip velocities of the order of 3 m/s^{-1}. When remote-clearance agitators are used in low-viscosity fluids, a turbulent region of high shear is generated near the impeller where the essential mixing processes occur as material is exchanged between different liquid streams. High shear levels close

to the impeller are also responsible for bubble breakup in sparged systems. Because good mixing should involve fluid from all parts of the vessel, as well as turbulence, the impeller must be able to generate circulatory currents with sufficient velocity to carry material from the furthermost reaches of the tank to the impeller. In viscous fluids, it is often not possible for mechanical and economic reasons to rotate the impeller fast enough to generate turbulence; therefore, impellers used for viscous mixing are usually designed instead to provide maximum bulk movement of material. Anchor and helical impellers are large agitators that are installed with small wall clearances and operated at low speeds to generate bulk fluid currents. For viscous fluids or when high shear rates must be avoided, slow-speed, low turbulence, high-flow impellers are preferred to high-speed, high-turbulence, low-flow impellers.

There is a wide range of impellers available commercially, some of which have been applied to plant cell culture. The general characteristics of agitators used in suspended plant cell reactors are described in the following sections.

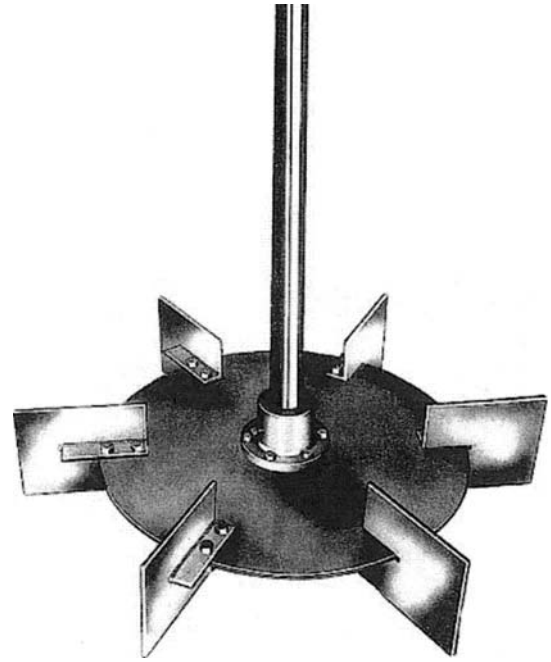


Figure 48.7. Rushton turbine.

48.4.3.1 Rushton Turbine. As shown in Fig. 48.7, the Rushton turbine is a disk turbine with six flat blades. This impeller has been the agitator of choice in the fermentation industry since the 1950s, largely because it has been well studied and characterized. Rushton impellers generate predominantly radial or horizontal flow, but have relatively low pumping efficiency resulting in low circulatory flows per unit power consumed (46,47). Rushton turbines are often chosen for their gas-handling capacity and perform well for gas dispersion. Bubble breakup is very effective near the impeller blades as air is forced into these high shear regions by the turbine disk. Changes in gas dispersion conditions with increasing stirrer speed or gas flow rate are illustrated in Fig. 48.8 (48). At high gassing rates or low stirrer speeds (Fig. 48.8a), the gas-handling capacity of the impeller is exceeded, the impeller ceases to pump the two-phase fluid, and the flow pattern is dominated by buoyant gas–liquid flow upwards the middle of the vessel as in a bubble column. This condition corresponds to impeller flooding. As the stirrer speed is increased or the gas flow rate reduced, the impeller starts to disperse the gas toward the walls of the tank (Fig. 48.8b). Complete gas dispersion below as well as above the impeller (Fig. 48.8c) is achieved at even higher stirrer speeds or lower gas flow rates; this is the desirable operating condition because it results in homogeneous dispersion of gas to all parts of the vessel. The ability to handle high gas velocities without flooding is an advantage for improving oxygen transfer conditions in the reactor. The gas-handling capacity of Rushton turbines can be improved by increasing the impeller-to-tank diameter ratio (49).

Pairs of low-pressure, high-speed trailing vortices are generated behind the flat blades of Rushton turbines (50,51). This hydrodynamic feature is responsible for the relatively high level of power drawn by Rushton turbines under nonaerated conditions. With sparging, gas readily accumulates in these low pressure regions, producing ventilated cavities behind the blades and causing a significant drop in power. The extent of this power reduction is a complex

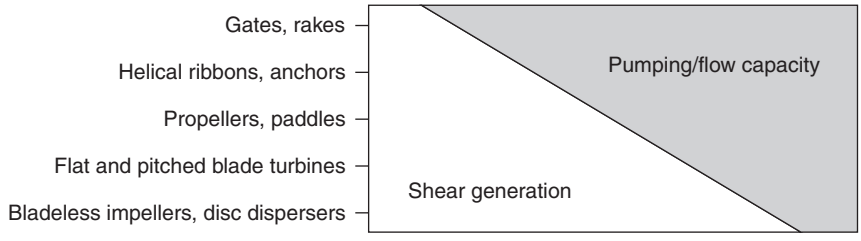


Figure 48.6. Characteristics of different impellers in terms of the ratio of shear generation to flow capacity.

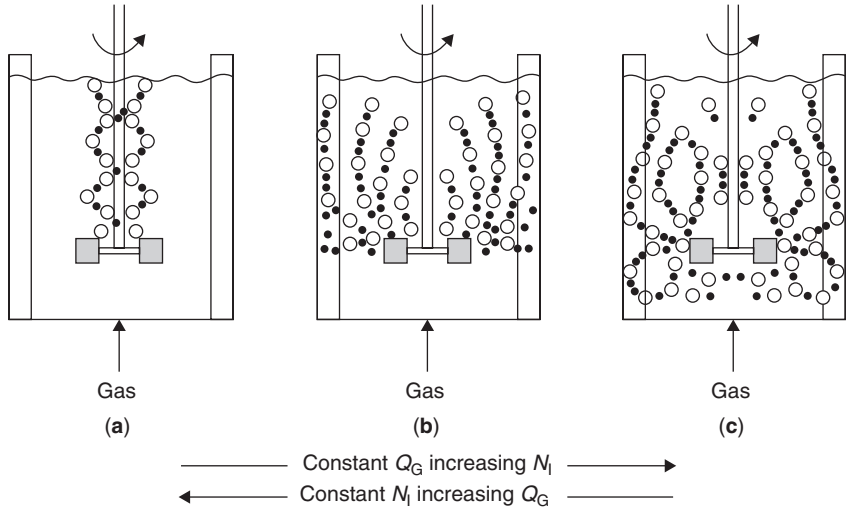


Figure 48.8. Flow patterns developed by a Rushton turbine under gassed conditions as a function of stirrer speed N_i and gas flow rate Q_G: (a) impeller flooding; (b) impeller loading, where the gas is dispersed by the impeller but poorly distributed throughout the vessel; (c) complete gas dispersion below as well as above the impeller. (Adapted from Ref. 48.)

function of the stirrer speed, air flow rate, vessel size, and fluid properties and cannot yet be accurately predicted (52). The rheological properties of the fluid exert considerable influence: practical operating conditions usually give a 40–50% loss of power with sparging in low-viscosity fluids (53), but this can increase to 80% or more in viscous or non-Newtonian fluids (49).

Rushton turbines are effective for solids suspension in three-phase systems. Suspension is generally improved by reducing the clearance between the impeller and the floor of the tank, but this can cause flow instabilities in aerated systems (54). An impeller off-bottom clearance of 1/4 the tank diameter is recommended because this allows gas dispersion under the impeller as well as adequate agitation in the upper parts of the vessel (44,55).

Single and multiple Rushton turbines have been applied for suspended plant cell culture in many experimental investigations, as indicated in Table 48.4. The suitability of Rushton turbines of different size for large-scale plant cell culture has also been analyzed in a theoretical engineering study based on a reactor size of 10 m^3 (32).

48.4.3.2 Other Disk Turbines. Disk turbines may have more or fewer blades than the Rushton turbine's standard six. Increasing the number of blades up to 18 reduces the rate at which the power drops with increasing gas flow and significantly improves the gas-handling capacity of the impeller (112). The unaerated power number also increases with the number of blades at constant impeller diameter (113). Even so, a 12-blade disk turbine has been shown to disperse about three times more gas than a larger Rushton impeller with six blades operating with the same power consumption and stirrer speed (112). Although turbine impellers with more than six blades have not been tested for plant cell culture, single and dual agitators with four flat blades have been used in several studies (Table 48.4). As an extrapolation of the above findings, decreasing the number of blades from six to four can be expected to reduce the gas-handling capacity of the impeller as well as the unaerated power number.

The blades on disk turbines may be pitched or angled rather than orthogonal to the disk. This reduces the unaerated power number by about 50% and generates impeller discharge currents with a more pronounced axial velocity component than the radial flows emanating from a Rushton turbine (54). At a given gas flow rate, lower stirrer speeds can be used without flooding compared with Rushton turbines of similar geometry; this has been attributed to the greater projected area of the pitched blades (47). The impeller discharge efficiency and gas holdup produced using pitched blade disk turbines are also improved relative to Rushton impellers (47). Disk turbines with angled blades have been applied for plant cell culture (Table 48.4).

48.4.3.3 Propellers. Propellers are usually of the three-blade marine type shown in Fig. 48.9. They generate a flow pattern with mainly axial velocity components. Propellers can be operated in either downward or upward pumping modes, downward being more common. They are generally installed with diameters of around 1/3 the tank diameter.

The unaerated power number for marine propellers is about 1/10 that for Rushton turbines, depending on the blade pitch and other geometric parameters (113).

TABLE 48.4. Examples of Stirred Bioreactor Configurations Applied for Suspended Plant Cell Culture[a]

Impeller	Bioreactor Specifications	Impeller Specifications	Stirrer Speed (rpm)	Sparger Specifications	Aeration Rate (vvm)	Bioreactor Operation	Maximum Cell Density	Plant Species	Reference
Rushton turbine	$V_L = 2$ L $D_T = 15$ cm Concave sides, flat bottom No baffles	$D_i/D_T = 0.50$ $W_B/D_i = 0.32$ $L_B/D_i = 0.32$ $D_D/D_i = 0.60$	1,000	—	—	Batch	6.4 g/L dry weight	*Catharanthus roseus*	56
Rushton turbine	$V_L = 1.45$ L	$D_i = 9$ cm	100–300	—	0.16	Chemostat, dilution rate = 0.35 day^{-1}	1.36 g/L dry weight (at 150 rpm)	*Daucus carota*	57
Six-flat-blade disk turbine	$V_L = 5$ L $D_T = 21$ cm No baffles	$D_i/D_T = 0.33$ $W_B/D_i = 0.19$ $L_B/D_i = 0.19$	200 and 300	—	0.06	Batch	18 g/L dry weight (at 200 rpm)	*Stizolobium hassjoo*	58
Dual Rushton turbines	$V_L = 8.5$ L $D_T = 23$ cm Concave sides, flat bottom	$D_i/D_T = 0.37$ $W_B/D_i = 0.22$ $C_S/D_T = 0.33$ $C_{i2}/H_L = 1$	100	Cross-shaped glass, 5-cm arms, two rows of 2-mm holes per arm; or 8-cm sintered glass disk, pore size 3	0.24	Batch	14 g/L dry weight (with cross-shaped sparger)	*Catharanthus roseus*	10
Dual Rushton turbines	$V_L = 11$ L $D_T = 23$ cm Concave sides, flat bottom No baffles	$D_i/D_T = 0.35$ or 0.52	100	Crucifix or sintered disk	0.009–0.2	Batch	14 g/L dry weight	*Catharanthus roseus*	59
Dual six-flat-blade disk turbines	Volume = 12 L $D_T = 23$ cm Concave sides, flat bottom No baffles, or three linked internals or baffles $W_{BF}/D_T = 0.08$	$D_i/D_T = 0.37$ $W_B/D_i = 0.035$ above disk $W_B/D_i = 0.21$ below disk $C_{i2}/H_L = 1$	300	In unbaffled vessel, sintered glass, 8-cm diameter; in baffled vessel, one of the three internals supplied air	—	Batch	13.6 g/L dry weight (unbaffled)	*Catharanthus roseus*	60

(*continued*)

TABLE 48.4. (*Continued*)

Impeller	Bioreactor Specifications	Impeller Specifications	Stirrer Speed (rpm)	Sparger Specifications	Aeration Rate (vvm)	Bioreactor Operation	Maximum Cell Density	Plant Species	Reference
Dual disk turbines: six blades lower, four blades upper	$V_L = 20$ L $D_T = 28.4$ cm Three baffles Foam breaker	$D_i/D_T = 0.50$	50	Cross-shaped stainless steel pipe with 21 × 1.0–1.5-mm holes	0.75–1.1	Semicontinuous	18.1 g/L dry weight	*Nicotiana tabacum*	61
Dual disk turbines	Volume = 2000 L $D_T = 125$ cm	$D_i/D_T = 0.34$	10–100	—	—	Batch	12 g/L dry weight	*Nicotiana tabacum*	36
Six-blade disk turbine with inclined vanes	$V_L = 2$ L $D_T = 15$ cm Concave sides, flat bottom No baffles	$D_i/D_T = 0.50$ Blades inclined 60° from the vertical	1000	—	—	Batch	7.7 g/L dry weight	*Catharanthus roseus*	56
Angled disk turbine	$V_L = 25$ L	—	100	—	0.25	Fed-batch	17 g/L dry weight	*Panax ginseng*	62
Six-flat-blade turbine	$V_L = 2.5$ L $D_T = 15$ cm $H_L/D_T = 0.93$ Four baffles	$D_i/D_T = 0.56$ $W_B/D_i = 0.20$	115	Ring, eight holes	1	Batch	17 g/L dry weight	*Vinca rosea*	63
Six-flat-blade turbine	$V_L = 1.8$ L $D_T = 13$ cm $H_L/D_T = 1.2$ Round bottom Four baffles $W_{BF}/D_T = 0.11$	$D_i/D_T = 0.35$ $W_B/D_i = 0.24$ $C_i/D_T = 0.23$	300	—	0.11	Batch	12.3 g/L dry weight	*Atropa belladonna*	64
Six-flat-blade turbine	$V_L = 5$ L $D_T = 21$ cm No baffles	$D_i/D_T = 0.29$ $W_B/D_i = 0.13$ $C_i/D_T = 0.14$	300	Sandstone, 2 cm long × 1.2 cm diameter	0.06	Batch	21.3 g/L dry weight	*Stizolobium hassjoo*	65
Six-blade impeller	$V_L = 3$ L $D_T = 15$ cm Concave sides, flat bottom	$D_i/D_T = 0.49$	480	—	0.033	Batch	8.2 g/L dry weight	*Helianthus annuus*	66
Six-blade turbine with magnet stirring plate	$V_L = 0.55$ L $D_T = 8.5$ cm $H_L/D_T = 1.14$ Flat bottom Three baffles $W_{BF}/D_T = 0.09$	$D_i/D_T = 0.59$ $W_B/D_i = 0.16$ $C_i/D_T = 0.47$	200–500	Surface aeration	0.18	—	—	*Carthamus tinctorius*	67
Dual six-flat-blade turbines	$V_L = 800$ L	—	60–80	—	0.063	Batch	135 g/L fresh weight	*Solanum demissum*	39
Dual six-flat-blade turbines	Volume = 13.5 L	—	200	Ring, 6 × 1-mm pores	0.2	Batch	15 g/L dry weight	*Perilla frutescens*	68

Dual six-blade turbines	$V_L = 1.8$ L Three baffles	—	250	Sintered steel	0.33	Batch with gas recirculation	8.1 ± 0.6 g/L dry weight	*Catharanthus roseus*	69
Dual six-blade turbines	$V_L = 2$ L Three baffles $H_{BF} = 14$ cm $W_{BF} = 1.4$ cm	$D_i = 4.5$ cm	250	Sintered steel	0.2	Two-stage batch	14 g/L dry weight	*Catharanthus roseus*	70
Dual six-blade turbines	$V_L = 1.8$ L	—	125	Sintered steel	0.28	Chemostat, dilution rate = 0.19 day^{-1}	2.8 g/L dry weight	*Catharanthus roseus*	71
Dual six-blade turbines	$V_L = 10$ L	—	120	—	Varied	Chemostat, dilution rate = 0.0083 h^{-1}	8.9 g/L dry weight	*Nicotiana tabacum* (transgenic)	72
Dual six-blade turbines	$V_L = 1.3$ L $D_T = 12$ cm $H_L = 13$ cm	$D_i/D_T = 0.46$ $C_{i1}/D_T = 0.17$ Clearance between impellers = 4.5 cm	100–250	Sintered stainless steel	0.05, 0.2, and 0.4	Batch	16.2 g/L dry weight (at 0.05 vvm)	*Taxus chinensis*	20
Triple six-flat-blade turbines	$V_L = 5{,}000$ L	—	30	—	0.010–0.017	Batch	11 g/L dry weight	*Catharanthus roseus*	38
Four-flat-blade disk turbine	$V_L = 1.4$ L $D_T = 13$ cm $H_L = 14$ cm	$D_i/D_T = 0.35$ $L_B/D_i = 0.24$ $C_i/D_T = 0.20$	400	Sintered stainless steel	0.1	Batch	11.9 g/L dry weight	*Uncaria tomentosa*	21
Four-blade turbine	$V_L = 3$ L $D_T = 14$ cm	$D_i/D_T = 0.56$ $W_B/D_i = 0.19$ $C_i/D_T = 0.36$	150	—	0.5	Batch	26 g/L dry weight	*Nicotiana tabacum*	73
Four-flat-blade impeller	$V_L = 3$ L $D_T = 14$ cm	$D_i/D_T = 0.54$ $W_B/D_i =$ 0.67–1.8 $L_B/D_i = 0.33$ $C_i/D_T = 0.27$	50–200	—	0.2	Batch	580 g/L fresh weight (at 150 rpm and $W_B/D_i = 1.8$)	*Nicotiana tabacum*	15
Four-flat-blade impeller	$V_L = 3$ L	$D_i = 5.6$ cm	150	One-hole nozzle	0.7	Batch	18.5 g/L dry weight	*Nicotiana tabacum*	74
Four-blade turbine	$V_L = 1.65$ L	$D_i/D_T = 0.46$ $C_i = 2.6$ cm	400	Ring	0.1	Batch	10.1 g/L dry weight	*Beta vulgaris*	4
Four-blade turbine	$V_L = 1.65$ L $D_T = 13$ cm	$D_i/D_T = 0.35$ $L_B/D_i = 0.24$ $C_i/D_T = 0.20$	400	Ring	0.1	Batch	10.7 g/L dry weight	*Solanum chrysotrichum*	5

(*continued*)

TABLE 48.4. (*Continued*)

Impeller	Bioreactor Specifications	Impeller Specifications	Stirrer Speed (rpm)	Sparger Specifications	Aeration Rate (vvm)	Bioreactor Operation	Maximum Cell Density	Plant Species	Reference
Four-blade impellers	$V_L = 1.7$ L	—	100	—	0.12	Batch	4.6 g/L dry weight	*Daucus carota* (embryo-genic)	75
Dual four-flat-blade turbines	$V_L = 3$ L $D_T = 14.8$ cm	$D_i/D_T = 0.51$	150–400	—	0.2	Batch	13 g/L dry weight	*Perilla frutescens*	76
Dual four-blade impellers	$V_L = 1.8$–3.6 L	—	80	—	0.3	Two-stage chemostat	6.0 g/L dry weight (at dilution rate = 0.10 day^{-1})	*Dioscorea deltoidea*	77
Dual flat-blade turbines; six blades lower, four blades upper	$V_L = 13$ L	$D_i = 10$ cm	100	17 × 1.0–1.8-mm holes	—	Batch	15 g/L dry weight	*Nicotiana tabacum*	78
Dual flat-blade turbines; six blades lower, four blades upper	$V_L = 34$ L $D_T = 35$ cm Magnetically coupled stirrer shaft	$D_i/D_T = 0.50$ $C_{i1}/D_T = 0.37$ $C_{i2}/D_T = 0.77$	100	—	0.7	Chemostat, dilution rate = 0.42 day^{-1}	15 g/L dry weight	*Nicotiana tabacum*	79
Flat-blade and 45° angle-blade turbines	$V_L = 10$ L	—	80	Three extra-course glass frits	Up to 0.6 (air) and up to 0.2 (pure oxygen)	Batch	8.2 g/L dry weight	*Dioscorea deltoidea*	80
Dual impellers; six-flat-blade turbine lower, three-pitched-blade turbine upper	$V_L = 5$ L $D_T = 21$ cm No baffles	$D_{i1}/D_T = 0.29$ $D_{i2}/D_T = 0.33$ $W_{B1}/D_{i1} = 0.13$ Distance between impellers = 8 cm Pitched blade angle = 30°	300	Sandstone, 2 cm long × 1.2 cm diameter	0.06	Batch	20 g/L dry weight	*Stizolobium hassjoo*	65
Triple turbines	Volume = 5 L	—	90	—	1.0	Batch	6.7 g/L dry weight	*Digitalis lanata*	81
Sail impeller	$V_L = 3$ L $D_T = 14$ cm	$D_i/D_T = 0.54$ $W_B/D_i = 1.8$ $L_B/D_i = 0.33$ $C_i/D_T = 0.27$	150	—	0.2	Batch	590 g/L fresh weight	*Nicotiana tabacum*	15

Dual six-flat-blade impellers connected by crossed Teflon ribbons	$V_L = 4$ L Baffles Bottom-entry stirrer shaft	$W_R = 2.5$ cm $L_R = 22$ cm	40	—	0.075	Batch	2.7 g/L dry weight	*Fragaria* × *ananassa* cv. Brighton	82
Marine blade impeller	$V_L = 0.5$ L Magnetically coupled stirrer shaft	—	150–180	—	1.2	Batch	9 g/L dry weight	*Medicago sativa*	83
Marine-type impeller	$V_L = 50$ L	$D_i = 15$ cm	150–420	—	0.20–0.45	Multicycle draw–fill	29 g/L dry weight	*Panax ginseng*	84
Marine three-blade impeller	$V_L = 2$ L $D_T = 13$ cm $H_L/D_T = 1.15$ Round bottom	$D_i/D_T = 0.35$ $H_i/D_i = 1.33$ $C_i/D_T = 0.23$ Blade pitch = 45°	100	Pipe with row of 7 × 1-mm holes	0.43	Batch	11.8 g/L dry weight	*Nicotiana tabacum*	85
Marine impeller	$V_L = 3$ L $D_T = 14.3$ cm	$D_i/D_T = 0.59$	120–170	—	0.033	Batch	15.5 g/L dry weight	*Perilla frutescens*	18
Propeller	$V_L = 2.3$ L	—	80–140	Bubble-free aeration	—	Semicontinuous perfusion	26 g/L dry weight	*Anchusa officinalis*	86
Three-bladed impeller	$V_L = 40$ L	—	50	—	0.1	Batch	~10 g/L dry weight	*Nicotiana tabacum* (transgenic)	87
Pitched blade impeller	$V_L = 5$ L	—	75	—	0.2 (intermittent)	Batch with medium exchange	4.1 g/L dry weight	*Oryza sativa* (transgenic)	88
Kaplan turbine	$V_L = 75$ L Draft-tube reactor	—	350	—	0.33	Batch	15.3 g/L dry weight	*Morinda citrifolia*	14
Perforated disk	Volume = 10 L	—	100	—	0.5	Batch	—	*Morinda citrifolia*	14
Six-blade paddles	$V_L = 4$ L Round bottom No baffles	—	90–160	Hollow stirrer shaft	0.25–0.50	Batch	8.4 g/L dry weight	*Daucus carota* (embryogenic)	89
Modified (gate-type) paddle	$V_L = 5$ L $D_T = 20$ cm $H_L/D_T = 0.80$ No baffles	$D_i/D_T = 0.67$ $W_B/D_i = 0.60$	60	Ring, eight holes	0.5–1.5	Fed-batch	30 g/L dry weight	*Cudrania tricuspidata*	24

(*continued*)

TABLE 48.4. (*Continued*)

Impeller	Bioreactor Specifications	Impeller Specifications	Stirrer Speed (rpm)	Sparger Specifications	Aeration Rate (vvm)	Bioreactor Operation	Maximum Cell Density	Plant Species	Reference
Modified (gate-type) paddle	$V_L = 2$ L $D_T = 13$ cm $H_L/D_T = 1.15$ Three baffles $W_{BF}/D_T = 0.12$ $H_{BF}/H_L = 0.20$	$D_i/D_T = 0.54$ $H_i/D_i = 1.0$ $C_i/H_L = 0.20$	175 or 280	Ring	0.5 or 0.25	Batch	9 g/L dry weight (at 175 rpm and 0.5 vvm)	*Catharanthus roseus*	90
Modified (gate-type) paddle	$V_L = 2$ L	—	50	—	1.0	Batch	11.6 g/L dry weight	*Panax ginseng* (embryo-genic)	91
Modified paddle (hollow stirring wing)	Volume = 2.5 L	—	—	—	0.05 (oxygen)	Fed-batch	75 g/L dry weight	*Coptis japonica*	92
Two-blade grid paddle	$V_L = 2$ L $D_T = 13$ cm $H_L/D_T = 1.23$ Four baffles	$D_i/D_T = 0.53$ $H_i/D_i = 2.1$	50	Spiral, 16 holes $D_S/D_T = 0.46$	0.3	Fed-batch	30 g/L dry weight	*Oryza sativa*	8
Dual angled four-blade paddles	Volume = 20,000 L $D_T = 250$ cm	$D_i/D_T = 0.50$ Blade angle = 45°	10–40	—	—	Batch	17 g/L dry weight	*Nicotiana tabacum*	36
Maxblend impeller	$V_L = 5$ L $D_T = 21$ cm No baffles	$D_i/D_T = 0.48$ $H_i/D_i = 1.2$	100	Sandstone, 2 cm long × 1.2 cm diameter	0.08	Batch	19 g/L dry weight	*Stizolobium hassjoo*	65
Anchor impeller	Volume = 15 L $D_T = 22$ cm	$D_i/D_T = 0.50$ $H_i/D_i = 2.5$	—	—	—	—	—	*Fragaria ananassa*	93
Anchor turbine	$V_L = 25$ L	—	100	—	0.25	Fed-batch	15.3 g/L dry weight	*Panax ginseng*	62
Anchor impeller	$V_L = 32$ L $D_T = 25.9$ cm $H_L/D_T \approx 3$	$D_i/D_T = 0.74$	40	—	0.6	Batch	—	*Coleus blumei*	25,94
Double helical ribbon impeller (upward pumping)	$V_L = 10$ L $D_T = 21$ cm Profiled base Three vertical surface baffles, 8 × 10 × 0.16 cm	$D_i/D_T = 0.90$ $W_R/D_i = 0.195$ $L_R/D_i = 4.12$	120	Surface aeration (air and oxygen-enriched air)	0.1	Batch	27.6 g/L dry weight	*Catharanthus roseus*	2
Double helical ribbon impeller (upward pumping)	$V_L = 10$ L $D_T = 21$ cm Profiled base Three vertical surface baffles, 8 × 10 × 0.16 cm	$D_i/D_T = 0.90$ $W_R/D_i = 0.195$ $L_R/D_i = 4.12$	60	Surface aeration (air and oxygen-enriched air)	0.05	Batch	10.4 g/L dry weight	*Eschscholtzia californica* (embryo-genic)	95

Double helical ribbon impeller (downward pumping)	$V_L = 2.5$ L $D_T = 12.6$ cm Four cell sedimentation columns within the bioreactor	$D_i/D_T = 0.91$ $H_i/D_i = 1.04$ $W_R/D_i = 0.19$	40	Porous (2 μm) stainless steel, 6 cm below the liquid surface	Varied	Perfusion	15.9 g/L dry weight (with antifoam)	*Eschscholtzia californica*	96
Helical agitator	$V_L = 32$ L $D_T = 25.9$ cm $H_L/D_T \approx 3$	$D_i/D_T = 0.89$ Seven helices Helix spacing $= 0.32\ D_i$	50	Ring, 16 × 1.5-mm holes $D_S/D_T = 0.39$	0.6	Batch	—	*Coleus blumei*	94
Helical stirrer (downward pumping)	—	—	100–300	—	—	Batch	—	*Berberis wilsoniae*	97
Helical stirrer	$V_L = 27$ L	—	100	—	0.15–0.74	Batch	27 g/L dry weight	*Digitalis lanata*	98
Spin stirrer	$V_L = 27$ L	—	100	—	0.15–0.55	Batch	27 g/L dry weight	*Digitalis lanata*	98
Cell-lift impeller	$V_L = 1.25$ or 2.5 L	—	60	Ceramic stone, off-center	—	Batch	6.5 g/L dry weight	*Glycine max* (photo-mixotrophic)	99
Cell-lift impeller	Volume = 5 L Dished base	—	—	Sintered stainless steel	—	Perfusion	27.6 g/L dry weight	*Thalictrum rugosum*	100
Centrifugal impeller (six blades)	$V_L = 2$ L $D_T = 14$ cm Round bottom	$D_i/D_T = 0.64$ $W_B/D_i = 0.20$ Blade angle = 60°	80–300	Sintered stainless steel	0.1	Batch	15.9 g/L dry weight (at a mixing time of 5 s)	*Taxus chinensis*	101
Centrifugal impeller (six blades)	$V_L = 21$ L	—	80	—	—	Fed-batch	30.3 g/L dry weight	*Panax notoginseng*	102

(*continued*)

TABLE 48.4. (*Continued*)

Impeller	Bioreactor Specifications	Impeller Specifications	Stirrer Speed (rpm)	Sparger Specifications	Aeration Rate (vvm)	Bioreactor Operation	Maximum Cell Density	Plant Species	Reference
Membrane stirrer	$V_L = 19$ L	Membrane tubing wound into a basket configuration	30–50	Bubble-free aeration with pulses of bubbling through the tubing (air and oxygen-enriched air)	—	Fed-batch	50 g/L dry weight	*Thalictrum rugosum*	103
Taylor–Couette membrane stirrer	$V_L = 2.2$ L Magnetically coupled stirrer	$D_i/D_T = 0.53$	200	Bubble-free aeration	0.95	Batch	93 g/L dry weight	*Beta vulgaris*	104
Spin filter	Magnetically coupled stirrer	—	—	—	—	Batch	10.3 g/L dry weight	*Daucus carota*	105
Magnetic stirrer bar	$V_L = 3$ L Dual carboys	$D_i = 7.5$ cm	90	Stainless steel, porosity 10 μm	1.5	Batch	5.2 g/L dry weight	*Mentha spicata*	106
Magnetic stirrer bar	$V_L = 2$ L Round-bottom flask Stirrer stabilizer rod	—	125	Fritted glass	0.025	Chemostat, dilution rate $= 0.36\ day^{-1}$	—	*Glycine max*	107
Magnetic stirrer bar	$V_L = 20$ L	$C_i = 1$ cm	200	—	0.05	Batch, turbidostat, and chemostat	7.3 g/L dry weight (batch)	*Acer pseudoplatanus*	108
Magnetic stirrer bar	$V_L = 4$ L Round-bottom flask	$D_i = 6$ cm	260	Pipe (1-mm diameter) or sintered glass, porosity 2	0.125	Turbidostat	3 g/L dry weight	*Acer pseudoplatanus*	109
Magnetic stirrer bar	$V_L = 3.5$ L	—	—	—	—	Multicycle draw–fill	1.7 g/L dry weight (batch)	*Haplopappus gracilis*	110
Double-bar magnetic stirrer	$V_L = 2$ L V-shaped flask	—	200–300	—	—	Multicycle draw-fill	8.4 g/L dry weight (batch)	*Phaseolus vulgaris*	111

[a]Symbols are defined in the section titled "Nomenclature".

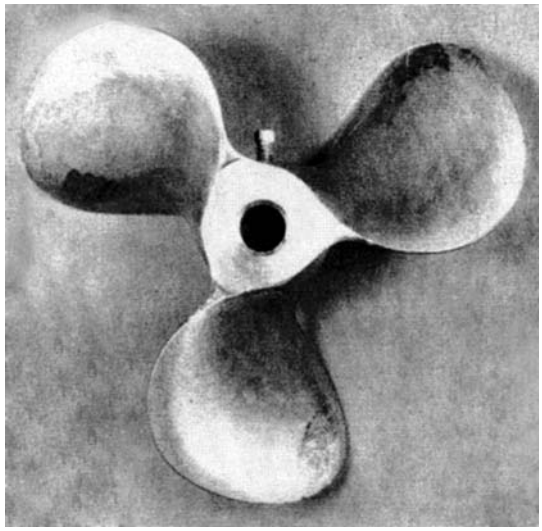


Figure 48.9. Marine propeller.

Significant power losses occur with gassing; aerated downward pumping propellers may also exhibit flow and power draw instabilities (54). Propellers are very effective for solids suspension with low power consumption and outperform disk turbines and paddles in this respect (114). Several investigators have used marine propellers for suspended plant cell culture (Table 48.4).

48.4.3.4 Axial Flow Impellers with Draft Tube. The use of a draft tube with an axial flow impeller such as a marine propeller can significantly improve particle suspension in systems containing solids (114,115). Two configurations for this type of stirring system are shown in Fig. 48.10. The position and size of the draft tube have a strong influence on the hydrodynamic conditions generated. For example, if the bottom of the tube restricts the impeller outflow, the loss of local pressure causes a marked increase in the energy dissipation rate required for solids suspension (114). The power saved by installing draft tubes to assist particle suspension is reported to be greatest at low solids concentrations (115). An axial-flow Kaplan turbine in a 75-L vessel with a draft tube performed satisfactorily for plant cell culture (Table 48.4) and compared well with other impeller configurations (14).

48.4.3.5 Perforated Disks. Rotating perforated disks are most commonly employed in two-phase liquid extraction systems, including aqueous extraction of biological molecules such as proteins (116,117). This type of contactor is very effective for high-shear liquid droplet dispersion and is associated with high mass transfer rates and separation efficiencies. Application of perforated disks for stirring in bioreactors is not well characterized in the literature; however, a perforated disk impeller operated at

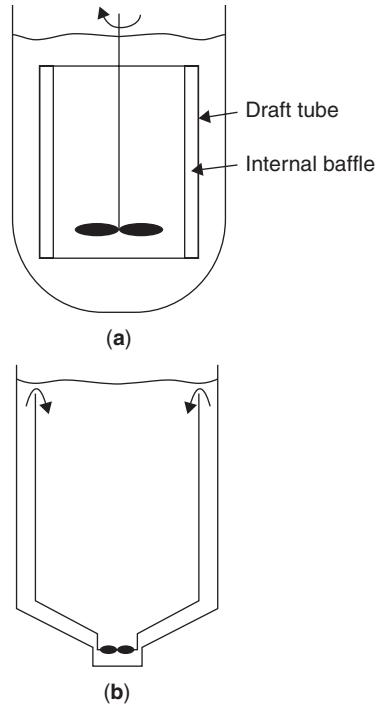
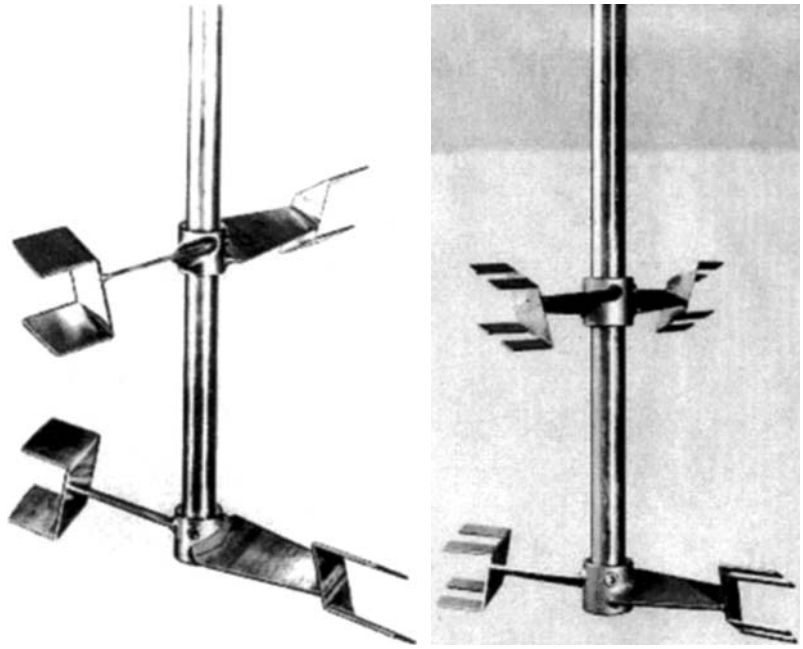


Figure 48.10. Axial flow impellers with draft tube. (a) Vessel with draft tube and internal baffles. The internal baffles prevent vortexing and liquid draw-down into the draft tube. (Adapted from Ref. 115.) (b) Draft tube reactor with Kaplan turbine used for culture of *Morinda citrifolia* plant cells. (Adapted from Ref. 14.)

a speed of 100 rpm was tested by Wagner and Vogelmann (14) for culturing *Morinda citrifolia* plant cells in a 10-L vessel. Its performance in terms of biomass and secondary metabolite production was similar to that of dual flat-blade turbines and a Kaplan turbine with draft tube.

48.4.3.6 Intermig Impellers. The Intermig is an impeller design of Ekato GmbH, Germany. As shown in Fig. 48.11, Intermig impellers are used in dual configuration, orthogonal to each other and positioned on the stirrer shaft about one impeller diameter apart. Each impeller has two large blades connected at the hub; each large blade supports smaller blades at its ends. The smaller blades may be either unslotted (Fig. 48.11a) or slotted to form four wing tips (Fig. 48.11b). The large and small blades pump in opposite directions; the recommended arrangement is for the small outer blades to pump downwards while the central blades pump upwards. Because the unaerated power number for each impeller is very low (about 0.35; Ref. 118), at least two Intermigs with diameter 0.6–0.7 times the tank diameter would be used instead of a single Rushton turbine.

The flow produced by ungassed Intermig impellers is very chaotic (119), and energy dissipation rates are reported to be more uniformly distributed throughout the vessel than with Rushton turbines (120). With aeration,



(a) (b)

Figure 48.11. Dual Intermig agitators with (a) unslotted wing tips and (b) slotted wing tips. (Photographs provided courtesy of Ekato Rühr- und Mischtechnik GmbH, Germany.)

the flow becomes radial due to the development of large ventilated cavities at the tips of each blade. These cavities extend back into the liquid, increase in size with increasing gas flow rate, and reduce the power draw by up to about 50% (49,52). Mixing of non-Newtonian fluids has been found to be equally satisfactory with Intermig and Rushton impellers under a range of operating conditions, with the presence or absence of slots on the blades having little effect (121). The energy dissipation rates required for particle suspension by dual Intermigs are higher than for Rushton turbines and significantly greater than for downward pumping axial flow impellers (45).

Unslotted Intermig impellers have been tested for pilot- and large-scale suspended plant cell culture (P. Forschner, Ekato GmbH, personal communication; Ref. 33). Advantages of low shearing force, good mixing, good gas dispersion, and low energy consumption have been cited (33), but more detailed quantitative information was not provided.

48.4.3.7 Paddles. Flat-blade paddles are simple in design and construction and commonly have two or four blades (Fig. 48.12a). Paddles generate radial flow patterns similar to those produced by Rushton turbines (122,123), and are intermediate between circulation- and dispersive-type impellers in their function and operating characteristics. They are often applied as large-blade-area, low-speed agitators that push or carry liquid around the vessel. Under these conditions, no high speed liquid streams are generated, and little top-to-bottom mixing takes place (124). Flat-blade paddles perform poorly compared with other impellers in terms of gas distribution, gas holdup, power consumption, and discharge efficiency, and have been reported to be unsuitable for use in gas–liquid systems (47). Their small projected blade area means that they flood relatively easily. Particle suspension efficiency in large-scale tanks is also lower with two-flat-blade paddles than with Rushton turbines (123).

A large variety of modified paddle geometries is used in industry for mixing applications; some examples are illustrated in Fig. 48.12b–d. The Maxblend impeller (Fig. 48.12d) by SHI Mechanical & Equipment Inc., Japan, is a wide impeller combining a lower paddle with a grid (125). The impellers shown in Fig. 48.12b–d are usually employed at low speeds for mixing viscous liquids. Several semiconventional paddle configurations, such as modified gate and hollow stirring wing paddles and the Maxblend impeller, have been investigated for use in plant cell reactors (Table 48.4). In most of these studies, the stirring speeds were higher (up to 630 rpm; Ref. 24) than those commonly used in viscous fluids, and cell densities of up to 75 g/L dry weight were supported without sedimentation (92). Because raising the gas flow rate reduced biomass levels, oxygen transfer rates with a wing-type paddle were increased by enriching the air supply with oxygen (92).

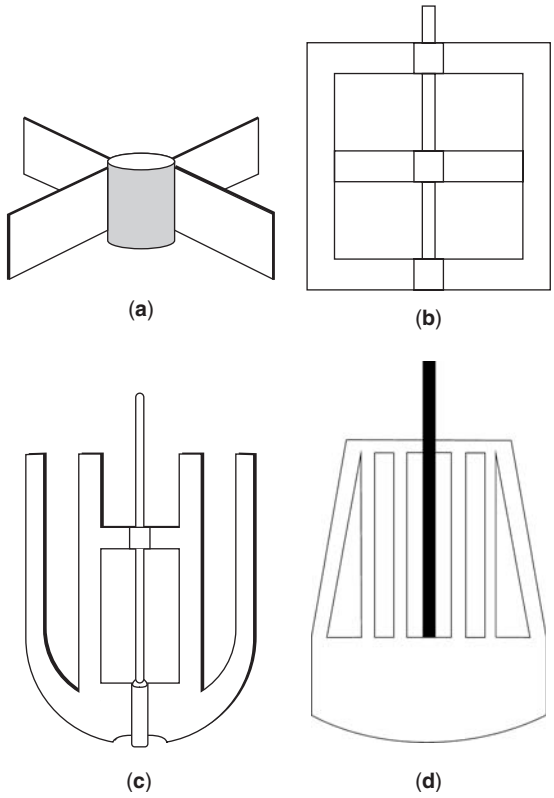


Figure 48.12. Flat-blade paddle and examples of modified paddle geometries: (a) four-flat-blade paddle, (b) frame- or wing-type paddle, (c) gate- or grid-type paddle, (d) Maxblend impeller.

48.4.3.8 Anchors. Anchor impellers such as that shown in Fig. 48.13 are applied when circulatory rather than dispersive mixing is required. Often used with high viscosity fluids for laminar blending and heat transfer applications, anchors are typically large-diameter agitators operated with small wall clearance (around 1–5% of the tank diameter) and low-speed (5–20 rpm). While producing highest shear levels near the wall, anchors generate a relatively uniform distribution of energy dissipation rates compared with small-diameter impellers (122). However, by creating primarily tangential flows, anchor impellers do not provide strong top-to-bottom mixing, although secondary axial flows may also develop at higher rotational speeds (126). Fluid near the stirrer shaft is relatively stagnant during anchor operation because there is little mixing from near the wall to the center of the vessel (127). Therefore, anchor impellers are not recommended if completely uniform mixing is required (128); breakup of bubbles sparged into the vessel is also not very effective. Wall clearance exerts a strong influence on the power requirements for mixing with anchors (129).

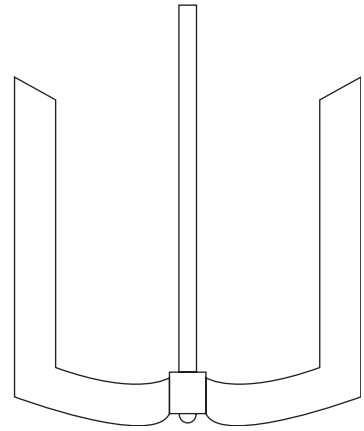


Figure 48.13. Anchor impeller.

Anchors with relatively small impeller-to-tank diameter ratios of 0.50–0.74 have been tested for plant cell culture at speeds of up to 100 rpm (Table 48.4), but have not performed as well as other agitators for secondary metabolite production (62,94).

48.4.3.9 Helical Ribbon Impellers. Helical ribbon impellers are large-diameter agitators with spiral-like motion operated at small clearance from the vessel wall to promote fluid mixing and minimize the formation of stagnant zones. Depending on the direction of rotation, upward or downward pumping can be achieved. As shown in Fig. 48.14, helical impellers may be constructed with either single or double helices. Like anchor impellers, helical ribbons are usually operated at low speeds and shear rates and have lower capacity for gas dispersion than turbines and other high-speed agitators. In non-Newtonian fluids, oxygen transfer depends more strongly on gas flow rate than power input or stirrer speed, reflecting the limited ability of helical impellers to disperse air bubbles (130). Aeration may be facilitated, however, by installing surface baffles (131), such as those illustrated in Fig. 48.14b. Circumferential flows are dominant in stirred tanks fitted with helical agitators; however, upward flows are also generated by the outer helix and downward flows are prominent along the stirrer shaft (132). Changes in impeller geometry can have a significant effect on mixing (133); for example, the mixing time may be doubled by increasing the blade width at constant impeller diameter (134). Overall, helical impellers give a positive top-to-bottom turnover without unmixed regions, thus representing a significant advantage over anchor agitators. Power requirements are similar to those for anchor impellers (135).

Helical impellers have been used for plant cell culture in several studies (Table 48.4). Biomass concentrations of

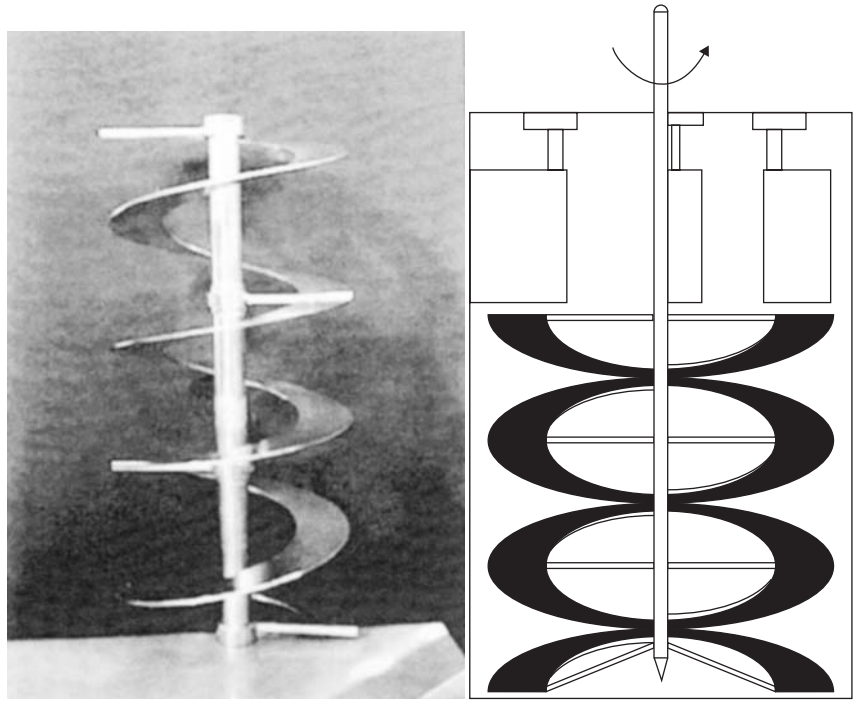


Figure 48.14. (a) Helical ribbon impeller. (Photograph provided courtesy of B. Braun Biotech International, Germany.) (b) Bioreactor with double helical ribbon impeller and three surface baffles. (Adapted from Ref. 2.)

27–28 g/L dry weight were supported using either air sparging below the impeller (98) or surface aeration only with oxygen-enriched air and surface baffles (2). For large-scale applications, oxygen transfer may present some difficulties. The success of helical impellers for plant cell culture has been attributed to their high pumping capacity and low mechanical shear forces; however, the investment costs associated with this type of stirrer are greater than for conventional equipment (2). The advantages associated with using impellers designed for mixing high viscosity fluids may be most apparent toward the end of batch plant cell cultures, when the cell density and suspension viscosity are highest.

48.4.3.10 Spin Stirrers. As illustrated in Fig. 48.15, spin stirrers consist of vertical stirrer blades that rotate independently on a stirring assembly. The length of the blades ensures that as much fluid as possible is kept in motion by the action of the stirrer. There is little general information in the literature about the performance characteristics of spin stirrers; however, they have been used for suspended plant cell culture (Table 48.4) at biomass concentrations up to 27 g/L dry weight (98). When applied for culture of *Berberis wilsoniae* cells, production of protoberberine alkaloids was lower than that achieved with a bladed turbine (97).

48.4.3.11 Cell-Lift Impellers. These novel impellers comprise a draft tube topped with radial or tangential exit ports, as shown in Fig. 48.16. With rotation, reduced

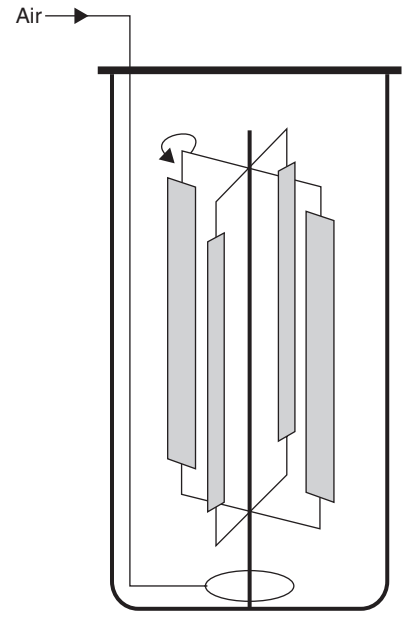


Figure 48.15. Bioreactor with spin stirrer, each blade capable of individual rotation. (Adapted from Ref. 98.)

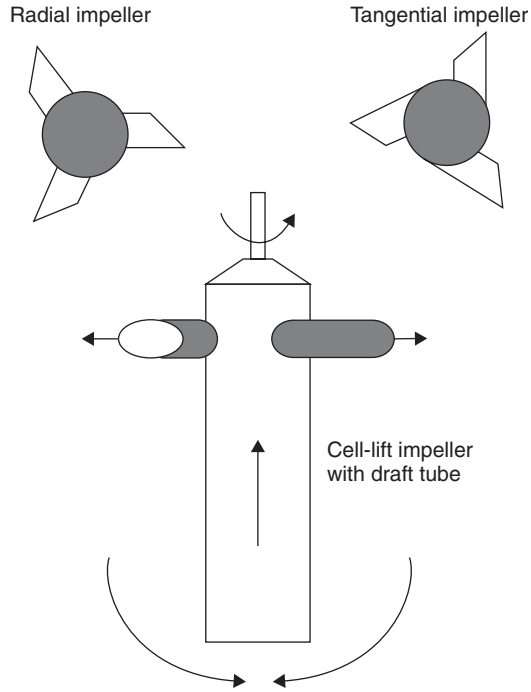


Figure 48.16. Cell-lift impeller, showing radial and tangential exit port configurations. (Adapted from Ref. 99.)

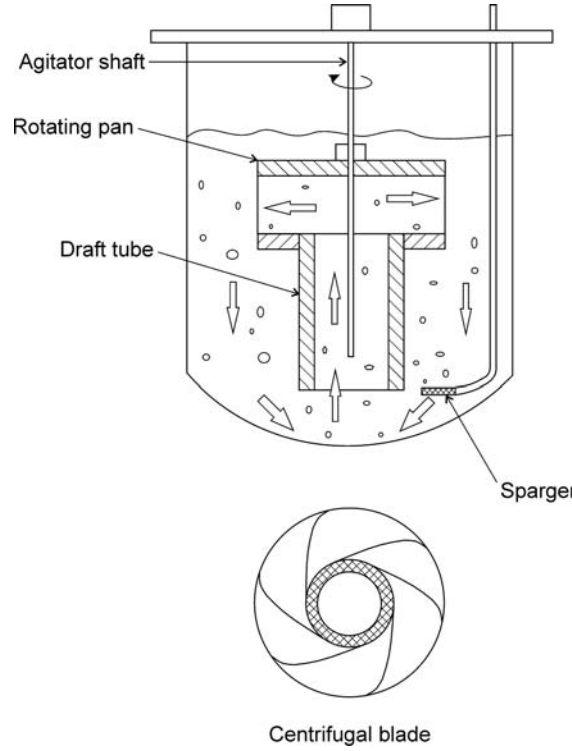


Figure 48.17. Centrifugal impeller in a sparged bioreactor. The rotating impeller consists of a draft tube topped with a centrifugal blade. (Adapted from Ref. 136.)

pressure is created at the tips of the exit ports, drawing liquid from the bottom of the reactor up the draft tube and out to the sides of the vessel for low-shear mixing. Mixing may be enhanced by installing a sparger at the base of the draft tube to generate additional airlift-type circulation (100). Cell-lift impellers have been tested for plant cell culture (Table 48.4). It was found in these studies that the tangential port configuration provided better lift than the radial design (99).

48.4.3.12 Centrifugal Impeller. As a variation on the cell-lift impeller, the centrifugal impeller (Fig. 48.17) consists of a draft tube topped with a bladed device that, when rotated with the draft tube, creates a pumping action similar to a submersible centrifugal pump (136). The centrifugal impeller was developed with the aim of reducing shear stress generation and surface liquid turbulence while maintaining liquid lift capacity. Liquid is drawn up the draft tube from the bottom of the reactor and is discharged through the bladed section of the impeller. Air is provided by sparging outside of the draft tube; this minimizes entrainment of bubbles inside the impeller, which could lead to cavitation effects at high impeller speeds. When the centrifugal impeller was applied for culture of suspended *Taxus chinensis* cells (Table 48.4), the reactor mixing time, which was dependent on both the impeller speed and suspended cell density, was identified as a critical parameter affecting taxoid production and cell aggregate size (101).

48.4.3.13 Membrane Stirrers. Membrane stirrers are used for bubble-free aeration when the effects of gas sparging, such as cell shear damage or foaming, must be avoided. To date, the major application of membrane stirrers has been in animal cell culture. Aeration is achieved by gas exchange through silicone or microporous polypropylene tubing immersed in the culture broth. For bubble-free aeration, the gas pressure inside the tubing must not exceed the bubble point, at which bubbles appear on the outside of the tube walls. Several different membrane stirrer devices have been developed (137,138). To prevent the cells from settling and to promote mixing, the tubing may be kept in motion as an effective stirrer; this also enhances mass transfer of oxygen from the air or oxygen-enriched air in the tubing to the culture fluid, and facilitates penetration of liquid into the inner sections of the tubing coil. Reactors with membrane stirrers have been used to culture plant cells to high-density (50 g/L dry weight) with little foaming and no cell flotation (Table 48.4).

An alternative reactor configuration using gas-permeable membranes and based on the Taylor–Couette flow principle has also been designed for suspended plant cell culture

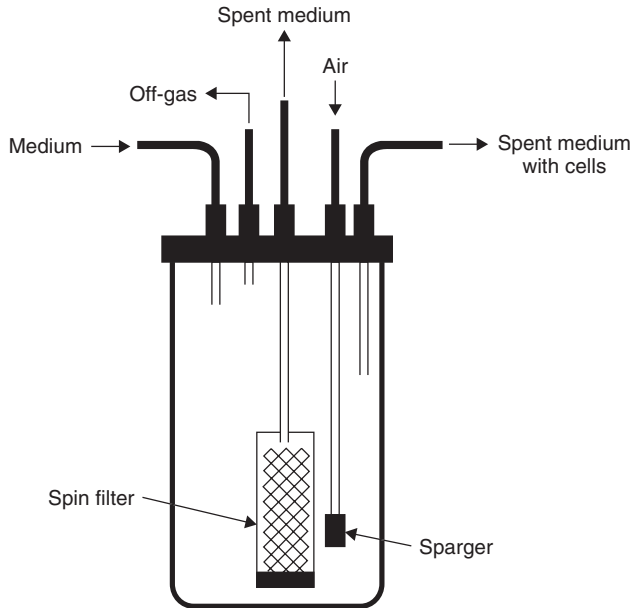


Figure 48.18. Bioreactor with spin filter unit for removal of medium in perfusion culture. The reactor also has provision for continuous whole broth removal. (Adapted with permission from Ref. 105.)

(Table 48.4). In this reactor, a perforated cylindrical glass tube covered with silicone membrane sheeting was rotated as a primitive type of stirrer generating vortex flow in the annulus between the tube and the walls of the bioreactor. The inside of the glass tube was maintained at high pressure relative to the annulus by using an air pump, so that bubble-free aeration of the culture was achieved. Some sedimentation of plant cells occurred in this reactor, prompting the investigators to suggest that the vessel could be operated with its axis horizontal (104).

48.4.3.14 Spin Filters. Spin filters are used in bioreactors for continuous perfusion culture at high cell densities. They have been applied mainly for intensive culture of animal cells. A simple spin filter system is shown in Fig. 48.18. Culture fluid is removed from inside the spin filter with minimal cell loss in the spent medium, while fouling is reduced by rotating the filter unit. Because spin filters are not designed to perform the normal mixing and gas dispersion functions of an impeller, problems with oxygen transfer may occur unless other devices, such as turbine agitators or membrane tubing aeration, are used to enhance mass transfer rates (139). As indicated in Table 48.4, spin filters have been used for culture of plant cells (105).

48.4.3.15 Magnetic Stirrers. Many of the first attempts to cultivate suspended plant cells in bioreactors involved the use of Teflon-coated magnetic stirrer bars driven by external drives at the base of the culture vessel (Table 48.4). However, because only limited power can be input by magnetic stirrers and the liquid currents generated are relatively weak, mixing was most likely inadequate in these reactors except at low cell densities. Magnetic stirrer bars are usually placed at the bottom of the vessel and rotate in contact with the reactor floor, so that the risk of plant cell damage by abrasion in this region is also high. This problem was avoided in one study by suspending the stirrer bar 1 cm from the bottom of the vessel using a flexible Teflon stalk (108). The usual position of magnetic stirrers also means that gas must be sparged into the liquid from above the stirrer. Because contact between the bubbles and agitator is minimized by this arrangement, gas dispersion and therefore oxygen transfer may be severely restricted. This is reflected in the relatively low biomass densities supported by plant cell reactors with magnetic stirrer bars, as indicated in Table 48.4.

48.4.4 Spargers

Several types of sparger are in common use. Porous spargers of sintered metal, glass, or ceramic are applied mainly in small-scale applications; gas throughput is limited because the sparger poses a high resistance to flow. Cells growing through the fine holes and blocking the sparger can also be a problem. Orifice spargers, also known as perforated pipes, are constructed by making small holes in piping, which is then fashioned into a ring or cross and placed at the base of the reactor. The individual holes on orifice spargers should be large enough to minimize blockages. Point or nozzle spargers are used in many agitated fermenters from laboratory to production scale. These spargers consist of a single open or partially closed pipe providing a point-source stream of air bubbles. Advantages compared with other sparger designs include low resistance to gas flow and small risk of blockage.

The design and location of the sparger have an important influence on gas–liquid hydrodynamics and power consumption in stirred vessels. With Rushton turbines, the fall in power with aeration can be reduced by installing a large sparger, for example, a ring sparger with diameter 1.2 times that of the impeller, rather than a small sparger (140). Use of a large ring sparger affects the formation of ventilated cavities behind the agitator blades, thus allowing a 50% increase in the aeration rate that could be used without flooding compared with a point or small ring sparger. The effect of sparger geometry is even more pronounced with downward pumping axial flow impellers: the use of point spargers increases the likelihood and severity of torque and power instabilities that can occur with these impellers in gassed systems (49). The gas-handling ability of downward pumping agitators can be improved and the stirrer speed required for complete solids suspension reduced by replacing point spargers with ring spargers of diameter about 0.8

times the impeller diameter, and increasing the separation between the sparger and impeller from 0.1 to up to 0.2 times the tank diameter (49,141).

48.5 PLANT CELL CULTURE IN STIRRED BIOREACTORS: EXPERIMENTAL FINDINGS

Studies of suspended plant cell culture in stirred vessels have been carried out for at least 40 years. A wide variety of reactor, impeller, and sparger geometries has been tested in batch, fed-batch, perfusion, draw-fill, chemostat, and turbidostat operations. A summary of the equipment and operating conditions used and the maximum cell densities achieved is shown in Table 48.4. The list includes results from vessels with working volumes of 0.5–20,000 L equipped with single or multiple impellers.

Stirrer systems for plant cell culture have often been evaluated in terms of biological rather than physical parameters: that is, cell growth and alkaloid levels are usually measured in preference to more direct indicators of stirrer performance, such as mixing time, power consumption, or gas holdup. Many papers that describe reactor culture of plant cells do not provide complete details of the vessel internals; for example, the number and width of the baffles, the diameter and position of the impeller, the type and position of the sparger, the vessel diameter, and the liquid height are often not specified. Yet, all of these geometric variables influence the effectiveness of fluid circulation and bubble dispersion in aerobic bioreactors. Despite the large number of experimental studies carried out, few general-purpose guidelines have emerged for designing and operating stirrers for plant cell culture. The lack of widely accepted design principles reflects in part the inherent complexity of stirring hydrodynamics, especially for three-phase systems such as aerobic cell suspensions, as well as the variation in critical properties, for example, rheology, cell shear sensitivity, and level of aggregation, among different plant cell suspensions.

48.5.1 Comparative Studies of Reactor Hardware: Impellers, Baffles, and Spargers

Several comparative studies have been carried out using the same cell line and vessel configuration to determine which impeller design produces the best outcome in terms of plant cell growth and/or production of valuable metabolites. These investigations are summarized in Table 48.5. The results highlight the difficulty associated with drawing general conclusions about impeller performance in plant cell systems: the relative outcomes obtained using the same or similar impellers may vary considerably between different studies. Because replicate bioreactor experiments are often not carried out, the statistical significance of any differences observed as a result of modifying the stirring equipment is also sometimes questionable.

Baffles in stirred tanks can be expected to increase levels of hydrodynamic shear as well as reduce vortexing and improve mixing. Experiments have been carried out to examine the effect of baffles on plant cell growth and product formation. Total protoberberine levels (gram per liter) produced by *Berberis wilsoniae* cells in a reactor stirred with a flat-blade turbine were about 35% greater with baffles than without (97). In other work with a cell-lift impeller, plant cells tended to accumulate in the space between the baffles and vessel wall, resulting in poor local mixing on both sides of the baffles. Removal of the baffles alleviated these fouling problems but did not significantly affect growth; only slight differences in biomass were observed for reactors with and without baffles (99). For *Catharanthus roseus* cultured in a 12-L reactor with dual 8.5-cm flat-blade turbines, the presence or absence of baffles did not have a significant effect on cell growth at most stirrer speeds. Alkaloid levels measured as milligrams per gram dry weight were similar in baffled and unbaffled vessels at 100 rpm; however at 700 rpm, specific alkaloid levels were 3.0–3.5 times higher in the baffled tank (60).

The effect of different sparger designs on *C. roseus* cultures was investigated using a 12.5-L bioreactor with dual Rushton turbines (10). When operated with the same aeration rate and stirrer speed, a sintered glass disk sparger of diameter 8 cm gave higher k_La values than a glass cross-shaped sparger with two rows of 2-mm holes. These spargers were employed at various air flow rates to produce initial k_La values ranging from 2.5 to 20 h^{-1} at a constant stirrer speed of 100 rpm. The highest biomass level was achieved with the sintered sparger at an intermediate initial k_La of 12.5 h^{-1}; k_La values above 12.5 h^{-1} obtained using the same sparger depressed growth. In a cell-lift reactor, replacing a single orifice sparger with a porous ceramic air stone resulted in the generation of smaller bubbles and an increase in k_La; changing the sparger position to slightly off-center also improved mixing in the vessel (99). A new type of spiral sparger with fine holes was used to produce small bubbles in a 2-L fermenter equipped with a two-blade grid paddle (8). High k_La values of 20 h^{-1} were obtained at a stirrer speed of 50 rpm, whereas 235 rpm was required to achieve the same k_La using a dual flat-blade turbine system and conventional ring sparger.

48.5.2 Mechanical Shear

Stirred tank reactors have been used in several studies to assess the sensitivity of plant cells to mechanical forces, and to determine the restrictions this property imposes on reactor operating conditions (17,18,58,60,67,90). Plant cell responses to short- (2–24 h) and long-term shear forces have been examined, and various criteria used to evaluate

TABLE 48.5. Results from Comparative Studies of Different Impellers Applied for Suspended Plant Cell Culture

Impeller and Operating Conditions	Performance Indicators	Bioreactor Specifications	Bioreactor Operation	Plant Species	Reference
Disk turbine (100 rpm, 0.25 vvm)	14.4 g/L dry weight cells and 50.1 mg/L saponins produced	$V_L = 25$ L	Fed-batch, 28 days	*Panax ginseng*	62
Anchor turbine (100 rpm, 0.25 vvm)	15.3 g/L dry weight cells and 43.5 mg/L saponins produced				
Angled disk turbine (100 rpm, 0.25 vvm)	17.0 g/L dry weight cells and 30.1 mg/L saponins produced				
Six-flat-blade turbine ($D_i = 6.4$ cm, $W_B = 1.4$ cm, 225 rpm, 1.0 vvm)	$k_La = 42$ h^{-1} at a cell concentration of 11 g/L dry weight Mixing and gas dispersion poor at cell densities above 20 g/L dry weight	$V_L = 1$ L $D_T = 11.3$ cm $H_L = 10$ cm Ring sparger, eight holes	—	*Cudrania tricuspidata*	24
Modified (gate-type) paddle ($D_i = 7.0$ cm, $H_i = 5.0$ cm, 400 rpm, 1.0 vvm)	$k_La \approx 52$ h^{-1} at a cell concentration of 11 g/L dry weight Mixing and gas dispersion satisfactory at cell densities above 20 g/L dry weight				
Rushton turbine ($D_i = 7.5$ cm, 1,000 rpm)	Biomass doubling time = 7.6 days Maximum cell concentration = 6.4 g/L dry weight Maximum alkaloid concentration = 10.4 mg/L	$V_L = 2$ L $D_T = 15$ cm Concave sides, flat bottom No baffles	Batch, up to 14 days	*Catharanthus roseus*	56
Vaned six-blade disk turbine, blades inclined 30° from the vertical ($D_i = 7.5$ cm, 1,000 rpm)	Biomass doubling time = 6.1 days Maximum cell concentration = 6.8 g/L dry weight Maximum alkaloid concentration = 5.5 mg/L				
Vaned six-blade disk turbine, blades inclined 60° from the vertical ($D_i = 7.5$ cm, 1,000 rpm)	Biomass doubling time = 4.5 days Maximum cell concentration = 7.7 g/L dry weight Maximum alkaloid concentration = 24.2 mg/L				
Flat-blade turbine (with baffles)	Concentration of protoberberine alkaloids produced = 3.0 g/L	Volume = 30 L	Batch	*Berberis wilsoniae*	97
Flat-blade turbine (without baffles)	Concentration of protoberberine alkaloids produced = 2.2 g/L				
Helical stirrer (upward pumping)	Concentration of protoberberine alkaloids produced = 2.3 g/L				
Spin stirrer	Lower maximum protoberberine alkaloid concentration than with the flat-blade turbine and baffles				

Six-flat-blade disk turbine (D_i = 7 cm, L_B = 1.3 cm, W_B = 1.3 cm, 200–300 rpm)	Maximum cell concentration = 18 g/L dry weight at 200 rpm Maximum L-DOPA content = 6.4% of dry weight at 200 rpm Higher levels of shear force intensity than with the six-flat-blade turbine	V_L = 5 L D_T = 21 cm No baffles	Batch	*Stizolobium hassjoo*	58
Six-flat-blade turbine (D_i = 6 cm, W_B = 0.8 cm, 100–500 rpm)	Maximum cell concentration = 21.5 g/L dry weight at 300 rpm Maximum L-DOPA content = 11.5% of dry weight at 400 rpm Lower levels of shear force intensity than with the six-flat-blade disk turbine				
Six-flat-blade turbine (D_i = 6 cm, W_B = 0.8 cm, 300 rpm, 0.06 vvm)	Maximum cell concentration = 21.3 g/L dry weight after 10 days Maximum L-DOPA content = 4% of dry weight after 11 days	V_L = 5 L D_T = 21 cm No baffles	Batch	*Stizolobium hassjoo*	65
Maxblend impeller (D_i = 10 cm, H_i = 12 cm, 100 rpm, 0.08 vvm)	Maximum cell concentration = 19 g/L dry weight after 15 days Maximum L-DOPA content = 2.3% of dry weight after 11 days				
Dual impellers; six-flat-blade turbine lower, three-pitched-blade turbine upper (D_{i1} = 6 cm, W_{B1} = 0.8 cm, D_{i2} = 7 cm, pitched blade angle = 30°, 300 rpm, 0.06 vvm)	Maximum cell concentration = 21 g/L dry weight after 13 days Maximum L-DOPA content = 2.0% of dry weight after 10 days				
Four-flat-blade impeller (D_i = 5.6 cm, W_B = 1.5 cm, 100–200 rpm, 0.2 vvm)	No growth at 200 rpm due to shear damage Poor mixing at 100 rpm Maximum cell concentration = 520 g/L fresh weight after 12 days at 150 rpm	V_L = 3 L D_T = 14 cm	Batch	*Nicotiana tabacum*	15
Large four-flat-blade impellers (D_i = 7.6 cm, W_B = 5.1–14 cm, 50–200 rpm, 0.2 vvm)	Growth rate increased with increasing blade width Maximum cell concentration = 580 g/L fresh weight after 7–8 days at 150 rpm with W_B = 14 cm Some cell damage				
Sail impeller (D_i = 7.6 cm, W_B = 14 cm, nylon cloth blades, 150 rpm, 0.2 vvm)	Longer lag phase Maximum cell concentration = 590 g/L fresh weight after 9 days at 150 rpm No cell damage Higher power requirements than for the large flat-blade impellers				

(*continued*)

TABLE 48.5. (*Continued*)

Impeller and Operating Conditions	Performance Indicators	Bioreactor Specifications	Bioreactor Operation	Plant Species	Reference
Dual Rushton turbines (60 rpm)	Maximum cell concentration = 75 g/L fresh weight after 15 days	V_L = 2.0–2.5 L	Batch	*Glycine max*	99
Dual marine impellers (60 rpm)	Maximum cell concentration = 15 g/L fresh weight after 11 days				
Cell-lift impeller (60 rpm)	Maximum cell concentration = 82 g/L fresh weight after 13 days Reduction in average biomass aggregate size				
Dual turbines (100 rpm, 0.5 vvm)	Lower biomass yield and productivity but higher anthraquinone yield than with perforated disk	Volume = 10 L	Batch	*Morinda citrifolia*	14
Perforated disk (100 rpm, 0.5 vvm)	Lower anthraquinone yield but higher biomass yield and productivity than with dual turbines				
Dual flat-blade turbines: six blades lower, four blades upper (D_i = 6.5 cm, W_B = 1.4 cm, 235 rpm, ring sparger, 0.3 vvm)	Maximum cell concentration = 9.5 g/L dry weight after 29 days Biomass yield from sugar = 0.29 g g^{-1} Cell damage observed	V_L = 2 L D_T = 13 cm H_L = 16 cm Four baffles	Batch, 29 days	*Catharanthus roseus*	8
Two-blade grid paddle (D_i = 6.9 cm, H_i = 14.8 cm, 50 rpm, spiral sparger, 0.3 vvm)	Maximum cell concentration = 19 g/L dry weight after 25 days Biomass yield from sugar = 0.43 g g^{-1} No cell damage observed				
Internal turbine (400 rpm, 1.0 vvm)	14.5 g dry weight cells and 65.7 mg total ginsenoside produced	V_L = 2 L	Batch, 42 days	*Panax ginseng* (embryogenic)	91
Paddle (50 rpm, 1.0 vvm)	23.2 g dry weight cells and 77.7 mg total ginsenoside produced				
Dual vaned six-flat-blade disk turbines (D_i = 12 cm, W_B = 1.8 cm, vane width = 0.3 cm, 100 rpm)	Biomass doubling time = 2.8 days Maximum cell concentration = 11.1 g/L dry weight Maximum alkaloid concentration = 21.8 mg/L	V_L = 7.5 L D_T = 23 cm H_L = 18.5 cm Concave sides, flat bottom No baffles C_{i1} = 7.5 cm C_{i2} = 18.5 cm	Batch	*Catharanthus roseus*	56
Dual vaned six-blade disk turbines, blades inclined 60° from the vertical (D_i = 8.5 cm, 100 rpm)	Biomass doubling time = 1.8 days Maximum cell concentration = 11.9 g/L dry weight Maximum alkaloid concentration = 25.8 mg/L				

Centrifugal impeller (six blades, $D_i = 8.5$ cm, blade angle = 60°, various stirrer speeds, 0.2–0.8 vvm)	Maximum cell concentration = 26.0 g/L dry weight Maximum saponin concentration = 0.80 g/L Lower stirrer speeds required to maintain higher dissolved oxygen tensions than with the turbine	$V_L = 2.5$ L $D_T = 12.5$ cm	Batch	*Panax notoginseng*	22
Turbine ($D_D = 6$ cm, various stirrer speeds, 0.2–0.8 vvm)	Maximum cell concentration = 22.7 g/L dry weight Maximum saponin concentration = 0.49 g/L Higher stirrer speeds required to maintain the dissolved oxygen tension above 15% air saturation than with the centrifugal impeller				
Anchor ($D_i = 19$ cm, 40 rpm, 0.6 vvm)	Maximum rosmarinic acid concentration = 2.1 g/L	$V_L = 32$ L $D_T = 25.9$ cm $H_L \approx 78$ cm	Batch	*Coleus blumei*	94
Helical agitator ($D_i = 23$ cm, 50 rpm, 0.6 vvm)	Maximum rosmarinic acid concentration = 3.3 g/L				
Spin stirrer (100 rpm, 0.15–0.55 vvm)	After 20 days, 25 g/L dry weight cells and 776 mg/L β-methyldigoxin produced	$V_L = 27$ L	Batch	*Digitalis lanata*	98
Helical stirrer (100 rpm, 0.15–0.74 vvm)	After 20 days, 23 g/L dry weight cells and 720 mg/L β-methyldigoxin produced				

[a]Symbols are defined in the section titled "Nomenclature".

shear effects. In some studies, the problem was viewed in terms of threshold values of shear rate (17,18,142) or shear stress (142,143), above which the growth rate, cell viability, product yield, or some other critical culture parameter was significantly altered. For this approach to be useful, the shear conditions present during cell culture must be quantified. Several methods have been applied to estimate shear levels in stirred bioreactors used for plant cell culture. Profiles of velocity and shear rate in an 11-L reactor stirred with dual Rushton turbines were determined using flow simulation methods; at a stirring rate of 100 rpm, shear rates varied from a maximum of 470 s^{-1} near the impeller to less than 5 s^{-1} in the bulk of the liquid (59). In other work, average and/or maximum shear rates were evaluated as a function of stirrer speed, impeller diameter, tank diameter, and blade width using correlations from the literature (56,60,144). The performance of different turbine impellers for suspended plant cell culture has also been correlated with several indirect indicators of shear force intensity, including the power input per unit mass and the Kolmogorov eddy scale, with reduced performance being associated with higher shear levels (58).

Because the hydrodynamic conditions in stirred reactors are ill-defined and spatially variable, it is difficult to predict the actual levels of shear experienced by suspended cells. Another limitation associated with the concept of threshold shear rate or shear stress for cell damage is that different threshold values may apply depending on the period of exposure of cells to the shear. If the response of plant cells to shear depends on the duration as well as the intensity of the shear forces, a parameter that takes the time of exposure into account would provide a better basis for predicting shear damage. The cumulative energy dissipated on the cells has been used as a correlating factor for shear effects in stirred plant cell reactors (32,57,64). This parameter can be calculated as the integral of the average power dissipated on the cells with respect to time. Under turbulent conditions, growth of *Atropa belladonna* suspensions in a baffled bioreactor stirred with a six-flat-blade turbine was observed to decline rapidly at energy dissipation values of about 10^8 J/m^3 (64). Sublytic effects such as changes in aggregate size, protein release, and mitochondrial activity may occur at lower cumulative dissipation energies (64,145).

Varying degrees of shear damage are known to be inflicted on plant cells by different types of impeller (8,15). If cumulative energy dissipation, as outlined above, is a satisfactory correlating parameter for shear damage irrespective of impeller design, it can be expected that of the remote-clearance impellers, low-power-number agitators such as pitched blade turbines, propellers, and hydrofoil impellers would be less damaging at the same stirrer speed and impeller diameter than high-power-number devices such as Rushton turbines. However, investigations with microbial cultures and a range of different impellers have indicated that the hydrodynamic forces generated in bioreactors and their shear effects on cells do not depend solely on overall energy dissipation levels. Additional factors, such as the distribution of energy dissipation rates within the vessel, the sweep volume of the impeller, and the trailing vortex structure behind the impeller blades, are responsible for generating local shear conditions close to the impeller where most cell damage takes place. In addition, impellers that generate strong circulation currents transport cells to the impeller region more frequently than agitators that do not promote rapid bulk liquid turnover, thus increasing the risk of shear effects. A correlating procedure for shear damage that takes all of these factors into account has been developed by Jüsten et al. (146,147) for mycelial cultures and applied to plant cell systems in a theoretical study (32). The utility of this approach for plant cultures remains to be tested experimentally.

The cell aggregate size distribution in plant cell cultures can vary significantly with stirring conditions and has been used as an indicator of shear effects in stirred reactors (5,8,17,56,64,67). Changes in aggregate size due to action of the impeller can influence cell growth and productivity in the culture. Not only is mass transfer of oxygen and nutrients affected (148,149), but a range of plant cell functions and properties including secondary metabolite synthesis, phenolic acid accumulation, enzyme activity, and levels of RNA, DNA, and protein has been found to depend on aggregate size (101,149–151). Forced breakup of aggregates, whether by shattering or attrition, may also affect viability if the plasmodesmata or cell walls are damaged. Although mechanisms of aggregate disruption have been investigated and predictive models developed for mycelial cultures in stirred reactors (152–154), similar analyses have not been carried out for plant cell systems. The factors affecting plant aggregate size appear to be complex; for example, aggregates may be larger in the presence of high shear levels (10), and complex cycles of aggregate growth, plasmolysis, and necrosis have been described in *Nicotiana tabacum* cell cultures under different agitation and aeration conditions (36). Lack of understanding in this area means that it is difficult to control cell aggregation in agitated reactors. Some models of cell damage predict that the effects of hydrodynamic shear are reduced with increasing scale (146). Consequently, it may not be possible to reproduce aggregate sizes at different equipment scales, thus affecting the success of plant reactor scale-up.

Contrary to most observations showing the deleterious effects of hydrodynamic shear on plant cell cultures, there is some evidence that increasing the average shear rate generated by turbine impellers in stirred reactors can improve secondary metabolite formation in plant cell suspensions. Increasing hydrodynamic stress was correlated with oxidative burst and transient synthesis of high levels of hydrogen peroxide in *Uncaria tomentosa* cells which, in turn, led

to a transient increase in monoterpenoid oxindole alkaloid production (144).

48.5.3 Mixing

Mixing is necessary in reactors to avoid concentration gradients and zones of oxygen and nutrient depletion. In vessels used for cell culture, the biomass represents a sink for substrates, and the sparger and medium inlet ports are oxygen and nutrient sources. Unless the cells are brought into regular and frequent contact with nutrients through good mixing, they experience deleterious physiological effects that cause a decline in overall culture performance. In the worst case, if bulk liquid velocities are very low, the cells settle out of suspension. This creates a region of high nutrient demand, rapid depletion of substrates, and high local concentration gradients at the bottom of the reactor. Because of the larger size of plant cells compared with microorganisms and their tendency to form macroscopic aggregates, cell settling is of greater concern in plant cell cultures than in most other fermentation processes.

Problems with incomplete mixing in stirred plant cell reactors have been reported in several studies (14,15,24,99). For continuous reactor operation, especially when culture overflow is used to maintain a constant liquid volume, unless special attention is given to the effluent removal, the cell concentration in the exit stream may be significantly different from that inside the vessel due to gradients of cell density developing in the broth (71,155–157). In most investigations of plant cell reactors, the adequacy of mixing has been judged qualitatively rather than measured, using visual observation of the absence of gross biomass settling or bulking. Although reported for plant cells in airlift contactors (158), spatial biomass distributions generally are not monitored in stirred reactors. However, even in plant cell broths that appear homogeneous, rates of mixing may not be adequate relative to the rates of other processes in the reactor, such as oxygen uptake and oxygen transfer. Because oxygen transfer takes place mainly in the impeller region in large stirred vessels, the time taken by cells to travel in bulk flow currents from the impeller through the remainder of the tank and back to the oxygen supply is an important consideration in assessing mixing performance.

The rate of mixing is generally quantified experimentally using tracer injection techniques (23,43), whereby the response of the system to a chemical or physical stimulus is recorded. The mixing time is the time required to achieve a given degree of homogeneity after the stimulus is imposed; the greater the mixing time, the slower is bulk mixing in the vessel and the greater is the likelihood that zones of nutrient depletion will develop. Mixing times for stirred plant cell reactors have been measured in a limited number of experimental investigations. Using a pulse of hot water as a tracer, Leckie et al. (60) estimated the mixing time in an unbaffled stirred tank of working volume 8.5 L used to culture *C. roseus* cells. With dual flat-blade turbines operated at 100 rpm, the mixing time determined from the measured temperature fluctuations was 3.6 s. In other work with an upward pumping double helical ribbon impeller, the mixing time was determined using an iodine decolorization method (2). In a flat-bottom vessel with a working volume of 11 L without baffles, mixing times of 18–25 s were measured as the stirrer speed was decreased from 150 to 120 rpm. Contouring the vessel base and installing surface baffles significantly reduced these mixing times to 4–9 s. Mixing time measured using decolorization techniques was also used to evaluate the performance of a centrifugal impeller bioreactor for *Taxus chinensis* culture (101). An increase in taxuyunnanine accumulation was correlated with a reduction in mixing time from 5 to 10 s in a 2-L stirred bioreactor. When mixing times were measured at the top and bottom of a 5-L stirred vessel containing plant pseudocells (granulated agar suspensions), the effectiveness of mixing was found to be location-dependent (65). The shortest mixing times (7–13 s) and most homogeneous mixing were found using a large Maxblend impeller; in contrast, mixing times observed using a more conventional flat- and pitched blade dual-impeller system at similar power inputs were 13–17 s.

The value of the mixing time can be used to determine whether mixing in a reactor is adequate relative to the rate of oxygen transfer or the cellular oxygen demand. Regime analysis or comparison of characteristic times (23,31) has been used for this purpose for other types of cell culture using experimental data (159), but its use with plant cell suspensions has been limited to theoretical analyses based on empirical correlations for mixing time (26,32).

48.5.4 Gas–Liquid Oxygen Transfer

An important function of reactors used for aerobic cell culture is providing adequate oxygen. Stirred plant cell reactors are most commonly aerated by bubbling air from spargers; however, surface aeration only (2) or bubble-free aeration using membrane tubing (86,104) may also be used (Table 48.4). The effectiveness of gas–liquid oxygen transfer is represented by the volumetric oxygen transfer coefficient $k_L a$; this parameter allows comparison of the oxygen transfer capacities of different reactors irrespective of their size and shape or the magnitude of the concentration difference driving force. When oxygen limits growth in cell cultures, the value of $k_L a$ determines the maximum biomass density that can be supported (43), so that increasing $k_L a$ is a common objective in reactor design and operation. Reports of higher final biomass concentrations with increasing initial $k_L a$ in batch cultures of tobacco cells (78) demonstrate this relationship. Oxygen transfer coefficients are measured experimentally using a variety of techniques (43); however, a common problem with all

k_La measurements is that it is necessary to assume that the reactor contents are perfectly mixed. If the dissolved oxygen concentration is not uniform in the vessel, measured k_La results are essentially meaningless. Because complete gas dispersion below as well as above the impeller requires relatively high power inputs for most agitators, gas-phase uniformity is often compromised in plant cell reactors to avoid the effects of shear damage (32). This means that dissolved oxygen levels, and therefore experimental k_La values, will vary depending on where in the reactor the dissolved oxygen level is measured. Practical estimation of k_La is also subject to several other common errors that affect the accuracy and value of the final results (160).

The power input, gas flow rate, and liquid properties are the principal determinants for k_La in stirred vessels. Dimensional correlations that are independent of agitator type have been developed in the following form (52,160):

$$k_La = A\left(\frac{P_T}{V_L}\right)^{\alpha} u_G^{\beta} \tag{48.1}$$

where k_La has units of s^{-1}, P_T has units of watts, V_L has units of cubic meters, and u_G has units of meters per second. The total power dissipation P_T is usually taken to be the sum of the aerated shaft power and the power provided by isothermal expansion of the gas (159,161). The values of α and β are largely insensitive to the properties of the culture broth (162) and usually fall in the range of 0.2–1.0. In contrast, liquid properties strongly influence the value of A, which includes a dependence on viscosity raised to a negative power of roughly 0.5–1 (12,161,163,164). The effects of other broth properties on k_La are complex and impossible to predict, with cell concentration and morphology, surface active agents, and coalescence-inhibiting substances such as salts, having a major influence on bubble size and gas–liquid interfacial conditions. Because changes in medium composition can alter k_La values by orders of magnitude, measurements using water or fluids other than the actual cell broth do not indicate the oxygen transfer rates achievable during reactor culture. Oxygen mass transfer coefficients have been measured in many studies of stirred plant cell reactors; examples of the results are summarized in Table 6. Because plant cells have lower specific oxygen requirements than most microbial cells, k_La values of 5–100 h^{-1} are sufficient for plant cell cultures, including those grown to high cell density (78,92,165). This range can be compared with 60–1000 h^{-1} for microbial cells and 0.1–25 h^{-1} for animal cells (166). At suboptimal k_La values, plant cell cultures may exhibit linear rather than exponential growth kinetics (78,167). The minimum k_La necessary to achieve exponential growth can be calculated using stoichiometric analysis (168).

Although the effect of suspended particles such as cells on k_La is highly variable (48), it is often found that suspended solids promote bubble coalescence, lower the gas holdup, dampen turbulence, and interfere with gas–liquid contact, thereby reducing k_La. In some cases, however, these effects are negligible below threshold particle concentrations (55,169). The data available for plant suspensions indicate that increasing the cell concentration to values as high as 20–60 g/L dry weight may have only a limited effect on k_La in stirred reactors (24,92). The influence of biomass concentration on the oxygen transfer coefficient can be expressed alternatively in terms of the relationship between k_La and the apparent viscosity of the broth (12). In other work, k_La at constant cell concentration was found to be sensitive to changes in osmotic pressure, apparent viscosity, and the biomass fresh weight to dry weight ratio. At a fixed cell density of 10.2 g/L dry weight, k_La increased from 4.8 to 5.7 h^{-1} as the fresh weight to dry weight ratio was reduced from 19.6 to 11.0 (170).

The efficiency of gas–liquid mass transfer in bioreactors depends to a large extent on the characteristics of the bubbles in the culture broth, in particular, their size. In stirred reactors with highly developed turbulent flow, the size of the bubbles produced by the sparger bears little relationship to those present in the vessel as bubble breakup and coalescence due to action of the impeller are the main influences on bubble size (171). However, because shear damage is a major concern in plant cell culture, stirred reactors will in most cases be restricted to operation at slow stirrer speeds, with the bubbles rising freely through the liquid after minimal interaction with the impeller. The same is true for large-diameter agitators such as anchors and helical impellers, which either cannot be operated at high speed because of the excessive power required or do not generate the high velocity turbulent flows needed for bubble disruption and dispersion. Because these conditions produce low gas holdups and k_La values, alternative low-shear strategies for improving the mass transfer coefficient are required. Particular attention may be given to design of the sparger because the delivery of small bubbles is advantageous for mass transfer when the impeller does not impart sufficient energy for continual bubble breakup. Improvements in k_La were achieved in plant cell reactors stirred with dual Rushton (10) or grid paddle (8) impellers using spargers that produce a greater number of smaller bubbles at the same gas flow rate. There may be practical limitations associated with this approach, however, because plant cells have a high tendency for wall growth and will invade and block porous or small-orifice spargers. Small bubbles also tend to coalesce rapidly in high-density cell suspensions. In large bioreactors affected by inadequate mixing due to stirrer speed restrictions, reducing the size of the bubbles cannot remedy the problem of poor gas distribution or the development of oxygen gradients in the vessel (32).

As indicated in Equation 48.1, the value of k_La in stirred reactors can be improved by increasing the gas flow rate at constant stirrer speed. Numerous studies have shown,

TABLE 48.6. Values of the Oxygen Transfer Coefficient (k_La) Measured in Stirred Plant Cell Bioreactors

Impeller	Stirrer Speed (rpm)	Aeration Rate (vvm)	Bioreactor Working Volume (L)	Liquid	Cell Concentration (g/L dry weight)	Plant Species	k_La (h^{-1})	Reference
Six-flat-blade turbine	225	1.0	1	Culture broth	0 and 11	*Cudrania tricuspidata*	43 and 42	24
Dual six-blade turbines	250	0.33	1.8	Sterilized culture broth with antifoam agent	—	*Catharanthus roseus*	40 ± 2	69
Marine impeller	100–325	0.43	2	Culture broth	2.5–12	*Nicotiana tabacum*	4.5–22	85
Modified paddle (hollow stirring wing)	—	0.2–1.0	2.5	Culture broth treated with formaldehyde	20–80	*Coptis japonica*	30–95	92
Modified (gate-type) paddle	400	1.0	1	Culture broth	0 and 21.6	*Cudrania tricuspidata*	55 and 48	24
—	200	—	—	Culture broth	—	*Nicotiana tabacum*	20–85	36
—	80	0.054–0.35	3.5	Medium, nonbiological	—	—	$k_La = 31.07\ (\text{vvm})^{0.792}$	167,168

however, that there are limits to which this strategy can be pursued, because reduced growth and metabolite production occur at high gas throughputs (20,27,65). This phenomenon has been attributed to stripping of carbon dioxide and other volatile components such as ethylene from the culture broth (28). The importance of gaseous metabolites in plant cell cultures was highlighted by Schlatmann et al. (69), who demonstrated that recirculating the reactor off-gas can be used to achieve a three- to fourfold increase in alkaloid concentrations in a stirred bioreactor, to reach product levels similar to those found in shake flasks. Because the mass transfer coefficient for stripping volatile compounds increases with any increase in the k_La for oxygen transfer, losses of these compounds are greater when the oxygen transfer capacity of the reactor is improved, for example, by increasing the gas flow rate or stirrer speed. Plant cell properties and metabolism may also be affected in other ways as a function of k_La. In a stirred bioreactor used for culturing *C. roseus* cells, ajmalicine was not produced at initial k_La values above 10 h^{-1}, whereas the rate of serpentine synthesis was enhanced with increasing k_La (10). The maximum specific oxygen uptake rate by cells grown at an initial k_La of 20 h^{-1} was higher than for cells grown at $k_La = 2.5$ h^{-1}. Dissolved oxygen concentrations in these reactors were not reported, although altered dissolved oxygen tension is the direct result of changes in k_La. The relationship between plant cell metabolism and oxygen concentration may be complex, with growth, secondary metabolite synthesis, and differentiation processes such as embryogenesis affected in different ways (74,75,95,172,173). The various influences of k_La on the performance of plant cell cultures reflect this complexity.

48.5.5 Gas–Liquid Hydrodynamics

For stirred bioreactors to perform their mixing and mass transfer functions satisfactorily, appropriate gas–liquid hydrodynamic conditions must be generated by the impeller. Neither bulk blending nor gas dispersion is effective when the impeller is flooded (Fig. 48.8a), and implicit in the application of k_La correlations such as Equation 48.1 is that the reactor is thoroughly mixed and of uniform composition. Impellers should be operated to achieve complete dispersion of gas bubbles above and below the impeller (Fig. 48.8c). For a given tank and agitator, the stirrer speed necessary to achieve this condition depends on the gas flow rate. The higher the gassing rate, the greater the stirring speed required.

Despite the importance of these hydrodynamic considerations, there are few reports in the literature that mention impeller flooding or are concerned with gas dispersion conditions in plant cell reactors (32). At the restricted stirrer speeds employed in many applications, adequate bubble dispersion must often be compromised to minimize shear damage. Using visual observations and computer simulation of bubble trajectories, Boysan et al. (59) demonstrated that an 11-L plant cell reactor stirred with dual Rushton turbines operated under flooded conditions at air flow rates as low as 0.009–0.2 vvm. Flooding was also reported using pitched blade and Maxblend impellers in a 5-L stirred vessel used for plant cell culture; in contrast, gas dispersion was satisfactory using a six-flat-blade turbine (65). Because the volumetric power input required to prevent flooding increases with reactor scale (49), many of the larger stirred reactors listed in Table 48.4 and operated at slow stirrer speeds are likely not to have achieved effective dispersion of the gas phase. This situation would be considered unacceptable and impractical in most applications of aerated stirred tanks.

48.5.6 Foaming

Foaming is particularly pronounced in plant cell suspensions, and its effects are exacerbated in reactor cultures by entrained cells attaching to the walls of the vessel and forming a thick meringue or crust in the reactor headspace. Plant cell meringues usually extend across the entire diameter of the vessel and prevent adequate circulation of medium, resulting in severe loss of culture performance. Foam development in plant suspensions is due mainly to the properties of the cell-free broth; the presence or absence of cells has a relatively minor influence (29). The volume of foam produced depends on the gas flow rate in the reactor; however, foam formation and stability at any given time during the culture are also strongly affected by broth properties such as pH (29). There are many reports of the use of chemical antifoam agents in stirred plant cell reactors (29,73,96,174), but a major disadvantage of antifoams is that they reduce the value of k_La and, consequently, the ability of the reactor to sustain high cell densities (29). Mechanical foam destruction is preferable if it can be made sufficiently effective, and various approaches to mechanical foam control have been reported for stirred plant cell reactors. Leckie et al. (56,60) installed a flat-blade turbine impeller at the liquid surface of a 12-L stirred bioreactor to act as a foam breaker; alternatively, periodic increases in stirring speed have been applied to clean off layers of plant cells attached to the reactor walls (57,155). For example, 2 s of high speed agitation every hour was effective in controlling meringue formation in a 2-L fermenter used for continuous culture of *Phaseolus vulgaris* cells. In other plant cell systems, foaming and wall growth were avoided by limiting the stirrer speed and air flow rate to relatively low levels (78).

48.6 PLANT CELL CULTURE IN STIRRED BIOREACTORS: THEORETICAL ANALYSIS

Although many bioreactor studies using conventional and novel impellers have been carried out to assess the effect

of impeller configuration on suspended plant cell culture, no definitive guidelines for impeller choice have emerged from this experimental work. Impeller selection affects a wide range of bioreactor functions including mixing, oxygen transfer, gas dispersion, solids suspension, and the generation of hydrodynamic shear forces.

An attempt to account for all these effects using a theoretical analysis of impeller function has been reported, based on equations and correlations from the literature (32). In this study, the performance of three different impeller designs or operating modes was compared. The impellers tested were a Rushton turbine, a downward pumping pitched blade turbine, and an upward pumping pitched blade turbine. Each impeller was fitted with six blades of width $^1/_5$ the impeller diameter; for the downward and upward pumping axial turbines, the blade angle was 45°. A model 10-m^3 bioreactor designed for mixing using a single impeller was used in the analysis; the geometric properties of the bioreactor system are listed in Table 7. The bioreactor was operated as a chemostat with a dilution rate of 0.2 day^{-1}, giving an average reactor residence time of 5 days. The plant cell broth in the reactor was assumed to contain 30 kg/m^3 dry weight of cells; other properties representative of plant cell cultures were assumed, as listed in Table 8.

Results from the theoretical analysis of impellers of diameter 1/2 that of the tank diameter are shown in Fig. 48.19 as regime maps for bioreactor operation (32). The maps indicate the performance features of the bioreactor system as a function of stirrer speed and sparging gas flow rate as operating variables. The maximum stirrer speeds allowed before shear damage affects the suspended plant cells were calculated using a typical threshold cumulative energy dissipation of 10^7 J/m^3 based on reported literature values; the effect of impeller geometry on shear damage was accounted for using the method of Jüsten et al. (146,147). As shown in Fig. 48.19, this approach allowed the maximum stirrer speeds to be estimated for each impeller type under unaerated conditions to avoid shear damage of the cells. The vertical shaded zones in Fig. 48.19a–c indicate the extent of uncertainty about the power drawn by the impellers when aerated. In general terms, to avoid cell shear damage in the model plant cell bioreactor, stirrer speeds are restricted to those in the "No damage" region to the left of the shaded zones.

The minimum gas flow rate required for adequate oxygen transfer in the bioreactors was calculated using analysis of characteristic times for oxygen uptake, mixing, and oxygen mass transfer. The results are shown as the horizontal lines across each of the regime maps in Fig. 48.19. For sufficient oxygen transfer, the bioreactor must be operated at gas flow rates above this value. Under these conditions, mixing in the bioreactor was adequate with each of the three impellers tested. The flooding/loading transition for the impellers and the conditions required for complete gas dispersion and solids suspension are also shown in the maps in Fig. 48.19. In each case, for optimum hydrodynamic performance, the impeller should be operated at stirrer speeds above those indicated by the curves representing these functions.

The results for the Rushton turbine are shown in Fig. 48.19a. At the maximum allowable stirrer speed of 0.41–0.51 s^{-1} and the minimum air flow rate of 0.13 vvm, the impeller is loaded and the cells completely suspended, but the gas bubbles are not completely dispersed. These operating conditions for the Rushton turbine are reasonably satisfactory but not ideal. The situation for the downward pumping pitched blade turbine is shown in Fig. 48.19b. Higher maximum stirrer speeds may be used with this impeller compared with the Rushton turbine while still avoiding cell damage, consistent with the lower power number for pitched blade turbines. However, the thickness of the shaded zone in Fig. 48.19b reflects the large uncertainty associated with estimating the power drawn by downward pumping turbines under aerated conditions. Because downward pumping impellers are subject to significant power and torque instabilities that can lead to mechanical damage at stirrer speeds just below those required for complete

TABLE 48.7. Properties of the Bioreactor System Used for Theoretical Analysis of Impeller Performance

Parameter	Specification
Reactor working volume	10 m^3
Tank diameter	2.3 m
Liquid height	2.3 m
Impeller type	Varies
Impeller diameter	1.15 m
Impeller clearance above the vessel floor	0.58 m
Sparger type	Ring
Sparger diameter	0.92 m
Clearance between the sparger and impeller	0.39 m
Number of baffles	4
Baffle width	0.23 m
Submerged baffle height	2.3 m

TABLE 48.8. Properties of the Plant Cell Culture Used for Theoretical Analysis of Impeller Performance

Parameter	Specification
Cell concentration	30 kg/m^3 dry weight
Cell fresh weight:dry weight ratio	15:1
Broth viscosity	30 mPa s
Suspending liquid viscosity	1 mPa s
Liquid density	1000 kg/m^3
Cell particle density	1030 kg/m^3
Cell particle diameter	500 μm

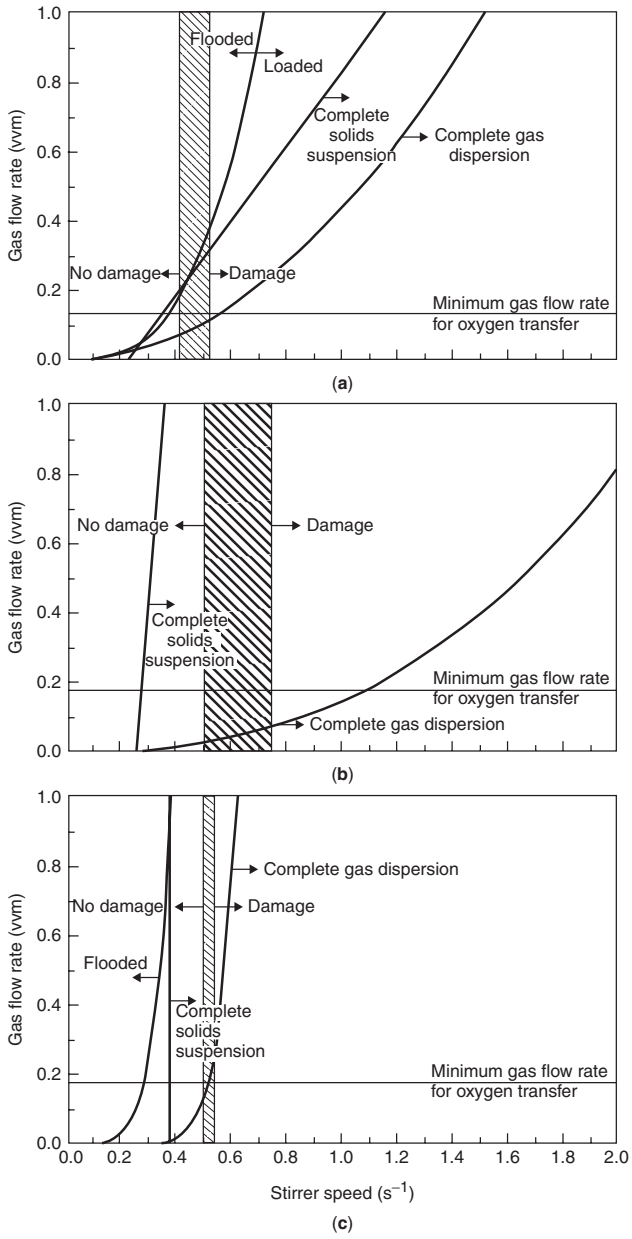


Figure 48.19. Bioreactor operating regime maps derived using theoretical analysis of the performance of different impellers for suspended plant cell culture: (a) Rushton turbine, (b) downward pumping pitched blade turbine, (c) upward pumping pitched blade turbine. The impellers were each of diameter 1/2 the tank diameter and were used to stir plant cell broth in a cylindrical vessel of working volume 10 m^3. (Data from Ref. 32.)

gas dispersion (54,163), ensuring that the gas bubbles are completely dispersed is of more practical importance than the flooding/loading transition. Accordingly, the curve for complete gas dispersion is shown in Fig. 48.19b but the flooding/loading transition is not. The results for the downward pumping pitched blade turbine show that this impeller is largely unsatisfactory for suspended plant cell culture. Although extremely effective for solids suspension, the impeller operates with far from complete gas dispersion at the minimum gas flow rate and maximum stirrer speed allowed. When the direction of rotation of the downward pumping pitched blade turbine is reversed, gas–liquid hydrodynamics in the vessel are substantially improved as shown in Fig. 48.19c for the upward pumping pitched blade impeller. Complete gas dispersion and solids suspension are achieved at relatively low stirrer speeds; at the maximum allowable stirrer speed and minimum air flow rate, all of the reactor functions are performed adequately or close to it by the upward pumping impeller. Another benefit with upward pumping impellers is that the power loss with gassing is much smaller than with Rushton or downward pumping impellers, so that the shaded region of uncertainty for the maximum allowable stirrer speed to avoid cell shear damage is reduced. An additional advantage compared with their downward pumping counterparts is that upward pumping turbines are not prone to power or torque fluctuations.

The overall conclusion from this theoretical analysis is that upward pumping axial flow impellers may offer substantial benefits for high-density plant cell culture in stirred bioreactors. The stirring speeds required to achieve complete gas dispersion and solids suspension are almost independent of aeration rate for this type of impeller. As indicated by the regime maps, this provides greater scope for effective, stable operation compared with Rushton and downward pumping impellers. Upward pumping impellers have not yet been used in any of the reported experimental studies of plant cell culture; yet the results of this analysis suggest that they deserve further investigation.

48.7 CONCLUSIONS

The ability to provide adequate mixing and oxygen transfer is the most important benefit of using stirred reactors for suspended plant cell culture. However, whether these conditions can be achieved depends on the extent to which cell shear sensitivity limits the stirrer speeds that can be employed. Other factors that play a major role in determining levels of plant cell growth and metabolite synthesis, such as aggregate formation and disruption, foam development, and stripping of volatile broth components, are also controlled by the operating conditions employed in stirred tank reactors. To date, few science-based, general-purpose rules have been developed to assist in the design of stirred vessels for plant cell culture. This reflects in large part the wide range of performance outcomes so far observed using different bioreactor hardware, operating regimes, and plant cell systems.

NOMENCLATURE

A	Dimensional constant in Equation 48.1
C_i	Impeller clearance above the vessel floor (m)
C_S	Clearance between the sparger and impeller (m)
D_D	Impeller disk diameter (m)
D_i	Impeller diameter (m)
D_S	Sparger diameter (ring-type sparger) (m)
D_T	Tank diameter (m)
H_{BF}	Baffle height (m)
H_i	Impeller height (m)
H_L	Height of liquid in reactor (m)
K	Consistency index (Pa s^n)
k_La	Oxygen mass transfer coefficient (s^{-1})
L_B	Impeller blade length (m)
L_R	Ribbon length (m)
N_i	Stirrer speed (s^{-1})
n	Flow behavior index
P_T	Total power input by agitation and gassing (W)
Q_G	Volumetric gas flow rate (m^3/s)
u_G	Superficial gas velocity (m/s)
V_L	Liquid volume in reactor (m^3)
W_B	Impeller blade width (m)
W_{BF}	Baffle width (m)
W_R	Ribbon width (m)
α, β	Exponents in Equation 48.1

Subscripts

1	Lower impeller in dual agitator system
2	Upper impeller in dual agitator system

REFERENCES

1. Ballica R, Ryu DDY. Biotechnol Bioeng 1993; 42: 1181–1189.
2. Jolicoeur M, Chavarie C, Carreau PJ, Archambault J. Biotechnol Bioeng 1992; 39: 511–521.
3. Kato A, Kawazoe S, Soh Y. J Ferment Technol 1978; 56: 224–228.
4. Rodríguez-Monroy M, Galindo E. Enzyme Microb Technol 1999; 24: 687–693.
5. Rodríguez-Monroy M, Trejo-Espino JL, Jiménez-Aparicio A, de la Luz Morante M, Villarreal ML, Trejo-Tapia G. Food Technol Biotechnol 2004; 42: 153–158.
6. Curtis WR, Emery AH. Biotechnol Bioeng 1993; 42: 520–526.
7. Scragg AH, Bond PA, Fowler MW. Proceedings of the 6th European Conference on Mixing; 1988 May 24–26; Pavia, Italy. Cranfield: BHRA, The Fluid Engineering Centre; 1988. pp. 457–464.
8. Yokoi H, Koga J, Yamamura K, Seike Y, Tanaka H. J Ferment Bioeng 1993; 75: 48–52.
9. Hoekstra SS, Harkes PAA, Verpoorte R, Libbenga KR. Plant Cell Rep 1990; 8: 571–574.
10. Leckie F, Scragg AH, Cliffe KC. Biotechnol Bioeng 1991; 37: 364–370.
11. Prenosil JE, Hegglin M, Baumann TW, Frischknecht PM, Kappeler AW, Brodelius P, Haldimann D. Enzyme Microb Technol 1987; 9: 450–458.
12. Tanaka H. Biotechnol Bioeng 1982; 24: 425–442.
13. Tsoulpha P, Doran PM. J Biotechnol 1991; 19: 99–110.
14. Wagner F, Vogelmann H. In: Barz W, Reinhard E, Zenk M, editors. Plant tissue culture and its bio-technological application. Berlin: Springer-Verlag; 1977. pp. 245–252.
15. Hooker BS, Lee JM, An G. Biotechnol Bioeng 1990; 35: 296–304.
16. Meijer JJ, ten Hoopen HJG, Luyben KChAM, Libbenga KR. Enzyme Microb Technol 1993; 15: 234–238.
17. Scragg AH, Allan EJ, Leckie F. Enzyme Microb Technol 1988; 10: 361–367.
18. Zhong J-J, Fujiyama K, Seki T, Yoshida T. Biotechnol Bioeng 1994; 44: 649–654.
19. Doran PM. Trends Biotechnol 2006; 24: 426–432.
20. Pan Z-W, Wang H-Q, Zhong J-J. Enzyme Microb Technol 2000; 27: 714–723.
21. Trejo-Tapia G, Cerda-García-Rojas CM, Rodríguez-Monroy M, Ramos-Valdivia AC. Biotechnol Prog 2005; 21: 786–792.
22. Zhong J-J, Chen F, Hu W-W. Process Biochem 1999; 35: 491–496.
23. van't Riet K, Tramper J. Basic bioreactor design. New York: Dekker; 1991. pp. 8–12, 204–207, 401–418.
24. Tanaka H. Biotechnol Bioeng 1981; 23: 1203–1218.
25. Ulbrich B, Wiesner W, Arens H. In: Neumann K-H, Barz W, Reinhard E, editors. Primary and secondary metabolism of plant cell cultures. Berlin: Springer-Verlag; 1985. pp. 293–303.
26. Doran PM. Adv Biochem Eng/Biotechnol 1993; 48: 115–168.
27. Hegarty PK, Smart NJ, Scragg AH, Fowler MW. J Exp Bot 1986; 37: 1911–1920.
28. Linden JC, Haigh JR, Mirjalili N, Phisaphalong M. Adv Biochem Eng/Biotechnol 2001; 72: 27–62.
29. Wongsamuth R, Doran PM. Biotechnol Bioeng 1994; 44: 481–488.
30. Kawase Y, Moo-Young M. Bioprocess Eng 1990; 5: 169–173.
31. Kossen NWF. Proceeding of the 3rd European congress on biotechnology, Volume 4. Weinheim: VCH; 1984. pp. IV-257–IV-282.
32. Doran PM. Biotechnol Prog 1999; 15: 319–335.
33. Rittershaus E, Ulrich J, Westphal K. Int Assoc Plant Tissue Cult Newsl 1990; 61: 2–10.
34. Ushiyama K. In: Komamine A, editor. Plant cell culture in Japan. Tokyo: CMC; 1991. pp. 92–98.
35. Ushiyama K, Hibino K. Abstract 213th American Chemical Society National Meeting; 1997; San Francisco (CA), Abstract No. AGFD057.

36. Hashimoto T, Azechi S. In: Bajaj YPS, editor. Biotechnology in agriculture and forestry, Volume 4. Berlin: Springer-Verlag; 1988. pp. 104–122.
37. Matsubara K, Fujita Y. In: Komamine A, editor. Plant cell culture in Japan. Tokyo: CMC; 1991. pp. 39–44.
38. Schiel O, Berlin J. Plant Cell Tissue Organ Cult 1987; 8: 153–161.
39. Berlin J, Wray V, Forche E, Reng H-G, Schüler H, Luckinger R, Mohlbach H-P. J Exp Bot 1985; 36: 1985–1995.
40. Curtin ME. Bio/technology 1983; 1: 649–657.
41. Fujita Y, Tabata M, Nishi A, Yamada Y. In: Fujiwara A, editor. Plant tissue culture 1982. Tokyo: Japanese Association for Plant Tissue Culture; 1982. pp. 399–400.
42. Shamkov NV, Zaitseva GV, Belousova IM, Strogov SE, Simonova GM, Butenko RG, Nosov AM. Biotekhnologiya 1991; 1: 32–34, Chem Abstr 115: 27653.
43. Doran PM. Bioprocess engineering principles. London: Academic Press; 1995. pp. 140–160, 201, 210–213.
44. Frijlink JJ, Bakker A, Smith JM. Chem Eng Sci 1990; 45: 1703–1718.
45. Ibrahim S, Nienow AW. Trans Inst Chem Eng, Part A 1996; 74: 679–688.
46. Hockey RM, Nouri JM. Chem Eng Sci 1996; 51: 4405–4421.
47. Xu GJ, Li YM, Hou ZZ, Feng LF, Wang K. Can J Chem Eng 1997; 75: 299–306.
48. Nienow AW, Konno M, Bujalski W. Chem Eng Res Des 1986; 64: 35–42.
49. Nienow AW. Chem Eng Prog 1990; 86(2): 61–71.
50. van't Riet K, Smith JM. Chem Eng Sci 1973; 28: 1031–1037.
51. van't Riet K, Smith JM. Chem Eng Sci 1975; 30: 1093–1105.
52. Nienow AW. Trans Inst Chem Eng, Part A 1996; 74: 417–423.
53. Nienow AW, Warmoeskerken MMCG, Smith JM, Konno M. Proceedings of the 5th European Conference on Mixing; 1985 Jun 10–12; Wurzburg, Germany. Cranfield: BHRA, The Fluid Engineering Centre; 1985. pp. 143–154.
54. Chapman CM, Nienow AW, Cooke M, Middleton JC. Chem Eng Res Des 1983; 61: 82–95.
55. Chapman CM, Nienow AW, Cooke M, Middleton JC. Chem Eng Res Des 1983; 61: 167–181.
56. Leckie F, Scragg AH, Cliffe KR. Enzyme Microb Technol 1991; 13: 801–810.
57. Dunlop EH, Namdev PK, Rosenberg MZ. Chem Eng Sci 1994; 49: 2263–2276.
58. Chen SY, Huang SY. Bioprocess Eng 2000; 22: 5–12.
59. Boysan F, Cliffe KR, Leckie F, Scragg AS. In: King R, editor. Bioreactor fluid dynamics. London: Elsevier Applied Science; 1988. pp. 245–258.
60. Leckie F, Scragg AH, Cliffe KC. Enzyme Microb Technol 1991; 13: 296–305.
61. Kato K, Shiozawa Y, Yamada A, Noguchi M, Nishida K. Agric Biol Chem 1972; 36: 899–902.
62. Furuya T, Yoshikawa T, Orihara Y, Oda H. J Nat Prod 1984; 47: 70–75.
63. Tanaka H, Nishijima F, Suwa M, Iwamoto T. Biotechnol Bioeng 1983; 25: 2359–2370.
64. Wongsamuth R, Doran PM. J Chem Technol Biotechnol 1997; 69: 15–26.
65. Huang S-Y, Shen Y-W, Chan H-S. Enzyme Microb Technol 2002; 30: 779–791.
66. Scragg AH. Enzyme Microb Technol 1990; 12: 82–85.
67. Takeda T, Seki M, Furusaki S. J Chem Eng Jpn 1994; 27: 466–471.
68. Zhong J-J, Fujiyama K, Seki T, Yoshida T. Biotechnol Bioeng 1993; 42: 542–546.
69. Schlatmann JE, Nuutila AM, van Gulik WM, ten Hoopen HJG, Verpoorte R, Heijnen JJ. Biotechnol Bioeng 1993; 41: 253–262.
70. Schlatmann JE, Moreno PRH, Sellés M, Vinke JL, ten Hoopen HJG, Verpoorte R, Heijnen JJ. Biotechnol Bioeng 1995; 47: 53–59.
71. van Gulik WM, Meijer JJ, ten Hoopen HJG, Luyben KChAM, Libbenga KR. Appl Microbiol Biotechnol 1989; 30: 270–275.
72. Verdelhan des Molles D, Gomord V, Bastin M, Faye L, Courtois D. J Biosci Bioeng 1999; 87: 302–306.
73. Li G-Q, Shin JH, Lee JM. Biotechnol Tech 1995; 9: 713–718.
74. Gao J, Lee JM. Biotechnol Prog 1992; 8: 285–290.
75. Jay V, Genestier S, Courduroux J-C. Plant Cell Rep 1992; 11: 605–608.
76. Zhong J-J, Konstantinov KB, Yoshida T. J Ferment Bioeng 1994; 77: 445–447.
77. Tal B, Rokem JS, Goldberg I. Plant Cell Rep 1983; 2: 219–222.
78. Kato A, Shimizu Y, Nagai S. J Ferment Technol 1975; 53: 744–751.
79. Kato A, Asakura A, Tsuji K, Ikeda F, Iijima M. J Ferment Technol 1980; 58: 373–382.
80. Drapeau D, Blanch HW, Wilke CR. Biotechnol Bioeng 1986; 28: 1555–1563.
81. Markkanen P, Idman T, Kauppinen V. Ann N Y Acad Sci 1984; 434: 491–495.
82. Hong YC, Labuza TP, Harlander SK. Biotechnol Prog 1989; 5: 137–143.
83. McDonald KA, Jackman AP. Plant Cell Rep 1989; 8: 455–458.
84. Lipsky AKh. J Biotechnol 1992; 26: 83–97.
85. Ho C-H, Henderson KA, Rorrer GL. Biotechnol Prog 1995; 11: 140–145.
86. Su WW, Humphrey AE. Biotechnol Lett 1991; 13: 889–892.
87. Fischer R, Emans N, Schuster F, Hellwig S, Drossard J. Biotechnol Appl Biochem 1999; 30: 109–112.
88. Trexler MM, McDonald KA, Jackman AP. Biotechnol Prog 2002; 18: 501–508.
89. Kessell RHJ, Carr AH. J Exp Bot 1972; 23: 996–1007.
90. Tanaka H, Semba H, Jitsufuchi T, Harada H. Biotechnol Lett 1988; 10: 485–490.
91. Asaka I, Ii I, Hirotani M, Asada Y, Furuya T. Biotechnol Lett 1993; 15: 1259–1264.

92. Matsubara K, Kitani S, Yoshioka T, Morimoto T, Fujita Y, Yamada Y. J Chem Technol Biotechnol 1989; 46: 61–69.
93. Kessler M, ten Hoopen HJG, Heijnen JJ, Furusaki S. Biotechnol Tech 1997; 11: 507–510.
94. Ulbrich B. Found Biotech Ind Ferment Res 1986; 4: 147–164.
95. Archambault J, Williams RD, Lavoie L, Pépin M-F, Chavarie C. Biotechnol Bioeng 1994; 44: 930–943.
96. De Dobbeleer C, Cloutier M, Fouilland M, Legros R, Jolicoeur M. Biotechnol Bioeng 2006; 95: 1126–1137.
97. Kreis W, Reinhard E. Planta Med 1989; 55: 409–416.
98. Spieler H, Alfermann AW, Reinhard E. Appl Microbiol Biotechnol 1985; 23: 1–4.
99. Treat WJ, Engler CR, Soltes EJ. Biotechnol Bioeng 1989; 34: 1191–1202.
100. Kim D-I, Cho GH, Pedersen H, Chin C-K. Appl Microbiol Biotechnol 1991; 34: 726–729.
101. Zhong J-J, Pan Z-W, Wang Z-Y, Wu J, Chen F, Takagi M, Yoshida T. J Biosci Bioeng 2002; 94: 244–250.
102. Zhang Z-Y, Zhong J-J. Biotechnol Prog 2004; 20: 1076–1081.
103. Piehl G-W, Berlin J, Mollenschott C, Lehmann J. Appl Microbiol Biotechnol 1988; 29: 456–461.
104. Janes DA, Thomas NH, Callow JA. Biotechnol Tech 1987; 1: 257–262.
105. Styer DJ. In: Henke RR, Hughes KW, Constantin MJ, Hollaender A, editors. Tissue culture in forestry and agriculture. New York: Plenum; 1985. pp. 117–130.
106. Wang C-J, Staba EJ. J Pharm Sci 1963; 52: 1058–1062.
107. Miller RA, Shyluk JP, Gamborg OL, Kirkpatrick JW. Science 1968; 159: 540–542.
108. Bligny R. Plant Physiol 1977; 59: 502–505.
109. Wilson SB, King PJ, Street HE. J Exp Bot 1971; 22: 177–207.
110. Constabel F, Shyluk JP, Gamborg OL. Planta 1971; 96: 306–316.
111. Veliky IA, Martin SM. Can J Microbiol 1970; 16: 223–226.
112. Bruijn W, van't Riet K, Smith JM. Trans Inst Chem Eng 1974; 52: 88–104.
113. Rushton JH, Costich EW, Everett HJ. Chem Eng Prog 1950; 46: 467–476.
114. Nienow AW. In: Harnby N, Edwards MF, Nienow AW, editors. Mixing in the process industries. 2nd ed. Oxford: Butterworth-Heinneman; 1992. pp. 364–393.
115. Cliff MJ, Edwards MF, Ohiaeri IN. Inst Chem Eng Symp Ser 1981; 64: M1–M11.
116. Coimbra JSR, Mojola F, Meirelles AJA. J Chem Eng Jpn 1998; 31: 277–280.
117. Porto ALF, Lima Filho JL, Aires Barros MR, Cabral JMS, Tambourgi EB. Biotechnol Tech 1997; 11: 641–643.
118. Nienow AW. Trends Biotechnol 1990; 8: 224–233.
119. Ibrahim S, Nienow AW. Trans Inst Chem Eng Part A 1995; 73: 485–491.
120. Laufhütte HD, Mersmann A. Chem Eng Technol 1987; 10: 56–63.
121. Galindo E, Argüello MA, Velasco D, Albiter V, Martínez A. Chem Eng Technol 1996; 19: 315–323.
122. Kaminoyama M, Arai K, Kamiwano M. J Chem Eng Jpn 1994; 27: 17–24.
123. Nienow AW, Miles D. Chem Eng J 1978; 15: 13–24.
124. Holland FA, Chapman FS. Liquid mixing and processing in stirred tanks. London: Reinhold; 1966. pp. 21–22.
125. Iranshahi A, Devals C, Heniche M, Fradette L, Tanguy PA, Takenaka K. Chem Eng Sci 2007; 62: 3641–3653.
126. Ohta M, Kuriyama M, Arai K, Saito S. J Chem Eng Jpn 1985; 18: 81–84.
127. Peters DC, Smith JM. Trans Inst Chem Eng 1967; 45: T360–T366.
128. Nagata S. Mixing: principles and applications. Tokyo: Kodansha; 1975. p. 198.
129. Beckner JL, Smith JM. Trans Inst Chem Eng 1966; 44: T224–T236.
130. Tecante A, Choplin L. Can J Chem Eng 1993; 71: 859–865.
131. Kamen AA, Chavarie C, André G, Archambault J. Chem Eng Sci 1992; 47: 2375–2380.
132. Kaminoyama M, Kamiwano M. Inst Chem Eng Symp Ser 1994; 136: 541–548.
133. Rieger F, Novák V, Havelková D. Chem Eng J 1986; 33: 143–150.
134. Carreau PJ, Patterson I, Yap CY. Can J Chem Eng 1976; 54: 135–142.
135. Zlokarnik M, Judat H. In: Gerhartz W, editor. Ullmann's encyclopedia of industrial chemistry. 5th ed. Weinheim: VCH; 1988. pp. 25-1–25-33.
136. Wang S-J, Zhong J-J. Biotechnol Bioeng 1996; 51: 511–519.
137. Lehmann J, Piehl GW, Schulz R. Dev Biol Stand 1987; 66: 227–240.
138. Lehmann J, Vorlop J, Büntemeyer H. In: Spier RE, Griffiths JB, editors. Animal cell biotechnology, Volume 3. Orlando (FL): Academic Press; 1988. pp. 221–237.
139. Emery AN, Jan DC-H, Al-Rubeai M. Appl Microbiol Biotechnol 1995; 43: 1028–1033.
140. Nienow AW, Liu H, Wang H, Allsford KV, Cronin D, Hudcova V. In: King R, editor. Bioreactor fluid dynamics. London: Elsevier Applied Science; 1988. pp. 159–177.
141. Frijlink JJ, Kolijn M, Smith JM. Inst Chem Eng Symp Ser 1984; 89: 49–58.
142. Chen H, Wang J-J, Liu Y-G. Abstract VIIth international congress on plant tissue and cell culture. Amsterdam: (IAPTC); 1990. p. 341.
143. Pareilleux A. NATO ASI Ser 1988; H 18: 313–328.
144. Trejo-Tapia G, Sepúlveda-Jiménez G, Trejo-Espino JL, Cerda-García-Rojas CM, de la Torre M, Rodríguez-Monroy M, Ramos-Valdivia AC. Biotechnol Bioeng 2007; 98: 230–238.
145. Namdev PK, Dunlop EH. Appl Biochem Biotechnol 1995; 54: 109–131.
146. Jüsten P, Paul GC, Nienow AW, Thomas CR. Biotechnol Bioeng 1996; 52: 672–684.
147. Jüsten P, Paul GC, Nienow AW, Thomas CR. Bioprocess Eng 1998; 18: 7–16.
148. Ananta I, Subroto MA, Doran PM. Biotechnol Bioeng 1995; 47: 541–549.

149. Hulst AC, Meyer MMT, Breteler H, Tramper J. Appl Microbiol Biotechnol 1989; 30: 18–25.
150. Kinnersley AM, Dougall DK. Planta 1980; 149: 200–204.
151. Kuboi T, Yamada Y. Phytochemistry 1976; 15: 397–400.
152. Taguchi H, Yoshida T, Tomita Y, Teramoto S. J Ferment Technol 1968; 46: 814–822.
153. Tanaka H, Takahashi J, Ueda K. J Ferment Technol 1975; 53: 18–26.
154. van Suijdam JC, Metz B. Biotechnol Bioeng 1981; 23: 111–148.
155. Bertola MA, Klis FM. J Exp Bot 1979; 30: 1223–1231.
156. Sahai OP, Shuler ML. Can J Bot 1982; 60: 692–700.
157. ten Hoopen HJG, van Gulik WM, Heijnen JJ. In Vitro Cell Dev Biol 1992; 28P: 115–120.
158. Assa A, Bar R. Biotechnol Bioeng 1991; 38: 1325–1330.
159. Nienow AW, Langheinrich C, Stevenson NC, Emery AN, Clayton TM, Slater NKH. Cytotechnology 1996; 22: 87–94.
160. van't Riet K. Ind Eng Chem Process Des Dev 1979; 18: 357–363.
161. Cooke M, Middleton JC, Bush JR. In: King R, editor. Bioreactor fluid dynamics. London: Elsevier Applied Science; 1988. pp. 37–64.
162. Martin T, McFarlane CM, Nienow AW. Proceedings of the 8th European Conference on Mixing; 1994 Sep 21–23; Cambridge. Rugby: Institution of Chemical Engineers; 1994. pp. 57–64.
163. Buckland BC, Gbewonyo K, Jain D, Glazomitsky K, Hunt G, Drew SW. In: King R, editor. Bioreactor fluid dynamics. London: Elsevier Applied Science; 1988. pp. 1–15.
164. Zhao X, Hu Z, Nienow AW, Kent CA, Chatwin S. Chin J Chem Eng 1994; 2: 198–209.
165. Smart NJ, Fowler MW. Biotechnol Lett 1981; 3: 171–176.
166. Spier RE, Griffiths B. Dev Biol Stand 1984; 55: 81–92.
167. Pareilleux A, Vinas R. J Ferment Technol 1983; 61: 429–433.
168. Pareilleux A, Chaubet N. Eur J Appl Microbiol Biotechnol 1981; 11: 222–225.
169. Greaves M, Loh VY. Proceedings of the 5th European Conference on Mixing; 1985 Jun 10–12; Wurzburg, Germany. Cranfield: BHRA, The Fluid Engineering Centre; 1985. pp. 451–467.
170. Zhang Y-H, Wang H-Q, Liu S, Yu J-T, Zhong J-J. Biotechnol Lett 1997; 19: 943–945.
171. Andrew SPS. Trans Inst Chem Eng 1982; 60: 3–13.
172. Kobayashi Y, Fukui H, Tabata M. Plant Cell Rep 1989; 8: 255–258.
173. Schlatmann JE, Vinke JL, ten Hoopen HJG, Heijnen JJ. Biotechnol Bioeng 1995; 45: 435–439.
174. Zhong J-J, Seki T, Kinoshita S-I, Yoshida T. World J Microbiol Biotechnol 1992; 8: 106–109.

49

CELL IMMOBILIZATION, ENGINEERING ASPECTS

RONNIE WILLAERT

Department of Ultrastructure, Flanders Interuniversity Institute for Biotechnology, Vrije Universiteit Brussel, Brussels, Belgium

49.1 INTRODUCTION

The immobilization of cells can be defined as "the physical confinement or localization of cells to a certain defined region of space with preservation of some desired activity" (1). The region in which the cells are localized is called the *immobilized cell system* or *immobilized cells aggregate*, which can be divided into three components: the cells, the support (or carrier or matrix) material, and the solution that fills the remainder of the space (interstitial solution). The immediate vicinity of the immobilized cells is also called the *microenvironment*. When cells are encapsulated in an immobilized cells system, the term *bioencapsulation* is usually used. Microencapsulation is used when the cells are immobilized in microcapsules, that is, micrometer-sized systems surrounded by a barrier membrane. In recent developments, active biologicals (i.e. proteins, DNA, etc.) are packed in nanoparticles of submicron or nanometer size range and is called *nanoencapsulation*.

Studies on immobilized biocatalysts were initiated by immobilizing single enzymes for simple reactions such as hydrolysis and isomerization. Subsequently, multienzyme systems, isolated cellular organelles, and treated (permeabilized) microbial cells have been used as biocatalysts for more complicated and conjugated reactions. Moreover, many applications have been developed utilizing living or growing microbial cells and cells of multicellular organisms (higher plants and animals) as well as genetically improved microbial cells. Table 48.1 lists the added beneficial characteristics cell systems obtain upon immobilization as well as the introduced drawbacks (1–11).

The successful application of immobilized cell systems relies on the proper choice of the cell system. This choice will be directed by the type of application and characteristics of the immobilization support. Accordingly, requirements will be different for each particular case. Common desirable requirements are high cell mass-loading capacity; easy access to nutrient media; simple "nontoxic" immobilization procedure; high surface area-to-volume ratio; optimum mass transfer distance from flowing media to center of support; mechanical (compression, abrasion) and chemical stability; sterilizable, reusable, or one-time use for very cheap carrier materials; low shear experienced by cells; easy separation of cells and carrier from media; suitable for conventional reactor systems; suitable for suspension as well as anchorage-dependent cells; biocompatibility with animal cells, immunoprotection barrier, and economic interesting (11,12).

49.2 INTERNAL MASS TRANSPORT

The analysis of the influence of mass transfer on the reactor performance in immobilized cell reactors is an important topic since the performance of these reactors may often be reduced by the rate of transport of reactants to and products from the immobilized cell system (external mass transfer limitation), and by the rate of transport inside the immobilized cell system (internal mass transfer limitation). External mass transfer limitations can usually be reduced or eliminated by a proper design/selection of the reactor and immobilized cell system. Several phenomena are involved

Upstream Industrial Biotechnology: Equipment, Process Design, Sensing, Control, and cGMP Operations, Volume 2, First Edition. Edited by Michael C. Flickinger.
© 2013 John Wiley & Sons, Inc. Published 2013 by John Wiley & Sons, Inc.

TABLE 49.1. Beneficial Characteristics and Drawbacks Created upon Immobilization of Cells (modified after (11))

Advantages
The density of immobilized cells is locally higher than that of freely suspended cells after cell growth and, consequently, results in higher productivities.
Immobilized growing cells are easily separated from the reaction system. Additionally, repeated or continuous use of immobilized growing cells is possible in various types of reactors.
Tailoring to the most efficient bioreactor is possible. Allows batch fermentors to be operated on a drain-and-fill basis.
The wash-out of cells during continuous fermentations can be avoided at high dilution rates.
Immobilized cells appear to be less susceptible to microbial contamination.
Immobilization can give rise to higher retention of plasmid-bearing cells and thus delay overgrowth by the corresponding plasmid-free cells.
Improved downstream processing: products can be recovered more easily as they are not or less contaminated by biomass.
Provides possibilities for the spatial location within reactors of different microbial populations.
Immobilizing cells can be better protected from their surroundings and thereby decrease problems to shear forces. This is especially important for shear-sensitive cells such as mammalian cells.
Immobilization can provide conditions conductive to cell differentiation and cell-to-cell communication, thereby encouraging production of high yields of secondary metabolites.
Mammalian cell immobilization behind a barrier membrane for transplantation therapy provides an effective immunoprotection. The controlled and continuous delivery of therapeutic products to the host is a potentially cost-effective method to treat a wide range of diseases.
The *in vivo* situation can be mimicked by immobilization, e.g. chondrocyte growth in Ca-alginate gel mimics the situation in the cartilage matrix.
Immobilization can have substantial effects on the physiology, resulting in higher productivities compared to free cells, e.g. production of secondary metabolites by gel immobilized plant cells, improved enzyme production by immobilized bacterial and fungal cells.
Properties of cell immobilization materials can be engineered for biocompatibility, selective permeability, mechanical and chemical stability, and other requirements as specified by the application including uniform cell distribution and a given membrane thickness or mechanical strength.
Cell immobilization can create a protective environment for the cells.
Disadvantages
Mass transfer limitations can reduce the efficiency of the reaction. The whole catalytic activity is not utilized due to restricted supply of substrate(s). Reduction of the efficiency can cause problems when high-density systems are scaled-up. Usually, this is because of oxygen transfer limitations and accumulation of toxic waste products.
The mechanical stability of some support materials limits its use.
Products are liable to be contaminated by cells leaking from the carriers. This problem can sometimes be solved by selection of a suitable carrier with a high cell-holding capacity and by limitation of excess cell proliferation.
Some immobilization techniques and materials can have an important negative impact on the economics of the bioprocess.
Biocompatibility of some immobilization matrices is not sufficient for transplantation therapy and results in fibrosis, which introduces supplementary diffusion limitation.

such as axial dispersion, convective flow, and macro- and micromixing. Internal mass transfer limitations are often more difficult to eliminate and their knowledge is a prerequisite to analyze and optimize the performance of the immobilized cell system.

Two physical phenomena are involved in the transport of molecules, that is diffusion and convection. Diffusion is the random motion of molecules that arise from thermal energy transferred by molecular collisions. Convection is a mechanism of transport resulting from the bulk motion of fluids.

49.2.1 Definition of Diffusion Coefficients

The relation between the diffusion flux and the concentration gradient was first quantified in 1855 by the German physiologist Adolf Fick (13). This relationship is known as *Fick's first law*, which states that the rate of transfer of the diffusing substance through a unit area is proportional to the concentration gradient measured normal to the section,

$$J = -D\frac{\partial C}{\partial x} \tag{49.1}$$

where J is the mass transfer rate per unit area of a section (diffusion flux), C the concentration of diffusing substance (amount per total volume of the system), x the space coordinate, and D is called the *diffusion coefficient*. D is sometimes expressed as the binary diffusion coefficient (or mass diffusivity) D_{AB}, where the subscript A refers to the solute A and B to the solvent B. In three dimensions, the flux $\mathbf{J}$ is a vector and flows can have components in all directions:

$$\mathbf{J} = -D\nabla C \tag{49.2}$$

In the biochemical engineering literature, it is general practice to use an effective diffusion coefficient (D_e), which can, for example, be readily used in the expression for the Thiele modulus and for the determination of the efficiency factor of a porous biocatalyst. When D is replaced by D_e in Equation 49.1, the corresponding concentration (C_L) is expressed as the amount of solute per unit volume of the liquid void phase. Concentration C may be correlated with C_L by using the void fraction (ε), which is the accessible fraction of a porous particle to the diffusion solute as $C = \varepsilon C_L$. Hence, the relationship between the effective diffusion coefficient and the diffusion coefficient is

$$D_e = \varepsilon D \tag{49.3}$$

Intraparticle forced convection can have a significant influence on the mass transport in a porous particle. The intraparticle convection depends on the external flow conditions and the degree of porosity, and can also be characterized by Fick's first law, where the "apparent" diffusion coefficient, which accounts for the convective mass transport, is used (14,15).

49.2.2 Internal Diffusion in Immobilized Cells Systems

The effective diffusion coefficient through a porous support material (matrix) is lower than the corresponding diffusion coefficient in the aqueous phase (D_a) due to the exclusion and obstruction effect. By the presence of the support, a fraction of the total volume ($1-\varepsilon$) is excluded for the diffusing solute. The impermeable support material obstructs the movement of the solute and results in a longer diffusional path length, which can be represented by a tortuosity factor (τ); τ equals the square of the tortuosity (16). The influence of both effects on the effective diffusion coefficient can be represented as

$$D_e = \frac{\varepsilon}{\tau} D_a \tag{49.4}$$

This equation holds as long as there is no specific interaction of the diffusion species with the porous carrier.

In the case of gel matrices, predictions using the polymer volume fractions are recommended, since, neither ε nor τ can be measured for a gel in a simple way (17–19):

$$D = \frac{(1-\phi_p)^2}{(1+\phi_p)^2} D_a \tag{49.5}$$

where ϕ_p is the polymer volume fraction. For low molecular weight (MW) solutes in cell-free gels, an approximate measure of ε can be given as

$$\varepsilon = 1 - \phi_p \tag{49.6}$$

D_e can also be expressed as a function ϕ_p by combining Eqs 49.2,49.4, and 49.5 (20–23) as

$$D_e = \frac{(1-\phi_p)^3}{(1+\phi_p)^2} D_a \tag{49.7}$$

Other physical models that have been proposed are the Phillies model, Equation 49.8 (24), and the Petit model (25), Equation 49.9:

$$D_e = e^{\left(-n_1 C_{gel}^{n_2}\right)} D_a \tag{49.8}$$

$$D_e = \left(1 + n_3 C_{gel}^{2n_4}\right) D_a \tag{49.9}$$

where C_{gel} is the gel concentration, n_1 and n_2 are parameters of the Phillies model, and n_3 and n_4 parameters of the Petit model. For example, the effect of the polyvinyl alcohol (PVA) concentration on the effective diffusion coefficient of an azo dye (Remazol Black B) could be described by the Phillies model (26).

49.2.3 Measurement Methods of Diffusion Coefficients

Both steady state and transient methods are used for measurements of diffusion coefficients; sometimes in combination as in the lag time method. A few researchers have used indirect methods, such as the use of a reaction–diffusion model, to determine the diffusion coefficient of gel immobilized cells (27–29) or biofilms (30–35). Westrin and coworkers (36) have reviewed in depth the methods for measuring diffusion coefficients. They compared different methods [including holographic laser interferometry and nuclear magnetic resonance (NMR)] with regard to accuracy, reproducibility, time, cost, and limitations.

The equation, which describes the transient diffusion, can be readily derived by writing the mass balance over the system:

$$\varepsilon \frac{\partial C_L}{\partial t} = x^{-n} \frac{\partial}{\partial x}\left(x^n D_e \frac{\partial C_L}{\partial x}\right) \tag{49.10}$$

where n is a shape factor which is 1 for planar, 2 for cylindrical or 3 for spherical geometry. In Table 48.2, the most popular methods to determine diffusion coefficients (in gels and dense cell masses) are listed. Recently, noninvasive microscopic and spectroscopic techniques have been developed. For example, Frazier *et al*. (37) used near-infrared spectroscopy to measure nutrients within a specially designed diffusion chamber that permits the noninvasive measurement of effective diffusivities in gels containing immobilized cells (e.g. D_e of glutamine in agarose gel).

TABLE 49.2. Experimental Methods to Determine Diffusion Coefficients

Method	Reference Examples
Concentration gradient methods: steady state	
True steady state diaphragm cell	38–46
Pseudo (quasi)-steady state diaphragm cell	20,45–51
Concentration gradient methods: transient	
Time-lag diaphragm cell	42,52–56
Uptake/release from particles dispersed in a stirred solution	26,57–90
Concentration profile in a material/cell mass	
Autoradiography	91
Electrode or mass spectrometric probe covering	92–95
Fixed ultrasonic probes	96
(Holographic) laser/light interferometry	97–99
Magnetic resonance imaging (MRI)	100,101
Microelectrodes in	
Gel phase or biofilm	21,22,32,93,102–107
Microcapsules	108
Fungal pellets	104,109–112
Spheroids	113
Infrared spectroscopy	37,114
Sectioning method	115–117
UV/VIS absorption scanning	61
Integrative optical imaging (IOI)	118
Confocal scanning microscopy	119–122
Multiphoton microscopy	123
Raman microscopy	114
Indirect methods	
Chromatographic curves	124,125
Instrumental methods	
Dynamic light scattering	126
Fluorescence correlation spectroscopy	127,128
Fluorescence recovery after photobleaching (FRAP)	129–136
NMR: pulsed gradient spin-echo (PGSE); radio-frequency field gradient	23,137–146
Holographic relaxation spectroscopy	147,148

Experimentally, a concentration disturbance is applied over the system and the change of the concentration as a function of time is followed until the steady state is reached. Diffusion coefficients are determined by fitting the theoretical curve to the experimental one, which is obtained after solving Equation 49.9 using the appropriate initial and boundary conditions. Analytical solutions for simple cases are described by Crank (149). Crank also gives the solution in terms of M_t, the amount of solute in the matrix at time t, as a fraction of M_∞, the equilibrium amount, which is practically more accessible.

Steady state measurements can be performed by using a "diaphragm-diffusion cell" (Table 48.2). Two liquid-filled well-stirred compartments are separated by a membrane under investigation, through which a steady state diffusional flux is set up (42–44,48,49,53,54). While in the steady state method, a constant upstream and different downstream solute concentration is employed, in the pseudo-steady state method, a change in solute concentration in the compartments is allowed.

If the diffusion coefficient is measured by the steady state method, the value of the equilibrium partition coefficient (K) should be known. Another approach is to determine directly the product of K and D, which equals the effective diffusion coefficient (150). Sun and coworkers (42) used a non-steady state method to immediately determine the product of K and D_e for oxygen in cell-free and cell-containing Ca-alginate and polyvinyl alcohol stilbazolium (PVA-SbQ) gels. The partition coefficient is defined as

$$K = \frac{C_m}{C_L} \tag{49.11}$$

where C_m is the solute concentration in the matrix (amount per volume matrix) and C_L the solute concentration in the liquid phase. In the absence of specific adsorption phenomena, the partition coefficient for cell-containing matrices can be predicted by the following equation (20,49,150) :

$$K = 1 - (\alpha\phi_c + \phi_p) \tag{49.12}$$

where α represents the volume fraction of the individual cell that is not accessible to the solute and ϕ_c is the volume fraction of the cells. If the outer cell membrane totally excludes the solute, the value of α will be unity. Axelsson and Persson (49) found a value of 1 for glucose, lactose, galactose, and ethanol for alginate gels containing yeast cells deactivated by iodoacetic acid. Chresand and coworkers (52) measured the partition coefficient of labeled sodium acetate between 1% (w/w) agar gel containing mammalian cells and the surrounding solution, and found a value that was unity. This result corresponds with a value of zero for α. It can also be assumed that the solute is excluded from a certain volume fraction of the individual cell: $0 < \alpha < 1$. This volume fraction may, for example, be approximately equal to the dry weight fraction of the cells, which can be assumed to be equal to 0.25 (20). If there are no immobilized cells present, Equation 49.11 is reduced to $1-\phi_p$ which equals ε (Eq. 49.7).

Values of experimentally determined partition coefficients for cell-free gels are in a lot of systems close to unity; for example, between 0.97 and 1.02 for glucose in 2% Ca-alginate (62); 0.98 for lactose in 2.75%/0.25% (w/w) κ-carrageenan/locust bean gum (69); 1.2 for lactose, 1.3 for glucose, 1.1 for galactose, and 1.32 for ethanol in

2.4–2.8% (w/w) alginate, the higher value for ethanol was explained as adsorption of ethanol on the alginate gel; and 1.14 for catechol, 0.99 for 3,4-dihydroxy-L-phenylalanine (L-DOPA), and 2.03 for dopamine in cross-linked gelatin (10% w/v) beads at pH 7.1 and 35°C (70). For solute molecules with a large MW, a low value for K was determined: 0.57 for ovalbumin (43.5 kDa), 0.37 for bovine serum albumin (BSA) (67 kDa), and 0.18 for IgG (155 kDa) in 3% Ca-alginate; 0.48 for ovalbumin, 0.23 for BSA, and 0.17 for immunoglobulin G (IgG) in 4% agarose (81). Owing to the obstruction effect of cells immobilized in κ-carrageenan/locust bean gum, partition coefficients decreased from 0.89 to 0.79 and from 0.98 to 0.87 for lactose and lactic acid, respectively (71); Øyaas *et al*. (79) found that K was constant for both lactose and lactic acid (1.00 and 1.16, respectively) with increasing cell concentration.

The partition coefficients of Remazol Black B (azo dye) in PVA decreased from 4.1 to 1.3 with an increase in ϕ_p values ranging from 0.0521 to 0.0954 m^3 PVA/m^3 gel (26). The gel pore size was greater than the size of the Remazol Black B molecules and a strong affinity existed between PVA and the azo dye molecules. The lipoglycopeptide antibiotic, A40926, and its deacetylated derivative showed markedly different partition (and diffusion) characteristics (87). When soybean meal and/or *Actinoplanes teichomyceticus* mycelium was present in Ca-alginate or κ-carrageenan gel beads, A40926 strongly partitions to the solid phase ($K > 10$).

In biofilms, the partition coefficient between the biomass and water is determined through isotherm experiments. For biofilms composed of *Xanthobacter autotrophicus* and *Pseudomonas* sp., a value of 1 was found for 1,1,2-trichloroethane (95). The partitioning coefficient of a model hydrophobic compound (α-pinene) was approximately 100 times smaller for the air/biofilm system (in a biofilter) compared to the air/water system, indicating that α-pinene has a higher degree of partitioning into the biofilm than into water due to the presence of solids (51).

49.2.4 Diffusion in Cell-Containing Matrices

The presence of immobilized cells in the immobilization matrix can have a substantial effect on the effective diffusion coefficient, especially at high biomass concentrations. Also, the effective diffusion coefficient decreases as a function of time in growing immobilized systems because the cell volume fraction increases. Diffusion in gels containing immobilized cells has been reviewed by Westrin and Axelsson (20). The influence of the cells on the effective diffusion coefficient can be described as

$$D_e = f(\phi_c, D_c) D_{e0} \tag{49.13}$$

where D_c is the effective diffusion coefficient within the cells and D_{e0} the effective diffusion coefficient in a cell-free matrix. Two theoretical approaches have been developed: (i) the cells are impermeable to the diffusing solute or (ii) the solute diffuses in the cells with a very low D_e. Suitable expressions have been derived for $f(\phi_c, D_c)$, which were based on heterogeneous media (151,152). Expressions could be classified into five model types: (i) the exclusion model, (ii) model of suspended impermeable spheres, (iii) model of suspended permeable spheres, (iv) capillary models, and (v) empirical models.

49.2.4.1 Exclusion Model. This model assumes that D_c is zero. The presence of the impermeable cells reduces the volume available for diffusion. Equation 49.12 can now be written as

$$D_e = (1 - \phi_c) D_{e0} \tag{49.14}$$

Using this equation, effective diffusion coefficients have been determined for substrate diffusion in Ca-alginate gel with entrapped deactivated yeast cells (49,72).

49.2.4.2 Model of Suspended Impermeable Spheres. This model regards the cells as impermeable spheres (D_c equals zero), which are suspended in a continuum. The expression for this model has been adapted from the expression derived by Maxwell (154) for effective conductivity in a composite medium of periodically spaced spheres:

$$D_e = \frac{1 - \phi_c}{1 + (\phi_c/2)} D_{e0} \tag{49.15}$$

This equation has been used to correlate experimental diffusion coefficients with immobilized mammalian cells in agar gel (52), coimmobilized *Aspergillus niger* and *Zymomonas mobilis* in Ca-alginate beads (83), *Saccharomyces cerevisiae* entrapped in Ca-alginate (155) and in artificial biofilms (agar containing inert polystyrene particles of the same size as bacteria) (21,22). Owing to limitations of Maxwell's model in other immobilized cell systems, a correlation was developed by using a scaling relationship (156):

$$D^*(\phi_c) = \frac{1 - D_e/D_{e0}}{1 - D_c/D_{e0}} \tag{49.16}$$

and a polynomial approximation to D^*:

$$D^*(\phi_c) = 1.7271\phi_c - 0.8177\phi_c^2 + 0.09075\phi_c^3 \tag{49.17}$$

Diffusivity values used for constructing the correlation were generated from Monte Carlo computer simulations.

49.2.4.3 Model of Suspended Permeable Spheres. This model assumes only permeable cells ($D_c > 0$). In this case, a more complex expression (adapted from (157)) has been derived:

$$D_e = \frac{2/D_c + 1/D_{e0} - 2\phi_c(1/D_c - 1/D_{e0})}{2/D_c + 1/D_{e0} + \phi_c(1/D_c - 1/D_{e0})} D_{e0} \quad (49.18)$$

Values for D_c/D_{e0} have been determined to be 0.31, 0.30, and 0.20 for fermentation media of *S. cerevisiae*, *Escherichia coli*, and *Penicillium chrysogenum*, respectively (158). Equation 49.17 has been used to correlate experimental diffusion coefficients in cell-containing gels (52) and dense cell suspensions (158,159).

49.2.4.4 Capillary Models. Capillary models have been developed to quantify the influence of the tortuosity on the effective diffusion coefficient, that is, the model of Kozeny (160) and the improved random pore model (161). This model has been adapted to immobilized cell systems where cells are considered as impermeable (i.e. $D_c = 0$):

$$D_e = (1 - \phi_c)^2 D_{e0} \quad (49.19)$$

Several investigators have used this equation to correlate the effective diffusion coefficient with the immobilized cell concentration (26,42,57,78,85,162–167). This random pore approach has been adapted to obtain an improved general diffusion model, which accurately includes systems containing impermeable or permeable cells (168):

$$\frac{D_e}{D_{e0}} = (1 - \phi_c)^2 + \phi_c^2 \frac{KD_c}{D_{e0}} + 4\phi_c (1 - \phi_c) \frac{KD_c}{D_{e0}} \left(1 + \frac{KD_c}{D_{e0}}\right)^{-1} \quad (49.20)$$

By introducing a complex tortuosity value, $\tau_c(\varepsilon_c) = 1/\varepsilon^\beta$ and $\tau_g(\varepsilon_c) = 1/\varepsilon^\gamma$ (where τ_c is the tortuosity created by the immobilized cells, τ_g the tortuosity of the gel matrix, and β and γ are order values ($\beta < 1$, $\gamma > 1$), Mota *et al*. (169) developed the following model:

$$\frac{D_e}{D_{e0}} = \frac{D_{eg}}{D_{e0}} (1 - \phi_c)^\alpha \quad (49.21)$$

with $\alpha = 1 + \beta + \gamma$ and where D_{eg} the effective diffusion coefficient in pure gel is. This model assumes a homogeneous cell distribution in the gel. For a nonhomogeneous cell distribution, composed of two layers (where the first layer contains all the immobilized cells and the second layer is free of cells), this model was rearranged to (170):

$$\frac{D_e}{D_{e0}} = \frac{(1 - \phi_{c1})^\alpha}{\delta + (1 - \phi_{c1})^\alpha (1 - \delta)} \quad (49.22)$$

where ϕ_{c1} is the cell volume fraction in the first layer and δ is the dimensionless thickness (= thickness of layer 1 divided by the total thickness).

49.2.4.5 Empirical Models. Prediction equations have been obtained by fitting some arbitrary function to experimental data (171). Empirical models are only valid for the studied gel material and immobilized cell type, and can only be used to predict D_e between the investigated boundaries. Ogston *et al*. (172) and Cukier (173) developed an empirical equation to describe the restricted diffusion of proteins in polymer gels:

$$\frac{D_e}{D_{e0}} = \exp\left(-Br_0 C_f^{1/2}\right) \quad (49.23)$$

where r_0 is the interaction radius between the protein and the polymer fibers, B a proportionality constant, and C_f the polymer (fiber) concentration in particles. This correlation allowed the estimation of several protein diffusivities in an agarose matrix based on the MW of the protein and the polymer concentration (125). Scott *et al*. (174) used the following correlation:

$$\frac{D_e}{D_{e0}} = 1 - 0.9\phi_c + 0.27\phi_c^2 \quad (49.24)$$

Korgel and coworkers (164) also developed the following empirical correlation:

$$\frac{D_e}{D_{e0}} = 1 - 2.23\phi_c + 1.40\phi_c^2 \quad (49.25)$$

49.2.4.6 Experimental Considerations. Some researchers have reported that the diffusivity was not influenced by the presence of cells. Kurosawa and coworkers (29) found that the oxygen diffusivity in Ca- and Ba-alginate was not influenced by the presence of immobilized yeast cells up to a cell density of 30 g DW/L. Estapé *et al*. (73) studied the influence of counterdiffusion of ethanol and glucose on the diffusion coefficients of glucose and ethanol respectively: there was no significant decrease of the diffusion coefficients in the presence of yeast cells when counterdiffusion was involved; without counterdiffusion the presence of cells resulted in a significant decrease of the diffusion coefficient for ethanol, but in contrast an increase was observed for the glucose diffusion coefficient.

In the determination of the effective diffusion coefficient in cell-containing matrices by methods based solely on diffusion, the solute may not react, or erroneous results would be obtained. In the literature, different methods have been described to deactivate living cells. Cells have been deactivated using ultraviolet radiation (30); heat (26,39,42,175–177); organic solvents like ethanol (53,72),

chloroform (178), and glutaraldehyde (52,179); (organic) acids like iodoacetic acid (49,155), ethyl acetate (180), and hydrochloric acid (78); toxins or inhibitors like mercuric chloride (21,22,30,181,182), dimethyl sulfoxide (58), and sodium azide (69,71); detergents, for example, Triton X-100 (159). Some researchers have investigated the effect of the deactivating agents on the effective diffusion coefficient. Matson (183) found that the deactivation process by mercuric chloride or heat had no effect on the diffusion process. The results of Dibdin (175) and McNee and coworkers (179) suggest that neither heat treatment nor glutaraldehyde fixation have a significant effect on the rate of diffusion through dental plaque. In contrast, Tatevossian (176,177) found a significant effect by using heat deactivation. Libicki and coworkers (159) found that the mass transport of nitrous oxide in aggregates of *E. coli* prepared from cells treated with detergents or disrupted by dehydration and grinding differed only slightly from the values obtained for aggregates formed from treated cells. Pu and Yang (58) observed that the permeabilization of apple cells with dimethyl sulfoxide led to an increase in effective diffusivity. Beuling *et al*. ((21,22) showed that glucose was excluded by deactivated (with mercuric chloride) *Micrococcus luteus* cells entrapped in agar, while the cells were somewhat permeable for oxygen.

Another strategy is to select a solute that will not be consumed by the microorganism, for example, nitrous oxide (159,185), inert gases (H_2, He, CH_4, C_2H_2, N_2O, $CHClF_2$, SF_6) (28), yohimbine, which is a secondary metabolite of plant cells (58); potassium chloride (44), galactose, which is not metabolized by *Z. mobilis* (162).

Itamunoala (116) compared three methods of determining D_e based on the shape of the matrix—designated (i) thin disc, (ii) cylinder, and (iii) beads types—and showed that, by using a sensitivity and error analysis, the thin disc and cylindrical techniques gave more accurate results than the bead method. Westrin and Zacchi (186) studied theoretically, the method of calculating diffusion coefficients in gel beads based on transient experiments of solute uptake from a finite volume. Monte Carlo simulations were used to investigate the effect of random errors on concentration measurements. The influence of sampling frequency and diffusion direction was investigated. Systematic errors derived from an assumption of constant diffusion coefficient and of monodisperse beads were also investigated.

49.2.5 Diffusion in Gels

A lot of research has been performed on the diffusion in polymeric gels with and without encapsulated cells. Various values of measurements of diffusion coefficients in cell-free and cell-containing gels are presented in Refs 20 and 159; Willaert and Baron (187–189,168).

Size exclusion chromatography (SEC) has been used to study the porosity of alginate gels (190–192). Smidsrød (190) studied the porosity of alginate gels using scanning electron microscopy and found that there was a very broad distribution in pore diameter, ranging from 5 to 200 nm. Globular proteins with radii of gyration of approximately 3 nm and with net negative charges should therefore not be trapped in the alginate network, but be able to diffuse at a rate dependent upon their sizes (76). In contrast, Klein *et al*. (191) showed, using SEC and dextrans of known size, that the pore diameters in Ca-alginate gels were fairly uniform. The exclusion volumes for standard macromolecules were recorded and values of 6.8, 14.1, and 16.6 nm were estimated for three different alginates. SEC with 2% Ca-alginate beads using proteins of known Stokes radii indicated a pore diameter of 8–10 nm when eluents of 30 and 150 m*M* $CaCl_2$ were used at pH 6.2 (192). The whey proteins, α-lactoalbumine and β-lactoglobulin, easily penetrated the alginate pores and no proteins had complete access to the total internal volume of the matrix. Polakovic (193) used SEC to evaluate the pore size distribution of 5% Ca-pectate gel and predicted—using a cylindrical and slit-pore model—pore diameters of 50 and 35 nm respectively.

From pore size distribution studies using electron microscopy (194), it was suggested that there is a more constricted network on the bead surface than in the gel core. Skjåk-Bræk and coworkers (195) found that the alginate structure is governed not only by the concentration and chemical structure of the gel material, but also by the kinetics of gel formation. They showed that gels with varying degrees of anisotropy (heterogeneity) can be prepared by controlling the kinetics of the process. Therefore, it is difficult to compare the different diffusion coefficients reported by different workers because of the considerable variations in the experimental conditions of preparing alginate gels. When gels were formed in the presence of antigelling cations, such as Na^+ or Mg^{2+}, isogeneous Ca-alginate gels were obtained (196). Such beads were mechanically stronger and had a higher porosity than those formed in the absence of antigelling ions. Klein and coworkers (191) have reported that glucoamylase is retained for many days in ferric-alginate gel, although it is lost from Ca-alginate or Al-alginate beads. Gray and Dowsett (197) showed that insulin may be entrapped in zinc alginate and Zn–Ca alginate gels.

The average pore diameters of alginate and agarose gels have been estimated from the following semiempirical expression, often used to describe the diffusion of solutes in porous materials and originally derived by Renkin (198) to characterize the diffusion of protein molecules through

cellulose membranes (81):

$$\frac{D_{gel}}{D_a} = \left(1 - \frac{d}{\delta_p}\right)^2 \left\{1 - 2.104\left(\frac{d}{\delta_p}\right) + 2.09\left(\frac{d}{\delta_p}\right)^3 - 0.95\left(\frac{d}{\delta_p}\right)^5\right\} \qquad (49.26)$$

where δ_p is the average pore diameter of the gel and d is the hydrodynamic diameter of the solute. This equation accounts for steric and frictional hindrance to diffusion under Stokes flow conditions, but neglects charge related interactions between solute and matrix. The effect of varying crosslinking condition, polymer concentration, and direction of diffusion on transport for alginate and agarose gels have been investigated (81). In general, 2–4% agarose gels offered little transport resistances for solutes up to 150 kDa, while 1.5–3% alginate gels offered significant transport resistances for solutes in MW range 44–155 kDa—lowering their diffusion rates from 10- to 100-fold as compared with their diffusion in water. Doubling the alginate concentration had a more significant effect on hindering diffusion of larger MW species than did doubling the agarose concentration. Average pore diameters of approximately 170 and 147 Å for 1.5% and 3% agarose gels, respectively, and 480 and 360 Å for 2% and 4% agarose gels, respectively, were estimated using Equation 49.25.

For the case where multiple cellular inclusions (e.g. bacterial or fungal microcolonies or mammalian spheroids) are distributed in a continuous phase (i.e. hydrogel), molecules diffuse more slowly in the cell phase than in the continuous phase. Numerical (finite difference) techniques have been developed to calculate the effective diffusivities (199).

49.2.5.1 Influence of Gel Type and Concentration. Studies on the diffusion of nicotinamide adenine dinucleotide (NAD) and hemoglobin in Ca and Ba-alginate gels showed that NAD diffusion characteristics are unaffected by alginate (from 2.5% to 4% w/v) and calcium chloride (from 0.125 to 0.5 M) concentrations. However, hemoglobin diffusion was affected by the alginate concentration (200). Hannoun and Stephanopoulos (53) demonstrated that D_e for ethanol and glucose decreased when the alginate concentration was increased from 1% to 4% (w/v). Itamunoala (115) showed that by increasing the concentration of either the calcium chloride (1–4% w/v) or Na-alginate (2–8% w/v) component used in Ca-alginate formation substantially decreased D_e, but the effect of the alginate was the greater of the two. A slight reduction of the product of K and D_e for oxygen was found when the alginate concentration was increased from 2% to 4% (w/v) by Sun and coworkers (42). In contrast, Tanaka *et al*. (60) demonstrated that the diffusion of solutes with a MW less than 2×10^4 (glucose, L-tryptophan, and α-lactoalbumin) was not disturbed by increasing the alginate concentration (2–4% w/v) and $CaCl_2$ concentration used in the gel preparation; and diffusion coefficients comparable with those in water were found. For larger molecules such as albumin, γ-globulins, and fibrinogen, the diffusion in the gel was retarded to an extent that depended upon the concentration of alginate and $CaCl_2$ concentration. Moreover, these proteins could diffuse out of, but not into the beads. Therefore, it was suggested that the structure of Ca-alginate gel formed in the presence of large protein molecules was different from that of the gels formed in their absence. Axelsson and Persson (49) also found that the dependence of D_e on the alginate concentration (in the range 1.4–3.8% w/w) for glucose, lactose, galactose, and ethanol was negligible. Hulst and coworkers (67) examined the influence of the concentration of Ca-alginate, gellan gum, κ-carrageenan, agarose, and agar on D_e for oxygen. For agarose and agar, D_e decreased when the gel concentration was increased from 2% to 8% (w/v). Gellan gum and alginate showed a remarkable maximum value for the diffusion coefficient with respect to the gel concentration: at 1% and 2% (w/v) respectively. κ-Carrageenan had a maximum at 5% (w/v) in the concentration range of 1–5% (w/v). The effective diffusion coefficient determined in pure 2% alginate beads was 10–25% lower than the diffusivity in water for various solutes, and a 4% alginate concentration decreased D_e, corresponding well with increased inclusion effect due to the increase in polymer concentration (79). Chen *et al*. (201) used a linear absorption model (LAM) and a shrinking core model (SCM) to interpret the diffusion data of Cu^{2+} in Ca-alginate over a biopolymer range from 2% to 5%. The diffusion coefficient of Cu^{2+} calculated from the LAM was independent of the biopolymer concentration. The LAM had theoretical advantages over the SCM; the latter calculated an unreasonable exponential increase in the diffusion coefficient as the density of the alginate concentration increased. The diffusivity of Cu^{2+} in Ca-alginate increased by a factor of 2 when the gel concentration was increased from 2% to 5% (w/v) (202,203). The decrease of D_e for Remazol Black B (azo dye) in PVA could be described by the Phillies model up to a ϕ_p value of 0.08 m^3 PVA/m^3 gel (26).

The diffusion of solutes in alginate gel is also affected by the chemical composition of the alginate. Martinsen and coworkers (76) showed that the diffusion coefficient of albumin in 4% *Laminaria digitata*, *Macrocyctis pyrifera*, and *L. hyperborea* Ca-alginate gels decreased with decreasing content of guluronic acid (GG) and with any decrease in the average length of the GG blocks. Itamunoala (115) found a glucose diffusion coefficient which was slightly higher for Manutex RS gel compared with Manutex RH gel.

The effective diffusivity of sucrose in agar (0.5%, 1.0%, and 1.5% w/v) was similar to that in water (50). Dextran fractions (MW range from 10.5 to 1950 kDa) displayed restricted diffusion in the agar membranes. Their D_e values were a decreasing function of the agar content of the gel membrane. The diffusivity in a given membrane decreased as the MW of the diffusing molecule increased. The diffusion data did not agree with the Renkin model for a hard sphere diffusing through a cylindrical pore. Beuling *et al*. (23) studied the influence of agar concentration on the diffusion coefficient of glucose by using pulsed field gradient-nuclear magnetic resonance (PFG-NMR). The obtained values corresponded with the ones predicted by the model of Mackie and Meares.

The diffusivity of glucose in κ-carrageenan was affected by the presence of other solutes in the glucose solution (61): electrolytes such as ammonium sulfate, potassium chloride, and calcium chloride were observed to enhance the diffusion coefficient. Estapé *et al*. (73) demonstrated that the effective diffusion coefficients of glucose and ethanol were significantly reduced in the presence of counterdiffusion of ethanol and glucose, respectively.

It was found that lactic acid modified the structure of κ-carrageenan (2.75% w/w)/locust bean gum (0.25% w/w) gel (71), since lactose diffusion characteristics (D_e and K) differed significantly from other studies. Øyaas *et al*. (79) found that D_e for lactose and lactic acid in Ca-alginate were constant between pH 5.5 and 6.5, but significantly reduced at pH 4.5.

Renneberg and coworkers (93) investigated the influence of different variables on the oxygen diffusivity in gels derived from prepolymers. A series of ENT-type (prepared from hydroxyethylacrylate) hydrophilic polymers showed a steady increase in water content and diffusivity with increasing chain length of the prepolymers from 10 to 60 nm. The slightly higher diffusivity of the anionic ENT-type polymer compared with the cationic type seemed to be due to the lower water content rather than to electronic charges. The PVA-SbQ gels have a higher water content and also a higher diffusivity than the polymers of ENT-type. The polymers with 22-nm distance between the photofunctional groups showed a higher O_2 diffusion than the polymers with 6.6 and 6.5-nm distance. The PVA-SbQ 1800-100 with the highest polymerization degree (1800) and the highest saponification (100%) had the highest water content (94.2%) and the highest O_2 diffusivity.

The diffusion of negatively charged nitrate, positively charged ammonium, and a noncharged heavier molecule (glycerol) through Ca-alginate beads at pH 7.5 have been studied (88). When the residence time of gel beads in $CaCl_2$ solution was increased from 10 to 30 min, 30% more nitrate diffused in the gel, and when the alginate concentration was increased from 3% to 6%, 25% less nitrate diffused out of the beads. The diffusion of glycerol was faster than for nitrate. On the contrary, significantly less diffusion through the gel was measured for the ammonium ion. These results suggest that electrostatic interactions affect the diffusion process through Ca-alginate.

49.2.5.2 Influence of the Temperature. The influence of the temperature on the glucose diffusion in 3% (w/v) κ-carrageenan has been investigated in a temperature interval between 10 and 33°C (61). The diffusivity remained unchanged in the interval from 10 to 25°C; from 25 to 32°C, the diffusivity increased linearly from 3.73×10^{-10} to 6.10×10^{-10} m^2/s. This behavior was explained by the fact that the diffusion in the gel system is governed by the bead pore size as well as by the viscosity of the gel. The κ-carrageenan gel viscosity remains unchanged at temperatures below 20°C, and the viscosity decreases when the temperature increases above 2°C. The D_e values of glucose and galactose in κ-carrageenan (2.5% w/v) increased when the temperature was increased from 10 to 25°C and 32°C (55). The diffusion coefficient of glucose, lactate, hydroquinone, and urea in 2% collagen and 1% agar increased when the temperature was raised from 25 to 37°C (52). The temperature dependence of glucose in 3% (w/v) Ca-alginate followed the Arrhenius relation with an activation energy of 4350 J/mol (204). D_e of glucose increased from 6.1×10^{-6} to $7.8 \times 10 - 6$ m^2/s and the value for ethanol from $1.0 \times 10 - 6$ to 1.2×10^{-6} m^2/s in 2% Ca-alginate, when the temperature was increased from 22 to 30°C (54). Martinsen *et al*. (76) calculated the activation energy as 23.5 kJ/mol for the Arrhenius temperature dependence of the diffusion of albumin in 4% (w/v) Ca-alginate. The temperature dependency of the diffusion coefficients for lactose and lactic acid in Ca-alginate were found to be well described by an Arrhenius-type equation (49.70). The activation energy was constant in the temperature range tested (10–55°C), and was found to be 20.0 kJ/mol for lactose and 19.1 kJ/mol for lactic acid.

49.2.5.3 Influence of the pH. Because the alginate gel matrix is negatively charged, the pH influences the diffusion of charged substrates and products. Most proteins are negatively charged at pH 7 and will not easily diffuse into the gel matrix. However, when immobilized in the gel, they tend to leak out more rapidly than would be expected from their free molecular diffusion. The rate of diffusion of BSA out of alginate beads increased with increasing pH, due to the increased negative charge of the protein (76).

49.2.5.4 Influence of the Concentration of the Diffusing Compound. Teo *et al*. (204) found that the effective diffusion coefficient of glucose in 3% (w/v) Ca-alginate is independent of the glucose concentration over the range from 10 to 150 g/L. Concentrations of glucose

in the range 2–100 g/L and ethanol in the range of 10–80 g/L did not affect their diffusion coefficients in Ca-alginate (53). In contrast, Itamunoala (115) showed that only at low glucose concentrations was the glucose diffusivity in Ca-alginate higher. The diffusion of glucose in κ-carrageenan decreased when the glucose concentration was increased from 6.5 to 65 g/L (61). There was a minimal change in the measured values of the diffusion coefficients of Remazol Black B (azo dye) in PVA gel beads in a concentration range of 50–1000 mg/L (26).

Most of the reported effects can be explained on the basis of: a change in tortuosity τ or porosity ε change in partition coefficient, interaction of large molecules with the polymer network of the matrix, interaction between different diffusing solutes, and effect of the temperature.

49.2.6 Diffusion in Dense Cell Masses

49.2.6.1 Diffusion in Biofilms. Table 48.3 gives values of relative effective diffusive permeabilities and Table 48.4 values for effective diffusion coefficients for biofilms. The relative effective permeability (D_e/D_a) is defined as the ratio of the effective diffusive coefficient D_e (is also called *effective diffusive permeability*) of the biofilm to the diffusion coefficient D_a in water (159). The relative effective diffusion coefficient ($\mathcal{D}_e/D_a$) is the ratio of the effective diffusion coefficient to the diffusion coefficient in water, where $\mathcal{D}_e$ is defined as

$$J = -\mathcal{D}_e \nabla C_L \tag{49.27}$$

Effective diffusion coefficients and effective diffusive permeabilities have different applications (241). For analysis of phenomena involving reaction–diffusion interactions, the effective diffusive permeability (coefficient) D_e is the correct parameter. The effective diffusion coefficient D_e is appropriate for the analysis of unsteady behavior of a nonreactive solute.

Experimental measurements of relative effective diffusive permeabilities in biofilms range widely, but most of the variation can be attributed to differences in solute physical chemistry and in biofilm density (cell and extracellular polymeric substances) (241). Three categories of solute physical chemistry were distinguished: ionic solutions (inorganic anions or cations), small solutes (nonpolar solutes with MWs of 44 or less), and large solutes (organic solutes of MW greater than 44). It was proposed that large solutes are effectively excluded from microbial cells, that small solutes partition into and diffuse within cells, and that ionic solutes are excluded from cells but exhibit increased diffusive permeability (but decreased effective diffusion coefficients) due to sorption to the biofilm biomass.

Diffusion coefficients were found to be dependent on the biomass concentration, C/N ratio in the growth medium, temperature (40), and sludge age (30). Diffusion studies of lactose in acidogenic biofilms revealed that the active biofilms had about 66% void volume made up of channels through which the lactose molecules were transported into the bacterial aggregate (35). The decrease in lactose diffusivity was mainly caused by the biofilm's solid biomass fraction rather than by the tortuosity of the channels. The influence of the diffusion potential and the Donnan potential in grown biofilms have been evaluated by comparing the diffusion coefficients of positively and negatively charged ions, and a neutral molecule in experiments with different background electrolyte concentrations (238). Mass transfer effects by electrostatic forces are negligible at the ionic strength of wastewater and tap water. Holden and coworkers (228) determined the diffusion coefficient of toluene as a function of the water potential through unsaturated *Pseudomonas putida* biofilms. The effective diffusion coefficient for toluene was approximately 2 orders of magnitude lower than the diffusivity in water and did not vary markedly with the water potential.

Diffusion coefficients have been evaluated using only particulate biomass filtered onto a membrane (30,222,242). Another technique is to use an inactivated biofilm. The diffusion coefficient of a model hydrophobic compound (α-pinene) through irradiated leachate from biofilters has been determined using a diffusion cell (51).

The biofilm has been assumed to be a homogeneous phase in which mass transport is described by Fickian diffusion. More recently, insight into biofilm structures have led to the recognition that the biofilm is heterogeneous, and mass transfer also occurs by eddy diffusion and convection in the voids or channels and diffusion through the bacterial cells (95,103,105,238–240,243–249).

A 2-D and 3-D model have been developed to evaluate the effect of convective and diffusive substrate transport on biofilm heterogeneity (250). It was found that in the absence of detachment, biofilm heterogeneity is mainly determined by internal mass transfer rate and by initial percentage of carrier-surface colonization. Model predictions showed that biofilm structures with highly irregular surface develop in the mass transfer-limited regime. As the nutrient availability increases, there is a gradual shift toward compact and smooth biofilms. A smaller fraction of colonized carrier-surface leads to a patchy biofilm. Biofilm surface irregularity and deep vertical channels are caused by the inability of the colonies to spread over the whole substratum surface. The maximum substrate flux to the biofilm was greatly influenced by both internal and external mass transfer rates, but not affected by the inoculation density.

A technique, which is based on microinjection of fluorescent dyes and analysis of the subsequent plume formation using confocal laser microscopy, has been used to study the liquid flow in aerobic biofilms (251), and to determine

TABLE 49.3. Relative Effective Permeabilities (D_e/D_a) for Biofilms

Biomass Type	Cell Density (kg/m^3)	Component	D_e/D_a (%)	References
Acidogenic culture	87	Lactose	66	35
Cyanobacterial mat	—	Oxygen	55	205
		Nitrous oxide	68	
Denitrifying culture	69	Valerate	50	206
Denitrifying culture	62.1	Nitrate	46	207
Denitrifying culture	—	Nitrate	68	208
Dental plaque	—	Acetate	21	174
		Propionate	20	
		Lactate	20	
		Glucose	22	
		Fructose	22	
		Sucrose	19	
		^3H_2O	31	
		Lactate	18	209
		^3H_2O	26	
Methanogenic culture	—	Lithium	7	210
Methanogenic culture	—	Acetate	33	211
		Propionate	41	
		Butyrate	28	
Mixed (microbial)	40	Oxygen	55	212
Mixed (microbial)	—	Glucose	110	213
		Ammonia	70	
Mixed (microbial)	—	Glucose	37	214
Mixed (microbial)	94	Glucose	38	34
Mixed (microbial)	—	Oxygen	39–62	30
		Glucose	27–52	
Mixed (microbial)	23.3–24.5	Glucose	50	215
	23.3–24.5	Oxygen	50	
Mixed (bacterial)	3–100	Glucose	100–87	40
		Oxygen	100–86	
Mixed (microbial)	29–84	Oxygen	31–36	181
Mixed culture	37	Valeric acid	34–67	216
Mixed (microbial)	—	Oxygen	39	217
Mixed (microbial)	72–152	Phenol	28–10	218
Mixed (microbial)	141	Phenol	88	219
	195	Phenol	30	
	217	Phenol	5	
	219	Phenol	16	
	223	Phenol	12	
Mixed (microbial)	—	Oxygen	88	220
Mixed (microbial)	25–140	Oxygen	40–90	107
Mixed (microbial)	—	Bromide	8–20	221
Nitrifying culture	42–109	Oxygen	85	222
		Ammonia	81–88	
		Nitrate	90–97	
		Nitrite	84	
Nitrifying culture	25	Oxygen	60	223
Photosynthetic culture	—	Oxygen	51	224
Photosynthetic culture	—	Oxygen	69	225
Photosynthetic culture	—	Oxygen	78	226
Pseudomonads culture	8	Oxygen	100	227
		Napthalene-2-sulfonate	100	
Pseudomonas	—	Trichloroethane	200[a]	95
			30[b]	
Pseudomonas putida	—	Toluene	0.9–2.3	228
Xanthobacter autotrophus	—	Trichloroethane	100	95
Zoogloea ramigera	35–86	Oxygen	48–29	229
	35–86	Glucose	34–13	
	35–86	Ammonia	96–48	

[a] Biofilm thickness **<1** mm.
[b] Biofilm thickness **>1** mm.

TABLE 49.4. Relative Effective Diffusion Coefficients ($\mathcal{D}_e/D_a$) for Biofilms

Biomass Type	Cell Density (kg/m^3)	Component	$D_e D_a$ (%)	References
Cyanobacterial mat	—	Sulfate	13	230
		Hydrogen sulfide	16	
Cyanobacterial mat	—	Oxygen	71	231
Dental plaque	—	Xenon	46	232
Dental plaque	—	Carbonate	5	233
		Acetate	9	
		Lactate	9	
		Butyrate	12	
		Sucrose	11	
Dental plaque	—	Sodium fluoride	23	234
Dental plaque	—	Acetate	31	179
		Lactate	31	
		Sucrose	43	
Dental plaque	200	Lactate	8	177
	200	Sucrose	4.5	176
Dental plaque	—	Acetate	29	209
		^3H_2O	30	
Dental plaque	—	TR-dextran (3 kDa)	3.6	121
		TR-dextran (10 kDa)	0.6	
		TR-dextran (40 kDa)	1.7	
		TR-dextran (70 kDa)	1.2	
		IgG (100 kDa)	0.4	
		IgG (150 kDa)	0.4	
		R-phycoerythrin (240 kDa)	0.2	
Dental plaque	—	Fluoride	43	117,235
Mixed (microbial)	—	Oxygen	4.8	236
		Glucose	27–52	
Mixed (microbial)		Oxygen	60	237
Mixed (bacterial)	19	Glucose	97	238
	26	Bromide	50	
	14–25	Sodium	50–70	
Mixed (microbial)	130–180	Phenol	39–13	68
Mixed (bacterial)	—	Fluorescein	2.3	239
Mixed (bacterial)	—	Fluorescein	97	240
Pseudomonas aeroginosa	—	Glycerol	34	144
Pseudomonas putida	—	Fluorescein	91	132
		Dextran (10 kDa)	28	
		Dextran (70 kDa)	15	
		Bovine serum albumin	54	
		Hexokinase	49	
		DNA	19	
Staphylococcus epidermidis	—	Rhodamine B	11	122
		Fluorescein	32	

[a] TR, Texas red

the local diffusion coefficients in biofilms (119). The diffusion coefficients of fluorescein (MW 332), tetramethyl rhodamine iso-thiocyanate (TRITC)-IgG (MW 150,000), and phycomerythrin (MW 240,000) were measured in the cell clusters and interstitial voids of a heterogeneous biofilm.

Zhang and coworkers (95) used a single tube extractive membrane bioreactor (STEMB) for the determination of the effective diffusion coefficient for a nonreactive tracer (1,1,2-trichloroethane). A video imaging technique was used for the *in situ* measurement of biofilm thickness and continuous monitoring and recording of biofilm growth during experiments.

Bryers and Drummond (132) refined an alternative analytical technique to determine the local diffusion coefficients on a microscale to avoid the errors created by the biofilm architectural irregularities. This technique is based upon fluorescence return after photobleaching (FRAP), which allows image analysis observation of the transport of fluorescently labeled macromolecules as they migrate into a microscale photobleaching zone. The technique allows mapping of the local diffusion coefficients of various solute molecules at different horizontal planes and depths in a biofilm. These mappings also directly indicate the distribution of water channels in

the biofilm. FRAP results indicate a significant reduction in the solute transport coefficients in biofilm polymer gel versus the same value in water, with the reduction being dependent on solute molecule size and shape.

Beuling *et al*. (23) used PFG-NMR to measure the water mobility inside complex heterogeneous systems like natural and active biofilms. Diffusion coefficients measured in both well-defined biofilms and spontaneously grown aggregates corresponded well to glucose diffusion coefficients determined in the same matrices. Diffusion coefficients of the natural biofilms could be related to their physical characteristics. The monitored PFG-NMR signal contained supplementary information on cell fraction or spatial organization, but quantitative analysis was not yet possible.

Wood and coworkers (252) developed a scheme for numerically calculating the effective diffusivity of cellular systems such as biofilms and tissues. A finite difference model was used to predict the effective diffusivity of a cellular system on the basis of subcellular scale geometry and transport parameters. These predictions were compared with predictions from simple analytical solutions (253,254) and experimental data. Their results indicate that under many practical experimental circumstances, the simple analytical solution can be used to provide reasonable estimates of the effective diffusivity.

49.2.6.2 Diffusion in Bioflocs. Microbial flocs have been reviewed by Atkinson and Daoud (255), and Kosaric and Blaszczyk (256). Yeast flocculation has been reviewed by Speers *et al*. (257), Stratford (258), Straver *et al*. (259), Teunissen and Steensma (260), and Dengis and Rouxhet (261). The growth and modeling of the growth of fungal pellets have been reviewed by Whitaker and Long (262), Metz and Kossen (263), Nielsen (264), Nielsen and Carlsen (265), and Nielsen *et al*. (266). Examples of diffusion data for bioflocs are shown in Table 48.5.

Smith and Coackley (182) used surface area determinations to calculate the mean pore radius of activated sludge flocs. This value was found to be between 108 and 130 Å. The tortuosity of the pores in activated sludge (3–9% solids) was also calculated and found to have an average value of 2.73. Libicki and coworkers (159) determined the effective diffusive permeability in aggregates of *E. coli* confined in hollow fiber reactors. It was found that the effective diffusive permeability decreased with increasing cell volume fraction to a value, for aggregates comprising 95% cells, of approximately 30%, than that obtained for cell-free buffer solution. The dependence on the cell volume fraction was described adequately by the Hashin–Shtrikman bounds for a two-phase medium (273):

$$K_2D_2 + \frac{f_1}{\dfrac{f_2}{3K_2D_2} + \dfrac{1}{K_1D_1 - K_2D_2}} \le D_e \le K_1D_1 + \frac{f_2}{\dfrac{f_1}{3K_1D_1} + \dfrac{1}{K_2D_2 - K_1D_1}} \tag{49.28}$$

where f_1 and f_2 are the volume fractions; K_1 and K_2 are the partition coefficients; and D_1 and D_2 are the solute diffusion coefficients for the two components (cells and interstitial fluid), with the indices chosen such that $K_2D_2 \le K_1D_1$.

Mass transfer limitations into fungal pellets is usually due to intraparticle diffusion (266). External mass transport resistance should be taken into account only when intraparticle mass transfer is severe. The average pellet density is found to increase with decreasing pellet radius, and the porosity is related to the pellet density (274):

$$\varepsilon = 1 - \frac{\rho_{\text{pellet}}}{\rho_{\text{hyph}}\,(1-\omega)} \tag{49.29}$$

where ρ_{pellet} is the average pellet density, ρ_{hyph} the hyphal density, and ω is the thickness of the active biomass layer

TABLE 49.5. Diffusion in Bioflocs

Biomass Type	Cell Density (kg/m^3)	Component	Relative Diffusivity (%)		References
Aspergillus niger pellet	12–200	Oxygen	D_e/D_a	4–93	267
A. niger pellet	15	Oxygen	$\mathcal{D}_e/D_a$	58	109
A. niger pellet	19	Oxygen	D_e/D_a	53	268
Escherichia coli aggregates	36–299	Nitrous oxide	D_e/D_a	100–27	159
Methanogenic floc	122	Lithium	D_e/D_a	28	269
Methanogenic floc	—	Acetate	D_e/D_a	11	270
		Ethanol	D_e/D_a	11	
		Hydrogen	D_e/D_a	23	
Mixed culture floc	—	Glucose	D_e/D_a	7–67	214
Mixed microbial floc	29–84	Oxygen	D_e/D_a	31–36	182
Saccharomyces cerevisiae flocs	—	Oxygen	D_e/D_a	0.1–1.0	180
	—	Glucose	D_e/D_a	17	
Zoogloea ramigera floc	400	Oxygen	D_e/D_a	8	271
	390	Glucose	D_e/D_a	5–12	272

in a pellet. Metz (274) found that for *P. chrysogenum*, the average density of the pellet varies between 15 and 100 kg/m^3, and the porosity is in the range of 0.70–0.95. Similar values for the density of *P. chrysogenum* (275–277) and *A. niger* (267) pellets have been reported. The critical pellet radius for various concentrations of these substrates in the medium have been calculated using the appropriate reaction–diffusion model (265). It was observed that except for low glucose concentrations, it is most often oxygen that becomes the limiting substrate in the pellet. For pellets with a radius larger than the critical radius, there is an active growth layer. The active layer thickness depends on the pellet size. Wittler *et al*. (110) recorded the oxygen concentration profile in *P. chrysogenum* pellets using a microelectrode and found that the critical radius was in the range of 100–400 μm depending on the pellet structure and operation conditions. It was found that—as a result of zero oxygen concentration in the center of the pellet—cell lysis occurred, which led to the appearance of hollow pellets. Microelectrode studies by Cronenberg *et al*. (112) also showed that internal mass transport properties of *P. chrysogenum* pellets were highly affected by their morphological structure. Relatively younger pellets possessed a homogeneous and dense structure. These pellets were partly penetrated by oxygen at air-saturated bulk conditions. Older pellets were stratified and fluffy. They were completely penetrated by oxygen due to a decreased activity and a higher diffusivity. Investigations with glucose microelectrodes revealed that glucose consumption inside pellets of all lifetimes exclusively occurred in the periphery, indicating that growth was restricted to these regions only.

Usually, it is assumed that intraparticle molecular diffusion is the only mass transfer mechanism (for earlier work, see e.g. Refs 109,267,268,279,280). However, despite the low density difference between pellets and the bulk medium, some convective flow into the pellets can occur (110,281).

49.2.6.3 Diffusion in Mammalian Cell Aggregates. The Krogh's diffusion constant and the diffusion coefficient of various inert gases have been determined in rat skeletal muscle (38) (Table 48.6). Graham's law (inverse proportionality between the diffusion coefficient and the square root of the molecular mass) was found to represent a useful approximation for these gases. However, a better correlation between the diffusion coefficient and the molecular diameter was found.

The diffusion of ^{3}H-inulin (which does not penetrate the intact cell membrane of mammalian cells) in two types of multicell tumor spheroids have been studied (59). It was found that the value of the diffusion coefficient in spheroids with a smaller extracellular space was significantly larger than in spheroids with a higher extracellular space. It was suggested that the way the cells attach to each other and the extracellular matrix is responsible for this difference.

The diffusion of fluorescein isothiocyanate conjugated BSA, a graded series of FITC-dextrans and sodium fluorescein in both normal tissue and tumors grown in a rabbit ear chamber have been determined (282). Apparent interstitial diffusion coefficients showed a relationship with molecular size, which progressively deviated from that of free diffusion in a single solute, single phase system with values of albumin being significantly reduced from that for a dextran of equivalent hydrodynamic radius. Macromolecular transport in tumor tissue was hindered to a lesser extent than in normal tissue, which was consistent with reports of reduced glycosaminoglycan (GAG) content of tumors.

49.2.7 Diffusion in Microcapsules

The permeable membrane of a microcapsule introduces a supplementary mass transfer barrier compared to gel beads. The core of the microcapsule can be composed of cells in a liquid solution, cells in gel phase, or a combination of both. In the latter case, three mass transfer layers are present. A model for the transient diffusion of proteins from a bulk solution into microcapsules has been developed (284,285). It was used to describe the experimental concentration profiles and to determine the membrane diffusion coefficient of alginate-poly-L-lysine-alginate capsules. By introducing an effective volume fraction as parameter in the model, microcapsules with different sizes of impermeable gel cores could be studied. It was found that the ability of proteins to diffuse into the capsule was not only controlled by the membrane diffusivity, but also by the amount of Ca-alginate core remaining in the microcapsule. Diffusion of glucose, lactose, tyrosine, glutamic acid, and phenylalanine into intrahollow Ca-alginate microcapsules has been studied (89). The combined (microcapsule membrane and core solution) diffusion coefficients were 2–12% smaller than the diffusion coefficients in pure water.

The permeability of the capsule membrane is often characterized by the MW cut-off. Encapsulated cells for tissue engineering applications are better protected from the host's immune system (286,287,409). The application of microcapsules for immunoisolation required a membrane with a MW cut-off of around 50,000 to prevent the permeability of cytotoxic antibodies (288). The permeability of a membrane for a certain compound is not only dependent on the pore size and structure but also on other physical characteristics such as the hydrophobicity/hydrophilicity and charge, and the nature of the solute molecule (e.g. electrostatic interactions between proteins and synthetic polymers).

Measurement of the rate of glucose diffusion from EUDRAGIT RL and hydroxyethyl methacrylate-methyl methacrylate (HEMA-MMA) microcapsules with a Thiele modulus/Biot number analysis of the glucose utilization

TABLE 49.6. Diffusion in Mammalian Cell Aggregates

Cell/Tissue Type	Component	D_e (m^2/s)	Relative Diffusivity (%)		References
Bone lacunar-canalicular system	Fluorescein	3.3×10^{-10}	$\mathcal{D}_e/D_a$	62	136
Normal rat tissue	FITC-BSA		D_e/D_a	1.2–1.7	282
FITC-dextran (20.5 kDa)				2–17	
FITC-dextran (44.2 kDa)				2.4–3.1	
FITC-dextran (71.8 kDa)				0.9–1.0	
Sodium fluorescein				29–34	
Rat skeletal muscle	Helium		D_e/D_a	62	38
	Hydrogen			49	
	Acetylene			52	
	Nitrous oxide			59	
Rat brain tissue	Nerve growth factor	2.75×10^{-11}	$\mathcal{D}_e/D_a$	22	123
Rat somatosensory cortex	Epidermal growth factor	5.18×10^{-11}	$\mathcal{D}_e/D_a$	31	118
Tumor tissue					
9L rat brain tumor spheroids	Glucose	1.5×10^{-10}	D_e/D_a	16	283
Breast tumors	Gd-DTPA	$0.9–1.2 \times 10^{-9}$			101
VX2 carcinoma	FITC-BSA		D_e/D_a	10	282
FITC-dextran (20.5 kDa)				71	
FITC-dextran (44.2 kDa)				56	
FITC-dextran (71.8 kDa)				31	
Sodium fluorescein				89	
EMT6 spheroids	L-glucose	5×10^{-10}			91
EMT6/Ro spheroids	Glucose	1.1×10^{-10}			63
Human squamous and colon carcinoma spheroids	Glucose	$2.3–5.5 \times 10^{-11}$			
EMT6/Ro spheroids	Oxygen	1.46×10^{-9}			113
V−79	Inulin	8.9×10^{-12}			59
EMT6/Ro	Inulin	3.3×10^{-12}			
Xenograft tissue	Fab'	2.7×10^{-11}	$\mathcal{D}_e/D_a$	41	131
	IgG	$1.3\ 10^{-11}$		32	

[a]FITC, fluorescein isothiocyanate; BSA, bovine serum albumin, Gd-DTPA, gadolinium-diethylene-triamino-pentaacetic acid.

rate suggested that pancreatic islets and CHO cells (at moderate to high cell densities) were not adversely affected by the diffusion restrictions associated with these capsule membranes (289). Oxygen transfer through a cellulose sulfate capsule membrane could be measured using a microcoaxial needle electrode (108). Additionally, it was measured that in the case of entrapped yeast cells in the liquid core of the microcapsule, the oxygen supply to the cells was (in the investigated case) not critically influenced by the thin polymeric wall of the capsule.

The evaluation of the mass transfer coefficient (k_s) value was proposed as a supplementary method for the characterization of microcapsules (and gel beads) with semipermeable membranes (290). Owing to a good linear correlation between k_s and the capsule diameter, each investigated capsule type could be characterized by a unique k_s/diameter value.

By manipulating the parameters involved in membrane manufacturing such as the MW and concentration of the membrane forming molecules, the reaction time, polymerization conditions (temperature, pH, ionic strength, ...), addition of (an) additional layer(s) at the outside of the capsule (usually to improve the biocompatibility). Permeation can also be influenced by changing size, swelling, and shape of the capsules (291).

A heterogeneous mixture of dextrans of different MWs (MW 10,000–500,000) has been used as a test solute to study the membrane permeability of alginate polylysine microcapsules (292). The diffusion experiment revealed that the permeability of alginate polylysine (APL) microcapsules decreased with dextrans with MW larger than 80,000. At equilibrium, dextrans of MW 104,000–112,000 represented only approximately 50% of dextrans of equivalent MW outside of microcapsules. The microcapsule membrane does not show a distinct MW cut-off to dextran, but spans a very wide range of at least 80,000–110,000. It is suggested that this can be due to differences in permeability between microcapsules within a batch or to a nonuniform membrane.

Awrey *et al*. (293) have constructed a series of genetically modified cell lines secreting recombinant gene products (human growth hormone, rat serum albumin, human arylsulfatase A, human immunoglobulin, mouse β-hexosaminidase, mouse β-glucuronidase) of different MWs ranging from 21 through 150–300 kDa. They investigated the delivery of these products by alginate-PLL-alginate microcapsules enclosing these

producer cell lines. It was found that the secretion rates of the gene product were similar between nonencapsulated and encapsulated cells with the exception of the largest molecule (the 300-kDa β-glucuronidase), which showed an eightfold reduced secretion. Increasing the thickness of the PLL-membrane did not provide a lower MW cut-off; and an additional coating with alginate reduced the leakage of the larger molecular species but the effect was short lived. Hence, they concluded that immunoisolation of encapsulated cells with alginate-PLL-alginate microcapsules cannot provide a MW cut-off below 300 kDa.

Bacterial cellulose membranes can be used for cell encapsulation since they possess excellent mechanical strength, are biocompatible and simple to produce. Diffusion coefficients of various dextrans (MW 44–260 kDa) in bacterial cellulose have been determined (294). Also the permeation and diffusion coefficients of three marker molecules (Vitamin B_{12}, lysozyme, and BSA) were measured. Using microaxial needle electrodes, oxygen kinetics in different penetration depths within cellulose sulfate hollow spheres loaded with and without yeast cells could be measured (108). On the basis of reaction kinetics, the diffusion coefficient for oxygen and the oxygen uptake rate were calculated.

49.2.8 Internal Mass Transfer by Convection

Most cell aggregates have a dense structure with either a microporous matrix material between the immobilized cells or with closely packed cells. No significant transport by convection through this type of aggregate can occur. There are two exceptions: membrane immobilization and preformed large pore carriers (295).

Membrane immobilized cells can easily be subjected to convective flow or perfusion by applying a pressure difference across the layer. When porous particles are exposed to a pressure gradient (e.g. packed bed), a flow through such particles can occur. Considering the strong diffusion limitations occurring even with very thin immobilized cell layers, convective transport can easily remove this limitation, even at low pressure drops. The flow velocity (v) through a layer of thickness L with a pressure drop (Δp) is given by Darcy's equation:

$$v = \frac{k}{\mu}\frac{\Delta p}{L} \tag{49.30}$$

where μ is the fluid dynamic viscosity and k the hydraulic permeability of the material. With a solute concentration of C_i, the convective flux (J_{conv}) is then given by

$$J_{\text{conv}} = v\, C_i \tag{49.31}$$

This flux should be compared with the diffusional flux, which is of the order:

$$J_{\text{diff}} = D_{\text{e}}\frac{C_i}{L} \tag{49.32}$$

Rewriting the convection equation (Eq. 49.29) in terms of diffusion, gives

$$J_{\text{conv}} = D_{\text{conv}}\frac{C_i}{L} \tag{49.33}$$

with

$$D_{\text{conv}} = \frac{k\,\Delta p}{\mu} \tag{49.34}$$

which should be compared to the effective diffusion coefficient (D_{e}) to determine which of them—the highest—dominates the transport. In the case of a layer with Δp across it, the estimation is simple. Measuring the flow through a slab for a known pressure difference allows for experimental determination of k with Equation 49.29. If we approximate the porous layer by a dense aggregate of spherical particles with diameter d_{p}, the permeability can be estimated from the Kozeny equation (160):

$$k = \frac{d_{\text{p}}^2\varepsilon^3}{180(1-\varepsilon)^2} \tag{49.35}$$

where ε is the porosity. Particle or pore size distribution and shape have a strong influence and d_{p} should be considered as an effective pore size parameter. To estimate the convective flux in a porous particle, say in a packed bed reactor, a similar equation can be used but a geometric correction factor has to be included. The flow will be larger in the outer layer of this particle and only a fraction of the flow will penetrate the central region. Although not exact, Equation 49.33 can be compared to D_{e} to verify if convection plays a role or not in the internal transport. A major difficulty is the estimation of k (or ε or d_{p}) when cells start to fill the pores.

It has been recognized that intraparticle convection can be significant for large pore (bio)catalysts, especially in the case of liquid phase reactions when intraparticle diffusion is too slow to provide full utilization of the internal catalytic capacity (281,296–298). The quantification of the intraparticle fluid velocities is not a straightforward matter. Only for some special cases, like creeping flow of Newtonian fluids relative to permeable spheres, the equations of motion and continuity can be solved analytically. The magnitude of the intraparticle fluid velocity will determine the relative importance of intraparticle convection in the

mass transfer process. Usually an intraparticle Peclet number is defined, which is the ratio between the convective and diffusive flows:

$$Pe = \frac{L v_{\text{int}}}{D_{\text{e}}} \tag{49.36}$$

where v_{int} is the intraparticle convection velocity, and L is the characteristic dimension of the biocatalyst. To explain the dependency of measured effective diffusion coefficients on the flow rate in packed beds of porous particles, an apparent effective diffusion coefficient ($D_{\text{e,app}}$) has been defined (297). $D_{\text{e,app}}$ lumps intraparticle convection and intraparticle diffusion. By comparing the results in packed beds of porous particles, the following simple relationship has been derived:

$$D_{\text{e,app}} = \frac{D_{\text{e}}}{f(Pe)} \tag{49.37}$$

with

$$f(Pe) = \frac{3}{Pe}\left(\frac{1}{\tanh(Pe)} - \frac{1}{Pe}\right) \tag{49.38}$$

or $f(Pe)$ can be any suitable function. Intraparticle convection in immobilized porous cell systems can be accounted for in a very simple manner by using an apparent effective diffusion coefficient instead of the real effective diffusivity in the mass balance equations (14,15,299).

Fluid flow and mass transfer phenomena in porous particles can be obtained from residence time distribution (RTD) experiments where a pulse or step in tracer concentration is applied at the inlet of a packed bed of porous particles and the tracer concentration is measured as a function of time in at least one location of the reactor (usually at the outlet of the reactor). The flow pattern in the interstitial spaces can be represented as axially dispersed plug flow (300). As the fluid velocities inside the porous particles are small compared to the interstitial fluid velocities, the fluid phase inside the porous particles can be considered as a stagnant volume. The solute (tracer or substrate) is exchanged between the extraparticle fluid phase and the stagnant volume by diffusion, convection, or a combination of both. However, the mass transfer process is described by a diffusion equation, which is characterized by the apparent effective diffusivity. RTD experiments have been performed to characterize mass transport in porous glass beads. The value of the apparent effective diffusivity for porous glass beads was obtained by fitting experimental data to model predictions (301). The RTD profiles obtained from experiments performed in the presence of immobilized *S. cerevisiae* cells were hardly influenced by the presence of these cells (302). Only for a high biomass loading at high liquid flow rates, was a noticeable change in RTD profiles observed. Computer simulations revealed that due to the presence of immobilized cells, the reduction in mass transfer rate between extraparticle and intraparticle fluid phase is compensated partially by a decrease in intraparticle porosity.

The effect of intraparticle convection on nutrient transport in porous biological pellets has been studied (281). It was shown that the intrapellet (Pe_{in}) and extrapellet Peclet numbers (Pe_{out}) are generally related by a linear scaling relationship—$Pe_{\text{in}} \sim \xi\, Pe_{\text{out}}$—where ξ is a small number proportional to the hydraulic permeability of the particle and inversely proportional to the square of the characteristic length. External transport was further studied and found to be unaffected by intraparticle flow.

Although internal convection in particles or perfusion in membrane systems is an excellent means to reduce or eliminate mass transfer limitations, it should be clear that this will occur only with exceptionally large pores or pressure drops, respectively.

49.3 EXTERNAL MASS TRANSPORT

Mass transport for solutes to the immobilized cells and the removal of products from the aggregate is usually by convection. In some special situations, like, for example, aggregates not in a mixed part of a bioreactor or encapsulated cells in human tissue, mass transport is only by diffusion. We will discuss the convective external mass transport in more detail.

External mass transfer is described in terms of a liquid phase mass transfer coefficient k_{s}, lumping convective, and diffusive mass transport in the boundary layer around a cell aggregate (295). The mass flux of compound i toward the surface is described by

$$J_i = k_{\text{s}}\,(C_{i\infty} - C_{is}) \tag{49.39}$$

where $C_{i\infty}$ is the bulk liquid concentration, and C_{is} is the concentration at the solid interface.

Several theoretical models describing mass transfer within the external liquid film at the liquid–solid interface have been described (303). The film theory is the simplest and most elementary theory, which assumes the presence of a fictitious laminar film next to the solid boundary. For a fluid flowing past a solid, the whole resistance to mass transfer is in the stagnant liquid film. The actual mass transfer coefficient k_{s} is related to the liquid film thickness δ as

$$k_s = \frac{D_{\text{L}}}{\delta} \tag{49.40}$$

where D_L is the molecular diffusivity of the compound in the liquid. The film theory is not correct since it has been shown through the Chilton–Colburn analogy that k_s is proportional to $D_L^{2/3}$ and not to D_L (304). In 1935, Higbie derived the penetration theory for diffusion into a laminar falling liquid film for short contact times. This theory assumes that the liquid surface is comprised of small fluid elements which contact the second phase for an average time, after which they penetrate into the bulk liquid. Each element is then replaced by another element from the bulk liquid phase. The penetration theory gives the following relation between k_s and D_L:

$$k_s = \sqrt{\frac{4D_L}{\pi t_L}} \tag{49.41}$$

where t_L is the time of penetration of the solute (in seconds). The penetration model was later improved by Danckwerts (305) by replacing the constant exposure time with an average exposure time calculated from an assumed time distribution (304):

$$k_s = \sqrt{D_L s} \tag{49.42}$$

where s is the mean surface renewal factor (in s^{-1}). It was assumed that the chance of an element being replaced on the surface was independent of the time during which it had been exposed. The boundary layer theory describes the formation of a hydrodynamic and concentration boundary layer around objects (303). In this case, the mass transfer coefficient k_s is usually correlated with the external flow velocity and the fluid properties by equations of the form (for particles)

$$Sh = \frac{k_s d_p}{D_L} = a + bRe^n Sc^m \tag{49.43}$$

where d_p is the particle diameter; a, b, n, and m are constants; Sh is the Sherwood number, Re is the Reynolds number, and Sc the Schmidt number which are defined as

$$Re = \frac{u_r d_p}{\nu} \tag{49.44}$$

$$Sc = \frac{\nu}{D_L} \tag{49.45}$$

where u_r is the relative velocity between the fluid and the aggregate and ν the kinematic viscosity.

In the case of permeable spheres, the effect of the external mass transfer resistance on the overall uptake and/or release rate by the beads may be quantitatively evaluated by calculating the time constant for the external film (τ_e), and to compare it to the time constant for diffusion in the sphere (τ_i) (306). The internal time constant can be calculated as (307)

$$\tau_i = \frac{R^2}{15D_e} \tag{49.46}$$

where R is the radius of the bead. Alternatively, the film thickness can be estimated according to the film theory (61). The external mass transfer resistance can also be neglected if the Biot number (Bi) is much larger than one (26,69,167,308). Bi for beads is defined as the ratio of the characteristic film transport rate to the characteristic intraparticle diffusion rate:

$$Bi = \frac{k_s R}{D_e} \tag{49.47}$$

An estimation of the external mass transfer coefficient (k_s) is required to calculate τ_e, Bi, or the film thickness. The value of k_s can be calculated by a procedure described by Harriot (309). Merchant and coworkers (62) determined Bi for a rotating sphere. Using the empirical correlation of Noordsij and Rotte (310), k_s was estimated using the following equation:

$$Sh = 10 + 0.43Re_r^{1/2}Sc^{1/3} \tag{49.48}$$

where Re_r the rotational Reynolds number. In the case of diffusion through a membrane or thin disc, Bi can also be calculated. For free-moving particles, k_s can be determined using the following correlations (83,309,311–314):

$$Sh = \sqrt{4 + 1.21\left(Re_p Sc\right)^{0.67}} \quad \text{for } Re_p Sc > 10^4 \tag{49.49}$$

$$Sh = 2 + 0.6Re_p^{0.5}Sc^{0.33} \quad \text{for } Re_p < 10^3 \tag{49.50}$$

where Re_p is the (particle) Reynolds number which can be estimated using the following correlations:

$$Re_p = \frac{Gr}{18} \quad \text{for} Gr < 36 \tag{49.51}$$

$$Re_p = 0.153Gr^{0.71} \quad \text{for } 36 < Gr < 810^4 \tag{49.52}$$

$$Re_p = 1.74Gr^{0.5} \quad \text{for } 810^4 < Gr < 310^9 \tag{49.53}$$

where Gr is the Grashof number. Another correlation which has been used to estimate k_s for gel beads in agitated reactors (80), is (315):

$$Sh = 2 + 0.52\left(\frac{e_s^{1/3}d_p^{4/3}}{\nu}\right)^{0.59} Sc^{1/3} \tag{49.54}$$

where d_p is the average diameter of the particle, ν is the kinematic viscosity, e_s is the energy dissipation given as $N_p n_i{}^3 D_i{}^5/V$ for a stirred tank (where N_p is the power

number, n_i the impeller speed, D_i the impeller diameter and V the volume of the reactor) . The ranges of validity for this correlation are:

$$10 < \left(\frac{e_s^{1/3} d_p^{4/3}}{\nu} \right) < 1500 \quad \text{and} \quad 120 < Sc < 1450 \tag{49.55}$$

A correlation, which was originally developed for fluidized particles (316), has also been recommended for agitated dispersions of small, low density solids (80,167,317,318):

$$k_s = \frac{2D_{e0}}{d_p} + 0.31\,(Sc)^{-2/3} \left(\frac{\Delta\rho v g}{\rho_l} \right)^{1/3} \tag{49.56}$$

where $\Delta\rho$ is the particle/liquid density difference and ρ_l the density of the bulk liquid.

For particles suspended in aerated reactors, Sh has been expressed as (319):

$$Sh = 2 + 0.545 \sqrt[3]{Sc} \left(\frac{\varepsilon_s d_p^4}{\nu} \right)^{0.264} \tag{49.57}$$

For spherical particles in a packed bed, k_s depends on the liquid velocity around the particles. For the range $10 < Re_p < 10^4$, the Sherwood number has been correlated by the following equation (320):

$$Sh = 0.95 Re_p^{0.5} Sc^{0.33} \tag{49.58}$$

Gutenwik *et al*. (155) used the following Sh-correlation (321):

$$Sh = 2 + 1.45 \mathrm{Re}^{1/2} Sc^{1/3} \tag{49.59}$$

An estimation of k_s can be calculated if the stirred chambers have the shape of flat cylinders (72) using the following correlation (309):

$$k_s = 0.62 D_a^{2/3} \nu^{-1/6} \omega^{1/2} \tag{49.60}$$

where ν is the kinematic viscosity and ω the rotational speed of the stirrer (in rad/s). Other correlations can be adapted from heat transfer correlations (48).

The external mass transfer limitation can be experimentally investigated by observing the concentration-time profile at different mixing regimes in the bioreactor (e.g. rotation speeds of the stirrer) (42).

49.4 REACTION AND DIFFUSION

In immobilized cell systems, cellular reactions can take place in the presence of significant concentration gradients. These reactions are also called *heterogeneous reactions*. Reactions can only take place when the substrate molecules are transported to the reaction place, that is, mass transport phenomena can have a profound effect on the overall conversion rate. The concentration in each internal position has to be known to determine the local rates. In most cases, these internal concentrations cannot be measured but can be estimated using reaction–diffusion model.

49.4.1 Intrinsic Kinetics

Intrinsic kinetics describes the growth and product formation rates of cells in the immobilized (or free) state as a function of the local concentrations. A typically simple unstructured ("black box") model of microbial kinetics for growth on a single substrate can be described by the following three equations:

$$\text{Biomass growth:} \quad \mu = f(C_S) \tag{49.61}$$

$$\text{Substrate consumption:} \quad q_s = \frac{1}{Y_{X/S}} \mu + m_s \tag{49.62}$$

$$\text{Product formation:} \quad q_p = \frac{1}{Y_{X/P}} \mu + m_p \tag{49.63}$$

where μ is the specific growth rate of the cells (g DW/g DW/h); C_S is the substrate concentration; q_s is the specific substrate utilization rate (g substrate used/g DW/h); q_p is the specific product formation rate (g product formed/g DW/h); $Y_{X/S}$ (g DW/g substrate) and $Y_{X/P}$ (g DW/g product) are the yield coefficients; m_s (g substrate/g DW/h) and m_p (g product/g DW/h) are the specific maintenance rates for substrate and product, respectively. In some cases, these maintenance coefficients may be omitted or combined with a "cell death coefficient". The specific growth rate is a function of the substrate concentration and is usually of the Monod kinetics form. The model can also be extended to include growth inhibition by the product (and biomass), and $f(C_S)$ becomes some function of substrate and product (and biomass). The Monod equation is bound by zero-order (at high substrate concentrations relative to the Monod constant K_S) and first-order (at vanishingly small substrate concentrations) kinetics. The solutions of reaction–diffusion problems with these two simple rate equations are valuable in that they can be applied as lower or upper bounds to the general problem without requiring detailed knowledge of the rate expressions and thus considerably facilitating the calculations.

In the interpretation of kinetic data for immobilized cells, it is important to assess the significance of mass transfer

limitations. If negligible mass transfer limitation is present, the externally observed kinetics are the intrinsic cell kinetics. Any external or internal mass transfer limitation will lead to externally observed lower conversion rates. Mass transfer limitations may appear either in the external film around the support matrix or within the gel matrix, or in both.

It has been reported that the physiology, as well as the observed growth rate of cells upon immobilization is changed compared to the one of free cells (11,322). For gel immobilized cell systems, it has been observed that the metabolic rates of gel immobilized cells depend usually only on the local solution concentrations, and are in this case identical to those for free cells if diffusional limitations are absent (322). Some researchers found no significant difference between the maximum specific growth rates for immobilized yeast and bacteria, and those for free cells. On the contrary, a significant decrease has been noted by other researchers for the same microorganisms. It has also been observed that for some cases the growth rate is much higher than that for free-living cells (323,324).

49.4.2 Mathematical Modeling

The major issues involved in modeling immobilized cell reactors are very similar to those in heterogeneous chemical reactors. This analogy has encouraged a rapid development in the model building for immobilized cell systems, even if the level of understanding of biocatalysts is lower than for chemical catalysis. The ability to predict the behavior of immobilized cell systems is required for the understanding, the design, and the optimization of an appropriate bioreactor. It is necessary to consider both the bioreactor performance and the microbial kinetics (266). Description of the bioreactor performance involves modeling of mass transfer effects and the flow pattern in both gas and liquid phases while microbial kinetics deals with the kinetics both on the individual cell level and on the level on the whole cell population. Single cell kinetics can be described either with an unstructured model (no intracellular components considered) or with a structured model (intracellular components considered). The population model may be either unstructured (all cells in the whole population assumed to be identical, that is only one morphological form), or morphologically structured (with an infinite number of morphological forms, the term *segregated population model* is often used (325)). The models describing immobilized cell behavior are usually of the unstructured type.

Models for diffusion and reaction in biofilms are reviewed by for example, Wanner and Reichert (249), Wood and Whitaker (326,327), and Martins Dos Santos *et al*. (328). Recently, a spatially multidimensional (2- and 3-D) particle–based approach has been described to model the dynamics of multispecies biofilms growing on multiple substrates (329–332). The model is based on diffusion–reaction mass balances for chemical species coupled with microbial growth and spreading of biomass represented by hard sphere particles.

49.4.2.1 Gel Entrapment. Initially, models, which described immobilized cell kinetics, were based on steady state models for immobilized enzymes. Steady state models can give valuable information for design purposes, but fail to describe transient phenomena (like the start-up dynamics and response to changing conditions) encountered in growing immobilized cell systems. Therefore, dynamic models have been developed to simulate the transient behavior of growing immobilized cells.

In general, gel immobilized cell systems are considered as effective continua. However, it has been observed that when gel beads are inoculated with a low cell concentration, each growing cell will be the origin of a microcolony and growth results in the formation of expanding microcolonies (e.g. (199,333–341). A rigorous modeling approach to this microcolonies system requires consideration of the microstructure of the immobilized cell system: diffusion in the gel phase, and reaction and diffusion in the microcolony ("two-phase" system).

By the entrapment of cells in gel matrices, an additional barrier to mass transfer relative to free cells is introduced. This tends to lower the overall reaction rate, as well as create a specific microenvironment around the cells. Immobilized cells can grow in the gel matrix and the mass transfer limitations on substrate delivery and product removal lead to time-dependent spatial variations in growth rates and biomass densities, which may be accompanied by alterations in cellular physiology and biocatalytic activity. Since the local effective diffusion coefficient depends on the local biomass density, this nonhomogeneous growth will influence the local diffusive rates. The existence of chemical environmental gradients in immobilized cell systems has been verified experimentally with various microprobe techniques.

49.4.2.1.1 Steady State Modeling. If the cell mass does not vary rapidly, or is fairly uniform, the concentration profiles in a gel matrix with entrapped cells can be simulated using a steady state model at any point in time. These models can give valuable information for design purposes or can be combined with experimental *in situ* measurements (e.g. microelectrodes). In this case, mathematical calculations can be very simple and straightforward analytical solutions can be obtained for simple reaction kinetics (e.g. zero- or first-order kinetics). Examples of these models for cell entrapment are presented in Table 48.7.

49.4.2.1.2 Pseudo-Steady State Modeling. Under certain conditions, the full dynamic modeling to describe transient

TABLE 49.7. Examples of Steady State Reaction–Diffusion Models for Entrapped Cell Systems

Immobilized Cell System	Microbial Kinetics	Comments[a]	References
Gel Systems			
Corynebacterium glutamicum in Sr-alginate beads	Michaelis–Menten	B, C	342,343
Daucus carota in gel beads	Zero order	C, F, H	344
Denitrifying bacterial population in agar beads	Michaelis–Menten	A, C, G	345,346
Escherichia coli in κ-carrageenan beads	Zero order	A, C, F	347
Gluconobacter oxydans in Ca-alginate beads	Michaelis–Menten	A, B, D, G	28
Gluconobacter oxydans in bilayer latex coating	Michaelis–Menten	A. B. C, G, H	345
Hansenula polymorpha in Ba-alginate beads	Michaelis–Menten	A, B, C, G	27
Mycobacterium sp. in Ca-alginate beads	Product inhibition	A, B, D, G	349
Pseudomonas luteola in polyacrylamide	First order	A, C, E, F	350
Pseudomonas putida in Ca-alginate beads	Michaelis–Menten	A, B, D, F, G	351
Ralstonia eutropha in Ca-alginate beads	Haldane kinetics	B, C, F, H	352
Saccharomyces cerevisiae in alginate beads	First order	B, D, E, F, H	353
S. cerevisiae in Ca-alginate			
Continuum model	Monod	B, C, G, H	306
Microcolony model	Zero order	B, C, G, H	306,337
S. cerevisiae in Ca-alginate beads	Monod modified for substrate and product inhibition	A, B, D, G	155
Thiosphaera pantotropha in agarose beads	Zero order	A, D, F	354,355
Trichosporon cutaneum in Ca-alginate beads	Michaelis–Menten	B, C, G	356
Zymomonas mobilis in κ-carrageenan beads	Noncompetitive substrate and product inhibition	B, C, G, H	357
Zymomonas mobilis in Ca-alginate beads	Monod modified for product inhibition	A, B, C, E, G, H	358
Zymomonas mobilis in Ca-alginate beads	Zero and first order	A, B, C, F, H	162
Zymomonas mobilis in gels (slab, cylinder, sphere)	General rate expression (function of substrate and product concentration)	B, D, G, H	359
General models			
Gas production by whole cells (slab, cylinder and sphere)	Zero order	C, F, E, H	360,361
Review of models for enzymes and cells	e.g. Michaelis–Menten, without and with substrate and product inhibition	A, B, D, E, G, H	362
Review: engineering principles of immobilized whole cells	General, e.g. Michaelis–Menten	B, D, F, G, H	1
Model to evaluate the center concentration (slab, cylinder, sphere)	Monod	B, C, F, G, H	363
Model for gel beads containing microcolonies	Zero and first order	B, C, F, G, H	334
Model to estimate oxygen penetration depth (slab, cylinder and sphere)	Zero order	B, D, A, H	364,365
Model to estimate critical bead diameter	Zero and first order	C, F	366
Intrinsic structured model of immobilized cell kinetics and RNA content	Monod	B, C, G, H	367,368
Model for immobilized nongrowing biocatalysts (sphere and slab)	Michaelis–Menten, noncompetitive substrate and product inhibition, competitive product inhibition, reversible Michaelis–Menten	B, D, F, G, H	369
Model for nongrowing spherical biocatalysts	Michaelis–Menten, third-order approximate solution	A, B, C, F, G	370
Model for growth of biomass films immobilized in or around carriers	First-order growth inhibition by one of the products	B, D, C, F	371,372

[a] A, comparison to experimental data; B, effectiveness factor calculation; C, internal mass transfer resistance only; D, internal and external mass transfer resistance; E, includes overall reactor performance model; F, analytical solution; G, numerical solution; H, Thiele modulus calculation.

behavior can be simplified to "pseudo (or quasi)-steady state" modeling. Therefore, the biomass growth and the substrate consumption rate and/or product formation rate are treated separately. This approach is valid as long as the time scale for growth is much larger than the time scale for consumption and product formation. Hence, a pseudo-steady state substrate/product distribution is assumed at each instant. As a result, the system of partial differential equations is reduced to a system of ordinary differential equations, which facilitates the numerical solution. Table 48.8 gives some examples for cells which are entrapped in hydrogels.

TABLE 49.8. Examples of Pseudo-Steady-State Models of Growing Cells Entrapped in Gels

Immobilized Cell System	Microbial Kinetics	D_e expression	Comments[a]	References
Aspergillus awamori	Zero order	$D_{app} = \frac{D_e}{1 + (K-1)\phi_c}$	A, C	104
Aspergillus niger biofilm in solid state fermentation	Zero order	X independent	A, C, D	373
Denitrification bacteria: general model	Zero order	—	A, C, D	374
Escherichia coli in Ca-alginate beads	Monod		A, C, D	335
Continuum model		X independent		
Colony expansion model		$\frac{D_{e\,col}}{D_a} = 0.25$		
Nitrobacter agilis in κ-carrageenan beads	Combination of growth models of Pirt and Herbert	$D_{e0}\left(1 - \frac{C_X}{C_{X_{max}}}\right)$	A, C	375–377
Nitrosomas europaea in κ-carrageenan beads: colony expansion model	Combination of growth models of Pirt and Herbert	$\frac{D_{e\,col}}{D_{e0}} = 0.25$	A, C	378–379
Zymomonas mobilis in Ca-alginate beads	Monod, substrate and product inhibition	$D_{e0}\,a_1(1 - a_2 C_X)^2$	A, B	380,381

[a] A, comparison to experimental data; B, internal mass transfer resistance only; C, internal and external mass transfer resistance; D, includes overall reactor performance model.

49.4.2.1.3 Dynamic Modeling. A general dynamic model, which describes the growth of the immobilized cells and the resulting time-dependent spatial variation of substrate and product in the system, can be constructed by writing the mass balances over the immobilization matrix (it is usually assumed that diffusion in the system is governed by Fick's law; the cells are initially distributed homogeneously over the carrier and there is no deformation of the matrix due to cell growth or gas production):

$$\frac{\partial}{\partial t}(\varepsilon\beta C_i) = z^{-n}\frac{\partial}{\partial z}\left(z^n\, D_{e,i}\frac{\partial C_i}{\partial z}\right) \pm \varepsilon\beta r_i \qquad (49.64)$$

where ε is the ratio of the volume of the pores of the matrix to the total volume; β is the ratio of the volume of the pores minus the volume of the cells to the volume of the pores in the matrix; C_i is the substrate ($i = S$) or product ($i = P$) concentration (expressed per volume available for substrate; n is a shape factor of value 0 for planar, 1 for cylindrical or 2 for spherical geometry; and $D_{e,i}$ is the effective diffusion coefficient for species i. The substrate consumption rate ($r_i = r_s$) and the product formation rate ($r_i = r_p$) are linked to the growth rate (r_x) by the following equations:

$$\frac{\partial}{\partial t}(\varepsilon C_X) = \varepsilon\, r_x = \varepsilon\,\mu\, C_X \qquad (49.65)$$

$$r_s = \frac{1}{Y_{X/S}}\, r_x \text{ and } r_p = \frac{1}{Y_{X/P}}\, r_x \qquad (49.66)$$

where C_X is the biomass concentration expressed per volume available for the cells. Since ε is constant with time, the left hand side of Equation 49.64 can be written as

$$\frac{\partial}{\partial t}(\varepsilon\beta C_i) = \varepsilon\beta\frac{\partial C_i}{\partial t} + \varepsilon C_i\frac{\partial \beta}{\partial t} \qquad (49.67)$$

If a dry weight cell density ρ_c is defined as the ratio of the cell dry mass per cell volume, β can be expressed as function of C_X:

$$\beta = 1 - \frac{C_X}{\rho_c} \qquad (49.68)$$

Using the relationship $Y_{X/S} = dC_X/dC_S$, the second term on the right side of Equation 49.59 is negligible when C_S is much smaller than $\beta\rho_c\, Y_{X/S}$, and under those conditions substitution into Equation 49.64 gives

$$\varepsilon\beta\frac{\partial C_i}{\partial t} = z^{-n}\frac{\partial}{\partial z}\left(z^n D_{e,i}\frac{\partial C_i}{\partial z}\right) \pm \varepsilon\beta r_i \qquad (49.69)$$

These equations can be integrated to yield the substrate and biomass profiles as a function of time (usually together with the reactor model) using the correct initial and boundary conditions. These equations are valid for a wide range of immobilized cell systems. Table 48.9 shows some examples for cells entrapped in hydrogel systems.

49.4.2.2 Microcapsules. Mathematical models have been developed to simulate the membrane formation of microcapsules. A pseudo-stationary state approximation has been used to simulate the membrane thickness as a function of the reaction time (393). The electrostatic droplet formation during microcapsule production was modeled and a reasonably good agreement was obtained between calculated and

TABLE 49.9. Examples of Dynamic Models of Hydrogel Immobilized Cell Systems

Microorganism	System	Substrate	Product	D_e expression	References
Aspergillus niger and *Zymomonas mobilis*	Ca-alginate beads (glucose), maltose (glucose), oxygen	Starch	Ethanol, CO_2, biomass	$D_e = \frac{1-\phi_c}{1+(\phi_c/2)} D_{e0}$	83
Cephalosporium acremonium	Ca-alginate beads	Glucose, sucrose	Constant value		308
Clostridium acetobutylicum	Gel beads (not specified)		Butanol, butyric acid, acetone, acetic acid, ethanol, biomass	Constant value	382
Escherichia coli	Agar membrane	Glucose	Acetic acid, biomass	D_{e0} when $C_x < 10^5$ cells/cm^3	383,384
Escherichia coli	Sr-alginate beads	Glucose,	Acetate, formate, biomass	$D_{e0}\left(1-\frac{C_X}{C_{X_{max}}}\right)+ D_X\left(\frac{C_X}{C_{X_{max}}}\right)$	385
Lactobacillus delbrueckii	κ-Carrageenan beads	Glucose	Lactic acid, biomass	Constant value	386
Nitrosomas europaea and *Nitrobacter agilis*	κ-Carrageenan beads	Ammonia, oxygen, nitrite	Biomass	Constant value	387
Propionibacterium acidipropionici	Ca-polygalacturonate beads	Lactose	Propionic acid, biomass	Constant value	86
Saccharomyces cerevisiae	Ca-alginate membrane	Glucose	Ethanol, biomass	Constant value	54
Saccharomyces cerevisiae	Ca-alginate beads/membrane	Glucose	Biomass	$(1-\phi_c)D_{e0}$	82,72
		Glucose, maltose, maltotriose	Biomass	$(1-\phi_c)D_{e0}$	388,389
Saccharomyces cerevisiae	κ-Carrageenan beads	Glucose	Ethanol, biomass	Constant value	390
Zymomonas mobilis	Ca-alginate beads	Glucose	Ethanol, biomass	$\gamma\xi D_0 + (1-\xi)D_{col}$	391,392

[a] ξ local volume fraction of biocatalyst occupied by microcolonies; col: microcolony.

experimental values of microbead diameter (394,395). Only a few models including mass transfer and reaction kinetics, have been developed. Steady state as well as transient models, with or without cell growth within the capsules, have been constructed.

49.4.2.2.1 Models without Cell Growth

49.4.2.2.1.1 Steady State Modeling. Heath and Belfort (396) constructed a steady state model to simulate glucose and oxygen concentration profiles in microcapsules. Assumptions included homogeneous cell suspension, Fickian diffusion, and kinetics described by the zero and first-order limits of the Monod equation. Furthermore, it was assumed that the capsule membrane provides negligible resistance to diffusion compared to the resistance of mass transfer in the cell suspension; there is no convective fluid motion inside the particles (the validity of this assumption depends on the rate of stirring of the solution and the permeability and flexibility of the capsules); diffusion within the spheres is a geometrical function of radius only; and the bulk solution is well mixed (no external mass transfer limitation) and is maintained at a constant substrate concentration. The simulated concentration profiles indicated the possibility of a necrotic core due to insufficient substrate in those cases where diffusion is low and/or uptake is high. The model equations provided a means of estimating the maximum capsule radius, which would allow adequate diffusion of nutrients to all contained cells.

Willaert and Baron (188) constructed a model, which describes the oxygen diffusion and consumption by microencapsulated islets of Langerhans. The model deals with the situation where the islets of Langerhans in the microcapsule core are embedded in a gel. The influence of the oxygen mass transfer on the oxygen consumption is evaluated by calculating concentration profiles and Thiele modulus versus effectiveness factor plots. The oxygen transfer process for microcapsules containing animal cells has been modeled and investigated in an air-lift bioreactor (395,397).

49.4.2.2.1.2 Dynamic Modeling. Morvan and Jaffrin (398) have constructed a bioartificial pancreas model, constituted by a microencapsulated islet of Langerhans implanted in the peritoneal cavity, to study the effect of

different physical parameters upon the glucose and insulin kinetics during their transfer between an implanted islet and an arteriole. For each solute (glucose and insulin), the mass conservation equations inside and outside the microcapsule were reduced to a set of coupled integral equations, which were solved numerically (boundary element method associated with subregions formulation). The insulin release localized on the islet of Langerhans was controlled by the local value of glycemia. The analysis was made for a two-dimensional geometry. The numerical experiments demonstrated that the insulin quantity diffusing through the arteriole wall depends on the resistance to diffusion of the medium located between the islet and arteriole wall. While the kinetics of glucose did not seem to be affected by a small modification to the transfer conditions between the islet and the arteriole, the kinetics of insulin were extremely sensitive to such conditions. The insulin available for diffusion in the vascular system was considerably reduced as the islet to arteriole wall distances increased, or when the diffusion coefficient between the islet and the arteriole decreased.

49.4.2.2.2 Models with Cell Growth A transient mathematical model describing animal cell growth in microcapsules has been developed and compared to experimental data (285,395,399,400). The modeling study was based on the scenario in which microcapsules with fluid intracapsular liquid are used in stationary culture, that is, cells initially settle to the bottom of the capsules and the cell population expands from the bottom up during the culture period. The model described (i) material transport from the bulk to the interior phase of the microcapsule and (ii) mass transfer and cell growth kinetics in the intracapsular region. An unstructured model was used to describe animal cell growth:

$$\frac{dC_X}{dt} = u(t - t_{lag}) \left[\mu C_X + \lambda \int_0^t C_X(r) dr \right] \qquad (49.70)$$

where

$$u(t - t_{lag}) = \begin{cases} 1 & \text{if} \quad t > t_{lag} \\ 0 & \text{if} \quad t < t_{lag} \end{cases} \qquad (49.71)$$

and where λ is the death constant and t_{lag} is the lag time which has to be determined experimentally. The specific growth rate (μ) depended on the rate limiting substrate concentrations (C_i) according to a Monod relation and the cell density was controlled according to a contact-inhibition model developed originally by Frame and Hu (401). The complete expression for μ was therefore proposed as follows:

$$\mu = \mu_{max} \prod_{i=1}^{m} \left(\frac{C_i}{K_{M,S} + C_i} \right) \left[1 - \exp\left(-B \frac{C_{X_{max}} - C_X}{C_X} \right) \right] \qquad (49.72)$$

where C_{Xmax} is the maximum density physically allowable in a microcapsule and B is an adjustable parameter. The numerical "control-volume" method was used to solve the model equations. This approach involves setting up one or more criteria. If these criteria are met in a certain control volume, the neighboring control volumes will be initialized with a certain cell density. Cell growth in the neighboring control volumes will then be based on these initial cell densities. The distribution of cells and nutrients in the microcapsule illustrated clearly the delicate balance between the supply and the demand of nutrients and oxygen in the microcapsule system. The highest growth rate was found in the boundary region at the top of the cell mass. This region received the most abundant supply of nutrients and oxygen across the membrane and from the upper half of the capsule. The cells at the bottom of the capsule close to the membrane had virtually stopped growing since the maximum cell density was reached, and no more space for cell division was left. The cells at the central region of the population were probably suffering from a lack of nutrients and oxygen, and therefore had only a very low specific growth rate. The simulation results agreed quite well with experimental data.

A three-parameter model, which has been used to describe tumor and bacterial growth (402,403), is the Gompertz model (404):

$$y = a \exp\left[-\exp(b - cx) \right] \qquad (49.73)$$

In order to design and fabricate optimized microencapsulated cell system, the Gompertz model was used and modified to describe the growth, substrate consumption and product formation (405).

The growth of hybridoma cells in alginate-poly-L-lysine microscapsules during cultivation in an air-lift bioreactor has been modeled using a mean field approach expressed as a Langevin class of equations for two different regions, that is the alginate microcapsule core and the annular region between the microcapsule core and the membrane (406). The model successfully predicted the impact of various microenvironmental restriction effects on the dynamics of cell growth and appeared useful for further optimization of microcapsule design in order to achieve higher intracapsular cell concentrations, which resulted in higher amounts of monoclonal antibody production.

49.4.2.3 Effectiveness Factor. The effectiveness factor (η) can be calculated to obtain a numerical measure of the influence of mass transfer on the reaction rate. The effectiveness factor is defined as (325):

$$\eta = \frac{\text{observed reaction rate}}{\text{rate that would be obtained without mass transfer resistance}} \qquad (49.74)$$

Usually, the effectiveness factor only includes the internal mass transfer effect. The corresponding η is called the *internal effectiveness factor* η_i (407):

$$\eta_i = \frac{\text{observed reaction rate}}{\begin{array}{c}\text{rate that would occur if} \\ C_i = C_{is} \text{ everywhere in the particle}\end{array}} \tag{49.75}$$

where C_{is} is the concentration of compound i at the surface of the particle. For reactions, which are affected by both internal and external mass transfer restrictions, a total effectiveness factor η_T can be defined:

$$\eta_T = \frac{\text{observed reaction rate}}{\begin{array}{c}\text{rate that would occur if} \\ C_i = C_{ib} \text{ everywhere in the particle}\end{array}} = \eta_i \eta_e \tag{49.76}$$

where C_{ib} is the bulk concentration of compound i, and η_e the external effectiveness factor defined as

$$\eta_e = \frac{\begin{array}{c}\text{rate that would occur} \\ if\ C_i = C_{is} \text{ everywhere in the particle}\end{array}}{\begin{array}{c}\text{rate that would occur} \\ if\ C_i = C_{ib} \text{ everywhere in the particle}\end{array}} \tag{49.77}$$

From the definition of the effectiveness factor it is clear that one expects that the value of η cannot exceed one. However, this is not the case for a substrate-inhibited reaction. For example, it has been shown that the maltose and maltotriose beer fermentation efficiency for entrapped brewer's yeast in Ca-alginate gel was improved compared to freely suspended cells (i.e. effectiveness factor for maltose and maltotriose was larger than 1), since the uptake of maltose is inhibited by glucose and the uptake of maltotriose is inhibited by glucose and maltose (388,389).

Effectiveness factor calculations can be based on steady state models with the assumption of a homogeneous distribution of cells over the carrier (6,26,84,362,369–372,388,389,408–407), steady state models with a cell profile in the particle (155) or dynamic reaction–diffusion models with the assumption of an initial homogeneous distribution of cells (82,408).

The effectiveness factor for substrate consumption can be mathematically expressed as the volume averaged reaction rate relative to the rate at bulk phase concentration:

$$\eta = (n+1)\frac{\left(D_e \frac{dC'_S}{dz'}\right)_{z'=1}}{r_s(1)} \tag{49.78}$$

or

$$\eta = (n+1)\frac{\int_0^1 z'^{n'} r_s(C'_S)dz'}{r_s(1)} \tag{49.79}$$

where n is a shape factor (0 for planar, 1 for cylindrical or 2 for spherical geometry) and z' is the dimensionless position coordinate; r_s is the substrate reaction rate which is a function of the dimensionless substrate concentration (C_S) (and also of the position in the case of transient effectiveness factor).

Acknowledgments

Financial support from the Belgian Federal Science Policy Office (DWTC) and the European Space Agency (Prodex program), the Flanders Interuniversity Institute for Biotechnology (VIB), and the Research Council of the Vrije Universiteit Brussel is acknowledged.

REFERENCES

1. Karel SF, Libicki SB, Robertson CR. Chem Eng Sci 1985; 40: 1321–1354.
2. Tanaka A, Nakajima H. Adv Biochem Eng Biotechnol 1990; 42: 97–131.
3. Champagne CP, Lacroix C, Sodini-Gallot I. Crit Rev Biotechnol 1994; 14: 109–134.
4. Fukuda H. In: Asenjo JA, Merchuk JC, editors. Bioreactor system design. New York: Marcel Dekker; 1995. pp. 339–375.
5. Jen AC, Wake C, Mikos AG. Biotechnol Bioeng 1996; 50: 357–364.
6. Toda K. J Gen Appl Microbiol 2003; 49: 219–233.
7. Lacroix C, Grattepanche F, Doleyres Y, Bergmaier D. In: Nedovic V, Willaert R, editors. Applications of cell immobilisation biotechnology. Dordrecht: Springer; 2005. pp. 295–319.
8. Soderquist R, Lee JM. In: Nedovic V, Willaert R, editors. Applications of cell immobilisation biotechnology. Dordrecht: Springer; 2005. pp. 469–478.
9. Warnock J, Al-Rubeai M. In: Nedovic V, Willaert R, editors. Applications of cell immobilisation biotechnology. Dordrecht: Springer; 2005. pp. 423–438.
10. Verbelen PJ, De Schutter DP, Delvaux F, Verstrepen KJ, Delvaux FR. Biotechnol Lett 2006; 28: 1515–1525.
11. Willaert R. In: El-Mansi EMT, Bryce CFA, Demain A, Allman AR, editors. Fermentation microbiology and biotechnology. 2nd ed. Boca Raton: CRC Press; 2006. pp. 289–362.
12. Looby D, Griffiths B. TIBTECH 1990; 8: 204–209.
13. Fick A. Philos Mag 1855; 10: 30.
14. De Backer L, Baron GV. Appl Microbiol Biotechnol 1993; 39: 281–285.
15. Baron GV, Willaert R. In Nedovic V, Willaert R, editors. Fundamentals of cell immobilisation biotechnology. Dordrecht: Kluwer Academic Publishers; 2004. pp. 229–244.
16. Epstein N. Chem Eng Sci 1989; 44: 777–779.
17. Mackie JS, Meares P Theory. Proc Roy Soc London 1955; A232: 498–509.
18. Brown W, Johnsen RM. Polymer 1981; 22: 185–190.
19. Muhr AH, Blanshard JMV. Polymer 1982; 23: 1012–1026.

20. Westrin BA, Axelsson A. Diffusion in gels containing immobilized cells: a critical review. Biotechnol Bioeng 1991; 38: 439–447.
21. Beuling EE, van den Heuvel JC, Ottengraf SPP. In: Wijffels RH, Buitelaar RM, Bucke C, Tramper J, editors. Immobilized cells: basic and applications. Amsterdam, The Netherlands: Elsevier Science; 1996a. pp. 31–38.
22. Beuling EE, van den Heuvel JC, Ottengraf SPP. In: Wijffels RH, Buitelaar RM, Bucke C, Tramper J, editors. Immobilized cells: basic and applications. Amsterdam, The Netherlands: Elsevier Science; 1996b. pp. 31–38.
23. Beuling EE, van Dusschoten D, Lens P, van den Heuvel JC, Van As H, Ottengraf SPP. Biotechnol Bioeng 1998; 60: 283–281.
24. Phillies GDJ. Macromolecules 1986; 19: 2367–2376.
25. Petit JM, Roux B, Zhu XX. Macromolecules 1996; 29: 6031–6036.
26. Chen K-C, Wu J-Y, Yang W-B, Hwang S-CJ. Biotechnol Bioeng 2003; 83: 821–832.
27. Hiemstra H, Dijkhuizen L, Harder W. Eur J Microbiol Biotechnol 1983; 18: 189–196.
28. Adlercreutz P. Biotechnol Bioeng 1986; 28: 223–232.
29. Kurosawa H, Matsumura M, Tanaka H. Biotechnol Bioeng 1989; 34: 926–932.
30. Matson JV, Characklis WG. Water Res 1976; 10: 877–885.
31. Benefield L, Molz F. Biotechnol Bioeng 1985; 27: 921–931.
32. Beyenal H, Tanyolac A, Lewandowski Z. Water Sci Technol 1998; 38: 171–178.
33. Cunningham AB, Visser E, Lewandowski Z, Abrahamson M. Water Sci Technol 1995; 32: 107–114.
34. LaMotta E. Environ Sci Technol 1976; 10: 765–769.
35. Yu J, Pinder KL. Biotechnol Bioeng 1993; 41: 736–744.
36. Westrin BA, Axelsson A, Zacchi G. J Control Release 1994; 30: 189–199.
37. Frazier BL, Larmour P, Riley MR. Biotechnol Bioeng 2001; 72: 364–368.
38. Kawashiro T, Carles AC, Perry SF, Piiper J. Pflugers Arch 1975; 359: 219–230.
39. Matsunaga T, Karube I, Suzuki S. Biotechnol Bioeng 1980; 22: 2607–2615.
40. Onuma M, Omura T. Water Sci Technol 1982; 14: 553–568.
41. Smith BAH, Sefton MV. J Biomed Mater Res 1988; 22: 637–685.
42. Sun Y, Furusaki S, Yamauchi A, Ichimura K. Biotechnol Bioeng 1989; 34: 55–58.
43. Mignot L, Junter GA. Appl Microbiol Biotechnol 1990a; 32: 418–423.
44. Mignot L, Junter GA. Appl Microbiol Biotechnol 1990b; 32: 167–171.
45. Converti A, Casagrande M, De Giovanni M, Rovatti M, Del Borghi M. Chem Eng Sci 1996; 51: 1023–1026.
46. Zhang W, Furusaki S. Biochem Eng J 2001; 9: 73–82.
47. Reinhart CT, Peppas NA. J Membr Sci 1984; 18: 227–239.
48. Axelsson A, Westrin B. Chem Eng Sci 1991; 46: 913–915.
49. Axelsson A, Persson B. Appl Biochem Biotechnol 1988; 18: 231–250.
50. Lebrun L, Junter G-A. Enzyme Microb Technol 1993; 15: 1057–1062.
51. Miller MJ, Allen DG. Chem Eng Sci 2004; 59: 3515–3525.
52. Chresand TJ, Dale BE, Hanson SL, Gillies RJ. Biotechnol Bioeng 1988; 32: 1029–1036.
53. Hannoun BJM, Stephanopoulos G. Biotechnol Bioeng 1986; 28: 829–835.
54. Hannoun BJM, Stephanopoulos G. Biotechnol Prog 1990; 6: 341–348.
55. Brito E, Don Juan J, Dominguez F, Casas LT. J Ferment Bioeng 1990; 69: 135–137.
56. Park TG, Hoffman AS. Biotechnol Bioeng 1990; 35: 152–159.
57. Furusaki S, Seki M. J Chem Eng Jpn 1985; 18: 389–393.
58. Pu HT, Yang RYK. Biotechnol Bioeng 1988; 32: 891–896.
59. Freyer JP, Sutherland RM. Adv Exp Med Biol 1983; 159: 463–475.
60. Tanaka H, Matsumura M, Veliky IA. Biotechnol Bioeng 1984; 26: 53–58.
61. Nguyen A, Luong JHT. Biotechnol Bioeng 1986; 28: 1261–1267.
62. Merchant FJA, Margaritis A, Wallace JB. Biotechnol Bioeng 1987; 30: 936–945.
63. Cascari JJ, Sotirchos SV, Sutherland RM. Cancer Res 1988; 14: 3905–3909.
64. Haggerty L, Sugarman JH, Prud'homme RK. Polymer 1988; 29: 1058–1063.
65. Kou JH, Amidon GL, Lee PI. Pharm Res 1988; 5: 592–597.
66. Miller DR, Peppas NA. Eur Polym J 1988; 24: 611–615.
67. Hulst AC, Hens HJH, Buitelaar RM, Tramper J. Biotechnol Tech 1989; 3: 199–204.
68. Fan L-S, Leyva-Ramos R, Wisecarver KD, Zehner BJ. Biotechnol Bioeng 1990; 35: 279–286.
69. Arnaud J-P, Lacroix C. Biotechnol Bioeng 1991; 38: 1041–1049.
70. Anderson WA, Reilly PM, Moo-Young M, Legge RL. Can J Chem Eng 1992; 70: 499–504.
71. Arnaud J-P, Lacroix C, Castaigne F. Enzyme Microb Technol 1992; 14: 715–724.
72. De Backer L, Devleminck S, Willaert R, Baron G, Biotechnol Bioeng 1992; 40: 322–328.
73. Estapé D, Gòdia F, Solà C. Enzyme Microb Technol 1992; 14: 396–401.
74. Longo MA, Novella IS, García LA, Díaz M. Enzyme Microb Technol 1992; 14: 586–590.
75. Martinsen A, Skjåk-Bræk G, Smidsrød O. Biotechnol Bioeng 1989; 33: 79–89.
76. Martinsen A, Storrø I, Skjåk-Bræk G. Biotechnol Bioeng 1992; 39: 186–194.
77. Takamura A, Ishii F, Hidaka H. J Control Release 1992; 20: 21–28.
78. Wu W, Sidhoum M, DeLancey GB. Biotechnol Bioeng 1994; 44: 1217–1227.
79. Øyaas J, Storrø I, Svendsen H, Levine DW. Biotechnol Bioeng 1995a; 47: 492–500.
80. Øyaas J, Storrø I, Lysberg M, Svendsen H, Levine DW. Biotechnol Bioeng 1995b; 47: 501–507.
81. Li RH, Altreuter DH, Gentile FT. Biotechnol Bioeng 1996; 50: 365–373.
82. Willaert RG, Baron GV. Biotechnol Tech 1994; 8: 695–700.
83. Meyerhoff J, John G, Bellgardt K-H, Schügerl K. Chem Eng Sci 1997; 52: 2313–2329.

84. Araujo MLGC, Giordano RC, Hokka CO. Biotechnol Bioeng 1999; 63: 593–600.
85. Mateus DMR, Alves SS, da Fonseca MMR. Biotechnol Bioeng 1999; 49: 625–631.
86. Coronado C, Botello JE, Herrera F. Biotechnol Prog 2001; 17: 669–675.
87. Jovetic S, Beeftink HH, Tramper J, Marinelli F. Enzyme Microb Technol 2001; 28: 510–514.
88. Garbayo I, León R, Vigara J, Vílchez C. Colloids Surf B 2002; 25: 1–9.
89. Chai Y, Mei L-M, Lin D-Q, Yao S-J. J Chem Eng Data 2004; 49: 475–478.
90. Wu D-Q, Zhang G-L, Shen C, Zhao Q, Li H, Meng Q. World J Gastroenterol 2005; 11: 1599–1604.
91. Groebe K, Erz S, Mueller-Klieser W. Adv Exp Med Biol 1994; 361: 619–625.
92. Ho CS, Ju L-K, Baddour RF. Biotechnol Bioeng 1988; 32: 8–17.
93. Renneberg R, Sonomoto K, Katoh S, Tanaka A. Appl Microbiol Biotechnol 1988; 28: 1–7.
94. Willaert R. In: Willaert RG, Baron GV, De Backer L, editors. Immobilised living cell systems: modelling and experimental methods. Chichester, UK: John Wiley & Sons; 1996. pp. 177–213.
95. Zhang S-F, Splendiani A, Freitas dos Santos LM, Livingston AG. Biotechnol Bioeng 1998; 59: 80–89.
96. Rassing J. J Control Release 1985; 1: 169–175.
97. Korthäuer W, Gelléri B, Sernetz M. Ann N Y Acad Sci 1987; 501: 517–521.
98. Robert MC, Lefaucheux F. J Cryst Growth 1988; 90: 358–367.
99. Ruiz-Beviá F, Fernández-Sempere J, Colom-Valiente J. AIChE J 1989; 35: 1895–1898.
100. Prasad PV, Nalcioglu O. Magn Res Medicine 1991; 18 116–131.
101. Dadiani M, Margalit R, Sela N, Degani H. Cancer Res 2004; 64: 3155–3161.
102. Ottengraf SPP, van den Heuvel JC. In: Willaert RG, Baron GV, De Backer L editors. Immobilised living cell systems: modelling and experimental techniques. Chichester, UK: John Wiley & Sons; 1996. pp. 147–176.
103. Yang SN, Lewandowski Z. Biotechnol Bioeng 1995; 48: 737–744.
104. Hellendoorn L, Mulder H, van den Heuvel JC, Ottengraf SPP. Biotechnol Bioeng 1998; 58: 478–485.
105. Rasmussen K, Lewandowski Z. Biotechnol Bioeng 1998; 59: 302–309.
106. Stewart PS, Rayner J, Roe F, Rees WM. J Appl Microbiol 2001; 91: 525–532.
107. Hibiya K, Nagai J, Tsuneda S, Hirata A. Biochem Eng J 2004; 19: 61–68.
108. Wiesmann R, Zimelka W, Baumgärtl H, Götz P, Buchholz R. J Biotechnol 1994; 32: 221–229.
109. Huang MY, Bungay HR. Biotechnol Bioeng 1973; 15: 1193–1197.
110. Wittler R, Baumgartl H, Lübbers DW, Schügerl K. Biotechnol Bioeng 1986; 28: 1024–1036.
111. Michel DC Jr., Grulke EA, Reddy CA. AIChE J 1992; 38: 1449–1460.
112. Cronenberg CCH, Ottengraf SPP, van den Heuvel JC, Pottel F, Sziele D, Schügerl K, Bellgradt KH. Bioprocess Eng 1994; 10: 209–216.
113. Nichols MG, Foster TH. Phys Med Biol 1994; 39: 2161–2181.
114. Suci PA, Geesey GG, Tyler BJ. J Microbiol Methods 2001; 46: 193–208.
115. Itamunoala GF. Biotechnol Prog 1987; 3: 115–120.
116. Itamunoala GF. Biotechnol Bioeng 1988; 31: 714–717.
117. Watson PS, Pontefract HA, Devine DA, Shore RC, Nattress BR, Kirkham J, Robinson C. J Dent Res 2005; 84: 451–455.
118. Thorne RG, Hrabetová S, Nicholson C. J Neurophysiol 2004; 92: 3471–3481.
119. de Beer D, Stoodley P, Lewandowski Z. Biotechnol Bioeng 1997; 53: 151–158.
120. Wussling MHP, Krannich K, Drygalla V, Podhaisky H. Biophys J 2001; 80: 2658–2666.
121. Thurnheer T, Gmür R, Shapiro S, Guggenheim B. Appl Environ Microbiol 2003; 69: 1702–1709.
122. Rani SA, Pitts B, Stewart PS. Antimicrob Agents Chemother 2005; 49: 728–732.
123. Stroh M, Zipfel WR, Williams RM, Webb WW, Saltzman WM. Biophys J 2003; 85: 581–588.
124. Davies PA. J Chromatogr 1989; 483: 221–252.
125. Boyer PM, Hsu JT. AIChE J 1992; 38: 259–272.
126. Fang L, Brown W. Macromolecules 1990; 23: 3284–3290.
127. Guiot E, georges P, Brun A, Fontaine-Aupart MP, Bellon-Fontaine MN, Briandet R. Photochem Photobiol 2002; 75: 570–578.
128. Lead JR, Wilkinson KJ. Environ Sci Technol 2003; 37: 482–487.
129. Poitevin E, Wahl P. Biophys Chem 1988; 31: 247–258.
130. Scalettar BA, Selvin PR, Axelrod D, Klein MP, Hearst JE. Biochemistry 1990; 29: 4790–4798.
131. Berk DA, Yuan F, Leunig M, Jain RK. Proc Natl Acad Sci U S A 1997; 94: 1785–1790.
132. Bryers JD, Drummond F. Biotechnol Bioeng 1998; 60: 462–473.
133. Pluen A, Netti PA, jain RK, Berk DA. Biophys J 1999; 77: 542–552.
134. Pluen A, Boucher Y, Ramanujan S, McKee TD, Gohongi T, di Tomaso E, Brown EB, Izumi Y, Campbell RB, Berk DA, Jain RK. Proc Natl Acad Sci U S A 2001; 98: 4628–4633.
135. Sniekers YH, Donkelaar CC. Biophys J 2005; 89: 1302–1307.
136. Wang L, Wang Y, Han Y, Henderson SC, Majeska RJ, Weinbaum S, Schaffler MB. Proc Natl Acad Sci U S A 2005; 102: 11911–11916.
137. Sellen DB. J Polym Sci 1987; B25: 699–716.
138. Nyström B, Moseley ME, Brown W, Roots J. J Appl Polym Sci 1981; 26: 2285–2294.
139. Everhart CH, Johnson CS Jr. J Magn Reson 1982; 48: 466–474.
140. Brown W, Stilbs P, Lindström T. J Appl Polym Sci 1984; 29: 823–827.
141. Stilbs P. Prog NMR spectrosc 1987; 19: 1–45.
142. Lundberg P, Kuchel PW. Magn Reson Med 1997; 37: 44–52.

143. Lens P, Vergeldt F, Lettinga G, Van As H. Water Sci Technol 1999; 39: 187–194.
144. Vogt M, Flemming H-C, Veeman WS. J Biotechnol 2000; 77: 137–146.
145. Humbert F. J Ind Microbiol Biotechnol 2001; 26: 53–61.
146. Smouha E, Neeman M. Magn Reson Med 2001; 46: 68–77.
147. Stewart UA, Bradley MS, Johnson CS Jr., Gabriel DA. Biopolymers 1988; 27: 173–185.
148. Park IH, Johnson CS Jr., Gabriel DA. Macromolecules 1990; 23: 1548–1553.
149. Crank J. The mathematics of diffusion. 2nd ed. Oxford, UK: Clarendon Press; 1975.
150. Westrin BA. Appl Microbiol Biotechnol 1990; 34: 189–190.
151. Neale GH, Nader WK. AIChE J 1973; 19: 112–119.
152. Akanni KA, Evans JW, Abramson IS. Chem Eng Sci 1987; 42: 1945–1954.
153. Maxwell JC. Electricity and magnetism. 2nd ed. Oxford, UK: Clarendon Press; 1892.
154. Gutenwik J, Nilsson B, Axelsson A. Biotechnol Bioeng 2002; 79: 664–673.
155. Riley MR, Muzzio FJ, Buettner HM, Reyes SC. Biotechnol Bioeng 1996; 49: 223–227.
156. Maxwell JC. A treatise on electricity and magnetism. 2nd ed. Oxford, UK: Clarendon Press; 1881.
157. Ho CS, Ju L-K. Biotechnol Bioeng 1988; 32: 313–325.
158. Libicki SB, Salmon PM, Robertson CR. Biotechnol Bioeng 1988; 32: 68–85.
159. Coulson JM, Richardson JF. Chemical engineering. 4th ed. Oxford, UK: Pergamon Press; 1991.
160. Wakao N, Smith JM. Chem Eng Sci 1962; 17: 825–834.
161. Sakaki K, Nozawa T, Furusaki S. Biotechnol Bioeng 1988; 31: 603–606.
162. Klein J, Schara P. Appl Biochem Biotechnol 1981; 6: 91–117.
163. Korgel BA, Rotem A, Monbouquette HG. Biotechnol Prog 1992; 8: 111–117.
164. Wang H, Seki M, Furusaki S. Biotechnol Prog 1995; 11: 558–564.
165. Banerjee I, Jayant M, Modak K, Bandopadhyay K, Das D, Maiti BR. J Biotechnol 2001; 87: 271–277.
166. Jia X, Wen J, Jiang Y, Bai J, Cheng X. AIChE J 2006; 52: 1294–1303.
167. Zhao Y, DeLancey GB. Biotechnol Bioeng 2000; 69: 639–647.
168. Mota M, Teixeira JA, Yelshin A. Biotechnol Prog 2001; 17: 860–865.
169. Mota M, Teixeira JA, Yelshin A. Biotechnol Prog 2002; 18: 807–814.
170. Klein J, Manecke G. In: Chibata I, Fukui S, Wingard LB Jr., editors. Volume 6, Enzyme engineering. New York, USA: Plenum Press; 1982.
171. Ogston AG, Preston BN, Wells JD. Proc R Soc London 1973; 333 A: 297.
172. Cukier RI. Macromolecules 1984; 17: 252.
173. Scott CD, Woodward CA, Thompson JE. Enzyme Microb Technol 1989; 11: 258–263.
174. Dibdin GH. Arch Oral Biol 1981; 26: 515–523.
175. Tatevossian A. Arch Oral Biol 1985a; 30: 141–146.
176. Tatevossian A. Arch Oral Biol 1985b; 30: 365–371.
177. Cronenberg CCH. PhD thesis. The Netherlands: University of Amsterdam; 1994.
178. McNee SG, Geddes DAM, Weetman DA. Arch Oral Biol 1982; 27: 975–979.
179. Vicente AA, Dluhy M, Ferreira EC, Mota M, Teixeira JA. Biochem Eng J 1998; 2: 35–43.
180. Beuling EE, van den Heuvel JC, Ottengraf SPP. Biotechnol Bioeng 2000; 67: 53–60.
181. Smith PG, Coackley P. Water Res 1984; 18: 117–122.
182. Matson JV. Diffusion through microbial aggregates [Doctoral dissertation]. Rice University, U.S.A; 1975.
183. Libicki SB, Salmon PM, Robertson CR. Ann N Y Acad Sci 1986; 469: 145–151.
184. Westrin BA, Zacchi G. Chem Eng Sci 1991; 46: 1911–1916.
185. Willaert RG, Baron GV. Rev Chem Eng 1996a; 12: 1–205.
186. Willaert R, Baron GV. In: Wijffels RH, Buitelaar RM, Bucke C, Tramper J, editors. Immobilized cells: basics and applications. Amsterdam: Elsevier Science; 1996b. pp. 362–369.
187. Pilkington PH, Margiritis A, Mensour NA. Crit Rev Biotechnol 1998; 18: 237–255.
188. Smidsrød O. Faraday Discuss Chem Soc 1974; 57: 263–274.
189. Klein J, Stock J, Vorlop K-D. Eur J Appl Microbiol Biotechnol 1983; 18: 86–91.
190. Stewart WW, Swaisgood HE. Enzyme Microb Technol 1993; 15: 922–927.
191. Polakovic M Wijffels. In: RH, Buitelaar RM, Bucke C, Tramper J, editors. Immobilized cells: basic and applications. Amsterdam, The Netherlands: Elsevier Science; 1996. pp. 62–69.
192. Andresen IL, Skipnes O, Smidsrød O, Østgaard K, Hemmer PC. ASC Symp. Ser. 1977; 48: 361–381.
193. Skjåk-Bræk G, Grasdalen H, Smidsrød O. Carbohyd Polym 1989; 10: 31–54.
194. Skjåk-Bræk G, Grasdalen H, Larsen B. Carbohyd Res 1986; 154: 239–250.
195. Gray CJ, Dowsett J. Biotechnol Bioeng 1988; 31: 607–612.
196. Renkin EM. J Gen Physiol 1954; 38: 225–243.
197. Riley MR, Muzzio FJ, Reyes SC. Comput Chem Eng 1998; 22: 525–534.
198. Kierstan M, Darcy G, Reilly J. Biotechnol Bioeng 1982; 24: 1507–1517.
199. Chen D, Lewandowski Z, Roe F, Surapaneni P. Biotechnol Bioeng 1993; 41: 755–760.
200. Jang LK. Biotechnol Bioeng 1994; 43: 183–185.
201. Lewandowski Z, Roe F. Biotechnol Bioeng 1994; 43: 186–187.
202. Teo WK, Ti HC, Tan WH. Proceedings World Congress III of Chemical Engineering; Tokyo; 1986. pp. 851–854.
203. Glud RN, Jensen K, Revsbech NP. Geochim Cosmochim Acta 1995; 59: 21–237.
204. Andrews GF, Tien C. AIChE J 1981; 27: 396–403.
205. Mulcahy LT, Shieh WK, LaMotta EJ. Biotechnol Bioeng 1981; 23: 2403.
206. Arvin E, Kristensen GH. Water Sci Technol 1982; 14: 833–848.
207. Dibdin GH. Arch Oral Biol 1993; 38: 251–254.

208. Kitsos HM, Roberts RS, Jones WJ, Tornabene TG. Biotechnol Bioeng 1992; 39: 1141–1146.
209. Yu J, Pinder KL. Bioresour Technol 1994; 48: 155–161.
210. Tomlinson TG, Snaddon DHM. Air Water Pollut Int J 1966; 10: 865–881.
211. Atkinson B, Davies IJ. Trans Inst Chem Eng 1974; 52: 248–259.
212. Pipes DM, Characklis WG, Matson JV. J Environ Eng 1974; 10: 225–226.
213. Fujie K, Tsukamoto T, Kubota H. J Ferment Technol 1979; 57: 539.
214. Wang S-CP, Tien C. AIChE J 1984; 30: 786–794.
215. la Cour Jensen J, Harremoës P. Water Sci Technol 1985; 17: 1–14.
216. Tang W-T, Fan L-S. AIChE J 1987; 33: 239–249.
217. Livingston AG, Chase HA. AIChE J 1989; 35: 1980–1992.
218. Lewandowski Z, Walser G, Characklis WG. Biotechnol Bioeng 1991; 38: 877–882.
219. Charbonneau A, Novakowski K, Ross N. J Contam Hydrol 2006; 85: 212–228.
220. Williamson K, McCarty PL. J Water Pollut Control Fed 1976; 48: 281–296.
221. Siegrist H, Gujer W. Water Res 1987; 21: 1481–1487.
222. Revsbech NP. J Microbiol Methods 1989; 9: 111–122.
223. Glud RN, Ramsing NB, Revsbech NP. J Phycol 1992; 28: 51–60.
224. Kühl M, Jørgensen BB. Appl Environ Microbiol 1992; 58: 1164–1174.
225. Wagner K, Hempel DC. Biotechnol Bioeng 1988; 31: 559–566.
226. Holden PA, Hunt JR, Firestone MK. Biotechnol Bioeng 1997; 56: 656–670.
227. Beyenal H, Tanyolaç A. Water Sci Technol 1994; 29: 463–470.
228. Jørgensen BB, Revsberg NP, Blackburn TH, Cohen Y. Appl Environ Microbiol 1979; 38: 46–58.
229. Revsbech NP, Madsen B, Jørgensen B. Limnol Oceanogr 1986; 31: 293–304.
230. McNee SG, Geddes DAM, Main C, Gillespie FC. Arch Oral Biol 1979; 24: 359–362.
231. Tatevossian A. Caries Res 1979; 13: 154–162.
232. McNee SG, Geddes DAM, Main C, Gillespie FC. Arch Oral Biol 1980; 25: 819–823.
233. Stewart PS. J Dent Res 2005; 84: 1087.
234. Bungay HR, Whalen WJ, Sanders WM. Biotechnol Bioeng 1969; 11: 765–772.
235. Chen YS, Bungay HR. Biotechnol Bioeng 1981; 23: 781–792.
236. Siegrist H, Gujer W. Water Res 1985; 19: 1369–1378.
237. Lawrence JR, Wolfaardt GM, Korber DR. Appl Environ Microbiol 1994; 60: 1166–1173.
238. de Beer D, Stoodley P. Water Sci Technol 1995; 32: 11–18.
239. Stewart PS. Biotechnol Bioeng 1998; 59: 261–272.
240. Onuma M, Omura T, Umita T, Aizawa J. Biotechnol Bioeng 1985; 27: 1533–1539.
241. San HA, Tanik A, Orhon D. J Chem Technol Biotechnol 1993; 58: 39–48.
242. Tanik A, Orhon D, San HA. J Chem Technol Biotechnol 1993; 58: 49–55.
243. Zhang TC, Bishop PL. Water Res 1994; 28: 2279–2287.
244. Bishop PL, Zhang TC, Fu YC. Water Sci Technol 1995; 31: 143–152.
245. Lewandowski Z, Stoodley P, Altobelli S. Water Sci Technol 1995; 31: 153–162.
246. van Loosdrecht MCM, Heijnen JJ. In: Willaert RG, Baron GV, De Backer L, editors. Immobilised living cell systems: modelling and experimental methods. Chichester, UK; John Wiley & Sons; 1996. pp. 255–271.
247. Wanner O, Reichert P. Biotechnol Bioeng 1996; 49: 172–184.
248. Picioreanu C, van Loosdrecht MCM, Heijnen JJ. Biotechnol Bioeng 2000; 69: 504–515.
249. de Beer D, Stoodley P, Lewandowski Z. Biotechnol Bioeng 1994; 44: 636–641.
250. Wood BD, Quintard M, Whitaker S. Biotechnol Bioeng 2002; 77: 495–516.
251. Ochoa-Tapia JA, Stroeve P, Whitaker S. Chem Eng Sci 1994; 49: 709–726.
252. Wood BD, Whitaker S. Chem Eng Sci 2000; 55: 3397–3418.
253. Atkinson B, Daoud IS. Adv Biochem Eng 1976; 4: 41–124.
254. Kosaric N, Blaszczyk R. Adv Biochem Eng Biotechnol 1990; 42: 27–62.
255. Speers RA, Tung MA, Durance TD, Stewart GG. J Inst Brew 1992; 98: 293–300.
256. Stratford M. Adv Microb Physiol 1992; 33: 2–71.
257. Straver MH, Kijne JW, Smit G. TIBTECH 1993; 11: 228–232.
258. Teunissen AW, Steensma HY. Yeast 1995; 11: 1001–1013.
259. Dengis PB, Rouxhet PG. J Inst Brew 1997; 103: 257–261.
260. Whitaker A, Long PA. Process Biochem 1973; 8: 27–31.
261. Metz B, Kossen NWF. Biotechnol Bioeng 1977; 19: 781–799.
262. Nielsen J. Adv Biochem Eng Biotechnol 1992; 46: 187–223.
263. Nielsen J, Carlsen M. In: Willaert RG, Baron GV, De Backer L, editors. Immobilised living cell systems: modelling and experimental methods. Chichester, UK: John Wiley & Sons; 1996. pp. 273–293.
264. Nielsen J, Villadsen J, Lidén G. Bioreaction engineering principles. New York, USA: Plenum Press; 2003.
265. Yano T, Kodama T, Yamada K. Agric Biol Chem 1961; 25: 580–584.
266. Ngian KF, Lin SH. Biotechnol Bioeng 1976; 18: 1623–1627.
267. Nilsson BK, Karlsson HT. J Chem Technol Biotechnol 1989; 44: 255–260.
268. Ozturk SS, Palsson BO, Thiele JH. Biotechnol Bioeng 1989; 33: 745–757.
269. Mueller JA, Boyle WC, Lightfoot EN. Biotechnol Bioeng 1968; 10: 331–358.
270. Baillod CR, Boyle WC. J Sanit Eng Div ASCE 1970; 96: 525–545.
271. Hashin Z, Shtrikman J. J Appl Phys 1962; 33: 3125–3131.
272. Metz B. Ph.D. thesis. Delft, The Netherlands: Technical University of Delft; 1976.

273. Phillips DH, Johnson MJ. J Biochem Microb Technol Eng 1961; 3: 277–309.
274. Pirt SJ. Proc R Soc B 1966; 166: 369–373.
275. Trinci APJ. Arch Mikrobiol 1970; 73: 353–348.
276. Phillips DH. Biotechnol Bioeng 1966; 8: 456–460.
277. Kobayashi T, van Dedem G, Moo-Young M. Biotechnol Bioeng 1973; 15: 27–45.
278. Stephanopoulos G, Tsiveriotis K. Chem Eng Sci 1989; 44: 2031–2039.
279. Nugent LJ, Jain RK. AIChE Symp Ser 1983; 227: 1–10.
280. Li CKN. Cancer 1982; 50: 2066–2073.
281. Kwok WY, Kiparissides C, Yuet P, Harris TJ, Goosen MFA. Can J Chem Eng 1991; 69: 361–370.
282. Yuet PK, Kwok W, Harris TJ, Goosen MFA. In: Goosen MFA, editor. Fundamentals of animal cell encapsulation and immobilisation. Boca Raton, Florida, USA: CRC Press; 1993. pp. 79–111.
283. Nastruzzi C, Luca G, Bata G, Calafiore R. In: Nedovic V, Willaert R, editors. Applications of cell immobilisation biotechnology. Dordrecht: Springer; 2005. pp. 17–37.
284. Orive G, Hernandez RM, Gascon AR, Pedraz JL. In: Nedovic V, Willaert R, editors. Applications of cell immobilisation biotechnology. Dordrecht: Springer; 2005. pp. 185–196.
285. Christenson L, Dionne KE, Lysaght MJ, Goosen MFA, editors. Fundamentals of animal cell encapsulation and immobilisation. Boca Raton, Florida, USA: CRC Press; 1993. pp. 7–41.
286. Douglas JA, Sefton MV. Biotechnol Bioeng 1990; 36: 653–664.
287. Lewinska D, Rosinski S, Hunkeler D, Poncelet D, Werynski A. J Membr Sci 2002; 209: 533–540.
288. Okhamafe, AO, Goosen MFA. In: Goosen MFA, editor. Fundamentals of animal cell encapsulation and immobilization. Boca Raton, USA: CRC Press; 1993. pp. 55–78.
289. Coromili V, Chang TMS. Biomater Artif Cells Immobilization Biotechnol 1993; 21: 427–444.
290. Awrey DE, Tse M, Hortelano G, Chang PL. Biotechnol Bioeng 1996; 52: 472–484.
291. Sokolnicki AM, Fisher RJ, Harrah TP, Kaplan DL. J Membrane Sci 2006; 272: 15–27.
292. Willaert RG, De Backer L, Baron GV. In: Willaert RG, Baron GV, De Backer L, editors. Immobilised living cell systems: modelling and experimental methods. Chichester: John Wiley & Sons; 1996. pp. 21–66.
293. Nir A, Pismen L. Chem Eng Sci 1977; 32: 35–41.
294. Rodrigues AE, Ahn B, Zoulalian A. AIChE J 1982; 28: 541–546.
295. Converti A, Sommariva C, Del Borghi M. Chem Eng Sci 1994; 49: 937–947.
296. Willaert RG, Baron GV. Appl Microbiol Biotechnol 1995; 42: 664–670.
297. Levenspiel O. Chemical reaction engineering. 2nd ed. New York: John Wiley & Sons; 1972.
298. De Backer L, Baron GV. J Chem Technol Biotechnol 1994; 59: 297–302.
299. De Backer L. [PhD dissertation]. Brussels, Belgium: Vrije Universiteit Brussel; 1994.
300. Bird RB, Stewart WE, Lightfoot EN. Transport phenomena. 2nd ed. New York: John Wiley & Sons; 2002.
301. Geankoplis CJ. Transport process and unit operations. 2nd ed. Boston: Allyn and Bacon; 1983.
302. Danckwerts PV. Gas-liquid reactions. New York: McGraw-Hill Book Company; 1970.
303. Willaert, RG. Reaction and diffusion in immobilised cell systems [PhD dissertation]. Brussel, Belgium: Vrije Universiteit Brussel; 1993.
304. Glueckauf E. Trans Faraday Soc 1955; 51: 1540–1551.
305. Cruz AJG, Pen T, Giordano RC, Araujo MLGC, Hokka CO. Biotechnol Bioeng 2004; 85: 96–102.
306. Sherwood TKA, Pigford RL, Wilke CR. Mass transfer. London, UK: McGraw-Hill Book Company; 1975.
307. Noordsij P, Rotte JW. Chem Eng Sci 1967; 22: 1475–1481.
308. Ranz WE, Marshall WR. Chem Eng Prog 1952; 48: 141–146, 173–180.
309. Brian PLT, Hales HB. AIChE J 1969; 15: 419–425.
310. McCabe WL, Smith JC. Unit operations of chemical engineering. New York, USA: McGraw-Hill; 1976.
311. van ‘t Riet K, Tramper J. Basic bioreactor design. New York, USA: Marcel Dekker; 1991.
312. Kikuchi KI, Sugarawa T, Ohashi H. Chem Eng Sci 1988; 43: 2533–2540.
313. Calderbank PH, Moo-Young MG. Chem Eng Sci 1961; 16: 39–54.
314. Horstmann BJ, Chase HA. Chem Eng Res Des 1989; 67: 243–254.
315. Zhang SP, Sun Y. AIChE J 2002; 48: 178–186.
316. Sänger P, Deckwer WD. Chem Eng J 1981; 22: 179–186.
317. Moo-Young M, Blanch HW. Adv Biochem Eng 1981; 19: 1–69.
318. Foo SC, Rice RG. AIChE J 1975; 21: 1149–1158.
319. Willaert RG, Nedovic V, Baron GV. In: Nedovic V, Willaert R, editors. Fundamentals of cell immobilisation biotechnology. The Netherlands: Kluwer Academic Publishers; 2004. pp. 469–492.
320. Karel SF, Robertson CR. Biotechnol Bioeng 1989a; 34: 320–336.
321. Karel SF, Robertson CR. Biotechnol Bioeng 1989b; 34: 337–356.
322. Bailey JE, Ollis DF. Bioreactor engineering fundamentals. 2nd ed. New York: McGraw-Hill; 1986.
323. Wood BD, Whitaker S. Chem Eng Sci 1998; 53: 397–425.
324. Wood BD, Whitaker S. Biotechnol Bioeng 1999; 64: 656–670.
325. Martins Dos Santos VAP, Tramper J, Wijffels RH. In: Nedovic V, Willaert R, editors. Fundamentals of cell immobilisation biotechnology. The Netherlands: Kluwer Academic Publishers; 2004. pp. 493–529.
326. Picioreanu C, Kreft J-U, van Loosdrecht MCM. Appl Environ Microbiol 2004; 70: 3024–3040.
327. Xavier JB, Picioreanu C, van Loosdrecht MCM. Environ Microbiol 2005a; 7: 1085–1103.
328. Xavier JB, Picioreanu C, van Loosdrecht MCM. Biotechnol Bioeng 2005b; 91: 651–669.
329. Alpkvist E, Picioreanu C, van Loosdrecht MCM. Biotechnol Bioeng 2006; 94: 961–979.

330. Bailliez C, Largeau C, Casadevall E. Appl Microbiol Biotechnol 1985; 23: 99–105.
331. Salmon PM, Robertson CR. J Theor Biol 1987; 125: 325–332.
332. Salmon PM. [PhD Dissertation]. Stanford, CA, USA: Stanford University; 1989.
333. Wijffels RH, Tramper J. Appl Microbiol Biotechnol 1989; 32: 108–112.
334. Willaert R, Baron G. Appl Microbiol Biotechnol 1993; 39: 347–352.
335. Riley MR, Muzzio FJ, Buettner HM, Reyes SC. Chem Eng Sci 1995; 50: 3357–3367.
336. Picioreanu C, van Loosdrecht MCM, Heijnen JJ. Biotechnol Bioeng 1998; 57: 718–731.
337. Vogelsang C, Schramm A, Piciorenu C, van Loosdrecht MCM, østgaard K. Hydrobiologica 2002; 469: 165–178.
338. Yari B, Khorasheh F, Kheirolomoom A. Chem Phys 2006; 321: 34–40.
339. Ogbonna JC, Matsumura M, Kataoka H. Bioprocess Eng 1991a; 7: 11–18.
340. Ogbonna JC, Matsumura M, Kataoka H. Process Biochem 1991b; 26: 109–121.
341. Hulst AC, Tramper J, Brodelius P, Eijkenboom LJC, Luyben KChAM. J Chem Technol Biotechnol 1985; 35: 198–204.
342. de Beer D, Sweerts J-PRA. Anal Chim Acta 1989; 219: 351–356.
343. de Beer D, van den Heuvel JC, Sweerts J-PRA. In: de Bont JAM, Visser J, Mattiasson B, Tramper J, editors. Physiology of immobilized cells. Amsterdam: Elsevier; 1990. pp. 613–624.
344. Hooijmans CM, Briasco CA, Huang J, Geraats SGM, Barbotin J-N, Thomas D, Luyben KChAM. Appl Microbiol Biotechnol 1990; 33: 611–618.
345. Fidaleo M, Charaniya S, Solheid C, Diel U, Laudon M, Ge H, Scriven LE, Flickinger MC. Biotechnol Bioeng 2006; 95: 446–458.
346. Brink LES, Tramper J. Enzyme Microb Technol 1986; 8: 334–340.
347. Chen B-Y, Chen S-Y, Chang j-S. Process Biochem 2005; 40: 3434–3440.
348. Bandhyopadhyay K, Das D, Bhattacharyya P, Maiti BR. Biochem Eng J 2001; 8: 179–186.
349. Dursun AY, Tepe O. J Hazard Mater 2005; 126: 105–111.
350. Ramakrishna SV, Prema P, Sai PST. Bioprocess Eng 1991; 6: 117–121.
351. Hooijmans CM, Geraats SGM, van Neil EWJ, Robertson LA, Heijnen JJ, Luyben KChAM. Biotechnol Bioeng 1990b; 36: 931–939.
352. Hooijmans CM, Geraats SGM, van Niel EWJ, Robertson LA, Heijnen JJ, Luyben KChAM. In: de Bont JAM, Visser J, Mattiasson B, Tramper J, editors. Physiology of immobilized cells. Amsterdam: Elsevier; 1990c. pp. 361–368.
353. Chen K-C, Huang C-T. Enzyme Microb Technol 1988; 10: 284–292.
354. Luong JHT. Biotechnol Bioeng 1985; 27: 1652–1661.
355. Melick MR, Karim MN, Linden JC, Dale BE, Mihaltz P. Biotechnol Bioeng 1987; 29: 370–382.
356. Webb C, Dervakos GA, Dean JF. Ann N Y Acad Sci 1990; 589: 593–598.
357. Krouwel PG, Kossen NWF. Biotechnol Bioeng 1980; 22: 681–687.
358. Krouwel PG, Kossen NWF. Biotechnol Bioeng 1981; 23: 651–655.
359. Kasche V. Enzyme Microb Technol 1983; 5: 2–13.
360. Dalili M, Chau PC. Appl Microbiol Biotechnol 1987; 26: 500–506.
361. Chang HN, Moo-Young M. Appl Microbiol Biotechnol 1988a; 29: 107–112.
362. Chang HN, Moo-Young M. In: Moo-Young M, editor. Bioreactor immobilized enzymes and cells: fundamentals and application. London, England: Elsevier Applied Science; 1988b. pp. 33–51.
363. Chen T-L, Humphrey AE. Biotechnol Lett 1988; 10: 699–702.
364. Monbouquette HG, Ollis DF. Ann N Y Acad Sci 1986; 469: 230–244.
365. Monbouquette HG, Ollis DF. In: Moo-Young M, editor. Bioreactor immobilized enzymes and cells: fundamentals and applications. London: Elsevier; 1988. pp. 9–31.
366. Vos HJ, Heederik PJ, Potters JJM, Luyben KChAM. Bioprocess Eng 1990; 5: 63–72.
367. Li X, Chen XD, Chen N. Biochem Eng J 2004; 17: 65–69.
368. Van Ede CJ, Dijkman H, Beenackers AACM. Can J Chem Eng 1992; 70: 534–542.
369. Van Ede CJ, Bollen AM, Beenackers AACM. Can J Chem Eng 1993; 71: 901–910.
370. Thibault J, Pouliot K, Agosin E, Pérez-Correa R. Process Biochem 2000; 36: 9–18.
371. Langley WG, Wu JS, Chao AC. J Environ Eng 2001; 127: 682–688. August.
372. de Gooijer CD, Wijffels RH, Tramper J. Biotechnol Bioeng 1991; 38: 224–231.
373. Wijffels RH, de Gooijer CD, Kortekaas S, Tramper J. Biotechnol Bioeng 1991; 38: 232–240.
374. Wijffels, RH. [PhD dissertation]. Wageningen, The Netherlands: Landbouwuniversiteit Wageningen; 1994.
375. de Gooijer CD, Wijffels RH, Tramper J. In: Melo LF, *et al*., editors. Biofilms-science and technology. Dordrecht: Kluwer Academic Publishers; 1992. pp. 291–296.
376. Wijffels RH, de Gooijer CD, Schepers AW, Beuling EE, Malée LF, Tramper J. Enzyme Microb Technol 1995; 17: 462–471.
377. Seki M, Furusaki S, Shigematsu K. Ann N Y Acad Sci 1990; 613: 290–302.
378. Furusaki S, Seki M. Adv Biochem Eng Biotechnol 1992; 46: 161–185.
379. Volesky B, Votruba J. Modelling of fermentation processes. Amsterdam: Elsevier; 1992.
380. Lefebvre J, Vincent J-C. Enzyme Microb Technol 1995; 17: 276–284.
381. Lefebvre J, Vincent J-C. Enzyme Microb Technol 1997; 20: 536–543.
382. Kuhn RH, Peretti SW, Ollis DF. Appl Biochem Biotechnol 1993; 39/40: 401–413.
383. Yabannavar VM, Wang DIC. Biotechnol Bioeng 1991; 37: 544–550.

384. Hunik JH, Bos CB, van den Hoogen MP, de Gooijer CD, Tramper J. Biotechnol Bioeng 1994; 43: 1153–1163.
385. Willaert R, Smets A, De Vuyst L. Biotechnol Tech 1999a; 13: 317–323.
386. Willaert R, Van de Winkel L, De Vuyst L. Proceedings European Brewery convention congress; Cannes, France; 1999b. pp. 663–670.
387. Nakasaki K, Murai T, Akiyama T. Biotechnol Bioeng 1989; 33: 1317–1323.
388. Sayles GD, Ollis DF. Biotechnol Bioeng 1989; 34: 160–170.
389. Monbouquette HG, Sayles GD, Ollis DF. Biotechnol Bioeng 1990; 35: 609–629.
390. Breguet V, Gugerli R, Pernetti M, van Stockar U, Marison IW. Langmuir 2005; 21: 9764–9772.
391. Al-Hajry HA, Al-Maskry SA, Al-Kharousi LM, El-Mardi O, Shayya WH, Goosen MFA. Biotechnol Prog 1999; 15: 768–774.
392. Goosen MFA. Ann N Y Acad Sci 1999; 875: 84–104.
393. Heath C, Belfort G. Adv Biochem Eng Biotechnol 1987; 34: 1–31.
394. Sharp NA, Daugulis AJ, Goosen MFA. Appl Biochem Biotechnol 1998; 73: 57–77.
395. Morvan D, Jaffrin MY. Int J Heat Mass Transfer 1989; 32: 995–1006.
396. Yuet PK, Harris TJ, Goosen MFA. J Arif Cells Blood Subst Immob Biotechn 1995; 23: 109–133.
397. Goosen MFA. In: Willaert RG, Baron GV, De Backer L, editors. Immobilised living cell systems: modelling and experimental methods. Chichester: John Wiley & Sons; 1995. pp. 295–322.
398. Frame KK, Hu WS. Biotechnol Bioeng 1988; 32: 1061–1066.
399. Zwietering MH, Jongerburger I, Roumbouts FM. Appl Environ Microbiol 1990; 56: 1875–1881.
400. Fan YZ, Wang YY, Qian PY, Gu JD. Int Biodeterior Biodegradation 2004; 53: 57–63.
401. Gompertz B. Philos Trans R Soc London, Ser A 1825; 115: 513–585.
402. Wen-Tao Q, Ying Z, Juan M, Yu-Bing X, Wei W, Xiaojun M. Biotechnol Bioeng 2006; 93: 887–895.
403. Pajic-Lijakovic I, Bugarski D, Plavsic M, Bugarski B. Process Biochem 2007; 42: 167–174.
404. Doran PM. Bioprocess engineering principles. London: Academic Press; 1997.
405. Luong JHT. Eur J Appl Microbiol Biotechnol 1983; 18: 249–253.
406. Radovich JM. Biotechnol Adv 1985a; 3: 1.
407. Radovich JM. Enzyme Microb Technol 1985b; 7: 2–10.
408. Gonzalez-Gil G, Seghezzo L, Lettinga G, Kleerebezem R. Biotechnol Bioeng 2001; 73: 125–134.
409. Orive G, Hernandez RM, Gascon AR, Calafiore R, Chang TMS, de Vos P, Hortelano G, Hunkeler DD, Lacic I, Pedraz JL. Trends Biotechnol 2004; 22: 87–92.

50

FERMENTER/BIOREACTOR DESIGN

MARVIN CHARLES
Lehigh University, Bethlehem, Pennsylvania
JACK WILSON
ABEC, Inc., Allentown, Pennsylvania

50.1 INTRODUCTION

50.1.1 Scope

The scope of this chapter is limited to design of agitated vessels used for aerobic, single-cell (bacteria and yeast), and filamentous (bacteria and fungi) fermentations. It presents general design principles, combining basic concepts with practical matters including regulatory compliance, safety, maintenance, cleanability, ease of use, and cost, all of which are strongly interrelated. It focuses primarily on fermenters used to produce human and animal health products or their precursors, but the general approaches discussed are applicable to other types of products (e.g., industrial enzymes, food products); the primary differences are emphasized.

Included in the presentation are fermenter vessels; agitation; aeration; heat transfer; sterilization; cleaning; and piping systems. Control and data acquisition are discussed only to the extent that they influence the items already noted.

It is assumed that the reader is familiar with the basics of fermentation, general fermenter construction, and nomenclature. Those not having such background are advised to consult basic references (1–3).

50.1.2 Design Philosophy

Our basic philosophy comprises the following simple principles:

1. Each design case has unique requirements and calls for individualized application of the basic design concepts and practices discussed herein. The one-size-fits-all approach usually results in sleeves that drape into your food, arm holes that cut off circulation, pant legs that are made to trip over, or some combination of these features and others. The magic number approach—all problems have simple solutions based on codified numbers such as fixed geometric ratios (4)—leads to the same place.
2. Successful design requires a systems approach. A fermenter is a system that is part of a process system, and the process is part of a plant system. All these systems interact with each other, with real people, with control systems, and with other systems related to regulatory compliance, safety, documentation (including protocols, SOPs, etc.), change control, maintenance, and so forth. Failure to take these interactions into account during fermenter design usually results in considerable pain, not only for those guilty of the omission, but also for innocents who were never asked for planning and/or design input, but who must live with the result. Note that appropriate documentation, protocols, SOPs, change control, and so on should be considered important elements of design and operation of any plant, licensed or not.
3. Compromise is always necessary. Nothing in any project is 100% right, and nothing has to be. He or she who looks for 100% of anything will hold up a

Upstream Industrial Biotechnology: Equipment, Process Design, Sensing, Control, and cGMP Operations, Volume 2, First Edition. Edited by Michael C. Flickinger.
© 2013 John Wiley & Sons, Inc. Published 2013 by John Wiley & Sons, Inc.

project needlessly and will generate a lot of animus. (The words actually used in such cases cannot be used here.)

4. The time to be thinking about all of these points is prior to and during design, not when you're standing on the plant floor trying to validate a continuous mixer that has only one port and no instrumentation.

We discuss next the bases for safety and regulatory considerations, primarily to sensitize readers to these issues early on. They are all too often overlooked during early stages of design, when the focus is on satisfying process requirements (e.g., oxygen transfer). Unfortunately, this frequently leads to important constraints being ignored and hence to designs that require expensive and often cumbersome "fixes."

50.2 SAFETY AND REGULATORY COMPLIANCE

All fermenter designs are influenced by safety and regulatory factors, the extent depends on (1) the nature of the product and its intended use, (2) the process, and (3) the nature and location of the facility. For example, even fermentation products not regulated by the U.S. Food and Drug Administration (FDA) must adhere to safety requirements, which in some cases are very strict. Furthermore, no professional design can escape the effects of a long list of code requirements, for example, the ASME pressure vessel code (5). By the same token, not all products that are FDA regulated are equally affected by safety, regulatory, and code requirements. We must consider each case on the basis of its own unique requirements.

Our objective in the rest of this section is to introduce some of the requirements and to provide some rational bases for their implementation, details of which are discussed later. Much of the discussion is directly applicable to fermenters used for production of human or animal health products or for their precursors, but also applies to other cases to varying extents.

50.2.1 Containment: Worker and Community Biosafety

A fermenter must be an integral part of a system designed to insure safety at three levels: product, worker, and community. Many of the methods used to protect the product also serve to protect the plant personnel and the community (e.g., use of closed systems and HEPA filters); however, there are potential points of conflict (6). For example, some containment practices that call for completely welded hard piping to a contained drain line for any condensate that could be exposed to culture fluid could expose the product to drain line contaminants. One resolution of this problem is to use steam locks in all such lines. All such conflicts encountered to date have been resolved, but not always easily or relatively inexpensively.

Insurance of product safety is tied primarily to compliance with FDA (or similar organizations) regulations. This will be considered in the subsection "Product Safety". Here we deal with worker and community safety.

Protection must be provided against potential ill effects of fermentation products (e.g., cytotoxins, allergens), organisms (e.g., pathogens, whether recombinant or not), fermentation byproducts (e.g., pharmacologically active precursors of the active product), or some combination. The practice of providing such protection is called *containment*, which is defined as insuring that deleterious fermentation components can't be transported to any area inside or outside the plant before they have been rendered harmless. To accomplish this, containment must be exercised at several levels (7). We consider in this chapter only direct or "primary" containment of fermenters; however, one should not lose sight of the fact that the other levels must be considered during fermenter design, if for no other reason than to ensure that the fermenter design and operation will be consistent with the overall containment strategy.

Containment levels have been defined by the National Institutes of Health (NIH) (8), based on the potential danger of organisms. These levels, in increasing order of potential danger are GILSP, BL1-LS, BL2-LS, BL3-LS, and BL4-LS. (BL4-LS must be handled on a case-by-case basis in consultation with the Centers for Disease Control and others. It is, thank goodness, well beyond our scope.) There are other classifications that have been developed in the United Kingdom (9), the European Union (10), and elsewhere, but these do not differ markedly from the U.S. scheme. It is important to know that (1) all of these guidelines address what must be accomplished but not how they should be accomplished, and (2) there is not complete agreement on what is actually required to implement the guidelines. In addition, the guidelines do not address containment of products. Although many of the considerations for product containment are the same or very similar to those for organism containment, there are some very important differences. Here, we confine our attention to organisms; the interested reader should consult the Refs 11–14 for more specific information concerning hazardous products. One also should consult U.S. Environmental Protection Agency (EPA) regulations applicable to microorganisms and their products.

Most existing processes use organisms that require either GILSP or BL1-LS containment; nevertheless, many plants are built to satisfy requirements for BL2-LS (actually, somewhere between BL2-LS and BL3-LS). The reasons for this include satisfying FDA requirements (e.g., safety of the product) and the fact that the additional cost is not large and is relatively cheap insurance. There also

is the oft-stated reason that such a route insures greater flexibility for future operation (15). One might add to this the fact that the rules are not well established and that requirements could change substantially between the time of design and the time production begins. It also is worth noting that there is growing interest in using organisms that do, in fact, require BL2-LS and even BL3-LS containment, which will probably focus greater attention on further development of acceptable implementation practices as well as changes in the guidelines. Note that equipment requirements and cost for BL2-LS and BL3-LS are currently about the same (this probably will change); BL3-LS facilities requirements and cost are very much greater than for BL2-LS.

Finally, it is important to note that containment is nothing new. Highly pathogenic organisms have long been used to produce therapeutics and biological warfare components; hence, there is a considerable body of experience dealing with the subject (11,16). There also is considerable guidance to be had from the nuclear industry; nevertheless, the natures, sizes, and large number of new commercial processes, along with new methods, materials, and so on, will force heightened awareness, scrutinity, review, and modernization or change.

50.2.2 Physical Safety

Most physical safety issues are addressed by U.S. Occupational Safety and Health Administration (OSHA) requirements (17) and by various national codes such as the ASME Pressure Vessel Code (5) and the National Electrical Code. There also are many local construction codes that must be satisfied. Among these are various earthquake-resistant construction codes that are also applicable to containment considerations. And then there are the requirements of the final arbitors: the insurance companies.

50.2.3 Product Safety

We focus here on FDA requirements, but the reader is urged to keep in mind that he or she also must consider those of other regulatory agencies and be aware of the unsettling facts that it is not always clear which agency has jurisdiction, and there often are conflicting requirements.

The primary purpose of FDA regulations is to insure product safety, purity, and efficacy. The legal bases for the regulations and their enforcement can be found in the *Code of Federal Regulations* (CFR) (18) and a number of other FDA documents such as *Points to Consider* (19,20), *Inspection Guides* (21,22), and *Guides to Industry* (23,24). Industrial implementation of all the regulations, along with ongoing improvements, is referred to as current good manufacturing practices (cGMP).

There is an endless stream of writings in professional journals, short courses, and such concerning the regulations and cGMP practice. Unfortunately, there is a great deal that is not covered clearly in writing, and there is a constant proliferation of new and/or revised guidelines followed closely by lots of (frequently conflicting) interpretations and opinions. In addition there has been a problem of nonuniform application. For example, regulatory scrutiny has been far stricter for fermenters used to produce active molecules directly than for those used to produce precursors; there has been considerable variation from product to product within a given class; and manufacture of human drugs has been regulated much more rigidly than manufacture of animal drugs. While understandable to some extent, such nonuniformity has caused considerable confusion. These gaps are beginning to be closed, and this may have considerable influence on the design of fermenters—particularly those used to produce precursors and animal drugs.

In simplest terms, cGMP requires that the combination of fermentation process equipment and operating protocols must consistently yield product that meets acceptable specifications and is capable of being converted/purified consistently to final product, meeting approved product specifications. From this general sense of intent it can be argued that failure to have control over the fermentation puts the final product at risk. Few would argue with this general concept; however, there is considerable debate as to interpretation and extent.

Requirements that flow from the need to have control are based on relatively simple ideas:

1. If an organism is subject to environmental, medium, or other conditions outside the range in which it is known to yield product meeting acceptable specifications and capable of being converted/purified consistently to final product meeting approved product specifications, then we have no guarantee that it does not produce other products with which the recovery system can not cope and that can escape detection by the analytical methods in place.
2. If a fermenter becomes contaminated with other microbes, said microbes could produce toxins that could be carried undetected to the final product. It is possible that this could occur without altering the behavior of the process organism. It also is possible that products of the contaminant could cause the process organism to make toxins that could go undetected into the final product. Given these possibilities, plus the fact that it is not possible to prove that the contaminant will always be the same, evidence of contamination is evidence for lack of control.
3. If a fermenter is not cleaned properly, deleterious microbial or nonmicrobial products could remain to

> contaminate the next batch in such a way that impurities could be carried undetected to the final product. Similar statements can be made about other contaminants introduced via other routes as a result of poor cleaning practices.

Again, it is unlikely that many would argue with these points, but again there is considerable debate as to interpretation and extent.

Requirements 1–3 can be translated to specific requirements for, among other things, controllability and reliability of fermentation conditions, sterilization, and aseptic and cleaning operations. Controllability requires that the fermenter and its subsystems be designed and constructed in ways that make possible control of environmental variables within the operational ranges required. This obviously means that mechanical design must be in harmony with control system design.

Sterilization/aseptic operation translates to (1) destroying any microbial contaminants that may be present in any part of the equipment that might contact process fluids and (2) insuring that no microbes (other than the production organism) can enter after the equipment has been sterilized. The latter embodies the concept of the "sterile barrier." To these ends, the following apply:

- The fermenter and all its ports and direct attachments must be sterilizable.
- All piping that will contact process fluids (including additives) and/or provide paths into the system (e.g., the air exhaust line) must be sterilizable initially. Some (e.g., sampling lines, addition lines) must also be sterilizable at any time during a fermentation.
- Inlet gases (e.g., air, oxygen) and all additives (e.g., medium components, acid, base, antifoam) must be sterilized before they contact any sterile process piping.
- All penetrations (e.g., drive shaft, probe ports) must be sterilizable.

The preferred sterilization method is automatic sterilization-in-place (SIP) with steam. This is discussed at length later.

Clean operation requires, among other things, the following:

- The system must be designed such that any surface that can contact a process stream can be cleaned consistently to a level that insures that the product will be free of soils resulting from a fermentation.
- Nothing in the system that comes in contact with process fluid can introduce unacceptable and unidentifiable materials.

Note (for example) that 21 CFR 211 (Part D) (guidelines for design of equipment for licensed facilities) does not have any specific requirements for fermenter sterilization or cleaning; however, the preceding discussion coupled with the intended use and cGMP concepts makes it difficult to to argue the point. But again, there remain the questions of rational interpretation and extent of application.

Riding along with cGMP is the practice of validation. This is an extensive, expensive, and controversial area for which and about which reams of reams have written. Following is the formal definition of validation:

> Establishing documented evidence that provides a high degree of assurance that a specific process will consistently produce a product meeting its predetermined specifications and quality attributes (25).

What this means is that not only does the equipment have to be designed, installed, and operated so as to run consistently within well-defined ranges of process variables to consistently yield product that meets acceptable specifications and is capable of being converted/purified consistently to final product, meeting approved product specifications, but that there must be adequate documentation to prove this before product can be sold. In addition, one must demonstrate that this goal can be achieved under so called worst-case conditions; there is often considerable debate as to what this really means (26). It is beyond our scope to consider validation in detail. Suffice it to say that it can translate to checking and testing every component of the equipment and documenting not only its proper function but also its history. The brave of heart are referred to the bulging literature on the subject; Refs 27–30 provide a start.

All of this means we must take great care to consider *all* the details, such as materials, corrosion issues, machining methods, vendors, welds, and types of steam and water, keeping in mind that all must be considered as part of a system that must interface "seamlessly" with the systems of cGMP and validation. Failure to consider this before and during design is almost always very costly. Design should be done so as to facilitate validation, and subsequently, routine cGMP operation, maintenance, and so forth. "Simple" things such as judicious placement of access valves and piping isolation can go a very long way to ensuring minimum pain and maximum operability. Having said all this, we reiterate that not all fermenters are subject to all these requirements, and even those that are, are subject to them in varying degrees (at least in practice).

50.3 DESIGN BASIS AND OTHER GENERAL CONSIDERATIONS

A design basis for fermentation equipment should derive from a facility/process design basis. The latter should

include (among other items) the general nature of the facility (e.g., research and development vs. production, single product vs. multiuse); product(s) specifications; regulatory, containment, and other requirements; level of automatic operation; general processing scheme (e.g., batch); nature of individual process steps; productivity, concentrations, and so forth; cleaning requirements; special considerations (e.g., earthquake-proof construction); critical valving and instrumentation; staffing requirements and constraints; architectural and general floor plan constraints; and utilities. Most of these will have some influence on fermenter design—some in more subtle ways than others.

It is difficult to overstate the importance of the initial definition that will derive from the design basis. Obviously, a rational design basis for a fermenter must also be based on fermentation characteristics as well as operating cycle and productivity required (which should derive from the overall process design basis). From these will flow the sizes and number of vessels, and definitions of oxygen transfer, heat transfer, power, and bulk mixing requirements. The design must satisfy these but must also satisfy requirements for regulatory compliance, safety, cleaning, facile operation, and maintenance. All of these factors are highly interactive (e.g., design for oxygen transfer affects design for cleaning); hence, responsible design will almost always require several iterations to ensure the greatest probability of success and to minimize lost time caused by installation, operation, and various problems. The iterative nature of the design (and, unfortunately, construction) process makes most important the existence of a well-crafted, well-implemented, and well-documented change control process. Finally, as with any engineering project, failure to have a solid basis of design, a complete scope, accurate process flow diagrams and piping and instrumentation diagrams (P&IDs), and accurate process timing will almost certainly result in added cost, lost time, and worse.

50.4 PROCESS REQUIREMENTS: BASICS

One of the first steps in fermenter design is translation of process demands to oxygen transfer, heat transfer, bulk mixing, and power requirements—the so-called transport processes (TPs). Sound translation is not straightforward because the TPs interact not only with each other, but also with vessel geometry and other design factors. The nature of each TP and the relationships among them vary with the process requirements. They also vary significantly with the basic nature of the organism and the culture broth. The major factors here are the rheological nature of the broth and the sensitivity of the organism to fluid mechanical forces. In some cases, sensitivity of the organism to temperature and other environmental factors, such as pH, impose tighter constraints (e.g., wall temperature control, uniformity of mixing).

Single-cell organisms (most bacteria and yeasts) tend to tolerate fluid forces very well (there are a few exceptions) and tend to have low-viscosity, Newtonian broths. Mycelial organisms (fungi and some mycelial bacteria such as streptomycetes) tend to be more prone to damage by fluid mechanical forces than are single-cell organisms and tend to have high-viscosity, non-Newtonian broths. Detailed discussion of all these factors is beyond the scope of this chapter; however, we now discuss a few points concerning rheological behavior, and point to fluid effects wherever appropriate in the remainder of the chapter.

50.4.1 Broth Rheology and Its Effects on Transport Processes

Newtonian viscosity depends only on composition and temperature; the nature of the fluid motion does not affect it. Non-Newtonian viscosity does depend on the nature of the fluid motion. This dependency is usually expressed in terms of fluid shear rate (a measure of how rapidly fluid velocity changes from one point to another point close by).

There are several types of non-Newtonian behavior (e.g., pseudopalstic, Bingham) that can be described quantitatively by a host of mathematical models. One model used frequently to describe non-Newtonian fermentation broths (31–33) is the so-called power law:

$$\eta = K\gamma^{(n-1)} \tag{50.1}$$

where η is viscosity, γ is shear rate, and n and K are constants. Such relationships can be useful if one has rheological data for the subject broth and if the design correlations used incorporate rheological properties in a meaningful and accurate way. It is seldom that either of these conditions is satisfied, and almost never that both are satisfied. Also, there is a considerable amount of misleading and/or inaccurate information in the literature concerning broth rheology, its measurement, and its use; the reader is cautioned to tread carefully in this area (4,34). If accurate viscosity information is available, it can be a valuable qualitative and sometimes semiquantitative guide, if interpreted and used properly.

Mass transfer (oxygen), heat transfer, and bulk fluid motion all depend strongly on rheological characteristics. Generally, all are poorer in non-Newtonian than in Newtonian broths; indeed, the rheological characteristics of mycelial broths can and do impose severe constraints. Two of many examples are the following:

1. Heat and oxygen transfer rates tend to be anywhere from 50 to 5% of what they would be for typical (e.g., *Escherichia coli*) bacterial fermentations.

2. Bulk mixing quality (homogeneity) is much poorer than in typical Newtonian broths; therefore, accurate monitoring and control are much more difficult.

Difficulties associated with viscous, non-Newtonian rheology also extend to other areas such as cleaning.

50.4.2 Oxygen Transfer/Aeration

Please note that in this and subsequent sections we include design and operating rules of thumb based on our experience and the experiences of others. They are intended to be helpful guides, not edicts.

50.4.2.1 Requirements. Oxygen transfer rate (OTR) requirements are usually dictated by conditions during the most active part of the growth phase (other phases require oxygen, but supply rate usually is not as high). The requirement is calculated from

$$\mathrm{OTR} = (Y_{x/\mathrm{o}})^{-1}(\mu X)_{\max} \tag{50.2}$$

where μ is the specific growth rate (h^{-1}), X is the cell mass concentration (g/L dw), and $Y_{x/\mathrm{o}}$ is the cell yield coefficient on oxygen (g cells dw/g O_2). Note that the maximum growth rate and maximum cell mass are not always reached simultaneously.

50.4.2.2 Satisfying the Oxygen Material Balance: Gas Flow and Linear Velocity. The very first thing we must do in satisfying an OTR requirement is to insure that we have a closed oxygen material balance. For most practical operating conditions, the rate of change of oxygen inventory in a fermenter is very small compared to oxygen flows in the inlet and outlet and to the OTR. It also can be demonstrated easily that the total molar flow rate of gas does not change enough to cause any loss of sleep. Given these practical realities, the oxygen material balance is

$$\mathrm{OTR} = (1,000 \times 60)\mathrm{F}(y_{\mathrm{in}} - y_{\mathrm{out}})/V_{\mathrm{L}} \tag{50.3}$$

where, F is the gas flow rate (mol/min), y is the mole fraction of oxygen in the gas, and V_{L} is the liquid volume (L). Note that the usual units for OTR are millimoles per liter per hour and that the factors of 1,000 and 60 in equation 50.3 are conversion factors needed to keep unit consistency.

The material balance also can be expressed as

$$F = \mathrm{OTR} \times V_{\mathrm{L}}/(1,000 \times 60\ \varepsilon y_{\mathrm{in}}) \tag{50.4}$$

where ε is the oxygen transfer efficiency and y_{in} is the oxygen mole fraction in the inlet gas. Equation 50.4 is a more useful form because we know that under practical conditions ε will be between 0.15 and 0.35 for typical Newtonian broths, and between 0.05 and 0.15 for typical non-Newtonian broths.

As a general rule, heroic efforts will be required to get OTRs over 300 mmol/(L h) in large fermenters (>5,000 L). Even if the effort is expended and it is successful, it will usually create heat transfer problems (see later) that will require even greater effort to overcome. Our advice is to consider other options very seriously.

The material balance provides information about the gas volumetric flow rate, which often is expressed as the standard flow, v_{std}, in units of standard liters per minute (SLPM):

$$v_{\mathrm{std}} = 22.4F \tag{50.5}$$

This is useful because most flow meters are calibrated in terms of standard flow; however, actual flow is more useful for fermenter design purposes. One problem encountered in calculating the actual flow is that it increases from the bottom to the top of the broth because of pressure change. As a practical matter, however, it is usually adequate to use the average pressure in the tank:

$$v_{\mathrm{act}} = v_{\mathrm{std}} \times (1/P_{\mathrm{avg}})(T_{\mathrm{f}}/298) \tag{50.6}$$

where v_{act} is the gas flow at average pressure (L/min), P_{avg} is the average pressure (atm, abs), and T_{f} is the fermentation temperature (K). One might want to revisit this for very tall vessels.

The standard gas flow rate also is expressed in standard gas volumes per liquid volume per minute (VVM).

Among the important information that can be obtained from v_{act} is the gas linear velocity, V_{S} (cm/min):

$$V_{\mathrm{S}} = 4 \times 1000\ v_{\mathrm{act}}/(\pi \times D_{\mathrm{t}}^2) \tag{50.7}$$

where D_{t} is the inside diameter of the fermenter. V_{S} affects mass transfer, deliverable power via the impellers, foaming, gas holdup, and aerosol formation. As a rule of thumb, V_{S} should be held below 200 cm/min to avoid problems associated with excessive gas holdup, foaming, and aerosol formation. These effects are discussed later.

50.4.2.3 Mass Transfer. The rate at which oxygen can be transferred is dictated by three factors: the driving force, the resistance to transfer, and the contact area between the gas and liquid phases. This is usually expressed as

$$\mathrm{OTR} = K_{\mathrm{g}}a(\Delta P)_{\mathrm{LM}} \tag{50.8}$$

where K_{g} is the mass transfer coefficient ([mmole M]/[L h atm]), and a is the interfacial area per unit volume (M^2/M^3). $(\Delta P)_{\mathrm{LM}}$ is the log mean pressure driving force, defined as

$$(\Delta P)_{\mathrm{LM}} = \left(P_{\mathrm{O,in}} - P_{\mathrm{O,out}}\right) / LN\left[\left(P_{\mathrm{O,in}} - P_{\mathrm{O}}^{*}\right) / \left(P_{\mathrm{O,out}} - P_{\mathrm{O}}^{*}\right)\right] \tag{50.9}$$

where $P_{O,in}$ is the partial pressure of oxygen in the gas inlet (atm, abs), $P_{O,out}$ is the partial pressure of oxygen in the gas outlet (atm, abs), and P_O^* is the partial pressure of oxygen that would be in equilibrium with the dissolved oxygen concentration in the existing liquid (atm, abs). Note that use of the log mean driving force assumes that the liquid is mixed perfectly (homogeneous liquid phase) and that the gas moves in plug flow through the fermenter. These assumptions are acceptable for most low-viscosity Newtonian broths, but they can be quite poor for high-viscosity, non-Newtonian broths. Unfortunately, no useful alternatives have yet been proposed; therefore, extra caution should be exercised in interpreting calculated results for non-Newtonian broths.

Other mass transfer coefficients are used for driving forces other than $(\Delta P)_{LM}$. The most common among these is $k_l a$ (min^{-1}), which is used in conjunction with a dissolved oxygen concentration driving force. The reader is cautioned that $K_g a$ and $k_l a$ are sometimes confused with each other—even in the literature.

A given OTR requirement can be satisfied by various combinations of driving force and mass transfer coefficient. It is important to note, however, the following:

- Factors that influence driving force also can influence $K_g a$.
- Each combination will have different effects on the ultimate design of the vessel, piping system, and support systems, as well as on operational factors related to regulatory compliance cleaning, maintenance, and so on. Such effects are discussed as we proceed.

Driving force is affected by total pressure, gas inlet oxygen mole fraction, total gas flow rate, and the dissolved oxygen concentration. Total pressure and oxygen mole fraction affect the oxygen partial pressure directly. The effect of total gas flow is a bit more subtle. For a given oxygen transfer rate, increasing the total gas (fixed inlet conditions, pressure, etc.) increases the mole fraction of the outlet gas flow, thereby increasing the average mole fraction of oxygen in the gas; hence, the average driving force is increased. This can be seen quantitatively via an oxygen material balance which gives

$$P_{O,out} = P_{O,in} - OTR \times P/(1,000\ F) \qquad (50.10)$$

where P is the total absolute pressure (atm) and F is the total molar flow (mmol/h) of gas.

The characteristics of K_g and a are complex and not completely understood. Our first clue to this is that $K_g a$ is expressed as a product in terms of empirical correlations (we don't understand enough about them to get reliable quantitative guidance from first principles). Typical correlations have the form

$$K_g a = \delta \times \left(P_g/V_L\right)^{\varphi} (V_S)^{\kappa} \qquad (50.11)$$

where P_g is the power delivered to aerated broth (HP), V_L is the unaerated liquid volume (L), and δ, ϕ, and κ are usually advertised as constants. There also a several variations on this form. A discussion of all the fine points of such correlations is beyond our scope; however, the the reader should take note of the fact that published correlations usually cannot be relied upon to provide accurate predictions. They should be used as qualitative or semiquantitative guides only. Reasons for this caveat include the following:

- They are usually applicable only under conditions at or near the ones used to develop them. Unfortunately, most are developed at scales and under conditions that are not realistic for production.
- They can have pronounced dependence on fermenter geometry.
- They do not scale up well, or at all. The "constants" in equation 50.11 and its relatives usually aren't constant.

These caveats should be made more emphatically for viscous non-Newtonian broths than for Newtonian broths because non-Newtonian rheological characteristics can have profound effects on $K_g a$ (as well as the other transport properties). Most $K_g a$ correlations do not account for broth rheology. Those that do, usually do so inadequately or in ways valid only for a particular broth. It also is important to note that the broth rheology can vary dramatically during a fermentation and that the rheological characteristics can be affected by the fermentation conditions, ranging from the nature of the inoculum to the history of the agitation speed.

As noted earlier, we can get some qualitative guidance from the form of equation 50.11. We'll do that, but please keep in mind that the relationships are highly nonlinear, the factors that influence $K_g a$ are dependent on each other in practical operation, and it is not always possible to control variables at the levels you would like. For example, equation 50.11 predicts that increasing power input per unit liquid volume will increase $K_g a$. This usually turns out to be true in practice if the power can actually be delivered to the fluid and delivered in a manner that will contribute to $K_g a$. Such might not be true in any given case.

The fact that a drive's power rating is 100 hp doesn't mean that 100 hp can be delivered to the broth. Deliverability depends on, among other things, geometry (vessel and agitator), rheology, agitator speed, and gas linear velocity (see later). The effects of all are complex and interactive; the interrelations are more complex for non-Newtonian broths than for Newtonian broths. The manner in which

power is delivered depends largely on impeller type and broth rheology. For example, oxygen transfer rates to highly viscous, non-Newtonian mycelial broths have been shown to be larger for A-315 (hydrofoil) impellers than for Rushton (disk turbine) impellers delivering the same power (35). There appears to be no meaningful difference for Newtonian broths.

The bottom line is that one should try to obtain experimentally determined correlations for the subject organism and broth at meaningful scales. Failing that (which usually is the case because of time and resource constraints), one should try to use correlations developed for systems as similar as possible to the one at hand. Considerable art is involved here.

The reader can find more about $K_g a$ in the literature (35–38).

50.4.3 Power

Power delivered to the broth is used for micromixing and gas dispersion, which are related to mass transfer, and macromixing, which provides overall homogeneity (discussed later). Agitated vessel power is delivered via two mechanisms: direct mechanical power from the impellers and gas expansion. The bulk (>90%) of the power comes from the impellers as long as the fluid motion is under their control, a condition that prevails so long as the impellers are not flooded. There are reasonably reliable correlations available to determine flooding conditions for Newtonian broths (39); however, flooding usually is not a problem under typical conditions used in most Newtonian broth fermentation. Flooding is more likely in highly viscous, pseudoplastic broths typical of mycelial and polysaccharide fermentations because the viscosity near the impeller is much lower than in the rest of the broth. As a result (assuming air is introduced under the impeller), air tends to channel toward the impeller, thereby enshrouding it and decreasing the deliverable power (4). This can dramatically decrease overall mass transfer (and heat transfer) rates and quality of bulk mixing quality (see later). Reliable flooding correlations for non-Newtonian broths have not been published, but some companies have accumulated a considerable amount of data for the fermentations they practice.

Calculation of power input relies on empirical correlations. As with $K_g a$, many correlations have been published (see for example Refs 40–42), but they are not particularly reliable for many of the same reasons given for the unreliability of $K_g a$ correlations; therefore, we give the same advice here as we did for $K_g a$.

Among the more popular approaches used is the one that relies on the aeration number, N_A (dimensionless), defined as

$$N_A = v/N D_i^3 \tag{50.12}$$

where v is the gas volumetric flow rate (m^3/min), N is the agitation speed (min^{-1}), and D_i is the impeller diameter (m). Published correlations give the ratio of gassed power to ungassed power as empirical functions of N_A:

$$P_g/P_{ug} = \text{Func}\,(N_A) \tag{50.13}$$

where P_{ug} is the power delivered to the same broth agitated under the same conditions but unaerated.

Each such correlation pertains to a specific impeller type, a single fermenter geometry, and a fairly narrow range of operating conditions. In some such correlations (40), a unique function is presented for each impeller type (Fig. 50.1). In others the relationship is shown not to be unique (43). In most cases, the correlations are for a single aerated impeller. The situation is more confusing for non-Newtonian broths.

Obviously, to use equation 50.13 one must be able to calculate the ungassed power. This can be done via other empirical correlations that give ungassed power in terms of the dimensionless power number (N_P), defined as

$$N_P = P_{ug} \times g_c/N^3 \times D_i^5 \times \rho \tag{50.14}$$

where g_c is Newton's law conversion factor, and ρ is the ungassed broth density (lb/ft^3). There are published correlations that give N_P as a function of Reynolds number for a wide range of single impellers (44). Each is specific to a particular vessel geometry, liquid height, and so forth. Interestingly enough, there are fairly reliable correlations for Newtonian and non-Newtonian fluids so long as the constraints of the correlations are observed.

It is important to note that some impellers that have high power numbers under unaerated conditions can "unload" considerably under aerated conditions. For example, it is fairly typical for a Rushton turbine to deliver, under aerated conditions, only 40% of the power it can deliver when unaerated. On the other hand, the

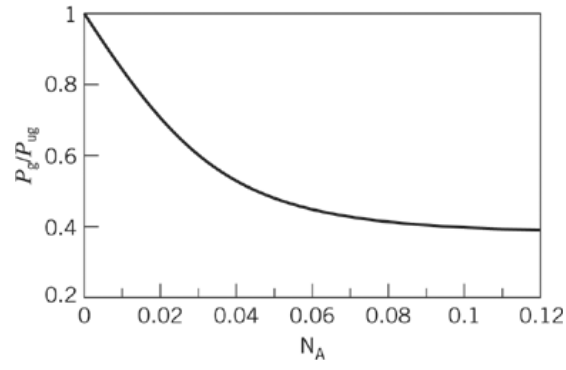


Figure 50.1. Power ratio as a function of aeration number for a Rushton turbine.

SCABA 6SRGT (45), which is a curved-blade disc turbine, does not tend to unload at all. Some hydrofoils also exhibit very little unloading. This is an important consideration when one is trying to rank impellers in terms of how much power they can deliver for oxygen transfer purposes. (Often the ranking tends to be done qualitatively or "semiquantitatively.")

50.4.3.1 Multiimpeller Systems. Most fermenters are equipped with more than one impeller. The reasons for this are to improve bulk mixing (see later) and power distribution and to avoid the need for very large impellers and/or very high agitator speeds. Impeller size is limited practically not only by vessel internals but also by the following:

- *Torque transmitted to the drive shaft*. The larger the torque, the stronger and thicker the shaft must be. This also translates to higher torque and more expensive gear boxes.
- *The size of the vessel manway*. This is particularly important if the impellers must be single piece for better cleaning/sterilization characteristics.

Agitator speed is limited by the natural frequency of the agitation system (4). This is because severe and potentially dangerous vibrations will occur if the rotational speed of the agitator approaches the natural frequency. We recommend that the maximum shaft speed not exceed 70% of the natural frequency.

Having said all this, we are left with the problem of doing the power calculations. This usually involves an iterative calculation in which the parameters are (assuming we have selected impeller types) number of impellers, impeller diameter(s), and shaft speed. (There are other considerations we discuss later.) To do this we use the power correlations already noted. But these usually apply only to single impellers. In most cases, they apply to the lowest impeller, which is the one under which inlet air is introduced. Several approaches have been suggested. The simplest is to treat all the impellers as though each is the only one present. Among other things, this assumes that the impellers do not interact with each other. There is empirical evidence (46 pp. 264–266) that Rushton turbines will not interact substantively in Newtonian broths if they are spaced at least an impeller diameter apart. Obviously, the assumption of noninteraction is not meaningful for impellers that produce significant axial flow (see later).

Another approach used frequently, but not recommended by the authors, is to use the correlations for the lowest impeller but to use them for the upper impellers:

$$P_g/P_{ug} = (1 + \mathrm{HU})^{-1} \tag{50.15}$$

where HU is the gas holdup. You guessed it: there are empirical correlations for HU. One example for Newtonian broths is (47)

$$\mathrm{HU} = 1.8\left(P_g/V_L\right)^{0.14} V_S^{0.75} \tag{50.16}$$

The usual caveats apply.

Typical values for gas holdup range from about 0.1 to 0.3; therefore, equation 50.15 predicts about 10–20% unloading for the upper impellers. Aeration number correlations predict around 50–60% unloading. Given the uncertainty in all this, and assuming that no other (reliable) information is available, we suggest the more conservative approach of applying the aeration number correlation to each impeller independently.

The added cost for the larger drive will not be a major factor for vessels up to about 5,000 L; this is fairly cheap insurance. One should do pilot agitation studies at a meaningful scale for much larger vessels.

50.4.3.2 Organism Sensitivity to Fluid Mechanical Forces. Finally, an additional constraint must be imposed if the organism is sensitive to fluid mechanical forces. This is seldom true of unicellular organisms. There are, however, some mycelial organisms that are sensitive. The extent of sensitivity and the nature of the forces that cause damage should be determined experimentally. One also should keep in mind that the character of fluid forces changes significantly with scale. For example, some turbulent forces that are negligible at small scale can be large and potentially destructive at large scale. Reliable guidance in this area is almost nonexistent. There is, however, a rough rule of thumb that states that damage will occur if impeller tip speed exceeds 1,500 ft/min. Bear in mind that this rule was developed almost 50 years ago and was based on information for organisms used at that time in vessels that had working volumes in the 30,000 to 50,000-gal range. It is clear that many factors (including broth rheology) will affect the potential for damage. Unfortunately, most of the information is seldom available when needed. In such cases, the "any port in a storm" approach to design usually becomes operable. Fortunately, we seldom encounter a circumstance in which the rule of thumb must be violated.

50.4.4 Bulk Mixing

Good bulk mixing is needed to insure homogeneity, which is required for reliable data acquisition and control. There are several important factors that affect mixing quality.

Broth rheology. This is the primary factor affecting our ability to provide good mixing quality, but we seldom have any control over it. We simply must recognize that we will have to go to greater and greater lengths as the

broth becomes more viscous and non-Newtonian. Also, one must bear in mind that the nonlinear behavior of most non-Newtonian fluids often results in nonobvious responses to various actions. For example, increasing agitator speed in a highly non-Newtonian, pseudoplastic broth often leads to a decrease in power input and a decrease in bulk mixing quality.

Type(s) of impeller(s). Impeller types fall into three basic categories: radial flow (e.g., Rushton turbine), axial flow (e.g., marine propellor), and mixed axial and radial flow (e.g., Lightnin' A-315). Radial flow impellers tend to deliver the high power required to enhance micromixing and mass transfer but do not promote top-to-bottom mixing; therefore, they are not the best choice for promoting homogeneity. Multiple radial flow impellers often are used in an attempt to compensate for poor bulk mixing. This can work fairly well for low-viscosity Newtonian broths when the ratio of liquid height to tank diameter does not exceed 1.7–2, but it is a very poor solution when the broth is very viscous and highly non-Newtonian. Anyone who has observed classical streptomycete or xanthan gum fermentations can attest to this fact. Pure axial flow impellers do not deliver much power but do tend to promote good top-to-bottom mixing and hence contribute significantly to bulk homogeneity. They do not, however, contribute much to mass transfer. Some mixed flow types appear to provide a good balance between bulk mixing and mass transfer requirements, particularly for non-Newtonian broths. We recommend that they be considered seriously for such cases. We also have had considerable success with combination systems, for example, those with turbines as the lower impellers and a hydrofoil on top. This appears to work well for Newtonian and non-Newtonian broths.

Impeller size(s). In most cases, large-diameter impellers distribute power better and promote bulk mixing better than do small-diameter impellers. As a rough rule of thumb, based on considerable empirical evidence, we recommend D_i/D_t ratios of between 0.4 and 0.5 unless some other constraint (e.g., torque) is violated. Exceptions to this are some cases in which an axial flow impeller is the top impeller. In such cases, the ratio should not exceed 0.35 to avoid the risk of vortexing. This is particularly true for low-viscosity Newtonian broths.

Vessel geometry. We suggest that the ratio of the aerated liquid height to the tank diameter be kept below 2.0 to minimize bulk mixing problems. This must be reconciled with impeller diameter and impeller spacing requirements (see later) and with architectural, shipping, and other constraints.

Impeller spacing. As noted earlier, there is a body of empirical evidence (48) that supports the spacing of Rushton turbines 1–1.5 impeller diameters apart in Newtonian broths. This spacing appears to provide a balance between preventing impellers from interfering with their neighbors and at the same time avoiding dead zones between them. The same sources of empirical data support placing the lowest impeller one impeller diameter from the bottom of the vessel (assuming a standard dished head) and placing the uppermost impeller one impeller diameter below the liquid surface. We have found these rules to work reasonably well for Newtonian broths and a few non-Newtonian broths, and for radial flow impellers other than Rushtons. Please note that these conclusions are based on limited observations. Finally, keep in mind that one cannot avoid interaction among impellers when at least one of them is an axial flow type or has a significant axial flow component, and that spacing effects in highly non-Newtonian broths are not well understood.

Baffling. Baffles are placed in vessels to minimize fluid swirling and vortex formation (see Ref. 48 for flow pattern diagrams). The usual approach is to use four baffles on 90° centers, each baffle having a width equal to 0.1 of the D_t. Baffling tends to increase transmittable power and to improve mixing (except for the dead spots, which tend to form behind the baffles). Elimination of significant vortexing is important for safety as well as for improved bulk mixing. A vortex can reach down to the impeller in an unbaffled vessel. When this happens, a sizable portion of the impeller becomes air enshrouded, thereby decreasing resistance on the impeller. This tends to drive up the impeller speed, at least briefly (or the speed may be increased intentionally in an attempt to increase the power input). Unfortunately, vortices are unstable and can collapse shortly after formation, resulting in very large and potentially catastrophic stresses (impulse) on the impeller, particularly if the impeller speed is increased significantly while it is enshrouded.

Gas flow. Gas flow has a complex effect on bulk mixing. The flow alone does tends to promote bulk mixing (as in bubble tanks), but it also tends to decrease the effect of the impellers, particularly at high values of gas linear velocity. Fortunately, this is not a major problem in most cases, but it can be for very large fermenters and for highly viscous non-Newtonian broths.

50.4.5 Gas Holdup, Foaming, and Aerosol

There are several problems that can interfere seriously with a fermentation. Gas holdup (discussed earlier) decreases the effective volume of a fermenter. Foaming and aerosol formation can constrain operation, cause major cleaning and asepsis problems, and in the extreme cause termination of a fermentation. All three are dependent on broth characteristics, power input, and gas flow rate. There is some information in the literature, but these points have not been given the attention that even begins to reflect their importance. In general, all one can say is that all three become bigger problems for a given fermentation as gas flow and power

input increase. Beyond that, each case is a new adventure. More will be said about the practical aspects later.

50.4.6 Heat Transfer

50.4.6.1 Heat Loads. Heat transfer is required during fermentation to maintain constant temperature conditions, and at other times (i.e., sterilization, induction) to increase or decrease broth temperature. In most cases, cooling is required during most of an active, aerobic fermentation. A good approximation to the total heat load, Q_{tot}, during such fermentations in which the primary carbon source is glucose or a similar carbohydrate is (49)

$$Q_{tot} = Q_{metab} + Q_{mech}$$
$$Q_{tot} = 0.48(\text{OTR})V_L/Y_{x/o} + 2545P_g \quad (50.17)$$

where Q_{metab} is the heat generated by metabolism (Btu/h), Q_{mech} is the heat generated by power input (Btu/h), and $Y_{x/o}$ is the yield of cells on oxygen (g dry wt cells per g oxygen consumed). Heat transfer can be more of a limiting factor in aerobic fermentations than is oxygen transfer—particularly in large fermenters. The major heat transfer demand is usually during the maximum growth period (i.e., when μX is greatest). It is always wise, however, to check other loads. For example, rapid cooldown after an induction phase could put enormous demands on the cooling system. Cooling a 10,000-L (wv) fermenter from 38°C (104°F) to 10°C (50°F) in 30 min would require an average heat transfer rate of approximately 2.4×10^6 Btu/h. The same heat transfer rate would support an oxygen transfer rate of approximately 495 mmol/L(h), which is very high by almost anyone's standards. Similarly, one should check other potentially high loads such as cooldown after sterilization (see later). In any case, careful thought and solid, empirical facts (e.g., product thermal degradation rates) should form the basis of any specification that will require extraordinary transfer rates.

50.4.6.2 Heat Transfer Rate. The rate at which heat can be transferred is dependent on (1) the driving force for heat transfer, (2) the area across which transfer must occur and, (3) the resistance to heat transfer:

$$Q = (1/\text{resistance}) \times (\text{area}) \times (\text{driving force}) \quad (50.18)$$

The driving force for agitated vessels is usually taken to be the log mean temperature difference, ΔT_{LM}, defined as

$$\Delta T_{LM} = (T_{c,o} - T_{c,i})/LN[(T_f - T_{c,i})/(T_f - T_{c,o})] \quad (50.19)$$

where $T_{c,o}$ is the coolant outlet temperature (°F), $T_{c,i}$ is the coolant inlet temperature (°F), and T_f is the fermentation temperature (°F). Note that use of equation 50.19 assumes that the broth is homogeneous and can be characterized by a single temperature.

The transfer area, A_{JA}, is the actual contact area (not necessarily the same as the available area) between the broth and the heat exchange surface, which is usually a jacket and/or an internal coil. The actual area can be found if the height of aerated liquid in the tank is known, along with the geometry of the jacket and any internal exchange area (e.g., a coil). The aerated liquid height measured along the centerline of the vessel, h_{LA} (ft), is

$$h_{LA} = [(1 + \text{HU})V_{LU} - V_D]/(0.785D_t^2) + \text{IDD} \quad (50.20)$$

where V_{LU} is the unaerated liquid volume (ft^3), V_D is the lower dish volume (ft^3), IDD is the inside depth of lower dish (ft), and D_t is the tank inside diameter (ft).

The resistance to heat transfer is a little more complicated. It is composed of five resistances in series and is expressed as

$$1/U = 1/h_i + 1/h_o + 1/h_{fi} + 1/h_{fo} + t/k \quad (50.21)$$

where U is the overall heat transfer coefficient (Btu/[h°F ft^2]), h_i is the broth film heat transfer coefficient (Btu/[h°F ft^2]), h_o is the jacket fluid heat transfer coefficient (Btu/[h°F ft^2]), h_{fi} is the broth fouling factor (Btu/[h°F ft^2]), h_{fo} is the jacket fluid fouling factor (Btu/[h°F ft^2]), t is the fermenter wall thickness (ft), and k is the fermenter wall thermal conductivity (Btu/[h°F ft]). The resistance of the tank wall can be predicted accurately because both k and wall thickness are known accurately. It should be noted that the k for stainless steel is very low (about 10 Btu/[°F h ft]). This means that the tank wall should be kept as thin as possible to minimize its contribution to heat transfer resistance (see later).

Correlations for h_o can be found in the literature (46 pp. 282–283) but are seldom as reliable as those available from vendors for the specific jackets they fabricate.

The problem in predicting U is in predicting reliable values of h_i, h_{fi}, and h_{fo} Published correlations (50) for h_i values for aerated, Newtonian fermentation broths have been published but are not very reliable. Correlations for non-Newtonian broths have also been published (51), but as was the case for mass transfer coefficients, h_i is strongly dependent on broth rheological characteristics. Unfortunately, existing correlations do not do a very good job of accounting adequately for broth rheology, a problem exacerbated by the fact that good rheological information is seldom available. Finally, the fouling factors are essentially impossible to predict. The best one can do is keep fouling to a minimum by means of good cleaning practices and proper filtration of coolants. Effects of individual resistances on U are illustrated in Fig. 50.2.

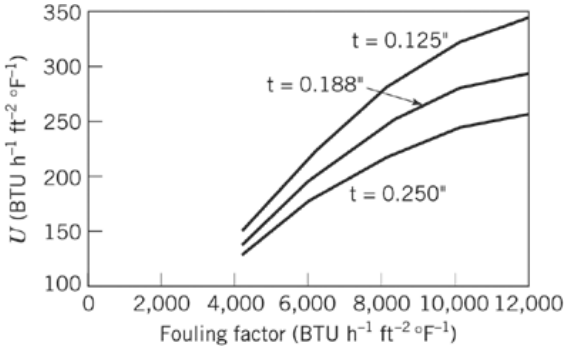


Figure 50.2. Effects of metal thickness and fouling resistances on the overall heat transfer coefficient.

The following rough guides (based on many years of experience) are offered because the authors are unable to offer any collection of reliable prediction tools:

1. U values for simple, low viscosity Newtonian broths usually range from about 120 to 150 Btu/(h°F ft^2) for new, clean stainless steel tanks.
2. U for viscous, non-Newtonian broths ranges from about 30 to 60 Btu/(h°F ft^2)

It also should be noted that U's for heating usually are a bit higher than U's for cooling.

The heat transfer rate can now be expressed as

$$Q = UA\Delta T_{LM} \tag{50.22}$$

Similar equations can be developed for heat transfer via an internal coil. The only difference is that the heat transfer coefficients for coils are usually a bit higher than those for jackets. That having been said, we will try everything possible to discourage you from using internal coils. The reasons relate primarily to mechanical and cleaning considerations and are discussed later.

In applying the preceding, we suggest that the reader consider the following suggestions:

- Avoid the use of internal cooling surfaces (e.g., coils). They make cleaning difficult to impossible, are potential sources of contamination (leaking of coolant), put a lot of mechanical strain on the vessel, and can cause deterioration of bulk mixing (particularly for viscous non-Newtonian broths).
- Avoid subfreezing coolant. Sooner or later, subfreezing coolant will cause severe valve freeze-up and worse.
- Try to keep coolant flow rates low enough to avoid pipe diameters greater than 3 in.; cost increases considerably and availability of fittings and so forth decreases as size increases.

Finally, there are some cases in which high wall temperatures have been cited as causing problems with temperature-sensitive organisms. The wall temperature, T_w, depends on the temperatures of the broth and of the jacket fluid, as well as on the relative values of the heat transfer resistances. A simple energy balance across the heat transfer path yields

$$T_w = (T_f + \beta T_j)/(1 + \beta) \tag{50.23}$$

where

$$\beta = k/h_i/(t + k/h_o) \tag{50.24}$$

Note that this does not account for locally high wall temperatures that would be caused by steam applied to steam locks during fermentation.

50.4.7 Sterilization

50.4.7.1 Introduction. Sterilization and aseptic operation taken together (as they must be) have a much greater influence on fermenter design and operation than does any other requirement.

In theory (1) sterilization destroys or removes all foreign organisms in all process equipment (including piping, seals, etc.) that might come into contact with the process fluid, and (2) aseptic operation insures that *no* contaminating organisms enter the fermenter after sterilization. These ideals are not attainable in practice because (among other reasons) (1) there is a finite probability that a very low concentration of contaminating organisms will not be captured in a sample used to test for contamination, and (2) there is a finite probability of false positives due to sample contamination and so forth. It also is important to note that there is a continuing debate concerning the definitions of pure culture and sterility (6,51).

The driving forces for sterilization and aseptic operation range from minimizing product losses to insuring strict compliance with regulatory requirements. Among the many specific problems that contamination can cause are the following:

- Production of a toxin that can't be removed by the purification system
- Production of an enzyme that degrades the product
- Decreased product yield due to use of substrate by contaminants
- Production of toxins that inhibit the producer strain
- Production of compounds (e.g., polysaccharides) that interfere with the operation of recovery and purification equipment

Which specific problems will exist and where in the spectrum a particular case will lie depend primarily on the product, its economic value, whether it is regulated, and how it will be used. Given all these variables and the fact that absolute sterility is an unachievable abstraction, the extents to which one should go should be considered on a case-by-case basis. As a practical matter, sterilization has to be interpreted as "effective sterilization," meaning that the design and procedures (including sampling and detection) are suitable for the specific case. For example, sterilization of fermenters used to produce parenterals should be held to a much higher standard than sterilization of fermenters used to produce amylases for starch hydrolysis. Unfortunately, there remains a lot of room for disagreement among well-intentioned people (see also the section "Product Safety").

50.4.7.2 Quantification of Sterilization. Mechanical details and other practical considerations of sterilization and aseptic operation are discussed in the subsection "Sterile Piping Systems".

Several methods have been developed to quantify sterilization. The simplest is based on the empirical observation that the death kinetics of many vegetative organisms and spores can be described by a simple first-order expression

$$dN/dt = -kN \tag{50.25}$$

where N is the number of viable organisms (or spores) at any time, t, and k is the thermal death constant. k is a function of most environmental variables but is most strongly affected by temperature. This dependence is very often expressible as an Arrhenius relationship

$$k = A \exp(-E_A/RT) \tag{50.26}$$

where A is the preexponential factor (min^{-1}), E_A is the thermal death activation energy (cal/mol), T is the absolute temperature (K), and R is the gas constant. The effect of temperature on k is pronounced for most organisms because their E_A's are so high (e.g., 65,000 cal/mol for *Bacillus stearothermophilus* spores).

Among other methods of quantifying sterilization concepts are the following:

- *Probability-based theories* (52). These are conceptually different from the first-order model, but give essentially the same results for the levels of kill that must be achieved practically.
- *Methods based on the "decimal reduction factor," D*. These are used widely (53). It is important to note, however, that the nature of temperature dependence has no rational, physical basis and differs considerably from an Arrhenius relationship: it is based primarily on an empirical observation for relatively small temperature ranges.

We use the first-order model for the rest of the discussion.

50.4.7.3 Medium Sterilization. The primary design basis for sterilization systems and procedures is usually the level of sterility that must be achieved. This is most frequently expressed in terms of the probability of sterilization failure (i.e., the probability that a single organism will survive). In most instances probabilities of 10^{-3} to 10^{-4} are quite adequate. This means 1 failure in 1,000 or 10,000 sterilization operations, respectively. It also is important to note that the probability of failure is numerically very close to the value of N in the first-order model.

The reader should also take note of the fact that in some quarters, sterilization criteria are stated in terms of "logs of kill." That is to say, a fixed number of logs (e.g., 12) is taken to be adequate. This is meaningless in that it does not take into account the initial contaminant loading.

Now we consider prediction of requirements for batch sterilizing a fermentation medium as part of the fermenter design process to ensure that we'll have adequate heating and cooling capacity. It should also be done as part of the process design to ensure adequate timing. Batch sterilization involves heating the medium in the fermenter to sterilization temperature (T_{ster}), holding the medium temperature constant at T_{ster} for an adequate time, and then cooling the medium down to fermentation temperature (see the section "Mechanical Design" for additional details). The medium is kept in the fermenter throughout.

It is assumed in what follows that (1) heating and cooling are via the jacket only, and (2) the energy and condensate contributed by the small amount of steam that flows into the vessel as a result of sterilizing piping, air filters, and so on is negligible for energy balance purposes.

The rate of kill at any instant during the sterilization process is

$$dN/dt = -kN = -A \exp(-E_A/RT)\, N \tag{50.27}$$

therefore,

$$N/N_o = A \int \exp(-E_A/RT)\, dt \tag{50.28}$$

where N_o is the number of contaminating organisms initially present. The integration of equation 50.26 must be performed over heating, hold, and cooling phases of sterilization. This is done by numerical integration of equation 50.28, coupled with the equations that describe broth temperature as a function of time.

For heating

$$T_f = T_{ST} - \left(T_{ST} - T_{F,O}\right) \exp\left(-U^* A^*_{JA} t / M^*_F C_{P,m}\right) \tag{50.29}$$

where T_f is the medium temperature (°F), T_{ST} is the steam temperature (°F), $T_{F,O}$ is the initial medium temperature (°F), A_{JA} is the active jacket area (ft^2), t is the time since beginning of heating (h), M_F is the medium mass (lb), and $C_{P,m}$ is the medium heat capacity (Btu/[lb°F]).

For cooling

$$T_f = T_{C,i} + (T_{ster} - T_{C,i}) \exp\left(t \left(W_J C_{P,c} / \left(M_F C_{P,m}\right)\right)\right) \cdot \left(\exp\left(U A_{JA} / \left(W_J C_{P,c}\right)\right) - 1\right) \tag{50.30}$$

where $T_{C,i}$ is the inlet coolant temperature (°F), T_{ster} is the sterilization temperature (°F), t is the time from beginning of cooling (h), W_J is the coolant flow (lb/h), and $C_{P,c}$ is the coolant heat capacity (Btu/[lb°F]). Equations 50.29 and 50.30 can be derived via energy balances.

One chooses times and temperatures such that the desired kill, N/N_o, is achieved. Unfortunately, one usually does not know the level of contamination or the nature of the contaminants. Indeed, it is very unlikely that contamination will remain constant from one fermentation to the next. The usual practice, therefore, is to design for what is thought to be the "worst case." This usually gives results that are quite satisfactory for design specifications. A "typical" worst case is a loading of 5×10^6 spores/mL of the organism *B. stearothermophilus*. Such spores are highly resistant and have the added advantage of being used widely to validate sterilization operations (see later). It is important to note that the purpose of the calculations is to provide a rational basis for obtaining reasonable design information and ensuring a high probability that the desired level of sterilization can be achieved over the whole range of anticipated operating conditions.

Fig. 50.3 illustrates the results of such calculations for the following case:

- Medium volume = 15,000 L
- Initial spore load = 5×10^6/mL
- Initial medium temperature = 70°F
- Steam temperature = 300°F
- Coolant temperature = 35°F
- Coolant flow rate = 100 gpm
- Fermentation temperature = 86°F
- Active jacket area = 225 ft^2
- U = 150 Btu/(h°F ft^2)
- $A = 2.1 \times 10^{36}$/min
- E_A = 65,000 cal/mol
- N (probability of failure) = 0.0001

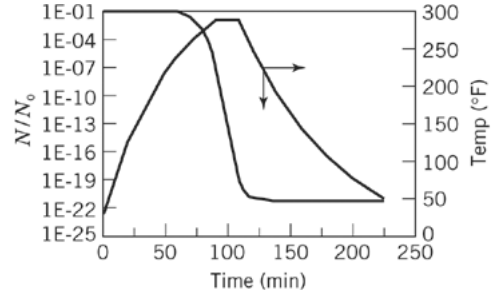


Figure 50.3. Temperature profile and kill ratio for a batch sterilization.

As seen in this example, heating and cooling phases usually contribute only a small fraction of the total sterilization kill, but they do affect turnaround time significantly. Long heating and cooling times can also have other effects:

- Cause damage to the fermentation medium to the extent that the fermentation can be compromised. The seriousness of this depends on some combination of economics and regulatory compliance.
- Cause medium changes that have negative effects on recovery and purification without causing fermentation problems. This includes the possibility of introducing foreign materials that may pass undetected into the final product.

The example also shows that cooling time is considerably longer than heating time. This results primarily from the lower temperature-driving forces during cooling. The problem is exacerbated considerably when the heat transfer coefficient is very low as is the case for viscous non-Newtonian broths. Another method used for batch sterilization is direct steam injection: live steam is injected directly into the medium as the main source of thermal energy. This decreases heating time as well as the overall steam requirement. It also increases the medium volume by about 20% (as a result of steam condensation), which can cause some problems, including the following:

- *Increased cooling time*.
- *Medium dilution*. This will be a significant problem if the initial medium cannot be made concentrated enough to account for the dilution. Some reasons include low solubility of medium components, increased viscosity, and increased reaction rates among medium components at elevated temperatures.
- *Introduction of impurities*. This depends primarily on the quality of the injected steam. In some cases plant steam is acceptable if boiler cleaning agents do not cause problems. At the other extreme is the requirement to use clean steam (WFI quality). It should be noted with regard to this point that some steam will

be injected directly even when jacket heating is used as the main energy source; therefore, one will always be in the position of having to evaluate the effects of contaminants carried by the steam.

For cases in which sterilization times are too long or medium alterations cause too many problems, one might consider continuous sterilization. The interested reader is directed to the literature for additional information (54 pp. 159–176).

50.4.7.4 Piping System Sterilization. Heating and cooling times are not usually significant issues for sterilizing piping; however, there can be some serious heat transfer problems related to piping length, diameter, and orientation. Some of these are discussed in the subsection "Vessel Design". The reader is also referred to literature reports of some practical experiments and theoretical analyses (55,56).

50.4.7.5 Air Sterilization. Theoretical aspects of air sterilization are not discussed here. Suffice it to say that modern filters, if sized, installed, and maintained properly, will provide very reliable results. We'll discuss some of these practical aspects in the section "Mechanical Design". See Refs 54 pp. 176–183 and 57 for additional information.

50.4.8 Cleaning

Scrupulous cleaning is necessary to decrease nonbiological contamination and prevent cross-contamination of batches. Experience also has shown that reliable sterilization is difficult or impossible to achieve in the absence of rigorous cleaning.

As noted earlier, fermenter cleaning is not mentioned specifically in 21 CFR, but the basis is provided in section 211.67, which requires equipment be cleaned as per a defined plan and by trained people. Furthermore, the FDA has made clear the importance it attaches to cleaning not only in various agency publications (58), but also in more stringent enforcement. This is particularly true in multiproduct facilities (a key issue for most modern biotech plants). This agency initiative and the desire to generally improve operation have caused the industry to develop more reliable cleaning systems and protocols and to move to fully automated cleaning-in-place (CIP) systems, which provide greater assurance of successful validation and long-term compliance.

Developing and designing reliable fermenter cleaning systems is not as straightforward as it might appear, and considerable controversy continues. Among the reasons for this is that while much is known about the basic science of cleaning in general, very little is known about the basic science of cleaning fermenters and little has been published. The approach taken is based primarily on experience derived from the dairy, food, and beverage industries. Such information is useful but is not directly applicable in general to pharmaceutical and biotech processes where soils are different and the cleaning requirements are far more stringent. What meager information there is concerning pharmaceutical and biotech soils has been obtained from experiments done on single soil components and/or studies done under conditions not truly representative of the process conditions (59,60). There have been no significant attempts to develop systematic analyses based on experiments done with complex mixtures typical of real fermentation soils under conditions found in real processes. As a result there are no reliable general methods, tools, or correlations on which to base the development of cleaning agents, protocols and CIP system design; decisions tend to be made based on arbitrary criteria (e.g., coupon bake on studies). In keeping with our general design philosophy, we think it important that such arbitrariness be avoided and that cleaning protocols be developed along with the fermentation. It is clear that this will help to ensure not only proper design but will also minimize cleaning validation studies and any questions concerning the presence of contaminants and/or cleaning residues in the commercial product that could not have been present in clinical trial material.

The selection of fermenter cleaning agents and protocols should be based not only on the specific soil but also on the materials of construction, surface finishes, and so on. In addition, one should consider the issues of (1) compatibility of each material with the cleaning agents and protocols, and (2) potential materials interaction during cleaning. These are decisions that usually are made during the design phase, but really should be defined much earlier. These issues are discussed in the subsection "Agitation Systems".

Fermenter cleaning validation is beyond the scope of this chapter; however, the design must be done so as to minimize validation problems and ensure maximum ease in ongoing compliance. The design team must therefore be aware of the procedures that will be used for validation and recognize that this is an issue that has not yet been resolved in the general community.

50.4.9 Putting It Together: Preliminary Design Calculations

We now begin to see some of the interactions that can arise among the transport processes, and between them and the operating variables. This is a necessary step in developing sound designs, and a precursor to preliminary design calculations. As an example, consider a case in which we are trying to find ways to increase the OTR above some base value. One approach would be to increase the gas flow rate (ν) keeping other variables constant:

- The overall driving force tends to increase (equation 50.10).

- V_s increases (equation 50.7).
- Increased V_s tends to increase $K_g a$ (equation 50.11).
- Increased v also increases N_A (equation 50.12).
- Increased N_A tends to decrease power input (Fig. 50.1).
- Decreased power input tends to decrease $K_g a$ (equation 50.11).

As another example, consider increasing the vessel pressure while keeping other variables constant:

- The overall driving force tends to increase (equation 50.10).
- The actual gas volumetric flow rate (v) tends to decrease (assuming constant molar flow rate) (equation 50.6).
- V_s tends to decrease (equation 50.7).
- The decrease in V_s tends to decrease $K_g a$ (equation 50.11).
- The decrease in v also tends to decrease N_A (equation 50.12).
- This tends to increase power input (Fig. 50.1).
- Increased power input tends to increase $K_g a$ (equation 50.11).

Such complex interrelationships develop regardless of what steps are taken to increase OTR. The nature of these will change depending on the approach taken and the system being considered. There will also be additional pluses and minuses related to factors such as cost, safety, cleaning, and regulatory compliance. For example, using pure oxygen to increase the driving force carries with it very distinct cost and safety problems. Many of these more practical implications are be discussed in the section "Mechanical Design".

Now let's carry the second approach a little further. We do this because increasing pressure is usually the easiest and seemingly least expensive way to increase OTR. The decrease in V_s caused by the increased pressure has the positive effects of decreasing foaming, aerosol formation, and gas holdup. But it has the negative effect of requiring thicker tank walls, thereby increasing heat transfer resistance in the face of an increased heat load due to increased metabolic activity. This will become a significant problem when the pressure desired is greater than that required for vessel sterilization. The larger the tank diameter, the greater the possible problem. It should also be noted that thicker walls can make it more difficult to get a good surface finish and therefore increases the possibility of cleaning problems. In addition, the higher the pressure and thicker the walls, the shorter the list of qualified vendors.

This type of reasoning process is applicable to any of the many permutations possible. We extend it after we consider some additional basic concepts, mechanical design practices, and a few more important practical constraints.

We now consider two examples of preliminary design calculations, the objectives of which are to, first, define vessel geometry to ensure that it will not violate architectural constraints and be able to satisfy general rules of thumb for good bulk mixing, impeller spacing, and so forth. Some of this will require checking calculations done later (see later) and may require some iteration.

The second objective is to establish ranges of air flow, pressure, oxygen enrichment, and power that will accomplish the following:

- Satisfy the design basis maximum OTR requirement.
- Keep V_S low enough to avoid foaming, holdup, and aerosol problems. We have found a limit of 200 cm/min to be a safe guide; however, there are cases (Newtonian broths) in which considerably higher values up to 300–350 cm/min tolerable and others (very viscous, highly non-Newtonian broths) in which it is not wise to go beyond 75–100 cm/min.
- Not violate compressor and other component constraints.
- Not require heroic efforts (e.g., extremes in pressure, power, etc.).

Please note that we are trying to establish reasonably broad ranges for each of the variables within which we can satisfy the requirements with a reasonable degree of comfort (based on experience). This is important because the correlations usually available have questionable accuracy, and it allows some breathing room for process improvements and so forth.

The third objective is to define impeller type(s), sizes, and speed that will do the following:

- Provide the power required
- Provide good bulk mixing
- Satisfy impeller spacing rules of thumb
- Not violate constraints related to the sensitivity of the organism
- Make possible single-piece impeller construction and so forth (see the section "Mechanical Design" for consideration of mechanical constraints)
- Not violate any other constraints specified

The fourth objective is to define heat exchange area and coolant flow and temperature that achieve the following:

- Satisfy peak heat transfer requirements

- Not violate coolant temperature and flow constraints and such
- Avoid internal heat exchange area
- Not require subfreezing coolant or flow that will require very large pipe diameters

(*Note*: One should check to make sure that other heat loads [e.g., cooling after fermentation] are not greater than the load during maximum growth activity. We assume that to be the case here.)

The fifth objective is to use the results of the calculations not only to define mechanical details (see the section "Mechanical Design"), but also as a basis for recommendations for rational changes in design basis.

Please note that experimentally derived correlations for the subject cases are used in the examples (this is a design gift as rare as hen's teeth). All were obtained at 500-L scale, and we are just within our comfort range concerning their scalability to 15,000 L (design scale). The reader is cautioned, however, that there is no basis to believe that the correlations would be applicable to other cases, nor would we recommend extrapolation to much larger scales. It also is worth noting that there are some good examples in the literature that might be applicable to the problems at hand or to others; however, one must exercise considerable caution if the conditions specified in the reference differ significantly from those for the case being analyzed. Unfortunately, it is often not possible to determine if significant differences exist.

50.4.9.1 Case 1.

Product	Intracellular protein
Organism	*E. coli*
Final broth volume	15,000 L
Maximum OTR	234 mmol/(L h)
Dissolved oxygen requirement	10% relative to atmospheric conditions
Broth rheological type	Newtonian
Maximum broth viscosity	5 cp
Regulation	CBER
Containment	BL2-LS
Maximum coolant flow	250 gpm
Minimum fluid temperature	35°F
Internal coils	No
Compressor max press/max flow	50 psig/25,000 SLPM
Minimum heat transfer coefficient	150 Btu/(h°F ft^2)
Ceiling height	336 in.
Floor space	1000 ft^2, unobstructed

The following experimental correlations are applicable:

$$K_g a = 108\left(P_g/V_L\right)^{0.6} V_S^{0.2}$$

$$P_g/P_{ug} = 1.0 - 18.56N_A + 215.64N_A^2 - 1082.66N_A^3 + 1859.68N_A^4$$

$$\mathrm{HU} = 0.0133\left(P_g/V_L\right)^{0.4}\left(60V_S/^{0.5}\right) - 0.0333$$

These were developed under the following conditions for single Rushton turbines:

- $0.8 < P_g/V_L < 2.9$ hp/100 gal
- $100 < V_S < 200$ cm/min
- $0 < N_A < 0.1$
- $0.33 < D_i/D_t < 0.45$

Vessel geometry calculations are the same for both cases. We start by assuming a vessel diameter and wall thickness. (Note that the thickness will probably be changed a bit later to satisfy code requirements. This will not have a significant effect on height and volume calculations to follow.) In this case we assume a 96-in. outside diameter and a 0.25-in. wall thickness. By straightforward geometry and using tabulated values of volumes and inside depth of dish (IDD) for standard ASME heads, we get the following:

Liquid height	134.2 in.
(Liquid height)/tank diameter	1.41
Total tank height	192.5 in.
Total volume	21.1 L
Percent fill (unaerated)	71.1%

This satisfies rules of thumb concerning liquid height-to-diameter ratio and fill percent. If we add about 72 in. for legs and 30 in. for opening the manway, we get a total height requirement of 294.5 in. We should be able to satisfy the maximum height limit.

The results of oxygen transfer calculations for several operating conditions are given in Table 50.1. From these results we conclude that the following will satisfy the OTR required and give us a reasonable amount of "breathing room."

Gassed power	100 hp (includes transmission efficiency)
Maximum operating pressure	40 psig
Maximum air flow	10,000 SLPM

We do not recommend oxygen enrichment at this point, but we do suggest that the "holes be punched" to facilitate future installation of an oxygen system. The agitation

TABLE 50.1. Oxygen Transfer Calculation Results (Single Cell)

Pressure (PSIG)	35	20	20	2
O_2 trans eff. (%)	21	30	28	28
O_2 (MOL % in)	21	21	40	40
Gas flow (in, SLPM)	29,762	20,833	11,719	11,719
VVM	1.98	1.39	0.78	0.78
Average V_s (cm/min)	186	183	103	200
hp/100 gal	1.3	2.7	1.0	2.6
Theor. P_g	52.8	105.6	41.1	103.8

TABLE 50.2. Citation System Calculation Results (Single Cell)

Shaft speed (rpm)	114	141	88	141
Turb imp dia (in)	40.00	40.00	40.00	40.00
Turb D_i/D_t ratio	0.42	0.42	0.42	0.42
Ungassed hp (turb)	123.1	233.0	56.6	233.0
N_a, aeration numb	0.071	0.057	0.051	0.062
P_g/P_o ratio	0.43	0.46	0.48	0.45
Gassed hp	53	106	42	104

TABLE 50.3. Heat Transfer Calculation Results (Single Cell)

Heat load (MMBtu/h)	1.808	1.943	1.779	1.938
Hold-up	0.199	0.271	0.123	0.282
Jacket area (ft^2)	297	317	276	320
UJKT (BTU/ft^2 h°F)	150	150	150	150
Coolant temp in (°F)	35	35	35	35
Coolant flow (GPM)	190	210	235	200

system calculations are based on the assumption of using two 40-in. diameter Rushton turbines. The results are given in Table 50.2. A maximum speed of 150 rpm should be adequate. Note also that the impellers can be spaced to satisfy the rules of thumb for bulk mixing rules discussed previously. Although this should give satisfactory results for such a low viscosity broth, we recommend consideration of a slightly larger turbine as the lower impeller and a hydrofoil (e.g., A-315) as the top impeller.

The results of the heat transfer calculations are given in Table 50.3. A minimum coolant temperature of 35°F was used in all cases. The results show that the heat loads can be handled, but the conditions are uncomfortably tight. For example, in no case will increasing the coolant flow to the maximum make up for a 10% decrease of the heat transfer coefficient. The potential consequences of inadequate heat transfer in this case should be considered seriously before final design commitments are made. Alternatives (e.g., lower coolant temperature) should be explored.

50.4.9.2 Case 2.

Product	Antibiotic
Organism	*Streptomyces* sp.
Final broth volume	15,000 L
Maximum OTR	50 mmol/(L h)
Dissolved oxygen requirement	10% relative to atmospheric conditions
Broth rheological type	Non-Newtonian (pseudoplastic)
Maximum broth viscosity	1,000–1,500 cp
Regulation	CDER
Containment	BL1-LS
Max coolant flow	250 gpm
Min fluid temperature	35°F
Internal coils	No
Compressor max press/max flow	50 psig/25,000 SLPM
Min heat transfer coefficient	40 btu/(h°F ft^2)
Ceiling height	336 in.
Floor space	1000 ft^2, unobstructed

The following empirical equations are applicable:

$$K_g a = 8.0\left(P_g/V_L\right)^{0.5} V_S^{0.4}$$

$$P_g/P_{ug} = 1.0 - 26.99N_A + 417.37N_A^2 - 2789.43N_A^3 + 6643.30N_A^4$$

$$\mathrm{HU} = 0.012\left(P_g/V_L\right)^{0.3}(60V_S/100)^{0.52} - 0.029$$

TABLE 50.4. Oxygen Transfer Calculation Results (Mycelial)

Pressure (PSIG)	35	25	20	10
Oxygen transfer eff (%)	6	6	6	6
O_2 mol % in	21	21	40	40
Gas flow IN (SLPM)	22,222	22,222	11,667	11,667
VVM	1.48	1.48	0.78	0.78
Average V_s (cm/min)	154	172	102	140
hp/100 gal required	1.7	2.0	1.0	1.6
Theoretical Pg	60.9	79.9	41.7	61.8

These were developed under the following conditions for single Rushton turbines:

- $1.0 < P_g/V_L < 2.3$ hp/100 gal
- $60 < V_S < 130$ cm/min
- $0 < N_A < 0.1$
- $0.36 < D_i/D_t < 0.42$

The results of oxygen transfer calculations for several operating conditions are given in Table 50.4. From these results we conclude that the following will satisfy the OTR required.

Gassed power	100 hp (includes transmission efficiency)
Maximum operating pressure	40 psig
Maximum air flow	25,000 SLPM

Oxygen enrichment should be considered in this case despite the fact that the calculations show that it is not necessary. The reason is that the gas flow rate, and hence V_S, is quite high without enrichment. This results primarily from the very low oxygen transfer efficiency typical of very viscous non-Newtonian broths. Although it is true that we haven't broken the rule of thumb for holdup, foaming, and aerosol we should take note of the fact that high air flows in pseudoplastic broths can exacerbate impeller unloading and cause flooding more readily than for non-Newtonian broths. It also is generally true that our correlations become less reliable as conditions become more extreme and further removed from the conditions under which they were developed. Note in particular that our correlations were not developed for the high values of V_S found in the calculations. It also is clear that we should specify higher pressures than shown in the results in Table 50.4. Additional calculations show that 40–45 psig would bring the V_S into a comfortable range. We suggest, therefore, the following:

Gassed power	100 hp (includes transmission efficiency)
Maximum operating pressure	45 psig
Maximum air flow	25,000 SLPM
Oxygen enrichment	40% oxygen in inlet stream

The agitation system calculations are based on the assumption of using two 40-in.-diameter Rushton turbines. The results are given in Table 50.5. A maximum speed of 140 rpm appears to be adequate. Note also that the impellers can be spaced to satisfy the bulk mixing rules of thumb discussed previously.

That's very nice, but we have significant reservations about the results. An alternative should be given serious consideration because of the rheological nature of the broth, the profound effect this can have on mixing, and the issues of scalability for such broths. At the very least, the lower turbine should be replaced by one having a D_i/D_t approaching 0.5, and the upper turbine should be replaced by a hydrofoil. The reader should understand that this is based on experience only: we have no solid correlations for this case. The best route to take would be to do a few pilot mixing studies in as large a vessel as possible with the real broth.

The results of the heat transfer calculations are given in Table 50.6. The minimum coolant temperature of 35°F was used in all cases. The results show that the heat loads can be handled. It also appears that we are well below the maximum available coolant flow. This may be comforting, but the reader should realize that there is not a lot of breathing

TABLE 50.5. Agitation System Calculation Results (Mycelial)

Shaft speed (rpm)	124	137	107	124
Ungassed hp	159	214	102	159
Aeration number	0.049	0.055	0.042	0.049
Gassed hp	61	80	42	62

TABLE 50.6. Heat Transfer Calculation Results (Mycelial)

Heat load (MMBtu/h)	0.533	0.560	0.463	0.515
Gas hold-up	0.202	0.230	0.124	0.182
Jacket area (ft^2)	298	306	276	292
UJKT [(Btu/ft^2 h°F)]	40	40	40	40
Coolant temp in (°F)	35	35	35	35
Coolant flow (GPM)	190	210	235	200

room for process improvement. In particular, an increase in OTR up to 60–65 mmol/(L h) would put us over the top even if there were no deterioration in heat transfer coefficient. Again, one should give this serious consideration before committing to a final design.

We trust that the discussion and examples in this section have helped the reader to understand not only the many interactions that must be considered, but also the nature of preliminary design calculations and their limitations. The results obtained here must now be translated into a mechanical design that must also take into consideration the items to be discussed in the next section.

50.5 MECHANICAL DESIGN

50.5.1 Mechanical Design Basis

Much of the mechanical design follows from the results of calculations discussed in the previous section Process Requirements: Basics; however, these must be tempered by other considerations that should be included in the process and/or facility design basis. Some of these (e.g., regulatory compliance, containment) have already been discussed and are revisited in greater detail in this section. Other items that should be included and will affect fermenter design include the following:

- *Extent of automation, nature of plant wide control system, etc.* Such items affect not only the instrumentation (beyond our scope) and similar factors, but also valving, piping, vessel ports, and so forth. Among some of the major issues here are identification of critical (as defined by cGMP requirements) valves and other components. It must be kept in mind that failure to identify critical instrumentation and control components frequently leads to very complex valving systems in which the failure of a single switch can bring everything to a grinding halt. Unfortunately, there are too many people who do not think this through (as a system) before final design begins. Much of this results from the human tendency to rationalize and/or push "problems" downstream, the kind of thinking that results in the thought "Why worry? We'll get it whether or not we need it." Such thinking is in no one's best interest (buyer or seller).
- *Staff requirements and the anticipated nature of the operating staff*. This can influence the complexity and physical layout of (among other things) the piping system(s).
- *Plant location*. This will have some affect on overall design and component selection if for no other than service issues.
- *Available utilities*. This can influence such things as the designs of the cooling and aeration systems.
- *Architectural constraints*. These can have profound effects on the ways in which process requirements will be satisfied. Floor space and ceiling height constraints often require that a fermenter be designed in such a way that it violates some or most or even all of the rules of thumb mentioned in the previous section. This is not good but is better than building a vessel that does not fit into the plant.
- *Transportation constraints*. The fermenter has to be moved from the fabricator's shop to the plant—at a cost not greater than the total project budget. This may require some thumb bending or breaking. In extreme cases it may be better to fabricate the fermenter on site; however, this can carry large penalties, particularly in licensed facilities.
- *Maintenance*. Many design decisions can have major effects on the ease of maintenance. It is also often true that some of the design features that ease maintenance are more costly than those that do not. In most cases, the savings in capital expenditure will not come near paying for losses that will result later because of maintenance problems. This is particularly true in licensed facilities where regulators view good, facile maintenance as an integral, indispensible part of cGMP operation.
- *Definition of standards*. Standards for welds, finishes, and so on should be standardized for all parts of the equipment that will contact process fluid. It does not, for example, make sense to call for a high-quality vessel finish (e.g., 320 grit, EP) and at the same time accept unpolished tubing and valves in inoculation and medium addition lines.

Finally, there are a few recurring themes that are encountered in fermenter design:

- *Building-in "versatility."* The types of versatility desired range from wanting a fermenter that can operate well over a very wide range of conditions but with a narrow range of organisms, to wanting a convertible bioreactor that can handle microbes, mammalian cells, and maybe (someday) transgenic animals. Most people understand the value of versatility, but many do not understand the attendant problems and costs. As a general rule, converting laboratory glassware directly into large, stainless steel equivalents usually costs more than any rational person should be willing to pay. Also as a general rule, versatility should decrease as a process goes from the lab to the production floor. Versatility in the laboratory is almost a requirement because change is in the nature of laboratory work. Versatility on the plant floor, however, leads to more procedures, more paper work, more testing, and more confusion, particularly when equipment modifications are required to achieve the versatility; change is not in the basic nature of most plant work. Equipment capital savings can justify the added costs of all the preceding for many cases in which the equipment is designed to handle multiple, similar fermentations on a campaign basis and without significant equipment modification. This statement becomes less true as the fermentations become less similar, as more modifications are necessary, and as regulatory scrutiny increases. Bottom line: analyze very carefully any inclination to want versatility built into plant equipment (or even pilot equipment, in some cases).
- *Retrofitting existing equipment*. The usual thinking is that capital and time savings can be had by refurbishing "old faithful." Just how true this is depends not only on the condition of the existing equipment but also on the intended application(s) of the reborn version. Comments similar to the ones made for versatility apply here. The chances of success decrease as one goes from a lab to licensed production facility. There are ample, expensive corpses to prove this point.

50.5.2 Vessel Design

Please note that Figures 50.4 and 50.5 are simplified vessel and piping diagrams intended to assist the reader in the discussions to follow.

50.5.2.1 Materials of Construction. The major choices that must be made are (1) the type of metal to be used for the vessel and nozzles, and (2) the type of elastomer to be used for static seals (see later for rotating seals). The selections should be based on compatibility with the organism, compatibility with the product, corrosion resistance, cleanability (also related to finish), welding characteristics, and cost and durability. All of these should be determined during process development but seldom are. In almost all cases, the metal selected will be some grade of stainless steel (usually SS304, SS304L, SS316, or SS316L). The choice is usually associated with the nature and value of the product, although some of the other factors noted earlier may be considered. SS304 is usually good enough for lower-value, unlicensed products, whereas SS316L is the material of choice for high-value, licensed products. L-grade is selected when better corrosion resistance and good multipass welding characteristics are required; it adds about 15% to the cost of the vessel.

It is important in making metal selection to keep in mind that clean steam, purified water, and WFI are all highly corrosive. The reader should note that there is considerable controversy concerning metal selection and is directed to Refs 61–63 for additional information and opinion.

Static seal (O-rings and gaskets) materials are usually limited to silicone, EPDM, Viton, or Teflon. Silicone and EPDM are the materials of choice for headplates and elsewhere, respectively. (The reader should be alert to the fact that there are several grades of both, not all of which are FDA approved.) Teflon has much better temperature resistance than either silicone or EPDM, but it doesn't stretch, and it cold flows. Viton hardens on use.

Finally, one should be aware of that some O-ring/gasket-forming processes can leave very small quantities of metals in the seals. These may not be enough to cause fermentation or product problems per se, but they can be the cause of considerable corrosion.

50.5.2.2 Finish. In most instances, the need for a high-quality finish is closely related to the need for high-quality cleaning: there is little question that CIP systems function better when surfaces are smoother. Smoothness is expressed on several scales, two of the more common being grit number and surface R_A. Grit number is related directly to the abrasive used to achieve the finish (mechanical); surface R_A is the actual surface roughness as measured by means of a profilometer and expressed in microns:

Grit	R_A (μm)
120	3.2
220	0.8
320	0.4

The two most common ways of achieving smoothness are mechanical polishing and electropolishing. Mechanical polishing is done by means of a series of continually decreasing abrasive particle sizes (grits). Electropolishing is achieved

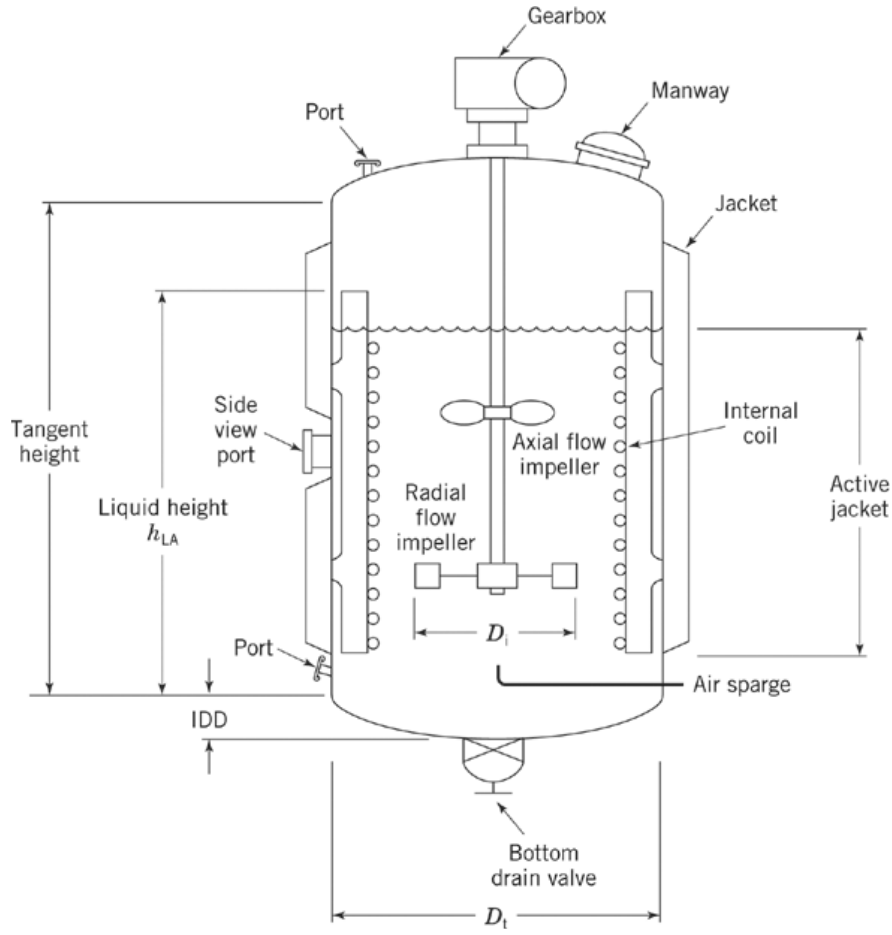


Figure 50.4. Fermenter vessel schematic and terminology.

by electrochemical removal of metal from high points on the surface. One is usually best advised to electropolish only after getting a good mechanical polish (240-grit minimum). It has long been held that the very good finishes required for vessels where cleaning is critical could be achieved only by electropolishing a 320-grit mechanical finish (although 240-grit EP is the most common practice). There is some evidence in the literature (62,63) to support this, but it is not overwhelmingly convincing. It also is important to note that recent advances in mechanical finishes have produced surfaces that easily rival the appearance of any electropolished surface (Lee Industries, personal communication, 1996).

It should be (but is not always) evident that cost increases with surface smoothness. It is also important to note that just because a surface is almost perfectly smooth does not guarantee that it will be easy to clean. Cleanability will also depend on the nature of the interaction between foulants and the surface material. The only way to know for sure is to try your broth on various surfaces and then make a specification based on rational evaluation of the experimental information. Surface material and finish, cleaning agents, and cleaning protocols must be considered together—preferably before design.

Passivation must also be considered. This is a treatment that restores oxides that protect stainless steel from corrosion but can be removed during vessel fabrication (primarily welding). The process is rather simple, but the surface chemistry is not and is not completely understood (64,65); hence, there is controversy as to which method is best and whether it is really as necessary for fermenters as it is for high-purity water systems where rouge formation is a serious problem (66). Two methods are in common use: (1) treatment with sodium hydroxide, citric acid, and nitric acid; and (2) treatment with chelating agents. The second is much milder and does not generate the noxious waste of the first. Both appear to be equally effective; hence, the chelating method is becoming more popular.

50.5.2.3 Nozzles. Ports for additions and probes must be designed to be sterilizable and cleanable. Among other things, this means they must have reliable seals and be free draining. The major debate here usually focuses on the choice between Ingold ports and those designed

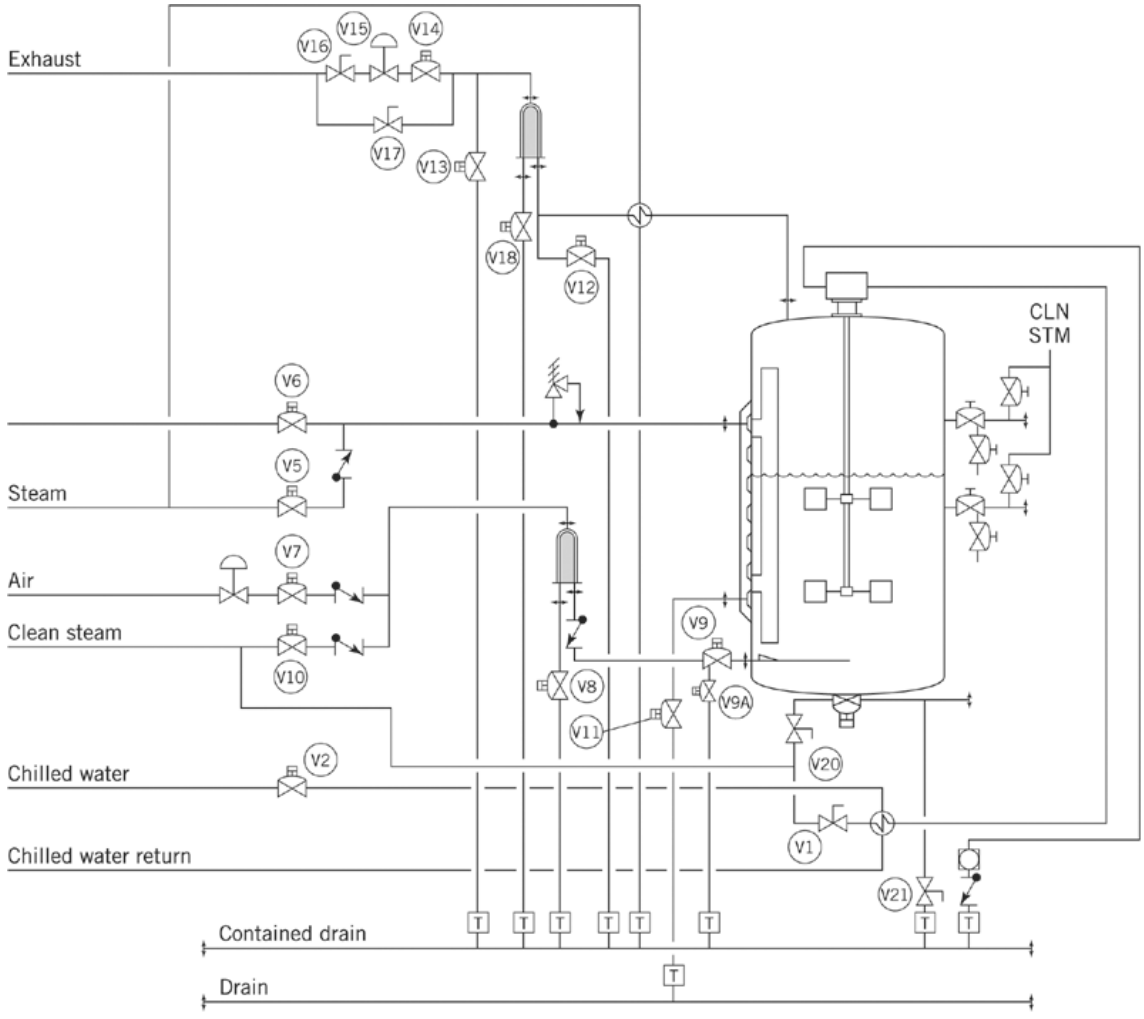


Figure 50.5. Simplified fermenter piping diagram.

for sanitary clamp connection (Fig. 50.6). There have been sterility problems with Ingolds, most of which have been traced to the ports being out of round as a result of distortions caused by welding. Such distortion causes obvious problems with the O-ring seals. This problem can be corrected quite easily by making the nozzle thick enough to avoid distortion. Our experience has been that such a correction yields nozzles that are just as reliable and more easily cleaned than are sanitary fittings when both are mounted at the usual 15°.

50.5.2.4 Side View Ports. The first word that comes to mind is "don't." Side view ports let the bugs see out more than they let you see in. The little that's gained by being able to see less than 1% of the total action does not seem to justify the expense, the jacket coving, and the cleaning and sterility problems caused by these little gems. If you must have one, we suggest the circular Metaglas™ type (Fig. 50.7) attached to the vessel with sanitary clamps; the glass is bonded directly to the metal, which avoids the sealing problems encountered with other types. It does, however, have the disadvantage of having a smaller viewing area than does a standard, circular view port, and it is more expensive. We recommend avoiding long rectangular view ports, which are very difficult to keep clean and free draining, and types in which the glass has to be sealed with gaskets and/or O-rings on both sides (Fig. 50.8). Keep in mind that tolerances for glass are measured in fractions of an inch, not thousandths. That, coupled with the fact that the gaskets will compress means that the probability of repeatedly achieving a good seal and good cleaning is lower than your odds of winning more than once at Atlantic City.

50.5.2.5 Baffles. Baffles are usually required in high-power systems to prevent swirling and vortexing, thereby increasing the power that can be delivered to the fluid. The usual practice is to use four baffles on 90°

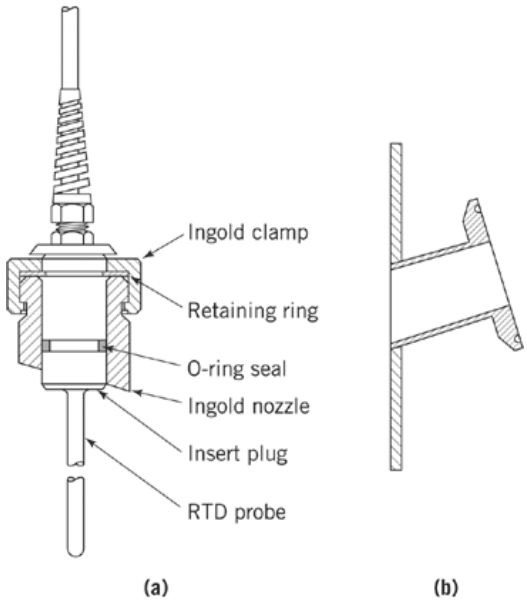


Figure 50.6. Ingold and sanitary clamp fittings.

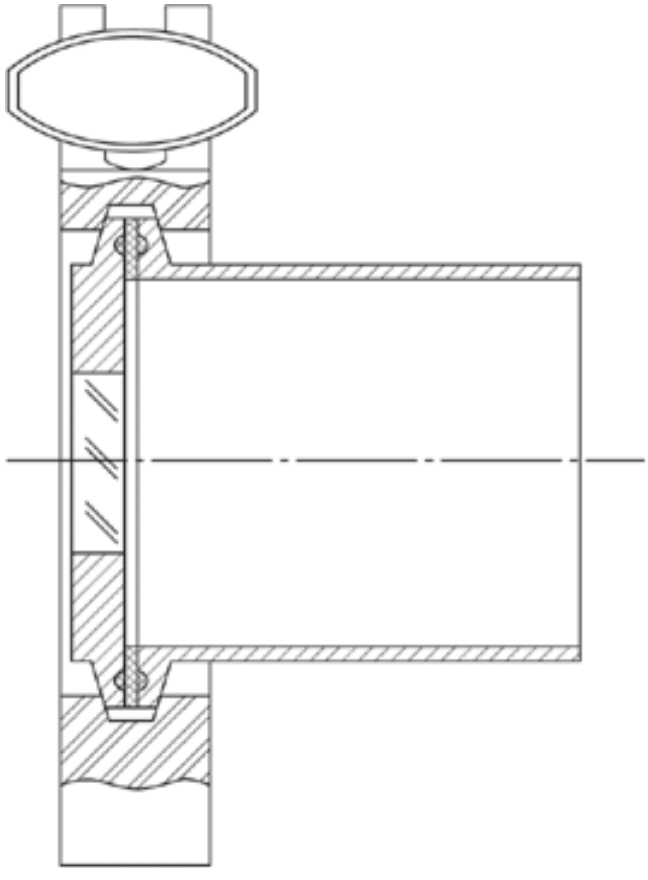


Figure 50.7. Metaglas™ side viewport.

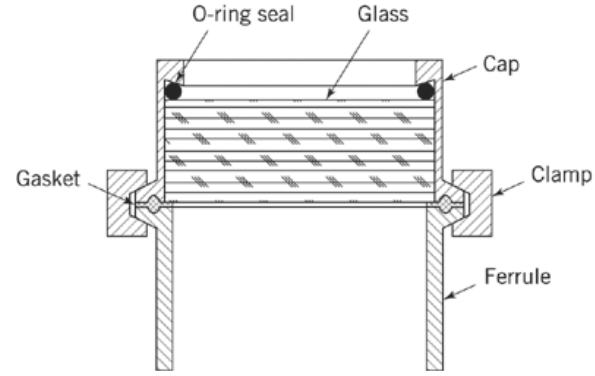


Figure 50.8. Side viewport with separate glass piece sealed by two gaskets.

centers welded directly to the wall. Each baffle should have a width equal to 10% of the tank diameter and should have long slots cut out of the edge facing the wall so as to prevent solids build up and to make cleaning easier. Removable baffles are used in some cases; however, we discourage this practice, particularly in cases where cleaning is a critical issue, simply because unsealed joints resulting from baffle removal make cleaning more difficult.

50.5.2.6 Jackets. Several types (67) of jacket are used on fermenters; the choice of type is usually not critical for heat transfer purposes and is best left to the vessel fabricater. In some cases, however, a jacket type (e.g., half pipe) may be chosen to increase the vessel pressure rating. The following have proven to be useful practices:

- The jacket should extend from the probe ring (about 2 in. above the bottom tangent line) to the top tangent line and should be zoned. This allows additional active surface area to come in contact with the broth as the volume increase due to additions and to increasing gas holdup, minimizing cooling-loop pressure drop, and minimizing medium bake-on.
- Connections to the jacket should be via sanitary clamps or flanges, not by screwed fittings. This minimizes possible damage to jacket welds when cooling lines are connected or disconnected.
- Coolant should be filtered to avoid solids buildup and/or jacket fouling.
- Bottom jackets should be considered only for vessels larger than 5,000 L. The additional area will be about 10% of the straight side jacket area (allowing for bottom drain, etc. and will add about 5% to the cost of the vessel). In cases where there is an internal coil, bottom jacketing isn't necessary or desirable.
- Jacket coving to accommodate view ports, decreases jacket area and effectiveness and increases cost considerably. It should be avoided.

50.5.2.7 Internal Cooling Surfaces. Coils are the most common internal cooling surfaces, although there are other types (68). They can easily double the available heat transfer area and tend to be more effective than jackets; however, they can have big disadvantages:

- They make cleaning very difficult.
- They can cause additional bulk mixing problems, particularly for very viscous non-Newtonian broths.
- They will eventually leak nonsterile coolant into the broth.
- They can add up to 25% to the cost of the vessel.

We recommend that every other alternative (including slight decreases in growth rate and/or cell mass) be considered before yielding to the temptation to use coils. Keep in mind that, once installed, they will be there for the life of the vessel. If you absolutely, positively must use a coil, there are several points to remember:

- Mount it in a way that will insure minimum stress during heat-up and cooldown.
- Weld cladding over the butt welds used to join the coil pipe sections.
- Leak test (69) after construction and build in design features that will simplify leak testing on a regular basis thereafter.
- Space coil turns at least 3 in. apart. Anything closer will insure major cleaning problems.

50.5.2.8 Spargers. There has been a lot of discussion concerning the pros and cons of ring and single-orifice spargers, and the details of design of each. We have seen both work well and have not found any evidence for the validity of claims concerning the importance of hole size (for example) for oxygen transfer per se. The primary focus should be on gas distribution (which will depend on other aspects of the agitation system) and on aseptic operation. We usually favor single-orifice spargers.

There also have been advocates of porous (frits) spargers. The rationale presented has focused primarily on the small bubble size such spargers produce. There is some basis for these claims in cases where little mechanical energy is available for bubble breakup (e.g., in mammalian cell systems). There might also be some value in cases for which bubble coalescence is not a problem (far and few between in practical systems). They can be extremely difficult to clean, particularly for mycelial organisms. We usually suggest they not be used except in very special cases, as just noted.

Finally, it is important that the sparger be made and mounted in such a way that it can be removed easily for cleaning.

50.5.3 Piping and Valving

Design and construction details of the piping system depend on process, sterility, cleaning, and containment requirements, taken together.

50.5.3.1 Service Lines for Non-Process-Contacting Fluids. All lines providing fluids that cannot contact process fluid surfaces (e.g., coolant lines, plant steam lines for heating only) fall into this category. Satisfactory service is provided by either copper or stainless steel piping along with a rational combination of welded and compression fittings. Durability, servicability, cost, and corrosion resistance are major considerations. Ball valves are satisfactory on lines not turned on and off frequently (diaphragm valves tend to withstand a greater number of on–off cycles prior to failure).

50.5.3.2 Sterile Piping Systems. Before we discuss design of sterile piping systems, we reiterate the importance of a systems approach to integrating vessel and piping design. Independent design almost always results in a lot of aggravation, as well as higher cost and lost time.

A sterile piping system can usually be divided into five major subsystems: process, steam/condensate, air, harvest, and seal lubrication. Each has specific requirements dependent on its unique functions as well as the specific demands of the process. None of these systems is completely independent of the others, and all share common components. All also interact with the CIP piping system, which is discussed later.

Details of each of these subsystems follow a simplified description of sterilization procedures (Fig. 50.5). The reader is advised that the procedure is one of several commonly practiced; there are, for example, different opinions as to when live steam to the air inlet line should be turned on.

Phase 1 . After the vessel is filled with set medium, steam flow is started through the jacket. The agitator is run at low speed, and particulate free steam lubricates the shaft seal. The exhaust line is open for venting to the atmosphere. All other valves are closed. During this time not only are the vessel and the set medium being heated, but air is being purged from the medium. If the air is not purged, the vessel pressure during sterilization can become dangerously high, and there will not be a reliable correlation between pressure and temperature. Phase 1 continues until the medium temperature reaches 100°C.

Phase 2 . Steam continues to flow through the jacket. The air exhaust line is closed; the only path out is via steam traps. Steam is now admitted through the air inlet line to sterilize the inlet filter; steam leaving the vessel through the air exhaust line sterilizes the exhaust line piping and the exhaust filter. Steam flow is started through subsurface

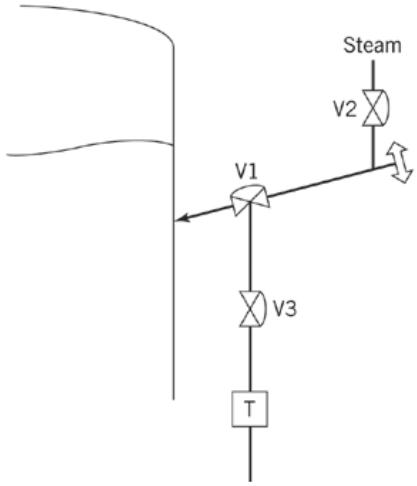


Figure 50.9. Sterilization of subsurface ports.

ports via steam lock assemblies (Fig. 50.9). (See later for further discussion of steam locks.) Ports above the liquid surface are sterilized by steam escaping through them from the vessel and then to condensate lines. Steam flow also is started through the bottom drain valve. All steam flows continue until the cooldown begins. Phase 2 continues until the medium temperature reaches 121°C.

Phase 3. Steam flow to the jacket is throttled to hold sterilization temperature constant until cooldown begins.

Phase 4. Cooldown. This is not discussed here.

50.5.3.2.1 General Principles. There are several general principles that should be applied to all sterile piping:

- Make all piping system components free draining. This requires special attention to the details of pipe pitches, valve orientations, and so forth
- Design all components and the piping layout so as to eliminate nooks and crannies where contamination (biological and nonbiological) can hide so as to escape cleaning and/or sterilization. Frequently overlooked problems include such things as deadlegs and ridges formed by welding operations.
- Make steam and condensate piping at least 3/8 in. diameter to insure proper steam flow and condensate draining.
- Make all piping lengths as short as possible without interfering with good fabrication practices (GFP), operability, and maintenance.
- Use check valves only when no other solution is possible (e.g., in overpressurized lines).
- Do not use sight glasses in condensate drain lines except in the seal lubricant drain line.
- Pay careful attention to piping orientation to avoid the possibility of air traps and inadequate heating (55,56).
- Make sure that bottom drain valves are flush-mounted diaphragm valves capable of being steamed in the closed position (Fig. 50.10). They must be free draining.
- Avoid dip tubes unless there is no other way (there almost always is).

Finally, the design should take into consideration the methods that will be used for validation of sterilization operations. These will vary considerably with the product and the organism. At one extreme is virtually no validation; at the other extreme is temperature mapping of the vessel and all the trap lines, as well as the use of spore strips and/or spore ampules in the vessel and in the trap lines. In some cases, tee sections have been included in drain lines for insertion of spore strips.

50.5.3.2.2 Welds. Orbital welding of the piping system produces the most reliable results with regard to aseptic operation and cleanability; it is essentially a requirement for many classes of regulated products, particularly those regulated by Center for Biologics Evaluation and Research (CBER). It also is the most expensive to build and to maintain. There are, however, many processes for which an economic combination of welded and compression fittings is acceptable. These can be operated quite satisfactorily if proper attention is paid to cleaning, sterilization, and maintenance protocols. The fact is that such systems have been used for many years to manufacture regulated products safely and efficaciously.

50.5.3.2.3 Valves. Diaphragm valves have become essentially required for most classes of regulated fermentation products. There is little argument that their design provides the greatest reliability for clean, aseptic operation. They have the added advantage of integral sterile access ports, which permit very short piping runs, particularly in valve clusters. Historically, diaphragm valves have been more expensive than have ball valves, but this has changed recently, particularly for some materials (e.g., SS316L). It therefore makes sense to use diaphragms for most applications. The primary exceptions are steam lines or other applications in which diaphragm life is a problem; in those cases one should consider ball valves or plug valves, as appropriate.

Another important consideration is the extent to which one uses valve actuators and position indicators. Obviously, this will depend in large measure on the nature of the control systems employed. In any event, one should consider very seriously the problems (e.g., space and orientation constraints, reliability) associated with valve "extras" while control system decisions are being made.

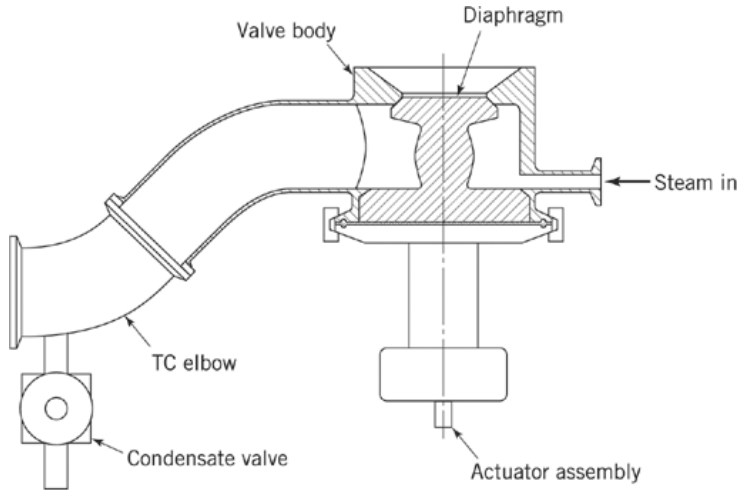


Figure 50.10. Bottom drain valve.

50.5.3.2.4 Steamlock Assemblies. The primary purpose of steamlocks (also known as block and bleed) is to allow sterilization of ports and process piping at any time during a fermentation in such a way that connections can be made and broken without risk of breaching the sterile barrier and/or the containment barrier. A basic steamlock assembly is illustrated in Fig. 50.11. In this case, vessel T1 contains presterilized nutrient that must be added at some time during the fermentation. T1 is connected to the fermenter by means of sanitary clamps (other means are possible). Steam flow is then started (open V1, V3, and V5) so as to sterilize the connecting hose and all the valving not previously sterilized. Condensate goes to drain (sanitary, if necessary) via V3 and V5. The steam and condensate valves are closed after sterilization is complete; process valves V2 and V4 can be opened anytime thereafter to make the sterile transfer. Note that the diaphragm valve sterile access ports make it much easier to sterilize the steam side of the valves than is possible with other valve types. Variations on this theme are better suited to cases involving long transfer lines or having other special requirements.

50.5.3.2.5 Air Inlet and Outlet. Fig. 50.12 is a simplified diagram of a "typical" air inlet/outlet system. The major problems for this system are related mainly to the filters. Chief among these (other than outright failure) is wetting of both filters caused by condensate during sterilization, and wetting and clogging of the exhaust filter by condensate and/or aerosol during fermentation. These problems are not all easy to resolve and should be dealt with most seriously during design. Wetting and/or clogging of the inlet filter by condensate and/or compressor oil during fermentation also can be a problem but is usually the result of not using proper quality air, having no or improper prefilters in the air inlet

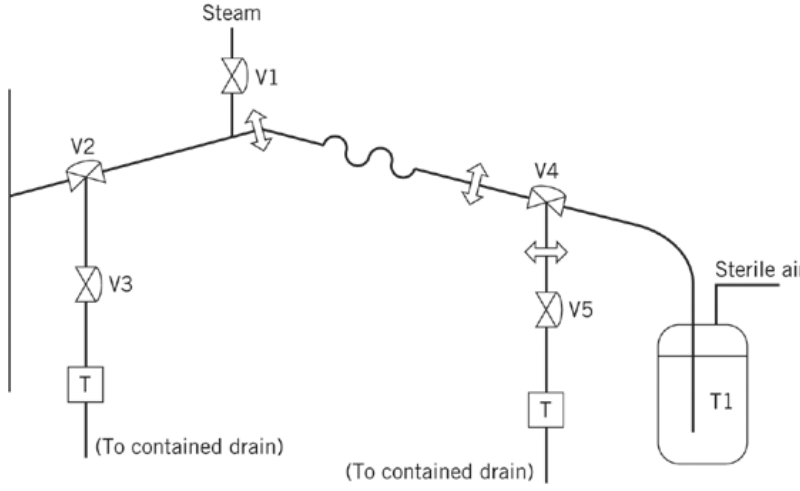


Figure 50.11. Steam lock assemblies for transfering sterile medium.

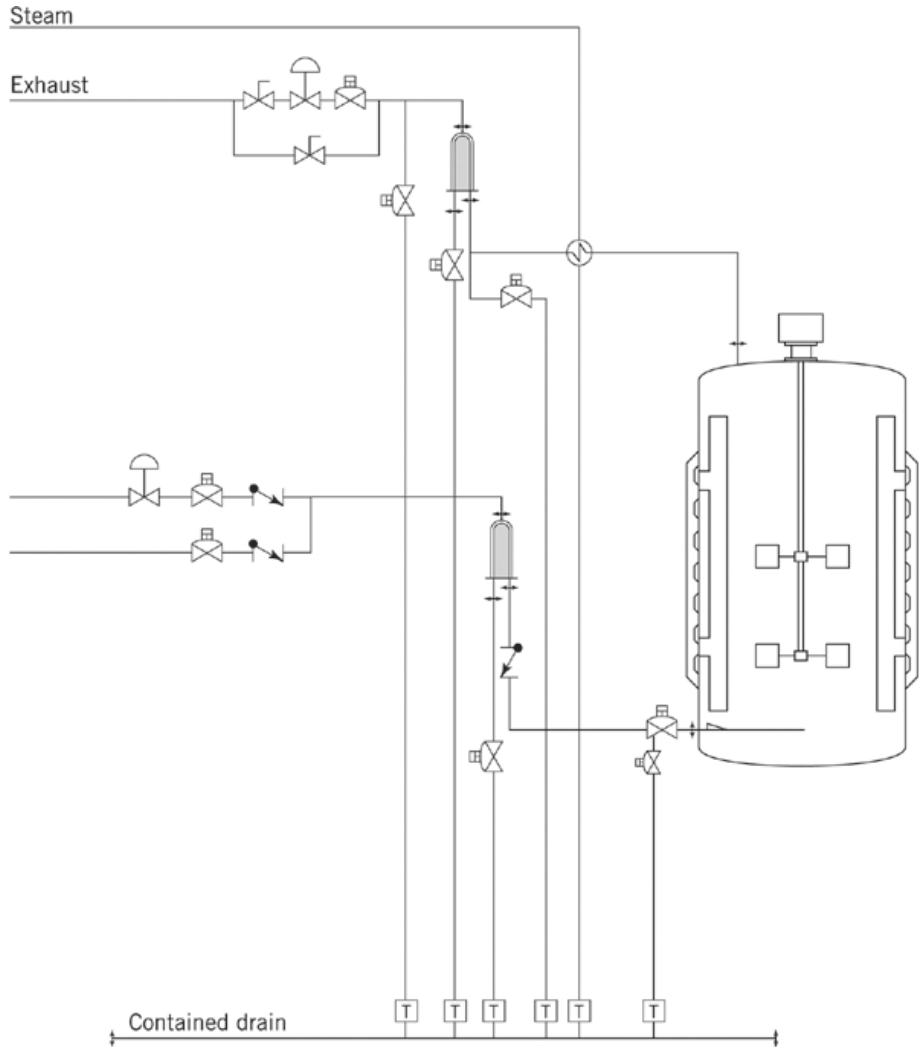


Figure 50.12. Simplified piping diagram illustrating air inlet and outlet systems.

line, and/or poor maintenance (e.g., of the compressor). All of these are easily remedied.

The extent of condensate problems during sterilization can be remedied best by ensuring that whatever condensate does form can drain freely. This can be complicated by the fact that it is undesirable to have the sterile side of the filter connected directly to the drain line. Another approach is to steam heat the filter housing such that condensation cannot occur. This is effective but has the disadvantages of adding cost and decreasing filter life.

Other factors that can affect condensate problems are the positioning and orientation of the housing. There are differing opinions concerning these; one is best advised to consider the advice the filter and the fermenter vendors for specific cases.

Plugging of the exhaust filter by condensate and aerosols during fermentation require special consideration. Air leaving the fermenter will be essentially saturated with water vapor at fermentation temperature. The exhaust line, filter, and so on usually are colder than the fermenter; therefore, condensation is inevitable. The amount of condensation will depend on temperature differences, air flow rate, and the nature of the surfaces of the components in the exhaust line (the maximum potential is easily calculable). Approaches that have been used to deal with these problems include (70):

- Condensers
- Heat exchangers; used before the exhaust filter to avoid condensation from the fermenter off gases and after the pressure control valve to prevent reflux from the exterior exhaust line
- Steam-heated filter housings
- Heated exhaust lines
- Coalescers
- All of the above

None of these is completely successful, and each has its proponents and detractors. Suffice it to say that each case should be considered on its own merits (e.g., fermentation temperature, duration, and air flow) and that combinations of the approaches should not be ignored.

The condensate problem is exacerbated by the aerosol problem. Aerosols will form in any aerobic fermentation and will carry liquid along with dissolved solids and particulates (including organisms) to the exhaust line. The only questions are how much and what problems they will cause. Among the problems are deposition of dissolved and particulate solids, not only on the filter, but also on heated surfaces or condenser surfaces. Among the problems deposition causes is reduction in heat exchange effectiveness, which reduces the capabilities of the previously mentioned devices to eliminate condensation. In severe cases, exhaust line blockage can lead to other problems related to pressure buildup and/or higher linear velocities in the exhaust line. The problem should be dealt with on a case-by-case basis during process development and fermenter design.

Provisions should be made for in situ integrity testing of sterile filters. This can be done by means of any of several commercial electronic testing devices that are based on liquid intrusion, diffusion, or some other well-established method for testing membrane filter integrity (71–73). One example of the piping necessary to perform the test on an exhaust filter is shown in Fig. 50.13.

Finally, two pressure control valves are required in the case of constant pressure sterilization (continuous flow of steam into the vessel and out to atmosphere). The reason is that the steam flow will be very much lower than the air flow during fermentation; hence, the valve C_v required to maintain steam pressure accurately will be far too small to control air pressure accurately.

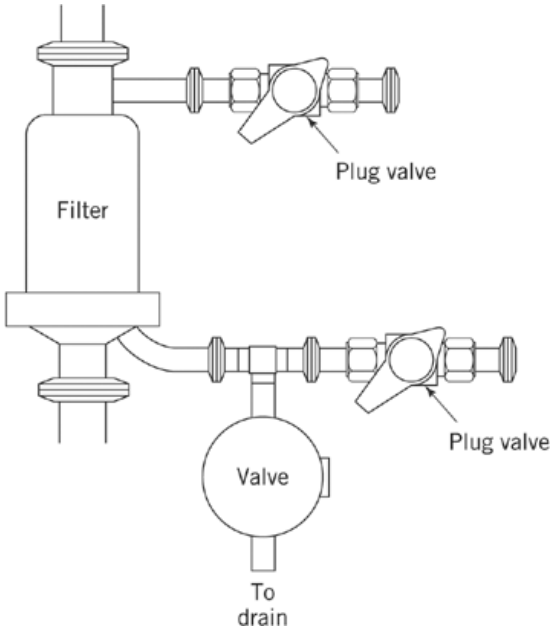


Figure 50.13. Piping diagram for in situ air outlet integrity test.

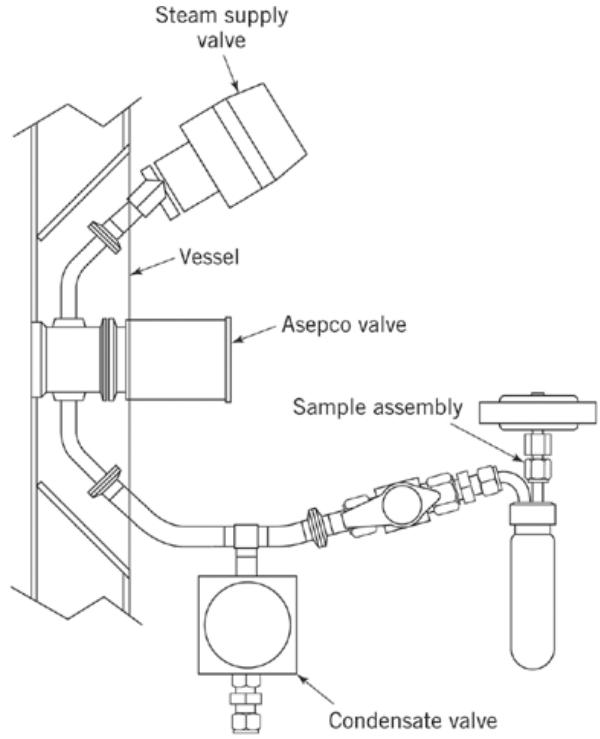


Figure 50.14. Aseptic sampling system.

50.5.3.2.6 Sampling Systems. One example of a simple aseptic sampling system is illustrated in Fig. 50.14. The sample vial, vent filter, and valve V1 are sterilized as a unit in an autoclave. The unit then is connected to the fermenter piping via a sanitary clamp. After the connection is made, steam is introduced via V3 and passes across the nonsterile sides of V2 and V1 and then to trap via V4. Once the valves and line are sterile, the steam and condensate valves are closed. Samples may be taken any time after the sampling system cools. Samples are taken via V1 and V2. Lines and valves are resterilized before the sanitary connection is broken.

The valves selected for this system will depend on the class of service required. We suggest that vessel sampling valve V3 be a flush-mounted diaphragm valve (e.g., Asepco™, NovaSeptic™) designed in such a way as to minimize dead volume and piping lengths; it is an excellent choice for service requiring very high levels of asepsis and cleanability. Less expensive valves can be used for less-demanding service, but we think that the initial extra cost will more than pay for itself. Diaphragm valves are suggested for V1, V3, and V4 in cases of demanding cGMP or containment requirements. This is not required for all classes of service; indeed, it is usually satisfactory

to use plug valves for steam and condensate lines even in many demanding circumstances. It should be noted, however, that you may encounter a perception problem if you use them for applications deemed to be sensitive.

There are several other designs that have been used successfully. A few have been designed specifically for systems requiring BL3-LS containment or higher. These are discussed later. Finally, please note that addition system design and operation are very similar to those for sample systems and are not discussed here.

50.5.4 Agitation Systems

Agitation can be done by direct mechanical coupling of the shaft to the drive or by magnetic coupling. The latter has been recommended for cases where high levels of containment are required (74). There also is the perception that magnetic drives are more suitable for maintaining more stringent levels of asepsis and cleanliness than is possible with direct drive. Neither claim has any substantive basis; indeed, there is good reason to believe that existing magnetic drives may present greater cleaning difficulties because of the manner in which the driven magnet must be mounted at the bottom of the vessel. In addition, power transfer by magnetic drive is quite low.

Direct drive is the predominant current choice at almost any scale of operation. The major mechanical decisions that must be made in this case (other than power) have been discussed at length elsewhere (4,75). The major arguments for bottom drive are ease of maintenance, shorter shafts, less support structure, and lower overall height. The arguments against bottom (and for top drive) focus primarily on the potential of catastrophic spills resulting from bottom seal failure, seal grinding as a result of broth particulates working into a bottom seal, and greater cleaning difficulties. If the seals are designed and maintained properly, none of these is a problem. We have seldom seen any real difference in aseptic operability between top and bottom drives, and we are reasonably certain that the organisms don't care. The choice probably will continue to be driven primarily by personal preference.

There are very few cases in which double mechanical seals are not (or should not) be used in fermenters. The major debate focuses on seal orientation and the details of individual seal designs. There are basically two orientations used: inline (Fig. 50.15) and back-to-back (Fig. 50.16). The

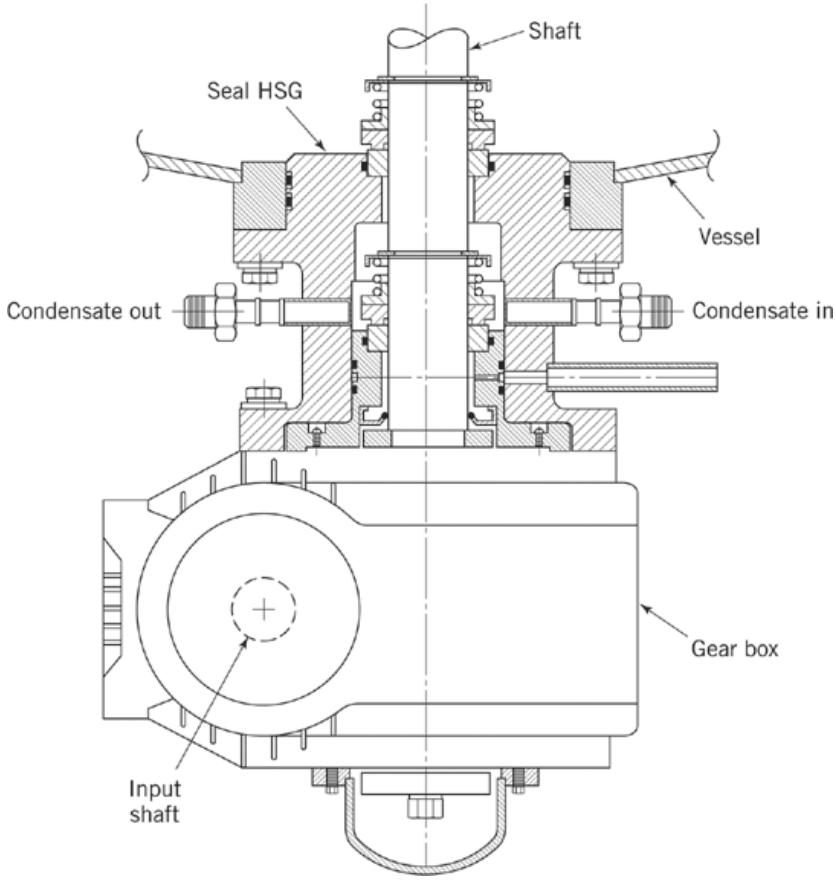


Figure 50.15. In-line double mechanical fermenter shaft seal.

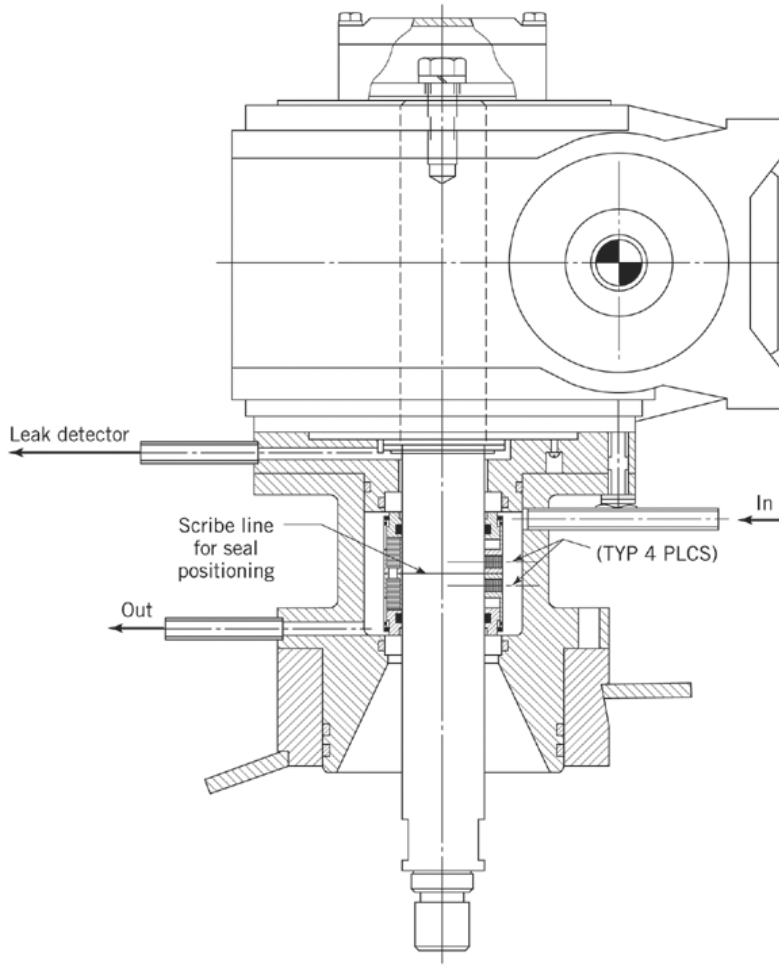


Figure 50.16. Back-to-back double mechanical fermenter shaft seal.

details are discussed in Refs 4 and 75. We recommend in-line design because we have found it to operate more cleanly and require a simpler sterilizing/lubricant system (4,75).

Seal lubrication is usually provided by means of sterile steam condensate. It is extremely important that this condensate be free of particulates: their presence guarantees rapid seal failure, contaminated fermentations, and a hyperactive maintenance program. It is also important to note that during sterilization live steam flows through the seal housing. There are some who insist on keeping the steam flowing throughout the fermentation. (Obviously, they have no faith in the seals.) The one thing this will guarantee is much more rapid wearing of the seals (perhaps supporting the lack of faith in the seals).

One must also decide on the means for controlling lubricant flow rate. Most use a valve for this purpose. We suggest an orifice sized to deliver the proper flow. This avoids the cost and maintenance of a valve and insures fiddle-proof operation. It does, however, require the use of particulate-free condensate, but then so does proper operation of the seals. We also recommend including a sight glass in the lubricant drain line as well as a seal leak detector (Fig. 50.17). Other more complex detection systems might be considered for specific circumstances (e.g., severe containment requirements).

Finally, preventing shaft vibration is another important factor in agitation system design. Shaft vibration is a safety hazard. It will also cause premature seal failure and other costly mechanical damage. Details have been presented elsewhere (4).

50.5.5 Cleaning Systems

As noted earlier, specific requirements for cleaning depend on several factors including the nature of the fermentation

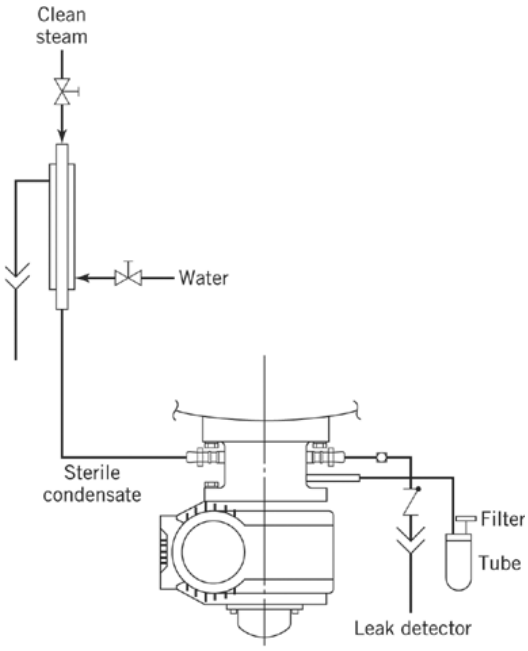


Figure 50.17. Piping diagram illustrating lubricant flow sight glass and seal leak detector.

broth. There is a major difference between most microbial broths and most mycelial broths. Single-cell microbial broths, with the exception of those containing a lot of undissolved particulates and high viscosity components (e.g., xanthan broths), tend to be free draining and readily amenable to cleaning based primarily on the physicochemical action of the cleaning agents. Many fungi and mycelial bacteria, on the other hand, tend to cling to fermenter internals and may require mechanical action (e.g., high-velocity jets) in addition to cleaning agents.

The following guidelines are applicable for most systems. These principles must be applied in light of the actual cleaning agents and protocols to be used:

- Eliminate internals and nooks and crannies to the greatest extent possible in the vessel and throughout the piping system. This practice is consistent with design for aseptic operation.
- Drill and position sprayballs to insure complete coverage of all surfaces inside the vessel. This usually requires an empirical approach. Coverage can be tested by means of the riboflavin test. The reader is cautioned, however, that complete coverage is a necessary but not sufficient condition for cleaning. Also, please note the following:
  - Spray balls designed for sanitary operation are self-draining and self-cleaning. They can be sterilized in situ. There is, however, considerable debate concerning whether they should be removed prior to fermentation.
  - High-velocity, rotating devices that may be necessary when large clumps of sticky residue must be removed (e.g., as with a fungus) are not designed to be inherently self-cleaning, self-draining, or sterilizable. They should not be mounted permanently.
- Eliminate deadlegs in piping and deadspaces in valves, fittings, and other system components. This is also consistent with design for aseptic operation.
- Specify the same materials and finishes for process and CIP piping as are specified for the fermenter. Obviously, these must be compatible with the cleansers and conditions used.
- Avoid threaded joints. A completely welded system is best, but compression fittings can be satisfactory when cost is a major consideration, particularly for nonregulated products.
- Make CIP piping as simple as possible. For example, make dual use of process and other piping as much as possible.
- Avoid complex, expensive transfer panels wherever possible. Use swing elbows wherever practical.
- Design and construct the system to facilitate validation and on-going testing for removal of contaminants, including the cleaning agents. This design should provide for swabbing, obtaining rinse samples, or whatever else the cleaning protocol requires.

A portion of one approach to integral CIP piping is illustrated in Fig. 50.18.

There are many cases for which a portable CIP system is preferable to an integral system. For such cases, the fermenter and the portable unit should be designed to allow simple mechanical attachment of the necessary hoses between the two units and with utilities, and a straightforward means for interfacing the instrumentation, logging data, and controlling the systems of the two units.

Finally, we note that classical CIP systems rely on continuous cleanser flow and the maintenance of a shallow puddle in the bottom of the fermenter. To achieve this they rely on special pumping devices such as eductors (74). Aside from the design, control, and other operating problems this causes, it has been observed in some facilities that the stable pool leads to the formation of "cleaning rings" at the bottom of the fermenter. These rings may not be real problems (additional evidence is still required), but they do cause perception problems. We suggest the use of a pulsed-flow system to overcome not only the need for special pumping devices but also the "cleaning ring" problem. Such pulsed systems have been found to accomplish both objectives in practice.

Additional details concerning fluid velocity, vortex elimination, and many other aspects of CIP system design and operation are described elsewhere (59).

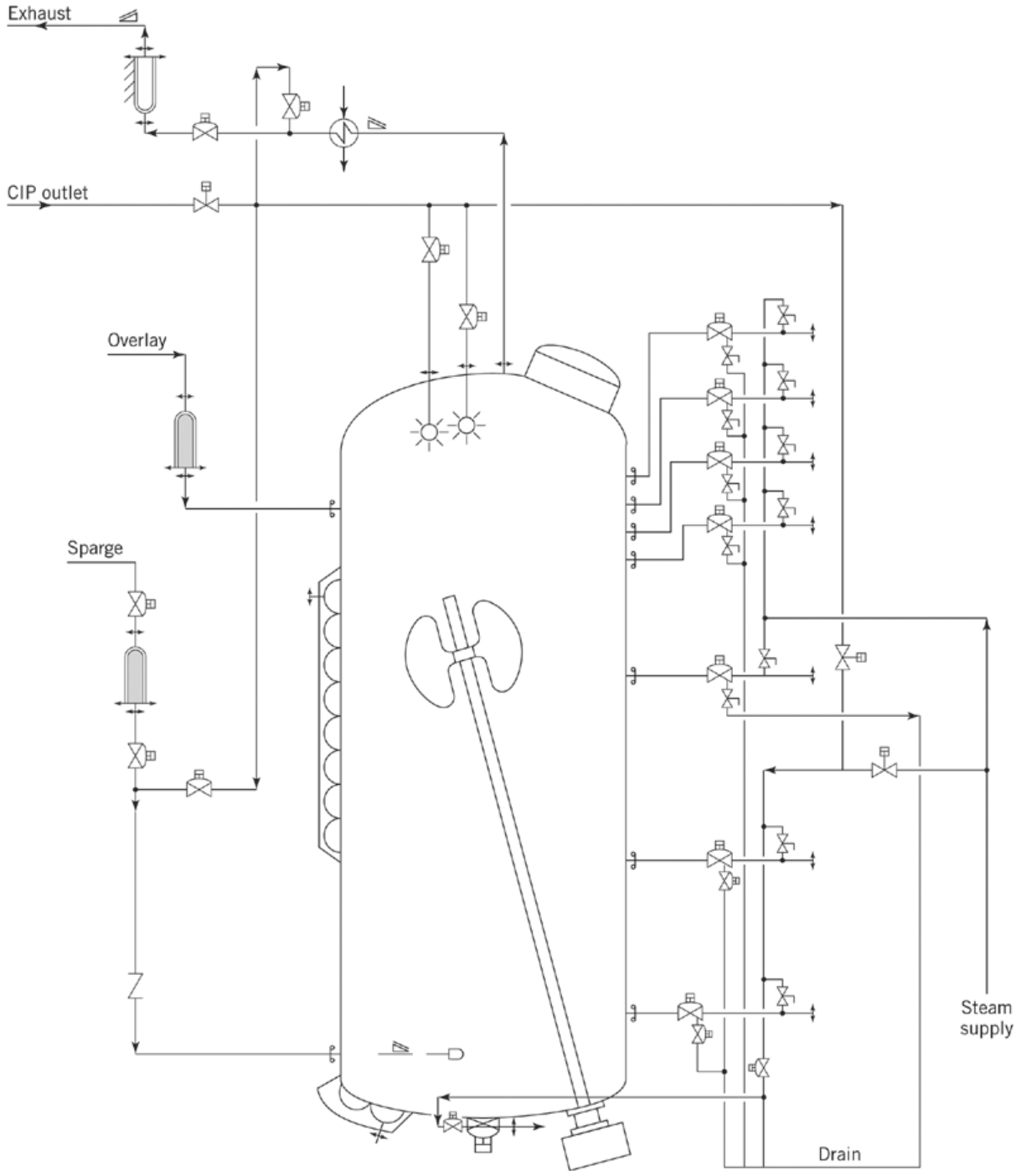


Figure 50.18. Simplified CIP piping diagram.

50.5.6 Containment

Our scope is limited to containment of fermenters; however, we reiterate here the importance of making certain that the equipment, the facility, and the operating protocols be considered simultaneously to ensure compatibility with regard to containment (just as in the cases of sterility and cleaning). As noted earlier, most new facilities for regulated products are being built to satisfy BL2-LS facility requirements and (in most cases) BL3-LS fermenter containment requirements. With few exceptions (about which there is no agreement) there is no difference with regard to the equipment containment requirements at the two levels—at present.

The guidelines require that BL2-LS/BL3-LS fermenters be designed and constructed to prevent organism release (primary containment) from the vessel and from any of the subsystems noted earlier; hence, they must be built as closed systems. (Note that it also is possible to enclose a fermenter in a biosafety "cabinet," but this is not usually practical or necessary.) Some areas that have been subject to greater scrutiny than has been required for cGMP compliance are as follows. In evaluating the discussion, the reader should bear in mind that there is not much information readily available concerning containment reliability data. Some progress is being made via the Industrial Biosafety Project in the United Kingdom.

- *Static seals*. It has been suggested that double static seals (e.g., in headplates) be used for BL2-LS and that double static seals with a steam trace between the seals be used for BL3-LS (76). There has been little to demonstrate that these are either needed or desirable. Indeed, there have been substantive arguments made against using such devices (76). There is as yet no consensus.
- *Rotating seals*. Arguments have been made in favor of using magnetic drives at anything higher than BL2-LS. This was discussed earlier. There are many who argue that only top drive be considered for BL2-;LS and above. Their reasons have mainly to do with avoiding the possibility of large spills in the event of catastrophic seal failure. Such a circumstance is possible but highly unlikely. Leak detectors (which would normally be installed for cGMP requirements) would almost certainly indicate a leak long before there was the remotest possibility of catastrophic failure. One also should consider that a leak in top drive seal might be more difficult to detect and could lead to release of a more insidious nature. Again there is no consensus. Finally, it has been suggested that a low-pressure sensor or flow sensor be used to detect lubricant flow failure. This could help to avoid seal failure (77).
- *Sampling systems*. One system recommended (78) for contained sampling is illustrated in Fig. 50.19. Note that it is similar to the system in Fig. 50.14 recommended for cGMP compliance. It is a bit more complicated and may provide some incremental benefit; however, this might be outweighed by the greater likelihood of operator error. There have also been more complex systems suggested that involve more intricate valving and/or biosafety cabinets. It is apparent that this is an area that needs considerably more development work.
- *Air exhaust system*. It has been suggested that two in-series sterile filters or a sterile filter followed by an incinerator be used at BL2-LS and higher. All other aspects are covered by the earlier discussion of exhaust lines.
- *Pressure relief*. This is an area of some controversy because of the need to satisfy physical and biological safety requirements simultaneously. It has been suggested by many that relief venting be done via a large kill tank protected by a HEPA filter; however, this could be in conflict with physical safety codes that require there be no devices in the relief path (79). We do not have anything approaching universal agreement here; however, it does seem fairly apparent that limiting the supply pressure would help to minimize the risk. There does appear to be agreement on the use of rupture disks rather than pressure relief valves; this is consistent with accepted practice for cGMP compliance. Rupture disks are cleaner and are not prone to sticking.

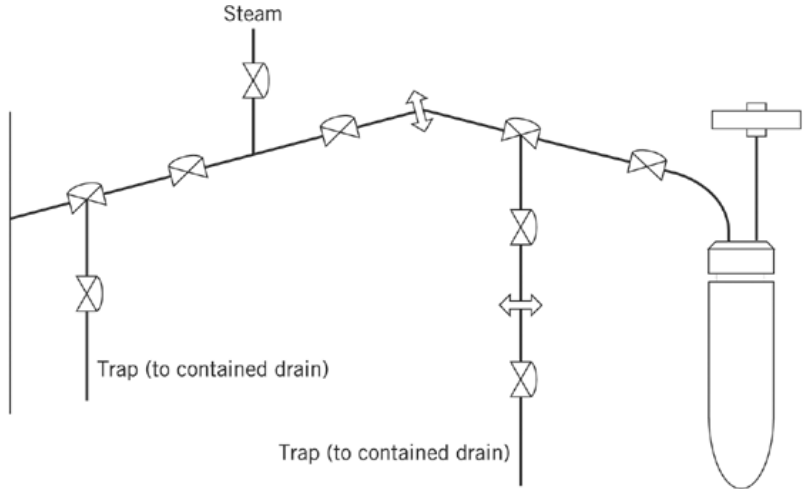


Figure 50.19. Contained sampling system. *Source*: Adapted from Van Houten (78).

Finally, HAZOP evaluations for fermenter containment have been recommended. Such analyses would evaluate potential hazards that might be caused by a wide range of incidents (e.g., fire) not limited to normal operation.

50.6 CONCLUSION

Our intent has been to present a balanced view of stirred-tank fermenter design and construction for microbial and and mycelial organisms. There are, however, several important aspects that space and scope considerations prevent us from considering in the depth they warrant. In particular, we would like to have included more information related to overall process considerations, instrumentation, and control; however, we believe that these are addressed elsewhere in this volume. We trust that we have conveyed the sense that fermenter design is very much an art and that we have convinced you to consider each case separately.

REFERENCES

1. D.I.C. Wang, C.L. Cooney, A.L. Demain, P. Dunill, and A.E. Humphrey, Fermentation and Enzyme Technology, Wiley, New York, 1979.
2. M.L. Schuler and F. Kargi, Bioprocess Engineering: Basic Concepts, Prentice-Hall, Englewood Cliffs, N.J., 1992.
3. H.W. Blanch and D.S. Clark, Biochemical Engineering, Marcel Dekker, New York, 1996.
4. M. Charles and J. Wilson, in B.K. Lydersen, N.A. D'Elia, and K.L. Nelson eds., Bioprocess Engineering, Wiley, New York, 1994.
5. S. Yokell, Chem. Eng. 93: 75–83 (1986).
6. S.P. Vranch, in W.C. Hyer ed., Bioprocessing Safety, Worker and Community Safety and Health Considerations, STP 1951, ASTM, Philadelphia, 1990, pp. 39–57.
7. C.H. Collins, in C.H. Collins and A.J. Beale eds., Safety in Industrial Microbiology and Biotechnology, Butterworth Heineman, Oxford, U.K. 1992, pp. 23–33.
8. Guidelines for Research Involving Recombinant DNA Molecules, Fed. Regist. 59(127): 34496–34547. (July 5 1994).
9. Management of Health and Safety at Work Regulations, HMSO Publication Centre, London, 1992.
10. Council Directives on the Protection of Workers from Risks Related to Exposure to Biological Agents at Work (90/679/EEC), Off. J. Eur. Commun. 33: 1–12 (1990).
11. M.C. Flickinger, E.B. Sansone, Biotech. Bioeng. 26: 860–870 (1984).
12. Design Criteria for Viral Oncology Research Facilities, DHEW 78-891, Department of Health, Education, and Welfare, Washington, D.C., 1978.
13. M. Dick and E. Hanel, Design Criteria for Microbiological Facilities, Fort Dietrick, Maryland, vols. 1 and 2; Dept. of the Army, Technical Engineering Division Project 1B662706A072, 1970.
14. R.S. Runkle and G.B. Phillips, Microbial Contamination Control Facilities, Van Nostrand Reinhold, New York, 1969.
15. C.A. Perkowski, in B.K. Lydersen, N.A. D'Elia, and K.L. Nelson eds., Bioprocess Engineering, Wiley, New York, 1994, pp. 730–743.
16. E.L. Paul, in W.C. Hyer ed., Bioprocessing Safety, Worker and Community Safety and Health Considerations, STP 1951, ASTM, Philadelphia, 1990, pp. 65–73.
17. Code of Federal Regulations, Title 29, Washington, D.C. 1996.
18. Code of Federal Regulations Title 21, Washington, D.C. 1996.
19. Points to Consider in the Production and Testing of New Drugs Produced by Recombinant DNA Technology, Food and Drug Administration, Washington, D.C., 1993.
20. Points to Consider in the Manufacture and Testing of Monoclonal Antibody Products for Human Use, Food and Drug Administration, Washington, D.C., 1991.
21. Biotechnology Inspection Guide, Food and Drug Administration, Division of Field Investigations, Washington, D.C., 1991.
22. Guide to Inspection of Bulk Pharmaceutical Chemicals, Food and Drug Administration, Washington, D.C., 1991.
23. Guidance for Industry for the Submission of Chemistry, Manufacturing, and Controls Information for a Therapeutic Recombinant DNA–Derived Product or a Monoclonal Antibody Product for In Vivo Use, Food and Drug Administration, Washington, D.C. 1996.
24. FDA Guidance Document Concerning Use of Pilot Plant Manufacturing Facilities for the Development and Manufacture of Biological Products, Food and Drug Administration, Washington, D.C., 1995.
25. Guidelines on the General Principles of Process Validation, Food and Drug Administration, Washington, D.C., 1987.
26. J.Y. Lee, in I.R. Berry and R.A. Nash eds., Pharmaceutical Process Validation, Marcel Dekker, New York, 1993, pp. 573–597.
27. T.J. Naglak, M.G. Keith, and D.R. Omstead, BioPharm 7(6): 28–36 1994.
28. R. Baird and P. De Santis, in B.K. Lydersen, N.A. D'Elia, and K.L. Nelson eds., Bioprocess Engineering, Wiley, New York, 1994.
29. E.K. White and D.M. Marks, in J.K. Shillenn ed., Validation Practices for Biotechnology Products, ASTM STP 1260, ASTM, Philadelphia, 1995.
30. M.G. Beatrice, in G. Stephanopoulos ed., Biotechnology: Bioprocessing, vol. 3, VCH, Weinheim, 1993.
31. L. Tuanchi and D. Yu, Biotechnol. Bioeng. 42: 777–784 (1993).
32. L. Leong-Poi and D.G. Allen, Biotechnol. Bioeng. 40: 403–412 (1992).
33. Y. Kawase and T. Kumagai, Bioprocess Eng. 71, 25–28 1991.
34. M. Charles, Adv. Biochem. Eng. 8: 1–62 (1978).
35. B.C. Buckland, K. Gwebonyo, D. DiMasi, G. Hunt, G. Westerfield, and A.W. Nienow, Biotechnol. Bioeng. 31: 737–742 (1988).
36. M. Reuss, in G. Stephanopoulos ed., Biotechnology: Bioprocessing, vol. 3, VCH, Weinheim, 1993.

37. Y. Kawase, B. Halard, and M. Moo-Young, Biotechnol. Bioeng. 39: 1133–1140 (1992).
38. J.M.T. Vasconcelos and S.S. Alves, Chem. Eng. J. 47: B35–B44 (1991).
39. D.S. Dickey, 72nd AIChE Ann. Meeting, San Francisco, November 25–29, 1979.
40. A. Bakker, J.M. Smith, and K.J. Myers, Chem. Eng. 101(12): 98–104. 1994.
41. C.M. McFarlane, X.-M. Zhao, and A.W. Nienow, Biotechnol. Prog. 11: 608–618 (1995).
42. G.J. Balmer, I.P.T. Moore, and A.W. Nienow, in C.S. Ho and J.Y. Oldshue eds., Biotechnology Processes, Scale-Up and Mixing, AIChE, New York, 1987, pp. 117–127.
43. N.M.G. Oosterhuis and N.W.F. Kossen, Biotechnol. Lett. 3(11): 645–650. 1981.
44. C.J. Geankopolis, Transport Processes and Unit Operations, Allyn and Bacon, Boston, Mass., 1983, pp. 154–157, 169–170.
45. A.W. Nienow, Trends Biotechnol., 8: 224–233 (1990).
46. J.Y. Oldshue, Fluid Mixing Technology, McGraw-Hill, New York, 1983.
47. M. Yasukawa, M. Onodero, K. Yamagiwa, and K. Ohkawa, Biotechnol. Bioeng. 39: 629–636 (1991).
48. D.G. Cronin, A.W. Nienow, and G.W. Moody, Trans. IChemE. 72 (part C), 35–40 1994.
49. C.L. Cooney, D.I.C. Wang, and R.I. Mateles, Biotechnol. Bioeng. 11: 269–281 (1968).
50. R. Pollard and H.H. Topiwala, Biotechnol. Bioeng. 18: 1517–1535 (1976).
51. P. Mohan, A.N. Emery, and T. Al-Hassan, Trans. IChemE. 70 (part C), 200–204 1992.
52. S. Aiba and K. Toda, J. Ferm. Tech. (Japan) 43: 527 (1965).
53. U. Pflug and R.G. Holcomb, in S.S. Block ed., Disinfection, Sterilization and Preservation, Lea and Feibiger, Philadelphia, 1991.
54. G.K. Raju and C.L. Cooney, in G. Stephanopoulos ed., Biotechnology: Bioprocessing, vol. 3, VCH, Weinheim, 1993.
55. J.H. Young, Biotechnol. Bioeng. 42: 125–132 (1993).
56. J.H. Young, W.C. Lasher, and R.P. Gaber, Bioprocess. Eng. 12: 293–304 (1995).
57. T. Oakley, in B.K. Lydersen, N.A. D'Elia, and K.L. Nelson eds., Bioprocess Engineering, Wiley, New York, 1994, pp. 500–521.
58. Guide to Inspection of Validation of Cleaning Processes, Food and Drug Administration, Division of Field Investigations, Washington, D.C., 1993.
59. R. Brunkow, D. DeLucia, S. Haft, J. Hyde, J. Lidsay, J. McEntire, R. Murphy, J. Myers, K. Nichols, B. Terranova, J. Voss, and E. White, in Cleaning and Cleaning Validation: A Biotechnology Perspective, PDA, Bethesda, Md., 1996, pp. 41–62.
60. S. Lombardo, P. Inampudi, A. Scotton, G. Ruezinsky, R. Rupp, and S. Nigam, Biotechnol. Bioeng. 48: 513–519 (1995).
61. C.P. Dillon, D.W. Rahoi, and A.H. Tuthill, BioProcessing 8(5): 32–35, 8(7): 31–33 1992.
62. J. Villafranca and E.M. Zambrano, Pharm. Eng. 5(6): 28–30 1985.
63. J. Butters and A. Reynolds, Process Eng. 71(2): 65–79 1990.
64. K.B. Balmer and M. Larter, Pharm. Eng. 13(3): 21–28 1993.
65. D.C. Coleman and R.W. Evans, Pharm. Eng. 10(2): 43–49 1990.
66. D.C. Coleman and R.W. Evans, Pharm. Eng. 11(4): 75–79. 1991.
67. R.E. Markovitz, Chem. Eng. 78(11): 156–163. 1971.
68. U.S. Pat. 4,670,397(July 2, 1987), E.H. Wegner and H.R. Hunt (to Phillips Petroleum).
69. C.A. Perkowski, Biotechnol. Bioeng. 26: 857 (1984).
70. M.A. Fogglesong, in W.C. Hyer ed., Bioprocessing Safety, Worker and Community Safety and Health Considerations, STP 1951, ASTM, Philadelphia, 1990, pp. 14–19.
71. T.H. Meltzer, M. Jornitz, P.J. Waibel, Pharm. Technol. 18(9): 76–84 1994.
72. S.F. Emory, Pharm. Technol. 13(9): 68–77 1989.
73. J.J. Errico, in F.J. Carleton and J.P. Agalloco eds., Validation of Aseptic Pharmaceutical Process, Marcel Dekker, New York, 1990, pp. 427–471.
74. P.D. Walker, T.J. Narendranathan, D.C. Brown, F. Woolhouse, and S.P. Vranch, in M.S. Verall and M.J. Hudson, eds., Separations for Biotechnology, Ellis Horwood, Chichester, U.K., 1987, pp. 469–479.
75. J.D. Wilson and T.E. Andrews, Biotechnol. Bioeng. 25: 1205–1214 (1983).
76. N.J. Titchener-Hooker, P.A. Sinclair, M. Hoare, S.P. Vranch, A. Cottman, and M.K. Turner, BioPharm 6(8): 32–37 1993.
77. S.R. Miller and D. Bergmann, J. Ind. Micro. 11: 223–234 (1993).
78. J. Van Houten, in W.C. Hyer ed., Bioprocessing Safety, Worker and Community Safety and Health Considerations, STP 1951, ASTM, Philadelphia, 1990, pp. 91–100.
79. G. Leaver, in P. Hambleton, J. Melling, and T.T. Salusbury, eds., Biosafety in Industrial Biotechnology, Blackie Academic and Professional, London, 1994, pp. 213–239.

51

GAS-HOLDUP IN BIOREACTORS

Christian Sieblist and Andreas Lübbert
Institute of Biotechnology; Centre of Bioengineering, Martin-Luther-University Halle-Wittenberg, Weinbergweg, Halle (Saale), Germany

51.1 BASIC DEFINITIONS

The gas holdup ε_G is an important bioprocess design variable, as it determines the maximal liquid culture volume $V_{L\,max}$ that can be processed in a given bioreactor of total vessel volume V_T.

Most production processes in biotechnology are performed as submerged cultures, where cells are suspended in a liquid medium of volume V_L. In order to support aerobic cultures with oxygen and to remove the carbon dioxide formed at sufficient rates, air is dispersed into the liquid medium. The total volume V_G of gas within the entire volume V_D of the dispersion is most often represented as its volume fraction ε_G. This is referred to as the gas holdup (Eq. 51.1).

$$\varepsilon_G = \frac{V_G}{V_L + V_G} = \frac{V_G}{V_D} \tag{51.1}$$

Dispersed gas also appears in anaerobic cultures, for example during beer fermentation. There, the gas holdup is made up by CO_2 bubbles. This gas is one of the main metabolic products during beer fermentation.

Obviously, the larger the gas holdup ε_G, the larger is the dispersion volume V_D occupying the total reactor or tank volume V_T. Particularly from this point of view we must distinguish two forms of gas–liquid dispersion within a bioreactor. The first is the dispersion of bubbles in the bulk of the culture, where bubbles rise relative to the liquid. The other is the foam that most often develops on top of the culture (1–3). Again, foam consists of gas dispersed within the continuous liquid phase, even though the gas bubbles no longer rise relative to the liquid. On the contrary, the liquid drains out of the foam, down into the bulk of the liquid. In foam, the gas holdup is quite high, sometimes larger than 99% of the total volume.

The gas volume fraction in the bioreactor is not homogeneously distributed across the bioreactor volume (27). Hence it is straightforward to distinguish between local gas holdup ε_{Gl} and the integral or total gas holdup ε_{Gt}. Whenever not directly specified, we mean the global or total gas holdup $\varepsilon_G = \varepsilon_{Gt}$. The local gas holdup, ε_{Gl}, is defined by the differential quotient (Eq. 51.2).

$$\varepsilon_{Gl} = \frac{dV_G}{dV_D} \tag{51.2}$$

In this case, we assume that we are allowed to speak about the dispersion as a quasi-homogeneous fluid. This is a reasonable assumption when we speak about technical bioreactors where the bubbles are generally very small as compared to the reactor dimensions. Of course, when we discuss effects on small scales, we should keep in mind that the gas-phase in gas–liquid dispersions is composed of individual bubbles of volume V_j. But when we are looking for effects on scales in the order of the mean bubble size, it does not make sense at all to speak of gas holdup. On such small scales, the gas–liquid two-phase flow system must be treated in a discontinuous way. In conclusion, discussions about the gas holdup in bioreactors are more or less restricted to scales which are large as compared to the bubble size.

With respect to the foam layer, we must discuss the foam formation and the stability of the already formed foam. Both

Upstream Industrial Biotechnology: Equipment, Process Design, Sensing, Control, and cGMP Operations, Volume 2, First Edition. Edited by Michael C. Flickinger.
© 2013 John Wiley & Sons, Inc. Published 2013 by John Wiley & Sons, Inc.

are of considerable practical relevance to the gas holdup in the fermenters used in bioprocess engineering. Foam formation is related to gas sparging or bubble generation. Only where bubbles are formed, can foam develop. When the bubbles rise in the continuous liquid phase they finally approach the upper surface of the dispersion. There they are slowed down before they can disengage from the dispersion. When the disengagement process is retarded, we observe a traffic jam effect, that is, a high bubble density. From this region, the liquid flows down and the gas holdup rises. Finally, the liquid phase forms only thin layers which separate the bubbles. Then we speak of foam: it is important to recognize that in a bioprocess with a foam layer on top of the dispersion, the local gas holdup rises from the upper part of the dispersion into the foam. In other words, in an actively aerated bioreactor we do not observe a sharp boundary layer between the bulk of the dispersion and the foam.

The bubbles in the foams which we are dealing with in bioreactors, are more or less stable. Usually, the bubbles coalesce after a shorter or longer time. When the number of bubbles entering the foam is smaller than the number of bubble coalescence processes, the foam layer will rise. Stable foams are persistent even if no bubbles are entering the foam layer from below. On the average, however, roughly the same amount of gas that arrives at the foam layer during cultivation processes is disappearing from the upper surface of the foam. Otherwise, the foam on top of a microbial culture, aerated with a gas flow rate of about 1 (vvm) would enter the reactor's vent line after a few seconds. There it would clog the off-gas filter so that the process would have to be stopped. In practice, foam layers increase comparably slowly so that there is time to act against foam stabilization.

51.2 BIOTECHNOLOGICAL RELEVANCE

51.2.1 Gas Holdup for Mass Transfer

One main reason for the importance of the gas holdup results from the reason why a gas holdup is established during gas–liquid mass transfer.

Most important to aerobic cultivations is the oxygen transfer from the dispersed air (in some cases enriched with oxygen), into the continuous liquid phase. It is essentially determined by the diffusion of oxygen across the liquid-side boundary layer around the bubbles, which is driven by the oxygen concentration difference O^*-O between the bulk concentration O and the concentration O^* directly at the physical interfacial area. With the corresponding volumetric transfer coefficient k_La, the corresponding transport law, the oxygen transfer rate (OTR) reads as given in Equation 51.3:

$$OTR = k_La(O^* - O) \tag{51.3}$$

A more detailed analysis shows that the coefficient k_La is composed of two factors, k_L and a. The first, k_L, considers the mean conductance of the boundary layer, around the bubble. The second, a, is the transport cross-section provided per unit volume.

The gas holdup is related to both factors: the size of the mass-transfer cross-sectional area per dispersion volume, a, and via the mean equivalent bubble diameter d, to the boundary layer conductance and thus k_L. The equivalent diameter d_j of the j-th bubble is defined as the diameter of the sphere of the volume V_j of the bubble gas. It is the preferred bubble size measure because it is more intuitive than the bubble volume V_j. The total gas volume V_G is composed of all individual bubbles (Eq. 51.4).

$$V_G = \sum V_j = \frac{\pi}{6}\sum d_j^3 \tag{51.4}$$

Using this bubble size definition, the integral transport cross-sectional area A for gas–liquid mass transfer can also be divided into the contributions from individual bubbles (Eq. 51.5):

$$A = \sum A_j = \pi \sum d_j^2 \tag{51.5}$$

where A_j is the surface area of the j-th bubble. In biochemical reaction engineering, one prefers to discuss the transport cross-section as a specific property of the dispersion. In this particular case it is a volume-related quantity. The specific interfacial area, a, is defined as the transport cross-section per unit volume of the culture (Eq. 51.6):

$$a = \frac{A}{V_D} = \frac{\sum A_j}{V_D} = \frac{\pi \sum d_j^2}{V_D} \tag{51.6}$$

With these definitions we are able to relate the gas holdup to the quantities of primary interest in biochemical reaction engineering. Starting from the definition (1), we get Equation 51.7.

$$\varepsilon_G = \frac{V_G}{V_D} = \frac{AV_G}{V_DA} = \frac{A}{V_D}\frac{\frac{\pi}{6}\sum d_j^3}{\pi \sum d_j^2} = a\frac{\frac{\pi}{6}\sum d_j^3}{\pi \sum d_j^2} \tag{51.7}$$

Since the bubbles in biotechnologically relevant dispersions are not of uniform diameter d_j, such expressions are of little practical use. It is straightforward to characterize the bubbles by a mean equivalent bubble diameter. In the light of the preceding discussion, it is convenient, as proposed by Sauter, to take the quantity d_s as such a (special!) mean of the bubble diameters (Eq. 51.8):

$$d_S = \frac{\sum d_j^3}{\sum d_j^2} \tag{51.8}$$

The sums are drawn over all bubbles j. In literature, d_s is referred to as the Sauter diameter.

An advantage of this definition of the Sauter diameter d_s is that we obtain a very simple relationship for the relevant gas-phase characteristics of bubble dispersions, as given in Eq. 51.9:

$$\varepsilon = a\frac{d_S}{6} \text{ or } a = \frac{6\varepsilon}{d_s} \tag{51.9}$$

This essentially says that the specific interfacial area a, the key quantity for mass transfer, increases proportionally to the gas holdup ε. The proportionality factor depends in a most simple way of the Sauter mean bubble diameter d_s. In other words: The specific interfacial area a, is formed by establishing a gas holdup ε and one is more effective, when the mean bubble size is kept smaller.

Only at first glance, the specific interfacial area, a, appears to be of primary importance to mass transfer. When, at the same gas holdup, ε_G, the mean bubble size d_S is too small then, although a large specific interfacial a appears and the bubbles do not have enough relative motion with respect to the continuous liquid phase. When they will stay within the dispersion, and after they became exhausted, they can no longer contribute to oxygen mass transfer. Then, in the same way as the foam, they must essentially be considered as dead volume that reduces the productivity of the reactor.

In practice, ε is primarily increased by increasing the aeration rate or gas throughput Q_G. The latter is often represented relative to the cross-sectional area A_{RCS} of the reactor. This quantity is referred to as the superficial gas velocity w_{sg} (Eq. 51.10), since it formally has the dimension of a velocity.

$$w_{sg} = \frac{Q_G}{A_{RCS}}[m^3/h/m^2 = m/h] \tag{51.10}$$

At lower superficial gas velocities of about $w_{sg} < 8$ [cm/s] the bubbles form a homogeneous dispersion with a narrow bubble size distribution, and they rise with a more or less constant velocity within the liquid phase. At superficial gas velocities larger than about 8 cm/s the bubble flow becomes heterogeneous. Additional larger bubbles are formed that rise with an enhanced velocity and the overall flow becomes turbulent. Then, one speaks of a churn-turbulent flow regime.

In bubble columns, the gas holdup ε shows a small decrease with increased column diameter. This effect is due to increased liquid recirculation with increasing scale. The volumetric mass-transfer coefficient, k_La, closely follows the trend in gas holdup (4). In the heterogeneous flow regime, that is at $w_{sg} > 8$ (cm/s), the value of k_La/ε was found to be practically independent of column diameter and superficial gas velocity w_{sg} (4).

51.2.2 Gas Holdup Determining Mixing

The second main aspect, influenced by the gas holdup, is the mixing of the dispersion. Mixing of the continuous liquid phase is a very important task for every bioreactor.

For mixing, the local gas holdup ε_{Gl} is important. This can most easily be understood, considering the important group of bubble column bioreactors. They are the preferred reactors for very large production processes such as citric acid production ($V_D > 500$ (m^3)). In bubble columns the gas is dispersed at the bottom by means of a sparger. The correspondingly enhanced local gas holdup in the sparger region leads to a reduced density ρ_D of the dispersion, which can be represented as a linear function of the local gas holdup ε_{Gl} (Eq. 51.11) where ρ_L is the density of the liquid phase:

$$\rho_D = (1 - \varepsilon_{Gl}) \cdot \rho_L \tag{51.11}$$

This immediately leads to convective flows by which the dispersion tries to counteract, that is, tries to degrade the density inversion. When the gas flow rate into the bioreactor becomes higher, the density around the sparger becomes even lower. Finally, the resulting convective flows become turbulent over the entire dispersion in the bubble column and this turbulence is required for an efficient mixing.

According to Freedman and Davidson (5) the mean fluid flow acquires the appearance of a gulf stream. This model shows a region of higher local gas holdup in the surroundings of the column axis where the mean flow velocity is rising. Corresponding to this flow, a downward-directed flow near the wall is compensating the rise. This is important for the top-to-bottom mixing in these bioreactors.

In airlift tower loop reactors (e.g. Bello *et al*. (6)) the gas holdup difference between the riser and the descender part is essential for the reactor to work, that is, to globally circulate the culture around the loop.

When the mean axial bubble velocity in the laboratory coordinate system is w_{bl} which is given by (Eq. 51.12):

$$w_{bl} = \frac{H_D}{\tau_B} \tag{51.12}$$

where τ_B is the mean residence time of the bubbles in the reactor, and Q_G is given by Equation 51.13.

$$Q_G = \frac{V_G}{\tau_B} \tag{51.13}$$

Then we get Equation 51.14:

$$\varepsilon_G = \frac{V_G}{V_D} = \frac{V_G}{A_{RCS}H_D} = \frac{V_G\tau_B}{\tau_B A_{RCS}H_D} = \frac{w_{sg}\tau_B}{H_D} = \frac{w_{sg}}{w_{bl}} \tag{51.14}$$

In other words, the gas holdup ε_G is proportional to the superficial gas velocity, the proportionality constant being the reciprocal value of the mean bubble rise velocity in the laboratory coordinate system. The superficial gas velocity w_{sg} is usually taken as the primary manipulated variable since, as will become clear soon, most important variables of gas–liquid reaction systems are primarily influenced by w_{sg}. The other important quantity in Equation 51.14, the effective bubble rise velocity, w_{bl}, depends on the fluid dynamic properties within the reactor as well of the broth rheology. Equation 51.14 has some practical consequences that will be discussed later.

The gas residence time distribution in the reactor may be influenced by the geometry of the reactor. The gas throughput and, where installed, the impeller system inducing re-circulated flows within the reactor. In order to estimate the mean gas residence time, the mean bubble rise velocity allows a first estimate. Correlations are only available for the rise velocities of single bubbles in a large basin (e.g., Clift *et al*. (7)). They must be corrected for bubble-bubble interactions in bubble swarms. Such corrections primarily depend on the gas holdup. Kendoush (8) presented a simple correction term (Eq. 51.15):

$$\frac{v_B}{v_{Bs}} = (1 - \varepsilon)^3 \tag{51.15}$$

An additional mixing effect, resulting from the gas holdup, is the local mixing made by individual bubble wakes. When bubbles rise, they carry along within their wakes some amount of liquid through the dispersion, relative to the liquid bulk. Of course, there is some liquid transfer between the wake and the bulk, but on the average, the rising bubbles carry the liquid for some seconds. This results in liquid displacements in the order of several decimeters. When the wake is roughly half the bubble volume, this means at a gas holdup of 20%, roughly 10% of the entire liquid is steadily being shifted relative to the bulk motion, by means of the bubbles. Hence, the local mixing due to the bubbles is primarily a function of the gas holdup.

In the most important bioreactors, the stirred tank reactors, the situation is not very different. Only when the impeller system works, it superimposes an additional mean flow on the bubble column flow. But in stirred tank bioreactors the gas holdup has another indirect influence on mixing: The larger the gas holdup, the lower the power that can be transferred from the agitator into the dispersion at the same stirrer speed. This results from gas cavities developing behind the impeller blades due to the lower pressures at these places which attract bubbles. The gas cavities reduce the effective flow resistance of the impeller blades and thus, at a predefined stirrer speed, less mechanical power will be transferred into the flow.

Another aspect to note is that the gas, which is sucked into the cavities behind the impeller blades, is redispersed into the bulk of the dispersion such that there is a constant gas flow through these cavities. The mean size of these secondary gas bubbles is determined by the impeller geometry, the stirrer speed, the gas holdup and the rheological properties of the fluids. The amount of gas redispersed in this way is larger than the gas delivered by the primary gas sparger, because it will be recirculated several times through the cavity system. Hence, in stirred tank reactors the mean bubble size and the gas holdup is determined more by the impeller system than by the sparger (25). From the practical point of view this means that it does not make much sense to optimize a sparger construction for stirred tank reactors with respect to small primary bubble sizes. Thus, in many production-scale bioreactors, an open tube is used for gas supply to the cultures.

51.2.3 Gas Holdup and Foam

The key problem with a foam layer on top of the dispersion is that when it becomes too high, it enters the vent line and reaches the off-gas sterile filter. After a short time, the filter will clog and finally prohibit the gas throughput. Foaming is not completely predictable. In order to avoid such situations, the headspace chosen must be quite large, allowing the development of rather large foam volumes before the foam can enter the vent line. This obviously restricts the culture volume, which can be operated in the vessel, to rather low values. In production-scale baker's yeast cultivations for instance, the average dispersed gas and foam sum up to roughly 30% of the liquid volume. Moreover, additional 10–20% must be reserved for situations in which extraordinary amounts of foam are being formed.

From the reactor design perspective, both parts, the dispersed bubble part and the foam layer on its top, influence the process performance in different ways. However, both must be discussed in the same context for a number of reasons:

(i) The size of the culture that can be operated in a given bioreactor is determined by both.

(ii) During the main cultivation phases both parts cannot sharply be separated from each other. In most reactors, their relative volumes can neither be determined nor controlled.

(iii) Most measures affecting one part immediately influence the other one. Antifoam agents, for example, reduce the foam but also the gas holdup in the bulk of the culture.

There are a few more important aspects where culture and foam interact. By virtue of their surface properties, some cells have the tendency to concentrate at gas–liquid

interfaces. There, they can be separated from fermentation broths by flotation into the foam. Factors affecting cell flotation include bubble size, aeration rate, pH, and cultivation conditions. Hydrophobicity of the cell surface has been found to be a significant parameter in a number of studies.

51.3 WHAT DETERMINES GAS HOLDUP?

In practical bioprocess engineering, we are primarily interested in the influences of the manipulatable or adjustable process variables on gas holdup.

51.3.1 Physical Influences

The height of a gas holdup in a culture is most easy to understand in terms of the gas residence time τ_b. When the bubbles are considered as vehicles moving the gas from the sparger or gas distributor into the headspace of the reactor, a slower rise, that is a longer mean residence time, leads to a higher gas holdup. At low bubble rise velocities we observe traffic jam or traffic holdup effects. If the bubbles are restricted to move at slow speeds, the bubble density and, thus, the gas holdup become high.

The bubble size is the most important variable affecting the resident time distribution. The primary bubble size, which is the size which is generated at the gas sparger, depends on many variables (26). Most important for the liquid properties are the surface tension σ, the density ρ_L, the viscosity μ, and the direct sparger properties. The key operating variable is the superficial gas velocity w_{sg}. Pohorecki *et al*. (9) proposed for Sauter's diameter d_s, the following equation (Eq. 51.16):

$$d_s = 0.889\rho_L^{-0.552}\mu^{-0.048}\sigma^{0.442}w_{sg}^{-0.124} \qquad (51.16)$$

Upon the appearance of surfactants, the bubble size in such solutions is smaller than in pure water, as the surface tension σ is usually reduced by these compounds.

The mean bubble size d_s immediately influences the bubble rise velocity, hence $w_B = w_B(d_s)$. Larger bubbles usually do rise faster than smaller ones (e.g., Abou-El-Hassan (10)). However, $w_B(d_s)$ is not a linear but a rather complex function of d_s.

The bubble rise velocity is also influenced by the mobility of molecules at the surface of the bubbles. The liquid media which are used in biotechnology most often contain surfactants and also most proteins work as surface-active substances. They reduce the surface mobility and thus lead to smaller bubble rise velocities.

Most importantly the gas hold in bioreactors is affected by the coalescence of smaller gas bubbles and redispersion of larger ones. These processes immediately change the bubble size, rise velocity, and number density. In real cultures coalescence and redispersion are rather complicated processes that are not yet completely understood. Both are dependent on a number of aspects such as composition of the liquid and the gas phase, motion of the liquid phase, process time, etc.

The basic physical process leading to bubble coalescence can be divided into three steps:

- Bubbles must come into *contact* and form a film of 1–10 μm thickness. This is mostly controlled by the hydrodynamics of the bulk liquid.
- Thinning down the films. The rate of *thinning* is controlled by the hydrodynamics within the liquid film.
- *Rupturing* occurs once the film is sufficiently thin.

The rupturing process is faster than the other two steps but will not occur if the contact time is shorter than the thinning process. So we can consider that rate of thinning in the liquid film is the rate-controlling step.

However, the coalescence repression may appear when the thinning process is retarded by changes in the rheology of the liquid, close to the surfaces or when the bubble collision frequency is reduced, for example by electrostatic repulsion of the bubbles in cases where polarization effects appear with the surfactants at the bubble surface.

During fermentation some of the metabolites and particularly, the components of lyses organisms may change the bubble surface properties and thus the frequency of coalescence and redispersion processes develops, with time, in a practically unpredictable way.

In stirred tank reactors, gas can also be drawn into the dispersion by an impeller. This is an important effect when the vessel does not wear baffles because then, whirling occurs at higher stirrer speeds. However, such operational modes are generally avoided in industrial bioreactors. Hence, when there is no active aeration, then the gas holdup is negligible.

Practically, the gas holdup within a biotechnical cultivation broth is first of all a function of the superficial gas velocity w_{sg}. One usually describes the relation in terms of the folllowing engineering correlation (Eq. 51.17):

$$\varepsilon_G = a \cdot w_{sg}^b \qquad (51.17)$$

The free parameters a and b are determined from experiments. Values are published for simple model media only. For tapwater typical values are $a = 0.6$ and $b = 0.7$ for the case that w_{sg} is measured in m/s. Chisti (11) found that parameters were dependent on the flow regime and flow behavior index of the fluid.

McManamey and Wase (12) proposed to relate volumetric mass transfer coefficients to gas holdup by

Equation 51.18:

$$k_L a = 0.2883 \cdot \varepsilon^{0.9562} \tag{51.18}$$

McManamey and Wase (13) and Prokop *et al*. (14) found that the exponent can vary between 0.8 and 1.1 depending on the medium properties. It is well known (11) that logarithmic scale plots of $k_L a$ vs. (ε/(1-ε)) for any particular data set should have a unit slope as given in Equation 51.19:

$$\ln k_L a = \ln\left(6\frac{k_L}{d_B}\right) + \ln\left(\frac{\varepsilon}{1-\varepsilon}\right) \tag{51.19}$$

where k_L is the mass-transfer coefficient and d_B is the bubble diameter.

In mechanically stirred bioreactors, which are the most used devices in biochemical engineering, a second influence parameter gains importance This is the mechanical power P_D transferred into the dispersion per culture volume. For this practically important case, Equation 51.20 was formulated as an experimental or engineering correlation.

$$\varepsilon \propto \left(\frac{P_D}{V_D}\right)^{0.47} w_{sg}^{0.53} \tag{51.20}$$

Both, (P_D/V_D) and w_{sg} represent power inputs to the dispersion. w_{sg} is related to the power P_c released by the rising bubbles (Eq. 51.21). This power is supplied by the air compressor against the static pressure of the liquid at the sparger location.

$$P_C = Q_G \cdot \Delta_p = w_{sg} \cdot W \tag{51.21}$$

Δp is the pressure difference between the surface of the dispersion and the position of the sparger. W is the weight of the dispersion above the sparger, i.e. essentially the weight of the liquid phase. The point to note is that the mechanical power, pneumatically introduced with the bubbling gas into the dispersion, is proportional to the superficial gas velocity w_{sg}. In bubble column bioreactors this is the only way of bringing mechanical power into the liquid.

What is the reason for the power dependency of the gas holdup? With the mechanical power input, two additional fluid mechanic effects become relevant to the gas holdup:

– The first effect is that with higher energy inputs, the velocities of the circulatory fluid flows within the reactors become more intense. That is why a larger part of the bubbles within the flow get recirculated. Thus, the mean residence time and, consequently, also by Equation 51.16, the gas holdup increases. In particular, intensive eddy motions with high local flow velocities may trap some smaller bubbles within the dispersion for some time.

– The second effect supports the first one. At higher power input levels, the chaotic eddy flow motions lead to higher shear rates in the liquid phase on the scale of the bubble size. This reduces the mean bubble diameter as characterized by the Sauter diameter due to redispersion. Consequently, even more bubbles closely follow the liquid motions and thus the gas holdup increases.

51.4 PHYSICO-CHEMICAL EFFECTS

51.4.1 Pure Versus Solutions

In pure liquids bubbles are prone to coalesce. Small impurities may suppress the coalescence probability considerably. The impurities may change the bubble–bubble interaction forces, for example by repulsing electrical surface charges, or by stabilizing the boundary layer around the bubbles, or both.

51.4.2 Solutions of Organics

It was shown by many investigators that contaminants had a significant impact on the gas holdup. Usually this effect is so high that it considerably overshadows the effect of many other physical influence variables (15).

The size of a spherical bubble, which contains a fixed amount of a gas, depends on the surface tension which is determined by pressure created by the surrounding liquid. Therefore we can say, the size depends on the gas compression within the bubble.

This, however, is not so relevant to the bubble size in technical devices, as the bubble sizes generated by a sparger are most often practically independent of the surface tension. It is more dependent on the viscosity of the liquid and the fluid flow conditions at the sparger's orifices. The reason is that these conditions significantly influence the coalescence and redispersion events of the bubbles after their release from the sparger. Coalescence effects increase the bubble size and redispersion effects, for instance, by means of the impellers in a stirred tank reactor they reduce the primary bubble size.

Hu *et al*. (16) showed that a marked minimum bubble size can be found at low concentrations of solutions of hydrophilic organics in water. These concentrations depend on the particular organic. With miscible hydrophobic or hydrophilic organics, a minimum bubble size could not be found.

51.4.3 Salt Effects

It has long been recognized that electrolytes influence bubble coalescence. Further, different electrolytes give rise to the coalescence behavior. Some electrolytes such as NaCl

or KNO_3 solutions inhibit bubble coalescence, while others such as sodium acetate or HCl do not. Where coalescence inhibition is observed, a transition between no inhibition of bubble coalescence and a constant inhibition appears over a narrow concentration range. Typically 0.01 *M* solutions show no effect relative to pure water, and coalescence inhibition reaches a maximum by 0.2 *M*.

Craig *et al*. (17) systematically investigated a large number of electrolytes and developed simple rules which can predict the bubble coalescence behavior for different electrolytes on the basis of assigned properties of the individual ions.

When free surfaces approach each other in pure water, very high surface free energy leads to an attractive interaction. In electrolyte solutions where both anions and cations are attracted to the surface (like H^+ and Cl^- in HCl solutions), van-der-Waals-attraction facilitates approach of the surfaces and the coalescence of air bubbles (18). When only one type of an ion, an anion or a cation, is attracted to the surface (like Cl^- in NaCl solutions), an electric double layer is formed. This results in repulsive interactions between free surfaces. This inhibits coalescence events.

The change of surface tension with concentration correlates weakly with the inhibition of coalescence (e.g., Marcelja (18)). Two features of the inhibition of coalescence point to the controlling role of the ionic contribution to the interaction between free surfaces. The effect is strongly ion-specific, and the transition concentration is well-defined.

51.4.4 Stabilizing Surfaces

A third class of substances, most important to gas holdup, is surfactants. Surfactants are chemical compounds which are preferentially adsorbed on an interface when they are dissolved or dispersed in a liquid. The molecules of the tenside surfactants have a hydrophobic (= lipophilic, i. e. water repellent = oil attracting) organic residual part, and a hydrophilic (= lipophobic, i. e. water attracting = oil repellent) group. The surfactant molecules settle on the water–air interface in such a way that the hydrophilic part of the molecule is in the water, and the hydrophobic part in the air. A monomolecular layer is formed—that is a thin film—of surfactant molecules. Due to reduction in the surface tension upon the appearance of surfactants, the bubble size in such solutions is smaller than in pure water (19).

This layer (film) is the precondition for the formation of stable foams. The high concentration at the water–air interface means that frequently, only very small quantities of surfactant (foaming agent) in relation to the total quantity of water, are sufficient to bring about considerable foam formation.

Most suspended microorganisms produce foam-producing agents by themselves. These agents include, for example:

- Proteins (e.g. gelatin, caesin and albumin)
- Polysaccharides (e.g. starch, pectins)
- Cellulose derivatives (e. g. cellulose ethers and carboxy-methyl-cellulose)
- Humic acids

Particularly when these compounds are part of the substrate, problems with foam are to be expected. In some cases extremely high stabilization of foams can be obtained by these substance components. These obstinate, stable and elastic foams are the so-called microbubble foams.

51.4.5 Antifoam Agents

Foam can be combated mechanically or chemically by means of antifoam agents (20,21). The mechanical approach usually applies turbines that fling the foam onto the reactor wall in order to break the lamellae between the foam bubbles. The chemical antifoam agents destabilize the lamellae. Defoamers must be specially chosen for each fermentation system. Screening and selection of suitable antifoam agents is a complex empirical task.

Antifoam agents do not only influence the main foam layer but also the bubbles in the bulk of the culture. In this respect, the principal disadvantage associated with chemical antifoams is a significant reduction in the gas–liquid mass-transfer coefficient. Two obvious mechanisms for this are:

(i) The average bubble size in the broth increases and gas holdup decreases due to antifoam-induced bubble coalescence. The consequence is a lower specific interfacial area, which in turn gives lower oxygen transport rates.

(ii) Surfactants from the defoamer are distributed as a spread film on the bubble surfaces, inhibiting oxygen diffusion.

Foaming tendencies and properties of biomedia vary considerably. Moreover, the surface properties of antifoam agents are not constant. Hence, foam suppression requires a balance between various surface-active components in the media including the antifoam agent. An agent capable of destroying foam in one case may well act as a foam stabilizer in another one (22). So we can note that screening is required for an effective antifoam agent.

Antifoam agents may also complicate downstream processing as these surface-active substances may interfere with filter membranes and the beads in chromatographs.

51.5 MEASUREMENT TECHNIQUES

In order to control the gas holdup, at least in the sense of keeping it below a critical value, it must be measured. Many techniques have been proposed in literature, however only a few of them can routinely be applied in biotechnical production practice (23,24).

The simplest way of monitoring situations in which the entire gas holdup including the foam are within the desired limits, is a foam detector in the headspace of the bioreactor. Conductivity probes, which make use of the fact that biotechnical culture media are electrically conductive, can be used as foam sensors. A single electrode placed at the critical height in the headspace of the bioreactor, connected with some counterelectrode in the dispersion (e.g. the wall of the reactor) via a voltage source, suffices. Only when the dispersion reaches the electrode, the current loop becomes closed. Then the flowing electric current indicates that the gas holdup has reached its maximally allowed value.

The most straightforward way to measure the gas holdup ε_G is to register the difference $\Delta H = H_D - H_L$ in the culture surface height with (H_D) and without (H_L) aeration (Eq. 51.22).

$$\varepsilon_G = \frac{V_G}{V_D} = \frac{\Delta H}{H_D} \tag{51.22}$$

However, since in most real bioprocesses the air supply cannot be switched off and it is not possible to remove the bubbles, the volume of liquid phase must be determined indirectly. The simplest way is to make use of the culture weight, which is often measured even at production reactors and some estimate on the density of the non-gas phase of the dispersion.

The most convenient method to estimate the mean gas holdup ε between two heights in large reactors is the volume expansion method. Measuring the static pressure differences Δp between the two heights of difference ΔH allows to determine the gas holdup (Eq. 51.23).

$$\varepsilon = 1 - \frac{\Delta p}{\left(\rho_l - \rho_g\right) \cdot g \cdot \Delta H} \tag{51.23}$$

The liquid and the gas phase densities ρ_l and ρ_g must be known. Reliable pressure sensors, which are sensitive and also robust enough for measurements in production reactors, are on the market. However, one must make sure that only the static pressure difference is measured.

Another measurement principle for local gas holdups uses point-like probes that can distinguish between gas- and liquid-phase. For instance, a point-like conductivity probe can be used for that purpose. Whenever the point electrode of this probe is within a bubble, the current flow between this and another electrode is interrupted. When the total measurement time t_{tm} was not chosen too short, the ratio of the sum of the time intervals Δt_j that the current is interrupted to the total measurement time t_{tm}, is exactly the local gas holdup. All other point-like sensors, which can distinguish between gas and liquid phase, can be used in the same way, for example, a light reflection probe.

There are other probes for local gas-hold measurements with larger measurement volumes, like the capacitance sensors which measure the local gas holdup by introducing a small capacitor into the dispersion, so that the dispersion forms the dielectric. The dielectricity constant is dependent on the gas holdup within this capacitor. After some calibration, this sensor can be used to monitor the local gas holdup, provided it can be made sure that the holdup between the plates of the capacitor is representative of the holdup in its surrounding.

REFERENCES

1. Hall MJ, Dickinson SD, Pritchard R, Evans JI. Foams and foam control in fermentation processes. Prog Ind Microbiol 1973; 12: 171–234.
2. Prins A, van't Riet K. Proteins and surface effects in fermentation: foam, antifoam and mass transfer. Trends Biotechnol 1987; 5: 296–301.
3. Wongsamuth R, Doran PM. Foaming and cell flotation in suspended plant cell cultures and the effect of chemical antifoams. Biotechnol Bioeng 1994; 44: 481–488.
4. Vandu CO, Krishna R. Influence of scale on the volumetric mass transfer coefficients in bubble columns. Chem Eng Proc 2004; 43: 575–579.
5. Freedman JF, Davidson JF. Hold-up and liquid circulation in bubble columns. Trans Inst Chem Eng 1969; 47: 251–261.
6. Bello RA, Robinson CW, Moo-Young M. Gas holdup and overall volumetric oxygen transfer coefficient in airlift contactors. Biotechnol Bioeng 1986; 27: 369–381.
7. Clift R, Grace JR, Weber ME. Bubbles, drops and particles. New York: Academic Press; 1978.
8. Kendoush AA. Hydrodynamic model for bubbles in a swarm. Chem Eng Sci 2001; 56: 235–238.
9. Pohorecki R, Moniuk W, Bielski P, Sobieszuk P, Dąbrowiecki G. Bubble diameter correlation via numerical experiment. Chem Eng Sci 2005; 113: 35–39.
10. Abou-El-Hassan ME. Correlations for bubble rise in gas-liquid systems. In: Cheremisinoff NP, editor. Volume 3, Encyclopedia of fluid mechanics, Gas-liquid flows. Houston (TX): Gulf Publishing Company; 1986, Chapter 6. pp. 110–120.
11. Chisti MY. Airlift bioreactors. London: Elsevier; 1989.
12. McManamey WJ, Wase DAJ. Relationship between the volumetric mass transfer coefficient and gas holdup in airlift fermentors. Biotechnol Bioeng 1986; 28: 1446–1448.
13. Akita K, Yoshida F. Gas holdup and volumetric mass transfer coefficient in bubble columns. Effects of liquid properties. Ind Eng Chem Process Des Dev 1973; 12: 76–80.
14. Prokop A, Janik P, Sobotka M, Krumphanzi V. Hydrodynamics, mass transfer, and yeast culture performance of a

column bioreactor with ejector. Biotechnol Bioeng 1983; 25: 114–1160.

15. Smith JM, Gao Z. Vertical void fraction distribution in gas-liquid reactors. Proceedings 3rd International Symposium on Mixing in Industrial Processes; 1999; Osaka, Japan. pp. 189–196.
16. Hu B, Nienow AW, Stitt EH, Pacek AW. Bubble sizes in agitated water-hydrophilic organic solvents for heterogeneous catalytic reactions, ACS Online. 2007.
17. Craig VSJ, Ninham BW, Pashley RM. Effect of electrolytes on bubble coalescence. J Phys Chem 1993; 97: 10192–10197.
18. Marcelja S. Selective coalescence of bubbles in simple electrolytes. J Phys Chem B 2006; 110: 13062–13067.
19. Sardeing R, Painmanakul P, Hébrard G. Effect of surfactants on liquid-side mass transfer coefficients in gas–liquid systems: a first step to modeling. Chem Eng Sci 2006; 61: 6249–6260.
20. Pelton R, Flaherty T. Review: defoamers: Linking fundamentals to formulations. Polym Int 2003; 52: 479–485.
21. Degussa. Antispumin, Brochure, Degussa Site Krefeld, Stockhause GmbH, Water Chemicals, Bäckerpfad 25, D-47805 Krefeld. 2007.
22. Vardar–Sukan F. Effects of natural oils on foam in bioprocesses. Biotechnol Lett 1991; 13: 107–112.
23. Hofmeester JJM. Gas holdup measurements in bioreactors. Tibtech 1988; 8: 19–22.
24. Laakkonen M, Moilanen P, Miettinen T, Saari K, Honkanen M, Sarenrinne P, Aittamaa J. Local bubble size distributions in agitated vessel combination of three experimental techniques. Chem Eng Res Des 2005; 83: 50–58.
25. Alves SS, Maia CI, Vasconcelos JMT, Serralheio AJ. Bubble size in aerated stirred tanks. Chem Eng J 2002; 89: 109–117.
26. Chisti Y. Animal cell culture in stirred bioreactors: observations on scale up. Bioprocess Eng 1993; 9: 191–196.
27. Joshi JB, Parasu Veera U, Parasad CV, Phanikumar DV, Desphande NS, Thakre SS, Thorat BN. Gas hold-up structure in bubble column reactors, review article. PINSA 1998; 64A (4): 441–567.

52

IMMOBILIZATION OF PROTEINS AND ENZYMES, MESOPOROUS SUPPORTS

Martin Hartmann and Dirk Jung
Advanced Materials Science, Department of Physics, University of Augsburg, Augsburg, Germany

52.1 INTRODUCTION

Immobilization of biocatalysts paves the way for their economic reuse and the development of continuous bioprocesses. For the preparation of heterogeneous biocatalysts, either isolated enzymes or whole cells are immobilized on suitable supports. Immobilization often results in stabilization and allows the use of enzymes under harsh environmental conditions of pH, temperature, and in the presence of organic solvents. Biotechnology is currently considered a suitable alternative to conventional process technology in industrial catalysis, sensing applications, and disease diagnostics. In the light of this development, immobilization of proteins on organic [e.g. polymers (1)] and inorganic support including controlled porous glass (CPG) and sol–gel materials has been extensively studied (2–6).

The encapsulation of enzymes and other proteins into ordered mesoporous inorganic hosts and related materials has attracted considerable attention over the past 10 years. Ordered mesoporous silicas prepared using a surfactant templating approach were discovered in the 1990s and are characterized by high specific surface areas and pore volumes as well as narrow pore size distribution. Their regular pore system consisting of tunable mesopores ($d = \sim 2–30$ nm) offers the possibility of immobilizing large biomolecules within their pores. The distinct order of the channels and cages as well as the possibility to tune structure, pore size and chemical composition over a wide range offers advantages over sol–gel or CPG materials. While the first report on enzyme immobilization on ordered mesoporous supports appeared as early as 1996 (7), the major developments in particular with respect to applications in biocatalysis have only come within the last 5 years. This research has demonstrated that biomolecules immobilized in inorganic matrices retain their functional characteristics to a large extent. These new materials are of interest for applications as (optically based) biosensors and biocatalysts. The present contribution intends to outline the basic principles of protein immobilization on (ordered) mesoporous molecular sieves, summarize the state of the art with respect to the application of the resulting bioinorganic hybrid materials in biocatalysis and highlight potential areas of future development.

52.2 IMMOBILIZATION OF PROTEINS ON MESOPOROUS SILICAS AND CARBONS

52.2.1 Materials

Porous solids have been classified by IUPAC (International Union of Pure and Applied Chemistry) based on their pore size into three groups (Fig. 52.1) (8). Porous solids with a pore diameter below 2 nm are named microporous. Zeolites and related materials with a pore diameter between 0.4 and 1.2 nm belong to this group of materials. Porous solids with a pore diameter between 2 and 50 nm are labeled mesoporous, while solids with a pore diameter above 50 nm are named macroporous. Typical macroporous solids with a broad pore size distribution are silica gel and active charcoal (Fig. 52.1).

Upstream Industrial Biotechnology: Equipment, Process Design, Sensing, Control, and cGMP Operations, Volume 2, First Edition. Edited by Michael C. Flickinger.
© 2013 John Wiley & Sons, Inc. Published 2013 by John Wiley & Sons, Inc.

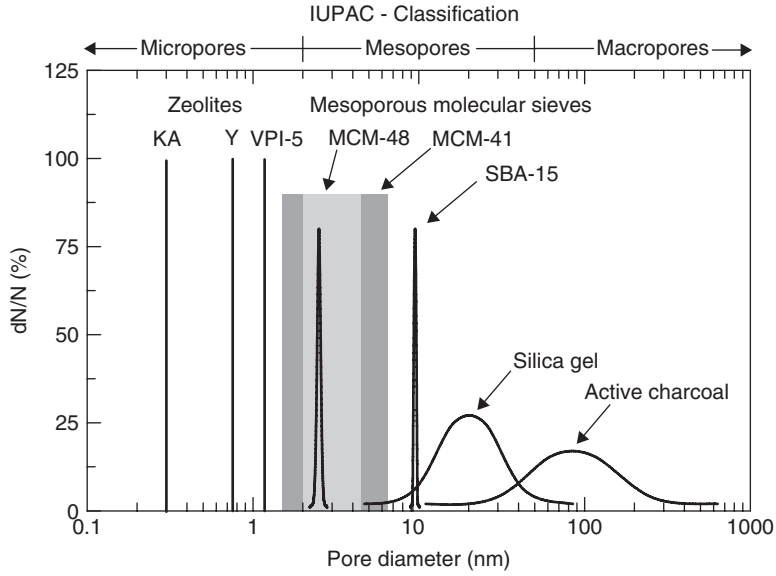


Figure 52.1. Pore size distribution of various micro-, meso- and macroporous materials.

The preparation of low density silica materials by hydrolysis of tetraethylorthosilicate (TEOS) in the presence of cationic surfactants, namely, hexadecyltrimethylammonium bromide, was patented by Chiola *et al*. in 1969 (9). However, the structural properties of these materials were not assessed. Di Renzo *et al*. (10) reported in 1997 that the patented preparation indeed results in the formation of mesoporous silicas of the Mobil Composition of Matter (MCM)-41 type, which were later rediscovered by researchers from Mobil Research and Development Corporation.

In 1990, Kuroda and coworkers (11) reported the synthesis of hexagonally arranged mesoporous silicas, which were obtained from kanemite in the presence of hexadecyl trimethylammonium bromide. These materials were prepared by exchange of the sodium ions in kanemite, a crystalline layered silicate, by hexadecyltrimethylammonium cations in aqueous solution and subsequent calcination to remove the organic template. Owing to the proposed synthesis mechanism, the novel materials were named *folded sheet materials (FSM-16)*. The transformation of kanemite in the presence of templates with different alkyl chain length into mesoporous materials with different pore size was later reported by Inagaki *et al*. (12).

The discovery of mesoporous molecular sieves of the M41S family was reported by researchers from the Mobil Research and Development Corporation in 1992 (13,14). The initial members of M41S family consisted of MCM-41 (hexagonal *p6mm* phase), MCM-48 (cubic *Ia-3d* phase) and MCM-50 (a stabilized lamellar phase). MCM-41 exhibits an X-ray diffraction pattern containing three or more peaks below $2\theta = 10^{\circ}$ that can be indexed in a hexagonal *hk*0 lattice (Fig. 52.2). The structure is proposed to have a hexagonal stacking of porous tubes with uniform diameter. MCM-48, the cubic phase, exhibits an X-Ray diffraction (XRD) pattern (Fig. 52.3) consisting of several peaks that can be assigned to the *Ia-3d* space group. The structure of MCM-48 has been proposed by Husson et al. (15) to be bicontinuous with a simple representation of two infinite three-dimensional, mutually intertwined, unconnected networks. A more sophisticated and perhaps more realistic model would be based on the concept of an infinite periodic minimal surface of the gyroid form, Q^{230}, proposed for water-surfactant systems (16). The proposed structure is also shown in Fig. 52.3. The lamellar phase MCM-50 is instable and collapses upon template removal.

In addition to the "classical" [$S^+ I^-$; cationic surfactant (S^+) and anionic inorganic species (I^-)] route to mesoporous molecular sieves such as MCM-41 and MCM-48, new synthesis concepts have been developed, which differ from the original one by the nature of the electrostatic interaction between the organic and the inorganic phases (Table 52.1). The ($S^- I^+$) pathway involves condensation of an anionic surfactant with cationic inorganic species (17). Two other routes were also developed in which the surfactant and the inorganic phase have similar charges, but are separated from each other by small ions with opposite charge: ($S^+X^- I^+$)($X^- = Cl^-$; Br^-) and ($S^- M^+I^-$) with $M^+ = Na^+$ or K^+ (17,18). At the same time, an elegant route to prepare mesoporous silicas at room temperature by a neutral (S^0I^0) templating route was proposed by Tanev and Pinnavaia (19). The materials prepared by using the S^0I^0 approach, so-called hexagonal mesoporous silica (HMS) materials, exhibit single d_{100} reflections accompanied by more or less pronounced diffuse scattering centered

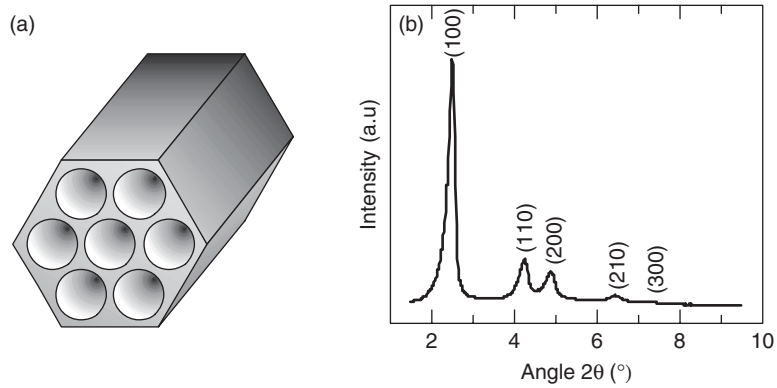


Figure 52.2. Schematic representation of the MCM-41 pore structure (a) and X-ray powder diffraction pattern (b).

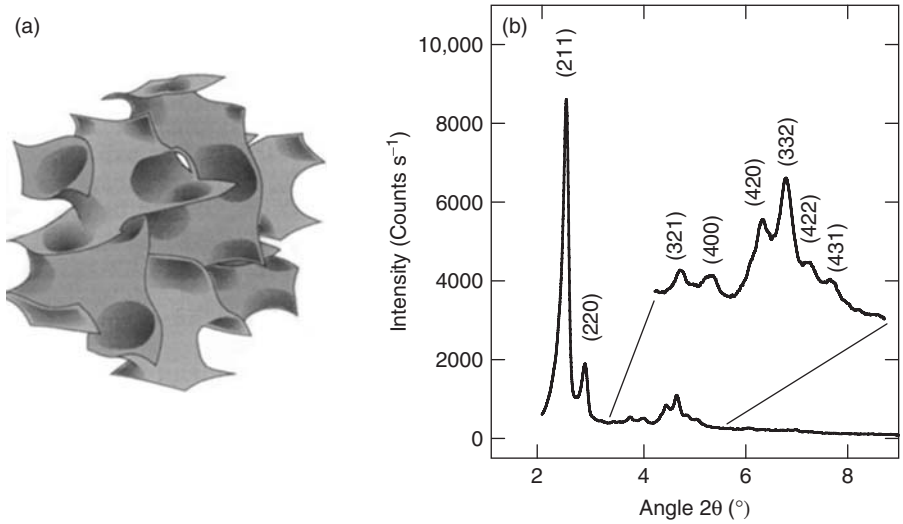


Figure 52.3. Schematic representation of the MCM-48 pore structure (a) and X-ray powder diffraction pattern (b).

at ~1.8 nm. Compared with the electrostatically templated MCM-41 silicas, HMS materials show a consistently larger wall thickness (1.7–3 nm), but a lower long-range hexagonal order (20).

Further studies led to the discovery of several other types of mesoporous silicas with high specific surface area, high specific pore volume and pores in the mesopores range with a narrow pore size distribution. A cubic phase SBA-1 (Santa Barbara advanced material no. 1), which was synthesized in acidic media, was suggested to have an ordered three-dimensional structure with two types of globular cages forming a continuous porous network (Fig. 52.4) (17,21). SBA-2 was shown to exhibit a three-dimensional periodic hexagonal array of mesoporous cages (21). Moreover, a hexagonal phase SBA-15 with pore sizes ranging from 5 to as large as 30 nm, and a variety of other cubic structures (i.e. SBA-2, SBA-7, and SBA-8) were prepared using oligomers and triblock copolymers as templates (22,23). The highly ordered large-pore mesoporous silica SBA-15, prepared by using the amphiphilic triblock copolymer $EO_{20}PO_{70}EO_{20}$ (Pluronic P123), possesses also a two-dimensional hexagonal structure comparable to MCM-41. However, the pore walls are substantially thicker (~2–6 nm) and the large mesopores are interconnected by micropores. This results in a somewhat higher thermal (>900°C) and hydrothermal stability compared to other mesoporous materials. SBA-15 may exhibit a large variety of morphologies depending on the synthesis conditions. Moreover, the pore size can be adjusted between ~4 and 30 nm by variation of the synthesis gel composition [e.g. addition of the swelling agent tetramethylbenzene (TMB)] and conditions [e.g. temperature (24)]. Stucky and his group also reported the preparation of mesocellular foams (MCF, Fig. 52.5)

TABLE 52.1. Structural Characteristics of Mesoporous Materials Employed for the Immobilization of Biomolecules

Pore System	Crystal System	Symmetry	Typical Material	Typical Template Used
Lamellar (no channel)	Hexagonal	—	MCM-50, KSW-2	Long-chain alkyl trimethyl ammonium salts (e.g. CTAB or CTACl)
Low-ordered channel	(Near hexagonal)	—	MSU-n, HMS, KIT-1, TUD-1	Long-chain primary amine, nonionic poly(ethylene oxide), CTB
1D-channel	Hexagonal	*p6mm*	MCM-41, FSM-16	CTAB; C_nTMA^+ ($n = 14–18$); $C_{16-n-16}$ ($n = 4,6,7,8,10$)
			SBA-3	C_nTMA^+ ($n = 14–18$); $C_{16-n-16}$ ($n = 3,4,6,7,8,10,12$)
			SBA-15	P123 ($EO_{20}PO_{70}EO_{20}$)
	Hexagonal	*c2mm*	SBA-8, KSW-2	Bola surfactant
3D-channel	Cubic	*Ia-3d*	MCM-48	C_nTMA^+ ($n = 14–18$); Gemini surfactants $C_{22-12-22}$ and $C_{16-12-16}$
			KIT-6	P123 ($EO_{20}PO_{70}EO_{20}$), *n*-butanol
3D-cage	Cubic	*Pm-3n*	SBA-1	$C_{16}TEABr$
			SBA-6	$18B_{4-3-1}$
		Im-3m	SBA-16	F127 ($EO_{106}PO_{70}EO_{106}$)
		Fm-3m	KIT-5	F127 ($EO_{106}PO_{70}EO_{106}$) + *n*-butanol
			FDU-12	F127 ($EO_{106}PO_{70}EO_{106}$) + TMB and KCl

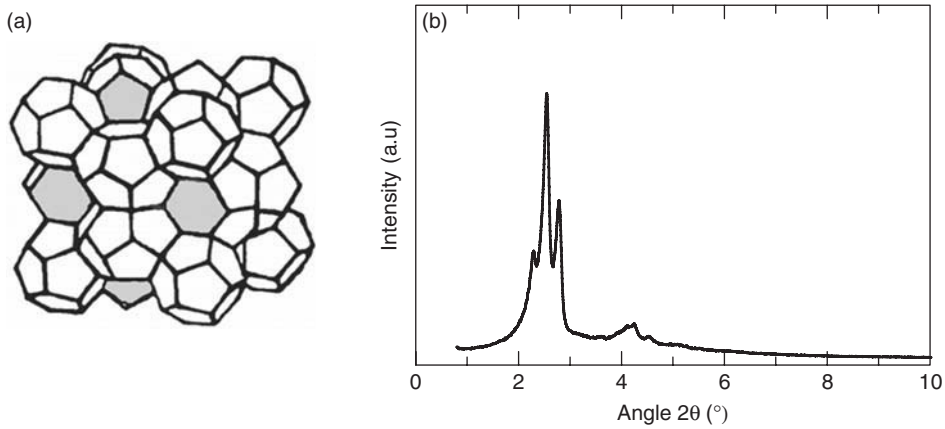


Figure 52.4. Schematic representation of the SBA-1 pore structure (a) and X-ray powder diffraction pattern (b).

employing triblock copolymers stabilized in oil in water emulsions (25). The large-pore system with open pores renders MCF materials that are interesting candidates for the immobilization of large biomolecules. MCF materials resemble aerogels, but offer the additional benefit of a simple and reliable synthesis protocol. Disordered materials such as LMU-1 (Ludwig-Maximilians Universität no. 1) (26) and KIT-1 (*K*orean Advanced *I*nstitute of Science and *T*echnology no. 1) (27) were also reported to have uniform channels.

SBA-16 is a mesoporous silica material with large cage-like mesopores arranged in a three-dimensional cubic-body-centered Im-3m symmetry. Analogous to SBA-15, the synthesis of SBA-16 is conducted under acidic conditions using a nonionic triblock copolymer as surfactant. The mesophase is created using mixtures of Pluronic P123 and F127 ($EO_{103}PO_{70}EO_{106}$) or employing mixtures of water, *tert*-butanol and F127. The cage diameter can be tuned between 5 and 15 nm by changing the composition of the polymer mixture. The structure of

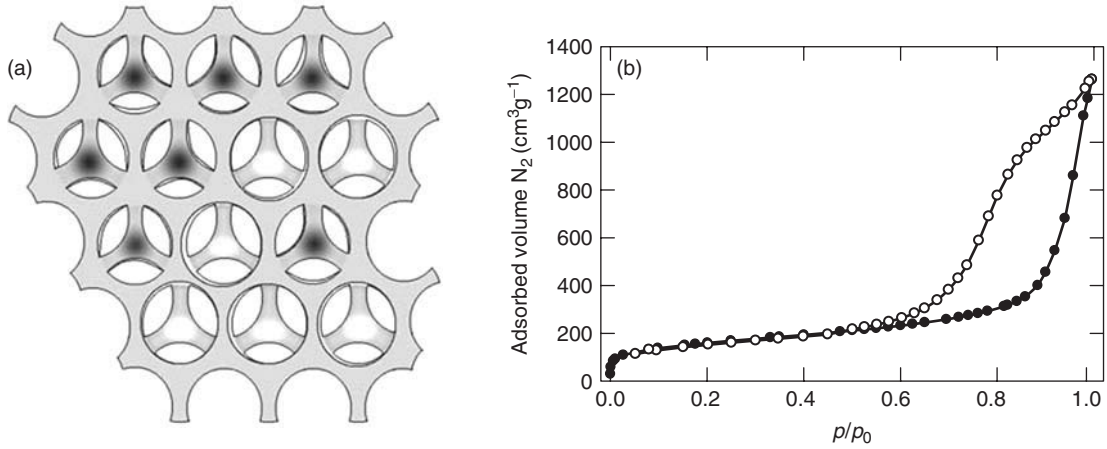


Figure 52.5. Schematic representation (a) of the mesocellular foam (MCF) materials and characteristic nitrogen adsorption isotherm (b).

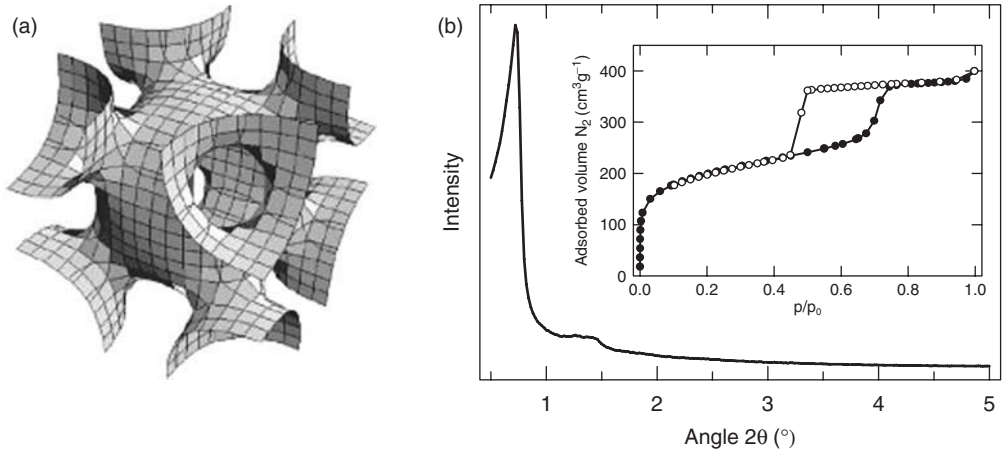


Figure 52.6. Schematic representation of the pore structure (a) and representative powder XRD pattern and nitrogen adsorption isotherm (b) of SBA-16.

SBA-16 is best described by a triply periodic minimal surface names I-WP (body centered wrapped package, Fig. 52.6) (28). As suggested by electron crystallography, each mesopore is connected to eight neighboring mesopores. The size of the pore entrances is significantly smaller than the diameter of the cages and may not exceed 5 nm.

KIT-5 is a porous silica material with properties similar to those of SBA-16; the mesopores are ordered in a cubic face-centered *Fm-3m* symmetry. Similar to SBA-16, KIT-5 is synthesized in a ternary water, *n*-butanol and Pluronic F127 surfactant system with emphasis on a low HCl concentration in aqueous solution (29). In contrast to the triply periodic bicontinuous minimal surface of the SBA-16 mesophase, KIT-5 may be represented by a cubic micellar mesophase. In this case, each mesopore would only be statistically connected to its neighbors, but arranged in a face-centered symmetry. FDU-12 also represents a cubic (*Fm-3m*) mesostructure with a large cavity size of 10–12 nm. Mesoporous silicas FDU-12 were synthesized using the block copolymer F127 or F108 assisted by TMB and inorganic salts, for example KCl (30). It has been reported that the synergistic role of TMB and KCl is critical for the synthesis of this material. Lowering the aging temperature and increasing the synthesis temperature can enlarge the pore sizes from 14 to 22 nm and the entrance diameters from 4 to ca. 9 nm (30,31). The approximate structure of FDU-12 prepared at low temperature can be regarded as face-centered cubic closed packing of spherical cages, each connected to 12 neighboring cages (32). A remarkable difference between the two materials FDU-12 and KIT-5 has been observed in the XRD pattern of the two materials with the same face-centered cubic *Fm-3m* symmetry. FDU-12 displays

strong (311) and unsolved (200) and (400) reflections, while KIT-5 exhibits a strong (220) and weak (200) and (311) diffraction lines. The structural implications to these structural differences are, however, not understood yet and subject to further investigations.

KIT-6 (33,34) is analogous to MCM-48 and possesses a three-dimensional *Ia-3d* structure. Again, the representation of the structure is a gyroid minimal surface as shown in Fig. 52.3. The gyroid structure, which can be interpreted as two interwoven cylindrical channel systems result in adsorption properties very similar to those observed for two-dimensional hexagonal systems. In contrast to MCM-48, these two intertwined systems of relatively large channels in KIT-6 can also be connected through irregular micropores present in the mesopore walls analogous to those present in SBA-15.

Owing to their potential application in various petroleum refining processes, aluminum-containing mesoporous materials have received considerable attention over the last years in both the patent and the open literature (35). In particular, two reviews by Sayari (36,37) give an overview of catalytic applications of AlMCM-41 and an exhaustive list of industrial patents on the catalytic applications of these materials reported until 1996. The degree of incorporation of aluminum into mesoporous silicas as well as the physical properties and stability of the obtained solids strongly depend on the synthesis conditions (38–40). MCM-41 materials with n_{Si}/n_{Al} ratios in the range from 2 to 100 can be obtained and ^{27}Al Magic Angle Spinning Nuclear Magnetic Resonance Spectroscopy (MAS NMR) shows that the aluminum species are exclusively in tetrahedral environment (41,42). The incorporation of aluminum into other phases, for example, MCM-48, SBA-15, and SBA-1, is more difficult and was studied to a lesser extent (43–48). Incorporation of other heteroatoms including Cu (49,50), Zn (49,50), B (51–56), Ga (57,58), Fe (51,59–63), Cr (64–67), Co (68), Nb (69–72), Ni (73), Mn (74–76), Mo (77,78), Ti (79–81), V (64,67,82–85), Sn (80,81), and Zr (86–90) has been widely investigated, however, the potential of these materials for protein adsorption is only rarely explored.

Inorganic-organic hybrid mesoporous materials offer the potential of tuning the chemical composition. There are three general methods of generating functionalized materials, (i) direct functionalization during synthesis, (ii) post-synthesis functionalization and (iii) incorporation of organic moieties into the pore walls using organic molecules possessing multiple alkoxysilane groups (Fig. 52.7). The synthesis of this so-called periodic mesoporous organosilicates (PMO) was independently reported by the groups of Inagaki (91), Ozin (92) and Stein (93). Chemical modification of the pore wall has also been reported (94–97). One of the most fascinating features of certain PMOs is the formation of crystalline pore walls. The first example was reported by Inagaki *et al*. who employed 1,4-bis(triethoxysilyl)benzene as precursor (98). Moreover, the condensation approach can be used to introduce a second functionality (94,99).

At the end of the 1990, the preparation of mesoporous carbon materials using mesoporous silicas as hard templates has been reported [for reviews see e.g. (100,101)]. Kyotani and coworkers prepared ordered microporous carbons using zeolite Y as a template (102,103). This concept has been extended by Ryoo *et al*. to the preparation of ordered mesoporous carbons employing ordered mesoporous silica molecular sieves such as MCM-48, SBA-1, and SBA-15 as templates (104–107). A similar approach was reported independently by Hyeon *et al*. (108,109); the obtained well-ordered mesoporous carbon materials were designated SNU-x. The use of the cubic mesoporous silica MCM-48 as template and sucrose as carbon source result in the formation of the mesoporous carbon CMK-1. SBA-15, which possesses a hexagonal array of cylindrical mesoporous interconnected by micropores, is used for the preparation of CMK-3. It was shown that the pore diameter of the mesoporous carbons CMK-3 can be tuned by using silica templates prepared at different temperatures (110). The use of the face-centered cubic mesoporous silica KIT-5 enables the formation of the more complex carbon nanostructure coined "carbon nanocage" by their inventors (Fig. 52.8) (111,112). The pore dimensions of this material can be tuned by using KIT-5 mesoporous silicas prepared at different temperatures and by variation of the sucrose to silica ratio. An overview of the reported ordered mesoporous carbons generated by nanocasting is given in Table 52.2.

Mesoporous oxides from other elements than silica have been reported as early as 1994. Huo *et al*. (21,113) found that metals such as Sb, Fe, Zn, Pb, W, and Mo also form mesoporous oxides. However, many of the obtained mesophases were lamellar and were not porous after template removal (calcination). Antonelli and Ying reported the transformation of titanium, niobium and tantalum alkoxides into stable mesophases (114–117). Subsequently, mesoporous oxides based on zirconium, hafnium, and manganese have been synthesized [for a recent review on these materials see (118)]. Bagshaw and Pinnavaia (119) prepared mesoporous alumina with worm-like pores and a specific surface area of more than 400 m^2/g. Mesoporous aluminas with surface areas above 700 m^2/g have been reported by Vaudry *et al*. (120).

The morphology of the mesoporous silicates is important for envisaged industrial application in catalysis, separation, and chromatography. In recent years, various morphologies such as fibers, discs, doughnuts, rods, vesicles, and helices have been reported (121,122). It has been found that several factors can affect the morphology of the final materials including hydrolysis and condensation of silicate species, the shape of the surfactant micelles, the interaction between them and the use of additives (inorganic salts, organic swelling agents, cosolvents, and

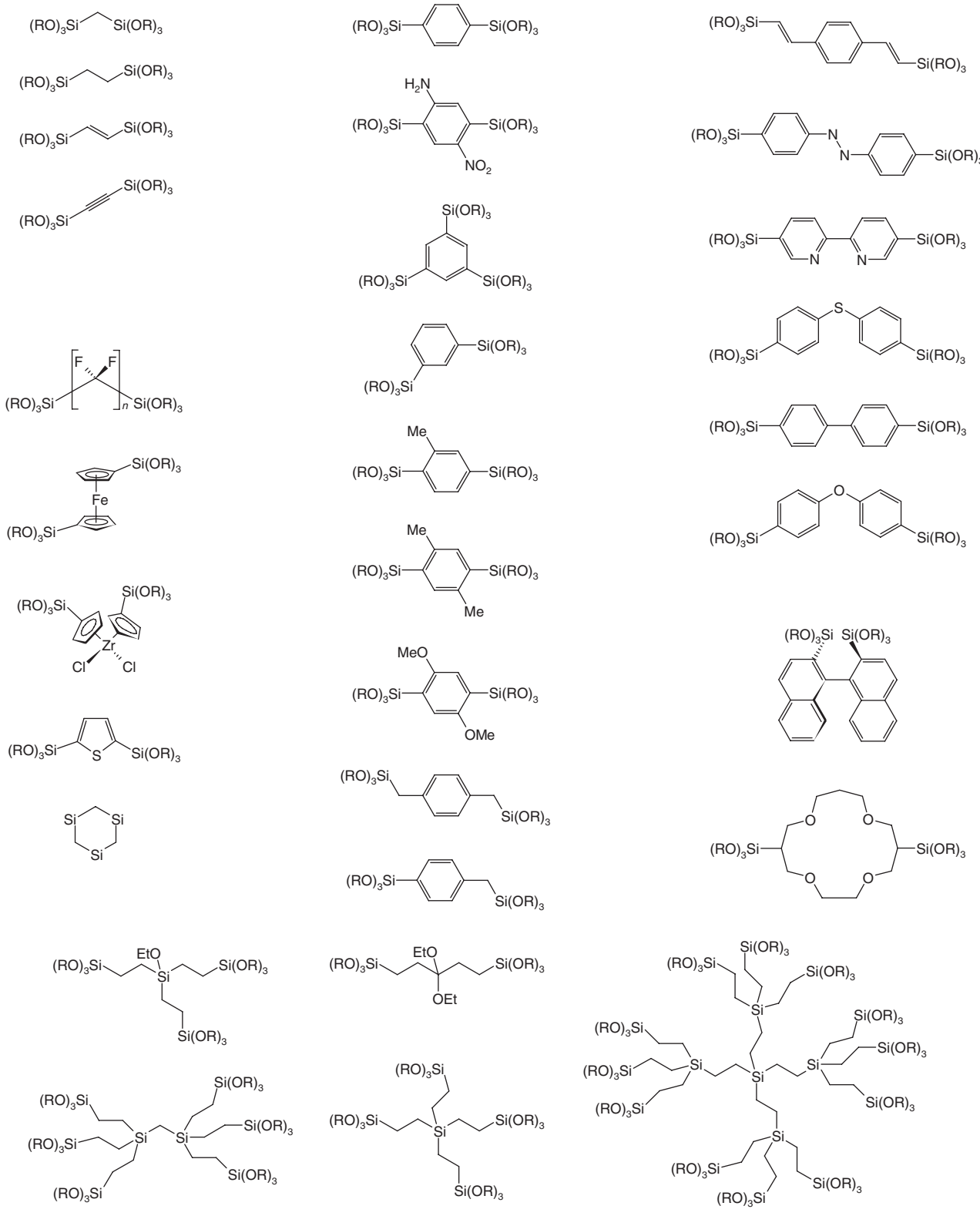


Figure 52.7. Si-alkoxy precursors for the synthesis of PMO materials.

TABLE 52.2. Overview of Reported Ordered Mesoporous Carbons Generated by Nanocasting

Carbon	Space Group	Template	Space Group	Precursor
CMK-1 (SNU-1)	*I4 1/a*	MCM-48	*Ia-3d*	Sucrose, phenol resin
CMK-2	Unknown cubic	SBA-1	*Pm-3n*	Sucrose
CMK-3	*p6mm*	SBA-15	*p6mm*	Sucrose, phenol resign,
CMK-4	*Ia-3d*	MCM-48	*Ia-3d*	Acetylene
CMK-5	*p6mm*	SBA-15	*p6mm*	Furfuryl alcohol
NCC-1	*p6mm*	SBA-15	*p6mm*	Furfuryl alcohol
CMK-8 (rodlike) CMK-9 (tubelike)	*Ia3-d*	KIT-6, FDU-5	*Ia-3d*	Sucrose, furfuryl alcohol
Cubic OMC	Unknown	FDU-12	*Fm-3m*	Sucrose
Cubic OMC	*Im-3m*	SBA-16	*Im-3m*	Sucrose, furfuryl alcohol, acenaphthene
Carbon nanocage	Unknown	KIT-5	*Fm-3m*	Sucrose

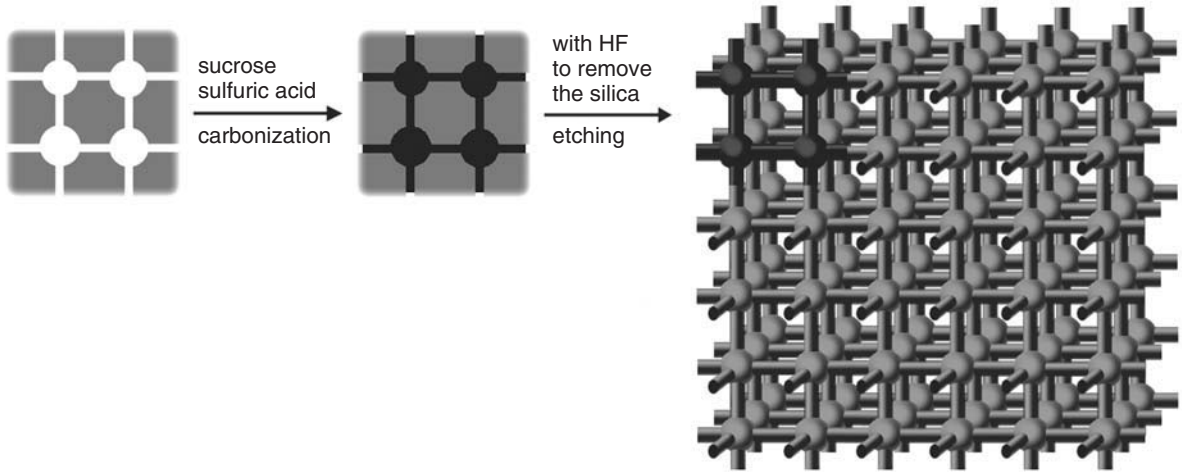


Figure 52.8. Nanoreplication of KIT-5 into carbon nanocage (CNC) material.

cosurfactants). Lamellar silicas with hierarchical vesicular structure are expected to provide optimal access to the pore walls under diffusion limited conditions (123,124). For the preparation of these materials, Pinnavia and coworkers employed electrically neutral and unsymmetrical Gemini surfactants of the type $C_nH_{2n+1}NH(CH_2)_mNH_2$ ($n = 12$, 14 and $m = 3$, 4). However, the achievable pore diameters are too small for the adsorption of larger biomolecules.

The development of tailor-made mesoporous silica supports has significantly advanced in recent years. Based on the understanding that an ordered array of mesopores is not required for the majority of applications in biocatalysis and biosensing, synthesis protocols for high surface area materials with narrow pore size distributions based on silica microspheres have been reported (125–128). Lecithin/dodecylamine mixed-micelles in an alcoholic/water media are reported to form sponge mesoporous silicas (coined SMS) through a self-assembly process between mixed micelles and TEOS (129,130). This synthesis strategy expands the classical sol–gel synthesis allowing to control the mesoporosity. SMS materials feature an isotropic three-dimensional pore structure analogous to SBA-16 but with a lower degree of mesoscopic structural order. Its porosity results from cavities and connecting channels, whose dimensions are controlled by the synthesis parameters (131).

Recently, the design of a novel biocompatible controlled- release motif including silica particles (d = ca. 400 nm) containing hexagonally arranged pores with a diameter of about 2 nm has been reported (132). The porous mesostructure is templated by CTAB (cetyltrimethyl-ammonium bromide) and particles synthesis is accomplished using a base-catalyzed sol–gel procedure. The snap-top consists of a [2] rotaxane tethered to the surface of a nanoparticle in which an α-cyclodextrin torus encircles a polyethylene glycol thread. The ester-linked adamantyl stopper is cleaved by porcine liver esterase and the payload is set free.

For further details on the preparation of mesoporous silicas and carbons, organic-inorganic hybrid materials (PMOs)

and mesoporous thin films, the reader is referred to extensive reviews published recently (133–136).

52.2.2 Nature of the Adsorption of Proteins on Surfaces

The various factors affecting the amount of protein adsorbed on a given (in the case of porous supports curved) surface are inevitably linked to the conformation adopted by the protein in the cages and channels. The reason is that a modification to a more disordered structure contributes to the driving force of adsorption as it increases the entropy of the systems. Thus, the Gibbs energy decreases which is the driving force for spontaneous adsorption. Moreover, the conformational modifications may also affect the maximum quantity of protein adsorbed since those changes may alter the area occupied by a single protein molecule in particular when the available space is restricted in three dimensions.

The adsorption of proteins at constant temperature and pressure leads to a decrease of the free enthalpy of the system according to the second law of thermodynamics (137,138). The change in free enthalpy $\Delta_{ads}G$ depends on the enthalpy (change) $\Delta_{ads}H$, which is a measure of the potential energy (i.e. the energy that has to be supplied to separate the molecular constituents from another) and the entropy change $\Delta_{ads}S$, which is related to the disorder of the system multiplied by the absolute temperature T:

$$\Delta_{ads}G = \Delta_{ads}H - T\Delta_{ads}S < 0$$

As pointed out by Quiquampoix (139), the difficulty in analyzing these processes lies in the fact that enthalpy effects and entropic effects are not totally independent. Enthalpic effects are typically related to intermolecular forces while entropic effects are related to the spatial arrangements of molecules. Moreover, intermolecular forces influence the molecule distribution and the potential energy is also dependent on the molecular structure of the system. Nevertheless, the enthalpic and entropic contributions will be discussed separately.

52.2.2.1 Enthalpic Effects

52.2.2.1.1 Coulomb Interactions. Proteins carry electrical charges resulting from the ionization of carboxylic, tyrosyl, amine, and imidazole groups of amino acid side chains. The electric charges of the mesoporous adsorbent surface may result from the isomorphous substitution of aluminum or other elements into the silica walls or from pH-dependent ionization of silanol or other surface groups. Coulomb forces are very strong and long-range interactions, which may even be as strong as covalent bonds. However, as the thermodynamic cost of an uncompensated electrical charge even in a small unit of volume is high, all charges of a given sign are compensated by an equal number of electrical charges of the opposite sign. Thus, a diffuse double layer is established around the biomacromolecule and the (curved) surfaces. The electrostatic interaction between proteins and the surfaces can be described as an overlap of their electrical double layers. The electrostatic part of the free enthalpy is given by the isothermal and isobaric work of charging the electrical double layer:

$$G_{el} = \int_0^{\sigma} \varphi(\sigma)d\sigma \qquad (52.1)$$

where ϕ is the variable electrostatic potential and σ is the variable surface density during the charging process.

52.2.2.1.2 Van der Waals Interactions. In addition to electrostatic interactions, van der Waals forces act on all molecules even if they are electrically neutral. These forces are composed of three different components and are considered short range forces. The main components are the dispersion (or London) forces, which originate from the instantaneous dipolar moment resulting from the fluctuation of the electrons around the nuclear protons in nonpolar molecules. Thus, an electric field is created that induces a dipole moment in nearby molecules, which in turn creates an instantaneous attractive interaction. The other two components are the induction (or Debye) forces, which are related to the interaction between a polar molecule and a nonpolar molecule, and the orientation (or Keesom) forces related to the interaction between two polar molecules.

52.2.2.2 Entropic Effects

52.2.2.2.1 Hydrophobic Interactions and Solvation Effects. Sometimes hydrophobic interactions are involved when proteins are adsorbed on mineral surfaces. One of the most important factors responsible for the stability of proteins in solution is the shielding of amino acids with a hydrophobic side chain in the core of the protein from contact with water. This phenomenon contributes to the decrease of the free enthalpie of the polypeptide chain that accompanies its folding. The shielding originates from the "hydrophobic effect" which causes water molecules to establish more hydrogen bonds among themselves in the presence of a nonpolar group than in the presence of a polar group. This process maximizes the mutual association of water molecules by hydrogen bonds and results in an increased order of the surrounding water and, thus, a favorable decrease in entropy of the system. It can be inferred that the presence of a surface with hydrophobic properties perturbs the spatial arrangement of nonpolar amino acids, and consequently the adsorption of proteins on surfaces cannot be analyzed without taking into account the interaction of water molecules with both the mineral surface and

the protein. Moreover, a gain in entropy is expected when water does not have to solubilize hydrophobic amino acids.

52.2.2.2.2 Modifications in Protein Molecular Structure. The interaction of proteins with surfaces in confined spaces is a more complex phenomenon than the interaction of ions or small more rigid molecules with surfaces. In the case of protein adsorption an entropic contribution can result from a modification of the protein conformation. This phenomenon is related to an increase in the rotational freedom of the peptide bonds engaged in the secondary structure, that is, α-helices and β-sheets. These ordered secondary structures represent an important part of the densely packed hydrophobic core of the protein. When a protein is adsorbed on a pore surface, internal hydrophobic amino acids can reach more external positions in contact with the surface, since the amino acid remains (partially) shielded from the contact with water molecules of the surrounding solvent phase (139). The breaking of hydrogen bonds that maintain the peptide chain in a given conformation results in an increase of conformational entropy. The gain in conformational entropy, S_{conf}, can be calculated under the assumption that four different conformations are possible for peptide units in random structures as compared with only one in α-helices and β-sheets:

$$\varepsilon\theta\nu\Delta_{\text{ads}}S_{\text{conf}} = R\ln(4^n) \tag{52.2}$$

In Equation 52.2, R is the gas constant and n is the number of peptide units involved in the transfer from an ordered secondary structure to a random secondary structure (140,141).

52.2.3 Strategies for Enzyme Immobilization

Different strategies have been developed for the immobilization of proteins on mesoporous supports. Figure 52.9 gives an overview on the immobilization methods available so far. Several parameters have to be considered when a suitable enzyme-carrier system is selected (Table 52.3). Physisorption of proteins onto oxide surfaces is governed by the interaction of amino acids with the solid surface. Proteins are highly complex and possess a wide variety of chemical properties originating from different surface groups including amines, carboxylates and disulfide bridges. The predominant binding forces of proteins to hydrated silica surfaces are electrostatic interactions, hydrogen bonding, and van der Waals interactions. Electrostatic protein-surface interactions are likely to be dominating when the adsorption is performed at a pH below the isoelectric point (pI) of the protein, that is, the point where the overall charge of the proteins is zero. Then the protein possesses a positive charge, while silica carries negative charges at a pH above ca. 3 (7). The larger the positive charge of the protein, the stronger the interaction between protein and surface, but the repulsion between adsorbed proteins is also increased. At a pH above the isoelectric point, the protein is negatively charged and repulsive interactions between the protein and the negatively charged surface will dominate. Consequently, surface adsorption capacities of proteins are found to vary with pH of the solution according to a bell-shaped curve with the maximum being near the isoelectric point of the protein (Fig. 52.10). Nevertheless, the pH dependence is very much dependent on the protein, that is, compare cytochrome *c* with chloroperoxidase (CPO).

Covalent binding is an extensively used technique for the immobilization of enzymes. The enzymes are covalently linked to the support using the functional groups of enzymes, which are not essential for their activity. The first step is the organic functionalization of the silica surface. The most potentially useful surface functional groups are alkyl chlorides, amines, carboxylic acids, and thiols. Other functional groups such as alkyl, phenyl, and vinyl can be added to modify the environment of the enzyme by increasing the hydrophobicity of the surface. Formation of covalent bonds with functionalized surfaces ensures strong binding and negligible leaching. It is often advisable to carry out the immobilization in the presence of the substrate or a competitive inhibitor in order to protect the active site. Moreover, the covalent binding has to be carried out in such a way that the conformational flexibility of the enzyme is not altered.

Another way of preventing leaching of the enzyme from the mesoporous support is physical encapsulation inside the pores. Several routes have been explored including silanation or coating with microporous silicas or organic layers. First, the protein is adsorbed from the solution and subsequently the pore entrance is reduced in size by, for example, silanation using 3-aminopropyltriethoxysilane (APTES) (142).

Biocatalysts can also be immobilized through chemical cross linking using homo- as well as hetero-bifunctional cross-linking agents. Chemical cross-linking of the enzymes preserves their catalytic activity even under harsh conditions such as high temperature, extreme pH values, the presence of organic solvents and radicals. Glutardealdehyde (GA) reacts with amino groups in a base-catalyzed reaction. GA has been used extensively due to low costs, high efficiency, and stability. Adsorption followed by cross-linking may allow encapsulation of proteins on porous support having a cage-like structure. The advantages and disadvantages of the four preferred immobilization methods are compared in Tables 52.4 and 52.5 (142).

52.2.4 Enzyme Immobilization on Ordered Mesoporous Materials

The unique advantages of ordered mesoporous solids over disordered, high surface area silicas, such as those prepared by sol–gel or aerosol methods, are their narrow pore size distribution and the well-defined pore geometry and connectivity. Diaz and Balkus were the first to publish work on the immobilization of globular proteins (cytochrome *c*, papain, and trypsin) on MCM-41 (7). A clear (almost linear) dependence of the protein size on the achieved loading was found. Since then, research in this area has developed rapidly and more than 200 papers have been published in this area up till now.

Initial adsorption studies were confined to small, stable, and readily available enzymes such as cytochrome *c*, lysozyme, trypsin, and lipase. Typically rather low loadings were obtained, which could only be increased significantly after thorough studies of different factors affecting protein adsorption including pH and ionic strength of the solution, surface charge and pore diameter of the support. Over the years, larger and less stable enzymes such as horseradish peroxidase (HRP) and CPO have also been studied. Recent studies also deal with the adsorption of even larger biomolecules including DNA (142).

Some general trends can be deduced from the adsorption studies published so far. Adsorption is dominated by weak

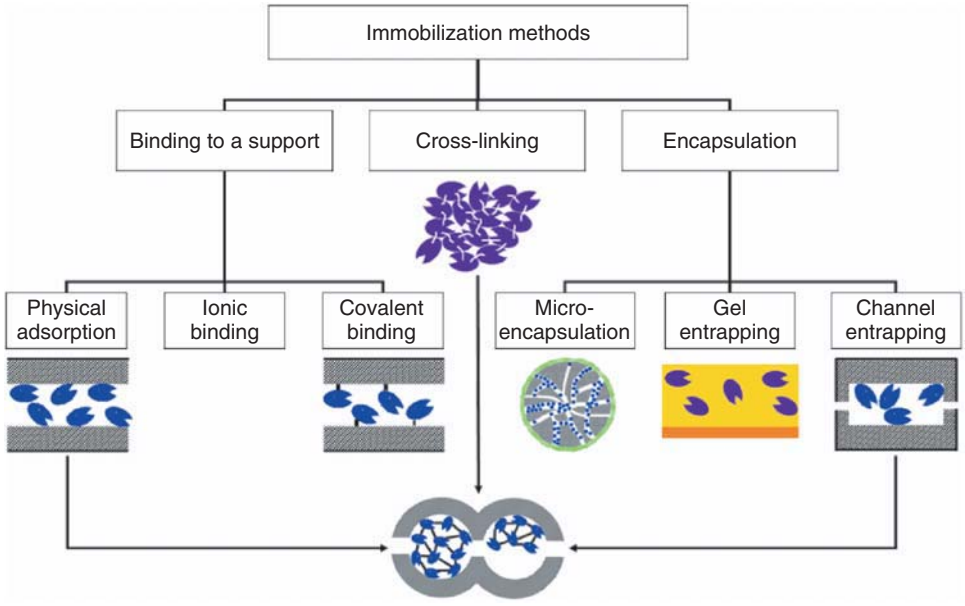


Figure 52.9. Overview of immobilization strategies on mesoporous supports. (This figure is available in full color at http://onlinelibrary.wiley.com/book/10.1002/9780470054581.)

TABLE 52.3. Parameters to be Considered for Enzyme Immobilization

	Parameters to be Considered	Examples
Enzyme	Biochemical properties	Molecular weight, functional groups on the surface, surface charge, purity, isoelectric point (p*I*)
	Kinetic parameters	Specific activity, pH and temperature profiles, solvents; stability against pH, temperature, solvents, contaminants and impurities
Carrier	Chemical characteristics	Composition, functional groups, swelling behavior, surface charge, pore size, stability
	Mechanical properties	Particle size, flow resistance (in case of fixed-bed application), single particle compression behavior, abrasion (for stirred tanks).
Immobilized enzyme	Immobilization methods	Bound protein, yield of active enzyme, intrinsic kinetic parameters
	Mass transfer effects	Buffer effect, film and pore diffusion
	Stability	Operational and storage stability
	Performance	Productivity (space–time yield), enzyme consumption and reuse

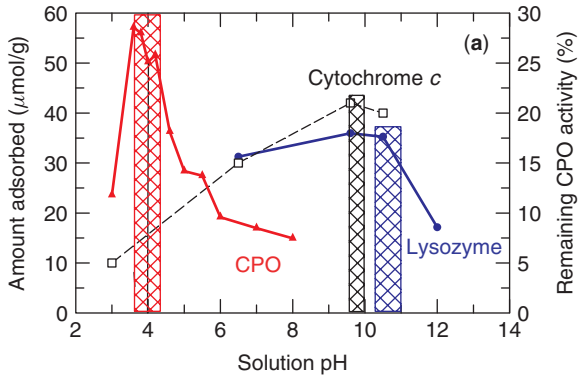


Figure 52.10. Dependence of the maximum of the enzyme adsorption on the pH of the solution. The shaded area represents the range of isoelectric points reported in the literature. (This figure is available in full color at http://onlinelibrary.wiley.com/book/10.1002/9780470054581.)

physical forces, that is, van der Waals or dispersion forces. It is shown in some studies that proteins tend to adsorb better, when strong electrostatic (charge) interactions occur between the (alumino) silica surface and the protein. Near the isoelectric point, the coulomb forces derived from the positive charges of the ionized protein and the negative charges at the silica surface are small. Under these circumstances, hydrophobic interactions between the protein and the adsorbent become more important. It is worth to mention that hydrophobic interactions are believed to be much weaker (by about 1/13 in water) than coulombic forces. These hydrophobic interactions may either originate from attraction of the nonpolar side chains of the amino acid residues on the surface of the protein or from protein–protein interactions between the hydrophobic side chains of neighboring protein molecules. It should be noted that the surface properties of the adsorbent are of paramount importance when adsorption occurs mainly by hydrophobic interactions. More work is needed in this area to gain full understanding and control. Under conditions of physical adsorption, the active site of the enzyme is often unaffected and nearly full activity is retained upon adsorption. However, desorption (leaching) of proteins is a common problem, in particular in the presence of a strong hydrodynamic force, since binding forces are weak. For a given pore size of the adsorbent, smaller proteins generally are adsorbed to a higher degree than larger ones, although the

TABLE 52.4. Advantages and Disadvantages of the Four Preferred Immobilization Methods

Immobilization Method	Advantages	Disadvantages
Encapsulation	Enzyme molecules retained; Enzyme molecules free to move inside channels	Complicated experimental procedure; Reactive species and toxic solvents may denature enzymes; Reduced pore opening may decrease diffusion rate of reactants and products
Physical adsorption	Simple (and cheap) experimental procedure; No toxic solvents; Little or no conformational changes of the enzyme or destruction of its active left	Leaching of enzymes during reaction resulting from changes in pH, temperature and ionic strength
Covalent binding	Enzyme molecules retained; Wide choice of organic linkers available	More expensive and complicated procedure in support preparation; Enzyme molecules immobile inside the channels
CLEA confinement	Concentration inside the pores prior to cross-linking; Size of the CLEAs is restricted by the cage size	Enzyme molecules immobile inside the channels

TABLE 52.5. Comparison Between Different Methods

Characteristics	Physical Adsorption	Covalent Binding	Encapsulation	CLEA Confinement
Preparation	Simple	Difficult	Difficult	Difficult
Cost	Low	High	Moderate	High
Binding force	Variable	Strong	Weak	Strong
Enzyme leakage	Yes	No	Yes	No
Applicability	Wide	Selective	Wide	Not yet known
Running problems	High	Low	High	Low
Matrix effects	Yes	Yes	Yes	No
Large diffusion barriers	No	No	Yes	Yes
Microbial protection	No	No	Yes	Yes

loading in many studies is low and far from complete filling of the mesopores. Moreover, it is unlikely that the proteins are evenly distributed in a given mesopore, but are more likely clustered at the pore entrance. For complete filling of the pore, (slow) single file diffusion (the proteins size is often similar to the pore diameter) might hinder rapid approach to thermodynamic equilibrium. Moreover, little is known regarding the geometry of the adsorption complex on mesoporous supports. Most proteins are somewhat ellipsoidal and might adsorb with either their long or their short axis with comparable probabilities. The molecule may also relax its orientation and may bind more strongly by moving its long axis from perpendicular to parallel. However, the relaxation is dependent on the surface coverage since it cannot take place if the neighboring area into which the molecule could expand is already occupied by another protein molecule. Finally, in many cases, it is furthermore found that adsorption is not completely reversible which also has a number of important implications as outlined in (143). However, more research work is needed to understand the fundamentals of this particular adsorption process. For further improvement of the adsorption process, different goals have been identified:

- Improvement of the adsorption capacity (loading).
- Adsorption kinetics (fast uptake).
- Immobilization rather than reversible adsorption.

The adsorption capacity is mainly dominated by the specific pore volume and the pore diameter, respectively, of a given support. While high loadings would be beneficial for catalysis in terms of reaction rate, the activity of immobilized enzymes is often loading dependent. Typically, the activity (in U/g) of the immobilized enzyme increases with increasing loading and finally reaches a plateau. Often, enzyme loading up to an amount sufficient to form a monolayer is beneficial in order to avoid conformational changes that result in reduced activity. Furthermore, the stabilization of the enzymes is associated with the pore diameter of the host and the size of the enzyme. In this context, different views are expressed in the literature whether the pore size should be significantly larger than the protein to allow for facile diffusion of protein and substrate down the pore or of similar size in order to increase stability and protection of the protein from the external environment. In addition, smaller pore dimensions allow a tight fit of the adsorbed enzymes and may reduce leaching. On the other hand, the use of mesocellular mesoporous silica with very large mesoporous cages connected by smaller mesoporous channels allows the encapsulation of cross-linked enzymes in the pore cavities. By cross-linking enzymes within mesocellular pores the resulting enzyme aggregates were successfully retained in the pores and high loading capacities were achieved (144–146).

A new strategy for enzyme immobilization, that is, the formation of cross-linked enzyme aggregates (CLEAs) was invented by Sheldon *et al*. (147–149). The addition of salts, water-miscible organic solvents or nonionic polymers to aqueous solutions of proteins leads to their precipitation as physical aggregates. Subsequent cross-linking of these physical aggregates make them permanently insoluble while maintaining their preorganized superstructure, and, hence their catalytic activity. The CLEA methodology essentially combines purification and immobilization into a single unit operation that does not require a highly pure enzyme. Since the discovery of CLEAs, this novel route is widely used for the heterogenization of a variety of enzymes ((150,151) and references therein).

Hyeon and coworkers (144,145) developed hierarchically ordered mesocellular mesoporous silica materials (HMMS) as a support for cross-linked enzymes. The final pore structure of HMMS is a combination of MCF pores and one-dimensional SBA-15 channels. α-chymotrypsin and lipase were immobilized in HMMS by enzyme adsorption followed by GA cross-linking. This results in the formation of CLEAs entrapped in the mesocellular pores of HMMS ($d_p = 37$ nm), which do not leach out through the narrow mesoporous channels ($d_c = 13$ nm). The formation of CLEAs of α-chymotrypsin in HMMS enables high enzyme loadings accompanied by significantly increased enzyme stability. No decrease in activity was observed for 2 weeks under rigorous shaking, while adsorbed and free α-chymotrypsin showed rapid inactivation due to enzyme leaching and presumably autolysis, respectively. The CLEAs of lipase in HMMS retained 30% of the specific activity of free lipase, but with significantly enhanced stability.

In a further study, the same authors applied the CLEA approach to enzyme immobilization in SBA-15, which has one-dimensional pores (146). It is not really clear, however, whether the use of SBA-15 instead of materials with bottle-neck pore structure presents an advantage with respect to enzyme leaching. In general, these initial studies demonstrate that the CLEA approach can efficiently be employed for enzyme immobilization resulting in enhanced stability of the immobilized enzymes with high loading and activity. The natural concentration of the enzymes by adsorption in the pores of the mesoporous material without the addition of additives and the restriction of the CLEA size by the pore diameter (thereby increasing the accessibility of the enzymes) are the most important advantages of this novel approach. However, the inherent shortcoming that the crosslinking step can deactivate the enzyme is still not solved. Regrettably, the applications of this approach to catalytic conversions and reaction engineering is still lacking up till now. In extension of the CLEA approach, multifunctional nanocomposites of enzymes and magnetic nanoparticles located in the pores of

HMMS materials were developed by Hyeon and coworkers (152). This approach involves a simple, two-step process comprising the coadsorption of enzyme and magnetic nanoparticles into HMMS followed by GA treatment. α-Chymotrypsin was immobilized via coadsorption of the enzyme and magnetite (Fe_3O_4) nanoparticles followed by cross-linking of the enzymes with GA. Under optimal conditions, the cross-linking of the enzymes resulted in the effective entrapment of the magnetite nanoparticles in the CLEAs. Furthermore, the composites of CLEAs and magnetite nanoparticles in the large mesocellular pores did not leach out from the HMMS through the narrow mesoporous channels. The authors inferred from their study that this ship-in-a-bottle approach for a magnetically separable and stable enzyme biocatalyst can be easily expanded to many other enzymes and has large potential in biotechnology applications such as bioremediation and bioconversion.

Han *et al*. (153) described a pressure-driven method for entrapping enzymes. Instead of stirring the MCF part- icles in the enzyme solution, high pressure (205–345 bar) was used to achieve high enzyme loading within the pores of the support (up to 275 mg/g of silica). The modified mesoporous silica was dispersed in 2-propanol and packed into a high-performance liquid chromatography (HPLC) column. After the 2-propanol in the column was removed thoroughly by washing with water, the enzyme stock solution was cycled through the prepacked silica column for 2 h under high pressure. Compared to the conventional approach, the pressure-driven method resulted in significantly higher enzyme loading on MCF and FDU-12 materials within a shorter period of time. For example, 24 h of stirring led to an enzyme loading of 92 mg/g onto MCF, whereas an enzyme loading of 275 mg/g onto MCF was achieved within 2 h with the pressure-driven method.

In order to reduce leaching, functionalization of the mesoporous silica support is another promising approach. An easy access to organic-inorganic hybrid materials based on SBA-15 is provided by surface modification (154,155). Thereby, surface silanol groups are condensed with an organotrialkoxysilane or with another reactive silane species to generate covalently bound organic moieties. There are two approaches to surface modification (142,156), that is postmodification, also known as *grafting*, and direct synthesis or co-condensation. Grafting is the method more commonly used in performing surface modification by covalently linking organosilane species with surface silanol groups.

However, the grafting method has several shortcomings as follows:

- The pore size is reduced due to the attachment of a layer of functional moieties on the surface.
- It is time-consuming, because two steps are required to accomplish the modification process.
- The number of accessible surface silanol groups on the mesoporous silica materials is limited.
- Difficulties in controlling the loading and position of the organosilane may arise.

In 1996, the co-condensation method was first independently reported by two research groups (157,158). This method allows surface modification of the mesoporous materials in a single step by copolymerization of organosilanes with silica or organosilica precursors in the presence of a surfactant. This approach enables a higher and more homogeneous surface coverage of organosilane functionalities. The disadvantage of the co-condensation is that the functionalized alkoxysilane (e.g. APTES) must hydrolyze at a similar rate as compared to the unfunctionalized alkoxysilane (e.g. tertaethylorthosilicate) otherwise a heterogeneous gel will be formed and, thus, the functional groups will not be homogenously distributed.

A variety of functional groups has been incorporated into mesoporous materials such as aliphatic hydrocarbons, thiol groups, vinyl groups, phenyl groups, amine groups, and perfluoro groups (142,154–159). Surface modification using APTES, producing a terminal amine group ($-NH_2$) has been found to be useful for covalent coupling of proteins to the surface of silica materials (142). An overview of commonly used functional groups for covalent enzyme linking is given in Table 52.6.

Yiu *et al*. (160) showed in their study that there is an essential difference between *in situ* synthesis and postmodification. The method of functionalization is found to be critical for using the resulting organosilica materials as support for trypsin immobilization. Thiol, chloride and acid functionalized solids are more active when the functional group has been incorporated during the synthesis of the mesoporous molecular sieve rather than by postsynthetic treatment. This study also shows that the nature of the functional group is critical. For example, amine-functionalized solids exhibit enhanced leaching characteristics, but the observed catalytic activity of trypsin is strongly reduced. The most promising support for trypsin in this study is a thiol-functionalized SBA-15 which was prepared by direct synthesis. This catalyst, which exhibits negligible leaching in the respective activity assays, possesses a catalytic activity that corresponds to 84% of the activity determined for the free enzyme. The differences between *in situ* synthesis and postmodification concerning the uptake of trypsin are illustrated in Table 52.7. It has to be pointed out that this study only applies to trypsin and may not be generalized. Consequently, this has to be investigated for the particular enzyme under study.

Furthermore, the immobilization of enzymes was affected not only by the functionalization with organo

TABLE 52.6. Assembling of Different Functional Groups for Covalent Enzyme Immobilization

Surface Functional Group	Enzyme	References
Amine groups	Trypsin	160
	Invertase	161
	Glucoamylase	161
	Penicillin G acylase	162,163
	Glucose oxidase	164
	α-Amylase	165,166
	Lipase	167
	Glucose isomerase	168
	Chloroperoxidase	169
	Organophosphorus hydrolase	170
Aminopropyl ethyl carbodiimde	Chloroperoxidase	171,172
	α-L-arabinofurano-sidase	173
Imino groups	Penicillin G acylase	174
	Chloroperoxidase	169
Thiole groups	Trypsin	160
	Cytochrome *c*, lysozyme, β-lactoglubulin, myoglobin	159
Chloride groups	Trypsin	160
Carboxylic acid groups	Trypsin	160
	Organophosphorus hydrolase	170
Propanal groups	α-Chymotrypsin	174

TABLE 52.7. Percentage of Trypsin Found in the Supernatant Solution after Immobilization and Percentage of Trypsin Leached from Support during the Leaching Test

Support	Residual Enzyme in Solution (%)	Amount of Enzyme Leached from Support (%)
Post synthesis		
PrSH-SBA-15	27	16
PrCl-SBA-15	6	0[a]
$PrNH_2$-SBA-15	18	20
PrCOOH-SBA-15	3	11
Ph-SBA-15	12	55
In situ		
PrSH-SBA-15	10	1
PrCl-SBA-15	7	1
$PrNH_2$-SBA-15	22	25
PrCOOH-SBA-15	30	2
Ph-SBA-15	9	19

[a]Below the detection limit.

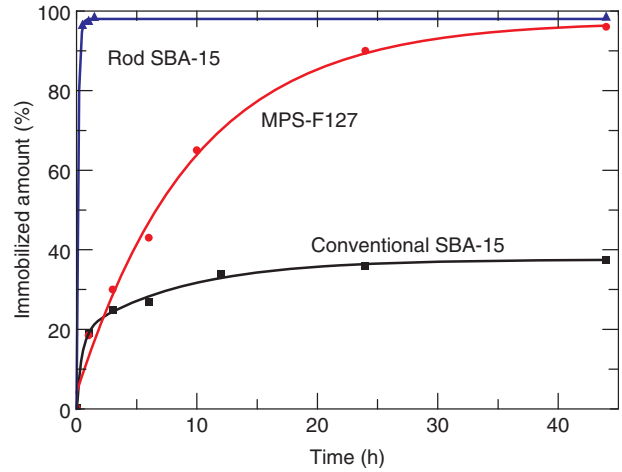


Figure 52.11. Uptake of lysozyme on rod-like and conventional SBA-15 in comparison to MPS-127 which possesses a three-dimensional cage structure (after Fan *et al*. (176)). (This figure is available in full color at http://onlinelibrary.wiley.com/book/10.1002/9780470054581.)

moieties but also the incorporation of metal ions. Aburto *et al*. (171) impregnated SBA-16 with Cs^+ ions which resulted in an increased activity of immobilized CPO compared to a sample prepared by physical adsorption. The authors suspect that the higher activity is due to the proper enzyme orientation on the Cs-doped surface leading to an orientation of the active site of the enzyme away from the silica wall. It cannot be ruled out that the higher activity is due to enzymes which are adsorbed on the outer surface of the material. Interactions between the enzymes and the Cs-doped outer surface may result in an increase in activity because diffusion of the substrate into the pore system is not required. However, a mechanistic understanding has not been achieved so far.

The adsorption kinetics, namely, the uptake rate of the enzyme, is influenced by the macrostructure (i.e. particle size and morphology) of the host material. Fan *et al*. (176) reported a correlation between the macrostructure of mesoporous silica and the rate and amount of enzyme uptake. Smaller particles possess a larger number of pore entrances compared to conventional larger particles, which results in an improved bioimmobilization performance (Fig. 52.11). For rod-like SBA-15, a very rapid (< 10 min to reach equilibrium) and large (up to 533 mg/g) uptake of the protein lysozyme was reported (176).

PMOs represent an exciting class of organic–inorganic hybrid supports. These materials are of interest, because they exhibit well-defined host–guest chemistry. The specific interactions between host and guest can be tuned for a desired application. Therefore, enzyme immobilization onto PMO is of current interest, but only little work was reported in this area up till now. For example, Hudson *et al*. (177) described the immobilization of cytochrome *c* and xylanase onto SBA-15 and a

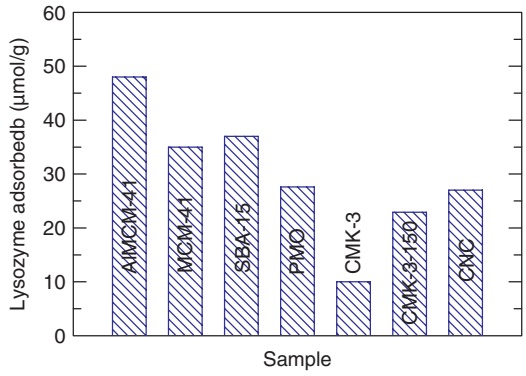


Figure 52.12. Comparison of the maximum lysozyme adsorption capacity for different mesoporous supports. (This figure is available in full color at http://onlinelibrary.wiley.com/book/10.1002/9780470054581.)

1,2bis(trimethoxysilyl)ethane-based PMO. They observed that electrostatic attraction dominated protein interactions with SBA-15, while weaker hydrophobic interactions are more prominent with PMO. The advantage of PMOs is the easy design of a solid support for any protein by simple variation of the organic bridging group. In two similar publications, Qiao *et al*. (178,179) describe the adsorption of bovine heart cytochrome *c* and lysozme onto a 1,2bis(trimethoxysilyl)ethane-based PMO in comparison to conventional SBA-15. As the amounts of enzyme adsorbed decrease with ionic strength of the solution, the authors concluded that the electrostatic interaction between the enzymes and support is much more important than the hydrophobic interaction.

In Fig. 52.12, the adsorption of lysozyme on different mesoporous supports is compared under optimized conditions. While the more hydrophilic silica-based supports still allow higher enzyme loadings, PMO materials as well as specially engineered mesoporous carbons might not be too far behind. However, the vast options in variation of the chemical composition and the possibility to introduce different functional groups will allow extraordinary freedom in tailoring the surface properties of the support.

Wang and Caruso developed a new method for enzyme encapsulation in mesoporous supports. They reported enzyme immobilization and encapsulation in bimodal mesoporous silica spheres (BMS) (180). The enzymes were immobilized in the BMS spheres, and a multilayer shell was then assembled on the sphere surface by the layer-by-layer (LbL) electrostatic assembly of oppositely charged species to encapsulate the enzymes. Nonporous silica spheres and mesoporous silica spheres with a series of pore sizes were used as enzyme immobilization hosts for comparison. Two systems were used to form dense coatings on the enzyme-loaded BMS spheres: (i) a polyelectrolyte (PE) multilayer shell formed through the alternate deposition of poly (diallyldimethylammonium chloride) and poly (sodium 4-styrenesulfonate) and (ii) a composite shell through the alternate deposition of poly (diallyldimethylammonium chloride) and the nonporous silica spheres. The authors described an effective method to encapsulate enzymes by using mesoporous silica particles with pore sizes between 10 and 40 nm and subsequent stepwise coating with nanoscale shells. Enzyme loadings in the range of 20–40 wt.% were obtained for small enzymes (diameter ca. 3 nm) with a high p*I* (>10) and ca. 8 wt.% for larger enzymes such as catalase. The lifetime of catalase was improved by encasing LbL assembled PE shells on the catalase-loaded BMS spheres. The encapsulated catalase can also be recycled 25 times with an associated loss of activity of 30%, which is significantly smaller than the loss in activity observed for catalase immobilized in the BMS spheres (ca. 65%). Additionally, ca. 98% of the activity of the encapsulated catalase was retained when subjected to proteolysis treatment. The enzyme-loaded particles prepared are expected to find future applications in industrial catalysis.

Apart from the studies exemplary discussed above, a large (and still increasing) number of studies is devoted to enzyme immobilization on (ordered) mesoporous supports (Table 52.8). It should be pointed out that characterization after immobilization of both the protein and the porous support after adsorption is very important in order to confirm that the protein and the support are stable under the prevailing immobilization conditions. For a more detailed discussion on enzyme immobilization on ordered mesoporous supports, the reader is referred to recent review chapters (142,181–183).

52.2.5 Biocatalysis

52.2.5.1 General Remarks. The use of enzymes in enzyme-catalyzed reactions is often hampered by three main drawbacks:

- Many enzymes are not sufficiently stable under the prevailing operation conditions and may loose their catalytic activity as a consequence of auto-oxidation, self-digestion, and/or denaturation by the reactants and the solvent or due to mechanical shear forces.
- Enzymes are water-soluble molecules and, thus, their repeated use (which is often required from an economical point of view) requires the recovery of the enzyme from aqueous solutions also containing the reactants.
- The space–time yield (a measure of the productivity of an industrial process) is often low due to the limited tolerance of enzymes to high concentration of the reactants.

TABLE 52.8. An Overview of Published Research in Protein Immobilization Using Mesoporous Molecular Sieves as Supports

Enzyme	Support	Activity Assay	Chemical Reaction	References
Encapsulation				
Cytochrome *c*, trypsin, papain, HRP	MCM-41	Cyclic voltammetry	Hydrolysis of BAPNA	7
Cytochrome *c*	MCM-41, AlMCM-41, MCM-48, SBA-15, Nb-TMS-1, Nb-TMS-4	Cyclic voltammetry	—	184,185
Lipase	MCM-41	Hydrolysis of triacetylglycerol	—	186
Lipase	MTS	—	Hydrolysis of ethylthiodecanoate	129
Lipase	Poly(hydroxy-methyl-siloxane)	—	Esterification of stearic acid	187
Lipase	Magnetic MCF	Hydrolysis of tributyrin	Resolution of 1-phenylethanol	188
Hemoglobin	FSM-16	Oxidation of ABTS	—	189
Physical adsorption				
Trypsin	SBA-15, MCM-41, MCM-48	Hydrolysis of BAPNA	—	190
Penicillin acylase	MCM-41	Hydrolysis of phenylacetic acid	—	191
Horseradish peroxidase	FSM-16, MCM-41, SBA-15	—	Oxidation of diaminobenzene	192,193
β-Lactoglobulin	SBA-15, thiol-modified SBA-15	—	—	158
Lipase	MCM-41, AlMCM-41	—	Esterification of acetic acid with ethanol	194
Crude lipase	SBA-15	Hydrolysis	Transesterification	195
Lipase	SBA-15	—	Acetylation of methyl(±)-mandelate	196
Trypsin	MCM-41	—	Transesterification	197
α-Chymotrypsin	MCM-1	—	Resolution of esters	165
Cytochrome P450	MCM-41, AlMCM-41	BCA assay	Oxidation of 2-propyl pentanoic acid	198
Lysozyme	MCM-41, surface- coated MCM-41	(No assay available)	—	199
Lysozyme	MCM-41, AlMCM-41, SBA-15, AlSBA-15, CMK-1, CMK-2, CMK-3	(No assay available)	—	200,201
Lysozyme	SBA-15, FDU-12, SBA-16	(No assay available)	—	30,175,202
Cytochrome *c*	MCM-41, MPS-127,	—	—	203–206
Cytochrome *c*	MCM-41, AlMCM-41, SBA-15, AlSBA-15, CMK-1, CMK-2, CMK-3	—	—	207,208
Cytochrome *c*	SBA-15, PMO	Oxidation of ABTS	—	177
Xylanase	SBA-15, PMO	—	—	177
RNase A	MCM-48	—	—	209
Hemoglobin	HMS	Cyclic voltammetry	—	210
Myoglobin	HMS	Cyclic voltammetry	—	211
Cytochrome *c*, protease, catalase	Bimodal mesoporous silica	Proteolysis	—	179
Trypsin	Modified MCM-41	Hydrolysis of BAPNA	—	212
Chloroperoxidase	SBA-15	MCD assay	Oxidation of indole	213

TABLE 52.8. (*Continued*)

Enzyme	Support	Activity Assay	Chemical Reaction	References
Chloroperoxidase	SBA-15, SBA-16, MCM-41, Al-MCM-41	—	Oxidation of 4,6-DMDBT	172,214
Bovine serum albumin	AlMCM-41	—	—	129
Manganese peroxidase	FSM-16	—	Pulp-free paper bleaching	215
Horseradish peroxidase	SBA-15	Cyclic voltammetry	—	216
Myoglobin	SBA-15, MCM-41	UV absorbance	—	217,218
Urease	MCM-41	Hydrolysis of urea	—	219
Glucose oxidase	MCM-41	Electrochemical	—	220
Glucose oxidase	Mesoporous silica	Oxidation of glucose	—	221
Lipase	KIT-6, SBA-16, FDU-12	Hydrolysis of *p*-NPA	—	222
Myoglobin	SBA-15, MCF, MSE, CNS, MCM-41	Oxidation of ABTS	—	223
Modified heme	FSM	Oxidation of ABTS	—	224
Lysozyme	PMO	*Micrococcus lysodeikticus* cell test	—	225
Serine protease	Mesoporous carbon gel	Conversion of casein	—	226
Laccase	Fe_3O_4@mesoporous silica	Oxidation of ABTS	—	227
Lipase	SBA-15	—	Resolution of 2-octanol	228
Covalent bonding				
Lipase	Modified CPS	Hydrolysis of olive oil	Esterification of butyric acid	229
Lipase	Modified MCF	—	Resolution of 1-phenylethanol	153
Lipase	Modified commercial mesoporous silica	Hydrolysis of *p*-NPP	N-Acylation of ethanolamine	230
Trypsin	Modified SBA-15	Hydrolysis of trypsin	—	160
α-Chymotrypsin	Modified SBA-15	Hydrolysis of SAAPPN	Transesterification of APEE	174
Organophosphorus hydrolase	Modified SBA-15	Paraoxon assay	—	169
Penicillin acylase	Modified SBA-15	Hydrolysis of penicillin G	—	231
Penicillin acylase	Modified SBA-15, KIT-6	Hydrolysis of penicillin G	—	232
Chloroperoxidase	MCF, SBA-15, SBA-16	MCD assay	—	233
Chloroperoxidase	Modified SBA-15	MCD assay	Oxidation of indole	169,234
Glucose oxidase	Modified SBA-15	Oxidation of glucose	Oxidation of indole	169,234
α-Amylase	MCM-41, MCF, SBA-15	—	Hydrolysis of starch	165
Glucose oxidase	MCF	Oxidation of glucose	—	164
Invertase	Modified MCF	Hydrolysis of succrose	—	235
Glucoamylase	Modified MCF	Hydrolysis of starch	—	235
Lysozyme	Modified CMK-3	(no assay available)	—	236
Glucose oxidase	Modified mesoporous silica	—	Conversion of D-fructose	237
Lipase	Modified mesoporous silica	Hydrolysis of olive oil	—	238

(*continued*)

TABLE 52.8. (*Continued*)

Enzyme	Support	Activity Assay	Chemical Reaction	References
Trypsin	Modified MCF	Conversion of BAPNA, casein	—	239
Methemoglobin	Modified FSM	—	Oxidation of guaiacol	240
Lipase	Modified SBA-15	—	Esterification of oleic acid in CO_2	241
Glucose oxidase	Gold-nanoparticles supported on mesoporous silica	Amperometry	—	242
γ-Glutamyl-transpeptidase	Meso-macroporous silica	Conversion of GPN	—	243
Penicillin G acylase	Modified KIT-6, SBA-15	Hydrolysis of penicillin G	—	232,244
Penicillin G acylase	Modified SBA-15	Hydrolysis of penicillin G	—	245
Glucose oxidase	Modified mesoporous silica	Oxidation of glucose	—	246
Trypsin	Modified SBA-15	Hydrolysis of BAPNA	—	247
Cross-linking				
α-Chymotrypsin	HMMS, SBA-15	Hydrolysis of N-Succinyl-Ala-Ala-Pro-Phe p-nitroanilide	—	144,145,151
Lipase	HMMS, SBA-15	Hydrolysis of 4-nitrophenyl butyrate	—	144,145,151
Lipase	Mesoporous oxides	—	Conversion of caprylic acid	248
Glucose oxidase	Pt/CMK-3	Amperometry	—	249

Depending on the immobilization technique, the properties of the biocatalyst such as stability, selectivity, kinetics, pH- and temperature characteristics may be significantly altered, which may result in (often) reduced or (sometimes) improved performance. However, at present predictions about the influence of the immobilization on the catalytic performance are difficult to make.

It is reasonable to assume that immobilization of the enzyme on a suitable support is a prerequisite for the use of biocatalysts in large-scale processing. Besides achieving retention of the biocatalyst, immobilization is often employed to stabilize the enzyme as translational motion as well as volume enhancing enfolding of enzymes is restricted. Moreover, encapsulation induces a change in microenvironment with respect to pH or hydrophobicity. However, in immobilized biocatalyst systems based on (meso) porous materials, film and pore diffusion might be rate determining instead of the catalytic reaction. It is, therefore, of utmost importance to establish the rate-determining step under the prevailing reaction conditions. Furthermore binding to the mesoporous carrier might cause changes in the active site of the enzyme often accompanied by significant loss in catalytic activity. Even when binding does not alter the enzyme structure, some enzymes may be bound to the carrier surface with the active site oriented away from the substrate solution and toward the surface, thereby hindering access of the substrate to the active site of the enzyme.

Although many cases of successful immobilization of enzymes using ordered mesoporous materials have been reported (cf. Tables 52.6 and 52.7) most of the research published only uses standard activity assays to monitor the catalytic performance. Up till now only a small effort has been made to test biocatalysts immobilized on mesoporous supports in real catalytic reactions. Thus, demonstration of their utility including the possibility to reuse the biocatalyst is of imminent importance. For industrial applications, a major obstacle to overcome is the low space–time yield in comparison to conventional (chemical) catalysts. Significant progress in this area would presumably increase the use of immobilized biocatalyst in industrial practice. Moreover, a unique feature of enzymes is their capability to catalyze reactions with high regio- and enantioselectivity.

The development of novel biocatalyst would be in particular useful for the production of pharmaceuticals and fine chemicals.

In the majority of studies devoted to the application of enzymes immobilize on mesoporous supports in catalysis, the catalytic activity is determined using standard activity assays. In this way, the relevant issues (i) enzyme activity after immobilization, (ii) stability during the reaction, and (iii) reusability after reaction are addressed for a large number of individual systems. Since these aspects have been thoroughly discussed in a recent review (181), here only a few representative examples with respect to potential industrial applications are discussed.

52.2.5.2 Case Studies. Many of the enzymes (e.g. lysozyme, papain, subtilisin Carlsberg, and trypsin) investigated so far are proteolytic enzymes that have large potential in the area of proteonomics owing to their potential to produce characteristic peptides that allow peptide mass finger printing. In particular, trypsin is one of the three principal digestive proteinases, the other two being pepsin and chymotrypsin. In the digestive process, trypsin acts with the other proteinases to break down dietary protein molecules to their component peptides and amino acids. Trypsin is the most discriminating of all the proteolytic enzymes in terms of the restricted number of chemical bonds that it will attack. Good use of this fact has been made by chemists interested in the determination of the amino acid sequence of proteins; trypsin is widely employed as a reagent for the orderly and unambiguous cleavage of such molecules.

Magner and coworkers (250) developed and studied a "nanoporous reactor" based on cyano-functionalized mesoporous silicates for efficient proteolysis employing trypsin. The trypsin-mediated digestion of proteins is reported to occur within its mesochannels. Mesoporous silica (d_p = 18 nm) is used as support for trypsin and rapid *in situ* digestion of the proteins cytochrome *c* and myoglobin is observed. After digestion, the generated peptides were analyzed by matrix-assisted laser desorption ionization time-of-flight mass spectrometry (MALDI-TOF MS). The authors pointed out that proteolysis by trypsin immobilized in the channels of mesoporous silica is much more efficient than digestion in solution. This observation is ascribed to the nanoscopic confinement and the concentration enrichment of the substrate within the mesopores. Thus, the invented "nanoreactor" combines the advantages of short digestion time with retention of enzymatic activity, thus providing a promising way to advance the development of proteomics.

The hydrolysis of *N*-α-benzoyl-DL-arginine-4-nitroanilide (BAPNA) is widely used for the activity determination of immobilized trypsin (7,160,251). Yiu *et al*. reported the immobilization of trypsin onto a variety of functionalized mesoporous SBA-15 materials (160). The most promising catalyst in this study is trypsin adsorbed on a thiol-functionalized SBA-15 support. The catalytic activity of this solid, which showed negligible leaching in catalytic assays, amounts to about 84% of the activity measured for the free enzyme. It was shown that reuse of the catalysts is also possible, even after a period of several days, although the initial activity of the recycled catalyst (trypsin supported on thiol-functionalized SBA-15) is only two-thirds of that displayed by the fresh catalyst.

Hodnett and his group (197) studied the transesterfication of *N*-acetyl-L-tyrosine ethyl ester with propane-1-ol by trypsin supported on MCM-41 (d_p = 4.5 nm). The catalytic experiments were performed in a batch reactor. The authors reported that the activity of the catalyst is not reduced after the second and third reuse. Under the prevailing experimental conditions, the turnover number (TON) amounts to 600, that is, 600 molecules of ethanol are formed per molecule of trypsin.

In vivo, chymotrypsin is a proteolytic enzyme acting in the digestive systems of mammals and other organisms. In enzymatic catalyzed experiments, chymotrypsin was found to be useful for resolutions of racemic mixtures and in transesterifications. Fadnavis *et al*. (166) immobilized the zymogen α-chymotrypsinogen A onto mesoporous silica MCM-41. After activation of the zymogen with trypsin, the active α-chymotrypsin immobilized on MCM-41 was obtained. The enzyme was tightly bound to the support and can be used in over 100 cycles over 1 week in aqueous as well as reverse micellar media. The immobilized α-chymotrypsin has been used for resolution of *N*-acetyl- DL -amino acid esters. The determination of enantiomeric purity showed that the racemic amino acid is completely resolved giving *N*-acetyl-L-amino acid and the unreacted D-ester with an enantiomeric excess (ee) > 99% and an ee of 98%, respectively.

The kinetic resolution and accordingly the transesterification of racemic (±)-*trans*-4-methoxy-3-phenylglycidic acid methyl ester is an industrially important process since the optically pure (2*R*,3*S*)-*trans*-4-methoxy-3-phenylglycidic acid methyl ester is used as an intermediate for the production of diltiazem, which is an important drug. It was observed that the immobilized α-chymotrypsin shows stereoselectivity toward the (2*S*,3*R*)-isomer, giving *trans*-(2S,3*R*)-*p*-methoxy-3-phenylglycidic acid butyl ester (ee = 75%) and *trans*-(2*R*,3*S*)-*p*-methoxy-3-phenylglycidic acid methyl ester with ee = 65% at a conversion of 45% (Fig. 52.13). Furthermore, the activity of immobilized α-chymotrypsin in aqueous buffer was found to be consistent for at least 100 recycles (20 recycles per day) over 1 week at room temperature and decreased gradually to 15% during the next 10 days. It was confirmed that the inherent properties of α-chymotrypsin do not change after immobilization in the pores of MCM-41 and the resulting

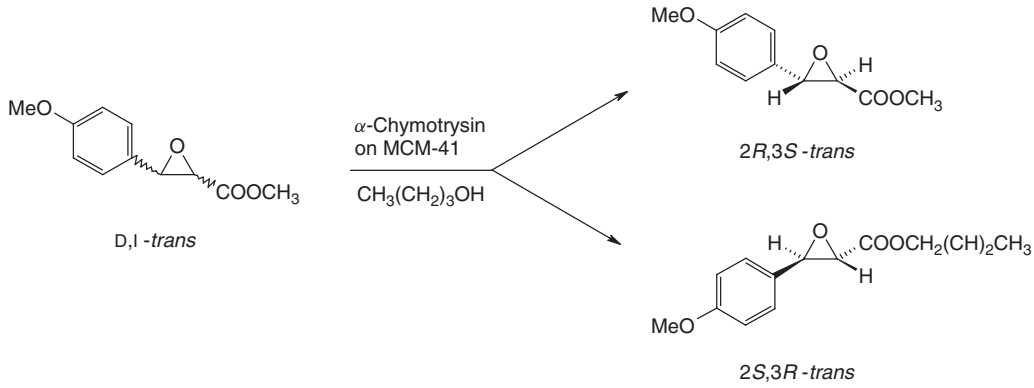


Figure 52.13. Kinetic resolution of racemic (±)-*trans*-4-methoxy-3-phenylglycidic acid methyl ester glycidate with α-chymotrypsin.

heterogeneous catalyst can be used in both aqueous and reverse micellar media for practical applications.

Transesterification reactions using immobilized α-chymotrypsin in organic solvents were conducted by Wang *et al*. (175). α-Chymotrypsin was immobilized by covalent anchoring onto an ordered mesoporous silica support (SBA-15-like with $d_p = 15$ nm) and its activity in the transesterification of *N*-acetyl-L-phenylalanine ethylester and *n*-propanol in hexane, acetonitrile, methanol, and *iso*-octane was tested. Although methanol is a potential reactant for the transesterification, no methylester product peak was detected and, thus, no transesterification with methanol occurs. The authors observed a much higher activity of the immobilized α-chymotrypsin compared to the native enzyme suspended in the same organic solvent. For hexane, a 110-fold enhancement was observed, while the highest activity was determined when *iso*-octane was used as a solvent. In contrast, the apparent activities of immobilized α-chrymotrypsin are usually much lower than those of their free parent enzyme as measured by the hydrolysis reaction.

A broad variety of esterifications is catalyzed by lipases. Lipases belong to the hydrolytic enzymes beside proteases, amylases, amidases, and esterases, which provide the major contingent of enzymes used for industrial processes. Lipases (triacylglycerol acylhydrolases, E.C. 3.1.1.3) have turned bit by bit to key enzymes in the growing biotechnology sector and find usage in a wide array of industrial applications including food technology, detergents, chemical industry, and biomedical sciences. Lipases are hydrolases which cleave the carboxyl ester bonds in triacylglycerols under aqueous conditions to liberate fatty acids and glycerol. The natural substrates of lipases are long-chain triacylglycerols with very low solubility in water. Therefore, the reaction is catalyzed at the lipid–water interface. Under microaqueous conditions, lipases possess the unique ability to carry out the reverse reaction, leading to esterification, alcoholysis, and acidolysis. Besides being lipolytic, lipases also possess esterolytic activity. In order to improve the catalytic potential of lipases and to enhance their utilization in industrial processes and for further applications, several strategies have been developed for efficient immobilization onto mesoporous silicas.

To exploit the lipolytic nature, studies of gas-phase enzymatic reactions catalyzed by supported lipases onto MCM-41 and Al-MCM-41 were carried out. Pires *et al*. (194) examined lipases produced by five different microorganisms in the esterification reaction of acetic acid with ethanol. The used lipases were extracted from: *Rhizopus oryzae*, *Rhizopus niveus*, *Mucor javanicus*, *Pseudomonas fluorescens*, and *Pseudomonas cepacia*. The transesterification of acetic acid catalyzed by free and immobilized lipases was tested in the liquid-phase in a batch reactor. In addition, the immobilized lipases were tested in gas-phase reactions in a continuously operated fixed-bed reactor. In general, Pires *et al*. observed an increase of the turnover number for the liquid-phase reactions carried out with the immobilized lipases compared to the homogeneous catalytic reaction. Although the results showed that the rates of liquid-phase reactions were higher than those measured for the gas-phase reactions, the authors avoided a comparison of the two systems because the concentration of reactants and the amount of catalyst used were lower in the gas-phase experiments. In addition, Pires *et al*. found a higher activity for the lipases immobilized in Al-MCM-41 than for those immobilized in MCM-41.

To enhance lipase activity by coimmobilization of different stabilizing additives was found to be a promising strategy. Soares *et al*. (229) reported that simultaneous immobilization of lipase and nonenzymatic proteins (e.g. albumin and lecithin) on the same mesoporous support enhanced the activity of the resulting catalyst. The solid catalysts were prepared by covalent immobilization of lipase together with albumin and lecithin, respectively. The mesoporous support was functionalized with APTES followed by the reaction

of the pretreated beads with glutaraldehyde and the proteins. The reaction mixture consisting of heptane, *n*-butanol, butyric acid, and immobilized lipase was incubated at 37°C for 24 h with continuous shaking at 150 rpm. The initial esterification activity of immobilized lipase without additive was 161 μmol/g·min, while for the catalyst prepared in the presence of lecithin or albumin the activity increased by about a factor of 2. The authors showed that the lipase catalyzed synthesis of butyl butyrate via esterification can be enhanced by nonenzymatic additives. In Fig. 52.14, the concentration of the synthesized butyl butyrate is plotted against the reaction time. The improved lipase activity was considered to be a consequence of the coimmobilization of lipase with the additives, which presumably prevents enzyme aggregation and increases the accessibility of active sites to the substrate.

A special case of an esterification, which is very common in the synthesis of natural products, is the acetylation. Because of its manifold applications in organic synthesis, the enzymatic catalyzed acetylation using immobilized lipases is also investigated. Here, methyl (±)-mandelate (methyl-α-hydroxyphenyl acetate) was chosen as a model substrate for the lipase-catalyzed reaction (196). This model reaction, shown in Fig. 52.15, was carried out in an ionic liquid as solvent, therefore, lipase PS was immobilized on a methacrylpropyl-modified SBA-15 (252).

Itoh *et al*. (196,252) showed that the acetylation of methyl (±)-mandelate results in the formation of (−)-methyl (*R*)-mandelate with an ee larger than 99%. The acetylation provided the product (+)-methyl (*S*)-α-acetoxyphenyl acetate in 71% yield with an ee of about 22%. This type of reaction is potentially interesting since it allows kinetic resolution of racemic mixtures.

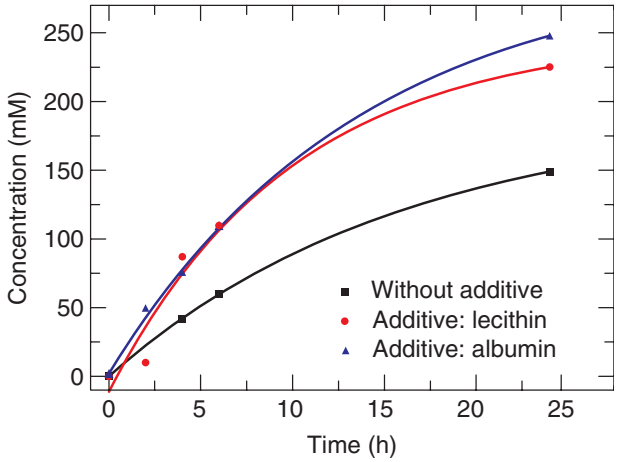


Figure 52.14. Synthesis of butyl bytyrate from butanol and butyric acid using immobilized lipase without (■) and with additives (lecithin (•) and albumin (▲)), respectively. The intial esterification activities for immobilized lipase without additive, with lecithin and with albumin amount 161, 306, and 338 μmol/g, respectively (after C.M.F. Soares *et al*. (229)). (This figure is available in full color at http://onlinelibrary.wiley.com/book/10.1002/9780470054581.)

Full resolution of the racemic mixture of 1-phenylethanol to (*R*)-1-phenylethanol and (*R*)-1-phenylethyl acetate was achieved in a packed fixed-bed reactor as described by Han *et al*. (153). A standard HPLC column was filled with a catalyst consisting of lipase *Candida antarctica* lipase B immobilized on modified silica MCF by the pressure-driven immobilization method (described in Section 2.4). The catalyst-packed column was tested for continuous conversion of 1-phenylethanol. The flow rate was adjusted to give full conversion of (*R*)-1-phenylethanol (i.e. 50% conversion of the (*R*)-1-phenylethanol and (*S*)-1-phenylethanol racemic mixture). The activity and enantioselectivity of the reaction remained constant in the beginning and decreased by 9% after 48 h of reaction. Unfortunately, the conversion of (*R*)-1-phenylethanol was 100% at the beginning and so deactivation cannot be detected in the early stage of the reaction. A multitude of experiments was carried in a batch reactor in order to determine the conversion of (*R*)-1-phenylethanol over immobilized lipase prepared by the pressure-driven method as well as the conventional method in comparison to the commercial catalyst Novozyme 435 and free lipase (CALB). After 5 h, a conversion of 50% based on the racemic mixture was achieved over the immobilized lipases, while only 45% were found over the free lipase. After a thermal treatment at 80°C, only the pressure-driven immobilized lipase reached a conversion of 50%. Moreover, leaching of the catalysts was reported to be a problem.

Another versatile and often employed reaction in organic synthesis is the acylation of, for example, amines, amides, and alcohols. A prominent example is the industrial production of the pain-killer aspirin. Thus, there is also an interest in performing lipase-catalyzed acylations under conditions which fulfill industrial requirements. Blanco *et al*. described the acylation of ethanolamine with lauric acid in acetonitrile catalyzed by lipase from *C. antarctica* B (230). The catalyst used was lipase immobilized onto a commercial mesoporous silica (with a surface area of 300–320 m^2/g and an average pore diameter of 30–40 nm), which was modified with octyltriethoxysilane prior to the immobilization step. The N-acylation of ethanolamine with lauric acid was conducted in a stirred-tank reactor, where the lipase-octyl-silica catalyst was added to the acetonitrile solution containing ethanolamine and lauric acid. After completion of the reaction, the solid catalyst was recovered by filtration and a new reaction was started. Following this procedure, the catalyst was reused up to 15 times. The catalyst remained fully active for these 15 cycles at 40°C, thus, exhibiting an excellent operational stability of the immobilized lipase.

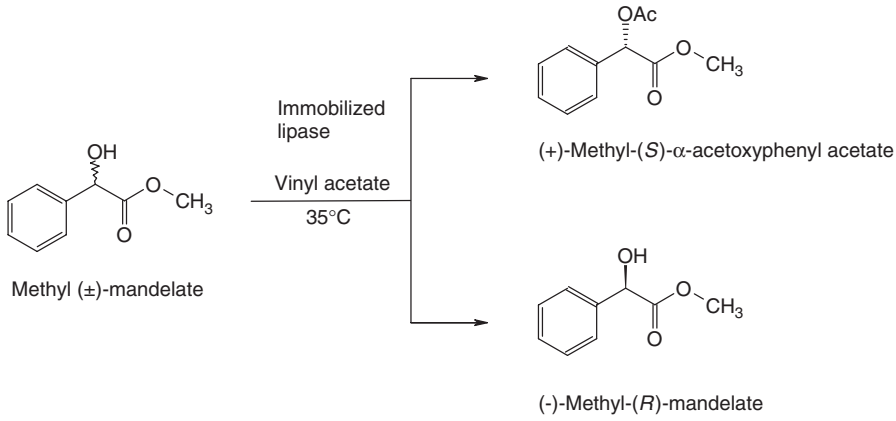


Figure 52.15. Transesterification of methyl (±)-mandelate and vinyl acetate in 1-butyl-3-methylimidazolium tetrafluoroborate or hexafluorophosphate catalyzed with immobilized lipase PS.

The hydrolysis of ethylthiodecanoate with encapsulated lipase was tested by Mureseanu *et al*. (134). The enzymatic catalysis tests were performed in a cuvette. The hydrolysis of the ethylthiodecanoate was selected because the thioethanol formed during this reaction can be easily detected by UV–Vis spectroscopy from the yellow colored product formed in the presence of 5,5-dithiobis(2-nitrobenzoic acid).

In the majority of the studies published so far, the activity of lipase is determined via an enzymatic activity assay, that is, the hydrolysis of olive oil and *para*-nitrophenyl palmitate, respectively. Owing to the lack of correlation between the hydrolytic and synthetic activity of lipases, high activities in hydrolysis reactions do not necessarily go along with high activities in synthetic reactions. Therefore, it is necessary to study more lipase-catalyzed reactions with respect to their applicability in organic synthesis and in industrial areas, for example, the production of pharmaceuticals.

Hydrolysis also plays an enormous role in the breakdown of starch into maltose molecules. Starch is the most common storage carbohydrate in plants. Since it is used by the plants themselves, by microbes and by higher organisms, a great diversity of enzymes is able to catalyze the hydrolysis of starch. Acidic hydrolysis of starch was widely used in the past and is now replaced by enzymatic processes step by step. Thus, there is a large interest in heterogeneous catalysts based on α-amylase to produce dextrin, glue, starchy syrup or other food ingredients such as glucose.

Pandya *et al*. (165) reported the immobilization of α-amylase into SBA-15, MCM-41, and MCF. The immobilization of α-amylase was carried out in a three-step process. In the first step, alkylamine was covalently bonded to the silanol groups of mesoporous silica. Further treatment with glutaraldehyde resulted in an imino function. In the last step, α-amylase was covalently anchored onto the mesoporous material. Owing to the inability of α-amylase to hydrolyze $\alpha(1-6)$ bonds, the actual reaction products are dextrins rather than maltose. The highest starch conversion with a specific activity of 80% of the free enzyme was observed for α-amylase immobilized on MCF possibly due to the higher enzyme loading. Furthermore, the structural features of MCF provide accessibility and more diffusional freedom for substrate and product molecules. Hence, the authors conclude that the two-dimensional pore structure of MCM-41 and SBA-15 might impose diffusional restrictions on substrate and product molecules. In conclusion, it was observed that the stability of immobilized α-amylase was enhanced with increasing pore sizes of the support and the catalyst retains its activity in starch hydrolysis for 140 min.

Vegetable raw materials are not only important for the production of food or food additives, but also for energy generation using biomass. Sulfur-containing compounds of biomass and petroleum are a well-known problem for industry and environment. The oil refining industry is a potential candidate for the use of enzymes in the production of clean fuels including diesel and gasoline in order to meet the present and future rigorous environmental regulations. The technological and economical feasibility of biocatalytic oxidation and subsequent separation of organosulfur compounds by distillation to obtain low-sulfur fuels is insufficient. Up till now, only few papers were published dealing with this topic, which provides an interesting area for future studies. The homogeneous enzymatic oxidation of dibenzothiophene by laccase (253) and the oxidation of 4,6-dimethyldibenzothiophene (4,6-DMDBT) by immobilized CPO from *Caldariomyces fumago* were recently investigated (172,214). CPO was immobilized on amorphous and ordered silica-based materials either by physical adsorption or covalent anchoring using an organosilane derivative; both catalysts were tested in the oxidation of

4,6-DMDBT with H_2O_2 as oxidant. The performance in this reaction was investigated with respect to the addition of organic solvents (e.g. acetonitrile) the thermal stability of the enzyme and the influence of the different supports. In addition, different supports were explored such as SBA-15, SBA-16, MCM-41, and Al-MCM-41. It was found that the activity is reduced by only 20% in the presence of 60 vol.% acetonitrile compared to the homogenously catalyzed reaction in a buffer solution containing 20 vol.% acetonitrile. Surprisingly, CPO immobilized on Al-MCM-41, which shows the highest activity at room temperature in a reaction mixtures containing 20 vol.% acetonitrile, is no longer active in the presence of higher concentrations of acetonitrile. Increase of the temperature from 24 to 35°C results in a 2.5-fold higher reaction rate for the immobilized CPO, while the rate of the native enzyme decreased by 20%. In summary, this study indicates that the immobilization of CPO on mesoporous materials might be a promising approach for this specific case in petroleum industry. However, major hurdles to overcome still are the cost of CPO and its low stability.

The oxidation of indole to 2-oxindole catalyzed by immobilized CPO was studied by Jung *et al*. (234) under flow conditions in a fixed-bed reactor. The nonenzymatic synthesis of 2-oxindole requires harsh conditions or complex inorganic catalysts to be successful, since oxidation of the electron-rich 3-position is typically favored. Preliminary studies on CPO immobilized SBA-15 by physical adsorption were carried out by *Hartmann et al*. (213). External H_2O_2 addition to the batch reactor results in deactivation of the immobilized CPO due to high local H_2O_2 concentrations. Deactivation was circumvented by *in situ* hydrogen peroxide generation. H_2O_2 was produced by oxidation of glucose with glucose oxidase (GOx) from *Aspergillus niger* immobilized on SBA-15. By the use of this tandem reaction, CPO deactivation was largely suppressed due to the "sensitive" hydrogen peroxide generation. The maximum indole conversion of 91% is observed at a pH of 5.5, which is also the pH where the highest average H_2O_2 formation rate was observed. Moreover, the tandem catalyst can be recycled several times without significant loss of activity (234).

Besides deactivation, leaching of the enzymes is a frequently encountered problem. In order to avoid leaching from the mesoporous support, CPO and GOx were covalently anchored to the carrier surface via chemical bonding. Jung *et al*. (169) have observed that under continuous operation in a fixed-bed reactor leaching of the covalently anchored enzymes is significantly reduced as compared to catalysts containing physically adsorbed enzymes (Fig. 52.16). By using immobilized CPO and GOx as catalysts in this tandem reaction, the final 2-oxindole yield amounts to 8.3% after 50 h time-on-stream which is more than twice the amount found for the physisorbed CPO and GOx at similar catalyst loadings.

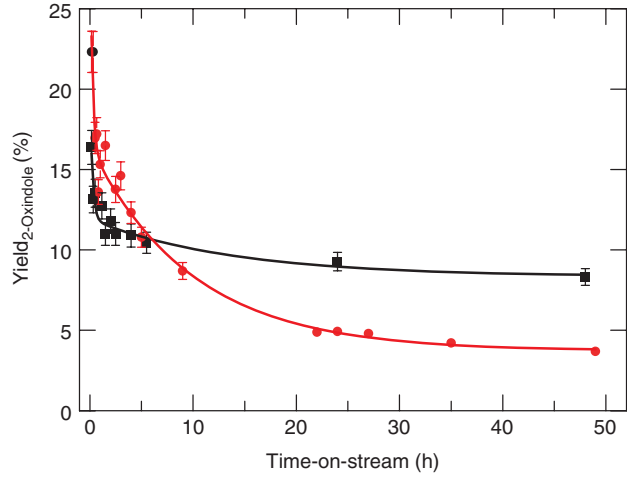


Figure 52.16. Oxidation of indole over 150 U CPO-GA-ATS-SBA-15 and 7 U GOx-GA-ATS-SBA-15 (•) and 150 U CPO-SBA-15 and 7 U GOx-SBA-15 (■) (after Jung *et al*. (169)). (This figure is available in full color at http://onlinelibrary.wiley.com/book/10.1002/9780470054581.)

Together with CPO, HRP belongs to the group of oxidoreductases. HRP is used as a reagent for organic synthesis, biotransformation and in coupled enzyme assays. Some applications of HRP are small-scale organic syntheses including N- and O-dealkylation, oxidative coupling, selective hydroxylation, and oxygen-transfer reactions. However, van de Velde *et al*. (254) raised the general point that scale-up of peroxidase-catalyzed enantioselective oxidations to industrial level will require a substantial reduction in the price of enzyme per unit of product. Solutions to this problem may include better process management of hydrogen peroxide to avoid enzyme inactivation (see paragraph on CPO) and use of engineered enzymes with improved stability and catalytic efficiency.

For evaluation of the catalytic activity and efficiency of HRP immobilized on mesoporous silica, the oxidation of 1,2-diaminobenzene in toluene was selected by Takahashi *et al*. (193) as test reaction. The experiments were performed in the absence of water; *tert*-butylhydroperoxide was used as the oxidant and HRP was immobilized on FSM-16, SBA-15, and MCM-41 materials with different pore diameters. The conversion over HRP immobilized on FSM-16 (d_p = 5.1 nm) and on MCM-41 (d_p = 5.0 nm) amounts to 75% and 63%, respectively, after 7 h. When HRP was immobilized on supports possessing pores smaller or larger pores than 5 nm, the conversion was lower. Thus, the authors concluded that the average mesopore sizes have to match the molecular dimensions of the enzymes in order to achieve immobilized enzymes exhibiting good stability and high activity.

The most abundant polymer on earth besides cellulose is lignin. About 65–75% of the dry mass of wood consists of lignin. It is extracted by the Kraft process, but for

further applications, for example, in the paper industry it has to be bleached. In an attempt to use manganese peroxidase (MnP) for chlorine-free pulp bioleaching, MnP from *Phanerochaete chrysosporium* has been immobilized on FSM-16 with a pore diameter of 7.0 nm (215). This support has nearly the same pore diameter than the size of the enzyme and the immobilized MnP exhibits high thermal stability and tolerance to H_2O_2. MnP immobilized on FSM-16 retained more than 80% of its initial activity even after 10 days of reaction. Moreover, a two-stage reactor system is proposed, in which the Mn^{3+} generation step and the pulp-bleaching step were separated. In the first step, the substrate solution comprising Mn^{2+}, H_2O_2, and malonic acid (as a chelating agent) was introduced in a column packed with FSM-16 supported MnP. In the next stage, the Mn^{3+} malonate complex generated by the immobilized MnP was transferred into the bleaching vessel containing unbleached treated kraft pulp. By using a two-stage reactor system, the conditions for the oxidation of Mn^{2+} to Mn^{3+} by MnP and the subsequent oxidation of lignin in pulp by Mn^{3+} can be optimized independently (215). The best results were obtained when the MnP reaction and the pulp-bleaching reaction were performed at 39 and 70°C, respectively, MnP activity was maintained throughout the reaction and the brightness of the pulp after 9 h had increased from 61% to 70%.

A further improvement of this process was achieved by combination of the bleaching process with a subsequent alkaline extraction. The enzyme-treated pulp was washed with deionized water and then suspended in a 2.5% NaOH solution. The enzyme treatment (55 min) and alkaline extraction (5 min) were repeated alternately for seven cycles. Seven hours after completion of the last treatment the brightness of the pulp has increased to about 88%.

Galarneau *et al*. (131) described the immobilization of alcohol dehydrogenase (ADH), which is known to be a fragile enzyme. ADH has been immobilized either alone or coimmobilized with its cofactor nicotinamide adenine dinucleotide (NAD^+) in SMS. The self-assembly of mixed-micelles of lecithin and dodecylamine in an alcoholic aqueous media allows to template the formation of SMS. The activity of this biocatalyst was tested in the oxidation of ethanol to acetaldehyde and compared to the activity of a similar catalyst prepared by coadsorption of ADH and NAD^+ on MCM-41 (Fig. 52.17). The authors concluded that this biocompatible method of SMS formation enhances enzymatic activity which allows the encapsulation of even very fragile enzymes for use in catalytic processes.

Penicillins are the most widely used β-lactam antibiotics, which hold a 19% share of the estimated worldwide antibiotic market. However, excessive use of these antibacterial drugs has led to the development of resistant pathogens. Currently, the only method of overcoming

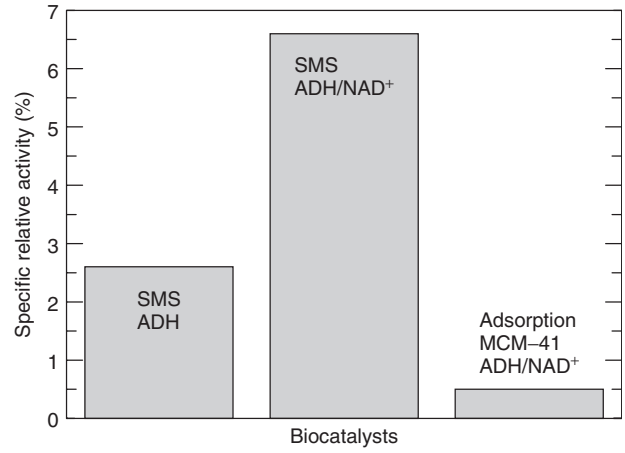


Figure 52.17. Relative specific activity of ADH encapsulated in SMS with and without its cofactor NAD^+. For comparison, relative activity of ADH immobilized with its cofactor NAD^+ by adsorption in a large-pore MCM-41-type material is given (after A. Galarneau *et al*. (131)).

the resistance problem is the use of newer semisynthetic antibiotics. 6-Aminopenicillanic acid (6-APA) is a key raw material for the production of semisynthetic penicillins and, thus, of increasing interest in pharmaceutical industries. 6-APA can be produced via hydrolysis of penicillin G by penicillin acylase (PA) (Fig. 52.18). Efforts to use PA have been hampered by its high cost, instability, and the difficulty in recovering the active enzyme for reuse. By immobilizing PA on a mesoporous support, it is hoped that the catalyst can be used in a continuous process and may also be readily separated from the reaction mixture and reused. Furthermore, the properties of PA may be enhanced or its lifetime may be increased, because immobilized PA is less susceptible to degradation, aggregation, or denaturation. He *et al*. (191) reported the immobilization of PA onto MCM-41 and Al-MCM-41 and its catalytic evaluation in penicillin G hydrolysis. The authors pointed out that PA can be immobilized on MCM-41 and Al-MCM-41 with different Si/Al ratios (Table 52.9) through either direct immobilization or covalent coupling with glutardialdehyde. Direct immobilization resulted in higher activities compared to covalent coupling.

7-Aminocephalosporanic acid (7-ACA) is an important starting material for the synthesis of semisynthetic cephalosporins (Fig. 52.19). The cephalosporins are a class of β-lactam antibiotics, which belong to a subgroup called *cephems*. The enzymatic transformation of cephalosporin C (CPC) into 7-ACA can be performed by a two-step process including the oxidative deamination of CPC to glutaryl-7-aminocephalosporanic acid (GL-7-ACA) catalyzed by a D-amino acid oxidase and the subsequent hydrolysis catalyzed by GL-7-ACA acylase (255). In this context, Park *et al*. (256,257) studied the immobilization of

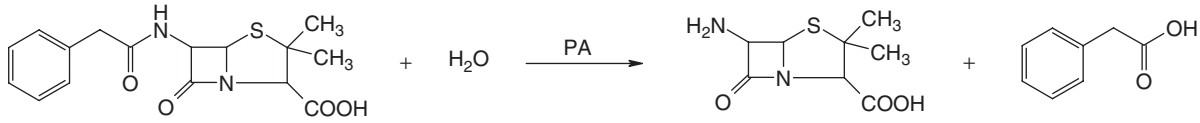


Figure 52.18. Hydrolysis of penicillin G with penicillin acylase to obtain 6-aminopenicillanic acid.

TABLE 52.9. Activity of Immobilized PA on MCM-41 with Different Si/Al Ratios

AlMCM-41 Support	Activity of the Resulting Biocatalyst (U/min/g)
Pure silica	364
Si/Al = 100	475
Si/Al = 50	491
Si/Al = 25	511

GL-7-ACA acylase on a conventional silica gel modified with APTES followed by glutaraldehyde coupling and studied the resulting catalyst in the production of 7-ACA.

The Michaelis–Menten kinetic parameters, K_m and V_{max}, for free and the immobilized GL-7-ACA acylase on siclica gel were determined to be 9.9 mM and 171.36 μg/min and 15.4 mM and 114.94 μg/min, respectively. The pH values for optimum activity of the free and immobilized GL-7-ACA acylase were almost identical. However, the pH-dependent activity profile for the immobilized GL-7-ACA acylase is considerably expanded. A similar finding has been reported, for example, for CPO immobilized on mesoporous silica (213). In order to investigate the thermal stability of the immobilized GL-7-ACA acylase, experiments were carried out at various temperatures (20–60°C).

The thermal inactivation rate constant (k_i) values of the immobilized GL-7-ACA acylase at all temperatures studied were lower than those of the free GL-7-ACA acylase, and the half-lives for inactivation of the immobilized GL-7-ACA acylase were higher than those of the free GL-7-ACA acylase (Table 52.10). Consequently, the thermal stability of the immobilized GL-7-ACA acylase was increased significantly compared to that of the free GL-7-ACA acylase. Therefore, the authors conclude, that the immobilization strategy used in their study should be applicable to the production of 7-ACA in large scales. Moreover, the use of a suitable mesoporous silica support might also be interesting.

The last example in this chapter is devoted to a multistep synthesis in microfluidic devices which involves enzymes immobilized on (meso)porous silica. Luckarift *et al*. (258) reported the combinatorial synthesis of 2-aminophenoxazin-3-one (APO) in a microfluidic device (Fig. 52.20). Microfluidic channels (40 mm long × 1.5 mm wide × 0.1 mm deep; 6 mL volume) were fabricated in

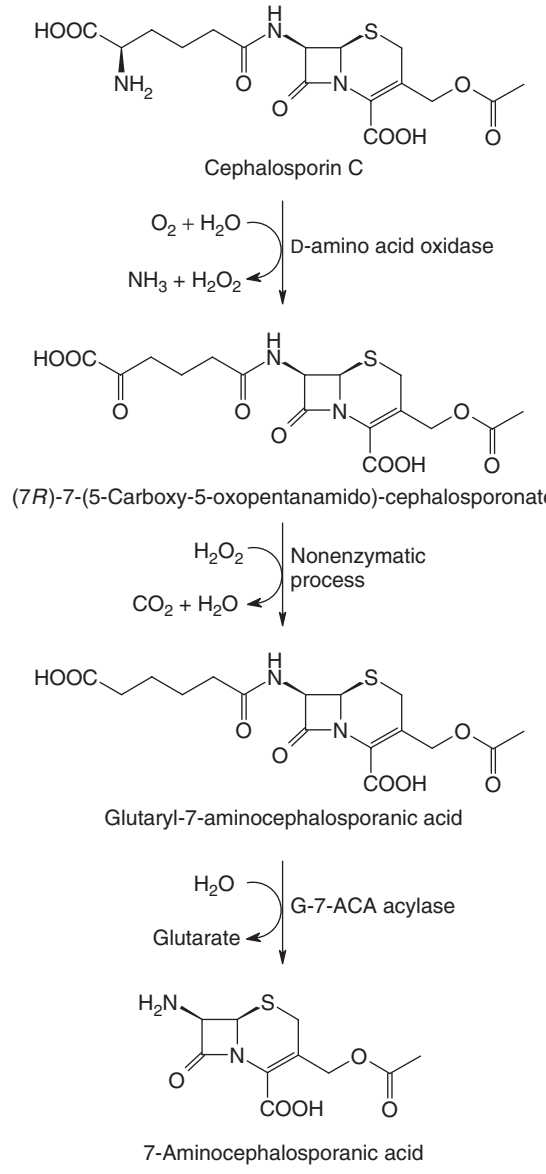


Figure 52.19. Synthesis route of 7-aminocephalosporanic acid for the production of semisynthetic cephalosporins with cephalosporin C as starting material.

polydimethylsiloxane. The resulting chip is fabricated with three 50 mm channels to form an exit network to retain the immobilized catalysts. The biocatalyst immobilized on silica was loaded into the channel by applying a vacuum to the product reservoir. Individual microfluidic chips containing

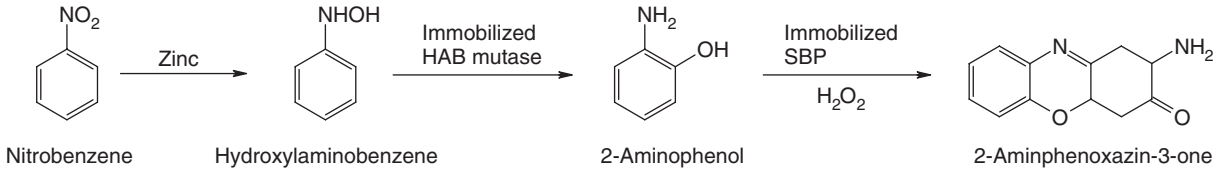


Figure 52.20. Multistep synthesis of 2-aminphenoxazin-3-one.

TABLE 52.10. Thermal Inactivation Rate Constants (k_i, min^{-1}) and Half-life Times ($t_{0.5}$, min) of the Free and Immobilized GL-7-ACA Acylase at Different Temperatures

Enzyme	37°C		45°C		50°C		55°C	
	$k_i \cdot 10^2$ (min^{-1})	$t_0.5$ (min)	$k_i \cdot 10^2$ (min^{-1})	$t_0.5$ (min)	$k_i \cdot 10^2$ (min^{-1})	$t_0.5$ (min)	$k_i \cdot 10^2$ (min^{-1})	$t_0.5$ (min)
Free GL-7-ACA acrylase	0.22	307.65	1.38	49.97	2.33	29.72	4.07	17.03
Immobilized GL-7-ACA acrylase	0.09	733.72	0.34	200	1.06	65.90	1.99	34.74

metallic zinc, silica-immobilized hydroxylaminobenzene mutase (HAB-mutase) and silica-immobilized soybean peroxidase (SBP) are connected in series to create a chemoenzymatic system for the synthesis. Zinc catalyzes the initial reduction of nitrobenzene to hydroxylaminobenzene (HAB), which undergoes a biocatalytic conversion to 2-aminophenol, followed by enzymatic polymerization to APO. The immobilization of the enzymes onto silica allows stabilization and a minimal preparation of the biocatalyst into the microfluidic device. The system proved suitable for synthesis of a complex natural product (APO) from a simple substrate (nitrobenzene) under continuous flow conditions.

This work is a fine example for a chemoenzymatic microfluidic device allowing synthesis of a natural product from nitrobenzene. The facile immobilization of the employed enzymes on silica provided stable heterogeneous catalysts, which can be easily incorporated into microfluidic chips. The invented flow-through system could, in principle, be applied to the transformation of a wide variety of nitroarene substrates into their corresponding phenoxazinone products, and provides an attractive alternative to conventional chemical synthesis. This example shall trigger more work in this area including the use of mesoporous silicas as support for immobilization of the enzyme. However, it is at present not clear whether an increase in performance will justify a potentially higher price of the device.

52.3 CONCLUSIONS AND OUTLOOK

Although quite young, the field of mesoporous silicas and carbons doped with biologically interesting molecules has already exhibited its diversity and potential applications at many frontiers of modern material science including biocatalysis, biosensing, drug release, and separation of biological molecules. It has been shown that ordered mesoporous materials are useful for stable entrapment of biofunctions and the stabilization of biological interesting molecules such as proteins and enzymes under severe conditions. For example, enzymes immobilized on ordered mesoporous supports often show higher stability as compared to the free enzyme. However, the activity of immobilized enzymes is often found to be lower than that of the free enzyme. Moreover, the access of a substrate to the enzyme confined in a mesoporous host might be orientation selective resulting in a unique selectivity of a reaction. While the activity of the immobilized enzymes is often assessed by a suitable assay, evaluation of the novel biocatalysts in reactions which are potentially interesting for an industrial application are rare. Moreover, tandem reactions which employ two or more enzymes in a one-pot reaction, which is one of the huge advantages of enzymatic biocatalysis, are seldom used. One of the major problems to be solved is the stability of mesoporous silicas upon prolonged exposure to aqueous solutions. Moreover, a possible reuse of these (at present cost-intensive) adsorbent/catalyst has to be investigated. For industrial applications, particle size and morphology of the mesoporous support are important issues with respect to reactor configuration, crystallization of reaction products, and intraparticle diffusions. Moreover, several critical points such as mechanical stability and shaping of (macroscopic) particles with well-defined properties have to be addressed in future work. Commercial issues such as cost of the support and scale-up of the preparation of a biocatalyst by immobilization of an enzyme have to be assessed in competition with existing materials. A major issue in biocatalysis is the low space–time yield in comparison to conventional "chemical routes." However, the high selectivity to the (enantiopure) target molecule might overcompensate this drawback. Although a number of ordered mesoporous materials

including PMOs and mesoporous carbons have been prepared, mesoporous silicas are still predominantly used. In particular PMOs offer the possibility of tailor-made functionalization of walls with suitable anchoring groups and tuning of the hydrophobicity of the support. In conclusion, the use of ordered mesoporous materials in biocatalysis, bioadsorption and biosensing is a young and growing but still challenging field with still high demand of new and improved materials and processes.

REFERENCES

1. Cao L. Carrier-bound immobilized enzymes. Weinheim: Wiley-VCH; 2005.
2. Weetall HH. Appl Biochem Biotechnol 1993; 41: 157–188.
3. Avnir D, Braun S, Lev O, Ottolenghi M. Chem Mater 1994; 6: 1605–1614.
4. Gill I. Chem Mater 2001; 13: 3404–3421.
5. Jin W, Brennan JD. Anal Chim Acta 2002; 461: 1–36.
6. Avenir D, Coradin T, Lev O, Livage J. J Mater Chem 2006; 16: 1013–1030.
7. Diaz JF, Balkus KF Jr. J Mol Catal B: Enzym 1996; 2: 115–126.
8. Sing KSW, Everett DH, Haul RAW, Moscou L, Pierotti RA, Rouquerol J, Siemienswska T. Pure Appl Chem 1985; 57: 603–619.
9. Chiola V, Ritsko JE, Vanderpool CD. US Patent 3 556 725. 1971.
10. Di Renzo F, Camion H, Dutartre R. Microporous Mater 1997; 10: 283–286.
11. Yanagisawa T, Shimizu T, Kuroda K, Kato C. Bull Chem Soc Jpn 1990; 63: 1535–1537.
12. Inagaki S, Fukushima Y, Kuroda K. J Chem Soc, Chem Commun 1993; 8: 680–682.
13. Kresge CT, Leonowicz ME, Roth WJ, Vartuli JC, Beck JS. Nature 1992; 359: 710–712.
14. Beck JS, Vartuli JC, Roth WJ, Leonowicz ME, Kresge CT, Schmidt KD, Chu CT-W, Olson DH, Sheppard EW, McCullen SB, Higgins JB, Schlenker JL. J Am Chem Soc 1992; 114: 10834–10843.
15. Husson F, Mustacchi H, Luzzati V. Acta Crystallogr 1960; 13: 668–677.
16. Mariani P, Luzzati V, Delacroix H. J Mol Biol 1988; 204: 165–189.
17. Huo Q, Margolese DI, Ciesla U, Feng P, Gier TE, Sieger P, Leon R, Petroff PM, Schüth F, Stucky GD. Nature 1994; 368: 317–321.
18. Huo Q, Margolese DI, Ciesla U, Demuth DG, Feng P, Gier TE, Sieger P, Leon R, Firouzi A, Chmelka BF, Schüth F, Stucky GD. Chem Mater 1994; 6: 1176–1191.
19. Tanev PT, Pinnavaia TJ. Science 1995; 267: 865–867.
20. Tanev PT, Pinnavaia TJ. Chem Mater 1996; 8: 2068–2079.
21. Huo Q, Leon R, Petroff PM, Stucky GD. Science 1995; 268: 1324–1327.
22. Zhao D, Huo Q, Feng J, Chmelka BF, Stucky GD. J Am Chem Soc 1998; 120: 6024–6036.
23. Zhao D, Feng J, Huo Q, Melosh N, Fredrickson GH, Chmelka BF, Stucky GD. Science 1998; 279: 548–552.
24. Hartmann M, Vinu A. Langmuir 2002; 18: 8010–8016.
25. Schmidt-Winkel P, Lukens WW, Zhao D, Yang P, Chmelka BF, Stucky GD. J Am Chem Soc 1999; 121: 254–255.
26. Behrens P, Glaue A, Haggenmüller C, Schechner G. Solid State Ionics 1997; 101-103: 255–260.
27. Ryoo R, Kim JM, Ho CH, Shin CH. J Phys Chem 1996; 100: 17718–17721.
28. Sakamoto Y, Kaneda M, Terasaki O, Zhao DY, Kim JM, Stucky GD, Shim HJ, Ryoo R. Nature 2000; 408: 449–453.
29. Kleitz F, Liu DN, Anilkumar GM, Park IS, Solovyov LA, Shmakov AN, Ryoo R. J Phys Chem B 2003; 107: 14296–14300.
30. Fan J, Yu CZ, Gao T, Lei J, Tian BZ, Wang LM, Luo Q, Tu B, Zhou WZ, Zhao DY. Angew Chem Int Ed Engl 2003; 42: 3146–3150.
31. Fan J, Yu CZ, Lei J, Zhang Q, Li TC, Tu B, Zhou WZ, Zhao DY. J Am Chem Soc 2005; 127: 10794–10795.
32. Yu T, Zhang H, Yan XW, Chen ZX, Zhou XD, Oleynikow P, Zhao DY. J Phys Chem B 2006; 110: 21467–21472.
33. Kleitz F, Choi SH, Ryoo R. Chem Commun 2003: 2136–2137.
34. Kim TW, Kleitz F, Paul B, Ryoo R. J Am Chem Soc 2005; 127: 7601–7610.
35. Corma A. Chem Rev 1997; 97: 2373–2420.
36. Sayari A. Stud Surf Sci Catal 1996; 102: 1–46.
37. Sayari A. Chem Mater 1996; 8: 1840–1852.
38. Chen CY, Li HX, Davis ME. Microporous Mater 1994; 2: 17–26.
39. Corma A, Fornes V, Navarro MT, Perez-Pariente J. J Catal 1994; 148: 569–574.
40. Luan Z, Cheng CF, Zhou W, Klinowski J. J Phys Chem 1995; 99: 1018–1024.
41. Borade RB, Clearfield A. Catal Lett 1995; 31: 267–272.
42. Hamdam H, Endud S, He H, Muhid MM, Klinowski J. J Chem Soc, Faraday Trans 1996; 92: 2311–2315.
43. Luan Z, Hartmann M, Zhao D, Zhou W, Kevan L. Chem Mater 1999; 11: 1621–1627.
44. Schmidt R, Junggreen H, Stöcker M. Chem Commun 1996: 875–876.
45. Romero AA, Alba MD, Zhou W, Klinowski J. J Phys Chem B 1997; 101: 5294–5300.
46. Gedeon A, Lassoued A, Bonardet JL, Fraissard J. Microporous Mesoporous Mater 2001; 44-45: 801–806.
47. Hartmann M, Vinu A, Elangovan SP, Murugesan V, Böhlmann W. Chem Commun 2002: 1238–1239.
48. Vinu A, Böhlmann W, Hartmann M. J Phys Chem B 2004; 108: 11496–11505.
49. Hartmann M, Racouchot S, Bischof C. Chem Commun 1997: 2221–2222.
50. Hartmann M, Racouchot S, Bischof C. Microporous Mesoporous Mater 1999; 27: 309–320.
51. Tuel A, Gontier S. Chem Mater 1996; 8: 114–122.
52. Sayari A, Moudrakovski I, Danumah C, Ratcliffe CI, Ripmeester JA, Preston KF. J Phys Chem 1995; 99: 16373–16379.
53. Sayari A, Danumah C, Moudrakovski I. Chem Mater 1995; 7: 813–815.
54. Chenite A, Le Page Y, Sayari A. Chem Mater 1995; 7: 1015–1019.

55. Liu S, He H, Luan Z, Klinowski J. J Chem Soc, Faraday Trans 1996; 92: 2011–2015.
56. Yuan ZY, Luo Q, Liu JQ, Chen TH, Wang JZ, Li HX. Microporous Mesoporous Mater 2001; 42: 289–297.
57. Kosslick H, Lischke G, Landmesser H, Parlitz B, Storek W, Fricke R. J Catal 1998; 176: 102–114.
58. Landmesser H, Kosslick H, Kürschner U, Fricke R. J Chem Soc, Faraday Trans 1998; 94: 971–977.
59. Kosslick H, Lischke G, Walther G, Storek W, Martin A, Fricke R. Microporous Mater 1997; 9: 13–33.
60. Alves M, Pastore HO. Microporous Mesoporous Mater 2001; 47: 397–406.
61. Tuel A, Arcon I, Millet JMM. J Chem Soc, Faraday Trans 1998; 94: 3501–3510.
62. Echchahed B, Moen A, Nicholson D, Bonneviot L. Chem Mater 1997; 9: 1716–1719.
63. Vinu A, Savant DP, Ariga K, Hossain KZ, Halligudi SB, Hartmann M, Nomura M. Chem Mater 2005; 17: 5339–5345.
64. Zhang W, Pinnavaia TJ. Catal Lett 1996; 38: 261–265.
65. Zhang W, Wang J, Tanev PT, Pinnavaia TJ. J Chem Soc, Chem Commun 1996: 979–980.
66. Ulagapan N, Rao CNR. J Chem Soc, Chem Commun 1996: 1047–1048.
67. Yuan ZY, Wang JZ, Zhang ZL, Chen TH, Li HX. Microporous Mesoporous Mater 2001; 43: 227–236.
68. Carvalho WA, Varaldo PB, Wallau M, Schuchardt U. Zeolites 1997; 18: 408–416.
69. Zhang L, Ying JY. AIChE J 1997; 43: 2793–2801.
70. Ziolek M, Novak I. Zeolites 1997; 18: 356–360.
71. Ziolek M, Novak I, Lavalley JC. Catal Lett 1997; 45: 259–265.
72. Hartmann M, Prakash AM, Kevan L. Catal Today 2003; 78: 467–475.
73. Hartmann M, Pöppl A, Kevan L. J Phys Chem 1995; 99: 17494–17496.
74. Zhao D, Goldfarb D. J Chem Soc, Chem Commun 1995: 875–876.
75. Xu J, Luan Z, Wasowicz T, Kevan L. Microporous Mesoporous Mater 1998; 22: 179–191.
76. Zhang J, Goldfarb D. J Am Chem Soc 2000; 122: 7034–7041.
77. Rana RK, Viswanathan B. Catal Lett 1998; 52: 25–29.
78. Che S, Sakamoto Y, Yoshitake H, Terasaki O, Tatsumi T. J Phys Chem B 2001; 105: 10565–10572.
79. Corma A, Navarro MT, Pariente JP. J Chem Soc, Chem Commun 1994: 147–148.
80. Das TK, Chaudari K, Chandwadkar AJ, Sivasanker S. J Chem Soc, Chem Commun 1995: 2495–2496.
81. Abdel-Fattah TM, Pinnavaia TJ. J Chem Soc, Chem Commun 1996: 665–666.
82. Luan Z, Xu J, He H, Klinowski J, Kevan L. J Phys Chem 1996; 100: 19595–19602.
83. Wei D, Wang H, Feng X, Chuch W-T, Ravikovitch P, Lynbovsky M, Li C, Takeguchi T, Haller GL. J Phys Chem B 1999; 103: 2113–2121.
84. Chatterjee M, Iwasaki T, Hayashi H, Onodera Y, Ebina T, Nagase T. Chem Mater 1999; 11: 1368–1375.
85. Luan Z, Bae JY, Kevan L. Chem Mater 2000; 12: 3202–3207.
86. Gontier S, Tuel A. Appl Catal A 1996; 143: 125–135.
87. Tuel A, Gontier S, Teissier J. J Chem Soc, Chem Commun 1996: 651–652.
88. Occelli ML, Biz S, Auroux A. Appl Catal A 1999; 183: 231–239.
89. Chaudhari K, Bal R, Das TK, Chandwadkar A, Srinivas D, Sivasanker S. J Phys Chem B 2000; 104: 11066–11074.
90. Wang XX, Lefebvre F, Patarin J, Basset JM. Microporous Mesoporous Mater. 2001; 42: 269–276.
91. Inagaki S, Giuan S, Fukushima Y, Ohsuna T, Terasaki O. J Am Chem Soc 1999; 121: 9611–9614.
92. Asefa T, MacLachlan MJ, Coombs N, Ozin G. Nature 1999; 402: 867–871.
93. Melde BJ, Holland BT, Blanford CF, Stein A. Chem Mater 1999; 11: 3302–3308.
94. Asefa T, Kruk M, MacLachlan MJ, Cooms MJ, Grondey H, Jaroniec M, Ozin GA. J Am Chem Soc 2001; 123: 8520–8530.
95. Burleigh MC, Markowitz MA, Spector MS, Gaber BP. Chem Mater 2001; 13: 4760–4766.
96. Yang Q, Kapoor MP, Inagaki S. J Am Chem Soc 2002; 124: 9694–9695.
97. Wang Z, Heising JM, Clearfield A. J Am Chem Soc 2003; 125: 10375–10383.
98. Inagaki S, Guan S, Ohsuna T, Terasaki O. Nature 2002; 416: 304–307.
99. Kapoor MP, Yang Q, Goto Y, Inagaki S. Chem Lett 2002; 32: 914–915.
100. Schüth F. Angew Chem Int Ed Engl 2003; 42: 3604–3622.
101. Lu AH, Schüth F. Adv Mater 2006; 18: 1793–1805.
102. Kyotani T, Nagai T, Inoue S, Tomita A. Chem Mater 1997; 9: 609–615.
103. Kyotani T. Carbon 2000; 38: 269–286.
104. Ryoo R, Joo SH, Jun S. J Phys Chem B 1999; 103: 7743–7746.
105. Jun S, Joo SH, Ryoo R, Kruk M, Jaroniec M, Liu Z, Ohsuna T, Terasaki O. J Am Chem Soc 2000; 122: 10712–10713.
106. Joo SH, Choi SJ, Oh I, Kwak J, Liu Z, Terasaki O, Ryoo R. Nature 2001; 412: 169–172.
107. Tiemann M. Chem Mater 2008; 20: 961–971.
108. Lee J, Yoon S, Hyeon T, Oh SM, Kim KB. Chem Commun 1999: 2177–2178.
109. Lee J, Yoon S, Oh SM, Shin CH, Hyeon T. Adv Mater 2000; 12: 359–362.
110. Vinu A, Hartmann M. Catal Today 2005; 102-103: 189–196.
111. Vinu A, Miyahara M, Sivamurugan V, Mori T, Ariga K. J Mater Chem 2005; 15: 5122–5127.
112. Vinu A, Miyahara M, Mori T, Ariga K. J Porous Mater 2006; 13: 379–383.
113. Ciesla U, Demuth DE, Leon R, Petroff P, Stucky G, Unger K, Schüth F. J Chem Soc, Chem Commun 1994: 1387–1388.
114. Antonelli DM, Ying JY. Angew Chem Int Ed Engl 1995; 34: 2014–2017.
115. Antonelli DM, Ying JY. Angew Chem Int Ed Engl 1996; 35: 426–430.

116. Antonelli DM, Nakahira A, Ying JY. Inorg Chem 1996; 35: 3126–3136.
117. Antonelli DM, Ying JY. Chem Mater 1996; 8: 874–881.
118. Antonelli DM, He X. Angew Chem 2002; 114: 222–238.
119. Bagshaw SA, Pinnavaia TJ. Angew Chem Int Ed Engl 1996; 35: 1102–1105.
120. Vaudry F, Khodabandeh S, Davis ME. Chem Mater 1996; 8: 1451–1464.
121. Zhao DY, Sun JY, Li QZ, Stucky GD. Chem Mater 2000; 12: 275–279.
122. Xu R, Pang W, Yu J, Huo Q, Chen J. Chemistry of zeolites and related porous materials - synthesis and structure. Singapore: Wiley; 2007. pp. 575–583.
123. Kim SS, Zhang WZ, Pinnavia TJ. Science 1998; 282: 1302–1305.
124. Karkamkar AJ, Kim SS, Mahanti SD, Pinnavaia TJ. Adv Funct Mater 2004; 14: 507–512.
125. Ma Y, Qi L, Ma J, Wu Y, Liu O, Cheng H. Colloids Surf A 2003; 229: 1–8.
126. Kosuge K, Kikukawa N, Takemore M. Chem Mater 2004; 16: 889–898.
127. Katiyar A, Yadav S, Smirniotis PG, Pinto NG. J Chromat A 2006; 1122: 13–20.
128. Chen Y, Wang YJ, Yang LM, Luo GS. AIChE J 2008; 54: 298–309.
129. Mureseanu M, Galarneau A, Renard G, Fajula F. Langmuir 2005; 21: 4648–4655.
130. Galarneau A, Muruseanu M, Atger S, Renard G, Fajula F. New J Chem 2006; 30: 562–571.
131. Galarneau A, Renard G, Mureseanu M, Tourette A, Biolly C, Choi M, Ryoo R, Di Renzo F, Fajula F. Microporous Mesoporous Mater 2007; 104: 103–114.
132. Patel K, Angelos S, Dichtel WR, Coskun A, Yang YW, Zink JI, Stoddart FF. J Am Chem Soc 2008; 130: 2382–2383.
133. Vinu A, Hossain KZ, Ariga K. J Nanosci Nanotechnol 2005; 5: 347–371.
134. Wan Y, Zhao D. Chem Rev 2007; 107: 2821–2860.
135. Hoffmann F, Cornelius M, Morell J, Fröba M. Angew Chem Int Ed Engl 2006; 45: 3216–3251.
136. Guliants VV, Carreon MA, Lin YS. J Membr Sci 2004; 235: 53–72.
137. Lyklema J. Colloids Surf 1984; 10: 33–43.
138. Norde W. J Dispersion Sci Technol 1992; 13: 363–377.
139. Quiquampoix H, Bollag JM, Stotzky G, editors. Soil biochemistry. Volume 10. New York: Marcel Dekker; 2000. pp. 171–206.
140. Norde W, Lyklema JJ. Biomater Sci, Polymer Edn 1991; 2: 183–202.
141. Haynes CA, Norde W. Colloids Surf B 1994; 2: 517–566.
142. Yiu HHP, Wright PA. J Mater Chem 2005; 15: 3690–3700.
143. Ramsden JJ. Chem Soc Rev 1995; 24: 73–78.
144. Kim MI, Kim J, Lee J, Jia H, Na HB, Youn JK, Kwak JH, Dohnalkova A, Grate JW, Wang P, Hyeon T, Park HG, Chang HN. Biotechnol Bioeng 2007; 96: 210–218.
145. Lee J, Kim J, Kim J, Jia H, Kim MI, Kwak JH, Jin S, Dohnalkova A, Park HG, Chang HN, Wang P, Grate JW, Hyeon T. Small 2005; 1: 744–753.
146. Kim MI, Kim J, Lee J, Shin S, Na HB, Hyeon T, Park HG, Chang HN. Microporous Mesoporous Mater 2008; 111: 18–23.
147. Cao L, van Rantwijk F, Sheldon RA. Org Lett 2000; 2: 1361–1364.
148. Cao L, van Langen LM, van Rantwijk F, Sheldon RA. J Mol Catal B: Enzymatic 2001; 11: 665–670.
149. van Langen LM, Oosthoek NHP, van Rantwijk F, Sheldon RA. Adv Synth Catal 2003; 345: 797–801.
150. Mateo C, Fernandes B, van Rantwijk F, Stolz A, Sheldon RA. J Mol Catal B: Enzymatic 2006; 38: 154–157.
151. Ruiz Toral A, de los Rios AP, Hernandez FJ, Janssen MHA, Schoevaart R, van Rantwijk F, Sheldon RA. Enzyme Microb Technol 2007; 40: 1095–1099.
152. Kim J, Lee J, Na HB, Kim BC, Youn JK, Kwak JH, Moon K, Lee E, Kim J, Park J, Dohnalkova A, Park HG, Gu MB, Chang HN, Grate JW, Hyeon T. small 2005; 1: 1203–1207.
153. Han Y, Lee SS, Ying JY. Chem Mater 2006; 18: 643–649.
154. Subramanian A, Kennel SJ, Oden PI, Jacobson KB, Woodward J, Doktycz MJ. Enzyme Microb Technol 1999; 24: 26–34.
155. Impens NREN, van der Voort P, Vansant EF. Microporous Mesoporous Mater 1999; 28: 217–232.
156. Chong ASM, Zhao XS. J Phys Chem B 2003; 107: 12650–12657.
157. Burkett SL, Sims SD, Mann S. Chem Commun 1996: 1367–1368.
158. Macquaire JD. Chem Commun 1996: 1961–1962.
159. Yiu HHP, Botting CH, Botting NP, Wright PA. Phys Chem, Chem Phys 2001; 3: 2983–2985.
160. Yiu HHP, Wright PA, Botting NP. J Mol Catal B: Enzym 2001; 15: 81–92.
161. Szymanska K, Bryjak J, Mrowiec-Bialon J, Jarzebski AB. Micropor Mesopor Mater 2007; 99: 167–175.
162. Chong ASM, Zhao XS. Catal Today 2004; 93-95: 293–299.
163. Jing H, Li X, Evans DG, Duan X, Li C. J Mol Catal B: Enzym 2000; 11: 45–53.
164. Zhang X, Guan RF, Wu DQ, Chan KY. J Mol Catal B: Enzym 2005; 33: 43–50.
165. Pandya PH, Jasra RV, Newwalkar BL, Bhatt PN. Microporous Mesoporous Mater 2005; 77: 67–77.
166. Fadnavis NW, Bhaskar V, Kantam ML, Choudary BM. Biotechnol Prog 2003; 19: 346–351.
167. Salis A, Meloni D, Ligas S, Monduzzi M, Solinas V, Dumitriu E. Langmuir 2005; 21: 5511–5516.
168. Lei C, Shin Y, Liu J, Ackerman EJ. Nanoletters 2007; 7: 1050–1053.
169. Jung D, Hartmann M. Stud Surf Sci Catal 2008; 174B: 1045–1050.
170. Lei Y, Shin Y, Liu J, Ackerman EJ. J Am Chem Soc 2002; 124: 11242–11243.
171. Aburto J, Ayala M, Bustos-Jaimes I, Montiel C, Terres E, Dominguez JM, Torres E. Microporous Mesoporous Mater 2005; 83: 193–200.
172. Montiel C, Terres E, Dominguez J-M, Aburto J. J Mol Catal B: Enzym 2007; 48: 90–98.
173. Tortajada M, Ramon D, Beltran D, Amoros P. J Mater Chem 2005; 15: 3859–3868.

174. Lü Y, Lu G, Wang Y, Guo Y, Guo Y, Zhang Z, Wang Y, Liu X. Adv Funct Mater 2007; 17: 2160–2166.
175. Wang P, Dai S, Waezsada SD, Tsao AY, Davison BH. Biotechnol Bioeng 2001; 74: 249–255.
176. Fan J, Lei J, Wang L, Yu C, Tu B, Zhao D. Chem Commun 2003: 2140–2141.
177. Hudson S, Magner E, Cooney J, Hodnett BK. J Phys Chem B 2005; 109: 19496–19506.
178. Qiao SZ, Yu CZ, Xing W, Hu QH, Djojoputro H, Lu GQ. Chem Mater 2005; 17: 6172–6176.
179. Qiao SZ, Djojoputro H, Hu QH, Lu GQ. Prog Solid State Chem 2006; 34: 249–256.
180. (a) Wang YJ, Caruso F. Chem Commun 2004: 1528–1529; (b) Yu A, Liang Z, Caruso F. Chem Mater 2005; 17: 171–175.
181. Hartmann M. Chem Mater 2005; 17: 4577–4593.
182. Vinu A, Miyahara M, Ariga K. J Nanosci Nanotechnol 2006; 6: 1510–1532.
183. Hudson S, Cooney J, Magner E. Angew Chem Int Ed Engl 2008; 47: 8582–8594.
184. Gimon-Kinsel ME, Jimenez VL, Washmon L, Balkus KJ Jr. Stud Surf Sci Catal 1998; 117: 373–380.
185. Washmon-Kriel L, Jimenez VL, Balkus KJ Jr. J Mol Catal B: Enzym 2000; 10: 453–469.
186. Ma H, He J, Evans DG, Duan XJ. Mol Catal B: Enzym 2004; 30: 209–217.
187. Hetflejs J, Kuncova G, Sabata S, Blechta V, Brus J. J Sol-Gel Sci Technol 2006; 38: 121–131.
188. Zhang Y, Li J, Han D, Zhang H, Liu P, Li C. Biochem Biophys Res Commun 2008; 365: 609–613.
189. Urabe Y, Shiomi T, Itoh TT, Kawai A, Tsunoda T, Mizukami F, Sakaguchi K. ChemBioChem 2007; 8: 668–674.
190. Yiu HHP, Wright PA, Botting NP. Microporous Mesoporous Mater 2001; 44-45: 763–768.
191. He J, Li X, Evans DG, Duan X, Li C. J Mol Catal B: Enzym 2000; 11: 45–53.
192. Takahashi H, Li B, Sasaki T, Miyazaki C, Kajino T, Inagaki S. Chem Mater 2000; 12: 3301–3305.
193. Takahashi H, Li B, Sasaki T, Miyazaki C, Kajino T, Inagaki S. Microporous Mesoporous Mater 2001; 44-45: 755–762.
194. Pires EL, Miranda EA, Valenca Paim G. Appl Biochem Biotechnol 2002; 100: 963–976.
195. Chen ZZ, Lei YM, Peng X, Huang FR, Zhao YF. J Mol Catal B: Enzym 2002; 18: 243–249.
196. Itoh T, Ouchi N, Nishimura Y, Hui HS, Katada N, Niwa M, Onaka M. Green Chem 2003; 5: 494–496.
197. Gomez JM, Deere J, Goradia D, Cooney J, Magner E, Hodnett BK. Catal Lett 2003; 88: 183–186.
198. Rosalez Hernandez MC, Mendieta Wejebe JE, Vazquez Alcantara JI, Miranda Ruvalcaba R, Garcia Serrano LA, Trujillo Ferrara J. Microporous Mesoporous Mater 2005; 80: 25–30.
199. Kisler JM, Stevens GW, O'Connor AJ. J Mater Phys Mech 2001; 4: 89–93.
200. Vinu A, Murugesan V, Hartmann M. J Phys Chem B 2004; 108: 7323–7330.
201. Vinu A, Miyahara M, Ariga K. J Phys Chem B 2005; 109: 6436–6441.
202. Lei J, Fan J, Yu C, Zhang L, Jiang S, Tu B, Zhao D. Microporous Mesoporous Mater 2004; 73: 121–128.
203. Deere J, Magner E, Wall JG, Hodnett BK. Chem Commun 2001: 465–466.
204. Deere J, Magner E, Wall JG, Hodnett BK. Stud Surf Sci Catal 2001; 135: 233.
205. Deere J, Magner E, Wall JG, Hodnett BK. J Phys Chem B 2002; 106: 7340–7347.
206. Deere J, Magner E, Wall JG, Hodnett BK. Catal Lett 2003; 85: 19–23.
207. Vinu A, Murugesan V, Tangermann O, Hartmann M. Chem Mater 2004; 16: 3056–3065.
208. Vinu A, Streb C, Murugesan V, Hartmann M. J Phys Chem B 2003; 107: 8297–8299.
209. Ravindra R, Zhao S, Gies H, Winter R. J Am Chem Soc 2004; 126: 12224–12225.
210. Dai Z, Liu S, Ju H, Chen H. Biosens Bioelectron 2004; 19: 861–867.
211. Dai Z, Xu X, Ju H. Anal Biochem 2004; 332: 23–31.
212. Goradia D, Cooney J, Hodnett BK, Magner EJ. J Mol Catal B: Enzym 2005; 32: 231–239.
213. Hartmann M, Streb C. J Porous Mater 2006; 13: 347–352.
214. Terres E, Montiel M, Le Borgne S, Torres E. Biotechnol Lett 2008; 30: 173–179.
215. Sasaki S, Kalino T, Li B, Sugiyama H, Takahashi H. Appl Environ Microbiol 2001; 67: 2208–2212.
216. Dai Z, Bao J, Yang X, Ju H. Biosens Bioelectron 2008; 23: 1070–1076.
217. Miyahara M, Vinu A, Ariga K. Mater Sci Eng C 2007; 27: 232–236.
218. Miyahara M, Vinu A, Hossain KZ, Nakanishi T, Ariga K. Thin Solid Films 2006; 499: 13–18.
219. Hossain KZ, Monreal CM, Sayari A. Colloids Surf B Biointerfaces 2008; 62: 42–50.
220. Dai ZH, Ni J, Huang XH, Lu GF, Bao JC. Bioelectrochemistry 2007; 70: 250–256.
221. Yao K, Zhu Y, Wang P, Yang X, Cheng P, Lu H. Mater Sci Eng C 2007; 27: 736–740.
222. Serra E, Mayoral A, Sakamoto Y, Blanco RM, Diaz I. Microporous Mesoporous Mater 2008; 114: 201–213.
223. Essa H, Magner E, Cooney J, Hodnett BK. J Mol Catal B: Enzym 2007; 49: 61–68.
224. Itoh T, Yano K, Kajino T, Inada Y, Fukushima Y. Biotechnol Bioeng 2006; 93: 476–484.
225. Wang X, Lu D, Austin R, Agarwal A, Mueller LJ, Liu Z, Wu J, Feng P. Langmuir 2007; 23: 5735–5739.
226. Chaijitrsakoola T, Tonanona N, Tanthapanichakoona W, Tamonb H, Prichanonta S. J Mol Catal B: Enzym 2008; 55: 137–141.
227. Zhu Y, Kaskel S, Shi J, Wage T, van Pée K-H. Chem Mater 2007; 19: 6408–6413.
228. Yu D, Wang Z, Zhao L, Cheng Y, Cao S. J Mol Catal B: Enzym 2007; 48: 64–69.
229. Soares CMF, Santana MHA, Zanin GM, de Castro HF. Biotechnol Prog 2003; 19: 803–807.
230. Blanco RM, Terreros P, Fernández-Pérez M, Otero C, Díaz-González G. J Mol Catal B: Enzym 2004; 30: 83–93.
231. Chong ASM, Zhao XS. Appl Surf Sci 2004; 237: 398–404.

232. Lü Y, Guo Y, Wang Y, Liu X, Wang Y, Guo Y, Zhang Z, Lu G. Microporous Mesoporous Mater 2008; 114: 507–510.
233. Han YJ, Watson JT, Stucky GD, Butler A. J Mol Catal B: Enzym 2002; 17: 1–8.
234. Jung D, Streb C, Hartmann M. Microporous Mesoporous Mater 2008; 113: 523–529.
235. Szymanska K, Bryjak J, Mrowiec-Bialon J, Jarzebski AB. Microporous Mesoporous Mater 2007; 99: 167–175.
236. Vinu A, Hossian KZ, Srinivasu P, Miyahara M, Anandan S, Gokulakrishnan N, Mori T, Ariga K, Balasubramanianc VV. J Mater Chem 2007; 17: 1819–1825.
237. Lei C, Shin Y, Magnuson JK, Fryxell G, Lasure LL, Elliott DC, Liu J, Ackerman EJ. Nanotechnology 2006; 17: 5531–5538.
238. Bai YX, Li YF, Yang Y, Yi LX. J Biotechnol 2006; 125: 574–582.
239. Jarzebski AB, Szymanska K, Bryjak J, Mrowiec-Bialon J. Catal Today 2007; 124: 2–10.
240. Itoh T, Ishii R, Ebina T, Hanaoka T, Fukushima Y, Mizukami F. Bioconjug Chem 2006; 17: 236–240.
241. Jackson MA, Mbaraka IK, Shanks BH. Appl Catal A: General 2006; 310: 48–53.
242. Bai Y, Yang H, Yang W, Li Y, Sun C. Sens Actuators B 2007; 124: 179–186.
243. Besanger TR, Hodgson RJ, Green JRA, Brennan JD. Anal Chim Acta 2006; 564: 106–115.
244. Lü Y, Zhao Q, Guo Y, Wang Y, Guo Y, Lu G. Stud Surf Sci Catal 2007; 165: 877–880.
245. Shah P, Sridevi N, Prabhune A, Ramaswamy V. Microporous Mesoporous Mater 2008; 116: 157–165.
246. Oha C, Lee JH, Lee YG, Lee YH, Kimb JW, Kang HH, Oha SG. Colloids Surf B Biointerfaces 2006; 53: 225–232.
247. Jang S, Kim D, Choi J, Row K, Ahn W. J Porous Mater 2006; 13: 385–391.
248. Reis P, Witula T, Holmberg K. Microporous Mesoporous Mater 2008; 110: 355–362.
249. Yu J, Yu D, Zhao T, Zeng B. Talanta 2008; 74: 1586–1591.
250. Qiao L, Liu Y, Hudson SP, Yang P, Magner E, Liu B. Chem Eur J 2008; 14: 151–157.
251. Gray CJ, Lee CM, Barker SA. Enzyme Microbiol Technol 1982; 4: 143–146.
252. Itoh T, Nishimura Y, Ouchi N, Hayase S. J Mol Catal B: Enzym 2003; 26: 41–45.
253. Villasenor F, Loera O, Campero A, Viniegra-Gonzalez G. Fuel Process Technol 2004; 86: 49–59.
254. van de Velde F, van Rantwijk F, Sheldon RA. Trends Biotechnol 2001; 19: 73–80.
255. Alfani F, Cantarella M, Cutarella N, Gallifuoco A, Golini P, Bianchi D. Biotechnol Lett 1997; 19: 175–178.
256. Park SW, Choi SY, Chungb KH, Honga SI, Kima SW. Biochem Eng J 2002; 11: 87–93.
257. Park SW, Choi SY, Chungb KH, Honga SI, Kima SW. J Mol Catal B: Enzym 2000; 11: 45–52.
258. Luckarift HR, Ku BS, Dordick JS, Spain JC. Biotechnol Bioeng 2007; 98: 701–705.

53

IMMOBILIZED CELLS

Manojlović Verica and Bugarski Branko
Department of Chemical Engineering, Faculty of Technology and Metallurgy, University of Belgrade, Belgrade, Republic of Serbia
Nedović Viktor
Department of Food Technology and Biochemistry, Faculty of Agriculture, University of Belgrade, Belgrade, Republic of Serbia

53.1 INTRODUCTION

Cell immobilization can be defined as entrapment or localization of living cells to a certain region of space with preservation of their metabolic and/or catabolic activity. Cell immobilization improves the efficiency of the cultures by mimicking cell natural environment. Numerous biotechnological processes are advantaged by the immobilization technology. There are numerous publications on immobilization of various cell types, emphasizing many advantages for biomass and metabolite productions compared with free cell systems, such as: high cell density, reuse of biocatalysts, improved resistance to contamination and other exterior influences, stimulation of production and secretion of secondary metabolites and physical and chemical protection of the cells. In addition, immobilized cell systems can be operated in continuous mode at higher dilution rates without the risk of cell washout. Especially attractive are the options for co-immobilization of different cell types for the simultaneous implementation of consecutive reactions. Another reason for co-immobilization is to promote growth of one species by co-immobilization with another type of microorganism. Moreover, the local oxygen environment can be manipulated by incorporating photosynthetic organisms for *in situ* generation, or conversely to provide a gradient, by binding aerobes externally to anaerobes to generate internal oxygen limitation. Except numerous benefits of immobilization, possible disadvantages like costs of immobilization, lowered specific activity of the biocatalyst, diffusion problems, or bad mechanical stability of the biocatalyst have to be considered and met by choosing the right immobilization technology.

So far, various types of living cells such as bacteria, yeast, plant, or mammalian cells have been successfully immobilized for applications in industry, medicine, and agriculture. The possible uses are numerous, ranging from ethanol and beverage production, food production, production of phytochemicals and biopharmaceuticals, treatment of waste water, soil and groundwater, construction of electronic devices to measure toxicity, such as biosensors, to disease treatment, tissue (pancreas, skin, liver, cartilage, heart, bone) engineering, and production of artificial seeds. Another attractive area of application of immobilized systems is the production of noncontaminant energy (such as H_2), intended to be explored in the next years. Issues of safety, simplicity, applicability, and price of immobilization technology may differ depending on the field of its application and purpose. The criteria for industrial acceptance of immobilization technology may be different from that for biomedical applications. The concept of immobilization is applied in both products and processes. Product examples include the bioactives in drug delivery. Encapsulation technology is widely used for stabilizing sensitive microorganisms (providing their metabolic activity after storage and intake by a new host), controlling the oxidative reactions, sustained or controlled release of active ingredients or to provide barriers between the sensitive bioactive materials and the environment. Process examples include the immobilization of biologically based catalysts, such as enzymes, cells,

Upstream Industrial Biotechnology: Equipment, Process Design, Sensing, Control, and cGMP Operations, Volume 2, First Edition. Edited by Michael C. Flickinger.
© 2013 John Wiley & Sons, Inc. Published 2013 by John Wiley & Sons, Inc.

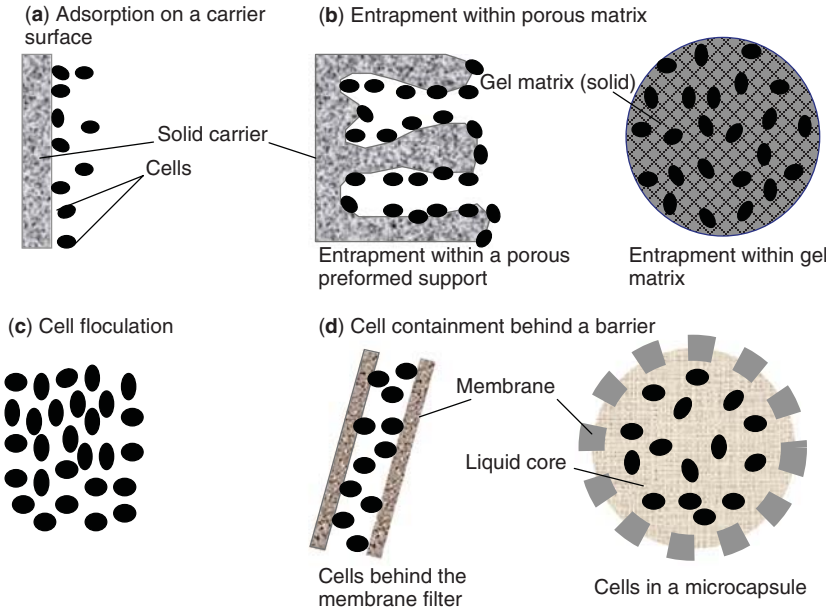


Figure 53.1. Methods for cell immobilization. (This figure is available in full color at http://onlinelibrary.wiley.com/book/10.1002/9780470054581.)

and biologically active components promoting tissue formation.

53.2 CELL IMMOBILIZATION: CARRIERS AND TECHNIQUES

The key elements of an immobilized cell system are: cell type, immobilization material and method, and bioreactor design. Immobilization methods can be classified into four major categories (Fig. 53.1) based on the mechanism of cell localization employed and the nature of support material: (i) attachment or adsorption on solid carrier surfaces, (ii) entrapment within a porous matrix, (iii) self-aggregation by natural flocculation or with cross-linking agents, and (iv) cell containment behind barriers (1). The purpose of this review is to describe recent developments in immobilized cell technology.

53.2.1 Immobilization on Solid Carrier Surfaces

Many microorganisms have a natural tendency to adsorb spontaneously and grow on a wide variety of organic and inorganic supports. For example, algal cells (2) and fungi (3) spontaneously attach to loofa sponges. This is a process of passive immobilization, easily reversible and contamination of an effluent with unstuck cells is unavoidable. Active cell immobilization on solid carriers is based on physical or chemical adsorption to a surface induced by van der Waals forces, ionic bonds, hydrogen bridges, or covalent interactions between the cell membrane and the carrier. Chemical attachment of sensitive living cells may cause damage in cellular surfaces and drastically reduce viability of cells. Principally, ion attraction is not harmful to living organisms, but effectiveness of the immobilization process depends of pH and ionic strength of the surrounding media. Microbial cells exhibit a dipolar character and behave as cations or anions depending on the cell type and environmental conditions such as pH of the solution. The thickness of cell layer ranges from one layer up to few millimeters. The immobilization procedure is usually cheap and simple and therefore, a very popular method and convenient for industrial large-scale applications. The interaction forces between cells and supports are weak, hence the detachment of cells to the surrounding medium is likely to be possible. Eventually, the equilibrium between immobilized and free cells is established during processes in bioreactor systems. Various solid carriers have been used as supports, such as cellulosic materials (DEAE-cellulose, wood, sawdust, delignified sawdust), clays, inorganic materials (porous glass, porcelain) etc.

Natural supports, when they are safe and of food-grade purity, seem to have great potential in food production. For example, fruit pieces are of food-grade purity, cheap, abundant, and could be easily accepted by consumers. Therefore, apple (4), quince (5), and pear pieces (6) were proposed as immobilization supports for wine making due to ease in the immobilization technique. They gave the distinctive aromatic potential and improved sensory characteristics of the produced wines. One promising technology is the combination of immobilization and freeze drying techniques for

the preparation of biocatalysts. It may solve the problem of supplying industrial units with preserved and marketable ready-to-use immobilized cells due to possibility of storage of freeze-dried immobilized biocatalysts for long time intervals without any loss of cell viability and fermentation activity. Lyophilized gluten (a cheap and abundant material as the main substance of cereals) in the form of pellets has already been successfully applied in glucose (7), beer (8), and wine fermentations (9–11). Also, delignified cellulosic material showed commercial potential in lyophylized form (12,13).

53.2.2 Entrapment within Porous Matrix

In this type of immobilization, cells penetrate into the pores and throughout the channels inside the immobilization matrix. A rigid network keeps the cells inside the carrier and allows diffusion of nutrients toward the cells and metabolic products from cells to the outside medium, thereby making possible the growth and maintenance of active cells. This is the most frequently used immobilization method, where polysaccharides gels like alginate, pectate, carrageenan, chitosan, agar, polygalacturonic acid, and polymers like gelatin, collagen, polyvinyl alcohol (PVA), polyacrylamide are the most often employed. These can be gelled into hydrophilic matrices under mild conditions, thus allowing cell entrapment with minimal loss of viability. Very high biomass loadings can be achieved, since the cells are well protected. In order to provide even better protection from cell release, an external layer can be formed around the internal gel core. This is the so-called microencapsulation technique, which is well-established and the most often-used immobilization technology. It will be discussed in more detail in one of the following sections. The main disadvantage of gels is a limited mechanical stability under conditions of a rapid cell growth, severe shear stresses, and prolonged exposure to some chemical compounds (for example, phosphates disturb the alginate structure during the process of wort fermentation to beer). Several methods have been proposed for reinforcement of gel structures. For example, alginate gel can be strengthened by reaction with polyethyleneimine, gluteraldehyde cross-linking, addition of silica, genepin, and polyvinylalcohol or by partial drying of the gel. Another drawback of gel systems is mass transfer limitations. Understanding mass transfer phenomena within entrapment matrices may allow one to simultaneously provide different conditions at the carrier surface and in the interior. In this way, the gel bead can be made more stable and less permeable. In addition, the gels with heterogeneous cores could be attractive for co-immobilization of different cell types performing consecutive processes.

Unlike gels, porous preformed supports can be inoculated directly from the bulk medium. In these systems, cells are not completely separated from the effluent, similar to the adsorption method. Cell immobilization occurs by attachment to the internal surfaces, self-aggregation and retention in dead-end pockets within the material. Ideally, the colonized porous particles should retain some void spaces for flow so that mass transport of substrates and products could be achieved by both molecular diffusion and convection. Consequently, mass transport limitations are less stringent under optimal conditions as compared to gel entrapment method. However, fluid flow within the support can be realized only if cell adhesion is not very strong so that excessive biomass could be washed out from the matrix. When high cell densities are obtained, convection is no longer possible and the particles behave as dense cell agglomerates with high diffusion limitations. Yet the cell densities represented per unit of support volume are lower than those achievable by gel entrapment since the porous matrix material takes up significant volume fraction. As compared to gel particles, preformed carriers provide better mechanical properties and higher resistances to compression and disintegration. Numerous inorganic and organic materials have been used as preformed carriers: reticulated polyurethane (PU) and polyvinyl formal foam, other polymers, plastics, stainless steel, ceramic, glass, synthetic ion exchange resins, activated charcoal, aluminum oxide, diatomaceous earth, sand, cellulose, lignocellulose, cellulose acetate, and others. In addition, a variety of mixtures of different materials are commercially available for immobilization purposes, such as cytopore (cellulose with *N*,*N*-diethylaminoethyl groups), cytoline (polyethylene and silica), Bio-Sep beads (25% aramid polymer and 75% powdered activated carbon) etc. The porosity of the carriers varies across a rather wide range to suit immobilization of various bacterial, yeast, fungal, plant, and animal cells and tissues. Depending on the cell and the carrier type, immobilization then takes place in a combination of filtration, adsorption, growth, and colonization processes. Surface-associated growth of microorganisms in nature usually leads to a formation of highly structured biofilms, which are in fact naturally immobilized cells (14). The type of forces involved with cell immobilization surface interactions can involve Lewis acid/base (hydrophobic), Lifshitz–van der Waals (electrodynamic) and Coulombic (electrostatic). Carrier surfaces can be modified in order to affect cell immobilization. The surface of most inorganic supports is mainly composed of oxide and hydroxyl groups (e.g. in glass are silanol groups), which provide a mildly reactive surface for activation and binding of cell-surface proteins. Pretreatments of carriers can be accomplished by an inorganic and/or a cross-linked organic coating. Microorganisms interact with surfaces through many specialized structures on their walls (e.g. piles and pilus-associated

adhesions), exopolymers (glycocalyx in the case of bacteria), and complex ligand interactions involving signaling molecules (15). They have quorum-sensing mechanisms, as well. Therefore sensing either a biotic or an abiotic surface triggers genetic switches that can change cells' metabolism, phenotype, and morphology (16,17). Immobilization of plant and animal cells in the preformed carriers requires pretreatment of a carrier surface. A carrier can be modified to mimic biological extracellular matrix (ECM) proteins such as fibronectin, collagen, vitronection, elastin, laminin, and growth factors. A surface morphology (smoothness, roughness, micropatterning) can also be modified by etching, using lasers and photolithography (18).

53.2.3 Cell Flocculation

Cell flocculation is an aggregation process of cells that forms large clusters and represents biomass which sediments under gravitation. The ability to aggregate is seen in just a few types of cells, such as fungi, yeast, and some plant cells. This is the simplest and the least expensive immobilization method. In naturally nonflocculating cultures, sometimes, chemical agents or cross-linkers can help to induce the cell aggregation process. Interactions between cells keeping them together are very sensitive to conditions in a reactor, and are not easily controllable. Yeast flocculation is a property of major importance for the brewing industry as it affects fermentation productivity throughout yeast removal and recovery (19). Packed-bed, fluidized-bed, and continuous stirred-tank reactors are the most suitable fermenter types to employ flocculation immobilization method. In 2005, ethanol fermentation with self-flocculating yeast was commercialized, and a fuel ethanol plant with an annual production capacity of 200,000 tones was established at BBCA, one of the three ethanol producers in China.

53.2.4 Cell Containment behind Barriers

Mechanical containment of cells behind the barriers implies localization of cells either behind the membrane filters or inside a material (solid or fluid) surrounded by a semipermeable membrane. In process industry, micro- and ultrafilters are integrated inside the membrane reactors. This technology is relatively expensive and has found some applications in cell recycling and continuous processes (20,21).

53.3 MICROENCAPSULATION OF CELLS

Microencapsulation consists of entrapping a biologically active substance or cells in an appropriate material, to improve its performance, enhance its shelf life, or develop customized, high margin products. In strict terms, microcapsules are spherical beads coated with a membrane, that is capsules with a diameter of about 100–1000 μm. Besides traditional capsules consisting of a core and well-defined shell, plain microbeads without a distinct membrane have also been successfully used for encapsulation of cells. The capsules or beads should be semipermeable to allow diffusion of oxygen and nutrients into the cell inside the beads and metabolic products out of beads. The membrane insures the protection of the internal, bioactive substance, or cells. Despite its nonphysiological nature, the permselective capsule environment has been shown to support cellular metabolism, proliferation, differentiation, and cellular morphogenesis.

The application of capsules imposes demands on specific properties of capsules. Many different materials, approaches, and techniques for microencapsulation have been studied and some of them are summarized in recent reports (e.g. 22). Microcapsules are most frequently produced from water-soluble polymers. The hydrophilic nature of the immobilization material provides low interfacial tension with surrounding media or tissues and minimizes the protein adsorption and cell adhesion. Furthermore, gel materials enable the permeation of low molecular nutrients and metabolites. Water-insoluble immobilization materials require usage of organic solvents, which in most cases are harmful for living cells. Polyanions and polycations may form a gel by covalent or ionic cross-linking. Combination of covalent and ionic cross-linking may also be used. However, covalent cross-linking involves reactive chemicals and their applications are mainly limited to enzymes, fast-growing cells, or dead cells. Among water-soluble polymers, natural polysaccharides have been most frequently used for encapsulation of living cells, such as alginate, agarose, κ-carrageenan, chitosan, pectin, pectates, gellan. Alginate, pectate, and chitosan form gels by ionic cross-linking, whereas gelation of agarose, κ-carrageenan, and pectin is based on thermal procedure. A combination of thermal gelation and ionic cross-linking is used to produce gellan gels.

There are few different approaches to create semipermeable membrane for cell encapsulation, such as phase inversion, polyelectrolyte coacervation, interfacial precipitation, to mention some of them. Phase separation occurs from initially homogeneous solution, either by temperature change or exposing of a polymer solution to a nonsolvent component. The second procedure can be performed in a bath (wet process) or a saturated atmosphere (dry process). The coacervation process consists of decreasing the solubility of the encapsulating polymer by addition of a third component to the polymer solution in an organic solution. This procedure enables the separation of an aqueous polymeric solution into two miscible liquid phases: a dense polymer containing coacervate phase

and a dilute, supernatant equilibrium phase depleted in polymer. The active compound (cells) dispersed/dissolved in polymer solution is coated by the coacervate. Complex coacervation can result spontaneously on mixing oppositely charged polyelectrolytes in aqueous media. The charges must be sufficiently large to induce interaction, but not large enough to cause precipitation. The formulation of the process is very complex and variables (such as pH, ionic strength, temperature, molecular weight, and concentration) significantly affect the kinetics of the entire process and ultimately characteristics of the final microspheres (23). The obtained membrane porosity varies in a rather wide range from 0.1 to 50 μm, depending on several factors, such as polymer–nonsolvent compatibility, polymer precipitation time, diluent concentration. Various cell types have been encapsulated in semipermeable capsules of polyacrylate. In series of investigations, different combinations of polyionic species have been studied, such as alginate with either protamine or spermine (24), cellulose sulphate with poly(diallyldimethyl ammonium chloride), carboximethyl cellulose with chitosan, or diehylaminoethil dextran (25). The porosity of the network can be easily controlled by adjusting the osmotic condition and the molecular weight distribution of the polyionic species. There is also a possibility to improve biocompatibility and reinforce the network by one or multiplied coating process. More complex structures contain multicomponent polyelectrolyte mixtures of both polyanionic and polycationic species. Gelatin is often used as one of the polyelectrolites in combination with gum arabic, polyphosphate, heparin, carrageenan, and chitosan (26).

Alginate systems are based on interfacial precipitation in calcium chloride solution. The gelation of alginate–cell suspension in calcium chloride bath creates matrix suitable for immobilization of living cells. The network formation is usually further followed by the coating step with poly-L-lysine (PLL). The described procedure gives a capsule with solid core of calcium alginate coated with a one-layer membrane. In order to liquefy the core of capsules, Ca-alginate gel is subsequently dissolved with sodium citrate. The obtained capsules can be further fortified by coating procedure with alginate or another polyanion (27,28). Formation of double and multilayer membrane capsules have been suggested in the literature (29,30). Furthermore, PLL can be modified or exchanged with other polycations (31,32). Properties of capsules depend on composition and molecular weight of core and coating material, as well as on a way of exposure to gelation and coating solution (duration of this processes and concentration of solutions).

Beside the composition, the size of capsules is another very important feature. Smaller capsules show better mass transfer properties of nutrients and metabolic products. Moreover, reduction in capsule size lowers the shear forces and may increase their long-time stability. For implantation purposes, smaller capsules are by themselves shown to be more biocompatible than bigger capsules (33) and can be more easily implanted since they occupy less space. However, small beads have larger surface-to-volume ratio compared to big particles and therefore can be more easily damaged by swelling or by exposure to oppositely charged ions (34). In addition, smaller spheres are more fragile to internal stresses caused by cell proliferation and expansion of cell colonies. The choice of capsule size depends on specific application and the cell type is going to be entrapped in. Numerous techniques for bead production have been developed up to now and are available to achieve the desired size of capsules.

Capsules can release their contents upon applying specific treatments or conditions (heating, salvation, diffusion, and pressure). Sealed capsules are coated with semipermeable, spherical, thin, strong membrane around the solid or liquid core. A coating can be designed to open in the specific areas of the body and microcapsules can then gradually release active ingredients. The choice of core and coating materials and capsule design should be established according to the requirements of their application. To give an example, for engineering probiotic contained capsules, a coating which can withstand acidic conditions in the stomach acids after consumption by gastrointestinal fluids is usually employed. In this way, the protection of the biological integrity of probiotic products is achieved during gastro-duodenal transit, which is prerequisite for delivery of a high concentration of viable cells to the jejunum and the ileum. Since capsules should provide protection to sensitive microorganisms, against harsh conditions in the gut environment, the produced microspheres should be tested on swelling, erosion, disintegration in simulated gastric/intestinal fluids prior to industrial and real-life applications.

The capsules may be designed in wet or dry forms. Encapsulation in the hydrocolloid beads entraps the cell within the matrix; this provides good protection against environmental effects. Encapsulation of cells in gel–particle systems has been investigated for improving their viability in various products and the intestinal tract (35), then for delivering of active compounds, as well as to restore, maintain or improve tissue function. The mechanical or tissue irritation to surrounding tissue is reduced by the soft and pliable features of the gel. As a consequence of the hydrophilic properties of the material, there is virtually no interfacial tension with surrounding fluids and tissues which minimizes the protein adsorption or cell adhesion. Hydrogels have also been mainly utilized for fermentation processes, such as fermentation of whey (36), yoghurt manufacture (37), beer (38), wine (39) and cider (40). Hydrogels provide a high degree of

permeability for low-molecular-mass (Mr) nutrients and metabolites.

Drying techniques are often applied to give microorganisms more stability and flexibility. The dry product, after milling and screening are powder particles of freeze-dried or spray-dried microorganisms and additives. Capsule fillings, sachets, and tablets are also very popular among consumers and inexpensive to produce, thus manufactured in the pharmaceutical area.

There are more problematic issues when considering microencapsulation of cells in contrast to encapsulation of other active compounds. One of them is their size (at least several microns in diameter) which immediately restricts the application of nanotechnologies. Furthermore, encapsulation techniques involving harsh conditions usually are not acceptable for encapsulation of sensitive cells. However, relatively mild conditions (e.g. process carried out in aqueous conditions without the use of reactive species) generally yield a less durable microcapsule. Harsher encapsulation conditions might compromise cell viability but the resultant capsule may be more resilient and cell capable of proliferation may be suitable for such conditions. Fragile cells can also be subjected to harsher conditions provided that the cells are compartmentalized from toxic chemical or conditions. Then, it is necessary to provide hygienic conditions during cell processing. This makes encapsulation process and equipment difficult to handle.

A number of aspects of encapsulated cells are critical for the success of the technology: the capsule permeability, mechanical properties, immune protection in case of tissue transplantation, and biocompatibility. There are numerous publications on penetration rate of particular elements. Effective oxygen penetration (the most important element for cell growth), for example, has been estimated to be 0.1–0.15 mm in alginate beads (41) and 0.08–0.1 mm (42) in carrageenan beads. The metabolic requirements of various cell types are different and, hence, optimal membrane permeability is expected to be dependent on the choice of cells. Although the role of permeability for particular elements essential for cell survival has been explored [e.g. oxygen (43)], no systematic approach has been taken to determine permeability requirements of particular cell types. An empirical approach has been typically taken to tailor capsule permeability for cell survival. The upper limit of capsule permeability, that is molecular weight cut-off (MWCO), will be application dependent. Besides permeability, the next important consideration is the availability of an ECM to encapsulated cells (44). The ECM not only allows the cells to express their differentiation function, but also helps to organize the cell mass within the capsules for optimal viability. Capsule biocompatibility is critical when encapsulated cells are intended for transplantation since it is the compatibility of a biomaterial with the host that ultimately determines the nature of host response and graft survival. The physicochemical nature of a biomaterial and exploration of different materials for this purpose have out of necessity, developed different encapsulation procedures to accommodate the varying physicochemical properties.

53.4 REQUIREMENTS FOR CELL IMMOBILIZATION

In order to achieve successful process by implementing a cell immobilization, certain prerequisites should be fulfilled. In general, those requirements depend on a specific purpose of cell immobilization and can be different from one field of application to another. However, there are few characteristics considered as favorable for carriers in general. It is better if a support has a high surface area-to-volume ratio and if it is renewable. In industrial processes, the immobilized biocatalyst has to keep operational stability for longer times. The biological or catalytic activity must not be adversely affected by immobilization. The carrier should retain good mechanical, chemical, and biological stability and not be easily degraded by enzymes, solvents, pressure changes, or shearing forces (19). For food applications, the carrier material should be of food-grade purity and readily accepted by consumers, while in case of biomedical applications, biodegradable supports have advantages over nonbiodegradable. A carrier design may also differ from one application to another. For example, for the replacement of a biochemical function, nanoporous, immunoisolatory polymer membranes are convenient. Their pores should be large enough to allow diffusion of nutrients, waste, and bioactive factors, but not large enough as to allow immune cells to attack the cells within. Another case is when it is necessary to promote the formation of a new tissue that is structurally and functionally integrated with the surrounding tissue; then, micro- or macro-porous polymer scaffolds are more suitable.

53.5 BIOMATERIALS FOR CELL IMMOBILIZATION

In order to provide the varying requirements for each specific application, a variety of naturally derived and synthetic biomaterials are used for cell encapsulation. These materials can be processed into many different physical forms and geometries. Natural polymers are attractive for cell immobilization due to their abundance and apparent biocompatibility. These polymers can provide a wide range of physical properties that offer unique characteristics for cell encapsulation technologies. In addition, biopolymers are easily subjected to biodegradation. On the other hand, instead of being inert, they can act as media compounds

for potentially contaminating organisms (mostly molds) and thus are cleaved and metabolized. This can lead to more or less deterioration of the complete immobilized biocatalyst when operating under nonsterile conditions. In contrast, some synthetic polymers are hardly biodegradable which lowers demands on the process' sterility. Moreover, synthetic polymers are attractive due to the resultant properties able to be created by controlling the formation and structure of these materials. One of the main challenges in development of materials for cell immobilization is the creation of materials with predefined pore structures and appropriate degradation and mechanical properties. This chapter briefly describes the most frequently used natural and synthetic materials in cell immobilization technology.

53.5.1 Alginate

Alginate is the most widely used material for encapsulation/immobilization of various types of cells. Alginate is used in a form of a salt of alginic acid. Alginates are naturally derived linear copolymers of 1,4-linked β-D-mannuronic acid (M) and α-L-guluronic acid (G) residues (45). The ratio and sequential distribution of uronic acid residues, along the length of the alginate chain vary in alginates of different origins (brown seaweeds, certain bacteria) (46). There is no regular repeat unit in alginate polymers, and the chains can be described as a varying sequence of regions which usually denotes as M blocks, G blocks, and MG blocks. Dissolving alginate in water gives a viscous solution of which the viscosity will increase with the length of alginate molecules, that is number of monomers. Water solutions of polysaccharides form hydrogels in the presence of divalent Ca^{2+} ions via ionic interactions between the acid groups on G blocks and the gelating ions. As a result, calcium alginate gels are physically cross-linked polymers with mechanical and hosting properties dependant on the alginate composition. Monovalent cations and Mg^{2+} ions do not induce gelation, while ions like Ba^{2+} and Sr^{2+} will produce stronger alginate gels than Ca^{2+}. Alginate can be also covalently cross-linked using bifunctional molecules such as adipic dihydrazide, methyl ester L-lysine, and poly(ethylene glycol) (PEG). A potential limitation to the use of alginate is its often uncontrollable and unpredictable dissolution, which occurs by a process involving the loss of divalent ions into surrounding fluids (47).

However, since alginates are heterogeneous group of polymers, with a wide range of functional properties, the success will rely on an appropriate choice of materials and methodology for each application. This must be based on knowledge of their chemical composition, the correlation between structural and functional properties, and a sufficient understanding of the behavior of polysaccharide formulations on a macroscopic as well as molecular level

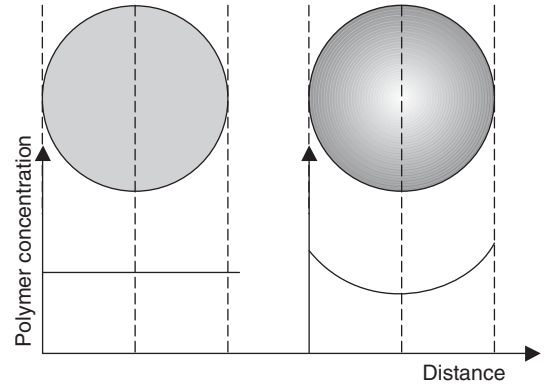


Figure 53.2. Polymer gradients in homogeneous and heterogeneous alginate gel beads [from (18)]. (This figure is available in full color at http://onlinelibrary.wiley.com/book/10.1002/9780470054581.)

(47). The mechanical properties of an alginate gel will to a large extent vary with the alginate composition. Thus, gels made of alginates with a high G-block content will be stronger and more stable as compared to low G-block content alginate gels. The physical properties of alginate gels can be improved by formation of an heterogeneous structure (Fig. 53.2). Gels with varying degrees of anisotropy with respect to polymer concentration can be formed by controlling the kinetics of the gel formation. This heterogeneity is governed by the relative rate of diffusion of calcium ions and the rate of diffusion of the sodium alginate molecules toward and inward moving gelling zone. Simply by adjusting the concentration of alginate and the cross-linking ions, the distribution of the polymer in the gel can be controlled, and alginate beads with a capsular structure (with a polymer concentration of about 10% on the surface and less than 0.2% in the core) have been made without adding polycations or any other nongelling polymer (48). Also, the composition of alginate influences the bead homogeneity: G high degree alginates form more homogeneous gels than high M alginates (22).

Both techniques (extrusion and emulsion) can be applied to generate alginate microspheres. When a droplet of alginate falls into a bath containing divalent cations like Ca^{2+}, the gelling process will start immediately at the contact zone between the alginate droplet and the aqueous gelling ions generating a gel bead. The gel formation process may be controlled and gels with different properties may be formed. In particular, bead homogeneity is dependent upon the way in which the gelling ions are added. The distribution of the gel within the bead may thus to a large extent be controlled and beads even with a capsular structure can be made (48). In order to produce more heterogeneous beads while retaining physiologic conditions, sodium may be replaced by noncharged molecules like mannitol to prevent osmotic

stress to the cells (28). In the emulsion technique the addition of an oil-soluble acid, such as acetic acid, reduces the alginate pH from 7.5 to approximately 6.5, enabling initiation of gelation with Ca^{2+} (49). The gelling speed is roughly around 100 μm/min in 50 m*M* $CaCl_2$, which means that a 500 μm bead is gelled in approximately 2.5 minutes. This is near the rate of freely diffusing calcium ions (45).

The survivability of cell cultures in alginate beads in general depends on many factors such as concentration of alginate and gelation solution ($CaCl_2$), the duration of gelation, and cell concentration. The type of alginate and the initial cellular concentration seem to be very important in maximum cellular density that can be reached in immobilized cultures. Coated alginate microcapsules prove to have better protective characteristics compared to uncoated. PLL is of great interest as the coating material due to its better biocompatibility and potential applications in biomedicine and food industry. Champagne and coworkers (50) suggested coating of alginate beads with double layer of PLL, claiming reducing the cell release by a factor of 50. PLL-cross-linked alginate microparticles loaded with bifidobacteria successfully protected cells against low pH media and in addition, showed to provide improved stability during storage in a refrigerator compared to free cultures (51). But the high cost of poly-lysine may limit the large-scale use of alginate-poly-lysine microcapsule in microorganism immobilization. Therefore, except conventional polymers, polysaccharides (fructo-oligosaccharides, isomalto-oligosaccharides) and peptides may also been used as an outer coating layer (52). To give an example, alginate–chitosan–alginate has attracted much attention for its good biocompatibility and the low cost of chitosan, which is about 2500 times lower than that of poly-lysine.

53.5.2 κ-Carrageenan

Carrageenan is a natural polysaccharides isolated from marine macroalgae, commonly used as food additive and immobilization matrix. Carrageenan dissolves at high temperatures (60–80°C) in concentrations 2 to 5% (53). Dispersion of the carrageenan gel into small droplets has to be carried out at elevated temperatures (40–45°C) and gelation occurs during cooling procedure down to room temperatures. After the beads are formed *K* ions in the form of KCl are used to stabilize the gel, prevent swelling or to induce gelation (54). Audet and coauthors (36) reported inhibitory effect of KCl on some bacteria strains such as *Streptococcus thermophilus* and *L. bulgaricus*. The presence of monovalent ions such as Rb^+, Cs^+, NH_4^+ makes stronger gels (55). Locus bean gum in ratio to carrageenan of 1:2 significantly increases the strength of the gel through specific interaction of its galactomannan chains with carrageenan. Carrageenan–locus bean gum mixture has been frequently tested for microbial encapsulation, e.g. (56,57). The treatment with $Al(NO_3)_3$ has also been used to increase mechanical stability of carrageenan-based matrices (58).

53.5.3 Chitosan

Chitosan is a positively charged linear polysaccharide formed by deaceylation of chitin. It is widely found in crustacean shells, fungi, insects, and mollusks. Chitosan is water soluble below pH 6, forms hydrogels by ionic or chemical cross-linking with glutaraldehyde and degrades via enzymatic hydrolysis. The terms chitin and chitosan refer not to specific compounds, but to two types of copolymers containing the two monomer residues anhydro-*N*-acetyl-D-glucosamine and amino-D-glucosamine, respectively. Chitin is a polymer of β-(1,4)-2-acetamido-2-deoxy-D-glucopyranose and one of the most abundant organic materials. Chitosan, a polycation with amine groups, can be cross-linked by anions and polyanions, such as polyphosphates (59), $[Fe(CN)_6]^{4-}$ and $[Fe(CN_6)]^{3-}$ (60), polyaldehydrocarbonic acid (53), and sodium alginate (61). It is important biomaterial in food and pharmaceutical applications due to its favorable properties, such as good biocompatibility, biodegradability, and nontoxicity. Chitosan is often combined with other materials (like calcium phosphate and collagen) to achieve more desirable mechanical properties. It has been mainly utilized for wound dressings, drug delivery systems, space-filling implants, micro- and macro-porous scaffolds.

However, chitosan exhibits inhibitory effects on different types of sensitive lactic acid bacteria (62). Thus, chitosan is mainly used as a coating for conventional alginate gel beads [e.g. (54)]. Alginate–chitosan microcapsules can be made by one- or two-step processes, based on the presence or absence of Ca^{2+} in the receiving chitosan solution (63). The beads can be prepared in a way to differ in a level of homogeneity of the alginate concentration gradient through the cross-section of the bead, by addition of sodium chloride to the calcium chloride solution. The capsule's mechanical strength and permeability strongly depend on the process of capsule preparation (64). In the one-stage process (in the absence of Ca^{2+} in chitosan solution), chitosan is located only at the interface, as a thin-alginate-chitosan membrane with a weak mechanical resistance. The capsules were much stronger when the two-stage protocol was used. This difference between the two protocols of capsule formation is due to the ability of chitosan to penetrate through the membrane (63). The kinetics of membrane formation and the capsule parameters (thickness, permeability, and mechanical strength) depend on the concentration of components, molar masses of both alginate and chitosan reaction times, pH, and ionic strength. Sprayed particles coated with chitosan are recommended as impressively effective vehicles in delivering viable bacterial cells.

53.5.4 Hyaluronic Acid

Hyaluronic acid gels can be formed by covalently cross-linking with various hydrazide derivatives and these gels are enzymatically degraded by hyaluronidase. Hyaluronic acid can be readily isolated from natural sources; however, it requires purification for impurities and endotoxins to be removed prior to usage. Hyaluronic acid has been widely applied in micro- and macro-porous cell encapsulation.

53.5.5 Proteins

Industrial (bulk) proteins are biopolymers derived from plants and animals. Proteins are composed of amino acids linked via amide bonds giving chain lengths ranging from about 50 up to more than 100,000 amino acids. Amino acids are amphoteric due to the presence of basic (NH_2) and acidic groups (COOH). The degree of hydrophobicity and hydrophilicity of the amino acids is one of the major determinants of the three-dimensional structure of proteins. Protein denaturation occurs at elevated temperatures (above 75°C in water medium) or in the presence of certain chemical compounds, denaturants (e.g. urea, guadinium). Relevant protein properties for encapsulation purposes include surface active properties, biodegrability, good film forming and mechanical properties, high gas barrier properties, and high resistance to organic solvents and oils/fats, natural emulsifying, dispersing and gelling properties, processability (in melt, aqueous solutions and dispersions), variety in source, composition and number of functional groups, and ease of modification (26,65). In principle, any protein capable of forming a film is suitable for microencapsulation. Film formation is based on separation of proteins from the solvent phase due to changes in solvent conditions, thermal treatment, or drying. It is possible to alter some of protein properties (e.g. to improve water resistance, to increase water solubility, or mechanical strength to increase lipophilicity) by physical, chemical, or enzymatic means. Examples of proteins produced on large scales and suitable for immobilization purposes are collagen, gelatin, whey protein, casein, keratin, and plant proteins like wheat gluten, soy protein, pea, and potato protein.

53.5.6 Collagen and Gelatin

Collagen is the major component of mammalian connective tissues such as tendon, skin, bone, cartilage, and ligament. Due to the natural ability to bind cells and its abundance in nature, biocompatibility and biodegradability, and high tensile strength, collagen has been widely used in cell immobilization. It may be gelled utilizing changes in pH value. Collagen has been processed into porous sponges, films, micro- and macro-porous scaffolds, mainly to engineer a variety of tissues (66). Gelatins are derived by particle hydrolysis of collagen and have subsequently a quite similar amino acid composition as collagen. Gelatin dissolves in warm water and upon cooling, a gel is formed. Gelatin is a potentially useful biomaterial mainly because of its advantageous gelating properties, melting temperature of 37°C, low price, easy availability, and biodegrability.

53.5.7 Starches

Starch consists of two types of molecules, amylose and amylopectin. Chemically modified starches and starch hydrolysates are used as microencapsulation matrices. Blending of syrups and/or sugars with modified or hydrolyzed starches has been claimed to lead to optimal encapsulating materials. The increased interest to use bioactive compounds as functional ingredients in formulations of novel foods is a challenging field to apply microencapsulation technologies. Starch occurs naturally as discrete particles, called granules. The size of the granules depends on the starch origin ranging from 1–100 μm (67). The granular structure is lost upon heating above 80°C and the starch creates polymer solution. Commercial starch hydrolysates called dextrins are manufactured by prolonged heating under dry conditions with or without the addition of an acid. Starches have been mainly used in food area to encapsulate flavors. A recent study showed that starches can be successfully applied for immobilization of living cells such as bifidobacteria strains [e.g. (68)].

53.5.8 Polyvinyl Alcohol

PVA is a hydrophilic polymer which can be gelled in an aqueous solution during prolonged storage period. The network is formed by hydrogen bounds between hydroxyl groups of neighboring polymer chains and therefore is not stable at temperatures above 0°C. During the freezing process, phase separation occurs resulting in the formation of stronger hydrogel, so called cryogel. PVA cryogel is mechanically very stable, hardly biodegradable, and not soluble at temperatures below 60°C. Parameters influencing the gel strength are the degree of deacetylation of the used PVA, the chain length of the polymer, its concentration in the solution, and the rate of thawing (69). The process of gel formation by freezing–thawing procedure may lead to a loss of a microbial activity when living cells are to be immobilized, due to temperature stresses involved in the process. To counteract this loss of biological activity the method of room-temperature gelation was developed by Vorlop and Jekel (70) and the resulting particles were named LentiKats®. LentiKats particles have specific lenticular shape (Fig. 53.3) due to which they combine the advantages of small (good diffusion properties) and large

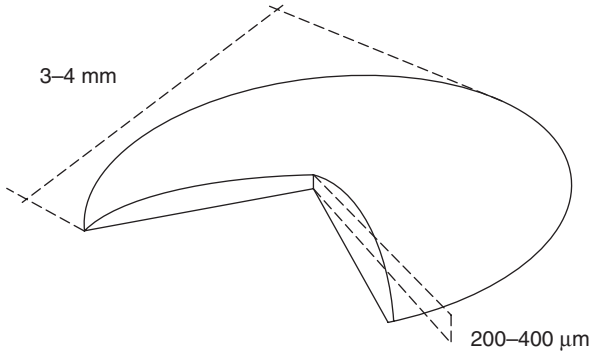


Figure 53.3. LentiKats® hydrogel particle based on PVA.

beads (easy retention and removal). Detailed information on preparation of LentiKats can be found in the literature (69) and on the Internet (71). Production of LentiKats particles is based on the usage of the specially designed LentiKats Printer on lab and industrial scales. Bacteria (72), fungi (73), yeast (74) and enzymes (75) have been successfully encapsulated in LentiKats particles up to now.

53.5.9 Poly(glycolide) and Poly(lactide)

The most widely used synthetic degradable polymer are poly(glycolide) (PGA), poly(lactide) (PLA), and their copolymer poly(lactide-co-glycolide) (PLGA). The degradation occurs via nonspecific hydrolysis of the ester linkage when lactic and glycolic acids are formed, which are naturally metabolized and easily cleared by the body (76). Poly(hydroxy esters) are mainly processed as scaffolds, where limited mechanical stability is the main problem.

53.5.10 Poly(ethylene oxide) and Poly(ethylene glycol)

Poly(ethylene oxide) (PEO) and PEG are synthesized by anionic or cationic polymerization of ethylene oxide. The surface of these polymers prevents the adsorption of nonspecific proteins, which makes them suitable for scaffold design. This attribute can also be useful when trying to pattern the biomaterial surface with specific signals that promote cellular attachment. PEG can be copolymerized with PLA to form a degradable, hydrophilic polymer that can be used as a hydrogel for cell immobilization.

53.5.11 Polyurethane Foam

PUs are formed by condensation of polycyanates (R-CNO) and polyols (R-OH) when carbon dioxide escapes from the matrix leaving pore spaces. Except for their open pore structure, they are convenient because of their inertness and mechanical strength. The pore size of PU foam matrices is usually expressed as the number of pores per linear inch (ppi).

53.6 TECHNIQUES FOR CELL IMMOBILIZATION

53.6.1 Gel–Particle Techniques

Extrusion or emulsification techniques may be applied to produce spherical polymer beads ranging from 0.3 to 3 mm in diameter. The first step in both gel–particle technologies (extrusion and emulsion) is mixing of cell culture with a polymer solution to create cell–polymer suspension (Fig. 53.4), which is then extruded through a needle to produce droplets collected in a bath where gelation occurs (ionotropic or thermal), or dispersed in a continuous phase applying mixing to create stable w/o emulsion.

Extrusion is the oldest and the most common approach to making capsules with hydrocolloids. It is based on forcing down a polymer-cell suspension through a nozzle to generate small droplets (Fig. 53.5). Extrusion bead production techniques (coaxial air flow, electrostatic, vibration, Jet Cutter, atomization) are based on applying the additional force to generate smaller spheres compare to those produce by simple dropping method. The polymer-cell droplets should fall directly into a continuously stirred gelling agent solution. The stirring can be maintained by a magnetic stirrer, or alternatively, a vessel containing the gelling agent solution is rotated by means of a motor. In case of the coaxial air flow, additional air flow through an outer concentric nozzle is applied to enhance dropping (Fig. 53.5a). The electrostatic extrusion is based on applying an electrostatic force to generate microdroplets (Fig. 53.5b). Even high electric fields (few thousand volts) do not adversely affect cell viability (77). A droplet generation by the vibration technology is achieved by adding a vibration on a laminar fluid jet which breaks apart definitely if the right wavelength has been applied (Fig. 53.5c). Jet Cutter technology is based on a mechanical cut of a liquid jet by rotating cutting wires installed in a cutting tool. The Jet Cutter may be operated in two different modes called the normal mode (Fig. 53.5di) or the soft-landing mode (Fig. 53.5dii). In the normal mode, the trajectory of the microspheres is top down in a rather direct way, whereas in the soft-landing mode it is diagonal bottom-up. In the soft-landing mode the velocity of the microspheres is dramatically reduced near the zenith of the trajectory where they are collected. Hence, the speed at which the microspheres enter a liquid collection bath is rather low so that the risk of microsphere deformation is reduced. The atomization technique applies a disk rotating at high velocity to atomize a liquid jet into fine microspheres (Fig. 53.5e).

The size of the particles can be adjusted by choosing the needle diameter and manipulating the distance between the outlet and the coagulation solution and other parameters of a technique. Extrusion technology is the most popular due to its simplicity, convinience of handling with the equipment, low cost, and gentle formulation conditions ensuring

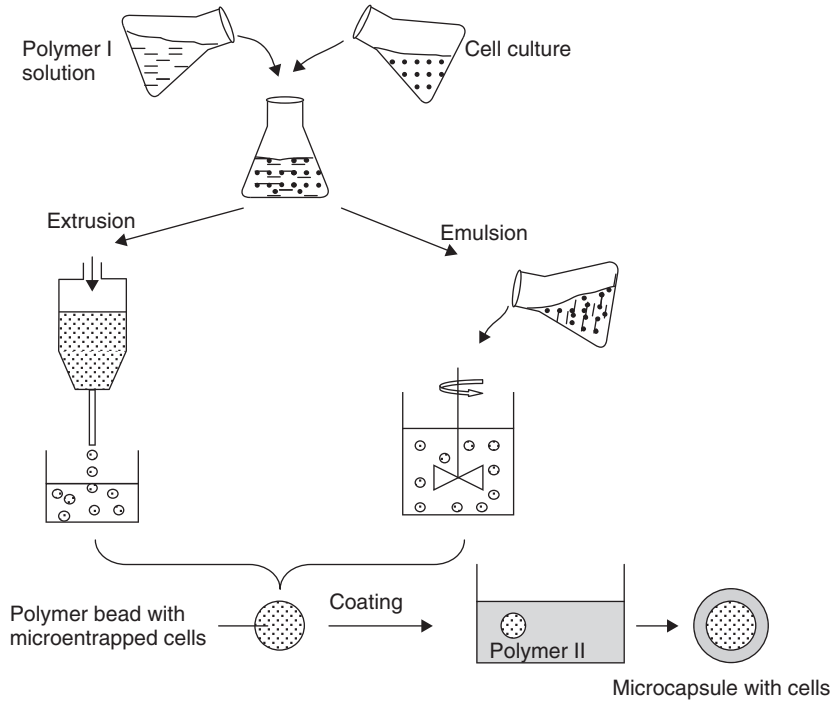


Figure 53.4. Gel–particle technologies for the microencapsulation of cells [from (44)].

high retention of cell viability. The lab devices are designed to work either with a single or a concentric nozzle. With the single nozzle, homogeneous beads with equally distributed cells over the whole cross-section could be obtained; for example, there are cells in the center and at the surface of the bead. With the concentric nozzle, it is possible to produce capsules with a defined core region having the cells and a shell region with pure polymer. In general, it is possible to process polymer solutions of wide range of viscosities (20–10,000 mPas) and to generate microspheres of the desired size with very narrow size distribution. For industrial-scale applications, multinozzle plants with multiplied productivity rates are more suitable than single-nozzle devices. In a recent report (78), several extrusion techniques were analyzed from the aspect of their advantages, limitations, and disadvantages and compared regarding the roundness and uniformity of obtained microspheres and with respect to the productivity and transferability of each technique.

In the emulsion technique, a small volume of cell–polymer suspension (discontinuous phase) is added to a large volume of an oil (continuous phase). The mixture is homogenized to form a water-in-oil (w/o) emulsion. In some cases emulsifiers are added to form more stable emulsions, since these agents lower the surface tension of droplets leading to smaller spheres. The most common emulsifier used is Tween 80 at low concentrations. Once the emulsion is formed, solidification occurs after the addition of an adequate solidifying agent to the emulsion. In the emulsion procedure, adjustment of agitation speed and phase ratio enables production of the targeted bead size. The size of the beads can vary between 25 μm and 2 mm. The double emulsion technique (water-in-oil-in-water, w/o/w), a modification of the basic technique in which an emulsion is made of an aqueous solution in a hydrophobic wall polymer can also be appropriate for incorporation of cells. The relative viability of the encapsulated cells depends on operating parameters, such as inner phase volume ratio and the median diameter of the oil droplets.

The obtained polymer beads with entrapped cells can be further introduced into the second polymer solution to create a coating layer which provides an extra protection to the cells and/or gives sensorial properties to the product (Fig. 53.3). Another way to perform coating is to use coextrusion devices, where beads formation and wrapping occur simultaneously. Coating can be performed with cationic (polyethilenimine, polypropileneimine, glutaraldehyde or combination of those) or other polymers. Formation of the membrane around the beads results in stronger microcapsules and minimized cell release.

53.6.2 Spray Coating

In spray coating, the core material needs to be in solid form and is kept in motion in a specially designed chamber,

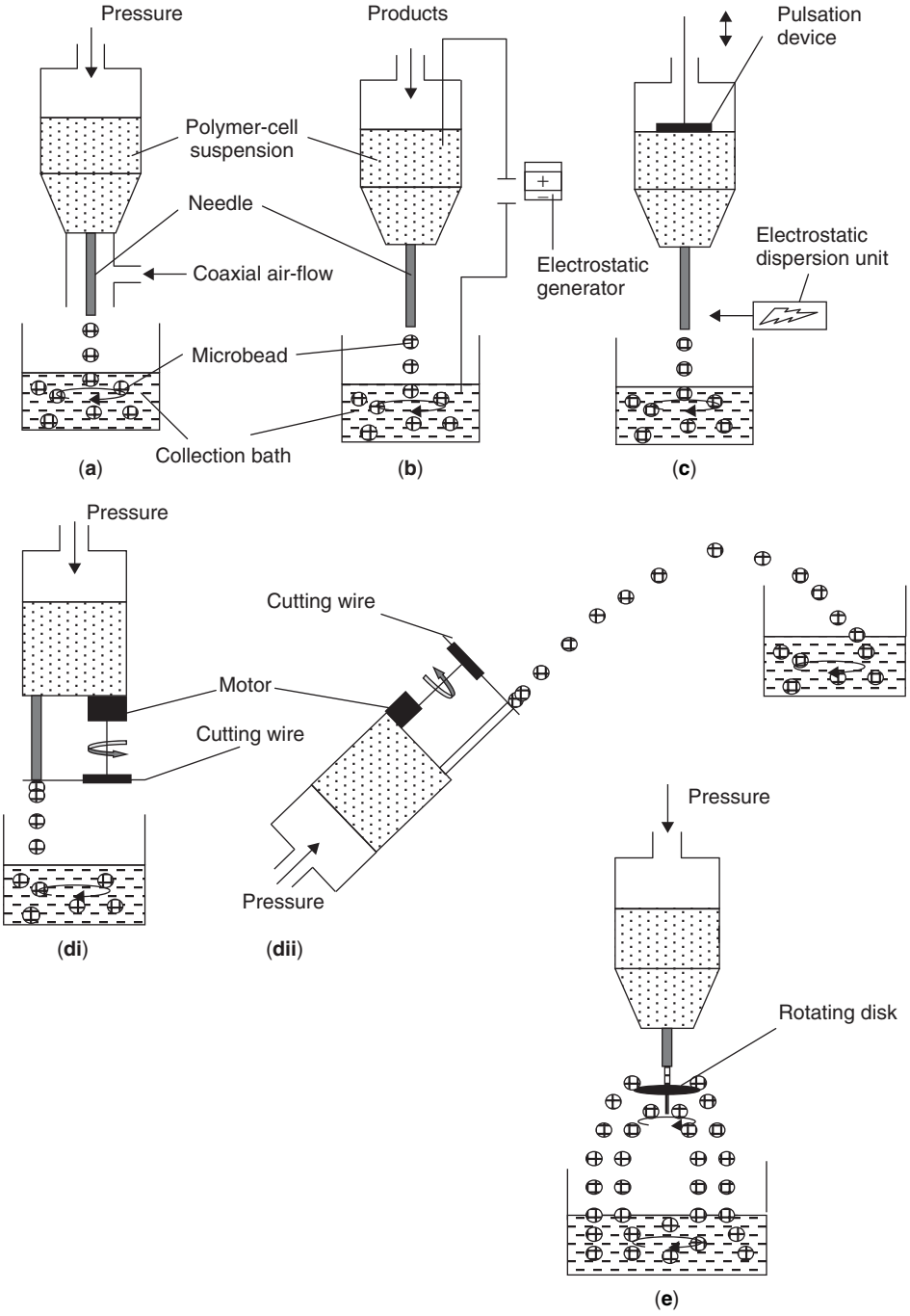


Figure 53.5. Extrusion techniques: (a) Coaxial air flow; (b) electrostatic extrusion; (c) vibration technique; (d) Jet Cutter with (i) normal mode, (ii) soft-landing mode; (e) atomization technique [from (68)].

either by injection of air at the bottom or by rotary action. A liquid coating material is sprayed through a nozzle over the core material, in a hot environment. The film formation begins, followed by successive wetting and drying stages which result in a solid, homogeneous layer on the surface of a core. The small droplets of the sprayed liquid contact the particle surface, spread on the surface and coalesce. The spray liquid, also referred to as shell, wall or coat material can be a solution, a suspension, an emulsion, or a melt. Any edible material, with a stable molten phase can be sprayed, allowing coatings with a thickness of 100 μm up to 10 mm, at high deposition rates. The coating

material can be injected from many angles and this influences the properties of the coating. In Fig. 53.6, the three spray coating technologies are presented; they principally differ in the type of air fluidization employed and the site in the vessel where the coating material is sprayed: the top spray, the bottom spray, and the tangential spray coating. The cells are presented in fine powder particles prepared by traditional methods (fermentation, concentration, freeze drying, and granulation). The coating material is introduced into the vessel under the compressed air. In food applications the coating is mostly lipid based (e.g. waxes, fatty acids, and specialty oils), but proteins (e.g. gluten and casein), or carbohydrates (cellulose derivatives, carrageenan, and alginate) can also be used (79).

Spray coating technique is suitable for particles with a diameter from 50 μm to 5 mm. Product quality characteristics depend on numerous variables, which affect different steps of the process. The film characteristics, through the evaporation rate are function of fluidization air velocity, temperature, and humidity (80). The coating homogeneity and success are influenced by the stickiness of the coating material, the wettability of particles by the coating liquid, and the operating conditions. The thickness of the final film coat is determined by the number of coating cycles (passages of the particles in the coating zone). An adequate choice of the coating material (with respect to viscosity and hydroscopicity), and control of the operating conditions, such as the particle velocity and bed moisture content, prevent collision between particles and agglomeration. During spraying process bubbles might form, due to shear, and be trapped in the coating film, which affects porosity, permeability, and mechanical properties of the shell layer.

In the top spray coating mode, the spray liquid and the air are in the counter current (Fig. 53.6a). Therefore, pulverization occurs at the top of the fluidized bed, involving a high risk of the droplets drying. Particles should travel fast to prevent agglomeration and the droplets should be small enough to sediment on the core and create dense coating film. In practical applications, the motions of fluidized core particles are random, resulting in a nonuniform coating. In the bottom spray coating, the spray liquid is introduced in the vessel through spray nozzles placed at the bottom, thus in the concurrent direction with the air (Fig. 53.6b). In 1950, Dr D. Wurster (81) improved the device by adding a cylindrical partition centrally placed and an air distribution plate. This improved device enables dense and homogeneous coating. Collision between droplets and particles is increased, resulting in higher coating efficiency, lower droplets drying, and minimal risk of agglomeration. In addition, the production capacity of the Wurster coating device is increased compared to a conventional top spray coating system. The tangential spray coating device is also called rotary-spray coating system (Fig. 53.6c). A rotary disk, placed at the bottom of the chamber maintains a complex fluidization pattern and the particles movement is influenced by centrifugal force, air stream, and gravity (80). The coating liquid is brought in tangentially, while air streams pass through the gap between the rotor disk and inside chamber wall, maintaining fluidization of the core particles. As with bottom spray device, the achieved coating is homogeneous. The main disadvantage of the technique is the high shear stress applied to the particles, thus it is limited to sturdy and resistant materials.

The spray coating is among all, the most applicable technique in industrial productions, since it is possible to achieve large batch volumes and high throughputs. Spray coating is widely used in industrial applications, mainly for microbial products. However, most of devices are proprietary and the information about how to control the process is very limited. Therefore, it is not easy for public scientists to design coated cultures and investigate their health effects in functional foods (79).

53.6.3 Spray and Freeze Drying

The first step of spray drying procedure involves the dispersion of the core (usually in oil) in a concentrated aqueous solution of the wall polymer, which is usually a water-soluble compound (such as gum arabic), to form an emulsion with droplets of few microns. The emulsion is then fed as droplets to the heated chamber of the spray drier where they are dehydrated to form solid capsules. The size of a spray-dried bead depends on both, physical and operating parameters, such as solution viscosity, density, surface tension, atomization pressure, nozzle type. The temperature of the sprayed emulsion must be optimized in order to avoid solidification prior to atomization on one side, and late solidification, resulting in odd-shaped sticky particles, on the other side (80).

Microencapsulation by spray drying is well-established technique suitable for large-scale industrial applications. However, the conventional procedure requires exposing of cells to severe temperature and osmotic stresses which results in relatively high cell mortality and/or viability and activity losses.

Freeze drying is preformed at low temperatures and under vacuum, avoiding water phase transition and oxidation. The obtained dried mixture must be grounded and the final particles are of wide size distribution and with low surface area. The freeze drying technology is very expensive and thus less frequently used compared to other encapsulation techniques.

One approach to improve cell survival during drying process is to use protectants added to media prior to drying. Hence, the addition of cryoprotectants helps to retain lacobacilis activity during freeze drying and stabilize them during storage.

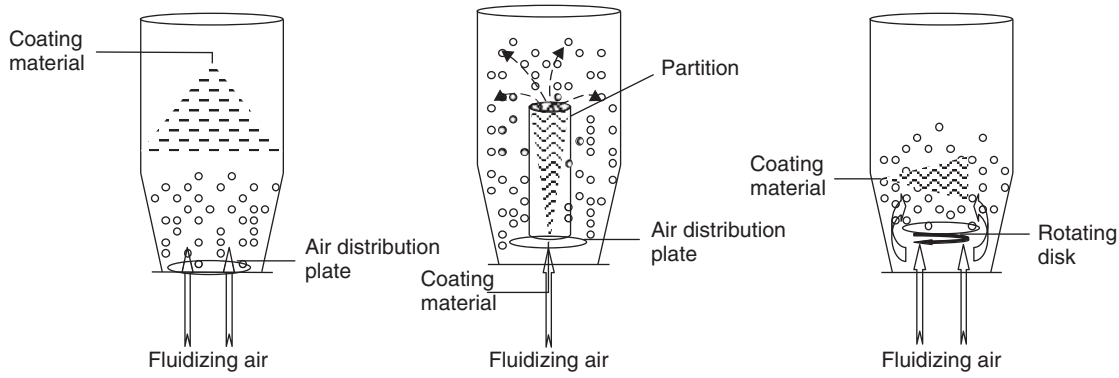


Figure 53.6. Spray coating methods for the microencapsulation of cells: (a) fluid-bed top spray coating, (b) fluid-bed bottom spray coating with the Wurster device, (c) fluid-bed tangential spray coating [from (69,70)].

Spray drying or freeze drying methods, followed by milling and other physical preparation steps are frequently used to produce technical powders of microorganisms aimed for commercial distribution. These powders have a large surface, are very hygroscopic and stable under adequate conditions.

53.6.4 Compression Coating

Recently, the compressing coating has been developed as a promising technique which permits the stabilization of lyophilized bacteria cells during storage (82). This technique involves compressing the lyophilized cell powder into a core tablet or a pallet and then compressing coating material around the core to form the final compact. The compressed cell pallet should be positioned on the center of the die before the rest of the coating material is poured on the top of it and the punch applied, as shown on Fig. 53.7. In this way, two coatings may be formed: the enteric and the outer coating layers. Sodium alginate or pectin can be used as coating material with the addition of a binder compound (such as hydroxypropyl cellulose) to make a more rigid compact. The viability of microbial culture after the compression to form a pallet gradually decreases with the pressure applied during compression procedure (upper punch pressure). Since the compression pressure could have harmful effects on the cells during compaction, careful selection of a pressure which will be employed is needed.

53.6.5 Spray Chilling

In spray chilling, a molten matrix with low melting point (32–42°C) containing the bioactive compound is atomized through a pneumatic nozzle into a vessel. This process is similar to spray drying with respect to the production of fine droplets. However, it is based on the injection of cold

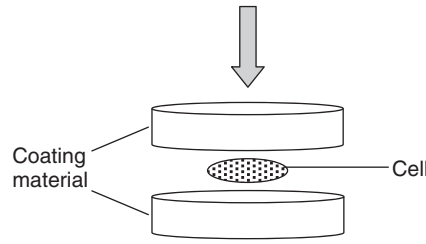


Figure 53.7. Compression coating of cells [from (72)].

air into the vessel to enable solidification of the gel particle, rather than on hot air which dries the droplet into a fine powder particle. The liquid droplet solidifies and entraps the bioactive product. Spray chilling is considered to be the least expensive encapsulation technology and offer few advantages over other encapsulation techniques. It may expand the range of matrices used. Further, it is possible to produce very small particles. However, so far it has been used rarely for cells (rather more suitable for encapsulation of active compounds, like water-soluble vitamins, fatty acids, antioxidants, fatty acids, yeasts, enzymes), since other technologies are easer to establish in laboratories.

53.6.6 Phase Separation (Coacervation)

Coacervates contain the core material suspended in the wall polymer. They are made by liquid–liquid phase separation induced by complex or salt coacervation. The only constraint is that the core material must be compatible with the polymer coating solution and insoluble or weakly soluble in the coacervation medium. There are several versions of the technique such as simple coacervation, salt coacervation, and complex coacervation. In the case of simple coacervation, only one polymer is involved and a phase separation is induced by an addition of an inducer such as ethanol or other water immiscible nonsolvent. In the case

of salt coacervation, phase separation is induced by an electrolyte such as sodium sulphate. The polymer absorbs on the surface of the hydrophobic oil droplets to form the capsule wall. The capsules have the tendency to aggregate. Thus, stabilization step must be provided which is usually based on the addition of cross-linking agents or variation of temperature and/or pH. Complex coacervation occurs through the interaction of two oppositely charged colloids in an aqueous solution, such as cationic gelatin and anionic gum arabic. Several factors determine the size and polydispersity of capsules, such as core material/wall polymer ratio, concentration of stabilizer, agitation speed, viscosity, temperature, and contact time.

53.7 EFFECTS OF IMMOBILIZATION ON CELLS

The study of immobilized cells requires specific experimental techniques. Many biophysical techniques have been used to study immobilized cells *in situ*. Only a few of theses techniques are noninvasive. Some involve the removal of the cells from the immobilization matrix and/or destruction of the sample. The biophysical methods for the direct examination of immobilized cells are overviewed by Willaert and coauthors in a recent report (83).

There are numerous reports on cell physiology, growth, morphology, metabolic activity that may be changed upon immobilization. The reasons for the altered metabolic behavior of cells may be various depending on the type of cells and immobilization method, as well as immobilization parameters. In case of microencapsulation technology, parameters such as microcapsules core status, initial cell density, microcapsule diameter, and membrane formation time influence on the growth, metabolism, and product secretion of microencapsulted microorganisms. Diverse effects on cells upon immobilization have been reported for a variety of type of cells. For example, in case of immobilization of yeast, mass transfer limitations by diffusion (84), disturbance in the growth pattern (85), surface pressure and osmotic pressure changes (86), reduced water activity (87), contacts between cells in limited space (88), changed membrane permeability (89) and availability of nutrients (90) have been attributed to be responsible for changes in cells properties. In specific, the immobilized *Saccharomyces cerevisiae* showed to have increased ethanol production and glucose consumption, higher ploidy and RNA content (85), lower internal pH value (91) and altered glucose catabolic pathways compared to free cells in suspensions, resulted in increased enzyme activity and therefore productivity (92). *Candida tropicalis* cells had higher intracellular levels of Na^+ and K^+ than suspended cells. Moreover, the intracellular environment was more viscous in immobilized cells (93). The immobilization reflected on metabolism of many other microbia cell types like *Propionibacterium acidi-propionici* (94), *Saccharomyces bayanus* (95), *Pichia stipitis* (93), *Escherichia coli* (96), *Pichia farinosa* (97), etc.

Physiology of mammalian cells is even more affected by immobilization than other cell types. However, no detailed investigation has been reported on the effect of both the immobilization matrix and its geometrical configuration on the medium-term viability and physiology of mammalian cells. In a recent study, it has been demonstrated that the shape of the calcium alginate immobilization matrix has considerably different effect on viability and physiology of neuroblastoma cells, whether the gel has a spherical or membrane form (98). Herein, a considerable decrease in the biosynthesis of reduced glutathione and RNA was observed in cell immobilized in thin membrane layers.

It has been demonstrated that cell immobilization has certain additional advantageous physiological effects. Herein, the immobilization reflects on plant cell differentiation and the production of secondary metabolites. In a recent study (99), an increased production of hydrogen peroxide and phenylalanine lyase was revealed in *Vitis vinifera* cells immobilized in pectin/chitosan coacervate capsules, while the immobilization process enhanced hydrogen peroxide and antraquinone synthesis by *Cruciata glabra* up to five times. Since cell growth was reduced in immobilized cultures, substrate consumption and flux of energy consumption were directed to the desired secondary metabolite pathway and improved product yield of the process. In general, the effect of stress factor caused by immobilization and elicitors (the matrix material works as an elicitor, a signal triggering the formation of secondary metabolites) is dependent on cell culture and metabolite pathway. This strategy may be used to improve the production efficiency of different kinds of secondary metabolites, extracellular enzymes, and recombinant proteins in plant cell cultures.

53.8 REACTOR DESIGN

The reactor design is another key factor of immobilized cell technology. It governs the overall fluid dynamic, mass, and heat transfer conditions at the biocatalyst surface. Reactor configuration is related to the choice of cell carrier and various modifications and combinations of stirred-tank, packed-bed, fluidized-bed, gas-lift, and membrane reactors have been proposed for different biotechnological processes. These types of bioreactors operating in a continuous operation mode are shown on Fig. 53.8.

The main issue when considering external mass transfer in immobilized cell systems is the choice between a packed-bed reactor and a fluidized or agitated reactor (100). Most of studies have been made in packed-bed bioreactor.

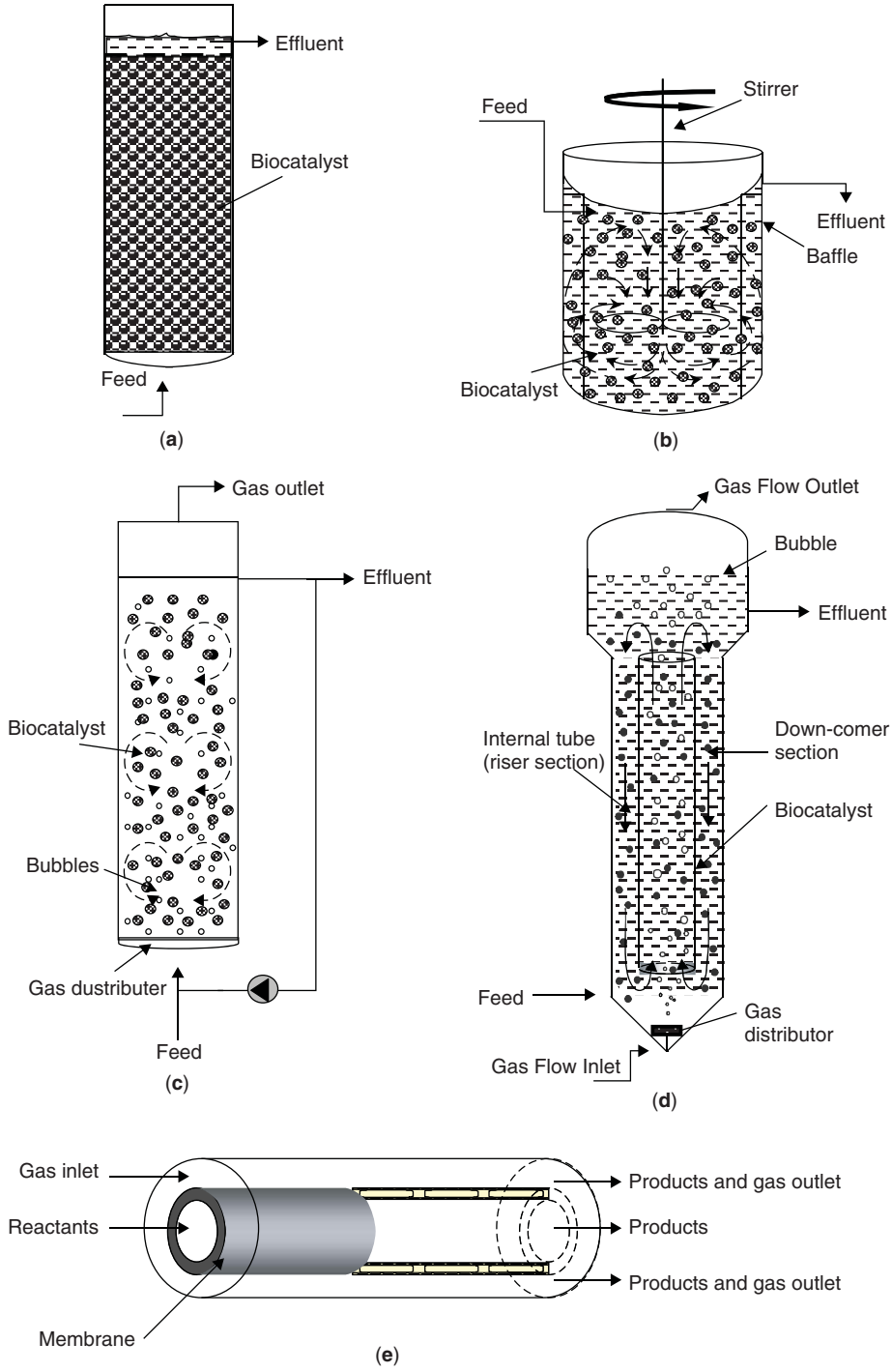


Figure 53.8. Bioreactor designs: (a) packed-bed reactor, (b) stirred-tank reactor, (c) fluidized-bed configuration: straight-bed configuration, (d) gas-lift reactors: internal-loop configuration. (This figure is available in full color at http://onlinelibrary.wiley.com/book/10.1002/9780470054581.)

This type of reactor is traditionally used in industrial-scale productions and fermentation processes. Packed-bed bioreactors are characterized by a simple design, consisting of a column, which is packed with biocatalyst (Fig. 53.8a). Optionally, the column packing can be perfused by the liquid phase or with liquid circulation. The liquid flow is close to plug regime causing low shear rates. This enables usage of various, even fragile materials for cell immobilization.

However, the use of mechanically week materials such as hydrogels can be limited to lower bed heights and liquid flow rates due to possible compression of beads. Therefore, few modifications of packed-bed reactors have been designed and nowadays a variety of packed-bed reactor typologies are available. In one of these, new configurations layers of alginate beads are separated by screens (101). In another one, biocatalysts bed is divided in several chambers. This bioreactor is called multistage fixed bed tower bioreactor (MFBT). The MFBT has been successfully tested both in laboratory and pilot scale in beverage production applications and it seemed to have a great potential (11,102,103). Industrial packed-bed bioreactors put up with several engineering problems linked to mass transfer limitations, the accumulation of evolved gas, (which can be in high concentrations mortal to living cells and reduces the useful volume), the formation of preferential paths or channeling (causing concentration and temperature gradients), excessive pressure drop, as well as short circuiting and clogging. Some of these problems have been reduced by applying the perturbation in the form of pulsation into the fixed bed reactor which generates the slow movements of the bed. These movements regenerate the interfacial area, improve the distribution of the substrate and help to eliminate gaseous metabolites that cause the dead zones. The strategy of bed pulsation has been tried on alcoholic fermentation (104) and the process of phenol biodegradation (105) where layers of immobilized glass beads are separated by perforating plates exposed to pulsation movements. In packed-bed type of reactor, both internal and external mass transfer limitations should be taken into consideration. Some pilot and industrial-scale applications of packed-bed reactors include denitrification of water using sand immobilized heterotropic bacteria (106), sulphate removal using bacteria immobilized on PU foam (107), H_2S removal using bacteria immobilized on Rasching rings (108), beer maturation and low alcohol beer production (109).

The stirred-tank bioreactor was one of the first reactor types used in biotechnology. It consists of a vessel with one or more stirrers (Fig. 53.8b). A stirrer can have a variety of designs to satisfy specific operation conditions. For immobilized cell systems, stirrers providing more gentle mixing (such as helical ribbon, screw or anchor, modified and centrifugal impellers) are preferred instead of turbines and propellers. A vessel is usually equipped with baffles, which facilitate mixing and prevent undesirable bulk rotation since it causes high mechanical stresses in the stirrer shaft, bearings and seal (101). The fluid flow is generally turbulent maintaining an almost ideal mixing of the fluid phase. The shear is highest near the stirrer and gradually decreases toward the walls. Intensive shear rates may cause cell death, therefore, low power inputs are required for shear-sensitive cells. Mechanically weak hydrogel materials can not withstand abrasion during long-term operations.

In the fluidized-bed bioreactors, particles with immobilized cells are fluidized in the liquid up-flow, while gas can be optionally supplied (Fig. 53.8c). It is difficult to maintain low density particles in fluidization and prevent their washout. There is a specific geometry of this type of reactor with the enlargement of the reactor diameter in the upper zone. This geometry provides higher liquid velocities only in the tapered zone (instead of high liquid rates along the whole bed height), therefore the risk of particle washout is decreased. In order to assure particle retention within the reactor, a settling zone is usually installed at the top of the reactor. In the inverse fluidized-bed configuration, biocatalyst particles are fluidized in liquid down-flow. An alternative is a pseudofluidized bed type, where biocatalyst particles are fluidized by gas up-flow. As a consequence of particle fluidization, moderate local mixing is established providing better mass and heat distribution with more uniform liquid flow throughout the reactor volume, as compared to packed-bed reactors. Particle movements and collisions in the fluidized state result in moderate shear stresses and abrasion, creating a need for relatively mechanically stable supports. The scaling up of fluidized-bed bioreactors meets problems due to the difficulties in controlling the bed expansion or biofilm thickness and may encounter hydrodynamic problems; enlargement of distribution devices and/or oxygen saturation systems is also demanding task. Some industrial-scale applications of fluidized-bed reactors include biofilm and sludge blanket reactors for the treatment of wastes (110,111).

Gas-lift bioreactors are very attractive for various applications in biotechnology, because they feature effective mixing, with respect to the liquid and solid phases, pneumatic agitation with no mechanical devices, effective tuning of liquid recirculation, moderate shear stress and good interphase mass transfer. The pressure difference between the gassed and nongassed sections of the reactor provides liquid and solid circulation and efficient mixing. Gas-lift reactors contain base, riser, down-comer and a top section (Fig. 53.8d). They can be constructed as internal-loop or external-loop configuration. Air is commonly used as a gas in aerobic applications, while in anaerobic processes the circulation is induced by an inert gas, alternatively by a gas produced in the reaction. Gas-lift reactors can operate at different flow regimes, and hydrodynamic characteristics under different operating conditions have to be closely examined to achieve optimal external mass transfer. In general, the flow in the riser and down-comer section can be described as plug flow with axial dispersion. Efficient mixing and low shear rates make gas-lift reactors as suitable for all types of immobilization materials. At a lab scale, gas-lift reactors have been utilized for different applications [e.g. for beverage fermentations (112,113), phenol bioconversion (114)], while at an industrial scale, aerobic wastewater

treatments have been preformed in them (110,111). Another commercial application is the production of single cell protein (115).

As compared to conventional reactor types, the design of membrane reactors is relatively more complex and more expensive, mainly due to the high cost of the membrane material. Membrane reactors provide simultaneous bioconversion and product separation. Their usage is payable for production of high value biological molecules. Membrane reactors can be designed as flat sheet or hollow fiber configurations. A simple hollow fiber module is shown on Fig. 53.8e. Polymeric (nylon, polysulfone, teflon, polypropylene) microfiltration or ultrafiltration membranes have been usually used, although other types of membranes have been also investigated, such as ceramic, silicone, or ion exchange membranes. Mass transfer through the membrane is dependent on the pore size and structure as well as on the hydrophobicity/hydrophilicity and surface charge. Cell immobilization can occur on the membrane (as a biofilm), within the membrane or in a cell compartment separated by the membrane.

53.9 CONCLUSIONS

Various types of living cells such as bacteria, yeast, plant, or mammalian cells have been so far successfully immobilized for different applications in industry, medicine, and agriculture. Advantages of immobilized cell technology are numerous, where higher productivities, reuse of biocatalysts, and cell protection are the most important benefits.

There are different approaches how to place cells in a discrete location of a carrier and herein we categorized and described immobilization methods and techniques. Numerous organic and inorganic materials have been used so far as carriers to immobilize cells, while we gave an overview on chemical structure and properties of the most important polymers and proteins used in immobilized cell technology. Microcapsules have specific shell-core design and are mainly used in biomedical application. The manufacture of microcapsules is usually long-term and complex process, and the choice of core and coating materials determines capsule properties (permeability, mechanical properties, biocompatibility).

Reactor configuration is related to the choice of cell carrier. It governs the overall fluid dynamic, mass and heat transfer conditions at the biocatalyst surface. Packed-bed reactors are still the first choice in the industrial sector, mainly due to the simplicity of the design. Other bioreactor types provide better mixing, but high mechanical stresses and shear rates, large power inputs, investment cost, and difficulties in scale up are still the main issues constraining their wider application.

The selection of the suitable carrier and bioreactor system is a challenge and many issues should be taken into account, such as product quality, safety and stability, processing, investment and operating costs, as well as matters of legality. The assessment of the industrial feasibility of the immobilized technology is mandatory for providing cost-effective, large-scale applications. Further application of immobilized cell technology will depend on research results upon preservation of immobilized cells, as well as development of processes that can be readily scaled-up. Thus, research should be oriented toward the evolvement of reliable preservation and storage techniques that could be easily adopted by the industrial sector. Incomplete knowledge of the effects of immobilization on the physiology of cells led to incomplete and partially empirical use of immobilized cell technology. Ongoing basic research is continuing to identify and characterize changes in cell physiology and metabolism upon immobilization. Further research will explore new materials as potential carriers for microbial cells, and develop new or modify existing encapsulation processes.

REFERENCES

1. Pilkington PH, Margaritis A, Mensour NA, Russel I. J Inst Brew 1998; 104: 19–31.
2. Akhtar N, Iqbal J, Iqbal M. J Hazard Mater B 2004; 108:85–94.
3. Ahmadi M, Vahabzadeh F, Bonakdarpour B, Mehranian M. Process Biochem 2006; 41:1148–1154.
4. Kourkoutas Y, Komaitis M, Koutinas AA, Kanellaki M. J Agric Food Chem 2001; 49:1417–1425.
5. Kourkoutas Y, Komaitis M, Koutinas AA, Kaliafas A, Kanellaki M, Marchant R, Banat IM. Food Chem 2003; 82:353–360.
6. Mallios P, Kourkoutas Y, Iconomopoulou M, Koutinas AA, Psarianos C, Marchant R, Banat IM. J Sci Food Agric 2004; 84:1615–1623.
7. Bekatorou A, Koutinas AA, Kaliafas P, Kanellaki M. Process Biochem 2001; 36:549–557.
8. Bekatorou A, Koutinas AA, Psarianos K, Kanellaki M. J Agric Food Chem 2001; 49:373–377.
9. Bardi E, Koutinas AA, Kanellaki M. Process Biochem 1997; 32:691–696.
10. Iconomopoulou M, Psarianos K, Kanellaki M, Koutinas AA. Process Biochem 2002; 37:707–717.
11. Sipsas V, Kolokythas G, Kourkoutas Y, Plessas S, Nedovic VA, Kanellaki M. J Food Eng 2009; 90:495–503.
12. Iconomou L, Kanellaki M, Voliotis S, Agelopoulos K, Koutinas AA. Appl Biochem Biotechnol 1996; 60:303–313.
13. Iconomopoulou M, Kanellaki M, Soupioni M, Koutinas AA. Appl Biochem Biotechnol 2003; 104:23–36.
14. O'Tolle G, Kaplan HB, Kolter R. Annu Rev Micribiol 2000; 54:49–79.
15. Mavituna F. In: Nedovic V, Willaert RG, editors. Volume 8a, Focus on biotechnology: fundamentals of cell

immobilisation biotechnology. Dordrecht: Kluwer Academic Publishers; 2004. pp. 121–139.
16. Eberl L, Molin S, Givskov M. J Bacteriol 1999; 181:1703–1712.
17. Loo CY, Corliss DA, Ganeskhumur N. J Bacteriol 2000; 182:1374–1382.
18. Chapekar MS, Biomed J. Mater Res (Appl Biomater) 2000; 53:617–620.
19. Kourkoutas Y, Bekatorou A, Banat IM, Marchant M, Koutinas AA. Food Microbiol 2004; 21:377–397.
20. Lebeau T, Jouenne T, Junter GA. Enzyme Microbiol Technol 1997; 21:265–272.
21. Kargupta K, Siddhartha D, Sanyal SK. Biochem Eng J 1998; 1:31–37.
22. Strand BL, Skjak-Braek G, Gasetrod O. In: Nedovic V, Willaert RG, editors. Volume 8b, Focus on biotechnology: applications of cell immobilisation biotechnology. Dordrecht: Kluwer Academic Publishers; 2004. pp. 165–183.
23. Burgess DJ. J Colloid Interface Sci 1990; 140:227–238.
24. Chaikof EL. Annu Rev Biomed Eng 1999; 1:103–127.
25. Dautzenberg H, Schuldt U, Grasnick G, Karle P, Muller P, Lohr M, Pelegrin M, Piechaczyk M, Rombs KV, Gunzburg WH, Salmons B, Saller RM. Ann N Y Acad Sci 1999; 875:46–63.
26. Vingerhoeds MH, Harmsen PFH. In: Nedovic V, Willaert RG, editors. Volume 8a, Focus on biotechnology: fundamentals of cell immobilisation biotechnology. Dordrecht: Kluwer Academic Publishers; 2004. pp. 73–102.
27. Vandenbossche GMR, Bracke ME, Cuvelier CA, Bortier HE, Mareel MM, Remon JP. J Pharm Pharmacol 1993; 45:115–120.
28. Thu B, Bruheim P, Espevik T, Smidsrod O, Soon-Shiong P, Skjak-Braek G. Biomaterials 1996; 17:1069–1079.
29. Sakai S, Ono T, Ijima H, Kawakami K. J Microencapsul 2000; 17:691–699.
30. Schneider S, Feillen PJ, Slotty V, Kampfner D, Preuss S, Berger S, Beyer J, Pommersheim R. Biomaterials 2001; 22:1961–1970.
31. Sawhney AS, Hubbell JA. Biomaterials 1992; 13:863–870.
32. Calafiore R, Basta G, Luca G, Boselli C, Bufalari A, Cassarani MP, Giustozzi GM, Brunetti P. Ann N Y Acad Sci 1999; 875:219–232.
33. Robitatille R, Pariseau JF, Leblond F, Lamoureux M, Lempage Y, Halle JP. J Biomed Mater Res 1999; 44:116–120.
34. Strand BL, Gaserod B, Kulseng B, Espevik T, Skjak-Braek G. J Microencapsul 2002; 19:615–630.
35. Rao AV, Shiwnarain N, Maharaj I. Can Inst Food Sci Technol J 1989; 22:345–349.
36. Audet P, Paquin C, Lacroix C. Appl Microbiol Biotechnol 1988; 29:11–18.
37. Kailasapathy K. Lebensm-Wiss Technol 2006; 39:1221–1227.
38. Willaert R, Nedovic V. J Chem Technol Biotechnol 2006; 81:1353–1367.
39. Durieux A, Nicolay X, Simon J-P. In: Nedovic V, Willaert RG, editors. Volume 8b, Focus on biotechnology: applications of cell immobilisation biotechnology. Dordrecht: Kluwer Academic Publishers; 2004. pp. 275–284.
40. Divies C, Cachon R. In: Nedovic V, Willaert RG, editors. Volume 8b, Focus on biotechnology: applications of cell immobilisation biotechnology. Dordrecht: Kluwer Academic Publishers; 2004. pp. 285–294.
41. Ogbonna JC, Matsumura M, Kataoka H. Process Biochem 1991; 26:109–121.
42. Huang J, Hooijmans CM, Briasco CA, Geraats SGM, Luyben KCAM, Thomas D, Barbotin JN. Appl Microbiol Biotechnol 1990; 33:619–623.
43. Yuet PK, Harris TJ, Goosen MFA. Artif Cells Blood Substit Immobil Biotechnol 1995; 23:109–133.
44. Uludag H, De Vos P, Tresco PA. Adv Drug Deliv Rev 2000; 42:29–64.
45. Martinsen A, Skjak-Braek G, Smidsrod O. Biotechnol Bioeng 1989; 33:79–89.
46. Gombotz WR, Wee S. Adv Drug Deliv Rev 1998; 31:267–285.
47. Melvik JE, Dornish M. In: Nedovic V, Willaert RG, editors. Volume 8b, Focus on biotechnology: applications of cell immobilisation biotechnology. Dordrecht: Kluwer Academic Publishers; 2004. pp. 33–51.
48. Thu B, Gaserod O, Paus D, Mikkelsen A, Skjak-Braek G, Toffanin R, Vittur F, Rizzo R. Biopolymers 2000; 53:60–71.
49. Poncelet D, Poncelet SB, Beaulieu C, Neufeld RJ. In: Goosen MFA, editor. Fundamentals of animal cell encapsulation and immobilization. Boca Raton (FL): CRC Press Inc.; 1993. pp. 532–547.
50. Champagne CP, Gaudy C, Poncelet D, Neufeld RJ. Appl Microbiol Biotechnol 1992; 58(5):1429–1434.
51. Cui JH, Goh JS, Kim PH, Choi SH, Lee BJ. Int J Pharm 2001; 210:51–59.
52. Chen KN, Chen MJ, Lui JR, Lin CW, Chiu HY. J Food Sci 2005; 70:260–266.
53. Klein J, Vorlop DK. In: Cooney CL, Humphrey AE, editors. Comprehensive biotechnology. Oxford: Pergamon Press; 1985. pp. 542–550.
54. Krasaekoopt W, Bhandari B, Deeth H. Int Dairy J 2003; 13:3–13.
55. Tosa T, Sato T, Mori T, Yamamoto K, Takata I, Nishida Y, Chibata I. Biotechnol Bioeng 1979; 21(2):1697–1700.
56. Audet P, Paquin C, Lacroix C. Appl Microbiol Biotechnol 1990; 32:662–668.
57. Doleyres Y, Fliss I, Lacrox C. Appl Microbiol Biotechnol 2002; 59:297–302.
58. Chamy R, Nunez MJ, Lema JM. Enzyme Microb Technol 1990; 12:749–754.
59. Anal AK, Stevens WF. Int J Pharm 2005; 290:45–54.
60. Anal AK, Singh H. Trends Food Sci Technol 2007; 18:240–251.
61. Anal AK, Bhopatkar D, Tokura S, Tamura H, Stevens WF. Drug Dev Ind Pharm 2003; 29:713–724.
62. Groboillot AF, Champagne CP, Darling GD, Poncelet D. Biotechnol Bioeng 1993; 42(10):1157–1163.
63. Lacik I. In: Nedovic V, Willaert RG, editors. Volume 8a, Focus on biotechnology: fundamentals of cell immobilisation biotechnology. Dordrecht: Kluwer Academic Publishers; 2004. pp. 103–120.
64. Gaserod O, Smidsrod O, Skjak-Braek G. Biomaterials 1998; 19:1815–1825.
65. de Graaf LA. J Biotechnol 2000; 79:299–306.

66. Riddle KW, Money DJ. In: Nedovic V, Willaert RG, editors. Volume 8a, Focus on biotechnology: fundamentals of cell immobilisation biotechnology. Dordrecht: Kluwer Academic Publishers; 2004. pp. 15–32.
67. Forssell P, Poutanen K, Mattila-Sandholm T, Myllaerinen P. In: Nedovic V, Willaert RG, editors. Volume 8a, Focus on biotechnology: fundamentals of cell immobilisation biotechnology. Dordrecht: Kluwer Academic Publishers; 2004. pp. 65–71.
68. Crittenden R, Laitila A, Forssell P, Maetoe J, Saarela M, Mattila-Sandholm T, Myllaerinen P. Appl Environ Microbiol 2001; 67:3469–3475.
69. Wittlich P, Capan E, Schlieker M, Vorlop K-D, Jahnz U. In: Nedovic V, Willaert RG, editors. Volume 8a, Focus on biotechnology: fundamentals of cell immobilisation biotechnology. Dordrecht: Kluwer Academic Publishers; 2004. pp. 53–63.
70. Jekel M, Buhr A, Willke T, Vorlop KD. Chem Eng Technol 1998; 21:275–278.
71. GeniaLab, Tips&Tricks manual. Available at http://www.geniaLab.de/download/tt-english.pdf. Accessed 2002.
72. Sievers M, Schaefer S, Jahnz U, Schlieker M, Vorlop K-D. Lanbauforschung Völkenrode SH 2001; 241:81–86.
73. Welter K. PhD thesis: Technical University of Braunschweig; 2000.
74. Parascandola P, Branduardi P, De Alteris E. Enzyme Microb Technol 2006; 38:184–189.
75. Groeger H, Capan E, Barthuber A, Vorlop K-D. Org Lett 2001; 3:(13):1969–1972.
76. Agrawal CM, Ray RB. J Biomed Mater Res 2001; 55(2):141–150.
77. Bugarski B, Obradovic B, Nedovic VA, Poncelet D. In: Nedovic V, Willaert RG, editors. Volume 8a, Focus on biotechnology: fundamentals of cell immobilisation biotechnology. Dordrecht: Kluwer Academic Publishers; 2004. pp. 277–294.
78. Pruesse U, Bilancetti L, Bucko M, Bugarski B, Bukowski J, Gemeiner P, Lewinska D, Manojlovic V, Massart B, Nastruzzi C, Nedovic V, Poncelet D, Siebenhaar S, Tobler L, Tosi A, Ikartovska VA, Vorlop K-D. Chem Pap 2008; 62(4):364–374.
79. Champagne CP, Fustier P. Curr Opin Biotechnol 2007; 18:184–190.
80. Jacquot M, Pernetti M. In: Nedovic V, Willaert RG, editors. Volume 8a, Focus on biotechnology: fundamentals of cell immobilisation biotechnology. Dordrecht: Kluwer Academic Publishers; 2004. pp. 343–356.
81. Wurster DE. J Am Pharm Assoc 1950; 48(8):451–460.
82. Chan ES, Zhang Z. Food Bioprod Process 2002; 80:78–82.
83. Willaert R, Verachtert H, Van Den Bremt K, Delvaux F, Derdenlickx G. In: Nedovic V, Willaert RG, editors. Volume 8a, Focus on biotechnology: fundamentals of cell immobilisation biotechnology. Dordrecht: Kluwer Academic Publishers; 2004b. pp. 469–492.
84. Webb C, Fukuda H, Alkinson B. Biotechnol Bioeng 1986; 28:41–50.
85. Doran M, Bailey JE. Biotechnol Bioeng 1986; 28:73–87.
86. Vijayalakshmi M, Marcipar A, Segard E, Broun GB. Ann N Y Acad Sci 1979; 326:249–254.
87. Mattiasson B, Larsson M, Hahn-Haegerdal B. Ann N Y Acad Sci Enzyme Eng 1984; 434:475–478.
88. Shuler ML. World Biotechnol Rep 1985; 2:231–239.
89. Brodelius P, Nilsson K. Eur J Appl Microbiol Biotechnol 1983; 17:275–280.
90. Chen C, Dale MC, Okos MR. Biotechnol Bioeng 1990; 36:993–1001.
91. Galazzo JL, Shanks JV, Bailey JE. Biotechnol Tech 1987; 1:1–6.
92. Galazzo J, Bailey JE. Biotechnol Bioeng 1990; 36:417–426.
93. Lohmeier-Vogel EM, McIntyre DD, Vogel HJ. In: de Bont JAM, Visser J, Mattiasson B, Tramper J, editors. Physiology of immobilized cells. Amsterdam, The Netherlands: Elsevier; 1990. pp. 661–676.
94. Santos H, Pereira H, Crespo JPSG, Moura MJ, Carrondo MJT, Xavier AV. In: de Bont JAM, Visser J, Mattiasson B, Tramper J, editors. Physiology of immobilized cells. Amsterdam, The Netherlands: Elsevier; 1990. pp. 685–687.
95. Taipa MA, Cabral JMS, Santos H. In: de Bont JAM, Visser J, Mattiasson B, Tramper J, editors. Physiology of immobilized cells. Amsterdam, The Netherlands: Elsevier; 1990. pp. 689–691.
96. Karel SF, Robertson CR. Biotechnol Bioeng 1989; 34:320–336.
97. Hoetmann U, Bisping B, Rehm HJ. Appl Microbiol Biotechnol 1991; 35:258–263.
98. Kintzios S, Yiakoumetis I, Moschopoulou G, Mangana O, Nomikou K, Simonian A. Biosens Bioelectron 2007; 23:543–548.
99. Doernenburg H. Process Biochem 2004; 39:1369–1375.
100. Obradovic B, Nedovic V, Bugarski B, Willaert RG, Vunjak-Novakovic G. In: Nedovic V, Willaert RG, editors. Volume 8a, Focus on biotechnology: fundamentals of cell immobilisation biotechnology. Dordrecht: Kluwer Academic Publishers; 2004b. pp. 411–436.
101. Chien NK, Sofer SS. Enzyme Microbiol Technol 1985; 7:538–542.
102. Koutinas AA, Bakaoyianis V, Voliotis S. Appl Biochem Biotechnol 1997; 66(2):121–131.
103. Bakoyianis V, Koutinas AA. Biotechnol Bioeng 1996; 49:197–203.
104. Sanroman A, Roca E, Nunez MJ, Lema JM. Bioprocess Eng 1994; 10:75–81.
105. Shetty KV, Kallifathulla I, Strinikethan G. J Hazard Mater 2007; 140:346–352.
106. Kappelhof JWNM, van der Hoek JP, Hijnen WAM. In: Proceedings of the IWSA International Workshop Inorganic Nitrogen Compounds and Water Supply; 1991 Nov 27–29; Hamburg, Germany. pp. 101–112.
107. Silva AJ, Varesche MB, Foresti E, Zaiat M. Process Biochem 2002; 37:927–935.
108. Giro MEA, Garcia O, Zaiat M. Biochem Eng J 2006; 28:201–207.
109. Lomi H. Brew Dist Int 1990; 55:22–23.
110. Nicolella C, van Loosdrecht MCM, Heijnen SJ. J Biotechnol 2000a; 80:1–33.
111. Nicolella C, van Loosdrecht MCM, Heijnen SJ. Trends Biotechnol 2000b; 18:312–320.
112. Nedovic VA, Obradovic B, Leskosek-Cukalovic I, Vunjak-Novakovic G. In: Thonart PH, Hoffman M, editors. Volume 4, Focus on biotechnology series: engineering and

manufacturing for biotechnology. Dordrecht: Kluwer Academic Publishers; 2001. pp. 277–292.

113. Bezbradica D, Stojanov V, Nedovic V, Obradovic B, Bugarski B, Leskosek-Cukalovic I. In: Proceedings of the 1st International Congress on Bioreactor Technology in Cell, Tissue Culture and Biomedical Applications; Tampere, Finland; 2003. pp. 210–217.
114. Viggiani A, Olivieri G, Siani L, Di Donato A, Marcocchella A, Salatino P, Barbieri P, Galli E. J Biotechnol 2006; 123:464–477.
115. Margaritis A, Wallace JB. Biotechnology 1984; 2:447–453.

FURTHER READING

Flickinger MC, Schottel JL, Bonds DR, Aksan A, Scriven LE Biotechnol Prog 2007 23: 2–17.

Mota M, Yelshin A, Fidaleo M, Flickigner MC 2007, Biochem Eng J 37: 285–293.

Srikanth S, Marsili E, Flickinger MC, Bond DR 2008, Biotechnol Bioeng 99: 1065–1073.

Schottel JL, Orwin PM, Anderson CR, Flickinger MC 2008 J Ind Microbiol Biotechnol 35: 283–290.

Gosse JL, Engel, BJ, Hui JCH, Harwood CS, Flickinger MC 2010 Biotechnol Prog 26: 907–918.

Gosse JL, Flickinger MC 2011 Meth Mol Biol 743: 2213–222.

Fidaleo M., Flickinger mC 2011 Chem Eng Sci 66: 3251–3257.

Jenkins, JS, Flickinger MC, Velev OD 2012 J Colloid INterface Sci 380: 192–200.

Gosse JL, Chinn MS, Grunden AM, Bernal, OI, Jenksin JS, Yeager, C, Kosourov S, Seibert, M Flickinger MC 2012 J Ind Microbiol Biotechnol 39: 1269–1278.

54

IMMOBILIZED ENZYMES

Jose M. Guisan, Lorena Betancor, and Gloria Fernandez-Lorente
Instituto de Catalisis, CSIC, Madrid, Spain

54.1 INTRODUCTION

54.1.1 Enzymes as Industrial Catalysts

Because of their excellent functional properties (activity, selectivity, and specificity), the enzymes are able to catalyze the most complex chemical processes under the most benign experimental and environmental conditions. In fact, enzymes are able to catalyze very fast modifications of a unique functional group among several similar groups from a single molecule (substrate) in the presence of other very similar molecules, under very mild conditions. Therefore, enzymes could be excellent industrial catalysts in a number of areas of the chemical industry: biofuels, fine chemistry, food chemistry, analysis, and so on (1,2). For example, enzymes could be used to (i) transform lignocellulosic wastes (e.g. by mild hydrolysis of cellulose) into simple and valuable organic compounds, (ii) produce biodiesel via transesterification of fats and oils with aliphatic alcohols, (iii) asymmetric synthesis from prochiral ketones or prochiral diesteres, (iv) perform selective oxidations, (v) transform protein wastes into bioactive peptides, and so on.

However, enzymes have been modified throughout the long process of biological evolution, in order to optimize their behavior in the framework of complex catalytic chains inside living beings under stress and regulation. Obviously, enzymes have not been optimized to work inside industrial reactors. Thus, in addition to their excellent catalytic properties, enzymes have also some characteristics that are not very suitable for their industrial application: they are soluble catalysts, they are usually very unstable, they may be strongly inhibited by substrates and products, they work very properly only on natural substrates and under physiological conditions, and so on.

In most cases, enzymes have to be greatly improved before being industrially applied. The engineering of enzymes, from the natural environment inside living beings to the final chemical reactors, is one of the most exciting, complex and interdisciplinary goals of biotechnology. The massive implementation of enzymes as industrial catalysts requires a multidisciplinary utilization of very different techniques (Fig. 54.1): (i) screening of the biodiversity for enzymes with improved properties, (ii) improvement of enzyme properties via techniques of molecular biology, (iii) improvement of enzyme properties via immobilization and postimmobilization techniques, (iv) improvement of enzyme properties via reaction and reactor engineering, and so on. The successful improvement of enzyme properties constitutes one of the key solutions for the development of a much more sustainable chemical industry able to synthesize very complex and useful compounds under very mild and cost-effective conditions.

54.2 IMMOBILIZED ENZYMES AS CATALYSTS OF INDUSTRIAL CHEMICAL PROCESSES

For technical and economical reasons the majority of chemical processes catalyzed by enzymes may be greatly improved by the reuse or the continuous use of the biocatalyst for a very long time (3–6) (Fig. 54.2). Immobilization of enzymes may be defined as any technique able to allow the reuse or continuous use of the biocatalysts. On one hand, from that industrial point of view, simplicity and

Upstream Industrial Biotechnology: Equipment, Process Design, Sensing, Control, and cGMP Operations, Volume 2, First Edition. Edited by Michael C. Flickinger.
© 2013 John Wiley & Sons, Inc. Published 2013 by John Wiley & Sons, Inc.

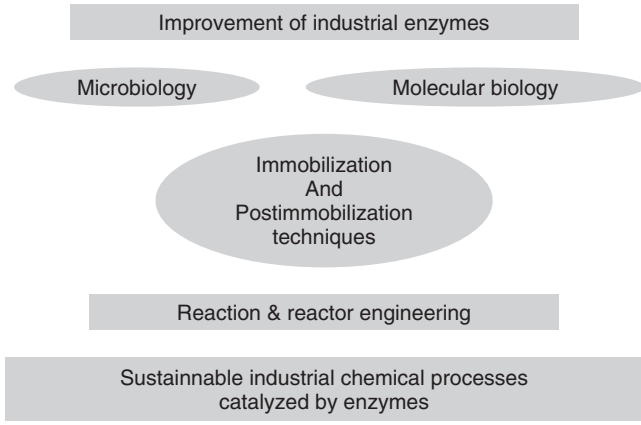


Figure 54.1. Summary of a number of techniques for improving the industrial implementation of immobilized enzymes.

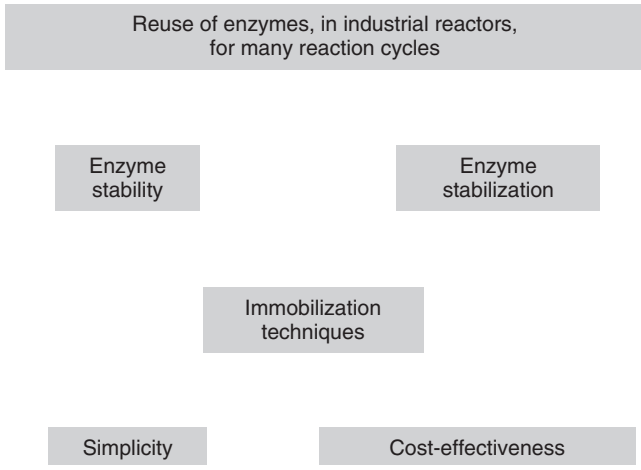


Figure 54.2. Some requisites for preparation of immobilized enzyme derivatives for industrial application.

cost effectiveness are key properties of immobilization techniques. On the other hand, a long-term industrial reuse of immobilized enzymes also requires the preparation of very stable derivatives with additional suitable functional properties for a given reaction (activity, selectivity, etc.) (7–10). At first glance, the practical development of protocols for immobilization of enzymes is intimately related to simplicity, cost-effectiveness, and stability and stabilization of enzymes (Fig. 54.3).

There are excellent revisions on immobilized enzymes and on a number of different protocols for enzyme immobilization. In this chapter, we focus our discussion mainly toward those protocols primarily related with industrial application. We will comment both on very simple protocols for enzyme immobilization and on the current and future protocols, which are able to greatly improve enzyme properties via immobilization techniques.

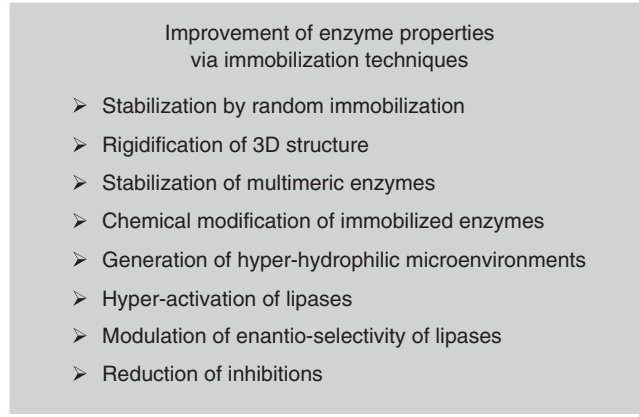


Figure 54.3. A summary of possible improvements of enzyme properties via immobilization techniques.

54.3 CURRENT INDUSTRIAL APPLICATIONS OF IMMOBILIZED ENZYMES

More than a hundred of different industrial biotransformations are catalyzed by immobilized enzymes used mostly for the production of pharmaceutical and agrochemical precursors (11). Some of the most relevant enzymes and products are summarized in Table 54.1 and Table 54.2. In the following sections we summarize the main processes that involve the use of immobilized enzymes.

54.3.1 Enantioselective Hydrolysis

The racemic resolution of *N*-acetyl amino acids via the enantioselective hydrolysis by amino acid acylase is perhaps one of the first industrial processes using isolated immobilized enzymes (11). Currently, immobilized lipases are being used for a number of enantioselective hydrolysis as well as the synthesis of racemic mixtures of chiral esters (containing chiral acyl donors or chiral alcohols). For example, methyl-*p*-methoxyphenyl glycidate is stereospecifically hydrolyzed by means of a lipase. Recently, a process to obtain (*S*)-1-phenylethylamine from the corresponding racemate was commercialized by BASF-Germany (12).

54.3.2 Chemioselective Hydrolysis

Another critical step in the industrial implementation of immobilized enzymes at large industrial scale is the production of 6-amino penicillanic acid from penicillin G using Penicillin G acylase (13). The enzymatic approach allowed the replacement of a complex and poorly sustainable chemical process. The production of acrylamide from acrylic acid using nitrile hydratase also benefited from the use of the immobilized enzyme (14). Immobilized commercial lipases (Novozymes, Amano,

TABLE 54.1. Some Relevant Products Industrially Synthesized with Immobilized Enzymes

Immobilized Enzyme	Product
Glucose isomerase	High fructose corn syrup
Amino acid acylase	Optically pure L-amino acids
Penicillin G acylase	Semi-synthetic penicillins
Nitrile hydrolase	Acrylamide
β-galactosidase	Hydrolyzed lactose
D-amino acid oxidase + glutaryl acylase	Semisynthetic cephalosporins
Thermolysin	Aspartame
Lipases	Lipids with improved properties
Lipases	Optically pure alcohols
Dehydrogenases	Optically pure secondary alcohols

TABLE 54.2. Some Examples of Immobilized Enzymes Commonly Used in Organic Synthesis at Laboratory Scale

Enzymes	Reactions
Esterase, lipases	Ester hydrolysis, synthesis
Amidases	Amide hydrolysis, formation
Dehydrogenases	Oxidoreduction of alcohols and ketones
Oxidases (mono- and dioxygenases)	Oxidation
Peroxidases	Oxidation, epoxidation,
Kinases	Phosphorylation
Aldolases, transketolases	Synthesis of (C–C bond)
Glycosidases, glycosyltransferases	Glycosidic bond formation
Sulphotransferases	Formation of sulphate esters
Transaminases	Synthesis (C–N bond)
Hydrolases	Hydrolysis
Isomerases	Isomerization

etc.) are also used for many processes of interesterification of fats and esterification of fatty acids (15).

54.3.3 Red-ox Processes

An isolated D-amino acid oxidase is used in the transformation of cephalosporin *C* to *R*-keto-adipyl-7-aminocephalosporinic acid, which is an intermediate in the acylase-catalyzed synthesis of 7-aminocephalosporanic acid (ACA) (16). Again, this transformation has successfully replaced a very complex and a poorly sustainable alternative chemical process.

Twenty years ago a process for the continuous regeneration of red-ox cofactors using isolated enzymes was developed (17). The reductive amination of trimethylpyruvate to L-*tert*-leucine was achieved using a combination of leucine dehydrogenase and formate dehydrogenase. This process has now reached ton-scale (18). A similar combination of a principal and an auxiliary dehydrogenase can be used for asymmetric reduction of prochiral ketones (e.g. alfa-keto acids) to optically pure secondary alcohols (e.g. the corresponding *R*-hydroxy acids). In this way, (*R*)-2-hydroxy-4-phenylbutyric acid (an important precursor for acetyl choline esterase inhibitors) can be obtained (19).

54.3.4 Transfer Processes

Glucose-6-phosphate is synthesized by means of a glucokinase starting from glucose in combination with an acetate kinase (20). This process is carried out in multikilogram scale by the Japanese company, Unitika.

54.3.5 Isomerization

The production of high fructose corn syrups by immobilized glucose isomerase is another classical industrial process catalyzed by an immobilized enzyme (21). In this case the enzymatic process comprises a breakthrough as the chemical alternatives are extremely complicated.

In some of the above examples, annual productions are higher than 1000 tons (acrylamide). In most cases the protocols for enzyme immobilization are very simple: adsorption on commercial resins, mild covalent attachement on glutaraldehyde and epoxy activated supports, and so on. In general, these simple immobilization protocols do not greatly improve the enzyme properties. These successful industrial applications are partially due to the good functional properties intrinsic to the enzyme. However, this is not the general case of thousands of very interesting biotransformations reported in the scientific literature (Fig. 54.2). In general, enzymes have to be greatly improved before their industrial implementation. For this reason, as we will propose in the second part of this chapter, the improvement of enzyme properties via immobilization methods could significantly improve the implementation of immobilized enzymes at industrial scale toward a much more sustainable chemistry.

54.4 IMMOBILIZATION PROTOCOLS

54.4.1 Very Simple Protocols for Enzyme Immobilization

Every day, new native enzymes showing good selectivity and stability properties become available (22,23). Under such circumstances, it will be possible to carry out many enzyme catalyzed reaction cycles without the need to improve the enzyme properties using immobilization and postimmobilization techniques. Therefore, it should be very interesting to develop very easy methods to prepare enzyme derivatives to be used at the industry scale.

Some desirable characteristics to develop very simple immobilization protocols can be summarized as follows:

1. Supports (even the whole reactors) should be reusable when the enzyme is inactivated. The inactive enzyme could also be desorbed from the support. Once the clean support has been recovered, fresh enzyme could be added and the whole biocatalysts should be used again. The chance for support reutilization has three important advantages: First, the industrial process becomes much cheaper. Second, high value supports (magnetic particles, macroporous supports with extremely good mechanical properties, etc.) could be used for extremely long periods of time (independent of enzyme stability). Finally, enzymes with a moderate stability (able to resist 20–30 reaction cycles) would become of high industrial interest if the support, and the whole reactor, can be easily recovered and reused.
2. Supports having very good mechanical properties will allow us to develop simple continuous reactors (e.g. high volumes of biodiesel can be produced by using continuous reactors with immobilized lipases). Another attractive industrial application could be the modification of solid substrates with enzymes (e.g. enzymes attached to magnetic particles could be applied to obtain glucose from cellulosic compounds).
3. Supports should be very stable (e.g. chemically inert supports used for physical adsorptions). Very inert/stable supports can be prepared and easily stored long before their use facilitating their transport between companies. This means that the whole enzymatic reactor could be prepared step-by-step in different companies even if they are far away from each other.
4. Immobilization processes should be fast and carried out under mild chemical and physical conditions (neutral pH, low temperature, etc.). Most enzymes are very stable in these conditions and very easy to handle.

The following sections highlight examples of very simple immobilization protocols.

54.5 ADSORPTION OF INDUSTRIAL ENZYMES ON IONIC EXCHANGERS

This is perhaps the simplest protocol for immobilization of enzymes on preexisting supports (24). The majority of the proteins become adsorbed (even at pH 7.0 and 4°C) either on anionic or cationic exchangers. Most of them (with a low isoelectric point) are mainly adsorbed on anionic exchangers. There are a number of organic and inorganic exchangers commercially available and able to strongly adsorb enzymes (e.g. agarose beads, Duolite, Levattit, Amberilite, porous glass, acrylic resins, etc.) (25). These supports containing high densities of quaternary ammonium salts or of sulfopropyl groups are the most suitable for a very intense anionic or cationic enzyme adsorption. Enzyme loadings on some macroporous commercial exchargers reach up to 100 mg of enzyme per gram of support. Commercial ion exchangers span a variety of mechanical properties: (i) some of them are very useful to be used in stirred tanks (e.g. agarose beads) and (ii) others are very useful to be used in packed beds (e.g. acrylic resins). The very high stability of ionic groups allows a full covering of the support surface with enzyme molecules and hence the preparation of very active immobilized biocatalysts.

At first glance, ionic adsorption does not improve the rigidity of immobilized enzyme molecules. However, enzyme molecules fully dispersed in the inner part of a porous structure are protected from some inactivation phenomena: aggregation, proteolysis, interaction with hydrophobic interfaces, and so on. Therefore, in many cases these immobilized derivatives are much more stable than the soluble enzymes.

These types of immobilized derivatives are very suitable for the immobilization of thermostable enzymes acting in anhydrous media or in aqueous media with very low salt concentration. In the presence of high concentrations of buffers or ionized substrates/products the enzyme may become desorbed from the support, for example, 90% of proteins of a crude extract from *Escherichia coli* are desorbed away from commercial DEAE-Sepaharose at 250 m*M* of NaCl (26).

Coating of the surface of a support with a deep and dense layer of ionic polymers [polyethylenimine (PEI), dextran-sulfate, etc.] constitutes an interesting alternative to get a much more intense ionic adsorption of enzymes. These supports, mimicking "ionic flexible and deep beds," have a much higher concentration of ionic groups than conventional supports and their flexible structure allows a better adaptability of the ionic layer to the immobilized enzyme (26–41) (Fig. 54.4). For example, a thermostable beta-galactosidase from *Thermus* sp. remains fully adsorbed of PEI agarose even at 400 m*M* of NaCl (28).

In addition, the very high hydrophilicity of these ionic polymers may also promote the stabilization of the immobilized enzyme against the deleterious effect of organic solvents since it is partially buried inside the hyper-hydrophilic bed (34). Moreover, the flexible structure of the ionic layer may also favor multisubunit adsorption of multimeric enzymes with their subsequent stabilization against dissociation (33).

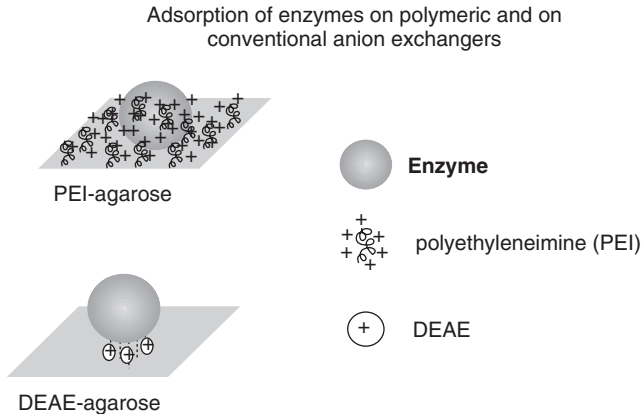


Figure 54.4. Schematic representation of the differences between anionic exchange on new polymeric layers and on conventional supports.

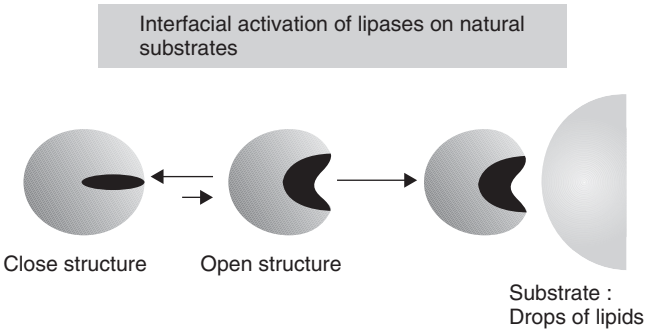


Figure 54.5. Interaction of soluble lipases on drops of lipids.

54.6 SELECTIVE ADSORPTION OF LIPASES ON HYDROPHOBIC SUPPORTS

Lipases interact with any hydrophobic surface like they do on fat surfaces: the enzyme adsorbs on the support surface with the active center lid wide open (35–38) (Fig. 54.5). In addition, this interaction is quite specific, lipases adsorb on hydrophobic surfaces at very low ionic strength and under these conditions most of the proteins are unable to adsorb on hydrophobic surfaces. Thus, purification and immobilization can be achieved in only one step (Fig. 54.6).

Additionally, the lipase-hydrophobic surface complex is fully stable and exhibits hyperactivation when acting on small esters in 100% aqueous media (Fig. 54.7). An important increase in catalytic activity of different lipases adsorbed on octyl-agarose was found by using p-nitrphenyl propionate as substrate (an hyperactivation ranged from 150% for a *Pseudomonas* lipase to 2000% for the *Thermomyces lanuginose* lipase) (37).

Lipases adsorbed on hydrophobic supports can be used both in aqueous and anhydrous media. However, lipases desorb away from the support when using water-cosolvent mixtures with a moderate or high concentration of organic

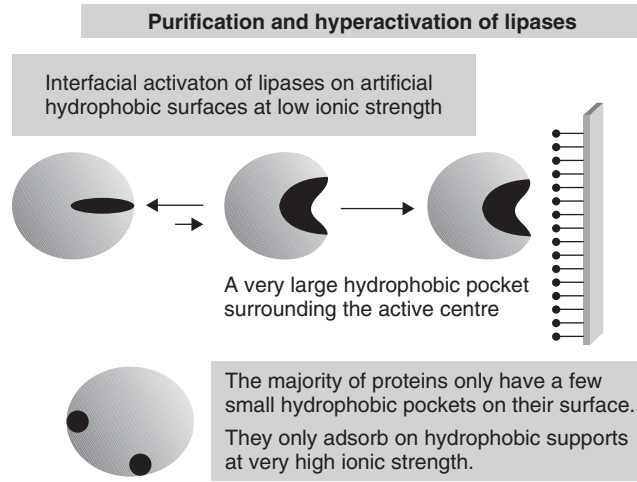


Figure 54.6. Interaction of soluble lipases on hydrophobic surfaces resembling drops of lipids.

Hyperactivation of microbial lipases by adsorption on octyl-agarose

Microbial source	Hyperactivation
C. antarctica - fracción B	200
T. lanuginosa	2000
M. javanicus	300
R. miehei	700
P. fluorescens	150
R. niveus	600

Activity of derivatives is compared with soluble enzymes and it is measured in a fully aqueous medium, at pH 7.0 and 25°C, by using p-nitrophenil propionate as substrate.

Figure 54.7. Hyperactivation (regarding to soluble enzymes) of some microbial lipases after adsorption on hydrophobic supports.

solvents. Other proteins (to be also used in anhydrous media) can also be dispersed on hydrophobic supports with no release of enzyme during such biotransformations (42).

54.7 BIOAFFINITY IMMOBILIZATION

The rationale behind this protocol is the selective adsorption of industrial enzymes on immobilized proteins or ligands. An excellent revision about this immobilization protocol has been recently published by Gupta *et al*. (43,44). The utility of this methodology is based on a number of advantages that are summarized as follows:

1. The purification and immobilization of a target enzyme may be achieved in unison, provided that the specificity of the biorecognition is high; for example, an enzyme adsorbed on its corresponding

immobilized antibody, adsorption of recombinant enzymes tagged with poly-His tails on immobilized metal chelates, and so on.

2. Biorecognition is generally performed under benign experimental conditions (e.g. pH 7.0 y 4°C), which allows for high recoveries of immobilized enzyme activies and the support can be fully loaded with immobilized enzyme.
3. In some cases, the stability of the immobilized enzyme may be enhanced [e.g. the interaction of concanavalin A (Con A) with some glycoproteins] (45).
4. Bioaffinity immobilization is reversible and the immobilized ligand could be reused after a partial inactivation of the immobilized enzyme. The immobilized inactivated enzyme could be then washed away from the support and the immobilized ligand used again to immobilize a new fresh enzyme solution.
5. A correct selection of the immobilized ligand (a lectin, a monoclonal antibody, etc.) may promote the adsorption of the enzyme through regions located far from the enzyme active center. In addition to that, the immobilized ligand may act as a spacer arm. Both effects could contribute to a better accessibility of the immobilized enzyme to macromolecular substrates and even insoluble substrates; for example, cellulases immobilized on nonporous magnetic nanoparticles acting on cellulose.

Some relevant examples of bioaffinity immobilization are as follows:

54.7.1 Adsorption of Enzymes on Immobilized Anti-enzyme Antibodies

Glucose oxidase and horseradish peroxidase have been adsorbed on their corresponding immobilized antibodies. These derivatives were very useful to design "flow injection analysis" of glucose and hydrogen peroxide. In both cases, immobilized enzymes were much more stable than their corresponding soluble counterparts allowing for their reuse in a number of analytical cycles (46). The production of monoclonal antibodies that strongly adsorb a target enzyme through regions far from the active center should allow the simultaneous purification, immobilization, correct orientation, and stabilization of industrial enzymes (47).

54.7.2 Adsorption of Glycosylated Enzymes on Immobilized Lectins

In 1991, Saleemuddin and Husain published an excellent review on the utilization of immobilized Con A for the adsorption of glycosylated molecules (48,49). Immobilized Con A presents itself as a very interesting alternative to tackle the difficult task of immobilizing glycosylated enzymes on preexisting supports. Immobilization on Con A is reversible and a partially inactivated enzyme may be removed by incubation of the derivative in the presence of high concentration of sugars. Very different glycoproteins have been successfully immobilized via this protocol (invertase (49), cellobiose (49), glucose, oxidase (49), etc.). In general, these derivatives are fully active and well-oriented because glycosidic chains are usually not involved in the active center of the enzyme. In some cases highly stable derivatives have also been prepared (49).

Bioaffinity layering (50) recently emerged as a new bioaffinity immobilization methodology. It was developed by immobilizing several superimposed layers of Con A-enzyme on the same support, which provided a significant increase in enzyme loading capacity and thereby highly active derivatives. Dalal and Gupta have applied this methodology for the preparation of very active derivatives of horseradish peroxidase able to be used for the treatment of phenolic wastewater.

54.7.3 Immobilization of Chimeras of Recombinant Proteins on Simple Immobilized Affinity Ligands

Recombinant proteins having a poly-His tail in either the amino or carboxyl terminus may be selectively adsorbed on tailor-made immobilized chelates (51,52). Again, this very selective adsorption may allow the purification and immobilization of industrial enzymes and the preparation of very active derivatives with a fully loaded support (under very mild condition) with pure enzyme (even using a highly impure crude protein extract as the source of the enzyme). The adsorption is very stable at neutral pH and it can be reversed after partial inactivation of enzyme by addition of imidazol (competing with His residues for the support) or by addition of chelating agents such as ethylenediaminetetraacetic acid (EDTA). Although significant stabilization factors should not be expected, a full multisubunit immobilization of dimeric or trimeric enzymes could be achieved if the different poly-His tails (one per subunit) are correctly oriented. As a result, immobilization of multimeric enzymes becomes much more intense and the dissociation of subunits now becomes impossible.

Other interesting chimeras may be constructed by using other tags. For example, a chimera of one industrial enzyme and a cellulose-binding domain can be directly and selectively adsorbed on cellulose supports (53).

54.8 COVALENT IMMOBILIZATION

54.8.1 Introduction

Covalent attachment of enzymes on preexisting supports containing reactive groups is perhaps the most popular protocol for enzyme immobilization. As commented before,

different macroporous supports able to immobilize up to 100 mg of enzyme per gram of support are commercially available. These commercial supports have different and excellent properties to be used in a variety of reactor configurations (stirred tank, packed beds, etc.) and in different reaction media.

A very stable covalent attachment of enzymes on these supports also allows the use of the biocatalysts in any reaction media without desorption of the enzyme: aqueous media at high ionic strength, aqueous media in the presence of high concentrations of cosolvents, organic media, ionic liquids, supercritical fluids, and so on.

The covalent one-point or multipoint immobilization of an enzyme promotes a full dispersion of isolated enzyme molecules on the inner surface of a porous support. This distribution avoids a number of effects that could potentially inactivate the enzyme: proteolysis, aggregation (by cosolvents, at the isoelectric point, etc.), interaction with hydrophobic interfaces (e.g. air bubbles in stirred tanks), and so on. It is for this reason that many authors often correlate immobilization with stabilization of enzymes. However, a real stabilization of the three-dimensional structure of enzymes requires a very careful design of the activated support and the immobilization protocol. In fact, only an intense multipoint covalent attachment of each enzyme molecule to the activated support accomplishes the dramatic stabilization required for the industrial application of immobilized enzymes.

Supports with covalently immobilized enzymes cannot be reused after enzyme inactivation. However, reactivation of the immobilized derivative after partial inactivation of the enzyme (e.g. by unfolding-refolding with urea or guanidine) could allow for reuse of the whole biocatalyst for many reaction cycles.

54.8.2 Immobilization Through the Amino Groups on the Protein Surface

Enzymes can be immobilized through different residues placed on their surface (e.g. Tyr react with diazonium salts, Cys react with reactive disulfide bridges, Asp and Glu (activated with carbodiimide) react with low pK amino groups, etc.). These and other immobilization protocols have been previously described in excellent reviews (54). However, in our opinion, the ideal functional groups for enzyme immobilization are the amino groups (amino terminal plus Lys). Nonionized amino groups are excellent nucleophiles without needing any kind of activation. In general, amino groups are also hydrophilic and abundant in the surface of industrial enzymes (Fig. 54.8).

We can consider two clases of amino groups on the protein surface:

1. Low-pKa amino groups (pK_a around 7.0–7.5). These groups are very reactive for enzyme immobilization (at neutral pH and even at 4°C) in the intermolecular process of reacting soluble enzymes with solid supports containing a high concentration of highly reactive groups. At first glance, only the terminal amino group has such a low pK. However, some Lys residues fairly exposed to the medium but surrounded by some special microenvironments could also exhibit a modified low pK and hence a good reactivity for immobilization.
2. High pK_a amino groups (pK_a around 10.5). Most of the Lys residues are very exposed to the medium and their ε-amino group has a very high pK_a. These Lys groups are poorly reactive for intermolecular immobilization at neutral pH even on highly reactive supports. However, these groups are usually abundant on the enzyme surfaces and they become very useful for further intramolecular multipoint attachment with stable groups on the support after the first process of enzyme immobilization.

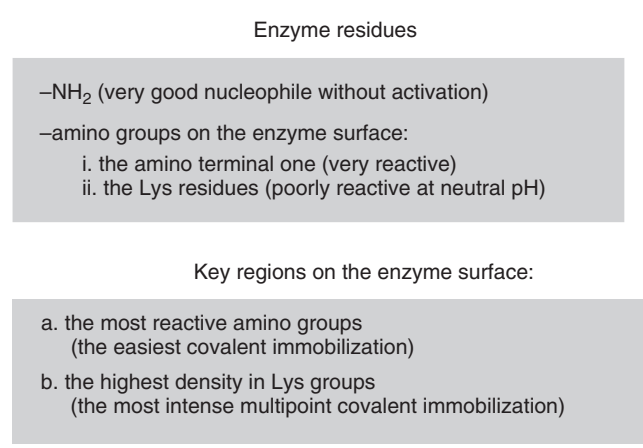


Figure 54.8. Main enzyme residues suitable for intermolecular and intramolecular covalent immobilization of industrial enzymes.

54.8.3 Activated Supports to React with Amino Groups of the Enzyme Surface

The different reactive groups able to react with amino groups of enzymes are shown in Table 54.3. At first glance, all these reactive groups could be useful for the immobilization of enzymes.

The most reactive groups allow the immobilization of a certain concentration of enzymes under very mild conditions. However, the most reactive groups are also very unstable in water and they are unable to allow a full loading of the support with immobilized enzyme molecules. In addition to that, the lack of stability of these highly reactive groups prevents an intense multipoint covalent immobilization with Lys residues (mainly under alkaline conditions where Lys are much more reactive).

TABLE 54.3. Covalent Immobilization Through Their Amino Groups on Differently Activated Supports

Reactive Group on the Support	Stabillity of Reactive Groups	Immobilization Rate at Neutral pH
Tresyl chloride	Very low	Very fast
Cyanogen bromide	Very low	Very fast
Epoxyde	Very high	Very slow
Glutaraldehyde	High	Fast
Glyoxyl	Very high	Very slow—very unstable bonds
N-hydroxy-succinimidyl	Low	Fast

On the other hand, the groups with a low intermolecular reactivity (epoxy, glyoxyl, etc.) are not very useful for simple enzyme immobilization. However, as discussed in subsequent sections, they are the most useful for obtaining very intense multipoint covalent immobilization and highly loaded derivatives.

54.8.4 Enzyme Immobilization on Agarose Beads Activated with Cyanogen Bromide

Agarose beads activated with cyanogen bromide are commercially available (CNBr-Sepharose™ from GE Healthcare). Its active groups are very reactive but also very unstable. In fact, they have to be stored after freeze-drying in the presence of dextran. As commented before this type of very reactive and unstable activated groups are not very suitable for the preparation of industrial biocatalysts. However, the utility of these supports lays in the determination of the industrial potential of a given enzyme (55). By using a diluted crude extract (without purification) a small amount of enzyme is immobilized via a single attachment or a very poor intense multipoint attachment (at pH 7.0, 4°C for 15 minutes and additional blocking with ethanolamine) Thus, fully dispersed immobilized enzyme molecules (without any interaction with interfaces, with proteases or with other proteins) will exhibit the exact functional properties (activity, selectivity, and stability) of the native enzyme. In fact, these derivatives should be used as the suitable control to compare the potential of novel immobilization protocols. On the contrary, the comparison of new immobilized derivatives with concentrated and impure preparations of the soluble enzyme may be influenced by a number of artifacts.

54.8.5 Enzyme Immobilization on Aminated Supports by Using Glutaraldehyde

1. *Aminated Supports Previously Activated With Glutaraldehyde.* Enzyme immobilization on amino-activated supports activated with glutaraldehyde is a straightforward process (56–58). Preactivated supports (amino-supports) are chemically very stable and can be stored, at 4°C, for very long time periods. Additionally, glutaraldehyde activation of these supports is simple and its Generally Recognized As Safe (GRAS) status allows for its utilization in food industry. Glutaraldehyde is attached to secondary amino moieties and hence these supports (at low or moderate ionic strength) have a high capacity to ionically adsorb proteins via anion exchange. In most cases, the first step of this immobilization, at low ionic strength, is a very fast ionic adsorption of the enzyme (pH 7.0, 4°C) on the amino-glutaraldehyde support. The region of the protein surface having a high density of negative charges becomes adsorbed on the secondary amino groups on the support. After the first adsorption, some amino group of the enzyme protein surface (having a low or high pK_a) can quickly react (via intramolecular reaction) with a high concentration of glutaraldehyde groups on the support. This immobilization method allows to immobilize enzymes (through the richest area in negative charges of the protein surface) that otherwise would be hardly adsorbed onto positive ionic supports. The second intramolecular- binding event is so fast that it shifts the adsorption equilibrium toward the full adsorption and reaction of the enzyme onto the aminated support. In fact, only 70% of the proteins from an *E. coli* extract adsorbs onto amine supports at pH 7.0, whereas, 100% of the protein from the same extract absorbs when the aminated support is activated with glutaraldehyde. It is noteworthing that this protocol is not very useful for a very intense multipoint covalent attachment, because of the instability of the glutaraldehyde groups under alkaline conditions necessary for the involvement of many Lys residues in the covalent attachment with the support (57). However, the first very rapid step of ionic adsorption allows the preparation of very highly loaded derivatives.
2. *Physical Adsorption of Enzymes on Inert Ionized Aminated Supports With Further Cross-Linking With Glutaraldehyde.* This protocol, although quite similar to the above mentioned one shows some additional advantages: (i) the enzymes can be adsorbed onto very stable amino-supports without any activation, (ii) enzymes may also be adsorbed on PEI of several sizes and having tertiary, secondary and primary amine groups, (iii) the further addition of soluble glutaraldehyde promotes a more intense multipoint covalent union between the amino groups of the protein surface and the amine groups of the support (58).

However, it must be borne in mind that the addition of soluble glutaraldehyde promotes the modification of all amino groups of the enzyme surface and this overall chemical modification may, in some case, have negative effects on enzyme activity and/or stability.

In general, derivatives obtained by using this second glutaraldehyde protocol are more stable than those obtained when using the first—more conventional—glutaraldehyde protocol (58).

54.8.6 Enzyme Immobilization on Commercial Supports Containing a High Concentration of Epoxy Groups

There are two commercial acrylic resins containing a high concentration of poorly reactive but very stable epoxy groups (Eupergit® C from Rohm Darmstadt and Sepabeads® from Residion-Mitsubishi Chem. Corp.) (6–59). Immobilization of enzymes on these supports is usually performed at very high ionic strength (e.g. 1 *M* phosphate buffer). The resins are moderately hydrophobic and hence enzymes are firstly adsorbed on the supports via hydrophobic adsorption (Fig. 54.9). After the first adsorption, any amino group of the enzyme surface placed in the vicinity of the hydrophobic pockets may become covalently attached (an intramolecular process) to the very dense layer of epoxy groups. The high stability of epoxy groups allows for a further incubation of the immobilized derivatives under alkaline conditions that increases the reactivity of all Lys residues existing in the vicinity of the hydrophobic pockets involved in the first adsorption of the enzyme. Finally, epoxy groups may be blocked with mercaptoethanol or glycine (59). The stability of epoxy supports also allows long time storages and transportation from the manufacturing company to the end-user company. Obviously these very stable supports permit a high loading of immobilized enzyme yielding very active biocatalyst with good prospects for industrial implementation. Again, as commented for glutaraldehyde, poorly reactive epoxy groups only act after a first adsorption of the enzyme, on the support in a second intramolecular event, leading to the covalent attachment of the already immobilized enzyme.

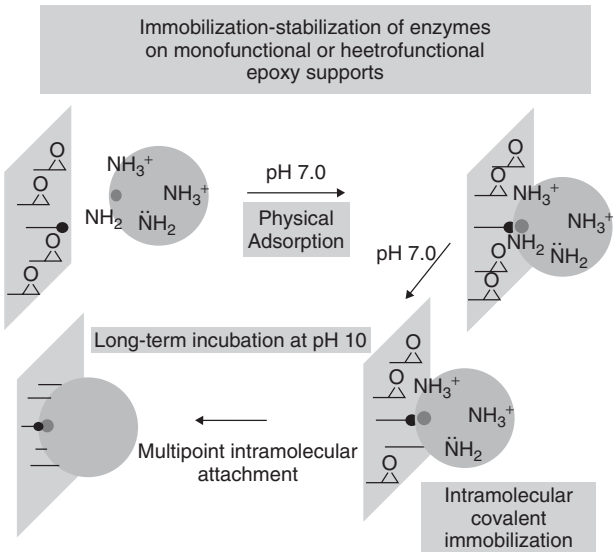


Figure 54.9. Schematic representation of a 2–3 steps process for a single or multipoint covalent immobilization of enzymes on epoxy supports. The Scheme is valid either for hydrophobic commercial supports or for heterofunctional supports reviewed below.

54.9 IMMOBILIZED ENZYMES WITHOUT SUPPORTS

Unsupported immobilized derivatives capitalize on their ease of preparation, their very high volumetric activities and their cost effectiveness. Many of them have industrial potential and in the following section we will summarize some examples of this type of immobilization.

54.9.1 Cross-linking of Soluble Enzymes With Glutaraldehyde (CLEs)

It is probably one of the first developed immobilization protocols that emerged around 1970 (60,61). They are easily prepared by cross-linking of an enzymatic solution with a high concentration of an inexpensive cross-linking agent (e.g. glutaraldehyde). The industrial application of cross-linked enzymes(CLEs) however may be restricted by their final gelatinous structure; for example, for their use in packed bed reactors or filtration steps. The reader is refered to a number of interesting reports on this immobilization protocol (60).

54.9.2 Freeze-Dried Enzymes

In 1980s, Klibanov promoted the use of enzymes in organic media (62). The idea was highly successful and in some cases very practical. The rationale was that because of their lack of solubility in organic media, freeze-dried enzymes (FDEs) or commercial enzyme powders could be used as heterogeneous biocatalyst without being immobilized. These extremely simple enzyme derivatives were very useful to work at laboratory scale, discovering exciting possibilities of industrial enzymes in organic media (63). However, FDEs also may exhibit a number of industrial limitations. For example, enzyme particles have poor mechanical properties, and catalytic activities per gram of solid biocatalyst are usually low (63).

54.9.3 Cross-Linked Enzyme Crystals (CLECs)

The cross-linking of crystallized enzymes with glutaraldehyde was firstly proposed by Quiocho and Richards in 1964 (64) with academic purposes. However, they discovered that these crystals preserved a good percentage of the initial catalytic activity. More than 25 years later, a company called Vertex used the same strategy to develop a method for the preparation of immobilized enzyme catalysts (65,66). These promising derivatives were further commercialized by Altus Biologics (65,66). The advantages of cross-linked enzyme crystals (CLECs) include mechanical robustness and high volumetric activities since almost 100% of their mass is composed by pure enzyme. In addition to that, CLECs usually are very stable, much more stable than soluble enzymes or one-point covalently immobilized derivatives. This stability may be due to the close contact among crystallized enzyme molecules and it is observed against any denaturing agent. On the other hand, CLECs are quite expensive because large amounts of pure and crystallized enzyme are required. Moreover, some enzymes are difficult to be crystallized and additionally the production of large crystal particles (e.g. 100 μm of diameter) is not easy limiting the industrial use of these immobilized derivatives. These extremely active catalyst may be very useful, however, both in aqueous or organic media as an alternative for enzymes exhibiting low intrinsic activity toward interesting nonnatural substrates.

54.9.4 Cross-Linked Enzyme Aggregates

Stable cross-linked enzyme aggregates (CLEAs) can be easily prepared in a two-step protocol (Fig. 54.10). Firstly, aggregation of soluble enzymes is performed in the presence of salts, organic solvents, polymers, and so on, under very mild experimental conditions (pH 7.0, 4°C), in order to be sure that every enzyme molecule remains fairly active. After a rapid aggregation, a strong stirring is promoted in order to get small particles of enzyme aggregates. Finally, enzyme aggregates are stabilized by using different cross-linking agents (i.e. glutaraldehyde). This method produces insoluble CLEAs once the aggregating agents are rinsed out. This methodology was first developed in Prof Sheldon′s laboratory and has allowed the easy preparation of a number of very active derivatives of industrial enzymes (67–71). The technique may also allow some interesting improvements of enzyme properties: (i) different enzymes can be coimmobilized if they must work close together, (ii) enzymes and highly hydrophilic polymers can be coimmobilized in order to improve the stability of enzymes against oxygen or organic solvents, (iii) enzymes and polymers containing a number of primary amino groups (i.e. PEI) can also be coimmobilized to enhance the intensity of chemical cross-linking (e.g. when using enzymes which are relatively poor in lysine residues), (iv) very complex quaternary structures of multimeric enzymes can be highly stabilized—avoiding subunit dissociation—as cross-linking agents keep the structure tightly joined.

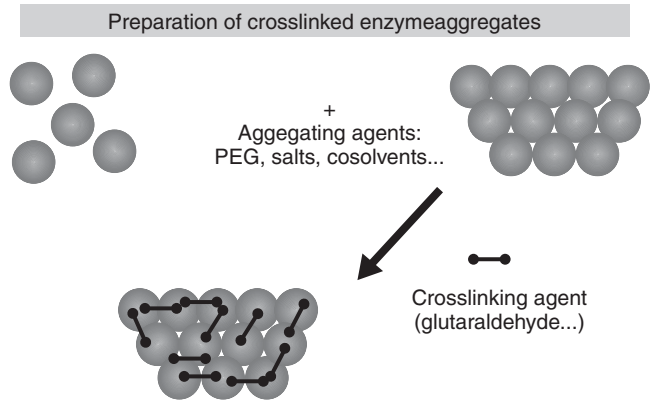


Figure 54.10. Schematic representation of the very simple preparation of cross-linked enzyme aggregates.

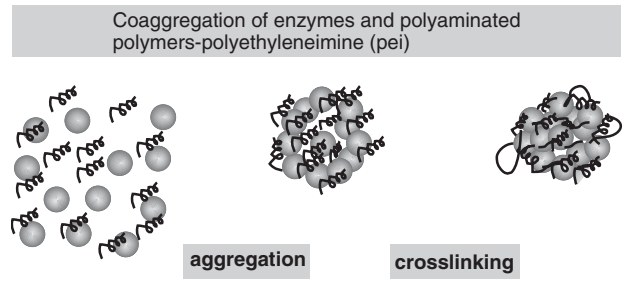


Figure 54.11. Coaggregation of enzymes and polyethylenimine.

This method can be applied to any enzyme and absolute purity is not necessary. Obviously, this method becomes much easier to use with enzymes from thermophilic microorganisms; these enzymes are more resistant toward aggregation processes and toward chemical modifications.

A scheme of the two main protocols for the preparation of CLEAs is shown in Fig. 54.10 and Fig. 54.11.

The CLE as a methodology is now reported by several research groups. The additional advantages of CLEAs are now more deeply commented:

1. *Stabilization of Multimeric Enzymes.* When multimeric enzymes are chemically cross-linked every enzyme subunit also becomes cross-linked avoiding dissociation. This advantage can be achieved even for complex multimeric enzymes (hexameric, heteromultimeric, etc.) that are difficult to stabilize

by immobilization on preexisting supports. Figure shows the stabilization of bovine liver catalase. Cross-linked derivatives are much more stable than their soluble counterparts. In addition to that, inactivation of cross-linked aggregates does not depend on dilution. When using nonstabilized derivatives a more diluted suspension inactivates much more rapidly because dissociation of subunits is favored. Similar stabilizations could be obtained via the CLEC methodology.

2. *Enzyme Stabilization Against Organic Solvents.* Coaggregation of enzymes and highly hydrophilic polymers (i.e. PEI) may produce a hydrophilic environment around the surface of every aggregated enzyme molecule. Thus, when the derivative is used in the presence of high concentrations of organic cosolvents there might be a partition effect of the cosolvent between the bulk solution and the enzyme environment. Owing to this partition effect the enzyme is in contact with a much lower concentration of organic cosolvent. In this way, the deleterious effect of the cosolvent becomes highly diminished (69) (Fig. 54.12). Obviously, cocrystallization of enzymes and polymers is not possible.
   In the best case, coaggregation of complex multimeric enzymes from thermophilic organisms and highly hydrophilic ionic polymers (with primary amines) will produce easy to prepare derivatives with high activity and stablity against dissociation and organic solvents.
3. *CoAggregation of Two Enzymes Acting in Tandem.* In some cases (e.g. oxidases plus catalases) two enzymes may act consecutively and the intermediate product (e.g. hydrogen peroxide) may be deleterious for the stability of both enzymes. In these cases, an instant removal of the product by the second enzyme is strictly necessary. Coaggregation may facilitate this instant removal of the toxic intermediate product. In other cases, the intermediate product may be very unstable hence its immediate modification may be strictly necessary. These "combi-CLEAs" may be an important practical alternative which again is not possible via cocrystalization of two very different enzymes (67).

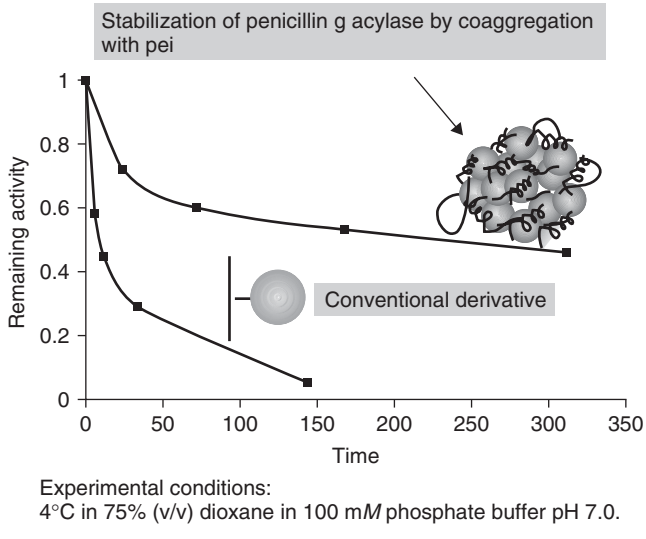


Figure 54.12. Time-course of inactivation by cosolvents of penicillin G acylase coaggregated with polyethyleneimine.

54.10 IMPROVEMENT OF ENZYME PROPERTIES BY IMMOBILIZATION TECHNIQUES

The majority of the enzymes of industrial interest are not very stable for reuse for long periods of time. In addition, enzymes may be poorly active and selective when acting on nonnatural substrates. For these reasons, as mentioned in the section titled Introduction, the additional improvement of enzyme properties through the necessary immobilization techniques became quite an exciting technological approach (72). Random immobilization of unstable or poorly active industrial enzymes is not very relevant from an industrial point of view. On the contrary, some interesting protocols to improve enzyme properties, with special emphasis in stabilization, will now be described:

54.10.1 Stabilization of Enzymes by Multipoint Covalent Immobilization: Glyoxyl-Agarose

The establishment of a number of attachments between every immobilized enzyme molecule and the support should exert very interesting stabilizing effects. When spacer arms (between the enzyme and the support) are very short and the support is very rigid, we can assume that all the relative positions among the enzyme residues involved in multipoint immobilization have to remain unmodified during any conformational change induced by any distorting agent (heat, organic cosolvents, etc.). Thus, the intensity of these conformational changes should be strongly diminished (Fig. 54.13). This very interesting hypothesis has been already established from the beginning of enzyme technology (around 1977) (73,74). However, currently, 40 years later, there are only very few immobilization protocols useful to promote very intense enzyme-support multipoint covalent immobilizations (75).

The internal morphology of agarose gels is composed of large highly hydrophilic fibers with a high geometrical congruence with proteins surfaces (76). At first glance, these gels when activated with glyoxyl groups (small

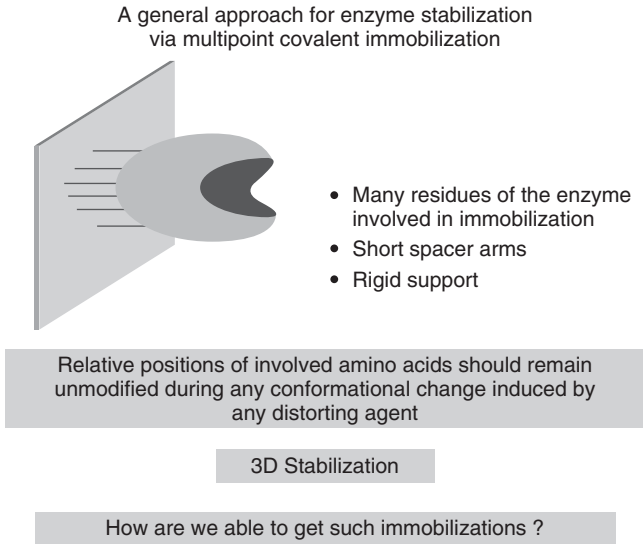


Figure 54.13. Rational explanation of the stabilizing effect promoted by multipoint covalent immobilization.

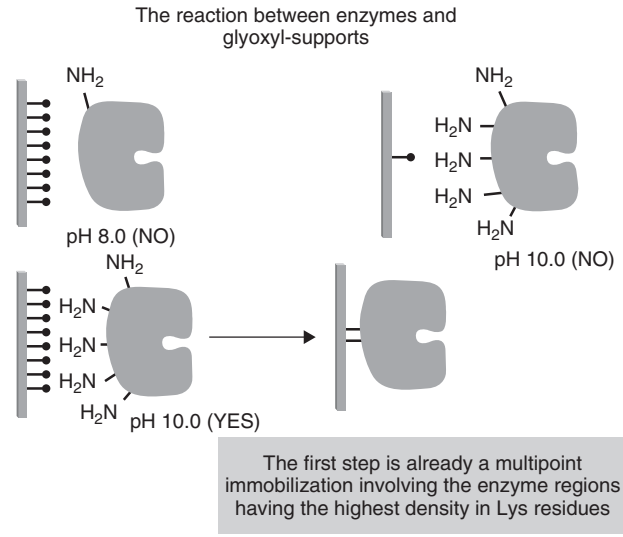


Figure 54.14. Some special features of immobilization of enzymes on glyoxyl activated supports.

aliphatic aldehydes) are very unsuitable for "enzyme immobilization." However, under "tailor-made" conditions, they seem to be the most adequate to get dramatic immobilization-stabilization of industrial enzymes. These activated gels are very easy to prepare and very stable (76) and they are commercially available from Biotica S.A. (76).

The binding between a unique glyoxyl group and a unique unionized amino group yields a very unstable Schiff's base, which tends to total dissociation. In fact, very highly activated glyoxyl-agarose (e.g. 100 μmols per mL of support) is not able to immobilize an enzyme at pH 7.0 (Fig. 54.14). Under these conditions, in most of the cases, enzymes have only one unionized amino group on their surface (perhaps the amino terminal one) since the pK of fairly exposed surface Lys groups is too high (higher than 10). On the other hand, poorly activated glyoxyl-agarose (e.g. 1 μmol per mL of support) is also not able to immobilize an enzyme at pH 10.0 (containing a number of reactive amino groups). However, the combination of very highly activated supports (100 μmols/mL) and very highly reactive enzymes (at pH 10.0) promotes a very rapid and irreversible immobilization of all enzymes (at least more than 50 different enzymes tested in our laboratory) (76–89). This result (and other experimental evidences already reported) seem to indicate that even the first immobilization process has to be a multipoint covalent attachment (77,78). Obviously, such type of immobilization should mainly occur through the region of enzyme surface having the highest density in Lys groups. That is, the best region to get a very intense multipoint covalent attachment after a long incubation (at

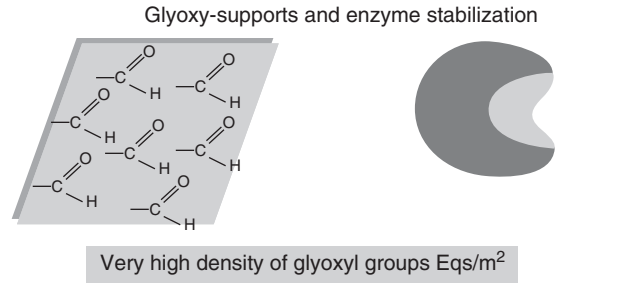


Figure 54.15. Overall advantages of glyoxyl supports to promote very intense and stabilizing multipoint covalent immobilizations.

pH 10 and 25°C) between the immobilized enzyme and the highly activated support containing very stable active groups. In fact, immobilized trypsin has formed seven linkages with the support per enzyme molecule having only 15 Lys residues on their surface (77).

In addition to that, the transformation of primary amino groups into secondary amino ones promotes a very small physicochemical modification of the enzyme surface, in

spite of a very intense multipoint attachment. For this reason, many enzymes have been dramatically stabilized with very small decrease of catalytic activity.

The overall characteristic of glyoxyl-agarose (Fig. 54.15) for multipoint covalent immobilization of enzymes cannot be found for more conventional immobilization protocols [cyanogen bromide (BrCN) supports, glutaraldehyde supports, National Health Service (NHS)-supports, etc.].

In fact very interesting stabilizations have been observed for different monomeric enzymes, which are associated with very small decrease of catalytic activities. Inactivation experiments made by comparison of stabilities of multipoint immobilized derivatives and stability of one-point immobilized ones (prepared by using very lowly activated supports). In this way, the stabilization factors reported in the Fig. 54.16 really represent the 3D rigidification of enzyme structures. Interesting stabilizing factors that are intrinsic to random immobilizations (no aggregation, no interaction with interfaces, etc.) are identical for the two types of derivatives. Similar stabilization factor for 3D structures of industrial enzymes are hardly reported in scientific literature.

Moreover, rigidification of enzymes by a very intense multipoint covalent immobilization should promote stabilization against any distorting agent (heat, organic cosolvents, saturating concentrations of organic solvents, pH, etc.) (89). Agarose beads are excellent supports for this type of stabilization. They are initially and finally very hydrophilic, they have a very high density of modifiable hydroxyl groups, they are very resistant to stirring and hence, very suitable to be used in stirred tank, and so on. However, this protocol for enzyme stabilization is not exclusive of agarose beads. Similar dense layers of glyoxyl groups can be also synthesized on the surface of very different solid supports (porous glass, polyacrylamides, cellulose, magnetic particles, etc.).

Some enzymes highly stabilized by multipoint covalent attchment on glyoxyl-agarose

Enzyme	Activity(%)	Stabilization
Trypsin	75%	10.000
Chymotrypsin	70%	60.000
Penicillin G acylase from *E. Coli*	70%	8.000
Penicillin G acylase from *K. citrophila*	70%	7.000
Ferredoxin NADP reductase from Anabaena	60%	1.000
Lipase from *C. rugosa*	50%	150
Glutamate racemase	70%	1.000
Esterase from *B. stearothermofilus*	70%	1.000
Thermolysin from *B. thermoproteolyticus*	100%	100

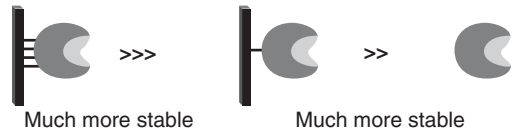


Figure 54.16. Some example of enzymes highly rigidified by multipoint covalent immobilization.

54.10.2 Stabilization of Enzymes by Multipoint Covalent Immobilization: Heterofunctional-Epoxy Supports

Immobilization on glyoxyl-agarose is, very likely, the most precise protocol to get very intense enzyme-support multipoint covalent attachments: the enzyme becomes immobilized through its surface region having the highest density of Lys (amino) groups. However, it is also probable that many enzymes may have different surface regions with different sensitivity against inactivation by different distorting agents. For example, a very flexible region close to the active center may be much more relevant to inactivation than a very robust one far from the catalytic site. On the other hand, sometimes multipoint attachment has to be promoted on the opposite side of the active center even with a less intense stabilization (e.g. enzymes acting on macromolecular substrates). Thus, the promotion of intense multipoint attachment on different regions of the enzyme surface may be quite interesting. As commented before, epoxy groups are very poorly reactive for immobilization (an intermolecular process) at neutral pH. The enzyme has to be adsorbed on the support before a covalent attachment between amino groups of the enzyme surface and a dense layer of epoxide groups on the support takes place. For this reason, in addition to monofunctional commercial epoxy supports (the enzyme is firstly adsorbed via hydrophobic adsorption), a number of hetero-functional epoxy supports can also be prepared, in order to promote different first adsorptions of the enzyme through different regions of the enzyme surface: (i) Immobilized Metal Affinity Chromatography (IMAC)-epoxy support promotes a first adsorption through the region containing the highest density of histidine groups, (ii) carboxy-epoxy support promotes a first adsorption through the region with the highest density of positively ionized groups, (iii) ionized amino–epoxy supports promote a first adsorption through the region with the highest density of negative charges, and so on. The amino-epoxy support is commercially available from Resindion-Mitsubishi Chem. Corp. and will be used as an example of this immobilization protocol.

We will now discuss the rigidification of enzymes, through the surface region with the highest density of negative charges (e.g. Asp + Glu), by using a highly activated commercial amino-epoxy supports (90–94).

The ideal amino groups on the support should have a pK around 9–10 in order to be easily modified with epoxy reagents and, after modification, to become ionized (as secondary amino groups) at pH 7.0 and 4°C. In this way, a very simple first adsorption of enzymes by anionic exchange may be achieved.

A three-step immobilization protocol on hetero-functional epoxy supports is represented in Figure 9.

This mechanism of immobilization is similar (the first two steps) to the one commented for glutaraldehyde activated supports. However, the stability under alkaline conditions of epoxy groups allows a third step of alkaline incubation that may now promote an intense multipoint covalent attachment, and much more intense enzyme stabilization. In general enzymes stabilized on amino-epoxy supports are much more stable than those immobilized via glutaraldehyde.

54.10.3 Stabilization of Multimeric Enzymes

Many enzymes of industrial interest have a quaternary structure and are composed of several subunits whose dissociation leads to the total loss of the catalytic activity (95). Prevention of subunit dissociation constitutes a key point to accomplish enzyme stabilization. A two-step protocol has been proposed to get such stabilization (Fig. 54.17): (i) first, an immobilization of the enzyme on highly activated supports involving the highest possible number of enzyme subunits and (ii) an additional cross-linking of all subunits (mainly those not immobilized on the support) by using polyfunctional flexible polymers (i.e. aldehyde-dextrane polymers of several sizes able to react with lysines located in different subunits of the enzyme). All the multimeric proteins from a crude extract from *E.coli* have been stabilized by this strategy. In addition, several successful stabilizations of relevant multimeric enzymes have also been reported (96,97).

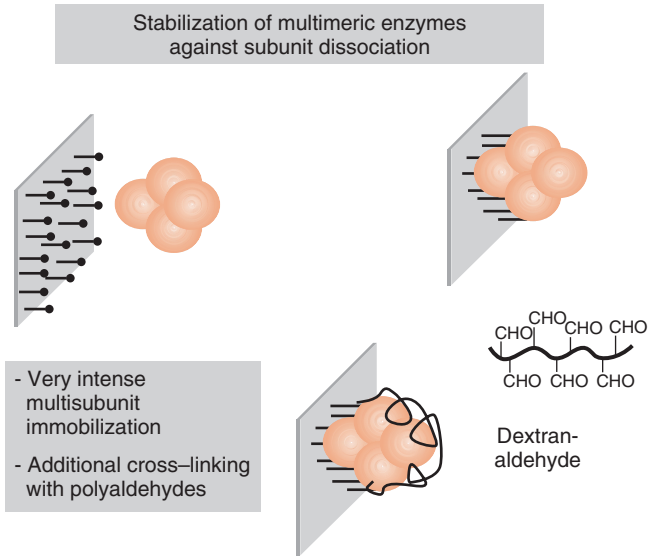


Figure 54.17. Schematic representation of a general strategy for stabilization of multimeric enzymes. (This figure is available in full color at http://onlinelibrary.wiley.com/book/10.1002/9780470054581.)

Glyoxyl supports have been used in the past to obtain a multisubunit immobilization of several enzymes with the additional advantage of a simultaneous rigidification of each immobilized subunit (97). This interesting complementary approach of multisubunit and multipoint immobilization requires the use of very highly activated support.

54.11 MODULATION OF SELECTIVITY OF LIPASES BY USING DIFFERENT IMMOBILIZATION METHODS

Lipases undergo important conformational changes during their catalytic action even in fully hydrophilic environments: an equilibrium is established between the close inactive form and the open active counterpart (98). Lipase open and close structures exhibit very different conformations even in regions quite far from the active center. Thus, the immobilization of the same lipase using different methods (e.g. via rigidification of different regions, etc.) would determine the degree of exposure of the active center. Therefore, by using different immobilization protocols it may be possible to involve different lipase regions, altering the mechanism of opening of the lipase as well as the exact conformation of the open active center. In fact, it has been observed that by using very different lipases, different immobilized derivatives of the same lipase may display very different enantio-selectivity, (from 1 to 100 *R* or 100 *S*) when hydrolyzing racemic mixtures of different chiral ester substrates (98–103).

54.11.1 Reactivation of Immobilized Enzymes

Reactivation of partially inactivated enzyme derivatives permits a much longer reuse of an immobilized enzyme catalyst. The most sustainable enzyme processes are developed under relatively mild conditions (moderate temperatures, moderate pH values, presence of inert solvents or cosolvents, etc.). Under these conditions, the primary structure of the immobilized enzyme should remain fully inalterated (104). Slight distortions of the 3D structure of the immobilized enzyme should be the only cause of its inactivation. A simple reincubation of the partially inactivated derivative under very mild conditions (pH 7.0, 25°C) for long incubations (24 hours) may in some cases promote the near full recovery of the initial activity (105). Each immobilized biocatalyst could then be reactivated several times and its operational stability would be strongly increased. In other cases, reactivation may be more complex and activity recovery may be low. It is possible that responding to the conformational changes promoted by a distorting agent the enzyme structure iterates until it encounters a fairly stable incorrect configuration. It has been described that complete disruption of

incorrect enzyme structures can be achieved via incubation of inactivated enzyme derivatives in the presence of urea or guanidine. Then, the further reincubation of the random-coiled immobilized enzyme molecule may promote a rapid and correct refolding up to the fully active structure.

The above-mentioned reactivation strategies are better developed using covalently immobilized enzymes on hydrophilic and inert support surfaces. In that case, unfolded enzymes do not desorb away from the support, interactions between several unfolded enzyme structures are impossible and new interactions between the distorted enzyme and the support are avoided. In addition to its stabilizing effect multipoint covalent immobilization also favors the correct refolding of inactivated enzymes (105).

54.12 FUTURE PROSPECTS: IMMOBILIZATION OF ENZYMES ACTING ON INSOLUBLE SUBSTRATES

Hydrolysis of cellulose, starch, solid proteins and other insoluble substrates are very relevant topics in Enzyme Biotechnology. Currently, the use of lignocellulosic wastes for the production of clean and renewable energy sources is of increasing interest (106). The possibility of reusing hydrolytic enzymes for many reaction cycles would greatly improve the practical potential of these processes. Considering that enzymes immobilized on porous supports are unable to hydrolyze these insoluble substrates new alternatives are required:

54.12.1 Immobilization of Enzymes on Nonporous Magnetic Nanoparticles

These supports (30–100 nm of bead diameter) have a similar loading capacity than conventional porous supports (40–100 mg of enzyme per gram of catalyst). A range of magnetic nanoparticles coated with different structures (polystyrene, polyvinyl alcohol, etc.) are currently available and can be activated for ionic, covalent or affinity immobilization of industrial enzymes. Magnetic particles should be resistant to abrasion and they are easily handled by using a magnet. They can be used as a support for all the immobilization techniques commented herein. However, in addition to a profitable stabilization (e.g. by multipoint covalent attachment of enzymes on the nanoparticles), a correct orientation of the active center of the enzyme accessible to insoluble substrates is in this case strictly necessary. Hetero-funcional epoxy or glyoxyl supports could be therefore an interesting alternative to get rigidification of a given enzyme with different orientation on magnetic nanoparticles (107).

54.12.2 Use of DNA Hybridization as a Thermo-Reversible Immobilization Protocol

Conjugation of an enzyme with a DNA probe and immobilization of the complementary probe on one support may allow the recovery of the soluble enzyme at high temperatures (e.g. required for cellulose hydrolysis). At the end of the process temperature is lowered and the enzyme becomes immobilized on the support via DNA–DNA hybridization (108).

54.12.3 Immobilization of Enzymes on Smart Polymers

Smart polymers are soluble molecules that can be precipitated by an appropriate stimulus such as changes in pH, temperature, and so on. The immobilization of enzymes on smart polymers has been excellently reviewed by Roy and Gupta (109). There are natural and synthetic smart polymers (alginates, Eudragit, etc.). Perhaps the synthetic polymers are more suitable for practical use. Then, during a reaction the polymer could be kept in solution while the enzyme (e.g. xylanase) is acting on the insoluble substrate (e.g. xylan). At the end of the reaction, the enzyme is precipitated, the reaction mixture is filtrated, and the enzyme could be then reused for new reaction cycles in a soluble manner (110–112).

54.13 CONCLUDING REMARKS

In this chapter, different protocols for enzyme immobilization have been commented. Rather than an exhaustive description of every immobilization protocol, we have selected those that, in our opinion, are the more suitable for industrial implementation. In general, the main advantages and possibilities of each protocol have been remarked. In some cases, we have also proposed some protocols that may now be quite complex and expensive: the utilization of magnetic nanoparticles as supports for immobilization, the use of monoclonal antibodies as immobilized affinity ligands, and so on. However, on the basis of the recent great advances in nanotechnology and immunology it could be assumed that these protocols will become economic and technologically suitable within the next few years. The existence of several interesting immobilization methods allows us to select the most suitable support and the most suitable immobilization protocol for each application. Different immobilization protocols should be selected depending on: (i) the added value of the corresponding reaction product, (ii) the stability and selectivity of the soluble enzyme, (iii) the reaction conditions (e.g. to use very high substrate concentrations), (iv) the environmental requirements, and so on.

In recent years, advances in a number of sciences such as microbiology, molecular boilogy and metagenomics have contributed to the availability of improved soluble enzymes. We anticipate that with such readily available better enzymes, very simple immobilization protocols will be used. For example, a very simple commercial derivative of one lipase (from *Rhizomucor miehi*e) can be used for 2 years catalyzing the esterification of fatty acids. In this and similar cases, the cost of the immobilized biocatalyst is minimized and the further improvement of enzyme properties (stabilization, reactivation, reuse of the support, etc.) may not be necessary. The mechanical properties of the support may then become a more critical parameter than the enzyme stability. However, in many instances the improvement of enzyme properties during and after immobilization will be strictly necessary: more inexpensive, more intensive or more selective processes will be necessary: biodiesel synthesis, hydrolysis of cellulose, bioactive ingredients, chemically improved foods, and so on. In these cases the availability of stable enzymes, the development of strategies for immobilization–stabilization (e.g. multipoint covalent immobilization), the design of strategies for reactivation of partially inactivated immobilized enzymes, and so on, will be strictly necessary for a much more massive implementation of enzyme processes at an industrial level.

REFERENCES

1. Koeller KM, Wong CH. Nature 2001; 409: 232–240.
2. Wong C-H, Whitesides GM. Enzymes in synthetic organic chemistry. Oxford: Pergamon Press; 1994.
3. Bickerstaff GF. Immobilization of enzymes and cells, Methods in biotechnology 1. Totowa (NJ): Humana Press; 1997.
4. Guisan JM. Immobilization of enzymes and cells, Methods in biotechnology 22. 2nd ed. Totowa (NJ): Humana Press; 2006.
5. Chibata I, Tosa T, Sato T. J Mol Catal 1986; 37: 1–24.
6. Katchalski-Katzir E, Kraemer DM. J Mol Catal B Enzym 2000; 10: 157–176.
7. Klibanov AM. Anal Biochem 1979; 93: 1–25.
8. Gianfreda L, Scarfi MR. Mol Cell Biochem 1991; 109: 97–128.
9. Cao L. Curr Opin Chem Biol 2005; 9: 217–226.
10. Bornscheuer UT. Angew Chem Int Ed Engl 2003; 42: 3336–3337.
11. Wandrey C, Liese A, Kihumbu D. Org Process Res Dev 2000; 4(4): 286–290.
12. Balkenhohl F, Ditrich K, Hauer B, Ladner W. J Prakt Chem 1997; 339: 381–384.
13. Rolinson GN, Batchelor FR, Butterworth D, Cameron-Wood J, Cole M, Eustace GC, Hart MV, Richards M, Chain EB. Nature 1960; 187(4733): 236–237.
14. Nagasawa T, Yamada H. Trends Biotechnol 1989; 7(6): 153–158.
15. Novozymes. Commercial Information http://www.novozymes.com/, Amano Enzyme Inc. Commercial Information http://www.amano-enzyme.co.jp/.
16. Tanaka A, Tosa T, Kobayashi T. Industrial application of immobilized biocatalysts. New York: Marcel Dekker; 1993.
17. Cordes A, Kula M-R. Methods Enzymol 1994; 228: 600–608.
18. Kragl U, Vasic-Racki D, Wandrey C. Bioprocess Eng 1996; 14(6): 291–297.
19. Schmidt E, Ghisalba O, Gygax D, Sedelmeier G. J Biotechnol 1992; 24(3): 315–327.
20. Tomita K, Nagata K, Kondo H, Shiraishi T, Tsubota H, Suzuki H, Ochi H. Ann N Y Acad Sci 1990; 613: 421–425.
21. Antrim R, Colilla W, Schnyder B. In: Wingard L, Katchalski-Katzir E, Goldstein L, editors. Volume 2, Enzyme Technology. New York: Academic Press; 1979. pp 97–207.
22. Koch-Schmidt A-C, Mosbach K. Biochemistry 1977; 16: 2101–2105.
23. Scandurra R, Consalvi V, Chiaraluce R, Politi L, Engel PC. Biochimie 1998; 80: 933–941.
24. Tosa T, Mori T, Fuse N, Chibata I. Enzymologia 1966; 31: 214–224.
25. Rohm and Hass. Commercial Information http://www.rohmhass.com/, Resindion-Mitsubishi Chem. Corp. Commercial information http://www.resindion.com.
26. Mateo C, Abian O, Fernandez-Lafuente R, Guisan JM. Biotechnol Bioeng 2000; 68: 98–105.
27. Abian O, Mateo C, Fernández-Lorente G, Palomo JM, Fernández-Lafuente R, Guisán JM. Biocatal Biotransformation 2001; 19: 489–503.
28. Pessela BCC, Fernández-Lafuente R, Fuentes M, Vian A, Garcia JL, Carrascosa AV, Mateo C, Guisan JM. Enzyme Microb Technol 2003; 32: 369–374.
29. Fuentes M, Maquiese JV, Pessela BCC, Abian O, Fernández-Lafuente R, Mateo C, Guisán JM. Biotechnol Prog 2004; 20: 284–288.
30. Alonso-Morales N, Lopez-Gallego F, Betancor L, Hidalgo A, Mateo C, Fernandez-Lafuente R, Guisan JM. Biotechnol Prog 2004; 20: 533–536.
31. Torres R, Pessela BCC, Mateo C, Ortiz C, Fuentes M, Guisan JM, Fernández-Lafuente R. Biotechnol Prog 2004; 20: 1297–1300.
32. Pessela BCC, Betancor L, Lopez-Gallego F, Torres R, Dellamora-Ortiz GM, Alonso-Morales N, Fuentes M, Fernández-Lafuente R, Guisán JM, Mateo C. Enzyme Microb Technol 2005; 37: 295–299.
33. Torres R, Mateo C, Fuentes M, Palomo JM, Ortiz C, Fernández-Lafuente R, Guisan JM, Tam A, Daminati M. Biotechnol Prog 2003; 18: 1221–1226.
34. Fuentes M, Pessela BCC, Maquiese JV, Ortiz C, Segura RL, Palomo JM, Abian O, Torres R, Mateo C, Fernández-Lafuente R, Guisán JM. Biotechnol Prog 2004; 20: 1134–1139.
35. Brady L, Brzozowski AM, Derewenda ZS, Dodson E, Dodson G, Tolley S, Turkenburg JP, Christiansen L, Huge-Jensen B, Norskov L, Thim L and Menge U, Nature 1990; 343: 767–770.
36. Brzozowski AM, Derewenda U, Derewenda ZS, Dodson GG, Lawson DM, Turkenburg JP, Bjorkling F, Huge-Jensen B, Patkar SA and Thim L. Nature 1991; 351: 491–494.

37. Fernández-Lafuente R, Armisén P, Sabuquillo P, Fernández-Lorente G, Guisan JM. Chem Phys Lipids 1998; 93: 185–197.
38. Reetz MT. Adv Mater 1997; 9: 943–954.
39. Mingarro I, Abad C, Braco L. Proc Natl Acad Sci U S A 1995; 92: 3308.
40. González-Navarro H, Bañó MC, Abad C. Biochemistry 2001; 40: 3174–3183.
41. López-Serrano P, Cao L, Van Rantwijk F, Sheldon RA. Biotechnol Lett 2002; 24: 1379–1383.
42. Carrea G, Riva S. Angew Chem Int Ed Engl 2000; 39(13): 2227–2254.
43. Gupta MN, Roy I. In: Gupta MN, editor. Methods for affinity-based separation of proteins/enzymes. Basel: Birkhauser Verlag; 2002. pp 1–15.
44. Roy I, Gupta MN. In: Guisan JM, editor. Immobilization of enzymes and cells, Methods in biotechnology 22. 2nd ed. Totowa (NJ): Humana Press; 2006.
45. Farooqi M, Saleemuddin M, Ulber R, Sosnitza P, Scheper T. J Biotechnol 1997; 55: 171–179.
46. Farooqi M, Sosnitza P, Saleemuddin M, Ulber R, Scheper T. Appl Microbiol Biotechnol 1999; 52: 373–379.
47. Bourdillon C, Demaile C, Moinrux J, Saveant JM. J Am Chem Soc 1984; 116: 1328–10329.
48. Saleemuddin M. Adv Biochem Eng Bioeng 1999; 64: 203–226.
49. Saleemuddin M, Husain Q. Enzyme Microb Technol 1991; 13: 290–295.
50. Dalal S, Gupta MN. Chemosphere 2007; 67: 741–747.
51. Sulkowski E. Trends Biotechnol 1985; 3: 1–8.
52. Hermanson GT, Mallia AK, Smith PK. Immobilized affinity ligand techniques. California: Academic Press, Inc.; 1992.
53. Ong E, Greenwood JM, Gilkes NR, Kilburn DG, Miller RC Jr, Warren RAJ. Trends Biotechnol 1989; 7: 239–243.
54. Brena B, Batista-Vieria F. In: Guisan JM, editor. Immobilization of enzymes and cells, Methods in biotechnology 22. 2nd ed. Totowa (NJ): Humana Press; 2006.
55. Axén R, Portath J, Ernback S. Nature 1067; 214: 1302–1304.
56. Monsan P, Puzo G, Mazarguil H. Biochimie 1975; 57: 1281–1292.
57. López-Gallego F, Betancor L, Hidalgo A, Alonso N, Fernandez-Lorente G, Guisan JM, Fernandez-Lafuente R. Enzyme Microb Technol 2005; 37: 750–756.
58. Alonso N, López-Gallego F, Betancor L, Hidalgo A, Mateo C, Guisan JM, Fernandez-Lafuente R. J Mol Catal, B Enzym 2005; 35: 57–61.
59. Mateo C, Abian O, Fernandez-Lorente G, Pedroche J, Fernandez-Lafuente R, Guisan JM. Biotechnol Prog 2002; 18: 629–634.
60. Rembaum A, Levy J, Gupta A, Margel S. Volume 19 (1), Reaction of polyglutaraldehyd with proteins: American Chemical Society, Polymer Preprints, Division of Polymer Chemistry; 1978. pp 648–653.
61. Rajput YS, Gupta MN. Enzyme Microb Technol 1987; 9(3): 161–163.
62. Klibanov AM. Nature 2001; 409(6817): 241–246.
63. Cao L, Langen LM, Sheldon RA. Curr Opin Biotechnol 2003; 14: 387–394.
64. Quiocho FA, Richards FM. Proc Natl Acad Sci U S A 1964; 114: 7314–7316.
65. Margolin AL, Navia MA. Angew Chem Int Ed Engl 2001; 40: 2204–2222; Lalonde J. Clecs. 2, 1997.
66. Häring D, Schreier P. Curr Opin Chem Biol 1999; 3: 35–38.
67. Cao L, Van Rantwijk F, Sheldon RA. Org Lett 2000; 2: 1361–1364.
68. Wilson L, Betancor L, Fernández-Lorente G, Fuentes M, Hidalgo A, Guisán JM, Pessela BCC, Fernández-Lafuente R. Biomacromolecules 2004; 5: 814–817.
69. Wilson L, Illanes A, Abián O, Pessela BCC, Guisan JM, Fernandez-Lafuente R. Biomacromolecules 2004; 5: 852–857.
70. Wilson L, Illanes A, Pessela BCC, Abián O, Fernandez-Lafuente R, Guisan JM. Biotechnol Bioeng 2004; 86: 558–562.
71. Mateo C, Fernandes B, Van Rantwijk F, Stolz A, Sheldon RA. J Mol Catal, B Enzym 2006; 38: 154–157.
72. Mateo C, Palomo JM, Fernandez-Lorente G, Guisan JM, Fernandez-Lafuente R. Enzyme Microb Technol 2007; 40(6): 1451–1463.
73. Martinek K, Klibanov AM, Goldmacher VS, Berezin IV. Biochim Biophys Acta 1977; 485: 1–12.
74. Mozhaev VV, Melik-Nubarov NS, Sergeeva MV, Sikrnis V, Martinek K. Biocatalysis 1990; 3: 179–187.
75. Guisan JM. Enzyme Microb Technol 1988; 10(6): 375–382.
76. Mateo C, Palomo JM, Fuentes M, Betancor L, Grazu V, López-Gallego F, Pessela BCC, Hidalgo A, Fernández-Lorente G, Fernández-Lafuente R, Guisán JM. Enzyme Microb Technol 2006; 39: 274–280.
77. Pedroche J, Yust MM, Mateo C, Fernández-Lafuente R, Girón-Calle J, Alaiz M, Vioque J, Guisán JM, Millán F. Enzyme Microb Technol. 2007; 40: 1160–1166.
78. Mateo C, Abian O, Bernedo M, Cuenca E, Fuentes M, Fernandez-Lorente G, Palomo JM, Grazu V, Pessela BCC, Giacomini C, et al. Enzyme Microb Technol 2005; 37: 456–462.
79. Blanco RM, Calvete JJ, Guisán JM. Enzyme Microb Technol 1988; 11: 353–359.
80. Blanco RM, Guisán JM. Enzyme Microb Technol 1988; 11: 360–366.
81. Guisán JM, Bastida A, Cuesta C, Fernández-Lafuente R, R osell CM. Biotechnol Bioeng 1991; 39: 75–84.
82. Betancor L, Hidalgo A, Fernández-Lorente G, Mateo C, Fernández-Lafuente R, Guisan JM. Biotechnol Prog 2003; 19: 763–767.
83. Suh C-W, Choi G-S, Lee E-K. Biotechnol Appl Biochem 2003; 37: 149–155.
84. Ichikawa S, Takano K, Kuroiwa T, Hiruta O, Sato S, Mukataka S. J Biosci Bioeng 2002; 93: 201–206.
85. Rocchietti S, Ubiali D, Terreni M, Albertini AM, Fernández-Lafuente R, Guisán JM, Pregnolato M. Biomacromolecules 2004; 5: 2195–2200.
86. Tardioli PW, Zanin GM, Morae FF. Enzyme Microb Technol 2006; 39: 1270–1278.
87. Megias C, Pedroche J, Yust MD, Alaiz M, Girón-Calle J, Millán F, Vioque J. J Agric Food Chem 2006; 54: 4641–4645.
88. Suau T, Calveras J, Clapes P, Benaiges MD, Alvaro G. Biocatal Biotransformation 2005; 23: 241–250.

89. Bes T, Gomez-Moreno C, Guisán JM, Fernández-Lafuente R. J Mol Catal 1995; 98: 161–169.
90. Mateo C, Grazu V, Palomo JM, Lopez-Gallego F, Fernandez-Lafuente R, Guisan JM. Nat Protoc 2007; 2(5): 1022–1033.
91. López-Gallego F, Betancor L, Hidalgo A, Mateo C, Guisan JM, Fernandez-Lafuente R. J Biotechnol 2004; 111: 219–227.
92. Mateo C, Abian O, Fernandez-Lafuente R, Guisan JM. Enzyme Microb Technol 2000; 26: 509–515.
93. Mateo C, Abian O, Fernández-Lorente G, Pedroche J, Fernánde-Lafuente R, Guisan JM, Tam A, Daminati M. Biotechnol Prog 2002; 18: 629–634.
94. Pessela BCC, Mateo C, Fuentes M, Vian A, García JL, Carrascosa AV, Guisán JM, Fernández-Lafuente R. Biotechnol Prog 2004; 20: 388–392.
95. Poltorak OM, Chukhray ES, Torshin IY. Biochemistry (Moscow) 1998; 63: 303–311.
96. Fernández-Lafuente R, Rodríguez V, Mateo C, Penzol G, Hernández-Justiz O, Irazoqui G, Villarino A, Ovsejevi K, Batista F, Guisán JM. J Mol Catal, B Enzym 1999; 7: 181–189.
97. Balcão VM, Mateo C, Fernández-Lafuente R, Malcata FX, Guins JM. Biotechnol Prog 2001; 17: 537–542.
98. Fernández-Lorente G, Terreni M, Mateo C, Bastida A, Fernández-Lafuente R, Dalmases P, Huguet J, Guisán JM. Enzyme Microb Technol 2001; 28: 389–396.
99. Palomo JM, Segura RL, Fernández-Lorente G, Guisán JM, Fernández-Lafuente R. Tetrahedron Asymmetry 2004; 15: 1157–1161.
100. Palomo JM, Fernández-Lorente G, Mateo C, Fuentes M, Fernández-Lafuente R, Guisan JM. Tetrahedron Asymmetry 2002; 13: 1337–1345.
101. Palomo JM, Fernández-Lorente G, Mateo C, Ortiz C, Fernandez-Lafuente R, Guinsa JM. Enzyme Microb Technol 2002; 31: 775–783.
102. Chaubey A, Parshad R, Koul S, Taneja SC, Qazi GN. J Mol Catal, B Enzym 2006; 42: 39–44.
103. Turner NJ. Curr Opin Biotechnol 2003; 14: 401–406.
104. Mozhaev VV, Berezin IV, Martinek K. Methods Enzymol 1987; 135: 586–596.
105. Soler G, Bastida A, Blanco RM, Fernández-Lafuente R, Guisán JM. Biochim Biophys Acta 1997; 1339(1): 167–175.
106. Kumar R, Singh S, Singh OV. J Ind Microbiol Biotechnol 2008; 35(5): 377–391.
107. Johnson AK, Zawadzka AM, Deobald LA, Crawford RL, Paszczynski AJ. J Nanoparticle Res 2008; 10(6): 1009–1025.
108. Pita M, Abad JM, Vaz-Dominguez C, Briones C, Mateo-Martí E, Martín-Gago JA, del Puerto Morales M, Fernández VM. J Colloid Interface Sci 2008; 321(2): 484–492.
109. Roy I, Sharma S, Gupta MN. Adv Biochem Eng Biotechnol 2003; 86: 159–189.
110. Hoffman AS. Clin Chem 2000; 46: 1478–1486.
111. Roy I, Gupta MN. Chem Biol 2003; 10: 1161–1171.
112. Tyagi R, Roy I, Agarwal R, Gupta MN. Biotechnol Appl Biochem 1998; 28: 201–206.

55

IMPELLER SELECTION, ANIMAL CELL CULTURE

Alvin W. Nienow
University of Birmingham, School of Chemical Engineering, Birmingham, United Kingdom

55.1 INTRODUCTION

As in all stirred bioreactors, the impeller(s) used in bioreactors for animal (mammalian or insect) cell culture have to be able to achieve a number of different tasks. These tasks are essentially describable in physical terms, all of which are related to the fluid motion imparted by the impeller(s). The tasks are listed in Table 55.1 and in order to obtain sufficient understanding of the link between impeller type and each task, they can initially be studied without the complexity of actually growing an organism. Such studies are very important if the impeller choice is to be made rationally. The type of information needed is listed in Table 55.2 and it is important to know how changes of scale affect these physical parameters too. Finally, it is also necessary to have as much information as possible on the characteristics of the biological species of interest. These biological aspects are listed in Table 55.3 and many of them can be evaluated at smaller scales, including shake and spinner flasks and microwell plates, especially if they are well instrumented. Others require work in stirred bioreactors, albeit at the bench or pilot scale. Given the right combination of small- and large-scale data in relation to the parameters listed in Tables 55.2 and 55.3, it then becomes possible to choose the appropriate impeller(s) and design the whole bioreactor. Impeller selection will now be considered on the basis of the special needs of animal cell culture. The selection applies equally well to both mammalian and insect cells.

55.2 THE MOST IMPORTANT ASPECTS IMPACTING IMPELLER SELECTION

For all microorganisms, the feature of greatest importance in determining the overall agitation conditions is the level of oxygen demand (OD). To meet this demand, oxygen has to be continuously supplied because of its limited solubility in the media. In the case of animal cells, the specific oxygen demand (SOD) is low (typical values of about $\sim 1 \times 10^{-17}$ to 1×10^{-16} mol/s/cell (2,3) and though the cell density, X, has steadily increased over the years to about 10^7 cells/mL, relative to many other organisms, the overall $\mathrm{OD} = (\mathrm{SOD} \cdot X)$ is also low. This low OD means that the oxygen transfer rate is low and therefore because it is linked to the specific power input from the agitator when aerated, $P_g/\rho V$, and the sparge rate, these two operating parameters are low too, typical values being $< \sim 0.05$ W/kg and $< 5 \times 10^{-3}$ vvm (2,3) to give $k_L a$ values $< 15 \mathrm{h}^{-1}$ (2,3). A corollary to meeting the OD is adequate stripping of CO_2, which must also be achieved by the same agitation and sparging conditions. This aspect is particularly important for cell culture and is discussed in more detail later.

The other critical and special feature of animal cell culture that has had an impact on agitator selection, and agitation and aeration intensity, is the perception that the cells are very "shear sensitive." This perception arises from the fact that these cells do not have a cell wall and that as a result they can be easily damaged. In the early days of commercial scale animal cell culture, it was believed that

Upstream Industrial Biotechnology: Equipment, Process Design, Sensing, Control, and cGMP Operations, Volume 2, First Edition. Edited by Michael C. Flickinger.
© 2013 John Wiley & Sons, Inc. Published 2013 by John Wiley & Sons, Inc.

TABLE 55.1. Process Tasks in Bioreactors that the Impeller must Ensure are Met

A. Homogenize (mix) the liquid phase
B. Bubble breakup
C. Oxygen transfer into the media
D. Carbon dioxide stripping
E. Heat transfer

TABLE 55.2. Physical Phenomena in Stirred Bioreactors to be Studied Including the Effect of Scale

A. Unaerated power draw, P (W) [or mean specific energy dissipation rate, $\overline{\varepsilon}_T$ (W/kg) or P/V (W/m^3)]
B. Aerated power draw, P_g (W) [or $(\overline{\varepsilon}_T)_g$ (W/kg) or P_g/V (W/m^3)]
C. Local specific energy dissipation rate, ε_T (W/kg) including the maximum near the impeller $(\varepsilon_T)_{max}$ (W/kg)
D. Flow structure near the impeller
E. Liquid-phase mixing time, θ_m (s)
F. Gas-phase mixing (plug flow or back-mixed) (1)
G. Flooding–loading transition
H. Mass transfer rates
I. Rheological properties—viscosity μ_a (Pas) or Reynolds no $\rho\, ND^2/\mu_a$ (dimensionless)
J. Microcarrier suspension (for attached cells)

TABLE 55.3. Biological Performance Parameters

A. Specific oxygen demand, cell density and respiratory quotient
B. Suitable temperature, pH, dO_2, pCO_2, and osmolality ranges.
C. Any product inhibition or sensitivity to high nutrient concentrations
D. Sensitivity to temporal and spatial variations in temperature, pH, dO_2, CO_2, osmolality, or nutrients.
E. Sensitivity to stresses due to turbulence and bubble rupture
F. Changes in D and E with changes in scale.

the cells would be most susceptible to stresses associated with agitation so that airlift and bubble columns were proposed as a replacement for stirred bioreactors because of the reduced level of "shear" (4). More recent work has shown that the stresses associated with bursting bubbles at the upper surface of the media are much greater than those associated with the fluid motion induced by the impeller. As animal cells tend to attach to the bubbles, these stresses are lethal to cells (2,5). However, with the addition of the polyol surfactant, Pluronic F68 (2,6,7), cells do not attach and damage is thus prevented. Hence, because of their enhanced flexibility compared to bubble-driven configurations, stirred bioreactors are now the preferred choice and a number of reactors with volumes up to 25 m^3 have been reported to have been built.

Taken together, the concern for cell damage and the need to only provide low oxygen transfer rates leads to the decision to use low agitation intensity and aeration rates in animal cell culture and this decision along with the search for a "low shear" agitator has essentially defined the agitator types used. In the remainder of this chapter, aspects of these special features of animal cell culture will be developed in more detail and their impact on the other physical and biological aspects listed in Tables 55.2 and 55.3 will be outlined in relation to impeller selection.

55.3 OXYGEN TRANSFER CONSIDERATIONS

For stable operation, the oxygen transfer rate needs to meet the OD or oxygen uptake rate (OUR) (1). Thus,

$$\mathrm{OD} = \mathrm{OUR} = \mathrm{OTR} = k_L a.\Delta C \qquad (55.1)$$

In Equation 55.1, ΔC is the driving force and represents the difference in oxygen concentration in the liquid phase (media) in equilibrium with the partial pressure of oxygen in the air bubble (allowing for back pressure or the use of oxygen-enriched air or even pure oxygen) and that in the bulk of the media. The latter oxygen concentration must be controlled to ensure that it lies within the range of concentrations at which the cells grow satisfactorily. This range (along with the SOD for the particular cell line) can be determined at very small scale with proper instrumentation.

The constant of proportionality, $k_L a$, is often called the *mass transfer coefficient*, though strictly k_L is the mass transfer coefficient and a is the specific surface area of bubbles in the media. However, these separate parameters are intimately connected, both being heavily dependent on the interfacial properties of the media and their impact on bubble breakup and coalescence. With the current state of knowledge, this dependence makes both the separate parameters and the combination impossible to predict. Hence, the combination, $k_L a$ [with units of $(\mathrm{time})^{-1}$], are usually measured. In practice, $k_L a$ is surprisingly difficult to determine experimentally and the reasons for this are set out in detail elsewhere (1). As a result, it has proved impossible to measure $k_L a$ sufficiently accurately to distinguish the efficacy of one impeller type compared with another with respect to oxygen transfer (1). Thus, starting with the work of Van't Riet (8), correlations of the form

$$k_L a = A(\overline{\varepsilon}_T)_g^{\alpha} v_s^{\beta} \qquad (55.2)$$

have become accepted and Hoeks *et al*. (9) showed the applicability of Equation 55.2 across the scales in 12, 500, and 20,000 L bioreactors using animal cell culture media. Here, $(\overline{\varepsilon}_T)_g$ (watts per kilogram) is the total mean specific energy dissipation rate imposed on the system, and v_s (meters per second) is the superficial air velocity which is equal to (vvm/60)(volume of broth)/(cross-sectional area of the bioreactor). $(\overline{\varepsilon}_T)_g$ is made up of that (i) from air sparging, $(\overline{\varepsilon}_T)_S \approx v_s g$, where g is the acceleration due to gravity (9.81 m^2/s) and which can often be neglected and (ii) from the impeller under sparged conditions, $(\overline{\varepsilon}_T)_{Ig}$, where

$$(\overline{\varepsilon}_T)_{Ig} = P_g/\rho V = Po_g N^3 D^5/V \tag{55.3}$$

and Po_g is the power number of the impeller under aerated conditions, N (per second) and D (meters), the impeller speed and diameter, respectively, and V (cubic meters), the volume of media in the bioreactor. The exponents in Equation 55.2 are typically about 0.5 ± 0.1 independent of the system of interest. On the other hand, A is extremely sensitive to composition and the addition of antifoam or Pluronic F68 both of which lower k_La or salts which increase it, may lead to a 20-fold difference in k_La for the same values of $(\overline{\varepsilon}_T)_g$ and v_s (1). A recent attempt to mimic a media (which included sodium chloride, sodium bicarbonate, and 1 g/L Pluronic F68) used in industry for Chinese hamster ovary (CHO) cell culture at 3000–4400 L volume with a pipe sparger (3) led to the following correlation for k_La

$$k_La = 0.075(P_g/V)^{0.47} v_s^{0.80} \tag{55.4}$$

where the mean specific energy input is used, P_g/V (watts per cubic meter) and

$$P_g = Po_g \rho N^3 D^5 \tag{55.5}$$

Since Equation 55.4 was obtained under conditions that closely mimic those used under realistic large-scale culture, it may be a good one to use if information is not available for the precise cell culture under consideration.

Overall, $(\overline{\varepsilon}_T)_g$ (or the equivalent in watts per cubic meter) and v_s must together be sufficient to produce the necessary k_La to meet the OD of the cells while maintaining the dO_2 concentration in the media in the desired range. However, Equations 55.3 and 55.4 both suggest that the choice of impeller is largely confined to ensuring that whichever is chosen, it is of sufficient size and aerated power number and is run at a speed that will enable the power input to be generated to achieve the required k_La.

55.4 "SHEAR SENSITIVITY" TO IMPELLER-GENERATED FLUID DYNAMIC STRESSES

55.4.1 Reynolds Number, Power Number, and Flow Patterns

As in all fluid flow situations, both laminar and turbulent flow can exist in a bioreactor. In turbulent flow, inertial forces dominate and in laminar flow, viscous ones. Conceptually the ratio of these two forces is the Reynolds number (Re). For a bioreactor with a media of viscosity, μ, (or kinematic viscosity, $\nu(=\mu/\rho)$), the Reynolds number is defined as

$$Re = \rho N D^2/\mu = N D^2/\nu \tag{55.6}$$

If $Re > \sim 2 \times 10^4$, the flow is turbulent and even with the relatively gentle agitation found in cell culture bioreactors, it is in all sizes from the bench scale to the industrial scale. Under unbaffled conditions, the main flow will be totally dominated by horizontal rotational flows (swirling flow) with a central vortex (Fig 55.1). Under the gentle conditions found in cell culture bioreactors, the vortex depth will be small. In addition, the presence of inserts such as dO_2 probes will tend to damp out the swirl and reduce the vortex but the flow will still approximate that shown in Fig 55.1 whichever impeller is chosen. Under these conditions, there is poor vertical mixing so that homogenization of the media takes a relatively long time, the power input is limited, and solids such as microcarriers are more difficult to suspend.

Introducing baffles overcomes these problems. Also, once baffles have been introduced, the flow pattern is dependent on the agitator type. The impellers (Fig 55.2) are usually described as axial, producing a mainly vertically downward flow approximately parallel to the agitator shaft (Fig. 55.2a) as with the Chemineer HE3 (Chemineer Inc., Dayton, Ohio) (Fig. 55.3a) or radial, giving horizontal flow and a figure-of-8 flow pattern (Fig. 55.2b) as with the Rushton turbine (Fig. 55.3b). Some impellers produce a flow somewhere between the two (Fig. 55.2c) and are called *axial flow* or *pitched blade turbines* (Fig. 55.3c). The power drawn by the impeller and imparted into the media, P (watts), can be determined from the power number, Po:

$$Po = P/\rho N^3 D^5 \tag{55.7}$$

It is of critical importance for the mechanical design of shafts, gear boxes, seals, and so on, and for sizing drive motors, which must be $> P$ to allow for friction

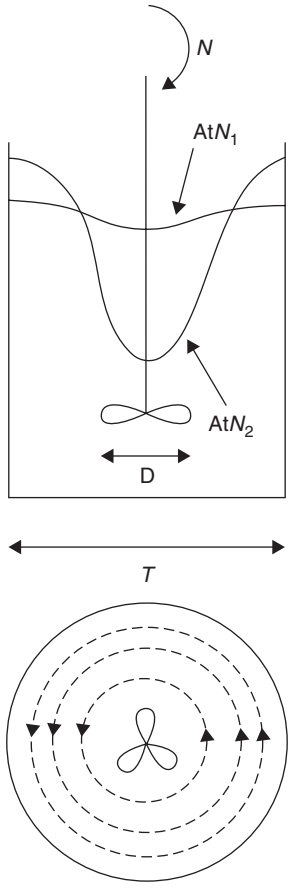


Figure 55.1. Flow patterns in an unbaffled cylindrical bioreactor, diameter T. ($N_1 < N_2$).

and energy losses in the motor, gear box, bearings, seal, and so on. Specific power based on the volume of media in the bioreactor, that is *P/V* (kilowatts per cubic meter) or *P/M* (watts per kilogram) is also used extensively to compare impeller performance. The latter is equivalent to the mean specific energy dissipation rate, $\overline{\varepsilon}_T$ (watts per kilogram or square meter per cubic second) in theoretical analysis of many phenomena in bioreactors and in scale-up considerations. *Po* is dependent on the impeller type and on its relative size, *D/T*, position in the tank, *C/T*, and so on, and impeller material thickness but in the turbulent region ($Re > \sim 10^4$), Po = constant, independent of *Re*. Most importantly, for geometrically similar systems (all length dimensions changed proportionally), it is essentially independent of scale.

55.4.2 High/Low "Shear" Impellers and Impeller Tip Speed

Another dimensionless group that can be used to characterize impellers is the flow number, $\mathrm{Fl} = Q/ND^3$, where Q is the volumetric flow rate of fluid generated by the impeller (10). Publications starting around the 1960s introduced the concept of considering impellers as having high "shear" or high flow characteristics based on the ratio of *Po/Fl*. Since flow numbers do not change very much, typically being between about 0.4 and 0.9 while *Po* values vary for agitators commonly found in bioreactors by a factor of about 20 (Table 55.4), it is essentially only *Po* that determines whether *Po/Fl* is high or low. Impellers with relatively high values of *Po* are often called *high shear impellers* while those with low values are considered *low shear ones*, especially by mixer manufacturers. The impeller most commonly called high "shear" whether in relation to cell culture or other purposes, for example the manufacture of oil in water dispersions with small oil drops, is the Rushton turbine, $Po = \sim 5$. Because of the perceived "shear" sensitivity of animal cells, therefore, the Rushton turbine has generally not been used for cell culture. Yet, that impeller was used successfully from the late 1960s to the mid-1980s in a bioreactor of 8 m^3 for the production of interferon from CHO cells at Wellcome Foundation (11). It also gave identical results to those obtained with a propeller agitator ($Po = \sim 0.3$) when used for growing a range of cell types

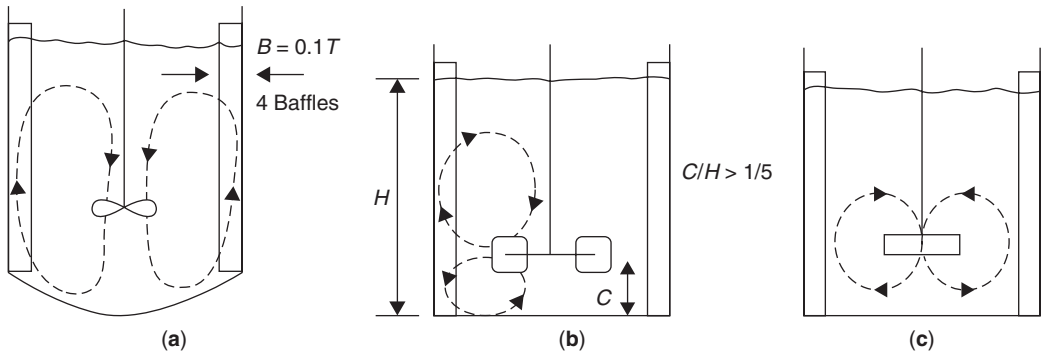


Figure 55.2. Flow patterns produced in an unaerated cylindrical baffled bioreactor by (a) down-pumping axial flow propellers or hydrofoils; (b) radial flow Rushton turbines; and (c) pitched blade or axial flow turbines.

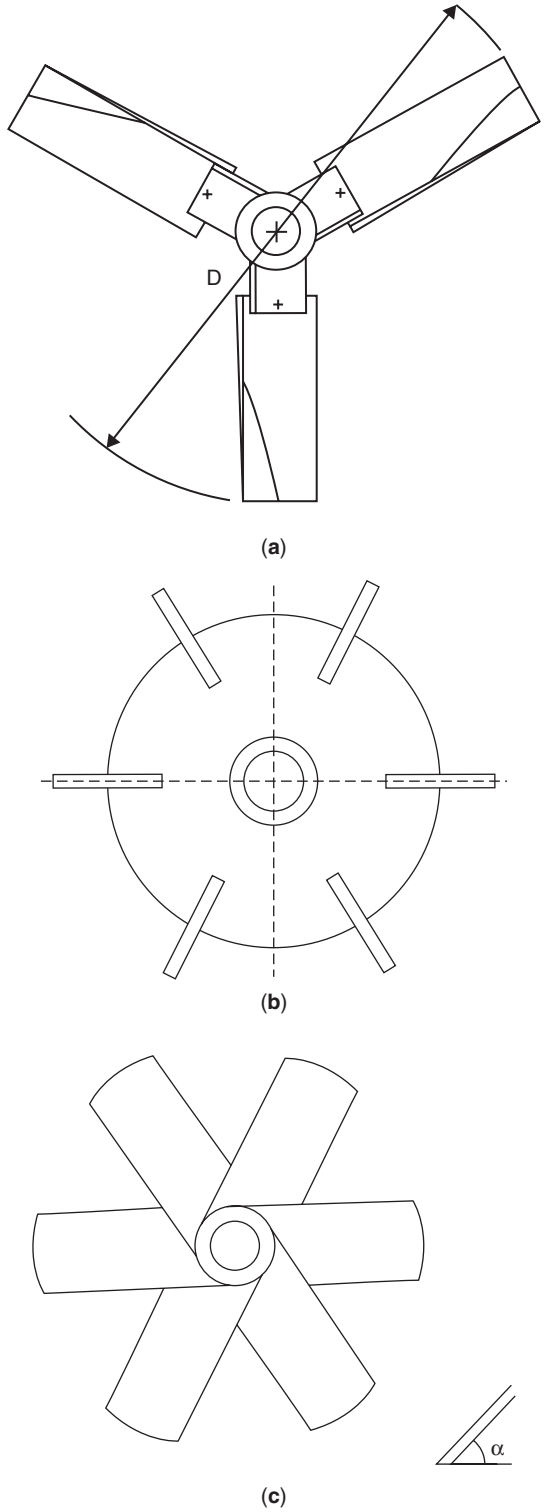


Figure 55.3. Different impeller types: (a) Chemineer HE3 (axial; "low shear"; $Po = \sim 0.3$); (b) Rushton turbine (radial; "high shear"; $Po = \sim 5.0$); (c) pitched blade turbine ($Po = \sim 1.7$, $\alpha = 45^\circ$).

TABLE 55.4. Power Numbers and Flow Numbers for Some Impellers in the Turbulent Regime in Baffled Bioreactors

Impeller Type	Shear Designation	Power Number	Flow Number
Rushton turbine	High shear	~5.0	~0.74
Chemineer HE3 hydrofoil	Low shear	~0.3	~0.41
6-blade, 45°-pitch turbine	Intermediate	~1.7	~0.73
Lightnin' A315 hydrofoil	Low shear	~0.84	~0.73
Applikon "Elephant ears"	Low shear	~1.7	~0.87

at the University of Birmingham (2) and also recently at Schering-Plough (12) for growing CHO cells to produce antibodies. It is also interesting to note that so-called low "shear" impellers cause greater disruption to mycelia than high "shear" Rushton turbines (13) and also produce smaller drops (14).

Another traditional way of considering the possibility of "shear" damage is to relate it to impeller tip speed which is equal to πND. For example, it has been stated (4) that "above 1.5 m/s, cell damage may begin." However, this statement was made without any referenced work to support it and from a fluid dynamic perspective, the dimensions of tip speed are not correct in relation to damage, and there is little or no evidence to support it (2). In addition, and somewhat strangely, the concept also suggests that the potential for "shear" damage increases with the use of low "shear" impellers if $(\overline{\varepsilon}_T)_I$ is held constant to maintain k_La! For similar reasons, it leads to the concept that "shear" damage increases with scale because tip speed increases with scale ($\propto$ (scale)$^{1/3}$) (10). Thus, maintaining tip speed $<$1.5 m/s is a major constraint on scale-up with severe implications for homogeneity (see below) as well as mass transfer. Indeed, in only one case has mechanical damage been clearly shown to occur under "normal" operating conditions of agitation intensity with any microorganism and that is in mycelial fermentations. Here, at equal $\overline{\varepsilon}_T$, that damage went down on scale-up in spite of the increase in tip speed (13). On balance, both tip speed and the low/high "shear" impeller concepts appear less than useful.

55.4.3 Kolmogoroff Eddy Size Concepts

Kolmogoroff's theory of homogeneous isotropic turbulence has been used extensively to predict the interaction between the turbulent structure of a flow in any type of equipment and its impact on dispersed entities. The equipment covered includes in-line static mixers, pipe flow as well as stirred vessels and the topics include the breakup of immiscible drops, bubbles, and flocs as well as damage to cells. More details can be found elsewhere (2,10). A critical feature of the theory is the Kolmogoroff or microscale of turbulence, λ_K, where

$$\lambda_K = ((\varepsilon_T)/\nu^3)^{-1/4} \tag{55.8}$$

where ε_T is the local specific energy dissipation rate in the flow and ν is the kinematic viscosity ($\approx 10^{-6}\text{m}^2/\text{s}$ for the cells suspended in media since the latter is water like). The mechanism of breakup depends on whether the dispersed entity is greater than or lesser than λ_K. Similarly, it is considered that if the cell of interest, in this case the animal cell, is $< \lambda_K$, damage due to flow associated stresses will not occur.

For all agitators, the maximum local specific energy dissipation rate, $(\varepsilon_T)_{\text{Imax}}$, is close to the impeller and is very high relative to the average $(\overline{\varepsilon}_T)_{\text{I}}$. However, most importantly, in relation to impeller selection, it also depends on the agitator type and probably its relative size, *D/T*. A typical example of the distribution of $(\varepsilon_T)_{\text{I}}/(\overline{\varepsilon}_T)_{\text{I}}$ where $(\varepsilon_T)_{\text{I}}$ is the local specific energy dissipation rate is shown in Fig 55.4, measured by laser Doppler anemometry (LDA). As can be seen, $(\varepsilon_T)_{\text{I}}/(\overline{\varepsilon}_T)_{\text{I}}$ varies enormously throughout the vessel (15). It is interesting to note that baffles were often excluded from animal cell culture bioreactors, again because of the perception that they would give rise to a region of high "shear." However, as can be seen in Fig 55.4, there is no indication that $(\varepsilon_T)_{\text{I}}/(\overline{\varepsilon}_T)_{\text{I}}$ increases in the region of the baffles. Their use is now not uncommon.

Table 55.5 shows some values of $(\varepsilon_T)_{\text{Imax}}/(\overline{\varepsilon}_T)_{\text{I}}$ for some other impellers covering both a "high" and a "low" shear impeller and a pitched blade turbine. As can be seen, the values are a strong function of *D/T* with all types, those of the low shear Chemineer HE3 being quite similar to those of the Rushton turbine while those with the pitched blade turbine are somewhat lower. It should be recognized that to obtain $(\varepsilon_T)_{\text{Imax}}/(\overline{\varepsilon}_T)_{\text{I}}$ requires certain assumptions to be made and considerable numerical manipulation of the raw LDA data and hence the absolute numbers should not be considered to be exact. In fact, values of $(\varepsilon_T)_{\text{Imax}}/(\overline{\varepsilon}_T)_{\text{I}}$ from about 20 to about 100 have been reported just for 1/3 *D/T* Rushton turbines (10). However, Table 55.5 certainly does not suggest that the "low shear" Chemineer HE3, even though it has the lowest *Po*, is superior to the Rushton impeller. On the other hand, there is a strong indication that a larger *D/T* ratio minimizes $(\varepsilon_T)_{\text{Imax}}/(\overline{\varepsilon}_T)_{\text{I}}$.

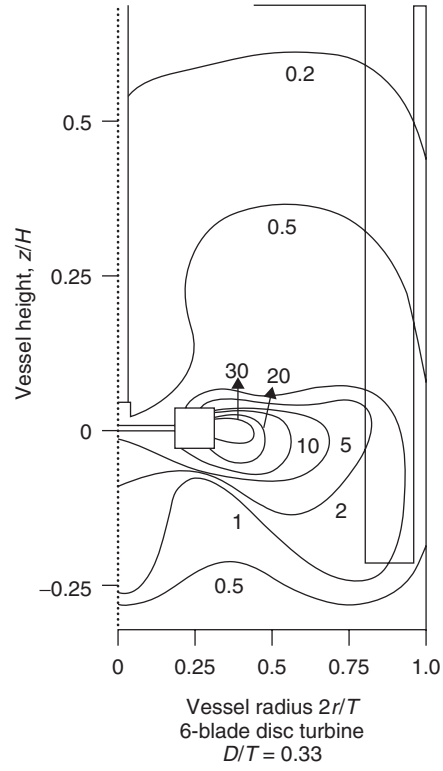


Figure 55.4. Contours of $(\varepsilon_T)_{\text{I}}/(\overline{\varepsilon}_T)_{\text{I}}$ in a vessel agitated by a Rushton turbine (15).

Since the value of $(\overline{\varepsilon}_T)_{\text{I}}$ must be set to give sufficient oxygen transfer whatever the agitator type following Equation 55.2, then the greater $(\varepsilon_T)_{\text{Imax}}/(\overline{\varepsilon}_T)_{\text{I}}$, the greater will be the $(\varepsilon_T)_{\text{Imax}}$ value experienced by the cells. If a typical value for $(\varepsilon_T)_{\text{Imax}}/(\overline{\varepsilon}_T)_{\text{I}}$ from Table 55.5 of 50 is taken for the commonly used *D/T* ratio of 1/3 along with the typical $(\overline{\varepsilon}_T)_{\text{I}}$ of 0.05 W/kg, then $(\varepsilon_T)_{\text{Imax}} = 2.5\text{W/kg}$ and from Equation 55.8, $\lambda_K = 25\ \mu\text{m}$. Since most animal cells are of the order of $14 - 18\ \mu\text{m}$ which is $< \lambda_K$, the lack of "shear damage" fits in with the Kolmogoroff eddy size concept. However, of course, it does not prove it.

Unfortunately, $(\varepsilon_T)_{\text{Imax}}/(\overline{\varepsilon}_T)_{\text{I}}$ has not been measured for many impellers. In that case, it has been estimated

TABLE 55.5. Values of $(\varepsilon_T)_{\text{Imax}}/(\overline{\varepsilon}_T)_{\text{I}}$ for Various Impellers as a Function of *D/T* (16)

Impeller Type	Shear Designation	*D/T*	$(\varepsilon_T)_{\text{Imax}}/(\overline{\varepsilon}_T)_{\text{I}}$
Rushton turbine	High shear	1/4	~147
		1/3	~48
		1/2	~23
Chemineer HE3 hydrofoil	Low shear	1/4	~135
		1/3	~99
		1/2	~14
6-blade, 45°-pitch turbine	Intermediate	1/4	~66
		1/3	~37
		1/2	~16

$(\overline{\varepsilon}_T)_{\text{I}} = P/\rho V = PoN^3D^5/V$

successfully when applying Kolmogoroff's theory to the breakage of immiscible drops by assuming that the power input was dissipated in the impeller swept volume, V_{swept}, that is $(\varepsilon_T)_{\text{Imax}}/(\overline{\varepsilon}_T)_{\text{I}} = P/\rho V_{\text{swept}}$ (10). This approach also suggests that the selection of a large D/T impeller would be beneficial in that it would lead to lower values of $(\varepsilon_T)_{\text{Imax}}$ for a given $(\overline{\varepsilon}_T)_{\text{I}}$. Another approach is to compare the impellers on the basis of turbulent kinetic energy which is easier to measure and is closely related to specific energy dissipation rate. This comparison has recently been done using particle image velocimetry (PIV). The impellers studied were an "elephant ears" impeller (Fig. 55.5a), which is currently being extensively used in industrial cell culture (17) because it is claimed to be a particularly low "shear" one, an up-pumping Hayward-Tyler B2 (Fig. 55.5b) (which is also designated a low "shear" impeller) and a pitched blade turbine. The work showed that essentially their turbulent kinetic energy characteristics (which mirrors ε_T) were all the same (18).

55.4.4 Energy Dissipation Rates and Cell Culture Performance with Different Impeller Types

There have also been some actual studies where the impact of specific energy dissipation rate on cell growth and other bioperformance parameters was measured. Work at Birmingham, first published in 1989 and recently summarized (2), showed that even at $(\overline{\varepsilon}_T)_{\text{I}}$ values up to 0.25 W/kg, a range of mammalian (TB/C3 mouse hybridomas, HPV cells producing antibodies, and CHO cells producing γ-interferon) and insect cell (Sf9 insect cells producing viruses) lines grew quite satisfactorily (same number of viable cells per ml and productivity) compared with culture at a typical industrial value of 0.01 W/kg both under unsparged and sparged conditions, the latter provided Pluronic F68 was present. These findings were obtained in bench-scale bioreactors up to ~5 L whether "low shear" propeller or "high shear" Rushton turbines were used. Another interesting experiment during these studies involved the removal of baffles. Removal reduced $(\overline{\varepsilon}_T)_{\text{I}}$ fivefold compared with the baffled case where satisfactory growth occurred without sparging. At the highest speed employed of 400 rpm, severe vortexing occurred, which led to air entrainment followed by bubbles bursting as it disengaged. The bursting bubbles caused cell damage, though it could be eliminated by the addition of Pluronic F68, as with normal sparging.

Meier (19) reported that at Genentech, Rushton turbines, Lightnin' A320s (Lightnin', Rochester, New York) and ABEC "Elephant ear" impellers (ABEC Inc., Bethlehem, Pennsylvania) had all been used successfully at $(\overline{\varepsilon}_T)_{\text{I}}$ values up to 0.1 W/kg at the industrial scale. Sandadi *et al*. (12) had equal success producing antibodies from CHO cells at Schering-Plough with a Rushton turbine and a propeller at 0.018 W/kg at the 30-L scale.



(a)



(b)

Figure 55.5. Two other "low shear" impellers: (a) an Applikon "elephant ears" impeller (Applikon Biotechnology B. V., Schiedam, Netherlands) used extensively in animal cell culture; (b) an up-pumping Hayward-Tyler B2 impeller. (This figure is available in full color at http://onlinelibrary.wiley.com/book/10.1002/9780470054581.)

55.4.5 Studies in Other Configurations and a Comparison with Cell Strength

It is worth just briefly summarizing work characterizing cell strength and other studies as they impact on the question of impeller selection. The mechanical properties have been measured extensively by Thomas and Zhang using micromanipulation (20) and on the basis of these measurements, they have successfully predicted when lethal damage should occur under turbulent flow conditions (21). With

TB/C3 hybridoma and NS1 myeloma cells in turbulent flow through capillary tubes, ($\overline{\varepsilon}_T$) values as high as $10^5 - 10^6$ W/kg were predicted and shown to be required to totally disrupt the cells.

For some time, Chalmers and coworkers have been passing cells under laminar flow conditions through an extensional flow chamber particularly looking for nonlethal effects associated with mechanically generated stresses on protein product quality, especially with respect to glycosolation. In their most recent study, CHO cells were grown in a 2-L fed-batch process (22). During the 14-day run, a suspension of cells was continuously removed from the bioreactor and pumped through the device at ($\overline{\varepsilon}_T$) values from 60 to 6000 W/kg. They compared the results with those found with circulation but without the flow device. For all these ($\overline{\varepsilon}_T$) conditions, they monitored viability, cell size, necrosis, and apoptosis (using flow cytometry), LDH, glucose metabolism, molecular weight distribution, methionine oxidation, charge distribution, and glycosolation. For all the parameters measured except glycosolation and at all ($\overline{\varepsilon}_T$) values except the highest of 6000 W/kg, the control and the flow chamber gave the same results. In the case of glycosolation, a pattern shift was observed, though somewhat strangely, it was the same at all ($\overline{\varepsilon}_T$) values. A similar study with NSO cells did not show any effects at ($\overline{\varepsilon}_T$) = 300 W/kg. As can be seen, all the ($\overline{\varepsilon}_T$) values used in this study are orders of magnitude greater than those currently being used or likely to be used in the foreseeable future for animal cell culture even with increasing cell density. These results essentially fitted in with all the previous papers from Chalmers group that used the flow device.

55.4.6 Conclusions

Overall, these studies strongly suggest an excessive concern for agitator-generated stresses in animal cell culture processes; and that they should not be of importance for agitator selection. It is also worth noting that though $(\overline{\varepsilon}_T)_{\mathrm{Imax}}/(\overline{\varepsilon}_T)_{\mathrm{I}}$ is dependent on agitator type and size as shown in Table 55.5, it is independent of scale. Therefore, the possibility of stress sensitivity of a cell line at the large scale can be assessed by using geometrically similar impellers at appropriate $(\overline{\varepsilon}_T)_{\mathrm{I}}$ values at the bench scale.

55.5 OTHER PARAMETERS DEPENDENT ON AGITATION AND BIOREACTOR CONFIGURATION: IMPLICATIONS FOR IMPELLER SELECTION

55.5.1 Homogeneity

Under turbulent flow conditions, the time required to homogenize the contents of a bioreactor, the mixing time, θ_m (s), is related to agitation parameters by (10):

$$\theta_{\mathrm{m}} = 5.9(\overline{\varepsilon}_T)_{\mathrm{g}}^{-1/3}(D/T)^{-1/3}T^{2/3} \qquad (55.9)$$

for bioreactors for $H = T$. For bioreactors with an aspect ratio (2,10) AR($= H/T$) > 1, then

$$\theta_{\mathrm{m}} \propto (H/D)^{2.43} \qquad (55.10)$$

The applicability of Equations 55.9 and 55.10 has been demonstrated in an 8 m^3 animal cell culture bioreactor of different ARs from 0.3 up to 1.3 with a single impeller working in the draw and fill mode (2). The work covered a "high shear, low flow" Rushton turbine and a low "shear, high flow" Lightnin' A310 hydrofoil ($Po = \sim 0.30$) (Fig. 55.6a), each of $D/T = \sim 0.23$. As predicted from Equation 55.9, equal mixing times were obtained. Thus, both "high/low shear" and "high/low flow" concepts in relation to impeller selection are generally misleading. However, to demonstrate the validity of Equation 55.9 under simulated culture conditions, it was shown that, though not reported to have been used for cell culture, a larger *D/T* Intermig impeller ($D/T = \sim 0.4$, $Po = \sim 0.35$) (Fig. 55.6b) gave a slightly shorter mixing time (2). [in passing, it should be noted that the Intermig impeller is not appropriate in high oxygen demanding fermentations, especially viscous ones, because they often give rise to severe equipment vibrations when aerated under high agitation and aeration rates (10)].

Equation 55.9 clearly shows that if $(\overline{\varepsilon}_T)_{\mathrm{I}}$ is held constant under conditions of geometric similarity across the scales, the mixing time increases significantly with $T^{2/3}$(or (linear scale)$^{2/3}$) and Equation (55.10) shows its great sensitivity if fill height is increased. Large increases in AR with scale are common with fermentations involving other microorganisms, and for such cases multiple impellers are used, typically dual wide-blade, high solidity ratio (plan area of impeller blades/area of circle swept out by blades as they rotate), axial flow impellers. Examples of such impellers are the Lightnin A315 (Fig. 55.6c) or Hayward-Tyler B2 (Hayward-Tyler plc, East Kilbride, Scotland) and they are preferred because they reduce mixing times by a factor of ~ 2 compared with radial flow impellers.

Often, the absolute value of the mixing time, *per se*, is not so important. It is the trend for θ_{m} to get longer with scale and height, which means cells will experience greater temporal or spatial differences on scale-up of the parameters listed in Table 55.3, line D such as dO_2 (3) compared with the bench scale. The variations in dO_2 are also dependent on the OUR of the culture and the k_La and can be analyzed via regime analysis (2). With batch systems, pH problems are enhanced with the tendency on the larger scale to use more concentrated chemicals to reduce the quantities to be sterilized and by the tendency to add them to the top surface

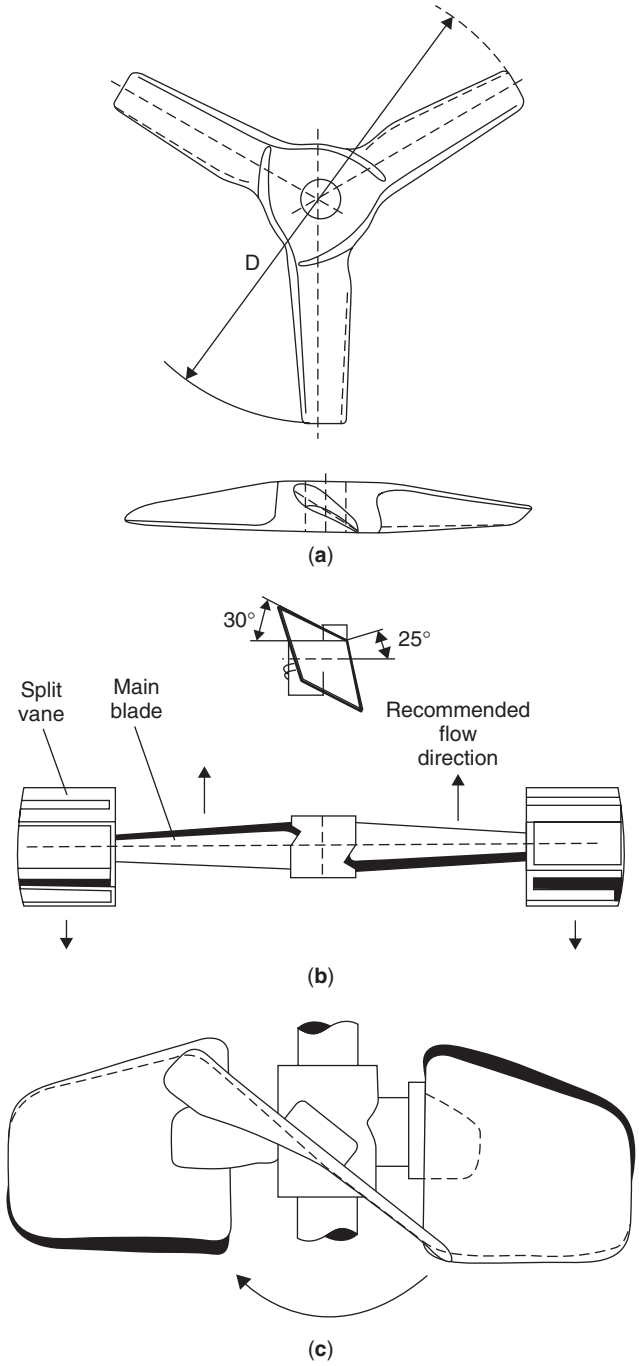


Figure 55.6. Some other impellers: (a) a Lightnin A310 impeller; (b) an Ekato Intermig impeller (Ekato, Schopfheim, Germany); (c) a Lightnin' A315 impeller.

of the media. With fed-batch operation, the need to add both pH control chemicals and nutrients to a surface, which may be a long way above the agitator as the bioreactor fills, only increases the problem (3). So far only the damage due to large spatial and temporal pH excursions from the mean has been clearly shown to exist and produce a reduction in performance in animal cell culture bioreactors. These points are discussed in detail elsewhere (2).

With respect to agitator selection and an operation strategy to help this inevitable loss of spatial and temporal homogeneity, it is suggested that dual axial flow impellers should be used. In addition, *H/T* should be ~1. Subsurface feeding of pH chemicals and nutrients during fed-batch operation is also recommended. Since that mode of operation is often objected to because of concerns for sterility, it has been shown that directing the feed at the surface where the discharge from an up-pumping impeller impacts is helpful in maximizing the rate of incorporation of the additive (23).

55.5.2 Aerated, P_g, and Unaerated, P, Power Input from the Agitator

These two aspects have already been discussed in some detail. However, the connection between them has not. In bioreactors with most other organisms (bacteria, yeast, mycelia) typical aeration rates are of the order of 1–2 vvm with power inputs between about 1 and ~5 W/kg from the impeller. These conditions are required to meet the much greater OD. In such cases, if the agitator speed is not fast enough the air is not dispersed and the system is flooded. It is important to avoid this condition and ensure that the system is loaded, that is the flow pattern is controlled by the agitator (Fig 55.7), if efficient mass transfer is to be achieved. Also, with most agitators, P_g/P is <1, often <0.5 and the relationship between the two is a complex function of impeller speed and aeration rate and depends on the agitator type. Because of their importance to these high oxygen demanding fermentations, aerated power draw and flooding–loading relationship is a critical consideration in impeller selection.

For insect and mammalian cell culture, such considerations are essentially unimportant. At the agitator speeds employed to give the desired power input to achieve adequate mass transfer, most of the dispersion is provided by the sparger and the impeller provides little or no additional effect. As a result, gas cavities do not form behind impeller blades (2) and the air passes through the impeller without significantly affecting the flow pattern close to the agitator; and $P_g \approx P$ and $Po_g \approx Po$ (2). Therefore, at present, this factor is unimportant for impeller selection for cell culture.

55.5.3 Heat Transfer

The OUR is very low compared to fermentations with other organisms. As a result, since the metabolic heat release Q_H (W/m^3) is proportional to the OUR (mol $O_2/m^3/s$) (24), that is,

$$Q_H = \sim 4.6 \times 10^5 \text{ OUR} \qquad (55.11)$$

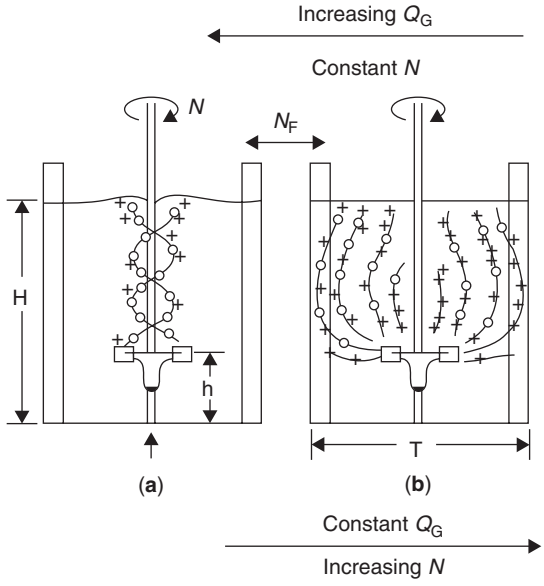


Figure 55.7. The flooding–loading transition with a radial flow impeller.

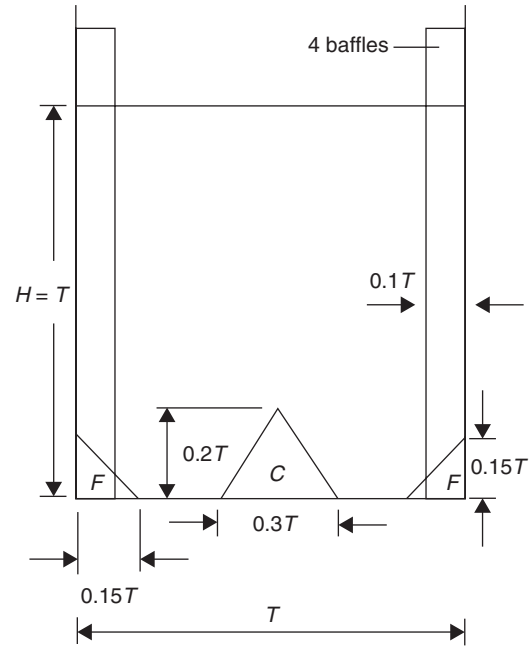


Figure 55.8. Modifications by the addition of a corner fillet (F) and a central cone (C) to a flat-based bioreactor to enable solids to be suspended at lower $(\overline{\varepsilon}_T)_{\mathrm{Ijs}}$ (the inverted cone can be used alone in a dished base). With this configuration, $C/T = 0.25$.

Thus, Q_{H} for animal cell culture is also relatively low. With other organisms, this cooling load at the commercial scale is often a problem as Q_{H} scales with the volume of the reactor, that is T^3, while cooling surface area scales with T^2. Hence, for such systems, cooling coils are often required. However, with animal cell culture bioreactors, simple cooling jackets are sufficient for good temperature control. In addition, agitation has little impact on overall heat transfer, though larger D/T ratios give a higher velocity at the inner surface of the bioreactor for a given $(\overline{\varepsilon}_T)_{\mathrm{I}}$ and hence they maximize the inner film heat transfer coefficient.

55.5.4 Microcarrier Culture

For adherent animal cells to be grown in large quantities in bioreactors, microcarriers are used. These are usually of the order of $150 - 200$ μm, either solid or macroporous, to give a large surface area for cell growth to enable a high cell density to be achieved. The most common ones commercially are Cytodex microcarriers with a density just greater than water (for Cytodex 3, it is 1040 kg/m^3). For the microcarriers to work efficiently, they must be fully suspended so that all of their surface area is available for cell growth. However, few of the papers on microcarrier culture have used impeller/vessel configurations that achieve suspension at low values of $(\overline{\varepsilon}_T)_{\mathrm{I}}$. In addition, all of the concerns discussed above with respect to oxygen transfer, homogenization and "shear" sensitivity also have to be considered once again.

The minimum agitator speed that keep the microcarriers suspended, N_{js}, and associated mean specific energy dissipation rate, $(\overline{\varepsilon}_T)_{\mathrm{Ijs}}$, are very sensitive to agitator type and precise vessel configurations. The use of a bioreactor with a hemispherical base has been recommended but in fact such a shape is not at all suitable if microcarriers are to be suspended at low values of $(\overline{\varepsilon}_T)_{\mathrm{Ijs}}$ in order to minimize the potential for damage to the cells growing on them. The presence of baffles is also important to avoid the swirling motion shown in Fig 55.1 and aid suspension (an off-center or angled impeller mounting without baffles might achieve the same effect on the small scale but it is mechanically not advisable at the industrial scale). A very efficient combination is to use an impeller such as the Chemineer HE3 (Fig. 55.6a) with a contoured base as shown in Fig 55.8. With this combination using D/T ratios from 0.44 to 0.35 at $C/T = 0.25$, it was possible to suspend Cytodex 3 microcarriers at $(\overline{\varepsilon}_T)_{\mathrm{Ijs}} <\sim 0.0005$ W/kg, though it took some time for full suspension to be reached. Even without the fillets and the flat base, $(\overline{\varepsilon}_T)_{\mathrm{Ijs}}$ was only a little higher (25). Thus, just placing a cone at the center of the dished base found in cell culture reactors would be expected to significantly lower $(\overline{\varepsilon}_T)_{\mathrm{Ijs}}$.

The reason for the desire to achieve such low values of $(\overline{\varepsilon}_T)_{\mathrm{Ijs}}$ is because it has been reported that cells on microcarriers are more sensitive to mechanical stress than when they are in free suspension (26,27). Thus, it has been suggested (26) that $(\overline{\varepsilon}_T)_{\mathrm{I}} < 0.001$ W/kg to avoid damage. This greater sensitivity is not unreasonable for two reasons. First, even at this $(\overline{\varepsilon}_T)_{\mathrm{Ijs}}$, λ_K is still only $\sim$180 μm and therefore less

than the size of many microcarriers so that cells on their surface might be damaged by turbulent eddies. Secondly, because of their size and density compared to free cells, microcarriers which are typically present at concentrations of about 5–15% of total culture volume may impact with each other or with the impeller. Such a problem is found with secondary nucleation with crystals in stirred reactors (28). Such impacts may damage cells directly or by dislodging them from the microcarrier surface. It has also been suggested that air bubbles may also dislodge cells from them.

The precise sensitivity of cells to damage on microcarriers is not well established. To reduce the possibility of damage by turbulent eddies or impacts, macroporous carriers where the cells may grow in the pores have been developed. In addition, reducing microcarrier size helps significantly to reduce damage by any mechanism. However, once a microcarrier is selected, if small-scale tests with the geometry suggested here (or with a similar down-pumping hydrofoil such as a Lightnin' A310 or even possibly an A315) show that cells can be grown successfully, since $(\overline{\varepsilon}_T)_{\mathrm{Ijs}}$ falls with increasing scale, then damage due to agitation should become less likely on scale-up.

Of course, it is quite possible that such low levels of $(\overline{\varepsilon}_T)_{\mathrm{I}}$ will cause oxygen transfer and homogenization concerns, though it can be easily increased by raising the agitator speed, and feeding into the impeller zone can enhance homogenization. However, these issues do not appear to have been addressed in the open literature. Therefore, choosing a geometry such as that recommended here that minimizes $(\overline{\varepsilon}_T)_{\mathrm{Ijs}}$ while ensuring higher speeds and $(\overline{\varepsilon}_T)_{\mathrm{I}}$ values can be obtained probably offers the best approach to culture on microcarriers at the present time.

55.6 IMPORTANT PARAMETERS NOT RELATED TO IMPELLER SELECTION

These are some very important issues in animal cell culture that are not associated with impeller selection but are worthy of a brief mention. They are discussed in more detail elsewhere (2).

55.6.1 Bubble Burst Phenomena

Bursting bubbles produce local specific energy dissipation rates up to $\sim 10^4$ to $\sim 10^5$ W/kg, with bubbles of 2 and 1 mm diameter, respectively. As stated earlier, Pluronic F68, as a result of preventing cell attachment is able to prevent damage in spite of these huge values. Nevertheless, since the impellers in animal cell culture bioreactors do not increase significantly bubble dispersion above that achieved by the sparger and the OD is relatively low, there is little need to produce such small bubbles anyway. However, it has been shown that if cell damage does occur, increasing the AR of a bioreactor reduces the proportion of the media in which it takes place (2). If a higher AR is chosen, the use of a second agitator becomes increasingly important at the commercial scale to minimize the increase in inhomogeneities.

55.6.2 pH, pCO_2, and Osmolality

pH, pCO_2 and osmolality are very important issues in animal cell culture. Under normal sparging conditions, impeller selection has no impact on CO_2 stripping rates since essentially the appropriate version of Equations 55.2 and 55.4 should apply and the k_La for O_2 transfer in and CO_2 out are approximately equal. However, largely because of the perception of shear sensitivity and bubble damage at the high superficial gas velocities implied by constant vvm scale-up, the OD at the large scale has often been met by increasing either a (and hence k_La) by producing small bubbles by sintered spargers or by enhancing ΔC by using oxygen-enriched air or a pure oxygen bleed. All these actions often lead to sparge rates that are unable to strip out the CO_2 produced at a respiratory quotient $\approx$1. As a result, pCO_2 may build up to levels $>\sim$150 mmHg, especially at the current largest scale being used ($\sim$20 m^3) at the cell densities ($\sim 10^7$ cells/mL) being achieved. As a result, pH falls, alkali must be added and osmolality increases. The low sparge rate and higher CO_2 level at the 5000 L scale has recently been considered to be one of the main reasons for the lower cell density achieved compared with those at the 5 and 20 L scale (3).

It is hoped that this discussion on the overreaction to the sensitivity of freely suspended animal cells to mechanical stresses associated with agitation and sparging will help reduce these approaches to scale up to meet the OD of the cells as they produce more problems than they solve.

55.7 SELECTION OF IMPELLER/GEOMETRY, SCALE-UP, AND OPERATIONAL STRATEGY

55.7.1 Free Suspension Culture

From the above analysis of the tasks required to be fulfilled by impeller(s) when undertaking animal cell culture and the special features involved in undertaking it, it can be concluded that many different impeller types could be used successfully. Indeed, many different types have been reported to have done so even at the commercial scale; Rushton turbines (2,12,19,29), Lightnin' A320s(19), propellers (3,12), and "elephant ear" impellers (19). This success is hardly surprising since it has been shown that both with respect to lethal (2,20) and sublethal (2,22) effects, animal cells

are much more robust (21) than their initial designation of "shear-sensitive" implied. It has also been shown here that the concept of "low" and "high shear" impellers is misleading. However, it is still possible to indicate which impeller(s) and associated geometry are likely to prove the most suitable. It is also important to point out that for ease of scale-up, the use of geometrically similar configurations at the different scales is recommended, especially if basic data like specific OUR for the particular cell line are not known. The relationships for the physical parameters that define the "mixing" conditions are much easier to match or determine across the scales if geometric similarity is followed.

Overall, based on the earlier analysis, the following general guidelines for the selection of impeller(s) and geometrically similar vessel geometry across the scales are recommended:

1. One of the major problems of scale-up in all bioprocessing is the decreasing homogeneity associated with increasing scale (Eq. 55.9) and vessel AR (Eq. 55.10). Because of the very low $(\overline{\varepsilon}_T)_{\mathrm{Ig}}$ value required to provide the k_La to meet the OD (Eq. 55.2), this issue is particularly significant in animal cell culture. Therefore, it is important to keep the vessel AR to a value $<\sim 1.3$.
2. Also for the best homogeneity for a given $(\overline{\varepsilon}_T)_{\mathrm{Ig}}$, use baffles (preferably four but three or even two are much better than none!). The use of baffles also ensures that if Po for the chosen impeller is known (and since at the low sparge rates used, Po_g can realistically assumed to be equal to Po), the speed to give $(\overline{\varepsilon}_T)_{\mathrm{Ig}}$ required for mass transfer can be calculated (Eq. 55.3).
3. Use subsurface feeding of pH control chemicals and nutrients if fed-batch operation is involved (2,29) to minimize spatial and temporal concentration variations. If concentration variations remain a problem, consider use of more dilute feeds (30).
4. Use dual, up-pumping, wide-blade axial flow hydrofoil or "elephant ear" impellers diameter of 0.4–0.5 of the vessel diameter with clearance between them of 0.33 to 0.5 T depending on the AR and the level changes (which may lead to splashing) associated with fed-batch operation if it is used. The lower impeller maximizes the level of air dispersion and though not important at present, as higher sparge rates will need to be utilized as cell densities increase further, they should continue to remain effective (31). The upper impeller improves homogeneity near the upper surface, especially if nutrients and pH control chemicals are added to the top surface (23,31). It also has been shown to reduce the amount of foaming compared with other impellers (31,32). The large D/T ratios also maximize the inner film heat transfer coefficient.
5. Estimate power requirements of the motor from the OD requirements of the organism (3). If the OD is not known, but small-scale operation in a bench-scale bioreactor has been achieved, use equivalent $(\overline{\varepsilon}_T)_{\mathrm{Ig}}$ on scale-up. Then select a variable speed motor capable of giving higher $(\overline{\varepsilon}_T)_{\mathrm{Ig}}$ values but with a large turn-down ratio. During the early stages of the culture when OD is low, this flexibility should allow less power to be used while maintaining dO_2 control. It also allows for the possibility of increased cell density and associated OD with improvements in animal cell culture technology elsewhere and if estimates of current operating requirements are under estimated.
6. Air/nitrogen should be introduced through a pipe (2,3,33) or ring sparger (2,34) [though exit velocities through the holes >30 m/s at the large scale should be avoided (34)] placed below the lower impeller. The total flow rate should approximate constant vvm across the scales and be balanced to give both the required k_La and dO_2 and the required CO_2 ventilation rate and pCO_2. If needed, oxygen can be introduced through a separate sparge pipe. This sparge strategy should also minimize foaming (2).
7. To minimize cell damage due to bubble bursts from aeration, use Pluronic F68 at concentrations ≥ 0.5 g/L.
8. Use antifoam to control foaming as appropriate. For a more detailed analysis of the use of antifoams and the optimum addition strategy, the papers of Denkov and Marinova are recommended (35).

55.7.2 Microcarrier Culture

All of the issues above apply to agitator choice for microcarrier culture. However, the issue of "shear damage" is almost certainly much more critical due to the size and to a lesser extent density of the microcarriers, increasing the chances of direct damage to the cells or to their removal from the microcarrier by bubbles, particle impacts or turbulence. The use of smaller microcarriers may help reduce this tendency. To minimize the possibility of damage due to agitation, a down-pumping hydrofoil is preferred with a contoured vessel base as shown in Fig 55.8. With the lack of literature available which report both successful microcarrier culture and details of the agitation system utilized on the commercial scale, it is therefore recommended that the considerations set out above be used generally to guide impeller and geometry selection. The major change would be to the lower impeller. It should be a down-pumping impeller, even possibly a thin blade hydrofoil such as the Chemineer HE3 which together with a shallow dished or

contoured base has been shown (25) to suspend microcarriers at very low values of $(\overline{\varepsilon}_T)_{Ijs}$, lower than those that have been reported elsewhere to prevent successful microcarrier growth (26,27). However, it must be recognized that if cell "damage" occurs as easily as has been suggested in the literature, problems due to other issues such as poor homogeneity, poor pCO_2 stripping and pH control, and osmolality buildup may well occur. In that case, whatever impeller is selected, there must be serious doubts about the viability of large-scale microcarrier cell culture.

The author's experience suggests that "shear sensitivity" has been frequently (and damagingly) overemphasized in the past and perhaps it has been again for microcarrier culture. Certainly, more work needs to be directed toward such systems; especially it is currently becoming an important issue for the scale-up of stem cell cultivation for regenerative medicine and for producing cells as an alternative to live animal testing. Such cells require the use of microcarriers as, at present, they cannot be grown in free suspension.

NOMENCLATURE

a	specific area of bubbles
A	dimensional constant
AR	aspect ratio, H/T
B	baffle width
C	clearance above vessel base
D	agitator diameter
Fl	flow number
g	gravitational constant
H	bioreactor fill level
k_L	mass transfer coefficient
k_La	specific mass transfer coefficient
M	mass of media
N	agitator speed
OD	oxygen demand
OTR	oxygen transfer rate
OUR	oxygen uptake rate
P	power
Po	power number
Q	liquid flow rate pumped by the impeller
Q_H	heat evolution rate
Re	Reynolds number
SOD	specific oxygen demand
T	bioreactor diameter
v_s	superficial gas velocity
vvm	specific volumetric flow rate
V	volume of media
X	cell density

Greek letters

α, β	exponents
α°	blade angle
ΔC	driving force
ε_T	local specific energy dissipation rate
$\overline{\varepsilon}_T$	mean specific energy dissipation rate
λ_K	Kolmogoroff turbulence scale
μ	viscosity
ν	kinematic viscosity
ρ	liquid density
θ_m	mixing time

Subscripts

g	when air is sparged
I	Impeller
js	just suspended
max	maximum
s	sparged
swept	impeller swept volume

REFERENCES

1. Nienow AW. Kirk Othmer. Encyclopedia of chemical technology (online). Hoboken: John Wiley & Sons, Inc.; 2005. http://www3.interscience.wiley.com/cgi-bin/mrwhome/104554789/HOME
2. Nienow AW. Cytotechnology 2006; 50: 9–33.
3. Xing Z, Kenty BM, Li ZJ, Lee SS. Biotechnol Bioeng 2009; 103: 733–746.
4. Varley J, Birch J. Cytotechnology 1999; 29: 177–205.
5. Handa-Corrigan A, Emery AN, Spier RE. Enzyme Microb Technol 1989; 11: 230–235.
6. Kilburn DG, Webb FC. Biotechnol Bioeng 1968; 10: 801–814.
7. Meier SJ, Hatton TA, Wang DIC. Biotechnol Bioeng 1999; 62: 468–478.
8. van't Riet K. Ind Eng Chem (Proc Des Dev) 1979; 18: 357–367.
9. Hoeks FWJMM, Khan M, Guter D, Willems M, Osman JJ, Mommers R., Wayte J. Industrial applications of mixing and mass transfer studies. Alvin W. Nienow's Day; Stirred, not Shaken Symposium; Sept. 2004; Birmingham, UK, University of Birmingham.
10. Nienow AW. In: Pohorecki R, editor. Fluid mechanics problems in biotechnology. App Mech Rev 1998; 51: 3–32.
11. Pullen KF, Johnson MD, Phillips AW, Ball GD, Finter NB. Dev Biol Std 1985; 60: 175–185.
12. Sandadi S, Rose P, Bowers J, Rendeiro D. Impact of impeller design on antibody production by Chinese Hamster Ovary Cells. AIChE Annual Meeting; Nov. 2007; Salt Lake City, Utah.
13. Amanullah A, Nienow AW, Buckland BC. In: Paul EL, Atiemo-Obeng VA, Kresta SM, editors. Handbook of industrial mixing; science and practice. New York: Wiley-Interscience; 2004. pp. 1071–1157.
14. Nienow AW. Adv Coll Interface Sci 2004; 108-109C: 95–103.
15. Geissler R, Krebs R, Forschner P. Proceedings of 8th European Mixing Conference. IChemE; 1994; Rugby, UK, pp. 241–251

16. Zhou G, Kresta SM. AIChEJ 1996; 42: 2476–2490.
17. Zhu H, Bujalski W, Nienow AW, Simmons MJH. Chem Eng Res Des (Trans I Chem E Part A) 2009; 87: 307–317.
18. Simmons MJH, Zhu H, Bujalski W, Hewitt CJ, Nienow AW. Chem Eng Res Des (Trans I Chem E part A) 2007; 85: 551–559.
19. Meier SJ. Cell culture scale-up: mixing, mass transfer, and use of appropriate scale-down models. Biochemical Engineering XIV; July 2005; Harrison Hot Springs, Canada.
20. Zhang Z, Ferenczi MA, Thomas CR. Chem Eng Sci 1992; 47: 1347–1354.
21. Thomas CR, Al-Rubeai M, Zhang Z. Cytotechnology 1994; 15: 329–335.
22. Godoy-Silva R, Mollet M, Chalmers JJ. Biotechnol Bioeng 2009; 102: 1119–1130. DOI: 10.1002/bit.22146.
23. Battacharya S, Kresta SM. Chem Eng Res Des (Trans I Chem E Part A) 2004; 82: 1153–1160.
24. Van't Riet K, Tramper J. Basic bioreactor design. New York: Marcel Dekker; 1991.
25. Ibrahim S, Nienow AW. Chem Eng Res Des (Trans I Chem E, Part A) 2004; 82: 1082–1088.
26. Aunins JG, Croughan MS, Wang DIC, Goldstein JM. Biotechnol Bioeng Symp 1986; 17: 699–723.
27. Croughan MS, Hamel JFP, Wang DIC. Biotechnol Bioeng 1987; 29: 130–141.
28. Nienow AW. In: Harnby N, Edwards MF, Nienow AW, editors. Mixing in the process industries. 2nd ed (paperback revision). London: Butterworth Heinemann; 1997. pp. 364–411.
29. Langheinrich C, Nienow AW. Biotechnol Bioeng 1999; 66: 171–179.
30. Assirelli M, Bujalski W, Eaglesham A, Nienow AW. Chem Eng Sci 2005; 60: 2333–2339.
31. Nienow AW, Bujalski W. Chem Eng Res Des (Trans I Chem E, Part A) 2004; 82: 1073–1081.
32. Boon LA, Hoeks FWJMM, van der Lans RJM, Bujalski W, Wolff MO, Nienow AW. Biochem Eng J 2002; 10: 183–195.
33. Mostafa SS, Gu X. Biotechnol Prog 2003; 19: 45–51.
34. Zhu Y, Cuenca JV, Zhou W, Varma A. Biotechnol Prog 2008; 101: 751–760.
35. Denkov ND, Marinova KG. In: Binks BP, Horozov TS, editors. Colloidal particles at liquid interfaces. Cambridge, UK: Cambridge University Press; 2006. pp. 383–444.

56

MAMMALIAN CELL BIOREACTORS

Weichang Zhou
Genzyme Corporation, Framingham, Massachusetts

Gargi Seth
Genentech, Inc., South San Francisco, California

Maria J. Guardia
Camino De Purchill, Puleva Biotech Department of Process Engineering, Granada, Spain

Wei-Shou Hu
University of Minnesota, Department of Chemical Engineering and Materials Science, Minneapolis, Minnesota

56.1 INTRODUCTION

The year 2012 marked the 25th anniversary of the introduction of the first recombinant mammalian cell culture produced therapeutic protein, tissue plasminogen activator (Activase®) by Genentech. The first Chinese hamster ovary (CHO) cell produced protein drug was followed by the introduction of erythropoietin (EPO) (by Amgen in 1989). In the past decade, a rapid expansion of recombinant antibody-based therapeutics has pushed the annual production amount of therapeutic protein to tens of thousands of kilograms and over 20 billion US dollars in revenue per annum (Tables 56.1 and 56.2). Before the advent of recombinant DNA technology, industrial mammalian cell culture was used primarily for the production of biologics using isolated transformed cells and viral vaccines using primary cells and normal diploid cell strains. The arrival of rDNA technology and the expression of heterologous proteins in mammalian cells completely transformed cell culture technology. Except for the production of attenuated or inactivated viral vaccines, virtually all mammalian cell culture processes now employ continuous cell lines, most of which have been adapted to grow in suspension, without a surface support. The adoption of the growth of suspension cells as the typical vehicle for the production of complex molecules requiring extensive posttranslational modification also transformed the concept of bioreactor selection.

Most research and many commercial efforts on developing bioreactors for mammalian cell culture occurred in the 1980s and early 1990s. The anticipation was that the potentially detrimental effect of the air sparging on mammalian cells would require a newly designed bioreactor to accommodate the manufacturing needs of the new mammalian cell-derived products. What was unanticipated to researchers and altered the landscape of bioprocessing technology was the extraordinary capability of cells to adapt to suspension growth, serum-free, even protein-free, and other culture conditions at very large scale (over 20,000 L). Over time the bioreactors used for industrial cell culture converge on a few basic configurations. This chapter focuses only on the main types used currently for industrial cell culture. It should be noted that many of the bioreactors developed in the 1980s, although not commonly used, might find specialized applications in other areas, such as tissue engineering, gene therapy, and cellular therapy.

Upstream Industrial Biotechnology: Equipment, Process Design, Sensing, Control, and cGMP Operations, Volume 2, First Edition. Edited by Michael C. Flickinger.
© 2013 John Wiley & Sons, Inc. Published 2013 by John Wiley & Sons, Inc.

TABLE 56.1. Major Licensed Recombinant Therapeutic Proteins Expressed by Mammalian Cells (as of 1997)

Protein	Cell Line Used	Therapeutic Use (Year Approved)
Tissue plasminogen activator (TPA)	CHO	Heart attack/embolism, stroke (1987)
Erythropoietin (EPO)	CHO	Anemia (1989)
Human growth hormone	C127	Growth deficiency, renal insufficiency (1989)
Granulocyte colony stimulating factor	CHO	Neutropenia (1991)
Factor VIII	CHO/BHK-2	Hemophilia A (1992 & 1993)
Deoxyribonuclease I (DNase)	CHO	Cystic fibrosis (1993)
Glucocerebrosidase	CHO	Gaucher's disease (1994)
Interferon-β	CHO	Multiple sclerosis (1996)
Factor IX	CHO	Hemophilia B (1997)

TABLE 56.2. Licensed Therapeutic Monoclonal Antibodies and Antibody Fusion Proteins in the United States (as of 2007)

Protein (Trade Name)	Cell Line Used	Therapeutic Use (Year Approved)
Anti-CD3 (Orthoclone OKT3)	Hybridoma	Allograft rejection (1986)
Anti-GPIIb/IIIa Fab fragment (ReoPro),	Sp2/0	Blood clots in angioplasty (1994)
Anti-IL 2 receptor a chain (CD25) (Zenapax)	NS0	Renal transplantation (1997)
Anti-CD20 (Rituxan)	CHO	Non-Hodgkin's lymphoma (1997)
Anti-IL 2 receptor a chain (CD25) (Simulect)	Sp2/0	Renal transplantation (1998)
Anti-respiratory syncytial virus (Synagis)	NS0	Respiratory syncytial virus (1998)
Anti-tumor necrosis factor a (Remicade)	Sp2/0	Crohn's disease (1998)
Anti-HER2 (Herceptin)	CHO	Metastatic breast cancer (1998)
Anti-tumor necrosis factor Fc fusion (Enbrel)	CHO	Rheumatoid arthritis (1998)
Anti-CD33 (Mylotarg)	NS0	Acute myeloid leukemia (2000)
Anti-CD52 (Campath)	CHO	B cell chronic lymphocytic leukemia (2001)
Anti-CD20 (Zevalin)	CHO	Non-Hodgkin's lymphoma (2002)
Anti-tumor necrosis factor a (Humira)	CHO	Rheumatoid arthritis (2002)
Anti-IgE (Xolair)	CHO	Asthma (2003)
Anti-CD20 (Bexxar)	Hybridoma	Non-Hodgkin's lymphoma (2003)
Anti-leukocyte function antigen-1 (Raptiva)	CHO	Psoriasis (2003)
Anti-leukocyte function antigen-3 (CD2) Fc fusion (Amevive)	CHO	Psoriasis (2003)
Anti-epidermal growth factor receptor (Erbitux)	Sp2/0	Colorectal cancer (2004)
Anti-vascular endothelial growth factor (Avastin)	CHO	Colorectal cancer (2004)
Anti-alpha4-subunit of alpha4beta1 and alpha4beta7 integrins (Tysabri)	NS0	Multiple sclerosis (2004)
Anti-CD80 and CD86 (Orencia), Fc fusion	CHO	Rheumatoid arthritis (2005)
Anti-epidermal growth factor receptor (Vectibix)	CHO	Metastatic colorectal cancer (2006)
Anti-C5 (the complement protein) (Soliris)	NS0	Paroxysmal nocturnal hemoglobinuria (PNH) (2007)

56.2 BASIC REACTOR OPERATION AND KINETICS

56.2.1 Basic Types of Reactors

Mammalian cell bioreactors can be generally categorized similarly to chemical reactors according to their mixing characteristics. It is instructive to review two ideal reactors: well-mixed stirred-tank- and plug-flow (tubular) reactor. In an ideal well-mixed bioreactor, the mixing is assumed to be intense enough that the fluid is homogeneous through the reactor. The mathematical description of ideal continuous flow stirred-tank reactor is described by the following first-order differential equation.

$$\frac{\mathrm{d}(VC_\mathrm{A})}{\mathrm{d}t} = F_\mathrm{i}C_\mathrm{Ai} - F_\mathrm{o}C_\mathrm{Ao} + r_\mathrm{A}^V \qquad (56.1)$$

V is the culture volume in the bioreactor, C_A the concentration of nutrient or product A, t is time, F is the flow rate, and r_A is the volumetric consumption rate of nutrient or production rate of product A.

In an ideal continuous stirred-tank reactor, there is no flow bypass and no shunt of substrate from inlet to outlet, no dead zones or clumps of undissolved solid substrate floating around. Any substrate added through feeding is instantaneously distributed throughout the entire reactor,

and when gas sparging is employed, the agitator provides an intimately mixed gas–liquid.

The basic model for the tubular reactor (such as hollow fiber and many other membrane bioreactor systems that are described later in this chapter) is that liquid phase moves as a plug-flow, meaning that there is neither variation of axial velocity over the cross section nor backmixing in the longitudinal direction. The mass balance for component A in a volume element $S\,\partial z$ that described an ideal plug-flow reactor is as follows:

$$\frac{\partial C_{\mathrm{A}}}{\partial t} = -\mathrm{v}_Z S \frac{\partial C_{\mathrm{A}}}{\partial z} + r_{\mathrm{A}} \tag{56.2}$$

where v_z is the linear velocity in the z direction and S is the cross-sectional area.

Given the initial condition in Equation 56.1, or both initial and boundary condition in Equation 56.2, one can obtain the concentration profiles over time; or for tubular reactors, the profile can be obtained over time and spatial position. At steady state (i.e. cell concentration and cellular activities are not changing with time), the equation for tubular reaction becomes

$$\frac{\partial C_{\mathrm{A}}}{\partial z} = \frac{r_{\mathrm{A}} \cdot S}{F} \tag{56.3}$$

which describes changes of concentration of A along the direction of fluid flow. It is clear that the nutrient concentration will decrease from inlet to the distal end of the reactor, while metabolite or product concentration increases. The length of the reactor is limited because eventually nutrient depletion or metabolite accumulation inhibits growth and metabolism.

These ideal cases of well-mixed tanks or plug-flow tubular reactors are situations that can be approximated in small-scale laboratory conditions. The conditions in larger scale reactors deviate significantly from these ideal conditions.

In a well-mixed bioreactor, there are no concentration gradients in either the gas or the liquid phase. In other words, none of the chemical species or cells is segregated in the reactor. The other extreme of mixing is total segregation where there is no interaction between different volume elements in the bioreactor. An ideal plug-flow reactor is assumed to be under conditions of total segregation. Most bioreactor systems have a mixing pattern between the two extremes and are under partially segregated conditions.

In general, laboratory and small pilot plant bioreactors are used for process development, optimization, and characterization. The fluid mixing characteristics are rather sensitive to the scale of the reactor. Furthermore, plug-flow bioreactors are intrinsically more difficult to scale up than mixing vessels, as the concentration gradient of essential nutrients, oxygen in particular, will inevitably become limiting in the downstream region of the reactor. In considering the selection of bioreactors for mammalian cell cultures, the mixing characteristics and their relationship to scale-up have to be kept in mind.

56.2.2 Batch/Fed-batch Versus Continuous/Perfusion Operations

Mammalian cell cultures can be operated in batch, fed-batch, and continuous modes. In a batch culture all nutrients are added at the beginning of a production cycle, except that oxygen is supplied continuously by diffusion through the interface with an oxygen carrying stream, which is part of the recirculating medium or air flowing through the culture. Using a conventional medium, the typical concentrations achieved in a batch culture are rather low, around $2-4\times10^6$ cells/mL. In many cases, batch operation tends to be run as extended batch processes that are sometimes referred to as *repeated batch cultures* with intermittent harvest. In this operation mode, spent medium with or without cells may be harvested periodically and replaced by an equal quantity of fresh medium. It allows a production process to be extended to a few weeks with an increased productivity for the reactor. With this technique it is possible to prevent the inhibitory products from accumulating to an exceedingly high level and to provide nutrients for cell growth and production.

To prolong the culture period, fed-batch operation is practised. The culture is started at less than full volume; after a short period of growth, concentrated nutrient stream containing amino acids, glucose, and some other nutrients is added continuously or intermittently until reaching maximum volume. The total amount of nutrients added to the reactor is typically substantially (a few fold) higher than if the reactor was filled with fresh basal medium at the beginning. Such fed-batch processes reach higher cell concentrations and prolong the product formation period. The final product concentration is substantially higher than that in a batch culture.

Continuous chemostat is a very useful research tool. Once a steady state is reached, the spent medium withdrawn is balanced by equal supply rate of fresh medium, and the amount of cells being continuously discharged from the bioreactor is balanced by growth. A drawback of a simple continuous culture is the low cell concentration, and the corresponding low product throughput of the system. To increase the cell concentration and the reactor throughput, a perfusion culture is more frequently used in industrial continuous operations. In a perfusion culture, a high medium flow rate (one much higher than the cell growth rate, which would wash out cells in a simple continuous culture) is used, but a cell retention device is used to prevent most of the cells from leaving the reactor. The cell concentration

in the reactor is many times higher than that for a simple continuous culture.

A cell retention device may be physically positioned inside or outside of the bioreactor vessel (1,2). The devices that have been used include settling tanks (3), external centrifuges (4) (5), external membrane filtration (6), internal microfiltration (7), rotating wire cage (spin filters) (8), and acoustic settling device (9). All these, or similar devices, have been shown to be effective at laboratory scale. On the industrial scale, bioreactors of up to hundreds of liters, centrifuges, settling devices, and spin filters appear to be the top choices. The employment of a centrifuge or a settling device necessitates a recirculation loop to return the concentrated cell stream back to the reactor, while discarding the purged cells along with the other stream. As the scale increases the holding time in the external recirculating loop also becomes longer and potential oxygen starvation must be avoided to minimize the risk of cell progression to apoptosis. Such concern may require the reduction of temperature in the external loop. Using an internal cell retention device minimizes such a concern. However, all cell retention devices may face occasional problems of cell clogging or mechanical failure. An external device is in general easier to be replaced or duplicated for alternating operation than an internal device. When a culture is operated in a continuous mode, it is desirable for the operation to last for months; a replaceable cell retention device can make the process more robust.

56.3 CELL SUPPORT FOR MIXING VESSELS

56.3.1 Microcarriers

The use of microcarriers for cell culture was first demonstrated four decades ago (10). The basic concept is to allow cells to attach to the surface of small suspended beads so that conventional stirred-tank bioreactors can be used for cell cultivation. The diameter and density of these cell-laden microcarriers are usually in the range of 100–300 μm and 1.02–1.05 g/cm^3 so that the settling velocity is in the order of centimeter per minute. This diameter range also gives a good growth surface area per reactor volume. Even at a moderate microcarrier concentration, in the range of 8–15% culture volume being occupied by microcarriers, a significantly larger surface area per reactor volume can be achieved in a microcarrier culture than in T-flasks, roller bottles, or other plastic reactors with flat surfaces.

Although even smaller microcarriers, less than 100 μm in diameter, can provide more surface area, they are not used often. Most adherent-dependent cells do not develop their normal morphology, and in many cases, do not multiply well on surfaces with an excessively high curvature. These cells do not grow well on small microcarriers. On the other hand, some cells, especially transformed cells, multiply well even though they are attached to small microcarriers and do not spread. These cells, after attaching to the small microcarriers, agglomerate to form aggregates and continue to grow to high density. The small microcarriers, usually with a diameter of about 50 μm, serve as nuclei for the initiation of aggregate formation (11).

The microcarriers can be made of many different materials, including dextran, gelatin (12), polystyrene (13,14), glass (15), and cellulose (16). Not all these are commercially available. In general, in addition to having a wettable surface, the backbone materials of microcarriers often need to be chemically modified to improve cell attachment. One of the most widely used microcarriers, the dextran based ones, are derivatized with charged molecules or collagen. Polystyrene microcarriers have also been coated with collagen or other adhesion molecules for better performance.

An advantage of microcarriers for the industrial-scale culture of anchorage-dependent cells is the ease of separating cells from culture medium. Many microcarrier cultures require medium exchanges during cultivation to remove accumulating lactate, ammonia, and other metabolites and to replenish nutrients. In many cases, the cell-laden microcarriers are simply allowed to settle and the spent medium is withdrawn and replenished. In large-scale operations, continuous or semicontinuous perfusion is more frequently used. This can be accomplished by withdrawing medium through a coarse screen that allows medium to pass through but retains microcarriers in the reactor. Many types of cells have been grown on microcarriers, including fibroblasts, kidney, epithelial, hepatocyte, neuroblastoma, and endothelial cells from various species. Overall, microcarrier culture is a convenient laboratory and research tool, and it has the advantage of being amenable to large-scale production if a large quantity of product is needed.

56.3.2 Macroporous Microcarriers

A variant of microcarriers is one with large pores of tens of micrometers in its interior. The void space inside allows cells to be cultivated not only on the external surface but also internally. Cells in the interior are less susceptible to mechanical damage caused by agitation and gas sparging. Of course, being in the interior of microcarriers, cells are more likely to be subject to oxygen limitation due to the long diffusional distance, especially since most macroporous microcarriers have a larger diameter (500 μm to a couple of millimeters). Macroporous microcarriers are made of different materials, including gelatin (17), collagen (18), and plastic (e.g. Cytoline®). Some macroporous microcarriers have apparent bulk density similar to that of conventional microcarriers. However, because of their larger particle size, the settling velocity is substantially higher. In some cases, the settling velocity is orders of

magnitude higher, in the order 100–1000 cm/min. These microcarriers are suitable for use in fluidized beds with a high fluid recirculation rate. Because of the high settling velocity even at high upward supervelocity, the carrier can be retained in the reactor. Similar to microcarriers many cell lines have been successfully grown on macroporous microcarriers including Vero, HepG2, CHO, and HEK293 cells. The final cell concentration achieved tends to be higher than that obtained with an equivalent volumetric concentration of conventional microcarriers. But, in some cases, the growth kinetics are a bit slower because the penetration of cells into the interior may be slowed or even retarded by restrictive opening of these pores.

Since the cells are protected inside the capsules, they are protected from hydrodynamic damage. The culture can be stirred at faster rates than conventional culture, which improves nutrient, metabolite, and gas exchange. Entrapped cells may be cultured in stirred-tank bioreactors, fixed-bed and fluidized-bed reactors. An airlift reactor could be used as well, provided that the beads are small and not significantly denser than the medium.

56.3.3 Aggregates

Some transformed cells that normally attach to or spread and grow on a surface can form aggregates when cultivated on less hydrophilic surfaces or in shaker flasks or stirred vessels (19). Different methods have been used to induce aggregate formation for cells. Aggregation can be promoted by manipulating the calcium concentration (20) in conjunction with the agitation rate. Aggregate cultures have advantages similar to microcarrier cultures. They can be cultivated in conventional stirred-tank reactors with environmental control. They can be allowed to settle relatively rapidly by stopping agitation. This permits medium replenishment readily.

For many cell types, one limitation for application of the aggregate culture is that the rate of aggregate formation is slow. One way to induce aggregate formation is to add microspheres, the small microcarriers with a diameter of about 50 μm, to cell suspension to allow for rapid agglomeration to the microspheres (11). If the aggregate diameters become too large, necrotic centers can be formed due to transport limitation. The aggregate size may influence the viral infection kinetic and yield for vaccine formation (21). Many cell lines, including BHK, CHO, 293, and ST cells, have been cultivated as aggregates with sizes ranging between 90 and 400 μm, without the formation of necrotic centers (11,22).

56.3.4 Cell Entrapment

Another method of cell cultivation, which enables the use of a stirred-tank reactor, is cell entrapment. This technique entails entrapping cells in polymeric spheres. The spheres can then be coated with another polymeric film with controlled cross-linking of the polymer to modulate the permeability to molecule according to their size. This is commonly referred to as *microencapsulation*. In other applications, the spheres with entrapped cells are cultivated in the same way as the beads suspended in medium to allow for cell growth. One of the polymers frequently used for cell entrapment is calcium alginate. Cell entrapment in calcium alginate is accomplished by preparing a cell suspension in sodium alginate and adding it, in a drop-wise fashion, into a solution of calcium chloride. A high calcium concentration promotes cross-linking of alginate, instantaneously forming beads containing entrapped cells. The alginate beads may be coated with polylysine for increased mechanical characteristics and structural integrity, but such treatment decreases the molecular weight cutoff (MWCO) and prohibits large-molecular weight proteins in the medium from reaching the cells. To prepare hollow spheres, the alginate gel inside a bead coated with a polylysine is liquefied by treatment with a calcium chelator such as EDTA (ethylenediaminetetraacetic acid) or citrate.

The diameter of these beads is often in the order of millimeters. The mechanical strength of the gel which constitutes the beads is relatively weak even with polymeric coating. Large-scale application using such techniques is not easy. On the other hand, the microcapsule provides a means of immunoisolation of transplanted cells or tissues (sometimes referred to as *artificial cells*) and could be suitable for some tissue engineering applications. Cell entrapment has been applied to hybridomas (23) and small clusters of adherent cells (24). It has also found applications in the cultivation of differentiated cells, such as insulin-secreting cells. For tissue engineering applications using differentiated cells, the enclosing membrane around the cells and the hydrogel must be biocompatible (25).

56.4 CELL CULTURE BIOREACTORS

Cells respond to fluid flow by changing their morphology, metabolism, and, in some cases, their signaling pathways. Excessive fluid shear causes cell damage and ultimately death. How cells respond to fluid flow is dependent on cell types, as well as the way they are cultivated. For cells capable of growing either in suspension or attached, the sensitivity to fluid flow may differ when grown in suspension or on a surface. Adherent cells may respond differently on a flat surface and on a curved surface such as microcarriers. Even surface roughness or adhesiveness may affect how they respond to fluid flow field. During the reactor selection process, the most fundamental consideration is that the reactor provides sufficient mixing and mass transfer

while minimizing potential cell damage. Cell damage from the interaction between microcarriers and turbulent eddies may be severe. Thus, fluid shear is of paramount consideration in microcarrier culture. This is especially of concern when the Kolmogorov length scale for the smallest turbulent eddies becomes comparable to the diameter of the microcarriers (26). The microcarrier–microcarrier collisions are also expected to increase in frequency and severity in the presence of eddies of size equal to the average interparticle distance. Suspended cells are generally less prone to hydrodynamic damage than cells on microcarriers. Overall, stirred-tank bioreactors are most commonly used for cell cultivation. The use of disposable cell culture devices (also referred to as a *single-use device*) suitable for process scale (up to hundreds of liters) has become common place in the past few years, especially in cell propagation for inoculum preparation.

56.4.1 Stirred-Tank Bioreactor

Stirred tanks have been widely used for culturing suspension cells since the 1960s. The basic configuration of stirred-tank bioreactors for mammalian cell culture is rather similar to that of microbial fermentors (Fig. 56.1). The aspect ratio (the height-to-diameter ratio) of bioreactors used for mammalian cell culture is often smaller than that for microbial cultivation. However, in recent years that distinction has become less apparent as the scale of cell culture bioreactors approaches tens of cubic meters in volume. However, the bioreactors used for microcarrier cultures generally have a low aspect ratio to provide a higher surface-to-volume ratio. The power input per unit volume of bioreactor is substantially lower in mammalian cell culture bioreactors. While the Rushton type impeller is the norm in microbial fermentors, mammalian cell culture bioreactors mostly employ pitched blade or marine type impeller. Like in microbial fermentors, multiple impellers are used in larger scale bioreactors for mammalian cell culture. The use of pitched blade, as opposed to Rushton turbine, reflects the different purposes of agitation. In microbial fermentation, agitation is needed at a higher power input to disperse air bubbles and to increase oxygen transfer efficiency, whereas in mammalian cell culture, a much lower agitation rate is sufficient to keep cells or microcarriers suspended in medium relatively uniformly and to support the oxygen demand of the culture. In general, the acceptable mixing time in a mammalian cell culture bioreactor is substantially higher than that in a microbial fermentor. The oxygen transfer capacity in a cell culture bioreactor is substantially lower than that in a microbial fermentor, since the typical oxygen demand in a mammalian cell culture is also much lower (10–50 times) due to lower cell mass than that in microbial fermentation.

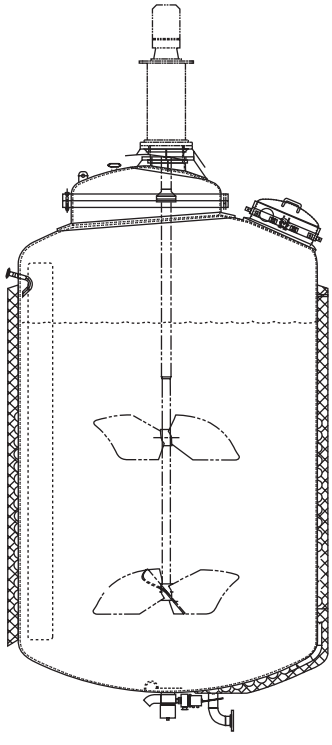


Figure 56.1. Schematic of a stirred-tank bioreactor. (Courtesy of Genentech, Inc.)

The most efficient way to supply oxygen, especially in large scale, is the direct sparging of air or oxygen-enriched air. Direct sparging, however, can potentially damage cells. Numerous studies have tried to clarify the mechanism of cell damage caused by direct gas sparging (27). The high energy released as the gas bubbles release from the liquid surface due to bubble ruptures appears to be responsible for its most damaging effects. These consequences can be partially alleviated by the addition of polyols in the culture medium to prevent cells from attaching to the bubble surface. It is, in fact, standard practice to include Pluronic F-68® in low protein or protein-free medium for suspension cultures. This effectively prevents cells from attaching to the bubble surface, thus minimizing cell damage or death due to bubble ruptures. Commonly used spargers include open pipe, ring sparger with multiple holes of a diameter of ~1/16 in., and microsparger made of sintered stainless steel. Microspargers create swarms of small bubbles and are efficient for oxygen transfer, as they create a larger interfacial area at a given air flow rate. With the use of microspargers, the gas flow rate required to supply oxygen to maintain certain dissolved oxygen levels tends to be smaller, leading to a lower CO_2 removal rate and a generally higher CO_2 concentration in culture. Furthermore, in larger vessels, bubble coalescence is unavoidable, thus offsetting the advantage of small bubbles. The open pipe or multiple-hole spargers are simple and are generally used in large reactors. In general, gas flow rates for sparging can

be scaled up by keeping the same superficial gas velocity. However, it is important to increase the number of holes for sparging linearly to the gas flow rates in order to keep the gas entrance velocity at the same levels as it has been reported recently that a high gas entrance velocity of more than 30 m/s may exert an adverse effect on NS0 cells (28).

56.4.2 Airlift Bioreactor

An airlift reactor is essentially a relatively high aspect ratio (tall and thin) tank with an internal concentric draft tube as a guide for fluid recirculation (Fig. 56.2). The internal liquid circulation is achieved by sparging at the bottom of the draft tube. The sparged section has a lower effective density than the bubble-free section, and the difference in hydrostatic pressure between the two sections induces the liquid circulation upward in the sparged section (riser) and downward in the bubble-free section (downcomer). The loop has the advantages of permitting high efficiency mass transfer and improving the flow and mixing properties in the vessel. A potential advantage of airlift reactors is the low capital costs because of their simple mechanical configuration. Although simple in construction, sound design is critical for optimal hydrodynamic behavior. Airlift reactors have been used successfully with suspension cultures of BHK 21, human lymphoblastoid, CHO, hybridomas, and insect cells. In the past decade, the cell concentration achieved in cell culture bioreactor increased substantially as fed-batch culture became the prevailing mode of operation. In a fed-batch mode, the culture is often initiated at about two thirds of the maximum volume. The other one third is gradually fed throughout the cultivation period. The initially low volume makes the use of airlift bioreactors impractical as the draft tube is not completely submerged in the medium. Furthermore, the increased oxygen consumption caused by the high cell concentration requires a faster mixing time provided by a stirred-tank reactor. As a result stirred-tank bioreactor has become the prevailing type used for cell culture.

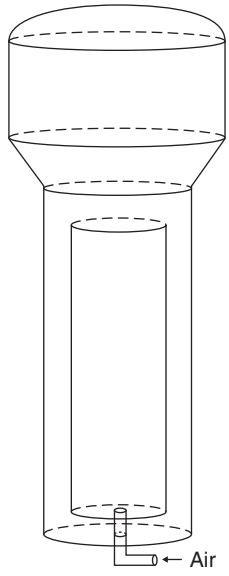


Figure 56.2. Schematic of an airlift bioreactor.

56.4.3 Disposable Single-Use Bioreactors

Many different types of disposable single-use plastic bioreactors including T-flasks, roller bottles, and multiple flat panels are commonly used for production of recombinant proteins and viral vaccines using both attachment-dependent and suspension cells. Their surface may be treated to facilitate attachment of adherent cell cultures. However, for suspension cells, it is usually more convenient to grow the cells in a stirred vessel, and disposable plastic bioreactors are used only at smaller scale when ease of operation is a more important consideration.

Roller bottles are cylindrical screw-capped bottles with a total volume ranging from 1 to 1.5 L suitable for a culture volume of 0.1–0.3 L. Stacks of bottles can be placed on a rack and can be rotated at 1–4 rpm. For small-scale operations, roller bottles provide many advantages for the cultivation of adherent cells. It is relatively inexpensive to set up. It allows for a rapid change of throughput in response to the need. Furthermore, replacing medium from cell growth medium to one designed for product formation is rather straightforward. It is particularly useful in the case that the serum-containing medium needs to be replaced by a serum-free or protein-free medium for the production of secreted proteins or viruses. The transparent glass or plastic wall allows visual or microscopic examination of the culture status. Microbial contaminated bottles can be readily spotted and discarded before being pooled together with others.

However, the drawbacks of roller bottles are numerous for large-scale production of biologics. On-line environmental monitoring and control is virtually impossible, or at least impractical. The aseptic bottle handling for inoculation—protease treatment for cell detachment and expansion, medium exchange, and product harvest—requires extensive well-trained labor to ensure a low failure rate. Each batch of manufacturing can easily involve hundreds or even thousands of bottles, and the large number of manual steps involved makes the risk of microbial contamination rather high. Despite these significant drawbacks, roller bottles are still widely used in the production of recombinant proteins and viral vaccines, often because the product involved has been approved by regulatory agencies and a process change would incur too high a cost and may result in product comparability issues. In some cases, roller bottles are selected because the process is easy to implement and the production capacity needed is manageable. Notable examples include

the production of EPO using recombinant CHO cells and the production of the live attenuated chickenpox (varicella) vaccine and herpes zoster (shingles) vaccine using adherent secondary human lung fibroblasts MRC-5 cells. Recent improvements include developing a fully automatic and continuous cell culture for a large number of roller bottles to make industrial-scale production by mammalian cell culture (29).

Nunc Cell Factories® (NCFs) are widely used in laboratories and in industrial production of viral vectors, vaccines, and recombinant proteins. They are ideal to support growth of adherent cells; however, they can also be used for suspension culture. A 40-tray NCF has a capacity of 25,280 cm^2 and ~8000 mL liquid volume. In one study adherent PER.C6® cells, grown on a single tray and transfected with adenovirus plasmid, produced 5×10^{10} of an adenovirus type 5 vector expressing HIV-1 gag gene (MRKAd5gag). Scale-up can be easily performed using multiple tray systems (30). For large-scale manufacturing using tray disposal device, a mechanical handling system can be used. One notable example is the production of a recently licensed multivalent Rotavirus vaccine using Vero cells, a continuous African green monkey kidney cell line. The vaccine is a live attenuated virus vaccine that contains five different human-bovine virus reassortants, each produced from a different process (31).

Another multiple plate system (CellCube Module) entails 9 $in.^2$ polystyrene plates stacked vertically at 1 mm spacing in an overmolding resin case. The space between stacks is completely filled with medium. Continuous medium circulation is used for oxygen and nutrient supply. It has been used in the cultivation of MRC-5 cells for the production of attenuated hepatitis A virus (HAV) and for the production of VA2TA, an inactivated HAV vaccine. These disposable bioreactors have also found some popularity for the production of cells and gene therapy vectors at intermediate scales of operation (32,33).

Disposable cell culture wares suitable for modest scale of suspension culture are increasingly being used for production of biopharmaceuticals. Most of them use disposable plastic bags as cell chambers. They are especially suitable for cell expansion before reaching the production scale. Wave™ mainly consists of a presterilized, disposable Cellbag and a special rocking platform. The rocking motion of this platform induces waves in the culture fluid. These waves provide mixing and oxygen/gas transfer to support over 20×10^6 cells/mL. With no cleaning or sterilization required, disposable bags simplify setup operations. Various systems at a culture volume from 0.1 to 500 L are available (http://www.wavebiotech.com/products/wave_bioreactor/index.html). pH, dissolved oxygen (DO), temperature sensors are designed for these single-use bioreactors. In manufacturing settings, validating the equipment for restart of the process contributes to a very significant part of overall operating cost. The use of disposable bag systems can significantly shorten the process development time, require much less capital investment than installing stirred-tank bioreactors, and reduce the cost associated with validation.

A more extreme case of single-use alternative to conventional fermentor is a retrofit product to mimic existing stainless steel bioreactor vessel. It consists of a reusable stainless steel outer support container and single-use BioProcess Container (BPC®) with a working volume of up to 1000 L, which can be integrated with the existing bioreactor control system. The integrated sparging system provides effective oxygen transfer (http://www.hyclone.com/bpc/new_prod/sub.php). Since all parts contacting the cell culture are single-use and tested, no cleaning or sterilization is needed.

56.4.4 Hollow Fiber Bioreactor

The use of hollow fiber reactors for cultivation of mammalian cells dates back to the early 1970s (34). A hollow fiber system can be used for anchorage-dependent and suspension cells. It consists of a bundle of capillary fibers sealed inside a cylindrical tube. The basic configuration is rather similar to the hollow fiber cartridge used in kidney dialysis. In fact, many hollow fiber bioreactors basically consist of a kidney dialysis hollow fiber unit connected to a medium recirculating reservoir. The hollow fiber, in most cases, consists of supporting polymeric porous materials for mechanical strength and a thin layer of membrane that provides selective passage of molecules depending on their size. The MWCO of the membrane differs according to applications, ranging from a few thousand to a hundred thousand daltons. In most cases, an ultrafiltration membrane is used (35). The ultrafiltration membrane prevents free diffusion of secreted product molecules from passing through the membrane and allows them to accumulate in the extracapillary space to a high concentration. The culture medium is pumped usually through the fiber lumen, and cells grow in the extracapillary space or the shell side. Supply of low molecular weight nutrients to the cells and the removal of waste products occur by diffusive transport across the membrane between the lumen and the shell spaces. Although the use of microfiltration hollow fiber membranes for cell culture is infrequent, it does find application in various research uses for studying metabolism and for the cultivation of anchorage-dependent or highly aggregated cells for which a convective flow of medium through the extracapillary space to bathe cells in medium is desired.

Most hollow fiber systems used for cell culture employ fibers of approximately 250–350 μm in outer diameter. The interfiber distance is at least as large. A factor limiting the potential of scaling-up of a hollow fiber system is mass transfer. In the radial direction, the nutrient (including

oxygen) diffuses through the hollow fiber wall and membrane to reach the site of cells for consumption by the cells. In the axial direction, the medium entrance region is exposed to fluid with higher oxygen, while the exit end inevitably sees a lower concentration of oxygen. Oxygen is of primary concern because it is usually the first nutrient to become growth limiting. To ensure ample oxygen supply, the recirculating medium is typically passed through an oxygenator (e.g. one used in surgery operations) before it enters the hollow fiber system. A typical setup of a hollow fiber system therefore includes not only a constant temperature incubator to house the hollow fiber bioreactors but also pH control, oxygenation and oxygen monitoring systems, and a medium reservoir for recirculating medium. In addition, frequently a small medium reservoir is used to supply high molecular weight nutrient supplements to the extracapillary space directly. A harvest reservoir is used to collect the product containing fluid from extracapillary space. In a hollow fiber bioreactor, a nonuniform growth of cell mass and product accumulation is often seen (36). This is usually caused by the small convective flow in the shell side, the difficulty to inoculate cells uniformly, and settling due to gravity.

Techniques to improve oxygen supply include the use of fiber or silicon tubing for oxygen supply into the shell side of the reactor. However, the use of mixed fibers in the bioreactor makes the bioreactor harder to manufacture. Another technique is to reverse the flow direction periodically to inverse the axial regions exposed to high and low oxygen concentration.

Despite its limitation in scaling-up, the hollow fiber system is a proven technology relatively easy to apply to processes requiring a modest amount of product. In some tissue engineering and cellular therapy applications, the product is often patient specific and the quantity of cells needed is relatively small. A hollow fiber system could be ideal for those applications.

56.4.5 Bioreactors for Scale-Down/High Throughput Operations

Cell culture has long been carried out in small scales, such as 96 well or even 384 well format, for various biological assays. Such small-scale systems are ideal for parallel cultures for testing medium components or other biologically active ingredients. They are also convenient for screening a large cell population to identify cell variants or clones that have certain desired characteristics. Although those small-scale systems are largely carried out as stationary cultures like T-flask, there are also deep well systems in such 96 or 384 well format for parallel culture of cells kept in suspension. The use of suspension system allows for larger quantities of cells be grown, which is important for some cases where the assay requires a larger sample volume. Such systems are also more amenable to optimization of culture conditions. The systems conform to the standard format of laboratory liquid handling robotic systems and are suitable for high throughput operations needed for drug screening, toxicity testing, or gene transfection studies. These high throughput formats are also employed in screening clones with high productivity as well as in media development and optimization.

In the past few years, smaller scale operations are increasingly being used in bioprocess industry as they enable reduction in labor and material costs and expand the number of variables that can be investigated as compared to conventional laboratory bioreactors with a culture volume varying from 0.5 to 10 L. Recent efforts on bioreactor miniaturization also aim to reproduce the conditions of process scale to render the studies at small scale more relevant to manufacturing conditions.

The key parameters of design and operation in those small-scale reactors are thus mixing, mass transfer, and other factors affecting environmental control (such as pH, dissolved oxygen, and nutrient levels). The most commonly used small-scale bioreactors that provide mixing is the shaker flask. Mixing is carried out simply by shaking the 'bioreactor' using various shaking diameters and angles. Although convenient for cultivating cells, conventional shaker flasks require large space for a given culture volume. The rotational speed that can be used is limited to avoid spillage. Furthermore, the rotary motion used in providing mixing does not provide a high oxygen transfer rate. In the past decade a number of culture tube small-scale systems became available commercially. The simple cylindrical shape and the relatively small volume of culture fluid allows a high shaking speed to be used. Oxygen transfer rate can possibly be improved by using square- versus round-shaped wells (37). A high $k_L a$ value has been reported in square-shaped shake tubes with gas permeable membrane for oxygen delivery (38). The volume of such tube-based culture system ranges from a couple to tens of milliliters. In some cases, mixing is provided by high frequency motion in a vertical direction, instead of the traditional rotary motion. Small tube cultures in 96 well format with mixing provide a mechanism amenable to robot-assisted high throughput operation. However, with a small culture volume and highly turbulent liquid mixing, evaporation can be seriously affecting the osmolality of culture. Evaporation in the plate formats is generally prevented by using low-evaporation lids.

From an operational standpoint of view, especially ease of sampling as well as lower risk of cross-contamination, 24 and 96 well plates are more commonly used for cell cultivation compared to plates with more densely packed wells (37,39). μ24 MBR (manufactured by Micro-Reactor Technologies, Inc., Mountain View, CA) and marketed by Applikon, Inc., Foster City, CA) is an example of

microbioreactor system made using special 24-well micro titer plate.

To mimic large-scale cultures, small bioreactors employing stirred agitation using impellers driven with a shaft or magnetic transmission are used. Stirred minibioreactors may be constructed using wide range of materials including glass and polymers, with a working volume in the order of 20–100 mL (40). Larger volume compared to miniature plates allows for ease of feeding, sampling, better instrumentation, and control. However, relatively higher cost of the stirred minibioreactors may limit their application for high throughput screening. The system needs to be better optimized to provide high quality instrumentation at a lower price.

Instead of employing ministirred bioreactors with tens of milliliters of culture volume, some have miniaturized mixing by employing lab-on-a-chip idea to allow for cultivation on polymer or glass plates (41,42). These reactors are typically very small with 5–150 μL working volume (47), and the capacity to measure critical process variables on-line and even perform chemostat cultivations (42,43). It is worthwhile to note that the small working volumes require analytical tools capable of analyzing correspondingly small samples. In the literature, microbioreactors and larger, liter-scale cultivations comparisons have reported equivalency for process parameters and optical density measurements (40,44).

To be better able to manipulate the environment to mimic large-scale operations, environmental monitoring and control is important. Because of the small culture volume and restriction on sample volume, on-line monitoring is highly desirable or even essential for high throughput operations. Typically on-line monitoring of bioreactors relies on *in situ* electrical probes that convert chemical state or reaction to an electric signal. Miniaturized pH and DO probes can be used with stirred minibioreactors (Frachon *et al*., 2006). Such wired, fix-position probes are cumbersome to use in high throughput systems employing culture tubes or shaker flasks and are too large for 96 well format based systems. For these microscale bioreactors, optical sensor technology that monitors pH and dissolved oxygen noninvasively and possibly transmits the signal remotely is preferred. Fluorescence measurement techniques for measuring dissolved oxygen and pH using dye in culture media and/or sensing patches are being developed (42,44–46). Biomass measurements can possibly be made by using simple transmission intensity measurement (42) or miniature capacitance probe. The availability of better on-line sensing will certainly facilitate the use of miniaturized cell culture systems.

56.4.6 Bioreactor Scale Translation and Intensification

As the mammalian cells become a major workhorse for the production of biopharmaceuticals, the focus of process research and development also shifted from the development of bioreactors to process optimization and intensification using existing bioreactors. In the past decade, we have witnessed a surge in the productivity, from 100s mg/L to 2–5 g/L, in the production of recombinant proteins from cell culture processes. This increased productivity has been the result of intensified optimization of fed-batch processes to increase cell concentration and to extend the high productivity stage of the culture. The advances have allowed a much higher demand of product be met without increasing physical manufacturing capacities and have saved large sums of capital investment. Such fed-batch cell culture processes are now commonly used for production of clinical and commercial supplies of antibody products at scales of up to 20,000 L. The continued advances are reliant on process productivity enhancement and scale-down efforts. Current protocol of generating a high producing cell line involves isolation and evaluation of cell clones derived from single cells after the introduction of transgene. Clonal variation renders their behavior difficult to predict under different culture environment. Rapid optimization of a high productivity process and successful bioreactor scale translation, especially predicting a particular producing cell line's behavior in manufacturing environment, is critical for the production of biopharmaceuticals. Cell line characterization and process optimization are invariably performed in small-scale- and pilot-scale bioreactors. A high confidence on the translatability of small- and pilot-scale results to manufacturing conditions will greatly fasten the timelines and reduce the drug development cost. In addition, a suitable scale-down model is needed to support process characterization, troubleshooting, and process validation.

A successful scale-up and scale-down depends on a good understanding of physical and chemical parameters affected by scale, their quantitative or qualitative relationship to scale, and the design of the scale-down model. It is the changes in the dynamics of these critical parameters in scale translation that eventually cause changes in cellular physiology and productivity. Mechanical agitation and shear, aeration, and oxygen (and carbon dioxide) transfer, which are the conventional subjects of scale-up studies, are apparently important parameters. Additionally, the parameter values for pH and gas flow control often scale nonlinearly causing subtle differences in chemical environment, such as dissolved carbon dioxide and osmolality. There have been few reports on scale-down models, which describe time profiles of scale-sensitive physical and chemical parameters. It is worth noting that key to scale-up studies is the comparison of the cellular physiology in both small and large scales. The profiles of cell growth, metabolism, and product formation have been the key parameters being compared in scale translation. However, in the past few years we have seen various omic tools, especially DNA microarrays, increasingly finding their applications in bioprocessing research.

Its potential in physiological comparative studies on scale translation is worth exploring.

56.5 CONCLUDING REMARKS

The reactors discussed above (see also Chapter 57 in this volume) are the ones commonly used in manufacturing of biopharmaceuticals. The selection of a reactor for a particular process is largely based on process needs, especially whether the cells employed are adherent or suspension cells. Large-scale bioreactors, whether they are used for fed-batch operations or perfusion cultures, are mostly stirred tanks. Their dominance is attributed to the robust performance gained through their wide use in various bioprocesses over the decades. However, many other considerations, especially low capital investment and ease in operations and validation, have rendered an increased usage of disposable devices in the past few years. Many processes of moderate scales and seed culture preparations of large-scale culture are increasingly being performed in disposable devices. Other types of reactors, many of which were innovated a couple of decades ago, although not commonly used in bioprocessing nowadays, are finding applications in tissue engineering. Furthermore, miniaturized bioreactors (see Chapter 32, volume 1) are increasingly being used in high throughput operations. In the near future, we may see that the experience gained in bioprocess technology begin to benefit high throughput technology.

REFERENCES

1. Kompala, D, Ozturk SS. Optimization of high cell density perfusion bioreactors. In: Ozturk SS, Hu W-S, editors. Cell culture technology for pharmaceutical and cell-based therapies. New York: Taylor and Francis; 2006. p 387–416.
2. Voisard D Meuwly F, *et al*. Biotechnol Bioeng 2003; 82(7): 751–765.
3. Kitano K, *et al*. Appl Microbiol Biotechnol 1986; 24: 282–286.
4. Tokashiki M, *et al*. Cytotechnology 1990; 3(3): 239–244.
5. Takamatsu H, *et al*. Appl Microbiol Biotechnol 1996; 45(4): 454–457.
6. Takazawa Y, Tokashiki M, Hamamoto K, Murakami H. Cytotechnology 1990; 1: 171–178.p.
7. Seamans TC, Hu W-S. J Ferment Bioeng 1990; 70: 241–245.
8. Yabannavar VM, Singh V, Connelly NV Biotechnol Bioeng 1994; 43: 159–164.
9. Gorenflo VM, *et al*. Biotechnol Prog 2003; 19(1): 30–36.
10. van Wezel AL. Nature 1967; 216: 64–65.p.
11. Goetghebeur S, Hu WS. Appl Microbiol Biotechnol 1991; 34:(6): 735–741.p.
12. Tao T-Y, Ji G-Y, Hu W-S. J Biotechnol 1987; 6: 9–12.p.
13. Zuhlke A, *et al*. J Biomater Sci Polym Ed 1993; 5(1-2): 65–78.
14. Roder B, *et al*. J Biomater Sci Polym Ed 1993; 5(1-2): 79–88.
15. Varani J, *et al*. J Biol Stand 1985; 13: 67–76.
16. Reuveny S, *et al*. Dev Biol Stand 1982; 50: 115–123.
17. Reiter M, *et al*. Cytotechnology 1990; 3: 271–277.
18. Runstadler PW Jr, *et al*. Bioprocess Technol 1990; 10: 363–391.
19. Tolbert W, Hitt MM, Feder J. In Vitro 1980; 16: 486–490.p.
20. Peshwa MV, Kyung Y-S, McClure DB, Hu W-S. Biotechnol Bioeng 1993; 41: 179–187.
21. Perusich CM, Goetghebeur S, Hu W-S. Biotechnol Tech 1991; 5: 145–148.
22. Moreira JL, Alves PM, Rodriguez JM, Cruz PE, Aunins JG, Carrondo MJT. Ann N Y Acad Sci 1994; 745: 122–133.
23. Nilsson K, Scheirer W, Horton OH, Osfberg L, Liedhl E, Katinger HWD, Mosbach K. Nature 1983; 302: 629–630.
24. Papas KK, Sambanis A. The characterization of the metabolic and secretory behaviour of suspended free and entrapped insulin-producing AtT-20 spheroids. Annual Meeting of the American Institute of Chemical Enginners. Miami Beach, FL; 1992
25. Jen AC, Wake MC, Mikos AG. Biotechnol Bioeng 1996; 50: 357–364.
26. Croughan MS, Hamel J-F, Wang DIC. Biotechnol Bioeng 1987; 29: 130–141.
27. Chalmers JJ, Bavarian F. Biotechnol Prog 1991; 70: 151–158.
28. Zhu Y, Cuenca JV, Zhou Q, Varna A. Biotechnol Bioeng 2008; 101: 751–760.
29. Kunitake R, Suzuki A, Ichihashi H, Matsuda S, Hirai O, Morimoto K. J Biotechnol 1997; 52: 289–294.
30. Subramanian S, *et al*. Biotechnol Prog 2007; 23(5): 1210–1217.
31. Buckland BC. Nat Med 2005; 11(4 Suppl):S16–S19.
32. Aunins JG, *et al*. Biotechnol Prog 2003; 19(1): 2–8.
33. Hagen AJA. J Bioprocess Biosys Eng 2000; 23:(5): 439–449.
34. Knazek RA, Gullino PM, Kohler PO, Dedrick RL. Science 1972; 178: 65–67.
35. Evans TL, Miller RA. BioTechniques 1988; 6: 766–767.
36. Piret JM, Devens DA, Cooney CL. Can J Chem Eng 1991; 69: 421–428.p.
37. Kumar S, *et al*. Biotechnol Lett 2004; 26: 1–10.
38. Kato I, *et al*. J Ferment Bioeng 1998; 85: 404–409.
39. Duetz WA, *et al*. Appl Environ Microbiol 2000; 66(6): 2641–2646.
40. Betts JI, Baganz F. Microb Cell Fact 2006; 5: 21.
41. Szita N, *et al*. Lab Chip 2005; 5: 819–826.
42. Zanzotto A, *et al*. Biotechnol Bioeng 2004; 87(2): 243–254.
43. Zhang Z, *et al*. Lab Chip 2006; 6: 906–913.
44. Kostov Y, *et al*. Biotechnol Bioeng 2001; 72(3): 346–352.
45. Kensy F, *et al*. Bioprocess Biosyst Eng 2005; 28(2): 75–81.
46. Arain S, *et al*. Sensor Actuat B-Chem 2006; 113: 639–648.
47. Zhang Z, *et al*. A well-mixed polymer-based microbioreactor with integrated optical measurements. Biotech Bioeng 2006b; 93: 286–296.

57

MAMMALIAN CELL CULTURE REACTORS, SCALE-UP

J. Bryan Griffiths
Scientific Consultancy & Publishing, Salisbury, United Kingdom

57.1 INTRODUCTION

Although mammalian cells have been grown in vitro since before 1907 (1) the factor that gave impetus to their current widespread laboratory and industrial use was the discovery by Enders (2) that human pathogenic viruses could be grown in cell cultures. Following this demonstration by Enders in 1949 it took only 5 years for the first cell-based vaccine to be licensed for clinical use (Salk polio vaccine in primary monkey kidney cells in 1954). This opened up 20 years of continuous development of human and veterinary viral vaccines and created the need for industrial-scale cell culture processes. The most effective large-scale process developed during this period was for foot-and-mouth disease virus (FMDV) based on suspension culture of baby hamster kidney (BHK) cells (3). Developments in processes for human vaccines were less dramatic because of the need to use biologically safe cell lines. This meant that the use of human diploid cell lines, such as WI-38 (4) and MRC-5 (5), because of their normality (i.e., they behaved as cells in vivo without tumorgenic transformation), only grew attached to a substrate (anchorage dependent) and only reached low cell densities. The wide range of animal cell reactors available is partly due to the dual development of systems for anchorage-dependent cells (ADCs) and free-suspension cells (6,7). ADCs were grown in small culture vessels, and a production batch constituted hundreds or even thousands of replicate cultures (i.e., a multiple-batch process) (8). The need for a unit batch process (one large culture vessel), such as the fermentors used for suspension cells, saw the development of a wide range of novel culture reactors (6,7), but the significant breakthrough came with the microcarrier system (9). This procedure, developed in 1967 by van Wezel (9), allowed cells to grow attached to small (200 μm) spheres that were stirred in a large tank fermentor analogous to suspension cells. This was the first successful large-scale unit process for ADCs.

Vaccines were the dominant product until the 1970s, but changes in regulatory and licensing procedures then allowed cells from sources other than normal tissues to be used for human medicinal products. This came about during the development of an interferon process using a cancer cell line, Namalva, by Wellcome (10). This company's pioneering work established the safety criteria, and thus acceptance, for using nonnormal (heteroploid, transformed, or tumor-derived cell lines) and the feasibility of scaling up an industrial cell culture process to 8,000 L. Cell culture then entered a new, or modern, phase in which a wide variety of cell products (Table 57.1) is produced from a range of cell types (Table 57.2). Two of these products can be highlighted as being significant milestones. First, the production of monoclonal antibodies from hybridoma cells (the fusion of a normal antibody producing cell and a hemopoitic cancer cell) (12) has given rise to hundreds of new products. Second, the development of recombinant tissue plasminogen activator (tPA) by Genentech (14) gave rise to the first genetically engineered clinical product from cell cultures. Currently applications are widening to include the cell itself as a product in tissue engineering, organ replacement, and gene therapy (15).

In this chapter the description of cell culture reactors is given against this historical evolution of cultures from small-scale virus production through scale-up to the more

Upstream Industrial Biotechnology: Equipment, Process Design, Sensing, Control, and cGMP Operations, Volume 2, First Edition. Edited by Michael C. Flickinger.
© 2013 John Wiley & Sons, Inc. Published 2013 by John Wiley & Sons, Inc.

TABLE 57.1. Mammalian Cell Products

	Native products
Human vaccines	Polio (1954), measles (1963), rabies (1964), mumps (1969)
Veterinary vaccines	Foot-and-mouth disease vaccine, rabies, Marek's, pseudorabies, BVD, louping ill, bluetongue, avian influenza, canine distemper (examples)
Interferon	Refs 10 and 56
	Engineered products
Monoclonal antibodies	OKT3/Orthoclone (1987), Centoxin (1990), Reopro (1994), Myoscint (1989), Oncoscint (1990)
Tissue-type plasminogen activator	Activase/actilyse (1987)
Erythropoeitin (EPO)	Epogen/Procrit/Eprex (1989), Epogin/Recormon (1990)
Human growth hormone	Saizen (1989)
HBsAg	GenHevac B Pasteur (1989), HBGamma (1990)
Interferon	Roferon (1991)
Colony stimulating factor (G-CSF)	Granocyte (1991), Neupogen (1991)
Blood factor VIII	Recombinate (1992), Kogenate (1993)
Dnase I	Pulmozyme (1993)
Glucocerebrosiduse	Cerezyme (1994)
Follicle-stimulating hormone	Gonal-F (1995)
	rDNA products in development/clinical trial
HIV vaccines (gp120, pg160, CD4)	
Herpes simplex vaccines (gB, gD)	
Chimeric monoclonal antibodies (her2, CD4, TNFa, CD20, Cd18, TAC, leukointegrin, CF54, RSV)	
Others (TSH, TNF, M-CSF, IL-6, IL-1)	
In vitro diagnostic monoclonal antibodies (1–200)	
Tissue engineering and replacement (e.g., skin, artificial kidneys)	

than 10,000-L unit processes that now play a dominant role in the health biotechnology industry, with hundreds of products either already available in the clinic or going through phase I through III clinical trials. The emphasis is on scale-up because of the relatively low biomass productivity of animal cells compared with bacteria, the low product expression rates (one clinical dose is often equivalent to 0.1 to 100 L of culture supernatant), and the need to introduce more efficient and economical industrial processes.

TABLE 57.2. Typically Used Cells in Biotechnology

Cell line	Derivation	Application
CHO	Chinese hamster ovary	Good product glycosylation
CHO dhfr	Mutant for genetic amplification	Principal substrate for recombinant products
BHK21	Syrian hamster	Viruses/veterinary vaccines
Vero	African green monkey	Viral vaccines
HeLa	Human cervical adenocarcinoma	Polio vaccine
MRC-5/WI-38	Human fetal lung fibroblasts	Human vaccines
MDCK	Cocker spaniel kidney	Viral vaccines
Namalwa	Human B lymphoblastoid	Interferon
COS 1/COS 7	African green monkey kidney	Recombinant products
NS0/NS1 and Sp2/0-Ag14	Myeloma	Fusion partners for monoclonal antibody production immunoglobulin
J558L	Mouse Balb/C myeloma	Secretes immunoglobulin A
NIH/3T3	Swiss mouse embryo	Sarcoma virus
GH3	Rat pituitary tumor	Hormone studies
293	Adenovirus transformed HEK	Gene therapy
X CRE/Y CRIP	Mouse NIH3/Moloney leukemia	Retrovirus packaging
		Insect
Sf9	Spodoptera frugipeda	Baculoviruses
Schneider-2	Drosophila melangogaster	Recombinant products

Source: Ref. 12.

57.2 BACKGROUND

57.2.1 Mammalian Cells

Major differences between single mammalian cells and microorganisms should be noted because they influence, and put constrictions on, the culture process. Cells do not have a cell wall but a thin cell membrane (a phospholipid bilayer) that mediates communication between the cell and the environment. They are thus very sensitive to environmental stimuli, such as pH, nutrients, oxygen, regulatory molecules, and hydrodynamic forces. Cell shape and morphology are controlled by cytoskeletal elements attached to the membrane and running through the viscous cytoplasmic gel. The degree of polymerization of the microtubular network regulates the shape, whether spherical or elongated, flattened or attached. Mammalian cells are on the order of 12–20 μm in diameter (i.e., 1,000-fold greater volume than microorganisms), which means diffusion into the cytoplasm is greatly reduced in the spherical state. When flattened, membrane folding and ruffling give a much greater surface area. Also, mammalian cells are far more fastidious in their nutrient requirements, with critical optimal chemical and physical environmental parameters. The consequence of these factors is that cells need more gentle stirring and aeration procedures than bacteria, which greatly reduces mass transfer and homogeneous mixing in the culture. This need for more moderate stirring and aeration procedures, together with greater sensitivity to nonoptimum or fluctuating culture conditions, slower growth rate (14–22 h average doubling time), and vulnerability to microorganism contamination, means that the culture system has to be extremely well controlled and contained. Some key issues in setting up successful cultures are as follows:

- Cells should be inoculated from the late logarithmic phase rather than stationary cultures.
- Cells should be prepared for inoculation as quickly as possible and the time they are exposed to trypsin, acidity, or low temperatures limited during harvesting.
- The new culture medium should be at the required temperature (37°C), pH (usually 7.1–7.3), and so forth before inoculating.
- The minimum inoculation density ($1–2 \times 10^5$/mL or 2×10^4/cm^2) should always be exceeded.

57.2.2 Scale-Up

57.2.2.1 Principles. Normally a culture process begins with an ampoule, stored at −196°C, of about 5 million cells put into 10 mL of medium, which can then be expanded up to a final volume of 10–20,000 L at 2 million cells per milliliter (i.e., a 1 to 2 million–fold scale-up). This expansion is achieved by a series of ever-increasing culture volumes (the seed train), each step bringing about a 5- to 10-fold volume increase and taking 4 to 5 days. Thus, before the final production culture is initiated, cells will have been passaged at least five times over 25 days. This investment in time and resources shows how important it is to keep sterility by strict attention to all aspects of the process (equipment, reagents, and handling procedures). The scale-up process involves many factors, including engineering (especially to maintain sterility and reliability), physiological (supply of oxygen and nutrients and critical maintenance of the correct environmental conditions), monitoring and control (biosensors, performance measurements, and computer control), logistics, and compliance with pharmaceutical licensing and health and safety regulations. The aim of such scale-up is to provide more cells and more cell product in as efficient and cost-effective a manner as possible while complying with all regulatory and health and safety criteria. This emphasizes the importance of moving from a multiple-unit (many replicate bottles, roller cultures, spinner flasks, etc.) to a high-volume-unit process. Such a shift allows economy in manpower (reduction in repetitive steps), space (expensive hot rooms), and time and an increased efficiency by being able to reproducibly control environmental factors, such as pH and oxygen, in a unit process. The wide range of alternative culture systems that are or have been available (6,7,16) is due (*1*) the need to find processes for both suspension and ADC cells and (*2*) various solutions to overcoming limiting factors in scale-up (17).

57.2.2.2 Limiting Factors in Scale-Up. The first problem in moving from a small, multiple unit process to a large unit process is usually oxygen limitation. To overcome this problem and supply oxygen without the damaging effects of air bubbles from sparging and the high stirring speeds needed to effect efficient mass transfer, bioreactors have been developed that oxygenate through a membrane. This bubble-free aeration has been achieved by means of long lengths of tubing in the bioreactor (18–20) or external medium loops through hollow fiber oxygenators. A related factor is mixing, and low-shear modifications to impellers and the airlift bioreactor concept (21) have been introduced. A problem for ADCs is the limitation on surface area during scale-up. A huge range of reactors have been developed (multiple plates, spirals, ceramic matrices, glass beads), but the most successful method has been the microcarrier (9,22). The large fermentor systems used for suspension cells thus became available for ADCs because the small microcarriers with cells attached behaved analogously to a suspension cell.

The next problem to be overcome is nutrient limitation and toxic metabolite buildup. Although media changes can be used (especially for attached cells), the most efficient

means of overcoming these problems is continuous medium perfusion. To perfuse suspension cells cells and waste medium have to be physically separated; this separation has been done by means of spin filters, external loops to filters or centrifuges, or gravitational settling devices (18). The use of perfusion resulted in the development of many immobilization procedures to prevent cell washout (e.g., encapsulation, hollow fiber devices, membrane reactors, gels, fibers, and porous microcarriers). Additional benefits to these developments were the provision of huge unit surface areas for cell attachment and the ability to grow cells at 50- to 100-fold higher densities than previously achieved in free suspension. Thus these developments mean that manufacturers have a choice in scale-up routes (6).

57.2.2.3 Scale-Up Strategies. Some scale-up strategies are as follows (22–24):

- High-volume (to 10–20,000 L) tank fermentor systems with conventional cell densities of $1–2 \times 10^6$/mL
- Low-volume (<1 L) but very-high-density ($1–2 \times 10^8$/mL) heterogeneous systems (e.g., hollow fiber bioreactors)
- Intermediate systems using spin filters to increase cell density to $1–2 \times 10^7$/mL but to a volumetric scale of only 500 L
- High-density (1×10^8/mL) scaleable systems (to 200 L) based on porous microcarriers

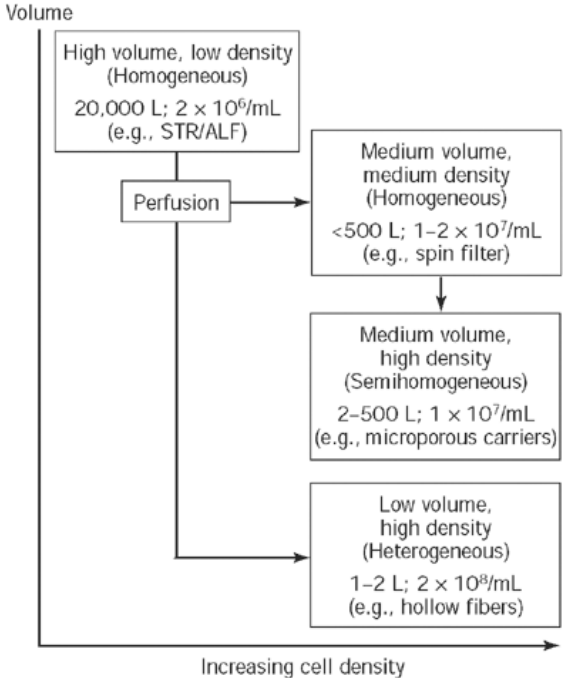


Figure 57.1. Scale-up strategies and the evolution of high cell density culture systems. STR, stirred-tank reactor; ALF, air-lift fermenter.

These systems are summarized conceptually in Figure 57.1. It should be emphasized at this stage that there is no ideal system, but the advantages of high-density systems, summarized in Table 57.3, show why a choice has to be made. Immobilized systems, such as porous microcarriers, also have the advantage of being equally suitable for suspension and anchorage-dependant cells (the Universal System?), protecting from shear, and having a three-dimensional structure that enhances productivity. Basically, the low-volume, high-density systems fill an important niche in manufacturing capability (e.g., gram amounts of monoclonal antibodies), whereas the high-volume systems are the most widely used scale-up route for pharmaceutical products.

57.2.3 Culture Modes

Suspension culture is the preferred method for scale-up because it is easier and cheaper to scale up, requires less space, can monitor cell growth, and can more easily control environmental parameters. However, many cell lines have higher specific productivity when attached to the substrate. In the urge to move to suspension systems the following advantages of anchorage-dependent systems should not be overlooked:

- They facilitate complete medium changes, which are often needed to wash out serum before adding serum-free production medium, for example.
- They are easier to perfuse and thus achieve higher cell densities and healthier cells.

TABLE 57.3. Comparison of High- and Low-Cell-Density Culture Systems

Advantages of high cell density
Smaller reactor volume and therefore reduced need for high-quality laboratory space
More concentrated product
Reduced requirement for expensive serum and growth factors
Long run lengths (50–100 days) and thus less downtime and seed preparation
Daily or continuous harvesting
Shorter residence time for products (and exposure to preteolytic degradation)
Cell debris washout
Disadvantages of high cell density
Volumetric scale-up more difficult and complex
Mass transfer problems leading to heterogeneity
Sterilization problems because some systems cannot be heat sterilized
Higher degree of process control needed (direct cell measurement impossible)
More validation and regulatory conditions for product licensing needed
Perceived as experimental and therefore not accepted as readily as traditional methods

- Media-to-cell ratios are more easily changed during an experiment, thus increasing product titre.

Microcarrier culture, especially porous microcarrier (25), has most of the advantages of both suspension and anchorage-dependent systems.

Different types of culture strategy can be employed; they are defined as follows:

Batch culture. Cells grow from seed to final density over a 4- to 7-day period and are then harvested (typical monoclonal antibody yield is 6 mg/L per batch run)

Fed-batch culture. Additional media or medium components are added to increase culture volume and density of cells as the culture progresses.

Semicontinuous batch culture. A batch culture is partially harvested (e.g., 70%), topped with fresh medium, allowed to grow up again, and reharvested. Typically three to four harvests can be made, although usually with diminishing returns at each harvest.

Continuous-flow (chemostat) culture. Because it is completely homogeneous for long periods of time while cells are in a steady state, this is an extremely useful tool for physiological studies but not very economical for production (by definition, cells are never at maximum density).

Continuous-perfusion culture. This type of culture differs from chemostat in that all nutrients are kept in excess and cells are retained within the bioreactor. This is the most productive culture system, with typical monoclonal antibody yields of 10 mg/L per day for 50–100 days.

There is no definitive answer as to the best system to use; the answer depends on the nature of the cell and product, the quantity of product, downstream processing capability, licensing regulations, and so forth. However, a rough guide to relative costs for producing monoclonal antibodies by perfusion, continuous-flow, and batch culture is 1:2:3.5 (26).

57.3 REACTORS FOR ADCS

57.3.1 Basic Culture Units

Tissue culture flasks and tubes giving surface areas of 5–200 cm^2 are the familiar stock items of any culture laboratory. The largest stationary flask routinely used is the Roux bottle (or disposable plastic equivalent), which gives a surface area of 175–200 cm^2 (depending on make and type), needs 100–150 mL medium, and utilizes 750–1,000 cm^3 of storage space. Such a vessel will yield 2×10^7 diploid, or 10^8 heteroploid cells; thus, to produce a modest 10^{10} cells, more than a hundred replicate cultures are needed (i.e., manipulations have to be repeated 100 times) and 100 L culture space is required. The need to move to larger units is obvious and is approached by increasing the surface-area-to-volume ratio. The first step in scale-up usually involves a change from stationary flasks to roller bottles (i.e., a dynamic system). Roller bottles can be up to 1,750 cm^2, use 350 mL medium, and have a volume of 2.5 L (i.e., a ninefold increase in surface area but only a threefold increase in medium and total volume). This is brought about by using the total internal surface area for cell growth and more efficient aeration as the cells move in and out of the culture fluid. However, this procedure has been used industrially for viral vaccines, veterinary vaccines in multiples of 28,000 (8), interferons, and EPO. It has a place in modern processes largely because it is automatable with robotic systems, such as the Cellmate (Automation Partnership, Royston, Herts, U.K.) and that described by Kunitake *et al*. (27). All the routine manipulations of cell seeding, media changing, bottle gassing, cell sheet rinsing, trypsinization, and cell collection by scraping can be carried out automatically, and reproducibly, with very precise volumes. Examples of products produced by this method are Varivax (Merck varicella vaccine) and Saizen (Serono recombinant human growth hormone).

Many modifications have been made to the roller bottle to increase the surface-area-to-volume ratio. Although some of the following adaptations are no longer commercially available, they are included to stimulate further innovation:

- *Disks*. A series of vertical disks placed along the horizontal axis of the roller bottle (28)
- *Spira-Cell Multi-Surface Roller Bottle (Bibby Sterlin Ltd.)*. A spiral polystyrene cartridge on which cells grow on both sides of the film, available in 2,000, 4,500, and 6,000 cm^2 sizes (29).
- *Glass tubes*. A roller bottle packed with a cluster of small glass tubes arranged in parallel and separated by silicone spacer rings, available in 1,000, 10,000, and 15,000 cm^2 sizes (Bellco-Corbeil Culture System) (30). The initial concept was developed by Chemap as the Gyrogen (31)
- *Extended surface area roller bottles (ESRB)*. A polystyrene roller bottle with a ribbed, or corrugated, surface that doubles the area of an 850-cm^2 bottle to 1,700 cm^2 (Bibby Sterlin Ltd.).
- *ImmobaSil*. Silicone rubber matrix–coated roller bottles that increase the surface area severalfold (Ashby Scientific Ltd., Coalville, U.K.).

Also, to increase cell productivity, roller bottle perfusion systems (32) with specially modified swivel caps (Bellco Autoharvester, New Brunswick Roller Apparatus) can be

used. The roller bottle is a well-established technique and is still widely used in both the research laboratory and the industrial plant. Some cell lines (particularly epithelial) may not be as successfully grown in roller bottles because of streaking, clumping, or inadequate spreading over the total surface (i.e., nonlocomotory cell lines) as in stationary bottles. An alternative scale-up route is to use multisurface plate stationary systems.

57.3.2 Multisurface Plate Units

There are two commercially available examples of multiple-layered polystyrene plates stacked within a polystyrene box. In the Cell Factory (A/S NUNC, Roskilde, Denmark), the trays are 335 × 205 mm (600 cm^2) and can be obtained in multiples of 1, 2, 10, and 40. The largest, therefore, has a surface area of 24,000 cm^2 and needs 8 L medium (i.e., it is equivalent to 14 large roller bottles but requires half the incubation space and no ancillary roller equipment). However, for convenience of handling, especially large numbers, the Cell Factory Manipulator is advantageous because it can be operated robotically.

Although the CellCube (Costar, Cambridge, Mass., USA) (33) also has parallel polystyrene trays, it is a modular closed-looped perfusion system, including an oxygenator, pumps, and a system controller (pH, O_2, level control). The unit is very compact, with the trays being only 1 mm apart; thus, the smallest unit of 21,250 cm^2 is less than 5 L total volume (1.25 L medium). Additional units of 42,500 cm^2 (2.5 L medium) and 85,000 cm^2 (5 L medium) are available, and four units can be run in parallel in the system, giving 340,000 cm^2 growth area.

57.3.3 High-Volume Units

High-volume units are true unit process systems, analogous in volume and performance to suspension cell fermentor vessel processes. Examples include (*1*) the multisurface propagator (34), with vertically stacked circular stainless steel plates on a central revolving shaft scaled up to 200 L (200,000 cm^2), and the titanium plate reactor (35); (*2*) the plate heat exchanger (36,37); (*3*) glass spheres (38–41); (*4*) microcarriers (9,42,43); (*5*) porous microcarriers (44–46); and (*6*) stainless steel wire coils (48).

57.3.3.1 Glass Bead Culture. Packed beds of 3- to 5-mm glass spheres through which medium is continuously perfused has a demonstrated scale-up to 100 L (49). Spheres of 3-mm diameter pack sufficiently tightly to prevent the bed from shifting but allow sufficient medium flow up the column so that fast flow rates, which would cause shear damage, are not needed. The physical properties of glass spheres are given in Table 57.4. Medium can be circulated by pump or by airlift (to give better oxygenation) (50). Although 3-mm beads are normally used to maximize the available surface area, the use of 5-mm spheres can actually give a higher total cell yield, despite the reduced surface area per unit volume, because of better physiochemical conditions (6,39). Scale-up has vertical limitations in that it is difficult to maintain a uniform plug flow without channeling. For inoculation, the use of a perforated tube placed centrally for the height of the bed allows even distribution of cells. Also, alternating the direction of medium flow on a daily basis increases homogeneity and thus scale-up potential. In conclusion, glass sphere packed beds constitute a simple system (that minimizes moving parts and the risk of mechanical failure) with an inexpensive and reusable substrate capable of considerable radial and reasonable vertical scale-up to operate beds of volumes more than 200 L using 5-mm spheres. The disadvantages are that it is a low-intensity system (spheres have the minimum surface area per unit volume) and is limited to secreted products because it is difficult to harvest cells from the bed (i.e., it is ideal for long-term continuous cultures rather than batch cultures, as demonstrated by Brown *et al*. (51)). Experimental protocols for using glass sphere technology have been published (52).

57.3.3.2 Microcarrier Culture. Microcarriers are small particles, usually spheres, 100 to 300 μm in size, that are suspended in stirred culture medium. The concept was initiated in 1967 (9); however, the chromatographic grade of dextran (Sephadex A-50) then used proved unsuitable for consistent and reliable growth. After considerable developmental work, Pharmacia produced a range of suitable microcarriers—the Cytodex series. The first industrial process based on microcarriers was for FMDV (43,53). Subsequently a wide range of microcarriers based on gelatin, collagen, polystyrene, glass, cellulose, polyacrylamide, and silica have been manufactured to meet all situations (23,54) (Table 57.5). The key criteria were to get the surface chemically and electrostatically correct for cell attachment, spreading, and growth. The power of the method is exemplified by the following data:

TABLE 57.4. Properties of Solid Glass Sphere Fixed-Bed Reactors

Glass sphere (diameter)	3 mm	5 mm
Weight, g	0.0375	
Surface area, cm^2/kg	7,546	4,570
Volume, mL/kg	990	625
Void fraction	0.46	0.40
Void volume, mL/kg	455	250
Channel size, mm^2	0.32	1.00
Vero cell yields		
$10^5/cm^2$	0.78	2.5/3.1[a]
10^8/kg	4.00	8.0/9.9
10^6/mL	1.6	3.2/4.0

[a] Yield in 1 kg/10 kg bed reactors.

TABLE 57.5. Microcarriers

Name	Manufacturer	Material	cm^2/g
	Solid microcarriers		
Bioglas	Solo Hill Engineering	Glass/latex	350
Bioplas	Solo Hill Engineering	Polystyrene	350
Biosilon	Nunc	Polystyrene	255
Cytodex 1, 2	Pharmacia	Dextran	6,000
Cytodex 3	Pharmacia	Collagen	4,600
Dormacell	Pfeifer & Langen	Dextran	7,000
Gelibead	Hazelton Laboratories	Gelatin	3,800
Micarcel G	Reactifs IBF	Polyacrylamide	5,000
Microdex	Dextran Products	Dextran	250
			Diameter (μg)
	Microporous microcarriers		
Cellsnow	Kirin Ltd	Cellulose	800–1,000
Cytocell	Pharmacia	Cellulose	180–210
Cultispher	Hyclone	Gelatin	170–270
Cytoline 1,2	Pharmacia	Polyethylene	1,200–1,500
ImmobaSil	Ashby Scientific	Silicone rubber	1,000
Siran	Schott Glaswerke	Glass	400–5,000

1 g Cytodex = 6,000 cm^2, which at 2 g/L = 12,000 cm^2/L (i.e., eight large roller bottles). Scale-up to 4,000 L (equivalent to 3,200 roller bottles) has been achieved in an environmentally controlled and optimized process. This method opened up industrial production opportunities (Table 57.6) and allowed research laboratories to easily produce substantial quantities of developmental products.

Experimental considerations and principles (54) are as follows:

- Because cells differ in their attachment requirements, a range of microcarriers should be assessed.
- Microcarriers vary in their density (1.01 to 1.06), mechanical robustness, hardness, and the concentration at which they can be used. These factors have implications for the choice of process (e.g., stirring system, need for rapid sedimentation due to frequent medium changes, and total unit surface area required: Cytodex 6,000 cm^2/g, glass or polystyrene 300 cm^2/g).
- Culture equipment is critical. Small-scale culture requires the use of specially designed spinner flasks rather than the conventional magnetic bar and siliconized glass to prevent microcarrier attachment.
- Culture initiation conditions are critical and should include a high-quality single-cell inoculum and a prewarmed and stabilized culture medium. Inoculation should not be undertaken below the minimum cell number per bead (usually five, optimally seven), and a nutritionally supplemented medium (e.g., with nonessential amino acids) might be necessary.
- Instead of counting by the trypan blue technique, after trypsinization the nuclei-counting method (57), should be used.
- Some microcarriers can be reused, and it may be possible to recolonize microcarriers in situ during scale-up (58).
- >Enzyme harvesting (e.g., trypsin) can be difficult or damaging, so consideration should be given to using a microcarrier that can be enzymically digested (e.g., by dextranase or collagenase), leaving the cells intact.

TABLE 57.6. Industrial Processes Using Microcarrier Technology (See also Chapter 32 in volume 1)

Product	Cell line	Scale (L)	Company	Reference
Foot-and-mouth disease vaccine	Pig kidney	235	Merrieux	50
Polio and rabies vaccines	PKMC	500	RIVM (Bilthoven)	55
Polio and rabies vaccines	Vero	1,000	Merrieux	43
Human IFN-β	HDC	50	Sclavo	11
Human IFN-β	HDC	4,000	Toray	
Human growth hormone	Vero	100	UNSW (Australia)	56
Tissue-type plasmingon activator	Bowes melanoma	40	RIVM (Bilthoven)	42

- Microcarriers, such as Cytodex, should be used between 1 and 3 g/L unless a perfusion system (e.g., using a spin filter) is employed, with which concentrations of 15 g/L are feasible (39).
- Inoculation in a reduced volume assists attachment and should be followed by topping up to the final working volume after 4–8 h.
- An advantage of microcarriers is the ease with which cell samples can be taken and analyzed.
- As the culture progresses, partial medium changes will have to be carried out and the stirring speed increased from 40–60 rpm to 75–90 rpm to prevent microcarrier aggregation.

In conclusion, microcarrier culture is the most versatile, reliable, and well-characterized procedure for unit volume scale-up of ADCs. It has had widespread use for industrial processes (Table 57.6), as well as many developmental uses (59), has been scaled up to 4,000 L, and has the potential for process intensification by perfusion with spin filters or by the use of microporous microcarriers.

57.4 REACTORS FOR SUSPENSION CELLS

57.4.1 Laboratory Scale

The basic culture unit for suspension cells is the spinner flask, so called because it has a magnetic bar operated by standing the unit on a magnetic stirrer. Initially a bar magnet was placed on the floor of the glass vessel, but spinner flasks now have the magnet suspended just above the bottom of the culture on a stirrer shaft fitted to the bottle top to prevent cells from being crushed. Side arms are usually fitted to allow gassing with CO_2/O_2 through a filter and for sampling. There are many variations in the design of spinner flasks, most affecting the size, number, and positioning of the stirrer bar (6,23). The spinner flask is usually glass, with a silicone- or Teflon-coated magnet and is available in sizes from 50 mL to 20 L, although 10 L should be considered the maximum practical size. The quality of the magnet stirrer (usually multibased to take at least four replicates) is extremely important because it must maintain a stable rpm between 30 and 300, an accurate tachometer, ability to restart after power interruptions at the set speed, a surface that does not become hot, and reliable operation for long periods in a 37°C environment. It is advisable to siliconize the culture vessel and add medium supplements, such as Pluronic F-68 (polyglycol) (BASF, Wyandot) at 0.1% to protect against mechanical damage, especially if low serum concentrations are used. Carboxymethyl cellulose (CMC, 15–20 cps) can also be used to protect cells (0.1%) and antifoam (6 ppm) if foaming is a problem (usually when serum is present at 5–10%). Stirring speeds for suspension cells are usually within the range of 100–250 rpm (depending on cell type and vessel geometry), and a culture will expand from $1–2 \times 10^5$/mL to $1–2 \times 10^6$/mL in 4 to 5 days before needing either harvesting or a medium change. Cell clumping is often a problem but can be reduced by using low Mg^{2+} and Ca^{2+} ion media. Conventional spinner flasks are available from a wide range of laboratory suppliers. The range includes ones with large-bladed paddles attached to the magnet. They are primarily designed for microcarrier culture to give better mixing at the lower speeds necessary. Modified spinner cultures include a radial stirring action (Techne) (60), a floating impeller (Techne BR-06 Bioreactor), the Superspinner (Braun Melsungen AG), CellSpin (Tecnomara AG, Switzerland), and a dual overhead drive system to allow perfusion (Bellco). Experimental details for using spinner flasks have been published (61).

57.4.2 Scale-Up

Suspension culture is the preferred method for scaling up cell cultures because it is easier to volumetrically increase the size of a single fermentor vessel than the specialized units used for ADCs. Although some cell lines will not grow in suspension (e.g., human diploid cell lines WI-38 and MRC-5), many lines can be adapted to grow in free suspension by recognized procedures (62).

Several physical factors must be satisfied for successful scale-up. Good mixing is essential for homogeneity and efficient mass transfer, but during scale-up the power needed to produce these conditions can cause problems. The energy generated at the tip of the stirrer blade is a limiting factor because it gives rise to damaging shear forces (created by fluctuating liquid velocities in turbulent areas); because mixing efficiency increases with turbulence, a compromise has to be reached to minimize cell damage. Thus cell cultures use large impellers running at relatively low speeds. Magnetic bars used in spinner flasks give only radial mixing, with no lift or turbulence, and scale-up means a move to marine (not turbine) impellers. Alternative systems developed to avoid stirring are as follows:

- *Airlift fermentor.* The airlift fermentor uses the bubble column principle to both agitate and aerate a culture (21,28,63,64). Air bubbles are introduced into the bottom of a culture vessel (aspect ratio 8–12:1) and rise up an inner draft tube. Aerated medium has a lower density than nonaerated medium so the medium rises through the draft tube and circulates down the outside of the vessel (upflow and downflow approximately equal volumes). The amount of energy needed is very low and shear forces are absent; thus it is an ideal method for fragile cells. Airflow rates of about 300 mL min^{-1} are used. Vessels are available from 2 L upward, with 2,000 L reactors used in industrial

manufacturing processes. However, scale-up is more or less linear, and a 90-L vessel requires 4 m headroom; special manufacturing suites are thus needed for large-scale operations.

- *Vibro-mixer.* The Vibro-mixer (65) is a nonrotating agitator that produces a stirring effect by a vertical reciprocating motion with a path of 0.1–3 mm at a frequency to 50 Hz. The mixing disk is fixed horizontally to the agitator shaft, and cone-shaped holes in the disk cause a pumping action as the shaft vibrates. This is a low energy system with reduced shear forces and foaming.
- *Celligen fermentor.* This fermentor (66,67) is available from New Brunswick Scientific and is designed so that the impeller acts as a fluid pump and aerator. Macrocirculation mixing is generated by the hollow central shaft filled with three rotating horizontal jet tubes in a low-shear bulk movement of cells and medium (cell-lift effect).

The other principal physical factor to be accommodated is aeration. Sparging can cause cellular damage unless carried out at very low rates. General guidelines are to use large bubbles (1–3 mm diameter) and low flow rates (5–10 cm^3/L/min), which means relatively inefficient mass transfer, especially at the low stirring rates used. Even though cell bioreactors have an aspect ratio of less than 2:1 to maximize surface diffusion, a means of increasing oxygen supply during scale-up is essential. Strategies for increasing the oxygen supply have included a surface aerator (68), multiple nozzle injection on the medium surface (69), caged aerator (70), spin exchange aerator (37), external and internal loop oxygenator (71), membrane tubing arranged in the vessel (19), and stirring system (20). The use of closed perfusion loops through external reservoirs is also an efficient means of oxygenation as long as the perfusion rate is fast enough (6), which requires a very efficient spin filter or other cell separation device in the culture.

Scale-up from laboratory spinner cultures to fermentors (1–10,000 L) has the following consequences:

- Change from glass to stainless steel vessels
- Change from mobile (autoclavable) to in situ system connected to steam, seed, medium holding and downstream harvesting vessels, and so forth
- Requirement for water jacket, or internal temperature control
- Greater sophistication in environmental control systems and engineering to preserve integrity

Animal cell bioreactors were adapted from the microbial fermentation tanks with only minor modifications:

- Suitable impeller (e.g., marine)
- No baffles and a curved base for better mixing at low speeds
- Water jacket rather than immersion heater type of temperature control (to avoid localized heating at low stirring speeds)
- Top-driven motor stirrer so that cells cannot become entangled between moving parts
- Mirror finish to internal surfaces to reduce mechanical damage and cell attachment

57.4.3 Large-Scale Bioreactors

Large-scale bioreactors described in the previous chapters are based on either the fermentor tank or the airlift principle. Stirred tanks have been operated at 8–10,000 L (14) for the production of interferon and tPA and airlift at 2,000 L principally for monoclonal antibodies. The preference is for the tank fermentor because this is a well-tried and familiar production method using conventional production plant facilities that have been refined over the past 30 years. However, most processes run at scales between 50 and 500 L. Airlift bioreactors are considered more flexible in that a greater range of cells (including extremely fastidious and fragile types) can be grown in them. However, scale-up is very dependent on tall buildings. A modification of the single-cell suspension system is to grow cells as aggregates or flocculants brought about by the addition of slightly positively charged polymers (e.g., poly-L-histidine) (72). Flocculants facilitate process operations such as filtration, centrifugation, perfusion, and sedimentation, and the microenvironment created within the cell aggregate can increase specific productivity (73).

Scale-up increases the complexity of equipment and the process and thus gives rise to greater risks of system failure, loss of integrity (sterility), and potential release of hazardous materials. Because the reason for scale-up is the production of therapeutic biological products, conditions have to comply with current good manufacturing practice (cGMP) standards acceptable to the relevant licensing authorities. Containment of the process to prevent ingress of contaminating factors and release of materials that may affect the process worker and environment are thus key factors in these processes. Microbiological containment of small-scale systems (below 20 L) in class III microbiological cabinets is possible (74), and larger-scale fermentation plants can be contained to P3 standards at least up to the 150-L scale (75).

The scale-up chain to the final production vessel is governed by the split ratio possible with the particular cell line at each subculture and is usually between 1:3 and 1:5. The chain starts with an ampoule of cells stored at $-196^{\circ}C$ (liquid nitrogen) in a master cell bank (MCB) that has been fully characterized for biological contaminants and cell line stability (76). All manipulations are carried out according

to standard operating procedures to obtain reproducibility between runs and to generate the necessary quality control data for acceptance of the final product.

The engineering complexity and considerable resource investment in money and time to build and operate a large-scale production process means that many new products are still brought to market using replicate small-scale systems. This provides for quicker market entry but requires complete reregistration of the product if the product is later moved to a large-scale production process. The experimental procedures for scaling up a stirred bioreactor process have been described (77).

57.5 HIGH-CELL-DENSITY BIOREACTORS

The alternative strategies for scale-up were outlined earlier. In this section the processes that support cells at significantly greater densities than the classical $2-3 \times 10^6$/mL level are described. In the human body cells in tissues are on the order of $2-3 \times 10^9$ cells/cm^3, and this has always been a target for in vitro systems. However, 2×10^8 cells/mL has so far been the practical limit of density scale-up; even so, this is a 100-fold increase over the conventional low-density methods described so far. The two critical factors needed to achieve higher unit cell density are (*1*) perfusion to supply nutrients and remove waste products (78) and (*2*) cell immobilization to perfuse media at a fast enough rate without damaging or washing the cells out of the culture. Many devices have been developed to meet these requirements (6,7,18,22) (Table 57.7), of which hollow fiber bioreactors, spin filter perfusion, and microporous microcarriers are the most successful in terms of acceptance and use.

57.5.1 Hollow Fiber Bioreactors

Use of hollow fiber bioreactors was pioneered by Knazek *et al*. (95) using ultrafiltration capillary fibers. They can be considered analogous to a blood vascular system because the fibers selectively (by molecular weight cutoff) allow passage of macromolecules through the spongy fiber wall (60 μm) as the medium flows continuously through the lumen (200 μm in diameter). Cells are kept in the extracapillary space. A unit consists of thousands of fibers potted at either end in a cylindrical housing and capable of supporting both ADCs and suspension cells at $1-2 \times 10^8$/mL. This concept has been widely developed, with many commercial units available, and has been used particularly for producing monoclonal antibodies. The principal limiting factor in its exploitation is the difficulty in scaling up beyond very small volumes (25 mL). The problem is due to transmembrane flux being directed back into the lumen for the latter half of the flow path (6,112). Methods of overcoming this gradient problem include the insertion of contraflow and aeration fibers (112), cyclical flushing of medium between the lumen and extracapillary compartment (113), use of flat-bed rather than cylindrical filtration cartridges (91), and use of a radial flow reactor (114). The concept of using pressure differentials to simulate in vivo arterial and venous flow is used in the Acusyst System (Cellex Biosciences, Inc.). This system is well documented (113), including experimental details (115), and is probably the most used and successful application of hollow fiber technology.

To allow ADCs to attach, special fibers can be used (e.g., Amicon 3S1000) to give a huge surface area (1-L cartridge has 1 m^2 surface area and supports 10^{10} suspension cells or 2×10^9 ADCs). Thus this method gives a very large surface-area-to-volume ratio, allows continuous removal of waste products and supply of nutrients, supports high cell densities with a tissuelike architecture, and allows a concentrated product to be harvested. The disadvantages are diffusional limitations that cause culture inhomogeneity and cell necrosis, process control complexity, and difficulty in sterilization.

TABLE 57.7. Devices Used for Immobilizing Animal Cells to Permit Medium Perfusion (see also Chapter 46 in this volume)

Device	Reference
Gravitational settling of cells in medium outflow	79–81
Spin filter	5,66,69,81–85
Centrifuge circulation loop	86,87
Filtration membrane	
Dialysis	88,90
Hollow fibers	91–95
Membranes	96,97
Encapsulation	98–100
Entrapment	
Textured ceramics	101
Tubular flow reactor	102
Cellulose or polyurethane sponges	103,104
Fibers	105,106
Polyester (Fibra-cel)	107
Microporous microcarriers	46,47,108–111

57.5.2 Spin Filters

Because all static filters within a culture eventually become blocked, the development of a rotating filter that creates a boundary effect, thus delaying cell attachment and filter clogging, has been a successful step forward. The principle was introduced by Himmelfarb in 1969 (82) using a 3-μm stainless steel mesh rotated at 300 rpm. Subsequently there have been many variations (reviewed in Ref. 6): polymers (84), ceramics, microfibers, porcelain, immersed cages, baskets semiimmersed in the culture or attached to the stirrer shaft, separate rotating shaft (to increase rpm), filter within a draft tube and so forth. They provide a simple technical solution to scaling up process intensity within well-established stirred fermentors. They are limited in

that clogging eventually occurs and in the perfusion rate that can be maintained. However, they are particularly useful for microcarriers because a far larger mesh can be used, thus reducing the onset of filter clogging and permitting cell densities of 2×10^7/mL to be attained.

57.5.3 Microporous Microcarriers

Microcarrier culture has proven to be the most effective scale-up method for ADCs, despite its limitations (critical procedures, low surface-area-to-volume ratio of a sphere). Attempts were made to increase the surface area by surface indenting techniques but were not successful until the fabrication of porous particles. The initial particle was the Verax microsphere (47,108), which was 500 μm in diameter and manufactured from bovine collagen; the interconning channels of 20–40 μm diameter gave an internal open volume of 80% of the sphere. They were designed for fluidized-bed reactors, and thus their specific gravity was artificially increased to 1.7 with the addition of small metallic weights incorporated into the matrix. The spheres were fluidized at 75 cm/min upward flow, and cell densities in excess of 10^8 per milliliter intrasphere volume were achieved (equivalent to 4×10^7/mL in the bioreactor). The sphere matrix provided a huge surface area for attachment of ADCs but was equally suitable for suspension cells (which were entrapped in the pores). The system was scaled up to 24 L routinely and 200 L in the company's production unit and used for more than 85 different cell lines producing many cell products (including tPA, pro-urokinase [proUK], EPO, interferon, interleukin, factor VIII, and various immunoglobulins).

Verax was initially a closed product in that you had to invest in the complete system. Thus other microporous beads were quickly developed (Table 57.5). Alternative systems are also available such as the Pharmacia Cytopilot using Cytoline porous microcarriers (110). Microporous microcarriers that could be used in stirred rather than fluidized bioreactors are preferred and now available (Cellsnow and ImmobaSil). ImmobaSil (116) is of particular value because it is extremely permeable to oxygen, a robust, nonanimal product safe from bovine contaminants that can be used in all culture modes. Because the concentration of spheres is far less, the total cell mass is greatly reduced in stirred systems. However, it allows manufacturers to use conventional stirred equipment and increases cell density in the microcarrier system from 2×10^6/mL to in excess of 5×10^7/mL (using spin filter perfusion and aeration).

An alternative to using stirred or fluidized microporous carriers is use of a fixed bed of porous glass spheres (e.g., Siran) (46,109). Fixed-bed reactors of solid glass spheres have many advantages (111), and the disadvantage of low cell density can be overcome by using 5-mm Siran spheres. These spheres have surface areas of 75 m^2/L with interconning pores and channels of 60–300 μm and can be stacked in 5-L beds and perfused at 5 linear cm/min to provide a high feed rate without washing out or damaging the cells (protected from shear within the particles). The versatility and usefulness of this technique has been demonstrated for a range of suspension and anchorage-dependent cells, resulting in a 10-fold higher productivity over equivalent systems (18,117–119). A characteristic of all microporous carrier systems is that cell specific productivity is always higher (18,117), presumably due to the favorable environment of cells packed together in almost tissuelike density. Details on experimental methods have been published; fluidized-bed (120), fixed-bed (121), and commercial fixed-bed reactors are available (Meredos GmbH, Bovenden).

The advantages of porous carrier culture are summarized in Table 57.8. This technology is truly universal in being equally suitable for suspension cells and ADCs and flexible in the range of bioreactor systems it can be in. It is the only truly scaleable high-cell-density system available and provides a microenvironment that stimulates cell product expression. As the need for high-quantity biopharmaceutical manufacture increases, this technology will become increasingly widespread in application and use (Table 57.9).

TABLE 57.8. Advantages of Microporous Microcarriers

Unit cell density 50- to 100-fold higher than that of free suspension
Suitable for both attached and suspended cells
Can be used in fluidized- and fixed-bed reactors and stirred suspension
In situ 100- to 250-fold seed expansion eliminates seed chain steps
Diffusion into a sphere efficient (30% diameter penetration = 70% of volume)
Cells protected from shear
Specific cell productivity increased three- to five-fold
Three-dimensional structure easily derivitized for specialized cells
Capable of long-term (>100 days) culture with continuous harvesting
Scale-up potential by comparison with analogous systems (microcarrier to 4,000 L)

TABLE 57.9. Necessary Conditions for the Acceptance of Scaleable Immobilized Bioreactors

Insufficient quantities produced by other methods
Product only produced by immobilized or specialized cells that need three-dimensional culture
End product price only attainable with scale-up economies possible with these systems
Increased production plant capacity when expansion is no longer possible
New company or product beginning registration process
Sufficient data and experience accumulated to give manufacturing confidence

57.6 COMPARISONS, CONCLUSIONS, AND FUTURE DEVELOPMENTS

Given the range of culture strategies and options mentioned in this chapter, how does one choose the system best suited to the problem at hand? In Figure 57.2, a flow sheet of the options is given by which a product manager can reach such a decision based on the cell line, the product type, the time table, the available plant and resources, the manpower, and the annual product requirement. The question of whether to take the high-volume or high-density option is based on the considerations summarized in Tables 57.3 and 57.8 and the range of total cell densities that various bioreactors will support (Fig. 57.3). The system chosen will be the one that fulfills the defined need at the minimum commercial risk, because there is no one ideal system to meet all needs.

The future of animal cell biotechnology as a production vehicle for therapeutic products is as an essential component in a range of biological processes. Recombinant microorganisms will be the first method of choice for simple, nonglycosylated products without complex three-dimensional configurations necessary for bioactivity. Transgenic production may take over for products needed in 50 to 100-kg quantities. However, society may demand that these products be produced even at greater considerable cost in culture systems to reduce the exploitation of animals; this will be the driving factor for high-volume high-density systems based on microporous microcarriers. Finally, engineering solutions (122) to scale-up are not the only means of increasing unit productivity and economy of cell manufacturing processes. Considerable advances are being made in increasing cell-specific productivity from a modest 0.2 mg/10^6 cells/day to nearer in vivo levels of 7 mg/10^6 cells/day by cell engineering (recombinant control of metabolic processes). Advances are also being made in development of media and the environment to

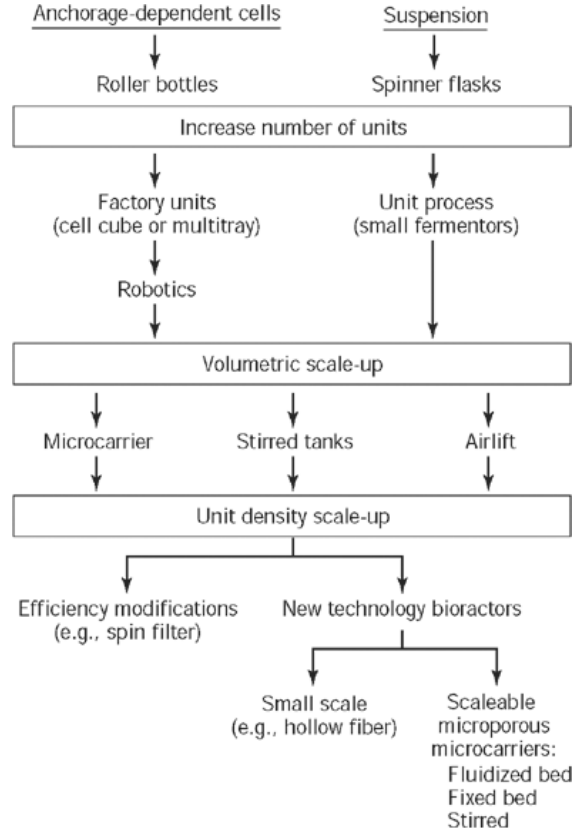


Figure 57.2. Scale-up: the decision process.

Scale (L)	System	Area (cm^2) (batch size)	Cells per batch (cells/L)
	Roller	1,750 (× 100)	2×10^{10} (2×10^{8})
	Multitray	24,000 (× 10)	3×10^{10} (3×10^{9})
	Cell cube	85,000 (× 4)	4×10^{10} (9×10^{9})
1	Hollow fiber	20,000	10^{10} (10^{11})
20	Microporous microcarrier	2.5×10^{6}	10^{12} (5×10^{10})
100	Glass sphere	10^{6}	10^{11} (10^{9})
200	Stacked plate	2×10^{5}	2×10^{10} (1×10^{8})
500	Microcarrier (with spin filter)	2×10^{10}	10^{13} (5×10^{10})
2,000	Airlift		4×10^{12} (2×10^{9})
4,000	Microcarrier	5×10^{6}	8×10^{12} (2×10^{9})
10,000	Stirred tank		2×10^{13} (2×10^{9})

Figure 57.3. Comparison of culture systems indicating volumetric size, unit, and system cell yields.

regulate cell growth, metabolism, and product expression in simpler (cheaper) media. There are also considerable improvements to be made in downstream scale and efficiency, where often only 20% of the product survives the purification process.

REFERENCES

1. R.G. Harrison, Proc. Soc. Exp. Biol. Med. 4: 140–143 (1907).
2. J.F. Enders, T.H. Weller, and F.C. Robbins, Science 109: 85–87 (1949).
3. P.J. Radlett, T.W.F. Pay, and A.J.M. Garland, Dev. Biol. Stand. 60: 163–170 (1985).
4. L. Hayflick and P.S. Moorhead, Exp. Cell Res. 25: 585–621 (1961).
5. J.P. Jacobs, Nature (London) 227: 168–170 (1970).
6. J.B. Griffiths, in R.E. Speir and J.B. Griffiths eds., Animal Cell Biotechnology, vol. 3, Academic Press, London, 1988, pp. 179–220.
7. A. Prokop and M.Z. Rosenberg, Advances in Biochemical Engineering/Biotechnology 39: 29–71 (1989).
8. G.F. Panina, Animal Cell Biotechnology, vol. 1, Academic Press, London, 1985, pp. 211–242.
9. A.L. van Wezel, Nature (London) 216: 64–65 (1967).
10. K.F. Pullen, M.D. Johnston, A.W. Phillips, G.D. Ball, and N.B. Finter, Dev. Biol. Stand. 60: 175–178 (1985).
11. M. Morandi and A. Valeri, Advances in Biochemical Engineering/Biotechnology 37: 57–72 (1988).
12. B. Clough, in A. Doyle and J.B. Griffiths eds., Cell and Tissue Culture: Laboratory Procedures for Biotechnologists, Wiley, Chichester, U.K., 1998, pp. 5–17.
13. G. Kohler and C. Milstein, Nature (London) 256: 495–497 (1975).
14. A. Lubiniecki, R. Arathoon, G. Polastri, J. Thomas, M. Wiebe, R. Garnick, A. Jones, R. van Reis, and S. Builder, in R.E. Speir, J.B. Griffiths, J. Stephenne, and P.J. Crooy eds., Animal Cell Biology and Technology for Bioprocesses, Butterworths, Guildford, U.K., 1989, pp. 442–451.
15. R.P. Lanza, J.L. Hayes, and W.L. Chick, Nature Biotechnology 14: 1107–1110 (1996).
16. M.W. Glacken, R.J. Fleischaker, and A.J. Sinskey, Trends Biotechnol. 1: 102–108 (1983).
17. J.B. Griffiths, Cytotechnology 3: 109–116 (1990).
18. J.B. Griffiths, in R.E. Spier and J.B. Griffiths eds., Animal Cell Biotechnology, vol. 4, Academic Press, London, 1990, pp. 149–166.
19. W. Kuhlmann, Dev. Biol. Stand. 66: 263–268 (1987).
20. J. Lehmann, G.W. Piehl, and R. Schulz, Dev. Biol. Stand. 66: 227–240 (1987).
21. J.C. Merchuk and M.H. Siegal, J. Chem. Technol. Biotechnol. 41: 105–120 (1988).
22. J.B. Griffiths, Biotechnol. 10: 30–32 (1991).
23. J.B. Griffiths, in R.I. Freshney ed., Animal Cell Culture: A Practical Approach, IRL Press, Oxford, 1992, pp. 47–93.
24. J.B. Griffiths, Ann. N.Y. Acad. Sci. 665: 364–370 (1992).
25. D. Looby and J.B. Griffiths, Trends Biotechnol. 8: 204–209 (1990).
26. J.B. Griffiths, J. Biotechnol. 22: 21–30 (1992).
27. R. Kunitake, A. Suzuki, H. Ichihashi, S. Matsuda, O. Hirai, and K. Morimto, J. Biotechnol. 52: 289–294 (1997).
28. H.G. MacMorine, G.D. Laurence, W. Parisius, and N.B. Cucakovich, Dev. Biol. Stand. 37: 139–142 (1977).
29. W. House, M. Shearer, and N.G. Maroudas, Exp. Cell Res. 71: 293–296 (1972).
30. M. Corbeil, M. Trundel, and P. Payment, J. Clin. Microbiol. 10: 91–95 (1979).
31. H.C. Girard, M. Sutcu, H. Erdem, and I. Gurhan, Biotechnol. Bioeng. 22: 477–493 (1980).
32. P.F. Kruse, L.N. Keen, and W.L. Whittle, In Vitro 6: 75–81 (1970).
33. I.A. Beeksma and R. Kompier, in E.C. Beuvery, J.B. Griffiths, and W.P. Zeijlemaker eds., Animal Cell Technology: Developments towards the 21st Century, Kluwer Academic, Dordrecht, 1995, pp. 661–663.
34. J.B. Schleicher and R.E. Weiss, Biotechnol. Bioeng. 10: 617–624 (1968).
35. O. Molin and C.G. Heden, Prog. Immunobiol. Stand. 3: 106–110 (1969).
36. C. Burbidge and I.K. Dacey, Dev. Biol. Stand. 55: 255–259 (1984).
37. J.B. Griffiths, D.R. Cameron, and D. Looby, Dev. Biol. Stand. 66: 331–338 (1987).
38. C. Burbidge, Dev. Biol. Stand. 46: 169–172 (1980).
39. D. Looby and J.B. Griffiths, in R.E. Spier and J.B. Griffiths eds., Modern Approaches to Animal Cell Technology, Butterworths, Guildford, U.K., 1987, pp. 342–352.
40. O.T. Ramirez and R. Mutharasan, Biotechnol. Bioeng. 33: 1072–1076 (1989).
41. J.H. Robinson, P.M. Butlin, and R.C. Imrie, Dev. Biol. Stand. 46: 173–181 (1980).
42. A.L. van Wezel, Dev. Biol. Stand. 55: 3–9 (1984).
43. B. Montagnon, J.C. Vincent-Falquet, and B. Fanget, Dev. Biol. Stand. 55: 37–42 (1984).
44. K. Nilsson, F. Buzsaky, and K. Mosbach, Biotechnology 4: 989–990 (1986).
45. D. Looby and J.B. Griffiths, Trends Biotechnol. 8: 204–209 (1990).
46. D. Looby and J.B. Griffiths, Cytotechnology 1: 339–346 (1988).
47. P.W. Runstadler and S.R. Cernek, in R.E. Spier and J.B. Griffiths eds., Animal Cell Biotechnology, vol. 3, Academic Press, London, 1988, pp. 305–320.
48. W. Noe, R. Bux, W. Berthold, and W. Werz, Cytotechnology 15: 169–176 (1994).
49. J.P. Whiteside and R.E. Spier, Biotechnol. Bioeng. 23: 551–556 (1981).
50. Y. Chisti and M. Moo-Young, Trans. Inst. Chem. Eng. 72C: 91–94 (1994).
51. P.C. Brown, C. Figueroa, M.A. Costello, and S.M. Maciukas, in R.E. Spier and J.B. Griffiths eds., Animal Cell Biotechnology, vol. 3, Academic Press, London, 1988, pp. 251–262.

52. D. Looby, in A. Doyle, J.B. Griffiths, and D. Newell eds., Cell and Tissue Culture: Laboratory Procedures, Wiley, Chichester, U.K., 1993, p. 28D:2.
53. B. Meignier, H. Mougeot, and H. Favre, Dev. Biol. Stand. 46: 249–256 (1980).
54. J.B. Griffiths, in A. Doyle, J.B. Griffiths, and D. Newell eds., Cell and Tissue Culture: Laboratory Procedures, Wiley, Chichester, 1993, p. 28C:1.1.
55. A.L. van Wezel, Dev. Biol. Stand. 46: 151–158 (1980).
56. J.S. Friedman, Biotechnology 7: 359–364 (1989).
57. K.K. Sanford, W.R. Earle, and V.J. Evans, J. Natl. Cancer Inst. 11: 773–795 (1951).
58. C.L. Crespi and W.G. Thilly, Biotechnol. Bioeng. 23: 983–993 (1981).
59. B.H. Junker, F. Wu, S. Wang, J. Waterbury, G. Hunt, J. Hennessey, J. Aunins, J. Lewis, M. Silberklang, and B.C. Buckland, Cytotechnology 9: 173–188 (1992).
60. N.A. de Bruyne, in R.E. Spier and J.B. Griffiths eds., Animal Cell Biotechnology, vol. 3, Academic Press, London, 1988, pp. 142–176.
61. J.B. Griffiths, in A. Doyle, J.B. Griffiths, and D. Newell eds., Cell and Tissue Culture, Laboratory Procedures, Wiley, Chichester, U.K., 1993, p. 28A:2.3.
62. P.B. Capstick, A.J. Garland, R.C. Masters, and W.G. Chapman, Exp. Cell Res. 44: 119–129 (1963).
63. H.W.D. Katinger, W. Scheirer, and E. Kromer, Ger. Chem. Eng. 2: 31–38 (1979).
64. M. Rhodes, S. Gardner, and D. Broad, in C.S. Ho and D.I.C. Wang eds., Animal Cell Bioreactors, Butterworth-Heinemann, Boston, Mass., 1991, pp. 253–268.
65. H.C. Girard, G. Okay, and Y. Kilvilcin, Bulletin of the Office of International Epizoology 79: 805–822 (1973).
66. S. Reuveny, Z.-B. Zheng, and L. Epstein, Am. Biotechnol. Lab. 28–36 (January/February 1986).
67. M. Johnson, G.A.C. Chavrie, and H. Archambault, Biotechnol. Bioeng. 35: 43–49 (1990).
68. W.-S. Hu and D.I.C. Wang, in W.G. Thilly ed., Mammalian Cell Technology, Butterworths, Boston, Mass., 1986, pp. 167–197.
69. A.L. van Wezel, J. Chem. Technol. Biotechnol. 32: 318–323 (1982).
70. J.P. Whiteside, S. Farmer, and R.E. Spier, Dev. Biol. Stand. 60: 283–290 (1985).
71. C. Leist, H.P. Meyer, and A. Fiechter, J. Biotechnol. 4: 235–246 (1986).
72. J.G. Aunins and D.I.C. Wang, Biotechnol. Bioeng. 34: 629–638 (1989).
73. A. Racher, J.L. Moreira, P.M. Alves, M. Wirth, U.H. Weidle, H. Hauser, M.J.T. Carrondo, and J.B. Griffiths, Appl. Microbiol. Biotechnol. 40: 851–856 (1994).
74. P. Hambleton and J. Melling, in P. Hambleton, J. Melling, and T.T. Salusbury eds., Biosafety in Industrial Biotechnology, Blackie Academic, London, 1994, pp. 129–148.
75. P. Hambleton, J.B. Griffiths, D.R. Cameron, and J. Melling, J. Chem. Technol. Biotechnol. 50: 167–186 (1991).
76. A. Doyle and J.B. Griffiths, in R.E. Spier and J.B. Griffiths eds., Animal Cell Biotechnology, vol. 5, Academic Press, London, 1992, pp. 75–96.
77. A.B. Lang and U. Schuerch, in A. Doyle, J.B. Griffiths, and D. Newell eds., Cell and Tissue Culture, Laboratory Procedures, Wiley, Chichester, U.K., 1993, p. 28B:1.1.
78. J.B. Griffiths, D. Looby, and A.J. Racher, Cytotechnology 9: 3–9 (1992).
79. S. Sato K. Kawamura, and N. Fujiyoshi, J. Tissue Culture Methods 8: 167–171 (1983).
80. M. Butler, T. Inamura, J. Thomas, and W.G. Thilly, J. Cell Sci. 61: 351–363 (1983).
81. J. Feder and W.R. Tolbert, Sci. Am. 248: 24–31 (1983).
82. P. Himmelfarb, P.S. Thayer, and H.E. Martin, Science 64: 555–557 (1969).
83. R. Varecka and W. Scheirer, Dev. Biol. Stand. 66: 269–272 (1987).
84. G.C. Avgerinos, D. Drapeau, J.S. Socolow, J. Mao, K. Hsiao, and R.J. Broeze, Biotechnology 8: 54–58 (1990).
85. E. Favre and T. Thaler, Cytotechnology 9: 11–19 (1992).
86. V. Jager, in R.E. Spier, J.B. Griffiths, and C. MacDonald eds., Animal Cell Biotechnology: Developments, Processes, and Products, Butterworth-Heinemann, Oxford, 1992, pp. 397–402.
87. K.O. Gronvik, H. Frieburg, and U. Malmstran, in R.E. Spier, J.B. Griffiths, J. Stephenne, and P.J. Crooy eds., Advances in Animal Cell Biology and Technology for Bioprocesses, Butterworths, Guildford, U.K., 1989, pp. 336–344.
88. G.B. Gori, Appl. Microbiol. 13: 93–97 (1965).
89. A. Bohmarn, R. Portner, J. Schmieding, V. Kasche, and H. Markl, Cytotechnology 9: 51–57 (1992).
90. H. Buntemeyer, C. Bohme, and J. Lehmann, Cytotechnology 15: 243–251 (1994).
91. K. Ku, M.J. Kuo, J. Delente, B.S. Wildi, and J. Feder, Biotechnol. Bioeng. 23: 79–95 (1981).
92. G. Klement, W. Scheirer, and H.W.D. Katinger, Dev. Biol. Stand. 66: 221–226 (1987).
93. G.L. Altshuler, D.M. Dziewulski, J.A. Sowek, and G. Belfort, Biotechnol. Bioeng. 28: 646–658 (1986).
94. P. Knight, Biotechnology 7: 459–461 (1989).
95. A. Knazek, P.M. Gallino, P.O. Kohler, and R.L. Dendrick, Science 178: 65–67 (1972).
96. F.W. Falkenberg, H. Weichert, M. Krane, I. Bartels, M. Palme, H.-O. Nagels, and H. Fiebig, J. Immunol. Methods 179: 13–29 (1995).
97. Tecnomouse, Integra Biosciences, AG, CH-8304 Wallisellen.
98. K. Nilsson, Trends Biotechnol. 5: 73–78 (1987).
99. R.G. Duff, Trends Biotechnol. 3: 167–170 (1985).
100. A. Tinto, P. Vila, C. Casca, and F. Godia, in M.J.T. Carrondo, J.B. Griffiths, and J.L.P. Moreira eds., Animal Cell Biotechnology: From Vaccines to Genetic Medicine, Kluwer Academic, Dordrecht, 1997, pp. 423–428.
101. G.J. Berg, Dev. Biol. Stand. 60: 297–307 (1985).
102. H.W.D. Katinger, Dev. Biol. Stand. 66: 195–209 (1987).
103. A. Lazar, L. Silberstein, A. Mizrahi, and S. Reuveny, Cytotechnology 1: 333–338 (1988).
104. H.A. Phillips, J.M. Scharer, N.C. Bols, and H. Moo-Young, Cytotechnology 9: 29–40 (1992).
105. H. Yamaji, H. Fukuada, Y. Nojima, and C. Webb, Appl. Microbiol. Biotechnol. 30: 609–613 (1989).

106. J. Litwin, Dev. Biol. Stand. 60: 237–242 (1985).
107. A. Kadouri, G. Wang, W. Zhang, C. Jacklin, and D. Friedman, in M.J.T. Carrondo, J.B. Griffiths, and J.L.P. Moreira eds., Animal Cell Biotechnology: From Vaccines to Genetic Medicine, Kluwer Academic, Dordrecht, 1997, pp. 307–312.
108. M.W. Young and R.C. Dean, Biotechnology 5: 835–837 (1987).
109. S. Pak and G. Stephanopoulas, Biotechnol. Bioeng. 41: 25–34 (1993).
110. G. Klima, G. Kreismayr, D. Muller, C. Schmatz, S. Wiederkum, W. Steinfellner, A. Assadian, G. Lhota, G. Bluml, O. Doblhoff-Dier, and H. Katinger, in M.J.T. Carrondo, J.B. Griffiths, and J.L.P. Moreira eds., Animal Cell Technology: From Vaccines to Genetic Medicines, Kluwer Academic, Dordrecht, 1997, pp. 447–454.
111. R.E. Spier, in R.E. Spier and J.B. Griffiths eds., Animal Cell Biotechnology, vol. 1, Academic Press, London, 1985, pp. 243–263.
112. J.P. Tharakan and P.C. Chau, Biotechnol. Bioeng. 28: 1064–1071 (1986).
113. M.L. Wolf and M.D. Hirschel, in R.E. Spier and J.B. Griffiths eds., Animal Cell Biotechnology, vol. 6, Academic Press, London, 1994, pp. 237–258.
114. J.P. Tharakan and P.C. Chau, Biotechnol. Bioeng. 29: 657–671 (1987).
115. J.A.J. Hanak and J.M. Davis, in A. Doyle, J.B. Griffiths, and D. Newell eds., Cell and Tissue Culture: Laboratory Procedures, Wiley, Chichester, U.K. 1993, pp. 28D:3.1–16.
116. D. Looby, A.J. Racher, J.P. Fuller, and J.B. Griffiths, in E.C. Beuvery, J.B. Griffiths, and W.P. Zeijlemaker eds., Animal Cell Technology: Developments Towards the 21st Century, Kluwer Academic, Dordrecht, 1995, pp. 783–786.
117. J.B. Griffiths and A.J. Racher, Cytotechnology 15: 3–9 (1994).
118. A.J. Racher and J.B. Griffiths, Cytotechnology 13: 125–131 (1993).
119. A.J. Racher, D. Looby, and J.B. Griffiths, J. Biotechnol. 15: 129–146 (1990).
120. D. Looby, in A. Doyle, J.B. Griffiths, and D. Newell eds., Cell and Tissue Culture: Laboratory Procedures, Wiley, Chichester, U.K., 1993, pp. 28D:1.1–16.
121. D. Looby, in A. Doyle, J.B. Griffiths, and D. Newell eds., Cell and Tissue Culture: Laboratory Procedures, Wiley, Chichester, U.K., 1993, pp. 28D:2.1–13.
122. S. Ozturk, Cytotechnology 22: 3–16 (1996).

58

MASS TRANSFER

YUSUF CHISTI
Massey University, School of Engineering, Palmerston North, New Zealand

58.1 INTRODUCTION

Mass transfer phenomena impact upon all facets of bioprocessing. Transport effects often determine the productivity of bioreactors and the downstream recovery operations. Gas–liquid mass transfer problems arise during supply of oxygen from a gas phase to liquid culture, and during removal of metabolically generated carbon dioxide from a culture fluid to a gas phase. Similarly, gas–liquid mass transfer issues must be faced again during recovery operations such as distillation. Liquid–liquid mass transfer occurs when oxygen is supplied through liquid carriers such as perfluorocarbons during liquid–liquid extraction, and during degradation of water immiscible liquid substrates. Solid–liquid mass transfer problems are faced during recovery by adsorption, during chromatographic separations, and in operations such as crystallization. Performance of solid-phase biocatalysts such as immobilized cells and enzymes is often limited by solid–liquid mass transfer. Solid–liquid mass transfer effects influence the workings of membrane separations such as microfiltration and ultrafiltration. Transport within solid particles or intraparticle mass transfer becomes limiting in certain cases. Gas–solid transport is seen during some drying situations. Some of these transport issues are the focus of this chapter.

Ultimately the transport of a solute through any fluid or space is governed by the molecular diffusivity or the diffusion coefficient of the solute in the fluid or solution. How diffusivity is affected by factors such as temperature and viscosity, and the estimation of diffusivities in various situations are discussed below.

58.2 DIFFUSION COEFFICIENT OR DIFFUSIVITY

Diffusion coefficient is a measure of a solute's mobility in a solvent. Diffusion coefficient depends on temperature, the type of solvent and its viscosity, and the concentration of solute in solution. Diffusivities in liquids and gases generally increase with temperature. Liquid-phase diffusivities are little affected by pressure, but in gases diffusivities decline as pressure increases. Typically, liquid-phase diffusivities are much lower, only about a hundredth, compared to those in gases. Diffusion coefficients of common solute–solvent combinations are available in handbooks. Tables 58.1 and 58.2 provide some bioprocess-relevant data. Methods of measuring diffusion coefficients have been described by Geankoplis (1) and Pratt (2). When diffusion coefficients are not available, they can be estimated.

Diffusivities of small solutes diffusing in dilute liquids can be estimated using the Wilke and Chang (3) equation,

$$D_{\mathrm{L}} = 1.173 \times 10^{-16} \frac{(\xi M_{\mathrm{L}})^{0.5}\, T}{\mu_{\mathrm{L}} V_{\mathrm{M}}^{0.6}} \qquad (58.1)$$

where M_{L} and μ_{L} are the molecular weight and the viscosity of the solvent, respectively; T is the absolute temperature, V_{M} is the molar volume of the solute at its boiling point, and ξ is the association parameter—a measure of polar interactions among molecules—of the solvent. Association parameters of some common solvents are noted in Table 58.3. The molar volumes are given in handbooks,

Upstream Industrial Biotechnology: Equipment, Process Design, Sensing, Control, and cGMP Operations, Volume 2, First Edition. Edited by Michael C. Flickinger.
© 2013 John Wiley & Sons, Inc. Published 2013 by John Wiley & Sons, Inc.

TABLE 58.1. Diffusivities of Some Common Solutes in Dilute Liquids

Solute	Solvent	Temperature (°C)	D_L ($\times 10^9$ m^2/s)
Acetic acid	Water	25	1.26
Acetic acid	Benzene	25	2.09
Acetone	Water	25	1.28
Benzoic acid	Water	25	1.21
Carbon dioxide	Water	20	1.50
Carbon dioxide	Water	25	2.00
Ethanol	Water	25	1.24
Glucose	Water	20	0.60
Glycerol	Water	20	0.83
Methanol	Water	15	1.26
Nitrogen	Water	20	1.64
Oxygen	Water	20	1.80
Oxygen	Water	25	2.41
Phenol	Water	20	0.84
Sucrose	Water	20	0.45
Urea	Water	25	1.38
Water	Ethanol	25	1.13

TABLE 58.2. Diffusivities of Some Globular Proteins in Dilute Aqueous Solutions

Protein	Molecular weight (kg/kmol)	Temperature (°C)	D_L ($\times 10^{11}$ m^2/s)
Bovine serum albumin	67,500	25	6.81
Urease	482,700	25	4.01
Human serum albumin	72,300	20	5.93
Human fibrinogen	339,700	20	1.98

TABLE 58.3. Association Parameters for Some Solvents

Solvent	Association Parameter, ξ
Water	2.6
Methanol	1.9
Ethanol	1.5
Benzene	1.0
Ether	1.0
Heptane	1.0
Other unassociated solvents	1.0

Based on Ref. 3.

or, for organic solutes, they are easily calculated by the group contribution method (1,2). Equation 58.1 is suitable for small solutes with $V_M \leq 0.500$ m^3/kmol. When molar volumes are larger, as with globular proteins, the Stokes–Einstein equation may be used to estimate diffusivities; thus,

$$D_L = \frac{9.96 \times 10^{-16}\, T}{\mu_L V_M^{1/3}} \tag{58.2}$$

Larger molecules diffuse more slowly than smaller ones. For example, the diffusivities of globular proteins (Table 58.2) are much lower than those of smaller solutes listed in Table 58.1.

Small solutes such as sugar or oxygen diffusing in solutions of proteins, move more slowly than in water. Diffusion coefficient D_P of a small solute in a solution of globular protein can be approximated as (1)

$$D_P = D_L(1 - 1.81 \times 10^{-3} C) \tag{58.3}$$

where D_L is the diffusivity of the solute in water and C (kilograms per cubic meter) is the concentration of protein in solution. Equation 58.3 is suitable only when the diffusing solute does not associate with the protein molecule. When a solute associates with the protein, a part of the observed diffusivity of the solute is due to diffusion of the protein molecules, and a part is due to diffusion of unassociated solute.

Small molecules diffusing through gels such as agar, gelatin, and alginate, diffuse more slowly than in water. The diffusion coefficient declines with increasing concentration of the gelling agent; however, in typically formulated gels, diffusivities are only 20–50% lower than in water. Inorganic salts and electrolytes that dissociate in water actually diffuse as "molecules" in the absence of electric fields. Diffusivities of electrolytes may be estimated using methods discussed by Pratt (2) and Knudsen *et al*. (4).

58.3 GAS–LIQUID MASS TRANSFER

Many industrial fermentations require oxygen. Oxygen supply must at least equal the oxygen demand or the fermentation will be oxygen limited. Oxygen demand is especially difficult to meet in viscous fermentation broths and in broths containing a large concentration of the oxygen consuming cells. In large fermenters, oxygen transfer becomes difficult when demand exceeds 4–5 kg/m^3 h (5). Above a critical concentration of dissolved oxygen, the amount of oxygen does not influence the specific growth rate. The critical dissolved oxygen level depends on the microorganism, the culture temperature, and the substrate being oxidized. The higher the critical dissolved oxygen value, the greater the likelihood that oxygen transfer will become limiting (5). Under typically used culture conditions, fungi such as *Penicillium chrysogenum* and *Aspergillus oryzae* have a critical dissolved oxygen value of about 3.2×10^{-4} kg/m^3. For baker's yeast and *Escherichia coli*, the critical dissolved oxygen values are 6.4×10^{-5} and 12.8×10^{-5} kg/m^3, respectively (5). For comparison, the dissolved oxygen concentration in an air saturated sterile medium is typically around 7×10^{-3} kg/m^3; hence, in terms of percentage of

air saturation, the minimum acceptable dissolved oxygen level in a fungal fermentation is about 5%.

Oxygen uptake rate of mammalian cells is typically $(0.8–8.0) \times 10^{-15}$ kg O_2/cell h. In suspension culture of animal cells, cell concentrations typically reach $(1–1.2) \times 10^6$ cells/mL; concentrations up to 1.2×10^7 cells/mL are attained in perfusion culture and even higher values occur in immobilized cell bioreactors. The critical dissolved oxygen concentration for animal cells tends to be low, for example, 0.5% of air saturation, or 0.035 kg/m^3.

The transport route of a soluble gas from the gas to the liquid phase is schematically illustrated in Figure 58.1. The gas may be imagined as passing through stagnant gas and liquid films on either side of the gas–liquid interface. The resistance to transfer is localized within the stagnant films and the gas–liquid interface is itself assumed to offer no resistance to mass transfer. Mass transfer in the films occurs solely by diffusion; therefore, at steady sate, linear concentration profiles exist in the films (Figure 58.1). The transport flux (J) of the diffusing species is related to the concentration gradient (ΔC) in the film and to the film thickness (δ) as follows:

$$J = \frac{D}{\delta}\Delta C \tag{58.4}$$

In Equation 58.4, D is the diffusivity of the transferring component in the film. The ratio D/δ is known as *the mass transfer coefficient*, k.

In the steady state, the flux of the diffusing component—or the rate of transfer per unit cross-sectional area—is the same through the gas and the liquid films; thus, Equation 58.4 may be written for each of the two films:

$$J = k_G(C_G - C_{Gi}) \tag{58.5}$$

$$= k_L(C_{Li} - C_L) \tag{58.6}$$

where k_G and k_L are the gas and the liquid film mass transfer coefficients, respectively. The overall mass flux from the gas to the liquid phase may be written as follows:

$$J = K_L(C^* - C_L) \tag{58.7}$$

where C^* is the saturation concentration (i.e. the maximum possible value) of the diffusing component in the liquid in equilibrium with the gas phase and K_L is the overall mass transfer coefficient based on the liquid film. The saturation concentration C^* in the liquid is related to the gas-phase concentration (C_G) of the diffusing component by Henry's law:

$$C_G = HC^* \tag{58.8}$$

where H is the dimensionless Henry's constant (6). Using Equations 5–8 and the knowledge that $C_{Gi} = HC_{Li}$ (i.e. equilibrium exists at the interface because the interface offers no resistance to mass transfer), the various mass transfer coefficients can be shown to be related as follows (6):

$$\frac{1}{K_L} = \frac{1}{k_L} + \frac{1}{Hk_G} \tag{58.9}$$

For a sparingly soluble gas such as oxygen, H is much greater than unity ($H \approx 30$ for oxygen in water); furthermore, the coefficient k_G is typically larger than k_L because the gas-phase diffusivities are vastly greater than those in liquids (e.g. $D_{oxygen/air} = 10^4\ D_{oxygen/water}$ at 20°C). Consequently, the second term on the right-hand side of Equation 58.9 is negligible relative to the first, and the equation becomes

$$\frac{1}{K_L} \approx \frac{1}{k_L} \tag{58.10}$$

This implies that essentially all resistance to interfacial mass transfer of a sparingly soluble gas is localized in the liquid film at the interface, that is, the mass transfer is liquid film controlled (6).

Because the transport flux J equals the rate of transfer per unit gas–liquid interfacial area, Equation 58.7 may be expressed in terms of rate as follows:

$$\frac{dC_L}{dt} = K_L a_L(C^* - C_L) \tag{58.11}$$

where C_L is the dissolved gas concentration at time t and a_L is the gas–liquid interfacial area per unit volume of the liquid.

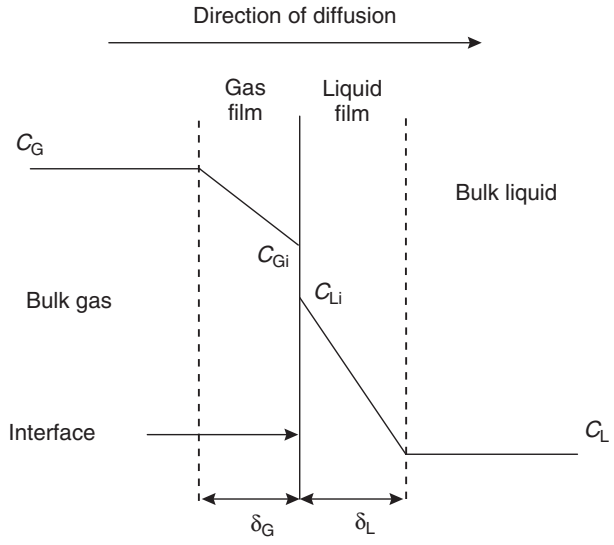


Figure 58.1. Steady state dissolved oxygen concentration profile in the vicinity of the gas–liquid interface.

58.3.1 Volumetric Gas–Liquid Oxygen Transfer Coefficient, $k_L a_L$

In view of approximation 10, the overall volumetric mass transfer coefficient $K_L a_L$ for gas–liquid mass transfer is often expressed as $k_L a_L$. The overall volumetric gas–liquid mass transfer coefficient $k_L a_L$ and the concentration driving force $(C^* - C_L)$ for mass transfer must be known if the rate of supply of oxygen or other soluble gases is to be quantified (6). The mass transfer driving force, which is easily determined, depends on temperature and pressure. The coefficient $k_L a_L$ depends on the properties of the fluid, the hydrodynamic regime, and the configuration of the bioreactor. The factors influencing $k_L a_L$ and mass transfer are summarized in Table 58.4. Prediction of $k_L a_L$ is an important part of bioreactor design. The individual terms in $k_L a_L$ are difficult to measure directly, but the product is relatively easily measured (6).

Usually the overall volumetric gas–liquid mass transfer coefficient is expressed in terms of the liquid volume in the fermenter; however, sometimes the basis of expression has been the gas–liquid dispersion volume (6). An identical basis is necessary for comparing mass transfer capabilities, and the coefficient expressed in one form may be converted to the other if the overall gas holdup (ε_G) is known.

$$k_L a_L = \frac{k_L a_D}{1 - \varepsilon_G} \tag{58.12}$$

Some typical $k_L a_L$ values seen in various types of bioprocesses are noted in Table 58.5.

As noted earlier, the rate of diffusive transport of a component through a unit area perpendicular to the direction of transport can be expressed as mass flux or molar flux, that is, kilogram or kilomole of component transferred per unit area per unit time. The flux J is proportional to a mass transfer driving force and a mass transfer coefficient K_L, or $J = K_L \times$ (driving force). Mass transfer is driven by differences in chemical potential. A species diffuses from regions of high potential to those of low potential until the difference has been eliminated. In practice, the driving force for mass transfer may be expressed as a concentration difference, partial pressure difference, or mole fraction difference. For example, when oxygen-free water is brought into contact with air, oxygen diffuses from air to water until the water becomes saturated. At this point the oxygen concentrations in the two phases are in dynamic equilibrium, but there is no net transfer. Note that the concentrations of oxygen in water and air are not equal, but the chemical potentials are. Depending on how the mass flux J and the driving force are expressed, the mass transfer coefficient may have different numerical values and different units as noted in Table 58.6 for a few cases. A coefficient expressed in one form may be easily converted to a different one.

TABLE 58.4. Factors Influencing Gas–Liquid Mass Transfer

Temperature	Concentration of solids
Pressure	Hydrophobicity of solids
Diffusivity	Morphology of solids
Viscosity	Shear rate or power input
Density	Aeration velocity
Surface tension	pH
Presence of surfactants and ions	Geometry of the bioreactor
Ionic strength	Flow parameters of non-Newtonian fluids

TABLE 58.5. Typical $k_L a_L$ Values Seen in Bioprocesses

Process	$k_L a_L$ (/s)
Fungal fermentations	10^{-2}
Bacterial and yeast fermentations	10^{-1}
Wastewater treatment	3×10^{-3}

From Ref. 6.

58.3.2 Measurement of $k_L a_L$

Several methods are available for measuring $k_L a_L$ values (1,6–8). Only a few of the more useful and common methods will be noted here.

TABLE 58.6. Possible Ways of Expressing Mass Flux and Mass Transfer Coefficient

Flux, J	Driving Force	Units of K_L
kg/s m^2	Concentration difference, kg/m^3	m/s
kg/s m^2	Mole fraction difference	kg/s m^2
kg/s m^2	Partial pressure difference	kg/s m^2
kmol/s m^2	Concentration difference, kg/m^3	m/s
kmol/s m^2	Mole fraction difference	kmol/s m^2
kmol/s m^2	Partial pressure difference	kmol/s m^2
m^3/m^2 s (for transfer of a gas)	Partial pressure difference	m/s

58.3.2.1 Sulfite Oxidation Method. The sulfite oxidation method has been extremely widely used, but it is suited to measurements only in physical systems (no live microorganisms) such as water or some polymer solutions. The method is subject to too many interferences (6,7) and, therefore, is not suitable for use in most culture media or in nonviable fermentation broths. Moreover, because of high ionic strength, the sulfite oxidation medium is strongly noncoalescing and rheologically quite different from fermentation systems. Consequently, the sulfite oxidation measurements are not readily translated to biologically relevant systems.

The sulfite oxidation method relies on oxidation of sulfite to sulfate using dissolved oxygen:

$$SO_3^{2-} + 1/2\ O_2 \xrightarrow{\text{catalyst}} SO_4^{2-}$$

The reaction is catalyzed by copper(II), cobalt(II), as well as other metal ions. The rate of sulfite oxidation is a measure of the rate of oxygen transfer to the liquid. The overall reaction generates H^+, and pH control is necessary because the reaction rate is pH-dependent. Also, the temperature needs to be controlled carefully to assure constant reaction kinetics. Impurities such as iron, manganese, and other transition metals in the parts per million range affect the reaction.

For k_La_L measurements, the reaction conditions should be such that the reaction occurs in the bulk liquid and not at the gas–liquid interface. Thus, Cu(II) catalysis is used with a sufficiently high sulfite concentration, such that the oxidation rate is independent of the sulfite level. The rate of sulfite consumption is given by

$$-\frac{d[SO_3^{2-}]}{dt} = k_La_L(C^* - C_L) \qquad (58.13)$$

where C^* and C_L are the saturation concentration of dissolved oxygen and the actual instantaneous concentration at time t, respectively. C_L is usually close to zero. The sulfite consumption rate, which should remain constant, is followed by quenching the samples taken at various times with excess iodine, and back titration of the residual iodine with thiosulfate (6).

Another oxygen consuming reaction is the oxidation of dithionite ($S_2O_4^{2-}$) in alkaline solutions; however, in view of uncertain kinetics and other factors, the usefulness of that reaction for k_La_L measurements remains questionable.

58.3.2.2 Chemical Absorption of Carbon Dioxide. This method is similar in principle to the sulfite oxidation procedure. Carbon dioxide is absorbed into a mildly alkaline or suitably buffered solution where it is converted to other species. Chemical absorption of carbon dioxide into Na_2CO_3–$NaHCO_3$ solution is sufficiently slow for use in k_La_L determinations when the ratio of carbonate to bicarbonate concentrations is between 3 and 5 (6). Other reaction conditions need to be controlled to ensure that the reaction rate does not enhance mass transfer. The method has limitations similar to those of the sulfite oxidation technique.

58.3.2.3 The Hydrazine Method. The hydrazine method makes use of the reaction

$$\underset{\text{hydrazine}}{N_2H_4} + O_2 \xrightarrow{\text{catalyst}} N_2 + H_2O$$

The reaction is best carried out at pH 11–12 using copper sulfate catalyst (6). A steady flow of hydrazine into an aerated reactor is used to maintain a constant concentration of dissolved oxygen. The amount of hydrazine consumed per unit time equals the oxygen absorption rate. The reaction does not produce any ionic species; hence, the ionic strength of solution can be kept lower than with the sulfite oxidation or the carbon dioxide absorption methods.

58.3.2.4 Oxygen Balance Method. This technique depends on measurement of mass flow rates of aeration gas into and out of the fermenter. The mass fraction of oxygen in the inlet and exhaust gas streams must also be determined (mass spectrometer, paramagnetic oxygen analyzer), in addition to the steady state dissolved oxygen concentration in the broth (dissolved oxygen electrode). The k_La_L value is obtained from the oxygen balance

$$F(x_i - x_o) = V_Lk_La_L(C^* - C_L) \qquad (58.14)$$

where F is the mass flow rate of gas, x_i and x_o are the mass fractions of oxygen in the gas (i = inlet, o = outlet), and V_L is the volume of the broth in the fermenter. Equation 58.14 assumes no evaporation and it does not correct for carbon dioxide production; however, the necessary corrections can be easily incorporated. For constant volume continuous culture, Equation 58.14 needs to be further modified to account for oxygen entering and leaving the fermenter via the liquid streams.

The oxygen balance method requires accurate measurements of gas flow rates and oxygen concentrations. The oxygen mass fraction in the inlet and outlet gas must differ measurably—that is, the oxygen consumption rate in the fermenter should be relatively large—for reliable k_La_L measurements. Under suitable conditions, the method is very reliable and it does not disturb the fermentation by interrupting the air supply (8).

58.3.2.5 Enzymatic Oxidation Method. Oxygen transfer may be followed by the formation of gluconic acid via oxidation with oxygen in presence of the enzyme glucose oxidase. The rate of absorption of oxygen is calculated from the rate of consumption of alkali that is needed to neutralize the acid. The liquid-phase oxygen concentration is determined with a dissolved oxygen electrode. The cost of the enzyme restricts the method to small-scale applications (6). Other similar methods have been described (9). Enzyme catalyzed oxidation can potentially be used only in the absence of microorganisms and under a restricted range of conditions.

58.3.2.6 The Dynamic Gassing-In Method. In a fermentation at steady state, the oxygen supply rate exactly matches the rate of consumption by the microorganisms and the concentration of dissolved oxygen does not change, that is,

$$\frac{dC_L}{dt} = \underbrace{k_L a_L (C^* - C_L)}_{\text{oxygen supply or mass transfer term}} - \underbrace{q_{O_2} X}_{\text{consumption term}} = 0 \qquad (58.15)$$

where q_{O_2} is the specific oxygen consumption rate and X is the concentration of viable biomass. If the oxygen supply is interrupted now, the mass transfer term in Equation 58.15 becomes zero and, as shown in Figure 58.2, the dissolved oxygen concentration declines linearly with time (8). The slope of C_L versus t line during the unaerated period provides $q_{O_2} X$. After a short period, before the oxygen concentration has dropped to the critical level, the oxygen supply must be resumed. Now, the dissolved oxygen level rises (Figure 58.2). During the rise period, the dissolved oxygen concentration as a function of time is given by

$$C_L = C^* - \frac{1}{k_L a_L}\left(q_{O_2} X + \frac{dC_L}{dt}\right) \qquad (58.16)$$

which is a rearranged form of Equation 58.15. Thus, $k_L a_L$ can be calculated from the slope of a plot of C_L versus $\left(q_{O_2} X + \frac{dC_L}{dt}\right)$. This procedure requires interrupting the oxygen flow to the fermenter and the dissolved oxygen electrode needs to be capable of a rapid response.

The gassing-in method is commonly applied also to physical systems (6). In such cases the dissolved oxygen in the liquid is first reduced to nearly zero by bubbling with nitrogen. The nitrogen flow is then stopped, the bubbles are allowed to leave the fluid, and the system is oxygenated by bubbling with air. The concentration of the dissolved oxygen in the liquid is followed as a function of time, and the $k_L a_L$ is calculated as the slope of the linear equation

$$\ln\left(\frac{C^* - C_{L0}}{C^* - C_L}\right) = k_L a_L t \qquad (58.17)$$

where C^* is the saturation concentration of dissolved oxygen, C_{L0} is the initial dissolved oxygen concentration at time t_0 when a hydrodynamic steady state has been reestablished upon commencement of aeration, and C_L is the dissolved oxygen concentration at any time t (5). Equation 58.17 is obtained by integration of Equation 58.15, assuming a well mixed liquid (i.e. uniform C_L), no change in gas-phase composition (i.e. a constant C^*), and an absence of oxygen consumption (i.e. $q_{O_2} = 0$) in the physical system.

Correct evaluation of $k_L a_L$ by this method requires attention to several factors including the response dynamics of the dissolved oxygen electrode and the nature of mixing in the gas and the liquid phases. In large intensely mixed fermenters, a well mixed liquid phase may still be assumed, but the gas-phase composition changes significantly from the inlet to exhaust. The gas is generally in plug flow and, thus, a log mean concentration driving force $(C^* - C_L)_{LM}$ should be used in Equation 58.15. The driving force is

$$(C^* - C_L)_{LM} = \frac{C^*_{in} - C^*_{out}}{\ln\left(\frac{C^*_{in} - C_L}{C^*_{out} - C_L}\right)} \qquad (58.18)$$

where C^*_{in} and C^*_{out} are the saturation concentrations in equilibrium with the gas-phase composition at the fermenter inlet and outlet, respectively.

Generally, the nature of mixing in the gas phase is inconsequential in $k_L a_L$ determinations so long as $1/k_L a_L$ is less than the residence time of the gas phase in the liquid.

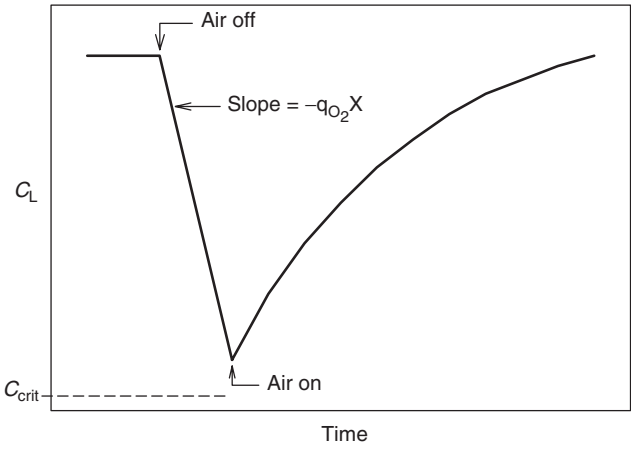


Figure 58.2. Dissolved oxygen concentration as a function of time during dynamic determination of the overall volumetric gas–liquid mass transfer coefficient in a fermentation.

The mean residence time t_R of the gas phase in bubble columns and stirred tanks can be estimated using (6)

$$t_R = \frac{h_L \varepsilon_G}{(1-\varepsilon_G)U_G} \tag{58.19}$$

where ε_G is the overall gas holdup. Equation 58.19 may also be applied to risers of airlift reactors when there is little or no gas in the downcomer. In the latter case, the U_G should be replaced with U_{Gr}—the superficial gas velocity based on the riser cross-section—and the gas holdup should be replaced with ε_{Gr}. When there is gas in the downcomer, Equation 58.19 may still be used because the downcomer gas holdup acts mostly as a dead volume.

The response characteristics of the dissolved oxygen electrode have little influence on the dynamic determination of $k_L a_L$ if the response time (63% of full response) is less than or equal to $1/k_L a_L$. Consult Chisti (6) for additional details. Other variations of the gassing-in technique exist. For example, methods have been developed to simultaneously determine $k_L a_L$ and the oxygen consumption rate without having to interrupt the flow of gas (10). Such schemes are especially useful for use in bubble columns and airlift bioreactors in which gas is the sole mechanism of achieving mixing.

58.3.3 Estimation of $k_L a_L$ for Gases Other Than Oxygen

Most of the available data and correlations for $k_L a_L$ were obtained for mass transfer of oxygen. The overall volumetric mass transfer coefficient for transfer of other gases can be estimated using the oxygen transfer data and the diffusion coefficients for oxygen and the other gases (6); thus,

$$(k_L a_L)_{gas} = \frac{D_{gas}}{D_{oxygen}} (k_L a_L)_{oxygen} \tag{58.20}$$

or

$$(k_L a_L)_{gas} = \sqrt{\frac{D_{gas}}{D_{oxygen}}} (k_L a_L)_{oxygen} \tag{58.21}$$

Equation 58.20 applies when the transfer can be ascribed to the film penetration mechanism of the two-film theory (6). Equation 58.21 is applicable when the surface renewal is the predominant mechanism of mass transfer (6). The difference between the two correction factors is small. The diffusivities used for the correction should be at the same temperature as the $k_L a_L$ data. The correction is satisfactory only for transfer in identical fluids at identical hydrodynamic conditions. Data on carbon dioxide mass transfer have been reviewed by Ho and Shanahan (11).

58.3.4 Solubility of Oxygen

Information on solubility of oxygen is needed for estimating the concentration difference driving force for mass transfer. Calculation of the saturation concentration C^* of dissolved oxygen (Eq. 58.8) requires a knowledge of the Henry's law constant, H. The dimensionless H for oxygen in pure water may be calculated as a function of temperature T (degrees Celsius) using the equation:

$$H = -9281.4 \times 10^{-3} + 4030.9 \times 10^{-3} T - 1403.5 \times 10^{-4} T^2 + 178.8 \times 10^{-5} T^3 \tag{58.22}$$

Equation 58.22 provides almost exact values of H over the range 20–30°C. Oxygen solubility in water at a pressure of 1 atm can be calculated with the equation,

$$C^* = 2178.549 \times 10^{-3} - 549.304 \times 10^{-4} T - 848.781 \times 10^{-6} T^2 - 483.785 \times 10^{-8} T^3 \tag{58.23}$$

where the temperature T is in degrees Celsius and C^* is in millimoles per liter. Equation 58.23 applies over 0–40°C. In addition to temperature, other factors influence oxygen solubility and the H value. Solubility declines with increasing ionic strength of solution. Solubility also depends on the types of ions in solution. For example, for the same molar concentrations of sodium chloride and hydrochloric acid in different samples of pure water, the oxygen solubility is lower in the salt solution. Solubility data for oxygen and other gases are available in handbooks. At 37°C, the saturation concentration of dissolved oxygen in a typical animal cell culture medium with serum is about 6.5×10^{-3} kg/m^3.

58.4 LIQUID–LIQUID MASS TRANSFER

Transfer of a solute from an immiscible liquid dispersed into another liquid (the continuous phase) can be analyzed using the two-film approach discussed for gas–liquid mass transfer. Now, the overall mass transfer coefficient K_L and the film coefficients for the dispersed (k_{Ld}) and the continuous (k_{Lc}) phases are related as follows:

$$\frac{1}{K_L} = \frac{1}{k_{Lc}} + \frac{K_p}{k_{Ld}} \tag{58.24}$$

In Equation 58.24, K_p is the partition coefficient of the solute between the two phases. The partition coefficient defines the equilibrium distribution of the solute between the phases; thus,

$$K_p = \frac{C_{Lc}}{C_{Ld}} \tag{58.25}$$

where C_{Lc} and C_{Ld} are the equilibrium concentrations of the solute in the continuous and the dispersed phases, respectively. Again, as for gas–liquid mass transfer, the interface between the phases is assumed to offer no resistance to mass transfer; hence, the equilibrium relationship determines the solute concentrations at the interface.

The overall volumetric mass transfer coefficient for liquid–liquid mass transfer is $K_L a_{Lc}$ where the specific interfacial area (a_{Lc}) is based on the volume (V_{Lc}) of the continuous phase. The rate of mass transfer from the dispersed to the continuous phase is given by

$$\frac{dC_{Lc}}{dt} = K_L a_{Lc}(C^* - C_{Lc}) \tag{58.26}$$

where C^* is the saturation concentration of the solute in the continuous phase in equilibrium with the dispersed phase.

58.5 SOLID–LIQUID MASS TRANSFER

Mass transfer to or from suspended solids is important in many bioprocess situations. Solid–liquid mass transfer may be rate limiting in immobilized enzyme and cell reactors, during dissolution of solids, adsorption, as well as in other cases. The rate of mass transfer to or from the suspended particle depends on the solid–liquid mass transfer coefficient (k_L), the total solid–liquid interfacial area (A_s), and the concentration driving force; thus,

$$V_L \frac{dC_L}{dt} = k_L A_s(C^* - C_L) \tag{58.27}$$

where C_L is the concentration of the transferring component in the liquid at time t, C^* is the saturation concentration (or solubility) of the transferring component, and V_L is the volume of the suspending liquid. Equation 58.27 is written for transfer from the solid to the liquid. By analogy with the film model of mass transfer, the coefficient k_L conceptually equals the diffusivity of the solute divided by the thickness of the stagnant liquid film at the solid–liquid interface; k_L is needed for quantifying the rate of mass transfer. Methods for estimating the solid–liquid or solid–gas (also gas–liquid if liquid is adsorbed as a very thin film on the surface of the solid) mass transfer coefficient k_L in various situations are discussed in a later section of this chapter.

58.6 MASS TRANSFER BEHAVIOR

58.6.1 General Aspects

Mass transport by diffusion and forced convection are influenced by the following variables: the mass transfer coefficient k_L, the molecular diffusivity of the transferring component D_L, the fluid density ρ_L and viscosity μ_L, a characteristic length d, and the velocity of flow U_L. Mass transfer by natural convection is also influenced by the gravitational acceleration g and the density difference $\Delta\rho$ between phases. These variables can be grouped into the following principal dimensionless groups or "numbers":

$$Re \text{ (Reynolds number)} = \frac{\text{inertial force}}{\text{viscous force}} = \frac{\rho_L U_L d}{\mu_L} \tag{58.28}$$

$$Sh \text{ (Sherwood number)} = \frac{\text{total mass transfer}}{\text{diffusive mass transfer}} = \frac{k_L d}{D_L} \tag{58.29}$$

$$Sc \text{ (Schmidt number)} = \frac{\text{momentum diffusivity}}{\text{mass diffusivity}} = \frac{\mu_L}{\rho_L D_L} \tag{58.30}$$

$$Gr \text{ (Grashof number)} = \frac{(\text{inertial force})(\text{bouyancy force})}{(\text{viscous force})^2} = \frac{d^3 \rho_L \Delta\rho g}{\mu_L^2} \tag{58.31}$$

$$Fr \text{ (Froude number)} = \frac{\text{inertial force}}{\text{gravitation force}} = \frac{U_L^2}{gd} \tag{58.32}$$

The above noted dimensionless numbers represent ratios of various factors that may play a role in a given situation. Grashof number is important in situations where density difference driven natural convection affects mass transfer. Reynolds number is employed in situations where forced convection is the predominant influence on transport processes. Froude number is useful in describing gravity-influenced flows. Schmidt number, or ratio of momentum diffusivity to mass diffusivity, is a measure of relative effectiveness of mass and momentum transfer. Some of those dimensionless numbers may be expressed in other forms depending on the situation. A few possible alternatives are noted in Table 58.7. In addition to the dimensionless groups discussed above, other groups relevant to mass transfer and related fluid mechanics are encountered in the literature. Some of the more common ones and their physical significance are noted in Table 58.8.

Grouping the many variables that affect mass transfer into a few dimensionless numbers greatly simplifies the process development experimentation and data correlation

TABLE 58.7. Alternative Methods of Expressing Dimensionless Groups

Group	Alternative Expressions
Reynolds number, *Re*	$\frac{\rho_L U_L d}{\mu_L}$ or $\frac{\rho_G U_G d}{\mu_G}$ (in pipes and channels)
	$\frac{\rho_L N d_i^2}{\mu_L}$ (stirred tanks)
	$\frac{\rho_L U_L L}{\mu_L}$ or $\frac{\rho_G U_G L}{\mu_G}$ (flow past a plate)
	$\frac{\rho_L U_L d_p}{(1-\phi)\mu_L}$ or $\frac{\rho_G U_G d_p}{(1-\phi)\mu_G}$ (flow past particles in packed beds)
Sherwood number, *Sh*	$\frac{k_L d}{D_L}$ or $\frac{k_G d}{D_G}$ (d may be diameter of a particle, flow channel, etc.)
Froude number, *Fr*	$\frac{U_L^2}{g h_L}$ or $\frac{U_G^2}{g h_L}$ (in bubble colums and airlift reactors)
	$\frac{N d_i^2}{g h_L}$ or $\frac{N^2 d_i}{g}$ (in stirred tanks)
Peclet number, *Pe*	$\frac{U_L h_L}{D_L}$ or $\frac{U_B d_B}{D_L}$ (in bubble colums and airlift reactors)
	$\frac{N d_i^2}{D_L}$ (in stirred tanks)

TABLE 58.8. Other Dimensionless Groups Relevant to Mass Transfer and Related Fluid Mechanics

Group	Definition	Physical Significance
Bond number, *Bo*	$\frac{g d_p^2 \Delta\rho}{\sigma_L}$	$\frac{\text{Gravity force}}{\text{Surface tension force}}$
Peclet number, *Pe*	$\frac{U_L L}{D_L}$	$\frac{\text{Bulk mass transport}}{\text{Diffusional mass transport}}$
Poiseuille number, *Ps*	$\frac{\mu_L U_p}{\rho_L g d_p^2 \Delta\rho}$	$\frac{\text{Viscous force}}{\text{Gravity force}}$
Power number, *Po*	$\frac{P}{\rho_L N^3 d_i^5}$	
Rayleigh number, *Ra*	*Gr Sc*	
Stanton number, *St*	$\frac{Sh}{ReSc}$	
Weber number, *We*	$\left(\frac{U_p^2 \rho_L d_p}{\sigma_L}\right)^{1/2}$	$\frac{\text{Inertial force}}{\text{Surface tension force}}$

for predicting the behavior of a system. For example, for fluids flowing in straight pipes the flow pattern changes from laminar to turbulent at a Reynolds number value of about 2300. This occurs irrespective of which specific fluid (e.g. air, water, milk, or thick glucose syrup) is being used so long as the combination of the fluid density, viscosity, flow velocity, and pipe diameter yields a Reynolds number value that exceeds 2300. Equations for correlating the mass transfer behavior of systems are often expressed in terms of dimensionless groups.

58.6.2 Behavior of Dispersions

A dispersion consists of one or more phases dispersed in a continuous phase. The continuous phase may be a gas or liquid. The dispersed phase may be liquid droplets, solid particles, or gas bubbles. The magnitude of the mass transfer coefficient inside and outside fluid particles depends on whether the particles behave as ridged spheres or are mobile. Small drops and bubbles behave as noncirculating ridged spheres. Larger bubbles and drops have internal fluid circulation and mobile interfaces because of relative motion between the particle and the surrounding fluid. Bubbles are immobile if the dimensionless diameter $d^* \leq 10$. The interface is nearly always mobile if d^* exceeds 50. Here, the dimensionless "diameter number" is

$$d^* = d_B \left(\frac{\mu_L^2}{\rho_L g(\rho_L - \rho_G)} \right)^{-1/3} \tag{58.33}$$

as defined by Wesselingh (6). Using this criterion, in air–water, bubbles smaller than 0.5 mm will always be ridged, whereas bubbles larger than about 2.5 mm will have mobile interfaces (6).

In certain cases, drops and bubbles may experience additional interfacial motions that are a consequence of mass transfer itself. Because the local mass transfer coefficient around a particle may be different at different locations, the local mass transfer rates may be different. In this situation, uneven transfer of a solute such as acetone or ethanol will generate solutions of different local concentrations and surface tensions. Adjacent films of different surface tensions lead to violent motions: regions of high surface tension contract and the film ruptures in regions of low surface tension. This effect is the well known Marangoni effect and it can significantly enhance mass transfer especially in liquid–liquid extraction processes.

For suspended solids, increasing agitation beyond that needed to achieve complete suspension has little impact on the mass transfer coefficient. The coefficient is influenced by relative velocity between the phases, which is determined by density differences. In gas–liquid dispersions too, the k_L is not substantially affected by increasing agitation, but the overall volumetric mass transfer coefficient ($k_L a_L$) increases because of the increase in gas–liquid interfacial area.

For freely suspended particles and bubbles, mass transfer to or from the bubble or particle obeys the general relationship

$$Sh = f(Gr, Sc) \tag{58.34}$$

For just suspended small particles ($d_p < 0.6$ mm) in stirred tanks, Calderbank and Moo-Young (12) recommended the equation

$$k_L = \frac{2D_L}{d_p} + 0.31 Sc^{-2/3} \left(\frac{\Delta\rho_L \mu_L g}{\rho_L^2} \right)^{1/3} \tag{58.35}$$

which is suitable for suspensions as well as gas–liquid dispersions of noncirculating bubbles ($d_p < 0.6$ mm). For larger circulating bubbles and liquid drops ($d_p > 2.5$ mm) in a just suspended state, the recommended equation is

$$k_L = 0.42 Sc^{-0.5} \left(\frac{\Delta\rho_L \mu_L g}{\rho_L^2} \right)^{1/3} \tag{58.36}$$

For bubbles in the 0.6–2.5-mm range, the k_L may be estimated as a linear function of bubble diameter.

Large spherical cap bubbles frequently occur in gas–liquid dispersions especially when the viscosity of liquid exceeds about 7×10^{-2} Pa s. Calderbank and Lochiel (13) correlated mass transfer from such bubbles using the equation

$$Sh = \frac{1.79(3R_b^2 + 4)^{2/3}}{R_b^2 + 4} (ReSc)^{1/2} \tag{58.37}$$

where R_b is the ratio of bubble width to bubble height. For spherical caps, R_b is about 3.5; hence, Equation 58.37 becomes

$$Sh = 1.31(ReSc)^{1/2} \tag{58.38}$$

Mass transfer to or from a particle suspended in a stagnant fluid occurs solely by diffusion. For a single spherical particle surrounded by a stagnant medium, the theoretical minimum value of the transfer coefficient is given by $Sh = 2$. For a single particle in the creeping flow regime ($Re < 0.1$), the specific relationship is

$$Sh = 0.39(GrSc)^{1/3} \tag{58.39}$$

Equation 58.39 applies to particles with ridged interfaces and this includes noncirculating small bubbles ($Re < 0.1$) in fermentation broths. Thus, compared to the case of a single noncirculating bubble (Eq. 58.39), the mass transfer coefficient in swarms of ridged bubbles (Eq. 58.35) is about 20% lower.

For power inputs greater than needed for just suspension, Calderbank and Moo-Young (12) have established the following equation in stirred tanks

$$k_L = 0.13 \left(\frac{\left(\frac{P_G}{V_L}\right) \mu_L}{\rho_L^2} \right)^{1/4} Sc^{-2/3} \tag{58.40}$$

where P_G / V_L is the power input per unit volume.

Transfer coefficient correlations generally require a knowledge of liquid properties such as viscosity and density. This is usually not a problem when dealing with Newtonian liquids, but difficulties arise with slurries and non-Newtonian media. Slurries of biomass solids may be usually treated as pseudohomogeneous fluids (6). Depending on the amount of suspended solids, slurries may behave as Newtonian or non-Newtonian power law fluids. For small amounts of spherical solid particles, Newtonian behavior is commonly observed, and in this case the viscosity of the slurry is independent of shear rate. The Newtonian viscosity may be estimated using equations of Einstein and Vand (8). Another suitable equation is that of Thomas:

$$\mu_{SL} = \mu_L(1 + 2.5\phi_S + 10.05\phi_S^2 + 0.00273e^{-16.6\phi_S}) \tag{58.41}$$

where ϕ_S is the volume fraction of suspended solids and μ_L is the viscosity of the suspending fluid.

When the slurry behaves as a non-Newtonian power law fluid, the apparent viscosity depends on shear rate; thus,

$$\mu_{ap} = K\gamma^{n-1} \tag{58.42}$$

where K is the consistency index or "thickness" of the fluid and n is its flow behavior index. The parameter γ is the shear rate. The shear rate is difficult to define in most realistic configurations of bioreactors under the usual operational conditions; nevertheless, the following expressions are commonly employed in estimating shear rates:

58.6.2.1 Bubble Columns and Airlift Devices

$$\gamma = \alpha U_G \tag{58.43}$$

where the constant α has been specified variously as 1000, 2800, 5000 m, and so on (14). Equation 58.43 has also been applied to airlift reactors, but that use is incorrect; for airlift reactors, the superficial gas velocity based on the cross-sectional area of the riser should be used in expressions such as Equation 58.43 as recommended by Chisti (6). Depending on the constant used, Equation 58.43 provides wildly different values of the supposed shear rate; hence, its use is not generally favored and it has been severely criticized (6,14,15). Another expression for shear rate in airlift reactors is

$$\gamma = 3.26 - 3.51 \times 10^2 U_{Gr} + 1.48 \times 10^4 U_{Gr}^2 \tag{58.44}$$

which was developed for $0.004 < U_{Gr}$ (meters per second) < 0.06 (16). Equation 58.44 also has significant problems as discussed elsewhere (15,17). Alternative approaches for estimating shear rates have been propounded by Molina Grima *et al*. (15). Methods of estimating shear rates in other process devices have been discussed exhaustively, elsewhere (18–20). An excessive shear rate can be damaging to some fragile biocatalysts and macromolecules (18–20).

58.6.2.2 Stirred Vessels.

The mean shear rate in impeller agitated tanks is usually given as

$$\gamma = k_i N \tag{58.45}$$

where k_i is an impeller-dependent constant (8). Some typical k_i values are: 11–13 for six–bladed turbines, 10–13 for paddles, ~10 for propellers, and ~30 for helical ribbon impellers. Again, as with pneumatically agitated bioreactors, much of the discrepancy among various predictive correlations that rely on a shear rate–dependent apparent viscosity has been associated with the use of equations such as Equation 58.45 (21). Equation 58.45, although empirically derived, has been shown to have a more fundamental basis (22).

The apparent viscosity of many fermentation fluids declines with increasing shear rate, that is, $n < 1$ (Eq. 58.42), and these fluids are known as *shear thinning* or *pseudoplastic*. Because shear rate is not easily defined in typical bioreactors (6,14,15,21), correlations employing solids holdup directly are preferred to those relying on a poorly established apparent viscosity of the slurry (6). As with viscosity, the density of a pseudohomogeneous slurry may be related to phase holdups as follows:

$$\rho_{SL} = \rho_L(1 - \phi_S) + \rho_S\phi_S \tag{58.46}$$

In some viscous fermentations, the principal resistance to oxygen transfer may be in the bulk fluid or at the cell–liquid interface and not at the gas–liquid interface. In such cases, dilution of the broth with water and increased agitation may slightly improve the transfer rate. In broths of filamentous fungi, promoting pelletlike growth as opposed to the usual pulplike morphology may substantially reduce the broth viscosity and improve mass transfer. Additional details on transport fundamentals of dispersions have been noted by Moo-Young and Blanch (23) and Knudsen *et al*. (4). Similar discussions with a focus on gas–liquid mass transfer in non-Newtonian media are due to Oolman and Blanch (24). Carbon dioxide mass transfer in bioreactors has been treated in depth by Ho and Shanahan (11). Mass transfer in gas–liquid dispersions and slurries can be substantially enhanced by the use of ultrasound, as reviewed by Chisti (25).

58.6.3 Gas–Liquid Mass Transfer

Either the bubble-free aeration of the liquid surface in a bioreactor may be used to provide the needed oxygen or the

aeration gas mixture may be bubbled or sparged through the body of the fluid. These schemes are discussed separately below.

58.6.4 Surface Aeration

Oxygen transfer through the surface of a fluid is useful in relatively small-scale devices, or in microaerophilic processes and certain wastewater treatment applications (26). Surface aeration is especially common in early stages of culture, for example, in shake flasks, tissue culture flasks, roller bottles, and spinner flasks. Understanding and characterization of surface aeration in small-scale devices is essential for process scale-up that minimally attempts to reproduce on larger scale the culture performance attained in the laboratory. Surface aeration is also employed in relatively small production bioreactors for growing cultures with extremely low oxygen requirements. Surface aeration in the principal types of laboratory and production culture devices is detailed in the following sections.

58.6.4.1 Laboratory Culture Devices

58.6.4.1.1 Shake Flasks. In 500-mL Erlenmeyer flasks placed on reciprocating and rotary shaker platforms, Yamada *et al*. (27) measured the volumetric rates of oxygen transfer in sulfite solutions and in *Acetobacter suboxydans* fermentations for converting sorbitol to sorbose. The rates were expressed in terms of the volumetric oxygen transfer coefficients through the flask closure (K_p) and across the gas–liquid interface (K_S):

$$\text{Volumetric rate of oxygen transfer} = (\text{mol } O_2/\text{mL h})\frac{1}{\left(\frac{1}{K_P}+\frac{1}{K_S}\right)}\frac{1}{V_L}(p_{atm}-p_L) \tag{58.47}$$

In Equation 58.47, V_L (milliliters) is the volume of liquid in the flask; p_{atm} (atmospheres) and p_L (atmospheres) are the partial pressures of oxygen in the atmosphere outside the flask and in the liquid in the flask, respectively. The units of K_p and K_S are moles of oxygen per atmosphere per hour. The mass transfer coefficient K_p through the closure declined with increasing weight (3–7 g) of cotton used to form the plug. The mean K_p value for cotton plugs was 2.87×10^{-2} mol O_2/atm h. Values for polyurethane foam and silicone foam plugs were a little lower. Compared to open flasks, cotton plugs restricted oxygen transfer. The K_S values in sulfite oxidation solutions agitated at 110–140 rpm ranged over $(2.04–4.63) \times 10^{-2}$ mol O_2/atm h. Under similar conditions in *A. suboxydans* fermentations, the K_S values were lower—only 50–60% of those obtained with sulfite oxidation. Various types of baffles and indentation in the flasks enhanced K_S by about 50% relative to the base case.

For mass transfer from liquid surface in unbaffled Erlenmeyer shake flasks, the following equation has been recommended (28)

$$k_L a_L\left(\frac{\mu_L}{\rho_L g^2}\right)^{1/3} = 0.5\left(\frac{\mu_L}{\rho_L D_L}\right)^{-1/2}\left(\frac{d_F}{V_L}\right)^{8/9}\left(\frac{\mu_L^2}{\rho_L^2 d_F^3 g}\right)^{8/27}\left(\frac{N^2\sqrt{\hat{e}d_F}}{g}\right)^{0.5} \tag{58.48}$$

where d_F is the maximum diameter of the flask, N is the speed of rotation, and $\hat{e}$ is the eccentricity of the shaker platform. Equation 58.48 applies to animal cell culture media when the liquid volume in the flask is 50–200 mL.

Open unbaffled shake flasks of 250 mL capacity filled to 100 mL with water at 37°C have been reported to have a $k_L a_L$ value of 30.8 ± 6.7/h when agitated at 250 rpm on an orbital shaker (29). For otherwise identical conditions, the measured $k_L a_L$ value in baffled flasks was 59.2 ± 7.4/h (29). Mass transfer data in shake flasks operated with various combinations of fill levels, agitation speed, and liquid viscosity have been published (30,31).

The type of closure used significantly affects oxygen absorption in Erlenmeyer flasks (32,33). Nikakhtari and Hill (34) correlated gas–liquid volumetric mass transfer coefficient in open Erlenmeyer flasks using the following equation:

$$k_L a_L = 2.584 T_L (V - V_L)^{2/3} \tag{58.49}$$

The variable T_L in Equation 58.49 is a liquid turbulence factor defined as follows:

$$T_L = \frac{V^{0.463}}{V_L} N \tag{58.50}$$

In Equations 58.49 and 58.50, $k_L a_L$ is in per hour, V is the volume of the flask in liters, V_L is the volume of the liquid in liters, and N (per second) is the shaking speed.

58.6.4.1.2 T-Flasks. Tissue culture flasks or T-flasks are commonly used in initial stages of animal cell culture. During typical culture conditions, the cells utilize the oxygen in the liquid layer, but the concentration of oxygen in the gas phase is little affected irrespective of whether the flask is fully closed or the cap is cracked open (35). Clearly, diffusion through the liquid layer controls mass transfer; thus, the shallower the liquid depth, the better. The oxygen transfer resistance of the deposited cell layer at the bottom of the flask is insignificant compared to the resistance

through the bulk liquid layer (35). The observed oxygen transfer rates through the liquid layer tend to be greater than if the transfer was purely by diffusion. This suggests that convection and micromixing (e.g. during sampling, opening or closing of incubator door) significantly contribute to transfer. In typical culture, the dissolved oxygen declines linearly with time until, by about 60 h, the dissolved oxygen level is reduced to below 10% of air saturation (35). Because T-flasks are typically inoculated and transferred every other day, the observed decline in oxygen may be of little real consequence; however, if the culture period is to exceed 60 h and dissolved oxygen levels of 10% or higher are wanted, then once or twice-daily gentle agitation of T-flasks is recommended.

58.6.4.1.3 Roller Bottles. Roller bottles are commonly used for initial stages of cell culture. Typically about 0.1 m in diameter and about 0.25 m tall, plastic roller bottles are filled to about a third of their height with culture fluid. The bottles are laid on their sides in a roller cabinet and rotated at 1–2 rpm. Roller bottles are used to culture both adherent cells as well as free suspension cells. The interfacial area for oxygen transfer is the surface of the culture fluid and the liquid film on walls that continuously enters and leaves the pool of liquid. Mechanized and automatic handling of a large number of roller bottles have extended this culture technique to commercial production scale in a few cases, but this kind of processing has a limited scope. The surface aeration capability of roller bottles, corrected for differences in surface-to-volume ratio, is somewhere between that of Erlenmeyer style shake flasks under typical conditions and the stationary T-flasks.

58.6.4.1.4 Spinner Flasks. Aunins *et al*. (36) reported k_La_L measurements (surface aeration) in 500-mL Corning spinner flasks (Figure 58.3) filled to a depth of 0.08 m with Dulbecco's Modified Eagle's Medium (DMEM), supplemented with 5% (vol/vol) fetal calf serum and 1 kg/m^3 ethylenediaminetetraacetic acid (EDTA). The data were obtained at 37°C and followed the equation

$$Sh = 1.08Re^{0.78} \tag{58.51}$$

where the Sherwood number is based on the vessel diameter and the Reynolds number is based on the impeller diameter. The measurements spanned the impeller speed range 25–150 rpm, impeller diameters of 0.0525 and 0.078 m, and impeller Reynolds number of 1500–20,000. Locating the impeller less than 0.01 m below the liquid surface dramatically enhanced the k_La_L value. At 50 rpm, with 0.078-m diameter paddle impeller placed at the liquid surface, the k_La_L value was about 9.72×10^{-4}/s. Moving the impeller to 0.01 m below the surface provided

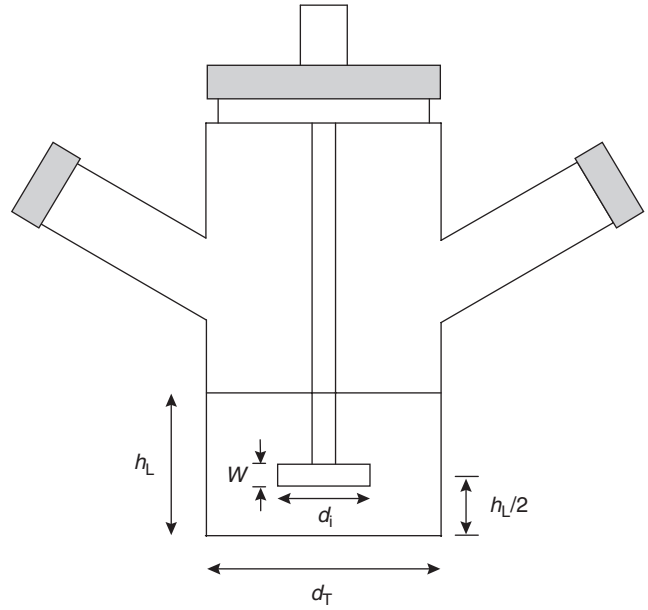


Figure 58.3. Geometry of 500-mL Corning spinner flasks: $h_L = 0.08$ m; $d_T = 0.096$ m; $d_i = 0.078$ m ($W = 0.025$ m), or $d_i = 0.053$ m ($W = 0.019$ m).

a k_La_L value of about 4.17×10^{-4}/s. Lowering the impeller further into the fluid did not affect the k_La_L value significantly.

58.6.4.1.5 Stirred Vessels. Lavery and Nienow (37) reported k_La_L measurements in water, RPMI 1640 basal cell culture medium, and the medium supplemented with 5% (vol/vol) fetal calf serum in a small, unbaffled, spherical cell culture vessel (1.5 L, static surface area of liquid $= 2.23 \times 10^{-2}$m^2) stirred with one or two, three-bladed propellers ($d_i = 0.060$ m, located 0.035 m apart). The lower impeller was positioned 0.003 m from the bottom of the vessel flask and the upper was 0.002 m below the surface of the liquid. The agitation speeds were 1.6–5.8/s (100–350 rpm). Air was sparged (100 mL/min) either in the liquid under the lower propeller or only through the headspace (i.e. surface aeration). The submerged aeration k_La_L values generally agreed with predictions of Van't Riet's correlation for nonionic solutions (i.e. Eq. 58.63). Relative to measurements in water, the serum and the basal medium had little effect on k_La_L values. The k_L for surface aeration was little affected by the number of impellers (whether 1 or 2). The k_La_L values for surface aeration were about 75% of those for submerged aeration in the reactor used. Addition of silicone antifoam (6 ppm) reduced the k_La_L values by about 50%. In the basal medium with the serum and the antifoam, the k_L values for surface aeration (no vortex) were $(1.18–3.54) \times 10^{-5}$ m/s. The k_La_L values for submerged aeration were $(2.8–8.5) \times 10^{-4}$/s.

58.6.4.1.6 Other Devices. For absorption of oxygen at the free surface of sodium sulfite solution in cylindrical containers placed on an orbital shaker platform, the volumetric mass transfer coefficient has been correlated (38) as follows:

$$k_L a_L = 6 \times 10^{-5} \left(\frac{P}{V_L}\right)^{0.4} d_T^{-0.25} h_L^{-0.6} \tag{58.52}$$

Equation 58.52 is independent of the gas flow rate in the headspace; it was determined for $20 \le P/V_L$ (watts per cubic meter) ≤ 500 and $0.5 \le h_L/d_T \le 1.5$ ($d_T = 0.12$ or 0.15 m). The agitation speed of the shaker platform varied over 1.2–3.3/s, and the moving vessel described a diameter of 0.01–0.04 m.

Sulfite oxidation method has been used to measure $k_L a_L$ in 48-well microtiter plates (39). The volumetric mass transfer coefficient depended on the fill volume, shaking frequency, and shaking diameter. Combinations of low fill volume and high shaking frequency generally produced high $k_L a_L$ values of up to 1600/h. Prediction of $k_L a_L$ values in microtiter plates is further discussed by Doig *et al*. (40). $k_L a_L$ values for various miniature bioreactors (0.15–500 mL) that are used typically in animal cell culture, have been provided by Betts and Baganz (41). Microliter bioreactors have been discussed by Fernandes and Cabral (42). Oxygen transfer in single-use disposable culture pouches is discussed by Kilani and Lebeaut (43).

58.6.4.2 Larger Systems

58.6.4.2.1 Stirred Tanks. Multibladed disc turbines located at the surface provide superior surface aeration relative to other types of impellers (44). To prevent entrainment of bubbles, the turbines must be operated such that (44)

$$N d_i \le 0.11 \left(\frac{d_i}{d_T}\right)^{-0.2} \tag{58.53}$$

As the tank diameter increases, the ability of a given impeller to agitate the entire liquid surface declines if the agitation speed is to remain below the bubble entrainment limit. The optimum impeller size for surface aeration is given by Henzler and Kauling (44)

$$\frac{d_i}{d_T} \approx 0.5 \tag{58.54}$$

Surface aeration is suited only to small reactors because $k_L a_L$ declines rapidly with increasing tank volume of surface aerated bioreactors. For subsurface impellers operated such that there is no entrainment of gas, the mass transfer coefficient k_L has been correlated with the impeller Reynolds number as follows (28):

$$Sh = 1.4 Re_i^{0.76} \tag{58.55}$$

which applies to waterlike media.

The contribution of the free surface to aeration in conventionally stirred, baffled tanks declines as the scale of operation increases. The liquid-phase mass transfer coefficient at the free surface (no vortex) in such tanks can be estimated using the correlations summarized in Table 58.9. A preferred correlation (45) is

$$k_L = 0.138 Sc^{-\frac{2}{3}} \left(\frac{4\mu_L Po N^3 d_i^5}{\pi d_T^2 h_L \rho_L}\right)^{\frac{1}{4}} \tag{58.56}$$

TABLE 58.9. Correlations for Liquid-Phase Mass Transfer Coefficient at Free Surface in Baffled Stirred Tanks (No Vortex)

$k_L = 5.11\times10^{-3}\left[\frac{11^{n-1}K}{\rho_L}\left(\frac{3n+1}{4n}\right)^n\right]^{-0.426} D_L^{0.5} d_i^{0.852} N^{1.352-0.426n}$	Perez and Sandall (46)
$k_L = 0.322 Sc^{-2/3} N^{0.7} d_i^{0.4} \left(\frac{\mu_L}{\rho_L}\right)^{0.3}$	Hikita and Ishikawa (45)
$k_L = 0.0256 Sc^{-1/2} \frac{Po^{1/3} N d_i^2}{\left(\frac{\pi d_T^2 h_L}{4}\right)^{1/3}}$	Farritor and Hughmark (47)
$k_L = \left\{0.432\left(\frac{d_i}{d_T}\right) - 0.13\right\}\left(\frac{E\rho_L}{\mu_L}\right)^{1/3} D_L^{1/2}$	Bin (48)
$\frac{k_L d_i}{D_L} = 0.04\left(\frac{N d_i^2 \rho_L}{\mu_L}\right)\left(\frac{N^2 d_i^3 \rho_L}{\sigma_L}\right)^{1/2}\left(\frac{\mu_L}{\rho_L D_L}\right)^{1/2}$	Kataoka and Miyauchi (45)

where Po is the power number ($Po = P/(\rho_L N^3 d_i^5)$), d_T and d_i are the diameters of the tank and the impeller, respectively, h_L is the height of liquid in the tank, N is the impeller rotational speed, and P is the power input. Equation 58.56 applies to Newtonian media without antifoams or surfactants. Added surfactants, fatty acids and proteins reduce k_L relative to values in clean liquids.

For a large (1.46 m^3) concentric draft-tube reactor with downward pumping five-bladed hydrofoil impellers located in the draft-tube, Chisti and Jauregui-Haza (49) correlated the $k_L a_L$ for surface aeration (air–water) with the impeller speed (N), as follows:

$$k_L a_L = 8.043 \times 10^{-6} e^{1.197N} \tag{58.57}$$

At the lowest aeration rate used (0.0156 m/s superficial aeration velocity in the annular zone) in the sparged mode of operation, the contribution of surface aeration to the total mass transfer varied from 1.5% to 11.6%, depending on the speed of the impeller (49).

58.6.4.2.2 Vortex Aeration. In unbaffled stirred tanks, agitation with a centrally located impeller creates a vortex that draws closer to the impeller as the rate of agitation increases (Figure 58.4). In a vortex aerated industrial fermenter (240 L) used in producing diphtheria vaccine, the following equation has been reported (26):

$$k_L a_L = 7.33 \times 10^{-4} + 1.36 \times 10^{-4} Q_G \tag{58.58}$$

where Q_G is the surface aeration rate (10–45 normal L/min). The equation was developed in aqueous sodium chloride (2.5 kg/m^3) and in the medium used in culturing the diphtheria bacterium. The tank was agitated with a six-bladed Rushton-type turbine (without disc) and the agitation rate was 300–800 rpm. The working aspect ratio was 0.74, which is substantially lower than values that are typically used in sparged microbial fermenters. Over the entire range of agitation rates used, the vortex was fully developed and reached the eye of the impeller (26). The conditions used in establishing Equation 58.58 were identical to those employed in commercial processes for producing the vaccine (26).

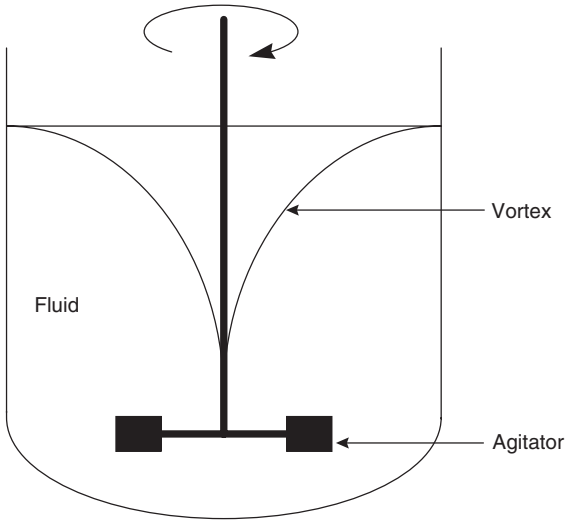


Figure 58.4. Vortex aeration in a stirred fermenter.

58.6.4.2.3 Wetted–Wall Columns. Mass transfer coefficient in liquid films in wetted-wall falling film columns can be estimate with the following equation (58.2)

$$k_L = 9.0 Re^{-0.40} Sc^{-0.67} U_L \tag{58.59}$$

where the Sc and Re are based on properties of the liquid. Depth of the film and the mean film velocity (U_L) are used to calculate the Reynolds number. Equation 58.59 is appropriate for $Re < 2000$ and $Sc < 100$. Another useful equation is

$$Sh = 0.023 Re^{0.8} Sc^{1/3} \tag{58.60}$$

The gas and liquid film coefficients in highly turbulent films ($Re > 4000$) in cocurrent wetted-wall columns can be estimated using the following equations (50):

$$Sh_L = 0.01613 Re_G^{0.664} Re_L^{0.426} Sc_L^{0.5} \tag{58.61}$$

$$Sh_G = 3.1 \times 10^{-4} Re_G^{1.05} Re_L^{0.207} Sc_G^{0.5} \tag{58.62}$$

These equations apply when $4000 \leq Re_L \leq 12{,}000$ and $7500 \leq Re_G \leq 18{,}300$. Other correlations for mass transfer in wetted-wall columns have been summarized by Spedding and Jones (51).

58.6.5 Submerged Aeration

Submerged aeration in which an oxygen containing gas is sparged or bubbled through the culture fluid is the norm in large-scale processes including animal cell culture. Typically, submerged cultivation is carried out in stirred tanks, bubble columns, and airlift bioreactors. Stirred vessels are relatively more common, but the number of airlift devices continues to increase. Bubble columns are employed less frequently (14). Typically, sparged aerated bubble columns and stirred tanks have aspect ratios between three and four. Airlift devices generally have higher aspect ratios, usually greater than six. Stirred vessels used in culturing animal cells are usually shorter with aspect ratios less than two. Microbial fermentations are aerated at high rates with superficial aeration velocities of up to 0.1 m/s in airlift vessels and somewhat lower maximum values in bubble columns. Aeration rates are substantially lower in stirred tanks to

prevent flooding of the impeller. A flooded impeller is a poor mixer and gas disperser.

Sparged aeration can potentially damage sensitive animal cells (15,52–55) and cells of certain cyanobacteria. Nevertheless, sparged aeration is successfully used quite widely in commercial culture of animal cells (56–58); however, the superficial aeration velocity in cell culture vessels is always low, usually well below 2.5×10^{-3} m/s. Supplementing the culture medium with serum, albumin, viscosity enhancers such as carboxymethyl cellulose, or surfactants such as Pluronic F68 is known to suppress the damaging effects of sparged aeration in cell culture (15,19,59).

As a rule, serum supplementation of basal animal cell culture media has little effect on mass transfer under conditions that are typically employed. Properties of serum supplemented media are usually quite similar to those of serum-free basal media. At 37°C, the surface tension of a typical cell culture medium with serum is about 0.060–0.064 N/m as compared to 0.071 N/m for water; and the viscosity is about 0.75×10^{-3} Pa s. This viscosity value is satisfactory for media containing 5–10% serum. In submerged aeration, serum-containing media tend to foam especially if a fine-pore sparger is employed for aeration (56); however, fine-pore aeration is not the norm.

58.6.5.1 Stirred Frmenters. The gas–liquid volumetric mass transfer coefficient in stirred vessels has generally shown good correlation with agitation power input and the superficial gas velocity; thus,

$$k_L a_L = \alpha \left(\frac{P_G}{V_L} \right)^{\beta} U_G^{\gamma} \tag{58.63}$$

where P_G/V_L (watts per cubic meter) is the gassed power input and U_G (meters per second) is the superficial aeration velocity; generally, $0.4 < \beta < 1$ and $0 < \gamma < 0.7$ (7). For pure water, α, β, and γ values are 2.6×10^{-2} ($s^{\beta+\gamma-1} m^{3\beta-\gamma} J^{-\beta}$), 0.4, and 0.5, respectively, when $500 < P_G/V_L$ (watts per cubic meter) $< 10,000$ (7). These values have been shown to apply over a wide scale: $0.002 \leq V_L$ (cubic meters) ≤ 2.6. In strongly ionic aqueous solutions, the α, β, and γ values become 2.0×10^{-3} ($s^{\beta+\gamma-1} m^{3\beta-\gamma} J^{-\beta}$), 0.7, and 0.2, respectively, when $500 < P_G/V_L$ (watts per cubic meter) $< 10,000$ and $0.002 \leq V_L$ (cubic meters) ≤ 4.4 (7). In pure water and ionic aqueous media, the volumetric mass transfer coefficient depends only on the specific power input irrespective of the type of stirrer—whether turbines, propellers, paddles, or self-sucking agitators—used for agitation. Neither does the number of impellers matter and nor does the location so long as it is within the usual ranges. Similarly, the height of liquid and the type of sparger have negligible influence under the usual operating conditions (7). The parameters values noted above assume an absence of flooding. Maximum aeration rates that still assure unflooded operation depend on the geometry of the impeller as discussed by Nienow (60).

For single impeller stirred air–water system, Bakker *et al*. (61) have recommended the following values of the constants in Equation 58.63: $\beta = \gamma = 0.6$, and $\alpha = 0.015 \pm 0.005$. The parameters noted apply only to the nonflooded state. At high gas flow rates, concave-bladed gas dispersion impellers (Figure 58.5) yield at least 20% higher $k_L a_L$ value than obtainable with Rushton turbines under the same conditions (61). The constants in Equation 58.63 can be strongly affected by fluid properties, presence of surfactants, and insoluble oils. For fluids other than water and for multi-impeller systems, Bakker *et al*. (61) recommended measuring α, β, and γ in a geometrically similar small-scale stirred fermenter. This data can be used in Equation 58.63 for scale-up.

For fermentations of *Endomyces* sp. in stirred fermenters, α, β, and γ values in Equation 58.63 have been reported to be 4.015×10^{-2} ($s^{\beta+\gamma-1} m^{3\beta-\gamma} J^{-\beta}$), 0.33, and 0.56, respectively, over a broad scale ($0.03 \leq V_L$ (cubic meters) ≤ 50). In a 5-L stirred fermenter operated with high density culture of a recombinant *E. coli*, Shin *et al*. (62) reported the following equation for $k_L a_L$

$$k_L a_L = 0.0195 \left(\frac{P_G}{V_L} \right)^{0.55} U_G^{0.64} (1 + 2.12X + 0.20X^2)^{-0.25} \tag{58.64}$$

where X (grams per liter) is the biomass concentration. The X values ranged over 0–75 g/L and the $k_L a_L$ values during culture varied over $(10–25) \times 10^{-3}$/s.

In stirred tank bioreactors for animal cell culture, the type of impeller used does not affect $k_L a_L$ so long as

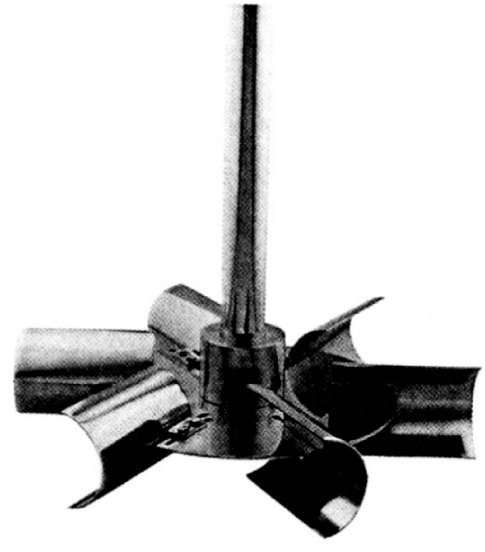


Figure 58.5. A concave-blade impeller for dispersing gases in liquids. Courtesy of Chemineer, Inc.

TABLE 58.10. Mass Transfer Correlations for Stirred Tanks

Correlation	Ranges
1. Taguchi *et al*. (64)	Pseudoplastic paper pulp slurries (1.6% wt/vol pulp). Disc turbine stirred vessel
$\frac{k_L a_L}{N} = 0.113\left(\frac{d_T^2 h_L}{W\ell(d_i - W)}\right)^{1.437}(Nt_m)^{-1.087}\left(\frac{d_i}{d_T}\right)^{1.021}$	
2. Yagi and Yoshida (65)	Viscous Newtonian and non-Newtonian liquids, including viscoelastic fluids
$\frac{k_L a_L d_i^2}{D_L} = 0.06\left(\frac{d_i^2 N\rho_L}{\mu_L}\right)^{1.5}\left(\frac{d_i N^2}{g}\right)^{0.19}\left(\frac{\mu_L}{\rho_L D_L}\right)^{0.5}\left(\frac{\mu_L U_G}{\sigma_L}\right)^{0.6} \times\left(\frac{N d_i}{U_G}\right)^{0.32}[1+2\sqrt{\lambda N}]^{-0.67}$	
For non-Newtonian fluids use apparent viscosity instead of μ_L. λ is the characteristic time or "relaxation time" of viscoelastic fluids; $\lambda = 0$ for nonviscoelastics	
3. Perez and Sandall (46)	Carbon dioxide absorption in water and non-Newtonian power law solutions
$\frac{k_L a_L d_i^2}{D_L} = 21.2\left(\frac{\rho_L N d_i^2}{\mu_{ap}}\right)^{1.11}\left(\frac{\mu_{ap}}{\rho_L D_L}\right)^{0.5}\left(\frac{U_G d_i}{\sigma_L}\right)^{0.447}\left(\frac{\mu_G}{\mu_{ap}}\right)^{0.694}$ $\mu_{ap} = K(11N)^{n-1}\left(\frac{3n+1}{4n}\right)^n$	
4. Kawase and Moo-Young (66)	Newtonian and non-Newtonian power law fluids
$k_L a_L = 0.675\sqrt{D_L}\frac{\rho_L^{3/5}E^{\frac{9+4n}{10(1+n)}}}{\left(\frac{K}{\rho_L}\right)^{\frac{1}{2(1+n)}}\sigma_L^{3/5}}\left(\frac{U_G}{U_B}\right)^{0.5}\left(\frac{\mu_{ap}}{\mu_w}\right)^{-0.25}$	
5. Niebelschütz (21)	Non-Newtonian power law fluids such as broths of *Aspergillus niger, Penicillium chrysogenum*, and xanthan fermentation.
$k_L a_L\left(\frac{V_L}{Q_G}\right)Sc^{0.3} = 0.103\left(\frac{P_G}{Q_G\rho_L\left(\frac{g\mu_L}{\rho_L}\right)^{2/3}}\right)^{0.53}$	$0.035 \le V_L\ (m^3) \le 0.070$, $0.02 \le \mu_L$ (Pa s) ≤ 3.1; μ_L was calculated at shear rate $= 10^4$/s
6. Reuss (21)	Newtonian broths of *Saccharomyces cerevisiae* and gluconic acid, glucose solutions, $\mu_L \le 12 \times 10^{-3}$ Pa s, $0.05 \le V_L\ (m^3) \le 1.9$
$\frac{k_L a_L}{U_G}\left(\frac{\mu_L^2}{g\rho_L^2}\right)^{1/3}Sc^{0.3} = 5.5\times10^{-4}\left(\frac{P_G}{V_L U_G\rho_L g}\right)^{0.7}$	
7. Chandrasekharan and Calderbank (67)	Air–water
$k_L a_L = \left(\frac{0.0248}{d_T^4}\right)\left(\frac{P_G}{V_L}\right)^{0.551}Q_G^{\frac{0.551}{\sqrt{d_T}}}$	

mixing is sufficient. For power inputs that are typical (< 25 W/m^3) better mixing is attained with relatively large ($d_i/d_T \sim 0.5$–0.6), slow moving, axial flow impellers. For typically used conditions, the $k_L a_L$ should be calculated as for bubble columns (Eq. 58.66) because for impeller power inputs less than about 40 W/m^3, the impeller has little effect on $k_L a_L$. Stirred tank design considerations for animal cell culture have been discussed by Chisti (56) and others (44).

Some of the main correlations for estimating gas–liquid volumetric mass transfer coefficient in stirred microbial fermenters are summarized in Table 58.10, which includes

equations suitable for relatively viscous power law broths. Methods for estimating the power input in mechanically agitated fermenters have been detailed by Chisti and Moo-Young (8) and Nienow (60) and Ascanio *et al*. (63).

58.6.5.2 Bubble Columns. For a given fluid in bubble columns the k_La_L is affected mainly by the superficial gas velocity, which also determines the specific power input (6). The specific power input can be calculated using the equation

$$\frac{P_G}{V_L} = \rho_L g U_G \tag{58.65}$$

where V_L is the volume of the liquid or slurry and ρ_L is its density. Properties of the fluid also affect k_La_L. In waterlike fluids, the aspect ratio of bubble columns does not affect k_La_L so long as the column diameter exceeds about 0.1 m (6). Similarly, liquid superficial velocities do not affect k_La_L provided $U_L \leq 0.1$ m/s.

For power inputs that are typically used in microbial culture, the k_La_L value in relatively coalescing media is little influenced by the design of the sparger because the turbulence in the fluid controls the bubble size. In strongly ionic low viscosity media, bubbles do not coalesce easily and the bubble size depends on the characteristics of the gas sparger. Porous plate spargers and those with smaller holes produce smaller bubbles and higher k_La_L values; however, small bubbles are rapidly exhausted of oxygen and have long residence times in the fluid. Small bubbles are produced also under highly turbulent conditions irrespective of the sparger hole size. Such bubbles are especially persistent in viscous media because the viscous drag prevents them from leaving the fluid. Persistent microbubbles are seen in broths of *Streptomyces*, mycelial fungi, and certain fermentations that produce extracellular polymers such as xanthan.

In coalescence inhibiting media typical of animal cell culture the k_La_L values in bubble columns at the very low superficial gas velocities that are normally used depends on the sparger hole diameter: the k_La_L value declines as the sparger hole diameter increases over the range 0.01–2 mm (44). Relative to values in clean fluids, surfactants and proteins reduce k_La_L value, but the reduction is greater in finer dispersions (i.e. in small, ridged bubbles) generated by small hole spargers than in dispersions of larger, circulating bubbles. For aeration rates relevant to cell culture, the k_La_L values for water may be calculated with the following equation (44):

$$\frac{k_La_L}{U_G}\left(\frac{\mu_L^2}{\rho_L^2 g}\right)^{\frac{1}{3}} = \alpha\left[\left(\frac{\mu_L g}{\rho_L}\right)^{-\frac{1}{3}} U_G\right]^{-\beta} \tag{58.66}$$

The values of α and β for use with various sparger hole sizes are noted in Table 58.11. The k_La_L values in culture media are only about 50% of those obtained with Equation 58.66 for water. Equation 58.66 was developed in bubble columns with aspect ratios $1 \leq (h_L/d_T) \leq 3$ when the specific power inputs were $3 \leq P_G/V_L$ (watts per cubic meter) ≤ 38.

Although the overall k_La_L in tall bioreactors may be little affected by the height, the overall mass transfer rates tend to be greater in taller systems because the mass transfer driving force increases with increasing hydrostatic pressure. Mass transfer in bubble columns is discussed further by Shah *et al*. (68), Chisti (6,17), and Deckwer (69), and Deckwer and Schumpe (70). The various correlations available for estimating k_La_L or k_L in bubble columns are summarized in Table 58.12. Those correlations apply to the relatively high gas flow rates that are typical of microbial fermentations. The correlation of Akita and Yoshida (71) is recommended for viscosities less than about 21×10^{-3} Pa s. The correlation of Kawase *et al*. (72) (Table 58.12) has also agreed well with independent measurements (73).

58.6.5.3 Airlift Bioreactors. Because of superior oxygen transfer performance airlift bioreactors have given excellent productivities with yeasts, bacteria, and filamentous fungi (6,17). Processes that produce highly viscous broths, including several biopolymer producing fermentations, have been successfully carried out in airlift devices (17). Similarly, many hybridoma cultures and plant cell suspensions have

TABLE 58.11. Values of α and β for use in Equation 58.66

Sparger	d_H (mm)	α	β	Range
Frit	0.01	6.0×10^{-5}	0.4	$0.001 \leq U_G\left(\frac{\mu_L g}{\rho_L}\right)^{-1/3} \leq 0.1$
	0.02	6.3×10^{-5}	0.2	
Perforated pipe	0.5	4.2×10^{-5}	0.2	$0.01 \leq U_G\left(\frac{\mu_L g}{\rho_L}\right)^{-1/3} \leq 0.2$
	2.0	2.2×10^{-5}	0.17	

From Ref. 44.

TABLE 58.12. Gas–Liquid Mass Transfer Correlations for Bubble Columns

Correlation	Ranges
1. Chisti (6)	Air–water, $d_T \geq 0.1$ m, $200 \leq P_G/V_L$ (W/m^3) ≤ 1000, h_L/d_T up to 25
$k_L a_L = 2.39\times10^{-4}\left(\frac{P_G}{V_L}\right)^{0.86}$	
2. Heijnen and Van't Riet (74)	Air–water at 20°C, $0.08 < d_T$ (m) < 11.6, $0 < U_G$ (m/s) < 0.3, $0.3 < h_L$ (m) < 21. Perforated pipe or perforated plate spargers producing 4–6-mm bubbles
$k_L a_L = 0.32 U_G^{0.7}$	
3. Fair (75)	Newtonian fluids
$k_L a_D = 3.31\left(\frac{D_L \varepsilon_G}{d_B^2}\right)\left(\frac{\mu_L}{\rho_L D_L}\right)^{1/3}\left(\frac{d_B \rho_L U_G}{\mu_L}\right)^{0.5}$	
4. Akita and Yoshida (71)	Air–water and other Newtonian fluids; $\mu_L \leq 21 \times 10^{-3}$ Pa s, U_G and U_L up to 0.4 m/s
$\frac{k_L a_D d_T^2}{D_L} = 0.6\left(\frac{\mu_L}{\rho_L D_L}\right)^{0.5}\left(\frac{g d_T^2 \rho_L}{\sigma_L}\right)^{0.62}\left(\frac{g d_T^3 \rho_L^2}{\mu_L^2}\right)^{0.31}\varepsilon_G^{1.1}$	
5. Akita and Yoshida (71)	Air–water and other Newtonian fluids, $\mu_L \leq 21 \times 10^{-3}$ Pa s, U_G and U_L up to 0.4 m/s
$\frac{k_L d_B}{D_L} = 0.5\left(\frac{\mu_L}{\rho_L D_L}\right)^{0.5}\left(\frac{g d_B^3 \rho_L^2}{\mu_L^2}\right)^{0.25}\left(\frac{g d_B^2 \rho_L}{\sigma_L}\right)^{3/8}$	
6. Chisti (6)	Air–water, and slurries of mycelia-like fibrous solids (paper pulp) in salt-solutions; bubble and churn turbulent flow; $0 \leq C_S$ (wt/vol%) ≤ 3
$k_L = 5.63\times10^{-5}\left(\frac{g\rho_L^2 D_L \sigma_L}{\mu_L^3}\right)^{0.5} d_B e^{-0.131 C_S^2}$	
7. Hughmark (76)	Newtonian fluids, $0.0009 \leq \mu_L$ (Pa s) ≤ 0.152
$\frac{k_L d_B}{D_L} = 2 + 0.0187\left[\left(\frac{\mu_L}{\rho_L D_L}\right)^{0.339}\left(\frac{d_B U_G \rho_L}{\mu_L}\right)^{0.484}\left(\frac{d_B g^{1/3}}{D_L^{2/3}}\right)^{0.072}\right]^{1.61}$	
8. Nakanoh and Yoshida (77)	Newtonian, non-Newtonian and viscoelastic fluids, $0.005 \leq \mu_L$ (Pa s) ≤ 0.06, $U_G < 0.1$ m/s
$\frac{k_L a_D d_T^2}{D_L} = 0.09\left(\frac{\mu_L}{\rho_L D_L}\right)^{0.5}\left(\frac{g d_T^2 \rho_L}{\sigma_L}\right)^{0.75}\left(\frac{g d_T^3 \rho_L^2}{\mu_L^2}\right)^{0.39}\left(\frac{U_G^2}{g d_T}\right) \times\left(1+\chi\left(\frac{U_B \lambda}{d_B}\right)\right)^{-0.45}$	
$\chi = 0$ (inelastic fluids) or 0.133 (elastic fluids). For non-Newtonian power law fluids $\mu_L = \mu_{ap} = K(5000U_G)^{n-1}$	
9. Schumpe *et al*. (78)	Non-Newtonian media
$\frac{k_L a_L d_T^2}{D_L} = 0.021\left(\frac{\mu_L}{\rho_L D_L}\right)^{0.5}\left(\frac{g d_T^2 \rho_L}{\sigma_L}\right)^{0.21}\left(\frac{g d_T^3 \rho_L^2}{\mu_L^2}\right)^{0.60}\left(\frac{U_G}{\sqrt{g d_T}}\right)^{0.49}$	
μ_L is the apparent viscosity of the power law fluid	

(*continued*)

TABLE 58.12. (*Continued*)

Correlation	Ranges
10. Kawase *et al*. (72) $\frac{k_L a_L d_T^2}{D_L} = 0.555 \left(\frac{K d_T^{1-n}}{\rho_L D_L U_G^{1-n}}\right)^{0.5} \left(\frac{g d_T^2 \rho_L}{\sigma_L}\right)^{3/5} \left(\frac{d_T^n U_G^{2-n}}{\frac{K}{\rho_L}}\right) \times \left(\frac{U_G^2}{g d_T}\right) \frac{(2+n)(2n-3)}{20(1+n)^2} \varepsilon_G^{0.5}$	Newtonian and non-Newtonian power law fluids. For Newtonian fluids $K = \mu_L$ and $n = 1$
11. Hikita *et al*. (79) $k_L a_L = \frac{14.9 g f}{U_G} \left(\frac{U_G \mu_L}{\sigma_L}\right)^{1.76} \left(\frac{\mu_L^4 g}{\rho_L \sigma_L^3}\right)^{-0.248} \left(\frac{\mu_G}{\mu_L}\right)^{0.243} \left(\frac{\mu_L}{\rho_L D_L}\right)^{-0.604}$ f is 1.0 for nonelectrolytes; $f = 10^{0.0681I}$ for ionic strength $I < 1.0$ kg ion/m^3; and $f = 1.114 \times 10^{0.021}$ for $I > 1.0$ kg ion/m^3	Low viscosity Newtonian media: water and various gases (air, oxygen, carbon dioxide, hydrogen, methane), sucrose solution, aqueous electrolytes, alcohols, $0.0008 \le \mu_L$ (Pa s) ≤ 0.011, $0.042 \le U_G$ (m/s) ≤ 0.38
12. Deckwer *et al*. (80) $k_L a_D = 3.15 \times 10^{-3} U_G^{0.59} [K (5000 U_G)^{n-1}]^{-0.84}$	Non-Newtonian power law fluids, slug flow ($U_G > 0.02$ m/s)
13. Godbole *et al*. (81) $k_L a_D = 8.35 \times 10^{-4} U_G^{0.44} [K (5000 U_G)^{n-1}]^{-1.01}$	Non-Newtonian power law fluids

given good results. As a general rule, the volumetric productivity of airlift bioreactors equals or betters that of conventional stirred tanks (17). Typically, this level of performance is achieved at substantially lower power input than in stirred vessels. Furthermore, the probability of mechanical failure and likelihood of loss of sterility are lower with airlift bioreactors. Airlift devices outperform bubble columns in suspending solids. Relative to bubble columns, the airlift reactors have a better defined flow pattern; airlift systems are better than bubble columns in heat transfer capabilities (17). The operational range of airlift bioreactors tends to be generally broader than similar bubble columns. Unlike in bubble columns, the overall height h_L of liquid in airlift reactors affects $k_L a_L$ because the height strongly influences the liquid circulation velocity and, hence, the gas holdup (17).

Many equations have been developed to relate the apparent viscosity of non-Newtonian media to the $k_L a_L$ in airlift reactors. Most authors agree that $k_L a_L$ generally declines with increasing apparent viscosity; however, there is great discrepancy on the precise magnitude of the viscosity effect (6,17). The exponent on the apparent viscosity term has been given variously as -0.255 (82), -0.66, -0.89, and other values (see Ref. 6). Such discrepancies are associated in part with the questionable practice of defining shear rate as an arbitrary linear function of the gas velocity (6,14). The viscosity associated decline in $k_L a_L$ is especially pronounced for viscosities exceeding about 2.5×10^{-2} Pa s. In highly viscous non-Newtonian fermentations, the use of a supplementary axial flow impeller in the draft-tube of airlift reactors is known to enhance fermentation performance.

Table 58.13 lists the correlations available for estimating the gas–liquid mass transfer coefficient in airlift bioreactors. Other correlations have been reviewed by Petersen and Margaritis (83) and Kilonzo and Margaritis. (84). These correlations are suitable only for initial estimates because the hydrodynamic and transport behavior of airlift devices is quite sensitive to the type of fluid, the reactor geometry, the distribution of gas holdup in the various zones, and the induced liquid circulation rate. Because of the numerous influences, a superior approach to prediction of mass transport for a more reliable design and scale-up relies on data measured at small-scale. This method is discussed below.

58.6.5.3.1 A General Method of Predicting $k_L a_L$ for Scale-up. Although various correlations can be used to directly estimate $k_L a_L$, the reliability of such estimates is often quite poor. A more reliable prediction of $k_L a_L$ for process scale-up is based on methodology that combines fundamental principles with small-scale experimentation. This proven approach is especially suited to prediction of $k_L a_L$ in complex media. Thus, based on purely analytical

TABLE 58.13. Gas–Liquid Volumetric Mass Transfer Coefficient Correlations for Airlift Bioreactors

Configuration	Equation	Ranges
Concentric-tube internal-loop vessels (annulus sparged)	$\frac{k_L a_D \sigma_L}{D_L g \rho_L} = 2.25\left(\frac{\mu_L}{\rho_L D_L}\right)^{0.500}\left(\frac{\rho_L \sigma_L^3}{g\mu_L^4}\right)^{0.136}\left(\frac{d_H}{d_T}\right)^{-0.0905}\varepsilon_G^{1.26}$ Average estimation error was 12% for 175 measurements Koide *et al*. (85)	Newtonian media, $3.71 \times 10^2 \le \mu_L/\rho_L D_L \le 6.00 \times 10^4$, $1.18 \times 10^6 \le \rho_L\sigma_L^3/g\mu_L^4 \le 5.93 \times 10^{10}$, $0.471 \le d_i/d_T \le 0.743$, $7.14 \times 10^{-3} \le d_H/d_o \le 2.86 \times 10^{-2}$, $0.0302 \le \varepsilon_G \le 0.305$, $6 \le$ aspect ratio ≤ 15, $0.52 \le A_d/A_r \le 1.23$
Concentric-tube internal-loop vessels (draft-tube sparged)	$\frac{k_L a_D d_T^2}{D_L} = 2.66\left(\frac{\mu_L}{\rho_L D_L}\right)^{0.500}\left(\frac{g d_T^2 \rho_L}{\sigma_L}\right)^{0.715}\left(\frac{g d_T^3 \rho_L^2}{\mu_L^2}\right)^{0.251}\left(\frac{d_i}{d_T}\right)^{-0.429}\varepsilon_G^{1.34}$ Koide *et al*. (86)	Newtonian media, $\rho_L = 997$–$1182\,\text{kg/m}^3$, $\mu_L = (0.894\text{–}17.0) \times 10^{-3}$ Pa s, $\sigma_L = (51.7 - 73.0) \times 10^{-3}$ N/m, $D_L = (0.145\text{–}2.42) \times 10^{-9}$ m^2/s, $A_r/A_d = 0.3$–0.8, aspect ratio = 6–15
External-loop reactor	$\frac{k_L a_L L}{U_{Lr}} = 14.5\left(\frac{U_{Gr}}{U_{Lr}}\right)^{0.83} Pe^{-0.6}$ *Pe* value is for the entire loop Verlaan *et al*. (87)	Air–water in 0.165 m^3 reactor, aspect ratio = 16 (based on riser), $A_r/A_d = 4$, no gas in downcomer, $0.01 \le U_{Gr}$ (m/s) ≤ 0.14, $Pe = U_L L/E_L$, $Pe = 40$–60 (increased with gas flow rate)
A bubble column and a draft-tube sparged concentric-tube airlift vessel	$\frac{k_L a_L d_T^2}{D_L} = 0.018\left(\frac{K(2800U_G)^{n-1}}{\rho_L D_L}\right)^{0.5}\left(\frac{g d_T^2 \rho_L}{\sigma_L}\right)^{0.20}\left(\frac{U_G}{\sqrt{g d_T}}\right)^{0.51} \times \left(\frac{g d_T^3 \rho_L^2}{[K(2800U_G)^{n-1}]^2}\right)^{0.62}(1 + 0.12Wi)^{-1}$ Suh *et al*. (88)	Non-Newtonian xanthan fermentation broths of the obligate aerobic bacterium *Xanthomonas campestris*. Bubble column (0.05 m^3, aspect ratio $\approx$ 19); airlift bioreactor (1.2 m^3, $A_r/A_d = 1$, aspect ratio $\approx$ 12)
Concentric-tube internal-loop (draft-tube sparged)	$k_L a_L = 3.43 \times 10^{-2} U_{Gr}^{0.524} \mu_{ap}^{-0.255}$ μ_{ap} was calculated by assuming the shear rate to equal $5000U_{Gr}$ for $U_{Gr} \ge 0.04$ m/s, or $1000(U_{Gr})^{0.5}$ for $U_{Gr} < 0.04$ m/s Li *et al*. (82)	Aqueous carboxymethyl cellulose ($K = 0.286 - 11.5$ Pa s^n; $n = 0.441 - 0.617$, 0.055 m^3 vessel, $A_r/A_d = 0.618$, aspect ratio $\sim$ 26.0.020 $\le \mu_{ap}$ (Pa s) ≤ 0.85
Concentric-tube internal-loops (draft-tube sparged)	$\frac{k_L a_D d_T^2}{D_L} = 2.66\left(\frac{\mu_L}{\rho_L D_L}\right)^{0.500}\left(\frac{g d_T^2 \rho_L}{\sigma_L}\right)^{0.715}\left(\frac{g d_T^3 \rho_L^2}{\mu_L^2}\right)^{0.251}\left(\frac{d_i}{d_T}\right)^{-0.429} \varepsilon_G^{1.34} \times \left(1 + 0.099\left(\frac{C_S}{\rho_S}\right)^{0.069}\left(\frac{\rho_L \sigma_L^3}{g\mu_L^4}\right)^{0.023}\left(\frac{U_t}{U_G}\right)^{0.046}\right)^{-1}$ Average estimation error was within 17% for 383 measurements Koide *et al*. (86)	Suspensions of glass or bronze spheres, $3.71 \times 10^2 \le \mu_L/\rho_L D_L \le 9.92 \times 10^4$, $1.36 \times 10^3 \le g d_T^2 \rho_L/\sigma_L \le 1.22 \times 10^4$, $1.29 \times 10^8 \le g d_T^3 \rho_L^2/\mu_L^2 \le 1.26 \times 10^{11}$, $0.471 \le d_i/d_T \le 0.743$, $3.99 \times 10^{-2} \le \varepsilon_G \le 2.73 \times 10^{-1}$, $1.69 \times 10^{-11} \le g\mu_L^4/\rho_L\sigma_L^3 \le 2.55 \times 10^{-6}$, $0 \le C_S/\rho_S \le 8.00 \times 10^{-2}$, $1.17 \times 10^{-2} \le U_t/U_G \le 0.844$, $A_r/A_d = 0.3$–0.8, aspect ratio = 6–15
Concentric-tube internal-loop reactors (draft-tube sparged)	$\frac{k_L a_D d_T^2}{D_L} = \frac{4.04}{1 + 2\phi_S^{1.3}}\left(\frac{\mu_L}{\rho_L D_L}\right)^{0.5}\left(\frac{g d_T^2 \rho_L}{\sigma_L}\right)^{0.67}\left(\frac{g d_T^3 \rho_L^2}{\mu_L^2}\right)^{0.26}\left(\frac{d_i}{d_T}\right)^{-0.047}\varepsilon_G^{1.34}$ Average error of estimation was 14% for 260 data; U_G is based on the diameter d_T of the outer column The $k_L a_D$ values in water and salt solutions were similar. Koide *et al*. (89)	Suspensions of relatively low density calcium alginate beads in water, aqueous glycerol and aqueous salt solutions (0.10 or 0.27 kmol/m^3 barium chloride; 0.4 kmol/m^3 sodium sulfate), 0–20% vol/vol solids, 1.88–3.98-mm bead diameter, $A_r/A_d = 0.3$–1.2, aspect ratios = 6–16, $\mu_L = (0.894\text{–}12.5) \times 10^{-3}$ Pa s, D_L of oxygen $= (0.194\text{–}2.42) \times 10^{-9}$ m^2/s, $3.71 \times 10^2 \le \mu_L/D_L\rho_L \le 5.52 \times 10^4$, $2.66 \times 10^3 \le \rho_L d_T^2 g/\sigma_L \le 1.22 \times 10^4$, $2.35 \times 10^8 \le \rho_L^2 d_T^3 g/\mu_L^2 \le 3.29 \times 10^{11}$, $0.471 \le d_i/d_T \le 0.743$, $1.69 \times 10^{-11} \le Mo \le 6.67 \times 10^{-7}$, $3.79 \times 10^{-2} \le \varepsilon_G \le 2.24 \times 10^{-1}$, $0 \le \phi_S \le 0.2$; where the Morton number is $Mo = \frac{g(\rho_L - \rho_G)}{\sigma_L^3 \rho_L^2} K^4 \left(\frac{8U_{Lr}}{d_r}\right)^{4(n-1)}\left(\frac{3n+1}{4n}\right)^{4n}$

reasoning, the volumetric mass transfer coefficient (k_La_L), gas holdup (ε_G), the Sauter mean bubble diameter (d_B), and the true mass transfer coefficient (k_L), have been related as follows (6):

$$\frac{k_L}{d_B} = \frac{k_La_L(1-\varepsilon_G)}{6\varepsilon_G} \tag{58.67}$$

Calculations of the k_L/d_B ratio from the measured k_La_L and gas holdup have shown that in bubble columns and airlift devices this ratio is constant for a given fluid irrespective of the aeration rate (6,90). The value of k_L/d_B depends on the properties of the fluid. Thus, in slurries of mycelia-like cellulose fiber particles, k_L/d_B is affected by the concentration of solids (Figure 58.6). For aqueous salt solution (0.15 *M* sodium chloride) with or without suspended cellulose fiber, the k_L/d_B ratio has been expressed as (6)

$$\frac{k_L}{d_B} = 5.63 \times 10^{-5}\left(\frac{g\rho_L^2\sigma_L D_L}{\mu_L^3}\right)^{\frac{1}{2}} e^{-0.131C_S^2} \tag{58.68}$$

where C_S is the concentration of solids (% wt/vol). Equation 58.68 applies to airlifts as well as bubble columns. Chisti's (6) observations of constant k_L/d_B ratio in pneumatically agitated reactors have also been confirmed by others (17).

The observed constancy of k_L/d_B provides a reliable method for predicting k_La_L in large-scale bioreactors from data easily measured in a small-scale model unit (6). This proven technique consists of the following steps:

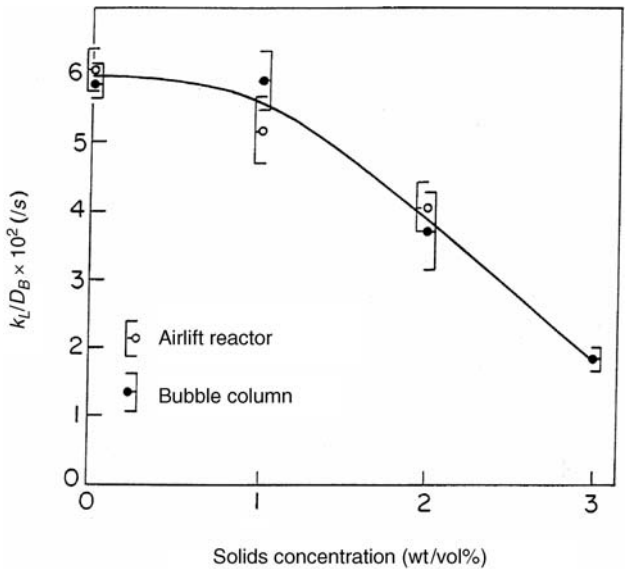


Figure 58.6. Effect of concentration of mycelia-like cellulose fiber particles on the k_L/d_B ratio in aqueous salt solution (0.15 M sodium chloride) (6).

1. Measure the gas holdup and the k_La_L in a small model reactor with the fluid of interest over the range of gas flow rates that are of interest.
2. Use the data from step 1 to calculate the constant k_L/d_B ratio (Eq. 58.67).
3. Measure or calculate the riser gas holdup (ε_{Gr}) in the full scale reactor. (See Refs 6,17)
4. Calculate the k_La_L value for the large reactor:

(a) for bubble columns

$$k_La_L = \frac{k_L}{d_B}\frac{\varepsilon_G}{(1-\varepsilon_G)} \tag{58.69}$$

(b) for airlift bioreactors

$$k_La_L = \frac{k_L}{d_B}\frac{\varepsilon_{Gr}}{(1-\varepsilon_{Gr})}\frac{A_r}{A_r + A_d} \tag{58.70}$$

In Equations 58.69 and 58.70 the gas holdup and the geometric parameters A_r and A_d are for the large reactor; the k_L/d_B value is from step 2. The rationale for Equations 58.69 and 58.70 has been discussed by Chisti (6).

Figure 58.7 compares the measured k_La_L values with prediction of the foregoing procedure for 11 reactors including bubble columns and external- and internal-loop airlift devices. The comparison spans waterlike media

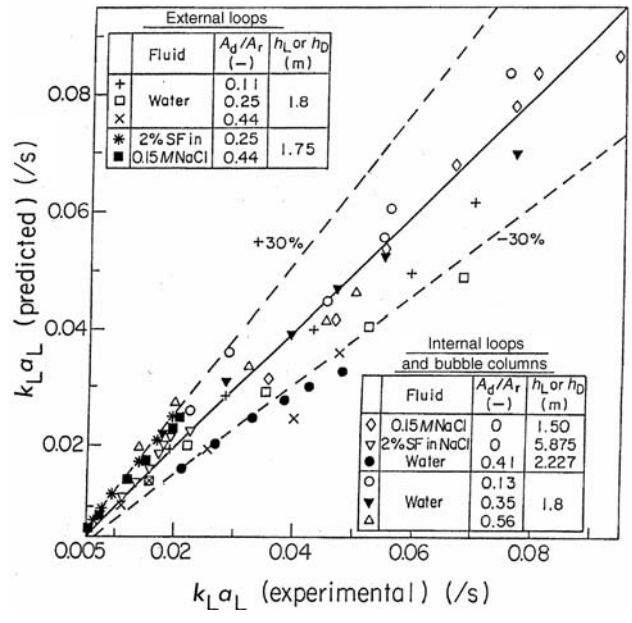


Figure 58.7. Predicted versus measured overall volumetric gas–liquid mass transfer coefficient in bubble columns, external-loop and internal-loop airlift devices in "Solka Floc" (SF) cellulose fiber slurries and solids–free media (6). The solid line represents exact prediction.

as well as pseudoplastic slurries of cellulose fiber. In all cases the predictions agree remarkably well with the measurements (Figure 58.7). Note that the "Solka Floc" cellulose fiber slurries in aqueous salt solutions used in Figures 58.6 and 58.7 were meant to simulate the fermentation broths of mycelial fungi and filamentous bacteria (6,90). Such broths are usually pseudoplastic. The non-Newtonian flow properties of cellulose fiber suspensions are quite close to those of the typical fungal fermentation broths (6).

For the low aeration rates typical of animal cell culture, the k_La_L in an internal-loop draft-tube airlift vessel is almost identical to that in an equivalent bubble column; hence, Equation 58.66 can be used for an estimation. Although the gas is sparged only in the draft-tube or in the annulus of an airlift bioreactor, for estimation of k_La_L with Equation 58.66 the superficial gas velocity should be calculated using the cross-sectional area of the outer column. For conditions typical of animal cell culture, whether the gas is sparged in the draft-tube or the annulus, does not affect k_La_L so long as the outer-to-inner tube diameter ratio is 1.6–2.1 and $2 \leq h_L/d_T \leq 5$. Large concentric draft-tube type of airlift bioreactors are used in commercial culture of animal cells (57,58). Various aspects of design of airlift bioreactors have been exhaustively treated in the literature (6,17). A few specifics are discussed in the following sections.

58.6.5.3.2 Axial Dissolved Oxygen Profiles. As clearly demonstrated (6,91,92), the steady state dissolved oxygen concentration varies axially in tall bubble columns and airlift reactors even in the absence of an oxygen consuming reaction. The exact nature of the concentration profile depends on the state of mixing in the reactor. During culture of baker's yeast in a draft-tube sparged concentric-tube internal-loop airlift reactor ($A_r/A_d = 0.8$; aspect ratio $\approx$ 10; 0.25 m^3), Russell *et al*. (93) observed that the steady state dissolved oxygen concentration in the riser and the downcomer increased with increasing aeration rate. The dissolved oxygen levels were always several fold higher in the downcomer than in the riser (93). In the riser, the dissolved oxygen levels tended to be $\leq$ 30% of air saturation. The oxygen concentration did not vary radially either in the riser or in the downcomer. Similarly, no significant variations were observed axially in the downcomer (93).

Using the annulus sparged mode of the same vessel as was employed by Russell *et al*. (93), Pollard *et al*. (94) found that the axial dissolved oxygen profiles in the riser showed a constant zero level of oxygen over a broad range of superficial gas velocities (0.036–0.136 m/s) during baker's yeast fermentations. Surprisingly, the dissolved oxygen concentration increased down the downcomer, peaking close the bottom of the draft-tube, and declining sharply to zero as the fluid moved into the riser. These anomalous results seemed to indicate better oxygen transfer in the downcomer relative to the riser (94). In view of the observed profile, the cells experienced extreme dissolved oxygen heterogeneity in the reactor; however, there seemed to be no effect on the culture performance. Installation and operation of a marine propeller (diameter = 0.16 m; 1000 rpm) near the bottom of the draft-tube, combined with a high level of aeration (0.358 m^3/ min), enhanced liquid circulation and oxygen transfer so much so that the dissolved oxygen level did not drop below 35% of saturation anywhere in the reactor.

58.6.5.3.3 Contributions of Various Zones to Overall k_La_L. Many airlift reactors consist of two hydrodynamically distinct zones—the riser and the downcomer—that contribute differently to the observed mass transfer (6). Sometimes a third zone—the gas–liquid separator (95)—may also exist with its own contribution toward mass transfer.

In airlift bioreactors that do not have gas–liquid separators, the measured k_La_L consists of contributions from the riser and the downcomer zones; thus,

$$(k_La_L)_{measured} = \frac{A_r(k_La_L)_r + A_d(k_La_L)_d}{A_r + A_d} \qquad (58.71)$$

Equation 58.71 is an analytical expression that relates the measured k_La_L to the separate, hypothetical, contributions of the riser and the downcomer (6). Equation 58.71 leads to the general conclusion that for any airlift device in which gas–liquid mass transfer is confined to the riser (i.e. no gas in the downcomer), the actual volumetric mass transfer coefficient in the riser would be larger than the apparent measured value; the difference being dependent on the A_r/A_d ratio. Equation 58.71 applies to reactors in which the riser and the downcomer have approximately equal heights. In cases in which a significant portion of the liquid resides in the head zone, Equation 58.71 should be modified to account for that volume (17); generally, $(k_La_L)_d < (k_La_L)_r$.

On the basis of data obtained in several concentric draft-tube airlift reactors that were sparged either in the draft-tube or the annulus (aspect ratios = 6–11; $U_G = 0.019$–0.12 m/s), Koide *et al*. (96) suggested that in air–water the contribution of the downcomer zone to gas–liquid mass transfer was "relatively large." Furthermore, in liquids such as aqueous salt solutions in which the bubbles are smaller, the riser and the downcomer were claimed to contribute to the total mass transfer in proportion to the fraction of the total volume occupied by those zones (96). These observations in relatively small reactors are not entirely consistent with other findings (6,17).

58.6.5.3.4 Mass Transfer Enhancement by Static Mixers. Installation of static mixer elements in airlift and bubble column bioreactors is known to enhance the gas–liquid mass transfer coefficient relative to mixer-free operation (17,97). The enhancement is mostly due to an increase in the gas–liquid interfacial area that is brought about by the bubble breaking action of the mixer elements. Improved productivity of cephalosporin C by *Cephalosporium acremonium* was observed (98) in an airlift reactor when static mixers were installed.

The mass transfer enhancing effect of static mixers is most pronounced in viscous fluids that give rise to large spherical cap bubbles (97); though less dramatic, large improvements are still observed with waterlike media. Generally, for a given fluid, the mass transfer coefficient and the gas velocity in the riser of a given airlift reactor may be correlated in the form

$$k_L a_L = \alpha U_{Gr}^{\beta} \tag{58.72}$$

For a given fluid, the exponent β in Equation 58.72 is not affected by the presence of static mixers in the reactor; however, the mixers significantly enhance the value of α (97). The improvement in α depends mainly on the consistency index (K) or the "thickness" of the fluid: generally, the thicker the fluid, the greater the effect of static mixers (97). The approximate relationship among α, α_M (the α value in presence of static mixers), and K has been established to be (97)

$$\frac{\alpha_M}{\alpha} = 4.43K^{0.12} \tag{58.73}$$

Equation 58.73 was determined for approximately 10^4-fold variation in K. The flow behavior index n (varied between 0.5 and 1.0) had no direct impact on enhancement of $k_L a_L$ by the mixers (97). Depending on the fluid, the static mixers were found to enhance $k_L a_L$ by 30–500% relative to mixer-free operation (97). The constants in Equation 58.73 are expected to depend on the type of static mixer used.

Installation of mixing elements in airlift bioreactors slows down the circulation of fluid; hence, fewest possible mixing elements should be used to satisfy the mass transfer needs while limiting the loss of liquid circulation. The optimal interval between elements depends on the type of fluid. The more coalescing the fluid, the closer the mixers must be positioned for maximum performance. There is an upper limit to the viscosity that may be used in airlift reactors with static mixers (97). In excessively viscous media, just a few mixing elements can slow down the liquid so much so that the reactor stagnates. Static mixers are further discussed by Thakur *et al*. (99).

58.6.5.4 Reciprocating Jet Fermenter. A reciprocating plate or reciprocating jet fermenter has been employed in a few laboratory studies. The device is similar to a pulsed extraction column. It consists of a cylindrical tank containing a central shaft that supports a frame of evenly spaced perforated plates or discs. The plates are mounted horizontally relative to the axis of the shaft. The plates or baffles remain clear of the fermenter walls; the interdisc space and the diameter of perforation varies. Typically, discs are placed 0.07–0.10 m apart and the perforations, 0.06–0.08 m in diameter, occupy a large proportion of the disc surface. The stack of discs oscillates up and down through the fluid. The liquid moves through the perforations as jets that change direction as the movement of stack reverses. The frequency of oscillation is usually a few cycles per second and the vertical movement is small. Brauer reported on these devices in the early 1980s and more gas–liquid mass transfer data have since appeared (100–102). The $k_L a_L$ in reciprocating jet reactors increases with increasing frequency and amplitude of oscillation of the baffles. The power input also increases. The $k_L a_L$ generally follows the equation

$$k_L a_L = \alpha \left(\frac{P}{V_L}\right)^{\beta} U_G^{\gamma} \tag{58.74}$$

where α, β, and γ depend on the bioreactor geometry, fluid properties, and the power input range. Some typical values for these variables are noted in Table 58.14. Commercial utility of reciprocating plate fermenters remains to be proven.

58.6.5.5 Tubular Loop Fermenters. Tubular loop fermenters employ cocurrent flow of gas and liquid in a pipe. The liquid is recirculated by a pump. This design is generally not practical except for low volume fermentations or unusual situations such as those seen in the tubular solar receivers of photobioreactors used in culturing microalgae (103–105). For a tubular loop (0.025 m tube diameter, 22 m length), Ziegler *et al*. (106) recommended the equation

$$k_L a_L = 5.321 \times 10^{-5} \left(\frac{P_G}{V_L}\right)^{0.9} U_G^{0.2} + 8.333 \times 10^{-3} \tag{58.75}$$

Equation 58.75 was obtained using the sulfite oxidation system. Gas–liquid mass transfer in loop reactors is further discussed by VandenHeuvel *et al*. (107).

58.6.5.6 Fluidized Beds. Gas–liquid–solid fluidized bed bioreactors are seen in immobilized cell culture and wastewater treatment processes. These reactors usually consist of a cylindrical vessel containing a suspension of

TABLE 58.14. The Parameters in Equation 58.74 for Pulsed Baffle Fermenters

Fluid	α ($s^{\beta+\gamma-1}m^{3\beta-\gamma}$ $J^{-\beta}$)	β	γ	Ranges
Water	4.86	0.364	1.55	$23 \le P/V_L$ (W/m^3) ≤ 3620 $0.0049 \le U_G$ (m/s) ≤ 0.0099 $h_L/d_T \approx 40$
Water	0.281	0.632	1.138	$35 \le P/V_L$ (W/m^3) ≤ 6600 $0.0005 \le U_G$ (m/s) ≤ 0.004 $h_L/d_T \approx 1.87$
Water–glycerol (1:1 by vol)	0.0039	0.735	0.668	$35 \le P/V_L$ (W/m^3) ≤ 6600 $0.0005 \le U_G$ (m/s) ≤ 0.004 $h_L/d_T \approx 1.87$
Aqueous yeast slurry	4.8	0.268	1.184	$d_T = 0.05$ m

immobilized biocatalyst. The solids are kept in suspension by continuous flow of a liquid and gas. A solid–liquid separator, usually a sedimentation device, located near the top of the reactor prevents washout of solids. Essential design features of gas–liquid–solid fluidized bed reactors are discussed by Muroyama and Fan (108). The gas–liquid mass transfer coefficients in three-phase fluidized beds may be estimated using the correlation:

$$\frac{k_L a_L d_p^2}{D_L} = \alpha \left(\frac{d_p U_t \rho_L}{\mu_L}\right)^{3.3} \left(\frac{\mu_L U_G}{\sigma_L}\right)^{0.7}$$
$$(\alpha = 2.33 \times 10^{-5} \text{ when } Re_t < 2000; \alpha = 3.946 \times 10^{-7} \text{ when } Re_t > 2000) \quad (58.76)$$

where U_t is the terminal settling velocity of the particle and Re_t is the Reynolds number based on the terminal settling velocity. Equation 58.76 was developed for carbon dioxide absorption in water containing porcelain beads, sand, lead shots, or iron shots. The terminal settling velocity of the solids ranged over 0.12–0.815 m/s. Other parameters were: $0 \le U_G$ (meters per second) ≤ 0.1; $0.05 \le U_L$ (meters per second) ≤ 0.172; $1.06 \le d_p$ (millimeters) ≤ 6.84; and $2400 \le \rho_S$ (kilograms per cubic meter) $\le 11{,}180$.

Another correlation for gas–liquid mass transfer in fluidized beds is due to Nguyen-Tien *et al*. (109):

$$k_L a_L = 0.394 \left(1 - \frac{\varepsilon_S}{0.58}\right) U_G^{0.67} \quad (58.77)$$

where ε_S is the volume fraction of solids. For three-phase circulating bed fermenters, Loh *et al*. (110) have recommended the following equation

$$k_L a_L = 1.4 \times 10^{-4} \left(\frac{P}{V_L}\right)^{0.91} \frac{(1 - 2.5\varepsilon_S)^{0.95}}{(1 - \varepsilon_S)^{4.3}} \quad (58.78)$$

Because $k_L a_L$ is generally not too sensitive to the liquid flow rate, the equations developed for slurry bubble columns may also be applied to fluidized beds. Consult Muroyama and Fan (108) for further details on gas–liquid mass transfer in fluidized beds.

58.6.5.7 Other Factors Affecting $k_L a_L$

58.6.5.7.1 Surfactants and Antifoam Agents. Relative to clean systems, addition of surfactants may reduce or enhance $k_L a_L$. The specific effect and its magnitude depend on the type of surfactant, its concentration, and the nature of the broth. The coalescence promotion effect of some surfactants reduces the specific interfacial area a_L and the $k_L a_L$. Addition of surface active agents such as ethanol to water generally increases a_L and $k_L a_L$. Surfactants such as sodium dodecyl sulfate (SDS) or sodium lauryl sulfate (SLS) accumulate at the gas–liquid interface and usually cause a reduction in k_L.

58.6.5.7.2 Temperature. The overall volumetric gas–liquid mass transfer coefficient $k_L a_L$, generally increases with increasing temperature. This is mainly because the diffusion coefficient increases with temperature. Also, the viscosity of the liquid declines with increasing temperature; hence, for a given energy input, the film thickness declines and the interfacial area may increase slightly. The $k_L a_L$ value at any temperature T (degree Celsius) may be calculated from the $k_L a_L$ at 20°C using the equation:

$$(k_L a_L)_T = (k_L a_L)_{20^\circ C} \theta^{(T-20)^\circ C} \quad (58.79)$$

where θ is 1.200–1.024.

58.6.5.7.3 Suspended Solids. How and how much suspended solids affect $k_L a_L$ depends on several factors including concentration of solids, the density difference between the solid and the suspending fluid, the particle diameter, the operating conditions of the reactor (i.e. the power input), and the hydrophobicity of the solids. Up to 15% (wt/wt) of particles smaller than about 50 μm have little effect on $k_L a_L$; however, much smaller amounts

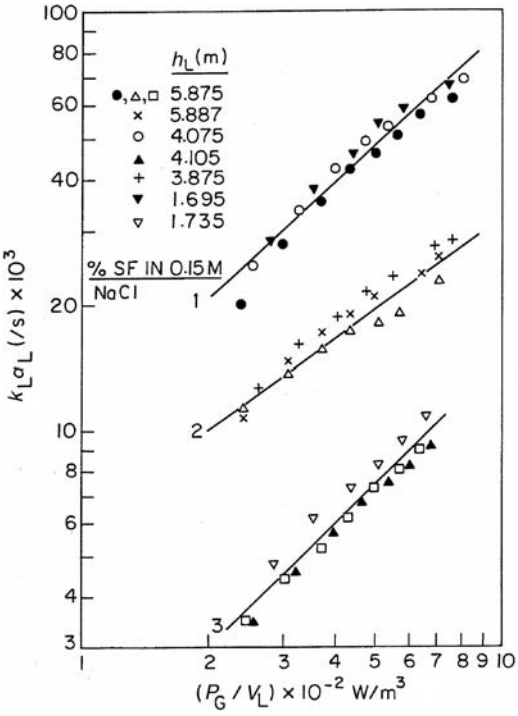


Figure 58.8. The effect of "Solka Floc" (SF) cellulose pulp fibers on gas–liquid mass transfer coefficient in bubble columns at various static slurry heights h_L. The fibers were suspended in 0.15 M sodium chloride in tap water (6). The $k_L a_L$ is shown as a function of the specific power input.

of larger particles can reduce $k_L a_L$ significantly. Very small concentrations of relatively high density solids may actually enhance $k_L a_L$ a little. Increasing amounts of low density filamentous or mycelial biomass rapidly increase the apparent viscosity of the slurry and the $k_L a_L$ may decline sharply (6). The effect of such solids on $k_L a_L$ is illustrated in Figure 58.8, which is for paper pulp fibers that simulate filamentous mycelial biomass.

In a draft-tube sparged concentric draft-tube airlift reactor for potential application to microbial desulfurization of coal, the mass transfer coefficient data in a simulated basal salt medium was reported by Smith and Skidmore (111). The medium contained a total 1.9 kg/m^3 of various salts in distilled water. Pulverized coal particles (74×10^{-6} m particle diameter; density = 1415 kg/m^3) were suspended in the fluid to a concentration of 0–40% wt (equivalent to 0–0.315 volume fraction of solids in gas-free medium). Over the temperature range 303–345 K, the $k_L a_L$ values were strongly enhanced by increasing temperature. Increasing concentration of solids over 0–5% wt (equivalent to ϕ_S of 0–0.035) increased the $k_L a_L$ values slightly, but further increase in solids loading strongly lowered the mass transfer coefficient (111). This phenomenon was explained as being due to penetration of fine solid particles in the stagnant liquid film around gas bubbles, thereby reducing the effective diffusion length (111). However, as the concentration of solids increased beyond 5% wt, the solids caused a blocking effect, which reduced the effective mass transfer area (6,111). In the region of enhanced mass transfer ($0 \leq \phi_S < 0.035$), the $k_L a_L$ was correlated with (111)

$$k_L a_L = (5.7 - 144.8\phi_S + 5048.3\phi_S^2) \times 10^4 U_{Gr}^{1.55} e^{-2990/T} \tag{58.80}$$

whereas in the "blocking" region ($0.035 \leq \phi_S \leq 0.315$), the following equation was obtained (111)

$$k_L a_L = (2.6 - 16.8\phi_S + 29.4\phi_S^2) \times 10^6 U_{Gr}^{1.45} e^{-4130/T} \tag{58.81}$$

Equations 58.80 and 58.81 agreed with the data to within about ±20%. These equations applied over the U_{Gr} range $(0.154–1.39) \times 10^{-1}$ m/s, when the A_r/A_d and the aspect ratios were 1.3 and about 5, respectively.

Mass transfer measurements in suspensions of agar-filled soft polyurethane foam particles ($d_p = 3$ mm; $\rho_p = 1030$ kg/m^3) in uninoculated penicillin culture medium ($\mu_L = 1.9 \times 10^{-1}$ Pa s) in draft-tube sparged concentric-tube airlift reactors have been reported (112). Increasing volume fraction of solids over the 0–0.1 range, enhanced the volumetric mass transfer coefficient by 15–20% over solids-free operation (112). Further increase in solids loading to 40% (vol/vol) caused a decline in $k_L a_L$ values. The mass transfer coefficient values in airlift reactors were up to threefold higher than in comparable fluidized beds.

In suspensions of relatively low density calcium alginate beads in water and other Newtonian fluids (0–20% vol/vol solids, 1.88–3.98 mm bead diameter) in draft-tube sparged concentric–tube airlift reactors, Koide *et al*. (89) noted that the mass transfer coefficient declined with increasing concentration of solids, but was not affected by the size of the particles.

58.6.6 Oxygen Transfer in Wastewater Treatment Processes

The typically used bioreactor in activated sludge treatment of wastewater consists of a relatively shallow (~4-m deep) rectangular basin aerated by sparging through perforated pipes or diffusers located at the bottom of the tank. The oxygen transfer capability of such systems is quite limited; hence, biodegradation is slow. Usually only about 0.5–2 kg O_2 can be transferred per kilowatt-hour of energy spent. The oxygen transfer capabilities of other conventional aeration systems have been detailed by Winkler (113).

Faster degradation of pollutants can be achieved with low volume high rate oxygen transfer systems. One such technology is the "deep shaft" reactor based on the airlift principle. This advanced activated sludge process relies on

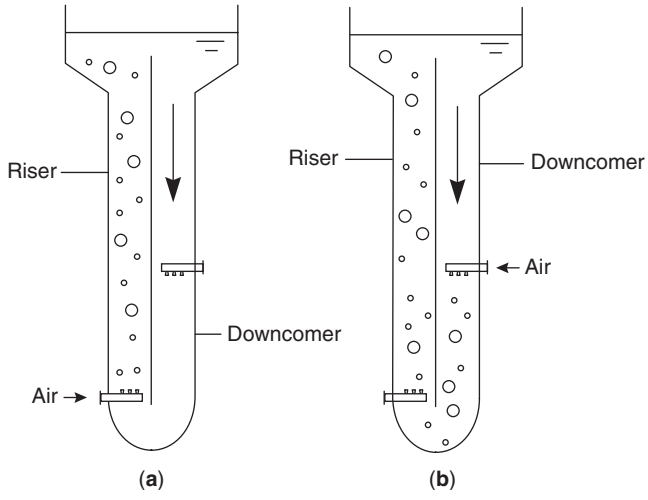


Figure 58.9. Deep shaft airlift reactor: (a) aeration in riser during start-up; (b) aeration in downcomer during normal operation. In case (b) no gas is being injected in the riser; all the gas bubbles in the riser are due to circulation from the downcomer.

high hydrostatic pressure in a deep airlift column to significantly enhance oxygen transfer. In comparison with conventional processes, oxygen transfer rates are up to 10-fold greater (113). The transfer rate at peak load is about 1 kg O_2/m^3 h (17). Several factors combine to yield this high level of performance, including long gas–liquid contact times and intense turbulence in the circulating fluid with Reynolds numbers of the order of 10^5 or higher (113). The shaft is 30–220 m deep (113), 0.5–10 m in diameter, and partitioned vertically into a riser and a downcomer. Air is injected into the downcomer, about 20–40 m below the surface (113), except during start-up when the riser is aerated (Figure 58.9). To ensure that air bubbles move down the downcomer, a superficial liquid velocity of 1–2 m/s must be generated in the downcomer zone. Because the gas is not recirculated, the downcomer region above the sparger is free of bubbles. Oxygen transfer efficiencies of 3–5.5 kg O_2/kWh can be attained (113). Up to 90% of the oxygen in the air is used up.

For deep shaft plants, Winkler (113) cites a biochemical oxygen demand (BOD) loading of 0.9 kg BOD/kg sludge solids per day. A retention time of about 1.5 h has been mentioned for 92% BOD removal (113). Volumetric BOD removal is of the order of 3.7–6.6 kg BOD/m^3 d, which is generally associated with high rate treatment processes. Sewage is treated without primary sedimentation; only preliminary de-gritting is needed (113). Sedimentation of grit at the bottom of the shaft is prevented by ensuring that the flow velocity at the bottom exceeds 1 m/s. See Chisti (17) for additional details.

In addition to the deep shaft, a "biotower" configuration is increasingly being used in wastewater treatment. The biotower units consist of a relatively shallow (18–20 m) above-ground pool of liquid with or without multiple draft-tubes (downcomers). The towers handle streams with 2–12 kg/m^3 chemical oxygen demand. The oxygen transfer efficiency ranges over 1.2–3.8 kg O_2/kWh (114). The biomass sludge produced rises to the top with the bubbles and is separated in an integral settling zone. Chisti (17) provides further details.

58.6.7 Liquid–Liquid Mass Transfer

Liquid–liquid dispersions are encountered in solvent extraction and in fermentations of hydrocarbons or other water immiscible liquid substrates. Liquid–liquid dispersions also occur in extractive fermentations where a product is continuously extracted into a water immiscible phase. Similarly, oxygen supply using water immiscible perfluorocarbons and other fluids utilizes liquid–liquid mass transfer. While in gas–liquid dispersions only the liquid film around the bubble is the principal resistance to mass transfer, in liquid–liquid dispersions the film inside the dispersed drops also affects the transport rate. Tables 58.15 and 58.16 list the correlations that are useful in calculating the mass transfer coefficients in the dispersed and continuous phases. Noncirculating small drops can be treated as ridged particles and solid–liquid mass transfer correlations (see later sections) developed for suspended spherical solids can be used. Presence of surfactants often renders drops nonmobile and solid-sphere correlations apply again. For larger, mobile, or oscillating droplets, both the continuous phase and the dispersed phase mass transfer coefficients are greater than for solid spheres.

58.6.8 Perfluorocarbons and Oxygen Vectors

Perfluorocarbons are water immiscible liquids that dissolve 10–20 times more oxygen than water. These fluids can be used for bubble-free oxygenation and removal of carbon dioxide in animal cell culture. Another potential application is stripping of inhibitory oxygen produced via photosynthesis in cultures of microalgae. Perfluorocarbons are biologically inert, and suitably selected ones are nontoxic to animal cells and microorganisms. Indeed, emulsified perfluorocarbons have been used to supplement blood to improve oxygen supply to human patients. In microbial culture, perfluorocarbon concentrations as low as 10% vol/vol have significantly enhanced culture performance.

One scheme for bubble-free oxygenation using perfluorocarbons is illustrated in Figure 58.10. A separate vessel is used to aerate the organic phase and strip the carbon dioxide. The oxygen enriched liquid is pumped to the fermenter and "sprayed" into the culture medium. As the droplets settle to the bottom in the relatively quiescent environment of animal cell bioreactors, the oxygen transfers to the aqueous phase. The oxygen depleted perfluorocarbon from the

TABLE 58.15. Mass Transfer Coefficient Inside Mobile or Oscillating Drops in Liquid–Liquid Dispersions

Correlation	Range
$Sh \approx 16.7$	$Re < 50$
$Sh = 0.320 Re^{0.68} \left(\frac{\sigma^3 \rho_C^2}{g \mu_C^4 \Delta\rho}\right)^{0.10} \left(\frac{4 D_D t_C}{d_D^2}\right)^{-0.14}$	$Re > 150$–200
$Sh = 0.32 Re^{0.63} Sc^{0.50} \left(1 + \frac{\mu_D}{\mu_C}\right)^{-0.5}$	$10 \le Re \le 1000$ Spherical drops
$Sh = 7.5 \times 10^{-5} Re_C^{2.0} Sc^{0.56} \left(1 + \frac{\mu_D}{\mu_C}\right)^{-0.5}$	$100 \le Re_C \le 1500$ Larger oblate drops

Re in these equations is based on drop diameter and relative velocity between phases; all other properties are for the drop phase unless otherwise noted. The density and viscosity in Re_C are for the continuous phase. The subscripts C and D refer to continuous and dispersed phases, respectively.

TABLE 58.16. Continuous Phase Mass Transfer Coefficient Correlations for Liquid–Liquid Dispersions

Small, noncirculating drops	$Sh = 2 + 0.79 Re^{0.5} Sc^{0.33}$ $Sh = 2 + 0.76 Re^{0.5} Sc^{0.33}$ $Sh = 0.562 Re^{0.5} Sc^{0.33}$
Larger, mobile drops	$Sh = \frac{2}{\sqrt{\pi}} \left[1 - Re^{-0.5} \left(2.89 + 2.15 \left(\frac{\mu_D}{\mu_C}\right)^{0.64}\right)\right]^{0.5} (ReSc)^{0.5}$ when $Re < 120$, $(\mu_D/\mu_C) \le 2$, and $0 \le (\rho_D/\rho_C) \le 4$ $Sh = -126 + 1.8 Re^{0.50} Sc^{0.33}$ when $8 \le Re \le 800$ $Sh = -178 + 3.62 Re^{0.50} Sc^{0.33}$

Re in these equations is based on drop diameter and relative velocity between phases; all other properties are for the continuous phase unless otherwise noted. The subscripts C and D refer to continuous and dispersed phases, respectively. Based on Pratt (2) and Schügerl (115).

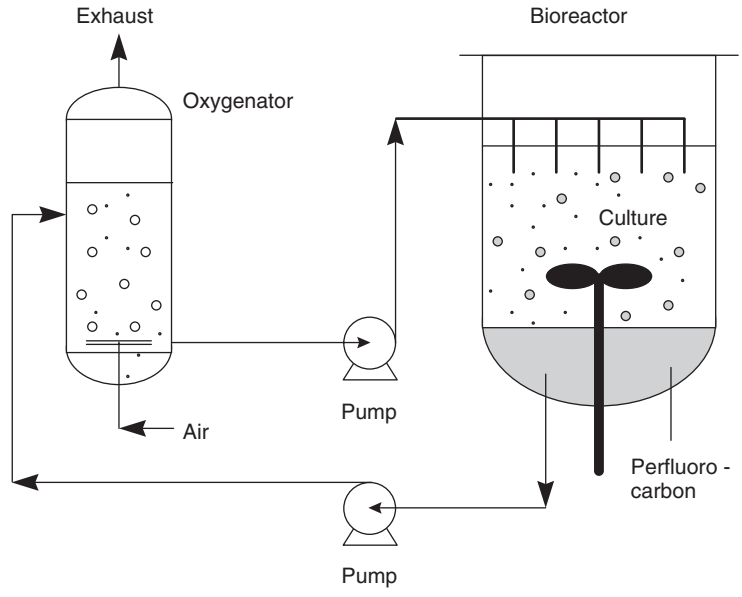


Figure 58.10. Bubble-free aeration with perfluorocarbon oxygen vector in a cell culture bioreactor.

bottom of the fermenter is recycled to the external aerator. Perfluorocarbons and other oxygen vectors enhance oxygen transfer performance, when added to an aerated reactor also. The oils extract more oxygen from the gas phase and effectively increase oxygen–culture contact time. In agitated continuous culture of *E. coli* operated at a dilution rate of 0.275/h and 35.5°C, an emulsified perfluorocarbon added to the feed at 50% volume fraction could provide 0.17 kg O_2/m^3 h when the biomass concentration was 0.74 kg/m^3 (116). The same system removed 0.23 kg/m^3 h of carbon dioxide.

With animal cells, clumping has been reported at the interface between the culture medium and the perfluorocarbon layer at the bottom of the fermenter, when the agitator is placed in the bottom layer. Cells generally do not adhere to perfluorocarbon droplets. Other oxygen carriers have been tested, including hemoglobin solutions and erythrocytes, hydrocarbons such as *n*-hexadecane and *n*-dodecane, silicone oil emulsions, and soybean oil. Relevant properties of two types of oxygen vectors are noted in Table 58.17. Gas–liquid mass transfer enhancement due to the presence of water immiscible oxygen vectors in aerated aqueous dispersions has been reviewed by Dumont and Delmas (117).

58.6.9 Aqueous Two-Phase Extractions

Aqueous two-phase extraction is used in bioprocessing to recover and purify bioactive proteins that are susceptible to denaturation during traditional solvent extraction that employs hydrophobic solvents. Save *et al*. (118) measured mass transfer coefficients of cytochrome-c, amyloglucosidase, and β-galactosidase in aqueous two-phase systems in a stirred cell with a flat interface between phases. In the poly(ethylene glycol) (PEG)–dextran system, the controlling resistance to mass transfer occurred in the heavy phase (the dextran-rich phase). This was correlated as

$$k_L = 3.9 \times 10^{17} D_L^{1.8} E^{0.42} \mu_L^{0.78} \tag{58.82}$$

For PEG–sodium sulfate systems, the controlling resistance lay in the light phase (PEG-rich phase) and the mass transfer coefficient was correlated as (118):

$$k_L = 0.17 D_L^{0.33} E^{0.38} \tag{58.83}$$

In Equations 58.82 and 58.83, μ_L is the viscosity of the phase and D_L is the estimated diffusivity of the protein in that phase. The agitation power input per unit phase mass is represented by E. The E values ranged over $\sim(2–32) \times 10^{-4}$ W/kg.

58.6.10 Solid–Liquid and Gas–Solid Mass Transfer

Dissolution or vaporization of a solid phase into a fluid, or crystallization from a liquid are problems of solid–fluid mass transfer. Other similar situations occur in adsorption/desorption of material and during reaction catalyzed by a solid-phase biocatalyst. Common examples of gas–solid mass transfer are seen in various kinds of drying operations. Mass transfer may occur to or from a fluid flowing past a stationary solid, or the solid may be suspended in the fluid. These cases are treated separately below.

58.6.11 Flow Past a Solid Surface

Material transport to or from a fluid moving past a stationary solid is encountered in packed beds of biocatalysts, chromatographic media, and solid adsorbents such as activated carbon. Other occurrences are in membrane processes, solid-state state fermentations (119–121), surfaces of biofilms, capillaries containing surface-immobilized enzymes, and biofilters for treating gaseous effluents. The rate of mass transfer in flow past a solid is controlled by the flow rate of the fluid, the geometry of the solid surface, the diffusivity of the solute, and the physical properties of the flowing fluid. Suitable correlations for estimating the mass transfer coefficient for flow past solids of various geometries (e.g. flat plate, sphere, pipe) are listed in Table 58.18. The correlations given are for smooth surfaces. Predictive equations such as those in Table 58.18 and others in this chapter are usually accurate to only about ±50% of the actual value. Some more important bioprocess-relevant cases of mass transfer in flow past stationary solids are discussed in greater depth in the following sections.

58.6.11.1 Packed Beds. External mass transfer to or from spherical solid particles in packed beds has been correlated

TABLE 58.17. Properties of Some Oxygen Vectors

Property	*n*-Dodecane	Perfluorocarbon
Oxygen solubility (mg/L)	59.4	118.0
Density (kg/m^3)	743	1750
Interfacial tension (liquid–air) (N/m)	24.6×10^{-3}	17.8
Interfacial tension (liquid–water) (N/m)	32.9×10^{-3}	25.0
Boiling point (degrees Celsius)	214	206

Oxygen solubility data at **35°**C; all other data at **30°**C.

TABLE 58.18. Relationships for Estimating Solid–Liquid Mass Transfer Coefficients

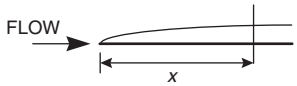
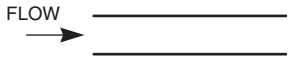
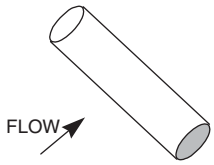
Flow Geometry	Laminar Flow	Flow Transition	Turbulent Flow
1. Flow parallel to a flat plate 	$Sh_x = 0.332 Re_x^{1/2} Sc^{1/3} (Sc \geq 0.5)$ $Sh = 0.66 Re^{1/2} Sc^{1/3} (Sc \geq 0.5)$ $Sh_x = 0.565 Re_x^{1/2} Sc^{1/2} (Sc \leq 0.025)$ Subscript x indicates *local* value a distance x (characteristic length) from the leading edge of plate. Mean coefficient is given by the second equation where the whole length of the plate is used to calculate Re	$Re_x \approx 5 \times 10^5$	$Sh_x = 0.0296 Re^{0.8} Sc^{0.6}$ $(10.0 \geq Sc \geq 0.5)$
2. Fully developed flow in straight pipe 	$Sh = 3.65 + \dfrac{0.0668\left(\dfrac{d}{L}\right) ReSc}{1 + 0.04\left[\left(\dfrac{d}{L}\right) ReSc\right]^{2/3}}$ Use hydraulic diameter d_h for noncircular section: $d_h = \dfrac{4 \times \text{flow area}}{\text{wetted perimeter}}$	$Re \approx 2300$	$Sh = 0.023 Re^{0.8} Sc^{0.33}$ $(Sc > 0.5)$ $Sh = 0.0102 Re^{9/10} Sc^{1/3}$ $(Sc \geq 10^3;\ Re \geq 3000)$
3. Fully developed flow between parallel plates 	$Sh = 7.54 + 0.0234 \dfrac{ReSc}{\left(\dfrac{L}{d}\right)}$	$Re \approx 2800$	$Sh = 0.023 Re^{0.8} Sc^{0.33}$ $(Sc > 0.5)$
4. Flow across a cylinder 	$Sh = 0.43 + \alpha Re^{\beta} Sc^{0.31}$ $1000 \leq Re \leq 4000$ $(\alpha = 0.53, \beta = 0.5)$ $4000 \leq \text{Re} < 40,000$ $(\alpha = 0.193, \beta = 0.618)$ $Sh = 0.600 Re^{0.513} Sc^{1/3}$ $0.6 \leq Sc \leq 2.6$(gases) $1000 \leq Sc \leq 3000$ (liquids) $50 \leq Re \leq 50,000$	$Re \approx 40,000$	$Sh = 0.43 + 0.0265 Re^{0.8} Sc^{0.31}$
5. Flow across a sphere 	$Sh = 2 + 0.37 Re^{0.6} Sc^{0.33}$ $Sh = 2 + 0.552 Re^{0.53} Sc^{1/3}$(gases) $0.6 \leq Sc \leq 2.7$ $1 \leq Re \leq 48{,}000$ $Sh = 2 + 0.95 Re^{0.50} Sc^{1/3}$(liquids) $2 \leq Re \leq 2000$ $Sh = 2 + 0.347 Re^{0.62} Sc^{1/3}$(liquids) $2000 \leq Re \leq 17,000$	$Re \approx 150,000$	

TABLE 58.18. (*Continued*)

	Flow Geometry	Laminar Flow	Flow Transition	Turbulent Flow
6.	Flow through a packed bed of spheres	$St\,Sc^{2/3} = 1.625 Re_d^{-1/2}$ $15 < Re_d < 120$ $Re_d = \frac{\rho_L U_L d_{hi}}{\mu_L}$, where $d_{hi} = \frac{6(1-\phi) \times \text{flow area}}{\text{wetted perimeter}}$ where ϕ is the void fraction and St is the Stanton number: $St = \frac{Sh}{ScRe} = \frac{K_L}{U_L}$	$Re_d = 120$	$St\,Sc^{2/3} = 0.687 Re_d^{-0.327}$ $120 < Re_d < 2000$

On the basis of Refs 1,122.

with the following equations:

$$Sh = \frac{0.4584}{\phi} Re^{0.5931} Sc^{\frac{1}{3}} \tag{58.84}$$

for gases when $10 \leq Re \leq 10{,}000$ (123);

$$Sh = \frac{1.09}{\phi} Re^{\frac{1}{3}} Sc^{\frac{1}{3}} \tag{58.85}$$

for liquids when $0.0016 \leq Re \leq 55$ and $165 \leq Sc \leq 70{,}600$ (1); and

$$Sh = \frac{0.250}{\phi} Re^{0.69} Sc^{\frac{1}{3}} \tag{58.86}$$

for liquids when $55 \leq Re \leq 15{,}000$ and $165 \leq Sc \leq 10{,}690$ (1). The Reynolds number in these equations is based on the particle diameter; the superficial fluid velocity is based on the total cross-section of the bed, and ϕ is the voidage of the packed bed. For nonspherical particles, these equations should be corrected: the Reynolds number should be calculated using the diameter of a sphere having the same surface area as the particle. Mass transfer in packed beds has been reviewed by Larachi *et al*. (124) and Wang *et al*. (125).

Chromatography columns are a form of packed bed. Mass transfer in chromatographic columns has been discussed by Li *et al*. (126). Mass transport aspects of high-performance liquid chromatography (HPLC) have been reviewed by Miyabe and Guiochon (127). Mass transfer of proteins in ion exchange media such as those used in many chromatographic separations, has been discussed by Carta *et al*. (128). During chromatography of macromolecules such as proteins, the combination of molecular diffusivities, particle size of the stationary phase, and elution velocity are such that separation is invariably controlled by mass transfer of the solute to the stationary phase.

58.6.11.2 Aeration Through Polymer Tubing. Bubble-free gas exchange through polymer tubing has been employed in animal cell culture and culture of microalgae. In the latter case, the gas inside the tube is carbon dioxide, which is used by photosynthetic cultures to generate carbohydrates and cell mass. For animal cell culture, the tube may be supplied with air, pure oxygen, or an atmosphere containing 5% (vol/vol) carbon dioxide for pH control.

Either microporous or nonporous tubing may be used for oxygenation of cultures having low oxygen demands. Microporous tubing is made of polytetrafluoroethylene or polypropylene, both of which are strongly hydrophobic. Micropores, 0.03–3.5 μm in diameter, occupy between 30% and 75% of the surface of the tube. The tubing is fairly ridged, with typical outer diameters of 2.5–4 mm and a wall thickness of about 0.5 mm. The pressure inside the tubing cannot exceed the bubble point pressure or else, the gas will issue through the pores as bubbles. The bubble point pressure tends to be low, of the order of 10 mbar. So long as the pores are gas-filled, they do not pose a significant resistance to mass transfer (28), which occurs only through the liquid film held outside the pores. Microporous tubing generally provides a better mass transfer performance than the nonporous silicone tubing, if the pores remain unwetted. Pore wetting can be a problem especially during prolonged use.

In homogeneous nonporous silicone tubing, also known as *solution-diffusion tubing*, the oxygen from inside the tube transfers to the outside by diffusion through the silicone tube wall; the transfer rate is quite slow compared to unwetted microporous tubing. The typical dimensions of silicone tubing are: inside diameter = 1.8 mm and outside diameter = 3.2 mm, or inside diameter = 3 mm and outside diameter = 4.6 mm. The silicone tubing may be internally pressurized. Because of stretching and internal gas pressure, the surface area of the installed tubing differs from that in the relaxed state. The entire surface of the tubing is effective in

mass transfer, except when the tubing has been reinforced. Solubilities and diffusivities of different gases are different in silicone; hence, transport is selective (28).

The mass transfer coefficient k_L outside the microporous tubing in agitated tanks has been correlated as (44)

$$Sh = (7.8 + 0.0021 Re^{1.2}) Sc^{\frac{1}{6}} \tag{58.87}$$

for $250 < Re < 6000$ and $200 < Sc < 500$. The Reynolds number in Equation 58.87 is based on the impeller tip speed and the outer diameter d_o of the tube; thus,

$$Re = \frac{\pi N \rho_L d_i d_o}{\mu_L} \tag{58.88}$$

The Sherwood number is based on d_o and oxygen diffusivity in the liquid. The d_i in Equation 58.88 is the impeller diameter. Equation 58.87 was developed in a cell culture vessel having the polymer tubing coiled into a cylindrical draft-tube configuration (Figure 58.11). A two-bladed anchor impeller located inside the "draft tube" was used for agitation. For any given Reynolds number, the anchor impeller yielded higher values of Sherwood number relative to propellers and screw impellers. Equation 58.87 is for a protein-free medium. For microporous tubes, the k_L values in protein-containing media are about 20% lower than in water. Presence of protein does not seem to affect the mass transfer coefficient of nonporous tubing (44). Equation 58.87 may also be used for homogeneous silicone tubing.

Depending on the porosity of tubing and its diameter, 1.8–3.0 m of polymer tubing is needed per liter of culture volume to meet the $k_L a_L$ demands (44). This length of tubing is close to the technical limits of accommodation in a given volume; therefore, aeration through polymer tubes is useful only for specific cases. The tubing is susceptible to fouling and requires periodic replacement. Anchorage-dependent cells sometimes attach to the surface of silicone tubing; hence, oxygen transfer to bulk fluid is prevented.

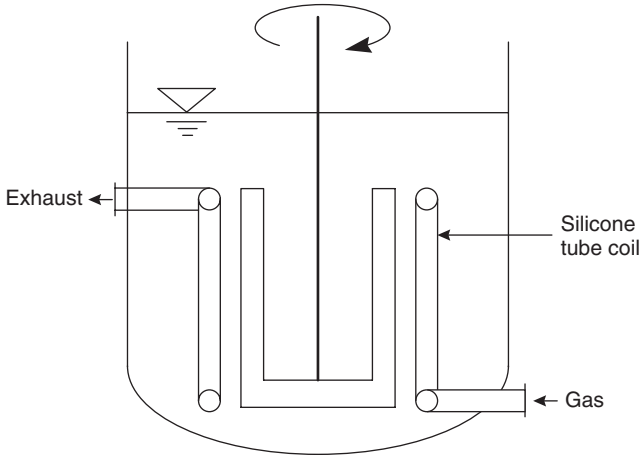


Figure 58.11. Oxygen supply via silicone tubing.

For transfer of carbon dioxide through nonporous silicone membranes and tubes (wall thickness of 1.5–2.0 mm), the diffusion coefficient (D) has been reported to be 1.92 ± 0.14 m^2/ min at 25°C (129). For mass transfer through such a tube to a highly agitated culture volume V_L, the transfer rate can be written as

$$\frac{dC_L}{dt} = \frac{AD(C^* - C_L)}{V_L \delta_w} \tag{58.89}$$

where A is the surface area of the tube, δ_w is its wall thickness, C_L is the instantaneous concentration of the diffusing gas in the liquid phase, and C^* is the saturation concentration of the diffusing component in a liquid sample that is in equilibrium with a gas phase having the same composition as in the silicone tube; C^* may be calculated using Henry's law. Note that Equation 58.89 assumes a constant composition of the gas within the tube (i.e. no diffusion of other dissolved gases from the liquid into the tube). This assumption may be valid for relatively short tubes and high flow rates within the tubes. Aeration through polymer tubing is discussed further by Aunins and Henzler (28).

58.6.11.3 Mass Transfer Effects in Membrane Processes. Membrane filtrations, particularly microfiltration and ultrafiltration, are commonly employed in bioprocessing to separate cells, particles, microemulsions, and macromolecules. Generally, a crossflow scheme is used in which the fluid being filtered flows parallel to the membrane but perpendicular to the direction of the permeate flux. The turbulence generated by the flow improves mass transfer at the membrane surface; consequently, the buildup of a solute layer or gel layer on the surface of the membrane is reduced to assure relatively high permeate or filtrate flux through the membrane. At steady state, a solute concentration profile develops on the upstream side of the membrane as shown in Figure 58.12. The permeate flux J is related to the concentration C_{Ge} of the solute in the gel layer, the concentration C_B in the bulk fluid, and the mass transfer coefficient k_L as follows:

$$J = k_L \ln \frac{C_{Ge}}{C_B} \tag{58.90}$$

The mass transfer coefficient depends on the Reynolds number on the slurry side of the membrane as follows:

$$Sh = \alpha Re^{\beta} Sc^{\frac{1}{3}} \tag{58.91}$$

where Sh and Re are based on the hydraulic diameter d_h of the flow channel. During ultrafiltration, β is 0.5 in laminar

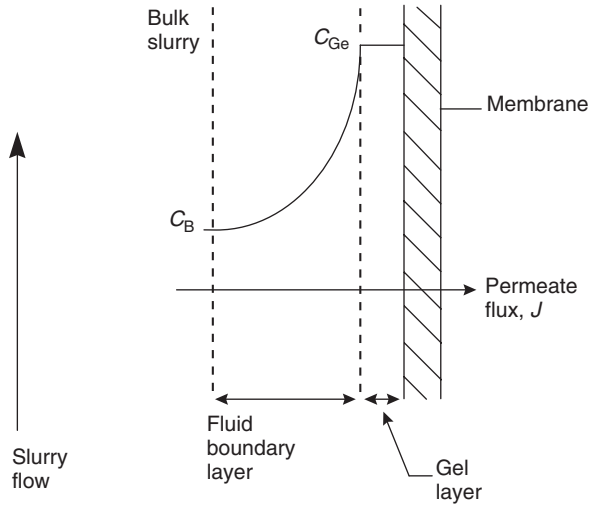


Figure 58.12. Steady state solute concentration profile in ultrafiltration and microfiltration processes.

flow and about 1.0 in turbulent flow. In crossflow microfiltration of particles and cells, β equals 0.8 in laminar flow, but increases to about 1.3 in turbulent flow (130). The α value is 0.023 in turbulent flow. Other expressions for Sherwood number are

$$Sh = 1.62\left(ReSc\frac{d_h}{L}\right)^{0.33} \tag{58.92}$$

$$Sh = 1.86\left(ReSc\frac{d_h}{L}\right)^{0.33} \tag{58.93}$$

and

$$Sh = 0.023Re^{0.875}Sc^{0.25} \tag{58.94}$$

Equations 58.92 and 93 are for laminar flow in tubes and channels, respectively; Equation 58.94 is for turbulent flow. For fully developed laminar flow in ultrafiltration, k_L may be related to shear rate γ by the Porter equation:

$$k_L = 0.816\gamma^{0.33}D_L^{0.67}L^{-0.33} \tag{58.95}$$

where L is the length of the flow channel and the shear rate depends on the channel geometry: $\gamma = \frac{8U_L}{d}$ for tubes with diameter d, and $\gamma = \frac{6U_L}{h}$ for rectangular channels of height h.

The crossflow velocity is the principal operating variable for enhancing the performance of a given filtration membrane module. The optimal crossflow velocity depends on the product and the configuration of the filtration module. For tubular microfiltration membranes with $\sim$ 5.5 mm inner diameter, the optimal crossflow velocity is about 2.5–5 m/s (131). The inner diameter of membrane tubes is usually 4–20 mm. Hollow fibers have much smaller diameters at 0.5–2 mm. Membranes are often deployed as flat sheets in a plate-and-frame configuration, in which the height of the flow channel is 0.5–1.5 mm (131).

Other methods for improving mass transfer in membrane processes include operation at higher temperature (i.e. higher diffusivity and lower viscosity), addition of large inert particles to the feed to agitate the gel layer, and use of pulsating flow. Module design may also be modified to enhance turbulence in the flow channel; hence, turbulence promoters such as static mixers (e.g. wire screens) may be used in tubes and channels, or membranes may be formed into a corrugated configuration. Another method of mass transfer enhancement is the use of dynamic filtration systems with rotating membranes, or agitators placed in close proximity to the membrane (8).

In both ultrafiltration and microfiltration, the mass transfer coefficient tends to be quite small because of the small diffusivities of the cells and macromolecules. Formation of the gel layer, also known as *concentration polarization*, reduces the permeate flux in microfiltration to only about 5% of the pure water flux. Unlike microfiltration and ultrafiltration, pervaporation processes use nonporous homogeneous membranes. Typically, the solute flux is low and the mass transfer coefficient k_L is relatively large in view of the higher diffusivities of small solutes such as ethanol. For additional information on mass transfer in membrane processes see Mulder (132), Ho and Sirkar (133), and Brindle and Stephenson (134).

58.6.11.4 Mass Transfer at Rough Surfaces. Compared to smooth surfaces, mass transfer from a geometrically similar rough surface is generally higher for otherwise identical conditions. Roughness induces an earlier transition to turbulence in flow past a surface. The effect of surface roughness on mass transfer coefficients in Newtonian fluids has been correlated by Kawase *et al*. (135) using the equation

$$Sh = 0.0093\left(\frac{e}{d}\right)^{0.15}ReSc^{0.5} \times \left(1.11 + 0.44Sc^{\frac{-1}{3}} - 0.70Sc^{\frac{-1}{6}}\right) \tag{58.96}$$

where e is the absolute roughness (mean height of projections from the surface) and d is pipe or channel diameter. The ratio e/d is known as *relative roughness*. Equation 58.96 is for the ranges: $5 \times 10^3 < Re < 5 \times 10^5$, $5 < Sc < 400$, and $0.003 \leq e/d \leq 0.056$.

Mass transfer in solid-state fermentation devices is relatively poorly understood. Relevant studies have been reviewed by Rahardjo *et al*. (120) and Mitchell *et al*. (121). Mass transfer in rotating drum solid-substrate bioreactors has been discussed by Hardin *et al*. (136) and Barrera-Cortes *et al*. (137). Mass transfer in biofilms under oscillatory flow conditions has been discussed by Nagaoka

(138). Surface mass transfer during air chilling and storage of food products is discussed by Kondjoyan (139).

58.6.12 Fluid–Solid Slurries

For mass transfer to or from suspended solids, energy dissipation in the vicinity of the particles is generally assumed to control mass transfer in an isotropically turbulent field. Under such conditions, the small energy dissipating eddies are independent of the nature of the bulk flow; the properties of those eddies depend only on energy dissipation rate per unit mass of fluid, E. In general, the liquid film mass transfer coefficient k_L at the solid–liquid interface is expressed in terms of E as follows (140):

$$Sh = \frac{k_L d_p}{D_L} = 2 + c\left(\frac{E^{1/3}\rho_L d_p^{4/3}}{\mu_L}\right)^a Sc^b \qquad (58.97)$$

where $(E^{1/3}\rho_L d_p^{4/3}/\mu_L)$ may be regarded as the energy dissipation Reynolds number (141). Notice that in a quiescent environment, purely diffusive mass transfer occurs and Equation 58.97 reverts to $Sh = 2$ as expected from theoretical considerations. Irrespective of the reactor configuration, solid–liquid mass transfer in slurries is not significantly influenced by the presence of gas bubbles. Solid–liquid mass transfer cases for the principal types of bioreactors are discussed in the following sections.

58.6.12.1 Stirred Tanks. Use the Calderbank and Moo-Young (12) Equation 58.35 noted earlier, or the Liepe and Möckel equations recommended by Hempel (142):

$$Sh = 2 + 0.67\left(\frac{P}{V_L}\frac{\rho_L^2 d_p^4}{\mu_L^3}\right)^{\frac{1}{8}} Sc^{\frac{1}{3}} \qquad (58.98)$$

which is valid when

$$d_p < 5.2\left(\frac{\Delta\rho}{\rho_L}\right)^{\frac{-5}{6}}\left(\frac{\mu_L^3 V_L}{P\rho_L^2}\right)^{\frac{1}{4}} \qquad (58.99)$$

When the particle diameter exceeds that given by inequality 99, the recommended equation is

$$Sh = 2 + 0.35\left(\frac{\Delta\rho}{\rho_L}\right)^{\frac{1}{3}}\left(\frac{P}{V_L}\frac{\rho_L^2 d_p^4}{\mu_L^3}\right)^{\frac{2}{3}} Sc^{\frac{1}{3}} \qquad (58.100)$$

Solid–liquid mass transfer coefficients in solid–liquid and gas–liquid–solid systems in stirred tanks have been reviewed by Pangarkar *et al*. (143).

58.6.12.2 Bubble Columns. The recommended correlation is

$$\frac{k_L d_p}{D_L} = 2 + 0.545 Sc^{\frac{1}{3}}\left(\frac{g d_p^4 \rho_L^3 U_G}{\mu_L^3}\right)^{0.264} \qquad (58.101)$$

which is due to Sänger and Deckwer (144). It is suitable for $137 \leq Sc \leq 50{,}000$.

58.6.12.3 Airlift Bioreactors. For typical operating conditions, solid–liquid mass transfer coefficient in airlift bioreactors is insensitive to the gas flow rate until such a point, where increasing the superficial gas velocity ceases to produce much increase in circulation of the slurry. If the aeration rate is increased further, the k_L increases rapidly (17,140). Pneumatic energy imparted to the slurry initially produces bulk circulation of fluid; only when circulation no longer improves, the energy is dissipated in microeddies that penetrate to the vicinity of the solid–liquid interface and enhance k_L. Slight variations in solids concentration (e.g. 0.2–4% wt/wt) do not affect k_L in airlift reactors (140,145).

Under similar conditions, solid–liquid mass transfer in external-loop airlift reactors exceeds that in stirred tanks and bubble columns; airlifts perform marginally better than fluidized beds (17). Performance of draft-tube internal-loop airlift devices also exceeds that of bubble columns. The solid–liquid mass transfer coefficient in both external- and internal-loop types of airlift reactors may be increased further by using static mixers. In draft-tube sparged reactors Kenics-type twisted ribbon static mixers placed in the draft-tube have been shown to enhance the mass transfer coefficient by about 20%, relative to operation without the mixers (17).

The various correlations developed for solid–liquid mass transfer coefficient in internal- and external-loop types of airlift reactors are noted in Table 58.19. These correlations require a knowledge of the energy dissipation rate per unit mass of fluid; E is calculated using the equation

$$E = \frac{g U_{Gr}}{1 + \frac{A_d}{A_r}} \qquad (58.102)$$

where U_{Gr} is the superficial gas velocity in the riser (6,90).

58.6.12.4 Fluidized Beds. Mass transfer coefficient for spherical particles suspended in a gas or liquid fluidized bed can be estimated using

$$Sh = \frac{0.4548 Re^{0.5931} Sc^{\frac{1}{3}}}{\phi} \qquad (58.103)$$

TABLE 58.19. Solid–Liquid Mass Transfer Coefficient in Airlift Reactors

Reactor Configuration	Correlation	Ranges
Internal-loop reactors (draft-tube sparged)	$Sh = 2 + 0.064\left(\frac{E\rho_L^3 d_p^4}{\mu_L^3}\right)^{0.165} Sc^{0.45}$ Kushalkar and Pangarkar (146)	0.5% wt benzoic acid granules, $d_p = 0.55$–3 mm, in air–water. $A_r/A_d = 0.17$–1.29, $U_G = 0.08$–0.35 m/s
Internal-loop reactors (draft-tube sparged)	$Sh = 2 + 1.01\left(\frac{E\rho_L^3 d_p^4}{\mu_L^3}\right)^{0.173} Sc^{0.33}$ Goto *et al*. (145)	Amberlyst 15 ion exchange resin, $d_p = 0.55$–0.92 mm, suspended in dilute aqueous sodium hydroxide. $A_r/A_d = 0.1$–1.4
Internal-loop reactors with static mixers (draft-tube sparged)	$Sh = 2 + 1.68\left(\frac{E\rho_L^3 d_p^4}{\mu_L^3}\right)^{0.133} Sc^{0.33}$ Gaspillo and Goto (147)	Kenics-type twisted ribbon static mixers were in draft-tube
External-loop reactors	$Sh = 2 + 0.48\left(\frac{E^{1/3}\rho_L d_p^{4/3}}{\mu_L}\right)^{0.72} Sc^{1/3}$ Mao *et al*. (140)	Benzoic acid coated particles, $d_p = 3.8$ mm, $\rho_S \approx$ 1080 kg/m^3, suspended in water

where ϕ is the void fraction of the bed. Equation 58.103 is suitable for $10 \leq Re \leq 4000$. Another correlation applicable only to liquid fluidized beds is

$$Sh = \frac{1.1068 Re^{0.28} Sc^{\frac{1}{3}}}{\phi} \tag{58.104}$$

which is suitable for $1 \leq Re \leq 10$. Gas–solid mass transfer in gas-fluidized beds has been discussed by Yusuf *et al*. (148).

Mass transfer from the vessel wall to the fluid in a liquid fluidized bed (no gas) is aided by suspended solids that disturb the boundary layer at the wall of the reactor. The liquid film mass transfer coefficient at the wall of such systems has been correlated (149) with the following equation:

$$\frac{k_L d_p}{D_L} = 0.14\left(\frac{d_p U_L \rho_L}{\mu_L}\right)^{1/3}\left(\frac{\mu_L}{\rho_L D_L}\right)^{1/3} + 0.13(1-\phi_f)(\phi_f - \phi_b)\left(\frac{\mu_L^2}{\rho_L^2 U_L d_p D_L}\right)^{1/3}\left(\frac{d_p^3(\rho_S - \rho_L)\rho_L g}{\mu_L^2}\right)^{1/3} \tag{58.105}$$

Equation 58.105 applies when $0.9 \leq \left(\frac{d_p U_L \rho_L}{\mu_L(1-\phi_f)}\right) \leq 1652$ and $151 \leq \left(\frac{\mu_L}{\rho_L D_L}\right) \leq 7021$. In Equation 58.105, ϕ_f is the bed voidage and ϕ_b is the void fraction of the settled bed.

58.6.13 External Mass Transfer and Heterogeneous Bioreaction

At steady state, the rate of mass transfer of a substrate being consumed at the surface of a nonporous particle equals the rate of consumption; thus,

$$k_L a_s (C_B - C_{Sb}) = R \tag{58.106}$$

where a_s is the solid–liquid interfacial area per unit liquid volume, R is the overall rate of reaction, and C_B and C_{Sb} are substrate concentrations in the bulk fluid and at the solid's surface, respectively. Because R is a function of the substrate concentration C_{Sb}, R tends to a maximum when the concentration at the interface approaches that in the bulk fluid, that is, the mass transfer rate or the $k_L a_s$ is large. In this situation, the rate of reaction is maximum and is controlled by the intrinsic kinetics and not by mass transfer effects. At the other extreme, when the mass transfer rate is low compared to the reaction rate, the substrate concentration at the interface approaches zero, and the reaction is mass transfer controlled. Because now $C_{Sb} = 0$, the reaction rate is

$$R = k_L a_s C_B \tag{58.107}$$

Thus, the observed rate of a mass transfer controlled reaction will be influenced by changes in C_B, k_L, or the specific solid–liquid interfacial area a_s. Indeed, observing influence of these variables on the reaction rate provides methods for determining if the reaction is mass transfer limited. In addition, because the activation energy for mass transfer is much smaller than that of biochemical reactions, the observed rate of a mass transfer controlled reaction is not as sensitive to temperature changes as the rate of reaction when it is not limited by transport effects. In a batch stirred vessel, an increase in the rate of a solid-phase catalyzed reaction with increasing agitation implies a mass transfer limited reaction. Similarly, in a packed bed reactor, the rate of a mass

transfer controlled reaction will increase as the flow rate is increased, but the contact time is kept unchanged (i.e. the depth of the bed is increased proportionately).

The solid–liquid mass transfer correlations given earlier in this chapter may be used to estimate k_L in bubble columns, packed beds, fluidized beds, and other geometries of bioreactors. External mass transfer in immobilized enzyme systems has been discussed in greater detail by Goldstein (150).

58.6.14 Intraparticle Mass Transfer

When a substrate is being consumed or a product is being produced inside a porous immobilization matrix or in homogeneous gels, an internal substrate (and product) concentration profile exists within the matrix at steady state. In microporous particles, in the absence of convective transport, the main internal mass transfer parameter is the effective diffusivity D_e in the particle. The effective diffusivity is related to the liquid- or gas-phase diffusivity in the pores as follows:

$$D_e = \frac{p}{\tau} D_L \tag{58.108}$$

In Equation 58.108, p is the porosity, and τ is the tortuosity of the immobilization matrix. The tortuosity corrects for changes in cross-sectional area of the pore. Equation 58.108 applies to gases and liquids when the ratio of the mean free path and the pore diameter (i.e. the dimensionless Knudsen number) is less than 0.01. Tortuosity of many porous solids (e.g. silica gel and alumina) are in the range $2 \leq \tau \leq 6$ (4). For activated carbon, $5 \leq \tau \leq 65$ (4). Intraparticle mass transfer is encountered in immobilized enzyme and cell particles, in chromatographic media, and during leaching of solubles from inert solids.

In macroporous particles, changes in local fluid velocity outside the particle create pressure fluctuations within the larger pores and this leads to some "agitation" of the fluid held in the pores. In this situation, the apparent effective diffusivity (D_{eap}) is greater than that predicted by Equation 58.108. For example, the apparent effective diffusivity of oxygen in pellets of *Aspergillus niger* has been reported to be $\sim 10^{-8}$ m^2/s, or about 10-fold greater than in water, which suggests a level of fluid movement within the pellet possibly because of turbulence induced elastic structural deformations of the loose floc.

For porous particles in packed beds, the apparent effective diffusivity has been observed to depend on the effective diffusivity (no convection) and the Peclet number; thus,

$$D_{e\,ap} = \frac{D_e}{\frac{3}{Pe}\left(\frac{1}{\tanh Pe} - \frac{1}{Pe}\right)} \tag{58.109}$$

where the Peclet number is given as

$$Pe = \frac{d_p U_L}{(1-\phi) D_e} \tag{58.110}$$

In Equation 58.110, d_p is the diameter of the particle, U_L is the superficial fluid velocity through the bed, and ϕ is its void fraction. More complete treatments of intraparticle mass transfer have been provided by Chisti and Moo-Young (8), Radovich (151), Willaert *et al*. (152), Pitcher (153), Bailey and Ollis (154) and Pilkington *et al*. (155). Mass transfer effects during osmotic dehydration of foods and other biological matrices have been discussed by Shi and Le Maguer (156). Mass transfer in frozen food matrices has been reviewed by Pham (157). Gervais and Beney (158) have discussed osmotic mass transfer in the yeast *Saccharomyces cerevisiae*. Combined heat and mass transfer during freezing processes such as those commonly encountered in the food industry, have been discussed by Delgado and Sun (159).

NOMENCLATURE

A	Surface area of tube (m^2)
A_d	Cross-sectional area of downcomer (m^2)
A_r	Cross-sectional area of riser (m^2)
A_s	Total solid–liquid interfacial area (m^2)
a_D	Gas–liquid interfacial area per unit volume of dispersion (/m)
a_L	Gas–liquid interfacial area per unit liquid volume (/m)
a_{Lc}	Liquid–liquid interfacial area per unit volume of continuous phase (/m)
a_s	Solid–liquid interfacial area per unit liquid volume (/m)
BOD	Biochemical oxygen demand
Bo	Bond number
C	Concentration (kg/m^3)
C^*	Saturation concentration of transferring gas or solute in liquid (kg/m^3)
ΔC	Concentration gradient (kg/m^3)
C_B	Solute or substrate concentration in bulk liquid (kg/m^3)
C_G	Concentration in the gas phase (kg/m^3)
C_{Ge}	Solute concentration in gel layer (kg/m^3)
C_{Gi}	Interfacial concentration of the diffusing component in the gas phase (kg/m^3)
C_L	Instantaneous concentration of transferring component in liquid (kg/m^3)
C_{L0}	Initial dissolved oxygen concentration at time t_0 (kg/m^3)
C_{Lc}	Equilibrium concentration of solute in continuous phase (kg/m^3)

C_{Ld}	Equilibrium concentration of solute in dispersed phase (kg/m^3)
C_{Li}	Interfacial concentration of the diffusing component in the liquid phase (kg/m^3)
C_S	Concentration of solids in slurry (% wt/vol or kg/m^3)
C_{Sb}	Substrate concentration at solid–liquid interface (kg/m^3)
C^*_{in}	Saturation concentration of oxygen in equilibrium with ingoing gas (kg/m^3)
C^*_{out}	Saturation concentration of oxygen in equilibrium with the exhaust gas (kg/m^3)
D	Diffusivity (m^2/s)
D_D	Diffusivity of dispersed phase (m^2/s)
D_e	Effective diffusivity in particle (m^2/s)
$D_{e\ ap}$	Apparent effective diffusivity in particle (m^2/s)
D_{gas}	Diffusivity of gas in liquid (m^2/s)
D_L	Diffusivity of gas or solute in liquid (m^2/s)
DMEM	Dulbecco's modified Eagle's medium
D_{oxygen}	Diffusivity of gas in liquid (m^2/s)
D_p	Diffusivity of small solute in protein solution (m^2/s)
d	Characteristic length dimension (m)
d^*	Diameter number defined by Equation 58.33
d_B	Sauter mean bubble diameter (m)
d_D	Diameter of drop (m)
d_F	Maximum diameter of flask (m)
d_H	Diameter of sparger hole (m)
d_h	Hydraulic diameter (m)
d_{hi}	Hydraulic diameter in packed bed as defined in Table 58.18 (m)
d_i	Diameter of impeller (m)
d_o	Outer diameter of tubing (m)
d_p	Diameter of particle (m)
d_r	Diameter of riser (m)
d_T	Diameter of tank or column (m)
E	Energy dissipation rate per unit mass (W/kg)
EDTA	Ethylenediaminetetraacetic acid
E_L	Overall axial dispersion coefficient of liquid (m^2/s)
e	Absolute roughness (m)
$\hat{e}$	Eccentricity of shaker platform
F	Mass flow rate of gas (kg/s)
Fr	Froude number
f	Parameter
Gr	Grashof number
g	Gravitational acceleration (m/s^2)
H	Dimensionless Henry's law constant
h	Height of channel (m)
h_D	Height of dispersion (m)
h_L	Height of gas-free liquid (m)
I	Ionic strength (kg ion/m^3)
J	Mass flux (kg/m^{2}s or kmol/m^{2}s) or permeate flux (m/s)
K	Consistency index of fluid (Pa s^n)
K_L	Overall mass transfer coefficient based on liquid film (m/s)
K_p	Mass transfer coefficient for plug (mol O_2/ atm/h)
K_p	Partition coefficient of solute defined by Equation 58.25
K_S	Mass transfer coefficient at surface (mol O_2/ atm h)
k	Mass transfer coefficient (m/s)
k_G	Gas film mass transfer coefficient (m/s)
k_i	Impeller-dependent constant in Equation 58.45
k_L	Liquid film mass transfer coefficient (m/s)
k_La_L	Overall gas–liquid volumetric mass transfer coefficient (/s)
$(k_La_L)_{r\ or\ d}$	Overall volumetric mass transfer coefficient in riser or downcomer (/s)
k_{Lc}	Liquid film mass transfer coefficient in continuous phase (m/s)
k_{Ld}	Liquid film mass transfer coefficient in dispersed phase (m/s)
L	Length of circulation loop, pipe, plate, or flow channel (m)
ℓ	Length of impeller blade (m)
M_L	Molecular weight of liquid (kg/kmol)
Mo	Morton number
N	Rotational speed (/s)
n	Flow behavior index
P	Power input (W)
PEG	Poly(ethylene glycol)
Pe	Peclet number
P_G	Gassed power input (W)
Po	Power number
Ps	Poiseuille number
p	Porosity of particle
p_{atm}	Partial pressure of oxygen in the atmosphere outside flask (atm)
p_L	Partial pressure of oxygen in liquid in flask (atm)
Q_G	Volume flow rate of gas (m^3/s)
q_{O_2}	Specific oxygen consumption rate (/s)
R	Overall rate of reaction (kg/m^3 s)
Ra	Rayleigh number
R_b	Ratio of bubble diameter to its width
Re	Reynolds number
Re_C	Reynolds number for the continuous phase
Re_d	Reynolds number based on d_{hi} as in Table 58.18
Re_G	Reynolds number of gas
Re_i	Reynolds number based on impeller

Re_L	Reynolds number of liquid
Re_t	Reynolds number based on terminal settling velocity of particle
Re_x	Local value of Reynolds number at distance x from leading edge
RPMI	Cell culture medium
Sc	Schmidt number
SDS	Sodium dodecyl sulfate
Sh	Sherwood number
Sh_x	Local value of Sherwood number at distance x from leading edge
Sh_G	Sherwood number of gas
Sh_L	Sherwood number of liquid
SLS	Sodium lauryl sulfate
St	Stanton number
T	Temperature (degree Celsius) or absolute temperature (K)
T_L	Turbulence factor defined by Equation 58.50 ($L^{-0.537}/s$)
t	Instantaneous time (s)
t_C	Contact time of droplets (s)
t_m	Mixing time (s)
t_R	Residence time of gas in liquid (s)
U_B	Bubble rise velocity (m/s)
U_G	Superficial gas velocity based on outer column cross-sectional area (m/s)
U_{Gr}	Superficial gas velocity in the riser (m/s)
U_L	Mean superficial liquid velocity in the reactor or pipe (m/s)
U_{Lr}	Superficial liquid velocity in the riser (m/s)
U_p	Velocity of particle (m/s)
U_t	Terminal settling velocity of a single particle in liquid (m/s)
V	Volume of shake flask (L)
V_L	Volume of liquid or slurry (m^3)
V_{Lc}	Volume of continuous phase (m^3)
V_M	Molar volume of solute at its boiling point (m^3/kmol)
W	Width of impeller blade (m)
We	Weber number
Wi	Weissenberg number
X	Viable biomass concentration (kg/m^3)
x	Distance (m)
x_i	Mass fraction of oxygen in inlet gas stream
x_o	Mass fraction of oxygen in exhaust gas

Greek Symbols

α	Parameter; parameter in Equation 58.72 ($m^{\beta}/s^{(\beta+1)}$)
α_M	Value of α (Eq. 58.72) in presence of static mixers ($m^{-\beta}/s^{(\beta+1)}$)
β	Parameter
γ	Parameter or shear rate (/s)
δ	Film thickness (m)
δ_G	Thickness of gas film (m)
δ_L	Thickness of liquid film (m)
δ_w	Wall thickness of tube (m)
ε_G	Overall gas holdup
ε_{Gr}	Gas holdup in the riser
ε_S	Volume fraction or holdup of solids in three-phase systems
θ	Parameter in Equation 58.79
λ	Characteristic time or relaxation time of viscoelastic fluid (s)
μ_{ap}	Apparent viscosity of non-Newtonian fluid (Pa s)
μ_C	Viscosity of the continuous phase (Pa s)
μ_D	Viscosity of the dispersed phase (Pa s)
μ_G	Viscosity of the gas (Pa s)
μ_L	Viscosity of the liquid (Pa s)
μ_{SL}	Viscosity of the slurry (Pa s)
μ_w	Viscosity of water (Pa s)
ξ	Association parameter
π	Pi
ρ_C	Density of continuous phase (kg/m^3)
ρ_D	Density of dispersed phase (kg/m^3)
ρ_G	Density of gas (kg/m^3)
ρ_L	Density of the liquid (kg/m^3)
ρ_p	Density of the particles (kg/m^3)
ρ_S	Density of solids (kg/m^3)
ρ_{SL}	Density of slurry (kg/m^3)
$\Delta\rho$	Density difference between phases (kg/m^3)
σ	Interfacial tension (liquid–liquid) (kg/s^2)
σ_L	Interfacial tension (kg/s^2)
τ	Tortuosity of pores
ϕ	Void fraction of the packed bed
ϕ_b	Voidage of settled bed
ϕ_f	Voidage of fluidized bed
ϕ_S	Volume fraction of solids in gas-free slurry
χ	Parameter

REFERENCES

1. Geankoplis CJ. Transport processes and unit operations. 3rd ed. Englewood Cliffs, NJ: Prentice Hall; 1993.
2. Pratt HRC. In: Lo TC, Baird MHI, Hanson C, editors. Handbook of solvent extraction. New York: Wiley; 1983. pp. 91–123.
3. Wilke CR, Chang P. AIChE J 1955; 1: 264–270.
4. Knudsen JG, Hottel HC, Sarofim AF, Wankat PC, Knaebel KC. In: Perry RH, Green DW, editors. Perry's chemical engineers' handbook. 7th ed. New York: McGraw-Hill; 1997. pp. 5.1–5.79.
5. Chisti Y. In: Robinson R, Batt C, Patel P, editors. Encyclopedia of food microbiology. London: Academic Press; 1999. pp. 663–674.
6. Chisti Y. Airlift bioreactors. London: Elsevier; 1989.

7. Van't Riet K. Ind Eng Chem Process Des Dev 1979; 18: 357–363.
8. Chisti Y, Moo-Young M. In: Moses V, Cape RE, editors. Biotechnology: the science and the business. New York: Harwood Academic Publishers; 1991. pp. 167–209.
9. Ortiz-Ochoa K, Doig SD, Ward JM, Baganz F. Biochem Eng J 2005; 25: 63–68.
10. Casas López JL, Rodríguez Porcel EM, Oller Alberola I, Ballesteros Martin MM, Sánchez Pérez JA, Fernández Sevilla JM, Chisti Y. Ind Eng Chem Res 2006; 45: 1167–1171.
11. Ho CS, Shanahan JF. Crit Rev Biotechnol 1986; 4: 185–252.
12. Calderbank PH, Moo-Young MB. Chem Eng Sci 1961; 16: 39–54.
13. Calderbank PH, Lochiel AC. Chem Eng Sci 1964; 19: 485–503.
14. Chisti Y, Moo-Young M. Biotechnol Bioeng 1989; 34: 1391–1392.
15. Molina Grima E, Chisti Y, Moo-Young M. J Biotechnol 1997; 54: 195–210.
16. Shi LK, Riba JP, Angelino H. Chem Eng Commun 1990; 89: 25–35.
17. Chisti Y. Appl Mech Rev 1998; 51: 33–112.
18. Chisti Y. In: Flickinger MC, Drew SW, editors. Volume 5, Encyclopedia of bioprocess technology: fermentation, biocatalysis, and bioseparation. New York: Wiley; 1999. pp. 2379–2406.
19. Chisti Y. Trends Biotechnol 2000; 18: 420–432.
20. Chisti Y. Crit Rev Biotechnol 2001; 21: 67–110.
21. Reuss M. In: Rehm H-J, Reed G, editors. Volume 3, Biotechnology. 2nd ed. Weinheim: VCH; 1993. pp. 185–217.
22. Sánchez Pérez JA, Rodríguez Porcel EM, Casas López JL, Fernández Sevilla JM, Chisti Y. Chem Eng J 2006; 124: 1–5.
23. Moo-Young M, Blanch HW. Adv Biochem Eng 1981; 19: 1–69.
24. Oolman T, Blanch HW. Crit Rev Biotechnol 1986; 4: 133–184.
25. Chisti Y. Trends Biotechnol 2003; 21: 89–93.
26. Chisti Y, Moo-Young M. J Chem Technol Biotechnol 1993; 58: 331–336.
27. Yamada S, Wada M, Chibata I. J Ferment Technol 1978; 56: 20–28.
28. Aunins JG, Henzler H-J. In: Rehm H-J, Reed G, editors. Volume. 3, Biotechnology, 2nd ed, Weinheim: VCH; 1993. pp. 219–281.
29. Gupta A, Rao G. Biotechnol Bioeng 2003; 84: 351–358.
30. Maier U, Büchs J. Biochem Eng J 2001; 7: 99–106.
31. Maier U, Losen M, Büchs J. Biochem Eng J 2004; 17: 155–167.
32. Mrotzek C, Anderlei T, Henzler HJ, Büchs J. Biochem Eng J 2001; 7: 107–112.
33. Nikakhtari H, Hill GA. Biotechnol Bioeng 2006; 95: 15–21.
34. Nikakhtari H, Hill GA. Can J Chem Eng 2005; 83: 493–499.
35. Randers-Eichhorn L, Bartlett RA, Frey DD, Rao G. Biotechnol Bioeng 1996; 51: 466–478.
36. Aunins JG, Woodson BA Jr, Hale TK, Wang DIC. Biotechnol Bioeng 1989; 34: 1127–1132.
37. Lavery M, Nienow AW. Biotechnol Bioeng 1987; 30: 368–373.
38. Kato Y, Hiraoka S, Tada Y, Sato K, Ohishi T. J Chem Eng Jpn 1997; 30: 362–365.
39. Kensy F, Zimmermann HF, Knabben I, Anderlei T, Trauthwein H, Dingerdissen U, Büchs J. Biotechnol Bioeng 2005; 89: 698–708.
40. Doig SD, Pickering SCR, Lye GJ, Baganz F. Chem Eng Sci 2005; 60: 2741–2750.
41. Betts JI, Baganz F. Microb Cell Fact 2006; 5: 21.
42. Fernandes P, Cabral JMS. Biocatal Biotransformation 2006; 24: 237–252.
43. Kilani J, Lebeault JM. Appl Microbiol Biotechnol 2007; 74: 324–330.
44. Henzler H-J, Kauling DJ. Bioprocess Eng 1993; 9: 61–75.
45. Kawase Y, Moo-Young M. Trans Inst Chem Eng 1990; 68: 189–194.
46. Perez JF, Sandall OC. AIChE J 1974; 20: 770–775.
47. Farritor RE, Hughmark GA. AIChE J 1974; 20: 1027–1028.
48. Bin KA. Chem Eng Commun 1984; 31: 155–183.
49. Chisti Y, Jauregui-Haza UJ. Biochem Eng J 2002; 10: 143–153.
50. Nielsen CHE, Kiil S, Thomsen HW, Dam-Johansen K. Chem Eng Sci 1998; 53: 495–503.
51. Spedding PL, Jones MT. Chem Eng J 1998; 37: 165–176.
52. Papoutsakis ET. Trends Biotechnol 1992; 9: 427–437.
53. Handa A, Emery AN, Spier RE. Dev Biol Stand 1987; 66: 241–253.
54. Handa-Corrigan A, Emery AN, Spier RE. Enzyme Microb Technol 1989; 11: 230–235.
55. Croughan MS, Hamel J-F, Wang DIC. Biotechnol Bioeng 1987; 29: 130–141.
56. Chisti Y. Bioprocess Eng 1993; 9: 191–196.
57. Arathoon WR, Birch JR. Science 1986; 232: 1390–1395.
58. Birch JR, Lambert K, Thompson PW, Kenney AC, Wood LA. In: Lydersen BK, editor. Large scale cell culture technology. New York: Hanser Publishers; 1987. pp. 1–20.
59. Zhang Z, Chisti Y, Moo-Young M. J Biotechnol 1995; 43: 33–40.
60. Nienow AW. Appl Mech Rev 1998; 51: 3–32.
61. Bakker A, Smith JM, Myers KJ. Chem Eng 1994; 101(12): 98–104.
62. Shin CS, Hong MS, Lee J. Biotechnol Tech 1996; 10: 679–682.
63. Ascanio G, Castro B, Galindo E. Chem Eng Res Des 2004; 82: 1282–1290.
64. Taguchi H, Yoshida T, Tomita Y, Teramoto S. J Ferment Technol 1968; 46: 814.
65. Yagi H, Yoshida F. Ind Eng Chem Process Des Dev 1975; 14: 488–493.
66. Kawase Y, Moo-Young M. Chem Eng Res Des 1988; 66: 284–288.
67. Chandrasekharan K, Calderbank PH. Chem Eng Sci 1981; 36: 819–823.
68. Shah YT, Kelkar BG, Godbole SP, Deckwer W-D. AIChE J 1982; 28: 353–379.

69. Deckwer W-D. Bubble column reactors. New York: Wiley; 1992.
70. Deckwer W-D, Schumpe A. Chem Eng Sci 1993; 48: 889–911.
71. Akita K, Yoshida F. Ind Eng Chem Process Des Dev 1973; 12: 76–80.
72. Kawase Y, Halard B, Moo-Young M. Chem Eng Sci 1987; 42: 1609–1617.
73. Dudley J. Water Res 1995; 29: 1129–1138.
74. Heijnen JJ, Van't Riet K. Chem Eng J 1984; 28: B21–B42.
75. Fair JR. Chem Eng (July 3) 1967; 74: 67.
76. Hughmark GA. Ind Eng Chem Process Des Dev 1967; 6: 218–220.
77. Nakanoh M, Yoshida F. Ind Eng Chem Process Des Dev 1980; 19: 190–195.
78. Schumpe A, Singh C, Deckwer W-D. Chem Ing Techn 1985; 57: 988–989.
79. Hikita H, Asai S, Tanigawa K, Segawa K, Kitao M. Chem Eng J 1981; 22: 61–69.
80. Deckwer W-D, Nguyen-Tien K, Schumpe A, Serpemen Y. Biotechnol Bioeng 1982; 24: 461–481.
81. Godbole SP, Schumpe A, Shah YT, Carr NL. AIChE J 1984; 30: 213–220.
82. Li G-Q, Yang S-Z, Cai Z-L, Chen J-Y. Chem Eng J 1995; 56: B101–B107.
83. Petersen EE, Margaritis A. Crit Rev Biotechnol 2001; 21: 233–294.
84. Kilonzo PA, Margaritis A. Biochem Eng J 2004; 17: 27–40.
85. Koide K, Sato H, Iwamoto S. J Chem Eng Jpn 1983; 16: 407–413.
86. Koide K, Horibe K, Kawabata H, Ito S. J Chem Eng Jpn 1985; 18: 248–254.
87. Verlaan P, Vos J-C, van't Riet K. J Chem Technol Biotechnol 1989; 45: 181–190.
88. Suh I-S, Schumpe A, Deckwer W-D. Biotechnol Bioeng 1992; 39: 85–94.
89. Koide K, Shibata K, Ito H, Kim SY, Ohtaguchi K. J Chem Eng Jpn 1992; 25: 11–16.
90. Chisti Y, Moo-Young M. Chem Eng Commun 1987; 60: 195–242.
91. Rubio FC, Garcia JL, Molina E, Chisti Y. Chem Eng Sci 1999; 54: 1711–1723.
92. Rubio FC, Garcia JL, Molina E, Chisti Y. Chem Eng J 2001; 84: 43–55.
93. Russell AB, Thomas CR, Lilly MD. Bioprocess Eng 1995; 12: 71–79.
94. Pollard DJ, Ison AP, Shamlou PA, Lilly MD. In: Galindo E, Ramírez OT, editors. Advances in bioprocess engineering. Dordrecht: Kluwer; 1994. pp. 163–170.
95. Chisti Y, Moo-Young M. Chem Eng Progress 1993; 89(6): 38–45.
96. Koide K, Horibe K, Kitaguchi H, Suzuki N. J Chem Eng Jpn 1984; 17: 547–549.
97. Chisti Y, Kasper M, Moo-Young M. Can J Chem Eng 1990; 68: 45–50.
98. Zhou W, Holzhaur-Rieger K, Schügerl K. J Biotechnol 1993; 28: 165–177.
99. Thakur RK, Vial C, Nigam KDP, Nauman EB, Djelveh G. Chem Eng Res Des 2003; 81: 787–826.
100. Audet J, Thibault J, LeDuy A. Biotechnol Bioeng 1996; 52: 507–517.
101. Lounes M, Audet J, Thibault J, LeDuy A. Bioprocess Eng 1995; 13: 1–11.
102. Ni X, Gao S, Pritchard DW. Biotechnol Bioeng 1995; 45: 165–175.
103. Grima EM, Fernández FGA, Camacho FG, Chisti Y. J Biotechnol 1999; 70: 231–247.
104. Grima EM, Fernández J, Fernández FGA, Chisti Y. J Biotechnol 2001; 92: 113–131.
105. Fernández FGA, Sevilla JMF, Pérez JAS, Grima EM, Chisti Y. Chem Eng Sci 2001; 56: 2721–2732.
106. Ziegler H, Dunn IJ, Bourne JR. Biotechnol Bioeng 1980; 22: 1613–1635.
107. VandenHeuvel JC, Verschuren PG, Ottengraf SPP. Water Sci Technol 1997; 36: 311–319.
108. Muroyama K, Fan L-S. AIChE J 1985; 31: 1–34.
109. Nguyen-Tien K, Patwari AN, Schumpe A, Deckwer W-D. AIChE J 1985; 31: 194–201.
110. Loh VY, Richards SR, Richmond P. Proceedings: international conference on bioreactor fluid dynamics. Cambridge, England: BHRA; 1986. 15–17 April.
111. Smith BC, Skidmore DR. Biotechnol Bioeng 1990; 35: 483–491.
112. Karamanev DG, Nagamune T, Endo I. Chem Eng Sci 1992; 47: 3581–3588.
113. Winkler MA. Biological treatment of waste-water. Chichester: Ellis Horwood; 1981.
114. Sittig W. J Chem Technol Biotechnol 1982; 32: 47–58.
115. Schügerl K. Solvent extraction in biotechnology: recovery of primary and secondary metabolites. New York: Springer-Verlag; 1994.
116. Martin S, Soucaille P, Condoret J-S. Bioprocess Eng 1995; 13: 293–300.
117. Dumont E, Delmas H. Chem Eng Process 2003; 42: 419–438.
118. Save SS, Desai RB, Sawant SB, Joshi JB. Trans Inst Chem Eng 1996; 74C: 171–177.
119. Chisti Y. In: Flickinger MC, Drew SW, editors. Encyclopedia of bioprocess technology, vol. 5. New York: Wiley; 1999. pp. 2446–2462.
120. Rahardjo YSP, Tramper J, Rinzema A. Biotechnol Adv 2006; 24: 161–177.
121. Mitchell DA, von Meien OF, Krieger N, Dalsenter FDH. Biochem Eng J 2004; 17: 15–26.
122. Edwards DK, Denny VE, Mills AF. Transfer processes. New York: Holt, Rinehart and Winston; 1973.
123. Dwivedi PN, Upadhyay SN. Ind Eng Chem Process Des Dev 1977; 16: 157–165.
124. Larachi F, Belfares L, Iliuta I, Grandjean BPA. Ind Eng Chem Res 2003; 42: 222–242.
125. Wang GQ, Yuan XG, Yu KT. Ind Eng Chem Res 2005; 44: 8715–8729.
126. Li Q, Grandmaison EW, Hu CC, Taylor D, Goosen MFA. Bioseparation 1995; 5: 189–202.
127. Miyabe K, Guiochon G. J Sep Sci 2003; 26: 155–173.
128. Carta G, Ubiera AR, Pabst TM. Chem Eng Technol 2005; 28: 1252–1264.

129. Lee Y-K, Hing H-K. Appl Microbiol Biotechnol 1989; 31: 298–301.
130. Tutunjian RS. Biotechnology 1985; 3: 615–626.
131. Ripperger S. Chem Eng Technol 1988; 11: 17–25.
132. Mulder MHV. In: Noble RD, Stern SA, editors. Membrane separations technology: principles and applications. Amsterdam: Elsevier; 1995. pp. 45–84.
133. Ho WSW, Sirkar KK, editors. Membrane handbook. New York: Van Nostrand Reinhold; 1992.
134. Brindle K, Stephenson T. Biotechnol Bioeng 1996; 49: 601–610.
135. Kawase Y, Shenoy AV, Wakabayashi K. Can J Chem Eng 1994; 72: 798–804.
136. Hardin MT, Howes T, Mitchell DA. J Biotechnol 2002; 97: 89–101.
137. Barrera-Cortes J, Manilla-Perez E, Poggi-Varaldo HM. Bioprocess Biosyst Eng 2006; 29: 391–398.
138. Nagaoka H. Water Sci Technol 1997; 36: 329–336.
139. Kondjoyan A. Int J Refrigeration 2006; 29: 863–875.
140. Mao HH, Chisti Y, Moo-Young M. Chem Eng Commun 1992; 113: 1–13.
141. Deckwer W-D, Schumpe A. Ger Chem Eng 1984; 7: 168–177.
142. Hempel DC. In: Finn RK, Präve P, Schlingmann M, Crueger W, Esser K, Thauer R, Wagner F, editors. Biotechnology focus 1: fundamentals, applications, information. New York: Hanser; 1988. pp. 51–94.
143. Pangarkar VG, Yawalkar AA, Sharma MM, Beenackers AACM. Ind Eng Chem Res 2002; 41: 4141–4167.
144. Sänger P, Deckwer W-D. Chem Eng J 1981; 22: 179–186.
145. Goto S, Matsumoto Y, Gaspillo P. Chem Eng Commun 1989; 85: 181–191.
146. Kushalkar KB, Pangarkar VG. Chem Eng Sci 1994; 49: 139–144.
147. Gaspillo PD, Goto S. J Chem Eng Jpn 1991; 24: 680–682.
148. Yusuf R, Melaaen MC, Mathiesen V. Chem Eng Technol 2005; 28: 13–24.
149. Schmidt S, Büchs J, Born C, Biselli M. Chem Eng Sci 1999; 54: 829–839.
150. Goldstein L. Meth Enzymol 1976; 44: 397–443.
151. Radovich JM. Enzyme Microb Technol 1985; 7: 2–10.
152. Willaert RG, Baron GV, De Backer L, editors. Immobilised living cell systems: modelling and experimental methods. Chichester: Wiley; 1996.
153. Pitcher WH Jr. Adv Biochem Eng 1978; 10: 1–26.
154. Bailey JE, Ollis DF. Biochemical engineering fundamentals. 2nd ed. New York: McGraw-Hill; 1986. pp. 204–220.
155. Pilkington FH, Margaritis A, Mensour NA. Crit Rev Biotechnol 1998; 18: 237–255.
156. Shi J, Le Maguer M. Food Rev. Int. 2002; 18: 305–335.
157. Pham QT. Int J Refrigeration 2006; 29: 876–888.
158. Gervais P, Beney L. Cell Mol Biol 2001; 47: 831–839.
159. Delgado AE, Sun DW. J Food Eng 2001; 47: 157–174.

59

OXYGEN TRANSFER RATE DETERMINATION METHODS

Felix Garcia-Ochoa and Emilio Gomez
Dept. Ingenieria Quimica, Facultad Quimicas, Universidad Complutense, Madrid, Spain

59.1 INTRODUCTION

A properly designed bioreactor must provide a controlled environment and a concentration of nutrients sufficient to achieve optimal cell growth allowing the formation of products, either biomass or a metabolite or the substrate, under fixed specifications. Several phases are involved in the bioprocesses: the substrates, nutrients, and products must be transferred from one phase to the other therefore, mass transfer between phases may often become the limiting step of the overall process rate and be a relevant factor in scale-up. Mixing, by aeration and agitation, is used to improve mass transfer and also to insure homogeneous distribution of the nutrients in the liquid phase. Hence, gas–liquid contact is a matter of decisive importance for the design, scale-up, and operation of bioreactors to carry out bioprocesses. This is true not only in aerobic systems, where oxygen transport from the air is necessary and obviously focused, but also in the case of anaerobic systems where the transport of other gases such as methane or carbon dioxide usually takes place.

Oxygen is one of the most important nutrients for aerobic cells that need oxygen dissolved in the broth for maintenance, growth and production of bioproducts. Due to its low solubility in broths, which are usually aqueous solutions (approximately 9 ppm at 25°C and 1 atm in pure water), oxygen must be continuously supplied by a gas phase (air or oxygen) with the purpose of achieving acceptable productivities, independent of the physical operational modes (batch, semi-batch, and continuous cultures). Frequently, in aerated bioreactors the critical limiting factor to providing the optimal environment is the oxygen transfer rate (OTR).

In shake flask scale, oxygen transport is accomplished by the rotary or reciprocating action of a shaker apparatus. In laboratory and pilot scales, oxygen is generally supplied by compressed air and distributed by a gas sparging, and mechanical devices are used to improve mixing of the broth for better distribution of gas bubbles and to rupture large bubbles into small ones, obtaining a large interfacial area. Thus in mechanically stirred-tank bioreactors, the impeller is the main gas-dispersing tool and stirrer speed and its design both have a pronounced effect on OTR. In this type of bioreactor, it is possible to alter the stirrer speed and thereby allowing a greater flexibility to deal with rheological changes in the medium. Mechanical agitation is however restricted by biological constraints, because the cells may be damaged by hydrodynamics stress when agitation and/or aeration are too vigorous.

In order to avoid mechanical agitation and to obtain a sufficiently high OTR to ensure that dissolved oxygen (DO) concentration can be maintained above a critical level, others types of bioreactors have been extended, the majority of which are pneumatically stirred bioreactors (bubble columns and airlifts). In these bioreactors, the supply of oxygen depends mainly on aeration, which is also responsible for the homogenization of the medium and for sweeping out the carbon dioxide and any volatile by-products formed, and therefore the system is less flexible than the mechanically stirred bioreactor. The main advantages of airlifts over bubble columns are the improved mixing and the increase of OTR.

Consequently, there are diverse ways of achieving a sufficient OTR in bioreactors. Hydrodynamics conditions and energy dissipated into bioreactor play an important

Upstream Industrial Biotechnology: Equipment, Process Design, Sensing, Control, and cGMP Operations, Volume 2, First Edition. Edited by Michael C. Flickinger.
© 2013 John Wiley & Sons, Inc. Published 2013 by John Wiley & Sons, Inc.

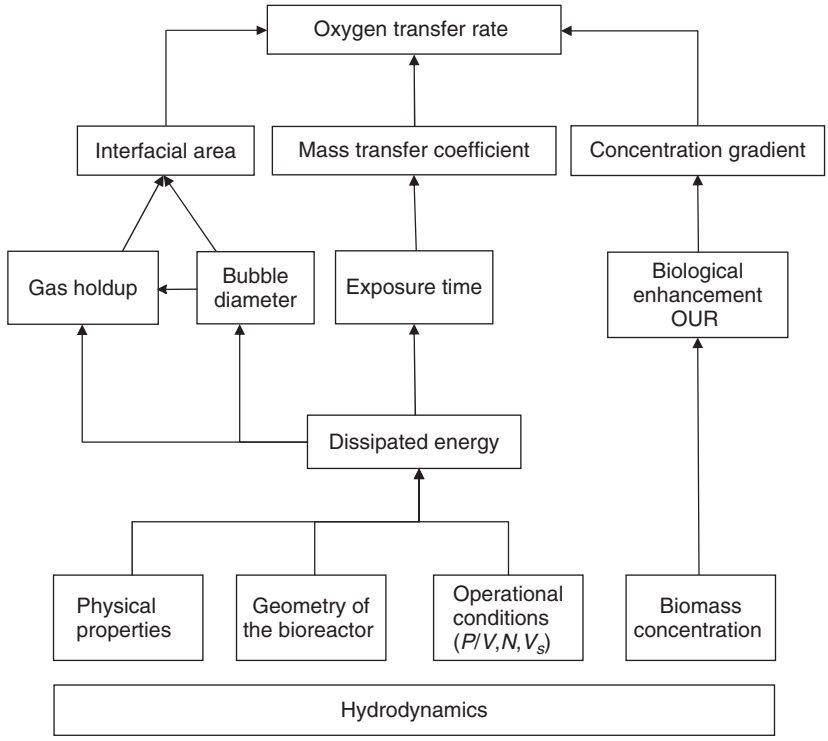


Figure 59.1. Factors influencing oxygen transfer rate at several levels in bioreactors. [Adapted from Garcia-Ochoa and Gomez (1).]

role because different phenomena are simultaneously taking place; also the relative importance of these phenomena changes with the scale, the type of bioreactor and so on. The interrelationship between factors influencing OTR is shown in Fig. 59.1.

Nonconventional methods for enhancing the oxygen supply to broth include introduction of chemicals (surfactants) (2,3), of an immiscible phase of inert hydrocarbons (4,5) or perflurocarbons with high oxygen solubility (6); coimmobilization or mixed culture of an oxygen-production photosynthetic alga (7,8); and by raising the oxygen partial pressure in the gas phase, using oxygen-enriched air (9) or increasing the pressure in the bioreactor head space (10).

Extensive literature on OTR in bioreactors is available and a considerable part of it has been published in recent years. Chapters of encyclopedias and books (11–14), several reviews (1,15–21), and many papers deal with different aspects of this phenomenon in stirred tanks (4,5,22–26), bubble columns, and airlifts (27–35). This chapter is devoted to the description of OTR in aerated bioreactors and to the different experimental techniques for the determination of k_La (the volumetric mass transfer coefficient). This information will be useful for better understanding the importance of OTR in aerobic microbial processes as well as for searching for better operational conditions for oxygen transfer and scale-up in bioreactors.

59.1.1 Oxygen Transfer Rate Description

Bioreactors carrying out microbial processes are gas–liquid–solid systems. In an aerated bioreactor, the oxygen is transferred from a gas bubble into a liquid phase, where it is taken up by the microorganism (which can be considered as a solid particle), and ultimately transported to the site of oxidative phosphorylation inside the cell. This transport can be represented by a number of steps and mass transfer resistances (36) at the following localization (schematized in Fig. 59.2): (r_1) transport from the interior of the bubble to the gas–liquid film; (r_2) movement at the gas–liquid interface; (r_3) diffusion in the liquid film surrounding the bubble; (r_4) transport in the bulk liquid; (r_5) diffusion through the relatively stagnant liquid film surrounding the cells; (r_6) movement across the liquid–solid interface and in the case of multicellular aggregates or solid particle, diffusion through the solid to the individual cell; (r_7) transport through the cytoplasm (r_8) at sites where biochemical reactions, involving oxygen consumption and production of carbon dioxide, take place.

It should be stressed that steps (r_1) to (r_7) correspond to physical phenomena that are in principle better known and easier to describe than biochemical phenomena and step (r_8), which is a complex reaction network. Not all these resistances are significant. Because oxygen is only slightly soluble in water, it can often be assumed that no

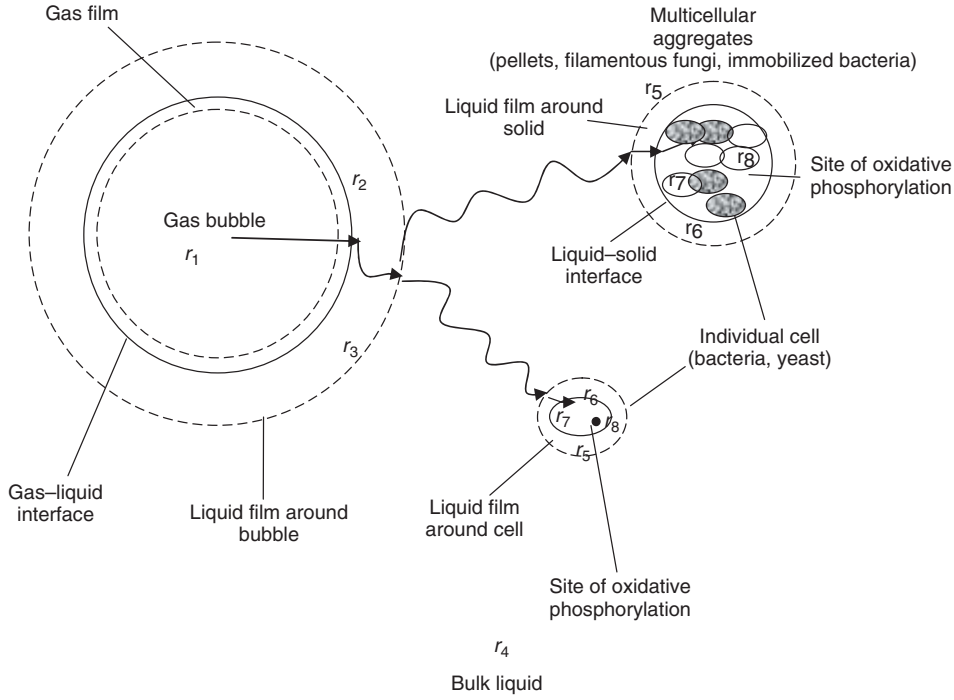


Figure 59.2. The pathway for transport of oxygen from gas bubble to cell in a bioreactor. [Adapted from Blanch and Clark (36).]

mass transfer limitation is observed within the gas phase. Provided that the liquid is well-mixed, transport through the bulk liquid is generally rapid and may be neglected as well. The resistance in the liquid film around the organism can be neglected since the organism (bacterium or yeast cell) is relatively small and thus, only an extremely small driving force is necessary to transport oxygen from the bulk liquid into the organism. Finally, in packed organisms (e.g. molds in pellet form, filamentous mycelia or immobilized bacteria) with a size comparable to that of a bubble, resistance in the liquid film surrounding the solid may dominate; also, the intraparticle resistance resulting from diffusion and oxygen consumption within the solid particles must be considered, but that is beyond the scope of this chapter. Intracellular oxygen transfer resistance must be negligible because of the short distances involved. The liquid film resistances around bubbles usually control the overall mass transfer rate and the oxygen transport problem is thus reduced to that of gas–liquid interfacial mass transfer (22,36).

The simplest theory on mass transfer is the two-film model (37) and usually the gas–liquid mass transfer rate is modeled according to this theory. In this model, the resistance to mass transfer in each phase is localized in the thin layer close to the interface, which is assumed to offer no resistance to transport. Mass transfer through the stagnant film of liquid around the bubble is transferred by molecular diffusion along a concentration gradient that can be assumed to be linear, as shown schematically in Fig. 59.3. In the steady state, the molar oxygen flux, J_0, through each of the two films, can be expressed as the product of the driving force times the mass transfer coefficient according to

$$J_0 = k_G \cdot (p_G - p_i) = k_L \cdot (C_i - C_L) \tag{59.1}$$

where k_G and k_L, are the local gas- and liquid-phase mass transfer coefficients, respectively; p_G is the oxygen partial pressure in the gas phase; and C_L the oxygen concentration in the liquid phase; index i refers to same magnitudes at the gas–liquid interface.

Considering Henry's law, an overall volumetric mass transfer coefficient can be used which includes the gas and liquid film resistances according to

$$J_0 = K_G \cdot (p_G - p^*) = K_L \cdot (C^* - C_L) \tag{59.2}$$

where K_G and K_L are the overall gas- and liquid-phase mass transfer coefficients, respectively; p^* is the oxygen pressure in equilibrium with liquid phase; C^* is the saturation oxygen concentration in the bulk liquid in equilibrium to the partial pressure of oxygen in the gas phase.

Combining Equations 59.1 and 59.2, the following relationship is obtained:

$$\frac{1}{K_L} = \frac{1}{H_e k_G} + \frac{1}{k_L} \tag{59.3}$$

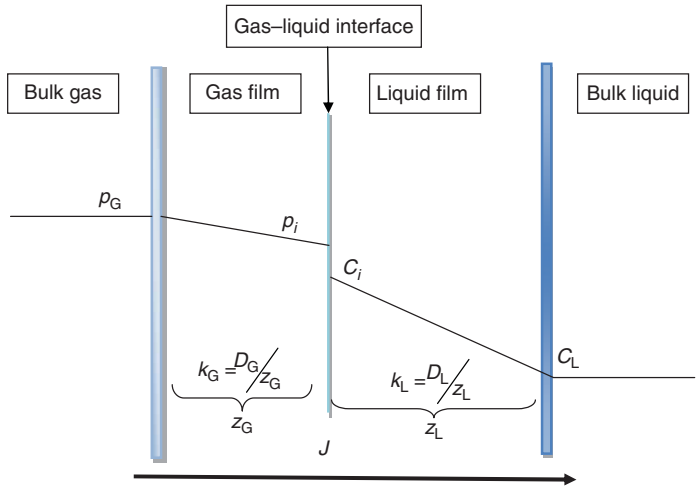


Figure 59.3. Schematic representation of the gas–liquid interface, concentrations, and mass transfer coefficients according to two-film theory. (This figure is available in full color at http://onlinelibrary.wiley.com/book/10.1002/9780470054581.)

where H_e is the Henry constant. This last equation represents the additive contribution of gas- and liquid-film resistances. Taking into account that H_e is very large for oxygen, it is commonly accepted that the greatest resistance for mass transfer is on the liquid side of the interface and the gas-phase resistance can usually be neglected and $K_L \approx k_L$.

The OTR is obtained by multiplying the flux by the gas–liquid interfacial area per unit of liquid volume, a:

$$\text{OTR} = a \cdot J_0 = k_L a \cdot (C^* - C_L) \qquad (59.4)$$

where $k_L a$ is the volumetric mass transfer coefficient.

Equation 59.4 implies that essentially all resistance to oxygen transfer is located at the interface in the liquid film and that OTR is dependent on the mass transfer coefficient, the gas–liquid interfacial area, and the gradient between the concentration of the oxygen at the interface and concentration in the bulk liquid (average concentration). The maximum value of the concentration gradient is limited due to the low solubility of oxygen. Therefore, the maximum OTR from the gas to the liquid in the bioreactor can be estimated by the product $k_L a C^*$. Gas solubility is mainly dependent on the temperature, pressure, concentration, and presence of salts and organic solutes (38). The gas solubility, in electrolyte solutions and organic solutes, is usually smaller than the gas solubility in pure water (solubility data are available in handbooks). As fermentation broths contain different salts, substrates, products and surfactants, reduction in OTR must be considered. Some of these effects are shown in Fig. 59.4 as an example. Due to the difficulty of measuring k_L and a separately, usually the product $k_L a$ is experimentally determined, and this parameter characterizes the transport from gas to liquid phase. Some of the measuring methods of oxygen transfer are applied to other gases, as well. To quantify the OTR for another gas, the relationship between the volumetric mass transfer coefficients and the diffusion coefficients for two different compounds can be employed according to

$$\frac{k_L a(\text{O}_2)}{k_L a(\text{gas})} = \frac{D_{\text{LO}_2}}{D_{\text{Lgas}}} \qquad (59.5)$$

The above relationship indicates a direct proportionality between the volumetric mass transfer coefficient and the diffusion coefficient and it applies when the transfer can be ascribed to the mechanism of the two-film model. Using other models, such as the penetration theory or the surface renewal theory, a direct proportionality is not obtained. However, since the ratio of the diffusion coefficients is close to 1, the error from using Equation 59.5 is small. The correction is satisfactory only for mass transfer for identical liquids under identical hydrodynamic conditions and the diffusion coefficients used for the correction should be at the same temperature as the $k_L a$ data.

The transport and the consumption of oxygen have usually not been described together, and have often been measured in different ways in the past. However, now it is usual to obtain both experimental values using the same technique, that is simultaneous determination of both, OTR (or $k_L a$) and oxygen uptake rate (OUR) in the same experiment.

59.2 EXPERIMENTAL DETERMINATION OF $k_L a$

There are several approaches to determine OTR in bioreactors. The most common methods can be classified

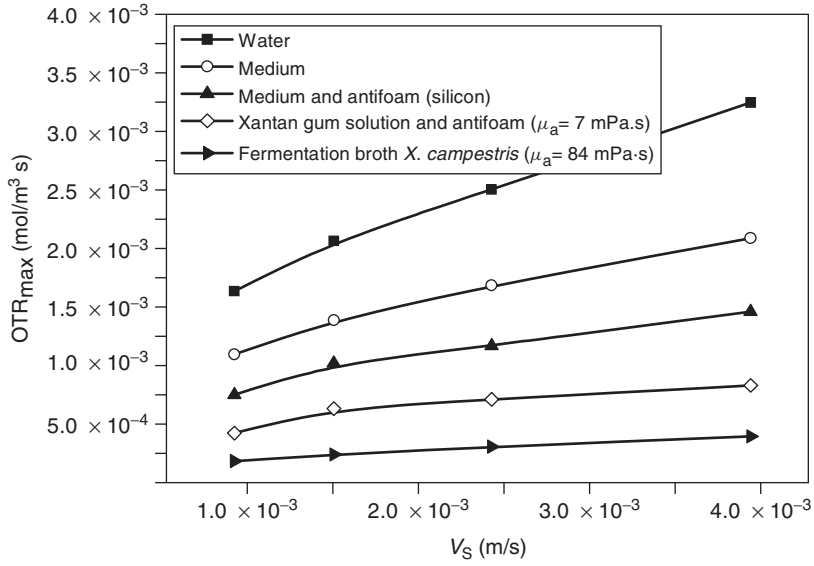


Figure 59.4. Comparison of oxygen transfer rate in different aqueous solutions for a 2 L bioreactor, and a stirrer speed of 350 rpm. Adapted from Garcia-Ochoa and Gomez (39).

depending on whether the determination is realized in the absence of microorganisms or with dead cells (chemical and physical methods) or in the presence of biomass that consumes oxygen at the same time that the measurement is carried out (biological methods). Chemical and biological methods require a reaction in the liquid phase to reduce the DO concentration to a level below saturation. In chemical methods it is usually a chemical oxidation, and in biological methods it is cellular respiration.

When selecting a method, several factors must be taken into account, mainly (i) the bioreactor type and its mechanical design, (ii) the aeration and mixing of the system (iii) the flow characteristics of gas and liquid phases, (iv) the composition of the fermentation medium, and (v) the type of microorganism and its morphology, due to the possible effect on measurements.

Whatever the method used for the experimental determination of $k_L a$, data generation is basically the same: the measured variable (usually oxygen concentration) is compared to the value predicted by a mathematical model that includes $k_L a$ as a parameter. It is thus obvious that the choice of the model is very important, and poor assumptions on flow characteristics of gas or liquid phases may lead to errors and deviations from the true values. All the models are a simplified description of the system and, therefore, $k_L a$ is not a property of the system, but a parameter of the model adopted (13).

The oxygen mass balance in the assumed well-mixed liquid phase can be written as

$$\frac{dC_L}{dt} = K_L a \cdot (C^* - C_L) - q_{O_2} \cdot C_X \qquad (59.6)$$

where dC_L/dt is the accumulation of oxygen in the liquid phase, the first term on the right-hand side is the OTR and the second term is the OUR. This last term is usually expressed by the product of the specific OUR of the microorganism, q_{O_2}, and the biomass concentration, C_X.

When biochemical reactions do not take place, OUR $= 0$, and the oxygen mass balance in the liquid phase can be simplified to

$$\frac{dC_L}{dt} = k_L a \cdot (C^* - C_L) \qquad (59.7)$$

Many methods for OTR determination are based on Equations 59.6 and 59.7 and different techniques from measuring the DO concentration can be used. Only the more useful and common chemical, physical, and biological methods will be examined here.

59.2.1 Chemical Methods

Chemical methods require a reaction in the liquid phase that consumes oxygen at a rate which is sufficiently fast so that transport of oxygen from the gas to the liquid phases through the liquid film around the gas bubbles is the limiting step of the overall process rate. Consequently, these methods cannot be applied to actual microbial processes. When a chemical is added to the system, there is the question of whether the addition has provoked changes in the physicochemical properties of the media, which have thus become different from the properties of the original system.

59.2.1.1 Sulfite Oxidation Method. This method is based on the reaction of sodium sulfite, a reducing agent, with the dissolved oxygen to produce sulfate, in the presence of a catalyst, usually a divalent cation (40); sulfite is oxidized according to the following equation:

$$2SO_4^{2-} - O_2 - 2SO_3^{2-} = 0 \qquad (59.8)$$

The kinetics of the sulfite oxidation is independent of the reactant concentration and sufficiently fast so as to assume that the overall rate is limited by OTR. The experimental procedure consists in first filling the bioreactor with sodium sulfite solution containing Co^{2+}, sparging the liquid with air, and allowing the oxidation reaction to continue for some minutes; after that, the air flow and the agitation are stopped and samples of the solution are removed at intervals of time. The concentration of nonreacted sulfite is determined by reaction of the sulfite in each sample with an excess of standard iodine reagent:

$$SO_4^{2-} + 2H^+ + 2I^- - SO_3^{2-} - I_2 - H_2O = 0 \qquad (59.9)$$

The amount of residual sulfite can also be estimated indirectly by the stoichiometry of the reaction (10) based on colorimetric determination of the iodine concentration (10) or by back-titration of the iodine with standard sodium thiosulfate solution ($Na_2S_2O_3$) to a starch indicator end point according to the following equation:

$$S_4O_6^{2-} + 2I^- - 2S_2O_3^{2-} - I_2 = 0 \qquad (59.10)$$

With respect to oxygen, the following balance can be written for a well-mixed liquid phase:

$$k_La(C^* - C_L) \cdot V - r \cdot V = 0 \qquad (59.11)$$

Once the sulfite concentration is measured versus time, the reaction rate is determined from the rate of sulfite disappearance, according to

$$-\frac{dC_{Na_2SO_3}}{dt} = 2 \cdot r \qquad (59.12)$$

The DO concentration in the bulk liquid C_L, will be essentially zero if the reaction rate is fast enough and k_La is calculated by measuring the observed reaction rate:

$$-\frac{dC_{Na_2SO_3}}{dt} = 2k_LaC^* \qquad (59.13)$$

This method is relatively easy to carry out and has been extensively used in the past but it has a number of drawbacks and several assumptions are involved in determining k_La in this way. First, the rate of reaction is assumed to be zero order with respect to sulfite concentration and catalyzed by heavy metal ions, usually Co^{2+}; the concentration of these ions must be kept carefully within narrow boundaries (5×10^{-6} M) in order to obtain an adequate reaction rate and avoid OTR enhancement due to the chemical reaction. Second, the physicochemical properties of the solution must be assumed to approximate the properties of the fermentation broth; this is an important limitation because some of its properties are very different from those of fermentation broths. The hydrodynamics of the solution is changed, mainly due to the influence on bubble size. This change makes k_La values obtained by this method bigger than those obtained by other techniques.

Linek and Vacek (41) and Ruchti *et al*. (42) have reviewed the use of the sulfite oxidation method, and its capacity for accurately determining mass transfer characteristics. This method has been criticized because the reaction rate is a complex function of the catalyst concentration (it is strongly dependent on the concentration and purity of the sulfite and catalyst employed) and the operational conditions that must be controlled in order to obtain reproducible measurements. However, the method has proved to be valuable in characterizing and comparing different aeration systems.

59.2.1.2 Chemical Absorption of Carbon Dioxide. The k_La can also be found by determination of mass transfer of carbon dioxide in different solutions. This method is similar, in principle, to the sulfite oxidation procedure.

59.2.1.2.1 Absorption in an Alkaline Solution. The technique involves the absorption of carbon dioxide in an alkaline solution (43). Carbon dioxide is considerably more soluble than oxygen and dissolution in water is more complex because of the liquid-phase reactions of CO_2. Alkaline solutions of CO_2 in water undergo two chemical reactions:

$$HCO_3^- - CO_2 - OH^- = 0 \qquad (59.14)$$

$$HCO_3^- + H^+ - CO_2 - H_2O = 0 \qquad (59.15)$$

According to Danckwerts (44), the reaction expressed by Equation 59.14 is of second order kinetics:

$$r = k \cdot C_{CO2} \cdot C_{OH^-} \qquad (59.16)$$

where the constant rate, k, takes a value of 5×10^3 L/mol/s (at 20°C).

On the other hand, Reaction 15 has a first-order kinetic equation:

$$r' = k' \cdot C_{CO_2} \qquad (59.17)$$

where the constant rate, k', takes a value of $2 \cdot 10^{-2} s^{-1}$ (at 20°C).

Therefore, in any solution in which the C_{OH}^- is higher than 10^{-4} mol/L (pH > 10), the rate of Reaction 59.14 will have a kinetic constant of pseudo-first order of, at least, 0.5 s^{-1}, 25 times higher than the kinetic constant of Equation 15. Therefore, it can be assumed that Reaction 15 is the limiting step controlling the absorption rate of carbon dioxide in alkaline solutions under pH > 10.

In order to be able to apply this method, it is necessary to work with a reaction of first order, whereas Reaction 59.14 is of second order. However, for gases in which the partial pressure of CO_2 is not high, the reaction behaves like one of pseudo-first order (45) and the mass transfer coefficient can be obtained from

$$-\frac{1}{2}\frac{dC_{CO2}}{dt} = k_L a \cdot C^* \sqrt{k \cdot C_{CO_2}} \tag{59.18}$$

In principle, this method uses a reaction more easily controllable than the sulfite oxidation technique. Nevertheless, it has disadvantages similar to the previous method, due to the need for using high concentrations of the ion OH^- that inhibits the coalescence of the bubbles and other reaction conditions need to be controlled to ensure that the reaction rate does not enhance the mass transfer rate.

59.2.1.2.2 Dynamic Measurement of pH. The change of pH by constant bubbling flow of carbon dioxide into the reactor can be used for measuring the overall mass transfer coefficient of carbon dioxide, as well. Upon dissolution in water, CO_2 undergoes three chemical reactions:

$$H_2CO_3 - CO_2 - H_2O = 0 \tag{59.19}$$

$$HCO_3^- + H^+ - H_2CO_3 = 0 \tag{59.20}$$

$$CO_3^{2-} + H^+ - HCO_3^- = 0 \tag{59.21}$$

The rates of reactions of Equations 59.19 and 59.21 are much faster than Reaction 20, which would be the rate-limiting reaction step determining the absorption rate of CO_2. Its equilibrium constant, K_1, is given by

$$K_1 = \frac{C_{H^+} C_{HCO_3^-}}{C_{H_2CO_3}} \tag{59.22}$$

The change of carbonic acid concentration (CO_2 and H_2CO_3 species) into liquid phase in a well-mixed reactor can then be modeled according to Hill (46):

$$\frac{dC_{H_2CO_3}}{dt} = k_L a \cdot \left(C^*_{H_2CO_3} - C_{H_2CO_3}\right) \cdot \left(1 - \frac{K_1}{K_1 + \left(K_1 \cdot C_{H_2CO_3}\right)^{1/2}}\right) \tag{59.23}$$

where $C^*_{H_2CO_3}$ represents the saturation carbonic acid concentration in the liquid phase.

Therefore, the following balance can be established:

$$C_{H^+} = C_{OH^-} + C_{HCO_3^-} + 2C_{CO_3^{2-}} \tag{59.24}$$

An equilibrium analysis shows that the CO_3^{2-} concentration is negligible for all partial pressure of CO_2 and taking into account that solution becomes acid, the OH^- concentration can also be overlooked. Under these conditions:

$$C_{H^+} \cong C_{HCO_3^-} \tag{59.25}$$

Since there is a simple relationship between carbonic acid and protons concentration, Equation 59.23 can be solved from the pH dynamics when carbon dioxide is bubbled into the reactor.

The experimental procedure consists in initially filling the bioreactor with water which is then brought to the correct temperature and stirring speed. At time zero, the gas flow is connected to the reactor and pH data are collected until a constant pH value is achieved. The pH probe response can affect the correct determination of the mass transfer coefficient if the time characteristic of the carbon dioxide transport is of the same order as the time response of the electrode.

59.2.1.3 Hydrazine Oxidation. Other techniques based on a chemical reaction have been proposed for measuring OTR, which improve some aspects of the above methods. One of them is hydrazine oxidation according to the following equation:

$$N_2 + 2H_2O - N_2H_4 - O_2 = 0 \tag{59.26}$$

In order to determine $k_L a$, a steady flow of hydrazine is fed into the bioreactor for maintaining a constant DO concentration. At steady state, the amount of hydrazine consumed per unit time equals the oxygen absorption rate

$$F_{Hy} - F_{O_2} = 0 \tag{59.27}$$

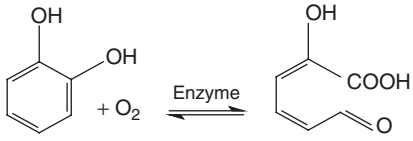
and $k_L a$ can be calculated from

$$k_L a = \frac{F_{Hy}}{V \cdot \Delta C_L} \tag{59.28}$$

Since at ambient temperature the hydrazine oxidation rate is very low, a catalyst is required. Onken *et al*. (47) developed a method based on homogeneous catalysis by several heavy metal complexes (Co, Cu, and Ni) and found that copper tetrasulfophthalocyanine (10^{-5} to 10^{-4} mol/L) was the best catalyst among those employed for $k_L a$ determination.

The applicability of this method is greater than others based on chemical reactions. The reaction rate is slow and it takes place in the liquid bulk, avoiding acceleration of oxygen uptake due to the chemical reaction. Hydrazine, a toxic chemical, is not accumulated. Thus this technique is more suitable for the k_La determinations in coalescing systems, because the reaction does not produce any ionic species which impact coalescence behavior, and the product is not accumulated.

59.2.1.4 Bio-oxidation of Catechol. The method involves the oxidation reaction of catechol forming 2-hydroxymuconic semialdehyde (2-HS) catalyzed by the enzyme catechol-2,3-dioxygenase, according to



(59.29)

If the enzyme concentration is in excess and the reaction rate is fast enough ($C_L = 0$), the kinetics of the biooxidation rate is zero order, and then the rate at which the product is formed will be equal to the OTR. With this assumption, k_La can be determined by measuring the rate of formation of brightly colored 2-HS, according to

$$\frac{dC_{2-HS}}{dt} = k_La \cdot C^* \tag{59.30}$$

The biooxidation of catechol is rapid and does not require any assumptions about its kinetic equations, but is limited to the evaluation of k_La in small-scale devices. Unlike sulfite oxidation, the biooxidation of catechol is controllable, kinetically robust, and simple to perform and yields similar k_La values when compared to the physical dynamic gassing-out method (48).

59.2.2 Physical Methods

The physical methods are based on the measurement of the oxygen concentration in the liquid or the exhaust gas during the absorption or desorption experiments in the absence of microorganisms (or nonrespiring systems that imitate the fermentation broth) under the unsteady state. The methods differ in the procedure of gas interchange (49–52), in the gas used (53), and in the model for the gas-phase description (54,55). Those methods based on the measurement of response of the DO probe during the absorption of oxygen in the solution are now the most commonly used methods of OTR determination.

59.2.2.1 Classical Dynamic Methods. The well-known dynamic techniques are based on oxygen mass balance in the liquid phase under unsteady-state conditions. After a step-change in the concentration in the inlet gas, the dynamic change in the DO concentration is analyzed. If the liquid phase is perfectly mixed and no chemical reaction takes place, Equation 59.7 can be integrated, yielding:

$$\ln \frac{C^* - C_{L1}}{C^* - C_{L2}} = k_La \cdot (t_2 - t_1) \tag{59.31}$$

where C_{L1} and C_{L2} are DO concentration at the beginning of experiment and at time t_1, t_2, respectively.

The dynamic desorption technique consists in supplying air until the saturation of oxygen concentration in the liquid is reached. Then, nitrogen is introduced downwards into the vessel and the decreasing DO concentration is recorded as a function of time. Under these conditions: $C_{L1} = C_{L0}$ at $t_1 = 0$, and from Equation 59.31, C_L can be expressed as

$$C_L = C_{L0} \cdot e^{-k_La \cdot t} \tag{59.32}$$

However, the most widely used dynamic technique is gassing out. The DO is first removed from the bioreactor by gassing out with nitrogen until the oxygen concentration falls to zero. The nitrogen flow is then stopped and bubbles are allowed to separate from the liquid. When the bioreactor has reached a hydrodynamic steady state, the system is then aerated and the increasing DO concentration, C_L, is measured as a function of time until the fluid becomes nearly saturated with oxygen. Now $C_{L1} = 0$ at $t_1 = 0$, and Equation 59.31 can be expressed as

$$C_L = C^* \cdot (1 - e^{-k_La \cdot t}) \tag{59.33}$$

Equations 59.32 and 59.33 describe the time course of DO concentration when it is removed from the media or from the restart of aeration (Fig. 59.5). In both cases, the slope of the straight line obtained from a plot of $\ln f(C_L)$ against time is numerically equal to k_La.

This technique has been widely employed (26,56–58) and the correct use of this method has been analyzed in depth by Linek *et al*. (59). It must be noted that in this method the dynamics of the oxygen electrode must be taken into account. The response time of the DO electrode, τ_r, is a critical parameter for the determination of accuracy values of oxygen concentration, because changes in the actual value of DO concentration in the media are not recorded until some later time. τ_r is defined as the time necessary to reach 63% of full response when exposed to a step-change of concentration (60) and it can be determined by transferring the oxygen electrode from a solution with sodium sulfite (whose oxygen concentration is zero) to another dissolution saturated with air (100% of saturation). When τ_r

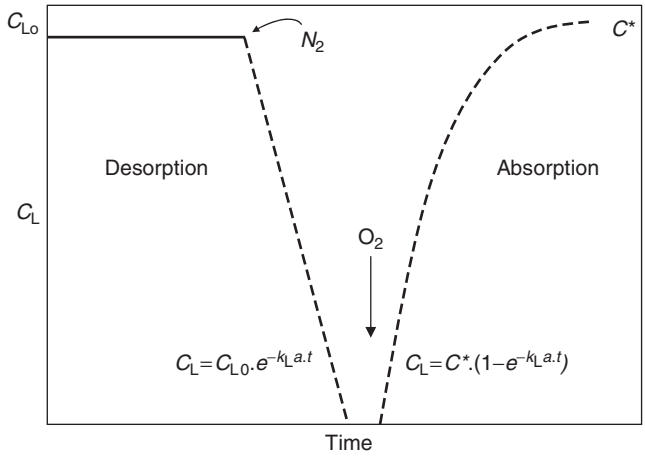


Figure 59.5. Schematic description of the dynamic technique of desorption–absorption of oxygen for inert condition measurements.

has a high value, the model of the dynamic behavior of the electrode should also be included for a correct analysis of measurement. A good approach is a first-order dynamic (61,62) according to

$$\frac{dC_{me}}{dt} = \frac{(C_L - C_{me})}{\tau_r} \tag{59.34}$$

Combining of Equations 59.7 and 59.34 permits the determination of the value of $k_L a$ from the DO concentration measurements; in the case of the gassing-out method, according to the following equation:

$$C_{me} = C^* + \frac{C^* - C_{L0}}{1 - \tau_r k_L a} \cdot \left(\tau_r k_L a \cdot e^{(-t/\tau_r)} - e^{(-k_L a \cdot t)}\right) \tag{59.35}$$

where C_{me} is the electrode output and C_{L0} is the DO concentration at the initial time of the aeration.

Assuming that the dynamic response of the electrode is of the first order, characterized by a constant time, a simple criterion for the suitable selection of the electrode, and despite this effect, would be $\tau_r < 1/k_L a$ (60,63). In pneumatically stirred bioreactors, when only one probe is used, this method is difficult to employ, because the results strongly depend on the modeling of probe dynamics, on the position of the probe in the reactor, and on the assumptions of the hydrodynamic conditions. These limitations have been discussed by Gourich *et al*. (64).

In order to simplify the above procedure, approximations based on the truncation of parts of the electrode response curve have been proposed. According to Merchuk *et al*. (65) for long time intervals ($t >> \tau_r$), the first term in the right-hand member of Equation 59.35 becomes irrelevant. As the electrode time constant approaches zero, Equation 59.35 further reduces to Equation 59.33. In addition, mass transfer data analysis for dynamic $k_L a$ determination can be simplified by truncation of the first part of the electrode response curve and applying the first-order approximation; nevertheless, truncating more than 30% of the lower end data is not recommended. It should be kept in mind that this simplification implies the loss of part of the information, and due care should be given to statistical analysis of the results.

59.2.2.2 Kr Method. This method is based on the injection of Kr-85 (a volatile radioisotope that emits β and γ radiation) into the medium and the measurement of the radioactivity in the outlet gas stream (53). To evaluate the response curve of radioactivity, a model for describing the concentrations of tracer in the liquid, bubble, and head space–gas is necessary. Two steps are involved in the gassing out of tracer. First, mass transfer from the liquid phase to the gas bubble and, second, mixing of the gas bubbles in the head space. The mass balance for the tracer in the liquid phase is given by Equation 59.7. Furthermore, the mass balance in the gas phase with the assumption of an ideally mixed head space is given by

$$V_G \frac{dC_L}{dt} = Q \cdot (C_b - C_G) \tag{59.36}$$

where V_G is the head space volume, Q is the gas flow rate and C_L, C_b, and C_G are the concentration of tracer in the liquid, bubble, and gas phase respectively.

To describe the concentration of tracer in the gas holdup, it is necessary to know the residence time distribution of the gas bubbles. Assuming a plug flow model, the Kr-85 concentration in the head space–gas of the bioreactor is given by

$$C_G = \frac{C_{L_0} \cdot V_L}{Q \cdot \xi - V_G} \cdot \left(e^{(t_b - t/\xi)} - e^{(Q(t_b - t)/V_G)}\right) \quad t \geq t_b \tag{59.37}$$

where C_{L0} is the concentration of tracer in the liquid at $t = 0$, t_b is the average residence time of gas bubbles, and the parameter ξ is defined by

$$\xi = \frac{1}{k_L a} + \frac{V_L}{Q \cdot H_e} \tag{59.38}$$

Equation 59.37 can be fitted to experimental response of radioactivity in the gas leaving the head space after the injection of Kr-85 pulse using a nonlinear regression with $k_L a$ as parameter. This method has been also used by Pedersen *et al*. (53) to obtain $k_L a$ values during bioprocesses involving different filamentous fungi, although the use of a radioactive isotope may cause some problems in an industrial application.

59.2.3 Biological Methods

Biological methods are those used while the microbial process is carried out; thus k_La values are directly determined in the suspension formed by the actual broth: substrates, nutrients, metabolites, products, and the cell population. In consequence, under suitable conditions, these methods provide values that are much more secure and realistic than others.

59.2.3.1 Biological Dynamic Gassing-Out Method. A modified physical gassing-out method is widely employed to determine both the k_La and the OUR values. The biological dynamic gassing-out method involves physical oxygen absorption combined with the oxygen consumption by microorganisms which are actively growing (and carrying out metabolic changes) inside the bioreactor. The application of the original method proposed by Taguchi and Humphrey (66), is illustrated in Fig. 59.6, and it requires the previous evaluation of the OUR by the culture. The air flow supplied to the fermentation broth is stopped (only for a short time in order to not affect the process evolution), and the decrease of DO concentration is recorded as a function of time. Under these conditions, during the nongassing period, the transport term disappears in Equation 59.6, being then simplified to

$$\left(-\frac{dC_L}{dt}\right) = q_{O_2} \cdot C_X = \text{OUR} \qquad (59.39)$$

obtaining OUR from the slope of the plot of DO concentration versus time after stopping air flow.

Before the DO concentration falls below the critical value, the air supply is resumed under the same previous operational conditions, thus ensuring equal OTR, and is then increased until the steady state is reached. The evolution of DO concentration is given by Equation 59.6, which can be rearranged to give

$$C_L = \frac{-1}{k_La} \cdot \left(q_{O_2} \cdot C_X + \frac{dC_L}{dt}\right) + C^* \qquad (59.40)$$

If DO where concentration is recorded as a function of time, the value of k_La can be obtained as the slope of the plot of C_L versus $(q_{O_2} \cdot C_X + dC_L/dt)$, and C^* value is obtained at the axis intersection. Due to the error accumulated by the necessary derivation of the experimental C_L versus time values, a better alternative is the integration of Equation 59.6, with the boundary conditions: $t = t_1 \therefore C_L = C_{L1}$ and $t = t_2 \therefore C_L = C_{L2}$, yielding

$$q_{O_2} \cdot C_x \cdot \Delta t + \Delta C_L = k_La \cdot \int_{t_1}^{t_2} \left(C^* - C_L\right) \cdot dt \qquad (59.41)$$

The k_La value is calculated by solving Equation 59.41 for each data set of experimental values of C_L versus time by an integration algorithm (67,68).

The biological dynamic method is now the most commonly employed, and it is used during an actual fermentation in large and small scales for determining k_La values due to its simplicity, reproducibility, and because gas analysis is not needed. The underlying assumption is that no interchange of oxygen between gas and liquid occurs during the nongassing period and that the culture is rapidly degassed when the air is switched off; but this is not always the case particularly for high viscous non-Newtonian fermentation broths. On the other hand, it is usually assumed that the change in hydrodynamic conditions associated with the stopping of the aeration stream does not affect the OUR; therefore, C_L must be sufficiently high so that q_{O2} value remains constant, and independent of DO concentration.

The probe characteristics are again crucial and, if the response time of the electrode is not negligible, it must be taken into account in the modeling and manipulation of the experimental data, as quoted above.

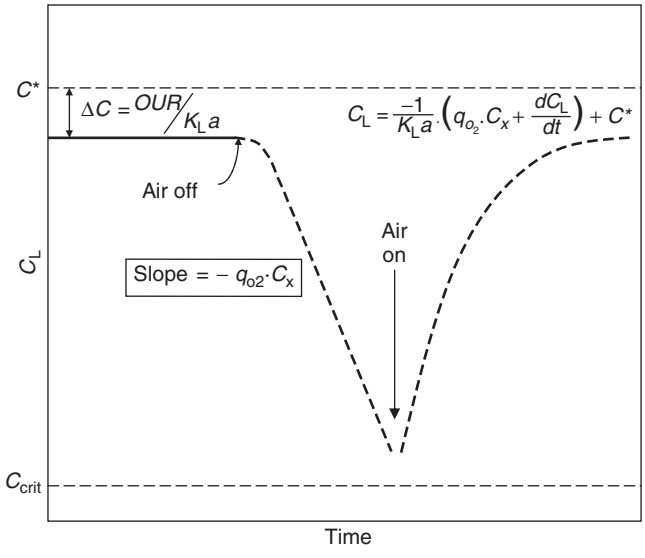


Figure 59.6. Schematic description of the direct measuring of K_La in bioprocess by the biological dynamic gassing-out method.

59.2.3.2 Biological Dynamic Method in Cultures with High OUR. In some cultures, oxygen demand is so high that the DO concentration decreases until it approaches zero and it is very difficult to increase it, even when OTR is improved (by increasing air flow, stirrer speed or the oxygen concentration in the gas phase). Consequently, the above technique can be difficult to apply. In this case, a modified dynamic method can be used. A possible modification consists in using a step-change of air to pure oxygen in the inlet gas stream or *vice versa*. Oxygen concentration changes as the result of both, physical oxygen absorption (or desorption) and oxygen consumption by the cells (69).

Assuming that OUR, C^*, and $k_L a$ are constants during the measurement time, Equation 59.6 can be expressed as

$$\frac{dC_L}{dt} = c - k_L a \cdot C_L \tag{59.42}$$

where c is given by

$$c = k_L a \cdot C^* - \text{OUR} \tag{59.43}$$

The integration of Equation 59.42, when oxygen is absorbed, with the boundary conditions: $t = 0 \therefore C^* = C_0^*$ and $C_L = C_{Lo}; t = t_1 \therefore C_L = C_L$, yields the following equation:

$$C_L = \left(C_0^* - \frac{\text{OUR}}{k_L a}\right) - \left(C_0^* - C_{L_0} - \frac{\text{OUR}}{k_L a}\right) \cdot e^{-k_L a \cdot t} \tag{59.44}$$

while, if the oxygen is desorbed, the integration of Equation 59.42, now with the boundary conditions: $t = t_1 \therefore C^* = C_1^*$ and $C = C_{L1}; t = t_2 \therefore C = C_L$, results in

$$C_L = \left(C_1^* - \frac{\text{OUR}}{k_L a}\right) + \left(C_{L_1} - C_1^* + \frac{\text{OUR}}{k_L a}\right) \cdot e^{-k_L a \cdot t} \tag{59.45}$$

Equations 59.44 and 59.45 describe the evolution in the time course of the DO concentration in the liquid phase from a starting concentration, C_{L0} or C_{L1}, after changing from air to pure oxygen or from pure oxygen to air for the gas flow through the bioreactor. According to the above procedure, $k_L a$ and OUR values can be determined during the bioprocess by fitting of the above equations to the experimental data using nonlinear regression techniques (Fig. 59.7).

Casas *et al*. (70) have discussed and compared this approach with the biological dynamic gassing-out method and found that $K_L a$ values are statistically identical. Therefore, this method can be a valuable tool for the determination of OTR in those systems and under operational conditions that would not tolerate the application of the classical dynamic gassing-out method.

59.2.3.3 Gaseous Oxygen Balance Method. The static method takes into account a gas oxygen balance in the bioreactor under steady-state conditions. This method uses a gaseous oxygen analyzer to measure the oxygen concentration in the gas streams, inlet and outlet, entering and leaving the bioreactor and a probe for measuring the DO concentration in the liquid phase. When the gas phase behaves like the liquid in a well-mixed bioreactor and there are no pressure variations, gas oxygen balance yields

$$F_{O_2}^{in} - F_{O_2}^{out} - V \cdot \text{OUR} = 0 \tag{59.46}$$

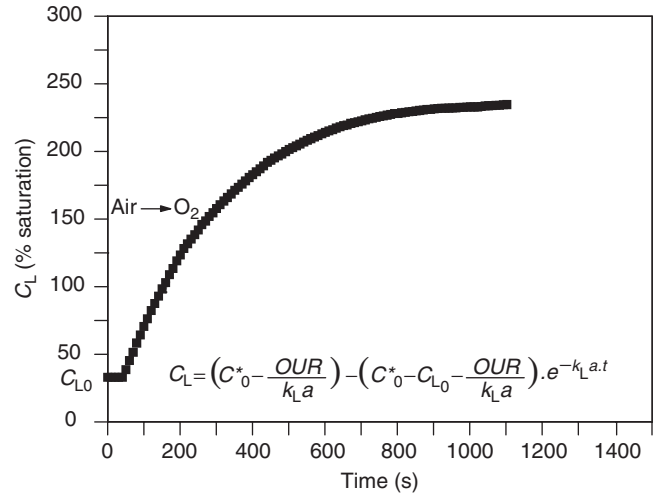


Figure 59.7. Evolution of DO concentration when the composition of the gas stream is modified changing from air to pure oxygen (absorption). [Adapted Gomez *et al*. (69).]

where F^{in} and F^{out} are the molar flow rates measured at bioreactor inlet and outlet, and V the bioreactor volume.

On the other hand, the OTR from the bubbles is equal to the rate of oxygen consumption by the cells:

$$k_L a \cdot (C^* - C_L) = \text{OUR} \tag{59.47}$$

Once the OUR is determined from the measurement of oxygen in the outlet gas and, at the same time, the DO concentration is measured in the broth, $k_L a$ can be calculated according to

$$k_L a = \frac{F_{O_2}^{in} - F_{O_2}^{out}}{V \cdot (C^* - C_L)} \tag{59.48}$$

This technique is very reliable under suitable conditions and it does not disturb the time course of fermentation by interrupting the air flow supply. However, accurate modeling of gas-phase mixing is required for the correct interpretation of data (60). It is also important to take into account the fraction of the oxygen consumed because, if OUR is low, the difference between F^{in} and F^{out} may be very small, and it becomes necessary to use very sensitive measuring equipment.

In this method, it is assumed that there is no significant variation of hydrostatic pressure within the bioreactor. In small-scale bioreactors there are insignificant static pressure differences and short mixing times, as a result of this C_L, C^*, and C_G values can be assumed to be constant in the whole reactor, and a single point determination of DO concentration will be sufficient, C^* can be determined using Henry's law, and C_G value can be assumed to be equal to the outlet gas concentration. However, in large-scale bioreactors (at $H > 1$ m), the hydrostatic pressure variation can

be relevant, and it may be necessary to read the DO concentration at several points and a logarithmic mean between the inlet and outlet gas streams must be considered. Moreover, due to the average bubble volume increase with height, the gas flow through the bioreactor can change (to approximate plug flow) and a combined model for the gas and liquid phase must be used to calculate OTR values (71).

59.2.3.4 Mass Balance from Growth Rate under Oxygen Limitation. Another method for the determination of OTR consists of the measurement of C_X versus time (growth curve) under oxygen-limited conditions (72). This technique employs the kinetic data for growth together with the biomass–oxygen yield (stoichiometric relationship).

According to Pirt (73), OUR can then be related with both oxygen necessary for biomass maintenance and oxygen necessary for growth, according to

$$\mathrm{OUR} = q_{O_2} \cdot C_X = m_{O_2} \cdot C_X + \frac{1}{Y_{XO}} \cdot \frac{dC_X}{dt} \qquad (59.49)$$

where m_{O_2} is the oxygen consumption coefficient for maintenance and Y_{XO} the yield of oxygen consumed for cell growth. From Equation 59.49, the rate of biomass growth during oxygen limitation (assuming no cell death and negligible maintenance requirement) can be written as

$$\frac{dC_X}{dt} = Y_{XO} \cdot \mathrm{OUR} \qquad (59.50)$$

As can be seen, the growth rate and OUR show a linear relationship. In steady-state conditions, OTR = OUR, and from Equation 59.50, the following relation is found:

$$\frac{dC_X}{dt} = Y_{XO} \cdot k_L a \cdot \left(C^* - C_L\right) \qquad (59.51)$$

and therefore

$$\mathrm{OTR} = k_L a \cdot \left(C^* - C_L\right) = \frac{\mu \cdot C_X}{Y_{XO}} \qquad (59.52)$$

In order to relate biomass growth rate with OTR, the yield of oxygen consumed for cell growth, Y_{XO}, must be known. This yield can be experimentally determined by an oxygen mass balance (73,74) or by an estimative model proposed by Heijnen and Roels (75). This method for OTR determination is very laborious and contains several doubtful assumptions.

59.3 COMPARISON OF $K_L A$ VALUES OBTAINED BY DIFFERENT METHODS

The different techniques for determination of $k_L a$ vary according to the accuracy required, and have advantages and disadvantages depending on the scale, availability of necessary analytical instruments and materials, assay time, and labor cost. In Table 59.1 a summary of different methods for $k_L a$ determination is shown. Chemical methods were the first to become widely accepted. In general, however, these methods are not recommended for $k_L a$ determination in the case of aerated bioreactors, due to the changes of physicochemical properties of liquids (especially decreasing the coalescence) produced by the addition of chemicals. High salt concentration as required for most chemical methods, which is known to lead to a lower solubility of oxygen, leads to systematic underestimation of the OTR values achievable in culture media. On the other hand, these methods can give values higher than the real ones, because the absorption rate may be enhanced by fast chemical reaction in the liquid phase, if the experimental conditions are not kept within certain limits. Thus, Pedersen *et al*. (53) found that $k_L a$ values were between 10–25% larger using the sulfite method as compared to values obtained using the Kr method.

Among physical methods to evaluate $k_L a$, the dynamic method has by far been the most commonly used in the last few decades due to its simplicity and relative accuracy. Both, the absorption and desorption measurements give equal values of $k_L a$ under identical hydrodynamic conditions (56) although, if the characteristic time for the oxygen electrode is of the same magnitude as the characteristic time for the oxygen transfer process ($1/k_L a$), the dynamic response of the electrode must be taken into account. Also, an incomplete modeling of the mixing and mass transfer in the bioreactor can give rise to inaccuracies in the determination of $k_L a$ (59).

In Fig. 59.8, for example, $k_L a$ values obtained by different methods as a function of stirrer speed in non-Newtonian solutions and 20 L vessels are compared from different studies ($V_S = 2 \cdot 10^{-3}$ m/s and $\mu_a = 8 \cdot 10^{-3}$

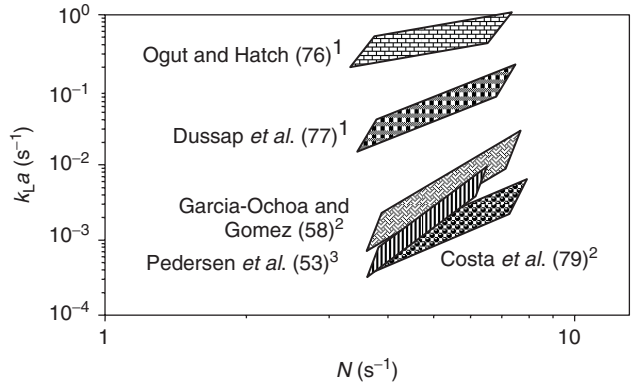


Figure 59.8. Comparison of $k_L a$ values obtained by different techniques as a function of stirrer speed in non-Newtonian liquids. Key: 1: sulfite oxidation method, 2: physical dynamic gassing-out method, 3: Kr method. [Adapted from Garcia-Ochoa and Gomez (58).]

TABLE 59.1. Summary of Different Methods for Volumetric Mass Transfer Coefficient Determination

Measuring Method			$k_L a \cdot 10^2$ Range (s^{-1})	Assay Time	Scale Applied	Assumptions/ Drawback
Chemical	Sulfite oxidation		0–0.3	Hours	Laboratory scale	The rate of reaction is assumed to be zero order in sulfite. Alteration of driving force, diffusion coefficient, and coalescence properties; complex kinetics boundary layer reduction. This method is fairly labor intensive
	Absorption of CO_2	Alkaline solution	0–0.1	Minutes	Laboratory scale	Assumptions about kinetic reaction must be made. Possible alteration of the driving force. Change of the coalescence behavior
		Dynamic measure of pH	0–0.03	Half an hour	Any scale	Assumptions about kinetic reaction must be made. Salt addition does not alter the mass transfer rate of CO_2
		Hydrazine oxidation	0–0.5	Minutes	Pilot plant	Hydrazine does not accumulate. No chemical enhancement
		Biooxidation of catechol	<0.8	Minutes	<100 mL	Available of oxidative enzyme; limited to small scales
Physical		Dynamic	0–0.1	Minutes	>100 mL	A nonrespiring system can be employed to simulate the fermentation broth. The response time of the electrode, τ_r, is a critical parameter. Gassing time can be significant at larger scales
		Kr method	0–0.3	Minutes	Any scale	The use of a radioactive isotope may cause some problems in an industrial application. Can be applied to microbial processes
Biological		Biological dynamic gassing out	0–0.1	Minutes	Any scale	High DO concentration is necessary. Nongassing period must be short and OUR independent of DO concentration. Invasive probes are necessary and response time must be considered. Hydrodynamic changes may disturb the microbial metabolism
		Biological dynamic method with high OUR	0–0.1	Minutes	Any scale	OUR independent of DO concentration. Invasive probes are necessary and response time must be considered
		Gas-phase analysis	0–0.3	Minutes	>100 mL	For large scales, the assumptions of well-mixed gas and liquid phase may not be valid. This method may not be the best choice in case of small bioreactors, where the difference between F^{in} and F^{out} may be very small because of the short contact time The accuracy depends on the precision of oxygen analyzer
		Mass balance from the growth rate under oxygen limitation	0.06–0.1	Hours	Any scale	Assuming a negligible maintenance requirement for the cells. The yield of oxygen consumed for cell growth, Y_{XO}, is required. Experimentally laborious

to $30 \cdot 10^{-3} Pa \cdot s \cdots$). It can be seen that $k_L a$ values obtained by Ogut and Hatch (76) and Dussap *et al*. (77), using the sulfite oxidation method, are much higher than those usually obtained for an electrolyte solution. The difference is greater for lower values of the stirrer speed; this is due in part, to the strong ionic state of the sulfite solution and in part, to the chemical reaction enhancement of transfer rate (78). The difference between the results obtained by other authors can be explained by the effect of certain distinctive features in the reactor used (e.g. D/T ratio, impeller and sparger type) on the $k_L a$ values (58). The next sections are devoted to anticipating variations of $k_L a$ among different systems and the equations for prediction of OTR will be presented.

59.4 CORRELATION OF $K_L A$ VALUES

In the literature, a high number of correlations for the volumetric mass transfer coefficient (in both dimensional and dimensionless equations) have been proposed. Values of $k_L a$ have been obtained by a variety of methods; as quoted above, there are considerable problems concerning the accuracy of $k_L a$ by experimental determination. Frequent discrepancies between experimental data and those estimated from these equations are found, mainly when $k_L a$ for actual broths are estimated from correlations proposed for aqueous solutions, that is in static systems with an invariable composition of the liquid media with time.

In mechanically stirred bioreactors, typical correlations for $k_L a$ have the form:

$$k_L a = C \cdot V_s^a \cdot \left(\frac{P}{V}\right)^b \cdot \mu_a^c \qquad (59.53)$$

where V_S is the superficial gas velocity, P/V is the power input per unit volume, and μ_a is the apparent viscosity of the liquid. Other authors have proposed substitute P/V by the stirrer speed, N. Some typical values given for the exponents are given in Table 59.2. As can be seen, the correlations show different influences of the operating variables, and the exponent values show a wide variation range in the different correlations: $0.3 \leq a \leq 0.7$; $0.4 \leq b \leq 1$; $-0.4 \leq c \leq -0.7$. This is due to the differences in the bioreactor geometry, fluid properties, and in power input range. Only in the equation proposed by Galaction *et al*. (25) is the biomass concentration considered as an alternative to viscosity. For nonviscous systems, the most frequently used correlation is that from Van't Riet (60).

One criticism of the dimensional equations is that no account is taken of all the properties of fluids and the geometric parameters of the bioreactor. There have been attempts to develop more complete relationships, using dimensional analysis. Dimensionless equations predict $k_L a$, included usually in the Sherwood number, as a function of other dimensionless numbers (Reynolds, Froude, Schmidt, Aeration, etc.), with the general form

$$\frac{k_L a T^2}{D_L} = C \cdot \left(\frac{\rho N T^2}{\mu_a}\right)^{\alpha} \cdot \left(\frac{N^2 T}{g}\right)^{\beta} \cdot \left(\frac{\mu_a}{\rho D_L}\right)^{\gamma} \cdot \left(\frac{NT}{V_s}\right)^{\delta} \qquad (59.54)$$

This approach presents certain advantages because, in principle, the correlation obtained for a known system can be used to estimate $k_L a$ in other bioreactors with different dimensions. Although a variety of dimensionless equations for $k_L a$ estimation are available, the complex correlations that have emerged have found few applications in microbial processes. Some of them, in mechanically stirred bioreactors for Newtonian and non-Newtonian liquids, are summarized in Table 59.3. The relationships may be divided into those which reflect the effect of the N directly and those which take into account the P/V effect. The correlation of Nishikawa *et al*. (82) is the only one to include both variables, differentiating between mass transfer resulting from stirring and from bubbling, although the latter contribution is usually negligible. Yagi and Yoshida (80) used various liquids and gases to deduce their correlations, although no effect of gas viscosity as implied in the equation of Perez and Sandall (90) could be observed. In addition, these authors take into account the effect of viscoelasticity by including the Deborah number (λN), but the method for the evaluation of characteristic material time (λ) from the shear rate, depending on the apparent viscosity, can be only applied to liquids approaching Newtonian flow behavior (91). The relationships proposed by Höcker *et al*. (92) and Schlüter and Deckwer (93) are the only approach considering the gas flow rate rather than superficial gas velocity. Finally, Garcia-Ochoa and Gomez (58) considered two rheological equations for liquid behavior (Ostwald–de Waele and Casson models), employing a similar approach to correlate $k_L a$ values in the production of the extracellular polysaccharide xanthan by *Xanthomonas campestris* (67).

In bubble columns, $k_L a$ is usually correlated by dimensional equations as Equation 59.55. For the internal loop airlift reactor, ascending flow by the circular and descendent crown by the central zone, Halard *et al*. (94) have verified that the equation proposed by Godbole *et al*. (61), for classic bubble columns, can be used for non-Newtonian fluids. In the case of external loop airlift reactor, expressions based on the ratio of down-comer to riser cross-sectional area (A_D/A_R), the effective viscosity of the dissolution and other fluid dynamic parameters have been proposed (95,96) as

$$k_L a = C \cdot V_s^{a} \mu_a^{b} \cdot \left(1 + \frac{A_D}{A_R}\right)^{c} \cdot V_{LR}^{d} \cdot \phi^{e} \qquad (59.55)$$

The (A_D/A_R) ratio is a key design parameter, which controls the hydrodynamics of the system, and thus also the

TABLE 59.2. Exponent Values in Equation 59.53 for Mechanically Stirred Bioreactors

Reference	V_S	P/V	N	μ_a	V (L)	System	Impeller Type
Yagi and Yoshida (80)	0.3	0.8				Water–glycerol CMC/PANa solutions	6FBT
	0.3	0.8	2.2	−0.4	12	Water–glycerol CMC/PANa solutions	6FBT
Figueiredo and Calderbank (81)	0.8	0.6	—	—	600	Water	FBT
Van't Riet (60)	0.5	0.4	—	—	2–2600	Water	Any
Nishikawa *et al*. (82)	0.33	0.8	2.4	−0.5	2.7–170	Water–Millet pulp/CMC solutions	FBT and FBP
Chandrasekharan and Calderbank (83)	$0.55 \cdot D^{-1/2}$	0.55	—	—	50–1430	Water	FBT
Kawase and Moo-Young (84)	0.5	1.0	—	—	—	Water–CMC	—
Ogut and Hatch (76)	0.7 0.5	—	0.9 0.5	−0.4	100	Water–Sodium sulphite and PANa	6FBP
Linek *et al*. (85)	0.4	0.65 1.1		—	20	Water	6FBT
Pedersen *et al*. (53)	0.5–0.7	—	2.7	—	15	Water–Xanthan	Two-6FBT
Garcia-Ochoa and Gomez (58)	0.5–0.67	0.6	2.0	-0.67 -1^a	2–25	Water/ Xanthan Solutions	1,2-FBT, CBT, FBP, CBP, PBP
Gagnon *et al*. (86)	0.5	0.6–0.8	—	—	22	Water	Agitated column 6FBT
Arjunwadkar *et al*. (19)	0.4–0.58	0.68	—	—	5	Water–Electrolytes CMC Solutions	FBT and PBT
Vasconcelos *et al*. (87)	0.49	0.62	—	—	5	Water	Two 6FBT
Garcia-Ochoa *et al*. (67)	0.5	0.6	2	−0.5	—	Xanthan fermentation broths	Two 4FBT
Chisti and Jauregui-Haza (88)	$0.41 \cdot (N\text{-}4.36)^{0.38}$ $1.57-0.12\ N$	2.67 0.18	—	—	1500	Water	Mechanically agitated airlift
Galaction *et al*. (25)	0.43	−0.03	—	-0.28^b	5	Nonrespiring biomass (bacteria)	Two 4FBT
Puthli *et al*. (26)	0.53	0.57–0.98	—	−0.84	2	Water–Electrolytes CMC Solutions	1,2-FBT, FBP, PBP
Kapic and Heindel (89)	0.93	—	1.34	—	7	Water	6FBT

Note: CMC, carboxymethylcellulose; PANa, sodium polyacrylate.

Casson viscosity.

Exponent on biomass concentration (C_X).

Acronyms for impellers: CBT, curved blade turbine; CBP, curved blade paddle; FBP, flat blade paddle; FBT, flat blade turbine; PBP, pitched blade paddle; PBT, pitched blade turbine.

TABLE 59.3. Selection of Dimensionless Correlations for k_La in Mechanically Stirred Bioreactors

Reference	Dimensionless Correlation	System
Yagi and Yoshida (80)	$\frac{k_La T^2}{D_L} = 0.06 \cdot \left(\frac{\mu_a}{\rho D_L}\right)^{0.5} \left(\frac{T^2 N \rho}{\mu_a}\right)^{1.5} \left(\frac{\mu_a V_s}{\sigma}\right)^{0.6} \left(\frac{N^2 T}{g}\right)^{0.19} \left(\frac{NT}{V_s}\right)^{0.32} \left(\frac{\mu_a V_s}{\sigma}\right)^{0.6} \cdot \left[1 + 2 \cdot (\lambda N)^{0.5}\right]^{-0.67}$	Viscous Newtonian and non-Newtonian
Perez and Sandall (90)	$\frac{k_La T^2}{D_L} = 21.2 \cdot \left(\frac{\rho N T^2}{\mu_a}\right)^{1.11} \cdot \left(\frac{\mu_a}{\rho D_L}\right)^{0.5} \cdot \left(\frac{V_s T}{\sigma}\right)^{0.45} \cdot \left(\frac{\mu_G}{\mu_a}\right)^{0.69}$	Non-Newtonian (Ostwald–de Waele model)
Höcker *et al*. (92)	$\frac{k_La V}{Q} = 0.105 \cdot \left(\frac{P}{Q\rho[g\mu_a/\rho]^{2/3}}\right)^{0.59} \cdot \left(\frac{\mu_a}{\rho D_L}\right)^{-0.3}$	Non-Newtonian (Ostwald–de Waele model)
Nishikawa *et al*. (82)	$\frac{k_La D^2}{D_L} = 0.115 \cdot \left(\frac{T^2 N_\rho}{\mu_a}\right)^{1.5} \cdot \left(\frac{\mu_a}{\rho D_L}\right)^{0.5} \cdot \left(\frac{\mu_a V_s}{\sigma}\right)^{0.5} \cdot \left(\frac{TN^2}{g}\right)^{0.37} \left(\frac{NT}{V_s}\right)^{0.17} \cdot \left(\frac{D}{T}\right)^2 \cdot \left(\frac{P_0}{N^3 T^5 \rho}\right)^{0.8} \cdot [1 + 2(\lambda N)^{0.5}]^{-0.67} + 0.112 \cdot \left(\frac{P/V}{N^3 T^5 \rho + P/V}\right) \cdot \left(\frac{V_s}{(gD)^{0.5}}\right) \cdot \left(\frac{k(CV_s)^{n-1}}{\rho D_L}\right)^{0.5} \cdot \left(\frac{gD^2\rho}{\sigma}\right)^{0.66} \left(\frac{gD^3\rho^2}{\left[k(CV_s)^{n-1}\right]}\right)^{0.42} \cdot \left[1 + 0.18\left(\lambda \frac{v_b}{d_b}\right)^{0.45}\right]^{-1}$	Newtonian and non-Newtonian liquids
Schlüter and Deckwer (93)	$k_La \left(\frac{\nu}{g^2}\right)^{1/3} = C \cdot \left[\frac{P/V}{\rho(\nu g^4)^{1/3}}\right]^{0.62} \cdot \left[\frac{Q}{V} \cdot \left(\frac{\nu}{g^2}\right)^{1/3}\right]^{0.23}$	Fermentation broths of yeast *Trichos-poron cutaneum*
Garcia-Ochoa and Gomez (58)	$\frac{k_La T^2}{D_L} = 6.86 \cdot \left(\frac{\rho N^{2-n} T^2}{k K^{n-1}}\right)^{2/3} \cdot \left(\frac{NT}{V_S}\right)^{-2/3} \cdot \left(\frac{\rho N^2 T^3}{\sigma}\right)^{1}$	
	$\frac{k_La T^2}{D_L} = 0.022 \cdot \left(\frac{\rho N T^2}{\mu_c}\right)^{1} \cdot \left(\frac{NT}{V_S}\right)^{-2/3} \cdot \left(\frac{\rho N^2 T^3}{\sigma}\right)^{1}$	Non-Newtonian liquids (Ostwald–de Waele and Casson models, respectively)
Garcia-Ochoa *et al*. (67)	$\frac{k_La T}{D_L} = C \cdot \left(\frac{\rho N T^2}{\mu_L}\right)^{1/2} \cdot \left(\frac{NT}{V_S}\right)^{-1/2} \cdot \left(\frac{\rho N^2 T^3}{\sigma}\right)^{1} \therefore \quad C_{\text{Ostwald}} = 11.96 \quad C_{\text{Casson}} = 9.78$	Fermentation broths of bacteria *X. campestris* (Ostwald–de Waele and Casson model s)

OTR in airlift reactors. Some values of exponents proposed in the literature for Newtonian and non-Newtonian fluids are noted in Table 59.4. As can be seen, the exponent on $1 + A_D/A_R$ is negative and therefore a decrease in k_La is predicted with increasing down-comer to riser cross-sectional area ratio (A_D/A_R). Furthermore, the correlations of Popovic and Robinson (95) and Li *et al*. (31) include a problematic definition of the apparent viscosity, defining shear rate as a linear function of the gas velocity. This approach can be questionable from a rheological point of view because it will predict the same shear rate for a certain superficial gas velocity, no matter which liquid is used (18,97).

On the other hand, in Table 59.5, a selection of dimensionless equations proposed for pneumatically stirred bioreactors is given; among these equations, that from Akita and Yoshida (103) is the most widely used, although it is limited to bubble columns with diameter less than 0.6 m and a simple gas sparger. The correlation proposed by Suh *et al*. (27) was successfully employed by these authors to correlate k_La values in the xanthan gum production by *X. campestris* (28). It should be emphasized that the validity and application of these correlations in non-Newtonian fluids depend very much on the measurements of the flow behavior of the liquid and also on the assumption regarding the estimation of a representative shear rate for predicting

TABLE 59.4. Exponent Values in Equation 59.55 for Pneumatically Stirred Bioreactors

Reference	V_S	$1+A_D/A_R$	V_{LR}	ϕ	μ_a	System	Bioreactor
Deckwer *et al*. (98,99)	0.7–1.3	—	—	—	—	Water–Electrolytes	Bubble column
Jackson and Shen (100)	1.2	—	—	—	—	Water	Tank
Bello *et al*. (96)	0.9	−1	0.1	—	—	Water–Electrolytes	Airlift
Godbole *et al*. (61)	0.44–0.59	–	—	—	−0.8 to −1	CMC Solutions	Bubble column
Popovic and Robinson (95)	0.52	−0.85	—	—	−0.89	CMC Solutions	Airlifts and bubble column
Li *et al*. (31)	0.52	—	—	—	−0.26	Non-Newtonian	Airlift
Al-Masry and Abasaeed (101)	0.76	−2.41	—	—	−0.76	Newtonian	Airlift
Sanchez *et al*. (56)	0.94–1.17	—	—	1	—	Tap and sea water	Bubble column and airlift
Bando *et al*. (102)	0.4	—	—	—	−1	Water and CMC Solutions	Bubble column

TABLE 59.5. Selection of Dimensionless Correlations for k_La in Pneumatically Stirred Bioreactors

Reference	Dimensionless Correlation	System
Akita and Yoshida (103)	$\frac{k_La D^2}{D_L} = 0.6\left(\frac{D^2\rho g}{\sigma}\right)^{0.62}\cdot\left(\frac{D^3\rho^2 g}{\mu^2}\right)^{0.3}\cdot\left(\frac{\mu}{\rho D_L}\right)^{0.5}\cdot\phi^{1.1}$	Water and Newtonian liquids
Nakanoh and Yoshida (104)	$\frac{k_La D^2}{D_L} = 0.09\cdot\left(\frac{D^2\rho g}{\sigma}\right)^{0.75}\cdot\left(\frac{D^3\rho^2 g}{\mu^2}\right)^{0.4}\cdot\left(\frac{\mu}{\rho D_L}\right)^{0.5}\cdot\left(\frac{V_S}{\sqrt{gD}}\right)^{1}\cdot\left[1+0.13\left(\frac{\lambda V_S(1-\phi)}{\phi\cdot d_b}\right)^{0.55}\right]$	Newtonian and non-Newtonian liquids
Kawase *et al*. (105)	$\frac{k_La D^2}{D_L} = 0.452\cdot\left(\frac{D^2\rho g}{\sigma}\right)^{0.6}\cdot\left(\frac{V_S}{gD}\right)^{0.3}\cdot\left(\frac{\mu}{\rho D_L}\right)^{0.5}\cdot\left(\frac{DV_S}{\nu_L}\right)$	Newtonian and non-Newtonian liquids
Uchida *et al*. (106)	$\frac{k_La D^2}{D_L} = 0.17\cdot\left(\frac{D^2\rho g}{\sigma}\right)^{0.62}\cdot\left(\frac{D^3\rho^2 g}{\mu^2}\right)^{0.3}\cdot\left(\frac{\mu}{\rho D_L}\right)^{0.5}\cdot\phi^{1.1}$	Newtonian liquids
Vatai and Tekic (107)	$\frac{k_La D^2}{D_L} = 0.031\cdot\left(\frac{D^2\rho g}{\sigma}\right)^{0.75}\cdot\left(\frac{D^3\rho^2 g}{\mu^2}\right)^{0.4}\cdot\left(\frac{\mu}{\rho D_L}\right)^{0.5}\cdot\left(\frac{V_S}{\sqrt{gD}}\right)^{1}$	Non-Newtonian liquids
Suh *et al*. (27,28)	$\frac{k_La D^2}{D_L} = 0.018\left(\frac{\mu}{\rho D_L}\right)^{0.5}\left(\frac{D^2\rho g}{\sigma}\right)^{0.2}\left(\frac{gD^3\rho^2}{\mu^2}\right)^{0.62}\left(\frac{V_S}{gD}\right)^{0.5}\left[\frac{1}{1+0.12\left(\frac{N_l}{\tau}\right)}\right]$	Non-Newtonian and xanthan fermentation broths
Zhao *et al*. (30)	$\frac{k_La D}{V_S} = 2.95\times10^{-3}\cdot\left(\frac{V_S\rho D}{\sigma}\right)^{-0.13}\left(\frac{DV_S\rho}{\mu}\right)^{0.37}\left(\frac{V_S}{\sqrt{gD}}\right)^{-0.31}\left(\frac{H}{D}\right)^{-0.5}\quad\therefore H<0.8\text{ m}$	Newtonian liquids
	$\frac{k_La D}{V_S} = 9.3\times10^{-5}\cdot\left(\frac{V_S\mu}{\sigma}\right)^{0.09}\left(\frac{DV_S\rho}{\mu}\right)^{0.56}\left(\frac{V_S}{\sqrt{gD}}\right)^{-0.86}\quad\therefore H\geq0.8\text{ m}$	

the apparent viscosity. Although various correlations can be used to directly estimate k_La, the reliability of such predictions is often quite poor. The correlations are suitable only for initial estimates because the hydrodynamic and transport behavior of bioreactors depends on the scale and is quite sensitive to the flow behavior of the liquid, concentration and morphology of the cells, reactor geometry, and, in airlift designs, to the distribution of gas holdup in the various zones, and the induced liquid circulation rate. Thus, the initial expectation to obtain a general correlation valid for different systems has not been reached and is perhaps scientifically unfounded.

In recent years, other types of models based on artificial intelligence such as the neural networks (108), or using support vector regression (109) have been developed but also with an empirical base. Because of the numerous influences, fundamental approaches to prediction of OTR have also been developed. Such approaches tend toward

generalization and enlargement of the range of applicability of the conclusions. These general methods are discussed in the next section.

59.5 A GENERAL METHOD FOR OTR PREDICTION

Although most literature reports empirical and semi-empirical equations on OTR, attempts have been made to theoretically predict k_La in pneumatically stirred (56,97,105,110,111) and mechanically stirred bioreactors (39,84,110,112). As a first step, it is necessary to separate k_La into the two terms, k_L and a, and estimate them under the conditions of the bioreactor.

The mass transfer coefficient, k_L, is usually estimated according to Higbie's penetration theory:

$$k_L = 2 \cdot \sqrt{\frac{D_L}{\pi \cdot t_e}} \tag{59.56}$$

The exposure time, t_e, that characterizes the residence time of microeddies at the interface is generally unknown, but can be estimated by an adequate model. The evaluation of that time can be done according to the Kolmogoroff's theory of isotropic turbulence, as the time spent by the bubble to travel a length equal to its diameter, and it is estimated using the ratio between the eddy length and the fluctuation velocity of Kolmogoroff. If the rheological model of Ostwald–de Waele is adopted for the description of non-Newtonian flow behavior of fluids, the following equations for t_e and k_L are obtained (105,112):

$$t_e = \left(\frac{k}{\varepsilon \cdot \rho}\right)^{\frac{1}{(1+n)}} \tag{59.57}$$

$$k_L = \frac{2}{\sqrt{\pi}} \cdot \sqrt{D_L} \left(\frac{\varepsilon \cdot \rho}{k}\right)^{\frac{1}{2\cdot(1+n)}} \tag{59.58}$$

The specific interfacial area, a, is a function of the hydrodynamic parameters, which depend on the fluid physicochemical properties and on the geometric parameter. Assuming spherical bubbles, it can be calculated from the average bubble size, d_b, and the gas holdup, ϕ, by the following equation:

$$a = \frac{6\phi}{d_b} \tag{59.59}$$

Bubble size, d_b can be estimated from the equation

$$d_b = C \cdot \frac{\sigma^{0.6}}{\left(\frac{P}{V}\right)^{0.4} \cdot \rho_L^{0.2}} \cdot \left(\frac{\mu_L}{\mu_G}\right)^{0.1} \tag{59.60}$$

where the constant C depends on the kind of fluid (112–114).

For mechanically stirred bioreactors, gas holdup can be estimated from (84)

$$\frac{\phi}{1-\phi} = 0.819 \cdot \frac{V_S^{2/3} N^{2/5} T^{4/15}}{g^{1/3}} \left(\frac{\rho_L}{\sigma}\right)^{1/5} \cdot \left(\frac{\rho_L}{\rho_L - \rho_G}\right) \cdot \left(\frac{\rho_L}{\rho_G}\right)^{-1/15} \cdot \left(\frac{\mu_L}{\mu_G}\right) \tag{59.61}$$

For pneumatically stirred bioreactors, the gas holdup is necessarily related to the superficial gas velocity, and the mean bubble rise velocity according to (115) is

$$\phi = \frac{V_S}{U_S + \frac{1}{2}V_{LC} + \overline{V}_{LR}} \tag{59.62}$$

where U_s is the terminal rise velocity of the bubble, V_{LC} is the average velocity in the core region and V_{LR} is the average linear velocity. For bubble column bioreactors, both terms, V_{LC} and V_{LR} disappear.

Therefore, the volumetric mass transfer coefficient in bioreactors can be predicted by taking into account the above equations: Equation 58 for the mass transfer coefficient, k_L, and Equation 59.59 for the specific interfacial area, a. In order to estimate both parameters, the power input in the bioreactor must be calculated. Methods for estimating the power input in mechanically and pneumatically agitated bioreactors have been detailed recently by Garcia-Ochoa and Gomez (1). In Fig. 59.9, k_La values predicted in mechanically stirred bioreactors for 2 and 20 L are shown as a function of the power input per unit volume.

59.5.1 Influence of Oxygen Consumption on OTR

The study of oxygen mass transfer in bioprocesses has usually been separated into the parameters related to transport (OTR, k_La) and the oxygen consumption by the cells (OUR). However, correct prediction of OTR in a bioprocess must take into account the relationship between both of them. Thus, oxygen absorption into a culture broth can be considered as the absorption of a gas into a liquid where it reacts, the suspended cells being the consumers of the oxygen, and therefore an enhancement of OTR can take place. A number of works have reported an enhancement on oxygen transfer in microbial system (57,116–120).

To take into account the possibility of an OTR enhancement in a microbial system, a biological enhancement factor, E, is defined as the ratio of the absorption flux of oxygen due to the oxygen consumption by the cells to the absorption flux in its absence under the same hydrodynamic

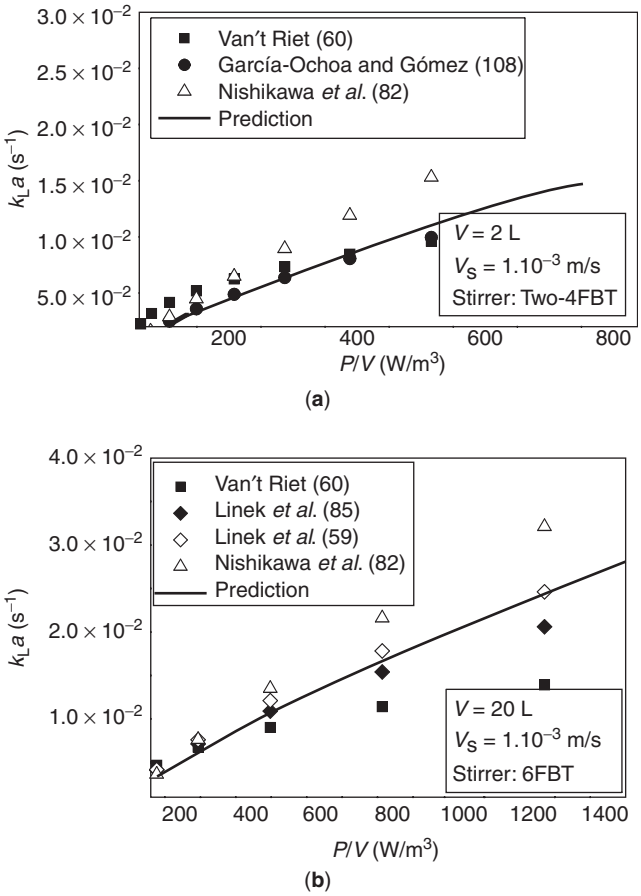


Figure 59.9. Comparison of k_La values predicted in mechanically stirred bioreactors for 2- and 20-L (4FBT and 6FBT = turbines of 4 and 6 flat blades, respectively). [Adapted from Garcia-Ochoa and Gomez (112).]

conditions and driving force according to

$$E = \frac{J}{J_0} = \frac{K_La}{k_La} \tag{59.63}$$

Some reports in the literature have discussed the biological enhancement factor for oxygen absorption into fermentation broths, and several models with different cell concentration distribution have been proposed (121–123). Garcia-Ochoa and Gomez (39) have proposed a model for estimation of the potential biological enhancement factor taking into account the substances usually added to the broths. This model considers three layers in series; therefore, to describe the oxygen mass transport, three mass transfer resistances are considered for the biological system: (i) the interfacial surfactant film resistance, (ii) the mono-layers of adsorbed microorganisms resistance, and (iii) the liquid film resistance. The different layer resistances are taken into account by the diffusion coefficient (D_i) and by layer thickness (z_i). According to this model, the biological enhancement factor, E, can be expressed as

$$E = \left[1 + \frac{q_{O_2} C_{X_m} z_m^2}{2D_m\,(C^* - C_L)} \cdot \left(1 + 2 \cdot \frac{z_l D_m}{z_m D_L} + \frac{2z_L^2}{3z_m^2}\right) + \frac{1}{3} \cdot \frac{q_{O_2} C_{X_L} z_L^2}{2D_l\,(C^* - C_L)}\right] \cdot \left[\frac{z_L / D_L}{\sum_i z_i / D_i}\right] \tag{59.64}$$

where C_X, i represents the cell concentration in the cell monolayer or in the continuous phase in liquid film; D_i is the molecular diffusion coefficient within a film of thickness z_i.

The first parenthesis in Equation 59.64 is always ≥ 1 and can be written as a function of the *Hatta* number, which takes into account the biological enhancement due to the oxygen consumption by the microorganisms in the different layers according to

$$\mathrm{Ha}_i = \frac{q_{O_2} C_{X,i} z_i^2}{2D_i \cdot (C^* - C_L)} \qquad (i = L, m) \tag{59.65}$$

The second parenthesis of Equation 59.64 is always ≤ 1, representing the resistance to diffusion exerted by each of the three films defined previously. Depending on the relative values of both terms in Equation 59.64, the enhancement factor E, can take values below, equal or above unity.

Now, the OTR can be determined as

$$\mathrm{OTR} = a \cdot J = a \cdot E \cdot J_0 = E \cdot k_La\,(C^* - C_L) \tag{59.66}$$

and

$$K_La = E \cdot k_La \tag{59.67}$$

Therefore, the overall volumetric mass transfer coefficient in the presence of a biochemical reaction, K_La, is a lumped parameter comprising the resistances to mass transport of oxygen due to several films around the gas–liquid interface and to the oxygen consumption; this last effect can be expressed by a biological enhancement factor, E. Figure 59.10 shows the evolutions of q_{O2} and E (experimental and predicted values by Eq. 59.64) with the biomass concentration of *Pseudomona putida* during a process-scale fermentation. As can be observed, the E values obtained in the presence of biomass can be higher than 1. The values $E < 1$ indicate that the OUR is low or that the transport resistance is high. In Fig. 59.11 the time course of biomass concentration and DO concentration are shown; here, experimental and predicted K_La values, according to Equations 58,59.59, and 59.64, are shown; it can be seen that the prediction method yields values of K_La close to the experimental ones.

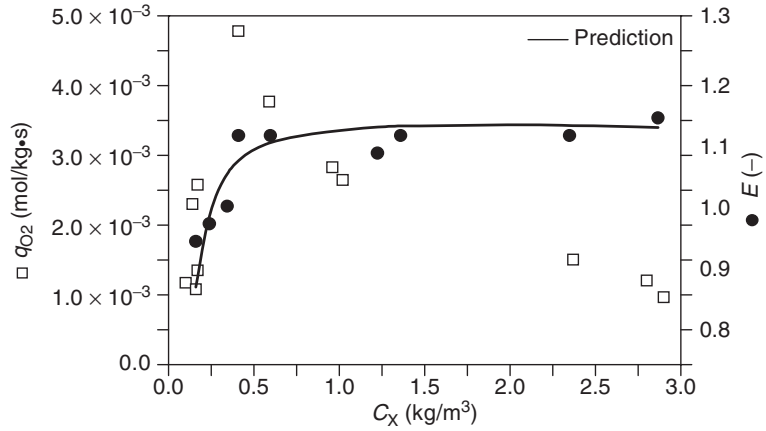


Figure 59.10. Evolution of specific OUR (□) and biological enhancement factor (experimental (•) and estimated (—) from Equation 59.64) in *Pseudomonas putida* culture applying the same stirrer speed (200 rpm) and gas flow rate (2 L/min).[Adapted from Gomez *et al*. (69).]

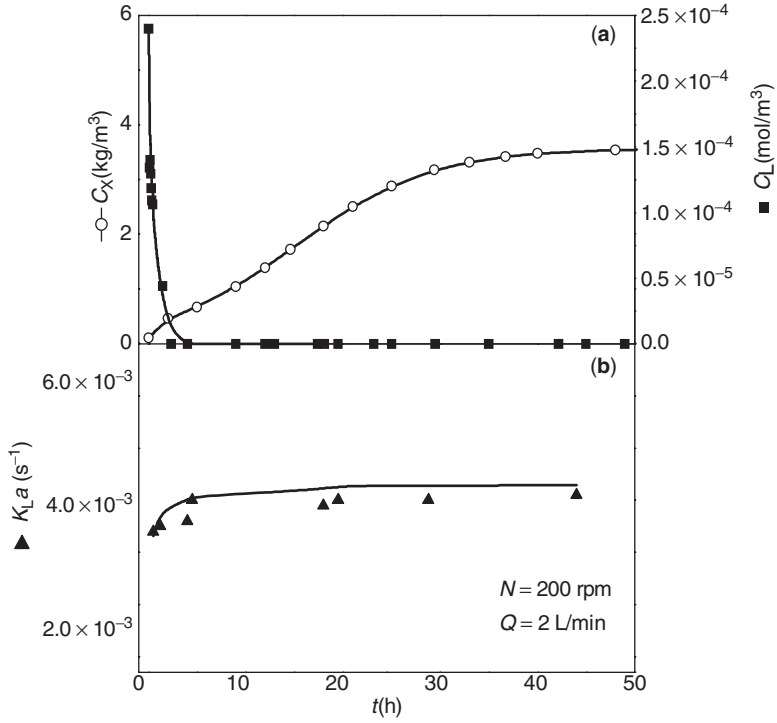


Figure 59.11. Time profile of biomass concentration (◯),dissolved oxygen concentration (■), and volumetric mass transfer coefficient (experimental (▲) and estimated (—) from Equations 58,59.59, and 59.64 of *Pseudomonas putida* culture applying the same stirrer speed (200 rpm) and gas flow rate (2 L/min). [Adapted from Gomez *et al*. (69).]

59.6 OTR IN MINIATURE BIOREACTORS (MINI- AND MICRO- DEVICES)

Bioprocess development (strain selection, strain enhancement, formulation and preparation of media, process optimization, biocatalyst production, etc.) has traditionally required the screening of large numbers of cell lines. The need for carrying out a vast number of cultures has resulted in the increasingly widespread development of s*hake flask* and *microscale* bioreactors. These devices offer a miniaturized high throughput solution to bioprocess development. It is important that such devices be very reliable so as to

accurately mimic laboratory and *pilot-scale* bioreactors when used for bioprocess development. Therefore, growth, product formation rates, and oxygen transfer capability, optimized at the *microscale*, can be expected to be easily scaled-up.

Several types of mini- and micro-devices have been described in the literature, which ca be classified according to the agitation system or to the device geometry. The main types are shaken devices (flask, microtiter and spin tubes) and miniature stirred tanks and bubble columns. The most commonly used culture vessel in bioprocess development is the shaken Erlenmeyer flask (0.1–2 L) filled with low volumes of media (10–25%) which are shaken to promote fluid mixing and oxygen transfer via surface aeration. They have a simple mechanical design, requiring only small amounts of material and power, and thus are inexpensive to operate. Nevertheless, the major limitation is their dependence on surface aeration, leading to reduced OTR as compared to that achieved in mechanically stirred bioreactors. Further, the oxygen consumption of microbial culture may become limiting if the oxygen demand exceeds the oxygen transfer capability through the shake flask closure or/and the gas–liquid interface.

Chemical, physical, and biological methods have been applied for the determination of k_La in miniature bioreactors. Liu *et al*. (124), using the sulfite oxidation method, found that k_La decreases with the liquid volume in the flask and increases with the shaker speed, the correlation being

$$k_La = 0.141 \cdot N^{0.88} \cdot \left(\frac{V_L}{V_0}\right)^{-0.80} \tag{59.68}$$

The small difference in absolute values of the exponents on N and V_L implies that the two variables have a similar influence on the OTR.

As a novel alternative to shaken vessels at a *small scale* and high throughput cell culture, miniaturized bioreactors have been developed. Lamping *et al*. (125) have measured (using the dynamic gassing-out method) and predicted (using the Higbie's model with the exposure time obtained from the computational fluid dynamics) k_La in a miniature stirred bioreactor, obtaining values in the range of 0.028–0.11 s^{-1}, typical of those reported for large-scale bioreactors. Doig *et al*. (74) estimated k_La in a miniaturized bubble column by three methods (the dynamic gassing-out method, the gas oxygen balance method, and the oxygen-limited growth method in *Bacillus subtilis* cultures). They found that all three methods provided values that were within 15% of each other and experimental data of k_La was fitted to the following:

$$k_La = 0.65 \cdot V_S^{0.6} \tag{59.69}$$

However, due to the problems associated with the classical methods for k_La determination, other specific methods have been developed in small-scale devices. Thus, Duetz *et al*. (72) estimated OTR using the mass balance from the growth rate under oxygen limitation method in *P. putida* broths. Hermann *et al*. (126) developed an optical method for determining OTR based on sulfite oxidation. More recently, Duetz and Witholt (127) used the reaction of formation of gluconic acid (via enzymatic oxidation of glucose with oxygen in the presence of glucose oxidase) for the determination of OTR in microtiter plates, by measuring the rate of consumption of alkali that is needed to neutralize the acid. Finally, Ortiz-Ochoa *et al*. (48) developed a chemical method based on the biooxidation of catechol by the enzyme catechol-2,3-dioxygenase for small-scale vessels. In both cases the cost of the enzymes restricts the methods to small-scale applications.

59.7 CONCLUSION

A proper mechanical design of the bioreactor is aimed at maintaining the environmental and nutritional conditions (temperature, pressure, pH, nutrients concentration, mixing, hydrodynamic stress, etc.) for optimal growth and/or a product formation. Among the various environmental and nutritional factors that influence the aerobic bioprocess, oxygen is a critical parameter since it is the only nutrient that has to be provided continuously, even in batch cultures.

The determination of OTR in bioreactors is essential in order to establish the aeration efficiency and quantify the effects of the operation variables on the requirement of oxygen, since DO concentration is dependent on transport processes. Under these conditions, OTR and k_La are two of the key parameters involved in the design, operation, and scale-up of bioreactors.

Among the methods used to determine OTR experimentally, the most desirable are biological methods, which determine OTR (k_La) and OUR (q_{O_2}) in the same experiment. Sometimes when OTR from a physical method is determined, it must take into account the enhancement factor, E, because oxygen absorption into a culture broth can be considered as the absorption of a gas into a liquid where it reacts, the microorganisms suspended being the consumers of the oxygen, and therefore an enhancement of oxygen mass transfer rate can take place.

In recent literature, predictive methods have been proposed to calculate k_La and E, and thus find the value of OTR, although it is necessary to measure OUR experimentally. This approach is much more reliable than those based on the use of empirical equations, which are usually developed for other systems, other bioprocesses, and to be carried out in different types or sizes of bioreactors.

NOMENCLATURE

a	specific interfacial area (m^{-1})
A_D	down-comer cross-sectional area (m^2)
A_R	riser cross-sectional area (m^2)
C	concentration (kg/m^3)
c	parameter defined by Equation 59.43 (mol $O_2/m^3 \cdot s$)
CMC	carboxymethyl cellulose
C_X	biomass concentration (kg/m^3)
D	diameter of bioreactor, vessel or column (m)
d_b	bubble diameter (m)
D_i	diffusivity (m^2/s)
DO	dissolved oxygen
F	molar flow rate (mol/s)
g	gravitational acceleration (m/s^2)
H	height (m)
H_e	Henry's constant ($mol/m^3 \cdot atm$)
J	flux density molar (mol $O_2/m^2 \cdot s$)
k	consistency index in Ostwald–de Waele model (Pa s^n)
k_L	liquid-side mass transfer coefficient (m/s)
k_La	volumetric oxygen mass transfer coefficient (s^{-1})
K_La	volumetric oxygen mass transfer coefficient in presence biotransformation (s^{-1})
N	stirrer speed (s^{-1} or rpm)
N_l	normal stress (N/m^2)
n	flow behavior index in Ostwald–de Waele model
OTR	oxygen transfer rate (mol $O_2/m^3 \cdot s$)
OUR	oxygen uptake rate (mol $O_2/m^3 \cdot s$)
P	power input (W)
Q	gas flow rate (m^3/s)
q_{O2}	specific oxygen uptake rate (mol $O_2/kg \cdot s$)
r	reaction rate (mol $O_2/m^3 \cdot s$)
T	stirrer diameter (m)
t	time (s)
t_e	exposure time (s)
U_s	terminal rise velocity of bubble liquid circulation velocity (m/s)
V	volume of the liquid in the vessel (m^3 or L)
V_0	volume of flask (m^3)
V_{LR}	average liquid circulation velocity (m/s)
V_{LC}	average velocity in the core region (m/s)
V_S	superficial gas velocity (m/s)
Y_{XO}	biomass yield on oxygen (kg X/mol O_2)
z	film thickness (m)

Greek Symbols

ε	energy dissipation rate (W/kg)
ϕ	gas holdup
ϕ_v	gas holdup in viscous system
λ	characteristic material time (s)
μ	viscosity (Pa·s)
μ_a	apparent viscosity according to Ostwald–de Waele model (Pa·s)
μ_c	viscosity according to Casson model (Pa·s)
ν	kinematic viscosity (m^2/s)
ρ	density (kg/m^3)
σ	surface tension (N/m)
τ	shear stress (N/m^2)
τ_r	electrode response time (s)
ξ	parameter defined by Equation 59.38 (s)

Subscripts or Superscripts

b	relative to the bubble phase
CO_2	relative to carbon dioxide
Crit	relative to critical value
G	relative to gas phase
Hy	hydrazine
L	relative to liquid phase
me	relative to measure by electrode
max	maximum value
O_2	relative to oxygen
In	relative to inlet
Out	relative to outlet
2-HS	2-hydroxymuconic semialdehyde
	*Relative to equilibrium value in each phase

REFERENCES

1. Garcia-Ochoa F, Gomez E. Biotechnol Adv 2009; 27: 153–176.
2. Dai Y, Deng T, Wang J, Xu K. Colloids Surf A 2004; 240: 165–171.
3. Ibrahim M, Schlegel HG. Biotechnol Bioeng 1980; 22: 1877–1894.
4. Dumon E, Delmas H. Chem Eng Process 2003; 42: 419–438.
5. Clarke K, Williams P, Smit M, Harrison S. Biochem Eng J 2006; 28: 237–242.
6. Van Sonsbeek HM, de Blank H, Tramper J. Biotechnol Bioeng 1992; 40: 713–718.
7. Adlercreutz P, Mattiasson B. Enzyme Microb Technol 1982; 4: 332–336.
8. Adlercreutz P, Holst O, Mattiasson B. Enzyme Microb Technol 1982; 4: 395–400.
9. Martin AB, Alcon A, Santos VE, Garcia-Ochoa F. Biochem Eng J 2005; 22: 229–237.
10. Yang JD, Wang N. Biotechnol Prog 1992; 8: 244–251.
11. Chisti Y. In: Flickinger MC, Drew, SW, editors. Encyclopedia of bioprocess technology, Mass transfer, vol. 3. New York: John Wiley & Sons; 1999. p 1607–1640.
12. Merchuk JC, Asenjo JA, editors. Bioreactor system design. New York: Marcel Dekker; 1995.

13. Merchuk J, Gluz M. In: Flickinger MC, Drew SW, editors. Encyclopedia of bioprocess technology, Airlift reactors. New York: John Wiley & Sons; 1999. p 340–342.
14. Mezaki R, Mochizuki M, Ogawa K, editors. Engineering data on mixing. Amsterdam: Elsevier Science; 2000.
15. Margaritis A, Zajic J. Biotechnol Bioeng 1978; 20: 939–1001.
16. Oldshue JY. Biotechnol Adv 1985; 3: 219–237.
17. Kawase Y, Moo-Young M. Chem Eng J 1990; 43: 405–429.
18. Chisty Y. Appl Mech Rev 1998; 51: 33–112.
19. Arjunwadkar S, Sarvanan A, Kulkarni P, Pandit A. Biochem Eng J 1998; 1: 99–106.
20. Kilonzo P, Margaritis A. Biochem Eng J 2004; 17: 27–40.
21. Clarke K, Correia L. Biochem Eng J 2008; 39: 405–429.
22. Van't Riet K. Trends Biotechnol 1983; 1: 113–119.
23. Arrua L, McCoy B, Smith J. AIChE J 1990; 36: 1768–1772.
24. Badino A, Facciotti M, Schmidell W. Biochem Eng J 2001; 8: 111–119.
25. Galaction A-I, Cascaval D, Onisco C, Turnea M. Biochem Eng J 2004; 20: 85–94.
26. Puthli M, Rathod V, Pandit A. Biochem Eng J 2005; 23: 25–30.
27. Suh I-S, Schumpe A, Deckwer W, Kulicke W. Can J Chem Eng 1991; 69: 506–512.
28. Suh I-S, Schumpe A, Deckwer W. Biotechnol Bioeng 1992; 39: 85–94.
29. Wilkinson P, Haringa H, Dierendonck LV. Chem Eng Sci 1994; 49: 1417–1427.
30. Zhao M, Niranjan K, Davidson J. Chem Eng Sci 1994; 49: 2359–2369.
31. Li G, Yan S, Cai Z, Chen J. Chem Eng J 1995; 56:B101–B107.
32. Eickenbusch H, Brunn P, Schumpe A. Chem Eng Process 1995; 34: 479–485.
33. Vasconcelos J, Rodrigues J, Orvalho S, Alves S, Mendes R, Reis A. Chem Eng Sci 2003; 58: 1431–1440.
34. Zhang T, Wang T, Wang J. Chinese J Chem Eng 2006; 14: 604–610.
35. Boltes K, Caro A, Leton P, Rodriguez A, Garcia-Calvo E. Chem Eng Process 2008; 47: 2408–2412.
36. Blanch HW, Clark DS, editors. Transport process in biochemical engineering. New York: Marcel Dekker; 1997.
37. Whitman W. Chem Metall Eng 1923; 29: 146–149.
38. Hermann C, Dewes I, Shumpe A. Chem Eng Sci 1995; 50: 1673–1675.
39. Garcia-Ochoa F, Gomez E. Biotechnol Bioeng 2005; 92: 761–772.
40. Cooper C, Fernstorm G, Miller S. Ind Eng Chem 1944; 36: 504–509.
41. Linek V, Vacek V. Chem Eng Sci 1981; 36: 1747–1768.
42. Ruchti G, Dunn J, Bourne JR, Stockar UV. Chem Eng J 1985; 30: 29–38.
43. Danckwerts P, Gillham A. Trans Inst Chem Eng 1966; 44: 42–54.
44. Danckwerts P. Gas-liquid reaction. New York: McGraw-Hill; 1970. p 239–250.
45. Sharma M, Danckwerts P. British Chem Eng 1970; 15: 522–527.
46. Hill G. Ind Eng Chem Res 2006; 45: 5796–5800.
47. Onken U, Sick R, Weiland P. Chem Eng Sci 1985; 40: 1990–1993.
48. Ortiz-Ochoa K, Doig S, Ward J, Baganz F. Biochem Eng J 2005; 25: 63–68.
49. Linek V, Benes P, Vacek V. Biotechnol Bioeng 1989; 33: 1406–1412.
50. Mignone C. Chem Eng Sci 1990; 45: 1583–1587.
51. Gauthier L, Thibault J, LeDuy A. Biotechnol Bioeng 1991; 37: 889–893.
52. Carbajal T, Tecante A. Biochem Eng J 2004; 18: 185–192.
53. Pedersen A, Andersen H, Nielsen J, Villadsen J. Chem Eng Sci 1994; 6: 803–810.
54. Stenberg O, Anderson B. Chem Eng Sci 1988; 43: 719–724.
55. Linek V, Sinkule J, Benes P. Chem Eng Sci 1992; 47: 3885–3894.
56. Sanchez A, Garcia F, Contreras A, Molina E, Chisti Y. AIChE J 2000; 46: 1872–1887.
57. Djelal H, Larher F, Martin G, Amrane A. J Biotechnol 2006; 125: 95–103.
58. Garcia-Ochoa F, Gomez E. Biochem Eng J 1998; 1: 1–10.
59. Linek V, Vacek V, Benes P. Chem Eng J 1987; 34: 11–34.
60. Van't Riet K. Ind Eng Chem Process Des Develop 1979; 18: 357–364.
61. Godbole S, Shumpe A, Shah Y, Carr N. AIChE J 1984; 30: 213–220.
62. Weiland P, Onken U. Ger Chem Eng 1981; 4: 42–50.
63. Johnson J, Andre G, Chavarie C, Archambault J. Biotechnol Bioeng 1990; 35: 43–49.
64. Gourich B, Vial C, Azher NE, Soulami MB, Ziyad M. Biochem Eng J 2008; 39: 1–14.
65. Merchuk J, Yona S, Siegel M, Zvi AB. Biotechnol Bioeng 1990; 35: 1161–1163.
66. Taguchi H, Humphrey A. J Ferment Technol 1966; 44: 881–889.
67. Garcia-Ochoa F, Gomez E, Santos V. Enzyme Microb Technol 2000; 27: 680–690.
68. Bandaiphet C, Prasertsan P. Carbohydr Polym 2006; 66: 216–228.
69. Gomez E, Santos VE, Alcon A, Martin AB, Garcia-Ochoa F. Energy Fuels 2006; 20: 1565–1571.
70. Casas JL, Rodriguez EM, Oller I, Ballesteros MM, Sanchez JA, Fernandez JM, Chisti Y. Ind Eng Chem Res 2006; 45: 1167–1171.
71. Merchuk JC, Stein Y. Biotechnol Bioeng 1981; 23: 1309–1324.
72. Duetz W, Ruedi L, Hermann R, O'Connor K, Buchs J, Witholt B. Appl Environ Microbiol 2000; 66: 2641–2646.
73. Pirt S. Arch Microbiol 1982; 133: 300–302.
74. Doig S, Diep A, Baganz F. Biochem Eng J 2005; 23: 97–105.
75. Heijnen J, Roels J. Biotechnol Bioeng 1981; 23: 739–763.
76. Ogut A, Hatch R. Can J Chem Eng 1988; 66: 79–85.
77. Dussap CG, Decorps J, Gros JB. Entropie 1985; 123: 11–20.
78. Thibault J, Leduy A, Denis A. Can J Chem Eng 1990; 68: 324–326.

79. Costa E, Lucas A, Aguado J, Avila JA. An Quim 1982; 78: 387–392.
80. Yagi H, Yoshida F. Ind Eng Chem Process Des Develop 1975; 14: 488–493.
81. Figueiredo L, Calderbank P. Chem Eng Sci 1979; 34: 1333–1338.
82. Nishikawa M, Nakamura M, Yagi H, Hashimoto K. J Chem Eng Jpn 1981; 14: 219–226.
83. Chandrasekharan K, Calderbank P. Chem Eng Sci 1981; 36: 819–823.
84. Kawase Y, Moo-Young M. Chem Eng Res Dev 1988; 66: 284–288.
85. Linek V, Sinkule J, Benes P. Biotechnol Bioeng 1991; 38: 323–330.
86. Gagnon H, Lounes M, Thibault J. Can J Chem Eng 1998; 76: 379–389.
87. Vasconcelos J, Orvalho S, Rodriguez A, Alves S. Ind Eng Chem Res 2000; 39: 203–208.
88. Chisti Y, Jauregui-Haza UJ. Biochem Eng J 2002; 10: 143–153.
89. Kapic A, Heindel TJ. Trans I Chem E Part A, Chem Eng Res Design 2006; 84: 239–245.
90. Perez J, Sandall O. AIChE J 1974; 20: 770–775.
91. Herbst H, Shumpe A, Deckwer W. Chem Eng Technol 1992; 15: 425–434.
92. Höcker H, Langer G, Werner U. Ger Chem Eng 1981; 4: 51–62.
93. Schlüter V, Deckwer W. Chem Eng Sci 1992; 47: 2357–2362.
94. Halard B, Kawase Y, Moo-Young M. Ind Eng Chem Res 1989; 28: 243–245.
95. Popovic M, Robinson C. AIChE J 1989; 35: 393–405.
96. Bello R, Robinson C, Moo-Young M. Can J Chem Eng 1984; 62: 573–577.
97. Kawase Y, Hashiguchi N. Chem Eng J 1996; 62: 35–42.
98. Deckwer W, Furckhart R, Zoll G. Chem Eng Sci 1974; 29: 2177–2188.
99. Deckwer W, Nguyen-Tien K, Kelkar B, Shah Y. AIChE J 1983; 29: 915915–915922.
100. Jackson M, Shen C. AIChE J 1978; 24: 63–71.
101. Al-Masry W, Abasaeed A. Chem Eng Sci 1998; 53: 4085–4094.
102. Bando Y, Chaya M, Hamano S-I, Yasuda K, Nakamura M, Osada K, Matsui M. Ind Eng Chem Res 2003; 36: 523–529.
103. Akita K, Yoshida F. Ind Eng Chem Process Des Dev 1973; 12: 76–80.
104. Nakanoh M, Yoshida F. Ind Eng Chem Process Des Dev 1980; 19: 190–195.
105. Kawase Y, Halard B, Moo-Young M. Chem Eng Sci 1987; 42: 1609–1617.
106. Uchida S, Tsuyutani S, Seno T. Can J Chem Eng 1989; 67: 866–869.
107. Vatai G, Tekic M. Chem Eng Sci 1989; 44: 2402–2407.
108. Garcia-Ochoa F, Gomez E. Enzyme Microb Technol 2001; 28: 560–569.
109. Gandhi AB, Gupta PP, Joshi JB, Jayaraman VK, Kulkarni BD. Ind Eng Chem Res 2009; 48: 4216–4236.
110. Kawase Y, Halard B, Moo-Young M. Biotechnol Bioeng 1992; 39: 1133–1140.
111. Tobajas M, Garcia-Calvo E, Siegel M, Apitz S. Chem Eng Sci 1999; 54: 5347–5354.
112. Garcia-Ochoa F, Gomez E. Chem Eng Sci 2004; 59: 2489–24501.
113. Calderbank P. Trans Inst Chem Eng 1958; 36: 443–463.
114. Bhavaraju S, Russell T, Blanch H. AIChE J 1978; 24: 454–466.
115. Garcia-Calvo E, Leton P. Chem Eng Sci 1991; 46: 2947–2951.
116. Calik G, Vural H, Özdamar T. Chem Eng J 1997; 65: 109–116.
117. Calik P, Yilgör P, Ayhan P, Demir A. Chem Eng Sci 2004; 59: 5075–5083.
118. Calik P, Yilgör P, Demir A. Enzyme Microb Technol 2006; 38: 617–627.
119. Kocabas P, Calìk P, Özdamar TH. Enzyme Microb Technol 2006; 39: 1077–1088.
120. Gomez E, Santos VE, Alcon A, Garcia-Ochoa F. Chem Eng Sci 2006; 61: 4595–4604.
121. Tsao G. Biotechnol Bioeng 1969; 11: 1071–1087.
122. Merchuk J. Biotechnol Bioeng 1977; 19: 1885–1889.
123. Ju L-K, Sundararajan A. Biotechnol Bioeng 1992; 40: 1343–1352.
124. Liu Y-S, Wu J-Y, Ho K-P. Biochem Eng J 2006; 27: 331–335.
125. Lamping S, Zhang H, Allen B, Shamlou P. Chem Eng Sci 2003; 58:747–758.
126. Hermann R, Walther N, Maier U, Büchs J. Biotechnol Bioeng 2001; 74: 355–363.
127. Duetz W, Witholt B. Biochem Eng J 2004; 17: 181–185.

60

PHOTOBIOREACTORS

Mario R. Tredici
Dipartimento di Biotecnologie Agrarie, Università degli Studi di Firenze, Firenze, Italy
Graziella Chini Zittelli and Liliana Rodolfi
CNR, Istituto per lo Studio degli Ecosistemi, Firenze, Italy

60.1 INTRODUCTION

Photobioreactors (PBR) are reactors specifically designed for the cultivation of phototrophic microbes (anoxigenic photosynthetic bacteria, cyanobacteria, microalgae) and plant cells, or to carry out a photobiological reaction (1).

In the last decades, PBR have much evolved and plenty of new designs have been proposed, most of them for research in the laboratory or small scale applications. This review will focus on pilot PBR and large-scale systems used for commercial cultivation of microalgae (including the cyanobacteria).

With few exceptions (e.g. *Crypthecodinium cohnii* and *Schizochytrium* sp. cultivated in fermenters, and the green stage of *Haematococcus* grown in PBR), large-scale commercial production of microalgae is limited to species (belonging to the genera *Arthrospira*, *Chlorella*, and *Dunaliella*), which are cultivated in open ponds taking advantage of their high growth rate or of a selective growth medium that limits contamination (2). The reason for this is that large (commercial) open ponds are easier and less expensive to build and operate, and more durable than large closed reactors. However, the majority of microalgae does not require a specific growth environment or a selective medium, and cannot be cultivated for prolonged periods in outdoor open systems because other microalgae tend to dominate the culture regardless of the species inoculated (2). PBR provide a close environment that, although not sterile, protects the culture from direct fall-out and invasion by unwanted species. This, together with a more accurate control of culture conditions (pH, temperature, pO_2, etc.), ensures dominance of the desired species, even in the absence of a selective pressure.

PBR have been reviewed by Lee (3), Chaumont (4), Prokop and Erickson (5), Torzillo (6), Tredici and Chini Zittelli (7), Pulz and Scheibenbogen (8), Tredici (1), Pulz (9), and more recently by Tredici (10), Carvalho *et al*. (11), and Ugwu *et al*. (12)

60.1.1 Photobioreactor Definition and Classification

PBR can be defined as culture systems for phototrophs in which photons, the main source of energy for growth, do not impinge directly on the culture surface but need to pass through the transparent walls of the reactor before reaching the cultivated cells (1,10). In PBR direct exchange of gases, liquids (e.g. rain) and particles (microbes, insects, dust) between the culture and the atmosphere is thus excluded or strongly limited.

PBR can be classified on the basis of both design and mode of operation. In design terms, the main categories of reactors are (i) flat or tubular; (ii) horizontal, inclined, vertical or spiral; and (iii) manifold or serpentine. An operational classification of PBR would include (i) air- or pump-mixed, and (ii) single-phase reactors (filled with media, with gas exchange taking place in a separate gas exchanger), or two-phase reactors (in which both gas and liquid are present and continuous gas mass transfer takes place in the reactor

Upstream Industrial Biotechnology: Equipment, Process Design, Sensing, Control, and cGMP Operations, Volume 2, First Edition. Edited by Michael C. Flickinger.
© 2013 John Wiley & Sons, Inc. Published 2013 by John Wiley & Sons, Inc.

itself). Construction materials provide additional subcategories: (i) glass or plastic and (ii) rigid or flexible PBR. Axenic PBR are exclusively those reactors intended for operation under sterile conditions and require sterilization (e.g. by steam) before operation.

60.1.2 Design Criteria for Photobioreactors

The main requisites of a commercial PBR are a high productivity (resulting from a high efficiency of conversion of light energy) combined with the necessary reliability, stability and cost-effectiveness of the cultivation process. An efficient photobioreactor cannot be properly designed without knowing the physiology of the organism to be cultivated. Since phototrophic microorganisms are highly diverse in their morphology, nutritional and light requirements, and resistance to stress, PBR cannot be designed so as to adapt to all organisms and conditions (1). Besides, we should not forget that in artificial culture systems conditions differ substantially from those found in nature, in terms of average distance between the cells, velocity of displacement, light regime, nutrient availability, and shear stress (9).

The main design criteria for PBR include: shape and structure, construction material, surface-to-volume ratio (S/V), orientation and inclination, mixing and degassing devices, and systems for cleaning and for temperature regulation. Ease of operation and construction and operating costs also take on particular relevance in relation to commercial PBR.

60.1.2.1 Materials for Photobioreactors. Glass and different types of transparent plastic and resin [polyethylene, polyvinyl chloride (PVC), polymethyl metacrilate, Teflon, polycarbonate, fiberglass] can be used for PBR construction. Materials for PBR must have high transparency, high mechanical strength, durability, chemical stability, and low cost. Ease of cleaning and lack of toxicity are also important requisites. Advantages and drawbacks of the most common tubular materials used for PBR have been described (1).

60.1.2.2 Light Regime and Surface-to-Volume Ratio (S/V). Light (photons) is the basic energy source for phototrophic growth. Light used in algal photosynthesis (and growth) is the so-called photosynthetically active radiation (PAR), which lies in the wavelength range 400–700 nm and typically represents between 43% and 45% of total solar radiation. Understanding how light quality and intensity influence growth and biochemical composition of microalgae is a basic requisite for their successful cultivation in a PBR. A main goal of PBR design is achieving the maximum photosynthetic efficiency (PE), that is the maximum conversion of light energy into the chemical energy of biomass. Outdoors, the maximum PE achievable is about 10% of total solar radiation (13). Because of mutual shading between the cells, light regime inside reactors exposed outdoors is very complex. The light effectively available for each cell in the reactor, the average irradiance (I_{av}), depends on both the irradiance at the culture surface (I_o) and the biomass concentration. Methods to evaluate I_{av} in tubular reactors, based on the Beer–Lambert law, have been developed (14,15).

Besides irradiance, it is the S/V that is, the ratio between the illuminated surface area of a reactor and its volume, that determines the amount of light that enters the system per unit volume. Generally, the higher the S/V, the higher the cell concentration at which the reactor can be operated and the higher the volumetric productivity attained. As found by Richmond *et al*. (16), the S/V also influences productivity per unit of illuminated surface area. There is an optimal S/V (or light path) at which maximum productivity per unit of illuminated surface area is obtained, and it changes with the species cultivated (see section on flat photobioreactors). High S/V PBR are generally preferred since high cell concentrations reduce the cost of harvesting as well as that of medium preparation and culture handling. It must be emphasized, however, that high S/V reactors may become highly inefficient systems when scaled up to industrial size, as the failure of the PBL plant set up in Spain well demonstrates (see section on flat photobioreactors). At high S/V, volumetric activities such as O_2 evolution, CO_2 absorption, nutrient depletion, and metabolite excretion change at a high rate and may quickly disrupt the stability of the culture. Problems such as biofouling and cell damage are also magnified in high S/V reactors.

60.1.2.3 Orientation and Inclination. Unlike horizontal systems, elevated PBR may be oriented and inclined at various angles to the sun and thus offer the possibility to vary irradiance at the culture surface. The effect of photobioreactor inclination on productivity outdoors has been investigated by Lee and Low (17), Tredici and Chini Zittelli (7), and Hu *et al*. (18). Sun-oriented systems (south-facing and tilted so as to intercept maximum solar radiation) achieve higher productivities, whereas vertical systems that intercept sun rays at large angles, and thus dilute sunlight, attain higher efficiencies of solar energy conversion. High temperatures may become a problem in sun-oriented reactors in the summer. Experimentation is required to define the best arrangement at large scale, which with difficulty can be inferred from experiments with single units (see section titled "Flat Photobioreactors").

60.1.2.4 Carbon Dioxide Supply and Oxygen Removal. Carbon dioxide supply and oxygen removal are related to mixing and to the mass transfer capacity of the system (11,15). Nearly 50% of the dry algal biomass is made up of carbon; consequently carbon nutrition is a major component

of the production cost of autotrophic biomass, unless waste CO_2 from flue gas or fermentation is available. Automatic pH control, in which CO_2 is injected when pH is above a desired value, is the most common system employed to both regulate pH and replenish CO_2. Supplying carbon dioxide in shallow suspensions at near neutral pH is not an easy task, the low residence time of the bubbles being in general not sufficient for complete absorption and resulting in great losses of CO_2 to the atmosphere. Gas injection as minute bubbles by use of sintered porous stones into a column of down-coming culture, in which the culture velocity is adjusted to that of the rising CO_2 bubbles, may increase the efficiency of absorption up to 70% (15). The response to CO_2 injection is much improved and the losses reduced with the use of model-based predictive control systems (11). As alternative to bubbling, diffusion through hollow-fiber membranes or silicon tubing has been successfully applied in microalgae cultures (11).

Photosynthetic oxygen production and accumulation are directly correlated with the volumetric productivity of the culture. Dissolved oxygen concentrations equivalent to more than four times saturation with respect to air (~30 mg oxygen/L), toxic to many microalgae, may be easily reached in outdoor cultures, especially in high S/V reactors. At maximal rates of photosynthesis, a 1-cm diameter reactor may accumulate 8–10-mg oxygen/L/min (19). In high S/V tubular reactors, the maintenance of oxygen levels below the toxic concentration requires frequent degassing and very high flow rates, making the serpentine design difficult to scale-up (see section on tubular PBR"). Vertical reactors (columns or flat panels) mixed by air-bubbling offer a significant advantage in this respect. A useful model for predicting dissolved oxygen and carbon dioxide concentration profiles in serpentine reactors has been developed by Camacho Rubio *et al*. (20) and gas transfer in PBR has been thoroughly described by Carvalho *et al*. (11).

60.1.2.5 Mixing. Mixing in PBR is necessary to provide uniform dispersion of the cells within the culture, to prevent thermal stratification, to distribute nutrients and break down diffusion gradients at the cell surface, to remove photosynthetically generated oxygen and above all to ensure that cells experience alternating periods of light and darkness of adequate length. The fluid dynamics of the culture medium and the type of mixing influence the average irradiance and the light regime to which the cells are exposed, which in turn determines productivity (15,21). Increasing mixing increases productivity, but damage may occur when the fluid microeddy sizes approach cellular dimension (22). For this, the choice of the mixing device and of the intensity of mixing should be based on the characteristics of the organism to be cultivated. Although even air-bubbling may damage the cells at the level of bubble formation and break-up (23), air-mixing causes in general less damage compared to pump-mixing, and therefore is recommended for fragile organisms. Camacho Rubio *et al*. (20) have well described gas–liquid mass transfer and mixing in serpentine airlift bioreactors.

60.1.2.6 Temperature Control. Maximum productivity can be achieved only at the optimal temperature for growth. While open ponds are limited by low temperatures in the morning, PBR generally require cooling at midday. Immersion in a water bath, water spraying, or the use of internal heat exchangers are the most common solutions adopted for temperature regulation in PBR outdoors. Cooling by immersion in a water pool is efficient, but its cost-effectiveness is rather doubtful. Water spraying may be reliable and cost-effective in dry climates. Economic considerations seem to favor evaporative cooling over the use of heat exchangers, although the latter have been found more efficient for controlling the culture temperature in a disposable panel reactor (24).

60.2 PHOTOBIOREACTOR CATEGORIES

60.2.1 Sleeves and Vertical Columns

An inexpensive disposable vertical reactor can be easily built by cutting a suitable length of transparent polyethylene tubing and heat-sealing one end. This "bag" or "sleeve" reactor can be suspended from a framework or supported within a mesh frame. The culture is mixed by bubbling air from the bottom. Such reactors are used indoors with artificial illumination (generally vertically mounted fluorescent lamps) or outdoors under sunlight. Polyethylene bags, from 50 to 500 L in volume are widely used to produce marine microalgae in the hatcheries. Polyethylene sleeves hung on an iron structure have been used to grow *Porphyridium* and *Dunaliella* outdoors at the Institute for Applied Research (Beer–Sheva, Israel) obtaining significantly higher productivities compared to open ponds (25) (Fig. 60.1). In 2000 MinaPro Ltd. was established at Nevatim (Beer–Sheva, Israel) (26) to exploit this technology for production of natural products from microalgae. The company was closed in 2002 (27). At Ketura Kibbutz (near Eilat, Israel) a small plant made of polyethylene sleeves is in operation to produce *Porphyridium* for the cosmetic market. NOVAgreen GmbH (Vechta–Langforden, Germany) develops and provides bioreactors based on the "bag system" for the production of microalgae for the food, cosmetics, and pharmaceutical industry (28) (Fig. 60.1). Sleeve reactors are used for inocula production at GreenFuel Technologies Corp. (Massachusetts, USA) (29). The main drawbacks of sleeve reactors are low S/V, biofouling and the need of large number of units for scaling-up.



(a) (b)

Figure 60.1. Polyethylene sleeves. (a) NOVAgreen GmbH (Vechta–Langforden, Germany) (courtesy of Prof. O. Pulz). (b) Institute for Applied Research (Beer–Sheva, Israel) (courtesy of Prof. S. Arad). (This figure is available in full color at http://onlinelibrary.wiley.com/book/10.1002/9780470054581.)

Vertical tubular reactors (or column reactors) are simple systems in which mixing is achieved by injecting compressed air at the bottom. The rigid vertical columns, typically 2–2.5 m in height and 30–50 cm in diameter, which are extensively used in hatcheries to produce algal biomass for feeding the larval stages of marine bivalves and fish must be included in this category. Most commonly, these systems are made of translucent glass fiber sheets formed into cylinders. Illumination is provided either by artificial or natural light.

Several vertical tubular PBR made of rigid material have been developed following Cook's first design set up at Stanford University in California in the late 1940s (30). Column reactors made of glass or Plexiglas® have been experimented with by Jüttner (31), Miyamoto *et al*. (32), Hu and Richmond (33), and García Camacho *et al*. (34). Volumetric productivities in the range of 0.5–1.5 g/L/d, mostly in inverse relationship with the column diameter, have been attained with different algae.

At the Department of Chemical Engineering of the University of Almeria, airlift and bubble-column vertical reactors, 9.6–19 cm in diameter and 2 m high were used to cultivate *Phaeodactylum tricornutum* outdoors (34–36). The systems compared favorably with horizontal serpentine reactors experimented with in the same location (22). On the other hand, when stress conditions (high pO_2, high irradiance) are required for the production of specific products (e.g. carotenoids) horizontal, higher S/V PBR may be necessary (37).

At the Energy Research Center of the Netherlands (ECN), a 64-L Plexiglas® bubble-column reactor, 21 cm in diameter and 2 m high, was used to cultivate *Monodus subterraneous* outdoors (38). The productivities attained (0.03 g/L/d in winter and 0.20 g/L/d in summer) constitute a good performance for *M. subterraneous* grown in this low S/V reactor under Dutch climate. Lu *et al*. (39) report comparable results for the same microalga grown in bubble columns of similar S/V under the climatic conditions of Southern Spain.

Vertical cylinders illuminated from inside, which may be considered a variation of the annular reactor devised by Jüttner (31), have been proposed for the production of marine microalgae in hatcheries. Internally lit cylinders typically attain higher volumetric productivities and greater efficiencies of light utilization compared to completely filled columns, since the photon flux provided is completely trapped by the culture (1).

A vertical annular column with internal illumination was developed at the University of Florence by Tredici and co-workers in 1997 (Fig. 60.2). The reactor consists of two 2m-high Plexiglas® cylinders of different diameter placed one inside the other so as to form a regular annular culture chamber, 3- to 5-cm thick and 120 to 150 L in volume. Compressed air is bubbled at the bottom of the annular chamber for mixing and gas exchange. CO_2 from cylinders is injected into the culture through a gas diffuser placed in an unaerated zone of the annular chamber to provide the carbon source and pH regulation. To operate the reactor with artificial illumination, lamps or fluorescent tubes can be placed inside the inner cylinder. These reactors have been used to cultivate various cyanobacteria and microalgae, among which bioactive *Nostoc* strains (40), *Nannochloropsis* sp. (41,42), *Isochrysis* sp. (T-ISO) (43), *Skeletonema* sp. (44) and *Tetraselmis suecica* (45) under artificial, natural or combined illumination. The potential of annular columns has been evaluated outdoors using units arranged to simulate a full-scale plant (45). High productivities (up to 38 g/m^2/d) and high PEs (up to 9.3% on PAR) were attained with *T. suecica* (45). The annular columns can produce high quality algae biomass on a regular basis, attaining 5–10 fold higher productivities and cell concentrations at harvesting than the traditional systems used in hatcheries. However, the small size and relatively high cost (more than €1000 for a 120-L unit) discourage the use of the annular column



(a) (b)

Figure 60.2. Plexiglas® (a) and polyethylene (b) annular columns commercialized by Fotosintetica & Microbiologica S.r.l. (from the company's web site). (This figure is available in full color at http://onlinelibrary.wiley.com/book/10.1002/9780470054581.)

in large scale production of algae biomass. Recently, at the University of Florence this design has been modified in order to reduce its cost by using a polyethylene film for the culture chamber, which is enclosed in a cylindrical wire structure (46) (Fig. 60.2). Annular columns of 30–230-L volume are commercialized by Fotosintetica & Microbiologica S.r.l. (Florence, Italy) (47), a spin-off company of the University of Florence, mainly as small cultivation units for research and microalgae production for aquaculture.

Horizontal annular columns, in which mixing is induced by air-bubbling in a half of the culture chamber that thus acts as a riser, have been developed by Yamaha Motor Co. Ltd. (Iwata, Japan) for the cultivation of *Chaetoceros calcitrans* under natural and artificial illumination (48).

In this category, the sterilizable PBR known as *Medusa*, developed for monoseptic (axenic) cultivation of microalgae (49), may be also included. The reactor consists of a U-shaped loop made of borosilicate glass tubes, 2 m long and 5 cm in diameter, vertically arranged and connected at the top to a stainless steel or glass vessel that acts as a degasser and houses electrodes and probes. One arm of the loop is gassed with air, thus the culture is circulated by an airlift system. Illumination is provided by fluorescent lamps regularly interspaced between the culture tubes. The reactor can be sterilized by steam injection or by *in-situ* sterilization at 121°C and an overpressure of 1 bar, and is thus suitable for mixotrophic cultivation of microalgae (50,51). At the University of Erlangen (Germany) units of 10, 25, and 100 L have been developed by combining a number of loops (52).

60.2.2 Tubular Photobioreactors

60.2.2.1 Serpentine Photobioreactors. Serpentine PBR are systems in which several straight transparent tubes are connected in series by U-bends to form a flat loop (the photostage) that can be arranged either vertically or horizontally. Gas exchange and nutrient addition normally take place in a separate vessel. Circulation between the photostage and the gas exchanger is achieved by the use of a pump or an airlift. Typically, in serpentine reactors the culture is circulated at flow rates between 20 and 30 cm/s. Several reactors of this type have been developed following the original design by Tamiya (53). After several months of experimentation with *Chlorella ellipsoidea*, this author concluded that a significant increase of productivity could be attained through cultivation of algae exhibiting higher temperature optima and through vigorous mixing aimed at increasing growth by providing intermittent illumination. These concepts still guide our research.

In the early 1950s, the Arthur D. Little Company at the Massachusetts Institute of Technology (USA) developed a horizontal tubular unit for the cultivation of *Chlorella* that may be considered the first pilot plant for microalgae production (54). The reactor, of a total surface area of about 56 m^2, consisted of polyethylene tubes that, once filled with algal culture, assumed a more or less elliptic shape of 1.2 m width and a maximum depth of about 8 cm. Leakage and contamination were the major problems encountered. In a 40-day run an average areal productivity of 9 $g/m^2/d$ was attained.

Following these initial studies, little work was carried out with PBR for several years. In the early 1980s, Gudin and co-workers (4,55), working at the Centre d'Etudes Nucléaires de Cadarache (France), devised a horizontal serpentine reactor that was immersed in a water pond to obtain temperature control. It was composed of five identical 20-m^2 units, each of which consisted of 20 polyethylene tubes, 20 m in length and 6 cm in diameter. Initially, the culture was circulated by means of a pump, but later, airlift systems were adopted to limit damage to shear-sensitive cells and, at the same time, provide CO_2 and obtain O_2 degassing. Productivities from 20 to 25 $g/m^2/d$ were obtained with *Porphyridium cruentum*. The use of rigid rather than flexible tubes permitted operating a self-cleaning system consisting of two plastic balls, one with higher density than the culture medium and one lighter, which were hydraulically pushed through the system. Although flotation and immersion in a water basin can provide efficient thermoregulation, the cost of such a system is prohibitive for most applications.

In the early 1980s, Pirt and co-workers developed a vertical serpentine tubular reactor at the University of London's Queen Elizabeth College (56,57). The photobioreactor consisted of a photostage formed of 52 Pyrex® glass tubes (each approximately 1 m long and with a 1 cm internal diameter) horizontally stacked and connected to glass U-bends by silicone-rubber tubing to form a vertical loop. The loop outlet was connected through a vertical riser to a degasser. A second tube connected the degasser to the inlet of the loop. The culture suspension was circulated either by a peristaltic pump, a rotary positive-displacement pump or an airlift; the latter method was preferred because of the adverse effects observed with the pumps. The work carried out by Pirt and co-workers was remarkable for three reasons: It provided the first detailed analysis of the fundamental engineering parameters of a closed photobioreactor, introduced the concept of high S/V reactors (127 m^{-1} in this case), and attained extremely high light-conversion efficiencies. Pirt's analysis, however, ignored the light saturation effect, assuming that the efficiencies observed at low light intensity could be achieved in full sunlight as well. Although Pirt's serpentine reactor did deal with many of the problems encountered in closed systems, the concept of very high S/V reactors revealed all its practical drawbacks when the experimental set-up was scaled up to industrial level by Photo Bioreactors Ltd. (PBL) (see section on large scale commercial PBR).

Reactors of the type developed by Gudin have been thoroughly investigated by Molina Grima and co-workers in Spain (15). The Spanish group has carried out extensive research with serpentine reactors on the influence of the principal parameters that regulate growth of photosynthetic cells, among which are average irradiance, gas–liquid mass transfer, temperature control, fluid dynamics and mixing (15,22,58–60).

Torzillo and co-workers developed and experimented with a 145-L two-plane serpentine reactor (61). A maximum areal productivity of 27.8 g/m^2/d was achieved with *Arthrospira platensis* in the summer. This study addressed fundamental engineering parameters such as the effect of the rheological behavior of the algal culture on the mixing characteristics of the system and the energy requirement for turbulent flow.

A similar two-layer design has been recently adopted and optimized at the University of Almeria to maximize light capture, achieve better exploitation of the occupied area and reduce oxygen accumulation (62,63). In 2004, a 4000-L two-layer serpentine PBR has been set up by Cajamar in a greenhouse near Almeria (Spain) (64). The system, made of 10-cm diameter Plexiglas® tubes connected by U-joints to form a single 400-m long loop, occupies an area of 80 m^2 (Fig. 60.3). Temperature regulation is provided by circulating tap water through a heat exchanger placed in the degasser. The reactor has been



(a)



(b)

Figure 60.3. (a) Double layer 4000-L serpentine PBR (Almeria, Spain) (courtesy of Prof. E. Grima). (b) Near-horizontal tubular reactor at the University of Florence (Italy) (photograph by the authors). (This figure is available in full color at http://onlinelibrary.wiley.com/book/10.1002/9780470054581.)

used for production of lutein-rich biomass of *Scenedesmus almeriensis* achieving a mean productivity of 290 mg lutein/m^2/d (65). More recently, a fence-type tubular photobioreactor (32,000 L total volume and 1000 m^2 occupied area) has been devised and set up for mass production of *S. almeriensis* (66).

A horizontal serpentine PBR cooled by immersion in a water pool is used to cultivate marine microalgae by Fitoplancton Marino S.L. (Cadiz, Spain). The company sells lyophilized biomass and slurries of several microalgae for aquaculture use (67).

A tubular photobioreactor that makes use of concentrated solar radiation has been devised at the Academic and University Centre of Nove Hrady (Czech Republic) (68). The photobioreactor is based on solar concentrators (linear Fresnel lenses), mounted in a climate-controlled greenhouse, that concentrate up to 3.5 times the direct component of incident sunlight on the cultivation tubes. The cultivation unit (a 24-m long loop made of six parallel horizontal glass

tubes connected by U-bends) is placed on a movable frame, which enables automatic focusing of direct solar radiation. The photobioreactor has been used to study acclimation of algae to supra-high solar irradiances.

60.2.2.2 Manifold Photobioreactors. In manifold PBR, a series of parallel tubes is connected at the ends by two manifolds, one for distribution and the other for collection of the culture suspension. The main advantages of these systems over serpentine loop reactors are the reduction of head losses and lower oxygen concentrations, two factors that facilitate scale-up to industrial size. As shown by Pirt *et al*. (57), more than 15% of the energy consumed for circulating the culture in serpentine reactors is spent in moving the culture suspension around the bends.

Richmond and co-workers (69) devised a system made of parallel sets of 20-m long tubes connected by manifolds in which the culture was circulated by an airlift. A productivity of 0.55 g/L/d was attained with *A. platensis*. A manifold elevated system called "α-type tubular photobioreactor" was developed and experimented with in Singapore (70).

Tredici and co-workers, working at the University of Florence (Italy), developed the near-horizontal tubular reactor (NHTR) (Fig. 60.3). Units made of rigid or flexible tubes of about 5 cm in diameter and ranging from 6 to 45 m in length have been built and used to grow different algal species outdoors (71,72). Typically, a NHTR consisted of 8–10 flexible tubes connected by two manifolds. The tubes were placed side-by-side on white corrugated plastic sheeting, facing south and inclined at a slight angle to the horizontal (4° to 6°). Mixing and degassing were achieved by injecting air at the base of 6–8 tubes (risers); the remaining unaerated tubes acted as return-flow tubes (downcomers). Temperature control was obtained by water spraying. The largest unit experimented with occupied an area of 60 m^2 and contained about 1200 L of culture. Volumetric productivities of up to 1.3 g/L/d and areal productivities of more than 28 g/m^2/d were obtained with *A. platensis* (7). A maximum productivity of 0.8 g/L/d was achieved with *Nannochloropsis* during the late spring (72). NHTRs can be scaled up by increasing the number and/or the length of the tubes. Adoption of tube lengths over 20–25 m are, however, not practical since it would require the preparation of land areas with a drop of more than 3 m in order to get the minimum inclination necessary for proper mixing through air-bubbling. Besides, low mass transfer may be a limiting factor in long NHTRs, unless mixing is improved (e.g. by static mixers) (73,74). A cost analysis for a large NHTR system developed for hydrogen production has been presented (75).

A vertical manifold PBR known as *BioFence* was developed by Applied Photosynthetics Limited (APL) (Manchester, UK) in the late 1990s. The BioFence consists of an array of rigid or flexible transparent tubes racked together in banks and connected by manifolds in a fence-like structure (76). The culture suspension is circulated between the photostage and a holding tank by a centrifugal pump or by an airlift. BioFence systems are currently commercialized by Varicon Aqua Solutions Ltd. (UK) (77), which offers several sizes of modular reactors that are used as small cultivation units for research and microalgae production for aquaculture (78). A BioFence unit of 1200 L was commercialized at about €36,000 (79).

Biofence PBR from 10 to 35,000 L are also distributed by B. Braun Biotech International GmbH (now incorporated in Sartorius Biotechnology Division). Industrial scale plants based on the biofence design have been built by Bioprodukte Prof. Steinberg GmbH (Germany) (80), Algaltechnologies Ltd. (Israel) (81) and, more recently, by Salata (Germany) (see section on large scale commercial photobioreactors).

60.2.2.3 Helical Photobioreactors. Helical PBR consist of small-diameter flexible tubes wound around an upright structure (biocoils). This design was used in the 1950s by Davis to grow *Chlorella* (82) and later adopted, in a flattened version made of glass tubes, by Setlik (83), Krüger and Eloff (84) and Jüttner (31).

A biocoil consisting of a photostage of polyethylene or PVC tubing (between 2.5 and 5 cm diameter) wound helically around a cylindrical support (typically 8 m in height with a core diameter of 2 m) was patented by Biotechna Ltd. (85). Several parallel bands of tubes were connected by manifolds to the pumping system, allowing more even flow and shorter tube length thus minimizing oxygen build-up.

A 120-L helical bubble reactor was used to grow *Anabaena siamensis* and *A. platensis* outdoors at the University of Florence (71). With *A. platensis*, a mean volumetric productivity of 0.9 g/L/d and a photosynthetic efficiency of 6.6% (PAR) were achieved. The cost of a 120-L unit of this type was estimated to be about US$150 (1).

Addavita Ltd. (Chesterfield, UK) commercialized a coiled reactor called Advanced Algal Production System (AAPS). In this reactor circulation of the culture is achieved through a pump or by an airlift accordingly to the type of algae grown. The culture is pumped at the base of the tubes and flows in the helical photostage up to the top degasser. From the degasser the cultures descend down to a water bath for thermoregulation. The slope of the tubes can be varied for flow optimization (86).

A flat coiled glass reactor named VGPR, similar to that developed by Setlik (83), of about 1000 L volume has been built in Nanchang (China) and used to grow *Arthrospira maxima* and *Haematoccocus* (87). One single module is 5 m high, 5 m long and 0.8 m wide. The tubular photostage is connected to two glass towers, one for deoxygenation, the second for CO_2 supply and thermoregulation. The culture

is circulated by a pump at a speed of 0.5 m/s. The system can be sterilized.

60.2.2.4 Vertical Columns vs. Horizontal Serpentine Photobioreactors. Horizontal serpentine PBR, especially those characterized by a high S/V, reveal limited scalability because as tube length increases, pH and dissolved oxygen rise to very high values. It has been suggested that also an inadequate light climate strongly limits this design (22). Oxygen removal is governed by the magnitude of the overall gas–liquid mass transfer capacity, which in bubbled columns is about four folds the estimated value for a horizontal serpentine. Vertical bubble columns and airlift cylinders have substantially greater gas hold-ups than horizontal reactors and a much more chaotic gas–liquid flow, and consequently can attain substantially increased radial movement of the fluid that is necessary for improved light–dark cycling (22). A limitation of vertical bubble columns may be seen in their cost and in the fact that, since diameter and height cannot be much increased, a large number of units is needed to set up an industrial plant.

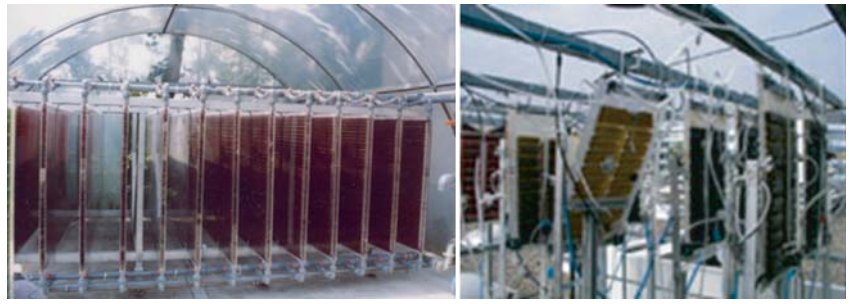
Vertical columns (and vertical reactors in general) are superior to horizontal reactors also in terms of PE, since they achieve higher light dilution because sun rays strike their surface with a large incidence angle. It has been demonstrated that light dilution reduces the negative effects of photosaturation and photoinhibition, leading to a significant increase of PE and productivity (71). Besides, the rear surface of a vertical reactor receives mainly disperse (diffuse and reflected) radiation of low intensity, which is known to be used with higher efficiency (16). In particular, during the central daylight hours, when the negative effect of excessive light upon outdoor cultures is maximal, the mean radiation incident on a vertical system undergoes about twofold dilution compared with that impinging on the horizontal. Besides, while the irradiance on the horizontal draws the well known bell-shaped curve centered at midday, the culture in a vertical column is exposed to a more homogeneous light environment for most of the day (45). However, the main advantage of this system (i.e. that around solar noon a large part of the direct radiation is reflected) can be seen also as a limitation, since it leads to significant losses of useful photons. These losses can be reduced at full-scale by closely spacing the different units so that a significant part of the photons reflected by the reactor walls (and then by the ground) are intercepted again by the reactors in the vicinity (45).

60.2.3 Flat Photobioreactors

Flat PBR have often been used in the laboratory because they are easy to be operated and provide a simple geometry that facilitates the measurement of irradiance at the culture surface. Despite their simplicity, few of such systems have been used for mass cultivation of algae until recently (1). Three main types of flat PBR have been experimented with at pilot level outdoors: alveolar panels, glass and acrylic plastic plates, and disposable panels.

60.2.3.1 Alveolar Panels. Interest in flat PBR sparkled in the 1980s when two groups working independently in France (88) and Italy (89) introduced alveolar panels for algae cultivation. The systems were constructed from commercially available, transparent PVC, polycarbonate or polymethyl methacrylate sheets internally partitioned to form narrow channels called *alveoli*. At the Centre d'Études Nucléaires de Grenoble (France) Ramos de Ortega and Roux (88) used 1.5 m^2, 4-cm thick, double layer PVC panels for growing *Chlorella*. The panels were laid horizontally on the ground; the upper layer of channels was used for algal growth, the lower for thermoregulation. The culture suspension was circulated through a pump. A productivity of 24 $g/m^2/d$ was achieved in the summer.

In 1988 Tredici and co-workers at the University of Florence developed vertical flat reactors made from commercially available, 16-mm thick Plexiglas® alveolar sheets (89). The sheets were placed vertically with the alveoli (and hence the culture flow) running parallel to the ground and pumps were used to circulate the algal suspension. A prototype of this design was presented at the exhibition ITALIA 2000 held in Moscow in 1988. In the same year, the Florence group started to experiment with a different design in which the panel was set up with the channels perpendicular or highly inclined to the ground so that mixing could be achieved by bubbling air at the bottom of the reactor (90). Several panels, with surface areas varying from 0.3 to 2.2 m^2 and different inclinations (from 20° to 50° to the horizontal) were experimented with by the Florence group and collaborating groups at Harbour Branch (Florida, USA), CSIRO (Hobart, Australia) and IFREMER (France) both under natural and artificial light with productivities of up to 24 g/m^2 (of illuminated panel surface) /d. The system proved adequate for growing different algal species, among which *A. platensis*, *Anabaena azollae*, *Isochrysis galbana*, *Pavlova lutheri*, *P. tricornutum*, *Nannochloropsis* sp., *T. suecica*, *Skeletonema* sp., and the fragile dinoflagellate *Alexandrium minutum* (7,44,71,90–94). Among the advantages of the system there is its high S/V (up to 160 m^{-1}), which allows to attain high volumetric productivities (> 2 g/L/d) and operation at high cell concentrations (4–6 g/L). Among the drawbacks, biofouling and the difficulty of scaling up seem to be the major ones. Besides, these systems, when placed near-horizontally (5°), have shown a lower performance compared to tubular reactors, which was attributed to the fact that tubular reactors achieve light dilution and reduce the negative effect of light saturation and photoinhibition (71).



(a) (b)

Figure 60.4. (a) alveolar panels at the IGV Institute für Getreideverarbeitung (Bergholz–Rehbrücke, Germany) (photograph by the authors). (b) airlift flat panel commercialized by Subitec GmbH (Stuttgart, Germany) (from the company's web site). (This figure is available in full color at http://onlinelibrary.wiley.com/book/10.1002/9780470054581.)

The design developed in Florence with pump-mixing was brought to industrial level by Pulz and co-workers at the IGV Institut für Getreideverarbeitung (Bergholz–Rehbrücke, Germany), who used 32-mm thick alveolar panels (8) (Fig. 60.4). Difficulty in maintaining an adequate turbulent flow, build-up of oxygen and fouling were among the problems encountered. The main merit of the reactors developed in Germany was the close spacing of the plates that provided an illuminated surface area of about 500 m^2 on a ground area of only 100 m^2. This design may seem weak at first sight, since in this configuration the panels strongly shade each other. However, despite the unfavorable climatic conditions of Germany, a record output of 130 g/m^2 (ground area)/d was reported with *Chlorella* (8). This very high productivity, which exceeds the maximum theoretical photosynthetic efficiency, may be partially explained by the fact that peripheral effects were not considered. It should be noted, however, that this arrangement allows a fivefold dilution of solar irradiance at the culture surface, compared to an horizontal surface, an effect called *culture lamination*, which enhances the efficiency of conversion of solar irradiance into biomass (95,96). Reactors based on this design are commercialized by B. Braun Biotech International GmbH (now incorporated in Sartorius Biotechnology Division) in sizes varying from 10 to 2000 L.

60.2.3.2 Glass Plates. In the mid 1990s Richmond and co-workers (97) developed an inclined modular photobioreactor consisting of a series of flat glass chambers, 0.7 m high and 0.9 m long, connected in cascade and tilted at an angle to maximize solar radiation capture. Reactors with light paths (thickness) from 1.3 to 10.4 cm were tested in the cultivation of *A. platensis*, *M. subterraneus* and *A. siamensis*. At the optimal population density and adopting vigorous mixing by air-bubbling, record productivities of about 50 g/m^2 /d of front illuminated reactor surface were achieved with *A. platensis*. When the back surface (that receives mainly reflected and diffuse radiation) of panels placed vertically was covered, culture productivity diminished of more than 50%, confirming the role played by diffuse and reflected light in elevated systems (97). Using glass panels with a light path ranging from 1.3 to 30 cm, Richmond and co-workers elucidated the influence of the light path on areal productivity (98–101). It was found that there is a precise light path at which areal productivity is maximal and that the optimal light path changes with the species cultivated: For example, it is 1–2 cm for *A. platensis*, 10 cm for *Nannochloropsis* and 20 cm for *Chaetoceros muelleri* var. *subsalsum* and *I. galbana*. A 500-L glass plate with 10-cm light path attained with *Nannochloropsis* an average productivity of 12 g/m^2 (total illuminated surface)/d (102). The same reactor design, but of 5-cm light path has been recently used for the cultivation of the green stage of *Haematococcus pluvialis* (103). In the summer a productivity of 0.37 g/L/d (9.3 g/m^2 of total illuminated surface/d) was attained. Another important result of the researches of the Israeli group was clearing the role of autoinhibition. Ultra-high cell densities (over 50 g/L) were achieved with *Nannochloropsis* and *A. platensis* in narrow (1–2 cm) light path plates exposed to high irradiance and under vigorous stirring, only when the exhaust growth medium was regularly replaced with fresh medium to remove inhibitory substances and replenish nutrients (16,104).

Glass panels have several advantages. Glass is highly transparent, easy to clean and resistant to weathering. Using glass sheets, reactors of any desired optical path can be assembled and tailored to meet the specific requirements of any algal species. However, glass excessive weight, fragility and cost discourage its use in large scale plants. Zhang *et al*. (102) calculated that for a 2000 L glass reactor, construction cost was US$8000. The cost of *Nannochloropsis* biomass production in this system was estimated to vary between US$50 and US$110 per kg dry wt, the dominant input being the cost of labor (102).

60.2.3.3 Plastic Plates. Vertical plates made of acrylic plastic and resembling those realized by Richmond and collaborators have been experimented with by the group of Miyachi (105,106). In some designs, vertical and horizontal baffles were inserted into the culture chamber to provide rigidity and improve mixing (107,108). In the laboratory with *Chlorococcum littorale* a cell density of up to 84 g/L was reached in a 1-cm light path reactor under 2000 μmol/photons m^2/s and by daily replacing the culture medium (106). With *Synechocystis aquatilis* the influence of the distance between reactors, reactor orientation and reactor size on productivity was evaluated (108,109). The productivity in an N-S oriented (east-west facing) set of parallel plates placed at a distance of 0.5 m was higher than the productivity obtained with E-W oriented (north-south facing) plates. These results differ from those attained by Rodolfi *et al*. (110) at similar latitudes in a different season with *T. suecica* (see section on disposable panels).

Small flat panels built from polycarbonate sheets held together in a steel frame with two chambers, one for the culture and the other for thermoregulation, have been used for the A-stat cultivation of *Dunaliella tertiolecta* (111) and to study the influence of autoinhibitory substances in high density cultures of *M. subterraneus* (112).

An airlift flat panel with a defined circulation path was patented and tested in the indoor cultivation of *Chlorella vulgaris* (113) and *P. tricornutum* (114). The reactors, made of Plexiglas® or PVC, were divided in a small downcomer zone and a larger riser zone, in which compressed air was injected. The riser was subdivided into interconnected chambers by means of horizontal baffles attached alternately to the two wider sides of the reactor. This arrangement allowed a more regular and defined mixing that significantly enhanced productivity in comparison with randomly mixed bubble columns (113,114). This design (Fig. 60.4) is commercialized by Subitec GmbH (115), a company founded in 2000 as a spin-off of the Fraunhofer Institute for Interfacial Engineering and Biotechnology (Stuttgart, Germany). A similar design made by molded plastic sheets is offered by PetroSUN Inc. (Arizona, USA) for production of biofuels (116). These reactors are an interesting development of plastic panels. However, low scalability and high cost (a 5–9 L unit is sold by Subitec GmbH for €1000) (115) limit their commercial application especially in the biofuel field.

A multi-compartment flat plate reactor made from acrylic plastic sheets was developed by Grobbelaar and Kurano (117). The idea was to have separate culture chambers with algal cells acclimated to different light conditions in order to allow better utilization of the entire light gradient found in dense cultures and maximize PE. A continuous-flow panel was tested in which the compartment facing the light source contained high-light acclimated cells, whereas low-light acclimated cells grew in the back compartment. With *S. aquatilis*, the double compartment plate yielded a 37% higher productivity compared to a traditional plate with a single compartment.

A 500-L Plexiglas® plate, with a 20-cm light path, based on Richmond's design (102) was tested with different microalgae used in aquaculture and compared with vertical columns and biofence-like tubular reactors at the Oceanic Institute of the University of Hawaii (78). The authors found that the hydrostatically limited height, the narrow width, the large internal surface area that hinders cleaning, and the high cost (about US$5000) were major drawbacks of this system.

60.2.3.4 Disposable Panels. In the early 2000s, two groups working independently in Italy (University of Florence) and Israel (Ben–Gurion University) developed and patented the concept of the disposable panel: a flat reactor consisting of a plastic culture chamber enclosed in a rectangular metal frame or cage (46,118) (Fig. 60.5). As in many of the previous designs, a tube inserted at the bottom provides mixing by air-bubbling, and water spraying, or a heating exchange unit, ensures temperature control. Different reasons prompted the two groups to develop the disposable panel design. While the Italian group aimed at



(a)



(b)

Figure 60.5. Disposable panels developed at the University of Florence, Italy (a) (photograph by the authors) and at the Ben–Gurion University, Israel (b) (courtesy of Prof. S. Boussiba). (This figure is available in full color at http://onlinelibrary.wiley.com/book/10.1002/9780470054581.)

a low-cost system for large scale applications, the main goal of the Israeli researchers was to have a clean and disposable culture chamber for the cultivation of those microalgae which suffer from contamination (Boussiba, personal communication). Disposable panels are simple to operate, have low construction cost and are capable to be scaled up. The plastic chamber can be either cleaned or replaced when necessary. They are currently used in hatcheries for microalgae feed production both in Israel and Italy.

In Italy, green wall (GW) panels, as the disposable reactors were called, 1 m high, 5 cm thick and from 2.5 to 10 m long (Fig. 60.5) have been used to grow *Tetraselmis*, *Isochrysis* and *Nannochloropsis* outdoors (93). These reactors have shown reliability, flexibility and good mass transfer capacity ($K_L a$ O_2 was 0.006 s^{-1} at an Ug of 0.004 m/s). With *T. suecica* it has been shown that while single units attain a higher productivity when they are N-S oriented (east-west facing), at full-scale an E-W orientation (north-south facing) is preferable (110). In the latter arrangement, overall areal productivities (OAP) (see section on evaluation of productivity) of about 30 $g/m^2/d$ were attained in a full-scale simulation with *T. suecica*, in September. With *Nannochloropsis* lipid productivities of more than 8 $g/m^2/d$ has been achieved, which represent a potential of more than 20 t/ha/y under the climatic conditions of Tuscany (Italy) and of 30 t/ha/y in sunny tropical regions (119,120).

Sierra *et al*. (24) evaluated the fluid dynamics and mass transfer characteristics of a 1.5-m high, 2.5-m long and 0.07-m thick disposable panel. The study concluded that the low power supply (53 W/m^3) and the high mass ($K_L a$ $O_2 = 0.007$ s^{-1}) and heat (500 W/m^2) transfer capacities were important advantages of the system, and make bubbled plates preferable to tubular PBR.

Recently the GW panel has been modified by the Italian group (119,120). A decrease of the culture chamber height from 1 to 0.7 m has permitted to use a much lighter metal frame and decreased construction cost from about €100 to about €30 for a 2-m long panel. Excluding accessory equipment (electrodes, tubing, valves, etc.), the cost of the new reactor (on a ground area basis) is within the range of construction costs of raceway ponds. The GW panels patented by the University of Florence are commercialized by Fotosintetica & Microbiologica S.r.l. (Florence, Italy) (47).

60.2.3.5 Critical Evaluation of Flat Systems. Vertical or inclined flat reactors represent very promising culture devices. Air-bubbling can be adopted attaining good mixing and high mass transfer capacity at relatively low power supply. Temperature control is efficient either through evaporative cooling by water spraying (in dry climates) or by heat exchangers. Some of the latter designs, especially the disposable panels, have shown good scalability. Disposable units of 1000–2000 L in volume have been built and successfully operated for long periods. Flat panels can be oriented and tilted at angles that maximize the amount of solar radiation intercepted and thus maximize productivity per reactor or, differently, inclined so as to reduce the amount of radiant energy impinging on the culture and increase the efficiency of light conversion and the productivity per unit of ground area. Which strategy is to be pursued depends on the objectives and local conditions. In contrast with horizontal reactors, the entire surface of elevated plates is illuminated. The front surface receives total radiation and the back surface is illuminated by a low energy photon flux made essentially of diffuse and reflected light, very effective for photosynthesis. They also offer the possibility to be closely packed together and thus attain, by a sort of "lamination" of the culture, high areal productivities.

60.2.4 Photobioreactors for Biofuels

Numerous companies have been established in the last 2–3 years in the field of microalgae biofuels, with interesting new ideas and innovative applications of old reactor designs. Here only three companies that have done some outdoor trials at pilot scale with proprietary designs will be shortly described. More information can be retrieved from http://peswiki.com/index.php/Directory:Biodiesel_from_Algae_Oil (121). The survey "Microalgae Biofuel & CO_2 Mitigation Ventures—Emerging New Business" (July 2006) prepared by Necton S.A. (Portugal) is also a useful source of information.

60.2.4.1 GreenFuel Technologies Corp. (GFT) (Massachusetts, USA) (122). GFT was founded in 2001 by MIT (Massachusetts Institute of Technology) and Harvard scientists. In 2004 its technology (the triangular airlift reactor) was tested at pilot level at MIT, and in 2006 a demonstration unit was set up at a coal-fired station in New York. The GFT bioreactor consisted of a series of riser tubes, gas separators and downcomers arranged in a triangular configuration (Fig. 60.6). GFT claimed the process was able to capture from the gas stream up to 82% CO_2 and reduce NOx by 86%. According to the reactor productivity, a biodiesel yield of up to 80 ton per ha per year was expected. Despite the high potential, this system has been not further developed and a different design, called the *3D Matrix System* (no details available at present), is currently under test at GFT facilities in the Arizona desert (Redhawk, Phoenix, Arizona). With the new technology in the summer 2007, an average areal productivity of 98 g (ash free dry wt) $/m^2/d$, with peak productivities of over 170 $g/m^2/d$ on good sunny days, was achieved (122). These numbers are unrealistic, even if



(a)



(b)

Figure 60.6. (a) GFT (Massachusetts, USA) triangular airlift reactor (from the company's web site). (b) AlgaeLink (The Netherlands) serpentine bioreactor (from the company's web site). (This figure is available in full color at http://onlinelibrary.wiley.com/book/10.1002/9780470054581.)

the 3D Matrix System, which is reported to have an S/V of 1500–2000 m^{-1} (20 times higher than in most PBR), maximizes the "light dilution effect". On sunny days, during the experiment, irradiances of about 870 μmol photons/m^2 /s (daily average) were measured, which in energy terms amount to about 9 MJ/m^2/d in the visible range. Given the peak productivity and an average energy content of the algal biomass of 22 kJ/g, a photosynthetic efficiency on PAR of more than 40% was attained, while the theoretical maximum is 22% (13).

60.2.4.2 Valcent Products, Inc. (Vancouver, Canada) (123). Valcent has developed a vertical bioreactor (named *Vertigro*) for the mass production of oil-rich algae. The system consists of a series of closely spaced vertical bioreactors made from thin plastic film membranes. The culture is pumped at the top of the reactor and circulates by gravity to the bottom in a meandering way. During a 90-day test carried out at Valcent's research center located at El Paso (Texas, USA), an algal suspension at 1 g/L was continuously harvested (123). The measured productivity was equivalent to more than 680 tons of dry biomass per ha and year, which is impossible. The system is interesting for its simplicity and verticality. Problems, however, might arise at high cell densities, that favor biofouling, and because of oxygen build-up. The cost of the single bioreactor may be low, but the system needs a heavy support structure and to be protected inside a greenhouse. In July 2007, Vertigro and SGCEnergia, the biofuel division of the SGC Group of Portugal, have agreed to form a joint venture company to build a Vertigro pilot plant near Lisbon, Portugal.

AlgaeLink N.V. (The Netherlands) (124). AlgaeLink N.V., based in The Netherlands, that currently commercializes PBR (Fig. 60.6) from demo up to 100 ton per day plants, is a good example of a growing, successful enterprise in the field of microalgae biofuel. The company has already sold several plants, in the USA, Asia, Europe, Australia and South America, based on a PC-controlled, large-diameter serpentine photobioreactor. The 3.5-m^3 demo is made of 36-m long, 30-cm diameter tubes, costs €69,000, occupies an area of 40 m^2, and produces between 3.5 and 5 kg dry biomass per day. Productivity is thus assumed to be between 1 and 1.4 g/L/d. The large scale reactors are made of 64-cm diameter tubes assembled on-site from transparent sheets. The expected volumetric productivity is 1.5 g/L/d. The AlgaeLink reactor is an example of a well developed (and well advertised) technology which is marketed on the basis of wrong assumptions: in this case that the algae will achieve a volumetric productivity of 1.5 g/L/d, which is impossible in such low S/V reactors under autotrophic conditions. According to http://www.algaelink.com (124), the 1 ton per day plant requires a ground area of 3327 m^2 (the installation area needed is wrongly reported to be 1782 m^2 in http://algaefuels.org). This means that the reactor is expected to produce 300 g/m^2/d and thus achieve, in energy terms, a daily output of about 6.6 MJ/m^2 (at an energy content of the algal biomass of 22 kJ/g). Given an average summer day of 23 MJ/m^2, this productivity will be equivalent to a PE on total solar radiation of about 30%, that is, three times the theoretical maximum, without considering irradiance losses because of reflection at the tubes' surface and the non-active empty spaces between tubes. AlgaeLink N.V. sells a 100 ton per day plant at about €300,000 ha^{-1} (€30 m^{-2}). This is an interestingly low price, even in comparison with raceway ponds (which will not cost much less if lined with a durable liner), for a completely-controlled, self-cleaning, pump-mixed closed system. The company also sells a prefabricated automatically controlled 1000-m^2 raceway-pond at the price of €45,500 (€45 per square meter), including tanks, pumps, valves, tubing and sensors (124).

Many other companies have been formed recently to exploit the interest on microalgae originated by the dramatic

problems of climate change and oil increasing price. In reality, no company in the field has at present a mature technology to be on the market and compete with fossil fuels. However, some of the proposed designs are worth being improved and tested at larger scale. It is not to exclude that, after adequate R&D, one of these or another system, very likely in combination with open ponds, might in the not far future produce algae biomass with the necessary efficiency so as to become a competitive source of renewable fuels.

60.3 LARGE SCALE COMMERCIAL PHOTOBIOREACTORS

60.3.1 Present Enterprises

With the exclusion of the plant built in Hawaii (USA) by MicroGaia Ltd. (now BioReal, Inc.) large industrial PBR are tubular, pump-mixed, one-phase systems. The photostage is typically made of plastic tubes, as in the Mera Growth Module (MGM) built by Mera Pharmaceuticals, Inc. (Hawaii, USA) or of glass tubes, as in the two largest commercial systems currently in operation, BPS (Germany) and Algatechnologies (Israel) plants.

60.3.1.1 BioReal, Inc., (USA) (125). In 2000 Micro Gaia, Ltd. (now BioReal, Inc. a subsidiary of Fuji Chemical Industry Co., Ltd., Japan) installed on an area of about 8 ha on the island of Maui (Hawaii) a plant based on its patented "bio-dome" (126). This is a rather elaborate system made by coupling two hemispheric transparent domes placed one on top of the other, convex surface up, so as to create a hemispheric culture chamber, from 2.5 to 10 cm wide. The culture is mixed and degassed by air-bubbling and by an apparatus that moves "jumping" along the circular bottom of the bio-dome. The air-tube, inserted from a top opening and connected to the moving device, cleans the dome walls by scraping their surface during its circular motion. Cooling is obtained by water spraying from the top of the reactor. Complexity, the need to build and connect thousands of units to realize a commercial plant, and difficulty of cleaning represent severe drawbacks of this system. BioReal, Inc. utilizes these dome-shaped reactors to grow *H. pluvialis* for production of astaxanthin (125).

60.3.1.2 Algatechnologies Ltd. (Israel) (81). Algatechnologies Ltd. was founded in 1999 to develop and commercialize microalgae derived products for the nutraceuticals and cosmeceuticals market (81). The plant, spread on an area of about 1.2 ha, is located at Kibbutz Ketura, 50 kilometres north of Eilat (Israel) (Fig. 60.7). Both horizontal manifold and biofence-like tubular systems are used to grow *H. pluvialis* based on the technology developed by Prof. Sammy Boussiba at the Microalgal Biotechnology Laboratory of Ben–Gurion University (127). Differently from Cyanotech Corp. and Mera Pharmaceuticals Inc., which use open ponds for the red stage, Algatechnologies Ltd. carries out both the green and the red stage in their closed system. A high quality product is obtained through strict control of growth parameters and inocula production under axenic conditions. Compared to the BPS and Salata plants in Germany (see following paragraph), productivity in this system is much advantaged by the high solar radiation available in the Arava desert (Southern Israel). Algatechnologies Ltd. has recently started collaboration with GreenFuel Technologies Corp. (Massachusetts, USA) for developing fuels from microalgae cultures using carbon dioxide emissions (128).



Figure 60.7. Algatechnologies Ltd. plant at Kibbutz Ketura (Israel) (courtesy of Prof. S. Boussiba). (This figure is available in full color at http://onlinelibrary.wiley.com/book/10.1002/9780470054581.)

Bioprodukte Prof. Steinberg GmbH (Klötze, Germany) and Salata GmbH (Ritschenhausen, Germany) (80). Among the large scale commercial plants currently in operation, special mention goes to the 700 m^3 PBR built by ÖPA GmbH at Klötze near Wolfsburg (Germany) (Fig. 60.8), now owned and operated by Bioprodukte Prof. Steinberg GmbH (BPS) (80). This plant consists of 20 modules, 35 m^3 each, installed in a 12,000 m^2 greenhouse. The photostage is made of 500 km of 48-mm diameter glass tubes running horizontally in a fence-like structure.



Figure 60.8. BPS plant at Klötze (Wolfsburg, Germany) (company's brochure). (This figure is available in full color at http://onlinelibrary.wiley.com/book/10.1002/9780470054581.)

Each unit is provided with an on-line control system. Mixing is achieved through centrifugal pumps. Harvesting is accomplished by Westfalia separators, and the biomass is spray dried. The expected productivity with *C. vulgaris* was 100–130 tons per year, which means achieving a volumetric productivity of 0.6–0.8 g/L/d during an 8-month operation period. Quality control of the *Chlorella* biomass produced at BPS has shown lower levels of heavy metals, pesticides and contaminating microorganisms compared to products attained in open ponds.

A similar design has been recently put in operation at Ritschenhausen (Germany) by Salata in cooperation with the Institut für Getreideverarbeitung GmbH. Salata cultivates, in modules of sizes ranging from 15,000 to 25,000 L, microalgae (*Nannochloropsis*, *Scenedesmus*, *Chlorella*, *Porphyridium*) and cyanobacteria (*Oscillatoria*, *Lyngbya*) mostly for the cosmetic market. Productivity is in the range of 0.2–0.8 g/L/d. Cost of production is high since artificial illumination is used to integrate solar radiation and to achieve year round production.

60.3.1.3 Mera Pharmaceuticals, Inc. (USA) (129). A 25,000 L polyethylene PBR, called *Aquasearch Growth Module* (AGM), was developed for astaxanthin production from *H. pluvialis* by Aquasearch, Inc. (now Mera Pharmaceuticals, Inc., Hawaii, USA) (129–131). The AGM (now MGM) consists of an unusually large (38 cm in diameter) serpentine reactor made up of a low-density polyethylene tube laid on an impermeable surface of about 200 m^2. The tubing is doubled back on itself several times so as to create a series of parallel tubes that are connected through a single end assembly. The end assembly incorporates a pump or an airlift, pH and temperature sensors, and fixtures to connect the PBR to tanks with nutrient media and to open ponds. The pump generates a velocity of the culture flow sufficient to attain a Reynold's number in the range of 2×10^3 to 2×10^4. Temperature is controlled by immersion in a water pond, which is cooled by addition of cold seawater. The reactor is sterilized by chlorination prior to inoculation. The system was operated continuously for several years. In the final year of operation an average areal productivity of 10.2 g/m^2/d was achieved. Given the low S/V, volumetric productivity was rather low (around 0.08 g/L/d). The PBR was used to inoculate ponds that, surprisingly, obtained a significantly higher productivity (15.1 g/m^2/d) (131).

60.3.2 Attempts of the Past

Among the several industrial PBR built in the last two decades and failed (1), two are worth to be illustrated here because they provide useful examples of technical and marketing mistakes that should not be repeated.

Photo Bioreactors Ltd. (PBL), set up in southern Spain in the late 1980s and based on two different designs patented by Queen Elizabeth College (UK) (56), represents one of the biggest failures in the field of microalgal biotechnology (Fig. 60.9). Despite the high quality of the work done by John Pirt and his collaborators at Queen Elizabeth College, several major technical errors were done in the full-scale plant, which was built without adequate piloting. The polyethylene tubes, about 50 m long, degraded quickly under sunlight and the tube diameter (1 cm) was too small for effective mixing and oxygen removal. Besides, temperature of the culture and wall growth were not adequately controlled. Together with improper management, the poor design led to heavy contamination of the culture, and in 1991 PBL closed without ever entering into production (132).

In 1996 Hidrobiologica SA, located at about 15 Km south of La Rioja (Argentina), started to cultivate *A. platensis* in one of the largest PBR known at that time (1). The plant consisted of 96 polyethylene tubes 120 m long and 25.5 cm in diameter laid parallel on the ground and arranged like a manifold with feeding and collecting channels made of concrete. The surface occupied by the whole plant was about 5000 m^2 and the total culture volume was 600 m^3 (Fig. 60.9). Some problems were apparent after the first years of operation, among which a limited capacity to control temperature and inadequate mixing, both consequent to low flow speed and unequal distribution of the culture among the tubes. The problems were approaching toward a solution when the plant was closed in 1999, when a hail storm destroyed part of the installation (Abdulqader, personal communication). It seems that the main problem that discouraged continuation was not technical, but it was the difficulty to compete with American and Asian companies using open raceways.



(a)



(b)

Figure 60.9. (a) PBL photobioreactor in Santa Ana (Murcia, Spain). (b) Hidrobiologica SA plant (La Rioja, Argentina). Photographs from Encyclopedia of Bioprocess Technology: Fermentation, Biocatalysis and Bioseparation. M.C. Flickinger and S.W. Drew, eds., J. Wiley & Sons, New York, 1999. (This figure is available in full color at http://onlinelibrary.wiley.com/book/10.1002/9780470054581.)

60.4 CONCLUDING REMARKS AND PROSPECTS

60.4.1 Evaluation of Productivity

Productivity in PBR can be evaluated as: (i) volumetric productivity (VP), that is, biomass produced per unit reactor volume per unit time (expressed as g/L/d); (ii) areal productivity (AP), that is, biomass produced per unit of ground area occupied by the reactor per unit time (expressed as $g/m^2/d$); or (iii) illuminated surface productivity (ISP), that is, biomass produced per unit of reactor illuminated surface area per unit time (expressed as $g/m^2/d$). VP is an important operational parameter that illustrates how efficiently the unit volume of the reactor is used. Being a function of the number of photons that enter the unit reactor volume in the unit time, it strictly depends on the S/V of the reactor. The higher the S/V, the higher the VP, but not necessarily a high VP translates into an efficient PBR. Care should be taken to discern between AP and ISP. In the case of ponds and horizontal flat reactors, the ground surface area occupied by the system and its illuminated surface area coincide, and so do AP and ISP. In the case of horizontal tubular reactors placed with tubes in contact, the illuminated surface area is 1.57 times the occupied surface area, so ISP will be always lower than AP. In the case of tubular reactors with tubes set up at a distance, the empty space among the tubes must be accounted for, and should be considered as occupied area when AP is calculated. The performance of elevated systems (i.e. reactors set at a high angle with the horizontal) is not easy to evaluate with these three parameters. For this it has been suggested to use a fourth parameter (10), the overall areal productivity (OAP) (expressed as $g/m^2/d$), which is obtained by summing the production of the reactors that constitute the plant and dividing the result by the total (including empty spaces) ground surface area occupied by all the reactors, carefully considering peripheral effects (10). When a plant of significant size cannot be set up, a simulation can be done by surrounding the experimental unit by an adequate number of dummy reactors arranged as in the planned industrial plant (45). OAP has greater meaning for scale-up and permits comparison between different kinds of reactors, and between reactors and ponds.

Commonly, VP and ISP, and sometimes also AP, are calculated from data obtained from the operation of a single unit. AP of an elevated reactor calculated on the basis of the area it projects on the ground is a meaningless parameter and should be avoided. A vertical or highly inclined reactor intercepts a much higher amount of radiation than that impinging on an area equivalent to its projection on the ground, and expressing productivity of vertical systems in terms of AP leads to unrealistic figures. When a single unit is experimented with to obtain data for scaling-up the system (to be essentially achieved by setting up a large number of units), it is necessary to understand that the data collected are of limited value, since the performance at large scale will be much influenced by the mode (essentially the distance) in which the several units in the field will be set up. Placing the reactors far apart and so that they do not significantly shade each other will maximize VP and ISP, which will not be too far from the values attained by experimenting with the single units. The OAP in this arrangement will be low because of the large non-productive space between the systems. If the reactors are placed closely packed, they will heavily shade each other, and VP and ISP will be reduced, generally in an inverse relationship with the distance. OAP on the contrary will be increased. Which strategy is to be chosen depends on many factors, among which are the cost of land, and capital and operating costs of the reactor.

An economic analysis providing the cost of biomass production in the system under consideration offers the best

evaluation of the performance of a PBR. However, economics evaluations are not valid for all situations, since many cost factors that have large impact on the final cost of the biomass (e.g. cost of labor, land, materials) change considerably from site to site even when the same species is cultivated.

60.4.2 Photobioreactors versus Ponds

The debate that opposes PBR and ponds is a false one. There is diffuse perception that open systems have reached their limit and there is little room for technological improvement (11). Together with their open surface, the major drawback of ponds is the fact that for practical reasons (reduction of flow and turbulence) the water level cannot be kept much lower than 15 cm (150 L/m^2). Optimal standing crops for algae are generally well below 100 g/m^2, hence the cell concentration of the culture in a 15-cm pond must be maintained below 0.65 g/L. Unless we are in the presence of some selective pressure (e.g. a specific chemical or physical requirement such as a high pH, salinity or temperature), these diluted, highly variable environments become readily contaminated by fast-growing microalgae, bacteria and protozoa, and do not ensure a durable and stable cultivation of the selected strain. Besides being closed, PBR have a much higher S/V (typically from 20 to 200 m^{-1}) than ponds (from 5 to 10 m^{-1}) and can sustain much higher cell concentrations. Together with the protected environment and tighter control over growth parameters (pH, pO_2, pCO_2 and temperature), the higher population density makes closed reactors relatively safe from invasion by competing microorganisms. However, growing algae in large raceway ponds is much cheaper than growing them in PBR, thus ponds are the systems of choice when the organism's requirements allow its cultivation in an open culture. In some cases a combination of PBR and ponds is worthy of consideration: the PBR for inoculum production and the ponds for bulk cultivation lasting for a period not long enough for contaminants to prevail. It is generally thought that PBR are more productive than ponds. This is true when the two systems are compared in terms of VP, unless PBR of unusual low S/V are used. On the contrary, when AP is the basis of comparison, it is difficult to reach any conclusion, the result depending on the algal species, the climate, the type of PBR used, and several other variables. Indeed, maximum short-term areal productivities of about 50 g/m^2/d have been reported for both ponds and PBR operated outdoors (65,133).

60.4.3 The Photobioreactor of the Future

PBR efficiency cannot be defined in general terms: any PBR that brings a product to the market making a profit must be considered efficient. In the future many other PBR designs (more or less efficient, more or less new) will be developed and, in much less number, exploited. However, two emerging opposite strategies can be foreseen in the future scenario of algal biotechnology: (i) very low-cost and (ii) high-tech systems. An example of the first type are the disposable panels (see section on flat reactors). These culture systems can be scaled up to large scale and set up with a capital investment of less than €200,000 ha^{-1} (120), much less than previously estimated (75) and not far from the construction cost of ponds.

A completely different approach is, for example, that of fiber optical–based systems, in which light capture and use are physically separated (Fig. 60.10). Visible solar light is collected by mirrors, concentrated through lenses and delivered into the bioreactor via an array of flexible, optical fibers (which transmit light via total internal reflection) and distributor rods or plates (21,134,135). Because the solar collectors track the sun, the main significant variation in photon flux is cloud cover (136). Wijffels and his team at the Agrotechnology and Food Sciences Group of Wageningen University (The Netherlands) envisaged a 10-m high, 250 m^3 in volume optical-fiber PBR, with the capability to produce about 200 t of dry algal biomass per year (21). Solar light is collected by parabolic dishes from a 2-ha field and conveyed through optical fibers to

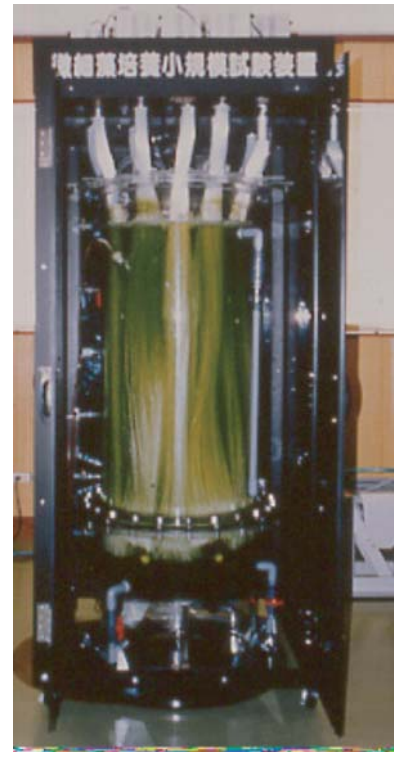


Figure 60.10. Optical fiber photobioreactor (courtesy of Prof. A. Richmond). (This figure is available in full color at http://onlinelibrary.wiley.com/book/10.1002/9780470054581.)

eighty 3-cm thick plates that re-distribute visible photons inside the culture at an irradiance of 1200 μmol/m^2/s. One main limitation of this technology is the efficiency of solar energy collection and transmission, but thanks to the much higher efficiency of liquid based cables, the efficiency of solar concentrating systems has significantly improved in recent years, exceeding 45% (136). Cultivation of microalgae in optical fiber PBR has been demonstrated only at the laboratory scale, and the very high cost of solar tracking devices and distribution systems seem prohibitive for most applications, but the potential of this technology is high and worth of further R&D efforts. (See also Chapter 18 in volume 1)

60.5 CONCLUSIONS

PBR are considered to have several advantages: They minimize contamination, offer better control over culture conditions, prevent evaporation, reduce CO_2 losses due to out-gassing, attain higher cell concentrations and volumetric productivities. Elevated reactors can be oriented and tilted at different angles and can use diffuse and reflected light, which plays an important role in productivity. PBR can be built with various light paths, a key issue to reach very high productivities and efficiencies of solar energy utilization, and can be mixed by either pumps or by air-bubbling. Many different materials can be used for their construction and many different designs are available. In conclusion, closed reactors are flexible systems that can be optimized according to the biological and physiological characteristics of the algal species being cultivated. The ultimate and most important advantage of closed systems, however, is that they permit cultivating algal species that cannot be grown in open ponds. On the other hand, the adoption of closed systems for large scale cultivation of microalgae requires that solutions are provided to the many problems that limit the technology (overheating, oxygen accumulation, biofouling, mixing generated shear-stress, deterioration of the construction material) and can lead to failures when not duly considered and solved. In the last years, even at commercial scale, these problems have been efficiently solved and some recent analyses support the conclusion that algae biomass production at large scale will be soon less expensive using PBR than open ponds (137).

REFERENCES

1. Tredici MR. In: Flickinger MC, Drew SW, editors. Encyclopedia of bioprocess technology: fermentation, biocatalysis and bioseparation. New York: John Wiley & Sons; 1999. pp. 395–419.
2. Richmond A. In: Cohen Z, editor. Chemicals from microalgae. London: Taylor & Francis; 1999. pp. 353–386.
3. Lee YK. Trends Biotechnol 1986; 4: 186–189.
4. Chamount D. J Appl Phycol 1993; 5: 593–604.
5. Prokop A, Erickson LE. In: Asenjo JA, Merchuk JC, editors. Bioreactor system design. New York: Marcel Dekker, Inc.; 1995. pp. 441–477.
6. Torzillo G. In: Vonshak A, editor. Spirulina platensis (Arthrospira): physiology, cell-biology and biotechnology. London: Taylor & Francis; 1997. pp. 101–115.
7. Tredici MR, Chini Zittelli G. In: Vonshak A, editor. Spirulina platensis (Arthrospira): physiology, cell-biology and biotechnology. London: Taylor & Francis; 1997. pp. 117–130.
8. Pulz O, Scheibenbogen K. In: Scheper T, editor. Advances in biochemical engineering/biotechnology. Berlin: Springer-Verlag; 1998. pp. 123–152.
9. Pulz O. Appl Microbiol Biotechnol 2001; 57: 287–293.
10. Tredici MR. In: Richmond A, editor. Handbook of microalgal cultures, biotechnology and applied phycology. Oxford: Blackwell; 2004. pp. 178–214.
11. Carvalho AP, Meireles LA, Malcata FX. Biotechnol Prog 2006; 22: 1490–1506.
12. Ugwu CU, Aoyagi H, Uchiyama H. Bioresour Technol 2008; 99: 4021–4023
13. Tredici MR. In: Zulpa G, Zaccaro MC, Conforti V, Storni MM, Maidana N, Stella AM, editors. Biotecnología algal: nuevas perspectivas para Latinoamérica: 1° Congreso Latinoamericano sobre botecnología algal. Buenos Aires, Argentina: Proyecto Editorial; 2004. pp. 27–30.
14. Evers EG. Biotechnol Bioeng 1991; 38: 254–259.
15. Molina Grima E. In: Flickinger MC, Drew SW, editors. Encyclopedia of bioprocess technology: fermentation, biocatalysis and bioseparation. New York: John Wiley & Sons; 1999. pp. 1753–1769.
16. Richmond A. In: Richmond A, editor. Handbook of microalgal cultures, biotechnology and applied phycology. Oxford: Blackwell; 2004. pp. 125–177.
17. Lee YK, Low CS. Biotechnol Bioeng 1991; 38: 995–1000.
18. Hu Q, Faiman D, Richmond A. J Ferment Bioeng 1998; 85: 230–236.
19. Weissman JC, Goebel RP, Benemann JR. Biotechnol Bioeng 1988; 31: 336–344.
20. Camacho Rubio F, Acién Fernández FG, Sánchez Pérez JA, García Camacho F, Molina Grima E. Biotechnol Bioeng 1999; 62: 71–86.
21. Janssen M, Tramper J, Mur LR, Wijffels RH. Biotechnol Bioeng 2003; 81: 193–210.
22. Sánchez Mirón A, Contreras Gómez A, García Camacho F, Molina Grima E, Chisti Y. J Biotechnol 1999; 70: 249–270.
23. Barbosa MJ, Hadiyanto H, Wijffels RH. Biotechnol Bioeng 2004; 85: 78–85.
24. Sierra E, Acién FG, Fernández JM, García JL, Gonzáles C, Molina E. Chem Eng J 2008; 138: 135–147.
25. Cohen E, Arad S (Malis). Biomass 1989; 18: 59–67.
26. Ben-Gurion University of the Negev web information. Available at http://www.bgu.ac.il/IAR/iaab/index.php. Accessed 2007 Sep 15.
27. Israel Venture Capital (IVC) Research Center web informa tion. Available at http://www.ivc-online.com/G_info.asp?fObjectID=5581&ObjectType. Accessed 2007 Sep 15.

28. NOVAgreen GmbH web information. Available at http://www.novagreen-microalgae.com/7.html. Accessed 2007 Sep 21.
29. GreenFuel Technologies Corporation web information. Available at http://www.greenfuelonline.com/gf_files/GF_Fortnightly.pdf. Accessed 2007 Oct 17.
30. Cook PM. In: Brunel J, Prescott GW, Tiffany LH, editors. The culturing of algae. Yellow Springs (OH): Charles F. Kettering Foundation; 1950. pp. 53–75.
31. Jüttner F. Process Biochem 1982; 17: 2–7.
32. Miyamoto K, Wable O, Benemann JR. Biotechnol Lett 1988; 10: 703–708.
33. Hu Q, Richmond A. J Appl Phycol 1994; 6: 391–396.
34. García Camacho F, Contreraz Gómez A, Acién Fernández FG, Fernández Sevilla JM, Molina Grima E. Enzyme Microb Technol 1999; 24: 164–172.
35. Sánchez Mirón A, Cerón García MC, García Camacho F, Molina Grima E, Chisti Y. Enzyme Microb Technol 2002; 31: 1015–1023.
36. Sánchez Mirón A, Cerón García MC, Contreraz Gómez A, García Camacho F, Molina Grima E, Chisti Y. Biochem Eng J 2003; 16: 287–297.
37. García-Malea López MC, Del Río Sánchez E, Casas López JL, Acién Fernández FG, Fernández Sevilla JM, Rivas J, Guerrero MG, Molina Grima E. J Biotechnol 2006; 123: 329–342.
38. Bosma R, van Zessen E, Reith JH, Tramper J, Wijffels RH. Biotechnol Bioeng 2007; 97: 1108–1120.
39. Lu C, Acién Fernández FG, Canizares Guerrero E, Hall DO, Molina Grima E. J Appl Phycol 2002; 14: 331–342.
40. Rodolfi L, Biondi N, Piccardi R, Ferroni P, Tredici MR. Book of Abstracts of the 9th International Conference on Applied Algology; 2002 May 26–30. Almeria, Spain. p. 21.
41. Chini Zittelli G, Rodolfi L, Tredici MR. J Appl Phycol 2003; 15: 107–114.
42. Rodolfi L, Chini Zittelli G, Barsanti L, Rosati G, Tredici MR. Biomol Eng 2003; 20: 243–248.
43. Chini Zittelli G, Somigli S, Rodolfi L, Tredici MR. In: Zulpa G, Zaccaro MC, Conforti V, Storni MM, Maidana N, Stella AM, editors. Biotecnología algal: nuevas perspectivas para Latinoamérica: 1° Congreso Latinoamericano sobre botecnología algal. Buenos Aires, Argentina: Proyecto Editorial; 2004. pp. 45–48.
44. Blackburn SI, Frampton DMF, Mansour MP, Gallori S, Tredici MR. Biomol Eng Abstr Mar Biotechnol Basics Appl 2003; 20: 63.
45. Chini Zittelli G, Rodolfi L, Biondi N, Tredici MR. Aquaculture 2006; 261: 932–943.
46. Tredici MR, Rodolfi L. WO patent 2004/074423. 2004 (to University of Florence).
47. Fotosintetica & Microbiologica S.r.l. web information. Available at http://www.femoline.it. Accessed 2007 Sep 21.
48. Yamaha Motor Co. Ltd. web information. Available at http://www.yamaha-motor.co.jp/global/news/2004/03/02/fukuroi.html. Accessed 2007 Sep 21.
49. Buchholz R. EP patent 0911386. 1999 (to Torsten Steinau Verfahrenstechnik Berlin).
50. Walter C, Steinau T, Gerbsch N, Buchholz R. Biomol Eng 2003; 20: 261–271.
51. Rechter S, Konig T, Auerochs S, Thulke S, Walter H, Dörnenburg H, Walter C, Marschall M. Antiviral Res 2006; 72: 197–206.
52. Institute of Bioprocess Engineering Friedrich Alexander University of Erlangen Nuremberg web information. Available at http://www.bvt.cbi.uni-erlangen.de. Accessed 2007 Sep 15.
53. Tamiya H, Hase E, Shibata K, Mituya A, Iwamura T, Nihei T, Sasa T. In: Burlew JS, editor. Algal culture from laboratory to pilot plant. Washington (DC): Carnegie Institution; 1953. pp. 204–232.
54. Anonymous. In: Burlew JS, editor. Algal culture from laboratory to pilot plant. Washington (DC): Carnegie Institution; 1953. pp. 235–272.
55. Chaumont D, Thepenier C, Gudin C. In: Stadler T, Morillon J, Verdus MC, Karamanos W, Morvan H, Christiaen D, editors. Algal biotechnology. London: Elsevier Applied Science; 1988. pp. 199–208.
56. Pirt SJ. UK patent 2,118,572. 1983 (to Queen Elizabeth College, University of London).
57. Pirt SJ, Lee YK, Walach MR, Pirt MW, Balyuzi HH, Bazin MJ. J Chem Technol Biotechnol 1983; 33B: 35–58.
58. Acién Fernández FG, García Camacho F, Sánchez Pérez JA, Fernández Sevilla JM, Molina Grima E. Biotechnol Bioeng 1997; 55: 701–714.
59. Acién Fernández FG, García Camacho F, Sánchez Pérez JA, Fernández Sevilla JM, Molina Grima E. Biotechnol Bioeng 1998; 58: 605–616.
60. Molina Grima E, Acién Fernández FG, García Camacho F, Chisti Y. J Biotechnol 1999; 70: 231–247.
61. Torzillo G, Carlozzi P, Pushparaj B, Montaini E, Materassi R. Biotechnol Bioeng 1993; 42: 891–898.
62. Molina Grima E, Fernández J, Acién Fernández FG, Chisti Y. J Biotechnol 2001; 92: 113–131.
63. Acién Fernández FG, Fernández Sevilla JM, Sánchez Pérez JA, Molina Grima E, Chisti Y. Chem Eng Sci 2001; 56: 2721–2732.
64. Molina Grima E, Fernández JM, Acién Fernández FG, Sáínchez JF, García J, Magan JJ, Pérez J. Book of Abstracts of the 10th International Conference on Applied Phycology; 2005 Aug 24–28; Kunming. p. 33.
65. Del Campo JA, Garcia-Gonzales M, Guerrero MG. Appl Microbiol Biotechnol 2007; 74: 1163–1174.
66. Acién Fernández FG, Molina Grima E, Parra JP, Magán JJ, Cerón MC. Book of Abstracts of the 7th European Workshop, Biotechnology of Microalgae; 2007 July 11–13; Nuthetal p.3.
67. Fitoplancton Marino S. L. web information. Available at http://www.easyalgae.com/index_ingles.asp. Accessed 2007 Sep 14.
68. Masojídek J, Papáček Š, Sergejevová M, Jirka V, Červený J, Kunc J, Korečko J, Verbovikova O, Kopecký J, Štys B, Torzillo G. J Appl Phycol 2003; 15: 239–248.
69. Richmond A, Boussiba S, Vonshak A, Kopel R. J Appl Phycol 1993; 5: 327–332.
70. Lee YK, Ding SY, Low CS, Chang YC, Forday WL, Chew PC. J Appl Phycol 1995; 7: 47–51.
71. Tredici MR, Chini Zittelli G. Biotechnol Bioeng 1998; 57: 187–197.
72. Chini Zittelli G, Lavista F, Bastianini A, Rodolfi L, Vincenzini M, Tredici MR. J Biotechnol 1999; 70: 299–312.

73. Babcock RW, Malda J, Radway JC. J Appl Phycol 2002; 14: 169–184.
74. Ugwu CU, Ogbonna JC, Tanaka H. Appl Microbiol Biotechnol 2002; 58: 600–607.
75. Tredici MR, Chini Zittelli G, Benemann JR. In: Zaborsky OR, Benemann JR, Matsunaga T, Miyake J, San Pietro A, editors. Biohydrogen. New York: Plenum Press; 1998. pp. 391–401.
76. Mortimer J, Thomas S, Temekenidis PA. WO patent 99/46360. 1999 (to Applied Photosynthetics Limited).
77. Varicon Aqua Solutions Ltd. web information. Available at http://www.variconaqua.com/bioreactors.htm. Accessed 2007 Sep 9.
78. Ellis AA, Laidley CW. In: Dennis K, editor. Regional notes. Honolulu (HI): CTSA; 2006. pp. 3–7, *(Online)*, http://www.ctsa.org/upload/note/RN_17_4633041079267810435.pdf.
79. Cellpharm Ltd. web information. Available at http://home.bt-webworld.com/cellpharm/. Accessed 2007 Sep 9.
80. Bioprodukte Prof. Steinberg GmbH web information. Available at http://www.bioprodukte-steinberg.de. Accessed 2007 Sep 20.
81. Algatechnologies Ltd. web information. Available at http://www.algatech.com/astax.htm. Accessed 2007 Sep 21.
82. Davis EA, Dedrick J, French CS, Milner HW, Myers J, Smith JHC, Spoehr HA. In: Burlew JS, editor. Algal culture from laboratory to pilot plant. Washington (DC): Carnegie Institution; 1953. pp. 105–153.
83. Setlik I, Komarek J, Prokes B. In: Necas J, Lhotsky O, editors. Annual report of the laboratory of experimental algology and department of applied algology for the year 1966. Praha, Czechoslovakia: Knihtisk; 1967. pp. 5–36.
84. Krüger GHJ. In: Grobbelaar JU, Soeder CJ, Toerien DF, editors. Wastwater for aquaculture. Bloemfontein: University of Orange Free State Publication; 1981. pp. 16–23.
85. Robinson LF, Morrison AW. EU patent 0239272. 1987 (to Biotechna Limited).
86. Burbidge IM, Harper JD. WO patent 00/12673. 2000 (to Addavita Limited).
87. Miao Jian Ren web information. Available at http://www.newbioreactor.com. Accessed 2007 Jun 4.
88. Ramos de Ortega A, Roux JC. Biomass 1986; 10: 141–156.
89. Tredici MR, Mannelli D, Materassi R. Italian patent CNR 9357. 1988 (to Consiglio Nazionale delle Ricerche).
90. Tredici MR, Carlozzi P, Chini Zittelli G, Materassi R. Bioresour Technol 1991; 38: 153–159.
91. Tredici MR, Materassi R. J Appl Phycol 1992; 4: 221–231.
92. Parker NS, Negri AP, Frampton DMF, Rodolfi L, Tredici MR, Blackburn SI. J Appl Phycol 2002; 14: 313–324.
93. Rodolfi L, Chini Zittelli G, Biondi N, Tredici MR. CD-R of Abstracts of the International Conference & Exhibition AQUA 2006; 2006 May 9–13; Florence.
94. Ponis E, Parisi G, Le Coz JR, Robert R, Chini Zittelli G, Tredici MR. Aquac Nutr 2006; 12: 322–329.
95. Carlozzi P. Biotechnol Bioeng 2003; 81: 307–315.
96. Richmond A, Zhang Z. J Biotechnol 2001; 85: 259–269.
97. Hu Q, Guterman H, Richmond A. Biotechnol Bioeng 1996; 51: 51–60.
98. Zou N, Richmond A. J Biotechnol 1999; 70: 351–356.
99. Richmond A, Zhang CW. J Biotechnol 2001; 85: 259–269.
100. Hu Q, Zarmi Y, Richmond A. Eur J Phycol 1998; 33: 165–171.
101. Zhang CW, Richmond A. Mar Biotechnol (NY) 2003; 5: 302–310.
102. Zhang CW, Zmora O, Kopel R, Richmond A. Aquaculture 2001; 195: 35–49.
103. Aflalo C, Meshulam Y, Zarka A, Boussiba S. Biotechnol Bioeng 2007; 98: 300–305.
104. Zou N, Zhang CW, Choen Z, Richmond A. Eur J Phycol 2000; 35: 127–133.
105. Zhang K, Kurano N, Miyachi S. Bioprocess Biosyst Eng 2002; 25: 97–101.
106. Hu Q, Kurano N, Kawachi M, Iwasaki I, Miyachi S. Appl Microbiol Biotechnol 1998; 49: 655–662.
107. Zhang K, Miyachi S, Kurano N. Biotechnol Lett 2001; 23: 21–26.
108. Zhang K, Miyachi S, Kurano N. Appl Microbiol Biotechnol 2001; 55: 428–433.
109. Zhang K, Kurano N, Miyachi S. Appl Microbiol Biotechnol 1999; 52: 781–786.
110. Rodolfi L, Chini Zittelli G, Tredici MR. Book of Abstracts of the 10th International Conference on Applied Phycology; 2005 Jul 24–28; Kunming. p. 32.
111. Barbosa MJ, Zijffers JW, Nisworo A, Waes W, van Schoonhoven J, Wijffels RH. Biotechnol Bioeng 2005; 89:233–242.
112. Wageningen University web information. Available at http://www.pre.wur.nl/UK/Research/Marine+Biotechnology/Engineering+aspects/. Accessed 2007 Sep 18.
113. Degen J, Uebele A, Retze A, Schmid-Staiger U, Trösch W. J Biotechnol 2001; 92: 89–94.
114. Meiser A, Schmid-Staiger U, Trösch W. J Appl Phycol 2004; 16: 215–225.
115. Subitec GmbH web information. Available at http://www.subitec.com/produkt5.html. Accesed 2007 Oct 16.
116. Innovacción BIIA web information. Available at http://biiainnovaccion.blogspot.com/2007/03/biodisel-con-algas-eeuu.html. Accessed 2007 May 12.
117. Grobbelaar JU, Kurano N. J Appl Phycol 2003; 15: 121–126.
118. Boussiba S, Zarka A. WO patent 2005/006838. 2005 (to Ben-Gurion University of the Negev).
119. Rodolfi L, Bassi N, Padovani G, Bonini G, Chini Zittelli G, Biondi N, Tredici MR. Book of Abstracts of the 7th European Workshop, Biotechnology of Microalgae; 2007 July 11–13; Nuthetal.
120. Rodolfi L, Bassi N, Parente I, Padovani G, Bonini G, Chini Zittelli G, Biondi N, Tredici MR. Book of Abstracts of the 8th International Marine Biotechnology Conference (IMBC 2007); 2007 Mar 11–16; Eilat. p. 87.
121. PESWiki web information. Available at http://peswiki.com/index.php/Directory: Biodiesel_from_Algae_Oil. Accessed 2007 Oct 17.
122. GreenFuel Technologies Corp. web information. Available at http://www.greenfuelonline.com. Accessed 2007 Oct 17.
123. Valcent Products, Inc. web information. Available at http://www.valcent.net. Accessed 2008 Jan 31.
124. AlgaeLink N.V. web information. Available at http://www.algaelink.com. Accessed 2008 Jan 22.

125. Bioreal, Inc. web information. Available at http://www.bioreal.com/BioRealHome.html. Accessed 2007 Sep 21.
126. Hirabayashi S. WO patent 99/50384. 1999 (to Micro Gaia Co. Ltd.).
127. Boussiba S, Vonshak A, Cohen Z, Richmond A. WO patent 97/28274. 1997 (to Ben-Gurion, University of the Negev).
128. The Israel Export & International Cooperation Institute-Environmental Technologies web information. Available at http://www.export.gov.il/Eng/_Articles/Article.asp?CategoryID=354&ArticleID=3686. Accessed 2007 Sep 21.
129. Mera Pharmaceuticals, Inc. web information. Available at http://www.merapharma.com/technology/mgm.html. Accessed 2007 Sep 21.
130. Olaizola M. Biomol Eng 2003; 20: 459–466.
131. Huntley ME, Redalje DG. Mitig Adapt Strateg Glob Change 2007; 12: 573–608.
132. Tredici MR, Chini Zittelli G. In: Kretschmer P, Pulz O, Gudin C, Semenenko V, editors. Proceedings of the second European workshop on biotechnology of microalgae. Bergholz-Rehbrucke: Institut für Getreideverarbeitung GmbH; 1995.
133. Grobbelaar JU. In: Grobbelaar JU, Soeder CJ, Toerien DF, editors. Wastewater for aquaculture, proceedings of a workshop on biological production system and waste treatment. Bloemfontein: University of the O.F.S.; 1981. pp. 24–30.
134. Mori K. Biotechnol Bioeng Symp 1985; 15: 331–345.
135. Ogbonna JC, Tanaka H. Chemtech 1997; 27: 43–49.
136. Ono E, Cuello J. Energy 2004; 29: 1651–1657.
137. Chisti Y. Biotechnology 2007; 25: 294–306.

61

RHEOLOGICAL BEHAVIOR OF FERMENTATION FLUIDS

COLIN R. THOMAS AND GRAINNE L. RILEY
School of Chemical Engineering, University of Birmingham, United Kingdom

61.1 INTRODUCTION

Rheology is the study of the deformation and flow of matter, while rheometry is the experimental characterization of rheology. Rheometers or viscometers are the instruments used for this purpose. The rheological behavior of fluids or suspensions such as fermentation broths is described in terms of viscosity, which is the ratio between shear stress and shear rate. A Newtonian fluid is one in which the viscosity is constant, so that the shear stress is proportional to the shear rate, and furthermore the only stresses generated during flow are shear stresses. Fluids or suspensions that do not conform to these criteria are described as non-Newtonian. It has been long been known that some fermentation broths exhibit non-Newtonian behavior, and this can happen in industrial fermentations for two main reasons. The first is if the microorganisms excrete an "exo-biopolymer". An exo-biopolymer such as xanthan or gellan consists of large, long molecules that can change shape or entangle to resist the flow of the liquid in which they are dissolved. The second reason is that filamentous fungi or filamentous bacteria consist of hyphae that are long, often branched, structures. Mycelia consist of many hyphae, and like exo-polymers, they can become entangled.

The viscosity of non-Newtonian broths is not constant, but depends on the shear rate. In this case, the ratio of the shear stress to the shear rate is called the *apparent viscosity*. The viscosity of water (and most fermentation media not containing filamentous microorganisms or exo-biopolymers) is around 10^{-3} Pa s (1 cP), while the apparent viscosity of some fermentation broths can be orders of magnitude higher than this. It is therefore typical for a broth to be Newtonian at the beginning of fermentation, but for it to become highly viscous and non-Newtonian as the biomass or exo-biopolymer concentration increases. This usually has deleterious effects on mixing and mass transfer, and hence productivity. It is therefore essential to be able to characterize the rheology of fermentation broths, but this is difficult because broths are suspensions of cells rather than homogeneous liquids. The way this is done and practical correlations for relating key rheological parameters to the biomass concentration and the morphology (shape) of mycelia are the subject of this chapter. The effects of high and non-Newtonian viscosity on mixing and flow of fermentation broths are also discussed.

61.2 RHEOLOGICAL MODELS

The common rheological models used to describe fermentation broths are given in Table 61.1, and shapes of some of the stress–strain curves are shown in Fig. 61.1. It should be noted that Bingham plastics, and Herschel-Bulkley and Casson fluids, have a "yield stress," that is, there is no flow until a certain stress is exceeded. The behavior of Power law fluids depends on the value of the consistency index n. For non-Newtonian fermentation broths, this is typically less than 1, in which case the fluid is described as "pseudoplastic" or "shear thinning" because the apparent viscosity decreases as the shear rate increases. For non-Newtonian fluids or suspensions, it is meaningless to quote an apparent viscosity without a corresponding shear rate.

Upstream Industrial Biotechnology: Equipment, Process Design, Sensing, Control, and cGMP Operations, Volume 2, First Edition. Edited by Michael C. Flickinger.
© 2013 John Wiley & Sons, Inc. Published 2013 by John Wiley & Sons, Inc.

TABLE 61.1. Common Rheological Models Used to Describe Fermentation Broth Rheology

	Rheological model
Newtonian fluid	$\tau = \mu\gamma$
Bingham plastic	$\tau = \tau_y + \mu\gamma$
Power law fluid	$\tau = K\gamma^n$
Herschel–Bulkley fluid	$\tau = \tau_y + K\gamma^n$
Casson fluid	$\tau^{0.5} = \tau_y^{0.5} + K\gamma^{0.5}$

τ, shear stress; γ, shear rate; μ, viscosity for a Newtonian fluid or plastic viscosity for a Bingham plastic; τ_y, yield stress; K, consistency index; n, flow behavior index.

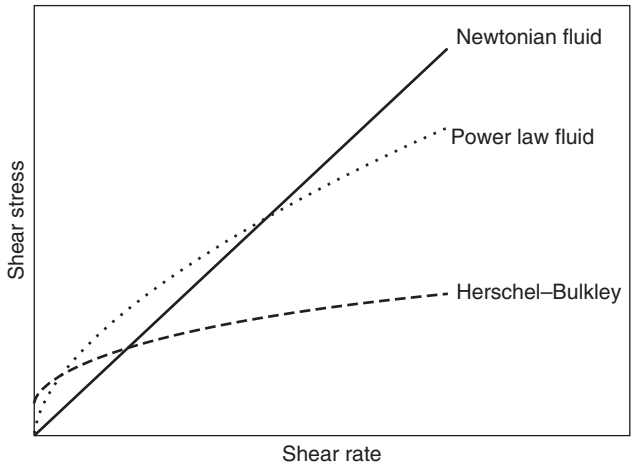


Figure 61.1. Some common models used to describe fermentation broth rheology.



Figure 61.2. Couette or cup and bob rheometer (Contraves Industrial Products Ltd.), sometimes called an annular gap rheometer because the bob fits concentrically in the cup leaving an annulus where the broth is sheared. Photograph: G. Wheeler, University of Birmingham.

It is important to recognize that the various rheological models are intended as empirical relationships between stresses and shear rates in the fluid or suspension. As such, more than one model may fit any given set of experimental data. The most commonly used model by far is the Power law because it has only two parameters, and fits most rheological data adequately.

61.3 RHEOMETRY

Conventional rheometers such as the "Couette" design, where a fluid or suspension is sheared in the annular gap between two concentric cylinders (Fig. 61.2), might be of limited value for suspensions of solids such as fermentation broths because of phase separation or "slip" at the smooth surfaces (1–3), and also because there might be gravity settling (3). Furthermore, geometries that have a narrow measuring gap such as cone and plate systems, where the material is sheared between a shallow cone and a flat plate, may incur the additional problem of particles of similar sizes to the gap jamming within it, destroying them and impairing accurate measurement. However, by careful design and choice of operating conditions, it may be possible to use such conventional rheometers to characterize fermentation broth rheology (4). A common industrial practice is to use very simple rheometers such as a flat disk rotating with a spindle (Fig. 61.3) in a beaker or cup of broth. The flows in these simple systems are usually ill-defined, and an empirical approach using test fluids must be used to calibrate the rheometer (5). That may be of little consequence in practice, because consistency and convenience of measurement often outweigh any need for fundamental understanding of the broth rheology, especially when monitoring an established fermentation.

To overcome the potential problems with conventional rheometers, the disk turbine impeller rheometer (Fig. 61.4) was developed (1,2). This is said to minimize particle settling and avoid particle jamming, and it might be particularly appropriate for fermentation broths as the flows might in some respects resemble those in a real fermenter (6). However, it is important that the flow remains laminar in this type of device, and this may limit the range of shear rates available. Even so, the flows around the impeller are too complex to model, and an empirical approach is used



Figure 61.3. Disk spindles (Viscometers UK Ltd.). The chosen spindle is rotated in a sample of broth, either in a cup supplied with the rheometer or in a beaker. Photograph: G. Riley, University of Birmingham.



Figure 61.4. Disk turbine impeller (purpose built). The impeller is rotated in a sample of broth, either in a cup supplied with a rheometer or in a beaker. Photograph: G. Wheeler, University of Birmingham.

to calibrate the rheometer. The calibration is based on the Metzner and Otto average shear rate concept (7). This proposes that the average shear rate near a disk turbine should be used to determine an average viscosity. The average shear rate is defined as

$$\gamma_{av} = k_s N \tag{61.1}$$

where γ_{av} is the average shear rate and k_s is a constant assumed to be dependent only on the geometry of the system, that is, independent of the rheology and impeller rotational speed, N. The shear stress corresponding to the average shear rate can be found from the torque on the impeller shaft as it rotates. The literature gives many descriptions of the method (e.g. (8)), although its validity has been criticized by some workers (4,9), particularly as it usually needs large sample volumes (10). It has recently been given a satisfactory theoretical underpinning, along with confirmation that k_s is a constant for Power law fluids in laminar flow (8). Turbine impeller rheometers have been used to give reproducible rheological measurements on various fungal fermentation broths (6,11–13). The calibration fluid is usually a viscous Newtonian fluid such as silicone oil or a pseudoplastic solution of a polymer such as Carbopol. At least for such calibration fluids, it has been confirmed that the assumption of an average shear rate is valid for the helical ribbon and disk turbine systems (12). It should be noted that the theory assumes a single phase fluid, and although this may be an acceptable approximation for mycelial suspensions, it might not be valid if gas bubbles are present in the broth. It may therefore be necessary to degas a sample before the measurements begin, for example, by sonication.

A common alternative to the turbine impeller rheometer is the vaned geometry (Fig. 61.5), which has become the universal choice for yield stress or very shear-thinning fluids (14), mainly in industries other than biotechnology.

It has been suggested that an impeller such as a helical ribbon (Fig. 61.6) with better mixing capabilities in the laminar flow region would be preferable to the disk turbine rheometer (4,15,16). An upward pumping helical ribbon impeller with a close clearance to the wall is used to create fluid motion all the way to the wall even for very viscous materials and to provide some top to bottom mixing, which is useful when suspended solids may settle. The use of this impeller can also increase the range of shear rates available for measurement by extending the laminar region. The determination of apparent viscosity for a helical ribbon rheometer is similar in method to that for the disk turbine (12).

Although it is probable that many non-Newtonian fermentation broths have a yield stress, it is often difficult to determine this without special techniques. It can be hard to distinguish between a highly shear-thinning fluid and one that yields, as can be seen in Fig. 61.1. This is another good reason for use of the Power law (Table 61.1), but it should be recognized that even small, nearly immeasurable, yield stresses may have deleterious consequences on fermenter mixing, as discussed later. Some workers use a "controlled shear stress" rheometer to attempt to measure yield stresses directly, but the geometry of such devices may well be inappropriate for broths containing larger particles. It is also

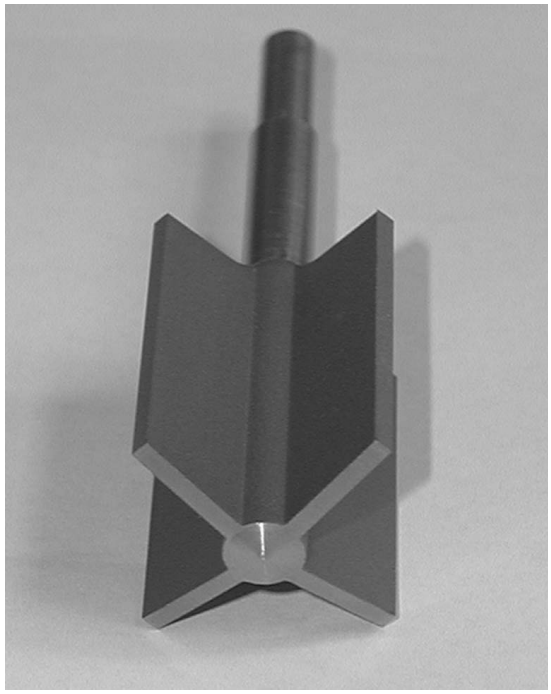


Figure 61.5. Vaned impeller (Bohlin Rheometers, Malvern Instruments Ltd). The impeller is rotated in a sample of broth held in a cup supplied with the rheometer, giving a close clearance. Photograph: G. Wheeler, University of Birmingham.

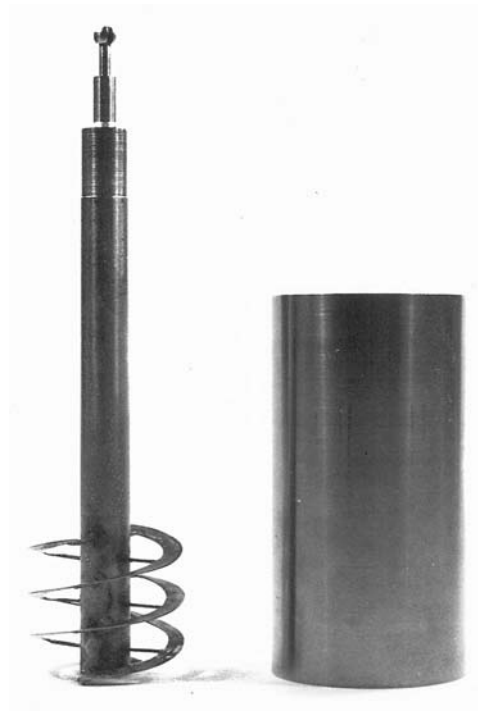


Figure 61.6. Helical ribbon impeller (purpose built). The impeller is rotated in a sample of broth held in a rheometer cup, giving a close clearance. Photograph: G. Wheeler, University of Birmingham.

possible that only the continuous phase (i.e. the medium) flows at very low shear rates, through any suspended solids, making it appear that there is no yield stress.

In rheometry in general, it is recognized that the temperature of the measurements may be important, as the (apparent) viscosity usually drops as the temperature rises. However, it is rare for the temperature to be quoted with rheological parameters for fermentation broths, and practical measurements are often at room temperature. Fortunately, many mycelial and exo-biopolymer fermentations are operated at or close to 25°C, and room temperature is adequate for rheological characterizations in these cases. This is because variabilities in sampling and rheological characterization are usually large enough to render temperature effects negligible or of the second order of importance. Furthermore, changes in apparent viscosity across mycelial and exo-biopolymer fermentations are usually orders of magnitude greater than any temperature effects.

It should be mentioned that on-line rheometry is possible (17,18), but has not been very popular in industrial fermentations, presumably because of contamination risks and the additional complexity. There are few published studies on the use of this method. A recent example was the use of such a rheometer as part of a process control strategy for an industrial, pilot-scale, fed-batch fermentation of *Aspergillus oryzae* (19).

61.4 EXO-BIOPOLYMER FERMENTATIONS

Xanthan and gellan are examples of microbial polysaccharides. Xanthan in particular is a major commercial biopolymer used extensively in the food industries (20) because its solutions are highly pseudoplastic and of high viscosity at low shear rates. This makes it an ideal suspending agent in food products. Gellan is an excellent gel-forming agent (20). The design of fermenters for production of these and other polysaccharides is very challenging, because high product concentrations are required to reduce downstream processing costs, and yet the resulting high viscosity, non-Newtonian, broths cause major mixing and oxygen transfer problems during the fermentations (20).

Mixing and oxygen transfer effects in fermentations of the bacterium *Xanthomonas campestris* have been studied in detail recently (21). The rheology of the broths was measured by cone and plate rheometer, and the Power law model was fitted to the data. In this application, the cone and plate rheometer is usable as the viscosity is caused by the dissolved polymer and there are no particles to jam in the device. Because of the production of xanthan to 26 g/L, the consistency index of the broth went from a very low value to over 30 Pa s^n and the value of the flow behavior index n dropped from 1 to 0.14 (shear rate range not

specified). This had serious consequences on the mixing and oxygen transfer in these stirred tank fermentations. The effects of changes in rheological behavior on mixing and mass transfer in fermentations are discussed later.

A comprehensive study of mixing and mass transfer conditions on gellan production by the bacterium *Auromonas elodea* (22) again showed that the fermentation broth was initially Newtonian and had low viscosity, but within a short time it had become highly shear thinning because of the excretion of the biopolymer. The broth had a yield stress, but this was difficult to determine and therefore the Power law (Table 61.1) was used to describe the rheology. It was discovered that the flow behavior index went from 1 to 0.3 within 9 h of a typically 32 h culture (shear rates ca. 2–200 s^{-1}) and the apparent viscosity could be as high as 20 Pa s (shear rate 0.1 s^{-1}).

A similar report of a low viscosity broth becoming viscous and pseudoplastic concerns scleroglucan production of *Sclerotium glucanicum* (23). In this case, there were deleterious effects on the performance of an airlift bioreactor with an internal circulation loop.

It is worth noting that highly viscous, non-Newtonian broths can also result from the release of deoxyribonucleic acid (DNA) from, for example, *Escherichia coli*, by alkaline cell lysis for plasmid recovery (24). Such suspensions have also been found to exhibit significant viscoelastic properties demonstrating the "Weissenberg effect" upon agitation. This is a phenomenon that occurs when entanglement causes polymer chains to be drawn toward a spinning agitator or spindle shaft, causing a surprising movement of the broth up the shaft. In DNA recovery, this viscoelasticity compounds the rheological challenges posed in processing.

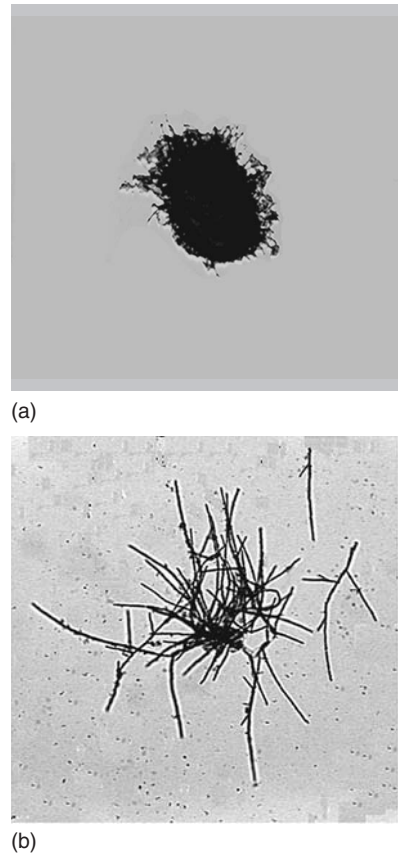


Figure 61.7. (a) Pellet of *Aspergillus niger*; (b) Dispersed forms of mycelia of *Penicillium chrysogenum*.

61.5 MYCELIAL FERMENTATIONS

Mycelial fermentations may be of filamentous fungi such as *Penicillium chrysogenum* (producing penicillin) or filamentous bacteria such as *Streptomyces* spp., from which come most antibiotics. In either case, the morphology has been shown to play a crucial role in submerged fermentations of these microorganisms. Most studies are on fungi, and the relationships between fungal morphology and metabolite production have been reviewed recently (25).

Commercial production of metabolites often requires that the microorganism is grown in one particular form, that is, morphology. In submerged culture, many filamentous microorganisms tend to aggregate into "pellets" (Fig. 61.7a), the size of which might be measured in millimeters or even centimeters. Although pelleted fermentation broths may remain Newtonian and of low viscosity throughout the entire time course of the fermentation, problems might arise with diffusion and transport of nutrients into pellet cores, thus reducing productivity. Nevertheless, the pellet form has been used traditionally for commercial production of citric acid and other metabolites. The dispersed form (Fig. 61.7b) can result in large increases in broth viscosity for only small increases in biomass concentration. Thus, even in the early stages of mycelial fermentations the broth can exhibit several non-Newtonian characteristics, possibly including a yield stress. This behavior of the broth is presumed to arise from the formation of complex entanglements of the mycelia (11). This may lead to difficulties with fermenter mixing, which in turn might affect mass and heat transfer deleteriously, causing a decrease in productivity and/or the production of undesirable metabolites (11,25). Problems with mixing can also affect process control, for example, pH control, by introducing a time lag between acid/alkali addition and the resulting signal from the pH electrode (11). These problems are compounded when a process is scaled up due to increased circulation times and generally lower agitation intensities. Nevertheless, dispersed mycelial fermentations are common and are found in the production of antibiotics.

The complex interactions between process conditions, morphology, productivity, growth, rheology, heat and mass transfer, mixing, and process control are summarized

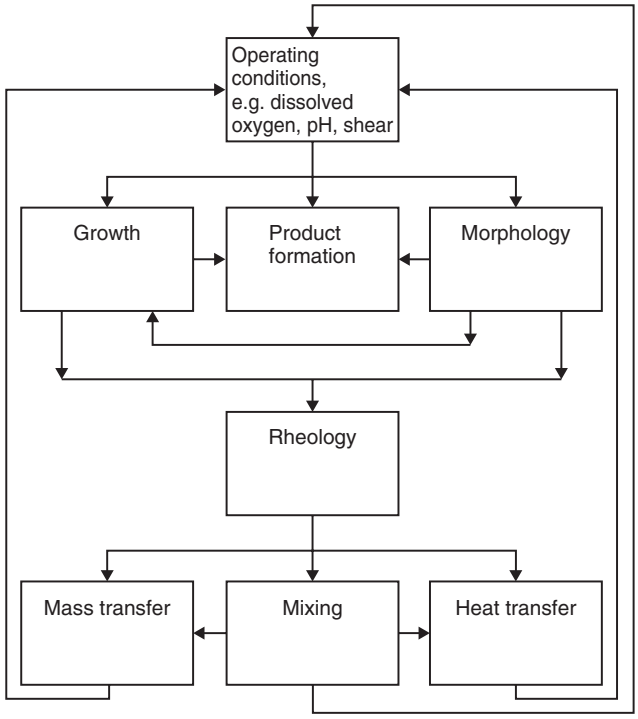


Figure 61.8. Complex interactions between process conditions, morphology, productivity, growth, rheology, heat and mass transfer, mixing and process control (after (11)).

in Fig. 61.8 (11). There is no doubt that the production of metabolites generally depends on the morphology (25), but the morphology depends on the process conditions including the agitation. The effects of agitation might be directly due to breakage of hyphae (26–30), or aggregation/disaggregation of mycelia (31), or might be indirect through changes in heat and mass transfer (particularly oxygen transfer). In either case, the morphology influences the rheology, and this in turn affects the mixing and transport processes, thus closing the loop, as shown in Fig. 61.8. Because of the complexity of this situation, the optimum process conditions for different fermentations vary considerably and are usually highly specific. Indeed, the optimum conditions may vary throughout a single fermentation. For example, conditions that are optimal for biomass growth may not be optimal for the production phase or *vice versa*. The means that has now been found to break into this loop is measurement of morphology by automatic image analysis (32–35). This method has allowed useful correlations to be sought between morphology and rheology, and studies on agitation effects on morphology to be undertaken, as described later.

61.5.1 Morphological Characterization

The development of image analysis techniques (32–35) has enabled methods for rapid and accurate characterization of mycelial morphology. These methods greatly extend the amount and type of data that can be obtained and have helped to describe the interactions between rheology and morphology more fully. Image analysis allows for the relatively rapid, fully or semiautomatic and reproducible extraction of quantitative data from mycelial broth samples, greatly extending the amount and type of data that can be obtained. In addition, the process allows a completely randomized field of view to be observed and measured thus reducing the dependency of the measurements on operator selection.

Some of the dispersed morphological forms found in mycelial cultures are illustrated in Fig. 61.9. Because the morphology usually requires microscopy and image analysis for its quantification, only two-dimensional projections of the objects are characterized. For example, the size of an object is often given as its "projected area," which is the area found in an image of the object as seen through a microscope. Pellets (Fig. 61.7a) are usually identified by the presence of a central core of highly entangled hyphae (34), and are sometimes classified into smooth and hairy types (34). The latter is sometimes described as "fluffy." Usually, the core of the pellet is identified and its size found

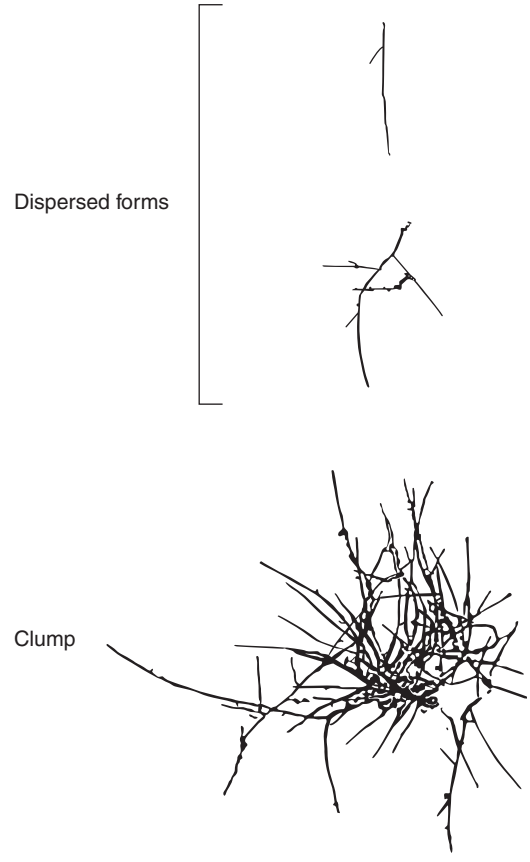


Figure 61.9. Dispersed morphological forms found in mycelial cultures.

as the projected area. This is probably a doubtful practice given pellets are not even approximately two-dimensional, but at least the characterization is consistent. For hairy pellets, the annular region is also characterized, often as a ratio of its projected area to the total projected area, sometimes called the *filament ratio* (36,37). Dispersed forms may be split into two groups; clumps and freely dispersed (Fig. 61.9). Clumps are loose aggregates of hyphae, which are not sufficiently tightly packed to be described as pellets (35). Hyphae are usually flexible enough for a clump to lie relatively flat on a microscope slide, and (except for hyphal overlapping) the projected area may indeed give a reasonable estimate of size. As clumps predominate in many mycelial fermentations (32,33), the characterization of this form is particularly significant. Typical morphological parameters for clumps beside projected area are roughness and compactness (35). In recent practice, it is usually considered better to have only one parameter to describe the morphology of all the dispersed forms. The obvious choice is the projected area, but the maximum dimension has also been suggested (13). These and other morphological parameters have been used in correlations of rheological parameters of mycelial fermentations, as described below.

61.5.2 Morphology and Rheology

61.5.2.1 Pelleted Forms. Lovastatin is an important cholesterol-reducing drug, which is made by fermentation of the filamentous fungus *Aspergillus terreus* growing in the pelleted form (36,37). In recent studies, large (ca. 2 mm) fluffy pellets gave high lovastatin titers but produced highly shear-thinning broths, which required the use of enriched oxygen to maintain sufficient oxygen transfer to the microorganism (36,37). Rheology was measured using a vane spindle device and it was assumed that the Power law was applied. Pellet morphology was quantified using the equivalent diameter of the total pellet projected area, that is, the diameter of the circle with the same area as the pellet, and the filament ratio. At low agitation rates (average shear rate of about 70 s^{-1}), which gave the desired morphology, the flow behavior index decreased and the consistency index substantially increased, as the biomass concentration and mean pellet size increased. However, at high intensity agitation where the pellets were much smaller, both the flow behavior index and the consistency index remained approximately constant with increasing biomass but decreasing pellet size. In the latter case, the flow behavior index exceeded 1, that is, the broths were shear thickening. Overall, it seemed that the main determinant of the rheological parameters was the pellet diameter (36,37). However, it was not clear from these papers whether there was little effect of biomass concentration (36) or that it was an important factor (37). In another work on *A. terreus* (38), the method of Tucker and Thomas (12), described later, was used to show the consistency index depended on the biomass concentration to the power of approximately 2. However, there was only a poor quality correlation if only the biomass concentration was considered. It seems essential that both the biomass concentration and the morphology are considered when trying to develop predictive correlations for rheological parameters.

Similar results have been obtained with *Aspergillus sojae* producing polygalacturonase (39), again showing dependence of the consistency index on the biomass concentration and pellet size, and the possibility that small compact pellets might lead to shear-thickening behavior. For this fermentation, it was found that careful choice of medium and seed culture could lead to high enzyme titers with a broth rheology close to Newtonian (40).

There is little reliable information on pelleted fermentations other than those of *Aspergillus* spp. The effects of morphology and rheology on neo-fructosyltransferase production by *Penicillium citrinum* have been reported recently (41). Once again, the rheology depended on the cell growth and morphology, but no correlations were presented.

Other workers have studied the rheology of pelleted fermentations, but have not characterized the morphology. Without such information, the results are difficult to interpret or use, except for a specific fermentation.

61.5.2.2 Dispersed Forms. Before the availability of comprehensive image analysis methods, there were a few attempts at correlating the rheological and morphological properties of mycelial broths. However, only the freely dispersed mycelia were characterized and there is no evidence that the morphology of hyphae within a clump is similar to that of the freely dispersed form. Indeed, no correlations between clump and freely dispersed morphologies have ever been found. Consequently, such work is generally flawed. However, it appears that some actinomycete fermentations contain only short, relatively unbranched, hyphae (42). In this case, it was possible to use the mean main hyphal length (the length of the longest or only hypha in a mycelium) as a reliable measurement of mycelial size. Rheological data were found using a disk-spindle rheometer, demonstrating a Power law relationship for shear rates from 0.3 to 100 s^{-1}. In all cases, the flow behavior index fell to 0.25 or lower, as soon as substantial growth occurred. The consistency index rose with the biomass concentration as the (fed-batch) fermentations progressed, and sometimes this was followed by a steep fall as cell lysis began. Unfortunately, it was concluded that there was no clear relationship between broth rheology and morphology.

The availability of comprehensive image analysis methods (32–35) now permits much more detailed studies of the effects of morphology on the rheology of mycelial

broths containing predominately dispersed forms. Most of this work has been on filamentous fungi. In an early study (12), the separate influences of biomass concentration and mycelial morphology on broth rheology was investigated, using an industrial strain of *P. chrysogenum*. To investigate the effect of biomass concentration separately to that of morphology, a large sample from the fermentation was split into a number of subsamples. These were reconstituted to a range of biomass concentrations by filtration and resuspension. The rheology and mycelial morphology of each subsample were then determined using a disk turbine impeller, assuming the Power law. By this procedure, sometimes called the *Tucker and Thomas* technique, each subsample possessed rheological properties due only to changes in biomass concentration. The rheological parameters could therefore be correlated with biomass concentration (X) assuming

$$\mathrm{RP} = \text{ constant} \times X^{\alpha} \tag{61.2}$$

where RP is a rheological parameter under examination and α is the exponent on the biomass concentration. Having established the effect of the biomass concentration, it was then possible to examine the effect of mycelial morphology independent of the biomass concentration. Table 61.2 shows some values of α found by direct correlations or the Tucker and Thomas technique. It should be noted that morphological analysis is not required to obtain such values. It can be seen that the value of α of around 2 is fairly typical. Figure 61.10 shows typical observations of the consistency index divided by the biomass concentration squared, that is, setting α equal to 2, for a *P. chrysogenum* fermentation broth (13). It is clear that the development of the rheology during such fermentations cannot be explained by changes in biomass concentration alone, and the morphology must also be considered. This is a common observation (e.g. 43,44).

Once α had been determined, morphological data from *P. chrysogenum* broths were used to estimate the constants in the correlation:

$$\mathrm{RP} = \text{constant} \times X^{\alpha} \times (\text{roughness})^{\beta} \times (\text{compactness})^{\gamma} \tag{61.3}$$

for each rheological parameter. The clump morphological parameters roughness and compactness were found by image analysis. The resulting correlations were fairly successful at predicting broth rheology for batch fermentations. It was later established that α was essentially constant throughout batch fermentations, and this allowed a mean value to be used. This method was also used on *Aspergillus niger* broths from chemostat cultures, and batch and fed-batch fermentations (17,18). The specific correlations are given in Table 61.3. In all these cases, the data were limited, and no indication was made concerning the statistical significance of the predictions made using the rheological parameter correlations. This lack is common to many published rheological correlations and makes the success of any particular correlation difficult to assess.

These problems were overcome in the subsequent extensive study on *P. chrysogenum* broths (13). No clear relationship between the flow behavior index and biomass concentration was found, at least for those phases of the fermentation in which the viscosities were high enough for the rheology to be characterized by a disk turbine

TABLE 61.2. Values of the Exponent α on the Biomass Concentration in Rheological Correlations from Dispersed Mycelial Fermentations (Eq. 61.3)

Reference	α	Microorganism	Rheological Measurement Method
40	2.3	*Aspergillus corymbifera*	Helical ribbon rheometer
41	0.315	*Aspergillus niger*	Pipe flow viscometer
4	3.3	*Aspergillus niger*	Cup and bob rheometer
	2.5	*Penicillium chrysogenum*	
	0.7	*Streptomyces levoris*	
12	2.8 ± 0.3 (sd)	*Penicillium chrysogenum*	Disk turbine rheometer
43,44	1.7, 2.9	*Aspergillus niger*	On-line impeller rheometer
13	2.0 ± 0.3 (sd)	*Penicillium chrysogenum*	Disk turbine rheometer
10	3.5–4.0	*Glarea lozoyensis*	Various
42	0.53, range 0.3–0.8	*Acremonium chrysogenum*	Disk spindle
45	~2	*Streptomyces olindensis*	Cup and bob rheometer

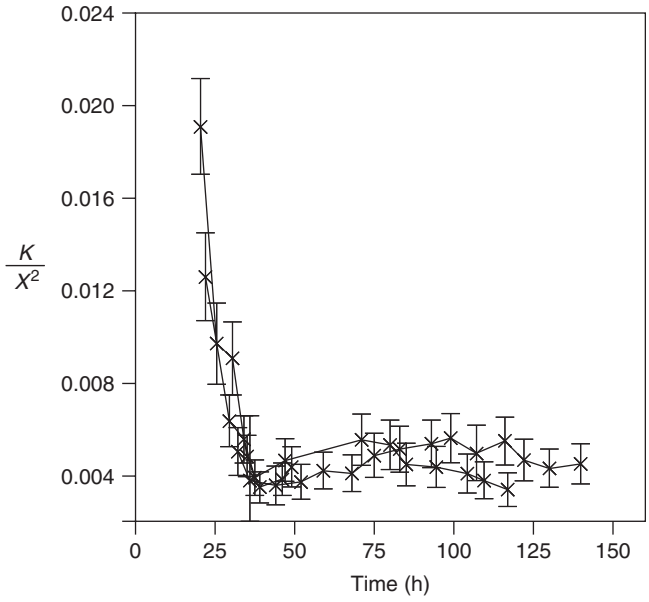


Figure 61.10. Time profiles of the consistency index, K (Pas^n) divided by the square of the biomass concentration X (g dry cell weight L^{-1}) i.e., for three *Penicillium chrysogenum* fermentations (13).

rheometer. The shear rate range was 3.5–75.8 s^{-1}, with lower rates impractical due to settling. The mean value of the flow behavior index was found to be 0.35 ± 0.1 (standard deviation) throughout both batch and fed-batch fermentations, although some significant deviations from this value were observed early and very late in the fermentations. Correlations for the consistency index, measured using a disc turbine rheometer and assuming the Power law, were based on the biomass concentration and the mean maximum dimension of the mycelia. These correlations were reasonably successful for both fed-batch and batch fermentations. The proposed correlation was

$$K = X^2 \times (5 \times 10^{-5}\ D - 10^{-3}) \qquad (61.4)$$

where K is the consistency index (Pa s^n), X is the biomass concentration as dry cell weight (g/L), and D is the mean maximum dimension (μm). Figure 61.11 shows a parity plot of the values of the consistency index K (Pa s^n) predicted from Equation 61.4 versus the experimentally determined values for three *P. chrysogenum* fermentations. The importance of Equation 61.4 is that it takes account of all dispersed morphological forms, not just clumps. This was a real advance on previous work. It was also shown by statistical analysis that the roughness and compactness of Equation 61.3 were not in fact independent variables, reducing the value of this correlation. It is clearly very important to consider the statistical validity of any proposed correlation between rheological and morphological parameters, although this is rarely done.

Mean maximum dimension, as used in Equation 61.4, is not the only morphological parameter that can collectively describe all the dispersed forms. Another possibility is the mean projected area (13). However, mean projected area measurements are significantly affected by the choice of magnification, unlike the mean maximum dimension. Therefore, correlations using the mean maximum dimension have been favored (13,46). This was especially significant when the correlations were extended to other fungal strains requiring different magnifications (46).

Given the wide range of rheometers used to measure mycelial broth theology, it is helpful that there has been a comprehensive comparison of the main choices (10). It was of particular value that broths were taken from production fermentations up to 19 m^3 scale.

In this work, the rheology of the broths of filamentous fungus *Glarea lozoyensis* was characterized using two spindles (Fig. 61.3) of different disk diameters, a disk turbine (Fig. 61.4), and a cup and bob device. The morphology of the fungus was dispersed and as might be expected, the broth was initially water-like, but eventually the apparent viscosity increased dramatically to over 10 times the value measured at the start of the fermentation.

For the smaller of the disk spindles, separation was observed around the spindle and there was some settling. On the other hand, values from the other disk spindle, the disk turbine, and the cup and bob were similar. Given the limited shear rate ranges available with the former two and their relative complexity, the cup and bob was chosen for further work. This was a very important observation and

TABLE 61.3. Correlations to Predict the Rheological Behavior of a Variety of Fungi, Measured Using Different Rheometric Techniques, from Measurements of the Morphology and Biomass Concentration

Reference	Correlation	Microorganism	Rheological Measurement Method
12	$K = X^{2.8} \times R^{0.7} \times C^{1.2} \times$ constant[a]	*Penicillium chrysogenum*	Disk turbine rheometer
43,44	$K = -0.56 + 0.0018 \times R \times X^{1.7}$ $K = 0.38 + 4.8 \times 10^{-5} \times R \times X^{2.9}$	*Aspergillus niger*	On-line impeller rheometer
13	$K = X^2 \times (5 \times 10^{-5} D - 10^{-3})$	*Penicillium chrysogenum*	Disk turbine rheometer
45	$K = 0.00043 \times X^{2.05} \times D^{0.82}$	*Streptomyces olindensis*	Cup and bob rheometer

K, consistency index (Pa s^n); X, biomass concentration (gram dry cell weight per liter); D, mean maximum dimension ((13); μm) or average clump dimension ((44); μm); R, roughness; C, compactness. *Value of constant not given.

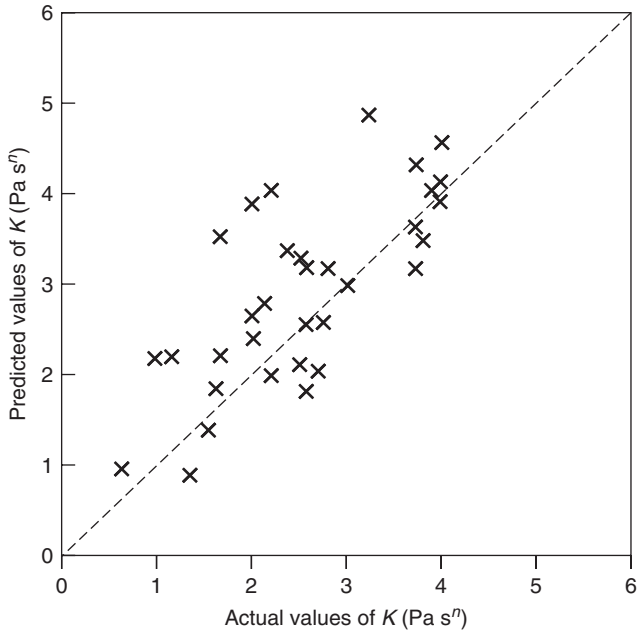


Figure 61.11. Parity plot of the values of the consistency index K (Pas^n) predicted from Equation 61.4 versus the experimentally determined values for three *Penicillium chrysogenum* fermentations (13).

conclusion, given that it is generally accepted that cup and bob systems are not appropriate for mycelial broths.

Yield stress experiments suggested that the Herschel–Bulkley model (Table 61.1) would fit the rheological data best, but because the Power law is in such common use, this was the eventual choice. Again this is important; essentially it was confirmed that the Power law is the most practical rheological model for mycelial fermentations.

There is limited morphological data from this study, but it is nevertheless an exemplar of good practice for rheological studies.

It is not necessary to use the Tucker and Thomas method to find α. An alternative approach is to gather a great deal of data and seek correlations directly. This was done in one of the few useful studies on an actinomycete, in this case *Streptomyces olindensis* (45). The morphology of all the dispersed forms in these fermentations was characterized by the average clump dimension (the average of the dimensions of the clumps in eight directions or "ferets"). The correlation for the consistency index K for a shear rate range of 0–330 s^{-1} was

$$K = 0.0043X^2D^{0.82}\text{dynes}s^n/\text{cm}^2 \qquad (61.5)$$

where X is the biomass concentration (g/L^1) and D is the average clump dimension (μm).

Image analysis is not the only way to characterize mycelial morphology; biomass particle size distributions may also be found by light scattering (47). This is an excellent, practical technique, which is fast and is inclusive as it does not classify particles into forms, and presumably can deal easily with other fermentation solids. This method was used to develop predictive correlations for the rheology of *A. oryzae* broths from 550 L fermentations (47). Principal component analysis was used to extract useful information from the data. The rheometer was a cone and plate system with a large gap width to "cope with the biomass particles in the broth". The shear rate range was 0–300 s^{-1}. The Herschel–Bulkley model was chosen (Table 61.1). It was discovered that the flow behavior index was not correlated with any other variables, and a constant value of 0.4131 (the mean measured value) was used. It was noted that estimates of other rheological parameters such as the consistency index were very sensitive to the choice of a value for n. This is an important practical point that should be considered when quoting consistency index values (for example).

Of course, to use this method one requires a suitable light scattering instrument, as no simple correlations are generated in this approach. It is probably best employed in a commercial environment, where its advantages outweigh any lack of a link to the detailed morphology of the microorganisms.

Finally, it is becoming clear that it may not be necessary to accept the morphology and hence rheology found in a conventional fed-batch, mycelial fermentation. Besides dilution of the broth with sterilized water, pulse-pause feeding (47,48) is known to reduce the viscosity of some fermentations by causing fragmentation of the mycelia.

61.6 MIXING

Some of the possible effects of high apparent viscosity and non-Newtonian broth rheology on fermenter mixing performance have been reviewed recently (49). For polysaccharide (exo-biopolymer) fermentations in which the polysaccharide concentration becomes high enough for the broth to have a yield stress, a "cavern" might form around the impeller. This is a region of relatively rapid motion, surrounded by a stagnant region. Its size can be predicted from the yield stress, but this requires careful determination. It might be that the Power law fits the rheological data well over a wide shear rate range, but a yield stress becomes apparent with more precise measurements over a narrower range. Of course, the existence of such a cavern may have a deleterious effect on oxygen mass transfer, thereby affecting productivity (50,51). In such a case, it might be preferable to use impellers with large diameters or novel impellers that improve bulk mixing (50).

As mentioned earlier, in an agitated mycelial fermentation, there are complex interactions between process conditions, morphology, productivity, growth, rheology, heat and mass transfer, mixing, and process control as summarized in Fig. 61.8. It might seem that reducing the broth apparent viscosity by increasing the impeller speed and hence the shear rate would be advantageous. However, an important issue here is the potential damage to mycelia caused by agitation. Fragmentation of mycelia can reduce the broth apparent viscosity, but may also reduce the fermentation productivity. It has been shown for several fungal fermentations that the (dispersed) morphology can be correlated using the "energy dissipation circulation" function (26–31). Again, much of this has been comprehensively reviewed elsewhere (49). Surprisingly, pellet sizes of *A. terreus* could also be correlated with this mixing parameter (36).

61.7 CONCLUSION

In choosing a particular rheometer, one has to consider both the intended use and prior art. In situations where consistency and ease of use are of paramount importance, for example, in routine monitoring of a well-established mycelial fermentation, a simple disk-spindle system might be the best choice. However, it is worthwhile reading the comprehensive comparison of the main choices that was mentioned earlier (10), from which it appears that a cup and bob system may also be feasible, with shear rates up to 100 s^{-1}. This may also be the best choice for a research environment, although the disk turbine rheometer has been in common use in laboratories for many years, and correlations with morphology obtained with this geometry are already available for some important fermentations.

It has been stated that "one of the most challenging tasks in the fermentation industry today is the design of bioreactors for highly shear-thinning, viscous fermentation broths" (49). It is through rheological studies on such broths, and the understanding of how the rheology is dependent on dissolved exo-biopolymers or suspended filamentous microorganisms, that progress is being made in understanding the complex interactions in such fermentations, with the prospect of their improved productivity.

NOMENCLATURE

C	compactness
D	mean maximum dimension or average clump dimension
k_s	constant in Metzner and Otto equation (Eq. 61.1)
K	consistency index
n	flow behavior index
N	impeller rotational speed
RP	any rheological parameter
R	roughness
X	biomass concentration
α	exponent on the biomass concentration (Eq. 61.2)
β	exponent on the biomass concentration (Eq. 61.3)
γ	shear rate or exponent on the biomass concentration (Eq. 61.3)
γ_{av}	average shear rate near an impeller
μ	viscosity for a Newtonian fluid or plastic viscosity for a Bingham plastic
τ	shear stress
τ_y	yield stress

REFERENCES

1. Bongenaar JJTM, Kossen NWF, Metz B, Meijboom FW. Biotechnol Bioeng 1973; 15: 201–206.
2. Roels JA, van Den Berg J, Voncken RM. Biotechnol Bioeng 1974; 16: 181–208.
3. Charles M. Adv Biochem Eng 1978; 8: 1–62.
4. Allen DG, Robinson CW. Chem Eng Sci 1990; 45: 37–48.
5. Mitschka P. Rheol Acta 1982; 21: 207–209.
6. Oolman T, Blanch HW. CRC Crit Rev Biotechnol 1986; 4: 133–184.
7. Metzner AB, Otto RE. AIChemE J 1957; 3: 3–10.
8. Sánchez Pérez JA, Rodríguez Porcel EM, Casas López JL, Fernández Sevilla JM, Chisti Y. Chem Eng J 2006; 124: 1–5.
9. Olsvik E, Kristiansen B. Biotechnol Adv 1994; 12: 1–39.
10. Pollard DJ, Hunt G, Kirschner TK, Salmon PM. Bioprocess Biosyst Eng 2002; 24: 373–383.
11. Metz B, Kossen NWF, van Suijdam JC. Adv Biochem Eng 1979; 11: 104–156.
12. Tucker KG, Thomas CR. Trans IChemE 1993; 71: 111–117.
13. Riley GL, Tucker KG, Paul GC, Thomas CR. Biotechnol Bioeng 2000; 68: 160–172.
14. Barnes HA, Nguyen QD. J Non-Newtonian Fluid Mech 2001; 98: 1–14.
15. Brito-de la Fuente E, Nava JA, Lopez LM, Medina L, Ascanio G, Tanguey PA. Can J Chem Eng 1998; 76: 689–695.
16. Chavez-Parga MC, Gonzalez-Ortega O, Negrete-Rodriguez MLX, Medina-Torres L, Escamilla Silva EM. World J Microbiol Biotechnol 2007; 23: 615–623.
17. Olsvik ES, Tucker KG, Thomas CR, Kristiansen B. Biotechnol Bioeng 1993; 42: 1046–1052.
18. Olsvik E, Kristiansen B. Biotechnol Adv 1994; 12: 1–39.
19. Bodizs L, Titica M, Faria N, Srinivasan B, Dochain D, Bonvin D. J Proc Control 2007; 17: 595–606.
20. Sutherland IW. Trends Biotechnol 1998; 16: 41–46.
21. Rocha-Valadez JA, Albiter V, Caro MA, Serrano-Carreón L, Galindo E. Bioprocess Biosyst Eng 2007; 30: 115–122.
22. Dreveton E, Monot F, Ballerini D, Lecourtier J, Choplin L. J Ferment Bioeng 1994; 77: 642–649.
23. Kang X, Wang H, Wang Y, Harvey LM, McNeil B. J Ind Microbiol Biotechnol 2001; 27: 208–214.
24. Chamsart S, Patel H, Hanak JAJ, Hitchcock AG, Nienow AW. Biotechnol Bioeng 2001; 75: 387–392.
25. Papagianni M. Biotechnol Adv 2004; 22: 189–259.

26. Jüsten P, Paul GC, Nienow AW, Thomas CR. Biotechnol Bioeng 1996; 52: 634–648.
27. Jüsten P, Paul GC, Nienow AW, Thomas CR. Bioprocess Eng 1998; 18: 7–16.
28. Amanullah A, Blair R, Nienow AW, Thomas CR. Biotechnol Bioeng 1999; 62: 434–446.
29. Amanullah A, Jüsten P, Davies A, Paul GC, Nienow AW, Thomas CR. Biochem Eng J 2000; 5: 109–114.
30. Amanullah A, Christensen LH, Hansen K, Nienow AW, Thomas CR. Biotechnol Bioeng 2002; 77: 815–826.
31. Amanullah A, Leonildi E, Nienow AW, Thomas CR. Bioprocess Biosyst Eng 2001; 24: 101–107.
32. Packer HL, Thomas CR. Biotechnol Bioeng 1990; 35: 870–881.
33. Tucker KG, Kelly T, Delgrazia P, Thomas CR. Biotechnol Prog 1992; 8: 353–359.
34. Cox PW, Thomas CR. Biotechnol Bioeng 1992; 39: 945–952.
35. Paul GC, Thomas CR. Adv Biochem Eng Biotechnol 1998; 60: 1–59.
36. Casas López JL, Sánchez Pérez JA, Fernández Sevilla JM, Rodríguez Porcel EM, Chisti Y. J Biotechnol 2005; 116: 61–77.
37. Rodríguez Porcel EM, Casas López JL, Sánchez Pérez JA, Fernández Sevilla JM, Chisti Y. Biochem Eng J 2005; 26: 139–144.
38. Gupta K, Mishra PK, Srivastava P. Biotechnol Bioprocess Eng 2007; 12: 140–146.
39. Oncu S, Tari C, Unluturk S. Biotechnol Prog 2007; 23: 836–845.
40. Gögus N, Tari C, Oncu S, Unluturk S, Tokatli F. Biochem Eng J 2006; 32: 171–178.
41. Lim JS, Kim JM, Park SW, Kim SW. Biotechnol Bioprocess Eng 2006; 11: 100–104.
42. Warren SJ, Keshavarz-Moore E, Ayazi-Shamlou P, Lilly MD, Thomas CR, Dixon K. Biotechnol Bioeng 1995; 45: 80–85.
43. Fatile IA. Appl Microbiol Biotechnol 1985; 21: 60–64.
44. Mishra P, Srivastava P, Kundu S. World J Microbiol Biotechnol 2005; 21: 525–530.
45. Pamboukian CRD, Facciotti MCR. Braz J Chem Eng 2005; 22: 31–40.
46. Riley GL. A study of the rheology of fungal fermentation broths. PhD thesis. University of Birmingham, Birmingham, UK; 1999.
47. Petersen N, Stocks S, Gernaey KV. Biotechnol Bioeng 2008; 100: 61–71.
48. Bhargava S, Wenger KS, Rane K, Rising V, Marten MR. Biotechnol Bioeng 2005; 89: 525–529.
49. Amanullah A, Buckland BC, Nienow AW. Mixing in the fermentation and cell culture industries. In: Paul EL, Atiemo-Obeng VA, Kresta SM, editors. Handbook of industrial mixing: science and practice: John Wiley & Sons; 2004.
50. Amanullah A, Serrano-Carreon L, Castro B, Galindo E, Nienow AW. Biotechnol Bioeng 1998; 57: 95–108.
51. Amanullah A, Tuttiett B, Nienow AW. Biotechnol Bioeng 1998; 57: 198–210.

62

RHEOLOGY OF FILAMENTOUS MICROORGANISMS, SUBMERGED CULTURE

Maria Papagianni
Aristotle University of Thessaloniki, Greece

62.1 INTRODUCTION

Rheology is the study of the deformation and flow of materials. The rheological characteristics of a fermentation broth directly affect its mixing behavior and all forms of mass and heat transfer (Fig. 62.1). This can have a profound influence on the course and outcome of fermentation as well as on the response of sensors used for monitoring and control. Beyond fermentation, the rheological properties of the final culture broth are a major determinant of the ease or difficulty of downstream processing.

Preinoculation media usually exhibit simple, water-like, Newtonian rheological behavior. With the progress of fermentation, broth rheology becomes more complex either by increases in biomass concentration or by both, increase of biomass and accumulation of high molecular weight products (e.g. extracellular polysaccharides) in considerable amounts. Biomass of most bacteria and yeasts, at the concentrations usually encountered, does not have much effect on rheological properties of culture broths (1). The effects of biomass are most pronounced for mycelial cultures (filamentous fungi and actinomycetes), in which the mycelia tend to give structure to the fluid (2). There are a number of economically important industrial processes that use filamentous microorganisms. Since the importance and influence of fluid flow properties on reactor performance is widely recognized, the physical properties of the suspensions involved in these processes should be accurately measured and correlated with the various transport phenomena.

The rheological behavior of mycelial suspensions arises from frictional and other energy losses which occur when suspensions are sheared. Mechanisms by which energy is dissipated include purely viscous frictional losses within the liquid phase and additional losses due to distortion of streamlines by the mycelial particles; flexing of hyphae resulting in distorted particle shapes; and fragmentation of hyphae or mycelial flocs (3). Mycelial morphology should therefore, exert a very profound effect on the nature of broth rheology. Morphology in submerged culture varies between two extreme forms: the filamentous and the pelleted (4,5). In the filamentous form, the mycelium has the form of hyphae with a varying degree of branching. Hyphae can be up to 500 μm in length and 2–10 μm in diameter. In the pelleted form, the mycelium develops as spherical particles of filaments intertwined around a core. These particles are stable and have a varying degree of compactness and roughness, while their diameters could be several millimeters (4,5).

In the first case of filamentous growth, a varying degree of filament entanglement is apparent. This may result in the formation of permanent aggregates without a core; they are referred to as mycelial clumps (6). A high degree of entanglement of filaments together with a high concentration of biomass in the reactor leads to very viscous suspensions in the order of several thousand centipoise (7–9). The rheological behavior in such cases is usually very non-Newtonian, leading to relatively low viscosities in regions of high shear rate (near the impeller) and very high viscosities in regions with low shear rate (near the

Upstream Industrial Biotechnology: Equipment, Process Design, Sensing, Control, and cGMP Operations, Volume 2, First Edition. Edited by Michael C. Flickinger.
© 2013 John Wiley & Sons, Inc. Published 2013 by John Wiley & Sons, Inc.

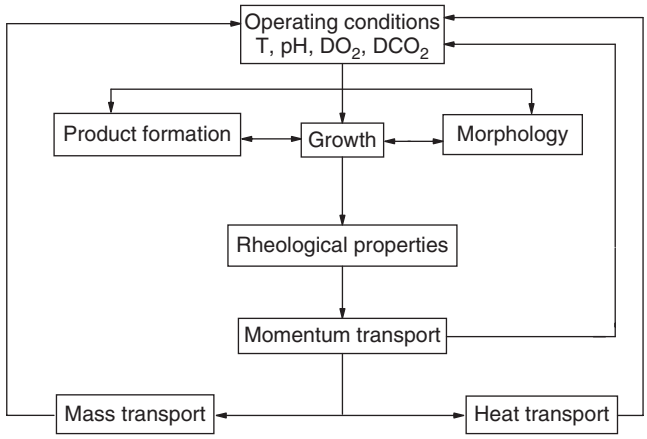


Figure 62.1. Interactions between process parameters in submerged mycelial fermentations.

wall). Suspensions of pellets are usually less viscous and their rheological behavior is more Newtonian-like although some degree of non-Newtonian response should be expected because the pellets are quite deformable or "hairy" (long filaments arise from the core) (1,7,10).

The effective size, shape, concentration, and size distribution of mycelial particles primarily affects the amount of energy dissipated through the particle–liquid interactions thus affecting the measured rheology. The analysis of rheological data is however, not a simple task and the superimposed effects of these parameters, and many others, on broth rheology can be difficult to simulate (11–13). Other parameters include the mode of fermentation, growth rate, dissolved oxygen concentration, pH, degree of mixing, and shear intensity as well as the presence of solid debris, impurities, additives, and surfactants (13). These parameters affect the properties of hyphae and the physicochemical interactions between them, and between hyphae and the continuous liquid phase. Disagreement in the area of rheology in filamentous fermentations is not uncommon, as well as difficulty in comparing results and a high level of ambiguity which makes it difficult to draw conclusions and establish useful generalities (14). Among the most important reasons for these difficulties are limited use of rheometry in fermentation processes, limited information on morphology, use of different types of viscometers and techniques by different investigators studying the same type of broth, the appropriate viscometer is not always used, and, instrument operating problems. Although considerable work has been done in recent years on fungal morphology and modeling in submerged fermentations, systematic studies which involved rheometry have been very limited. The wide range of parameters that affect both morphology and rheology have prevented construction of general predictive equations and modeling. These uncertainties have their impact on process design and scale-up.

This chapter discusses the factors that affect the rheological behavior of filamentous fermentation broths, rheological measurements, rheological models, control of the rheological properties of filamentous fermentations, and instrumentation.

62.2 RHEOLOGICAL MEASUREMENTS IN FILAMENTOUS FERMENTATION BROTHS

Deindorfer and Gaden (15), Chain and Gualandi (16), and Brierly and Steel (17) were among the first who reported a significant reduction of oxygen transfer rates in *Aspergillus* and *Penicillium* cultures as the mycelial concentration increased. Deindorfer and West (18), and Richards (19) discussed the influence of broth rheology on oxygen transfer rates and power consumption and reported differences on the type of rheological behavior of various fermentation broths. Deindorfer and West (18) pointed out the need for design and scale-up correlations for non-Newtonian broths as well as correlations of rheological properties with biomass concentration and mycelial morphology. A decade later, in 1971, Taguchi (20) discussed in his review chapter the rheology of fermentation broths but it seemed that no solutions had been found in the meantime to the problems addressed by Deindorfer and West (18).

The reviews of Blanch and Bhavaraju (21), Charles (1), and Metz *et al*. (7), give fundamental information on rheology of filamentous fermentation broths and still make the basis for any work in this area. Metz *et al*. (7) presented ways of relating the biomass and morphology of fungal cultures to broth rheology and discussed the factors that affect the behavior of viscometers with mold suspensions. Bongenaar *et al*. (22) and Roels *et al*. (2) were the first who pointed out the difficulties of using conventional viscometers in measuring the rheological properties of filamentous fermentation broths and presented new impeller viscometers which would prevent settling of the hyphae in the measuring cylinder and destruction of the flocs in the annulus of the apparatus. Problems with settling of hyphae however, were not avoided (7).

Online instruments for continuous automatic measurements of rheological properties were developed and presented by Kemblowski *et al*. (23,24). The first *in situ* instruments were also developed but not used with mycelial fermentations (25,26). The online system developed by Kemblowski *et al*. (23) was then used by Olsvik in the early 1990s (11,13,27) in the most important studies ever since in the area of online rheological measurements and control in fungal fermentations. Although the system developed by Kemblowski *et al*. (24) gives empirical results, these were consistent and reproducible. Based on the original instrumentation by Kemblowski and

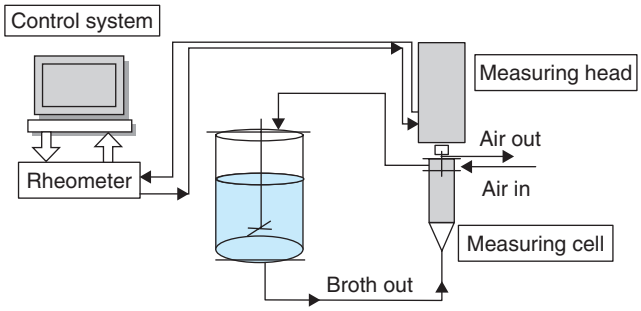


Figure 62.2. Schematic representation of an online rheometer system. (This figure is available in full color at http://onlinelibrary.wiley.com/book/10.1002/9780470054581.)

Kristiansen (12), Badino *et al*. (28) constructed a device for online rheological measurements which again produced experimental results of high accuracy that were successfully used for modeling purposes (29). Figure 62.2 gives a schematic representation of the setup for online rheological measurements.

For the study of flow properties, one has to experimentally develop the flow curve, or shear diagram, which is a plot of shear stress τ against shear rate γ in the laminar region. This information is usually obtained in a conventional laboratory viscometer, such as the concentric cylinder or a cone-and-plate viscometer. The difficulties in measuring rheological properties of a mycelial fermentation broth (and other biological suspensions) result from the fact that it is not a homogeneous liquid. Measurements with conventional viscometers are of rather limited value because of gravity settling of the suspended mycelia. In rotational rheometers, concentric cylinder or cone-and-plate instruments, additional difficulties arise from the fact that large particles may be of the same size as the measuring gap of the instrument and this causes destruction of particles in the shear field, impairing accurate measurements. In such cases useful rheological data can be generated indirectly in laminar flow by using a calibrated, scaled-down, "engineering" viscometer such as an instrumented pipe-flow viscometer or an impeller viscometer. Bongenaar *et al*. (22) were the first to propose the impeller type of viscometer, where the measuring unit consisted of a standard six-blade Rushton turbine or some other type of impeller rotating in a beaker, for rheology measurements in viscous fermentation broths. A Haake–Rotovisko rheometer was used for the measurement of impeller torque as a function of rotational speed. The same measuring technique was used by Roels *et al*. (2) and a similar approach was adopted by Kemblowski and Kristiansen (12). Engineering viscometers are used in research (11,13,27,29–32) and in the biochemical industry for flow characterization and they are essentially cup-and-bob viscometers except that the rotating inner cylinder is replaced by a mixer, such as a turbine, paddle, disc, or helical ribbon.

The basic problem with using engineering viscometers is that they do not provide a well-defined and uniform shear field and individual elements in the fluid may undergo periods of exposure to different levels of shear during measurements (33). In the case of the impeller viscometer, the evaluation of the average shear rate in the cup is based on the empirical technique originally developed by Metzner and Otto (34) for mechanically agitated vessels. The average shear rate around the impeller may be written as:

$$\gamma_{av} = kN \tag{62.1}$$

where N is the rotational speed of the impeller, and k, a constant that depends on the geometry of the system.

The viscosity, η, is by definition equal to the ratio of shear stress to shear rate and the shear-dependent viscosity can be expressed as:

$$\eta = \frac{2\pi M}{CNd^3} \tag{62.2}$$

with M, the torque on the impeller; C, a constant (shape factor) that depends on the geometry of the system; and d, the diameter of the impeller.

The average shear stress can be expressed as:

$$\tau_{av} = \frac{2\pi KM}{Cd^3} \tag{62.3}$$

In most early studies, shear rate was correlated with the rotational speed of the impeller as in Equation 62.1, or with the power input that depends on impeller speed. Recently, Sánchez Pérez *et al*. (35) proceeded to a rigorous theoretical analysis of the shear rate in stirred tank and bubble column bioreactors and showed that for both Newtonian and non-Newtonian power law fluids agitated mechanically, the average shear rate γ_{av} in the fluid is a function of the rotational speed N of the impeller, as follows:

$$\gamma_{av} = \text{constant } N, \text{ for laminar flow} \tag{62.4}$$

and

$$\gamma_{av} = \text{constant } N^{3/2}, \text{ for turbulent flow} \tag{62.5}$$

In turbulent flow and in the case of power law fluids, the constant depends on the flow behavior index and the consistency index of the power law fluid (refer to section titled "Rheological Models"). These equations were found to be in excellent agreement with the long-established empirical equation (Eq. 62.1) of Metzner and Otto (34), thus revealing a previously unknown theoretical foundation for that equation.

Sánchez Pérez *et al*. (35) extended their theoretical analysis to bubble column bioreactors for which the following

equation was given:

$$\gamma_{av} = \text{constant } U_g^{1/(n+1)} \tag{62.6}$$

where, U_g is the superficial gas velocity and n, the flow behavior index of the power law fluid. The constant in the above equation for bubble columns is a function of the flow index, the consistency index, and the density of the fluid.

A practical consideration of great importance is the selection of the appropriate type of rheometer (e.g. a rotating viscometer or a capillary flow rheometer). Flow-through cells for rheological measurements have been developed using a Rushton turbine (12,23) or a helical ribbon impeller (24,36) to get a uniform treatment of samples before measurement and to minimize aligning and settling of hyphae in the measuring cell. Rheological measurements are carried out under laminar flow conditions and in this context, the helical ribbon impeller system has been an improvement on the Rushton turbine version because the laminar shear rate is increased, thus allowing more accurate measurements (13,24). Pipeline systems have also been used for online measurements of the rheological properties of fungal fermentation broths (30,37). Of the applied systems, the flow field in an impeller system is more homogeneous and closer to what is found in the reactor itself. This should not be significant, as the rheological properties are intrinsic properties of the fluid and should not be influenced by the measuring system. This however, appears not to be the case with filamentous fermentation broths, with significant divergence in the classification of the fluids when based on their measured rheological properties. It must be remembered however, that determination of rheological properties in non-Newtonian broths are related to the measuring system and its calibration. Different methods give different results because the flow fields are different in different devices and the response of a non-Newtonian liquid depends on the flow field to which it is exposed. It is difficult therefore to compare results on rheological measurements from different publications.

In situ measurements of rheological properties during a bioprocess would be valuable, especially in terms of process control. Available literature on filamentous microorganisms is limited to the work of Wang and Fewkes (38) in which the bioreactor itself was used as a rheometer. Using a technique similar to Bongenaar's method to measure the rheological properties of a *Streptomyces niveus* culture *in situ*, they stated that effective measurements were accomplished by reducing the agitator speed to ensure "laminar" flow and then measuring the power input as a function of the agitator speed. Discussing their results, Charles (1) found the method promising but mentioned a number of parameters that did not allow for consistent measurements or for valid correlations; for example the failure to shut off the air flow during measurements, the applied narrow range of shear rate at the impeller tip, or the execution of the measurements themselves which influenced the mixing pattern and hence the reactor performance. Although instruments for *in situ* measurements are available today for commercial process applications, no reports have been published on their use in bioreactors.

Rheological characterization of filamentous fermentation broths remains a difficult task in biochemical engineering studies. Despite the industrial importance of viscous fermentations and in particular filamentous fermentations, few studies have considered the systematic characterization of filamentous broth rheology, particularly during scale-up, and its effect on process performance. Online measurements have been limited in the studies of Olsvik and coworkers (11,13,27,31) and Badino *et al*. (28). Most recent work, such as the studies by Müller *et al*. (39,40), and Pollard *et al*. (41) were based on data from off-line measurements. The applicability of the reported studies is limited by the practical difficulties encountered in rheological measurements, with no standard methodology and the use of elaborate devices.

62.3 RHEOLOGICAL MODELS

Newton's law is the simplest rheological model. It describes viscosity η as the ratio of shear stress to the applied shear rate:

$$\eta = \tau\gamma^{-1} \tag{62.7}$$

where η, viscosity (Newton per square meter per second); τ, shear stress (newton per square meter); and γ, shear rate (per second).

Viscosity in this model is defined as the relationship between the applied shear stress and the resulting movement (shear rate) of the fluid. The viscosity of a Newtonian fluid is independent of the shear rate.

Mycelial broths generally have pronounced non-Newtonian rheological characteristics showing shear-thinning or pseudoplastic behavior (15,18,42). Pseudoplastic fluids exhibit a decrease in viscosity with increasing shear rate. The viscosity of pseudoplastic fluids is therefore shear-dependent, and is referred to as apparent viscosity. A number of different mathematical models have been proposed to describe the rheology of mold suspensions. Most models describe a time-independent shear-thinning rheological behavior which can be described adequately by a two-parameter power law equation (8,30,43). Only a few researchers have reported time-dependent rheology and viscoelastic behavior for filamentous fermentations (2,18,21,22,41,44). Since it is impossible to have complete knowledge of shear

stress or shear rate relations and the elastic properties in the different flow fields for non-Newtonial fluids (7), rheological models may be regarded as an empirical fit for the experimental data (43). Reviews on rheological models have been given by Blanch and Bhavaraju (21), Metz *et al*. (7), and Charles (1). The three models most often used to describe the rheological properties of mycelial fermentation broths are the following:

62.3.1 Bingham Model

A number of authors (15,18,45–47) have described the rheological behavior of mold suspensions in terms of the so-called Bingham plastics. The Bingham model includes the often observed yield stress which has to be exceeded before the fluid will flow. The existence of yield stress is important because it determines whether there is flow in regions of low shear (47). At higher shear stresses, flow behavior is Newtonian. In mathematical terms, the Bingham model is expressed by the following equation:

$$\tau = \tau_o + \eta\,\gamma \tag{62.8}$$

where τ_o is the yield stress (newton per square meter).

62.3.2 Pseudoplastic Model

This model is very commonly used to describe the rheological behavior of filamentous fermentation broths (1,7,8,11,18,41,48–50). It is expressed by the equation:

$$\tau = K\gamma^n \tag{62.9}$$

where K is the consistency index (N s^n per square meter), and n is the power law index ($n < 1$).

This model does not include a yield stress and certain authors (18,51) modified the above equation and included the yield stress:

$$\tau = K\gamma^n + \tau_o \tag{62.10}$$

62.3.3 Casson Model

This model, originally formulated by Casson (52) for pigment-oil suspensions, has been applied successfully to a large variety of suspensions (7). Bongenaar *et al*. (22) and Roels *et al*. (2) were the first who applied the Casson model to mycelial suspensions. The mathematical expression for the model is the following:

$$\sqrt{\tau} = \sqrt{\tau_o} + K_c\sqrt{\gamma}$$

where K_c is "Casson" viscosity $(N/m^2\ s)^{1/2}$.

In many reported cases, the Casson model gave better fits to experimental data at lower shear rates than the power law model (2,7,22,41,43,53).

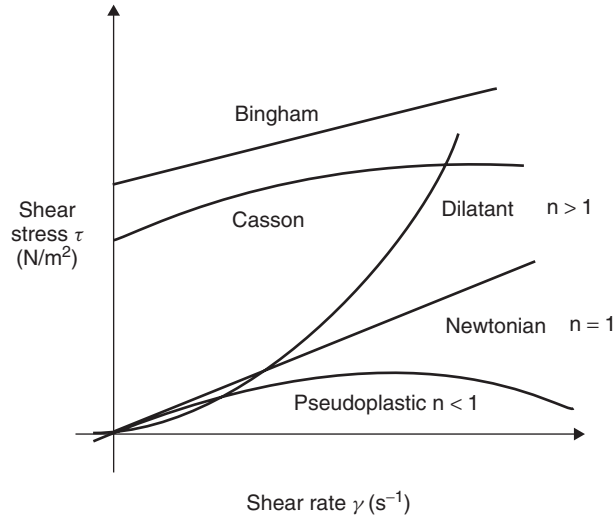


Figure 62.3. Rheological models.

The different rheological models are shown in Fig. 62.3.

Flow equations recommended for filamentous fermentation cultures based on the Bingham, Casson, or Herschel–Bulkley models include a yield stress parameter that needs to be evaluated from experimental data. However, in the case of a low shear rate, it becomes difficult to differentiate between the power law and models that contain a yield stress parameter. Scott Blair (54) demonstrated through statistical testing, that in cases in which the data ranges over only one or one and a half decades, alternative models can be used since they can describe the data equally well. Comparisons between the Casson, Herschel and Bulkley, and the power law models for the apparent viscosity of *P. chrysogenum* suspensions made by Reuss *et al*. (55), showed that in the small range of shear rates that can be measured with an impeller viscometer, discrimination between models was almost impossible. Very accurate data at low shear rates would be required to prove or disprove the existence of a true yield stress (43,56). Therefore, in the absence of such information it seems reasonable to use the power law model to describe rheological data of filamentous fermentations over a specified range of shear rates.

62.4 VISCOSITY AS AN ENGINEERING PROBLEM IN FILAMENTOUS FERMENTATIONS

The viscosity of a fluid influences the turbulence as expressed by the Reynolds number:

$$R_e = \frac{D^2 N\rho}{\eta_\alpha} \tag{62.11}$$

where R_e, is the Reynolds number; D, impeller diameter (meter); N, impeller speed (per second); ρ, broth density

(gram per liter); and η_α, shear-dependent viscosity (newton per square meter per second).

High turbulence in a fermentation system is needed to promote mass and heat transfer, and the lower the turbulence, the poorer the heat and mass transfer rates (14). As the viscosity in fungal fermentations may increase a hundredfold through the course of a batch process, the mass and heat transfer rates and the degree of mixing are adversely affected. The most critical transfer operation in aerobic fermentations is supplying enough oxygen to the microorganisms. The solubility of oxygen in water systems is very low and it can be assimilated by the organisms in a few seconds. The high viscosity of the suspension causes problems with the transfer of oxygen from the gas to the liquid phase. Coalescence of air bubbles in the reactor vessel is very pronounced and therefore, effective oxygen transfer takes place only in the impeller region. Another mass transfer problem arises from the tendency of the mycelia to agglomerate. Nutrients and oxygen must diffuse into the agglomerates and limited diffusion rates may result in a loss of productivity (57). The low DOT in the reactor may itself affect the morphology which in turn affects the rheological behavior. However, reports on the effect of oxygen on fungal morphology are contradictory (4).

The shear rates and power dissipation rates are very high near the impeller and decrease rapidly with distance from the impeller in viscous fermentation broths. Therefore, oxygen supply in the periphery of the vessel must be achieved by mixing. A higher viscosity causes longer mixing times and stagnant zones in the vessel (7). Mycelial microorganisms may thus experience severe oxygen starvation in viscous fermentation broths where the mixing times may be in the order of minutes. Apart from oxygen transport, mixing is important for sugar transport especially in continuous or fed-batch cultures operated at low sugar concentration levels in which sugar exhaustion can take place within a minute. Nutrient depletion can easily affect the process productivity. Mixing is also important for pH and temperature control in the bioreactor. In viscous fermentation broths, difficulties in mixing can cause instabilities in the control system due to a lag period between acid or alkali addition and the resulting signal from the pH electrode. Similarly, temperature control becomes difficult due to the fact that viscosity is highest in regions of low shear, where cooling coils are normally placed.

62.4.1 Oxygen Transfer Correlations ($K_L\alpha$-Correlations) in Filamentous Fermentation Broths

Oxygen transfer is a critical parameter that determines the outcome of aerobic fermentations. Methods for measurement and evaluation of the volumetric oxygen transfer coefficient K_La and the development of correlations useful for design and scale-up of industrial processes are always of great interest. Carcia-Ochoa and Gomez (58) in their most recent review give extensive information on literature and examine the oxygen transfer in microbial processes in different reactors, for example, stirred tanks and bubble columns, taking into account the effects of changes in viscosity, addition of substances that affect the hydrodynamics of the systems, and other aspects such as the consumption of oxygen by the microorganism. Owing to the importance of $K_L\alpha$ in the performance and scale-up of conventional bioreactors, the literature describing various correlations for $K_L\alpha$ in Newtonian fluids is rather extensive. However the situation is different with non-Newtonian and in particular filamentous fermentation broths.

Most published correlations for the calculation of $K_L\alpha$ in non-Newtonian fluids that incorporate a term for rheology have the following general form (59–65):

$$K_La = (P/V)^a (V_s)^\beta (\eta_a)^c \tag{62.12}$$

where K_La is the overall oxygen transfer coefficient (per hour); P, power consumption (Watt); V, volume (liter); V_s, superficial gas velocity (meter per second); η_α, shear-dependent viscosity newton per square meter per second); and a, b, and c, constants.

Correlations like Eq. 62.12, do not make use of any dimensional criterion but another type of correlation for $K_L\alpha$ is based on dimensional analysis. This approach presents certain advantages because the correlations obtained for a system can be applied for K_La estimations in other systems with different dimensions. Yagi and Yoshida (66) proposed the following correlation for the standard six-bladed turbine impeller in a vessel of 0.25-m diameter:

$$Sh^* = 0.060(R_{e_m})^{1.50}(Sc)^{0.50}(Fr)^{0.19} \times \left(\frac{\mu_{ap} v_s}{\sigma}\right)^{0.60} \left(\frac{N D_i}{v_s}\right)^{0.32} \tag{62.13}$$

where Sh^* is the modified Sherwood number $K_L\alpha\ D_i^2/D_{O_2}(-)$; R_{em}, modified Reynolds number (–); Sc, Schmidt number $\mu_{ap}/\rho D_{O_2}(-)$; Fr, Froude number $D_iN^2/g(-)$; μ_{ap}, apparent dynamic viscosity (Pascal second); V_s, superficial gas velocity $4Q/(\pi D_t^2)$ (meter per second); σ, surface tension (newton per square meter); N, impeller speed (revolutions per minute); and D_i, impeller diameter (meter).

Equation 62.13 was valid for Newtonian and non-Newtonian fluids and fitted the experimental data to a reasonable extent. Li *et al*. (67) proposed a relationship for $K_L\alpha$, the impeller speed, and apparent viscosity for fermentation broths of *Aureobasidium pullulans* in a 100-L reactor which correlated well a variety of experimental

data:

$$Sh^* = 5.40 \times 10^4 (Fr)^{0.45} \left(\frac{\mu_{ap}}{\mu_w}\right)^{-0.33} \quad (62.14)$$

where all terms are as in Eq. 62.13 and μ_w is the viscosity of water (Pascal second).

Zlokarnik (68) also applied dimensional analysis and suggested the following relationship:

$$K_L a \left(\frac{Q}{V_i}\right)^{-1} \alpha \left[\left(\frac{P_{gi}}{Q}\right)^*\right]^{\alpha^3} (Sc)^{b^3} (\sigma^*)^{c^3} (S_i^*)^{d^3} \quad (62.15)$$

where Q is the air flow rate (cubic meter per second); V_i, broth volume per impeller (cubic meter); α, constant of proportionality; P_{gi}, gassed power consumption per impeller (Watt); and S_i^*, dimensionless group.

The important characteristics of the relationship described by Eq. 62.15 are the term P_{gi} which is not found in any other proposed correlations, the dimensionless group S_i^*, which is related to the coalescence behavior of solutions, and the estimation of various terms per impeller which make possible its application in systems with different numbers of impellers and therefore, different geometries.

Badino and co-workers (29) applied four classical correlations, two of the first group that do not make use of any dimensionless criterion and two correlations based on dimensional analysis, in investigations of the influence of operating conditions on the rheological properties of *A. awamori* broths. These correlations were the proposed by Cooper *et al.* (65) and Ryu and Humphrey (66) for the first case, and the proposed by Yagi and Yoshida (67) and Zlokarnik (69) for the second case. In order to obtain accurate and reliable data, the authors developed their own methodologies for online rheological measurements and for determination of power consumption and $K_L\alpha$. Good fits were obtained for all four correlations tested with quite distinct operational conditions. The fits however were better with the more complex correlations which take into account the physical properties of the broth. The authors pointed out that good fits were obtained as a consequence of the quality and accuracy of the generated experimental values which were the result of the applied methodologies.

In their review, Garcia-Ochoa and Gomez (58) give a number of dimensionless correlations available in the literature for Newtonian and non-Newtonian fluids. In general, these can be divided into those which reflect the effect of the stirrer speed directly (N) and those which take into account the power input (P).

As in stirred tank bioreactors, many empirical equations have been proposed to estimate $K_L\alpha$ values in bubble columns and airlift reactors. Dimensional equations establish relationships between $K_L\alpha$ and superficial gas velocity, the properties of the fluid, and geometric factors of the bioreactor although the last two seem to have relatively little influence (58). The volumetric mass transfer coefficient is expressed by dimensional equations generally in the form:

$$K_L a = C \cdot V_s^a \cdot \mu_a^b \quad (62.16)$$

where C is constant, V_s superficial gas velocity, and μ_α the apparent viscosity.

In the same way as in stirred tanks, a number of dimensionless correlations have been proposed to express $K_L\alpha$ in bubble columns and airlift bioreactors (58).

Oxygen transfer rates increase with the superficial gas velocity, V_s, or with increasing impeller speed until maximum oxygen transfer rates are reached for the studied system (17,68). Increasing the gas flow rate has been reported to be less effective in increasing $K_L\alpha$ with increasing mold concentrations and viscosity due to coalescence of air bubbles and the consequent reduction in the interfacial gas–liquid area. Deindorfer and Gaden (15) noted an 85% reduction in $K_L\alpha$ as the mycelial biomass concentration increased. This was explained by the 100% increase in the viscosity of broth during fermentation. Decrease in oxygen transfer rate with increasing mycelial biomass concentration has been shown in many cases (6,7,11,15).

Despite the importance of oxygen transfer, there is considerable shortage of experimental data in filamentous fermentations. To develop reliable oxygen transfer and rheology correlations, mixing conditions and the development of morphology cannot be ignored and this represents the serious problem that results in the available data being limited. Difficulties involved in quantifying the rheological properties of fermentation broths may result in widely different values obtained from the $K_L a$ correlations (1,7,32,33) and difficulties involved in quantifying the morphology of a filamentous culture in real time make the task of developing such correlations very complicated and difficult. The use of model media in earlier studies (30,69,70), such as homogeneous polymer solutions, to simulate the flow behavior of heterogeneous fermentation broths offered no solution to the problem since none of these media could simulate well the course of $K_L\alpha$ in fungal fermentations. Moo-Young *et al*. (70) have, however, reported that the correlations obtained from model media may agree with data from fungal fermentation broths if no yield stress exists in culture broths.

62.5 VISCOSITY AS A FUNCTION OF SUSPENSION CHARACTERISTICS

During the first hours of a mycelial fermentation, viscosity is low while the rheological behavior of the broth is

Newtonian. Later during the process, viscosity increases and the rheological behavior of the broth becomes highly non-Newtonian. These are caused by the growth of the microorganism and the increase of the concentration of biomass, its morphology which develops into various forms and by changes in the composition of the broth. The latter may have a pronounced influence on the rheological characteristics of the broth in the case of production of biopolymers (e.g. extracellular polysaccharides).

62.5.1 Influence of Biomass Concentration

Several studies have shown that fermentation broths containing high concentrations of filamentous microorganisms are highly viscous and characterized by shear rate-dependent viscosities and by yield stress (1,13,20,27,48,55,71,72). Several authors have also proposed correlations between the biomass concentration and viscosity. Some of them are shown in Table 62.1.

The effects of biomass and mycelial morphology on rheology cannot be separated easily. Morphology effects were ignored in early studies and as shown in Table 62.1, the proposed correlations did not include any terms related to mycelial morphology. Roels *et al*. (2) included a general term δ for morphology, but later, the equations given by Metz *et al*. (7) included both, the effect of the length of hyphae L_e and the length of the hyphal growth unit L_{hgu} (hyphal length per branch) on the Casson model parameters τ_o and K_c. However, these equations were found to be inadequate for continuous culture experiments and that was attributed to differences in the flexibility of hyphae caused by the differences in culture conditions in batch and continuous experiments.

Tucker and Thomas (74) investigated the separate effects of biomass concentration and mycelial morphology on broth rheology of *P. chrysogenum* cultures. They proposed that rheology should be related mainly to clump properties since clumps account for almost 90% of the morphological forms in free filamentous broths. To investigate the effect of biomass concentration separately from that of morphology, a sample was divided into subsamples with biomass ranging from 10 g/L to 35 g/L and for each one the rheology and morphology were determined. The procedure allowed the evaluation of the biomass effects and rheological parameters (RP) that were correlated with biomass concentration with the equation given in Table 62.1, where RP is the rheological parameter under examination and α is the exponent on biomass concentration. The relationship was later complemented with terms related to morphological characteristics, like the roughness and compactness of the mycelial clumps of *P. chrysogenum*. Later, Tucker (76), via multiple reconstitution experiments, established that α was essentially constant during batch fermentations and a mean value was calculated.

Another correlation shown in Table 62.1 is the one proposed by Olsvik *et al*. (31) for *A. niger* in chemostat cultures operated at various dilution rates and dissolved oxygen concentrations. Image analysis studies revealed that more than 89% of the mycelia were in the form of clumps and apart from biomass concentration, clump roughness was the other determinant of rheological properties. Changes in the rheological properties of the broths were represented by the power law consistency index. Later, Olsvik and Kristiansen (77) presented a similar correlation for batch and

TABLE 62.1. Correlations between Rheological Parameters, Biomass Concentration, and Morphological Parameters

References	Correlation	Microorganism
Deindorfer and Gaden (15)	$\tau = X^{2.3-2.5}$	*Penicillium chrysogenum*
Takahashi and Yamada (73)	$\eta = X^{-1}$	Filamentous fungi
Solomons and Weston (45)	$\eta = X^{2.65}$	*Aspergillus niger*
Roels *et al*. (2)	$\tau_o = \delta \times X^{2.5}$	*Penicillium chrysogenum*
Metz *et al*. (7)	$\tau_o = 1.67 \times 10^{-4} \times 2.5 L_e^{0.8}$ $K_c = 5.45 \times L_{hgu}$	*Penicillium chrysogenum*
Tucker and Thomas (74)	$RP = \text{constant} \times C_m^a$ $K = C_m^{2.8} \times R^{0.7} \times C^{1.2} \times \text{constant}^\alpha$	*Penicillium chrysogenum*
Tucker (76)	$K = C_m^{2.3} \times R^{-0.96} \times C^{0.79} \times 6.6 \times 10^{-5}$	*Penicillium chrysogenum*
Olsvik *et al*. (31)	$K = -0.56 + 0.0018 \times R \times C_m^{1.7}$	*Aspergillus niger*
Olsvik and Kristiansen (77)	$K = 0.38 + 4.8 \times 10^{-5} \times R \times C_m^{2.9}$	*Aspergillus niger*
Mohseni and Allen (56)	$\tau_y = 4.2 \times 10^{-6} C_m^{2.6} \times L_e^{2.2}$ $\tau_y = 7.2 \times 10^{-6} C_m^{2.2} \times L_{hgu}^{0.65}$ $\tau_y = 4.8 \times 10^{-7} R^{3.2} \times C_m^{2.5}$	*Aspergillus niger* and *Streptomyces levoris*
Goudar *et al*. (48)	$K = \dfrac{K_0 e^{cX}}{1 - \frac{K_0}{K_f}(1 - e^{cX})}$	*Penicillium chrysogenum*
Riley *et al*. (71)	$k = C_m^2 \times (5 \times 10^{-5} D - 10^{-3})$	*Penicillium chrysogenum*

Biomass is denoted either as X or as $\boldsymbol{C_m}$.

fed-batch *A. niger* cultures (Table 62.1). Mohseni and Allen (56) also examined the influence of biomass concentration and mycelial morphology on the rheological properties of *Streptomyces levoris* and *A. niger* and proposed a set of correlations with the freely dispersed form using the biomass concentration, the mean dimensionless length, and the mean hyphal growth unit (Table 62.1).

Several authors have presented plots of the rheological parameters n and K versus the biomass concentration for various filamentous fermentations (30,48,72,78). Figure 62.4 gives the plot presented by Goudar *et al*. (48) of the apparent viscosity versus the shear rate of a *P. chrysogenum* fermentation broth at different biomass concentrations (5.07, 10.55, and 17.71 g/L). The flow behavior of the system (batch fermentations) was characterized at various fermentation times and was adequately described by the power law model. The apparent viscosity of the fermentation broth was significantly affected by the concentration of biomass in the reactor. Broths containing 17.71 g/L biomass had an apparent viscosity of 0.25 Pa s at a shear rate of 50 s^{-1}. Biomass concentration also affected the power law flow behavior index and the consistency index, which ranged from 0.002 Pa s^n at 0.1 g/L biomass to 6.14 Pa s^n at 17.71 g/L biomass concentration. The flow behavior index decreased from the initial value of 1 to the final value of 0.17. The relationship between K and the biomass concentration X was described by the three-parameter logistic equation shown in Table 62.1, where K_0 and K_f were the initial and final values of K, and c, a constant. Using experimental K and X values for *P. chrysogenum*, K_0, K_f, and c were estimated by nonlinear least-squares analysis. Experimental data obtained in that study were accurately described by the empirical correlation shown in Table 62.1. The general applicability of the relationship was assumed after testing with previously published rheological data on *A. awamori* and *A. niger* broths and obtaining good agreement between the experimental data and the equation-derived predictions. Ju *et al*. (72) however, reported that plotting the apparent viscosity versus biomass concentration could not be used to obtain a general relationship between the biomass concentration and viscosity since different plots could be obtained under different fermentation conditions; the differences were due to changes in morphology.

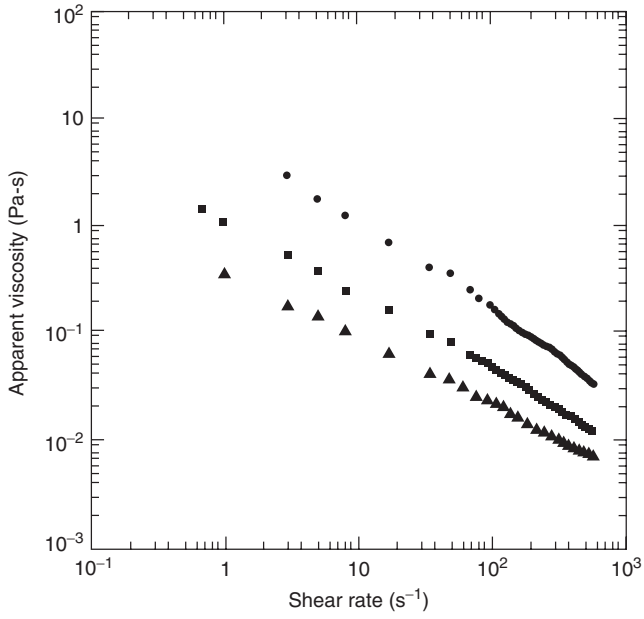


Figure 62.4. Apparent viscosity of a *Penicillium chrysogenum* broth at different biomass concentrations. ▼ 5.07 g/L, ■ 10.55 g/L, • 17.71 g/L. [From Goudar *et al*. (75)].

The relationship between the rheological behavior of *P. chrysogenum* fermentation broths and biomass concentration in batch and fed-batch cultures was studied extensively by Riley *et al*. (71). From the results of multiple reconstitution experiments, the consistency index was found to correlate strongly with the biomass concentration. The values of the exponents on the biomass concentration, α, were found to be constant throughout batch and fed-batch experiments and the use of an average α value permitted the separation of the effects of biomass and morphology. The value of the term K/C_m^a was found to be changing during fermentation and that confirmed that use of correlations to predict rheological characteristics of mycelial broths which are based solely on biomass concentration are intrinsically flawed. The proposed correlation for the consistency index K, biomass concentration, and morphology of *P. chrysogenum* in batch and fed-batch cultures is shown in Table 62.1. In that correlation, a mean maximum dimension D (micrometer) (the longest feret across the convex area of a mycelial particle) was used instead of the compactness and roughness of the aggregates. The correlation proposed by Riley *et al*. (71) was found to be successful with both batch and fed-batch fermentations. The authors pointed out that small changes in the exponent on the biomass concentration may dramatically affect any predictions.

62.5.2 Influence of Morphology

van Suijdam (79) used the terms microscopic and macroscopic morphology to refer to the external form and structure of an organism and to the nature of the microbiological system, consisting of the mycelial network and the homogeneous phase respectively. Microscopic morphology can be determined by microscopic examination, while macroscopic morphology involves determination of viscosity. In submerged culture, a large number of factors contribute to the development of any particular morphological form. Such factors include the

type and concentration of the carbon source, the levels of nitrogen and phosphate, trace minerals, dissolved oxygen and carbon dioxide tension, the pH and temperature, and the type and amount of the inoculum. Physical factors that affect mycelial morphology include the bioreactor geometry and agitation system, the degree of mixing, the viscosity of the broth, and the culture mode (batch, fed-batch or continuous). Microscopic and macroscopic morphology may respond differently to changes in some of these factors. Fungal morphology is related to metabolite production and this relationship has been discussed extensively (4). There are many fermentation cases in which particular morphological forms are associated with increased productivities. The large number of parameters that affect mycelial morphology in submerged fermentation and the interrelationships between them make it a very difficult task to deduce unequivocal general relationships between process variables, product formation, and mycelial morphology. However, the use of image analysis systems during the 1990s provided a valuable tool for characterization and quantification of complex morphologies, physiological states of mycelia, and relationships between morphology and productivity. Systematic morphological studies of fermentation broths through image analysis also made possible the development of correlations between morphological parameters and rheological behavior of the broths.

The influence of morphology on the viscosity of a culture was first reported by Deindorfer and West (18). Carilli *et al*. (80) found viscosity in a filamentous *A. niger* broth to be 3 times higher than in a broth containing large pellets. Similar observations were made by Takahashi and Yamada (73). As discussed in the previous section of rheology and biomass concentration, correlations between parameters describing the rheological properties of a broth and its biomass concentration have been suggested by many investigators. For the dispersed (free filamentous) growth forms, it has been suggested that in case the broth has power law-like behavior, the consistency index K will vary with biomass concentration, typically to the power of 0.3 to 3.3 (30,31,74,77,81,82). However, the large variability in morphological forms as well as the lack (in most reported cases) of appropriate instrumentation for performing morphological measurements resulted in comparatively fewer reports on correlations between morphological parameters and broth rheological properties. Using image analysis, Paul and Thomas (83) showed that for many strains of *P. chysogenum*, aggregated mycelia in the form of clumps may account for more than 90% (in terms of percentage projected area) of the biomass within the broth and this is also true for other fungi (4,6). It was suggested therefore, that the rheology of fungal fermentation broths should be related to clump properties rather than to morphology of the free filamentous mycelia that are dispersed in the broth in small amounts (74).

The microscopic morphology is determined by geometric descriptions of the hyphae and the mycelial aggregates. Information is extracted automatically by various image analysis techniques (84,85). Morphological parameters that have been used in rheology and morphology studies include the length and diameter of individual filaments, the branching frequency, the size and shape of aggregates (clumps and pellets), and various combinations of individual dimensions. By using image analysis techniques it is possible to differentiate quantitatively the freely dispersed from the aggregated mycelium (74,84).

Quite often, the term K/X (the consistency index divided by the biomass concentration), is used in plots against fermentation time or other variables and can be regarded as a simple description of the structure or morphology of the mycelia. By dividing K with the biomass, the effect of biomass concentration is eliminated and the term K/X represents the pure effect of the impeller speed on the system. Since morphology of filamentous microorganisms is directly affected by the impeller speed (4), morphological changes are included. The term K/X has been used by Roels *et al*. (2), Metz *et al*. (7), Olsvik and Kristiansen (27), and other investigators. Figure 62.5 shows the course of K/X as a function of fermentation time for three different impeller speeds, as presented by Olsvik and Kristiansen (27). It appears from these plots that the "morphology" parameter K/X is lowered by increasing the impeller speed.

Quantitative studies on morphology and rheology include the work of Roels *et al*. (2), Metz *et al*. (7), Fatile (81), Kim and Yoo (82), Liu and Yu (86), Olsvik *et al*. (31), Tucker and Thomas (74), Olsvik and Kristiansen (27), Olsvik (11), Tucker (76), Mohseni and Allen (56), Johansen *et al*. (9), Bocking *et al*. (87), Riley *et al*. (71), Sinha *et al*. (88,89), and Pollard *et al*. (41).

Metz *et al*. (7), based on batch fermentations, suggested the correlations shown in Table 62.1 between the Casson parameters τ_o and K_c and the morphological parameters of the freely dispersed form length of hyphae L_e, and length of hyphal growth unit L_{hgu}. These correlations gave a close fit for a number of strains in batch experiments in different bioreactors and under different mixing conditions, in different media with different pHs, but were not adequate for describing the relationship between morphology and rheology in continuous cultures. Morphological changes encountered were not quantified because of the lack of appropriate instrumentation then and the failure of the correlations to describe continuous cultures was attributed to changes in hyphal flexibility. This may be due to changes in cell wall composition, changes in the diameter of hyphae or changes in their degree of branching.

In Roels *et al*.'s (2) correlation (Table 62.1), the morphology parameter denoted as δ, was determined from

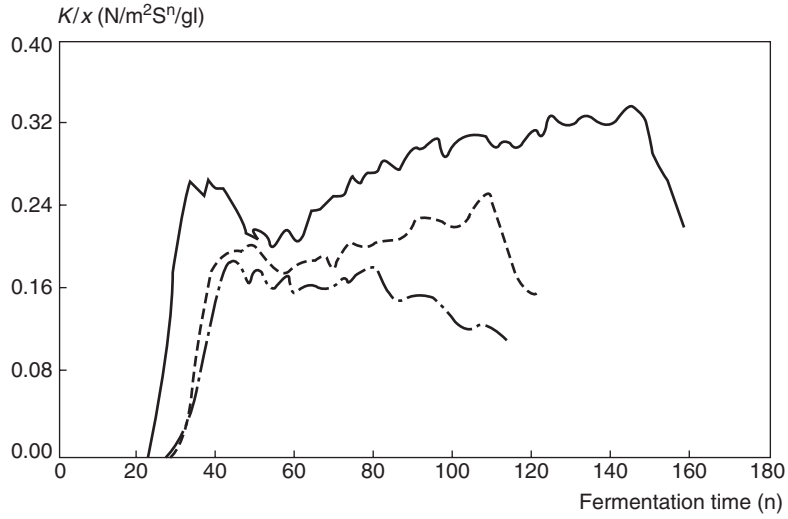


Figure 62.5. K values for three 10-l batch experiments run at different impeller speeds: (—) 300 rpm, (---) 360 rpm, (—.—) 420 rpm. [From Olsvik and Kristiansen (27).]

viscosity measurements of undiluted fermentation broth combined with mycelial dry weight determinations. van Suijdam (79) also included a general morphological parameter, which is defined as the apparent morphology factor M_F:

$$M_F = \lim_{x \to 0} (\eta/\eta_0 - 1)/x \tag{62.17}$$

The M_F factor was estimated through viscosity measurements of the broth which was diluted to biomass concentrations at which hyphal–hyphal interactions could be excluded.

Fatile (81), using the power law model, correlated the rheological properties of the fermentation broth with the biomass concentration X and the diameter of the mycelial aggregates d_p in the following equations:

$$K = 0.3X^{0.3} \times d_p^{0.2}, \tag{62.18}$$

and

$$n = 0.5X^{-0.06} \times d_p^{-0.08} \tag{62.19}$$

Apart from the diameter of the aggregates, which was measured according to Roels *et al*. (2), no other morphological parameters related to aggregated mycelia were considered.

Tucker and Thomas (74) having established the effect of biomass concentration on RP, the rheological parameter under examination, as shown in Table 62.1 and discussed in the previous section, proceeded in the estimation of the exponents β and γ, and the constant in the following correlation:

$$RP = \text{constant} \times C_m^{\alpha} \times (\text{roughness})^{\beta} \times (\text{compactness})^{\gamma} \tag{62.20}$$

Exponents β and γ, and the constant were estimated in 75-h samples of *P. chrysogenum* fermentation broths. The resulting correlations were fairly successful in predicting broth rheology for batch fermentations.

Olsvik *et al*. (31) correlated the shape of mycelial aggregates with the rheological properties and the biomass concentration for continuous fermentations of *A. niger* (Table 62.1). Changes in the roughness R of clumps were found to correspond to changes in the measured consistency index K. Later, Olsvik and Kristiansen (77) proposed a similar correlation for batch and fed-batch *A. niger* fermentations (Table 62.1). Values for the roughness parameter R were in the range of 15 to 40. As already discussed, the consistency index depends on biomass concentration. The exponent on biomass was found to vary according to the cultivation mode within the range of 0.7 to 4 as had been suggested by Metz *et al*. (7) and Allen and Robinson (30).

The studies made by Mohseni and Allen (56), Olsvik *et al*. (31), Olsvik and Kristiansen (77), Tucker and Thomas (74), and Tucker (76), established that clump morphology and in particular the roughness of clumps, is an important factor in determining broth rheology of fungal fermentations. Riley *et al*. (71) introduced error analysis and increased the amount of data to propose the correlation shown in Table 62.1. From the broader range of experimental data available and statistical analysis (F-test carried out at the 0.05 significance level), it became obvious that clump compactness and roughness were not independent

from each other and therefore they cannot be included in a single correlation. A new relationship had to be developed that took this into account, but also used morphological variables averaged over both clumped and freely dispersed forms. Having first determined the influence of the biomass concentration C_m, the authors looked for a correlation between morphology and the values of K/C_m^a. Mean values of roughness, compactness, projected area, and maximum dimension were measured for the combined, freely dispersed, and clumped forms and the following correlations were proposed:

$$K = C_m^a \times (\beta_1 \times A + \gamma_1), \tag{62.21}$$

and

$$K = C_m^a \times (\beta_2 \times D + \gamma_2) \tag{62.22}$$

where A, is the mean projected area (square micrometer); D, the mean maximum dimension (micrometer); β_1, β_2, γ_1, and γ_2, the constants of the regression lines in the plots of K/C_m^a against the mean projected area and the mean maximum dimension.

The plots of K/C_m^a against the mean projected area and the mean maximum dimension presented by Riley *et al*. are shown in Fig. 62.6. According to the data presented there, the value of K/C_m^a appeared to be nearly constant up to a mean projected area of about 5000 μm^2 or a mean maximum dimension of about 200 μm, suggesting that below a critical size this value is not a significant determinant of broth rheology. Both correlations of equations 62.21 and 62.22 were successful in describing the rheological behavior in batch and fed-batch fermentations. However, the second one that included the magnification-independent mean maximum dimension was preferable by authors. As a morphological parameter, the mean maximum dimension is more robust than other magnification-sensitive parameters and it is easy to measure even without image analysis equipment.

62.6 CONTROL OF THE RHEOLOGICAL PROPERTIES OF FILAMENTOUS FERMENTATION BROTHS

62.6.1 Influence of Operating Parameters on Broth Rheology

Different reactor configurations such as stirred tank, airlift, and loop reactors involve different flow patterns and mixing regimes which induce the development of different morphological forms and thus influence the viscosity of fermentation broths (90–92). The level of the applied agitation, either as impeller speed in stirred tank reactors, or as circulation time in loop reactors, has a great impact on the characteristics of the fermentation broth and hence, rheology. Agitation applied during fermentation creates shear forces which can affect microorganisms in several ways; for example, damage to cell structures, morphological changes, as well as variations in growth rate and product formation. The pellet size is influenced to a large extent by the level of agitation applied to the mycelial suspension. Strong agitation results in smaller and more compact pellets. The magnitude and variation of shear and other forces

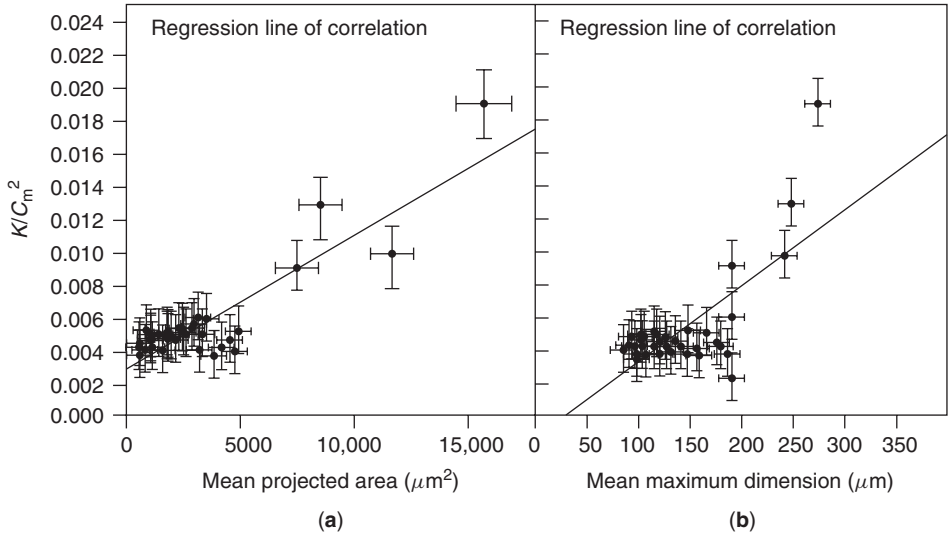


Figure 62.6. The consistency index K divided by the squared biomass concentration versus (a) the mean projected area and (b) the mean maximum dimension of clumps and freely dispersed hyphae. [From Riley *et al*. (71).]

in submerged mycelial fermentations have been discussed extensively in the literature (4).

For a stirred tank bioreactor, high viscosity and non-Newtonian behavior result in decreased homogeneity and poor process performance. Since good bulk mixing of mycelial cultures is important but difficult to achieve, it has been demonstrated earlier by several authors such as Phillips and Johnson (93), Maxon (94), and Steel and Maxon (95) that development of correlations between mixing parameters, impeller characteristics, and broth rheological properties would be valuable. Such correlations however, have been rare and the relevant literature has been very limited. The type of bioreactor employed and its mixing device influence the mixing and rheological properties of a fermentation fluid. The use of bioreactor designs other than the conventional stirred tank has received considerable interest. On the other hand, the application of alternative impeller configurations in mycelial fermentations has attracted little research interest (96); the subject has been reviewed by Charles (1) and more recently by Gibbs *et al*. (96). It is a general perception that for industrial production, increasing the mixing and the oxygen transfer rate by lowering the broth viscosity may be more profitable than trying out mechanical improvements (77).

Attempts have been made to influence the viscosity of a fermentation broth by diluting it (14,21,51,97,98). A 10% to 15% dilution of an *Endomyces* spp. broth in the work of Taguchi and Myamato (97) resulted in a significant reduction in viscosity with reducing the consistency index to a half. Similar results were presented by Sato (51) and Buckland *et al*. (98) with several actinomycete fermentation broths. For a shear-thinning broth of *Nocardia*, Buckland *et al*. (98) observed a large improvement in $K_L\alpha$ by addition of water to reduce broth viscosity. Sato achieved a 20% increase in product yield (kanamycin) by diluting the fermentation broth with water to 5% v/v. Blanch and Bhavaraju (21) suggested a strategy for dilution of viscous fermentation broths: periodic addition of water followed by removal of the same volume of broth was suggested as being more appropriate than continuous dilution. But these studies do not mention whether the observed improvements in viscosity were temporary or permanent. Olsvik and Kristiansen (27) working with *A. niger* showed that the effect of dilution on broth viscosity was only temporal and an inverse relationship between the initial broth viscosity and the duration of viscosity reduction existed.

Addition of salts is known to lower the viscosity in solutions of polyelectrolytes (99) and also to affect pellet formation in mycelial fermentations (57). Sodium salt additions have been shown to reduce significantly the viscosity in *P. chrysogenum* broths (7). Viscosity reductions mediated from the addition of various salts are always the result of morphological changes.

Other process parameters, such as the pH, dissolved oxygen and carbon dioxide tensions, and antifoam agent addition, also affect broth rheological properties and their effect is again through mediating morphological changes. The effects of these parameters on mycelial morphology are long-known and extensively discussed (4).

62.6.2 Influence of Operating Parameters on Mycelial Morphology

The development of a particular morphological form in submerged fermentation is the result of a genetic background that is influenced by a number of process parameters. These parameters can be controlled to a certain extent in most fermentation processes and include shear stress, pH, medium composition, dissolve oxygen tension, and growth rate. Both micro- and macro-morphology are affected by most operating parameters. In their classical review, Braun and Vecht-Lifshitz (57) distinguished the factors that affect mycelial aggregation in submerged culture between microbiological and physicochemical ones. The first include genetic factors, cell wall composition, size of inoculum, growth rate, nutritional factors, carbon to nitrogen ratio, and carbon dioxide tension. Physicochemical factors include the shear forces, pH, ionic strength, temperature, surface-active agents, Ca^{2+} ions, and presence of suspended solids. Some of these factors may be more important than others for mycelial aggregation. Such factors are the composition of cell wall, presence of suspended solids and surface-active agents, and divalent cations such as Ca^{2+} ions. Mycelial morphology in submerged fermentation has been the subject of a large number of studies (4). In this chapter, discussion will be limited to the most important process-engineering parameters, the influence of which has been studied with respect to both morphology and rheology.

62.6.2.1 Effects of Shear Stress. Shear induced micromorphological changes include reduced length of filaments, increased diameters, and increased branching frequencies while macromorphological changes include reduction in size of aggregates, increased compactness, and decreased roughness (92,100–103). Mycelial fragmentation is also induced by shear forces (104) and it is more intense in cases of increased vacuolation that results from aging of hyphae and limited nutrition (e.g. carbon exhaustion) (105,106). Badino *et al*. (29) observed a sharp decrease of the consistency index K in *A. awamori* cultures after exhaustion of the carbon source as a consequence of both hyphal fragmentation and autolysis. Although a large amount of information exists on the effects of shear stress

on mycelial morphology, only a few studies included rheological measurements.

Olsvik and Kristiansen (27) observed a small reduction in *A. niger* broth viscosity with increasing impeller speed in batch culture. Reduction of the process operating volume from 10 to 6l, and subsequent increase of the intensity of mixing, resulted in significant reductions of K/X. Morphology was not studied and the authors attributed these effects mainly to changes caused in the hyphal network or hyphal–hyphal interactions and to a lesser extent, to changes in the length of filaments assuming it to not be very sensitive to impeller speed changes as according to van Suijdam and Metz (101). However, both van Suijdam and Metz (101) and Smith *et al*. (102) reported a decrease in the mean length of filaments with increased power input per unit mass for a *P. chrysogenum* culture. A decrease in the mean length of hyphae with increasing impeller speed was also reported by Dion (103) for *Aspergillus* and *Penicillium* cultures. van Suijdam and Metz (101) reported that the effect of increasing shear stress on the hyphal growth unit is small and therefore they considered it to be of limited value in increasing the power input per unit mass as a means of reducing viscosity. The report by Johansen *et al*. (9) who observed that a 3-fold increase in hyphal length caused an increase in apparent viscosity by a factor of 7 is contradictory but this was independent of the stirrer speed. In experiments with *Aspergillus* and *Penicillium* and stirrer speeds ranging from 100–1100 rpm the authors noticed that the average hyphal length increase was independent of the stirrer speed.

Another important observation made by Olsvik and Kristiansen (27) was that the effect of changing the impeller speed on broth rheology was influenced by the composition of the medium. In an oxygen-limited culture, increasing the impeller speed resulted in an increased oxygen supply to the culture, an increase in the biomass concentration, and an increase in the consistency index K. In a nitrogen-limited culture, increasing the impeller speed led to a small reduction in broth viscosity.

62.6.2.2 Effects of Growth Rate. The growth rate of fungi in submerged culture is influenced by genetic factors, nutritional factors (e.g. the carbon source, nitrogen, and phosphate), growth temperature, dissolved carbon dioxide tension, culture mode, and perhaps other factors (5). The influence of the growth rate on mycelial morphology has been the subject of many studies but results are often contradictory as it appears that the same change in the growth rate can lead to either an increase or a decrease or even have no effect at all on morphological parameters, depending on strain and operating conditions (107). Growth rate was varied by varying the temperature, incorporating inhibitors in the medium, or changing the carbon source. The method used for altering the growth rate may have influenced the morphology and/or the viscosity of the broth. Therefore it is rather difficult to isolate the effects of growth rate on the rheological properties of a mycelial broth from the effects of the factors affecting the growth rate itself. Many earlier studies on the effects of the growth rate on fungal morphology in submerged cultures have not considered rheological measurements.

It appears from the literature that only Olsvik (11) and Olsvik and coworkers (13,27,31) studied the effects of growth rate on morphology and culture viscosity on mycelial cultures (*A. niger*). From continuous culture experiments, it was observed that the specific growth rate influenced the viscosity of the culture but the consistency index K was found to be very dependent on the dissolved oxygen tension (DOT) of the broth. The growth rate and the DOT were found to influence the roughness and compactness of the clumps and these influenced the consistency index. However, both K and clump roughness increased with time in one experiment and decreased in another. A close relationship between clump roughness and viscosity was suggested and also that prediction of viscosity based on the length and branching frequency of the hyphae is process-specific and not as universal as often suggested. By changing the DOT in the broth, the compactness of clumps appeared to change while no changes were observed in the hyphal geometry.

62.6.2.3 Effects of Dissolved Oxygen Tension. Industrial production of various metabolites by filamentous fungi is susceptible to regulation by the DOT of the medium. As these products are produced in most cases by differentiated cells, it is evident that the critical DOT for growth and the critical DOT for product formation are distinct parameters and in general, the latter is significantly higher (4). The described effects of DOT on mycelial morphology vary considerably among various reports, but it appears that in most cases morphology remains unaffected by changes in DOT. van Suijdam and Metz (101) varied the oxygen tension in continuous experiments with *P. chrysogenum* and observed no effect on the measured morphological parameters. Zetelaki and Vas (108) also found that morphology of *A. nidulans* remained unaffected by DOT changes while the apparent viscosity of the culture was reduced when increasing the DOT. This was attributed by the authors to changes in cell walls (thinner walls under increased DOT conditions) and thus, in hyphal flexibility that in turn constitutes macromorphological changes.

Metz *et al*. (7) suggested that low DOT in the reactor's vessel would result in changes in the mycelial properties and an increase in broth viscosity. This would result in a further drop of DOT, initiating a negative feedback loop. Similar observations were made by Olsvik and Kristiansen (13). They observed that in continuous *A. niger* fermentations, an increase in the consistency index K resulted in a

reduction of DOT which led to a further increase in K even if biomass concentration was kept constant. Also, shifts from low to high DOT in continuous cultures resulted in decreases of K while shifts from high to low DOT resulted in increased K. This large effect of DOT on K led to the need for a strict control of the DOT in continuous culture experiments. At low growth rate and DOT, a 2% change in DOT resulted in a 25% change in the consistency index.

62.6.2.4 Effects of Cell Wall Changes. As it represents the major determinant of the rheological behavior of mycelial submerged fermentations, attempts have been made to engineer the morphology of mycelial microorganisms. Such an approach could offer the desirable morphological form without altering the operating conditions in the bioreactor. Traditional screening and selection procedures would tend to select for less viscous and less highly branched cultures, as in the work of Warren *et al*. (8) with the actinomyces *Saccharopolyspora erythracea*, *Actinomadura roseorufa*, and *S. rimosus*. Bocking *et al*. (87) selected through mutagenesis highly branched strains of *A. oryzae* that appeared to give less viscous broths than the parental strains. This seems to be contradictory, but it is not the degree of branching alone that contributes to the rheological properties of the broth; the length of hyphae and the degree of interaction between them also play a role.

Another option to the approach of engineering the properties of cell walls is manipulation of the expression of genes associated with morphology. Deletion of chitin synthase genes (*chsB* and *csmA*) in *A. oryzae* by Müller and coworkers (39,40) resulted in lower values of K without affecting the overall process productivity. As the authors pointed out, the applicability of their results to other fungal strains remains to be proved. If proven, manipulation of chitin synthases can represent a simple, efficient, and inexpensive means to reduce viscosity during industrial filamentous-fungal fermentations.

62.7 EQUIPMENT USED FOR MEASURING RHEOLOGICAL PROPERTIES OF NON-NEWTONIAN BROTHS

62.7.1 Research Viscometers or Rheometers

Concentric cylinder or the cone-and-plate are the most commonly used types of viscometers in determination of rheological properties of mycelial fermentation broths, but the value of the results these instruments give is limited. The main problems associated with these viscometers are (2,22) as follows:

- particles in the suspension (e.g. pellets) may be of the same order of magnitude as the annulus of the apparatus, resulting in the destruction of pellets and other aggregated material;
- formation of layers of different densities such as less dense layers next to the surface of the measuring bodies;
- settling of particles and particle–particle interactions produce heterogeneous suspensions.

Tube viscometers with large pipe diameters handle larger volumes of samples and cope with the first of the listed problems, but the others may still be significant (2,7,22). The impeller type viscometer (2,22) provided a solution to the problems of settling and water layers next to the surfaces. According to Metz *et al*. (7), treatment of samples before measurement and the lag time between sampling, as well as the sampling timing, would all influence the results in turbine impeller rheometers. Settling of the mycelia was also observed during measurements. The disadvantages of using impeller systems, such as helical ribbon or Rushton turbine, is that they establish complex flow patterns with no straightforward calculation of shear, and results arebreak empirical.

Flow-through cells for rheological measurements have been developed using a Rushton turbine (23,24) or a helical ribbon impeller (36) and the problem of settling of hyphae was minimized. Pipeline systems have also been used for online measurements of the rheological properties of fungal fermentation broths (30,37).

Allen and Robinson (30) compared different types of viscometers with *A. niger* fermentation broths and found that measurements with Rushton-type impellers gave higher readings than helical ribbon impeller systems, concentric cylinder systems, and pipeline viscometers. The effect was more pronounced at high biomass concentrations. A problem with slip-in pipeline viscometers was shown to be that measurements were effective only at very low pipe diameters. Allen and Robinson's work was carried out using online pipeline systems, while the other tested types of viscometers were all off-line. Blakebrough *et al*. (78) also found significant differences between pipeline measurements and Rushton impeller measurements. The explanation given was that pipe-flow instruments make the measurements at the wall of the measuring device, whereas the turbine systems do so in the bulk of the fluid. Pace (3) suggested that high readings in impeller viscometers may be due to distortion of streamlines which then leads to energy dissipation.

In situ measurements of rheological properties have been reported by various investigators but the only work involving mycelial fermentations was the work carried out by Wang and Fewkes (38) who used the fermenter itself as a viscometer (discussed in the section "Rheological Measurements in Filamentous Fermentation Broths").

62.7.2 Commercial Viscometers or Rheometers

Brookfield, Rheomat, Haake, Bohlin, Rheomatrics, Paar Physica, are just a few of the manufacturers of devices used for rheological measurements on fluids. Viscometers are available in laboratory and portable forms and some are suitable for online applications (e.g. Brookfield). Major technology improvements over the past two decades have led to the development of instruments of various configurations, which can perform a variety of measurements including controlled stress and controlled strain, or yield measurements. Such devices are therefore suitable for a variety of applications with complex types of motion imposed on samples, such as oscillatory motion from which information can be extracted on the viscoelastic properties of a fluid. In studies with non-Newtonian fluids, these rheometers can be used to develop flow curves directly over a wide range of shear rates of interest to most process-engineering operations. A wide variety of viscometers or rheometers is available in the market today, from simple, easy-to-use devices to more sophisticated ones with a large choice of accessories, built-in thermometers and temperature control facilities, and software options to automate data collection, plotting and so on, and in some cases, process control.

62.8 CONCLUSION

The performance of a submerged mycelial fermentation process is greatly influenced by the rheological properties of the broth. These properties are determined mainly by the concentration of biomass and morphology. The filamentous growth form is the dominant morphological form in most processes. Long, thin, branched filaments create a network that gives very viscous fermentation broths with a pronounced non-Newtonian character. Although the influence on the rheological properties of the broth on bioreactor performance is widely recognized, systematic studies of the rheological properties and the use of rheometry in fermentation processes are still limited. Advances made in image analysis techniques in the early 1990s permitted the extraction of quantitative information on mycelial morphology and in combination with online rheological studies, resulted in a better understanding of the relationship between rheology and morphology. Comparison of rheological data from various sources is rather problematic. The main reasons for this are the different types of instruments used, the different methods applied, and the different morphological parameters evaluated or unstated differences in the morphology of a culture. Control of broth rheology has been attempted by either diluting the broth or by manipulating the morphology. Broth dilution offers only a short-term reduction of apparent viscosity and it is of little value for process control purposes. The latter approach has been extended beyond manipulation through varying process parameters, to genetic engineering of the genes associated with morphology. Further investigations with different microorganisms are needed to ensure the general validity of such attempts. A wide variety of rheometers is available in the market today but in research, measurements are still normally taken off-line introducing the added problem of sample treatment that influences measurements. These could be overcome with dynamic, online measurements which unfortunately have not found widespread application in fermentation technology. It is also possible and expected, that the area of fermentation broth rheology will be benefited in the future from advances in micro- and nano-fluidics applications. Such applications are expected to provide precise control over experimental conditions and in-depth rheological information on the studied systems (109,110).

NOMENCLATURE

a, b, and c	Constants in Eq. 62.12
C	Constant, shape factor in Eq. 62.2
C_m^a	Biomass in eqns of Table 62.1 (g/l[1])
d (or d_i, D, d_i)	Impeller diameter (m)
d_p	Diameter of mycelial aggregates (mm)
Fr	Froude number ($D_i N^2/g$)
K	Consistency index ($N/m^2 s^n$)
K_c	Casson viscosity $(N/m^2 s)^{0.5}$
k	Coefficient in Eq. 62.1
$K_L\alpha$	Overall oxygen transfer coefficient (h^{-1})
L_e	Length of hyphae (μm)
L_{hgu}	Length of hyphal growth unit (μm)
M	The torque on the impeller
M_F	Morphology factor
N	Impeller speed (s^{-1})
N	Flow behavior index
P	Power consumption (W), power input
P_{gi}	Gassed power consumption per impeller (W)
Q	Air flow rate (m^3/s)
R	Roughness of mycelial aggregates
R_e	Reynolds number
R_{em}	Modified Reynolds number
RP	Rheology parameter
Sc	Schmidt number ($\mu_{ap}/\rho D_{O_2}$)
Sh^*	Modified Sherwood number ($K_L a D_i^2/D_{O_2}$)
S_i	Dimensionless group in Eq. 62.15
U_g	Superficial gas velocity (m/s[1])
V	Volume (l)
V_i	Broth volume per impeller (m^3)
v_s	Superficial gas velocity (m/s[1])

X	Biomass (g/l^1)
γ	Shear rate (s^{-1})
γ_{av}	Average shear rate (s^{-1})
δ	Morphology factor
η	Viscosity (N m^{-2} s)
η_α	Sheardependent viscosity ($N/m^2/s^1$)
μ_{ap}, μ_α	Apparent viscosity (Pa s)
μ_w	Viscosity of water (Pa s)
ρ	Broth density (g/l^1)
σ	Surface tension (N/m^2)
τ	Shear stress (N/m^2)
τ_{av}	Average shear stress (N/m^2)
τ_0	Yield stress (N/m^2)

REFERENCES

1. Charles M. Adv Biochem Eng 1978; 8: 1–62.
2. Roels JA, van den Berg J, Voncken RM. Biotechnol Bioeng 1974; 16: 181–208.
3. Pace GW. Fungal biotechnology. London: Academic Press; 1980. pp. 95–110.
4. Papagianni M. Biotechnol Adv 2004; 22: 189–259.
5. Carlile MJ, Watkinson SC, Gooday GW. The fungi. London: Elsevier Academic Press; 2001.
6. Papagianni M. PhD thesis. Glasgow: University of Strathclyde; 1995.
7. Metz B, Kossen NWF, van Suijdam JC. Adv Biochem Eng 1979; 11: 103–156.
8. Warren SJ, Keshavarz-Moore E, Ayazi Shamlou P, Lilly MD, Thomas CR, Dixon K. Biotechnol Bioeng 1995; 45: 80–85.
9. Johansen CL, Coolen L, Hunik JH. Biotechnol Prog 1998; 14: 233–240.
10. Rodriguez Porcel EM, Casas Lopez JL, Sanchez Perez JA, Fernandez Sevilla JM, Chisti Y. Biochem Eng J 2005; 26: 139–144.
11. Olsvik ES. PhD thesis. Glasgow: University of Strathclyde; 1992.
12. Kemblowski Z, Kristiansen B. Biotechnol Bioeng 1986; 28: 1474–1483.
13. Olsvik ES, Kristiansen B. Biotechnol Bioeng 1992; 40: 1293–1299.
14. Solomons GL. Fungal biotechnology. London: Academic Press; 1980. pp. 55–80.
15. Deindorfer FH, Gaden EL. Appl Microbiol 1955; 3: 253–257.
16. Chain EB, Gualandi G. Rend Ist Sup Sanit 1954; 17: 5–60.
17. Brierly MR, Steel R. Appl Microbiol 1959; 7: 57–57.
18. Deindorfer FH, West JH. Adv Appl Microbiol 1960; 2: 165–175.
19. Richards JW. Prog Ind Microbiol 1961; 3: 141–172.
20. Taguchi H. Adv Biochem Eng 1970; 1: 1–30.
21. Blanch HW, Bharavaju SM. Biotechnol Bioeng 1976; 18: 745–790.
22. Bongenaar JJTM, Kossen NWF, Metz B, Meijboom FW. Biotechnol Bioeng 1973; 15: 201–206.
23. Kemblowski Z, Kristiansen B, Ajayi O. Biotechnol Lett 1985; 7: 85–98.
24. Kemblowski Z, Budzynski P, Owczarz P. Rheol Acta 1988; 27: 82–91.
25. Picque D, Corrieu G. Biotechnol Bioeng 1988; 31: 19–23.
26. Endo H, Sode K, Karube I, Muramatsu H. Biotechnol Bioeng 1990; 36: 636–641.
27. Olsvik ES, Kristiansen B. Biotechnol Bioeng 1992; 40: 375–387.
28. Badino AC, Facciotti MCR, Schmidell W. Braz J Chem Eng 1997; 14: 359–359.
29. Badino AC, Facciotti MCR, Schmidell W. Biochem Eng J 2001; 8: 111–119.
30. Allen DG, Robinson CW. Chem Eng Sci 1990; 45: 37–48.
31. Olsvik ES, Tucker KG, Thomas CR, Kristiansen B. Biotechnol Bioeng 1993; 42: 1046–1052.
32. Treskatis SK, Oregeldinger V, Wolf H, Gilles ED. Biotechnol Bioeng 1997; 53: 191–201.
33. Heydarian SM, Ison AP, Ayazi Shamlou P. Encyclopedia of bioprocess technology, fermentation, biocatalysis and bioseparation. Hoboken, NJ: John Wiley & Sons; 1999.
34. Metzner AB, Otto RE. AIChE J 1957; 3: 3–10.
35. Sanchez Perez JA, Rodriguez Porcel EM, Casas Lopez JL, Fernandez Sevilla JM, Chisti Y. Chem Eng J 2006; 124: 1–5.
36. Kemblowski Z, Budzynski P, Owczarz P. Rheol Acta 1990; 29: 588–593.
37. Björkman U. Biotechnol Bioeng 1987; 29: 101–113.
38. Wang DIC, Fewkes RCI. Dev Ind Microbiol 1977; 18: 38–56.
39. Müller C, Hansen K, Szabo P, Nielsen J. Biotechnol Bioeng 2002; 81: 525–534.
40. Müller C, McIntyre M, Hansen K, Nielsen J. Appl Environ Microbiol 2002; 68: 1827–1836.
41. Pollard DJ, Hunt G, Salmon PM. Bioprocess Biosyst Eng 2002; 24: 373–383.
42. Steel R, Maxon WD. Biotechnol Bioeng 1966; 8: 97–108.
43. Oalman T, Blanch HW. Crit Rev Biotechnol 1986; 4: 133–184.
44. Mohseni M, Kautola H, Allen DG. J Ferment Bioeng 1977; 83: 281–286.
45. Solomons GL, Perkin MP. J Appl Chem 1958; 8: 251–259.
46. Solomons GL, Weston GO. Biotechnol Bioeng 1961; 3: 1–6.
47. Karow EO, Bartholomew WH, Sfat MR. J Agric Food Chem 1953; 1: 302–306.
48. Goudar CT, Strevett KA, Shah SN. Appl Microbiol Biotechnol 1999; 51: 310–315.
49. Kang X, Wang H, Wang Y, Harvey LM, McNeil B. J Ind Microbiol Biotechnol 2001; 27: 208–214.
50. Gupta K, Mishra PK, Srivastava P. Biotechnol Bioprocess Eng 2007; 12: 140–146.
51. Sato K. Proceedings Congress Antibiotics; 1964; Prague. p. 740.
52. Casson N. Rheology of disperse systems. Oxford: Pergamon Press; 1959. pp. 84–102.
53. Childyal NP, Thakur MS, Srikanta S, Jaleel SA, Prapulla SG, Prasad MS, Devi PN, Lonsane BK. J Chem Technol Biotechnol 1987; 38: 221–234.

54. Scott Blair GW. Rheol Acta 1966; 5: 184–187.
55. Reuss M, Debus D, Zoll D. Chem Eng 1982; 381: 233–236.
56. Mohseni M, Allen DG. Biotechnol Bioeng 1995; 48: 257–265.
57. Braun S, Vecht-Lifshitz SE. TIBIOTECH 1991; 9: 63–68.
58. Garcia-Ochoa F, Gomez E. Biotechnol Adv 2009; 27: 153–176.
59. Henzler HJ. Chem Eng Technol 1980; 52: 643–680.
60. Nakanoh M, Yoshida F. Ind Eng Chem Process Des Dev 1980; 19: 190–195.
61. Deckwer WD, Nguyen-Tien K, Schumpe A, Serpemen Y. Biotechnol Bioeng 1982; 24: 461–481.
62. Hecht J, Voigt J, Schugerl K. Chem Eng Sci 1980; 35: 1325–1332.
63. Popovic M, Robinson CW. AIChE J 1989; 35: 393–405.
64. Cooper C, Fernstrom GA, Miller SA. Ind Eng Chem 1944; 36: 504–509.
65. Ryu DY, Humphrey AE. J Ferment Technol 1972; 50: 424–431.
66. Yagi H, Yoshida F. Ind Eng Chem Process Des Dev 1975; 14: 488–493.
67. Li G-Q, Qiu H-W, Cai Z-L, Yang S-Z. J Chem Technol Biotechnol 1995; 62: 385–391.
68. Zlokarnik M. Adv Biochem Eng 1978; 8: 133–151.
69. Chisti MY, Moo-Young M. Biotechnol Bioeng 1988; 31: 487–494.
70. Moo-Young M, Halard B, Allen DG, Burrell R, Kawase Y. Biotechnol Bioeng 1987; 30: 746–753.
71. Riley GL, Tucker KG, Paul GC, Thomas CR. Biotechnol Bioeng 2000; 68: 160–172.
72. Ju L, Ho CS, Shanahan JF. Biotechnol Bioeng 1991; 38: 1223–1232.
73. Takahashi J, Yamada K. J Ferment Technol Jpn 1960; 34: 100–103.
74. Tucker KG, Thomas CR. Trans IChemE Part C 1993; 71: 111–117.
75. Anderson C, LeGrys GA, Solomons GL. Biochem Eng 1982; 377: 43–49.
76. Tucker KG. PhD thesis. Birmingham: University of Birmingham; 1994.
77. Olsvik E, Kristiansen B. Biotechnol Adv 1994; 12: 1–39.
78. Blakebrough N, McManamey WJ, Tart KR. J Appl Chem Biotechnol 1978; 28: 453–461.
79. van Suijdam H. DECHEMA 1987; 6: 107–120.
80. Carilli A, Chain EB, Gaulandi G, Morisi G. Sci Rep Super Sanita 1961; 1: 177–189.
81. Fatile IA. Appl Microbiol Biotechnol 1985; 21: 60–64.
82. Kim EJ, Yoo YJ. Biotechnol Technol 1992; 6: 501–506.
83. Paul GC, Thomas CR. Biotechnol Bioeng 1996; 51: 558–572.
84. Paul GC, Thomas CR. Adv Biochem Eng Biotechnol 1998; 60: 1–59.
85. Papagianni M. Focus on biotechnology research. New york: Nova Publishers; 2006. pp. 179–212.
86. Liu T, Yu D. Biotechnol Bioeng 1993; 42: 777–784.
87. Bocking SP, Wiebe MG, Robseon GD, Hansen K, Christiansen LH, Trinci AP. Biotechnol Bioeng 1999; 65: 638–648.
88. Sinha J, Bae JT, Park JP, Kim KH, Song CH, Yun JW. Appl Microbiol Biotechnol 2001; 56: 88–92.
89. Sinha J, Bae JT, Park JP, Song CH, Yun JW. Enzyme Microb Technol 2001; 29: 392–399.
90. Träger M, Qazi GN, Onken U, Chopra CL. J Ferment Bioeng 1989; 68: 112–116.
91. Priede MA, Vanags JJ, Viestrus UE, Tucker KG, Bujalski W, Thomas CR. Biotechnol Bioeng 1995; 48: 266–277.
92. Papagianni M, Mattey M, Kristiansen B. Biochem Eng J 1998; 2: 197–205.
93. Phillips DH, Johnson MJ. Biotechnol Bioeng 1961; 3: 277–309.
94. Maxon WD. Biotechnol Bioeng 1959; 1: 311–324.
95. Steel R, Maxon WD. Biotechnol Bioeng 1966; 8: 109–115.
96. Gibbs PA, Seviour RJ, Schmid F. Crit Rev Biotechnol 2000; 20: 17–48.
97. Taguchi H, Myamato S. Biotechnol Bioeng 1966; 8: 43–54.
98. Buckland BC, Gbewonyo K, Dimasi D, Hunt G, Westerfield G, Nienow AW. Biotechnol Bioeng 1987; 31: 737–742.
99. Eiki H, Gushima H, Ishida H, Saito O, Oka Y, Osono T. J Ferment Bioeng 1989; 67: 345–349.
100. Papagianni M, Mattey M, Kristiansen B. Biotechnol Lett 1994; 16: 923–934.
101. van Suijdam H, Metz B. Biotechnol Bioeng 1981; 23: 111–147.
102. Smith JJ, Lilly MD, Fox RI. Biotechnol Bioeng 1990; 35: 1011–1023.
103. Dion WM, Carilli A, Sermonti G, Chain EB. Rend Ist Super Sanita 1954; 17: 187–205.
104. Belmar-Beiny MT, Thomas CR. Biotechnol Bioeng 1991; 37: 456–462.
105. Paul GC, Kent CA, Thomas CR. Trans IChemE 1992; 70: 13–20.
106. Papagianni M, Mattey M, Kristiansen B. Process Biochem 1999; 35: 359–366.
107. Wiebe MG, Trinci APJ. Biotechnol Bioeng 1990; 38: 75–81.
108. Zetelaki K, Vas K. Biotechnol Bioeng 1968; 10: 45–59.
109. Breedvelt V, Pine DJ. J Mater Sci 2003; 38: 4461–4470.
110. Hohne DN, Younger JG, Solomon MJ. Langmuir 2009; 25(13): 7743–7751.

63

SAMPLING AND SAMPLE HANDLING FOR PROCESS CONTROL

Bo Mattiasson and Martin Hedström
Department of Biotechnology, Lund University, Lund, Sweden

The need for process control in biotechnology is increasing. The initiative by FDA to stimulate the use of process analytical technology (PAT) among the pharmaceutical industries has strongly contributed to the growing interest. With PAT, the main emphasis is to encourage the implementation of advanced and innovative process-monitoring solutions within pharmaceutical manufacturing (1).

Another factor that contributes to place efficient sampling and sample handling in focus is the development of industrial biotechnology where bulk chemicals are being produced using biocatalytic processes either by using whole cells or separated enzymes. In order to obtain economy in such processes, it is imperative to efficiently utilize the substrate and also to obtain high volumetric productivities. Besides these two areas, several others can be mentioned from, for example environmental monitoring and food processing. Thus, sampling and sample handling are essential operations and more interest is now being focused on developing these into efficient and convenient operations that anyone can utilize.

Sampling and sample handling can be divided into several steps:

- taking a representative sample;
- sampling under sterile conditions;
- treatment of the sample in order to prepare it for analysis.

The sampling challenges are more or less the same over time, but the sample handling has changed with the increased interest in monitoring compounds present at low concentrations.

Monitoring and control is very often used during development of a process, during optimization, and when evaluating proper media components. However, when the process comes in production, fewer analyses are often done since, at this stage, the process will be well known. However, because of the need for better documentation of industrial processes, more monitoring is introduced in the production stage also.

The present review summarizes the state of the art and also indicates some trends in the development.

Process monitoring and control involves many different steps. It is, sometimes, difficult to discuss one separate step without mentioning the others since they are often interconnected. However, focus in this review lies on sampling and sample handling.

63.1 SAMPLING

63.1.1 The Sterility Barrier

In Table 63.1 some typical examples are listed on how the sterility issue has been treated over the years.

There are essentially three main strategies—the mechanical, the chemical/physical, and the heat barrier. The mechanical barrier has been dominating and it often involves the use of membranes as sterile barriers through which a particle-free solution can be taken out for future analysis. These membranes can be applied in many

Upstream Industrial Biotechnology: Equipment, Process Design, Sensing, Control, and cGMP Operations, Volume 2, First Edition. Edited by Michael C. Flickinger.
© 2013 John Wiley & Sons, Inc. Published 2013 by John Wiley & Sons, Inc.

TABLE 63.1. Means to Maintain Sterility when Sampling from Bioreactors

Type	References
Mechanical means	
Dialysis membrane	2
Microdialysis	3
Membrane probe	4
Membrane with high shear force in order to avoid fouling	5
Membrane loop outside the bioreactor	6
Chemical means	
Coaxial catheter	7
Chemical sanitation of sampling port	8
Physical means	
Heat	9

different modes, either within the bioreactor or in close proximity to the bioreactor connected via a sampling loop. Figure 63.1 illustrates some of the different membrane configuration applied.

63.1.1.1 Dialysis Membrane. The dialysis probe was initially developed to be used in medical studies where only very small samples could be taken. Thin dialysis tubing was connected to a continuous flow system and the tubing was continuously perfused with dialysis solution (10). When placed in the tissue/body cavity that was to be analyzed, small molecules were diffused through the membrane and then were transported away with the perfusion solution.

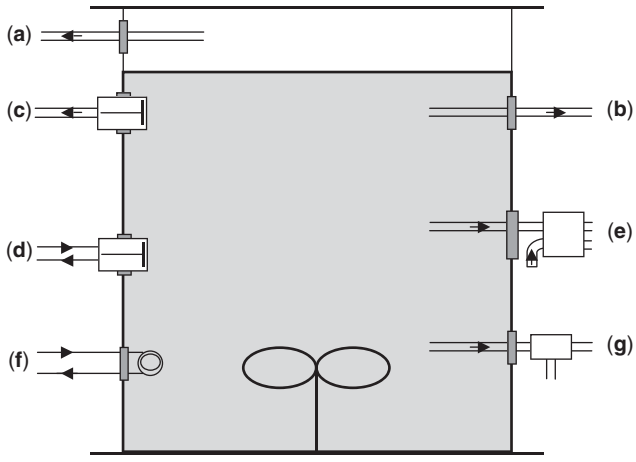


Figure 63.1. Modes of sampling from a bioreactor (a) sampling of headspace, (b) direct sampling, (c) membrane unit for sampling of particulate-free solution, (d) membrane dialysis probe with pumped-through receiving buffer, (e) sampling with an external filtering step outside the reactor, (f) dialysis, (g) sampling via filtering with collected permeate.

This latter was used for *in vivo* analysis of neurotransmitters in human brain tissue (3).

Besides being utilized in biomedical applications, the dialysis probe has also been applied in bioreactor surveillance with good success (2). Its characteristics are that the device is relatively slow, it takes very small volumes and it is only suitable for sampling low molecular weight compounds (Fig. 63.2). However, when utilizing the microdialysis equipment in an automated fashion, it is possible to gain real-time process information and hence the opportunity to eliminate the potential for contamination and error induced by the operator, as well as to reduce labor and improve yield (11).

63.1.1.2 Membrane Probe. Some different devices of membrane probes have been developed and presented. The ABC-probe seems to be the most reliable one and it is based on a mechanically robust membrane mounted in a holder that is inserted in the fermentor via one of the holes in the lid.

63.1.1.3 Membrane with High Shear Force in Order to Avoid Fouling. Sometimes it is needed to sample from very viscous media and then fouling is a serious problem.

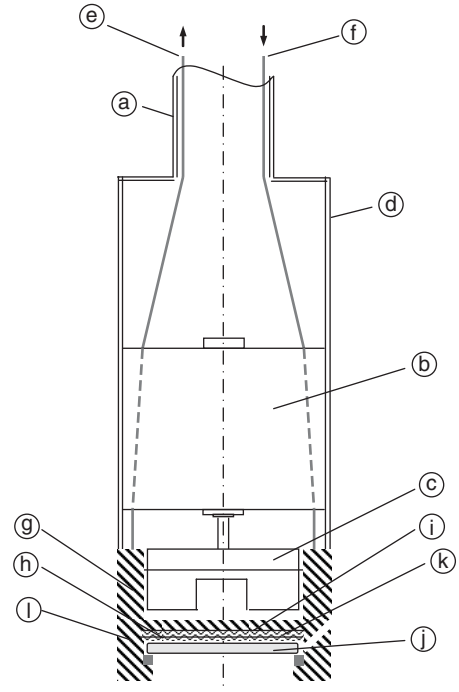


Figure 63.2. Cross-section of dialysis probe (a) stainless steel shaft, (b) autoclavable motor, (c) magnet, (d) stainless steel housing, (e, f) in- and outgoing dialysis solution, (g) polycarbonate membrane holder, (h) membrane, (i) membrane support with spiral groove, (j) magnetic stirrer bar, (k) thin Teflon washer, (l) channels for improved circulation. [Source: Reproduced with permission from Ref. 2].

Fouling will retard the passage over the membrane, thereby affecting the reproducibility of mass transfer of the analyte and later on give false values in the analysis. Fouling is a common phenomenon that appears on all membrane devices in contact with solutions containing macromolecules. The soluble molecules may form a secondary layer on the membrane thereby changing the characteristics of the membrane and thus of the sampling device. To compensate for such effects, one is trying to operate with shear forces. This could be to place the membrane probe close to the impeller where the shear forces are strong, or alternatively, may use a membrane probe with a built-in stirring that generates strong shear forces.

When biomass hydrolysate is being converted into biofuels and/or chemicals, it is important to operate with as concentrated solutions as possible, and then the risks of fouling of membrane units will be especially pronounced. The device shown in Fig. 63.2 was proven to function very well even when sampling from a hydrolysate of willow with a dry matter content of up to 15% (2).

63.1.1.4 Membrane Loop Outside the Bioreactor. When membrane filtering of fermentation broth was first used as a sampling method, the membrane was used for treating discrete samples, and later on it was applied in an external loop to the fermentor. This latter case was causing frequent sterility problems.

63.2 CHEMICAL MEANS

Beside the mechanical hindrance as sterility barrier, use of chemicals is efficient. There are at least two different methods presented:

63.2.1 The Coaxial Catheter

The coaxial catheter is based upon use of a double lumen catheter with the inner part slightly shorter than the outer part, thereby creating a small volume at the tip of the catheter. The sample is sucked into the inner catheter while an inhibiting solution is pumped in the reverse direction in the space between the inner and the outer catheter. Thus, one liquid stream with inhibitor is fed toward the tip of the coaxial catheter while the main stream is the sample being pumped in the other direction. By adjusting the flow rates such that the inhibitor stream is a fraction of that of the sampling stream, the two liquids will mix in the small volume created at the tip of the catheter, after which they are jointly sucked into the inner catheter for further treatment. The concept has been used in medical applications when continuously sucking blood from patients for on-line monitoring of blood glucose, and then heparin is fed as inhibitor of the blood-clotting process. When it comes to fermentation, it is fully possible to operate with toxic compounds that will arrest the metabolism of cells in the sample instantaneously. In one example, potassium cyanide (KCN) was successfully used to stop metabolism of yeast cells (12). An attractive feature with this concept is the instantaneous interaction between the sample containing cells and the inhibitor. There is, in some of the cases studied, a total volume at the tip of the catheter of approximately 20 μL, and when operating with a sampling rate of 1 mL/min, there will be a very short time for metabolism to continue after the sample is taken from the bulk (13). Potential leakage of inhibitor was carefully evaluated by FDA before the system was approved for continuous sampling from humans, and similar studies have been carried out on fermentation broth (13). A security system has been used in the sense that if the sampling tubing breaks, then the pump feeding the other channel will also stop.

63.2.2 Sanitation of Sampling Port

When sampling is done for off-line analysis, it is very common to use special procedures in order to secure that sterility is maintained during and after sampling. The sample is most often withdrawn from the bioreactor via a port and the zone of the port that might have been infected is sterilized in order to avoid backward infection and also to have a sterile port for the next sampling occasion (8).

63.3 PHYSICAL MEANS

63.3.1 Heat

The most common method to sterilize the sampling port is the use of steam. Such heat treatment might, of course, be automated so that a standardized procedure is connected to each sampling event. Figure 63.3 shows a steam-sterilized sample valve connected to regular fermentation equipment. The automated refrigerated sampling control unit is in close proximity to the fermentor (Fig. 63.4). Steam sterilization eliminates the often-used needle-puncturing system thereby improving the operator safety.

63.4 CHEMICAL MEANS

Strong oxidative toxic compounds are used to sterilize the sampling port. This is especially the case when automatic sampling is done and frequent intermittent assays are to be performed. Toxic chemicals can also be used as a chemical barrier to prevent infection of the bioreactor via the sampling port. In one system studied, a part of the tubing at the sampling port was intermittently filled with 5% formaldehyde, a concentration enough to kill any microbe (8). Similar effects were also obtained when using 3–6% hydrogen peroxide as sterilizing medium.



Figure 63.3. Sampling port from a fermentor where steam is used to secure sterilization prior to and after sampling [Source: Courtesy of Golden LEAF Biomanufacturing Training and Education Center (BTEC), North Carolina State University, Raleigh, NC USA]. (This figure is available in full color at http://onlinelibrary.wiley.com/book/10.1002/9780470054581.)



Figure 63.4. Automatic aseptic sampling system located next to a 30-L bioreactor [Courtesy of Golden LEAF Biomanufacturing Training and Education Center (BTEC), North Carolina State University, Raleigh, NC USA]. (This figure is available in full color at http://onlinelibrary.wiley.com/book/10.1002/9780470054581.)

63.5 SAMPLING FROM GAS PHASE

When volatile samples are to be analyzed, it is possible to sample from the gas phase in the bioreactor. This is relatively easy to do, since one can draw out a sample from the airspace and connect the flow to a gas chromatograph (GC) or a mass spectrometer (MS).

Volatile compounds may also be dissolved in the liquid phase and then sampling can be done from there. It has been shown that, it takes quite some time for equilibration between the aqueous phase and the gas phase, so that if a process is to be followed, it might be preferable to sample from the liquid phase.

A device for such sampling was developed and applied in monitoring ethanol fermentation. The device is relatively simple in the sense that it is a Teflon tubing that is immersed in the fermentation broth and that an inert gas, usually nitrogen, is flushed inside the tubing. Volatile compounds are dissolved in the Teflon material and are diffused through the walls and are then carried away by the flushing nitrogen gas. The sample containing the compound to be analyzed is transported to a semiconductor sensor where it reacts and gives rise to a signal, the amplitude of which is proportional to the concentration of the substance in the gas phase. By using calibration solutions, it is possible to determine the actual concentration in a fermentation broth (14).

The same device was later used to quantify the amounts of hydrogen produced during anaerobic digestion of organic material (15).

Problems with such a sampling device are the potential risk of fouling. When dealing with relatively well-defined media, that is not a major problem but when it comes to anaerobic digestion of, for example, sludge from wastewater treatment plants, it was shown that the fouling became a problem already after 6 h, and the device had to be cleaned.

Another approach to monitor volatile compounds in complex media was developed for analyzing the content of volatile fatty acids in digesters treating pig manure. There, a sample was taken and the aliquot was acidified thereby pushing the volatile fatty acids to the gas phase. Analysis of the gas phase gave reliable readings (16).

63.6 REPRESENTATIVE SAMPLES

No analysis is better than the sampling preceding it. When sampling is done from bioreactors, there are obvious problems in taking representative samples. Heterogeneity in the fermentation broth may be severe and will thus cause variations in the samples and thus in the analytical results. This is something that cannot be avoided, but the effects can be minimized by proper routines.

The heterogeneity in a broth during active fermentation is well studied (17). An often used strategy is to sample in the medium close to the impeller since that is an area where mixing is intense. If the sample is not perfectly representative of the whole reactor volume, it will anyway be relatively reproducible over time, and then any error will be more or less constant over time.

For solid substrates or heterogeneous material with liquid as well as solid material, the sampling becomes even more complex (18). Then, it is possible either to take one big sample and homogenize it before analysis, or one may take several smaller samples, pool them, and then treat them as one sample.

63.7 REPRODUCIBILITY IN SAMPLING

It is important to get reproducibility in the sampling process, such that if no reaction is on-going in the sample, the analytical result from samples taken at different occasions should be constant. This would be expected if no reaction takes place and no physical obstacles appear. However, heterogeneity in a bioreactor due to improper mixing might give misleading results with scattered data over time (19). Still another possible disturbance might lead to successive decrease in the analytical result, even if the concentration is constant. Very often, fouling of membranes involved in the sampling will cause a decreased mass-transport over the membrane thereby resulting in nonreproducibility in the sampling.

As discussed above concerning membrane-based sampling devices, it is important to operate with tangential flow in order not to allow fouling layer to be formed.

Still another potential problem is that, on continuous processing, there might be risks of microbial on-growth of the inner surface of the sampling device, and when a subsequent sample is transported through the device, metabolism might occur and then change to analytical read out. Such a case was reported on when yeast cells were growing as a dense biofilm inside the sampling device used for monitoring a cultivation of Baker's yeast (20).

The most common error is by far heterogeneity in the reaction medium, and that is also the most difficult problem to deal with.

63.8 SAMPLE HANDLING

Any sample taken from a complex medium needs some kind of treatment before being analyzed. Often, additions are used in order to arrest any metabolism going on in the sample. When particulate matter present will disturb the readings, then filtration or centrifugation is carried out, and when cells are present and intracellular compounds are to be analyzed, cell breakage must take place and the cell debris being removed.

63.8.1 Discrete Sample Handling

All unit operations, as described above, can be carried out on discrete samples. Time consumption is often too high and the reproducibility in the assays may be strongly influenced by many manual handling steps.

63.8.2 On-Line Handling

When a sample has left the reactor, a range of possibilities to handle it is available. Very much depends on the character of the sample and on the nature of the analyte to be quantified. In Fig. 63.5 is schematically illustrated the treatment needed for a sample taken from a fermentation and in which one is interested to analyze an intracellular protein in the microorganism. As seen from the figure, there is a whole sequence of activities that need to take place, and each of them will represent inaccuracy in handling and thus affecting the accuracy in the final reading of the analytical outcome. Provided, this could be done automatically, it would be possible to reduce the inaccuracies caused by the human factor, and one could expect a far better accuracy and reproducibility. That it is advantageous to eliminate many manual steps and to try to introduce automation was clearly shown for ELISAs. While the standard variation of the manual analyses was in the order of $\pm 15\%$ for the inexperienced person and $\pm 7\%$ for a skilled laboratory technician, it was possible to carry out the same analyses in an automated fashion with a standard variation of $\pm$ 1.5–2% (21).

63.8.3 Flow Injection as a Tool in Sample Handling

When flow injection analysis (FIA) was first introduced, it was claimed to have a great advantage in the sense that additions of an aliquot of liquid could be done very accurately and be reproducible. Later on, it was shown to be suitable for on-line dilution in a reproducible way (22) and for dialysis, and even for incubation for a fixed period of time before the sample was read could be carried out using the FIA-approach. Different unit operations can be integrated into a continuous flow system, thereby simplifying sample handling even if it consists of many different steps. In Table 63.2 are listed some of the different operations that have been reported to be integrated in the continuous flow system.

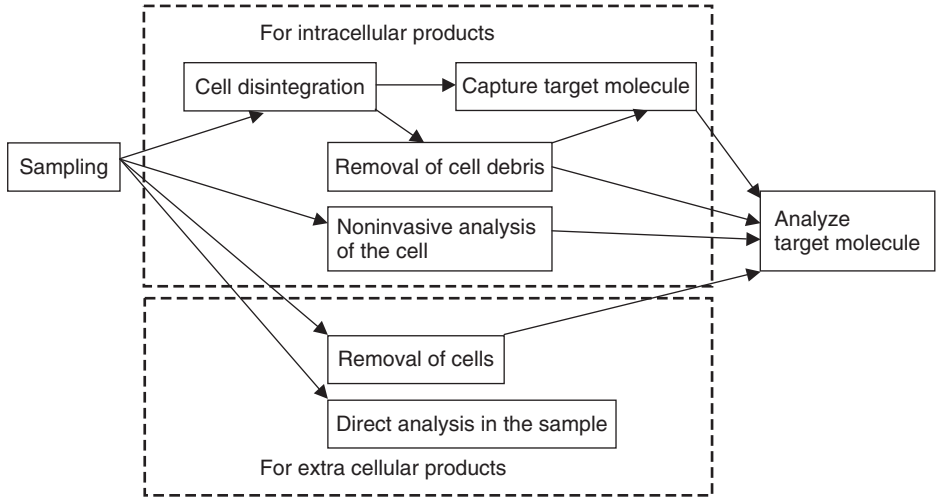


Figure 63.5. Schematic presentation of different options for analysis after sampling has been done.

TABLE 63.2. Unit operations in Sample Handling Integrated with Flow-Injection Systems

Unit Operation	Analysis	References
Dialysis	Penicillin V	23
Dilution	Many different	22
Enzymatic reaction	Cutinase	24
Binding reaction HSA	Human serum albumin (HSA)	25
	Gentamycine	26
	Amylase	21
Extraction	Ethanol	27
Cell homogenization	β-Galactosidease	28
	Plasmid DNA	29,30
Permeabilization	Plasmid DNA, alkaline phosphatase, intracellular target protein	31

63.8.4 Substances Present at High Concentrations: Dilution

When industrial processes are monitored, there may be situations when the target molecule is present in far too high concentrations to allow accurate assay. Then dilution is necessary, and that can easily be achieved using a flow-injection system (22).

The need for dilution is especially obvious when the assay falls far outside a linear range of a standard curve. This may be the case for immunoassays, since often such assays are set up to monitor low concentrations of substances (21). As long as it is the target molecule, one can expect high concentrations and needs for dilution. However, for impurities, especially impurities in pharmaceutical products, there is a need for enrichment.

63.8.5 Substances Present in Very Low Concentrations: Enrichment

When a substance is present in very low concentrations, it might be advantageous to enrich it on an adsorbent before analysis. Such adsorbents might be selective and then the substance is released by a less selective elution, or in some cases a nonselective adsorbent and a specific elution is used. Still, there might be a nonselective adsorbent and a nonselective elution and then a selective analysis. Some examples are given in Table 63.3. Examples on substances that are analyzed using enrichment strategies are listed in Table 63.4.

63.8.6 Cell-Free Solutions

The membrane units described above for sampling inside a fermentor, or from an external loop are all suitable to create cell-free solutions that can be used for further analysis.

63.8.7 Special Arrangements for Intracellular Substances

When intracellular substances are to be quantified, the cell walls need to be destroyed in order to release the intracellular material. There are many options on how to carry out such cell destruction. A crucial point is, of course, not to destroy the intracellular compounds that are of interest to analyze. When choosing suitable strategy for cell disruption, one needs to consider possible effects of addition of chemicals on the subsequent analysis.

In one example, a fermentation broth containing cells of *E. coli* was treated with lysozyme in order to enzymatically modify the cell wall before the pretreated cells were exposed to an ultrasound treatment as shown in Fig. 63.6

TABLE 63.3. Adsorbents Used for Enrichment of Analyte

Adsorbent	Analyte	Elution	Detection	References
Chelex-100	Heavy metal ions	Ammonium acetate, pH 9.5	Atomic absorption	32
pAAm-Cryogel	Urokinase	Imidazol	Enzymatic activity	33
IMAC-column	His-tagged protein	Imidazol	Enzymatic activity	34
Molecular imprinted polymer (MIP)	Hormones	pH	Diod-array detection	35

TABLE 63.4. Compounds Enriched in the Sample Handling Step Preceding the Assay

Target molecules
Host cell proteins (HCP)
Truncated target proteins
Modified target protein
Media components
DNA
Bacterial toxins
Endocrine disruptors
Explosives
Drugs

(28). All this was carried out in an integrated flow system and the results were analyzed in an immunochemical binding assay. A difficult task in such a situation is to know when the cell breakage is sufficient, since if the treatment is too brutal, then the proteins of interest to analyze will be denatured. On the other hand, if the destruction of cell walls is not complete, then a lower value of the intracellular target will be observed in the subsequent assay.

An interesting new methodology for on-line monitoring of intracellular products involves laser-induced disruption of the microbial cells. This technique, even not fully explored yet, has proven both rapid and efficient as well as clean for use as sample preparation in bioanalytical detection systems (36).

63.9 NONINVASIVE MONITORING METHODS

A dream for any biotechnologist would be to be able to follow the bioprocess without having to take samples and to carry out a range of analytical procedures. Novel sensing devices are being developed and some of them are possible to use *in situ* in the reactor and to read data that later on can be processed to a form that will give information about the physiological statues of the cells studied. Such methods are, for example, near-infrared spectroscopy (NIR), fluorescence spectroscopy, and to some extent NMR.

These methods do not yet have resolution enough to make it possible to register many specific metabolites. However, some useful information can certainly be achieved,

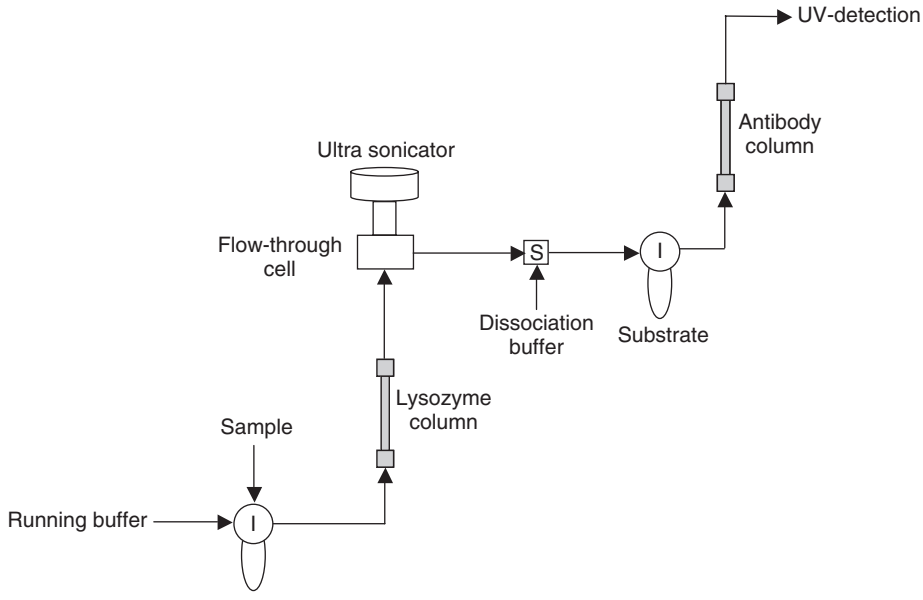


Figure 63.6. Schematic setup of the analytical system. I, injectors; S, switch valve [Source: Reproduced with permission from Ref. 28].

and the forecast is that such nonspecific analytical procedures combined with powerful computer programs will grow in importance in the future.

63.10 INTEGRATED PROCESSES

Flow-injection systems offer many attractive features. After sampling from the bioreactor has taken place, it is easy to retract well-refined and reproducible volumes of the aliquot for further processing. Moreover, the use of sample loops with fixed volumes could reduce sample volume inaccuracies in this step to a minimum (37).

A range of unit operations can be combined, and that makes it possible to build almost any kind of sample-handling procedure. Dialysis and/or dilution can be made in reproducible manners. A range of reports are available on these unit operations and it is obvious that they operate to satisfaction in most cases (23,28). Figure 63.7 illustrates one method for sampling from a bioreactor using a sample carousel. The samples collected are refrigerated at 4°C for later analysis.

When it comes to separation of macromolecules from a heterogeneous sample, it may be a little more problematic. Here dialysis will not do. If cells and cell debris are present, then an adsorption step might be useful for capturing the target molecules while the particulate matter is washed away. This can be done by using expanded bed adsorbents (38), or by using supermacroporous adsorbents connected in-line with the analysis system (39). By using selective adsorbents, it may even be possible to enrich the target molecule while most of the other molecules are removed.

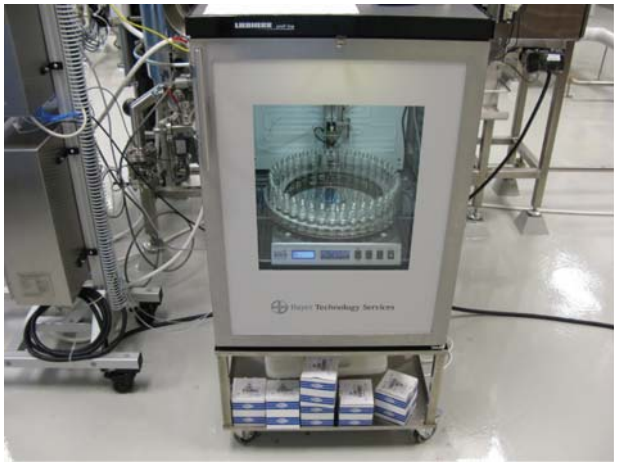


Figure 63.7. Automatic refrigerated aseptic sampling unit (BaychroMAT®, Bayer Technology Services) [Source: Courtesy of Golden LEAF Biomanufacturing Training and Education Center (BTEC), North Carolina State University, Raleigh, NC USA]. (This figure is available in full color at http://onlinelibrary.wiley.com/book/10.1002/9780470054581.)

Still, other possibilities in this connection would be to use magnetic trapment, that is, to have adsorbents with certain functionalities to trap the target molecule and at the same time have magnetic material in the adsorbent such that it will be possible to add the adsorbent to the sample and after binding has taken place, isolate the magnetic particles with their bound target molecules.

When it comes to monitoring intracellular compounds, very little on-line experience exists. However, a few reports in literature clearly show the possibility. Breaking the cells is the crucial step and depending on the type of cells different strategies may be used. When dealing with *E. coli*, it turned out to be efficient to let the organisms pass through a column with immobilized lysozyme and a subsequent step with ultrasound (39). When establishing this unit operation, it was a bit problematic to properly optimize the step. When is the optimum number of cells opened to release their content to the environment, without the effect that the target molecules get denatured by the ultrasound treatment? One has to make some trials and just decide the conditions yielding the best activity.

When nucleic acids are to be quantified, alkali treatment combined with adsorption chromatography turned out to be successful. This was exploited when monitoring the content of plasmids during a cultivation (29,30).

A different strategy based on sample handling in a flow-injection system involves the use of permeabilization of the cell walls and then monitoring of intracellular activities when substrate is supplied from outside. This was utilized in a model study when quantifying plasmids carrying the gene for alkaline phosphatase as well as cell density in the samples were studied. It was found that, there was a good correlation between the plasmid copy number and the monitored activity of the indicator enzyme. When one more enzyme was cloned into the plasmid, the expression of the target gene could be monitored (31).

There is always a risk that fouling and other disturbances might ruin the analyses. Calibration of the system is needed, preferably, all the way from the sampling point to the detector. In most cases, only some of the separation steps are evaluated, but not the whole system. However, when using a coaxial catheter (Fig. 63.8) for sampling, it turned out to be practically feasible to add a calibration solution to the system at the sampling point and then let it pass through all the different unit operations before being analyzed (40).

Besides flow-injection analysis, sequential injection analysis seems very attractive and useful. However, this later technique is of more recent date and not so many applications have been presented. The inventor of this technology is the same as of flow-injection analysis. Dr Ruzicka and his group have shown it possible to handle cells and to carry out a range of different unit operation in the sequential injection analysis.

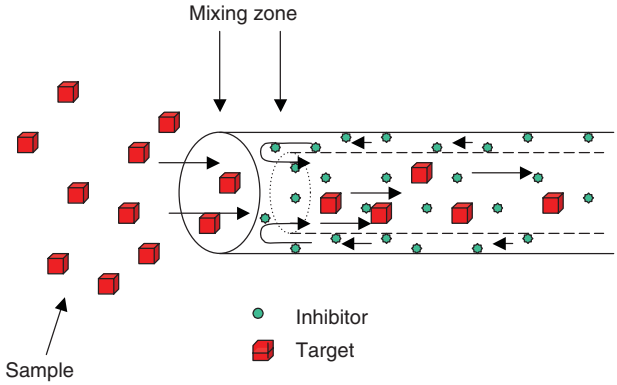


Figure 63.8. Schematic operation of a coaxial catheter unit during the *in situ* sampling step from a bioreactor [Source: Reproduced with permission from Ref. 13]. (This figure is available in full color at http://onlinelibrary.wiley.com/book/10.1002/9780470054581.)

63.11 COMMERCIAL SYSTEMS

With an increasing demand for time-efficient ways of extracting specific information from each step in the process, the development of techniques for direct sampling in bioprocess situations has shifted from being a typical academic discipline to become a factual concern to the industry. Typically, pharmaceutical production is performed by batch processing with concomitant off-line analysis of collected samples from the different steps throughout the purification process. However, rising public demands for shortened time-to-market for the development and production of critical drugs and accessibility to more affordable medicines have put strains on both regulatory agencies and manufacturers to change this situation.

There are, at present, only few methods offered for direct and noninvasive sampling from a bioreactor. Some systems have, however, been commercialized and are today used as tools in industrial large-scale bioproduction**:**

Microdialysis	CMA microdialysis AB	www.microdialysis.se 3,41
Oxygen analyzer (ABC-unit)	Daiichi Nekken Co. Ltd.	www.daiichinekken.co.jp
Biosensor	Biosensor Application AB	www.biosensor.se
FIA	Foss A/S	www.foss.dk

63.12 CONCLUSION

Much effort has been put into developing biotechnological processes, both with regard to upstream and downstream. There is, however, a lack of suitable analytical information concerning on-line monitoring of the processes. This is, especially, clear in the downstream area.

When more efficient and better controlled bioprocesses are to be set up, improved process control is a must. To reach that, one must have better analytical systems and well-functioning sampling and sample-handling routines. It seems that the industry is starting to realize the problem, and the potential benefits from improving process monitoring and control, and therefore, one can expect that focus for the development will shift from the academic laboratories toward industrial units. With such a development, it is expected that this part of analytical activities will become more in focus, thereby attracting more interest, and therefore develop faster.

The technology presented in this review forms a sound basis for future development, but what is required now is that the analytical systems are implemented on real industrial processes, thereby making it possible to get figures on the impact of applying suitable sampling, sample handling, and subsequent analysis and control.

REFERENCES

1. U.S. Food and Drug Administration. Washington (DC); 2004. Available at http://www.fda.gov/cder/OPS/PAT.htm.
2. Mandenius CF, Hedman T, Mattiasson B. J Inst Brew 1984; 90: 77–80.
3. Meyerson BA, Linderoth B, Karlsson H, Ungerstedt U. Life Sci 1990; 46: 301–308.
4. Kyrölåinen M, Hakånson H, Mattiasson B, Vadgama P. Biosens Bioelectron 1997; 12: 1073–1081.
5. Rice M, Roeraade J, Holmbom B. Nord Pulp Pap Res 1999; 14: 292–299.
6. Nielsen J. Proc Control Qual 1992; 2: 371–384.
7. Håkanson H, Holst O, Mattiasson B. Proc Eur Congr Biotechnol 1990; 1: 535–538.
8. Appelqvist R, Johansson G, Holst O, Mattiasson Bo. Anal Chim Acta 1989; 216: 299–306.
9. Seifert GKE, Matteau PP. Biotechnol Bioeng 1988; 32: 923–926.
10. Ungerstedt U. J Intern Med 1991; 230: 365–373.
11. Torto N, Gorton L, Laurell T, Marko-Varga G. Trends Anal Chem 1999; 1: 252–260.
12. Holst O, Håkanson H, Miyabayashi A, Mattiasson B. Appl Microbiol Biotechnol 1988; 28: 32–36.
13. Håkanson H, Nilsson M, Mattiasson B. Anal Chim Acta 1991; 249: 61–65.
14. Mandenius CF, Danielsson B, Mattiasson B. Anal Chim Acta 1984; 163: 135–141.
15. Björnsson L, Hörnsten EG, Mattiasson B. Biotechnol Bioeng 2001; 73: 35–43.
16. Boe K, Batstone DJ, Angelidaki I. Water Sci Technol 2005; 52: 473–478.
17. Pollard D, Ison AP, Shamlou A, Lilly MD. Adv Bioprocess Eng 1994; 1: 163–170.

18. Allen D, Robinson G, Campbell W. Chem Eng Sci 1990; 45: 37–48.
19. Larson G, Törnkvist M, Ståhl-Wernersson E, Trädgårdh C, Noorman H, Enfors SO. Bioprocess Eng 1996; 14: 281–289.
20. Mandenius CF, Holst O, Mattiasson B. Org Chem Biochem 1983; B37: 746–748.
21. Nilsson M, Vijayakumar AR, Holst O, Schornack C, Håkanson H, Mattiasson B. J Ferment Bioeng 1994; 78: 356–360.
22. Ruzicka J, Hansen EH. Anal Chim Acta 1978; 99: 37–76.
23. Scheper T, Brandes W, Maschke H, Plotz F, Muller C. J Biotechnol 1993; 31: 345–356.
24. Almeida CF, Cabral JMS, Fonseca LP. Anal Chim Acta 2004; 502: 115–124.
25. Mattiasson B, Borrebaeck C, Sanfridsson B, Mosbach K. Biochim Biophys Acta 1977; 483: 221–227.
26. Mattiasson B, Svensson K, Borrebaeck C, Jonsson S, Kronvall G. Clin Chem 1978; 24: 1770–1773.
27. Ogbomo I, Steffl A, Schuhmann W, Prinzing U, Schmidt HL. J Biotechnol 1993; 31: 317–325.
28. Nandakumar MP, Tocaj A, Mattiasson B. Bioseparation 1999; 8: 247–254.
29. Nandakumar MP, Karlsson-Nordberg E, Mattiasson B. Biotechnol Bioeng 2001; 73: 406–411.
30. Nandakumar MP, Karlsson–Nordberg E, Mattiasson B. Biotechnol Lett 2001; 23: 1135–1140.
31. Schendel FJ, Baude EJ, Flickinger MC. Biotechnol Bioeng 1989; 34: 1023–1036.
32. Ellis LA, Roberts DJ. J Anal At Spectrom 1998; 13: 631–634.
33. Kumar A, Bansal V, Nandakumar KS, Galaev IYu, Roychoudhury PK, Holmdahl R, Mattiasson B. Biotechnol Bioeng 2006; 93: 636–646.
34. Rios C, Salvado V, Hidalgo M. J Sep Sci 2004; 27: 602–606.
35. Le Noir M, Lepeuple AS, Guieysse B, Mattiasson B. Water Res 2007; 41: 2825–2831.
36. Dhawan M, Wise F, Baeumner A. Anal Bioanal Chem 2002; 374: 421–426.
37. Gardner WS, Malczyk JM. Anal Chem 1983; 55: 1645–1647.
38. Mattiasson B, Nandakumar MP. Bioseparation 1999; 8: 237–245.
39. Hedström M, Plieva F, Galaev YuI, Mattiasson B. Anal Bioanal Chem 2008; 390: 907–912.
40. Kyröläinen M, Håkanson H, Mattiasson B. Biotechnol Bioeng 1995; 45: 122–128.
41. Richards DA, Tolias CM, Sgouros S, Bowery NG. Pharm Res 2003; 48: 101–109.

64

SOLID STATE FERMENTATION, KINETICS

David A. Mitchell
Universidade Federal do Parana, Curitiba, Brazil
Deidre M. Stuart
Queensland University of Technology, Brisbane, Australia
Robert D. Tanner
Vanderbilt University, Nashville, Tennessee

64.1 INTRODUCTION

Solid-state fermentation (SSF) involves the growth of microorganisms on moist solid substrates in the absence of free water. The absence of free water makes the system quite different from submerged liquid fermentations and makes SSF superior for the production of some products. However, compared with submerged liquid fermentation, relatively little is known about how to design and operate bioreactors for large-scale SSF processes.

Despite this, there are commercially successful large-scale SSF processes for the production of soy sauce koji and other traditional fermented foods, citric and gluconic acids, and fungal enzymes such as cellulases, amylases, lipases, and pectinases (1,2). In addition, fungal spores have been produced by SSF for use in steroid transformations and as inocula for production of blue-vein cheeses (2). Composting is another SSF application that is widely practiced, although composting is different from other SSF processes, because self-heating of the fermenting substrate is desired in composting processes, whereas avoidance of overheating is a key problem in most SSF processes.

In addition to these commercial processes, over the last 20 years there has been a growing interest in other SSF applications (2), including the following:

- Upgrading of solid wastes from agriculture and food processing for use as fermented animal feeds. In some cases the microorganism is used to enrich the protein content; in other cases it is used to degrade toxic substances in the waste.
- Production of fungal spores for use as mycopesticides. SSF is superior for the production of fungal spores because most fungi do not sporulate well in liquid culture, and even when they do, spores produced in SSF tend to be more robust.
- Production of other enzymes such as dehairing enzymes, fungal rennets, beta-glucanases and xylanases.
- Biopulping of woodchips during the production of paper.
- Production of various other products such as gibberellic acid, aroma and flavor compounds, antibiotics, and ethanol.

Unlike the situation with submerged liquid fermentations, there is no systematic framework guiding the design and operation of large-scale bioreactors for SSF. As a result, there has been relatively little success in developing successful large-scale processes for these newer SSF products, although large-scale bioreactors have been used to make

Upstream Industrial Biotechnology: Equipment, Process Design, Sensing, Control, and cGMP Operations, Volume 2, First Edition. Edited by Michael C. Flickinger.
© 2013 John Wiley & Sons, Inc. Published 2013 by John Wiley & Sons, Inc.

soy sauce koji. Intermediate-scale processes can be carried out using tray fermentations, but such operations are quite labor intensive. Mathematical models of bioreactor operation will be key tools in the development of strategies for the design and operation of large-scale SSF bioreactors. This chapter summarizes the current state of development of modeling of SSF processes.

64.2 AIMS OF THIS CHAPTER

This chapter addresses the importance, to the development of large-scale SSF technology, of understanding and modeling microbial growth kinetics and transport phenomena, which combine to determine the overall performance of a solid-state bioreactor. Transport phenomena are of special importance in SSF due to the unavoidable heterogeneity of SSF systems. Good reactor performance will be achieved only through an understanding of these transport phenomena and how they interact with the microbial growth kinetics. Mathematical models represent a convenient, concise, and powerful way of describing these phenomena and their interactions and provide a sound foundation for process development, control, and optimization. They can also guide us in learning where the problems are and how to attack them.

The main message of this chapter is that modeling of phenomena in SSF and of the performance of SSF bioreactors has not yet progressed to a stage where it can be usefully applied to industrial applications. In fact, it was only in 1990 that the first model was proposed for SSF bioreactor operation (3). Although advances have been made since then, currently we still do not have mechanistic models of SSF that are able to make accurate predictions based fully on independently determined parameter values. To date the focus has been on appropriate model structures. Relatively little attention has been given to parameter estimation, with many parameters being borrowed from other systems, systems that often involve different substrates, organisms, and cultivation systems. As a result, none of the models has been properly validated against experimental data, and although the models are now being used to predict improved operating conditions, they have not yet been used to improve operation of actual bioreactors. In most cases some of the model parameters have been estimated by adjusting them to enable the model to fit the experimental data. Furthermore, although the ultimate aim of SSF processes is to produce useful products industrially, to date models have focused on growth. In fact, in some cases the main aim has been to predict temperatures rather than growth itself.

The aim of this chapter is to draw together the basic principles from the work that has been done so far, to show the general concepts that underpin all models, to identify the features that will make models most useful for application in industrial processes, and thereby to provide a foundation for continued progress in the modeling of SSF.

64.3 ORGANIZATION AND SCOPE

Filamentous fungi are the most important group of microorganisms used in SSF, and most processes are aerobic. Most of the work discussed in this chapter addresses this type of system, although other systems are mentioned as appropriate.

The chapter begins by describing the biological and transport phenomena occurring in an SSF bioreactor and identifying the various phenomena that can potentially limit the kinetic performance of the bioreactor:

- Microbial growth phenomena
- Local transport phenomena (occurring at the level of a single particle)
- Bulk transport phenomena (occurring at the level of the whole bioreactor)

Current models of SSF address the influence of either local or bulk transport phenomena on growth and are therefore labeled as microscopic or macroscopic models. The general aims and usefulness of these two types of models are discussed. The mathematical expressions appropriate for describing the three types of phenomena that may be incorporated into these models are discussed in turn.

Readers interested in modeling of SSF processes are urged to consult the original references because no attempt has been made to present the complete models of individual workers. The original chapters do that better than we could hope to do. Rather we have organized this chapter around the ways in which the various kinetic and transport phenomena have been handled. Therefore, where we present equations, these have been separated from the author's discussion of their underlying assumptions and the notation and units they have used.

64.4 DESCRIPTION OF KEY FEATURES OF SOLID-STATE FERMENTATION

Growth in an SSF bioreactor results from and is influenced by processes operating at different scales (Fig. 64.1): microbial processes and local and bulk transport processes. Figure 64.1 also highlights some of the complex interactions between these phenomena during SSF. This chapter addresses the approaches that have been made to modeling the various phenomena shown in Figure 64.1, and the interactions between the various phenomena. Thermodynamic phenomena, such as the ability of solid substrates to absorb

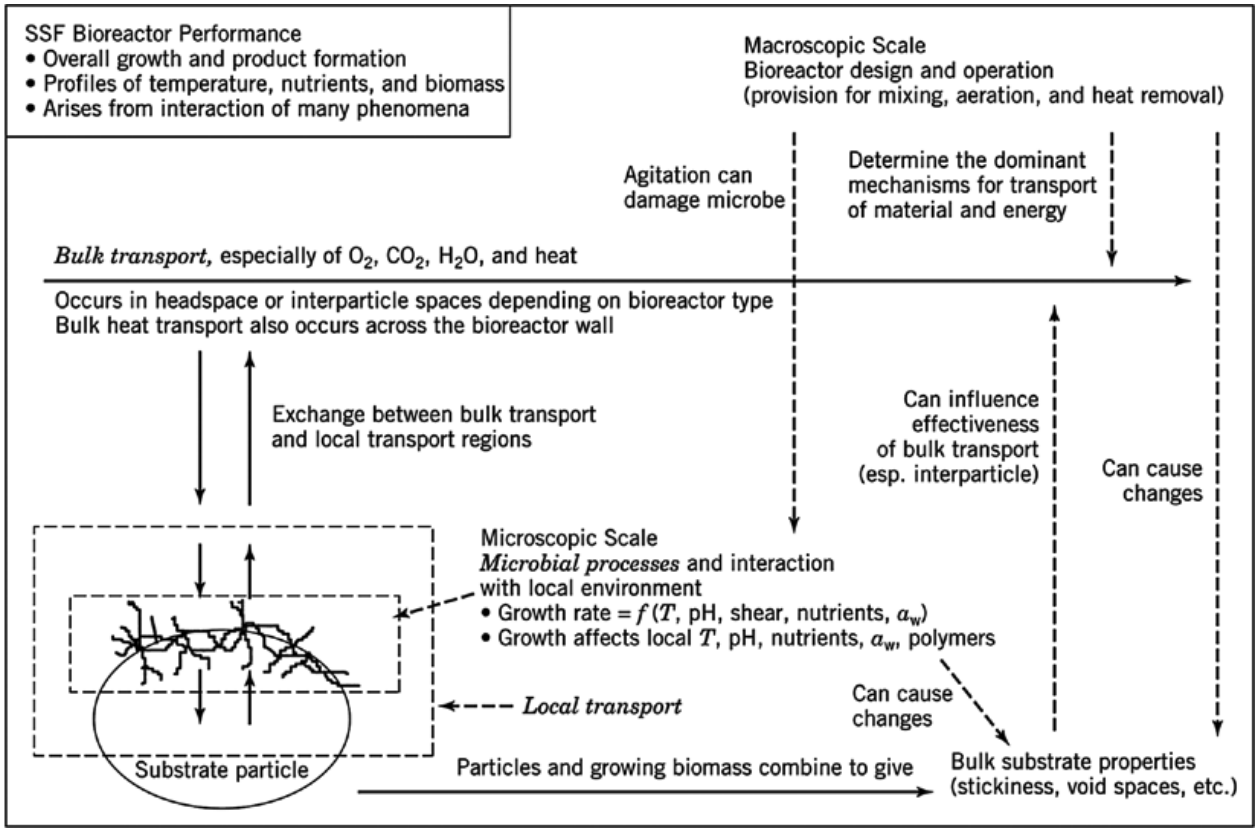


Figure 64.1. An overview of the microscopic and macroscopic processes that combine to determine the overall performance of an SSF bioreactor. This diagram describes transport processes in general terms and does not identify all the individual mass and heat transfer processes occurring. Although the diagram represents an SSF bioreactor, it is not drawn to scale. The nature and extent of the local and bulk transport regions depend on the particular bioreactor and how it is operated.

heat and the ability of gases to carry water vapor, also affect the overall bioreactor performance; however, these phenomena are not addressed in this chapter.

In developing a mathematical model, it is important to identify the processes occurring before attempting to describe them mathematically. This focuses attention on the processes that are potentially rate limiting. An understanding of the rate-limiting processes facilitates development of strategies to overcome the limitation, although SSF processes can be difficult to optimize because the limiting step might be different under different conditions, and at different stages of an SSF process the growth rate may be limited by different phenomena. Therefore this section provides a qualitative description of our current understanding of the phenomena occurring in SSF.

64.4.1 The Physical Nature Of Solid-State Fermentation Systems

From a macroscopic viewpoint, up to four subsystems are apparent (Fig. 64.2), depending on the bioreactor type:

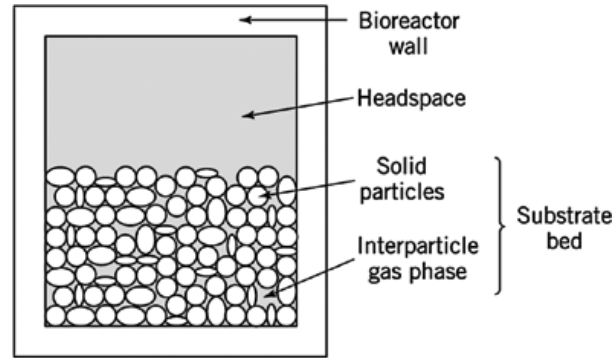


Figure 64.2. Subsystems within a solid-state fermentation bioreactor.

the material from which the bioreactor is constructed, a headspace containing gases, the solid particles themselves, and the interparticle gas phase entrapped between the solid particles. It is often appropriate to think of the solid particles and interparticle gas as a pseudohomogeneous "substrate bed."

From a microscopic perspective the system is considered in greater detail. The description focuses on the region near an individual particle and can include (Fig. 64.3) the following:

- The biomass, the majority of which is concentrated as a layer at the particle surface. Part of the fungal mycelium is immersed in the liquid film at the surface, but many hyphae extend into the gaseous region. These aerial hyphae may support films or droplets of water. Other hyphae may penetrate into the substrate particle. In contrast, yeasts and bacteria form a compact moist layer on the particle surface.
- The solid matrix, which provides the physical support for the liquid and biomass phases, and which may or may not be degraded during the fermentation.
- A liquid phase consisting of a stagnant liquid film at the substrate surface and the moisture inside the particle. This phase may be continuous, depending on the internal structure of the substrate particle.
- A gaseous phase. Although this gas phase is continuous, it may be conceived as comprising up to three regions. First, the aerial hyphae of the biomass are surrounded by regions of stagnant gas, and there will be a stagnant gas film adjacent to the liquid film. Second, there may be a stagnant gas region above the biomass region (i.e., part of the interparticle space). Third, there

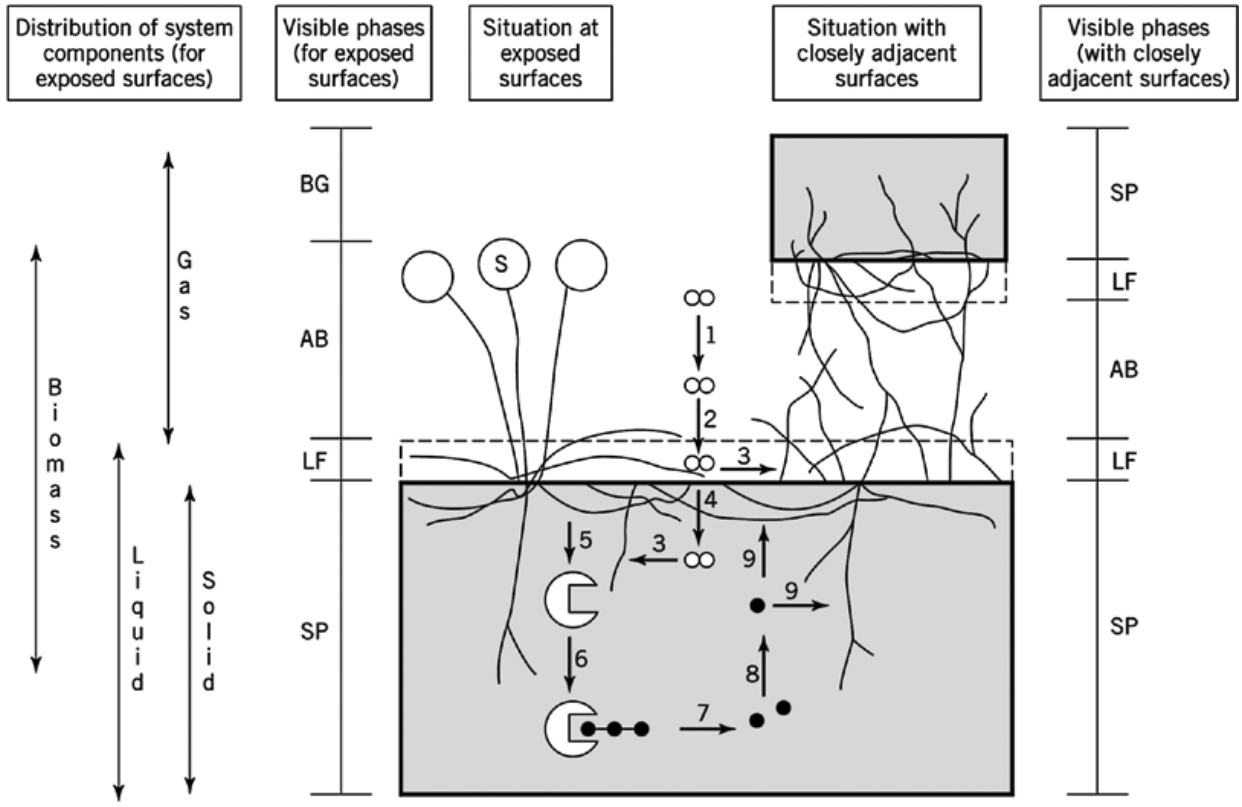


Figure 64.3. Structure of SSF systems at the microscopic scale and local mass transport processes. The example is for growth of a filamentous fungus, such as *Rhizopus* sp., on a starchy substrate. The diagram represents a cross-sectional view near the surfaces of the substrate particles and indicates the difference between substrate particles exposed to the bulk gas phase and substrate particles that are packed closely together. Simplifications, such as the absence of penetrative hyphae, and the liquid film as the only site of O_2 uptake, have been used in modeling studies. ∞, oxygen; •, glucose; •—•—•, starch; S, sporangium; SP, substrate particle; LF, liquid film; AB, aerial biomass; BG, bulk gas. The processes occurring are 1, bulk transport of oxygen; 2, diffusion of O_2 through stagnant gas regions and diffusion across the gas–liquid interface; 3, uptake of oxygen by hyphae; 4, diffusion of oxygen through the liquid phase of the substrate; 5, release of glucoamylase from the hyphae; 6, diffusion of glucoamylase through the solid substrate particle; 7, hydrolysis of starch by the glucoamylase; 8, diffusion of the released glucose through the solid substrate particle; 9, uptake of glucose by the hyphae.

may be a mobile region in which there is bulk flow. The locations and extents of the stagnant and mobile gas regions will depend on whether the substrate bed is agitated and how it is aerated. For example, in static packed beds the interparticle spaces are filled with a network of hyphae, but there is still bulk gas flow through parts of this region. On the other hand, in tray bioreactors, the gas phase within the substrate bed is relatively stagnant, although there may be some free convection due to thermal gradients.

64.4.2 The Processes Occurring During Solid-State Fermentation

Aufeuvre and Raimbault (4) described the changes in morphology during growth of the filamentous fungus *Aspergillus niger* in a packed bed bioreactor, on a granular substrate prepared from cassava flour. Initially, the spores used as inoculum are spread across the substrate surface. During the germination period of about 8 h, the spores swell and then extend germ tubes across the substrate surface. These germ tubes extend for up to 50 μm before branching begins. Branching of these germ tubes then rapidly leads to a loose covering of hyphae across the whole surface. As branching continues, the hyphal density increases, and it is soon impossible to distinguish individual mycelia. The network of hyphae increases in thickness, so that many hyphae are not in contact with the substrate surface. Some hyphae form together into multihyphal filaments, which can extend up to 80 μm above the substrate surface. These filaments form bridges between the substrate granules and bind the whole bed of substrate particles together into a single compact mass.

This description addresses only the features of the growth process that can be seen with a microscope. Many less obvious processes are occurring and influencing growth (Fig. 64.3). The growth activities of the microbe are determined by the local environment experienced by the microbe, especially the local temperature, pH, water activity (a_w), oxygen concentration, and nutrient concentrations. In turn, growth processes also affect the local environment, for example, hydrolytic enzymes are secreted, carbon and nitrogen substrates are absorbed into the mycelium, oxygen is consumed, and various products are excreted. In addition, waste metabolic heat is released by the microorganism. Therefore the temperature, pH, water activity, and oxygen and nutrient concentrations in the local environment are affected by the microorganism. This induces the transport processes, which tend to equilibrate chemical potential and temperature throughout a material. Within solid particles and within stagnant gas regions, mass transfer is limited to diffusion and the exchange of gases (O_2, CO_2, and water vapor) at gas–liquid interfaces, and heat transfer is limited to conduction, free-convection, and evaporation of water at the gas–liquid interface. These dissipative processes can be relatively slow compared with the rate of the microbial processes, leading to the establishment of local concentration and temperature gradients around the microbe.

The purpose of a bioreactor is to maintain an optimal local environment for the desired microbial activity, within the limits of physical and economical constraints. In SSF the ability to control the local environment is largely limited to manipulating either the bulk gas flow or agitation of the substrate, or both, providing oxygen for aerobic processes, removing carbon dioxide and evaporated water, and removing heat. Almost nothing can be done during the fermentation to prevent nutrient concentration gradients within individual substrate particles, because it is not possible to have bulk mixing below the scale of the substrate particles. This is an intrinsic consequence of the physical form of SSF systems.

Given that control of the environment is achieved by manipulating the bulk phases, the rate of removal of heat and the rate of supply of oxygen can be maximized by minimizing gradients within the bulk gas phase and minimizing the thickness of the stagnant gas film that separates the bulk gas phase from the local environment. Different reactor types enable this to be achieved to different extents. In bioreactors with bulk flow of air past the solids, due either to forced airflow or to mixing of the substrate bed, gases diffuse from the stagnant gas regions into the bulk flow and are carried away. Heat can be removed by convection and by evaporation of water into this air. Evaporative heat removal can be maximized by aerating with dry air, but this will tend to dry the substrate. Depending on the bioreactor operation there might be significant gas concentration gradients and temperature gradients in the bulk air phase across the bioreactor. Plug flow of gas (and maybe substrate) will tend to favor macroscopic gradients, whereas mixing of the gas phase and of the substrate bed will tend to minimize such gradients. In bioreactors without bulk flow of air past the solids (i.e., trays), mass transfer and heat transfer occur mainly by diffusion and conduction, respectively. In addition to heat and mass transfer within the bioreactor, there are also heat transfers between the substrate bed and the bioreactor wall, the headspace gases and the bioreactor wall, and the bioreactor walls and the surroundings (Fig. 64.1).

During microbial growth in SSF, growth activities and the aeration and agitation strategies can affect the bulk substrate properties, which in turn can influence the bulk transport processes, as indicated in Figure 64.1. For example, in an unstirred packed bed, fungal mycelia grow in the interparticle spaces and can significantly increase the pressure drop through the bed, affecting airflow patterns within the bed (5). Microbial activities on the substrate

may decrease the strength or increase the stickiness of the particles, leading to compaction or cohesion of particles when the substrate is agitated, thereby eliminating interparticle spaces and preventing bulk transport to or from the microbes within the bed.

In conclusion, there can be significant profiles of temperature, nutrients, and biomass at both the microscopic scale (looking at a single particle with a microbe growing on it, as shown in Figure 64.3) and the macroscopic scale (looking across the bioreactor as a whole, as shown in Figure 64.1). The success of transport processes at both these scales in dissipating thermal and concentration gradients determines how readily the local conditions can be maintained near the optimal state for the desired microbial activity. Therefore, the overall performance of an SSF bioreactor arises from the interaction of biological growth kinetics, local transport processes, and bulk transport processes. The next section discusses the nature of models of SSF in general terms, whereas the remaining sections address how the underlying phenomena have been described in mathematical models of SSF processes.

64.4.3 Approaches to Modeling Solid-State Fermentation

A fully mechanistic description of the bulk and local transport processes occurring within SSF (Figs. 64.1 and 64.3), when combined with the growth kinetics, would lead to a very complex model of the system. Models of SSF to date have focused on either local or bulk transport phenomena, and therefore it is convenient to classify the models as being either microscopic models or macroscopic models. Microscopic models concern themselves with growth at the level of individual particles, whereas macroscopic models describe overall bioreactor performance. Both types of models have a role to play in the development of SSF technology. However, in the future, models should be developed that integrate mechanistic descriptions of both local and bulk transport phenomena, although this will depend on further advances in computing power and methods for constructing and solving complex dynamic models. Such models will describe performance under a wide range of operating conditions. This trade-off between the power of the model and the ease of model solution should be kept in mind. As well, the purpose of the model and the ability to estimate parameters should be considered when developing models that incorporate both microscopic and macroscopic phenomena. Because microscopic and macroscopic models are currently developed separately, the modeling work usually has related but different aims.

Microscopic models combine local transport phenomena (Fig. 64.3) and the effect of the local environment on growth, in an attempt to identify the mechanisms by which these may control the growth rate and the total amount of growth that occurs during SSF. For example, due to the absence of mixing at the microscopic scale, diffusive phenomena within the substrate particle can limit the growth rate (6). Microscopic models tend to consider the biomass in more detail than do macroscopic models, and it may be appropriate to describe variations in hyphal density in space, or the presence of differentiated forms of biomass. However, for the modeling of bioreactor performance, it is not appropriate to describe the extension and branching of individual fungal hyphae. Models incorporating these growth phenomena are powerful tools for fundamental studies aimed at understanding the mechanisms of fungal growth but are not discussed in this chapter.

Macroscopic models attempt to describe the performance of the whole bioreactor (Fig. 64.1). Such models may be developed to contribute to various aspects of bioreactor development such as design, operation, scale-up, control, and optimization. The main aim is to describe growth, although this may require prediction of temperature or nutrient or oxygen concentrations, or properties of the substrate bed. Their level of sophistication is in keeping with the ability or lack of ability to measure fermentation parameters such as biomass, nutrient concentrations, gas concentrations, temperature, and pH. Macroscopic models should describe the phenomena controlling the bioreactor performance, but current macroscopic models simply combine bulk transport phenomena with empirical descriptions of microbial growth. They do not address local transport phenomena, because of the complexity that these introduce. Simple empirical descriptions of growth may subsume biological and local transport limitations on growth but conceal the mechanisms of the limitation. Therefore, current macroscopic models are most useful for determining whether bioreactor performance is limited by gas or heat exchange, and guiding bioreactor design and operation to overcome any such limitations.

Several other characteristics of SSF lead to common features of models:

- The vast majority of SSF processes are batch processes, and the few continuous processes involve plug flow systems rather than well-stirred vessels. Therefore dynamic models are most useful for describing SSF. Steady-state models are usually not appropriate.
- The presence of mass and thermal gradients means that in most cases it is desirable to include spatial coordinates in addition to the temporal coordinate. Unfortunately this makes the equation sets more complicated to set up and solve.
- Balances are commonly set up over more than one of the subsystems shown in Figure 64.2.

- Depending on what is expected to limit growth, either heat or mass transfer may be described. Models incorporating both of these transport phenomena will be most flexible in describing what controls the rate of growth under a wide range of operating conditions.
- Due to the complexity that transport phenomena introduce into problems, plus the difficulties of measuring biomass and metabolic states, the majority of models for SSF are unstructured and nonsegregated, although some do have very simple structure or segregation.

The remaining sections discuss the various expressions that have been used within models of SSF to describe microbial, local transport, and bulk transport phenomena in SSF.

64.5 MODELING OF MICROBIAL PHENOMENA

This section addresses microbial phenomena and how models of SSF have treated these phenomena. It focuses on studies of either SSF itself or similar systems involving overculture on solid nutrient media. Overculture occurs when a fungus is inoculated across the whole surface, and therefore the mycelium develops simultaneously from many points. This contrasts with colony growth, where the organism is inoculated at one point, and a colony spreads outward across the surface. The kinetics of colony growth on agar plates are not considered in this chapter. Note also that the word biomass is used here in the restrictive sense of microbial biomass, and not in the broad sense of agricultural biomass. This distinction is important because many substrates are of agricultural origin.

A word of warning is appropriate about modeling growth kinetics. The basis for expression of the microbial biomass must be clear (e.g., total biomass in the bioreactor, or biomass per kilogram of initial dry substrate, or biomass per kilogram of wet substrate present, etc.), and conservation equations must originally be formulated on a conserved quantity (i.e., absolute amounts of biomass rather than biomass concentrations). This is crucial in SSF because there is a significant decrease in substrate mass due to conversion of dry matter to CO_2, and therefore increases in biomass concentration result from two effects: the increase in the overall amount of biomass, plus the decrease in the overall amount of dry matter. Water transfer between the substrate and gas phases causes further complications if concentrations are expressed on a wet substrate basis. Due to the wide range of ways that different workers have expressed biomass, we have used general equations in which the variables X and S represent absolute amounts of biomass and substrate respectively, whereas the variables C_X and C_S represent concentrations. Rates are expressed as mass or energy per unit time and are represented by the symbol r with a subscript. Readers should refer to original chapters to find the units and nomenclature used by the authors.

64.5.1 Substrate-Independent Growth Kinetic Equations

Sangsurasak *et al*. (7) note that four general shapes of growth kinetic profiles in SSF have been reported. In SSF models the simplest kinetic expressions describing these profiles relate the growth rate (r_g) directly to the biomass:

- Linear growth kinetics, described by

$$r_g = \text{constant} \tag{64.1}$$

  where r_g is the rate of growth.
- Exponential growth kinetics, described by

$$r_g = \mu_m X \tag{64.2}$$

  where μ_m is the observed maximal specific growth rate.
- Early acceleration followed by deceleration, with the rates of acceleration and deceleration being nearly equal, such that the biomass profile is symmetrical by rotation around the transition point. These kinetics are described by the logistic equation

$$r_g = \mu_m X \left(1 - \frac{X}{X_m}\right) \tag{64.3}$$

  where X_m is the maximum possible amount of biomass.
- Early rapid acceleration, followed by an extended period during which growth decelerates slowly. This profile can be approximated by raising the ratio X/X_m to an exponent n to give the power-law logistic model (8,9)

$$r_g = \mu_m X \left(1 - \left(\frac{X}{X_m}\right)^n\right) \tag{64.4}$$

This allows the logistic curve to be skewed (i.e., for the rates of acceleration and deceleration to be different). The value of n is a measure of the relative sensitivity of the culture to self-inhibition at high biomass densities (8). For values of n less than 1, the organism is relatively sensitive to self-inhibition, and self-inhibition occurs for quite low values of X. For $n = 1$ the logistic equation is obtained. Finally, for values of n greater than 1 the organism is relatively resistant to self-inhibition, and significant self-inhibition occurs only at values of X close to X_m. The exponent n may have biological significance. The mycelium

arising from a spore undergoes a maximum number (k_m) of branching events before growth ceases, and mycelia arising from a large number of different spores have a distribution of k_m values. If n is less than 1 then many of the mycelia have low k_m values, whereas if n is greater than 1 then many of the mycelia have high k_m values (8).

The expressions for both the linear and exponential growth kinetics do not describe any limitation on growth and are of little use for incorporating into models of growth in SSF. On the other hand, the logistic equation (and by extension, its power-law modification) describes a limitation on growth, and for this reason has quite commonly been incorporated into models of growth in SSF (10–12), especially macroscopic models. However, the significance of X_m is not clear. Growth might potentially be limited by the amount of substrate or diffusional limitations, but it can also be limited sterically.

Assumption of symmetric branching enables a simplified description of the mycelial mode of growth and enables the macroscopic parameter μ_m in the logistic equation to be related to the specific growth rate of a segment of biomass just before it is about to divide (μ'_m). The value of μ'_m can be determined from microscopic observation of extending hyphae. After a few branching events the following equation holds (8,9):

$$\mu_m = \mu'_m \frac{(X + X_c)}{2X} \approx \frac{\mu'_m}{2} \tag{64.5}$$

where X_c is the biomass in one hyphal segment just prior to a branching event. The approximation arises because X_c is small compared with the total biomass. This relationship between the two specific growth rates occurs because, after a few symmetric branchings, the biomass in the actively extending segments of a mycelium comprises approximately half the total biomass. The remaining biomass is in the older section of the mycelium where there are no actively extending hyphal tips. The microscopic growth parameters (X_c and μ'_m) can be determined by image analysis, which might even be used to monitor growth during SSF itself (9). If the effect of environmental parameters on growth and branching is known, some prediction can be made about how the environment will influence macroscopic growth kinetics.

64.5.2 Substrate-Dependent Growth Kinetic Equations

Kinetic expressions that rely only on biomass are simple but lack flexibility in describing different systems because new values for the parameters must be determined for each new system. Another approach is to assume that growth is related to the concentration of a growth-limiting substrate (such as a soluble sugar or oxygen) by the Monod equation (6,13,14),

$$r_g = \mu_m X \left(\frac{C_S}{K_S + C_S} \right) \tag{64.6}$$

where K_S is the saturation constant for the substrate. The models of Muck *et al*. (13) and Kaiser (14), which are based on the Monod equation, are relatively complex because they describe composting processes involving several organisms and several substrates. Muck *et al*. have four microbial groups (fungi and yeasts, each of which is divided into thermophilic and mesophilic subgroups), each with different Monod growth parameters, and there are several substrates that are assumed to be used sequentially.

The substrate concentration in the Monod equation must be the actual concentration that the microorganism experiences, which may not be simple to define due to the presence of both solids and water. Due to the concentration gradients that arise during growth, substrate concentrations at the surface of a substrate where the microorganism is located can be quite low compared with the average concentration (6). Therefore the effect of substrate concentration should be incorporated into kinetic models only if the growth equations are coupled with local transport equations. Neither Muck *et al*. (13) nor Kaiser (14) modeled local transport, which limits the usefulness of their models.

Various modifications of simple Monod kinetics have been used by different workers:

- Simultaneous limitation of growth by oxygen according to Monod kinetics and self-inhibition by the biomass according to the logistic equation (15)

$$r_g = \mu_m \left(\frac{C_{o_2}}{K_{o_2} + C_{o_2}} \right) X \left(1 - \frac{X}{X_m} \right) \tag{64.7}$$

- Simultaneous limitation by oxygen and glucose (16)

$$r_g = \mu_m X \left(\frac{C_{o_2}}{K_{o_2} + C_{o_2}} \right) \left(\frac{C_G}{K_G + C_G} \right) \tag{64.8}$$

- Self-inhibition of growth by biomass late in growth (according to logistic kinetics) combined with substrate inhibition kinetics (17)

$$r_g = \mu_m \left(\frac{C_S}{K_S + C_S + C_S^2/K_i} \right) X \left(1 - \frac{X}{X_m} \right) \tag{64.9}$$

where K_i is the inhibition constant for the substrate.

64.5.3 Modeling Effects of Microbial Activities on the Environment

Microbial activities affect the environment in SSF, and the changes in the local environment in turn affect growth. The effect of microbial activities on the local pH and water activity in SSF have received almost no attention, with the exception of Muck *et al*. (13) who related pH changes to acetic and lactic acid production rates and the buffer index of the solids. This section therefore is restricted to describing how workers have modeled consumption of nutrients (either the carbon source or oxygen), the generation of metabolic heat, and effects of growth on porosity in the substrate bed.

In models that describe the dependence of the growth rate on substrate concentration, it is also important to describe the effect of the growth activities on the substrate (i.e., substrate consumption). Sometimes a constant growth yield coefficient has been assumed,

$$r_s = -\frac{1}{Y_{XS}} r_g \tag{64.10}$$

where Y_{XS} is the observed yield coefficient. The negative sign indicates that substrate is consumed during the growth reaction. However, many workers have assumed that substrate is used for both growth and maintenance and have assumed the relationship

$$r_s = -\frac{1}{Y'_{XS}} r_g - m_s X \tag{64.11}$$

where Y'_{XS} is the true growth yield on the substrate, and m_s is the maintenance coefficient. This equation has been applied both to nutrients within the substrate and to oxygen.

If the particle structure is provided by a macromolecule that is degraded by the microorganism, such as during the utilization of predominantly starchy materials by amylolytic microbes, or the degradation of cellulosic substrates by cellulolytic organisms, then the particle will shrink during the fermentation. This can affect bioreactor performance through effects on bulk transport. For example, a decrease in particle size caused the substrate bed in a packed-bed bioreactor to pull away from the walls, allowing the air to bypass the bed and reducing the availability of oxygen within the bed (18). A simple model for particle size reduction assumes that oxygen is the limiting substrate and that it is consumed at the substrate–biomass interface (19,20). As the fermentation proceeds, the oxygen must diffuse through a biomass layer that increases in thickness, lowering the rate of diffusion and therefore the rate of reaction. Further developments of shrinking-substrate models are necessary because most substrates have complex compositions, and microbes can produce a range of enzymes, often in sequential order according to preferences for different macromolecules.

The generation of large amounts of metabolic waste heat can cause overheating of the substrate, and the kinetics of waste heat generation must be described in models of heat transfer in SSF. The simplest approach is to assume a constant relationship between the rate of production of new biomass and the rate of generation of metabolic heat, r_Q (11,15):

$$r_Q = Y_{QX} r_g \tag{64.12}$$

where Y_{QX} is the differential yield coefficient for waste heat production during growth. However, if maintenance metabolism is significant, then a growth and maintenance model is appropriate (21),

$$r_Q = Y'_{QX} r_g + m_Q X \tag{64.13}$$

where Y'_{QX} is the differential yield of heat from the metabolism associated with growth, and m_Q is the maintenance coefficient for heat production.

The rate of metabolic heat production does not have to be directly related to the growth rate. Saucedo-Castaneda *et al*. (3) related heat generation to the carbon dioxide evolution rate, which in turn was related to the substrate utilization rate by a constant yield,

$$r_Q = Y_{QCO_2} r_{CO_2} = Y_{QCO_2}[Y_{CO_2S}(-r_s)] \tag{64.14}$$

where Y_{QCO_2} is the differential relationship between heat released and CO_2 evolved (J/g), and Y_{CO_2S} is the yield of carbon dioxide from the substrate (g/g). This equation was indirectly related to the growth equation because logistic growth kinetics were assumed, and substrate consumption was modeled by a growth and maintenance model.

Instead of simply using experimentally determined heat yield coefficients (e.g., Y_{QX}) several workers have applied a bioenergetic approach. Gutierrez-Rojas *et al*. (17) proposed a stoichiometric equation for microbial growth on sucrose and estimated the enthalpy change associated with the growth reaction from the enthalpies of formation of the reactants and products. Larroche and Gros (22) considered the energetics of growth in SSF in even greater detail, estimating ATP generation and expenditure during growth. Muck *et al*. (13) related the rate of energy release to the rate of consumption of each of four substrates (water-soluble carbohydrate, ethanol, lactic acid, and acetic acid), estimating the fraction of the energy of combustion of the substrates that is actually released as waste metabolic heat. Finally, Rodriguez Leon *et al*. (23) estimated the heat yield coefficient from considerations of the degree of reductance of the substrate and biomass.

The growth of the microorganism into the interparticle voids affects the porosity of the substrate bed according to the relationship (24)

$$E = E_0 - X/(\rho_x W_s V_r) \tag{64.15}$$

where ρ_x is the wet biomass density (g/cm^3); W_s is the biomass dry matter content (g/g); V_r is the reactor volume, and E_0 is the initial porosity. This reduction in void fraction affects the pressure drop through packed beds (5) and reduces the effective diffusion coefficient within the substrate bed in tray bioreactors (24).

64.5.4 Death Kinetics

Overheating is a common problem in SSF, and several models have attempted to describe both growth and death of microorganisms. To date, death kinetics have largely been assumed to be first order (11,12),

$$r_d = k_d X_v \tag{64.16}$$

where the specific death rate, k_d, is a function of temperature. The effect of temperature on the parameters in growth and death kinetic expressions will be discussed later. The incorporation of death kinetics into a model divides the population into viable (X_v) and dead (X_d) subpopulations, representing a very simple level of segregation. On the other hand, Sargantanis *et al*. (21) assumed that their organism was killed instantly when the temperature reached 43°C. Not all models considering the effect of temperature actually have death kinetics in them; some describe only a decrease in net growth rate with temperature (3).

64.5.5 Effects of Environmental Variables on Growth and Death Kinetics

The effect of the environment on kinetic parameters is quite important because it is difficult to control environmental variables; some may change quite significantly during growth, and some might limit growth. The effect of nutrient concentrations (including O_2) have already been considered. Of most interest here are temperature, water activity, and pH. Of these, temperature has received most attention due to the overheating problems that are commonly encountered in SSF. For bioreactors with large temperature gradients, heat transport equations must be built into the model if growth is to be adequately described.

Regarding the effect of temperature, most attention has been given to the effect of the temperature on the rate constants μ_m and k_d. Simple empirical equations are normally fitted by least squares regression to growth rate data collected between the minimum and maximum growth temperatures. Polynomial expressions (11,14,15) or double exponential expressions (3,17) have been used to describe the variation in specific growth rate with temperature. Arrhenius-type relationships have also been used to describe the effect of temperature on both the specific growth rate and the specific death rate (12),

$$\mu_m = \mu_{mo}\exp\left(\frac{-E_g}{RT}\right) - k_{do}\exp\left(\frac{-E_d}{RT}\right) \tag{64.17}$$

where R is the universal gas constant, T is the absolute temperature, E_g and E_d are the activation energies for growth and death, and μ_{mo} and k_{do} are rate constants. Least squares regression usually allows an adequate fit of such equations, although the biological significance of the parameters is not clear because the equations are not formulated on any theoretical basis.

Other growth parameters may be expressed as functions of the environmental conditions. Sargantanis *et al*. (21) expressed not only μ_m but also X_m in the logistic equation as empirically fitted functions of temperature and moisture content. Saucedo-Castaneda *et al*. (3) expressed the maximum biomass, X_m, in the logistic equation as an empirically fitted fourth-order polynomial function of temperature.

The model of Muck *et al*. (13) has described the effect of the environment on growth in most detail. In addition to using Arrhenius-type equations to describe the specific growth and death rates, with different parameter values for the different microbial groups, they also described the effect of pH and water activity on growth. However, for both these environmental variables the effects on the specific growth rates of the various microbial groups were incorporated simply by using empirical equations, fitted to experimental kinetic data, to modify the maximum specific growth rate. Gervais and Simatos (25) have addressed the effect of water activity on growth on solid surfaces in greater depth, although they consider the radial extension rates of fungal colonies. The effect of water activity on the overculture situation in SSF has not been addressed.

64.5.6 Modeling Branching, Penetration, and Differentiation

Fundamental phenomena in the growth of filamentous fungi on solid surfaces have received some attention. Some models address extension of the hyphal tip at a very fundamental level, but these models have not been extended to describe morphological development. Others can describe branching and certain aspects of hyphal morphogenesis but have not been extended to describe overall growth kinetics (8). In any case, models describing the extension and branching of individual hyphae describe the system in far more detail than is required in models of bioreactor performance, where only overall mycelial concentrations are of interest.

However, models describing hyphal phenomena might be useful if they concern themselves with the overall population of hyphae or hyphal tips, and this section addresses such models briefly. The equations are not presented but can be found in the original chapters.

The symmetric branching model of Viniegra-Gonzalez *et al*. (8,9), described earlier in conjunction with the logistic equation, makes many simplifying assumptions about the branching process, essentially that all hyphae branch after reaching a certain length, and the two branches arising are identical. These do not happen in practice but may be approximated on average in the large population of hyphae within a mycelium. As shown in equation 64.5, on this basis the relationship between some microscopic and macroscopic growth parameters can be derived.

Edelstein and Segel (26) used a modeling approach based on average tip and hyphal concentrations per unit area of substrate surface and describing the generation of tips by branching and the movement of hyphal tips across the surface due to hyphal extension. Growth of tips depended on the local nutrient concentration. This approach avoids the great complexity that would be involved in constructing a model on the basis of intracellular events, tip extension, and branching events, and some of the parameters such as tip densities can be estimated experimentally (27). Laszlo and Silman (28) used a cellular automata approach to model mycelial densities during fungal colony expansion over solid surfaces. In this approach a matrix of small squares is superimposed on a flat substrate surface. Initially, one or more squares are designated as living, to represent an inoculum. The fungus can then grow into adjacent squares, with simple rules based on the number of occupied squares adjacent to a vacant square being used to determine whether that vacant square will be colonized. This approach can give insights into density patterns within fungal colonies (28) but otherwise is of limited usefulness for modeling growth kinetics in bioreactors. Edelstein (29) developed a model describing colony expansion, assuming no nutrient limitations, but based on processes of branching, anastomosis, tip death, and hyphal death. Only the average frequencies of these processes need to be known. Different frequencies for the various processes can lead to very different colony morphologies. These approaches could be adapted to describe growth during overculture in SSF.

Penetration into the substrate is an interesting aspect that has not received much attention, although Jurus and Sundberg (30) gave a qualitative account of the penetration of *Rhizopus oligosporus* into soybeans. More recently Ito *et al*. (31) observed an exponential decrease in the concentration of hyphae below the surface of the rice in koji. Experimentally they observed that the quality of the koji was strongly correlated with the degree of mycelial penetration: at lower degrees of penetration, the activities of undesirable enzymes was high, leading to poorer quality koji. Although they proposed a mathematical equation to describe the decrease in hyphal concentration with depth, it was simply fitted to the data collected at each time point. A dynamic model describing the increase in concentration of penetrative hyphae as a function of time and distance was not proposed. Such dynamic models might be important because penetration into the substrate has the potential to increase substrate degradation.

Differentiation can be quite important in SSF processes as an essential step in the production of spores or secondary metabolites (32). Georgiou and Shuler (33) modeled growth and differentiation of *Aspergillus nidulans* on a solid medium containing glucose. The model could predict the increases in density of the various types of biomass (vegetative, competent, differentiated, and conidial) during overculture.

64.6 MODELING OF LOCAL TRANSPORT PHENOMENA

Local mass transfer processes have the potential to limit the rate of growth in solid-state fermentation. Most of the local transport phenomena occurring in SSF, such as diffusion through porous media and stagnant films, have been well studied in other systems. However, the translocation of nutrients within the fungal mycelium itself is poorly understood. The work done on nutrient diffusion during radial expansion of colonies on agar surfaces will not be described here because SSF usually involves overculture of the organism across the whole surface, for which nutrient diffusion horizontally toward the organism is not important. In overculture the key spatial dimension is the one passing vertically through the substrate (Fig. 64.3).

This section indicates how modeling of these local transport phenomena has improved our understanding of what controls growth in SSF. Emphasis is placed on the mathematical descriptions of the phenomena. Model predictions about system behavior are mentioned but not discussed in detail. This section concentrates on mass transport phenomena because local heat transfer has not been considered in any mathematical model of SSF to date. Indeed, local heat transport is less likely than local mass transfer to limit SSF performance, although it might have unknown significance, for example, through indirect effects on mass transfer coefficients.

64.6.1 Diffusion and Reaction

Early modeling studies relevant to SSF considered the overculture of microorganisms on solid agar media, with

glucose as the substrate (33,34). Two growth periods are predicted: an early period during which the glucose concentration at the substrate surface is relatively high and consequently the microbe grows at its maximum specific growth rate (i.e., exponential growth), followed by diffusion-limited growth during which the glucose concentration at the substrate surface is very low and the growth rate depends on the flux of glucose to the surface. The duration of the exponential growth phase depends strongly on the initial concentration of glucose because this determines how long it takes for the surface glucose concentration to fall to limiting levels. Analytical solutions to the diffusion equation can be obtained for short time periods but cannot describe the whole growth period. In any case, the usefulness of these models is limited because relatively few SSF processes contain a soluble sugar as the major carbon source.

Mitchell *et al*. (6) proposed and solved numerically a model for growth of *R. oligosporus* in overculture with starch as the carbon source. This allows some insight as to how mass transfer within the substrate itself can limit growth. In the experimental system a membrane filter prevented penetration of hyphae into the substrate. Five steps in the growth process were modeled (these correspond to processes 5 to 9 in Figure 64.3):

- Glucoamylase release into the substrate by the fungus located in a plane at the substrate surface; an empirical equation was used
- Diffusion of glucoamylase through the substrate according to Fick's law
- Hydrolysis of starch by the glucoamylase according to Michaelis–Menten kinetics
- Generation of glucose by the glucoamylase according to Michaelis–Menten kinetics and the diffusion of the glucose through the substrate; this is a process of simultaneous reaction and diffusion
- The uptake of glucose by the fungus at the substrate surface according to Monod kinetics based on the surface glucose concentration.

The expression of interest here is that for simultaneous reaction and diffusion. For diffusion in an overculture system in which net diffusion occurs only in the vertical direction, as shown in Figure 64.3, the balance equation for compound A has the general form

$$\frac{\partial A}{\partial t} = r_a + D_a \frac{\partial^2 A}{\partial z^2} \tag{64.18}$$

where r_a is the rate of generation of compound A, D_a is the diffusivity of A, and z is the vertical spatial coordinate. This equation, with the appropriate sign on the reaction term, can refer to the generation and diffusion of hydrolysis products within the substrate, or to the diffusion and consumption of nutrients within a biomass layer.

Microscopic models incorporating local transport equations are useful tools for understanding the role of local transport phenomena in limiting growth in SSF. The model of Mitchell *et al*. (6) predicts a short phase of exponential growth during the early period when the glucoamylase is still near the surface and the surface glucose concentration is much higher than the saturation constant for growth. As the biomass at the surface increases, the increased glucose uptake rate causes the surface glucose concentration to fall below the saturation constant. This is followed by a period of slow deceleration of growth. This kinetic profile has been observed in SSF by several workers. The model is able to explain how such kinetics might arise from interactions among the processes of glucoamylase diffusion, starch hydrolysis, and glucose diffusion.

Recently, Rajagopalan and coworkers have made two extensions to this model. Rajagopalan and Modak (16) incorporated an expanding biomass film of constant density, with simultaneous reaction and diffusion of oxygen from the bulk air above the biomass layer and of glucose from the substrate below the biomass layer. This model suggests that at different times during growth either glucose or oxygen may be limiting, but that overall oxygen limitation might be more important than glucose limitation. They ran simulations under different bulk oxygen concentrations, such as might occur in different positions in a bioreactor, foreshadowing the linking of both local and bulk transport equations in a single model. Rajagopalan *et al*. (35) then further modified the model to describe a decrease in particle size as glucose is used up. Their predictions agreed reasonably well with the experimental data of Nandakumar *et al*. (20), who measured decreases in particle size during growth of *Bacillus coagulans* on wheat bran particles. The predictions also confirm the observations of Mitchell *et al*. (6) that glucoamylase diffusion plays a crucial role. At low diffusivities most of the glucoamylase remains near the surface. This quickly depletes the starch at the surface, leaving much of the enzyme without substrate to act upon. As a consequence, the rate of glucose production within the substrate particle falls, and growth becomes limited by the rate of glucose production in the deeper regions of the particles.

These modeling studies have used homogeneous gel substrates with very high water contents in which diffusion is the major mass transport phenomenon. However, SSF substrates may have high solute concentrations and contain cellular structures. Sorption phenomena may restrict diffusion (25), capillary action may occur, and cell walls may present an impermeable barrier. The mechanisms of mass transport within real solid substrates deserve greater attention.

64.6.2 Film Transfer of Oxygen

Another important local transport process is that of diffusion of oxygen across the stagnant gas film into the thin liquid film at the substrate surface (Fig. 64.3). If the biomass is assumed to be surrounded by a thin liquid film that offers the major resistance to mass transfer, then the oxygen transfer rate, N, can be expressed as (36)

$$N = K_{\mathrm{L}}a(C^* - C) \tag{64.19}$$

where C^* is the concentration of oxygen in the bulk gas phase, C is the concentration of oxygen at the biomass–liquid interface, a is the area over which mass transfer occurs, and K_{L} is the mass transfer coefficient. This equation was used to estimate the overall mass transfer coefficient ($K_{\mathrm{L}}a$) for a packed-bed bioreactor. It can be applied also at the microscopic scale, although it can be difficult to measure local oxygen consumption rates and oxygen concentrations (36).

Alternatively, the biomass film can be assumed to be directly in contact with the gas phase, with the transport resistance residing in a stagnant gas film. In this case the variable C in the above equation is replaced by $HC_{\mathrm{O_2,F}}$, where H is Henry's constant, and $C_{\mathrm{O_2,F}}$ is the concentration of oxygen in the biomass film. This expression has been used to describe oxygen transfer to the biomass in a tray bioreactor (15). Film transfer of oxygen in SSF needs more attention because significant amounts of fungal mycelium are in direct contact with the air phase and are not immersed in the liquid film at the substrate surface (37).

64.7 MODELING OF BULK TRANSPORT PHENOMENA

64.7.1 Recognizing Subsystems within SSF Bioreactors

In developing a model of bulk transport phenomena occurring during SSF, we must consider the level of detail to be modeled and identify simplifications of the model structure. As pointed out earlier, at the macroscopic scale, up to four subsystems can be identified in SSF bioreactors: the bioreactor wall, the headspace gases, the solid particles themselves, and the interparticle gases (Fig. 64.2). The presence and arrangement of these various subsystems and whether the subsystems themselves are homogeneous or have concentration or temperature gradients depend on the particular bioreactor and how it is operated. Macroscopic models contain transport equations to describe the heat and mass transfer processes within and between the subsystems recognized by the model, and between the subsystems and the surroundings.

It is often convenient to ignore the bioreactor wall in order to simplify the model. This may be appropriate if the wall is maintained at a constant temperature by a cooling system, making the bioreactor wall part of the surroundings. Alternatively, if the resistance to heat transfer between the bioreactor wall and the outside air is much greater than the resistance to heat transfer from the substrate material to the bioreactor, the overall heat transfer coefficient can be assumed to be similar to the outside heat transfer coefficient. This also has the implicit assumption that the energy stored in the bioreactor wall is negligible.

It is usually convenient and appropriate in macroscopic models to lump two or more of the phases together as a pseudohomogeneous subsystem having the mass or volume-averaged properties of the individual phases (Table 64.1). Most commonly, a substrate bed consisting of the moist solid particles and the interparticle gases is defined as a single subsystem. In the pseudohomogeneous matrix that comprises this system, the temperatures and water potentials of the gas and solid at the same location are assumed to be the same. The validity of this assumption depends on whether the bioreactor operation allows the gas and solid to approach equilibrium. In addition, note that the temperature and water potential of this pseudohomogeneous matrix can vary from position to position.

Depending on how well subsystems are mixed, macroscopic models may only need to describe transfer between subsystems, or they may also need to describe transfer within subsystems. If a subsystem is well mixed, then there will be no thermal and concentration gradients across the subsystem, and there will only be transfer equations to describe the transport between subsystems. Therefore the spatial coordinate does not appear in the transfer equations for such subsystems. For subsystems that are static or poorly mixed, there will also be transfer equations to describe the transfer processes within subsystems. For example, equations incorporating the spatial coordinate may be required to describe solid or gas flow patterns in the bioreactor, and to describe temperature and concentration gradients within the substrate bed. Such models can be used to explore bioreactor design and operation strategies to minimize these gradients.

64.7.2 The Bulk Transport Phenomena Occurring in SSF Bioreactors

Through their interactions with local transport processes, bulk transport processes determine the local environment experienced by the microorganism and therefore influence the performance of SSF bioreactors. Macroscopic models predict bioreactor performance by combining empirical descriptions of growth kinetics with expressions describing bulk transport between and within the subsystems (solid,

TABLE 64.1. Subsystems in SSF Bioreactors and Their Simplification

Subsystem and References	Detailed view of the System (Macroscopic Viewpoint)	Simplification of the System Appropriate for Modeling	Mixing
Trays: may be stirred (the whole room is the bioreactor) (10,15,24)	Headspace gas (flowing around tray)	Headspace gas	Assume headspace infinite and well mixed, such that one tray represents all trays
	Solid particles (static) Interparticle gas (no forced flow)	Assume the bed consists of a pseudohomogeneous matrix	May be intermittently mixed, but usually not appropriate to assume that the bed is well mixed; gradients will exist
Packed beds and similar stirred reactors (3,38,39)	Solid particles (mostly static) Interparticle gas (flowing due to movement within bed)	Assume the bed consists of a pseudohomogeneous matrix	If mixed, usually intermittently; therefore will still have end-to-end gradients within the bed
Rotating drums and similar stirred reactors (21,40)	Headspace gas (flowing) Solid particles (flowing) Interparticle gas (flow depends on movement within bed)	Headspace gas Assume the bed consists of a pseudohomogeneous matrix	Depending on operation may assume these two subsystems are each well mixed, or may allow for axial variation; if well mixed, may assume that headspace and bed are in equilibrium (i.e., 1 subsystem)
Air–solid fluidized beds (growth in this bioreactor has not yet been modeled)	Solid particles (flowing) Interparticle gas (flowing)	Assume a pseudohomogeneous matrix, with mixing keeping the whole bed homogeneous, and that aeration air is moist so that system is close to moisture equilibrium	Typically well mixed

Note: Subsystems are in addition to the bioreactor wall itself.

gas, and bioreactor wall), and between these subsystems and the surroundings. Local transfer mechanisms are currently ignored in these models. Momentum transfer, heat transfer, and mass transfer may be involved, and any of these may potentially limit the performance of an SSF bioreactor. Table 64.2 indicates the mechanisms for these phenomena in various SSF bioreactor types. Of these phenomena, heat transfer has received the most attention.

Conversely, there is very little information regarding momentum transfer processes, that is, those processes involving material flow and that affect mixing and shear phenomena. Within bioreactors, both mixing of gas molecules within the gas phases in the bioreactor and mixing of solid substrate particles may be important. To date, the mixing of solids in agitated SSF systems has not been studied, and there are only two investigations of gas mixing and flow behavior (40,42). Residence time distributions for gas molecules indicate that operational parameters such as the gas velocity and solids loading affect the presence and extent of stagnant gas regions within the substrate bed and the homogeneity of the headspace gas phase (40,42). Further, such investigations are crucial because these flows underlie the other transport phenomena, such as heat and mass transfer. Due to the paucity of information, current macroscopic models assume ideal flow behavior such as plug flow of gases in packed beds or perfect mixing of the solids and gases in rotating drums.

The flow of solids leads to shear forces due to interactions of the solid substrate particles with each other and with the bioreactor wall. These shear forces are complex and therefore difficult to characterize. Thus, despite their potential to affect substrate characteristics and adversely affect microbial growth, and significant speculation regarding their importance in SSF systems, shear forces are not described in any macroscopic model of SSF.

Heat transfer processes have received attention because overheating due to release of metabolic waste heat is a very significant problem in SSF even at small scales. Rates of metabolic heat production reported in SSF range from about 3 to 330 kJ (kg dry matter)$^{-1}$ h^{-1}. Removal of metabolic heat is more difficult in SSF than in liquid fermentation

TABLE 64.2. Important Transport Phenomena within SSF Bioreactors

Bioreactor and Subsystem	Heat Transport Phenomena	Mass Transport Phenomena	Momentum Transport Phenomena
All bioreactor systems: the microscopic phenomena within the substrate particle are usually greatly simplified in macroscopic models describing bioreactor performance. Also, as noted in Table 64.1, *the solid and gas subsystems are often assumed to form a single pseudohomogeneous matrix.*			
Within the solid particle	This is the site of heat generation by the microbe growing at the surface of the solid particles.	Diffusion of enzymes and nutrients within the solid particle (6,11,33,34)	
Between the solid and gas subsystems within the substrate bed	Conduction, evaporation of water, and free or forced convection (depending on bioreactor operation) from solids to interparticle air	Evaporation of water, and transfer of O_2 and CO_2 between the solid particles and the interparticle air (15)	
After assumption of a pseudohomogeneous matrix	Solid and gas in thermal and moisture equilibrium	Transfer of O_2 and CO_2 between solid particles and interparticle air Transfer of water to maintain saturated air (38,39)	
Trays: the solid particles and interparticle air may or may not be considered as a single pseudohomogeneous substrate bed. The whole room is taken as the bioreactor. Individual trays are assumed to be open at the top and to have perforated bases.			
Transfer across the substrate bed	Conduction (15) and natural convection within the bed, leading to spatial gradients	Diffusion (10,15) and free convection of gases and water vapor within the bed, leading to spatial gradients	
Involving the tray wall or the headspace gases	Conduction to the tray walls, conduction within the tray wall, and then convection between the tray wall and the headspaces	Convection of gases (15) from the exposed bed surfaces into the headspace	Flow of headspace gases around the trays (15)
	Evaporation and free or forced convection (depending on airflow), between the exposed bed surfaces and the headspace gases	Evaporation of water from the substrate into the headspace at the exposed bed surfaces	
At inner surface of the room walls	Convection to the tray room walls Condensation on room walls		
Packed beds and similar stirred reactors, assumed to be vertical cylinders			
Transport through the pseudohomogeneous matrix	Conduction, convection and evaporation axially along the substrate bed (38,39) Conduction radially within the substrate bed (3,38) Both axial and radial gradients may exist (38)	Convection of air in the axial direction due to the forced aeration of the bed. Although axial O_2 gradients occur, they are usually not as important as the temperature gradients Radial mass transfer should be negligible	Gas flow patterns through the bed (plug flow without dispersion is often assumed) (3,38,39) Pressure drop between the bottom and top of the substrate bed (40)
At the inner surface of the bioreactor wall	Conduction radially between the substrate and the inside surface of the bioreactor wall (3,38)		

(*continued*)

TABLE 64.2. ***(Continued)***

Bioreactor and Subsystem	Heat Transport Phenomena	Mass Transport Phenomena	Momentum Transport Phenomena
Rotating drums and similar stirred reactors, assumed to be horizontal cylindrical drums			
Transport through the pseudohomogeneous matrix	The role of conduction depends on the degree of mixing; may assume that bed is well mixed (21,41) Convective flow within the bed due to mixing Usually well mixed radially, but axial gradients may exist	The role of diffusion depends on the degree of mixing Convection of gases within substrate voids due to mixing Axial O_2 gradients may occur but are usually not important	Mixing and flow of the solid substrate Shear forces; impact and abrasion due to solids interacting with each other
Between the bed and the headspace	Convection between the substrate bed surface and the headspace (41) Evaporative cooling at the surface of the substrate bed (41) Bulk flows of gases between the interparticle voids and the headspace carry sensible energy	Gas and water vapor exchange between the substrate bed and headspace gases (41).This may involve bulk flows exchanging gas between the headspace and interparticle voids.	Bulk gas flows between the interparticle voids and the headspace
Within the headspace	Convective flow of the headspace gases, carrying sensible energy (41)	Convective flow of the headspace gases (41)	Flow patterns of the headspace gases (41)
At the inner surface of the drum wall	Conduction from the substrate to the drum wall and convection between the headspace gases and the inside surface of the drum wall (41)		Shear forces, impact, and abrasion due to solids interacting with the drum wall
Air–solid fluidized beds, assumed to be vertical cylinders. The aeration air is assumed to be moist so that the bed is close to moisture equilibrium. Growth in these bioreactors has not yet been modeled.			
Within the well-mixed substrate bed	Whole bed well mixed such that there are no thermal or moisture gradients	Whole bed well mixed, such that there are no water vapor, CO_2, or O_2 gradients	Pressure drop across the bed itself, fluidization phenomena Shear, impact, and abrasion due to interactions between particles in the bed
At the inner surface of the bioreactor wall	Convection from the bed to the bioreactor wall		Shear, impact, and abrasion due to interactions between the solid particles and the wall
All bioreactors			
Involving the entry and exit of the airstream	Energy enters and leaves the system in the airstream blown through the bioreactor (3,21,38,41).	Gases and water vapor enter and leave the system in the airstream blown through the bioreactor (21,41)	Pressure drop between air pump and air exhaust
Within the bioreactor wall and between the wall and the surroundings	Conduction through the wall (the room wall for the tray system) and loss to the surroundings, often by free convection to air (21,41) or forced convection to cooling water (3,38)		

Note: These are phenomena that should be considered in the construction of mathematical models of bioreactor performance. As discussed in the text, most models greatly simplify the system by including only the most important transport phenomena or lumping phenomena together. In this table not all phenomena have been mentioned. In some places where transport processes occur in parallel, minor contributors have been ignored. In addition, the importance of the transport phenomena mentioned will depend on how the particular bioreactor is designed and operated. After identifying the phenomena to be modeled, the next task in modeling is to find appropriate expressions to include in the mass and energy balances that describe the system. Expressions that have been used to date in macroscopic models of SSF bioreactors are discussed in the text. Numbers in parentheses indicate references.

processes for a number of reasons. First, compared to liquid media, solid substrates have low heat capacities and low thermal conductivities, which means that although less heat is required to raise the temperature of the solid substrate by the same increment, the solid substrate loses heat less readily than liquid media. As well, due to the concentrated nature of SSF systems, biomass concentrations are higher and heat production on a volumetric basis is therefore also correspondingly higher. Heat removal in SSF system occurs by convection, conduction, and evaporative cooling, with the contributions of each mechanism depending on the bioreactor design and operation.

The important bulk mass transfers in SSF bioreactors involve the gas phase: oxygen supply and carbon dioxide removal for aerobic processes, and the removal of water vapor during evaporative cooling. The transfer processes described by macroscopic models may include transfer across interfaces, diffusion within stagnant gas regions, and convection by bulk gas flow. As noted in Table 64.1, it may be appropriate to divide the gas phase into a headspace gas phase and an interparticle gas phase. The degree of continuity between these phases depends on the type of bioreactor and how it is operated.

Solid-state bioreactors differ in the types of mixing that they provide and in the relative importance of flow and diffusion processes in the bulk transport phenomena that occur. This section discusses mathematical modeling of bulk transport in tray, packed-bed, and rotating drum bioreactors. Models have not been developed to describe transport phenomena within other bioreactor types. The following sections discuss, for each bioreactor, the approaches to modeling the transport phenomena identified in Table 64.2. Although these transport phenomena have also been studied in non-SSF systems, the discussion is limited to SSF itself.

64.7.3 Macroscopic Transport Phenomena in Tray Bioreactors

Tray bioreactors often consist of a large number of individual trays incubated within a room in which the temperature and the humidity of the air may be controlled. However, mathematical models of trays usually describe only a single tray, assuming homogeneous conditions within the headspace surrounding the multiple trays in the bioreactor. This single tray comprises either an intact or a perforated tray on which rests a thin layer of static solid substrate. Two distinct gas phases exist in tray SSF systems: the first is the interparticle voids within the substrate itself; the second is the bulk gas phase, which consists of the headspaces above and below the tray.

64.7.3.1 Heat Transfer in Tray Bioreactors. Only Rajagopalan and Modak (15) have described heat transfer during tray SSFs. In their model, sensible heat transfer occurs in the vertical direction by conduction through the substrate,

$$\frac{\partial T}{\partial t} = \frac{k}{\rho_s C_p}\frac{\partial^2 T}{\partial y^2} + \frac{\Delta H r_g}{C_p} \tag{64.20}$$

and by convection from the substrate surfaces to the headspaces above and below the substrate bed (the base of the tray was assumed to be open),

$$-k\frac{\partial T}{\partial y} = h(T_0 - T) \tag{64.21}$$

where T is the temperature of the bed; t is time; k, C_p and ρ_s are the thermal conductivity, heat capacity, and density of the bed, respectively; ΔH is the enthalpy of the growth reaction; y is the spatial coordinate; T_0 is the temperature of the surrounding air, and h is the heat transfer coefficient between the bed and the surroundings. The model predicted that substrate temperatures would be highest in the center of the tray, and that the incubation temperature and substrate depth were critical to the success of tray SSFs. For a tray bed 6.35 cm high, an incubation temperature of 30°C produced the greatest total biomass, although the maximum specific growth rate occurred at 40°C. Likewise, substrate depths of 3 cm and under gave significantly better growth when incubated at 38°C than when incubated at 40°C. Simulations involving simultaneous changes of incubation temperature and substrate depth indicate that, as the bed height decreases, the incubation temperature supporting optimal growth increases and overall growth is optimal in trays less than 1 cm high. Clearly, such shallow trays would not be practical at large scales. Gas flow velocity around the trays had little effect on heat transfer between the gas phase and the bed. This model did not describe evaporative cooling, convective heat transfer through the substrate bed due to free convection, or heat removal through the tray material.

64.7.3.2 Mass Transfer in Tray Bioreactors. A number of workers (10,15,24) have modeled mass transfer in trays. All of these models describe mass transfer within the interparticle voids; however, only the model of Rajagopalan and Modak (15) describes mass exchange between the interparticle voids and the bulk headspace.

In describing mass transfer within the interparticle voids, all three models consider transfer by diffusion in the vertical direction only. The models consider transfer of either oxygen only (10) or both oxygen and carbon dioxide (15,24). None of the models describes the mass transfer of water. All three models neglect the possibility of convective mass transfer due to thermal gradients within the substrate. The equations used in these models for mass transfer within the

substrate bed take the general form of a balance of compound A (either O_2 or CO_2) in the interparticle gas phase,

$$\frac{\partial \varepsilon C_a}{\partial t} = D_a \frac{\partial^2 C_a}{\partial y^2} - R_a \tag{64.22}$$

where t is time, y is vertical distance within the bed, ε is the porosity, and D_a and C_a are the diffusivity and the concentration, respectively, of A in the bed. In the case where A is oxygen, R_a is the rate of oxygen consumption (10,24) or the rate of oxygen dissolution into a liquid film layer on the substrate particles (15). For film transfer, $R_a = K_a(C_{o_2} - HC_{o_2,F})$, where K_a is an overall gas side mass transfer coefficient, H is Henry's constant for oxygen and $C_{o_2,F}$ is the oxygen concentration in the film liquid. In the case where A is carbon dioxide, the minus sign in front of R_a in the previous equation is changed to a plus sign, and R_a is the rate of carbon dioxide production (15,24).

The porosity in the previous equation is an important term and received further attention within the models of Rajagopalan and Modak (15) and Auria *et al*. (24). Rajagopalan and Modak (15) calculated D for the oxygen and carbon dioxide gases as

$$D_i^b = \frac{\varepsilon}{\tau} D_i' \tag{64.23}$$

where ε is the porosity of the substrate bed, τ is the tortuosity factor (taken to equal 1.7), i is the gas (either carbon dioxide or oxygen), and D^b and D' are the diffusivities in the bed and in air. However, the porosity was held constant for any one simulation; therefore porosity changes caused by growth were neglected. Auria *et al*. (24) used their model to estimate the diffusivity within static beds consisting of *A. niger* growing on beads of ion exchange resin impregnated with a nutrient medium. The diffusivity decreased with increasing biomass concentration, and at high biomass concentrations of 27 mg g^{-1} dry matter, the diffusivities of oxygen and carbon dioxide were less than 5% of their bulk diffusivities in air. The effect of growth on porosity and gas diffusivity deserves further attention.

The tray models of Auria and Rajagopalan are dynamic models. The model developed by Ragheva Rao *et al*. (10) is different in that it consists of only a single pseudo-steady-state equation. From a balance for oxygen within the bed, they developed an equation for the maximum thickness, H_c, that a tray could be without becoming depleted of oxygen at any depth within the substrate layer during the fermentation,

$$H_c = \sqrt{\frac{2D_e C_{O_2} Y}{\mu_m X_m}} \tag{64.24}$$

where μ_m and X_m are the maximum specific growth rate (h^{-1}) and maximum biomass concentration (mg cm^{-3}), respectively. Use of μ_m and X_m represents the worst case scenario for which the rate of oxygen demand would be greatest. This model has a number of implications for the design and operation of tray SSFs. First, with the use of perforated rather than unperforated trays, the critical bed thickness, H_c, could be increased by a factor of up to two, depending on the fraction of the area of the underside of the bed exposed to air. Second, greater substrate depths can be used if the air above the bed is oxygen enriched or if the headspace is continually replenished during operation (thereby keeping C_{o_2} as high as possible). This model is one that could be readily applied in practice, requiring only values of the D and kinetic parameters μ_m and X_m, although it has not yet been tested experimentally.

The model of Rajagopalan and Modak (15) goes further than the other models in not only describing diffusion within the bed, but also the convection of gases from the upper and lower bed surfaces into the headspaces. Headspace air is assumed to move horizontally across the substrate surface, being well mixed normal to the flow direction but with no axial dispersion. At the plane of contact with the substrate, gases diffuse into or out of the bed. The balance of oxygen or carbon dioxide at the bed surface is given by

$$\frac{\partial C_a^h}{\partial t} = -v_x \frac{\partial C_a^h}{\partial x} - \frac{D_a}{z} \frac{\partial C}{\partial y}\Big|_{y=L} \tag{64.25}$$

where A is either carbon dioxide or oxygen, x is the horizontal coordinate, y is the vertical coordinate, L is the thickness of the substrate, z is the thickness of the headspace above the bed, C_a^h is the headspace concentration, and v_x is the headspace gas flow velocity. Model simulations showed that substrate depth and porosity greatly affected mass transfer within the bed; however, the gas flow velocity around the trays had little effect on mass transfer between the headspaces and the bed. These predictions can guide design and operation of tray bioreactors.

64.7.3.3 Combined Heat and Mass Transfer in Tray Bioreactors. Finally, both heat and mass transfer processes may be important at different times during SSFs in trays. Therefore, mathematical models describing these systems will need to describe both transport mechanisms. Currently, only the model by Rajagopalan and Modak (15) does this. The phenomena described by their model are shown in Figure 64.4. The predictions of this model for substrate temperature, biomass, and gas phase concentrations of oxygen and carbon dioxide showed trends similar to those noted experimentally by Rathbun and Shuler (43) during the tempe fermentation of soybeans by *R. oligosporus*.

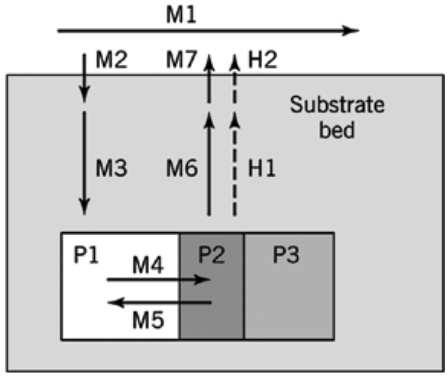


Figure 64.4. Diagrammatic representation of the tray bioreactor as modeled by Rajagopalan and Modak (15), indicating the three phases within the substrate bed. P1, Interparticle gas phase; P2, thin water film on the surface of substrate particles, which is the location of oxygen consumption, carbon dioxide production, and generation of waste metabolic heat; P3, solid substrate particle. The heat and mass transfer processes occurring are M1, bulk flow of air above the tray surface; M2, transfer of oxygen into the bed; M3, diffusion of oxygen within the bed; M4, transfer of oxygen from the interparticle air phase to the liquid film; M5, transfer of carbon dioxide from the liquid film to the interparticle air phase; M6, diffusion of carbon dioxide within the bed; M7, transfer of carbon dioxide from the bed to the surrounding air; H1, conduction of heat through the bed; H2, convective removal of heat at the bed surface.

The model predicts that the substrate temperature is the dominant influence on growth in the initial and final stages of the fermentation. During intermediate stages of the fermentation, oxygen has a large effect at the bottom of the bed (in an unperforated tray), whereas temperature effects are more important in the center of the bed.

64.7.4 Macroscopic Transport Phenomena in Packed-Bed Bioreactors

64.7.4.1 Heat Transfer in Packed-Bed Bioreactors. Heat transfer in packed beds has received most modeling attention because the temperature gradients obtained are more important than the gas concentration gradients, and if aeration satisfies the heat removal requirements it will also satisfy aeration requirements (44,45). In bioreactors of different designs and operated under different conditions, both axial and radial temperature gradients have been observed (45–47). Under some operating conditions, temperatures in the middle of the bed can be over 20°C higher than the temperature of the inlet air, leading to large variations in growth and product formation across the bioreactor (46).

Saucedo-Castaneda *et al*. in 1990 (3) modeled radial heat transfer in an experimental packed bed in which *A. niger* was grown on cassava meal. This model was later extended by Sangsurasak to describe both axial and radial heat transfer (38). A general expression for heat transfer in a pseudohomogeneous substrate bed within a cylindrical packed-bed bioreactor, which takes into account the heat transfer processes shown in Figure 64.5, can be expressed as (38)

$$\rho_b C_{pb}\frac{\partial T}{\partial t} + (\rho_{ma}C_{pma} + \rho_a f \Delta H_v)V_z\frac{\partial T}{\partial z} = \frac{k_b}{r}\frac{\partial T}{\partial r} + k_b\frac{\partial^2 T}{\partial r^2} + k_b\frac{\partial T}{\partial z^2} + r_Q \qquad (64.26)$$

where ρ_a, ρ_{ma}, and ρ_b are the densities of air, moist air, and the bed, respectively; C_{pma} is the heat capacity of moist air; C_{pb} the heat capacity of the bed; f describes the relationship between saturation humidity and temperature; ΔH_v is the enthalpy of vaporization of water; k_b is the thermal conductivity of the bed; V_z is the superficial air velocity; z and r are the axial and radial spatial coordinates; and r_Q is the rate of heat generation from the growth reaction. The factor $\rho_a f \lambda$ arises because the equilibrium assumed between the substrate and air means that the evaporation of water to keep the air saturated as the air temperature increases gives the air a higher apparent heat capacity. This is a simplified approach to handling evaporative cooling, which can contribute as much as 65% of the heat removal from a packed bed (47).

For thin packed-bed bioreactors of about 6 cm diameter, operated with low superficial air velocities (e.g., 0.01 m s^{-1}), radial conduction is the major heat removal mechanism (3). In this particular case the terms for convection and evaporation and axial conduction can be omitted.

In addition to transfer phenomena within the bed, the other important transfer process is from the outer edge of the substrate bed to the surroundings (the bioreactor wall itself has been assumed to offer negligible resistance to heat transfer). Convective cooling at this boundary has been assumed (3,38):

$$\left.\frac{\partial T}{\partial r}\right|_{wall} = \frac{ha}{k_b}(T_{surr} - T_{wall}) \qquad (64.27)$$

Overheating problems occur at the top of the column when it is aerated from the bottom because the air reaching higher regions has been prewarmed in the lower regions and therefore does not cool the top as effectively. Even for quite small columns, when they are operated with the cross-sectional airflow rates of 0.01 to 0.025 m s^{-1} that are commonly used in packed-bed bioreactors, temperatures that can cause significant microbial death are predicted. The model of Sangsurasak (38) can be used as a tool in bioreactor design, operation, and scale-up. Sangsurasak used the model to explore strategies for minimizing the overheating problem at large scale. Higher aeration rates and lower height-to-diameter ratios appear to be the best strategies. However, the model has not yet been used in the actual construction of a larger-scale packed bed.

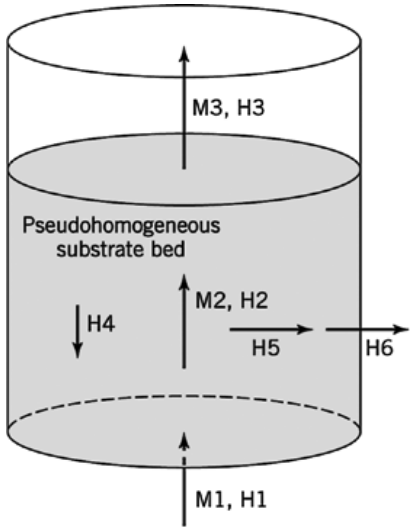


Figure 64.5. Diagrammatic representation of the packed-bed bioreactor as modeled by Sangsurasak (38). The substrate bed is treated as a single pseudohomogeneous phase. The microbe grows in the bed and releases waste metabolic heat. The heat and mass transfer processes occurring are M1, flow of moist air into the pseudohomogeneous bed; M2, flow of moist air within the bed, with the air being saturated at the bed temperature; M3, flow of moist air out of the pseudohomogeneous bed; H1, bulk transfer of energy into bioreactor with airflow; H2, convective heat transfer within the bed; H3, bulk transfer of energy out of bioreactor with airflow; H4, axial conduction within the bed (opposes the temperature gradient caused by convection); H5, radial conduction within the bed; H6, conduction across the bioreactor wall and convective removal by cooling water.

Gutierrez-Rojas *et al*. (17) used a different approach to modeling heat transfer during growth of *A. niger* in a packed bed on beads of ion exchange resin impregnated with nutrient medium. They defined an "elementary representative volume" of 20 mL, over which scale variations in the process variables were assumed to be negligible. However, they modeled only an individual elementary representative volume, and although their model was able to describe the experimental results obtained in a 20-mL packed bed, it is not able to describe the gas concentration and temperature profiles that occur across larger-scale packed-bed bioreactors (46).

64.7.4.2 Heat and Mass Transfer in Packed-Bed Bioreactors. The reliance on evaporative cooling means that water balances over the bed are important (45). A combined heat and mass transfer model is required to take these into account. Such a model, considering only gradients in the vertical direction, was proposed by Van Lier *et al*. (39), who modeled the composting of a mixture of wheat straw and horse manure. The energy balance is similar to that used by Sangsurasak (38), but because a material balance was also done for water, a simplified description of evaporation was not required. The equation was of the form

$$\rho_b C_{pb}\frac{\partial T}{\partial t} + \rho_{ma} C_{pma} V_z \frac{\partial T}{\partial z} = k_b \frac{\partial^2 T}{\partial z^2} - h(T - T_0) - \Delta H_v r_w + r_Q \quad (64.28)$$

where h is the heat transfer coefficient for conduction through the side wall to the surroundings at temperature T_0, and r_W is the rate of evaporation of water from the solid phase into the gas phase.

A general mass balance equation for compound A in the gas phase, for example, oxygen or water, can be written in the following form with terms for axial convection, axial diffusion, and exchange with the metabolizing organism attached to the solid phase:

$$\frac{\partial(\varepsilon C_A)}{\partial t} = -V_Z \frac{\partial C_A}{\partial z} + \frac{\varepsilon}{\beta^2} D_A \frac{\partial^2 C_A}{\partial z^2} + r_A \quad (64.29)$$

where C_A is the concentration of A at a location, D_A is the diffusivity of A in air, ϵ is the bed void fraction, β is the tortuosity and r_A is the rate of exchange of A with the solid phase. In the water balance Van Lier *et al*. assumed that the vapor phase remained saturated with water at the local temperature in the bed, and used this equation to calculate the evaporation rate (r_W). Film transfer of oxygen was not incorporated into the equations.

Solution of the equation set was complicated because the porosity and height of the bed changed during the composting process. However, good agreement was achieved between the model predictions and measured temperatures and bed heights. In composting, unlike other SSF processes, some self-heating is desired, and this reduces problems with overheating. Despite this, the aeration rate required to remove excess heat is still about 10-fold greater than that required to supply oxygen (39).

64.7.4.3 Other Phenomena in Packed-Bed Bioreactors. As air flows through the porous bed in a packed-bed bioreactor, there are viscous and kinetic phenomena (5). Substantial pressure drops can occur in packed-bed bioreactors (5,18,41). To date characterization of this phenomenon has been limited to demonstrating the relationship between pressure drop and the bed void fraction, which decreases as the microbe fills in the interparticle spaces. At high biomass densities, the microorganism can occupy up to 34% of the free interparticular space, reducing the relative permeability of the bed to around 1% of the original value (40). In the future, such considerations could be built into momentum balances to describe how the flow through the bed changes during the fermentation.

64.7.5 Macroscopic Transport Phenomena in Rotating-Drum Bioreactors

Only heat transfer phenomena (and the related mass transfer of water) have been modeled in rotating-drum bioreactors and the related rocking-drum bioreactor (RDBs). As in packed-bed systems, it is likely that in order to achieve adequate heat removal in RDBs, aeration requirements will already be met. Neither of the models developed so far (21,40) describes all of the heat transfer processes mentioned in Table 64.2.

Sargantanis *et al*. (21) modeled heat transfer during growth of *R. oligosporus* on corn grit in a rocking-drum bioreactor with a 1.2-L working volume. They described heat removal very simplistically by assuming equilibrium between the headspace and the substrate bed; in essence, this was a single homogeneous subsystem. The model was useful for determining better operation of their rocking-drum bioreactor system; however, it is not very versatile and can not readily be adapted to describe larger-scale SSFs in RDBs, where the assumption of thermal and moisture equilibrium between the solid substrate and the headspace could be unreasonable, particularly if high aeration rates are used. For such cases a model predicting heat removal in terms of heat transfer rather than equilibrium relationships is likely to be more useful.

Stuart (41) modeled heat transfer in a 20-L rotating-drum bioreactor in which *A. oryzae* was grown on both an artificial gel substrate and on wheat bran. The model is more mechanistic than that of Sargantanis *et al*. (21) and considers several of the heat transfer processes listed in Table 64.2. As shown in Figure 64.6, it simplifies the bioreactor system into three subsystems: the two internal subsystems, the fermenting substrate and the headspace gas, which are contained by the third subsystem, the fermenter wall. Each subsystem is assumed to be homogeneous with respect to composition and temperature in both the radial and axial directions. The model, therefore, does not describe heat transfer processes within any of the subsystems, and the temperature of each subsystem is represented by a single time-dependent value. Stuart (41) neglected water mass transfer within the substrate bed by assuming that water at 25°C is added to maintain the water activity within this pseudohomogeneous subsystem close to unity. Mass transfer from this bed to the headspace gas is assumed to be limited by the rate at which water vapor in the gas sublayer of the substrate bed diffuses into the bulk headspace gas.

Three energy balance equations, one for each subsystem, describe heat transfer phenomena within the RDB system, and heat exchange between the RDB system and the surroundings (41). Metabolic heat is generated within the substrate and then dissipated by conduction to the bioreactor wall and by convection and evaporative cooling to

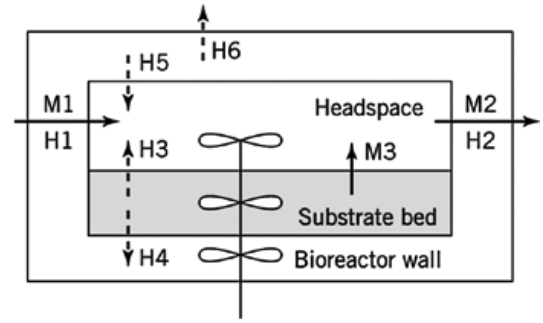


Figure 64.6. Diagrammatic representation of the rotating-drum bioreactor as modeled by Stuart (41), showing the three subsystems that were assumed. The pseudohomogeneous substrate bed is the site of generation of water and waste metabolic heat during growth. The mixer indicates that each subsystem is assumed to be at the same temperature at all locations within the subsystem. The heat and mass transfer processes occurring are M1, flow of moist air into the headspace; M2, flow of moist air out of the headspace; M3, transfer of water from the substrate bed to the bioreactor headspace; H1, bulk transfer of energy into bioreactor with airflow; H2, bulk transfer of energy out of bioreactor with airflow; H3, convection from the substrate bed to the headspace; H4, conduction from the substrate bed to the bioreactor wall; H5, convection from the bioreactor wall to the headspace; H6, convection from the bioreactor wall to the surroundings.

the headspace gases. The overall energy balance for the substrate is

$$\begin{aligned}\frac{d[T_s M(C_{pm} + C_{pw}W)]}{dt} &= r_Q - h_{sf}A_{sf}(T_s - T_f) \\ &\quad - h_{sa}A_{sa}(T_s - T_a) \\ &\quad - (1.2 \times 25)C_{pw}(W_i - W)M \\ &\quad - kA_{sa}(C_I - C_B)[T_s C_{pw} + \Delta H_v \\ &\quad - (T_s - T_a)C_{ph}] \qquad (64.30)\end{aligned}$$

Energy enters the headspace gas with the evaporated water from the substrate and with incoming aeration gases, and through convection from the substrate and from the bioreactor wall:

$$\begin{aligned}\frac{d[T_a G(C_{pg} + C_{ph}H)]}{dt} &= T_i F_i(C_{pg} + C_{ph}H_i) \\ &\quad + kA_{sa}(C_I - C_B)T_a C_{ph} \\ &\quad - T_a F_o(C_{pg} + C_{ph}H) \\ &\quad + h_{sa}A_{sa}(T_s - T_a) \\ &\quad + h_{fa}A_{fa}(T_f - T_a) \qquad (64.31)\end{aligned}$$

The exiting air flow carries energy out of the headspace and thereby away from the RDB system. During fermentation, the bioreactor wall heats up due to its contact with the

substrate. Energy, when it leaves the bioreactor wall, passes either to the surroundings or to the headspace gas inside the RDB:

$$\frac{d(T_f V_f \rho_f C_{pf})}{dt} = h_{sf}A_{sf}(T_s - T_f) - h_{fa}A_{fa}(T_f - T_a) - h_{fe}A_{fe}(T_f - T_e) \quad (64.32)$$

Thus there are two overall routes by which metabolic heat is removed from the substrate subsystem to the surroundings: with the exiting air stream or as heat lost through the bioreactor wall.

In these equations, T is temperature, M is the mass of dry solid, W is the mass of water per mass of dry solid, G is the mass of dry gas, H is the mass of water per mass of dry gas, V_f and ρ_f are the volume and density of the bioreactor material, respectively, C_P is a heat capacity, r_Q is the rate of production of metabolic heat, h is a heat transfer coefficient, A is an area of heat or mass transfer, k is a mass transfer coefficient, C is a concentration of water at either the interface (subscript I) or within the headspace bulk (subscript B), ΔH_v is the heat of vaporization of water, F is a flow of dry gas either entering (i) or leaving (o) the bioreactor system during aeration. The subscripts S, A, and F denote the three subsystems: the substrate, headspace gas, and fermenter wall, respectively. Combinations of these subsystem subscripts indicate heat or mass transfer between these materials, for example, the subscript combination "SF" represents heat transfer from the substrate to the bioreactor wall. The other subscript terms denote dry solid matter (m), dry gases (g), liquid water (w), water vapor (h), and the external surroundings (e).

Estimation of the coefficients and areas involved in the heat and mass transfer processes during SSF in RDBs is difficult, Stuart (41) used empirical equations to estimate transfer coefficients and assumed that the substrate and headspace gas subsystems occupy constant volumes throughout the fermentation. Likewise, transfer areas were assumed to be constant and were calculated based on the interfacial areas between the substrate, headspace gas, and the bioreactor wall, when the surface of the substrate bed forms a flat plane. Heat and mass transfer coefficients and interfacial areas of contact urgently require experimental attention in SSF systems.

In order to incorporate evaporative cooling into a model of heat transfer during SSF, water balances must be determined over the substrate and headspace gas subsystems. Stuart (41) assumed that the substrate and headspace gas subsystems each consist of a water component and a dry component. Therefore four material balance equations were written, two equations to describe each subsystem.

- Balance of dry matter in the substrate:

$$\frac{dM}{dt} = r_m \quad (64.33)$$

- Balance of liquid water in the substrate:

$$\frac{d\,(MW)}{dt} = -kA_{sa}(C_I - C_B) + r_w + 1.2(W_i - W)M \quad (64.34)$$

- Balance of dry gas in the headspace gas subsystem:

$$\frac{dG}{dt} = F_i - F_o + r_{dg} \quad (64.35)$$

- Balance of water vapor in the headspace gas subsystem:

$$\frac{d\,(GH)}{dt} = F_i H_i - F_o H_o + kA_{sa}(C_I - C_B) \quad (64.36)$$

In these equations, r_m, r_w, and r_{dg} are the net rates due to microbial metabolism of substrate dry matter consumption, water production, and dry gas production, respectively.

Due to consumption of substrate dry matter during microbial growth in SSF and loss of water from the substrate to the headspace gas, the flow of gases out of the RDB ($F_o[1 + H]$) will often be greater than the air flow into the RDB ($F_i[1 + H_i]$). Because RDBs are open systems and large pressure variations in the headspace are unlikely, ideal gas behavior and a constant pressure within the headspace gas are assumed. This gives an equation (not shown) for the flow of gas out of the bioreactor (F_o) and enables the calculation of C_B (the headspace concentration of water vapor).

This model was used to explore SSF performance in RDBs over a range of scales, operations, and designs. The model predictions of temperature profiles for the substrate, bioreactor wall, and headspace gas agreed reasonably well with experimental results for SSFs in real small-scale RDB systems (41). Model simulations indicate that, whereas at small scales heat removal from the substrate bed through the bioreactor wall is most important, the required contribution of evaporative cooling increases with scale. This requires very high aeration rates with relatively dry air: simulations showed that the aeration rate in air volumes per bioreactor volume per minute (vvm) required to achieve adequate heat removal from the substrate might increase by a factor of 25 over a scale change of 1,000. Such high aeration rates would be costly. Therefore heat transfer through the bioreactor wall should be maximized to minimize reliance on evaporative cooling and to limit the amount of water that needs to be added to the system during the fermentation. At all scales, heat removal from the substrate to the headspace gases by sensible heat transfer was insignificant compared with heat transport from the substrate subsystem

by conduction and evaporative cooling. However, sensible heat transfer to the headspace gases was always indirectly important in the model predictions because it affected the temperature of the headspace gases and thereby determined the amount of moisture that the headspace could hold and the driving force for evaporative cooling. This investigation of RDB performance demonstrates how models can be used as tools to explore interactions between important processes occurring during SSFs as well as operation and control options for the design of larger-scale bioreactors. This model, with its mechanistic basis, represents a first step toward developing semifundamental scale-up criteria for SSF in RDBs.

64.8 PARAMETER ESTIMATION

As highlighted in the introduction to this chapter, much more attention needs to be given to the estimation of the parameters involved in models of SSF systems. Models involve four main types of parameters: operational and design parameters, microbial parameters, transport parameters, and thermodynamic parameters. In the modeling work to date, many of these parameters have not been independently determined. In some cases parameters have been allowed to vary to enable the model to fit the experimental data. In other cases parameters have been borrowed from other systems involving different substrates and microorganisms, and even from work done in submerged liquid culture. Even physical parameters may depend on the substrate and its preparation and the bioreactor and how it is operated, making it important for parameters to be measured in the actual system studied. This section describes the work that has been done to determine model parameters in SSF systems.

64.8.1 Operational and Design Parameters

Operational and design parameters come directly from the experimental system being modeled. They include bioreactor geometry, air temperatures and flow rates, and rotation or mixing rates. These parameters are important in optimizing bioreactor performance, but these considerations are beyond the scope of this chapter. For modeling purposes, these parameters are easy to obtain because they are determined by the operator.

64.8.2 Microbial Parameters

Microbial parameters include specific growth and death rates, saturation constants, yields, activation energies, lag periods, and biomass composition. Ideally these parameters should be measured in SSF systems, although this is difficult for those parameters requiring direct measurement of biomass because it is usually impossible to remove the biomass from the substrate particles. Parameters such as specific growth rates and yields are often based on indirect indicators of growth, such as oxygen uptake or protein content, but the relationship of these indicators to growth can often vary during the growth phase. In other cases, parameter values determined in liquid culture have been used, but due to the different physical environment in SSF, these values may not be appropriate for SSF.

Specific growth rates depend on the particular system used. A wide range of values have been reported, from very low values of 0.05 h^{-1} to values as high as 0.5 h^{-1} (45). In some modeling work the specific growth rate has been used as one of the fitting parameters (3,6). The stoichiometry of growth will also be highly variable, and most models consider overall yields and do not balance elements. Only Larroche and Gros (22) have done detailed stoichiometric analyses (for growth and sporulation of *Penicillium roqueforti* on buckwheat seeds). For the anabolic reactions during biomass production from starch they obtained

$$1.104CH_{1.667}O_{0.833} + 0.087NH_3 \rightarrow CH_{1.882}O_{0.603}N_{0.087} + 0.014CO_2 + 0.109H_2O \quad (64.37)$$

Because a range of different empirical equations have been used to describe the effect of temperature on growth, the values of the parameters do not have general significance. In any case, these parameters are typically determined by incubating cultures at different temperatures, but with any one culture being held isothermally throughout the whole growth phase. The models of Stuart (41) and Saucedo-Castaneda *et al*. (3) suggest that the relationships obtained from such experiments may not describe the situation in SSF where the organism is subjected to high temperatures after an initial period at the optimum temperature for growth, because their models could describe their data only if the specific growth rate was maintained unchanged at the value for the optimum temperature as the temperature increased.

64.8.3 Transport Parameters

Transport parameters include heat and mass transfer coefficients, diffusivities, and thermal conductivities. Relatively few efforts have been made to determine these in SSF systems. With respect to mass transfer, Auria *et al*. (24) estimated the diffusivities of oxygen and carbon dioxide within substrate beds as 2 to 25% of their diffusivities in air, with the values decreasing with increasing biomass content. For transfer of oxygen into the moisture films on substrate surfaces, values of $K_L a$ have been estimated by a sulfite oxidation method to range from 1,140 to 3,050 h^{-1}, with the value increasing with increasing airflow rate (48). For

nutrient diffusion within particles, Mitchell *et al*. (6) estimated the diffusivity of glucose at 37°C as 8.2×10^{-3} $cm^2\ h^{-1}$ compared with a bulk diffusivity in water of $2.5 \times 10^{-2}\ h^{-1}$. However, because they used an artificial gel substrate, this value is not of general applicability. They were not able to measure glucoamylase diffusivity using their experimental system. Diffusion has not been investigated for real SSF substrates containing structures such as fibers and cell walls.

With respect to heat transfer, coefficients for heat transfer between subsystems in SSF bioreactors have typically been estimated from literature values for non-SSF systems. However, because these coefficients can depend strongly on bioreactor design and operation, they need to be determined experimentally for the particular system used. Thermal conductivities of composts varied from 0.25 $W\ m^{-1}\ K^{-1}$ at 20% moisture content to 1.0 $W\ m^{-1}\ K^{-1}$ at 70% moisture content (39).

64.8.4 Thermodynamic and Physical Parameters

Thermodynamic parameters include enthalpies of vaporization and saturation humidities that are usually straightforward to obtain from thermodynamic databases. However, it may be difficult to estimate other parameters such as the heat capacities of substrates with complex compositions, and therefore experimental measurements should be made. Physical parameters such as substrate densities and bulk packing densities are readily measured experimentally. They vary widely between different systems.

64.9 SUMMARY AND NEEDS FOR THE FUTURE

Growth in SSF results from the interaction of three types of phenomena: microbial growth, local transport, and bulk transport. This chapter has surveyed the ways in which these phenomena have been described in mathematical models of SSF processes. In these models, many simplifications are made, reducing both the complexity of the system and the complexity of the processes occurring within the system. Despite these simplifications and assumptions, the usefulness of the models has been identified. Microscopic models give insights into how diffusion of enzymes, their hydrolysis products, and oxygen can limit growth. Macroscopic models give insights into how interparticle oxygen transport, and more importantly, how heat transport can limit growth within bioreactors.

SSF and traditional liquid culture systems are quite different: compared with liquid culture systems, in SSF systems water availability is more restricted, and diffusional limitations play a greater role. It is these differences that can give SSF advantages over liquid culture in certain cases; the unique SSF environment can stimulate certain products, and the low water content can lead to higher concentrations and therefore higher volumetric productivities and reduced recovery costs. These differences also lead to some differences in approaches to modelling SSF and liquid culture. Due to the heterogeneity of SSF systems, differential equations must often be formulated and solved for each of several subsystems, and due to the importance of transport processes, many of the equations involve partial differential terms. Also, due to diffusional limitations within substrate particles, it is not simple to measure the substrate concentration experienced by the microbe. For this reason, growth kinetic expressions for the majority of models in SSF will continue to be substrate independent. This is in contrast to liquid culture, where even simple models usually take substrate concentration into account, often assuming a Monod-type relationship. However, in the future, some models will be developed that integrate the microscopic- and macroscopic-scale processes occurring within SSF. These models will give interesting insights into how the interactions among the various phenomena control growth at various stages during SSF.

More work needs to be done in establishing the validity and flexibility of current models. Due to the difficulties of measuring key process parameters in SSF, many of the parameters used in these models have been estimated, or borrowed from other systems. Therefore, more effort is required to measure model parameters in SSF systems. More attention must be paid to microbial physiology. Current expressions describing the effect of elevated temperatures on microbial growth are based on experiments where a number of cultures have been incubated isothermally at a range of temperatures. Better expressions will be developed from experiments that mimic the temporal temperature profiles characteristic of SSF systems. In addition, product formation is usually the main objective of an SSF process. Accurate description of product formation kinetics will require an understanding of how the SSF environment influences microbial product formation.

Our current ability to apply SSF technology at large scale is limited by our relatively poor knowledge of the basic engineering principles underlying SSF bioreactor performance. Rational rules for the design and operation of large-scale SSF bioreactors are crucial to the future commercial success of SSF technology, and mathematical models of bioreactor performance will be essential tools in the development of such rules. The power of the modeling approach is obvious. Modeling is a more cost-effective way of searching for optimal bioreactor designs than building large bioreactors and encountering problems experimentally. It does not replace the need to experiment, but can reduce the experimental program by avoiding poor designs and can guide the program by raising questions about the dominant mechanisms and the key process

variables. However, because the models to date have been based on laboratory-scale systems, work needs to be done to confirm that the mechanisms incorporated into the models remain dominant at large scale. Several of the bioreactor designs, such as stirred bioreactors and air solid fluidized beds, have not received any modeling attention. Air solid fluidized beds have the potential to overcome many of the problems faced in other SSF bioreactors, and therefore urgently need modeling attention.

REFERENCES

1. R.E. Mudgett, in A.L. Demain and N.A. Solomon eds., Manual of Industrial Microbiology and Biotechnology, American Society for Microbiology, Washington, D.C., 1986, pp. 66–83.
2. A. Pandey, Process Biochem. 27: 109–117 (1992).
3. G. Saucedo-Casteneda, M. Gutierrez-Rojas, G. Bacquet, M. Raimbault, and G. Viniegra-Gonzalez, Biotechnol. Bioeng. 35: 802–808 (1990).
4. M.A. Aufeuvre and M. Raimbault, Comptes Rendus des Seances de L'Academie des Sciences, Serie III Sciences de la Vie 294: 949–956 (1982).
5. R. Auria, M. Morales, M.E. Villegas, and S. Revah, Biotechnol. Bioeng. 41: 1007–1013 (1993).
6. D.A. Mitchell, D.D. Do, P.F. Greenfield, and H.W. Doelle, Biotechnol. Bioeng. 38: 353–362 (1991).
7. Sangsurasak, M. Nopharatana, and D.A. Mitchell, J. Sci. Ind. Res. 55: 333–342 (1996).
8. G. Viniegra-Gonzalez, G. Saucedo-Castaneda, F. Lopez-Isunza, and E. Favela-Torres, Biotechnol. Bioeng. 42: 1–10 (1993).
9. G. Viniegra-Gonzalez, C.P. Larralde-Corona, and F. Lopez-Isunza, Adv. Bioprocess Eng. 11: 183–189 (1994).
10. K.S.M.S. Ragheva Rao, M.K. Gowthaman, N.P. Ghildyal, and N.G. Karanth, Bioprocess Eng. 8: 255–262 (1993).
11. P. Sangsurasak and D.A. Mitchell, J. Chem. Technol. Biotechnol. 64: 253–260 (1995).
12. K.W. Szewczyk and L. Myszka, Bioprocess Eng. 10: 123–126 (1994).
13. R.E. Muck, R.E. Pitt, and R.Y. Leibensperger, Grass Forage Sci. 46: 283–299 (1991).
14. J. Kaiser, Ecol. Model. 91: 25–37 (1996).
15. S. Rajagopalan and J.M. Modak, Chem. Eng. Sci. 49: 2187–2193 (1994).
16. S. Rajagopalan and J.M. Modak, Chem. Eng. Sci. 50: 803–811 (1995).
17. M. Gutierrez-Rojas, R. Auria, J.C. Benet, and S. Revah, Chem. Eng. J. 60: 189–198 (1995).
18. E. Gumbira-Sa'id, P.F. Greenfield, D.A. Mitchell, and H.W. Doelle, Biotechnol. Adv. 11: 599–610 (1993).
19. M.P. Nandakumar, M.S. Thakur, K.S.M.S. Raghavarao, and N.P. Ghildyal, Process Biochem. 29: 545–551 (1994).
20. M.P. Nandakumar, M.S. Thakur, K.S.M.S. Raghavarao, and N.P. Ghildyal, Enzyme Microb. Technol. 18: 121–125 (1996).
21. J. Sargantanis, M.N. Karim, V.G. Murphy, D. Ryoo, and R.P. Tengerdy, Biotechnol. Bioeng. 42: 149–158 (1993).
22. C. Larroche and J.B. Gros, Biotechnol. Bioeng. 39: 815–827 (1992).
23. J.A. Rodriguez Leon, A. Torres, J. Echevarria, and G. Saura, Acta Biotechnol. 11: 9–14 (1991).
24. R. Auria, J. Palacios, and S. Revah, Biotechnol. Bioeng. 39: 898–902 (1992).
25. P. Gervais and D. Simatos, in S. Thorne ed., Mathematical Modelling of Food Processing Operations, Elsevier, London, 1992, pp. 137–183.
26. L. Edelstein and L.A. Segel, J. Theor. Biol. 104: 187–210 (1983).
27. L. Edelstein, Y. Hadar, I. Chet, Y. Henis, and L.A. Segel, J. Gen. Microbiol. 129: 1873–1881 (1983).
28. J.A. Laszlo and R.W. Silman, Biotechnol. Adv. 11: 621–633 (1993).
29. L. Edelstein, J. Theor. Biol. 98: 679–701 (1982).
30. A.M. Jurus and W.J. Sundberg, Appl. Environ. Microbiol. 32: 284–287 (1976).
31. K. Ito, A. Kimizuka, N. Okazaki, and S. Kobayashi, J. Ferment. Bioeng. 68: 7–13 (1989).
32. C. Larroche, J. Sci. Ind. Res. 55: 408–423 (1996).
33. G. Georgiou and M.L. Shuler, Biotechnol. Bioeng. 28: 405–416 (1986).
34. G. Lazarova, M. Kancheva, and I. Panayotov, Acta Microbiol. Bulgarica 15: 63–71 (1984).
35. S. Rajagopalan, D.A. Rockstraw, and S.H. Munson-McGee, Bioresource Technol. 61: 175–183 (1997).
36. M.K. Gowthaman, K.S.M.S. Ragheva Rao, N.P. Ghildyal, and N.G. Karanth, Process Biochem. 30: 9–15 (1995).
37. D.A. Mitchell, P.F. Greenfield, and H.W. Doelle, World J. Microbiol. Biotechnol. 6: 201–208 (1990).
38. P. Sangsurasak, Ph.D. Thesis, The University of Queensland, Brisbane, Australia, 1996.
39. J.J.C. Van Lier, J.T. Van Ginkel, G. Straatsma, J.P.G. Gerrits, and L.J.L.D. Van Griensven, Netherlands J. Agric. Sci. 42: 271–292 (1994).
40. R. Auria, I. Ortiz, E. Villegas, and S. Revah, Process Biochem. 30: 751–756 (1995).
41. D.M. Stuart, Ph.D. Thesis, The University of Queensland, Brisbane, Australia, 1996.
42. P. Gervais, C. Bazelin, and A. Voilley, Biotechnol. Bioeng. 28: 1540–1543 (1986).
43. B.L. Rathbun and M.L. Shuler, Biotechnol. Bioeng. 25: 929–937 (1983).
44. M.K. Gowthaman, N.P. Ghildyal, K.S.M.S. Raghava Rao, and N.G. Karanth, J. Chem. Technol. Biotechnol. 56: 233–239 (1993).
45. G. Saucedo-Castaneda, B.K. Lonsane, M.M. Krishnaiah, J.M. Navarro, S. Roussos, and M. Raimbault, Process Biochem. 27: 97–107 (1992).
46. N.P. Ghildyal, M.K. Gowthaman, K.S.M.S. Raghava Rao, and N.G. Karanth, Enzyme Microb. Technol. 16: 253–257 (1994).
47. M. Gutierrez-Rojas, S. Amar Aboul Hosn, R. Auria, S. Revah, and E. Favela-Torres, Process Biochem. 31: 363–369 (1996).
48. A. Durand, P. Pichon, and C. Desgranges, Biotechnol. Tech. 2: 11–16 (1988).

65

SOLID SUBSTRATE FERMENTATION, AUTOMATION

Mario Fernández-fernández
Industrial Technologies Department, Universidad de Talca, Talca, Región del Maule, Chile
J. Ricardo Pérez-correa
Chemical and Bioprocess Engineering Department, Pontificia Universidad Católica de Chile, Santiago, Chile

65.1 INTRODUCTION

Solid substrate fermentations (SSF) normally refer to processes where microorganisms grow in beds of water-insoluble moist solid particles, where the interparticle space is filled with a gas phase, and almost no visible liquid water (1,2). The gas phase is usually humid air that flows through the solid bed, providing oxygen and removing heat and carbon dioxide, whereas the solid particles provide the necessary nutrients for growth and metabolite production. The microorganism grows over and inside the support covered by a liquid film, and in the interparticle free space.

SSF has been used by man since ancient times (3,4) to produce fermented foods, such as bread and cheese all around the world, or typical oriental foods and alcoholic beverages, such as "koji" in Japan and China, "tempeh" and "ontjom" in Indonesia, "shao-hsing" wine and "kao-liang" liquor in China, and "ragi" in India. In addition, SSF has been used to produce vinegar, to preserve meat and fish, and for composting. More recently, SSF technology has been applied to bioremediation and to produce antibiotics, aromas, biofuels, biopesticides, enzymes, organic acids, mycotoxins, and secondary metabolites (3–6).

It is usually argued that in many cases SSF is superior to submerged fermentation (SmF) (5,7,8). Commonly mentioned advantages of SSF are its use of low cost agroindustrial wastes, low capital and processing costs, low demand on sterility, good oxygen circulation, differential expression of certain microbial metabolites with respect to SmF, high volumetric yields, high end-concentration products, lower catabolic repression, and simpler to carry out mixed cultivations (3,4,6,9). However, only few large-scale applications of SSF processes are currently running in industry.

Most of the advantages above are evident at laboratory scale but not at large production scales, where heat and mass transfer are insufficient, resulting in bed overheating, bed drying, and nutrients and oxygen limitations (3,10). For example, in fungi cultivation (2), fungal hyphae can dry out when they are exposed to unsaturated air streams. In addition, bed temperature during cultivation can vary widely and take on high values, far beyond those for optimum growth or production, or ultimately high enough to damage the microorganism. Finally, diffusion of oxygen and nutrients through the liquid film to supply the microorganism is very slow and sometimes insufficient to ensure optimum growth or viability. Other important factors that complicate the design and operation of large-scale SSF bioreactors are the lack of affordable and readily available sensors appropriate for monitoring this type of process, limited availability of experimentally validated SSF reactor models, and the need for robust and generally applicable control strategies that take into account the heterogeneous characteristic of this type of cultivation (9,11,12).

This chapter will focus in the latter topics, which we think are unavoidable for large-scale SSF processing. First, the most critical operating variables in SSF bioreactors and how we can measure them are discussed. Then, a brief description of SSF bioreactors commonly used for commercial-scale production together with suggested

Upstream Industrial Biotechnology: Equipment, Process Design, Sensing, Control, and cGMP Operations, Volume 2, First Edition. Edited by Michael C. Flickinger.
© 2013 John Wiley & Sons, Inc. Published 2013 by John Wiley & Sons, Inc.

control strategies is provided. Finally, the production of gibberellic acid by the filamentous fungus *Gibberella fujikuroi* is used to illustrate the design and performance of an automated SSF bioreactor.

65.2 MEASUREMENT AND CONTROL OF CRITICAL OPERATING VARIABLES

To build and put in operation an industrial-scale SSF bioreactor is challenging, mainly due to its complex dynamic behavior and the lack of affordable and reliable instrumentation for measuring key variables inside the solid bed. These hinder the development of supervision and automatic control systems to operate the bioreactor efficiently. Most of the instrumentation used in SSF bioreactors up to now is associated with the gaseous phase, whereas there is very little for the solid phase.

Measuring microorganism environmental variables such as temperature, water content, and pH of the solid bed is critical to ensure optimum growth and production. In addition, effective supervision and control of the bioreactor require measurements of inlet and outlet air condition (temperature and humidity) and composition (O_2 and CO_2), air flow rate, and bed pressure drop (13).

Next, each of them is briefly analyzed. Measurement of nutrients, biomass, and product composition would be beneficial; however, measuring them on-line is very difficult. For example, biomass sensors have been developed, but tested in small scale only (14). We have not found reports of applications of on-line biomass sensors in large-scale SSF bioreactors.

Possible measurements inside the solid substrate are as follows:

1. *Temperature.* Microorganism's growth produces metabolic heat. If this is not dissipated effectively, high temperatures (over 40°C) and significant temperature gradients will be developed (up to 3°C/cm). High temperatures reduce growth and production rates, and in extreme cases can cause loss of microorganism viability. In turn, temperature gradients impede optimum growth all over the bed. These phenomena can be observed in practically all static large-scale SSF bioreactors (15). Measuring bed temperatures is relatively simple in SSF bioreactors by means of thermocouples or resistance temperature detectors (RTDs) such as PT-100 (13,16,17). It is advisable to measure the temperature at different heights and radius to detect and control hot spots (18–20). If this is the case, the problem then is deciding which temperature to control. Reasonable choices are the maximum or average temperatures (19,21). In addition, an auctioneering control scheme (22) can be used. In this case, the average temperature is controlled during normal operation. However, the maximum temperature (hot spot) becomes the controlled variable when it surpasses a given threshold.
2. *Water Content.* Solid's bed water content directly affects growth and production rates; hence, it must be carefully controlled to achieve optimum bioreactor performance. Still, it is difficult to control the water content of the solid bed, since available on-line sensors are expensive and unreliable for SSF applications. Although TDR (time domain reflectometry) (23) has not been used in SSF bioreactors, there are many successful applications in porous solids (13); therefore, this kind of sensors may be a good option. Alternatively, water content can be estimated through soft-sensors (see below) (11,12,21,24) using other related measurements, such as bed weight or air measurements (13). The simplest option to measure water content, although not necessarily the best, is periodic sampling in different points of the bed followed by dry weight determination in the laboratory (19).
3. *pH.* It is rather difficult to get a good on-line measurement of the pH of the solid bed in SSF bioreactors. Although there are sharp or flat end (17,25) probes, specially designed for solids, it is not possible to ensure a good contact with the type of substrate normally used in SSF. This prevents a suitable diffusion of the ions through the sensible membrane of the probe. Experimental tests at laboratory (26) and pilot (19) scales have not been encouraging with these probes; on-line pH measurements in the solid phase were significantly different from those obtained from extracts of the solid samples. Despite this, pH control in SSF bioreactors is not that difficult due to the large buffer capacity of the solid bed. In standard practice, pH is initially adjusted to the optimal growth value (27) and then measured periodically from samples taken from the bioreactor. It is also possible to incorporate, initially or sporadically during the cultivation, nutrients like mixtures of ammonium salt and urea to keep the pH of the solid substrate at optimum values (4,28). Additionally, optic pH sensors that have been applied successfully in SmFs (29) could be adapted to SSF bioreactors in the future.
4. *Biomass.* Even though this is perhaps the most important variable, it is not measured in large-scale SSF bioreactors. In recent years several innovative sensors for biomass measurement have been developed. Although these are too expensive, not sufficiently reliable for large-scale commercial application or have been tested in SmF bioreactors only; a review on some of these sensors can be found in Ref. 30. Available biomass probes make use

of electric impedance (31–33), electric capacitance (14), and redox potential (34). Soft-sensors (see below) are a good option for now.

Variables that are not measured in the solid bed, but are relevant to monitor the state of the process are discussed next:

1. *Gas Flow Rate.* Bed aeration is required for microorganism's respiration, for removal of CO_2 and metabolic heat, and for bed humidity regulation (35). Therefore, measuring airflow rate is crucial for bioreactor monitoring and control. The diversity of probes available measure either the air velocity or the airflow rate (mass or volumetric) (13). It is rather difficult to select an appropriate airflow rate instrument. A detailed guide is provided in Ref. 36 to ensure that, for a given application, an accurate, reliable, and reasonable cost instrument is chosen.
2. *Relative Humidity of Inlet Air.* When the evaporative cooling strategy (see below) is used to control the bed temperature, it is advisable to measure and manipulate the inlet air humidity (19). Capacitive instruments that comprise a dielectric hygroscopic membrane are frequently used for this purpose (17). Air is assumed to be saturated when leaving the bioreactor, therefore it is usually not measured.
3. *Pressure Drop.* When flowing through the bioreactor, air suffers a pressure drop that depends on how compact the solid bed is, which in turn is affected by the growth of filamentous fungi. Therefore, differential pressure measurements have been used to estimate the permeability or porosity of the bed (1,37) and the biomass concentration (13,38,39). In addition, these measurements have been used to decide when to agitate in intermittently mixed bioreactors (25,40) or to detect gas channeling when the differential pressure falls without apparent reasons. Piezoelectric sensors are recommended for SSF applications, since they are fast, insensitive to temperature, and measure over a wide range (41).
4. *Off-Gas Analysis.* The analysis of the outlet air provides significant information regarding the state of the cultivation. For example, by measuring CO_2 and O_2, important respirometric parameters can be calculated on-line, like CO_2 production rate (CPR), oxygen uptake rate (OUR), or respiration quotient (RQ). These, in turn, can be used to infer the amount of viable biomass (17,42–44) and to assess the physiological state of the culture (25,45,46). The production of aromas and volatile metabolites can also be tracked through off-gas analysis (47). Measurements can be carried out using different techniques, such as gas chromatography (13,17,48), infrared spectroscopy (46), special sensors for respirometric gases (49,50), and tailor-made sensors called *electronic noses* for specific metabolites (13,51), which have been tested in fungus cultivations (52).
5. *Soft-Sensors.* These are computer algorithms that use a process model and auxiliary measurements (usually corrupted with noise) to infer the value of an unmeasured variable of interest. All kind of models, such as static or dynamic, empirical (black box), purely phenomenological (first principles) or hybrid models (gray box) have been applied in soft-sensors. One of the most widely used soft-sensor algorithms in fermentation biotechnology is the Kalman filter (KF) state estimator (53). Here, a dynamic phenomenological mathematical model, typically derived from mass and energy balances, is required. The KF algorithm uses feedback to provide reliable estimations of the real values of the unmeasured variables, taking into account both, model predictions and process measurements. The KF has been successfully used for many years in SmF bioreactors, and has been applied in a laboratory-scale SSF bioreactor (54) and in realistic simulations with a pilot-scale SSF model (55). Details of this algorithm are beyond the scope of this chapter, but a simplified description can be found in Ref. 55 and a detailed description in Ref. 56.
   Table 65.1 provides a quick reference for instrumentation useful in large-scale SSF bioreactors.
6. *Signal Processing.* All measurements have associated errors, which may prove detrimental for the operation and control of SSF bioreactors. High and medium frequency noise, systematic bias, and outliers (or gross errors) are the most common type of measurement errors found in this process (16). Systematic bias can be minimized by periodic calibration of the instruments, while noise and outliers should be reduced with analog circuits (usually incorporated in the instruments) or digital algorithms (when on-line data is stored in a computer). In the latter, signal processing techniques, such as digital filtering and peak shaving, are typically applied (57).
7. *Control Algorithms.* Automatic control involves a measurement (controlled variable), comparison with a predefined optimum value (set point), and implementation of a corrective action (manipulated variable). Several mathematical procedures (control algorithms) can be used to compute the corrective actions in terms of deviations (errors) from the set point. The easiest algorithm is on–off control, applicable when the corrective action can take only two possible states, such as "open/closed" or "high/low", like a thermostat for example. This algorithm is useful when the controlled variable just

TABLE 65.1. Instrumentation for Large-Scale SSF Bioreactors

Measured Variable	Sensor Type	Main Characteristics of the Method	Application and References
Temperature	Thermocouple	Seebeck effect produced in two different joined wires	Solid bed, inlet and outlet air (on-line), all scales (13,16,17)
	RTD (Pt100)	Variation of electrical resistance of a long wire	Solid bed, inlet and outlet air (on-line), all scales (58,59)
Water content	Dry weight	Weight difference between a wet and a dried sample	Solid bed samples (off-line), all scales (25,60)
	Capacitance	Variation of dielectric property	It must be used carefully in porous medium (61). No application in SSF bioreactors was found
	Conductivity	Variation of electric conductivity	Applications in solid medium (62). No application in SSF bioreactors was found
	TDR	Variation of the travel time of a high frequency, electromagnetic pulse	This technology has been used to measure soil (63) and substrates (64) water content. No application in SSF bioreactors was found
pH	Combination electrode	A pH electrode and a reference electrode, built into a single body or housing. Sense H^+ ions concentration	To correct solid medium pH, taking samples at the beginning or during a fermentation run (27). It is also used on-line to establish the fermentation state (26)
	Optic sensors	Fluorescent dyes immobilized in a water-permeable polymer layer inside an optical fiber	Used only in SmF (30,65). No application in SSF bioreactors was found
Biomass	Electric impedance	Measure the electric impedance of a given medium at different frequencies	Applied in SmF (31–33). No application in SSF bioreactors was found
	Capacitance and conductivity	Dielectric and conductivity measured at different frequencies (Aber Instrument Ltd)	Good results in Petri dishes (14,60,66). No application in SSF bioreactors was found
	Redox potential	Measure the relative affinity for electrons of a given substance compared with hydrogen	Applied in SmF (34). No application in SSF bioreactors was found.
Gas flow rate	Velocity sensors	Measure gas velocity in a representative point inside a duct	Air flow rate in pilot-scale SSF bioreactor (49). Applicable at all scales
	Flow sensors	Many options; see a selection guide in Ref. 67	Applicable at all scales. No application in SSF bioreactors was found
Relative humidity	Hygrometers sensors	A capacity sensor with a hygroscopic dielectric film	Commonly used in SSF bioreactors (49,68,69). Applicable at all scales
	Wet and dry bulb temperatures	Wet bulb temperature is a measure of relative humidity	Indirect measurement. Has been used in SSF bioreactors (19). Applicable at all scales
Pressure drop	Piezoelectric sensor	Deformation, produced by applied pressure, induces an electrical potential.	Used in SSF bioreactors to estimate the state of the fermentation (70), bed compactness (1,37) and biomass (13,38,39). Applicable at all scales
Off-gas analysis	Concentration of respiratory gases	Gas chromatography, mass spectrometry, infrared spectroscopy, optical sensors, paramagnetic, and electrochemical cells	Used to measure CO_2 and O_2 in exit gas in SSF bioreactors. Useful to assess state of the culture. Commonly used in SSF (46,71,72). Applicable at all scales (13,17,46,48–50,73–76)
	Electronics noses	Adsorption of some volatile metabolites of the exit gas produces an electrical signal	Used in SmF (52). No application in SSF bioreactors was found
Soft-sensors	Kalman filter, neural nets, fuzzy models, etc.	Also known as *virtual sensor*. Relate measured with unmeasured variables using a mathematical algorithm	Useful to estimate water content, biomass and fermentation products (11,12,19,21,24,55,77). Applicable at all scales

need to be near the set point. A more sophisticated algorithm is PID (proportional integrative derivative) control; a standard in the process industries. Here, the control action (u) is proportional to the error (e), the derivative of the error, and the integral of the error:

$$u(t) = P \cdot e(t) + I \cdot \int_0^t e(t)\ \mathrm{d}t + D\frac{\mathrm{d}e(t)}{\mathrm{d}t}$$

The parameters P, I, and D should be "tuned" to ensure stability, fast response, and no steady-state error (offset) (78). Many advanced control algorithms make use of process models to compute the corrective actions. For example, model predictive controllers (79) are widely used in the process industries and have been applied in pilot-scale SSF bioreactors (80). These controllers predict future values of the controlled variables and use an optimization algorithm to compute control actions that minimize set point deviations subject to constraints on controlled and manipulated variables.

65.3 AUTOMATIC CONTROL STRATEGIES FOR COMMERCIAL-SCALE SSF BIOREACTORS

To achieve optimum performance, the microorganisms in the solid bed should face a favorable environment. High temperatures, inadequate water content, and low available oxygen are common limitations that preclude optimum growth and production in large-scale SSF bioreactors. Next, control strategies that can be applied to minimize the impact of such limitations in the performance of the most common types of commercial-scale SSF bioreactors are described.

65.3.1 Tray Bioreactors

This is the first kind of SSF bioreactor used for commercial production and has been employed in the Far East for many years. In these bioreactors, individual trays are arranged one on top of the other with sufficient space between them to allow free circulation of air (81). Tray bioreactors have evolved from very simple designs, where an air-conditioned chamber contains several stacks of trays and solids handling is manual. In these, trays are normally open at the top and made of wood, bamboo, or plastic, with solids layers of 5 cm height or less (82) due to heat transfer limitations. More advanced designs consider heat exchanger surfaces and perforated metal trays to improve heat dissipation and aeration. Even more sophisticated designs nowadays comprise closed columns and complete automatic operation, including solids handling (47).

A reasonably good control strategy for tray bioreactors involve temperature regulation in predefined "hot spots" by manipulating inlet air temperature or flow rate, keeping the inlet air saturated to minimize evaporation from the solid bed. If that is not good enough to avoid overheating or over drying, other options for manipulation are air recirculation, vapor addition, cooling water flow rate and temperature, or periodic mixing of the solid layer in the trays. In addition, it has been shown that air pulsation is extremely effective to control solids temperature in industrial-scale tray bioreactors (83). Using this technique, the solids layer were increased to 9 cm height, the maximum temperature in the trays were reduced to 20°C, and the temperature gradient were reduced to one-third (18).

If temperature can be controlled effectively with just one operating variable, on/off or PID algorithms should suffice. However, if many operating variables need simultaneous manipulation to avoid overheating, model predictive control (MPC) is better. Mathematical modeling, as described in Ref. 27, can be useful to design a proper control strategy before building the bioreactor.

65.3.2 Packed Bed Bioreactors Without Mixing

These are cylindrical or rectangular tanks, filled with a solid substrate suspended on a perforated surface. Traditionally, air is forced through the perforated surface from the bottom, but to improve aeration air may be forced from either ends or perforated tubes can be immersed in the solid bed (84). Metabolic heat dissipation can be enhanced with a cooling jacket or immersed cooling plates (85) or tubes. In most cases, the main limitation for optimum performance in packed bed SSF bioreactors is temperature, since the high aeration rates required for heat removal ensure sufficient oxygen supply to solid particles (35). In some cases, though, this rule does not apply. For example, in bioremediation applications, where temperature control is not a concern, oxygen supply may affect bioreactor performance (86).

To regulate temperature, many probes can be inserted in the solid bed; however, we are concerned with the maximum temperature, which is normally found in the top of the bed. In addition, the outlet air is in equilibrium with the solids in the top; therefore, the outlet air temperature is a good candidate for control. In traditional designs (no inner tubes or plates), the only useful manipulated variables are aeration rate and inlet air temperature. In extreme cases, when temperature gradients can be as much as 20°C, pulsed aeration may be as effective here as in tray bioreactors. It is not advisable to manipulate inlet air humidity, since this will lead to bed drying and there is no effective way to replenish evaporated water without bed mixing. Therefore, inlet air should be saturated to minimize water loss from the bed. In addition, manipulating flow rate or temperature of the cooling water in the jacket is useless in large-scale bioreactors, since these will influence at most the solids within 20 cm from the wall (35).

Using a packed bed bioreactor model (87) have shown that manipulating either inlet air temperature or flow rate with a proportional control algorithm is effective to minimize the outlet air temperature. Using inner cooling plates makes bed temperature control much easier. It was found by simulations that a simple proportional control, manipulating cooling water temperature in a bioreactor with a 6 cm gap between plates, achieved almost optimal performance (87).

65.3.3 Packed Bed Bioreactors with Periodic Mixing

These are probably the most widely used type of SSF bioreactor at industrial large scale of production. Here screws, blades, or other mechanical devices agitate the solid bed. Agitation is intermittent, and its frequency, intensity, and duration can be varied during the process. These bioreactors may be either vertical or horizontal. Among the former, the most popular are the Japanese Fujiwara bioreactors (88). These are specifically designed and mostly used for Koji production in the Far East and United States. Among the latter, the best known is the INRA-Dijon bioreactor (89) that has been used in France for the production of enzymes and biopesticides. This open and rectangular reactor is based on a design for a barley malting process. The solid bed rests on a perforated plate through which air is forced. Rotating screws mounted on a conveyer that moves back and forth across the main axis of the tank provide agitation. The shape and size of the screws need to be designed specifically for each substrate and microorganism, in order to minimize abrasion and breakup damage. Both bioreactors have been redesigned for aseptic operation (88,90), and some applications of pilot stirred bioreactors with aseptic operation have been published (25,91,92). Packed bed bioreactors with periodic mixing require a high degree of automation. This complex engineering problem has to be resolved satisfactorily before scaling up the process.

In these bioreactors, addition of water, nutrients, and preservatives can be done by aspersion over the solid mass. Air can be conditioned at the inlet, while the temperature and pH of the solid may be measured at several places within the tank. Many of the difficulties complicating the operation and control of these bioreactors concern the regulation of temperature and water content in the solid bed. Especially hard is the ability to overcome the limited dissipation capacity of the metabolic heat generated during the cultivation. For example, temperature gradients can be as high as 20°C during the exponential growth period. The main manipulated variables for temperature control are flow rate, humidity, and temperature of the inlet air. Although bed agitation can reduce temperature gradients, metabolic heat cannot be removed by vigorous or frequent agitation, as it has a negative impact on microbial growth.

Perhaps, evaporative cooling is the most effective strategy to control bed temperature in periodically stirred bioreactors. In this technique, inlet air temperature or relative humidity (or both) is manipulated to control the rate of evaporation from the solid bed, thereby governing the amount of heat removed by the air stream. At certain point of the process, however, very dry inlet air may be required. This prompts the main drawback of this method—its excessive drying of the solid bed, necessitating the inclusion of efficient water content regulation in the control system. However, control of the water content is difficult since on-line sensors are scarce, expensive, and unreliable. This results in water content regulation being difficult, slow, and imprecise. However, this limitation can be overcome using soft-sensors based on secondary on-line measurements (12). Periodic samples could also be taken manually and analyzed in the laboratory to define the addition of fresh water based on the water balance or heuristics (25). Full details regarding automation of a pilot packed bed bioreactor with periodic mixing are given below.

65.4 CASE STUDY: AUTOMATION OF A PILOT PACKED BED BIOREACTOR WITH PERIODIC MIXING

65.4.1 General Features of the Process

Since most systems proposed in the literature to control SSF processes have been developed at lab scale, they do not take into account the complexity of the dynamic behavior of large-scale SSF bioreactors, such as bed heterogeneity, steep temperature gradients, limiting cooling capacity, multiple sensors and noisy measurements. Consequently, these lab-scale control systems are hardly applicable at industrial scale. In order to develop control systems suitable for commercial scale, we built and put in operation two pilot SSF bioreactors, one of 50 kg dry mass nominal capacity and then one of 250 kg capacity. The control system was similar in both reactors; therefore, only the large bioreactor is described here. The control system of the 50-kg bioreactor is described in Ref. 25.

The bioreactor and its control system consist of (Fig. 65.1) (a) a bioreactor chamber, (b) an air preparation system, (c) a power cabinet, (d) an instrumentation and control cabinet, (e) and a control room with a PC for remote monitoring and control. The bioreactor is made of stainless steel with a perforated base revolving body that can contain up to 250 kg of substrate (dry base). The bioreactor was designed to operate aseptically; hence, the upper and lower parts of the revolving body contain water seals. A hermetic lid supports two motor drives, a spray feeding system (fresh water, nutrients, and inoculation), and solid bed thermocouples. Below the revolving body, there is an air-mixing chamber to homogenize the air before passing through the solid bed.

In the mixing chamber, we placed the inlet air temperature and relative humidity probes. Additional type K thermocouples measure the temperature distribution (six) inside the solid bed and the temperature of the outlet air. The pressure drop through the solid bed, the outlet airflow rate (off-line), and the outlet air composition (O_2 and CO_2)

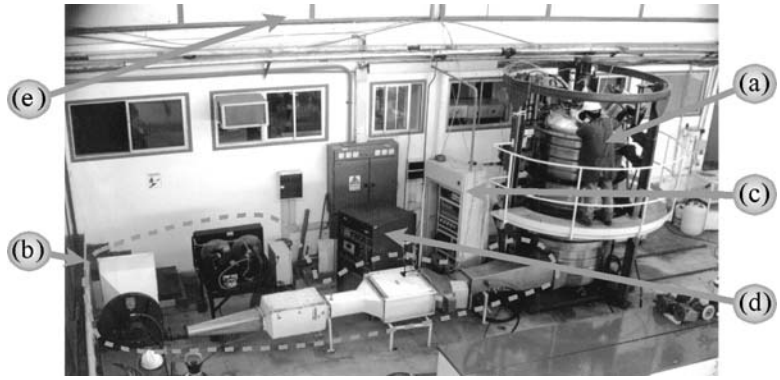


Figure 65.1. General view of the bioreactor and control system: (a) bioreactor chamber, (b) air preparation system, (c) power cabinet, (d) control cabinet, (e) control room.

are also measured. An electric fan drives the air through the preparation system duct containing a pre-filter, an absolute filter, ultraviolet (UV) radiation lamps, cooling fins, electric heaters, and a steam addition system. In this duct, a hot wire probe measured the air velocity.

65.4.2 Control System

As stated above, the main control goals in SSF bioreactors are temperature and water content of the solid bed. In large-scale bioreactors, we should try to minimize bed compactation and temperature gradients. An evaporative cooling strategy (25,93,94) with a cascade configuration was used to control the average bed temperature in this bioreactor. A discrete PID algorithm, based on the average bed temperature, defines the set point for the inlet air humidity. In turn, an on–off algorithm drives a solenoid valve that feeds steam into the air duct (Fig. 65.2). To enhance bed cooling, the inlet air temperature and the air flow rate were also manipulated at the peak heat generation

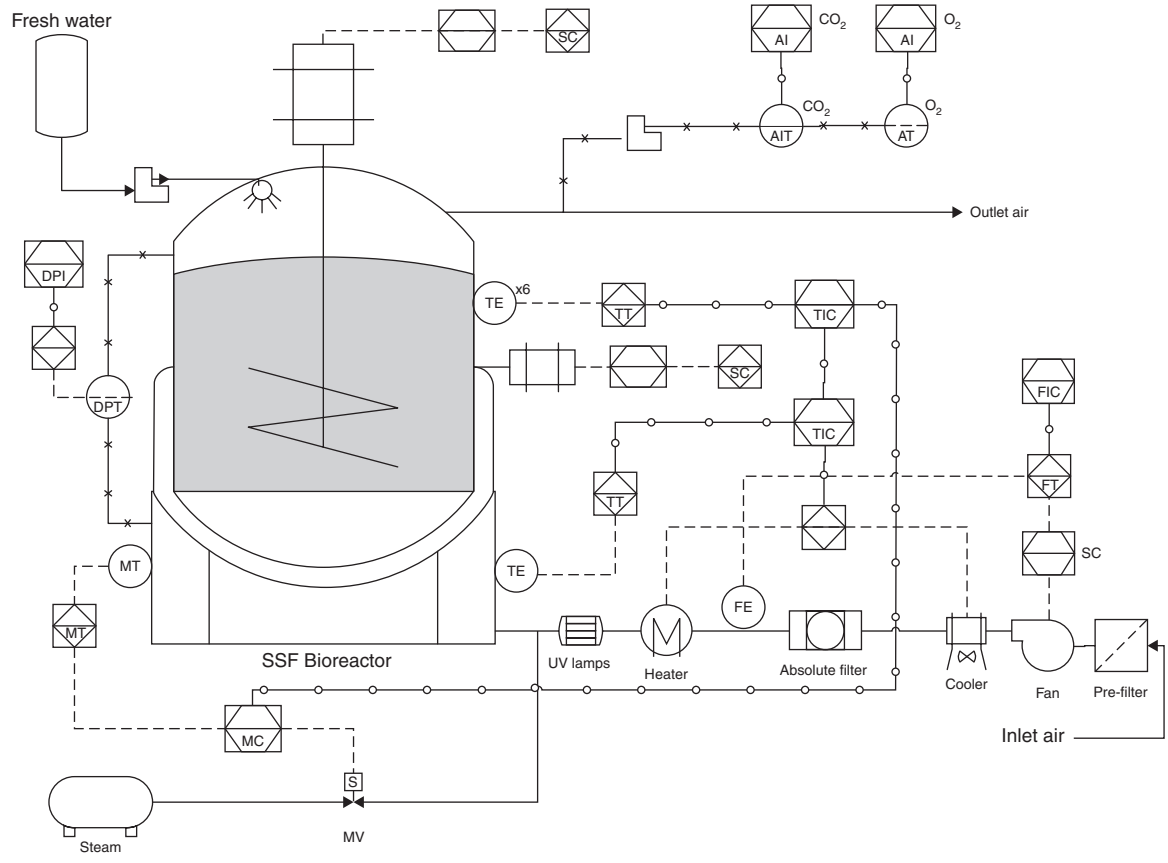


Figure 65.2. Process and instrumentation diagram (P&ID) of the system (Abbreviations are related to ISA 5.1 and ISA 5.3 standards, see Ref. 36).

period. Air flow rate was manipulated by changing the fan speed through an inverter drive, while air temperature was controlled with a split range arrangement that commanded two on–off algorithms; one for the cooling system and the other for the electric heaters.

The main drawback of the evaporative cooling strategy is that the solid bed gets dry. Therefore, we had to add fresh water periodically to replenish that lost by evaporation. It is important to agitate the bed during water addition to ensure good distribution of the water through the bed. The required amount of water was computed based on manual water content measurements and a water balance. In addition, bed agitation was turned on to reduce temperature gradients and bed compactation. A special purpose software with a graphics interface was developed to monitor, operate, and control the process from the PC.

65.4.3 Control Performance

Figure 65.3 shows the performance of the control strategy just described during cultivations of the filamentous fungus *G. fujikuroi* to produce gibberellins. During the first 80 h, the PID controller drove the relative humidity set point and the operator manipulated the inlet air temperature set point. After that, the PID loop manipulated the inlet temperature set point and the operator the relative humidity set point. In turn, both manipulated variables were adjusted to their respective set points by on–off algorithms, explaining the highly oscillatory behavior and offset shown in Fig. 65.3a. Despite this, a reasonably good bed temperature control was obtained most of the time with both configurations (Fig. 65.3b). However, a significant bed temperature gradient is observed along the whole fermentation, where for long periods the differences surpassed 15°C. It should

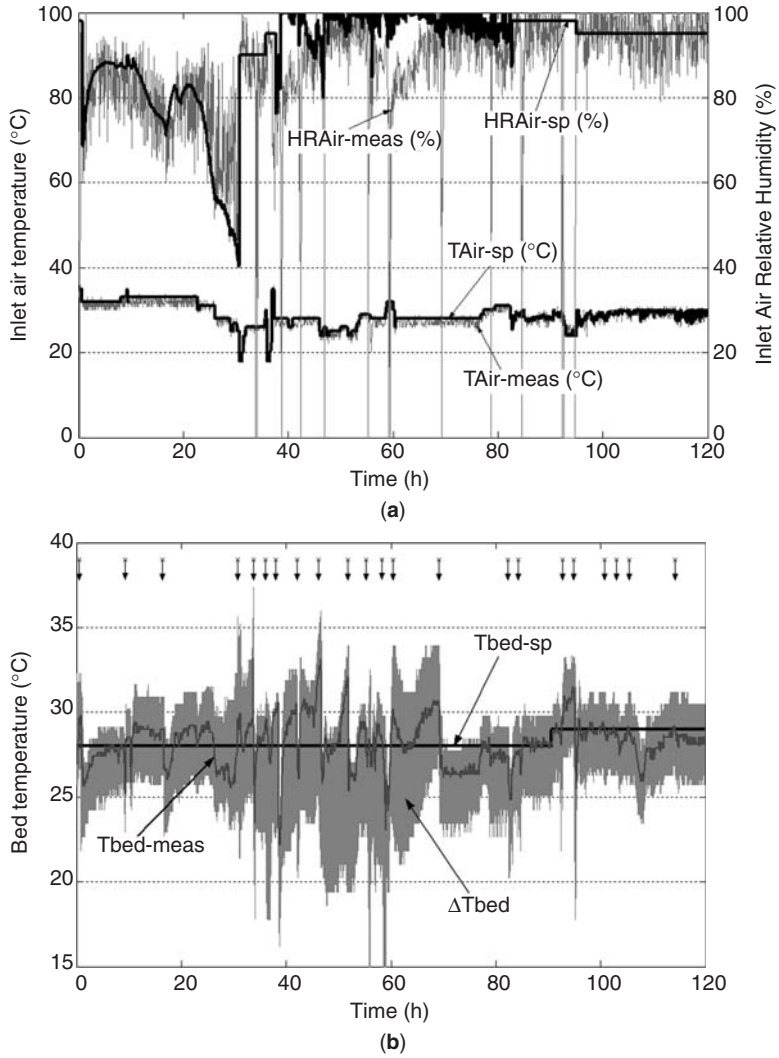


Figure 65.3. Main variables involved in bed temperature control: (a) manipulated variables and (b) bed temperature (↓ mixing events).

be noted, however, that the large temperature peaks that appear during mixing are not due to bad performance of the control system. To avoid damaging the probes during mixing, they are taken out of the bed; thus, in these instances they measure the headspace air temperature instead of the bed temperature. The figure also shows that at the peak of the metabolic heat generation (20–40 h), both manipulated variables saturate at their minimum (19°C, 40%) to achieve maximum heat removal rate. This means that, in this bioreactor, we could not achieve the required cooling by just inlet air temperature manipulation.

As Fig. 65.4 shows, the control system described above allowed us to operate the bioreactor reproducibly since four fermentation runs presented almost the same performance in terms of GA3 production. It is worthwhile noting that the performance shown in the figure does not differ much from that obtained at lab-scale cultivations (not shown here).

In conventional feedback algorithms, such as PID, control loops include one input and one output only (single input single output, SISO). Nevertheless, many large-scale processes need more complicated control configurations. For example, in the pilot bioreactor just described, manipulating the relative humidity was not enough to ensure good bed temperature control along the whole fermentation run. Consequently, the operator had to manipulate the inlet air temperature and sometimes the flow rate to aid the automatic bed temperature control.

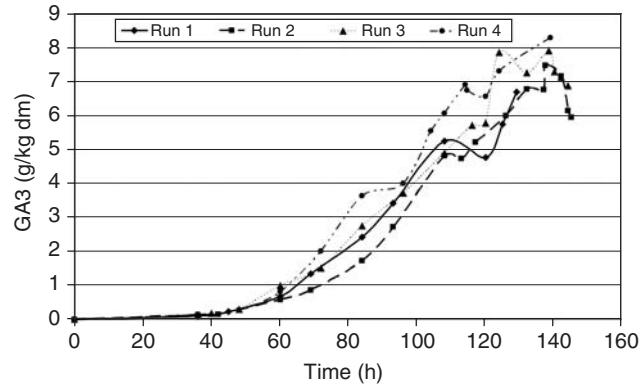


Figure 65.4. Production of GA3 in fourth different SSF cultures.

Figure 65.5 shows a typical 24-h bioreactor operation, where the inlet airflow rate was kept constant, while the

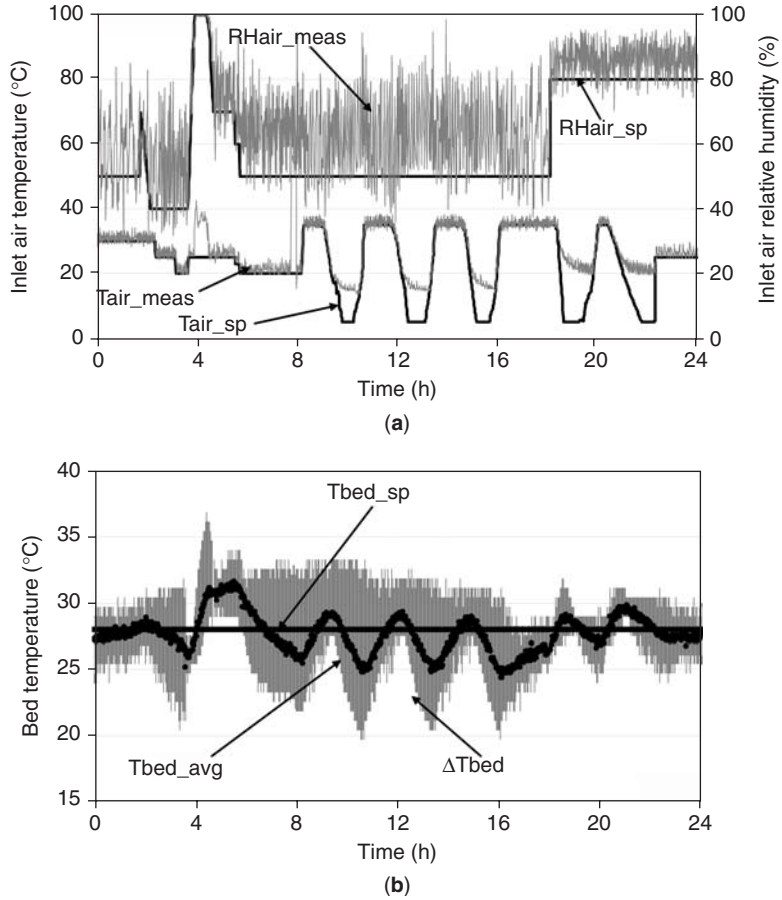


Figure 65.5. Bed temperature control using cascade-PID algorithms: (a) fixed and manipulated variables and (b) controlled variable.

operator manipulated the inlet air relative humidity when needed and the PID algorithm, based on average bed temperature measurements (Fig. 65.2), set the inlet air temperature. The first 8 h the bioreactor was operated manually, that is, the operator established both the inlet air temperature and relative humidity. Large temperature deviations are observed, revealing how difficult controlling this process is. Then, the relative humidity was set at a minimum value (50%) and the control loop was closed. In this case, the loop behaved extremely oscillatory, although temperature deviations were smaller than before. The figure also shows the limitation of the air cooling system that cannot achieve the low temperatures required by the control loop. When the operator set the inlet air humidity at a larger value (80%), the control performance improved significantly, showing smaller bed temperature deviations and finally achieving a steady condition. It is worthwhile noting also the large temperature gradients observed when the relative humidity was set to 50%. Saturation and interaction among different manipulated variables, as shown in Fig. 65.5, make automatic SISO control difficult, calling for manual intervention. At commercial production scale, this is undesirable since the result of each fermentation run will depend on the respective operator skill, affecting the reproducibility of the processes.

A good option is MPC algorithms that can deal with control saturations and inputs interactions easily. One of the simplest and most used at industrial-scale MPC algorithms is dynamic matrix control (DMC) developed by Shell Oil in the 1970s (95). DMC uses a dynamic linear model of the process and minimizes, without constraints, the sum of the square deviations between the set point and the controlled variable. This results in an analytical solution that can be coded in few lines in a standard computer language. To illustrate the potential benefits that DMC can provide in developing a control system for a large-scale SSF bioreactor, Fig. 65.6 shows a 24-h fermentation run controlled with DMC. In this run, the inlet air temperature and relative humidity were manipulated simultaneously, but the algorithm was tuned to manipulate the temperature more strongly. It is clear that DMC achieved a better performance; most of the time significantly smaller bed temperature deviations and temperature gradients are observed. It is important to mention that this was the first

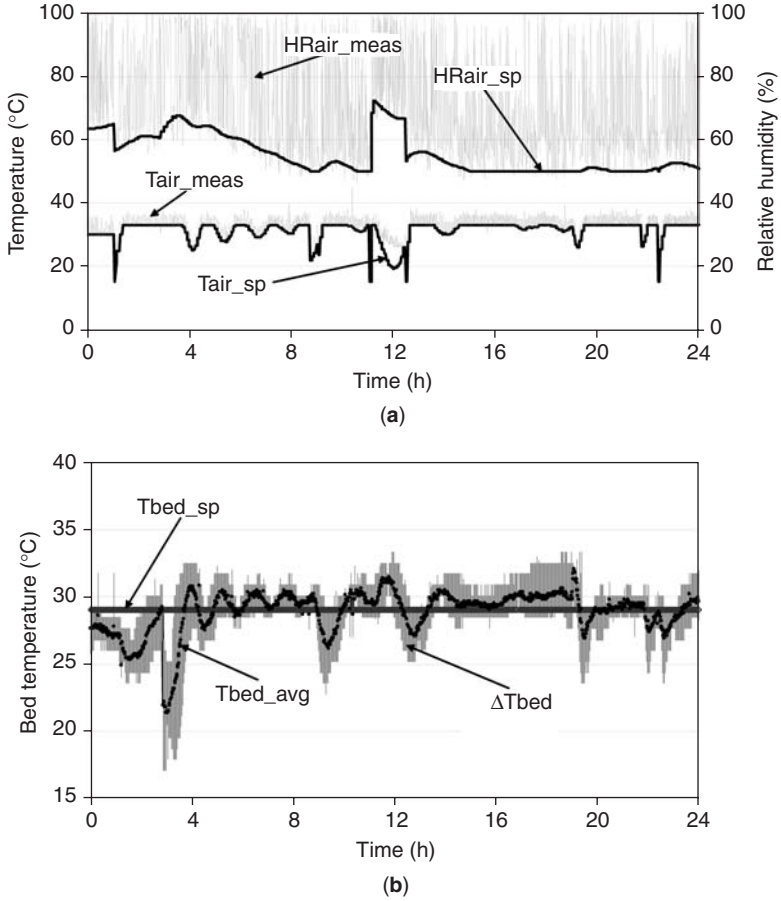


Figure 65.6. Bed temperature control using a DMC algorithm: (a) manipulated variables and (b) controlled variable.

fermentation run with DMC in this bioreactor therefore its performance was not optimized, whereas the PID fermentation runs shown here are the result of a thorough and time consuming tuning exercise.

Without doubt, optimizing the design and performance of a control system for commercial-scale SSF bioreactors is difficult, costly, and time consuming. Computer simulation provides a convenient option. In turn, this requires reliable mathematical models that are able to reproduce the main dynamic features observed in industrial-scale SSF bioreactors. One such model that represents the bioreactor described above has been recently presented by Fernández-Fernández and Pérez-Correa (56) and used to design, tune, and compare different MPC algorithms (96). The model can be adapted to reproduce the dynamic behavior of other kind of SSF bioreactors.

REFERENCES

1. Auria R, Morales M, Villegas E, Revah S. Biotechnol Bioeng 1993; 41(11): 1007–1013. DOI: 10.1002/bit.260411102.
2. Mitchell D, Berovič M, Krieger N. In: Mitchell DA, Krieger N, Berovic M, editors. Solid-state fermentation bioreactors: fundamentals of design and operation. Heidelberg, Germany: Springer; 2006. pp. 1–12. DOI: 10.1007/3-540-31286-2_1.
3. Krishna C. In: Steward GG, Rusell I, editors. Critical reviews in biotechnology; London: Taylor & Francis; 2005. pp. 1–30. DOI: 10.1080/07388550590925383.
4. Raimbault M. Electronic journal of biotechnology (Online). Valparaíso: Universidad Católica de Valparaíso; 1998. http://www.ejb.org.
5. Robinson T, Singh D, Nigam P. Appl Microbiol Biotechnol 2001; 55: 284–289. DOI: 10.1007/s002530000565.
6. Rodríguez Couto S, Sanromán MÁ. J Food Process Eng 2006; 76(3): 291–302. DOI: 10.1016/j.jfoodeng.2005.05.022.
7. Castilho LR, Alves TLM, Medronho RA. Bioresour Technol 2000; 71(1): 45–50. DOI: 10.1016/S0960-8524(99)00058-9.
8. Castilho LR, Polato CMS, Baruque EA, Sant'Anna GL, Freire DMG. Biochem Eng J 2000; 4(3): 239–247. DOI: 10.1016/S1369-703X(99)00052-2.
9. Hölker U, Lenz J. Curr Opin Microbiol 2005; 8: 301–306. DOI: 10.1016/j.mib.2005.04.006.
10. Mitchell D, Meien Ov, Luz L, Berovič M. In: Mitchell DA, Krieger N, Berovic M, editors. Solid-state fermentation bioreactors: fundamentals of design and operation. Heidelberg, Germany: Springer; 2006. pp. 57–64. DOI: 10.1007/3-540-31286-2_5.
11. Lenz J, Höfer M, Krasenbrink J-B, Hölker U. Appl Microbiol Biotechnol 2004; 65: 9–17. DOI: 10.1007/s00253-004-1592-8.
12. Peña y Lillo M, Pérez-Correa R, Agosin E, Latrille E. Biotechnol Bioeng 2001; 76: 44–51. DOI: 10.1002/bit.1024.
13. Bellon-Maurel V, Orliaca O, Christenb P. Process Biochem 2003; 38(6): 881–896. DOI: 10.1016/S0032-9592(02)00093-6.
14. Davey CL, Kell DB. Bioelectrochem Bioenerg 1998; 46(1): 91–103. DOI: 10.1016/S0302-4598(98)00132-9.
15. Weber FJ, Oostra J, Tramper J, Rinzema A. Biotechnol Bioeng 2002; 77(4): 381–393. DOI: 10.1002/bit.10087.
16. Fernández M, Pérez-Correa J. In: Mitchell DA, Krieger N, Berovic M, editors. Solid-state fermentation bioreactors: fundamentals of design and operation. Heidelberg: Springer; 2006. pp. 363–374. DOI: 10.1007/3-540-31286-2_26.
17. Raghavarao KSMS, Ranganathana TV, Karanth NG. Biochem Eng J 2003; 13(2–3): 127–135. DOI: 10.1016/S1369-703X(02)00125-0.
18. Chen H-Z, Xua J, Lia Z-H. Biochem Eng J 2005; 23: 117–122. DOI: 10.1016/j.bej.2004.11.003.
19. Fernández MA. Control automático de un bio-reactor piloto para cultivos sobre substrato sólido (in Spanish): Santiago, Chile: Deparamento de Ingeniería Eléctrica, Universidad de Chile; 2001. p. 247.
20. Ghildyal NP, Ramakrishna SV, Devi PN, Lonsane BK, Asthana HN. Enzyme Microb Technol 1994; 16(3): 253–257. DOI: 10.1016/0141-0229(94)90051-5.
21. Khanahmadi M, Roostaazad R, Mitchell DA, Miranzadeh M, Bozorgmehri R, Safekordi A. Chem Eng Sci 2006; 61(17): 5654–5663. DOI: 10.1016/j.ces.2006.04.039.
22. Ogunnaike BA, Ray WH. Process dynamics, modeling and control. New York: Oxford University Press; 1994.
23. ASTM. Standard test method for determination of water (Moisture) content of soil by the Time-Domain Reflectometry (TDR) method. 2006. Copyright 2006 ASTM International.
24. Mitchell DA, Meien OFv, Krieger N. Biochem Eng J 2003; 13(2–3): 137–147. DOI: 10.1016/S1369-703X(02)00126-2.
25. Fernández M, Pérez-Correa JR, Solar I, Agosin E. Bioprocess Eng 1996; 16(1): 1–4. DOI: 10.1007/s004490050278.
26. Durand A, de la Broise D, Blachere H. J Biotechnol 1988; 8: 59–66.
27. Mitchell D, Berovič M, Krieger N. Solid-state fermentation bioreactors: fundamentals of design and operation. Berlin Heidelberg: Springer; 2006. DOI: 10.1007/3-540-31286-2.
28. Pérez-Guerra N, Torrado-Agrasar A, López-Macias C, Pastrana L. Electron J Environ Agric Food Chem 2003; 2(3): 343–350.
29. Weidgans BM. New fluorescent optical pH sensors with minimal effects of ionic strength. Naturwissenschaftlichen fakultät IV–chemie und pharmazie. Regensburg: Universität; 2004. p. 138.
30. Vojinovic V, Cabral JMS, Fonseca LP. Sens Actuators, A 2006; 114: 1083–1091. DOI: 10.1016/j.snb.2005.07.059.
31. Bragos R, Gamez X, Cairo J, Riu PJ, Gòdia F. Ann N Y Acad Sci 1999; 873(1): 299–305.
32. November EJ, Van Impe JF. Water Sci Technol 2001; 43(7): 97–104.
33. Soley A, Lecina M, Gámez X, Cairó JJ, Riu P, Rosell X, Bragós R, Gòdia F. J Biotechnol 2005; 118(4): 398–405. DOI: 10.1016/j.jbiotec.2005.05.022.
34. Escalante-Minakata P, Ibarra-Junquera V, Rosu HC, De León-Rodríguez A, González-García R. Bioprocess Biosyst Eng 2008; 32(1): 47–52. DOI: 10.1007/s00449-008-0219-3.
35. Mitchell D, Srinophakun P, Krieger N, Meien Ov. In: Mitchell DA, Krieger N, Berovic M, editors. Solid-state fermentation bioreactors: fundamentals of design and operation. Heidelberg, Germany: Springer; 2006. pp. 77–94. DOI: 10.1007/3-540-31286-2_7.

36. Lipták G-B. Instrument engineers' handbook: process control. Radnor, Pennsylvania: Chilton Book Company; 1995.
37. Richard TL, Veeken AHM, Wilde Vd, Hamelers HVMB. Biotechnol Prog 2004; 20(5): 1372–1381. DOI: 10.1021/bp0499505.
38. Auria R, Ortiz I, Villegas E, Revah S. Process Biochem 1995; 30(8): 751–756. DOI: 10.1016/0032-9592(95)00004-F.
39. Koutinas AA, Wang R, Webb C. Biochem Eng J 2003; 14(2): 93–100. DOI: 10.1016/S1369-703X(02)00154-7.
40. von Meien O, Luz LF, Mitchell DA, Pérez-Correa JR, Agosin E, Fernández-Fernández M, Arcas JA. Chem Eng Sci 2004; 59(21): 4493–4504. DOI: 10.1016/j.ces.2004.06.027.
41. Liptak BG. In: Liptak BG, editor. Instrument engineers' handbook: process measurement and analysis, Radnor, Pennsylvania: Chilton Book Company; 1995. pp. 523–601.
42. Camargo Prado F, Porto de Souza Vandenberghe L, Soccol CR. Braz Arch Biol Technol 2005; 48: 29–36.
43. Ooijkaas LP, Tramper J, Buitelaar RM. Enzyme Microb Technol 1998; 22(6): 480–486. DOI: 10.1016/S0141-0229(97)00246-9.
44. Sato K, Yoshizawa K. J Ferment Technol 1988; 66: 667–673.
45. González-Sepúlveda M. Producción de acido giberélico mediante cultivo sobre substrato sólido (in Spanish): Santiago, Chile: Departamento Ingeniería Química y Bioprocesos, Pontificia Universidad Católica de Chile; 2000. p. 141.
46. Smidt E, Meissl K. Waste Manage 2007; 27: 268–276. DOI: 10.1016/j.wasman.2006.01.016.
47. Suryanarayan S. Biochem Eng J 2003; 13: 189–195. DOI: S1369-703X(02)00131-6.
48. Saucedo-Castañeda G, Trejo-Hernandez MR, Lonsanme BK, Navarro JM, Roussos S, Dufor D, Raimbault M. Process Biochem 1994; 29(1): 13–24.
49. Fernández M, Ananías J, Solar I, Pérez R, Chang L, Agosin E, Roussos E, Raimbault M, Viniegra-Gonzalez G, editors. Advances in the development of a control system for a solid substrate pilot bioreactor. Advances in solid state fermentation. Dordrecht: Kluwer Academic Publishers; 1997. pp. 155–168.
50. Smits JP, Rinzema A, Tramper J, Schlösser EE, Knol W. Process Biochem 1996; 31(7): 669–678.
51. Wang H-H. Biotech Adv 1993; 11: 701–710.
52. Olsson J. Modern methods in cereal grain mycology. Uppsala: Department of Microbiology Swedish University of Agricultural Sciences; 2000. p. 37.
53. Montague G. Monitoring and control of fermenters. Rugby (UK): Institution of Chemical Engineering; 1997. pp. 36–45.
54. Sargantanis J, Karim M. Ind Eng Chem Res 1994; 33(4): 878–888.
55. Pérez-Correa JR, Fernández-Fernández M, Bustamante-Merino C. In: Rai R, Bhat R, editors. Biotechnology: concepts and applications. Daryaganj, New Delhi, INDIA: Narosa Publishing House; 2008. p. 300.
56. Welch G, Bishop G. An introduction to the Kalman Filter; Chapel Hill: University of North Carolina at Chapel Hill; 1995.
57. Fernández-Fernández M, Pérez-Correa JR. Process Biochem 2007; 42(2): 224–234. DOI: 10.1016/j.procbio.2006.08.003.
58. de Reu JC, Swietering MH, Rombouts FM. Appl Microbiol Biotechnol 1993; 40(2–3): 261–265. DOI: 10.1007/BF00170377.
59. Fenice M, Sermanni GG, Federici F, D'Annibale A. J Biotechnol 2002; 100(1): 77–85.
60. Peñaloza W, Davey CL, Hedger JN, Kell DB. J Sci Food Agric 1992; 59(2): 227–235.
61. Li X, Lei T, Wanga W, Xua Q, Zhao J. Catena 2005; 60(3): 227–237. DOI: 10.1016/j.catena.2005.01.001.
62. Vlachos NA, Karapantsios TD. J Food Process Eng 2000; 46(2): 91–98. DOI: 10.1016/S0260-8774(00)00073-X.
63. Robinson DA, Jones SB, Wraith JM, Ord D, Friedmane SP. Vadose Zone J 2003; 2: 444–475.
64. Kritz G, Khaled T. Acta Hortic 2004; 644: 313–318.
65. Agayn VI, Walt DR. Nat Biotechnol 1993; 11: 726–729. DOI: 10.1038/nbt0693-726.
66. Davey CL, Peñaloza W, Kell DB, Hedger JN. World J Microbiol Biotechnol 1991; 7(2): 246–259. DOI: 10.1007/BF00328998.
67. ABB. Available at http://www.abb.co.uk/cawp/seitp202/12439c2f1ac1a1a180256c800037b15d.aspx. Accessed, 2008.
68. Gervais P, Bazelin C. Biotechnol Lett 1986; 8: 191–196.
69. Mason IG. A study of power, kinetics, and modelling in the composting process. New Zealand: University of Canterbury; 2007. p. 436.
70. Auria R, Revah S. In: Galindo E, Ramírez OT, editors. Advances in bioprocess engineering. The Netherlands: Kluwer Academic Publishers; 1994. p. 289–294.
71. Pollard D, Buccino R, Connors N, Kirschner T, Olewinski R, Saini K, Salmon P. Bioprocess Biosyst Eng 2004; 24(1): 13–24. DOI: 10.1007/s004490100226.
72. Wissler MD, Tengerdy RP, Murphy VG. Dev Ind Microbiol 1983; 24: 527–538.
73. Richard TL, Walker LP, Gossett JM. Biotechnol Prog 2006; 22: 60–69.
74. Sipior J, Randers-Eichhorn L, Lakowicz JR, Carter GM, Rao G. Biotechnol Prog 1996; 12: 266–271.
75. Bajracharya R, Mudgett RE. Biotechnol Bioeng 1980; 25: 2219–2235.
76. Narahara H, Koyama Y, Yoshida T, Atthasampunna P, Taguchi H. J Ferment Technol 1984; 62(5): 453–459.
77. Sundström H, Enfors S-O. Bioprocess Biosyst Eng 2008; 32(2): 145–152. DOI: 10.1007/s00449-007-0157-5.
78. Smith CA, Corripio AB. Principles and practice of automatic process control. 2nd ed. Toronto: John Wiley & Sons Canada, Ltd.; 1997.
79. Maciejowski JM. Predictive control with constraints. Harlow, Essex, UK: Prentice-Hall; 2002.
80. Pérez-Correa J, Fernández M, Meien Ov, Luz L, Mitchell D. In: Mitchell DA, Krieger N, Berovic M, editors. Solid-state fermentation bioreactors: fundamentals of design and operation. Heidelberg: Springer; 2006. pp. 387–402. DOI: 10.1007/3-540-31286-2_28.
81. Mitchell DA, Krieger N, Stuart DM, Pandey A. Process Biochem 2000; 35(10): 1211–1225. DOI: 10.1016/S0032-9592(00)00157-6.
82. Mitchell D, Krieger N, Berovič M. In: Mitchell DA, Krieger N, Berovic M, editors. Solid-state fermentation bioreactors: fundamentals of design and operation. Heidelberg: Springer; 2006. pp. 65–76. DOI: 10.1007/3-540-31286-2_6.
83. Chen H, Xu F, Tian Z, Li Z. J Biosci Bioeng 2002; 93(2): 211–214. DOI: 10.1263/jbb.93.211.
84. Hoelker U. Patent 20,000,960,656. 2000.

85. Roussos S, Raimbault M, Prebois J-P, Lonsane BK. Appl Biochem Biotechnol 1993; 42: 37–52.
86. Troquet J, Larroche C, Dussap C-G. Biochem Eng J 2003; 13: 103–112. DOI: S1369-703X(02)00123-7.
87. Mitchell D, Srinophakun P, Meien Ov, Luz L, Krieger N. In: Mitchell DA, Krieger N, Berovic M, editors. Solid-state fermentation bioreactors: fundamentals of design and operation. Heidelberg: Springer; 2006. pp. 331–348. DOI: 10.1007/3-540-31286-2_24.
88. Fujiwara Techno-Art Co. Tomiyoshi, Okayama City 701-1133 Japan. Available at http://www.fujiwara-jp.com/product5_1_e.html. Accessed 2007 June 28.
89. Chamilec Y, Renaud R, Maratray J, Almanza S, Diez M, Durand A. Biotechnol Tech 1994; 8(4): 245–248. DOI: 10.1007/BF00155415.
90. Durand A. Biochem Eng J 2003; 13(2–3): 113–125. DOI: 10.1016/S1369-703X(02)00124-9.
91. Bandelier S, Renaud R, Durand A. Process Biochem 1997; 32(2): 141–145. DOI: 10.1016/S0032-9592(96)00063-5.
92. Vrije Td, Antoine N, Buitelaar RM, Bruckner S, Dissevelt M, Durand A, Gerlagh M, Jones EE, Lüth P, Oostra J, Ravensberg WJ, Renaud R, Rinzema A, Weber FJ, Whipps JM. Appl Microbiol Biotechnol 2001; 56(1–2): 58–68. DOI: 10.1007/s002530100678.
93. Ryoo D On-line estimation and control in solid substrate fermentation. Fort Collins: Colorado State University; 1990. pp. 56–80.
94. Barstow LM, Dale BE, Tengerdy RP. Biotechnol Tech 1988; 2(4): 237–242. DOI: 10.1007/BF01875535.
95. Cutler CR, Ramaker BL. Dynamix matrix control - a computer control algorithm. AIChE National Meeting; Houston, TX; 1979
96. Pérez-Correa JR, Fernández-Fernández M. Bioprocess Biosyst Eng 2006; 29(5–6): 399–407. DOI: 10.1007/s00449-006-0089-5.

FURTHER READING

A complete and up to date discussion regarding SSF bioreactor engineering, including automation, can be found in:
Mitchell D, Berovic M, Krieger N. In: Mitchell DA, Krieger N, Berovic M, editors. Solid-state fermentation bioreactors: fundamentals of design and operation. Heidelberg: Springer; 2006.
This book provides a broad and readable coverage of control theory and algorithms applicable to the process industries:

Ogunnaike BA, Ray WH. Process dynamics, modeling, and control. New York: Oxford University Press; 1994.
A detailed and up to date description of instrumentation and devices for automatic process control is in these books:

Lipták B.G. Volume 1, Instrument engineers' handbook, Process measurement and analysis. 4th ed. Boca Raton (FL): CRC Press; 2003.

Lipták B.G. Volume 2, Instrument engineers' handbook, Process control and optimization. 4th ed. Boca Raton (FL): Taylor & Francis/CRC Press; 2005.

66

STAINLESS STEELS

C.P. Dillon
C.P. Dillon & Associates, Hurricane, West Virginia

Stainless steels offer an unusual combination of strength, ductility, formability, weldability, corrosion resistance, and amenability to cleaning that makes them uniquely suitable for pharmaceutical and bioprocessing operations. This chapter discusses the origin and nature of stainless steels, the several groups and many grades of stainless steels, together with the fundamentals of the metallurgical differences. Specific corrosion phenomena that pose potential problems, together with preventive and remedial measures, are presented. I explain the basic nominal workhorse compositions, together with their potential weaknesses, and discuss the possible utilization of other more highly alloyed substitute alloys. Particular emphasis is laid upon measures for quality assurance, postfabrication cleanup procedures, and passivation treatments to ensure improved resistance toward specific types of localized corrosion.

66.1 THE NATURE OF STAINLESS STEELS

As a whole, stainless steels and similar chromium-rich alloys are characterized by their *passivity*. Passivity is a condition in which a base metal, such as iron, exhibits the corrosion behavior of a more noble metal or alloy. As described further here, passivity cannot be maintained under some specific conditions.

Steel is an alloy of iron and carbon plus other minor elements and is notorious for susceptibility to rusting. With even minimal corrosion, it is a source of iron contamination and is therefore objectionable in many services. However, when a minimum of 12% chromium (Cr) is alloyed with steel, the resulting metal is generally not susceptible to rusting under ordinary circumstances of exposure to the atmosphere or in substantially neutral aqueous solutions. (Certain exceptions, however, are described further here.) Actually, several types of stainless steels, which are characterized by specific properties, have been developed.

66.2 TYPES OF STAINLESS STEELS

The 12% Cr grades of stainless steels are predominantly "martensitic." Martensite is a needlelike structure resulting from heating and quenching iron-base alloys, which gives increased hardness and strength with a concurrent diminution of ductility. (A certain amount of ductility is restored by tempering, i.e., heating to some intermediate temperature.) The martensitic grades are exemplified by Type 410 (UNS S41000) (1) and are characteristically magnetic.

When the chromium is increased to about 17%, the material is magnetic but not amenable to hardening by heat treatment. Such alloys, exemplified by Type 430 (S43000), are classified as "ferritic" and are more corrosion resistant than the martensitic grades by virtue of their higher chromium content, although they have lower strength than heat-treated martensitic grades.

The "workhorse" materials for the process industries, however, are the "austenitic" grades, often loosely called "18-8" stainless steels. When about 8% nickel (Ni) is added to an 18% Cr steel, a face-centered crystal structure called austenite is formed that is characteristically nonmagnetic. (This structure exists only at elevated temperatures with steels and the straight chromium grades.) Austenitic stainless steels, exemplified by Type 304 (S30400) and Type

Upstream Industrial Biotechnology: Equipment, Process Design, Sensing, Control, and cGMP Operations, Volume 2, First Edition. Edited by Michael C. Flickinger.
© 2013 John Wiley & Sons, Inc. Published 2013 by John Wiley & Sons, Inc.

316 (S31600), have in general a remarkable combination of properties that occasion widespread use in the process industries as compared with the martensitic and ferritic grades, which are used much less frequently.

Stainless steels that contain 18% Cr or more are also alloyed with a lesser amount of nickel (about 5%) to form "duplex" grades, which are about 50:50 austenite and ferrite. This method results in alloys of higher strength than Types 304 (S30400), 316 (S31600), and so forth, with an improved resistance in aqueous environments of high chloride content. The newer duplex grades are exemplified by Alloys 2205 (S31803) and 255 (S32550).

Finally, there are "superferritic" grades such as Alloy 26-1 (S44626) and several "superaustenitic" alloys, exemplified by Alloys 254SMO (S31254) and 6XN (N08367). The superaustenitic grades have superior resistance to localized corrosion such as pitting, crevice corrosion, and stress corrosion cracking (SCC) in chloride-bearing environments. Also, they are as strong as duplex grades by virtue of nitrogen addition.

The compositions of some typical specific grades in these basic categories are given in Table 66.1, wherein the midrange of major elements is given with the maximum allowable concentration for minor elements. More detailed listings of stainless steel types and compositions are available (2–4).

66.3 CORROSION MECHANISMS

Corrosion of metals is electrochemical in nature, metal ions being formed at anodic sites by oxidation, accompanied by a discharge of electrons through the external (metallic) circuit. At cathodic sites, electrons provide reduction of specific species (e.g., dissolved oxygen, cations) in the electrolyte to complete the reaction equilibrium. This change is most apparent in galvanic (i.e., bimetallic) corrosion in which the anodes and cathodes are different materials (e.g., the galvanic corrosion of steel by contact with copper, or of zinc by contact with steel). However, it also occurs in monometallic corrosion, such as steel in water, wherein discrete local anodes and cathodes of a transient nature provide the reactions.

$$Fe^{\circ} \rightarrow Fe^{2+} + 2e \text{ (anodic)}$$

$$2H^{+} + 1/2O_2 \rightarrow H_2O \text{ (cathodic)}$$

The formation and dissipation of discrete anodes and cathodes cause the general, uniform corrosion typical of base metals.

When a metal or alloy is protected by a superficial layer of a composition different from the substrate (mill-scale on steel; oxide films on copper-, nickel-, or chromium-bearing alloys), anodic sites may be relatively stable at defects in the otherwise protective film, causing a more localized type

TABLE 66.1. Composition of Typical Stainless Steels

Grade	UNS #	C	Cr	Ni	Mo	Other
			Martensitic grades			
410	S41000	0.15	12.5	—	—	1 Si
420	S42000	>0.15	13.0	—	—	1 Si
			Ferritic grades			
409	S40900	0.08	11.0	—	—	1 Si, Ti 6 × C
430	S43000	0.12	17	—	—	1 Si
444	S44000	0.025	18.5	1.0	2.0	Ti, Nb, N
			Austenitic grades			
304	S30400	0.08	19	9	—	1 Si
304L	S30403	0.03	19	10	—	1 Si
316	S31600	0.08	17	12	2.5	1 Si
316L	S31603	0.03	17	12	2.5	1 Si
317L	S31703	0.03	19	13	3.5	1 Si
Duplex grades						
329	S32900	0.08	25	3.5	1.5	0.75 Si
2205	S31803	0.03	22	5.5	3.0	0.08–0.20 N
255	S32550	0.04	25	5.5	3.0	1.5–2.5 Cu
			Superaustenitic grades			
254SMO	S31254	0.02	20	18	6.0	0.8 Cu, 0.20 N
367XN	N08367	0.03	21	24.5	6.5	1 Si
28	N08028	0.03	27	31	3.5	1.0 Cu
20Mo6	N08026	0.03	26	35	5.5	0.5 Si

of attack. This reaction is somewhat analogous to galvanic corrosion, the film acting as a cathode to the more anodic substrate.

66.4 CORROSION SUSCEPTIBILITY OF STAINLESS STEELS

The stainless steels in general resist corrosion because of the formation of an invisible oxide film that renders them passive in oxidizing environments. The semipermanent surface passive film is very thin (about 0.1 nm), analogous to ice on a pond. This passive film of chromic and silicon oxides plus adsorbed oxygen can be increased in thickness by exposing it to oxidizing solutions or by anodic passivation using an electrochemical technique. (Note: Electropolishing is followed by another electrochemical treatment to reform and enhance the passive film following anodic dissolution of the alloy. If the film is solubilized, as by reducing acids such as hydrochloric or dilute sulfuric, stainless steels change from a passive to an active state and are actually less resistant than ordinary iron and steel.) Most applications of stainless steels are in air, aerated water, and other oxidizing media wherein the passive film is retained. It should be noted that stainless steels are *autopassivating*; the film reforms immediately if removed by mechanical means (e.g., abrasion) when the alloy is subsequently exposed to air, water, or other oxidizing environments. They do not demonstrate the active state except under continuous abrasion or conditions of immersion in reducing environments.

Stainless steels are resistant to general corrosion in most applications, with corrosion rates <4–5 mpy. When data are reported showing general corrosion rates of 10, 20, or 50 mpy, this indicates that the alloy is fluctuating between an active and a passive state and should not be used in that specific environment. Unfortunately, despite their passive nature, stainless steels are subject to several forms of localized attack. These are described further for the austenitic grades, which are the primary alloys for bioprocessing applications (5).

66.5 FORMS OF LOCALIZED CORROSION

66.5.1 Pitting

Pitting can occur on boldly exposed surfaces in high-chloride environments, such as brackish cooling waters or dilute hypochlorite solutions (e.g., during sanitizing operations). The molybdenum-free alloys such as Type 304L (S30403) are more susceptible to pitting than molybdenum-bearing alloys in chloride-bearing environments, and the problem is combated by specifying successively higher grades, that is, Type 316L, Type 317L (S31703), and the 6% Mo grades as required by the severity of the environment.

66.5.2 Crevice Corrosion

Crevice corrosion is a special form of pitting occurring in physical or mechanical crevices (e.g., flanges, threaded fasteners) or under surface films. When it occurs under calcareous deposits, biomasses, or other foreign material, it is known as "under-deposit corrosion" or UDC. Typically, crevice corrosion is driven by a dissolved oxygen (DO) cell, the oxygen-starved crevice functioning as an anode to the boldly exposed cathodic area where the DO constitutes a cathodic depolarizer. However, the cell can also be driven by dissolved sulfur (DS) or by differences in metal ion concentrations. Crevice corrosion is aggravated by chloride contamination, the chlorides being attracted to the anodic sites and producing a locally low pH (e.g., pH 2) from acid chlorides within the crevice.

66.5.3 Sensitization

When the regular carbon grades such as Types 304 (S30400; 18 Cr–8 Ni–0.08 C maximum) or 316 (S31600) are heated in the temperature range from about 800° to 1,500°F (as by slow cooling from the annealing process or from thermal stress-relieving treatment, or in the heat-affected zones of welds), carbon migrates to the grain boundaries and precipitates as chromium carbides. This leaves a chromium-depleted zone around each grain and causes a susceptibility to intergranular corrosion (IGA) in many environments. When IGA is observed in the heat-affected zone of welds, it is commonly called by the misnomer "weld decay," although it is not the weld itself that suffers corrosion. Sensitized areas are also more prone to chloride pitting than are unaffected areas such as those at some distance from welds.

Conventional sensitization by chromium carbide precipitation was originally combatted by addition of stabilizing elements, that is, columbium (niobium) or titanium, to an 18-8 alloy such as Type 304 (S30400). When stabilizing elements are present in concentrations several times the carbon content, it is their carbides that precipitate, thereby avoiding chromium depletion. The stabilized grades such as Types 321 (S32100) and 347 (S34700) are therefore derivatives of Type 304 containing Ti and Cb, respectively, and are still used in some special applications. It should be noted that titanium-stabilized grades such as S32100 require a stabilizing anneal at about 1,600°F to tie up the carbon in the form of titanium carbides before welding. IGA may occur

even in stabilized or low-carbon grades if weldments are carbon-contaminated by oil or grease.

The stabilized grades can themselves become sensitized by multipass welding or cross-welding, causing knife-line attack (KLA); this is caused by a resolubilizing of the columbium or titanium carbides by the heat of welding, followed by slow cooling. This step requires about 1,250°C (2,300°F) reheating in 18-8 grades, moving the susceptible area to the fusion zone, and permitting a very narrow band of corrosion immediately adjacent to the weld (KLA). With higher nickel content, the resolubilization temperature drops; Alloy 20Cb3 (N08020) and Alloy 825 (N08825) with nickel contents in the 35% range are more easily sensitized to KLA (about 980°C or 1,800°F) than is type 347.

In modern practice, the problems of sensitization have been largely alleviated by use of low-carbon grades (Type 316L, S31603; 17 Cr–12 Ni–2.5 Mo–0.030 C maximum), although sensitization will occur with very prolonged exposure in the sensitizing range (e.g., in long-time service >800°F or when stainless steel–clad vessels are thermally stress relieved). Modern-day steel-making practice using argon–oxygen decarbonation (AOD) makes very low carbon grades of stainless steels routinely available.

IGA may also occur due to mechanisms other than carbide precipitation. A ferrite phase, if present for any reason, may be selectively attacked by reducing acids such as hydrochloric or sulfuric; its thermal conversion product, sigma phase, is selectively attacked by oxidizing acids (e.g., nitric). Chi phase can form in molybdenum-bearing grades (S31603) as the result of prolonged heating in the sensitizing range (e.g., thermal stress relief of clad-steel vessels), producing IGA in alloys of <0.030% carbon in certain aggressive environments.

66.5.4 Selective Weld Corrosion

Selective or preferential attack is sometimes encountered in weldments, particularly in the molybdenum-bearing grades. This can occur either in conventional welds or autogenous welds (i.e., welds made without the addition of filler metal) in some environments. This type of attack is ascribed to microsegregation, which causes a maldistribution of the molybdenum component of the alloy.

Selective weld corrosion is the reason for the cold-work requirement for welded stainless steel condenser tubes (see ASTM A249). Cold-working to minimum requirements before the final anneal allows the weld to recrystallize and homogenize, alleviating the microsegregation.

For butt welds in piping and fabrication welds in tanks and vessels, no such cold-work is feasible. Instead, an overmatching rod is used to confer higher resistance to the weld itself, for example, alloy 254SMO (S31254) to weld S31603 or S31703 or alloy 625 (N06625) to weld S31254.

66.5.5 Stress Corrosion Cracking

The predominant form of environmental stress cracking (ESC) in the 18-8 varieties of stainless steels is anodic stress corrosion cracking (SCC) under either applied or residual tensile stress. Compressive stress will not cause SCC, and indeed application of *compressive* surface stress, as by shot-peening, is sometimes used as a palliative surface treatment against SCC. Only the martensitic grades are subject to hydrogen-assisted cracking (HAC), a form of ESC found, for example, in "sour" service due to hydrogen sulfide effects.

The most common form of SCC of 18-8 austenitic grades is caused by chloride contamination. The ubiquitous chloride is sodium chloride (NaCl, table salt), as found in water and atmospheric exposures. NaCl usually causes SCC only between about 50°C (120°F) and 200°C (390°F). However, SCC can occur at room temperature and even at cryogenic temperatures in the presence of other chlorides, such as ferric chloride, sulfuric–NaCl mixtures, aqueous solutions of hydrogen sulfide–NaCl, and hydrogen chloride (HCl). For boldly exposed surfaces, there are rough correlations between pH and chloride concentration at which SCC may be anticipated. There is no minimum chloride concentration below which SCC will not occur if there is any possibility of concentration, either by evaporation or by occlusion or adsorption in films adhering to the stainless surface (e.g., mill scale, heat tints, welding slag, rust deposits, calcareous deposits, biomasses).

External stress corrosion cracking (ESCC) occurs when chlorides from the atmosphere, water leaks, or insulation concentrate on the surface of an 18-8 type stainless steel pipe or vessel. This is best combatted by coating vessels and piping that are more than 4 in in diameter and that operate between 60 and 200°C, using a zinc-free and chloride-free paint system (6,7).

Hot caustic can also cause SCC of 18-8 stainless steels, as frequently happens when high-pressure steam is contaminated by carryover of alkaline boiler-treating chemicals. This is a potential problem in steam lines and during sterilization procedures. Use of nickel-base alloys such as N06625 or better (but not N08800 or N08825) is effective against caustic SCC.

66.5.6 Rouging in High-Purity Water

Austenitic stainless steels are subject to superficial rusting under some circumstances, either because of tramp iron embedded in the surface or from chloride contamination by corrosive atmospheres or water environments. The former problem is addressed through standard cleaning and passivation techniques described further next.

An apparently separate problem, "rouging," is sometimes observed with clean stainless steels in high-purity water at about 80°C (175°F) (8). Strictly speaking, rouge

consists of a thin red deposit of α-Fe_2O_3 which is usually loosely adherent, wiping off easily. Generally, very little corrosion of the surface is evident. Typically, rouging is experienced in high-purity deionized water such as WFI ("water for injection") in the pharmaceutical industry, and UHPW ("ultrahigh-purity water") in the electronics industry and in nuclear reactor systems. When the U.S. Food and Drug Administration and solutions for human injection are involved, the presence of red-colored oxide on the surfaces of stainless steel equipment is not acceptable. Also, the standards for ultrahigh-purity water in the electronics industry do not permit this sort of condition.

One explanation that has been advanced to explain the fairly recent development of this phenomenon relates to modern steel-making processes. The AOD process itself gives a precise control that permits the manufacturer to work at the lowest ranges permissible for alloying elements, for example, chromium, within the nominal range specified. During long-time hot-working and annealing, the stainless steels form a chromium oxide scale that depletes the metal substrate of Cr. Modern short-time "spray pickling" may not be adequate to dissolve the depleted layer, leaving a surface of somewhat lesser corrosion resistance than the nominal analysis. However, even minor mechanical abrasion restores the proper surface chemistry, and electropolishing, although not simple nitric acid "passivation," which does not attack alloys with as little as 11% Cr, also does so.

A rouge of loose ferric oxide has been developed on Type 304L in laboratory tests in deionized water at 250°C, simulating a reactor loop. When the water was cooled for sampling and filtered through a 0.1-μm PTFE filter supported on a 0.2-μm silver filter, no deposits were found on the PTFE but large crystals of spinel ferric oxide (with traces of Cr and Ni) had developed on the silver filter and grown back into the PTFE from the backside. This reaction suggests either soluble or colloidal iron in the nearly supercritical (288°C or higher) water. Loose rouge has also been observed in hot aggressive waters (e.g., WFI) as low as 80°C (175°F) from sterilizing procedures with stainless steels in the pharmaceutical industry. Some operators have used solutions of sodium hydrosulfite ($NaHSO_3$) to reduce and remove rouge from their systems.

Some authorities state that the term *rouging* is a misnomer because the films may be either the powdery red iron oxide or adherent films of various colors including gray, black, purple, blue, and even yellowish green. In practice, it is often difficult to distinguish between superficial corrosion (involving a black substrate under a reddish-brown crust, associated with craters and white debris) and extraneous deposits (9). Heat tints and similar films exhibit colors related to their thickness and, although they can occlude and concentrated corrosive species such as chlorides, should not be considered rouge.

In one case, an electropolished Type 316L filter plate developed a blue-black tint, with no apparent corrosion of the parent metal, in ultrahigh-purity water of reportedly ambient temperature or at least not more than about 55°C (130°F). Analysis determined that the film contained more than 85% iron as a black oxide, probably derived from equipment upstream and entering the system, perhaps during regeneration of the mixed ion exchange beds.

66.6 FACTORS CONTRIBUTING TO LOCALIZED CORROSION

Some factors that contribute to the occurrence of localized corrosion in the stainless steels are surface defects or foreign matter. Surface defects are undercut welds, scratches, and grinding marks, which can initiate localized attack.

Foreign matter constitutes embedded iron or iron oxides (usually from mill or shop contamination of the stainless steel surface), the bluish heat tints adjacent to welds, weld splatter or arc strikes, and paint or crayon markings. Iron oxides and heat tints can occlude and concentrate chlorides and are themselves susceptible to corrosive attack. Weld splatter and arc strikes weaken the surface film and may constitute crevices for the initiation of attack. Paints and crayon markings may contain organic chlorides, which can hydrolyze or thermally degrade to release traces of hydrochloric acid and promote localized attack.

Bacterial effects in unsterile water, for example, residual hydrotest water, can also cause localized attack. The production of traces of hydrogen sulfide by sulfate-reducing bacteria (SRBs) and the excretion of iron or manganese oxides by aerobic strains can cause serious pitting in a very short time. Sulfides compete with oxygen and weaken the passive film, contributing to pitting and SCC. Microbiologically induced corrosion (MIC) has attracted increasing interest in the process industries.

66.7 PREVENTION OF LOCALIZED ATTACK

To prevent or minimize the possibility of localized corrosion, a specific sequence of events must be established. The methodology for this starts with proper materials and design and the establishment of certain procurement details in the materials selection, specification, and inspection phases, plus postfabrication cleanup and preservice sanitizing or other preparatory steps.

66.7.1 Materials

Materials must be properly chosen for the expected conditions of fabrication and service. The alloys chosen should be indicated by the proper alloy designation or

corresponding UNS number, and these should be allied with an appropriate ASTM or ASME specification and any necessary supplements.

For best results, cast components, such as pumps and valves (which are predominantly CF8M and CF3M, the cast equivalents of types 316 and 316L), should be purchased to ASTM A743 with a special annealing temperature requirement. Annealing at about 1,120°C reduces the tendency toward molybdenum gradients within the casting, ensuring a more uniform corrosion resistance.

To avoid materials mixups, such as may occur either at the manufacturer's plant or in warehousing, the composition of the alloy should be verified not only by checking the mill analysis but also by spot-test or nondestructive metal identification procedures; this is particularly necessary when a molybdenum-bearing alloy has been chosen. Inadvertent substitution of Type 304L for 316L has caused many problems in process applications. The fact that a piece of stainless steel is clearly marked as Type 316L, Heat No. *X*, is not a guarantee.

Finally, special finishes may be required. The several commercial finishes (in decreasing order of surface roughness) are numbered 1 (hot-rolled, annealed, and pickled) through 8 (a mechanically polished and buffed specular finish, with no visible abrasive scratches). For bioprocessing applications, a number 2B finish (cold-rolled, annealed, pickled, and temper-rolled) or a number 4 (which adds a 150-grit abrasive belt grinding to the 2 B finish) is usually specified.

For extra smoothness in special nonstick applications or to facilitate removal of bacterial contaminants, stainless steel may be electropolished to a mirror finish in lieu of a number 8 finish. Electropolishing aids surface homogenization and autopassivation, and an actual anodizing can be added as the final step to enhance the passive film.

66.7.2 Design

Because localized corrosion causes about 90% of the failures experienced with stainless steels in process applications, vessels, piping, and ancillary equipment must be designed, purchased, and maintained to minimize the risk of such attack. This requires that crevices, pockets, and traps should be avoided, thereby minimizing the probability of localized corrosion.

All fabrication steps, such as bending, forming, and welding, should conform to standard procedures. The welds must be full penetration to prevent crevice corrosion in incompletely fused joints. Fillet welds should be smooth and continuous, with no undercutting. Butt welds should be smooth and corner welds should be avoided if possible; side-wall welds in tanks are preferable. Lines and vessels should be sloped and self-draining, and top nozzles, side ports, and bottom nozzles must be accessible for cleaning.

A postweld chemical cleaning with an ammoniated citric acid solution, as described next, will remove the heat tints from the welded heat-affected zones (HAZ).

66.8 REMEDIAL MEASURES

66.8.1 Pickling

Because stainless steels are chosen for appearance, corrosion resistance, and freedom from product contamination in storage and shipment, pickling (to remove contaminants) or passivation (to augment the naturally occurring surface film) is often required. A surface of assured cleanliness, uniformity, and corrosion resistance is desirable and, in some services, absolutely required.

During fabrication, stainless steels are subject to contamination by embedded steel particles or iron oxides, as well as heat tints caused by welding. The alloy surface may be cleaned with acid solutions or pastes, mechanically cleaned with a stainless steel wire brush or a clean abrasive disk, or hydroblasted with high-pressure water of potable water quality (i.e., <250 ppm Cl^-). ASTM A 380, "Cleaning and Descaling Stainless Steel Parts, Equipment, and Systems," provides detailed procedures. Demineralized water is usually specified for critical services, but a 25-ppm maximum chloride limit should be adequate.

Embedded iron is subject to air oxidation to hydrated ferric oxide ($Fe_2O_3 \cdot H_2O$). Foreign rust particles or mill scale (Fe_3O_4) may also be present. "Pickling" (see following) is intended to effect the desired cleanliness while simultaneously homogenizing the surface. A solution of 10–15% nitric acid and 1–3% hydrofluoric (HF) acid has been used as a "bright pickle" to remove visible oxides, while pastes of similar composition are available for localized application. Such solutions and pastes constitute somewhat of a safety hazard to personnel, as well as potential disposal problems, but are very effective. (Note: There is increasing resistance to using HF mixtures today because of the safety concerns and disposal problems related to environmental considerations.)

A HNO_3–HF mixture, unlike nitric acid itself, is a reducing acid intended to remove iron oxides and other metallic oxides by chemical reduction. This mixture is not a passivating medium, and corrosion rates are high during the actual exposure. However, a uniform passive oxide film will reform over the freshly cleaned surface after removal of the pickling environment by autopassivation.

Heat tints from welding tend to adsorb chlorides, with attendant pitting or stress corrosion cracking. They may be removed by abrasive disks or with a nitric–HF paste. Citric acid solutions, such as a 5% solution adjusted to pH 3.5 with ammonia and used at about 80°C, are very effective and are to be preferred for removing heat tint from bioprocessing equipment. This solution is a chelating agent

as well as an acid cleaning medium. Unlike the nitric–HF materials, citric acid solutions are benign and quite readily disposable from the environmental standpoint. However, chelants incorporate the metal ions within a clawlike ringed structure that may pass through conventional waste treatment systems. When heavy metals (i.e., chromium, copper, nickel, and zinc) are involved, special waste treatment systems, rather than simple sanitary drain systems, may be employed.

Antisplatter pastes are sometimes used to minimize weld-splatter sticking. If such splatter has adhered to the adjacent areas, it should be removed by a flapper wheel, wire-brushing, or hydroblasting. A cleaning operation with organic reducing acids may be followed with an alkaline sodium nitrite neutralizing–oxidizing rinse. (Note: Adequate provision must be made for proper disposal of the chemical solutions in accordance with environmental regulations.)

Electropolishing, in which the work serves as the anode during electrochemical dissolution to produce a highly polished nonstick and uncontaminated surface, is a specialized form of chemical cleaning in which the surface is actively corroded during the operation. Although the stainless steel surface will passivate on rinsing and exposure to air, many users specify a final anodizing step, which is tantamount to chemical passivation.

66.8.2 Passivation

Cleaning and pickling, as described, and passivation of stainless steels, particularly in the widely used austenitic 300 series, for example, Types 304 (S30400), 304L (S30403), 321 (S32100), 347 (S34700), 316 (S31600), 316L (S31603), and 317L (S31703), are widely misunderstood.

Cleaning and pickling are intended to remove foreign materials and permit the surface to equilibrate or homogenize, effecting an electrochemically uniform surface for resistance to localized corrosion. Passivation has been defined as a reduction in the rate of the anodic reaction of an electrode involved in corrosion, as by formation of a protective oxide film.

As previously noted, stainless steels are self-passivating on exposure to air and moisture as the result of their high chromium content (i.e., >11%). Passivation treatment consists of augmenting the naturally occurring protective oxide film by chemical or electrochemical methods. The enhanced passive film is somewhat thicker and more persistent than that formed by autopassivation. For example, in some iron-sensitive organic chemicals (e.g., acetoacetanilide, glyoxal), stainless steel vessels are specially passivated and repassivated at intervals thereafter whenever chromophoric corrosion products are detected in the chemical product. This practice suggests a gradual diminution in thickness (or localized weakening of) the passive film with time in some services. Passivating is accomplished by treatment with oxidizing solutions, such as warm dilute nitric acid (not nitric-HF), ammonium persulfate (which is very safe to handle), dilute hydrogen peroxide, and citric acid–sodium nitrate mixtures.

Table A2.1 of ASTM A 380, Part II, recommends passivation with 20–50% nitric acid at 49–71°C (120–160°F) for 10–30 min or 21–38°C (70–100°F) for 30–60 min for dull or nonreflective surfaces. In the latter case, a 10% caustic–4% potassium permanganate solution is suggested for smut removal after the final rinse. A 20–40% nitric acid with 2–6% sodium dichromate is suggested for bright-machined or polished surfaces, instead of straight nitric acid. Such solutions are also used for precipitation-hardening (PH) grades, 12–14% chromium grades, and high-carbon martensitic grades, such as Type 440 (S44000). However, chromates are not compatible with pharmaceutical products. (Note: In chemical plants, large tanks or vessels are usually passivated with 10–15% nitric acid at 66°C (150°F) for about 4 h.) A 1% citric acid–1% sodium nitrate solution at 21°C (70°F) is discussed in ASTM A 380, Part III. The dairy industry has used a 0.5–1.0% nitric acid for 10 min at 65–82°C (150–180°F).

A special sequence of alkaline–acid–alkaline (A-A-A) treatment is recommended for free-machining grades (10). Because oil or grease interferes with passivation and because attack on sulfur or selenium inclusions in Type 303 (S30300) and its variants can leave minute pits with residual corrodents on the metal surface, the machined parts are (*1*) degreased for 30 min in 5% sodium hydroxide at about 70–80°C (160–180°F) and rinsed, (*2*) immersed in 20% nitric plus 3 oz. per gallon sodium dichromate at 50–60°C (120–140°F) for 30 min and rinsed, and finally (*3*) neutralized in the original caustic solution.

Because oil or grease can interfere with self-passivation by preventing ready access of water and oxygen to the metal surface, degreasing may be required. Such contamination occurs primarily from machining operations and should be removed by degreasing with nonchlorinated solvents before passivation is attempted. (Note: Chlorinated solvents may introduce inorganic chloride ions, Cl^-, by hydrolysis or by thermal degradation, and are proscribed.)

Note that nonoxidizing solutions, such as ammonium citrate, hydroxyacetic–formic acid mixtures, and EDTA (ethylenediaminetetraacetic acid) instead of a nitric acid passivation are described in ASTM A 380, Part III. The dairy industry uses a 0.5–1.0% phosphoric acid solution at 65–82°C (150–180°F) for 10 min. These nonoxidizing solutions used to remove iron or iron oxides only equilibrate the surface, facilitating autopassivation. They do not actually enhance the film as do the true passivation procedures.

66.8.3 Sanitizing

As a final step (or between batch operations), it is frequently desirable or even necessary to sterilize stainless steel equipment. Sodium or calcium hypochlorite is most frequently utilized, but the oxidizing capacity and chloride content pose serious potential dangers for pitting or crevice corrosion. The conditions and time of exposure and the proper steps to flush the hypochlorites from the system, including low spots, is of paramount importance. Serious failures have occurred in numerous stainless steel installations when adequate measures to preclude attack during treatment or by residual hypochlorites were not taken. Treatment with ozone or dilute hydrogen peroxide, as well as by ultraviolet light, seems to provide useful alternatives.

66.9 STANDARD OPERATING PROCEDURES

To summarize, the recommended sequence of treatment of fabricated stainless steel equipment for pharmaceutical applications should embrace the following steps:

1. A pretreatment with solvent or detergent to remove oil, grease, and the like
2. A rinse with water of suitable quality (deionized water being preferred)
3. Necessary pickling or other cleaning operations
4. Passivation
5. Water rinsing
6. Sanitizing
7. Final water rinse; drain and dry

A proper understanding of service conditions and requirements is essential if the several possible cleaning, pickling, and passivation treatments are to be successfully employed for their respective end purposes.

The most valuable resources for practical information on corrosion and corrosion prevention of stainless steels are as follows:

- NACE International (standards and publications), Houston, Tex.
- The Nickel Development Institute (AISI, INCO, and NiDI publications), Toronto, Ontario, Canada
- ASTM International (specifications), Barr Harbor, Pa.
- The Materials Technology Institute of the Chemical Process Industries, Inc. (publications), St. Louis, Mo.

REFERENCES

1. Metals & Alloys in the Unified Numbering System, SAE HS-1086, ASTM DS-56 E, 6th ed., American Soc. for Testing and Materials, Philadelphia, 1993.
2. C.P. Dillon, Corrosion Resistance of Stainless Steels, Dekker, New York, 1995.
3. High-Performance Stainless Steels, NiDI Reference Book Series No. 11021, Nickel Development Institute, Toronto, 2000.
4. Castings: Stainless Steel and Nickel-Base, NiDI Reference Book Series No. 11022, Nickel Development Institute, Toronto, 2001.
5. C.P. Dillon, D.W. Rahoi, and A.H. Tuthill, BioPharm 5: 3–6 (1992).
6. C.P. Dillon, Corrosion Control in the Chemical Process Industries, 2nd ed., Publ. 45, MTI, St. Louis, Mo., 1994.
7. Guidelines for Preventing Stress Corrosion Cracking in the Chemical Process Industries, Materials Technology Institute of the Chemical Process Industries, St. Louis, Mo., 1985.
8. P.H. Banes, Bioprocess Eng. 1993.
9. D.C. Coleman and R. Evans, Pharm. Eng. 11: 1991.
10. T. DeBold, Machine and Tool Blue Book, November 1986.

67

STATIC MIXING, FERMENTATION PROCESSES

Radu Z. Tudose
Technical University Gh.Asachi Iaşi, Iaşi, Romania
Maria Gavrilescu
Research Centre for Antibiotics, Iaşi, Romania

67.1 INTRODUCTION

The intensification of transfer processes in bioreactors using techniques that do not require additional energy costs is of great interest in biotechnology. Traditionally, most bioprocesses, especially aerobic fermentations, are conducted in stirred-tank bioreactors, which require considerable power input to attain adequate oxygen transfer rates. Besides the conventional mechanically agitated fermenters, other types of gas–liquid contactors are used, as pneumatic or jet bioreactors with or without a loop. Advantages of these nonmechanically agitated bioreactors are known to include efficient use of energy for aeration, simple design, and construction. To improve transfer processes in these bioreactors, considerable efforts have been made to study all the essentials of the major relationship for flow, mass and heat transfer over plates, cylinders, baffles, and spheres as well as through sieves and trays. These are the simplest and the oldest contacting bodies, and also are the basic shapes for other contacting devices of practical interest. Both theoretical and experimental studies on flow around these internals together with heat and mass transfer approaches are available (1–4).

Recently, new constructive types of internals known as static mixers or motionless mixers have been developed that supply spectacular effects concerning transfer rate increase. The first of these unconventional mixers was developed for viscous fluids about 30 years ago (5). After a slow start, the development of static mixers has been proceeding since 1970. Static mixers are applied in many operations in heterogeneous systems that require larger contact areas, thermal homogenization, and mass transfer. Today, these devices placed in column bioreactors are increasingly considered for use in fermentation industries, sometimes replacing the traditional mechanically agitated bioreactor design. Static mixers are suitable particularly for use in shear-sensitive cell cultures because of their lower shear rates, compared to those in mechanically agitated bioreactors. They proved to consider some specific criteria in the design of a bioreactor system for a definite process: population damage, energy distribution, and oxygen demand of a culture. The relatively numerous investigations and works that refer to static mixers are concerned with their influence on different process transfer parameters not only in fermentation systems, most of them being performed in model systems, in monophasic and polydispersed laminar or turbulent flow (usually gas–liquid dispersions), using low and viscous liquids, with Newtonian or non-Newtonian rheological behavior.

Static mixers frequently require no additional space (in-line assembly) and can be used as compact inserts or with a distance between the elements. They act on hydrodynamic conditions for turbulence development, the increase of contact areas, or the intensification of driving forces, separately or simultaneously. In all cases, the energy for process intensification is extracted from the fluid flowing through the mixers.

Upstream Industrial Biotechnology: Equipment, Process Design, Sensing, Control, and cGMP Operations, Volume 2, First Edition. Edited by Michael C. Flickinger.
© 2013 John Wiley & Sons, Inc. Published 2013 by John Wiley & Sons, Inc.

67.2 STRUCTURAL TYPES AND CONSTRUCTION

Static mixers can be of numerous constructive types, made of tubes, sheets, helixes, or wire matrix. They can be manufactured by steel, ceramic, or plastics. Their effect depends on the construction of the mixing element and the capacity to produce continuous separation, distribution, and reuniting the fluid stream. Besides their multiple advantages, static mixers often have the difficulty of a complicated structure. At the present time, most of the problems in the construction of static mixers have already been solved, and a number of different types of static mixing systems are being manufactured on an industrial scale, so that about 30 types of static mixers are known today. One of the most important moments in static mixing presentation was the ACHEMA '79 Exhibition in Frankfurt/Main (5). This section discusses some of the most interesting, familiar and, at the same time, most structurally dissimilar static mixers.

67.2.1 Static Mixers from Tubes or Short Pipes

Static mixers from tubes or short pipes generally affect the spatial distribution of the fluid by twisting, distorsion, and expansion of fluid elements in specially designed flow arrangements. For instance, the Ross-ISG static mixer (Aachener Misch- und Knetfabrik) is made by elements turned through 90°, placed one behind other. Over the cross-section of an element there are four obliquely sloped channels twisted with an angle of 120° (Fig. 67.1a), forming a tetrahedral space between elements. The PRM mixer (Prematechnik, Frankfurt/Main) consists of a tubular packet containing obliquely arranged partial tube sections (Fig. 67.1b), which change the direction of the fluid stream (5). Another static mixer used in laminar flow conditions, especially to equalize the distribution of the flow residence time, consists of six guiding holes, directed in the direction of flow (Fig. 67.1c). A portion of the fluid stream, which flows through the central section in front of the device, has a higher mean velocity and crosses the channels that direct it to a zone with a low mean velocity. Other parts of the fluid stream that flow near the pipe wall cross over the channels that direct them to the central zone of the pipe behind the static mixer. Therefore, the positions of the fluid streams that flow with different velocities are inverted (6–8).

67.2.2 Static Mixers of Plates or Sheets

The effects of these static mixers depend on the continuous cutting, subdividing, distribution, and reuniting the stream of fluid. The PSM mixer (Petzhold, Frankfurt/Main) (Fig. 67.2a) contains rectangular and conical channels combined with conical holes resulted from a special arrangement of

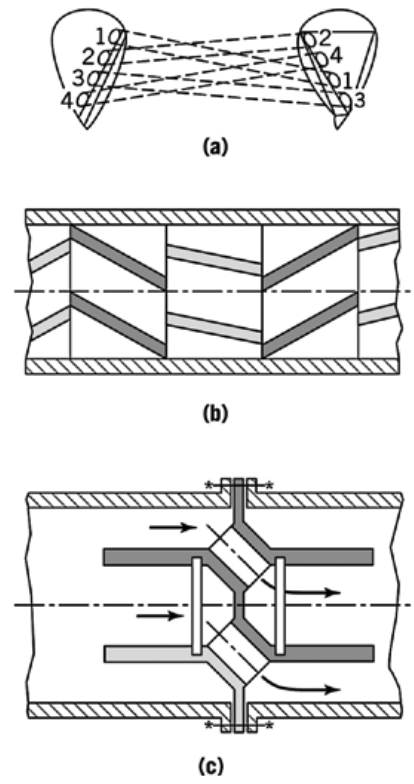


Figure 67.1. Static mixers made from tubes or short pipes. *Source*: Reprinted from Ref. 5, with permission from VCH Verlagsgesellschaft mbH, and from Ref. 7, with permission from Wiley-VCH.

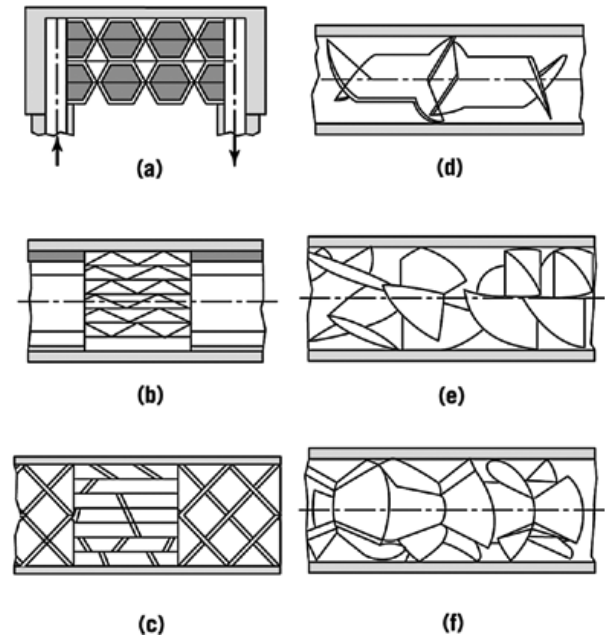


Figure 67.2. Static mixers made from plates and sheets. *Source*: Reprinted from Ref. 5, with permission from VCH Verlagsgesellschaft mbH and from Ref. 7, with permission from Wiley-VCH.

individual plates. The fluid flows from the entry to the exit of the static mixing element, being subdivided through a central hole, a conical space created by tangentially arranged slots and furthermore through other channels and openings (5). Sulzer mixers (Sulzer Brothers Ltd., Switzerland) are adequate for both laminar and turbulent regimes. They are constructed in many different ways (SMV, Fig. 67.2b; SMX, Fig. 67.2c) from stacks of corrugate sheets with open crossing channels. The SMX mixer consists of strips inclined to one another that form frameworks with the axis perpendicular to the column axis. The mixing elements are arranged successively in the column turned through 90° one to another. The SMLX mixer type is constructed from corrugate sheets with a distance between the strips increasing in the flow direction. The crossing angle of the sheets is 60°. These static mixers made of corrugate sheets can be mounted in packed form in compact arrangement or with distance between packets in different nonmechanical bioreactors (9). The Komax mixer (Long Beach, Calif.) contains triangular-shaped channels, made by the bent ends of the slotted sheets that form the mixing element (Fig. 67.2d). The Koch mixer (10,11) contains a numer of in-line elements mounted alternately at right angles to each other. The mixing elements are made from layers of corrugate metal sheets joined one to another, forming opened intersecting channels. C_1 and C_2 mixer types (12) (Figs. 67.2e and f, respectively) developed in the Central Institute of Physical Chemistry of the German Academy of Sciences and the Pyrapak 480 type developed at the CLG Leipzig-Grimma were also manufactured out of metal sheets.

67.2.3 Helical Static Mixers

The Kenics mixer (Ott Vertriebsgeselschaft, Leonberg) is made of counterclockwise and clockwise rotational elements twisted at 180°, being mounted in tubes alternating left and right with perpendicular leading edges (Fig. 67.3a). A particular form of this helical static mixer consists of an unbroken continuous helical surface that may have the diameter of a screw identical or smaller than the inner diameter of the tube (13) (Fig. 67.3b). Helical static mixers can be disposed in columns as in-line elements or in packed form (14). The Erestat mixer (Yxzet, Dr. Karg GmbH, Affalterbach) consists of four baffles twisted in an alternate manner arranged in a left- or right-handed arrangement on an inner support (Fig. 67.3c). This assembly creates various flowing channels. The N-shaped mixer (Bran and Lübbe, Norderstadt) consists of twisted mixing elements (Fig. 67.3d) that determine variable cross-sectional areas, owing to the formation of variable channels. The Lightin type (Lightin, Rochester, NY) combined in-line mixers obtained by assembling three-bladed elements to form helixes with different senses of rotation (Fig. 67.3e).

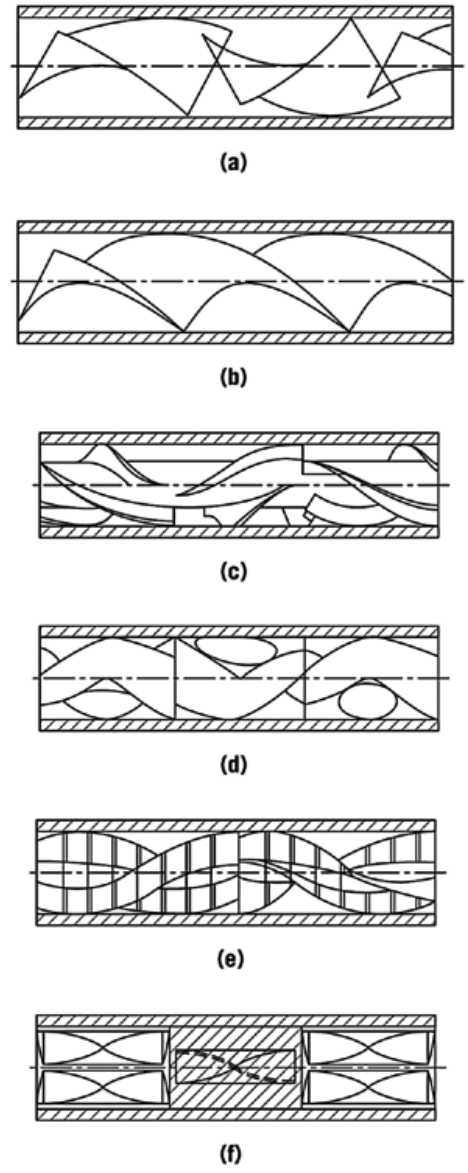


Figure 67.3. Helical static mixers. *Source*: Reprinted from Ref. 5, with permission from VCH Verlagsgesellschaft mbH, and from Ref. 7, with permission from Wiley-VCH.

The HI mixer (Toray, Tokyo) is constructed by helixes twisted at 180°, fitted into holes performed parallel to the axis in a solid cylinder (Fig. 67.3f).

67.2.4 Wire Matrix Turbulators

The Heatex inserts (15) consist of a central wire core onto which are wound a series of wire loops. Each loop is inclined at a certain angle to the core. These inserts are pulled into a tube, the loops being so inclined as to be oversized for the tube and come into a close contact with the tube wall in the form of an arc (Fig. 67.4). A degree

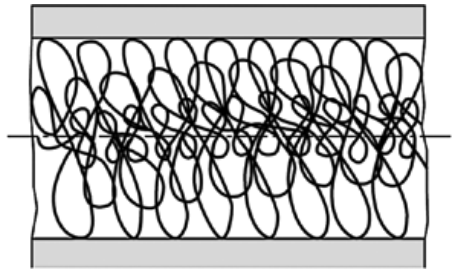


Figure 67.4. Static mixers of wire matrix. *Source*: Reprinted from Ref. 7, with permission from Wiley-VCH.

of resistance is offered as the insert is pulled into the tube, indicating that some wall contact is achieved and that the insert is self-supporting. Heatex inserts may have different loop densities, characterized by the number of tube wall contacts achieved per unit insert length.

67.3 EFFECTS OF STATIC MIXERS ON MOMENTUM TRANSFER

67.3.1 Flow Structure

Static mixers produce variations in the flowing cross-sectional area that result in modifications of velocity profiles. The fluid is split into individual streams at the open intersecting channels of the mixing element. At each intersection, a partial quantity is sheared off into a crossing channel and stagnant zones are usually eliminated. Also, most of the static mixers divide and reunite continually the main fluid stream and give rise to the formation of elementary layers of fluid. The number of n elementary layers or partial streams produced in laminar flow over a static mixer resulted through assembly of N mixing elements can be calculated from the following expression (16):

$$n = ca^{\mathrm{N}} \tag{67.1}$$

where c and a are parameters characteristic for the static mixer in discussion that are usually given in the literature (16). In the laminar regime, the flow profiles are modified by cutting and twisting, displacement and distortion, or separation and expansion. In the turbulent flow, additional effects occur (5). For instance, the fluid streams are alternating directed from the center to the wall of the column and from the wall to the center in the Ross-ISG mixer (Fig. 67.1a) or in the static presented in Fig. 67.1c. The presence of Heatex inserts (Fig. 67.4) causes a tube wall–fluid disturbance, and radial mixing is expected to be produced as the fluid flows through the mesh of loops nearer the pipe axis (15). In a Kenics mixer (Fig. 67.3a) a tracer injected below the first element in a certain point can perform a helical rotation strictly geometrically and reach the element edge in an opposite point situated on the same diameter, or it flows along a shortened path after a distortion and arrives at the end of the helix in a intermediate position on the diameter (5). The flow pattern in a Sulzer SMV mixer was presented by Pahl and Muschelknautz (5) using a model that consists in two triangular opened ducts crossing at 90° (Fig. 67.5) forming two intersected channels. Tracer introduced at the entrance of the channel I flows up to the intersection of the channels, and then about two-thirds of the tracer stream takes the shortest path flowing into duct II owing to the displacement that is produced at the crossing point. The trajectory of the tracer is also distorted; the fluid that exists along the left cathetus of the triangle representing the cross-section of the duct I shifts to the right side of duct I at the exit, performing a rotation. Also, the stream that starts from the opposite position at the entrance of duct I is greatly distorted at the crossing point and flows into both ducts I and II. In gas–liquid dispersions, a reasonably uniform distribution of the gas velocity over the cross-section of a column with static mixers is one of the favorable results. An equalizing effect is achieved by the resistance to flow, which forces the gas to spread out gradually in the direction of flow. This fact is very important in bioreactors with viscous non-Newtonian fermentation fluids, where the bubbles coalesce in the sparged vertical columns, leading to the formation of large bubbles, even at very low gas flow rates. In absence of static mixers, these bubbles rose with large velocities and their size distribution is controlled by bubble coalescence. The velocity profile of a fluid flowing through a tube containing motionless mixers is also considerably altered. There are some works in the literature that give information about radial and axial velocity profiles in the presence of static mixers (13,17,18). The axial

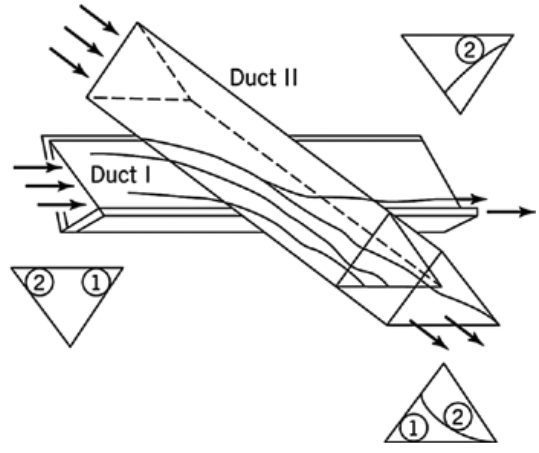


Figure 67.5. Flow path in a Sulzer-SMV static mixer (two triangular channels crossing at 90°). *Source*: Reprinted from Ref. 5, with permission from VCH Verlagsgesellschaft mbH, and from Ref. 7, with permission from Wiley-VCH.

and radial velocity profiles in a Kenics mixer change periodically owing to the use of alternating elements of right- and left-hand pitch that results in more intensive mixing of fluids. The screw having the form of a continuous helical surface divides the inside of the tube into two parallel channels, which causes a secondary motion of the fluid in the tube (13). In these motionless mixers, circulating flow occurs in the r-θ plane (r and θ being radial and tangential coordinates, respectively), which is caused by a slow twist in the partitioning chord so that it forms a helix. The actual velocity profiles can be calculated using a complex procedure (17), but an approximation can be made, leading to the following expressions:

$$\upsilon_r = \frac{dr}{dt} = \beta r(1 - r^{\upsilon}) \sin 2\theta \tag{67.2}$$

$$\upsilon_\theta = \frac{d\theta}{dt} = \beta[2 - (2 + \upsilon)r^{\upsilon}] \sin^2\theta \tag{67.3}$$

where

$$\upsilon = \left(\frac{11}{3}\right)^{0.5} - 1 \tag{67.4}$$

and β is a parameter that governs the intensity of circulation (17).

67.3.2 Pressure Drop

The changes in the velocity field caused by the static mixers cause modifications in the pressure loss as well. The pressure drop in static mixers depends very strongly on the geometrical arrangement of the packed elements, the nature of the flowing fluids, and the flow regime (19,20). A simple form representing the pressure loss equation can be referred to the empty tube, together with a geometrical correction factor (5,7,13). For Newtonian media, the equation for calculating the pressure drop is in the following form:

$$\frac{\Delta p_M}{\rho \upsilon_{SL}^2} \frac{2D}{L} = f_D(Re_D, \text{ geometry}) \tag{67.5}$$

The mean liquid superficial velocity υ_{SL} can be calculated on the basis of the empty tube cross-section as follows:

$$\upsilon_{SL} = \frac{4\dot{V}_L}{\pi D^2} \tag{67.6}$$

In laminar flow, $f_D\, Re_D =$ constant. Rearranging equation 67.5, a relationship is obtained whose denominator becomes the pressure drop for laminar flow through an empty pipe:

$$\frac{\Delta p_M}{\Delta p_L} = \frac{\Delta p_M}{32\eta\upsilon/D^2} \tag{67.7}$$

Defining a pressure drop factor as

$$z = f_D \frac{Re_D}{64} \tag{67.8}$$

it follows that

$$\Delta p_M = z\Delta p_L \tag{67.9}$$

In Figures 67.6 and 67.7, the pressure drop and friction factors for different static mixers are presented (5,7). The plot $f_D - Re_D$ could be also used for comparing static mixers in the turbulent flow regime, since f_D is then approximately independent of the Reynolds number

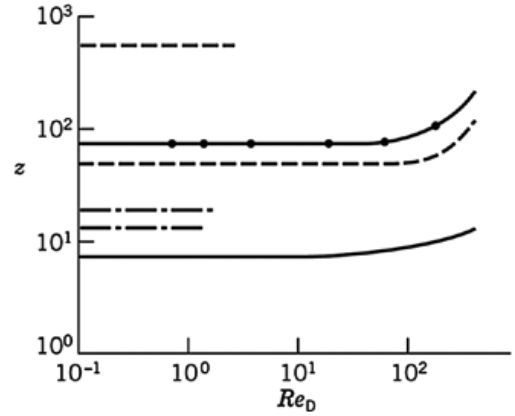


Figure 67.6. Relative pressure drop for different static mixers versus Reynolds number. — = Kenics; —·— = Erestat; —··— = N-shaped; — — — = HI; — □ — □ — = Sulzer-SMX; - - - - - - = Ross-ISG. *Source*: Reprinted from Ref. 5, with permission from VCH Verlagsgesellschaft mbH, and from Ref. 7, with permission from Wiley-VCH.

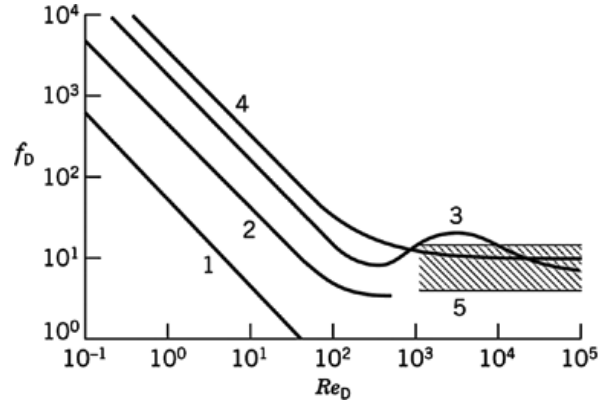


Figure 67.7. Friction factor as a function of Reynolds number for some static mixers. 1 = empty pipe; 2 = Kenics; 3 = HI; 4 = Sulzer-SMX; 5 = Sulzer-SMV. *Source*: Reprinted from Ref. 5, with permission from VCH Verlagsgesellschaft mbH, and from Ref. 7, with permission from Wiley-VCH.

(Fig. 67.7). Compared with an empty tube, the pressure drop in static mixers is 7 to 200 times greater for laminar flow and 100 to 600 times greater for turbulent flow. Kenics mixers show the smallest pressure drop, and the Ross-ISG affords the largest pressure drop (5,16). Also, the pressure losses in a tube containing continuous screws calculated using equation 67.5 are lower than those corresponding to a tube containing Kenics mixers for the same value of the parameter h/d. The following analytical expressions were developed for the different types of helical static mixers (13). For Kenics type (for $15 \leq Re_D \leq 1{,}200$):

$$f_D = \frac{213.5 + 224.0(h/d)^{-1}}{Re_D} + \left[-0.549 + 4.775(h/d)^{-1}\right] \quad (67.10)$$

For static mixer with a continuous screw surface for $15 \leq Re_D \leq 90$,

$$f_D = \frac{191.3 + 229.0(h/d)^{-1}}{Re_D} \quad (67.11)$$

for $90 \leq Re_D \leq 5{,}000$,

$$f_D = \frac{79.8}{Re_D^{0.839-0.454(h/d)^{-1}}} \quad (67.12)$$

With increasing of h/d, the pressure loss decreases for any given type of fittings (Fig. 67.8). The specification of notation is given in Table 67.1.

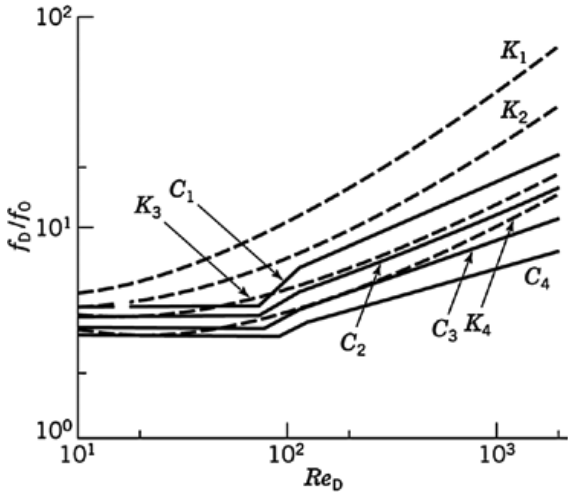


Figure 67.8. Dependence of the ratio between the friction coefficient in a tube with a screw f_D and that in the same tube without a screw f_0, on the Reynolds number, Re_D, and h/d (specification of C and K in Table 67.1). *Source*: Reprinted from Ref. 13, with permission from Elsevier Science, and from Ref. 7, with permission from Wiley-VCH.

TABLE 67.1. Geometrical Characteristics and Notations for Helical Static Mixers

Type of Screw	Notation	h/d	s/d	l/d
Continuous screw	C_1	2.28	0.095	46.85
	C_2	2.95	0.095	47.57
	C_3	3.85	0.095	47.57
	C_4	4.71	0.095	47.69
Kenics	K_1	2.02	0.095	48.26
	K_2	3.03	0.095	49.14
	K_3	4.05	0.095	47.86
	K_4	5.02	0.095	47.86

Source: Reprinted from Ref. 7, with permission from Wiley-VCH.

In Newtonian liquids, the presence of wire matrix turbulators caused an increase in pressure drop by factors up to 20 compared with the empty tube case (15). In non-Newtonian fluids, the pressure drop in a static mixer assembly can be correlated as follows:

$$\Delta p_M = \frac{A}{Re_D} + \frac{B}{Re_D^m} \quad (67.13)$$

where the values of A, B, and m are dependent on rheological behavior of the liquid phase (7,21). Olivier and Oosterhuis (22) studied the pressure drop in the laminar flow regime for a Sulzer-SMV-type in the xanthan fermentation and found that the pressure drop is approximately 15 times greater than that in an empty tube. Fan *et al*. (23) studied the pressure drop in a gas–liquid system in a bubble column packed with Sulzer-Koch mixing elements and observed that the ratio of the pressure drop through the packed column to that of the empty one was slightly greater than 1. Data referring to the pressure drop in a column equipped with a static mixer of the Kenics type were obtained for a single (gaseous) phase and two-phase countercurrent flow, respectively (14,24). For one mixing element, the pressure drop, which is a function of the Reynolds number for the gaseous phase, Re_G, is assessed as follows:

$$\Delta p' = \frac{\Delta p_M}{N} \quad (67.14)$$

The pressure drop in the system was calculated using the gas dynamic pressure for the single phase as

$$\Delta p' = f_{Do}\,\rho\,\frac{v_{SG}^2}{2} \quad (67.15)$$

and for the diphasic flow:

$$\Delta p'_{TP} = f_{DTP}\rho\,\frac{v_{SG}^2}{2} \quad (67.16)$$

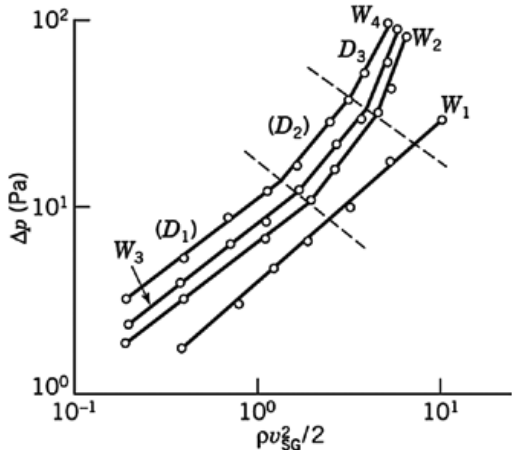


Figure 67.9. Pressure drop through a single static mixing element as a function of the dynamic pressure of the gaseous phase for different spraying intensities. $W_1 = 0$; $W_2 = 60.93$ m^3/m^{2}h; $W_3 = 81.24$ m^3/m^{2}h; $W_4 = 101.56$ m^3/m^{2}h. *Source*: Reprinted from Ref. 7, with permission from Wiley-VCH.

The plots show three domains with different slopes (Fig. 67.9). The friction factor also differs in the domains. For a single phase flow, it was correlated as follows:

$$\text{Domain D}_1: \quad f_{\text{Do}} = 12.86 Re_{\text{G}}^{-0.1708} \tag{67.17}$$

$$\text{Domain D}_2: \quad f_{\text{Do}} = 1.039 Re_{\text{G}}^{0.1062} \tag{67.18}$$

$$\text{Domain D}_3: \quad f_{\text{Do}} = 0.9742 Re_{\text{G}}^{0.1137} \tag{67.19}$$

For a diphasic flow, the following relation was established (24):

$$\frac{\Delta p'_{\text{TP}}}{\Delta p'} = B'^{\text{W}(1+b' Re_{\text{G}})} \tag{67.20}$$

The values of the spraying intensity, B', and of the parameter b', are different in the three domains of the curves (Table 67.2) (24).

For a two-phase flow, Shah and Khale (21) applied a correction factor for the manometer reading, assuming the gas holdup to be proportional with $\dot{V}_{\text{G}}/(\dot{V}_{\text{G}} + \dot{V}_{\text{L}})$. For an empty tube, the correction factor was found to be 0.83. They presented their data in the form of a Lockhart-Martinelli correlation for three types of static mixers, Kenics, Sulzer, and Komax, for two-phase non-Newtonian liquid–air systems in the following form:

$$\Delta p_{\text{TP}} = \varphi_{\text{L}}^2 \Delta p_{\text{L}} = \varphi_{\text{G}}^2 \Delta p_{\text{G}} \tag{67.21}$$

$$\varphi_{\text{L}}^2 = 1 + (c'/X) + (1/X^2) \tag{67.22}$$

$$X = (\Delta p_{\text{L}}/\Delta p_{\text{G}})^{0.5} \tag{67.23}$$

with $c' = 2.5 \pm 0.3$ for glycerol solution–air and $c' = 3.27 \pm 0.1$ for CMC solution–air diphasic systems, respectively. Generally speaking, the pressure drop in the gas–liquid systems decreases as the gas flow rate increases (10).

67.3.3 Gas-Holdup

In tower bioreactors with or without a loop (bubble columns, airlifts, jet contactors), liquid flow and gas holdup are of basic importance in the determination of their performance (25). Because microbial aerobic cultures often behave as non-Newtonian fluids, much attention was directed toward the performance of these gas–liquid contactors equipped with static mixers, especially when they handle non-Newtonian fermentation liquids. The rheological behavior of biofluids plays an important role in bubble coalescence and breakup, because the large velocities of coalesced bubbles lead to gas holdup decreasing (26). The presence of static mixers in diphasic flow diminishes the bubble coalescence rates owing to their shear effect. Therefore, the average bubble size should decrease and gas holdup is enhanced (7,10) (Fig. 67.10). The results of MacLean *et al*. (27) confirm these findings, suggesting that the motionless mixers help to retain more gas in the column. Similar effects can be obtained in triphasic sparged reactors (28). By using Ross-LPD and Sulzer SMV static mixers, larger gas holdup values resulted, compared with the empty contactor (Fig. 67.11). Kenics mixers mounted in an airlift bioreactor contribute to increase gas holdup values during the batch fermentation of a yeast culture (29). Gas holdup in downcomer (annular section) decreased because of a lower liquid recirculation rate, which implied a more intense gas disengagement at the upper part of the bioreactor, reducing the quantity of the recirculated gas. In the region of greater airflow rates (the riser), gas holdup values are, however, improved. This

TABLE 67.2. The Values of Parameters B' and b' from Equation 67.20

Domain	B'	b'
1	1.0150	$-5.596 \cdot 10^{-5}$
2	1.00925	$2.2348 \cdot 10^{-5}$
3	$0.947 + 2.6217 \cdot 10^{-4}$ W	$-8.5243 \cdot 10^{-9}$ W$^2 + 8.262 \cdot 10^{-7}$ W $- 1.4499 \cdot 10^{-4}$

Source: Reprinted from Ref. 7, with permission from Wiley-VCH.

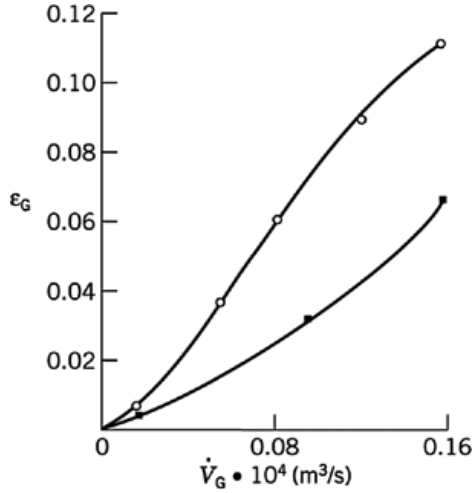


Figure 67.10. Gas holdup in a Koch mixer column in comparison to the witness one. ● = without static mixers; ◯ = with static mixers. *Source*: Reprinted from Ref. 7, with permission from Wiley-VCH.

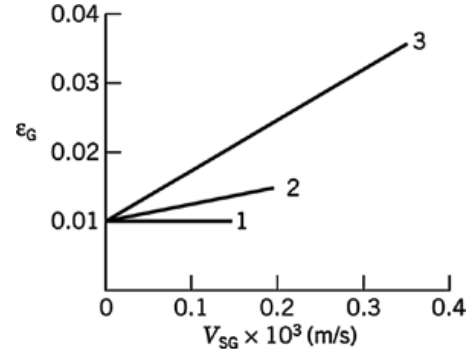


Figure 67.11. Gas holdup in a triphasic sparged reactor. 1 = witness reactor, 2 = Ross-LPD static mixers; 3 = Sulzer-SMV static mixer. *Source*: Reprinted from Ref. 7, with permission from Wiley-VCH.

behavior had a favorable influence on oxygen transfer rates (29,30). The presence of static mixers does not change the correlation between gas holdup and gas superficial velocity, which was established in the following form:

$$\varepsilon_G = a\upsilon_{SG}^{b} \tag{67.24}$$

For example, static mixers manufactured through assembly of corrugated stainless steel sheets and mounted in the riser section in an external-loop airlift bioreactor can contribute to gas holdup intensification at any given gas flow rate and liquid phase properties, relative to bioreactor configuration without static mixers (Fig. 67.12), also proved by the modified values of the parameters a and b in equation 67.24. This effect is found in low-viscous Newtonian and viscous non-Newtonian liquids as well (Table 67.3) (25). It is evident from Table 67.3 that static mixers show an increased efficiency in more viscous

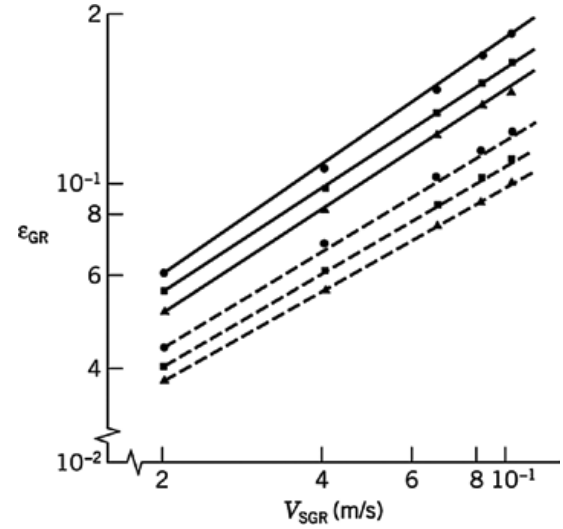


Figure 67.12. Gas holdup in an external-loop airlift bioreactor without (--------) and with (——) static mixers, in non-Newtonian starch solutions. ● = 0.5% w/v × 2.5 w/v; ▲ = 4.0 w/v. *Source*: Reprinted from Ref. 25, with permission from Springer-Verlag, Germany.

TABLE 67.3. Ratios Between Parameters a and b in Equation 67.24 in the Configuration with and without Static Mixers for an External-Loop Airlift Bioreactor

Ratio between parameters in equation 67.24	K (Pa s^n)		
	0.061	0.438	3.518
a_M/a	1.600	1.845	1.911
b_M/b	1.085	1.159	1.134

Source: Reprinted from Ref. 25, with permission from Springer Verlag.

liquids. Also, they affect the values of the coefficient a in equation 67.24 in a greater measure than those of b. Therefore, larger values of gas holdup in columns with static mixers resulted because of smaller bubble sizes and hindering action of the packing, which contribute to increasing the gas phase residence time (21,31).

67.3.4 Liquid Velocity

The presence of static mixers changes the liquid circulation rates, because they act as supplementary resistances in the flow path. Besides changes in gas flow pattern, the presence of static mixers in gas–liquid contactors having a net liquid flow (continuous bubble columns, airlifts, contactors with a liquid jet) changes the liquid circulation velocities, their effects being complementary to those of several other parameters, including gas superficial velocity, gas holdup, liquid phase viscosity, pressure drop along the flow path, reactor geometry. For instance, the static mixers mounted in an external-loop airlift bioreactor diminish the liquid

superficial velocity in the riser section both in Newtonian and non-Newtonian liquids. The parallel lines in the diagram presented in Fig. 67.13 show that in all cases the liquid velocity increases with gas superficial velocity. This behavior can be expressed by the following mathematical expression as:

$$\upsilon_{SL} = f\upsilon_{SG}^{m} \tag{67.25}$$

In non-Newtonian liquids, it was found that the presence of static mixers affects f and m values, dependent on consistency index values (25) (Table 67.4).

The relationship between the ratio of f values with and without static mixers, respectively, and the consistency index in an airlift contactor can be represented by the following relationship (25):

$$\frac{f_M}{f} = 0.85K^{0.008} \tag{67.26}$$

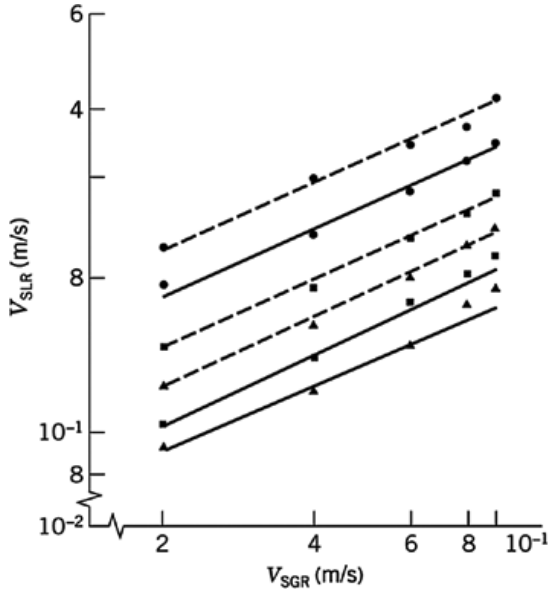


Figure 67.13. Liquid superficial velocity versus gas superficial velocity in an external-loop airlift bioreactor without (--------) and with (——) static mixers. Symbols as in Figure 67.12. *Source*: Reprinted from Ref. 25, with permission from Springer-Verlag, Germany.

TABLE 67.4. Ratios between the Parameters f and m in Equation 67.25 in an External-Loop Airlift Bioreactor with and without Static Mixers, in Non-Newtonian Liquids

Ratio between parameters in equation 67.25	K (Pa s^n)		
	0.061	0.438	3.518
f_M/f	0.829	0.841	0.856
m/m	0.997	0.994	0.994

Source: Reprinted from Ref. 25, with permission from Springer Verlag.

The effects of the consistency index on the liquid velocity could be considered as being less significant proving that static mixers are effective in viscous liquids. Popovic and Robinson (32) found that the circulating liquid velocity in the riser section of an airlift reactor is dependent mainly on the downcomer-to-riser cross-sectional areas ratio, A_D/A_R, the apparent viscosity, η_{ap} and gas superficial velocity, as described by the following correlation:

$$\upsilon_{SLR} = c'\upsilon_{SGR}^{0.32}(A_D/A_R)^{0.97}\eta_{ap}^{-0.39} \tag{67.27}$$

Considering that equation 67.27 correlates well a large number of experimental data, it was found that the differences in the values of υ_{SLR} should be treated as particular cases of diminuation up to 40% of the geometrical parameter A_D/A_R, as a result of the presence of static mixers (25).

67.3.5 Mixing

As shown, homogenization in static mixers is attained by means of motionless elements using the flow energy of the fluids. The mixing effect depends on the continuous separation, distribution, and reuniting streams of material (5,7). The energy requirements of static mixers when used for mixing are lower than those of conventional dynamic mixers and, moreover, they are of simple construction. In the case of two components, the two quantities are related to each other by the volumetric flow rate ratio, $\dot{V}_2/\dot{V}_1$. The degree of mixing may be described using the variation coefficient $s/\overline{C}_V$ or the relative standard deviation s/τ_0 (5). For component 1, the following expression held:

$$s_1/\overline{C}_V = \sqrt{\dot{V}_2/\dot{V}_1}s_1/\tau_0 \tag{67.28}$$

where

$$s_1^2 = \frac{1}{n-1}\sum_{i=1}^{n}(C_{V_i} - \overline{C}_{V_1})^2 \tag{67.29}$$

$$\tau_0 = [\overline{C}_{V_1}(1 - \overline{C}_{V_1})]^{0.5} \tag{67.30}$$

$$\overline{C}_{V_1} = \frac{1}{n}\sum_{i=1}^{n} C_{V_{1,i}} \tag{67.31}$$

$$C_{V_{1,l}} = \dot{V}_{1,i}/(\dot{V}_{1,i} + \dot{V}_{2,i}) \tag{67.32}$$

The degree of mixing is strongly dependent on the static mixer type and normalized mixing length, L/D (Fig. 67.14). It can be seen that the Sulzer-SMX mixer and HI-mixer require shorter homogenization lengths. Also, the degree of mixing is dependent on the entry point

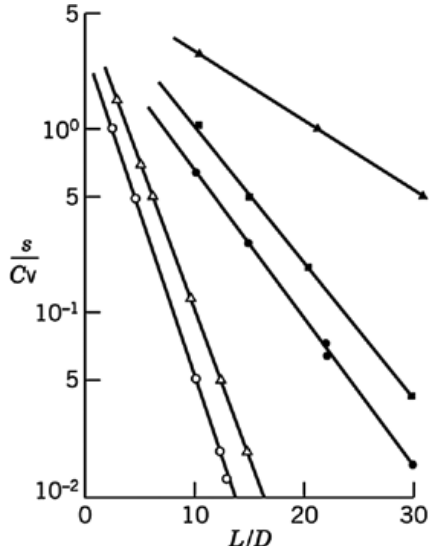


Figure 67.14. Variation coefficient as a function of the normalized mixing length for various static mixers. ● = Kenics; ◯ = Sulzer; ■ = Komax; ▲ = Lightin; △ = HI. $C_{V_1}^{-} = 0.1$; $Re_D < 1$. *Source*: Reprinted from Ref. 5, with permission from VCH Verlagsgesellschaft mbH, and from Ref. 7, with permission from Wiley-VCH.

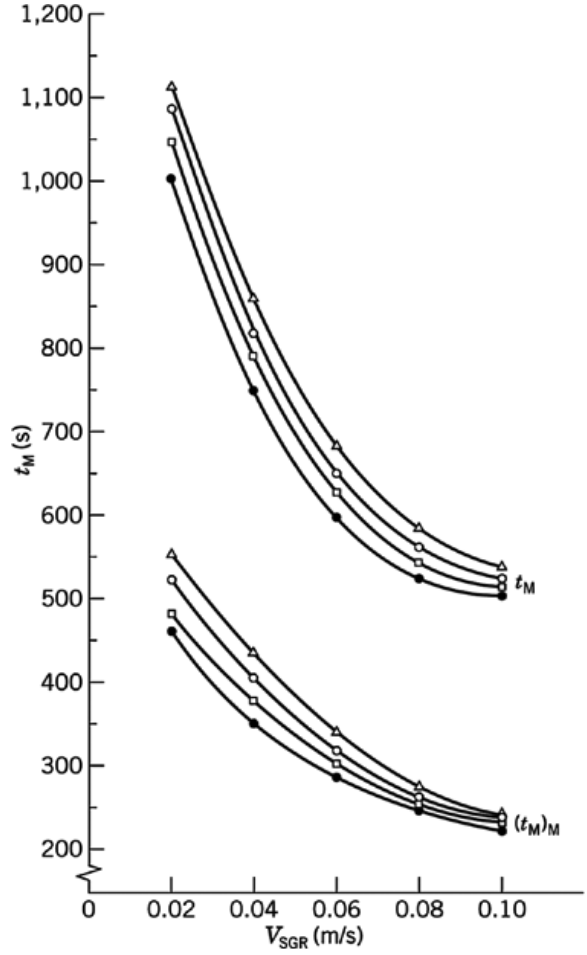


Figure 67.15. Mixing time versus gas superficial velocity in an external-loop airlift bioreactor without and with static mixers, operating with starch non-Newtonian solutions as liquid phase. ● = water; Starch solutions: □ = 0.5% w/v; ◯ = 2.5% w/v; △ = 4% w/v; *Source*: Reprinted from Ref. 34, with permission from Wiley-VCH.

of fluids to be mixed as well as by the operation scale (5). Static mixers achieve rapid mixing of fluids with low energy requirements, and the fluids may have either similar or different viscosity. Operation in fermentation processes involves very viscous fluids, and the flow will be predominantly in the laminar region for both liquid and gaseous phases. Suitability of static mixers to mix fluids of different viscosities was investigated in the literature (12,22,33,34).

Mixing behavior is usually described by mixing time, t_M, which is defined as the time required to achieve a definite degree of homogeneity after a trace pulse has been injected into the reactor (35). The mixing time is highly dependent on the presence of static mixers (34). In gas–liquid dispersions, the mixing time is dependent to a great extent on the gas superficial velocity and the presence of static mixers and to a low extent on the liquid phase properties. In Figure 67.15 the mixing time in water and starch solutions is plotted against superficial velocity. With static mixers, mixing times at a given superficial velocity are essentially up to 50% shorter than in the reactor without static mixers. The dependence of mixing time on gas superficial velocity can be expressed by the following equation:

$$t_M = k\upsilon_{SG}^{q} \tag{67.33}$$

The presence of static mixers does not affect q very much, but significantly influences k. Mixing times increase with increasing pseudoplasticity, but not very greatly (Fig. 67.15). In non-Newtonian systems, the consistency index had no significant influence on these parameters in the presence of static mixers (Fig. 67.16).

Other properties of a suitable static mixer are good radial mixing on as short as possible flow path and as low as possible axial mixing. Some static mixers contribute to diminish axial dispersion and influence the residence time distribution in laminar monophasic liquid flow, dependent on the Reynolds values (6). In the presence of static mixer seen in Figure 67.1c, the pulse response at the tube exit indicates a smaller axial dispersion (Fig. 67.17) (6). Also, the dead zones are diminished, and the distribution function of the elements of fluids with ages less than the residence time indicates an evident equalization of the residence times in laminar flow (Fig. 67.18) (6). In turbulent flow regimes, this effect is not very important. A good radial mixing

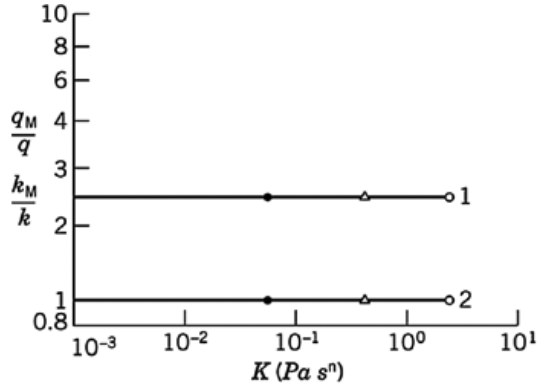


Figure 67.16. The influence of the consistency index K on the parameters in equation 67.33. ($1 = k_M/k$; $2 = q_M/q$. Symbols as in Figure 67.15. *Source*: Reprinted from Ref. 34, with permission from Wiley-VCH).

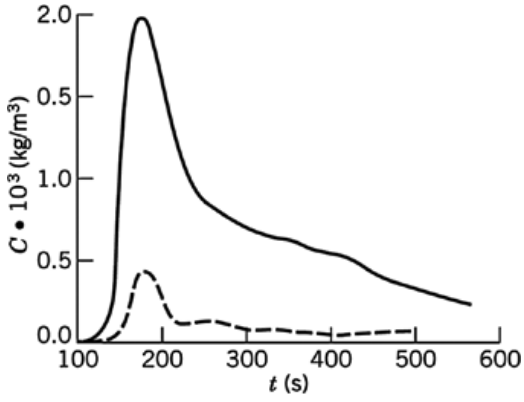


Figure 67.17. Pulse response at the exit of a tube equipped with the static mixer in Figure 67.1**c**, - - - - - - = without static mixer; — = with static mixer.

of a static mixer does not imply in all cases also low axial mixing. The individual static mixers display a different dependence of the axial dispersion on the flow rate of the phases both for single and two-phase flow system. A good static mixer from the standpoint of axial dispersion in single-phase flow does not necessary display a low axial dispersion in two-phase flow (12). Data on axial mixing for the individual types of static mixers are usually missing in the literature. Fialova *et al*. (12) presented the value of the Péclet number given by Sulzer for its SMX product ($Pé > 110$, $d = 0.1$ m; $L/D = 22$). These properties can be ascertained by experimental means.

67.4 MASS TRANSFER IN PRESENCE OF STATIC MIXERS

The application of the static mixers built in nonmechanically bioreactors, especially in aerobic bioprocesses, should

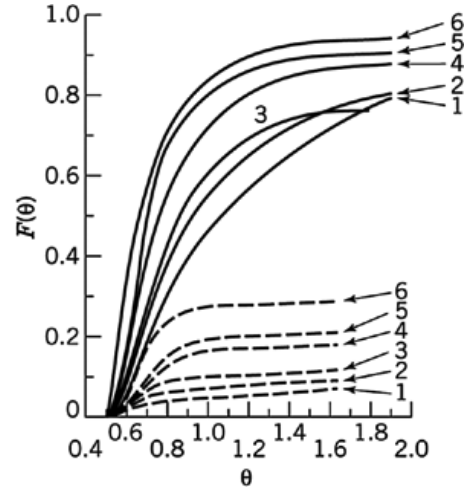


Figure 67.18. The distribution function of the fluid elements with the age less than the residence time versus Reynolds number in the tube without and with the static mixer from Figure 67.1**c**. $1 = Re_D = 630$; $2 = Re_D = 950$; $3 = Re_D = 1,260$; $4 = Re_D = 1,580$; $5 = Re_D = 1,890$; $6 = Re_D = 2,2000$. - - - - - - = without static mixer; — = with static mixer.

lead to attain the most extensive transport rate of oxygen into the liquid phase at the low possible energetic requirement. The influence of static mixers on hydrodynamic behavior has an important impact on mass and heat transfer characteristics and transfer rate intensification. The improvement of the oxygen mass transfer in bioreactors depends on a number of factors, such as bubble formation, bubble size distribution, bubble shear, gas holdup, rate of coalescence, and breakup. Also, bubble or drop coalescence behavior in gas–liquid dispersions, especially in viscous fluids, demonstrates the necessity for redispersing the gaseous or liquid phase to prevent the reduction of interfacial areas and mass transfer rates. A general solution to the mass transfer problems that appear in gas–liquid systems can be the use of static mixers installed at different intervals for increasing the degree of the gas dispersion and mass transfer rates (7,33,36). Usually, the intensity of oxygen transfer is characterized by its volumetric mass transfer coefficient, *Kla*. Static mixers improve *Kla* at any given gas flow rate relative to the bioreactor configuration without static mixer (7). The mass transfer rates are very high during bubble formation, and the values of mass transfer coefficient vary significantly being associated with large surface renewal rates. Coalescence and break-up, bubble formation, bubble shear, and turbulent liquid surface are examples of conditions where mass transfer coefficient is large. The introduction of static mixers has two important roles in *Kla* enhancement:

1. Bubble redispersion produces increased values of interfacial areas, a.

2. The interfacial turbulence during bubble coalescence and redispersion increases Kl.

At low gas flow rates, the latter mechanism becomes important (37). Small bubble size can be obtained with a homogeneous bubble distribution over the column cross-section and with a narrow size distribution. However, small rigid bubbles less than 2 mm in diameter have frequently been found to have much smaller mass transfer coefficients (38). Several studies were presented concerning the influence of the Sulzer type (22,33,36,39), Koch (10,11,20,24,40), Kenics (29,30) on *Kla* in bubble columns and external-loop airlift bioreactors in waterlike fluids as well as in non-Newtonian pseudoplastic media. Static mixers significantly enhance the mass transfer rates in waterlike fluids (Fig. 67.19). In non-Newtonian systems, the improvement in *Kla* due to static mixers depends on the rheological parameters. Stejskal and Potucek (30) and Chisti *et al*. (39) mounted static mixing elements in the risers of internal- and external-loop airlift reactors that enhanced mass transfer in viscous pseudoplastic CMC aqueous solutions that simulated the rheological behavior of filamentous biofluids. In pseudoplastic liquids, the thicker the fluid was, that is, the higher its value of the consistency index, K, the greater the effect of the static mixer was on *Kla* (36,39). Usually, the accumulation of biomass or product in the culture medium leads to increased viscosity and non-Newtonian flow characteristics that contribute to diminish *Kla* (26). This leads to a drastic decrease in oxygen transfer capability, and the aerobic culture eventually becomes oxygen limited (33,41). The significant decrease in *Kla* is mainly attributed to the formation of large bubbles and a decrease in specific interfacial areas that can be counterbalanced by the static mixers presence. The values of *Kla* can be correlated with the gas superficial velocity, v_{SG}, in tower bioreactors as

$$Kla = u v_{SG}^{t'} \tag{67.34}$$

The presence of static mixers affects u and t' values. They do not affect t' very much, but significantly enhance u dependent on the consistency index (Fig. 67.20) (36). The degree of *Kla* enhancement depends on the fluid viscosity and the pattern of fluid circulation through the reactor. The results of Hsu *et al*. (20) also show that mass transfer coefficient in a bubble column in the presence of Koch type static mixers is improved. A comparison of the oxygen transfer efficiency in terms of kilograms of oxygen transferred per kilowatt hour consumed at low flow rates indicated that the Koch mixed column was almost twofold as efficient as the empty column. However, at high gas flow rates, the efficiency was about the same for the two columns. Also, the ratio Kla/P_G can be used to characterize the efficiency of energy utilization for mass transfer per unit volume of the liquid phase or dispersion. Potucek (29) found that an airlift bioreactor with static mixers showed higher Kla/P_G values for absorption of oxygen in water or polyacrylamid solutions in the region of gas velocities of $v_{SGR} = 0.01 - 0.06$ m/s. Also, in the batch yeast cultivation, Kla/P_G was larger than in the witness bioreactor; gas superficial velocities ranged from $v_{SGR} = 0.03 - 0.06$ m/s, whereas with $v_{SGR} = 0.01 - 0.03$ m/s, lower values of Kla/P_G were obtained. As energy costs increase, more capital should be allocated to motionless mixers that increase the mass transfer efficiency. Olivier and Oosterhuis (22) considered that by keeping liquid and gas velocities as well as the volume ratio of empty tube parts and internals constant, the oxygen transfer would be higher and nearly independent on the scale. They also considered that oxygen transfer takes place not only in the internals, but also in the empty tube parts, and correlated the overall oxygen transfer coefficient as (22):

$$Kla = \frac{(Kla\, V_M)_{\text{internals}} + (Kla\, V_E)_{\text{empty tube}}}{(V_M)_{\text{internals}} + (V_E)_{\text{empty tube}}} \tag{67.35}$$

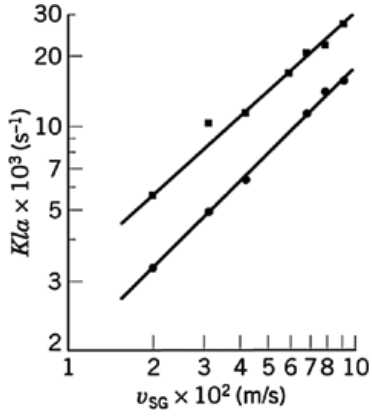


Figure 67.19. Effects of static mixers on the mass transfer coefficient in aqueous salt solutions. ● = without static mixers, ■ = with static mixers. *Source*: Reprinted from Ref. 7, with permission from Wiley-VCH.

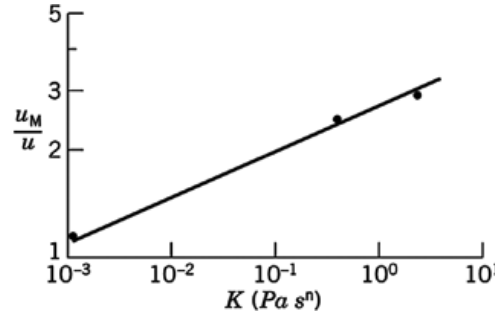


Figure 67.20. Variation of the ratio u_M/u with the consistency index.

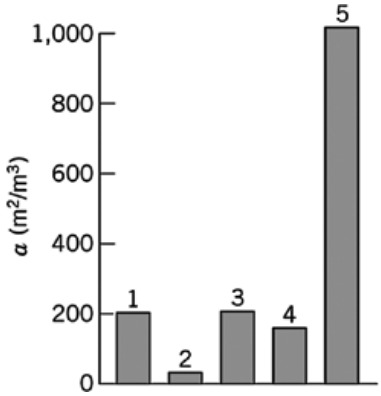


Figure 67.21. Comparison of specific interfacial areas in different gas–liquid contacting devices. 1 = Baffled agitated tank; 2 = bubble column; 3 = packed tower; 4 = plate tower; 5 = static mixers. *Source*: Data from Ref. 42.

The results obtained in different gas–liquid contactors show larger interfacial areas in the systems with static mixers (42) (Fig. 67.21). Data also indicate that the static mixer contactors are superior to other nonmechanically contacting devices, regarding mass transfer coefficient. Hsu *et al*. (20) investigated mass transfer in a bubble column with Koch mixers comparative to that with sieve trays. They found a different dependence of *Kla* on gas superficial velocity:

$$\text{for KOCH mixed column} : Kla \approx \upsilon_{SG}^{0.95} \tag{67.36}$$

$$\text{For sieve-tray bubble column} : Kla \approx \upsilon_{SG}^{0.89} \tag{67.37}$$

Also, data presented by Atkinson and Mavituna (42) show that in static mixed gas–liquid contactors a larger range of high Kla/V values was obtained, compared to those resulted in other gas–liquid contacting devices (Fig. 67.22).

The optimization of the number of motionless mixing elements and their positioning can enhance the mass transfer rates.

67.5 HEAT TRANSFER USING STATIC MIXERS

The role of the static mixers in heat transfer to flowing homogeneous or heterogeneous or heterogeneous fluids consists in fetching fresh fluid to the surface of the heat exchanger by promoting secondary flow, mixing, and turbulence (15). Most heat exchanger performances depend on hydrodynamics, and there are evident advantages that heat transfer may be enhanced by using built-in elements that change the velocity fields inside the tubes. Several studies investigated the heat transfer enhancement by using twisted strip inserts (43), helical static mixers (44,45), and wire matrix (15). The static mixers mostly used for heat transfer enhancement were helical static mixers,

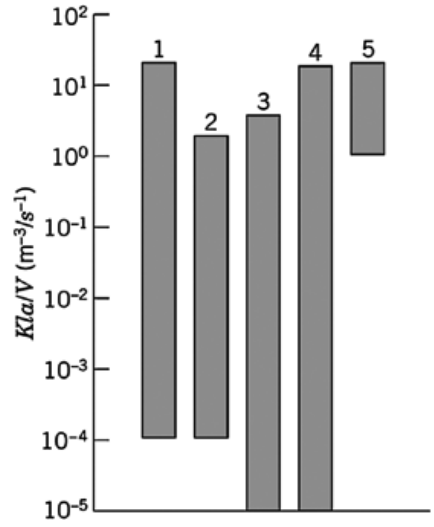


Figure 67.22. Comparison of different gas–liquid contacting devices regarding Kla/V values (significance of numbers as in Figure 67.21. *Source*: Data from Ref. 42.

which promote a secondary motion in the fluid, increasing the heat transfer between the fluid and the tube wall by convection.

The heat transfer performances of a given piece of equipment is usually estimated in terms of a Nusselt number, *Nu*, which is then related to the fluid properties and the Reynolds number, *Re*, characterizing the fluid environment. For instance, the individual heat transfer coefficient α_1 for the inside surface of a tube equipped with a helical static mixer is assessed from the following expression (44):

$$Nu_1 = \frac{\alpha_1 D}{\lambda_1} = \phi(Re_1, Pr_1, h/d, \eta W_1/\eta_1) \tag{67.38}$$

with

$$Re_1 = \frac{D\upsilon_1\rho_1}{\eta_1} \tag{67.39}$$

$$Pr_1 = \frac{c_{p1}\eta_1}{\lambda_1} \tag{67.40}$$

The overall heat transfer coefficient, K_T, of a tubular heat exchanger is related to the individual coefficients as follows:

$$K_T = \frac{1}{\frac{1}{\alpha_1}\frac{D_e}{D} + \frac{D_e}{2\lambda_s}\ln\frac{D_e}{D} + \frac{1}{\alpha_2}} \tag{67.41}$$

The values of K_T in a double-tube heat exchanger with hot water flowing through the annular space and cold water–glycerol solutions circulating through the inner tube containing helical static mixers were determined

using the individual heat transfer coefficients calculated with the following equations (67.44): For the tube ($90 \leq Re_1 \leq 5800$; $6 \leq Pr_1 \leq 5800$);

$$\mathrm{Nu_1} = 1.86\left(\mathrm{Re_1 Pr_1}\frac{\mathrm{d}}{\mathrm{L_T}}\right)^{0.33}\left(\frac{\eta_1}{\eta_{\mathrm{W_1}}}\right)^{0.14} \tag{67.42}$$

For the annular space ($Re_2 = 1520$):

$$Nu_2 = 1.02 Re_2^{0.45} Pr_2^{0.50}\left(\frac{D_e - D}{L_T}\right)^{0.40} \cdot \left(\frac{D_e}{D}\right)^{0.80} Gr^{0.05}\left(\frac{\eta_2}{\eta_{W_2}}\right)^{0.14} \tag{67.43}$$

Lecjacks *et al*. (44) reported the following relationship for helical elements of continuous and Kenics type:

$$Nu_1 Pr_1^{-1/3}\left(\frac{\eta_{W_1}}{\eta_1}\right)^{0.14} = \alpha_1 Re_1^{n_1} \tag{67.44}$$

with

$$\alpha_1 = \phi_a\left(Re_1, \frac{h}{D}\right) \tag{67.45}$$

and

$$n_1 = \phi_n\left(Re_1, \frac{h}{D}\right) \tag{67.46}$$

Also, they extended their investigations in the turbulent flow regime, which allowed them to assess the favorable effect of the built-in elements on heat transfer, especially in the laminar regime, for low values of h/d in Kenics static mixer. In the continuous helical static mixer, an increase in friction factor and heat transfer coefficient of 4.4% and 5.3% was obtained, whereas in the Kenics insert this increase was of 19.3% and 10.2%, respectively, comparative with the empty tube (45). Therefore, the heat transfer coefficient was found to be dependent on the flow conditions and geometrical properties of the internals. Olivier and Aldington (15) found a noticeable heat transfer enhancement by factors up to five in round tubes containing wire matrix turbulators, comparative to the empty tube, in laminar regime. Also, the wires caused the falling of the effective viscosity in non-Newtonian solutions at high liquid flow rates. Static mixers are used for thermal homogenization when a breakdown can occur on the heat transfer surface, especially in viscous media. Shear-thinning fluids should give good heat transfer/pressure drop behavior in the presence of tube inserts because the viscosity is reduced in the higher shear rates that are obtained. Static mixers are insensitive and nonresponsive to temperature. They can be well sealed against the surroundings. Maintenance and wear are small, and they are very economical, because they do not require additional space (in-line disposed).

67.6 SCALE-UP CONSIDERATIONS

Static mixers are used for many monophasic or gas–liquid, two-phase operations, which involve momentum, mass, and heat transfer. They are largely used in biotechnology and other applications such as processing of natural gases, wastewater treatment, dissolution of gases, continuous mixing of mutually soluble fluids of different viscosities, and so on. It is widely agreed that static mixers are suitable to mix fluids of very widely different viscosities, being especially effective for use with highly viscous fluids. They also could remove any mistakes made by the equipment designed for heat and mass transfer.

As shown in the fermentation field, factors taken into consideration on the choice and the design of an equipment for a definite process, besides the general factors, should include the population safety and damage, the uniform distribution of the phases and energy in phase transfers, the oxygen demand of the aerobic cultures, and so on (4,7). Static mixers can fulfill these objectives. Their action gives rise to elementary fluid layer formation. The maximum thickness of an elementary layer is given by the following expression (16):

$$\delta = \frac{D}{n} = \frac{D}{ca^{\mathrm{N}}} \tag{67.47}$$

As in the case of any apparatus, the static mixer behavior is tested first in small-scale equipment and then designed for large-scale operation, on the basis of the experimental data acquired for the model. For geometric similarity between the model and the actual mixer, the same degree of mixing means that (16):

$$\delta_m = \delta_a \tag{67.48}$$

or

$$\frac{D_m}{ca^{N_m}} = \frac{D_a}{ca^{N_a}} \tag{67.49}$$

Boss and Czastkievicz (16) introduced a linear scale-up coefficient, expressed as follows:

$$S = \frac{D_m}{D_a} \tag{67.50}$$

when equation 67.49 becomes

$$N_a = N_m + \frac{lgS}{lga} \tag{67.51}$$

This reasoning is valid in the laminar flow regime. For constant physicochemical properties of the fluids that flow through the model and the actual mixer, the changes in Reynolds number for the actual mixer relative to the model can be attributed to modifications occurring in the flow rate of the fluids or in the diameter of the static mixer. The relationships between the volumetric flow rates and Reynolds numbers in the model and the actual mixers, respectively, are as follows (16):

$$\dot{V}_a = \frac{z_m}{z_a} \frac{S^3}{1 + \lg S/N_m \, lga} \dot{V}_m \tag{67.52}$$

$$Re_a = \frac{z_m}{z_a} \frac{N_m}{N_a} S^2 Re_m \tag{67.53}$$

These general equations, applicable to scale-up of mixing processes in static mixers, are inferred starting from the pressure drops associated with laminar flow of a Newtonian fluid through circular pipes, which are taken into account by the pressure drop coefficient z, defined in equation 67.9. Boss and Czastkievicz (16) gave several examples of scale-up calculations for some types of static mixers, namely Kenics, Ross-ISG, and Sulzer.

67.7 CONCLUDING REMARKS

An overview of the published results on transfer processes in fluid flow through static mixers has been presented in the preceding pages. The velocity fields inside a tube containing motionless mixers can be modified using static mixers. As a result, a significant enhancement in mixing, mass, and heat transfer are achieved. Static mixers can be used in chemical and biochemical processes to perform a rapid mixing of monophasic, diphasic, and poliphasic systems with low energy requirements, and the fluids may have similar or different viscosities. The energy for mixing is extracted from the fluid flowing through the mixers. Static mixer effects result from specially designed flow arrangements, cutting and twisting, displacement and distortion, or separation and expansion. Significant efforts are devoted by specialists for developing new static mixers and optimal strategies for using minimum number of static mixers located at different positions in tubes, to ensure greater efficiency on transfer processes intensification, especially mixing and oxygen transfer in aerobic fermentation processes.

NOMENCLATURE

A	Cross-sectional area [m^2] (1 $in^2 = 6.4516.10^{-4}$ m^2; 1 $ft^2 = 9.290304.10^{-2}$ m^2)
a	Specific interfacial area [m^2/m^3]
c_p	Specific heat at constant pressure [J/kg °K] (1 ft pdl $°R^{-1}$ $lb^{-1} = 0.1672255$ J/kg °K)
D	ID of the tube [m] (1 in $= 2.54.10^{-2}$ m; 1 ft $= 3.084.10^{-1}$ m)
D_e	Outside tube diameter [m]
d	Diameter of static mixing element [m]
f_D	Friction factor
Gr	Grashof number
h	Height (length) of a static mixing element [m]
K	Consistency index in power-law rheological model [Pa s^n] (1 lb s $ft^{-2} = 1.488163944.10$ Pa s)
K_T	Overall heat transfer coefficient [W/m^2 °K] (1 lb $s^{-3}°R^{-1} = 0.816466266$ $W/m^2°K$)
L	Length of the tube [m]
N	Number of static mixing elements
Nu	Nusselt number
n	Number of elementary layers produced in laminar flow over a static mixer
Pr	Prandtl number
Δp	Pressure drop [Pa] (1 lb $in^{-2} = 6.89476.10^{-3}$ Pa)
Re	Reynolds number
Re_D	Reynolds number in a tube with inner diameter D
t_M	Mixing time [s]
V	Volume [m^3] (1 $ft^3 = 2.83168$ 10^{-2} m^3)
$\dot{V}$	Volumetric flow rate [m^3/s] (1 ft^3 $s^{-1} = 2.83168.10^{-2}$ m^3/s)
v_S	Superficial velocity ($v = 4\dot{V}/\phi D$) [m/s] (1 ft $s^{-1} = 3.048$ m/s)
α	Individual coefficient of heat transfer [$W/m^2°K$]
ε_G	Gas holdup
δ	Maximum thickness of an elementary layer [m]
λ	Thermal conductivity [W/m°K] (1 ft lb $s^{-3}°R^{-1} = 0.248858918$ W/m°K)
η	Dynamic viscosity [Pa s]
ρ	Density [kg/m^3] (1 lb $ft^{-3} = 1.60185$ 10 kg/m^3)

Indices

a	Referring to an actual static mixer
D	Downcomer section of an airlift reactor
E	Referring to the empty tube
G	Gaseous phase
L	Liquid phase
M	Referring to static mixer presence
m	Referring to model static mixer
o	Referring to a single phase
R	Riser section of an airlift reactor
s	Referring to solid surface

T	Referring to heat transfer
T P	Referring to diphasic flow
W	Referring to wall temperature
1	Fluid 1
2	Fluid 2

REFERENCES

1. B.H. Chen, Ind. Eng. Chem. Process Des. Dev. 9: 20–24; 121–126 (1970).
2. C.J. Slattery, AlChE J. 16: 345–352 (1970).
3. H. Brauer and D. Sucker, Int. Chem. Eng. 18: 367–380 (1978).
4. V.D. Prokopenki and U.E. Viesturs, Acta Biotechnol. 6: 325–338 (1986).
5. M.H. Pahl and E. Muschelknautz, Chem.-Ing.-Tech. 52: 285–291 (1980).
6. R.Z. Tudose and A. Moise, in Proc. of the First Natl. Symposium of Inventing Sept. 7–9, Iasi, Romania, 1984, pp. 209–212.
7. M. Gavrilescu and R.Z. Tudose, Acta Biotechnol. 15: 3–26 (1995).
8. Pat. RO 73630 (1979), R.Z. Tudose, F. Vitan, and L. Bujor (to Technical University of Iasi).
9. Pat. RO 98240 (1989), M. Ionescu, R.V. Roman, M. Gavrilescu, A. Sauciuc, A. Pintilie, A. Pascal, S. Matache and T. Rez (to Chemical-Pharmaceutical Research Institute of Bucharest).
10. K.H. Hsu, L.E. Erickson, and L.T. Fan, Biotechnol. Bioeng. 19: 247–265 (1977).
11. J.R. Gutierrez and L.E. Erickson, Biotechnol. Bioeng. 20: 487–501 (1978).
12. M. Fialova, K.H. Redlich, and K. Winkler, Collect. Czech. Chem. Commun. 51: 1925–1932 (1986).
13. Z. Lecjaks, I. Machak, and J. Sir, Chem. Eng. Process. 18: 67–72 (1984).
14. Pat. RO 83269 (1983), R.Z. Tudose, A. Bacaoanu, and L. Bujor (to Technical University of Iasi).
15. D.R. Olivier and R.W.J. Aldington, Chem. Eng. Res. Des. 66: 555–565 (1988).
16. J. Boss and W. Czaskievics, Int. J. Chem. Eng. 22: 362–367 (1982).
17. E.B. Naumann, Chem. Eng. J. (London) 47: 141–148 (1991).
18. R. Daraktschiev, Int. Chem. Eng. 30: 222–227 (1990).
19. F. Gross-Roll, Int. Chem. Eng. 20: 542–553 (1980).
20. K.H. Hsu, L.E. Robinson, and L.-T. Fan, Biotechnol. Bioeng. 27: 499–514 (1975).
21. N.F. Shah and D.D. Khale, AlChE J. 38: 308–310 (1992).
22. A.A.P.C. Olivier and N.M.G. Oosterhuis, in D.G. Bobichon and J. Florent eds., 8th International Biotechnology Symposium, Société Française de Microbiologie, Paris, 1998, pp. 388–409.
23. L.T. Fan, H.H. Hsu, and K.B. Wang, J. Chem. Eng. Data 20: 26–32 (1975).
24. R.Z. Tudose and F. Vitan, Rev. Chim. (Romania) 32: 1003–1006 (1981).
25. M. Gavrilescu and R.Z. Tudose, Bioprocess Eng. 16: 93–99 (1997).
26. M. Gavrilescu and R.V. Roman, Acta Biotechnol. 14: 27–36 (1994).
27. G.T. MacLean, L.E. Robinson, K.H. Hsu, and L.T. Fan, Biotechnol. Bioeng. 19: 493–505 (1977).
28. L. Rusnak and R. Vladea, Rev. Chim. (Romania) 42: 597–601 (1990).
29. F. Potucek, Collect Czech. Chem. Commun. 54: 3213–3219 (1989).
30. J. Stejskal and F. Potucek, Biotechnol. Bioeng. 18: 1552–1572 (1976).
31. K.B. Wang and L.T. Fan, Chem. Eng. Sci. 33: 945–952 (1978).
32. M. Popovic and C.W. Robinson, Biotechnol. Bioeng. 32: 301–312 (1988).
33. M. Gavrilescu and R.V. Roman, Acta Biotechnol. 15: 323–335 (1995).
34. M. Gavrilescu and R.V. Roman, Acta Biotechnol. 16: 145–153 (1996).
35. O. Levenspiel, Chemical Reaction Engineering, John Wiley, New York, 1972.
36. M. Gavrilescu, R.V. Roman, and A. Sauciuc, Biotechnol. Bioequip. (Bulgaria) 6: 60–64 (1992).
37. Y. Kawase and M. Tsujimura, Biotechnol. Bioeng. 44: 1115–1121 (1994).
38. P.H. Calderbank, in N. Blakebrough ed., Biochemical and Biological Engineering Science, Academic Press, London, 1967, pp. 101–180.
39. Y. Chisti, M. Kasper, and M. Moo-Young, Can. J. Chem. Eng. 68: 45–50 (1990).
40. C.H. Lin, B.S. Fang, C.S. Wu, H.Y. Fang, T.F. Kuo, and C.Y. Hsu, Biotechnol. Bioeng. 18: 1552–1572 (1976).
41. M. Gavrilescu, R.V. Roman, and V. Efimov, Acta Biotechnol. 13: 59–70 (1993).
42. B. Atkinson and F. Mavituna, Biotechnical Engineering and Biotechnology Handbook, Stockton Press, New York, 1991, p. 711.
43. A. Date, Int. J. Heat Mass Transfer 17: 845–859 (1974).
44. Z. Lecjaks, I. Machac, and J. Sir, Int. Chem. Eng. 27: 210–217 (1987).
45. D. Burfoot and P. Rice, Chem. Eng. Res. Des. 62: 128–132 (1984).

68

TRANSFER PHENOMENA IN MULTIPHASE SYSTEMS

RODICA-VIORICA ROMAN
Chemical Pharmaceutical Research Institute, Iaşi, Romania

68.1 INTRODUCTION

The dispersion of gases and solids in liquids is one of the most commonly applied processes of chemical engineering, and the fully baffled stirred vessel is one of many types of equipment used for this purpose. The hydrodynamic regime of the impeller controls the mixing performance of the whole reactor, as is reflected in phases of homogenization, the intensity of local energy dissipation distribution in the region of severe shear conditions, the retained gas fraction, bubble size, solid concentration distribution, mass transfer, and heat transfer (1–3). Good understanding of the dispersion mechanism of the impeller is indispensable for a reliable prediction of the behavior of the multiphase system flow in the reactor as a whole.

In multiphase processes carried out in stirred vessels, interphase mass transfer is often an important step and may be rate determining for the overall process. In aerobic fermentation systems, the oxygen transfer from the gas phase to the surface of the microbial cells is of primary importance, especially at high cell densities when microbial growth is likely to be limited by the availability of oxygen in the liquid phase (4–6). For many years, a set of radial flow Rushton disk turbine impellers of roughly one-third of the standard reactor diameter has been considered the optimum design for the multiphase system mixing, including fermentation processes. Mass transfer cannot be improved by increasing the specific power consumption or the aeration rate above certain limits, both of which lead to increased overall costs, but only by a modification of the blades of the impellers or by the development of impellers that allow a better bulk mixing with a minimum power consumption.

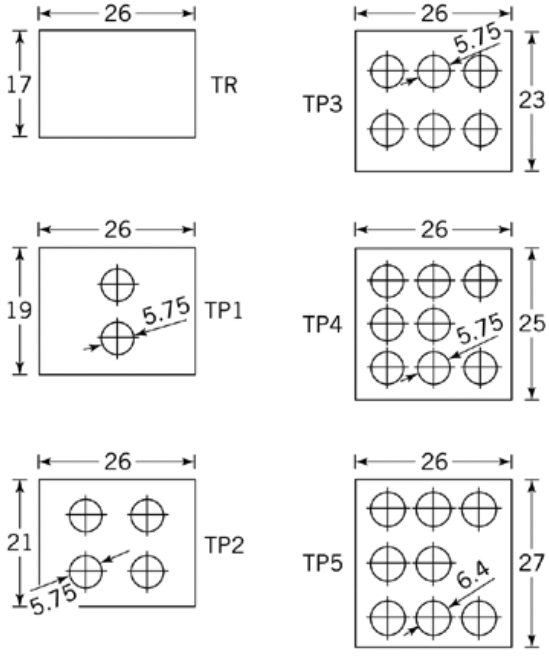
It has been reported (7) that a simple modification of the blades of a Rushton turbine through increase in the blade height simultaneously with perforation of the blade surface could significantly diminish power consumption and improve oxygen transfer efficiency in either a nonbiological system or in an antibiotic biosynthesis process.

68.2 DESCRIPTION OF THE MODIFIED RUSHTON TURBINE AGITATORS

The modified blades were obtained by increase in the conventional (standard) blade height simultaneously with perforation of the blade surface. Five modified blade turbine types (denoted TP1–TP5) were investigated; these are characterized by the fact that the number of perforations and their size varied and that the filled surface of the modified blades is equal to the blade surface of the standard Rushton turbine (TR) (Fig. 68.1) (7,8).

The application of perforations to the modified blades decreases the pathway between successive shearing actions on the liquid streams, increasing the number of times that the fluid is sheared. This effect has direct implications on local bubble size distribution in a gas–liquid mixture, which develops as a result of the balance between the complementary processes of dispersion and coalescence. The surface fraction of the perforations, defined as the ratio between the area S_G of the perforations on the surface and the full surface area S_C of the blade is in the range of 0 to 0.588. The

Upstream Industrial Biotechnology: Equipment, Process Design, Sensing, Control, and cGMP Operations, Volume 2, First Edition. Edited by Michael C. Flickinger.
© 2013 John Wiley & Sons, Inc. Published 2013 by John Wiley & Sons, Inc.



Agitator S_G/S_C	TR	TP1	TP2	TP3	TP4	TP5
	0	0.117	0.235	0.353	0.470	0.588

Figure 68.1. Schematic representation of the standard (TR) and modified (TP1–TP5) blades of the Rushton turbine. (*Source*: From Ref. 8, with permission.)

modified blade turbines do not require any modification in the electrical motor and drive assemblies and are simple to manufacture. The experiments were carried out in a transparent vessel of inside diameter $D = 0.25$ m, with a flat bottom and four symmetrical wall baffles of width $w = 0.1\,D$. Fluid mixing was carried out by conventional and modified blade turbines, positioned singly (1TR, 1TP1–1TP5) or doubly (2TR, 2TP1–2TP5) on the same shaft.

68.3 MULTIPHASE SYSTEM HYDRODYNAMICS

68.3.1 Gas–Liquid Dispersing Characteristics

The hydrodynamic regimes were defined by reference to the distribution of the gas phase in the vessel. For an air–water system, the flow regimes were detected through visual observation of the zone close to the outer edge of the TR and TP1–TP5 turbines (8). In the single-turbine configurations, the three classical regimes (9,10) were observed: flooding (F), loading (L), and complete dispersion (CD). For a double-turbine system, two hydrodynamic configurations were defined in the upper zone: ineffective dispersion (DI) and effective dispersion (DE), respectively; the transition between the hydrodynamic regimes corresponds to the rotational speed at which the bubbles have a radial velocity sufficient to reach the vessel wall. The gassed power consumption, P_g, is usually determined by varying the operational parameters: the volumetric flow rate, Q_g, and the impeller speed, N.

The curve representing the ratio P_g/P as related to the gas flow number presents maximum and minimum points when the volumetric gas flow rate is kept constant. Each of these extreme points corresponds to a gas–liquid hydrodynamic regime in the impeller region. The power curves change notably when the power consumption is expressed as a power number. Interesting results were obtained by plotting the gassed power number $(\mathrm{Ne})_g$ against the impeller speed N, when the aeration rate Q'_g, expressed as volumetric flow rate of gas per minute/volume of liquid (vvm) was kept constant. These results are presented in Figures 68.2 and 68.3 for mixing systems having one or two turbines, respectively. Table 68.1 explains the symbols used in Figures 68.2 and 68.3.

In the range of low N values, the power number for a single turbine decreased with increasing impeller speed until a certain point: subsequently, it increased suddenly in the case of the standard blade turbine and slowly in the case of the modified blade turbines. The impeller speed at which the transition between these two zones occurred was very close to the transition impeller speed between flooding and loading of the turbine. For two turbines on the same shaft, clear delimitation between the two zones of the impeller speed was not apparent (Fig. 68.3). The $(\mathrm{Ne})_g$ values decreased slowly with increasing impeller speed until the agitation system exceed the flooding state of the bottom turbine. In the range of large N values, when the gas dispersed uniformly through the entire vessel section, the gassed power number became independent of the impeller speed, as it was a function of aeration rate and geometrical configuration of the mixing system only. The variation in the power number depending on the surface fraction of the perforations, which indicates the geometry of the mixing system, is presented in Figure 68.4.

The range of power number for an individual Rushton turbine reported in the literature (11) is $\mathrm{Ne} = 4.8 - 6.3$ for

TABLE 68.1. Symbols used in Figures 68.2 and 68.3

Symbol	Aeration rate, Q'_g (vvm)	Volumetric gas flow rate, $Q_g\ 10^4$ (m^3/s) One turbine ($V = 0.0125$ m^3)	Two turbines ($V = 0.020$ m^3)
×	0.30	0.625	1.0
◯	0.50	1.042	1.666
▲	0.75	1.555	2.500
*	1.00	2.083	3.33
■	1.25	2.611	4.166
▼	1.50	3.125	—

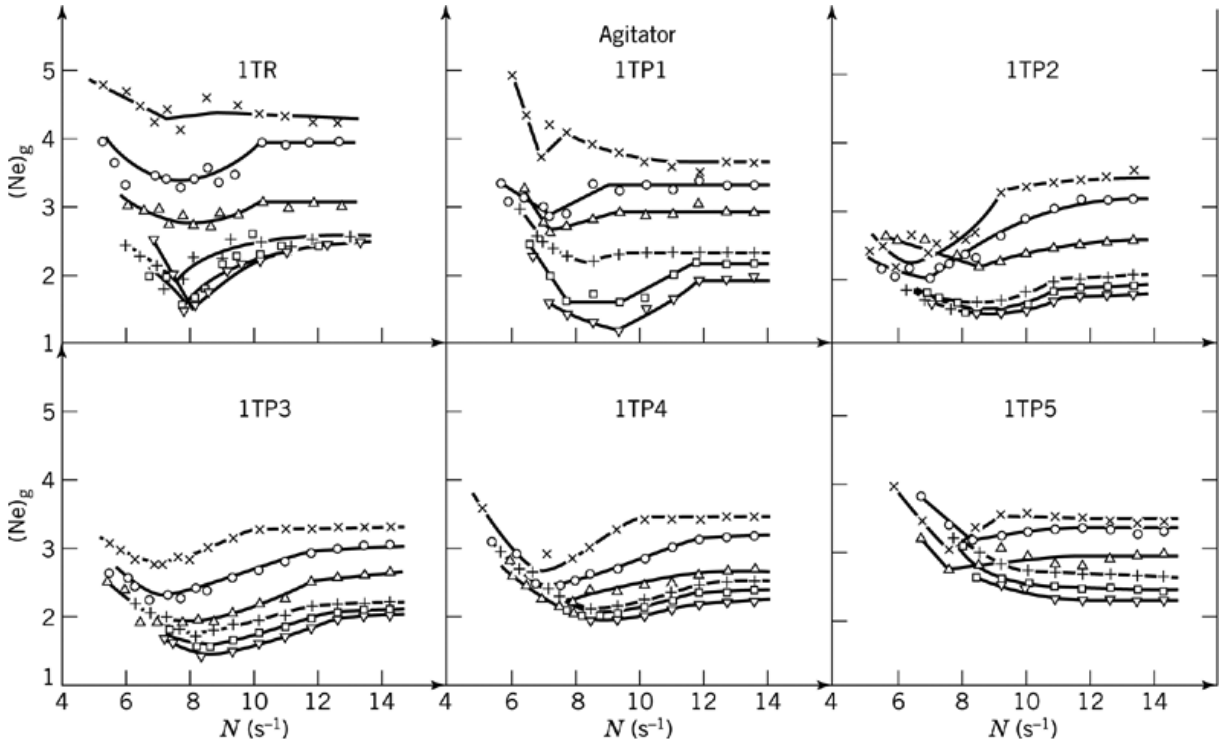


Figure 68.2. Variation in the gassed power number $(Ne)_g$, depending on the impeller speed (N) at various gas flow rates for single standard and modified Rushton turbines (symbols are defined in Table 68.1). (*Source:* From Ref. 8, with permission.)

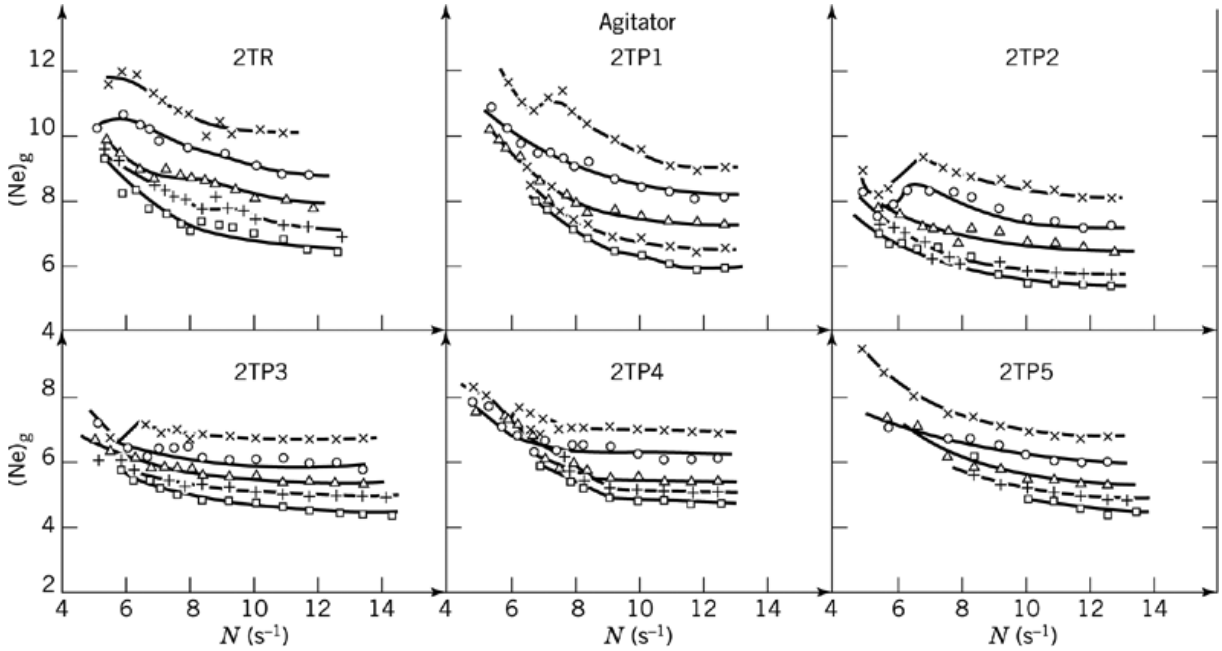


Figure 68.3. Variation in the gassed power number $(Ne)_g$ depending on the impeller speed (N) at various gas flow rates for double standard and modified Rushton turbines (symbols are defined in Table 68.1). (*Source*: From Ref. 8, with permission.)

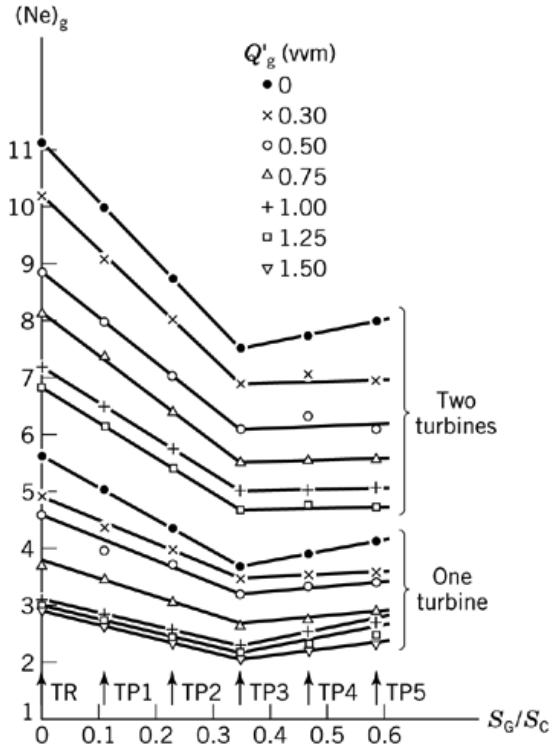


Figure 68.4. Variation in the power number depending on the surface fraction of the perforations (S_G/S_C) at various aeration rates ($Q_g^{'}$). (*Source*: From Ref. 8, with permission.)

$Q'_g = 0$. In our case, the value Ne = 5.5 for a single Rushton turbine is in good agreement with these data. The Ne values for Rushton turbines are dependent on a scale (12), and for a mixing system in which the geometrical symplexes deviate from the standard values, the introduction of a correction factor of the power number is recommended (13,14). The Ne and $(Ne)_g$ values for all the modified blade turbines are smaller than those for the Rushton turbine, as a result of the change in fluid flow around and over the blades and of the minimization of the drag forces associated with the motion of blades such that the energy losses due to form drag are very low. These results imply that it is possible to rotate the modified blade turbines much faster than the standard Rushton turbine at an equal specific power consumption. The TP3 modified blade turbine, with the surface fraction S_G/S_C of the perforations equal to 0.353, has the smallest gassed and ungassed power number values, these being reduced by approximately 50% in comparison with the standard Rushton turbine. The increase in the surface fraction of the perforations over $S_G/S_C = 0.353$ is not justified on the basis of the power consumption.

For double turbines, the power number values are approximately twice those obtained for the single turbines, irrespective of the turbine type, at constant aeration rate Q'_g. This shows that, in the case of two identical turbines, the power consumption P_g is twice that obtained using a single turbine: this is possible because, if Q'_g is kept constant, the volumetric gas flow rate, Q_g, ($m^3\ s^{-1}$) is 60% higher when the liquid volume is higher (Table 68.1). Also, the power consumption of two TP3 modified turbines is reduced by 50% in comparison with the double standard Rushton turbines. Because the surface of each modified blade increases simultaneously with the S_G/S_C ratio, it is to be expected that a larger gas volume is retained in the ventilated cavities behind the modified blades and dispersed afterward. Therefore, the modified blades have a greatly increased gas-handling capacity: the TP3 turbines handle more than 35% more gas than do the standard Rushton turbines at the same specific ungassed power consumption, before flooding or ineffective dispersion.

68.3.2 Suspension of Solid Particles in Liquid

Three suspension states can be defined, as follows (15):

1. Incomplete suspension, in which a part of the solid phase is deposited on the bottom of the vessels
2. Complete suspension, in which all particles are in suspension
3. Homogeneous suspension, in which the particle concentration is uniform throughout the vessel

Many earlier investigations concentrated on the impeller speed for complete suspension, when the maximum surface area available for processing is achieved (15–18). The most widely used criterion to describe solids suspension in mechanically agitated vessels is the just-off-the-bottom suspension condition, first described by Zwietering (19).

In this section, an attempt is made to understand the effects of the physical and rheological properties of the suspensions and number and turbine types on the complete suspension speed and on the power dissipation at complete and homogeneous suspension states of the solid particles (20). The solid particles used are $CaCO_3$, a cation exchange resin (Amberlite IR-120 type), and an anion exchange resin (Amberlite IRA-410 type). A range of density differences $\Delta\rho = (\rho_s - \rho_L)$ between 150 and 1,200 kg/m^3 was examined. The ion exchange resin particle shape is spherical, the particle size distribution being measured by a microscopic method. The change in particle size during the experimental run was negligible. The surface-to-volume (Sauter) mean diameter of the particles, d_p, was calculated for the ion exchange resin particles. In the $CaCO_3$ suspension, the mean diameter of the particles was 15 μm (21). The particle concentration, X, was between 20 and 150 kg/m^3 for each particle type used. The physical properties are given in Table 68.2. The suspensions used are pseudoplastic in behavior. The rheological properties of suspensions depend

TABLE 68.2. Physical and Rheological Properties of Solid Particles

Particle type	Symbol	Physical parameters			Rheological parameters		
		d_p (μm)	ρ_s (kg/m^3)	X (kg/m^3)	ρ_{sp} (kg/m^3)	K (Pa s^n)	n (−)
$CaCO_3$	S1	15	2,200	20	1,026	0.105	0.834
				50	1,065	0.118	0.815
				100	1,130	0.133	0.812
				150	1,195	0.186	0.751
Amberlite IR-120	S2	680	1,350	20	1,008	0.135	0.760
				50	1,020	0.149	0.741
				100	1,040	0.164	0.729
				150	1,060	0.204	0.721
Amberlite IR-120	S3	860	1,350	20	1,008	0.140	0.811
				50	1,020	0.150	0.789
				100	1,040	0.220	0.710
				150	1,060	0.382	0.609
Amberlite IRA-410	S4	600	1,150	20	1,002	0.194	0.730
				50	1,005	0.244	0.686
				100	1,010	0.355	0.611
				150	1,015	0.530	0.570
Amberlite IRA-410	S5	1,000	1,150	20	1,002	0.235	0.662
				50	1,005	0.292	0.651
				100	1,010	0.428	0.568
				150	1,015	0.753	0.553

Source: Ref. 20.

on the particle size and the concentration of solids. Rheological data of the suspensions were obtained with a rotational cylinder viscosimeter (Rheotest-2.1) and were fitted according to the power law model (22). The rheological parameters, consistency index, K, and flow behavior index, n, are also presented in Table 68.2. The definition of complete suspension speed, N_{js}, was taken as the speed at which no particles were visually observed to remain at rest on the vessel bottom for more than 1 or 2 s (19). The last particles to be suspended were located near the center of the vessel base and also behind the baffles. The experimental relationships between complete suspension speed and solid concentrations are shown in Figure 68.5 for each of the five particle types and for modified and standard turbines positioned singly or doubly on the same shaft.

For the same operation conditions, the N_{js} values for the TP3 modified turbine are slightly higher than those for the standard turbine. Also, Figure 68.5 shows that, independent of the agitator type, N_{js} actually is increased when two turbines are used, as was also observed by Armenante (23). Although the phenomenon of solid suspension off the vessel bottom is largely dominated by the lower impeller, the presence of two turbines modifies the flow pattern in the vessel.

In all geometrical systems, the N_{js} values are found to increase with solid concentration. This increase of the N_{js} value may result from an increase of probability to find particles at rest on the bottom as the number of particles in suspension increases. It was observed that at N_{js} the concentration of the solid particles in the zone near the bottom is considerably higher than the average value in the vessel. The physical background of the concentration effect is the increased power dissipation by presence of solid particles in the turbulent field (24). The particles can interfere with the turbulent field via two routes. (*1*) Because of their inertia, particles do not follow the motion of the liquid. Consequently, the kinetic energy of a particle changes continuously. Acceleration of a particle occurs at the expense of energy from the turbulent eddies, whereas deceleration leads to energy dissipation in the form of heat. (*2*) At high solids concentration, the particles will also interfere with each other (collison and/or hindrance). In a similar way, this will lead to increased dissipation of the energy of the turbulent eddies. Thus, for the point of complete suspension to be maintained, a higher solid concentration requires a higher power input to the systems.

Figure 68.6, where the power consumption expressed as power number for complete suspension condition $(Ne)_{js}$, is plotted against the Reynolds number Re, demonstrates that in the vessel equipped with the modified blade turbines, single or double, the $(Ne)_{js}$ values are approximately 30% lower than those in the standard vessel. In these plots, $(Ne)_{js}$ and Re numbers are calculated using the properties of the suspensions. The $(Ne)_{js}$–Re representation based solely on liquid properties is inadequate (25), because at the highest solids concentration laminar or transition range appear to persist up to very high Reynolds numbers. By using a suitable apparent viscosity for the solid–liquid suspension, it is possible to condense all the data in the adequate range. In our case, the Reynolds number values

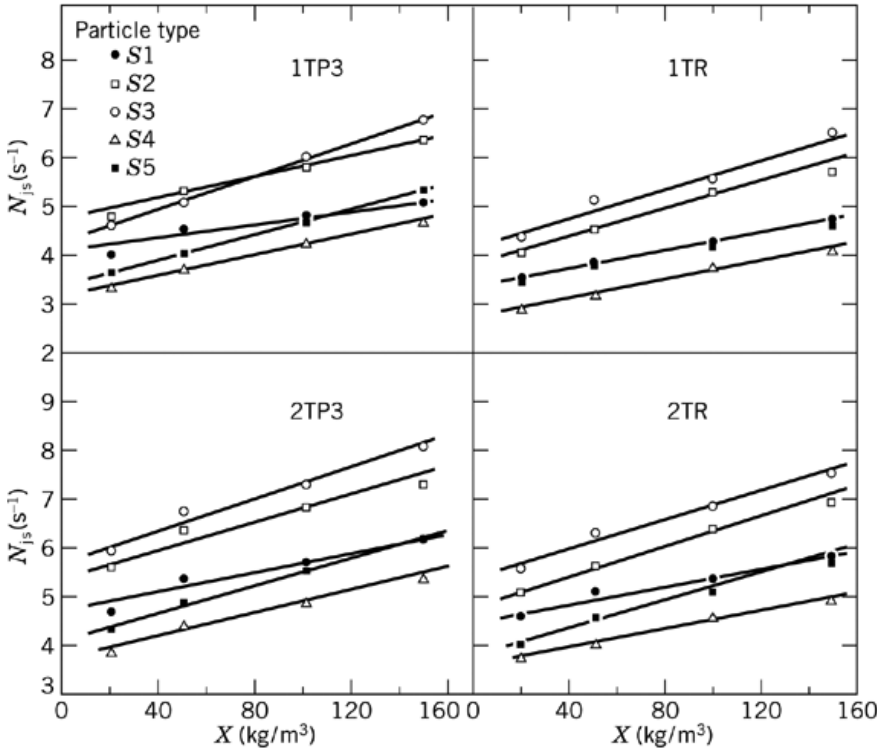


Figure 68.5. Effect of solid concentration on complete suspension speed for standard and modified Rushton turbines, positioned singly or doubly on the same shaft. S1–S5, particle types (see Table 68.2). (*Source*: From Ref. 20, with permission.)

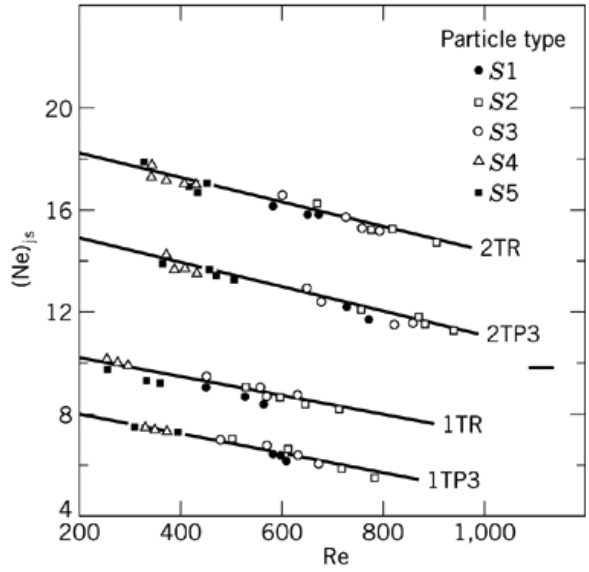


Figure 68.6. Relation between the power number and Reynolds number (Re) at the complete suspension state, for standard and modified Rushton turbines, single or double. (*Source*: From Ref. 20, with permission.)

for complete suspension condition are in the transition range ($Re < 1000$); the $(Ne)_{js}$–Re dependency has a negative slope.

The main reason for the smaller power number of modified blade turbines is the change of suspension flow around and over the blades. The fluid flow around the blades of the standard Rushton turbine was studied by Vant' Riet (26). Dead zones behind each turbine blade are formed. From these dead zones with the stagnation lines, the trailing vortex pair originates as a combined effect of the vortex motion at the rear of the vertical inner edge of the blade and the wrapping of the vortex sheets behind both horizontal edges. In the case of the modified blade turbines, the fluid jets penetrating the perforations, eliminate the stagnation lines and change the conditions of the trailing vortex formation.

When all the observation are combined, the following correlation is evident between complete suspension speed and the physical and rheological properties of the solid particles:

$$N_{js} = c d_p^{0.2} \Delta\rho^{0.45} X^{0.13} K^{0.1} \tag{68.1}$$

The exponents of d_p, $\Delta\rho$, and X are essentially the same as those reported by Zwietering. The correlation, equation 68.1, includes the consistency index K as a pseudo-viscosity of the suspensions. The value of the dimensionless constant, c, is specific for each of the geometrical configurations studied. The influence of the turbine type and number of the turbines on N_{js} can be

expressed by incorporation of two dimensionless groups, namely $(1 + S_G/S_C)$ and $n_p/6$ (S_G/S_C is the surface fraction of the perforation and n_p is the number of blades of the mixing system). Using nonlinear least squares regression, the following correlation was established:

$$N_{js} = 1.1 d_p^{0.2} \Delta\rho^{0.45} X^{0.13} K^{0.1} (1 + S_G/S_C)^{0.2} (n_p/6)^{0.25} \quad (68.2)$$

In the turbulent range (Re > 1000), when $N > N_{js}$, the particle concentration is uniform throughout the vessel, and power number in solid–liquid system, $(Ne)_s$, is constant.

In the vessel equipped with a standard turbine, the maximum value of the Reynolds number is 1,800; for the modified blade turbine, the maximum Reynolds number is 2,400. This is possible because the modified blade turbine rotates much faster than the standard turbine at an equal specific power input (11). The relation between the mean values of the power number and the physical properties of the solid particle, in the turbulent range, is

$$(Ne)_3 = 5.6175(n_p/6)(1 + S_G/S_C)^{-1.3867} \cdot (1 + 10 d_p^{0.2} \Delta\rho^{-0.45}) \quad (68.3)$$

The estimated error using equations 68.2 and 68.3 lies within ±10%.

68.3.3 Effect of Particles on Gas–Liquid Hydrodynamics

Establishment of the major interactions between gas dispersion and particle suspension mechanisms is a basis for examining in detail the effect of the major variables on the minimum agitator speed for particle suspension under gassed conditions and on the minimum agitator speed for gas dispersion to all parts of the vessel in the three-phase systems.

The manner in which the presence of the particles affects the gas dispersion is inferred from the variation of the relative power consumption P_{gs}/P_s (P_{gs} and P_s are power consumption in gas–liquid–solid and solid–liquid systems, respectively), with gas flow rate, Fl, which is associated with different stages of cavity growth behind the impeller blades. In the curves presented in Figure 68.7, for various volumetric gas flow rates and concentrations of the S5 type solid particles for 1TR and 1TP3 turbines, the transition to complete gas dispersion is obtained when a minimum occurs in P_{gs}/P_s and the cavity sizes are maximum (27). For the 1TR turbine, the maximum values of P_{gs}/P_s are between 0.5 and 0.3 for all solid concentrations and depend on the volumetric gas flow rate. The 1TP3 turbine shows a behavior similar to that of 1TR turbine but only at $X = 20$ kg/m^3 and $X = 50$ kg/m^3. At $X = 100$ kg/m^3 and $X = 150$ kg/m^3, the minimum values of the P_{gs}/P_s for 1TP3 are approximately 0.5, irrespective of the volumetric gas flow rate. This confirms previous observations (8) as regards the fact that the modified blades have a greatly increased gas-handling capacity.

Effect of particle concentration on power number in a three-phase system, $(Ne)_{gs}$, at constant superficial gas velocity is presented in Figure 68.8 for the S2 type ion exchange resin, in modified turbines, single or double. A decrease in power number at $N < N_{jsg}$ (jsg is the moment of complete solid suspension) is due to the "false bottom" formed by the particles effectively reducing impeller clearance at low speeds. As the agitator speed N tends to N_{jsg} (as indicated in Fig. 68.8), the particles were suspended, the false bottom removed, and the power number tended to the common value. The power number generally increased as particle concentration increased before complete particle suspension had been obtained.

In the case of the 1TP3 turbine, the moment of the complete gas dispersion N_{CD} shifts into the range of smaller gas flow rates when the particle concentration increases. For two turbines (2TP3), the variation $(Ne)_{gs} = f$ (Fl) showed the following transition points: the transition to effective dispersion of the gas at the upper impeller (minimum point of the each curve) and also the flooding–loading transition of the bottom impeller (maximum point of each curve). The transition at complete gas dispersion does not show in Figure 68.8, probably because, once the particles are suspended, the increasing suspension density in the impeller region (and of the power consumption) compensates the decrease in power consumption because of large cavity formation.

The examination of the experimental data in correlation with the Reynolds number shows the following (27):

- For Re < 1,000, mixing is in the transition range, in which the $(Ne)_{gs}$–Re dependence has a negative slope.
- In the range 1,000–1,400 of the Reynolds number, the $(Ne)_{gs}$ values for 1TR attain a minimum point more pronounced for the lower solids concentration. In the case of the 1TP3 turbine, the variation of $(Ne)_{gs}$ with Re is negligible, as a result of the change in fluid flow around and over the perforated blade. The formation of the ventilated cavities behind the modified blades was influenced by the impact of the jets that come through the blade perforations.
- For Re > 1,400, $(Ne)_{gs}$ becomes independent of the Reynolds number, but depends on particle and agitator types. The mixing is in the turbulent range and the phases are uniformly dispersed within the entire vessel section.

The relation between the power number and the physical and rheological properties of solid particles is presented in Figure 68.9 for the 1TR turbine at various aeration

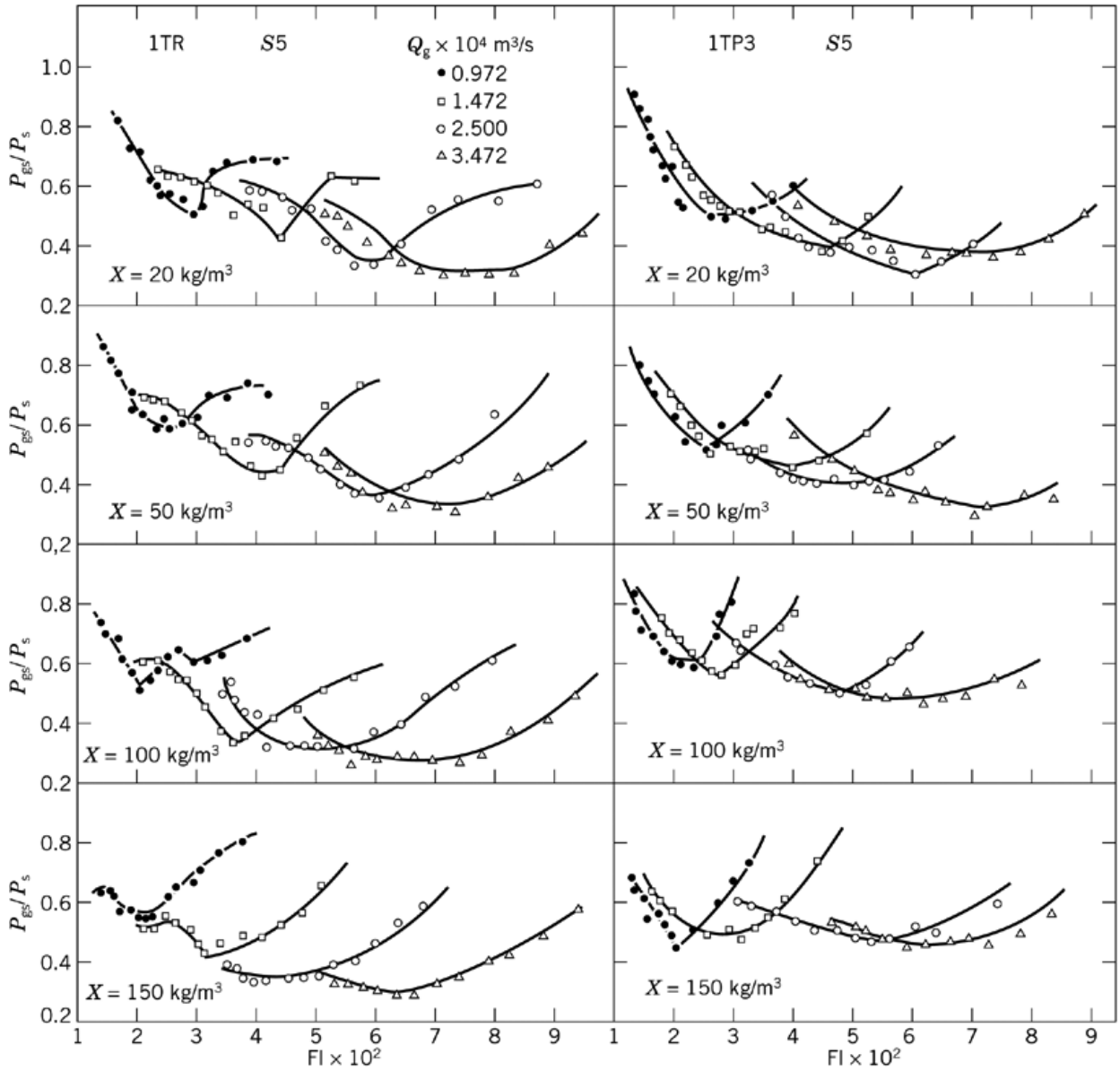


Figure 68.7. Relation between relative power consumption (P_{gs}/P_s) and gas flow number (Fl) for the S5 particles using single standard and modified turbines. (*Source*: From Ref. 27, with permission.)

conditions and for 1TP3, 2TP3, and 2TR turbines at constant aeration rate. For the same operation conditions, the modified blade turbines are more efficient, the power number $(Ne)_{gs}$ being reduced by 50% in comparison with the standard Rushton turbine.

68.3.4 Effect of Gas on Solid–Liquid Hydrodynamics

The effect of gas on solid–liquid hydrodynamics in mixing vessels was studied to determine the agitation speed required to just completely suspend all the particles under gassed conditions, N_{jsg} (28). The introduction of a small amount of gas into a solid–liquid system, for the just-suspended condition, causes slight sedimentation such that, for the same impeller speed, the particles were no longer just suspended (i.e., $N < N_{jsg}$). Further increases in the volumetric gas flow rate led to more sedimentation because the pumping capacity and ability of the impeller to circulate fluid and the power input decrease. Any decrease in pumping capacity and power input will decrease all the parameters that cause particle suspension: drag forces, energy dissipation, and associated turbulent eddies. An increase of the agitator speed to N_{jsg} ensured complete resuspension. Similarly, under gassed

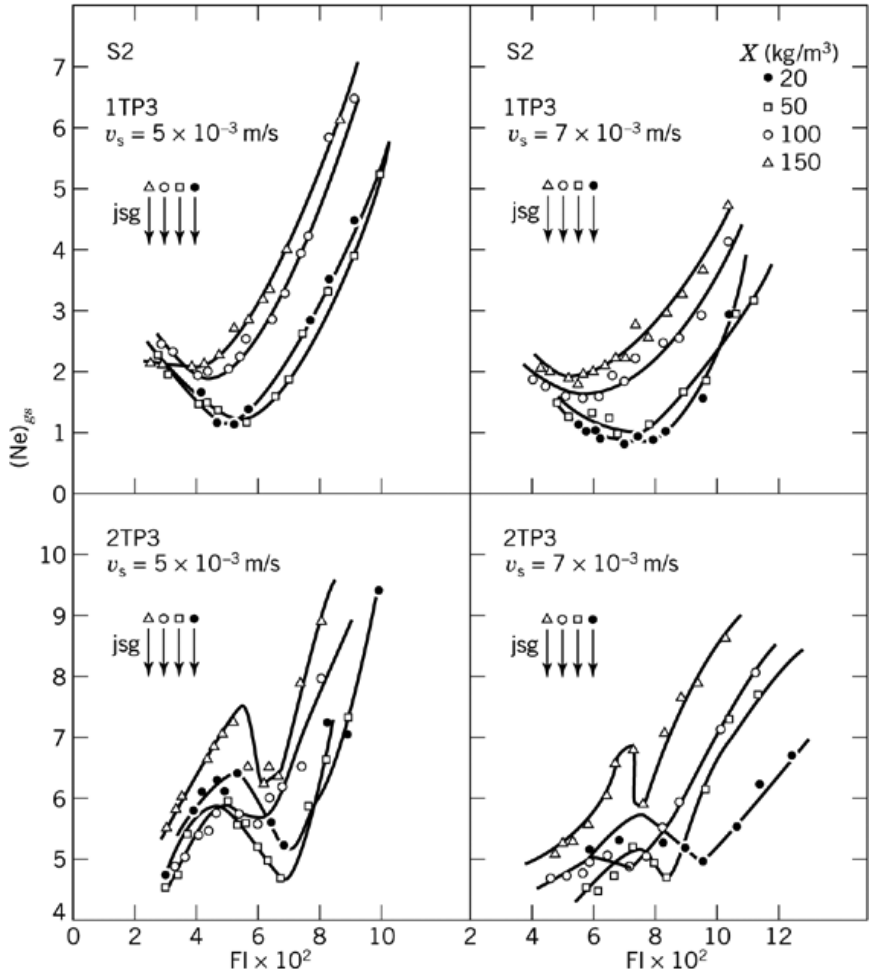


Figure 68.8. Variation of the power number with gas flow number for the S2 particles using modified turbines, single and double. (*Source*: From Ref. 27, with permission.)

conditions, if $N < N_{jsg}$, a reduction in volumetric gas flow rate gave complete resuspension. In fact, there is a unique combination of gas rate and impeller speed at which the just-suspended condition is achieved and which depends on the agitator type used.

If N_{jsg} is plotted against superficial gas velocity, v_s, the form of the curves is slowly parabolical, for any particle concentration (Figure 68.10). At superficial gas velocity of approximately 4×10^{-3} m/s, the slope of the dependence $N_{jsg} = f(v_s)$ decreases, demonstrating that the mechanism of the solid suspension changes. Indeed, this value of the superficial gas velocity is found around a gas flow number Fl = 0.03, when in gas–liquid systems, transition occurs between the clinging cavity regime and the large cavity regime (29,30). The presence of particles has no measurable effect on the formation of the gas-filled cavities.

As showed previously, for complete suspension to be maintained, a higher solid concentration requires a higher power input to the systems. The presence of the gas amplifies the effects mentioned, such that with increasing aeration rate, associated with increasing particle concentration, the agitator speed N_{jsg} must be larger (Fig. 68.11). The relationship for evaluation of the agitation speed required to just completely suspend all the particles under gassed conditions, N_{jsg}, takes into account the physical and rheological properties of suspensions, the aeration rate, and the equipment configuration (28).

68.4 MASS TRANSFER

The mass transfer process from the gas phase to the liquid phase is usually expressed in terms of the volumetric mass transfer coefficient, Kla. The determination methods of the volumetric oxygen transfer coefficient are divided by Rainer (31) into indirect methods, applied without biological system (gassing-out, electrode momentum, sulfite oxidation, carbon dioxide, and glucose oxidase

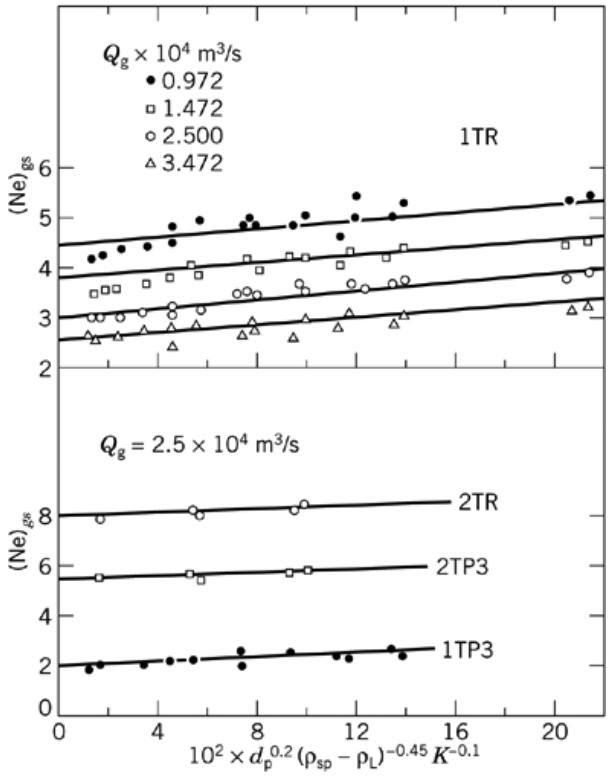


Figure 68.9. Relation between the power number and the physical and rheological properties of the suspension agitated by various agitator geometries. (*Source*: From Ref. 27, with permission.)

methods), and direct methods (method of gas balance, dynamic method, continuous culture method). The Kla values in mechanically agitated reactors depend on various parameters such as system properties, vessel and stirrer dimensions and arrangement, and operating conditions (32). To examine the behavior of the modified turbines regarding mass transfer, the Kla coefficients were determined in the presence and absence of the solid particles by the sulfite oxidation method.

68.4.1 Gas–Liquid Mass Transfer Characteristics

Figure 68.12 shows the measured Kla values as a function of gas flow number, Fl, for single and double turbine agitator of TP3 type, having as parameter the agitator speed (curves indicated in Figure 68.12 by the continual line) or the aeration rate (curves indicated by the dotted line). The same variation, Kla $= f$(Fl), was also observed for the other modified turbines and the Rushton turbine (33). The dependence of Kla on Fl, when N is constant, is greater at lower gas flow rates (lower gas flow numbers). At higher gas flow numbers, the curves tend to constant Kla values for all agitator speed values and single turbine types (Fig. 68.12a). In the case of double turbines (Fig. 68.12b), this tendency of the curves Kla $= f$(Fl) appears only at values $N < 10$ s^{-1}. This dependence of Kla on Fl can be explained by the prism of various hydrodynamic regimes, considering the value Fl $= 0.03$ as the transition point between the vortex-clinging cavity regime and large cavity regime (33). When the Kla values are represented depending on the gas flow number at a constant aeration rate (curves indicated by the dotted line in Figure 68.12), these increase slowly once with increasing the rotational speed when the agitator works in flooding regime (below line noted F/L in Figure 68.12). When the agitator works in the loading regime (over line F/L), the volumetric oxygen mass transfer coefficient increases considerably with the decreasing gas flow number.

One procedure for evaluating the volumetric oxygen mass transfer coefficient is based on knowledge of the specific power consumption (P_g/V) and the superficial gas velocity (v_s) (34):

$$\text{Kla} = c(P_g/V)^{0.95}(v_s)^{0.67} \tag{68.4}$$

The relationship between Kla and the product of the variables $(P_g/V)^{0.95}$ $(v_s)^{0.67}$ for all turbine types and their geometrical disposition is linear, the average value of the dimensional constant c being specific for each of the geometrical configurations studied.

The influence of the mixing system geometry on gas–liquid mass transfer is quantified by including, in equation 68.4, the geometrical elements $(n_p/6)$ and $(1 + S_G/S_C)$, which indicate the number of turbines and their type. The following correlations were obtained for the evaluations of the volumetric mass transfer coefficient:

$$\text{Kla} = 7.2202 \times 10^{-4}(1 + S_G/S_C)^{1.753}(n_p/6)^{-0.126} \cdot (P_g/V)^{0.95}(v_s)^{0.67} \text{ for } S_G/S_C \leq 0.353; r = 0.9843 \tag{68.5}$$

$$\text{Kla} = 2.721 \times 10^{-3}(1 + S_G/S_C)^{-2.73}(n_p/6)^{-0.141} \cdot (P_g/V)^{0.95}(v_s)^{0.67} \text{ for } S_G/S_C)0.353; r = 0.9629 \tag{68.6}$$

To obtain the same value of the volumetric mass transfer coefficient, the power consumption in the vessel equipped with the TR agitator is higher than that in the vessel equipped with the TP3 agitator. Therefore, the oxygen transfer efficiency E (m^3O_2/W h) (the oxygen volume transferred into the liquid phase for 1 W h of energy consumption for mixing) for one and two TP3 modified Rushton turbines, for any value of the aeration rate (Fig. 68.13), is more than 30% higher than those obtained with the TR turbines. The TR and TP5 turbines are similar as regards mass transfer efficiency.

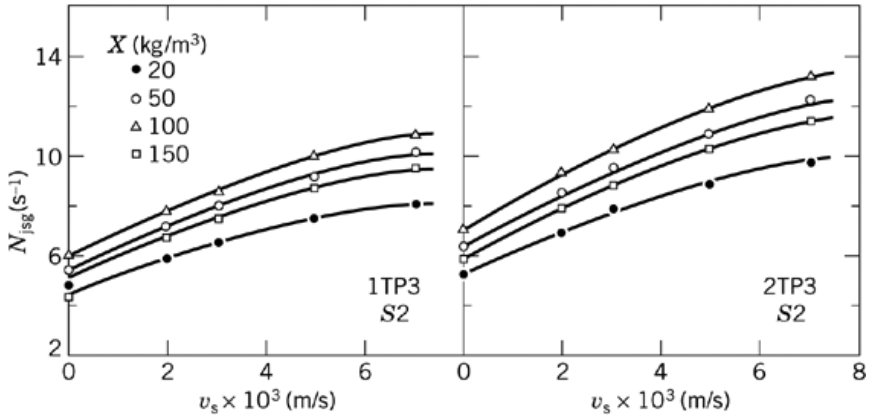


Figure 68.10. Relation between N_{jsg} and the superficial gas velocity (V_s) for the S2 suspension mixing with modified turbines. (*Source*: From Ref. 28, with permission.)

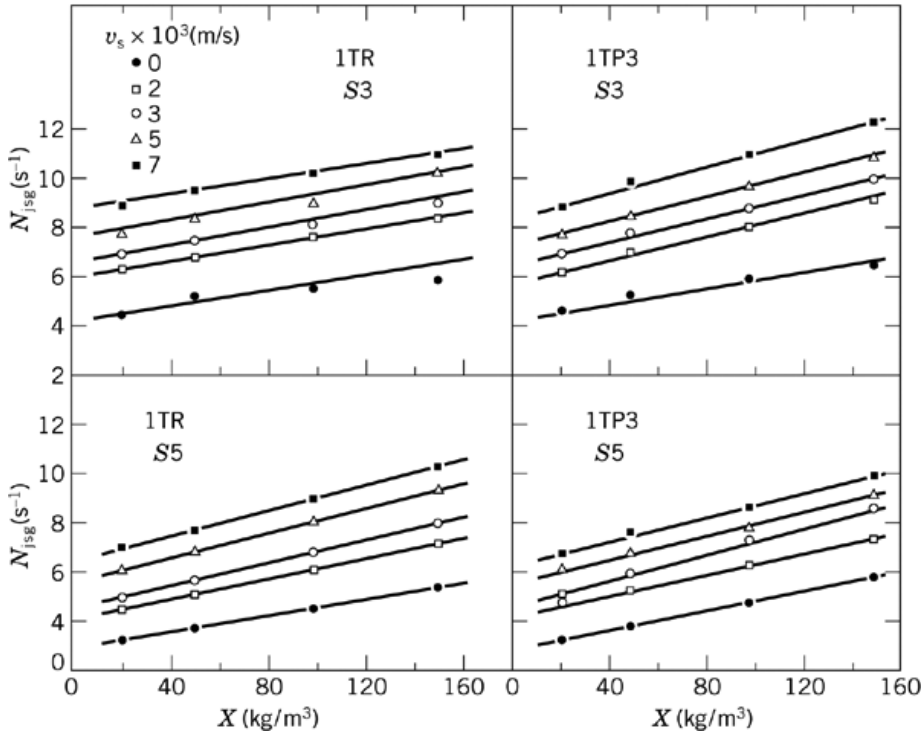


Figure 68.11. Relation between N_{jsg} (jsg, moment of complete solid suspension) and the solid concentration for various values of the superficial gas velocity. (*Source*: From Ref. 28, with permission.)

68.4.2 Effect of Particles on Gas–Liquid Mass Transfer

It has been observed that the addition of solids has an influence on gas–liquid mass transfer characteristics, even if these particles are not reactive and do not show increased adsorption of dissolved gases. The inert solid particles used in our work are $CaCO_3$ (S1) and cation exchange resin Amberlite IR-120 type (S3) (35). The experiments were carried out in the range of three-phase homogeneous mixing. The presence of the solid phase, with the concentration between 20 and 50 kg/m^3, influences the gas–liquid mass transfer as shown in Figure 68.14 for the standard (TR) and modified (TP3) turbines, single or double, at various values of superficial gas velocity. All curves show the same general trend.

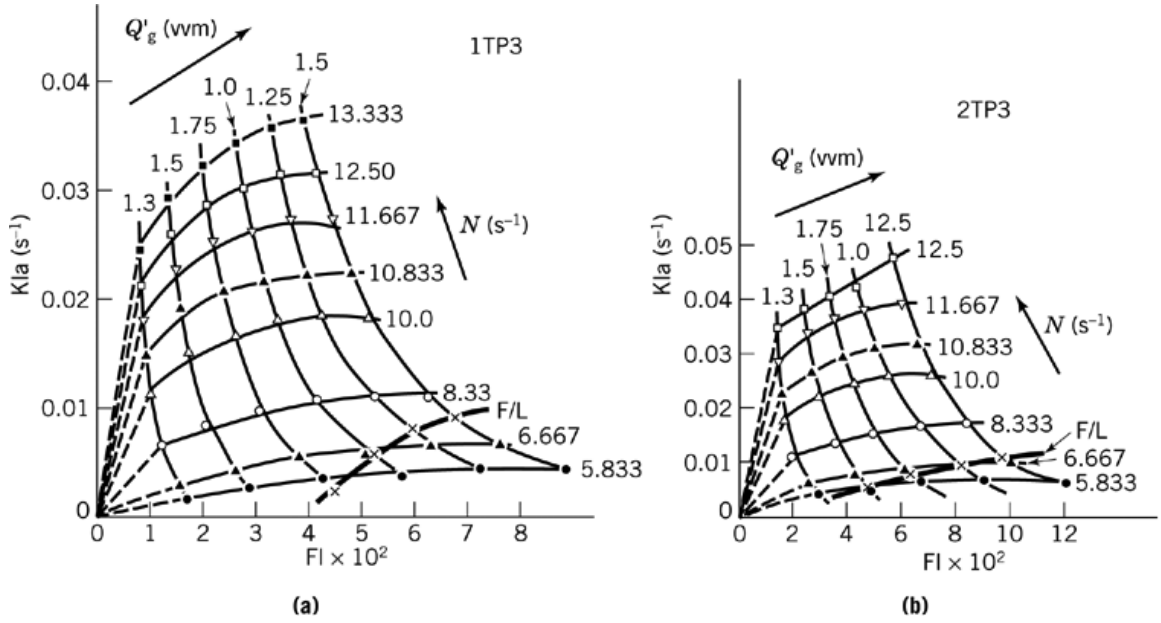


Figure 68.12. Variation of the volumetric mass transfer coefficient (Kla) depending on the gas flow number: (**a**) single TP3 modified Rushton turbine; (**b**) double TP3 modified Rushton turbines. (*Source*: From Ref. 33, with permission.)

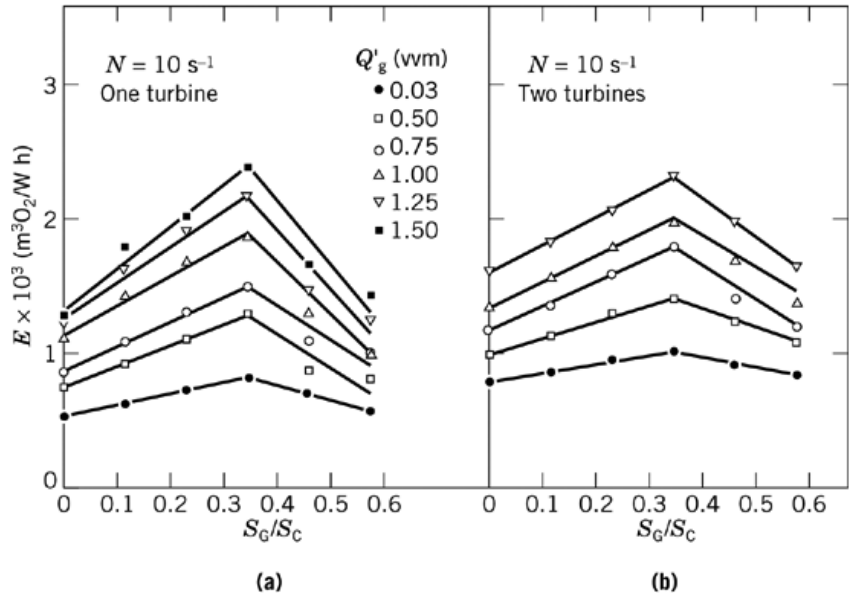


Figure 68.13. Variation of the oxygen transfer efficiency (E) depending on the surface fraction of the perforation at various values of the aeration rate: (**a**) single turbine; (**b**) double turbines. (*Source*: From Ref. 33, with permission.)

For $CaCO_3$ particles (S1 solid), a very slight increase of the Kla coefficient is observed until $X = 50$ kg/m^3, while the addition of the cation exchange resin in a proportion of 20 kg/m^3 leads to a pronounced increase of the Kla value, particularly at $N = 11.667$ s^{-1} and at higher values of the superficial gas velocity. This trend of the Kla coefficient to increase in the range of small solid concentration was explained by Brehm (36) that at the moderate agitator speed ($N < 15$ s^{-1}) the solid particles can move independently of fluid elements and break up the gas–liquid interface, which leads to decreasing thickness of the boundary layer. When increasing the solid concentration beyond the values

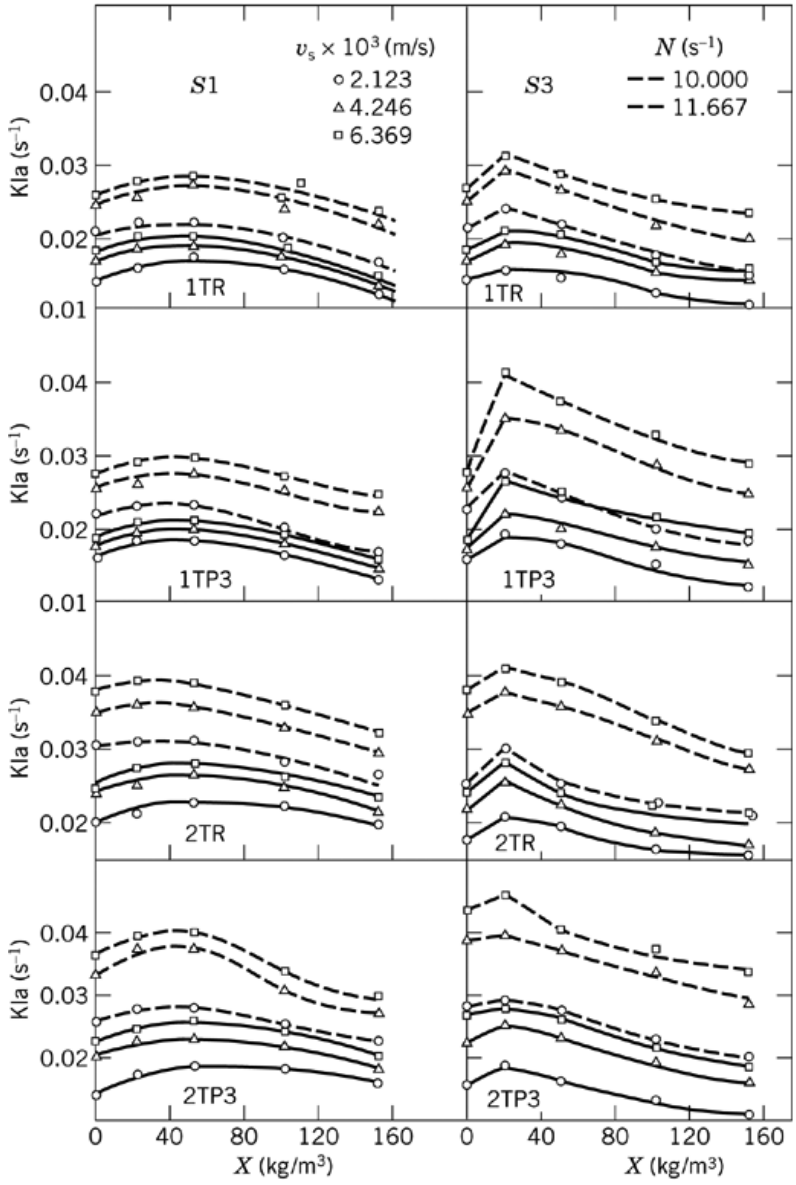


Figure 68.14. Effect of solid concentration on volumetric mass transfer coefficient for standard and modified Rushton turbine, positioned singly or doubly on the same shaft. (*Source*: From Ref. 35, with permission.)

mentioned, the Kla coefficient gradually decreases toward values smaller than those obtained in gas–liquid systems.

Two main factors are responsible for this reduction of the Kla values (37): one factor is the change of the rheological properties of the suspensions and the other is enhanced bubble coalescence, which is caused by turbulence intensity damping. The higher Kla values for mixing with two turbines (Fig. 68.14) are due to the their higher power consumption for the same operation conditions.

In the three-phase system, the oxygen transfer efficiency, E, decreases with increase of solid concentration, irrespective of the agitator type (Fig. 68.15), but for mixing with the TP3 modified turbines, the E values are more than 45% higher than those obtained using TR turbines. The experimental data regarding the mass transfer in gas–liquid suspensions demonstrate that the Kla values depend on the physical and rheological properties. The effect of the solid particles on Kla value is given by the group $K^{-0.15}X^{-0.1}$, which includes the consistency index K as a pseudo-viscosity of the suspensions. Therefore:

$$\text{Kla} = 7.2202 \times 10^{-4}(1 + S_G/S_C)^{1.753}(n_p/6)^{-0.126} \cdot (P_g/V)^{0.95}(v_s)^{0.67}K^{-0.15}X^{-0.1} \qquad (68.7)$$

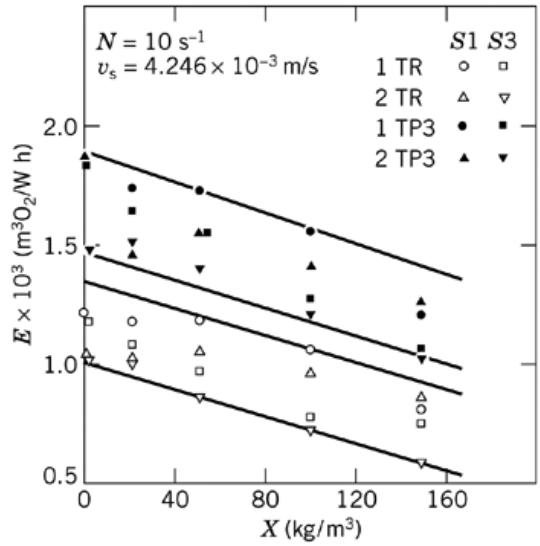


Figure 68.15. Relation between oxygen transfer efficiency and solid concentration for various agitators. (*Source*: From Ref. 35, with permission.)

Equation 68.7 describes the experimental data with an average error of 20%.

68.5 PERFORMANCE OF THE MODIFIED AGITATORS IN BIOSYNTHESIS OF ANTIBIOTICS

The transport phenomena in submerged aerobic fermentation involve mixing and mass and heat transfer in three-phase systems consisting of gas bubbles and suspended microorganisms in a liquid phase and are strongly influenced by the rheological properties of the medium used. The rheology of the broth is affected by the composition of the original medium and its modification by the growing culture, the concentration and morphology of the biomass, and the concentration of microbial products. Complex interaction between transport phenomena and reaction kinetics characterizes bioreactors and determines their performance. The modified turbine TP3 with the surface fraction S_G/S_C of perforations equal to 0.353, considered an optimum in dispersion of the gas and solids in liquid, was investigated in antibiotic biosynthesis liquids in semiindustrial and industrial bioreactors.

68.5.1 Biosynthesis of Antibiotics in Semiindustrial-Scale Bioreactors

The experiments were carried out in two 20-m^3 stainless steel stirred tank bioreactors, equipped with three modified Rushton turbines (TP3) (blade width × blade length = 0.306 × 0.225 m), and three witness Rushton turbines (TR) (blade width × blade length = 0.225 × 0.225 m), respectively, having the same diameter and rotating with the same agitator speed (38). The experimental data in the biological systems were obtained using four different microorganisms: *Streptomyces erithreus*, *S. griseus*, *S. noursei*, and *Nocardia mediterranei*, producing erythromycin, streptomycin, nystatin, and rifamycin, respectively. During the four parallel fermentations, the specific power consumption, the volumetric oxygen mass transfer coefficient, the oxygen transfer efficiency, and the antibiotic concentrations were investigated. For each fermentation type, the power consumption for the TP3 agitator is diminished by a factor of 1.18 (streptomycin) to 1.6 (erythromycin) compared to that for the TR agitator (Fig. 68.16). Therefore, in the viscous mycelial fermentation, the TP3 agitator minimizes the drag forces associated with the motion of the blades, confirming the observations presented for a nonbiological system.

The Kla values, as measured by the dynamic method, decrease during the fermentation processes, depending on the microorganism growing in the liquid (Fig. 68.17). The fermentation media for *S. erithreus* and *S. noursei*, producing erythromycin and nystatin, respectively, contain starch as a degradable component (22,39), which confers a high

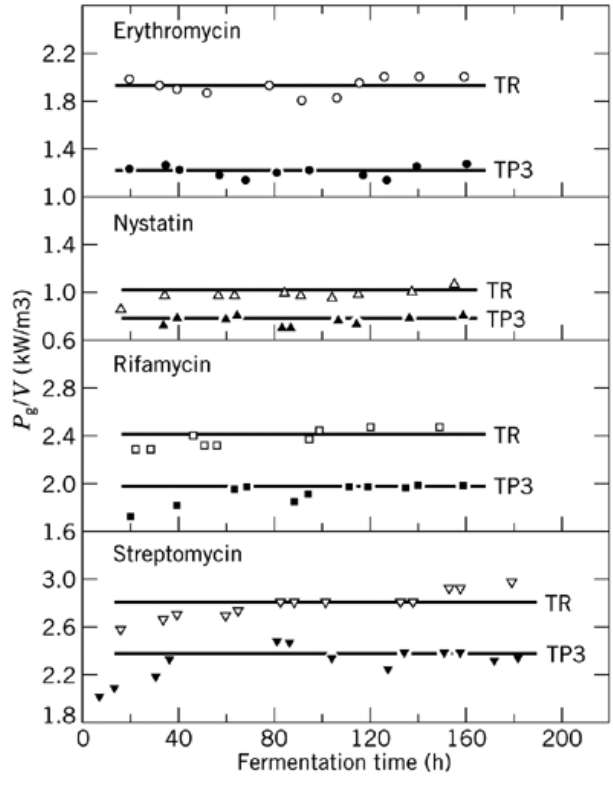


Figure 68.16. Comparison of TP3 and TR agitators with respect to specific power consumption in the course of processes in the biosynthesis of antibiotics. (*Source*: From Ref. 38, with permission.)

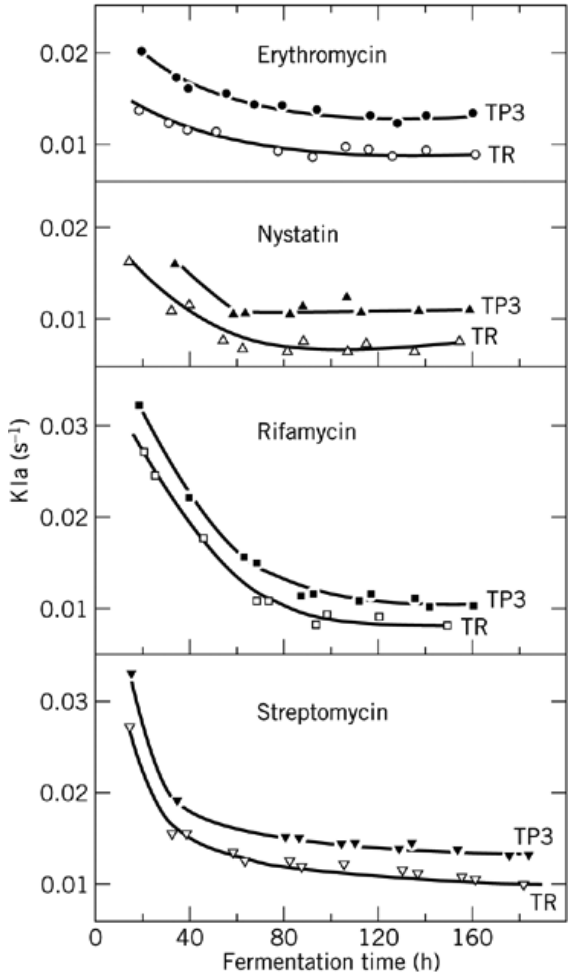


Figure 68.17. Comparison of TP3 and TR agitators with respect to the volumetric oxygen mass transfer coefficient in the course of processes in the biosynthesis of antibiotics. (*Source*: From Ref. 38, with permission.)

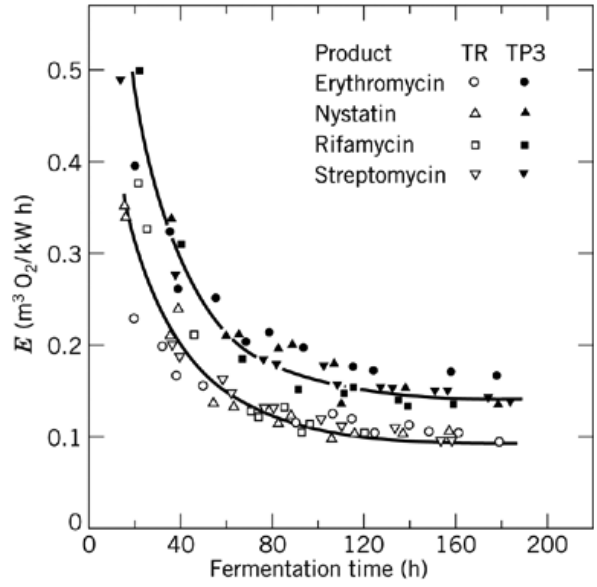


Figure 68.18. Comparison of TP3 and TR agitators with respect to oxygen transfer efficiency in the course of processes in the biosynthesis of antibiotics. (*Source*: From Ref. 38, with permission.)

viscosity on the initial medium; thus, Kla is smaller at the beginning of biosynthesis, compared to the initial medium for *S. noursei* and *N. mediterranei* without this component. The Kla values obtained under mixing conditions with the TP3 agitator are 25% (streptomycin) to 50% (nystatin) higher than those obtained by using the TR agitator. This effect can be explained by the improvement of the dispersion of the gas bubbles as a result of the impact of the jets that come through the perforations in the TP3 blades onto the relatively surface in the back of large cavities.

Because the TP3 blades are higher by 36% in comparison with the witness blades, the size of the well-mixed, low-viscosity, and high-Kla region is effectively increased. In the micromixing region, excellent bubble breakup and shear thinning of the viscous medium occurs, which results in oxygen transfer improving in accordance with the concepts of Bajpai and Reuss (40). Also, the macromixing region, away from the impeller where the oxygen transfer is relatively poor, is much smaller.

In the investigated biological systems, for 1 W h of energy consumption (for agitation and air compression), the oxygen volume transferred into the liquid phase is approximately 30% higher in the bioreactor equipped with a TP3 agitator (Fig. 68.18). The oxygen transferred into the medium is consumed mainly in the combustion reaction that takes place within the biomass, on which the antibiotic production depends. The relative antibiotic concentrations measured over the entire course of the fermentations are plotted in Figure 68.19.

The efficiency of the TP3 agitator was confirmed in that antibiotic production increased up to 35% in nystatin biosynthesis, as much as 9% in rifamycin biosynthesis, and up to 20% in streptomycin biosynthesis as well. No difference in erythromycin production was observed between the two parallel fermentations, but efficiency occurs from the energy savings. Therefore, using the TP3 agitator in the biosynthesis of antibiotics, it is possible to minimize the power consumption and to increase the antibiotic production for the same operating conditions as well as the TR agitator.

68.5.2 Biosynthesis of Antibiotics in Industrial-Scale Bioreactors

In the biosynthesis of antibiotics in semiindustrial-scale bioreactors, it was demonstrated that when the modified agitator has the same diameter and rotates with the same

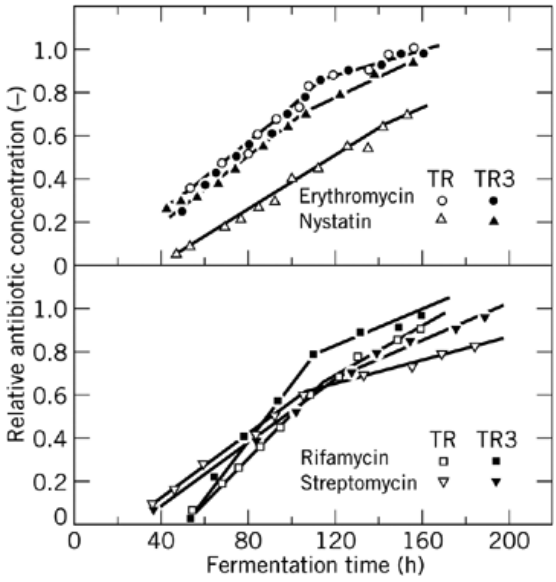


Figure 68.19. Relative antibiotic concentration profiles during the biosynthesis process using the TP3 and TR agitators in semiindustrial-scale bioreactors. (*Source*: From Ref. 38, with permission.)

agitator speed as the standard agitator, the power consumption is reduced by a factor of 1.18 to 1.6 (38). Therefore, the use of a modified agitator in biosynthesis of the antibiotics may improve the productivity for a given power input by increasing the TP3 impeller diameter and keeping the agitator speed as high as for the TR agitator, and by increasing the TP3 agitator speed and keeping the impeller diameter as large as for the TR agitator.

The improved agitation performance by modified Rushton turbine agitators corresponding to the two aforementioned cases (if the specific power consumption is constant) was verified experimentally in industrial-scale bioreactors, as follows (41):

- In parallel fermentations of *S. aureofaciens* and *S. rimosus*, producing tetracycline and oxytetracycline, respectively, in two 100-m^3 stainless steel stirred tank bioreactors equipped with four modified impellers (TP3) and four standard impellers (TR), respectively (first case)
- In parallel fermentations of *Penicillium chrysogenum* producing penicillin, in two 63-m^3 stainless steel stirred tank bioreactors equipped with three modified impellers (TP3) and three standard impellers (TR), respectively (second case)

The morphology of molds is a function of shear stresses in the bioreactor. The growth rate and partial pressure of oxygen, and the following elements, play a role: the growth of hyphae, the branching of hyphae, the dispersion (breakup) of hyphae caused by the shear stress in the vessel, and the tensile strength of hyphae. The breakup frequency (λ/k_o) is proportional to the frequency that a particle will have in the so-called dispersion zone (V_{disp}), that is, the volume at which the turbulent shear forces are greater than the forces necessary to break the hyphal cell wall (42). The λ/k_o and V_{disp} values for the agitators investigated are presented in Table 68.3.

Therefore, by using the TP3 agitators, the size of the well-mixed region is effectively increased up to 27% and the breakup frequency of the mycelial hyphae is increased up to 75%. The relative antibiotic production and variation of the specific antibiotic production rate, Q_p, during the cultivation time, are plotted in Figures 68.20 and 68.21, respectively. The improvement in antibiotic production by more than 30% by using modified agitators can be explained by creating a better hydrodynamic microclimate, and effectively increasing the well-mixed region, oxygen mass transfer, discharge efficiency, and the breakup frequency of mycelial hyphae.

The Q_p values reach a maximum in the early exponential phase of batch growth, although the cell mass concentration is small. The maximum values of the specific antibiotic

TABLE 68.3. Breakup Frequency of the Mycelial Hyphae and the Dispersion Zone of TP3 and TR Agitators

Product	Agitator	V_{disp} (m^3)	$\lambda/k_0 10^2 (s^{-1})$
Tetracycline and oxytetracycline	TR	1.846	1.688
	TP3	3.522	4.808
Penicillin	TR	1.948	2.255
	TF3	2.474	3.937

Source: Ref. 41.

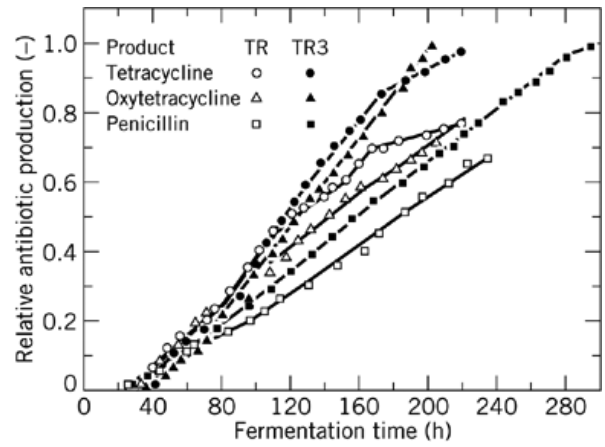


Figure 68.20. Relative antibiotic concentration profiles during the biosynthesis process using the TP3 and TR agitators in industrial-scale bioreactors. (*Source*: From Ref. 41, with permission.)

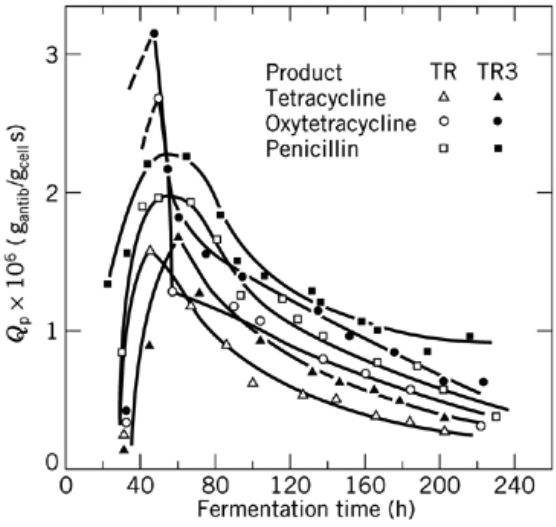


Figure 68.21. Specific antibiotic production rate profiles during the biosynthesis process using TP3 and TR agitators. (*Source*: From Ref. 41, with permission.)

production rate and the fermentation time at which these maximum points are reached depend on the type of producing microorganism and the type of agitator. Therefore, the standard and modified agitators create various types of environmental conditions under which the cells appear to adapt by structural and functional changes.

REFERENCES

1. M.M.C.G. Warmoeskerken, Ph.D. Thesis, University of Delft, The Netherlands, 1985.
2. J.M. Smith, in J.J. Ulbrecht and G.K. Patterson eds., Mixing of Liquid by Mechanical Agitation, Gordon and Breach, New York, 1985, pp. 139–202.
3. A.W. Nienow and J.J. Ulbrecht, in J.J. Ulbrecht and G.K. Patterson eds., Mixing of Liquid by Mechanical Agitation, Gordon and Breach, New York, 1985, pp. 203–237.
4. F. Kargi and M. Moo-Young, in M. Moo-Young, ed., Comprehensive Biotechnology, vol. 2, Pergamon Press, Oxford, 1985, pp. 5–56.
5. R.V. Roman and R.Z. Tudose, Rev. Chim. 46: 547–564 (1995).
6. R.V. Roman and R.Z. Tudose, Roum. Chem. Q. Rev. 4: 269–293 (1996).
7. R.V. Roman, Ph.D. Thesis, Technical University, Iasi, Roumania, 1997.
8. R.V. Roman and R.Z. Tudose, Chem. Eng. J. 61: 83–93 (1996).
9. R.V. Roman and M. Gavrilescu, Hung. J. Ind. Chem. 22: 87–93 (1994).
10. V. Abrardi, G. Rovero, G. Baldi, S. Sicardi, and R. Conti, Trans. Inst. Chem. Eng. A 68: 516–521 (1990).
11. R.V. Roman and R.Z. Tudose, Rev. Roum. Chim. 41: 309–319 (1996).
12. W. Bujalski, A.W. Nienow, S. Chatwin, and M. Cooke, Chem. Eng. Sci. 42: 317–326 (1987).
13. E.A. Bratu, Operatii Unitare în Industria Chimică, vol. 2, Editura Technică, Bucharest, 1985, p. 20.
14. R.V. Roman, M. Gavrilescu, and V. Efimov, Hung. J. Ind. Chem. 20: 155–160 (1992).
15. R.K. Geisler, R.K. Buurman, and A.B. Mersmann, Chem. Eng. J. 51: 29–39 (1993).
16. K. Takahashi, H. Fujita, and T. Yokota, Chem. Eng. Jpn. 26: 98–100 (1993).
17. A. Barresi and G. Baldi, Chem. Eng. Sci. 42: 2949–2956 (1987).
18. K.J. Myers, Can. J. Chem. Eng. 72: 745–748 (1994).
19. T.N. Zwietering, Chem. Eng. Sci. 8: 244–253 (1958).
20. R.V. Roman and R.Z. Tudose, Bioprocess Eng. 15: 221–229 (1996).
21. T. Koloini, I. Plazi, and M. Zumer, Chem. Eng. Res. Des. 67: 526–536 (1989).
22. M. Gavrilescu, R.V. Roman, and V. Efimov, Acta Biotechnol. 12: 383–396 (1992).
23. P.M. Armenante and T. Li, AIChE Symp. Ser. 293: 105–111 (1993).
24. C. Buurman, I. Chem. E. Symp. Ser. 121: 343–350 (1990).
25. M. Greaves and V.Y. Loh, I. Chem. E. Symp. Ser. 89: 69–96 (1984).
26. K. Vant Riet, Ph.D. Thesis, University of Delft, The Netherlands, 1975.
27. R.V. Roman and R.Z. Tudose, Bioprocess Eng. 16: 135–144 (1997).
28. R.V. Roman and R.Z. Tudose, Bioprocess Eng. 17: 55–60 (1997).
29. R.V. Roman and R.Z. Tudose, Hung. J. Ind. Chem. 24: 161–169 (1996).
30. R.V. Roman and R.Z. Tudose, Bioprocess Eng. 17: 307–316 (1997).
31. B.W. Rainer, Chem. Biochem. Eng. Q4: 185–196 (1990).
32. H. Oguz, A. Brehm, and W.D. Deckwer, Chem. Eng. Sci. 42: 1815–1822 (1987).
33. R.V. Roman and R.Z. Tudose, Hung. J. Ind. Chem. 24: 185–192 (1996).
34. N.M.G. Oosterhuis, Ph.D. Thesis, University of Delft, The Netherlands, 1984.
35. R.V. Roman and R.Z. Tudose, Bioprocess Eng. 17: 361–365 (1997).
36. A. Brehm, S. Ledakowicz, and R. Kokuun, Proc. 8th Int. Cong. CHISA, Praha, 1984.
37. W.M. Lu, R.C. Hsu, and H.S. Chou, J. Chim. I. Ch. E. 24: 31–39 (1993).
38. R.V. Roman and M. Gavrilescu, Acta Biotechnol. 14: 181–192 (1994).
39. M. Gavrilescu, R.V. Roman, and V. Efimov, Acta Biotechnol. 13: 59–70 (1993).
40. R.K. Bajpai and M. Reuss, Can. J. Chem. Eng. 60: 384–392 (1982).
41. R.V. Roman, R.Z. Tudose, M. Gavrilescu, M. Cojocaru, and S. Luca, Acta Biotechnol. 16: 43–56 (1996).
42. J.C. Van Suijdam and B. Metz, Biotechnol. Bioeng. 23: 111–148 (1981).

PART V

PROCESS ANALYTICAL TECHNOLOGIES (PAT)

69

BIOPROCESS AND FERMENTATION MONITORING

Michael Pohlscheidt, Salim Charaniya, and Christopher Bork
Genentech Inc., Manufacturing Science and Technology, Oceanside, California, USA
Marco Jenzsch and Tim L. Noetzel
Roche Diagnostics GmbH, Pharma Biotech, Penzberg, Germany
Andreas Luebbert
Martin Luther University, Halle, Germany

69.1 INTRODUCTION

The monitoring and control of processes is of key importance in all industries. Effective methods of monitoring are required to develop, optimize, and maintain processes at a maximum efficiency and desired product quality. Biotechnological processes are no exception to this (1,2).

Biotechnology processes are used to produce a large variety of products, such as primary and secondary metabolites, cells, tissues, vaccines, and therapeutic proteins (2). Different host cell systems are used in the modern biotechnology, for example, bacterial cells, plant cells, and eukaryotic cells, with specific requirements for bioreactor design, media composition, and process control. Especially the production of recombinant proteins and antibodies has become a major source of revenue during the past 30 years, which are typically produced by genetically engineered mammalian cells. The cultivation of mammalian cells requires, among other factors, complex media composition, specialized bioreactor design, and the control of various parameters in narrow ranges to obtain the desired productivity and product quality. Therefore, more research has been devoted to develop specifically designed sensors, sampling strategies, and integrated data management systems to allow better and more detailed process monitoring (3). Advanced analytical technologies are required in all phases of a product and process life cycle. During the development stage, it is needed to create knowledge and understanding of the process and therefore optimize the process with accelerated timelines (e.g. high throughput screening and design of experiments). During process characterization and validation, it is essential to understand and determine control limits, set points, and critical process parameters, which have an influence on process performance and, more importantly, affect product quality. In routine production, it is essential to control the process at the set points within the operating ranges. These process parameters are defined during process development and characterization to achieve the desired product quantity and quality and support ongoing process monitoring/validation as required by the health authorities.

The process analytical technology (PAT) framework published by the Food and Drug Administration (FDA) in 2004 describes PAT as a mechanism to design, analyze, and control pharmaceutical manufacturing processes through the measurement of (critical) process parameters that affect quality attributes of the product (4). The concept is based on building quality through deep understanding and control of the process, especially critical quality attributes and their interactions/dependencies to other parameters. This requires a comprehensive detection system to measure, analyze,

Upstream Industrial Biotechnology: Equipment, Process Design, Sensing, Control, and cGMP Operations, Volume 2, First Edition. Edited by Michael C. Flickinger.
© 2013 John Wiley & Sons, Inc. Published 2013 by John Wiley & Sons, Inc.

monitor, and control all important attributes of a bioprocess and the employment of feedback-based control systems, including integrated data management and analysis. Over the past several years, there has been a lot of effort in analytical technologies to enable these stringent controls (5).

The chapter describes general operational aspects of sensors, sampling technologies, and methods of process monitoring, examples for different controls and advanced applications such as soft sensors and metabolic controls. Some aspects are based on a previous article published in 2010 (1).

69.2 GENERAL ASPECTS OF SENSORS AND MONITORING

Several bioprocess sensors have been designed and are employed for routine applications. For bioprocesses monitoring, the following areas for physical, chemical, and biological parameters are commonly monitored (Fig. 69.1).

For any measuring technique, there are a number of criteria that the measuring device must satisfy to enable its deployment in commercial bioprocess manufacturing. The following list of characteristic is not exclusive, but does cover the main aspects of sensor attributes and characteristics (see also Ref. 1 for more details).

69.2.1 Measurement Frequency and Costs

In most cases—especially in context of the PAT initiative—real-time measurements at a high frequency are highly desirable. However, in some cases, this is not necessary and the kinetics of the reaction, consumption, and evolution must be considered in determining the frequency of measurements. In addition, differences in the life cycle of the process and cost aspects must be evaluated during the selection of one or more monitoring techniques. For research and development (R&D) purposes, in general, more data are obtained and collected to gain deeper process understanding and optimize process robustness and yield. At this stage, higher costs are often more acceptable compared with commercial bioprocessing. For routine operations, critical and important variables must be monitored and controlled within predefined intervals. A secondary aspect is cost; measurements that are resource and time intensive, but not critical to the process from a product quality and quantity perspective, may not be implemented. In general, high frequency at low costs, time, and resource consumption is desired, including automated data handling and analysis.

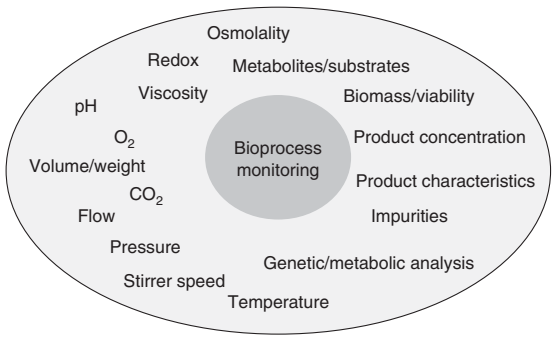


Figure 69.1. Major areas for bioprocess and fermentation monitoring.

For biological processes, the growth rates, substrate depletion rates, and evolution rates of products, by-products, and impurities are most relevant for the measurement frequency. Animal cells, for example, display a doubling time of approximately 1/ day. Bacterial cultures such as *Escherichia coli* display a doubling time of 20–30 min, also reflecting their metabolic activities. It becomes obvious that the measurement frequency to control feed rates and other physical parameters has to be much higher in bacterial cultures compared with animal cell cultures. Therefore, some fully automated systems have been developed for off-line or online analysis. *In situ* probes (discussed later) with fully automated analysis, such as spectral analysis, *in situ* microscopes, and off-gas analysis, have also been established.

69.2.2 Ease of Validation and Implementation

If operated in a regulated environment, the method and sensor should be easy to validate and qualify. Efforts required to validate and implement the sensor should not be complex as this could also affect project timelines, for example, implementation of a new sensor during a technology transfer project. Standard platforms that have been assessed toward this factor are often used for bioprocess operations at a large scale. In recent years, the aspects of leachables and extractables have become more important in the industry and should be considered as well because these can affect cells or even product quality attributes.

69.2.3 Easy to Use and Maintain

A sensor should be easy to maintain and easy to use (e.g. calibration and exchange of membranes). This may not be a primary focus during research and development. However, for routine operations, this is an important factor in terms of reliable execution: manufacturing schedule impacts for planned and predictable performance of operations. In general, calibration of the sensor and other preventive maintenance activities should be part of routine operations with intervals: calibration ranges and other requirements specified in operating procedures.

69.2.4 Cleaning Aspects and Sterility

When operated in an aseptic or sterile environment, the sensor must be amenable to clean in place (CIP) and steam

in place (SIP) without nonpredictable effects to performance of the sensor. This can be a threat because aggressive chemicals as well as high temperatures may be used to obtain sufficient cleaning and sterility/aseptic conditions. In biotech processes, temperatures in the range of 121–130°C are common for sterilization, and treatment of surfaces with hot base or acid is common for cleaning. The general acceptance and impact on lifetimes and performance for various probes can be found in vendor recommendations. Nevertheless, the standard probes currently applied in most routine (GMP) production biotech processes, such as pH or dO_2, are able to cope with these conditions quite well. Sensor drifts affected by caustic solution or heat treatment my occur, but are usually not an issue because most often these probes are operated in a single-use mode or at least only for a few batches with appropriate calibration cycles that assure the desired sensor performance.

Beside, the possibility of *in situ* sterilization probes and their fittings into the bioreactor are a critical point with respect to the sterile boundary. This is one of the key aspects, which has to be considered when introducing new probes into a (GMP) manufacturing environment.

69.2.5 Reliability, Accuracy, and Reproducibility

A sensor, especially when used online, has to provide reliable performance over a large span of time. Mammalian cell culture processes, for example, have operating times of up to several weeks (or months in perfusion systems) and therefore the probe/sensor has to deliver reliable performance to avoid failures and batch losses. The sensor should always provide sufficient accuracy in the desired control range. A low error between actual value and measured value is a prerequisite for adequate control. Measurement should be reproducible and drift only in an acceptable range for the measurement.

69.2.6 Linearity, Sensitivity, and Specificity

A measurement signal in most cases is directly proportional to the concentration of the component. Sometimes, there need to be corrections, and sample dilution has to be performed to overcome the effect of nonlinearity. A sensor has to deliver appropriate sensitivity to measure changes in the concentrations. The lowest level of detection is related to the sensitivity and the signal-to-noise ratio. Specificity is a statistical measure of how well a test correctly identifies the negative cases or those cases that do not meet the condition under study. Specificity is defined as the number of true negatives divided by the total sum of true negatives and false positives. A sensor with high sensitivity and specificity is capable of identifying and possibly quantifying a small signal, while still differentiating between a true signal and noise.

69.2.7 Response Time

The measurement of any process variable will entail a time delay between change in the parameter and display of the measured value. The response time should be appropriate for the progress of the bioprocess, particularly if the measurements are linked to a control action. For tight control limits and fast reaction times, an off-line sensor may not be appropriate. *In situ* measurement or online monitoring might be more appropriate. The response time of the sensor also depends on the control requirements of the bioprocess. For example, in a high cell density culture, dissolved oxygen (DO) will be depleted in a few minutes. Hence, DO is almost always monitored using an *in situ* sensor with a response time in seconds.

The importance of these aspects and factors varies and is different from R&D to a routine manufacturing application (6). Table 69.1 shows the importance of different aspects during the life cycle of a process (+ = low; ++ = medium; +++ = high).

69.3 METHODS OF MONITORING

In principle, analytics can be performed in two ways: withdraw a sample and perform off-line analysis or by integrating the sensor in the process, for example, bioreactor, peripheral equipment, and external loops, to enable online or *in situ* monitoring (Fig. 69.2). In some cases, a combination with auto sampling devices can lead to an "*in situ* sampling and *ex situ* sensor" (3,5).

TABLE 69.1. Aspects of Sensor and Their Importance During the Life Cycle of a Process from Research to Commercial Manufacturing (6)

Factors/Aspect	Research	Process Development	Manufacturing
Reliability, accuracy, reproducibility	+++	+++	+++
Selectivity, sensitivity, linearity	+++	+++	+++
Calibration	+/++	++	+++
Ease of validation and implementation	++	++	+++
Cleaning aspects and sterility	+/+++	+/+++	+++
Analysis frequency and costs	++	++	+++
Robust and easy to maintain	+	++	+++

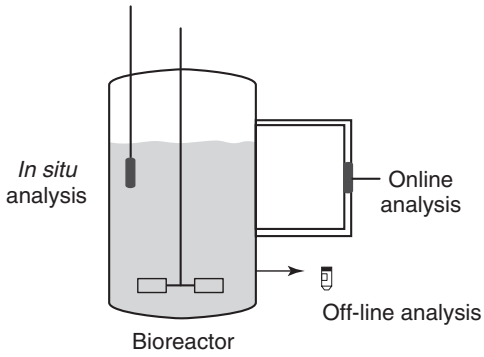


Figure 69.2. Different methods of monitoring and sensor interfaces with the process.

69.3.1 Off-Line Monitoring

For off-line monitoring, a sample is withdrawn from the bioreactor/vessel and analyzed after sample preparation in a suitable device. The preparation and handling of the sample is of crucial importance because it may affect the accuracy of the measurement. For example, for cell counts, homogeneous mixing after sampling and short lead times can be important. For pH and CO_2, rapid measurement is needed to avoid drifting due to off-gassing. This is especially important for pH to avoid offsets between *in situ* and off-line control measurements because pH is often controlled in a narrow range for bioprocesses. An important aspect (especially for bioburden monitoring) can be the aseptic treatment of the sample. For all off-line samples, detailed procedures, trained staff, and suitable laboratory are required. Off-line analytics always has a delay and affects the frequency of the measurement.

69.3.2 *In situ* or In-Line Monitoring

In Situ and in-line monitoring involves the use of sensors placed directly in the vessel or the flow lines associated with it or the unit operation (e.g. conductivity or pH monitoring in purification steps). The use of *in situ* sensors are well established, especially for chemical or physical parameters (pH, redox potential, O_2, CO_2, conductivity, and turbidity) (7). *In Situ* monitoring allows rapid measurement in high frequency and therefore enables real-time measurement and direct control. Robustness, long-term stability, aseptic design, and SIP/CIP capability are a prerequisite (and sometimes a pitfall) for these sensors and probes. Sometimes, *in situ* probes can be placed in external loops. The use of bypasses and additional peripheral equipment always adds potential risks to the process (e.g. sterile barriers, pumping of cells and protein and associated shear force, and cells outside a controlled environment) and therefore need to be carefully considered.

69.3.3 Online Monitoring

A compromise between *in situ* and off-line monitoring can be found with online monitoring, where a sample is automatically withdrawn and analyzed. One example of this has been the development (since the early 1980s) of flow injection analysis (FIA). This is a liquid handling technique that has proved flexible and adaptable to most chemical and biochemical reaction procedures (8), representing an effective compromise between the desirability of *in situ* monitoring and the technical ease of off-line measurements. The principal advantages of online methods are that sensor sterilization can be readily accomplished, sample pretreatment (e.g. gassing, dilution, and removal of interferences) is readily achievable, and sensor calibration can be built into the system. The main disadvantages are a need for an effective and reliable sampling system and the fact that the signal is discontinuous; the frequency of measurement is determined by the overall FIA design and the inherent limitation of the approach (3).

69.4 SENSOR, DEVICES, AND TECHNOLOGIES

69.4.1 pH Measurement

pH is a critical factor in most bioprocesses (5,6). As the impact on performance and in some cases impact on product quality has been described, an *in situ* monitoring and control is needed. In addition, a risk mitigation strategy is widely used by comparing *in situ* measurement with periodic off-line measurements. The most common form of pH sensor used for fermentation monitoring is based on the electrode design introduced by Ingold in 1947. The detailed design of a pH electrode and functional principles can be found elsewhere (1). A large variety of pH probes based on the electrochemical design are commercially available. pH probes can be autoclaved and cleaned in place. However, a reduction in lifetime and robustness needs to be taken into account. Steam sterilization can affect the glass membrane potential, thereby adversely affecting the robustness of these conventional pH probes (9). Also, optical pH sensor, which uses pH indicators immobilized on waveguides such as optical fibers, is available. Measurement of pH changes can be detected with a good precision by the change in absorption or in fluorescence. With the development of disposable bioreactors, the need for disposable sensors has also evolved. Several companies have developed disposable sensors for pH, DO, and dissolved CO_2 (DCO_2). In these sensors, a fluorescence dye sensitive to the analyte is immobilized in a matrix or patch, which can be miniaturized to a few millimeters. This enables monitoring and control with presterilized/γ-irradiated systems, even of miniature system (e.g. shake flasks and microplates) (1,5,6)

TABLE 69.2. Types and Principals of Temperature Probes

Type	Principle
Thermistors	Type of resistor measuring the change in resistance. The output response from thermistors is of a nonlinear temperature versus resistance curve, with the resistance decreasing as the temperature increases
Resistance thermometer	Based on the changes in the electrical resistance of metallic conductors (mostly platinum), with changing temperature (10). A platinum wire of 100-Ω resistance at 0°C is typically used—platinum sensors are stable under both sterilization and fermentation conditions
Bimetallic thermometers	Consist of a bimetallic helical coil surrounded by a protective tube or wall. The coil winds or unwinds with changes in temperature and causes movement of a fixed pointer (11)

69.4.2 Temperature

Temperature is a well understood and a well-controlled parameter in bioprocesses. Bioprocesses are monitored and controlled usually in a tight range of 0–121°C, including sterilization cycles. Several devices and principles are available to control temperature. Table 69.2 shows three of the most common applications.

Other applications and more details can be found in Refs 1 and 11.

69.4.3 Pressure

Pressure is an important control parameter because it affects not only the bioprocess but also safety. Pressure, in general, influences the saturation concentration of gases dissolved in the liquid phase. Therefore, the conditions for calibration (if not automatically pressure corrected) need to be taken into account. In some bacterial fermentations, pressure increase is sometimes used to enable higher mass transfer. For cell culture applications, this can lead to higher carbon dioxide levels, which can negatively influence the process. Pressurizing the fermenter also mitigates the risk of undesired contaminations. Pressure monitoring is also essential for sterilization of bioreactors. Several devices and principles are described (e.g. Bourdon tube pressure gauge and strain gauge). Most common applications are piezoelectric manometers and diaphragm-type sensors.

69.4.4 Viscosity

Information on rheology, or viscosity, can help in ensuring the efficiency of a biological process and understanding the behavior of mixture, flow, mass transfer, and heat transfer. Animal cell culture media are mostly Newtonian fluids. However, for high protein concentrations in formulation processes and bacterial fermentations for the production of polysaccharides and DNA, the liquid can depict non-Newtonian characteristics. These can have severe inputs on power characteristic, mass transfer, shear stress, pumping, bioreactor design, and so on. The viscosity can be determined by using commercial available viscometers, for example, cone and plate viscometers, coaxial cylinders viscometers, and impeller viscometers. Viscosity is especially important in the production of high protein concentration, for example, in *subcutaneous* formulation of antibodies (12).

69.4.5 Redox Potential

Monitoring the redox potential of a bioprocess medium can provide information about the equilibrium between oxidizing and reducing species (electron acceptors and donors, respectively) present. The redox potential plays a significant role in understanding and optimizing secretion of proteins from mammalian cells (13,14). Typically, the metal electrode can be gold, iridium, or platinum; with platinum being the usual choice. The reference electrode is either Ag/AgCl or calomel. The redox sensor is linked to a pH meter that is fitted to provide readout in millivolts. During operations, the redox potential (measured between the metal and reference electrodes) varies as the logarithm of the ratio of oxidizable and reducible components in the media. The redox value varies linearly with the pH of the media and with the logarithm of DO tension via chemical reactions of the media components or culture components. This can lead to complication when trying to interpret the readout from the sensor. A full description of the use and problems associated with the redox sensor was outlined by Kjaergard (13). New and more reliable sensors have been published by Pluschkel and Flickinger (14), including a case study on mammalian cells.

69.4.6 Osmolality

Osmolality is a measure to describe the solute concentration defined as number of osmoles per liter of solution. The osmolality is therefore a result of dissolved components in a media. Freezing point depression, a phenomenon where the freezing point of a solvent decreases due to the presence of a non-volatile solute, is the commonly used method to

determine the osmolality of culture broth in bioprocesses. Mammalian cells are typically cultured in conditions where the osmolality is in the range of 300–450 mOsm/kg. Higher osmolality can increase the specific productivity of recombinant proteins in mammalians (15). However, this is often accompanied by an impact on cell growth. Although not directly controlled, osmolality is an important parameter for monitoring mammalian bioprocesses.

69.4.7 Oxygen

Oxygen is an essential control parameter for all aerobic bioprocesses and can have influence on culture performance—the oxygen demand of cultures varies significantly. For cell culture, ranges from 20 to 200 mg/L/h have been reported (20). Impacts on metabolism and effects on cell culture have been described in high and low oxygen concentration—as well as on recovery process steps (21–24).

The control of oxygen is a simple feedback loop. DO is measured by an *in situ* oxygen probe in most cases. Mammalian cell culture processes are typically robust to changes in DO in the range of 20–60% of air saturation. Transient low (<10%) as well a high (>60%) perturbations are also well tolerated by Chinese hamster ovary (CHO) cells, the commonly use host cell line for production of recombinant proteins. DO is typically controlled at 30–40% of air saturation to ensure sufficient "driving force" for oxygen transfer. The driving force is determined as the difference between saturation concentration (in equilibrium with the gas phase) and the control set point of DO (20).

The control is based on the set point, and therefore, (dissolved) mass transfer for oxygen is controlled by gas flow rate, power input, and/or changes in gas composition. For cell cultures, the common practice is to keep gas flow constant at low power inputs and add more oxygen to the gas flow—this is feasible due to the low oxygen uptake rates (OURs) of mammalian cells. For bacterial fermentations, this is not the case. Here, high power inputs (>1 kW/m^3) and high gas flow rates are used (combined with overpressure) to achieve high mass transfer characteristics in the bioreactor. Most differences for cell culture bioreactors and bacterial bioreactors are driven by this unit operation. Although high power inputs and high shear is desired in bacterial fermentations to achieve high mass transfer and low mixing times, this is the opposite in cell culture processes due to their shear sensitivity (lack of cell wall). In cell culture processes, power inputs between 10 and 100 W/m^3 are typically used. In addition, several low shear–high mixing impeller types have been developed by retrofitting bacterial bioreactor operations. For high density cell cultures, often pure oxygen is used to achieve the necessary mass transfer rates without high power inputs. Specific sparger types (e.g. microsparger and open pipe sparger) are also used to avoid CO_2 build up and high shear force due to bursting of gas bubbles at the air–liquid interface (16–19).

Oxygen (and carbon dioxide) can also be measured in the vent lines at the exit of bioreactors. This "off-gas" measurement can be used to decipher the metabolic state of the cell. The difference in the oxygen and carbon dioxide level between the inlet and the outlet of a bioreactor can be utilized to estimate the OUR and carbon dioxide production rate (CPR) in real time. These parameters, especially OUR, can be used to adapt feed rates (21,22). In general, off-gas analysis requires a certain change in gas concentration in order to estimate the consumption of oxygen and buildup of carbon dioxide. For bacterial cells the difference between inlet gas concentrations and off-gas concentration is big enough for differential measurement using mass spectrometers. For mammalian cells this is not the case. Therefore, off-gas analysis is not common in mammalian cell culture processes. Recently, due to availability of more sensitive detectors, examples of off-gas analysis have been reported for mammalian cells (21,22).

Table 69.3 shows the most common methods to determine oxygen (dissolved as well as off-gas oxygen levels). A large variety of oxygen probes are available. The probes are easy to maintain and reliable, with sufficient specificity and reliability. The probes can be used in sterilization processes. Sometimes, long-term use after CIP/SIP can be an issue. Therefore, redundant electrodes are often used in processes to provide backup. However, preventive maintenance and preventive exchange of the *in situ* probes has been successfully applied of the past few years. For disposable application also, sensors are available based on fluorescence as described earlier (see pH).

Beside, the critical role of oxygen in aerobic fermentation, impact of dissolve oxygen on product quality in downstream processing has also been reported. Pizarro et al. (23) describe the relevance of DO concentration during a refolding process of recombinant human vascular endothelial growth factor (rhVEGF). Kao *et al*. (24) described the reduction in interchain disulfide bonds in a therapeutic antibody, in a CHO-based manufacturing process after the harvest operations, resulting in observation of antibody fragments in protein A pool. As a result, certain measures were introduced, one of which was air sparging of the harvest tank (24).

Despite their differences in operation and measurement principles, there are some constraints for electrodes. All electrodes need to have sufficient movement at the surface, including movement of oxygen through the bulk of the fermentation media and diffusion across the membrane and through the supporting electrolyte. An incorrect placing of the electrode in a highly viscous media displaying non-Newtonian characteristics might be an issue. If the electrode is situated in an area of quiescent fluid, the received signal may not be an accurate representation of oxygen partial pressure throughout the bioreactor. Pressure difference might play a significant role, as well

TABLE 69.3. Device and Principle for Oxygen Measurement

Type	Principle
DO Probes	Based on galvanic or polarographic principle. Measurement of partial oxygen pressure (19,26–28)
Optodes (DO)	Optical sensors for oxygen are constructed using an immobilized fluorophore that undergoes dynamic quenching of the luminescence of a ruthenium complex. The change in fluorescence signal is measured by optical measurement device. Also available as single-use sensors
Exit gas analysis	There are a number of methods available for determining the oxygen concentration of exit gas from a bioreactor. Several of these are based on exploiting the strong affinity shown by oxygen to a magnetic field. Paramagnetic gases, such as oxygen, display a positive magnetic susceptibility. There are two types of detectors based on this phenomenon: the magnetopneumatic and thermomagnetic analyzers consist of a bimetallic helical coil surrounded by a protective tube or wall. The coil winds or unwinds with changes in temperature and causes movement of a fixed pointer (11)

as temperature control and compensation. Fouling of the sensor membrane surface by components of the bioprocess media can lead to erroneous signals. With continued use, this could include the growth of microorganisms on the membrane surface, especially when cultivating adherent cell lines. DO electrodes are also susceptible to signal drift during operation. In addition, gas bubbles and restricted flow toward the sensor can affect the received signal. Other important considerations are the effect of sterilization on the sensor and its calibration. Typically, calibration is carried out after sterilization, using medium gassing to obtain the full range of sensor values. However, in some cases, this might lead to excessive foaming or reduction/oxidation of media components and therefore needs to be considered carefully. For fast reactions, especially with high mass transfer and oxygen consumption rates, the response time of the probe and potential calculation need to be taken into account as well.

69.4.8 Carbon Dioxide

For many bioprocesses, the measurement of CO_2 is an important feature. Media in bioprocesses is typically buffered by CO_2/bicarbonate buffer in addition to other buffers such as HEPES (16,20,21). Carbon dioxide is utilized for pH control in mammalian bioprocesses. In addition, carbon dioxide is also required for cellular processes such as fatty acid synthesis. At smaller scales, such as spinners and shake flasks, mammalian cells are typically cultured in incubators with 5% CO_2. However, increased levels of dissolved carbon dioxide can inhibit growth and reduce the production of secondary metabolites. Especially in cell culture processes, carbon dioxide is critical at certain concentration and has demonstrated impacts on product quantity and process performance. Hence, DCO_2 is typically maintained between 5% and 10%.

Cells produce CO_2 during respiration, which is stripped off by air (or oxygen) sparged in the bioreactor. Carbon dioxide build up must be considered carefully during scale-up. Due to geometric similarity during scale-up, the surface-to-volume ratio decreases. Hence, the volumetric air/oxygen flow rate is reduced to avoid excessive foaming. For oxygen supply, this is addressed by supplying oxygen-enriched air or pure oxygen. However, this causes a reduction in CO_2 stripping rate, resulting in an increase in DCO_2 concentration. DCO_2 levels above 20% are often growth inhibitory for mammalian cells. Hence, the aeration strategy should be carefully considered during scale-up of bioprocesses. In addition, the concentration of bicarbonate in the medium will affect the DCO_2 levels.

Carbon dioxide probes are commercially available. In principle, these are steamable and cleanable as described for pH and DO probes. These function in a similar way to oxygen probes and are based on a pH sensor immersed in a saturated bicarbonate buffer, separated from the bioreactor fluid by a hydrophobic membrane. DCO_2 gas molecules diffuse from the bioreactor media, through the hydrophobic membrane into the carbonate buffer (e.g. InPro 5000i by Mettler Toledo). *In situ* fiber optic probes are also available for DCO_2 measurement (e.g. YSI 8500 by YSI Life Sciences).

69.4.9 Weight and Liquid Levels

Weight and liquid levels are widely used to measure contents, nutrient additions and consumptions for mass balances, addition of base, flow rates, and so on. In most cases, load cells (measuring the strain on the device) or direct liquid level measurements are applied. The liquid level is also important from several perspectives (e.g. safety and total mass of product). In addition to load cells, several methods to determine liquid levels are known (e.g. measuring hydrostatic pressure) (29).

If the culture media shows excessive foaming, the exhaust filters may foul. Hence, conductivity sensors are widely used to monitor foam formation. If liquid or foam levels rise and contact the nonisolated tip of the probe,

the liquid or foam acts as an electrolyte—in most cases, this is used to control foam by addition of antifoam. Capacitance sensors detect the relative dielectric constant of the media compared with air. Acoustic sensors operate via transducers that generate and detect ultrasonic waves. Guided wave radar technologies are used as well. Guided wave radar is based on the principle of time domain reflectometry (TDR). TDR is a measurement technique used to determine the characteristics of electrical lines by observing reflected waveform pulses of electromagnetic energy that are transmitted down a probe and the pulse is reflected when it reaches a liquid surface. The distance to the reflecting surface is determined by the return time of the pulse to the source (30). Also, techniques of measuring temperature differences in the vessel can be applied (1).

69.4.10 Flow Measurement and Control of Liquids and Gas

Flows need to be measured at the inlet and the outlet of a bioreactor, vessel, filter, or column. Flow control is important for process robustness and safety. In upstream processes, flow control is applied, for example, in fed-batch processes (potentially combined with weight measurements) or the control of airflow. In recovery operations, it is important to maintain flow rates in chromatography and filtration operations—especially viral validations and filter integrity might be affected because flow can be correlated to pressure and therefore in most cases is controlled. Calibrated rotameters or flow meters are typically used for flow measurement. Also, thermal mass flow controllers play an important role. For liquids, the characteristics of liquid (especially viscosity and conductivity) and the process requirements (sensitivity, accuracy, sterility, etc.) are used to determine the measurement device.

69.4.11 Biomass

In bioprocesses, the monitoring of biomass, cell densities (or cell volumes), is of crucial importance for the process. A wide array of techniques are available, usually carried out using microscopic method, volume measurements, dry weight, and so on (31,32). These are routinely performed off-line. *In situ* or online methods have been described as well (turbidity, *in situ* microscopes, capacity probes, etc.) for direct measurement of cell counts, and so on. Of particular interest is the development of real-time online methods. Generally, methods for determining biomass concentration can be divided into two classifications: direct and indirect. The former is based on determining the physical properties of the cell and its components. In contrast, indirect methods measure factors related to the cell and its activity (e.g. respiration, electrochemical behavior, and nutrient fluctuation).

Quantification of cell number concentration is performed ubiquitously in cell culture operations. Trypan blue exclusion method is most commonly used to differentiate between viable and dead cells, although other staining methods that use ethidium bromide or propidium iodide can also be used. Viable cell density (VCD) and viability (percentage of total cells that are viable) can be measured either manually (using hemacytometer) or using automated cell counters (e.g. Bioprofile® CDV from Nova Biomedical or the Cedex HiRes Cell Analyzer from Roche Innovatis), although the latter results in greater consistency. Automated cell counters can also provide statistics related to cell size and cellular aggregation levels. Cell concentration can also be measured indirectly by cell volume. A fixed volume of cell culture fluid is typically centrifuged in a graduated tube at a predetermined gravitational force for 5–10 min to estimate the volume of packed cells, referred to as the *packed cell volume* (PCV). In exponential growth phase, when cell viability is high, PCV is strongly correlated with VCD. However, due to the inability of PCV to differentiate between alive and dead cells, the correlation between PCV and VCD is weak at low cell viabilities.

A primary disadvantage of these methods is their off-line nature. For mammalian cell culture process, a culture sample is drawn, typically every 12–24 h for each measurement. This limits the frequency at which cell growth can be monitored. Developing technologies to monitor cell growth in real-time has been an aggressive pursuit in the past two decades. Methods based on nuclear magnetic resonance spectroscopy, conductivity, capacitance, fluorescence, and optical absorbance have been tested in bioprocess (for review see Refs 5 and 32).

Among these methods, capacitance-based cell density measurement appears promising. Cells behave as capacitors due to the presence of charged molecules both inside (cytoplasm) and outside (culture broth), separated by a plasma membrane. Capacitance, measured by application of an electric field, is directly proportional to the cell concentration. An important advantage of the method is its ability to differentiate between live and dead cells, because dead cells without intact membranes do not contribute to charge polarization. Good correlations between VCD and capacitance measurement have been demonstrated in several reports (reviewed in Ref. 33). Real-time viable cell mass estimation was used to optimize the perfusion rates in CHO-based recombinant protein production process (34). For large-scale applications, the sensitivity, especially at low cell densities, and linearity of capacitance-based cell density measurements should be carefully considered, because nonlinear correlations between capacitance and cell mass have also been reported in the fermentation of yeast (35). In-line optical density probes have also been employed to monitor total biomass concentration in

TABLE 69.4. Examples for Optical Probes Used in Mammalian and Bacterial Fermentation Processes (5)

Sensor	Mechanism	Application
Aquasant AF44 SIR	Back scattering	Bacterial and mammalian
BE 2100	Back scattering	Bacterial
InPro 8100	Back scattering	Bacterial
Optek	Forward scattering	Not specified

bioprocesses. Table 69.4 shows the examples of optical probes in bacterial and mammalian fermentations. These probes rely on light scattering and absorbance properties of cells to estimate cell concentration. However, their application is limited due to their inability to distinguish between viable and dead cells. An *in situ* microscopic system was also developed for CHO-based process in a feasibility report (36). Despite its distinct advantage to enable real-time microscopic examination, a staining method could not be used with this technique to measure cell viability. Cell concentration can also be measured real time indirectly using indicators of cellular metabolism such as oxygen consumption rate, ATP production rate, or CO_2 production rate (32). Among these indirect methods, oxygen-consumption-based estimate is most promising because DO probes are routinely used in cell culture unit operations. Empirical correlations of oxygen transfer coefficient ($k_L a$) in stirred-tank bioreactors can be used to estimate approximate OUR. OUR can also be estimated periodically in the bioreactor by ceasing oxygen supply for short durations. Alternatively, the output of DO controller can be correlated to VCD (or PCV) in a bioreactor. As the cells divide and consume more oxygen, the output of the DO control will increase to maintain a constant DO level in the bioreactor, as shown in Fig. 69.3. However, DO-based methods assume that the specific oxygen update rate is relatively constant. Although this parameter depends on the physiological state of the cells, it is likely to be relatively constant during growth phases in seed and inoculum trains. Care should be taken, however, as these correlations may be cell line specific. Exit gas analysis can be applied as well, while using OURs displaying more accuracy.

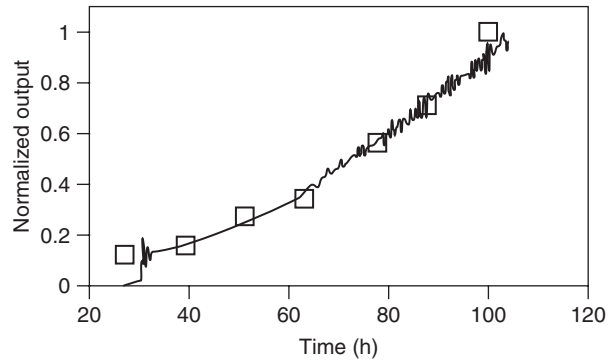


Figure 69.3. Robust correlation between DO controller output (black line) and PCV (open black square) for a CHO process. The *Y*-axis is normalized. DO output is represented as the ratio of the controller output (%) and the maximum output recorded at this bioreactor stage based on more than 100 batches. PCV is represented as percentage of the total volume.

The "health" of a cell culture operation can be monitored by other indicators such as viability and apoptosis. Assays based on extracellular quantification of lactate dehydrogenase (LDH), the reversible enzyme that converts pyruvate to lactate, is a commonly used method to estimate viability indirectly. Viability is measured from the extracellular levels of LDH in membrane-compromised, damaged cells. However, this is a very indirect measure for viability. Programmed cell death or apoptosis can also be used to understand the physiological state of mammalian cells. High recombinant antibody production levels, often accounting for more than 20% of cellular protein levels, can result in stress responses that induce apoptosis. A variety of colorimetric assay kits are available to detect early as well as late apoptotic cells. Many of these assays quantify the active levels of one of the many caspase enzymes that are activated during apoptosis. These assays can be used in conjunction with a flow cytometry device (such as a Guava Easycte) to observe distribution of cell populations. A flow injection instrument used in conjunction with flow cytometry allows real-time monitoring of cell subpopulations (38). Broger *et al*. (37) characterized different high and low EGF-producing populations of *Pichia pastoris* in small-scale bioreactors using real-time flow injection flow cytometry. Flow cytometry is a measuring technique based on the irradiation of a flowing sample solution (containing a cell population) with a suitable light source, followed by monitoring of the scattered or adsorbed light. In addition, fluorescence can be used as the measuring parameter. This technique can be used to ascertain a number of cellular features, such as the accumulation of cellular components (e.g. DNA, RNA, and proteins) and cell dynamics (e.g. cell size distribution). Furthermore, flow cytometry can be used to differentiate and quantify a range of species populations present in a mixed medium. Although such process

instrumentation can be very valuable to further our understanding of cell population heterogeneity in bioprocesses and its impact on process variability, their use in large-scale manufacturing processes has been limited thus far. Their use is often limited to screening and selection of high protein producing cell lines during cell line development.

69.4.12 Monitoring of Other Process Indicators and Product

Measuring and analyzing various metabolic parameters during fermentation is crucial for process control, to achieve and maintain a reproducible fermentation process, and to gain a deep process understanding to characterize, validate, and further improve fermentation processes. Conventionally, substrates, specific proteins, and the metabolites of fermentation media are analyzed using different methodologies depending on the nature of the analyte: that is, amperometric (enzyme membrane based), enzyme linked immunosorbent assay (ELISA), and/or high performance liquid chromatography (HPLC). For mammalian cell culture processes, the parameters typically monitored are glucose, lactate, ammonium, and glutamine. Glucose, lactate, glutamine, and glutamate are commonly measured using an enzyme-based biosensor that converts the substrate to hydrogen peroxide, which is oxidized to produce an amperometric signal proportional to substrate concentration. Examples include Nova Bioprofile Flex (Nova Biomedical) and YSI biochemistry analyzer (YSI Life Sciences). These bioprocess analyzers are most commonly used as off-line, standalone instruments for periodic nutrient measurements. However, autosampling technologies have been developed and successfully applied for cell culture. For bacterial fermentations, autosampling is challenging due to high viscosity, cleaning requirements, and so on. In all cases, comparable performance and reliability needs are to be demonstrated.

The Nova Bioprofile Flex has been applied with autosampling technologies. It can combine three analyzers (metabolite—glucose, lactate, glutamine, glutamate), cell counter, as well as gases and electrolytes (pH, PO_2, pCO_2, ammonium, potassium, sodium) by using a reactor valve module. Details can be found in Refs 5 and 39.

Methods based on photometric quantitation of nutrients such as glucose, glutamine, and other parameters have recently been commercialized (e.g. Cedex Bio by Roche Diagnostics GmbH Germany) to overcome potential disadvantages of other technologies. The Cedex Bio is shown in Fig. 69.4.

In addition to the already mentioned substrates and metabolites, the Cedex Bio can analyze IgG concentration from cell culture broth without any small-scale purification. LDH activity can also be determined using Cedex Bio. LDH is a cytosolic protein released on the lysis of cells, which can be representative to the amount of released proteases, glucosidase, nucleases, or host cell protein (HCP) detrimental to product.

Other chemical parameters such as sodium and potassium concentration are also periodically monitored. As all these parameters are only measured once every 12–24 h, it is desirable to have a high degree of accuracy and precision in their measurement. However, the level of accuracy necessary for process control is different for different parameters. For example, if feed addition is based on controlling glucose at low concentrations, then the instrument must be capable of measuring glucose concentration in the low range (e.g. 0.1–2 g/L) accurately. On the other hand, parameters such as sodium and potassium concentration are typically not utilized for processing decisions, but are useful for troubleshooting purposes. A high degree of accuracy may not be necessary for such parameters.

69.4.13 *In Situ* Process Monitoring Using Spectrometry

Autosampling can minimize disadvantages associated with off-line analysis and sampling procedures. However, this poses risks to sterility and robustness, while increasing complexity. *In Situ* sensors are therefore more advantageous. Several technologies are being developed for real-time estimation of nutrient levels. Technologies including Raman spectroscopy (41,42), infrared spectroscopy (43), UV spectroscopy (42), and fluorescence spectroscopy can monitor a wide array of species, including glucose, lactate, various amino acids, and NAD(P)H. Near infrared (NIR), mid infrared, and Raman spectroscopy have demonstrated successful applications in mammalian cell culture, yeast, and bacterial fermentations (5). In most cases, multivariate data analysis of large data sets from historical fermentations, model evaluation, and training were necessary to establish suitable models. Among all these technologies, NIR spectroscopy offers practical advantages with respect to cost and ease of use (for review see Ref. 44). However, interpretation of NIR absorbance spectra is rendered difficult due to the overlapping spectra of multiple species and the absorption of water in the NIR spectrum. Dimensionality reduction methods such as principal component analysis (PCA) and partial least squares (PLS) are commonly used to identify spectral correlations and express them as linear combinations of a small number of orthogonal dimensions. Pattern recognition methods [e.g. artificial neural network (ANN)] are also necessary to generate calibration or training data sets.

69.4.14 DNA Microarrays

The technology to examine the gene expression level of thousands of genes in a host cell (e.g. *E. coli* and CHO),



Figure 69.4. Cedex Bio by Roche Diagnostics GmbH.

using a single chip called *DNA microarray* was developed less than two decades ago (45). A DNA microarray comprises thousands of probes, each of which is designed to bind with messenger RNA (mRNA) of a particular gene with high specificity. The probe is designed to be complementary to the nucleic acid sequence of the mRNA of a gene. DNA microarrays are commercially available for several species (e.g. mouse and human) from Roche Nimblegen, Affymetrix, or Agilent Technologies. These oligonucleotide microarrays typically comprise 25–60 base pair-long probes that are deposited on the microarray surface by *in situ* synthesis using photolithography

Microarrays provide a valuable tool to decipher the physiological basis of traits that are biopharmaceutically relevant, such as high productivity of recombinant proteins in mammalian cells. Through direct comparison of the host cells under high productivity conditions and control conditions, the genes that are differentially up- or downregulated under the high productivity conditions can be identified. The biological function of the differentially expressed genes (e.g. role in cell cycle and protein synthesis and secretion) facilitates the correlation between the molecular snapshot obtained using microarray and the observed phenotype. Microarrays have been utilized as tools to identify the gene expression signature associated with high recombinant protein producing cells lines (46), as well as high productivity conditions (47). These signatures provide useful targets for engineering cells with relevant traits. The applications of this technology in development of biopharmaceutical processes is reviewed elsewhere (48). Real-time quantitative polymerase chain reaction (Q-PCR) can also be used to quantify the transcript level of genes. Although Q-PCR assay has greater sensitivity and accuracy compared with DNA microarrays, it has significantly lower throughput (e.g. 96-well plate-based assay format). Q-PCR-based expression analysis is often useful when the number of genes are small and known (e.g. all the genes encoding proteins involved in a specific metabolic pathway).

Microarrays can be used as diagnostic tools in cell culture processes. For example, investigations associated with lower productivity and adverse product quality trends during scale-up, technology transfer, and routine manufacturing can utilize a genome-scale survey tool such as microarray to facilitate product and process understanding, leading to possible corrective actions. Recently, the entire 2.45-Gb genome CHO-K1 parental cell line has been sequenced, which is publicly available (49,50). This development is likely to accelerate the use of whole-genome "omics" tools (e.g. a commercially

available DNA microarray for CHO) in a wide array of bioprocess applications.

Advent of massively parallel sequencing technologies has promoted development of several sequencing-based high throughput assays such as detection of noncoding microRNAs (79) and ChIP-Seq for detection of DNA sites that interact with proteins. As the cost of high throughput sequencing plummets, additional applications in cell engineering and bioprocessing will emerge.

69.4.15 Chromatography and Recovery Operations

After production in the fermentation process, the desired product has to be purified. The major goal of the recovery operations is to remove impurities (DNA, HCPs, etc.), potential viruses, and by-products. Therefore, chromatography has been widely used in the industry. The principle is based on the separation of a mixture of compounds by specific interactions with the matrix of a mobile and stationary phase.

Process monitoring for recovery operations is usually made up of two components—in-process analytical tests and real-time measurements via in-line sensors and probes. In-process analytical tests are designed to provide information on product quality attributes at various stages throughout the purification process. Some of these tests (i.e. pH or UV absorbance) can be performed quickly by the operators on the manufacturing floor with little set-up time, while others (i.e. bioburden) may take several days to obtain results and usually require the expertise of a separate analytical group. Currently, most real-time measurements are designed to provide information about the process. With modern manufacturing control systems and data historians, large amounts of continuous data can be collected during a purification process. Sensors located on the process equipment provide information about key process indicators such as pH, conductivity, pressure, and UV absorbance. These process indicators can be visualized during the process itself or examined retrospectively and provide information on the performance of chromatography steps or filtration operations. They can also be trended versus historical limits to identify subtle process changes over time. Although most real-time measurements are currently being used to provide data about the process performance, recent advances in PAT can now allow a direct correlation to product quality as well. To control the process, several analysis and detection methods have been established. Especially the production of therapeutic proteins and antibodies requires a wide range of analytical methods to determine the concentration, purity, identity, integrity, and activity. A large number of operations and detectors have been developed for these purposes (flame, UV detectors, electrochemical detectors, IR and refractive index detectors, conductivity, and mass spectrometry). Also, a large number of chromatographic methods are available for sample analysis. Most of the chromatographic analysis is carried out off-line. Table 69.5 shows exemplary analytics performed in a pharmaceutical antibody production process. Details can be found in the study by Flatman *et al*. (51). A state-of-the-art monoclonal antibody process can be found in the study by Shukla and Thömmes (52).

Some real-time testing of product quantity can be performed online. Other operation monitoring parameters can be performed online as well. For example, one factor that can have a significant effect on chromatographic performance is the quality of the column packing. The current standard procedure for testing the quality of a packed bed liquid chromatography column is to use a nonabsorbed tracer to perform a pulse-injection experiment. The injected tracer solution is assumed to be a Dirac pulse. The pulse exits the column as a peak due to axial dispersion. Plate number, N, describes the degree of the dispersion, which is influenced by the packing quality of the column bed. A related term, Height Equivalent to a Theoretical Plate (HETP), provides a measure of peak broadening in relation to the distance the tracer has traveled in the chromatography column. The mathematical definitions of N and HETP are given by the following equations:

$$N = V_r^2/\sigma^2$$

$$\text{HETP} = L/N$$

where V_r is the retention volume, which is defined as the volume that has passed through the column from the time when half the tracer is applied to the time when half the tracer has exited the column. In other words, V_r is the mean exit volume of the injected tracer, σ^2 the variance of the exit volume distribution, and L the column length.

Based on the normal density function, the width of a curve at half peak height, W_h, is equal to $2\sigma(2\ln 2)^{1/2}$. Because the peak generated by the tracer as it exits the column is assumed to follow a Gaussian distribution, N is usually calculated with the simplified formula shown in Fig. 69.5.

In recent years, efforts have been made to directly use process chromatography data to determine column efficiency to achieve real-time monitoring (53,54). The common approach taken in these studies is to utilize information from step transitions between buffers of different conductivities to describe the same dispersion parameters as the traditional pulse-injection method. One method is to transform a breakthrough curve or a washout curve into a peak by taking the first derivative (53). The dispersion parameters are then derived from the peak position and shape. To avoid the inaccuracy of calculation caused by assuming a normal distribution, algebraic functions other than the normal probability density function were evaluated, and a function that can describe

TABLE 69.5. Examples of Analytical Methods Performed in a Pharmaceutical Antibody Production Process (51)

Product Characteristic	Analysis Property	Method
Physical and chemical characteristics	Purity	Electrophoresis
		Reverse-phase HPLC
		Size-exclusion HPLC
	Integrity/molecular weight	Electrophoresis
		Mass spectrometry
		Size-exclusion HPLC
		Light scatter
	Identity	Isoelectric focusing
		Peptide mapping
		Ion-exchange HPLC
Potency/activity	Antigen binding	Immunoassay
	Biological methods	Cell proliferation
		Complement-mediated cytotoxicity
		Reporter-gene assays
Product-related impurities	Aggregation/fragments	Electrophoresis
		Size-exclusion HPLC
Process-related impurities and contaminants	Host Cell Protein (HCP)	Immunoassay
	Host cell DNA	DNA hybridization
		Q-PCR
		DNA binding threshold
		Fluorescent—picogreen
	Protein A	Immunoassay
	Cell culture medium proteins	Immunoassay
	Viruses	Q-PCR
		Electron microscopy
		In vivo/*in vitro* assays
	Microorganisms	Bioburden Endotoxin—LAL test
	Others: column, vessel, filters, bags, leachables/ extractables, cell, culture medium additives, reagents, chemicals, etc.	Various, for example, reverse, phase HPLC, ion chromatography, GC-MS, and spectral analysis

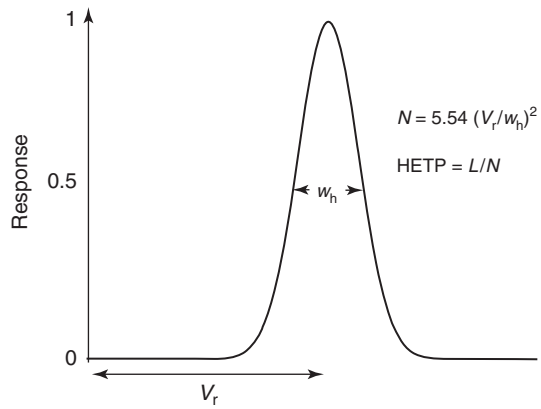


Figure 69.5. Plate calculation via traditional pulse-injection method.

a large number of step transitions has been identified. However, arbitrarily assigning a predetermined function to represent unknown distributions has disadvantages. Depending on the column packing quality and the running conditions of the chromatography, there are transitions that differ significantly from the chosen function and cannot be adequately represented by it. In these cases, the forced fitting of transitional data to the function would cause loss of information. Another method is to treat the exit volume of the solution that is replacing the original solution in the column as a discrete random variable (54). The incremental change in a response signal, such as conductivity, serves as the frequency of each exit volume. The starting point for the transition occurs when 0 L of the displacing buffer has flowed onto the column. The conductivity recorded at this point corresponds to that of the buffer on the column at that time ($C_{\min}$). After a sufficient amount of the displacing buffer has flowed through the column, the conductivity will reach a new equilibrium ($C_{\max}$).$C_{\max}$ is equal to the sum of $C_{\min}$ and the definite integral of dC, which is integrated from $C = C_{\min}$ to $C = C_{\max}$. To simplify the calculations, C

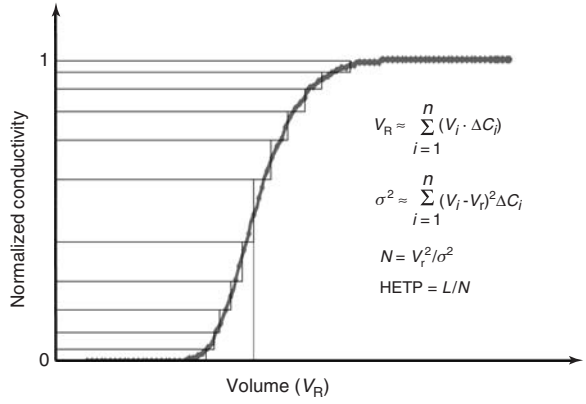


Figure 69.6. Plate calculation via transition analysis method.

may be first normalized using the following equation:

$$C_{\text{normal}} = \frac{(C_i - C_{\min})}{(C_{\max} - C_{\min})}$$

As shown in Fig. 69.6, V_r and σ^2 can be calculated from the transition curve using the rectangular approximations of their integral forms. As the numeric data used in the analysis is discrete, V_r and σ^2 can be calculated using the following equations:

$$V_r = \Sigma(V_i \Delta C_i)$$
$$\sigma^2 = \Sigma(V_i - V_r)^2 \Delta C_i$$

Note that the influence of each V_i on the output values of V_r and σ^2 is weighed by the magnitude of the corresponding ΔC_i. The largest value for ΔC_i usually occurs when its corresponding V_i is close to V_r. The values for N and HETP are calculated using equations shown later. Both breakthrough curves and washout curves can be analyzed in a similar fashion.

Monitoring the integrity of large-scale packed bed liquid chromatography columns using transition analysis can provide useful information about the process. Figure 69.7 provides an example of how the HETP value derived from the transition analysis of a protein A chromatography column changed over multiple cycles of processing. The values increased with time after initial column packing (A). Increased measurement variability was also observed as integrity decreased. This was later determined to be caused by the formation of a headspace on the column. When the top flow adapter was lowered to eliminate the headspace, the HETP values were restored to their original values (B). However, subsequent repacking of the column once again revealed rapid degradation of the column integrity due to insufficient consolidation of the resin during the packing procedure (C and E). The flow adapter was lowered again after the second packing (D) to improve column performance.

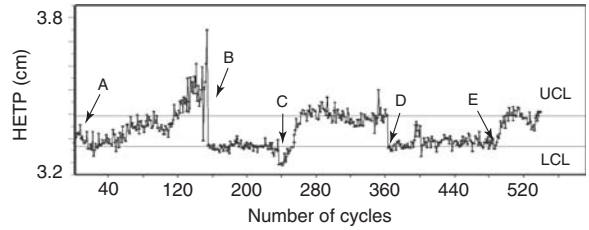


Figure 69.7. Control chart of protein A column HETP derived from transition analysis. UCL, upper control limit; LCL, lower control limit.

69.4.16 Data Technologies and Artificial Intelligence

The data obtained have to be analyzed to derive powerful and scientific sound conclusions, define interdependencies, and derive enhanced control strategies. Several approaches have been discussed in the literature, for example, hybrid modeling (55,56) and multivariate modeling, including principle component analysis, PLS, and ANNs (57,58).

Recent developments in the field of artificial intelligence have led to investigations into the use of such systems for improving bioprocess control, based on the received measurement output signals. This has included the use of both knowledge-based expert systems and neural networks, during bioprocess operation. Robotics is also an important way to manage millions of chemical assays. Undoubtedly, the adaptation of such "intelligent" systems will develop over the coming years and will play an important role in the precise control of bioprocess applications.

Multivariate tools are widely used to increase process understanding and optimization. Application in fermentations (including raw material screening) to analyze metabolic effects, estimations of final productivity in bioreactors, root cause analysis tools, real-time process monitoring, and so on have been described. Also, in recovery processes, this technology has been reported to add value. Chromatographic operations are often characterized by different phases that produce specific patterns and signals. For robust automation, these patterns have to be detected and discrete decisions need to be made at key points. Structured models are frequently used to perform online diagnosis and fault detection, and chromatogram overlays are often used to monitor interbatch performance. Early detection of process perturbations makes it easier to identify root causes and adjust control parameters or correct deficiencies to ensure high product quality and prevent batch loss. One method that has been described frequently in the literature for analyzing production data and gaining process understanding is multivariate statistical process control (MSPC) (59–62). Several papers have described the use of MSPC for monitoring batch processes to not only ensure acceptable product quality but also improve overall process performance and output

(63–65). In MSPC, multivariate models are first developed for "good batches" using PCA and PLS. These models can then be used to evaluate the performance of new batches in real time using commercially available software packages. When applying MSPC to chromatographic process data, a large number of factors can affect when certain events occur. Variations in the mobile phase composition, gradient reproducibility, temperature variations, and column packing variability can lead to shifts in the chromatographic patterns making objective analysis and comparison difficult. The unsynchronized nature of chromatographic data, therefore, implies the need for chromatogram alignment before analysis. Fortunately, most alignment problems can be resolved by normalizing the data based on the cumulative volume of buffer passed through the column. More sophisticated alignment techniques, such as dynamic time warping and correlation optimized warping, have also been used (66,67).

69.4.17 Softsensors

From a process engineering perspective, a software sensor, or in short, a softsensor is an estimation algorithm for a quantity that cannot be easily detected online. Information from other online sensors being utilized in the process can be used to estimate this quantity. Hence, a softsensor associates sensor hardware and an estimation method, that is, a software routine (70). Typically, softsensors were developed for online measurements of biomass concentrations, product concentrations, or specific biomass growth rates. The topic has also been reviewed elsewhere (75). At production scale bioreactors, the options for online measurement devices are rather restricted. Only a few basic devices can be validated such as sensors for pressure, temperature, pH, DO, and the off-gas volume ratios of O_2 and CO_2. Hence, softsensors are essentially a software challenge. Softsensors most often do not take their information from a single sensor. Instead, they pool and condense the information from several ones, thus performing a multivariate analysis of the bioprocess to provide accurate estimates. This gives them a decisive advantage over single sensors: By means of simple balances, data consistency checks can be performed. This is important because decisions can only be made on measurement data that have good accuracy. Thus, it is not only the possibility to measure quantities that cannot be measured directly that makes softsensors attractive, the software can also be employed to perform tasks beyond the actual estimation. For instance, the software can perform fault analysis with respect to the sensor and the process. The complexity of signal processing may vary from simple code conversion to sophisticated extraction of pattern hidden in the data. The focus in this section is the estimation part of softsensor. In this respect, the softsensors are classified by the sophistication of the model relating the available sensor signals to the quantities to be estimated. Two basic categories are distinguished: data-driven and first principle models.

69.4.18 Basic Estimation Models

69.4.18.1 Data-Driven Models

69.4.18.1.1 Utilization of Correlations. Simple engineering correlations are traditionally the first approach when process quantities must be related to each other. For instance, to track the biomass within a bioreactor with quantities that are measured online, a first choice is to look for the respiration rate of the cells.

The OUR or the CPR can reliably be determined from the volume fractions of O_2 and CO_2 in the reactor's vent line. They are related to biomass x by a simple relation similar to Luedeking and Piret's (77) expression:

$$\mathrm{OUR} = Y_{\mathrm{ox}}\mu X + m_0 X$$

This relation can be used to form a softsensor by converting it into an ordinary differential equation in biomass and solving it using a simple Euler algorithm. With an initial biomass $x_0 = x(t_0)$, the final expression to be iteratively determined at each sampling time t_i for OUR and culture mass W measurements:

$$x(t_i) = x(t_{i-1}) + \mathrm{d}t\left(\frac{\mathrm{OUR}(t_i)W(t_i) - m_0 x(t_{i-1})}{Y_{\mathrm{ox}}}\right)$$

An equivalent sensor can also be obtained for the relation between biomass and the CPR, which can be measured online as well.

Computationally, with softsensors we are faced with two different problems, we must distinguish between the computing power required during the online estimations (measurements). For the above example, this is the computing power needed for the stepwise solution of the Euler formula. On the other hand, we must consider the implementation expenses. In this particular case, it is the identification of the parameter values Y_{ox} and m_0 from a set of training data measured beforehand for the process under consideration by means of nonlinear optimization procedures. While the first task is usually time critical, the second is performed off-line using optimization routines and is thus uncritical concerning computing time.

69.4.18.1.2 Polynomials. An improvement can be obtained by pooling the information from several measurements. In the simplest case, the following linear relation can be used:

$$X = a_0 + a_1\mathrm{OUR} + a_2\mathrm{CPR} + \cdots$$

The parameters can simply be determined with multivariate regression algorithms available in all standard software libraries.

Simple improvements of this basic linear approach can be obtained when OUR and CPR are replaced by their cumulative rates cOUR and cCPR. This measure acts as a powerful noise filter. In addition, another cumulative signal that is usually available at fermenters can be added. This is the total mass of base added to the culture during pH control as measured online with a simple balance under the base reservoir. This enlarges the linear equation to

$$x = a_0 + a_1 \mathrm{cOUR} + a_2 \mathrm{cCPR} + a_3 \mathrm{Base}$$

The parameters a_i can be determined in the same way as before using a set of training data.

As the cultivation processes are intrinsically nonlinear, the linear relations can be extended to polynomials. A first approach is

$$\begin{aligned} x = {} & a_0 + a_1 \sum \mathrm{CPR} + a_2 \sum \mathrm{OUR} + a_3 \sum \mathrm{Base} \\ & + a_4 \left(\sum \mathrm{CPR}\right)^2 + a_5 \left(\sum \mathrm{OUR}\right)^2 + a_6 \left(\sum \mathrm{Base}\right)^2 \\ & + a_7 \sum \mathrm{CPR} \sum \mathrm{OUR} + a_8 \sum \mathrm{CPR} \sum \mathrm{Base} \\ & + a_9\ \mathrm{OUR} \sum \mathrm{Base} + a_{10} \sum \mathrm{CPR} \sum \mathrm{Our} \sum \mathrm{Base} \end{aligned}$$

With respect to the parameters a_i, this equation is still linear; hence, the parameters can once again be identified with multiple linear regression routines.

69.4.18.1.3 Principal Components. Another linear technique often applied in multivariate data analysis is PCA. This technique is particularly important when many different measurements are to be exploited within the analysis, because the main idea is to transform the input data matrix composed of the signals from n input variables into a matrix of signals for a lower number of latent variables ($< n$) that essentially carry the same measurement information (62,72,74). As with multiple linear regression, PCA can easily be performed using general PC software. Ready to used subroutines are included in all common software packages (e.g. MATLAB® subroutine *princomp*).

As many online process variables in a fermentation process are correlated (e.g. lactate concentration and base addition), a notable reduction in variables is possible. However, this can only be performed at the cost that the latent variables or scores obtained no longer depict a physical meaning. In fermentation processes where the number of online variables is rather low, the benefit of such an approach is thus questionable.

69.4.18.1.4 Artificial Neural Networks. A general approach of representing nonlinear relationships between several input and output variables is using ANNs. Even simple feed-forward networks with a single hidden layer proved to be able to represent the mappings that are of interest in softsensors.

The term *artificial neural network* can be considered a catchword that is derived from the dataflow in a very simple algorithm. In the case of the simple feed-forward network with a single hidden layer with m nodes, it loses its myth when represented as a simple expression in term of a logistic function $1/[1 - \exp(s)]$. For the biomass x

$$x(t) = w_\mathrm{h} \frac{1}{1 + \exp[-w_\mathrm{i} s(t)]}$$

This is a simple deterministic scalar product. The coefficients w_h, referred to as *weights*, form the first (row) vector, which is multiplied with a second (column) vector composed by elements that are logistic functions with argument $w_\mathrm{i} s$, where w_i is a weight matrix with m rows and n columns and $s(t)$ the n-dimensional input (column) signal vector at time instant t.

The coefficients of this representation, compiled in the vector w_h and the matrix w_i, can be determined in various ways. The easiest way is using the nonlinear optimization routines offered by the various software libraries (in MATLAB® the equation can be fitted to process data with *lsqcurvefit*).

An important point to be considered is that it is not reasonable to feed all available online signals to the input of an ANN biomass estimator. It must be made sure that every input signal will more significantly contribute information to the biomass estimate than just putting noise into the analysis. This requires knowledge about the cultivation process (Fig. 69.8).

More sophisticated versions of ANNs can be constructed by transferring the idea behind PCAs into the domain of nonlinear relationships. This is done in "autoassociative artificial neural networks" (aANNs). As with PCA, a set of $k < n$ latent variables is produced. For this purpose, a regular ANN with n input nodes is used. Then, in addition, these k signals are mapped back into the original data space by means of two further feed-forward network layers. After determining all coefficients or weights, the entire aANN should be able to map all reasonable input vector combinations of the process under consideration onto themselves. In this way, the layer with the latent variables is directly related to the input variables, that is, a nonlinear version of the linear PCA is generated.

Different estimators are often compared in terms of a performance measure, which is usually an average estimation error. Most often, the root-mean-square error (RMSE) is used for this purpose (73). A quantitative

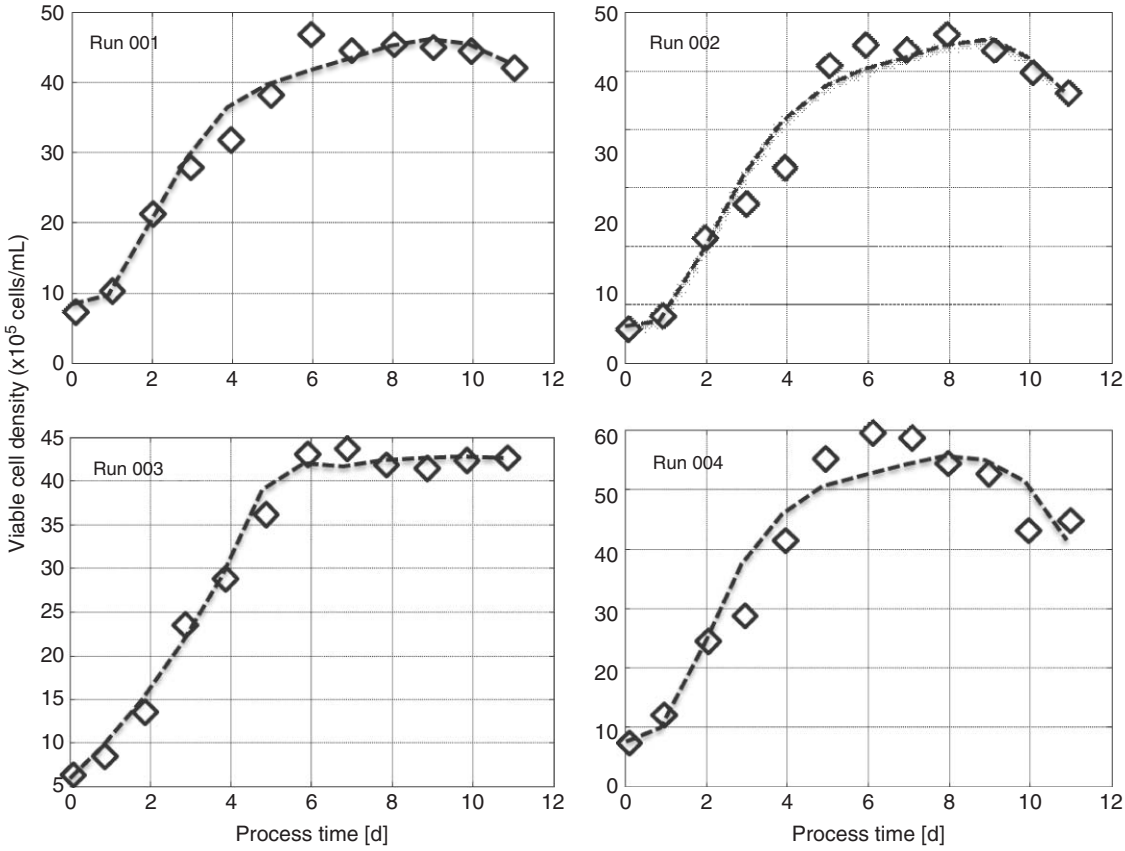


Figure 69.8. Viable cell count off-line data (symbols) from four individual batches of a CHO recombinant protein production process together with the online estimates of an ANN (lines). Input variables are several signals from the DO controller of the bioreactor as well as base consumption and reactor weight.

TABLE 69.6. RMSE Values for the Different Biomass Estimation Methods as Described in Text

Estimation Procedure Applied to VCD Data From a Production Cell Culture Process	Biomass Estimation Error, RMSE (%)
Biomass estimation by a feed-forward ANN	3.24
Polynomial regression	4.76
Multivariable nonlinear regression	4.12
Luedeking/Piret-like relationship and OUR measurements	4.41

comparison of the various approaches discussed here is shown in Table 69.6. All the estimators mentioned can be evaluated online, while the corresponding parameter optimization procedures can be rather time consuming.

The ranking of the methods mentioned clearly shows that the best estimation quality can be obtained with simple feed-forward ANNs with a single hidden layer. This result proved to be valid in microbial and animal cell cultures at various scales from the small liter scale-up to several cubic meters.

69.4.18.1.5 Support Vector Machines. Support vector machine (SVM) is an attractive alternative to ANNs. Compared with ANNs, SVMs find the global minimum, what cannot be guaranteed with neural networks.

The basic idea behind SVM is to map the training data from the input space into a higher dimensional feature space. This transformation allows constructing a separating hyperplane with maximal margins in the feature space. Consequently, although we cannot determine linear function in the input space to decide what class a given data element belongs to, we can easily determine a hyperplane that can discriminate between two classes of data. The accuracy of the SVM regression is at least about the same as the result obtained from the ANNs discussed earlier.

69.4.18.1.6 Bayesian Approaches. As the performance of computers increased significantly over the years, more computationally demanding algorithms can be employed for

analysis of online data. Thus, more practical applications of Bayes statistics (71) appear in the literature.

Instead of looking at single parameter values within an estimation algorithm, it considers probability density distributions of the parameters to characterize the actual knowledge about their values. When the density function is tight, that is, the variance is small; we have a rather concrete knowledge about its value. Bayes' law shows how the current prior knowledge about a parameter θ becomes sharper when we employ concrete measurement data from the process to obtain an improved *a posteriori* density function.

Additional techniques such as clustering, decision trees, and *k*-nearest neighbors can also be employed for mining bioprocess data (reviewed in Ref. 80).

69.4.19 First Principle Models

69.4.19.1.7 Virtual Plant. When there is not enough data available from the process, the measurement information used to estimate the quantity under consideration can be supplemented by a priori knowledge about the process in form of first principle models. Although full dynamic models of the process are an attractive option to relate online signals to key performance parameters of the process, they are not considered to be typical for softsensors as the online solution of the models might be expensive. Moreover, the behavior of the solvers of dynamic equation systems for combination of noisy input signals is difficult to keep under control. Nevertheless, developments of online simulations of the processes are under way and are referred to as *virtual plants*. Versions that are able to simultaneously run with the process are used for process supervision (68).

69.4.19.1.8 Extended Kalman Filters. Simpler first principle models can be employed in softsensors when they are exploited in the so-called observers or filters. The extended Kalman filters (EKFs) are an advanced variant that has been applied to recombinant protein production processes (68,76,78).

EKFs are one-step-ahead predictors: At each data sampling time, the EKF determines a new estimate as a weighted average from the previous estimate, the value predicted by the model and the measurements. When, for example, the measurement values are considered more accurate than the model predictions, they influence the estimate more than the values predicted by the model. A scheme for online estimating the biomass (X) and substrate (S) concentrations as well as the specific growth rates (μ) in a fed-batch process from OUR, CPR, and Base is depicted in Fig. 69.9.

Basis is the first principle model based on the mass balances for X, S, and W, under the assumption that specific growth rate is to be kept constant, is shown on the left. Measurements H performed online are shown on the right. The connection between both is established by means of the measurement equation. The measurement equation transforms the actual state vector c into the measurement vector H. The EKF then provides a weight matrix K_g, referred to as the *Kalman gain*, which determines a correction Δc to state c_{pred} predicted by the model from the difference between the actually measured values H and those (H_{pred}) predicted from the model, to provide a new estimate c_{est}.

An example is shown in Fig. 69.10 for an *E. coli* culture producing a recombinant protein.

69.4.19.1.9 Hybrid Models. A compromise between full dynamic process models and data-driven models can be made by combining the best of both approaches. From the full dynamic models, one can take the basic mass balance equations, which are simple to formulate, while the kinetic

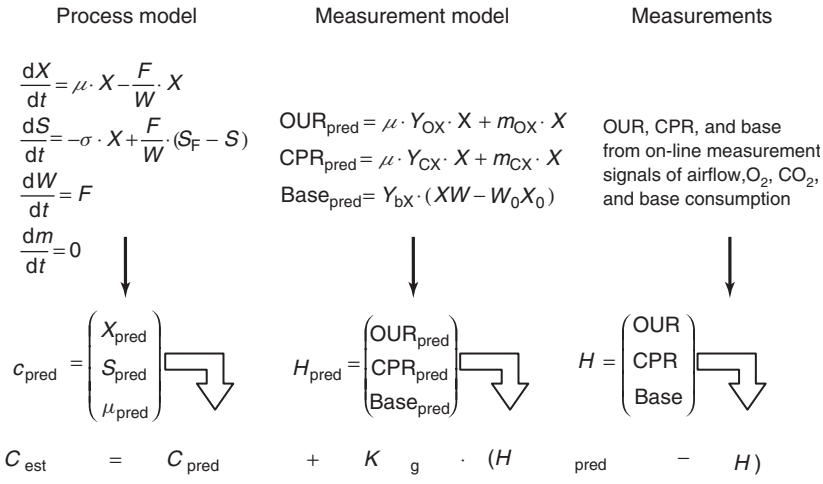


Figure 69.9. Concrete scheme of an EKF estimating biomass and substrate concentrations as well as the specific biomass growth rate from OUR, CPR, and Base consumption measurement values.

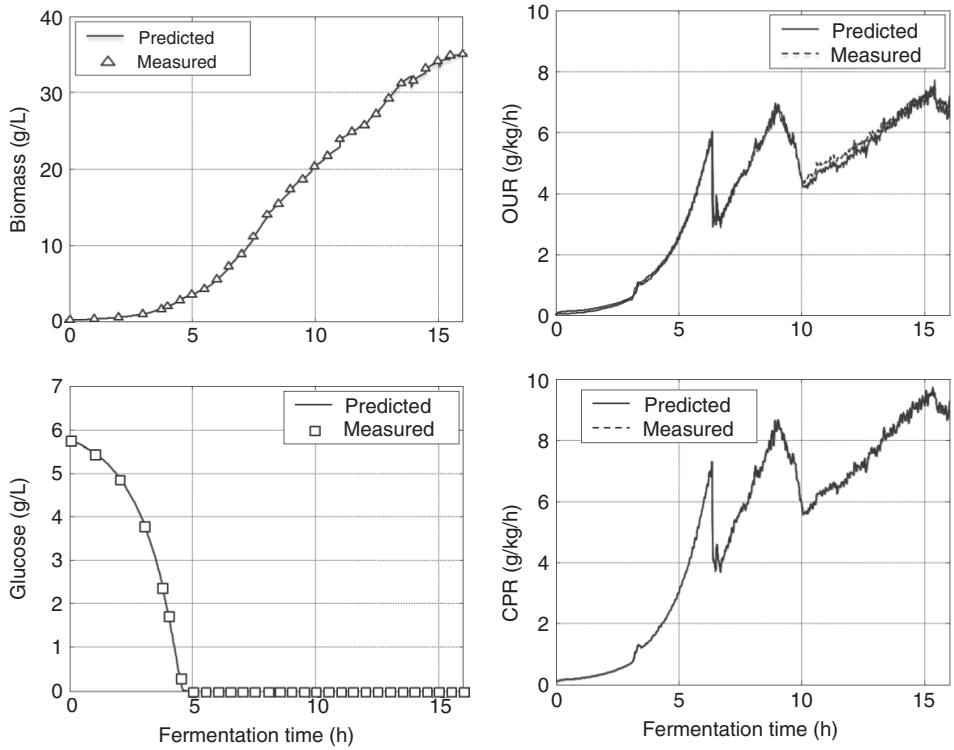


Figure 69.10. Typical example of EKF estimates of the biomass concentration X, the substrate concentration S, the OUR, and the CPR together with measured values.

submodels, which are much more difficult to establish, are represented in a data-driven way (e.g. by means of ANNs; Fig. 69.11.

69.5 CONCLUSION

A wide variety of sensor and instruments for process monitoring are available. Tremendous efforts have been made in the recent years to enable PATs in bioprocesses. Several *in situ* and online technologies and sensor are on their way into commercial manufacturing to enhance processes and enable more advanced control systems. Most of them have been used in other industries for years and have evolved to meet the demands of the biotechnology industry. The application of new sensors, with the right selectivity, robustness, ease of use, and so on, will lead to enhanced process understanding and drive more advanced

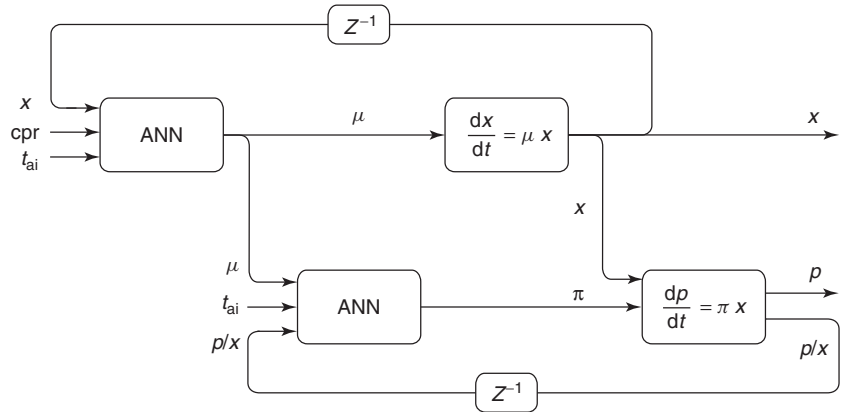


Figure 69.11. Scheme of an ANN-based approach of deriving the $\pi(\mu)$ relationship, that is, the product formation rate π as a function of the specific biomass growth rate μ.

process controls as a PAT application. New and advanced sensors combined with strong data analysis tools will drive toward a next level of process control. Multivariate data analysis techniques and softsensors will provide a valuable toolkit in our efforts to better understand and monitor bioprocess and to improve their consistency. In general, the following trends can be seen in applications of softsensors:

- an available sensor is not fast enough or not sensitive enough or displays adverse signal drifts;
- a sensor allowing direct measurements at sufficient accuracy is not available;
- a direct measurement is physically impossible;
- the employment of a direct measuring device is too expensive; and
- a direct measurement would require too much supervision or maintenance.

The choice of the estimation algorithm depends on the accuracy and the computing time in online applications required for a particular task. For control purposes, smaller response times are mandatory, while for process supervision, usually more time is available.

While the cost of sensing and computation has been decreasing drastically in the past, softsensor systems still require some development expenses. Hence, costs and benefits must carefully be balanced. Finally, it should be stressed that multivariate data mining techniques can discover patterns that are hidden within the process data sets and therefore lead to opportunities to increase robustness and yields. Software estimators do not generate new information. Hence, development and implementation of more accurate and reliable online sensors for production processes will be in important pursuit.

REFERENCES

1. Carloni A, Turner APF. Encyclopedia of industrial biotechnology. john wiley & sons; 2010. p 766–782
2. Nielsen J. Encyclopedia of industrial biotechnology. john wiley & sons; 2010. p 1–10.
3. Schepers TH, Lammers F. *Curr Opin Biotechnol* 1994; 5: 187–191.
4. FAD(http://www.fda.gov/cvm/guidance/published.html).
5. Arroyo AY. In: Baltz RH, Davies JE, Demain AL, editors. Manual of industrial microbiology and biotechnology. 3rd ed. ASM press 2010.
6. Olsson L, Schulze U, Nielsen J. *Trends Anal Chem* 1998; 17(2): 88–94.
7. Brooks SL, Higgins IJ, Newman JD, Turner APF. *Enzyme Microb Technol* 1991; 13: 946–955.
8. Ruzicka J, Hansen EH *Flow injection analysis*. 2nd ed. New York: Wiley; 1978.
9. Saucedo V, *et al*. *Biotechnol Prog* 2011; 27(3): 885–890.
10. Pons MN. In: Pons MN, editor. *Bioprocess monitoring and control*. Munich: Carl Hanser Verlag; 1991. p 4–28.
11. Stanbury PF, Whitaker A *Principles of fermentation technology*. Oxford: Pergamon Press; 1984.
12. Harris RJ, Shire SJ, Winter C. *Drug Dev Res. Special Issue: Monoclonal Antibodies Drugs* 2004; 61(3): 137–154.
13. Kjaergard L. In: Ghose TK, editor. *Advanced biochemical engineering*. New York: Springer-Verlag; 1977. p 131–145.
14. Pluschkel SB, Flickinger MC. *Cytotechnology* 1996; 19: 11–26.
15. Lee MS, *et al*. *Biotechnol Prog* 2003; 19: 1734–1741.
16. Sieblist C, Jenzsch M, Pohlscheidt M, Luebbert A. Underlying principles—bioreactor fluid dynamics. In: Moo-Young M, editor. *Comprehensive biotechnology*. 2nd ed, Volume 2. Elsevier 2011. p 47–62.
17. Pohlscheidt M, *et al*. *Chem Ing Technol* 2008; 80(6): 821–830.
18. Pohlscheidt M, *et al*. *Vaccine* 2008; 26: 1552–1565.
19. Hu WS, Aunins JG. *Curr Opin Biotechnol* 1997; 8(2): 148–153.
20. Aunins JG, Henzler HJ. In: Rehm HJ, Reed G, editors. *Biotechnology*. Stephanopolous G, Series editor. Volume 3, Bioprocessing. VCH publisher 1993. p 219–281.
21. Aehle M, *et al*. *Biotechnol Lett* 2011; 33: 2103–2110.
22. Kowollik S, *et al*. *Chem Ing Technol* 2010; 82(9): 1505–1506.
23. Pizarro SA, *et al*. *Biotechnol Bioeng* 2009; 104(2): 340–351.
24. Kao YH, *et al*. *Biotechnol Bioeng* 2010; 107(4): 622–632.
25. Lee YH, Tsao GT. *Adv Biochem Eng* 1997; 13: 35–58.
26. Atkinson B, Mavituna F Biochemical engineering and biotechnology handbook. 2nd ed. Chapter 1. Basingstoke, UK: MacMillan; 1991.
27. Carr-Brion KG. In: Carr-Brion KC, editor. *Measurement and control in bioprocessing*. New York: Elsevier Science; 1991. p 37–66.
28. Clark LC, Lyon C. *Ann N Y Acad Sci* 1962; 102: 29–45.
29. Reuss M. In: Finn RK, Prave P, editors. *Biotechnology focus I: fundamentals, applications, information*. New York: Oxford University Press; 1988. p 153–190.
30. Bean B, *et al*. *Pharmaceut Manufact* 2009; 9(1): 28–31.
31. Sonnleitner B, Locher G, Fiechter A. *J Biotechnol* 1992; 25: 5–22.
32. Konstantinov K, *et al*. *Trends Biotechnol* 1994; 12: 324–333.
33. Carvell J, Dowd J. *Cytotechnology* 2006; 50: 35–48.
34. Dowd J. *Cytotechnology* 2003; 42: 35–45.
35. Maskow T, *et al*. *Biosens Bioelectronics* 2008;; 24: 123–128.
36. Joeris K, *et al*. *Cytotechnology* 2002; 38: 129–134.
37. Broger M, *et al*. *J Biotechnol* 2011; 154: 240–247.
38. Lindberg W, *et al*. *Cytometry* 1993; 14: 230–236.
39. Derfus GE. *Biotechnol Prog* 2010; 26(1): 284–292.
40. Shaw A, *et al*. *Appl Spectrosc* 1999; 53: 1419–1428.
41. Lee H, *et al*. *Vibrat Spectrosc* 2004; 35: 131–137.
42. Noui L, *et al*. *Chem Eng Process* 2002; 41: 107–114.
43. Riley MR, *et al*. *Biotechnol Prog* 2001; 17: 376–378.
44. Scarff M, *et al*. *Crit Rev Biotechnol* 2006; 26: 17–39.
45. Schena M, *et al*. *Science* 1995; 270: 467–470.

46. Charaniya S, *et al*. *Biotechnol Bioeng* 2010; 102(6): 1654–1669.
47. Kantardjieff A, *et al*. *J Biotechnol* 2010; 145(2): 143–159.
48. Gupta P, Lee KH. *Trends Biotechnol* 2007; 25(7): 324–330.
49. Xu X, *et al*. *Nat Biotechnol* 2011; 29(8): 735–742.
50. Hammond S, *et al*. *Biotechnol Bioeng*. 2012; 109(6): 1353–1356.
51. Flatman S, *et al*. *J Chromatogr* 2007; 848: 79–87.
52. Shukla A, Thömmes J. *Trend Biotechnol* 2010; 28(5): 253–261.
53. Larson T, *et al*. *Biotech Prog* 2003; 19: 485–492.
54. Chang Y, Bork C, Thömmes J. *International Forum for Process Analytical Technology*, Arlington, VA; 2005.
55. Chen L, *et al*. *Control Eng Pract* 2000; 8: 821–827.
56. Azevedo S, Dahm B, Oliveira FR. *Comput Chem Eng* 1997; 21: 751–756.
57. Schügerl K. *J Biotechnol* 2001;(85): 149–173.
58. Kirdar A, *et al*. *Biotechnol Prog* 2007; 23: 61–67.
59. Kourti T. *Process Anal Technol* 2005; 2(1): 24–29.
60. Dushesne C, *et al*. *AIChE J* 2002; 48(12): 2890–2901.
61. Kourti T. *J Chemometr* 2003; 17(1): 93–109.
62. Kourti T, *et al*. *Comput Chem Eng* 1996;(20): 745–750.
63. Kourti T. *Process Anal Technol* 2004; 1(1): 13–19.
64. Kourti T. *Int J Adapt Control Signal Process* 2005; 19: 213–246.
65. Kourti. *Annu Rev Control* 2003; 27: 131–139.
66. Sakoe H, Chiba S. *IEEE Trans ASSP* 1978; 26: 43–49.
67. Nielsen N, *et al*. *J Chromatogr* 1998; A 805: 17–35.
68. Kuprijanov K. *Professional software toolbox advancing bioreactor performance*. Running PhD Project, Martin-Luther-University, Halle-Wittenberg, Germany; 2011.
69. Arndt M, Hitzmann B. *Biotechnol Prog* 2004; 20: 377–383.
70. Chéruy A. *J Biotechnol* 1997; 52: 193–199.
71. Eddy SR. *Nat Biotechnol* 2004; 22: 1177–1178.
72. Jackson JE *A user's guide to principal components*. New York: Wiley; 2003.
73. Jenzsch M, *et al*. *Bioproc Biosyst Eng* 2006; 29(1): 19–27.
74. Jolliffe IT. *Principal component analysis*. 2002; 2nd ed. New York: Springer.
75. Kiviharju K, *et al*. *J Ind Microbiol Biotechnol* 2008; 35: 657–665.
76. Lübbert A, Simutis R. *Trends Biotechnol* 1994; 12: 304–311.
77. Luedeking R, Pieret EL. *J Biochem Microb Technol* 1959; 1: 393–412.
78. Simutis R, Lübbert A. *Biotechnol Prog* 1997; 13(4): 479–487.
79. Johnson KC, *et al*. *Biotechnol Bioeng* 2011; 108(2): 475–480.
80. Charaniya SC, *et al*. *Trends Biotechnol* 2008; 26(12): 690–699.

70

FLOW INJECTION ANALYSIS IN INDUSTRIAL BIOTECHNOLOGY

ELO HARALD HANSEN
Department of Chemistry Technical University of Denmark Lyngby, Denmark
MANUEL MIRÓ
Department of Chemistry Faculty of Sciences, University of the Balearic Islands Carretera de Valldemossa, Illes Balears, Spain

70.1 INTRODUCTION

Introduced in 1975, flow injection analysis (FIA) was an entirely new approach to perform chemical analysis (1). While such assays for centuries had been based on thorough mixing of sample with appropriate reagent(s), and waiting for chemical equilibrium to be obtained (i.e. both physical and chemical homogenization), FIA was, as illustrated in Fig. 70.1(a), founded on injection of a well-defined volume of sample into an inert or reagent-containing carrier stream, to which additional reagents, if called for, could be added downstream, thereby accomplishing partial mixing of the components to promote chemical reaction, the result of which subsequently could be monitored by a suitable flow-through cell, which may continuously observe an absorbance, an electrode potential, or any other physical parameter as it changes on passage of the sample material through the flow cell. Thus, the physical and chemical homogenization, which, in fact, had been the key stones in batch assays and also in the then existing (predominantly clinical) automated analyzers, were not any more necessary, which, in turn, opened up entirely new avenues to perform chemical assays, where non-steady state conditions could be exploited. The ensuing years have amply proven these advantages, as clearly evidenced in the large number of FIA publications which have been published, counting at the beginning of 2008 altogether more than 17,500, to which should be added ca. 20 dedicated monographs and hundreds of Ph. D. theses (2).

During its existence, FIA has undergone certain changes and modifications, that is, it was in 1990 supplemented by Sequential Injection Analysis (SIA), also termed the second generation of FIA (3,4), and in 2000 by the Lab-on-Valve (LOV), the third generation of FIA (5). Thus, the present chapter will focus on these three generations of FIA, their characteristics and their applications, that is, initially outlining the distinctive features of FIA when compared to conventional continuous flow analysis (CFA) and via selected examples demonstrate some of its unique capabilities, while in the following sections emphasis will be placed on the ensuing generations of FIA, detailing their distinct advantages (and limitations) as compared to FIA. In selecting the examples given, attention has been given to show the versatility of FIA and its sequels particularly within the biotechnological field, including process-monitoring. What is of importance in the present context is, to demonstrate that the FIA approach, besides allowing automation of chemical assays with high sampling frequencies and minute consumptions of sample and reagent solutions, offers potentials to implement novel applications. As one of these authors previously wrote in characterizing FIA: "the ultimate test for an analytical approach is not that it can do better what

Upstream Industrial Biotechnology: Equipment, Process Design, Sensing, Control, and cGMP Operations, Volume 2, First Edition. Edited by Michael C. Flickinger.
© 2013 John Wiley & Sons, Inc. Published 2013 by John Wiley & Sons, Inc.

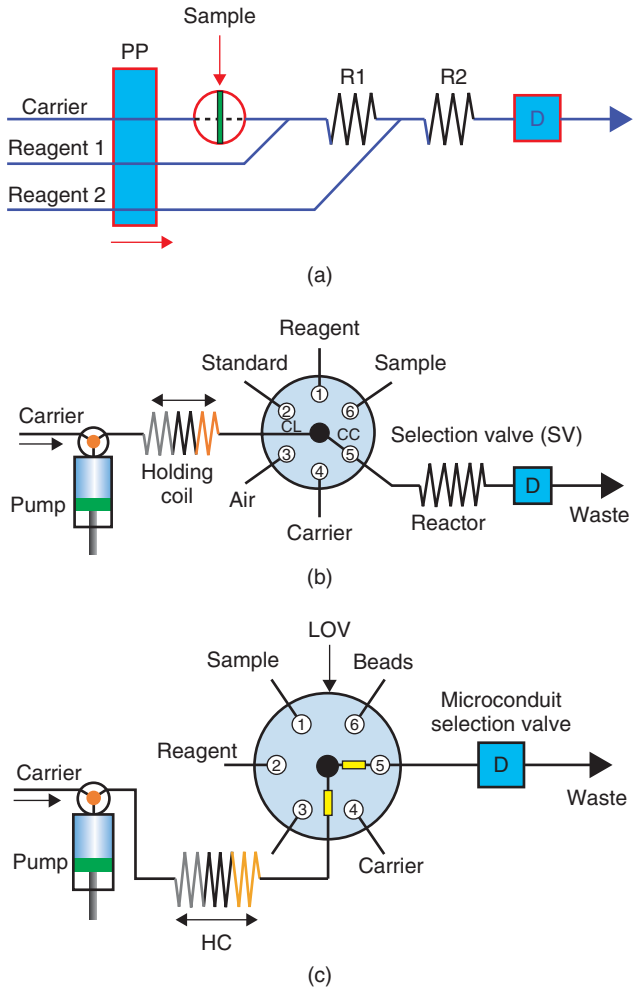


Figure 70.1. (a) Flow injection system, where the sample (S) is injected into a carrier stream as propelled by a peristaltic pump (PP), which downstream is merged with reagent(s), the transient signal from the product generated by passing the reaction coil(s) (R) being measured by a suitable detector (D). (b) Sequential injection system as based on using a selection valve, the central communication channel (CC) of which can be programmed to address each of the external ports. Via the central communication line (CL), sample and reagents can by means of the syringe pump be aspirated into the holding coil and afterwards propelled to the detector which monitors the ongoing chemical reaction. (c) Lab-on-valve (LOV) system, the concept of which is a microconduit placed atop a selection valve (as shown in Fig. 70.5). Ideally containing all means for facilitating the chemical assay, including a flow-through detection cell, the microconduit is also amenable to externally attached components, such as detectors or bead reservoirs for integrating small packed column reactors within the valve. (This figure is available in full color at http://onlinelibrary.wiley.com/book/10.1002/9780470054581.)

can be done by other means, but that it allows us to do something that we cannot do in any other way" (6). And FIA does exactly that. The only limitation is simply our own ingenuity.

70.2 FUNDAMENTALS OF FLOW INJECTION ANALYSIS

As mentioned above, FIA is based on injection, or insertion, of a discrete, well-defined volume of sample solution (usually 20–100 μL) into a flowing carrier stream. Yet as already verbalized in the very first FIA publication, it relies on two additional cornerstones, namely: (i) reproducible and precise timing of the manipulation that the injected sample zone is subjected to in the system, from the point of injection to the point of detection, that is, the so-called controlled, or rather controllable, dispersion, and (ii) the creation of a concentration gradient of the injected sample, providing a transient, but strictly reproducible readout of the recorded signal. The eventual peak-shaped readout, as monitored by a suitable detection device, is therefore always the result of two kinetic processes that occur simultaneously, namely the *physical* process of zone dispersion and the superimposed *chemical* processes resulting from reaction between analyte and reagent species. It is the combination of these features that makes it unnecessary to achieve steady-state conditions, as they are essential in conventional CFA. Any point on the path toward the steady-state signal is as good a measure as the steady-state itself, provided that this point can be reproduced repeatedly, and this is certainly feasible in FIA with its inherently exact timing. This, in turn, has not only allowed to perform chemical assays much faster, and hence facilitate higher sampling rates, than in conventional procedures, but more importantly it has permitted to implement procedures which are difficult, or, in fact, impossible, to effect by traditional means.

Being modular in its operational set-up, virtually any unit operation can be incorporated into an FIA system in order to facilitate the optimal manipulations and ultimate detection of the analyte. Thus, the sample might be subjected to appropriate pretreatments to separate the analyte species from interfering constituents (e.g. by dialysis or extraction). It can be heated/cooled, suitable chemical reagents can be added downstream to facilitate the desired chemical reaction(s) under optimal conditions, and almost any detection device is amenable to be used. In biotechnological applications, sampling is performed by exploiting a sterile barrier for removal of suspended matter, high molecular weight species or cells (7). The immediate consequences of this sample pretreatment is the effective stopping of any further metabolism in the collected sample and the feasibility to inject a preset volume of sample directly into the detection system without the need for further sample clean-up. The sterile barrier is usually composed of a flow-through concentric microdialysis probe operating under convective-controlled transport (8,9). The microdialysis probe can be introduced either directly into the reactor or implemented into an external by-pass loop in order to minimize membrane fouling.

When monitoring parameters in fermentation broths, it is however important to reduce both residence time in the loop and the ratio of loop volume to working volume in the bioreactor to prevent any effect on the performance of the microbial culture in terms of substrate availability (10). It should be borne in mind that yields of flow-through dialysis are frequently below 15% wherefore, dialysis modules/probes have been tailored successfully to bioreactors for in-line dilution of target species (11,12).

Moreover, since only one sample is handled at a time in FI set-ups, the inter-sample washout is efficient and there is no cross sample contamination. In addition, because the wash-to-sample ratio is high, the sample contact time with the detector is short, which is especially advantageous for biosensor applications, as the analytical reaction often reduces the life of the sensor (sensor wear-off) (7).

While much of the attention in using FIA (or just FI, to emphasize that it is a conceptual approach, in addition to a means of performing analysis) initially was set on the feasibility of achieving high sampling rates, as facilitated by exploiting transient rather than conventional steady-state signals, the focus was soon shifted to exploitation of the concentration gradient created, which, as a result of the axial and radial dispersion processes, in reality corresponds to an innumerable number of sequential liquid segments, representing all concentrations from zero to the maximum of the FI peak readout, each of which, as related to a fixed delay time (as measured from the time of injection), potentially can be used for the analytical readout. This, in turn, gave rise to a number of gradient methods (13) as briefly outlined in Table 70.1, among which especially should be highlighted the stopped-flow method (Fig. 70.2), which either can be used to gain increased reaction time without dilution (dispersion) of the injected sample, or, when stopping a part of the sample/reagent mixture within the flow-through cell, for sensitivity improvement as well as for measurement of reaction rates. The second approach has proven to be a very powerful tool in many contexts and implemented in the various generations of flow injection (14). Not the least for bioanalytical assays encompassing investigation of cellular activities (15,16) and enzymatic procedures for determination of both substrates and enzymatic activities (17,18), where the latter one traditionally has been very difficult to execute.

Later followed the introduction of methods relying on detection by bio- and chemiluminescence, allowing to relate the maximum intensity of the generated transient light emission to the analyte concentration (see below). These very sensitive analytical procedures, which prior to the introduction of FI virtually were nonexistent, have blossomed to the extent that more than 2000 publications have emerged in the scientific literature over the years, thus accounting for about 11.5% of all the published FI articles (2). Essentially, these assays are all based on enzymatic conversion procedures, and these types of kinetic *modus operandi* are, in fact, some of the most frequently encountered ones. In the beginning, primarily relying on the use of solubilized enzymes, but later predominantly via immobilized enzymes, taking advantage of the fact that the costly enzymes, even though they are participating in the reactions with the substrate, are not consumed and thus can be reused.

Exploiting the precise and reproducible timing in FI, the formation of intermediate/metastable constituents, which, in contrast to the ultimately generated products, exhibit specifically attractive analytical characteristics, have been utilized to serve for the analytical readout (14), an approach that is totally impossible to make use of in a batch system. Among the many exciting novel techniques are also found the so-called kinetic discriminating schemes, where, even subtle differences in the reaction rates of occurring

TABLE 70.1. Examples of FIA Gradient Techniques

Gradient dilution	
	Selecting and using for the analytical readout specific fluid elements along the concentration gradient, the concentration being $C = C^{o}/D(t_i)$. To be used, for instance, to accommodate the concentration of sample to the dynamic range of a detector.
Gradient calibration	
	Identifying and exploiting a number of elements along the gradient, the concentrations of which are given through the dispersion coefficient of the individual elements. A multipoint calibration curve can be obtained from a single injection of a concentrated sample.
Gradient scanning	
	Combining the use of gradient dilution with the use of a dynamic detector which, for each concentration level, is able continuously to scan a physical parameter, such as wavelength or potential.
Stopped-flow	
	Increase of sensitivity of measurement by increasing residence time, or quantifying sample concentration by measuring a reaction rate under pseudo-zero-order reaction conditions (Fig. 70.2).
Titration	
	Identifying elements of fluids on the ascending and descending parts of the concentration gradient where equivalence between titrand and titrant is obtained, and relating the time difference between these elements to the concentration of injected analyte.
Penetrating zones	
	Exploitation of the response curves from the concentration gradients formed when two or more zones are injected simultaneously. In addition to acting as an economical way of introducing sample and reagent solutions, it can be used for measuring selectivity coefficients, and to make standard addition over a wide, controllable range of standard/analyte concentration ratios.

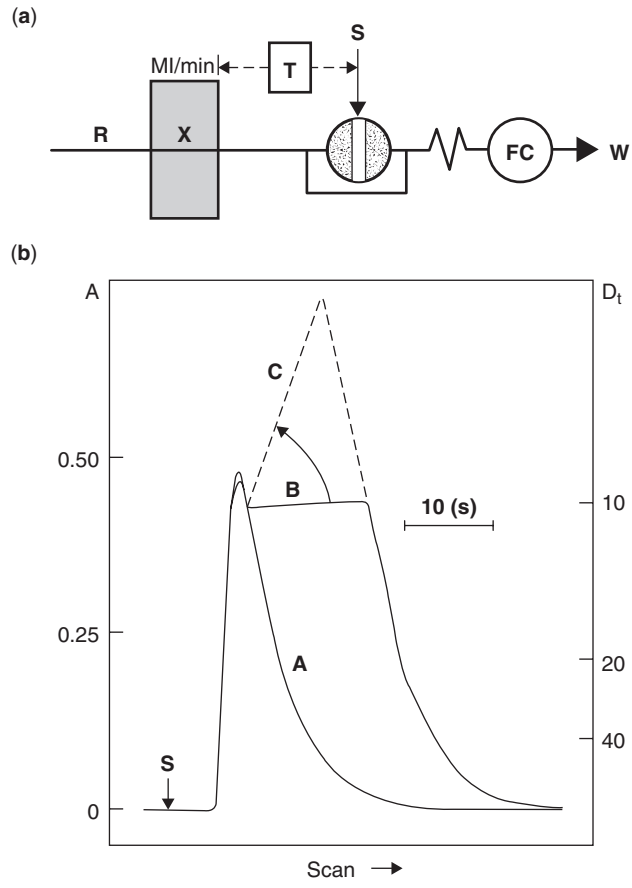


Figure 70.2. (a) Simple stopped-flow FI manifold, where the timer (T) can be set to stop the liquid stream at a preset time. (b) As demonstrated for a spectrophotometric measurement of absorbance, curve (A) shows the signal for continuous pumping, curve (B) for a fast (instantaneous) chemical reaction, while the dashed line (C) indicates the signal output that would be registered if a zero-order or pseudo-zero-order reaction had taken place within the stop interval. (From Ref. 14, courtesy John Wiley & Sons.)

chemical reactions judiciously are exploited (19,20) (see section below).

70.2.1 Dispersion and Dispersion Coefficient

The dispersion in an FI system is quantified by the dispersion coefficient D, which is defined as the ratio of the concentrations of sample material before (C^o) and after (C) the dispersion has taken place in that element of fluid that yields the analytical readout, that is: $D = C^o/C$ (14). The dispersion can be manipulated by the physical dimensions of the FI manifold used (e.g. length and i.d. of tube, pumping rate and number of merging points), as dictated by the analytical task to be fulfilled. Thus, *limited* dispersion ($D = 1-2$) is used when the injected sample is to be carried to a detector in undiluted form, that is, the FIA system serves as a means of rigorous and precise transport and sample presentation to the detection device (such as an ion-selective electrode or an atomic absorption spectrometer). *Medium* dispersion ($D = 2-10$) is employed when the analyte must mix and react with the carrier/reagent stream to form a product to be detected, while *large* dispersion ($D > 10$) is used only when the sample must be diluted to bring it within the dynamic measurement range of the detection device, which is imperative in a vast number of analyzers for determination of target species in cultivation media (7,11). *Reduced* dispersion ($D < 1$) implies that the concentration of the sample detected is higher than the concentration of the sample injected, that is, on-line preconcentration is effected (e.g. by means of liquid or by solid-phase extraction or by coprecipitation). The latter procedures have especially gained momentum for selective determination of ultralow levels of metals acting as potential inhibitors of enzyme reactions (see section below on SI-LOV).

70.3 SELECTED BIOANALYTICAL APPLICATIONS EXPLOITING FI

In the following will be mentioned some bioassays where the conditions of the FI system are manipulated so that the dispersion is optimal for the given purpose. As a good example of systems exploiting limited to small medium dispersion may serve the use of sensors (ion-selective electrodes (ISEs) or biosensors) (7,21). In potentiometry, it is observed that many ISEs operated in the dynamic mode facilitate fast and reproducible readout. ISEs are, however, generally characterized by fairly long response times to reach steady-state conditions, and therefore it can be difficult to ascertain exactly when to make the readout by manual operation. In FI, this decision is left entirely to the system, because the sample reaches the detector after a time governed exclusively by the manifold used. Besides, the well-known fact that many ISEs are more or less prone to interference from other ions can in many cases be eliminated, or considerably reduced, when making the measurement under FI conditions. Thus, by taking advantage of the short residence time and exposure time of the sample in the FI system, it is often possible, via kinetic discrimination between the ion under investigation and the interfering species (which frequently exhibit longer response times), to improve the selectivity and hence the detection limit of the sensor.

The same concept of manipulating the sample exposure time can be extended to more complex sensors such as enzyme sensors, in which a membrane containing one or more immobilized enzymes is placed in front of the active surface of a transducing element. The analyte is transported by diffusion into the membrane and here degraded enzymatically, forming a product which can then

be sensed by the transducer. Flow-injection biosensors for bioreactor monitoring usually combine oxidase or dehydrogenase-linked enzymic reactions with amperometric detection of molecular oxygen depleted or hydrogen peroxide generated (22–24). A common configuration for single parameter measurement involves a sandwich-type membrane configuration with the enzyme embedded in the intermediate layer in order to minimize enzyme leaching and microbial attack while preventing reducing or oxidizing interfering species from reaching the electrode surface (21). Sequential or simultaneous multiparametric detection can be accomplished by the use of either various enzymic sensors in a parallel or series configuration (23) or integrated electrode arrays (25–27), respectively.

A condition for obtaining a linear relationship between the concentration of analyte and analytical signal is, however, that pseudo-first-order reaction conditions are fulfilled, that is, the concentration of converted analyte reaching the detector surface must be much smaller than the Michaelis–Menten constant. Since this constant for most enzyme systems is of the order of 1 m*M*, and many sample matrices (e.g. substrates for culture broths) contain much higher analyte concentrations, the use of enzyme sensors in static (batch) systems often calls for complicated use of additional membrane layers aimed at restricting diffusion of analyte to the underlying enzyme layer, which in turn implies slow response, or, in case of electrochemical detectors, calls for chemically modified electrodes where the electron transfer is governed by appropriate mediators.

However, when operated in FI, the degree of conversion can be simply adjusted by the *time* the analyte is exposed to the enzyme layer, and therefore the amount of converted analyte can be regulated directly by adjusting the flow rate of the FI system (28). Thus in an FI system, used for the determinations of glucose by means of an amperometric sensor incorporating glucose oxidase, it was shown (Fig. 70.3), that by increasing the flow rate from 0.5 to 1.0 mL/min the linear measuring range could readily be expanded from 20 to 40 m*M* glucose (28). Of course there is a price to be paid for this convenience, and as seen in Fig. 70.3, it is that the sensitivity is slightly decreased. This approach has found much use in ensuing years. Thus, for instance Tsukatini and Matsumoto (29) have used it for the fluorometric determination of pyruvate, and in turn for the assay of acetate, citrate and L-lactate.

Additionally, the exposure time can be tuned for kinetic discrimination, taking advantage of differences in diffusion rates of analyte and interfering species within the membrane layer of the electrode. This was very elegantly demonstrated in the above-mentioned system (28), where temporal resolution of the signals due to glucose and paracetamol could be achieved, even when paracetamol was added at excessive levels. Besides, attention should be drawn to the fact that the operation of a (bio) sensor in the FI mode ensures a constant monitoring of the sensor itself, that is, while the recorded signal is a measure of the concentration measured, the baseline readout indicates directly the stability of the sensor.

In this context, it should be mentioned that considering the diversity of the chemical and physical events that can be involved in the function of a biosensor, in addition to satisfying individually dictated reaction parameters, it is not surprising that operational compromises frequently have to

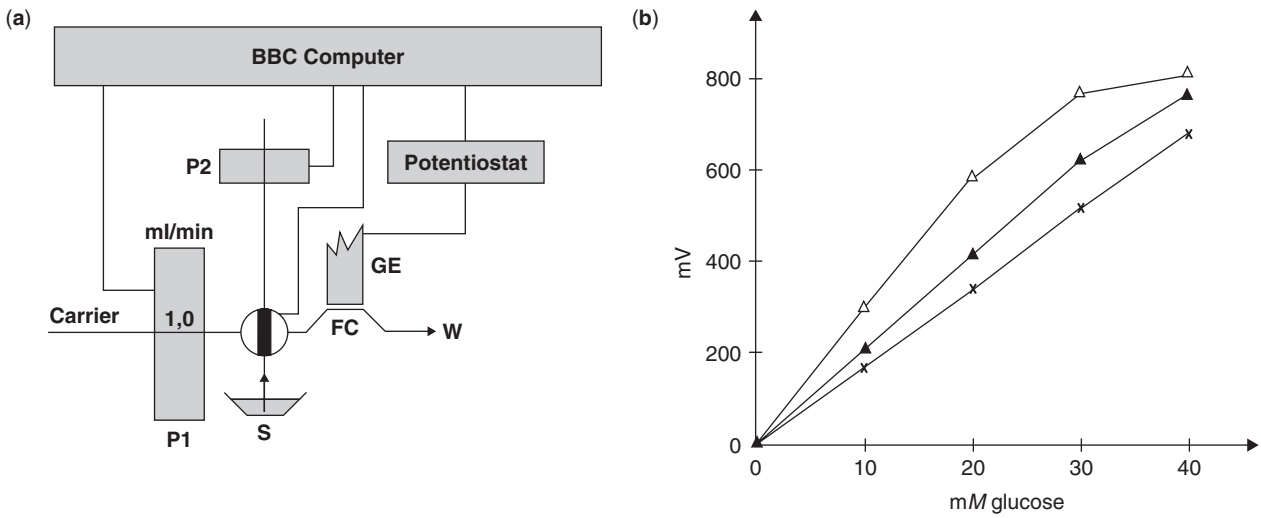


Figure 70.3. (a) FI manifold for the detection of glucose with an amperometric sensor to detect enzymatically generated hydrogen peroxide; (b) Calibration graphs for glucose in the concentration range 0–40 m*M* at three different flow rates: (Δ) 0.50, (▲) 0.75, and (x) 1 mL/min. (From Ref. 28, courtesy Taylor & Francis.)

be made for practical synchronization of all the processes required (30). Thus, the optimal pH used for the enzymatic degradation process might not (as is often the case) be identical to the preferential pH value for detection of the product generated. For example, if a gas sensor covered with a membrane of glutaminase is employed for determination of L-glutamine, the measurement of the ammonia evolved will require a pH value 2–3 units higher than that of the enzymic reaction. Furthermore, and in order to implement functions such as periodic calibration, conditioning and possible regeneration of the biosensor, and, very importantly, to yield the freedom to select the optimum detection means, it is advantageous to use these devices in the FI mode (31). Besides, utilization of biosensors in FI manifolds allows the sample to be modified/manipulated as required for execution of various unit operations such as separation, automatic dilution, or (bio) chemical derivatization prior to the final detection step. In fact, the ideal solution is to use an FI system where the enzymatic degradation of the sample and the detection step are separated and can be individually optimized, that is, the entire flow system is to be considered as a biosensor/biosensing device (32). For the very same reason, the emphasis on the development of biosensors has in recent years shifted from fabricating devices which can be used as probe sensors, similarly to the approach of ISEs in batch assays, to the development of flow-through sensor systems.

When applied in the FI mode, the use of immobilized enzymes offers not only the selectivity, economy and stability gained by immobilization, but also ensures that strict repetition, and hence a fixed degree of turnover from cycle to cycle, is maintained. Two types of reactors have been incorporated and evaluated in flow set-ups, namely, packed-bed reactors with the enzyme immobilized on controlled-pore glass (33–35), and wall-coated open tubular reactor with the enzyme attached to the inner surface of nylon tubing or silica-fused capillaries (36–38). The former features larger surface area and therefore larger enzyme load per unit volume, yet progressively tighter packing of the reactor might lead to increased backpressure with the consequent deterioration of the analytical performance of the analyzer. Thus, whenever several enzymic reactions are involved, co-immobilization strategies are preferred over coupling of various reactors in series. Several examples are found in the literature referring to biotechnological applications, mostly comprising the oxidase/peroxidase (35,39) or dehydrogenase/aminotransferase (34,40) pairs. Both optical and electrochemical detectors can be used to monitor the reaction(s). Thus, for dehydrogenases, involving NAD^+/NADH, spectrophotometry (34,40) or fluorometry (29) is directly applicable, while for oxidases, which give rise to the generation of hydrogen peroxide, amperometric measurements or spectrophotometric detection of a chromogenic redox reagent can also be employed (35,39).

In open reactors, the surface area per unit volume is orders of magnitude lower than that of the packed reactors and thus the enzyme load is much lower. Longer reactors are needed for attaining similar sensitivity, yet compromise should be taken to prevent undue sample/reaction product dispersion. The most relevant asset is the negligible flow impedance increase even after long operational protocols (41). Therefore, this alternative has found applications for monitoring high concentrations of dissolved substrate components, and also for products of bacteria or yeast cultivations when coupled to highly sensitive detection systems such as those involving luminol-based chemiluminescence reactions (35,36). Analyte detection via chemiluminescence is particularly fascinating and attractive, not merely because of the potentially high sensitivity achieved, but because of the wide dynamic range of luminescent procedures and fairly simple instrumentation needed. Furthermore, luminescence has an added advantage over most optical procedures, as light is produced and measured only when sample is present, there is generally no problem with blanking. However, the radiation in luminescence reactions is most often emitted as a flash which rapidly decreases, and for this reason, the conventional approach of quantification has been to integrate the intensity over a fixed period of time and relate this to the amount of analyte. It is obvious, however, that if the measurement of the intensity of light (dE/dt) can be made under precisely defined and reproducibly maintained conditions so that all samples are treated, physically and chemically, in exactly the same manner (i.e. the measurements can be taken repetitively at identical delay times t_i, Fig. 70.4), it is possible directly to relate any dE/dt value (and preferably the one corresponding to the maximum emission, Δt, Fig. 70.4) to the analyte concentration. This is feasible by means of FI, and therefore the combination of luminescence and FI has, in fact, revolutionized the application of bio- and chemiluminescence as analytical chemical detection procedures (42).

Numerous applications of enzyme assays in FI have been reported, advantage being taken of the fact that these components constitute the selective link in the analytical chain which therefore becomes selective overall (43). Some recent reviews contain extensive up-to-date FI enzymic assays and FI biosensing (7,21). Seen in this context, it is apparent that FI not only constitutes a complimentary facility to (bio) sensors, but in many cases offers itself as an attractive alternative.

70.4 THE ROLE OF FI FOR PROCESS ANALYSIS/MONITORING

In emphasizing the many analytical chemical possibilities that FI offers, it is of interest to end this section by drawing attention to an application of this concept that at an early

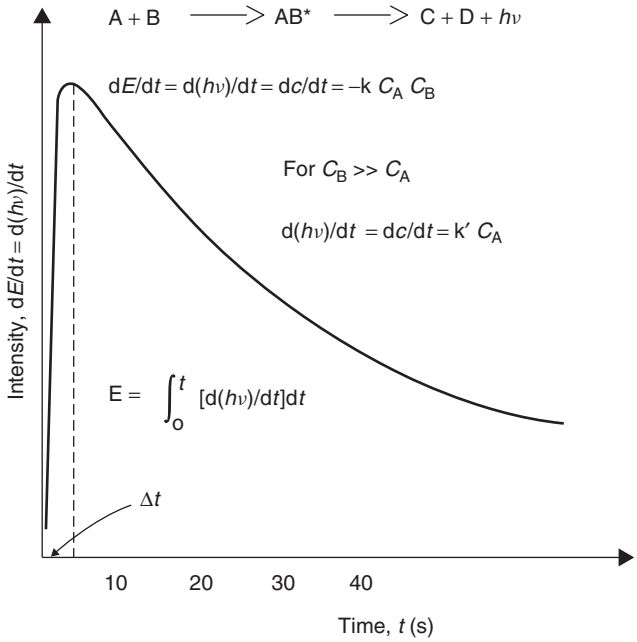


Figure 70.4. Typical course of light generation ($h\nu$) in a bio- or chemiluminescent reaction as a function of time. Quantification can be accomplished either by relating the amount of analyte to the energy released (i.e. integrating the area under the curve), or by using FI and determining the intensity (dE/dt) after a fixed period of time (Δt), which, if pseudo-first reaction conditions are fulfilled ($C_B \gg C_A$), is directly proportional to the concentration of the analyte (A).

stage promised to become very important, that is, its use for monitoring purposes notably in areas such as process control/development and optimizations. Traditionally, most industrial processes have been surveyed off-line in the laboratory after withdrawal of separate samples. However, for an efficient process monitoring and control, the time delay, the limited reliability, and the man power needed for analysis of a large number of samples are crucial parameters. Already in 1982, the first article on utilization of FI for process control appeared (44), and in their FI monograph, Ruzicka and Hansen (14) predicted that FI would turn out to play a major role in this area, because it potentially offered a number of advantages, the most significant ones being: (i) Because every FI readout inherently consists of a peak that goes from the baseline, through a maximum, and back to the baseline again, one cannot only monitor the analyte species via the reaction taking place in the manifold (i.e. via the peak maximum), but one can at the same time control the performance of the analytical system itself (i.e. by the baseline); (ii) FI allows occasional recalibrations or updates/checks of the calibration curve at will, that is, standards can be injected at any time desired, which is a necessity particularly if very complex samples are to be analyzed; (iii) FI is very economical in sample consumption—which not the least is important when used in pilot plant scale experiments—even if the procedure applied calls for the use of a reversed FIA assay (rFIA, i.e. where the reagent is injected into the sample); and (iv) FI permits appropriate pre-treatment of the sample prior to analyte detection, that is, subjecting the sample to dialysis, filtration, extraction or other separation procedures, thereby eliminating potentially interfering species.

The ideal solution for process monitoring would be, of course, to implement an *in situ* totally selective (in fact, "specific") detection device (sensor). As this is virtually impossible (a pH electrode and a thermometer possibly constituting the only exceptions coming close to meet this criteria), and considering the remarks stated above, near real-time monitoring must necessarily be made in an *ex situ* set-up (7). Facilitating this has in the literature been called by several names, such as "on-line" or "in-line" (which in this context are obviously wrong). Since a sample must be in some manner withdrawn from the system (e.g. using microdialysis probes) and then analyzed, the proper tag would be either "off-line" or "at-line" detection. When using FI as the analysis system, the latter term is preferential, because it implies that the determination is made at the site and is as close as possible to real-time.

In 2001 and 2003 Workman *et al*. (45,46) presented comprehensive compilations of FI literature for process control applications. Although some additional articles have appeared in the literature since then (e.g. (35)), it is evident that FI has not played the role expected in this field. Seen in retrospect, the reason for this is simply that the commercial (and homemade) FI apparatus available often was designed for the laboratory environment, where continuous supervision of its function was a norm, and therefore was not sufficiently reliable for application in industrial settings (47). In fact, it took two decades and the development of SIA to resurrect the idea in earnest, that is, by replacing the peristaltic pumps with a single syringe pump, the injection valve with a multiposition valve, continuous flow with reagent saving programmable flow, and human supervision with computer control (4). Autonomous SI systems are now deployed in industry as well as in remote locations to provide 24/7 (24 h/7 days a week) monitoring of variety of analytes ranging from spectrophotometric determinations of dyes to fluorescence/enzymatic assays of *bacteria coli* (48).

70.5 FUNDAMENTALS OF SEQUENTIAL INJECTION ANALYSIS

While most FI procedures employ continuous, unidirectional pumping of carrier and reagent streams irrespective of whether a sample is injected or not, which from the point of view of reagent consumption is a

drawback, sequential injection analysis (SIA or just SI) is based on using programmable, bidirectional discontinuous flow as precisely coordinated and controlled by a computer (3,4)). A sketch of a typical SI-manifold is reproduced in Fig. 70.1(b).

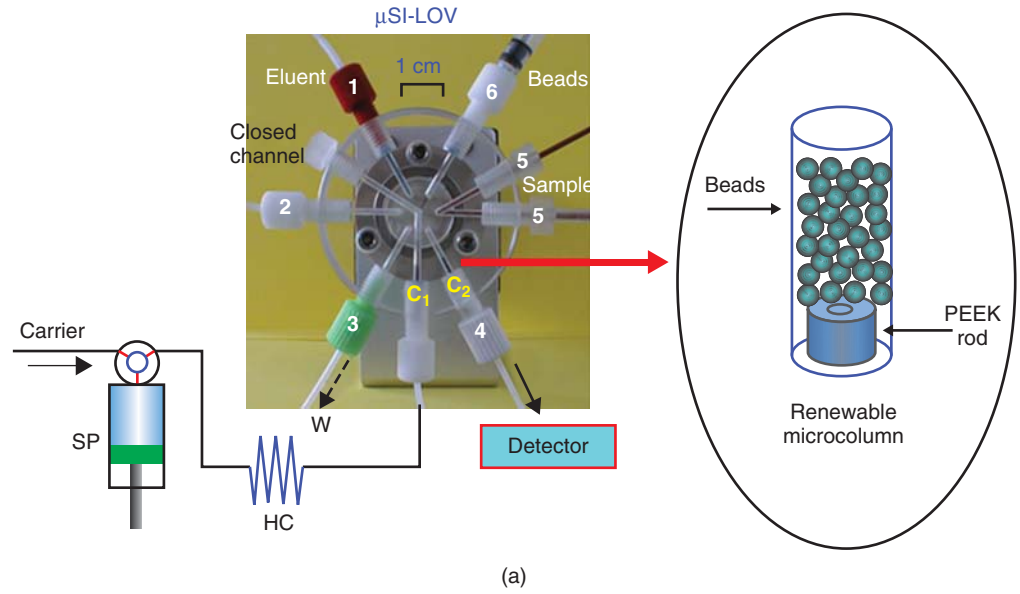
The core of the system is a multiposition selection valve (here shown as a six-port valve), furnished with a central rotary communication channel (CC) that can be made to address each of the peripheral ports (1–6), and a central communication line (CL) which, via a holding coil (HC), is connected to a syringe pump operating as the liquid driver. By directing the central communication channel to the individual ports, well-defined and precisely metered sample and reagent zones (typically 5–25 μL) are initially time-based aspirated sequentially into the HC where they are stacked one after the other. Afterwards, the selection valve is switched to the outlet port (here position 5), and the segments are propelled forward toward the detector, undergoing on their way dispersion and thereby partial mixing with each other, and hence promoting chemical reaction, the result of which is monitored by the detector. Notable advantages of SI as compared to FI are in particular that it allows the exact metering of even smaller volumetric volumes (of the order of a few microliters), which fostered the use of liquid enzymes (49,50) and costly cofactors as demanded in NAD-linked enzymic assays (40). Further, thanks to the use of a syringe pump, SI is much better suited for stopped-flow procedures where a very precisely selected delay time is necessary, and that it readily and reproducibly permits flow reversals, which, in fact, in addition as a mere means of transport, also might be used to promote mixing of sample and reagent(s) and to facilitate controlled sample dilution within the HC.

Besides, it is extremely economical as to the consumption of sample and reagents, and hence in waste generation, which nowadays is an important parameter since it is becoming increasingly expensive to dispose chemical wastes. And since all manipulations are computer-controlled, it is easy and simple to reprogram the system from one application to another, providing great versatility for monitoring multiple variables in fermentation broths (12,37) since all operating protocols such as sample injection, mixing, and separation are controlled precisely by the software without the need for physical reconfiguration of the system. However, it is generally difficult to accommodate (stack) more than two reagents along with the sample, although additional reagents might be added further downstream, that is, by making an FI/SI-hybrid. And due to the use of a syringe pump, SI has a somewhat limited operating capacity, although this in practice is rarely a constricting factor.

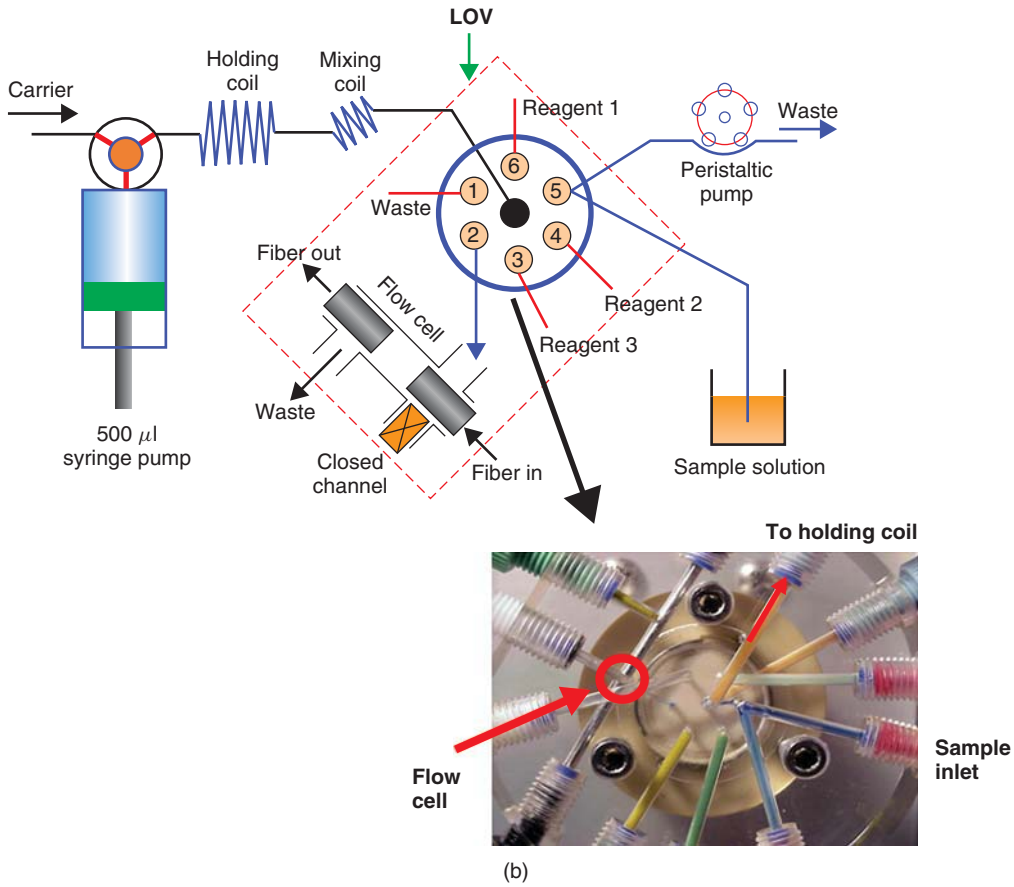
Allowing the communication to various peripheral ports at will, SI has proven itself especially useful for monitoring of fermentation processes as facilitated by automated recalibration of the system, injection of quality control standards, performing of standard addition methods, injection of samples from different sampling sites on a time basis and real-time calculation of actual concentrations of substrates and products as well (27,51). Besides, it has found notable use in pharmaceutical industries, allowing not only for analysis of drug formulations, but particularly facilitating monitoring of drug-dissolution profiles, *in vitro* drug-release testing and functional assays for screening of potential drugs (52–54).

70.6 MICROFLUIDIC DEVICES: LAB-ON-VALVE

In the LOV concept, (Fig. 70.1(c)) advantage is taken of using an integrated micromachined structure (5). The microconduit monolith (which has a diameter of about 5 cm, a thickness of about 10 mm; a photo of it is shown in Fig. 70.5(a)), made initially of Perspex, but more recently of hard polyvinylchloride, polyetheretherketone (PEEK) or polyetherimide (ULTEM) for improved chemical resistance to a wide range of organic solvents, is mounted atop of a 6- or 10-port selection valve. Allowing further downscaling of conventional SI systems, and designed to incorporate all necessary laboratory facilities for a variety of analytical chemical assays, hence the name *lab-on-a-valve*, it is made to contain mixing points for sample and reagents, working channels for sample dilution, overlapping of zones, sample and reagent(s) incubation and sample purification, and a multipurpose flow-through cell for real-time monitoring of the development of the chemical reactions (55). Thus, the LOV unit can readily be devised to incorporate optical detection facilities, that is, devices [namely, diode-array spectrophotometers, USB charged-coupled devices (CCDs), laser-induced spectrofluorimeters or luminometers] where the communications to the detector and/or the light source are made via optical fibers (Fig. 70.5(b)), and where the position of the fibers can be used to adjust the optical light path of the cell (5). Electrochemical detection has been recently proven feasible by use of the flow-through cell for housing a three-electrode voltammetric unit (16). The micro-fabricated channel system (typically 1.6 mm i.d.) is also amenable to admit conventional sized peripheral devices, thus facilitating the hyphenation with a plethora of optical detection techniques and modern analytical instruments (Fig. 70.5(a)), such as electrothermal atomic absorption spectrometry (56), inductively coupled plasma-atomic emission spectroscopy or mass spectrometry (57), cold-vapor atomic absorption spectrometry (58), electrospray ionization mass spectrometry (59,60), atomic fluorescence spectrometry (61), and, what is especially important for bioseparations and cell technology, to chromatographic/electrophoretic column separation systems coupled to UV–Vis or mass spectrometric detection for



(a)



(b)

Figure 70.5. (a) Close-up of LOV system for bead injection (BI) incorporating two microcolumn positions (C_1 and C_2), along with a diagram of a packed renewable microcolumn (from Ref. 55, courtesy Elsevier Science Publishers). (b) Schematic diagram and magnified close-up of an SI-LOV microsystem incorporating a multipurpose flow cell configured for measurement of absorbance. (Adapted from Ref. 65, courtesy Royal Society of Chemistry.) (This figure is available in full color at http://onlinelibrary.wiley.com/book/10.1002/9780470054581.)

multiparametric assays (62–64). Thus, the role of the LOV is here to serve as a "front end" to execute appropriate sample pretreatments aimed at introducing the analyte optimally into the detection instrument.

A valuable asset of the microchannel structure is the microfluidic handling of not only metered volumes of solutions but also of solid suspensions as well for exploitation of heterogeneous chemical reactions (Fig. 70.5(b)). The LOV approach fosters the in-valve manipulation of sorbent materials carrying suitable surface moieties in order to generate packed column reactors for microscale solid-phase extraction (66,67), or micro-affinity chromatography (68), in a permanent or a renewable flow fashion, that is, the so-called bead injection (BI) scheme (69,70), depending on the particular chemical assay. In short, microcolumns are *in situ* generated by aspirating beads with particular surface characteristics and particle sizes, advantage being taken of the fact that the sorbent can be manipulated exactly as and when handling liquids. The solid entities can even be automatically transported between different column positions within the LOV, their retention within the columns, as reported elsewhere (66), being facilitated by fitting the column positions with appropriate stoppers (Fig. 70.5(a)), which will keep hold of the beads, yet allow solutions to flow freely. Following sample loading and clean-up protocols, appropriate eluents can be aspirated, and the eluate propelled to either the flow-through cell or an external detection device, as sandwiched by air or immiscible liquid segments in order to preserve its integrity (71,72).

To be operated in the BI-LOV fashion, there are some requirements to the bead materials, that is, they should be perfectly spherical (i.e. in the form of globe-shaped particles); they should be uniform in size distribution (falling within a range of 40–150 μm); and they should possess a density close to that of water. Nowadays, a wide array of bead particles (predominantly with a core of Sephadex type copolymers) with various surface characteristics are commercially available, and in the following section will be described the procedures for real-time monitoring of cellular activities via immobilized live cells (15,73), isolation and on-column fluorimetric detection of DNA (15), optimization of immobilization protocols for proteins (74), as well as investigation of biomolecular association and dissociation processes as exploited in enzyme-linked immunosorbent assays (75) and affinity chromatographic methods (59,60,76). Yet before that, it might be of interest to compare the LOV with the so-called micro total analysis systems (μTAS) (77), or as they lately have been termed Lab-on-a-Chips (LOC), which are frequently used in bionanotechnological applications (78,79).

The interest for μTAS/LOC microstructures was actually stimulated in the early 90s by electrical and mechanical engineers, who parallelly and intensively focused on miniaturization of flow devices (77). The channel network, which is made by various sophisticated procedures, such as micro-drilling, etching, photolithography, or laser erasing, is impressively exact and reproducible, allowing different channel profiles to be obtained. In many instances it can be made in inexpensive materials, namely silicon, glass, polymethyl methacrylate and polydimethylsiloxane, and mass-produced at low cost, in fact, at much lower expenditures than the LOV. However, the microfluidic devices are usually dedicated, that is, they have fixed architecture for predetermined chemistries. However, as opposed to what applies for LOC systems, LOV practitioners are not being dictated by a fixed architecture of their microfluidic devices in order to implement chemical assays, but are able to control the parameters at will in order to adapt the physical movements of the liquids to the chemistries to be implemented. This, very importantly, implies that they can intelligently exploit the interplay between thermodynamics and kinetics, which is of utmost relevance when dealing with chemistries that are not fast or instantaneous, or even require stepwise reaction sequences. In this context, it is interesting to note that the authors of microfluidic devices are customarily demonstrating the capacity of their LOCs for fast, single step bioassays (80,81), which leaves a multitude of very interesting and intriguing chemistries unexplored. Further, the small dimensions of the microchip channels pose a severe problem for sensitive and reliable absorbance measurements (82).

LOV practitioners possess the ability to manipulate the conditions in such a manner that the axial dispersion is minimized at the expense of the radial dispersion, thereby ensuring good mixing of sample and reagent within the individual microfluidic segments. This can readily be accomplished by destabilizing the laminar flow pattern via the geometry of the flow conduit, for example, the sample/reagent path is made to be nonlinear and/or nonuniform in diameter (5,83), and, as opposed to LOCs, by designing appropriate flow programming protocols which might comprise flow reversals, flow acceleration, stopped-flow and bursts of high flow velocity. These tools promote fast radial mixing, while axial mixing is controlled by choice of the injected volumes, and by the length travelled by the plug in forward and reverse direction. Since incubation times are promoted by stopping the flow (either in the HC or better yet in the LOV flow-through cell), the length of the conduit through which the sample will travel can be minimized. At the same time, by increasing the conventional narrow flow channels in LOCs from 10–100 μm up to 1.6 mm in LOV, the surface to volume ratio in LOV is reduced, thus minimizing adsorption of macromolecules on the walls of the microbore conduit. In addition, the low flow resistance of short and wide flow conduits allows precise flow manipulation, and the use of ultra-fast bursts of

flow that can wash out the channels rapidly and easily remove stray air bubbles or clogging particles. Readers are referred to a recently published comprehensive review article for a detailed and critical comparison of LOV and LOC micromachined units (84).

In the following are detailed a few practical examples of using the SI-LOV approach for biochemical assays and bioseparations.

70.7 SELECTED BIOANALYTICAL APPLICATIONS EXPLOITING SI-LOV

70.7.1 Exploiting the Stopped-Flow Approach

As mentioned earlier, the stopped-flow technique (Fig. 70.2) is a very powerful tool for determining analyte species participating in enzymatic or cellular assays (14). Relying on manipulating the concentrations of the constituents participating in the chemical reaction so that these can be considered constant during the measurement (for instance by recording absorbance as depicted in Fig. 70.2), that is, pseudo-zero reaction conditions are met ($dA/dt = k'C$, where C is the concentration of analyte), the slope of a plot of the analytical signal (*in casu* absorbance, A) against the time will be directly proportional to the concentration of analyte at least within a certain time frame, which is also why the procedure is termed *measurement of initial reaction rates*. In practice, the progression in the recorded detector signal (Δsignal) over a fixed period of time (Δt) is used. Furthermore, the plot will directly reveal within which range the reaction conditions are fulfilled (i.e. slope is constant), and which time interval is thus applicable for measurement. An added and unique advantage of this approach is that automatic blanking is obtained, because only the generated signal (Δsignal) within the time interval is utilized for quantification. When incorporated within the LOV format, where very minute consumptions of sample and reagents are required, and where one can take advantage of the extremely accurate operation of the incorporated syringe pump for aspiration and propelling of solutions, the approach presents itself as an ideal solution for process monitoring of both large and small scale bioreactors (5,85).

Several LOV applications of the stopped-flow approach have appeared in the literature. Thus, with an LOV system as depicted in Fig. 70.5(b) and using detection by spectrophotometry, Wu *et al*. (65) monitored ammonia, glycerol, glucose and free iron in a fermentor, while Chen and Ruzicka (18) determined glucose and ethanol. While the glucose assay was based on catalytic degradation of glucose oxidase leading to the generation of hydrogen peroxide, which was subsequently reacted with 4-aminoantipyrine to form a quinoneimine dye (18), ammonia was assayed via the Berthelot indophenol blue method with salicylate and hypochlorite as reagents. In Fig. 70.6 is shown the sequence of the aspirated sample and reagents, where NH_3 represents the sample, the reagent is salicylate, while the spacer is a plug of carrier solution (diluted aqueous solution of detergent) inserted for promoting sufficiently partial mixing of sample and reagents and allowing a suitable delay time before the stopped-flow measurements. As shown in the lower part of the Fig. 70.6, the stopped-flow readouts are very reproducible.

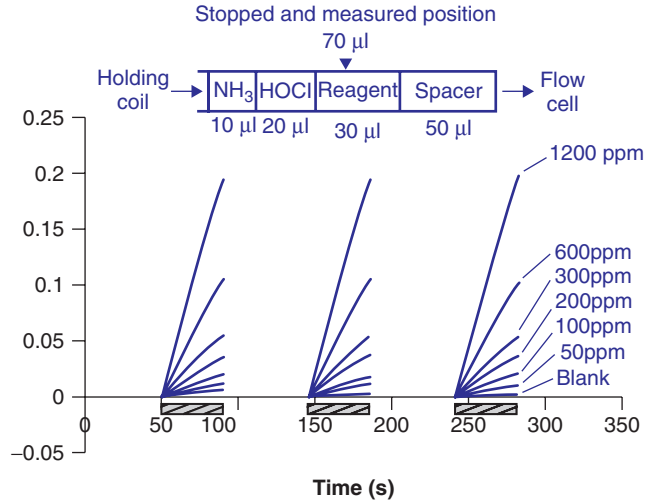


Figure 70.6. (Top) Sequence of the stacked zones of sample, reagents and spacer for the determination of ammonia. (Bottom) Stopped-flow readouts as shown in triplicate for different concentrations (0–1200 ppm) of ammonia, revealing the high reproducibility of measurements. The hatched rectangles indicate the stopped-flow measuring periods. (From Ref. 86, courtesy of the author.) (This figure is available in full color at http://onlinelibrary.wiley.com/book/10.1002/9780470054581.)

70.7.2 Bioseparations and Cellular Assays

Combining LOV and bead injection (BI), Ruzicka and coworkers have in particular focused on cellular analyses and immunoassays (15,68,74–76). The former are being used for screening of potential drugs by *in vitro* evaluation of biological responses. Cells are cultivated onto polysaccharide microbeads and thus a representative number of cells within the LOV is ensured using a minute volume of bead suspension. Cellular responses are evaluated by determination of different parameters, such as release of cytosolic calcium, intracellular or extracellular pH (15), metabolic oxygen consumption (16), lactate extrusion (73) or glucose consumption (65).

Immunoassays have been miniaturized within microfluidic devices for quantification of biomolecules by either monitoring them as they are captured on microbeads bearing antigen species as entrapped within the LOV flow cell

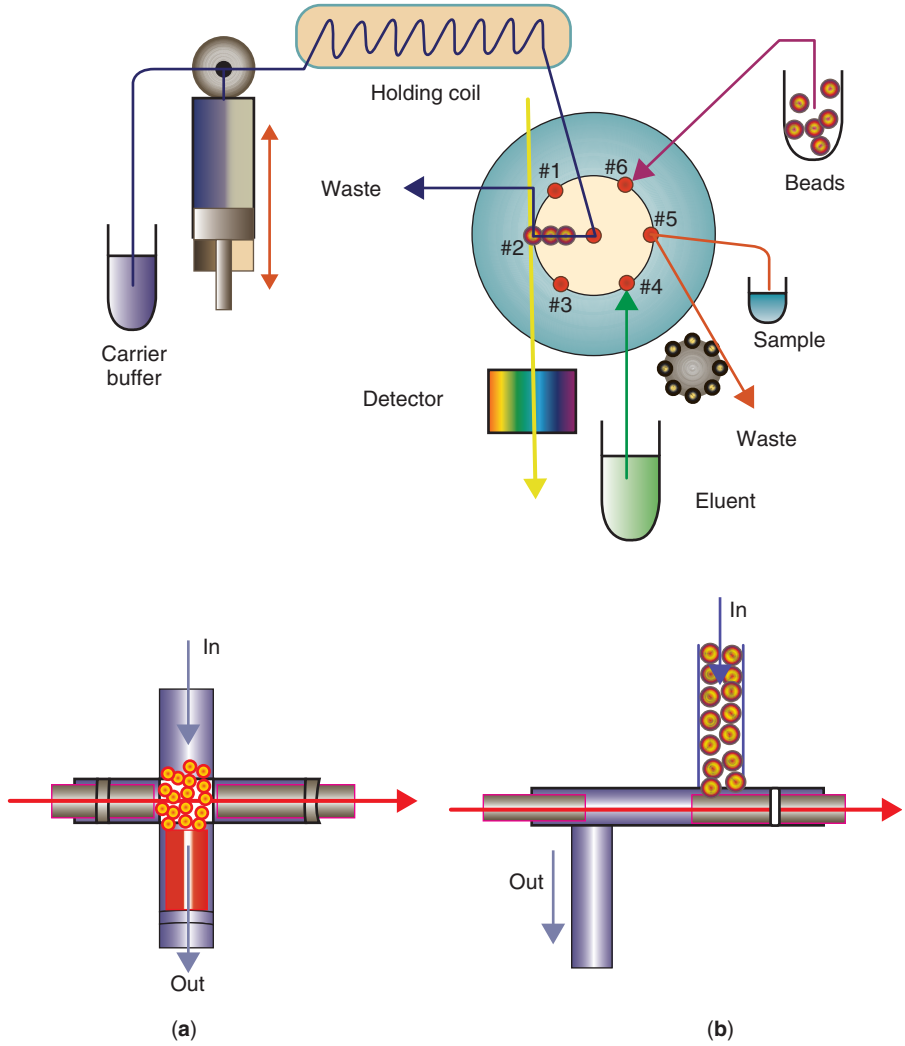


Figure 70.7. Experimental set-up for bead injection spectroscopy and micro-affinity chromatography. At the bottom is shown in (a) the configuration of the flow cell for capturing and monitoring of beads by UV–Vis spectrophotometry; and in (b) the configuration of the flow cell for micro-affinity chromatography. The beads are retained as a microcolumn by a sheath of optical fiber, designed to allow the mobile phase to pass freely into the flow cell (light path 10 mm). (From Ref. 86, courtesy of the author.) (This figure is available in full color at http://onlinelibrary.wiley.com/book/10.1002/9780470054581.)

via UV/VIS spectrophotometry or fluorometry (Fig. 70.7a) or by detecting them as they are eluted from the beads (Fig. 70.7b). While the first approach can be viewed as "on-column spectroscopy" (15,74,75), the latter one can be considered as miniaturized bioaffinity chromatography (59,60,68). Both methods employ in-valve bead injection analysis with renewable microcolumns and identical analytical instrumentation, whereby they can be exploited in a complementary fashion to get further knowledge on biomolecular association and dissociation reactions (76,87). The micro-affinity chromatography in the LOV format has been demonstrated for separation of immunoglobulins or nucleic acids, as based on molecular recognition between a site fixed on the stationary phase and the target species that is being captured, while unwanted matrix components, such as salts and proteins, are washed out by the mobile phase. In contrast to conventional immunoaffinity chromatography, it is readily feasible to control the operational pH, which is a very critical parameter, and compared to on-column spectroscopy, LOV-chromatography on a renewable bead column is more robust, since the volume of the beads captured within the microcolumn is far less critical, and also because the target analyte is eluted and monitored in solution and not on bead surfaces, thus precluding light scattering effects (68,76). Furthermore, by using a short pulse of eluant, the front elution contains almost all target

molecules, yielding excellent limits of detection. Yet, the most severe limitation of micro-affinity chromatography is that it cannot monitor antibodies when remaining immobilized irreversibly on the bioligand bearing beads. On the contrary, bead injection spectroscopy monitors the sorption process, whereby the elution of target species is not a must since beads can be automatically withdrawn following recording of the spectroscopic readout (74,76).

In this context it should also be mentioned that the SI-LOV system has been interfaced to capillary electrophoresis (CE) with UV detection for inorganic anion and protein separation (62,63). In this case, the multipurpose flow cell was reconfigured to act as a front end between the microfluidic device and the CE separation module. The microfluidic property of LOV did not merely provide an efficient sample delivery conduit for the CE system with various sample injection modes, including electrokinetic, hydrodynamic and head column field amplification sample stacking (62), but at the same time served as a versatile means of sample pre-treatment and chemical derivatization (e.g. protein labeling) (63) to facilitate the ensuing CE separation.

A detailed compilation of the work by Ruzicka and his coworkers can be found on the CD-ROM published by Ruzicka (86).

70.7.3 DNA Assays

A very active research group at Northeastern University in Shenyang, China, headed by Professor Jianhua Wang, has over the past few years published a series of articles focused on determination and/or purification of DNA exploiting the inherent features of LOV. In the first communication (88), using a LOV similar to the one shown in Fig. 70.8, they described a spectrophotometric procedure for DNA assay, where a small amount of crystal violet solution (10 μL) was de-coloured inside the flow cell of the LOV in the presence of 5 μL λ-DNA/*Hin*dIII within a certain pH range, the decrease in absorbance of the crystal violet solution being measured at 591 nm via optical fibers and employed as the basis of quantification. Obtaining a detection limit of 0.07 μg/mL, this work was supplemented by a procedure based on fluorescence measurement (89), where sub-nanoliter to a few microliters of DNA sample and ethidium bromide (EB) solutions were introduced into the LOV, resulting in the formation of a DNA–EB adduct, which afterwards was excited in the versatile flow cell of the LOV by a 473 nm laser beam, the emitted fluorescence being monitored *in situ* via optical fibers. By using this approach the detection limit was further decreased, that is, to 0.006 μg/mL by affixing the aspirated sample volume to 2.0 μL.

In a very recent publication (90), this research group has exploited the LOV for DNA separation/purification via solid-phase extraction with a silica microcolumn packed

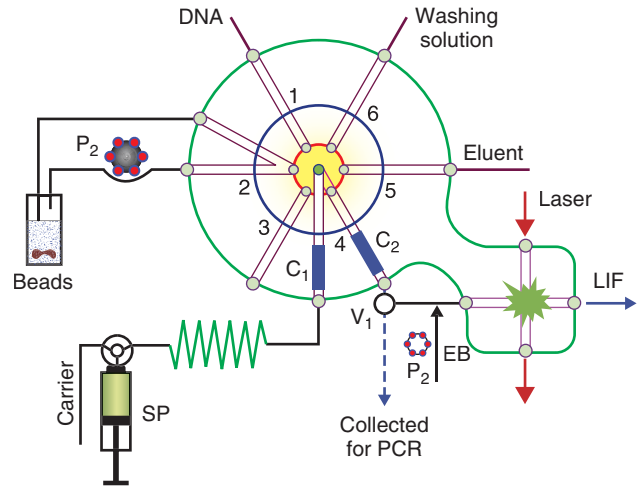


Figure 70.8. LOV system employed for DNA separation and purification from human blood, integrating a demountable fluorescence flow cell. EB, ethidium bromide; LIF, laser-induced fluorescence; P_1 and P_2, peristaltic pumps; SP, syringe pump; V_1, three-way valve; and C_1 and C_2, microcolumns. (From Ref. 90, courtesy of Springer Science and Business Media.) (This figure is available in full color at http://onlinelibrary.wiley.com/book/10.1002/9780470054581.)

within an LOV microchannel. By proper selection of the sample loading and the elution media, the complex matrix components in human whole blood, including proteins, could be completely eliminated. The DNA purification process was monitored on-line by using LIF at 610 nm in a demountable side part of the LOV unit incorporating optical fibers (Fig. 70.8). The practical applicability of the entire system was demonstrated by separation/purification of λ-DNA in a simulated matrix and human blood genetic DNA by performing in-valve SPE, *in situ* monitoring of the purified products via fluorometric detection of DNA–EB, and postcolumn PCR amplification. It was demonstrated to offer significant advantages over chip-based separation/purification systems based on the same principle in terms of precision, sampling frequency as well as robustness. The employment of the bead injection technique facilitated automatic injection and withdrawal of the solid-phase material in the LOV-based purification system, as opposed to LOC microdevices where renewal of solid substrates is not feasible and thus the entire microchip should be discarded and replaced by a new one after short term operation.

The Chinese group (91) and the one headed by Professor Luque de Castro (92) in Spain have most recently compiled comprehensive reviews on bioanalytical applications of LOV, including cellular analysis, immunoassays, affinity chromatography, DNA separation/purification, and enzymatic assays. Readers are encouraged to consult these articles for further details.

TABLE 70.2. Analytical Performance of Selected Flow Methods Involving Enzymic Reactions for Monitoring Fermentation and Culture Broths

Analyte	Microorganism	Flow approach	Detection technique	Linear range	Detection limit	Precision (RSD, %)	Reference
Glucose	*Penicillium chrysogenum*	FI	CL	5-700 mg/L	5 mg/L	<2	10
Ammonia	*Penicillium chrysogenum*	FI	SP	0-10.8 mg/L	NR	NR	10
Glucose	NR	SI	Amp	5-750 mg/L	15 μg/L (H_2O_2)	<1.2	12
Ethanol	NR	SI	Amp	0.15-30 mg/L	15 μg/L (H_2O_2)	<2.2	12
Ethanol	*Saccharomyces cerevisiae*	FI/SI	Amp	0.05-11.5 mg/L	50 μg/L	7.4	22
Glucose	*Lactobacillus casei*	FI	Amp	2-100 g/L	2 g/L	NR	23
L-lactate	*Lactobacillus casei*	FI	Amp	1-60 g/L	1 g/L	NR	23
Lactic acid	Mammalian cell 293S (kidney)	FI	Amp	0- 0.27 g/L	4.5 mg/L	1.5	24
Glucose	*Lactococcus lactis*	FI	Amp	0.01-0.1 g/L	10 mg/L	NR	25
L-lactate	*Lactococcus lactis*	FI	Amp	0.01-0.5 g/L	10 mg/L	NR	25
Glucose	*Torulopsis versatilis*	FI	Amp	5-50 g/L	5 g/L	NR	33
Ethanol	*Torulopsis versatilis*	FI	Amp	5-50 g/L	5 g/L	NR	33
Glutamate	*Torulopsis versatilis*	FI	Amp	1-20 g/L	1 g/L	NR	33
Glutamine	Mammalian cell culture	FI	SP	0-0.44 g/L	NR	<1	34
Glutamate	Mammalian cell culture	FI	SP	0-1.0 g/L	NR	<1	34
Glucose	Animal cells (Langerhans islets), *Escherichia coli* and *Saccharomyces cerevisiae*	FI	Amp	0-1.1 g/L	10 mg/L	1	35
Glucose	*Penicillium chrysogenum*	SI	CL	0-100 mg/L	5 mg/L	2.06	37
Lactic acid	*Penicillium chrysogenum*	SI	CL	0-100 mg/L	5 mg/L	2.56	37
Penicillin	*Penicillium chrysogenum*	SI	CL	0-100 mg/L	10 mg/L	<2	37
Glucose	*Escherichia coli*	FI	SP	0-1.5 g/L	11 mg/L	<1	39
Lactate	Mesenchymal stem cells	FI	SP	0-0.42 g/L	5 mg/L	<1	39
Ethanol	*Escherichia coli* and *Saccharomyces cerevisiae*	FI	SP	0-1.2 g/L	16 mg/L	<1	39
L-aminoacids	*Escherichia coli*	FI	SP	0-5 g/L (L-leucine)	5 mg/L	<1	39
D-lactic acid	*Lactobacillus-delbrueckii*	SI	SP	0.18-2.25 g/L	90 mg/L	NR	40
Glucose	*Streptococcu-scremoris*	FI	CL	1-2000 mg/L	5 mg/L	≤1	41

TABLE 70.2. (*Continued*)

Analyte	Microorganism	Flow approach	Detection technique	Linear range	Detection limit	Precision (RSD, %)	Reference
Lactose	*Streptococcu-scremoris*	FI	CL	0.025-5000 mg/L	0.1 mg/L	≤1	41
Galactose	*Streptococcu-scremoris*	FI	CL	3-3000 mg/L	3 mg/L	≤1	41
Lactic acid	*Streptococcu-scremoris*	FI	CL	0-8000 mg/L	0.1 mg/L	2	41
Methanol	*Pichia pastoris*	SI	SP	0-2 g/L	0.12 g/L	<4	50
Ammonium	*Escherichia coli*	LOV	SP	3-1200 mg/L	3 mg/L	0.9	65
Glucose	*Escherichia coli*	LOV	SP	35-1000 mg/L	35 mg/L	1.1	65
Glycerol	*Escherichia coli*	LOV	SP	20-120 mg/L	20 mg/L	1.1	65
Free iron	*Escherichia coli*	LOV	SP	80-400 mg/L	80 mg/L	1.5	65
Alkaline phosphatase	*Escherichia coli*	FI	SP	0.005-0.1 U/mL	NR	NR	93

Abbreviations: FI, Flow Injection; SI, Sequential Injection; LOV, Lab-on-a-Valve; SP, Spectrophotometry; Amp, Amperometry; CL, Chemiluminescence; RSD, Relative standard deviation; NR: Not reported.

70.8 CONCLUSION AND PERSPECTIVES

Being based on transient measurements and exact and reproducible timing, FIA and its sequels SIA and LOV have turned out to open an array of novel possibilities within bioanalytical sciences. A compilation of recently published automatic procedures for monitoring of fermentation broths are presented in Table 70.2. Although not exhaustive, it gives a rather good impression of the variability of the species determined and the techniques applied. In general it should be stressed that not only do the procedures consume very small amounts of sample and reagent solutions, and thus lead to generation of minute volumes of waste, but, more importantly, they allow entirely new and unique approaches to be implemented, which are not possible with conventional batch or continuous flow procedures.

The ultimate goal in modern (bio)chemical analysis is to identify individual analyte species in a given complex sample with sufficient selectivity and sensitivity which, in turn, often calls for appropriate sample pre-treatments or hyphenation of various selective detectors. Such schemes might entail physical/temporal separation of individual compounds via chromatographic or electrophoretic techniques or coupling of enzyme-based sensors in series, but might also involve the separation of the analytes from potentially interfering matrix constituents, or the execution of sample preconcentration protocols or, in fact, as most often encountered in practice, a combination of all strategies. Here, the SI-LOV approach presents itself as an ideal vehicle to act as the 'heart' of the system, because it is totally automated, miniaturized and fully computer-controlled. In SI-LOV, one has the advantage of being able to attach external units to facilitate individual operations, such as chromatographic columns for spatial separation of individual (bio) components, or the application of external energy sources such as UV light, or ultrasound radiation in order to effect desired reactions. But most importantly, a proper hyphenation will allow the implementation of intelligent chemistries, where advantage can be taken by the fact that the on-line systems operate under dynamic conditions so that one can exploit the interplay between thermodynamics and kinetics. Thus, what is needed in future applications is a realization of what this interplay implies, particularly in terms of facilitating the determination of (bio)chemical species in culture media or live cells, because this is exactly what differentiates the on-line LOV microanalysers from their batchwise counterparts—and, in fact, the LOCs. An eloquent alternative is to genetically engineer microbes to continuously report on their intracellular protein concentration with detection using FIA methods (93).

REFERENCES

1. Ruzicka J, Hansen EH. Anal Chim Acta 1975; 78: 145–157.
2. Hansen EH. Flow Injection Bibliography, http://www.fialab.com/, 2008.
3. Ruzicka J, Marshall GD. Anal Chim Acta 1990; 237: 329–343.
4. Lenehan CE, Barnett NW, Simon SW. Analyst 2002; 127: 997–1020.
5. Ruzicka J. Analyst 2000; 125: 1053–1060.
6. Hansen EH. Quim Anal 1989; 8: 139–150.
7. Vojinovic V, Cabral JMS, Fonseca LP. Chem Ind Chem Eng Q 2007; 13: 103–116.
8. Torto N, Gorton L, Laurell T, Marko-Varga G. Trends Anal Chem 1999; 18: 252–260.
9. Torto N, Laurell T, Gorton L, Marko-Varga G. Anal Chim Acta 1999; 379: 281–305.

10. Christensen LH, Nielsen J, Villadsen J. Anal Chim Acta 1991; 249: 123–136.
11. Ogbomo I, Kittsteiner-Eberle R, Englbrecht U, Prinzing U, Danzer J, Schmidt HL. Anal Chim Acta 1991; 249: 137–143.
12. Lapa RAS, Lima JLFC, Pinto IVOS. Food Chem 2003; 81: 141–146.
13. Hansen EH. Fresenius' Z Anal Chem 1988; 329: 656–659.
14. Ruzicka J, Hansen EH. Flow Injection Analysis. 2nd ed. New York: Wiley-Interscience; 1988.
15. Erxleben HA, Manion MK, Hockenbery DM, Scampavia L, Ruzicka J. Analyst 2004; 129: 205–212.
16. Lähdesmäki I, Park YK, Carroll AD, Decuir M, Ruzicka J. Analyst 2007; 132: 811–817.
17. Cos O, Montesinos JL, Lafuente J, Sola C, Valero F. Biotechnol Lett 2000; 22: 1783–1788.
18. Chen Y, Ruzicka J. Analyst 2004; 129: 597–601.
19. Fang Z-L. Gas-liquid separation. In: Flow-injection separation and preconcentration. Weinheim: VCH Verlagsgesellschaft mbh; 1993. Ch. 5, pp. 129–157.
20. Hansen EH, Miró M. Trends Anal Chem 2007; 26: 18–26.
21. Prodromidis MI, Karayannis MI. J Flow Inject Anal 2004; 21: 5–10.
22. Niculescu M, Erichsen T, Sukharev V, Kerenyi Z, Csoregi E, Schuhmann W. Anal Chim Acta 2002; 463: 39–51.
23. Kumar MA, Thakur MS, Senthuran A, Senthuran V, Karanth NG, Hatti-Kaul R, Mattiasson B. World J Microbiol Biotechnol 2001; 17: 23–29.
24. Male KB, Gartu PO, Kamen AA, Luong JHT. Anal Chim Acta 1997; 351: 159–167.
25. Min RW, Rajendran V, Larson N, Gorton L, Planas J, Hahn-Hägerdal B. Anal Chim Acta 1998; 366: 127–135.
26. Held M, Schuhmann W, Jahreis K, Schmidt HL. Biosens Bioelectron 2002; 17: 1089–1094.
27. Schuhmann W, Wohlschlaeger H, Huber J, Schmidt HL, Stadler H. Anal Chim Acta 1995; 315: 113–122.
28. Petersson BA, Andersen HH, Hansen EH. Anal Lett 1987; 20: 1977–1994.
29. Tsukatani T, Matsumoto K. Talanta 2006; 69: 637–642.
30. Hansen EH. Talanta 1994; 41: 939–948.
31. Lau K. Sensors: Overview, In: Encyclopedia of Analytical Science, 2nd ed. Netherlands: Elsevier; 2005. pp. 224–231.
32. Hansen EH. J Mol Recogn 1996; 9: 316–325.
33. Chen RLC, Matsumoto K. Anal Chim Acta 1995; 308: 145–151.
34. Mayer C, Frauer A, Schalkhammer T, Pittner F. Anal Biochem 1999; 268: 110–116.
35. Vojinovic V, Calado CR, Silva AI, Mateus M, Cabral JMS, Fonseca LP. Biosens Bioelectron 2005; 20: 1955–1961.
36. Benthin S, Nielsen J, Villadsen J. Anal Chim Acta 1992; 261: 145–153.
37. Min RW, Nielsen J, Villadsen J. Anal Chim Acta 1995; 312: 149–156.
38. Wu L-C, Cheng C-M. Anal Biochem 2005; 346: 234–240.
39. Vojinovic V, Esteves FMF, Cabral JMS, Fonseca LP. Anal Chim Acta 2006; 565: 240–249.
40. Shu H-C, Hakanson H, Mattiasson B. Anal Chim Acta 1995; 300: 277–285.
41. Nielsen J, Nikolajsen K, Benthin S, Villadsen J. Anal Chim Acta 1990; 237: 165–175.
42. Calokerinos AC, Palilis LP. Chemiluminescence in flow injection analysis. In: García-Campaña AM, Baeyens WRG, editors. Chemiluminescence in analytical chemistry. New York: Marcel Dekker; 2001. Ch. 12, pp. 321–348.
43. Hansen EH. Anal Chim Acta 1989; 216: 257–273.
44. Korenaga T, Ikatsu H. Bunseki Kagaku 1982; 31: 135–140.
45. Workman J, Creasy KE, Doherty S, Bond L, Koch M, Ullman A, Veltkamp DJ. Anal Chem 2001; 73: 2705–2718.
46. Workman J, Koch M, Veltkamp DJ. Anal Chem 2003; 75: 2859–2876.
47. Dantan N, Frenzel W. Poster No. 80, Proceedings of the International Conference on Flow Injection Analysis (ICFIA); Berlin; 2007. p. 173.
48. Ruzicka J, Hansen EH. Trends Anal Chem 2008; 27: 390–393.
49. Rhee JI. Biotechnol Bioprocess Eng 2007; 12: 289–294.
50. Surribas A, Cos O, Montesinos JL, Valero F. Biotechnol Lett 2003; 25: 1795–1800.
51. Chung SC, Christian GD, Ruzicka J. Process Control Qual 1992; 3: 115–125.
52. Pimenta AM, Montenegro MSCBM, Araujo AN, Martínez-Calatayud J. J Pharm Biomed Anal 2006; 40: 16–34.
53. Tzanavaras PD, Themelis GD. Anal Chim Acta 2007; 588: 1–9.
54. Motz SA, Klimundova J, Schaefer UF, Balbach S, Eichinger T, Solich P, Lehr C-M. Anal Chim Acta 2007; 581: 174–180.
55. Wang J-H, Hansen EH. Trends Anal Chem 2003; 22: 225–231.
56. Wang Y, Chen M-L, Wang J-H. Appl Spectrosc Rev 2007; 42: 103–118.
57. Wang J-H, Hansen EH. J Anal At Spectrom 2001; 16: 1349–1355.
58. Erxleben H, Ruzicka J. Anal Chem 2005; 77: 5124–5128.
59. Ogata Y, Scampavia L, Ruzicka J, Scott CR, Gelb MH, Turecek F. Anal Chem 2002; 74: 4702–4708.
60. Ogata Y, Scampavia L, Carter TL, Fan E, Turecek F. Anal Biochem 2004; 331: 161–168.
61. Long X-B, Miró M, Hansen EH, Estela JM, Cerdà V. Anal Chem 2006; 78: 8290–8298.
62. Wu C-H, Scampavia L, Ruzicka J. Analyst 2002; 127: 898–905.
63. Wu C-H, Scampavia L, Ruzicka J. Analyst 2003; 128: 1123–1130.
64. Quintana JB, Miró M, Estela JM, Cerdà V. Anal Chem 2006; 78: 2832–2840.
65. Wu C-H, Scampavia L, Ruzicka J, Zamost B. Analyst 2001; 126: 291–297.
66. Wang J-H, Hansen EH, Miró M. Anal Chim Acta 2003; 499: 139–147.
67. Miró M, Hansen EH. Trends Anal Chem 2006; 25: 267–281.
68. Erxleben H, Ruzicka J. Analyst 2005; 130: 469–471.
69. Ruzicka J, Scampavia L. Anal Chem 1999; 71:257A–263A.
70. Miró M, Kradtap-Hartwell S, Jakmunee J, Grudpan K, Hansen EH. Trends Anal Chem 2008; 27:749–761.
71. Hansen EH, Miró M. Appl Spectrosc Rev 2008; 43: 1–23.
72. Hansen EH, Miró M, Long X-B, Pedersen R. Anal Lett 2006; 39: 1243–1259.
73. Schulz CM, Scampavia L, Ruzicka J. Analyst 2002; 127: 1583–1588.

74. Ruzicka J, Carroll AD, Lähdesmäki I. Analyst 2006; 131: 799–808.
75. Carroll AD, Scampavia L, Luo D, Lernmark Å, Ruzicka J. Analyst 2003; 128: 1157–1162.
76. Gutzman Y, Carroll AD, Ruzicka J. Analyst 2006; 131: 809–815.
77. Manz A, Graber N, Widmer HM. Sens Actuators, B 1990; 1: 244–248.
78. Dempsey E, Diamond D, Smyth MR, Urban G, Jobst G, Moser I, Verpoorte EMJ, Manz A, Widmer HM, Rabenstein K, Freaney R. Anal Chim Acta 1997; 346: 341–349.
79. Sanders GHW, Manz A. Trends Anal Chem 2000; 19: 364–378.
80. Nguyen N-T, Wereley S. Fundamental and applications of microfluidics. Boston, MA: Artech House; 2002.
81. Oosterbroek RE, van den Berg A. Lab-on-chip: miniaturized systems for bio(chemical) analysis and synthesis. Amsterdam: Elsevier Science; 2003.
82. Kuswandi B, Nuriman, Huskens J, Verboom W. Anal Chim Acta 2007; 601: 141–155.
83. van den Berg A, Bergveld P, editors. Micro total analysis systems 2000. Proceedings of μTAS '2000 Symposium, Enschede, Netherlands; London: Kluwer Academic Publishers; 2000.
84. Miró M, Hansen EH. Anal Chim Acta 2007; 600: 46–57.
85. Wu C-H, Liu JL. PAT–J Process Anal Technol 2006; 3: 25–30.
86. Ruzicka J. Flow injection analysis CD-ROM tutorial. 3rd ed. FIAlab Instruments, Inc. available free of charge at www.flowinjection.com. 2004.
87. Edwards KA, Baeumner AJ. Anal Chem 2006; 78: 1958–1966.
88. Chen X-W, Wang J-H, Fang Z-L. Talanta 2005; 67: 227–232.
89. Chen X-W, Wang W-X, Wang J-H. Analyst 2005; 130: 1240–1244.
90. Chen X-W, Xu Z-R, Qu B-Y, Wu Y-F, Zhou J, Zhang H-D, Fang Z-L, Wang J-H. Anal Bioanal Chem 2007; 388: 157–163.
91. Chen X-W, Wang J-H. Anal Chim Acta 2007; 602: 173–180.
92. Luque de Castro MD, Ruiz-Jiménez J, Pérez-Serradilla JA. Trends Anal Chem 2008; 27: 118–126.
93. Schendel FJ, Baude EJ, Flickinger MC. Biotechnol. Bioeng., 1989; 34: 1023–1036.

71

FLUORESCENCE TECHNIQUES FOR BIOPROCESS MONITORING

Fabienne Anton
Institut für Technische Chemie, Gottfried Wilhelm Leibniz Universität Hannover, Hannover, Germany

Carsten Lindemann
Boehringer Ingelheim Pharma GmbH & Co. Biberach/ Riß, Germany

Bernd Hitzmann
Institut für Technische Chemie, Gottfried Wilhelm Leibniz Universität Hannover, Hannover, Germany

Kenneth F. Reardon
Department of Chemical and Biological Engineering, Colorado State University, Fort Collins, Colorado

Thomas Scheper
Institut für Technische Chemie, Gottfried Wilhelm Leibniz Universität Hannover, Hannover, Germany

71.1 INTRODUCTION

Monitoring and control of bioprocesses is of main interest in bioprocess engineering especially in the pharmaceutical industry because bioprocess efficiency, productivity, and optimization are essential. In this regard, the U.S. Food and Drug Administration (FDA) defined regulatory affairs like the process analytical technology (PAT) initiative in 2004. The main purpose of PAT is the implementation of innovative measurement techniques in the manufacturing processes, in order to increase the knowledge of process interactions directly and thus, to realize better on-line process monitoring along with a better understanding of the process (1). Due to the complex nature of microbial growth and product formation in bioprocesses, powerful analytical techniques for monitoring and control result in an increased efficiency, productivity and reproducibility, reduced costs, and improved quality control. With the implementation of capable analytical tools, deviations from the expected process run should be detected as early as possible. Thus, significant variations from the main route of the production process can be avoided and the final product quality and quantity can be ensured by realization of optimal conditions for growth, biosynthesis, and/or downstream processing.

In all stages of the manufacturing bioprocess, physical and chemical parameters for example, temperature, pH, dissolved oxygen, and CO_2 are traditionally measured directly on-line without time delay. However, monitoring of important biological/biochemical parameters such as cell density, metabolic activity, substrate consumption as well as product concentration is rather difficult due to the complexity of the sample composition. Thus, the determination of these parameters is mostly performed by complex analytical off-line techniques.

Ideal technologies for bioprocess monitoring of chemical and physical as well as important biological process variables and metabolic interactions should operate *in situ*, be noninvasive, and generate on-line information simultaneously without any time delay.

In recent years, various bioanalytical systems have been developed and investigated for improved on-line bioprocess monitoring and control. The application of such

Upstream Industrial Biotechnology: Equipment, Process Design, Sensing, Control, and cGMP Operations, Volume 2, First Edition. Edited by Michael C. Flickinger.
© 2013 John Wiley & Sons, Inc. Published 2013 by John Wiley & Sons, Inc.

on-line sensor systems in pilot facilities and production plants can provide a better understanding of different types of bioprocesses including cultivation, biotransformation, degradation processes as well as downstreaming operations. Most of these sensor techniques are still invasive and can disturb the current process. To overcome these limitations, a lot of research groups are involved in the development of new analytical tools, which can be interfaced into the bioprocess without extra risk of contamination for noninvasive bioprocess monitoring and control.

In this regard, spectroscopic techniques became a powerful tool for application in bioprocess monitoring (2). They provide information directly related to the molecular nature of the process. Spectroscopic sensors offer the advantage of noninvasive, non-destructive, continuous, and simultaneous multianalyte monitoring without a risk of contamination and no consumption of the analyte. They can be easily interfaced to the bioprocess via glass fiber systems or liquid light conductors. Due to the short response time of this spectro-optical system, signals can be obtained instantaneously.

Among noninvasive optical techniques, fluorescence spectroscopy is an attractive option in the development of on-line methods for bioprocess monitoring because many cellular constituents and media components are biogenic fluorophors. Therefore, many applications of fluorescence spectroscopy have been investigated intensively over the last 25 years in many categories of biotechnology processes in order to analyze the suitability of this technique of bioprocess monitoring and control. Based on this fact, special fluorescence sensors have been developed and optimized in regard to an improved bioprocess monitoring.

71.2 PRINCIPLES OF ON-LINE FLUORESCENCE SENSORS FOR BIOPROCESS MONITORING

Fluorescence sensors are fiber optical measuring instruments which can be used for the determination of bioprocess key variables such as biomass, substrate and product concentration, for bioreactor characterization, and metabolic studies in general. The development of such sensor systems started with the application of simple single wavelength sensors in the early 1970s and was continuously improved to the point of multiwavelength sensor systems for industrial application in bioprocess monitoring and control.

71.2.1 Single Wavelength Fluorescence

The principle of single wavelength fluorescence sensors is based on the fluorescence studies of Duysens and Amesz (3). They demonstrated that the reduced forms of nicotinamid adenine dinucleotide (NADH and NADPH) exhibit fluorescence at a wavelength of 450 nm when excited with UV light at a wavelength of 360 nm. This coenzyme is involved in the main metabolic reactions. By measuring the emitted light via this optical technique, the monitoring of the NAD(P)H pool inside living microorganisms is possible. The intensity of the fluorescence signal is affected by the amount of viable biomass concentration, the metabolic state of the cells as well as abiotic factors such as air bubbles or other fluorescent components in the medium.

The first *in situ* fluorescence sensors were able to measure one single excitation/emission wavelength pair in particular for the determination of intracellular NAD(P)H. Harrison and Chance (4) were the first to design a spectrometer device for biotechnology application based on NAD(P)H fluorescence for *in situ* on-line monitoring of cultivation in glass bioreactors. The light source for excitation and the photomultiplier holder were placed at an angle of 60°. The excitation as well as the emission light was passed directly though the reactor wall. Since the excitation light must penetrate a few centimetres into the cultivation broth, measurements are mainly limited to low biomass concentrations. With this setup, changes from anaerobic to aerobic conditions of *Klebsiella aerogenes* can be observed. Zabriskie *et al*. (5) used the same setup for the estimation of biomass in cultivations of different microorganisms. In the following years, other applications were published by several research groups (6).

On the basis of these experiments, smaller miniaturized process fluorometers were built which can be interfaced with bioreactors via standard ports (7). These sensors are arranged as open-ended detectors to measure the emission in the backward direction. The excitation light of 360 nm as well as the 180 backward fluorescence signal passes the reactor through a quartz glass window (Fig. 71.1). The advantage of this setup is the elimination of the inner filter effect by measuring the surface fluorescence directly at the observation window.

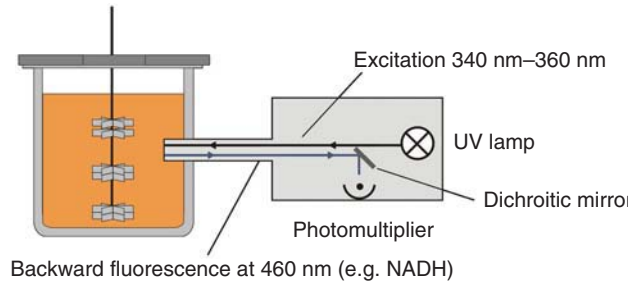


Figure 71.1. Principle setup of miniaturized single wavelength fluorescence spectrofluorometer for *in situ*, on-line measurements at a wavelength combination of ex350 nm/ em460 nm. (This figure is available in full color at http://onlinelibrary.wiley.com/book/10.1002/9780470054581.)

Commercially open-ended instruments were available by BioChem Technology, USA (FluoroMeasure) and Mettler Toledo, Switzerland (Fluorosensor). Both systems were restricted to the NAD(P)H fluorescence and culture fluorescence or fluorophors with the same fluorescence properties.

All these sensors have one disadvantage in common: they are restricted to one single wavelength pair and thus no verification of signals in regard to interfering fluorophors or disturbing factors (air bubbles, scattering particles) is possible.

One modification of these miniaturized fluorescence sensors was realized by Scheper and Schügerl in 1986 (8) for the simultaneous detection of two different emission wavelengths. The sensor was equipped with lenses, an optical filter system, and a special decoupled glass fiber optic for the emission light which is separated into two cables. Thus, a simultaneous detection of two different wavelengths is possible. The change of filters for excitation and emission wavelength offers the possibility of multiwavelength monitoring.

Single wavelength fluorescence sensors, developed for the determination of the NAD(P)H fluorescence, were tested for various applications regarding the bioprocess itself. Different cultivation processes including suspended or immobilized microorganisms were investigated mainly with regard to the determination of viable biomass or for on-line detection of metabolic changes during the cultivation process.

Several researchers correlated measured culture fluorescence to biomass concentration due to the fact that the fluorescence of the NAD(P)H pool inside the cells increases with an increase of cell concentration. Either a simple linear correlation is given or the fluorescence signal has to be linearized to biomass data in order to find a direct function between the coenzyme-dependent culture fluorescence and the biomass concentration. Under strictly defined conditions, on-line estimation of biomass is possible. Examples for biomass determination via single wavelength fluorescence for the growth in suspension are for example, *Saccharomyces cerevisiae*, a species of *Streptomyces*, *Zymomonas mobilis*, *Methylomonas mucosa* as well as *Pseudomonas putida*. Moreover, there are some applications for immobilized cell growth in regard to biomass estimation for example, *Clostridium acetobutylicum* and *S. cerevisiae*. A direct correlation with the culture fluorescence signal was not possible but an increase in fluorescence signal during cell growth has been observed.

However, as soon as limiting conditions occurred or the culture conditions were changed, deviations of the intracellular NAD(P)H pool were observed. Thus, not all attempts to correlate the biomass concentration with the fluorescence signal have been successful. An overview about the estimation of biomass via culture fluorescence in cultivations of different microorganism is given in (9). An updated summary concerning culture fluorescence is given in Table 71.1.

Monitoring of the NADH fluorescence inside the cells, the observation of the culture fluorescence can be used as indicator for environmental and metabolic changes during the cultivation process. Different applications are presented in the relevant literature (9,12).

Fluorescence and metabolic responses during aerobic and anaerobic transitions in the course of cultivation experiments of multiple microorganisms can be observed. The addition of substrates to starved cells or inhibitory reagents resulted in a metabolic change. The dynamic behavior of the initiated shift can be followed instantaneously. In chemostat cultures of *Escherichia coli* and *P. putida*, a change in dilution rate became obvious in the fluorescence signal, indicating that the intracellular redox state changes depending on the dilution rate. Based on the metabolic changes caused by external effects, Meyer and Beyeler (13) developed a system for the optimal control of the dilution rate for a continuous yeast cultivation process. Metabolic shifts during *Clostridium acetobutylium* growth, diauxic growth, or the glycolytic oscillations during the cell growth of *S. cerevisiae* can be measured as a function of the culture fluorescence.

The different applications of single wavelength fluorescence measurements are listed in Table 71.1. The broad applicability indicates that culture fluorescence provides much information on the metabolic state of the cells. Based on this information, further control strategies can be realized.

In conclusion, single wavelength fluorescence, measured at an excitation/emission wavelength pair of 360 nm/450 nm have been used as an indirect method to monitor biomass as well as metabolic changes along the bioprocess for different kinds of microorganisms over the last years. However, some application of these single wavelength measures showed that the interpretation of NAD(P)H fluorescence data is not always straightforward especially in regard to biomass estimation. The culture fluorescence is influenced by cellular metabolic changes. Furthermore, other medium components may fluoresce in the same region. Thus, interactions and overlapping effects with the fluorescence spectra of other fluorophors which are not detectable in a limited measuring range due to the very broad formation of the fluorescence peaks in general can occur. Especially in complex, turbid media which are common in biotechnological processes the interpretation of the data are difficult. Peak shifts and quenching effects due to other molecules as well as changes in chemical and physical parameters (like bubbles, pH, or dissolved oxygen) can influence the signal. Thus, broad applicability of the commercially available single wavelength fluorescence sensor in biotechnological processes is limited.

TABLE 71.1. On-line Estimation of Bioprocess Relevant Variables and Metabolic Studies of Different Organisms by Using Single and Multiwavelength Fluorescence (9–11)

Organism	Metabolic Studies	Monitored Bioprocess Variables	Single Wavelength	Multi Wavelength	Process Control
Procaryotic systems					
E. coli	Aerobic-anaerobic transition		X		
	Addition of carbon source to starved cells		X		
	Dilution rate changes		X		
	Addition of metabolic uncoupler			X	
	Strain stability			X	
	Biotransformation process			X	
		Biomass	X	X	
		Acetate		X	
		Target protein		X	X
		Plasmid copy number		X	
		CO_2 in exhaust gas		X	
Pseudomonas putida	Dilution rate changes		X		
		Biomass	X		
Zymomonas mobilis	Metabolic shifts		X		
		Biomass	X		
Bacillus subtilis		Biomass	X		
Bacilus polymyxa		Biomass		X	
		Target protein		X	
Alcaligenes eutrophus		Biomass	X		
C.lostridium acetobutylicum	Metabolic shifts		X		
		Biomass	X		
Streptomyces species		Biomass	X		
Thermoactinomyces species	Metabolic shifts		X		
Mucor mucosa		Biomass	X		
Klebsiella aerogenes	Aerobic-anaerobic transition		X		
Alcaligenese eutrophus	Metabolic shifts		X		
		Biomass	X		
Enterobacter aerogenes	Aerobic-anaerobic transition		X	X	
Spihingomonas yanoikuyae	Degradation process			X	
Pseudomonas fluorescenca		Biomass		X	
		CO_2 and O_2 in exhaust gas		X	
		Nitrate		X	
		Succinate		X	
		Total protein		X	
Pseudomonas aeruginosa	Aerobic-anaerobic transition		X		
Eucaryotic systems					
Fungi					
Sporotrichum thermophile		Biomass	X		
Penicillium chrysogenum	Aeration rate		X		
	Physiological effects		X		
		Biomass	X		
Cephalosporium acremonium		Biomass	X		
Claviceps purpurea		Biomass		X	
		Product formation (alkaloid)		X	
		Total protein		X	
Aspergillus niger	Spore germination			X	
	Metabolic activity (e.g. respiratory activity)			X	
		Product formation (mutant GFP)		X	

TABLE 71.1. (*Continued*)

Organism	Metabolic Studies	Monitored Bioprocess Variables	Single Wavelength	Multi Wavelength	Process Control
Aspergillus oryzae		Biomass		X	
		Lipase activity		X	
Yeast					
Saccharomyces cerevisiae	Aerobic-anaerobic transition		X	X	
	Addition of carbon source to starved cells		X		
	Diauxic growth		X		
	Dilution rate changes		X		
	Glycolytic oscillations		X		
	Addition of metabolic uncoupler		X		
		Biomass	X	X	X
		Glucose		X	X
		Ethanol		X	X
		Product		X	
Candida utilis		Biomass	X	X	
Candida tropicalis	Aerobic-anaerobic transition		X		
	Addition of carbon source to starved cells		X		
		Biomass	X		
Candida guilliermondi	Aerobic-anaerobic transition		X		
Pichia stipitis	Aerobic-anaerobic transition		X		
Pachysolen tannophilus	Aerobic-anaerobic transition		X		
Pichia pastoris		Biomass		X	X
		Glycerol		X	X
		Methanol		X	
Nicotiana tabacum		Recombinant GFP		X	
Plant cells					
Catharanthus roseus	Aerobic-anaerobic transition		X		
		Biomass		X	
		Secondary metabolites		X	
Podophyllum hexandrum		Biomass	X		
Eschscholzia californica		Biomass		X	
		Total alkaloid content		X	
		Secondary metabolites		X	
Azadirachta indica		Biomass	X		
Mammalian cells					
Human melanoma cells		Biomass	X		
Mouse hybridoma cells	Aerobic-anaerobic transition		X		
	Addition of carbon source to starved cells		X		
		Viable cell density	X		
NSO-cells		Recombinant GFP		X	
BHK cells		Viable cell density		X	
		Target protein		X	
Insect cells					
Spodoptera frugiperda		Biomass	X		

71.2.2 MultiWavelength Fluorescence

As bioprocesses are very complex systems, a detailed monitoring is required. Therefore, fluorescence measurements should be performed in a wide spectral range for both excitation and emission in order to get as much information as possible. More and more research groups developed and investigated measurement devices based on multiwavelength fluorescence in order to circumvent the restriction of single wavelength monitoring. Pioneering work was done by the research group of Humphrey (14) in 1991. They reported on the development of a multiple excitation fluorometric system with five different excitation light sources (289 nm, 313 nm, 334 nm, 365 nm, and 404 nm) in order to get a more detailed insight into the cultivation process of *Candida utilis*, *Pseudomonas putina*, and *S. cerevisiae*. Other important fluorophores besides NAD(P)H such as pyridoxine, riboflavin, and tryptophan were measured. These fluorophors are key vitamins and aromatic amino acids involved in cell growth and metabolism and in several cases their monitoring resulted in more reliable biomass estimation than the measurement of NAD(P)H. A major reason for this is the higher stability of these metabolites against diverse stresses such as oxygen limitations. Based on tryptophan monitoring, the amino acid concentration and protein expression can be followed. Measuring the fluorescence signal of tryptophan, a better correlation to cell mass concentration of *S. cerevisiae* was possible when compared to the determination based on NAD(P)H fluorescence. Further devices like the scanning fluorometer LS 5B (PerkinElmer/USA) were applied to a bioreactor via optical fibers (15). With these devices the scanning of a whole fluorescence spectrum can be realized by varying both excitation and emission wavelength independently in a wide spectral range. Problems of signal interpretation still remain, but in comparison to common single wavelength fluorescence sensors more reliable information on cell metabolic state and different processes variables can be gained.

The measuring of multiwavelength fluorescence generates a high density of information. In this case, the fluorescence is described by three parameters: the excitation wavelength, the emission wavelength, and the resulting fluorescence intensity. A full description requires an excitation-emission data matrix containing the data in numerical values. To visualize the fluorescence, a two dimensional (2D) spectrum can be generated based on the prepared matrix which represents the fluorescence intensity of the emission spectra at different excitation wavelengths. In this spectrum of excitation versus emission, different compounds can be identified by their position. Furthermore, an area free of fluorescence can be identifed in the spectrum. In the area where emission equals excitation wavelength, the scattered light is represented. Two illustrations of 2D spectrums are common. The contour plot shown in Fig. 71.2(a) is the most common projection in which fluorescence peaks are visualized by bright shadings. The isometric plot shown in Fig. 71.2(b) is more illustrative because the intensity of the fluorescence peaks is directly visual.

71.2.3 Biogenic Fluorophors

It is well known that many media components and cellular substances such as important vitamins like riboflavin and pyridoxine, aromatic amino acids like tryptophan, tyrosine and phenylalanine, enzymes and coenzymes like NAD(P)H as well as some proteins such as the green fluorescent protein (GFP) are biogenic fluorophors. A classification of these fluorophors can be done due to their intrinsic fluorescence in a characteristic spectral range (Fig. 71.3). By application of 2D fluorescence spectroscopy, it is possible to monitor all these fluorophors, which occur outside and inside the cell, simultaneously. A detailed insight into the metabolic state can be given based on these data and a better correlation to important process variables like biomass, substrate, or product concentration should be accessible.

In this context, the GFP is of great interest. The natural protein can be excited at wavelengths of 395 nm and 475 nm and has its maximum fluorescence emission intensity at a wavelength of 509 nm. GFP can be utilized as a reporter of gene expression and protein localization or folding. For this purpose it is used in bacteria, mammalian cells, plant cells, and yeasts. Due to its intrinsic fluorescence, it offers the possibility for on-line monitoring of product formation in recombinant protein production processes (16).

71.2.4 Chemometrics for the Evaluation of 2D Spectra

If 2D spectra from a process are considered, many intensity values representing different excitation and emission wavelength combinations of the spectrum are collinear, that is, the values are highly related and carrying the same information but with different sensitivity and specificity. However, the goal of the on-line measurement of such spectra is frequently the prediction of important process variables, which cannot be measured directly or just with extraordinary effort. To calculate a calibration model, off-line measurements of these process variables have to be carried out. However, a usual multilinear regression with all the data of the spectra and the off-line measurements is not recommendable to obtain a robust calibration model, because of the highly related data in a spectrum. Consequently, a special evaluation technique is required that allows obtaining independent variables out of the spectra, and results in a robust calibration model. The most prominent evaluation methods for this purpose are principal component regression (PCR) and partial least squares regression (PLSR).

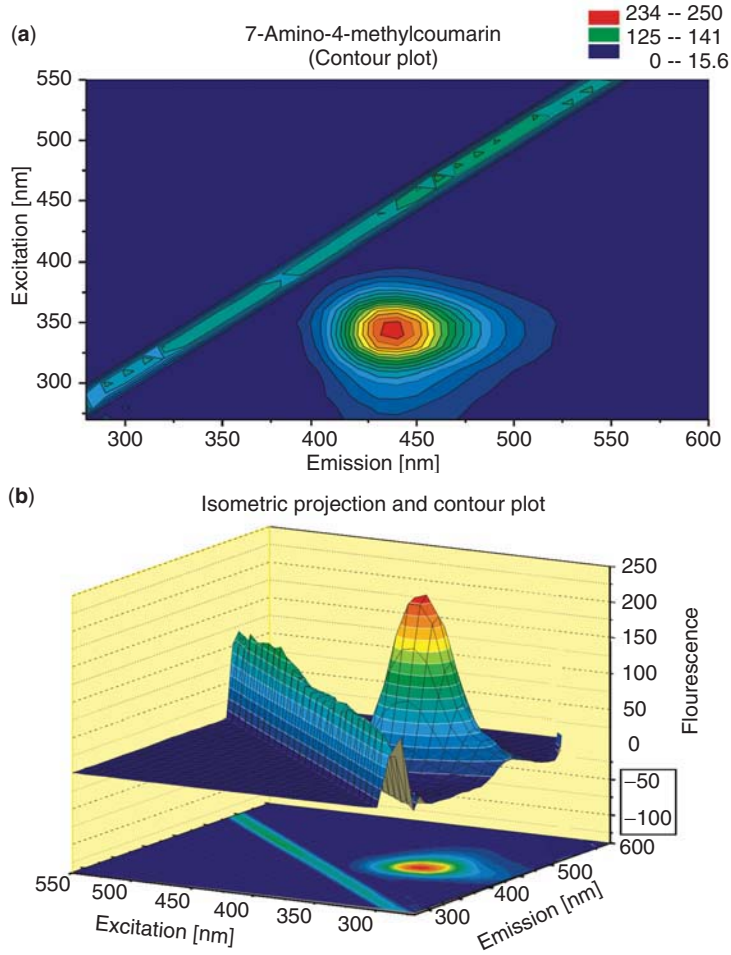


Figure 71.2. Contour plot (a) and the corresponding isomeric projection (b) of a fluorescence spectrum of 7-amino-4-methylcoumarin. (This figure is available in full color at http://onlinelibrary.wiley.com/book/10.1002/9780470054581.)

PCR is performed in a two step process. During the first step which is called principal component analysis (PCA) the mean centered data of the spectra are processed by using a successive variance maximizing rotational transformation of the coordinate system. During this transformation, the so-called principal components are calculated one after the other. To calculate the first component, which is the first determined axis of the new coordinate system, an axis is rotated around the origin of the mean centered data until it carries as much of the variance of the spectra data as possible. Then, the second axis is calculated in a way that it is perpendicular to the first axis and carries as much of the remaining variance of the data as possible. The third axis has to be perpendicular to the already calculated axis and represents as much of the remaining variance as possible. This procedure is repeated, until only noise is left in the residual data set. As a consequence, a new coordinate system is obtained, whose axis have decreasing variance. The number of the new axes is usually much less than the number of different excitation-emission wavelength combinations in a spectrum. Using the data represented in the new coordinate system by the principal components, a multilinear regression model can be calculated in the second step of the evaluation. The calibration model obtained by this method will robustly relate the spectra to values of important process variables.

Using PLSR the transformation, which is now performed with respect to the covariance of the spectra data and the off-line measurement data, and the regression are performed in a single step. PLSR gives for some applications better calibration models than PCR. The PLSR models can be calculated in two different ways. Using PLS1 to calculate a model to predict process variables, the transformation and regression is done for each process variable independently. As a result, one has to perform the calculation several times, whereas for a PLS2 model this calculation is performed together to get a single vector model. Here, the covariances

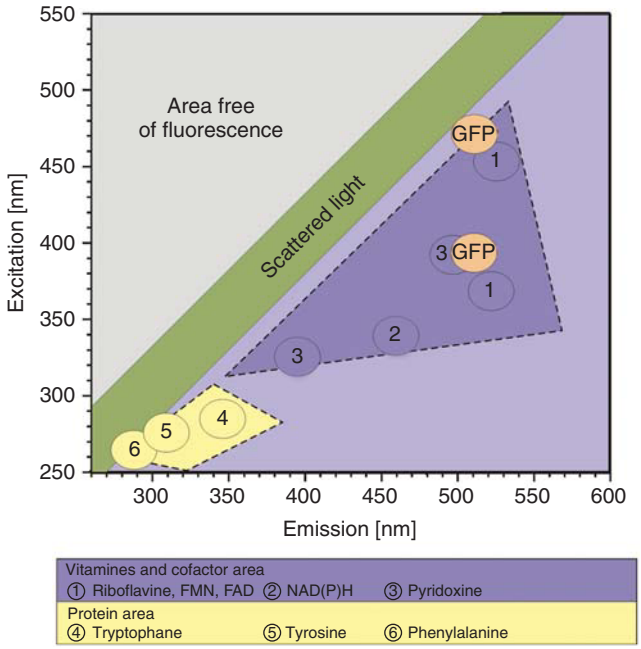


Figure 71.3. Biogenic fluorophors in a 2D fluorescence spectrum (17). Green flourescent protein (GFP), flavin adenine dinucleotide (FAD), flavin mononucleotide (FMN). (This figure is available in full color at http://onlinelibrary.wiley.com/book/10.1002/9780470054581.)

of the spectra data and all of the off-line data are used altogether simultaneously to calculate the calibration model.

For some applications it is advantageous not to use the full spectra for the above evaluation but just a few combinations of excitation and emission wavelengths intensity values. The reason for this is that some intensity values might not carry any information about the process but only noise. However, this has to be analyzed by calculating many calibration models and choosing the best validated one.

If the relation between the spectra data and the process variables are nonlinear, PCA and PLSR have to be modified. A simple approach is to use the original data set of the spectrum as well as the squared intensity values. Alternatively, the transformed data of PCA can also be used as input variables of a neural network, which will estimate the process variables (18).

Due to the fact that all the above mentioned modeling techniques are data driven, many calibration measurements are usually necessary to calculate the corresponding chemometric calibration model. This is a big drawback in almost all process spectrometers and not just the ones based on fluorescence measurements. However, a possible solution of this problem might be presented by Oliveira *et al*. (19), who used a theoretical process model to calculate the calibration model of a biotransformation process. The parameter values of the theoretical process model will be estimated inherently during the calibration procedure and are not required to be known beforehand.

A detailed discussion of the latest developments in multivariate statistical process control and its application to industrial processes as well as a critical review of the methodology and a description of how it is transferred to the industrial environment is given by Kourti (20).

71.2.5 Laboratory 2D Spectrofluorometer and Industrial Process Systems

For the measurement of 2D fluorescence several commercially available spectrofluorometers can be used. Different kinds of spectrofluorometers are available, commonly used in laboratories. These spectrofluorometer can be used either for off-line applications or, equipped with optical fiber for remote scanning, if on-line monitoring is preferred. Two commercially available examples are the ones produced by PerkinElmer, USA (Model LS 50B) and the one produced by Hitachi, Japan (Model F4500).

The fluorescence spectrophotometer Model F4500 is a very sensitive measurement device especially for laboratory application. Spectra can be generated in a range of 250 nm to 550 nm for excitation (10 nm step size) and 260 nm to 600 nm for emission (20 nm step size). The spectrometer allows a very fast scanning speed of 30,000 nm s^{-1}. An entire 2D spectrum can be measured within 1 min. For the selection of excitation and emission wavelengths, reflection grating monochromators are used on both excitation and emission sides. Excitation and emissions slits are selectable manually from a range of 2.5 nm, 5 nm, 10 nm, or 20 nm. A Xenon lamp is used for excitation. A reference photomultiplier is installed in order to compensate variations in the intensity of the excitation light source. A second photomultiplier (700 V) is used for the detection of the emission fluorescence signals. The configuration of the measuring setup is shown in Fig. 71.4.

After the sterilization of the reactor, the measuring chamber (place of cuvette holder in Fig. 71.4) of the spectrofluorometer can be connected with a bifurcated liquid light conductor (Lumatec, Germany) in an open-end-arrangement to a quartz window utilizing a 25 mm port of the bioreactor. For fluorescence measurement, the excitation light is guided via the fiber optic into the reactor and the emission light is guided via the second fiber optic to the detector. A computer with appropriate software is used for the configuration and control of the spectrofluorometer, data acquisition, and storing. With this setup, the sensor is not in contact with the medium and therefore a noninvasive, *in situ*, on-line measurement without the risk of contamination is possible.

A fluorescence sensor especially developed for fully automated industrial measurements and applications in bioprocess engineering is the BioView® sensor (DELTA, Denmark). The BioView® sensor is a very robust

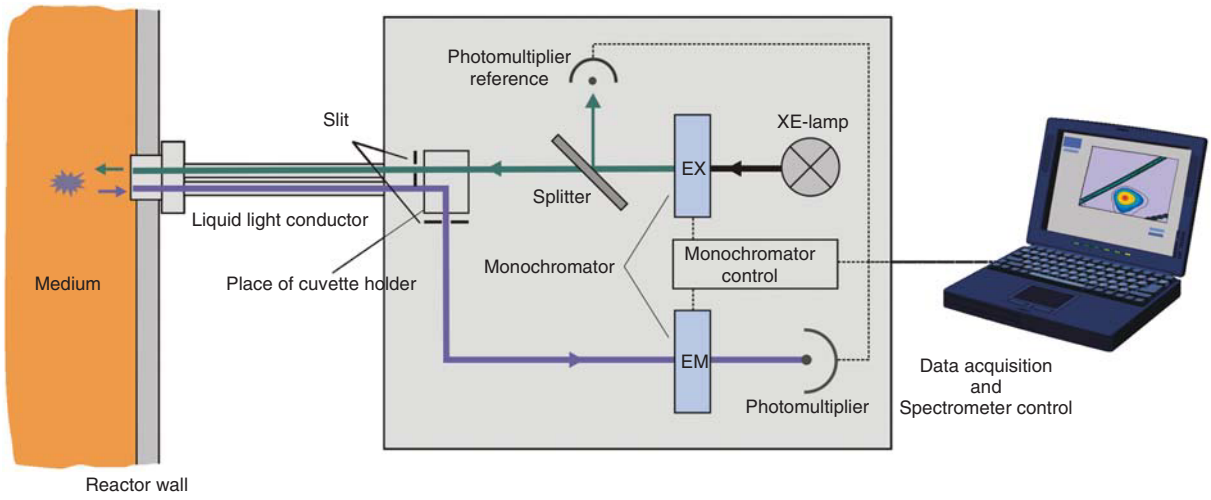


Figure 71.4. Measuring setup of a laboratory 2D fluorescence spectrometer (Hitachi F4500). (This figure is available in full color at http://onlinelibrary.wiley.com/book/10.1002/9780470054581.)

device that is encapsulated in a high-grade steel box for protection against harsh industrial environments such as high temperature, moisture as well as electromagnetic interference. In industrial facilities, long distance has often to be overcome for data transfer between the computer and the spectrometer. Therefore, a single-fiber asynchronous modem is used, which overcomes a distance of up to several hundred meters.

The sensor is solely designed for *in situ* on-line measurements. Therefore, the sensor is connected by a 2 m bifurcated liquid light conductor to a 25 mm standard port of the bioreactor. The port contains an adapter with a quartz glass window to ensure the noninvasive monitoring and thus, to eliminate the risk of contamination.

The optical part of the sensor is also optimized for the use in biotechnology processes. Instead of a grating monochromator, the sensor is equipped with two independently rotating filter wheels, one for excitation and one for emission, with 16 interference filters (DELTA, Denmark) for excitation (270–550 nm) and emission (310–590 nm). These filters can be chosen individually to meet the requirements of each individual process. The recording of a whole spectrum takes 90 s with a resolution of 20 nm. The measuring setup of the BioView® sensor is presented in Fig. 71.5. A Xenon flash lamp is used for excitation. The excitation filter wheel is set to the first filter position and the excitation light passes the first filter. The restricted light is guided via the liquid light conductor into the reactor. The emission signals of all excited fluorophores are guided backwards via the second light conductor and are monitored separately after passing each of the rotating emission filters. Afterwards, the excitation filter switches to the next position and the next data set is obtained. If the excitation wheel performed a complete cycle, the measurement of a whole spectrum is finished. This high measurement frequency enables the collection of information with no significant time delay and thus permits an estimation of different bioprocess variables simultaneously. In order to cover most of the information potential, properties and steps of filters can be adjust individually. Furthermore, the time of measurement can be minimized by reducing the number of filters used in a spectrum, for example, depending on the available or suitable fluorophores.

71.3 APPLICATION OF ON-LINE 2D FLUORESCENCE SPECTROSCOPY

2D fluorescence spectroscopy offers the possibility of simultaneous analysis of several fluorphores. Thus, the disadvantages of single wavelength spectroscopy can be overcome and important information based on multiwavelength fluorescence measurement can be obtained.

With 2D fluorescence spectroscopy, a closer insight into the bioprocess can be realized and a more detailed study of metabolic phenomenon is possible.

For monitoring of bioprocesses especially in the pharmaceutical industry, it is of great interest to get as much information as possible in order to guarantee optimal cultivation conditions for best bioprocess performance. Besides the on-line estimation of metabolic processes (e.g. aerobic-anaerobic transition, effect of metabolic uncoupler, diauxic growth, and the effect of pulse addition of substrate) a noninvasive simultaneous analysis of important bioprocess variables like cell density, substrate consumption as well as product concentration is essential. The application of fluorescence spectroscopy restricted

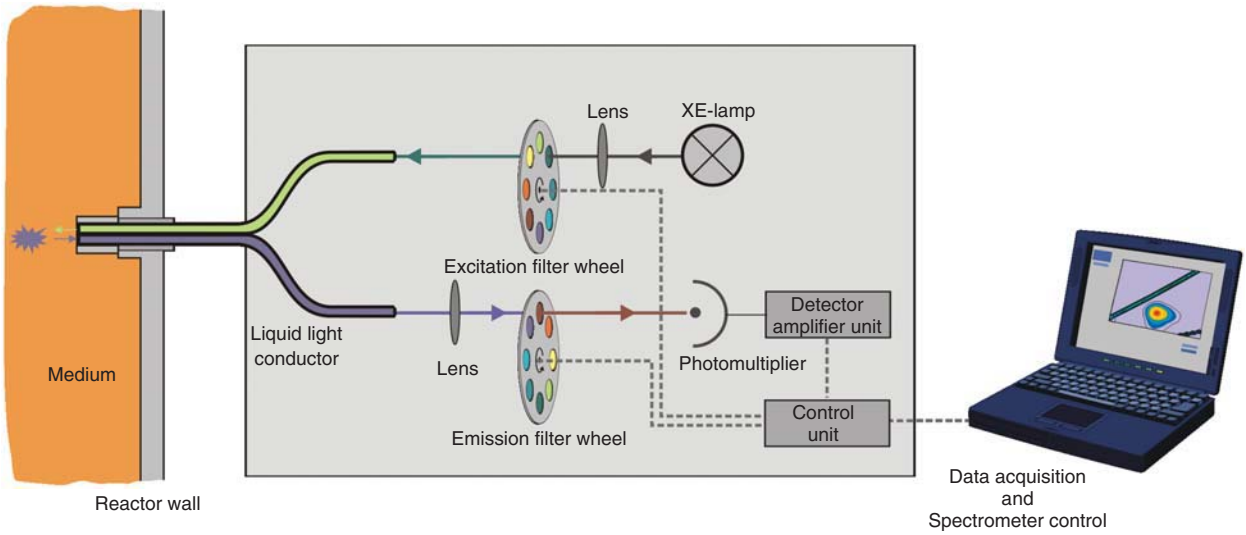


Figure 71.5. Measuring setup of industrial 2D fluorescence spectrometer (BioView® sensor). (This figure is available in full color at http://onlinelibrary.wiley.com/book/10.1002/9780470054581.)

to a single wavelength offers the possibility of biomass estimation in some cases under strictly defined conditions. For example, the NAD(P)H or tryptophan fluorescence showed a good correlation to the determined biomass concentration. However, multiwavelength fluorescence offers the possibility of determining various factors important for bioprocess monitoring and control.

Large-scale culture processes in combination with recombinant DNA technology have enabled the biotechnological production of proteins for pharmaceutical applications in a number of different hosts. Therefore, the potential of the application of 2D fluorescence spectroscopy for optimal process monitoring and control has been investigated for various organisms. Besides prokaryotic and eukaryotic systems like fungi, yeasts, and plant cells, the potential of the application of 2D fluorescence for process monitoring and control was also investigated for mammalian cells due to its increased application in the recombinant protein production processes. It is shown that this technique offers a good possibility for the monitoring of cultivation process of various organisms.

Table 71.1 gives a detailed overview of noninvasive on-line applications used in the last 25 years, for single and in particular, multiwavelength fluorescence spectroscopy with regard to metabolic studies and analysis of bioprocess relevant variables classified in prokaryotic and eukaryotic systems. It has been shown that the prediction of many process variables is possible utilizing multiwavelength fluorescence spectroscopy either due to direct correlation of the fluorescence signal of a single wavelength with the predictable relevant process variable, or by means of chemometric modeling as described in the previous section of this chapter. Moreover, determination of nonfluorescence process variables such as the glucose concentration is also possible. In high cell density cultivations (HCDC) in particular, 2D fluorescence seems to be a useful tool for on-line control and modeling of bioprocesses (9).

In a 2D fluorescence spectrum, various excitation-emission regions can be correlated to biomass concentration for several organisms as summarized in Table 71.1. Correlations to off-line cell mass concentrations during *S. cerevisiae* cultivations with the culture fluorescence in different regions of protein, cofactor, and vitamin area were performed. Information about cell growth and metabolism were obtained by correlations to fluorescent products and substrates (17).

Mycelia growth complicates common methods for biomass estimation. But even for the filamenteous fungi *Claviceps pupurea*, the on-line estimation of the biomass by 2D fluorescence spectroscopy is possible (17). Utilizing 2D fluorescence spectroscopy in combination with chemometric analysis, the estimation of ergotalkaloids which have a variety of pharmaceutical applications was achieved with only a minor error margin of 3%–4% (21). In contrast to common methods of alkaloid determination which are very time-consuming, 2D fluorescence spectroscopy enables on-line monitoring of ergotalkaloid concentration.

Accurate determination of viable cell density and glycoprotein concentration in batch and fed-batch cultivations of baby hamster kidney cells (BHK) confirm that multiwavelength spectroscopy seems to be a reliable method for on-line monitoring of bioprocesses (10). In fed-batch processes, the control of the substrate concentration at a low level is often required in order to prevent the production of overflow metabolites and to optimize the biomass

yield. In this context, Hantelmann *et al*. have developed a glucose feeding strategy for *S. cerevisiae* fed-batch cultivations based on the prediction of the metabolic state directly from fluorescence intensity. This approach avoids ethanol production while increasing the biomass yield (22).

Besides the determination of relevant process variables other studies based on metabolic changes were performed. For instance, strain stability of recombinant organisms is essential for consistent production in industrial applications. Johannson *et al*. demonstrated that on-line 2D fluorescence measurements provide information about metabolic changes useful for studying strain stability of plasmid containing *E coli*. This technique gave quicker and more extensive information in comparison to traditional time-consuming methods without influencing the cultivation process (23).

Investigation of *Aspergillus niger* cultivations demonstrated the potential of 2D fluorescence spectroscopy to detect the onset of spore germination, which represents a critical time-point in fungal bioprocesses. Furthermore, the quantitative formation of a mutant GFP in fed-batch cultivation as well as metabolic activity was determined (24).

During the last years, other applications of this noninvasive technique were investigated. Using fluorescent tracers, on-line characterization of bioreactors (e.g. mixing time experiments) can be performed under bioprocess relevant conditions in all types of bioreactors.

On-line monitoring of an industrial chromatographic desugarization process of molasses was realized by using 2D fluorescence technique. A noninvasive monitoring and prediction of different molasses compounds for a better process control were established (25).

Furthermore *in situ* fluorometry is a promising tool for monitoring anaerobic digestion processes in waste water treatments because waste water contains large amounts of proteins, amino acids, and other fluorescent compounds. Also, for various cultivations of microbial degradation processes of pollutants like chlorinated organic compounds 2D spectroscopy was used.

Since biocatalysis is of great interest for the production of industrial products, novel enzymes which show the ability to discriminate among many potential substrates are investigated. In this case, 2D fluorescence offers the possibility for a fast and effective on-line estimation of enantioselectivity of enzyme catalyzed reactions in aqueous and organic systems. Furthermore, the application of this technique for monitoring these reactions in supercritical carbon dioxide ($SSCO_2$) has been demonstrated (26).

71.4 CONCLUSION

2D fluorescence spectroscopy offers interesting applications in various fields of biotechnology. A noninvasive on-line monitoring and control of different process relevant variables as well as metabolic changes in bioprocesses can be performed simultaneously by using this optical analysis technique. In combination with chemometric modeling, a highly sophisticated process monitoring and control can be achieved, resulting in an improved economical process management. Thus, the implementation of 2D fluorescence spectroscopy in standard bioprocesses is a particularly useful tool for further bioprocess optimization and control in a wide range of applications.

REFERENCES

1. FDA U.S. Food and Drug Administration (2009) OPS process analytical technology- (PAT Initiative). Available at http://www.fda.gov/AboutFDA/CentersOffices/CDER/ucm088 828.htm. Accessed 2009 July 2.
2. Ulber R, Frerichs JG, Beutel S. Anal Bioanal Chem 2003; 376: 342–348. DOI: 10.1007/s00216-003-1930-1.
3. Duysens LN, Amesz J. Biochim Biophys Acta 1957; 24: 19–26.
4. Harrison DE, Chance B. Appl Microbiol 1970; 19: 446–450.
5. Zabriskie DW, Humphrey AE. Appl Environ Microbiol 1978; 35: 337–343.
6. Reardon KF, Scheper T, Rehm H-J, Reed G, editors. Biotechnology. Weinheim Germany: VCH; 1991. pp. 179–233.
7. Beyeler W, Einsele A, Fiechetr A. Eur Appl Microbiol 1981; 13: 10–14.
8. Scheper T, Schügerl K. J Biotechnol 1986; 3: 221–229.
9. Stärk E, Hitzmann B, Schügerl K, Scheper T, Fuchs C, Köster D, Märkl H Scheper T, editors. Advances in biotechnology engineering/biotechnology. Volume 74, Heidelberg Germany: Springer Verlag Berlin; 2002. pp. 21–38.
10. Teixeira AP, Partugal CA, Carinhas N, Dias JM, Crespo JP, Alves PM, Carrondo MJ, Oliveira R. Biotechnol Bioeng 2009; 102: 1098–1106. DOI: 10.1002/bit.22125.
11. Marose S, Lindemann C, Ulber R, Scheper T. Trends Biotechnol 1999; 17: 30–34.
12. Lindemann C, Marose S, Scheper T, Nielsen H-O, Reardon KF. In: Flickinger MC, Drew SW, editors, Encyclopedia of bioprocess technology –fermentation, biocatalyis and bioseparation, 1999, pp. 1239–1244.
13. Meyer C, Beyeler W. Biotech Bioeng 1984; 26: 916–925.
14. Li JK, Asali EC, Humphrey AE. Biotech Prog 1991; 7: 21–27.
15. Tarakovsky B, Sheintuch M, Hilmer J, Scheper T. Biotechnol Prog 1996; 12: 126–131.
16. Hisiger S, Jolicoeur M. J Biotechnol 2005; 117: 325–336. DOI: 10.1016/j.jbiotec.2005.03.004.
17. Marose S, Lindemann C, Scheper T. Biotechnol Prog 1998; 14: 63–74.
18. Wolf G, Almeida SJ, Crespo GJ, Reis MAM. J Biotechn 2007; 128: 801–812. DOI: 10.1016/j.jbiotec.2006.12.029.
19. Oliveira FRP, Goldberg K, Liese A, Hitzmann B. Chemometr Intell Lab Syst 2008; 94: 118–122. DOI: 10.1016/j.chemolab.2008.07.001.
20. Kourti T. Int J Adapt Control Signal Process 2005; 19: 213–246. DOI: 10.1002/acs.859.

21. Böhl D, Solle D, Hitzmann B, Scheper T. J Biotechnol 2003; 105: 179–188. DOI: 10.1016/S0168-1656(03)00189-5.
22. Hantelmann K, Kollecker M, Hull D, Hitzmann B, Scheper T. J Biotechnol 2006; 121: 410–417. DOI: 10.1016/j.jbiotec.2005.07.016.
23. Johansson L, Liden G. Biotechnol Prog 2006; 22: 1132–1139. DOI: 10.1021/bp060061m.
24. Ganzlin M, Marose S, Lu X, Hitzmann B, Scheper T, Rinas U. J Biotechnol 2007; 132: 461–468. DOI: 10.1016/j.jbiotec.2007.08.032.
25. Ulber R, Faurie R, Sosnitza P, Fischer L, Stärk E, Harbeck C, Scheper T. J Chromatogr A 2000; 882: 329–334.
26. Knüttel T, Meyer H, Scheper T. Anal Chem 2005; 77: 6184–6189. DOI: 10.1021/ac050747d.

72

OFF-LINE ANALYSIS IN ANIMAL CELL CULTURE

HEINO BÜNTEMEYER
Institute of Cell Culture Technology, University of Bielefeld, Bielefeld, Germany

72.1 INTRODUCTION

The cultivation of mammalian cells *in vitro* requires special environmental conditions. Except primary cells taken directly from an organ, cultured cells usually derive from immortal or immortalized cell lines. The cells may be genetically engineered or manipulated by transfection or fusion techniques. The behavior of this new cell depends very much on the origin of the basal cell line.

While some requirements are general for every cell, others can be very special for one cell line. All cells need isotonic conditions of about 300 mosmol/kg. Usually the cells need oxygen and also a carbon source (mostly glucose). As the cells cannot synthesize the essential amino acids and vitamins, they have to be supplied. Some additional components may basically not be needed for surveillance, but they can support the cells to optimize cell growth and productivity. This knowledge leads to complex media formulations that seldom contain less than 40 different components. During optimization of culture conditions and process strategies a detailed analysis of the nutrient requirements has to be performed. Many different analysis methods have to be established in a laboratory to comply with this extensive task.

In this chapter methods for almost all media compounds are described. All methodsthat are described in detail in this chapter, were developed, adapted, or checked in the laboratory for suitability of analysis of cell culture media and supernatants. They should be easily transferable to similar laboratory conditions. In this chapter, the methods for the analysis of proteins are only very briefly described. For each protein, special conditions and methods may apply. In general, the characterization of proteins includes a variety of steps. Methods for the analysis of amino acid sequence, glycosylation, molecular weight, heterogeneity, and activity have to be employed. A description of all these procedures would be beyond the scope of this chapter. For this reason, protein separation methods such as electrophoresis and protein and peptide chromatography are not included here.

For almost all suppliers of special equipment or chemicals cited in this chapter, a listing of the home pages (World Wide Web) can be found at the end of this chapter. All other products may be delivered by local suppliers. When a method is described in detail, an equivalent apparatus of any supplier may also be suitable.

72.1.1 Composition of Cell Culture Media

Cell culture media contain a multitude of components. In most cases a complete medium consists of a chemically well-defined basal medium with additions of more or less defined additives. The basal medium contains low molecular weight substances, such as inorganic ions, amino acids, vitamins, and some other components (e.g. glucose, pyruvate, etc.). In Table 72.1 the formulations of the three main basal media are listed. All three media contain roughly the same substances. Differences can be found in the individual concentrations. Often some low molecular weight compounds like ethanolamine, diaminobutane, selene dioxide,

Upstream Industrial Biotechnology: Equipment, Process Design, Sensing, Control, and cGMP Operations, Volume 2, First Edition. Edited by Michael C. Flickinger.
© 2013 John Wiley & Sons, Inc. Published 2013 by John Wiley & Sons, Inc.

TABLE 72.1. List of Ingredients for the Three Basal Cell Culture Media DMEM, Ham's F12 and RPMI 1640 (Reproduced from Cell Culture Catalogue, Life Technologies, Paisley, UK)

Substance	DMEM (mg/L)	HAM F12 (mg/L)	RPMI 1640 (mg/L)
Inorganic Salts			
$Ca(NO_3)_2 \cdot 4\ H_2O$	—	—	100.00
$CaCl_2$ (anhyd.)	200.00	33.22	—
$CuSO_4 \cdot 5\ H_2O$	—	0.003	—
$FeSO_4 \cdot 7\ H_2O$	—	0.834	—
$Fe(NO_3)_2 \cdot 9\ H_2O$	0.10	—	—
KCl	400.00	223.60	400.00
$MgSO_4$ (anhydrated)	97.67	57.22	48.84
NaCl	6400.00	7599.00	6000.00
$NaHCO_3$	3700.00	1176.00	2000.00
Na_2HPO_4 (anhydrated)	—	142.04	800.00
$ZnSO_4 \cdot 7\ H_2O$	—	0.863	—
Other Components			
Glucose	4500.00	1802.00	2000.00
Phenol red	15.00	1.20	5.00
Na-pyruvate	—	110.00	—
Hypoxanthine (Na—salt)	—	4.77	—
Thymidine	—	0.73	—
Linolic acid	—	0.084	—
Liponic acid	—	0.21	—
Putrescine · 2 HCl	—	0.161	—
Glutathione	—	—	1.00
Amino Acids			
Alanine	—	8.90	—
Arginine · HCl	84.00	211.00	241.86
Asparagine	—	15.01	50.00
Aspartic acid	—	13.30	20.00
Cysteine HCl · H_2O	—	35.12	—
Cystine· 2 H_2O	62.75	—	65.15
Glutamic acid	—	14.70	20.00
Glutamine	584.00	146.00	300.00
Glycine	30.00	7.50	10.00
Histidine HCl · H_2O	42.00	20.96	15.00
Hydroxyproline	—	—	20.00
Isoleucine	105.00	3.94	50.00
Leucine	105.00	13.10	50.00
Lysine · HCl	146.00	36.50	40.00
Methionine	30.00	4.48	15.00
Phenylalanine	66.00	4.96	15.00
Proline	—	34.50	20.00
Serine	42.0.0	10.50	30.00
Threonine	95.00	11.90	20.00
Tryptophan	16.00	2.04	5.00
Tyrosine (Na_2 salt)	104.20	7.81	28.94
Valine	94.00	11.70	20.00
Vitamins			
Biotin	—	0.007	0.20
Ca-pantothenate	4.00	0.48	0.25
Choline chloride	4.00	13.96	3.00
Folic acid	4.00	1.30	1.00
i-Inositol	7.20	18.00	35.00
Nicotinamide	4.00	0.037	1.00
Pyridoxine HCl	—	0.062	—
Pyridoxal HCl	4.00	—	1.00
Riboflavin	0.40	0.038	0.20
Thiamine HCl	4.00	0.34	1.00
Vitamin B_{12}	—	1.36	0.005
p-Aminobenzoic acid	—	—	1.00

glutathione, taurine, ascorbic acid, fatty acids, cholesterol, and so on are added to support the cells for distinct biochemical pathways. Particularly for continuous and high density processes, the concentrations of the main nutrients (glucose and amino acids) are elevated and animal- or plant-derived peptones are often added. High molecular weight supplements, in particular proteins, are sometimes added to fulfill the requirements of certain cell lines. Besides proteins, these supplements may also contain peptides, lipoproteins, phospholipids, or lipids. Sometimes it is necessary to use serum or serum substitutes as an additive to the basal medium, especially during development and establishment of new cell lines when the behavior and the requirements of the new cells are not known. The function of some of the proteins is known. Insulin stimulates the glucose metabolism, transferrin acts as the carrier for iron ions and possibly other trace elements, and albumin actsas an adsorbent for free lipids and toxic pollutions. Lipoproteins supply the cells with cholesterol and fatty acids. All in all, mammalian cells *in vitro* require a complex medium that consists of many chemically different components.

72.2 ANALYSIS OF CELL DENSITY

The determination of cell numbers is the main task during the monitoring of cultivation progress. Besides total cell number, the ratio of viable and dead cells is also of particular interest. Methods using cell staining and optical means are faced methods measuring particle size or volume.

72.2.1 Cell Density Determination by Cell Staining

The most common method of cell staining is the trypan blue exclusion method. A cell suspension is mixed with a 0.4% trypan blue solution (isotonic, 0.81% sodium chloride, 0.06% potassium dihydrogen phosphate) and placed in a calibrated hemocytometer chamber (Neubauer chamber). Anchorage-dependent cells have to be removed from the surface prior to the staining procedure. For this removal the cells are incubated with a trypsin solution for some minutes. The cells are manually counted by using a phase contrast microscope at a magnification of 100–400 times. The dye cannot pass the intact cell membrane. Therefore, viable cells are not stained. Dead cells are dyed blue. From cell count and calibrated chamber size the cell density and viability can be calculated.

In some special cases a direct cell counting is impossible. When the cells grow in aggregates (spheroids) or inside of macroporous carriers, a representative aliquot cannot be taken to ensure correct counting. In those cases it may be useful to lyse the cells and stain the nucleus. For this purpose a cell pellet is resuspended in a crystal violet solution (0.08% crystal violet in 0.1 M citrate) and incubated at 37°C for at least 3 h. Subsequently the nuclei can be counted microscopically using a hemocytometer chamber.

72.2.2 Automated Cell Density Examination Systems (Innovates, Beckman Coulter)

An improvement of the cell staining method has been made in regard to automation procedures. The Cedex and Cedex HiRes systems (both innovates AG, Germany) and the Vi-CELL series systems (Beckman Coulter, IN) use the trypan blue exclusion method in a fully automated liquid handling system with flow-through chamber combined with video microscopy and image processing. The algorithms of the image recognition technology are able to classify the mapped objects, discriminate living cells from dead ones, and detect cells aggregates, debris, and other objects. The necessary sample sizes are between 0.3 and 1 mL and the analysis time including automated image examination is below 5 min. The instruments differ furthermore in their hardware setup. While the Cedex instrument uses a microscope stative with a 4 × magnification lens, in the Cedex HiRes instrument the principle of a dynamic microscope (8.75 × magnification) is realized. This enables the Cedex HiRes to analyze objects from 1 to 90 μm and the Cedex from 4 to 40 μm, respectively. The Vi-CELL series systems are able to analyze objects from 2 to 70 μm. Some further cell parameterssuch as diameter spectrum, eccentricity histogram, and tendency of aggregation are available from the data on user request. In addition to the cell densities and viability, these parameters are helpful to assess the condition of the culture. The automation of the trypan blue method leads to a much higher precision and accuracy compared to the manual hemacytometer results. While deviation up to 35% are possible in the results of manual counts, the automated systems reduce this to 5%.

72.2.3 Coulter Particle Counter (Beckman Coulter)

The Coulter method of sizing and counting particles is based on measurable changes in electrical resistance produced by nonconductive particles suspended in an electrolyte. A small opening (aperture) between anode and cathode is the sensing zone through which suspended particles pass. In the sensing zone, each particle displaces its own volume of electrolyte. The volume displaced is measured as a voltage pulse. The height of each pulse is proportional to the volume of the particle, independent of shape, color, and density of the particle. The quantity of suspension drawn through the aperture is controlled to allow exact counting and sizing of particles for a reproducible volume. A differentiation between viable and dead cells can only be performed by examination of the particle (cell) size.

72.2.4 CASY Particle Counter (Innovates, Formerly Schärfe System)

This system combines the established resistance measuring principle with the pulse area signal processing method. This allows a very high dynamic range, high resolution, and excellent reproducibility for the volume determination. The cells are suspended in a weak electrolyte and driven through a capillary of predefined geometry at a constant stream velocity. Electricity is supplied to the capillary across two platinum electrodes. While passing through the capillary, the cell displaces an amount of electrolyte equal to its own volume. This change in resistance level becomes an indication of cell volume. The measuring signal is scanned by the system at a frequency of 1 MHz. The amplitude and width of the pulse are captured and the integral is determined (pulse area analysis). These integrals are stored for each particle. A size distribution over all particles is computed in a resolution of 1024 channels from the stored pulse area values (integrals) (1). Viable and dead cells can only be differentiated by their cell volume and/or size. The size ranges for viable and dead cells may vary from cell line to cell line. An adjustment has to be made by the analyst to compare the data.

72.3 ANALYSIS OF MEDIUM COMPONENTS

72.3.1 Analysis of Nutrients

72.3.1.1 Glucose. Glucose is the main nutrient for almost all mammalian cells. Therefore, the quantitative determination of the glucose concentration is very important. A multitude of established chemical and biochemical methods are there, but not all of them can be employed for a direct quantification in a complex mixture such as cell culture medium. Only a specific method that is insensitive to interference with other compounds can be used. All common methods use enzymes as specific agents. Two of the most often employed determination methods are described in this chapter.

72.3.1.1.1 Photometric Glucose Assay (e.g. R-Biopharm, formerly Boehringer Mannheim). D-glucose is converted in the presence of adenosine triphosphate (ATP) by the enzyme hexokinase to D-glucose-6-phosphate. This product is then converted by the second enzyme glucose-6-phosphate-dehydrogenase in the presence of $NADP^+$ to D-gluconate-6-phosphate. During this last reaction NADPH is formed. The concentration of NADPH can be easily monitored at a wavelength of 340 nm. The concentrations of produced NADPH and assayed glucose are proportional (2).

Reactions:

$$\text{D-GLUCOSE} + \text{ATP} \xrightarrow{\text{Hexokinase}} \text{D-GLUCOSE-6} + \text{ADP}$$

$$\text{D-GLUCOSE-6-P} + \text{NADP}^+ \xrightarrow{\text{Glucose-6-phosphate-dehydrogenase}} \text{D-GLUCONATE-6-P} + \text{NADPH} + \text{H}^+$$

This assay test kit is desired to be used in a cuvette UV spectrophotometer and needs no further laboratory equipment. The method can be recommended when only few or sporadic measurements are necessary. Otherwise, the analysis is too time consuming and expensive in labor. In that case, the acquisition of an automatic analyzer should be considered.

72.3.1.1.2 Enzyme electrode-based biosensor (e.g. Model YSI 2700, Yellow Springs Instruments; BioProfile Analyzer Series, Nova Biomedical). In both analyzers enzyme electrodes are used as glucose-specific parts. The following description explains the situation for the YSI 2700 analyzer. The enzyme electrode consists of an amperometric hydrogen peroxide sensitive electrode combined with immobilized glucose oxidase trapped between synthetic membranes. The electrode itself consists of a platinum anode and a Ag/AgCl cathode. The platinum anode is polarized at +700 mV relative to the cathode. At the electrodes, a current results from decomposition of hydrogen peroxide to water and oxygen. The membrane covering the electrodes consists of three layers. The outer layer, made of polycarbonate, is in direct contact with the sample. The next layer is the immobilized glucose oxidase enzyme followed by a cellulose acetate membrane, which readily passes H_2O_2 but excludes chemical compounds with a molecular weight above approximately 200 Da. This last cellulose acetate film also protects the electrode from fouling caused by proteins, detergents, lipids and other substances (3). After applying a sample that contains glucose, a dynamic equilibrium is achieved very rapidly, when the rate of peroxide production and peroxide diffusion to the electrode is equivalent, indicated by a steady state current response from the electrode. The current is proportional to the hydrogen peroxide conversion and the glucose oxidation (reactions).

Reactions:

$$\text{D-GLUCOSE} + \text{O}_2\ \text{ATP} \xrightarrow{\text{Glucoseoxidase}} \text{Glucono-}\delta\text{-lactone} + \text{H}_2\text{O}_2$$

$$\text{H}_2\text{O}_2 \xrightarrow{\text{Pt anode}} 2\text{H}^+ + \text{O}_2 + 2\text{e}^-$$

The enzyme electrode is placed in a small chamber in the automatic system. Calibration and maintenance procedures are performed routinely by a liquid handling system. The sample volume needed is typically 25 μL (5–65 μL, adjustable) and the minimal sample glucose concentration is 0.05–0.1 g/L. The analysis of one sample lasts about 1 min. The sample can be applied without any prior preparation. Nevertheless, a removal of cells (e.g. by centrifugation) is strongly recommended in order to prolong the stability of the enzyme membrane. The membrane, once placed on the electrode, normally runs stable for some weeks. All in all, this method (and the apparatus) is a reliable glucose quantification method that can be recommended when a variable number of samples have to be analyzed daily. Further automation can be set up by installing autoinjectors or connecting the instruments to online sampling probes.

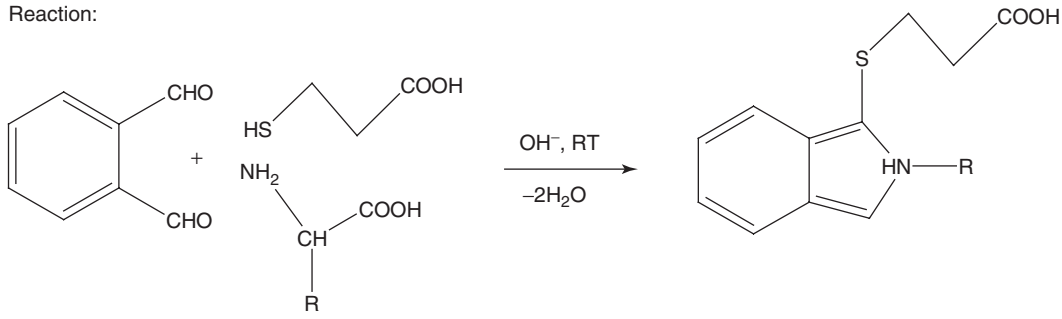
72.3.1.2 Amino Acids. Besides glucose, other sugars, or peptides, amino acids are the major group of medium compounds from which cells generate energy and carbon. The amino acids can be divided into two groups, essential and nonessential amino acids. This classification comes from a gradation made for animals and human beings. This might not be completely valid for mammalian cells cultured *in vitro*. Depending on donor and organ origin of each cell line, one or more amino acids, formerly classified as nonessential, might also be essential. Therefore, almost all amino acids are present in the defined basal medium formulations (Table 72.1), some in high and some in low concentrations. The amino acid with the highest medium concentration is glutamine, classified as a nonessential amino acid. But for all cell lines that do not express the glutamine synthetase gene, glutamine is essential. The cells can convert glutamine to α-ketoglutarate, which is introduced directly into the tricarboxylic acid (TCA) cycle.

From a chemical point of view, the amino acids are a very heterogeneous group of chemicals. Aliphatic, aromatic, polar, nonpolar, acidic, basic, and cyclic amino acids are present. Common for all acids is the carboxy and the primary (except proline and hydroxyproline) amino groups at the α-carbon. Except the three aromatic amino acids phenylalanine, tyrosine, and tryptophan, all other amino acids cannot be reasonably detected by spectrophotometrical means. An analysis method capable of quantification of all amino acids usually includes a separation procedure and a derivatization procedure to introduce a detectable group to the amino acid molecule. A multitude of methods have been developed using different derivatization reagents and chromatographic separation techniques. Two principles have been established: the pre-column and the post-column derivatization technique. In a pre-column method the amino acids are chemically modified first to introduce a chromophore or a fluorophore. The derivatization products are then separated on a chromatographic column and detected by an optical detector (spectrophotometer and fluorimeter). Usually an aromatic group is introduced to the amino acid molecule. The derivatives can be separated on a reversed phase column and monitored with an UV or fluorescence detector. In a post-column method the amino acids are separated first on an ion-exchange column and then modified just before detection. Almost every derivatization procedure modifies the amino acid in the amino group, which is much more reactive in an aqueous solution, especially at alkaline pH. In this chapter only the most important and commonly used methods are described in more detail.

72.3.1.2.1 Ninhydrin Method. This method is the only commonly used post-column derivatization method (4,5). The amino acids are separated on specially developed cation exchange columns (heated to temperatures of 40–70°C) by eluting stepwise with five different acidic lithium citrate buffers (containing also methanol and phenol) at pH of 2.5–5.0. At the end of the column the elution stream is merged with the ninhydrin reagent (20 g ninhydrin, 1.7 g hydrindantin in 65% dimethyl sulfoxide, and 35% 4 M lithium acetate buffer), passed through a reaction coil (T = 90–120°C) and applied to a VIS detector. Chromatograms are taken at wavelengths of 570 and 440 nm. Ninhydrin reacts under these conditions with all primary amino groups to form a dye which can be detected best at 570 nm. During this reaction only the amino group stays as part of the dye molecule (Ruhemann's purple). Secondary amino groups (proline, hydroxyproline) form other derivatives (yellow chromophores) than primary amino groups. These derivatives are detectable best at 440 nm. Although almost all biogenic amines and amino acids can be detected with this method it is replaced more and more by pre-column derivatization methods because of its very long analyzing time of more than 2 h, the unstable ninhydrin reagent, and the toxic and corrosive elution buffers.

72.3.1.2.2 o-Phthaldialdehyde Method. Primary amino groups react at alkaline pH in the presence of selected thiol compounds with *o*-phthaldialdehyde (OPA) to form unstable isoindoles. These isoindoles can be immediately separated on C_{18} (ODS)-reversed phase columns and detected with a fluorescence detector (6,7).

Dependent on the thiol used, the resulting derivative is more or less hydrophobic. Therefore, different elution buffers and profiles have to be used. The more hydrophilic the thiol is, the less hydrophobic the elution buffers can be. The following thiols were tested: 2-mercaptoethanol, mercaptoacetic acid, 2-mercaptopropionic acid and 3-mercaptopropionic acid. Good fluorescence yields can only be achieved when using 2-mercaptoethanol or 3-mercaptopropionic acid.



Only primary amino groups of amino acids and amines can react with OPA. Secondary amino groups will not be modified. Therefore, proline and hydroxyproline cannot be analyzed. But it is possible to employ a second derivatization with NBD chloride (7-chloro-4-nitrobenzofurazan) after OPA derivatization to form other fluorescent active products. Owing to the fluorescence quenching effect of sulfur, cysteine and cystine give only very poor fluorescent derivatives that are not quantitatively detectable. To overcome this problem it is possible to oxidise cysteine and cystine with an oxidant such as performic acid prior to OPA derivatization and quantify both together as cysteic acid. The OPA derivative of cysteic acid is very well detectable. The reagent OPA itself is not fluorescent and produces no interfering signals.

Procedure: The complete analysis of amino acid in samples from cell cultures can be performed with an automated high performance liquid chromatography (HPLC) system. A programmable autoinjector first mixes the prepared sample with the reagent mixture (OPA reagent) and then injects an aliquot onto a C_{18}-reversed phase HPLC column after a reaction time of 1.5 min. The OPA derivatives are eluted in a binary gradient in less than 30 min and passed through a fluorescence detector. Data recording, evaluation, calculation, and device control are done with a chromatography software (e.g. Galaxie CDS, Varian). A detailed description of this method follows.

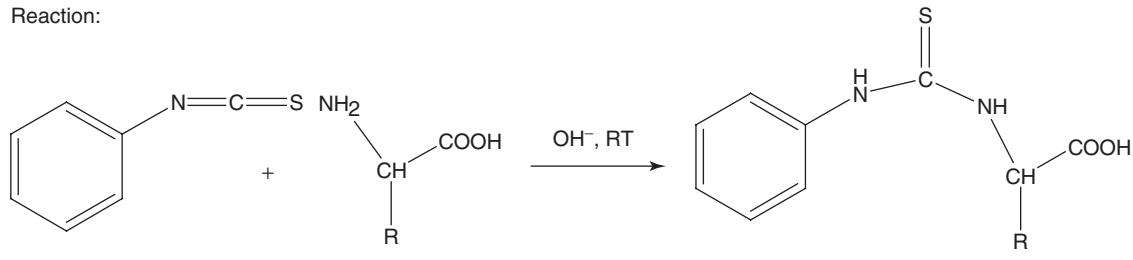
Sample Preparation: Cell-free supernatant is mixed 1:1 with 10% $HClO_4$ containing 300 μM of norvaline as an internal standard. The mixture is centrifuged for 5 min to remove the precipitated proteins. An aliquot is mixed with two aliquots of 0.4 M potassium borate buffer pH 10.4 to alkalize and dilute the sample.

Derivatization: 20 μL of the prepared sample is filled into a sampler vial. The sampler mixes with 70 μL of reagent (50 mg OPA, 1 mL methanol, 100 μL 3-mercaptopropionic acid, and 9 mL 0.6 M sodium borate buffer pH 10.4) and injects 20 μL onto the column after 1.5 min reaction time.

Elution: The mixture is separated on a C_{18}-reversed phase column (Kromasil C18, 5μ, 4.6 × 150 mm, Eka Nobel) with a multistep binary gradient in less than 30 min. The column temperature is set to 30°C. Buffer A consists of 89% 0.085 M sodium acetate pH 7.5 and 10% methanol and1% tetrahydrofurane. Buffer B is a mixture of 85% methanol and 15% 0.085 M sodium acetate pH 5.2. Total flow is set to 1.2 mL/min. The gradient is set as follows: 3% B at time 0, linear increase to 10% B in 8.2 min, linear increase to 34% B in 1 min, linear increase to 37% B in 9.5 min, linear increase to 77% B in 7.5 min, hold 77% B for 1 min, linear increase to 0% B in 1 min, and hold for 2 min.

Detection: The OPA derivatives are detected with a fluorescence detector set to excitation and emission wavelengths of 350 nm and 450 nm, respectively.

Figure 72.1 shows an example chromatogram obtained for a standard mixture. All amino acids are baseline separated and can be quantified by peak area integration.



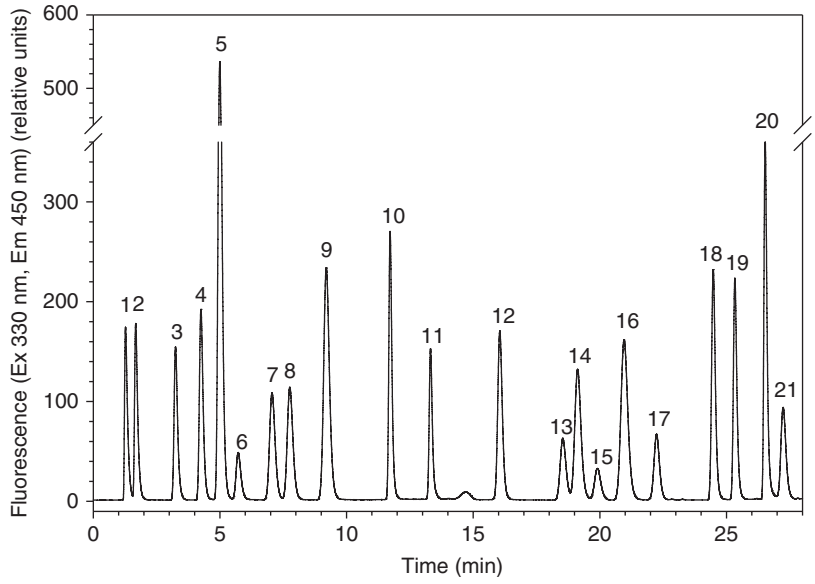


Figure 72.1. Standard chromatogram of amino acids processing the OPA method. Separation conditions apply as described in the text. List of amino acids: (1) aspartic acid, (2) glutamic acid, (3) asparagine, (4) serine, (5) glutamine, (6) histidine, (7) glycine, (8) threonine, (9) arginine, (10) alanine, (11) tyrosine, (12) ethanolamine, (13) methionine, (14) valine, (15) tryptophan, (16) norvaline (internal standard), (17) phenylalanine, (18) isoleucine, (19) leucine, (20) lysine, (21) by-product.

72.3.1.2.3 Phenylisothiocyanate Method. Phenylisothiocyanate (PITC) reacts under alkaline conditions with both primary and secondary amino groups (Edman reaction). The derivatives can be separated on C_{18} (ODS)-reversed phase columns and detected with a UV detector at 254 nm (8).

The method of sample preparation and derivatization follows a stringent procedure that involves many labour-intensive steps and cannot be completely automated. An improvement was made by introducing the PicoTaq system (Waters), a semi-automatic apparatus to perform the drying and derivatization of the sample (9,10). However, the resulting phenylthiocarbamyl derivatives are very stable and easy to handle.

Procedure: The analysis of samples from cell cultures is done with an automated HPLC system. An autosampler injects an aliquot of the prepared sample onto a C_{18}-reversed phase HPLC column. The PITC derivatives are eluted in a binary gradient in less than 50 min and passed through a UV detector. Data recording, evaluation, calculation and device control are done with a chromatography software. A detailed description of this method follows.

Sample preparation:Cell-free supernatant is mixed 1:1 with an internal standard solution of 300 μM norleucine. An aliquot of 100 μL is lyophilized with a vacuum concentrator.

Derivatization: 20 μL of mixture 1 (2:1:1 methanol: water:triethylamine) is added to the lyophilizate, vortexed and dried again. For derivatization, 20 μL of mixture 2 (7:1:1:1 methanol:water:triethylamine:PITC) is added and mixed during a reaction time of 20 min at room temperature (22°C). The mixture is lyophilized again to remove excess of PITC. The lyophilizate is dissolved in 100 μL elution buffer A and 40 μL are injected onto the column.

Elution: The mixture is separated on a C_{18}-reversed phase column (ODS Hypersil, 5μ, 4.6 × 250 mm, Hypersil) with a multistep binary gradient in less than 50 min. The temperature of the column is set to 39.5°C using a water bath. Buffer A consists of 98% 0.085 M sodium acetate pH 5.2, 2% acetonitrile. Buffer B is a mixture of 70% acetonitrile and 30% 0.085 M sodium acetate pH 5.2. The total flow is set to 1.4 mL/min. The gradient is set as follows: 2% B at time 0, hold 2% for 9 min, linear increase to 4% B in 1 min, linear increase to 10% B in 10 min, linear increase to 25% B in 9 min, linear increase to 31% B in 8 min, linear increase to 90% B in 3 min, and hold 90% B for 4 min.

Detection: The PITC derivatives are detected with a UV detector set to a wavelength of 254 nm. Figure 72.2 shows an example chromatogram obtained for a standard mixture. All amino acids are baseline separated and can be quantified by peak area integration.

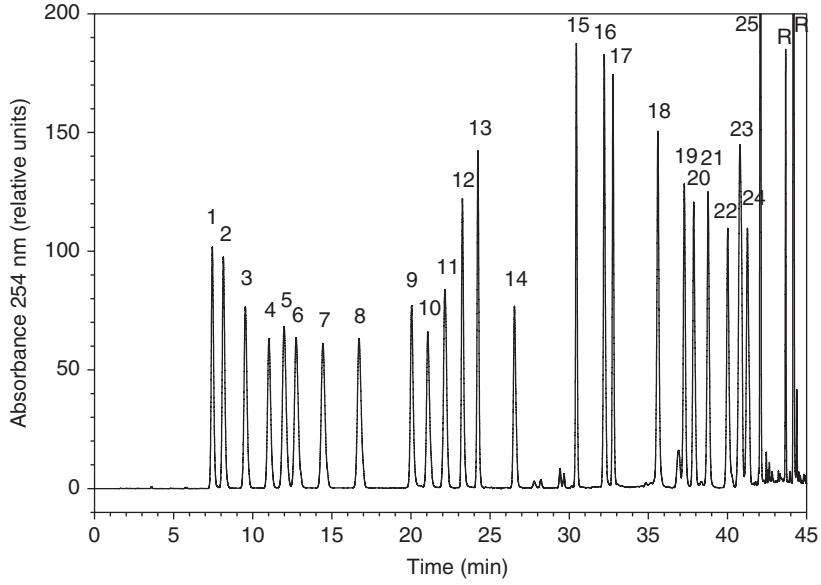


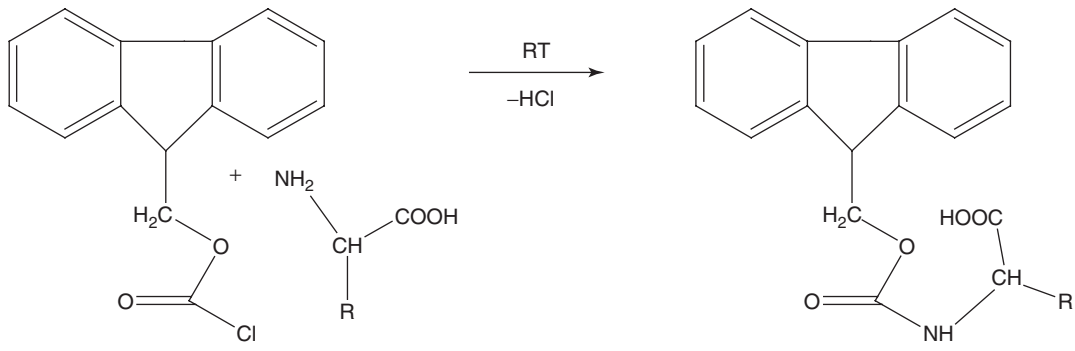
Figure 72.2. Separation of standard mixture amino acids using the PITC method. Amino acids identified as follows: (1) aspartic acid, (2) hydroxyproline, (3) glutamic acid, (4) serine, (5) asparagine, (6) glycine, (7) glutamine, (8) taurine, (9) histidine, (10) threonine, (11) alanine, (12) arginine, (13) proline, (14) ethanolamine, (15) tyrosine, (16) valine, (17) methionine, (18) cystine, (19) isoleucine, (20) leucine, (21) norleucine (internal standard), (22) phenylalanine, (23) ornithine, (24) tryptophan, (25) lysine, R reagent.

72.3.2 FMOC Method

9-Fluorenylmethoxycarbonyl chloride (FMOC) reacts with both primary and secondary amino groups. Owing to the introduction of the large hydrophobic fluorenylmethyl group, the derivatives can already be separated on a C_8-reversed phase column. Detection is done with a fluorescence detector at excitation and emission wavelengths of 260 nm and 310 nm, respectively.

FMOC offers a sensitivity comparable to the OPA method when used with fluorescence detection. But, FMOC and its hydrolysis products have similar fluorescence spectra to the FMOC amino acids. Excess FMOC remaining after derivatization reacts with water to form FMOC-OH (9-fluorenylmethyl alcohol), which elutes as a large broad peak. Removal of FMOC-OH can be achieved by liquid–liquid extraction into pentane. A more elegant method of preventing interference of FMOC-OH is to reactivate excess FMOC with a very hydrophobic amine (e.g. aminoadamantane) to form a derivative that elutes after all amino acids.

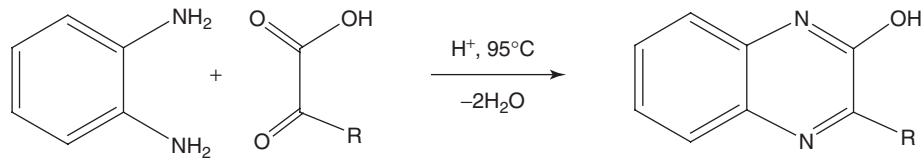
Reaction:



72.3.3 Analysis of Other Ingredients

72.3.3.1 Pyruvate. Pyruvate is the end product of aerobic glycolysis. At this point it can undergo several reactions, especially oxidative decarboxylation to produce acetyl-CoA or reduction to lactate (the end product of anaerobic metabolism). It was shown that free pyruvate is consumed by some mammalian cells rapidly, probably to bypass glycolysis. Other cell lines were observed to produce pyruvate to a certain extent. Nevertheless, no significant effect on cell growth and productivity was reported yet. Some basal medium formulations (e.g. F12) contain pyruvate in a concentration of 1 or 2 m*M*.

Reaction:



The determination of pyruvate cannot be performed without any molecule modification since no chromophore is present, except when employing an enzyme assay (using lactate dehydrogenase). On the other hand, pyruvate possesses an α-keto group which is reactive enough to react with primary amines under aqueous conditions. With *o*-phenylenediamine (OPD) (11) or 1,2-diamino-4,5-dimethoxybenzene (DMB) (12) fluorescent products (2-quinoxalinol derivatives) are formed, which can be separated on reversed phase columns and detected in a fluorescence detector.

Procedure: The analysis of pyruvate in samples from cell cultures can be performed with an automated HPLC system. The OPD derivatives are eluted in a binary gradient in less than 20 min and passed through a fluorescence detector.

Sample preparation: Cell-free supernatant is mixed 1:1 with 3% $HClO_4$ containing α-ketoglutarate as an internal standard. The mixture is centrifuged for 5 min to remove the precipitated proteins.

Derivatization: 50 μL of prepared sample is mixed with 500 μL of the OPD reagent (0.1 g OPD and 250 μL 2-mercaptoethanol in 100 m*M* 2 N hydrochloric acid) and derivatized for 2 h at 95°C. After cooling, 100 μL of the solution is mixed with 100 μL of 0.4 M sodium borate buffer pH 9.5 and 20 μL is injected onto the column.

Elution: The mixture is separated on a C_{18}-reversed phase column (Ultrasphere ODS, 5μ, 4.6 × 150 mm, Beckman Coulter Inc.) with a binary gradient in less than 20 min. The column temperature is set to 27°C. Buffer A consists of 0.085 M sodium acetate pH 7.5 and 1% tetrahydrofurane. Buffer B is a mixture of 70% methanol and 30% 0.085 M sodium acetate pH 5.2. Total flow is set to 1.0 mL/min. The gradient is set as follows: 20% B at time 0, linear increase to 100% B in 9 min, and hold 100% B for 4 min.

Detection: The OPD derivatives are detected with a fluorescence detector set to excitation and emission wavelengths of 340 nm and 412 nm, respectively (Fig. 72.3).

72.3.3.2 Inorganic Salts. Cell culture media contain inorganic cations and anions. The predominant salt in the medium is sodium chloride in a concentration of 6–7.5 g/L. This high concentration is necessary to maintain an osmotic pressure of about 300 mosmol/kg to ensure isotonic conditions for the cells. Besides sodium, only potassium, magnesium, and calcium cations are present in considerable concentrations. Sulfate, phosphate, and nitrate are the anions along with chloride. Some trace

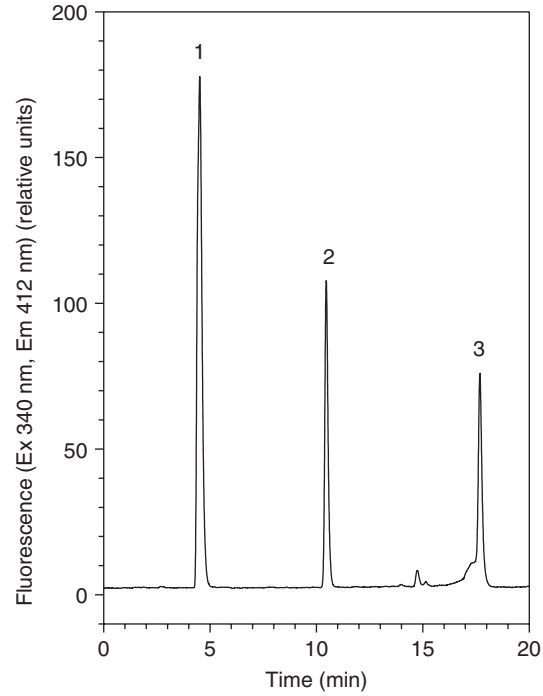


Figure 72.3. Separation of pyruvate (2) and ascorbic acid (3) standard solution on RP18 column after o-phenylendiamine derivatization (using α-ketoglutarate (1) as internal standard, concentration of each substance 1 m*M*).

elements like iron, zinc, copper, and selenium, each in very low concentration, may also be present. Sodium bicarbonate/carbon dioxide is usually the main pH buffer of the medium.

Ionic substances including inorganic cations and anions can be well separated by ion-exchange chromatography. The separated ions can easily be detected by using a conductivity detector, if the ion concentration is high enough to compensate the poor sensitivity. Conductivity detection is not suitable for the detection of trace elements. In that case methods like mass spectrometry (ICP-MS) or atomic absorption spectroscopy may apply.

Procedure: The ion separation can be performed with an ion chromatograph (e.g. Dionex, Metrohm) or any HPLC system equipped with a conductivity detector. The temperature of the column and of the flow cell of the detector has to be controlled very constantly since conductivity is extremely temperature sensitive.

Sample preparation: Cell-free supernatant is mixed with an internal standard (e.g. cesium bromide) and filtered (0.45 μm). The mixture has to be diluted with ion-free water to meet the detection range (e.g. 1:100).

72.3.3.2.1 Cation Separation. Inorganic cations can be separated on a cation exchange column [IC Cation SuperSep (silica, polybutadiene—malic acid), 125 mm × 4,0 mm, Metrohm] and eluted isocratically with a buffer consisting of 4 m*M* tartaric acid and 0.7 m*M* pyridine-2,6-dicarboxylic acid in less than 20 min. The column temperature is set to 30°C and total flow is set to 1.0 mL/min. A chromatogram obtained under these conditions is shown in Figure 72.4.

72.3.3.2.2 Anion Separation. The anions are separated on an anion exchange column (Anion/R (polystyrene, $-N(CH_3)^{3+}$), 10μ, 0,19 meq/g, 250 mm × 4.1 mm,

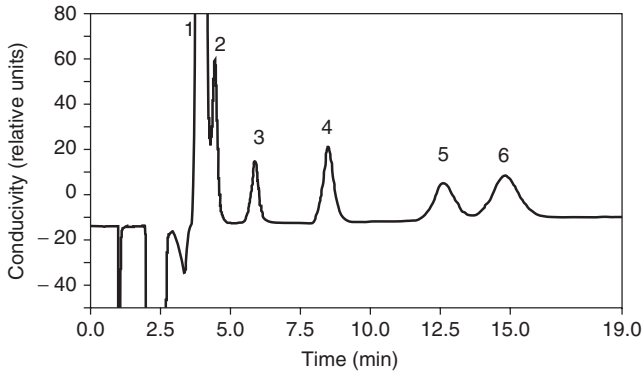


Figure 72.4. Separation of cations on a cation exchange column. Cell culture basal medium was diluted 1:100 prior injection. Identified cations are (1) sodium, (2) ammonium, (3) potassium, (4) cesium (internal standard), (5) calcium, (6) magnesium.

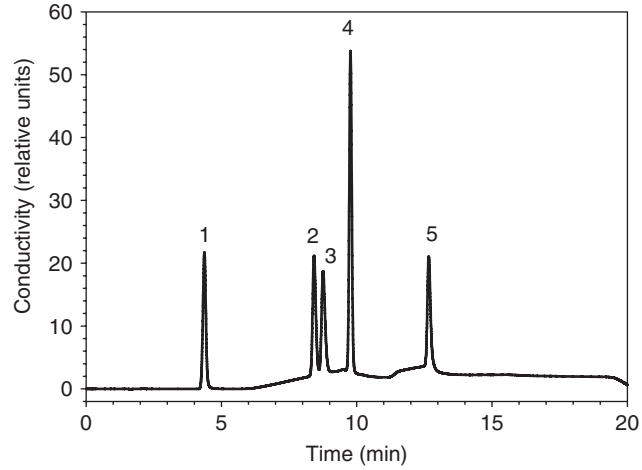


Figure 72.5. Anion separation by anion exchange chromatography. Separated anions of 1 m*M* standard calibrator are identified as follows: (1) chloride, (2) bromide, (3) nitrate, (4) sulphate, (5) phosphate.

Alltech) and eluted with 5 m*M* *p*-hydroxy benzoic acid, pH 8.5 (adjusted with LiOH) in 30 min. The column temperature and total flow are set to 30°C and 2.5 mL/min, respectively. Good results can also be obtained by using a Dionex ion chromatograph with suppressor technology equipped with an anion exchange column AS11 and a gradient elution with 10 and 100 m*M* sodium hydroxide solutions. Figure 72.5 shows an example of a standard chromatogram.

72.3.3.3 Vitamins. Cell culture basal media contain about 10 different vitamins and precursors (Table 72.1). Sometimes, special media recipes contain additional vitamins or provitamins such as Vitamin C (ascorbic acid), retinoic acid (Vitamin A acid), or E (α-tocopherol). From a chemical point of view, the group of vitamins is an extremely heterogeneous collection of substances with different chemical properties. Most of the vitamins are water soluble, but some are only fat soluble. Hence, a uniform analysis method cannot be achieved. A second problem for the determination derives from the very low concentrations, generally far below 10 mg/L. Nevertheless, the knowledge of vitamin requirements during cell cultivation (especially long term and high density cultures) may improve cell growth and productivity.

The analysis of vitamins is often performed in the food industry for quality control of multivitamin preparations, juices, engineered food, and other materials. In general, the vitamin concentrations in these matrices are much higher than in culture medium. However, some progress has been made in adapting methods for the analysis of certain vitamins to cell culture conditions. In the following

text, determination methods for some vitamins, which have been recently developed in our laboratory, are described.

72.3.3.3.1 Ascorbic acid. Ascorbic acid (Vitamin C) is often used in media as antioxidant and is known to be important for the cultivation of primary (embryonic) cells. It can be present to a concentration of 0.5–1 m*M*, sometimes much less. Vitamin C can be analyzed using the method and reagent described for pyruvate. It elutes considerably after ketoglutarate and pyruvate (Fig. 72.3).

72.3.3.3.2 Pantothenate. Pantothenate, a member of the vitamin B_2 group, is a dipeptide formed from 2,4-dihydroxy-3,3-dimethyl butyric acid and β-alanine. In conjunction with cysteamine, adenosine, and diphosphate, pantothenate forms the coenzyme A. The pantothenate molecule contains no chromophore or fluorophore. An analysis method was developed using a refractometer as detector (13). The low concentration in medium in a range of 0.4–4 mg/L and many other medium ingredients make the use of such a detection method impossible. Direct analysis of pantothenate from cell culture medium may be performed using liquid chromatography coupled to a mass spectrometer with electrospray ionization (ESI-MS) or by gas chromatography with mass spectrometry (GC-MS) detection after sialylation. If such equipment is not available, a promising alternative can be an acidic hydrolysis with later analysis of the released β-alanine. The β-amino acid β-alanine can be derivatized with one of the reagents described in the amino acid section. The second product of the hydrolysis is pantolactone. Pantolactone may be analyzed by gas chromatography after liquid–liquid extraction from the hydrolysis mixture using dichloromethane as organic solvent.

Procedure: The quantification of β-alanine after hydrolysis of pantothenate can be carried out with an HPLC system.

Sample preparation: 100 μL of sample and 200 μL concentrated hydrochloric acid is boiled for 15 min in a water bath. The mixture is lyophilized in a vacuum concentrator and resolved in 100 μL of 0.4 M sodium borate buffer pH 9.5.

Derivatization: 40 μL of the prepared sample is filled into a sampler vial. The sampler mixes with 70 μL of reagent (50 mg OPA, 1 mL methanol, 100 μL 2-mercaptoethanol, 9 mL 0.6 M sodium borate buffer pH 10.4) and injects 60 μL onto the column after 1.5-min reaction time.

Elution: The mixture is separated on a C_{18}-reversed phase column (e.g. Ultrasphere ODS, 5μ, 4.6 × 150 mm, Beckman Coulter Inc.) with a multistep binary gradient in less than 20 min. The column temperature is set to 39.5°C. Buffer A consists of 0.1 M sodium acetate pH 7.5, 1% tetrahydrofurane. Buffer B is a mixture of 70% methanol and 30% 0.1 M sodium acetate pH 5.2. Total flow is set to 1.8 mL/min. The gradient is set as follows: 25% B at time 0, linear increase to 50% B in 3 min, hold 50% B for 10 min, linear increase to 80% B in 1 min, and hold 80% B for 4 min. This gradient has to be chosen to separate the β-alanine derivative from all other amino acid derivatives present in the sample at much higher concentrations.

Detection: The OPA derivatives are detected with a fluorescence detector set to excitation and emission wavelengths of 330 nm and 450 nm, respectively.

72.3.3.3.3 Riboflavin. Riboflavin (7,8-dimethyl-10-ribityl-isoalloxazine), a member of the Vitamin B_2 group, is contained in prosthetic groups (FMN, FAD) of flavoprotein. Aerobic and anaerobic dehydrogenases often belong to the group of flavoproteins. Such enzymes are involved especially in the respiratory chain. The isoalloxazine structure in riboflavin acts in this context as a reversible redox system.

Riboflavin itself is fluorescent without any modification and an analysis is easy when the concentration is high enough (14–16). Usually the riboflavin concentration in cell culture media is in the range of 0.04 to 0.4 mg/L, which is too low for direct measurement. But a 10-fold concentration is sufficient for quantitative determination.

Procedure: The quantification of riboflavin can be performed with an HPLC system. Riboflavin is separated from disturbing substances on a C_{18} column and detected with a fluorescence detector.

Sample preparation: 1 mL of sample is lyophilized in a vacuum concentrator and resolved in 100 μL buffer.

Elution. The concentrated sample is injected onto a C_{18}-reversed phase column (e.g. Ultrasphere ODS, 5μ, 4.6 × 150 mm, Beckman Coulter Inc.) and eluted with a buffer consisting of 99% 0.01 M sodium acetate pH 7.4 and 1% tetrahydrofurane. Total flow is set to 1 mL/min.

Detection. Riboflavin is detected in a fluorescence detector set to excitation and emission wavelengths of 436 nm and 535 nm, respectively. At these wavelengths only a low interference was observed.

72.3.3.3.4 Thiamine. Thiamine, the Vitamin B_1, is in form of its diphosphate, the prosthetic group of the enzyme decarboxylase-dehydrogenase, one of the three units of a multienzyme complex performing the oxidative decarboxylation.

The thiamine concentration in cell culture media is in the range of 0.3–4 mg/L which is sufficient for quantitative determination, if a sensitive detection method is used. Although thiamine contains a pyrimidine and thiazole ring in the molecule a much more sensitive detection can be achieved when the thiazole ring is oxidised. The resulting thiochrome is fluorescent (17–19).

Procedure: The quantification of thiamine can be carried out with an HPLC system. Thiamine is oxidized by potassium hexacyanoferrate in alkaline solution to thiochrome. Thiochrome can be separated on a C_{18} column and detected with a fluorescence detector.

Sample preparation: 0.5 mL of sample is mixed with 0.5 mL of 1% $K_3Fe(CN)_6$ in 15% NaOH. After 45 s the reaction is stopped by adding 75 μL phosphoric acid.

Elution: The reaction mixture is injected immediately onto a C_{18}-reversed phase column (Ultrasphere ODS, 5μ, 4.6 × 150 mm, Beckman Coulter Inc.) and eluted with a buffer consisting of 99% 0.01 M sodium acetate pH 7.4 and 1% tetrahydrofurane. Total flow is set to 1 mL/min.

Detection: Thiochrome is detected in a fluorescence detector set to excitation and emission wavelengths of 364 nm and 436 nm, respectively.

72.3.3.4 Lipids. The cell membrane of mammalian cells consists basically of a lipid bilayer of phospholipids. The phospholipids (e.g. phosphatidyl choline, phosphatidyl ethanolamine, and phosphatidyl-serine) themselves are diesters of phosphoric acid with glycerin on one side and choline, ethanolamine, or serine on the other side. Glycerin is esterified at its two other hydroxyl groups with fatty acids. The fatty acids (saturated and unsaturated) can be synthesized by an enzyme complex (fatty acid synthetase complex) located in the cytosol starting from acetyl-CoA. Another main component of the cell membrane is the steroid cholesterol. It has a rigid structure and can strengthen the cell membrane if it is incorporated into the lipid bilayer. Cholesterol can also be synthesized from acetyl-CoA by another pathway.

Although the cells can prepare their lipids need, special additives to basal cell culture media can contain fatty acids, cholesterol and phospholipids to support the cell status. In medium additives like serum, lipoprotein mixtures, and protein/fatty acid mixtures these components may be included.

72.3.3.4.1 Fatty acids. Fatty acids may be analyzed either by liquid or by gas chromatography. Generally present in low concentrations, a concentration step is necessary. This concentration can be carried out by liquid–liquid extraction with a lipophilic solvent and subsequent lyophilization.

Procedure: The lyophilized fatty acids can either be dissolved and applied directly to a gas chromatograph equipped with a special column or have to be derivatized prior to HPLC analysis (13). In each case the same sample preparation procedure may be used.

Sample preparation: 0.4 mL of sample, 10 μL internal standard solution (5 m*M* heptadecanoic acid) and 1 mL of extracting agent (Dole mixture; isopropanol/*n*-heptane/2 M phosphoric acid 40:10:1) are vortexed for 10 min. 0.4 mL *n*-heptane and 0.6 mL pure water are added and mixed again. 0.4 mL of the upper (organic) phase are taken and lyophilized.

GC analysis: The lyophilized fatty acids are dissolved in *n*-heptane, dried with sodium sulphate and applied to the gas chromatograph. The gas chromatograph may be equipped with a split injector, an FID (flame ionization detector), and a polar capillary column (e.g. FFAP-CB, 25 m, Chrompack). The temperatures of injector and detector are both set to 300°C. The fatty acids elute at temperatures of 200 to 270°C.

HPLC analysis: Before injection the fatty acids have to be derivatized to add a chromophore. The lyophilized fatty acids are dissolved in 200 μL acetonitrile. 12 μL of reagent (50 m*M* p-bromophenacyl bromide, 5 m*M* 18-crowne-6) and 1 mg $KHCO_3$ are added and held for 45 min at 85°C. The fatty acid derivatives can be separated on a C_8-reversed phase column (Kromasil Octyl, 5μ, 125 × 4.6 mm, Eka Nobel) by binary gradient elution in less than 30 min. Solvent A consists of 50% acetonitrile, 50% water and solvent B of 99% acetonitrile, 1% water. The total flow is set to 1.3 mL/min. The gradient is set as follows: 0% B at time 0, linear increase to 100% B in 30 min, and hold 100% B for 2 min. Detection is carried out by UV absorption at 254 nm. Figure 72.6 shows an example chromatogram.

72.3.3.4.2 Cholesterol and Cholesteryl Esters. Cholesterol may be analyzed by gas chromatography. After liquid–liquid extraction from the aqueous sample with an organic solvent and subsequent lyophilization it can be acetylated and chromatographed on a nonpolar column. Cholesteryl esters can be hydrolyzed prior to acetylation.

The analysis of cholesterol acetate may be carried out with a normal gas chromatograph equipped with a split injector, an FID (flame ionization detector), and a nonpolar capillary column (e.g. CP-5-Sil CB, 10 m, Chrompack).

Sample preparation: 2 mL of sample is added to 2 mL of extracting agent (75% diisoproylether, 25% *n*-butanole) and mixed for 3 h in an end-over-end mixer. The nonaqueous phase is taken and lyophilized. The cholesteryl esters can now be hydrolyzed with ethanolic KOH (0.6 mL 33% KOH, 9.4 mL ethanol) for 1 h at 60°C. After neutralization (HCl) and extraction (hexane, three times) cholesterol can be derivatized.

Derivatization: The solvent (hexane) is removed and acetic anhydride is added. After 1 h at 100°C the reaction is stopped by adding ice water. Cholesterol acetate is extracted into hexane (three times). The joined organic phases are washed with pure water and lyophilized afterwards.

Chromatography: The dried extract is dissolved in hexane and an aliquot is applied to the gas chromatograph. The temperatures of injector and detector should be set to 270°C and 300°C, respectively. Cholesterol acetate elutes

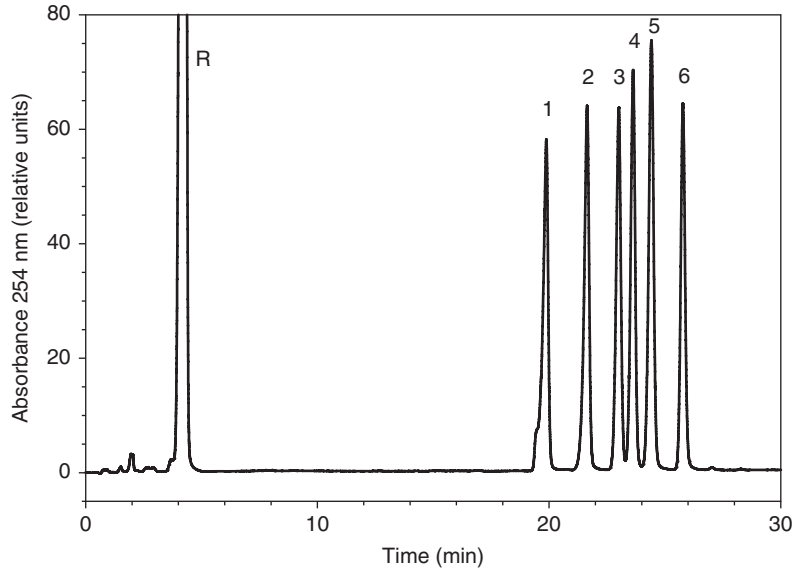


Figure 72.6. HPLC separation of standard mixture of predominant fatty acids. All conditions as described in the text. Identified fatty acids: (1) linolenic acid (18:3), (2) linoleic acid (18:2), (3) palmitic acid (16:0), oleic acid (18:1), heptadecanoic acid (17:0) (internal standard), (6) stearic acid (18:0), R reagent.

at a temperature of 240–270°C. For improved reproducibility an internal standard (e.g. stigmasterol acetate) may be added early during sample preparation.

72.4 ANALYSIS OF METABOLIC END PRODUCTS

During metabolization of glucose, amino acids, and other compounds, the cells also produce substances that are released into the surrounding medium. The main end products of metabolism are lactic acid (lactate) and ammonia. Both substances are known to affect cell viability and product formation. Therefore, it is necessary to monitor the concentrations in the culture supernatant to be able to maintain low concentrations through special means or process procedures.

72.4.1 Lactate

Lactate is the end product of anaerobic metabolism of glucose. Almost all cells *in vitro* produce lactate also under aerobic conditions. Lactate is formed from pyruvate by the enzyme lactate dehydrogenase. A maximum of two moles of lactate can be produced from 1 mole of glucose under completely anaerobic conditions. Additionally, lactate may also be synthesized by other pathways, especially amino acid metabolism. The two most common methods of lactate analysis are described below.

72.4.1.1 Photometric Lactate Assay (e.g. R-Biopharm, formerly Boehringer Mannheim). Lactate is converted in the presence of NAD^+ BY THE ENZYME L-lactate dehydrogenase to pyruvate. During this reaction NADH is formed, which can be monitored at a wavelength of 340 nm. The reaction is reversible and the equilibrium is more on the lactate side than on the pyruvate side. Therefore pyruvate has to be removed. This can be achieved by adding the second enzyme glutamate-pyruvate-transaminase, which converts pyruvate in the presence of glutamate to alanine and 2-oxoglutarate. The assay is desired to be used in a cuvette UV spectrophotometer and needs no further laboratory equipment (20,21).

Reactions:

$$\text{L-Lactate} + \text{NAD}^+ \xrightarrow{\text{L-Lactate dehydrogenase}} \text{Pyruvate} + \text{NADH} + \text{H}^+$$

$$\text{Pyruvate} + \text{L-Glutamate} \xrightarrow{\text{Glutamate-pyruvate-transaminase}} \text{L-Alanine} + \text{2-Oxoglutarate}$$

Enzyme electrode-based biosensor (e.g. Model YSI 2700, Yellow Springs Instruments, BioProfile Analyzer Series, Nova Biomedical): The principle of these systems is already described in detail in the section titled Glucose. In case of lactate determination the immobilized enzyme

is lactate oxidase, which oxidizes lactate and generates hydrogen peroxide.

Reactions:

$$\text{L-Lactate} + O_2 \xrightarrow{\text{Lactate oxidase}} \text{Pyruvate} + H_2O_2$$

$$H_2O_2 \xrightarrow{\text{Pt anode}} 2H^+ + O_2 + 2e^-$$

The YSI 2700 analyzer is capable of holding and maintaining two enzyme electrodes in its chamber. Therefore, from the same sample volume (25 μL) two determinations (e.g. glucose and lactate) can be made at the same time.

72.4.2 Ammonia

In animal cell culture, other than in mammals, ammonia is the main end product of nitrogen metabolism. Besides ammonia, alanine is also produced in a remarkable amount while only little urea is secreted by the cells. Especially, when high glutamine and other amino acid concentrations have to be used to supply the cells, an ammonia concentration of several millimolars can be found. High ammonia concentrations can affect cell growth, productivity, and product integrity very drastically. Several analytical methods have been used for the quantification of ammonia including enzyme assay systems (e.g. R-Biopharm, formerly Boehringer Mannheim) (22,23), gas sensitive electrodes (e.g. Mettler–Toledo), ion chromatography (e.g. Metrohm, Dionex), and derivatization. The methods are discussed in the following text. Each of these methods has its advantages and disadvantages.

72.4.2.1 Enzyme Assay. Owing to the use of a special enzymatic reaction (glutamate dehydrogenase), the enzyme assay is highly specific for ammonia. The concentration of NADH can be easily monitored at a wavelength of 340 nm. The concentrations of reacted NADH and assayed ammonium are inversely proportional. The necessity of the coenzyme NADH and the consumption of enzyme make this method a cost-intensive analysis procedure.

Reaction:

$$\text{2-Oxoglutarate} + \text{NADH} + NH_4^+ \xrightarrow{\text{Glutamate- dehydrogenase}} \text{L-Glutamate} + NAD^+ + H_2O$$

This assay test kit is desired to be used in a cuvette UV spectrophotometer and needs no further laboratory equipment. The method can be recommended when only few or sporadic measurements are necessary.

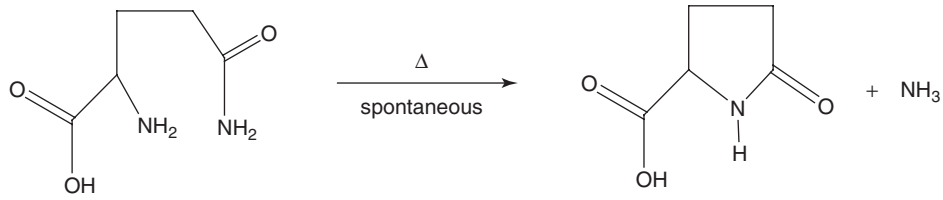
72.4.2.2 Gas-Sensitive Ammonia Electrode. An ammonia electrode works by the principle that under alkaline conditions ammonia degasses from aqueous solutions, passes through a hydrophobic membrane [polytetrafluoroethylene (PTFE)], and dissolves in an acidic solution where the resulting pH shift can be measured and quantitatively evaluated. In most cases this is also a specific detection method. The main disadvantages are the size of the electrode and the fragile membrane adapter. Depending on the ammonia concentration in the sample and a predilution possibility, a sample volume of up to 10–20 mL may be necessary for analysis.

Procedure: 2 mL of cell-free sample are diluted with water to a volume of 20 mL. The ammonia electrode is placed into the solution. After obtaining a stable value, 0.5 mL of 10 M NaOH is added and the highest value is registered.

72.4.2.3 Ion Chromatography. The ion chromatography analysis of ammonia is based on cation exchange chromatography (24) and conductivity detection. Owing to the chemical similarity of ammonium and potassium cations and the high sodium concentration, a good resolution may be difficult to obtain. A small sample volume requirement and an automatic analysis procedure are advantages of this method, whereas the high equipment requirement (chromatography system) is the main disadvantage.

72.4.2.4 Derivatization with Fluorescence Detection. OPA reacts with primary amines including ammonia in the presence of mercaptoacetic acid (thioglycolic acid) at basic conditions to unstable, fluorescent isoindole derivatives. The reaction product is analogous to the products formed with 3-mercaptopropionic acid and amino acids, but its fluorescent property is quite different. Whereas the fluorescence intensity at excitation and emission wavelengths of 330 nm and 450 nm (amino acids), respectively, is very poor, the fluorescence yield can be increased very much by shifting to wavelengths of 415 nm and 485 nm, respectively. On the other hand, the fluorescence intensity of the amino acid derivatives is negligible at those wavelengths. Therefore, this method has good selectivity for ammonium quantification.

Procedure: The reagent is prepared by dissolving 1.85 mmol OPA and 4 mmol mercaptoacetic acid (thioglycolic acid) in 2 mL methanol and adding 100 mL 0.4 M sodium borate buffer pH 10.4. The mixture can be stored at 4°C in 10 mL aliquots. Before measurement one aliquot was allowed to reach room temperature (20°C). The reaction is directly carried out in half micro quartz cuvettes by adding 1–1.3 mL reagent to 20 μL of cell-free sample. After a brief mixing the cuvette is immediately placed in a spectrofluorimeter (RF551, Shimadzu) set to excitation and emission wavelengths of 415 nm and 485 nm, respectively.



72.4.3 Urea

Urea is the end product of nitrogen metabolism in mammals. Normally it is produced in the liver and secreted by the kidney into the urine. Cells *in vitro* are usually not able to synthesize urea. Therefore, the predicted urea concentration in the supernatant may be very low. On the other hand, a considerable amount of urea may be found in medium additives like serum or plasma.

Urea may be quantified by using a two-step enzyme assay (25,26). The reaction may be monitored by following the NADH conversion at 340 nm. The reaction is specific for urea, but the method is not very sensitive.

Reaction:

$$\text{Urea} + H_2O \xrightarrow{\text{Urease}} 2NH_3 + CO_2$$

$$\text{2-Oxoglutarate} + \text{NADH} + NH_4^+ \xrightarrow{\text{Glutamate- dehydrogenase}} \text{L-Glutamate} + NAD^+ + H_2O$$

72.5 ANALYSIS OF OTHER SUBSTANCES AND PARAMETERS

72.5.1 Pyroglutamic Acid

Pyroglutamic acid (5-oxo-2-pyrollidone carboxylic acid) is a molecule, which is formed from glutamine in a spontaneous thermal intramolecular cyclization reaction.

Under cultivation conditions glutamine has a half-life of about 6–8 days (27). Therefore, when high glutamine concentrations are used and maintained under such conditions (e.g. high density batch and perfusion cultivations) a considerable amount of pyroglutamate is produced.

In principle, pyroglutamate can be analyzed by using the same derivatization procedure as described for HPLC analysis of fatty acids. But sample preparation and elution conditions distinguish clearly because the formed derivative is much more hydrophilic and cannot be separated on a C_8-reversed phase column.

Procedure: The analysis may be carried out using a binary gradient HPLC system with UV detection.

Sample preparation: The cell-free sample is adjusted to pH 3.50 μL thereof are lyophilized and resolved in 180 μL acetonitrile.

Derivatization: 20 μL reagent (50 m*M* p-bromophenacyl bromide, 5 m*M* 18-crowne-6) and 1 mg $KHCO_3$ are added to the solution and heated for 90 min to 85°C. The reaction mixture is rapidly cooled with ice water and 15–30 μL is injected.

Elution: The pyroglutamate derivative can be separated on a C_{18}-reversed phase column (Ultrasphere ODS, 5μ, 4.6 × 150 mm, Beckman Coulter Inc.) by binary gradient elution in less than 30 min. Solvent A consists of 20% acetonitrile, 80% water; and solvent B of 90% acetonitrile, 10% water.

The total flow is set to 1.3 mL/min. The gradient is set as follows: 0% B at time 0, linear increase to 100% B in 30 min, and hold 100% B for 2 min. Detection is carried out by UV absorption at 254 nm. Besides pyroglutamate, lactate can also be analyzed quantitatively with this method. Figure 72.7 shows an example chromatogram.

72.5.2 Enzyme Activities

Several enzymes are released from necrotic and apoptotic cells and cell membranes into the cell culture medium during cultivation. These enzymes may also be active in medium influencing cell behavior or product quality. Monitoring these enzyme activities may be necessary to assess culture status or product quality.

72.5.2.1 Lactate Dehydrogenase Activity. Lactate dehydrogenase is a cytosolic enzyme. The detection of lactate dehydrogenase activity in the cell culture supernatant indicates cell damage by defective membranes or cell lysis. This enzyme is often used as marker enzyme for cell death. As described in the section Lactate, lactate dehydrogenase converts pyruvate in the presence of NADH into lactate (or *vice versa*). The enzyme activity can be monitored by following the NADH conversion in a temperature-controlled spectrophotometer at a wavelength of 340 nm. A standardized procedure can be performed as follows. 100 μL cell-free supernatant is mixed with 700 μL of 30 m*M* sodium phosphate buffer pH 7.4, 100 μL of 10 m*M* sodium pyruvate solution (in phosphate buffer), and 100 μL 2.7 m*M* NADH solution (in phosphate buffer) in a quartz half micro cuvette. The cuvette is placed in a temperature-controlled (37°C) photometer. The linear extinction decrease at 340 nm is monitored for 1 min. The enzyme activity can be calculated

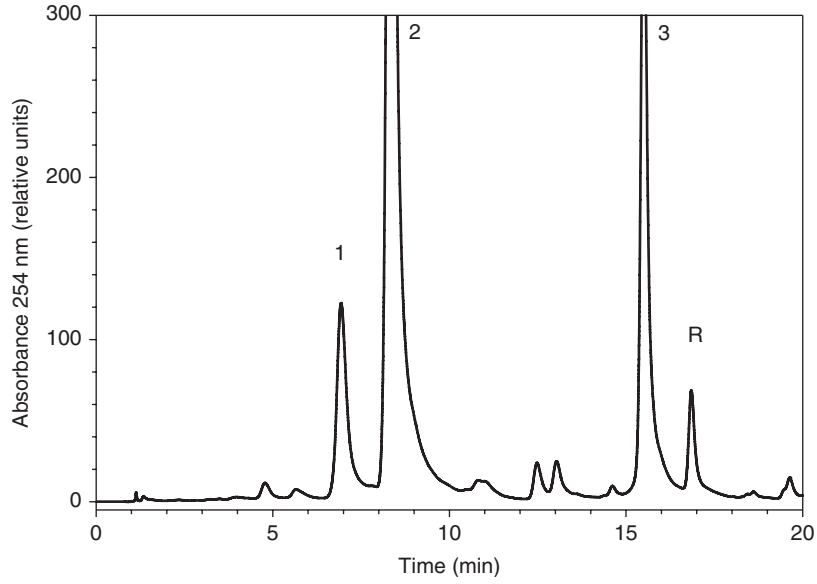


Figure 72.7. Chromatogram obtained by following the pyroglutamate derivatization procedure. Derivatization and separation conditions apply as described in the text. Identified substances are (1) pyroglutamate, (2) lactate, (3) unresolved amino acids (mainly glutamine), R reagent.

from the slope in comparison to the autolytic decomposition of NADH in a reference experiment.

72.5.2.2 Neuraminidase Activity and Sialic Acids. Many of the therapeutical proteins produced by cell culture are glycosylated. Variability in the oligosaccharide pattern can affect their behavior after application to a patient (half-time, biodistribution, and biological activity). Terminally linked sialic acids are particularly involved in various biological events. Sialic acids are easily cleaved off the oligosaccharide by neuraminidases. Neuraminidase activity has been localized on the subcellular level in the plasma membrane, the Golgi apparatus, the lysosomes and the cytosol. Moreover, neuraminidase activity has also been detected in cell culture fluids (28).

72.5.2.3 Determination of Neuraminidase Activity. The neuraminidase activity is determined fluorometrically with 4-methylumbelliferyl-α-D-N-acetylneuraminic acid substrate (MUF-NeuAc5) (29). A standardized assay can be performed as follows (30). After centrifugation (15,000 $\times$ g, 15 min), 250 μL of supernatant, 25 μL of 4 m*M* MUF-NeuAc5 solution, and 25 μL of 1 M phosphate buffer pH 7.0 are mixed and heated for 1 h at 37°C. The reaction is stopped by adding 700 μL 0.375 glycine/KOH buffer pH 10.4. The mixture is centrifuged again (15000 $\times$ g, 5 min), and the fluorescence is determined at excitation and emission wavelengths of 362 nm and 448 nm, respectively.

72.5.2.4 Determination of Sialic Acids. Free sialic acids can be derivatized with 1,2-diamino-4,5-methylenedioxy benzene (DMB) into fluorescent derivatives which can be separated on a C_{18}-reversed phase column (31,32). 20 μL of cell-free supernatant is mixed with 40 μL ice-cold acetone to precipitate soluble proteins. After centrifugation (15,000*g*, 5 min) 15 μL of the mixture is lyophilized in a vacuum concentrator. The lyophilizate is dissolved in 200 μL of 25 m*M* H_2SO_4. 200 μL of DMB reagent (7 m*M* DMB, 18 m*M* disodium dithionite, 1 M 2-mercaptoethanol in water) are added and heated for 2.5 h at 60°C. The reaction is stopped by cooling to 0°C (ice water). After centrifugation (15,000*g*, 5 min) 20 μL of the mixture is injected onto the column (Kromasil C18, 5μ, 4.6 $\times$ 150 mm, Eka Nobel). The sialic acid derivatives are eluted isocratically (1.2 mL/min) with a solvent consisting of 5% acetonitrile, 7% methanol, and 88% water and quantitatively detected with a fluorescence detector at excitation and emission wavelengths of 373 nm and 448 nm, respectively.

72.5.3 Osmolality

The cytosol interacts with the medium through the water permeable cell membrane. Depending on the concentration ratio of all substances on both sides of the cell membrane, the cell is exposed to an osmotic pressure. The osmotic pressure of a solution is given by its osmolality. The osmolality of the medium should be in the range of approximately 300 mosmol/kg $\pm$ 50 mosmol/L to provide isotonic conditions. For the determination of the osmolality, the

molar lowering of the freezing point (Raoult's law) by a dissolved substance can be measured. The osmolality is independent of the kind of the dissolved substance, but cumulative for all dissolved substances. The measurement can be performed with a freezing point osmometer (e.g. semi-automatic half micro osmometer, Knauer). 150 μL of cell-free supernatant is needed for the process.

72.6 ANALYSIS OF PROTEINS

There are several proteins present in cell culture fluids. Some are added to the medium to support cell growth and product formation. The others are produced by the cells, among which the desired product can be found. For this reason an overall, unspecific protein assay can usually not be used to determine product quantity. For each product a special assay, regarding the properties of that protein, has to be established; if not only quantity but also activity has to be analyzed. Nevertheless, the total protein content in the medium is often a useful parameter.

72.6.1 Unspecific Protein Assays

A number of methods have been developed to determine total protein concentration. Besides direct UV absorbance and fluorescence, dye staining and reaction with a copper containing reagent are the most common methods. The main problem of all those methods is that the response for different proteins may vary widely. With a complex mixture of unknown proteins this may lead to completely wrong results. Much care must be taken when choosing a method for a special purpose. The most common methods are discussed briefly in the following overview. A very detailed description of all methods including working instruction can be found in Dunn (33).

UV absorbance at 280 nm. Determination of absorbance of aromatic amino acids in the protein (phenylalanine, tyrosine, and tryptophan).

UV Absorbance at 205 nm. Determination of absorbance of peptide bonds.

Fluorescence (excitation 280 nm and emission 340 nm). Determination of tryptophan fluorescence in the protein.

Dye staining. The dye coomassie blue G 250 binds in strong acidic solution to positively charged protein molecules forming a blue product that can be determined at 595 nm (34).

Biuret reaction. Copper (II)—ions in alkaline solution form a purple complex with proteins (peptide bonds). Detection at 540 nm (35).

Lowry method. The method is based on the Biuret reaction and the Folin-Ciocalteau phosphormolybdicphosphotungstic acid reduction to heteropolymolybdeum blue by the copper-catalysed oxidation of aromatic amino acids (36). Detection at 750 nm.

BCA reagent. An alternative detection reagent, bicinchoninic acid (available from Pierce), has been developed for use with the Lowry method. Detection at 562 nm (37).

Protein Assay ESL. The method is an improvement of the Biuret method. Spare copper(II) ions are reduced to copper(I) ions by ascorbic acid. These copper(I) ions form a complex with bathocuproin which can be detected at 485 nm (38). Since spare copper ions are measured the extinction is inversely proportional to the protein concentration. An assay kit is commercially available (Roche Diagnostics).

72.6.2 Enzme Linked Immunoassays

For highly specific determinations the antibody–antigen binding is very useful. Whenever an antibody against a substance (protein) is available or can be produced, an immunoassay is the method of choice. An immunoassay may be performed in a multi-well micro titer plate as an enzyme-linked immunosorbent assay (ELISA), as a radio immunoassay (RIA), as an affinity chromatographic analysis or even otherwise (39).

A standard sandwich ELISA procedure usually provides sufficient selectivity and sensitivity. Sensitivity may be improved by use of the (strep)avidin biotin amplification method. The sandwich ELISA is performed in four steps. First, the multi-well micro titer plate is coated with a primary antibody. Remaining binding sites on the plate are saturated with inert protein (albumin, casein). Secondly, the samples and standards containing the desired protein are applied. After incubation and removal of supernatant, an enzyme-labeled antibody (secondary antibody, conjugate), is added at the third step. The fourth step is carried out by adding a substrate of the enzyme. The conversion of the substrate by time is monitored photometrically. By comparison to standard concentrations a quantitative determination can be obtained. Commonly labeled enzymes are horse radish peroxidase and alkaline phosphatase. The most appropriate substrates for the peroxidase may be OPD or ABTS (2,2′-azino-di-[3-ethylbenzthiazoline sulfonate(6)] diammonium salt). For the phosphatase *p*-nitrophenylphosphate is a useful substrate.

72.7 ANALYSIS WITH CLINICAL ANALYZERS

Fully automated analyzers are widely used in central hospital laboratories. These systems often have a sample

throughput of up to several hundred measurements per hour. A wide variety of parameters of clinical interest can be analyzed. These parameters can be categorized in groups of basal substrates, enzymes, electrolytes, or immunochemicals. In the group of basal substrates the following substances and parameters are compiled: albumin, bilirubin, cholesterol, creatinine, glucose, urea, uric acid, triglycerides, and total protein. Among others, the activity of the following important enzymes can be quantified: alkaline phosphatase (ALP), amylase (AMYL), cholinesterase (CHE), creatin kinase (CK), glutamate dehydrogenase (GLDH), aspartate aminotransferase (AST/GOT), alanine aminotransferase (ALT/GPT), γ-glutamyl transferase (GGT), lactate dehydrogenase (LDH), lipase (LIP). Additionally, analytical methods for electrolytes such as sodium, potassium, calcium, magnesium, chloride, iron, and inorganic phosphate are integrated in the clinical autoanalyzer systems. Some of these analyzers are also able to perform immunological quantifications for immunoglobolins (A, G, M), lipoproteins (APO), transferrin etc. All of these methods are based either on reactions followed by photometrical detection or on measurements with ion-selective electrodes.

An alternative to these methods based on liquid chemistry are systems using strip technology. All chemicals needed for one special detection are placed and fixed on a prepared area on the strip. The strip is dipped into the sample or wetted with a sample drop. With ongoing reaction a color or change in color is produced. Depending on the special strip used, this color can be evaluated either by comparison with a color table or by using a strip photometer. Fully automated analyzers based on this strip technology have also been developed for use in a clinical laboratory.

To explain each method in detail in this chapter would lead too far, but a complete description of each detection and quantification method can be obtained from the manufacturers of the clinical analyzers. These clinical systems are offered from companies such as Roche Diagnostics/Hitachi Instruments, Siemens Medical Solutions (formerly Bayer Diagnostics), Beckman Coulter, Randox, or Olympus Diagnostica.

All methods used in the clinical analyzer systems, as described above in this chapter, are optimized and established to meet the requirements of clinical samples such as whole blood, serum, plasma, urine or other body liquids. If these conditions are also satisfying a cell culture technologist to analyze his samples from culture supernatants or cell extracts has to be exactly and independently proven for each single method. Special attention has to be drawn to detection limit, sensitivity, reproducibility and presence of disturbing substances. When all these parameters are satisfactory, the use of a clinical analyzer may be a substantial help for routine analysis. Some methods used in the autoanalyzers are also offered as complete analyzing kits optimized for manual operation (Roche Diagnostics). Randox has adapted some of the parameter on their RX daytona analysis system to meet the requirement in cell culture.

Acknowledgments

The excellent technical assistance of Mrs Angela Ehrlich, Mrs Ute Bürstenbinder, Mrs Gesche Rottmann, Mrs Anja Ehrlich and Mrs Jana Schäfer and the help of Mrs Ulrike Baillie during the preparation of this manuscript are gratefully acknowledged. Furthermore, I thank all other current and former members of the institute who contributed to the development of certain methods.

72.8 SERVICE INFORMATION

Most of the suppliers cited in this chapter are present in the internet. Following is a list of the internet home pages:

Alltech, now Grace: http://www.discoverysciences.com

Beckman Coulter, Inc.: http://www.beckmancoulter.com

Chrompack, now Varian: http://www.varianinc.com

Dionex Corporation: http://www.dionex.com

Thermo Hypersil: http://www.thermo.com

Innovatis AG: http://www.innovatis.com

Knauer GmbH: http://www.knauer.net

Metrohm Ltd.: http://www.metrohm.com

Mettler-Toledo: http://www.mt.com

Nova Biomedical Corp.: http://www.novabiomedical.com

Olympus Diagnostica; http://www.olympus-diagnostica.com/

Pierce; http://www.piercenet.com/

Randox: http://www.randox.com

R-Biopharm: http://www.r-biopharm.com

Roche Diagnostics: http://labsystems.roche.com

Schärfe System GmbH: http://www.casy-technology.com/

Shimadzu, Inc.: http://www.shimadzu.com

Siemens Medical Solutions: http://diagnostics.siemens.com

Waters Corporation: http://www.waters.com

Yellow Springs Instrument Inc.: http://www.ysilifesciences.com

REFERENCES

1. Schärfe System. Operations manual, CASY® 1 Cell Counter TTC, Schärfe System.
2. R-Biopharm, D-Glucose Kit No. 10 716 251 035.

3. Operations manual, biochemical analyser YSI 2700. Yellow Springs Instrument Inc.
4. Moore S, Spackman DH, Stein WH. Anal Chem 1958; 30: 1185.
5. Hamilton PB. Anal Chem 1963; 35: 2055.
6. Roth M. Anal Chem 1971; 43: 880.
7. Büntemeyer H, Lütkemeyer D, Lehmann J. Cytotechnology 1991; 5: 57.
8. Koop DR, morgan ET, Tarr GE, Coon MJ. J Biol Chem 1982; 257: 8472.
9. Bidlingmeyer BA, Cohen SA, Tarvin TL. J Chromatogr 1984; 336: 93.
10. Reid S, Randerson DH, Greenfield PF. Aust J Biotechnol 1987; 2: 69.
11. Hayashi T, Tsuchiya H, Naruse H. J Chromatogr 1983; 273: 245.
12. Hara S, Takemori Y, Yamaguchi M, Nakamura M. J Chromatogr 1985; 344: 33.
13. Püttmann M, Krug H, von Ochsenstein E, Kattermann R. Clin Chem 1993; 39: 825.
14. Smith MD. J Chromatogr 1980; 182: 285.
15. Gatautis VJ, Naito HK. Clin Chem 1981; 27: 1672.
16. Pietta P, Calatroni A, Rava A. J Chromatogr 1983; 229: 445.
17. Bontemps J, Philippe P, Bettendorf L, Lombet J, Dandrifoss G, Schoffeniels E. J Chromatogr 1984; 307: 283.
18. Wielders JPM, Mink CJK. J Chromatogr 1983; 277: 145.
19. Fernando SM, Murphy PA. J Agric Food Chem 1990; 38: 163.
20. Gutmann I, Wahlefeld AW. In: Bergmeyer HU, *et al*., editors, Methods of enzymatic analysis. Volume 3, Weinheim: Verlag Chemie; 1974. p. 1464.
21. R-Biopharm, L-Lactic Acid Kit No. 10 139 084 035.
22. R-Biopharm, Ammonia Kit No. 11 112 732 035.
23. Bergmeyer HU, Beutler H-O. In: Bergmeyer HU, *et al*., editors, Methods of enzymatic analysis VIII. Weinheim: Verlag Chemie; 1985. p. 454.
24. Gardner WS, Bootsma HA, Evans C, St. John PA. Mar Chem 1995; 48: 271.
25. Gutmann I, Bergmeyer HU. In: Bergmeyer HU *et al*., editors. Methods of enzymatic analysis. Volume 2, Weinheim: Verlag Chemie; 1974. p. 1794.
26. Roche Diagnostics. Biochem. Catalogue 1998: 629.
27. Tritsch GL, Moore GE. Exp Cell Res 1962; 28: 360.
28. Munzert E, Heidemann R, Büntemeyer H, Lehmann J, Müthing J. Biotechnol Bioeng 1997; 56: 441.
29. Potier M, Mameli L, Bélisle M, Dallaire L, Melançon SB. Anal Biochem 1979; 94: 287.
30. Munzert E, Müthing J, Büntemeyer H, Lehmann J. Biotechnol Prog 1996; 12: 559.
31. Hara S, Takemori Y, Yamaguchi M, Nakamura M, Ohkura Y. Anal Biochem 1987; 194: 138.
32. Munzert E. Ph.D. thesis. University of Bielefeld; 1996.
33. Dunn MJ. In: Harris ELV, Angel S, editors. Protein purification methods: A practical approach. IRL Press; 1989. p. 10.
34. Bradford MB. Anal Biochem 1976; 72: 248.
35. Goldberg ML. Anal Biochem 1973; 51: 240.
36. Lowry OH, Rosenbrough NJ, Farr AL, Randall RJ. J Biol Chem 1951; 193: 265.
37. Smith PK, Krohn RI, Hermanson GT, Mallia AK, Gartner FH, Provenzano MD, Fujimoto EK, Goeke BJ, Olson BJ, Klenk DC. Anal Biochem 1985; 150: 76.
38. Matsushita M, Irino T, Komoda T, Sakagishi Y. Clin Chim Acta 1993; 216: 103.
39. Tijssen P. Laboratory techniques in biochemistry and molecular biology. Volume 15, Amsterdam: Elsevier; 1988.

73

PROCESS ANALYTICAL TECHNOLOGY: STRATEGIES FOR BIOPHARMACEUTICALS

Anurag S. Rathore and Gautam Kapoor
Department of Chemical Engineering, Indian Institute of Technology, Hauz Khas, New Delhi, India

73.1 INTRODUCTION

The topic of process analytical technology (PAT) with respect to applications in the pharmaceutical sector was first discussed at the Federal Drug Administration (FDA)'s Advisory Committee for Pharmaceutical Science (ACPS) meeting in 2001. A subcommittee on PAT consisting of experts from industry and academia was formed with the objective(s) of identifying potential technologies and strategies for implementation of PAT in pharmaceutical development and manufacturing (1). Both general principles and case studies were discussed at this meeting (2). On the basis of the recommendations of the ACPS PAT subcommittee, the FDA released the Guidance for Industry PAT—A Framework for Innovative Pharmaceutical Development, Manufacturing and Quality Assurance (3) in September 2004. This was a result of collaborative work between several divisions, including the Center for Drug Evaluation and Research (CDER), Center of Veterinary Medicine (CVM), and Office of Regulatory Affairs (ORA).

The guideline defines PAT as "a system for designing, analyzing, and controlling manufacturing through timely measurements (i.e. during processing) of critical quality and performance attributes of raw and in-process materials and processes, with the goal of ensuring final product quality" (3). It should be mentioned that the term *analytical* in the PAT context was viewed broadly to include chemical, physical, microbiological, mathematical, and risk analysis that are conducted in an integrated manner. The purpose of the guidance was to "1. Improve the scientific basis for establishing regulatory specifications, 2. Promote continuous improvement and 3. Improve manufacturing while maintaining or improving the current level of product quality" (3). The PAT initiative has also been adopted by several organizations to support its implementation, with the most prominent being the International Conference on Harmonization (ICH) and the American Society for Testing and Materials (ASTM) International Committee E55 (4).

The concept of PAT is in alignment with those of another important regulatory initiative, namely, quality by design (QbD). The latter was introduced later for pharmaceutical manufacturing in 2004 in the "Pharmaceutical Current Good Manufacturing Practices of the 21st Century—A Risk Based Approach" (5) initiative by the US FDA and has received a lot of attention lately. The general approach involves defining the target product profile (TPP), identification of the critical quality attributes (CQAs) that are of significant importance to product's safety and/or efficacy, definition of product design space via drug substance and drug product specifications, establishment of process design space for producing product that meets the expectations of quality, creation of control strategy that ensures consistent process performance, validation and filing of the process to demonstrate the effectiveness of these elements and their documentation, and finally, monitoring to ensure robust process performance over life cycle of the product (1,6). The concepts of risk assessment and management, raw material management, and use of statistical approaches provide a foundation to these activities. Table 73.1 shows the key enablers essential for successful implementation of PAT in the QbD paradigm.

Upstream Industrial Biotechnology: Equipment, Process Design, Sensing, Control, and cGMP Operations, Volume 2, First Edition. Edited by Michael C. Flickinger.
© 2013 John Wiley & Sons, Inc. Published 2013 by John Wiley & Sons, Inc.

TABLE 73.1. Enablers of PAT Implementation (3)

Enabler	Objective
Multivariate tools for design, data acquisition, and analysis	1. To identify and study the effects of and interactions among various product and process variables 2. To identify potential failure modes
Process analyzers	1. To make univariate process measurements such as pH, temperature, and pressure 2. To measure product quality attributes
Process control tools	1. To monitor the state of the process
Continuous improvement and knowledge management tools	1. To perform data collection and analysis over the life cycle of the product 2. To understand relevant multifactorial relationships

73.1.1 Definition and Objectives

As mentioned earlier, PAT has been defined as "a system for designing, analyzing and controlling manufacturing through timely measurements (i.e. during processing) of critical quality and performance attributes of raw and in-process materials and processes, with the goal of ensuring final product quality" (3).

The objectives of introducing such a scheme in pharmaceutical manufacturing could be several and include (1,3)

1. Better process understanding
2. Improved yield due to prevention of scrap, rejects, and reprocessing
3. Reduction in the production cycle time
4. Decrease in energy consumption and improved efficiency from conversion of batch process into a continuous process
5. Cost reduction due to reduced waste and energy consumption
6. Real-time release of batches
7. Improved operator safety and reduced human errors due to more automation.

73.1.2 Implementation of PAT

Implementation of PAT involves a thorough understanding of the process and the CQAs of the product. Figure 73.1 outlines the steps in the implementation of PAT and how it contributes to overall product and process understanding (7,8).

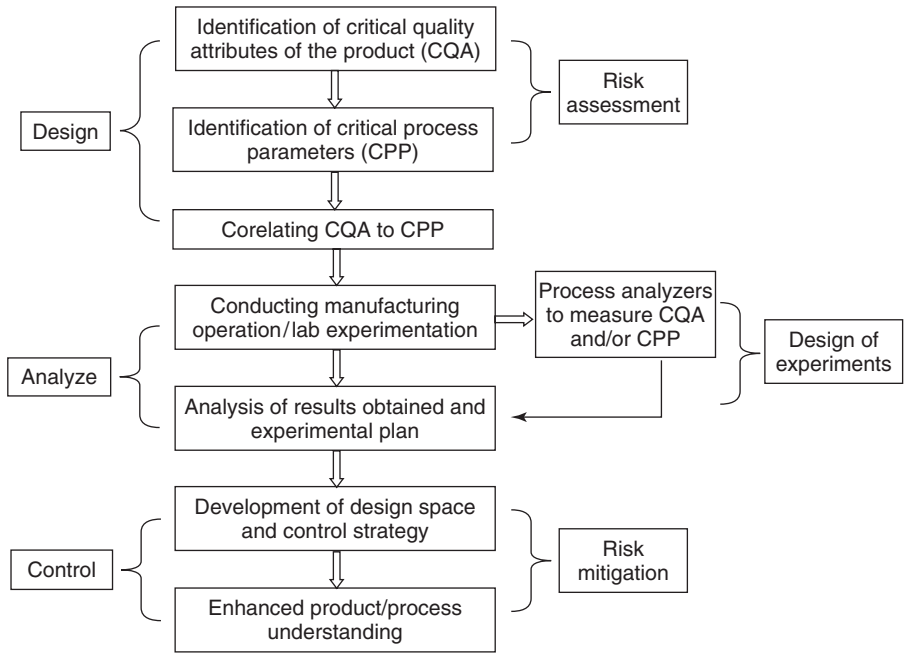


Figure 73.1. Overall scheme of PAT implementation: The three key phases of "design," "analyze," and "control" are shown along with the various steps that are required for making the implementation successful

A process is considered well understood when all critical sources of variability are identified and explained, variability is managed by the process, and product quality attributes can be accurately and reliably predicted over the design space established for materials used, process conditions, manufacturing, and environmental and other conditions (1).

On the other hand, a CQA is defined in the ICH guideline as (9) "physical, chemical, biological or microbiological property or characteristic that should be maintained within an appropriate limit, range or distribution to ensure the desired product quality." Implementation of PAT involves the following steps (7,8):

1. *Design:* The first activity in this step is identification of the CQAs of the product using the risk assessment tools, mentioned in the ICH Q9 guideline, based on information gathered from literature review and clinical and nonclinical studies with the molecule (10,11). Next, the manufacturing process is examined to understand which of the CQAs are affected by each unit operation of the process. Finally, CPPs are identified for each unit operation, which are found to affect the CQAs and a process model is created relating the CQAs to the CPPs.
2. *Analyze:* This step involves identification and development of analytical method for performing (7):
   (a) Real-time direct measurement of a product (or raw material) CQAs
   (b) Real-time measurement of CPPs
   (c) Real-time measurement of any other parameters that confirm that a unit operation/piece of equipment continues to be fit for purpose (e.g. filter back pressure, column integrity).

   Table 73.2 lists the process analyzers commonly used in a PAT-based scheme. Furthermore, these measurements can be online (sample is diverted from the manufacturing process and may be returned to the process stream), at-line (sample is removed, isolated from, and analyzed in close proximity to the process stream), in-line (sample is not removed from the process stream and the analyzer can be invasive or noninvasive), or off-line (sample is removed, isolated, and analyzed far from the process stream) (3).
3. *Control:* The data acquired in the analyze step is processed by various data analysis techniques to extract useful information. Techniques such as principal component analysis (PCA), partial least squares (PLS), and parallel factor analysis (PARAFAC) are used to decipher multivariate data sets, reduce redundancy, and eliminate noise (10,12,13). Empirical relationship between the CQAs and the CPPs can thus be formed and these can be used to establish the design space (acceptable operating range) for process parameters (14). A dynamic process control strategy can be established, where the process parameters can be suitably altered within the design space to nullify the variability caused by process inputs, thus resulting in consistent

TABLE 73.2. Process Analyzers Commonly Used in PAT (15)

Type of Analyzer	Subtypes	Typical Use
Sampling units	Membrane based (dialysis and ultra-/microfiltration)	To withdraw cell-free samples from the process equipment
	Flow injection analysis (FIA)	To inject into carrier stream that transports the sample to the analyzer
	Sequential injection analysis (SIA)	Advanced form of FIA, where reagent and sample quantity required is less. Used in association with flow cytometry
	Lab on valve (LOV)	Integrated microconduit that can conduct all unit operations of a given assay (immunoassays/enzymatic assays)
Spectroscopy	NIR spectroscopy	To monitor fermentation process and measure concentration of organic species in complex media
	Infrared and Raman spectroscopy	To monitor fermentation process and measure concentration of organic species in complex media
	FTIR	To monitor fermentation process (water-based samples)
	Photoacoustic spectroscopy	To measure gas concentration
	2D fluorescence spectroscopy	To detect trace compounds and determine biomass concentration
	Dielectric spectroscopy	To estimate biomass and viable cell count
Biosensors	Electrochemical Thermal Optical	To detect analyte using a bioanalytical method
Mass spectrometry	—	To monitor simple organic compounds
Machine vision and real-time imaging	—	To estimate cell density, cell size, and cell aggregation
Soft sensors	—	For state estimation and prediction

product quality. Most modern manufacturing equipments are capable of maintaining the process variables close to desired set-point values. Thus, it is feasible to design a process control scheme that can determine the appropriate control action to be taken to achieve the desired product quality.

4. *Optimize and monitor:* Multivariate statistical process control (MSPC) techniques are used to monitor process performance and report deviations from ideal performance. Data are collected throughout the life cycle of the product, stored using knowledge management tools, and analyzed by sophisticated statistical approaches to optimize the process.

Furthermore, Fig. 73.2 depicts the different configurations of bioprocess analyzers.

73.1.3 PAT Challenges in Biopharmaceutical Production

Biopharmaceutical production processes involve a series of unit operations. The upstream stage involves growing the cells in large production tanks in a defined media. The cells may be engineered to produce the protein either internally or secrete it into the culture media. The protein is then harvested. Downstream processing involves multiple purification steps to capture the target protein and remove endogenous and adventitious contaminants. The protein is then formulated with appropriate excipients to make it fit for use.

Biotech processes and products present unique challenges with respect to PAT implementation (7,8,11):

1. Biopharmaceuticals are produced in complicated cell-based systems that are sensitive to external factors such as temperature and pH.
2. In-process intermediates are often complex mixtures that contain impurities and other host cell-derived proteins along with the protein of interest. They may also contain adventitious contaminants such as viruses, which may not be detectable by process analyzers.
3. Raw materials are complex and variable and in many cases known to affect the final product quality.

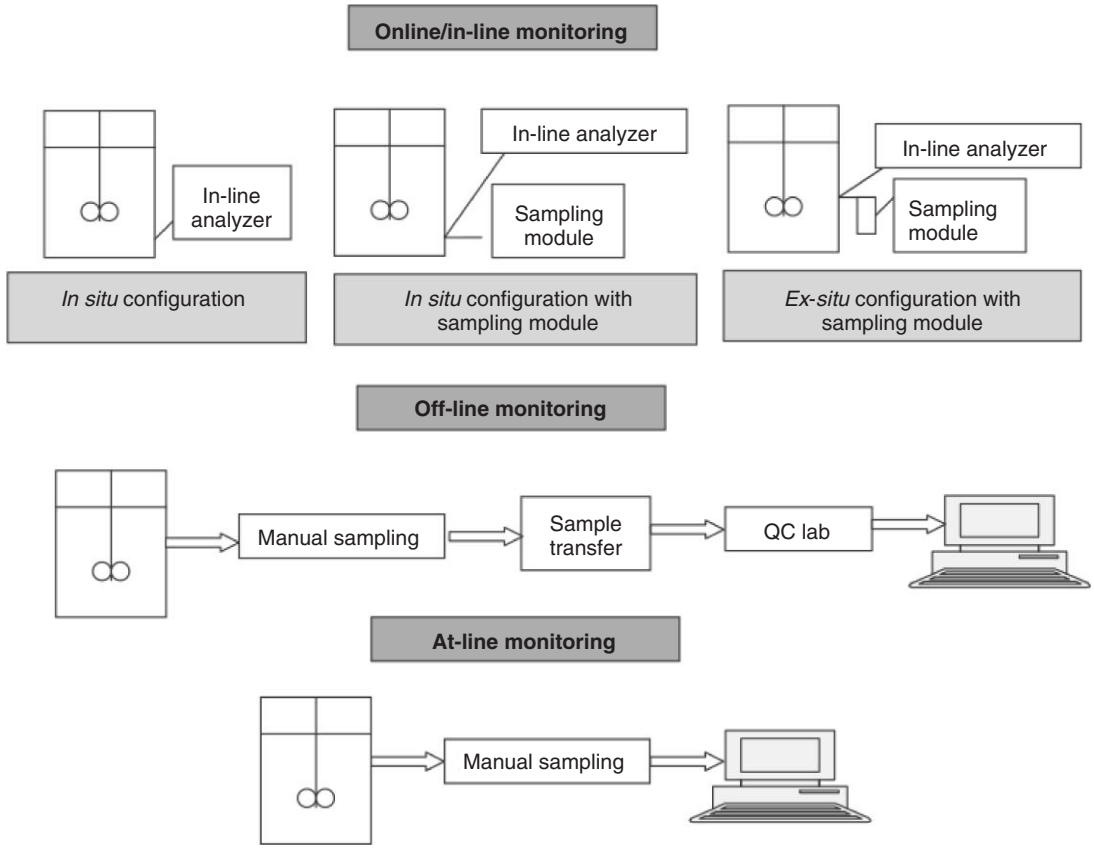


Figure 73.2. Different configurations of bioprocess analyzers: The time delay between sampling and analysis ranges from fast timescales of 1 s for in-line analysis to as long as 1 day for off-line methods. The data generated from the analyzers are sent to a data acquisition and control system

4. Minor excursions in the manufacturing process may drastically affect the final product quality.
5. Production process is complicated in terms of the number of process steps, in-process controls, and supporting documentation.
6. The understanding of the link between presence and level of product variants and other impurities and the product's clinical safety and efficacy is generally limited (1).

Table 73.3 summarizes the major unit operations in a biopharmaceutical manufacturing process along with the process and analysis times for each. The decision to transition from one unit operation to the next in a production process is made at definite decision points. The decision is taken based on real-time information that is provided. For each operation, ratio of the time taken to take the decision to the time needed for analysis is taken. This ratio serves as an indicator for the ease of PAT implementation for a given unit operation. Operations where the time for taking decision is more with respect to the time needed for analysis, the ease of PAT implementation is high (1). Figure 73.3 illustrates a plot of the ratio of the decision time and the analysis time for different process steps.

73.2 PAT APPLICATIONS FOR UPSTREAM OPERATIONS

Upstream operations of microbial and mammalian cell culture comprise media preparation, seed cell culture, and production cell culture.

In general, medium development for a fed-batch process involves batch medium and feed concentrate development, as well as optimization of the feeding strategy. The latter is often regarded as cell line dependent and is, therefore, based on the metabolism and nutrient consumption of a specific cell line (16). Several approaches can be used systematically for medium optimization, such as single component titration, spent medium analysis, and medium blending. During medium preparation, pH and/or temperature may require adjustment to ensure complete dissolution. The optimal feeding strategy involves giving consideration to nutrient consumption, by-product accumulation, and the balance between growth and production (16). Statistical design of experiments (DOEs) integrated with a high throughput platform are generally used to develop suitable media for the process.

A typical cell culture process starts with thawing a frozen vial of a working cell bank (WCB), which contains mammalian or microbial cells, followed by expanding the cell population through a series of seed trains in different culture vessels. Biomass concentration and specific biomass growth rate greatly affect the final product yield and quality during the seed production stage (16). The culture is then transferred to a production bioreactor where the cells continue to grow and the expressed product accumulates in the culture broth. To achieve a high product titer, high cell mass and cell viability need to be maintained in the production bioreactor. Two of the most popular process modes are fed-batch (feeding concentrated nutrient solutions to a batch production bioreactor) and perfusion (maintaining and recycling the cells to a bioreactor while continuously replacing spent media with a fresh supply). The fed-batch process is

TABLE 73.3. Listing of Typical Process Times, Decision Time, Quality/Process Attribute, Analytical Method, Analysis Time and Ratio of the Decision Time to Analysis Time, for the Various Process Segments, Namely Upstream, Harvest, Downstream, and Drug Product Processing [a]

Process Segment	Major Process Steps	Typical Process Time, t_p (h)	Typical Decision Time, t_d (h)	Quality Attribute (QA) or Process Attribute (PA)	Analytical Method	Typical Analysis Time, t_a (h)	Ratio (t_d/t_a)
Upstream	Microbial fermentation (production)	24	2	Misincorporation	HPLC	1	2
	Mammalian cell culture (production)	240	10	Glycosylation	Oligosaccharide profile	1	10
Harvest	Centrifugation	8	1	Recovery	HPLC	1	1
Downstream	Refolding	20	2	Misfolds	HPLC	0.5	4
	Chromatography	8	0.5	Aggregation	HPLC	1	0.5
Drug product processing	Formulation	6	0.5	Protein concentration	A280	0.1	5
	Lyophilization	24	1	Moisture	NIR	0.1	10
	Filling	12	2	Foreign particles	Visible particles	0.5	4

[a] aIt is seen that downstream unit operations offer the biggest challenges in PAT implementation, while upstream and drug product processing offer the least in most cases. Reprinted with permission from Ref. 1.

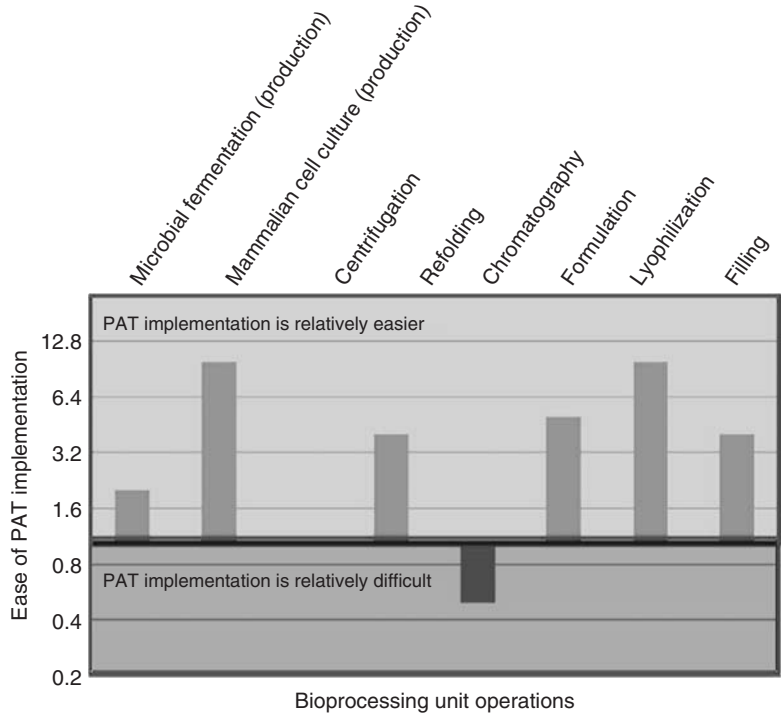


Figure 73.3. Ease of PAT implementation for some of the commonly used unit operations in biotech processes (Reprinted with permission from Ref. (1)): When the ratio is <1, PAT implementation is difficult. It is evident that most unit operations are amenable for PAT applications

often used due to its scalability, ease of operation, and high volumetric productivity.

Culture conditions need to be optimized within the bioreactor by balancing cell growth with product formation. A preferred cell growth condition may not be the optimal condition for product expression and vice versa. Although a bioreactor's physical environmental parameters such as pH, dissolved oxygen (DO), and temperature can be monitored online and controlled, monitoring of chemical and biological parameters is limited due to the lack of reliable online sensors. The measurement of cell density, metabolites, and protein concentrations usually occurs through daily bioreactor sampling and subsequent analysis by off-line methods. It is extremely important to monitor and control this stage of the production process as this is where the product and product-related impurities are produced (1). Posttranslational modifications such as glycosylation and deamidation generate product-related variants that have equivalent potency and safety profile, whereas aggregates and truncated forms generate variants that do not have an equivalent potency and safety. Thus, it is important to control the process parameters to obtain a product with the desired quality attributes.

Several examples illustrate the application of PAT in microbial and mammalian cell culture unit operations.

1. *Measurement of cell metabolites:* Monitoring of metabolic activity of mammalian cells and thus estimation of specific growth rate has been made possible by use of techniques such as nuclear magnetic resonance (NMR), mass spectroscopy, and radioactive tracers (17). High density perfusion cultures of Chinese Hamster ovary (CHO) cells employ C-glucose and two-dimensional (2D) NMR spectroscopy to control metabolic activity and predict the flux (18). Several strategies have been adopted to control specific growth rate and product quality in mammalian cell culture. These include utilization of multiwavelength fluorescence (MVF), software sensors, and multivariate data analysis (MVDA) to estimate glucose and biomass concentrations (19) and near infrared (NIR) spectroscopy to estimate biomass, glucose, and acetate concentrations (20). Ion chromatography with piezoelectric quartz crystal has been used for online monitoring of lactic acid for control of production rate (21).
2. *Estimation of biomass: In situ* microscopy has been used for estimation of hybridoma cell concentration in mammalian cell cultures (22). Amperometric sensors have been used online for measurement of viable cells and control of their metabolic activity (17). Conductance- and capacitance-based biomass

probes have been utilized to monitor specific growth rate and product formation to determine onset of stationary phase and cell lysis (23).

3. *Process control:* NIR spectroscopy has also been used for at-line control and fault analysis in fermentation processes (24). Flow injection systems have been extensively used in recent times in conjunction with online sensors to monitor ammonia and control feed addition rate in fed-batch penicillin fermentation (25). Similar system has been used for measurement of glucose concentration and control of cell growth when coupled with biosensors (26). Ion chromatography has emerged as an analytical tool of choice for measuring concentration of cations (Na^+, K^+, Ca^{2+}, NH_4^+) for control of cell growth in an in-line mode in association with double chamber acoustic wave detector (27).
4. *Media screening:* A combination of NIR spectroscopy and MVDA has been successfully used for screening many basal medium powders used in a mammalian cell culture process (28).

A summary of the process analyzers for microbial and mammalian cell culture is provided in Table 73.4.

As is seen from Table 73.4 , several sensors have been developed to monitor the upstream processing in microbial and mammalian processes and thus facilitate PAT. The upstream stage is arguably the most crucial with respect to impact on product quality and it also allows sufficient time for decision making to the next stage (Table 73.3). This makes implementation of PAT relatively simpler and of high impact. However, the biggest challenge is our limited ability in performing real-time testing of product titer or quality due to the significant quantity, as well as diversity of impurities that are present in the typical cell culture broth. Another challenge is the complexity of this step. Even if one is able to detect an underperformance with respect to product quality while a cell culture is being performed, it is not very straightforward to identify the root cause and the corrective measure that can be taken. As a result, most of the applications so far have focused on using pseudomarkers for product titer and quality and these have their own limitations. The upstream stage holds the greatest promise for development of PAT tools in the future. There is significant scope of improvement in our understanding of this step and then utilizing this understanding in designing robust PAT applications.

73.3 PAT APPLICATIONS IN HARVEST OPERATIONS

The harvest stage is an intermediate stage that marks the end of the upstream operations and beginning of the downstream operations. The decision to commence the harvest operations is typically based on measurement of biomass concentration and/or product titer. The harvest stage involves isolation of the target protein by clarification, often achieved by centrifugation, tangential flow filtration, or expanded bed adsorption. The clarified supernatant then undergoes primary purification by depth filtration to remove unwanted residual impurities. Flocculation, precipitation, and extraction methods have also been used to isolate the product of interest from the broth containing a plethora of impurities. PAT applications have been developed for real-time monitoring of these unit operations and are described later.

73.3.1 Centrifugation

Centrifugation involves clarification of particulate matter (cellular debris, protein, nucleic acids, etc.) suspended in a liquid medium based on sedimentation rates using centrifugal force. It is a versatile technique capable of performing applications varying significantly in their need of resolution of separation and throughput. On one hand, it is commonly used as a first step to separate whole cells from the supernatant. On the other, it can also separate protein aggregates from the supernatant after a precipitation step. NIR spectroscopy has been utilized to estimate sedimentation velocity during centrifugation (50). NIR transmission data from horizontally inserted samples has been used for measurement of separation/sedimentation kinetics of bentham/xantham gum mixtures during centrifugation. This information enabled optimization of concentration of excipients to be added in the final formulation (51).

73.3.2 Flocculation

Addition of flocculating agents such as chitosan, polyethyleneimine, and other polyelectrolytes assists in agglutination of cell debris and other fine particles, thus reducing turbidity. PAT has been applied to monitor and control the concentration of flocculating agents such as chitosan for achieving higher clarification throughput of the product of interest. Absorbance at 600 nm, estimation of flocculant strength, and filter resistance have been used as tools to control the addition of the flocculant (51).

73.3.3 Precipitation

Precipitation aids in removal of the product of interest from the broth containing other contaminants. Spectroscopic methods such as infrared (IR) and Raman spectroscopy have been applied to control the precipitation process by real-time measurement of solid–liquid suspensions (51). A microcentrifuge designed for autosampling and washing out of solids from the bowl has been proposed to monitor

TABLE 73.4. PAT Enabling Sensors for Cell Culture Unit Operations

Sensor	Application	Examples				References
		Tool	Status	Application	Type of Cell Culture	
Surface plasmon resonance	Assess product concentration and affinity	Same as sensor	Automated	Detection of antigen antibody complexes	Mammalian	(29)
HPLC			At-line	Analysis of metabolites for control of product formation	Microbial	(30)
Dielectric spectroscopy	Determine biomass	Same as sensor	Online	Closed-loop control of medium feed rate in fluidized bed fermenters	Mammalian	(31)
		Dielectric spectroscopy with NIR	Online	To estimate the biomass concentration during bacterial cultivations	Microbial	(32)
In situ microscopy	Characterize cell population	Microscopes with image processors and computer control	In situ	Specific growth rate used to control product formation in agitated cell broth cultivation	Mammalian	(20)
Flow cytometry		Flow cytometry (automated cell culture system)	Automated	To detect variability in cell surface markers during seed processing	Mammalian	(33)
		Flow injection flow cytometry (FI-FCM)	Online	Expression level of target protein on a single cell level using green fluorescent protein	—	(34)
		Flow cytometry	Automated	Monitoring culture homogeneity over time	Mammalian	(35)
IR spectroscopy	Detect media components and metabolic end products, sense metabolic process failure	NIR	In-line	Monitoring and control of the fermentation process of *Staphylococcus xylosus* ES13	Microbial	(36)
		ATR-MIR	Online	Monitoring production and accumulation of biomass for gluconacetan production	Microbial	(37)
		FT-MIR and ATR	Online	Investigation of fed-batch cultivations of the methylotrophic yeast *Pichia pastoris*	Microbial	(38)
In situ 2D fluorometry	Detect media components and metabolic end products	In situ 2D fluorometry with chemometrics	Online	Monitoring of key bioprocess variables for mammalian cell culture processes. Viable cell density and recombinant protein concentrations were monitored	Mammalian	(39)
		2D fluorescence spectroscopy	Online	Monitoring of chemometric model and control of metabolic changes in fermentation	Microbial	(40)

Raman spectroscopy		FT-MIR, NIR, FT-Raman spectroscopy	—	Mathematical modeling of *Lactobacillus casei* cultivation process with the goal of predicting the concentrations of glucose, lactate, and biomass	Microbial	(41)
UV spectroscopy	Measure homogenate components	Optic turbidimetric sensors	Online	Biomass/cell concentration and automatic regulation of substrate and nutrient feed rate	Microbial	(42)
Mass spectroscopy	Detect metabolic end products	Mass spectrometry	Online	Gas analysis (CO_2, O_2, CH_4) and control of metabolic rate	Microbial	(43)
		Mass spectroscopy membrane sensor	Online	Monitoring of acetone, butanol, and ethanol concentrations and control of fed-batch fermentation of acetone–butanol fermentation	Microbial	(44)
		Automatic membrane inlet mass spectroscopy (MIMS)	Online	Aromatic compound analysis and monitoring of changes for a two-phase process	Microbial	(45)
pH	Influence cell growth and productivity	Luminescence-based pH optrode	Online	pH control in fermentation	Microbial	(46)
Carbon dioxide	Influence intracellular and extracellular pH	CO_2 sensors	Online	Dissolved CO_2 concentration and control of medium feed rate	Microbial	(47)
Dissolved oxygen	Cells require oxygen for the production of energy from organic carbon sources	Mass-balance technique for measuring kLa, dissolved O_2 concentration	—	Control of physiological state of cells and cellular activity	Mammalian	(48)
Temperature	Effects biological reactions	Thermal biosensor with FIA system	Online	Monitoring and control for penicillin V production	Microbial	(49)

precipitation. Kinetics of precipitation has been estimated by sensors such as attenuated total reflection-Fourier transform infrared (ATR-FTIR) associated with proportional integral derivative (PID) controllers for controlling the feed rate of the precipitant (51).

73.3.4 Extraction

Extraction involves separation of the components on the basis of their relative solubility in two different immiscible liquids (aqueous and organic phase). NMR and IR spectroscopy have been used to monitor and thus optimize the proportion of organic solvent mixtures (51). A scheme to monitor the harvest process of a monoclonal antibody using hollow fiber membrane has been presented where the permeate was analyzed using chromatography and the results obtained were used to monitor the harvest process (52).

In summary, typical harvest unit operations have shorter process times when compared with upstream unit operations and this offers challenges with respect to creating successful PAT applications (Table 73.3). The issues associated to complexity of the sample matrix when analyzing for titer or product quality apply here as well. Furthermore, as, typically, the product quality is not affected to a great extent at this stage, creation of PAT applications may not be as impactful as for upstream or downstream stage. However, for cases where the product is known to degrade if held in harvest for too long due to presence of proteases or other reasons, developing PAT applications for these unit operations may be of significant value.

73.4 PAT APPLICATIONS IN DOWNSTREAM OPERATIONS

As most of the therapeutic proteins are parenteral, they require high purity and must be free of viruses, other proteins, nucleic acids, and pyrogens. Downstream operations must ensure that the product of interest is recovered in sufficient quantity with an acceptable impurity profile. The purification process should be capable of removing process-related (host cell proteins, DNA, etc.) and product-related (aggregates, fragments, etc.) impurities. Each unit operation in the downstream process serves a unique purpose and is capable of removing particular impurity/impurities.

73.4.1 Filtration

Filtration is an integral part of the purification process. It may be operated as normal flow filtration (depth filtration, nanofiltration, and sterile filtration) or as tangential flow filtration [ultrafiltration–diafiltration (UF-DF) and microfiltration]. Common applications include desalting, concentration, and buffer exchange of proteins. Typically, the operating conditions to be controlled include flow rate and pressure. High values of flow rate and transmembrane pressure (TMP) across the filter membrane may lead to denaturation/loss of the product on the filter surface. Sensors for real-time monitoring of these parameters include pressure gauge and flow meters installed with the filtration setup, which ensure smooth operation of the process with optimal yield.

Applications include

1. *Measurement of CQA:* Absorbance of the filtrate at 410 nm has also been used as a tool to monitor the depth filtration of host cell proteins (53).
2. *Monitoring of membrane fouling:* A series of techniques have been used to monitor cake formation and membrane fouling (which cause blockage of the membrane) during filtration. Formation of the deposition layer on the membrane has been tracked by image analyzers (54) and laser triangulometry (55). These techniques, however, are unable to measure cake porosity and can only track monolayer formation. However, this has been overcome by optic laser sensors, which can measure a cake layer of thickness of up to 30μm (56). Ultrasonic time domain reflectometry has been used to measure membrane fouling, though it is not specific to porous structure or membrane skin layer (57). Light deflection techniques such as shadowgraphy (58) and refractography (59) have been used to measure the concentration profile within medium and concentration gradient, respectively. This helps in monitoring concentration polarization. Magnetic resonance imaging has been used to measure the concentration polarization in colloidal suspensions (60) and electron diode array microscopy has been used in case of ultrafiltration and microfiltration (61). Adoption of the techniques mentioned earlier can help avoid blockage of the filter membrane by providing information to predict the timing of back-flushing the membrane, thus ensuring constant flux and greater retention.
3. *Monitoring process parameters in lieu of CQAs:* UF-DF offers unique challenges toward implementation of PAT. Diafiltration is currently carried out using fixed volumes. There are cases when there is a need to restrict the excessive consumption of costly diafiltration buffer and also to reduce the process time for maintaining product stability. PAT has been applied to signal the end of a diafiltration process by monitoring different species collected in the permeate after each diafiltration volume (62). A control species was identified and a correlation between its concentration and pH was established and verified at multiple concentrations.

73.4.2 Refolding

The expression of proteins in certain microbial systems (e.g. *Escherichia coli*) results in the formation of inclusion bodies that contain the product in an inactive and insoluble form. These inclusion bodies need to be solubilized using chaotropic/reducing agents to disrupt noncovalent interactions and break interchain disulfide bonds. Subsequently, in the refolding step, the concentration of the solubilizing agents is decreased, resulting in protein refolding (63). This can be achieved by buffer exchange via batch dilution or liquid chromatography. In such a process, the time required for refolding is critical and the process should be stopped when refolding is complete to ensure consistent product quality. The time of refolding is dependent on the refolding rate, which in turn is dependent on the characteristics of the feed material and the operating conditions. A PAT-based control scheme utilizing high performance liquid chromatography (HPLC) has been proposed (62), wherein the purity of the product as well as the levels of different product-related variants and impurities were monitored as a function of time, allowing effective decision making on when to stop the process. Such a scheme is practical to implement for cases when exceeding the refold time will lead to an increase in the level of one or more impurities. A different PAT approach has been applied to monitor the refolding of recombinant human vascular endothelial growth factor (rhVEGF) (64). As refolding process is dependent on oxygen, the DO profile was used as a tool to understand the oxygen needs of the reaction and its impact on product quality. An in-line DO probe was used to monitor the oxygen levels in the reaction vessel and reverse-phase high performance liquid chromatography (RP-HPLC) was used to assess product quality and a correlation was established between them (64). The aeration parameters were scaled up to manufacturing tanks of capacity 2000 and 15,000 L, and the DO profiles showed similar trends across scales; hence, this method was successfully used to control process performance at commercial manufacturing scale.

73.4.3 Chromatography

Process chromatography, commonly used in batch-wise mode, involves separation of a mixture of species based on differential interactions between the sample components and the resin particles (stationary phase) packed in the column in the presence of the mobile phase. Chromatography encompasses a wide range of separation modes that can be categorized as nonadsorptive (e.g. size-exclusion) or adsorptive (e.g. ion-exchange). The adsorptive modes of chromatography include but are not limited to ion-exchange, hydrophobic interaction, reversed-phase, affinity, and immunoaffinity (16).

Conventionally, pooling of chromatography columns is performed on the basis of absorbance at 280 nm. However, ultraviolet absorbance is unable to differentiate between product- and other protein-based impurities as both of them have similar absorbance profiles (7). Use of online RP-HPLC for separating recombinant human insulin-like growth factor-I (IGF) and IGF aggregates to facilitate real-time pooling based on product quality has been successfully demonstrated (65). A similar application using chromatographic separation with protein A-immobilized media has been shown to reliably control antibody loading on a protein A column in a CHO-derived recombinant antibody purification process (66). Stopped flow analysis has been used as an at-line tool to provide a visual description of product levels and real-time representation of yield during the production of alcohol dehydrogenase via hydrophobic interaction chromatography (HIC) in *Saccharomyces cerevisiae* (67). Implementation of PAT in a chromatographic step is most difficult in comparison with other unit operations due to the short window of decision that it normally offers (Table 73.3). The analysis time has to be reduced considerably to make an informed decision of proceeding further in the process. Very recently, the feasibility of utilizing online HPLC (68), online ultra-performance liquid chromatography (UPLC) (69) and at-line tryptophan fluorescence (70) has been assessed to facilitate real-time analysis and decision making in process chromatography. A case study pertaining to the use of online HPLC with process chromatography is presented later in the chapter.

73.4.4 In-Line Mixing

In-line mixing systems are often used to blend large volumes of premixed buffer solutions. A programmable logic controller (PLC) can be used as a PAT tool to monitor the composition of the blend during mixing and prevent release of the blend to the process until its composition accurately matches the set point (8). A similar technology has been implemented in Technikrom's patented in-line buffer dilution technology (71), where water for injection (WFI) and buffer concentrate are pumped into a mixing loop, where the buffer concentrate is diluted down The molarity of the buffer has a specific conductivity that can be monitored and controlled by an in-line process analyzer (conductivity sensor) that interfaces with a process control feedback loop. The sensor continually monitors conductivity of the buffer blend in the mixing loop and sends an output signal to the process control feedback loop. That loop then references the current process value to a user-defined conductivity target set point for the diluted buffer. It sends a signal to adjust the pump speeds accordingly so that the dynamic ratio of WFI to salt buffer in the mixing loop is continually adjusted toward the set point. When conductivity is sufficiently close

to the set point (within specification), buffer is released to a product collection vessel. When the buffer is not within specification, it is diverted to waste until the conductivity process value comes back into specification. In this manner, process conditions are always known and out-of-spec buffer cannot reach the product. For a process chromatography unit operation, a small decrease in variability of the mobile phase prepared in a PAT-controlled in-line mixing system or tank blending system can greatly improve separation efficiency, thus affecting product quality.

73.4.5 PEGylation of Proteins

PEGylation reaction involves association of PEG onto one or more accessible lysine residues or the N-terminal amino groups of the protein to stabilize the protein and increase its solubility. A PAT-based control strategy consisting of an online analytical HPLC system has been used to monitor and control the reaction so as to produce homogenous/active product (7).

73.4.6 Viral Filtration

Viral filtration is carried out to reduce the virus load in the process stream. For certain filter types such as the Viresolve NFP, the instantaneous clearance capacity has been shown to be tightly associated with the flux. Thus, the extent of fouling or alternatively the flux decay (which is easy to measure) has been considered as the critical process parameter and used to ensure effective and consistent viral clearance (7). Table 73.5 summarizes the process monitoring tools for downstream operations.

In summary, the downstream operations in most cases directly and significantly affect quality of the final product. While the process chromatography is the primary work horse of purification, it is challenging to design PAT applications due to the short decision time it offers (Table 73.3). The situation is marginally better with other unit operations, especially refolding. Along with the upstream operations, it is evident that PAT could have a very significant impact in ensuring that the final product is of acceptable quality and that the quality is consistently achieved lot after lot.

73.5 PAT APPLICATIONS IN DRUG PRODUCT OPERATIONS

Drug product unit operations are needed to turn a purified drug substance into the final dosage form, the finished product. The formulation step involves taking the purified protein at the desired concentration and dispensing it with the correct excipients that can ensure product quality and integrity during the subsequent fill/finish steps that may include filtration, filling, lyophilization, inspection, packaging, storage, transport, and delivery.

73.5.1 Bulk Freeze-Thaw

Bulk freeze-thaw is commonly employed during biopharmaceutical manufacturing to gain operational flexibility while maintaining product quality. A frozen drug substance provides several advantages over liquid storage, including increased product stability, reduced microbial growth, and reduced foaming during transportation. However, in such cases, the frozen bulk needs to be thawed before it can be formulated and processed. Thawing can cause further stress and damage to the protein. Excessive freezing and thawing rates can lead to shear-induced and surface-mediated protein denaturation. Temperature–time profiles can be obtained experimentally by freezing the bulk (or placebo because the actual product may not be available for such studies) in the selected container and freezer, and positioning temperature recorders at different places in the solution and control on the freezing/thawing rate may be achieved circulating a heat transfer fluid that allows rapid heating and cooling of vessel contents (72).

73.5.2 Formulation

The first step after thawing the bulk is to formulate it with the pertinent buffer and to the target concentration. The formulation step involves adding the desired excipients at target concentration and adjusting pH, conductivity, and protein concentration. Mixing speeds and times are critical during the mixing of the purified protein bulk and the formulation buffer. Inadequate mixing can leave the solution heterogeneous, while excessive mixing can result in the protein undergoing shear-related stress. The speed needs to be, therefore, continuously monitored and adjusted.

73.5.3 Sterile Filtration

After formulation, the active product is sterile filtered (using 0.22-μm pore size membrane) to ensure that the product is free of bioburden. Critical parameters that require careful consideration include allowable pressure drop across the filter, the duration over which filtered formulated product can be held to maintain protein integrity and product sterility, temperature of operation, and the mode of liquid transfer during filtration. These parameters can be conveniently measured by pressure gauges and flow meters.

73.5.4 Filling

Once the drug substance has been formulated and sterile filtered, it is filled into the primary drug product containers, which are usually vials, or syringes for prefilled injectables. Excessive fill speeds can result in foaming and subsequently in protein denaturation. Over extended periods of filling, it is possible that proteins/excipients interact with the

TABLE 73.5. Process Monitoring Tools for Downstream Operations (8)

Unit Operation	Sensor	Objective	Measurement Principle
Ultrafiltration/diafiltration	pH, conductivity probes, and OD probes	To timely terminate the process	Measure product concentration of the desired species directly using OD probes or alternatively establish a correlation between the pH and conductivity of the species (obtained in the permeate) and its concentration
	Pressure gauge to calculate transmembrane pressure, flux feed/permeate/retentate	To ensure the membrane integrity	Damage to the membrane will reduce the transmembrane pressure across the membrane
Chromatography	In-line analytical methods, online detectors, as UV, RI	For pooling	Product of interest will absorb light in the UV range and give a distinct peak in the chromatogram
	System control	For performing gradient elution	Controller within the chromatographic system automatically proportions the mobile phase constituents
	pH, concentration (System control)	For performing column equilibration	Chromatographic system automatically adjusts the pH and concentration to the desired set point
	Mock eluate	For performing column cleaning and regeneration	To collect the eluate, analyze it, and make sure it is free from impurities
	Height equivalent of theoretical plate (HETP)	For deciding when to repack	Analyze by test method using acetone and manual computation
In-line mixing	System control	For monitoring flow rate	In-built flow meter
	pH, concentration, conductivity	For deciding when blending is done	Programmable logic controller can be used to monitor the composition of the blend during mixing
Refolding steps	Addition control	For measuring concentration of reagents	Controlling the addition manually
Conjugation reactions	Product quality, reaction time	For indicating end of reaction	Monitor the reaction using online analytical HPLC

tubing/pumping surfaces. Therefore, it is necessary to characterize and prevent such interactions. Most manufacturing facilities use automatic fill machines with multiple needles. Automatic fill machines typically have the capabilities to periodically test fill-weights online. Fill parameters, including the filler speed and nozzle design, are controlled to avoid other issues such as dripping and liquid spurting (72,73).

73.5.5 Lyophilization

Most biopharmaceuticals show limited stability toward physicochemical degradation. To achieve acceptable shelf life, protein drug products are often lyophilized. Lyophilization is the process by which the moisture content of the product is reduced by freezing followed by sublimation under vacuum. The lyophilization process primarily consists of three stages. The first stage involves freezing the product and creating a frozen matrix suitable for drying. The second stage is that of primary drying and involves removal of ice by sublimation caused by reduction in pressure (to typically around 50–500 mm Hg) while maintaining the product temperature at a low, desirable level. The third stage in the process is called *secondary drying* where the bound water is removed until the residual moisture content reaches below the target level. The critical process parameters to be monitored during freeze drying include degree of undercooling, product temperature, sublimation rate, and primary drying endpoint determination (51). A series of tools have been developed to monitor the lyophilization process that include single-vial and batch monitoring tools. The preferred attributes of these tools include (51)

1. Provide absolute measurements representative of a batch, and not of a single vial
2. Capability of monitoring the slowest drying vials in the batch
3. Compatible with process procedures and flow (loading and unloading of vials/trays)
4. Compatible with cleaning and steam sterilization
5. No impact on lyophilizer stability and vacuum
6. Scalable for use and integration with laboratory through a production-scale freeze drying equipment.

Table 73.6 provides the monitoring tools for the lyophilization process. Two different approaches have been proposed to monitor the freeze drying process. The first involves a soft-sensor that allows for monitoring a single vial using a temperature measurement. It measures the temperature of the product (or of the vial) and uses a mathematical model of the process to provide a real-time estimation of some parameters or state variables such as the temperature profile in the product and the mass and heat transfer coefficients.

The second tool is called as the *dynamic parameters estimation* (DPE) algorithm and it allows for monitoring the whole batch by measuring the pressure rise that occurs when the valve placed between the drying chamber and the condenser is closed for a short time interval [pressure rise test (PRT)] (74). The DPE algorithm is a nonintrusive method useful for estimating the average state of the whole batch. It uses an unsteady mathematical model to interpret the pressure rise curve experimentally acquired and it supplies a full-state estimation of the system, that is, the moving front temperature and position, the temperature profile in the product, and the mass and heat transfer coefficients. *LyoDriver* is a control system that uses DPE, process variables, and an unsteady-state mathematical model for the time when the product temperature is varying and predicts potentially damaging temperature overshoots and anticipates the control actions accordingly (74).

A widespread technique for monitoring primary drying is the PRT. Several model-based methods were investigated using the PRT to monitor the primary drying of a lyophilization process. These included manometric temperature measurement (MTM), pressure rise analysis (PRA), and DPE and an optimization algorithm was used to estimate the product temperature and the residual water content looking for the best fit between the pressure measurement and the values obtained by mathematical simulation. Other parameters such as the heat transfer coefficient between the shelf and the vials and the resistance of the dried product to vapor flow can also be estimated from the PRT but require modern control tools to deliver process optimization and desirable product quality (75).

73.5.6 Inspection

Filled vials are inspected to ensure the absence of foreign contaminants. Automated inspection can be used at this stage to inspect the filled vials or syringes for presence of visible particles (73).

In summary, process analyzers for monitoring drug product operations are able to provide results well within the decision period required for forward processing. Hence, the current level of technology is well equipped to facilitate a PAT-based control scheme for drug product unit operations. This is also an area where PAT implementation is furthest ahead at present.

73.6 PAT AND RAPID MICROBIOLOGICAL METHODS

Traditional culture-based in-process microbiological analysis techniques have very limited value in PAT due to the

TABLE 73.6. Process Monitoring Tools for Lyophilization (51)

Tool	Method	Comments	Commercial Viability	Product Temperature	Sublimation Rate	Primary Drying Endpoint Indicator
TEMPRIS	Single vial	Sterilizable wireless battery-free temperature sensors that can be used in both laboratory and manufacturing scale	Yes	Yes	No	Yes
Thermocouples	Single vial	Positioned bottom-center in the vial. Used mainly in laboratory scale	Yes	Yes	No	Yes
RTD	Single vial	Reliable, easy to sterilize. Accurate positioning is difficult, limited validity due to measurement of temperature. Used in manufacturing scale	Yes	Yes	No	Yes
Microbalance	Single vial	Determines the loss of weight of a sample vial during freeze drying by intermittent or continuous weighing information about sublimation rate and process step endpoints	No	No	Yes	Yes
Pirani	Batch	Dependent on type of gas, calibrated for a specific gas (usually N_2)	Yes	No	No	Yes
MTM	Batch	Pressure rise tests are performed periodically by rapid closing (<0.1 s) of the isolation valve between chamber and condenser (laboratory scale)	Yes	Yes	Yes	Yes
Dewpoint	Batch	Determination of concentration of water vapor in a gas	Yes	No	No	Yes
Lyotrack (plasma emission spectroscopy)	Batch	Spectroscopic measurement of water concentration in the chamber atmosphere using a cold plasma source connected to the chamber	Yes	No	No	Yes
Residual gas analyzer (mass spectroscopy)	Batch	Measures water vapor, N_2, and also any additional residual solvents and volatiles	Yes, but cannot be steam sterilized	No	No	Yes s
Tunable diode laser absorption spectroscopy (TDLAS)	Batch	NIR-spectroscopic method for the determination of trace concentrations of a gas. No contact to the product. Used in sterile processes (manufacturing) and in all scales of freeze dryers	Yes	Yes	Yes	Yes
Infrared Spectroscopy	Single vial	NIR: for residual moisture measurements in vials through continuous measurements during secondary drying. Raman: for determination of physical product characteristics	No	No	No	Yes

TABLE 73.7. Common Rapid Microbiology Methods Used in Bioprocessing

Objective	Tools	Principle
Growth-based detection of biochemical or physiological growth indicators		
	ATP bioluminescence	Breakdown of ATP from microbial cells to produce light
	Colorimetric detection	Color change in growth medium due to microbial metabolism
	Autofluorescence detection	Fluorescence emission by microbial colonies growing on solid surface
	Headspace pressure measurement	Positive/negative pressure changes in headspace detected by electronic transducers
	Impedance	Change in electrical conductivity of growth media when AC is passed across two electrodes
	Turbidimetry	Difference in opacity at specified wavelength
Viability-based cell labeling techniques to detect and quantify viable microorganisms		
	Flow cytometry	Detection of a fluorescently labeled viable cell
	Microcalorimetry	Measurement of heat resulting from microbial catabolism
	Solid-phase cytometry	Filtration of potential microbial contaminants before detection of a fluorescently labeled viable cell
Molecular methods	Polymerase chain reaction (PCR)	Amplification of specific sections of microbial nucleic acids
Endotoxin testing limulus amebocyte lysate (LAL) assay		
Cell component-based technology	Biochemical assays, antigen–antibody interaction by enzyme-linked immunosorbent assay (ELISA), fatty acid profiling, gram staining, mass spectrometry, and immunological and spectroscopic techniques	To establish identity of microorganism

lengthy analysis time (2–28 days). Rapid microbiological methods (RMMs) are capable of producing results in real time, and thus are far more useful, because timely microbiological data are often critical not only for product release but also for continuous process monitoring and control. The most visible application for RMM in pharmaceutical manufacturing is in the release of finished products, where the shorter "time to result" may generate considerable cost savings. But RMM can also play a key role in other routine tests, including raw material testing, in-process testing, microbial limit testing, bioburden assessment, process water testing, environmental monitoring, and sterility testing. These applications have the potential to contribute to PAT, and in the near future, it is very likely that continuous real-time monitoring of microbiologicals in the manufacturing process will be feasible, resulting in very significant savings in both time and production costs. One may have to compromise on sensitivity over speed of the method chosen as the level of sensitivity required for the RMM is dependent on the level of sterility essential at that step in the process (8). Table 73.7 outlines some of the RMM that are commonly used in manufacturing facilities.

73.7 APPLICATIONS OF CHEMOMETRICS IN PAT

Chemometrics can be defined as the use of statistical tools toward analysis of complex data sets for uncovering information about the product or the process. Such information may be useful for process monitoring, control, and endpoint determination. Chemometrics encompasses many important fields of chemical data analysis, notably statistical analysis, optimization, signal processing, multivariate curve resolution, multivariate calibration, regression, pattern recognition, parameter estimation, structure–property relationships, cluster analysis, discrimination analysis, multiway analysis, factor analysis, library search, informatics, and artificial intelligence (4). These numerical techniques serve different roles in their diverse applications. In process development and scale-up, their primary goal is for process understanding, which is achieved by elucidating process-related physicochemical correlations and information such as kinetics, thermodynamics, product/process stability, and safety. In manufacturing scenarios, the computational methods may be used for MSPC, fault diagnosis, and continuous process knowledge management. Use

of statistical tools to analyze data from biopharmaceutical manufacturing is gaining popularity as the data obtained is very complex and subjecting the data sets from manufacturing to univariate or bivariate analysis can often be inefficient and result in misleading conclusions (76,77). Moreover, qualitative data analysis using chemometrics has been shown to aid in identification of patterns in data via trend analysis and to help in eliminating outliers, whereas quantitative data analysis using regression methods is useful for predicting relationships between independent and dependent variables (1).

Several applications involving the use of chemometric tools in biotech production have been published recently (Table 73.8). MVDA has been evaluated for scale-up, process comparability, process characterization, and fault diagnosis of a cell culture process. Several input parameters (pCO_2, pO_2, glucose, pH, lactate, and ammonium ions) and output parameters [purity, viable cell density (VCD), viability, and osmolality] for cell culture unit operation were evaluated in this analysis (78). MVDA has been used as a tool to identify process parameters that affect cell culture performance and their interactions. A PLS model has been shown to predict the concentration of glucose and ethanol during yeast fermentation by utilizing spectral data from mid-infrared (MIR) spectroscopy (79). Such models have been used to monitor and control fed-batch fermentation processes and are capable of detecting fault conditions and inferencing quality variables that are otherwise hard to estimate (80). Artificial neural network (ANN) has been employed to improve the fermentation process of docosahexaenoic acid production by predicting optimal conditions for fermentation using gas chromatography data as input (81). A flexible process monitoring method for fault detection and diagnosis was developed for an industrial cell culture pilot plant (82). Faults that were identified included differences in equipment, operational issues, and imminent batch failure. The study demonstrated that data from even a small number of batches (approximately 20) can still be used to monitor for a wide range of process faults and develop a control strategy to avoid them. NMR-PLS has been used to analyze spectral data for prediction of cell culture titer for a given peptone lot to optimize efficiency and consistency of protein production (83). Chemometrics analysis has also been used for optimizing and predicting protein–ligand binding conditions in affinity capillary electrophoresis (84,85).

Response surface methodology (Box–Behnken design) has been used to model the effect of injection time, voltage, and ligand concentration on protein–neutral ligand binding. The model was subsequently validated by a series of experimental runs (82). Combination of PLS and NIR has been used for monitoring a process that involves selectively removing contaminants such as cell debris, host cell proteins, and nucleic acids by flocculation of yeast cell homogenate. The approach was very cost effective and yielded a 90% correlation between the predicted and the actual data (99). Data pertaining to chromatographic behavior of conjugates of benzoic acid measured using high performance size-exclusion chromatography was analyzed by PCA. Analysis was performed on the data matrix of 18 conjugates described by 19 variables and the 6 principal components. The resulting model could explain 85.7% of the total variance in the data and was able to describe the structural behavior of each conjugate compound (100).

73.8 CASE STUDIES ON IMPLEMENTATION OF PAT

There are numerous case studies that demonstrate the successful application of PAT in biotech unit operations (56). Two of them are highlighted below:

73.8.1 Case Study 1: Real-Time Monitoring of Multiple Parameters in Mammalian Cell Culture Bioreactors Using an In-Line Raman Spectroscopy Probe

Raman spectroscopy is a highly specific method for establishing molecular identity (101). It measures the amount of light scattered inelastically at different frequencies by molecular vibrations. This case study demonstrates the feasibility of using a Raman probe for continuous acquisition of real-time data for process monitoring at large-scale mammalian cell culture (500-L bioreactor). For this purpose, a total of four bioreactors were operated in the fed-batch mode. Multiple Raman immersion probes were coupled to a Raman spectrometer for in-line collection of spectra, while at-line sampling was carried out daily in parallel for measurement of glucose, glutamine, glutamate, lactate, ammonium, VCD, and total cell density (TCD). The Raman spectra were correlated with at-line measurements using PLS modeling. Of the four bioreactor runs that were conducted, data from the first three were used in the calibration data set and data from the last lot were used to validate the models. The predictions from the model based on Raman spectra matched the measured and calculated values for glutamine, glutamate, glucose, lactate, and ammonium throughout the course of the run and also the increases in nutrient levels and decreases in metabolite levels after feeding. Similarly, VCD and TCD predictions also matched at-line measurements with slight deviations. Hence, in-line Raman spectroscopy was capable of successfully monitoring process conditions in a large-scale mammalian cell culture and has the potential to develop into a major PAT tool due to its favorable characteristics such as

TABLE 73.8. Chemometrics Applications in Biotech Production

Application	Process Analyzer	Chemometric Application	Observations	References
Scanning unprocessed culture fluid samples from a complex antibiotic production process	NIR	PCA	Process diagnosis and rapid assessment of process performance	(86)
Quality prediction and fault diagnosis for simulated fed-batch fermentation of penicillin	—	Multivariate statistical process monitoring	Enabled prediction of the end-of-batch quality during progress of the batch; this was useful for anticipating effects of excursions on final quality	(87)
To predict in advance the final quality of fermentation of antibiotic from *Streptomycetes*	FT-NIR reflectance spectroscopy	PCA (Kohonen network)	Kohonen network did predict successfully approximately 70% of the examples	(88)
Monitoring, detection, and diagnosis of small and embedded impurity peaks appearing in analytical chromatography	UV absorbance	MSPC based on PCA modeling	Applying this procedure for the detection of new peaks makes a fully automatic monitoring of complex chromatograms	(89)
Detection and diagnosis of abnormal process conditions in an industrial fed-batch cell culture process	NIR	PCA	The model was successfully able to detect abnormal process conditions, which resulted from three known fault types, namely, irregular thermal heating, elevated dissolved oxygen values, and large variation in agitation	(82)
Measurement of glucose, lactate, glutamine, and ammonia in undiluted serum-based cell culture media	NIR	PCA	Robust, analyte-specific models were generated	(90)
Monitoring the concentration of viable cells and the concentration of recombinant proteins in mammalian cell culture	2D fluorometry	PCA and PLS	Both viable cell density and glycoprotein concentration were accurately estimated	(91)
Monitoring concentrations of key analytes in a *Streptomyces clavuligerus* bioprocess for the synthesis of clavulanic acid	ATR-MIR	PLS	Quantitative, at-line models having low prediction error were developed and validated	(92)
Monitoring of fractionation of a whey protein isolate (WPI) during dead-end membrane filtration	Fluorescence spectroscopy	PLS models	Good agreement was obtained between predicted and measured values	(93)
Extract useful information from the manufacturing data for potential use in process optimization and enhancement of efficiency and robustness	—	PLS	Specific activity could be predicted reasonably well from the process data	(94)
Measurement of multiple analytes in undiluted serum-based cell culture media	NIR spectroscopy	PLS	Robust, analyte-specific models were generated with low prediction errors	(90)

Online batch fermentation process monitoring	NIR	PCA, PLS, MSPC charts	Easy and efficient identification of abnormal fermentation runs at an early stage of the fermentation	(95)
Yeast fermentations	MIR spectroscopy	PLS	Prediction of concentrations of glucose and ethanol	(79)
Use of online HPLC for making real-time decisions for pooling of process-scale chromatography columns based on product quality attributes to get consistent product quality	HPLC	Linear regression	Scalability demonstrated using online anion exchange HPLC for operations at pilot scale and eventually at manufacturing scale for pooling of a hydrophobic HIC column	(96)
	UPLC	Linear regression	UPLC offered significantly faster separations (7 min) while retaining the separation efficiency	(69)
	HPLC	Linear regression	Feasibility of using a commercially available online HPLC system for real-time pooling of process chromatography column	(68)
Real-time control of antibody loading during protein A affinity chromatography	Online HPLC, off-line ELISA	Linear regression	Accurate control of antibody loading on a protein A column in a CHO-derived recombinant antibody purification process and assessment of chromatography column performance	(97)
Thin layer chromatography for analysis of amino acids	NIR spectroscopy	PCA	Fast and easy method for classification of L-form amino acids either in dissolved or solid condition in blood samples	(98)

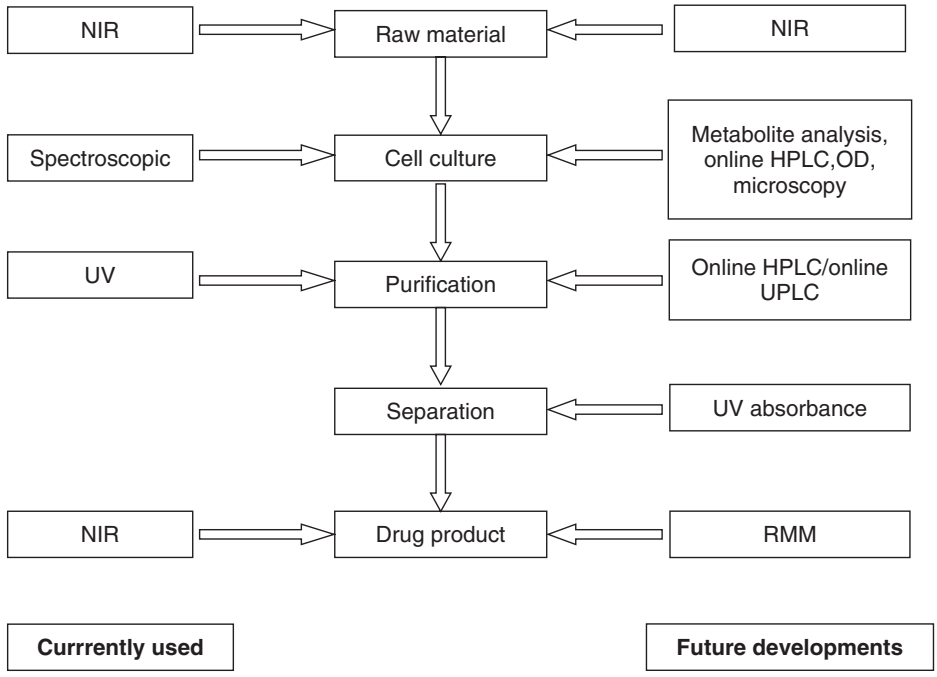


Figure 73.4. Status of PAT implementation in biopharmaceutical manufacturing: The left part shows tools that are currently used, primarily for monitoring. The right part shows tools that will possibly be used in the future to create true PAT applications

ease of sampling and potential to measure multiple analytes simultaneously.

73.8.2 Case Study 2: Use of Online HPLC for Making Real-Time Pooling Decisions for Process Chromatography

In this case study, a hydroxyapatite column was used for the separation of monomeric form of the product from higher molecular weight impurities (68). Product quality was determined using size-exclusion high performance liquid chromatography (SE-HPLC). The sample was collected directly from the hydroxyapatite column and its real-time analysis was performed. To achieve real-time decision making for pooling, it was necessary to not only decrease the elution flow rate for the Hydroxyapatite column but also to reduce the analysis time of the online SE-HPLC assay. As a result, implementation of this PAT application requires the ability to model the purity data in such a way that we can use the data from purity analysis of a fraction (x) to predict the pool purity if pooling was terminated at the next fraction ($x + 1$).The application can be extended to other modes of process chromatography and/or HPLC analysis. However, achieving this on the manufacturing floor would require a higher level of process understanding for designing such an approach and increased operational complexity.

73.9 CONCLUSION AND FUTURE PERSPECTIVE

PAT aims at improved monitoring and control for biopharmaceutical manufacturing processes. Figure 73.4 summarizes the current status of PAT for biopharmaceutical manufacturing. The focus in PAT implementation is on the principles of building quality into the product and process as well as continuous process improvement. This involves the use of multivariate tools, process analyzers, process control tools, and continuous improvement and knowledge management tools for manufacturing of the biopharmaceuticals. Control of the process by making real-time decisions based on measurement of product quality attributes would result in a more consistent product quality and a more efficient use of manufacturing capacity. However, this requires thorough understanding of the process and more specifically of the unit operation. While the emphasis has been on analysis and monitoring of the CQAs of the product or the critical process parameters, a greater degree of understanding is required of how process control (e.g. feedback and/or feedforward) can be achieved to ensure consistent process outputs. The recent development of chemometric tools has aided in deciphering useful information from data generated by process analyzers. Hence, the implementation of PAT is likely to result in a significant decrease in variability of product quality in the industry.

LIST OF ABBREVIATIONS

ACPS	Advisory Committee for Pharmaceutical Science
ASTM	American Society for Testing and Materials
ANN	Artificial neural network
ATP	Adenosine triphosphate
ATR-FTIR	Attenuated total reflection-Fourier transform infrared
ATR-MIR	Attenuated total reflection-mid-infrared
CDER	Center for Drug Evaluation and Research
CHO	Chinese Hamster ovary
CPP	Critical process parameters
CQA	Critical quality attribute
CVM	Center of Veterinary Medicine
2D	Two-dimensional
DOE	Design of experiments
DO	Dissolved oxygen
DPE	Dynamic parameters estimation
ELISA	Enzyme-linked immunosorbent assay
FDA	Federal Drug Administration
FIA	Flow injection analysis
FI-FCM	Flow injection flow cytometry
FTIR	Fourier transform infrared
FT-MIR	Fourier transform mid-infrared
HETP	Height equivalent of theoretical plate
HIC	Hydrophobic interaction chromatography
HPLC	High performance liquid chromatography
ICH	International Conference on Harmonization
IGF	Insulin-like growth factor
IR	Infrared
LAL	Limulus amebocyte lysate
LOV	Lab on valve
MIMS	Membrane inlet mass spectroscopy
MIR	Mid-infrared
MSPC	Multivariate statistical process control
MTM	Manometric temperature measurement
MVDA	Multivariate data analysis
MVF	Multiwavelength fluorescence
NIR	Near infrared
NMR	Nuclear magnetic resonance
OD	Optical density
ORA	Office of Regulatory Affairs
PA	Process attribute
PAT	Process analytical technology
PARAFAC	Parallel factor analysis
PCA	Principal component analysis
PCR	Polymerase chain reaction
PEG	Polyethylene glycol
PID	Proportional integral derivative
PLC	Programmable logic controller
PLS	Partial least squares
PRA	Pressure rise analysis
PRT	Pressure rise test
QA	Quality attribute
QbD	Quality by design
rhVEGF	Recombinant human vascular endothelial growth factor
RMM	Rapid microbiological methods
RP-HPLC	Reverse-phase high performance liquid chromatography
RTD	Resistance temperature diode
SE-HPLC	Size-exclusion high performance liquid chromatography
SIA	Sequential injection analysis
t_a	Analysis time
TCD	Total cell density
t_d	Decision time
TDLAS	Tunable diode laser absorption spectroscopy
TMP	Transmembrane pressure
TPP	Target product profile
t_p	Process time
UF-DF	Ultrafiltration-diafiltration
UPLC	Ultra-performance liquid chromatography
VCD	Viable cell density
WCB	Working cell bank
WFI	Water for injection
WPI	Whey protein isolate

REFERENCES

1. Rathore AS, Bhambure R, Ghare V. Anal Bioanal Chem 2010. DOI: 10.1007/s00216-010-3781-x.
2. Hinz DC. Anal Bioanal Chem 2006; 384: 1036–1042.
3. Guidance for industry PAT—a framework for innovative pharmaceutical development, manufacturing, and quality assurance. Available at http://www.fda.gov/cder/guidance/index.htm. September 2004.
4. Chew W, Sharratt P. Anal Methods 2010; 2: 1412–1438.
5. US Food and Drug Administration. Pharmaceutical cGMPS for the 21st century—a risk-based approach (Final Report); September 2004.
6. Rathore AS. Trends Biotechnol 2009; 27: 546–553.

7. Read EK, Park JT, Shah RB, Riley BS, Brorson KA, Rathore AS. Biotechnol Bioeng 2010; 105: 276–284.
8. Read EK, Shah RB, Riley BS, Park JT, Brorson KA, Rathore AS. Biotechnol Bioeng 2010; 105: 285–295.
9. Guidance for industry PAT—a framework for innovative pharmaceutical development, manufacturing, and quality assurance. Available at www.ich.org/fileadmin/Public.../Quality/Q9/.../Q9_Guideline.pdf.
10. Rathore AS, Winkle H. Nat Biotechnol 2009; 27: 26–34.
11. Rathore AS. Trends Biotechnol 2009; 27: 698–705.
12. Kirdar AO, Chen G, Rathore AS. Biotechnol Prog 2010; 26: 527–531.
13. Bhushan N, Hadpe S, Rathore AS. Biotechnol Prog 2012; 28: 121–128.
14. Junker BH, Wang HY. Biotechnol Bioeng 2006; 95: 226–261.
15. ISSN 1459.7683 (URL: http://www.vtt.fi/publications/index.jsp)
16. Ozturk S, Hu W, editors. Cell culture technology for pharmaceutical and cell-based therapies. CRC Press, Taylor & Francis; Boca Raton, FL, 2006.
17. Pescheck M, Schrader J, Sell D. Bioelectrochemistry 2005; 67: 47–55.
18. Goudar C, Biener R, Boisart C, Heidemann R, Piret J, Graaf A, Konstantinov K. Metab Eng 2009. DOI: 10.1016/j.ymben.2009.10.007.
19. Odman P, Johansen CL, Olsson L, Gernaey K, Lantz AE. J Biotechnol 2009; 144: 102–112.
20. Navratil M, Norberg A, Lamben M, Mandenius C. J Biotechnol 2005; 115: 67–79.
21. Zhang J, Xie Y, Dia X, Wei W. J Microbiol Meth 2001; 44: 105–111.
22. Guez JS, Cassar JPh, Wartelle F, Hulster D, Suhr H. Process Biochem 2009; 45(2): 288–291.
23. Guez JS, Cassar JPh, Wartelle F, Hulster D, Suhr H. J Biotechnol 2009; 111: 335–341.
24. Junker BH, Wang HY. Biotechnol Bioeng 2006; 95(2): 226–261.
25. Johansen C, Christensen LH, Nielsen J. J Villadsen Comp Chem Eng 1992; 16:S297–S304.
26. Ferreira LS, Desouza MB, Folly ROM. Sens Actuator B 2001; 75: 166–171.
27. Xie Y, Zeng H, Yao S, Wei W. Talanta 1999; 50: 1019–1025.
28. Kirdar AO, Green KD, Rathore AS. Biotechnol Prog 2008; 24: 720–726.
29. Reinecke M, Scheper T. J Biotechnol 1997; 59: 145–153.
30. Morovjan G, Szakacs G, Fekete J. J Chromatogr A 1997; 763: 165–172.
31. Noll T, Biselli M. J Biotechnol 1998; 63: 187–198.
32. Kiviharju K, Salonen K, Moilanen U, Meskanen E, Leisola M, Eerikäinen T, Eerikäinen T. J Ind Microbiol Biotechnol 2007; 34: 561–566.
33. Thomas RJ, Anderson D, Chandra A, Smith NM, Young LE, Williams D, Denning C. Biotechnol Bioeng 2009; 102: 1636–1644.
34. Broger T, Odermatt RP, Huber P, Sonnleitner B. J Biotechnol 2011; 154: 240–247.
35. Sitton G, Srienc F. J Biotechnol 2008; 135: 174–180.
36. Tosi S, Rossi M, Tamburini E, Vaccari G, Amaretti A, Matteuzzi D. Biotechnol Prog 2003; 19: 1816–1821.
37. Kornmann H, Valentinotti S, Duboc P, Marison I, von Stockar U. J Biotechnol 2004; 113: 231–245.
38. Schenk J, Marison I, von Stockar U. J Biotechnol 2006; 128: 344–353.
39. Teixeira AP, Portugal CA, Carrinhas N, Dias JM, Crespo JP, Alves PM, Carrondo MJ, Oliveira R. Biotechnol Bioeng 2008; 102: 1098–1106.
40. Rhee J, Kang T. Process Biochem 2007; 42: 1124–1134.
41. Sivakesava S, Irudayaraj J, Ali D. Process Biochem 2001; 37: 371–378.
42. Salgado AM, Folly ROM, Valdman B. Sens Actuator B 2001; 75: 24–28.
43. Heinzle E, Oeggerli A, Dettwiler B. Anal Chim Acta 1990; 238: 101–115.
44. Chauvatcharins S, Seki T, Fujiyama K, Yoshida T. J Ferment Bioeng 1995; 79(3): 264–269.
45. Tarkiainen V, Kotiaho T, Mattila I, Virkajarvi I, Aristidou A, Ketola R. Talanta 2005; 65: 1254–1263.
46. Chan C, Lo W, Wong KY. Biosens Bioelectron 2000; 15: 7–11.
47. Chen Y, Krol J, Huang W, Cino JP, Vyas R, Mirro R, Vaillancourt B. Process Biochem 2008; 43: 351–355.
48. Konstantinov K, Chuppa S, Sajan E, Tsai Y, Yoon S. F Golini Tibtech 1994; 12: 324–333.
49. Rank M, Danielsson B. Biosens Bioelectron 1992; 7: 631–635.
50. Kuentz M, Rothlisberger D. Eur J Pharm Biopharm 2003; 56(3): 355–361.
51. Undey C, Low D, Menezes JC, Koch M, editors. PAT applied in biopharmaceutical process development and manufacturing—an enabling tool for quality-by-design. CRC Press, Taylor & Francis; Boca Raton, FL, 2012
52. Zhang J, Zhou H, Ji Z, Regnier F. J Chromatogr B 1998; 707: 257–265.
53. Yigzaw Y, Piper R, Tran M, Shukla A. Biotechnol Prog 2006; 22: 288–296.
54. Mores WD, Davis RH. J Membr Sci 2001; 189: 217–230.
55. Altmann J, Ripperger S. J Membr Sci 1997; 124: 119–128.
56. Hamachi M, Mietton-Peuchot M. Chem Eng Res Des 2001; 79: 151–155.
57. Mairal AP, Greenberg AR, Krantz WB. Desalination 2000; 130: 45–60.
58. Chen J, Li Q, Elimelche M. Adv Colloid Interface Sci 2004; 107: 83–108.
59. Gowman L, Ethier CR. J Membr Sci 1997; 131: 95–105.
60. Yao S, Costello M, Fane AG, Pope JM. J Membr Sci 1995; 99: 207–216.
61. Mc-Donough RM, Bauser H, Stroh N, Chmeil H. Chem Eng Sci 1992; 47: 271–279.
62. Rathore AS, Sharma A, Chilin D. Biopharm Int 2006; 19: 48–57.
63. Freydell EJ, van der Wielen LAM, Eppink MHM, Ottens M. Biotechnol Prog 2011; 27: 1315–1328.
64. Pizarro SA, Dinges R, Adams R, Sanchez A, Winter C. Biotechnol Bioeng 2009; 104: 340–351.
65. Fahrner RA, Lester PM, Blank GS, Reifsnyder DH. J Chromatogr A 1998; 827: 37–43.

66. Fahrner RA, Blank GS. J Chromatogr A 1999; 849: 191–196.
67. Ündey C, Ertunc S, Mistretta T, Looze B. J Process Control 2010; 20: 1009–1018.
68. Rathore AS, Yu M, Yeboah S, Sharma A. Biotechnol Bioeng 2008; 100: 306–316.
69. Rathore AS, Wood R, Sharma A, Dermawan S. Biotechnol Bioeng 2008; 101: 1366–1374.
70. Rathore AS, Li X, Bartkowski W, Sharma A, Lu Y. Biotechnol Prog 2009; 25: 1433–1439.
71. Malone T, Li M. Bioproc Int 2010. 8:40–49.
72. Patro SY, Freund E, Chang BS. Biotechnol Annu Rev 2002; 8: 55–84.
73. Rathore N, Rajan RS. Biotechnol Prog 2008; 24: 504–514.
74. Fissore D, Pisano R, Rasetto V, Marchisio D, Barresi AA, Vallan A, Corbellini S. Chem Today 2009; 2. 7–11.
75. Fissore D, Pisano R, Barresi A. Dry Technol 2011; 29: 73–90.
76. Kourti T. Process Anal Technol 2004; 1: 13–19.
77. Martin EB, Morris AJ. J Biotechnol 2002; 99: 223–235.
78. Johnson R, Yu O, Kirdar AO, Annamalai A, Ahuja S, Ram K, Rathore AS. Biopharm Int 2007; 20: 130–144.
79. Mazarevica G, Diewok J, Baena JR, Rosenberg E, Lendl B. Appl Spectrosc 2004; 58: 804–810.
80. Zhang H, Lennox B. J Process Control 2004; 14: 41–50.
81. Rosa SM, Soria MA, Ve'lez CG, Galvagno MA. Bioresour Technol 2010; 101: 2367–2374.
82. Gunther JC, Conner JS, Seborg DE. Biotechnol Prog 2007; 23: 851–857.
83. Luo Y, Chen G. Biotechnol Bioeng 2007; 97: 1654–1659.
84. Montes RE, Hanrahan G, Gomez FA. Electrophoresis 2008; 29: 3325–3332.
85. Hanrahan G, Montes RE, Pao A, Johnson A, Gomez FA. Electrophoresis 2007; 28: 2853–2860.
86. Vaidyanathan S, Arnold SA, Matheson L, Mohan P, McNeil B, Harvey LM. Biotechnol Bioeng 2001; 74: 376–388.
87. Undey C, Ertunc S, Cinar AI. Eng Chem Res 2003; 42: 4645–4558.
88. Lopes JA, Costa PF, Alves TP, Menezes JC. Chemom Intell Lab Syst 2004; 74: 269–275.
89. Laursena K, Frederiksenb SS, Leuenhagenb C, Broa R. J Chromatogr A 2010; 1217: 6503–6510.
90. Rhiel M, Cohen MB, Murhammer DW, Arnold MA. Biotechnol Bioeng 2002; 77: 73–82.
91. Teixeira AP, Portugal CAM, Carinhas N, Dias JML, Crespo JP, Alves PM, Carrondo MJT, Oliveira R. Biotechnol Bioeng 2009; 102: 1098–1106.
92. Roychoudhury P, Harvey LM, McNeil B. Anal Chim Acta 2006; 561: 218–224.
93. Elshereef R, Budman H, Moresoli C, Legge RL. Biotechnol Prog 2010; 26: 168–178.
94. Thomassen YE, van Sprang ENM, van der Pol LA, Bakker WAM. Biotechnol Bioeng 2010; 107: 96–104.
95. Jorgensen P, Pederson JG, Jensen EP, Esbensen KH. J Chemom 2004; 18: 81–91.
96. Rathore AS, Parr L, Dermawan S, Lawson K, Lu Y. Biotechnol Prog 2010; 26: 448–457.
97. Fahrner RL, Blank GS. J Chromatogr A 1999; 849: 191–196.
98. Heigl N, Huck CW, Rainer M, Najam-ul-Haq M, Bonn GK. Amino Acids 2006; 31: 45–53.
99. Yeung KSY, Hoare M, Thornhill NF, Williams T, Vaghjiani JD. Biotechnol Bioeng 1999; 63: 684–693.
100. Bolzacchini E, Consonni V, Lucini R, Orlandi M, Rindone B. J Chromatogr A 1998; 813: 255–265.
101. Abu-Absi NR, Kenty BM, Cuellar ME, Borys MC, Sakhamuri S, Strachan DJ, Hausladen MC, Li ZJ. Biotechnol Bioeng 2011; 108: 1215–1221.

74

VENT GAS ANALYSIS

David Pollard and Jens Christensen
Merck & Co. Inc., Rahway, New Jersey

74.1 INTRODUCTION

Most biological processes involve the exchange or consumption of gases and volatile compounds, which makes the monitoring of exhaust gas an invaluable tool for the research or monitoring of fermentation processes. The monitoring of gas concentrations, such as CO_2 and O_2, in the inlet and outlet gas streams, and incorporating them into liquid and gas balances, makes it possible to quantify rates of gas utilization and respiratory quotient (RQ). The use of this data in conjunction with the fast response of the analyzers, provides an invaluable tool for on-line, real-time monitoring of the physiological state of the fermentation including growth kinetics, substrate consumption, and product formation (1,2). The aqueous concentration of organic volatile compounds, such as ethanol, butanol, and methanol, can also be determined from vent gas analysis and have been used to optimize productivity in industrial processes (3,4).

74.2 METHODS OF VENT GAS ANALYSIS

There are a variety of methods available for monitoring gases, however, only the methods most applicable for bioprocesses are described. These include thermal conductivity, flame ionization, gas chromatography (GC), electrochemical sensors, infrared absorption, and paramagnetism but by far, the most versatile and widely used is mass spectrometry which is why a considerable portion of this chapter is devoted to this widely used technology.

74.2.1 Gas Chromatography with Detection by Flame Ionization or Thermal Conductivity

GC combined with thermal conductivity or flame ionization detectors, has been used to determine H_2, CO_2, O_2, N_2, and organic volatiles. An analysis time of around 5–30 min is typical for each sample. This is much longer than other simpler, faster, and less expensive methods. GC is the phase separation of gas components by adsorption equilibrium differences between the stationary and mobile phases (5). The stationary phase is coated on small, solid particles (typically silica or polystyrene) packed or coated onto the walls of highly efficient fused silica columns (several meters in length). The particles have an affinity for the chosen gas analysis to achieve separation of gas components based on equilibrium differences. The system requires a carrier gas to transport the gas sample through the stationary phase (typically oxygen-free dry helium), a sample injection system, column temperature controller, and detector.

Thermal conductivity provides a resistance temperature detector whereby gas is passed over a heated filament and the magnitude of cooling is measured by the change of resistance of the filament as measured by a Wheatstone bridge (6). Typical units contain a bypass with two flows; one path houses the sensor with two heated coils. The heated gas is transported from upstream to downstream coils, changing their resistance. The bridge circuit with constant current input gives an output voltage in direct proportion to the difference in resistance, with heat input and specific heat assumed constant. For detectors used in GC, the heat transfer of the sample gas is compared with the

Upstream Industrial Biotechnology: Equipment, Process Design, Sensing, Control, and cGMP Operations, Volume 2, First Edition. Edited by Michael C. Flickinger.
© 2013 John Wiley & Sons, Inc. Published 2013 by John Wiley & Sons, Inc.

transfer of the carrier gas. The rate of transfer depends on the thermal conductivity of the gas which is proportional to the square root of molecular weight. The Wheatstone bridge balances the current through the sample element to restore its temperature to that of the reference. Instruments are calibrated for the gas to be used and can have a fast response time of 1 s, detection threshold of 30 ppm and accuracy of 2%. Carbon dioxide is often measured with this technique as the thermal conductivity of CO_2 is around two-thirds that of oxygen and nitrogen. The bypass units where the bulk of the flow bypasses the sensor are less sensitive to gas flow rate fluctuations but have larger response times, 20 s compared to 1 s. Although this technology has been used for many years it does not provide accuracy or long-term reproducibility. It is sensitive to gas flow rate, temperature, and mechanical vibration. Contamination of the sample cell can lead to drift and frequent calibration of these inexpensive devices is required. Sample pretreatment is often required to remove contaminants by condensation and drying.

An alternative is flame ionization, which is limited to the analysis of ethanol and organic volatiles because O_2, N_2, H_2, CO_2, Ar, H_2O, and NH_3 have no response. The sample gas is burned in a hydrogen- or air-induced flame and an electrical voltage is applied across two electrodes to remove the resulting ions from the flame. The current created across the two electrodes is a measure of the ion concentration (6). The detector has high linearity and sensitivity (ppb) with a short response time. This makes the method universal for organic analysis by GC, especially as contaminants, water, air, and ammonia, are not detected.

74.2.2 Electrochemical Sensors

Amperometric gas sensors can be used to measure oxygen concentration in vent gas. The sensor, 10–30 mm in length, measures the current across a working and counter-electrode as a function of analyte concentration in an electrochemical cell. The gold or platinum electrode hase a porous coating to allow the analyte gas to diffuse to the electrode surface which acts as a catalyst for electrochemical redox reactions. The oxygen diffusion results in a temperature-sensitive process and sensors are prone to drift from membrane fouling (7–9).

The electronic nose, an array of semiselective chemical gas sensors coupled with a pattern recognition algorithm, have been employed to analyze the volatile organic compounds (VOCs) and gases of fermentation vent gas (9,10). Typically, the arrays include 10–20 metal oxide sensors (MOS) operated at 300–500°C and 20–30 metal oxide semiconductor field effect transistors (MOSFETs) at 140–170°C. The MOS are ceramic cylinders <10 mm in length, containing a heating coil mounted onto a holder. The outside of the pellet is coated with metal oxide, usually SnO_2 doped with a small amount of Pd or Pt (Fig. 74.1). VOCs take part in redox reactions on the surface of the MOS while gases act as oxidizing agents at MOS operating temperatures. This results in a change in resistance of the sensor upon exposure to the VOC or gas. Selectivity of the sensor is fixed by changing the catalyst type or the operating temperature, which typically requires careful control to achieve sensitivities of 5–500 ppm. The MOSFETs typically use SiO_2 as the insulator and the common transistor configuration operates with three contacts: the source, drain, and gate (Fig. 74.1) (9). Applying a potential at the metal gate (typically platinum, palladium or iridium) determines the current. An inversion at the semiconductor–insulator boundary creates a channel that allows electrical current to flow from the source to the drain. This current of the transistor is controlled by the surface potential of the semiconductor. This in turn, determines the size of the depletion region as well as the concentration of charge carriers at the surface. Any gas reaction that causes a change in the metal gate or insulator properties will result in a change in the MOSFET sensor's electrical properties and a change in the drain current. The sensor response is measured by the change in gate voltage required to keep the drain current constant. Changing the temperature, gate metal type, thickness, and porosity of the metal gate will change the operation and selectivity. Sensor size is typically <1.5 mm and it operates around 150°C. Combinations of sensors allow good sensitivity but have slow response times, typically in the 5–10 min range. The data profiles are analyzed by principle component analysis and data sets require extensive validation of up to 10 repeated batches (10). The generated batch profiles can provide a real-time method of recognizing deviations from normal cultivation behavior (11). This can lead to methods for early contamination detection, providing a potentially powerful method to ensure product and process quality (12–14).

74.2.3 Infrared Absorption

The fundamental frequencies of vibration and rotation of a particular compound exposed to radiation, can be used to identify it from a mixture. IR (infrared) analyzers can only be used to monitor CO_2 and organic volatiles such as ethanol (15) since oxygen and nitrogen contain only one element. They are also sensitive to interference from other components of the gas, such as water. Most commonly used analyzers are nondispersive; they exclude most wavelengths apart from a few narrow bands of radiation. They are less selective than dispersive analyzers but more sensitive, simple, and reliable (16). Sources of radiation include quartz iodide lamps, tungsten filaments, and nichrome wires (6). A specific interference filter assembly, a monochromator, is chosen to filter out all wavelengths except for a desired wavelength band. The resulting radiation is a narrow band based around the mean of the desired wavelength

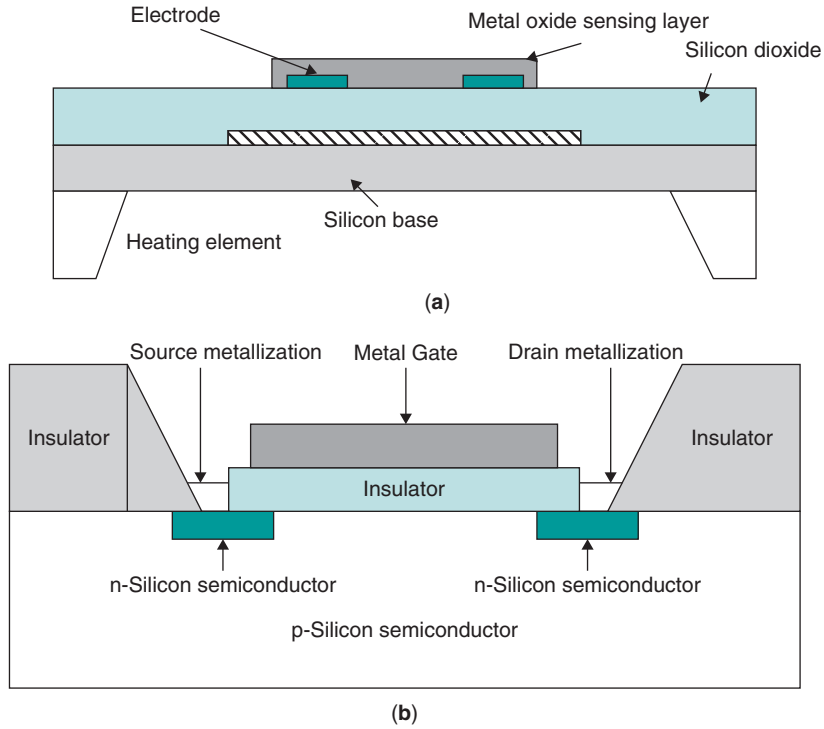


Figure 74.1. Schematic of (a) the metal oxide semiconductor (MOS) gas sensor and (b) the metal oxide semiconductor field effect transistor (MOSFET). [Adapted from 9]. (This figure is available in full color at http://onlinelibrary.wiley.com/book/10.1002/9780470054581.)

(4200–4400 nm for CO_2). Alternatively, a cell containing the gas of interest is used to isolate the desired wavelength source.

In a typical optical arrangement, such as the Luft analyzer, an optical beam splitter is used to split the single radiation source into two beams which pass into two separate chambers (Fig. 74.2). One chamber houses the sample cell and the other the reference cell. Both chambers contain a gas that absorbs at the desired wavelength and the detector gas is usually the same as the desired gas for analysis. Differences in IR absorption occur between the two chambers, reference and sample, which generates pressure imbalances. This distorts a diaphragm which separates the two chambers in the detector and forms part of a condenser microphone. A chopper wheel, that is a perforated or segmented disc, is used to block the radiation from one chamber and allow radiation to reach the detector through the other chamber. The alternate blocking of the reference and sample chambers allows each radiation to be sampled at their appropriate side of the detector. The alternating flow of radiation produces an oscillating effect on the diaphragm. The amplitude of the oscillations is measured by the capacitance of the condenser microphone which is correlated to the concentration of absorbed gas. The accuracy of IR analyzers is reasonable for fermentation processes, typically around 1% of range, but are prone to drift (up to 1% full-scale per day for both the zero and span). The calibration curve is typically nonlinear which gives added difficulty to the frequent recalibration required to counteract drift. However, the 0–90% response time of 0.5–5 secs is reasonably fast compared to other technologies already discussed.

A number of low-cost systems have become available in the last few years, which combine the IR absorption sensor with an amperometric electrochemical gas sensor or paramagnetic sensor for dual analysis of CO_2 and O_2 for a single fermenter. Magellan Instruments provide a unit with IR sensor and electrochemical sensor (17) while other similar technologies exist from Bluesens, Servomex, and Dasgip. While these units may provide a low-cost solution for a single fermentor they don't necessarily provide cost effectiveness for a large research or manufacturing facility. The units are prone to daily drift and sensors usually have to be replaced at least once a year.

74.2.4 Paramagnetism

When a magnetic field is applied to a gas, the atoms orientate themselves in the direction of the field. The thermomagnetic analyzer uses the principle that the magnetic susceptibility is proportional to the difference between sample temperature and the Curie point of 80°C for oxygen (6). A typical instrument is the Quincke-type analyzer which

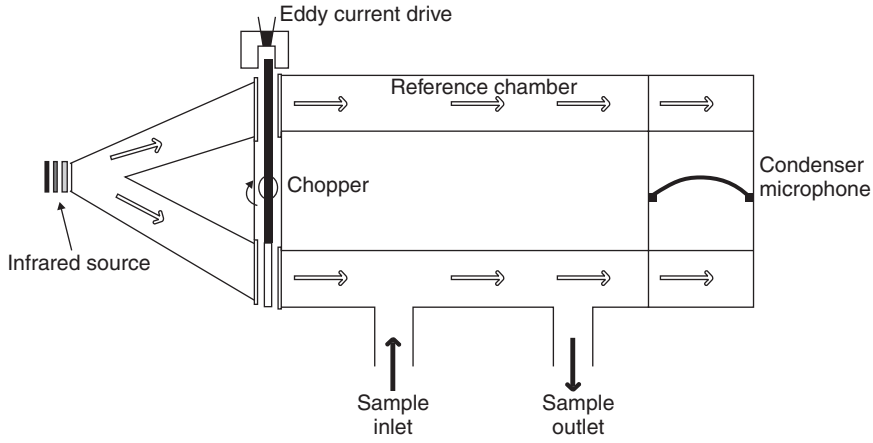


Figure 74.2. The Luft nondispersive IR analyzer with microphone sensor.

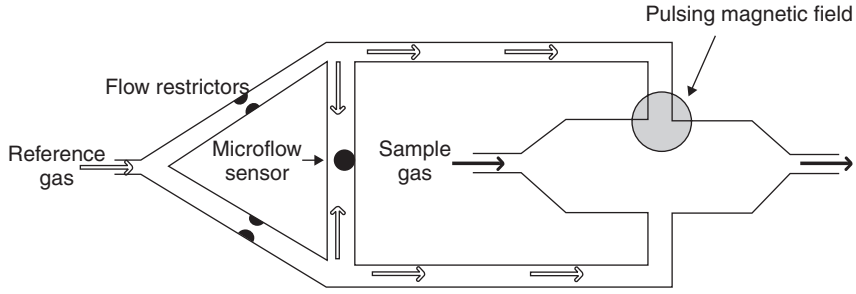


Figure 74.3. Quincke-type oxygen analyzer with capacitance sensor.

measures the pressure difference when two gases with different oxygen concentrations come together in the magnetic field. The reference gas (N_2, O_2, air) flows through two restrictions, so the gas entering either side of the sample chamber has equal flows (Fig. 74.3). One section of the reference gas is subjected to a pulsating magnetic field and if oxygen is present then a pressure difference is created between the two reference flows. The Luft capacitance sensor has been used as a detector. Alternatively, Siemans AG developed an analyzer with a microflow detector in a connecting channel which detects the pulsing flow, producing a current proportional to the oxygen concentration (Fig. 74.3). The separation of the sample from the detector reduces the possibilities of drift and instrument failure from contamination or corrosion of parts.

These paramagnetic analyzers have been found to be susceptible to vibration, pressure, and sample conditions with respect to moisture content and flow rate, resulting in frequent calibration to compensate for drift (2). Nevertheless, Quincke-type analyzers have been found to be more robust and have been widely used, including in the Merck & Co. Inc. production facilities. However, they are used only for single component analysis and are susceptible to moisture and high sample flow requirement. They have poor accuracy (1–2% of range) with slow response times (5–100 s) (18). The units require calibration from drift, the frequency of which depends upon care upon calibration, maintenance of the machine, and sample treatment (19). The use of microfluidics has renewed interest in paramagnetism, for the miniaturization of the oxygen sensor. A multilayer ceramic technology has been proposed with the integration of the magnetic coil into the fluidic system (20). This may provide a future source of inexpensive sensors.

74.2.5 Mass Spectrometry

This technology allows simultaneous measurement of both, air gases (e.g. Ar, O_2, N_2, CO_2) and volatile substances (including ethanol, acetone, and acetic acid (21,22) present in the fermenter headspace. A mass spectrometer with multipoint analysis and fast response times (in seconds) allows many fermentors and different processes to be monitored using the same instrument. This makes a cost-effective device for multifermenter sampling despite the high purchase cost of an individual unit. The analysis involves admitting a gas stream to an ion source and then ionizing the molecules by electron bombardment under a high vacuum. The ions produced are subsequently

separated according to their mass-to-charge ratio, by either a magnetic sector or a quadrupole mass filter, and detected sequentially. A typical magnetic sector mass spectrometer instrument has excellent repeatability of ±0.1% of range at calibration, zero and gain drift less than 1% of range/month and a response time of 1 sec (1,19,23). The limiting step of the response time becomes the passage through the sampling system, rather than the mass spectrometer itself. Maintenance is usually associated with contamination of the inlet device and filament and ion pump replacement. This is offset by the rapid analysis for polar organic species, excellent long-term accuracy, and precision plus flexibility of analysis. These features make mass spectrometry the most flexible and versatile instrument for vent gas analysis.

74.2.5.1 Vacuum System. A high vacuum (between 10^{-6} and 10^{-8} mmHg) is required to minimize collisions between particles in the analyzer chamber. At this pressure, the mean free path of particles will be long enough, 50 m as opposed to <0.01 m at atmospheric pressure, and the number of collisions small enough for good analysis (6). Particle collision reduces instrument resolution and sensitivity by increasing kinetic energy distribution of the ions, inducing fragmentation or preventing ions from reaching the detector (24). The vacuum is created in two stages: a roughing pump, which drives the vacuum down to 10^{-3} mmHg then a diffusion or turbomolecular pump is used to obtain pressure as low as 10^{-9} mmHg. The roughing pump is usually a reciprocating mechanical pump lubricated with low vapor pressure oil to prevent contamination of the mass spectrometer (6). The diffusion pump uses an oil, often polyphenol ether, to force molecules out of the vacuum chamber. The oil is heated at the bottom of the pump causing it to vaporize, and water-cooled coils at the top of pump then allow the oil to cool and condense. Large oil molecules force the smaller molecules down into the pump via momentum exchange and smaller gaseous molecules exit through the mechanical pump, around 200 L/sec. The disadvantage is that diffusion pumps are selective as noble gases are pumped at reduced rates (25). Turbomolecular pumping is mechanical where molecules are forced into the fins of the turbomolecular pump by momentum exchange. Fins revolve at around 10,000 rpm and produce an effective pumping capacity of about 400 L/sec. Turbomolecular pumps are often preferred to diffusion types as they give a very low contamination by hydrocarbons and high vacuum is obtained very fast on start-up. However, turbomolecular pumps are noisy (this can be muffled to some degree) and highly mechanical, requiring regular servicing.

74.2.5.2 Sample Inlet. The most popular design is the capillary inlet where a small representative sample flows from the main sample gas stream which is continually venting, and "leaked" into the instrument, typically at 20 mL/min (26,27). The constant flow of gas stream from sample line to vent and to the leak of the analyzer means that line-flushing can be ignored. The capillary is heated at 80–120°C to preserve the vapor state of the sample. The rotary pump draws the sample by creating a pressure drop through the capillary. At the outlet, before the ionization chamber, the molecules cross a fritted glass or metal filter to further reduce pressure (16). The response times of such an inlet system can be around 0.5 s, achieved by low dead volumes and maintaining the whole system at 80°C (22). Volatile components in the gas stream can contaminate the stainless steel capillary by adsorption and desorption, causing larger response times and memory effects from long transition times through the capillary (18,27). These factors can be reduced by using a capillary (diameter 3 mm and length 1–3 cm) lined with borosilicate glass which is heated resistively through a stainless steel outer sheath to 150°C.

74.2.5.3 Ionization. Electron impact ionization is the most common technique where the gas passes into an electron beam, resulting in electron ejection and a degree of fragmentation (2). Electrons ejected from a heated tungsten filament are accelerated through an electric field at 70 V to form an electron beam. The vacuum system draws molecules through the sample leak into the ionization chamber. Neutral molecules pass freely through the negatively charged ion-repeller in front of the leak and are thermally desorbed into the electron beam, transferring kinetic energy to the sample molecule (M). The ionization (electron ejection) results in parent ions with the same mass-to-charge, to molecular weight (MW) with 6 eV of excess energy (Fig. 74.4). The excess energy in the molecule leads to some degree of fragmentation of molecular ions, fragment ions, and neutral fragments. A negative ionization step (electron capture) also occurs but is 100 times less efficient than electron ejection. Electron bombardment is most stable and reliable but is complicated by the excessive fragmentation. Hence, other soft ionization techniques have been developed which produce only a few fragments: fast atom or ion bombardment, matrix-assisted laser desorption or ionization, and electrospray ionization. These methods give greater sensitivity and mass range but have primarily been developed for analysis of large molecules and solids (24).

74.2.5.4 Ion Separation. Separation of the ions of mass m from the ions of m' is most commonly done by the magnetic analyzer or the quadrupole filter as they are compact and easy to operate (28). The magnetic analyzer uses a magnetic field to separate the different ions. A moving charge passing through a magnetic field will experience a force, and travel in a circular direction with the radius of

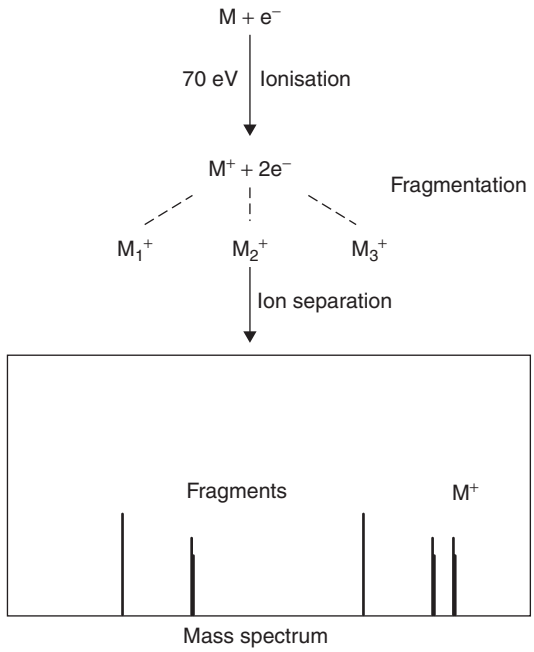


Figure 74.4. Ionization of molecules (M) producing fragment ions (M_1^+, M_2^+, and M_3^+).

curvature depending upon the mass charge ratio *m/z* of the ion. A magnetic analyzer separates ions according to their radii of curvature and therefore, only ions of given *m/z* will be able to reach a point detector in any given magnetic field (Fig. 74.5) (28). In a single detector system, an electromagnet is used to adjust the magnetic field to detect any *m/z* peak of interest (2). Alternatively, a multicollector system is set up, whereby each ion fragment is measured by a small number of Faraday bucket collector assemblies located along the focal plane according to which particular signals are of interest. Single detector systems are more common as they allow the combined use of the secondary electron multiplier (SEM) that is too large to be used in conjunction with multiple detector systems.

An alternative is the quadrupole filter that is a set of four cylindrical rods, typically 125–300 mm long and 6–16 mm in diameter, held in a square array to which an RF and DC potential are applied (25,29). Two rods are connected, and two are kept 180° out of phase (Fig. 74.6). This forms crossed, oscillating electric fields, perpendicular to the line of travel of the ions between the source and the detector. If the oscillating motion of the ion is out of resonance, the ions strike the walls and are not detected. Application a certain voltage and RF can control the trajectory of a known mass-to-charge ratio to selectively strike the detector (28). Scanning RF and DC voltages from zero, allows ions to be transmitted through the quad-filter sequentially, in order of their *m/z* values with constant resolution allowing multiple ion analysis. Resolution attained is determined by the accuracy of control of the parameters U (amplifier output amplitude), f (output frequency), V (amplifier voltage output) and α radius within the quad-rods (28).

Quadrupole systems are known to be faster, less expensive, and smaller than magnetic sector instruments. Yet, the resolution is lower, easily contaminated, and less stable over time, making the magnetic sector a superior choice for industrial on-line monitoring (18,28). The response times of both systems are comparable as the magnetic hysteresis associated with magnetic sectors has been eliminated using laminated magnets. The precision from magnetic sectors comes from the flat-topped peak profiles of ion current versus the magnetic field strength that they exhibit (Fig. 74.5). Thus peak center and peak height can be precisely determined. Any minor drifting that may occur due to temperature fluctuations has no effect. This results in high stability, accurate peak jumping, and long periods between recalibration (up to several weeks for fermentation applications). Absolute accuracy is <0.05% for O_2, <0.1% for N_2. Quadrupole filters exhibit a Gaussian-type peak profile and are more susceptible to drift (Fig. 74.6) and temperature variation; reduced accuracy and precision results in more frequent calibration. Insufficient resolution leads to an 'abundance sensitivity' problem whereby at low concentrations, peak discrimination is difficult with adjacent peaks. Comparisons between the quadrupoles and magnetic sectors have shown the improved accuracy and drift by a factor of 2 for magnetic sectors over the quadrupole systems (27,30). Although a considerable amount of useful applications for fermentation vent gas analysis have been demonstrated using quadrupole systems (31,32), the experience at Merck & Co. Inc. over the last three decades, favors magnetic sectors as opposed to quadrupoles. Suitable magnetic sector instruments for process monitoring are manufactured by Thermo Fisher Scientific (Prima δb) and by Applied Instruments (Hamilton Sundstrand, MGA series).

74.2.5.5 Detectors. The Faraday cup is a common detector used for mass spectrometry, where the ions pass the beam-defining slit of the cup and strike a metal dynode plate of a secondary emitting material such as BeO, GaP or CsSb. This induces several secondary electrons to be ejected and temporarily displaced. This temporary emission of electrons induces a current in the cup and provides for a small amplification of signal when an ion strikes the cup (24). The signal is measured by an electrometer and is directly proportional to the ion concentration. For the single collector system, with single amplifier and auto-gain switching, high precision can be maintained over the widest range. In this arrangement, any such drift is equal for all components and can therefore be compensated for by using any internal standard (2).

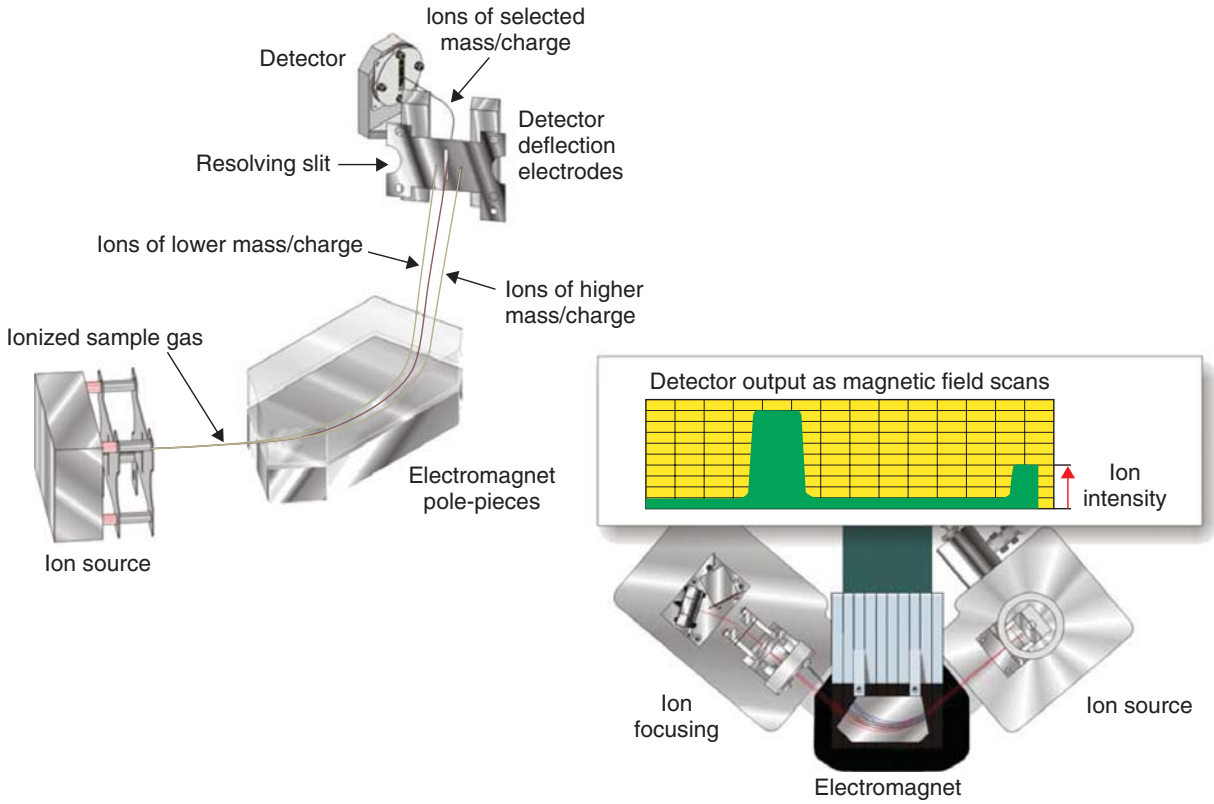


Figure 74.5. Magnetic sector mass spectrometer showing ion trajectory through magnetic field and the flat-top type of profile of the ion current versus magnetic field strength. [Thermo Fisher Scientific.]. (This figure is available in full color at http://onlinelibrary.wiley.com/book/10.1002/9780470054581.)

A second detector is the SEM, which is a series of dynodes (around 10) maintained at ever-increasing potentials. Ions strike the dynode surface, resulting in emission of secondary electrons which are attracted to the next dynode where again, secondary electrons are generated. This produces a cascade of electrons transferring from plate to plate, in a cycloidal flow path between two glass plates. The signal amplification or current gain of an electron multiplier is 10^6 with a lifetime of 1 to 2 yr. This is limited due to surface contamination from incident ions or poor vacuum (18). The Faraday cup is considered rugged, reliable, and is typically capable of measurements down to 1–10 ppm concentration levels (23). However, the SEM detector offers greater sensitivity (sub-ppm) with a faster response but has poorer long-term stability and is generally less accurate (2). SEM can be sensitive to repeated air exposure, background noise increases when the gain decreases, and is far less rugged than the Faraday cup (16). In a single collector arrangement with either a magnetic sector or quad, it is common to have remotely switchable Faraday cup and SEM assemblies. The appropriate detector is selected by the software, allowing all species to be monitored from 100% to ppm (25). For example, a Faraday cup is used for air components and a secondary system for volatiles such as ethanol, acetone or butanediol (22).

74.2.5.6 Spectral Analysis. To calculate the individual component concentrations c_1, c_2 ... c_n of a mixture of ion-fragment intensities with n components, requires a series of linear equations to be solved. The ion current signal, S_1, for each mass/charge is considered to be the sum of the contributions of all components, which are proportional to the concentration of each component:

$$s_1 = c_1 m_{11} + c_2 m_{12} + \cdots + c_q m_{1q}$$

$$\cdots$$

$$\cdots$$

$$\cdots$$

$$s_p = c_1 m_{p1} + c_2 m_{p2} + \ldots + c_q m_{pq}$$

or

$$\vec{s} = \mathbf{M}\,\vec{c}$$

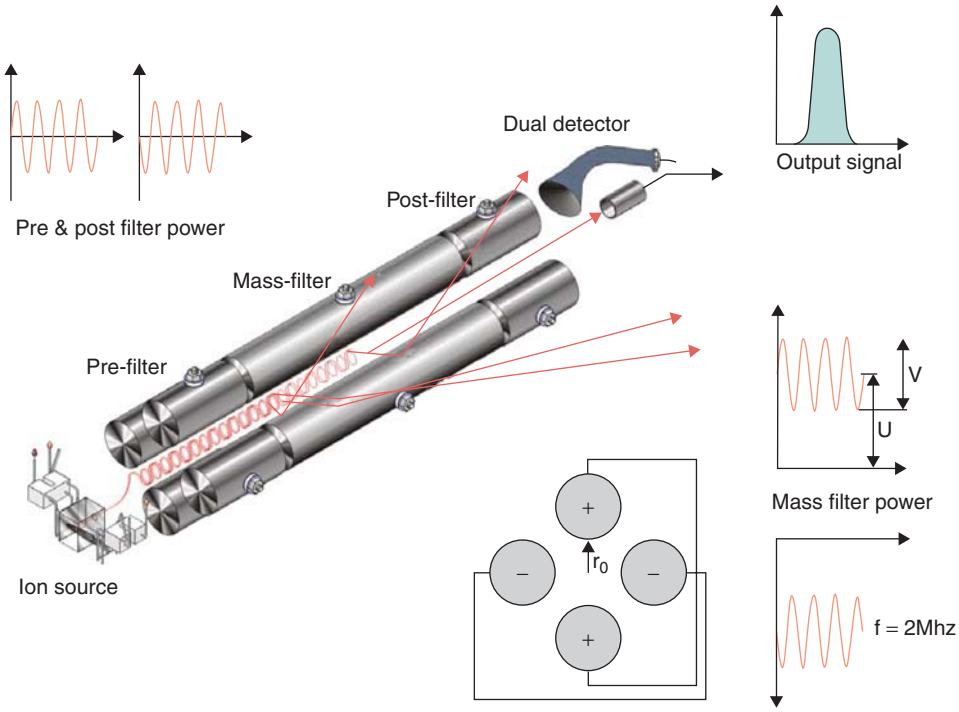


Figure 74.6. Magnetic sector mass spectrometer showing ion trajectory through magnetic field and the flat-top type of profile of the ion current versus magnetic field strength. [Thermo Fisher Scientific.]. (This figure is available in full color at http://onlinelibrary.wiley.com/book/10.1002/9780470054581.)

where s is the signal, **M** is the fragmentation pattern or sensitivity factor matrix determined by calibration with individual pure components, and c is the desired concentration (23).

Most species produce several peaks due to fragmentation or double ionization. For instance, nitrogen has peaks at nominal m/z values 28, 14, 29, and 15. So a set of linear equations is over-determined and solved using an iterative route of multidimensional least squares technique (33). The best fit is then made between the observed spectrum and that which can be synthesized following small adjustments of the species concentration. These adjustments use the known fragmentation patterns of various species. Therefore, all of the mass spectral information is made available by the single detector instrument which is most effectively used in achieving the concentration analysis.

74.3 INSTALLATION AND OPERATION

The design of a sampling system for vent gas analysis requires careful consideration and usually involves the multiplexing of one analyzer to a variety of fermenters. A sample handling system incorporates gas transport from the fermenter, followed by pretreatment, before passing through the multipoint sampling manifold into the analyzer. The design of such a system must minimize the response time of sample analysis. Most applications require removal of moisture and contaminating species from the vent gas which involves steps such as filtering and heating, before the analyzer. The materials of construction for transport lines, line purging, sample flow rate, and minimizing tubing lengths must all be considered.

74.3.1 Fermenter Sampling Location

If fermenter overpressure is to be used for gas transport to the mass spectrometer, then it is pertinent to have the sample port between the head plate and the back pressure control valve. The vent line of fermenters often contain a condenser, double piped steam heater or vent filters which are steam-dried from a jacket. These techniques can remove volatile compounds from the exhaust gas, so the sampling point should be upstream of these devices if organic volatile analysis is desired. Moisture must be removed before the analyzer, so sampling after the condenser may be advantageous. Foaming and liquid entrainment can occur into the vent line. Entrainment into the sampling system can be prevented to some extent by facing the sample port downstream of the gas flow (33). Gas has to make a 180° turn to the sample port while tending to exclude liquid, as its inertia prevents it from turning. Foam detection systems can

also prevent sample-line contamination. The foam sensor using capacitance or conductivity between two elements, usually probe and tank wall or two elements in the probe, can be mounted on the fermenter headplate. This can be part of an automatic defoamer addition system upon foam detection. A second probe can be mounted in the vent gas line to close off the gas sample valve upon foam detection.

74.3.2 Sample Delivery and Pretreatment

The fermenter headplate, over pressure, is often used to transport gas to the analyzer. However for laboratory-scale vessels, a gas membrane or piston pump may be required. A 0.1 bar pressure is sufficient for a 100-m length of standard 6-mm nylon tubing (or 1/4-inch tubing) (23). The tube can be stainless steel, nylon or preferably, polytetrafluoroethylene (PTFE) for volatile samples. The tubing is heated to between 60 to 160 °C to ensure compounds remain in the vapor phase, which avoids their removal via condensation. This can be done electrically, by steam or by jacketed hot water (29). For volatile analysis, the tube is heated to around 150°C and the use of Teflon is essential for fast response times (34). Adsorption or desorption effects of volatile components with the stainless steel tubing walls can hinder response times (>5 min) and cause memory effects.

The vent gas is often passed through a (0.2 μm) hydrophobic filter (PTFE) as a final particulate protector before the analyzer. For unheated lines, moisture removal occurs by condensation. Knockout pots are used in combination with a coalescing filter whereby large drops form and settle by gravity (33). A graded porosity hydrophilic matrix is used with a drain layer to direct coalescing liquids into a sump at the base of the housing. Automatic draining of the pot is ideal via solenoid actuation, periodically or upon liquid detection. If further moisture removal is required, various technologies are available including small concentric tube or coil in shell-heat exchangers with refrigerated coolant. Other systems include the Peltier effect cylindrical gas cooler with a sealed tube containing a pure fluid. A wick lines the inner walls, which ensures the fluid return by capillary action. One end of the tube is heated, liquid evaporates and the gas flow displaces the steam toward the end of the tube. The steam expands and condenses back to the heated end (16). Desiccants such as anhydrous calcium chloride, alumina or silica gel can be used for further sample drying but this is rarely necessary.

74.3.3 Sample Handling Manifolds

A single mass spectrometer for vent gas analysis is usually applied to an array of fermenters (>10). This requires a fast, cross-contamination and leak-free manifold system to automatically switch between fermenter samples and calibration gases. A typical system has the sampling streams from all tanks under permanent flow in order to guarantee instant sampling availability and avoiding line purging (Fig. 74.7). Three-way valves can eliminate dead legs and two valves per sample stream allow gas to flow to the drain, rather than contaminate other streams if both valves fail. Solenoid valves are often used as they are inexpensive and

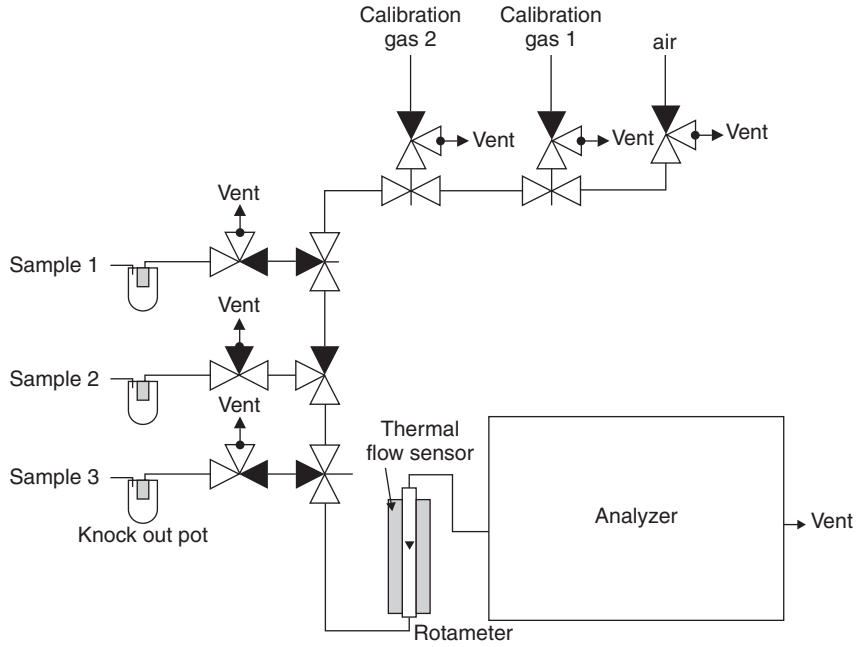


Figure 74.7. Multistream sample switching system. (Solid segments indicate valve's closed position).

compact compared to air-actuated ball valves. Rotameters can be used to verify flow at the vent side of the three-way valve. The manifold is mounted in a cabinet with heat control, to a temperature above the process temperature or to the 110°C required for organic volatiles. Multistream rotary valves have been designed using an actuated electric stepper motor for cross-contamination sampling (23,27). The RMS (rapid multistream sampler) unit designed by Thermo Fisher Scientific, can be configured for 32 or 64 sample streams connected to the periphery of a circular, flat, distribution plate which vents into a cylindrical housing with a common exhaust (Fig. 74.8 and 74.9). The electric stepper motor drives the rotary arm to position at a sample stream and the sample flows directly into the sample transfer tube. Cross-contamination of other gases is inhibited by a spring-loaded face-sealing sleeve (2). A single analyzer can hold two RMS units to enable analysis of a total of 127 streams. The response time of the manifold system can be reduced by minimizing tubing lengths. The time required to flush the lines should be 4 times the gas residence time (2). This is estimated using plug flow, but experimental measurements are preferred because of back-mixing through valves and regulators.

74.3.4 Sample Flow Control and System Monitoring

Sample pressure will directly influence vent gas analysis as the signal from a gas analyzer is proportional to volumetric concentration of the component of interest. This can be remedied by measuring internal standards (typically N_2, or Ar), then the concentration for all other components, followed by completion of a mole fraction. Alternatively, the pressure can be measured and the data corrected using the ideal gas law or by controlling the pressure at the fixed value (33). Pressure control can be overcome by simply venting the instrument outlet to the atmosphere. An upstream needle valve can be used to reduce the pressure and control sample flow rate through the instrument. Locating the valve as far upstream as possible reduces the lag time, as the gas velocity is increased after the pressure reduction. However, this leaves a 2–3% variation due to atmospheric pressure. If this is unacceptable error, then an absolute back-pressure regulator must be employed on the outlet (33). Temperature is controlled within the analyzer but it is useful to control temperature of the manifold cabinet by an electric heater. A temperature greater than 60°C will prevent condensation unless moisture has been removed, and minimize adsorption of compounds. Water can be detected in a manifold system by a U-shaped liquid trap with a sensor to detect water in the sample lines. The low electrical conductivity of water in the sample means that the sensor must monitor either the dielectric constant or the refractive index of the stream, or even the thermal dissipation from a self-heated thermistor or electric coil. The sample flow rate (greater than 1 mL/s) can be controlled by a simple needle valve and rotameter. The thermal sensor and autocontrol valve will ensure sample flow rate is adequate and stable. Leak testing is done by pressuring the system from instrument air and closing the valves.

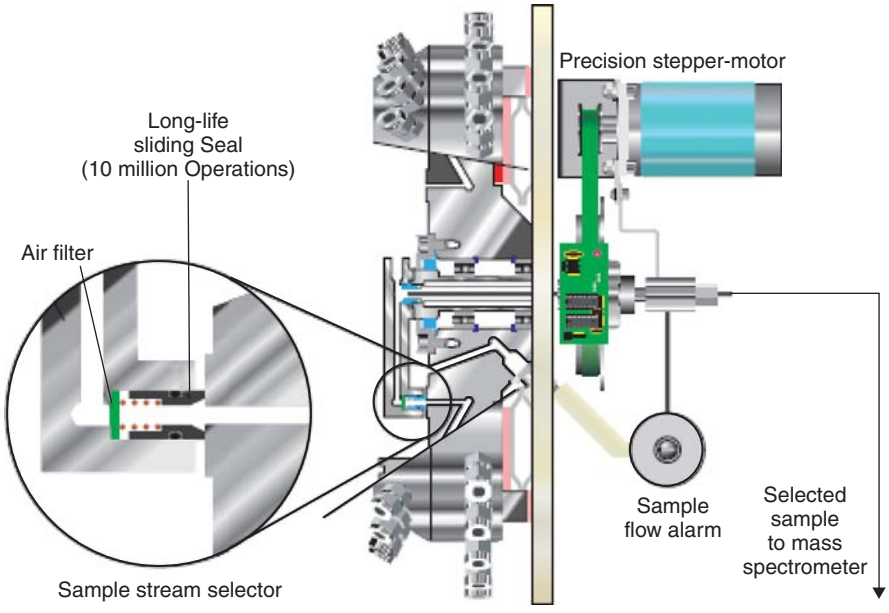


Figure 74.8. Rapid multistream sampler: rotary sampling system. by Thermo Fischer Scientific. (This figure is available in full color at http://onlinelibrary.wiley.com/book/10.1002/9780470054581.)



Figure 74.9. Magnetic sector mass spectrometer unit from Thermo Fischer Scientific fitted with the rotary motor sample device. (This figure is available in full color at http://onlinelibrary.wiley.com/book/10.1002/9780470054581.)

Alternatively, the pressure can be monitored while the sample system is evacuated if this step is part of the sampling sequence. Diagnostic packages are supplied with most analyzers, which will sound an alarm for problems associated with the capillary, filament, vacuum, and power supply.

74.3.5 Process Measurements Required for Variable Calculation and Data Acquisition

To calculate useful fermentation variables such as oxygen uptake rate (OUR), carbon evolution rate (CER), and RQ measurements of pressure, volume, airflow, and dissolved oxygen are required. Broth volume can be determined by load cell or differential pressure transducers. Airflow rate can be measured by a mass flow meter and dissolved oxygen concentration by polarographic probe whose response should be checked systematically by varying the headspace pressure or degassing with N_2. Strain gauge, piezoresistive, capacitance or resonant wire transducers can be used for pressure measurements. For a number of fermenters connected to a multistream manifold, such as an RMS, fast turnover of samples is required although accurate measurements must be made. Therefore data acquisition must occur after a suitable line purge time. Multiple measurements can subsequently be made and filtered or smoothed to reduce noise (2). A typical approach is to use an algorithm to produce a stable reading (33). A linear exponential filter is used where each successive measured value c_t is used to update a smoothed estimate as $\hat{c}_t = \kappa c_t + (1-\kappa)\hat{c}_{t-1}$ where k is a filtering parameter. The trend in the smoothed data is estimated as $\hat{S}_t = \lambda(\hat{c}_t - \hat{c}_{t-1}) + (1-\lambda)\hat{S}_{t-1}$, where λ is another parameter. A typical algorithm acquires at least $1/\kappa$ values and continues until the absolute value of the trend $\hat{S}_t$ is less than a target tolerance δ, indicating that a stable result has been obtained. The values of κ, λ, and δ depend on the rate of data acquisition and on instrument performance (33). Vent gas analysis processes gases on a dry gas basis, whereas the actual gases from the fermenter are saturated with water vapor. Standard handbooks can be used to correct this data (35). Most vent gas analysis is expressed as a mole fraction. If this is not the case, then data should be adjusted using the ideal gas law, to standard conditions of temperature and pressure, to allow mass balances to be performed. Good precision is achieved if signals are noise-free with no drift. However, the combination of vent gas data with on-line data such as airflow rate and dissolved oxygen for mass balancing introduces noise. These errors of measurement can dramatically enlarge errors in the data. Low pass filters can be used to smooth the data and many acquisition systems have built-in analog filters used for this purpose.

74.4 PARAMETER CALCULATION

The microbial physiology of a fermentation can be characterized using the consumption rates and metabolic factors which require equation balances for the gas and liquid phases. The following balance equations (Eqs 74.1 and 74.2) for species 'i' in the gas and liquid phases, are written assuming well-mixed phases in the fermenter. This assumes that concentrations are uniform throughout the liquid phase, and that mole fractions are uniform throughout the gas phase. The assumption is accepted for small-scale stirred reactors but is less valid at large scales >100 L. Axial volumetric concentration gradients of species in the gas phase, as a consequence of the hydrostatic pressure gradient, have been observed at a large scale. This leads to alternatives for large-scale vessels; these are discussed in the next section. For low pressure and dilute concentrations of interest, the ideal gas law and the simplest form of Henry's law (relating equilibrium gas- and liquid-phase concentrations through a simple proportionality constant) can be used. The equations have been given by Heinzle and Dunn (1991) (2), and modified by Salmon and Buckland (33). It is assumed that the

fermenter is isothermal and has a uniform cross-sectional area.

$$\frac{dV_G C_{G_{e,i}}}{dt} = G_o C_{G_{o,i}} - G_e C_{G_{e,i}} - k_{L_i} a V_L (C^*_{L_{e,i}} - C_{L_{e,i}}) \quad (74.1)$$

$$\frac{dV_L C_{L_{e,i}}}{dt} = L_o C_{L_{o,i}} - L_e C_{L_{e,i}} + k_{L_i} a\ V_L (C^*_{L_{e,i}} - C_{L_{e,i}}) - V_L \sum r_i \quad (74.2)$$

where $C_{G_{o,i}}$, $C_{G_{e,i}}$, $C_{L_{o,i}}$, and $C_{L_{e,i}}$ are the gas and liquid phase concentrations, subscripts o and e refer to the influent and effluent, and subscripts G and L refer to the gas and liquid phases. V_G and V_L are the gas- and liquid-phase volumes, G_o, G_e, L_o, and L_e are the influent and effluent gas and liquid flow rates, $k_{L_i}a$ is a mass-transfer coefficient, $C^*_{L_{e,i}}$ is the liquid-phase concentration that would be in equilibrium with $C_{G_{e,i}}$, and $\sum r_i$ is the total consumption rate of species i in the liquid phase. Standard conditions of pressure and temperature (typically $P_{ref} = 1$ atmosphere, $T_{ref} = 25^\circ C$) have been used for gas-phase concentrations, volumes, and flow rates.

An expression can be written for $C^*_{L_{e,i}}$, liquid-phase concentration, using Henry's law and integrating over the fermentation broth volume (33):

$$C^*_{L_{e,i}} = (RT_{ref}/H_i P_{ref})(P_h + V_L \rho_L g/2A) C_{G_{e,i}} \quad (74.3)$$

where H_i is the Henry coefficient, P_h is the headspace pressure, ρ_L is the liquid-phase density, and A is the cross-sectional area of the fermenter. It is usual to assume that the liquid-phase supply, removal, and accumulation terms in Equation 74.1 are negligible for gases such as oxygen which have low aqueous solubility. The gas-phase accumulation term in Equation 74.1 is also ignored as gas holdup is small and changes in oxygen utilization occur slowly. However, this simplification may not be valid for rapidly growing cultures (36) or when sudden metabolic changes occur (36), in which case the calculated results will lag behind actual events in the fermenter. Using the discussed assumptions, Equations 74.1 and 2 can be added and rearranged to obtain an expression for $OUR = r_{O_2}$, the net oxygen utilization rate:

$$OUR = G_o \left(C_{G_{o,O_2}} - G_e/G_o C_{G_{e,O_2}} \right) / V_L \quad (74.4)$$

An expression for the mass-transfer coefficient, in a dimensionless form, can also be derived from Equation 74.1.

$$\alpha_{O_2} = \frac{k_{L_{O_2}} a V_L}{G_o} = \frac{C_{G_{o,O_2}} - G_e/G_o\ C_{G_{e,O_2}}}{\beta_{O_2}(1+\gamma/2) C_{G_{e,O_2}} - C_{L_{e,O_2}}} \quad (74.5)$$

where $\beta_{O_2} = RT_{ref} P_h / H_{O_2} P_{ref}$, and $\gamma = V_L \rho_L g / A P_h$. Values of the Henry coefficient, H_{O_2}, can be obtained from the literature (37). The aqueous oxygen concentration $C_{L_{e,O_2}}$, found in Equation 74.5, can be measured on-line using a polarographic probe calibrated to read $\beta_{O_2}(1+\gamma/2) C_{G_{o,O_2}}$ before inoculation. The constant, 1, assumes that the difference of oxygen solubility in the fermentation medium is negligible when compared to water. This assumption is reasonable as the constant can be estimated for most fermentation broths (37,38) and a value of 0.945 is achieved for a typical broth containing, salts, yeast extract, and glucose.

Inert gas species (such as Ar or N_2) are monitored to compensate for gas-flow changes due to the presence of moisture and volatiles in the exhaust gas. The net utilization for the inert gas is zero and consequently $G_e/G_o = C_{G_{o,inert}}/C_{G_{e,inert}}$ by using the simplifications for oxygen.

For carbon dioxide, the situation is more complex as its high solubility (H_{CO_2} of 34 L bar/mol compared to H_{O_2} of 856.9 L bar/mol) means that the liquid-phase accumulation cannot be ignored. Also carbon dioxide reacts with water to give to biocarbonate at pH >6.5.

$$CO_2 + H_2O \underset{k_b}{\overset{k_f}{\rightleftarrows}} H_2CO_3 \overset{K_a}{\longleftrightarrow} H^+ + HCO_3^- \longleftrightarrow 2H^+ + CO_3^{2-} \quad (74.6)$$

The hydration of CO_2 to $H_2CO_3^-$ has a slow rate constant, however its concentration is low (<0.3% of CO_2 present) (39) as it is almost instantaneously dissociated to HCO_3^-. At the pH range of 4–8 for fermentation processes, the concentration of carbonate ions is negligible; complexing of CO_2 with amine groups can be ignored and the reaction of dissolved CO_2 with OH^- is negligible (40). Bicarbonate accumulations increase with pH and at pH 6.3, the concentration can be equal to the dissolved CO_2. Thus the basic liquid phase Equation 74.2 must be modified to include accumulation of bicarbonate:

$$\frac{dV_L C_{L_{e,CO_2}}}{dt} = L_o C_{L_{o,CO_2}} - L_e C_{L_{e,CO_2}} + k_{L_{CO_2}} a V_L (C^*_{L_{e,CO_2}} - C_{L_{e,CO_2}}) + V_L \left(CER - r_{HCO_3^-} \right) \quad (74.7)$$

$$\frac{dV_L C_{L_{e,HCO_3^-}}}{dt} = L_o C_{L_{o,HCO_3^-}} - L_e C_{L_{e,HCO_3^-}} + V_L r_{HCO_3^-} \quad (74.8)$$

where $CER = -r_{CO_2}$ is the net carbon dioxide evolution rate from the biomass, and $r_{HCO_3^-}$ is the net rate of bicarbonate formation given by:

$$r_{HCO_3^-} = k_f C_{L_{e,CO_2}} - k_b / K_a C_{L_{e,H^+}} C_{L_{e,HCO_3^-}}. \quad (74.9)$$

Values for the constants k_f, k_b, and K_a can be obtained from the literature (41). Rearrangement of Equation74.1, gas-phase balance, and neglecting accumulation terms as before, can produce this balance:

$$k_{L_{CO_2}} a V_L (C^*_{L_{e,CO_2}} - C_{L_{e,CO_2}}) = G_o C_{G_{o,CO_2}} - G_e C_{G_{e,CO_2}}. \quad (74.10)$$

and solved for the liquid-phase CO_2 concentration,

$$C_{L_{e,CO_2}} = \left\{ \frac{1}{\alpha_{CO_2}} \frac{G_e}{G_o} + \beta_{CO_2}(1 + \gamma/2) \right\} C_{G_{e,CO_2}} - \frac{1}{\alpha_{CO_2}} C_{G_{o,CO_2}} \quad (74.11)$$

where $\alpha_{CO_2} = k_{L_{CO_2}} a V_L / G_o$, and $\beta_{CO_2} = RT_{ref} P_h / H_{CO_2} P_{ref}$. Henry coefficient H_{CO_2} estimates are found from the literature (38). Combining Equations 74.7, 74.8, and 74.10, rearrangement gives:

$$CER = \frac{1}{V_L} \left\{ \begin{array}{c} \dfrac{dV_L \left(C_{L_{e,CO_2}} + C_{L_{e,HCO_3^-}} \right)}{dt} \\ - L_o \left(C_{L_{o,CO_2}} + C_{L_{o,HCO_3^-}} \right) + L_e \left(C_{L_{e,CO_2}} + C_{L_{e,HCO_3^-}} \right) \\ -G_o \left(C_{G_{o,CO_2}} - G_e / G_o C_{G_{e,CO_2}} \right) \end{array} \right\}. \quad (74.12)$$

The evaluation of $C_{L_{e,HCO_3^-}}$ can be considered in three algorithms of complexity (32). Equations 74.8 and 74.12 can be solved progressively as the fermentation proceeds, using current and past data. This enables monitoring of CO_2 evolution under dynamic conditions, as long as the rate of data acquisition by the analyzer is sufficiently rapid. This may be a problem when acid is introduced intermittently for pH control because after each addition, the CO_2 concentration in the vent gas will increase for a short period (42). A second approach can be applied if the time constant for process changes is greater than 5 min. In this case, the hydration reaction can be assumed to be at equilibrium, yielding $C_{L_{e,HCO_3^-}} \approx (k_f/k_b) K_a 10^{pH} C_{L_{e,CO_2}}$. Substituting this expression into Equation 74.12 allows the value of *CER* to be calculated directly if the rate of change of the dissolved CO_2 concentration is estimated using current and past data (32). Lastly, it is common practice to ignore the transient terms as long as changes of pH and CER are slow. Heinzle *et al*. (1990) demonstrated that including dynamic changes of CO_2 and HCO_3^- into a simulation only produced relative errors of $<2\%$ in the CER.

74.4.1 Large-Scale Mixing Models

Upon scale-up to manufacturing (100 to 10,000 L), axial gradients and large mixing time are observed and so previous equations for oxygen transfer rate, OTR and OUR based on the well-mixed system may not be valid. Hydrostatic pressure gradients in tall fermenters will cause large differences in oxygen solubility C_L from liquid surface to tank bottom. The dissolved oxygen concentration in a stirred tank can vary linearly from 5.4 mg/L at surface to 12.1 mg/L at a depth of 10 m. At the bottom of the tank, the oxygen solubility for a given gas composition is twice, as a consequence of the doubled hydrostatic pressure as shown by Henry's law. This will double the maximum OTR and hence, dissolved oxygen concentrations, oxygen solubilities, gas holdup, and transfer parameters may vary with depth in tall reactors. There is limited experimental data available for concentration heterogeneity within large fermenters, but radial and axial gradients of pH, conductivity and dissolved oxygen have been observed (43–45). Residence-time distribution data using liquid and gas transfers have characterized the mixing to produce a variety of models (46–51). Various models have been determined for large-scale mixing where axial back-mixing has been described by dispersion theory or a tank in series with recirculation based on the measurement of residence time distribution. Other research groups compartmentalize the reactor into distinct zones, such as a well mixed zone at the impeller and a second zone for the remainder of the reactor. The pumping power of the impellers (43,50) dictates the transport between the two compartments. The model behavior is described through simulations of the coupled material balance equations for OTR, mixing, and kinetics. The importance of back-mixing and hydrostatic pressure upon scale-up was demonstrated by using a three-phase multimixed compartment model (48). The flow conditions of these models fall between extremes of well-mixed and plug flow. Simplification for large-scale reactors involves assuming that the liquid phase is well-mixed but that the gas-phase moves in plug flow (no back-mixing) from inlet to outlet (52). The gas-phase concentration of species '*i*' was described by Salmon and Buckland (33) using the equation given below:

$$\frac{dC_{G_i}}{dx} - \alpha_i \left\{ \beta_i \left[1 + \gamma(1 - x) \right] C_{G_i} - C_{L_{e,i}} \right\} = 0 \quad (74.13)$$

where α_i, β_i, and γ are defined in the previous section. For the gas-phase concentration of species i: a closed-form solution to this equation was used to calculate $C_{G_{e,i}} = C_{G_i}(1)$ from the inlet condition of $C_{G_i}(0) = C_{G_{o,i}}$. Salmon and Buckland (33) used this solution to produce a comparison between the estimates of equilibrium between liquid and gas phases at two scales, 0.15 and 60 m^3 (where differences are solely due to hydrostatic pressure), and between

the two models of well-mixed phases and a gas phase with plug flow. For a given mass transfer coefficient, the predicted liquid-phase concentrations were closer to equilibrium with the effluent gas for the plug-flow model than with the well-mixed system. This difference was accentuated with the large-scale tank (where hydrostatic pressure is significant). This seems reasonable as the mass-transfer coefficient required to achieve a desired liquid-phase concentration is lower for a production vessel than for a small, laboratory fermenter. So for a given mass-transfer coefficient, the gas-phase and liquid-phase concentrations in a large vessel will be closer to equilibrium than those in a small vessel. This agrees with the observation that the dissolved carbon dioxide in a large tank can be calculated by presuming equilibrium with the vent gas, whereas this assumption is not appropriate for small fermenters.

74.4.2 Aqueous Concentration Estimation for Volatile Organic Compounds

Assuming a well-mixed system, then the liquid-phase concentration for an organic species can be calculated as for $C_{L_{e,CO_2}}$(Eq. 74.11) (35):

$$C_{L_{e,i}} = \beta_i \left\{ \frac{1}{\alpha_i \beta_i} \frac{G_e}{G_o} + (1 + \gamma/2) \right\} C_{G_{e,i}}. \qquad (74.14)$$

As $\alpha_i \beta_i \rightarrow 8$, the liquid-phase concentration approaches $\beta_i(1 + \gamma/2)\ C_{G_{e,i}}$, which is the concentration in equilibrium with the gas phase at the average fermenter pressure. Equilibrium constants can be attained for any volatile compound under most conditions (22), as most compounds have a high affinity for the liquid phase and a low Henry's coefficient (ethanol 10^{-2} bar/L/mol) compared to gas. Camelbeeck *et al*. (30) have experimentally confirmed this conclusion by demonstrating that changes in the rates of agitation and aeration have no influence on the vent gas measurements. The ability to monitor a specific organic compound depends on concentration, volatility, and analyzer sensitivity. Oeggerli and Heinzle (22) compared partial pressures above an aqueous solution at a concentration of 0.1 g/L at 30°C. Compounds were considered analyzable if the partial pressure was above 1 μbar hence, ethanol at 22.24 μbar and acetone at 181 μbar could be monitored (oxygen was $> 10^6$ μbar). However 2,3-mesobutanediol was considered undetectable as the partial pressure was 0.0174 μbar, and its limit of detection was found to be 5 g/L with a quadrupole mass spectrometer. Calibration is usually by adding a known amount of compound to the fermenter before inoculation, and measuring concentrations off-line from liquid samples by HPLC (high performance liquid chromatography) or GC. Most volatiles require an SEM for accurate detection as volatiles are in the ppm level in the headspace (22,27).

74.4.3 Growth Kinetics

The yield of biomass from oxygen consumed Y_{x/O_2}, from carbon dioxide evolution, Y_{x/CO_2} and the specific growth rate (51,52) can be simply determined using vent gas analysis:

$$Y_{x/O_2} = \frac{d(TOC)/dt}{dx/dt} \qquad (74.15)$$

$$X = Y_{x/O_2}(TOC) \qquad (74.16)$$

where *TOC* is the total oxygen consumed estimated from the summation of the *OUR* versus time, *X* the biomass concentration from oxygen. Linear regression from a curve of biomass concentration (determined off-line) versus *TOC* and total carbon dioxide evolution (TCE) can then lead to the respective yield factors for biomass from oxygen and carbon dioxide. The specific growth rate can be determined by:

$$\mu = \frac{d(TOC)/dt}{TOC} = \frac{OUR}{TOC} \qquad (74.17)$$

where the Y_{x/O_2} is assumed to be constant. Good agreement can be made between specific growth rates as calculated on line using *TOC* data and off line data from experimental dry cell weight (53). This provides a useful on-line tool for analyzing growth rate during process and development. The control of specific growth is important for the synthesis of secondary metabolites such as avermectin by *Streptomyces avermitilis* (53) (Fig. 74.10). The impact of a decrease of temperature by a few degrees at 12 h into the fermentation clearly showed a dramatic decrease in specific growth rate when compared to the control, as measured by the on-line method.

74.4.4 Mass Balancing and RQ

Vent gas analysis can be used to describe the substrate utilization and production kinetics of a fermentation via mass balancing (2,33). A typical fermentation could involve:

$$CH_{h_S}N_{n_S}O_{o_S} + aNH_3 + bO_2 \rightarrow Y_{X/S}CH_{h_X}N_{n_X}O_{o_X} + Y_{P/S}CH_{h_P}N_{n_P}O_{o_P} + cCO_2 + dH_2O$$

where biomass $CH_{h_X}N_{n_X}O_{o_X}$ and product $CH_{h_P}N_{n_P}O_{o_P}$ are formed from substrate $CH_{h_S}N_{n_S}O_{o_S}$. The coefficients a, b, c, and d can be solved from elemental balances for carbon, hydrogen, nitrogen, and oxygen. Coefficients for oxygen and carbon dioxide are $b = (\gamma_s' - Y_{X/S}\,\gamma_x' - Y_{P/S}\,\gamma_p')/4$ and $c = 1 - Y_{X/S} - Y_{P/S}$, where $\gamma_i' = 4 + h_i - 3n_i - 2o_i$ is the so-called generalized degree of reduction for compound $CH_{h_i}N_{n_i}O_{o_i}$. The value of γ for biomass is consistently about 4.2, and the values for some common

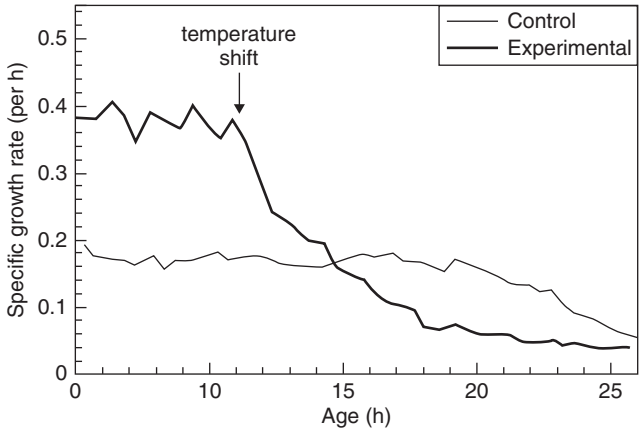


Figure 74.10. Impact of temperature shift on estimated specific growth rate (on-line) of *Streptomyces avermitilis* at 800 L (52).

substrates and products can be found in the literature (8). An expression can then derived for the RQ, the ratio between the rates of CO_2 evolution and oxygen utilization, as $\mathrm{RQ} = 4(1 - Y_{X/S} - Y_{P/S})/(\gamma'_s - Y_{X/S}\,\gamma'_x - Y_{P/S}\,\gamma'_p)$. Thus for a given fermentation the RQ, defined from vent gas analysis, CER/OUR, can be used along with off-line analysis of biomass, carbon, nitrogen, and production concentrations to define the yield coefficients for substrate and product (31). It is recommended that elemental balancing use high precision gas analysis with 0.01% accuracy, because a 1% error relative offset calibration error for oxygen can result in an error for product estimation of >50% (2).

Vent gas analysis is a valuable tool for studying process kinetics and metabolism. For recombinant protein expression it is common to limit feed rates to control the growth, preventing formation of overflow metabolites such as acetate, which are often inhibitory to growth and protein expression. During a yeast fermentation the OUR, CER and RQ can be seen responding to adjustments of the nutrient feed rate (Fig. 74.11). The rapid growth rate on the initial nutrient charge (batch phase) is seen on the off gas profiles. When the initial charge is depleted and after a transition phase, a nutrient feed is started. The rapid response to the feed rate adjustments is easily observed by the vent gas profile. The change in RQ indicates the switch to a different carbon source. After the adjustments, the second feed rate is increased exponentially and finally, kept at a constant rate to control the growth of the culture.

The scale-up of fermentations requires a good understanding of the impact of the chemical and physical environment on cell physiology. This is often hindered when little is known about the new organisms. For instance, the production of pneumocandin B_0 from the filamentous fungus *Glarea lozoyensis* was impacted by a range of unwanted pneumocandin analogs (54). Dissolved oxygen was suspected to affect the levels of these unwanted analogs but it is historically difficult to separate this from the effects of operating conditions such as agitation, or a changing microbial morphology. Gas blending experiments were designed to separate the effects of dissolved oxygen from agitation (55). Vent gas analysis was a key element of this experimental gas-blending design. In separate reactors, ranges of dissolved oxygen levels were controlled

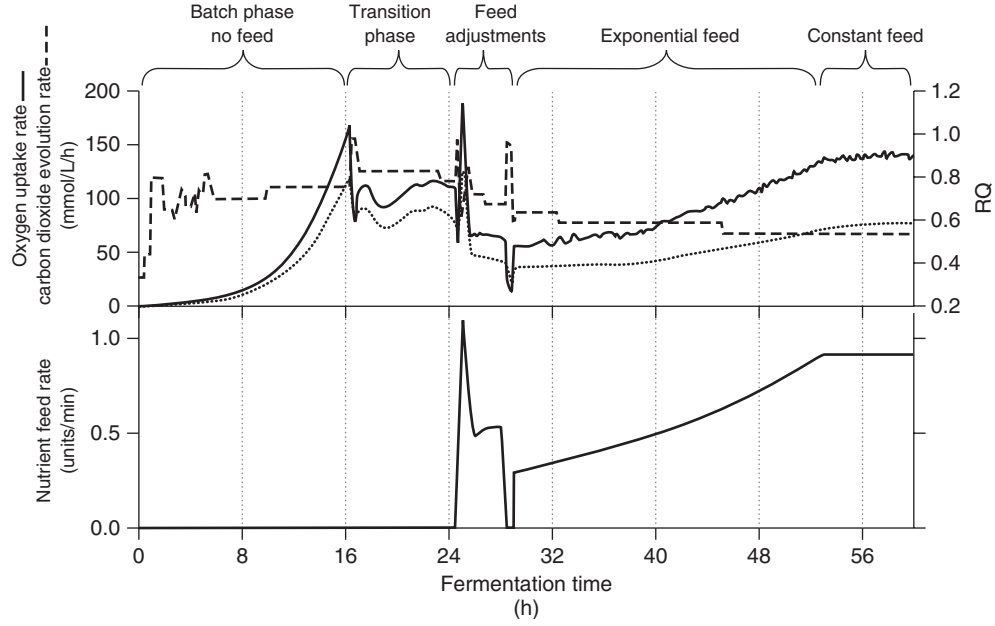


Figure 74.11. Comparison of vent gas analysis to off-line substrate data for a fungal fermentation at 1600 L.

at single setup points for the duration of the fermentation, using a combination of nitrogen and oxygen sparges into the fermentation inlet air. The control of the inlet gas composition was done from a combination of dissolved oxygen (DO) and the vent gas analysis. The experiment determined a relationship of pneumocandin analog formation with DO, and defined an operating range of DO to maintain the unwanted analogs at acceptable levels (54,55). Another example is from whole cell biocatalysis for the bioreduction of a pharmaceutically important unsaturated ketone (56). Yeast cells were exposed to the substrate in the presence of excess nutrients. During the rapid reaction there was a dramatic reduction in the OUR. This indicated a possible toxic effect of the substrate which was later confirmed with viable cell studies. This information led to process designs to minimize the effect of the toxic substrate, maximize conditions to maintain the OUR, and extend the duration of viable cells.

It is not possible to outline examples for all the applications of vent gas analysis. However, it is clear that the technology has provided tremendous value to all areas of fermentation including continuous culture (57), high cell density fermentation (58), the formation of metabolic models for metabolic and pathway engineering (59), systems biology models (60,61), and to even cell culture (62).

REFERENCES

1. Buckland B, Brix T, Fastert H, Gbewonyo K, Hunt G, Jain D. Bio/Technology 1985; 3: 982–988.
2. Heinzle E, Dunn IJ. Methods and instruments in fermentation gas analysis. In: Rehm H-J, Reed G, Schugerl K, editors. Biotechnology:measuring, modelling and control. Weinheim: VCH Verlagsgesellschaft; 1991, pp 27–74.
3. Aiba S, Nagai S, Nishizawa Y. Biotechnol Bioeng 1976; 18: 1001–1006.
4. Fieschki C, Egan KM, Ritch T, Koski RA, Jones M. Biotechnol Bioeng 1987; 29: 1113–1118.
5. Sevcik J. Detectors in gas chromatography. New York: Elsvier; 1976, pp 39–101.
6. Nichols GD. On-line process analyzers. New York: J.Wiley; 1988, pp 3–136.
7. Lee YH, Tsao GT. Adv Biochem Eng 1979; 15: 30–42.
8. Atkinson B, Mavituna F. Biochemical engineering and biotechnology handbook. New York: Stockton Press; 1991, pp 1032–1038.
9. James D, Scott S, Ali Z, O'Hare WT. Microchim Acta 2005; 149: 1–17.
10. Scott S, James D, Ali Z. Microchim Acta 2007; 156: 183–207 (data analysts for elec noses).
11. Cimander C, Bachinger T, Mandenius C-F. Biotechnol Prog 2002; 18: 380–386.
12. Bhattacharyya N, Seth S Sens Actuators 2007; 122: 627–634.
13. Bachinger T, Riese U, Eriksson R, Mandenius C-F. J Biotechnol 2000; 76: 61–71.
14. Navratil M, Norberg A, Lembren L, Mandenius C-F. J Biotechnol 2005; 115: 67–79.
15. Rottenbacher L, Behlau L, Bauer W. J Biotechnol 1985; 2: 137–147.
16. Pons M-N. Bioprocess monitoring and control. Munich: Carl Hanser Verlag; 1992, pp 1–63.
17. Bonham-Carter J, Ives P, Reeks D. BioProcess Int 2004; 9: 76–79.
18. Dadd AT. Am Biotechnol Lab 1990; 8: 35–38.
19. Swartz JR, Cooney CL. Process Biochem 1978; 13: 3–7.
20. Schmid U, Seidel H, Mueller G, Becker Th Sens Actuators B 2006; 116: 213–220.
21. Chauvatcharin S, Seki T, Fujiuyama K, Yoshida T. J Ferment Bioeng 1995; 79: 264–269.
22. Oeggerli A, Heinzle E. Biotechnol Prog 1994; 10: 284–290.
23. Winter MJ. The applications of single detector magnetic sector mass spectrometer systems in fermentation off-gas and liquid analysis. In: Henizle E, Reuss M, editors. Mass spectrometry in biotechnological process analysis and control. New York: Plenum Press; 1987, pp 17–38.
24. Suizdak G. Mass spectrometry for biotechnology. New York: Academic Press; 1996, pp 4–55.
25. Degn H, Cox RP, Lloyd D. Methods Biochem Anal 1985; 31: 165–194.
26. Schaefer K, Schultis. A micro-processor controlled multiple inlet system for mass spectrometers in biotechnology. In Henizle E, Reuss M, editors. Mass spectrometry in biotechnological process analysis and control. New York: Plenum Press; 1987, pp 39–48.
27. Camelbeeck JP, Comberbach DM, Goossens J, Roelants P. Biotechnol Tech 1988; 2: 183–188.
28. Schmid ER. Developments in mass spectrometric instrumentation relevant to biotechnology. In Henizle E, Reuss M, editors. Mass spectrometry in biotechnological process analysis and control. New York: Plenum Press; 1987, pp 7–16.
29. Bartman CD. The application of quadrupole mass spectrometer to biotechnology process control. In Henizle E, Reuss M, editors. Mass spectrometry in biotechnological process analysis and control. New York: Plenum Press; 1987, pp 49–62.
30. Camelbeeck JP, Comberbach DM, Orval M, Petre JO, Roelants P. Biotechnol Tech 1991; 5: 443–452.
31. Heinzle E J Biotechnol 1992; 25: 81–114.
32. Coppella SJ, Dhurjati P. Biotechnol Bioeng 1987; 29: 679–689.
33. Salmon P, Buckland BC. Fermenter vent gas analysis. In Rhodes PM, Stanbury PF, editors. Applied microbial physiology. New York: Oxford University Press; 1997, pp 131–163.
34. Heinzle H. Adv Biochem Eng Biotechnol 1987; 35: 1–46.
35. Perry RH, Green DW, Maloney JO. Chemical Engineers Handbook. New York: McGraw-Hill; 1984.
36. Aiba S, Furuse H. Biotechnol Bioeng 1990; 36: 534–538.
37. Schumpe A, Quicker G, Deckwer WD. Adv Biochem Eng 1982; 24: 1–38.
38. Popovic M, Niebelschutz H, Reuss M. Eur J Appl Microbiol 1979; 8: 1–15.
39. Smith J, Davison SW, Payne GF. Biotechnol Bioeng 1990; 35: 1088–1101.
40. Royce PNC, Thornhill NF. AIChE J 1991; 37: 1680–1686.

41. Harned HS, Owen BB. The physical chemistry of electrolyte solutions. New York: Reinhold; 1958.
42. Yegneswaran PK, Gray MR, Thompson BG. Biotechnol Bioeng 1990; 36: 92–96.
43. Oosterhuis NMG, Kossen NWF. Biotechnol Bioeng 1984; 26: 546–550.
44. Larsson G, Tornkvist M, Stahl Wernersson E, Tragardh C, Noorman H, Enfors S-O. Bioprocess Eng 1996; 14: 281–289.
45. Enfors SO, Rozkov JM. J Biotechnol 2001; 85: 175–185.
46. Ruffer HM, Petho A, Schugerl K, Lubbert A, Ross A, Dekwer WD. Bioprocess Eng 1994; 11: 145–152.
47. Lubbert A. Characterisation of bioreactors. In Rehm H-J, Reed G, Schugerl K, editors. Biotechnology: measuring, modelling and control. Weinheim: VCH Verlagsgesellschaft; 1991, pp 107–148.
48. Reuss M, Bajpai R. Stirred tank models. In Rehm H-J, Reed G, Schugerl K, editors. Biotechnology: measuring, modelling and control. Weinheim: VCH Verlagsgesellschaft; 1991, pp 299–348.
49. George S, Larsson G, Olsson K, Enfors S-O. Bioprocess Eng 1998; 18: 135–143.
50. Delvigne F, Lejeune A, Destain J, Thonart P. Chem Eng Sci 2006; 120: 157–167.
51. Hewitt C, Onyeaka H, Lewis G, Taylor IW, Nienow AW. Biotechnol Bioeng 2003; 96: 495–505.
52. Zabriskie DW, Humphrey AE. AICHE J 1978; 24: 138–142.
53. Gbewonyo K, Jain D, Hunt G, Drew SW, Buckland BC. Biotechnol Bioeng 1989; 34: 234–241.
54. Pollard DJ, Kirschner TF, Hunt GR, Tong I-T, Stieber R, Salmon PM. Biotechnol Bioeng 2007; 96: 308–317.
55. Pollard DJ, Kirschner TF, Hernandez D, Hunt G, Olweinski R, Salmon PM. Biotechnol Bioeng 2003; 78: 270–279.
56. Pollard DJ, Telari K, Lane J, Humphrey G, McWilliams C, Nidositko S, Salmon P, Moore J. Biotechnol Bioeng 2006; 93: 674–686.
57. Dahiya P. Agric Biol Res 2008; 24: 18–24.
58. Junker B, Mann Z, Seeley A, Zhang J, Greasham R. Appl Biochem Biotechnol 2002; 97: 63–78.
59. Wang W, Sun J, Hartlep M, Deckwer W-D, Zeng A-P. Biotechnol Bioeng 2003; 83: 525–536.
60. Nookaew I, Bhumiratana S. Biotechnol Bioeng 2007; 97: 1535–1549.
61. Nielson J, Jewett MC. FEMS Yeast Res 2008; 8: 122–131.
62. Kussow CM, Zhou W, Gryte DM, Hu W-S. Enzyme Microb Technol 1995; 17: 779–783.
63. Dekkers RM. Proceedings of the first IFAC workshop on modelling and control of biotechnical processes. Oxford: Pergamon Press; 1982, p 211.

PART VI

UPSTREAM cGMP OPERATIONS

75

ANTIBODY MANUFACTURE, DISPOSABLE SYSTEMS

Regine Eibl and Dieter Eibl
Zurich University of Applied Sciences, School of Life Sciences and Facility Management, Institute of Biotechnology, Wädenswil, Switzerland

75.1 INTRODUCTION

Monoclonal antibodies (MAbs) are considered to be a mainstream class of biopharmaceuticals and the most rapidly growing segment among modern life science products (1). The market launch of such potent products (for example, MabThera, Avastin, Herceptin, Erbitux, Remicade, and Synagis) has greatly revolutionized therapies for several types of cancer and immune disorders. Whereas hybridomas and murine lymphoid cells were the biocatalysts of choice in the early days of biotechnological MAb productions, more robust production vehicles [e.g. transfected Chinese hamster ovary (CHO) cells and human embryonic retinal (PERC.6) cells] have become established and widely used over the last 10 years (2). By increasing the availability of high-productivity cell lines and optimal culture media that are serum-free, protein-free or even chemically defined, cell productivity has moved from tens of milligrams per liter to a double-digit gram level (3–6).

This success has contributed to a rise in antibody therapeutics, which is predicted to continue. Total sales of MAbs are projected to reach $30 billion by 2010 (2). In order to respond to the needs of international markets, developers, biopharmaceutical manufacturers, and contract manufacturing organizations (CMOs) have striven for faster design, construction, and commissioning, and more efficient operation of MAb production facilities while improving process economy. Hybrid facilities in which disposable components are implemented have been identified as a sound way of achieving these aims. Devices that are typically accepted in disposable format are flexible tubing, connectors, sterile liquid containment bags, mixing systems, bioprocess containers for solution preparation and storage, single-use filters, chromatography equipment, sampling and transfer systems, pumps, centrifuges, and bioreactors (sensors included).

As the term *disposable* or *single-use* implies, the components used are nonreusable. They are mainly composed of Food and Drug Administration-approved plastics such as polyethylene, polystyrene, polytetrafluorethylene, polypropylene, or ethyl vinyl acetate (7). In contrast to their counterparts made of stainless steel, which always need to be steam sterilized (autoclaving or sterilization in place, SIP) by the applier prior to use, the majority of disposable components are gamma irradiated (dose levels between 25 and 50 kGy) by the manufacturer and can therefore be quickly put into operation (8,9). After process operations have finished, the disposables are decontaminated and discarded. Thus, time-consuming, expensive cleaning procedures are reduced and sterilization procedures are no longer required. Higher flexibility (easier process and product change) as well as reduced microbial and cross-contaminations are further benefits of disposables, along with additional time and cost savings (e.g. development time, setup time, time to market, production turnaround time, costs related to capital investment, and cost of goods) (10–12).

Limitations arise from short-term experience of using them, their material strength (chemical and physical compatibility, breakage), and their scalability. However, the most frequently discussed aspect of disposables is

Upstream Industrial Biotechnology: Equipment, Process Design, Sensing, Control, and cGMP Operations, Volume 2, First Edition. Edited by Michael C. Flickinger.
© 2013 John Wiley & Sons, Inc. Published 2013 by John Wiley & Sons, Inc.

the way they react and leach undesirable substances (leachables and extractables), which can interact with the product (13–16). Another critical factor which should be considered is the continual renewal of the disposable component, which increases the cost of solid waste disposal and consumables, and ultimately, running costs. In addition, high-level automation solutions are precluded. A further limiting issue is the restricted availability of disposable sensors (17) and some peripheral elements such as valves, connectors, and fittings. Finally, extra training for staff is required as the capacity of a manufacturing facility increases.

Starting with a general overview of single-use devices in antibody production processes, this chapter focuses on disposable bioreactors dominating the market. In MAb upstream processing, disposable bioreactors have become well established at the preclinical, clinical, and production scales during recent years (18). Interestingly, of all the disposable devices available, disposable bioreactors achieved the highest growth rate in 2008 (19). We present frequently used disposable bioreactor types, their characteristics and obtainable results, and suggest general trends for disposables in antibody manufacture.

75.2 SINGLE-USE DEVICES IN ANTIBODY PRODUCTION PROCESSES: AN OVERVIEW

An antibody production process has three main process stages: upstreaming, downstreaming, and the final formulation and filling. In the upstream stage, the culture medium is prepared (mixing, sterilization, storage), and the seed and inoculum train of the cells is produced. Cells and medium are introduced to a production bioreactor or fermentor in which the target molecule is generated. It is contained in the culture broth, separated from cells and clarified using centrifugation, depth filtration (lenticular filtration), and/or cross-flow filtration (microfiltration) (20). In the following downstream procedures, the isolated target molecule is subjected to a series of further separation, purification, and concentration steps in order to produce a purified antibody with high quality and quantity (21–24). These steps include chromatography processes (e.g. ion exchange membrane chromatography, gel filtration chromatography, affinity chromatography, hydrophobic interaction chromatography, and immobilized metal affinity chromatography) and cross-flow filtrations (ultrafiltration, UF or diafiltration, DF). In addition, intermediate liquid storage and buffer preparation are performed during downstream processing. Finally, the purified antibody is formulated by adding stabilizers to the liquid solution, then sterilized by filtration and/or aseptically poured into sterile containers.

All of the previously delineated main processing steps for MAb production have to date, become partly disposable. However, an MAb facility operating exclusively with disposables is not realistic in the near future. While in media preparation and its storage, cell cultivation steps, product hold, transfer and product storage, disposables are fully established up to commercial biomanufacturing at middle-volume scales; the application of disposables is less common in polishing, filtration, and mixing steps (24,25). Moreover, protein A affinity steps (frequently employed as a capture step to meet the purity, yield, and throughput requirements for antibody purification) are reusable (5,25), a fact which is not expected to change soon. As depicted in Fig. 75.1, the disposable systems available can be divided into three categories, namely expendable laboratory items (protective clothing, syringes, pipettes, vent and liquid filters, etc.); simple peripheral elements (stand-alone components) for single-use; and disposable multicomponent systems for unit operations (26,27).

Flexible tubing, fittings, valves, tri-clamps, protective caps, and aseptic transfer systems are typical disposable products in the category of peripheral elements. In addition, numerous types of disposable connectors (which differ in quality) are sold by various suppliers (e.g. Sartorius Stedim Biotech, Millipore, GE Healthcare, Colder, Pall). The customer can choose from laminar flow connectors (connection under laminar flow conditions), steam-in-place connectors (*in situ* sterilized), and aseptic connectors (connection in an unclassified environment). Instead of sterile coupling with a connector type listed above, fully automated heat weld tubing devices can be used without laminar flow. For thermal production of permanent and consistent leak-free seals on thermoplastic tubing, transportable disconnection devices are applicable. Dispensing and sampling bag manifold systems are further important peripheral elements with disposable design. Their main advantage is the significant reduction in the number of manipulations in the process. For example, dispensing manifolds allow a volume of liquid made up for a given batch to be dispensed into several bags of smaller volume. These bags are then stored and used according to process needs. Sampling manifolds permit multiple sampling for quality control purposes over a defined period of time. Simple liquid containment bags have also been considered as peripheral elements. To date, the volume of the bags ranges from a few millilitres up to 3000 L (7). However, when powdered culture medium is to be transferred, special bags should be used.

A basic requirement for a fully disposable design of unit operations and main process stages was the engineering of further disposable equipment for transport, storage, and heating as well as cooling, mixing, downstreaming, cell production, and protein expression. For this reason, bioprocess container systems (BPCS) have been in use

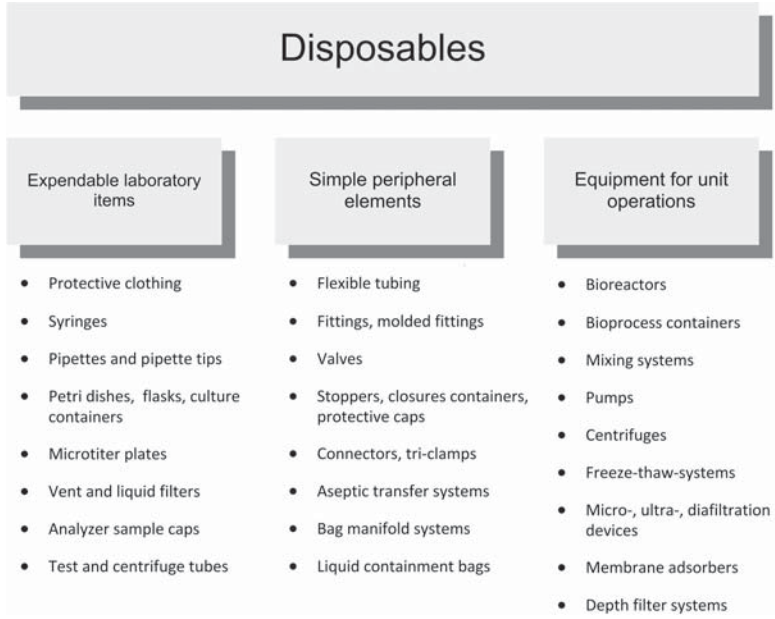


Figure 75.1. Categorization and overview of main disposables used in antibody manufacture.

for more than 10 years (5,7). Nowadays they consist of a flexible two- or three- dimensional bag and a pallet tank, and may also be equipped with cooling and mixing devices. The user can choose between more than 10 disposable mixing systems (27). The majority operate with a rotating or tumbling stirrer integrated into the bag, exceptions being the Wave Mixer (GE Healthcare), the BayShake (Bayer Technologies), the FlexMixer (GE Healthcare), and the VibroMixer (Meissner). Mixing in the Wave Mixer (Fig. 75.2a) is achieved by horizontal oscillation of the bag and in the BayShake (Fig. 75.2b) by the bag's vertical oscillation. In contrast, mixing in the FlexMixer (Fig. 75.2c) is accomplished by up and down movement of an integral perforated diaphragm in the bellow-like bag. In the VibroMixer (Fig. 75.2d), the movement of a conically perforated disk (which is fixed on a vertically oscillating hollow shaft) induces mixing. It is generally assumed that disposable mixing systems will become increasingly accepted and scaled up to 10,000 L.

New to the disposable equipment portfolio are disposable pumps and freeze–thaw systems with a maximum volume of around 16 L and maximum freezing temperatures of -60°C (5,28). This also applies to disposable centrifuges and UF or DF devices. However, disposable membrane absorbers (which remove high molecular weight contaminants such as DNA and viruses by flow-through anion exchange chromatography) and disposable depth filter systems are better known and commonly used up to the production scale (5,24,25). Finally, disposable bioreactors with a flexible or rigid plastic cultivation container have become increasingly influential in MAb productions during the last 10 years (26), even though non- or less-instrumented, small-scale membrane bioreactor systems were already described in the 1980s (29).

75.3 DISPOSABLE BIOREACTORS IN MAb PRODUCTION PROCESSES

75.3.1 Membrane Bioreactors

The introduction of hollow fiber technology by Knazek and his team (30) resulted in the development of hydraulically driven hollow fiber bioreactor systems (HFBS), as shown in Fig. 75.3a. In the 1980s and 1990s, they were favored for continuous *in vitro* productions of hybridoma-derived MAbs at low volume scale (29–31). This is explained by the high cell density levels provided (10^7–10^9 cells/mL) and high concentrations of MAbs (100 mg to several grams), which both arise from the perfusion mode in HFBSs.

Thousands of semipermeable hollow fibers that have been embedded in the cylindrical production cartridge allow adherent or suspension cells to grow on their outside. This is known as the *extracapillary space* and is where high molecular weight secreted proteins (such as antibodies) are also retained. At the fiber's molecular weight cutoff (MWCO), which is considerably less than the molecular weight of the target molecule, the passage of macromolecules through the fiber wall is affected as the oxygen-enriched culture medium flows through the fibers

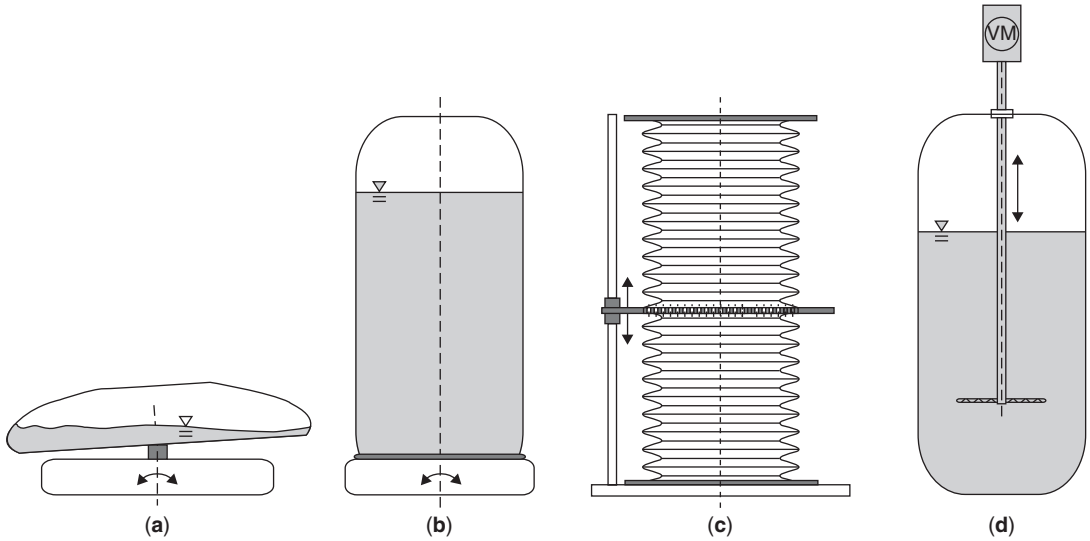


Figure 75.2. Working principles of nonstirred disposable mixing systems: (a) Wave Mixer, (b) BayShake, (c) FlexMixer, and (d) VibroMixer.

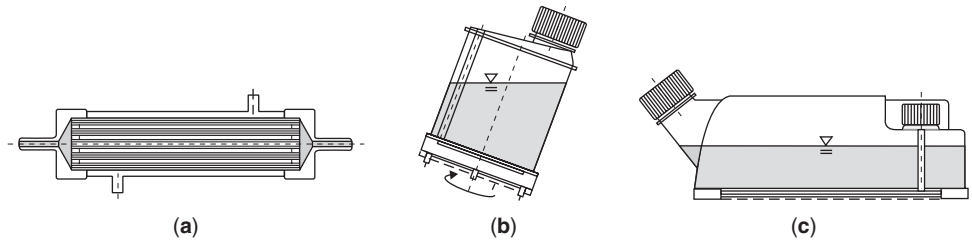


Figure 75.3. Schematic diagrams of different types of membrane bioreactors: (a) HFBS, (b) rotating two-compartment dialysis bioreactor, (c) T-flask-based two-compartment dialysis bioreactor.

(intracapillary space). However, due to restrictions (32) pertaining to the homogeneity of the culture environment and scale-up (one production module is limited to 110 mL with a maximum of 20 multiple modules), HFBSs play a subordinate role among disposable bioreactors in MAb production processes today. Nevertheless, they are still in use in R&D and the manufacturing of diagnostic antibodies (e.g. ProstaScint) required in small amounts of between 1 and 2 kg per year (33–35).

In the late 1990s, a rotating and a static two-compartment dialysis membrane bioreactor entered the cell culture labs: the roller bottle-like MiniPerm (Fig. 75.3b) and the T-flask-based CELLine (Fig. 75.3c). As in the case of HFBSs, a semipermeable membrane separates the cells from the medium and permits quasi-perfusion mode. Unlike HFBSs, they should be kept in a CO_2 incubator in order to ensure an optimum growth and production environment. A silicone membrane on the outside of both the CeLLine and the MiniPerm guarantees efficient gas transfer for culture volumes ranging from 5 to 35 mL and supports high cell density growth ($>1 \times 10^7$ cells/mL) as well as antibody production, generally in double-digit milligram range (36–39). As handling of the MiniPerm is more laborious, CeLLine systems are more popular in preclinical and clinical sample productions of MAbs at the milliliter scale (39–41). It therefore comes as no surprise that current efforts are aimed at further development of CeLLine systems with, for example, the installation of disposable sensors.

75.3.2 Wave-Mixed Bag Bioreactors

In 1998, the first version of a disposable wave-mixed bag bioreactor, the Wave Bioreactor System 20, was launched. By rocking its platform, a wave is induced in the fixed bag which contains culture medium and cells. In this way, mixing is enabled and bubble-free surface aeration takes place. Mass and energy transfer, which both have an influence on cell growth and product formation in this bioreactor system, are highly

dependent on wave development and propagation (42). These features can be adjusted via rocking angle, rocking rate, and filling level. Initially, many cell culture specialists were skeptical about this new mixing method, that is, the wave-induced motion (WIM), and the suitability of the originally less-instrumented plastic bag for cell and protein productions. However, promising results from early engineering and biological studies have demonstrated the potential of the Wave Bioreactor System 20 in animal and human cell-based processes as well as further possible uses (42,43). In comparison to reusable stirred bioreactors (the gold standard in cell cultivation processes), similar or higher cell densities and product titers have been achieved, which has lead to the scaling-up of the Wave Bioreactor System 20. In 2000 the first Good Manufacturing Practice (GMP) version of a wave-mixed bag bioreactor (100 L maximum culture volume) came onto the market. An improved system (resonance operation) with 500 L culture volume was patented in 2004 (44). This patent resulted in the Wave Bioreactor System 500/1000 from GE Healthcare which has till date, the largest bag size (500 L maximum culture volume) per rocker platform among wave-mixed bag bioreactors.

The first generation of wave-mixed bag bioreactors was mainly used for MAb productions with stably transfected and transient mammalian cell lines cultivated in batch, fed-batch, and perfusion modes (45–49). Internal perfusion up to 100 L culture volume can now be provided by perfusion bags with a floating or bottom-side fixed membrane in combination with a weight-based or volume flow rate–perfusion controller which balances culture medium renewal with the harvest rate. However, for culture volumes exceeding 100 L, external cell separation devices (e.g. cross-flow filtration units using hollow fiber modules, spin filters, gravity settlers, centrifuges, and hydrocyclones) should be used (50).

There is no doubt that the development of further wave-mixed bag bioreactor types such as Applikon's AppliFlex Bioreactor (51), CatchMab's Tsunami Bioreactor (52), Sartorius Stedim's BIOSTAT CultiBag RM series, and Cellution's CELL-tainer (18) can be ascribed to the triumphant success of the BioWave and Wave Bioreactor. They differ from each other in their control units, number of platforms and movement, as well as in culture bag design (material, scale, dimension, kind of sensor probes). Currently, it is possible to fit their bags with standard or disposable noninvasive sensors for dissolved oxygen (DO) and for on-line measurement and control of pH (17,53). It is also worth mentioning that, in only one decade, disposable wave-mixed bag bioreactors have secured a solid position in mammalian cell-based process developments and in small and middle scale manufacture of recombinant proteins and antibodies.

75.3.3 Stirred Bioreactors

In 2006, Hyclone and Xcellerec produced the first stirred bag bioreactors, which have a customized steel support container in order to assure the bag's cylindrical shape. A sparger, an excentrically mounted axial flow impeller, gas filters, and ports for the integration of sensor probes and line sets are included in the temperature-controlled cultivation bag. Currently, SUBs (single-use bioreactors) from ThermoFisher Scientific (which have been developed for antibody production processes at Baxter in cooperation with Hyclone) hold market-leading positions among stirred disposable systems. The 50, 100, 250, and 1000 L versions of the SUB are top-driven and have mechanical seals. Similarities in their engineering parameters, product quantities (middle to high cell densities, antibody titers in *g*-range) and product quality with stirred cell culture bioreactors made of stainless steel have been reported for CHO and PERC.6 cultivations (18). Cell growth and protein titers comparable to those in reusable cell culture bioreactors have also been found in disposable stirred tank bioreactor (XDR) SUBs from Xcellerex (54). XDR systems have bottom-driven magnetic impellers and can be operated with the largest culture bags available until now (2000 L).

A cubical bag shape and a tumbling impeller (based on the Pad-Drive Mixing System) are features of ATMI Life Science's Nucleo Bioreactors (Fig. 75.4a), which can be obtained up to 1000 L scale. Results of fed-batch and continuous cultivations with different kinds of mammalian cells were acceptable and reproducible (55). The BIOSTAT Cultibag STR series (Sartorius Stedim), available as 50, 200 (Fig. 75.4b), and 1000 L systems, comes as close as possible to the classical configuration of a reusable stirred cell culture bioreactor (56,57). Here a height/diameter ratio of 2:1 (typical for animal cell performances) can be realized. For aeration, it is possible to implement microspargers and ring spargers, the most frequently applied aeration devices for mammalian cells. Aeration and mixing is provided by centrically positioned three-blade segment impellers as well as by six-blade disk impellers.

All these stirred bag bioreactors have mainly been implemented in the labs and production facilities of process developers and CMOs, whose products are MAbs in the first instance. They have been primarily equipped with standard sensors for the measurement of temperature, DO, and pH. Meanwhile, single-use sensors have also come onto the market. At the same time as stirred bag bioreactors were gaining a foothold, noninstrumented disposable spinner flasks from different suppliers as well as Sartorius Stedim's SuperSpinner D 1000 became more and more popular for cell expansions. The SuperSpinner enables higher cell densities due to membrane aeration (58,59).



Figure 75.4. Product pictures of different types of fully controlled stirred bioreactors with disposable cultivation unit: (a) Nucleo-1000, (b) BIOSTAT CultiBag STR 200, (c) Mobius CellReady 3 L Bioreactor (with kind permission of ATMI Life Sciences, Sartorius Stedim, and Millipore).

The gap in the lower L-range for fully instrumented disposable stirred bioreactors was bridged with the introduction of the 3 L Mobius CellReady Bioreactor (Fig. 75.4c) in summer 2009 (60). This disposable bioreactor, developed by Millipore and Applikon, has a rigid plastic cultivation vessel. Measurement and control of key process parameters are feasible with standard sensors.

75.3.4 Orbitally Shaken and Pneumatically Driven Bioreactors

The finding that mammalian cells are not as sensitive to shear stress as originally presumed has resulted in increasing usage of surface aerated, orbitally shaken containers for process developments. Shaken multiwell plates and classical "Erlenmeyer" flasks have become the workhorses for high-throughput screening experiments at microliter- and milliliter scales (61). Fortunately, advanced adaptations (e.g. μ24 Microbioreactor from Applikon, the BioLector from mp2-labs, and Sartorius Stedim's Sensolux) have recently become available. These downscale systems are stand-alone versions enabling on-line measurement of pH and DO with disposable sensors during cultivation (62).

Following the discovery of Wurm and his team that mammalian cells are non-oxygen limited when grown in noninstrumented 50 mL centrifuge tubes with ventilated caps (the TubeSpin cultivation vessels), a new wave in orbital shaking began. These tubes (commercially available under the trade name CultiFlask 50 disposable bioreactors, distributor Sartorius Stedim) have to be vertically mounted on the platform of a shaker incubator. At agitation speeds between 180 and 220 rpm (25 mm displacement radius) and culture volumes between 20 and 40 mL, their volumetric oxygen mass transfer coefficients range between 5 and 30 h^{-1} (63). Consequently, the comparability of the high cell densities achieved ($>10^7$ cells/mL) for transfected CHO cells (64,65) and further cell lines (66) to the values of nondisposable stirred and disposable wave-mixed bioreactors comes as no surprise to experienced cell culture technologists. Owing to the ample oxygen supply and low mechanical stress, the feasibility of scaling-up orbital shaking technology (OrbShake technology) for mammalian cells up to 1000 L culture volume was demonstrated by Zhang *et al*. (63). This culminated in the design of the recently presented SB200-X Disposable Shaken Bioreactor System (see also http://www.shakingtechnology.com), which was developed in cooperation with ExcellGene, Adolf Kühner, and Sartorius Stedim (67). AmProtein's Current Bioreactor line (ranging from 20 mL to 300 L) is based on a similar approach (68,69).

Promising results have also been reported on cultivations in a novel, pneumatically driven bag bioreactor and in a hybrid system, both of which have special bag shapes deviating from the common cylindrical and cubical bags. In the pneumatic bioreactor system (PBS) there is an air-wheel design and a dual sparger system to facilitate mixing and aeration. At 2, 10, 50, and 250 L scales, high cell density growth (comparable to that in conventional stirred cell culture bioreactors) is guaranteed for a CHO cell line (Brian Lee, PBS, personal communication). In the case of the hybrid CellMaker Plus (18,70), mixing and aeration is achieved by using the air flow from a sparger tube and two magnetic impellers. The aeration is realized in the slim part of the bag, which is the lower area. As the air bubbles rise, "riser" flow is generated

and intensified by the impellers. The result is a transverse liquid movement which provides satisfactory mixing of aerated medium and cells. To minimize or even eliminate excessive foam formation (which is a well-known problem in pneumatically driven bubble columns), pressure to the headspace may be applied. Again, these bioreactors allow appropriate sensors to be implemented.

75.4 CONCLUSIONS AND APPARENT TRENDS

This chapter shows the wide variety of disposables that are employed in all process stages in the development and manufacture of MAbs. In addition to BPCs for buffers, media and bulk products, filtration and chromatography equipment, and mixing systems, disposable bioreactors are being increasingly used. They are implemented as both seed and production bioreactors, and are mainly stirred or wave-mixed. Driven by the successful scale-up of orbital shaking and the availability of the first suitable single-use shaking bioreactors, it is expected that this technology will have greater influence in the future. Provided that desired cell densities, product titers, and qualities are achieved while guaranteeing high process safety and cost savings, radical new concepts for disposable bioreactors are conceivable. Owing to strong international competition in the field of biotherapeutics and worldwide cost pressure in the healthcare sector, developers and manufacturers are increasingly willing to deviate from the "gold standard," that is, the stirring.

The development stage of disposable technology achieved, together with its connectivity, means that hybrid solutions are available for production facilities. Because of greater antibody titers, realization of fully disposable upstream processing is occasionally or even generally possible, as in the case of the manufacture of personalized and diagnostic antibodies (where only amounts in one-digit *g*-range are required). However, limitations such as the lack of technically mature in-process-control (IPC) with single-use sensors should not be overlooked. Nevertheless, pH and DO sensor technologies have proven favorable and additional sensor variations, which could potentially be utilized on obtainable controllers, are in the pipeline. At the time of writing, the lack of fully disposable facilities for MAb manufacturing at large scales can be attributed to the affinity purification step in downstream processing. Currently, there is no alternative to stainless steel (60).

Ongoing research by manufacturers of disposables focuses on the characterization of disposables and the elimination of present limitations. A promising tool for generating data on local and temporary components, temperature and velocity distributions, mixing times, shear and dissipation rates in the disposable systems investigated is computational fluid dynamics (CFD) (71–74). Successfully verified CFD data will allow the scale-up as well as comparison of different systems and support optimized bioprocessing in the long term. Further activities are aimed to make disposable systems the end user in a modular design available. By integration of gamma-sterilizable radio frequency identification (RFID) tags, rapid paperless identification of system parameters (e.g. part number, lot number, description, manufacture, and expiration dates) can be made. Furthermore, their combination with single-use sensors controlling critical process parameters appears to be feasible in the future. In conclusion, RFID-based connections may facilitate rapid setup and running of hybrid facilities as well as the realization of complete single-use manufacturing processes (5,75).

REFERENCES

1. Ball P, Brown C, Lindström K. Bioprocess Int 2009; 4: 18–28.
2. Morrow KJ. Gen Eng Biotechnol News 2008; 12: 36–39.
3. Percivia. Press release: DSM and Crucell announce record achievement in PERC.6 technology, Heerlen/Leiden, The Netherlands. 2008 Jun 16.
4. Coco-Martin JM, Harmsen MM. Bioprocess Int 2008; 4: 28–33.
5. Anicetti V. Bioprocess Int 2009; 7; Suppl 1: 18–23.
6. DePalma A. Gen Eng Biotechnol News 2009; 5: 42–46.
7. Pora H, Rawlings B. Bioprocess Int 2009; 4: 9–16.
8. BSPA Subcommittee. Bioprocess Int 2007; 8: 32–39.
9. BSPA Subcommittee. Bioprocess Int 2007; 9: 60–70.
10. Novais JL, Titchener-Hooker NJ, Hoare M. Biotechnol Bioeng 2001; 75: 143–153.
11. Lim JAC, Sinclair A. Am Pharm Rev 2007; 10: 114–121.
12. Foulon A, Trach F, Pralong A, Proctor M, Lim J. Bioprocess Int 2008; 6; Suppl 3: 12–18.
13. Altaras GM, Eklund C, Ranucci C, Maheswari G. Biotechnol Bioeng 2007; 96: 999–1007.
14. Jenke D. J Pharm Sci 2007; 96: 2566–2581.
15. Okonkowski J, Balasubramanian U, Seamans C, Fischrogen Z, Zhang J, Lachs P, Robinson D, Chartrains M. J Biosci Bioeng 2007; 103: 50–59.
16. Bestwick D, Colton R. Bioprocess Int 2009; 7; Suppl 1: 88–94.
17. Rao G, Kostov Y, Moreira A, Frey D, Hanson M, Jornitz M, Reif OW, Baumfalk R, Qualitz J. Bioprocess Int 2009; 7; Suppl 1: 24–27.
18. Eibl R, Eibl D. In: Kasper C, van Griensven M, Pörtner R, editors. Bioreactor systems for tissue engineering. Berlin: Springer; 2009. pp. 183–207.
19. Langer ES. Bioprocess Int 2009; 7; Suppl 1: 6–8.
20. Hill P, Bender J. In: Stacey G, Davis J, editors. Medicines from animal cell culture. Chichester: John Wiley & Sons; 2007. pp. 305–330.
21. Bender J. In: Stacey G, Davis J, editors. Medicines from animal cell culture. Chichester: John Wiley & Sons; 2007. pp. 331–346.

22. Wilson M. In: Stacey G, Davis J, editors. Medicines from animal cell culture. Chichester: John Wiley & Sons; 2007. pp. 347–370.
23. Schmidt FR. In: Gad SC, editor. Handbook of pharmaceutical biotechnology. Hobooken (NJ): John Wiley & Sons; 2007. pp. 1–52.
24. Behme S. Manufacturing of pharmaceutical proteins. Weinheim: Wiley VCH; 2009.
25. Vogt R, Paust T. Bioprocess Int 2009; 7; Suppl 1: 72–77.
26. Eibl R, Eibl D. Einwegkultivierungstechnologie für biotechnische pharmaproduktionen, BioWorld 2005; 1; Suppl 3: 1–2.
27. Eibl D. Concept Heidelberg ed., 2nd conference about usage of disposables; 2009; Mannheim. pp. 1–35.
28. Glaser V. Gen Eng Biotechnol News 2008; 9. Available at htpp:// www.genengnews.com/articles/chitem.aspx?aid = 2454.
29. Hopkinson J. Biotechnology 1985; 3: 225–230.
30. Knazek RA, Gullino PM, Kohler PO, Dedrick RL. Science 1972; 178: 65–67.
31. Marx U. Res Immunol 1998; 6: 557–559.
32. Fenge C, Lüllau E. In: Ozturk SS, Hu WS, editors. Cell culture technology for pharmaceutical and cell-based therapies. New York: CRC Press; 2006. pp. 155–224.
33. Norris BJ, Gramer MJ, Hirschek MD. In: Howard GC, Bethel DR, editors. Basic methods in antibody production and characterization. Bocca Raton (FL): CRC Press; 2000. pp. 87–104.
34. Davis JM. In: Pörtner R, editor. Animal cell biotechnology: methods and protocols. Totowa (NJ): Humana Press; 2007. pp. 337–352.
35. Davis JM. In: Stacey G, Davis JM, editors. Medicines from animal cell culture. Chichester: John Wiley & Sons; 2007. pp. 145–171.
36. Falkenberg FW. Res Immunol 1998; 6: 560–570.
37. McArdle J. ATLA 2004; 32 Suppl 1: 119–122.
38. Trebak M, Chong JM, Herlyn D, Speicher DW. J Immunol Methods 1999; 230: 59–70.
39. Bruce MP, Boyd V, Duch C, White JR. J Immunol Methods 2002; 264: 59–68.
40. Nagel A, Koch S, Valley U, Emmrich F, Marx U. Dev Biol Stand 1999; 101: 57–64.
41. Scott LE, Aggett H, Glencross DK. Biotechniques 2001; 31: 666–668.
42. Eibl R, Eibl D. In: Gutta Dupta S, Ibaraki Y, editors. Plant tissue culture engineering. Dordrecht: Springer; 2006. pp. 203–227.
43. Singh V. Cytotechnology 1999; 30: 149–158.
44. Singh V. Die wave bioreactor geschichte. Cork: Wave Europe Pvt. Ltd.; 2005.
45. Oashi R, Singh V, Hamel JFP. Gen Eng Biotechnol News 2001; 7: 40, 78.
46. Haldankar R, Li D, Saremi Z, Baikalov C, Desphande R. Mol Biotechnol 2006; 34: 191–199.
47. Fries S, Glazomitsky K, Woods A, Forrest G, Hsu A, Olewinski R, Robinson D, Chartrain M. Bioprocess Int 2005; 3; Suppl 6: 36–44.
48. Tang YI, Oashi R, Hamel JP. Biotechnol Prog 2007; 23: 255–264.
49. Pierce LN, Shabram PW. Bioprocess J 2004; 4: 51–56.
50. Eibl R, Werner S, Eibl D. In: Eibl R, Eibl D, editors. Disposable bioreactors. Berlin: Springer; 2009. pp. 55–87.
51. Morrow KJ. Gen Eng Biotechnol News 2006; 12: 42–45.
52. Houtzager E, van der Linden R, de Roo G, Huurman S, Priem P, Sijmons PC. Bioprocess Int 2005; 6: 60–66.
53. Liebsch G, Klimant I, Krause C, Wolfbeis OS. Anal Chem 2001; 73: 4354–4363.
54. Mardirosian D, Guertin P, Crowell J, Yetz-Aldape J, Hall M, Hodge G, Jonnalagadda K, Holmgren A, Galliher P. Bioprocess Int 2009; 7; Suppl 4: 30–35.
55. Castillo J, Vanhamel S. Gen Eng Biotechnol News 2007; 16: 40–41.
56. DeWilde D, Noack U, Kahlert W, Barbaroux M, Greller G. Bioprocess Int 2009; 7; Suppl 4: 36–41.
57. Greller G, Baumfalk R. Pharmatec 2009; 3: 24–25.
58. Eibl R, Eibl D. Bioprocess Int 2009; 7; Suppl 1: 18–23.
59. Schmale K. An Nat Methods 2008; 8: 217–218.
60. Glaser V. Gen Eng Biotechnol News 2009; 5: 48–53.
61. De Jesus MJ, Wurm FM. Bioprocess Int 2009; 7; Suppl 1: 12–17.
62. Eibl R, Kaiser S, Lombriser R, Eibl R. Appl Microbiol Biotechnol 2009. In press.
63. Zhang X, Bürki CA, Stettler M, De Sanctis D, Perrone M, Discacciati M, Parolini N, DeJesus M, Hacker DL, Quarteroni A, Wurm FM. Biochem Eng J 2009; 45: 41–47.
64. De Jesus MJ, Girard P, Bourgeois M, Baumgartner G, Kacko B, Amstutz H, Wurm FM. Biochem Eng J 2004; 17: 217–223.
65. Muller N, Girard P, Hacker D, Jordan M, Wurm FM. Biotechnol Bioeng 2004; 89: 400–406.
66. Ries C, John C, Eibl R. Bioforum 2009; 3: 11–13.
67. ExcellGene. Press release. ExcellGene SA offers contract manufacturing in 250 L OrbShake Bioreactor. Monthey, Switzerland 2009 May 19.
68. Jia Q, Li H, Hui M, Hui N, Joudi A, Rishton G, Bao L, Shi M, Zhang X, Luanfeng L, Xu J, Leng G. Bioprocess Int 2008; 6: 66–78.
69. Potera C. Gen Eng Biotechnol News 2009; 7: 20–21.
70. Eibl R, Eibl D. ACHEMA Worldw News 2007; 2: 8–10.
71. Pordal HS, Matice CJ, Fry TJ. Pharm Technol North Am 2002; 1: 72–79.
72. Paschedag A. Computational fluid dynamics in der verfahrenstechnik. Weinheim: Wiley VCH, 2004.
73. Dhanasekharan K. Bioprocess Int 2006; 3: 34–40.
74. Singh H, Hutmacher DW. In: Kasper C, van Griensven M, Pörtner R, editors. Bioreactor systems for tissue engineering. Berlin: Springer; 2009. pp. 231–249.
75. Cappia J-M, Chevalier E, Durand C, Priebe P, Johnson J, Tangretti M. Bioprocess Int 2009; 7; Suppl 1: 38–43.

76

BIOREACTOR OPERATIONS

David R. Gray
Chiron Corporation, Emeryville, California

76.1 PREPARATION

Bioreactor operations may be segregated into two different areas that constitute the overall production cycle. The first area includes operations involved with the preparation of the bioreactor system before the production phase. The second area deals with the operation and control of the bioreactor when cells are present, the production phase. This section describes operations in the first of these categories, the activities of harvesting, cleaning, sterilization and instrumenting of the reactor before inoculation. These operations encompass the physical and chemical processes that govern the cleaning, sanitization of the process contacting surfaces, sterilization of equipment and media, instrumentation, aseptic addition of sterile media components, calibration of measurement devices, preinoculation preparation, system checks for sterile operation (contamination control), and some aspects of fundamental maintenance. The sequences of events that must occur in starting up a bioreactor system are shown in Figure 76.1. Following cleaning to remove residual cell product and media components from the system, the equipment is sterilized using pressurized, saturated, clean steam at temperatures that inactivate any residual live bacteria. Media components, which may be degraded by exposure to high temperature, must be sterilized by filtration followed by aseptic transfer to the reactor. All sensors and probes used in monitoring or controlling the production phase must be installed, sterilized, and calibrated.

The precise methods used in bioreactor operations are a function of the scale of the reactor and the objectives of the process. The process may be required for manufacturing, development, proof of concept, or research. The scale of operation of a bioreactor is a function of the product demand (kg/yr.), process productivity (kg/m^3), and the facility occupancy (fractional yr.). In process development, the scale of operation may be 1–10% of the putative manufacturing scale and may feature a flexible, highly instrumented reactor. Cell culture bioreactors range from 10 L for simple development scale operation, 100–500 L for pilot- scale operation, and may be as large as 10,000 L for manufacturing (1). Plant-cell culture reactors of 20,000 L and greater are used in tobacco cell suspension culture (2,3). Process economics strongly affects the choice of scale in commercial manufacturing and can dictate the use of high volume bioreactors for the industrial production of low-value market products.

Bioreactors and process vessels up to 500 L in volume can be mobile and autoclavable and are amenable to manual cleaning procedures (referred to as cleaning out of place or COP). Tanks of 1000 L and greater are normally fixed-in-place, immobile, with hard-piped systems to supply nutrients, gases, and utilities to the bioreactor skid. (Note: A skid refers to the integrated bioreactor system including the associated piping, instrumentation, and point of use utility connections). Associated process recovery equipment and utility equipment would be also fixed-in-place. Fixed piping facilities are operated without long lengths of hoses on the floor, and spills and leakage from connections are minimized or avoided. A fixed piping layout requires installation of a large number of valves and components to direct the flow of fluids. These systems require a large initial capital expense. Cleaning-in-place (CIP) procedures are required to ensure that all process components are effectively cleaned.

Upstream Industrial Biotechnology: Equipment, Process Design, Sensing, Control, and cGMP Operations, Volume 2, First Edition. Edited by Michael C. Flickinger.
© 2013 John Wiley & Sons, Inc. Published 2013 by John Wiley & Sons, Inc.

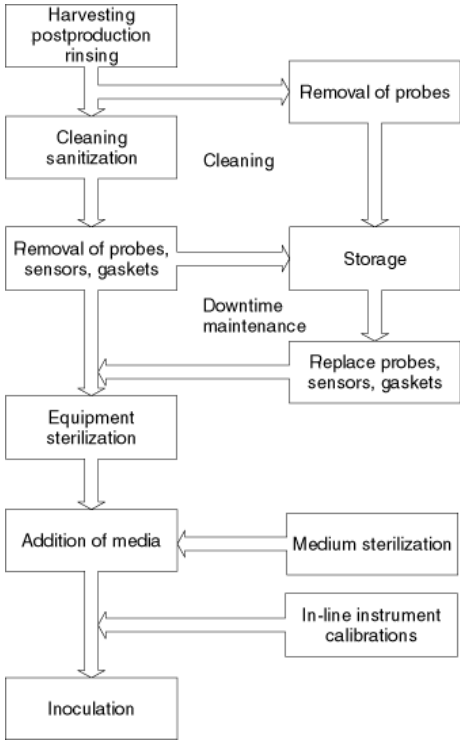


Figure 76.1. Bioreactor operations. Preparation of the bioreactor and associated skid components following the production phase through to inoculation. The sequence of activities are shown with reference to their location section numbers in this discussion of bioreactor operations.

Consistent optimal performance in bioreactor processes requires operation within narrow ranges of environmental parameters. In this respect, bioreactors are often equipped for automatic process control. Feedback control systems require output signals from the bioreactor sensors to provide information for determining controller outputs to actuate valves, pumps, and other devices remotely. Consequently, instrumentation of the bioreactor, calibration of probes, maintenance, and procedures for testing important sensors are important set-up operations. Sterilization of the equipment to provide asepsis is a key requirement. This is achieved by using pressurized (15 psig) steam at 121°C. The sterilization procedure is usually designed as an automatic process that uses sequentially programmed actuation of valves. For small and simple bioreactors, sterilization can be a manual or a semiautomatic process. Heat-sensitive media components are sterilized by submicron filtration. Sterilization of heat-sensitive plant tissue may be accomplished by chemical sterilization. Maintenance of asepsis requires careful control procedures following the SIP process, for example, good sterile (aseptic) technique, avoidance of low internal pressure relative to the environment, and the use of aseptic connections.

76.1.1 Cleaning

Cleaning is an important unit operation in the process industry. In the chemical process industries, the term cleaning refers to the removal of deposits in the form of scale or sediment following the prolonged use of such equipment. This is considered part of a scheduled maintenance program. These cleaning procedures are important in preserving and maintaining process surfaces, but may be equally important in many cases to prevent corrosion or scale buildup, which could decrease the efficiency of operation. Such cleaning may not be obligatory after every process batch and may be driven by economic factors. In the food processing industry, cleaning is absolutely required for producing clean and sterile equipment surfaces to avoid product spoilage. In the biotechnology industry, cleaning is a mandatory process which must achieve high standards of cleaning, sanitization, and reproducibility. Large-scale systems require cleaning in place (CIP) methods.

A simple cleaning procedure, after termination of a development bioreactor process, may be used when strict cleaning is not demanded. The basic procedure first involves disabling the controller alarms and information-gathering processors, such as chart recorders. Addition pumps are set to manual and output set to zero, or else switched to the off mode. The pH control is set to manual or off, and the sparger airflow rate lowered to a minimum flow to prevent debris from entering the sparger holes. The agitator should be set for general mixing during harvesting of the broth and during the rinsing and cleaning procedure. After the evacuation of the cells and product from the reactor, the inside surfaces are rinsed with DI water. After rinsing, the pH and DOT probes are removed from the vessel ports and replaced with blind plugs. The vessel is filled to operational volume with DI water, and concentrated sodium hydroxide is added to a final concentration of 0.5 N. The reactor is sanitized by using caustic for 1–4 hours at 40–60°C. During caustic cleaning, the agitator is operated at maximum rpm, and the spargers should be operated at a low airflow rate.

For small-scale vessels, the agitator motor and external disposable tubing connections would be removed. The top dish is opened and the internal surfaces rinsed with DI water. All O-rings are removed and discarded. Probes are removed and replaced with blind plugs. pH probes are placed in buffer. The empty vessel is rinsed with DI water several times through the top ports. The equipment can be washed with 7X detergent and finally rinsed with DI water. Spargers and small bore SS tubing are cleaned by circulating of 0.5 N NaOH for 30–60 minutes. After final DI water rinsing, the vessels and components are dried by using air.

Large-scale bioreactor systems are cleaned in place (CIP). In a CIP process all product-contacting surfaces are cleaned by circulating cleaning agents within the process equipment. Some of the equipment components may be

removed and cleaned out of place. This may be required for hard to clean equipment where adequate flow of CIP cleaning reagents is not possible, (e.g., internal settlers, spargers, and threaded components).

In clinical product manufacturing processes, the cleaning procedures must be validated to demonstrate their ability to remove cellular components, products, and solutes from the equipment surfaces. This becomes increasingly stringent for biotechnological manufacturing process equipment in which multiple products are produced. Absence of batch-to-batch and product-to-product carryover must be demonstrated in clinical product production. Thus CIP is also concerned with minimizing the risk of batch carryover.

The principles and standards used for cleaning and sanitization in the biotechnology and pharmaceutical industry originated in the dairy industry (4). The fundamental principles of CIP unit operation are based on the 3-A dairy standards (5). The important keys to successful CIP are given here:

- Construct equipment with cleanable smooth surfaces. In biotechnology, 316L stainless steel (SS316L) has become the standard. Seamless tubing is preferred.
- Design piping and other ancillary process equipment to ensure direct contact with the cleaning reagents. This requires excluding hard to clean valves, dead legs, and instruments from the bioreactor skid design.
- Select cleaning reagents capable of dissolving organic residues (proteins, lipids, carbohydrates).

Figure 76.2 provides a view of the important elements in CIP processes.

Typical CIP cleaning agents (shown in Table 76.1) are caustic soda (organic dissolving power and bactericidal power), sodium carbonate (limited organic dissolving power but compatible with brass), sodium metasilicate (dispersing and rinsing), trisodium phosphate (dispersing power), nonionic detergents (wetting agents, dispersing and rinsing, organic dissolving power), sodium tripolyphosphate (sequestering power), and EDTA and sodium gluconate (sequestering power and calcium dissolving power). A discussion of CIP reagents is given in Ref. 6 for the difficult cleaning challenges experienced in the brewing industry. The choice of reagent depends on the nature of the process residue and soil. In biotechnology applications, circulation of sodium hydroxide (0.1 N) at 50°C is normally suitable for cleaning and may be coupled in series with a detergent (1% Triton X100 or 1% SDBS) to enhance the organic dissolving power.

76.1.1.1 CIP. CIP methods are commonplace in the food, brewing, and pharmaceutical industries. In the food industry and in particular the dairy sector, a number of guidelines were established many years ago. The foremost of these is the document entitled "3-A Accepted Practices for Permanently Installed Sanitary Products, Pipelines, and Cleaning Systems (5)," which provides a basic guide for designing process systems and cleaning procedures used to clean such equipment. Discussions of CIP relating to bioreactor skid systems have described the importance of selecting effective cleaning chemistry (7), materials of construction (8,9), and sanitary valves and components (10,11).

CIP is a process for cleaning process equipment without dismantling it. CIP is the procedure by which flushing, washing, rinsing, and sanitizing solutions are brought into immediate contact with all soiled surfaces and continuously replenished. The cleaning process is essentially chemical, and in large-scale generally requires recirculating cleaning reagents to minimize water and chemical costs. CIP is the expedient choice for large-scale processing equipment because it is a reproducible, labor-saving process that provides consistency with minimal equipment damage. CIP is achieved by contacting all process surfaces with the cleaning solution at a correct flow rate. For piping, adequate flow rate and exposure to the cleaning agent is needed. If piping of several different diameters is present in the system, the larger tubing will be the path of least resistance, and special design considerations may be required.

In designing a CIP process for cleaning cell-culture equipment, some basic guidelines can be followed. The equipment and piping should be arranged to physically circulate the liquid across product contacting surfaces at velocities that promote liquid turbulence in piping and sufficient flow across all of the internal surfaces of vessels. Suitable cleaning reagents should be chosen for effectiveness in solubilizing the components of the cell membranes and product and in eliminating any potential process solutes that may reside in equipment.

The general process equipment design requirements for efficient cleaning are as follows:

- Use 316L stainless steel for all process contacting equipment surfaces (see Table 76.2).
- The equipment should confine the cleaning solutions.
- Use seamless SS316L tubing.
- Pitch the bottoms of flat vessels not less than 1/4″ per ft from rear to front and 1/2″ per ft from side to center to provide reasonable flow for moving of suspended solids.
- Pitch flat top surfaces approximately 1/2″ per ft from center to sidewalls to encourage the continual flow of water sprayed on the surfaces toward the sidewalls.
- A minimum radius of 1″ is desirable at all tank corners, whether vertical or horizontal.
- Equip the vessel with an adequate permanent vent to protect against all changes in pressure or vacuum resulting from the heating and cooling associated with the cleaning process or design it with appropriate vacuum and pressure ratings.

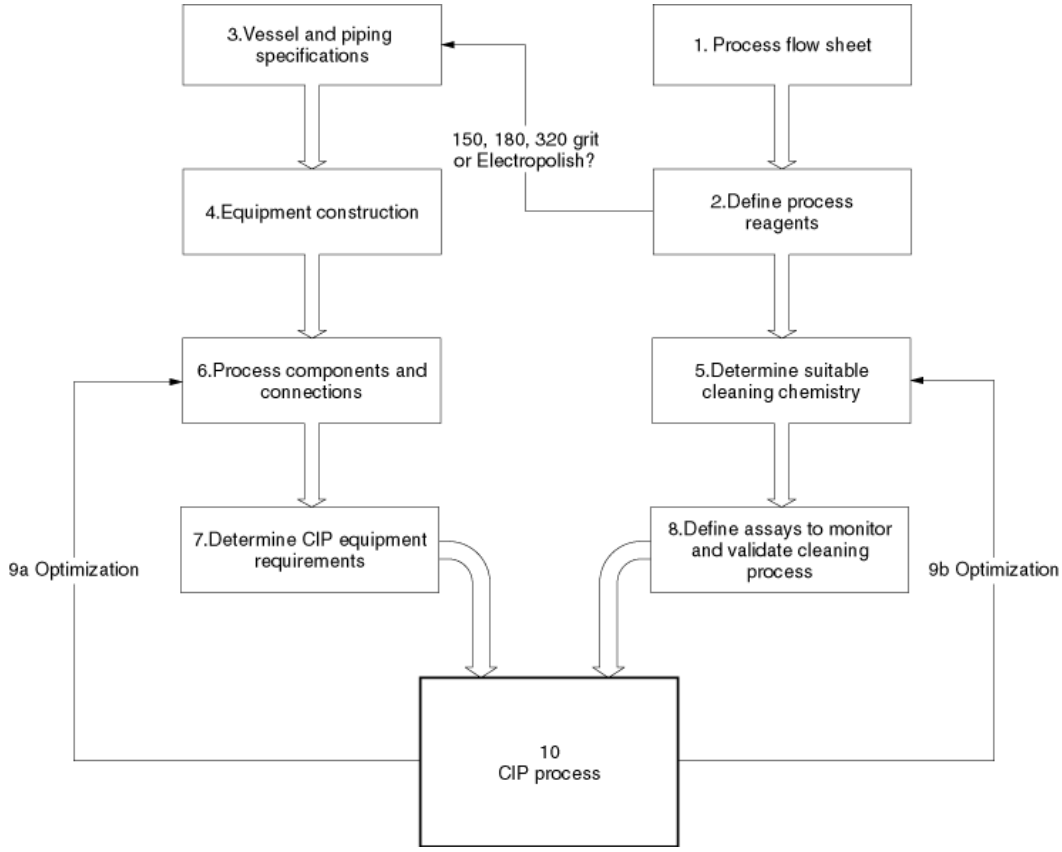


Figure 76.2. Fundamental elements for developing a CIP process for effective cleaning of bioreactor systems. The process flow sheet provides information for specifying of the process equipment and cleaning chemistry for the likely process residuals. Specification of electropolished surfaces may be based on the potential difficulty of cleaning the process, equipment. Numbers reflect the time sequence of the activities.

TABLE 76.1. Composition of CIP Reagents Used in Large-Scale Cell Culture Equipment Cleaning

Category	Compound	Comments
Prerinsing	Sodium phosphate buffer (50–100 m*M*, pH 6–8) DI water	Removal of loose protein and cellular material before cleaning
Caustic	0.1–1 N Sodium hydroxide 30–60°C	Strong organic dissolving power
Caustic detergents	0.1–1 N Sodium hydroxide+0.04% Sodium dodecyl benzene sulfonate (SDBS)	SDBS helps solubilize oil/lipid material and is easier to remove than SDS
Alkaline detergents	Trisodium phosphate and sodium hydroxide	Improved dispersion of soils; not used often in fermenters
Chlorinated caustic and alkaline detergents	Sodium hypochlorite (50–100 ppm Cl_2) with) trisodium phosphate and sodium hydroxide	Inceased cleaning and sanitization; has been used in filration membrane cleaning; requires extensive flushing with DI water to remove chlorine (can destroy oxide layer and lead to pitting)
Neutral detergents	0.1–1% Triton X-100, 0.1% Tween 80	Occasionally used as a orthogonal choice to caustic for hard to clean protein precipitates
Acids	Phosphoric acid	Used in neutralization step

TABLE 76.2. Composition of Common AISI Grades of Austenitic Stainless Steels

Grade	% Carbon by weight	% Chromium by weight	% Nickel by weight	% Titanium by weight	% Molybdenum by weight
304	0.08	18–20	8–11		
304L	0.03	18–20	8–12		
321	0.08	17–19	9–12	≥5 × Carbon	
316	0.08	16–18	10–14		2–3
316L	0.03	16–18	10–14		2–3

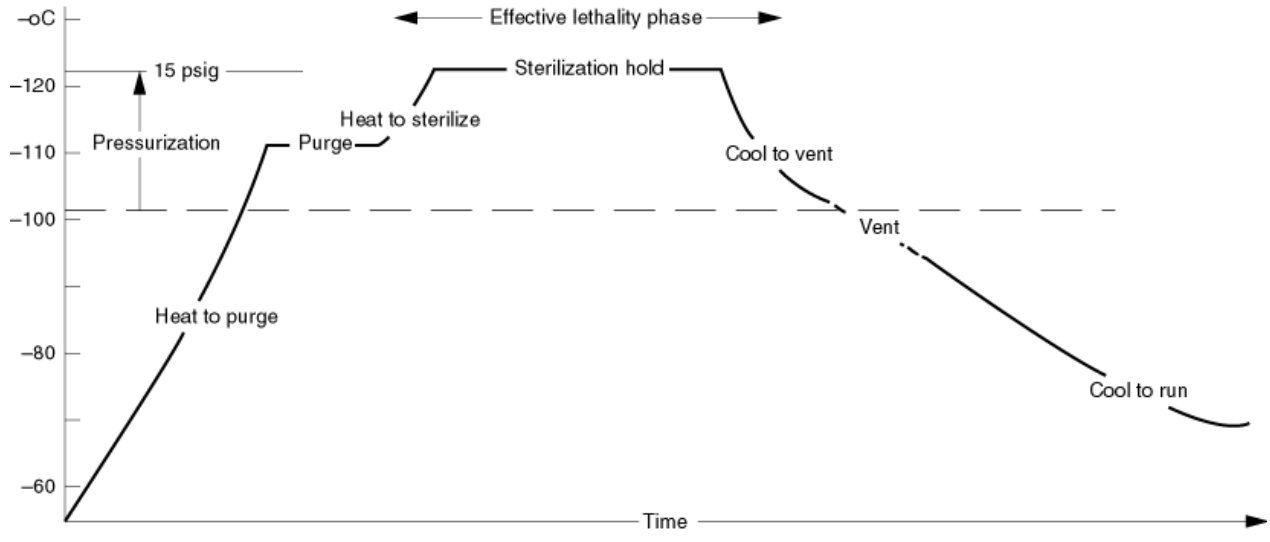


Figure 76.3. Typical sterilization temperature–time profile.

- Inert-gas fusion-welded joints are the most suitable for all permanent connections in transfer systems constructed of 316L stainless steel.
- Clamp-type joints of CIP design are acceptable for semipermanent connections. Such joints should maintain the alignment of the interconnecting fittings, have gaskets which remain flush with interior surfaces, and be designed to ensure that pressure exists on each side of the gasket to avoid product buildup that might occur in joints that are otherwise watertight.
- Pitch piping at 1/16″ to 1/8″ per ft sloping to the drain ports. The pitch must be continuous.
- Avoid dead-ends and branches in piping. Locate any required branches or tees in a horizontal position and limit them to not more than three pipe diameters long. Vertical dead-ends are undesirable because trapped air prevents cleaning solution from reaching the upper portion of the fitting.
- Use valves of diaphragm, pinch, or metal bellows sealed stem designs (12,13). Other designs such as ball valves are prone to accumulate particles and debris in the vicinity of the gasket (14).
- Construct equipment of components and materials which meet 3-A standards. Use appropriate materials such as EPDM, Teflon EPDM-backed silicone, and Teflon for gaskets.
- Polish contact surfaces to a #4 finish (RMS surface roughness factor of Ra 30–35 μinch) or better finish. This may also be specified as 150 grit (See Table 76.3) and for a Ra of 15–30 μinch 180 grit. Electropolishing, although not mandatory, may be a good choice to facilitate easy cleaning. Electropolishing involves polishing to at least a 180-grit finish followed by anodic electrochemical dissolution of vessel surface irregularities. The electropolishing process produces a smoother surface finish, reducing the surface roughness (Ra) to 0.18–0.22 μm (<10 μinch), and improves cleanability by removing pockets, that might retain solutes and microbes (15). Electropolishing passivates the stainless steel surfaces by forming a stable oxide layer that renders the surface resistant to corrosion. Chemical repassivation is necessary periodically using nitric acid or chelating solutions (16).
- For large-scale systems (>1000-L bioreactor) the CIP unit should operate reliably with minimal quantities of solutions in the total system to reduce water, chemical, and steam requirements and the cost of treating aqueous waste.

TABLE 76.3. Specified Stainless Steel Surface Finishes

Finish/Polish	Grit	Ra[a] (μinch)	AppearanceProcess Uses	Relative Cost		
No. 1 finish	80–120	40–50	Rough, dull, Imperfections	Hot rolled, annealed, and descaled	Not used in biotechnology	
No. 2D finish			Dull	Cold rolled, annealed, and descaled		
No. 2B finish			Bright gray	Cold rolled, annealed, descaled, and rolled through polish roll	A preliminary step to higher quality finishes; nonproduct contacting areas; media preparation tanks	1.00
No. 3 polish			Semipolished			1.04
No. 4 polish	150–180	15–30	Bright finish with grain marks; no surface imperfections		Standard 3-A polish Common dairy finish; bioreactors	1.05
No. 6 polish	240	10–15	Dull satin	Brushed in a medium of abrasives and oil	ms	1.07
No. 7 polish	320	<10	Highly reflective but some grit lines	Buffed, finely ground surfaces; a high-quality SS	Tissue cultures and QWFI system	1.08
No. 8 polish	320	<10	Mirror finish	Successive stage polishing with finer abrasives; extensive buffing with rouges to remove grit lines; high-quality SS	Bioreactors	
Electropolished	320	<10	Smooth, bright finish	Removal of a thin layer 0.01″ to 0.0001″ deep	WFI process equipment; bioreactors	1.10

[a]The average Ra is derived from readings taken at four cross sections approximately 90° apart. Ra readings taken across grain

The process of CIP may also be assigned some basic operational guidelines to ensure success. These are as follows:

- During CIP, the equipment remains assembled.
- Piping systems can be effectively cleaned via recirculation of flush, wash, and rinse solutions at flow rates that produce a velocity of ≥ 5 ft.s^{-1} in the largest diameter piping in a CIP circuit. A minimum Reynolds number of 10,000 leads to good radial mixing of solutes and soil, efficient heat transfer, effective mass transfer for removal of solutes, and a level of momentum that scours the equipment surfaces.
- Tanks can be effectively cleaned by distributing flush, wash and rinse solutions on the upper surfaces at pumping rates equivalent to 2.0–2.5 gpm/ft^2 of circumference for vertical vessels or at 0.2–0.3 gpm ft^2 of internal surface for horizontal and rectangular tanks.
- Use of one or more spray balls inside vessels, to distribute the cleaning fluids evenly across all the inside surfaces of the vessel and to avoid producing a "bathtub ring" that results from simply filling and draining a vessel.
- Use multiple spray balls in tanks that contain baffles and other internals that may interfere with the CIP fluid flow.

The essential cleaning problem is typical for all vessels. Vertical sight glasses, side ports for pH, dO_2 and temperature probes are present in the vessel sidewalls and present horizontal ledges. Inlet ports exist above the liquid level for acid, alkali, and antifoam addition, that may be vulnerable to aerosol deposition and drying. Spargers for efficient oxygenation and CO_2 and ammonia addition must be CIP cleanable. Agitators are top or bottom entry designs

requiring seals at the point of vessel entry. Magnetic drive agitators with simple internal ceramic seals can be used for mixing in small-scale suspension bioreactors. These mixers should be removed periodically to check and renew worn seal surfaces. Additional bearings within the vessel zone are needed for large-scale reactors with long agitator shafts. Foam at the liquid surface as a result of bubble aeration may lead to a dry biomass ring on the vessel surface. Pressure vessels are designed to operate at a maximum of 40–45 psig (150–180°C) and are equipped with pressure rupture disks. These disks may be in a remote location inside a nozzle outlet and require periodic maintenance and cleaning if foaming occurs. The vessel top-dish may also contain entry ports for sensors such as foam probes and pressure sensors, which will be fouled by foam and aerosol-entrained debris. Such problems may require spray-ball installations to access such locations with CIP reagents.

The degree of difficulty of cleaning is a function of the quality of the equipment surfaces, sanitary design, and the type of organism or biological material that causes the soiling. A mycelial polysaccharide-type soil will be harder to clean than a yeast or bacterial soil. Caustic, detergent, and water (Reverse Osmosis (RO water), Water For Injection (WFI)) rinses are generally suitable reagents for cleaning in cell culture reactors. Occasional nitric acid rinses for repassivation are performed. Rinsing of hydroxide can be monitored by pH, and rinsing of detergent can be monitored by a shake/foam test. From the standpoint of water usage, it is more efficient to use repeated low-volume rinses versus a few large-volume rinses.

Sanitary design of equipment is a fundamental requirement. The surface texture of equipment should be 180 grit or higher for vessels and 150 grit or higher for piping. In constructing the bioreactor, the surface quality should be preserved. Following mechanical polishing, the surfaces are washed and dried, oxides are removed by passivation, and surfaces maybe electropolished. Avoidance of dead legs in piping, use of high-quality welding to avoid hard to clean pits in cracks, and the use of diaphragm valves, and regular maintenance are fundamental to CIP. With electropolished vessels, CIP prevents damage to the surface that may be inflicted during COP operations. In addition to the aforementioned principle related to process equipment and CIP flow parameters, it is necessary to consider the design of the CIP recirculation equipment. The CIP systems consist of a centrifugal recirculation pump, heat exchanger, piping, and valves and tanks for storing CIP reagents. A waste collection vessel may be present for spent cleaning reagents enabling pH adjustment prior to evacuation to a sewer. In CIP systems, the multiple tank approach involves using a single tank per CIP solution. A single tank for each reagent utilizes more floor space but enables faster cleaning of many pieces of equipment. The single-tank approach, where one tank is used for all solutions, takes up less space, provides more flexibility, and will cost less but is less economical in the use of cleaning solutions (17). In medium-scale systems, it is usual to use the bioprocess tanks as CIP storage tanks. In this mode of operation, the bioreactor is rinsed and cleaned first and is then used as the CIP storage vessel for the external system cleaning. A vessel that is used for storing CIP reagent should possess a suitably sized drain port to allow an adequate flow rate from the supply tank to the inlet of the CIP pump. An NPSH calculation indicates the maximum frictional losses tolerable.

$$\mathrm{NPSH} = P_a + P_z + P_{vp} + P_f$$

where NPSH is the net positive suction head

P_a is the atmospheric pressure
P_z is the difference in vertical elevation between the supply tank liquid level and the pump inlet
P_{vp} is the vapor pressure of the liquid
P_f is the pressure drop due to frictional losses

Minimizing frictional losses by oversizing the supply tank outlet and adequately elevating of the supply tank are important. Tanks should be fitted with a vortex breaker above the tank outlet to avoid air entrainment and pump cavitation. Avoidance of cavitation and vortex formation will enable effective tank drainage and emptying. This is most important in the final water rinsing steps.

Validation of the CIP process is required in clinical product manufacturing processes but is a useful exercise in most situations. IQ and OQ Validation involves inspecting the installation of the valves and equipment to eliminate dead legs in the assemblies and to ensure that the cleaning fluid circulates at appropriate velocity of through the system. The PQ involves measuring the process residuals after cleaning. A minimum volume of sequestering solution is circulated through the equipment to contact and solubilize any residuals. The detection of residual is by a Lowry Petersen protein assay (18), which can detect ≥ 2 μg/mL protein. A total organic carbon (TOC) assay measures low quantities (0.5 ppm) of organic carbon containing residuals and has been applied in measuring residuals following CIP (19). Direct surface swabbing, in conjunction with TOC, can be used to investigate specific harder to clean surfaces such as gaskets. Acceptance criteria for process residuals depend on the potential level likely to associate with the flow of product through the process. Typically CIP should reduce the residual protein level to <100 ppm.

76.1.1.2 SIP. The steam-in-place (SIP) process has developed from the requirement to sterilize equipment that is too bulky or heavy to be moved into autoclaves or ovens. Although sterilization may be accomplished by wet heat, dry heat or chemicals, SIP has become synonymous with "sterilize-in-place." The biotechnology industry

has adopted saturated steam as the effective sterilizing agent for fixed-in-place equipment and autoclaving bioreactors and other tanks involved in parenteral filling operations (20).

Feed lines, inlet gas, exhaust lines, sensors, liquid feed filters, gas filters and vessels must be SIP compatible. A typical SIP cycle for a vessel involves several stages:

- Heat to purge (raising the temperature from ambient to ~105°C)
- Purge (eliminate air by steam at ~105°C). Air purging in SIP must be achieved by displacing the air with steam. In the air purge and initial heating stage, steam is introduced into the top of the vessel ports and the top port of the vessel heating/cooling jacket. In the example of a simple skid in Figure 76.4, the vessel drain port BRHV-1 on the base of the vessel, the steam solenoid valves SV-1 through SV-4, diaphragm valves D8, D10, D12 and D14, and exhaust line pressure regulating valve NV-1 are opened. The steam line to the vessel jacket, SV6, and the steam trap solenoid valve SV-7 are open and external steam/steam condensate heats the vessel walls and minimizes condensate buildup on the interior walls. The steam displaces the air from the vessel through the harvest drain line for several minutes, and the harvest line diaphragm valve D17 is closed to direct the steam condensate to the steam trap through the open diaphragm valve 18. If the air is not effectively removed by the air purge, the vessel will develop an air barrier, which increases the heat transfer resistance from the jacket. If this occurs, the mixture of air and steam will lower the saturation pressure of the steam resulting in a sterilization temperature below the targeted value of 121°C for a 15-psig sterilization pressure.
- Heat to sterilize (elevate temperature from 105°C to 121°C). In the heating period, the pressure in the system is allowed to approach the supply steam pressure (15 psig) by closing exit valves D14. Condensation is produced during the heating phase and is removed from the system through steam traps placed in drains, vents or the harvest line at the base of the vessel. Removal of condensate is very important because it may have the opportunity to supercool on the walls of the equipment.
- As the temperature increases, the steam flow through the system is reduced to the amount consumed by the traps and orifices plus the amount needed for heating. A manual steam pressure reduction valve (PRV-S) regulates steam pressure (18–25 psig).
- Sterilization (hold at 121°C for a designated duration of between 15 and 60 minutes). When the sterilization temperature is reached, the time and temperature are monitored. When the sterilization hold period is completed, steam valves SV1-SV-4 are closed, shutting off the steam. Vent valve NV-1 is used to reduce the system pressure after opening valve D14.
- Cool to vent (reduce temperature from 121°C to 100–105°C). After shutting off the steam supply, the pressure in the system decreases as a result of steam condensation and flow through the vessel vent filter.
- Vent sterile air (open D15) is used to displace the condensing steam vapor to avoid vacuum formation and to maintain a slight internal positive pressure to prevent possible ingress of gaskets, probe components, and nonsterile air. Allow the temperature to reach <100°C. The vessel drain valve BRHV-1 is closed, and the steam trace is initiated through solenoid valve SV-5. Residual heat in the vessel evaporates the cooling condensate as the pressure is reduced.
- Cool to run (reduce temperature to run temperature of 20–37°C, and maintain positive pressure inside the vessel).

Dead legs are most likely to be present somewhere in hard-piped systems. They may be present in tee connections for instrument housings, valves, or short pipe lengths before isolation valves. Unlike conditions in a straight pipe or a tank, air cannot be displaced by convection or a washout process. In the worst-case analysis, we assume that the air would be eliminated by diffusion from the dead leg into the main path. Orientation of the dead leg should allow condensate to drain into the sloped main path.

Autoclaves purge air through a slow vacuum cycle prior to the heating phase. Use of vacuum purging of air for large-scale process equipment is limited by the expense required to install a plant-wide vacuum system and the vacuum pressure rating of the process vessels and equipment. Bioreactors are typically built as pressure vessels rated for 3-bar internal pressure and for full internal vacuum at 150°C. In SIP, the relative positive pressure in the vessel is always maintained. In autoclaving, it is necessary to ensure that non-pressure-rated vessels are fitted with large enough vent filters to accommodate the rate of pressure change during vacuum/steam cycling and slow vent cool down.

Very few detailed engineering descriptions of the SIP process are provided in the literature. However, a singular detailed analysis has been provided by Noble (21). The following discussion of steam-sterilization design is taken from Noble's topical paper.

76.1.1.2.1 Air purging. During the purge phase, air is mixed with steam by convection and is removed as an air/steam mixture. The mixing process is poorly defined because forced circulation is not present. In practice, the

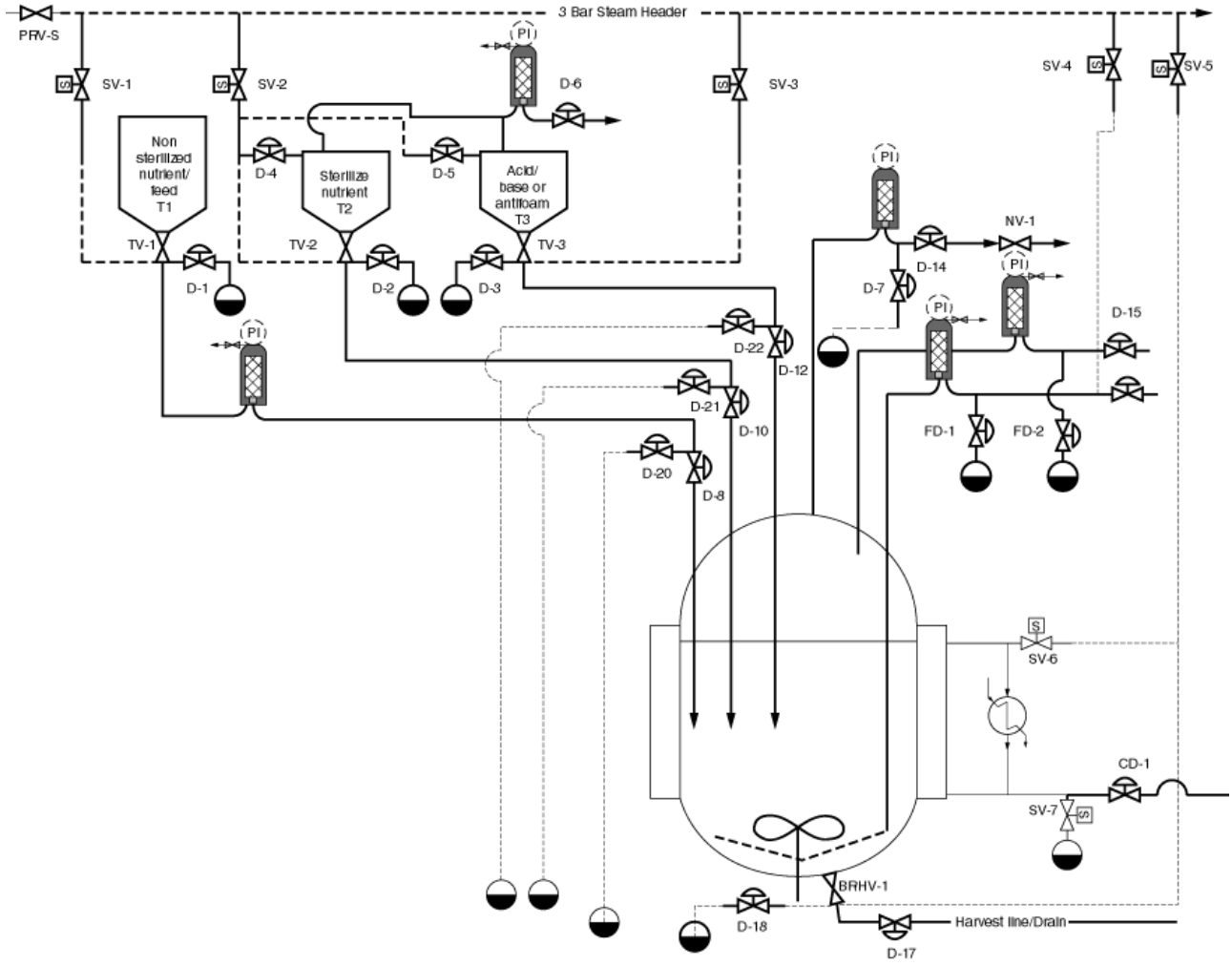


Figure 76.4. Bioreactor-skid pipe and valve arrangements. Representation of a fixed-in-place bioreactor showing interconnections with nutrient supply, inlet gases, and exhaust gas supplies. T1 piping is an example of filter sterilization of a nutrient to be fed to the bioreactor. T2 and T3 piping layouts are typical examples of direct addition of sterile components. TV-1, TV-2, and TV-3 are flush-mounted, steam-sterilizable, piston-design, tank harvest valves.

momentum of the in-flowing steam provides the mixing energy. The fastest removal of air can be anticipated when the agitation and flow approximate to an ideal Continuous Stirred Tank Reactor (CSTR). For this to occur, the mixing time (t_H) must be much less than the space-time (τ). For design purposes assume that

$$t_H = 0.1\tau \tag{76.1}$$

For a turbulent steam jet (Re_N range of 10,000–90,000), t_H can be estimated from an experimental correlation given by Henzler (22):

$$t_H = \frac{C_H d_i}{v_i} \tag{76.2}$$

where the subscript (i) refers to the diameter d and velocity v of the inflowing jet. The dimensionless mixing number C_H is (in the turbulent range) a function only of the geometry:

$$C_H = 1.1\left(\frac{D}{d_i}\right)^{2.75} \tag{76.3}$$

for $L = D$. For this geometry, the space-time is defined by

$$\tau = \frac{D^3}{(v_i)d_i^2} \tag{76.4}$$

In this case it is assumed that the steam is not condensing. In actual reality, the value is then larger because condensation

reduces the flow. Substituting these relations equation 76.6, there is no ratio of d_I/D that also ensures turbulent jet flow. The relationship in equation 76.1 is not feasible and this infers that, in practice, good mixing, provided by steam inflow, cannot be created in tanks unless special nozzle developments can improve jet-mixing performance. In reality, the mixing time is less than the space-time so that some mixing is to be expected. From a design perspective, d_i should be minimized and v_i should be maximized to reduce processing time and create a turbulent steam jet.

At maximum steam flow, the operation can be characterized by

$$\tau = \frac{4V}{\pi d_i^2(v_i)} = 0.0364\frac{V}{d_i^2} \tag{76.5}$$

and

$$w_s = \frac{\rho V}{\tau} \tag{76.6}$$

For a 1-inch steam inlet supplying a 1000 L bioreactor

$$\tau = 56.4 \text{ S}$$

and the steam flow is given as

$$w_s = 0.1213 \text{ kg} \cdot \text{s}^{-1} = 76.6 \text{ kg} \cdot \text{hr}^{-1}$$

for saturated steam at 1-bar gauge pressure.

It is recommended in practice that the air-purge step should be allowed a factor of 4 times τ.

Air is transported down to the harvest valve at the base of the vessel air and radially to the vessel wall where it may form a boundary layer. Cold air is denser than steam (ρ air is 1.225 kg m^{-3} at STP, steam 0.013 kg m^{-3} at 121°C). Trapped air may be found predominantly in the base of the vessel. This raises the importance of bottom vent purging.

In the equation of motion, the driving force for forced convection was described in Bird (23) as ∇P. The corresponding driving force for free convection is $\Delta\rho g$, which is related to the Grashof number. For the extreme combination of air at 25°C and steam at 121°C,

$$\Delta\rho g \approx 12 \text{ Nm}^3$$

whereas the average pressure gradient, assuming a 2-atm steam supply and a drain at 1 atm is

$$\nabla P \approx \frac{\Delta P}{L} \approx \frac{10^5}{5} = 2 \cdot 10^4 \text{ Nm}^3$$

Providing that the steam flow is not largely throttled during the air purge, free convection should be of minor importance, and an intact air body should not remain in the vessel. When the steam and air become mixed, a gravity-induced polarization will not be a measurable phenomenon. Gradients will be insignificant, as predicted using the relationship from Bird *et al*. (23, p. 576) employed for a similar situation.

$$\left(\frac{X_s}{X_{s0}}\right)^{\overline{V_a}}\left(\frac{X_{a0}}{X_a}\right)^{\overline{V_s}} = \exp\left[(\overline{V}_s M_a - \overline{V}_a M_s)\frac{gL}{RT}\right] \tag{76.7}$$

After mixing, the air purging will occur when steam mixes with the air and exits through both the drain and vent lines.

76.1.1.2.2 Heating. Heating the vessel space by displacing colder gas and by sending heat through the vessel wall will increase the temperature of the internal surfaces of the equipment. In this situation, heat transfer resistance becomes relevant. Insulation of vessels and pipe will reduce condensate load.

Thermal response time is estimated from

$$t_T = \frac{\Delta x^2}{2\alpha} \tag{76.8}$$

where α is the thermal diffusivity and the thermal resistance is calculated from

$$R_S = \frac{\Delta x}{k} \tag{76.9}$$

The temperature changes are very rapid in the wall and condensate film compared to the insulation. The condensate film plays a critical role, and a change in its thickness can have a large impact on the response of the system. This is a result of its relatively low thermal diffusivity.

76.1.1.2.3 Sterilization Hold. In this stage, a pseudosteady state can be assumed. Temperature is constant, and concentrations do not change significantly. Because temperature nonuniformities are minimal, normal convection will be unimportant. Transport of heat and mass will depend on diffusive driving forces.

Under these conditions the heat transport can be estimated. In a pipe it is required that the pipe wall temperature be at 121°C. For a well-insulated pipe, the heat flux becomes

$$\left(\frac{Q}{A}\right)_{INS} = \frac{(121-25)2k_{INS}}{D\ln(D + 2\Delta x_{INS}/D)} \tag{76.10}$$

Ignoring curvature, equation 76.15 gives

$$\left(\frac{Q}{A}\right)_{INS} = 344 \text{ W} \cdot \text{m}^{-2}$$

which is calculated when $\Delta x = D$ and $D = 2.54$ cm, $K_{INS} = 0.05$ W·m^{-1}·°C^{-1}, $\Delta x_{INS} = 0.0254$ m.

A correlation is available from Perry and Green (24) for convective and radiative heat transfer coefficient for noninsulated and insulated steel pipe in a room at 80°F. The result for a 1-inch diameter pipe is 16.1 W · m^{-2}·°C^{-1} which can be used to calculate Q/A below

$$\left(\frac{Q}{A}\right)_{\text{bare}} = h\delta T = 16.1(121 - 25) = 1550 \text{ W} \cdot \text{m}^{-2} \tag{76.11}$$

The fluxes correspond to the required minimum steam flow from which the expected condensate flow can be estimated. The minimum flow w_s is the entering steam flow and exiting condensate flow:

$$w_s = \left(\frac{Q}{A}\right) \cdot \frac{\pi DL}{H} \tag{76.12}$$

Laminar flow will prevail at the pipe exit. At the entrance of the pipe, turbulent flow will arise if the pipe exceeds a critical length, corresponding to a value of Re = 2000 at the entrance:

$$L_{\text{crit}} = \frac{500\mu_s H}{(Q/A)} \tag{76.13}$$

L_{crit} is in the range of 10–50 m for the heat flux determined in equation 76.10. Assuming a worst case of laminar steam flow and horizontal stratified flow of condensate, the depth of liquid (Δx_c) condensate in a round pipe is hard to calculate. Rectangular channel models have been described (25) and may provide a relevant solution, considering the low depth of condensate likely in SIP where curvature effects are not so important:

$$w_s = \frac{4a\Delta x_c^3 N}{K} \tag{76.14}$$

where a is the channel width, K is a geometric constant,

$$N = \frac{\rho^2 g(\sin\beta)}{\mu c} \tag{76.15}$$

and β is the angle between the pipe and the horizontal. For pipes with a diameter of 1 inch, a good approximation is $a = 10\Delta x_c$, and substituting equation 76.12 gives

$$\Delta x_c \propto \left[\frac{(Q/A)DL}{\sin\beta}\right]^{1/4} \tag{76.16}$$

76.1.1.2.4 Steady-State Models and Analysis. A one-dimensional model is depicted in Figure 76.5 for a region at a horizontal wall. During the sterilization hold period, the largest nonuniformities in properties would be expected in this region.

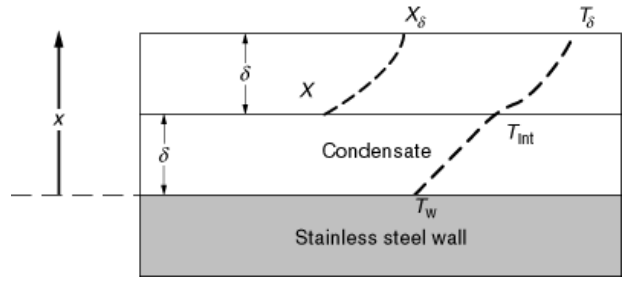


Figure 76.5. One-dimensional model of temperature profile for condensate layer at pipe wall. Adapted from Ref. 21.

Heat transfer in the condensate layer occurs only by conduction. This is described by

$$\left(\frac{Q}{A}\right) = k_c \frac{(T_{INT} - T_W)}{\delta_C} \tag{76.17}$$

Assuming that the maximum allowable temperature difference is limited to 0.5°C, a maximum condensate layer may be derived using the heat fluxes defined earlier.

$$(\delta_{C,max})_{INS} = 1.0 \cdot 10^{-3} \text{ m}$$

$$(\delta_{C,max})_{bare} = 2.2 \cdot 10^{-4} \text{ m}$$

Relating equation 76.17 to equation 76.16, a design aid for placing steam traps or orifices can be determined as

$$\Delta L = \frac{(9.28 \cdot 10^{16})k_c \sin\beta}{(Q/A)^5 D\Delta T^4} \tag{76.18}$$

Using a 1″ pipe sloped to 1/8″/ft as an example, the length at which the buildup of condensate creates a 0.5°C drop is given below:

$$(\Delta L_{max})_{INS} = 110 \text{ m}$$

and

$$(\Delta L_{max})_{bare} = 0.057 \text{ m}$$

Clearly, the result shows the importance of insulating piping. A similar result is obtained by using flow relationships for round channels instead of equation 76.12. Because liquid flow in this model is laminar, it will not thermally mix. A temperature probe in the drain will measure the mixed condensate stream. From this average temperature measurement, it will be difficult to measure the extent of subcooling. This average temperature can be computed from

$$\langle T \rangle = \frac{\int_0^{\delta_c} T v_z dx}{\int_0^{\delta_c} v_z dx} \tag{76.19}$$

In a rectangular flow model, the velocity profile is well known and is given as

$$\langle T \rangle = T_{\mathrm{INT}} - (T_{\mathrm{INT}} - T_{\mathrm{w}})/6 \tag{76.20}$$

Where the cold spot is associated with T_{w}, the equation indicates that the temperature deviations are damped severely in the resultant T.

76.1.1.2.5 Gas Phase. A model for one-dimensional condensation of vapor in the presence of a noncondensable gas is well-known and used in psychrometric calculations (see Ref. 23, example 18.5-1). The basic equations to be solved are heat transport, mass transport, air properties, (assuming ideal gas), and steam properties (obtained from curve fits to the steam tables). The sum of mole fractions is limited to one, and the pressure is constrained to be constant over the boundary layer. The heat transport equation is then given by

$$-\left(\frac{Q}{A}\right) = -k\frac{dT}{dx} + N_{\mathrm{s}}M_{\mathrm{s}}[C_{\mathrm{p}}(T - T_{\mathrm{INT}}) + H] \tag{76.21}$$

where the constant N_{s} is the molar flux of steam to the wall. The molar flux is constant in this model and is the solution for diffusion through the stagnant film:

$$N_{\mathrm{s}} = \frac{c_{\mathrm{ln}}\wp_{\mathrm{as}}}{\delta}\ln\left(\frac{1 - X_{\mathrm{s},\delta}}{1 - X_{\mathrm{s,INT}}}\right) \tag{76.22}$$

Constant concentration has been assumed and set to the log mean average. The variation in concentration is normally insignificant. There are two degrees of freedom in this model. The wall temperature can be fixed at a suitable sterilization temperature (121°C). The other variable is the amount of air in the boundary layer. A simple analytical solution may be obtained if a value of N_{s} is assumed. The value is constrained between zero and $N_{\mathrm{s,\,max}}$:

$$N_{\mathrm{s,max}} = -\frac{(Q/A)}{HM_{\mathrm{s}}} \tag{76.23}$$

which would exist when no resistance to mass transfer in the gas phase exists.

With the constant B defined as

$$B = \frac{(Q/A)}{N_{\mathrm{s}}M_{\mathrm{s}}C_{\mathrm{p}}} + \frac{H - C_{\mathrm{p}}T_{\mathrm{INT}}}{C_{\mathrm{p}}} \tag{76.24}$$

the integration of equation 76.21 can be expressed as

$$T_{\delta} = (T_{\mathrm{INT}} + B)\exp\left(\frac{N_{\mathrm{S}}M_{\mathrm{S}}C_{\mathrm{p}}\delta}{k}\right) - B \tag{76.25}$$

Given the temperatures at the boundaries, the partial pressures of steam can be evaluated from the following quadratic fit to the steam table over the range of 120–141°C:

$$P_{\mathrm{s}} = (8.91534 \cdot 10^5) - (1.76864 \cdot 10^4)T + 99.28\,T^2[P_{\mathrm{a}}] \tag{76.26}$$

The molar concentrations of steam can also be determined by a similar curve fit:

$$c_{\mathrm{x}} = \frac{0.8892}{134.829 - 1.60466\,T + 0.004999\,T^2}(\mathrm{kg \cdot mol \cdot m^{-3}}) \tag{76.27}$$

The concentration of air can be expressed from the ideal gas law, yielding the following relationship:

$$c_{\mathrm{a},\delta} = \frac{(P_{\mathrm{s,INT}} - P_{\mathrm{s},\delta}) + c_{\mathrm{a,INT}}R(T_{\mathrm{INT}} + 273.16)}{R(T_{\delta} + 273.16)} \tag{76.28}$$

Converting mole fractions to concentrations with

$$X_s = \frac{c_{\mathrm{s}}}{(c_{\mathrm{s}} + c_{\mathrm{a}})} \tag{76.29}$$

these relations can be solved simultaneously with equation 76.27 to find the concentrations at the two limits.

The total system pressure is then

$$P_{\mathrm{tot}} = P_{\mathrm{s,INT}} + 8313.7c_{\mathrm{a,INT}}(T_{\mathrm{INT}} + 272.16) \tag{76.30}$$

which is an approximate measure of the air trapped in the system. The exact fraction of the original air that is trapped can be expressed as

$$f_{\mathrm{a}} = \frac{\int_0^{\delta} c_{\mathrm{a}}dx}{\delta(P/RT)} \tag{76.31}$$

From equation 76.22, this can be derived as

$$f_{\mathrm{a}} = c_{\mathrm{a,INT}}\left[\exp\left(\frac{\delta N_{\mathrm{s}}}{c_{\mathrm{ln}}\wp_{\mathrm{as}}}\right) - 1\right] \cdot \frac{c_{\mathrm{ln}}\wp_{\mathrm{as}}}{\delta N_{\mathrm{s}}} \cdot \frac{298\,R}{1.015 \cdot 10^5} \tag{76.32}$$

Examining the equations, the solution space can be defined by two parameters δN_{s} and $(Q/A)/N_{\mathrm{s}}$. As these parameters increase, the gas-phase resistance increases. Because N_{s} is not of particular interest, the space is shown in terms of f_{a}, (Q/A), and D. Under the stated assumptions, the boundary layer thickness is related simply to D by

$$\delta = \frac{D}{2} \tag{76.33}$$

The parameters used in the analysis are shown in the list of symbols at the end of the section and reflect steam

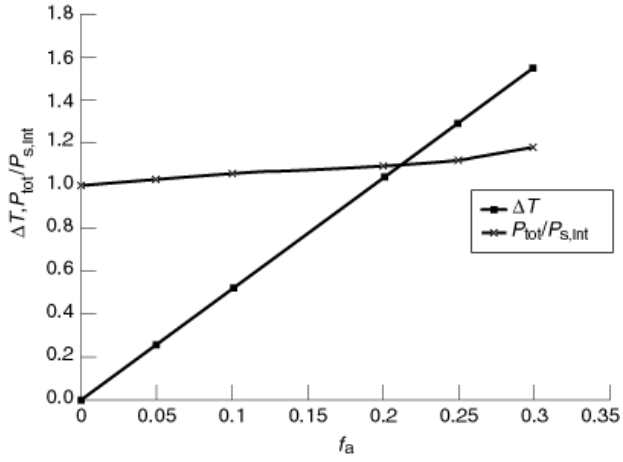


Figure 76.6. Magnitude of the gas-phase heat-transfer resistance. Conditions for pipe diameter D = 1 inch; T_{int} = 121°C; Q/A = 1550 W·m^{-2} (bare pipe). The air fraction f_a is calculated from equation 76.31. ΔT is the temperature span in the gas phase, and $P_{tot}/P_{a,\,int}$ shows the contribution of air to the total pressure. Adapted from Ref. 21.

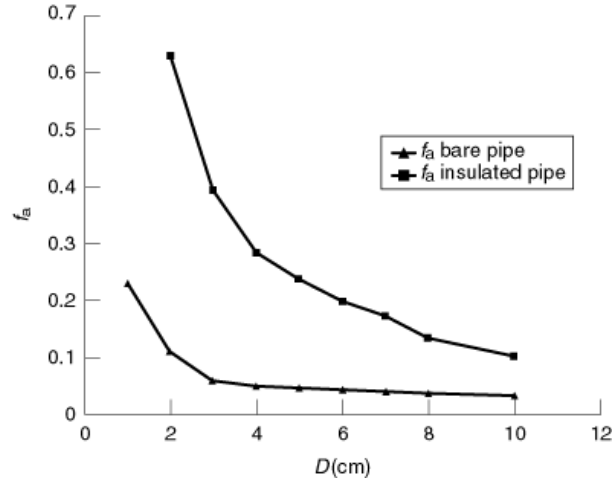


Figure 76.7. Limits of trapped air as a function of pipe diameter for a temperature drop of 0.5°C. For the gas-phase temperature span of 0.5°C, the interface temperature was fixed at 121°C. The trapped air is expressed as f_a, which is calculated from equation 76.31. Adapted from Ref. 21.

properties at 121°C. The diffusivity is estimated from a prediction developed by Slattery and Bird for low-pressure mixtures of steam and nonpolar gases, available in Bird *et al*. (23).

Figure 76.6 shows the magnitude of the gas-phase resistance. It is concluded that the amount of air trapped in a pipe would be low and $f_a < 0.1$. In Figure 76.7, it is shown that the gas-phase resistance in smaller pipes can be neglected because the air removal requirements are not large. In tanks it may be considered that gas-phase resistances may be significant, thereby resulting in nonhomogeneity of temperature. In reality, the gas layer would be close to the vertical walls. The lower temperature would be measured by an RTD thermometer at the vessel wall or else could be mapped using thermocouples attached to the vessel surfaces.

Dead legs in ports, nozzles and piping may harbor air which will cause significant gas-phase heat transfer resistance. When condensate can drain from dead legs, it can increase the mixing of steam and air through convection and aid in purging. In the worst case, dead-leg pockets will eventually reach temperature through diffusive heat transfer. Minimization of the *L*/*D* ratio at ≤6 is recommended to facilitate air purging and the ability to reach sterilization temperature in the dead-leg zone.

Use of double steam blocks on vessel inlet lines will enable sterilization through valves and longer lengths of piping.

Steam traps are important components in SIP and should be used in all low-point locations where condensate can accumulate.

In the final analysis steam-sterilization cycles are designed to provide significant overkill, providing greater than 30 logs of kill for a spore-forming organism. Through adherence to high standards for cleaning equipment, maintenance, and diligence in operation, the probability of contamination is virtually negligible. Small discrepancies in temperature (0.5°C) will have no significant effect on increasing or decreasing the very low probability that a contaminant survives the SIP process. Contamination is most frequently a result of operational errors during sampling and production. Equipment related contamination is usually through waterborne sources, for example, as a result of leaking cooling coils or faulty seals and gaskets.

76.1.2 Instrumentation

Instruments measure the parameters in the bioreactor and provide a means for adjusting the conditions. Adjustments are through manual intervention or by automated control of the bioreactor. A variety of sensors and probes are available (see Table 76.4).

Instrumentation has been an important part of bioreactor operation for over thirty years. At the start of the era, in-line instruments were confined to temperature control and simple indications of DOT and pH, enabling manual adjustments of aeration and acid/base addition. At that time, sensors were leading the control envelope. Computer-assisted bioreactor control applications emerged in the mid 1960s and then increased rapidly during the 1970s. Currently, powerful, compact computer systems provide an ideal partnership for the wide variety of the instruments that are available for use in bioreactors. The early concerns for

TABLE 76.4. Sensors and Measurement Devices

Physical Parameter	Sensor Principle	Features
Gas flowrate	Rotameter	Bouyancy position	Simple but limited use
	Mass flowmeters (Porter)	Temperature difference	Automatic, accurate, requires calibration; gas specific (C_p)
Liquid Flow Rate	Turbine, gear, and helical flowmeters (e.g., Hoffer,)	Positive displacement volume rpm	Common, simple, low–high flow rates
	Mass flowmeters (e.g., Porter)	Temperature difference	Automatic, accurate, requires calibration
	Load cells/Scales	Δ weight/time	
	Peristaltic pumps	Volume delivered/rpm	Requires calibration; tubing creep and wear can occur in prolonged use
	Platinum resistance RTD	Change in resistance with T ($^\circ$C)	Reliable linear response of resistance and temperature
	Thermocouple		
Temperature	Hg-glass thermometer	Expansion of fluid with increasing temperature	Standard for cross-checking using thermowell in vessel
	Galvanic DOT in-tank probe	Electrochemical reaction at cathode	Requires maintenance, post-SIP calibration, and checking
	In-tank probe	Change of pH in bicarbonate electrolyte (combined with pH probe)	Slow response; requires post-SIP calibration and checking
DOT (dO_2)	In-tank probe	Electrochemical	Requires pre-SIP calibration; check during run
pCO_2	In-tank probe	CO_2 diffusion and pH change in bicarbonate buffer	Calibration using known pCO_2
pH	In-tank probe	Hydrogen ion passage across ceramic pore	Requires calibration before sterilization Checking required off-line

the increased risk of contamination or failure through the use of multiple in-line devices are compensated for by the increases in productivity gained with reliable and reproducible process control. Nowadays, the use of control loops using mass spectrometer-based off-gas analysis is common in industrial manufacturing processes (26).

Data analysis, process control, and determination of physiological parameters in bioreactors depend on measuring chemical and physical variables. Measurements are obtained either by manual off-line measurements or else monitored by in-tank sensors. pH and DOT probes have been widely used in the industry for many years. Many new probe devices are available for in-tank sensing of pCO_2 and biomass, and new autosamplers can facilitate rapid in-line measurement of metabolites (glucose, glutamine) and waste products (lactate, ammonia).

Bioreactors include nozzles and ports for inserting probes and sensors and connecting lines for adding or removing liquids and gases. The number and type of ports are specified before the construction of the bioreactors. In jacketed bioreactors built as pressure vessels, the insertion of probes through the vessel wall results in a decrease in the jacketed surface area available for heat transfer. This is not a serious restriction for plant and cell culture with low metabolic heat generation compared to bacteria. Ports are placed to enable locating sensors and probes in appropriate positions in the vessel for monitoring the designated parameters. Ports designated for pH and DOT probes are located near the bottom of the tank so that the probes are submerged in media at all times during the process. This requires side entry ports on vessels 50 L or greater in volume. In fed-batch reactors, the initial volume could be 0.2–0.6 of the total vessel volume, and the minimum liquid height should cover the probes. In small-scale bioreactors ($\leq$20 L), it is possible to use a top-head plate probe insertion in combination with long probes to access the liquid media. Vessels with many internal features such as aeration tubing, baffles, agitators,

spin filters, or internal settlers impose limitations on probe location.

For larger scale vessels, probes are inserted through the side of the vessel at the base of the cylindrical section. In large, tall vessels, additional probes are placed at the middle or higher section of the cylinder. The commonly used probes, pH, DOT, and newer probe types, are designed to fit into the Ingold 25-mm probe port. The guide tube is stainless steel (SS316L) and is specified as DIN 1 4435. The probes are inserted in a metal support cage that fits the 25-mm port. The probe tip is exposed to the bioreactor media and the probe stem is sealed by an O-ring. The metal sleeve is sealed in the Ingold probe holder by O-rings and is secured by a threaded, drilled cap at the end of the probe holder cylinder. A typical arrangement is shown in Figure 76.8.

76.1.2.1 pH. Growth and production rates may be strongly influenced by pH. Components of the media may have limited stability outside of the physiological pH range. Degradation of glutamine in cell culture media is influenced by pH with a rate constant of degradation of 2.2×10^{-4} hr^{-1} at pH 7.0 and 2.8×10^{-3} at pH 8.0 at 37°C which is equivalent to a half-life of 7–8 days (27). Thus it is important to control the pH of the medium before inoculation, as well as during the production phase. Probes for measuring of pH were developed by Ingold in 1947. In-vessel, steam-sterilizable pH probes have been available for nearly 50 years. Use of an in-line pH electrode in a fermenter was reported in 1959 (28).

The glass probes used for insertion in bioreactors consist of combined reference and indicator electrodes. Probes are available 13, 16, 21, 26, 31 and 36 cm long. The range of measurement is 1–14 pH with a temperature range of −5 to 135°C and a pressure range (in housing) of 100 psig at 25°C and 30 psig at 135°C. The reference electrolyte is a silver chloride/potassium chloride solution. Internal temperature correction is achieved through an integral thermistor temperature sensor. The outer glass body of the probe is constructed of potash soda lead glass. The terminal glass bulb is a proprietary silica glass made with small percentages of alkali metals and rare earth metals. The porous ceramic liquid junction, through which the process and probe are connected, is made of silica plus complex mineral compounds, fired at high temperature to form an inert, porous ceramic matrix. The internal electrolyte gel is 3.8 M potassium chloride, a cellulose thickening agent, and butylparaben (0.005%), an antifungal preservative.

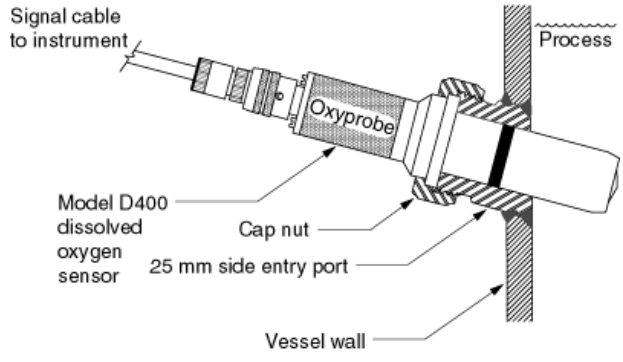


Figure 76.8. Vessel side port.

A standard Ingold probe measures pH with an accuracy of 0.04 pH ±0.01 and a reproducibility of 0.01–0.02 pH units. A drift of the pH signal may occur in a solution of constant (H+) concentration but should be less than 0.02 pH units hr^{-1}. Gel electrolyte (containing cellulose in the electrolyte) probes are the current, preferred choice, when SIP or autoclaving is required. Nongel electrolyte probes require housing pressurization to avoid boiling of the electrolyte during sterilization.

Following the insertion of the probe in the vessel port, the probe is ready for SIP or autoclaving. Control of pH is accomplished through a PID controller. Ideally, pH controllers should be split-range PID loop controllers. Split-range controllers have range-specific set points and provide separate PID outputs for actuating acid and base peristaltic pumps or valves. Split-range loop controllers are suited to pH control because they enable separation of the PID constants for the acid and base additions. With standard PID controllers, it is possible to have the acid pump overshoot the set point leading to a demand for base addition. This often leads to overadjustment of pH with a consequence of increased osmolality and potentially decreased productivity. When a common PID controller is used, a significant deadband and/or a decrease in the maximum addition rate of the acid and base can prevent the acid/base overcorrection. For large-scale reactors, acid and base may be added by using pneumatic tank pressure with actuating pulse-modulated solenoid valves.

76.1.2.2 DOT (dO_2 Probes). DOT is an important parameter to monitor and generally will be controlled in a bioreactor. Oxygen is required for cellular energy production and biosynthesis of product and cellular constituents. It is consumed at a rate of approximately 12×10^{-17} mol. $cell^{-1} \cdot s^{-1}$ (29). Oxygen is sparingly soluble in aqueous media (10 ppm or 260 μM) and may become limiting in high cell-density cultures. A high level of dissolved oxygen (hyperbaric DOT) is associated with oxygen-radical cell death (30). Two types of electrodes, galvanic and polarographic probes, are currently used for measuring dissolved oxygen. The major difference between polarographic and galvanic sensors is the source of the polarization voltage. The most commonly used probe is the polarographic probe, obtainable originally from Ingold, in which the voltage is supplied by a power supply in the amplifier. In the galvanic probe, the voltage is supplied by a separate electrochemical

reaction. In the polarographic probe, the cathode is platinum and the anode is a silver/silver chloride half-cell.

Cathode reaction (Pt):

$$O_2 + 2H_2O + 2e^- \rightarrow H_2O_2 + 2OH^-$$

Anode reaction (Ag/AgCl):

$$4Ag + 4Cl^- \rightarrow 4AgCl + 4e^-$$

Overall reaction:

$$4Ag + O_2 + 2H_2O + 4Cl^- \rightarrow 4AgCl + 4OH^-$$

The overall reaction produces alkaline conditions and consumes chloride ions. Silver chloride accumulates at the anode but does not impair the electrode. The chloride ions have to be replenished through periodic addition of fresh KCl. The electrode current depends on the oxygen partial pressure, not on the oxygen solubility in the solution. For a specific solution, the O_2 concentration C is proportional to its partial pressure (pO_2) according to Henry's law:

$$C = Kap O_2$$

where a = solubility factor of the solution and K is Henry's constant. The solubility factor is strongly influenced by the temperature and composition of the solution (illustrated in Table 76.5).

The cathode, anode, and the electrolyte of polarographic electrodes are separated from the measuring medium by a membrane permeable to oxygen but impermeable to most ions. The rate-controlling step is the diffusion of oxygen from the liquid medium through the membrane to the surface of the cathode. The current output of the probe is proportional to the activity or the partial pressure of the oxygen in the liquid medium.

DOT is controlled by using a staged control strategy. As the overall oxygen uptake rate increases, the DOT falls. In the first stage of DOT control, the agitation rate will be increased stepwise up to a maximum designated rpm. The next stage involves an increase in the airflow rate up to a designated maximum Lpm. The third stage involves decreasing the air flow rate and supplementing with oxygen gas up to a maximum Lpm. A fourth stage involves an increase in the bioreactor operating pressure. In cell culture, the rpm is generally fixed, and the DOT is controlled only through an increase in airflow rate and oxygen supplementation. Thus a DOT PID controller must provide output signals for rpm control and valve positioning for gas flow-rate control.

For lengthy perfusion mode operation, it is advisable to install a backup probe. In-line DOT probes may be readjusted by using off-line blood gas analyzer measurements. Daily off-line checks should be performed to monitor probe drift during culture processes.

TABLE 76.5. Oxygen Solubility and DOT Measurement

Medium Saturated with Air	Solubility of O_2 at 20°C and 760 mmHg (mg O_2/L)	% DOT (100% in water at 20°C and 760 mmHg)
Water	9.2	100
4 mol/L KCl	2.0	100
50% methanol/H_2O	21.9	100

76.1.2.3 Temperature Probes. Platinum 100-Ω resistance thermometers are used extensively in bioreactors. They can be inserted into an Ingold 25-mm standard probe holder. They may also be placed in the inlet and outlet of bioreactor cooling jackets to monitor heat removal/generation during culture operation. They need to be calibrated periodically to avoid large offsets. A temperature measurement accuracy of 0.1–0.2°C is achievable with RTD probes. Platinum RTD temperature sensors exhibit a linear, stable resistance versus temperature relationship. They are available in sanitary designs that conform to 3-A Sanitary Standards and feature product contact surfaces designed for CIP applications. Temperature control requires PID control of cooling jacket valves. In general, cooling is more likely to be required for large-scale vessels with lower surface area to volume ratios. Small vessels operating with animal or plant cells have low metabolic heat production, and control of culture temperature is likely to require heating the jacket. Unjacketed tanks may be fitted with heating bands (31) which operate as on/off devices and can be used with a pulse-modulating on/off PID controller. (Pulse modulation involves variation of the on-time/off-time and number of events/unit time).

76.1.2.4 pCO_2. CO_2 is toxic to CHO cells at levels >105 mmHg which is evidenced by reduced growth rate and productivity (32). It is likely that aqueous dissolved CO_2 influences the internal pH of the cell (pH_i). CO_2 may accumulate to high levels in bioreactors at high cell density and where removal of CO_2 from the broth is low due to low sparging rates and microbubble oxygenation. Absence of CO_2 or bicarbonate ions in cell culture media can also lead to repression of growth of animal cells (33). Therefore, it is important to monitor the CO_2 level in a bioreactor. Control of dCO_2 is usually not automated and is regulated through manipulation of sparging rates or vessel head-sweep airflow rate to reduce the headspace pCO_2. In sparged reactors, the total removal rate of CO_2 is limited by the maximum sparge rate that can be tolerated before foam or cell/bubble damage rates become limiting.

Cell culture media often use a bicarbonate buffer system. The reactions of the CO_2/bicarbonate buffer system are as follows:

$$CO_2 + H_2O \longleftrightarrow H_2CO_3 \text{ (at pH} < 8.0 \text{ reversible, forward reaction rate is slow)}$$

$$H_2CO_3 \longleftrightarrow HCO_3^- + H^+ \text{(rapid rate)}$$

$$CO_2 + H_2O \longleftrightarrow HCO_3^- + H^+ \text{(overall reaction } K_a = 5.2 \times 10^{-7} \text{ M)}$$

If a bicarbonate-buffered medium is allowed to stand in air, the carbon dioxide will leave solution, and the pH of the medium will increase. To prevent this, media should be stored below a 5% v/v CO_2 air mixture.

CO_2 can been measured off-line using blood gas analyzers (34) or by in-line sterilizable pCO_2 probes. In-line probes were described in 1980 (35). The Severinghaus type pCO_2 probe is essentially a combination of a pH probe with a CO_2 permeable silicone membrane. Dissolved CO_2 passes through the membrane into the NaCl/$NaHCO_3$ electrolyte where it dissociates and increases the H^+ concentration and hence decreases the pH. Response time is relatively slow (1–2 minutes) but decreases at higher pCO_2 levels. The probes are compatible with the standard 25-mm Ingold port. The probe is SIP and autoclave compatible.

Another approach has been the use of in-liquid silicone tubing through which N_2 is purged at a low flow rate (36). A mass spectrometer is used to determine the CO_2 concentration. This approach requires inserting silicone tubing into the liquid medium by using a modified 19-mm or 25-mm DIN 1 4435 Ingold-style fitting which is drilled and fitted to provide a SS316L tube connection inside the vessel and a sanitary connector externally. The tubing is connected on the inside and sterilized with the reactor.

76.1.2.5 Biomass Probes. Biomass is most often measured off-line using turbidity or direct visual counting to determine cell concentration. In-line measurement devices are now available and have been used in mammalian-cell bioreactors (37). The back-scattering in-line probes show a linear response to cell density in the range of 2–15 million cells per mL (38). Transmission laser probe types such as the Cerex (Cerex Corp., USA), Wedgewood (Wedgewood Technologies, CA, USA) and Monitek (Monitek Technologies, CA, USA), perform well in hybridoma suspension culture (39). The probes are Ingold 25-mm type design and are SIP compatible. Another in-line laser turbidimeter (ASR Co. Ltd., Tokyo) has been used to continuously monitor microbial culture (40) and can also be applied in cell-culture reactors.

Capacitance sensors have been examined for on-line biomass determination of attachment-dependent HeLa cells on Cytodex carrier beads (41). The biomass determination is based on the capacitance imparted by cell membranes. This type of sensor can distinguish biomass from the inert carrier matrix. Concentrations in the range of 2–3 million cells per mL were measured.

Biomass probes are calibrated outside of the bioreactor by using a high-density suspension of cells. The medium is used to zero (offset) the probe and a high concentration cell sample provides the span measurement. Calibration information is cell-specific and can be stored in the controller memory.

76.1.2.6 Flow-Rate Sensors. Flow measurement devices are required to control gas and liquid flow rates. In manual systems, gas flow rate can be adjusted and monitored by using rotameters. In automated control, gas mass flowmeters are used. These meters use a thermal sensing device, which is influenced by the gas density and specific heat capacity, to determine flow rate. Mass flowmeters require periodic calibration.

Precise liquid flowmeters are needed for perfusion culture feeds. Feed rates may be as low as 5 Lpd and cell removal rates in continuous culture may be as little as 1 Lpd. Turbine positive displacement meters and mass flowmeters can be used for measuring and controlling of flow rate.

The gas flowmeters are placed before the sterilizing filters and are not sterilized. The liquid mass flowmeters may have to be placed in the sterile fluid circuit and would have to be SIP or autoclave compatible.

76.1.2.7 Nutrient/Metabolite Sensing. External off-line analyzers such as the YSI Biolyzer are used for determining of glucose, glutamine, and ammonia. In-line detection requires using an external low-volume recirculation loop with a microporous tangential cross-flow filter. External loop recirculation rates of 50–100 mL/min are used to effect permeation of the soluble media across the membrane. The clarified filtrate is sent to an aseptic sampling module and then sequentially loaded to an off-line YSI type analyzer. A 12-L perfusion system was operated with a Millipore 0.22-μm cross-flow filter in an Applikon minimum holdup volume external cross-flow holder (38). At a laboratory scale (20 L), the device can be operated aseptically in-line. The vessel/device connection is made by using autoclaved tubing which is connected aseptically to the sterilized membrane device. Connection with a large-scale SIP-based bioreactor requires producing SIP compatible sample loop devices.

76.1.2.8 Pressure. Pressure influences the DOT and pCO_2 in the medium. Bioreactors are operated with

pressures in the range of nominal 0–10 psig. Inlet gas flowrate and outlet pipe diameter and filtration sizing must be compatible to prevent pressure buildup and thus enable control of pressure using a sterilizable, needle design control valve (42). Pressure should be measured in the vessel headspace and before the exhaust filter. Pressure sensors (43) are available in Ingold style fittings or in sanitary flush-mounted Triclamp designs. A simple pressure-indicating gauge can be installed at a vessel top-plate nozzle where simple pressure indication is desired. This may be useful in addition to a sensor for local and immediate indication for operators. Sanitary 3-A design gauges with flush-mounted designs are available (44).

76.1.2.9 Liquid Level. Liquid Level probes are used to measure liquid level and provide the sensor to control the bioreactor medium level. Control of medium level is important in perfusion-based cultures where a constant bioreactor volume is desired. Long batch runs should also be monitored for liquid level to provide a measurement for replacing evaporative loss or for monitoring vessel volume during fed-batch bioreactor processes.

The following approaches are available:

- determination of bioreactor weight using a load cell (45) for large reactors or floor-mounted scales for smaller reactors (46)
- magnetostrictive sensors (47)
- capacitance sensors (48)

Capacitance sensors measure the change in dielectric constant between the vessel wall and the probe and detect the liquid/air interface. They are fitted through the top-plate of the vessel through a 19-mm Ingold type or sanitary clamp fitting. They are steam-sterilizable and are fitted before SIP.

76.1.2.10 Others. Process control loops require actuators to respond to output signals from the controller. Peristaltic pumps can be activated and regulated by external signals. The flow rate must be calibrated with rpm to enable precise tuning of the control loop. Remote actuating valves and metering pumps play some part in large-scale process control loops. In regulating the gas flow rate, proportional valves are placed outside the sterile boundary with a sterile air filter between the nonsterilizable device and the bioreactor. A representation of a basic controlled-perfusion bioreactor is shown in Figure 76.9.

The level of sophistication of bioreactor sensors and instrumentation depends on goal. In manufacturing, the trend is more toward conservatism and minimal failure risk whereas in research, maximization of the information accrual rate dominates the strategy.

76.1.3 Maintenance of Valves and Changing of O-Rings and Gaskets

Valves are an essential element of any bioreactor system. They divert fluids through fixed piping manifolds and delivery lines in bioreactor skids. They isolate fluids from product and equipment in the production phase and are fundamental in ensuring the direction of steam, nutrients, gases, and product during the phases of the production cycle. Valves that are part of the primary product contacting system and the sterilizable zones of the bioreactor should comply with sanitary design standards. Several valve designs are used in a bioreactor system.

Diaphragm valves (49) are the most usual choice for on/off selection in the sanitary flow path. Ball valves are available in SS316L three-piece designs (50) and are used as absolute shut-off valves for utilities and to a smaller extent in the sanitary flow path. Simple plug valves (51) are useful in small diameter utility line applications and can operate with steam but are not regarded as a sanitary design. Several specialized valves are used for sampling, harvesting, and in automated CIP skids. Aseptic-designed tank harvest valves (52) have a steamable piston design and provide a flush-mounted, drainable face inside the vessel. The piston design produces a steam barrier while the valve is closed. When the valve is opened, the steam supply to the valve stem is cut off, and samples or product can flow out of the vessel. Sample valves are similar in design to harvest valves but are located in the vessel sidewall.

Diaphragm valves feature a smooth, crevice-free flow path free of any entrapment areas, and a self-draining design which is the key choice for SIP/CIP applications. The isolating diaphragm protects flow medium from external contamination while containing the medium within the valve bore.

All moving parts are isolated from contacting the flow medium. In addition to the standard two-way forged and cast valve bodies, the manufacturers of sanitary diaphragm valves offer many important process-related features:

- Multiport diverter valves divert or combine process streams.
- Close-coupled branch valves minimize the dead leg on sampling valve lines.
- Tee pattern valves provide excellent drainability and minimal deadleg for process sampling.
- The standard forged valve body provides the highest available surface finish and the optimum surface for electropolishing. Because these bodies are forged from wrought stainless steel bar (ASTM A -182 grade 316L), they have minimum porosity and low ferrite content (0.5% maximum). As a result, the migration of oxides throughout the system is minimized. These bodies comply with FDA guidelines as well as cGMP

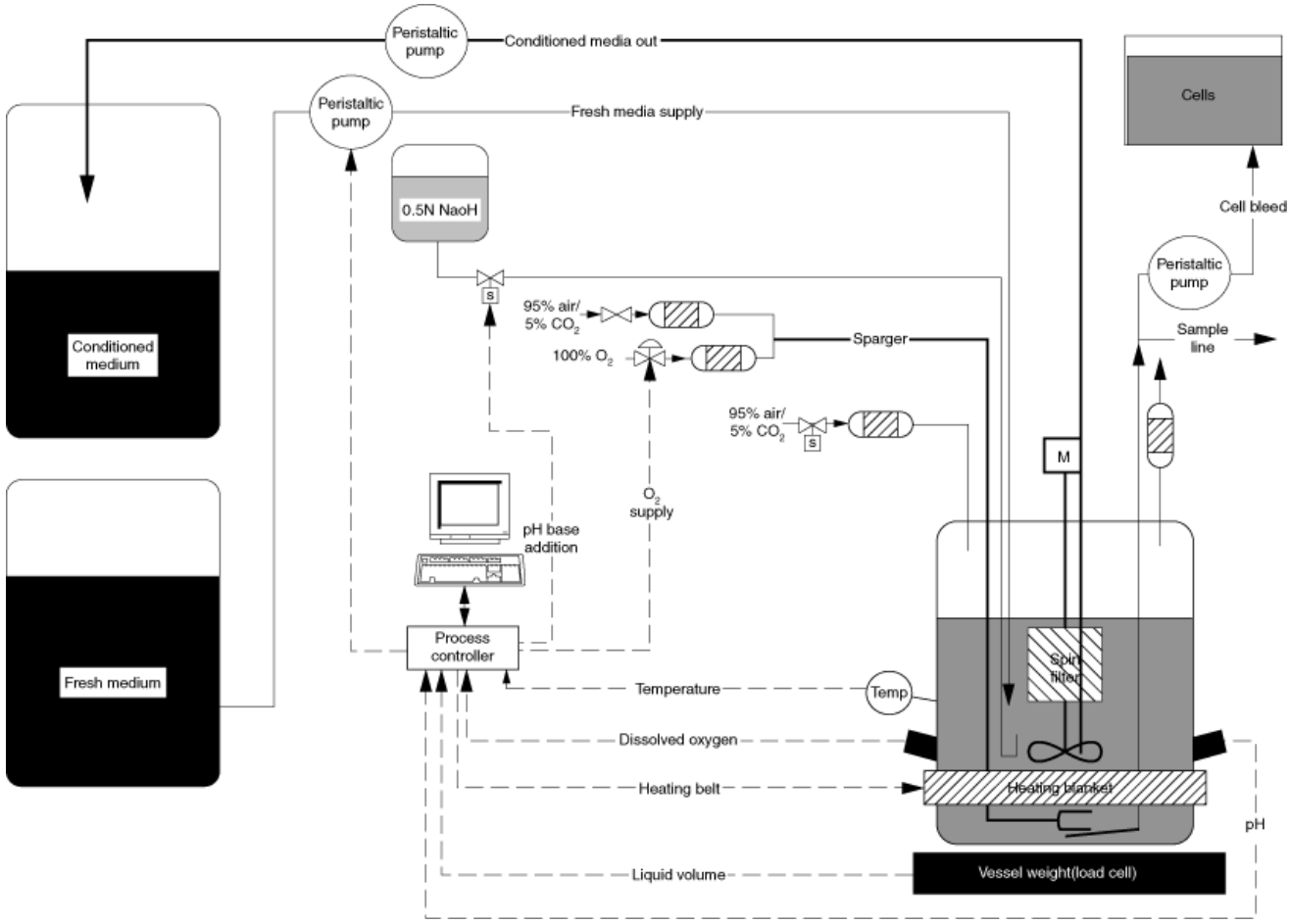


Figure 76.9. A perfusion bioreactor system. Liquid level control using a vessel load cell and regulation of a medium inlet pump.

principles and are ideal for high purity applications in the bioprocessing industry.

In addition to the stainless steel valve body, the diaphragm contacts the process stream and/or utilities. A variety of elastomers are available for bioreactor use in valves and as gaskets. The major elastomers used are given in Table 76.6. In bioproduct processes it may be important to pick an elastomer that possesses the right physical properties for the application and is also acceptable to the FDA for safety and nonleachables.

- EPDM is available for valve diaphragms and flat gaskets, but not in an O-ring format without the use of additives that render it unacceptable by the FDA for use in product-contacting applications in biopharmaceutical production. In this case EPR O-rings are used. An important consideration is the potential for toxicity of the materials to the cells in the bioreactor. Some materials such as PVC may be toxic to the cells in the reactor. Tests can be performed in shake flasks to evaluate the toxicity of particular polymeric elastomers. It has been shown that silicone, C-flex, and Teflon are noninhibitory to the growth of hybridomas (53).
- Teflon/EPDM-backed diaphragms are used in Saunders-type diaphragm valves for product-contacting vessels and lines.
- Buna-N material will handle most food, dairy, pharmaceutical, and sanitary services. It is the backbone of elastomer for the food and edibles industries and has excellent resistance to compression set, tear, and abrasion. It has good acid and mild alkali resistance.
- EPDM (ethylene propylene rubber) is excellent for hot water and steam service up to 325°F, and in addition it is very abrasion resistant and has excellent resistance to ozone, sunlight, weather, and deionized water. EPDM also has good tensile strength and good resistance to mild acids, alkalis, and alcohols (rated −65°F to 350°F and short term to 400°F).

TABLE 76.6. O-Ring and Gasket Elastomers

Elastomer Valve Diaphragms and GasketsColor	Lower	Temperature Range (°F)		Regulatory Acceptance	
		Upper	FDA	USP	
Butyl rubber	Black	−22	266	√	√
Black EPDM Peroxide-cured	Black	−40	266	√	√
Black EPDM Post peroxide-cured	Black	−40	266	√	√
Clack EPDM sulfur-cured	Black	−40	266	√	
White EPDM sulfur-cured	White	−40	248	√	
TFE butyl-backed	White face Black backing	−4	302	√	√
TFE Viton-backed	White face Black backing	23	347		
Steam grade TFE Viton-backed	White face Black backing	23	347		
TFE EPDM-backed	White face Black backing	−4	320	√	√
Sream grade TFE EPDM-Backed	White face Black backing	−4	320	√	√
Silicone FDA	White	−40	302	√	
White Butyl FDA	White	−40	230	√	

- Viton(fluorocarbon rubber) material has excellent mechanical, chemical, and heat resistance. It is particularly well suited for hot, fatty, and oil products. Viton has poor serviceability in steam contact application. EPDM is favored, for steam service. Viton is especially good for hard vacuum service because of its high molecular weight and low gas permeability. It has been used to −65°F in some static seals due to its high flexibility (temperature ranges 0°F to 400°F under continuous duty and will take 600°F for short periods of time).
- Silicone is known for its purity and nonleaching characteristics. Its ability to withstand many chemicals and combination of chemicals makes it a good choice in the pharmaceutical industry. Silicone has excellent low-temperature flexibility.

Harvest valves should be steam-sterilizable, piston-type valves with O-ring seals and should be flush-mounted to provide a smooth join with the vessel interior surface to eliminate dead pockets. In several designs, the valve housing can be pressurized with steam between operations to reduce the risk of contamination. A harvest valve should be sized to allow harvesting of the bioreactor and recirculation of CIP fluids.

In skid systems, there are many valves and gaskets which must be checked and installed before each batch run. EPDM-type gaskets, present in utility lines, are likely to be stable for months and are replaced during planned maintenance activities. The vessel and cell-culture-contacting gasket materials should be carefully inspected after each run. Flat Teflon gaskets are normally replaced after each process because they are prone to cold flow and deformation. Silicone rubber O-rings can be used for several cycles without problems and simple inspection and replacement are usual rather than regular replacement. After reinstalling gaskets, a low-pressure leak test will detect poorly seated gaskets and O-rings.

When replacing O-rings, it is important to clean the surfaces to eliminate small debris such as gasket particulates. Where circular O-rings are required to fit inside a tight sleeve, it is necessary to place a small amount of silicone gel on the O-ring to prevent any damage. If O-ring damage is persistent, then steel surfaces should be inspected. Any burrs or aberrations should be carefully machined away. Probe holders and other O-ring sealing systems are engineered to provide suitable seats and grooves. For O-rings, straight-sided grooves are best to prevent extrusion or nibbling, but 5° sloping sides are easier to machine and are suitable for very high pressure (15,000 psig.). The sides should be finished to a 32 μinch RMS (root mean square) with no burrs, nicks, or scratches. Any rubbing surfaces should be 8–16 μinch RMS.

When replacing flat gaskets, for example, sight glass gaskets, take care to prevent crimping the gasket. Tighten faces evenly by working with geometrically diapositioned nuts in a sequenced tightening procedure. Use a torque wrench that is correctly adjusted when it is stipulated that nuts are to be tightened to a set torque value.

76.1.4 Connections to Receive Charging Fluids

Several line connections are required for autoclaved and mobile vessels, after sterilization. For acid, base, antifoam, nutrients, inlet gases, and inoculation. Pilot-scale bioreactors may contain components that are disposable or are assembled using sterilized-silicone tubing. Assembly of components is specific to the vessel's particular design. In general, flexible silicone tubing can be used to link CO_2, air, oxygen, nutrient, and some utility lines to the reactor. These components need to be sterilizable by autoclaving because they will not tolerate steam under pressure in an SIP process. Tubing connections can be made to attach vessel stainless steel ferrules or dip tubes. These connections are secured by attaching external Tygon ties. The tubing is assembled and connected to the vessel before autoclaving. Sterilizing gas filters and liquid filters used in operating the bioreactor are also attached to the appropriate tubing and autoclaved. Final connections are made to the utility lines outside of the sterile boundary, for example, between the air filter inlet and the air utility line. When direct sterile tubing connections are to be made, a hot tubing weld must be used. This is accomplished by a sterile-tubing welder (Sterile Connection Devices-SCD) (54). The SCD device makes a sterile heat-fused connection of C-flex tubing. A vessel can be autoclaved with tubing, fitted with a terminal piece of C-flex tubing and a guarding sterile vent filter, and attached to various connections. A remote, sterile, C-flex capped line may be fused to the vessel C-flex line to form a complete assembly connection. This can be used for small-scale vessels on small tubing (up to size 16).

Larger bioreactor skid designs are made up of numerous connections for transferring the liquid medium, alkali and acid for pH control, antifoam, sterile quality air, carbon dioxide, and oxygen. Peripheral hard-piped connections, to be made within the sterile zone of the skid, must be from a sanitary design and must be steam-sterilizable. Instrument air, indirect utility lines, heating/cooling jacket water, and other non-process-contacting materials are also associated with the skid. Non-process-contacting connections are usually made with typical threaded pipe connections, swaged connections, or with plastic PVC glued pipe of ferrule or threaded design. Deionized water lines are usually constructed of schedule 80 plastic PVC (1–2″ pipe) which delivers the deionized water to tanks where it is batch-sterilized or else transferred to a stainless steel piped sterilizable filter unit to be sterile-filtered into aseptic equipment. Teflon-lined flexible hose with sanitary connectors can be used to transfer products, nutrients and other sterile components between equipment. Utility lines may be joined to process piping through quick-coupling fittings.

Sterile connectors are available in various forms, the most common of which is the Tri-clamp fitting. Pressure gauges, valves, pumps and other associated important skid equipment are available with sanitary design connections. The connectors most commonly used are described here and are illustrated in Figure 76.10.

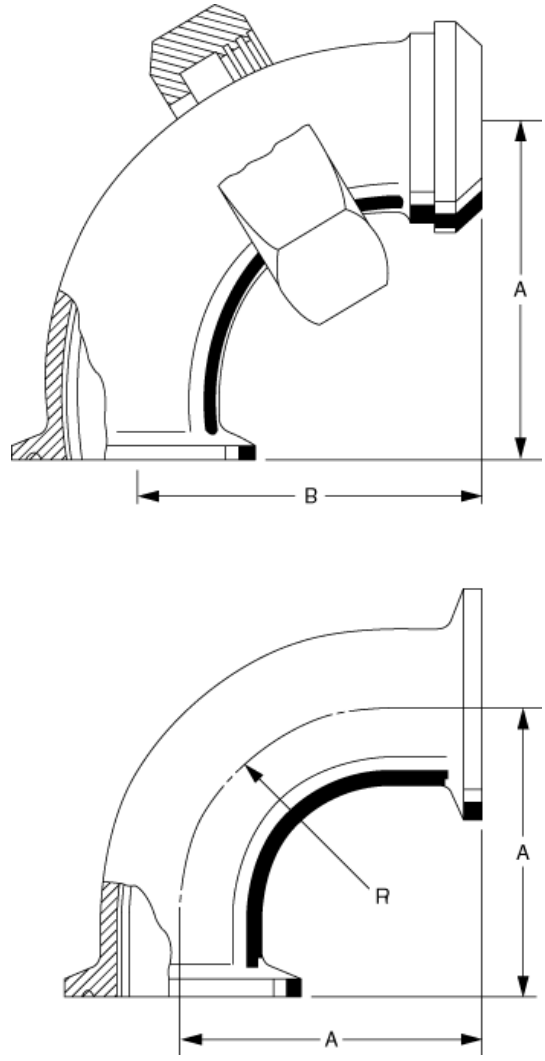


Figure 76.10. Sanitary design connectors.

76.1.4.1 Tri-Clamp. The Tri-clamp (TC) type fitting consist of a grooved, 316L stainless flange, an annular elastomeric gasket with a built-in O-ring that fits the flange groove, and a three-piece hinged 304 or 316 stainless clamp that fits around the assembled flanges and gasket. The fitting is self-aligning and easy to assemble or disassemble and in the 1.5–4 inch pipe diameter range provides a flush inside surface suitable for CIP. The fractional 0.5 and 0.75 inch fittings are useful in assembling small, fixed, stainless tubing. However, it is advisable to fit the 0.75-inch gasket into a 0.5-inch ferrule to facilitate CIP reagent access to the flat face of the ferrule (similarly fit a 1-inch ferrule with a 1.5-inch gasket).

76.1.4.2 Bevel Seat. Bevel seat fittings employ union nut assembly and Acme sanitary threads for connection (55). This fitting is more difficult to align and assemble than the Tri-clamp, and it is important to check the tightening of the exterior nut in lengths of pipe subject to vibration. The fitting is suitable for CIP, and the alignment and vibrational problems may be alleviated through correct use of pipe supports.

76.2 STERILIZATION

Sterilization inactivates potential contaminants and provides asepsis (the absence of bacterial contamination). Sterilization processes are designed to reduce the probability of survival of a single bacterial spore to less than 10^{-3}. The ability to achieve the low probability ($p \leq 0.001$) of contamination is met by the steam-sterilization procedure. In addition to wet heat sterilization with pressurized steam, dry heat (1800°C) for small equipment components, hot air (170°C for 2 h), radiation (γ rays, X rays, high-energy electron beams,) for serum medium, and nonionizing radiation (UV rays) for surface sterilization are potentially useful. Where high temperature sterilization is not feasible, such as where the vegetative organism surfaces must be sterilized (seeds, plant materials), chemical sterilization methods are required.

Empty vessel sterilization is used when cell culture media, containing temperature-sensitive nutrients and potentially cross-reactive components (glucose and amino acids). In this situation, the presterilization microbial loads are lower than situations in which an unsterilized medium is present in the bioreactor before sterilization.

Vessels which are in the 10 to 100-L range may fit into autoclaves and hence undergo programmed sterilization using a slow vacuum/steam cycle heat-up, a 60-minute sterilization cycle at 121°C, and a slow venting cool-down cycle. The vessel probes, addition line connectors, or silicone tube lines are unclamped and open but protected by a terminal, 47-mm, 0.45-μm gas-sterilizing grade disc filter.

SIP is the method for sterilizing vessels that are skid-mounted.

76.2.1 Theory

The destruction of microorganisms by heat implies loss of viability. The destruction of organisms by heat at a constant temperature follows a first-order rate equation given by

$$\frac{dN}{dt} = -kN$$

where k = Reaction rate constant, min^{-1}, $k = f(T)$ and N = number of viable organisms.

$$N = N_0 e^{-kt}$$

t = time (min)

76.2.1.1 Decimal Reduction Time (D). D is the time (min) of exposure to heat to reduce viable microbes by 90% at temperature T.

$$\frac{N}{N_0} = 0.1 = e^{-kD}$$

Thus

$$D = \frac{2.303}{k}$$

Spores are more resistant to thermal inactivation than vegetative organisms. The k value for spores is less than for vegetative cells. The rate constant k is a strong function of temperature. At 121°C, the value of k for *Bacillus stearothermophilus* is around 0.77 min^{-1} (56). The D value would then be calculated as 3.0 minutes. In other words, a log reduction in viable *Bacillus stearothermophilus* cell number would be obtained every 3 minutes during the sterilization hold period at 121°C. By contrast, the k values for heat intolerant organisms like *Escherichia coli* are very large at 121°C. The D values for *E. coli* RV308 in the temperature range of 56–62°C are shown in Table 76.7. The k values from this data are 0.75 min^{-1} at 56°C and 12.6 min^{-1} at 62°C, indicating a very steep curve for k versus temperature and clearly showing that such organisms are undetectable at 121°C.

The rate constant k is a function of temperature, and an Arhenius type expression can be used as follows:

$$k = ae^{-E/RT}$$

where

a = empirical constant, min^{-1}
T = absolute temperature, K
E = activation energy, $\text{cal} \cdot \text{g}^{-1} \cdot \text{mole}^{-1}$.
R is the gas constant = 1.98 $\text{cal} \cdot \text{g}^{-1} \cdot \text{mole}^{-1} \cdot \text{K}^{-1}$

On the basis of Eyring's theory of absolute reaction rate;

$$k = gTe^{\frac{-\Delta H}{RT}} e^{R\frac{\Delta S}{}}$$

where

g = factor including Boltzmann constant and Planck's constant

TABLE 76.7. Heat Kill *D* Values for *E.Coli* RV308

Temperature (°C)	*D* Value (s)
56	185
58	63
60	26
62	11

$\Delta H =$ heat of reaction activation
$\Delta S =$ entropy change of activation

In 1921 Bieglow published the Q_{10} theory (57) which said that

$$D = ae^{-b'}$$

where a' and b' are empirical constants.

Thus the reaction rate constant can be calculated.

76.2.1.2 Z-Value. The Z-value represents the number of degrees of temperature required to change the D-value by a factor of 10. The Z-value is defined as the slope of log D versus temperature. This is a straight-line graph.

$$\frac{\Delta \log_{10} D}{\Delta T} = \frac{1}{Z}$$

The D values determined for the various temperatures can then be used to calculate the Z-value for a sterilization process. Knowing the Z-value allows determining lethality at a particular temperature compared to a known lethality delivered at a reference temperature:

$$F_R = [\Delta T] \cdot 10^{\frac{(T-R)}{Z}}$$

where
$R =$ reference temperature having a known D-value (lethality)
$T =$ temperature
$F_R =$ the equivalent time at the reference temperature required to produce the level of lethality delivered at temperature T.

Dividing F_R by D_R gives the log reduction achieved at temperature T per unit time.

76.2.1.3 Del Value (∇). The Del value is frequently used in analyzing sterilization. The heating up and cooling down phases provide a finite kill effect of contaminant in addition to the sterilization hold phase. (The Del value accounts for this effect and can be described as the $\log_e$ of the population survival ratio throughout the whole sterilization cycle.)

$$\ln \frac{N}{N_0} = -Ae^{-E/RT \cdot t}$$

$$\ln \frac{N}{N_0} = \nabla$$

and,

$$\nabla = A \int_0^T e^{-E/RT} dT$$

Note that

$$N = \frac{N_0}{e^{\nabla}}$$

For a complete cycle, the overall Del value is determined according to the following equations:

$$\nabla_{TOTAL} = \ln \frac{N_0}{N} = \nabla_{HEATING} + \nabla_{HOLDING} + \nabla_{COOLING}$$

$$\nabla_{TOTAL} = a \int_T^{121} e^{-E/RT} dT + ae^{-E/RT} T_{121} + a \int_{121}^T e^{-E/RT} dT$$

In practice, the heating and cooling curves are integrated, and Del may be determined. Del factors represent the number of $\log_e$ (or $\log_{10}/2.303$) reductions in population throughout the whole sterilization cycle.

76.2.2 Principles (Unambiguous Flow of Steam)

The multiple addition lines and integral components that must be sterilized to ensure aseptic operation during the production phase complicate sterilization of fixed-in-place systems. It is important to design a sterilization cycle to ensure that saturated steam at 121°C contacts all of the equipment surfaces and areas for a specific duration to guarantee achieving design ∇ factor at all locations. It is not possible to sterilize all skid components concurrently because steam would be required to flow in multiple directions and would be difficult to direct. Sequential sterilization of systems is likely to be needed. Many valves will be needed to enable the flow of steam in the correct direction. The commonly used steam block valve arrangement is a key element in SIP. Steam blocks may be unidirectional or bidirectional (Fig. 76.11).

During the heat-up phase, condensate is produced and must be eliminated from the system to prevent cool spots and hindering steam flow. Steam traps are used at suitable points in the system, and piping is arranged with slopes to enable condensate drainage to the steam traps. Vents are placed at equipment high points to accelerate air displacement by steam. Steam supply pressure should be regulated to 20–30 psig to ensure that steam can enter sterilizing areas at 15–psig pressure when pulse control valves are opened.

76.2.2.1 Manual. Manual sterilization involves sequential operation of steam supply, steam trap bypass, and vessel-associated valves by an operator. The following simplified operations are the basic elements for achieving empty vessel sterilization.

- Open vessel drain valve.
- Open gas exhaust line valves (if pressure-regulating valve is in-line, open the valve manually at the controller).

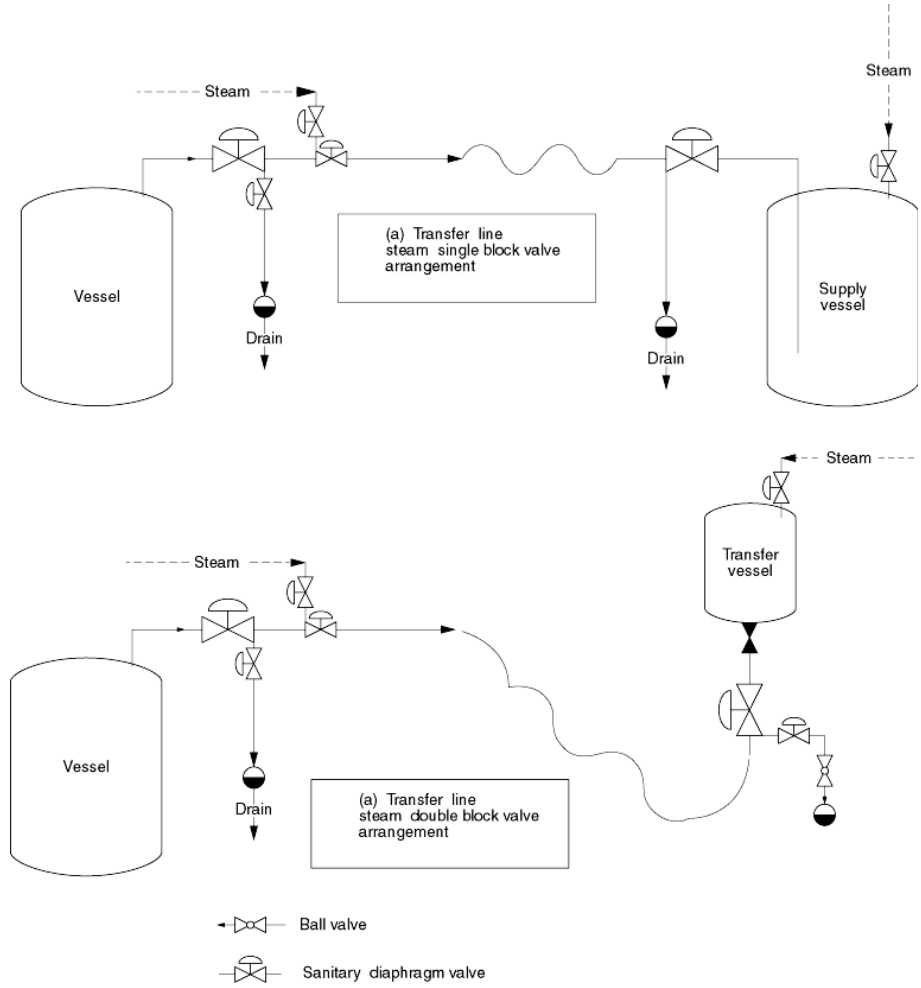


Figure 76.11. Steam block assemblies. Single block assembly (a) for sterilization of a media addition line. Double block assembly (b) for sterilization of a transfer line pre transfer and tank and transfer line post-transfer.

- Open all steam trap valves, and open steam trap bypass lines.
- Open up steam lines to vessel inlet nozzles (gas inlets, nutrient, acid/base) and the vessel jacket top valve.
- Close the exhaust line valve and steam trap bypass lines when steam is exiting the steam trap bypass lines and the vent lines.
- Ensure that steam is flowing into the vessel and is exiting through the drain-line steam trap and the exhaust filter line steam trap. Check that the individual TD steam traps are functioning correctly.
- Monitor the temperature during heat-up (use an external thermowell thermocouple or thermometer).
- After 5 minutes at 100°C close the exhaust line valve, and regulate the inlet steam supply pressure at 15–20 psig at the steam PRV valve.
- As the vessel temperature approaches 121°C regulate the supply steam pressure to 15 psig.
- Sterilize for 30–60 minutes for empty vessel sterilization.
- After sterilization shut off the steam supply, and allow the vessel to cool to 110°C. If there is a cooling jacket start the flow of cooling water through the jacket. Open the exhaust valve, and close the harvest valves.
- When the vessel temperature reaches 105–110°C, flow sterile air into the vessel to maintain 5–10 psig pressure during cool down.
- Cool the vessel to the desired run temperature using the jacket temperature control loop.

76.2.2.2 Automatic. Automatic SIP is most commonly used on skid systems where many valves are in the sterilizable zone. A sequential program that automatically opens

and closes valves during the progressive stages of the SIP cycle drives the sterilization cycle. Purging of air from the system can be accelerated by incorporating steam trap bypass lines that include a pulse open/closed solenoid valve. This is a suitable feature for automated systems. The pulsed valves open in the early heat-up phase and then close as the air and condensate are removed. A temperature sensor in the purge line could provide the threshold signal for opening/closing the solenoid valve. The valves are of the fail-closed design option, that is in the absence of electrical or pneumatic actuation they are closed.

A sequential program cycle for a bioreactor may be divided into the following nine stages.

76.2.2.2.1 Idle. This represents the vessel downtime configuration when SIP is inactive.

76.2.2.2.2 Heat to Purge. Vessel temperature is raised from ambient to a purge temperature (100–105°C). The next stage is initiated when the temperature reaches the purge temperature.

76.2.2.2.3 Purge. The vessel temperature is maintained at the purge temperature for a specified period of time. The trigger to move to the next stage is when the elapsed time equals the purge time entered in the controller. Purge time is in the range of 2–10 minutes.

76.2.2.2.4 Heat to Sterilize. In this stage, the air exhaust system is closed, and the vessel temperature is increased from the purge temperature up to the sterilization temperature. Steam passes into the vessel and vessel jacket, and condensate is removed through the steam traps. When the sterilization temperature (121°C) is reached, the next stage is initiated.

76.2.2.2.5 Sterilization. The vessel temperature is maintained at the sterilization temperature for a designated period of time. When the timer clock indicates that the designated duration has elapsed, the next stage is initiated.

76.2.2.2.6 Cool to Vent. The steam supply to the jacket of the vessel is shut off, and chilled water enters the jacket. The circulation loop is initiated, and the vessel temperature decreases to the stipulated vent temperature (∼105°C).

76.2.2.2.7 Vent. The air inlet valve opens to allow air to enter the vessel thereby preventing the possibility of a vacuum forming on further cooling.

76.2.2.2.8 Cool to Run. Temperature is decreased to the stipulated operating temperature.

76.2.2.2.9 Run. Run is the initial fermentation configuration, and the valves are positioned to allow the control loops to function. The system-specific valve-sequencing program is established, and a step logic program is entered into the sequence controller.

76.2.2.3 Steam. Some basic definitions for steam follow:

- Live steam is steam at temperatures greater than 100°C or greater than 1 atmosphere pressure.
- Saturated steam is steam at the dew point.
- Superheated steam is steam above the dew point.
- Service steam is steam used for general purposes; it may be contaminated with dissolved components of the feed water, rust, scale, water treatment chemicals, feed-water additives used to purify the boiler water, and volatile organic additives, typically amines and ammonia derivatives that help prevent corrosion. Examples of boiler water additives are sodium hydroxide (pH 13.2), sodium bisulfite, sodium sulfite, morpholine (pH 11.4), cyclohexylamide, and diethylaminoethanol (pH 11.2). The impurities present can be pyrogenic, (i.e., cause increased temperature) if present in pharmaceutical drug substances that are injected.
- Clean steam is steam free of pyrogens and chemicals, that is produced from demineralized and prepurified feed waters. Clean steam should be generated from stainless steel stills with stainless steel condensers and tubing.

Clean steam is characterized as dry saturated steam, having no additives, relatively low pH, and equal in purity (when condensed) to the water purity acceptable for final rinsing of drug contact surfaces.

When water changes phase from liquid to vapor in the form of steam at a given pressure, heat is added without changing the temperature of the fluid. By increasing the heat input into the water, the amount of steam produced is increased. Under constant pressure, the enthalpy value increases in proportion to the temperature until the boiling point is reached. While the water is changing phase, the temperature remains constant, but the enthalpy is increasing.

For a given pressure, enthalpy of water at the boiling point is commonly referred to as h_f. This is the value of enthalpy for water that is on the verge of boiling, also known as saturated water.

The temperature at which the phase change occurs is known as the saturation temperature.

At this point, heat can be added until all of the water is changed into steam without changing temperature. When this happens, the value of enthalpy is referred to as h_g, and

TABLE 76.8. Steam Table

Gauge Pressure (psig)	Absolute Pressure (psia)	Temperature (°C)	Heat Content			Volume Steam
			Sensible h_f (kJ/Kg)	Latent h_{fg} (kJ/Kg)	Total h_f (kJ/Kg)	V_g (m^3/Kg)
0	14.7	100.00	419.0	2257.1	2676.1	1.673
1	15.7	101.89	427.0	2252.0	2678.9	1.573
2	16.7	103.61	434.4	2247.3	2681.7	1.486
3	17.7	105.28	441.4	2242.9	2684.3	1.405
4	18.7	106.94	448.1	2238.5	2686.6	1.336
5	19.7	108.56	454.6	2234.3	2688.9	1.274
6	20.7	110.00	460.7	2230.6	2691.2	1.211
7	21.7	111.33	466.5	2226.8	2693.3	1.161
8	22.7	112.67	472.3	2223.1	2695.4	1.117
9	23.7	113.94	477.9	2219.6	2697.5	1.074
10	24.7	115.22	483.5	2215.9	2699.4	1.030
11	25.7	116.44	488.6	2212.7	2701.2	0.993
12	26.7	117.61	493.7	2209.4	2702.9	0.955
13	27.7	118.78	498.6	2205.9	2704.5	0.924
14	28.7	119.94	503.2	2202.9	2706.1	0.893
15	29.7	121.00	507.9	2199.9	2707.8	0.868
16	30.7	122.06	512.3	2197.1	2709.4	0.837
17	31.7	123.11	516.7	2194.1	2710.8	0.812
18	32.7	124.11	520.9	2191.5	2712.4	0.793
19	33.7	125.11	525.1	2188.7	2713.8	0.768
20	34.7	126.00	529.0	2186.2	2715.2	0.749

this is known as saturated steam. The values of h_f and h_g are tabulated in standard steam tables (Table 76.8).

Additionally, there is a value h_{fg} that indicates the amount of steam necessary to go from saturated water to saturated steam. This value relates to the quality of steam. When the amount of steam is half of the total weight, the steam quality is said to be 50%. When the amount of steam is equal to the total weight, the steam quality is 100%. Because this quality is generally not achievable in real circumstances, the accepted industry standard for steam quality is 99.5%.

76.2.2.4 Steam Traps and Drains. Steam traps are a critical component in SIP systems. A steam trap is a self-actuating valve that opens in the presence of condensate and/or noncondensable gases (air, CO_2, H_2 present in steam) and closes in the presence of steam (58). Steam traps are present in equipment that uses steam for sterilization. They are placed in lines draining condensate from the bioreactor. Several types of steam traps are available. Mechanical traps operate by the difference in density between steam and condensate. This category includes float and thermostatic traps and inverted bucket traps. Thermostatic traps operate on the principle that saturated process steam is hotter than either its condensate or steam mixed with noncondensable gas. When separated from steam, condensate cools below the steam temperature. A thermostatic trap opens its valve to discharge condensate when it detects a lower temperature. Balanced pressure and bimetallic traps and liquid and wax expansion thermostatic traps are included in this category.

Thermodynamic traps (TD traps) are the most commonly used traps in biotechnology applications. The TD trap uses the velocity and pressure of flash steam to operate the condensate discharge valve. The discharge valve is a simple flat disc (see Fig. 76.12). When closed, the flat disc is lying on the flat seat covering both the inlet and discharge orifices. Cool condensate at process pressure readily flows through the orifice, lifts the disk, and flows over the seat to the discharge orifices. When condensate reaches steam temperature, it flashes, which causes a decrease in pressure below the disk as the gas velocity increases, and the disk is forced down onto the seat which then seals the orifices. A TD trap can remove air from the system at startup but not if the system pressure increases very quickly because high velocity air, like flash steam, can force the disc closed and seal the orifice. Thus TD traps often require a separate air vent or bypass when used on batch applications that shut down and start up frequently and rapidly, for example, batch bioreactors. Because the TD trap has only one moving part, the disc, it is extremely rugged. TD disc traps are available in SS316L and with NPT or tube ends for ¼″, ⅜″, ½″, ¾″ and 1″ tubing (59). They may be installed in any position and are compact and easy to maintain.

Steam condensate is collected in the drain pan. A drain is essentially a fluid collection device that is separated

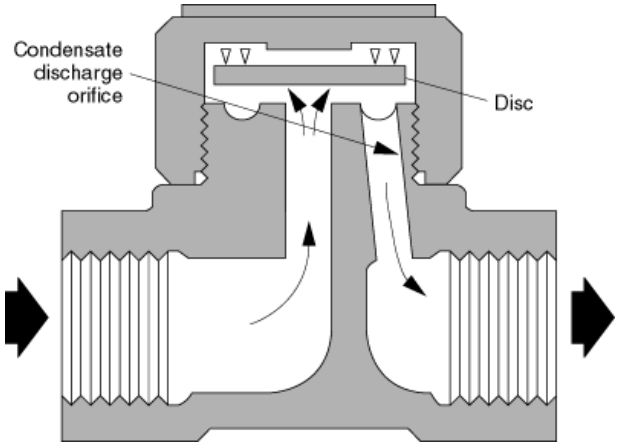


Figure 76.12. Representation of a TD steam trap.

from the process piping by an air gap which prevents pressure backup into the system. Drains should have sufficient capacity to handle full flow of fluids. Drains are connected to the facility floor drains. The air gap in a drain also prevents back-siphoning of waste into process equipment.

76.2.2.5 Ethylene Oxide. Ethylene oxide (EtO) can be used to sterilize materials that cannot be sterilized by heat. This may be performed by direct batch exposure to EtO or in a suitably designed gas-diffusion system (60). In a gas-diffusion system, a package is wrapped in a permeable material typically of low-density polyethylene (LDPE) film.

The direct batch gas sterilization process loses efficiency as product lot size increases as a result of the progressive increase in the load density. By comparison, product sterilized in a biological indicator evaluation resistometer (BIER vessel) has only one layer of protective barrier that separates the product from the critical process elements (temperature, humidity, and EtO concentration).

Ethylene oxide sterilization is effective only in defined humidity ranges. Moisture levels of 20–40% were used to inactivate spore samples (61). These levels are rarely employed by the sterilization industry. The original Kaye and Phillips experiment was performed directly on a microbial site that did not include multiple layers of packaging to hinder gas permeation.

A modern, industrial-size vessel typically injects steam into the headspace until a relative humidity of 50–80% is achieved. Additional steam is used to maintain the high level of humidity throughout the conditioning dwell. The same holds true for EtO concentration. Although a BIER vessel may inactivate spores with a sterilant concentration of 350 mg/L, industrial vessels use 600–1000 mg/L.

EtO gas-diffusion technology is a safety-conscious, effective, and efficient way for routine terminal EtO sterilization of small components. By controlling temperature and humidity and selecting packaging materials with compatible EtO permeation properties, a gas-diffusion sterilization system can be installed, validated, and operated to deliver six logs of lethality (SAL) in 10–12 hours of exposure.

76.2.2.6 Hypochlorite. Hypochlorite has frequently been used for surface disinfection. It has broad antimicrobial activity, rapid bacteriacidal action, is stable in water. Other advantages are high solubility and nontoxicity at use concentration. The active species is hypochlorous acid (HOCl). Spore-forming organisms are more resistant than vegetative organisms and viruses. It should be noted that heavy metals can reduce its sterilizing ability. Hypochlorite is used in water to prevent bacterial colonization. Hypochlorite contains chloride ions that can cause pitting of stainless steel or stress corrosion cracking around welds at temperatures greater than 50°C. In general, bleach is used reluctantly for the cleaning and sanitizing of stainless steel equipment. If fermenter cooling water is chlorinated, care should be exercised to drain and flush the cooling system before sterilization. In large vessels, the coils may be left filled with water during sterilization.

Vapor-phase sterilization of seeds can be accomplished by overnight chlorination. Seeds are incubated in the vapor phase of acid-treated bleach in a fume hood. Such procedures are limited to very small-scale operation due to the toxicity of chlorine.

76.2.3 Monitoring and Control

A bioreactor is a complex system that requires preventive maintenance to assure smooth operation. Leaky seals resulting from faulty O-rings and gaskets may result in loss of the process through contamination. Contamination control in production is based on initial good design and high standards of fabrication for the equipment and its support systems, piping, valves and seals. Operator training, adequate sterilization procedures, and ongoing preventive maintenance programs go a long way toward minimizing the risk of contamination. A laboratory logbook is useful for recording maintenance activity. Bioreactor skid supply lines contain numerous connections that depend on gaskets for correct functioning and maintenance of asepsis. Careful selection and checking of gaskets is important. All flanges and fittings should be checked routinely to ensure correct sealing and operation.

Once the basic procedures for SIP are in place, it is important to investigate the procedures through a testing method that will detect any potential flaws in the equipment setup or method. Flaws may exist in the components in the system, aberrant procedures, and operator errors, or in utility deficiencies.

Thermocouples can be placed inside equipment to monitor the SIP process. Special gaskets are available with

features that enable inserting a thermocouple through a sanitary standard flange (62). For example, it is possible to insert four probes through a single gasket-clamp connector. These devices, along with the temperature probes and data logging equipment, enable thermal mapping and validation of the sterilization process. Special gaskets, which accommodate biological indicator (BI) devices such as *Bacillus stearothermophilus* bacterial spore strips, can be used to investigate the SAL values at various places during the SIP cycle.

76.2.3.1 Dummy Runs with Bacterial Culture Media. System integrity may be tested using a sterile run method. This involves incubating the bioreactor system with a suitable bacterial growth medium to allow investigating system integrity. A carefully planned sterility test will enable the user to investigate the equipment and associated operational procedures. Growing bacteria doubling times range from 20 minutes for wild type *E. coli* to 6 hours for some yeasts and fungi in nonoptimal conditions.

Cell-culture media provide a rich nutritional environment for potential contaminating microbes. Using cell-culture medium is an expensive proposition for large-scale sterility testing at a cost of \$10 L^{-1}. Sterility can be checked economically by using simple microbial growth media in the bioreactor. Lauria Broth (LB) requires few components, involves simple preparation, is cheap, and will provide adequate nutrition for a range of bacteria. The LB medium consists of

- 10 g·L^{-1} Bacto tryptone
- 5 g·L^{-1} Bacto yeast extract
- 10 g·L^{-1} NaCl

To prepare the LB medium, fill the vessel to approximately 70% of the final operating volume, and add the solid media components with mixing. Heat the medium to 50°C to dissolve the components.

Adjust the pH with NaOH to 7.0, and add further DI water to final operating volume. The bioreactor should be set up with probes and associated systems in the same way as the intended culture process. The LB medium can be sterilized in place in the vessel at 121°C for 20 minutes. After sterilization the LB medium is cooled to 30°C. Add sterile glucose to the vessel to give a final 10 g/L concentration. The agitation is set to provide surface aeration, and the vessel is incubated for 1–2 days. A 250–1000 mL sample of medium can be removed after each stage of the test. This sample can be further incubated in a shaker flask to increase the sensitivity of detecting of contaminants in the bioreactor. In the subsequent step of the bioreactor sterility test, the aeration is activated (if it is part of the process being tested), and the vessel is incubated for a further 1–2 days. In the third stage the nutrient additions are activated, and a defined volume (0.1% v/V–1% v/V) of nutrient is added to the LB medium. Contamination is evident by growth in the shake flask samples followed by decreasing DOT in the bioreactor because O_2 is taken up by contaminating organisms. The sensitivity of the detection method depends on the contamination level that may be present after sterilization or after initiating the subsequent stages of the test.

Given:

- SOUR is approximately 1.5 mM. hr^{-1}· A 650^{-1} for bacterial contaminant (63).
- 1.0 OD 650 is $\sim 2 \times 10^6$ cell·mL^{-1}.
- Specific growth rate μ of contaminant of 1.0 hr^{-1} (i.e., a doubling time of 0.693 hr).
- DOT of 100% air saturation is 240 μM O_2 for air-saturated water.

We calculate that an A 650 of 0.02 (4×10^4 cells mL^{-1}) is required to give a 10% decrease of DOT per hour. This is a sensitive test of contamination in conditions where aeration is not provided.

Incubating samples from the reactor in shakers may increase contaminant detection resolution. The bigger the proportion of the sample relative to the bioreactor, the higher the sensitivity of the assay. If a single viable contaminant is present in the sample, it will be evidenced by the development of turbidity over the 7-day duration of the test. The most sensitive test would be to filter the entire test medium through a 0.2 μm sterile filter and then incubate the filter in nutrient agar to detect a single contaminant colony. This would be problematic because it may not be possible to filter the large volume of media aseptically and with typical test filters, and the test would be limited to one time. Removing a large volume into a shaker or sterile bag may increase sensitivity to 1–2 contaminants/L.

The LB medium does not provide a universal growth medium that supports a wide range of contaminants. This may be addressed by incubating the LB medium sample in small volumes of cell culture media after sampling or else into other selective media. Aliquots removed from the sterility test can be incubated under different conditions in other media such as indicated in Table 76.9. Tests should be incubated for at least 7 days.

Contamination can be detected by visual checking (A_{650}) or with a microscope at 400 × magnification. Contaminants detected should be typed using a commercial microbial identification kit. Typically, *Pseudomonas* sp. are of aqueous origin, *Bacillus* sp. airborne, and *Staphylococcus* sp. are typical of handling contamination.

76.2.3.2 Leak Testing. After completing the assembly of the empty clean bioreactor vessel, it is wise to perform

TABLE 76.9. Media and Conditions for Sterile Test

Medium	Temperature 20°C	Temperature 37°C	Aerobic	Anaerobic
Thioglycollate broth	+	+	+	
Sabouraud's medium	+	+	+	
Blood agar plate (streaked sample)		+	+	+
Deoxycholate plate (streaked sample)		+	+	+
Cell-culture medium (250-mL shake flask)		+	+	

a simple pressure test before the sterilization process to ensure that seals and gaskets are providing the necessary sealing. Internal vessel surfaces should be dry before a pressure test because small deformities may be filled with water, which is held by capillary action and will not be displaced by the 10–15 psig overpressure used in the test. First, make sure that all vessel fittings are securely fastened, caps are tightened, and silicone tubing is clamped shut. Attach a pressure gauge to the exit exhaust gas filter. Connect a 12-psig, regulated air supply line to the inlet air filter, and pressurize the vessel to 10 psig. When the vessel pressure has reached 10 psig, clamp the inlet gas line, and hold for 30 minutes. The pressure should not drop by more than 1 psig for a vessel of approximately 100 L in volume. For larger vessels, a longer period of time will be necessary to detect the drop in pressure caused by a small leak. During the pressure test, connections and probe holders can be inspected using a soapy-liquid squirt bottle. Dispense the soap around potentially suspect components, for example, probe insert ports, top port connections, and silicone tubing connections. A leak is detected by observing a foam layer around the leak. After pressure testing, slowly release the pressure in the reactor through the exhaust line.

A pressure test will indicate a poorly seated gasket and other faulty leaking components before sterilization, and so is worthwhile in leading to greater certainity of achieving successful asepsis after sterilization. For large-scale skid systems of high volume, a pressure hold test may not be entirely successful in identifying problems. Very sensitive testing is possible using tracer gases such as Freon or sulfur hexafluoride. Indeed such methods have been used for integrity testing of large-scale fermenters in the pharmaceutical industry and can detect the presence of microscopic leaks. The cooling coils in large industrial fermenters are likely to contain many welded sites that may develop microscopic leaks which can cause contamination of the bioreactor through ingress of cooling water contaminants. The coils can be pressurized (20–30 pisig) with a Freon 12 gas mixture. Leaks are indicated by the accumulation of Freon in the fermenter which is detected by a halogen gas detector (64).

76.3 CHARGING

Bioreactors and ancillary feed tanks are charged with liquid media components. Typical bacterial, yeast, and plant cell culture media can be autoclaved or sterilized in place. Some components, for example, vitamins, are heat-sensitive and would be added as poststerilization sterile additions. The cell-culture medium is not autoclaved and must be sterilized by filtration. Sterile media may be stored in commercially available (65) γ-irradiated polyethylene-vinyl acetate sterile bags or transferred to the bioreactor. Sterile media would normally be stored at cold room temperature (2–10°C). Sera supplied by various manufacturers are triple-filtered sterile solutions. Other manufacturers may supply γ-irradiated sterile serum. When serum is required in the medium, it is added to the bioreactor as a sterile addition using a sterile addition vessel through a sterile connection. Filter-sterilized protein additions, for example, growth factors, are similarly added as sterile additions.

Ancillary tanks are charged with base for pH control, specific nutrients for batch-fed and perfusion bioreactors, and may be antifoam. Addition tanks may be empty vessel-sterilized or autoclaved, and the component is added aseptically to the sterile tanks or vessel. Sodium hydroxide (0.1–1 N) is filter-sterilized into the storage vessel using a polysulfone-based 0.2-μm sterilizing filter. Potassium hydroxide is sterilized in place or autoclaved if it is to be used (rarely used in pH control). Antifoams such as PPG 2000 are diluted and sterilized in place or are autoclaved. If ammonium hydroxide is used, it is obtained as a sterile concentrated ammonia solution that can be diluted with sterile water and aseptically transferred to a presterilized vessel. Fluid is transferred by various simple methods, which are described in the following sections. The equipment layouts are illustrated in Figure 76.13.

76.3.1 Fluid Transfers

Following SIP or autoclaving, media can be transferred to the bioreactor. Small-scale bioreactors are assembled with sterile tubing connected to the inlet ports. This tubing will consist of a length of silicone tubing (size 15, 16, or 24) attached to a length of Pharmed tubing (size 15 or 24) and finally a short length of C-flex tubing (size 16) which is fitted with a terminal sterile 47-mm disposable vent-type filter that prevents ingress of contaminants after sterilization. This standard setup is present on all lines that use a peristaltic pump with a size 15, 16, or 24 head and require sterile connection to media or base or other fed tanks. Pharmed tubing is robust and suited for use in peristaltic pump heads. The soft C-Flex tubing can be sterilely welded to other tubes fitted with terminal C-Flex. In small-scale

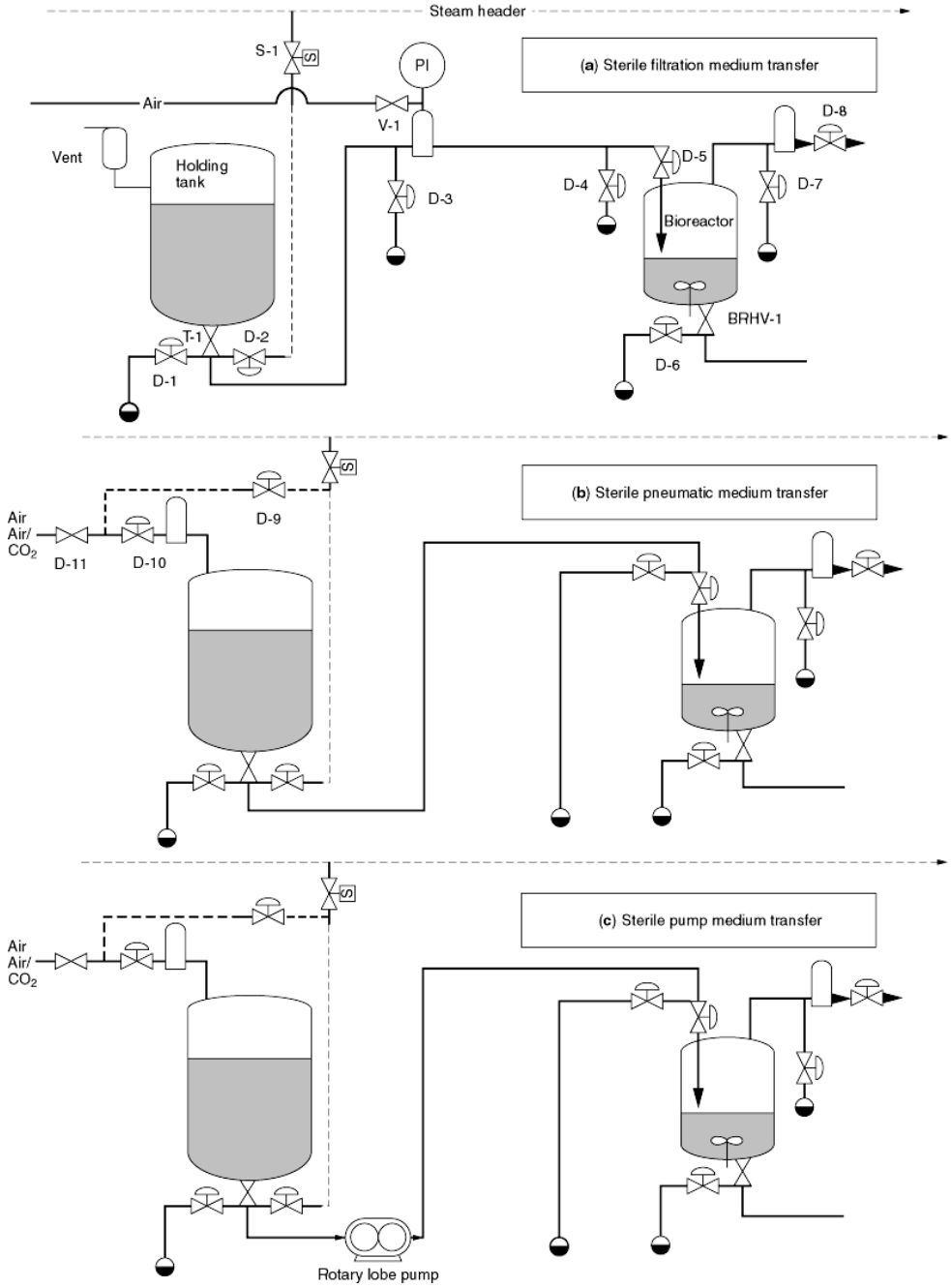


Figure 76.13. Charging media to bioreactor. Tank overpressure, pumping, and filtration are used for transferring media to the sterilized vessel. Valve arrangements provide a means to sterilize addition lines pretransfer.

and pilot-scale operation, medium may be stored in sterile bags thereby saving capital for the purchase of tanks. The sterile gamma irradiated bags have found much use in recent years for small-scale cell culture operation in conjunction with the sterile-welding technology. In larger scale systems, the media would be stored in sterilizable tanks or made fresh and 0.2-μm filter-sterilized into the bioreactor.

76.3.1.1 Overpressure or Sterile Air. Sterile media can be transferred from the sterile storage tank to the bioreactor using gas pressure as the driving force. This requires that the storage tank be designed as a pressure vessel. Because the storage tank would most likely possess a cooling jacket to preserve media at 2–12°C, it would already be rated for external pressure and be capable of

meeting the design criteria for internal positive pressure. Bicarbonate-containing cell-culture media are stored under 95% v/v/air, 5% v/v CO_2 to maintain the bicarbonate buffer system at a stable pH (7.2–7.4). The gas mixture is delivered through a steam-sterilized 0.2-μm hydrophobic gas filter to the top dish port. A pressure of 10–15 psig is applied to the vessel headspace. A steam-sterilizable transfer line is present between the medium vessel and the bioreactor. The fundamental operations for sterile transfer are as follows. (Fig. 76.13a):

- Charge the medium vessel with sterile medium, and close the drain port valve. The bioreactor media transfer port inlet valve D-5 is closed.
- Open steam supply valves S-1 and D-2 to medium vessel drain port and transfer line. Open the steam trap valve D-1 on the bioreactor transfer port steam block assembly and D-4 at the bioreactor inlet port.
- Steam the transfer line for 30 minutes at 121°C.
- Shut off the steam supply to transfer line valves S-1 and D-2, and allow the line to cool to ambient temperature. Pressurize the empty bioreactor with sterile air at 10 psig and open valve D-5, close D4, and allow air to push condensate out through D-1 until the temperature falls below 100°C.
- Close the steam trap isolation valve D-1 at the medium vessel.
- Maintain positive pressure (5–10 psig) in the transfer line during cooling.
- Pressurize the medium vessel to 15 psig with a sterile air/CO_2 mixture (if not, bicarbonate-based medium system air can used).
- When the line is cooled to ambient temperature, begin the medium transfer. Open the medium vessel drain port T-1 and the bioreactor inlet port D-5. Open the bioreactor exhaust line valve D-8.
- When the prescribed volume has transferred (indicated by bioreactor or media vessel load cell or level sensors), close the medium vessel drain port valve and allow the line pressure to dissipate into the bioreactor.
- When the transfer is complete, close both the bioreactor inlet port valve D-5 and the medium tank valve T-1.

76.3.1.2 Pump (Sterilized). Small volumes of sterile media may be transferred between vessels or from sterile media bags through sterilized silicone/Pharmed tubing. A peristaltic pump is used for the transfer. Flow rates are relatively slow, and this method may not be suitable for large scale operations. In small-scale operation, the method allows precise volume transfers. The highest flow rate possible with a peristaltic pump is 1000 Lph with large tubing sizes. More typically, flow rates for common peristaltic pumps are in the range of 0.1–1 Lpm.

In larger systems, the pump must be sterilizable in place. A steam-sterilizable rotary lobe pump can be used for this application (66). Transfer line steam-sterilization is as described in the example of pneumatic transfer.

76.3.1.3 Through Sterilizing Filter. Nonparticulate liquid media may be sterilized by filtration through an absolute 0.2-μm liquid filter. Manufacturers supply presterilized liquid filters. For small-scale operations, these filters may be setup with sterilized silicone/Pharmed tubing and used in a transfer line to the bioreactor. In large-scale operations, it is usual to insert the filter in a stainless steel housing located in the sterilizable transfer line. The filter is steam-sterilized in the forward direction and cooled with concomitant air pressurization on the upstream side of the filter cartridge to prevent backpressure on the cartridge. In clinical manufacturing, sterilizing filters must be validated by an integrity test after use (67). The integrity test is performed by either a bubble-point or diffusion-forward-flow measurement (68). In a bubble-point test, the filter is removed and placed in a test housing and wet. The micropores of the filter contain water held by strong capillary forces. Upstream air pressure is increased stagewise and held for a short period of time. At some pressure, the water will be pushed out of the capillaries by the air pressure, and the upstream pressure will collapse as air bubbles pass through the filter. The pressure at which this occurs is known as the bubble-point pressure and is a function of the size of the pores:

$$P = \frac{4k \cos\theta\sigma}{d}$$

where

P	= bubble-point pressure
d	= pore diameter
k	= shape factor corection
$\cos\theta$	= liquid-solid contact angle
σ	= surface tension

A 0.2-μm filter has a bubble point between 40–50 psig depending on the specific materials and manufacturer. In another test, the decrease in pressure as oxygen diffuses across a wetted membrane is measured over a fixed time period.

$$\Delta P = \frac{D \cdot (t) \cdot (P_a)}{V_h}$$

where

$D =$	diffusion rate (ml.min^{-1})
$t =$	time (mins)
$P_a =$	atmospheric pressure (psi)
$V_h =$	upstream reservoir volume of apparatus (ml)
$\Delta P =$	pressure drop (psig)

Filter integrity is validated by a suitable bubble-point result or by a diffusion test pressure drop within the manufacturer's specification.

Filters are available as 4″ and 10″–30″ pleated cartridges which provide approximately 5 to 15 ft^2 of surface area (69–71). Low protein binding filter materials should be used when filtering media that contain low levels of growth factors or other medium proteins. Bio-inert type materials are available from manufacturers (e.g., Pall with nylon 6, 6 polyamide.) Clean water flow rates of these cartridge style membranes are in the range of 0.2–0.5 $L \cdot min^{-1} \cdot ft^{-2} \cdot psig^{-1}$. Sanitary 3-A design housings are available with a double O-ring cartridge seal.

76.3.2 Volume Control (Weight, Level)

During transfer of media to the bioreactor, it is desirable to monitor the progress of the transfer by measuring the volume or mass transferred. As liquid enters the bioreactor, the weight increases as mass is added. A load cell can measure the mass of the reactor. Alternatively, a capacitance level probe (72) could be used to indicate when the liquid has reached a predetermined level and provide a signal to stop the transfer pump or close valves in the transfer circuit.

A floor load scale can be used for mobile vessels up to 500 L in operating volume. Fixed-in-place tanks require skid-mounted load cells to measure the vessel weight. Volume control can be achieved by activating of a feed pump to maintain a fixed volume. A common method of volume control in a perfusion system is to set the tank dilution rate by controlling the medium outlet continuous pump at a set flow rate and using a level sensor or load cell to regulate the flow rate from the fresh medium inlet pump. The flow control may be by PID pulsed on/off control or by PID regulated continuous flow rate. Continuous flow control is recommended in high-density cell culture.

Typical arrangements for simple liquid level control are shown in Figure 76.9.

76.3.3 Foam/Tangential Inlets

Foam results when bubbles persist at the liquid surface. Because the medium will contain proteins and other foam-generating materials (high surface tension), it is usual to experience foam in bioreactors that are sparged. When frit spargers are used, a stable fine textured foam may persist throughout a run (73). The foam layer will provide a gas mass transfer resistance between the headspace and the liquid surface. This may lead to a small increase of the pCO_2 of the culture during the production phase. Larger diameter bubbles do not tend to form stable foam packs and can be used to break down the foam layer to a certain extent. Foam may be entrained in the exhaust lines where it may coat and block exhaust filters and lead to a failure to control the bioreactor at optimal conditions. To avoid catastrophic foam-out problems, a break tank can be installed between the vessel and the exhaust filter. Foam may lead to specific CIP complications when the foam transports cellular material and media into the filter housing and top-plate nozzles.

Foam can be detected by a conductivity probe that can send a signal to alert operators or to initiate addition of antifoam in standard type bacterial culture. Antifoam agents are potentially toxic to cell culture and are rarely used in foam control. Mechanical devices are most often the choice for cell culture foam separation during the production phase. Defoaming has been achieved by inserting a preformed polysiloxane hydrophobic screen at the top of the liquid surface in an ascites suspension culture (74).

During transfer of the medium in the preparative phase, it useful to add the liquid components through vessel side ports. Ideally, these ports would be arranged tangentially on the side of the vessel. This minimizes the degree of splashing and air entrainment during addition and the formation of a foam layer on the surface of the media. There are also designs in the patent literature that describe abatement of foam using tangential inlets coupled with a low rpm centrifugal separator (75). Foam layers may impede the ability to adjust pH correctly if base is retained in the foam layer after addition through a top-plate nozzle. It is advisable to set the pH controller on manual or the integral function at a low value in attempting to adjust the pH when a foam pack exists.

76.3.4 Sterile Connections/Disconnections

Following sterilization, it is necessary to connect feed tanks, base tanks, sample lines, and perhaps gas lines to the bioreactor. Small autoclaved systems are usually set up with flexible tubing for later connections. Sterile tubing may be connected by using a sterile tubing welder. These devices are supplied as medical devices for connecting tubes aseptically (Terumo Medical Corporation Elkton, MD 21921 USA SCD IIB Sterile Tubing Welder). The type of tubing used to make a sterile connection can be PVC with a nominal OD of 0.21 inches and a wall thickness of 0.030 inches. Users of this equipment have had successful results in fusing thermoplastic tubing such as C-Flex (size 16). The equipment is portable and can be operated inside a class 100 hood if required. The SCD welder makes a sterile connection between the two lengths of tubing by thermal welding. Two pieces of tubing are placed in the tubing holder on the machine. The welding wafer heats to approximately 500°F ensuring sterility and melts through both pieces of tubing. With the wafer maintaining a functionally closed system, one tubing holder moves back to align the two pieces of tubing being connected. The instrument then simultaneously retracts the wafer and welds the tubes together. The two

pieces of tubing to be welded together should be previously autoclaved and have a terminal 0.2-μm 47-mm disc air filter. Because the tubing size is limited to size 16 with a nominal ID of 0.21 inches the flow rate of fluids is restricted. Exhaust gas flow rates of >5 Lpm may cause some pressure buildup in this small diameter tubing. If a line is to be severed or removed, place two tubing clamps over the line, and cut distally from the fermenter. If the line is to be reused, use a tubing welder to join a short C-flex tubing length to the vessel C-flex line.

For larger vessels, larger diameter tubing connections must be made. It is not possible to make a strict sterile connection between two hoses without steaming afterward. Where aseptic connections are required to link equipment, such as tanks, it is important to include steam-block arrangements in the interconnecting lines (Fig. 76.11). Steam-block arrangements enable sterilization of the transfer lines independently of the vessel sterilization cycle.

76.3.5 pH Priming

Before initiating automatic pH control, it is important to prime the acid and base lines. This involves filling the lines between the supply tank and bioreactor with acid or base, setting the controller to manual mode, and manually pulsing the addition pump or regulating valve to allow the base or acid to flow up to the vessel. An operator would have to visually observe the process of priming to assure that the lines are filled. In very large scale, use of a closed circulation loop or of an in-line conductivity probe could automate systems priming. A simplified example of a pH control loop is shown in Figure 76.14.

If priming is not done, it is possible that the initial pH control will overshoot and may cause the cells to experience wide pH fluctuations. Process control of pH is best achieved using PID process loop controllers. In PID control, the difference between the set-point pH and the actual measured pH would be used to generate a controller output signal for actuating of the base or acid pump. In a split PID control loop, the acid and base systems have individual PID controllers. In a standard PID control loop, the output signal is calculated from a control algorithm PID equation.

$$\text{Output} = K_c \cdot E + \frac{1}{t_i}\int_0 E dt + t_d \frac{dE}{dt}$$

where

E = set-point measurement value
K_c = controller gain (proportional)
t_i = integral time (integral)
t_d = derivative time (derivative)

This expression explains that an unprimed line will lead to an artificial delay in the change of the pH because base or acid is not present through the line. This will lead to an increase in the influence of the integral term, and a high output value will be calculated, which will likely lead to an overshoot in pH. To prevent this, the controller should be set in manual mode during priming and installation.

76.3.6 Instrumentation Checks

Sterilization may affect the calibration of various probes. Simple poststerilization checks can be made and any necessary readjustments can be made.

76.3.6.1 Temperature. The RTD probe can be checked by measuring the temperature of the medium with a mercury in glass thermometer in a thermowell port filled with a nonvolatile liquid such as glycerol.

76.3.6.2 pH. As mentioned earlier, a standard Ingold probe measures pH with an accuracy of 0.04 pH ± 0.01 and a reproducibility of 0.01–0.02 pH units. A drift of the pH signal may occur in a solution of constant (H^+)

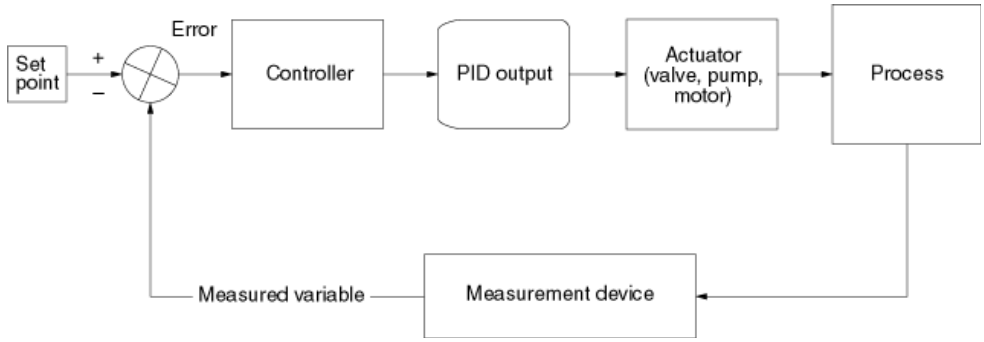


Figure 76.14. Process control loop. Feedback control loop showing PID controller. Comparison of the process pH to the set point value generates an error value. This electronic value feeds into a PID algorithmic calculation which generates a PID output to open a valve or to activate a pump motor resulting in the addition of acid (CO_2) or base to the process tank.

concentration. However, the rate of drift should be less than 0.02 pH units hr^{-1}. Larger rates of drift are usually due to clogging of the liquid junction.

The response of a pH probe should be 59.19 mV/pH at 25°C. The response time should be less than 30 seconds. Slow response time indicates thickening of the gel layer and accompanies increased electrical resistance, low slope, and zero-point drift. The aging of the probe is markedly increased by increased temperature. Normal probe life is 1–3 years at 20°C and less than a week at 120°C. Repeated dehydration, resulting from leaving a probe inside a dry vessel before or after a process, decreases the effective probe life. A dry probe gel layer may require days to rehydrate. The reference electrode is also adversely affected when the probe is allowed to dry out. Salt crystals may form in the reference electrode liquid junction causing an increase in the reference electrode impedance. Soaking in 3.8 M KCl may reverse this effect.

Because of potential problems due to poor storage and maintenance of probes, several points for maintaining and checking probes are provided here.

- During downtime, immerse the pH probe tips in 3.8 M KCl. Do not store at pH > 10 or in nonionic solutions for a prolonged time because pH sensitization of the glass may occur which renders the probe sluggish at low pH.
- When changing electrolyte or during cleaning, use an aspirator to remove the entire electrolyte from the inner and outer reservoirs.
- Clean diaphragm junctions regularly (2–3 process cycles) when immersion in high protein media occurs. Place the cleaning solution (supplied by manufacturer) in a probe cap over the tip, and invert the probe overnight. The inversion causes the small hydrostatic pressure to push the cleaning solution through the diaphragm ceramic frit. Rinse thoroughly and replenish the probe electrolyte. Allow 1–2 hours for stabilization before calibration and use. Preferably, leave the probe overnight in 3.8 M KCl.
- Never clean the probe with tissue. It can create a static charge that will render the probe very sluggish.

Probes are calibrated by a two-point calibration method. The probe is immersed in a pH 7.0 standard. The standard electrolyte is pH 7.0 ± 0.2 pH units at 20°C. The probe reading is adjusted to this value by adjusting the meter zero. The probe is rinsed and placed in pH 4.0 ± 0.2 pH unit buffer, and the meter span is adjusted to read pH 4.0. The process should be repeated once. At this point, the probe is inserted into the 25-mm Ingold-type vessel port. In lengthy perfusion-mode bioreactor processes, it is usual to install more than one probe as backup sensors. Probes are steam-sterilizable in place.

Several useful diagnostic tests can indicate the state of a before deciding whether it is reliable and suitable for in-line duty. Some practical tests are given here:

- A probe that gives a stable reading at pH 7.0 ± 0.2 pH should indicate a value of pH 4.0–4.15 within 30 seconds after placement in a pH 4.0 calibration buffer.
- An mV slope of <35 mV/pH unit indicates that a probe has an internal short circuit and should be discarded. This may be indicated by an unusually high span value (>140% normal new probe).
- Place a high impedance ohmmeter (10 MΩ) in parallel with the probe, which is immersed in 3.8 M KCl, by placing one electrode in the beaker of 3.8 M KCl and locating the other electrode in the probe electrolyte through the fill hole. Use only Ag/AgCl wires to prevent half-cell formation. The resistance should typically be 3–15 kΩ. If the reading is 20 kΩ or greater, the junction is blocked and needs cleaning.
- Electrical resistance between the reference element and the lead out signal wire should be too great to measure. However, any detected measurable resistance indicates cracking of the isolating glass and electrolyte leakage. This results in an inoperative probe.

Other indications and cautions for nongel electrolyte probes are as follows:

- Ensure that the sealing plug is removed from the probe before use to equalize the pressure of the probe within the housing. During sterilization at 121°C, the pressure will increase in the probe as the equilibrium vapor pressure increases.
- Maintain positive pressure on the probe housing to create a flow of electrolyte out of the electrode junction. The probe housing pressure should be approximately 6–8 psig greater than the sum of the positional hydrostatic plus vessel head pressure during operation. Note: A drop of electrolyte should form at the probe junction at positive housing pressure if the junction is not blocked. The electrolyte leak rate is 0.5–1.0 mL/day at 2-bar overpressure.
- For all pH probes, a normal drift of 0.05 pH/day can occur and is usually corrected by off-line grab sample and calibration measurement. It is important in this method that the sampling technique does not impart an error to the pH correction. This may be a problem in high cell-density cultures, high pCO_2 and changing sample temperature. To minimize errors of this nature, a contained sampling device such as a siliconized syringe is used.

76.3.6.3 DO_2. Ingold DOT probes give a current of 60 nA at air-saturation DOT. In N_2 saturated solution, the current should be less than 1% of the air saturation value. Response time from saturation to N_2 should be 45–90 seconds. Probes are stable at constant temperature and pressure, and the change in output in air saturated solution is less than 2%/week. The dissolved oxygen (DO) probe should be plugged in to the amplifier with the power to the control box on. If the probe has been unplugged from the amplifier or the power to the control box is off for more than one hour, the probe must be repolarized for 12 to 24 hours. Probes that have been unplugged or have had power interrupted for less than one hour must be repolarized for approximately two times the power off/unplugged time period.

Place the probe in air-saturated water, and record the dissolved oxygen value. This can be set-up using a 2000-mL graduated cylinder filled with deionized water and sparging the flask with air at approximately 5 Lpm for about 10 minutes. Next, place the probe in an oxygen-free atmosphere, that is, pure nitrogen. Use an empty 500-ml Erlenmeyer flask sparged with nitrogen at approximately 1 Lpm. The dissolved oxygen reading should drop to less than 2 to 5% of the saturated air value.

Leave the probe in the nitrogen atmosphere, and record the minimum steady-state dissolved oxygen value and the output current or amplifier voltage. If the voltage is greater than 0.04 volts, the probe must be rejected. If the probe passes the test, set the DO to zero. Placing the probe in air-saturated water can check the response time of the probe. On changing from nitrogen to air-saturated water, the probe should attain 98% of the air value within 45 to 90 seconds.

The DOT probe is calibrated in the vessel after sterilization and addition of sterile media. The bioreactor should be at the run temperature and sufficient media should be in the vessel to cover the probe. The rpm is set at a level that gives good bulk mixing. Attach a 95% v/v N_2/5% CO_2 gas line to the inlet sparger and headspace inlet filters. Sparge the mixture until the output signal is asymptotic for >30 minutes. Then adjust the probe zero on the DO controller amplifier. After the zero adjustment is completed, disconnect the N_2/CO_2 line, and flow 95% air/5% CO_2 through the gas inlet lines. When an asymptotic maximum is achieved, set the span to 95% airsaturation.

76.4 CULTURE INITIATION

76.4.1 Transfer of Cell Inoculum

Inoculum transfer essentially involves transferring an actively growing culture of cells from one growth vessel to another larger growth vessel containing fresh medium. The operation of transferring the culture should impose little or no physiological stress on the cells. The important aspects of inoculum transfer are as follows:

- Transfer in minimum time.
- Avoid DOT <20%.
- Avoid foam generation in transfer equipment.
- Preset receiving environmental conditions to run conditions.
  - Set pH at set-point value.
  - Set DOT at 95% saturation.
  - Set temperature at set point.
  - Set an initial low agitation rate (for bulk mixing).
- Sterilize transfer lines and allow them to cool ahead of time.

Ensure that the vessel valves are in the correct open/closed positions for the culture run conditions. Particular attention should be given to ensuring that the receiving vessel airflow rate is set at a low rate and that the gas vent (exhaust) line is open to avoid any elevation of backpressure toward the inoculum vessel or container. Any backflow of gas could result in foam production in the transfer lines or overpressurization of the inoculum vessel and subsequent breakage of connecting joints.

In small-scale vessels, it is possible to locate the inoculum inlet line below the initial liquid level line. This avoids the possibility that vessel headspace internal devices will hinder the inoculum. For larger vessels, a subsurface transfer line may impart hydrostatic pressure which must be overcome by pressurizing the inoculum sufficiently.

Overpressurizing an inoculum vessel can lead to transient high pCO_2 and O_2 concentrations and potential physiological shock to the cells. Transfer is achieved by using gravity feed or a peristaltic pump to avoid this problem. Small-scale cultures may be grown in small spinner jars or flasks that are set up with internal stainless tubing to facilitate transfer (Fig. 76.15). The inoculum can be transferred by gravity feed or by using a peristaltic pump. The spinner flask should be agitated by gentle swirling during the procedure. It is generally not possible to maintain the flasks at temperature in an incubator during the procedure when the vessels are separated by distance. The flask could be wrapped in insulating foam for the short inoculation duration if desired. Larger scale inoculum transfer may require using a slight gas overpressure to convey the inoculum. Using a minimum pressure, avoiding any large pressure gradients, and avoiding foaming are key design parameters.

76.4.2 Initial Mixing/Planting Conditions

After inoculation, a number of checks and controls are performed. The control and monitoring systems are

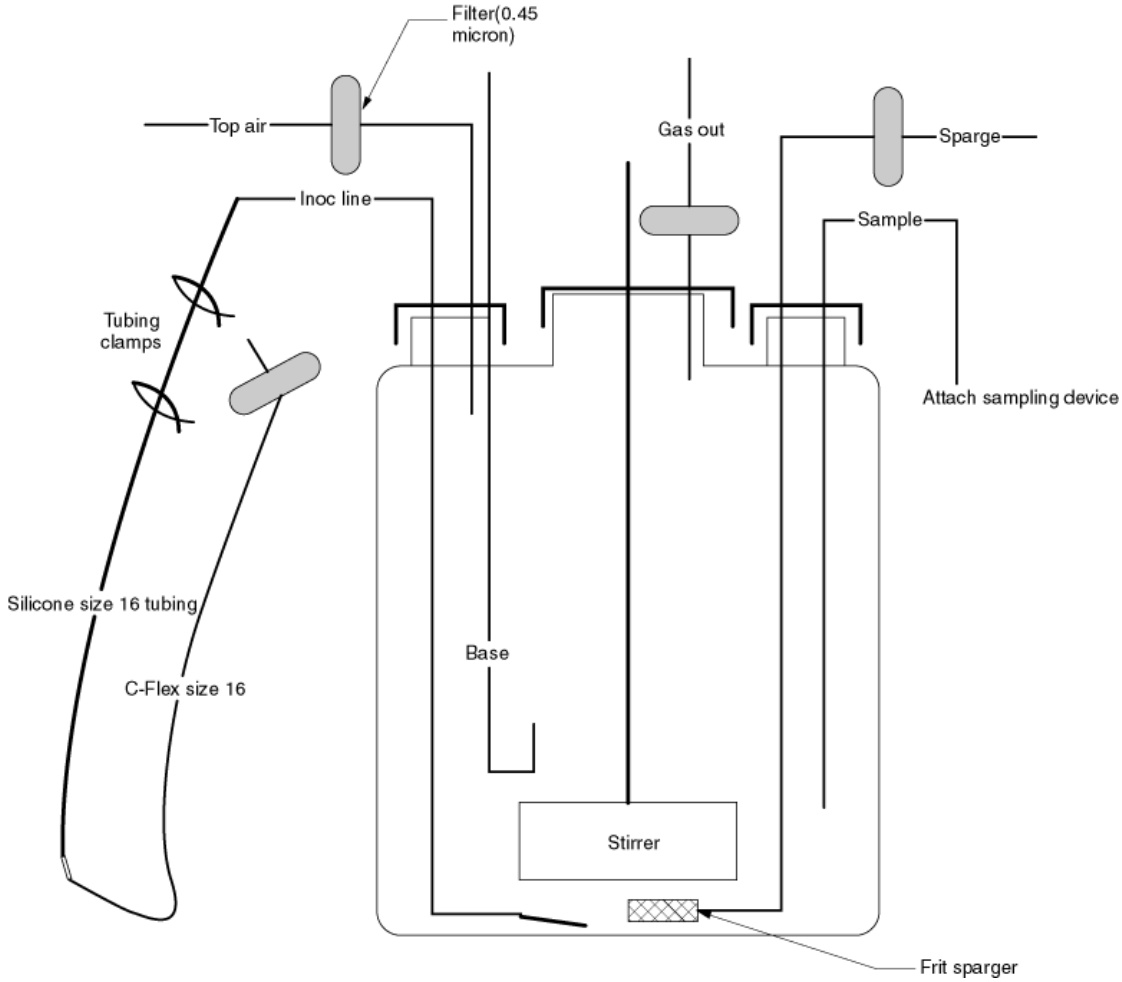


Figure 76.15. Inoculum transfer apparatus. A spinner jar (1 L–20 L) can be used to propagate and transfer an inoculum. The use of C-Flex tubing facilitates attachment to the bioreactor by using a SCD tubing welder.

switched from manual to automatic remote control mode. Initial aeration conditions are set for minimal flow rate to maintain the DOT and pH (CO_2). Overaeration during and just after inoculation can lead to production of a foam layer at the liquid surface which can trap cells and potentially inactivate them. In general, bubbles can inflict serious forces as they disengage at the liquid/gas surface, and through interfacial tension forces. These forces may irreversibly damage cells (76). In cell culture adding a low quantity of Pluronic Polyol F68 to the medium may very significantly decrease the rate of bubble damage (77). When cell density is low, this can lead to a significant lag phase through the reduction in viable cell concentration following an increased specific death rate. The agitation rate should be set to the lowest Rpm that keeps the cells suspended. The DOT will usually remain unchanged because the overall OUR is low relative to the volumetric OTR (Oxygen Transfer Rate).

The pCO_2 is a function of the % CO_2 in the aeration mixture and can be verified by checking the mixture component flow rates and the liquid pCO_2 using a BGA. In batch bioreactor operation, the volume will change only by a small amount, which would be the balance of loss through evaporation and entrainment and gain through the addition of base and other reagents. Nutrient feed should be initiated soon after the inoculation. The pump and hardware are checked to ensure that the lines are set up for the flow of nutrient feed to the vessel.

76.4.3 Initial Sampling

Samples are removed for sterility testing and off-line chemistry checks. A 100–200 mL sample of preinoculation medium is taken and stored at 2°–10°C before inoculation with postinoculation cells from the bioreactor. A small aliquot of the fresh sampled bioreactor medium is used to

TABLE 76.10. Postinoculation Sampling Matrix

	Sample	Medium (additions present)	Inoculation Cells	Comments
1.	Sterile sampling of medium	Sterile medium from supply vessel or bag pretransfer to bioreactor	None	Observe for any contaminant growth over 7 days
2.	Sterile sample of medium from bioreactor	Preinoculation medium from bioreactor	None	Observe for any contaminant growth over 7 days
3.	Test of growth medium	Sterile medium from supply vessel or bag pretransfer to bioreactor	Healthy growing stock cells (from culture deposit or research source)	Test medium for growth (specific growth rate μ and capacity—cell yield)
4.	Test of growth medium after transfer manipulations and residence in bioreactor	Preinoculation medium from bioreactor	Healthy growing stock cells (from culture deposit or research source)	Test for possible medium transfer effect on medium and bioreactor/medium interactions; any decrease in μ and yield from test 3 may indicate that changes to medium have occured
5.	Test of growth medium after inoculation manipulations	Postinoculation medium; aseptically centrifuge out cells, and decant and save medium	Healthy growing stock cells (from culture deposit or research source)	Test for possible inoculation effect on medium; any decrease in μ and yield from test 3 and 4 may indicate that changes to the medium have occured
6.	Test cells preinoculation	Sterile medium from supply vessel or bag pretransfer to bioreactor	Cells from inoculum vessel sample diluted to original inoculation density	Examine μ of cells to determine any decrease in cell function; tests health of inoculum
7.	Test cells postinoculation	Sterile medium from supply vessel or bag pretransfer to bioreactor	Cells from bioreactor postinoculation aseptically centrifuged to concentrate and then diluted to original inoculation density	Examine μ of cells to determine any decrease in cell function; compare with (7) to determine any effect on cell health during the inoculation process

determine preinoculation glucose, glutamine, ammonia, lactate, pCO_2 (BGA), DOT (BGA), and pH (BGA) values.

After completing the inoculation, a small sample of the inoculum is retained to determine viable cell concentration. The bioreactor is sampled to provide measure postinoculation viable cell count, pH (BGA), and pCO_2 (BGA). The culture is visually examined under a phase-contrast microscope to determine cell count and viability and to inspect the morphology of the cells.

76.4.4 Control Cultures Set Up

Various shake flask or small-scale incubation tests are setup. The tests are designed to detect any source of contamination that occurs during the inoculation and to compare and possibly troubleshoot differences in the cell growth rate in the bioreactor and the shake flask controls. The tests are depicted in Table 76.10.

76.5 HARVESTING

In cell culture, where the product of interest is secreted into the medium, the harvesting process should not result in cell damage or lysis. Operation at low temperature (4–12°C) is used to minimize enzymatic degradation of glycoproteins. In cell culture, sialadase may be active and cause degradation. It may be possible to minimize the degradation process by using inhibitors such as 2,3-dehydro-2-deoxy-*N*-acetyl neuramic acid (78). Prevention of mechanical damage and lysis involves chilling and using low-shear transfer systems. Peristaltic pumps with silicone tubing, pneumatic transfer through overpressure of the reactor, or gravity transfer in small-scale vessels are recommended. Additionally, static laboratory centrifugation is a gentle approach useful for clarifying relatively small volumes of culture liquid. The largest laboratory rotor capacities are 5 liters. The researcher can gauge the time needed to process the material with such an approach. It would be feasible to process up to 30 liters of culture broth in ~2.5 h using a laboratory batch centrifuge.

Filtration techniques may be used to separate the cells from the product. When cross-flow filtration is employed to separate cells and medium, it is important to minimize cell lysis, which could result in a decrease in yield and purity of the product, as well as decreased performance of the membrane system. Avoidance of average wall shear rates greater than 3000 s^{-1}, using membrane pore sizes of 0.2 um, and minimizing of shear rates (less than 25 $dyn \cdot cm^{-2}$) minimize the potential cell damage in cross-flow filtration

(79). Addition of Pluronic polyol F68 (0.1%w/v) prevents damage from gas bubbles generated by mixing and shearing. If small membrane systems of 1 ft^2 are used, then peristaltic pumps (Watson-Marlow or Cole-Palmer) are adequate. For larger systems, larger gap rotary positive-displacement pumps are employed (Flowtech, Waukesha). Cross-linked cellulosic membranes are available (Sartorius Hydrosart) which are useful in minimizing surface fouling and for facilitating high protein flux.

76.5.1 Discharge

The simplest methods for transferring the bioreactor contents from the bioreactor are mentioned in the next sections.

76.5.1.1 Gravity. In a facility in which tanks are arranged at multiple levels, gravitational force may be used to drain the bioreactor. The harvest valve is designed to allow sufficient flow from the tank. Harvest valve designs are flush-mounted with the vessel internal dish surface and use piston-type operation to open the closed positioning (Fig. 76.16). The flow rate from the tank will drop as the liquid height decreases. The following equation relates the time for reducing of the liquid height from the original height (H) to the empty vessel height designated as the reference height of zero.

$$T = \frac{1}{C_D}\sqrt{\frac{2}{g}} \cdot \left(\frac{D}{d}\right)^{0.5} \cdot (H^{0.5})$$

where D is the tank diameter, d is the outlet valve and piping diameter, and C_D is the discharge coefficient of the harvest orifice. Time restrictions limit this operation to small-volume systems (<500 L).

76.5.1.2 Sterile Air Overpressure. Sterile air overpressure at the bioreactor is frequently used to make liquid transfers. An air supply feeds a sterilizing inlet filter. The exhaust gas lines, inlet nutrient, and base lines are closed, and the vessel head pressure is increased to between 10–20 psig. Transfer is initiated by opening the harvest valve and the receiving vessel inlet and vent valves. When processing fragile cells, a minimum overpressure is chosen to minimize potential lysis caused by rapid pressure decreases through valves and fittings.

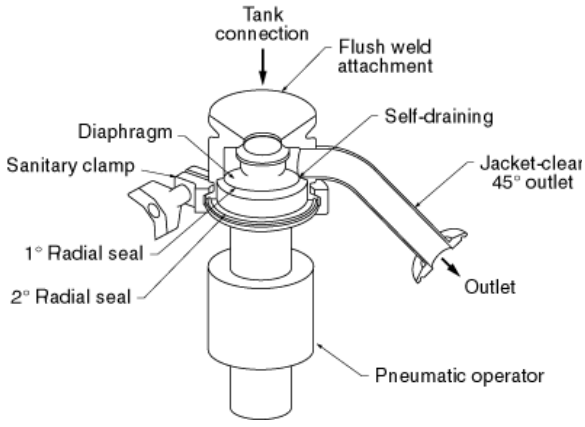


Figure 76.16. Typical flush-mounted tank harvest valve design.

76.5.1.3 Pump. To transfer small-scale bioreactor contents, it is possible to use a peristaltic pump with silicone tubing. Although peristaltic pumps are available up to 4″ in diameter and with deliverable flow rates of 1000 Lph it is generally not feasible to operate such systems smoothly. Placing persistaltic pumps at a distance from the reactor outlet may cause pressure losses that result in restriction of flow to the pump and subsequent tubing collapse. Rotary lobe pumps have been used for liquid transfer in cell culture. Recirculation of hybridoma cells through a recirculation loop of 0.75″ diameter and 8 ft long for 1 hour at flow rates up to 16.7 gpm did not cause any decrease in cell viability in the presence of Pluronic F68. The turbulent shear associated with flow through the system did not damage cells over a range of Reynolds numbers up to 71000, corresponding to a Kolomogorov eddy length of 12 μm (79). Cell damage at Kolomogorov eddy lengths of 3.5 μm or less at high power dissipation rates have been reported (80). Circulation of hybridoma cells through a rotary lobe pump showed cell damage at tip speeds of 350 $cm \cdot s^{-1}$ (79). When cell damage is to be avoided, the choice of pump should enable operation at low rpm with maximum tip speed in the region of 250 $cm \cdot s^{-1}$.

REFERENCES

1. W.R. Arathoon and J.R. Birch, Science 232: 1390–1395 (1986).
2. A.E. Humphrey, E. Galindo, and O.T. Ramirez, eds., Advances in Bioprocess Engineering, Kluwer Academic Publishers, Dordrecht, The Netherlands, 1994, pp. 103–107.
3. T. Hashimoto, in S. Azechi, S. Sugita, and K. Suziki, Proc. 5th Int. Plant Tissue Cell Culture, Tokyo, July 1982, p. 403.
4. D.A. Seiberling, Spec. Tech. Publ. ASTM STP 538: 196–209 (1973).
5. International Association of Milk, Food and Environmental Sanitarians, The United States Public Health Service, The Dairy Industry Committee, J. Milk Food Technol. 37(1): 605–02 1974.
6. D. Parry, Process Biochem., July/August, pp. 27–29 (1974).
7. D.G. Adams and D. Agarwal, Pharm. Eng. 10: 9–15 (1990).
8. C.T. Cowan and C.R. Thomas, Process Biochem. February, pp. 5–11 (1988).
9. E. Grave, Biopharmacology pp. 22–28 (1988).
10. A.K. Lloyd, Food Manuf. February, pp. 37–42 (1972).
11. D.A. Seiberling and W.J. Harper, Am. Milk Rev. 19(1): 30–31, 34 (1957).

12. Y. Christi, Chem Eng. Prog. 88(9): 80–85 (1992).
13. G. Hauser, Inst. Chem. Eng. Symp. Ser. 126: 435–445 (1992).
14. A. Grasshoff, Trans. Inst. Chem Eng. 70(C2): 69–77 (1992).
15. J. Villafranca and E.M. Zambrano, Pharm. Eng. 5(6): 28–30 (1985).
16. D.C. Coleman and R.W. Evans, Pharm. Eng. 10(2): 43–49 (1990).
17. T. Myers, T. Kasica, and S. Chrai, J. Parenter. Sci. Technol. 41: 9–15 (1987).
18. G.L. Petersen, Anal. Biochem. 100: 201–220 (1979).
19. R. Baffi *et al*., J. Parenter. Sci. Technol. 45(1): 13–19 (1991).
20. J. Agalloco, J. Parenter. Sci. Technol. 44(5): 253–256 (1990).
21. P.T. Noble, Biotechnol. Prog. 8(4): 275–284 (1992).
22. H.J. Henzler, Untersuchungen Zum Homogenisieren Von Fluesigkeiten Oder Gasen VDI-Forschungsh. 587: VDI Verslag, Dusseldort (1978).
23. R.B. Bird, W.E. Stewart, and E.N. Lightfoot, Transport Phenomena, Wiley, New York, 1960.
24. R.H. Perry and D.W. Green, Chemical Engineers Handbook, McGraw-Hill, New York, 1984.
25. L.G. Straub, E. Silberman, and H.C. Nelson, Trans. Am. Soc. Civ. Eng. 123: 685–717 (1958).
26. J. Alford *et al*., Ann. N.Y. Acad. Sci. 721: 326–336 (1994).
27. S.S. Seaver, J.L. Rudolph, and J.E. Gabriels, Bio Techniques 2(4): 254–260 (1984).
28. G. Gualandi, E. Caldorola, and E.B. Chain, Sci. Rep. Ist. Super. Sanita 2: 50, (1959).
29. H.P.J. Bonarius, C.D. de Gooijer, J. Tramper, and G. Schmid, in R.E. Spiers, ed., Animal Cell Technology, Proc. 13th ESACT Meet., Butterworth-Heinemann, Wiltshire, U.K., 1995.
30. L. Packer, ed., Methods in Enzymology, Vol. 105: Academic Press, New York, 1984.
31. Heating Belt systems available from Watlow, St. Louis, MO.
32. D.R. Gray *et al*., Cytotechnology 22: 65–78 (1996).
33. A. Itagaki and G. Kimura, Exp. Cell Res. 83(2): 351–361 (1974).
34. Blood Gas Analyzer available from Ciba Corning Diagnostics, Corning, NY.
35. E. Puhar, A. Einele, H. Buhler, and W. Ingold, Botechnol. Bioeng. 22: 2411–2416 (1980).
36. S.K. Dahod, Biotechnol. Prog. 9: 655–660 (1993).
37. Available from Aquasant-Messtechnik AG, Switzerland.
38. K.B. Konstantinov, Y.-S. Tsai, D. Moles, and R. Metanguihan, Biotechnol. Prog., 12: 100–109 (1996).
39. P. Wu *et al*., Biotechnol. Bioeng. 45: 495–502 (1994).
40. T. Yamane, Biotechnol. Prog. 9: 81–85 (1993).
41. R.M. Mantanguihan, Bioprocess Eng. 11: 213–222 (1994).
42. Supplied by Badger Meter Inc., Research Control Valve (Orion), Tulsa, Okla.
43. Supplied by Sensortronics, Covina, Calif.
44. Pressure gauges supplied by Andersen Instruments Co. Inc., Fultonville, N.Y.
45. Load Cells supplied by Sensortronics, Covina, Calif.
46. Floor scales supplied by Fairbanks Scales, Kansas City, Mo.
47. Mag-Flow meters available from Yokogawa Corporation, Newnan, Ga.
48. Capacitance probes from Endress and Hauser, Greenwood, Ind.
49. Diaphragm valves supplied by Tri-Clover Inc., Kenosha, Wis.
50. Sanitary design ball valves from Worcester Controls, Marlborough, Mass.
51. Plug valves available from Nupro, Willoughby, Ohio.
52. Sanitary design valves supplied by Triclover Inc., Kenosha, Wis.
53. W.M. Miller, A.A. Lin, C.R. Wilke, and H.W. Blanch, Biotechnol. Letts. 8(7): 463–468 (1986).
54. SCD IIB Sterile Tubing Welder available from Terumo Medical Corporation Elkton, Md.
55. Clamp and Bevel seat fittings available from Tri-Clover Inc., Kenosha, Wis.
56. S. Aiba, A.E. Humphrey, and N.F. Millis, Biochemical Engineering, Academic Press, New York, 1965, Chapter 8, p. 194, Table 76.8.1.
57. W.E. Bigelow, J. Infect. Dis. 29: 528 (1921).
58. J. Radle, L.R. O'Dell, and B. Mackay, Chem. Eng. Prog. January, pp. 30–47 (1992).
59. Steam Traps supplied by Spirax Sarco Inc., Blythewood, S.C.
60. Ethylene Oxide Sterijet System supplied by Andersen Products, Inc., Haw River, N.C.
61. S. Kaye and C.R. Phillips, Am. J Hyg. 50: 296–306 (1949).
62. Tri-Clamp fitting validation gaskets available from Rubberfab Mold and Gasket, Andover, N.J.
63. S. Chen, Chiron Corporation, Calif. (personal communication) (1999).
64. C.A. Perkowski, G.R. Daransky, and J. Williams, Biotechnol. Bioeng. 26: 857–859 (1984).
65. Sterilized polyethylene vinyl acetate clear Bio-Pharm bags supplied by Stedim Laboratories, Concord, Calif.
66. Steam Sterilizable Positive displacement pumps supplied by Waukesha Cherry -Burrell, Charlotte, N.C.
67. S.S. Chrai, 1988, Pharm. Technol., October, pp. 62–71 (1988).
68. A. Kononov, Pharm. Eng. 13: 30–35 (1993).
69. Sartorius Corporation, Edgewood, N.Y.
70. Millipore Corporaton, Bedford, Mass.
71. Pall Corporation, East Hills, N.Y.
72. 3-A Sanitary Capacitance probes supplied by Garner Industries Inc., Lincoln, Neb.
73. S. Zhang, A. Handa-Corrigan, and R.E. Spier, Biotechnol. Bioeng. 41: 685–692 (1993).
74. M. Ishida *et al*., Cytotechnology 4: 215–225 (1990).
75. U.S. Pat. 4,553,990 (November 19, 1985), A. Hofmann (to, Linde AG).
76. A. Handa-Corrigan, A.N. Emery, and R.E. Spier, Enzyme Microb. Technol. 11: 230–235 (1989).
77. B.L. Maioella, D. Inlow, A. Shauger, and D. Harano, Bio/Technology 6: 1406–1410 (1988).
78. M.J. Gramer *et al*., Bio/Technology 13: 692–698 (1995).
79. B. Maiorella, G. Dorin, A. Carion, and D. Harano, Biotechnol. Bioeng. 37: 121–126 (1991).
80. A. McQuen, E. Meilhoc, and J.E. Bailey, Biotechnol. Lett. 9(12): 831–836 (1987).

77

BIOREACTORS, CELL CULTURE, COMMERCIAL PRODUCTION

TAN-CHE ZHOU AND WEN-WEN ZHOU
Molecular Biochemical Engineering Group, Key Laboratory of Microbial Metabolism, Ministry of Education, School of Life Sciences & Biotechnology, Shanghai Jiao Tong University, Shanghai, China

WEIWEI HU
Cell Culture Development, Biogen Idec Inc., San Diego, California

JIAN-JIANG ZHONG
Molecular Biochemical Engineering Group, Key Laboratory of Microbial Metabolism, Ministry of Education, School of Life Sciences & Biotechnology, Shanghai Jiao Tong University, Shanghai, China

77.1 INTRODUCTION

77.1.1 Animal Cell Culture

Animal cells are widely used to produce recombinant glycoproteins such as hormones, enzymes, cytokines, and antibodies for human therapy (1). There has been a rapid increase in the demand for approved biopharmaceuticals produced from animal cell culture processes, especially the monoclonal antibodies (mAbs), which have become the most successful molecule modality in the development of modern biological medicine (2–4). In 2007, US sales of mAbs reached US$14 billion with an annual growth rate of 22% (5). MAbs also represent the second largest single category of biopharmaceutical substances under investigation as therapeutic drugs. Representative products from mammalian cell culture are listed in Table 77.1.

In the early 1980s, with the development of genetic engineering, it was possible to stably insert target DNA into mammalian cells and produce recombinant proteins, which were new kind of products in the pharmaceutical industry. Compared to the microbial expression systems, mammalian cell systems can produce larger, more complex proteins, which often require extensive posttranslational modifications, particularly glycosylation (7). About 60–70% of all recombinant protein therapeutics are produced by mammalian cells, primarily Chinese hamster ovary (CHO) cells (8).

Although animal cell culture technology has more than 100 years' history at the laboratory scale, its application as commercial bioprocess started from 1950s for the production of human viral vaccines (particularly for poliomyelitis) (9,10). In 1965, Telling and Elsworth demonstrated that baby hamster kidney (BHK) cells can be cultured in suspension by using a 30-L agitated, stainless steel bioreactor (11). The first commercial production of therapeutic recombinant protein from animal cells on a large scale was the human tissue plasminogen activator (tPA) by Genentech in 1986, which used suspended CHO cells in stirred-tank bioreactors (STRs) with sparger aeration. With the increase in the number and demand for biopharmaceutical products from animal cell cultures, the production capacity has significantly increased during last few years. Currently, a number of companies have a total capacity greater than 75 000 L (12). Nevertheless, for large-scale animal cell culture, key barriers including mass transfer limitations, shear sensitivity, the need for more sophisticated process control, and the challenges of growing adherent cell lines should generally be considered (6).

Upstream Industrial Biotechnology: Equipment, Process Design, Sensing, Control, and cGMP Operations, Volume 2, First Edition. Edited by Michael C. Flickinger.
© 2013 John Wiley & Sons, Inc. Published 2013 by John Wiley & Sons, Inc.

TABLE 77.1. Representative Products Generated In Mammalian Cell Culture Systems (Adapted from (6))

Product NameType of Product Cell Line Use			
Recombinant therapeutics			
Tenecteplase	Recombinant glycoprotein	CHO	Reduction of mortality associated with acute myocardial infarction
Antihemophilic factor(recombinant)	Recombinant glycoprotein	CHO	Control of hemorrhagic episodes
Interferon α-n1, lymphoblastoid	Endogenous glycoprotein	Human lymphoblastoid cell line	Treatment of chronic hepatitis C
Coagulation factor VIIa (recombinant)	Recombinant glycoprotein	BHK	Treatment of bleeding in hemophilia A or B patients
Etanercept	IgG1 fusion with TNF receptor	CHO	Treatment of rheumatoid arthritis
Trastuzumab	mAb, humanized IgG1, κ with murine CDRs	CHO	Treatment of metastatic breast cancer
Infliximab	mAb, mouse/human chimeric IgG1, κ	Murine myeloma cell line recombinant (NS0 based on medium components)	Treatment of Crohn's disease
Palivizumab	mAb	NS0, recombinant	Prophylaxis of respiratory syncytial virus
Basiliximab	mAb, mouse/human chimeric IgG1, κ	Murine myeoma cell line recombinant	Prophylaxis of acute organ rejection
Daclizumab	mAb, mouse/human chimeric IgG1	SP2/0	Prophylaxis of acute organ rejection
Rituximab	mAb, mouse/human chimeric IgG1, κ	CHO	Treatment of B-cell non-Hodgkin's lymphoma
Coagulation factor IX (recombinant)	Recombinant glycoprotein	CHO	Control of hemorrhagic episodes in patients with hemophilia B
Vaccines			
Rotavirus vaccine, live, oral, Tetravalent	Live viral vaccine	FRhL-2	Immunization for rotavirus
Rabies vaccine	Vaccine	Not revealed	Immunization for rabies
Hepatitis A vaccine, inactivated	Inactivated virus	Human MRC-5 diploid fibroblasts	Immunization for hepatitis A
Tissue-culture products			
Autologous cultured chondrocytes	Autologous cells	Chondrocytes	Repair of cartilaginous defects
Diagnostic products			
Human T-lymphotropic virus types I and II	mAb	Chronically infected human T and B lymphocytes	Enzyme immunoassay
Capromab pendetide	mAb, murine IgG1, κ	Murine hybridoma cell line	Cancer imaging agent
Nofetumomab	mAb, murine IgG2b FAb fragment	Mammalian cells	Cancer imaging agent
Imciromab pentetate	mAb, murine IgG1-κ FAb fragment	Murine hybridoma cell line	Cardiac imaging agent

BHK, baby hamster kidney; CHO, Chinese hamster ovary; mAb, monoclonal antibody. CDR, complementarity-determining region; FAb, fragment of antigen binding; FRhL-2, fetal rhesus diploid cell line; TNF, tumor necrosis factor.

77.1.2 Plant Cell Culture

Plant secondary metabolites are valuable, rich sources of various bioactive molecules, which play an important role in human medicine (13–15). Approximately 10% of all drugs considered to be "basic and essential" by the WHO are from plants (16). According to their biosynthetic pathways, the secondary metabolites are usually classified as three large molecule families: phenolics, terpenes, and steroids (17). Table 77.2 shows the plant-derived pharmaceuticals.

Many natural products are isolated from wild or field-cultivated plants; however, plants typically produce these compounds in low quantities, and purifying plant natural products is generally expensive, time-consuming, and not environmentally friendly. Compared to the traditional

TABLE 77.2. Important Plant-Derived Pharmaceuticals (Adapted from (18,19))

Product TypePlant Species		Therapeutic Use
Alkaloids		
Ajmalicine	*Catharanthus roseus*	Antihypertensive
Ajmaline	*Rauvolfia serpentine*	Antimalarial
Atropine, hyoscyamine, scopolamine	*Solanaceous*	Anticholinergic
Camptothecin	*Camptotheca acuminata* Decne	Antineoplastic
Capsaicin	*Capsicum*	Topical analgesic
Codeine, morphine	*Papaver somniferum*	Analgesic, antitussive
Cocaine	*Erythroxylum coca*	Local anaesthetic
Colchicine	*Colchicum autumnale*	Antigout
Ellipticine	*Orchrosia elliptica*	Antitumor
Emetine	*Cephaelis ipecacuanha*	Antiamoebic
Galanthamine	*Leucojum aestivum*	Cholinesterase inhibitor
Morphine	*Papaver somniferum*	Sedative
Nicotine	*Nicotiana*	Smoking cessation therapy
Physostigmine	*Physostigma venenosum*	Cholinergic
Pilocarpine	*Pilocarpus jaborandi*	Cholinergic
Quinine	*Cinchona*	Antimalarial
Quinidine	*Cinchona*	Cardiac depressant
Reserpine	*Rauwolfia serpentine*	Antihypertensive, psychotropic
Tubocurarine	*Chondodendron tomentosum, Strychnos toxifera*	Skeletal muscle relaxant
Vinblastine, vincristine	*C. roseus*	Antineoplastic
Yohimbine	*Apocynaceae, Rubiaceae*	Aphrodisiac
Terpenes and steroids		
Artemisinin	*Artemisia annua*	Antimalarial
Diosgenin, hecogenin, stigmasterol	*Dioscorea*	Oral contraceptives and hormonal drugs
Taxol and other taxoids	*Taxus brevifolia*	Antineoplastic
Glycosides		
Digoxin, digitoxin	*Digitalis*	Cardiotonic
Sennosides A and B	*Cassia angustifolia*	Laxative
Others and mixtures		
Ipecac	*Cephaelis ipecacuanha*	Emetic
Podophyllotoxin	*Podophyllum peltatum*	Antineoplastic
Shikonin	*Lithospermum erythrorhizon*	Antibacterial

methods of plantation, large-scale plant cell culture is more competitive as it offers two advantages: (i) controlled culture conditions without the variations in growing conditions that inevitably occur with plants grown in the wild, such as climate, pests, and pathogens; (2) well-defined production systems that result in higher yields and more consistent quality of the products (20). Furthermore, plant cell cultures have other advantages such as their intrinsic safety without foreign gene dissemination in the environment or contamination by mammalian pathogens, cost-effective bioprocessing, and the capability for posttranslation modifications. Recently, with the advances in culture technology, physiology, metabolism, and molecular biology of plant cells (21–23), plant cell cultures are being considered as a possible means for the production of various recombinant proteins. Such proteins include antibodies (24,25), industrial enzymes (e.g. trypsin) (26), technical proteins that are used in research (27), milk proteins that are suitable nutritional supplements (28), and new protein polymers with both medical and industrial uses (29). The first pharmaceutically relevant protein made in plants was the human growth hormone, which was expressed in transgenic tobacco in 1986 (30). Table 77.3 shows examples of recombinant proteins produced by plant cell suspension cultures.

The use of plant cell culture methodology as a means of producing medicinal metabolites has a long history. In the 1930s, it was first reported that plant cells could be cultivated in a synthetic medium in an undifferentiated state, and this achieved unlimited growth (56). In the 1970s, scientists began to make great efforts to use plant cell culture to produce natural products (57). At the laboratory scale, shake flask cultures are commonly used. However, the industrial scale requires a highly controlled culture environment, and various process variables such as mixing, shear force, and

TABLE 77.3. Examples of Recombinant Proteins Produced using Plant Cell Suspension Cultures (Adapted from (31,32))

Recombinant Protein	Expression Host	Promoter System	Localization	References
Human biopharmaceuticals				
Human serum albumin (HSA)	*Nicotiana tabacum* cv NT-1 (tobacco)	Modified CaMV 35S	Secreted, extracellular	33
	Oryza sativa (rice)	RAmy 3D: inducible	Secreted, extracellular	34
Human erythropoietin	*N. benthamiana* cv BY-2 (tobacco)	CaMV 35S	Secreted, extracellular	35
Human α1-antitrypsin (AAT)	*O. sativa* (rice)	RAmy 3D: inducible	Secreted, extracellular	36,37
	N. icotiana benthamiana (tobacco)	CaMV 35S	Secreted, extracellular	38
Human granulocyte–macrophage colony-stimulating factor (hGM-CSF)	*N. tabacum* cv NT-1 (tobacco)	CaMV 35S	Secreted, extracellular	39
Human interleukin-2 and interleukin-4	*N. tabacum* cv NT-1 (tobacco)	CaMV 35S	Secreted, extracellular	40
Human lysozyme	*O. sativa* (rice)	*RAmy3D*	Intracellular	41
Antigens				
Hepatitis B surface antigen (HBsAg)	*Glycine max* cv Williams 82 (soybean) and *N. tabacum* cv NT-1 (tobacco)	Chimeric $(ocs)_3$mas	Intracellular	42
HBsAg	*N. tabacum* cv NT-1	*A. thaliana* ubq3	Secreted, extracellular	43
Single-chain variable fragments (scFv)				
Anti-HBsAg single-chain Fv	*N. tabacum* cv NT-1 (tobacco)	CaMV 35S	Apoplast targeting	44
Anti-CEA antigen single-chain Fv	*O. sativa* (rice)	Maize ubiquitin	Apoplast targeting and ER-retention	45
Heavy-chain mAb anti-Ars	*N. tabacum* cv NT-1 (tobacco)	CaMV 35S	Secreted, extracellular	46
biscFv antibody fragment	*N. tabacum* cv BY-2	Enhanced CaMV 35S	Intracellular	47
Antibodies				
mAb against HBsAg	*N. tabacum* cv BY-2	CaMV 35S	Secreted, extracellular	48
Mouse mAb IgG anti-TMV	*N. tabacum* cv NT-1 (tobacco)	CaMV 35S	Secreted, extracellular	49 50
Human anti-rabies virus mAb	*N. tabacum* cv Xanthi (tobacco)	CaMV 35S	Apoplast targeting and ER-retention	51
Mouse IgG anti *Streptococcus* surface antigen	*N. tabacum* cv NT-1 (tobacco)	CaMV 35S	Secreted, extracellular	52
Report proteins				
Carrot invertase	*N. tabacum* cv NT-1 (tobacco)	CaMV 35S	Secreted, extracellular	53
GUS (β-glucuronidase)	*N. tabacum* cv BY-2 (tobacco)	Heat shock (HSP18.2): heat inducible	Intracellular	54
Acid phosphatase (APase)	*Anchusa officinulis*	APase- inducible by phosphate starvation	Secreted, extracellular	55

gas content should be well controlled when the plant cell cultures are grown at different volumes (58).

77.1.3 Typical Bioreactors for Cell Cultures

In general, bioreactor systems for both animal and plant cell cultures can be classified into five main types as follows.

77.1.3.1 STRs. STRs are one of the most conventional bioreactors. Owing to its advantages such as easy scale-up, good fluid mixing, oxygen transfer ability, and alternative impellers and easy compliance with current good manufacture practice (cGMP) requirements, STRs are commonly used in cell cultures. However, this type

of bioreactor also has several limitations, such as high power consumption, high shear, and the concerns about sealing and stability of shafts in tall bioreactors. Compared to microorganisms, both animal cells and plant cells are shear sensitive, which results in remarkable efforts to modify and optimize the impeller system in order to balance mixing and mass transfer requirements and potential damage by hydrodynamic forces. Numerous modifications of conventional STRs have been made by developing new impeller designs (Fig. 77.1) (59–63). Several biopharmaceutical manufacturers have successfully implemented STRs at the 10 000–20 000-L scale for large-scale animal cell cultures (9).

77.1.3.2 Pneumatically Agitated Bioreactors. The pneumatic bioreactor is a type of gas–liquid dispersion reactor consisting of a cylindrical vessel, where compressed air or gas mixture is usually introduced at the bottom of the vessel through nozzles, perforated plates, or a ring sparger for aeration, mixing, and fluid circulation without moving mechanical parts (64,65). There are two main types of pneumatically agitated bioreactors: air-lift and bubble-column bioreactors, which are generally of low shear stress and simple design and construction. They consist of a main body, air bubbling device, steam generator for sterilization, air inlet, air vent system, various control systems for monitoring temperature, oxygen, and pH, and pipeline systems for transportation of steam, air, medium and product masses.

Air-lift bioreactors (Fig. 77.2 A, B, C, D) have some advantages over STRs: they distribute shear stress more gently as they do not have a mixer or impeller and they are easy to construct and scale-up at low cost. However, the lack of an impeller also brings some disadvantages such as poor fluid mixing for highly viscous culture and excessive foaming under high aeration (53). Air-lift bioreactors have been widely used in plant cell culture (66,67). Their application in animal cell culture has also been reported (68).

Compared to air-lift bioreactors, bubble-column bioreactors (Fig. 77.2 E,F and Fig. 77.3) have some disadvantages: backmixing in the continuous liquid phase and the decrease in interfacial area due to bubble coalescence in viscous liquids. These characteristics limit its application to a certain degree (69).

77.1.3.3 Membrane Bioreactors. Membrane bioreactors (Fig. 77.4), which utilize specialized membranes to retain cells in the reactors, are designed for *in situ* separation of cells from the medium and to integrate production and separation into a single step. The main advantages of membrane bioreactors are high cell density, high volumetric productivity, and low shear stress; therefore, membrane bioreactors are widely used in cell cultures (71–73). However, the disadvantages such as poor cell viability, poor process stability (membrane fouling and

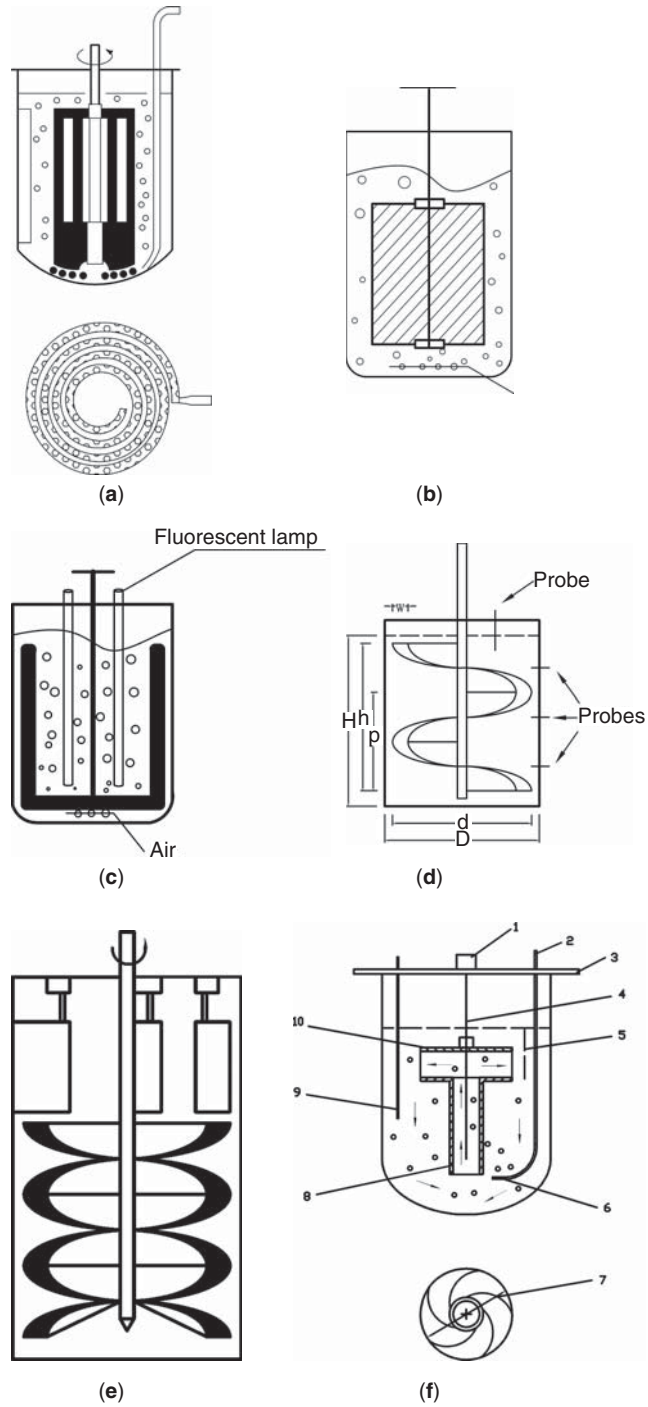


Figure 77.1. Schematic diagram of STRs with different impellers. (a) Gate paddle bioreactor with a spiral sparger (59); (b) large flat-bladed impeller bioreactor; (c) internally illuminated bioreactor (60); (d) helical ribbon impeller bioreactor with bubble aeration (61); (e) helical ribbon impeller bioreactor with surface aeration and surface baffles (62); (f) centrifugal impeller bioreactor (63). 1-Stirrer, 2-gas in, 3-head plate, 4-shaft, 5-measuring points for liquid velocity, 6-sparger, 7-blade, 8-draft tube, 9-DO probe, and 10-rotating pan.

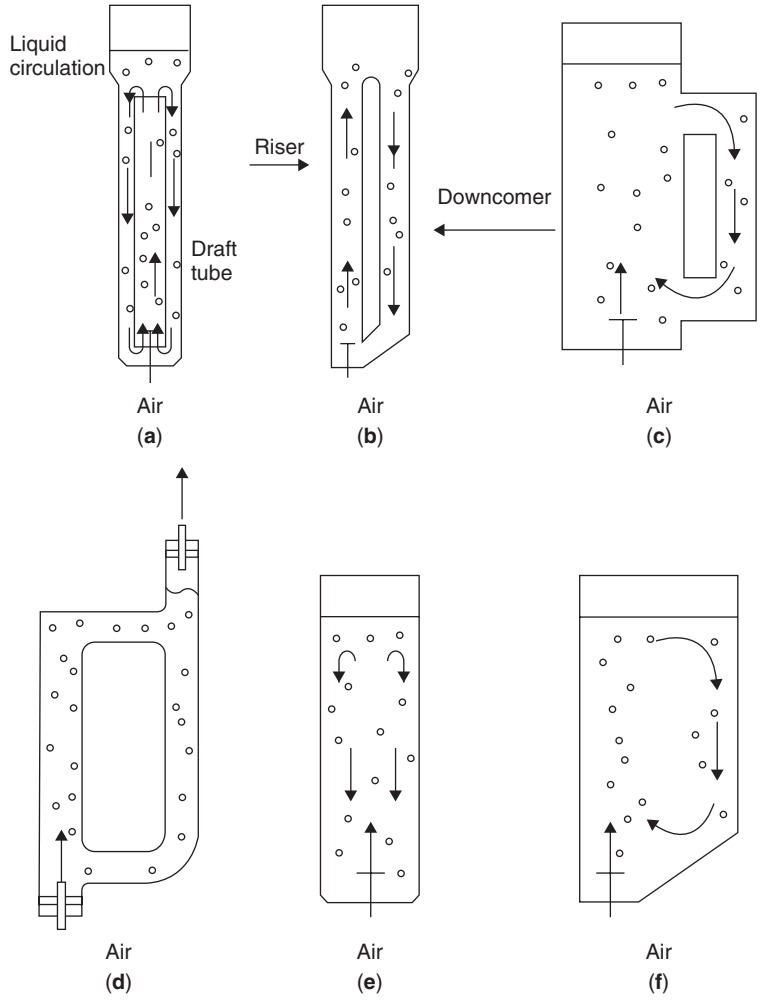


Figure 77.2. Air-lift bioreactors and bubble-column bioreactors (BCB). (a) Air-lift with internal loop; (b), (c), and (d) Air-lift with external loop; (e) Bubble-column; (f) Slanted-bottom bubble column.

clogging), product inhomogeneity, and diffusion gradients limit their large-scale applications. Despite the weaknesses, many membrane configurations have been tested (such as flat sheet and rotating bioreactors), and, among them, the hollow fiber configuration is a particularly interesting one (Fig. 77.5). It has been used for the commercial production of Capromab pendetide/ProstaScint™ (a cancer-imaging agent) with mAb, and murine IgG1 using murine hybridoma cells. It has been proved to be a good and economical alternative to *in vivo* production of antibodies at the lab scale or in large quantities required for diagnostic purposes (74). The bioreactors can reach high cell density with high product concentration. This type of reactor is generally used for small- and medium-scale antibody production. Oxygen delivery is considered to be the main factor limiting cell growth in hollow fiber reactors (75,76).

77.1.3.4 Packed and Fluidized-Bed Bioreactors. For the immobilization systems, packed and fluidized-bed bioreactors are frequently employed.

77.1.3.4.1 Packed-Bed Bioreactors (PBRs). PBRs, also called *fixed-bed bioreactors*, have been used for the cultivation and production of a wide range of cell lines and biologics such as mAbs, recombinant proteins, etc. (78,79). Typically, a PBR (Fig. 77.6) consists of a packed-bed that supports the cells on or within carriers and a reservoir that is used to recirculate the oxygenated nutrient medium through the bed. There are possibly two major configurations, with the packed-bed compartment located either external to, or within, the reservoir of the medium (80). Compared to STR, this type of bioreactor has the advantage of generating high cell densities with a low concentration of free cells in suspension, possibly due to the low shear forces present in the system, hence

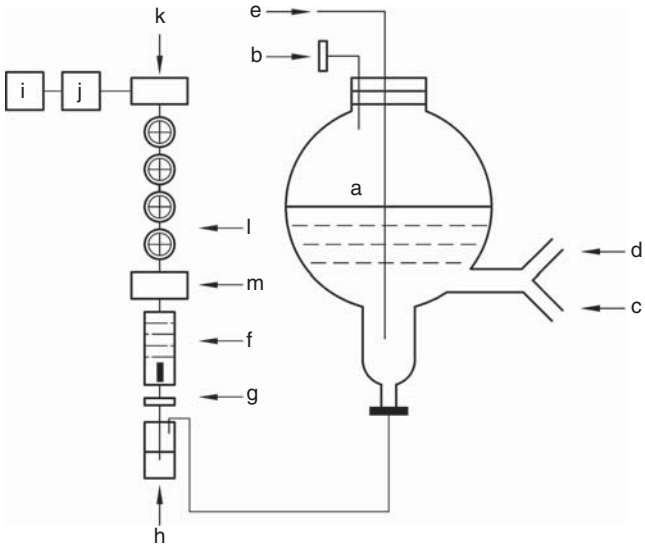


Figure 77.3. Schematic of balloon-type bubble bioreactor (70). (a) Body of balloon type bubble bioreactor, (b) air vent, (c) inoculum port, (d) sampling port, (e) medium exchange port, (f) air flow meter, (g) membrane filter, (h) water column, (i) air compressor, (j) air reservoir, (k) air cooler, (l) filter system, (m) air dryer.

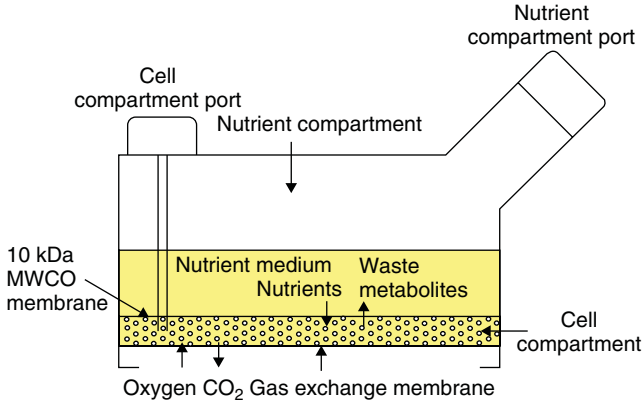


Figure 77.4. Schematic diagram of membrane bioreactor (71). (This figure is available in full color at http://onlinelibrary.wiley.com/book/10.1002/9780470054581.)

high cell density and high productivity can be achieved. Yang *et al*. (81) reported that a fixed-bed bioreactor showed advantages in achieving high cell density and mAb concentration when using different culture systems for mAb production. The major problems of the PBR are their relatively poor mass and heat transfer coefficients due to low liquid velocities. By using intraparticle convective flow technology, this problem could be overcome, thereby significantly improving the transport of oxygen in the fixed bed (82).

77.1.3.4.2 Fluidized-Bed Bioreactors. The fluidized-bed bioreactor is the most widely used culture system for

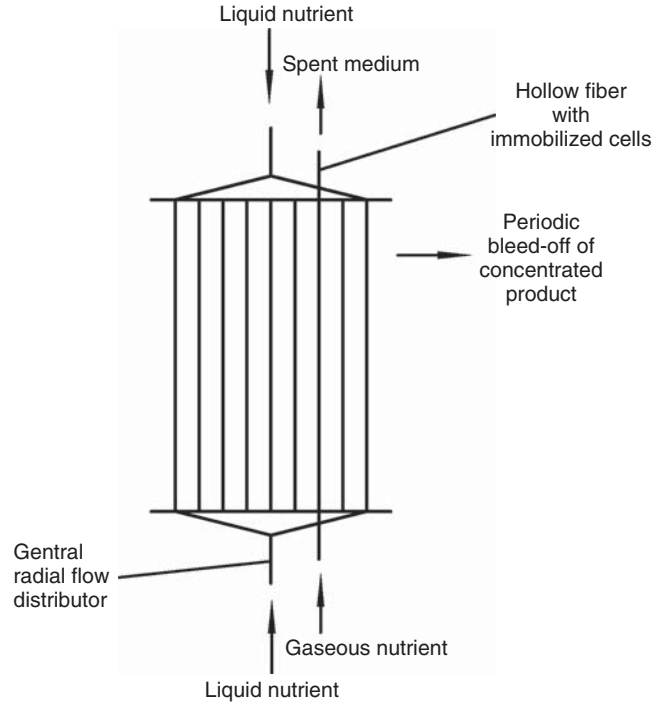


Figure 77.5. Hollow fiber bioreactor (77).

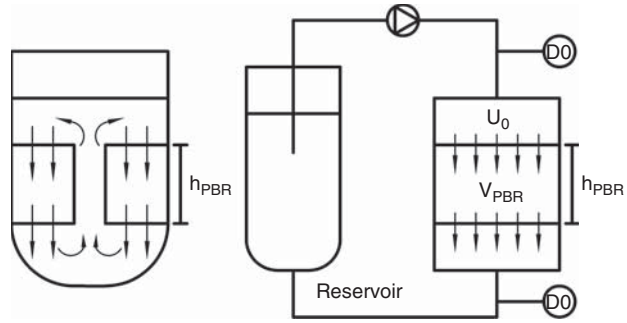


Figure 77.6. Packed-bed reactors with external and internal recirculation of nutrient medium (80). The main design variables for the packed-bed are its volume (V_{PBR}), height (h_{PBR}), and the linear velocity of the medium at the entrance of the bed (U_0). DO: dissolved oxygen sensor.

porous microcarriers (83). Because the density of the microcarriers is higher than that of the culture medium, the upward flow of the medium can suspend the microcarriers, which then circulate through the bed; therefore, the carriers are separated from direct aeration and agitation. As a result, the carriers can avoid local high shear forces. Furthermore, as both cells and fluid can move, fluidized-bed bioreactors provide a very high mass transfer interface, making it suitable for larger-scale production (84).

Goldman *et al*. (85) specifically used macroporous microcarriers in a perfused, fluidized-bed bioreactor

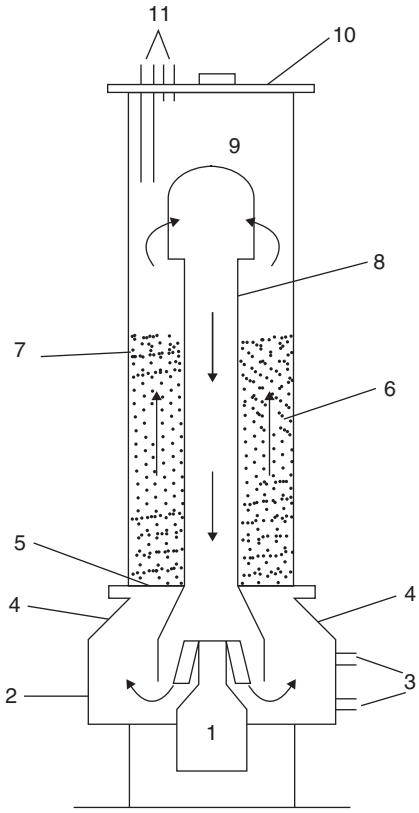


Figure 77.7. Schematic representation of Cytopilot mini fluidized-bed bioreactor (85). 1-magnetic stirrer, 2-stainless-steel double jacketed housing, 3-inlet and outlet for heating circuit, 4-probe nozzles, 5-porous gas/liquid distribution plate, 6-macroporous microcarriers, 7-glass cylinder, 8-downflow section of draft tube, 9-retention sieve, 10-headplate, 11-medium inlet and outlet for continuous-mode operation.

(Fig. 77.7), which have offered great potentials for the production of recombinant human interferon-γ (IFN-γ).

However, a major problem is that, with the fluidized-bed bioreactor, it is not easy to predict the back-mixing and fluidization patterns as it is quite difficult to maintain the nonfluctuating operation. This problem has made operation difficult and has hampered the efforts to scale up this type of bioreactors.

77.1.3.5 Wave Bioreactors. Wave reactors (Fig. 77.8) (86) have emerged and have been applied for cell culture in recent years. These reactors can generate a wave motion by mechanically rocking a culture-containing bag back and forth. These waves provide mixing and mass transfer, resulting in a suitable environment for suspension culture of both plant and animal cells. Several cell lines including CHO cells, NS0 cells, hybridoma cells, insect cells, as well as anchorage-dependant cells using microcarriers have been tested in the system.

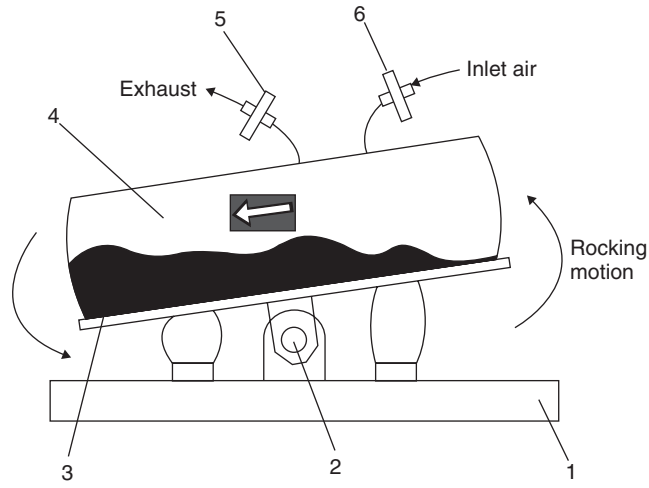


Figure 77.8. Schematic of disposable wave bioreactor (86).1-Base, 2-Pivot, 3-Cell culture media in bag, 4-Inflated plastic bag forms a disposable cultivation chamber, 5-Exhaust vent filter, 6-Inlet air filter.

In addition, the reactor uses a presterilized, plastic, disposable chamber, providing the ultimate ease in operation and protection against cross contamination. The chamber is placed on a special rocking platform that facilitates the compliance of cGMP regulations (87). On the basis of a similar principle, Terrier and coworkers (88) designed a wave and undertow (WU) bioreactor (Fig. 77.9) and a slug bubble (SB) bioreactor (Fig. 77.10). The WU bioreactor provides agitation while offering convenient mixing and aeration to the cell culture in the bioreactor. The SB bioreactor is a high-aspect-ratio bubble-column bioreactor, whose mixing and aeration are achieved through the intermittent generation of large-diameter bubbles. Both bioreactors can have application in various cell cultures on small-to-medium scales. Recently, such wave bioreactor systems have been scaled up to a capacity of 1000 L, and a cell density as high as 10^7 cells/mL was achieved (86,89).

In the following sections, the basic design principles for cell culture bioreactors, the process used to operate these bioreactors, and methods of scale-up for production are introduced and discussed.

77.2 DESIGN OF BIOREACTORS

77.2.1 Fundamental Design Principles

The basic function of a bioreactor is to provide optimum conditions for cell physiology and metabolism by regulating various chemical and/or physical factors. The design and selection of each type of bioreactors is unique but there are some basic fundamental principles. In general, the main

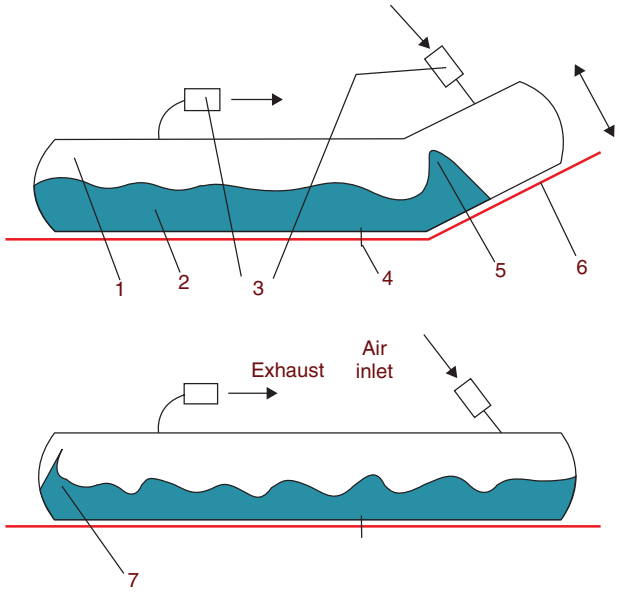


Figure 77.9. Schematic diagram of wave and undertow (WU) bioreactor (88). 1-Headspace, 2-cell culture, 3-filters, 4-harvest, 5-wave induction, 6-raising platform, 7-undertow formation. (This figure is available in full color at http://onlinelibrary.wiley.com/book/10.1002/9780470054581.)

criteria for designing bioreactors should be adequate oxygen transfer, low shear stress, and adequate mixing (69).

77.2.2 Oxygen Supply

Oxygen is one of the most important nutrients for cells as it is a major factor in all aerobic metabolic cycles (90,91). Most nutrients required for cellular growth and metabolism are highly soluble in water, and sufficient and timely supply of these nutrients can be achieved in a well-mixed bioreactor; in contrast, oxygen is only sparingly soluble in aqueous solutions, especially in high-density and high-viscosity cell suspensions. Its supply to cells in liquid cultures usually becomes a limiting step to the optimal performance of biological systems and to the scale-up of cell culture processes (92). Maintaining a suitable oxygen concentration in the culture medium is equally important. Oxygen requirements of plant cells are relatively low, but may significantly increase during cultivation with increase of cell density (93).The optimal dissolved oxygen (DO) concentration may be different for cell growth and product formation in both plant and animal cells. In suspended cultures of *Perilla frutescens* for production of anthocyanin (red pigments) in a 2.6-L aerated and agitated bioreactor with a six-flat-bladed turbine, Zhong *et al*. (94) found that the oxygen supply and light irradiation exhibited significant influence on the production of anthocyanin by the plant cells. When the initial volumetric oxygen transfer coefficient ($k_L a$) value

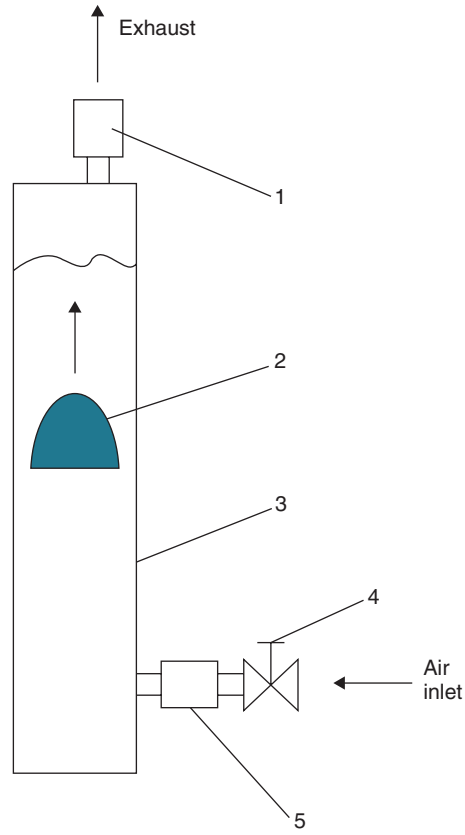


Figure 77.10. Schematic of slug bubble (SB) bioreactor (88). 1-Filter, 2-SB, 3-cell culture, 4-valve, 5-filter. (This figure is available in full color at http://onlinelibrary.wiley.com/book/10.1002/9780470054581.)

was below 10 h^{-1} and light was not irradiated, the anthocyanin production was never over 0.6 g/L. By modifying a gas sparger, the oxygen supply capability of the STR was remarkably improved, and 1.65 g/L of anthocyanin was obtained at an enhanced $k_L a$ value of 15.4 h^{-1} (94). For bioreactor-based ginseng cultures, oxygen supplementation was also beneficial for biomass accumulation and saponin production (95).

Oxygen supply is also important for animal cell cultures, and recent developments in high cell density and high productivity fed-batch animal cell cultures have placed a high demand on oxygen supply and carbon dioxide removal in bioreactors. Usually, the high oxygen demand is met by increasing agitation speeds and sparging rates of air/O_2 in bioreactors. However, Zhu *et al*. (96) found that an increase in sparging resulted in cell damage at the sparger site due to high gas entrance velocities. The critical velocity for their NS0 cell line was found to be 30 m/s, above which low cell growth, low viability, and consequently reduced antibody production were observed. Increase in addition of pluronic F-68, a protective surfactant, from 0.5 to 2 g/L

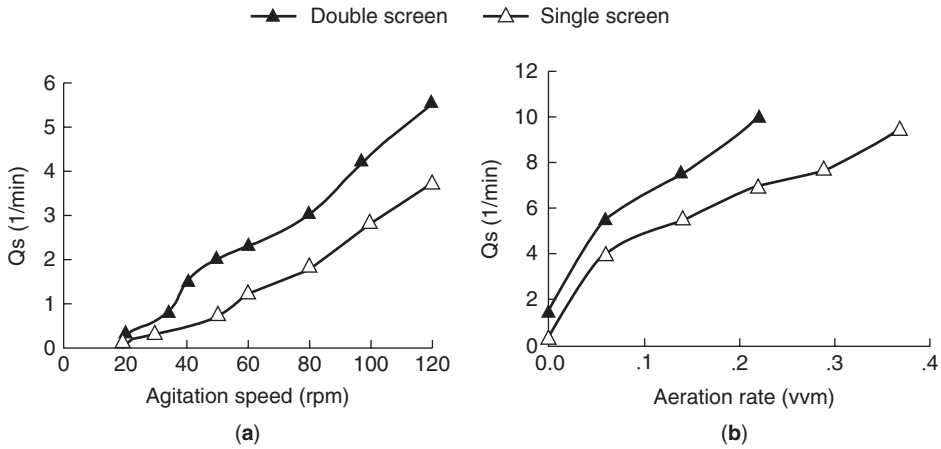


Figure 77.11. Effects of agitation speed (without aeration) (**a**) and aeration rate (at 50 rpm) (**b**) on the liquid exchange rate (Q_s) through the screen of a 20-L modified cell-lift bioreactor (13.5 L of working volume) with a double-screen cage (CellCul-20A) (103).

did not solve the problem. The sparger nozzle should also be carefully designed at pilot and large scale in order to accommodate high gas flow rate. The results of gas velocity analysis for cell damage helped a troubleshooting study in a 600-L bioreactor and successful scale-up of a process to a large-scale bioreactor (e.g. 10 000 L) for antibody manufacturing (96).

High cell culture density often causes a lower k_La value. The parameter k_La is so important in supplying oxygen to the medium that a very critical aspect of bioreactor design is to achieve a sufficiently high k_La. To meet a general oxygen uptake rate (OUR) of 5–10 mmol O_2/(L h), a typical k_La value required in bioreactor operation for plant cell culture is between 10 and 50 h^{-1} (97), while that for mammalian cell culture is around 0.25–10 h^{-1}. In addition, aeration rates in the range of 0.01–0.5 vvm (volume of gas per volume of culture per minute) are typically used in a STR and 0.1–2 vvm is applied in a pneumatic bioreactor. High aeration rates may result in severe foaming and gas stripping (of CO_2, ethylene or other volatile metabolites), which may inhibit plant cell growth (98,99). In another aspect, k_La is affected by many factors, including the geometrical and operational characteristics of the reactor vessel, agitation speed, aeration rate, fluid hydrodynamics, medium composition, cell type, morphology, and concentration. In mammalian cell cultures, gas sparge is also related to another issue: bubble-associated cell damage, which is mostly caused by high energy dissipation rate released during bubble rupture. Extensive studies have been conducted to investigate the mechanism and how to prevent it. Now preventative additives such as pluronic F-68 have been commonly used to alleviate it (100–102). However, aeration strategy still needs to be carefully considered.

For a better understanding of mass transfer mechanisms in the bioreactor, the effects of temperature, agitation speed, aeration rate, and the configuration of the cage screen on the k_La were investigated in a 20-L modified cell-lift bioreactor with a double-screen cage (CellCul-20A) by Wang *et al*. (103). Using a mathematical model based on the oxygen transfer in deep aeration, the value of k_La inside the cage was obtained, and the mass transfer resistances for the bubbling inside the cage and the transfer of liquid across the screen of the cage were also compared. Figure 77.11A shows the effects of agitation speed on the liquid exchange rate (Q_S) through the screen without aeration. The following correlations can be obtained through regression analysis:

$$\text{For the double screen: } Q_S = 3.42 \times 10^{-5}\, N^{1.49}$$
$$\text{For the single screen: } Q_S = 1.93 \times 10^{-5}\, N^{1.81}$$

where N is the agitation speed (1/s).

Figure 77.11B shows the effect of the aeration rate on the rate of liquid exchange through the screen. Under aeration and agitation, the liquid exchange through the cage screen can be regarded as the synergistic effect of these two factors.

Wen and Zhong (104) developed a simple and convenient technique for measuring OUR and CO_2 evolution rate (CER) of plant suspended cells in shake flask cultures, which are very essential and critical to bioprocess control and optimization on a reactor scale. This method was successfully applied to suspension cultures of rice (*Oryza sativa*) and *Panax notoginseng* cells, and some important bioprocess parameters, such as OUR, CER, respiratory quotient (RQ), specific oxygen uptake rate (SOUR) and specific CO_2 evolution rate (SCER), were quantitatively obtained (104). A model was developed for oxygenation in a PBR system, which was used to cultivate CHO cells at a high density of 6.1×10^7 cell/mL (Fig. 77.12), and, with

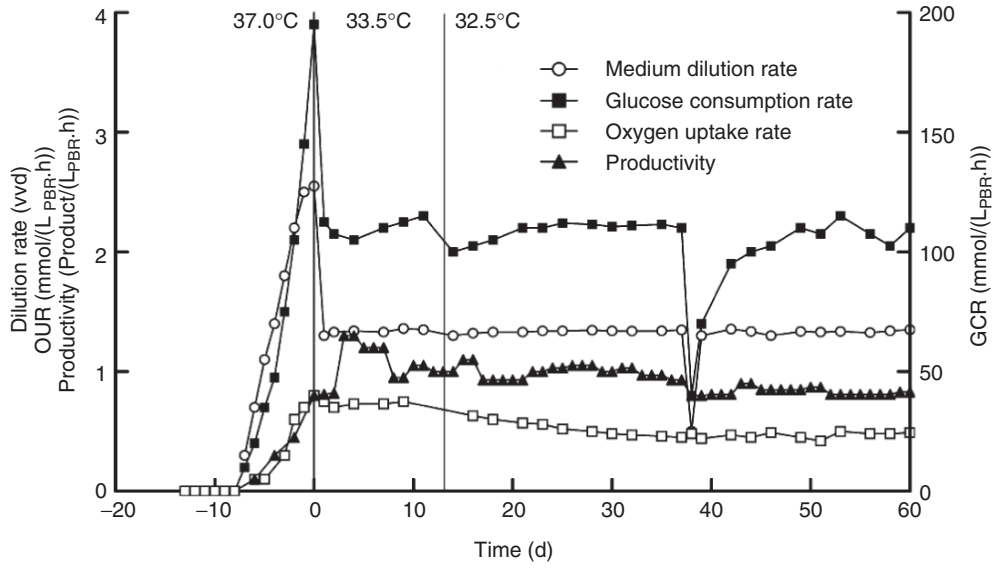


Figure 77.12. Time profiles of glucose consumption rate (GCR), oxygen uptake rate (OUR) productivity, and medium dilution rate during continuous culture of CHO cells in a fixed-bed bioreactor (105). Time 0 corresponded to the start of the production phase at 33.5/32.5°C; a deviation of dilution rate occurred on day 38 due to a technical failure of the feeding pump.

the help of this model, it was possible to identify if a PBR system is operated in optimal or suboptimal conditions. On the basis of this model, two options were proposed that could improve the performance of the basal system about twofold by increasing the density of immobilized cells from 6.1×10^7 to 1.2×10^8 cell/mL, or by increasing the packed-bed height from 0.2 to 0.4 m. Compared to the basal conditions, it would be possible to achieve a substantial improvement of about twofold higher productivity (105).

77.2.3 Shear Force

In order to maintain a homogeneous cell suspension and to provide effective nutrients (especially oxygen) transfer/supply, the cell culture system requires good mixing. Compared to microorganisms, both plant and animal cells are much bigger and more sensitive to shear force. Shear has been mainly considered in the technical literature as a destructive element, especially for plant cells. As cultured plant cells range from 20–40 μm in diameter and from 100–200 μm in length and embrace vacuoles up to 95% or more of cell volume (106), the primary cell wall contains parallel cellulose microfibrils embedded in a polysaccharide matrix. These features have led to the general belief that plant cells are shear sensitive, especially during the late exponential growth and early stationary phases when the cells are of relatively large size and contain large vacuoles (107). The shear sensitivity of plant cells has been observed in a number of cases (106,108–113). For example, Takeda *et al*. (114) reported a decreases in respiration rate, ATP content, and membrane integrity of both eucalyptus and safflower cells under hydrodynamic stress in a STR.

A couple of parameters are related to the shear-induced cell death, such as shear stress, shear time, power dissipation, and the growth phase of the cells. As mentioned earlier, sparging can also cause the shear damage, which can occur at different locations in a bioreactor: bubble generation zone at the sparger; the rising zone through the bulk liquid; and the surface of the suspension (it can either be covered with foam layer or be free of foam). The mechanism of cell damage at bubble disengagement zone is as follows: cells attach to the bubble surface (115), and then the bubble bursts at the suspension surface, which causes high shear (116). Small bubbles cause more severe damage than large bubbles (117). To analyze the effects of shear stress on plant cell cultures, a quantitative investigation of the influence of hydrodynamic shear on the cell growth and anthocyanin pigment production by *P. frutescens* was demonstrated by using a plant cell bioreactor with marine impeller of larger (85 mm) or smaller (65 mm) diameter (Fig. 77.13) (118). Figure 77.14A and B shows the effect of the average and maximum (represented by the impeller tip speed) shear rates on the specific growth rate of *P. frutescens* cells in a bioreactor. The specific growth rate was apparently reduced at an average shear rate over 30 s^{-1} or at an impeller tip speed of over 8 dm/s. Figure 77.14C and D shows the influence of shear on the maximum cell concentration. The maximum cell concentration was relatively higher at an an average shear rate of 20–30 s^{-1} or

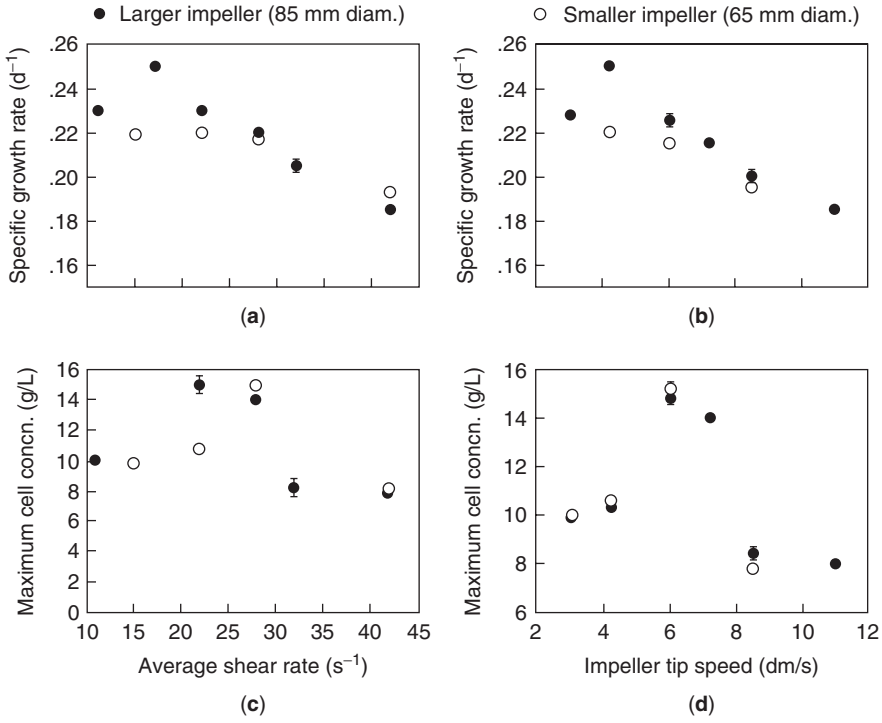


Figure 77.13. Influences of shear on specific growth rate and maximum cell concentration of *Perilla frutescens* cells in a plant cell reactor with a marine impeller (118). (**a**) and (**b**) show the effect of the average and maximum (represented by the impeller tip speed) shear rates on the specific growth rate of *P. frutescens* cells in the reactor. (**c**) and (**d**) show the influence of shear on the maximum cell concentration.

an impeller tip speed of 5–8 dm/s, and the pigment production and productivity as well as the yield coefficient of anthocyanin showed the same trends (data not shown). There have been abundant reports on shear damage suffered by animal cells grown in suspension, especially damaged by disengaging bubbles (119–123). Moreover, in the case of cells attached to microcarriers, limitations in the degrees of freedom for deformation lead to an increased sensitivity toward shear damage. Koynov *et al*. performed a detailed, high-resolution numerical simulation of bubble flows to analyze the stress and oxygen transport on a microscale (90). Different parameters such as gas holdup as well as bubble Reynolds, Morton, and Eotvos numbers were characterized. Better knowledge of the magnitude of the shear forces and DO distribution in sparged bioreactors can have a significant impact on their future design and optimization (90).

For shear-sensitive cell cultures, therefore, reducing the shear stress intensity by decreasing the agitation speed of the impeller is a general solution. However, this can also bring inadequate mixing and may conflict with enhancing oxygen and heat transfer rates in a high-viscosity cell culture broth. Furthermore, at high biomass concentrations, low agitation rates can also enhance the clumping of cells into cell aggregates of various sizes. However, appropriate bioreactor design and control can minimize shear damage from agitation and aeration. Wagner *et al*. (107) reported that anthraquinone production by *Morinda citrifolia* cells was lower in a STR than in an air-lift bioreactor, which implies the detrimental effect of shear force on plant cells. Wang and Zhong successfully designed a novel centrifugal impeller bioreactor (CIB) (Fig. 77.1F) for shear-sensitive biological systems including animal and plant cell cultures (63,125). As shown in Fig. 77.1F, this new impeller was designed on the basis of the principle of a centrifugal pump. During the impeller rotation, the center of impeller generates a negative pressure, drawing liquid and cells from the reactor bottom through the draft tube and centrifuging them toward the liquid bulk. This new type of impeller-reduced shear force, created much better mixing, and improved oxygen transfer capacity compared to the conventional STR with flat turbine and even with a relatively new, commercially available cell-lift impeller. This CIB has been demonstrated to be very successful in high cell density plant cell cultures (65,126–129). For example, in high-density cultivation of *P. notoginseng* cells, the production of the major, individual ginsenosides Rg_1, Re, and Rb_1 was significantly

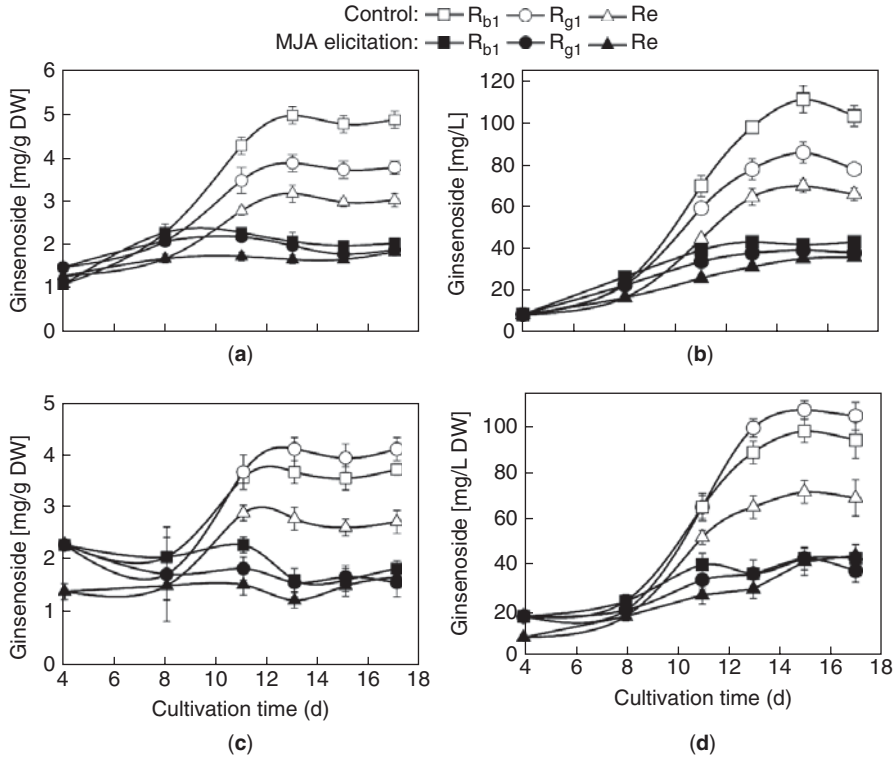


Figure 77.14. Effects of methyl jasmonate (MJA) elicitation (at 200 μM) on the content and production of the Rg_1, Re, and Rb_1 ginsenoside in high-density cultivation of *Panax notoginseng* cells in 3 L (**a**,**b**) and 30 L (**c**,**d**) CIBs (124).

enhanced in both 3- and 30-L CIBs (Fig. 77.14). The advantages of CIB were also confirmed by Prakash *et al*. They claimed that the CIB was less shearing and had higher O_2 transfer rate (OTR) than the setric impeller (a specially designed low-shear impeller (130)) bioreactor with respect to biomass and azadirachtin production in *Azadirachta indica* suspension cultures (124). Korin and coworkers designed a micro-wells/grooves bioreactor, which could protect sensitive cells from the detrimental effects of fluid shear stress by its microtopographical features. This is a promising approach to culture sensitive cells in perfusion microsystems (131). As mentioned earlier, based on advantages of wave-induced agitation, disposable wave bioreactors are also suitable for secondary metabolite production from suspension cultures, hairy roots, and embryogenic cultures (86–89).

Another possibility to overcome the problem of the rising air bubbles is bubble-free aeration using membranes for indirect aeration, in which the supply of oxygen is diffusion controlled and no bubbles arise. As the length of the membrane is limited, the average OTR is low. Also, the pressure inside the tubing has limitations. Therefore, this type of bioreactor is quite suitable for small-scale cell cultures but limited for large-scale cell cultures (10).

77.2.4 Fluid Mixing

In bioreactors, fluid mixing is another key variable because adequate mixing is essential to ensure a sufficient supply of nutrients (especially oxygen) and to prevent the accumulation of toxic or undesired metabolites like CO_2 in cultures. To maintain uniform concentration of chemical species (e.g. pH, gases, and nutrients) in the bulk phase and to increase the rates of mass transfer, mixing is normally carried out by sparging, mechanical agitation, or their combination (132). Global mixing quality in a bioreactor is usually characterized by measuring mixing time, which is defined as the time required in reaching a certain arbitrary level of uniformity in the mixed fluid (133). For the same power input per unit volume, mixing time in air-lift reactors is generally higher than that in STRs. On the basis of the time constants for oxygen conversion, oxygen transfer, and mixing, Doran compared the performance of air-lift and STRs and concluded that mixing became the limiting factor for pneumatically agitated reactors at high plant cell densities (134).

It is easy to maintain a homogeneous condition in a small-scale reactor; however, mixing often becomes one of the constraints during scale-up, as the magnitudes of hydrodynamic forces associated with mixing should be low enough so that they do not to cause cell damage.

In large-scale bioreactors, poor mixing often leads to undesirable concentration gradients and a decrease in mass transfer efficiency. In animal and plant cell cultures, which are typical shear sensitive biological systems, mixing could be enhanced by increasing agitation speeds and/or aeration rates in agitated bioreactors, but it has to balance with the increase of shear stress because shear force caused by intense agitation or aeration can bring damage to living cells. Furthermore, animal cells are very sensitive to pH changes. In large-scale suspension cell culture reactors, pH can also cause damage to cells, as a fast adjustment of bioreactor pH cannot be quickly mixed well with bulk liquid (135,136). Therefore, how to find the maximum agitation speed without causing cell damage is important. Baffles are recommended to be installed to increase mixing performance and eliminate detrimental center vortex. Cell damage in baffle zone should not be a concern generally as its hydrodynamic force is lower than that at impeller zone (137).

In the design of STR for cell suspensions, mixing has always been the focus of much attention. Doran (138) used an engineering analysis to identify whether the mixing situation in large-scale plant cell reactors can be improved by making different choices of impeller design, tank configuration, and operating conditions. On the basis of a novel mixing principle, Zhang *et al*. developed a new scalable helical track reactor for large-scale cultivation of mammalian cells. By simply using air for surface aeration, liquid-gas transfer was increased compared to standard STRs. This new type reactor with k_La around 10 h^{-1}, and capacity to support $8-10 \times 10^6$ cells mL^{-1}, meets the essential requirements for a cell culture system, that is, mixing without damaging shear-sensitive cells, sufficient gas transfer, and easy scale-up and process control (139). A novel wavy-walled bioreactor (WWB) was designed for tissue engineering (140). This bioreactor possesses a new geometry comprising walls with sinusoidal waves, which act as baffles and can potentially improve mixing and provide a lower shear stress.

77.3 PROCESS OPERATIONS

The design of a bioreactor system is an optimization procedure of balancing biological and engineering factors to obtain the required capacity and product quality at minimum production costs. At the heart of bioreactor control is the ability to monitor important process variables such as pH, DO, temperature, OUR, CER, and specific gravity. Mixing, oxygen transfer, and shear stress are the biggest challenges as far as the scale-up to industrial-size cell culture bioreactors is concerned (141). Control strategies, which range from the maintenance of basic parameters at constant levels to sophisticated computer-aided adaptive control systems, can often determine the overall output of the bioreactor. The important target of commercial process development and optimization is to minimize production cost by increasing product output and maintaining product quality. To realize this, unit operation studies are necessary toward maximum productivity. A comprehensive characterization of operational parameters must be conducted to support a robust commercial process.

77.3.1 Effects of Process Variables

77.3.1.1 Oxygen and Mass Transfer. Oxygen transfer is always a concern in aerobic biological systems. Most nutrients required for cellular growth and metabolism are highly soluble in water; sufficient and timely supply of these nutrients can be achieved in a well-mixed bioreactor. However, oxygen transfer often becomes a limiting step to the optimal performance of biological systems and also for scale-up because oxygen is only sparingly soluble in aqueous solutions. When oxygen supply is limited, both cell growth and product formation can be severely affected. Mass transfer is also an important factor for cell culture process; however, the overall mass transfer rate is not easy to measure because different phenomena are simultaneously taking place; also, the relative importance of these phenomena changes with the scale, the type of bioreactor, and so on. Therefore, the OTR is influenced by quite a number of factors (physical properties of gas and liquid, operational conditions, and geometrical parameters of bioreactor) and also by the presence of biomass, namely, the consumption of oxygen by the cells (139). Zhu *et al*. (142) were able to increase the mass-transfer rate by 17% by changing the impeller, and Puthli *et al*. (143) found that k_La value was affected by the stirrer configuration.

For animal or plant cell cultures, shortage of oxygen can be expected at a high cell density. As k_La is very important in supplying oxygen to the medium, a very critical aspect of bioreactor design is to achieve a sufficiently high k_La, which is affected by many factors, including the geometrical and operational characteristics of the reactor vessel, agitation speed, aeration rate, fluid hydrodynamics, medium composition, and biocatalyst properties, such as cell type, morphology, and concentration. It was estimated that oxygen transfer management accounts for about 15–20% of all operating costs for aerobic cultivation (144). Very high oxygen levels may become toxic to cells and cause localized oxidative stress (145).

For typical animal cell types, specific OUR is between 3×10^{-10} and 2×10^{-8} mg/(cell·h) (146). Generally, animal cell metabolism and productivity is consistent at a DO level between 10% and 100% of air saturation. Chotigeat *et al*. (147) studied the effect of environmental conditions, including the DO concentration and the level of sodium butyrate, on the expression levels, glycoform pattern, and

the levels of sialytransferase for human follicle stimulating hormone (hFSH) production by recombinant CHO cells. In steady-state perfusion cultures in an STR at different DO concentrations, it was found that both the specific productivity of hFSH and specific activity of sialyl transferase were increased from 0.7 to 2.6 ng $(10^6 \text{cells})^{-1}$ h^{-1} and from 1.0 to 4.9 mol (mg protein)$^{-1}$ h^{-1}, respectively, when the DO was increased from 10% to 90% of air saturation. The number of viable cells was found to be relatively constant, ranging from 4.5–5.7x10^6 cells/mL over the DO levels studied. Tang *et al*. (148) studied the effects of dissolved oxygen tension (DOT) and agitation speed on the Meth A tumor cell suspension culture process in a STR, and found that the heat-shock protein glycoprotein (gp96) biosynthesis was very sensitive to DOT and agitation speed. Compared to 50% of DOT, the production and specific productivity of gp96 was increased by 27% and 66% at 10% of DOT, respectively. Compared to the agitation rate of 100 rpm, the production and volumetric productivity of gp96 was increased by 48% and 144% at an agitation rate of 200 rpm, respectively. Low DOT (i.e. 10% of air saturation) and a relatively high agitation rate (i.e. 200 rpm) were identified to be favorable for gp96 biosynthesis. Low cell growth, low glucose/glutamine consumption, and high lactate production were observed when the DO level dropped below 10% (149). High DO level at 125% favored glucose consumption than glutamine and increased lactate yield (150), in which the shift toward anaerobic metabolism at high DO could be explained by oxygen toxicity. High DO also increased reactive oxygen species causing oxidative damage to cells and products.

In plant cell cultures, the deleterious effects of an oversupply of oxygen were demonstrated by Smart and Fowler (151). In suspension cultures of *Catharanthus roseus* in air-lift bioreactors, when the $k_L a$ value was 14.5 h^{-1}, a maximum biomass density of 14.3 g dry weight (DW)/L was achieved; however, it was only 8.9 g DW/L when $k_L a$ was increased to 39 h^{-1} (151).

77.3.1.2 Fluid Mixing. In bioreactors, adequate mixing is important to ensure sufficient supply of nutrients, especially oxygen (69). In cell culture processes, mixing has often been evaluated in terms of biological performance, such as cell growth rate and productivity. The control of temperature, pH, and substrate concentration is dependent on good mixing in the bioreactor. In plant cell cultures, Zhong *et al*. (128) studied the effect of mixing time on taxoid production in a novel CIB. In the agitation intensity range without damage to the cultured cells, two different mixing times (5 and 10 s) were applied by adjusting impeller agitation speeds. A higher cell density and taxoid productivity were obtained under a shorter mixing time. Poor mixing limited oxygen transfer and led to the formation of larger cell aggregates.

Many techniques and algorithms have been employed to solve fluid-based problems (152). Both Porter *et al*. (153) and Raimondi *et al*. (154) modeled the effects of perfusion to better comprehend the influence of perfusion and hence shear stresses on 3D cultures. Porter *et al*. used a code based on the Lattice–Boltzmann principle to approximately obtain solutions to the Navier–Stokes equations (153), whereas Raimondi *et al*. modeled their flows with the aid of a commercially available FLUENT package (154). Lappa (155) also developed equations based on the level-set principle to model fluid flow as well as to estimate soft tissue growth within a bioreactor. While the level-set method may provide higher levels of accuracy, it tends to be quite complex and might not always be feasible to apply.

77.3.1.3 Temperature. Temperature is one of the most critical parameters to be carefully controlled in a bioreactor. Regardless of the cell type, cell culture always has a quite narrow optimal temperature range for growth. According to van't Hoff's law, an increase in temperature causes an increase in the rate of endothermic reactions. Hence, an increase in the temperature should enhance the speed of conversions in the cells and contribute to the economy of the process (156). However, excessive increases in temperature lead to the enzyme (which catalyzes the reactions) denaturation, and hence reduce the speed of the reactions they catalyze. Therefore, there is an optimum temperature for any biological conversion process. The optimal temperature for plant cell culture (generally 23–30°C) depends on the plant species (157,158). Both the growth of plant cells and the biosynthesis of desired metabolites are influenced by the cultivation temperature with varied optimal values. Georgiev *et al*. found that the optimal temperature for growth of *Lavandula vera* cells was 30°C but the highest volumetric production of rosmarinic acid was at 28°C (159). The same trends were also found by Zhong *et al*. (160), who investigated the effect of temperature on suspended cultures of *P. frutescens* for optimizing the production of anthocyanin pigments. A higher (specific) growth rate was obtained at higher temperatures in a range of 22–28°C, while 25°C was optimal for the volumetric productivity of anthocyanin and the pigment production was remarkably reduced at the a relatively high temperature of 28°C. For animal cell cultures, typical operating temperatures are cell line specific. It varies between 36 and 38°C for mammalian cells, while it lies between 25 and 30°C for insect cells (161).

There are a number of reports on the effects of temperature on cell growth rates and product formation rates for different culture processes. In a conventional process, once the optimal temperature is determined, it is always maintained. This, however, may not always be the case for mammalian cell culture processes. In mammalian cell cultures, a large portion of the protein product is synthesized

during the post growth phase. As the cell viability drops quickly after the cell density approaches maximum in most cases, the cultivation of cells at a reduced temperature has been proposed to improve culture performances. It has been consistently reported that a decrease in cultivation temperature leads to prolonged culture viability (162,163). In CHO cell cultures, sometimes changes in temperature can induce desired effects as it can affect the cell cycle and a temperature shift from 37 to 30°C after 48-h postinoculation can retain cells in the G1 phase (a period in the cell cycle from the end of cell division to the beginning of DNA replication) longer and therefore delay the onset of apoptosis (163). The temperature shift was also successfully proposed by Ahn *et al*. to produce erythropoietin (EPO) (164). The CHO cells were cultivated using a perfusion bioreactor at 37°C until its viable cell concentration reached 1×10^7 cells/mL, and then the culture temperature was shifted to 25, 28, 30, 32, and 37°C (control), respectively. Lowering the culture temperature suppressed cell growth but was beneficial in maintaining high cell viability for a longer period. In a control culture at 37°C, cell viability gradually decreased and fell below 80% on Day 18, while it remained over 90% throughout the culture at a low culture temperature. The cumulative EPO production and specific EPO productivity q_{EPO} increased at low culture temperature and reached the maxima at 32 and 30°C, respectively (164).

77.3.1.4 pH. Medium pH affects the transport of ionized molecules between the cells and the medium. The buffering capacity of the medium and concentration of hydrogen ions in the medium affect the intracellular pH profile, the activity of the intracellular enzyme systems, and also the rate of diffusion of ionized molecules in the electrical field of the cells. The starvation of cells for several minutes brings about a prolonged change in the electrical field of the cells (165). Different biological systems have different optimal pH ranges. Most cells grow best at pH 7.2. During cultivation, the pH usually changes. As the cells grow, metabolites are released into the medium, and substrate consumption also changes the pH value of the medium. For example, ammonium is a common nitrogen source; when ammonium is utilized during cell cultivation, pH decreases. Therefore, the medium pH must be monitored and adjusted by base or acid addition in order to constantly maintain it at an optimum level (69). The pH monitoring and control is important to animal cell cultures, but it is not so in plant cell cultures as the medium pH value generally does not change so much in the latter case.

During plant cell cultivation for recombinant protein production, one of the main obstacles is product degradation by proteases that are produced by cells and/or the loss of biological activity of secreted (extracellular) products as a result of alteration in the recombinant protein conformation. To minimize these effects, Huang *et al*. (38) proposed a bioreactor strategy using a protocol involving pH adjustment and medium exchange during plant cell culture for improving the production of functional recombinant α1-antitrypsin (rAAT), a human blood protein. It was found that higher medium pH helped reduce protease activity derived from cell cultures and improve the inherent stability of rAAT as well, and both the productivity of extracellular functional rAAT and the ratio of functional rAAT to total rAAT were increased. Figure 77.15 shows the effect of pH control on the total and functional rAAT production for a chemically inducible, estrogen receptor-based promoter (XVE) expression system. Under pH control, extracellular functional rAAT reached approximately 60 mg/L in 9 days, compared to that of only negligible levels observed without pH control.

In animal cell culture processes, culture pH is often controlled by adding an alkaline reagent such as $NaCO_3$, $NaHCO_3$, or NaOH to neutralize the acidic effects of lactate and CO_2 production during cultivation (166). Another scheme for pH control in animal cell culture process is CO_2 aeration to decrease pH at the beginning of culture. Its usage decreases and ceases with the increase of lactate and dissolved CO_2 level in culture medium. Gramer and Ogorzalek (167) developed a mathematic model to correlate lactate concentration, pH, dissolved CO_2, and base addition, which helped them identify the reason for the need to add more base at pilot and large scale.

The medium pH is one of the most important process parameters in mammalian cell culture because of the cells' sensitivity. In hybridoma cultures, a pH value of 7.2 was found to be optimal for cell growth. When the pH value was decreased from 7.2 to 6.9, a twofold decrease in specific growth rate, specific glucose consumption rate, and specific lactate production rate was observed (168). On the other hand, Wayte *et al*. (166) reported that the final antibody concentration of two different murine hybridoma cell lines was increased 1.5-fold when the bioreactor pH was slightly reduced from 7.2 to 7.1. Xie *et al*. (169) studied PER.C6® cell growth, metabolism, and adenovirus production in STRs under different pH conditions. It was found that cell metabolism, in both infected and uninfected cultures, was very sensitive to culture pH. Dramatic changes were observed in glucose/glutamine consumption and lactate/ammonium production under different pH conditions. A more than twofold increase in adenovirus productivity was observed by reducing the pH from 7.6 to 7.3. Culture pH is an important environmental factor that should be precisely controlled to ensure the quality of a desired product. Its importance has been demonstrated in T-flask cultures without pH control. Borys *et al*. (170) found that culture pH significantly affected the expression rates and glycosylation of recombinant mouse placental lactogen-I (mPL-I) in CHO cells. Zanghi *et al*. (171) demonstrated the importance of culture pH and pCO_2 interactions, which altered

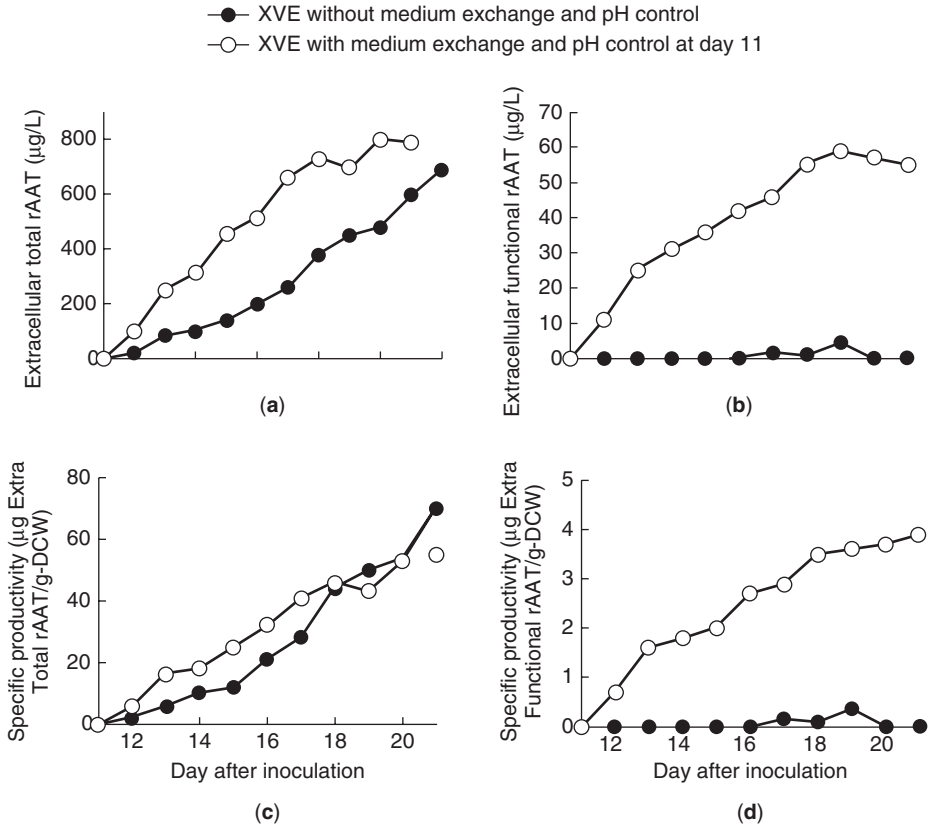


Figure 77.15. Effects of pH control on cell growth and recombinant α1-antitrypsin (rAAT) production in XVE cell cultures in a bioreactor (induction timing at day 11 after inoculation) (38).Extracellular functional rAAT reached approximately 60 mg/L in 9 days under medium exchange and pH control.

glycosylation of recombinant protein in CHO cells. Yoon *et al*. (172) studied the effect of culture pH on cell growth and EPO production at two different culture temperatures (32.5 and 37.0°C) in serum-free suspension cultures of recombinant CHO (rCHO) cells in a bioreactor with pH control (Fig. 77.16). At 32.5°C, q_{EPO} was significantly influenced by the culture pH, and it reached the highest [0.31 ± 0.02 μg/(10^6 cells h)] at pH 7.00, which was approximately 1.8-fold higher than that at pH 6.85, 7.60, or 7.80. At 37.0°C, however, the culture pH did not affect q_{EPO}, which suggested that the cells at low culture temperature were more susceptible to the pH change.

77.3.1.5 Light Irradiation. Light is usually important in affecting growth, organogenesis, and formation of plant products including primary and secondary metabolites. The spectral quality, intensity, and period of light irradiation have been shown to have significant effects on the secondary metabolism of plant cell cultures. Sakamoto *et al*. (173) demonstrated the stimulatory effect of light irradiation on the formation of compounds such as anthocyanins, vindoline, catharanthine, and caffeine in cell suspension cultures. The accumulation of anthocyanin was strongly stimulated by light in cell cultures of *Daucus carota* and *Vitis vinifera* (174). Mulder-Krieger *et al*. (175) found that illumination affected the composition of sesquiterpenes in callus cultures of *Marticaria chamomilla*. Illumination of *Coffea arabica* cell suspensions enhanced caffeine biosynthesis by a factor of 10 (176). Light irradiation had remarkable effects on callus growth of *Oldenlandia affinis* and biosynthesis of kalata B1 with an optimum intensity of 35 μmol/(m^2·s) (177). However, light can also have an inhibitory effect on the accumulation of secondary metabolites such as nicotine and shikonin (178). In addition, the biosyntheses of some metabolites, such as anthraquinone and ubiquinone, are not significantly influenced by light irradiation.

Zhong *et al*. found that the light irradiation and period under daylight irradiation greatly affected anthocyanin production by suspended cultures of *P. frutescens* (179). At a light irradiation intensity of 27.2 W/m^2, a high amount of anthocyanin pigments, 3.0 g/L, was obtained in a bubble-column bioreactor after 10 days of cultivation at an aeration rate of 0.1 vvm, while 2 g/L was obtained at

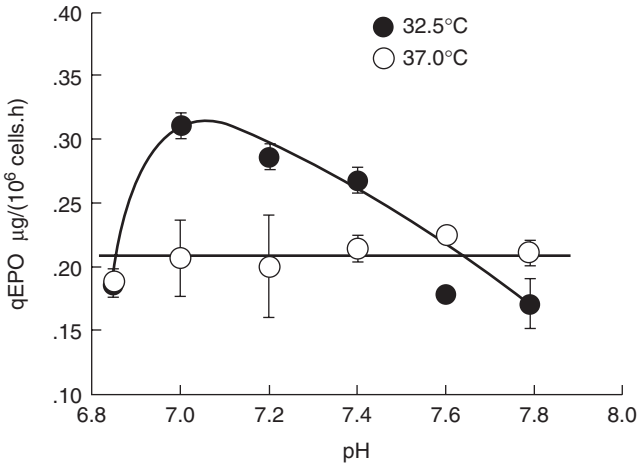


Figure 77.16. Specific erythropoietin (EPO) productivity in batch cultures of rCHO cells at different culture pH values and temperatures (adapted from (172)).

13.6 W/m^2, and very little at 54.4 W/m^2 (Fig. 77.17). A high amount of anthocyanin pigments, 2.9 g/L, was also produced using an aerated and agitated bioreactor with a marine impeller at an agitation speed of 130 rpm, an aeration rate of 0.1 vvm, and light irradiation intensity of 27.2 W/m^2 (179). The amount of anthocyanin produced was more than twice that without light irradiation.

Different types of spectral radiance can also influence the cell growth and secondary metabolite production. After 21 days of callus cultivation of *Saussurea medusa*, red light significantly improved its growth, but inhibited the biosynthesis of flavonoids (180). However, blue light was found to enhance the flavonoids' biosynthesis, although callus growth under this spectrum was comparable to that under white and other color spectra such as green and yellow. The accumulation of flavonoids in the cultures was related to the L-phenylalanine ammonia-lyase (PAL) activity, which was stimulated by the spectral composition of irradiation. Yu *et al*. found that the biomass of hairy roots was highest in the cultures grown under dark or red light, while ginsenoside accumulation was optimum in the cultures grown under fluorescent light during hairy root cultures of *Panax ginseng* (181). Similarly, the growth of hairy roots and betalain accumulation in *Beta vulgaris* (red beet) was also affected by different radiation sources—blue (B), red (R), R plus B (RB), B plus far red (BFr), and R plus far red (RFr), and Shin *et al*. found that BFr treatment induced betalain pigmentation in hairy roots (182).

77.3.2 Bioreactor Operation Strategy

An effective bioreactor operating strategy should provide a high volumetric productivity, which means more products can be formed per unit time per unit reactor volume. A major disadvantage of standard batch processes is that significant amount of time is taken up by the sterilization of system and medium, filling, emptying, and cleaning of the system. Thus, to improve the cost effectiveness of cell culture processes, various operational modes such as multistage batch, fed-batch, single- or multistage continuous (chemostat), semicontinuous (draw-and-fill or repeated batch), and perfusion (chemostat with cell retention) cultivations have been applied or developed so far (156,183–185).

77.3.2.1 Fed-Batch Culture. Generally, the final product concentration is primarily affected by the specific productivity of cells and integrated cell growth. Batch cultivations are characterized by constantly changing environmental conditions, and are capable of producing metabolites associated with any kinetic pattern. Batch studies are used to determine the conditions for maximum productivity. However, depletion of nutrients and a steady increase in toxic metabolites limits the final cell and product concentrations. With the resources available in a typical growth medium, cells are simply unable to attain and sustain high cell densities (133).

To overcome nutrient limitation, fed-batch processes have been widely practiced. This involves the addition of one or more nutrients continuously or intermittently to the initial medium after the start of cultivation, or from certain point during the batch process (13). Fed-batch cultures are currently the norm for most cell culture processes, especially for intracellular products of cell cultures that are stored within the cells. For intracellular products, a culture strategy that gives a high biomass output rate is most desirable (186). For example, in *P. ginseng* cell culture for ginsenoside production (187) and *Taxus chinensis* (188) cell culture for taxoid production, fed-batch cultivation has been successfully demonstrated. During the cultivation of *Coptis japonica* to produce berberine in STR, the biomass concentration was reduced due to high osmotic pressure of the culture medium and accumulation of inhibitory products during cell growth, and this problem was solved by a suitable fed-batch operation that enhanced both cell growth and berberine production at high cell density (189,190). Hu *et al*. (191) performed fed-batch cultivation of *P. notoginseng* cells in a concentric-tube air-lift reactor to study the effects of bottom clearance on cell growth and the production of ginseng saponin and polysaccharide. A fed-batch operational mode was also developed, in which sucrose was fed just prior to a sharp decrease in the specific OUR [>0.20 mmol/(g DW h)] (192). By applying this feeding policy to *P. notoginseng* cell suspensions, cultivated in a 10-L air-lift bioreactor (192) and a 30-L CIB (126), very high biomass productivity of approximately 1.5 g/(L·d) was achieved, and both saponins

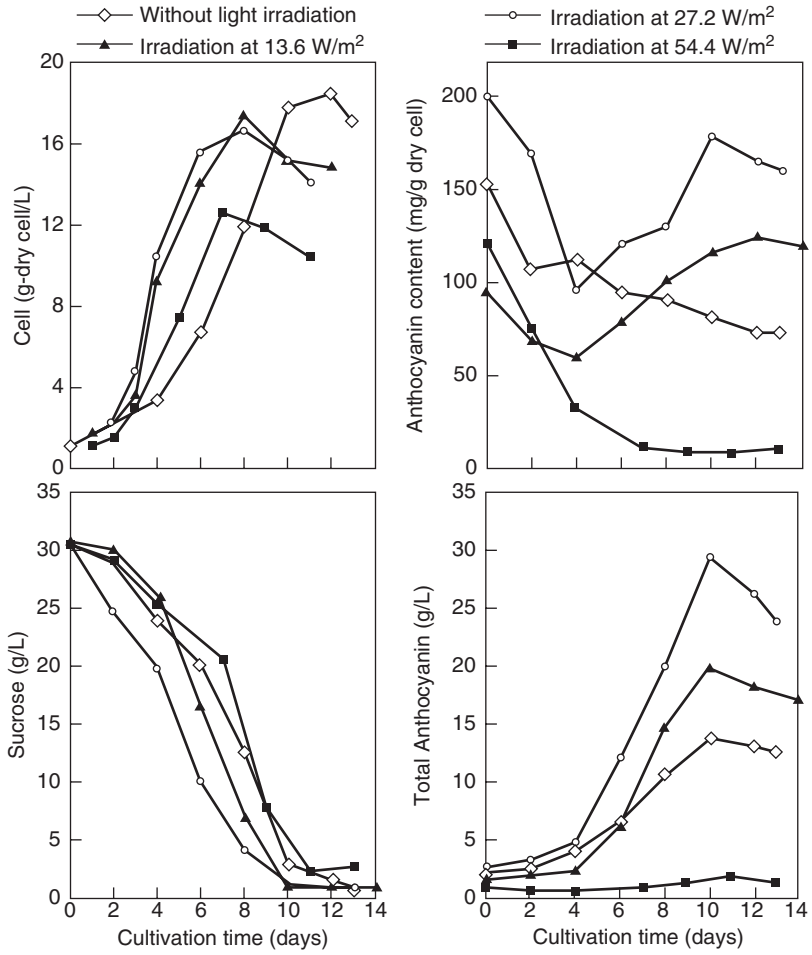


Figure 77.17. Effects of light irradiation intensity on production of anthocyanin pigments by suspension cultures of *P. frutescens* cells in a bubble-column bioreactor at an aeration rate of 0.1 vvm (adapted from (179)).

and polysaccharide productivities were also higher than those in a comparative batch process.

Fed-batch processes are also common in animal cell cultures and have been operated at scales up to 25 000 L working volume for large-scale antibody production (193). The titer from fed-batch mammalian cell culture has increased dramatically in recent years due to the improvement in cellular engineering, culture medium, and feeding strategy (8). High density of 3×10^7 cells/mL has been reached (194). Huang *et al*. recently reported up to 13 g/L of final titer and high volumetric productivity of 800 mg/(L·d) in an 18-day fed-batch process using a CHO cell line without the antiapoptosis gene (195). It can be predicted that more companies can achieve this level in future, which will increase the manufacturing capability dramatically and will put a positive pressure on downstream purification. In another case, because the forecasted market demand is beyond the designed capability of the first-generation process using packed-bed perfusion technology, Meuwly *et al*. (196) converted it to a fed-batch model at $15m^3$ and increased product output by 18-fold while maintaining a comparable product quality.

A comparison of different feeding modes is presented in Table 77.4. Among these, the most popular and successfully used ones are fed-batch and perfusion.

77.3.2.2 Continuous and Semicontinuous Culture. Theoretically speaking, continuous culture is the most promising mode for obtaining high culture productivity. In a continuous culture, the nutrients consumed by the cells are continuously replenished by an inflow of fresh medium. A constant inflow of fresh medium is balanced by a constant efflux of spent medium plus cells. Consequently, a steady state is developed at a dilution rate (equal to outflow rate/volume) less than the maximum specific growth rate of the culture. Under steady-state conditions, the average specific growth rate in the culture is identical to the dilution

TABLE 77.4. Comparison of Some Commonly Used Modes of Feeding Based on Product Yield and Process Economics (Modified from (197))

Culture Mode	Product Yield	Process Manipulation	Cost (Capital Investment and Labor)	Throughput
Batch	Low	Low	Low	Low
Repeated batch	Low	Medium	Medium	Medium
Fed-batch	High	Medium	Low	Low
Chemostat	Low	Medium	Low	Low
Perfusion	Medium	High	Medium	High

rate. The biomass concentration of the culture is then determined by the concentration of the growth-limiting nutrient in the influent. All culture parameters (biomass, biomass composition, and nutrients) remain constant for prolonged periods of time in a steady state. This "balanced growth" is a very attractive tool in studies on growth and production kinetics or cell physiology (185).

Seki *et al*. (198,199) and Phisalaphong and Linden (200) demonstrated the enhancement of paclitaxel production by continuous plant cell culture of *Taxus cuspidata* and by using a semicontinuous culture of *Taxus canadensis* with total cell recycle, respectively. However, due to the practical problems of cell line stability and requirement for long-term sterile operation of bioreactors, such work is still limited in the laboratory. On the other hand, as shown by Van Gulik *et al*. (201), a chemostat culture technique is useful in obtaining reliable data on the stoichiometry of the growth of plant cells in bioreactor. Several other groups have also studied growth kinetics, stoichiometry, and modeling of the growth of suspension-cultured plant cells by using semicontinuous or fed-batch cultures to achieve steady-state growth. In addition, Westgate *et al*. (202) presented fed-batch cultivation kinetics for continuous approximation in *Cephalotaxus harringtonia* cultures. Trexler *et al*. (203) used a cyclical, semicontinuous operation to produce rAAT in the transgenic rice culture; the process consisted of three cycles over a 25–28-day period, with each of the growth phases lasting 4–6 days and each of the protein expression phases lasting 2.5–5 days.

In animal cell culture, little work has been done by continuous cultivation. Nyberg *et al*. studied the glycosylation of IFN-γ produced in continuous culture of CHO cells to investigate the relationship between metabolism and glycosylation site occupancy (204).

77.3.2.3 Perfusion Culture. Perfusion model is normally chosen for the production of unstable proteins. This is because perfusion culture has low resident time in bioreactor and the product can be harvested and purified promptly (205). In addition, it can avoid the accumulation of toxic or inhibitory metabolites that might have a negative impact on the productivity of fed-batch cultures. Perfusion cultivation is carried out by continuously feeding fresh medium to the bioreactor and constantly removing the cell-free spent medium while retaining the cells in the reactor, thus a much higher cell density can be obtained in perfusion cultures compared to that in continuous cultures, as cells are retained within the reactor via a cell-retention device (206). The perfusion rate depends on the demand of the cell line, the concentration of nutrients in the feed, and the level of toxification. Table 77.5 summarizes the key assumptions in process inputs between fed-batch and perfusion modes of operation (207).

The overall advantage of perfusion cultures is that it requires a smaller scale compared to that required in batch cultures in order to obtain the desired amount of product, thus perfusion culture has been used in mammalian cell processes to produce at least seven commercialized products (208). However, it has low product titer compared to fed-batch culture, which brings challenges to downstream purification. Konstantinov *et al*. (209) proposed a "push-to-low" method, decreasing the perfusion rate until it failed to maintain high viability, in order to reach comparable titer as batch or fed-batch culture. Using transient gene expression (TGE) to produce large amounts of recombinant proteins within a short period of time has recently attracted considerable interest (210). Compared to the batch modes, in which the transfections are conducted at a low cell density, high-density perfusion culture has been used in the production of recombinant adenovirus with a significantly higher production (211,212). The cell densities achieved in perfusion culture (10^7–10^8 cells/mL) are typically higher than most fed-batch processes ((1–30) $\times$ 10^6 cells/mL). In specific cases, it has been demonstrated that continuous perfusion offers an approximately 10-fold

TABLE 77.5. Chemical and Physical Methods Used for Cell Synchronization

Assumption	Fed-Batch	Perfusion
Size of production bioreactor (L) (working volume)	5000	1000
Seed bioreactor train (L)	20; 100;500	20; 100
Duration of cultivation (days)	15	35
Cultivation titer (g/L)	1.0	0.35

improvement in volumetric productivities compared to that in fed-batch culture (207,213). Jardin *et al*. designed high cell density fed batch and continuous perfusion processes to maximize the productivity of stably transformed cell (Sf-9SEAP), with a total yield of 17.6 IU in batch process, of 46.1 IU in fed batch process, and of 394 IU in perfusion process (214). Deo *et al*. (215) reported a 500-L-scale spin filter perfusion hybridoma culture for antibody production that was run for 15–35 days. They estimated that the volumetric productivity of the perfusion process was approximately 10 times that of batch or fed-batch cultures. Coagulation factor VIII, licensed by Bayer, was the first biopharmaceutical produced by recombinant BHK cells using continuous perfusion culture. Bayer validated a 185-day production process. Compared to the batch culture, the advantage of Bayer's production process is a 30-fold increase in cell density that results in a 30-fold higher yield of factor VIII. This leads to significantly reduced requirements for plant capacity: a 100–500 L perfusion reactor versus a 5000–15 000 L batch reactor (216). Sun *et al*. established a high-density perfusion culture of 293 EBNA1 cells in a 2-L bioreactor. The process resulted in a longer posttransfection production phase and higher protein production (217).

Perfusion culture is also used in plant cell culture. Su and Humphrey (218) adopted the perfusion strategy for high cell density culture and enhanced secondary metabolite production. Chen and Lin used a fibrous scaffold from *Luffa cylindrica* in a PBR for dynamic seeding and perfusion culture of rat hepatocytes (219). In order to investigate the effects on the transgenic *Nicotiana tabacum* cell physiology and the human granulocyte-macrophage colony-stimulating factor (hGM-CSF) production, a perfusion culture was carried out in a 5-L STR with three different perfusion rates (0.5, 1.0 and 2.0 per day) by Lee *et al*. Owing to the lower protease activity caused by the perfusion, in all the cases, the hGM-CSF in the medium was significantly increased during the overall culture period (16 days), with maximum values 3.0-, 9.4-, and 6.0-fold higher than those obtained in batch cultures, respectively. Su *et al*. (55) grew *Anchusa officinalis* cells in a perfusion bioreactor with perfusion rates up to 0.4 L/(L day). With complete cell retention, the dry cell weight exceeded 20 g/L, and the packed cell volume exceeded 70%. It was concluded that perfusion bioreactor system showed high potential as an alternative to immobilized plant bioreactors.

77.3.3 Process Monitoring and Control

The maintenance of optimal conditions for cell culture in a bioreactor requires systematic qualitative and quantitative descriptions of cell culture processes by on-line and off-line process monitoring methods (31). Currently, process monitoring for cell culture processes is mainly applied for detecting cell growth and the related physiological status such as biomass concentration, nutrient consumption, OUR (220), CER, RQ, DO, and pH. To accurately characterize several plant suspension cultures (*O. sativa*, *Nicotiana benthamiana*, and *Trichosanthes kirilowii*), including biomass concentration and aggregate size, McDonald *et al*. (221) successfully applied a focused beam-reflectance method (FBRM developed by Lasentec Inc., Redmond, WA). By using a laser turbidimeter (at 780nm), the cell concentration of *P. frutescens* was successfully measured on-line and *in situ* (222). Furthermore, Zhong *et al*. established a computer-aided on-line monitoring system to analyze the response of *P. frutescens* cells during cultivation. The physiological and metabolic aspects such as cell growth and respiratory activity under different agitation speeds were also investigated (223). The system was useful for the selection of some informative process variables and for the identification of physiological states of plant cells during bioreactor cultivation. The process variables, such as RQ, pH, and SCER, could be used for the identification of the growth phase of the cells during cultivation. The experimental results also suggest that the process variables, that is, OUR and SOUR, may be related to the accumulation of anthocyanin in *P. frutescens* cell cultures (Fig. 77.18). Monitoring of the above variables including OUR and SOUR during bioreactor cultivation may be very useful for effective feeding and control in a high-density cell culture to optimize the product accumulation. The information provided by the work could be helpful for the control and optimization of plant cell bioprocesses (223). Zhou *et al*. (224) used on-line OUR measurement to determine the time for feeding as OUR dropped dramatically when nutrients depleted. Schoenherr *et al*. (225) found that the on-line OUR measurement was a sensitive and convenient way to determine the end of exponential growth phase, which can help optimize transfer time for inoculum expansion.

Spectroscopy is a useful tool for on-line monitoring of many biological species. Near-infrared (NIR) spectroscopy can be used to measure various chemicals in cell culture mediums such as glucose, glutamine, ammonia, lactate, and glutamate (226). Recently, Rhiel *et al*. (227) reported the application of mid-infrared (MIR) spectroscopy to detect glucose and lactate in CHO cell culture without recalibration in 60 days. With advances in electro-optics and computing power, two-dimensional fluorescence spectra can also provide information on many fluorescent species simultaneously (228). The recombinant protein that fused with green fluorescent protein (GFP) can provide an on-line monitoring method to rapidly observe the recombinant protein production kinetics as well as cellular dynamic responses (229). Schulze-Horsel *et al*. (230) utilized a sensitive and quantitative method for the flow cytometric detection of influenza A virus infection

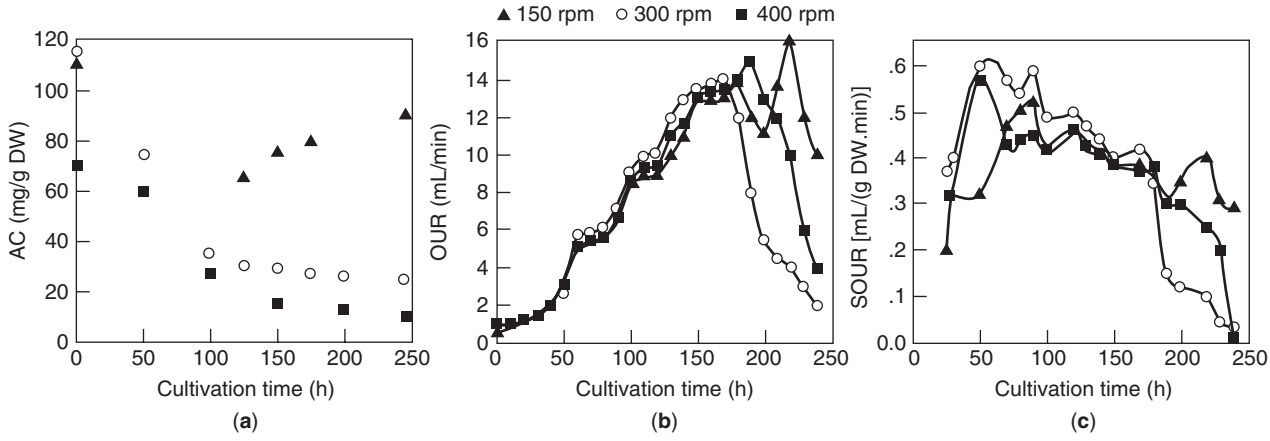


Figure 77.18. Dynamic behaviors of anthocyanin content (AC), OUR, and SOUR in a stirred bioreactor (adapted from (223)).

with mAbs in adherent MDCK cells fixed in ethanol and PFA/ethanol, and they demonstrated that this method was a valuable addition to other detection methods of influenza virus infection such as immunotitration and RNA hybridization. By using fluorescence probe, Srivastava *et al*. (231) investigated on-line biomass measurement during bioreactor batch cultivation of *A. indica* cells for azadirachtin (biopesticide) production; they established a linear correlation between viable cell concentration and net NADH fluorescence under balanced growth condition.

For mammalian cell culture, capacitance probe or dielectric spectroscopy is becoming a useful tool to monitor viable biomass. Under an electric field, the capacitance output is proportional to intact nonconducting cell membrane area where charge can be built up. Dowd *et al*. (232) applied it in a CHO perfusion process to assess viable cell concentration and adjusted the perfusion feeding rate accordingly.

In situ microscopy (233) has proven to be a suitable method for real-time inline monitoring in mammalian suspension cell lines (234–236). Important process parameters [such as cell concentration, cell size distribution, cell volume, and culture aggregation state that are distributed into single cells, double cells, and cell clusters (with more than two cells), respectively] can be measured. Rudolph *et al*. (237) utilized *in situ* microscope to measure the level of colonization of fibroblasts on microcarrier surfaces during cultivation, and then developed a neural-network-based algorithm for the estimation of the process parameters of plating efficiency (PE) and the level of colonization (LOC) from the segmented image regions of the microcarriers.

For production of antibodies, an upcoming trend in process control and online measurement is immunoanalysis of the produced antibodies to analyze the product characteristics regularly. The process can be monitored according to the concentration and quality of the desired product (238,239).

77.4 PROCESS SCALE-UP FOR PRODUCTION

The major challenge of process scale-up has been how to translate the laboratory-scale product designs into large-scale production. Bioreactor culture is the key step toward commercial production of bioactive therapeutics (145). During the scale-up of cell culture processes, reduced productivity has often been reported, which can be attributable to any of a couple of factors including shear stress, oxygen supply, and gas composition. With the aim of implementing an industrial-scale process, the behavior of cell cultures in bioreactors has been receiving much attention (127).

Bioreactors in general can be evaluated by the following physical characteristics: mixing time, shear, pH, heat transfer, and mass (oxygen) transfer. Although the physical characteristics are interrelated, in scale-up and reactor design, the mixing time, shear, and mass transfer aspects are coupled, while pH and heat transfer are considered separately (240).

Unlike mass transfer, which takes place throughout the broth, heat transfer occurs only at the boundary surfaces of heat exchange. It is possible to provide the required heat transfer capacity of a large-scale bioreactor by methods independent of process scale-up, such as by using a refrigerant rather than cooling water or by using an external heat exchanger. Consequently, traditionally equal heat transfer capacity has not been used as a basis for translating experimental results between different scales of operation. Similarly, proper pH control can be achieved independently by automatic addition of concentrated acids or bases into culture systems. Assuming an adequate mixing, pH itself does not constrain scale-up. pH gradient is an issue related to mixing on a large scale.

The process characteristics that have been suggested to be maintained constant or similar during scale-up include the following:

1. Reactor geometry
2. Volumetric oxygen transfer coefficient, $k_L a$
3. Maximum shear
4. Power input per unit volume of liquid, P_g/V
5. Volumetric gas flow rate per unit volume of liquid, Q/V or vvm
6. Superficial gas velocity, v_s
7. Mixing time
8. Impeller Reynolds number
9. Momentum factor.

To combat the problems of poor mixing in large bioreactors, especially with viscous non-Newtonian systems, people employ equal mixing times in bioreactors of different scales (241). Although important for fast chemical reactions, the requirement of constant mixing time is unnecessary for normal cell cultures. Furthermore, the volumetric power input required to maintain equal mixing time increases as the 2/3-th power of the system volume and can become prohibitive on scale-up. Experience proves that the power input thus determined is much more than that required for practical scale-up. Constant power input per volume commonly used in microbial fermentation, criterion 4, is also applicable to cell culture process as it has a great impact on mass transfer and hydrodynamic force distribution in a bioreactor (135). Criteria 8 and 9 are generally not used. One main reason is that no consideration is given to the effect of aeration on the process results. Consequently, only criteria 1–6 are commonly considered for scale-up of cell culture bioreactors.

Criterion 1 is based on the fact that almost all of the existent empirical or semiempirical correlations for scale-up are developed experimentally with geometrically similar reactors of different scales. When translating experimental results between reactors with different geometries, one needs to consider the validity of correlations chosen from the literature and the necessity of developing or modifying the correlations for the specific situation.

Criteria 5 and 6 address the importance of aeration rate to scale-up of aerobic cell cultures. Volumetric gas flow rate per unit liquid volume, due to its influence on mass transfer in bioreactors subjected to bubble aeration without mechanical agitation, has been accepted as a traditional scale-up criterion even for mechanically agitated vessels (242). On the other hand, the superficial gas velocity is also an important factor in reactor design. It strongly affects the mixing energy required to disperse the gas stream, and, in all the cases, has an upper limit before impeller overloading or liquid blow-out action begins. The upper limit of v_s is strongly system dependent. When overloaded, the impeller cannot disperse all the gas supplied, short-circuiting occurs, the gas rises as big bubbles to the surface, and the pumping action of the impeller diminishes.

Unfortunately, criteria 5 and 6 are contradictory to each other when applied to scale-up of geometrically similar bioreactors. If it is desirable to maintain equal vvm, then the superficial gas velocity through the vessel increases directly with the scale ratio, and consequently may lead to impeller overloading or liquid blowout. Therefore, the choice and/or compromise between criteria 5 and 6 has to be carefully evaluated for the individual process involved.

As mentioned above, without doubt, the bioreactor scale-up technology is critical to industrial application, for example, in plant root cultures (145). In some cases, the scaling-up factor may be quite different from the above-mentioned conventional ones. For example, in plant cell suspension cultures of *T. chinensis*, it was noted that a considerable drop in taxuyunnanine C (Tc, a novel bioactive compound) accumulation occurred when the cells were transferred from shake flasks to bioreactors; and, after a series of investigations, interestingly ethylene was finally identified as a key factor in scaling up the process (243).

77.4.1 Animal Cell Culture Scale-Up

Owing to high dose and multiple indications, the requirement of certain commercialized mAbs reaches 500–1000 kg per year. Therefore, large-scale manufacture with high productivity is of vital importance. Until the mid-1980s, the largest scale reported was 8000 L for the production of interferon from Namalwa cells (244). Currently, the manufacture scale can reach 25 000 L for a fed-batch process and 2000 L for a perfusion process. Table 77.6 shows large-scale processes of animal cells (10).

Even though large-scale mammalian cell culture has been routinely performed by biopharmaceutical companies, the literatures about scale-up are still limiting. Moran *et al*. (245) and Schenerman *et al*. (246) showed that very similar process performance and product characteristics are achieved for suspension cultures conducted at scales ranging from 3 to 10 000 L. Yang *et al*. (247) focused on the scale-up of a Sp2/0 mouse myeloma cell line–based fed-batch bioreactor process, from the initial 3-L bench scale to a 2500-L scale. A stepwise scale-up strategy that involved several intermediate steps in increasing the bioreactor volume was adopted. Consideration was also given to scale-up of the nutrient feeding, inoculation, and the set points of operational parameters such as temperature, pH, DO, dissolved carbon dioxide, and aeration in an integrated manner. They chose 65 rpm in the end to balance the mixing time and tip speed. The 2500-L process is currently in use for the routine clinical production of Epratuzumab in support of two global Phase III clinical trials in patients with lupus.

Xing *et al*. (248) performed cell-free mixing and mass transfer studies in production scale 5000-L bioreactors

TABLE 77.6. Large-Scale Processes of Animal Cells (Adapted from (10))

Cell LineScale (L) Reactor Product			
BHK 21	10,000	Agitated tank	Foot and mouth disease vaccine
CHO	10,000	Agitated tank	tPA
Namalwa cells	8,000	Agitated tank	Lymphoblastoid interferon
Bowes melanoma	7,000	Agitated tank/microcarrier	tPA
Murine hybridoma	2,000	Air-lift	mAbs
Vero cells	1,000	Agitated tank/microcarrriers	Killed polio vaccine
Murine hybridomas	1,000	Stirred-tank	mAbs against cell-surface antigens of adenocarcinomas
BHK	500	Agitated tank/perfusion	Factor VIII

with three Lightnin A100 impellers. It was found that pH and oxygen gradients might exist based on the difference between top and bottom probes. The oxygen transfer threshold analysis indicated that the current 5000-L configuration could only support a maximum viable cell density of 7×10^6 cells/mL. Empirical equations were developed to predict mixing time, oxygen transfer coefficient, and carbon dioxide removal rate. These equations indicated that increasing bottom air sparging rate was more efficient than increasing power input in improving oxygen transfer and carbon dioxide removal.

Van Berkel *et al*. (249) performed glutamine synthetase selection technology in suspension growing CHO-K1SV cells to test antibody expression. The N-linked glycosylation was highly consistent for the same cell line when grown extensively, indicating the robustness of the production and glycan analysis procedure. The N-linked glycosylation altered when batch production in a shake flask was changed to fed-batch production in a bioreactor, but was consistent again when the process was scaled from 130 to 5000 L. It may be due to uncontrolled environments in a shake flask such as pH and DO.

The level of dissolved CO_2 (dCO_2) should be carefully monitored during scale-up of mammalian cell cultures. Compared to O_2, CO_2 has high solubility, which also increases with scale because of hydrostatic pressure. For a single bubble, the gas composition changes, resulting from ongoing mass transfer while the bubble rises. The driving force to remove dCO_2 decreases more quickly than that to supply O_2. Mostafa and Gu (250) mentioned that dCO_2 level increased from the 68 to 179 mmHg level when scaling up a process from 4 to 1000 L resulting in a 40% decrease in productivity. The authors found that a decrease in the top impeller position and increase in the aeration rate could help lower the pCO_2 level and increase the final titer by 100%. Zhu *et al*. (251) also reported a high dCO_2 level of 120–150 mmHg observed in production scale as well as high osmolality, which caused quick viability drop and low titer compared to bench scale data. Therefore, the aeration and agitation strategy needs to be carefully designed to prevent dCO_2 accumulation on a large scale.

77.4.2 Plant Cell Culture Scale-Up

In 1959, it was first reported that plant cells were cultured in a 10-L bioreactor made of glass or steel (252). The first large-scale production of *N. tabacum* cells in a 20 000-L STR was reported in 1977 (253). Plant cell culture was industrially accomplished up to the 75 000-L scale (254).

Adventitious roots of *Echinacea purpurea* were cultured in air-lift bioreactors (20- and 500-L balloon-type bubble bioreactors and 1000-L drum-type bubble bioreactor) for production of chichoric acid, chlorogenic acid, and caftaric acid (255). On the basis of studies in a 20-L bioreactor, pilot-scale cultures were established and 3.6 kg and 5.1 kg dry biomasses were achieved in the 500- and 1000-L bioreactors, respectively. The accumulation of 5 mg of chlorogenic acid/g DW, 22 mg of chichoric acid/g DW, and 4 mg of caftaric acids/g DW were achieved with adventitious roots grown in a 1000-L bioreactor (255). OTR and the corresponding power requirement are vital for design and scale-up of surface aerators. Rao *et al*. (256) developed a simulation or scale-up criterion correlating the oxygen transfer coefficient and power number along with a parameter governing the theoretical power per unit volume. It has been demonstrated that energy can be saved substantially if the aeration tanks are run at relatively higher input powers. It is also demonstrated that smaller-sized tanks are more energy conservative and economical when compared to big sized tanks. The results presented have application in biotechnology areas with a particular emphasis on the design of appropriate surface aeration systems. Son *et al*. (257) demonstrated a novel type of bioreactor for the production of paclitaxel and its precursors by culturing cells of *Taxus cuspidata* on a pilot scale. The cells were inoculated in 20-L-capacity bioreactors of different types to test the growth performance, including a balloon-type bubble bioreactor (BTBB), a bubble-column bioreactor (BCB), a BCB with a split-plate internal loop, a BCB with a concentric draught-tube internal loop, a BCB with a fluidized bed bioreactor, and two different models of STRs. Among the reactors, BTBB appeared to be the most efficient in promoting cell growth. When yew tree cells were grown in

different sizes (100–500 L) of BTBBs, more than 70% cell viability was recorded at the time of harvest. The growth pattern of the cells in the pilot-scale BTBB appeared to be the same as that in a 20-L bioreactor. Approximately 3 mg/L of paclitaxel and 74 mg/L of total taxanes were obtained after 27 days of cultivation.

77.5 CONCLUSIONS

Currently, cell culture technology has had rapid development in application and technological innovation. It is used to produce a series of mAbs, hormones, cytokines, antiviral vaccines, effector cells, and so on. Cell culture at the laboratory scale does not seem to meet the production need; therefore, the bioreactor technology is necessary to meet the market need to get sufficient amounts of useful products. Most cell culture systems can be classified into one of the following types: STRs, pneumatically agitated bioreactors, membrane bioreactors, fixed and fluidized-bed bioreactors, as well as wave bioreactors. In bioreactor design, the mass (especially oxygen) transfer rate, production intensity, and dynamic characteristics should be considered. Biomedical research institute, pharmaceutical companies, and bioengineering companies combine different methods and bioreactor instruments to produce cells for different purposes, which also become the important driving force for bioreactor development, and here the cell or tissue could also be seen as a "super bioreactor" (69).

As we know, plant-derived natural products play a critical role in modern medicine. However, harvesting these products from the parent plant is expensive, requires large amounts of plant material, and is often harmful to the environment. Plant cell cultures have been established for a wide variety of species using nominal amounts of plant material, a particularly useful strategy for the production of valuable metabolites from endangered or rare plants. Although plant cell culture represents an important alternative for natural product production, at present only a small fraction of plant products are produced by cell culture on an industrial scale. However, with the development of biosynthesis and biochemical studies at cellular and molecular levels, metabolic engineering of plant cells is becoming more feasible, and the commercial prospects of plant cell culture will be improved. Further studies are also needed to develop correlations between cell physiology/metabolism and operating variables such as hydrodynamic forces in the *in vitro* culture environment, and to identify fluid dynamic parameters that are optimal for product accumulation and release, and so on. Such correlations will help improve our understanding of plant cell responses to cultivation conditions, and will provide a basis for more effective approaches to bioreactor design and optimization.

It is evident that the transfer of successful laboratory-scale results to large-scale industrial processes is still a challenge. Products from animal cell cultures such as vaccines, antibodies for therapeutic use, and recombinant proteins are mainly produced in batch reactors up to the 25 000-L scale. High amounts of antibodies and vaccines are in demand throughout the world to meet therapeutic or diagnostic needs. Ongoing development and optimization of fed-batch and perfusion processes are required to meet the worldwide market at an economically and socially acceptable price. For large-scale cell culture processes, cell retention and separation is still ineffective; the devices undergo fouling very quickly; the cells are stressed to some extent by retention or separation, and viability drops. The latter is also a problem for batch cultures when the product is harvested and separated from the cells. Dead cells release a variety of proteins into the supernatant, which might alter the product quality and DNA might also contaminate the product and has to be carefully removed.

Meanwhile, the bioreactors for mass production of regenerated tissues and organs have already been proposed by a few companies. New horizons have been opened, and clinicians, scientists, engineers, and other individuals, whether in private or in public industries, should begin to work in teams as a multidisciplinary approach is required. Numerous applications have been proposed, but many more are expected. Biomaterials and artificial organs increase life expectancy and improve the quality of life of millions. Currently, bioreactor engineering is also moving forward toward new challenges and aims to turn them into industrialization achievements for the benefit of human beings and the society.

NOMENCLATURE

$k_L a$	Volumetric oxygen mass transfer coefficient, h^{-1} (or s^{-1})
N	agitation speed, s^{-1}
Pg/V	power input per unit volume of liquid, kW/m^3
Qs	liquid exchange rate, m^3/s
Q/V	volumetric gas flow rate per unit volume of liquid, $m^3/(m^3\ s)$
v_s	superficial gas velocity, m/s

ACKNOWLEDGMENTS

The experimental results from the JJ Zhong Lab (Molecular Biochemical Engineering Group) were mainly obtained by Wei-Wei Hu, Zhi-Wei Pan, Zhi-Gang Qian, Hong-Qiang Wang, Si-Jing Wang, Zhi-You Wen, Cai-Jun Yue, and Zhan-Ying Zhang. Financial aids from National Natural

Science Foundation of China, Ministry of Education of China, Shanghai Municipal Science & Technology Commission, ECUST, and SJTU are also appreciated. The authors also thank the referees for their constructive comments.

REFERENCES

1. Meuwly F, Ruffieux PA, Kadouri A, von Stockar U. Biotechnol Adv 2007; 25: 45–56.
2. Zhou JX, Tressel T, Yang X, Seewoester T. J Biotechnol 2008; 3: 1185–1200.
3. Chadd HE, Chamow SM. Curr Opin Biotechnol 2001; 12: 188–194.
4. Walsh G. Biopharm Int 2005; 18: 58–65.
5. Aggarwal S. Nat Biotechnol 2008; 26: 1227–1233.
6. Chu L, Robinson DK. Curr Opin Biotechnol 2001; 12: 180–187.
7. Dingermann T. J Biotechnol 2008; 3: 90–97.
8. Wurm FM. Nat Biotechnol 2004; 22: 1393–1398.
9. Butler M. Appl Microbiol Biotechnol 2005; 68: 283–291.
10. Kretzmer G. Appl Microbiol Biotechnol 2002; 59: 135–142.
11. Telling RC, Elsworth R. Biotechnol Bioeng 1965; 7: 417–434.
12. Warnock JN, Al-Rubeai M. Biotechnol Appl Biochem 2006; 45: 1–12.
13. Zhong JJ. Adv Biochem Eng Biotechnol 2001; 72: 1–26.
14. Wu J, Zhong JJ. J Biotechnol 1999; 68: 89–99.
15. Mulabagal V, Tsay HS. Int J Appl Sci Eng 2004; 2: 29–48.
16. Rates SM. Toxicon 2001; 39: 603–613.
17. Harborne JB. In: Walton NJ, Brown DE, editors. Chemicals from plants, perspectives on secondary plant products. London: Imperial College Press; 1999. pp. 1–25.
18. Ramachandra Rao S, Ravishankar GA. Biotechnol Adv 2002; 20: 101–153.
19. Smetanska I. Adv Biochem Eng Biotechnol 2008; 111: 187–228.
20. Fowler MW. In: Neumann KH, Barz W, Reinhardt E, editors. Primary and secondary metabolism of plant cell cultures. Berlin, Heidelberg: Springer; 1985. pp. 362–378.
21. Twyman RM, Stoger E, Schillberg S, Christou P, Fischer R. Trends Biotechnol 2003; 21: 570–578.
22. Schillberg S, Twyman RM, Fischer R. Vaccine 2005; 23: 1764–1769.
23. Streatfield SJ. Plant Biotechnol J 2007; 5: 2–15.
24. Hiatt A, Cafferkey R, Bowdish K. Nature 1989; 342: 76–78.
25. During K, Hippe S, Kreuzaler F, Schell J. Plant Mol Biol 1990; 15: 281–293.
26. Hood EE, Bailey MR, Beifuss K, Magallanes-Lundback M, Horn ME, Callaway E, Drees C, Delaney DE, Clough R, Howard JA. Plant Biotechnol J 2003; 1: 129–140.
27. Hood EE, Witcher DR, Maddock S, Meyer T, Baszczynski C, Bailey M, Flynn P, Register J, Marshall L, Bond D, Kulisek E, Kusnadi A, Evangelista R, Nikolov Z, Wooge C, Mehigh RJ, Hernan R, Kappel WK, Ritland D, Li CP, Howard JA. Mol Breed 1997; 3: 291–306.
28. Chong DK, Roberts W, Arakawa T, Illes K, Bagi G, Slattery CW, Langridge WH. Transgenic Res 1997; 6: 289–296.
29. Ruggiero F, Exposito JY, Bournat P, Gruber V, Perret S, Comte J, Olagnier B, Garrone R, Theisen M. FEBS Lett 2000; 469: 132–136.
30. Barta A, Sommergruber K, Thompson D, Hartmuth K, Matzke MA, Matzke AJ. Plant Mol Biol 1986; 6: 347–357.
31. Huang TK, McDonald KA. Biochem Eng J 2009; 45: 168–184.
32. Hellwig S, Drossard J, Twyman RM, Fischer R. Nat Biotechnol 2004; 22: 1415–1422.
33. Sijmons PC, Dekker BMM, Schrammeijer B, Verwoerd TC, Vandenelzen PJM, Hoekema A. Biotechnology 1990; 8: 217–221.
34. Huang LF, Liu YK, Lu CA, Hsieh SL, Yu SM. Transgenic Res 2005; 14: 569–581.
35. Matsumoto S, Ikura K, Ueda M, Sasaki R. Plant Mol Biol 1995; 27: 1163–1172.
36. Huang J, Sutliff TD, Wu L, Nandi S, Benge K, Terashima M, Ralston AH, Drohan W, Huang N, Rodriguez RL. Biotechnol Prog 2001; 17: 126–133.
37. Terashima M, Murai Y, Kawamura M, Nakanishi S, Stoltz T, Chen L, Drohan W, Rodriguez RL, Katoh S. Appl Microbiol Biotechnol 1999; 52: 516–523.
38. Huang TK, Plesha MA, Falk BW, Dandekar AM, McDonald KA. Biotechnol Bioeng 2009; 102: 508–520.
39. James EA, Wang C, Wang Z, Reeves R, Shin JH, Magnuson NS, Lee JM. Protein Expr Purif 2000; 19: 131–138.
40. Magnuson NS, Linzmaier PM, Reeves R, HayGlass AnGK, Lee JM. Protein Expr Purif 1998; 13: 45–52.
41. Huang J, Wu L, Yalda D, Adkins Y, Kelleher SL, Crane M, Lonnerdal B, Rodriguez RL, Huang N. Transgenic Res 2002; 11: 229–239.
42. Smith ML, Mason HS, Shuler ML. Biotechnol Bioeng 2002; 80: 812–822.
43. Sunil Kumar GB, Ganapathi TR, Revathi C-J, Prasad KSN, Bapat VA. Protein Expr Purif 2003; 32: 10–17.
44. Ramírez N, Lorenzo D, Palenzuela D, Herrera L, Ayala M, Fuentes A, Pérez M, Gavilondo J, Oramas P. Biotechnol Lett 2000; 22: 1233–1236.
45. Torres E, Vaquero C, Nicholson L, Sack M, Stoger E, Drossard J, Christou P, Fischer R, Fischer R, Perrin Y. Transgenic Res 1999; 8: 441–449.
46. Magnuson NS, Linzmaier PM, Gao JW, Reeves R, An GH, Lee JM. Protein Expr Purif 1996; 7: 220–228.
47. Fischer R, Schumann D, Zimmermann S, Drossard J, Sack M, Schillberg S. Eur J Biochem 1999; 262: 810–816.
48. Yano A, Maeda F, Takekoshi M. J Med Virol 2004; 73: 208–215.
49. Fischer R, Liao YC, Drossard J. J Immunol Methods 1999; 226: 1–10.
50. Sharp JM, Doran PM. Biotechnol Prog 2001; 17: 979–992.
51. Girard LS, Fabis MJ, Bastin M, Courtois D, Petiard V, Koprowski H. Biochem Biophys Res Commun 2006; 345: 602–607.
52. Wongsamuth R, Doran PM. Biotechnol Bioeng 1997; 54: 401–415.
53. Des Molles DV, Gomord V, Bastin M, Faye L, Courtois D. J Biosci Bioeng 1999; 87: 302–306.
54. Yoshida K, Kasai T, Garcia MRC, Sawada S, Shoji T, Shimizu S, Yamazaki K, Komeda Y, Shinmyo A. Appl Microbiol Biotechnol 1995; 44: 466–472.

55. Su WW, Arias R. J Biosci Bioeng 2003; 95: 13–20.
56. White PR. Plant Physiol 1934; 9: 585–600.
57. Heinstein PF. J Nat Prod 1985; 48: 1–9.
58. McCoy E, O'Connor SE. In: Petersen F, Amstutz R, editors. Progress in drug research. Basel: Birkhäuser; 2008. pp. 330–370.
59. Yokoi H, Koga J, Yamamura K, Seike Y, Tanaka H. J Ferment Bioeng 1993; 75: 48–53.
60. Ogbonna JC, Yada H, Masui H, Tanaka H. J Ferment Bioeng 1996; 82: 61–67.
61. Cheng J, Carreau PJ. Can J Chem Eng 1994; 72: 418–430.
62. Kamen AA, Tom RL, Caron AW, Chavarie C, Massie B, Archambault J. Biotechnol Bioeng 1991; 38: 619–628.
63. Wang SJ, Zhong JJ. Biotechnol Bioeng 1996; 51: 511–519.
64. Wang PM, Huang TK, Cheng HP, Chien YH, Wu WT. J Chem Eng Jpn 2002; 35: 354–359.
65. Huang T, Wang P, Wu W. Biochem Eng J 2001; 7: 35–39.
66. Yue CJ, Zhong JJ. Bioprocess Biosyst Eng 2008; 31: 95–100.
67. Qian ZG, Zhao ZJ, Xu Y, Qian X, Zhong JJ. Biotechnol Bioeng 2005; 90: 516–521.
68. Neves JM, Teixeira JA, Simões N, Mota M. Biotechnol Bioeng 2001; 72: 369–373.
69. Wang SJ, Zhong JJ. In: Yang ST, editor. Bioprocessing for value-added products from renewable resources. Amsterdam: Elsevier; 2006. pp. 131–161.
70. Thanh NT, Murthy HN, Yu KW, Hahn EJ, Paek KY. Appl Microbiol Biotechnol 2005; 67: 197–201.
71. McDonald KA, Hong LM, Trombly DM, Xie Q, Jackman AP. Biotechnol Prog 2005; 21: 728–734.
72. Chresand TJ, Gillies RJ, Dale BE. Biotechnol Bioeng 1988; 32: 983–992.
73. Knazek RA, Gullino PM, Kohler PO, Dedrick RL. Science 1972; 178: 65–66.
74. Yazaki PJ, Shively L, Clark C, Cheung CW, Le W, Szpikowska B, Shively JE, Raubitschek AA, Wu AM. J Immunol Methods 2001; 253: 195–208.
75. Shi Y, Ryu DD, Park SH. Biotechnol Bioeng 1993; 42: 430–439.
76. Piret JM, Cooney CL. Biotechnol Bioeng 1991; 37: 80–92.
77. Tharakan JP, Chau PC. Biotechnol Bioeng 1986; 28: 329–348.
78. Hu YC, Kaufman J, Cho MW, Golding H, Shiloach J. Biotechnol Prog 2000; 16: 744–750.
79. Kaufman JB, Wang G, Zhang W, Valle MA, Shiloach J. Cytotechnology 2000; 33: 3–11.
80. Wang G, Zhang W, Jacklin C, Freedman D, Eppstein L, Kadouri A. Cytotechnology 1992; 9: 41–49.
81. Yang ST, Luo J, Chen C. Adv Biochem Eng Biotechnol 2004; 87: 61–96.
82. Park S, Stephanopoulos G. Biotechnol Bioeng 1993; 41: 25–34.
83. Kratje RB, Wagner R. Biotechnol Bioeng 1992; 39: 233–242.
84. Preissmann A, Wiesmann R, Buchholz R, Werner RG, Noe W. Cytotechnology 1997; 24: 121–134.
85. Goldman MH, James DC, Rendall M, Ison AP, Hoare M, Bull AT. Biotechnol Bioeng 1998; 60: 596–607.
86. Singh V. Cytotechnology 1999; 30: 149–158.
87. Eibl R, Eibl D. In: Gupta SD, Ibaraki Y, editors. Plant tissue culture engineering (Focus on biotechnology). Dordrecht: Springer; 2006. pp. 203–227.
88. Terrier B, Courtois D, Henault N, Cuvier A, Bastin M, Aknin A, Dubreuil J, Pétiard V. Biotechnol Bioeng 2007; 96: 914–923.
89. Jain E, Kumar A. Biotechnol Adv 2008; 26: 46–72.
90. Koynov A, Tryggvason G, Khinast JG. Biotechnol Bioeng 2007; 97: 317–331.
91. Curran SJ, Black RA. Biotechnol Bioeng 2005; 89: 766–774.
92. Williams SN, Callies RM, Brindle KM. Biotechnol Bioeng 1997; 56: 56–61.
93. Schlatmann JE, Vinke JL, Ten Hoopen HJ, Heijnen JJ. Biotechnol Bioeng 1995; 45: 435–439.
94. Zhong JJ, Yoshida M, Fujiyama K, Seki T, Yoshida T. J Ferment Bioeng 1993; 75: 299–303.
95. Thanh NT, Murthy HN, Yu KW, Seung Jeong C, Hahn EJ, Paek KY. J Plant Physiol 2006; 163: 1337–1341.
96. Zhu Y, Cuenca JV, Zhou W, Varma A. Biotechnol Bioeng 2008; 101: 751–760.
97. Curtis WR, Tuerk AL. In: Gupta Dutta S, Ibaraki Y, editors. Plant tissue culture engineering. The Netherlands: Springer; 2006.p 173–186.
98. Mirjalili N, Linden JC. Biotechnol Bioeng 1995; 48: 123–132.
99. Hohe A, Winkelmann T, Schwenkel HG. Plant Cell Rep 1999; 18: 863–867.
100. Cherry RS. Biotechnol Adv 1993; 11: 279–299.
101. Meier SJ, Hatton TA, Wang DI. Biotechnol Bioeng 1999; 62: 468–478.
102. Dey D, Emery AN. Biotechnol Bioeng 1999; 65: 240–245.
103. Wang SJ, Zhong JJ, Chen YL, Yu JT. J Ferment Bioeng 1995; 80: 71–77.
104. Wen ZY, Zhong JJ. Biotechnol Tech 1995; 9: 521–526.
105. Meuwly F, Loviat F, Ruffieux PA, Bernard AR, Kadouri A, von Stockar U. Biotechnol Bioeng 2006; 93: 791–800.
106. Dunlop EH, Namdev PK, Rosenberg MZ. Chem Eng Sci 1994; 49: 2263–2276.
107. Wagner F, Vogelmann H, Barz W, Reinhard E, Zenk MH. Plant tissue culture and its biotechnological application. Berlin: Springer; 1977. pp. 245–252.
108. Leckie F, Scragg AH, Cliffe KC. Enzyme Microb Technol 1991; 13: 296–305.
109. Ho CH, Henderson KA, Rorrer GL. Biotechnol Prog 1995; 11: 140–145.
110. Hooker BS, Lee JM, An G. Enzyme Microb Technol 1989; 11: 484–490.
111. Kieran PM, O'Donnell HJ, Malone DM, MacLoughlin PF. Biotechnol Bioeng 1995; 45: 415–425.
112. MacLoughlin PF, Malone DM, Murtagh JT, Kieran PM. Biotechnol Bioeng 1998; 58: 595–604.
113. Meijer J, ten Hoopen H, van-Gameren Y, Luyben K, Libbenga K. Enzyme Microb Technol 1994; 16: 467–477.
114. Takeda T, Kitagawa T, Takeuchi Y, Seki M, Furusaki S. Can J Chem Eng 1998; 76: 267–275.
115. Jordan M, Sucker H, Einsele A, Widmer F, Eppenberger HM. Biotechnol Bioeng 1994; 43: 446–454.
116. Papoutsakis ET. Trends Biotechnol 1991; 9: 316–397.

117. Boulton-stone JM, Blake JR. J Fluid Mech 1993; 302: 231–257.
118. Zhong JJ, Fujiyama K, Seki T, Yoshida T. Biotechnol Bioeng 1994; 44: 649–654.
119. Chalmers JJ, Bavarian F. Biotechnol Prog 1991; 7: 151–158.
120. Cherry RS, Hull CT. Biotechnol Prog 1992; 8: 11–18.
121. Handa-Corrigan AN, Emery AN, Spier RE. Enzyme Microb Technol 1989; 11: 230–235.
122. Jobses I, Martens D, Tramper J. Biotechnol Bioeng 1991; 37: 484–490.
123. Chisti Y. Crit Rev Biotechnol 2001; 21: 67–110.
124. Prakash G, Srivastava AK. Process Biochem 2007; 42: 93–97.
125. Wang SJ, Zhong JJ. Biotechnol Bioeng 1996; 51: 520–527.
126. Zhang ZY, Zhong JJ. Biotechnol Prog 2004; 20: 1076–1081.
127. Zhong JJ. J Biosci Bioeng 2002; 94: 591–599.
128. Zhong JJ, Pan ZW, Wang ZY, Wu JY, Chen F, Takagi M, Yoshida T. J Biosci Bioeng 2002; 94: 244–250.
129. Zhong JJ, Chen F, Hu WW. Process Biochem 1999; 35: 491–496.
130. Chattopadhyay S, Srivastava AK, Bhojwani SS, Bisaria VS. J Biosci Bioeng 2002; 93: 215–220.
131. Korin N, Bransky A, Khoury M, Dinnar U, Levenberg S. Biotechnol Bioeng 2009; 102: 1222–1230.
132. Sajc L, Grubisic D, Vunjak-Novakovic G. Biochem Eng J 2000; 4: 89–99.
133. Su WW. Appl Biochem Biotechnol 1995; 50: 189–230.
134. Doran PM. Adv Biochem Eng Biotechnol 1993; 48: 115–168.
135. Langheinrich C, Nienow AW. Biotechnol Bioeng 1999; 66: 171–179.
136. Nienow AW, Drain SM, Boyes AP, Carpenter KJ. Ind Eng Chem Res 1997; 36: 2984–2989.
137. Vakili MH, Esfahanny MN. Chem Eng Sci 2009; 64: 351–362.
138. Doran PM. Biotechnol Prog 1999; 15: 319–335.
139. Zhang XW, Stettler M, Reif O, Kocourek A, DeJesus M, Hacker DL, Wurm FM. New Biotechnol 2008; 25: 68–75.
140. Bilgen B, Chang-Mateu IM, Barabino GA. Biotechnol Bioeng 2005; 92: 907–919.
141. Lu JT, Chung YC, Chan ZR, Hu YC. Biotechnol Lett 2005; 27: 1059–1065.
142. Zhu Y, Bandopadhayay PC, Wu J. J Chem Eng Jpn 2001; 34: 579–584.
143. Puthli MS, Rathod VK, Pandit AB. Biochem Eng J 2005; 23: 25–30.
144. Junker BH, Stanik M, Barna C, Salmon P, Buckland BC. Bioprocess Eng 1998; 19: 403–413.
145. Sivakumar G. Biotechnol J 2006; 1: 1419–1427.
146. Aunins JG, Henzler HJ. In: Rehm HJ, Reed G, editors. Biotechnology. Birlin: VCH; 1993. pp. 219–281.
147. Chotigeat W, Watanapokasin Y, Mahler S, Gray PP. Cytotechnology 1994; 15: 217–221.
148. Tang YJ, Li HM, Hamel JFP. Bioprocess Biosyst Eng 2009; 32: 475–484.
149. Godia F, Cairo JJ. Biotechnol Bioeng 2006; 30: 81–112.
150. Jan DCH, Petch DA, Huzel N, Butler M. Biotechnol Bioeng 1997; 54: 153–164.
151. Smart NJ, Fowler MW. Appl Biochem Biotechnol 1984; 9: 209–216.
152. Garcia-Ochoa F, Gomez E. Biotechnol Adv 2009; 27: 153–167.
153. Porter B, Zauel R, Stockman H, Guldberg R, Fyhrie D. J Biomech 2005; 38: 543–549.
154. Raimondi MT, Boschetti F, Falcone L, Migliavacca F, Remuzzi A, Dubini G. Biorheology 2004; 41: 401–410.
155. Lappa M. J Biomech 2006; 38: 185–190.
156. Georgiev MI, Weber J, Maciuk A. Appl Microbiol Biotechnol 2009; 83: 809–823.
157. Zhao D, Xing J, Li M, Lu D, Zhao Q. Plant Cell Tissue Organ Cult 2001; 67: 227–234.
158. ten Hoopen HJG, Vinke JL, Moreno PRH, Verpoorte R, Heijnen JJ. Enzyme Microb Technol 2002; 30: 56–65.
159. Georgiev M, Pavlov A, Ilieva M. Biotechnol Lett 2004; 26: 855–856.
160. Zhong JJ, Yoshida T. J Ferment Bioeng 1993; 76: 530–531.
161. Nienow AW. Cytotechnology 2006; 50: 9–33.
162. Ducommun P, Rueux PA, Kadouri A, von Stockar U, Marison IW. Biotechnol Bioeng 2002; 77: 838–842.
163. Moore A, Mercer J, Dutina G, Donahue J, Bauer K, Mather J, Etcheverry T, Ryll T. Cytotechnology 1997; 23: 47–54.
164. Ahn WS, Jeon JJ, Jeong YR, Lee SJ, Yoon SK. Biotechnol Bioeng 2008; 101: 1234–1244.
165. Votruba J, Sobotka M. Folia Microbiol 1992; 37: 331–345.
166. Wayte J, Boraston R, Bland H, Varley J, Brown M. Gen Eng Biotechnol 1997; 17: 125–132.
167. Gramer MJ, Ogorzalek T. Biotechnol Appl Biochem 2007; 47: 197–204.
168. Ozturk SS, Palsson BO. Biotechnol Prog 1991; 7: 481–494.
169. Xie L, Pilbrough W, Metallo C, Zhong T, Pikus L, Leung J, Aunins JG, Zhou W. Biotechnol Bioeng 2002; 80: 569–579.
170. Borys MC, Linzer DIH, Papoutsakis ET. Biotechnology 1993; 11: 720–724.
171. Zanghi JA, Schmelzer AE, Mendoza TP, Knop RH, Miller WM. Biotechnol Bioeng 1999; 65: 182–191.
172. Yoon SK, Choi SL, Song JY, Lee GM. Biotechnol Bioeng 2005; 89: 345–356.
173. Sakamoto K, Iida K, Sawamura K, Hajiro K, Asada Y, Yoshikawa T, Furuya T. Plant Cell Tissue Organ Cult 1994; 36: 21–26.
174. Curtin C, Zhang W, Franco C. Biotechnol Lett 2003; 25: 1131–1135.
175. Mulder-Krieger T, Verpoorte R, Svendse A, Scheffer J. Plant Cell Tissue Organ Cult 1988; 13: 85–114.
176. Kurata H, Achioku T, Okuda N, Furusaki S. Biotechnol Prog 1998; 14: 797–799.
177. Dörnenburg H, Seydel P. Plant Cell Tissue Organ Cult 2008; 92: 93–99.
178. Tabata M, Mizukami H, Hiraoka N, Konoshima M. Phytochemistry 1974; 13: 927–932.
179. Zhong JJ, Seki T, Kinoshita S, Yoshida T. Biotechnol Bioeng 1991; 38: 653–658.
180. Guo B, Liu YG, Yan Q, Liu CZ. Plant Growth Regul 2007; 52: 259–263.

181. Yu KW, Murthy HN, Hahn EJ, Paek KY. Biochem Eng J 2005; 23: 53–56.
182. Shin KS, Murthy HN, Heo JW, Paek KY. Biol Plant 2003; 47: 149–152.
183. ten Hoopen HJG, van Gulik WM, Heijnen JJ. In Vitro Cell Dev Biol 1992; 28: 115–120.
184. Chang HN, Sim SJ. Curr Opin Biotechnol 1995; 6: 209–212.
185. van Gulik WM, ten Hoopen HJG, Heijnen JJ. Enzyme Microb Technol 2001; 28: 796–805.
186. Suehara KI, Takao S, Nakamura K, Uozumi N, Kobayashi T. J Ferment Bioeng 1996; 82: 51–55.
187. Wu J, Ho KP. Appl Biochem Biotechnol 1999; 82: 17–26.
188. Wang HQ, Yu JT, Zhong JJ. Process Biochem 1999; 35: 479–483.
189. Matsubara K, Kitani S, Yoshioka T, Morimoto T, Fujita Y, Yamada Y. J Chem Technol Biotechnol 1989; 46: 61–69.
190. Hara Y. In: DiCosmo F, Misawa M, editors. Plant cell culture secondary metabolism toward industrial application. New York: CRC Press; 1996. pp. 187–201.
191. Hu WW, Zhong JJ. J Biosci Bioeng 2001; 92: 389–392.
192. Hu WW, Yao H, Zhong JJ. Biotechnol Prog 2001; 17: 838–846.
193. Birch JR, Racher AJ. Adv Drug Deliv Rev 2006; 58: 671–685.
194. Kelly B. Biotechnol Prog 2007; 23: 995–1008.
195. Huang YM, Hu WW, Rustandi E, Yusuf-Makagainsar H, Ryll T. Submitted for publication.
196. Meuwly F, Weber U, Ziegler T, Gervais A, Mastrangeli R, Crisci C, Rossi M, Bernard A, von Stockar U, Kadouri A. J Biotechnol 2006; 123: 106–116.
197. Ahuja S. Handbook of bioseparations. Academic Press, San Diego, CA; 2000.
198. Seki M, Takeda M, Furusaki S. J Chem Eng Jpn 1995; 28: 488–490.
199. Seki M, Ohzora C, Takeda M, Furusaki S. Biotechnol Bioeng 1997; 53: 214–219.
200. Phisalaphong M, Linden JC. Biotechnol Prog 1999; 15: 1072–1077.
201. Van Gulik WM, ten Hoopen HJG, Heijnen JJ. Biotechnol Bioeng 1992; 40: 863–874.
202. Westgate PJ, Curtis WR, Emery AH, Hasegawa PM, Heinstein PF. Biotechnol Bioeng 1991; 38: 241–246.
203. Trexler MM, McDonald KA, Jackman AP. Biotechnol Prog 2005; 21: 321–328.
204. Nyberg GB, Balcarcel RR, Follstad BD, Stephanopoulos G, Wang DIC. Biotechnol Bioeng 1999; 62: 336–347.
205. Kadouri A, Spier RE. Cytotechnology 1997; 24: 89–98.
206. Farid SS. Adv Biochem Eng Biotechnol 2006; 101: 1–42.
207. Lim AC, Washbrook J, Titchener-Hooker NJ, Farid SS. Biotechnol Bioeng 2006; 93: 687–697.
208. Kompala DS, Ozturk SS. In: Ozturk SS, Hu WS, editors. Cell culture technology for pharmaceutical and cellular therapies. London: Taylor & Francis; 2005. pp. 387–416.
209. Konstantinov K. Adv Biochem Eng Biotechnol 2006; 101: 75–98.
210. Pham PL, Kamen A, Durocher Y. Mol Biotechnol 2006; 34: 225–237.
211. Cortin V, Thibault J, Jacob D, Garnier A. Biotechnol Prog 2004; 20: 858–863.
212. Henry O, Dormond E, Perrier M, Kamen A. Biotechnol Bioeng 2004; 86: 765–774.
213. Bibila TA, Robinson DK. Biotechnol Prog 1995; 11: 1–13.
214. Jardin BA, Montes J, Lanthier S, Tran R, Elias C. Biotechnol Bioeng 2007; 97: 332–345.
215. Deo YM, Mahadevan MD, Fuchs R. Biotechnol Prog 1996; 12: 57–64.
216. Boedecker BGD, Newcomb R, Yuan P, Braufman A, Kelsey W. In: Spier RE, Griffiths JB, Berthold W, editors. Animal cell technology: products of today, prospects for tomorrow. Oxford: Butterworth Heinemann; 1994. pp. 580–583.
217. Sun X, Hia HC, Goh PE, Yap MGS. Biotechnol Bioeng 2008; 99: 108–116.
218. Su WW, Humphrey AE. Biotechnol Lett 1990; 12: 793–798.
219. Chen JP, Lin TC. Biochem Eng J 2006; 30: 192–198.
220. Lecina M, Soley A, Gràcia J, Espunya E, Lázaro B, Cairó JJ, Gòdia F. J Biotechnol 2006; 125: 385–394.
221. McDonald KA, Jackman AP, Hurst S. Biotechnol Lett 2001; 23: 317–324.
222. Zhong JJ, Fujiyama K, Seki T, Yoshida T. Biotechnol Bioeng 1993; 42: 542–546.
223. Zhong JJ, Konstantinov KB, Yoshida T. J Ferment Bioeng 1994; 77: 445–447.
224. Zhou W, Chen CC, Buckland B, Aunins J. Biotechnol Bioeng 1997; 55: 783–792.
225. Schoenherr I, Stapp T, Ryll T. Biotechnol Prog 2000; 16: 815–821.
226. Chung H, Arnold MA, Rhiel M. J Appl Spectrosc 1996; 50: 270–276.
227. Rhiel M, Ducommun P, Bolzonella I, Marison I, von Stockar U. Biotechnol Bioeng 2002; 77: 174–185.
228. Simon D, Müller RH, Groβe HJ, Bley TH, Babel W. Bioprocess Eng 2000; 23: 1–10.
229. Su WW, Guan P, Bugos RC. Biotechnol Bioeng 2004; 85: 610–619.
230. Schulze-Horsel J, Genzel Y, Reichl U. BMC Biotechnol 2008; 8: 45.
231. Srivastava S, Harsh S, Srivastava AK. Process Biochem 2008; 43: 1121–1123.
232. Dowd JE, Jubb A, Kwok KE, Piret JM. Cytotechnology 2003; 42: 35–45.
233. Bittner C, Wehnert G, Scheper T. Biotechnol Bioeng 1998; 60: 24–35.
234. Frerichs JG, Joeris K, Konstantinov K, Scheper T. Chem Eng Technol 2002; 74: 1629–1633.
235. Guez JS, Cassar JP, Wartelle F, Dhulster P, Suhr H. J Biotechnol 2004; 111: 335–343.
236. Joeris K, Frerichs JG, Konstantinov K, Scheper T. Cytotechnology 2002; 38: 129–134.
237. Rudolph G, Lindner P, Gierse A, Bluma A, Martinez G, Hitzmann B, Scheper T. Biotechnol Bioeng 2008; 99: 136–145.
238. Zhang J, Zhou H, Ji Z, Regnier F. J Chromatogr B Biomed Sci Appl 1998; 707: 257–265.

239. van der Pol JJ, Machnik M, Biselli M, Portela-Klein T, de Gooijer CD, Tramper J, Wandrey C. Cytotechnology 1997; 24: 19–30.
240. Ju LK, Chase GG. Bioprocess Eng 1992; 8: 49–53.
241. Fox FA, Gex VE. AIChE J 1956; 2: 539–544.
242. Wang DIC, Cooney CL, Demain AL, Dunnill P, Humphrey AE, Lilly MD. In: Wang DIC, Cooney CL, Demain AL, Dunnill P, Humphrey AE, Lilly MD, editors. Fermentation and enzyme technology. New York: John Wiley & Sons, Inc.; 1979. pp. 194–211.
243. Pan ZW, Wang HQ, Zhong JJ. Enzyme Microb Technol 2000; 27: 714–723.
244. Pullen KF, Johnson MD, Phillips AW, Ball GD, Finter NB. Dev Biol Stand 1985; 60: 175–185.
245. Moran EB, McGowan ST, McGuire JM, Frankland JE, Oyebade IA, Waller W, Archer LC, Morris LO, Pandya J, Nathan SR, Smith L, Cadette ML, Michalowski JT. Biotechnol Bioeng 2000; 69: 242–255.
246. Schenerman MA, Hope JN, Kletke C, Singh JK, Kimura R, Tsao E, Folena-Wasserman G. Biologicals 1999; 27: 203–215.
247. Yang JD, Lu C, Stasny B, Henley J, Guinto W, Gonzalez C, Gleason J, Fung M, Collopy B, Benjamino M, Gangi J, Hanson M, Ille E. Biotechnol Bioeng 2007; 98: 141–154.
248. Xing Z, Kenty BM, Li ZJ, Lee SS. Biotechnol Bioeng 2009; 103: 733–946.
249. van Berkel PH, Gerritsen J, Perdok G, Valbjørn J, Vink T, van de Winkel JG, Parren PW. Biotechnol Prog 2009; 25: 244–251.
250. Mostafa SS, Gu X. Biotechnol Prog 2003; 19: 45–51.
251. Zhu MM, Goyal A, Rank DL, Gupta SK, Vanden Boom T, Lee SS. Biotechnol Prog 2005; 21: 70–77.
252. Tulecke W, Nickell LG. Science 1959; 130: 863–864.
253. Noguchi M, Matsumoto T, Hirata Y, Yamamoto K, Katsuyama A, Kato A, Azechi S, Kato K. In: Barz W, Reinhard E, Zenk MH, editors. Plant tissue culture and its biotechnological application. Berlin, Heidelberg: Springer; 1977. pp. 85–94.
254. Eible R, Eibl D. In: Oksman–Caldentey KM, Barx WH, editors. Plant biotechnology and transgenic plants. New York: Marcel Dekker; 2002. pp. 163–199.
255. Wu CH, Murthy HN, Hahn EJ, Paek KY. Biotechnol Lett 2007; 29: 1179–1182.
256. Rao AR, Kumar B. Biotechnol Bioeng 2007; 96: 464–470.
257. Son SH, Choi SM, Lee YH, Choi KB, Yun SR, Kim JK, Park HJ, Kwo OW, Noh EW, Seon JH, Park YG. Plant Cell Rep 2000; 19: 628–633.

FURTHER READING

See also numerous chapters in this volume and in volume 1 on industrial plant cell bioreactors, photo bioreactors for cultivation of algae, and the design and operation of industrial mammalian cell bioreactors.

78

BIOTRANSFORMATION, PROCESS OPTIMIZATION

Lutz Hilterhaus and Andreas Liese
Institute of Technical Biocatalysis, Hamburg University of Technology, Hamburg, Germany
Udo Kragl
Department of Chemistry, Rostock University, Rostock, Germany

78.1 INTRODUCTION

The use of biotransformations in the food, pharmaceutical, and chemical industries has increased steadily since the early 1970s. Applications range from synthesis in the milligram scale for precious oligosaccharides up to multiton scale for bulk chemicals either using whole cells or isolated enzymes. These processes have been documented in numerous reviews and textbooks (1–5). When new processes are being developed, the special properties of the biocatalyst must be considered, as well as the basic elements of chemical engineering. There is a strong interaction among the individual aspects, which may be considered for process optimization. These are summarized in Fig. 78.1.

The intention of this contribution is to outline the basic strategy for the development of industrial process of biotransformation including the beneficial role of biochemical engineering. For some selected examples the beneficial role of biochemical engineering is demonstrated. A more detailed description can be found in textbooks of biochemical engineering (1,3,6–8).

78.2 WHOLE CELLS OR ISOLATED ENZYMES?

Whole microorganisms or their components, enzymes, may be used for biotransformations. Both approaches have specific advantages and requirements, as summarized in Table 78.1. Commonly, the word *biotransformation* is used to describe the transformation of a substrate or precursor into a certain product in only a few steps. Fermentation processes, for example, production of amino acids from glucose and ammonia or production of (recombinant) proteins, are normally not regarded as biotransformation. Literature describing those processes can be found elsewhere in this volume or in external references (2,9–13).

Examples for industrial biotransformations using whole cells or isolated enzymes are given in Table 78.2. Some special information about process characteristics is given as well. When isolated enzymes are used for biotransformations, the purity must only be such that no side reactions occur. There is no need to purify the enzyme to homogeneity, as required for biochemical characterization. On the contrary, many enzymes show reduced stability with increasing purity. In some cases, the addition of inert proteins, such as bovine serum albumin, may be used as a simple way to increase the stability of the production enzyme. In others, the enzyme stability may be increased by immobilization on a support. Covalent attachment fixes the conformation of the enzyme often preventing denaturation. However, the increase of stability has to be balanced against the losses during the immobilization step, as well as the additional work and materials costs. A method introduced in the 1990s for the stabilization of enzymes and their immobilization is the formation of cross-linked enzyme crystals (CLECs) (21). A simpler approach uses cross-linked enzyme aggregates, as they are easier to obtain.

Reactors for immobilized enzymes are discussed elsewhere. However, the engineering approach as outlined in

Upstream Industrial Biotechnology: Equipment, Process Design, Sensing, Control, and cGMP Operations, Volume 2, First Edition. Edited by Michael C. Flickinger.
© 2013 John Wiley & Sons, Inc. Published 2013 by John Wiley & Sons, Inc.

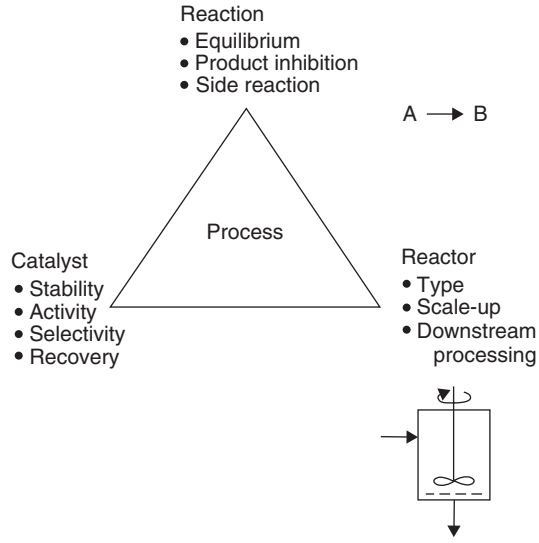


Figure 78.1. Elements of process development.

the following sections is the same for all forms of biocatalysts. Specific requirements and properties such as oxygen delivery, mass transport limitations, or particle size must be considered for individual cases.

78.3 CLASSIFICATION OF DIFFERENT REACTORS

There are three basic types of reactors, which have several variations (Fig. 78.2):

1. Stirred tank reactors (STRs) or batch reactors
2. Continuously operated stirred-tank reactors (CSTRs)
3. Plug-flow reactor s (PFRs)

Unlike the STR, which is operated batchwise, the latter two are operated continuously. By knowing the main characteristics of these fundamental reactors and some of their variations, for example, the cascade reactor of Fig. 78.2, it is possible to choose the appropriate reactor for a specific application. This is especially important when dealing with a kinetically or thermodynamically limited system, as demonstrated later. In the following analyses only the basic terms are explained. For more details the reader is referred to textbooks (6–8).

The STR is operated in a nonsteady state (Fig. 78.2a). Assuming ideal mixing characteristics, the instantaneous concentration of every species is the same in every volume element. With advancing conversion, the substrate concentration is decreased and the product concentration is increased. A steady state is only reached at equilibrium conversion.

TABLE 78.1. Comparison of Biotransformations Using Whole Cells or Isolated Enzymes

Whole Cells	Isolated Enzymes
Large amounts of catalyst easily available	Additional step for obtaining the catalyst required
No stability problem when growing cells are used	Catalyst stability strongly influenced by reaction conditions
Limited volumetric catalyst activity	High volumetric catalyst activity possible
Multistep processes	Multistep processes difficult
Cofactor recycling solved	Cofactor recycling so far only for NADH and ATP
Side reactions may occur	No side reactions
Toxicity of substrate/product	Enzyme stability may be influenced by substrate or product, but can be enhanced choosing the appropriate reactor
Problem of oxygen supply	Nonnatural substrates and reaction conditions possible
Normally no cosolvent possible leading to low concentration of hydrophobic compounds	Cosolvents possible, but often reducing enzyme stability
Transport in and out of the cell may be limit	Mass transport limitations only with immobilized enzymes

In the PFR, the product concentration increases slowly over the length of the reactor (Fig. 78.2b). Therefore, the average reaction velocity is faster than in the CSTR. In each single volume element in the reactor, the concentration is constant in the steady state, whereas in different volume elements along the reactor the concentrations are different. In other words, the dimension of time is exchanged with the dimension of place in comparison to the STR.

The CSTR works under product outflow conditions, meaning that the concentrations in every volume element are the same as those at the outlet of the reactor (Fig. 78.2c). If the steady state is reached, the concentrations are independent of time and place. The conversion is controlled by the catalyst concentration and the residence time, τ.

$$\tau = \frac{V}{F}$$

where τ (hour) is the residence time, V (liter) is the total reactor volume, and F is the (liter/hour) substrate feed rate.

One very common variation of the CSTR is the cascade of n CSTRs (Fig. 78.2d). With an increasing number, n, of reaction vessels, the cascade approximates the PFR (22). The product concentration is increased stepwise from vessel to vessel.

78.3.1.1 Mass Balances. The performances of the different reactor types concerning the reaction can be simulated

TABLE 78.2. Examples for Industrial Biotransformations

Product	Substrate	Catalyst	Comments	References
Acrylamide	Acrylnitrile, H_2O	Nitril hydratase in whole cells of *Rhodococcus rhodochrous*	Very high substrate concentration	14
Chiral hydrophobic alcohol	Ketone	Whole cells of *Zygosaccharomyces rouxii*	XAD-resin as substrate reservoir	15
β-Tetralol derivative	β-Tetralone derivative	Whole cells of *Trichosporon capitatum*	—	16
Trimegestone	Corresponding ketone	Baker's yeast	In water	17
KDN[a]	Mannose, pyruvate	Neuraminic acid aldolase	Continuously operated enzyme-membrane reactor	18
Fructose	Glucose	Fructose glucose isomerase	Immobilized thermostable enzyme	4
Aspartame	L-Phenylalanine-OMe, Z-L-asparaginic acid	Thermolysine	Precipitation of the product	18
(S)-Phenylethyl amine	Rac. phenylethyl amine	Lipase from *Pseudomonas* sp.	Activation of enzyme by lyophilization with fatty acids	19
L-*tert*-Leucine	2-Oxo-3,3-dimethylbuturic acid, NH_4COOH	Leucine dehydrogenase, formate dehydrogenase	NADH regeneration	20

[a] KDN = ketodeoxynonulosonic acid

mathematically. This is also the verification of the kinetic model of the reaction, because it should describe the course of the concentration for each compound with only a small error. The main part of the simulation model is the coupled system of differential equations of first order, which are the mass balances of all substrates and products. The change in the concentration of one compound in time and in a volume element (called the accumulation) is the sum out of convection, reaction, and diffusion (Eq. 78.1).

$$\text{accumulation} = \text{convection} + \text{reaction} + \text{diffusion} \quad (78.1)$$

The convection term describes the change of the concentration of one compound in the reactor as difference of the influx into the reactor and the efflux. The reaction term describes by use of the kinetic model the change of the concentration of one compound as result of the reaction. The reaction velocity, v_S, is the sum of individual reaction velocities describing consumption of a substrate or formation of a product. Diffusion occurs only in the case where no ideal mixing is stated.

With regard to the chosen reactor type the mass balance can be simplified assuming ideal mixing or ideal plug-flow behavior.

Stirred-Tank Reactor.

Diffusion = 0 At a defined time the concentrations are the same in every volume element.

Convection = 0 There is no influx or efflux of substrates or products to a single volume element in time.

The mass balance is simplified to:

$$-\frac{dc_S}{dt} = v_s \rightarrow t = c_{S,0} \int_0^{\text{desired conversion}} 1/v \; dx \quad (78.2)$$

Continuously Operated Stirred-Tank Reactor.

Diffusion = 0 At a defined time the concentrations are the same in every volume element.

Accumulation = 0 In the steady state the concentrations will not change with time.

The mass balance is simplified to:

$$0 = -\frac{dc_S}{dt} = \frac{c_{S,0} - c_S}{t} + v_S \quad (78.3)$$

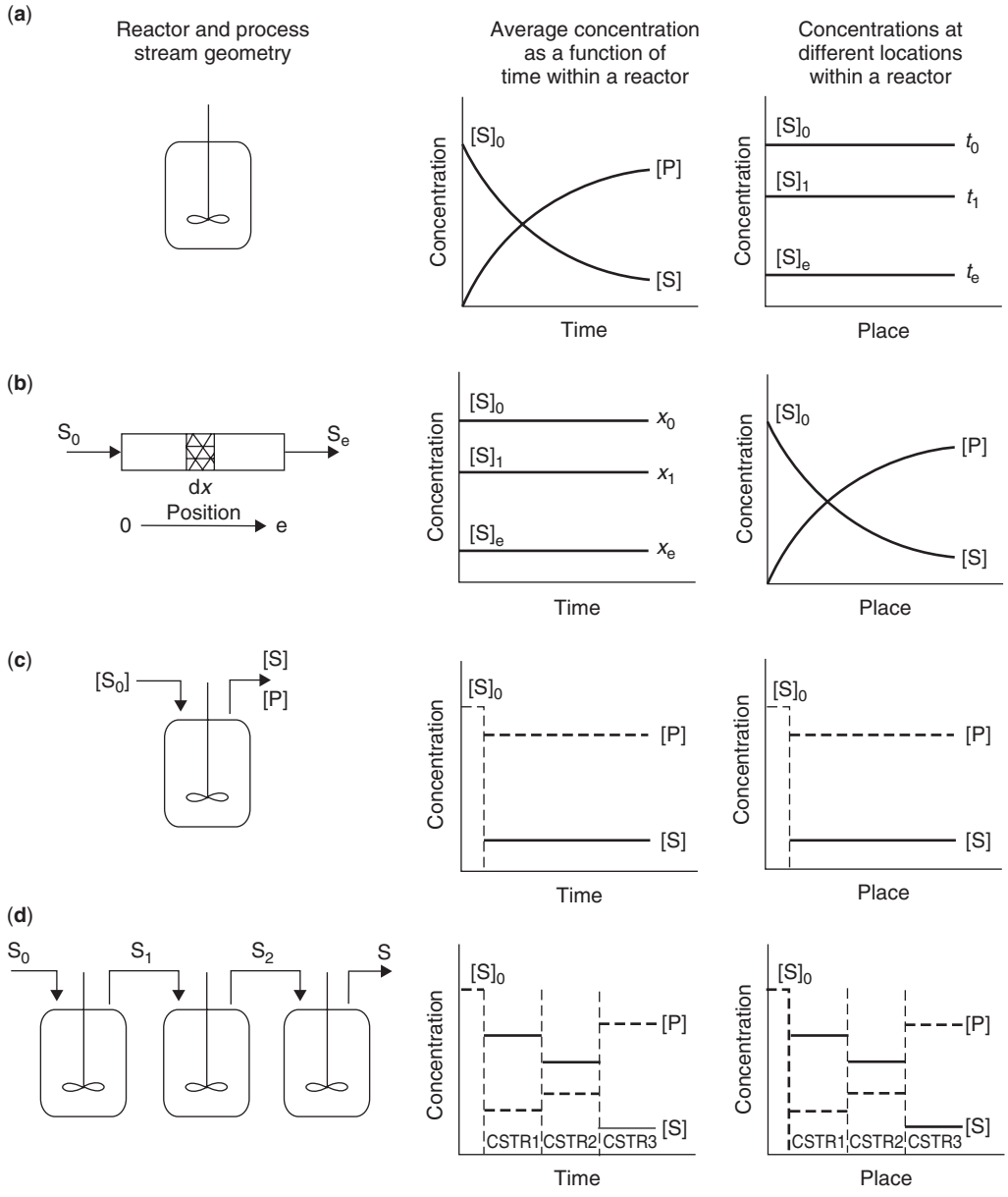


Figure 78.2. Characterization of different reactors.

Plug-Flow Reactor.

$$\text{Diffusion} = 0 \quad \text{Diffusion is neglected in an ideal PFR.}$$

$$\text{Accumulation} = 0 \quad \text{In the steady state the concentrations will not change with time.}$$

The mass balance is the same as for the STR. In the integrated form the time, t, has to be replaced by the residence time, τ.

78.3.1.2 Kinetics. The fundamental equation (Eq. 78.4) for the description of enzyme kinetics was derived by Michaelis and Menten (24).

$$v = c_{\mathrm{E}} \times \frac{v_{\max} \times c_{\mathrm{A}}}{K_{\mathrm{M}} + c_{\mathrm{A}}} \tag{78.4}$$

The enzyme activity is expressed as a function of the substrate concentration for an irreversible one-substrate reaction without inhibition. As this is hardly found in nature, Equation 78.5 gives the rate for a reversible reaction A $\rightleftharpoons$ B. In this form the product inhibition is considered as a competition of A and B for the active sites, as expressed by the two K_{M} values. This form might

be extended to cover substrate surplus inhibition as well as multisubstrate reactions by adding additional terms to the numerator and denominator (6,25–27).

$$v = c_E \times \frac{\frac{v_{max,\ A} \times c_A}{K_{M,A}} - \frac{v_{max,\ B} \times c_B}{K_{M,B}}}{1 + \frac{c_A}{K_{M,A}} + \frac{c_B}{K_{M,B}}} \qquad (78.5)$$

The determination of the kinetic parameters can be performed either by initial reaction velocity measurements or by batch experiments at different substrate concentrations. The kinetic parameters are determined by fitting the kinetic model to the experimental data by use of nonlinear regression; in the case of the batch experiments, numerical integration of the reaction velocity equations is required.

78.4 PROCESS DEVELOPMENT STEP BY STEP

Figure 78.3 shows different phases and topics to be addressed during development and optimization of a biotransformation. The main focus is on the use of isolated enzymes, but for whole cell processes a similar scheme must be followed. A more detailed description can be found in (6). In practice, some of the investigations listed here stepwise will be performed simultaneously. For example, experiments should first hint possible problems from side reactions. Other factors may be considered as well.

- Buffer compounds may be important for enzyme stability, but must be removed during product isolation. Avoiding them may simplify product isolation and save costs.
- Any reaction exhibiting substrate surplus inhibition should not be carried out in a batch-reactor setup, since this results in longer reaction times due to the high substrate concentration at start-up which lowers the initial reaction velocity. In such a case, a CSTR that is operated at a high conversion in the steady state is preferred, resulting in a low substrate concentration. Another possibility is the use of a fed batch, which means that the substrate is added in small portions as a function of time, also resulting in a small substrate concentration. One example for such systems is the enzymatic synthesis of L-phenylalanine by reductive amination, which can be found in literature (24,28).
- If product inhibition occurs, either an STR, a PFR or a cascade of n CSTRs should be chosen. In all these reactors, the product concentration increases over time. Another possibility is the use of a differential reactor with integrated product separation (29). These two possibilities will be discussed in detail in the section titled "Examples."

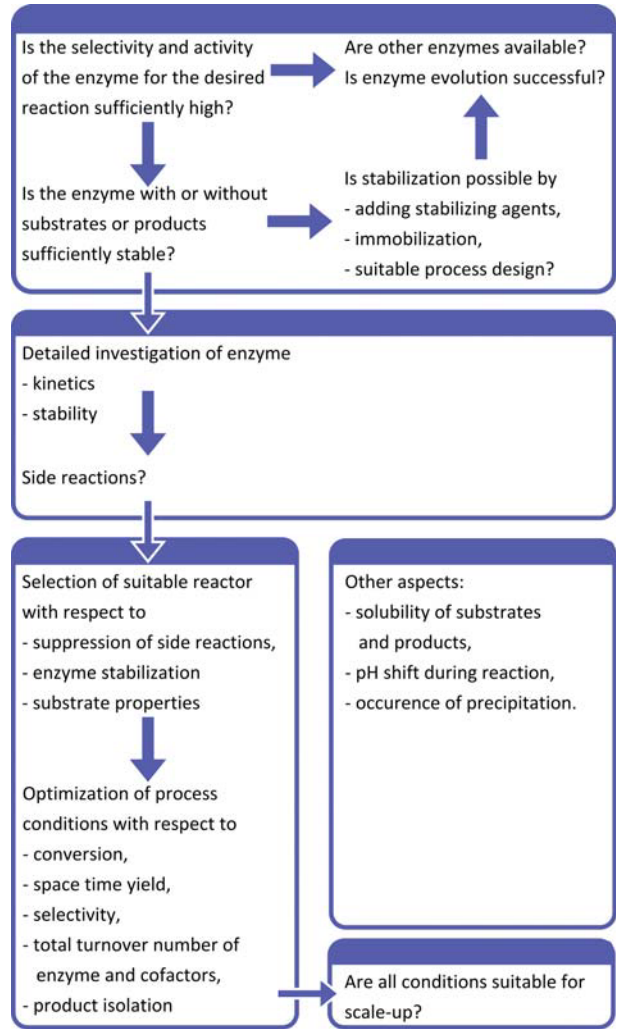


Figure 78.3. Process development step by step. (This figure is available in full color at http://onlinelibrary.wiley.com/book/10.1002/9780470054581.)

- The biocatalyst may be recirculated in and between the reactors by various means to enhance catalyst concentration. Whole cells are often concentrated by microfiltration membranes or centrifugation. Isolated enzymes are much smaller, but can be retained by an ultrafiltration membrane. This type of equipment is commercially available for the processing of volumes of a few microliters up to the cubic meter scale. If the enzyme is immobilized on a support, its size determines the separation step. For example, penicillin amidase is immobilized on a support suitable for separation using a stainless steel mesh in an STR. Also, whole cells might be immobilized on a support, most often simply by adsorption, or by entrapment in alginate gel or similar material.
- The optimization process shown here and discussed later (see section titled "Examples") is based on a

kinetic model of the whole reactions system, including side reactions. This model, together with the mass balance for the reactor, can be used for simulation. By a variation of feed concentrations, catalyst concentration, and residence time, conditions can be found that result in high conversion and space-time yield. When enzyme deactivation is known, the product-specific catalyst consumption may be calculated as well. Alternatively, an empirical optimization can be performed using a simplex method or a generic algorithm. The latter have been successfully applied to fermentation processes (30), but only tested preliminary for optimization of multienzyme systems. These methods are especially powerful for optimization of processes where a direct connection between input- and output-values cannot be given.

- A discussion of the influence of organic solvents onto the solubility of reactants and on enzyme stability can be found in literature (31–35).

Figure 78.4 summarizes some measures that can be taken to overcome or modulate against enzyme deactivation caused either by thermal inactivation or by the reaction partners. Whereas in the first case lowering of the temperature, application of stabilizers, or immobilization on a support may be helpful, the deactivation caused by the reaction partners, may be overcome with the help of the tools of reaction engineering. For the deactivation caused by substrates or products, different tools can be used. The different reactor types are discussed in section titled "Classification of Different Reactors."

78.5 EXAMPLES

By choosing the appropriate fundamental reactor type on the basis of the individual reaction kinetics, the production of the fine as well as bulk chemicals as given in Table 78.3 is possible even in processes that exhibit either a strong inhibition by one of the reaction compounds or limitation by thermodynamics.

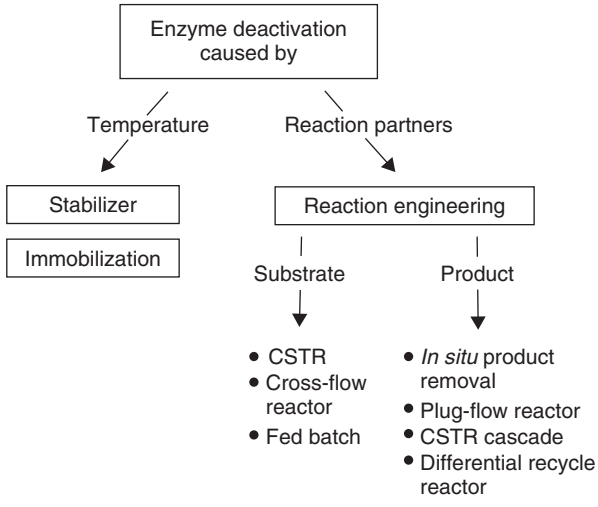


Figure 78.4. Tools to overcome enzyme deactivation.

78.5.1 Product Inhibition

The product inhibition is the consequence of the competition of a substrate and a product for complexation in the active site of a catalyst. This kind of inhibition is not only observed in enzymes, but is also found in reactions which are catalyzed by homogeneous soluble and heterogeneous chemocatalysts (27). Whereas the reaction velocity is reduced by product bonding in the case of an irreversible reaction, the situation is more complex for reversible reaction (*principle of the microscopic reversibility*). In terms of the mathematics, product inhibition is expressed as an additional term in the denominator of the Michaelis–Menten equation (Eq. 78.6). This form of the equation describes competitive inhibition. An explicit discussion of other types of inhibition can be found in the textbooks of enzyme kinetics (6,24,25). By transformation of Equation 78.6, Equation 78.7 can be obtained, which is similar in its structure to the common reaction velocity equation (Eq. 78.5), derived for chemical systems by Hougen and Watson in 1947 (40,27).

$$v = c_E \times \frac{v_{max} \times c_S}{K_M^{substrate} \times \left(1 + \frac{c_P}{K_i^{product}}\right) + c_S} \tag{78.6}$$

where v (catalytic activity/liter) is reaction velocity (1 kat = 1 mol/s), c_E(gram/liter) is enzyme concentration, c_S(mole/liter) is concentration of substrate, v_{max}(catalytic activity/gram, Unit/milligram) is maximal mass specific activity of the reaction, $K_M^{substrate}$ (mole/liter) is Michaelis–Menten-constant of substrate, and $K_i^{product}$ (mole/liter) is competitive product inhibition.

$$v = c_E \times \frac{\frac{v_{max}}{K_M^{substrate}} \times c_S}{1 + \frac{c_S}{K_M^{substrate}} + \frac{c_P}{K_i^{product}}} \tag{78.7}$$

$$v = \frac{(\text{kinetic term}) \times (\text{potential term})}{(\text{adsorption term})^n} \tag{78.8}$$

where n is the number of centers, which are part of a velocity limiting elementary reaction

The decrease of the reaction velocity with increasing product concentration is described by the ratio of K_M to K_i. The relative reaction velocity is plotted as function of the conversion in Fig. 78.5. Three different ratios of K_M to K_i are plotted, which relate to a strong (curve A), moderate (curve B), and weak (curve C) product inhibition.

TABLE 78.3. Examples for the Contribution of Biochemicalengineering

Product	Catalyst	Problems	Solution	References
(S)-1-Phenyl-1,2-ethanediol	Glycerol dehydrogenase	• Product inhibition • Chemical side reaction	Differential batch with continuous product extraction	29
GDP-mannose	GDP-Man pyrophosphorylase	• Product inhibition • Chemical complexation of reaction compounds	Cascade of continuously operated stirred-tank reactors	36
CMP-Neu5Ac	CMP-Neu5Ac synthethase	• Substrate surplus inhibition	Fed-batch reactor	37
Oxindol, chiral sulfoxide	Chloroperoxidase	• Catalyst deactivation	H_2O_2-dosing with closed loop control	38
Chiral lactone	Mono-oxygenase	• Oxygen delivery	Bubble-free aeration using silicone tubing	39

In 1985, Lee and Whitesides suggested, using the example of an oxidoreductase-catalyzed alcohol oxidation, that the feasibility of a process can be judged by the ratio of $K_M^{substrate}$ to $K_i^{product}$ (41):

- If $K_M^{substrate} : K_i^{product} \leq 1$, it is, in principle possible that the reaction can proceed with practicable conversions (Fig. 78.5, curves B and C).
- If $K_M^{substrate} : K_i^{product} > 1$, the reaction is unusable with regard to preparative syntheses (Fig. 78.5, curve A).

This is clearly a simplified view. It is also important to note that the kinetic parameters of a given reaction cannot be changed.

78.5.2 Overcoming Product Inhibition by Product Extraction

Chiral diols are important building blocks, for example, for the synthesis of chiral ligands, agrochemicals and pharmaceutical intermediates (42–44). Using the example of the oxidative resolution of 1-phenyl-1,2-ethanediol, it is demonstrated how the product inhibition can be overcome in case of hydrophobic products.

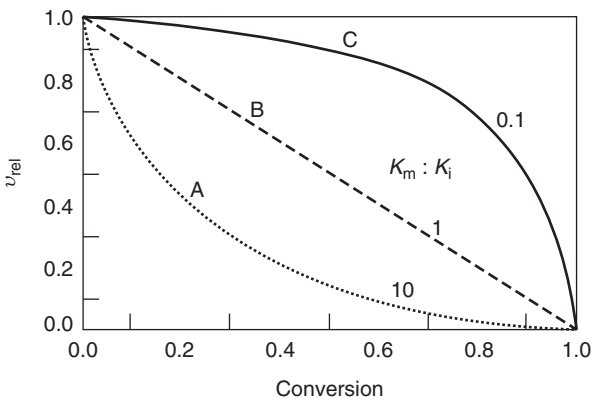


Figure 78.5. Influence of product inhibition on reaction velocity as function of conversion and ratio of K_M and K_i.

The enantioselective oxidation of the (*R*)-enantiomer to ω-hydroxyacetophenone (1-oxo-1-phenyl-2-hydroxyethane) is catalyzed by the glycerol dehydrogenase (GDH) from *Enterobacter aerogenes* (EC 1.1.1.6) (45). Because the GDH needs β-nicotinamide adenine dinucleotide (NAD^+) as a cofactor, a cofactor regeneration carried out by lactate dehydrogenase (LDH) (EC 1.1.1.27) was incorporated as depicted in Fig. 78.6. LDH reduces pyruvate to (L)-lactate enantioselectively. The cofactor regeneration must proceed faster than the racemic resolution in order not to become the limiting step. The remaining (*S*)-enantiomer of the diol is the desired product for further synthesis.

The detailed investigation of the reaction conditions and the kinetics revealed that a strong product inhibition by the hydroxyketone as well as by the NADH was given (29). This resulted in a ratio of $K_M^{substrate} : K_i^{product} = 43.2$ for the ω-hydroxyacetophenone. The inhibition by NADH was not taken into account, because NADH is converted *in situ* to NAD^+ by LDH. Utilizing the above determined criteria, the reaction as investigated here would never proceed efficiently. Additionally, it was observed that the hydroxyketone reacted in a chemical side reaction with NAD^+. Thus, ω-hydroxyacetophenone not only reduced the GDH activity due to its inhibition, it furthermore reduced the available NAD^+ concentration. Therefore it is very important, that the ω-hydroxyacetophenone concentration is kept as low as possible. One possibility is an integrated extraction of the inhibiting compound. Best results were obtained for hexane. In contrast to phenylethanediol which was not extracted, up to 98% of the hydroxyketone was extracted after eight extraction steps.

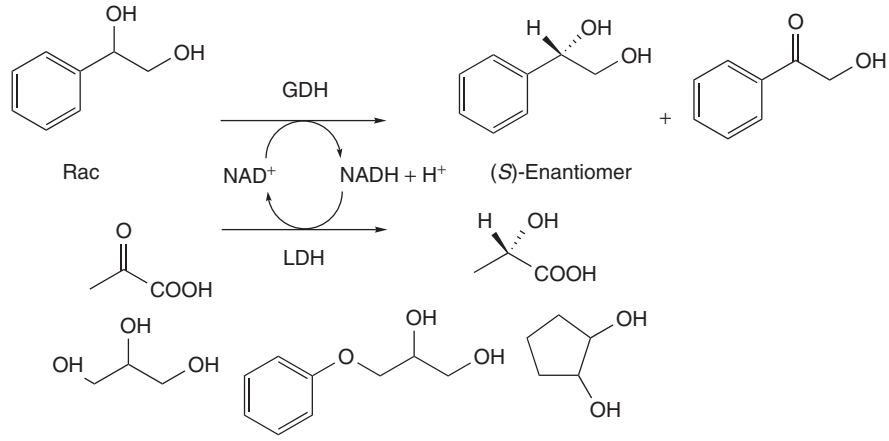


Figure 78.6. Enzymatic resolution of racemic 1-phenylethan-1,2-diol; GDH = glycerin dehydrogenase; LDH = lactate dehydrogenase. Relative activities: glycerol 100%, 3-phenoxypropan-1,2-diol 31%, 1-phenylethan-1,2-diol 8%, *trans*-cyclopentan-1,2-diol 3%.

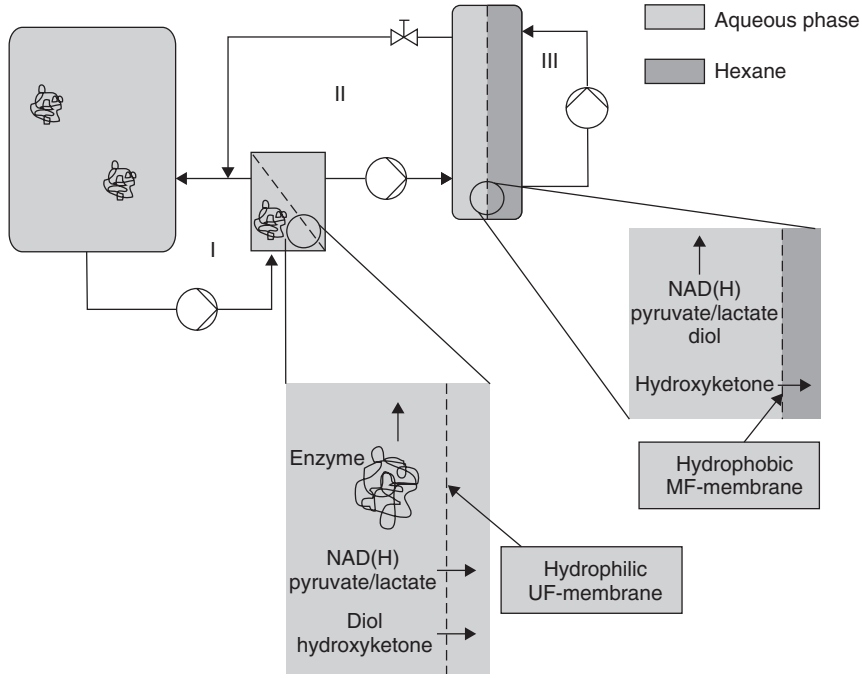


Figure 78.7. Flowsheet of the two-phase membrane reactor; I membrane reactor loop, II extraction loop, aqueous phase, III extraction loop, organic phase. For details refer to (46,53).

The flow sheet of the two-phase membrane reactor is shown in Fig. 78.7. The reactor consists of three different loops. The membrane reactor (loop I) integrates the stirred-reaction vessel and the membrane module (47,48). A hydrophilic ultrafiltration membrane (YM 10, cutoff 10,000 Da, Amicon GmbH, Witten, Germany) is used to retain the GDH and the LDH. The consequence is the decoupling of the residence times of the catalysts and the reactants. Prior to the membrane reactor, an extraction module was positioned in a closed loop arrangement (loop II). The aqueous phase is continuously extracted by means of liquid/liquid extraction, using a hollow fiber module (Liqui-Cel® 5PCM-106, Hoechst, Frankfurt, Germany), consisting of Celgard® microporous, hydrophobic hollow fiber membranes (49). The module was circulated countercurrently by a hexane stream. The best ratio of the flow rates of the aqueous phase to the organic phase was determined to be 1: 6. To reduce the amount of organic solvent used, a distillation (not shown) is incorporated in the extraction loop III. The oxidation

product ω-hydroxyacetophenone is collected in the bottom of the distillation.

The entire reactor behaves as a batch reactor with recirculation, meaning that only a low conversion per cycle is reached corresponding to a small amount of oxidation product, which is directly extracted (29). The consequence is a continuous low concentration of the ω-hydroxyacetophenone in the membrane reactor. This reactor represents a modification of the continuously operated bimembrane reactor which was constructed for the conversion of sparingly soluble substrates (46,50,51).

In Fig. 78.8, two experiments are compared, one with the integrated extraction and the other one without. When no extraction is incorporated, an enantiomeric excess of only 58% and a conversion of 37% was reached after 170 h. The reason for this unsatisfactory result was the accumulation of the reaction product, which lowers the reaction velocity of the GDH and also reduces the concentration of the NAD^+ by the chemical side reaction. With integrated product extraction a conversion of 50% and an enantiomeric excess >99% is reached after 64 h.

This process example demonstrates that by means of reaction engineering, kinetically unfavorable reaction can still be used on a preparative scale. By application of the integrated extraction, a transition from curve A to curve C in Fig. 78.5 is reached.

78.5.3 Overcoming Product Inhibition by a CSTR Cascade

D-Mannose can be found as building block of numerous glycoproteins and glycolipids, for example, in the

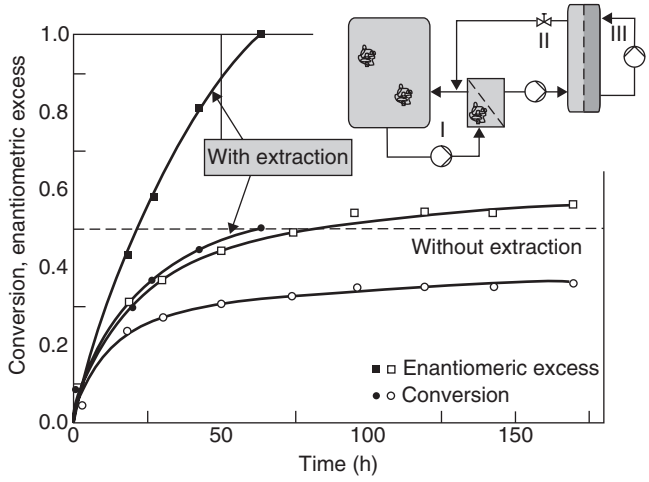


Figure 78.8. Increase of enantiomeric excess and conversion for the kinetic resolution of 1-phenyl-1,2-ethanediol due to product extraction. Residence time in the membrane reactor: 15 min; pressure difference: 2 bar; total volume 500 mL; 100 m*M* glycine/KOH buffer; pH 9; $T = 25^{\circ}C$; 0.054 U/mL GDH; 0.6 U/mL LDH; 200 m*M* ammonia; 40 m*M* (R,S) 1-phenyl-1,2-ethanediol; 2 m*M* NAD^+; 25 m*M* pyruvate).

common core structure of *N*-glycans (52). For the enzymatic *in vitro* synthesis of oligosaccharides guanosine-5′-diphospho-α-D-mannose GDP-Man is used as donor for mannosyltransferases. Recombinant mannosyltransferases have been used for the synthesis of the trisaccharide Man β1-4GlcNAcβ1-4GlcNAc (53). The enzymatic synthesis of GDP-Man starting from mannose-1-phosphate (Man-1-P) and guanosine-5′-triphosphate (GTP) using a recombinant GDP-Man pyrophosphorylase (E.C. 2.7.7.13) has been described (54) (Fig. 78.9). Both reaction products show a very strong inhibition on the GDP-Man pyrophosphorylase. The inhibition by pyrophosphate can be overcome by cleaving it to phosphate using an inorganic pyrophosphatase (E.C. 3.6.1.1). The product inhibition by the product GDP-Man itself can be reduced in a CSTR cascade as shown below. Additionally, the cofactor Mg^{2+}, required by the GDP-Man pyrophosphorylase, is complexed by the substrate GTP. Its influence of the enzyme activity and the preferable use of a continuously operated reactor to establish a constant Mg^{2+} to GTP ratio, together with a complete set of kinetic data for the pyrophosphorylase, has been published (42). For the ratio $K_M^{Man-1-P}/K_i^{GDP-Man}$, a value of 4.4 is obtained. According to the classification outlined in the section "Product Inhibition," this reaction would be only of limited use. Unfortunately, the substrates and products are quite similar with respect to size, hydrophilicity, or charge, prohibiting a selective removal of the inhibiting product. However, simulations on the basis of the kinetic model and various reactor configurations revealed, that a cascade of two CSTRs in series is reducing the required amount of enzyme by >50% (22). A two-stage cascade is a good compromise: plug-flow behavior is approximated to a large extent, whereas the experimental setup does not require too much effort (7). Figure 78.10 compares the conversion of Man-1-P as function of the product of enzyme concentration and residence time for a single CSTR and a two-stage CSTR cascade. In a two-stage cascade 98% conversion is reached for 4.5 (U/mL)min, whereas a single CSTR requires 9.0 (U/mL) min. That means that at a constant enzyme concentration the residence time can be cut in half, resulting in a doubling of the space-time yield. When the enzyme deactivation is only a function of time, by an increase of the space-time yield at constant enzyme concentration, the product-specific enzyme consumption can be decreased. The experimental verification revealed a good agreement between calculated and experimental values (36). At a conversion at 98%, a space-time yield of 28 g(L day) and an enzyme consumption of 900 $U/kg_{product}$ was obtained. For a single CSTR, an enzyme consumption of 2000 $U/kg_{product}$ was reached due to the higher enzyme concentration required to reach the desired conversion under otherwise identical conditions. The relatively low space-time yield is caused by the low substrate concentrations. Complex interactions

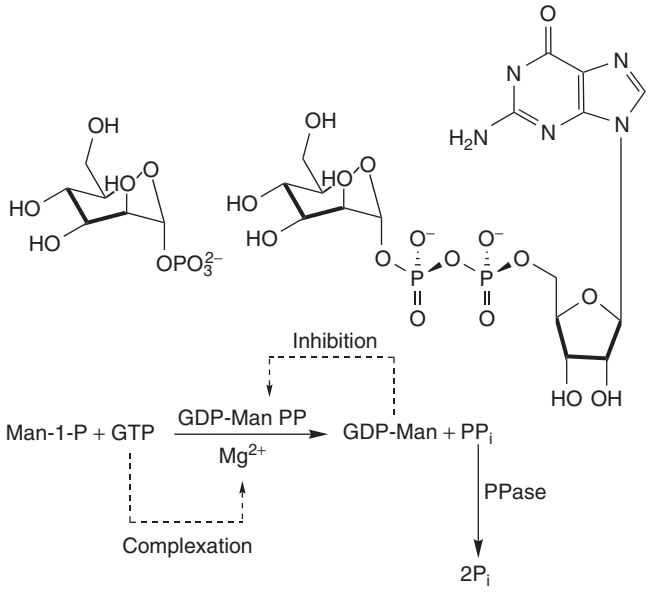


Figure 78.9. Enzymatic synthesis of GDP-Man starting from Man-1-phosphate and GTP; GDP-Man PP = GDP-Man pyrophosphorylase, PPase = inorganic pyrophosphate.

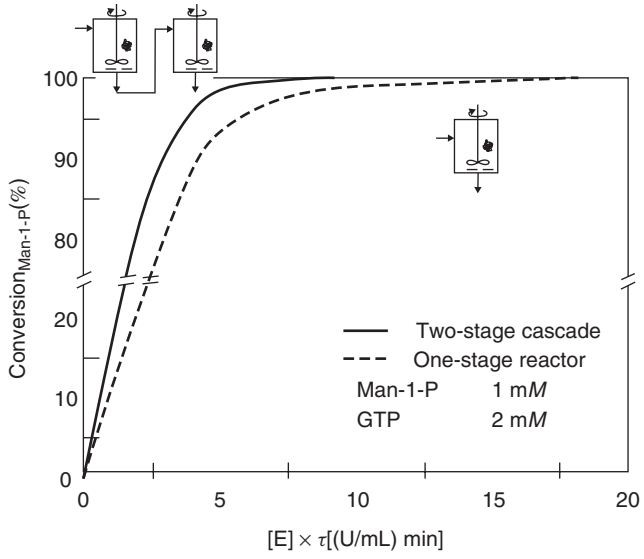


Figure 78.10. Simulation of GDP-Man synthesis in a one-stage CSTR and a two-stage CSTR cascades.

between K_M values of the substrates and the K_i of GDP-Man require simulation to show that the space-time yield can be increased 10-fold by a corresponding increase of the substrate concentration (Fig. 78.11). In order to keep a high conversion at >98%, the enzyme concentration must be increased at the same time, but only 2.5-fold. This clearly demonstrates the potential of process optimization based on a model and a complete set of kinetic data.

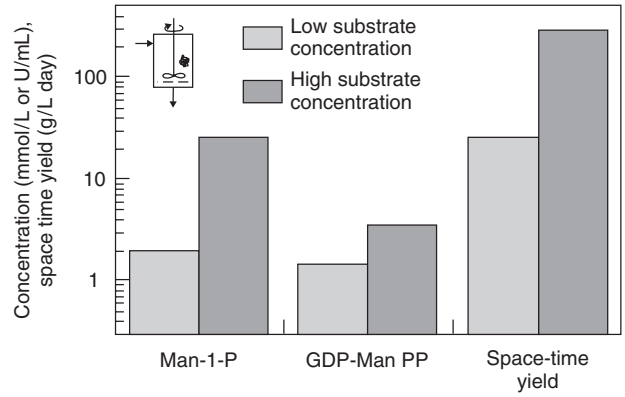


Figure 78.11. Improvement of space-time yield of GDP-Man by higher substrate and enzyme concentration in a one-stage CSTR; (GTP) 2.5 mmol/L or 25 mmol/L, (Mg^{2+}) 1 mmol/L or 9 mmol/L, residence time 1 h; conversion >98%.

78.5.4 Overcoming Thermodynamic Equilibrium by Side-Product Removal

The production of surfactants from high-viscous or high-melting reactants, for example, diglycerol, polyglycerol, or other polyols, illustrates the need to overcome limitations caused by thermodynamic equilibrium. The enzymatic synthesis of fatty acid esters can be carried out as a solvent-free reaction in a PFR. However, the produced water has to be removed from the reaction medium to obtain total conversion by shifting the thermodynamic equilibrium. This is possible by a sequence of a PFR containing the biocatalyst and an evacuated stirred-tank reactor for water removal. In this case the reaction progress is limited by the liquid/gas interface. Additionally, a PFR is restricted to raw materials and products having a viscosity which is low enough to allow its pumping through the bed of immobilized enzyme, resulting in a low differential pressure drop.

The enzymatic synthesis of polyglycerol-3-esters starting from polyglycerol-3 and lauric acid using an immobilized lipase B from *Candida antarctica* (Novozym 435) has been described in detail (55) (Fig. 78.15). Both substrate and the product show a very high viscosity, therefore, removal of the formed water by vacuum only is not sufficient. The limitation of the low surface to volume ratio applying vacuum can be overcome by using a bubble column reactor. The side-product removal can be enhanced in this reactor type but is strongly dependent on the aeration rate and size of the formed gas bubbles (Fig. 78.13). Additionally, aeration enables mixing of the two liquid reactants as well as of the immobilized biocatalyst. The detailed description of the benefit of the bubble column reactor regarding reaching minimal reaction time and the preferable use also for low viscous products like myristyl myristate was recently published (56). Comparing the effective reaction times ER_n

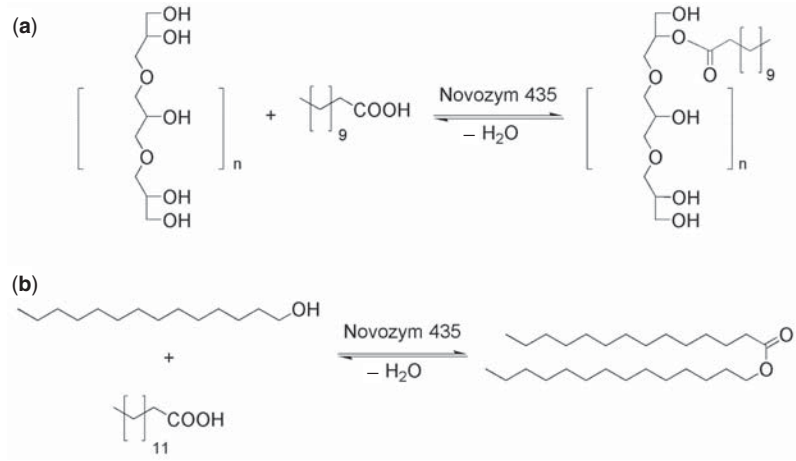


Figure 78.12. Reaction systems carried out within the bubble reactor: (a) polyglycerol-3/lauric acid; (b) myristic alcohol/myristic acid.

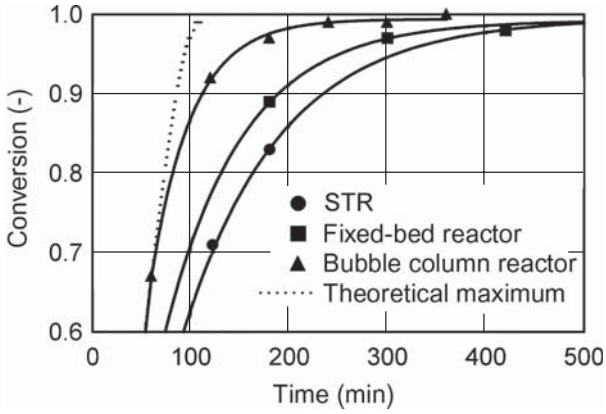


Figure 78.13. Comparison of different reactor setups for the synthesis of myristyl myristate with the theoretically calculated reaction time. All reactions with 0.4% (w/w) of Novozym 435 at 60°C.

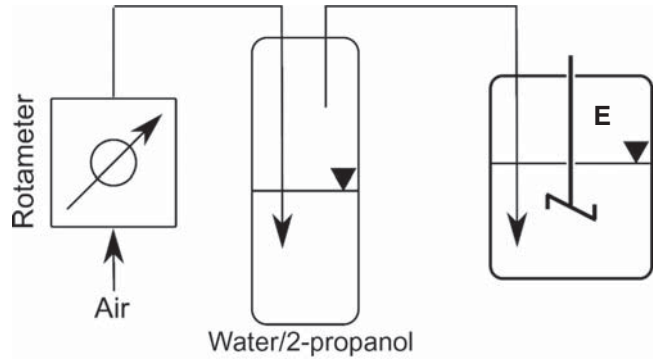


Figure 78.14. Flow scheme of the stripping process.

with the theoretical reaction times TR_n and calculating the efficiency quotients EQ_n revealed the high efficiency of this reactor setup in the case of enzymatic esterifications for a given conversion n:

$$TR_n = \frac{c_{S,0} - c_S}{v_{max}} + \frac{K_m}{v_{max}} \times \ln\left(\frac{c_{S,0}}{c_S}\right)$$

$$EQ_n = \frac{ER_n}{TR_n}$$

The efficiency quotients $EQ_{99.6}$ of 8.3 when using a PFR are significantly reduced to 3.3 when applying the developed bubble column reactor. This means that at a constant enzyme concentration the space-time yield can be doubled. At a conversion at 99.6%, a space-time yield of 6.7 kg(L day) and a biocatalyst consumption of less than 4 $mg/g_{product}$ was obtained.

A second example for overcoming thermodynamic limitations by reaction engineering is the asymmetric reduction of prochiral ketones with alcohol dehydrogenases and substrate-coupled cofactor regeneration. Here, the maximum conversion in ketone reduction depends on the thermodynamic properties of the system (57). A possibility to overcome this limitation in the case of 2-propanol/acetone as coupled reactants is the integration of an ISPR technique, thereby shifting the equilibrium toward the desired product (58,59). As the coproduct acetone is the most volatile compound in the reaction system, it is possible to remove it by applying the stripping process (Fig. 78.14).

A continuous air stream—saturated with water and 2-propanol—is passed through the reaction mixture. Moreover, the air flow causes a mixing of all components, so that additional stirring is not required. To prevent an excessive foaming of the protein suspension, polypropylene glycol was added as polymeric additive. The efficiency of the method on the asymmetric reductions of acetophenone catalyzed by *E. coli*/ADH-"A" was evaluated. The conversion increases up to over 99% in comparison to

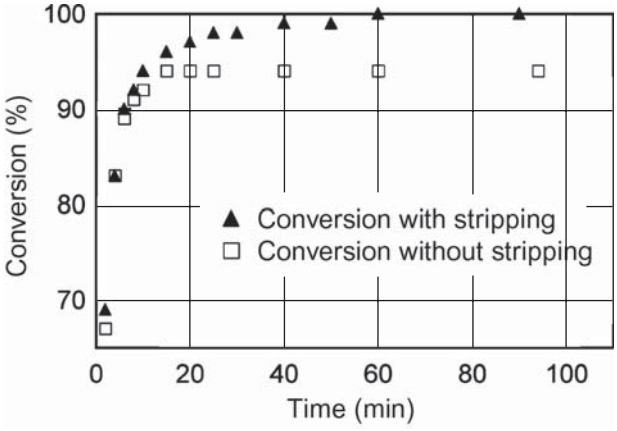


Figure 78.15. Conversions as a function of time. Asymmetric reduction of acetophenone (80 m*M*) with recombinant *E. coli* cells (80 mg) at 30°C in phosphate buffer (50 m*M*, pH 7.5) containing 1 m*M* NADH with a 2-propanol concentration of 2.355 *M* in an overall reaction volume of 20 mL. The biotransformations are carried out with and without stripping.

94% without applying the outgassing method (Fig. 78.15). During the reaction no substrate or product was outgassed from the reaction vessel, which could be proven by determining the mass balances for these compounds during the course of the biotransformation. The technical complexity of the coproduct separation via application of the stripping process is rather low.

REFERENCES

1. Faber K. Biotransformations in organic chemistry. Berlin: Springer Verlag; 2004.
2. Liese A, Seelbach K, Wandrey, C, editors. Industrial biotransformations. Weinheim: VCH; 2006.
3. Drauz K, Waldmann H, editors. Enzyme catalysis in organic synthesis. Weinheim: VCH; 2002.
4. Godfrey T, West S, editors. Industrial enzymology –application of enzymes in industry. 2nd ed. London: Macmillan; 1996.
5. Sheldon RA. Chirotechnology: industrial synthesis of optically active compounds. New York: Marcel Decker; 1993.
6. Biselli M, Kragl U, Wandrey C. Reaction engineering for enzyme catalyzed biotransformations. In: Drauz K, Waldmann H, editors. Enzyme catalysis in organic synthesis. 2nd ed. Weinheim: Wiley-VCH; 2002. p 185–257.
7. Levenspiel O. Chemical reaction engineering, New York: John Wiley & Sons; 1999.
8. Bailey JE, Ollis DF. Biochemical Engineering Fundamentals. New York: McGraw-Hill; 1986.
9. Rozzell D, Wagner F Biocatalytic production of amino acids & derivatives. München: Hanser; 1992.
10. Kelley WS. Bio/Technology 1996; 14: 28–31.
11. Grobiollot A, Boadi DK, Poncelet D, Neufeld R Critical Rev. Biotechnol. 1994; 14: 75–107.
12. Norton S, Vuillemard JC. Critcal Rev Biotechnol 1994; 14: 193–224.
13. Nagasawa T, Yamada H. Trends Biotechnol 1985; 7: 153–158.
14. Anderson BA, Hansen MM, Harkness AR, Henry CL, Vicenzi JT, Zmijewski MJ. J Am Chem Soc 1995; 117: 12358–12359.
15. Reddy J, Tschaen D, Shi Y-J, Pecore V, Katz L, Greasham R, Chartrain M. J Ferment Bioeng 1986; 81: 304–309.
16. Crocq V, Masson C, Winter J, Richard C, Lemaitre G, Lenay J, Vivat M, Buendia J, Prat D. Org Process Res Dev 1982; 1: 2–13.
17. Salagnad C, Gödde A, Ernst B, Kragl U. Biotechnol Progress 1997; 13: 810–813.
18. Elferink VHM. Progress in the application of biocatalysis in the industrial scale manufacture of chiral molecules. Reprints of Chiral USA '96, Boston. London: Spring Innovations Ltd.; 1996, p 79–80.
19. Balkenhol F, Ditrich K, Hauer B, Ladner W. J Prakt Chem 1997; 339: 381–384.
20. Bommarius AS, Schwarm M, Stingl K, Kottenhahn M, Huthmacher K, Drauz K. Tetrahedron: Asymmetry 1995; 6: 2851–2888.
21. Zelinski T, Waldmann H. Angew Chem 1997; 109: 746–748, and cited lit.
22. Kragl U, Vasic-Racki D, Wandrey C. Bioprocess Eng 1996; 14: 291–297.
23. Michaelis L, Menten ML. Biochem Z 1913; 49: 333–369.
24. Cornish-Bowden A. Fundamentals of enzyme kinetics. London: Butterworth & Co Ltd.; 2004.
25. Segel IH. Enzyme kinetics. New York: John Wiley & Sons, Inc.; 1975.
26. Bisswanger H. Enzyme kinetics: principles and methods, Weinheim: Wiley-VCH; 2008.
27. Baerns M, Hofmann H, Renken A. Chemische reaktionstechnik. Stuttgart: Thieme Verlag; 1999.
28. Schmidt E, Fiolitakis E, Wandrey C. Ann N Y Acad Sci 1988; 501: 434–437.
29. Liese A, Karutz M, Kamphuis J, Wandrey C, Kragl U. Biotechnol Bioeng 1996; 51: 544–550.
30. Weuster-Botz D, Wandrey C. Process Biochem 1995; 30: 563–571.
31. Koskinen AMP, Klibanov AM, editors. Enzymatic reactions in organic media. London: Chapman & Hall; 1996.
32. Adlerkreutz P. Biocatal Biotrans 1996; 14: 1–30.
33. Kvittingen L. Tetrahedron 1994; 50: 8253–8274.
34. Carrea G, Ottolina G, Riva S. Trends Biotechnol 1995; 13: 63–70.
35. Gutmann AL, Shapira M. Adv Biochem Eng Biotechnol 1995; 52: 87–128.
36. Fey S, Elling L, Kragl U. Carbohydr Res 1997; 305: 475–481.
37. Kragl U, Klein T, Vasic-Racki D, Kittelmann M, Ghisalba O, Wandrey C. Ann N Y Acad Sci 1996; 709: 577–583.
38. Seelbach K, van Deurzen MPJ, van Rantwijk F, Sheldon RA, Kragl U. Biotechnol Bioeng 1997; 55: 283–288.
39. Rissom S, Schwarz-Linek U, Vogel M, Tishkov VI, Kragl U. Tetrahedron: Asymmetry 1997; 8: 2523–2526.

40. Hougen OA, Watson KM. Chemical process principles. New York: John Wiley; 1947.
41. Lee LG, Whitesides GM. J Am Chem Soc 1985; 107: 6999–7008.
42. Hasegawa J, Ogura M, Tsuda S, Maemoto S, Kutsuki H, Ohashi T. Agric Biol Chem 1990; 54: 1819–1827.
43. Bosetti A, Bianchi D, Cest P, Golini P, Spezia S. J Chem Soc Perkin Trans 1992; I: 2395–2398.
44. Kündig PE, Dupre C, Bourdin B, Cunningham A Jr, Pons D. Helv Chim Acta 1994; 77: 421–428.
45. Webb EC. Enzyme nomenclature. New York: Academic Press, Inc.; 1992.
46. Kruse W, Hummel W, Kragl U. Recl Trav Chim Pays-Bas 1996; 115: 239–243.
47. Kula M-R, Wandrey C. Methods Enzymol 1987; 136: 9–21.
48. Wichmann R, Wandrey C, Bückmann AF, Kula M-R. Biotechnol Bioeng 1981; 23: 2789–2802.
49. Daiminger U, Plucinski P, Nitsch W. Chem Ing Tech 1995; 67: 217–220.
50. Kragl U, Kruse W, Hummel W, Wandrey C. Biotechnol Bioeng 1996; 52: 309–319.
51. Kise S, Hayashida M. J Biotechnol 1990; 14: 221–228.
52. Fukuda M, Hindsgaul O, editors. Molecular glycobiology. Oxford: Oxford University Press; 1994.
53. Flitsch SL, Goodridge DM, Builbert B, Revers L, Webberly MC, Wilson IBH. Bioorg Med Chem 1994; 2: 1243–1250.
54. Elling L, Ritter JE, Verseck S. Glycobiology 1996; 6: 591–597.
55. Hilterhaus L, Thum O, Liese A. Org Process Res Dev 2008; 12(4): 618–625.
56. Thum O, Hilterhaus L, Liese A. DE102008004725A1, 2009.
57. Goldberg K, Edegger K, Kroutil W, Liese A. Biotechnol Bioeng 2006; 95(1): 192–198.
58. Stillger T, Bonitz M, Villela M, Liese A. Chem Ing Techn 2002; 74(7): 1035–1039.
59. Stillger T, Villela M, Liese A, Wandrey C. DE 100 60 602, 2005.

79

FOAM FORMATION AND CONTROL IN BIOREACTORS

Frank Delvigne
Fond de la Recherche Scientifique (FRNS-FRS), Bruxelles, Belgium
Faculté Universitaire des Sciences Agronomiques, Unité de Bio-industries/CWBI, Gembloux, Belgium

Jean-Paul Lecomte
Dow Corning S.A., Seneffe, Belgium

As outlined by Prins and van't Riet (1), foam in bioprocess operations has received little attention compared to other engineering problems such as mixing and mass transfer.Hence, as reported in a recent review, the problem of foam formation in fermentation processes is not yet well controlled (2). Most of the progress has been made at the level of the knowledge of the physicochemical mechanisms and only a few experiments have been performed on the tools needed to control foaming during a bioprocess. This knowledge has notably led to the conception of chemical antifoams. However, the use of such chemicals in bioprocesses must be carefully monitored considering the microorganisms' sensitivity to extracellular changes. A second source of important data comes from the investigation of the hydrodynamic effect leading to the appearance of foam in bioreactors.

79.1 AN OVERVIEW OF THE MECHANISMS OF FOAM FORMATION IN BIOREACTORS

In bioreactors, the intensification of the aeration process and the protein content of the broth are at the basis of foam formation. Indeed, in aerobic cultures, oxygen is provided by the injection of compressed air into the lower part of the reactor. Oxygen solubility being very low in aqueous media (about 7–8 mg/L in fermentation conditions) and oxygen requirement by the microorganisms being very high, the oxygen transfer from air bubbles to the liquid phase must be strongly optimized. This is achieved in practice by increasing the air flow rate through the reactor and, in the case of stirred bioreactors, by increasing the stirrer speed. In all cases, the oxygen transfer process is optimized by increasing the gas–liquid dispersion inside the vessel. The rising bubbles (being as fine as possible) cross the surface of the liquid inside the reactor and in the presence of surface-active molecules, induce the formation of foam. In general, the surface-active molecules found in fermentation media are proteins that are at the basis of most of the industrial complex media or being released by cell autolysis during the process (3). Other compounds exhibiting a surface-active behavior can also be secreted by microorganisms, for example, Escherichia coli, which is known to release lipopolysaccharides (LPS) in a culture when exposed to starvation stress (4), and Bacillus subtilis, which is able to synthesize several lipopeptides (5). A wide variety of compounds excreted during the culture of Penicillium herqueii have been characterized. These include pigments and non-identified lipophilic surfactants released from cell lysis and accumulated in the foam (6). However, proteins are the most frequent surface-active agents encountered in bioprocesses. Proteins are adsorbed at the gas–liquid interfaces, and according to their surface-active properties (i.e. the constituent

Upstream Industrial Biotechnology: Equipment, Process Design, Sensing, Control, and cGMP Operations, Volume 2, First Edition. Edited by Michael C. Flickinger.
© 2013 John Wiley & Sons, Inc. Published 2013 by John Wiley & Sons, Inc.

chains of amino acids each exhibiting hydrophobic or hydrophilic properties) are able to promote foam at very low concentrations (as low as 1 mg/L (1)). In addition, it has been shown that the sterilization procedure of a protein solution significantly increases the foaming capacity of the medium (3). Considering the isoelectric point of the protein, that is the pH for which the global charge of the protein is null, the pH of the medium plays an important role on foam formation. However, the pH is also an important parameter which affects microbial growth and is usually controlled during the culture; therefore, in practice, it cannot be modified to limit foam. In some specific cases, surface-active molecules, named *biosurfactants*, can be released by the microorganisms' secondary metabolism (7,8), leading to an increase of the process difficulties promoted by the foaming media. To illustrate this problem, some research involving a Bacillus subtilis strain overproducing a surfactin (a surface-active molecule belonging to the lipopeptide class), has necessitated a special reactor configuration where oxygen is provided by surface aeration in order to avoid the problem associated with air injection (9). Foam, owing to the amount of precautions to be taken to prevent its formation, is a big challenge for the process engineer. The problems generated by a foaming medium are multiple (10): decrease of the working volume of the reactor, removal of microbial cells and metabolites, contamination, decrease of the oxygen transfer rate subsequent to the addition of antifoam, toxic effects on cell physiology, and so on.

Two spatial scales are involved in the understanding of the underlying mechanisms associated with foam formation in bioreactors. First, the microscopic scale involving molecular arrangement at the gas–liquid interfaces. Second, the macroscopic scale involving gas–liquid flows at the level of the bioreactor.

79.2 DESCRIPTION OF THE FOAM AT THE MICROSCOPIC LEVEL: MOLECULAR MECHANISMS AT THE INTERFACES

An extensive amount of data involving the physical and molecular mechanisms of foam formation is available in the literature. In this section, only the basic molecular mechanisms will be presented. The molecules comprising a hydrophobic and a hydrophilic part are termed as surface-active and are preferentially located at the interfaces. The surface tension, that is the interfacial free energy per unit area, represents the force of cohesion that maintains the molecules in each phase. A surface-active molecule is able to significantly reduce the surface tension after adsorption at the interface. One of the major macroscopic effects resulting from this adsorption, is the stabilization of the dispersion of one phase into the other. In aqueous solutions, when the air–water interface is saturated the adsorption stops and the surface excess of surface-active molecules is arranged in micelles in the solution. This point corresponds to the critical micellar concentration (CMC), that is the surfactant concentration leading to the saturation of the interfacial film. Above the CMC, the surfactant concentration has no influence on the surface tension (Fig. 79.1). The formation of micelles is also a mechanism by which the contact between water and hydrophobic parts of molecules is minimized, leading to a reduction of the free energy of the system. However, this is not the magnitude of the surface tension drop that influences formation of foam. Indeed, there are surface-active molecules that greatly reduce the surface tension but lead to unstable foams. The concept of foam stability is thus important and appears to be strongly correlated to the rate of surface tension variation $d\sigma$ (11). An important parameter controlling the stability of the interface against mechanical action is the force of elasticity (12,13). The effect of surface dilational elasticity (N/m and generally in the range of 10–100 mN/m for protein solutions) was first described by Gibbs, using the following equation:

$$E = \frac{d\sigma}{d\ln A} \tag{79.1}$$

With σ being the surface tension (N/m) and $d\ln A$ the relative change in surface area. Surface elasticity is a parameter allowing the quantification of mechanisms conferring mechanical strength to an interface stabilized by proteins or small molecular weight surfactants. Proteins are able to form a strong viscoelastic network at the interface because of their ability to modify their conformation to readjust the surface equilibrium after a perturbation. But in the case of small molecular weight surfactants, surface elasticity has a different origin. Indeed, in this case, the readjustment of

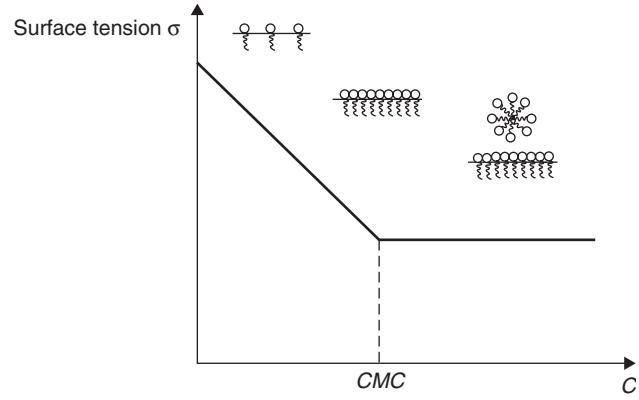


Figure 79.1. Ideal system in which the surface tension σ decreases linearly with the surfactant concentration C.

surface properties is attributed to the mobility of these small surface-active molecules at the interface. Equation (79.1) is very relevant since the flow properties of liquid/air interfaces are strongly influenced by elastic forces. As pointed out above, it is important to highlight the molecular differences between foam produced by low molecular weight surfactants and by proteins. Indeed, proteins differ from low molecular weight surface-active molecules in several aspects: it is very difficult to desorb a protein from an interface except with a low molecular weight surfactant; proteins can change their conformation at the interface conferring some amount of elasticity to the foam and consequently increasing the foam stability; more than one layer of protein can adsorb at the interface (1). In summary, the interfacial effect induced by protein adsorption is strongly linked with its conformation at the interface. (Fig. 79.2 for a comparison of the conformation of a low molecular weight surfactant and a protein, at an interface.) Under dynamic conditions, such as those encountered in bioreactors where bubbles continually flow through the media and burst at the free surface, proteins can change their conformation in order to readjust the surface tension and equilibrium. This effect is enhanced by the sterilization process leading to a loss of conformation at the level of the protein structure. This is a good example of elasticity leading to foam with high stability which can be quantified by the Gibbs dilational modulus (Eq. 79.1). Indeed, in the case of protein-stabilized foam, this modulus is very high, which means that the surface tension gradient can persist for a long time in a surface onto which a protein is adsorbed. However, the adsorption of surfactants at the interface is not the only condition required for the formation of foam. Depending on the intensification of the aeration process in the reactor, the gas–liquid mixture is a very important factor, the surfactant being required only in order to stabilize the bubbles bursting at the level of the free surface. These hydrodynamic phenomena will be described in the next section.

79.3 DESCRIPTION OF THE FOAM AT THE MACROSCOPIC LEVEL: GAS–LIQUID DISPERSION IN THE REACTOR

In the previous section, it has been shown that at the gas–liquid interface the adsorption of surfactant molecules is required to produce foam. However, this is not the only condition. Indeed, the gas–liquid mixture inside the bioreactor is also important, the surfactant being required only to stabilize the bubbles bursting at the liquid free surface. Several authors have pointed out the fact that the turbulent motions in the reactor are important, these motions being strongly linked with the dispersion of bubbles and other gas–liquid phenomena (14).

From a chemical engineering point of view, the foam is considered a special case of gas–liquid dispersion with a large air/liquid ratio (15). Foam formation in a sparged bioreactor is a dynamic phenomenon involving two competing processes, that is the rate of disintegration of bubbles in the foam and the rate of bubbles entering the foam. Freshly formed foam is composed of spherical bubbles separated by liquid films which are up to a few millimeters in thickness.Foam stabilization occurs if the bubbles remain separated from each other by a liquid lamella, a mechanism favored by the presence of surface-active molecules. During ascension of the foam column in the headspace of the bioreactor, the liquid contained in the lamella is drained. At this stage, the aged foam is morphologically different from the fresh foam as it contains polyhedrals in which three bubbles intersect at a corner with an angle of 120° (15) (these corners are called *Plateau borders*). The drainage of the liquid in this lamella is responsible for the collapse of the foam. Like other gas–liquid dispersions, the destabilization of foam involves the aggregation of gas bubbles known as the *coalescence phenomenon*. The evolution of gas bubbles from the bulk of the reactor to the headspace, as well as shape modification of the air bubbles entrapped in the foam phase, is depicted in Fig. 79.3. As shown in this figure, the generation of foam depends on the rate of

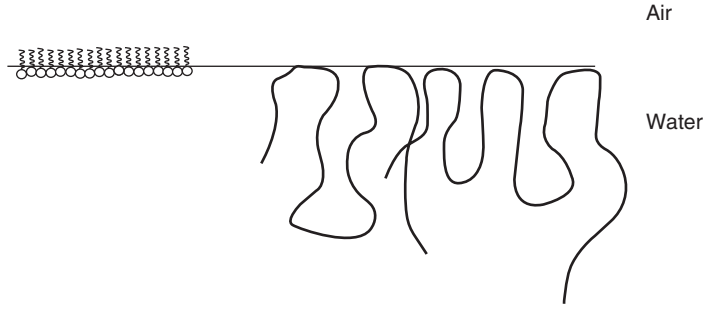


Figure 79.2. Difference of conformation of low molecular weight surfactant (left) and protein (right) at an air/water interface.

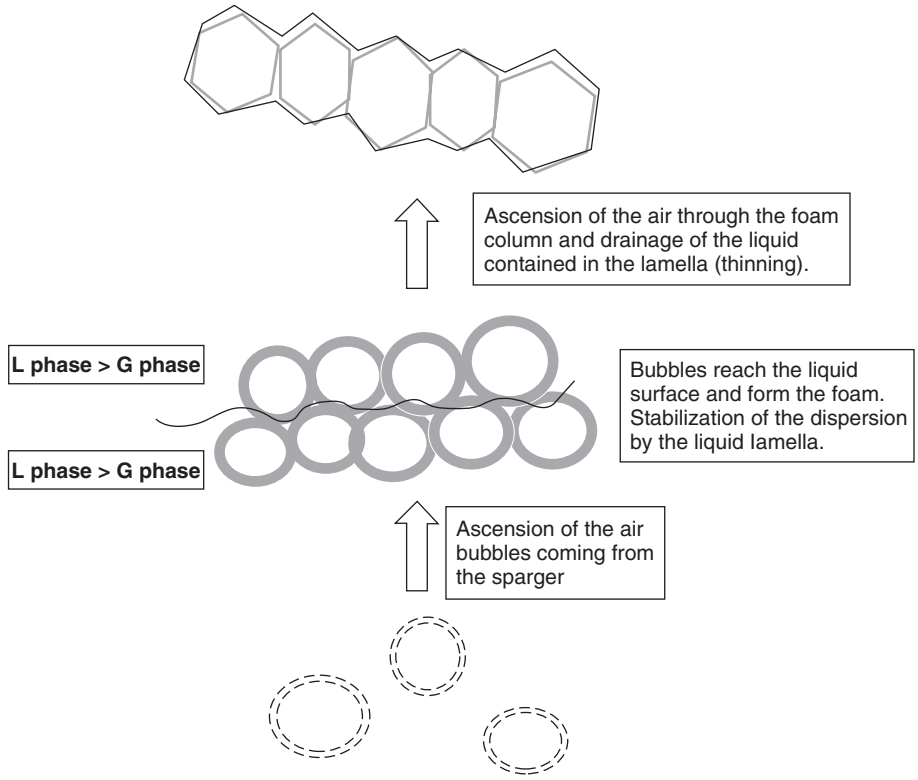


Figure 79.3. Macroscopic mechanisms involved in the generation and the aging of foam in an aerated bioreactor.

alimentation of air bubbles through the liquid surface. The foam rise velocity in the headspace of the reactor is thus strongly dependent on the gas rise velocity in the bulk of the reactor.

$$V_{\text{foam}} = f(V_{\text{g}}) = f\left(\frac{G}{S}\right) \tag{79.2}$$

The gas superficial velocity is described as the ratio of the air flow rate G (m^3/s) to the reactor's cross-sectional area S (m^2).

To limit the foam formation in bioreactors, that is the gas–liquid dispersion at low liquid fractions occurring in the headspace of the reactor, it is important to understand gas–liquid dispersion at high liquid fractions occurring in the bulk of the reactor. This is a large problem owing to the incompatible nature of the two dispersions. Indeed, the gas–liquid dispersion is favored in order to maximize oxygen transfer, but in turn, this dispersion induces the appearance of foam. These two phenomena will be discussed in the following lines by highlighting the interactions between oxygen transfer efficiency and foam intensity. Air is injected into the bioreactor in order to ensure a continuous oxygen supply, with oxygen playing the role of final electron acceptor in microorganisms involved in aerobic processes. The oxygen transfer in bioreactors is described by the general equation:

$$\frac{\mathrm{d}C_L}{\mathrm{dt}} = K_L a(C_L^0 - C_L) \tag{79.3}$$

With $K_L a$ (s^{-1}), defined as the volumetric rate of oxygen transfer, and being the main performance parameter used to estimate the gas–liquid transfer efficiency, C_L^0 being the dissolved oxygen concentration at saturation (typically around 8 mg/L) and C_L being the actual dissolved oxygen concentration. The bioreactor gas–liquid hydrodynamics is optimized to minimize the bubble size and to increase the specific surface available to transfer oxygen (represented by a in the $K_L a$). In the literature, two kinds of correlations using $K_L a$ in function of the operating parameters of the bioreactor have been proposed (16).

For bubble column or airlift bioreactors:

$$K_L a = C\left(\frac{G}{S}\right)^{\alpha} \tag{79.4}$$

For stirred tank reactors:

$$K_L a = C\left(\frac{P}{V}\right)^{\alpha}\left(\frac{G}{S}\right)^{\beta} \tag{79.5}$$

With G being the air flow rate (m^3/s), S being the reactor's cross-sectional area (m^2), P being the power drawn at the level of the impeller (W) and V being the volume of the reactor (m^3).

The gas–liquid dispersion in relation to K_La is far better described in literature than the foaminess, owing to the strong relation existing between the two kinds of dispersion (17) and the operational parameters influencing oxygen transfer that can be used to discuss about foam-influencing parameters at the process scale. In general, the critical condition for foaming in a bioreactor (with or without stirrer) is reached when the gas velocity exceeds a critical value depending on the liquid velocity in the bulk of the reactor (14). The ratio between these two velocities can be modified by the operational parameters. In pneumatic reactors (e.g. bubble column and airlift), the gas–liquid dispersion is quite simple to describe because the air flow rate alone can be considered in order to improve oxygen transfer (Eq. 79.4). It has been shown that the foam appears in a bubble column bioreactor when the gas superficial velocity V_g is larger than a critical value for a fixed liquid velocity V_l (14). Thus the difference between the gas superficial velocity and the liquid flow rate is correlated to the turbulent motions in the reactor which are, in turn, governing the appearance and ascension of foam in the headspace of the reactor. The critical gas superficial velocity above which foam appears can be described by Equation (79.6):

$$V_g = a \cdot V_l + b \tag{79.6}$$

With a and b depending on the nature of the foaming solution.

From this equation, the foam increases when V_g increases for a fixed V_l, and the foam decreases when V_g decreases for a fixed V_l; no foam is produced when V_l is large enough. Similar results have been obtained in the case of 10 m^3 jet loop bioreactors with a draft tube for which a stronger liquid circulation is correlated to a reduction in the foaminess of the medium (18).

The situation is a little bit more complicated in the case of a stirred bioreactor for which the gas–liquid dispersion is governed by two operational parameters: the stirrer speed and the air flow rate (Eq. 79.5). These two parameters must be considered together in order to describe the quality of gas–liquid dispersion (19). If the air flow rate is too important and/or if the stirrer speed is insufficient, the reactor is in the flooding regime. The air bubbles coming from the sparger cross the impeller cross-sectional area without being dispersed, leading to a weak specific area (a) and thus a low K_La. The dispersion can be optimized by increasing the stirrer speed and/or by lowering the air flow rate. At this stage, the reactor is in the loading regime and the bubbles are mechanically broken when passing the vicinity of the impeller, leading to an effective gas–liquid dispersion. Our personal findings suggest that there is a direct relationship between the foam rise velocity in the headspace of the reactor and the gas–liquid dispersion regime in stirred bioreactors (Fig. 79.4). These considerations suggest that the operational parameters of bioreactors can be optimized in order to reach an acceptable level of oxygen transfer and to limit the foaminess to some extent. It has led, for example, to the "stirring as foam disruption" (SAFD) concept (20) that will be discussed in detail later in the text.

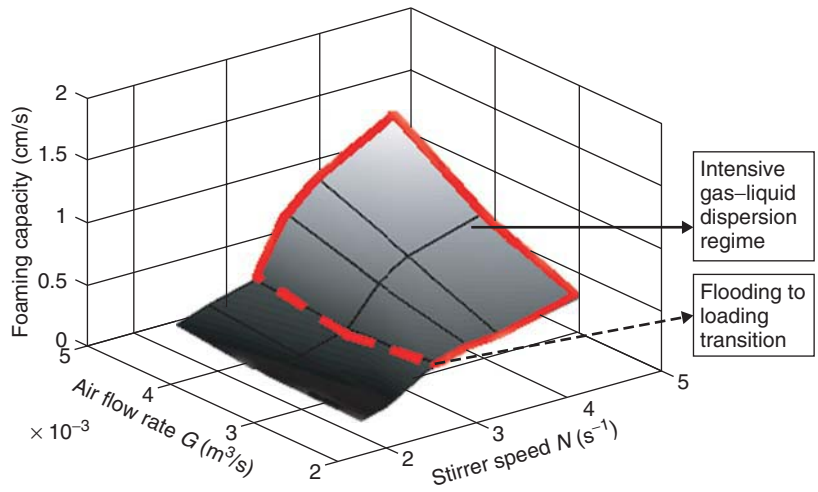


Figure 79.4. Relation between foam rise velocity in a stirred bioreactor as a function of the air flow rate and stirrer speed. The transition between the flooding and loading regime of the impeller has been highlighted. Experiments have been performed in a 300 L stirred tank reactor equipped with a Rushton disk turbine having six blades. (This figure is available in full color at http://onlinelibrary.wiley.com/book/10.1002/9780470054581.)

However, in case of intensive foaming, a foam control procedure has to be considered (as is discussed in the sections on Chemical Methods Used to Prevent Foamand Physical Methods Used To Prevent or Reduce Foam Formation in Bioreactors).

79.4 METHODS USED TO EVALUATE THE FOAMING PROPERTIES OF A SOLUTION

To estimate the problems associated with the formation of foam, it is important to have a technique for measuring some parameters linked with foaming intensity. The foaming properties of proteins or surfactant solutions can be classified into two main categories: the foaming intensity (foaminess or foamability) and the foam stability. These two properties seem to be complementary, but can diverge under some conditions. For instance, increase in temperature leads to an increase of foaminess and decrease of foam stability (21). In general, the foamability of a surfactant solution refers to its overall capacity to produce foam, irrespective of some given characteristic of this foam (e.g. its liquid content and bubble size distribution). On the other hand, the foam stability is a parameter that takes into account the rate of change of foam properties (13). It is thus important to consider these two properties in order to characterize the foaming behavior of solutions.

Three main techniques have been used to determine the foaming properties of surfactant solutions. The first one, based on the volume of foam generated as a function of time, is known as the *Bikerman method* (22). The foam can be generated by whipping or bubbling, but considering the lack of reproducibility of the former, the bubbling apparatus is preferred (23). This apparatus comprises of a glass column equipped with a porous sparger in order to uniformly disperse the air bubbles at the base of the column. The second method is based on the measurement of the liquid drainage from the foam (23). This method can be used only to measure stability of foam and not foaming intensity of a medium. The third one is based on the conductivity of foam, since foam with a high water content exhibits a higher conductivity. A more sophisticated method involves the combination of both the volume and conductivity measurements, the two techniques being known to produce complementary results (5,23). The conductivity method is the most sophisticated and permits the measurement of conductivity at multiple points of the foam column allowing us, for example, to have a precise description of foam behavior in the headspace of a bioreactor (24). This principle is currently under investigation in order to elaborate probe able to measure on line the development of foam inside a reactor (more details are given in the next section). This kind of probe is based not only on foaminess (which is related to the height of foam inside the reactor), but also on foam stability, giving a clearer picture of what can be done to destroy the foam.

These techniques can also be used to test the efficiency of chemical antifoam (25). In this case, foam is generated and when it reaches the top of the column, given quantities of an antifoam are added. The frequency of antifoam addition within a given time interval can be exploited in order to measure the efficiency of the antifoam, the frequency of addition being inversely proportional to this efficiency.

79.5 DETECTION AND REGULATION OF FOAM IN BIOPROCESSES

The detection of foam is generally performed by using a resistivity probe located in the headspace of the bioreactor. The foam level is then detected by a contact probe inducing the automatic delivery of the antifoam. The contact between the probe and the foam close the electrical circuit supplying the antifoam delivery pump. However, this simple on/off control does not take into account the dynamics of foam formation and can lead to the delivery of an inappropriate dose of antifoam. Current research involves more sophisticated probes that are able to measure the conductivity at different levels of the foam column. The conductivity value can be exploited to measure the liquid content of the foam at a given point (24); this method is used mainly to estimate the foaming properties of solutions, as explained in the section on "Methods Used to Evaluate the Foaming Properties of a Solution". This measure is more representative of the properties of foam especially its stability, and gives a robust parameter that can be exploited to improve the dynamic control of foam during a bioprocess. However, such types of sensors are sensitive to fouling by the residual foam. This problem can be avoided by an appropriate processing of the signal at the level of the transmitter. In this way, some companies (e.g. Charis) propose a sensor technology that will be able to detect foam intensity and deliver a precise dose of antifoam. For example, combination of the multi-conductivity probe with a neural network processing of the signal, has allowed effective control of the foam during Pseudomonas sp. cultivations performed in laboratory-scale stirred bioreactors (26).

When using a physical defoamer, the automatic controls can be based on the power input variation required by the turbine of the foam breaker, when being exposed to foam (15).

79.6 CHEMICAL METHODS USED TO PREVENT FOAM

An agent that inhibits initial foam formation is often called *antifoam* whereas an agent that ruptures already-formed

foam is called a *defoamer* (27). We will however use the word "antifoam" in a general way, whether it is used as antifoam or defoamer. Typical antifoams or defoamers consist of oil, hydrophobic solid particles or a mixture of both (28–31). Nonpolar and polar oils have been described while solid particles can be either organic or inorganic. Nonpolar oils are based either on silicone oils (PDMS, see *vide infra*) or organic oils. The most important organic nonpolar oils are water-insoluble paraffinic mineral oils, vegetable oils (such as tall oil, soybean oil, or rape seed oil) or polymeric oils (such as polyisobutylene). Although some nonpolar oils may exhibit some antifoaming performance on their own, mixtures of nonpolar oils with hydrophobic solid particles perform much better than each component, which in some cases can be ineffective when used alone. Hydrophobic solid particles which are the most widely used in the making of antifoam formulations, consist of treated silica (either fumed or precipitated) (32,33), organic waxes (such as ethylene bis-stearamide) or so-called metallic soaps (Aluminum or Calcium stearate) (34). There is a whole class of soluble foam control agents, mostly based on polypropylene (PO) or polyethylene-oxide (EO) (or copolymers such as EO-PO-EO or ethoxylated fatty alcohols) which function by phase separating above their cloud point to form insoluble droplets of a hydrophobic liquid (35). Some soluble polymeric surfactants are thought to destabilize the foam stabilized by proteins or macromolecules by entering the surface as a soluble surface-active species and decreasing the surface elasticity. Antifoam with surfactant structures use this principle (36). A list of selected antifoam agents is presented in Table 79.1. This table includes the main antifoam classes found in the market and for each class, several examples of commercial products are given.

79.6.1 Modes of Action of a Chemical Defoamer

Many foam control agents are added to the foaming medium after being predispersed in water, either as self-dispersible neat materials, oil-in-water emulsions, or self-dispersible mixtures and compounds. The main reason justifying this kind of formulation comes from the fact that, to be efficient, the antifoam must be dispersed as small droplets in the liquid medium. Indeed, in order to destroy a foam film, it is critical that a hydrophobic particle droplet emerges from the aqueous phase into the air/water interface (this process is termed as *entering*). Subsequently, after the entering process, the oil coming from the droplet is able to spread on the air/liquid interface. The two phenomena are not independent as spreading of the oil at the solution/air surface can change the so-called "barrier to entry", which is related to the forces which prevent the emergence of predispersed oil drops on the foam film surface (37,38). Two coefficients, that is the entering and the spreading coefficients, are thus used to characterize the change in free energy of the system when the antifoam droplets emerge from the

TABLE 79.1. List of Selected Antifoam Materials (Neat oil, Emulsion and Powder)

Antifoam Class	Trade Name	Vendor
100% Silicone-based active		
	Dow Corning® Antifoam 1500	Dow Corning
	Silfar® 100	Wacker
Oxylated fatty alcohol or acid		
	Range of Clerol or Agnique defoamer	Cognis
	Acepol 42 Ester	Emerald
	Range of ethoxylated fatty alcohol material	OUVRIE
Organic oil based		
	Acepol 183E	Emerald
Polypropylene glycol or polyethyleneglycol polypropylene glycol copolymer		
	Range of Pluronic	BASF
	Range of Genapol	Clariant
	Range of Polyglycol	Dow
	Polypropylene glycol	BASF, Dow
Emulsion of polydimethylsiloxane		
	Dow Corning Antifoam 1510	Dow Corning
	Silfar SE 4	Wacker
	Acepol 15	Emerald
	Antifoam FD 30	Basildon
Powdered antifoam		
	Dow Corning 1920 Powdered Antifoam	Dow Corning
	Agnique Soap L	Cognis

This list is not exhaustive and is given only as an example of material currently available on the market.

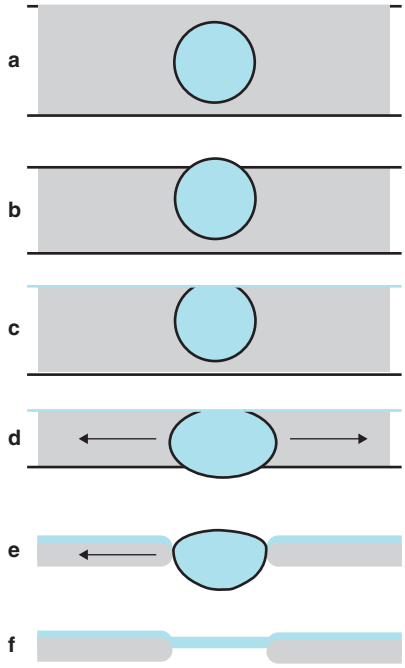


Figure 79.5. Schematic presentation of the bridging of a foam film by a spherical antifoam droplet. (a) The antifoam droplet is entirely in the liquid film. (b) The antifoam droplet has entered the surface. (c) The antifoam droplet bridges the film. (d) The process of bridge de-wetting occurs, leading to destabilization of the foam film and eventually to foam rupture (E and F). (This figure is available in full color at http://onlinelibrary.wiley.com/book/10.1002/9780470054581.)

solution to the solution/air surface (entering, see step B in Fig. 79.5) and when oil from the droplets spreads on the solution-air surface (step C, Fig. 79.5). In the latter process, solution-air surface is replaced by solution-oil interface and oil-air surface.

The entering coefficient can be described by the following equation:

$$C_{\text{entering}} = \sigma_{A/W} + \sigma_{O/W} + \sigma_{O/A} \qquad (79.7)$$

A positive value for this coefficient means that the surface tension of the antifoam liquid ($\sigma_{O/A}$) is lower than the sum of the surface tension of the foaming solution ($\sigma_{A/W}$) and the interfacial tension between the antifoam and the foaming solution ($\sigma_{O/W}$). This also means that the change in free energy of the system when the antifoam droplets emerge from the solution to the solution/air surface, is negative.

When oil from an emerged drop spreads over the air/water interface (step C, Fig. 79.5), it leads to a change of free energy which is the opposite of the spreading coefficient given by the following equation:

$$C_{\text{spreading}} = \sigma_{A/W} - \sigma_{O/W} - \sigma_{O/A} \qquad (79.8)$$

During this step, the water surface is progressively replaced by the oil. A positive value for the spreading coefficient means that the surface tension of the foaming liquid ($\sigma_{O/W}$) is greater than the sum of the surface tension of the antifoam ($\sigma_{O/A}$) and the interfacial tension between the antifoam and the foaming liquid ($\sigma_{O/W}$). Entering is obviously essential to rupture the foam, and it is generally recognized that the entering coefficient must be positive to cause this rupture. A recent study suggests that the spreading of a layer of oils facilitates the foam breaking mechanism, suggesting that the ability to spread is an important property for an oil used in an antifoam formulation (37). To get a positive value for both the entering and the spreading coefficient, it is important to have a liquid with a low surface tension condition which is met for example, in the case of silicone oils. It has been shown that hydrophobic particles facilitate the penetration of the antifoam droplets in foam films, explaining the benefit associated with their addition to antifoam formulations. Hydrophobic particles were shown to decrease the so-called "barrier to entry", thus the barrier which prevent the droplet to emerge from the solution (39). On the other hand, the dispersion of hydrophobic particles in a reactor is an efficient method to control foam (40). After a silicone droplet has penetrated the double air-water interface, a bridge is formed between the two surfaces of the foam film (Fig. 79.5). At this stage, one of the mechanisms invoked in the literature involves the de-wetting of the solution, away from the antifoam droplet associated with the low surface tension of the oil and eventually leading to the rupture of the film (Step E, Fig. 79.5). By no means, is this the only mechanism proposed in the literature, but it helps to better understand how antifoam droplets can eventually lead to foam rupture. For example, another mechanism proposed in literature is "Bridging-stretching" which is illustrated in Step F (Fig. 79.5). In this mechanism, the bridge stretches till a thin, unstable oil film forms in the center of the bridge. Rupture of this oil film results in the perforation of the entire foam lamella (41,42).

79.6.2 Polydimethylsiloxanes as Surface-Active Ingredients in Antifoams

Silicone oils, and more specifically polydimethylsiloxane (PDMS) materials, because of their molecular characteristics, combine many unusual properties such as the flexibility of the Silicium-Oxygen-Silicium backbone and the very low cohesive energy existing between methyl groups (Fig. 79.6). PDMS polymers have low surface tension, and most of them are nonvolatile and remain liquid even at fairly high molecular weights. They are also highly insoluble in water (43). Because of the extreme flexibility of the siloxane backbone and ease with which various polymer

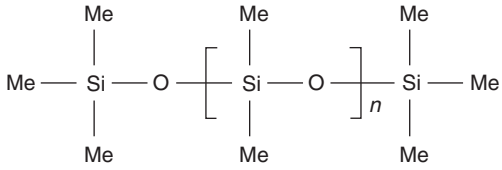


Figure 79.6. Polydimethylsiloxane backbone of a silicon-based antifoam.

configurations can be adopted (despite the siloxane backbone's considerable polarity), it is the side groups that are the primary surface-active entities in the polymer structure. The pendant groups in PDMS are methyl groups, which show the weakest intermolecular interactions known: the London dispersion forces. The low surface tension, which is a direct manifestation of low intermolecular forces, confirms that the interactions between two PDMS chains occur only through their methyl groups. The polymer backbone controls the organization of the side groups at the surface, and its flexibility has a major effect on the ease with which the pendant groups can adopt preferred configurations. Thus, from a surface tension standpoint, the more flexible the backbone, the more readily will the lowest surface energy configurations be adopted. PDMS is a particularly favored case of very low intermolecular force pendant groups anchored along the most flexible backbone, thus allowing the methyl groups to be ideally presented to the external world (44). It is often observed that neat silicone oil shows low efficiency as an antifoaming agent. But mixtures of such oils with hydrophobic particles such as treated silica or finely divided high melting point waxes, are generally much more effective than the individual components (27–29,39). In fact, the mixture performs well even if each component is ineffective when used alone. This synergy is observed for most combinations of oils and solids and in various types of foaming media. It is now widely accepted that the main role of solid particles in antifoam formulations is to facilitate the entry of antifoam droplets. The "barrier to entry" is much lower when the oil drop contains hydrophobic particles. The main role of solid particles is then, to facilitate the entry of the antifoam droplets (39). Effective foam control agents continue to be developed using such combinations to adjust for different types of foam problems.

79.6.3 Formulation Trends

The delivery vehicles, by which the antifoam is delivered to the foaming system, are a key aspect of the antifoam formulation. Practical aspects such as the physical state of the foam control agent (liquid, pasty, or solid), its viscosity (which can be a limit for the pumping or dosing systems), the required cost efficiency, and the addition method will all impact the way the foam control can or need to be added in the fermentation system. There are interactions between the parameters which control foam formation (air incorporation, chemical composition of the broth, presence of surface-active species or pH of the solution) and the antifoam's characteristics (formulation of the antifoam) and how it is delivered to the foaming system. These interactions are illustrated in Fig. 79.7.

79.6.3.1 Neat. Almost all foam control agents sold and used on the market are liquid. As discussed in a different section, they can belong to different chemical families (silicone, aliphatic oil, triglyceride, polyglycols, ethoxylated fatty alcohols, etc.). Their chemical composition will drive

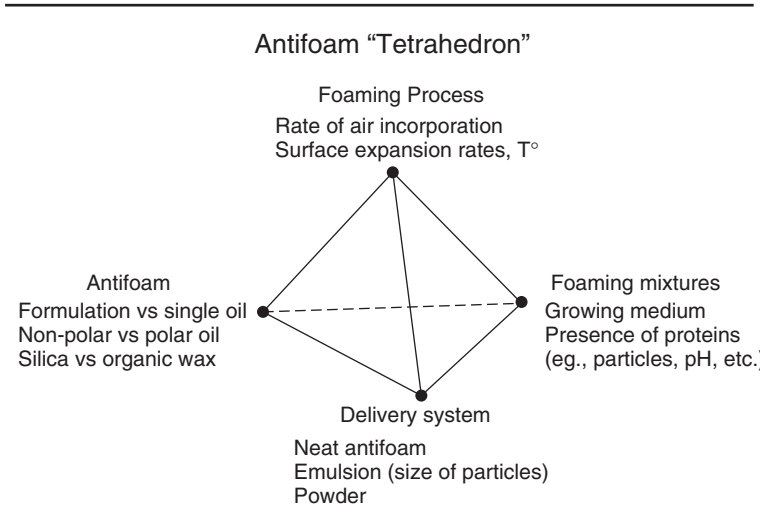


Figure 79.7. Scheme illustrating the different parameters taken into account in the elaboration of a chemical antifoam.

the physicochemical properties, especially the ease of dispersion into water. This is the main characteristic which will dictate if the foam control agent needs to be further formulated or can be used as such; we will characterize this as the neat active agent. If the foam control agent has a low interfacial tension with water (or with the foaming solution), it may be used as such, as it may "disperse" in such a way that it can reach the desired particle size and start to control the foam. If the foam control agent shows a high interfacial tension with water (like PDMS or aliphatic oil with water), some further formulation will be required, such as the addition of surfactant for the making of self-dispersible blends or as emulsion for easier handling.

79.6.3.2 Emulsions. Emulsions are dispersed systems consisting of two (or more) mutually insoluble or sparingly soluble liquids (45). The liquid, usually present in excess, is termed the *continuous* or *external phase*, while the liquid dispersed in it is termed the *internal* or *dispersed phase*. If the external phase consists of water and the internal phase of an organic liquid, for example mineral oil, the term *oil-in-water* (o/w) emulsion is used. In the field of foam control agents, emulsions are generally aqueous, which means they are made by dispersing a nonaqueous foam control agent (dispersed phase) into water (the continuous phase).

Emulsions are prepared industrially to improve the effect of the foam control active substance during the application, by using it in a more or less finely dispersed form. The external phase assumes the role of a transporting and/or diluting agent while the dispersed foam control agent is present as tiny droplets.

Emulsions are used for easy handling of foam control agents which are sometime greasy, highly viscous, organic liquids. Stability of the emulsion is obtained from the proper use of surface-active agents (surfactant) which reduce the interfacial tension between water and the foam control agent in such a way that, the high interfacial area between the dispersed phase and water can be achieved. Thickeners such as functionalised cellulose or some other natural or synthetic materials reduce creaming and further stabilise the emulsion. The latter can have some detrimental impact on downstream treatment of the fermentation broth.

79.6.3.3 Self-Emulsifiable or Self-Dispersible Systems. Self-dispersible systems are blends of foam control agents with surfactants which are designed to readily disperse into the foaming system or, readily emulsify and stabilize the foam control agent in aqueous solutions prior to addition in the foaming liquid. Various systems are described in the literature such as dispersion of antifoam in silicone polyether (46), glycols (47) or organic surfactant (48). Although apparently simple, the compatibility between the foam control agent and the surface-active agent needs to be good enough to achieve stability of the self-dispersible systems, and yet effective enough to ensure ready dispersion during the final application.

79.6.3.4 Powdered Antifoam. The last means by which a foam control agent can be added is as a solid form, most often this will be a powdery material which can be conveniently dosed or handled. Various methods exist to transform a liquid foam control agent into a solid powder. A simple adsorption of a liquid on an absorbing solid is sometime enough to obtain a nice free-flowing powder (49). When improvement of the physical properties of the powder is required (i.e. free-flowing powder with improved shelf stability), more complex formulations and methods of manufacturing will be used. This can imply the preliminary dispersion of the foam control active followed by spraying on a powder acting as carrier and water evaporation (50).

79.7 PHYSICAL METHODS USED TO PREVENT OR REDUCE FOAM FORMATION IN BIOREACTORS

Various physical principles have been proposed in order to prevent foam formation (10). It includes thermal, ultrasound methods and more classically, the mechanical method which involves a special turbine designed to break the foam bubbles by rotating. Considering that the latter is by far the most widely used at the process scale, only this method will be investigated here (the ultrasonic method is actually under investigation but presents some adverse effects notably at the level of the influence of ultrasound on the viability of the microorganisms). To reduce the costs associated with the electrical motor, several turbines have been designed in order to be effective when placed directly on the shaft of the bioreactor. Finally, a new method, based on the management of the bioreactor hydrodynamics in stirred tanks (to reduce foam formation), will be considered. This new method is termed *stirring as foam disruption* (SAFD). These three physical alternatives are presented at Fig. 79.8.

It is important to point out the fact that the first method proposed in this section can be used in order to suppress foam, whereas the second and third methods can only be used to limit its formation.

79.7.1 Mechanical Foam Breakers

79.7.1.1 Classical Mechanical Foam Breaker. Considering the limitations associated with the chemical antifoams (see section on "Impact of Foam Formation and Prevention"), the use of a mechanical foam breaker can in certain cases be a good alternative. It can be used simultaneously with the addition of chemical antifoam

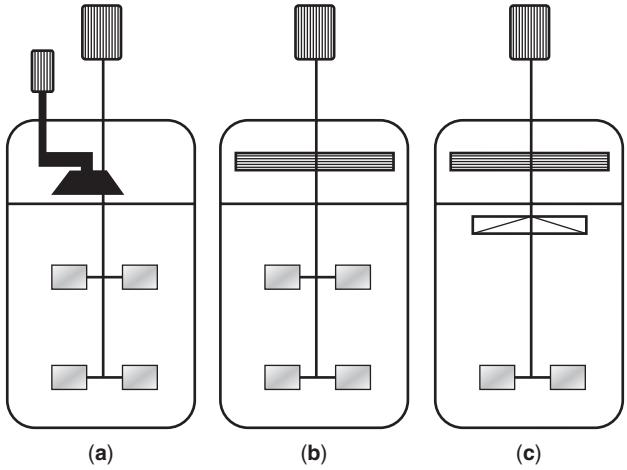


Figure 79.8. Different concepts of mechanical foam breaker. (a) classical concept with the defoamer mounted on a separate shaft, (b) defoamer with the turbine mounted on the shaft of the bioreactor, and (c) "stirring as foam disruption" (SAFD) concept for which the liquid flow pattern generated by the upper impeller tends to destabilize the foam.

in order to reduce the amount of antifoam added in the bioreactor. There are numerous systems available which have been extensively reviewed in the literature (10), and their actions are based on pressure change, shear force and compressive force leading to the destabilization of the foam film. A good example of commercially available and effective mechanical foam breaker is the Fundafom system developed by Chemap (Fig. 79.9) for which the turbines (inverted cones) have been especially designed in order to enhance the shear effect. This apparatus is typically centrally mounted on the bioreactor cover and allows an effective separation of the gas and liquid phase (the volatile part of the collapsed liquid film is collected in a cooled condenser and injected back into the reactor). Other systems including foam breakers with rotating disks (51) have also been experimentally investigated. The main limitations of the mechanical systems is the energy cost associated with the motor of the defoamer. In the case of a stirred vessel, two motors are required, one for the mixing system and another for the defoamer, leading to a significant increase in the installation, functioning and maintenance costs. These costs become unacceptable in large-scale bioprocesses (1). The following sections involve the description of some low cost alternatives to this system.

79.7.1.2 Mechanical Foam Breaker and Mixing System Mounted on the Same Shaft. To reduce the costs associated with power consumption, the turbine of the mechanical defoamer can be mounted directly on the shaft of the impeller system of the bioreactor. In addition, this method presents a lower risk of contamination because the foam

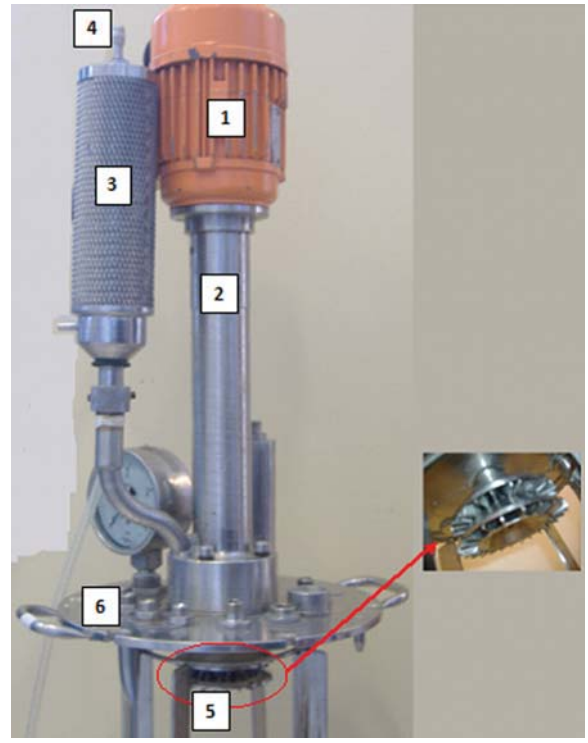


Figure 79.9. Classical mechanical foam breaker equipped with a rotating turbine and installed on a 20 L bioreactor. (1) motor, (2) shaft, (3) cooled condenser, (4) condenser outlet back to the reactor, (5) turbine (conical disks), (6) cover part of the bioreactor. (This figure is available in full color at http://onlinelibrary.wiley.com/book/10.1002/9780470054581.)

breaking apparatus is directly integrated on the shaft of the bioreactor (no mechanical seals are required). Considering the strong interrelation existing between oxygen transfer and foam generation (as reported in the section "Description of the Foam at the Macroscopic Level: Gas–Liquid Dispersion in the Reactor"), this method is only valid if the critical speed for foam control is lower than the required speed for gas dispersion in the bulk of the bioreactor (52). In this context, the turbine of the defoamer must be appropriately designed. A comparison has been done between classical impellers (originally used for the mixing operation in the bulk of the reactor) and some newly designed turbines. It has been shown that these new turbines (thin needles and large paddle turbines) were more efficient in the sense that they lead to a significantly reduced critical speed for foam control (52–55). A more recent system based on hollow inverted cones has been tested in a pilot bioreactor (56). This system is derived from the autonomous foam breaker Fundafom (see section "Classical Mechanical Foam Beaker") and has allowed efficient foam control during a Bacillus culture (a culture generally associated with strong foam problems considering the surfactant synthesis capabilities of this microorganism) at a 0.5 m^3 scale.

79.7.2 Stirring as Foam Disruption (SAFD) Techniques

As discussed before, the bioreactor's hydrodynamics can be optimized to limit foam formation and ensure a given level of oxygen transfer. Further studies have led to the consideration of hydrodynamics as a primary factor in preventing foam in stirred bioreactors this is known as the *stirring as foam disruption* (SAFD) concept. As mentioned before, the foaming intensity in relation to the gas–liquid dispersion in the reactor is governed by the ratio V_L/V_G. The SAFD technique consists simply of designing the impeller system to enhance the liquid velocity near the free surface. To achieve this, the impeller configuration must be modified, that is the height of the upper impeller must be increased for it to be closer to the free surface. Several impeller geometries have been tested (20,57,58) and it has been shown that up-pumping hydrofoils (and notably the A340 hydrofoil commercialized by Lightnin) are the most effective because their flow pattern gives rise to high liquid velocities in the vicinity of the free surface. Considering the complexity of gas–liquid dynamics inside stirred bioreactors, the SAFD mechanism is not completely understood. In addition to the shear effects induced by the liquid flowing through the dispersion surface, the distortion of this surface under the action of liquid waves propelled by the hydrofoils can also play a role in the mechanism of foam rupture (59,60).

79.8 IMPACT OF FOAM FORMATION AND PREVENTION

Foam formation has several impacts at the level of a bioprocess design. In this section, the impact of foam formation will be reviewed by considering three distinct parts of the process: the cell growth and metabolites production, the bioreactor optimization and scale-up and the downstream processing operations. The appearance of foam induces a direct and an indirect negative effect on the bioprocess. The direct effect is attributed to the appearance of the foam which induces cell loss and sterility problems. Indeed, the flow of foam outside the reactor can lead to a significant reduction in reacting volume (and in some extreme cases, to the loss of the entire volume), and can lead to the incorporation of contaminating microorganisms. Subsequently it can result in obstruction of the filters, valves, piping, and so on, by the foam itself and/or the liquid from the collapsing foam. The indirect effects are linked with the antifoam strategy. Mechanical foam breakers can induce shear damages at the level of the cell membrane. Like the other stirrer dependent variables, the shear damages are proportional to the specific power input $\varepsilon = P/\rho V$ [P being the power dissipated by the stirring device (W), ρ being the fluid density (kg/m^3) and V being the volume of the agitated fluid (m^3)] (19). It is generally assumed that the microbial cells are exposed to shear effect when they are of a size approaching the Kolmogoroff microscale of turbulence λ_K. This scale can be directly calculated from the local specific power dissipation:

$$\lambda_K = \left(\frac{\varepsilon}{\upsilon^3}\right)^{-1/4} \tag{79.9}$$

where υ is the kinematic viscosity (m^2/s).

Hewitt and Nienow (61) have calculated that, for water-like media and for a specific power dissipation of 1 KW/kg, the Kolmogoroff microscale has a value of 30 μm, which is largely below the mean size of a bacterial cell (about 1 μm). This result suggests that, in most cases, the shear stress has no effect on the microbial cell. However, the picture is not the same if the power drawn by the impeller is increased in order to improve the mixing and the oxygen transfer efficiency of the bioreactor. Differences can also be noted for microorganisms other than bacteria and for which the average size can approach the critical size for shear damage (e.g. budding yeast and filamentous fungi). This effect is also enhanced in the case of a mechanical foam breaker designed to destroy the foam by shear effect. However, in this case the application of the Kolmogoroff equation (Eq. 79.9) is not straightforward, since the nature of the foaming medium is difficult to characterize.

On the other hand, the chemical antifoams also exhibit several problems as they can alter the microbial metabolism, reduce the oxygen transfer efficiency and compromise the downstream processing operation.

79.8.1 Impact of Foam Formation and Prevention on Microbial Growth

The direct and indirect effects of foam on the bioprocess have to be distinguished. Foam directly affects the process by removing the cells from the medium by flotation. In addition, foam indirectly affects the process performance by the elaboration of a foam suppression strategy. Indeed, the addition of chemical antifoam has an impact on the microbial growth process. The non-metabolizable antifoams, such as silicone oils and polyglycols, have little effect on microbial metabolism (11), although a noticeable exception occurs in the case of exopolysaccharides production with the addition of a polypropylene glycol antifoam (62). However, the process-related problems associated with the use of such antifoam agents (i.e. principally oxygen transfer limitation and membrane fouling as it will be explained in the next sections), has led to the consideration of natural oils as an alternative. In particular, the use of vegetable oils has been investigated (63). As the organic compounds contained in the oils (e.g. triglycerides and free fatty acids) can be used as a carbon source, the course of fermentation is altered when using

such products as antifoam agents. Their impact at the level of the metabolism depends on the microorganism cultivated and the composition of the oil: in certain cases, they can increase the cell mass yield because they are incorporated as carbon sources (63), and in other cases they can induce toxic effects related to the release of specific fatty acids (11). A major disadvantage related to the use of natural oils as antifoam agents is their relatively low efficiency when compared to their synthetic alternatives. In addition, the natural oil has to be added continuously during the culture as it is metabolized by the microorganism. Vardar-Sukan (63) has made a comparison of the efficiency of several natural oils (castor, corn, cotton seed, linseed, olive, sesame, soybean, and sunflower) and has found large variations in their efficiency which is a function of the composition of the culture media, suggesting that the use of natural oils must be carefully tested before being applied to large-scale bioprocess.

79.8.2 Impact of Foam Formation and Prevention on Bioreactor Performances and Scale-Up

The use of chemical antifoam is known to reduce the oxygen transfer efficiency and in general, the gas–liquid dispersion performance of the reactor. Indeed, the adsorption of antifoam molecules at the gas–liquid interface induces a resistance to oxygen diffusion. In addition to this surface effect, antifoam addition has a bulk effect interfering with the mixing mechanism and leading to reduced gas–liquid dispersion, larger bubbles and reduced gas hold up and interfacial area (64). As mentioned before (section 2), many surface-active agents are added as emulsions of suspended oil droplets in order to break the foam structure by formation of hydrophobic bridges and displacement of proteins at the interface. However, these conditions induce, at the same time, the coalescence of air bubbles in the bulk of the reactor (65). This adverse effect is enhanced at higher aeration rates, leading to problems when the aeration process has to be scaled up (3). This effect has been investigated and confirmed on 55 and 770 L external loop airlift bioreactors with the addition of silicone-based antifoams (65) and on bubble column bioreactors (66). During the culture of plant cells, a significant decrease of K_La (see Eq. 79.2) has been observed in laboratory bubble column reactors and stirred tank reactors when little quantities (as low as 20 ppm) of polypropylene glycol and Pluronic PE6100 were added to the culture to control foam (67).

79.8.3 Impact of Foam Formation and Prevention on the Downstream Processing Operation

In general, the addition of antifoam during the culture leads to several problems at the level of recovery procedures. The addition of antifoam modifies the suspension capabilities of the cells, leading to problems during centrifugation and induces fouling of the micro and ultra filtration membranes (68,69). Considering their surface-active properties, antifoams tend to stay at the interface, increasing their tendency to accumulate onto the membrane surface or pore walls. The antifoam polymers can easily spread on this surface, inducing the formation of a gel layer which causes fouling of the membrane. From a physicochemical standpoint, several mechanisms are involved in membrane fouling by antifoams, for example, hydrophobic interactions between emulsified antifoam and the membrane, cloud point effects of polyglycols, and formation of a gel layer at the surface of the filtration membrane (70,71). The prevalence of one of these mechanisms over the others depends on the nature of the filtration surface and the antifoam used. Pretreatment of polysulfone membrane surfaces has been proposed in order to reduce the fouling effect (72). The treatment of the membrane with a wetting agent tends to decrease the hydrophobicity of the surface of the membrane. The hydrophylisation of the membrane can be achieved by chemical modification of the surface charge or by physical precoat of the membrane.

On the other hand, in some specific cases, the foaming behavior of the broth can be exploited to perform a downstream processing operation. Indeed, proteins of interest can be recovered by foam fractionation (73). Specific methods for the direct purification of biosurfactants based on foam generation from the culture media have also been proposed (74,75). Along the same lines, the process of foam separation has been applied to separate microbial cells from the fermented medium in order to reduce the costs associated with centrifugation (76).

79.9 FOAM IN BIOTECHNOLOGICAL PROCESSES: PRESENT KNOWLEDGE AND FUTURE PROSPECTS

It is clear that foam formation in bioreactors is a complex physicobiochemical phenomenon that may induce a huge amount of technological problems. Foam prevention in biotechnological processes requires a thorough understanding of the microscopic, as well as the macroscopic, mechanisms involved in foam generation. The microscopic mechanisms are based on the molecular interactions of the surfactant with the gas–liquid interfaces. The picture is more complicated in the presence of microorganisms since the biomass leads to a modification of the nature of the broth and subsequently to substrate consumption and the release of metabolites; some efforts must be allocated to the investigation of the effect of the biophase on evolution of foaminess of the broth. The latter is of particular importance to better understand the impact of addition of

chemical antifoam on the course of the bioprocess. Indeed, silicone-based antifoams are actually the best alternative for an effective antifoam strategy, but in several cases they cannot be used due to biological constraints (toxic effect on the microorganisms, reduction of the oxygen transfer efficiency, etc.). At this stage, some efforts remain to be made at the level of antifoam formulation in order to increase their efficiency along with low adverse effects on the culture. On the other hand, the macroscopic mechanisms are related to the gas–liquid hydrodynamics of the bioreactor. It has been shown that bioreactor hydrodynamics (e.g. by the inclusion of a SAFD strategy) and/or operational parameters can be adjusted in order to reduce the generation of foam. However, these changes can only be performed on a limited range, since they directly affect the transfer performances (i.e. oxygen transfer, heat transfer and homogenization efficiency) of the bioreactor. A lot of experimental methods are available to study the gas–liquid dispersion in the bulk of the reactor (e.g. local gas hold up and K_La measurements), but only few are available to make similar observations at the level of the gas–liquid dispersion below the liquid free surface. It is important to have some techniques to better characterize the foam generated in the bioreactor, and not simply consider the level of foam. At present, they are several techniques that can be used at the laboratory scale to measure the liquid content of the foam. This principle has been adapted at the level of the bioreactor by a specially-designed probe for the online monitoring of foam characteristics during a bioprocess (i.e. the foam level, as well as the foam stability at different levels of the foam column in the headspace of the reactor). This kind of probe will be very useful in the future for the control of addition of antifoam and will allow the combination of chemically-based antifoam strategy (microscopic mechanisms) with those based on the knowledge of gas–liquid efficiency of the reactor (macroscopic mechanisms) such as adjustment of the air flow rate and/or stirrer speed.

In conclusion, at this point in time, foam still poses a serious threat to biotechnological applications, but a reasoned application of antifoam strategy along with a precise characterization of foam properties and integration of biological constraints associated with the process, would lead to better control over this problem.

REFERENCES

1. Prins A, van't Riet K. Trends Biotechnol 1987; 5: 296–301.
2. Junker B. Biotechnol Prog 2007; 23: 767–784.
3. Schügerl K. Process Biochem 1985; 20: 122–123.
4. Ling H, Enfors SO, Häggström L. Bioprocess Biosyst Eng 2003; 25: 205–212.
5. Razafindralambo H, Paquot M, Baniel A, Popineau Y, Hbid C, Jacques P, Thonart P. J Am Oil Chem Soc 1996; 73: 149–151.
6. Noble I, Collins M, Porter N, Varley J. Biotechnol Bioeng 1994; 44: 801–807.
7. Lin SC. J Chem Technol Biotechnol 1996; 66: 109–120.
8. Healy MG, Devine CM, Murphy R. Resour Conserv Recy 1996; 18: 41–57.
9. Guez JS, Müller C, Danze PM, Büchs J, Jacques P. J Biotechnol 2008; 134: 121–126.
10. Ghildyal NP, Lonsane BK, Karanth NG. Adv Appl Microbiol 1988; 33: 173–222.
11. Hall MJ, Dickinson SD, Pritchard R, Evans JI. Prog Ind Microbiol 1971; 12: 171–231.
12. Dukhin SS, Kretzschmar G, Miller R. Dynamics of adsorption at liquid interfaces: theory, experiment, application. Amsterdam: Elsevier; 1995.
13. Malysa K, Lukenheimer K. Curr Opin Colloid Interface Sci 2008; 13: 150–162.
14. Guitian J, Joseph D. Int J Multiphase Flow 1998; 24: 1–16.
15. Perry RH, Green DW, editors. Perry's chemical engineers' handbook. New York: McGraw-Hill; 1997.
16. Van't Riet K, Tramper J. Basic bioreactor design. New York: Marcel Dekker; 1991.
17. Van't Riet K, van Sonsbeek HM. In: Ladisch MR, Bose A, editors. Harnessing biotechnology for the 21st century. Washington (DC): American Chemical Society; 1992. pp. 189–192.
18. Flores-Cotera LB, Garcia-Salas S. J Biotechnol 2005; 116: 387–396.
19. Nienow AW. Appl Mech Rev 1998; 51: 3–32.
20. Hoeks FWJMM, Van Wees-Tangerman C, Gasser K, Mommers HM, Schmid S, Luyben KCAM. Can J Chem Eng 1997; 75: 1018–1029.
21. Bumbullis W, Schügerl K. Eur J Appl Microbiol Biotechnol 1981; 11: 106–109.
22. Bikerman JJ. Trans Faraday Soc 1938; 34: 634–638.
23. Baniel A, Fains A, Popineau Y. J Food Sci 1997; 62: 377–381.
24. Varley J, Brown AK, Boyd JWR, Dodd PW, Gallagher S. Biochem Eng J 2004; 20: 61–72.
25. Etoc A, Delvigne F, Lecomte JP, Thonart P. Appl Biochem Biotechnol 2006; 129–132: 392–404.
26. Brown AK, Gallagher CI, Dodd PW, Varley J. Trans IChemE 2001; 79: 114–121.
27. Wasan DT, Christiano SP. Foams and antifoams: a thin film approach. In: Birdi KS, editor. Handbook of surface and colloid chemistry. New York: CRC Press; 1997.
28. Garret PR. The mode of action of antifoams. In: Garrett PR, editor. Defoaming: theory and industrial applications. New York: Marcel Dekker; 1993.
29. Kulkarni RD, Goddart ED, Chandar P. Science and technology of silicone antifoam. In: Prud'homme RK, Khan SA, editors. Foams: theory, measurements and applications. New York: Marcel Dekker; 1996.
30. Owen MJ. Defoamers. Kirk-othmer encyclopedia of chemical technology: John Wiley & Sons.
31. Höfer R, Jost F, Schwuger MJ, Scharf R, Geke J, Kresse J, Lingmann H, Veitenhansl R, Erwied W. Foams and foam control. Ullmann's encyclopedia of Industrial Chemistry: Wiley.
32. Marinova K, Denkov N, Tcholakova S, Deruelle M. Langmuir 2002; 18: 8761–8769.

33. Marinova K, Denkov N, Branlard P, Giraud Y, Deruelle M. Langmuir 2002; 18: 3399–3403.
34. Nora A, Szczepanek A, Koenen G. Metallic soaps. Ullmann's encyclopedia of industrial chemistry: Wiley.
35. Joshi K, Jeelani S, Bicenstorfer C, Naegeli C, Oliviero C, Windhab E. Langmuir 2006; 22: 6893–6904.
36. Calik P, Ileri N, Erdinc B. Langmuir 2005; 21: 8613–8619.
37. Denkov ND, Tcholakova S, Marinova K, Hadjiiski A. Langmuir 2002; 18: 5810–5817.
38. Arnaudov L, Denkov N, Surcheva I, Durbut P, Broze G, Mehreteab A. Langmuir 2001; 17: 6999–7010.
39. Denkov ND. Langmuir 2004; 20: 9463–9505.
40. Mata S, Joseph DD. Int J Multiphase Flow 1999; 25: 63–85.
41. Denkov N, Cooper P, Martin J-Y. Langmuir 1999; 15: 8514–8529.
42. Denkov N. Langmuir 1999; 15: 8530–8542.
43. Moretto H-H, Schulze M, Wagner G. Silicones. Ullmann's encyclopedia of industrial chemistry: Wiley.
44. Owen MJ. Siloxane surface-activity. Adv Chem Ser 1990; 224: 705–739.
45. Heusch R. Emulsion. Ullmann's encyclopedia of industrial chemistry: Wiley.
46. Tonge L. EP patent 663225B1. 1994.
47. Keil J. US patent 3984347A. 1974.
48. Koczo K. EP patent EP879628B1. 1998.
49. Ziemelis M. EP patent EP339958B1. 1989.
50. Kolaitis L. US patent US5668101A. 1994.
51. Yasukawa M, Onodera M, Yamagiwa K, Ohkawa A. Biotechnol Bioeng 1991; 38: 629–636.
52. Deshpande NS, Barigou M. J Chem Technol Biotechnol 1999; 79: 979–987.
53. Takesono S, Onodera M, Nagai J, Yamagiwa K, Mori A, Ohkawa A. J Ferment Bioeng 1993; 75: 314–318.
54. Takesono S, Onodera M, Yamagiwa K, Mori A, Ohkawa A. J Ferment Bioeng 1994; 77: 221–223.
55. Takesono S, Onodera M, Yoshida M, Yamagiwa K, Ohkawa A. J Chem Technol Biotechnol 2002; 78: 48–55.
56. Stocks SM, Cookeb M, Heggs PJ. Chem Eng Sci 2005; 60: 2231–2238.
57. Boon LA, Hoeks FWJMM, van der Lans RGJM, Bujalski W, Nienow AW. Can J Chem Eng 2000; 78: 884–891.
58. Boon LA, Hoeks FWJMM, van der Lans RGJM, Bujalski W, Wolff MO, Nienow AW. Biochem Eng J 2002; 10: 183–195.
59. Malysa K. Adv Colloid Interface Sci 1992; 40: 37–83.
60. Malysa K, Warszinsky P. Adv Colloid Interface Sci 1995; 56: 105–139.
61. Hewitt CJ, Nienow AW. The scale-up of microbial batch and fed-batch fermentation processes. Adv Appl Microbiol 2007; 62: 105–135.
62. Stasinopoulos SJ, Seviour RJ, Auer DF. Lett Appl Microbiol 1988; 8: 91–93.
63. Vardar-Sukan F. Biotechnol Adv 1998; 16: 913–948.
64. Al-Masry WA, Dukkan AR. Chem Eng J 1997; 65: 263–271.
65. Al-Masry WA. Chem Eng Process 1999; 38: 197–201.
66. Al-Masry WA, Ali EM, Aqeel YM. Chem Eng Sci 2006; 61: 3610–3622.
67. Wongsamuth R, Doran PM. Biotechnol Bioeng 1994; 44: 481–488.
68. Mc Gregor WC, Weaver JF, Tansey SP. Biotechnol Bioeng 1988; 31: 385–389.
69. Cabral JMS, Casale B, Cooney CL. Biotechnol Lett 1985; 7: 749–752.
70. Liew MKH, Fane AG, Rogers PL. Biotechnol Bioeng 1997; 56: 90–98.
71. Penticoff A. Fluid/Part Sep J 1990; 3: 145–147.
72. Yamagiwa K, Kobayashi H, Onodera M, Ohkawa A. Biotechnol Bioeng 1994; 43: 301–308.
73. Brown AK, Kaul A, Varley J. Biotechnol Bioeng 1999; 62: 278–290.
74. Georgiou G, Lin SC, Sharma MM. Biotechnology 1992; 10: 60–65.
75. Chai J, Loha V, Prokop A, Tanner RD. J Agric Food Chem 1998; 46: 2868–2872.
76. Parthasarathy S, Das TR, Kumar R, Gopalakrishnan KS. Biotechnol Bioeng 1988; 32: 174–183.

FURTHER READING

See also Chapter 31 in volume 1.

80

PILOT PLANTS, DESIGN AND OPERATION

Beth H. Junker
Bioprocess R&D, Merck Research Laboratories, Rahway, New Jersey

80.1 INTRODUCTION

Several diverse roles, objectives, and purposes are associated with a bioprocessing, biochemical, or biopharmaceutical pilot plant. These include, but are not limited to, the manufacture of early- and late-phase clinical supplies, process development (including process characterization, validation, and comparability (1)) for new products in the company pipeline, process improvement including technical support for existing products in the market, and production of biologically produced materials (which are not intended for the clinic) to support basic research efforts such as screening, assays, and disease mechanism elucidation. Despite desires to design pilot facilities for diverse differences in scale, products, processes, clinical phases, and capacity, limited capital and operating budgets force value engineering decisions about "must have" and "nice to have" capabilities (2). Unlike chemical pilot plants, pharmaceutical pilot plants are used not only to scale-up laboratory processes, but also to produce developmental quantities of chemicals (and biological substances) for safety, toxicological, and clinical studies (3). Thus, balancing of the demands for scale-up and development research with those for clinical production is a key dilemma for pilot plant operation (4). This tension has resulted in an increased recent attention to the development of scale-down models to mimic larger scale performance and thus reduce demands for pilot scale process development runs (5). Another challenge is to determine what proportion of the material requirements for each phase of a product's development has to be outsourced to contract manufacturing organizations (CMOs). Some CMOs are even targeting clinical-scale production clients, essentially building pilot plants for hire (6). The timing and reliability of clinical material production is critical as expensive and time-consuming clinical programs can be delayed, thus postponing product application filings, approvals, and launches (7). Although traditionally pilot plants have not manufactured material for sale, accelerated launch dates, deferred manufacturing facility capital commitments, and other areas of project uncertainty have prompted consideration and use of pilot plants for manufacturing in recent years. In addition, rising fermentation titers, isolation yields, and overall process streamlining has expanded the capabilities of smaller sized facilities to satisfy larger kilogram material demands (5).

The types of products manufactured using biologically based methodologies include primary metabolites, secondary metabolites (ranging from pharmaceuticals to biopolymers), constitutive proteins, recombinant proteins, intracellular/extracellular enzymes and biocatalysts, antigens, viruses, polysaccharides, and plasmid DNA itself. These products are made using a wide range of cell cultivation and isolation techniques suitable for bacteria, yeast, fungi, actinomycetes, suspension animal cells, anchorage dependent animal cells, insect cells, and plant cells. Processing equipment considerably varies among these diverse systems.

Designing for extensive processing flexibility can be expensive, potentially in excess of $100 million, depending on the specific process requirements, size, and intended use of the pilot plant. In addition, processing requirements can change drastically as products are de-emphasized

Upstream Industrial Biotechnology: Equipment, Process Design, Sensing, Control, and cGMP Operations, Volume 2, First Edition. Edited by Michael C. Flickinger.
© 2013 John Wiley & Sons, Inc. Published 2013 by John Wiley & Sons, Inc.

and re-emphasized in development. These decisions on priorities often are not usually caused by process robustness but rather by the state of the clinical data or potential market share. The ability to process multiple products in an acceptable manner is typically desirable to maximize facility use. Although designers may need to predict future types of processes and products, they should be cautious about over designing the facility in terms of containment and flexibility (8). Designing for future expansion with minimal disruption to operations can help in reducing initial capital expenditures (9).

The general areas required in a pilot plant might include support labs for bench scale development and quality control, production suites for scale-up, utility areas, personnel offices, as well as ample storage areas for raw materials, supplies, product, samples, and documentation (4). There should be a clear division between controlled and noncontrolled areas utilizing signs at a minimum and perhaps by physically restricting access. General design criteria might focus on modularity, simplicity, future growth provisions, redundancy, construction costs, operating costs, and air/water waste containment (10). Future operating costs are important considerations for pilot plants as ample funds are necessary for raw materials, staffing, maintenance, and additional capital modifications to permit improvements.

80.2 OPERATIONAL CONCEPTS AND PROCESSING REQUIREMENTS

Several operational concepts influencing design requirements need to be agreed upon prior to the initiation of design activities. Agreement should be sought among end users, operations staff, compliance auditors, environmental consultants, safety officers, as well as appropriate levels of management who are directly or indirectly influencing or controlling capital expenditures. A written document summarizing consensus on these issues may then become the basis for conceptual design activities.

Major decisions influencing pilot plant capabilities include whether the facility will produce bulk drugs (thus falling under the regulation of Center for Drug Evaluation and Research (CDER) and following guidelines from 21CFR 210/211) or biologics (thus falling under the regulation of Center for Biologics Evaluation and Research (CBER) and following guidelines from 21CFR 210/211 and 600) (11). The level of validation and the validation philosophy are directly related to the end use of the resulting pilot plant products, specifically whether they are used for process development, clinical supplies (presafety/basic research, safety, phase I, phase IIa, IIB, phase III), or material for sale. Validation strategies, as well as other operational and design issues, are also influenced by whether the pilot plant is administratively located within the manufacturing or research division. Individual company preferences and guidelines for similarity between manufacturing and pilot plant areas need to be identified and evaluated for their impact on the proposed pilot plant facility. Typical areas targeted for standardization within a company might include vessel designs, computer systems and interfaces, equipment vendors, and construction specifications.

Design requirements center on the desired initial and end product stages of processing, specifically the forms of the pilot plant inputs and outputs, as well as in-process hold steps. Example stages include master/working seed preparation, fermentation broth, initial captured product (e.g. microfiltration retentate, ultrafiltration concentrate, cell paste), crude product (e.g. rich ion-exchange fraction), finished isolated/sterile bulk, and filled vials. Ambient, refrigerated, and frozen storage requirements based on these inputs/outputs then need to be addressed in the areas of seed, raw materials, intermediates, clinical supplies, and process samples.

The scale of the pilot plant relative to current or proposed manufacturing scale and relative to laboratory scale needs to be established. Generally, a 1:5 or 1:10 scale-up is common (1), but smaller ratios can be advantageous in terms of minimizing risk during factory start-up. The appropriate level of biosafety also must be considered with GLSP being sufficient for most recombinant work. Some pilot plant areas may require BL1-LS and/or BL2-LS, and careful consideration of multiple use/decon issues for BL1 and BL2 containing facilities is necessary. Solvent-use areas need to be identified and minimized if possible as cost implications for explosion proof design can be substantial.

Primary motivations to design a multiuse pilot plant are the conservation of capital and improved response time for clinical manufacturing requirements for new product development. The strategy for multiuse should be identified and considered throughout the design process. Common strategies (12) include (i) using totally dedicated equipment and limiting production to one product at one particular production stage, (ii) using campaigned equipment in which multiple products are sequentially processed in the same equipment "campaign style," with documented product changeover procedures completed to minimize cross-contamination potential, and (iii) conducting concurrent manufacturing in dedicated equipment in which several products are simultaneously produced in segregated areas with segregation achieved via physical separation or closed systems. These strategies result in the minimization of cross-contamination potential through engineering controls, SOPs, and/or temporal segregation (13). Typical pilot plants combine the second and third strategies by providing segregated and dedicated areas for certain types of processing (e.g. virus and nonvirus

areas, GLSP versus BL1/BL2 areas, beta-lactam antibiotic processing, heat-resistant spore former cultivation) (14), and maintaining flexible areas that can be reconfigured efficiently to suit their multiproduct portfolio needs. Example layouts for product-specific and common areas depending upon the strategy selected have been described (15).

To increase the speed and number of products entering clinical trials, platform processes are becoming increasingly more common to achieve high throughput for early-phase products, avoiding large amounts of individualized process development effort. Platform processes are based on classes of products with similar processing requirements and/or properties. Less optimized processes (e.g., lower yields, longer cycle times, higher cost) are accepted for early material deliveries (i.e. prior to Phase IIB) in exchange for reduced resource requirements. A platform for cell cultivation for monoclonal antibody production has been developed by IDEC based on their own in-house medium and feed formulations (16). In addition, a platform for monoclonal antibody downstream processing based on Protein A capture has been described by Amgen in which a flexible, generic process is used, which predefines most operating parameters and requires only a small subset of other operating parameters to be defined via product-specific process development (17–19).

Guidelines concerning the use of open versus closed systems for various processing stages need to be devised and justified based on available and cost-effective technologies as well as quality requirements. In a closed system, the product is not exposed to the immediate environment. The quality of materials entering a closed system (such as water, steam, and air entering a bioreactor) is controlled by its quality as well as the manner in which these materials are entering the closed system (such as filter sterilization, autoclaving, and/or steam sterilization of system connections) (12). In an open system, the product is directly exposed to the surrounding environment, thus necessitating the creation of a controlled or sometimes even a closed system around the open system. One example of this latter strategy is the transfer of seed vial contents in a biosafety cabinet. Other examples might include the supply of higher quality filtered area to areas for the cool down of autoclaved materials and assembly of clean equipment. Thus, levels of containment can be constructed until all open systems are contained within controlled or closed systems to meet quality requirements for the specific processing stage.

The specific issue of potential exposure of product to spore-forming organisms has been extensively debated. The closed system concept appears to minimize the concern for airborne spores that are typically found in the environment. Cultivation guidelines for spore-forming organisms within a multiuse facility appear to have been redefined to evaluate the robustness of the spore type formed. The careful consideration of segregation has been given when cultivating organisms that form spores that are difficult to be killed, such as *Bacillus*. A separate, self-contained area with no shared equipment, air systems, or entrances minimizes exposure concerns for other products. The relatively heat-sensitive, substantially larger, fungal spores have not been highlighted as a substantial cross-contamination concern. Thus, segregation of these types of processes is not as critical, though it still might be implemented due to company preferences for separate bulk drug and biologics processing areas.

80.3 DESIGN

The initial generation of flow charts for a bioprocessing, fermentation, and/or isolation pilot plant is best conducted based on model processes that are developed and critiqued by several end users of the equipment and facility. These model processes are carefully selected so that they give adequate and appropriate representation to current and reasonable future needs of the pilot plant. Specifically, current and future projections for fermentation titers should be modeled to establish the potential operating range for downstream steps. Because model processes form a preliminary but sound basis for equipment and utility sizing, they should include specific unit operations, equipment scales, and expected cycle times. In some cases, simulation (17,20–23) and/or actual laboratory/pilot scale testing (24) of critical equipment under typical processing conditions or with expected process streams may be warranted to further define design specifications. Time and effort expended to identify and change the design on paper is more efficient (i.e. causing fewer delays) and less expensive than modifications during construction or after start-up (25,26). The proper level of criticality must be assigned to each system; attention to too many critical systems results in unnecessary expenses and too few critical systems results in design changes, delivery delays, and validation challenges (25). Example model processes and throughput evaluations have been published for vaccines, antibodies, and other intracellular/extracellular products (26–31). Resulting flow charts can focus on raw materials for fermentation/isolation, seed development, fermentation, recovery, crude product isolation, final product isolation, product finishing, buffers, utilities, and waste (including chemical waste, biological waste and any necessary off-gas treatment) (27).

The requirements for these model processes, coupled with an estimate of the required facility output, can be used to construct a preliminary architectural layout that divides the facility into sections (commonly termed as *modules, cubes, or suites*). These sections are surrounded by controlled corridors and accessed via airlocks (8). On the basis of this initial layout, flow patterns are developed to permit the logical, usually unidirectional, flow of personnel,

raw materials, product, waste, and clean/used equipment throughout the facility. Flows are primarily designed to minimize cross contamination from multiple products and from used equipment while maintaining access and flexibility (8). This separation is often accomplished using clean and return corridors located on either side of the processing area as well as via temporal segregation using appropriate SOPs. Evaluation of these flow patterns should be conducted carefully and incorporate end users as well as quality auditors. In some cases, companies may solicit outside GMP reviews of the project at this time from external consultants, a second design firm, or even FDA representatives. Gathering and organizing up-to-date, accurate information and comments about the design's impact on model process requirements are critical factors in forming a successful basis of design (32).

Example layouts for process flows for biotech facilities have been published (6,12,33,34). An extensive reference (including piping and instrument diagrams (P&IDs), layouts, and flow diagrams) for the design of biopharmaceutical plant equipment, utilities, heating, ventilation, and airconditioning (HVAC), and waste treatment also has been published (35). Although it was based on acceptable practices in 1991, the strategies and concepts for design presented are still relevant. Adequate space around the equipment needs to be reserved for operations and maintenance access as well as for process-related portable equipment. Specifically, the movement, segregation, storage, and cleaning of portable equipment such as vessels, skids, hoses and carts should be fully examined.

Various reports of successful and problematic aspects of facility design, construction, start-up, and validation have been published. Often, cost estimation for pilot plants is more difficult than that for manufacturing plants owing to incomplete understanding of processes, equipment, and technology (36). Pressure to meet initial schedules and budgets can result in higher initial and subsequent costs, particularly for retrofitting projects. Cost control issues and the benefits of formulating a master schedule (37) need to be reviewed in terms of their potential validation impact. Construction concerns and "lessons learned" from multiple biotech installations also have been summarized (38). One case study of a laboratory facility highlights the need for teamwork among the client, design firm, and construction manager (39). This trio can be extended to include validation contractor in an effort to minimize "finger pointing" and "blame storming" when unforeseen problems are uncovered. Regardless of who may actually be perceived as being "at fault," the company owning the facility ultimately is adversely affected by substantial start-up and validation delays. A comprehensive overview of biochemical pilot plant design and operational guidelines appeared in the mid-1980s (40). A more recent review focuses on best practices for design and operation to reduce bioreactor contamination, a key type of abnormality typically resulting in batch termination (41).

80.3.1 Process Equipment

For a pilot plant, the major decision regarding process equipment is that of similarity versus diversity as it applies to multiple process steps as well as multiple products. The extent of commonality required in equipment specifications is an important operational factor to be considered, as equipment specifications are devised based on the inputs from model processes. For a pilot plant to accept a manufacturing interface role, at least a portion of the equipment (and automation) design and selection should be representative of the factory that the pilot plant is intended to support (1). For example, if the factory is intending to use continuously sterilized medium for large scale fermentation, then there should be provisions in the pilot plant to perform continuous sterilization as products get closer to their transfer to production. Alternatively, depending on individual company preferences for the pilot plant role, later clinical batches (Phase IIB and beyond) might be manufactured in the factory to facilitate eventual process transfer upon commercialization and ensure consistency of equipment.

Skid-mounted or packaged equipment is a common selection in recent pilot plant installations because it puts the design, delivery, and start-up burden entirely on one vendor (25), who specifies the appropriate quality, supply rate, and/or pressure of the required utilities (e.g. steam, cooling water, instrument air). Skid-mounted equipment can be fixed or portable, the latter permitting different types of processing to occur in the same space as necessary. Several skid-mounted unit operations can be mounted together to create "super skids," further streamlining construction, start-up and validation, and placing even more responsibility on the vendor (9). Customization of skid designs with respect to components and spare parts may be a drawback as vendors might not be willing to build skids to individual company specifications without added costs. This situation can be particularly problematic if the skid manufacturer has arranged a low cost deal with a vendor (e.g. diaphragm valves) or developed a programmed software on a PLC that may not be the vendor of choice for the rest of the facility. There also may be incompatibilities in piping, utility requirements, or software when the skid is connected (42) if miscommunications occurred between the skid vendor and the facility designer. Typically, a team, consisting of representatives from the vendor, facility owner, facility user, validator, procurement, engineering/construction management firms, and facility maintenance organization, is assembled.

The traditional alternative to skid-mounted designs is to request the facility designer to purchase the equipment

components separately and assemble the piping and equipment on site (25). One advantage to this "stick build" approach is that total flexibility in equipment selection now rests with the pilot plant designers who may be quite confident in their ability to design the equipment based on their extensive prior experience. Drawbacks of this approach include placement of the design burden on the facility as well as added design costs for one-of-a-kind systems. Specific references for fermentation equipment flow charts, detailed design, and qualification are available (43–46) as well as for filtration units (47), chromatographic equipment (33,48–50) and centrifuges (51,52). A list of typical process, utility and support equipment that might be required in a bioprocessing pilot plant has been compiled (Table 80.1).

A third alternative for pilot plants is the use of disposable, single-use equipment now available for solution preparation and storage, bioreactors, filtration, and chromatography (53,54). Several authors describe how disposables reduce fixed capital costs (often at the expense of variable operating costs), operational effort (recleaning and often sterilization are not needed which decreases turnaround time and effort) as well as space and utility requirements (2,53,55–57). Specific analysis tools for stainless versus disposable equipment selection for clinical material preparation based on manufacturing strategy have been developed (58,59). In fact, one company has designed a biopharmaceutical pilot plant based on disposable systems to maximize flexibility and speed of cell line process development and early-phase clinical material supply (60).

For any type of bioprocessing facility, certain aspects of equipment and piping specifications should be uniform throughout the installation where possible; this goal is particularly challenging for a pilot plant containing a large variety of equipment from multiple vendors. These specifications might include requirements for orbital welding of lines, documented weld inspections, passivation, pressure testing, self draining (sloped) piping, minimal lengths for dead legs and pockets, restricted use of flanged connections, level of polish on product-contact surfaces, stainless steel quality (typically 316 L for product-contact surfaces) and use of FDA-approved polymers in specific applications (gasket, o-rings, valve seats, and distribution piping) (61). Proper storage of fabricated piping awaiting installation as well as prominent identification of valves and lines also

TABLE 80.1. Types of Processing Equipment and Utilities Possibly Required for a Bioprocessing Pilot Plant

Fermentation and Harvest	Isolation	Utilities	Support
Culture storage freezer	Low pressure chromatography	Clean steam generator	Sterilizing autoclave
Incubator/shaker	High pressure chromatography	USP-purified water system	Decontamination autoclave
Biosafety cabinet	Membrane chromatrograhy	WFI system	Depyrogenation oven
Laminar flow hood	Solvent blending and delivery	Deionized water	Laminar flow hoods for cool down and equip. assembly
Seed fermenter	Viral filter	Process (city) water	Glasswasher (glassware, vial, stopper)
Production fermenter	Sterile filter	Compressed clean air	Buffer preparation tank
Nutrient feed tank	Laminar flow hood	Compressed instrument air	Media preparation tank
Harvest tank	Liquid transfer pumps	Compressed plant air	In-line mixer
Microfilter	Dispensing machines	Compressed gases (O_2, N_2, CO_2, NH_3)	In-process sample refrigerator/freezer
Ultrafilter	Chemical fume hood	Electricity	Raw material cold/frozen storage
Centrifuge	Portable tanks	Chilled water	Floor and bench scale
Depth filter	Laboratory scale centrifuge	Cooling tower water	Process and equipment monitoring/alarm system
Expanded bed absorption	Ultrafilter/ultracentrifuge	Plant steam	Uninterrupted power source (UPS)
Homogenizer	In-process refrigerator/cold room/freezer	Glycol	Off-gas analyzer (mass spectrometer)
Continuous sterilizer	Product refrigerator/freezer	HVAC and building automation system	Bar code system
Filter integrity tester	Syringe/vial filling equipment	CIP skid	
Sterile tubing welder	Lyophilizer	Biowaste inactivation system	
		Environmentally potent chemical destruction system	
		Dust collection system	

must be considered. Valve specifications can be important to determine early in the design cost estimation phase (62). Valve capital cost contribution is high due to the large numbers required and any installed valves (either diaphragm or ball) require subsequent maintenance. Consideration should be given as to whether live steam, set up as a steam block, should be used to continually purge the back side of product-contact valves and/or whether live steam should be used for tracing between double o-rings on a port or manway (43). Although such designs traditionally have increased sterility assurance for lengthy secondary metabolite fermentations, they may create detrimental localized hot spots during animal cell cultivations conducted in the same pilot plant fermenters. Neither the equipment itself nor its disposable/replaceable parts should release any extractable substances (after the initial postinstallation rinsing and cleaning steps) into the product (43). An overview of sanitary piping design, installation, and validation concerns is available (63).

Transfer piping strategy is another major design decision. One common strategy for several transfer lines is to meet at a transfer panel or process manifold, typically located at a high point between two or more areas, and be connected using spool or "jumper" pieces to move material in the desired fashion (8). Steam entry is at the high point and condensate drainage at the low point for steam-in-place (SIP) during sterile transfers. Clean-in place (CIP) solutions are passed along the direction of the previous transfer. Advantages of this approach include reduced piping distribution costs and space requirements (which can multiply fast when multiple tanks and multiple types of process transfers are required). Disadvantages center on operational restrictions concerning the elapsed time between successive transfers through a common manifold system, as well as cross contamination associated with transfers of nonsterile media/buffer, sterile media/buffer, inoculum, harvested broth, CIP solutions, and/or water through common lines. Ring headers with automated or multiport valves are one recent alternative design being introduced to avoid "jumper" connections (53). A listing of product and nonproduct transfer line/utility piping that might be required in a bioprocessing pilot plant has been compiled (Table 80.2).

Sterilization, sanitization, cleaning, and draining sequences need to be carefully defined and documented during the equipment and transfer piping specifications because retrofits postinstallation can be time consuming and expensive. P&IDs should be traced through these process sequences prior to approval by both operational and validation personnel. Requirements for validation testing and in-use monitoring of equipment operation also need to be identified during the equipment specification phase. Examples include sizing condensate lines to permit adequate drainage of condensate when spore strips are present, specification of additional validation ports for thermocouples on vessels and condensate lines, installation of product-contact utility sampling stations (especially at worst-case locations), and installation of temperature sensors on critical lines to monitor sterilization and/or proper trap operation.

TABLE 80.2. Transfer Lines and Utility Piping Possibly Required for a Bioprocessing Pilot Plant

Product Contact	Nonproduct Contact
Utilities	**Utilities**
Clean water	Chilled/cooling water and/or glycol
Clean air	Instrument/plant air
Clean steam	Plant steam
CIP solutions	Contained sewer
Other compressed gasses (CO_2, O_2, N_2, NH_3)	Chemical (noncontained) sewer
Process	Sanitary sewer
Sterilized medium or buffer	Vacuum system
Sterilized nutrient/acid/base/antifoam feeding	Natural gas
Nonsterilized medium or buffer	
Inoculum	
Harvest	

80.3.2 Utilities

Similar to any bioprocessing facility, product-contact utilities in a pilot plant might include water, clean steam, compressed air and other gases, and CIP systems. Nonproduct-contact utilities generally include chilled water, instrument air, plant steam and plant air, although for some products plant steam may be appropriate for product contact based on its quality (Table 80.3). A listing of product and nonproduct-contact utilities is compiled in Table 80.2. Multiple utility use points are located within and among suites for both product and nonproduct utilities. These are organized into utility stations for each equipment skid. To minimize piping, it might seem convenient to use product-contact utilities in nonproduct-contact applications

TABLE 80.3. Comparisons of Example Plant Steam and Clean Steam Achievable Quality

Quality Attribute	Clean Steam	Plant Steam
Bioburden	<0.1 cfu/mL	<0.1 cfu/mL
TOC	<0.5 ppm	<2.0 ppm
Endotoxin	<0.25 EU/mL	<0.5 EU/mL
pH	5–7	5–8
Conductivity	Meets USP 23 supplement 5 standards	N/A

such as compressed clean air on a vessel jacket, relying on a check valve for back flow prevention. This approach can risk disaster because the operation and quality of product-contact utilities can affect processing throughout the entire facility.

Peak utility loads should be based on carefully investigated assumptions for anticipated pilot plant processing portfolios, which are transferred from design directly to validation testing. Although it may be probable to operate several large fermenters simultaneously each at their maximum air flow rate, it may be less likely that several large fermenters will be cooled simultaneously after completion of sterilization. Thus, air compressors might be sized assuming maximum load, while process chillers might be sized based on an operationally realistic fractional load. Assumptions about processing cycle times and fermenter working volumes are important particularly when sizing CIP and liquid waste decontamination systems. Shorter (50 h) *Escherichia coli* fermentations might require a smaller tank volume (5000 L) but are run more frequently, compared with longer (400 h) animal cell or fungal fermentations, which might require a larger tank volume (20,000 L) but are run less often.

80.3.2.1 Product Contact. The most critical product-contact utility for a bioprocessing facility often is water due to the sheer volume required during typical processing steps. It is well known that the quality of water needs to be appropriate for the intended application, but higher than the necessary water quality often is designed and system capacities underestimated, particularly when actual pilot plant processing portfolios exceed the design basis. In many installations, purified water is utilized for upstream processes and early CIP steps, and WFI is reserved for cultures that are sensitive to endotoxin such as animal cells and for downstream isolation steps (64). A brief overview of various methods to produce pure water is available (65).

Water for injection (WFI) is often favored for the entire pilot plant facility for uniformity and to avoid mix-up. Specifications are set for parameters such as bioburden (typically 0.1 CFU/mL), endotoxin (typically 0.25 EU/mL), conductivity (1.3 μScm at 25°C), and total organic carbon (TOC) (<500 ppb). WFI systems containing stills are the most predominant and are generally designed as a hot 80°C loop (66). Recently, 65°C loops have been sanctioned to reduce cooling costs and to permit the use of thermostable plastics in construction (67,68). Point-of-use coolers provide water at a user-selected temperature. These coolers can form deadlegs and require substantial flushing prior to use, thus increasing waste water. It is also possible to design a cold or ambient WFI loop with periodic (typically daily) heating to 80°C or ozonization for sanitization purposes.

USP-purified water is an attractive alternative to WFI for various applications that do not require WFI. Specifications include bioburden (typically 100 CFU/mL), conductivity (1.3 μScm at 25°C), and TOC (<500 ppb) (69). Ion-exchange, distillation, and/or reverse osmosis (RO) systems are used (66). Although such systems can be operated hot or cold, success with ambient systems that are sanitized with ozone or chemically (70) has been reported. Examples of the design and validation of two ambient USP-purified water systems for pilot plant use are available (70,71).

Other noncompendial grades of water also may be utilized. In these cases, quality attributes are typically set by the facility to address the requirements of specific processing steps (Table 80.4). Examples might be deionized water with bioburden (<500 cfu/mL) and resistivity (>1 Mohm) specifications or process water (municipal water passing through a break tank) with TOC (<10 ppm) or particulate (≤ disk #1 standard) specifications. Using the lowest quality of water appropriate for the quality of the process step reduces operating costs, assuming running multiple water systems in the facility is acceptable (68).

General design elements for water systems include the desired flowrate at each use point and the expected number of simultaneous use points in operation. These values are combined to obtain the total "take-off" flow rate; the system and piping are then sized such that velocity of remaining flow rate is sufficient to minimize bioburden and biofilm growth. Suggested methods for obtaining this residual velocity have been outlined (72). Use point positioning should consider the height of the take-off valve, automation of take-off valves, sink or sewer location for flushing, as well as cleaning, sanitization, and acceptable noncoiled storage racks for associated use-point hoses. In addition, water systems should be designed with specific sanitization procedures identified at the outset. Steam, ozone, or chemical sanitization methods are most common, although steam

TABLE 80.4. Comparison of Example USP-Purified Water, Deionized Water, and Process Water Achievable Quality Attributes

Quality Attribute	USP-Purified Water	Deionized Water	Process (City) Water
Bioburden	<100 cfu/mL	<500 cfu/mL	<500 cfu/mL
Coliforms	Absent	Absent	Absent
TOC	<0.5 ppm	<2.5 ppm	<5 ppm
Endotoxin	<0.25 EU/mL (for info. only)	N/A	N/A
pH	5–7	5–8	5–8
Conductivity/resistivity	Meets USP 23 suppl. 5 standards	>1 Mohm	N/A

sanitization is generally not recommended for plastic loop systems due to concerns about distribution pipe sagging. Plastic systems utilizing PVDF instead of stainless steel are becoming more common and effective for achieving even WFI conditions. A direct comparison of plastic piping with stainless steel with respect to ion leaching, smoothness, and CFU counts has been made (73).

By using plant steam for supplying heat of vaporization, clean steam can be generated from a purified water feed. Increased heat exchanger fouling may occur if a controlled feed water supply is not utilized. Clean steam distribution piping is designed with regulators to reduce the pressure from 5 atm down to about 2–2.5 atm needed for typical SIP operations. Sanitary pressure gauges, placed near or on equipment skids, can assist in monitoring dynamic pressures during SIP cycles. Steam sampling stations generally encompass a removable sanitary trap to which a sample cooling device (typically a heat exchanger) is attached. Consequently, a source of cooling water is necessary, either piped from local lines or transported by gravity via a portable holding tank about 20 L in volume. Steam traps are placed in header branches and equipment supply lines such that when skid equipment is isolated for repair, condensate buildup does not occur. Most importantly, steam traps and pressure regulating/control valves should be selected and sized properly to remove excess condensate during SIP operation (74). Periodic cleaning of the clean steam system assists in cleaning fouled heat exchange surfaces and minimizing rouging.

Compressed air in product contact is generally used for fermentation sparger air supply, pressurized transfers, and other positive pressure requirements. Oil-free compressors are favored with intakes positioned away from other building effluents. Heating up to and holding at 200°F (93°C), typically accomplished by design of the compression ratio and residence time in a receiver, is desirable to minimize airborne biological contaminants such as bacteriophage, although there is some evidence that submicron (0.1 μ) filtration also can be effective (41). Humidity then can be reduced from the compressed air using refrigeration and/or desiccant dryers. Moisture removal is desirable down to a dew point of −40°C. Air then is microfiltered (0.2 μ) at the point of use to remove microbes/particulates. Compressed air may be sampled for any or all of the following depending on the application: identity, hydrocarbon level, microbial content, and particulates. Other gases may be required for the facility such as oxygen enrichment for microbial cells, carbon dioxide for pH control of bicarbonate-buffered animal cell media, nitrogen, and oxygen supplementation for animal/insect cells, along with appropriate gas blending and control systems. Planning should consider the storage of bottled gas cylinders or tanks outside the facility or in segregated maintenance areas to minimize the transport of unclean cylinders into controlled locations.

Clean-in-place (CIP) skids can be portable and moved into place in the suite at a designated utility location and/or one or more fixed supply skids can be located permanently in the utility area. CIP systems are composed of supply and return pumps, one or more cleaning agent dilution tanks, provisions for heating cleaning agents, and a PLC for sequence control and associated data acquisition. Specific aspects of CIP design guidelines, cleaning agents, and step sequences are documented (75). Owing to the tankage and pumps required (33), these skids often are located in utility areas where acid/caustic-based cleaning agents arriving in drums can be suitably diluted. More than one CIP skid may be necessary to provide product segregation and minimize cross contamination. Multiple skid requirements depend on design decisions concerning the level of containment and product segregation (8), as well as capacity.

80.3.2.2 Nonproduct Contact. The type of vessel jacket cooling/heating system selected, although not in product contact, has widespread design implications, and ultimately may limit pilot plant fermenter versatility. Recirculating temperature control loops, containing high surface area/unit volume heating and cooling heat exchangers, an expansion tank, and a circulation pump, are common. These systems rely on indirect heating/cooling of jacket fluid so that their response can be slow, particularly if heat exchangers were not sized according to user expectations. The involvement of heat exchangers suggests that practical application may be limited to vessels of few thousand liters in size. Jacket fluids can be water, glycol, or novel fluids with wide temperature ranges. Reliable operation of the circulation pump and internal (as well as external) integrity of the heat exchangers are also critical. Cooling heat exchangers can use either chilled water and/or glycol, while heating heat exchangers generally use plant steam. Dual parallel filter housings, containing 10–50 μm elements, are advantageous to reduce cooling heat exchanger fouling. Sediment buildup on filters can be monitored using measured pressure differentials across the filters, and the assembly can be designed so that one filter set may be replaced while maintaining flow to the second filter set.

Direct application of heating or cooling fluids to process jackets is the traditional alternative. Consecutive application of chilled water and steam on the jacket is acceptable if the design evacuates the jacket using higher pressure compressed air such that banging is minimized. Regardless of the indirect/direct mode of heating/cooling fluid application, jacket design can greatly affect the effectiveness of heat transfer. Dimple or straight jackets are preferred for smaller vessels, and external half-pipe cooling coils are used in larger vessels. The largest manufacturing scale vessels utilize internal cooling coils, but these coils present

additional internals for cleaning and increased sterility risks, particularly at welds, because cooling water can be at a higher pressure than the fermenter contents.

Filtered dried instrument air, typically at a pressure near 100 psi, is required for solenoids valves on bioprocessing skids. Pressure specifications for control valve operation considerably vary among vendors and inversely affect valve actuator size. Plastic hosing, although convenient and cost effective, should be carefully evaluated for instrument air lines, especially on hot equipment where heat-induced leaks can develop and in solenoid cabinets where crimping can slice the tubing. A back-up instrument air compressor and expansion tank can minimize operational consequences from supply pressure dips. A separate compressed air source, at a higher pressure than chilled/cooling water and jacket steam, is desirable for the evacuation of vessel jackets to minimize risk of backflow into the instrument air system.

Natural gas usage, if required, might be best addressed using bottled gas for safety reasons, which discourage distribution piping throughout the facility. Favored for flaming of openings in many microbiological procedures, the use of Bunsen burners or propane torches in a biosafety cabinet or laminar flow hood should be examined with company safety department representatives. Care should be taken to minimize the potential for reaching the lower explosive limit near the motor of the cabinet or hood. Compatibility of plastic laboratoryware with flames also should be insured.

80.3.2.3 HVAC. HVAC is the key and costly component of a pilot plant facility owing to its multiproduct nature. Its design and operation needs to be understood by operating, maintenance, and quality personnel. Requirements for air cleanliness, as well as the ability to achieve them, are determined by HEPA filtration, airflow volume, pressurization room design as well as the type of operation being conducted (Table 80.5) (8). HEPA filters are oftrn used for inlet air but only used for exit air when required by biosafety containment.

The specific classification of processing areas depends on processing step quality requirements as they are related to equipment design. Where possible, support equipment (or portions of thereof) is located in cheaper gray utility space, reducing disruptions for alterations needed as pilot plant processes change. Gray space does not require classification and thus has reduced gowning, cleaning, and monitoring requirements, as well as lowered HVAC construction and operating costs (53,56). As closed system operation in processing spaces increases, trends toward smaller classified core areas enveloped in nonclassified space are emerging (9,53,76). The use of contained sampling devices that permit sampling by maintaining a closed system also helps in supporting this trend.

Classification level, representing the maximum number of particles permitted per cubic foot of air sampled, of an area increases from fermentation (class 10,000–100,000; 20–40 room changes per hour) to purification (class 1000–10,000; up to 100 room changes per hour) (8). Within a room, there are cleaner areas surrounding open transfers (e.g. biosafety cabinets or laminar flow hoods) which are class 100 (540 changes per hour) (77). For viable particles, the range is from class 100,000 which permits 2.5 cfu/ft^3 down to class 100 which permits 0.1 cfu/ft^3 with intervening levels that are generally determined by the individual processing application being conducted (77). Sufficient air velocities also are necessary to dilute particulate contaminants. In some cases, separate air handlers are considered for critical sterile areas, inoculum preparation areas, high particle or dust areas, and segregated product areas. In most other instances, air flow is designed in a once-through pathway which may substantially increase heating and cooling utility costs.

Inlet air enters from the top of the room, flows downward, and exits from ducts near the floor. Any recirculation, which may be desirable to minimize the capital costs for heating and cooling equipment as well as operational costs, should be only from the room where the air originated, limited to areas that do not generate substantial amounts of particles, and pass through inlet HEPA filters again. This strategy is beneficial to the life span of the HEPA filters and the ease of maintaining constant temperature and humidity (8). Exit ducts should be placed near equipment within a

TABLE 80.5. Comparisons of Example Controlled and Noncontrolled Area Achievable quality Based On Room Design in a Pilot Plant Facility

Type of Area	Pressurization	Airflow Changes (#/h)	Inlet Filtration	Nonviable (#/ft^3)	Viable (cfu/ft^3)
Bulk fermentation processing	None	5–7	Coarse	<250,000	<25
Laboratory	Positive	60	Coarse	<100,000	<2.5
Laboratory	Positive	10	HEPA	<100,000	<2.5
Laboratory-clean construction	Positive	25	HEPA	<100,000	<2.5
Laboratory-clean construction	Positive	20	HEPA	<10,000	<0.5
Laboratory-contains autoclave	Positive	100	HEPA	<100,000	<2.5
Laboratory-contains glasswasher	Negative	50	HEPA	<100,000	<2.5

processing area, which generates the most particulates or aerosols so as not to spread them throughout the area. Specific examples include autoclaves, glass washers, and cell disrupting homogenizers.

Room pressurizations should be higher for cleaner areas and lower for areas that generate particles (8). Higher pressurization levels should be assigned to airlocks between adjacent areas for which it is desired to minimize cross contamination. Relative pressurizations between rooms sharing a common wall should be considered to supplement and/or minimize reliance on completely sealing rooms during their construction. The use of door sweeps and gasketted ceiling tiles to achieve and maintain pressurization should be evaluated relative to floor cleanability and ceiling maintenance access, respectively. Pressure differentials might be as high as 0.03 inches water between classified areas and as high as 0.05 in. water between classified and nonclassified areas. Lower pressure differentials might be acceptable depending on the specific product as long as the direction of airflow remains consistent. Interlocks, control, monitoring, and alarm building automation systems may be designed to reduce pressure losses when doors are opened and to alert users to unsatisfactory conditions. When desired pressurization has been lost, affected areas are recleaned and in-process materials are evaluated for quality impact, delaying schedules, and increasing manpower.

Facility temperature is generally maintained on the cool side because gowning requirements tend to make workers warm. Inaccurate assumptions concerning the impact of radiant heating from windows may cause higher than desired temperatures on certain days of operation. Humidity should be comfortable to avoid drying of workers' respiratory membranes during extended processing hours. Care should be taken to specify tolerance limits that have quality implications appropriate for the processing steps expected to be conducted in the area to avoid unnecessary additional facility costs. Although specific example guidelines are 23 $\pm$ 3°C and 40–60% relative humidity (78), substantially larger ranges may be acceptable for many processing applications. An extensive P&ID of HVAC design for clean spaces is available as a published Ref. 77. In addition, consideration should be given to Federal Standard 209E, Airborne Particulate Cleanliness Classes in Clean Rooms and Clean Zones, as well as EC regulations which establish parallel categories of Grade D (100,000), Grade C (10,000), and Grades A+B (different designs of class 100) (77,79).

80.3.3 Containment

Similar issues exist for product, environmental, and personnel protection, and these issues are heightened due to constantly changing pilot plant processes. Often the resulting design specifications overlap with those items necessary for sterile or sanitary operation. This concept is addressed in the literature (80), which compares solutions to prevent microbial transport to attain containment with those to maintain sterility for fermenters. A unified approach is recommended to minimize unnecessarily stringent specifications, which can substantially augment capital and operating costs. Environmental and personnel protection issues are evaluated for each new pilot plant process undertaken by the facility, along with product protection quality concerns. Samples of broth, and other product, intermediate, and waste streams, are submitted for aquatic (and sometimes human) toxicity testing in advance of processing in the pilot plant when appropriate. Preliminary test data might be then available to evaluate potential hazards in conjunction with published documentation concerning the similarity of the questionable compounds, raw materials, or organism to known hazards.

80.3.3.1 Product Protection. The major concept surrounding product protection is the closed system in which all material entering or leaving the process must be controlled in a specified and documented manner. This requirement extends to product-contact utilities such as purified water, clean steam, compressed air, and controlled/monitored room air so that when equipment is opened for cleaning the quality of surrounding environment is consistently at a known and documented level. The equipment is then cleaned to an acceptable quality level. Several elements are typically included as part of closed system operation. After sterilization, material enters the closed system via a sterilizing filter, steamed connection to an autoclaved bottle assembly, and/or sterilized transfer line. Off-gas passes through a 0.2 μ steam-sterilized vent filter, often contained in a low pressure, steam-jacketed housing preceded by a coalescing filter, condenser, and/or vent heater to avoid pluggage from moisture. Double mechanical seals are utilized with a barrier fluid of a controlled quality (typically condensed clean steam) at a higher pressure than the vessel. A closed system also can be used to surround an open operation such as the use of isolator technology (i.e. glove box) as an alternative to clean rooms or biosafety cabinets (81,82).

80.3.3.2 Environmental Protection. Environmental protection concerns focus on emissions from air, liquid, and solid waste. Typically, state air permits are required for new vessels and need to be altered if additional air treatment devices such as vent filters, incinerators, or scrubbers are added to existing vessels. Hydrophobic vent filters can provide emergency foam control and prevent external product or organism release. These filters can be monitored for pluggage over cultivation time using pressure differentials with plugged filters replaceable during a run only if a bypass line exists. Liquid emissions include accidental spills/sewerings, which can be minimized by locking vessel

bottom valves, blocking open sewer connections, collecting sample line flush waste, and providing clear written instructions to personnel regarding batch disposition. Dikes, troughs, and vaults can be used to contain large spills or divert inadvertently sewered material. Sample waste can be minimized using low volume sampling devices. Thermal or chemical (less common) batch or continuous kill tanks need to be considered for biological hazards. For chemical hazards, other appropriate waste destruction and minimization systems may include hot caustic hydrolysis, reverse osmosis, and evaporative condensers. Batch leakage into cooling water utility systems can be minimized by operating utility systems at a pressure higher than the batch, but this differential might introduce contamination if jacket cooling coils develop leaks. Alternatively, the utility system return headers can be isolated from general use until their contents are treated and/or tested. This solution might be attractive for cooling water as well as condensate, especially when it is returned to river sources. Care must be taken to avoid sequestering large quantities of potential waste for long periods of time. Solid waste can be controlled procedurally using clearly labeled containers.

80.3.3.3 Personnel Protection. Personnel protection requirements are reduced now that several recombinant organisms can be grown under typical operating conditions of GLSP. For other pilot plant processes requiring personnel protection, either the culture is rated at or above BL1-LS or a compound produced by the culture adversely affects human heath (e.g. a genotoxin, mutagen, teratogen, or carcinogen). Environmental monitoring of the operating area is necessary for the compound or culture of interest using air and/or swab sampling techniques. For optimal recovery, swabs should be soaked in a solvent that is known to dissolve the compound of interest. Screening and monitoring of personnel potentially in contact with the process (operator, mechanics, janitors, engineers, visitors) must be arranged and notification must be given to those personnel at unacceptable levels of risk. A key element of personnel protection is personal protective equipment (PPE). This equipment can include gowns, uniforms, safety glasses, lab coats, and gloves at a minimum, but can be extended to include face shields, goggles, and respirators as required. Spill response equipment, procedures, and training are also necessary.

Reduction to practice techniques are presented in the literature for general biocontainment issues (83) as well as biocontainment regulations and requirements (84,85). Specific examples are available for the design of waste inactivation systems (86,87), contained facility design and operation (88,89), design details for cleanliness and containment for floors, walls, ceilings and penetrations (90), and contained sampling systems (91).

80.3.4 Instrumentation

The main purpose of a pilot plant is to collect data as comprehensively as possible. Thus, a large fraction of the pilot plant capital allocation might be devoted to instrumentation. Use of in-process measurements and controls to improve product quality is a key foundation of the FDA's recent process analytical technology (PAT) initiative (92). Traditional instruments for on-line monitoring, particularly for fermentation, include pH (93), dissolved oxygen (DO) (94–96), temperature, agitator speed, agitator power draw, back pressure, foam detection, batch level or weight, air flow rate, and vent gas analysis via mass spectrometry (97). Redundant instrumentation is desirable for critical parameters such as pH and DO. Instrumentation for isolation processes includes the monitoring of conductivity, pH, ultraviolet wavelength intensity, and refractive index. Useful utility instrumentation includes on-line TOC analysis and resistivity/conductivity meters. Local readouts of transmitter values can be particularly useful for pressure and possibly temperature, although the potential for differences between field and control room values may have to be addressed.

Many novel sensors have been developed including dissolved carbon dioxide probes (93,98), redox sensors (93), glucose sensors (99), near infrared detectors (100,101), fiber optic biosensors (102), fluorometry of intracellular NADPH (103) and cell density probes (104–106). Another novel measurement device example incorporates fermenter side streams to measure viscosity on line (106). A description of useful sensors may be found in the literature (92,107). Characteristics of on-line and *in-situ* devices include cleanability, minimal drift, minimal interferences, versatility, sterilizability, and ease of calibration. Implementation of any sensor should be evaluated for its effect on bioreactor sterility as well as product quality.

80.3.5 Automation and Control

Automation and control can reduce manual work and operator errors, as well as raise operational consistency (9). The need for flexibility and change within a pilot plant (as compared with production) needs to be apparent in control schemes, event sequencing, data collection and presentation, and alarming (108). Increased amounts of automation restrict the abilities of the end user to implement changes, but do reduce the number of manual operations and thus possibly headcount. Specifically, the control system should readily permit set-point and alarm changes. Control systems can be distributed or centralized with distributed control systems (DCS) favored because there are individual controllers/computers for each unit connected via a high speed network. Thus, the loss of one centralized computer is not catastrophic (108).

Although there can be "islands of automation" within a pilot plant owing to automated skids purchased from different manufacturers, connectivity in a centralized location for data monitoring, set point/alarm changes, and data archiving typically is desirable. Substantial advantages exist for localized controls on skids when there are large numbers of inputs required based on an operator's evaluation of field conditions. A local readout of data versus a centralized "control room style" monitoring area (or even both) is dependent on the expected degree of operator supervision versus intervention required during processing. This decision is directly related to the flexibility of operators to move in and out of the field in terms of gowning procedures and access restrictions. The ability to remotely input set point and/or alarm changes can be useful when containment and/or product protection levels are high. Multiple areas for setting parameter values should be carefully considered from an operational control viewpoint to avoid duplication of desired changes and to batch record log omissions. Verbal communications between the field and control room using hand-held radios, intercoms, or phones also can minimize unnecessary movement within the facility.

Distributed control systems are favored for process management in some pilot plants. System architecture requirements vary depending on the processing requirements, but examples for a non-PC-based system are present in the literature (109). Distributed control systems also can be PC-based using commercial PC control/data acquisition software (110). In either case, some type of process-level controller is required such as a PLC (programmable logic controller), LC (loop controller), or PCBC (personal computer-based controller) (47). The ability for the noncomputer expert to easily modify and understand control sequences using newly developed, commercial control software is attractive but requires effective change control and documentation procedures. The ability to readily configure the data acquisition system to download and archive data is an important consideration for process performance evaluation.

There are several types of computer inputs/outputs (108) which include: (i) digital inputs in the form of an on/off signal used for foam probe, pressure, flow, and/or temperature switches, (ii) digital outputs in the form of an on/off signal used for the flow of antifoam, open/close valves, and/or pump/motor start/stops, (iii) analog inputs in the form of an amplified output in the range of 4–20 ma used for temperature, pressure, pH, dissolved oxygen, flow, and power draw, and (iv) analog outputs in the form of a proportional signal which controls the valve opening via an I/P conversion (typically used for back pressure, cooling, and/or airflow valves) or else signals such as motor speed.

The most frequently utilized type of control is the PID (proportional integral differential) control loop. It is tuned using three parameters to minimize oscillations, which can change depending on the specific process (e.g. for dissolved oxygen cascade control of a fermenter cultivating faster growing *E. coli* versus slower growing animal cells) or over the course of the same process (e.g., for glucose and ethanol consumption phases of a Bakers' yeast fermentation (111)). These three parameters are the (i) size of the error relative to proportional band with smaller bands resulting in more sensitive systems, (ii) integral of the error over time with longer error durations resulting in greater corrections, and (iii) rate of error change with time with larger increases in correction with time calculated the faster the error is growing with time (107). Typically, the third parameter is at a minimal value near zero for the optimally tuned loop.

A conscious decision needs to be made concerning the level of automation for CIP, SIP, and vessel-to-vessel transfers desired for a pilot plant. Higher levels of automation may insure reproducibility of operation, reduce reliance on operational staff, and simplify SOPs. However, raising the level of automation increases capital, validation, and maintenance costs, while reducing flexibility to quickly adapt to changing pilot plant processes. Familiarity with the details of automated versus manual equipment operational sequences may be lower among operating personnel routinely observing automated processing steps. A domino effect may exist in that automation of one valve may lead to the automation of several related valves, severely increasing design complexity and cost. Limit switches are often installed which confirm to the control system that the desired automatic valve has opened or shut as requested. Automatic pulsed diaphragm valves have been successful for nutrient feeding as well as for sterilization of transfer lines in automatic plants (112). A prominent example of a highly automated but apparently reliable fermentation facility is operated for the manufacture of cephamycins as well as for pilot use (113). Typical diagrams for the monitoring and control of a fermenter (33,108) and for the monitoring and control of an ultrafiltration unit (47) have been published.

80.3.6 Data Acquisition and Archiving

The collection and management of data obtained during pilot plant operations (as well as laboratory experiments) is a critical facet of knowledge management for the speeding implementation of cost-effective manufacturing processes (114). Capture, storage, and retrieval of critical product/process knowledge, including pilot scale process development and scale-up data, also is a key challenge to implementing quality by design strategies (115). The data collection interval is dependent upon the nature of the processing step. For fermentations, intervals might be in every 15–20 min during secondary metabolite or animal cell cultivations but might shrink to 5–10 min for faster growing bacterial or yeast cultures, especially when a key

process addition or change is planned based on off-gas or dissolved oxygen measurements. Typically, 5–10 min intervals are appropriate for microfiltration or centrifugation operations and continuously for chromatography systems especially during loading and elution. Smaller data collection intervals may create substantial data archiving demands, which may be alleviated by only saving those data substantially different from previous values based on some user-defined value.

In-process trending of data is attractive to permit the timely evaluation of process status and trouble shooting of processing problems, which are the two factors critical to continuous improvement efforts. Specifically, multivariate analyses can be performed for critical variables and results can be used to adjust the process (116). Automatic recording of alarms and changes to the control system, preferably sorted according to the equipment and/or batch for which they occurred, also can help to trace back processing problems and actions taken. On-line data might be archived on a common server by some unique batch delimiter, according to the established facility SOP for archiving data. Two formidable challenges are to capture off-line data electronically (without manual re-entry) and then incorporate it within the same or a closely related reference database, which is preferably located in a central repository. Otherwise, this off-line data can get fragmented among the notebooks and files of individual researchers. Novel customized systems for bar-coding samples taken from the field and creating a database for results can be helpful, permitting possible use of robotic systems for sample analysis. Remote access is an attractive option for monitoring process performance from off-site locations. Remote alarming can be triggered to a satellite pager thus removing the necessity for round-the-clock on-site coverage. Remote control of operations can be administratively challenging to regulate and document as well as a potential safety issue. Security issues must always be considered for any established remote capability.

80.3.7 Warehousing

Warehousing requirements for the facility need to be determined based on expected pilot plant production capacity and desired batch lead times. Common items that might be stored include ambient, cold and/or frozen solid/liquid hazardous and nonhazardous raw materials (controlled temperature and/or relative humidity storage), disposables, equipment, spare parts, as well as sample and product storage. Computerized inventory systems, organized by process or equipment, can be useful for most of these items with reminders to reorder when supplies decline to a critical level or discard when items expire. Marker equipment also might be purchased for long lead replacement parts for which redundancy was not desired during the original facility design. Sizing of these storage areas should match typical lot volumes of prepared culture media and solids to minimize repetitive release testing for multiple lots. For a pilot plant, in which several diverse processes may be run, additional process-specific storage often is required. The relative amount of storage necessary within or near the building should be compared with other available on-site and off-site options. Vendor manufacturing schedules often require the purchasing of larger quantities of rare raw materials to avoid future shortages. In this instance, if on-site storage is not available, vendor storage, or a third party warehouse alternative may be required. Warehouse access may need to be restricted depending upon the nature of its contents. Within the warehouse, there should be segregation for released, unreleased, and quarantined materials either by physical separation or by designated labels.

Although the entire facility should have a comprehensive pest monitoring program (as well as an SOP), there may be a need to directly address pest control, particularly for flours and meals used in certain secondary metabolite fermentations. These food ingredients when purchased for pilot scale fermentation purposes may not pass through fumigation unless specifically requested on the purchase order. Typically, larger customers in the food industry have invested capital for on-site fumigators, but commercial nutrient vendors may not have this type of equipment due to their high rate of inventory turnover.

Staging areas should be available for collecting raw materials and supplies in advance of a specific batch. Some method of inventory assessment and control should be available; one convenient method is to use computerized bar coding to check inventory as well as to confirm the use of specified materials when charging occurs. In addition, controlled sampling areas (to provide raw material, environmental, and/or personnel protection) for the sampling of raw materials may be necessary.

80.3.8 Back-up Systems/Redundancy

A critical design decision centers on the level of backup and/or redundancy required in the pilot plant. Equipment sharing to reduce services for less critical tasks can be cost effective to increase the amount of backup available for critical tasks (117). Although typically none of the material created in the pilot plant is "for sale," mechanical problems can delay processing and thus material production, which may interrupt clinical supplies and compromise the success of ongoing studies. Even if no clinical material is at risk, process development efforts are hampered when experiments are frequently interrupted for mechanical support-type equipment failures (10). Scenarios that might be protected against include loss of clean steam lubrication to agitator seals, positive air pressure on a sterile tank, and electrical power to a controller. Corresponding equipment

needs might include redundant clean air compressors, clean steam generators, and/or purified/WFI water generation systems with the peak plant capacity requirements split between two systems rather than relying on a single system sized for peak usage. Such redundancy usually is achievable because utility costs are low compared to equipment costs (10). A UPS system sized to include the most critical equipment (typically controllers and data acquisition devices) might also be installed. Back-up power for large electrical loads such as motors might not be economical; however, consideration might be given to installing connections for a gas-powered generator if future evaluations altered the economic assessment.

80.3.9 Future Expansion/Modification

As future processing needs may change, the pilot plant must adapt to maintain its usefulness to the company. Large initially underutilized spaces might be outfitted with utility headers to minimize processing disruption during future installation. Oversizing of utilities for anticipated future loads (10), as well as unforeseen procedural modifications warranted based on future validation testing results (such as additional rinsing cycles), assures subsequent flexibility. Selection of portable equipment permits exchanges for new pilot plant processes, provided there are procedures developed for storage, cleaning, and start-up of this equipment.

Modular design and central spine approaches facilitate expansion and adaptability with minimal impact on existing operations when new components are added (9,117). One aggressive approach to increase versatility is a modular, mobile, validated pilot plant (118), comprised of a system of interconnected and integrated modules. Modules are selected according to processing needs and can be rapidly assembled to form a processing plant capable of undergoing validation. Example processing modules include fermentation, recovery, and purification; the utility module includes clean water and clean steam; the personnel support module includes lockers and changing areas; and the HVAC module houses the air handling and filtration equipment. Additional modules can be then added or deleted as required.

80.4 OPERATION

Each pilot plant facility must decide for itself whether it is required to operate in a continuous mode of GMP compliance or whether it can selectively apply GMP practices to certain batches (but not to other concurrently run batches) or during certain specific processing periods. A conservative solution might be to operate continually in GMP compliance, thus insuring facility readiness and preventing the omission of a required procedure for an actual batch destined for the clinic. Dual GMP and nonGMP operation serves to create two standards and may cause confusion among operating and maintenance staff. If dual operating modes are implemented, then a clear distinction between GMP and nonGMP operation must be established, documented, and maintained.

80.4.1 Maintenance

80.4.1.1 Preventative. Preventive maintenance, performed during an annual facility shutdown, is probably the most important factor influencing smooth pilot plant operation throughout the upcoming year. The scheduling of an annual facility shutdown is desirable for several reasons including the ease of lock out of hazardous energy sources, the time economies of concentrating several maintenance workers in a single area, and the ability to supervise and document completion of a large fraction of maintenance work at one time. This yearly PM documentation can then serve as the model for maintenance personnel for the following year's shutdown. Individual PM work orders, spread over the course of a year, result in substantial time and effort expended in scheduling, preparing, and documenting the work done. Interspersing of annual PM work among batch processing inevitably results in PM delays due to equipment and/or manpower unavailability. Guidelines for planning and executing an annual plant shutdown are available (119).

All PM work orders can be categorized and then listed according to trade, equipment, material, or time requirements. They can be reviewed prior to the facility shutdown and augmented with any modifications or "one-time" replacement work orders that are requested. As PM work is completed, documentation should be signed by the tradesperson as applicable and reviewed by mechanical and operational staff for completeness. Problems that are identified with equipment or instrumentation should be highlighted as they occur and then entered into change control work order systems so that they can be tracked for their effect on validation.

Before the annual shutdown, transfer line manifolds and/or utility supply lines, that typically cannot be shutdown entirely for maintenance throughout the year, might be leak tested to identify faulty valves in need of replacement. After the annual shutdown, equipment start-up procedures should be documented, preferably through the use of equipment start-up batch sheets. These procedures might include equipment cleaning, testing of instrument calibrations such as level, temperature, and pressure (120) and vessel integrity testing for leaky valves. Instrument calibration accuracy should be evaluated for random or systematic errors with random error within accepted tolerances being the expected outcome.

Some general PM procedures can be applied to several areas in a pilot plant, both product and nonproduct contact.

Sanitary fittings, which tend to loosen during repeated heating and cooling cycles, should be checked, gaskets replaced, and clamps tightened as required. Any flanges in product contact should be tightened to a specified torque. PM inspections of vessel internals should be conducted and lock washers installed on external nuts that may loosen due to repeated heating and cooling. A PM should be developed for the inspection of vessel cooling coils for leaks, which can result in inadvertent cooling water contact with product (121). For agitated systems, there should be a regular examination of foot bearings, motor/drive vibration, oil analysis, and shaft runout. Double mechanical seals, the failure of which can lead to condensate buildup and/or batch contamination, should be tested regularly and replaced preventatively based on a minimum life expectancy (122). An outline of specific PM procedures for laboratory fermenters can be applied to larger scale fermenters (123). An example of the documentation for the maintenance of horizontal laminar flow hoods is also available (124) which can be readily adapted to other HEPA filter units. PMs should be conducted on all utility systems and may include the rebuild of air compressor heads, descaling of heat exchange surfaces, and replacing of air dryer desiccant, among other items recommended by the equipment manufacturer. Finally, novel predictive maintenance evaluation techniques should be explored and implemented as appropriate to identify imminent equipment failures (125).

It is most appropriate to perform any annual validation work (e.g. fermenter SIP, autoclave load pattern, controlled temperature unit) at the conclusion of the annual PM shutdown. In this manner, proper equipment operation can be documented and the effectiveness of PM procedures can be evaluated. Often inadvertent mistakes or omissions during maintenance can be identified prior to having an adverse, and possibly widespread, quality impact on pilot plant batches destined for clinical trials.

80.4.1.2 Ongoing. A reliable system of tracking outstanding maintenance by equipment or by process should be designed and implemented, particularly for a pilot plant in which equipment is used less regularly. Each piece of equipment has a clearly distinguished tag name. Work orders are initiated, evaluated for their effect on validation, marked as complete when mechanical work done, then finalized when process personnel have checked the job. A computerized database can readily track maintenance and identify repetitive maintenance problems. Such a system permits easy review of outstanding work orders for each piece of equipment prior to getting it ready for service. All maintenance work orders need to be tracked within one system; care should be taken not to bypass the operations area when maintenance needs are identified by those directly controlling the mechanical staff.

Interim maintenance work, such as calibrations and subannual preventative maintenance (PM) activities, should be documented and filed in a manner equivalent to the yearly PM results. PM schedules should be reviewed based on the frequency and results of interim maintenance work. Unusually common equipment failures can be identified through maintenance database searches and appropriate longer term repair efforts or replacement justified and undertaken.

80.4.1.3 Calibrations. Calibrations of pilot plant equipment have additional concerns associated with them because important processing decisions for early scale-up batches may be based on the accuracy of the instrument readings. In some cases, specific instruments are designated as "critical" for a processing step; in other cases, desired specification ranges for the processing step are targeted based on certain noncritical instruments. These two methods provide assurance that product quality is not compromised if any of the other instruments that are present in the equipment utilized fail.

Although some facilities distinguish between calibration procedures for "critical" and "noncritical" instrumentation, it may be prudent for a pilot plant to calibrate all instruments in a reliable and documented manner because their accuracy ensures useful process development data. Calibrations should be performed using NIST traceable instruments and include full loop calibration to the process monitor as appropriate. A specific calibration and maintenance SOP for the instrument is most desirable but a general SOP referencing vendor manuals might also be acceptable, particularly in the interim period while instrument calibration SOPs are being developed. The "as found" (or "before") and "as left" conditions should be documented along with the serial number of the standard used (126). Establishment of an acceptable tolerance for each instrument insures consistency. When an instrument is found outside the tolerance specified, the impact of this calibration "as found" error on previously executed batches may need to be evaluated. Thus, a confirmation of the error might be warranted prior to correcting the calibration. Records should be evaluated for the amount of instrument drift, which may indicate the need to either recalibrate on a more frequent basis or else replace/upgrade aging equipment. An example calibration sheet is available (127).

80.4.1.4 Modifications/Change Control. Any validated facility needs to devise procedures for tracking changes on equipment as well as on processes and computers. This requirement is heightened for a pilot plant because a large number of changes are expected owing to its rapidly changing portfolio and processes. Incomplete documentation of changes can obviate extensive time and money spent on validation testing. Although the exact contents may change, such a procedure starts during the

initial design phase as equipment specifications are altered, continues through the facility start-up and qualification phases, and then moves directly into the facility operational phase. Adherence to change control procedures may be difficult during facility start-up as many unexpected items are found to be incorrect and management pressure may mount to have the facility operational quickly. Depending upon the philosophy of the individual facility, the scope of this change control procedure may include product and nonproduct equipment to varying degrees. The procedure identifies the individuals who need to approve changes and determine prior to or in concert with the change implementation what additional validation testing is required. Often, processing personnel, being most familiar with the equipment being modified and the reason for its modification, can provide valuable leadership in this area and initiate contact with quality and validation personnel as required for input.

Generally, replacements of this kind are accepted without additional testing unless the item being replaced was specifically tested or calibrated during the initial validation effort. Example items and associated testing might include a replacement or rebuilt motor or associated drive (measure motor amperage draw at various agitator speed settings) or replacement instrumentation (calibrate sensor and transmitter). Replacement items in this category need to be tagged appropriately in the field with the same tag number as the original item and serial numbers updated in any centralized maintenance data bank as well as recorded on installation documentation.

Modifications or obvious changes in equipment or instrumentation need to be evaluated for their potential impact on the validated state of the equipment. This impact is particularly important for SIP and CIP cycles. Such modifications may be minor, such as a change in gasket or o-ring material of construction, or major, such as a change in piping. An example procedure is available which can insure proposed changes are reviewed by operations, maintenance, and quality for their potential impact (128). Specific attention should be given to alterations needed in P&IDs, SOPs, PMs, batch sheets, and/or training programs. Equipment modifications, necessary to accommodate a new process, need to be identified early on and their impact also should be evaluated (4). It is critical to balance the request for change with an evaluation of its validation impact. Changes cannot be discouraged in a multipurpose pilot plant, but they need to be controlled and managed in a logical yet expedient manner.

80.4.2 Staffing

Personnel requirements are best defined based on the production process (129) but in a pilot plant setting, production processes change rapidly and substantially (130). Both short- and long-term planning tools and models are necessary to plan manpower for the preparation, execution, and finalization of various campaign efforts (130). A decision needs to be made early in the design process concerning the level of off-shift activity that is reasonably expected in the facility as it can severely impact items such as utility capacity and operation. Round-the-clock coverage, although demanding for personnel involved, may be necessary almost throughout the process to insure success and timeliness of production. The use of unionized personnel, technicians, or process development staff should be incorporated into the educational requirements and manual workload expectations for the operating staff to ensure appropriate job fits and reduce potential drivers for turnover. A core operations group, responsible for the facility, can insure continuity in areas such as SOP updates, maintenance work order tracking, batch sheet content, and equipment operation. Such a group might be supervised by an area manager, responsible for coordination and scheduling, who might interface with those directly involved in process development. Then, the processing groups might rotate through the pilot plant as their projects demanded are accompanied by a member of the operations group. Alternatively, a dedicated pilot production process development staff might be instituted, responsible for the translation of laboratory processes into GMP batches.

80.4.3 Laboratory Support

To provide adequate and accurate sample analyses, laboratory support needs to be identified and addressed through either on-site or contract laboratories. Targets for testing might include final product, in-process samples, raw materials, sterility, culture purity, environmental quality of controlled environments, and utility quality (Table 80.6). Although the goal of these laboratories may be to work toward using validated methods and approved SOPs for all assays, this goal might not be attainable for project-specific assays until the later stages of a successful development project. Initially, in the early project stages, only notebook procedures might be available to guide laboratory testing. Information directly impacting quality should be communicated directly to both quality and operating personnel and appropriate investigations conducted both in the field and laboratory for failing or out-of-specification (OOS) results.

A microbiological laboratory is critical for fermentation-based operations to prepare seed cultures and test new culture seed vials for culture purity and productivity in lab-scale processes. An examination of up-to-date sterility/culture purity results prior to vessel-to-vessel transfers should be undertaken as close to possible to the time of transfer to minimize the adverse impacts of contaminated cultures. In a pilot plant setting, tension may exist between

TABLE 80.6. Types of Testing (Sampling and Analysis) Possibly Required by On-Site or Off-Site Support Laboratories for a Bioprocessing Pilot Plant

Facility Monitoring	Sterilization Cycle Validation	Cleaning Cycle Validation	Process Monitoring
Total organic carbon (TOC)	Indicator spore strip incubation	Total organic carbon (TOC) (swab and rinsewater)	Spectrophotometer
pH	Indicator water spore suspension incubation	pH	pH meter
Conductivity	Indicator media spore suspension incubation	Conductivity	HPLC for organic acids, amino acids, sugars
Endotoxin (LAL)	Sterility	Endotoxin (LAL)	HPLC for product/impurity analysis
Bioburden and coliforms	Bacterial and fungal culture purity-	Bioburden (swab and rinsewater)	LC-mass spec
Airborne viable particles	Filter integrity testing	Ultraviolet light absorbance	Protein gel analysis
Airborne total particles	Microbial identification	Visible light absorbance	Osmometer
Surface viable particles	Gram stains	Filtered solids	Microscope
Compressed gas viable particles		Dissolved solids	Cell counter/viability monitor
Compressed gas nonviable particles			Conductivity
Compressed gas identity			Metabolite analyzer
Noncondensable gases in steam condensate			Plate readers
			Blood gas analyzer
			Laboratory scale-down control/trouble-shooting experiments

the time required to adequately test new cultures and development pressure to use the latest mutant or transformant in a pilot scale cultivation to evaluate its capabilities. Reasonable procedures need to be established in advance for the introduction of new processes and/or new cultures into the pilot plant. Laboratory prepared nutrients, trace ingredients, and/or sterilized additions should be evaluated for their quality impact and the procedures used for their preparation should be documented where possible.

80.4.4 Standard Operating Procedures (SOPs)

SOPs are essential for the planning and standardization of various procedures conducted by operational staff and maintenance personnel that need to be completed before, during, and after pilot plant batches (4). Typical categories include SOPs for equipment operation, facility and equipment cleaning, sampling, sterilization/sanitization, maintenance, and documentation procedures for tasks such as product changeover, change control, and batch sheets (Table 80.7). When referencing SOPs as part of the batch record, working versions of SOPs can be helpful to track progress and ensure accuracy of step execution in the field. An SOP on the requirements for writing, issuing, and inactivating an SOP also is useful. SOPs focus operation, guide operations staff, document the order and scope of activities, standardize approaches, define regulatory needs and constraints, and increase the speed of new personnel training (4). They should be written by a person familiar with the facility or equipment operation that is the subject of the SOP, reviewed by another person who might be asked to follow the SOP, and approved by a quality group. Each SOP should have an effective date of issue, be available to those who need it, and be archived when a future revision is created.

The need for structure and consistency within an SOP must be balanced by the need for flexibility in a pilot plant when unexpected process requirements arise. Procedures must be defined for what to do when an SOP is altered intentionally to accommodate a new process or an unexpected development in an existing process. Consideration of SOPs should be given during the equipment design phase so that tasks can be performed in a logical clockwise or counterclockwise fashion (129). SOPs should be clear so that the expected outcome is insured. Specific examples of often omitted details include (i) statements regarding settings for pressure switches and acceptable calibration error tolerances, (ii) diagrams, part numbers, and manual references to aid in following the procedure, and (iii) relying solely on valve numbers, not valve purposes, to describe the procedure. Although SOPs should be reviewed periodically in every few years to determine if they are in need of clarification, care should be taken to minimize the number and frequency of similar versions of the same SOP issued to the field. Operational clarification memos, issued to all operational staff and signed off when read, might be used to provide additional noncritical SOP clarification without

TABLE 80.7. List of Example Types of Procedures that are Possibly Required for a Bioprocessing Pilot Plant

Administrative	Process Equipment	Lab Equipment	Maintenance	Operations
Processing abnormality	Sterilization-in-place	Autoclave operation-sterilization and decon	Instrument calibration	Gowning
Investigation of contamination	Cleaning-in-place	Autoclave load patterns	Equipment preventative maintenance	Water system flushing/sampling
Product changeover	Sanitization	Glasswasher operation	Utility preventative maintenance	Steam system sampling
Writing of an SOP	Vessel set-up and operation	Glasswasher load patterns	HVAC preventative maintenance	Spill containment
Personnel training on equipment/operations	Transfer line/panel operations	Working in biosafety cabinet	Equipment change control	Facility housekeeping and cleaning
Personnel training on assays	Batch harvest (noncontained)	Working in laminar flow hood	Equipment start-up after processing hiatus	Facility start-up after processing hiatus
Personnel training on computers	Batch harvest (contained)	Incubator/shaker operation	Equipment start-up after major mechanical work	Daily utility checkout
Issuing and review of batch sheets	Equipment integrity test	Freezer	Equip. storage during processing hiatus	In-process sampling and analysis
Raw material release and storage	Utility systems operation	Refrigerator/cold room	Computer system change control	Data archiving
Investigation of monitoring excursions	HVAC systems operation	Tubing welder use and cleaning	Computer system failure recovery	Computer system operation
Forklift certification	Media/buffer preparation	Manual washing	Shutdown/interim maintenance document	Monitoring- controlled environments
Pest control	Specific equipment SOPs	Usage of scales and checkweights	Equipment isolation for maintenance	Tracking of process/equipment status
Ongoing validation testing		Calibration of pH meter	Issuing and tracking of work orders	
Ongoing facility monitoring		Facility monitoring assays		
Introduction of new products/processes		In-process monitoring assays		
		Fume hood use		
		Seed preparation		

reissuing the SOP during the interim period between SOP reviews. All major SOPs changes should be documented, evaluated for their effect on validation, and communicated to staff in a documented manner.

80.4.5 Safety

Because concerns regarding product exposure to personnel are similar to concerns for personnel exposure to product, GMP guidelines overlap with safety regulations in many respects such as training, SOPs, preventative maintenance including calibrations, and validation/change control (4). In fact, specific procedures for managing change to conform to process safety requirements (131) match the rigor of those required to confirm with GMP requirements. By the definition of a pilot plant's mission, change is an integral part of its existence. Consequently, comprehensive yet reasonable safety procedures must be established.

Safety captions can be required for certain raw materials based on the review of MSDS documentation. Broths, as well as isolated compounds, might be submitted for toxicity testing as soon as they are cultivated in laboratory bioreactors so that results are available prior to pilot plant scale-up. Safety is a component of installation qualification(IQ) because pressure vessel documentation and utility connections are reviewed. HAZOP (hazard operability) reviews for pressure vessels (e.g. fermenters, autoclaves) and utilities (e.g. clean steam generators) often are required by company policy and summaries included within equipment qualification reports. HAZOP action items need to be addressed promptly and any necessary modifications to equipment and/or procedures made to minimize risk. Equipment design needs to be reviewed for the ease of lockout and removal of hazardous energy sources (e.g. bleed valves for the evacuation of process and utility lines, local field-mounted pressure gauges to confirm depressurization), as well as the individual

isolation of skids/units for maintenance. In addition, equipment-specific SOPs for preparing the equipment for maintenance might be required.

Regular safety inspections with documented action items that are communicated to all affected personnel (i.e. operating staff, technicians, engineers, management) can identify and correct nonoptimal working conditions and cluttered processing areas. Tracking systems can be effective to ensure that corrective actions are taken and are effective. Specific attention should be given to the purchase of ergonomic lifting devices such as material elevators, drum lifters, and vacuum assist arms. Exposure of personnel to excessive sound, heat, or dust also should be considered during facility design as well as monitored during facility operation. Although personal protective equipment is available such as ear plugs, heat-resistant gloves, and respirators, when possible engineering controls such as sound dampeners, insulation, and dust collectors may be better solutions. Safety during validation testing should always be considered, particularly when groups outside of operations are involved in setting up/operating equipment and when sources of hazardous energy are involved. Whether during validation testing or operational use, fittings of any sort should be tightly secured and should not be tightened when equipment is under pressure and/or hot, specifically during SIP and CIP procedures. Summaries of generally accepted laboratory and pilot plant safety procedures to consider are available (132).

According to ASME code, overpressurization protection using relief devices is required for vessels over six inches in diameter. The background for this regulation as well as details of pressure relief valves and rupture disks is available (133). Although sanitary rupture disks are most desirable for product contact, once blown, processing must stop until they are replaced. Sometimes, a rupture disk may be installed followed by a pop-safety valve rated at a slightly higher pressure with a pressure gauge or other type of sensor in between to indicate rupture of the disk (84). If this arrangement is used, then the cleanliness of the area between the rupture disk and the pop-safety valve must be demonstrated for the batch quality not to be adversely impacted if the disk ruptures but the pop-safety valve does not release. Removal of entire rupture disk assembly (not the removal of the disk out from the assembly) for cleaning should be checked with company policy but may be acceptable in most cases.

Another key concentration is that the outlets of safety relief devices (which might be unexpectedly spewing steam, hot water, or broth after relief) should be oriented such that personnel safety is considered for those who may be standing near them. One method is to pipe outlets to outside containment troughs, but it may not be desirable to have a potential connection to the outside. A second alternative is to create a designated area within the pilot plant processing area. Although piping outlets to the floor beside the equipment should be minimized, if they are found to be necessary, they should be carefully situated outside the normal path of personnel.

80.4.6 Training

Initial and ongoing training programs need to be developed and documented for each individual associated with the facility based on the facility needs. The number of different individuals associated with pilot plant processing can be high unless a dedicated group is established regardless of product. A training SOP should be established, which might include a training manual containing useful items such as copies of key SOPs, facility layouts, equipment diagrams, and policies. Initial training might include items ranging from vendor supplied training sessions to validated load pattern arrangements. Often this training falls at a peak workload period during the facility start-up and validation (or during subsequent batch preparation) when attentions can be diverted into seemingly more urgent areas. In other cases, more individuals require training than can be reasonably accommodated in the area surrounding the equipment. When permitted, such training might be recorded for later review by the staff once they have fully assumed responsibility for operation. Another alternative is for those just trained to provide training to others, which may be suitable for certain operations. For best results, training should occur with written reference documentation available to those being trained.

Ongoing training should be done on a regular basis with sessions once in every one or two months, which seems to be most appropriate for an active pilot plant facility. Training should include supervisors, operators, engineers, and maintenance personnel, as well as validation and GMP staff. Training might include a process review that highlights critical steps and equipments, SOP reviews, identification of personnel safety and environmental containment issues, review of PM and ongoing maintenance needs, as well as what operational personnel should anticipate with respect to proper equipment function (127). Training sessions are one method to communicate recent SOP changes and to explain why certain procedures are necessary. They also might be used for periodic SOP reviews to obtain feedback from those using the SOP frequently. Attendance should be required, sessions recorded when possible, and those new to the facility should review prior training sessions for the past few years as applicable.

80.4.7 Validation

When manufacturing clinical materials, pilot plants are evaluated under the guidelines for investigational new drug

products, among other regulations, which clearly state that GMPs applying for drug products are approved for clinical trials in humans and animals (134). The recent guideline issued by the FDA (135) makes pilot plants eligible for product licensure should company needs require a product launch from a pilot plant facility. Individual company philosophies vary on the suitability or desirability of their pilot plants for this task because using a pilot facility for manufacturing reduces its availability for the production of clinical material. The level of validation effort required is best considered during the initial facility design. Prospective validation is the preferred option, owing to the association of document collection and equipment testing with facility start-up. Validation can be done retrospectively although the collection of the required documentation may be more challenging and modifications that are necessary for testing may be costly.

The major steps for validation ensure that installed equipment and utilities operate in a manner acceptable for the process to be run in that equipment. Because multiple processes, many of which are not necessarily identified at the time of validation, may be conducted in a pilot plant, operational ranges need to be set to accommodate a wide range of reasonably expected processes. For example, an incubator might be validated for temperatures between 25 and 37°C to accommodate common bacterial, yeast, and fungal cultures, but not necessarily at 45°C to accommodate unusual thermophiles. The selection of "worst-case" scenarios can be difficult for a pilot plant if the associated "worst-case" conditions are unduly burdensome for normal operation. Specifically, the cleaning procedures required after a three week fungal production cultivation are significantly more involved than those required after a two day fungal seed cultivation of the same culture or for a two week animal cell cultivation. Similarly, the sterilization cycle hold time for a concentrated sugar solution is substantially longer than that required for a heat-sensitive waterlike growth medium (136). Approaches for efficiently resolving these multiproduct validation issues can be complicated by desires to follow manufacturing validation guidelines, which most likely were established based on a single product.

Often validation, qualification, verification, commissioning, and start-up are used with specific definitions in mind for individual facilities and organizations. Generally, validation implies the highest rigor of direct reproducible testing of a specific procedure. Qualification encompasses a wider range of documentation collection and testing of capabilities. Verification might imply a single test against an identified standard. Commissioning can refer to documented trouble shooting of newly installed equipment, and start-up might refer to initial equipment checkouts directly after installation. The major validation phases are divided to focus on qualification followed by validation. IQ focuses of the verification of proper installation, appropriate utility connections, and adherence to manufacturers' and purchase order specifications (137). Operational qualification (OQ) includes testing of equipment function and an acceptance criteria for equipment performance (135). Performance qualification (PQ) centers on process-specific testing for SIP, CIP, and autoclave sterilization and decontamination load patterns. For computers, a system life cycle methodology incorporating specifications, program design, coding, testing, start-up, operation, and maintenance has been adopted (137,138).

Process validation centers on the reproducibility of the process in the manufacturing area (139). Parameters influencing this reproducibility might be initially identified at the laboratory scale then studied in the pilot plant to obtain acceptable operating ranges for those processing parameters, such as cultivation temperature, pH, and dissolved oxygen, are found to influence product quality. The set of criteria for proceeding to the next processing step, specifically volumetric/specific productivity, yield and purity, must be validated in a documented fashion. The critical processing steps important to process quality should be identified and validated (137). Other noncritical process steps may be studied for their impact on manufacturing productivity. Process validation may require multiple identical pieces of equipment (such as fermenters) at the laboratory and process scales to define acceptable processing ranges in a parallel rather than sequential manner.

80.4.8 Facility Records and Manufacturing Execution Systems (MES)

Documentation associated with a new pilot plant facility and its equipment can be extensive initially and increases substantially during the time that the facility operates. Although centralizing all documentation in a single archive can be attractive, duplicate copies of some items are often needed in other locations during every day operation. For example, equipment manuals and facility drawings may be needed near the actual location of the equipment, in the maintenance shop, and archived in the centralized documentation repository. Validation documentation, consisting of IQ/OQ, PQ, and load pattern/SIP/CIP reports, is generated both during the initial validation and during annual retesting and ongoing environmental monitoring programs. Storage of change control documentation might be accomplished through notebooks/file folders designated for individual pieces of equipment or individual suites. SOPs might be archived in a centralized location but also posted near equipment for ready reference. Access and sign-out procedures for the control of documentation need to be developed. Electronic on-line access is one way

to minimize space requirements and facilitate locating documentation.

A robust system for batch records needs to be created, based on individual batch sheets for processing steps or for individual pieces of equipment or for some appropriate combination of the two approaches. Issued batch sheets should be tracked by a unique sequential number with the product, processing step, and/or equipment number clearly identified. There is a need to track the use of equipment by product and batch, particularly for multipurpose pilot plant facilities. Although this might be done through individual equipment use logs, it is also helpful to include such tracking within the batch record itself.

Newly authored or completed batch sheets should be reviewed by the pilot plant operations area and may be required to be approved by a quality group prior to execution. Batch sheets should have clear written instructions as well as a signature, date and time, as required, for each step. Handwritten instructions, likely to be added during the processing of pilot scale batches, may need to be reviewed by representatives from operation and/or quality groups. Brief justifications for alterations in batch sheet instructions also should be considered. A written explanation documenting that the material from the current step is acceptable for continued processing in a subsequent step is recommended. Care should be taken to use common templates wherever possible to simplify successive batch sheet differences and minimize the review effort. Executed batch sheets should be reviewed for completeness by the operations area, by those in charge of the batch, and by a quality group as required. A tracking system should be instituted to monitor the review of completed batch sheets as well as to ensure that all issued batch numbers are accounted for in the batch record filing cabinets. Photocopying, microfilming, or scanning of completed batch sheets serve to provide a backup in case of loss or damage. Paperless electronic batch records, as well as electronic signatures, can minimize documentation volume and guidelines for implementation and validation are published (140).

Manufacturing execution systems (MES) control manufacturing processes. These include areas such as inventory, batch sheets, scheduling, and calibration management (141), as well as mechanical and operational status of equipment. Bioprocess facilities in general have been slow to implement these systems owing to their large initial costs, need for knowledgeable IT support, challenges with melding with paper-based systems, and validation requirements (55). Bioprocessing pilot plants have been even slower because their inherent need for flexibility can make scoping of MES systems difficult. However, there are several benefits deriving from MES tools and they should attain successful implementation and be readily maintainable (142). In the case of a pilot plant, frequent changes in batch-associated procedures make it challenging to gain the benefits of electronic batch records that utilize computerized cross-checking to ensure that steps are completed in the proper order (55).

REFERENCES

1. O'Leary RM, Etcheverry T, Bezy P, Anicetti V, Burton LE. PDA J Pharm Sci Technol 2001; 55: 230–234.
2. Levin J. Bioprocess Int 2004; 2: 26, 28, 30, 32, 74.
3. Basu P, Quaadgras J, Holleman J, Mack R, Noren A. Chem Eng Prog 1997; 96(6): 66–75.
4. Basu P, Quaadgras J, Mack R, Noren A. Chem Eng Prog 1998; 94(2): 67–74.
5. DePalma A. Genet News 2007; 27(9): 48–52.
6. Lias RJ, Perry SD. Bioprocess Int 2006; 4: 12–18.
7. Burnett M, Santamarina V, Omstead D. Ann NY Acad Sci 1991; 646: 357–366.
8. Tulsi B. Pharm Process 2007; 23(6): 10–12.
9. Barrer P. Biotechnology (NY) 1983; 1(8): 661–666.
10. Bader F. In: Ladisch M, Bose A, editors. Harnessing biotechnology for the 21st century. Washington (DC): American Chemical Society; 1992; pp. 228–231.
11. Odum J. Pharm Eng 1995; 15: 8, 10–18, 20.
12. Bader F, Blum A, Garfinkle B, MacFarlane D, Massa T, Copmann T. BioPharm 1992; 5(7): 32–40.
13. Hamers M. Biotechnology (NY) 1993; 11: 561–570.
14. Fitzpatrick S, Ma'ayan A, Wagget J. Chem Eng Prog 1990; 86(12): 26–31.
15. Narodoslawsky M. Chem Biochem Eng Q 1991; 5(4): 183–187.
16. Samsatli N, Shah N. Trans IChemE 1996; 74(4)C: 221–231.
17. Sofer G, Chirica LC. Biopharm Int 2006; 19(11): 48–54.
18. Shukla A, Hubbard B, Tressel T, Guhan S, Low D. J Chromatogr B 2007; 848: 28–39.
19. Chang DYH, Garza P, Huang Y-M, Talabardon M, Rahmati S, Fallon E, Noe W. In: Godia F, Fussenegger M, editors. Animal cell technology meets genomics. Netherlands: Springer; 2005; pp. 459–464.
20. Samsatli N, Shah N. Trans IChemE 1996; 74(4)C: 232–242.
21. Shanklin T, Roper K, Yegneswaran PK, Marten MR. Biotechnol Bioeng 2001; 72(4): 484–489.
22. Bader RA, Weiss J, Rumsey T. Bioprocess Int 2004; 2(5): 66–73.
23. Schell D. Appl Biochem and Biotechnol 1995; 51/52: 549–557.
24. Marks DM. Bioprocess Int 2003; 1: 50–57.
25. Cannales M, Enriquez A, Ramos E, Cabrera D, Dandie H, Soto A, Falcon V, Rodriguez M, de la Fuente J. Vaccine 1997; 15(4): 414–422.
26. Eliezer E. Biopharm 1993; 6(4): 24–29.
27. Sato R, da Costa M. Biotechnol Lett 1996; 18(3): 275–280.
28. Petrides D, Sapidou E, Calandranis J. Biotechnol Bioeng 1995; 48: 529–541.
29. Titchener-Hooker N, Gritsis D, Mannweiler K, Olbrich R, Gardiner S, Fish N, Hoare M. Biopharm 1991; 4(7): 34–38.
30. Kemp G, O'Neil P. In: Subramanian G, editor. Antibodies. New York: Kluwer Academic/Plenum Publishers; 2004; pp. 75–100.

31. Zawistowski J, Rago J. Pharm Eng 1994; 14:24+.
32. Shahidi A, Torregrossa R, Zelmanovich Y. Pharm Eng 1995; 15: 72–83.
33. Doblhoff-Dier O, Huss S, Litos R, Plail R, Unterluggauer F, Reiter M, Katinger H. Process Biochem 1991; 26(4): 201–207.
34. Nelson K. In: Prokop A, Bajpai R, Ho C, editors. Recombinant DNA Technology and Applications. New York: McGraw-Hill Inc.; 1991.
35. Palluzi R. Chem Eng 2005; 112(11): 40–45.
36. Leach K. Pharm Eng 1993; 13: 54–62.
37. Odum J. Biopharm 1992; 5(6): 36–38.
38. Scutti L, Stark S. Pharm Eng 1993; 13(1): 47–52.
39. Hamilton BK, Schruben JJ, Montgomery JP. In: Demain A, Solomon N, editors. Manual of industrial microbiology and biotechnology. Washington (DC): American Society for Microbiology; 1986; pp. 321–344.
40. Junker B, Lester M, Leporati J, Schmitt J, Kovatch M, Borysewicz S, Maciejak W, Seeley A, Hesse M, Connors N, Brix T, Creveling E, Salmon P. J Biosci Bioeng 2006; 102(4): 251–268.
41. James P. Pharm Eng 1998; 18: 72–82.
42. Wisniewski R, Burman C. In: Lubiniecki A, Vargo S, editors. Regulatory practice in biopharmaceutical production. New York: Wiley-Liss; 1994; pp. 407–445.
43. Charles M, Wilson J. In: Lydersen B, D'Elia N, Nelson K, editors. Bioprocess engineering: systems, equipment and facilities. New York: Wiley; 1994; pp. 3–67.
44. Chisti Y. Chem Eng Prog 1992; 88(1): 55–58.
45. Alford J, Allen B, Bisch S, Brill L, Clapp D, Danaher L. Ann NY Acad Sci 1994; 721: 326–336.
46. Ransohoff T, Murphy M, Levine H. Biopharm 1990; 3(3): 20–26.
47. Barry A, Chojnacki R. Biopharm 1994; 7(9): 43–47.
48. Fulton S, Shahidi A, Gordon N, Afeyan N. Biotechnology (NY) 1992; 10: 635–639.
49. Rathore AS, Kennedy RM, O'Donnell JK, Bomberis I, Kaltenbrunner O. Biopharm Int 2003; 16(3): 30–40.
50. Aronsson G, Zadorecki P. Aust J Biotechnol 1987; 1(2): 17–20.
51. Mahar J. Biopharm 1993; 6(7): 42–51.
52. Huang W. Genet Eng News 2005; 25(19): 42–44, 46.
53. Houtzager E, van der Linden R, de Roo G, Huurman S, Priem P, Sijmons PC. BioProcess Int 2005; 3: 60–66.
54. Hodge G. Bioprocess Int 2004; 2(5): 74–80.
55. Carson KL. Nat Biotechnol 2005; 23(9): 1054–1058.
56. Pora H. Biopharm Int 2006; 19(6): 72–75.
57. Farid SS, Washbrook J, Titchener-Hooker NJ. Biotechnology 2005; 21: 486–497.
58. Sinclair A, Monge M. Pharm Eng 2002; 22(3): 20–34.
59. Brecht R, Sandig V, Koch S, Riedel M. Biopharm Int 2005; 18(7): 22–30.
60. Stadler EL, Henon BK, Koiro D. Bioprocess Int 2007; 5(6): 78–82.
61. Sahoo T. Chem Eng 2004; 5: 34–39.
62. Odum J. Pharmaceutical Engineering 1992; 12(1): 8–12.
63. Nelson K. Biopharm 1988; 1(3): 34+.
64. Williams J. Biotechnology (NY) 1989; 7: 75–76.
65. Collentro A. Pharm Process 2004; 20: 14–20.
66. Dabbah R. Bioprocess Int 2006; 4(5): 18–23.
67. Glaser V. Genet Eng News 2006; 26(1): 38, 40, 41, 43.
68. Baird A, Williams R. Chem Eng 2005; 112(5): 36–43.
69. Junker B, Stanik M, Adamca J, LaRiviere K, Abbatiello M, Salmon P. Bioprocess Eng 1997; 17: 277–286.
70. Tunner J, Katsoulis G, Denoncourt J, Murphy S. Pharm Eng 2006; 26(4): 58–70.
71. Gray G. Pharm Eng 1997; 17(6): 28–33.
72. Burkhart M, Wermelinger J, Setz W, Muller D. PDA J Pharm Sci Technol 1996; 50(4): 246–251.
73. Grunenberg D. Valve Mag 2006; 18(2): 12–19.
74. Chisti Y. In: Robinson R, Batt C, Patel P, editors. Encyclopedia of food microbiology. London: Academic Press; 1999; pp. 1806–1815.
75. DePalma A. Pharm Manuf 2003; 2: 32–38.
76. Del Valle M. Pharm Eng 1995; 15: 14–22.
77. Petrossian A, Smart N, Projetto R. Biopharm 1993; 6(6): 40–45.
78. Sharp J. Good pharmaceutical manufacturing practice rationale and compliance. New York: CRC Press; 2005; p. 358.
79. Brooks CH, Russell PD. Process Biochem 1986; 21(3): 77–80.
80. Akers J. Biopharm 1994; 7(6): 43–47.
81. Akers J. J Pharm Technol 1995; 19(3): 28+.
82. Miller S, Bergmann D. J Ind Microbiol 1993; 11: 223–234.
83. Van Houten J, Fleming DO. J Ind Microbiol 1993; 11: 209–215.
84. Chisti Y. In: Subramanian G, editor. Volume 2, Bioseparation and bioprocessing: a handbook. 2nd ed. New York: Wiley-VCH; 2007; pp. 533–574.
85. Janssen D, Lovejoy P, Simpson M, Kennedy L. In: Yu P, editor. Fermentation technologies: industrial applications. New York: Elsevier; 1990; pp. 388–393.
86. Kossik J. Genet Eng News 1998; 18(6): 21.
87. Kennedy L, Boland M, Janssen D, Frude M. In: Yu P, editor. Fermentation technologies: industrial applications. New York: Elsevier; 1990; pp. 383–387.
88. Maigetter R, Bailey F, Miller B. Biopharm 1990; 3(2): 22–29.
89. Odum J. Biopharm 1993; 6(1): 42+.
90. Hodgson J. Biotechnology (NY) 1994; 12(10): 983–987.
91. Junker BH, Wang HY. Biotechnol Bioeng 2006; 95(2): 226–261.
92. Gary K. Am Biotechnol Lab 1989; 7(2): 26–33.
93. Lee Y, Tsao G. In: Ghose T, Fiechter A, Blakebrough N, editors. Volume 13, Advances in biochemical engineering. New York: Springer-Verlag; 1979; pp. 35–86.
94. Johnson M, Borkowski J, Engblom C. Biotechnol Bioeng 1964; 6: 457–468.
95. Elsworth R. Chem Eng 1972; 258: 63–71.
96. Salmon P, Buckland B. In: Rhodes M, Stanbury P, editors. Applied microbial physiology. Oxford: Oxford University Press; 1997; pp. 131–163.
97. Uttamlal M, Walt D. Biotechnology (NY) 1995; 13: 597–601.
98. Bradley J, Kidd A, Anderson P, Dear A, Ashby R, Turner A. Analyst 1989; 114: 375–379.

99. Macaloney G, Hall J, Rollins M, Draper I, Thompson B, McNeil B. Biotechnol Tech 1994; 8(4): 281–286.
100. Macaloney G, Hall J, Rollins M, Draper I, Anderson K, Preston J, Thompson B, McNeil B. Bioprocess Eng 1997; 17(3): 157–167.
101. Agayn V, Walt D. Biotechnology (NY) 1993; 11: 726–729.
102. Humphrey A, Brown K, Horvath J, Semerjian H. In: Fiechter A, Okada H, Tanner R, editors. Bioproducts and bioprocesses. Chapter 3. Berlin: Springer-Verlag; 1989; pp. 309–320.
103. Kell D, Markx G, Davey C, Todd R. Trends Anal Chem 1990; 9(6): 190–194.
104. Olsson L, Nielsen J. Trends Biotechnol 1997; 15(12): 517–522.
105. Groot W, Mijnhart R, van der Lans R, Luyben K. Biotechnol Tech 1991; 5(5): 371–376.
106. Collins S. In: Rhodes M, Stanbury P, editors. Applied microbial physiology—a practical approach. Oxford: Oxford University Press; 1997; pp. 75–101.
107. Petersen J. Pharm Technol 1988; 12(7): 42+.
108. Doblhoff-Dier O, Huss S, Litos R, Plail R, Unterluggauer F, Reiter M, Katinger H. Process Biochem 1991; 26: 201–207.
109. Blachere H. Genet Eng News 1998; 18(7): 23.
110. Jones K, Williams D, Phipps D, Montgomery P. On-line automatic tuning PID control of dissolved oxygen. In: IFAC Symposium Series 8 on Advanced Control of Chemical Processes; Toulouse, France. 1992; pp. 35–40.
111. Wilde F. Genet Eng News 1998; 18(3): 24.
112. Eiki H, Kishi I, Gomi T, Ogawa M. In: Ladisch M, Bose A, editors. Harnessing biotechnology for the 21st century. Washington (DC): American Chemical Society; 1992; pp. 223–227.
113. Hill C, Sinclair A. Biopharm Int 2007; 20(7): 38–42.
114. Kataria AR. Pharm Process 2007; 23(7): 14–16.
115. Dittmer M. Pharm Technol Eur 2006; 18: 48–40.
116. Yakren M. Biopharm Int 2006; 19(5): 34–38.
117. Bardone E, Lani B, Cassani G. Pharm Eng 1994; 14: 34–38.
118. Williams G. Plant Serv 1998; 19(3): 115–118.
119. Junker B, Lynch J, Leporati J, Schmitt J, Gieger J, Garah T, Stober M, Salmon P. Bioprocess Eng 1995; 17: 279–287.
120. Perkowski C. Biotechnol Bioeng 1984; 26: 857–859.
121. Todhunter D. Bioprocess Eng Symp 1989; 20: 97–103.
122. Kleppinger F. Int Biotechnol Lab 1987; 5(3): 28.
123. Kleppinger F. Int J Pharm Compound 1997; 1(5): 344–345.
124. Mobley K. Plant Serv 1998; 19(4): 147+.
125. Sorensen C. Pharm Process 2005; 21.
126. Wade D. Maintenance Technol 1989: 44–46.
127. Kennedy C. Biopharm 1995; 8(3): 34–37.
128. Perkowski C. Biopharm 1987; 1: 62–65.
129. Mockus L, Vinson JM, Luo K. Comput Chem Eng 2002; 26: 697–702.
130. Eastman MMR, Sawers JR. Chem Process 1998; 61(11): 15–22.
131. Singh V. Chem Age India 1988; 39(6): 387–388.
132. Kossik J. Genet Eng News 1998; 18(4): 25.
133. Guideline on the preparation of investigational new drug products (human and animal). Washington (DC): CDER, FDA; 1991.
134. Fed Regist 1995; 60(132): 35750–35753.
135. Junker B. Biotechnol Bioeng 2001; 74(1): 49–61.
136. Werner RG, Langlouis-Gau H, Walz F, Allgaier H, Hoffman H. Arzneim Forsch 1988; 38(6): 855–862.
137. Junker B, Kardos P, Smizaski W, Brix T. In: Langer ES, editor. Advances in large-scale biopharmaceutical manufacturing and scale-up production. Washington (DC): ASM Press; 2004; pp. 510–554.
138. Junker B. In: Gad SC, editor. Handbook of pharmaceuticals biotechnology. New York: John Wiley and Sons; 2007; pp. 319–370.
139. Junker B. Fed Regist 1997; 62(54): 13429–13466.
140. Fry S. Quality 2005; 44(1): 56–61.
141. Vinson JM, Keck DD, Basu PK, Houston RB, Mockus L, Noren AR. AICHE Symp Ser 1998; 320: 171–177.
142. Junker B, Reddy J, Gbewonyo K, Greasham R. Bioprocess Eng 1994; 10: 195–207.

81

SHEAR SENSITIVITY

YUSUF CHISTI
School of Engineering, Massey University, Palmerston North, New Zealand

81.1 INTRODUCTION

Depending on its intensity, a shear field may be stimulatory, inhibitory, or outright destructive. Intense shear fields will disintegrate even the most robust of microorganisms (1). Lesser levels of turbulence impact upon cellular morphology (2,3), biochemistry and physiology (4), floc size (5), and attachment and detachment from surfaces (6,7). These influences of shear stresses are reflected in the industrially important aspects of production rate, productivity, product spectrum, and characteristics. Among the most susceptible to shear effects are the animal cells, plant cells, and cells of some microalgae and cyanobacteria. Shear-associated problems have the greatest economic impact in the animal cell culture industry because it is the largest amongst ones based on shear-sensitive cells and because of the high-value nature of most cell culture–derived products (8). Damaging consequences of intense shear fields are well documented for other microorganisms also. For example, shear effects may alter characteristics of extracellular microbial polysaccharides by affecting the secretory processes in some bacteria (9,10). Considerations of shear stress levels are also important in design and operation of biomedical devices such as dialysis machines, heart–lung machines, and transfusion filters. The shear stress associated with implanted devices such as artificial heart valves can have medically significant implications. Increasingly, shear-sensitive human cells are being used to regenerate damaged tissue *in vitro* for later implanting or grafting. In other instances, susceptibility to shear may be beneficial; for example, during recovery of intracellular material by mechanical disruption (1,11,12). Some of the factors that determine shear sensitivity are summarized in Table 81.1. In the future, it might be possible to correlate the mechanical properties of cells with their susceptibility to damage by shear stress. Data is becoming increasingly available on mechanical strength of cells and organelles (13–16).

81.2 SHEAR FORCES IN BIOREACTORS

Substantial information exists on the effects of hydrodynamic forces on cells in defined flow geometries such as viscometers and capillaries (5,17–22), but little is known about shear fields in bioreactors (23–25). While selection

TABLE 81.1. Factors Determining Shear Sensitivity

1. Type of cell and species
2. Composition and thickness of cell wall when present
3. Size and morphology of cell
4. The intensity and nature of shear stress, whether turbulent or laminar, or associated with interfaces (e.g. during bubble rise and rupture)
5. Growth history, both short-term (e.g. starvation) and long-term adaptation
6. Growth environment (pH, temperature, agitation intensity, light in photosynthetic cultures)
7. Growth medium (trace elements, vitamins, carbon and nitrogen sources)
8. Growth rate
9. Growth stage
10. Type and concentration of shear protective agents if present

Upstream Industrial Biotechnology: Equipment, Process Design, Sensing, Control, and cGMP Operations, Volume 2, First Edition. Edited by Michael C. Flickinger.
© 2013 John Wiley & Sons, Inc. Published 2013 by John Wiley & Sons, Inc.

of more shear-tolerant cell lines can be helpful, successful culture of shear-sensitive biocatalysts requires attention to bioreactor design and operation.

The magnitude of the fluid mechanical forces is often expressed as shear stress τ or shear rate γ. These quantities are related; thus, in laminar Newtonian flow,

$$\tau = \gamma \mu_{\mathrm{L}} \tag{81.1}$$

where μ_{L} is the viscosity of the fluid. Shear rate is a measure of spatial variation in local velocities in a fluid. Cell damage in a moving fluid is sometimes associated with the magnitude of the prevailing shear rate or the associated shear stress, but these quantities are neither easily defined nor easily measured in the relatively turbulent environment of most bioreactors. Moreover, shear rate varies with location within a vessel. Attempts have been made to characterize an average or a maximum shear rate in various types of bioreactors and process flow devices, as discussed in the following text for the more common cases.

81.2.1 Bubble Columns and Airlift Bioreactors

Expressions for mean shear rate in bubble columns have been summarized by Chisti (25), Chisti and Moo-Young (23), and Shi *et al*. (26). These expressions generally correlate the average shear rate with the superficial gas velocity; thus,

$$\gamma = kU_{\mathrm{G}}^{a} \tag{81.2}$$

where the parameter a equals 1.0 in most cases, but the k value has been reported variously as 1000, 1500, 2800, 5000 m^{-1}, and so on (24). The enormous disagreement among various authorities is obvious in Fig. 81.1, where the shear rate calculated according to several available equations is shown as a function of the superficial aeration velocity in an air–water system in a bubble column. Theoretical analysis suggests the following dependence between average shear rate and superficial gas velocity in bubble columns (27):

$$\gamma = \left(\frac{g \rho_{\mathrm{L}} U_{\mathrm{G}}}{K} \right)^{1/(n+1)} \tag{81.3}$$

where U_{G} is the superficial gas velocity, g is gravitational acceleration, ρ_{L} is the density of the fluid, K is the consistency index, and n is the flow index.

Equation 81.2, which was originally developed for bubble columns, has been applied also to airlift bioreactors using the superficial gas velocity in the riser zone as a correlating parameter; however, that usage is incorrect (23). A more suitable form of equation 81.2 for airlift reactors is

$$\gamma = \frac{kU_{\mathrm{Gr}}}{1 + \dfrac{A_{\mathrm{d}}}{A_{\mathrm{r}}}} \tag{81.4}$$

where U_{Gr} is the superficial gas velocity in the riser, A_{r} is the cross-sectional area of the riser, and A_{d} is the

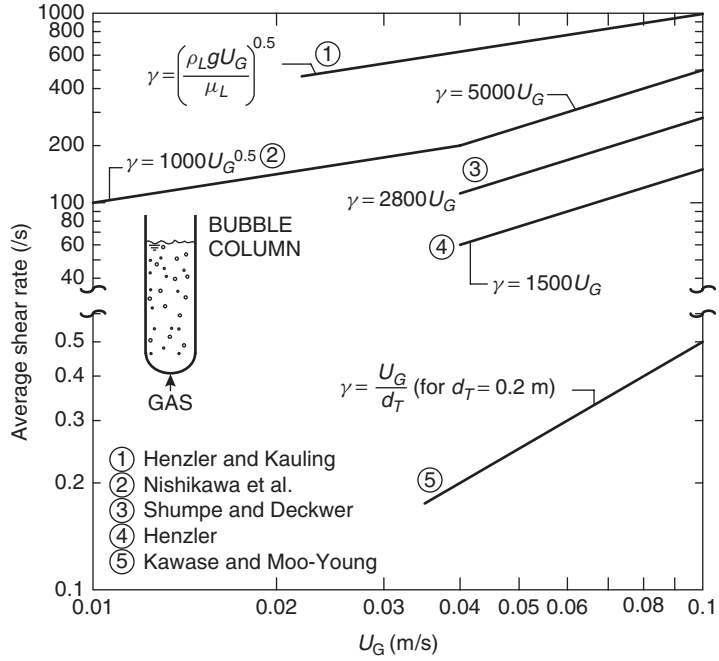


Figure 81.1. Average shear rate in air–water system in a bubble column according to various sources. Based on Ref. (25).

cross-sectional area of the downcomer. In addition to the discrepancies already noted (Fig. 81.1), Equations 81.2 and 81.4 have other significant flaws. The shear rate should depend also on the momentum transfer capability of a fluid, that is, on the density and the viscosity of the fluid;but Equations 81.2 and 81.4 show no such dependence. Indeed, it is well known that the bubble size in a turbulent field depends on the viscosity and the density of the fluid as well as on the specific energy input rate. It is therefore reasonable to assume that correlations that express the shear rate as a function of U_G (or U_{Gr}) alone are incomplete (23). Furthermore, correlations such as Equation 81.2 have generally been based on observations of phenomena at solid–liquid interfaces (e.g. heat transfer from coils or jackets), and their extension to phenomena at gas–liquid interfaces or the bulk fluid is absurd at best. Shear stress and, hence, shear rate at walls of riser and downcomer zones of an airlift device are readily calculated using methods developed for pipes and channels as discussed in a later section.

Another equation for estimation of an "effective" shear rate in airlift reactors is

$$\gamma = 3.26 - 3.51 \times 10^2\, U_{Gr} + 1.48 \times 10^4\, U_{Gr}^2 \qquad (81.5)$$

which was developed for $0.004 < U_{Gr}$ (m/s) < 0.06 (26); the shear rate range covered was 2–35 s^{-1}. Equation 81.5 was developed in an external-loop airlift reactor. First, the effect of viscosity on the induced liquid circulation velocity in the downcomer was established using Newtonian glycerol solutions at various gas flow rates. The maximum Reynolds number in the downcomer was about 3200 or barely in the turbulent regime. In a second step, pseudoplastic media were used in the reactor, and the effective viscosity (μ_{ap}) of these fluids in the circulation loop was determined as being equal to the viscosity of the Newtonian glycerol solutions when the two systems were at identical aeration and liquid circulation rates. The effective viscosity and the known values of K and n were used in the power law equation to calculate the prevailing shear rate:

$$\gamma = \left(\frac{\mu_{ap}}{K}\right)^{\frac{1}{n-1}} \qquad (81.6)$$

The calculated shear rates were correlated with the superficial gas velocity in the riser as noted in Equation 81.5 (26). Although written in terms of the superficial gas velocity in the riser, Equation 81.5 may be usefully expressed in terms of the specific power input in the reactor, as recommended elsewhere (23).

Because the procedure employed by Shi *et al*. (26) equated the viscosity-associated reduction in the liquid circulation velocity in different fluids, it gave in some sense a shear rate in the vicinity of the interface between the fluid and the walls of the reactor; shear rate in the bulk flow, which is the quantity of interest in most cases, was not quantified. Furthermore, the method of analysis used (26) applies strictly to a laminar flow regime, quite unlike the flow situations encountered in most practical operations.

Compared with bubble columns, Equation 81.5 yields quite low values for shear rates in airlift reactors, as noted by Shi *et al*. (26). In such comparisons, care needs to be taken to ensure that the devices are being compared at identical values of specific power inputs (23,25). Although Shi *et al*. (26) did not adhere to this criterion, the specific geometry of the reactor they used was such that the error was small. Unlike what Shi *et al*. (26) concluded, Equation 81.5 is not suitable for correlating mass transfer from gas bubbles or suspended solids because it does not give shear rates at gas–liquid or particle–liquid interfaces. Similarly, the usefulness of the shear rate calculated using Equation 81.5 for correlating survival of fragile biocatalysts remains questionable.

Following a methodology identical to that of Shi *et al*. (26) but in a 0.7 m^3 external-loop airlift device, Al-Masry (28) obtained the equation

$$\gamma_w = 14.9 + 11.1\, U_{Gr} + 24.392 \times 10^3\, U_{Gr}^2 \qquad (81.7)$$

for an A_d/A_r value of unity, in a 1.6-m tall reactor operated such that the superficial gas velocity in the riser remained below 0.07 m/s (28). The wall shear rate values were almost always less than 120 s^{-1}. Equation 81.7 is subject to the same criticisms as Equation 81.5. To account for effects of reactor geometry, Al-Masry (28) correlated their data and that of Shi *et al*. (26) with the equation

$$\gamma_w = 3.36\,(1 - U_{Gr})^{-32.56}\left(1 + \frac{A_d}{A_r}\right)^{0.89} h_D^{0.44} \qquad (81.8)$$

which applied to $0.0018 \le U_{Gr}$ (m/s) ≤ 0.07; $0.11 \le A_d/A_r \le 1.0$; and $1.4 \le h_D$ (m) ≤ 6. Equations 81.7 and 81.8 disregard effects of momentum transport properties on shear rate, even though such effects are known to exist (29–32).

An alternative, mechanistic approach to quantifying the bulk shear rate in various zones of airlift bioreactors has been advanced by Molina Grima *et al*. (18). Because the hydrodynamic environment in various zones of airlift reactors tends to be quite different, characterization of shear rate by a single global value is not sensible. The overall shear rates can be deceptively low even though damaging levels may be experienced in the high shear zones (18); hence, the approach of Molina Grima *et al*. (18) is preferred. This method computes shear rates using reliable expressions for energy dissipation in various zones of airlift reactors (25,33).

Some directly measured shear rate data in an airlift bioreactor for hybridoma culture have become available (34). At aeration power input of ~9 W/m^3 in the

BSA-supplemented medium (bovine serum albumin (BSA) concentration = 1 g/L), the mean shear rate values in the downcomer were ~100 s^{-1}, and were independent of height (34). For the same conditions, the mean wall shear rate values in the riser zone varied axially from a high of ~600 s^{-1} at 0.06 m from the sparger to ~100 s^{-1} about midway up the riser. Measured average wall shear rate values were reduced by BSA supplementation; but this effect was largely independent of the BSA concentration over the range 0.1–1 g/L. Although the BSA concentration over the range 0.1–1 g/L did not further affect the mean wall shear rate value, the concentration affected the probability distribution of the shear rates 0.06 m above the sparger; higher concentrations produced narrower distributions (34). These results were obtained in a concentric draft-tube airlift device that was sparged in the draft-tube. The aspect ratio of the vessel was ~7 and the A_r/A_d ratio was ~0.7. Significantly, these observations regarding the axial variation in the mean wall shear rate (γ_w) do not agree with Equation 81.8, which predicts a hyperbolic increase in γ_w with increasing height h_D of dispersion.

Other attempts at characterizing the hydrodynamic forces relied on measurement of noises associated with events such as bubble formation at the sparger, bubble disengagement at the surface, and liquid flow over the baffle into the downcomer (35). Spectra of acoustic signals were measured in water, a salt solution, and aqueous glycerol media in a bubble column and split-cylinder airlift reactor (35). Because several events occur simultaneously in bubbling reactors, there were substantial ambiguities in assignment of the noise signals to specific events. The practical significance of the results was unclear even though the intended aim was to somehow relate the data to damage of fragile cells that has been reported by others in such reactors. Other work (36) examined the structure of turbulence in water and power law solutions ($K = 0.0194^{0.973}$ Pa $s^{0.973}$ and 0.0596 Pa $s^{0.958}$) in an external-loop airlift reactor. The reactor achieved complete gas–liquid separation, and there was no gas in the downcomer. Measurements of local root mean square velocity fluctuations as an indicator of turbulence intensity showed a slight decrease from the center of the riser to the wall. These measurements were at a constant gas velocity of 2.05×10^{-2} m/s. The magnitudes of the velocity fluctuations were similar for all media; however, the velocity fluctuations were much lower in the gas-free downcomer than in the riser despite similar values of Reynolds numbers in the two zones. On the basis of measurements of one-dimensional energy spectra in the center of the riser (36), turbulence could not be considered isotropic, particularly in power law fluids. Other substantial evidence for the absence of isotropic turbulence in airlift and bubble column reactors has been documented (37,38).

81.2.2 Stirred Tank Fermenters

The local velocity at a fixed position in any vessel fluctuates around a mean value; hence, the shear rate fluctuates. The extent of fluctuations is position dependent. In stirred tanks with radial flow impellers such as Rushton turbines, the velocity fluctuations are greatest near the impeller tip and decline rapidly as one moves radially outward from the tip. Elsewhere in the vessel, the velocity fluctuations are reduced even further. The time-averaged mean shear rate generated by a six-bladed Rushton turbine agitating a Newtonian fluid in a baffled vessel of diameter d_T is given as (39):

$$\gamma_{av} = 4.2N \left(\frac{d_i}{d_T}\right)^{0.3} \frac{d_i}{W} \tag{81.9}$$

where W is the width of the impeller blade, d_i is the impeller diameter, and N is its rotational speed. The time-averaged maximum shear rate value is 2.3 times γ_{av} (39). Another expression for the maximum shear rate at Rushton turbine blades is (30):

$$\gamma_{max} = 3.3N^{1.5} d_i \left(\frac{\rho_L}{\mu_L}\right)^{1/2} \tag{81.10}$$

which applies to Newtonian and non-Newtonian liquids when $100 \le \left(N d_i^2 \rho_L / \mu_L\right) \le 29,000$. The uncertainty in the coefficient (Eq. 81.10) is said to be ±20%. For non-Newtonian fluids, μ_L in Equation 81.10 is the zero shear viscosity. A different equation has been proposed by Wichterle *et al*. (30):

$$\gamma_{max} = N\,(1 + 5.3n)^{1/n} \left(\frac{N^{2-n} d_i^2 \rho_L}{K}\right)^{1/1+n} \tag{81.11}$$

Equation 81.11 provides the maximum shear rate on a Rushton turbine blade. An average shear rate expression applicable to a broader range of impellers and media is (40)

$$\gamma_{av} = k_i \left(\frac{4n}{3n+1}\right)^{n/n-1} N \tag{81.12}$$

where n, the flow index of a fluid, equals 1.0 for a Newtonian liquid. In Equation 81.12, k_i is an impeller-dependent constant. Some typical k_i values are noted in Table 81.2.

TABLE 81.2. The k_i Values for Use in Equation 81.12

Impeller	k_i
Six-bladed disc turbines	11–13
Paddle impellers	10–13
Propellers	~10
Helical ribbon impellers	~30

Shear stress encountered near the wall of a stirred tank is discussed by Wichterle *et al*. (41,42). According to Wichterle *et al*. (41), the friction factor C_f and the wall shear stress τ_w in a stirred tank are related as follows:

$$C_f = \frac{\tau_w}{\rho_L N^2 d_i^2} \left(\frac{d_T}{d_i}\right)^2 \tag{81.13}$$

The value of the friction factor was found to depend on position at the tank wall (42). In both Newtonian and pseudoplastic media, the maximum value of the friction factor correlated with the impeller Reynolds number, as follows:

$$C_{f\,max} = (15n + 1)\, Re_i^{-1/(1+n)} \left(\frac{d_T}{d_i}\right)^{2(1-n)/(1+n)} \tag{81.14}$$

where the Reynolds number is $Re_i = \frac{N^{2-n} d_i^2 \rho_L}{K}$. According to Equation 81.14, the maximum shear rate at the wall in a standard stirred tank ($d_i/d_T = 1/3$) containing a Newtonian fluid ($n = 1$) is nearly 30% of the maximum shear rate near the impeller, calculated with Equation 81.11.

The various shear rate correlations discussed here are compared in Fig. 81.2, for water in a standard stirred tank (43) agitated with a 0.1-m diameter six-bladed Rushton turbine. For some context, the shear rate around a rising bubble may be approximated as the ratio of the terminal rise velocity to the bubble diameter (or radius); hence,

$$\gamma_{av} = \frac{2U_B}{d_B} \tag{81.15}$$

In air–water, under conditions typical of bubble columns and airlift reactors, the bubble rise velocity is about 0.2 m/s and the bubble diameter is about 0.006 m. Thus, the interfacial shear rate approximates to 67 s^{-1} if the interface is nonmobile. Lower shear rates are expected at circulating interfaces. Shear rate in stirred tanks is further discussed elsewhere (27,41,42,44).

81.2.3 Spin Filter

Spin filters—rotating cylinders made of wire screen with openings that are significantly bigger (e.g. 25 μm openings) than the cells—are used to retain suspended animal cells in perfusion culture continuous bioreactors. Most of the cells are kept on the upstream side of the wire mesh by a hydrodynamic mechanism that depends on rapid rotation (e.g. 500 rpm) of the cylindrical screen (Fig. 81.3). The spent, largely cell-free medium is withdrawn from the zone within the rotating screen. Shear stresses associated with rotation of spin filters do not generally damage animal cells (45). Sometimes the cell-free zone within the confines of the screen are also used for submerged aeration.

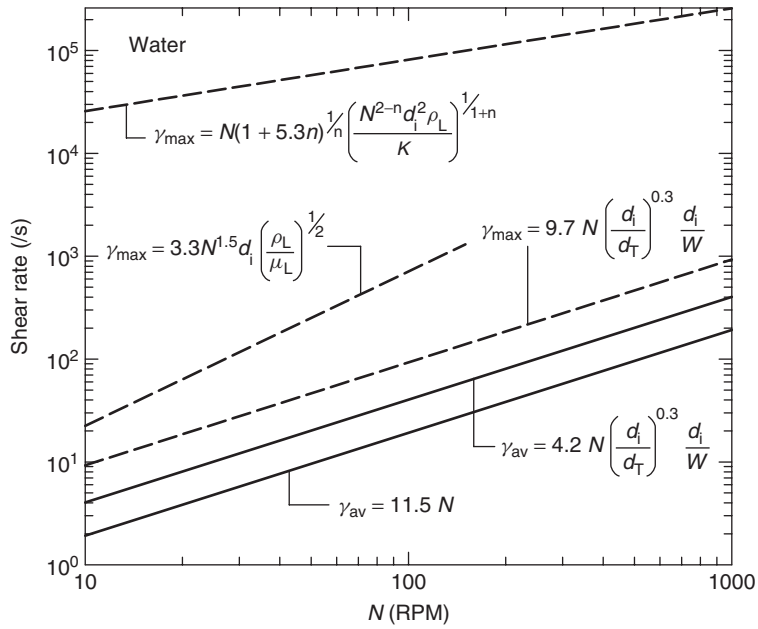


Figure 81.2. Comparison of the various shear rate correlations for water in a standard stirred tank agitated with a 0.1-m diameter, six-bladed Rushton turbine. The dashed lines are for the maximum shear rate; the solid ones are for the average shear rate. See text for additional details.

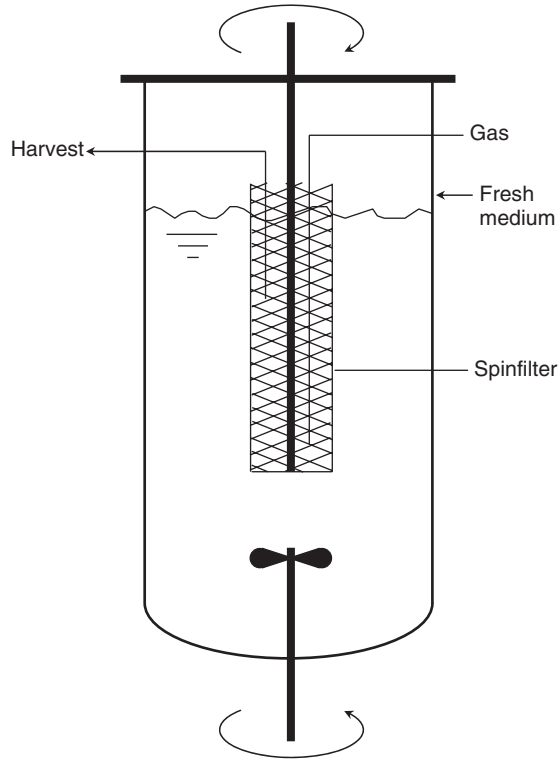


Figure 81.3. Perfusion culture with spin filter for hydrodynamics-based cell retention in bioreactors.

81.2.4 Other Flow Devices

Bioreactors and process vessels are where much of the shear-sensitive material is processed; however, at least part of the processing usually requires transfer of material between vessels. Transfer is accomplished through pipe work and centrifugal pumps are sometimes used. Methods of estimating shear stress levels in these devices are briefly summarized next.

81.2.4.1 Pipes, Tubings, and Flow Channels

81.2.4.1.1 Newtonian Fluids. In developed laminar flow of a Newtonian fluid through a straight tube of diameter d, the wall shear rate is given as

$$\gamma_w = \frac{8U_L}{d} \tag{81.16}$$

where U_L is the mean flow velocity. For rectangular channels of height h, the maximum or wall shear rate in developed laminar flow is

$$\gamma_w = \frac{6U_L}{h} \tag{81.17}$$

where U_L is again the mean flow velocity.

The wall shear stress, that is, the maximum value, in a flow channel such as the riser of an airlift reactor is related to the pressure drop (ΔP), the length L of channel, and the hydraulic diameter (24); thus,

$$\tau_w = \frac{d}{4L}\Delta P \tag{81.18}$$

Consequently, in turbulent flow, the wall shear stress is

$$\tau_w = \frac{1}{2}C_f \rho_L U_L^2 \tag{81.19}$$

where ρ_L is the liquid density and C_f is the Fanning friction factor. The latter is related with the Reynolds number as follows:

$$C_f = 0.0792\left(\frac{\rho_L U_L d}{\mu_L}\right)^{-0.25} \tag{81.20}$$

where d is the hydraulic diameter of the flow channel or pipe. From Equations 81.19 and 81.20, the wall shear stress can be shown to depend on Newtonian viscosity of the fluid: $\tau_w \propto \mu_L^{-0.75}$ (18). A typical variation of the wall shear rate and the isotropic turbulence shear rate (see a later section) during flow of a cell culture broth through a pipe is shown in Fig. 81.4. The wall shear rate greatly exceeds that in the bulk fluid; nonetheless, as discussed in a later section, conditions in the bulk volume are usually the relevant ones with regard to cell damage. Use of Equations 81.16 and 81.17 and similar others given later presupposes that the liquid velocity is known. This is normally the case in pipes and channels; however, with airlift vessels, the induced liquid circulation rate will often need to be estimated using available methods (24,25,33).

81.2.4.1.2 Non-Newtonian Power Law Fluids. Methods for calculation of wall shear stress in laminar and turbulent flow of power law fluids with and without dispersed gas have been discussed by Chisti (25) and Chisti and Moo-Young (46). For a non-Newtonian pseudoplastic medium flowing through a tube such as the riser or the downcomer of an airlift bioreactor, the flow is laminar when (47)

$$Re \leq 2300\frac{3n+1}{4n} \tag{81.21}$$

where the Reynolds number is calculated using the equation

$$Re = \frac{8\,U_L^{2-n}\,d^n\,\rho_L}{K\left(\frac{6n+2}{n}\right)^n} \tag{81.22}$$

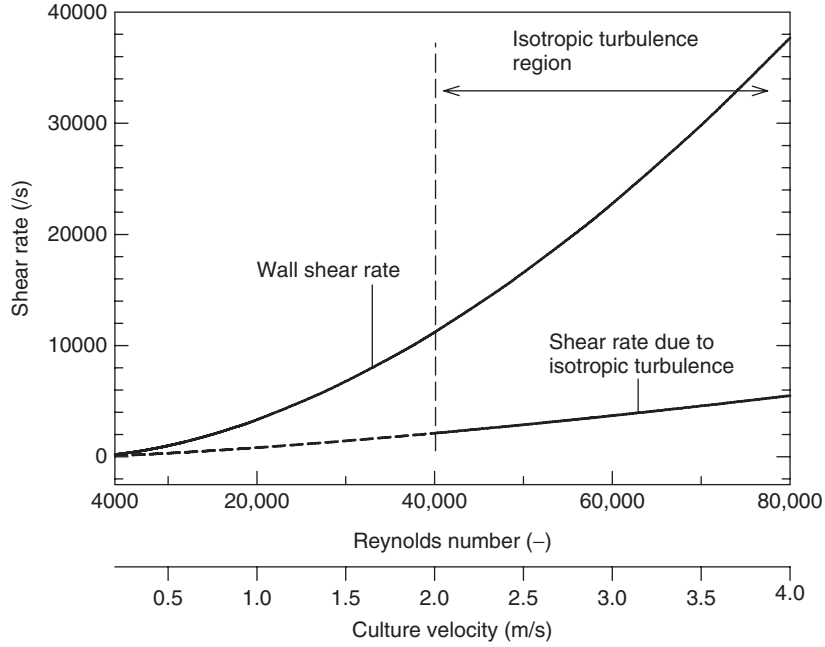


Figure 81.4. Variation of shear rate at pipe wall and in the bulk culture during turbulent flow through a 0.02 m diameter smooth pipe at various Reynolds numbers. The culture velocity is also shown. Density and viscosity of the culture fluid were 10^3 kg/m^3 and 10^{-3} Pa s, respectively. Turbulence was considered to be isotropic when the length scale of the terminal microeddies was smaller than or equal to a thousandth of the diameter of the pipe. The latter was taken as the scale of the primary eddy.

In the laminar regime, the wall shear stress for flow of a gas-free liquid has been expressed as (48)

$$\tau_w = \frac{8\,\rho_L\,U_L^2}{Re} \tag{81.23}$$

When the flow is turbulent, that is, the Reynolds number exceeds the value calculated with Equation 81.21, the wall shear stress in a gas-free liquid is (47,48)

$$\tau_w = \frac{0.316n^{0.121}\rho_L U_L^2}{8Re^{2/n(x-1)+2}} \tag{81.24}$$

In presence of a gas, the shear stress is a complex function of τ_w, the gas holdup, the properties of the liquid (ρ_L, K, n), and the superficial velocities of the gas and the liquid phases as discussed elsewhere (25,46). In Equations 21–24, d is the channel diameter, U_L is the superficial liquid velocity, K is the consistency index, and n is the flow behavior index. The parameter x in Equation 81.24 is given as

$$x = 0.70n^{-0.591} \tag{81.25}$$

as reported by Chisti and Moo-Young (46) based on data of Sokolov and Metkin (47).

81.2.4.2 Turbulent Submerged Jets. Submerged jets are encountered wherever a pipe or nozzle discharges a fluid beneath the surface of the same fluid in a larger reservoir. For example, culture broth recirculating from a tank to an ultrafiltration module and back to the tank could form a submerged jet. If the cross-sectional area of the discharge nozzle is less than about 25% of that of the reservoir, the wall effects can be neglected, and the jet is said to be "free". In a stable, submerged, turbulent jet, the maximum shear stress occurs in the direction of discharge, six to seven nozzle diameters downstream from the orifice. This shear stress is given as

$$\tau_{max} = 0.018\rho_L u_o^2 \tag{81.26}$$

where u_o is the velocity at the orifice.

A turbulent jet consists of two regions (Fig. 81.5). A conical core of fluid next to the orifice retains the discharge velocity of the orifice. This region of potential flow extends about six nozzle diameters from the discharge orifice, and within this region shear stresses are minimal. The potential core is surrounded by an expanding zone of developed turbulence. Quiescent fluid surrounds the turbulent flow field (Fig. 81.5). The total mass flow rate at any cross-section in the turbulent flow field of a jet increases linearly with

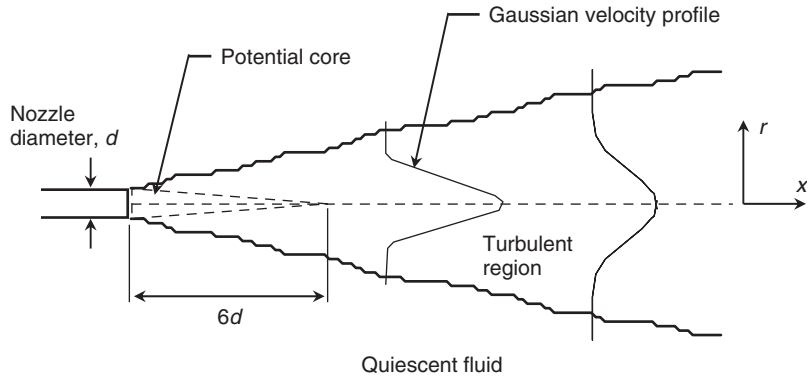


Figure 81.5. A submerged turbulent jet.

distance from the orifice, as the surrounding quiescent fluid is entrained in the jet. The velocity profile in the turbulent region is Gaussian and it is described by the equation

$$\frac{u_1}{u_{max}} = e^{-\beta(r/x)^2} \tag{81.27}$$

where β is about 75.2, r/x is the dimensionless radial distance (Fig. 81.5), u_1 is the local velocity at position r, and u_{max} is the maximum or the centerline velocity. The Gaussian profile persists until the centerline velocity declines to that of the surrounding flow. The maximum velocity, u_{max}, depends on the exit velocity at the nozzle and the axial distance:

$$\frac{u_{max}}{u_o} = C\left(\frac{d}{x}\right) \tag{81.28}$$

In Equation 81.28, d is the orifice diameter, x is the axial distance, and the constant C is about 6.06. The constants β and C may be influenced by the operating conditions.

If the nozzle discharge velocity is the same as in the pipe, the maximum shear stress at the pipe wall is always less than in the jet. The ratio of these shear stresses is given as

$$\frac{\tau_{max\,J}}{\tau_w} = 0.455\left(\frac{\rho_L U_L d}{\mu_L}\right)^{0.25} \tag{81.29}$$

The ratio τ_{maxJ}/τ_w increases with increasing velocity of discharge as shown in Fig. 81.6 for discharge of a cell culture fluid from a 0.02-m diameter pipe. Consequently, damage to fragile cells may occur during transfer operations such as inoculation of a bioreactor, even though the velocity in the transfer pipe may be relatively low. These effects

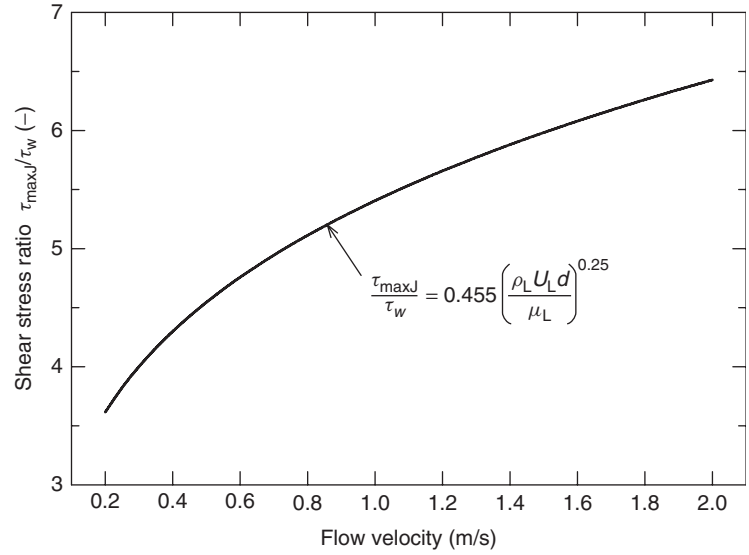


Figure 81.6. Ratio of the maximum shear stress in the jet to that at pipe wall for flow of animal cell culture fluid (density = 10^3 kg/m^3, viscosity = 10^{-3} Pa s) from a 0.02-m diameter pipe ending in same diameter opening to form a free jet.

may be avoided by discharging the jet above the level of the receiving fluid such that the liquid flows down the vessel wall.

Energy dissipation rates in turbulent jets are nonuniform. Dissipation is greatest near the axis of the jet and declines radially outward, becoming negligible at dimensionless radial distances (r/x) of greater than 0.2. In the fully developed turbulent region, the radially averaged energy dissipation rate E declines with axial location as follows:

$$E = \eta \left(\frac{d u_o}{x^{4/3}} \right)^3 \tag{81.30}$$

where the constant η is about 50 (49,50).

81.2.4.3 Centrifugal Pumps. Centrifugal pumps are commonly employed in bioprocessing; hence, knowledge of the shear rate in these devices is essential to assessing their suitability for a given use. The shear rate in a Newtonian fluid adjacent to the rotating impeller of a centrifugal pump depends on the radial position. The local shear rate at any position has been expressed as

$$\gamma = 6.30 N Re_L^{0.5} \tag{81.31}$$

where the local Reynolds number at the local diameter d_L is

$$Re_L = \frac{N d_L^2 \rho_L}{\mu_L} \tag{81.32}$$

Equation 81.31 is based on theoretical considerations, but it has closely correlated with the measured shear rate data over the range $10^2 \leq Re_L \leq 2 \times 10^6$ in a centrifugal pump with the impeller rotating in a standard volute casing (51). Over the approximate impeller rotational speed range of 0.01–100 s^{-1}, the shear rate values ranged over 1–10^5 s^{-1} in aqueous electrolyte solutions (51).

As a general guideline, centrifugal pumps may be used to transfer most low viscosity microbial broths and enzyme solutions so long as gas–liquid interfaces are rigorously excluded. Centrifugal pumps should not be used for animal cells, biofilm-supporting particles, soft immobilized enzyme supports, suspensions of nematodes and protozoa, protein precipitates, and plant cells. These pumps will be satisfactory for some microalgae, but not for others.

81.2.5 Shear Rate in Isotropic Turbulence

Irrespective of the bioreactor configuration, a turbulence field is deemed isotropic when the size of the primary eddies generated by the turbulence-producing mechanism is a 1000-fold or more compared to the size of the energy-dissipating microeddies. The length scale of the primary eddies is often approximated as the width of the impeller blade or the diameter of the impeller in a stirred tank. In bubble columns and airlift bioreactors, the length scale of primary eddies is approximated as the diameter of the column (or the riser tube) or the diameter of the bubble issuing from the gas sparger.

Shear stress, shear rate, the dimensions of microeddies, and other characteristics of flow are linked ultimately to the energy input and dissipation rates in the fluid. The local shear rate in the vicinity of an eddy in an isotropically turbulent field may be estimated as the ratio of the velocity and the length of the eddy; hence,

$$\gamma_i = \frac{u}{\ell} = \frac{\mu_L}{\rho_L \ell^2} \tag{81.33}$$

where ρ_L and μ_L are the density and the viscosity of the fluid, respectively. The mean length ℓ and the velocity u of the microeddies are related with the energy dissipation in the turbulence field; thus,

$$\ell = \left(\frac{\mu_L}{\rho_L} \right)^{3/4} E^{-1/4} \tag{81.34}$$

and

$$u = \left(\frac{\mu_L E}{\rho_L} \right)^{1/4} \tag{81.35}$$

where E is the rate of energy dissipation per unit mass of fluid. In most cases, all the energy input to the fluid is dissipated in fluid eddies, and E equals the rate of energy input. Equations 33–35 apply when local isotropic turbulence prevails.

For single-phase pipe flow, the specific energy dissipation rate is

$$E = \frac{U_L \Delta P}{\rho_L L} \tag{81.36}$$

where ΔP is the pressure drop over the tube length L, and U_L is the mean flow velocity. The pressure drop may be computed using Equations 18–20. The energy dissipation rate in bubble columns and airlift vessels is a function of the superficial aeration velocity (24,25); thus

$$E = g U_G \qquad \text{(bubble columns)} \tag{81.37}$$

and

$$E = g \frac{U_{Gr}}{1 + \dfrac{A_d}{A_r}} \qquad \text{(airlift bioreactors)} \tag{81.38}$$

Methods for calculating the specific energy dissipation rate in stirred vessels have been discussed elsewhere

(43,52). The energy dissipation varies greatly from the mean value in a stirred tank. The maximum energy dissipation occurs in the vicinity of the impellers. This maximum value can be calculated using the equation:

$$E = \frac{PoN^3 d_i^2}{\rho_L} \tag{81.39}$$

where Po is the power number, d_i is the diameter of the impeller, and N is the rotation speed (s^{-1}). In developed turbulent flow in stirred vessels, that is, when the impeller Reynolds number ($Nd_i^2\rho_L/\mu_L$) exceeds 10^4, the power number is generally constant for a given type of impeller and tank geometry. The constant power number values are noted in Table 81.3 for some common types of impellers in baffled stirred tanks. The energy dissipation rate in presence of aeration is generally less than in the equivalent ungassed state. The extent of reduction depends on the aeration rate used. In typically aerated conditions in microbial culture, the energy dissipated is generally 50–60% of the nonsparged case; however, in animal cell culture the aeration rates are so small that power number is barely affected by aeration.

Equation 81.39 assumes that dissipation occurs in the volume around the impeller; but it disregards flow through that volume. If the volume flowing through the impeller zone in 1 s is taken into account, the maximum specific energy dissipation will reduce by a factor that depends on the rotational speed and the geometry of the impeller.

As noted in Fig. 81.7, the same relationship exists between the isotropic turbulence shear rate and the specific energy dissipation rate in various culture devices; however, because the different devices operate in different ranges of specific energy dissipation rates, the shear rates experienced by cells are different under typically used culture conditions.

TABLE 81.3. Turbulent Power Number (Po) in Baffled Stirred Tanks

Impeller	Po
Propeller (square pitch, three-bladed)	0.32
45° Pitched blade turbine (six blades, pumping down)	1.90
Lightnin' A310 hydrofoil	0.31
Turbine (six-bladed)	6.30
Turbine (six curved blades)	4.80
Flat paddle (two blades)	1.70
Scaba agitator	1.45
Prochem impeller (five blades, $d_i = d_T/2$)	1.0

Source: Ref. 43.

Generally, if the dimensions of the biocatalyst particle are much smaller than the calculated length ℓ of the microeddies, the particle is simply carried around by the fluid eddy; the particle does not experience any disruptive force. On the other hand, a particle that is larger than the length scale of the eddy will experience pressure differentials on its surface, and if the particle is not strong enough it could be broken by the resulting forces.

In addition to turbulence within the fluid, other damage-causing phenomena in a bioreactor include interparticle collisions; collisions with walls, other stationary surfaces, an the impeller; shear forces associated with bubble rupture at the surface of the fluid; phenomena linked with bubble coalescence and breakup; and bubble formation

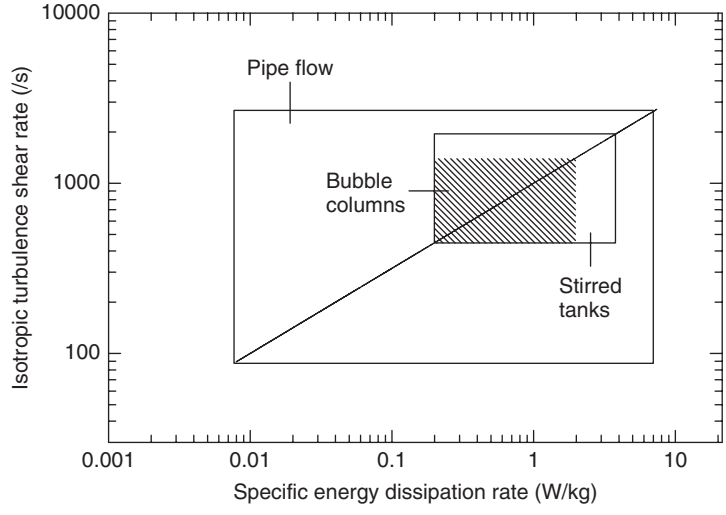


Figure 81.7. The relationship between isotropic turbulence shear rate and the specific energy dissipation rate is the same (solid line) in various culture devices, but the devices operate in different ranges of specific energy dissipation rates (boxes) along the diagonal line. The plot is for a waterlike culture fluid (10^3 kg/m^3 density, 10^{-3} Pa s viscosity).

at the gas sparger. Some of these aspects are discussed elsewhere in this chapter. Summarizing, several possible shear rate values may be calculated for a given situation in a bioprocess device. Not every calculated value is appropriate or relevant to the problem at hand. For pneumatically agitated bioreactors, when the turbulence characteristics in the bulk fluid are the relevant ones, the preferred approach is to use Equation 81.33 for shear rates in the vicinity of eddies. The same applies to mechanically stirred tanks. In some cases, the relevant shear rate may be that at the interface of a rising bubble unless turbulence is so intense that bubbles do not rise freely. Other situations would be controlled by the bubble rupture events as discussed later. In some other cases, the fluid eddy shear rate and the maximum shear rate at the impeller will need to be taken into account. Factors such as the frequency of passage of a sensitive biocatalyst through high shear regions may need consideration. Shear rates in the vicinity of particles and bubbles may be greatly accentuated by the presence of ultrasound (53).

81.3 RESPONSE TO SHEAR

Response to shear has been characterized using various indices, including growth rate (54–56), cell viability (57), and regrowth potential (58); release of intracellular material (54,59,60); changes in oxygen uptake rate, adenosine triphosphate (ATP), productivity of metabolites, and biochemical composition of the cells; and alterations in morphology of cells and cell aggregates (2,58,59).

Most studies of shear response of cells have utilized batch culture with or without aeration. Such cultures contain cells at different stages of growth; hence, the size and metabolic state of cells are nonuniform. In contrast, continuous culture is time consuming (54), differs substantially from the culture methodologies that are typically employed commercially, and, through natural selection, the cells in continuous culture adapt to shear fields, hence masking the effect of shear. For example, Wu *et al*. (61) noted for insect cells that the beneficial effect of shear-protective agents (serum, methyl cellulose, Pluronic F68) were not as important as the effect of passage number. Similar results have been alluded to for plant cells (54). To overcome problems associated with cell growth and shear adaptation, Zhang *et al*. (59) recommended the use erythrocytes for comparative evaluation of the hydrodynamic environment in bioreactors. A nongrowing, well-defined, and shear-susceptible cell population such as those provided by erythrocytes can help identify suitable regimes of operation of a given reactor. In addition, shear damaging potential of different bioreactor configurations can be assessed on a common basis using cells such as erythrocytes. Specific information on shear susceptibility of animal, plant, and various microbial cells is discussed in the following sections.

81.3.1 Bacteria, Yeasts, and Mycelial Microfungi

Yeasts, bacteria, and mycelial microfungi are generally quite robust and not easily damaged under typical processing conditions; however, even the most robust cells are broken when subjected to suitable combinations of high stress and exposure time (1). Often, genetically modified strains of an otherwise robust microorganism are less shear tolerant (1,10,62–64). With microorganisms, the composition of the growth medium and the specific growth rate used for the culture are known to influence the robustness of the cell (1). Cells grown in fully defined media that may lack one or more component essential for the synthesis of normal cell wall are often less robust (1). Growth at a higher specific rate will often produce weaker cells (1). When the shear field is not intense enough to damage cells, it may still affect product formation and characteristics (9,10). In one case, properties of a shear-sensitive polymer were affected, but not the producing bacterial cells (10). Cells experiencing physiological stress—for example, starvation—are more susceptible to shear stress–related damage (60).

Fragmentation of fungal hyphae and filamentous bacteria by mechanical agitation in stirred fermenters has been widely reported (55,56,65–69). Reports cited by Märkl *et al*. (60) document increasing release of intracellular material from mycelium of *Rhizopus javanicus* and *Mucor javanicus* as the stirrer speed increased. Increasing release of nucleotides was noted with increasing speed of agitation or with increasing agitation time at a constant agitation speed. Effect of Rushton turbine tip speed on performance of a process for converting cellulose to protein-enriched microbial biomass was clearly demonstrated by Moo-Young *et al*. (55). The process utilized the filamentous microfungus *Neurospora sitophila* for the conversion. Increasing impeller tip speed from 2.35 to 3.29 m/s reduced the specific protein production rate and the final yield (Fig. 81.8). In addition, a distinct lag phase was observed at the higher agitation rate (Fig. 81.8) when the inoculum grown in a more quiescent environment was transferred to the fermenter. At the highest tip speed shown in Fig. 81.8, the specific protein production rate was only 55% of that at the lowest tip speed. Similarly, the yield of crude microbial protein was reduced to ~67% of the value obtained at the lowest agitation speed used (55). Further work revealed that agitation-associated damage could be reduced substantially by replacing the Rushton turbines with axial flow hydrofoil impellers (55), thus confirming that different types of impellers generate very different shear fields at identical tip speeds. For equal or lower power draw, hydrofoil impellers are typically better bulk mixers than Rushton turbines (43,52).

In *Penicillium chrysogenum* fermentations performed in turbine impeller–agitated vessels of 0.005–1 m^3 working volumes, operated at impeller tip speeds of 2.5–6.3 m/s, the specific penicillin production rate and the mean length

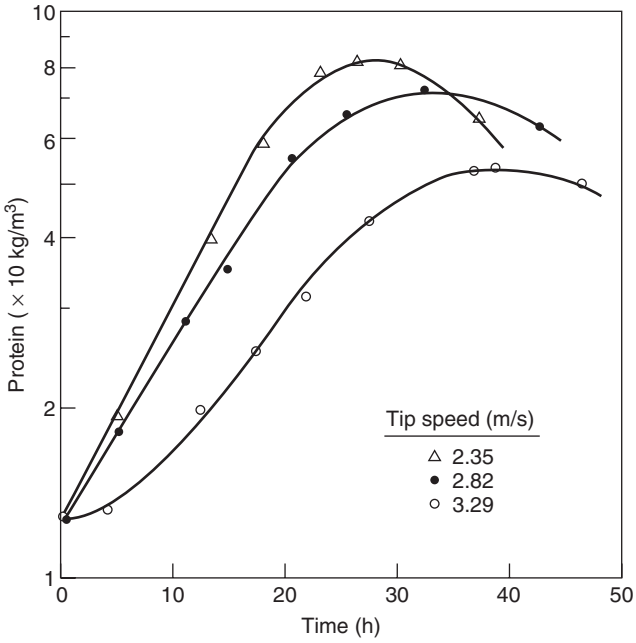


Figure 81.8. Effect of Rushton turbine tip speed on protein production by the mold *N. sitophila*. *Source:* Refs 55 and 56.

of the main hyphae were lower at high agitation intensities (2). High agitation speeds affected the fungal morphology, promoting mycelial fragmentation and a greater frequency of branching (2). The behavior of the fermentation at various scales correlated poorly with the impeller tip speed, but correlation was superior in terms of a parameter that took into account the frequency of passage of the culture through the intensely agitated zones around the impellers (2). This behavior suggests that the degree of hyphal damage in stirred bioreactors depends on a combination of the shear intensity in the impeller zone and the cumulative time of exposure of the microbial solids to the shear field.

Sometimes, especially with certain mycelial microfungi, the biomass yield may not be affected by agitation rate, but the cell morphology and production of metabolites may be influenced greatly. Using different strains of citric acid-producing *Aspergillus niger*, Ujcova *et al*. (3) showed that the yield of citric acid first increased with increasing agitation rate presumably because of improved oxygen supply, but the yield declined because of cell damage if the agitation speed was increased further. The yield maxima occurred at different agitation rates for different strains, and the sensitivity to agitation differed among strains. Other morphological effects of non-damaging shear levels include changes in growth form, whether pellet or pulplike; changes in the degree of branching; the extent of entanglement; whether growth occurs in filamentous or spherical cell form in certain dimorphic species; as well as others.

Evidence suggests that even a supposedly robust cell such as *Saccharomyces cerevisiae* (1,11) is susceptible to mechanical shear damage in fermenters (70–72). In one study, *S. cerevisiae* suspended in isotonic saline lost viability at increasing rate over a 25-h period, as the agitation speed of the paddle impeller was increased (71). At 1.43 m/s impeller tip speed, >90% of the cells were dead over 25 h. In contrast, at 0.66 m/s tip speed, only about 15% of the cells died over the same period (71). Excessive shear has been alleged to also influence the productivity of ethanol in fermentations employing *S. cerevisiae* (70). Shear stress in stirred fermenters has been claimed to affect production of thuringiensin by the bacterium *Bacillus thuringiensis* during stationary phase of culture (73).

Among methane bacteria, *Methanobacterium thermoautotrophicum* with rodlike cells that exceeded 2 μm in length was highly resistant to shear stress (60). In contrast, and surprisingly, the relatively smaller (<2 μm) spheroidal cells of *Methanococcus vaniellii* were quite sensitive to shear stresses (60). Supplementing the medium with carboxymethyl cellulose viscosity enhancer increased the extent of the cell damage (60). Failure to provide an essential nutrient, selenium in this case, also enhanced shear susceptibility of the culture (60). Although many authors have successfully correlated cell damage with the tip speed of the impeller, Märkl *et al*. (60) believe that power input per unit culture volume is a superior correlating parameter, which is also suitable for comparing the cell damage effects of mechanically stirred and other nonmechanically agitated bioreactors. A constant power input per unit culture volume has also been suggested as a bioreactor scaleup criterion for fragile biocatalysts (60). This recommendation notwithstanding, average power input alone cannot be a universally satisfactory determinant of cell damage; as noted in an earlier section, the maximum shear rate and the frequency of passage (or cumulative exposure) through the high shear zone need to be taken into account, especially when the shear rate in a given device is strongly position dependent. Several studies confirm that frequency of passes through high shear environment has a clear impact on biocatalyst survival (1,2,11,12,20,24,74). Effects of variously intense shear fields on microbial cells are further discussed by Thomas (5,75), Prokop and Bajpai (76), and Chisti and Moo-Young (1). Shear effects on microbial flocs and pellets are treated in a separate section of this chapter. Table 81.4 summarizes the damaging threshold values of impeller tip speed and specific power input for some microorganisms.

81.3.2 Microalgae and Cyanobacteria

Cell fragility has been referred to as the key problem of culture of microalgae in photobioreactors (77); however, the real situation is not quite as bad. Among microalgae, the sensitivity to shear varies greatly with the species. Algae

TABLE 81.4. Damaging Threshold Values of Impeller Tip Speed or Specific Power Input for Some Microorganisms

Stirred fermenters	**Impeller tip speed** (m/s)
Saccharopolyspora erythraea	>1.07
Methanococcus jannaschii	>2.35
Microalga *Ochromonas malhamensis* (8–20 μm average diameter cells)	≤1.4 with low level sparging
Ciliated protozoan *Tetrahymena pyriformis* (~80 μm cell diameter)	≤0.5
Saccharomyces cerevisiae suspended in isotonic saline	<1.43
Recombinant *Aspergillus oryzae*	Power inputs between 2.2 and 12.6 kW/m^3
Penicillium chrysogenum	>2.5
Neurospora sitophila	~2.35
Trichoderma harzianum	~0.4
Airlift bioreactors	**Power input** (W/m^3)
Microalga *Phaeodactylum tricornutum*	~270
Bubble columns	**Power input** (W/m^3)
Microalga *Dunaliella tertiolecta*	98

such as *Dunaliella* are indeed extremely fragile, but many other species will tolerate high levels of turbulence and sparging with gas. Thus, gas sparged airlift devices are commonly used to circulate algal cultures through solar receivers of photobioreactors (24,78–80). Similarly, relatively low shear positive displacement rotary pumps have been successfully employed. High shear centrifugal pumps have also been used; however, at least in some cases, the centrifugal pumps are known to be more damaging than the other fluid moving systems. In one case, for otherwise equivalent conditions, replacement of the centrifugal pump with a positive displacement device doubled the productivity of *Porphyridium cruentum* (77), a producer of phycoerythrin and polyunsaturated fatty acids. Irrespective of the method used to circulate the culture, the culture flow velocities through tubular solar receivers typically range over 0.3–0.5 m/s in tubes up to 0.06 m in diameter. These conditions have been used with a variety of algae.

Damage to cells of the marine microalgae *Skeletonema costatum* and *Haslea ostrearia* has been reported during passage through pumps and valves (81). The extent of damage depended on the characteristics of the device and the operational parameters such as the opening of the valve (i.e. the pressure drop and hence the energy dissipation rate) and the rotational speed of the pump. *H. ostrearia* is a single-celled diatom, whereas *S. costatum* grows as chains of connected cells. Both centrifugal and positive displacement rotary vane pumps reduced the chain length of *S. costatum*. Centrifugal pump was more damaging than the positive displacement device. Larger algal filaments were the most susceptible to damage. The rate of decrease in chain length was greater for chains with a longer initial length (Fig. 81.9). In the positive displacement pump, the percentage cell damage D_p correlated (81) with the number of passes N_d through the pump and the initial length L_i (μm) of the algal filaments as follows:

$$D_p(\%) = 2.54 N_d^{0.21} L_i^{0.55} \tag{81.40}$$

Equation 81.40 applied to filaments with initial modal lengths of 37.1, 65.5, and 77.8 μm. In a monoscrew pump, the percentage cell damage increased (81) with

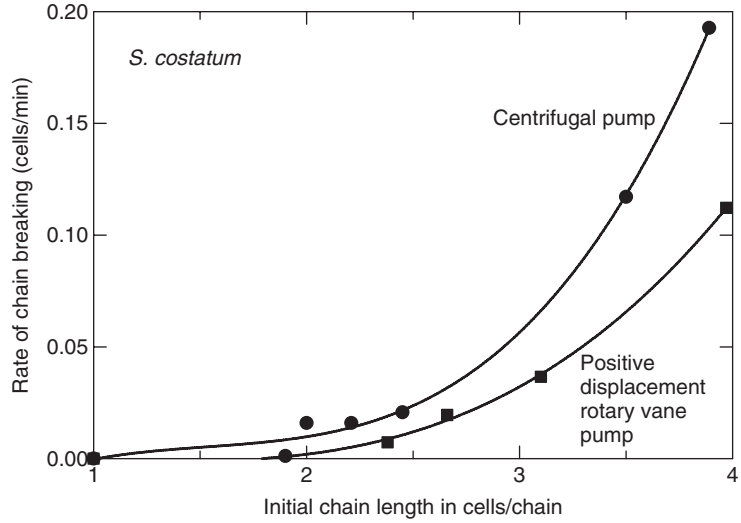


Figure 81.9. Rate of breakage of *S. costatum* chains as a function of the initial chain length (number of cells) for two types of pumps. The flow rate was 12 L/min in both cases. *Source:* Ref. 81.

increasing frequency of passes through the device; for a given frequency F, the damage increased with cumulative exposure time t as follows:

$$D_p(\%) = 1.8\,(Ft)^{0.64} \qquad (81.41)$$

For similar number of passes and taking into account pump leakage, the monoscrew pump was less damaging than the centrifugal device (81). Similarly, for *H. ostrearia*, the monoscrew pump was less disruptive than both the centrifugal and the positive displacement rotary vane machines (81). In other similar work with the highly motile microalga *Tetraselmis suecica*, Jaouen *et al*. (82) observed a loss of motility on passage of culture suspension through centrifugal and rotary vane positive displacement pumps but not through a peristaltic pump.

In cultures of *Haematococcus pluvialis*, a producer of astaxanthin, early onset of the stationary phase has been associated with turbulence-induced deflagelation of the cells (77). Fragility of species such as *H. pluvialis* depends also on the phase of growth; thus, tailoring the bioreactor operational regime to the growth phase can improve overall productivity (77). The stationary phase red cysts of *H. pluvialis* are significantly more robust than the green vegetative cells (77).

The cyanobacterium *Spirulina*—a health food and source of the food colorant phycocyanin—is another species that is susceptible to damage by excessive shear forces. Shear stress applied to optically dilute cultures of *Spirulina platensis* and *Chlorella vulgaris* in a Couette flow device, affected the rate of photosynthesis of the cells (83). Depending on the temperature and the intensity of irradiance, the increasing shear stress over the range of 0–0.6 Pa initially enhanced the rate of oxygen evolution by *Spirulina*; but beyond a "critical shear stress," the rate of photosynthesis plateaued and declined. The initial enhancement was apparently due to better illumination of the helically coiled bacterial trichome because of rotation in the flow field. Microscopic observations confirmed a shear stress–dependent reduction in the "straightened" trichome length of the bacterium, as shown in Fig. 81.10. The critical shear stress declined with increasing test temperature over the range of 25–40°C, suggesting a loss of mechanical strength of trichome with increasing temperature (83). In view of the short duration (16 min), the test temperature could not have altered the composition of the cell wall, only its strength. The growth temperature had little effect on shear susceptibility of the cells (Fig. 81.10). Shear stress values of 0.4 Pa and greater did not further affect the final trichome length (~50 μm), presumably because the trichome size had become too small to be further affected by the prevailing eddies.

In contrast to observations with *Spirulina*, increasing shear stress did not enhance the rate of photosynthesis in *Chlorella* (83); the rate of photosynthesis declined consistently with increasing shear stress, irrespective of the illumination intensity used (Fig. 81.11). *Chlorella* is known to be a relatively robust alga, so the results in Fig. 81.11 cannot be attributed to physical destruction of the cells. Indeed, the loss in photosynthesis was substantially reversible upon removal of the shear stress stimulus (83). A lack of any shear-induced enhancement in photosynthesis was apparently because a small spherical cell of *Chlorella* could not shade itself; hence, in an optically dilute suspension, increasing shear stress (turbulence) may have produced no

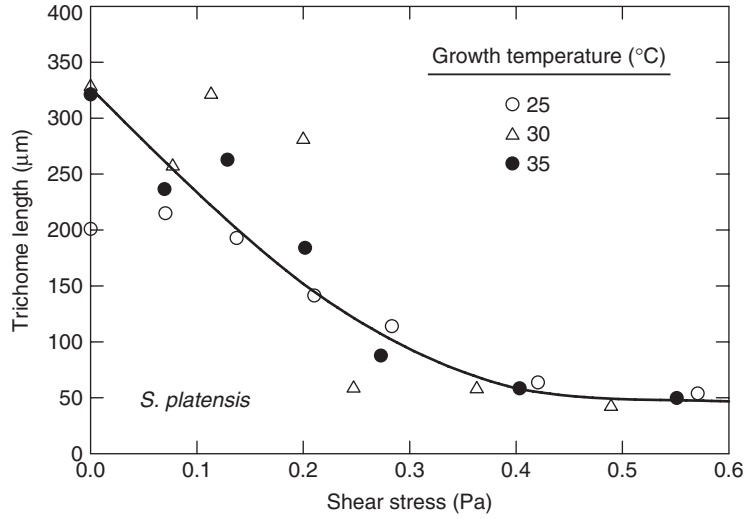


Figure 81.10. Effect of shear stress on average straightened trichome length of *S. platensis*. The shear stress was applied for 16 min at 30°C on cultures grown at various temperatures. *Source:* Ref. 83.

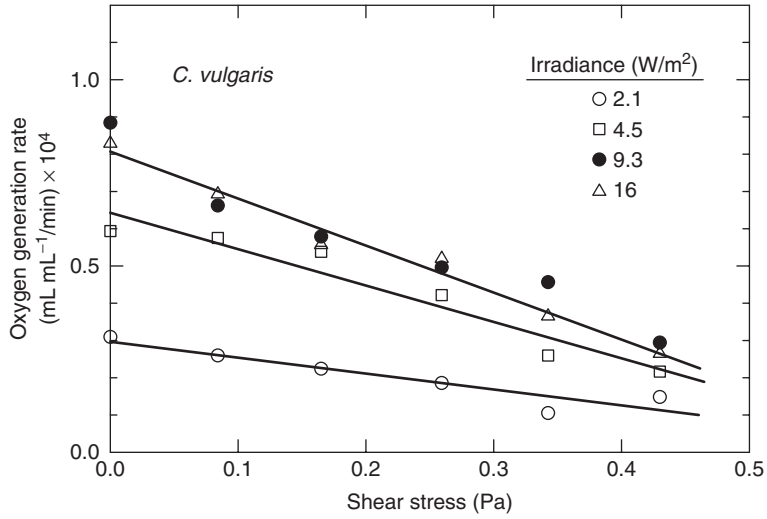


Figure 81.11. Rate of oxygen generation declines with increasing shear stress in Couette flow of *C. vulgaris*. Data are shown for various intensities of irradiance at 30°C test temperature. *Source:* Ref. 83.

improvement in light availability. Also, the 5–6 μm spherical cells of *Chlorella* are much smaller than the 50 μm stable trichome size attained by *Spirulina* trichomes exposed to shear stress (Fig. 81.10). In view of all this, the data in Fig. 81.10 have only one plausible explanation; at least in some species, the sublethal shear stress stimulus affects the photosynthetic capability of the cell.

The marine alga *Dunaliella* is particularly fragile: the cell lacks a ridged wall; only a thin cytoplasmic membrane encloses it. *Dunaliella* is a good source of natural β-carotene; hence, it is commercially useful. The cell also produces glycerol. Silva *et al*. (84) showed that *Dunaliella* was susceptible to damage by gas bubbles as well as by turbulence in the liquid. Supplementing the culture with carboxymethyl cellulose or agar improved cell survival.

In one study with *Dunaliella tertiolecta*, culture in a bubble column was quite successful; but when the bubble column was converted to an airlift device by inserting a vertical baffle, the productivity declined (85). Under conditions that were earlier identified as optimal, no growth was observed in the airlift reactor whereas good growth occurred in the bubble column. Microscopic examination showed significant disruption of the cells in the airlift device (85). This was associated with the hydrodynamic stresses generated as the culture flowed over the upper edge of the baffle into the downcomer (85). This effect could have been avoided, or at least minimized, by hydrodynamic smoothing of the upper and lower parts of the baffle to prevent flow separation (24). In the bubble column, the growth was sensitive to aeration rate: growth rate increased with increasing superficial gas velocity up to a velocity of about 0.6 m/min. Further increase in aeration rate reduced growth, apparently because of hydrodynamic stresses in the fluid (85). Under nongrowth conditions (no light), the specific death rate in the bubble column was shown to increase with superficial gas velocity for velocities exceeding 0.6 m/min (85). At a fixed aeration velocity ($U_G = 1$ m/min), the specific death rate decreased with increasing height of the culture fluid in the column (85), probably because the specific power input and, hence, the turbulence intensity declined (24). Similar behavior has been reported with animal cells in bubble columns (86–90).

For otherwise fixed conditions, increasing the number of aeration nozzles—that is, decreasing the gas jet velocity—caused a marginal reduction in the specific death rate of *D. tertiolecta* (85). This led to the conclusion that the events at the gas sparger did contribute to cell death (85), although the effect was minimal. Unlike Suzuki *et al*. (85), others (79,80) have quite successfully cultured various microalgae in pilot-scale airlift devices. Continuous culture of the green alga *Chlorella pyrenoidosa* in a rectangular airlift device with multiple light-emitting diodes was reported by Matthijs *et al*. (91). With a relatively robust photosynthetic organism such as *Chlorella*, increasing turbulence within limits improves productivity in photobioreactors because of enhanced fluid interchange between the dimly lit interior and the better illuminated exterior parts of a photobioreactor.

In addition to an organism's morphology, the biochemical composition of the cell wall has been associated at least qualitatively with the cell's susceptibility to hydrodynamic stresses. The microalga *C. vulgaris*, which is shear tolerant, has a thick (100–200 nm) cell wall composed of cellulose, pectin, and sporopollenin (60). The somewhat more sensitive alga *Chlamydomonas reinhardii* has only glycoproteins in its relatively thin (40 nm) cell

wall (60), whereas a highly sensitive cell wall–defective mutant of *C. reinhardii* is devoid of cell wall (60). Similarly, the cyanobacterium *Synechococcus* with murein-containing cell wall and the methane bacterium *M. thermoautotrophicum* with pseudomurine-containing wall are noticeably more resistant than methane bacteria such as *M. vaniellii*, which has a protein-based wall.

Although earlier work with the mold *M. javanicus* showed a reduced extent of damage to mycelia as the viscosity was increased at constant agitation rate, and similar reports exist with animal cells (92,93) and the halotolerant alga *Dunaliella* (84), Märkl *et al*. (60) observed an opposite effect: with a highly shear-sensitive strain of *C. reinhardii*, even a slight increase in viscosity enhanced cell damage (60). The viscosity was increased by adding carboxymethyl cellulose to the culture broth. With a relatively less shear-sensitive strain of *C. reinhardii*, increasing the viscosity reduced the impeller agitation speed at which the damaging effects were first discerned (60). Apparently, at least with the less sensitive strain, supplementing the medium with the viscosity enhancer caused the cells to grow in clumps, and aggregation supposedly was an effective shield against cell damage (60). Increasing shear damage with increasing culture viscosity has been seen before with a protozoan (94). These apparently contradictory results are easily explained: whether changes in viscosity increase or reduce shear damage depends on the peculiarities of the mechanism causing the damage. For a given impeller tip speed, increasing viscosity will not affect the tip speed-associated shear rate, but the turbulence will be reduced; hence, the shear rate in the fluid should be lower. However, the shear stress around a particle may increase if the fluid eddy length scale remains comparable to the dimensions of the particle. In other cases, increased viscosity may reduce both shear rate and shear stress; only eddies that are larger than the particle may survive and there may be little or no relative motion between the fluid and the particle. In other cases, the frequency of passage through high shear zones may decline with increasing viscosity.

Dinoflagellates are a group of microalgae. Biotechnological potential of dinoflagellates has been discussed by Garcia Camacho *et al*. (95). Small-scale turbulence is known to affect the growth rate and morphology of dinoflagellates (96–99). Agitation, shaking, aeration, and stirring have inhibited growth in laboratory cultures (100–105). The shear stress levels that dinoflagellates may withstand are generally one or two orders of magnitude lower than the levels that generally damage most animal and plant cells. The shear stress threshold of some dinoflagellates is even lower than that of erythrocytes (0.029 N/m^2). For example, a continuous laminar shear stress level of only 0.0044 N/m^2 (equivalent to a shear rate of 2.2 s^{-1}) has proved lethal to the dinoflagellate *Gonyaulax polyedra* Stein (103–105). Like animal and plant cells, *G. polyedra* responds differently to laminar and turbulent shear stresses. The observed response depends also on the intensity, duration, and frequency of exposure to shear field. Growth phase during which exposure occurs, prevailing irradiance level, and light–dark cycling also appear to influence shear tolerance. Other dinoflagellate species behave similarly (106,107). Shear stress levels can influence the production of dinoflagellate toxins (106).

Engineering problems of dinoflagellate culture notwithstanding, dinoflagellates can potentially contribute to improved understanding of shear stresses and other turbulence phenomena in bioreactors. For example, many morphologically diverse dinoflagellates are bioluminescent (e.g. *Lingulodium polyedrum*, *Ceratocorys horrida*, *Pyrocystis fusiformis*, *G. polyedra*), and turbulence appears to stimulate bioluminescence. Dinoflagellate bioluminescence is easily visualized and quantified (108). This provides a powerful tool for flow visualization under conditions not amenable to conventional methods (108–111). Bioluminescence stimulation and suppression under different conditions of turbulence may assist in establishing mechanisms of cell damage in bioreactors (112). Potentially, dinoflagellates can be used to map regions of high shear in biomedical devices such as prosthetic heart valves. Bioluminescence response of dinoflagellates to developed and developing turbulent flow in pipes has been discussed (113,114). Similar work in Couette flow devices has been reported (115,116).

Effects of hydrodynamic forces on microalgae and protection of the cells against damage are further discussed elsewhere (117–121).

81.3.3 Plant Cells

Cultured plant cells are a potential source of numerous high value compounds, although few production processes have been commercialized (17,122). Low culture productivities continue to be the primary limitation. Investigational culture in large bioreactors has been carried out since at least 1959. A variety of reactors have been used, including bubble columns, airlift devices, stirred vessels, rotary drum reactors, and immobilized cell systems (17). Airlift bioreactors have proved especially effective for large-scale culture of heterotrophic, photomixotrophic, and photosynthetic plant cell suspensions (24,123). Relatively low values of pneumatic power inputs have given satisfactory results during cultivation of plant cells. For example, Fischer and Alfermann (123) obtained good results with about 13 W/m^3 specific power input during culture of *Chenopodium rubrum* cells in a concentric draft-tube airlift device. Similarly, Ballica and Ryu (124) obtained maximum biomass and product yield at an approximate power input value of 35 W/m^3, also in a draft-tube airlift

reactor while culturing *Datura stramonium* cells. In the latter case, power inputs above ~60 W/m^3 caused large declines in biomass and product yields. The size of the cell aggregates declined with increasing specific power input (124). Reinhard *et al*. (125) described culture of *Digitalis lanata* in a 300-L airlift bioreactor for producing β-methyldigoxin.

Plant cells in suspension tend to be large: 20–50 μm in diameter and 100–500 μm in length. The cells have a cellulose-based wall. Most of the cell's volume is taken up by a vacuole that may occupy >95% of the available space. The fluid in the vacuole is much less viscous than the cytoplasm; hence, a cell with a large vacuole is likely to be less resistant to certain types of deformations than one with a smaller vacuole. Cells frequently occur as aggregates of up to a hundred cells. The aggregates settle easily. Plant cells grow slowly with doubling times of the order of 20–100 h. Cells may secrete extracellular polysaccharides, producing non-Newtonian broths. Also, the biomass concentration may be high, up to 70 kg/m^3. Heterotrophically growing plant cells require oxygen, but demands are low, of the order of 10^{-6} kg O_2/kg cell/s. Critical dissolved oxygen concentration generally tends to be ≤20% of air saturation. The polysaccharide-containing cultures tend to foam a lot when aerated. Also, excessive aeration may reduce productivity by stripping carbon dioxide and other essential volatiles produced by the cells themselves (5,122).

As has been demonstrated with some microorganisms (1), the composition of the culture medium, the culture conditions, and the specific growth rate of cells may affect the wall strength of plant cells also. For otherwise identical conditions, agitation intensity is reported to influence the composition of plant cell walls. Thus, the relative amounts of pectin, cellulose, and hemicellulose in walls of *Catharanthus roseus* were affected by the intensity of agitation in one case (126). In another case, cited by Doran (17), the mass ratio of cell wall relative to the whole cell increased with increasing intensity to shear, suggesting adaptation of the cell to the prevailing environment even over short periods. Even though the turbulence level may be insufficient to affect individual cells, aggregates may be affected; hence, a shear-related metabolic response may occur because of altered cell–cell interactions (122) and changes in nutrient supply (127). This indirectly affects metabolism.

On the basis of laminar flow viscometric measurements, a critical shear stress level of 80–200 N/m^2 has been suggested for *Morinda citrifolia* cells. For suspended cells of the same species exposed to turbulent shear stress, a damage threshold energy dissipation rate of 50 W/kg broth has been reported (128), while for *Daucus carota* a shear stress level of 50 N/m^2 has been associated with cell damage. In another study, carrot cells in a laminar flow Couette viscometer lost the ability to grow and divide in the shear stress range of 0.5–100 N/m^2 (76). The intracellular enzyme activity was impaired at shear stress levels above 3000 N/m^2, but significant lysis did not occur until a shear stress level of 10,000 N/m^2 applied over a prolonged period (≥1 h) (76). In contrast to the behavior in laminar flow, the cells were quite sensitive to turbulent impeller agitation. Impeller tip speeds of ~1.1 m/s lysed a significant proportion of the cells within 40 min (76).

In studies with *Perilla frutescens* cell suspensions, Zhong *et al*. (129) noted that the cell viability declined with increasing shear rate (constant exposure time) or increasing shear time at a constant rate of shear in a concentric cylinder shearing device. A constant shear rate of about 140 s^{-1} produced a noticeable loss of viability within 20 min. At a higher shear rate of ~860 s^{-1}, less than 75% of the cells were viable after 20 min (129). In marine propeller agitated fermenters, the impeller tip speed affected the specific growth rate and the yield of the cells (129). Tip speeds of >0.6 m/s reduced the specific growth rate and the cell biomass yield (129). In other cases, impeller tip speeds as low as 0.35 m/s have extensively lysed certain plant cells.

With *M. citrifolia* cells subjected to 25–350 N/m^2 turbulent shear stress in a capillary, the viability decline followed first-order kinetics in which the rate constant increased with the applied shear stress (130). The culture was circulated through the capillary by a peristaltic pump, which also contributed to cell damage (130). The specific death rate constant was linearly related with the cumulative energy dissipated (130). Cell aggregates subjected to shear were reduced in size. For the same species, damage was reported when cells grown in a quiescent environment were subjected to turbulent jet flow through 1- and 2-mm nozzles (74). Cells lost viability with increasing number of passes through the nozzles. The viability loss was of first-order in the number of passes (74). For a fixed number of nozzle passes, increased nozzle flow velocity enhanced the death rate constant. Similarly, the maximum and the mean aggregate size reduced when the suspension was subjected to jet flows (74). The average aggregate size was lower for higher jet velocities. The average energy dissipation rates in the jet ranged over 10^3–10^5 W/kg (74).

Meijer *et al*. (54) assessed the hydrodynamic stress sensitivity of *C. roseus*, *Nicotiana tabacum*, *Tabernaemontana divaricata*, and *Cinchona robusta* in a 3-L Rushton turbine-stirred vessel. Effects of stress were quantified in terms of culture growth rate, respiration rate, and release of organic compounds from the cells. Cultures of *C. roseus* carried out at 0.59 m/s and 2.36 m/s impeller tip speed showed identical behavior in terms of biomass growth rate and glucose consumption rate; hence, it was concluded that hydrodynamics-associated stress did not affect the cells over the ranges examined (54). Similarly, *N. tabacum* was little affected by different agitation rates, although the growth rate and the final yield were noticeably

greater at the lower agitation speed. Cells of *C. robusta* responded differently: at 0.59 m/s impeller tip speed, the cells grew and there was little release of intracellular protein; however, at 2.36 m/s, there was no growth and the specific protein concentration increased with culture time, indicating leakage from damaged cells (54). The *T. divaricata* cells also were damaged at 2.36 m/s, but less than the cells of *C. robusta*. The damage to *T. divaricata* was reduced at a lower impeller tip speed of 0.59 m/s. In separate experiments, cells of *N. tabacum* that had earlier withstood higher shear stress levels were shown to be more susceptible to damage after a prolonged period (10 days) of starvation (54). This effect is similar to that noted with other cells (60).

Increasingly, plant tissue is being cultured as hairy roots (131). Growing tips of hairy roots are damaged by elevated shear stress level, but can be acclimatized to tolerate relatively high shear forces (132,133). In column cultures (Fig. 81.12), superficial velocity of flow affects the rate of elongation and the viability at tip meristems (132). In studies that varied the medium flow velocity from 2 to 28 m/h, optimal growth occurred at a velocity of 15 m/h in column culture of red beet hairy roots (132).

Table 81.5 is a summary of the damage thresholds levels—either impeller tip speed or the specific power input due to aeration—noted for various plant cell suspensions in stirred fermenters and airlift bioreactors. The studies referenced earlier clearly affirm that the susceptibility to shearing forces varies a great deal with cell line. Moreover, for the same cell line, cultivation history (e.g. prolonged starvation) and age of cell affect the cell's response to shear fields (54,60,122), which is consistent with similar findings for microorganisms (1). That plant cells adapt to shear fields is also well known—cells cultured in high shear environments better withstand hydrodynamic forces after many generations. Shear sensitivity can depend on the age of the cell (134). Shear sensitivity of plant cells has been further reviewed by others (13,58,86,122,135–137).

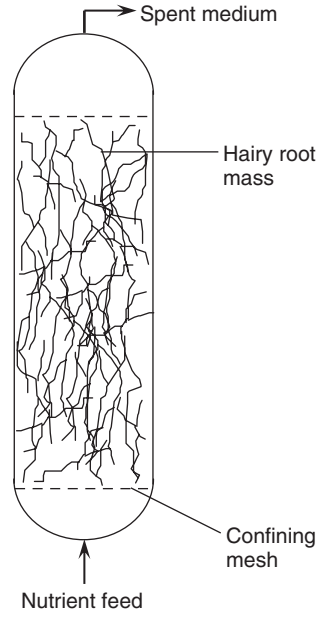


Figure 81.12. In hairy root culture the growth of root mass is confined within a column, and a nutrient medium flowing past the biomass supplies oxygen and other nutrients.

TABLE 81.5. Damaging Threshold Values of Impeller Tip Speed or Specific Power Input for Some Plant Cells

Stirred fermenters	**Impeller tip speed** (m/s)
Catharanthus roseus	≥2.36
Nicotiana tabacum	~2.36
Cinchona robusta	<2.36
Daucus carota	<1.10
Tabernaemontana divaricata	~0.59
Perilla frutescens	0.60
Others	≤0.35
Airlift bioreactors	**Power input** (W/m^3)
Chenopodium rubrum	≥13
Datura stramonium	~60

81.3.4 Protozoa

Strong shear fields have long been known to damage large protozoa. The ciliated protozoan *Tetrahymena* is certainly sensitive to high intensity shear forces (94), with and without gas–liquid interfaces. Low density cultures appear to be damaged by gentle agitation (138) and static gas–liquid interfaces (139). Higher density cultures can be more shear tolerant, and resistance to shear can be increased by using suitable protective additives in the culture medium (138,140).

In agitated suspension of *Tetrahymena pyriformis* (~80 μm cell diameter), lysis correlated with impeller tip speed (94), and most of the cells were destroyed once the tip speed equaled or exceeded 0.5 m/s. In a Couette viscometer, the critical shear stress for incipient lysis was ~24 N/m^2 (94). Eighty percent of the cells lysed within the first minute when exposed to a shear stress of 10^3 N/m^2. The damage increased with shear stress level and exposure time. At a given shear rate, increasing the broth viscosity made the protozoan more susceptible to shear damage, implying that the damage was associated with shear stress rather than with shear rate (94). The cells were more sensitive to turbulent shear stress: an average turbulent shear stress of ~10 N/m^2 lysed over half the population within 10 min. In contrast, in laminar flow, a similar level of damage occurred at shear stress levels of almost 300 N/m^2. Note that *T. pyriformis* cells are larger than most animal cells, but smaller than most cultured plant cells.

Low density ($<10^4$ cells/mL) cultures of *T. pyriformis*, *Tetrahymena thermophila*, and *Tetrahymena pigmentosa* in Erlenmeyer flasks were adversely affected by gyratory shaking (138). Also, air sparging of the flasks increased the doubling time of the cells. The damaging effect of gyratory agitation disappeared once the cell concentration exceeded 10^4 cells/mL (138). The damaging effect of agitation could be reduced by supplementing the broth with dextran (138), Pluronic F68 (141), and certain fatty acids (140). The protective effect of fatty acids such as 9 μM oleic acid and 140 μM linoleic acid appeared to be biochemically based rather than being purely physical (140). *T. pyriformis* cells under gyratory shaking undergo ultrastructural changes. These changes are not suppressed by supplementation of the culture with fatty acids, even though a protective effect occurs. Cell protective effect has also been observed with ergosterol and cholesterol supplementation, but not with octanoic acid, palmitic acid, and palmitoleic acid (140).

Surprisingly, even a static gas–liquid interface has been associated with lysis of *T. thermophila* cells (139). Lysis is suppressed by adding a small amount of a surfactant (e.g. Sodium dodecylsulfate (SDS), Pluronic F68, Tween 80) to the culture medium (139). The damaging effect of a static interface certainly cannot be ascribed to shear phenomena and biochemical factors must play a role. Indeed, the lytic effect of a static surface is abolished if the medium is simply diluted or reformulated without added surfactants (142). Apparently, certain constituents of a poorly formulated medium make the cells unduly susceptible to a gas–liquid interface.

Despite a claimed low tolerance for shear (138), *T. thermophila* has been successfully cultured in a 15-L stirred tank and a 1.5-m^3 airlift bioreactor (143). Cell concentration values of up to 3×10^6 mL^{-1} were easily attained in the stirred tank that was agitated with three, six-bladed paddle impellers (~7 cm diameter, 50–150 rpm, 0.05 vvm aeration rate, 13 L working volume). In the airlift device, the maximum cell concentration attained was 2×10^6 mL^{-1}, when the specific power input during cultivation ranged from 50 to 250 W/m^3 (143). Stepwise increases in the agitation speed and the aeration rate to maintain dissolved oxygen at ~50% of air saturation caused no obvious change in the growth profiles, as shown in Figs 81.13 and 81.14. Mass cultivation of another protozoan, *Paramecium tetraurelia*, has been reported (144).

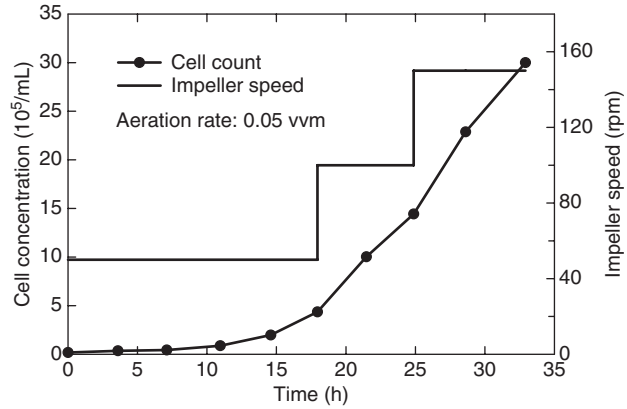


Figure 81.13. Growth profile of *Tetrahymena thermophila* in a stirred tank bioreactor (13 L working volume, three six-bladed paddle impellers, impeller diameter ~7 cm, 0.2 m tank diameter). *Source:* Ref. 143.

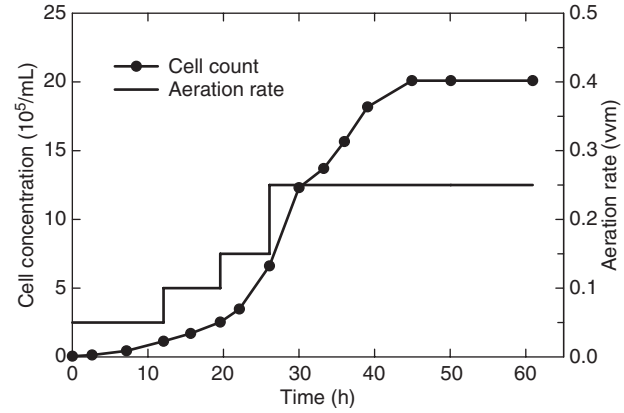


Figure 81.14. Growth profile of *Tetrahymena thermophila* in an airlift bioreactor (vessel diameter 0.5 m, 1.2 m^3 working volume). *Source:* Ref. 143.

81.3.5 Animal Cells

Animal cells are among the most shear-susceptible of biocatalysts. Animal cells are relative large—typically 10–20 μm in diameter—and they lack a protective cell wall. Osmotic shock is often sufficient to lyse animal cells. Other than blood cells, most normal animal cells are anchorage dependent. Cancerous cells, hybridomas, and established lines will normally grow in suspension. Because of these distinct growth characteristics, two types of culture methods are employed in industrial practice: free suspension culture in which cells are freely suspended in a nutrient broth and microcarrier culture in which anchorage-dependent cells grow on surfaces of solid carriers that are suspended in a culture fluid. Irrespective of the culture method, the suspending fluid is invariably directly sparged with air or other gas mixtures to supply the cells with oxygen. Although other aeration alternatives are available (145), direct sparging with a gas is likely to remain the dominant method of providing oxygen to animal cells (146). Both stirred tanks and airlift devices have been successfully employed for commercial processing of animal cells (147–149). Anchorage-dependent cells may also be cultured on surfaces of large static particles held

in packed beds (150,151), but this method is uncommon. Devices used in generation of implantable tissue typically grow normal cells supported on stationary surfaces or within a static matrix of gel or woven fabric (152). The supporting surface may be flat or variously shaped.

Cells in bioreactors are subject to two main kinds of fluid mechanical forces: (i) those due to turbulence within the liquid and (ii) forces associated with the gas–liquid interface. The latter category includes effects of bubble formation, rise, and rupture. In addition, in microcarrier culture, collisions among carriers and carrier–impeller (or carrier–wall) interactions may play a role. Furthermore, in tall bioreactors, cells may be subjected to substantial changes in hydrostatic pressure as they circulate with the fluid. Cells in tissue regeneration bioreactors experience the same kind of forces as occurring in flow past a flat plate, wall, or other submerged object. The specific considerations relevant to the various culture methodologies are treated in the following sections.

Resistance to shear stress is determined at least partly by the cytoskeletal structure of the cell. Cytoskeleton determines a cell's mechanical properties, its shape, and movements such as those that occur during phagocytosis. Cytoskeleton is made of protein filaments, mainly of actin. The filaments interact closely with the cell membrane by anchoring to specific membrane proteins. A cell exposed to mechanical forces undergoes cytoskeletal reorganization. Cytoskeleton-mediated stress signal transmission to intracellular organelles (Fig. 81.15) has been associated with various biochemical, physiological, and gene-level responses in vascular cells (4). Some cells are known to have surface stress receptors (e.g. Ca^{2+} ion channels) that have been implicated in biochemical responses (4,153,154) independent of cytoskeletal mediation (Fig. 81.15). Cytoskeletal properties are known to affect shear tolerance of hybridomas. Effects of turbulence on cytoskeleton and other biological responses have been treated by several authors (4,76,155). The work cited by Al-Rubeai *et al*. (156) suggests that inhibitors of actin polymerization decrease a cell's resistance to shear forces, while inducers of polymerization make the cells more robust. Thus, supplementing the culture medium with actin polymerization inducers may be one way of improving performance of bioreactor-cultured animal cells so long as the requisite production biochemistry is not adversely affected.

Plasma membrane fluidity (PMF)—a measure of the degree of packing of the membrane and its constituent's freedom to move about laterally through the bilayer membrane, to rotate about their major axes, and to oscillate in the plane of the membrane—is another factor that appears to influence shear susceptibility of cells (57). Increasing membrane fluidity correlates with increasing shear sensitivity (57). PMF increases with increasing temperature and can be manipulated in both directions using various additives. In studies with a freely suspended mouse–mouse hybridoma in a laminar shear stress Couette flow device, conditions that yielded higher membrane fluidity produced more fragile cells (57). For example, cells sheared at elevated temperatures showed greater loss of viability than unsheared controls at the same temperature (57). Effects of shearing of insect cells in a Couette flow device have been discussed by O'Connor and coworkers (157).

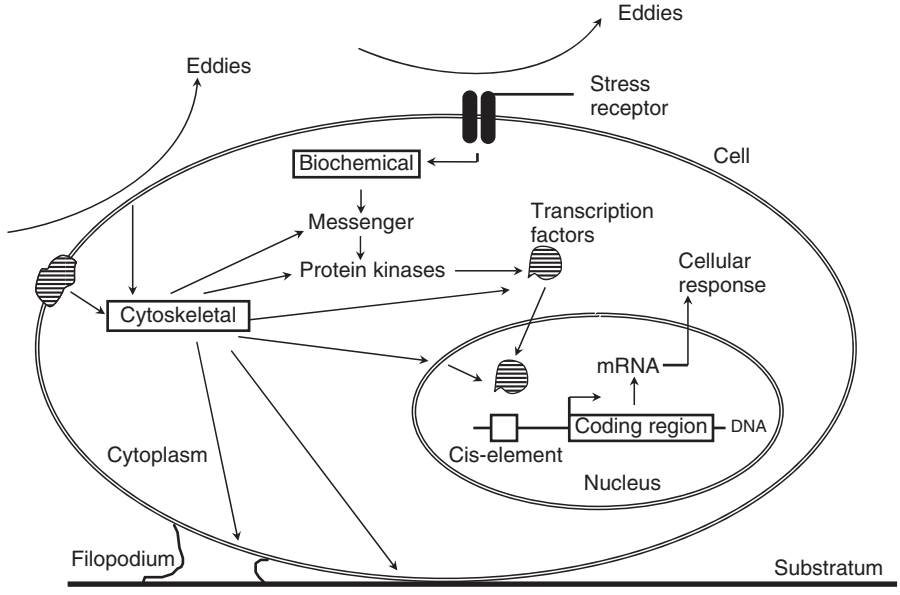


Figure 81.15. Stress signal transmission and transduction via cytoskeletal and biochemical routs in an anchored cell. Adapted from Ref. 4.

81.3.5.1 Shear Effects in Bubble-Free Environments

81.3.5.1.1 Suspended Cells. Freely suspended cells in bubble-free bioreactors are not damaged by mechanical agitation even at intensities much greater than the ones used in typical processing. Exceptions occur in extensional or elongational flow in certain high shear devices even when the flow is laminar. Extensional or elongational flow occurs whenever the cross-sectional area of the flow channel reduces, for example, at an orifice on the wall of a tank or at the entrance of a capillary connected to a larger reservoir. The fluid elements undergoing extensional flow stretch and thin. Suspended particles also experience elongational forces in the direction of flow and compression perpendicular to the flow streamlines. Drops subjected to extension flow can rupture. Similarly, extensional flow through orifices of high pressure homogenizers contributes to rupture of even the very robust microbial cells (1). Rupture of erythrocytes at entrances to capillaries is well known (158). Shear effects on suspended erythrocytes are discussed in detail in a later section. Shear susceptibility of suspended marine sponge cells has been discussed by García Camacho *et al*. (159). Shear-associated damage during cross-flow filtration (160) and centrifugation (161) of suspended mammalian cells have been discussed.

For a hybridoma line, Born *et al*. (162) reported that exposure to laminar shear stress (208 N/m^2) in unaerated flow in a cone-and-plate viscometer led to substantial loss in cell count and viability within 20 min. At a constant 180 s exposure, increasing shear stress over 100–350 N/m^2 linearly enhanced cell disruption, with >90% of the cells being destroyed at 350 N/m^2 stress level (162). Shear stress levels associated with bubble rupture at the surface of a bioreactor may range over 100–300 N/m^2 (17). These values are remarkably consistent with shear rates that damaged hybridomas in *unaerated* laminar flow experiments (162).

For a suspended mouse myeloma line in turbulent capillary flow, McQueen *et al*. (22) noted a threshold average wall shear stress value of 180 N/m^2, when lysis first commenced. Although the flow caused lysis, it had no effect on viability (22), suggesting that cells at various growth stages were equally affected. The sudden flow contraction at the entrance to the capillary may have contributed to cell lysis, but the residence time in the capillary also had an effect at otherwise constant average wall shear stress level. The rate of lysis was first-order in cell number. Above the threshold shear stress value, the specific lysis rate increased with increasing level of shear stress (22). The growth rate and the DNA synthesis rate of the cells exposed to the shearing environment were unaffected when the surviving cells were returned to a normal quiescent growth environment (22). In other studies cited by McQueen *et al*. (22), the shear stress threshold for damage has been reported as 0.87 N/m^2 for a mouse hybridoma and 1.5 N/m^2 for insect cells. Higher shear sensitivity of another mouse cell line relative to a human carcinoma has been reported (20).

For human cervical carcinoma HeLa S3 and mouse abdominal fibroblast L929, Augenstein *et al*. (20) observed lysis of suspended cells in turbulent flow through stainless steel capillaries. Cell death could be correlated with the average wall shear stress level or the power dissipation within the capillaries. The L929 line was more sensitive than the human cell. Control experiments showed that the positive displacement pumps used to circulate the cells through capillaries contributed little to cell lysis (20). Average wall shear stress levels of $0.1–2.0 \times 10^3$ N/m^2 were sufficient to induce cell inactivation for the two lines. According to Shiragami (21), the mean shear stress acting on cells suspended in capillary flow is 4/3 the shear stress at the capillary walls, so long as the ratio of the cell's diameter to that of the capillary is <0.08.

For a hybridoma examined by Shiragami (163), the specific rate of monoclonal antibody production in a surface-aerated spinner flask depended on the agitation speed. In a 250-mL spinner vessel an agitation rate of ~180 rpm gave the highest specific antibody production rate. The specific productivities were reduced at higher or lower values of agitation speed. The increased antibody production with increasing agitation was associated supposedly with enhanced secretion in a more turbulent environment (163). Oxygen transfer effects may have better explained the observations (see Chisti 145), but no data were reported on this aspect.

Damage to murine hybridomas was observed by Jan *et al*. (45) in stirred tanks equipped with marine impellers agitated at sufficiently high speeds that vortexing occurred and gas entrained into the medium. Even at these high speeds damage could be prevented by baffling the tank, which suppressed vortex formation. Usually though, vortexing is not a problem in large-scale cell culture. Unbaffled, marine impeller-stirred tanks were successfully used by Chisti (148) in industrial culture of several hybridoma lines. Effects of agitation on hybridoma culture in the absence of sparging or surface entrainment were further examined by Smith and Greenfield (164). Culture growth was unaffected by agitation intensity (100 or 600 rpm) in the RPMI medium supplemented with fetal bovine serum (FBS) (10% vol/vol). However, in PFHM II medium supplemented with Pluronic F68, FBS, or BSA, and agitated at 600 rpm (impeller tip speed = 1.6 m/s, power input = 1 kW/m^3), the results were different: the agitation intensity did not affect the exponential growth rate, but once growth had ceased, the decline phase was substantially faster than in control experiments (164).

A certain level of hydrodynamic shear is generally beneficial to culture processes, especially in intraparticle immobilized culture where mass transfer limitations can be severe. In producing engineered tissue of smooth muscle

cells/polymer matrices (biodegradable 2-mm diameter fibers of polyglycolic acid assembled into a nonwoven matrix), Kim *et al*. (151) noted that seeding of the matrix under agitation led to significantly higher intramatrix cell densities than when cell were seeded under static conditions. Moreover, the higher cell densities were attained more rapidly than the lower densities of static culture. In addition, the relative rates of synthesis of elastin and collagen were significantly greater in seeded matrices cultured with agitation than in ones grown statically (151). A lower possible supply of oxygen or other nutrients may have reduced the performance of static seeding methodology.

In view of the studies referenced earlier and similar others, sufficiently intense fluid mechanical forces other than those associated with aeration do affect cells. In culturing animal cells in stirred bioreactors, the average energy dissipation rate should not exceed about 50 W/m^3, even when low shear impellers are used.

81.3.5.1.2 Adherent Cells. Quite low shear stress levels—for example, between 0.25 and 0.6 N/m^2 in laminar flow (165)—can interfere with the process of cell attachment to surfaces; however, once the cells are attached and spread out, they may tolerate higher stresses. Laminar shear stress of the order of 0.5–10 N/m^2 may remove adherent cells from surfaces (166), but even lower values, for example, 0.1–1.0 N/m^2, are known to affect cellular morphology, permeability, and gene expression (166). Sublethal shear stress levels cause no obvious physical damage, but are known to produce various biochemical and physiological responses (4,153,154,167). In studies with rat aortic endothelial cells anchored on internal walls of glass capillaries, laminar shear stress was shown to affect the cytosolic pH because of preferential leakage of certain ions out of the cells into the buffer saline (154). This reversible permeability enhancement occurred even at stress levels as low as 0.05 N/m^2 applied over short durations ($\sim$2 min). Similar effects were noted with human aortic endothelial cells, but not with human skin fibroblasts or rat intestinal epithelial cells exposed to shear stress levels of up to 1.34 N/m^2 (154). With rat aortic cells, the flow-induced cytosolic acidification could be maintained for at least 30 min at 1.34 N/m^2 shear stress level, but the cytosolic pH returned to unstressed levels within about 15 min, when the sustained shear stress was $\leq$0.027 N/m^2 (154).

In studies with anchorage-dependent cells attached to the flat glass walls of a rectangular flow channel, Shiragami and Unno (168) observed increased activity of lactate dehydrogenase (LDH) in cells that had been exposed to a steady state shear stress of 0.5 N/m^2 for 12 h: the activity was fourfold greater relative to controls. The LDH activity correlated with the transmission of energy from the fluid to the attached cells (168).

In vivo hemodynamic forces have been implicated in various physiological and pathophysiological processes (4). Atherosclerotic lesions in humans tend to develop in zones of flow separation (4) such as regions of arterial branching and sharp curvature. Arteries adapt to chronic changes in blood flow, increasing in circumference under high flow and declining under reduced flow (4). Shear stress signals transmitted throughout the vascular cell via cytoskeletal and biochemical elements result in changes to structure, metabolism, and gene expression (4).

Moderate shear intensities can benefit virus production from some anchorage-dependent cells but not from others. For example, moderate shear levels improved the productivity of Japanese encephalitis virus (JEV) in microcarrier-supported Vero cells but not in similarly supported BHK-21 cells (169).

Shear effects need to be considered also in perfusion devices that retain cells over long periods in continuous culture (170). Shear effects on adhering erythrocytes and leukocytes are treated separately.

81.3.5.2 Erythrocytes and Leukocytes. Mammalian erythrocytes or red blood cells are among the best studied of animal cells. Properties of erythrocytes and other blood cells are relevant to various pathologies and biomedical processes. Erythrocytes and leukocytes being suspended cells *in vivo* likely experience the kind of stresses encountered in bioreactors and various other industrial processing devices; hence, these cells may provide a broad general insight into mechanical behavior of other cells of mammalian origin. The normal lifetime of a human erythrocyte in circulation is 121 days. The normal daily destruction rate is about 2×10^{11} cells (158). Some cells lyse during circulation; most are destroyed in the spleen. Aging cells resist deformation more than the younger ones. All cells unable to deform in the 3-μm openings of the splenic circulation are delayed and ultimately phagocytized (158).

Erythrocytes are highly deformable cells that orient in laminar flow so that the least possible surface area of the disc-shaped cell is perpendicular to the flow. Cytoplasm of erythrocytes is a viscous Newtonian fluid (171). The cell membrane behaves as an elastic solid: the cell deforms but almost instantly recovers its shape when the deforming force is removed. The membrane has little resistance to bending, but substantially resists increase in area (171). Erythrocytes suspended in turbulent isotonic saline (viscosity $\sim 1 \times 10^{-3}$ Pa s) have been observed to undergo elongation and deformation; however, the cell appears to be less vulnerable to turbulent shear stress than a cell at the same stress level in a viscous suspending medium (158). On the basis of measurements in turbulent jets, a critical lytic shear stress level of 4000 N/m^2 has been reported for very brief exposures ($\sim 10^{-5}$ s) (158). Measurements on erythrocytes of different mammals reveal that the critical

shear stress increases dramatically as the cell volume declines.

According to Blackshear and Blackshear (158), "Areal change occurs when the cell membrane is subjected to stress; hemolysis occurs when the area increases by approximately 6.4 percent." Hemolysis is associated at least in part with physical factors and flow, which produce the hemolysis threshold strain in membranes of erythrocytes (158). Once the threshold strain is exceeded, membrane pores open and the membrane eventually tears (158). A briefly (e.g. 10 ms) imposed uniaxial tension of 0.058 N/m is a sufficient criterion for lysis (158). When the cell is subjected to biaxial stress, a tension of about 0.029 N/m may produce lysis. In viscometric stressing for prescribed periods, time to lysis declines as the imposed stress is increased. However, it has been conclusively shown that shear stress alone is not a sufficient predictor of hemolysis rate or thresholds (158); cell shape and tumbling also play a role. Membrane shear appears to be far lower when the cells are suspended in higher viscosity media in viscometric studies.

Erythrocytes allowed to adhere to a glass surface and then subjected to a fluid shear commence movement when the fluid shear force exceeds about 10^{-11} N (171). During this process the cell gradually moves downstream, but the membrane may remain attached to the surface (171). The membrane can be deformed permanently when the deforming force persists for more than a few minutes (171). Shear elasticities of nonnucleated mammalian red cells are generally similar, but elasticities are about an order of magnitude greater for cells of nucleated species. Small amounts of thiol reagents are known to decrease the elongation of human red cells suspended in a shear field (171), presumably by producing some sort of cross-linking. Potentially, this methodology may improve survival of any fragile cell with significant amounts of cross-linkable protein in the membrane. Other additives may render the cell more susceptible to shear damage. Certain chemical lysins and some antigen–antibody reactions cause perforation of cell membrane and leakage of intracellular material (158). Cholesterol enrichment or depletion of the human erythrocyte membrane does not affect its viscosity.

Hemolysis of red cells is known to occur intravascularly *in vivo* as well as in various *in vitro* flow systems (158). A number of studies have correlated hemolysis to flow in pumps, valves, heart–lung machines, blood dialyzers, and transfusion filters. In flow through tubes, wall roughness of the scale of erythrocyte correlates with hemolysis (158). Bubbles trapped in surface imperfections appear to aid lysis. In flow through tubes, hemolysis correlates with the shear rate and the surface-to-volume ratio (158). This type of lysis occurs at shear stress thresholds lower than the ones required to produce lysis in a fluid shear field. Wall contact-associated lysis has been observed to depend on the chemical nature of the wall material. Lysis may decline with time as surfaces become passivated by prolonged contact with plasma proteins (158).

In capillaries of ~1 mm diameter, an upper limit on the mean tube velocity of 6 m/s has been suggested for capillaries with sharp-edged entrances and blood with a viscosity of 4×10^{-3} Pa s (158). This corresponds to a Reynolds number of 1500 inside the capillary and an average wall shear rate of about 4800 s^{-1}. Velocities as high as 17 m/s may be employed inside capillaries with carefully flared entrances (158). As with other animal cells, erythrocytes subjected to bubbling are susceptible to bubble rupture–associated damage (59). Agitation in the absence of gas sparging can damage erythrocytes. In surface-aerated shake flasks, increasing shaker platform speed over 100–400 rpm increased the specific cell lysis rate (Fig. 81.16). The slight decline in lysis rate at 100 rpm (Fig. 81.16) was associated with improved surface aeration relative to static flask. Because erythrocytes do not multiply *in vitro*, the effects of cell damaging forces are not masked by growth-associated adaptation, changes in cell size, and stages of growth; hence, suitably chosen erythrocytes provide a well-defined cell population for comparative assessment of the damaging potential of various hydrodynamic environments (59).

In comparison with erythrocytes, the cytoplasm of leukocytes has markedly different rheological properties (172), but the properties of its membrane are similar to those of the red cells. Leukocytes adhering to vascular endothelium detach when the shear stress is between 26.5 and 106.0 N/m^2 (172). According to work cited by Prokop and Bajpai (76), a shear stress level of 60 N/m^2 applied over 10 min should lyse about a quarter of a leukocyte population. In another study, sublethal shear stresses of 10 and 20 N/m^2 applied over 10 min in a Couette viscometer affected the biochemical response of human T cells relative to unsheared controls (153). It seems, therefore, that cells

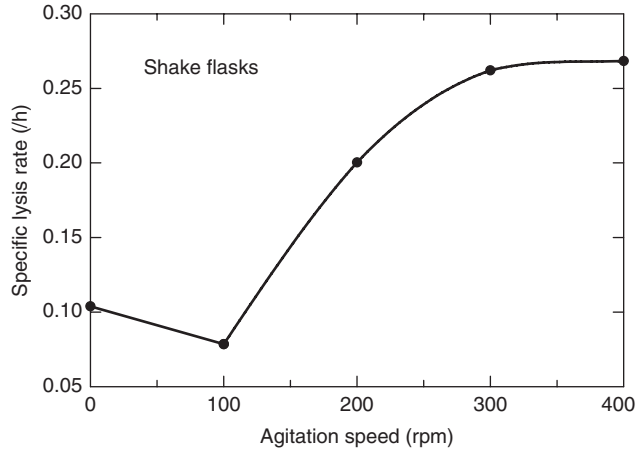


Figure 81.16. Effect of shaker platform agitation speed on specific lysis rate of suspended porcine erythrocytes in surface-aerated shake flasks. *Source:* Ref. 59.

in *in vivo* circulation are apparently more shear resistant than ones studied *in vitro*.

81.3.5.3 Microcarrier Culture. Both stirred tank and airlift bioreactors (173) may be used for suspended microcarrier culture. Microcarrier-supported cells likely experience hydrodynamic forces of greater magnitude than do freely suspended cells. This is because in highly agitated or aerated systems, the length scale of fluid eddies can be of the same order as the dimensions of microcarriers, resulting in high local relative velocities between the solid and the liquid phases (19,148,174). Furthermore, the carriers have greater inertia than free cells; hence, collisions among microcarriers, and between the impeller and microcarriers likely damage attached cells. Similarly, the fluid eddy impact and shear stress forces on a high inertia particle are greater than on free cells.

Resistance of a cell to rupture by impact, that is, burst resistance, is a possible measure of the cell's survivability in culture environment. Measurements of burst force are potentially useful also for comparative assessment of cell strength and in establishing culture conditions that give rise to more robust cells. It may eventually be possible to correlate the sensitivity to shear of a cell to its resistance to mechanical rupture (175). Burst strength may be directly relevant in microcarrier culture where impact-associated damage is likely; however, in view of the cytoskeleton-mediated pressure signal transmission to internal parts of a cell, a more likely scenario is that the force required to cause impact-associated damage is far lower than the rupture threshold. These issues notwithstanding, resistance to rupture of a mouse hybridoma grown in continuous serum-containing culture has been measured by squeezing single cells between flat surfaces of micromanipulator arms (176). The bursting strength increased with cell size (177). The bursting force correlated with the initial cell diameter as follows:

$$S = 0.2d_c - 0.1 \times 10^{-6} \tag{81.42}$$

where the intercept was not significantly different from zero (176). The cell diameter ranged over $\sim(10-17) \times 10^{-6}$ m. Other similar data (177) have been correlated (175) as follows:

$$S = 0.27d_c - 0.86 \times 10^{-6} \tag{81.43}$$

where the burst strength S is in newtons and the hybridoma cell diameter d_c is in micrometers. The calculated bursting tension had a mean value of $(1.8 \pm 0.5) \times 10^{-3}$ N/m, which was essentially independent of cell size (176). Because the bursting tension was size independent, the bursting pressure fell with increasing cell diameter. At $(0.8 \pm 0.3) \times 10^{-3}$ N/m, the calculated mean compressibility modulus of the cells was roughly independent of cell diameter (176).

Sinskey *et al*. (178) advanced the concept of "integrated shear factor" (ISF)—a measure of the strength of the shear field between the impeller and the spinner vessel walls—to correlate shear damage to mammalian cells. The ISF was defined as

$$ISF = \frac{2\pi N d_i}{d_T - d_i} \tag{81.44}$$

or effectively the laminar shear rate between the impeller tip and the walls. For a range of stirred vessels (0.25–2.0 L, $0.032 \leq d_i$ (m) ≤ 0.085), cell damage occurred once the *ISF* value exceeded about 18 s^{-1}, during culture of microcarrier-supported human fibroblasts (179). Damage could also be correlated with the impeller tip speed, but unlike the ISF, the damaging value of the tip speed depended on the size of the culture vessel (179).

Relying on earlier work of Nagata, Croughan *et al*. (179) arrived at the following expression for a time-averaged shear rate

$$\gamma_{av\,T} = \frac{112.8 r_i^{1.8} \left(r_T^{0.2} - r_i^{0.2}\right) (r_c/r_i)^{1.8}}{r_T^2 - r_i^2} \tag{81.45}$$

where r_i and r_T are the impeller and the tank radii, respectively. The radius r_c of the formed vortex zone would need to be estimated using Nagata's expression:

$$\frac{r_c}{r_i} = \frac{Re_i}{1000 + 1.6Re_i} \tag{81.46}$$

The impeller Reynolds number in Equation 81.46 is calculated as follows,

$$Re_i = \frac{N d_i^2 \rho_L}{\mu_L} \tag{81.47}$$

Equation 81.45 was developed for unbaffled stirred tanks operated in the turbulent regime (179). For human fibroblasts on microcarriers in various stirred vessels, cell damage occurred when the time-averaged shear rate exceeded about 2.5 s^{-1} (179). For chicken embryo fibroblasts, also on microcarriers, the damage threshold was 6 s^{-1} time-averaged shear rate (179). Cell damage correlated also with the Kolmogoroff eddy length scale (ℓ); for human fibroblasts the cell damage occurred when the length scale declined to approximately below 125 μm, whereas for the chicken embryo cells damage was observed when the ℓ value declined to below 100 μm (179).

Analyzing data from several sources, Croughan *et al*. (179) further showed that the specific death rate correlated with the average energy dissipation rate per unit mass;

thus,

$$k_d \propto E^m \tag{81.48}$$

where m was 0.72, 0.76, and 0.82, respectively, for microcarrier-supported Vero cells, similarly supported human fibroblasts, and a freely suspended protozoan. For attaining a more homogeneous shear field in stirred culture vessels, that is, for the minimum value of the maximum-to-average shear rate ratio, Croughan *et al*. (179) noted an optimal vessel geometry corresponding to $r_i/r_T = 0.74$.

Damage to microcarrier-supported Chinese hamster ovary cells during an abrupt contraction in laminar flow began to be detected at the energy dissipation value of 10^4 cm^2/s^3 (180). This value of energy dissipation is orders of magnitude lower than the values reported to cause damage to suspended animals cells (180).

In microcarrier culture, collisions between microcarriers and interactions between carriers and internals of a reactor are other possible causes of cell damage, particularly in stirred bioreactors (19,181,182). Cherry and Papoutsakis (174,181,182) advanced the concept of "severity of collision" to account for at least some of the damage to cells in suspended microcarrier culture in stirred vessels. Severity of collision combined collision frequency and energy of the impact. Two collision severities were defined: a "turbulent collision severity" (TCS) for turbulence-associated particle-to-particle impacts and an "impeller collision severity" (ICS) for particle-to-impeller collisions; thus,

$$TCS = \left(\frac{E\rho_L}{\mu_L}\right)^{3/2}\left(\frac{\pi^2\rho_S d_p^5 \varepsilon_S}{72}\right) \tag{81.49}$$

and

$$ICS = \frac{9\pi^4\rho_S n_B N^3 d_i^4 d_p^4}{512 V_L} \tag{81.50}$$

where E is the energy dissipation rate per unit liquid mass, ρ_S and d_p are the density and diameter of the microcarriers, ε_S is the volume fraction of the carriers, n_B is the number of impeller blades, N and d_i are the impeller rotational speed and diameter, and V_L is the volume of the liquid in the vessel. Improved cell growth was observed with smaller microcarriers as predicted by Equations 81.49 and 81.50. The specific cell death rate increased with increasing values of TCS and ICS (181,182); however, the influence of hydrodynamic forces on culture performance correlated also in terms of the ratio of Kolmogoroff eddy scale to bead diameter: the specific death rate declined as ℓ/d_p increased. As culture viscosity was raised, damage to cells declined in conformance with Equation 81.51 and in agreement with interpretations based on the ℓ/d_p ratio (182).

Unlike in stirred tanks, animal cell microcarriers suspended in airlift bioreactors under typical operating conditions do not significantly interact with each other or with the walls of the vessel (183); instead, the microcarrier particles follow the laminar streamlines of the fluid (183). Consequently, in airlift reactors at least, the effects of particle–particle or particle–wall collisions on monolayers of cells may be disregarded. Observations of Ganzeveld *et al*. (183) spanned microcarrier loadings of up to 30 kg/m^3, with carriers of 150–300 μm diameter, and 1030–1050 kg/m^3 density. The observations covered a power input value of up to 33 W/m^3, which is about the upper limit for cell culture in pneumatically agitated bioreactors. These results applied to a split-cylinder airlift bioreactor with an aspect ratio of 7.6, which would not normally be exceeded in large-scale cell culture systems. As an additional design constraint, the Reynolds number in the riser and the downcomer should not exceed about 3000, or the flow will be more chaotic (183).

Numerical analysis of forces exerted by laminar flow on anchorage-dependent cells attached to flat surfaces suggests that shear stress between 0.25 and 0.6 N/m^2 is sufficient to detach round cells, but much higher values are needed to dislodge spread out cells (165). These observations are relevant to microcarrier culture where, during inoculation, the round cells must first attach to microcarriers before spreading on the solid surface. During proliferation, bead-to-bead transfer of cells may also require a level of turbulence that is not so high as to hinder the reattachment process, yet not so low that bead-to-cell encounters are few.

Typically, the shear rate values in airlift bioreactors range over 250–4000 s^{-1} for operational conditions that are relevant to animal cell culture (18). These shear rates are substantially lower than $\sim 10^5$ s^{-1} that would be needed to damage cells if a 100-N/m^2 shear stress value (17,162) is taken as the threshold of mechanical damage. However, based on the shear stress data of Olivier and Truskey (165), during the process of attachment of cells to microcarriers, shear rate levels of 250–600 s^{-1} may well be detrimental. Thus, during initial attachment of cells, the reactor would need to be operated at reduced aeration rates—a practice that is well established through empirical experience, but previously explained only intuitively (18).

Under conditions typical of microcarrier culture in airlift bioreactors, the specific energy dissipation rates are different in different zones of the vessel. The specific energy dissipation rates increase in the order: downcomer < riser < bottom, for any fixed value of the aeration rate (18). The dissipation rates in all zones decline with increasing loading of microcarriers; however, the prevailing shear rates are not particularly sensitive to the density or the diameter of microcarriers within the ranges that are relevant to anchorage-dependent cell culture.

In one case, typical shear rates ranged over 250–4000 s^{-1} in microcarrier-containing systems, but much higher values, up to 12,000 s^{-1} could occur in solids-free media (18). These values compare favorably with shear rates of $\sim 10^5$ s^{-1} that have been reported as the threshold of damage to cells. Cells in airlift bioreactors would experience a substantial increase in the riser shear rate only when the fluid eddy length-to-microcarrier diameter ratio declines to ~1 (18).

Effects of shear stress on adherent cells are further discussed by Kretzmer (184). Effects of mixing intensity on cell seeding and proliferation in three-dimensional fibrous matrices have been discussed (185). Many adherent cells *in vivo* are known to be affected by shear stress (186).

81.3.5.4 Hydrostatic Pressure. As the scale of operation increases, suspended animal cells will inevitably experience substantial hydrostatic pressure changes as they move with fluid elements in a large bioreactor. At least for hybridomas, artificially imposed pressure cycling of up to 1.2 atm (18 psig) has shown no harmful effect (149). This level of pressure fluctuation will be encountered in bioreactors that are about 12 m tall; hence, for a 2:1 aspect ratio, an animal cell culture vessel could be scaled up to about 340 m^3. If, as recommended for airlift and bubble column bioreactors (24,25), an aspect ratio of 5:1 is employed, a maximum vessel volume of about 50 m^3 should be feasible. Suspension cell culture vessels in current commercial use do not generally exceed 10 m^3, or about 20% of the feasible volume based on hydrostatic pressure considerations.

81.3.5.5 Bubble-Associated Damage. That sparging damaged cells has been known since the 1960s; however, the specific events responsible for the damage—whether bubble formation at the sparger, bubble detachment, rise through the fluid, or events at the disengagement surface—and the mechanism(s) of damage remained unclear until recently.

The growth rate, viability, and antibody productivity of a mouse hybridoma in a surface-aerated stirred vessel were not affected by the agitation rate, but damage occurred when gas was sparged through the culture (187). In surface-aerated operation, the average and the maximum shear stress values varied over the respective ranges of 0.001–0.4 N/m^2 and 0.06–6.4 N/m^2. Subsequent work showed that bubbles larger than 5 mm were significantly less damaging to cells than smaller bubbles (188). Furthermore, placing the sparger below the impeller enhanced cell damage presumably because the impeller-associated bubble breakup gave rise to the more damaging smaller bubbles (188).

Cell lines differ tremendously in sensitivity to aeration as was demonstrated by Handa *et al*. (189). At constant aeration rates in geometrically identical bubble columns, smaller diameter bubbles (0.2 mm diameter) were shown to be significantly more damaging to a hybridoma than larger bubbles (1.62 mm diameter). In industrial scale culture of several hybridomas, Chisti (148) preferred even larger bubbles (10–20 mm diameter) for aeration. Similarly, Tramper *et al*. (89) observed that smaller bubbles were more damaging to insect cells than larger ones. However, the effect of bubble size may not be prevalent across cell types. Thus, in another study, baby hamster kidney (BHK-21) cells were not sensitive to the size of gas bubbles (190). Over a superficial gas velocity range of (0.42-8.5) $\times$ 10^{-4} m/s, higher velocities led to faster decline in cell viability of a hybridoma (189), which is consistent with other similar observations (87).

In commercial stirred tank culture of several hybridoma lines at up to 0.3 m^3, Chisti (148) employed submerged aeration with bubbles of 0.01–0.02 m diameter. Because of high rise velocities and mobile interfaces, such bubbles did not carry many attached cells to the surface. In contrast, during aeration with sintered metal spargers that produced slower rising bubbles of ~0.002–0.003 m diameter, the cells were rapidly carried into a persistent foam layer at the top by a froth floatation mechanism (148). The foam produced by larger bubbles collapsed soon after the bubbles rose to the surface. The reactors employed were agitated by magnetically coupled agitators with support bearings submerged in the culture. Reactors with submerged mechanical seals were also used. No loss in culture performance occurred relative to roller bottles. The impeller tip speeds >1 m/s produced no ill effects. Under typical operating conditions, the length scale of the microeddies was about 130 μm, or about 10-fold greater than the dimensions of the cells (148).

On the basis of energetics of bubble-associated damage to freely suspended cells, Wang *et al*. (191) concluded that the principal determinants of cell damage were cell-bubble encounter rate, the rate of bubble breakup within the fluid, and the bursting rate at the surface. Cell death correlated linearly with specific gas–liquid interfacial area, with the proportionality constant being 0.0125 m/h for a murine hybridoma (191). For a bubble larger than about 7 mm, microeddies in the wake of the rising bubble are incapable of damaging freely suspended animal cells (192).

Using an elegant mechanistic analysis, Tramper *et al*. (88,89) related the first-order rate constant for cell death due to all causes to aeration rate in a bubble column; thus,

$$k_d = \frac{24 Q V_k}{\pi^2 d_B^3 d_T^2 h_L} \tag{81.51}$$

where k_d is the first-order death rate constant, Q is the volumetric aeration rate, h_L is the height of fluid, d_T is the column diameter, and V_k is a hypothetical killing volume associated with the bubbles. The latter is actually the total

volume of fluid associated mainly with the bubble wakes; the cells entrapped in the circulating wake are carried with the bubble to the surface where most of the damaging events take place. According to Equation 81.51, the specific cell death rate is proportional to the frequency of bubble generation or $6Q/\pi d_B^3$. Alternatively, because at hydrodynamic steady state the bubble generation frequency equals the frequency of rupture at the surface, the death rate may be interpreted as being dependent on the frequency of bubble rupture and the killing volume associated with the bubbles.

On the basis of Equation 81.51, the death rate constant should decline with increasing height of fluid as experimentally confirmed. For otherwise fixed conditions, increasing liquid height in bubble columns improved survival of insect cells (88,89), myelomas, and hybridomas (86,90,190), supporting the view that cell death occurred predominantly in the bubble disengagement zone at the surface (189,190). For a myeloma grown in serum-supplemented medium, the minimum culture height that provided a performance equivalent to that of surface-aerated flasks, was ~0.7 m, corresponding to a bubble column aspect ratio of ~14 (90). The 0.05 m diameter column was aerated through a sintered disc sparger (150–250 μm pore size). The aeration rate was 5 mL/min (90), corresponding to a specific power input of about 0.42 W/m^3.

If bubble rise were to predominantly contribute to cell death, then the specific cell death rate should be independent of the height of fluid (193). Because this is contrary to experimental observations, the rise events may be disregarded as principal contributors to cell damage (193). If gas entry at the sparger contributed predominantly to cell damage, then at a given gas flow rate in the reactor, decreasing the number of sparger holes should enhance the specific cell death rate constant (193). In bubble columns, Jöbses *et al*. (193) noted that increasing the sparger hole gas velocity over 0.6–2.5 m/s at a constant volumetric gas flow in the reactors had no effect on the first-order rate constant for cell death; hence, events at the sparger could be disregarded as contributing to cell damage. This process of elimination identified bubble breakup at the culture surface as the principal cause of damage to suspended cells in sparged bioreactors such as bubble columns (193). Equation 81.51 applies also to airlift devices (87), especially ones in which gas is not carried into the downcomer. Because most agitated tanks used in animal cell culture operate at quite low mechanical power input and the impeller does not usually serve as a bubble breaking device, Equation 81.51 should provide a lower limit on k_d also in such tanks.

Using a hybridoma culture van der Pol *et al*. (86) showed that the first-order death rate constant increased with increasing $1/d_T^2$ in bubble columns as expected from Equation 81.51. Equation 81.51 suggests that cell damage increases in direct proportion to the superficial gas velocity in the column, or in direct proportion to the specific power input. Note that increasing the liquid level at constant aeration rate in a column of fixed diameter decreases the specific power input (18,24,25). Equation 81.51 further suggests that for a given V_k, larger bubbles should be less damaging than smaller ones. This agrees with substantial empirical evidence (88,89,148,188,190,194).

That the death rate increases linearly with increasing aeration rate has been proved (88,89,194). Also, the killing volume V_k has been shown to be independent of the aeration rate and the height of fluid, so long as the bubble diameter is not affected (88,89). The killing volume apparently depends on bubble diameter, increasing with diameter but in such a way that the ratio V_k/d_B^3 declines as the bubble diameter increases. This has been confirmed by Wu and Goosen (194) using *Spodoptera frugiperda* insect cells in bubble columns that were sparged with bubbles of different mean diameters while maintaining a constant volumetric gas flow rate. Increasing bubble diameter reduced the specific death rate as shown in Fig. 81.17. In view of the numerous contrary observations, analyses suggesting lesser cell damage with smaller bubbles are clearly flawed.

The dimensionless specific killing volume, or $6V_k/\pi d_B^3$ in Equation 81.51, depends on the concentration of serum in the culture medium. Van der Pol *et al*. (86) showed that the dimensionless killing volume declined as the serum concentration was raised over the range 0–2.5% (vol/vol); the dimensionless killing volume in the absence of serum was ~2.7-fold compared to that at 2.5% serum in a hybridoma culture (86). This and other similar observations (86) at least partly explain the well-known protective effect of serum. Cell-protective effects of other proteins may be similarly explained. Serum-free media with 1 g protein/L—equivalent to supplementing the medium with 2% vol/vol serum—are commercially used in sparged airlift culture vessels (149).

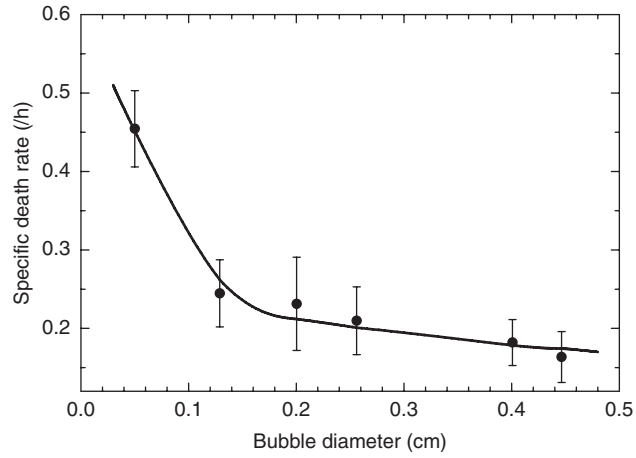


Figure 81.17. Effect of bubble diameter on the specific death rate of *S. frugiperda* insect cells in bubble columns aerated at a constant volumetric gas flow rate of 10 mL/min. Adapted from Ref. 194.

The reason for rupture of larger bubbles being less damaging to cells than breakup of smaller ones has become clear through analyses of mechanics of rupture (195,196). Numerical simulations and experimental observations of bubble rupture at air–water interface confirm that smaller bubbles rupture much more violently than larger ones (195,196). A bubble reaching the surface rises to different heights above the flat liquid surface before rupturing. For a bubble that is stationary at the surface, a part is always submerged below the flat surface of the liquid. The degree of submergence is generally greater for smaller bubbles.

During rupture, the liquid drains from the film between the raised liquid surface and the bubble (197,198). As the film thins, a hole develops in the center of the dome and the film rapidly retreats into the bulk liquid (Fig. 81.18). The rupture of the film and consequent elongational and accelerational flow have been postulated to damage cells in the film and those adhering to the bubble cavity (197). A cell on the surface of a rupturing film would apparently not experience any motion until struck by the toroidal ring of fluid at the receding edge of the film (197). The force experienced by the cell will depend on the film thickness at the instance of rupture (197). Rupture of thinner films is likely to be less damaging than when a thicker film breaks.

Once the bubble ruptures, fluid rapidly accelerates and moves down the interior walls of the bubble cavity (Fig. 81.18). The flow from around the walls impacts at a stagnation point located immediately below where the bubble had been (Fig. 81.18). The high pressure produced by the impacting streams forces a jet of fluid upward into the gas phase above the liquid surface (Fig. 81.18). A second opposing jet is forced into the fluid below the stagnation point. Intense accelerational flows around the bubble cavity and formation of liquid jets occur mostly during rupture of small bubbles. Bubbles larger than about 6 mm rupture much less violently.

According to Boulton-Stone and Blake (195), "...one of the most important factors determining the motion following film rupture, in terms of the energy released, is the height of the top of the bubble above the equilibrium free-surface" of the liquid. Bubbles rupturing from a lower position beneath the equilibrium surface of the liquid release more energy because of their higher internal pressure. The energy is released as high-speed liquid jets. Bubbles larger than about 6 mm bursting at the surface do not form significant jets (195), which is consistent with numerous observations dating from the 1950s and earlier. When a jet is produced, the speed of the jet declines as the size of the rupturing bubble increases: for example, for air bubbles rupturing on water, a maximum jet speed of 6.4 m/s has been calculated for rupture of a 1-mm bubble; for rupture of a 6-mm bubble, the maximum jet speed declines to 0.94 m/s (195). In addition to a liquid jet rising into the atmosphere above the liquid, a second liquid jet moves down into the fluid from the region which had been below the base of the bubble. The maximum pressure produced during bursting of bubbles of various sizes declines with increasing bubble diameter as illustrated in Fig. 81.19. The maximum energy dissipation rate occurs just beneath the bubble, immediately before the jet forms (195). The calculated maximum energy dissipation rates for the smallest bubbles are equivalent to a stress of about 10.4 N/m^2 (195). The maximum energy dissipation rates

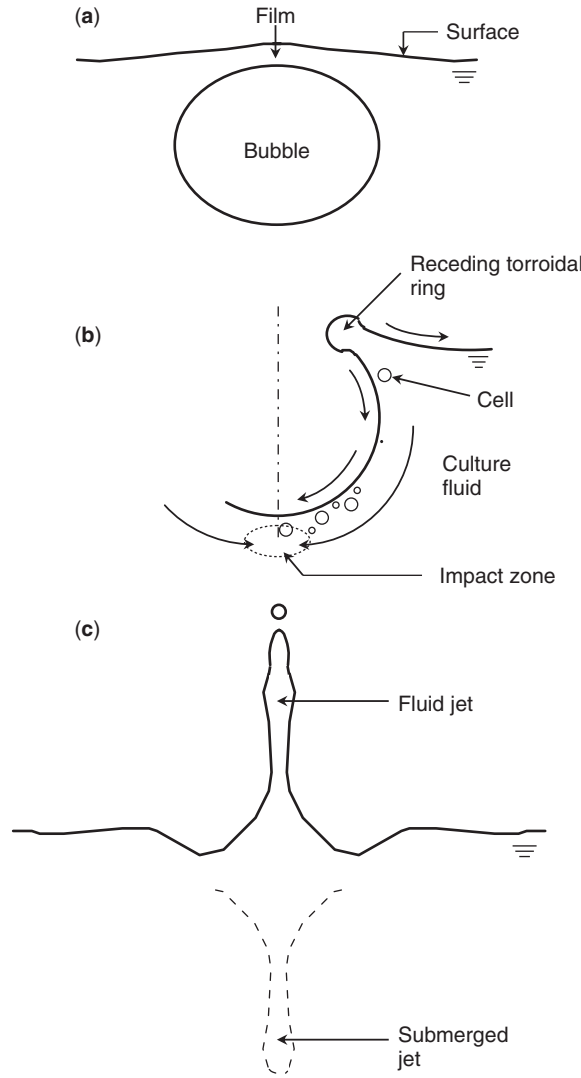


Figure 81.18. Events during the rupture of a bubble. (a) Bubble arrives at the surface and rises so that the film between the bubble and the surface thins. The height of the rise and the film thickness depend on the bubble size; smaller bubbles rupture deeper. (b) A hole develops in the film and the toroidal ring of the rupture vent expands and recedes into the bulk fluid. Streams of fluid draining into the bulk fluid impact beneath the bubble, generating intense local turbulence and creating a jet of fluid (c); a similar jet is produced underneath the liquid surface. When produced, the jet might rupture near the top to form droplets.

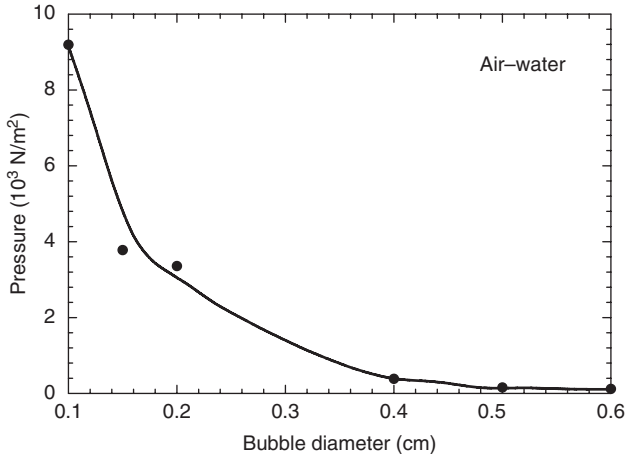


Figure 81.19. The maximum pressure produced during bursting of air bubbles of various sizes on the surface of water. Adapted from Ref. 195.

decline with increasing bubble diameter as depicted in Fig. 81.20.

Even a violent bubble rupture event would be inconsequential if there were no cells in the vicinity. Unfortunately, cells attach to rising bubbles and the fluid behind bubbles is especially rich in cells. That some animal cells will attach to rising bubbles has been shown with *Trichoplusia ni* and *S. frugiperda* insect cells (197,199). The cells adhered to rising microbubbles (diameter $\leq$ 3 mm) of the type used commonly in froth flotation. Hydrophobic interactions are apparently responsible for cell attachment—a mechanism observed also with ore particles attaching to bubbles during foam flotation. Although very small bubbles are generally not suited to aeration of cell cultures (148), larger bubbles also transport cells to the surface, but not predominantly as

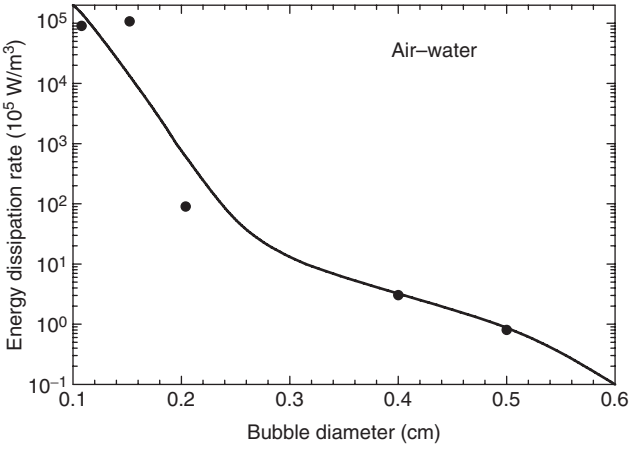


Figure 81.20. The maximum energy dissipation rates produced during bursting of air bubbles of various sizes on the surface of water. Adapted from Ref. 195.

adhering cells. Instead, the cells are trapped in the circulating wake carried behind large bubbles. The fluid associated with the wakes is known to be richer in particles than the bulk fluid.

More than 95% of the cells in the liquid ejected as a jet during rupture of bubbles have been shown to be nonviable even when the cells in the bulk culture contained fewer than 10% dead cells (196). Clearly, the cells carried in the bubble wake are destroyed by the rupture event. On the basis of simulations of rupture of bubbles with diameters of 0.77, 1.70, and 6.32 mm, Garcia-Briones *et al*. (196) calculated maximum energy dissipation rate values of 9.52×10^7, 1.66×10^7, and 9.40×10^4 W/m^3, respectively. Comparing these values with energy dissipation rates that have damaged cells in various unaerated flow devices (capillaries and viscometers), Garcia-Briones *et al*. (196) noted that values of the order of 5.81×10^2 W/m^3 did not damage the cells significantly, whereas appreciable damage occurred when the energy dissipation rate exceeded about 2.25×10^4 W/m^3. Clearly, therefore, a 6.32-mm bubble still has a significant potential to damage cells, and smaller bubble would produce instantaneous damage. For example, in gas-free capillary flow in experiments reported by Augenstein *et al*. (20), more than 80% of the cells died within 0.3 s of exposure to energy dissipation rates of about 4.80×10^7 W/m^3 (196). Interpreting data from several sources, Garcia-Briones *et al*. (196) further note that average energy dissipation rates of the order of 2990–29,000 W/m^3 have generally produced a significant decline in growth rate in impeller agitated bioreactors. These dissipation rates are average values; the cells probably experienced much higher local energy dissipation rates in the vicinity of the impellers.

If stable foam is not allowed to form, and relatively large bubbles (diameter $\approx$ 10–20 mm) are used for aeration so that the energy dissipated during rupture remains below the cell-damaging threshold, then the cells carried in the wake will not be damaged or removed into a foam layer. For bubbles of a given size, the volume of the circulating wake can be reduced by increasing the viscosity of the culture broth. Small increases will reduce the rise velocity of the bubbles and the circulation in the wakes will be slowed down. Consequently, slight enhancements in viscosity could reduce the transport of particles in the wake. This may indeed be one explanation of why viscosifying additives have been frequently observed to reduce cell damage. Also, for a given volumetric aeration rate, use of larger bubbles reduces bubbling frequency; hence, the frequency of bubble rupture is reduced.

On the basis of the studies reviewed, several important observations can be made regarding freely suspended animal cells in sparged and agitated bioreactors: (i) the aeration rate should be kept as low as possible; (ii) the mean bubble size should larger than 7 mm, preferably about 10–20 mm;

(iii) the location of the sparger should be such that the rising bubbles do not interact with any impellers; (iv) with small airlift and bubble column reactors the aspect ratio should be about 14; however, in larger columns where the sparged portion of the cross-section can be a small fraction of the total cross-sectional area, more realistic aspect ratios of about six or seven are satisfactory; (v) when an impeller is used, the average energy dissipation (input) rate should remain below about 1.0×10^3 W/m^3. Observations (i)–(iii) are consistent with industrial practice (148). The sole purpose of the impeller should be to suspend the cells and mix the fluid gently so that the oxygen transferred from the bubbles is distributed throughout the vessel. Consistent with this purpose, the impeller should be of a kind that does not produce excessively high local rates of energy dissipation. For example, relatively large axial flow hydrofoils are the preferred impellers (43,148). In addition, a suitably selected additive such as Pluronic F68 should be used whenever feasible.

81.3.5.6 Mitigation of Shear Damage. Various approaches have been used to reduce bubble rupture-associated damage to cells. Some common approaches are the use of cell protective additives as noted here; compartmentalization of the culture into cell-free and cell-containing zones with sparging confined to cell-free regions (150,151); use of bubble-free oxygenation through microporous or diffusion tubing made of silicone rubber or other polymers (145); use of liquid oxygen vectors such as perfluorocarbons (145); and surface aeration (145). Alternatives to bubbling are suited typically only to specific cases; direct sparging remains the predominant method of aeration of cell cultures and it is not likely to be displaced in the foreseeable future (146).

One adaptation of submerged aeration is the "bubble bed" bioreactor that can substantially reduce surface rupture of bubbles in short-term batch culture (200). The bubble bed device (Fig. 81.21) is similar to a concentric draft-tube airlift bioreactor, but a downward pumping axial flow impeller located in the draft-tube circulates the fluid. The downward liquid flow in the draft-tube is sufficiently fast that gas bubbles injected into the draft-tube cannot escape; hence, the bubbles do not rupture at the surface of the culture. Pure oxygen or oxygen-enriched gas is used to reduce the needed gas injection rate to very low values. The gas holdup in the downcomer increases during batch operation and a noncirculating bed of bubbles develops. The cross-sectional area of the draft-tube increases downward (Fig. 81.21) so that the superficial velocity of the liquid declines as it moves down; consequently, the downflowing liquid cannot drag the bubbles out of the draft-tube and into the bubble-free annular zone. According to Sucker *et al*. (200), the cell growth and antibody production in bubble bed devices is comparable to values

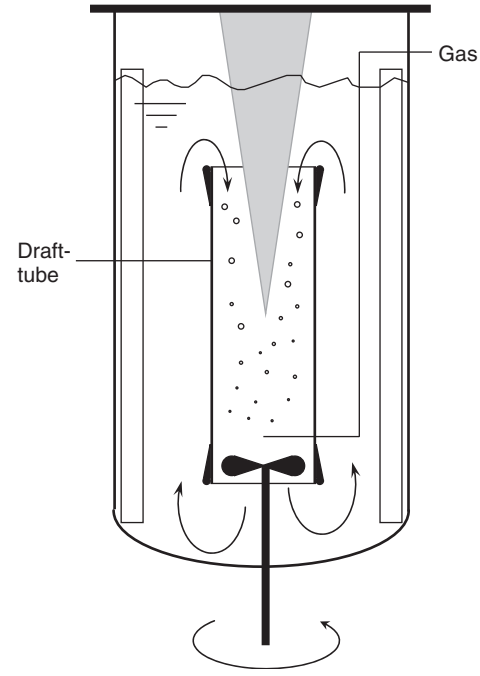


Figure 81.21. A bubble bed reactor.

obtained in surface-aerated spinner flasks even when the sparged culture in the bubble bed units is not supplemented with serum, Pluronic F68, or other protective additives.

81.3.5.6.1 Shear Protectants. Bubble-associated damage can be significantly reduced by adding shear protective substances to the culture medium. Many additives have been examined for shear protective function (201). Some of the protective additives are noted in Table 81.6. The protective effect depends on the properties of the specific additives, the concentration used, the type of cell, and the mechanism(s) of protection. Some common protective agents and their mechanisms of protection are discussed in the following text.

81.3.5.6.1.1 Serum. A concentration-dependent protective effect of fetal calf serum, horse serum, and others has been widely observed in aerated and bubble-free suspension cultures of many types of animal cells (57,86,87,92,190,201–203). Typically, protection increases

TABLE 81.6. Media Additives Associated with a Cell Protective Effect

Serum	Pluronics
Proteins (e.g. serum albumin)	Polyvinyl alcohols
Derivatized celluloses (e.g. methyl cellulose)	Polyvinyl pyrrolidone
Derivatized starches (e.g. hydroxyethyl starch)	Polyethylene glycols
Dextrans	

with increasing serum concentration up to about 10% (vol/vol) serum. In one study reduction in fetal calf serum level from 2.5% to 0% substantially increased the death rate constant of a hybridoma in aerated culture (86). Investigations revealed that serum had no long-term biological effect, but only a direct nonspecific physical protective effect (86). Thus, cells growing in low serum medium were immediately protected upon transfer to a medium with 2.5% serum. A physical protective effect of serum has been claimed to originate in its ability to reduce PMF (57,202). According to Martens *et al*. (87), serum has an immediate physical protective effect, and also a physiological protective effect that takes longer to become effective. The latter finding concurs with Michaels *et al*. (203). In bubble-free experiments in a Couette viscometer (shear rate = 5000 s^{-1}, shear stress = 5 N/m^2), prolonged exposure of cells to FBS reduced their shear sensitivity in laminar flow studies (203); however, shorter (30–120 min) exposure to FBS did not affect shear tolerance of cells. On the basis of these results, the protective effect of FBS was claimed to have both physical and biological (biochemical) origins (203).

The precise nature of the physical protective effect of serum is not clear. Supplementation with serum enhances the viscosity of the culture medium, but the effect is small (166,204). Nevertheless, Croughan *et al*. (92) and others (93,181) have associated the observed protection to the turbulence dampening effect of serum. In contrast, other evidence suggests a lack of relationship between the amount of protection afforded by the serum and enhancement of viscosity (205,206). In addition to dampening turbulence, the serum proteins may coat the cells so that the fluid eddies no longer penetrate to the vicinity of the cell membrane (92). In one study, increasing concentration of FBS over 0–10% (vol/vol) reduced PMF of a hybridoma line, making the cells more resistant to shear damage (57,202).

81.3.5.6.1.2 Pluronic® F68. Another well-known shear protectant is the nonionic surfactant polyol Pluronic® F68, a block copolymer of poly(oxyethylene) and poly(oxypropylene). Highly pure Pluronic F68 is added to cell culture media, typically at 0.5–3 kg/m^3 (166,189,190,193,201,203). The protective effect of the surfactant is concentration dependent, increasing with concentration, but leveling off at ~0.5 g/L (Fig. 81.22).

The protective effect of Pluronic F68 is commonly associated with its ability to suppress attachment of cells to bubbles (190): in presence of the surfactant fewer cells are carried to the surface where much of the cell damage occurs in aerated culture. However, evidence exists for other protective mechanisms. For example, a cell protective effect of Pluronic F68 has been observed even in unaerated culture (57,193). In one case, this effect was observed in a strongly agitated culture sample (193). Although no bubbles were present, a deep vortex was drawn into the fluid by the marine impeller used. Extensive cell damage occurred, but the damage was significantly reduced when the culture was supplemented with Pluronic F68. On the basis of these observations, Jöbses *et al*. (193) concluded that the protective effect of Pluronic F68 was due to its direct influence on cells and due to some effect of the surfactant on the gas–liquid interface. One possible explanation for the protection observed by Jöbses *et al*. (193) in the absence of the bubbles follows: the damage may have been occurring at the rapidly moving surface of the vortex (207) and supplementation of the culture with Pluronic F68 may have reduced surface adherent tendency of the cells; hence, fewer cells may have attached to the surface during its formation at the periphery of the vessel.

Using flow cytometry, Al-Rubeai *et al*. (156) showed that leakage of a positively charged dye, fluorescein diacetate, from murine hybridomas increased with rising intensity of agitation, hence suggesting a possible link between permeability of cell membrane and shear rate. However, because intense agitation was accompanied by entrainment of gas bubbles into the culture (156), the observed leakage could not be conclusively associated with fluid turbulence. The authors noted that for otherwise fixed agitation conditions, the leakage of the dye reduced when the culture medium was formulated with 1% Pluronic F68. The protective effect of the surfactant was apparently linked at least partly with its biochemical association with the cell membrane. The agitation- and vortex-associated hydrodynamic forces were reported to also affect the antigen receptors embedded in the membrane of the hybridoma (156). The number of active surface receptors declined with increasing intensity of agitation and the accompanying increase in the size of the vortex; however, the viability of the cells

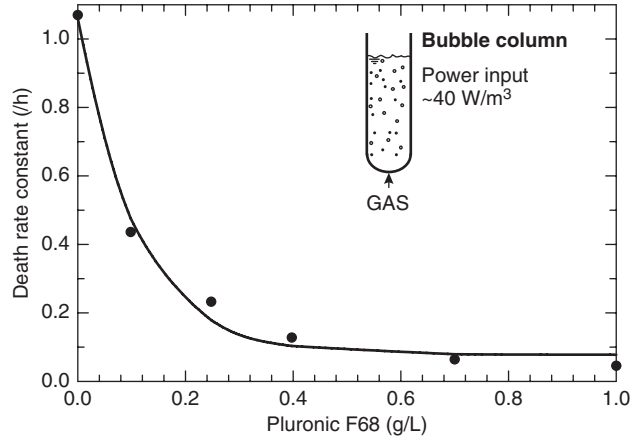


Figure 81.22. Cell protective effect of Pluronic F68 in a bubble column. The specific first-order cell death rate constant is plotted as a function of the concentration of Pluronic F68 in the medium. All data were obtained at a constant specific power input of ~40 W/m^3. Adapted from Ref. 193.

was unaffected. Pluronic F68 had a protective effect on the receptors.

Pluronic F68 is known to reduce the PMF of cells and this has been suggested as a possible mechanism of protection (57,202). Other additives that affect PMF also affect a cell's shear tolerance; for example, in one case, cholesterol enrichment of the culture medium reduced membrane fluidity and enhanced the shear resistance of hybridomas, whereas supplementing the culture with benzyl alcohol increased PMF and made cells more shear sensitive relative to controls (57,202).

Other protective mechanisms speculated for Pluronic F68 include its stabilizing action on the gas–liquid interface and consequent slower film drainage during bubble rupture (190), improved nutritional transport because of a reduced cell–fluid interfacial tension, and incorporation of the surfactant into the cell membrane accompanied with membrane-stabilization (208,209). Although the protective effect of Pluronic F68 is said to be solely due to physical factors (203), the surfactant is known to produce other physiological and biochemical effects in some cases at least. Growth suppressory and stimulatory effects of Pluronic F68 have been seen even in some static cultures. Such effects are sometimes associated with impurities in Pluronic F68 samples. Pluronic F68 affects permeability of some cells. Exposure of *S. cerevisiae* to 0.2% (wt/vol) for 30 min at 20°C made the cells more permeable and they became susceptible to otherwise nonlethal doses of certain antibiotics (210). The mean activity of alcohol dehydrogenase in permeablized cells was more than 3.5-fold of that in normal cells. Although Pluronic F68 could permeablize the yeast cells, it did not inhibit growth or affect cell viability relative to controls when added to culture media at up to 1% (wt/vol), which was the highest concentration tested (210).

Other data suggest that the cell-protective effect of Pluronic F68 may not be quite general (59). For porcine erythrocytes suspended in isotonic buffer, Zhang *et al*. (59) noted that addition of Pluronic F68 actually increased cell lysis in agitated environments relative to results in the surfactant-free medium. Whether Pluronic F68 incorporates into erythrocyte's membrane is not known; however, cholesterol enrichment or depletion of erythrocyte membrane is reported to not affect its viscosity and presumably, therefore, its fluidity. In addition to Pluronic F68, several other pluronics are known to have a shear protective capability. Shear tolerance of plant cells is improved in presence of Pluronic F68 (211).

81.3.5.6.1.3 Poly(ethylene glycol) (PEG). Poly(ethylene glycol) (PEG) supplementation of the medium has a protective effect on some cells but not on others. In one study (212) that employed different PEGs of molecular weights of 400–35,000 Da in the concentration range of 0–2 kg/m^3, the polymer had a protective effect in sparged cultures when the molecular weight and the concentration exceeded 1000 Da and 0.25 kg/m^3, respectively. The extent of protection afforded depended on the molecular weight and the concentration used. Under the best conditions, the PEG supplementation reduced the first-order cell death rate constant to 0.5% of the value in the PEG-free medium (212). The PEG additives affected the surface tension of the culture medium; however, in extreme cases the surface tension varied only over $\sim$(60-70) $\times$ 10^{-3} N/m (212). The pattern of variation (but not the magnitude) in surface tension with the addition of PEG was similar to the pattern of change in the death rate constant. This led the authors to suggest that the presence of PEG at the gas–liquid interface was somehow related to the protective mechanism.

Michaels *et al*. (203) showed that in sparged bioreactors supplementing the culture medium with Pluronic F68, FBS, or PEG (8000-Da molecular weight, 1 kg/m^3) protected cells irrespective of whether the CRL-8018 hybridomas were grown in the presence of the additive or the additive was added after the damaging levels of agitation were imposed.

81.3.6 Composite Particles and Cell Aggregates

81.3.6.1 Microbial Biofilms on Suspended Particles. Gas–liquid–solid three-phase suspension reactors are increasingly being used in wastewater treatment (24,213). The suspended solid phase (usually sand, glass beads, or carbon particles) supports a biofilm of waste-degrading microorganisms (214). The hydrodynamic environment of such systems must be tailored to control the biofilm thickness without dislodging it altogether (24). Biofilm slurry reactors are conceptually similar to microcarrier-supported suspension culture of animal cells, but there the similarity ends. Unlike animal cell microcarrier suspensions, the biofilm reactors are much more turbulent, the solids loading is generally higher, the density difference between the solid and the liquid phase is much greater, and the biofilm is typically four or five times thicker than the monolayer of cells on microcarriers.

In studies of degradation of naphthalene-2-sulfonate by *Pseudomonads* immobilized as biofilms on sand particles suspended in an external-loop airlift bioreactor, Wagner and Hempel (215) noted that at solids loadings of 20–30 kg/m^3, only about 15–20% of the particles were covered with biofilm, but high solid loadings were necessary to control the film thickness at 75 $\pm$ 10 μm by providing a high attrition environment (215). These observations were for particles about 200 μm in diameter, covered with $\sim$75-μm thick biofilm, suspended in the reactor under fairly turbulent conditions (230–440 W/m^3

specific power inputs). Even when oxygen limitation is not an issue, diffusion of other substrates limits the useful thickness of microbial biofilm to less than 400 μm in most wastewater treatment operations (213).

The development of microbial biofilms on static surfaces and carriers suspended in airlift bioreactors has been investigated quite extensively (6,7,214,216–222). In one case, 21 carriers were tested at a constant carrier loading of 125 kg/m^3 (214). The superficial gas velocity was constant at 0.038 m/s. The hydraulic retention time of wastewater was 1 or 2 h. On the basis of the tests, carrier diameter and surface roughness were the major factors that influenced biofilm formation (214). Smaller particles, 0.1–0.3 mm in diameter, tended to show better biofilm development. This was said to be due to more frequent collisions among larger particles causing biofilm detachment (214); however, with larger particles, a greater *severity* of collisions would have been a better explanation (24). For equal mass loadings of solids in two systems, the system with larger particles should have fewer particles per unit volume and, therefore, a lower frequency of particle–particle collisions. Cell disruption experiments in agitated slurries of glass beads confirm this (11). The explanation for the impact of surface roughness on biofilm formation lies in the fact that a rough surface provided many relatively protected, low shear sites where microbial colonies could take hold in the process of gradually spreading over the whole surface. On the basis of the criteria of surface roughness, particle size, cost, and the requirement of a high density carrier for ease of separation, basalt ($\rho_S = 2900$ kg/m^3) was the best carrier (214).

Irrespective of carrier type, biofilm formation is favored at relatively high dilution rates when any detached cells are rapidly washed out (214,218). Tijhuis *et al*. (218) have shown that during start-up at high dilution rates, the concentration of bare carriers declines as an increasing number are covered with the biofilm. The total amount of the biomass in the reactor increases, but the amount per carrier remains constant until most of the carriers are covered. With few bare carriers remaining, the extent of abrasive loss of film declines and the film thickness begins to increase until a stable thickness is reached (218). These observations suggest that varying the reactor operation to suit different stages of film development may be worthwhile (24).

In other similar work, detachment of biomass from nongrowing biofilms supported on carriers suspended in four configurations of draft-tube sparged internal-loop airlift reactors was examined (221). The superficial aeration velocity in the riser varied over the approximate range 0.03–0.09 m/s. The detachment of biomass from biofilm-covered carriers in presence of bare solids was dominated by collisions between bare carriers and the covered particles (221,222). The concentration of bare solids and the particle roughness strongly influenced the detachment rate (221). For otherwise identical conditions, biofilm detachment due to bare carriers increased in the order: glass, sand, basalt. The glass particles were the most round and smooth; the basalt carriers were the roughest. While biofilms develop more easily on rough surfaces (214), once developed, the film is readily damaged by biofilm-free rough carriers. Gjaltema *et al*. (221) observed that a "change in flow regime from bubbling to slug flow considerably increased the detachment rate." This change apparently occurred at a U_{Gr}-value of ~0.06 m/s. The "slug flow" regime noted by Gjaltema *et al*. (221) was more likely the highly chaotic churn turbulent regime in which particle-to-particle collisions are more frequent and severe than in the bubble flow regime. The bottom clearance of the draft-tube had no effect on detachment rate (221), but only a small range of the A_d/A_b ratios was investigated. The volume fraction of carriers was 3.3–3.8% and other properties were basalt, $d_p = 0.32$ mm, $\rho_S = 3010$ kg/m^3; sand, $d_p = 0.31$ mm, $\rho_S = 2606$ kg/m^3; and glass, $d_p = 0.28$ mm, $\rho_S = 2887$ kg/m^3 (221). Another similar study focused on the effects of particle shape, structure, and concentration on biofilm detachment (222).

Strategies for development of biofilms with nitrification activity on carriers suspended in draft-tube sparged internal-loop airlift reactors were investigated by Tijhuis *et al*. (220) and van Benthum *et al*. (223). The development of the nitrifying films was similar to what had been reported for heterotrophic biofilms (216–219); however, the nitrifying films were more robust (223). This suggests that biofilms formed by different microorganisms can have markedly different physical properties and strength of attachment to substrate (24); hence, the operating regime of the reactor and, in extreme cases, the design peculiarities are likely to be affected.

In further studies of the dynamics of biofilm detachment from carriers suspended in airlift reactors, Tijhuis *et al*. (217,218) noted that the common assumptions of uniform growth and detachment of biomass over the surface of the film under fixed hydrodynamic conditions were inconsistent with observations. Instead, nonuniform local detachment of biofilm with formation of cracks and fissures on its surface and rapid filling of the spaces formed with new growing biomass was proposed as a more realistic picture of film dynamics (217).

During development of mixed bacterial biofilm on static glass surface in a rectangular turbulent flow cell, Stoodley *et al*. (7) noted that parts of the biofilm sloughed off at a wall shear stress level of 1.32 N/m^2. In the region of detachment, pieces of the biofilm were still attached to the surface, suggesting that the glass-to-biofilm bond was stronger than the biofilm structure (7). Relative to the clean flow cell, the pressure drop through the channel was higher in presence of the biofilm (7) presumably because a patchy development of the film increased the effective surface roughness.

81.3.6.2 Flocs and Agglomerates. Microbial flocs are encountered in several commercially relevant processes, especially in wastewater treatment and beer fermentation with autoflocculating yeasts. Similarly, agglomerates of protein precipitates form during certain recovery operations. The size of flocs and agglomerates often needs to be preserved or increased during processing. The stable size of aggregates and flocs and whether the flocculated mass further increases in size or breaks up depend on the level of turbulence in the suspending fluid. Turbulent stress levels below about 0.75 N/m^2 are generally too mild to break aggregates (224). Physical disruption of aggregates commences at stress levels of ~2.6 N/m^2 and especially when the stress level exceeds about 5 N/m^2 (224). In a turbulent field, aggregates may deform or breakup because of the influence of instantaneous velocity differences acting on different parts of the floc (225). Also, turbulent drag forces originating from the local motion of the fluid relative to the aggregate may contribute to fragmentation (224). The shear force across the aggregate due to instantaneous velocity difference is related to the energy dissipation rate in the fluid and the size of the aggregate (224); thus,

$$F_s = \frac{\pi}{4}(\rho_L \mu_L E)^{1/2} d_F^2 \tag{81.52}$$

The dynamic pressure fluctuations acting on opposite sides of the floc create a normal stress. Assuming that the eddy size is in the Kolmogoroff microscale range and that the particle dimensions are similar to those of the eddies, the normal force can be expressed as follows (224):

$$F_n \propto \left(\frac{E}{\mu_L}\right) \rho_L^2 d_F^2 \tag{81.53}$$

The turbulent drag force acting on an aggregate may be calculated using the following expression (224):

$$F_D \propto \frac{C_D}{2}\left(\frac{d_F}{2}\right)^3 (\Delta u d_F)^2 \rho_L \tag{81.54}$$

where Δu is the difference in velocities of the particle and the fluid, and C_D is the drag coefficient. For low density particles in the Stokes regime ($Re < 1$), the drag coefficient equals $24/Re$, where Re is the Reynolds number, or $(\rho_L \Delta u d_F)/\mu_L$. Reynolds shear stresses—that is, turbulent stresses associated with the fluctuating component of the mean velocity—may be calculated using the equation (226):

$$\tau = 0.37 \rho_L \left(\frac{E \rho_L}{\mu_L}\right) d_p^2 \tag{81.55}$$

which applies to stresses around a spherical particle. Reynolds stresses are independent of viscosity.

The maximum stable size of the aggregate in a turbulent field can be established by a force balance on a particle: at stable size the instantaneous turbulence force accelerating the particle just equals its mechanical strength (224). In the inertial subrange of turbulence when the eddy size is greater than the Kolmogoroff scale (ℓ),

$$d_{F\,max} \propto \left(\frac{\rho_L \sigma_M}{\mu_L}\right)^{1/3} E^{-1} \tag{81.56}$$

whereas in the viscous subrange of turbulence when the eddy size is $\leq \ell$, we have

$$d_{F\,max} \propto \left(\frac{\sigma_M \mu_L}{\rho_L^2 E}\right)^{1/2} \tag{81.57}$$

where σ_M is the mechanical strength of the aggregate. In practice, the maximum stable floc size has correlated with the energy dissipation per unit mass of fluid as follows:

$$d_{F\,max} \propto \Gamma E^{-m} \tag{81.58}$$

where the coefficient Γ depends on the nature of the particle and m is usually between 0.2 and 0.4 (227).

In stirred tanks, the maximum floc size for particles of uniform composition has been theoretically and experimentally correlated with the rotational speed of the impeller (225); thus,

$$d_{F\,max} \propto N^{-1.5} \tag{81.59}$$

which applies to particles smaller than the microscale of turbulence. The dependence shown in Equation 81.59 can be expressed in terms of the energy dissipation per unit mass; hence,

$$d_{F\,max} \propto E^{-0.5} \tag{81.60}$$

Expression (81.60) is consistent with that reported by Thomas (225), but the exponent on E is somewhat stronger than the values noted by Gregory (227) (see Eq. 81.58). In precipitation vessels, shear rate values of ~80 s^{-1} appear to be a damaging threshold for soy protein precipitate particles of 20–30 μm initial size (5). Particles exposed to approximate shear rates of ≥80 s^{-1} over 10–12 min would be reduced to 5–8 μm. The shear rate numbers were calculated from the specific energy dissipation rates in the vessels, as follows:

$$\gamma = \left(\frac{\rho_L E}{\mu_L}\right)^{0.5} \tag{81.61}$$

Protein precipitates are easily damaged by pumping. Moyno screw pumps, centrifugal pumps, and gear pumps all damage precipitates to similar levels (5). Peristaltic pumps are

apparently the only suitable ones. Shear-induced break up of protein precipitates during acceleration in a centrifugal field can greatly (>10-fold) reduce the recovery capacity of centrifugal separators (228). In the entrance region of a disc stack centrifuge, the shear rate can approach 10^5–10^6 s^{-1} (229). Effects of agitation during precipitation and processing of α-lactalbumin enriched whey protein precipitates have been discussed by Byrne and Fitzpatrick (230).

Size, morphology, and density of mycelial pellets depend on agitation intensity (231–235). Fragmentation of mycelial pellets of the molds *Lentinus edodes* and *A. niger* in a standard Rushton turbine-stirred tank was examined by Taguchi *et al*. (236). Two types of pellet fragmentation patterns were noted: (i) decrease in diameter by erosion of surface; and (ii) direct rupture of the spherical pellet. The rates of these processes were expressed as

$$-\frac{\mathrm{d}d_\mathrm{p}}{\mathrm{d}t} = k_\mathrm{j}\,(N d_\mathrm{i})^{5.5}\, d_\mathrm{p}^{5.7} \qquad (81.62)$$

for pellet surface erosion, and

$$-\frac{\mathrm{d}N_\mathrm{p}}{\mathrm{d}t} = k' N_\mathrm{p} = \alpha \left(d_\mathrm{p}^{3.2} N^{6.65} d_\mathrm{i}^{8.72}\right)^{5.5} N_\mathrm{p} \qquad (81.63)$$

for rupture of the particle. In Equations 81.62 and 81.63, d_p is the pellet diameter at time t, N is the rotational speed of the impeller, d_i is the impeller diameter, N_p is the concentration of unbroken pellets at time t, and k_j, k', and α are constants. The rates of pellet erosion and rupture depend strongly on the agitation intensity–associated factors (i.e. on N and d_i) and on the dimensions of the pellet. As shown in Fig. 81.23, the pellet diameter declined with increasing agitation speed and with increasing elapsed time at a given speed. The decline slowed as the pellet attained a stable size with respect to given conditions of agitation (Fig. 81.23).

In submerged stirred tank culture of the filamentous fungus *Aspergillus awamori*, Cui *et al*. (237) correlated the pellet size with the specific energy dissipation rate; thus,

$$d_\mathrm{p} \propto E^{-0.16} \qquad (81.64)$$

The E values varied over 0.2–5.7 W/kg (237), whereas the pellet diameter ranged roughly over 1–2 mm. The length of the "hairy" hyphal extensions from the well-defined surface of the denser pell*et al*so correlated with the specific energy dissipation rate (237); thus,

$$L_\mathrm{h} = 1.17 \times 10^{-4} E^{-0.25} \qquad (81.65)$$

where L_h (m) is the length of the hairy extensions.

In studies with aggregates of *Corynebacterium glutamicum* in a stirred tank and a capillary loop shear device, Illing and Harrison (238) correlated the break up of cell aggregates with the magnitude of the turbulent

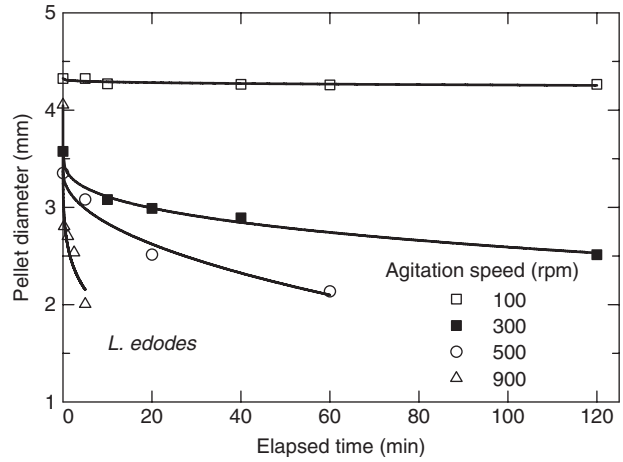


Figure 81.23. Effect of impeller agitation speed and elapsed time on pellet diameter of *L. edodes*. Pellets were 3.4–4.3 mm in initial diameter. A conventional stirred tank with a Rushton turbine ($d_\mathrm{i}/d_\mathrm{T} = 3$) was used for agitation. *Source:* Ref. 236.

forces and the total duration of the force event. Effects of hydrodynamic stresses on particles are further discussed by Henzler (239) and others (240). Shear sensitivity of activated sludge flocs is discussed by Mikkelsen (241).

81.3.7 Nematodes

Nematodes or round worms are the most abundant multicelled animals that occur widely in soil. Many nematodes are free living, thriving on bacteria and fungi, but some are parasites. Insect parasitic (or entomopathogenic) nematodes are potentially useful for biocontrol of insect pests (242). Entomopathogenic nematodes are generally quite small (e.g. 0.5 mm in length). Nematode preparations for use as molluscicide for control of garden slugs have been developed (243). Nematodes lack well-defined circulatory and respiratory systems and oxygen is absorbed directly through the body surface in contact with the surrounding medium.

Nematodes for use in insect control can be mass produced using solid-state culture techniques (242), but these methods are labor intensive and submerged culture is preferred for large-scale propagation. For use in biocontrol, a submerged culture needs to generate a large quantity of the "infective juvenile" stage of the worm's life cycle. Infective juveniles are highly sensitive to shear forces (243,244). Shear sensitivity and other process-relevant properties of nematode broths depend on the species being cultured (243). Methods for large-scale submerged culture of various species have been described (243,245–247).

81.3.8 Bioactive Proteins and Polymers

The biological activity of large molecules such as proteins, enzymes, and antibodies is a function of the molecular

structure, and any change to structure can produce irreversible loss of bioactivity. Large molecules are susceptible to structural disruption by hydrodynamic and other physicochemical forces. In general, the likelihood of a molecule being affected by shear forces increases with molecular size. Also, hydrodynamic forces can greatly affect the physical characteristics of some physiologically inactive biopolymers by influencing their synthesis by the producing organisms, although the organisms themselves may remain unaffected (9,10). For example, the morphology of bacterial cellulose produced in cultures of *Acetobacter* sp. is affected by mechanical agitation (10,62,248). Cellulose microfibers produced under intense agitation tend to be shorter because they break off earlier from the surface of the producing cell (10).

Bioactive proteins consist of one or more polypeptide chains that are folded into a globular shape. Molecular dimensions of globular proteins in solution depend mainly on the molecular weight, that is, the number and the lengths of the polymer chains contained in the globule. Globular protein molecules are typically 3–10 nm in diameter and the dimensions of the fluid microeddies do not approach that size in most realistic processing situations. Solution properties such as ionic strength and water activity are other factors that affect protein size by affecting the tightness of the globule. Because the hydrodynamic diameter of a protein globule is affected by the properties of the solvent, the globule's resistance to shear damage is also affected. Under given conditions of intense turbulence, damage is more likely in solvents that force the protein to adopt a loosely folded configuration with a large hydrodynamic diameter. Most eukaryotic proteins also have large carbohydrate groups attached and these groups can influence or modulate bioactivity (249). Certain proteins are associated with membranes, for example, with the endoplasmic reticulum, mitochondrial folds, and lamellae of chloroplasts, and functionality depends on maintaining the necessary association.

A seemingly minor alteration of the protein structure can greatly affect its ability to withstand hydrodynamic shear. For example, normal hemoglobin is relatively shear tolerant but the variant form found in patients with inherited sickle cell anemia is sensitive to shear. This shear sensitivity is clinically manifested in the denaturation of the protein and consequent hardening of the erythrocytes (250).

Shear-associated inactivation has been reported for numerous enzymes including catalase, rennet, carboxypeptidase, fibrinogen, urease, cellulase, ribulose-1,5-biphosphate carboxylase, lipase, yeast alcohol dehydrogenase, and horse liver dehydrogenase. Generally, the activity loss was irreversible and could be correlated with the dimensionless product of the shear rate and the time of exposure. Many of these studies did not rigorously suppress the formation of gas–liquid interfaces and the observed shear effects were really the effects of shear in presence of a gas–liquid interface (5). The apparent shear damage can be greatly reduced or prevented if a gas–liquid interface is not allowed to form in the shearing device, as demonstrated by various authors (251–254). Proteins adsorb and unfold at the gas–liquid interface and such unfolded proteins are susceptible to damage. Development of gas–liquid interfaces cannot be completely suppressed in most processing scenarios, and therefore, some loss of protein activity is inevitable. Protein inactivation at interfaces has been reviewed by Sadana (255).

Most enzymes withstand the shear rates that are commonly encountered during processing including high shear operations such as cell disruption (1). Exceptions occur when shear stresses are applied in presence of gas–liquid interfaces (1,8,256,257) or liquid–liquid interfaces (258,259), or when the bioactivity of the enzyme is linked with its association with a membrane or organelle. Membrane-associated proteins are more prone to shear damage (1). The globular structure of proteins unravels at least partly at gas–liquid interfaces and other hydrophilic–hydrophobic boundaries. Such unfolded proteins are especially susceptible to irreversible damage by aggregation and other mechanisms. Some protein solutions become turbid when shaken vigorously. This phenomenon is caused by protein aggregation that is facilitated by the enhancement in the gas–liquid interfacial area that occurs during shaking (260,261). In addition to processes such as high pressure homogenization and pumping, high shear processing of proteins occurs during liquid–liquid emulsification, which is used to produce microencapsulated proteins for drug delivery systems (262). Shear and interface-associated damage to proteins in delivery devices such as implantable pumps for insulin (263) can be a problem. Stability problems can also arise during parenteral administration of proteins by needleless injectors.

For *Trichoderma reesei* cellulase solution in a stirred reactor, agitation-related enzyme inactivation was observed in presence of surface aeration and also when the surface was eliminated; however, denaturation was much faster in gas-entrained operation (264). In both cases, the rate of enzyme denaturation increased with increasing speed of agitation. Under given conditions of agitation, increasing the concentration of the dissolved enzyme reduced the rate of inactivation in both surface-aerated and gas-free systems (264). This contrasts with several earlier observations and suggests that aggregation of the unfolded protein was not a major contributor to the observed denaturation. The activity loss was influenced by the pH of the solution (264). Also, the type of buffer used at a given pH value affected the enzyme stability in the agitated reactor (Fig. 81.24). The agitation-associated activity loss could be reduced by increasing the ionic strength (buffer concentration) of the enzyme solution (264). Nitrogen sparging of the enzyme

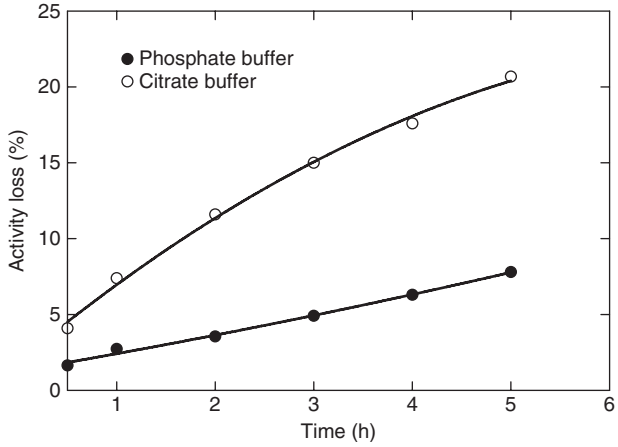


Figure 81.24. Cellulase activity loss by agitation (six-bladed turbine, ~1.6 m/s impeller tip speed) in a surface-aerated vessel using different buffer systems at pH 4.8 and 50°C. *Source:* Ref. 264.

solution enhanced the deactivation rate compared to the nonsparged (surface-aerated) reactor. The denaturation rate depended on gas holdup and, therefore, on the impeller speed (264).

Effects of extremely high shear rate levels ($>10^5$ s^{-1}) on recombinant human growth hormone (rhGH) and recombinant human deoxyribonuclease (rhDNase) were examined by Maa and Hsu (262). The rhGH and rhDNase had respective molecular masses of 22.13 and 32.74 kDa. The shearing was done at a controlled temperature of 20°C. The aggregation and the bioactivity of the two proteins were not significantly affected at shear rates greater than 10^5 s^{-1} applied over 60 min in the absence of gas–liquid interfaces (257,262). Thermodynamic properties of the proteins were determined before and after shearing using scanning microcalorimetry (SM). Alterations in secondary and tertiary structure of a protein are manifested in its scanning calorimetry data. The SM thermograms of rhDNase were not significantly affected by shearing; however, for rhGH, the SM indicated possible conformational changes (262). The silver-stained sodium dodecylsulfate-poly(acrylamide) gel electrophoresis (SDS-PAGE) gels of rhGH showed no significant differences in the high molecular weight region, but low molecular weight fragments were observed in the sheared sample, which suggested some clipping of rhGH in the intense shear field. No significant changes were noted in the SDS-PAGE gels of sheared and unsheared rhDNase (262). If a globular protein's molecular weight is assumed to indicate its size, the rhDNase molecule should be larger by a factor of approximately $(32.74/22.13)^{1/3}$, or 1.14 relative to the rhGH. It seems, therefore, that the molecular size is not the sole determinant of a protein's susceptibility to damage; the specific structure or morphology also appears to play a role.

The damaging effect of shear in presence of gas–liquid and solid–liquid interfaces may be reduced by supplementing the protein solution with a surfactant. Added surfactants tend to reduce gas–liquid interface-induced aggregation and precipitation of rhGH (257). Proteins adsorb also on hydrophobic solid surfaces. Adsorption of insulin at hydrophobic surfaces accompanied by denaturation is well known. Similarly, tPA is known to adhere to solid surfaces (249), but the surface adherent tendency is reduced in the presence of surfactants such as Tween-80 (polyoxyethylene sorbitan monooleate) added at 0.01% typical concentration (249). Shear susceptibility of proteins is further discussed elsewhere (5,265).

Plasmids (229,266) and linear double-stranded DNA (267–273) are susceptible to damage by shear forces. Consideration of shear effects is necessary in the processing of DNA, for example, during microencapsulation for making DNA vaccines (273). Plasmids being evaluated for use as vaccines and in gene therapy are generally obtained from recombinant bacteria, typically *Escherichia coli*. For isolating the native undamaged supercoiled circular plasmid DNA, the cells are lysed by thermal or chemical methods, as mechanical means of cell disruption tend to damage the DNA (226,274).

Damage to a 10.4-kb plasmid was observed during recovery from the *E. coli* host by various methods of mechanical disruption of the cell (226). The methods tested included several variants of high pressure homogenization, ultrasonication, and bead milling (1,226). Homogenization and ultrasound were the most destructive to the plasmid. Although sonication fully lysed the cells within 2 min under the conditions used, no intact plasmid was obtained in the lysate (226). Bead milling was relatively less damaging and more than 95% of the plasmid in the cells could be recovered intact under relatively mild processing conditions. The conditions for maximum recovery were a nominal bead loading of ~84% of the volume of the grinding chamber; 0.5-mm diameter glass beads; 1910-rpm agitation with a six-bladed polyurethane impeller; and six passes through the mill with an average residence time of ~1 min per pass (226).

A plasmid is of course substantially larger in size than the protein it codes. Also, unlike globular proteins, plasmids adopt stringlike shapes with an average hydrodynamic diameter of 150–250 nm for 5- to 10-kb plasmids (274). For larger plasmids, the hydrodynamic diameter may potentially exceed 1 μm (274). As a consequence of the size, plasmid and other DNA are susceptible to hydrodynamic shear forces (274). Compared to the plasmid DNA, the much larger chromosomal DNA (e.g. 4000–4500 kb for *E. coli*) is even less shear tolerant, and this has important implications for recovery of the plasmid; overzealous processing can reduce the size of chromosomal DNA compared to that of the plasmid, making separation difficult (274).

Even short-duration exposure to sufficiently intense shear fields will undesirably convert the native supercoiled circular plasmid DNA to the open circular and linear forms (274). A plasmid's susceptibility to shear forces is critically dependent on its size and the ionic strength of solution (274,275). Plasmids of 13, 20, and 29-kb size are prone to shear degradation (229). Shear sensitivity increases rapidly with increasing plasmid size (Fig. 81.25). For plasmids $\geq$20 kb, degradation is observed within a few seconds of exposure to shear rates of $>1 \times 10^6$ s^{-1} generated by a rotating disc (274,275). At a shear rate of 1×10^6 s^{-1}, more than 80% of the native plasmid structure may be lost within 5 s for a plasmid of $\geq$30 kb. The degradation typically obeys first-order kinetics. Degradation occurs in the absence of gas–liquid interfaces, but is accelerated by such interfaces. In Fig. 81.25, the 13-kb plasmid is relatively shear tolerant in the absence of a gas–liquid interface; however, much smaller plasmids are damaged when sheared in presence of a gas. Damage has been reported during nebulization of a 6.5-kb plasmid (276). The rate of degradation is lower in media with a high ionic strength, presumably because the ionic strength affects the hydrodynamic diameter of the plasmid. DNA adopts a more compact shape in media with high ionic strengths. Also, the ions may interact with the plasmid DNA to increase its resistance to uncoiling. In studies with a 20-kb plasmid, increasing ionic strength to a physiological value (equivalent to ionic strength of 150 m*M* sodium chloride) reduced the damaging effect (229,275). This protective influence of the ionic strength was observed only at relatively high shear rate values ($\sim 1.2 \times 10^6$ s^{-1}). Shear damage to a 20-kb plasmid was independent of the plasmid DNA concentration over the concentration range from 0.2 to 20 μg/mL (229).

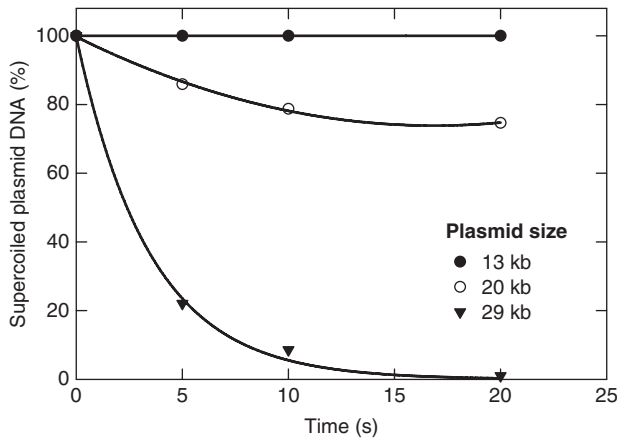


Figure 81.25. Percentage of initial native supercoiled plasmid DNA remaining after various periods of exposure to an average shear rate of $\sim 1.2 \times 10^6$ s^{-1} in a rotating disc chamber. The measurements were at room temperature. *Source:* Ref. 229.

Damage to plasmid DNA has been reported also during centrifugal clarification of the flocculated cell lysate. This damage is apparently associated with the acceleration of the fluid entering the rotating bowl of the centrifuge (274).

In drug delivery formulations, the shear susceptibility of the plasmid DNA can be reduced by formulating with complexing additives (e.g. polylysine, lipids) that cause compaction of the molecule into relatively shear-tolerant particles (274). Effects of shear stress on linear double-stranded DNA are similar to those discussed here for the plasmid DNA.

81.4 CONCLUDING REMARKS

Biocatalysts, especially molds, filamentous bacteria, certain microalgae, and plant and animal cells are susceptible to damage by hydrodynamic and mechanical forces encountered in bioprocessing. Typically, recombinant strains are more prone to shear damage than equivalent wild types. Extent of damage depends on the cell and the specific damaging mechanism operating. Often, the damage may be reduced by one or more of several approaches: adaptation of cells, supplementing culture media with shear protectants, modification of processing operations and equipment, as well as other methods. In many cases, the mechanisms of protection and damage are not entirely clear, but multiple mechanisms seem to operate. As noted throughout this chapter, some sound guidance is available for engineering and operation of fragile culture processes; nevertheless, *a priori* quantitative prediction of culture behavior is not reliably possible. Empirical approaches must continue to be relied upon in engineering practice.

NOMENCLATURE

A_b	Cross-sectional area under the baffle or draft-tube (m^2)
A_d	Cross-sectional area of the downcomer (m^2)
A_r	Cross-sectional area of the riser (m^2)
ATP	Adenosine triphosphate
a	Parameter in Equation 81.2
BSA	Bovine serum albumin
C	Parameter in Equation 81.28
C_D	Drag coefficient
C_f	Fanning friction factor
C_{fmax}	Maximum value of friction factor
D_p	Percentage cell damage (%)
d	Diameter or hydraulic diameter (m)
d_B	Bubble diameter (m)
d_c	Cell diameter (μm)
d_F	Floc diameter (m)
d_{Fmax}	Maximum stable diameter (m)

d_i	Impeller diameter (m)
d_L	Local diameter (m)
d_p	Microcarrier or particle diameter (m)
d_T	Tank or column diameter (m)
E	Energy dissipation rate per unit mass (W/kg)
F	Frequency (s^{-1})
FBS	Fetal bovine serum
F_D	Turbulent drag force on a particle (N)
F_n	Normal force on a particle (N)
F_s	Shear force across the aggregate due to instantaneous velocity difference (N)
g	Gravitational acceleration (m/s^2)
h	Channel height (m)
h_D	Height of dispersion (m)
h_L	Height of liquid (m)
ICS	Impeller collision severity defined by Equation 81.50 (kg/m^2s^3)
ISF	Integrated shear factor defined by Equation 81.44 (s^{-1})
K	Consistency index (Pa s^n)
k	Parameter in Equation 81.2 (m^{-1})
$k\prime$	Constant in Equation 81.63 (s^{-1})
k_d	Death rate constant (s^{-1})
k_i	Constant in Equation 81.12
k_j	Constant in Equation 81.62 ($s^{4.5}/m^{10.2}$)
L	Channel length (m)
LDH	Lactate dehydrogenase
L_h	Length of hairy extensions from pellet surface (m)
L_i	Initial length of filament (μm)
ℓ	Mean microeddy length (m)
m	General exponent
N	Rotational speed (s^{-1}) or cell concentration (m^{-3})
N_d	Number of passes through pump
N_o	Initial cell concentration (m^{-3})
N_p	Concentration of unbroken pellets at time t (m^{-3})
n	Flow behavior index
n_B	Number of impeller blades
PEG	Poly(ethylene glycol)
PMF	Plasma membrane fluidity
Po	Power number
ΔP	Pressure drop (Pa)
Q	Volume flow rate of gas (m^3/s)
Re	Reynolds number
Re_i	Impeller Reynolds number defined by Equation 81.47
Re_L	Local Reynolds number defined by Equation 81.32
r	Radial distance (m)
r_c	Radius of the vortex zone defined by Equation 81.46 (m)
rhDNase	Recombinant human deoxyribonuclease
rhGH	Recombinant human growth hormone
r_i	Impeller radius (m)
r_T	Tank radius (m)
S	Burst strength (N)
SDS-PAGE	Sodium dodecylsulfate-poly(acrylamide) gel electrophoresis
SM	Scanning microcalorimetry
TCS	Turbulent collision severity for particle-to-particle collisions (kg/m^2s^3)
t	Time (s)
U_B	Bubble rise velocity (m/s)
U_G	Superficial gas velocity (m/s)
U_{Gr}	Superficial gas velocity in riser (m/s)
U_L	Average liquid velocity (m/s)
u	Mean velocity of the microeddies (m/s)
Δu	Difference in velocities of the particle and the fluid (m/s)
u_l	Local velocity at position r (m/s)
u_{max}	Maximum velocity at centerline (m/s)
u_o	Jet velocity at orifice (m/s)
V_k	Dimensionless hypothetical specific killing volume
V_L	Volume of liquid (m^3)
W	Width of the impeller blade (m)
x	Parameter in Equation 81.24 or axial distance (m)

GREEK SYMBOLS

α	Constant in Equation 81.63 ($s^{35.575}/m^{65.56}$)
β	Parameter in Equation 81.27
Γ	Coefficient in Equation 81.58
γ	Shear rate (s^{-1})
γ_{av}	Average rate (s^{-1})
γ_{avT}	Time-averaged shear rate (s^{-1})
γ_i	Isotropic turbulence shear rate defined by Equation 81.33 (s^{-1})
γ_{max}	Time-averaged maximum shear rate (s^{-1})
γ_w	Wall shear rate (s^{-1})
ε_S	Volume fraction of microcarriers or solids
η	Constant in Equation 81.30
μ_{ap}	Effective or apparent viscosity (Pa s)
μ_L	Viscosity of liquid (Pa s)
π	Pi
ρ_L	Density of liquid (kg/m^3)
ρ_S	Density of microcarriers or solid (kg/m^3)
σ_M	Mechanical strength of aggregate (N/m^2)
τ	Shear stress (N/m^2)
$\tau_{max\ J}$	Maximum shear stress in submerged free jet (N/m^2)
τ_w	Wall shear stress (N/m^2)

REFERENCES

1. Chisti Y, Moo-Young M. Enzyme Microb Technol 1986; 8: 194–204.
2. Makagiansar HY, Shamlou PA, Thomas CR, Lilly MD. Bioprocess Eng 1993; 9: 83–90.
3. Ujcová E, Fencl Z, Musi'lková M, Seichert L. Biotechnol Bioeng 1980; 22: 237–241.
4. Papadaki M, Eskin SG. Biotechnol Prog 1997; 13: 209–221.
5. Thomas CR. In Winkler MR, editor, Chemical engineering problems in biotechnology. London: Elsevier; 1990. p. 23–93.
6. Kwok WK, Picioreanu C, Ong SL, van Loosdrecht MCM, Ng WJ, Heijnen JJ. Biotechnol Bioeng 1998; 58: 400–407.
7. Stoodley P, Lewandowski Z, Boyle JD, Lappin-Scott HM. Biotechnol Bioeng 1998; 57: 536–544.
8. Chisti Y. In: Subramanian G, editor. Bioseparation and bioprocessing: a handbook, Vol. 2. New York: Wiley-VCH; 1998. pp. 3–30.
9. Dreveton E, Monot F, Lecourtier J, Ballerini D, Choplin L. J Ferment Bioeng 1996; 82: 272–276.
10. Moo-Young M, Chisti Y. Biotechnology 1988; 6(11): 1291–1296.
11. Garrido F, Banerjee UC, Chisti Y, Moo-Young M. Bioseparation 1994; 4: 319–328.
12. Tamer IM, Moo-Young M, Chisti Y. Ind Eng Chem Res 1998; 37: 1807–1814.
13. Yamada T, Arakawa H, Okajima T, Shimada T, Ikai A. Ultramicroscopy 2002; 91: 261–268.
14. Alcaraz J, Buscemi L, Grabulosa M, Trepat X, Fabry B, Farré R, Navajas D. Biophys J 2003; 84: 2071–2079.
15. Rabinovich Y, Esayanur M, Daosukho S, Byer K, El-Shall H, Khan S. J Colloid Interface Sci 2005; 285: 125–135.
16. Hilal N, Bowen WR, Alkhatib L, Ogunbiyi O. Chem Eng Res Des 2006; 84A: 282–292.
17. Doran PM. Adv Biochem Eng Biotechnol 1993; 48: 115–168.
18. Molina Grima E, Chisti Y, Moo-Young M. J Biotechnol 1997; 54: 195–210.
19. Papoutsakis ET. Trends Biotechnol 1991; 9: 427–437.
20. Augenstein DC, Sinskey AJ, Wang DIC. Biotechnol Bioeng 1971; 13: 409–418.
21. Shiragami N. Bioprocess Eng 1994; 10: 47–51.
22. McQueen A, Meilhoc E, Bailey JE. Biotechnol Lett 1987; 9: 831–836.
23. Chisti Y, Moo-Young M. Biotechnol Bioeng 1989; 34: 1391–1392.
24. Chisti Y. Appl Mech Rev 1998; 51: 33–112.
25. Chisti Y Airlift bioreactors. London: Elsevier; 1989.
26. Shi LK, Riba JP, Angelino H. Chem Eng Commun 1990; 89: 25–35.
27. Sánchez Pérez JA, Rodríguez Porcel EM, Casas López JL, Fernández Sevilla JM, Chisti Y. Chem Eng J 2006; 124: 1–5.
28. Al-Masry WA. Biotechnol Bioeng 1999; 62: 494–498.
29. Henzler HJ, Kauling J, Scale-up of mass transfer in highly viscous liquids. Presented at the 5th European Conference on Mixing, Würzberg, paper 30, BHRA, Cranfield, 1985, pp. 303–312.
30. Robertson B, Ulbrecht JJ. In: Ho CS, Oldshue JY, editors. Biotechnology processes: scale-up and mixing. New York: American Institute of Chemical Engineers; 1987. pp. 31–35.
31. Kawase Y, Kumagai T. Bioprocess Eng 1991; 7: 25–28.
32. Hoffmann J, Buescher K, Hempel DC. Chem -Ing -Tech 1995; 67: 210–214.
33. Chisti Y, Halard B, Moo-Young M. Chem Eng Sci 1988; 43: 451–457.
34. Hülscher M, Pauli J, Onken U. Food Biotechnol 1990; 4(1): 157–166.
35. Glasgow LA, Hua J, Yiin T-Y, Erickson LE. Chem Eng Commun 1992; 113: 155–181.
36. Okada K, Shibano S, Akagi Y. J Chem Eng Jpn 1993; 26: 637–643.
37. Lübbert A, Larson B. Chem Eng Sci 1990; 45: 3047–3053.
38. Lübbert A, Larson B, Wan LW, Bröring S. Inst Chem Eng Symp Ser 1990; 121: 203–213.
39. Bowen R. Chem Eng June 9, 1986; 55–63.
40. Calderbank PH, Moo-Young MB. Trans Inst Chem Eng 1959; 37: 26.
41. Wichterle K, Zák L, Mitschka P. Chem Eng Commun 1985; 32: 289–305.
42. Wichterle K, Mitschka P, Hájek J, Zák L. Chem Eng Res Des 1988; 66: 102–106.
43. Chisti, Y, Moo-Young, M. In: Moses V, Cape RE, Springham DG, editors. Biotechnology: the science and the business, 2nd ed. New York: Harwood Academic Publishers; 1999. pp. 177–222.
44. Chisti Y. Crit Rev Biotechnol 2001; 21: 67–110.
45. Jan DC-H, Emery AN, Al-Rubeai M. Biotechnol Tech 1993; 7: 351–356.
46. Chisti Y, Moo-Young M. J Chem Technol Biotechnol 1988; 42: 211–219.
47. (a) Sokolov VN, Metkin VP. Zh Prikl Khim 1981; 54: 1321–1326; (b) Sokolov VN, Metkin VP. J Appl Chem USSR 1981; 54: 1103–1107.
48. Metkin VP, Sokolov VN. J Appl Chem USSR 1982; 55: 558–563.
49. Baldyga J, Bourne JR, Zimmerman B. Chem Eng Sci 1994; 49: 1937–1946.
50. Baldyga J, Bourne JR, Gholap RV. Chem Eng Sci 1995; 50: 1877–1880.
51. Wichterle K, Sobolík V, Lutz M, Denk V. Chem Eng Sci 1996; 51: 5227–5228.
52. Nienow AW. Appl Mech Rev 1998; 51: 3–32.
53. Chisti Y. Trends Biotechnol 2003; 21: 89–93.
54. Meijer JJ, ten Hoopen HJG, van Gameren YM, Luyben KChAM, Libbenga KR. Enzyme Microb Technol 1994; 16: 467–477.
55. Moo-Young M, Chisti Y, Vlach D. Biotechnol Lett 1992; 14: 863–868.
56. Moo-Young M, Chisti Y, Vlach D. Biotechnol Adv 1993; 11: 469–479.
57. Ramírez OT, Mutharasan R. Biotechnol Bioeng 1990; 36: 911–920.
58. Dunlop EH, Namdev PK, Rosenberg MZ. Chem Eng Sci 1994; 49: 2263–2276.

59. Zhang Z, Chisti Y, Moo-Young M. J Biotechnol 1995; 43: 33–40.
60. Märkl H, Bronnenmeier R, Wittek B. Int Chem Eng 1991; 31: 185–197.
61. Wu J, King G, Daugulis AJ, Faulkner P, Bone DH, Goosen MFA. J Ferment Bioeng 1990; 70: 90–93.
62. Chisti Y, Moo-Young M. Trans Inst Chem Eng 1996; 74A: 575–583.
63. Moo-Young M, Chisti Y In: Durand G, Bobichon L, Florent J, editors. Proceedings, 8th international biotechnology symposium, Vol. 1. Paris: Société Française de Microbiologie; 1988. pp. 454–466.
64. Moo-Young M, Chisti Y, Zhang Z, Garrido F, Banerjee U, Vlach D. Ann N Y Acad Sci 1996; 782: 391–401.
65. Nielsen J, Krabben P. Biotechnol Bioeng 1995; 46: 588–598.
66. Heydarian SM, Ison AP, Lilly MD, Shamlou PA. Chem Eng Sci 2000; 55: 1775–1784.
67. Li ZJ, Shukla V, Fordyce AP, Pedersen AG, Wenger KS, Marten MR. Biotechnol Bioeng 2000; 70: 300–312.
68. Li ZJ, Shukla V, Wenger K, Fordyce A, Pedersen AG, Marten M. Biotechnol Bioeng 2002; 77: 601–613.
69. Mantzouridou F, Roukas T, Kotzekidou P. Biochem Eng J 2002; 10: 123–135.
70. Converti A, Sommariva C, Borghi MD, Ferraiolo G. Bioprocess Eng 1993; 9: 183–189.
71. Converti A, Borghi MD, Ferraiolo G, Sommariva C. Chem Eng J 1996; 62: 155–167.
72. Stoupis T, Stewart GG, Stafford RA. J Am Soc Brew Chem 2003; 61: 219–225.
73. Wu W-T, Hsu Y-L, Ko Y-F, Yao L-L. Appl Microbiol Biotechnol 2002; 58: 175–177.
74. MacLoughlin PF, Malone DM, Murtagh JT, Kieran PM. Biotechnol Bioeng 1998; 58: 595–604.
75. Thomas CR. In: Shamlou PA, editor. Processing of solid-liquid suspensions. Oxford: Butterworth-Heinemann; 1993. pp. 158–191.
76. Prokop A, Bajpai RK. Adv Appl Microbiol 1992; 37: 165–232.
77. Gudin C, Chaumont D. Bioresour Technol 1991; 38: 145–151.
78. Watanabe Y, de la Noüe J, Hall DO. Biotechnol Bioeng 1995; 47: 261–269.
79. Molina Grima E, Sánchez Pérez JA, García Camacho F, García Sánchez JL, Acién Fernández FG, López Alonso D. J Biotechnol 1994; 37: 159–166.
80. Molina Grima E, Sánchez Pérez JA, García Camacho F, Fernández Sevilla JM, Acién Fernández FG, Urda Cardona J. Appl Microbiol Biotechnol 1995; 42: 658–663.
81. Vandanjon L, Rossignol N, Jaouen P, Roberts JM, Quéméneur F. Biotechnol Bioeng 1999; 63: 1–9.
82. Jaouen P, Vandanjon L, Quemeneur F. Bioresource Technol 1999; 68: 149–154.
83. Mitsuhashi S, Hosaka K, Tomonaga E, Muramatsu H, Tanishita K. Appl Microbiol Biotechnol 1995; 42: 744–749.
84. Silva HJ, Cortiñas T, Ertola RJ. J Chem Technol Biotechnol 1987; 40: 41–49.
85. Suzuki T, Matsuo T, Ohtaguchi K, Koide K. J Chem Technol Biotechnol 1995; 62: 351–358.
86. van der Pol L, Bakker WAM, Tramper J. Biotechnol Bioeng 1992; 40: 179–182.
87. Martens DE, de Gooijer CD, Beuvery EC, Tramper J. Biotechnol Bioeng 1992; 39: 891–897.
88. Tramper J, Joustra D, Vlak JM. In: Webb C, Mavituna F, editors. Plant and animal cells: process possibilities. Chichester: Ellis Horwood; 1987. pp. 125–136.
89. Tramper J, Smit D, Straatman J, Vlak JM. Bioprocess Eng 1987; 2: 37–41.
90. Emery AN, Lavery M, Williams B, Handa A. In Webb C, Mavituna F, editors. Plant and animal cells: process possibilities. Chichester: Ellis Horwood; 1987. pp. 137–146.
91. Matthijs HCP, Balke H, Van Hes UM, Kroon BMA, Mur LR, Binot RA. Biotechnol Bioeng 1996; 50: 98–107.
92. Croughan MS, Sayre ES, Wang DIC. Biotechnol Bioeng 1989; 33: 862–872.
93. McQueen A, Bailey JE. Biotechnol Lett 1989; 11: 531–536.
94. Midler M, Finn RK. Biotechnol Bioeng 1966; 8: 71–84.
95. Garcia Camacho F, Gallardo Rodríguez J, Sánchez Mirón A, Cerón García MC, Belarbi EH, Chisti Y, Molina Grima E. Biotechnol Adv 2007; 25: 176–194.
96. Berdalet E, Estrada M. In: Smayda TJ, Shimizu Y, editors. Effects phytoplankton blooms in the sea. Amsterdam: Elsevier; 1993. pp. 737–740.
97. Sullivan JM, Swift E. J Phycol 2003; 39: 83–94.
98. Sullivan JM, Swift E, Donaghay PL, Rines JEB. Harmful Algae 2003; 2: 183–199.
99. Stoecker DK, Long A, Suttles SE, Sanford LP. Harmful Algae 2006; 5: 407–418.
100. White AW. J Fish Res Board Can 1976; 33: 2598–2602.
101. Pollingher U, Zemel E. Br Phycol J 1981; 16: 281–287.
102. Berdalet E. J Phycol 1992; 28: 267–272.
103. Thomas WH, Gibson CH. J Appl Phycol 1990; 2: 71–77.
104. Thomas WH, Gibson CH. J Phycol 1995; 30: 50–59.
105. Juhl AR, Velásquez V, Latz MI. Limnol Oceanogr 2000; 45: 905–915.
106. Juhl AR, Trainer VL, Latz MI. Limnol Oceanogr 2001; 46: 758–764.
107. Juhl AR, Latz M. J Phycol 2002; 3: 683–694.
108. Latz MI, Juhl AR, Ahmed AM, Elghobashi SE, Rohr J. J Exp Biol 2004; 207: 1941–1951.
109. Latz MI, Rohr J, Hoyt J. IEEE J Oceanic Eng 1995; 20: 144–147.
110. Rohr J, Allen J, Losee J, Latz MI. Phys Lett A 1997; 228: 408–416.
111. Blaser S, Kurisu F, Satoh H, Mino T. Luminescence 2002; 17: 370–380.
112. Chen AK, Latz MI, Frangos JA. Biotechnol Bioeng 2003; 83: 93–103.
113. Latz MI, Nauen JC, Rohr J. J Plankton Res 2004; 26: 1529–1546.
114. von Dassow P, Bearon RN, Latz MI. Limnol Oceanogr 2005; 50: 607–619.
115. Cussatlegras A-S, Le Gal P. J Exp Mar Biol Ecol 2004; 310: 227–246.
116. Cussatlegras A-S, Le Gal P. Nonlinear Proc Geophys 2005; 12: 337–343.
117. Mazzuca Sobczuk T, García Camacho F, Molina Grima E, Chisti Y. Bioprocess Biosys Eng 2006; 28: 243–250.

118. Sánchez Mirón A, Cerón García MC, Contreras Gómez A, García Camacho F, Molina Grima E, Chisti Y. Biochem Eng J 2003; 16: 287–297.
119. Barbosa MJ, Albrecht M, Wijffels RH. Biotechnol Bioeng 2003; 83: 112–120.
120. García Camacho F, Contraras Gómez A, Mazzuca Sobczuk T, Molina Grima E. Process Biochem 2000; 35: 1045–1050.
121. García Camacho F, Molina Grima E, Sánchez Mirón A, González Pascual V, Chisti Y. Enzyme Microb Technol 2001; 29: 602–610.
122. Kieran PM, MacLoughlin PF, Malone DM. J Biotechnol 1997; 59: 39–52.
123. Fischer U, Alfermann AW. J Biotechnol 1995; 41: 19–28.
124. Ballica R, Ryu DDY. Biotechnol Bioeng 1993; 42: 1181–1189.
125. Reinhard E, Kreis W, Barthlen U, Helmbold U. Biotechnol Bioeng 1989; 34: 502–508.
126. Tanaka H. Biotechnol Bioeng 1981; 23: 1203–1218.
127. Keβler M, ten Hoopen HJG, Furusaki S. Enzyme Microb Technol 1999; 24: 308–315.
128. Sowana DD, Williams DRG, Dunlop EH, Dally BB, O'Neill BK, Fletcher DF. Trans Inst Chem Eng 2001; 79A: 867–875.
129. Zhong J-J, Fujiyama K, Seki T, Yoshida T. Biotechnol Bioeng 1994; 44: 649–654.
130. Kieran PM, O'Donnell HJ, Malone DM, MacLoughlin PF. Biotechnol Bioeng 1995; 45: 415–425.
131. Guillon S, Trémouillaux-Guiller J, Pati PK, Rideau M, Gantet P. Trends Biotechnol 2006; 24: 403–409.
132. Kino-Oka M, Hitaka Y, Taya M, Tone S. Chem Eng Sci 1999; 54: 3179–3186.
133. Hitaka Y, Takahashi Y, Kino-oka M, Taya M, Tone S. Biochem Eng J 2000; 6: 1–6.
134. Gong YW, Li SY, Han RB, Yuan YJ. Biochem Eng J 2006; 32: 113–118.
135. Doran PM. Biotechnol Prog 1999; 15: 319–335.
136. Namdev PK, Dunlop EH. Appl Biochem Biotechnol 1995; 54: 109–131.
137. Kieran PM, Malone DM, MacLoughlin PF. Adv Biochem Eng Biotechnol 2000; 67: 139–177.
138. Hellung-Larsen P, Lyhne I. J Protozool 1992; 39: 345–349.
139. Kristiansen TB, Hagemeister JJ, Grave M, Hellung-Larsen P. J Cell Physiol 1996; 169: 139–148.
140. Hellung-Larsen P, Lyhne I. Microbios 1993; 75: 241–247.
141. Hellung-Larsen P, Assaad F, Pankratova S, Saietz BL, Skovgaard LT. J Biotechnol 2000; 76: 185–195.
142. Hagemeister JJ, Grave M, Kristiansen TB, Assaad F, Hellung-Larsen P. J Eukaryot Microbiol 1999; 46: 6–11.
143. Hellenbroich D, Valley U, Ryll T, Wagner R, Tekkanat N, Kessler W, Ross A, Deckwer W-D. Appl Microbiol Biotechnol 1999; 51: 447–455.
144. Schönefeld U, Alfermann AW, Schultz JE. J Protozool 1986; 33: 222–225.
145. Chisti Y. In: Flickinger MC, Drew SW, editors. Encyclopedia of bioprocess technology. New York: Wiley; 1999. pp. 1607–1640.
146. Chalmers JJ. Appl Mech Rev 1998; 51: 113–120.
147. Arathoon WR, Birch JR. Science 1986; 232: 1390–1395.
148. Chisti Y. Bioprocess Eng 1993; 9: 191–196.
149. Birch JR, Lambert K, Thompson PW, Kenney AC, Wood LA. In: Lydersen BK, editor. Large scale cell culture technology. New York: Hanser Publishers; 1987. pp. 1–20.
150. Chisti Y, Moo-Young M. Trans Inst Chem Eng 1993; 71C: 209–214.
151. Chisti Y, Moo-Young M. Trans Inst Chem Eng 1994; 72C: 92–94.
152. Kim B-Y, Putnam AJ, Kulik TJ, Mooney DJ. Biotechnol Bioeng 1998; 57: 46–54.
153. Chittur KK, McIntire LV, Rich RR. Biotechnol Prog 1988; 4:(2): 89–96.
154. Ziegelstein RC, Cheng L, Capogrossi MC. Science 1992; 258: 656–659.
155. Cherry RS. Biotechnol Adv 1993; 11: 279–299.
156. Al-Rubeai M, Emery AN, Chalder S, Goldman MH. J Biotechnol 1993; 31: 161–177.
157. O'Connor KC, Cowger NL, De Kee DCR, Schwarz RP. Enzyme Microb Technol 2002; 31: 600–608.
158. Blackshear PL, Blackshear GL. In: Skalak R, Chien S, editors. Handbook of bioengineering. New York: McGraw-Hill; 1987. pp. 15.1–15.19.
159. García Camacho F, Belarbi EH, Cerón García MC, Sánchez Mirón A, Chile T, Chisti Y, Molina Grima E. Biochem Eng J 2005; 26: 115–121.
160. Vickroy B, Lorenz K, Kelly W. Biotechnol Prog 2007; 23: 194–199.
161. Hutchinson N, Bingham N, Murrell N, Farid S, Hoare M. Biotechnol Bioeng 2006; 95: 483–491.
162. Born C, Zhang Z, Al-Rubeai M, Thomas CR. Biotechnol Bioeng 1992; 40: 1004–1010.
163. Shiragami N. Bioprocess Eng 1997; 16: 345–347.
164. Smith CG, Greenfield PF. Biotechnol Bioeng 1992; 40: 1045–1055.
165. Olivier LA, Truskey GA. Biotechnol Bioeng 1993; 42: 963–973.
166. Aunins JG, Henzler H-J. In: Rehm H-J, Reed G, editors. Biotechnology, Vol. 3, 2nd ed. Weinheim: VCH; 1993. pp. 219–281.
167. Keane JT, Ryan D, Gray PP. Biotechnol Bioeng 2003; 81: 211–220.
168. Shiragami N, Unno H. Bioprocess Eng 1994; 10: 43–45.
169. Wu S-C, Huang Y-L. Bioprocess Eng 2000; 23: 229–233.
170. LaPorte TL, Shevitz J, Kim Y, Wang SS. Bioprocess Eng 1996; 15: 1–7.
171. Hochmuth RM. In: Skalak R, Chien S, editors. Handbook of bioengineering. New York: McGraw-Hill; 1987. pp. 12.1–12.17.
172. Schmid-Schönbein GW. In: Skalak R, Chien S, editors. Handbook of bioengineering, New York: McGraw-Hill; 1987. pp. 13.1–13.25.
173. Dai X, Ouyang F, Qi Y. In: Teo WK, Yap MGS, Oh SKW, editors. Better living through biochemical engineering, Singapore: University of Singapore; 1994. pp. 408–410.
174. Cherry RS, Papoutsakis ET. Bioprocess Eng 1986; 1: 29–41.
175. Chisti Y, Moo-Young M. Chim Oggi 1993; 11(3–4): 25–27.

176. Zhang Z, Ferenczi MA, Thomas CR. Chem Eng Sci 1992; 47: 1347–1354.
177. Zhang Z, Ferenczi MF, Lush AC, Thomas CR. Appl Microbiol Biotechnol 1991; 36: 208–210.
178. Sinskey AJ, Fleishaker RJ, Tyo MA, Giard D-J, Wang DIC. Ann N Y Acad Sci 1981; 369: 47–59.
179. Croughan MS, Hamel J-F, Wang DIC. Biotechnol Bioeng 1987; 29: 130–141.
180. Gregoriades N, Clay J, Ma N, Koelling K, Chalmers JJ. Biotechnol Bioeng 2000; 69: 171–182.
181. Cherry RS, Papoutsakis ET. Biotechnol Bioeng 1988; 32: 1001–1014.
182. Cherry RS, Papoutsakis ET. Bioprocess Eng 1989; 4: 81–89.
183. Ganzeveld KJ, Chisti Y, Moo-Young M. Bioprocess Eng 1995; 12: 239–247.
184. Kretzmer G. Adv Biochem Eng Biotechnol 2000; 67: 123–137.
185. Ouyang A, Yang ST. Biotechnol Bioeng 2007; 96: 371–380.
186. Langille BL. Microcirculation 2001; 8: 195–206.
187. Oh SKW, Nienow AW, Al-Rubeai M, Emery AN. J Biotechnol 1989; 12: 45–62.
188. Oh SKW, Nienow AW, Al-Rubeai M, Emery AN. J Biotechnol 1992; 22: 245–270.
189. Handa A, Emery AN, Spier RE. Dev Biol Stand 1987; 66: 241–253.
190. Handa-Corrigan A, Emery AN, Spier RE. Enzyme Microb Technol 1989; 11: 230–235.
191. Wang NS, Yang J-D, Calabrese RV, Chang K-C. J Biotechnol 1994; 33: 107–122.
192. Chisti Y. Trends Biotechnol 2000; 18: 420–432.
193. Jöbses I, Martens D, Tramper J. Biotechnol Bioeng 1991; 37: 484–490.
194. Wu J, Goosen FA. Enzyme Microb Technol 1995; 17: 1036–1042.
195. Boulton-Stone JM, Blake JR. J Fluid Mech 1993; 254: 473–466.
196. Garcia-Briones MA, Brodkey RS, Chalmers JJ. Chem Eng Sci 1994; 49: 2301–2320.
197. Chalmers JJ, Bavarian F. Biotechnol Prog 1991; 7: 151–158.
198. Cherry RS, Hulle CT. Biotechnol Prog 1992; 8: 11–18.
199. Bavarian F, Fan LS, Chalmers JJ. Biotechnol Prog 1991; 7: 140–150.
200. Sucker HG, Jordan M, Eppenberger HM, Widmer F. Biotechnol Bioeng 1994; 44: 1246–1254.
201. Papoutsakis ET. Trends Biotechnol 1991; 9: 316–324.
202. Ramirez OT, Mutharasan R. Biotechnol Prog 1992; 8: 40–50.
203. Michaels JD, Petersen JF, McIntire LV, Papoutsakis ET. Biotechnol Bioeng 1991; 38: 169–180.
204. Lavery M, Nienow AW. Biotechnol Bioeng 1987; 30: 368–373.
205. Kunas KT, Papoutsakis ET. J Biotechnol 1990; 15: 57–70.
206. Goldblum S, Bae Y-K, Hink WF, Chalmers JJ. Biotechnol Prog 1990; 6: 383–390.
207. Chisti Y, Moo-Young M. J Chem Technol Biotechnol 1993; 58: 331–336.
208. Murhammer DW, Goochee CF. Biotechnology 1988; 6: 1411–1418.
209. Murhammer DW, Goochee CF. Biotechnol Prog 1990; 6: 142–148.
210. Laouar L, Lowe KC, Mulligan BJ. Enzyme Microb Technol 1996; 18: 433–438.
211. Sowana DD, Williams DRG, O'Neill BK, Dunlop EH. Biochem Eng J 2002; 12: 165–173.
212. van der Pol LA, Beeksma I, Tramper J. Enzyme Microb Technol 1995; 17: 401–407.
213. van Loosdrecht MCM, Heijnen SJ. Trends Biotechnol 1993; 11: 117–121.
214. Heijnen JJ, van Loosdrecht MCM, Mulder A, Tijhuis L. Water Sci Technol 1992; 26: 647–654.
215. Wagner K, Hempel DC. Biotechnol Bioeng 1988; 31: 559–566.
216. Tijhuis L, Zwols H, van Meekeren K-H, van Loosdrecht MCM, Heijnen JJ. In: Alberghina L, Frontali L, Sensi P, editors. Progress in biotechnology, Proceedings of the 6th european congress on biotechnology, Vol. 9. Amsterdam: Elsevier; 1994. pp. 953–956.
217. Tijhuis L, van Benthum WAJ, van Loosdrecht MCM, Heijnen JJ. Biotechnol Bioeng 1994; 44: 867–879.
218. Tijhuis L, van Loosdrecht MCM, Heijnen JJ. Biotechnol Bioeng 1994; 44: 595–608.
219. Tijhuis L, van Loosdrecht MCM, Heijnen JJ. Biotechnol Bioeng 1995; 45: 481–487.
220. van Benthum WAJ, Garrido-Fernández JM, Tijhuis L, van Loosdrecht MCM, Heijnen JJ. Biotechnol Prog 1996; 12: 764–772.
221. Gjaltema A, Tijhuis L, van Loosdrecht MCM, Heijnen JJ. Biotechnol Bioeng 1995; 46: 258–269.
222. Gjaltema A, Vinke JL, van Loosdrecht MCM, Heijnen JJ. Biotechnol Bioeng 1997; 53: 88–99.
223. Tijhuis L, Huisman JL, Hekkelman HD, van Loosdrecht MCM, Heijnen JJ. Biotechnol Bioeng 1995; 47: 585–595.
224. Shamlou PA, Titchener-Hooker N. In: Shamlou PA, editor. Processing of solid-liquid suspensions. Oxford: Butterworth-Heinemann; 1993. pp. 1–25.
225. Bagster DF. In: Shamlou PA, editor. Processing of solid-liquid suspensions. Oxford: Butterworth-Heinemann; 1993. pp. 26–58.
226. Matsuo T, Unno H. J Env Eng Div Am Soc Civ Eng 1981; 107: 527–545.
227. Gregory J. In: Shamlou PA, editor. Processing of solid-liquid suspensions. Oxford: Butterworth-Heinemann; 1993. pp. 59–92.
228. Maybury JP, Hoare M, Dunnill P. Biotechnol Bioeng 2000; 67: 265–273.
229. Levy MS, Collins IJ, Yim SS, Ward JM, Titchener-Hooker N, Shamlou PA, Dunnill P. Bioprocess Eng 1999; 20: 7–13.
230. Byrne EP, Fitzpatrick JJ. Biochem Eng J 2002; 10: 17–25.
231. Wang L, Ridgway D, Gu TY, Moo-Young M. J Chem Technol Biotechnol 2003; 78: 1259–1266.
232. Rodríguez Porcel EM, Casas López JL, Sánchez Pérez JA, Fernández Sevilla JM, Chisti Y. Biochem Eng J 2005; 26: 139–144.
233. Rodríguez Porcel EM, Casas López JL, Sánchez Pérez JA, Fernández Sevilla JM, García Sánchez JL, Chisti Y. Ind Eng Chem Res 2006; 45: 4837–4843.

234. Casas López JL, Sánchez Pérez JA, Fernández Sevilla JM, Rodríguez Porcel EM, Chisti Y. J Biotechnol 2005; 116: 61–77.
235. El-Enshasy H, Kleine J, Rinas U. Process Biochem 2006; 41: 2103–2112.
236. Taguchi H, Yoshida T, Tomita Y, Teramoto S. J Ferment Technol 1968; 46: 814–822.
237. Cui YQ, van der Lans RGJM, Luyben KChAM. Biotechnol Bioeng 1998; 57: 409–419.
238. Illing S, Harrison STL. Chem Eng Sci 1999; 54: 441–454.
239. Henzler H-J. Adv Biochem Eng Biotechnol 2000; 67: 35–82.
240. Yim SS, Shamlou PA. Adv Biochem Eng Biotechnol 2000; 67: 83–122.
241. Mikkelsen LH. Colloids Surf A 2001; 182: 1–14.
242. Smart GC Jr. J Nematol Suppl 1995; 27(4S): 529–534.
243. Young JM, Dunnill P, Pearce JD. Bioprocess Eng 1998; 19: 121–127.
244. Fife JP, Derksen RC, Ozkan HE, Grewal PS, Chalmers JJ, Krause CR. Biotechnol Bioeng 2004; 86: 96–107.
245. Friedman MJ. In: Gaugler R, Kaya HK, editors. Entomopathogenic nematodes in biological control. Boca Raton, FL: CRC Press; 1990. pp. 153–172.
246. Friedman MJ, Langston SE, Pollitt S, US Patent 5,023,183, 1991.
247. Lewis JA, Fleming JT. In: Epstein HF, Shakes DC, editors. *Caenorhabditis elegans*—modern biological analysis of an organism. San Diego, CA: Academic Press; 1995. pp. 4–29.
248. Chao Y, Ishida T, Sugano Y, Shoda M. Biotechnol Bioeng 2000; 68: 345–352.
249. Rouf SA, Moo-Young M, Chisti Y. Biotechnol Adv 1996; 14: 239–266.
250. Asakura T, Agarwal PL, Relman DA, McCray JA, Chance B, Schwartz E, Friedman S, Lubin B. Nature 1973; 244: 437–438.
251. Thomas CR, Nienow AW, Dunnill P. Biotechnol Bioeng 1979; 21: 2263–2278.
252. Thomas CR, Dunnill P. Biotechnol Bioeng 1979; 21: 2279–2302.
253. Virkar PD, Narendranathan TJ, Hoare M, Dunnill P. Biotechnol Bioeng 1981; 23: 425–429.
254. Narendranathan TJ, Dunnill P. Biotechnol Bioeng 1982; 24: 2103–2107.
255. Sadana A. Bioseparation 1993; 3: 297–320.
256. Harrison JS, Gill A, Hoare M. Biotechnol Bioeng 1998; 59: 517–519.
257. Maa Y-F, Hsu CC. Biotechnol Bioeng 1997; 54: 503–512.
258. Cassells JM, Halling PJ. Enzyme Microb Technol 1990; 12: 755–759.
259. Fan K-K, Ouyang P, Wu X, Lu Z. Enzyme Microb Technol 2001; 28: 3–7.
260. Adamson AW. Physical chemistry of surfaces, 2nd ed. New York: Interscience; 1960.
261. Henson AF, Mitchell JR, Musselwhite PR. J Colloid Interface Sci 1970; 32: 162–165.
262. Maa Y-F, Hsu CC. Biotechnol Bioeng 1996; 51: 458–465.
263. Brennan JR, Gebhart SSP, Blackard WG. Diabetes 1985; 34: 353–359.
264. Ganesh K, Joshi JB, Sawant SB. Biochem Eng J 2000; 4: 137–141.
265. Bell DJ, Hoare M, Dunnill P. Adv Biochem Eng 1983; 26: 1–72.
266. Carlson A, Signs M, Liermann L, Boor R, Jim Jem K. Biotechnol Bioeng 1995; 48: 303–315.
267. Davison PF. Proc Natl Acad Sci USA 1959; 45: 1560–1568.
268. Levinthal C, Davison PF. J Mol Biol 1961; 3: 674–683.
269. Bowman RD, Davidson N. Biopolymers 1972; 11: 2601–2624.
270. Adam RE, Zimm BH. Nucleic Acids Res 1977; 4: 1513–1537.
271. Reese HR, Zimm BH. J Chem Phys 1990; 92: 2650–2662.
272. Odell JA, Taylor MA. Biopolymers 1994; 34: 1483–1493.
273. Walter E, Moelling K, Pavlovic J, Merkle HP. J Control Release 1999; 61: 361–374.
274. Levy MS, O'Kennedy RD, Ayazi-Shamlou P, Dunnill P. Trends Biotechnol 2000; 18: 296–305.
275. Levy MS, Ciccolini LAS, Yim SSS, Tsai JT, Titchener-Hooker N, Shamlou PA, Dunnill P. Chem Eng Sci 1999; 54: 3171–3178.
276. Eastman SJ, Tousignant JD, Lukason MJ, Murray H, Siegel CS, Constantino P, Harris DJ, Cheng SH, Scheule RK. Hum Gene Ther 1997; 8: 313–322.

82

STERILIZATION AND DECONTAMINATION, BIOPROCESS EQUIPMENT

PETER L. ROBERTS
R&D Department, Bio Products Laboratory, Elstree, Hertfordshire, United Kingdom

82.1 INTRODUCTION

Sterilization and decontamination methods are used during the development and manufacture of biological and other pharmaceuticals in order to remove microbiological agents. For instance, in the case of biologicals products derived by fermentation in bacterial or cell cultures, this involves ensuring that all components that are added to the culture, for example, the growth medium and all items of equipment that the cells come into contact with, are sterile. In addition, in the case of animal cells, the possibility of the presence of endogenous viruses needs to be considered. The classical sterilization methods used in hospitals and the pharmaceutical industry, for example, autoclaving and sterile filtration, are able to inactivate or remove microorganisms very effectively. However, it may be necessary to accept a lower degree of sterility assurance with cell culture or human derived material, or when the specific clinical application is taken into account.

In the case of cell culture systems, the presence of microorganisms can lead to gross and obvious destruction of the cells or difficulties in their culture, although contamination may not be obvious or easily detectable. Increasingly, cells have been recognized as being a potential source of endogenous infectious agents, for example, persistent/latent viruses such as retroviruses or herpesviruses. Moreover, viruses may be used for the immortalization of primary cell lines and for engineering cells to produce biological products using recombinant DNA technology. Thus, biologicals pose a threat to the recipient of any such product as well as to all those that handle such material, whether in a laboratory or on an industrial scale. In addition, consideration must be given to the disposal of potentially contaminated waste materials. All these safety aspects are becoming increasingly subject to legislation by governments.

The range of microbial agents that may potentially contaminate a cell culture include protozoa, fungi, bacteria, mycoplasma, and viruses. The range is further extended by the so-called unconventional agents that cause prion-associated diseases in animals and man, for example, bovine spongiform encephalopathy (BSE), Creutzfeldt–Jakob disease (CJD), and scrapie, that is, the spongiform encephalopathies. These infectious agents are unusual in that they are considered to be infectious proteins, that is, prions (1,2). The sensitivity to inactivation of all these microbiological agents varies widely, although, in general all can be inactivated by heat treatment using a standard autoclave or dry heat oven, or they can be removed by filter sterilization. Exceptions to this include highly resistant prions (3) and bacterial endospores, for example, the *Bacillus* and *Clostridium* species. Also, smaller microorganisms, that is, mycoplasma and small viruses, can pass through conventional bacterial retentive filters. Further general background on this topic can be found in Refs 4–9.

82.2 STERILIZATION BY HEAT

The use of heat, either in the form of dry heat treatment in an oven at about 160°C or by treatment with steam

Upstream Industrial Biotechnology: Equipment, Process Design, Sensing, Control, and cGMP Operations, Volume 2, First Edition. Edited by Michael C. Flickinger.
© 2013 John Wiley & Sons, Inc. Published 2013 by John Wiley & Sons, Inc.

at about 121°C, that is, autoclaving, are two of the most commonly used methods of sterilization (10,11). In general, autoclaving is the more severe of the two methods, but to be performed successfully requires an efficient, well-maintained, and validated machine. It may not be possible to use these standard sterilization methods for some materials due to their heat sensitivity. Less effective conditions may be acceptable, for example, treatment with boiling water or steam at about 100°C. For instance, cell culture incubators are commonly fitted with the ability to be heated at about 80°C for decontamination purposes. The recommended procedure in this case is to repeat the heat treatment on several successive occasions. It is preferable to keep the incubator in a humid state to maximize the sterilizing effect. Heat treatments such as these can be very effective, but fall short of conditions that are accepted as true sterilization. In particular, agents such as bacterial endospores or even standard vegetative bacteria may not be inactivated at these temperatures.

82.2.1 Autoclaves

Almost all microorganisms, apart from some bacterial endospores and prions, are readily inactivated by moist heat at about 121°C, such as that generated in an autoclave (Fig. 82.1). Various standard cycle conditions may be used, for example, 115°C for 30 min, 121°C for 15 min, 126°C for 10 min, or 134°C for 3 min. These times and temperatures are those that should be actually found in the load during the sterilization phase and exclude the machine and load warm-up phase. These standard cycles are not strictly equivalent, with that at 115°C being the least effective and that at 134°C being the most effective. The efficiency of these cycles is tested by determining the survival of highly heat-resistant endospores of *Bacillus stearothermophilus* at a given temperature after various time intervals. The cycle of 121°C for 15 min is most commonly used and is capable of inactivating 1×10^8 cfu of *B. stearothermophilus*. While it is possible to use other cycles with a similar sterilizing capability, these would in fact be either excessively long, for example, 115°C for 60 min, or excessively short, for example, 126°C for 5 min or 134°C for 1 min. In practice, cycles of 115°C for 30 min, 121°C for 15 min, 126°C for 10 min, and 134°C for 3 min have become the accepted standard cycles. These cycles are capable of killing in the order of 1×10^4, 1×10^8, 1×10^{17}, or 1×10^{32} cfu of *B. stearothermophilus*. For routine cell culture applications, the 121°C for 15 min cycle is commonly used. A more severe cycle is currently recommended for the inactivation of prions, 132°C for 1 h, or 134°C to 138°C for 18 min (12). This latter cycle is only applicable if an adequate porous load cycle can be used. Even these extreme cycles may not be fully effective for certain strains/types of agents. To operate the autoclave, steam must be generated either in the equipment itself, as in the case of a small bench top model, or from an external boiler in the case of a large capacity machine as used in industries, hospitals, or microbiology departments. It is critical to operate these machines correctly to ensure that a sterile load is produced. In addition, due to the use of high pressure and high temperature in the equipment, appropriate safety precautions must be followed, as directed by the manufacturers.

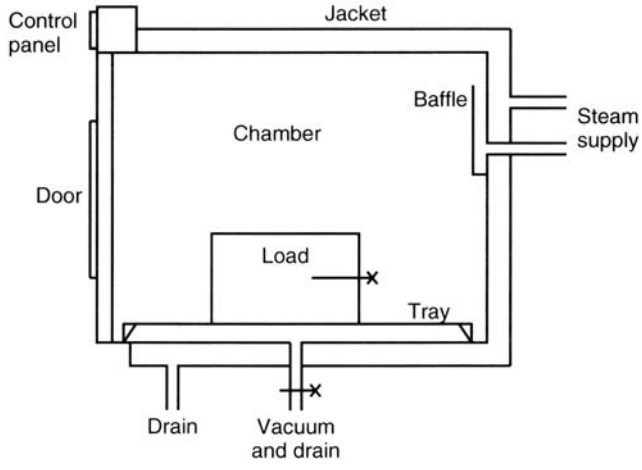


Figure 82.1. Diagrammatic representation of a multipurpose laboratory autoclave. The sterilization phase of the cycle is controlled by thermocouple probes placed in the chamber drain or in the load. The control panel contains temperature and pressure and cycle stage indicators as well as various recording instruments such as a chart recorder or printer. A filter is usually placed on the vacuum line to prevent any microorganisms from leaving the chamber.

82.2.1.1 Laboratory Autoclaves. At their most basic, these are simply small domestic pressure cookers with a capacity of about 0.01 m^3. To operate such a machine, open the lid and fill with water to the required depth. The items to be sterilized are then placed in the machine on shelves or in a basket as appropriate. The lid is then closed and tightly sealed. The water is heated to boiling point and the steam, which is generated, is allowed to purge the chamber for several minutes before the pressure valve is closed. This pressure valve may close automatically in some models. The timer is started when the required pressure/temperature is reached. At the end of the cycle, the heater is turned off and the pressure allowed to fall. When a temperature of about 80°C and atmospheric pressure is reached, the door is opened and the sterilized items are removed. Horizontal models of portable bench top autoclaves are often more sophisticated and have additional controls and safety features. They may have more than one cycle, for example, 121°C and 134°C, a drying option at the end of the sterilization process,

and safety features such as a temperature lock to prevent access during the process. In addition, an automatic timer and various cycle stage indicators may be present.

There are various limitations associated with using such small bench top machines. Generally, they lack adequate air removal methods and are therefore not suitable for porous loads, such as wrapped items, or laboratory discards. If they do not possess an adequate drying stage after sterilization, items may be wet. Because the temperature/pressure in the load is not monitored and there is no printed cycle record, documentation and assurance of sterility may be difficult to demonstrate. In addition, because of the absence of a cooling phase the load may cool slowly and the cycle may take excessively long to complete. There may also be concerns about the safety of the operator using the more basic models of such equipment. In conclusion, their use in the cell culture laboratory is limited to small items that have not been wrapped and bottled fluids. They should not be used for very critical applications, wrapped or difficult items, or contaminated laboratory discards.

82.2.1.2 Large Capacity Autoclaves. Larger autoclaves have a chamber size of at least 1 m^3 and use an external steam supply. In the case of a single cycle gravity displacement autoclave, air is displaced from the bottom of the chamber by the steam of lower density that enters at the top. A system for cooling the load at the end of the cycle via a jacket or spray cooling system is included. There is often a drying stage, using vacuum and heat, at the end of the run. This type of autoclave is useful for items that are easily exposed to steam, that is, not wrapped, and for bottled fluids. However, they are not really suitable for porous loads and wrapped items because air removal is probably not adequate to ensure complete steam penetration, and thus, sterilization. To overcome these limitations and to ensure maximum flexibility in use, a multicycle porous load autoclave is preferable in a cell culture laboratory. It is essential that such a machine includes a porous load cycle, in which air is removed from the load and chamber using vacuum and pressure pulsing stages. The basic steps in such a cycle generally include air removal, sterilization, cooling, and drying using heat and vacuum. The precise details of the stages involved depend upon the exact type of cycle and machine as each is dedicated to a specific type of load. A standard gravity displacement cycle is also included for bottled fluids. Examples of various cycles are given in Fig. 82.2. In contrast to the standard gravity displacement cycle (Fig. 82.2d), the use of a vacuum pump and steam pressure to produce pulses of pressure in the chamber is a more effective method for removing air from difficult loads and wrapped items. There are a wide range of cycles specifically dedicated for this purpose and examples are given in Fig. 82.2a–c. The inclusion of a single high vacuum step at the start of the cycle (Fig. 82.2a) is the simplest approach; however, other methods are generally more effective. The use of a cycle that includes a number of pulses at negative and/or positive pressure is preferable (Fig. 82.2b and c) for ensuring effective air removal. Such cycles should be used for sterilizing/decontaminating critical loads such as contaminated laboratory discards and well wrapped items. Relevant aspects of each cycle programme are generally predetermined by the manufacturer.

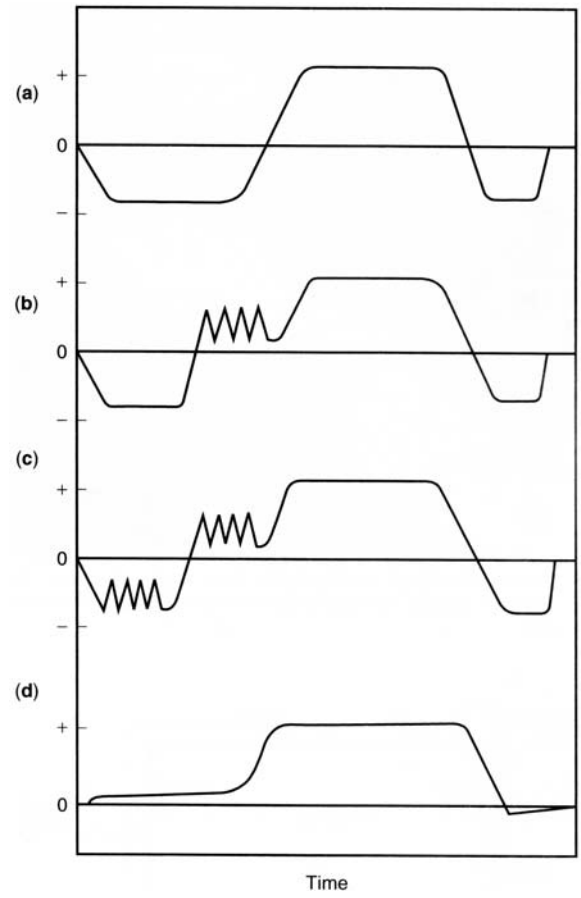


Figure 82.2. Autoclave cycles available on a multipurpose laboratory autoclave. For difficult porous loads, wrapped items, or laboratory discards, a cycle using air removal must be used. Various different methods are available for achieving this and some of these are illustrated. Positive (+) and negative (–) pressure conditions are indicated. In the simplest approach a single initial vacuum pulse is used at the start of the cycle (a). However cycles with a combination of negative and positive pressure pulsing stages as shown in (b) and (c) are generally more effective for air removal. A combination of both negative and positive pulsing stages as shown in (c) is particularly effective. A cycle in which the air is simply removed by gravity displacement and steam flow is shown in (d). This type of cycle is only suitable for bottled fluids and unwrapped items. At the end of the sterilizing phase, a vacuum is created, while the load is still warm in order to dry porous loads. The exact details of pressures, times, and resulting temperatures depend on the specific nature of the cycle.

Dials and/or digital meters on the equipment indicate the stage of the cycle and the current operating conditions in terms of pressure and temperature. This information is also recorded via a printer or chart recorder. An air detector is usually fitted and this monitors the efficiency of air removal from the load and chamber. The cycle will not start unless this is adequate. There are many advantages in using a multicycle autoclave with a porous load cycle. For instance:

- there is good steam penetration into wrapped items, thus ensuring sterility;
- several cycles are available allowing flexibility of use;
- the equipment has a large capacity;
- items will be free of moisture at the end of the cycle.

In general, large capacity/industrial-scale autoclaves are tailored to the customer's specific requirements. They are used in hospitals, the pharmaceutical industry and are preferable for cell culture and microbiology.

After the machine has been installed and initial tests carried out, it may be necessary to conduct further tests and validate critical loads. The heat sensitivity of items should be considered and tested if necessary. Most plastics can withstand the standard 121°C cycle, although polystyrene will not. Only a relatively few cell culture media or supplements are capable of being autoclaved. Autoclavable formulations of some media do exist and these have glutamine omitted, because of its heat sensitivity. The suppliers of cell culture reagents should be consulted for further information.

It is best to add temperature indicators to every item in the load. This is essential where autoclaves do not have a temperature recorder. Autoclave-sensitive tape, autoclave tubes (Browne's tubes) or indicator strips can be used. Such indicators only provide an approximate indication that sterilization conditions have been met. Items of equipment to be sterilized are usually placed in paper sterilization bags or wrapped in aluminum foil or paper. The wrapping is sealed by folding and taping; however, care must be taken not to completely seal the package in order to ensure that satisfactory air removal and steam penetration is accomplished. In the case of empty bottles/containers with caps, the cap should be loosened. Although some autoclave bag manufacturers claim that steam can penetrate directly into sterilization bags, it is best to completely open the neck of the bag prior to autoclaving to ensure adequate air removal and effective steam penetration. Bottled fluids are best autoclaved with the lids tightly closed in order to prevent any possibility of the fluid boiling over. Suitable bottles should be used that can withstand the autoclave cycle when used in this way; alternatively, the lids can be loosened. The ability of the container or bottle/cap combination to withstand autoclaving should also be checked. The manufacturer's/sterilization engineer's instructions and Standard Operating Procedures (SOP) should always be followed. These are different for each autoclave. Logbooks on the servicing, testing, and use of the machines must be maintained.

82.2.1.3 Testing. While in theory it may be possible to directly confirm the sterility of every autoclave load, by for example, incubating the complete batch of product or by inoculating suitable culture media in the case of critical therapeutic products, this is rarely done in practice. Instead, the performance of the autoclave is confirmed by a comprehensive programme of routine testing and validation by autoclave engineers. Testing should be carried out on a regular basis and records kept. This is essential to ensure efficient and safe operation of the machine and to meet regulatory requirements, for example, Health and Safety; Good Manufacturing Practice (GMP) and Good Laboratory Practice (GLP) guidelines. The user should record details of all the runs in a logbook and a leak rate test should be carried out at least weekly. At the end of every run, the autoclave recorder should be checked to ensure a satisfactory cycle, for example, pulsing profiles, temperature, and time. A steam penetration test into a standardized load of towels or cotton sheets, that is, the Bowie–Dick Test, is usually done daily or weekly (13). Servicing must be carried out at regular and agreed intervals, for example, every 3–6 months. Before the machine is first used, the testing of critical worst-case loads should be validated by thermocouple studies. The types of load to be tested might include a mixed load of contaminated laboratory discard. To ensure the worst case is tested, the autoclave should be filled to capacity and thermocouple probes placed in those items where steam will have difficulty penetrating. When carrying out a testing programme, a standard test pack of towels, as used in the Bowie–Dick Test, should be monitored with a thermocouple placed in the center of the test pack. The temperature should be maintained at an acceptable limit, for example, 0–2°C above the target temperature throughout the cycle. The temperature indicated on charts and displays should correspond with this. Important critical loads are best tested using the worst-case situations and critical or difficult items, for example, filters used in sterilization, must also be specifically validated. The operation of the door lock, which prevents entry into the machine until the load has cooled to a safe level, that is, 80°C, should be checked. In the case of liquids, a similar testing procedure is used and the temperature of all bottles within the load should agree to within set limits, for example, ±1°C. Full details of the current requirements for sterilizers are given in various published standards and guidelines (9,14,15).

82.2.2 Hot Air Ovens and Incineration

Heating in the dry state by incineration or treatment in a hot air oven is an alternative method of sterilization (10,11,14). In general, higher temperatures and longer times must be used, compared to autoclaving. Incineration may be used during routine aseptic techniques, for example, the mouth and lids of bottles may be briefly flamed directly in a Bunsen burner. Metal items and scissors, as used during the preparation of primary tissue cultures, can be sterilized in ethanol and subsequently flamed. Waste that is contaminated with microorganisms is considered as clinical waste. This is also true for biological materials, which include cell cultures. Various guidelines control the safe disposal of such waste (12,16). Incineration of microbiologically contaminated material is best carried out after the material has been made safe by autoclaving or chemical treatment directly in the laboratory. The waste material can then be sent for incineration. Where incineration is the only means of decontamination and is outside the user's control, health and safety issues regarding the use of contractors will need to be considered. Incineration is effective when a temperature of about 350°C is reached and thus the operation and type of incinerator is important. The incinerator used must be effective and able to ensure that no unburned material remains or escapes in the smoke.

Ovens are simple and cheap alternatives to the use of autoclaves. They are routinely used to sterilize glassware and metal objects; however, they are generally unsuitable for plastic items. In an oven, heat may be distributed by convection or more effectively by the use of a fan. A filter can be fitted to the air vent to prevent any recontamination of the load by air gaining access to the chamber during the cooling process. The actual time of the load at sterilizing conditions is the critical factor for ensuring effective sterilization. The timer fitted to the oven may start either when the machine is switched on or when the interior of the chamber reaches a predetermined temperature. In more sophisticated cases, thermocouple probes placed in the load provide the controlling parameter for the sterilizing phase. Where this is not the case, an estimate for the load warm-up period must be included when setting the timer. The treatment process can be monitored by chart or digital recorders. In the pharmaceutical industry, tunnel sterilizers may be used to increase capacity. In these, items of equipment, for example, bottles, are continuously fed through the oven on a conveyor system. This type of equipment requires extensive validation to ensure effective sterilization.

The most common heat treatment cycle is 170°C for 1 h, however alternative combinations are 160°C for 2 h or 180°C for 0.5 h. In all cases, this represents the actual temperature within the load during the sterilization phase. Other cycles exist, for example, 150°C for 2.5 h, 140°C for 3 h, and 120°C for 18 h, but these are less effective. These are much less commonly used but may be suitable for less critical applications or where the material is heat-sensitive, for example, plasticware. The basic steps involved in using an oven for sterilization are relatively straightforward and much simpler than for an autoclave. Care must be taken not to overfill the oven, so as to ensure good air circulation. As with autoclaves, suitable indicators can be included to confirm that items have been heat-treated. Heat-sensitive tape is available, which changes color at 160°C to reveal dark stripes. Other strip indicators are available, which indicate that other temperatures have been reached.

Because of their simplicity, the need for extensive engineering maintenance and validation is reduced. However, it is wise to test the performance of the instrument as part of the commissioning process. Further, ongoing testing on a routine basis will be required for critical use in pharmaceutical and hospital applications. Testing may include the use of thermocouples placed in the oven, next to the oven temperature probe, to confirm that the warm-up phase and any temperature overshoot is not excessive, for example, warm up <135 min, overshoot <2°C. Slight fluctuations during the sterilization phase and the general drift in temperature must also be within acceptable limits, for example, 1°C and 2°C respectively. Thermocouples placed around and within the load should confirm that the load temperature agrees with the oven temperature indicator, for example, within 5°C. The appropriate guidelines for sterilizers should be checked for details of the exact current requirements (14,17).

82.3 FILTRATION

Filtration is used in the cell culture laboratory to remove cellular microbial agents from liquids and gases (18–20). Special filters are also now available for removing viruses (see the section on Virus Filtration) and are commonly used for the sterilization of cell culture media and additives, because of the heat sensitivity of such items. With filtration there is the added risk of recontamination between the actual filter sterilization step and dispensing the sterile material into the sterile final container. Because of the critical nature of this process, commercial sterile filtration/final filling operations need to be closely monitored and controlled, and there are extensive regulatory and GMP requirements, which must be complied with. In practice, many of the commonly used materials in cell culture are filter-sterilized. Standard filtration processes commonly use filters with a pore size of 0.2 μm, which are suitable for removing bacteria, yeast, and fungi. There are essentially two types of filters—membrane filters that trap microorganisms on their surface, and depth filters with a less defined pore size that trap microorganisms in the depth of the matrix. Both types are considered in more detail below. Membrane filters are preferred for critical

sterilizing applications, because they have a defined pore size and mode of action, that is, trapping bacteria on the surface. However, the use of depth filters is often very useful for prefiltering a product and thus, reducing the bioburden of microorganisms present, prior to the final sterile filtration step. Recently, filters with a pore size small enough to remove viruses, that is, about 15 nm, have become available (21–26). However, this is a relatively new area and its application in cell culture and bioproducts has thus far been limited. This technology is being used by some manufacturers of calf serum–based products, as well as for treatment of bioproducts for therapeutic use. Recently, plasma-derived products that use this technology have become available (26). In addition to removing conventional microbial agents, filtration may be a useful method for removing prions (27). This is because these agents normally exist in a highly aggregated state and even the minimal infectious unit comprises a large number of individual prion protein units. The range of filters and filtration equipment available is very large. However, the manufacturers produce a range of technical literature and are happy to provide technical advice. In some cases they are willing to optimize/test filtration systems for a specific user's application in their own testing laboratory.

82.3.1 Depth Filters

This type of filter is often made of glass fiber, but other materials may be used. Depth filters operate by trapping microorganisms in the depth of the filter matrix. This may involve physical trapping or be due to electrostatic, or other, interactions. It is possible, at least in theory, to saturate the capacity of this type of filter with regard to microbial binding. For this reason, membrane filters are normally used for situations where the absolute sterilization of liquids is critical. However, with extensive validation it may be possible to justify the use of specific depth filters/product combinations. Depth filters are more commonly used for reducing the microbial content/bioburden, both at various stages in a manufacturing process, for example, prior to specific purification stages, and immediately prior to the final sterile filtration step. The efficiency of the purification process and the capacity of the final sterile filtration step can thus be enhanced.

Depth filters are commonly used for filtering gases (28). The simplest example of the use of this type of filter is the cotton wool used for plugging pipettes used in liquid transfer. In addition, micropipette tips, tubes, and flasks are available with integral depth filters. One type of depth filter that is extensively used in cell culture situations is the so-called HEPA (high efficiency particulate air) filter. These are used to filter air in laminar airflow or microbiological safety cabinets, as well as sterile rooms. In addition, they can be used as vent filters on cell culture fermentation equipment or to filter gases supplied to cell cultures. They remove particles of 0.3 μm or larger at >99.97% efficiency. They are effective for all types of microorganisms, including viruses, even though these agents are much smaller than the nominal filter pore size. This is by virtue of the fact that these agents exist in the atmosphere, attached to liquid droplets in aerosols or attached to dust particles. For pharmaceutical use, there are standards for the quality of air permitted for any particular class of clean room or cabinet. For filter sterilization and aseptic filling there should be no more than 3500 particles/m^3 (29). Relevant standards/classifications should be consulted for the current requirements.

82.3.2 Membrane Filters

Membrane filters are preferable to depth filters for critical sterilization applications where a high level of assurance regarding sterility is required. Membrane filters are made from a range of materials, including cellulose (acetate, nitrate or a mixture), nylon, polysulfone, polyvinylidene fluoride, or polycarbonate. Filters made with low protein-binding properties such as polyvinylidene fluoride, may also be useful in some circumstances. In the case of polycarbonate filters, the pores are of a particularly discrete size because they are produced by a radiation etch method. Because membrane filters act exclusively by retaining microorganisms on their surface due to the pores being of a defined size, there is no risk of exceeding the capacity of the filter and allowing microorganisms to pass through.

Filters with a nominal pore size of 0.2 μm are the current standard for sterilizing liquids and removing cellular microorganisms. If the effective removal of mycoplasmas is essential, the use of membrane filters with a pore size of 0.1 μm should be considered. These are now commonly used by most manufacturers of serum-based additives for cell culture. Such filters may also help by removing any large animal viruses that may be present. Low residual levels of the chemicals used during the filter manufacturing process, for example, detergent, ethylene oxide if used as the sterilizing method, can affect cell growth (30,31). Filter manufacturers can usually provide data on the levels of extractable chemicals as determined using standard solutions/solvents. In the case of pharmaceutical products, such data may not be sufficient and product-specific testing may be required by the regulatory agencies. For cell culture applications it is preferable to use filters with low extractable levels, which have been sterilized by gamma irradiation or autoclaving rather than by ethylene oxide. In critical applications, the first volume of liquid through the filter can be discarded. Membrane filters can also be used for filtering the gases, that is, CO_2 or air that may be used when culturing cells that is, with incubators or

fomenters. Cell culture flasks are available with integral membranes, which allow gaseous exchange without having to leave the cap partially open. For sterilizing gases, it is possible to use a filter with a pore size of 0.02 μm (32), which is small enough to remove viruses. Membrane filters may also be used to protect pipette-handling devices from contamination.

A wide range of types of apparatus for filtration are available. In the simplest systems, a filter of 11 or 25-mm diameter can be attached to a syringe. On a larger scale, cartridges of various sizes (which may be pleated to maximize filtration area with a given device) are used for filtering large volumes of at least several liters. Filter units, comprising the filter membrane in a plastic housing, often come presterilized or may be autoclavable. The unit is designed for single use. In some cases, the filter cartridge must be inserted into a metal housing to produce the complete unit. In the case of filter discs, these need to be assembled in metal or plastic holders prior to sterilization. Complete preassembled and presterilized filter units have the advantage that they are convenient and pretested by the filter manufacturer, whereas filters that require assembly in housings, particularly filter discs, are more prone to failure.

82.3.3 Using Filters

Although filtration can be carried out using positive or negative pressure, it is best carried out using positive pressure. This is because in some situations, for example, when filtering buffers/medium with bicarbonate, the pH may rise during filtration. In addition, frothing and protein denaturation may occur if protein solutions are filtered under negative pressure. On a small scale, the apparatus may simply involve the use of a syringe, but on a larger scale air or nitrogen at positive pressure can be used. An alternative approach is to use a peristaltic pump (Fig. 82.3a). Metal vessels dedicated for filter applications and which can be pressurized are commercially available.

The exact details for using filters vary widely and are dependent upon the type of filtration system used. In the case of commonly used stainless steel filter housings and filter discs (Fig. 82.3b), the method used is as follows.

Disassemble the unit and place the filter on top of the metal grid. Care must be taken to ensure that the filter is used in the correct orientation. To increase the capacity of the filtration system, appropriate prefilters (depth or membrane) can be included with the use of appropriate separators between the layers. The assembly of the unit is a critical process and the manufacturer's instructions must be carefully followed in order not to damage the filter. The assembled unit, along with any associated plastic tubing, is then autoclaved. The standard conditions for this are 121°C for 15 min, although some types of filter are able to withstand higher temperatures. The manufacturer's instructions must be consulted. The filtration process itself is carried out in a laminar airflow cabinet or sterile room using appropriate aseptic procedures. The liquid to be filtered may be placed in a pressure vessel or alternatively a peristaltic pump may be used. An air vent may be present on the housing to allow any air bubbles present in the system to be bled off at the start of the filtration process.

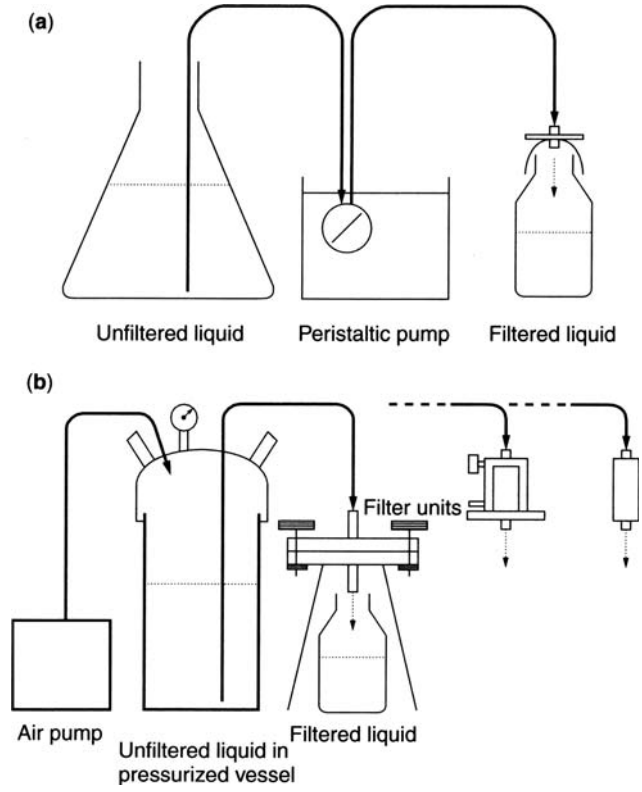


Figure 82.3. Methods used for sterilizing liquids by filtration. The systems shown are designed to filter volumes of a minimum of 1 L, but are usually used for volumes of 5 L or more. In system (a), a peristaltic pump is used to force the liquid through a disposable sterile disc filter. In system (b), a pump is used to pressurize the vessel holding the liquid to be sterilized. This can then be filtered in one of several ways, for example, disc filter, cartridge filter in a stainless steel metal housing that has been autoclaved by the user. Alternatively a presterilized cartridge filter or disc filter that requires no special housing can be used.

82.3.4 Integrity Testing

The manufacturer of the filter will confirm its integrity prior to release. In addition, it is possible for the user to test the integrity of filters. This monitoring is essential in the pharmaceutical industry for sterile filling operations. It must be carried out after using the filter, but may also be performed before use. There are various methods available, including the bubble point, diffusion airflow (or forward flow), or pressure hold tests. The filter manufacturers have

correlated these tests with filter performance for removing microbial agents and provide acceptance limits for the test. The industry standard for this is the use of a particularly small bacterium, for example, *Pseudomonas diminuta* in the case of 0.2-μm filters, which provides a severe test of the filter's efficiency. The test method used should preferably confirm the integrity of the complete filter system, that is, with the housing where relevant. The different integrity test methods are considered below:

1. *Bubble Point Test.* Relatively simple tests may be sufficient, for instance, testing the bubble point by trying to force air forwards or backwards through a wet filter unit attached to a syringe. If air passes through unhindered, then the filter is damaged. During the filtration operation itself, the presence of backpressure also provides some assurance of filter integrity. More sophisticated quantitative procedures can also be used. The manufacturers provide appropriate values for the pass/fail limit which are dependent on the exact filter type and size and the filter system in use.
2. *Diffusion Airflow (Forward Flow) Test.* An alternative approach is that based on determining the airflow across the filter. This method is known as the *diffusion airflow* or *forward flow method* and involves testing the airflow across the wet filter at a specified pressure, usually at about 80% of the bubble point pressure.
3. *Pressure Hold Test.* A third method is the pressure hold test. For this, the filter is pressurized and the pressure decay against time measured.

In addition to all these methods, the actual sterility of the final product can be tested directly, simply by incubating the final product at an appropriate temperature and inspecting for microbial growth. This may be carried out on the complete batch or samples can be taken and inoculated into appropriate microbiological growth media. The sensitivity of such methods will depend on the sample size and use of suitable growth media. This approach is routinely carried out in critical applications such as with therapeutic products. This is because the sterilization step itself is not carried out on the product in its final container, as with for example, autoclaving, and thus, there exists the risk of contamination during the final sterile filling operation itself. Testing for viruses is not generally carried out due to the wide range of virus types in existence. Instead, these agents are usually controlled by testing and controlling the start materials, that is, the cell cultures and growth media.

For critical applications in the pharmaceutical industry, there may be a requirement to test the filter performance with the specific product in use. While this may not be essential for filters that remove bacteria, product-specific testing is likely to be required to confirm the effectiveness of virus filters. This is because virus removal systems have only recently been developed and experience in their use is limited. In contrast, bacterial filters have been in use for a long period of time and so an extensive knowledge of filter performance in relation to a wide range of specific types of test products has been built up. This is sometimes referred to as the *matrix approach* and may be used to justify the efficiency of a specific product/filter combination without recourse to specific bacterial challenge testing with a particular new product. In the case of the HEPA filters used in microbiological safety cabinets and the filtration of air in sterile rooms or containment rooms, smoke challenge tests are used. For this, dioctyl-phthalate particles of about 0.3 μm diameter are used. Testing should be carried out approximately every year.

82.4 FUMIGATION

An alternative sterilization method involves the use of disinfectants in the gaseous state, that is, fumigation. Either formaldehyde gas or ethylene oxide are commonly used (5,9,33). They are, in general, effective against most types of microorganisms although bacterial endospores are somewhat more resistant. These agents are more effective at temperatures over 37°C and high humidity levels, for example, 75–100%. Fumigation is less effective if conditions reduce the accessibility of the microorganisms to the gas, for example, being dried in organic or inorganic material. Fumigation is not used for decontaminating general laboratory waste due to the difficulty in penetrating the load and the presence of organic materials.

82.4.1 Formaldehyde

Formaldehyde gas is commonly used to decontaminate or sterilize laminar airflow cabinets and rooms used for handling cell cultures (6,9). It can also be used for sterilizing items of equipment. Formaldehyde gas is toxic and appropriate safety precautions must be observed and it may be necessary to use breathing apparatus.

Before fumigating a sterile room, all unnecessary items must be removed, particularly those items, which would or might be harmed by exposure to the gas, for example, cell cultures and sensitive electrical or electronic equipment such as computers. The room must then be cleaned to minimize the level of microbial contamination and to remove substances that may hinder penetration of the gas. In the laboratory a dedicated formaldehyde-generating kettle can be used. A simpler method involves filled a pan with formaldehyde and placing this on a hot plate connected to a timer. For this, formalin solution (20 mL/m^3 room volume) is used. Alternatively, paraformaldehyde (10 g/m^3 room volume) can be heated. Formaldehyde

gas can also be generated directly by mixing formalin solution, or paraformaldehyde and water, with potassium permanganate. However, caution must be exercised when using this method as the reaction can be very rapid and may be violent. Equipment that generates a mist of formaldehyde droplets can also be used. With the environmental air handling system for the room turned off, the formaldehyde generator is turned on and the room is evacuated. The door is then locked and fully taped up and sealed and a safety warning notice placed on the door. The room should be left until the next day. Before entering the room, the total exhaust cabinet and/or air extracting system, operating in total exhaust mode, should be turned on remotely. If this is not possible, the room should be entered by someone wearing breathing apparatus that can turn on the cabinet and air handling system. The room should be left until the formaldehyde reaches an acceptable safe level. Testing equipment can be used to monitor the level of formaldehyde. It may be necessary to clean the room to remove deposits of paraformaldehyde that will emit formaldehyde gas. It may take several days to fully remove residues of the formaldehyde gas from the area. In view of the safety implications, fumigation is considered as a fairly specialist procedure and as a last resort, for example, for major spills of high risk microbial agents and in sterile filling rooms in the pharmaceutical industry.

Microbiological laminar airflow/safety cabinets used for handling cell cultures should be decontaminated on a regular basis or after it has become apparent that contaminated cultures have been handled. The use of appropriate respiratory protective clothing is not necessary for this procedure. Only cabinets that can be sealed and, which are ducted to the outside can be decontaminated using formaldehyde. The cabinet must first be thoroughly cleaned before fumigation, particularly if spillages of cell culture media or reagents are likely to have occurred. This should include the area below the removable work surface. In some cases, the cabinets may have integral formaldehyde generators that can be filled from outside the cabinet; otherwise a small dedicated portable formaldehyde generator can be placed inside the cabinet. The generator should be filled with about 25 mL of formalin solution; however, this will depend on the size of the cabinet. Where appropriate, follow the manufacturer's instructions. The cabinet door should be closed and sealed with masking tape. The generator should be turned on and a warning notice placed on the cabinet. The cabinet should be left overnight for the fumigant to act. The next day, the air-exhaust system should be switched on while gradually opening the door to the cabinet. The cabinet should be left running for about half an hour to remove residues of formaldehyde gas. Deposits of paraformaldehyde should preferably be cleaned from the cabinet. However, the operator must take care not to be exposed to formaldehyde when carrying out this task, as residual levels can remain high for a considerable period of time. Full cleaning of the cabinet, involving removal of the work surface and opening of the glass front panel are preferably carried out several hours later.

Items of equipment can be conveniently sterilized at the time the room or cabinet is fumigated by leaving them inside the room/cabinet. An alternative procedure is to place the items in a suitable plastic bag or box together with some formalin liquid. Items used very regularly for cell culture procedures such as pipette aids and micropipettes should be treated on a regular basis and prior to their return to the equipment manufacturer for calibration or servicing.

82.4.2 Ethylene Oxide

Ethylene oxide is used for sterilizing items of clean equipment in so-called cold-temperature autoclaves or in combination with steam, particularly in the hospital environment (33). It is not commonly used in the laboratory. However, it is possible to buy some items of plasticware, which have been presterilized with ethylene oxide, for example, syringes and filters. However, this method of sterilization can leave behind toxic residues; so items sterilized by alternative methods, for example, gamma irradiation, may be preferable. As with formaldehyde, it is also important to remember that ethylene oxide gas is very toxic and operator exposure needs to be minimized.

82.4.3 Hydrogen Peroxide

As an alternative low temperature sterilization agent, hydrogen peroxide is becoming more commonly used. This has the advantage that it will inactivate endospores, leave no toxic residues or significant moisture, and is relatively rapid that is, 2 h versus 14 h for ethylene oxide. This method is routinely used for sensitive items of hospital equipment, as well as for sterile isolators. However, it has been reported that the penetration of the gas into difficult loads can be a problem (34), and thus suitable validated sterilizing cycle must be used.

82.5 GAMMA IRRADIATION

Gamma irradiation is a very common method of sterilization (35). Most presterilized items of equipment are treated in this way, for example, tissue culture flasks, filters, plastic pipettes, pipette tips, and syringes. It is frequently used to sterilize items that cannot be heated. It has good penetrating powers and thus, has the advantage that items can be completely sealed and packaged before being sterilized. Items are exposed to 2.5 Mrad, the accepted standard dose, in a ^{60}cobalt plant. Some chemicals can also be purchased that have been sterilized in this way, for example, antibiotics.

This level of exposure has been in industrial use for a considerable time and has been found to be acceptable as long as there are only low levels of contamination by microorganisms. It is thus suitable for items that are essentially sterile before final irradiation, that is, items made in a factory environment. This method may not eradicate the more resistant bacterial spores and viruses. Both γ and ultraviolet (UV) irradiation have almost no effect on prions (2,3), an observation suggesting they either have no nucleic acid or have a very small and highly resistant genome.

82.6 ULTRAVIOLET LIGHT

UV light at a wavelength of about 260 nm will inactivate microorganisms and viruses (35). However, its usefulness as a method of sterilization is limited because of its poor powers of penetration. UV light can be used to sterilize the air in cell culture cabinets and rooms and to sterilize surfaces once they have been cleaned. The power of UV lamps decreases with use; so, they must be checked regularly. Bacterial spores and prions are highly resistant and bacteria possess DNA repair mechanisms, which can overcome limited damage. Irradiation with UV light is used in some high purity/pyrogen-free water systems to keep the level of viable microorganisms to a low level. This approach can also be used in combination with other chemical methods to decontaminate water, for example, in swimming pools. Recent developments using high intensity visible/UV light sources have allowed this method to be used for sterilizing simple pharmaceutical products such as water or saline. However, more complex bioproducts may be too sensitive to allow this method to be used.

82.7 LIQUID DISINFECTANTS

Many types of liquid disinfectants are available and play a useful role in the cell culture laboratory (4,5,9). A summary of common disinfectants, their effectiveness and use is given in Table 82.1. Disinfectants can be either prepared using laboratory reagents or purchased in the form of proprietary formulations. Various factors should be taken into account when using or selecting a suitable disinfectant. The use of disinfectants is not considered an absolute method of sterilization compared to such methods as autoclaving. They have limitations in terms of their spectrum of antimicrobial activity (Table 82.1). All disinfectants, some more than others, are less effective in the presence of organic matter. Although the concentrated stock disinfectant is stable, the stability of the working dilution varies with the type of disinfectant. Nevertheless, diluted disinfectants are used in the laboratory for the routine disinfection of equipment and surfaces in rooms and cabinets, routine hygiene within the laboratory, disinfection of cell culture items after use and before washing and resterilizing for recycling, for example, glassware, and treating used or contaminated cell culture media before disposal. However, care must be taken to ensure that they are effectively used. For instance, when treating items by immersion, care must be taken to fully immerse the equipment and to prevent pockets of air being trapped, which can prevent all surfaces being exposed to the disinfectant. For this reason, and to ensure that all organic material is removed, exposing the item to the disinfectant in two separate steps is a preferable approach to ensure effective decontamination in more critical situations. Disinfectants can be applied to surfaces using a cloth or by a hand-held sprayer. Paper towels should be used to cover liquid spills and then disinfectant applied. This must be allowed to act for the recommended time before disposal and the surface must then be retreated with the disinfectant. Some disinfectants are available in powder form, which can be directly applied to liquid spills so that they can be contained, absorbed, and treated in one step.

Disinfectants can be used to disinfect clean rooms on a routine basis prior to fumigation. For this a "knapsack" or large volume sprayer with a long lance is used. Appropriate safety precautions must be taken to avoid exposure of the face, eyes, and lungs to the disinfectant.

TABLE 82.1. Use of Common Disinfectants

	Recommended Conditions[a]		Effective Inactivation[b]			
Type of Disinfectant	Concentration	Time (min)	Bacteria	Bacterial Endospores	Fungi	Viruses
Alcohol	70%	30[c]	+	–	–	±
Phenolics	2–5%	30	+	–	+	±
Hypochlorite	10,000 ppm	30	+	+	+	+
Aldehydes	2–4%	30	+	+	+	+

[a] The specific manufacturer's recommendations should be followed for proprietary products.

[b] Agents that are inactivated at the recommended concentration are indicated by (+). In the case of viruses, the agent may be effective against enveloped viruses, but its effect on nonenveloped viruses may be only partial (±).

[c] In practice, it may require repeated applications to achieve a sufficient exposure time.

82.7.1 Formaldehyde and Glutaraldehyde

Formaldehyde and glutaraldehyde can both be used as liquid disinfectants, although glutaraldehyde is more commonly used and is probably more effective. Their advantage is that they are relatively insensitive to the presence of organic matter and are both able to inactivate bacterial endospores. However, there are health and safety implications regarding their use. For glutaraldehyde, in particular, there is pressure to limit exposure. Formaldehyde is used at about 4% and this is easily prepared by diluting the commercially available solution, that is, 40% formaldehyde solution (formalin). Glutaraldehyde is used at 2% and this is available as a component of many commercial formulations. The typical treatment time is at least 30 min, but longer times are advised to obtain full sporicidal activity. Proprietary glutaraldehyde-based disinfectants need the addition of an activator before use and then have a recommended life of about 7 days. Aldehyde vapors are considered to be relatively toxic because they are able to sensitize and also have mutagenic and carcinogenic properties. Steps to limit exposure must therefore be taken by for example, the use of a fume cupboard or appropriate microbiological safety cabinet.

82.7.2 Hypochlorite

Hypochlorite has a relatively low cost and is readily available, for example, household bleach and Chloros. Its disadvantage is that it is not so effective in the presence of high levels of organic matter. It corrodes metals and therefore, must not be used to sterilize centrifuge rotors or cell culture cabinets. Although the concentrate is stable, dilute hypochlorite is not and should be changed after 24 h. The recommended concentration when high levels of organic matter are present or for critical situations when contamination is known to be present, is 10,000 ppm available chlorine. Lower concentrations of 2500 ppm are recommended for routine hygiene. The recommended exposure time is at least 30 min, although overnight exposure may be preferable. Extended exposure to hypochlorite at 20,000 ppm available chlorine is currently a recommended procedure for inactivating prions. Sodium dichloroisocyanurate powder can be used for treating spills by absorbing the liquid and rapidly releasing high levels of chlorine.

82.7.3 Phenolics

Clear phenolic disinfectants such as Hycolin, used at a concentration of 2–5%, are effective against most common microorganisms; although, they are less effective against bacterial endospores. They are largely unaffected by the presence of organic matter and are commonly used in bacteriology laboratories. One disadvantage is that they tend to leave sticky residues when used for cleaning surfaces.

82.7.4 Alcohol

Alcohol, usually in the form of ethanol, is frequently used for disinfecting surfaces, protective gloves, and hands. For optimal effect it should be used at a concentration of about 70%. It can be readily applied using a hand-held sprayer. Surfaces must be fully saturated to ensure that the exposure time is sufficient. The ethanol/water mixture is then left to evaporate off naturally. Its rapid rate of evaporation, enhanced in a cabinet due to the airflow, may make it difficult to ensure an adequate exposure time. In such situations, more than one application of the alcohol may be preferable. Its advantage is that it has low toxicity, is convenient, easy to use, and leaves no residue. However, it is not very effective against fungi, bacterial endospores, and nonenveloped viruses. Also, care must be taken when handling it due to its flammability. It is therefore best used as a cleaning agent or disinfectant for less critical applications. In the case of cell culture procedures, it can be used as a precautionary measure for treating work surfaces and the exterior of cell culture flasks prior to and during work. For critical use or where contamination is suspected, it is best to decontaminate first with a more effective disinfectant and then to treat or spray surfaces with an alcohol solution as an additional precautionary measure.

82.7.5 Others

There are many other useful disinfectants, which can be prepared in the laboratory or purchased as commercial formulations. Some examples are hydrogen peroxide at 5–10%; acids or alkali; ethanol (70%) mixed with 4% formaldehyde or 2000 ppm hypochlorite; ethanol/propanol/aldehyde mixtures. The proprietary disinfectant Virkon has been shown to inactivate a wide range of viruses and other microorganisms, and is made up of three components: an oxidizing agent (peroxide), acid at pH 2.6, and detergent. This is used as a 1% solution and requires an exposure time of at least 10 min. In the pharmaceutical industry, chemical "clean in place" systems are used to clean and disinfect pipe systems and vessels. This procedure usually involves wash cycles with sodium hydroxide (0.5 *M*), followed by an acid rinse, and extensive washing with water. Final sterilization is usually accomplished using steam.

82.8 VIRUS TESTING AND ELIMINATION FROM BIOLOGICAL PRODUCTS

The presence of viruses is a common problem in biological products. Due to their small size, conventional sterilizing filters cannot easily remove viruses. The approach used is a combination of testing and the incorporation of specific virus reduction steps in the manufacturing process.

82.8.1 Virus Screening

The range of viruses that may potentially be present in biological material is extensive. This is made more difficult by the ability of some viruses to exist in a latent/persistent state without any obvious cytopathic effect. Thus, retroviruses such as the human immunodeficiency viruses (HIV-1 and -2), the human T-cell lymphotropic viruses (HTLV-1 and -2), or mouse retrovirus should be tested for. Similar considerations apply to herpesviruses such as herpes simplex virus (HSV-1 and -2), Epstein–Barr virus, cytomegalovirus, varicella zoster, and human herpes virus 6 (HHV-6). In the case of rodent cells, viruses that are potentially pathogenic to man that may be present include rat rotavirus, reovirus type 3, Sendai virus, lymphocyte choriomeningitis virus, and hantavirus. For bovine cells or those that have been grown with bovine serum, tests are commonly performed for viruses such as bovine viral diarrhea, infectious bovine rhinotracheitis, parainfluenza, bovine parvovirus, and bovine adenovirus. Various strategies may be employed in virus testing, including detection in animals, eggs, or cell culture. The induction of virus-specific antibodies in animals in the so-called mouse, rat, or hamster antibody production tests, are also commonly used. Increasingly, molecular techniques based on the detection of viral nucleic acid by the polymerase chain reaction (PCR) are used. Master and extended cell banks produced at the end of the manufacturing run are tested. In order to assure the worst-case situation, a passage number well in excess of that which is likely to be used in the final full-scale manufacturing process should be tested. The sensitivity of detecting certain latent viruses, such as herpesvirus and retroviruses, can be increased by the inclusion of appropriate chemical agents that induce virus replication.

82.8.2 Virus Elimination Methods

A complementary approach to screening and testing for viruses is to treat the product in order to physically remove or inactivate any viruses that might be present (36–39). A virus reduction step may be part of the standard purification process for the product, that may fortuitously remove viruses, or alternatively, a specific or dedicated step may be added.

The minimum level of virus elimination that is considered effective for any given virus elimination step is about 10^4-fold (4 logs). Enveloped viruses are in general more susceptible than nonenveloped viruses. The incorporation of more than one step is needed in order to provide a sufficient level of assurance with regard to virus safety. When several steps are included in a process, elimination figures of around 10 logs for resistant viruses and 20 logs or more for viruses of low to medium resistance can be expected. Quantitative risk assessment taking into account the level of virus that is likely to be present in the start material, can be used to determine if the level of virus reduction is sufficient. Because of the limitation of any particular removal or inactivation method with regard to the range of viruses affected, there has been pressure to include two or more specific virus reduction steps in a purification process. In addition, the methods used should be complementary in that they act by different mechanisms, for instance, the combination of a physical step such as virus filtration and a chemical inactivation step such as solvent/detergent. The inclusion of several virus elimination steps also has the advantage that in the unlikely case of one step failing, there should still remain an adequate margin of virus safety. The use of specific virus elimination steps, rather than simply relying on the standard manufacturing process steps, is preferred. This is because dedicated steps are generally more readily controlled, can be specifically optimized for virus reduction, and can be more readily validated. Virus elimination values for a range of viruses by various steps in a typical manufacturing process are given in Table 82.2.

In addition to the inclusion of effective virus reduction steps, it is essential to ensure that virus safety is not subsequently compromised by recontaminating the product by exogenous viruses during the manufacturing process. The various precautions taken to prevent recontamination are part of the GMP and include the use of closed processing systems and/or physical separation in different rooms or areas. Effective cleaning and sterilization procedures for equipment are also used as described previously.

A major factor that must be considered with any virus removal/inactivation method is the possibility that the step may have adversely affected the product. Most effective virus inactivation methods are relatively severe, and a compromise between maximum virus elimination and minimum product yield/activity loss must be reached. Even in the case of virus filtration, which is a very gentle procedure, product losses on the filter membrane can be high if the size of the protein is too near to that of the filter pores.

Some of the most commonly used virus elimination techniques are considered below. However their effectiveness may be dependent on the specific conditions in the material in question. For this reason product-specific virus elimination studies are necessary (see section titled Validating Virus Reduction Steps).

82.8.2.1 Downstream Processing. The purification steps used during the manufacturing process may provide some degree of virus elimination. Filtration steps using a pore size of 0.2 μm, used for removing cellular microorganisms and debris, will remove larger viruses to some degree. Filters of a smaller pore size, for example, 0.1 μm, used for removing mycoplasma and particulates, are capable of removing larger viruses even more effectively as well as removing

TABLE 82.2. Example of Virus Elimination During the Purification of a Monoclonal Antibody

Step[b]	Virus Reduction (log_{10})[a]					
	Sindbis	SFV	HSV-1	Vaccinia	MLV	Polio-1
Solvent/Detergent[c]	>5.7	>6.7	>5.7	nd	>3.6	0[d]
Protein-G Chromatography[e]	6.0	nd	7.1	nd	nd	3.1
Ion-Exchange Chromatography	nd	nd	5.5	nd	nd	2.4
Size-Exclusion Chromatography	nd	nd	2.7	nd	nd	1.2
Virus Filtration (50 nm)[f]	6.7	6.7	>7.6	6.8	nd	1.0
Total Reduction	>18.4	>13.4	>28.6	6.8	>3.6	7.7

[a] All are enveloped except polio-1. Sindbis and Semliki Forest viruses (SFV) as representative enveloped virues, and models for the hepatitis C virus and the West Nile virus (WNV). Herpes simplex as a representative herpes virus. Murine leukemia virus as a retrovirus, a common endogenous contaminant of rodent cells. Polio-1 as a representative nonenveloped virus.
[b] Purification of human anti-D monoclonal antibody BRAD-3 (39).
[c] 0.3% tri-*n*-butyl phosphate/1% Triton X-100 for 1 h at 20°C.
[d] Nonenveloped virus, thus not susceptible to solvent/detergent treatment.
[e] Step includes column elution at acid pH, which contributes to virus elimination by inactivation
[f] Ultipor DV-50 (Pall) was used. Alternatives such as Viresolve-180 (Millipore) or Planova 35 (Asahi) should be equally effective. Filters with a smaller pore size will be effective for removing small viruses such as polio-1 and encephalomyocarditis (EMC).
nd, not determined.

some smaller viruses. Precipitation methods used to concentrate the product from the bulk harvest will, in some cases, separate virus into the waste material. For instance, this occurs during the cold-ethanol fractionation steps that are used during the preparation of albumin and immunoglobulin from plasma (41,42). The chemical reagents that are used may themselves inactivate viruses (43). In view of the variables associated with the process, this is generally not considered a robust elimination step. However, it almost certainly contributes to the safety of the product.

Chromatographic methods used in the preparation of high purity products also make a significant contribution to the virus safety of the product (44). Affinity or ion-exchange methods have been reported to give significant virus reduction in some manufacturing processes (45–47). However, for any given chromatographic system, the degree of virus elimination cannot be predicted. Reduction values ranging from 2 to 7 logs have been reported for different viruses in different chromatography systems. This variation is not surprising in view of the diversity of surface characteristics associated with different viruses and the column resins involved. Virus reduction during chromatography is largely due to virus removal, and procedures that enhance this, such as extensive washing or the use of buffers of varying ionic strength and pH, can enhance virus elimination. In addition, virus inactivation by chemicals used during washing or elution for example, low pH or isothiocyanate can occur during the process.

82.8.2.2 Virus Filtration. Virus filters have now become widely used in the pharmaceutical industry for eliminating viruses from biological products. This is due to the development of filters that have a sufficiently small pore size that they are effective for virus removal (48–52). Ultipor VF (22,53,54), Planova (23,26,55–58), and Viresolve (25,59–61) filters have been used (Table 82.3). These filters are available in a range of formats and have been shown to remove viruses in a size-dependent fashion. Some of these filters can be used in either a dead-end or recirculating mode. The filter types come in a range of pore-sizes

TABLE 82.3. Examples of Virus Filters

Manufacturer	Filter Type	Grade	Pore-Size[a]	Material	Mode of Use[b]	Mechanism	Integrity Testing
Asahi	Planova	15N 35N	15 nm 35 nm	Regenerated Cellulose	T or D	Depth	Liquid–liquid intrusion
Millipore	Viresolve	70 180	70 kDa 180 kDa	PVDF[c]	T	Membrane	Gold particle
Pall	Ultipor VF	DV-20 DV-50	70–160 kDa 160–200 kDa	PVDF	E	Membrane[d]	Forward flow

[a] Nominal pore size or molecular weight cutoff alone is given.
[b] T, tangential or D, dead-end.
[c] PVDF, polyvinyl deoxyfluoride.
[d] Triple layer membrane.

and the most appropriate type that gives the highest virus reduction without affecting product yields should be used. When filters of the smallest size are used, viruses ranging from the smallest of ca. 20 nm that is, parvoviruses to the largest of ca. 150 nm that is, herpes virus, can be used. If it is necessary to use filters with a medium pore size in order to ensure the passage of product through the filter, then virus removal will be limited to only those of medium to large size that is, >50 nm.

As with sterilizing filters that are designed to remove bacteria, it is essential that integrity testing is carried out on virus filters. Different test methods are available depending on the type of filter involved. The filter manufacturer may also use supplementary test methods for the quality control and release of the product. In all cases, the performance of the filter in the integrity tests has been correlated with the removal of a representative virus, which has been selected to have a size close to that of the filter pore size. The filter manufacturers have generally used bacteriophages such as PR772 (53 nm) as size models for this purpose. The filter manufacturer provides an acceptable pass limit, which correlates with the removal of about 4 log of virus.

The integrity of virus filters is tested by various types of integrity tests, depending on the filter manufacturer. In the case of the Planova filters, a gold particle tester is used. This test involves evaluating the removal of gold particles, slightly larger than the pore size of the filter, from a solution. The optical absorbance of pre- and postfiltration samples are measured on a spectrophotometer and their ratio calculated. This method is destructive, and thus can only be performed after filter use and allows no possibility of retesting the filter. In the liquid/liquid intrusion test, the filter is first treated with a liquid, for example, polyethylene glycol 800, to lower the pressure required to force a second immiscible liquid, for example, ammonium sulphate solution, through the filter. The second immiscible liquid is then introduced and the pressure increased to a specified level. The flow-rate under these conditions is then determined. The forward flow test is a variation on the familiar bubble point method. It involves treating the filter with isopropanol in order to reduce the pressure required to force air through the filter. The pressure is then increased and the pressure needed to force air through the filter is measured.

82.8.2.3 Solvent/Detergent Treatment. The most widely used method for virus inactivation is the solvent/detergent procedure. This involves treatment with a mixture of an organic solvent tri-n-butyl phosphate (TNBP) and a nonionic detergent in order to destroy enveloped viruses (62–65). Polysorbate 80 (Tween® 80) or Triton® X-100 at 1% are the detergents most commonly used at present. It should be noted that polysorbate 80 may be manufactured from bovine sources, but the use of vegetable-derived polysorbate 80 is equally effective, (66) and is to be preferred in view of concerns over prions (see section titled Prions). Solvent/detergent treatment is best carried out early in the standard purification process, so that subsequent purification steps, particularly those involving chromatography, may be sufficient to remove the chemicals to acceptably low levels. Initial treatment with soybean oil is sometimes used for the partial removal of TNBP, and specific chromatographic resins are available to remove the detergent if needed. The solvent/detergent procedure is gentle, generally having no apparent effect on structure, activity, or immunogenicity of proteins. The rate of virus inactivation is dependent on the particular nonionic detergent used and increases with temperature. The inactivation of >9–11 log of virus has been demonstrated. The method is robust and relatively insensitive to small changes in manufacturing conditions such as temperature, solvent/detergent concentration, pH, ionic strength, and protein concentration (67).

82.8.2.4 Pasteurization. Heat treatment in solution at 60°C for 10 h in the final container has long been used as a virus inactivation method (68). In the case of albumin, the fatty acid caprylate (octanoate) and/or acetyl tryptophan is used at low concentration as a stabilizer and does not need to be removed after treatment. In other cases it may be necessary to treat the product in bulk solution, often after the addition of a general stabilizer such as a sugar, amino acid, or salt. These are generally added at a high concentration and need to be removed after treatment. During pasteurization, the inactivation of most viruses occurs rapidly, that is, within 10–30 min. However, inactivation can be slower or incomplete for the heat-resistant viruses such as hepatitis A virus or some parvoviruses. There is evidence that the composition of the product can effect virus inactivation for such viruses as parvovirus B19.

82.8.2.5 Dry Heat Treatment. Products that are freeze-dried and treated at 80°C for 72 h have a good safety record with regard to virus transmission (69–72). Higher temperatures, for example, 100°C (73–75) have also been used. Some virus elimination also occurs during the freeze-drying process, a necessary prelude to the virus inactivation step itself. Several factors may influence virus inactivation by this method, particularly residual moisture content (72). However, a loss of product activity due to denaturation may occur. Also, there is the possible production of neo-antigens in the product by such extreme heating conditions. This may lead to the induction of an immune response against the product in recipients.

82.8.2.6 Extreme pH. Treatment at low pH, usually of about pH 3.5–4 for 30 min–2 h, has been used for virus

inactivation in various biological products (40,76–81). Virus inactivation is more effective at a lower pH and a higher temperature. Even a pH as high as 5.0 can be very effective, provided a long incubation period is used. Some nonenveloped viruses such as hepatitis A and parvoviruses are relatively resistant to acid conditions and may not be inactivated by this method.

82.8.2.7 Irradiation. Irradiation with UV light can be used as a method for virus inactivation (82–87). Because of the poor penetrating power of UV light, it is necessary to use a system that ensures all the liquid is effectively exposed to the light. This may involve the use of a thin film of liquid or a static mixer. Light in the UV-C wavelength that is, of 200–290 nm appears to be the most effective and is able to inactivate both enveloped and nonenveloped viruses. Damage or alterations to proteins by free radicals and reactive oxygen species can be a problem. However, this can be prevented by the inclusion of a quencher such as the flavonoid rutin (88,89).

γ irradiation has also been used for virus inactivation. Irradiation from a cobalt-60 γ irradiation source, as available in commercial irradiation facility is used. A loss of protein activity may occur at the high doses required for effective virus inactivation (90,91). However, if the dose-rate and total exposure dose are well controlled, effective virus inactivation can be achieved with only a limited effect on the product (80). The inclusion of protectants, such as the antioxidant ascorbate, to removes the free radicals and reactive oxygen that can damage the product, can improve the process (92–95). Freezing or lowering the moisture content of the product by freeze drying prior to irradiation maybe necessary to further prevent damage to the product.

82.8.2.8 Validating Virus Reduction Steps. While published information on the effectiveness of any virus elimination procedure is useful, product-specific studies are also required. This is in order to confirm and optimize the virus reduction step and to satisfy the requirements of regulatory agencies (96).

This involves the deliberate addition of virus to a small-scale version of the purification process, and following the virus through the process. The laboratory model must be demonstrated to be an exact scaled-down model of the full-scale manufacturing process. The product intermediate is then spiked with the virus and the process step performed. The amount of virus present at the start and end of the process is quantified by assaying infectivity or by detecting viral nucleic acid by PCR as appropriate.

Various viruses can be used for spiking studies including those that are of particular concern in the product. In addition viruses that are related to any viruses of concern are also included for example, bovine viral diarrhoea (BVDV) virus or Sindbis is a specific model for hepatitis C virus (HCV). In addition, other general model viruses are used in order to increase the range of virus types being tested and to include viruses with particular properties, for example, enveloped or nonenveloped, small or large size, or high resistance to physicochemical damage. Possible model viruses have been suggested by regulatory authorities (96).

While an estimate of the total virus reduction capability of the manufacturing process can be made. This is only really practical for processes with relatively low virus reduction capabilities. However, adding up the individual reduction values for each stage of the process can give an estimate for the total process. Although this approach is only strictly applicable where the individual steps are orthogonal, that is, based on different principles, this method has become widely used. Also, the effect of various parameters on the process, for example, protein concentration, residual moisture content, stabilizer concentration, pH, ionic strength, temperature, and chromatographic parameters, should be investigated. From such studies, an idea of the robustness of the inactivation process can be obtained and suitable limits set for relevant process parameters.

82.9 PRIONS

Screening for prions is not generally carried out on biological products at present. However, current concerns over prions and evidence that lymphocytes are involved in their spread and pathogenesis, may lead to routine testing for such agents in the future. At present, the most sensitive detection methods for prions are based on infectivity; however such testing may take at least 1 year to be completed and are very expensive to conduct. An alternative approach is to screen for the abnormal form of the prion protein, which appears to coexist with infectivity. This can be done by Immuno Western blotting or immunoassay; but these are less sensitive than infectivity assay. However, further developments in this area are likely, given public and regulatory concerns over BSE and its possible human derivative, the new variant Creutzfeldt–Jakob disease (vCJD). Prions are extremely stable to many physical and chemical inactivation procedures. However, they are removed by many manufacturing processes including filtration, chemical precipitation, and chromatography. At present, the screening and/or sourcing of the biological start material is the standard approach recommended for controlling such agents and preventing their presence in therapeutic products (104). Where it is essential to use bovine-derived material, such as fetal-calf serum, source material should be obtained from countries where BSE is absent. In addition, manufacturing procedures themselves have been shown to eliminate prions (98).

82.10 REGULATORY AND SAFETY ISSUES

The safety of individuals involved in manufacturing biological and other products is controlled, for example by the Control of Substances Hazardous to Health (COSHH) regulations in the United Kingdom. Codes of practice are published, which provide practical guidance on how to meet such legal requirements, covering hazards from both chemical as well as biological agents that may pose a safety risk, for instance chemical agents that are used as disinfectants, for example, glutaraldehyde and formaldehyde, as well as cells, microorganisms, and viruses. Detailed guidance on these aspects is given in such documents as the Categorisation of Biological Agents According to Hazard and Categories of Containment, which is regularly updated. More specific guidance may exist for specific groups of agents such as HIV and prions. From a legal point of view, the COSHH regulations put the onus for safety on the employer. From a practical point of view, this means that the manager of those individuals involved is responsible for their safety. This involves assessing the associated risks, developing and implementing safe working practices and ensuring these are followed. In turn, the worker himself must ensure that such safe working procedures are followed and must also ensure the safety of other individuals.

Appropriate guidelines for the sterilization and decontamination of equipment and contaminated waste materials must be followed in order to protect individuals receiving products, to protect the environment and to ensure safe practice. This also applies to the effective operation of equipment designed to sterilize and decontaminate, that is, autoclaves and ovens. Such aspects are covered by documents including Health Technical Memorandum 2010 (14) and appropriate British Standards (15).

The manufacturers of sterile pharmaceutical products are required by regulatory authorities to follow GMP guidelines (29). GMP is defined by regulatory bodies such as the Medicines and Heathcare products Regulatory Agency (MHRA) in the United Kingdom, the European Medicines Agency (EMEA) in the European Union, the Food and Drug Administration in the United States, or equivalent bodies in other countries. These regulators are required to ensure that products are safe and effective to the public. They must therefore be free of bacteria and other microorganisms and, in addition, the risks from viruses and prions must be reduced to an acceptable minimum. Guidelines have been issued and are regularly updated on the testing of cell lines for viruses and other infectious agents (99–101), methods for the removal and inactivation of viruses from cell culture and other biological products, and the validation of such procedures (96,98).

The use of the principles of GLP may also be relevant when developing biological products. In the case of the safety studies required for new pharmaceutical products, their use may be mandatory. Details of the approaches to be followed have been published (102,103). The use of the principles of GLP is designed to ensure the quality and integrity of scientific data generated in the laboratory. They are designed to ensure that all the methods used are adequately described, the results accurately recorded and fully traceable. All aspects of the study are covered, including the planning, performance, recording, and independent monitoring and archiving of the data generated. SOP can be used for routine activities. In the context of sterilization in the laboratory, this may include sterile filtration, the use of disinfectants, and the operation of ovens/autoclaves. There must also be an independent Quality Assurance programme. A Study Director is required to take overall responsibility for any particular safety study. It is also a requirement that all the equipment, such as autoclaves and ovens, used must be well maintained, regularly serviced, and calibrated at suitable intervals and records kept. In addition to official documents on GLP, practical guidance on its interpretation in the context of the cell culture laboratory has been published (104). Working to GLP is only mandantory in limited situations such as studies designed to ensure the safety of therapeutic products; these include animal toxicity testing of cell lines and products, the screening of cell lines for viruses; and the evaluation of virus inactivation/removal methods used in biological products. However, many or all of the principles involved may be usefully applied in the research or R&D laboratory, particularly, if for instance a cell line is subsequently used for manufacturing a therapeutic product.

REFERENCES

1. Prusiner SB. Dev Biol Stand 1991; 75: 55–74.
2. Kimberli RH. In: Collier LH, Timbury MC, editors. Topley and Wilson's principles of bacteriology, virology and immunity. 8th ed. London: Edward Donald; 1990. pp. 671–693.
3. Taylor DM. Dev Biol Stand 1991; 75: 97–102.
4. Russell AD, Hugo WB, Ayliffe GAJ. Principles and practice of disinfection, preservation and sterilization. 2nd ed. Oxford: Blackwell Scientific Publications; 1992.
5. Block SS. Disinfection, sterilization and preservation. 3rd ed. Philadelphia, PA: Lea and Febiger; 1983.
6. Doyle A, Griffiths JB, Newell DG. Cell and tissue culture: laboratory procedures. Chichester: John Wiley & Sons; 1996.
7. Davis JM. Basic cell culture: a practical approach. 2nd ed. Oxford: Oxford University Press; 2002.
8. Spier RE, Griffiths JB. Volume 2, Animal cell biotechnology. London: Academic Press; 1984.
9. Collins CH, Lyne PM, Grange JM. Collins and Lyne's microbiological methods. 7th ed. Oxford. Butterworth Heinemann; 1995.

10. Alder VG, Simpson RA. In: Russell AD, Hugo WB, Ayliffe GAJ, editors. Principles and practice of disinfection, preservation and sterilization. Oxford: Blackwell Scientific Publications; 1992. pp. 483–511.
11. Josyln L. In: Block SS, editor. Disinfection, sterilization and preservation. 3rd ed. Philadelphia, PA: Lea and Febiger; 1983. pp. 3–46.
12. Advisory Committee on Dangerous Pathogens. Categorisation of biological agents according to hazard and categories of containment. 4th ed. London: HMSO; 1995.
13. Bowie JH, Kelsey JC, Thompson GR. Lancet 1963; 281: 586–587.
14. Department of Health. Sterilizers, Health Technical Memorandum No. 2010. London: HMSO; 1994.
15. British Standards Institute. Autoclaves for sterilization in Laboratories, BS2646. London: British Standards Institute; 1993.
16. Health Services Advisory Committee. Safe disposal of clinical waste. London: HMSO; 1992.
17. British Standards Institute. Specification for the performance of electrically heated sterilizing ovens, BS3421. London: British Standards Institute; 1961.
18. Brock TD. Membrane filtration. Berlin: Springer Verlag; 1983.
19. Fifield CW, Leahy TJ. In: Block SS, editor. Disinfection, sterilization and preservation. 3rd ed. Philadelphia, PA: Lea and Febiger; 1983. pp. 125–153.
20. Denyer SP. In: Russell AD, Hugo WB, Ayliffe GAJ, editors. Principles and practice of disinfection, preservation and sterilization. 2nd ed. Oxford: Blackwell Scientific Publications; 1992. pp. 573–603.
21. Roberts PL. Vox Sang 1995; 69: 82–83.
22. Roberts P. J Virol Methods 1997; 65: 27–31.
23. Burnouf-Radosevich M, Apourchaux P, Huart JJ, Burnouf T. Vox Sang 1994; 67: 132–138.
24. DiLeo AJ, Allegrezza AE Jr, Builder SE. Biotechnology 1992; 10: 182–188.
25. DiLeo AJ, Vacante DA, Deane EF. Biologicals 1993; 21: 287–293.
26. Crombie D, Bramall D, Winkelman L, Feldman P, Roberts P. Thromb Haemost 1995; 73: 1023.
27. Tateishi J, Kitamoto T, Ishikawa G, Manabe SI. Membrane 1993; 18: 101–106.
28. Harper GJ. In: Spier RE, Griffiths JB, editors. Volume 1, Animal cell biotechnology. London: Academic Press; 1985. pp. 141–164.
29. Medicines Control Agency. Rules and guidance for pharmaceutical manufacturers and distributors. London: Pharmaceutical Press; 2007.
30. Harrison KL, Sherrin DA, Hawthorne TA, Breen TM, West GA, Wilson LM. J In Vitro Fert Emb Transf 1990; 7: 347–350.
31. Knight DE. Nature 1990; 343: 218.
32. Pall Process Filtration Ltd. Retention of viral contaminants by 0.04 μm Nylon 66 Filters, Pall Scientific and Technical Report STR 1358, Portsmouth: Pall Process Filtration Ltd..
33. Christensen EA, Kristenson H. In: Russell AD, Hugo WB, Ayliffe GAJ, editors. Principles and practice of disinfection, preservation and sterilization. 2nd ed. Oxford: Blackwell Scientific Publications; 1992. pp. 557–572.
34. Kanemitsu K, Imasaka T, Ishikawa S, Kunishima H, Harigae H, Ueno K, Takemura H, Hirayama Y, Kaku M. Infect Control Hosp Epidemiol 2005; 26: 486–489.
35. Christensen EA, Kristenson H, Miller A. In: Russell AD, Hugo WB, Ayliffe GAJ, editors. Principles and practice of disinfection, preservation and sterilization. 2nd ed. Oxford: Blackwell Scientific Publications; 1992. pp. 528–556.
36. Roberts P. Rev Med Virol 1996; 6: 25–38.
37. Burnouf T. Biologicals 1992; 20: 91–100.
38. Foster PR, Cuthbertson B. In: Madhok R, Forbes CD, Evatt BL, editors. Blood, blood products and HIV. London: Chapman and Hall; 1994. pp. 207–248.
39. Roberts PL, Walker CP, Feldman PA. Vox Sang 1994; 67(l Suppl): 132–138.
40. Baker RM, Brady AM, Combridge BS, Ejim LJ, Kingland SL, Lloyd DA, Roberts PL. In: Pyle DL, editor. Separations for biotechnology 3. Cambridge: Royal Society of Chemistry; 1994. pp. 53–59.
41. Morgenthaler JJ, Omar A. Dev Biol Stand 1993; 81: 185–190.
42. Yei S, Yu MW, Tankersley DL. Transfusion 1992; 32: 824–828.
43. Morgenthaler JJ. Curr Stud Hematol Blood Transfus 1989; 56: 109–121.
44. Burnouf T. Dev Biol Stand 1993; 81: 197–199.
45. Hrinda ME, Huang C, Tarr GC, Weeks R. Semin Hematol 1991; 28: 6–14.
46. Lawrence JE. Dev Biol Stand 1993; 81: 191–197.
47. Roberts PL. In: Pyle DL, editor. Separations for biotechnology 3. Cambridge: Royal Society of Chemistry; 1994. pp. 420–426.
48. Aranha H. BioPharm 2001: 32–42.
49. Burnouf T, Radosevich M. Haemophilia 2003; 9: 24–37.
50. Carter J, Lutz H. Eur J Parenter Sci 2002; 7: 72–78.
51. Levy RV, Phillips MW, Lutz H. In: Meltzer TH, Jornitz MW, editors. Filtration in the biopharmaceutical industry. New York: Marcel Dekker; 1998. pp. 619–646.
52. Roberts P. Eur J Parenter Sci 2000; 5: 3–9.
53. Pall Process Filtration Ltd. Virus retention by Ultipor VF grade DV50 membrane filters. New York: Pall Europe Ltd.; 1996.
54. Oshima KH, Evans-Strickfaden TT, Hightsmith AK, Ade EW. Biologicals 1996; 24: 137–145.
55. Hamamoto Y, Harada S, Kobayashi S, Yamaguchi K, Iijima H, Manabe S, Tsurumi T, Alzawa H, Yamamoto N. Vox Sang 1989; 56: 230–236.
56. Manabe S. Dev Biol Stand 1996; 88: 81–90.
57. Oshima KH, Evans-Strickfaden TT, Hightsmith AK, Ades EW. Biologicals 1996; 24: 137–145.
58. Yokoyama T, Murai K, Murozuka A, Tanifuji M, Fuji N, Tomono T. Vox Sang 2004; 86: 225–229.
59. Levy RV, Phillips MW, Lutz H. In: Meltzer TH, Jornitz MW, editors. Filtration in the biopharmaceutical industry. New York: Marcel Dekker; 1998. pp. 619–646.
60. Maerz H, Hahn SO, Maassen A, Meisel H, Roggenbuck D, Sato T, Tanzmann H, Emmrich F, Marx V. Nat Biotechnol 1996; 14: 651–652.
61. Hughes B, Bradburne A, Sheppard D, Young D. Dev Biol Stand 1996; 88: 91–98.

62. Horowitz B, Weibe ME, Lippin A, Stryker MH. Transfusion 1985; 25: 516–522.
63. Horowitz B, Prince AM, Horowitz MS, Watklevicz C. Dev Biol Stand 1993; 81: 147–161.
64. Prince AM, Horowitz B, Brotman B, Huima T, Richardson L, van der Ende MC. Vox Sang 1984; 46: 36–43.
65. Prince AM, Horowitz B, Brotman B. Lancet 1996; 1: 706–710.
66. Roberts P, Sims G. Biologicals 1999; 27: 263–264.
67. Roberts PL, Dunkerley C. Vox Sang 2003; 84: 170–175.
68. Nowak T, Niedrig M, Bernhardt D, Hilfenhaus J. J Biol Stand 1993; 81: 169–176.
69. Hart HF, Hart WG, Crossley J, Perrie AM, Wood DJ, John A, McOmish F. Vox Sang 1994; 67: 345–350.
70. Roberts PL, Hart H. Biologicals 2000; 28: 185–188.
71. Winkelman L, Feldman PA, Evans DR. Curr Stud Hematol Blood Transfus 1989; 56: 55–69.
72. Roberts PL, Dunkerley A, McAuley A, Winkelman L. Vox Sang 2007; 92: 56–63.
73. Dichtelmuller H, Rudnick D, Breuer B, Kotitschke R, Kloft M, Darling A, Watson E, Flehmig B, Lawson S, Frosner G. Biologicals 1996; 24: 125–130.
74. Roberts PL. Vox Sang 1995; 68: 61–62.
75. Santagostino E, Mannucci PM, Gringeri AA, Morfini M, Musso R, Santoro R, Schiavoni M. Transfusion 1997; 37: 517–522.
76. Bos OJ, Sunye DG, Nieuweboer CE, van Engelenburg FA, Schuitemaker H, Over J. Biologicals 1998; 4: 267–276.
77. Hamalainen E, Suomela H, Ukkonen P. Vox Sang 1992; 63: 6–11.
78. Kempf C, Jentsch P, Poirier B. Transfusion 1991; 31: 423–427.
79. Louie RE, Galloway CJ, Dumas ML, Wong MF, Mitra G. Biologicals 1994; 22: 13–19.
80. Reid BD. Biologicals 1998; 26: 125–130.
81. Brorson K, Krejci S, Lee K, Hamilton E, Stein K, Xu Y. Biotechnol Bioeng 2003; 82: 321–329.
82. Caillet-Fauquet P, Di Giambattistra M, Draps ML, Sandras F, Branckaert T, de Launoit Y, Laub R. J Virol Methods 2004; 15: 131–139.
83. Hart H, Reid K, Hart W. Vox Sang 1993; 64: 82–88.
84. Kallenbach NR, Cornelium PA, Negus D, Montgomerie D, Englander S. Curr Stud Hematol Blood Transfus 1989; 56: 70–82.
85. MacLeod AJ. Dev Biol 2004; 118: 139–147.
86. Wang J, Mauser A, Chao SF, Remington K, Treckmann R, Kaiser K, Pifat D, Hotta J. Vox Sang 2004; 86: 230–238.
87. Roberts P, Hope A, Virol J. Methods 2003; 110: 61–65.
88. Chin S, Williams B, Gottlieb P, Margolis-Nunno H, Ben-Hur E, Hamman J, Jin R, Dobovi E, Horrowitz B. Blood 1995; 86: 4431–4436.
89. Chin S, Jin R, Wang XL, Hamman J, Marx G, Mou X, Andersson I, Lindquist LO, Horowitz B. Photochem Photobiol 1997; 65: 432–435.
90. Hiemstra H, Tersmette M, Vox AHV, Over J, van Berkel MP, DeBree H. Transfusion 1991; 31: 32–39.
91. Kitchen AD, Mann GF, Harrison JF, Zuckerman AJ. Vox Sang 1989; 56: 223–229.
92. Amareld RW Jr, Wersocki M, Drohan M, Drohan WN, Burgess WH, Mann DM, Forng R-Y. Biologicals 2003; 31: 261–264.
93. Grieb T, Forng R-Y, Brown R, Owolabi T, Maddox E, McBain A, Drohan WN, Mann DM, Burgess WN. Biologicals 2002; 30: 207–216.
94. Miekka SI, Forng R-O, Rohwer RG, MacAuley C, Stafford RE, Flack SL, MacPhee M, Kent RS, Drohan WN. Vox Sang 2003; 84: 36–44.
95. Tran H, Marlowe K, McKenney K, Petrosian G, Griko Y, Burgess WH, Drohan WN, Imboden MA, Kempf C, Boschetti N, Mann DM. Biologicals 2004; 32: 94–104.
96. Committee for Proprietary Medicinal Products, European Medicines Evaluation Agency. Note for guidance on virus validation studies: the design, contribution and interpretation of studies validating the inactivation and removal of viruses, CPMP/BWP/268/95, 1996.
97. European Agency for the Evaluation of Medicinal Products. CHMP position statement on Creutzfeldt-Jakob disease and plasma-derived and urine-derived medicinal products, EMEA/CPMP/BWP/2879/02/rev1.2004.
98. European Agency for the Evaluation of Medicinal Products. CHMP guideline on the investigation of manufacturing processes for plasma-derived medicinal products with regards to vCJD Risk, CPMP/BWP/CPMP/5136/03.2004.
99. US Food and Drug Administration. Points to consider in the characterization of cell lines used to produce biologicals. 1987.
100. US Food and Drug Administration. Points to consider in the manufacture and testing of monoclonal antibody products for human use. 1987.
101. Committee for Proprietary Medicinal Products, European Medicines Evaluation Agency. Note for guidance on the quality of biotechnological products: viral safety evaluation of biotechnology products derived from cell lines of human or animal origin, CPMP/ICH/295/95, 1995.
102. Department of Health. Good laboratory practice: The United Kingdom Compliance Programme. London: HMSO; 1989.
103. The Organization for Economic Co-Operation and Development. OECD principles of good laboratory practice. Paris: OECD Publications; 1998.
104. Clitherow B, Froud SJ, Luker J. Good laboratory practice in the cell culture laboratory. In: Davis JM, editor. Basic cell culture: a practical approach 2nd ed. Oxford: Oxford University Press; 2002 pp. 273–286.

INDEX

2,3,5-triphenyltetrazolium chloride (TTC), 757
2,4-dichlorophenoxyacetic acid (2,4-D), 751
2-isopentyl adenine, 752
3-(4,5-dimethylthiazol-2-yl)-2, 5-diphenyltetrazolium bromide (MTT), 98
[^{3}H]proline, 98
[^{3}H]thymidine, 77
[^{3}H]uridine, 98
3D Matrix System, 1337–1338
4′-6-diamidino-2-phenylindole (DAPI), 476
4-hydroxy-3-methyl-trans-2-butenylaminopurine, 752
5-azacytidine, 738
5-cyano-2,3-ditolyl tetrazolium chloride (CTC), 98
6-aminopenicillanic acid (6-APA), 1171
6-benzylaminopurine (BA/BAP), 752
6-furfurylaminopurine (kinetin), 752
6-methylpurine deoxyriboside (6-MPDR), 475
7-aminocephalosporanic acid (7-ACA), 1171
9-fluorenylmethoxycarbonyl chloride (FMOC), 1530
^{51}chromium (Cr), 98
[^{75}Se]selenomethionine, 98

abciximab, 636
abscisic acid (ABA), 752
absolute reaction rate, 1616–1617
absorbed photon flux, 392–393
Academic and University Centre of Nove Hrady (Czech Republic), 1332
acceleration due to gravity, 765–766
Accumax™, 299
Accustase™, 300, 720
Acholeplasma, 469
Acholeplasma laidlawii, 471
acoustic sensors, 1478
acoustic settlers, 1006, 1007, 1008
Acridine Orange (AO), 97
Acusyst System (Cellex Biosciences, Inc.), 1254
acute transforming retrovirus, 247
Addavita Ltd. (Chesterfield, UK), 1333
adeno-associated virus (AAV) vectors, 240
  molecular biology, 240–241
  recombinant, 241
adenosine triphosphate (ATP), 79, 98, 468, 589
adenovirus vectors, 238
  molecular biology, 238–239
  recombinant, 239–240
adherent cells, 1740
adsorption
  enzymes on anti-enzyme antibodies, 1206
  glycosylated enzymes on immobilized lectins, 1206
  industrial enzymes on ionic exchangers, 1204
  selective lipase, on hydrophobic supports, 1205
Advanced Algal Production System (AAPS), 1333
Aequoria victoria, 451
aeration, 792–794
  carbon dioxide accumulation and removal, 797–798
  effect, 569
  membrane, 796–797
  oxygen carriers, 796
  perfluorocarbons, 795–796
  sparger design, 797
  sparging, 797
  surface, 795
aeration number, 1108, 1109, 1316
affinity tags, for protein purification, 171
agar, 121, 429
agarose, 429, 1208
age density function, 360
agitation, 792
Agrotechnology and Food Sciences Group, Wageningen University (The Netherlands), 1342
airborne contamination, control of, 68
air cleanliness, ISO classification, 67
air exhaust system, 1134
air inlet and outlet, 1127–1129
air-lift bioreactors, 1639, 1658
airlift external circulation membrane bioreactor (AECMBR), 942
airlift fermenter, 1252–1253
airlift pump, special designs based on, 934–935

Upstream Industrial Biotechnology: Equipment, Process Design, Sensing, Control, and cGMP Operations, Volume 2, First Edition. Edited by Michael C. Flickinger.

© 2013 John Wiley & Sons, Inc. Published 2013 by John Wiley & Sons, Inc.

airlift reactors (ALRs), 11, 887, 1239, 1278, 1280–1284, 1294
advantages, 888–890
bioprocesses
biopolymers, 938–939
drugs, 938
food additives, 939
heavy metals removal, 939
hydrocarbons in groundwater, 939
lignocellulosic wastes exploitation, 939
waste gas treatment, 939
wastewater treatment, 940–942
external loop, 895–898, 900
fluid dynamics, 890
energy dissipation and shear rate, 909–911
flow configuration, 890–892
gas holdup, 892–901
gas recirculation, 901
and integrated kinetics, 920
liquid mixing, 904–908
liquid velocity, 901–904
mixing in gas phase, 908–909
heat transfer, 915–917
internal loop, 893–895
liquid level effect, 899–901
liquid rheology effects, 898–899
mass transfer, 911
bubble size and interfacial area, 914
data correlation for rate, 914–915
rate measurement, 911–914
models, 935–938
morphology, 887–888
multiphase, 917, 927–928
four-phase, 918–920
three-phase, 917–918, 937
selection and design
design improvements, 927–935
scale-up, 920–927
with static mixers, 929–930
using mechanically moved internals, 928–929
airlift systems, 385
air pulsation, 1417
air sterilization, 1115
alanine, 425
albuferon, 201
Alcian Blue, 97
alcohol, 1773
light-weight, 426
alcohol dehydrogenase (ADH), 1171
Aldurazyme™, 725
alemtuzumab, 636
AlgaeLink N.V. (The Netherlands), 1338
Algatechnologies Ltd. (Israel), 1339–1340
alginate, 1185–1186
alginic acid and κ-carrageenan, 430
alkaline solution, absorption, 1308–1309
alkosense probe (Frings America, Illinois), 204
Allegra®, 838
alphabaculoviruses, 19
alphavirus vectors, 241–243
alternating tangential flow (ATF), 726, 997, 1002
alveolar panels, 1335–1336
American Society for Testing and Materials (ASTM) International Committee E55, 1543
American Type Culture Collection (ATCC), 155, 159
amino acids, 1527–1529
ammonia, 521, 589, 590
enzyme assay, 1536
fluorescence detection derivatization, 1536
gas-sensitive electrode, 1536
ion chromatography, 1536
ammonium ions supply, in plant culture, 749
amperometric gas sensors, 1568
amplicons, 238, 240, 248
amplifiable marker, 227
anabolic substrates, 333
Anaeroplasma, 469
anchorage-dependent cells (ADCs), 1245, 1247, 1254
reactors for
basic culture units, 1249–1250
high-volume units, 1250–1252
multisurface plate units, 1250
anchor impellers, 1049
Anchusa officinalis, 1655
aneuploidy, 618
animals as bioreactors, 284–285
animal cell bioreactors, 791
aeration, 792–794
carbon dioxide accumulation and removal, 797–798
membrane, 796–797
oxygen carriers, 796
perfluorocarbons, 795–796
sparger design, 797
sparging, 797
surface, 795
animal cells relationship with hydrodynamic forces, 804
cell damage mechanisms, 807–809
cell damage quantification, 809–811
molecular mechanism, 805–807
sparging detrimental effects, 811–814
mixing, 798
baffles, 801
geometry, 799
impellers, 799–801
mixing times and energy dissipation rates, 801–804
stirred tank reactors, 799
aimal cell cultures, 663
animal cell culture media, 581–582
basal medium development, 584–585
chemically defined development strategies, 585–587
feed medium development, 587
strategy, 588–589
industrial considerations for basal and feed media optimization and implementation
liquid media stability and scalability, 594
platform and customized process, 592–594
nutrients, 582
amino acids, 582–583
carbohydrates, 582
cofactors and substrates, 583
growth factors and carrier proteins, 584
lipids and lipid precursors, 583–584
nucleosides, 584
organic salts, metals, and trace elements, 583
osmolality, 584
vitamins, 583
product quality, 589–591
small-scale models and high throughput systems, 591–592
animal cells and shear sensitivity response, 1737–1750
animal cell stability, 617
consequences of genetic instability on recombinant protein quality, 624–627
factors that affect genetic stability of endogenous genes, 618
DNA-dependent protein kinase, 620–621
molecular regulation of genetic stability, 618
oncogenic transformation, aneuploidy, and genetic stability, 618
p53 tumor suppressor gene, 619
phenotypic change due to DNA methylation and gene silencing, 619
poly(ADP-ribose) polymerase, 620
proto-oncogenes and genomic instability, 619
retinoblastoma tumor suppressor gene, 619
telomeres and telomerase, 621
tumor suppressor genes and proto-oncogenes, 618–619

genotypic and phenotypic stability of recombinant cell lines, 621
genetic and epigenetic manipulation of cell phenotypes, 623–624
phenotypic heterogeneity and population dynamics, 622–623
stable integration of heterologous genes in animal cell genomes, 621–622
genotypic characterization and validation of genetic stability, 627
genetic stability, 630–631
gross structural evaluation of genes and transcripts, 628–629
sequence analysis of genes and transcripts encoding the product, 629–630
animal cell types
alternatives to antibodies for use in human beings, 642–643
antibody production by animal cells *in vitro*, 637
hybridoma technique, 638–640
production of human antibodies, 640–641
biotechnological production of proteins, for biomedical use, 635
cultivation methods, 636–637
human antibody production, new methods for, 641–642
for industrial protein expression, 635–636
animal cloning, 290
anion exchange chromatography, 501–502
anthocyanin, 1651–1652
anthraquinone, 1651
anti-auxins, 752
antibiotic resistance genes, 169
antibiotics biosynthesis, modified agitator performance in, 1464
industrial-scale bioreactors, 1465–1467
semiindustrial-scale bioreactors, 1464–1465
antibodies with improved functions and properties, creating, 647
antibody dependent cellular cytotoxicity (ADCC), 183, 645, 735
antibody-derived TNF antagonists, 648
antibody libraries, 652
antibody manufacture and disposable systems, 1587–1588
disposable bioreactors in MAb production processes
membrane bioreactors, 1589–1590
orbitally shaken and pneumatically driven bioreactors, 1592–1593
stirred bioreactors, 1591–1592
wave-mixed bag bioreactors, 1590–1591
single-use devices, 1588–1589
antibody production, by animal cells *in vitro*, 637
human antibodies, production of, 640–641
hybridoma technique, 638–640
antibody production, human recombinant, 645, 649, 654
antibodies with improved functions and properties, creating, 647
human antibodies *in vitro,* selection of, 651–654
recombinant antibody gene repertoires, 652
selection systems for recombinant antibodies, 652–654
human monospecific antibodies, 646–647
making hybridoma-derived antibodies more human, 648
chimerization, 649
humanization, 649
in silico humanization, 649
production systems for, 650–651
recombinant antibodies, applications of, 659
cross reactivity, avoiding, 659
intracellular antibodies, 660
proteomics and interactomics, recombinant antibodies for, 660
recombinant antibodies, production of, 654
recombinant antibody variants, 655
antibodies with new functions, 657
disulfide-stabilized Fv fragments (dsFv), 656
Fab fragments, 656
oligovalent and bispecific antibodies, 657–659
single chain antibody fragments (scFv), 656
single chain Fab fragments (scFab), 656
V_H and camel antibodies, 656–657
transgenic mice, 651
antibody production
intracellular, rate expression for, 87
rate, 86
antibody secretion rates, effect of hyperosmolar stress on, 604
anticalins, 642
antifoam agents, 1285, 1143, 1626, 1684–1685, 1686
antigen-binding fragment (Fv), 646
antisense RNA constructs, and gene silencing, 276–277
antisense suppression, 258
antisplatter pastes, 1433
apoptosis, 81–82
Applied Instruments (Hamilton Sundstrand, MGA series), 1572
Applied Photosynthetics Limited (APL) (Manchester, UK), 1333
AppliFlex, 305
AppliFlex Bioreactor (Applikon), 1591
Applikon, 682
aptamer, 278
APTES, 1160, 1167
Aquasearch Growth Module (AGM), 1340
aqueous two-phase extractions, 1289
Arabidopsis seeds, 754
Arabidopsis thaliana, 743
Archaeoglobus spp., 414
Archimedes number, 968, 977
areal productivity(AP), 1341
arginine, 425
argon–oxygen decarbonation (AOD), 1430, 1431
Armed Forces Epidemiology Board (AFEB), US, 185
Arrhenius equation, 347, 385, 1113, 1616
Arthrospira platensis, 1332, 1333, 1335, 1340
Arthur D. Little Company, Massachusetts Institute of Technology (USA), 1331
artificial intelligence and data technologies, 1484–1485
artificial membranes, 821
artificial neural networks, 925–926, 1486–1487, 1559
"as-built" state, 67–68
ascorbic acid, 1533
Asepco™, 1129
aseptic techniques, in cell culture , 49
basic procedures, 53
aseptic manipulation of equipment, 55–56
manipulation of cells and liquid reagents, 53–55
biohazards, 49–50
capping, 52
cell culture environments, 50
cellular cross-contamination, 49
cleanrooms for cell culture use, 66
design and operation, 66–69
clothing, 52
culture equipment, 50–51
flaming, 52
HEPA filtration, 56
construction, 57–58
efficiency, 57
hoods and cabinets employing, 58
mechanism, 56–57
microbial safety cabinets, 59–60
specification, 68
testing, 58

aseptic techniques, in cell culture (*continued*)
unidirectional airflow cabinets, 58–59
microbial contamination, 49
microbial safety cabinets, 60
class I, 61
class II, 61–62
class III, 62
testing, 62, 64–66
personal hygiene, 51–52
pipetting, 52–53
pouring, 52
swabbing and spraying, 52
unidirectional airflow cabinets, 60
horizontal, 61
vertical, 61
working area, 51
Asian Consortium for the Conservation and Sustainable Use of Microbial Resources, 146
Aspergillus awamori, 1365, 1367, 1753
Aspergillus nidulans, 1397
Aspergillus niger, 1366, 1367, 1368, 1369, 1371, 1372, 1391, 1521, 1730
Aspergillus sojae, 1353
Aspergillus terreus, 1353
Asteroleplasma, 469
asynchronous infection kinetic model, 42
attachment, internalization, and infection, 42–43
mass balances, 44
population balance, 48
solving, 44–45
usage, 45–47
ATG, 22
atomic force microscopy (AFM), 438, 454
atomization technique, 1188
"at-rest" state, 68
Auromonas elodea, 1351
austenitic stainless steels, 1427, 1430
common AISI grades composition, 1599
autoclaves, 426, 431, 1602
cycles, 1764, 1765
laboratory, 1764–1765
large capacity, 1765–1766
testing, 1766
Autographa californica multicapsid nucleopolyhedrovirus (AcMNPV), 19, 20, 21, 22, 29, 30, 243, 311, 312, 316
Autographa californica nuclear polyhedrosis virus ((AcNPV), 34, 41
automated cell counters, 1478
automated cell density examination systems, 1525
automatic steam-in-place, 1618–1619
autopassivation, 1429, 1432
autoradiography, 77
autosampling technologies, 1480
autotrophs, 415
auxins, 751–752
available electrons, 334
Avastin®, 305, 659
average shear rate, 1349, 1361, 1720
average shear stress, 1361
avidity, 657
axial dispersion model, 905
axial dissolved oxygen profiles, 1283
axial flow/pitched blade turbines, 1221
axial flow impellers, 1110
with draft tube, 1047
Azadirachta indica, 1656
Azotobacter, 416

B. Braun Biotech International GmbH, 1333, 1335
baby hamster kidney (BHK) cells, 10, 89, 109, 724, 742, 1245, 1635, 1655
Bacillus, 163
advantages of, 163
in industry, 164
major industrial strains, 164–165
megaterium, 165–176
Bacillus amyloliquefaciens, 165
Bacillus clausii, 165
Bacillus coagulans, 1398
Bacillus licheniformis, 165, 174
Bacillus megaterium, 165–167
commercial protein production systems, 173
culture heterogeneity, 173
DSM319, 167–168
and derivatives protoplast transformation, 175–176
genomics and systems biotechnology, 173–174
QM B1551, 167
and derivatives electrotransformation, 174–175
toolbox for recombinant protein production, 168–173
Bacillus stearothermophilus, 431, 1616, 1764
Bacillus subtilis, 164–174, 546, 550, 552, 561, 563, 673
growth, simulation model of, 355
Bacillus thuringiensis, 1730
back-flushing approach, 1007, 1009–1010
back-propagation neural network (BPNN), 926
back-to-back double mechanical fermenter shaft seal, 1131
BacMam technology, 30–31
bacmids, *E. coli*, 21
BacPAK6, 21
bacteria. See also protein expression, in bacteria
culture preservation
long-term methods, 154–158
short-term culture, 153–154
and fungi, 123
Bacteroides forsythus, 422
Bac-to-Bac™, 21, 245
transfer vectors for, 28
BaculoDirect, 22, 28
baculovirus, 19, 313
gene expression, 314–315
in mammalian cells, 30–31
genome modification, for protein production improvement, 28
insect cell culture, 28
modification for recombinant protein production, 29–30
scaling up of, 30
in serum-containing medium, 28–29
in serum-free medium, 29
recombinant, production of, 20
circular virus genomic DNA, 21
DNA manipulation *in vitro*, 21–22
linear baculovirus DNA, 21
selection within bacterial host, 21
recombinant construction, 315–317
structure and replication, 19–20
transfer vectors, 22
for Bac-to-Bac system, 28
for BaculoDirect, 28
with circular and linear virus genomes, 22, 28
commercially available, 23–27
vectors, 243–244
AcMNPV molecular biology, 244
recombinant, 244–245
baculovirus expression vector system (BEVS), 605
baculovirus kinetics, 33, 34–35
asynchronous infection model, 42
attachment, internalization, and infection, 42–43
mass balances, 44
population balance, 48
solving, 44–45
usage, 45–47
cell yield, 35–36
history and challenge, 33–34
synchronous infection model, 36–37
modeling of infection cycle, 37–42
noninfected cell growth, 37
qualitative aspects of infection cycle, 37
baffles, 801, 998, 1003, 1014, 1035–1036, 1053, 1110, 1123–1124, 1221, 1224
split, 931–932
balanced growth, 354

balloon-type bubble bioreactor (BTBB), 1658–1659
ball valves, 1126, 1612
barrier to entry process, 1685, 1686, 1687
basal promoter, 253
basic quantity, 760
basiliximab, 636
batch culture, 1249
batch culture kinetics
  experimental data, 85–86
  model simulation comparison with experimental data, 87–88
  unstructured kinetic models, 86–87
batch/fed-batch culture, 11–13
  versus continuous/perfusion operations, 1235–1236
batch sterilization, 1113, 1114
Bayesian approaches, 1487–1488
BayShake, 1589
bead injection, 1502
Beer's law, 409
Beer–Lambert's law, use of, 380
Belgian Co-ordinated Collections of Microorganisms (BCCM™), 147, 148
Bellco Glass Inc, 720
Bernoulli force, 1006
betabaculoviruses, 19
β-galactosidase, 39
Beta vulgaris, 1652
Betula verrucosa, 565
bevel seat fittings, 1616
Bexxar® (tositumomab-I131), 659
bicarbonate buffers, 427
bifunctional antibodies, 647
Bikerman method, 1684
bimodal mesoporous silica spheres (BMS), 1162
binding, significance of, 43
Bingham model, 1363
bioactive proteins and polymers, 1753–1756
bioaffinity immobilization, 1205–1206
  enzyme adsorption on anti-enzyme antibodies, 1206
  glycosylated adsorption on immobilized lectins, 1206
  recombinant protein chimeras immobilization, 1206
biocatalysis, 1162, 1165–1166
  case studies, 1166–1173
biocatalyst, 1156, 1669
  membrane reactors, 829–831
  stability, 828
biochemical engineering, 1671
biochemical oxygen demand (BOD), 1017, 1020, 1287
BioChem Technology, USA (FluoroMeasure), 1513
bioencapsulation, 1069
BioFence, 1333
biofilms, 367–368, 1073
  characteristics, 1022–1023
  diffusion in, 1078–1079
  reactors, 832
biofilm airlift suspension reactors (BASRS), 918, 919, 940
biofilters, 982, 991
bioflocs, diffusion in, 1081–1082
biofuels, photobioreactors for, 1337
  GreenFuel Technologies Corp. (GFT) (Massachusetts, USA), 1337–1338
  Valcent Products, Inc. (Vancouver, Canada), 1338–1339
biogenic fluorophors, 1516
biohazards, 49–50
bioinformatics, 134
  resources, for glycans analysis and assignment, 506
biological indicator evaluation resistometer (BIER vessel), 1621
biological mutagens, 221
biological resource centers (BRCS), 131
  and anticipated income streams, 134
  culture collection funding, 134–135
  and existing income streams, 133–134
  operation, 135
    biological resource management and laws, 137–140
    holding preservation, 135
  quality management, 141–143
  services, 143–145
    Asian Consortium for the Conservation and Sustainable Use of Microbial Resources, 146
    European Culture Collection Curators Organisation, 147
    Microbial Resource Centres (MIRCEN), 147
    national federations and affiliations, 147–148
    organization and information resources, 145
    WFCC, 145–146
  sustainability, 133
  transition towards, 131–133
bioluminescence, 1734
  assay, 98
biomass, 1478–1480
  concentration influence, 1366–1367
  estimation, 1548–1549
  phototrophic, 955
biomass productivity, 383–385
biomedical applications, 839–841
biominiaturization, of bioreactors, 639, 669–670, 687, 689
  bubble column reactors, 689, 691–692
  convective mixing methods, 692
  microfabricated reactors, 671–672
  monitoring tools, 670
  shaken systems, 672
    multi-well plates, 677, 680–683
    roller bottles, 685
    shake flasks, 672–677
    tubes, 683, 685
  static systems
    T flasks, 670–671
  stirred systems
    cuvette, 686
    plate type, 686–687
    spinner flasks, 685–686
biomolecules immobilization, mesoporous materials for, 1150
biopanning, 641
biopharmaceuticals, 106
biopolymers, 938–939, 1184–1185
bioprocess analyzers, 1480
bioprocess and fermentation monitoring, 1471–1472
  basic estimation models
    data-driven models, 1485–1488
    first principle models, 1488–1489
  biomass, 1478–1480
  carbon dioxide, 1477
  chromatography and recovery operations, 1482–1484
  data technologies and artificial intelligence, 1484–1485
  DNA microarrays, 1480–1482
  in situ process monitoring using spectrometry, 1480
  liquids and gas flow measurement and control, 1478
  monitoring methods, 1473
    in situ and in-line monitoring, 1474
    off-line monitoring, 1474
    online monitoring, 1474
  osmolality, 1475–1476
  oxygen, 1476–1477
  pH measurement, 1474
  pressure, 1475
  process indicators and product monitoring, 1480
  redox potential, 1475
  sensors and monitoring aspects, 1472
    cleaning aspects and sterility, 1472–1473
    linearity, sensitivity, and specificity, 1473
    measurement frequency and costs, 1472
    reliability, accuracy, and reproducibility, 1473
    response time, 1473
    use and maintenance ease, 1472
    validation and implementation ease, 1472

bioprocess and fermentation monitoring, (*continued*)
softsensors, 1485
temperature, 1475
viscosity, 1475
weight and liquid levels, 1477–1478
BioProcess Container (BPC®), 1240
bioprocess container systems (BPCS), 1588
bioprocesses, 979
biopolymers, 938–939
drugs, 938
food additives, 939
heavy metals removal, 939
hydrocarbons in groundwater, 939
lignocellulosic wastes exploitation, 939
waste gas treatment, 939
wastewater treatment, 940–942
Bioprodukte Prof. Steinberg GmbH (BPS), 1339
bioreactor operations, 1595–1596
charging, 1623
fluid transfers, 1623–1626
foam/tangential inlets, 1626
instrumentation checks, 1627–1629
pH priming, 1627
sterile connections and disconnections, 1626–1627
volume control, 1626
cleaning, 1596–1601
instrumentation, 1607–1612
steam-in-place (SIP), 1601–1607
culture initiation
cell inoculum transfer, 1629
control culture set up, 1631
initial mixing and planting conditions, 1629–1630
initial sampling, 1630–1631
harvesting, 1631–1632
gravity, 1632
pump, 1632
sterile air overpressure, 1632
sterilization, 1616
monitoring and control, 1621–1622
principles, 1617–1621
theory, 1616–1617
valve maintenance and o-rings and gaskets change, 1612–1614
connections to receive charging fluids, 1615–1616
bioreactor scale-down, 847–849
application, 852–853
studies in cell culture, 853–855
studies in microbial fermentations, 855
approach, 849
experimental configurations, 855–856
dissolved oxygen and carbon dioxide gradients simulation, 856–858
optimization and modeling, 851–852
regime analysis, 849–851
scale-down approach, 849
simulation, 851
simultaneous environmental gradients simulation, 859
substrate and pH gradients simulation, 858–859
bioreactor scale-up, 863–864
aspect ratio, homogeneity, and gradients
airlift and bubble column bioreactors, 868–871
disposable reactors, 867–868
heterogeneous bioreactors, 871–873
stirred tanks, 865–867
heating and cooling, 873–874
heat transfer, 874–880
practical cases, 880–881
BioReal, Inc., (USA), 1339
bioscrubbers, 983
bioseparations and cellular assays, 1503
BioSep system (AppliSens), 1007
BIOSTAT®, 305
BIOSTAT CultiBag RM series (Sartorius Stedim), 1591
biosurfactants, 1680
Biotechna Ltd., 1333
biotechnological processes scale-up, 759
dimension analysis, 759–760
advantages, 772
applicability area, 772
basic and derived quantities and dimensional constants, 760
dimensional system, 760
example, 761–762
fundamental principle, 759
heat transfer process treatment, 779–782
mass transfer process treatment, 782–785
physical content dimensional homogeneity, 761
physical quantity, 760
variable physical properties treatment, 773–779
fundamentals
model experiments and scale-up in process point, 764–765
theory of models, 764
pi
determination by matrix calculation, 762–764
theorem, 762
procedures to establish relevance list
acceleration due to gravity, 765–766
examples, 766–767, 768–771
intermediate quantities, 767–768
material systems of unknown properties, 770
scale-up experimental methods, 772–773
biotechnology, fluidized bed reactors, 964
Biotechnology Solution, 1005
Biot number, 1086
biotransformation and process optimization, 1665
examples, 1670
overcoming product inhibition by CSTR cascade, 1673–1674
overcoming product inhibition by product extraction, 1671–1673
overcoming thermodynamic equilibrium by side-product removal, 1674–1676
product inhibition, 1670–1671
reactor classification, 1666
kinetics, 1668–1669
mass balances, 1666–1668
step by step process development, 1669–1670
whole cells and isolated enzymes, 1665–1666
biotransformations, 828
biotrickling filters, 983
BioView® sensor (DELTA, Denmark), 1518–1519
BioWAVE®, 305
birefringence, 445
bisbenzimide, 476
bispecific antibodies, 647, 657–659
bistat, 364
BK virus, 224, 231
black box model, 1087
Blasius equation, 386, 389
blue–white selection, 217
“Blutserumtherapie”, 646
BM-Cyclin, 483
Bottleneck concept, 351–352
bottom spray coating, 1191
bottom-up approach, 587
boundary layer theory, 1086
bovine papillomavirus (BPV), 224, 231–232
bovine polyomavirus (BPyV), 109
bovine spongiform encephalopathy (BSE), 50, 420
bovine viral contaminants, tests for, 118–119
bovine viral diarrhoea virus (BVDV), 109, 118
Bowie–Dick Test, 1766
Bradyrhizobium, 416
Brevibacillus brevis, 165
bridging-stretching mechanism, 1686
bright-field microscopy, 441–442
bromodeoxyuridine (BrdU), 77, 473

broth procedures, 121, 155, 156. *See also individual entries*
broth rheology, 1109–1110
  effects on transport processes, 1105–1106
bubble-associated damage, 1744–1748
bubble bursting, 387
bubble burst phenomena, 1229
bubble coalescence, 1141, 1278
  unknown numbers for, 784
bubble-column bioreactor (BCB), 1658
bubble columns, 374–375, 766, 1139, 1294, 1316
  and airlift, 868–871, 1720–1722
  bioreactors, 689, 691–692, 696
bubble free environments, shear effects in, 1739–1740
bubble-gasified reactors, 983
bubble point test, 1770
bubble size, 1138, 1141
  and interfacial area, 914
bubbling apparatus, 1684
Budapest Treaty, 145, 147
budded virus (BV), 20
buffers, 427
  natural buffering agents, 427–428
  synthetic buffers, 428
bulk aeration, 783, 784–785
bulk mixing, 1109–1110
bulk transport phenomena modeling and solid state fermentation
  bioreactors, 1399–1403
  macroscopic transport phenomena
    packed-bed bioreactors, 1405–1406
    rotating-drum bioreactors, 1407–1409
    tray bioreactors, 1403–1405
  subsystem recognition within bioreactors, 1399
Buna-N material, 1613
Bunsen, working with, 55
bursting force, 1742
butyrate, 521

caffeine, 1651
calcium phosphate, 234
calcium supply, in plant culture, 750
callus cultures and cell suspensions, 754–756
Campath®(alemtuzumab), 659
Candida antarctica, 1674
Candida tropicalis, 1193
capacitance, 1478
  sensors, 1478, 1611, 1612
capillary electrophoresis, 504
  direct UV detection, following, 504
  indirect UV detection following, 504
capillary inlet, 1571
capping, 52, 256–257
capromab pendetide/ProstaScint™, 1640
capsules, 1183, 1186
  biocompatibility, 1184
carbon, 415
  and energy sources, 425–426
  reduction degree, 334
  source, for plant culture, 751
carbon dioxide accumulation and removal, 797–798
carbon dioxide chemical absorption, 1265
carbon dioxide evolution rates (CERs), 321
carbon dioxide gas (CO_2), 415
carbon dioxide production rate (CPR), 1476, 1485, 1486
carbon dioxide transfer rate (CTR), 673
carbon nanocage, 1152
Carbopol, 1349
Carboseed™, 716
carboxy-epoxy support, 1213
Cardizem®, 838
κ-carrageenan, 1186
carrier fixed enzymes, characterization of, 964
carrier proteins, 552
Casson model, 1363
CASY particle counter, 1526
catabolic substrates, 333
catalytic constant, 343
catechol bio-oxidation, 1310
Categorisation of Biological Agents According to Hazard and Categories of Containment, 1778
Catharanthus roseus, 1053, 1059, 1649, 1735
cathepsin, 20, 28
Cedex, 1525
  HiRes systems, 1525
Cedex Bio (Roche Diagnostics GmbH Germany), 1480
cell-based gene transfer procedures advantages, 286–287
cell-containing matrices, diffusion in, 1073
  capillary models, 1074
  empirical models, 1074
  exclusion model, 1073
  experimental considerations, 1074
  model for suspended impermeable spheres, 1073
  model for suspended permeable spheres, 1074
CellCube, 1250
cell cultures, bioreactors for, 1638
  fluidized-bed bioreactors, 1641–1642
  membrane bioreactors, 1639–1640
  packed-bed bioreactors, 1640–1641
  pneumatically agitated bioreactors, 1639
  STRs, 1638–1639
  wave bioreactors, 1642
cell cycle, 71
  external influence, 76–77
  gap phases, 73–74, 76
  in biotechnology
    analysis as proliferation predictor, 81
    apoptosis, 81–82
    cultural proliferation and growth, 79–80
    production in relation to cell cycle phase, 80–81
    susceptibility to hydrodynamic damage, 81
  methods
    DNA content measurement, 78
    flow cytometry, 78
    labeled nucleotide uptake in S phase, 77
    mitotic index, 77
  mitosis, 75
  overview, 71–73
  synthesis phase, 74
cell damage, 1720
  due to bubbles in ALRs, 910
  mechanisms, 807–809
  quantification, 809–811
cell density
  automated cell density examination systems, 1525
  CASY particle counter, 1526
  Coulter particle counter, 1525
  determination by cell staining, 1525
cell entrapment, 1237
cell expansion
  for adherent cell cultures, 300–301
  in seed bioreactors, 301
    batch processes, 301
    perfusion process, 301–302
    process parameters, 302–303
  for suspension cell cultures, 299
    agitated cultures, 299
    processed parameters, 299–300
    static cultures, 299
cell fragility, 1730
cell growth, assessing, 756. See also protein expression kinetics and cell growth
celligen fermenter, 1253
CelliGen™, 726
cell immobilization , 1069, 1179–1180
  beneficial characteristics and drawbacks, 1070
  biomaterials, 1184–1185
    alginate, 1185–1186
    κ-carrageenan, 1186
    chitosan, 1186
    collagen and gelatin, 1187
    hyaluronic acid, 1187

cell immobilization (*continued*)
poly(ethylene oxide) and poly(ethylene glycol), 1188
poly(glycolide) and poly(lactide), 1188
polyurethane (PU) foam, 1188
polyvinyl alcohol (PVA), 1187–1188
proteins, 1187
starches, 1187
cell containment behind barriers, 1182
cell flocculation, 1182
compression coating, 1192
effects, 1193
entrapment within porous matrix, 1181–1182
external mass transport, 1085–1087
gel-particle techniques, 1188–1189
internal mass transport, 1069–1070
diffusion coefficient measurement methods, 1071–1073
diffusion coefficients, 1070–1071, 1078
diffusion in biofilms, 1078–1079
diffusion in bioflocs, 1081–1082
diffusion in cell-containing matrices, 1073–1075
diffusion in gels, 1075–1078
diffusion in mammalian cell aggregates, 1082
diffusion in microcapsules, 1082–1083
internal diffusion, 1071
internal mass transfer by convection, 1084–1085
microencapsulation, 1182–1184
phase separation (coacervation), 1192–1193
reaction and diffusion, 1087
intrinsic kinetics, 1087–1088
mathematical modeling, 1088–1093
reactor design, 1193–1196
requirements, 1184
on solid carrier surfaces, 1180–1181
spray and freeze drying, 1191–1192
spray chilling, 1192
spray coating, 1189–1191
CELLine systems, 1590
cell-lift impellers, 1050–1051, 1053
cell lines, in monoclonal antibody production, 733
mammalian cell lines, properties of, 737, 739–742
baby hamster kidney, 742
cell line engineering, 739
Chinese hamster ovary (CHO), 740–741
human cell lines, 741–742
hybridomas, 741
mammalian cell expression vectors, 737–738
mouse myeloma, 741
transfection, selection, and screening methods, 738–739
productivity, 736–737
product quality, 735–736
antibody dissociation, 736
clonal variability, 736
glycosylation, 735–736
proteolytic and glycolytic activity, 736
regulatory acceptability of, 733–734
safety, 734–735
cell-loaded membranes, in regenerative medicine, 841
cell lysis, maintaining solubility during, 569–570
CellMaker Plus, 1592
cell number, 756
cell phenotypes, genetic and epigenetic manipulation of, 623–624
cell quota, 333
cell suspension, 160
cultures, synchronization of, 757
CELL-tainer®, 305, 1591
cell transfection overview, 223–224
cellular cross-contamination, 49
cellular prion protein (PrP^c), 126, 127
cellular responses to osmolality perturbations, 599
cellular signaling, 600
cytoskeletal reorganization, 600
volume-regulatory responses, 599–600
cell viability, 521, 719
assessing, 756–757
cell viability measurement, 97
flow cytometry, 100–101
functional assays
bioluminescence assay, 98
permeability assays, 97
DNA gel electrophoresis for apoptosis analysis, 100
exclusion, 97
FISH methods, 98
FUN-1 assay, 99–100
inclusion, 98
membrane potential assay, 98–99
release, 98
RT-PCR methods, 99
tetrazolium assay, 98
physical methods
dielectrophoresis, 101–102
image analysis, 102
impedance measurement, 102
in situ microscopy, 101
cell wall changes, effects of, 1373
cell yield, 35–36, 46
Center for Biologics Evaluation and Research (CBER), 107, 121, 187, 1126, 1696
Center for Drug Evaluation and Research (CDER), 1696
Centers for Disease Control, 1102
centrifugal forces and separators, 1007
centrifugal freeze-drying, 136, 154–155
centrifugal impeller bioreactor (CIB), 1646–1647
centrifugal impellers, 1051
centrifugal pumps, 1727, 1731
Centritech centrifuge, 1007
cephalosporins, 1171
Cephalosporium spp., 415
Cephalotaxus harringtonia, 1654
Cerex (Cerex Corp., USA), 1611
Cervarix, 319
C-flex, 1613, 1615, 1623
chaperone proteins, 739
characteristic times, 849–850, 1033
charge-coupled device (CCD) images, 403
chemical absorption, of carbon dioxide, 1308–1309
chemical and enzyme reactions, microbial growth kinetics of, 340
basic kinetic equations derivation for enzymatic reactions, 342
cooperativity, 345–346
equilibrium approach, 342
general non-steady-state approach, 343–344
inhibitors and activators, 345
Michaelis–Menten equation kinetic parameters experimental determination, 344
order and molecularity, 340–341
order of reactions and numeric values of kinetic constants, 342
pH effects, 346–347
rate constant dimensions, 341
reaction dynamics, 341
reaction half-time, 341
reversible enzymatic reactions, 344–345
steady-state approximation, 342–343
temperature effects, 347
chemical defoamer action modes, 1685–1686
chemically induced dimerization (CID), 256, 260, 261
chemical oxygen demand (COD), 1019
chemical transfection techniques, 233
chemioselective hydrolysis, 1202–1203
chemolithotrophic organisms, 414
chemometrics for 2D spectra evaluation, 1516–1518
chemoorganotrophs, 414

chemostat, 13, 89, 335, 340, 351, 364, 955, 959, 961, 1654
  continuous, 1235
  culture physiological state, 355–356
  non-steady state culture, 353
  steady-state culture, 353
  synthetic chemostat model (SCM), 356–358
Chenopodium rubrum, 1734
chimeric and humanized antibodies, 640–641
Chinese hamster ovary (CHO) lines, 9, 12, 91–92, 109, 182, 183, 184, 188, 191, 297, 307, 496, 509, 515, 582, 584, 618, 719, 725, 727, 728, 739, 740–741
Chinese hamster ovary (CHO) lines, 798, 809, 850, 867, 1221, 1233, 1476, 1548, 1587, 1592, 1635, 1650, 1653, 1654, 1655, 1743
chitin, 1186
chitinase, 20, 28
chitosan, 1186
Chlamydomonas reinhardii, 1733, 1734
chloramphenicol, 169
Chlorella pyrenoidosa, 1733
Chlorella vulgaris, 1336, 1340, 1732, 1733
Chlorococcum littorale, 1336
chloroperoxidase (CPO), 1156, 1161, 1169, 1170
chloroquine, 235
cholesterol, 1534
cholesteryl esters, 1534
choline chloride, 583
chromatin, 263
chromatographic profiling, 501
  anion exchange chromatography, 501–502
  frontal affinity chromatography (FAC), 504
  hydrophilic-interaction liquid chromatography, 502
  multidimensional liquid chromatography, 502–503
  reversed-phase chromatography, 502
chymotrypsin, 1166–1167
Cimzia®(certolizumab pegol), 659
Cinchona robusta, 1735, 1736
Circe Biomedical Inc., 840
circulation time, 848–849, 858, 869
  effects, 855
Clarinex®, 838
classical dynamic methods and OTR, 1310–1311
cleaning-in-place (CIP), 1115, 1121, 1125, 1132, 1472, 1595, 1596–1612, 1615, 1700, 1702
  clamp-type joints, 1599
  development, fundamental elements, 1598
  instrumentation, 1607–1609
    biomass probes, 1611
    DOT, 1609–1610
    flow-rate sensors, 1611
    liquid level, 1612
    nutrient/metabolite sensing, 1611
    pCO_2, 1610–1611
    pH, 1609
    pressure, 1611–1612
    temperature probes, 1610
  reagents composition, in large-scale cell culture equipment cleaning, 1598
  simplified piping diagram, 1133
  steam-in-place (SIP), 1601–1607
clean mutations, 273
clean steam, 1619, 1702
Clean Water Act (CWA), 842
clinical analyzers, 1539–1540
clinically approved antibody products, 659
clonal selection, 645
Clostridium acetobutylicum, 705
Clostridium aminovalericum, 415
Clostridium butylicum, 705
clothing, 52
clumps, 1353, 1354
CMP-*N*-acetylneuraminic acids (NANA), 183
CMP-*N*-glycolylneuraminic acid (NGNA), 183, 188
CNBr-Sepharose™, 1208
CO_2 sparking, 415
coacervation, 1192–1193
coaggregation of enzymes, acting in tandem, 1211
coalescence phenomenon, 1681
coaxial air flow technique, 1188
coaxial catheter, 1379
co-condensation, 1160
Code of Federal Regulations (CFR), US, 118, 119, 123
codon adaptation index (CAI), 172
codon choice, 258
codon usage, of recombinant genes, 172–173
Coffea Arabica, 1651
coils and internal cooling surfaces, 1125
coimmobilization process, 1167–1168
collagen, 1187
collision induced dissociation (CID), 498
colony-forming units (CFU), 399
Colwellia psychroerythrus, 422
commercial freeze-dryer, 155
commercial production, 1635
  animal cell culture, 1635–1636
  bioreactor design
    fluid mixing, 1647–1648
    fundamental design principles, 1642–1643
    oxygen supply, 1643–1645
    shear force, 1645–1647
  cell cultures, bioreactors for, 1638
    fluidized-bed bioreactors, 1641–1642
    membrane bioreactors, 1639–1640
    packed-bed bioreactors, 1640–1641
    pneumatically agitated bioreactors, 1639
    STRs, 1638–1639
    wave bioreactors, 1642
  plant cell culture, 1636–1638
  process operations, 1648
    fluid mixing, 1649
    light irradiation, 1651–1652
    oxygen and mass transfer, 1648–1649
    pH, 1650–1651
    process monitoring and control, 1655–1656
    strategy, 1652–1655
    temperature, 1649–1650
  process scale-up, 1656–1657
    animal cell culture scale-up, 1657–1658
    plant cell culture scale-up, 1658–1659
commercial viscometers and rheometers, 1374
Committee for Proprietary Medicinal Products (CPMP), 107
Common Access to Biological Resources and Information (CABRI), 141, 147, 148
complementary lines, 238
component freeze-dryer, 155
composite particles and cell aggregates, 1750–1753
compression coating, 1192
computational fluid dynamics (CFD), 368
computational fluid dynamics (CFD), 852, 867, 908, 915, 923–925, 938, 1593
concentration polarization, 826, 830, 1293
condenser, 439
conditional gene silencing, 278
conductivity, of foam, 1684
conductivity probes, 1144
confocal laser microscopy, 1078
confocal microscopy, 451–452
Congo Red, 97
conical settlers, 1003
conserved substrates. See anabolic substrates
constitutive promoters, 547–548
containment, 1102–1103, 1133–1135, 1253
  cell, behind barriers, 1182
  environmental protection, 1704–1705

containment (*continued*)
personnel protection, 1705
product protection, 1704
contamination detection, in animal cell culture, 105
bacteria and fungi, 123
bovine viral contaminants, tests for, 118–119
endotoxin detection, 124
historical perspectives, 105–106
manufacturing and safety testing standards, 108
mycoplasmal detection, 120–121
agar and broth procedures, 121
enhanced cell culture procedure, 121
indicator cell culture procedure, 121
using Gen-Probe Inc., 121–123
oxygen uptake rate, 123–124
porcine viral contaminants, tests for, 119–120
prions detection, 126
in vivo assays, 127
in vitro assays, 127
regulatory issues, 106–108
statistical analysis, 124
minimum detectable level, 124–125
virus quantitation by $TCID_{50}$, 125–126
viral contaminants detection in cell lines, 109–110
in vitro assays, 115–117
polymerase chain reaction (PCR), 117–118
retroviral detection, 110–115
viral contaminants, examples of, 108–109
continuous and semicontinuous cultures, 1653
continuous cell culture kinetics
cell cycle models, 91–92
experimental data, 88–90
segregated models, 92
structured kinetic models, 90–91
continuous culture of plant cells, 955–956
application, 960–961
assumptions and pitfalls, 956–957
mathematical description, 959–960
practical setup, 957–959
continuous culture systems, 13–14
continuous fermentation, 205–206
continuous flow analysis (CFA), 1493
continuous-flow culture, 1249
continuous labeling, 77
continuously operated stirred tank reactor (CSTR), 827, 1016, 1603, 1666, 1673–1674, 1667, 1669, 1673
continuous-perfusion culture, 1249
continuous stirred-tank reactor (CSTR), 325
Contois equation, 353
contract manufacturing organizations (CMOs), 1695
control algorithms, 1415
controlled cell biosynthesis, 351
Control of Substances Hazardous to Health (COSHH), 1778
control-volume method, numerical, 1092
convection, 1070, 1139, 1667
cooling, 1405
internal mass transfer, 1084–1085
intraparticle, 1071, 1085
convective flushing, 101
convective mixing methods, 692
conventional SEMs (CSEM), 459
Convention on Biological Diversity (CBD), 139
Coptis japonica, 1652
correlations, utilization of, 1485
Corynebacterium glutamicum, 340, 1753
cosuppression, 266
cotransformation, 227
Couette design, 1348
Couette viscometer, 1736
Coulomb interactions, 1155
Coulter particle counter, 1525
Coulter™, 321
counterdiffusion, 1074
covalent binding, 1156
covalent immobilization, 1206–1207
activated supports to react with enzyme surface amino groups, 1207–1208
agarose beads enzyme immobilization activated with cyanogens bromide, 1208
aminated supports enzyme immobilization using glutaraldehyde, 1208–1209
through amino groups on protein surface, 1207
commercial supports containing epoxy groups high concentration, 1209
Creutzfeldt–Jakob disease (CJD), 126
critical dilution rate, 351
critical gas superficial velocity, 1683
critical micellar concentration (CMC), 1680
critical quality attributes (CQAs), 1543, 1545, 1552, 1562
process parameter monitoring in lieu of, 1552
cross-flow filtration, 1631–1632
cross-flow microfiltration, 839
crossflow velocity, 1293
cross-linking
chemical, 1156
cross-linked enzyme aggregates (CLEAs), 1159, 1210–1211
cross-linked enzyme crystals (CLECs), 1210, 1665
soluble enzyme with glutaraldehyde, 1209
crossover event, 270
cross reactivity, avoiding, 659
Cruciata glabra, 1193
cryopreservation, 135, 137, 157–158, 159, 160
CultiBag RM, 305
CultiBag STR, 305
cultured mammalian cells, effect of osmotic stress on, 600
culture media osmolality effect on hybridoma cell size, 602
on protein posttranslational modification, 602–603
on protein productivity, 600–601
hypoosmotic conditions effect on specific protein productivity, 603
osmoprotective compounds use, to mitigate inhibitory effects, 601–602
culture lamination, 1335
culture preservation, 153
of bacteria
long-term methods, 154–158
short-term culture, 153–154
of cell cultures
long-term preservation, 160
of fungi and yeast
long-term methods, 159–160
short-term preservation, 158–159
Cunninghamella echinulta, 705
Current Bioreactor (AmProtein), 1592
current good manufacturing practices (cGMP), 1103, 1253, 1638
cuvette, 686
cyanobacteria, 414
Cyanotech Corp., 1339
cyclic fed-batch culture (CFBC), 206
cyclin-dependent kinases (Cdks), 73
cylindrical intravacuolar structures (CIVS), 100
cysteine, 583, 594
cystic fibrosis transmembrane conductance regulator (CFTR), 283
cystine, 582–583, 594
cytochrome P450 monooxygenase (CYP1A1), 809
Cytodex™, 712
cytokinins, 752
Cytoline™, 716
cytomegalovirus (CMV), 30, 31
cytometer, 100
Cytopore™, 719
cytoskeleton, 805, 1738

daclizumab, 636
Damköhler number, 825
Darcy's equation, 1084
dark-field microscopy, 442–443
data-driven models, 1485–1488
Datura stramonium, 1734
Daucus carota, 1651, 1735
dead legs, 1601, 1602, 1607
dead zones, 1456
DEAE Sephadex™, 711–712
decimal reduction factor, 1113
decimal reduction time, 1616–1617
deep freeze, 156–157
deep shaft reactor, 1286
defective interfering particles (DIPs), 42, 324, 326
defoamer, 1685. See also antifoam agents
deglycosylation methods
  chemical methods, 498–499
  enzymatic methods, 499–500
DELFIA (dissociation enhanced lanthanide fluoroimmunoassay), 127
Del value, 1617
denaturation, 347
dendritic cells, 637
depth filters, 1768
derivatization, 504
derived quantity, 760
designed ankyrin repeat protein (DARPins), 642
design of experiment (DoE) principle, 586
Desulfovibrio sp., 426
Detachin™, 300
deterministic growth models, 347
detoxifiers, 423
dextran, 1737
DG44, 740
diabody, 657, 658
dialysis membrane, 1378
diameter number, dimensionless, 1270
diaphragm valves, 1126, 1129, 1612
dielectrophoresis, 101–102
diethylaminoethyl–dextran, 234–235
differential interference microscopy, 439, 446
differential interference optics, 284
diffusion, 1070, 1667
  coefficient measurement methods, 1071–1073
  coefficients, 1070–1071, 1078
  biofilms, 1078–1079
  bioflocs, 1081–1082
  cell-containing matrices, 1073–1075
  gels, 1075–1078
  mammalian cell aggregates, 1082
  microcapsules, 1082–1083
  internal, 1071
  and reaction, 1087
    intrinsic kinetics, 1087–1088
    mathematical modeling, 1088–1093
diffusion airflow (forward flow) test, 1770
diffusion coefficient and diffusivity, 1261–1262
diffusion effects, 354
diffusion limited attachment rate, 43
diffusion-limited regime, 825
diffusive retention, 56
Digitalis lanata, 1734
dihydrofolate reductase (DHFR) amplification, 607, 622
dimethyl sulfoxide (DMSO), 137, 156, 157, 298–299, 701
dinoflagellates, 1734
dioctylphthalate (DOP) test, 58
Dirac pulse, 1482
direct steam injection, 1114
discrete sampling, 1381
disease models, 283
disk turbines, 1038
Dispase™, 720
dispersion and dispersion coefficient, 1496
dispersion behavior, 1270–1271
  bubble columns and airlift devices, 1271
  stirred vessels, 1271
dispersion forces, 1155
disposable panels, 1336–1337
disposable reactors, 11, 867–868
disposable single-use bioreactors, 1239–1240
dissolved carbon dioxide concentration, 14–15
dissolved oxygen (DO), 792, 848, 852, 853, 854, 857, 858, 873, 1303, 1310, 1312, 1429, 1473, 1476, 1479, 1553, 1648–1649
  levels, 1021–1022
dissolved oxygen (DO) concentration, 14, 375, 389, 393, 521, 670, 675, 682, 686
  control, 203
  methanol control schemes, 204–205
dissolved oxygen tension (DOT), 321, 854, 1372–1373, 1608, 1609–1610, 1629, 1630, 1649
distributed control systems (DCS), 1705, 1706
disulfide-stabilized Fv fragments (dsFv), 656
D-mannose, 1673
DNA assays, 1505
DNA content measurement, 78
DNA-dependent protein kinase, 620–621
DNA fluorochrome staining, 476–477
DNA gel electrophoresis for apoptosis analysis, 100
DNA hybridization, as thermo-reversible immobilization protocol, 1215
DNA methylation
  and gene silencing, phenotypic change due to, 619
  and homology-dependent gene silencing, 265–266
DNA microarrays, 1480–1482
DNA transfer
  direct
    cell transfection overview, 223–224
    reporter genes in transfection analysis, 225
    selectable markers used in mammalian cell lines, 227–230
    stable transfection using episomally maintained vectors, 231–232
    stable transfection using nonreplicating DNA, 225, 227
    transgene expression maximization by gene amplification, 230–231
    transient transfection, 224–225
  introduced into animal cells, 215–216
domain swapping, 566
domestic wastewater, 940–941
dominant selectable markers, 227
donor nuclei source, 288–289
dosage effects, gene, 261
double minutes, 230
downstream processing, for virus elimination, 1774–1775
draft tube airlift reactor (DT-ALR), 890, 895, 900, 932, 939
  and external loop, 930–931
drag force, 970
drain, 1620–1621
drift flux model, 896, 903
Drosophila, 221, 223, 256, 263, 266, 278
Drosophila-SFM, 322
dry heat sterilization, 432–433
dry heat treatment, for virus elimination, 1776
dry weight, 406
  determination, 756
dual-particle liquid–solid circulating fluidized bed (DP-LSCFB), 965
duck hepatitis B virus (DHBV), 605
Dulbecco's Modified Eagle's Medium (DMEM), 111, 112, 189, 585
Dunaliella tertiolecta, 1336, 1733
DXB11, 740
dynamic desorption technique, 1310
dynamic gassing-in method, 1266–1267
dynamic matrix control (DMC), 1422–1423
dynamic parameters estimation (DPE), 1556

EBx™, 10
ecdysone, 256
Echinacea purpurea, 1658

economic coefficient, 332
edrecolomab, 636
effective diffusion coefficient, 976, 1078
effectiveness factor, 825, 1092–1093
effective viscosity, 778
effluent and solid circulation, 1022
effluent efficiency, 956
effluent removal system, 958
Elaprase™, 183, 508
electrochemical sensors, 1568
electrodialysis, 838
electronic enumeration, 403–404
electronic nose, 1568
electron impact ionization, 1571
electron microscopy, 114–115, 438, 457–459
electrophoresis, 505
electropolishing, 1121–1122, 1429, 1433, 1599
electroporation and laser transfection, 235
electrospray ionization (ESI), 500, 504
electrostatic extrusion, 1188
embryonic cells, ruminant, 287–288
embryonic germ cells (EGs), 280, 287
embryonic stem (ES) cells, 213, 274, 280
emulsions, 1688
  technique, 1189
enantioselective hydrolysis, 1202
encapsulation, 1156, 1162, 1179, 1183
endogeneous and constitutive viral promoters, 253
endogenous genes, factors that affect genetic stability of, 618
  molecular regulation of genetic stability, 618
    DNA-dependent protein kinase, 620–621
    p53 tumor suppressor gene, 619
    phenotypic change due to DNA methylation and gene silencing, 619
    poly(ADP-ribose) polymerase, 620
    proto-oncogenes and genomic instability, 619
    retinoblastoma tumor suppressor gene, 619
    telomeres and telomerase, 621
    tumor suppressor genes and proto-oncogenes, 618–619
  oncogenic transformation, aneuploidy, and genetic stability, 618
endogenous marker, 227
endogenous respiration, 335
endothelial cells (ECs), 805
endotoxin detection, 124
energetic growth yield, 334
energetic product yield, 334
energy, for microorganisms, 414
energy dissipation, 973
energy dissipation rates (EDRs), 677, 793, 802–804, 809, 810–811, 813, 1225, 1727–1728
  and shear rate, 909–911
engineering viscometers, 1361
enhancer, 253
enhancer probe vectors, 217
Entamoeba histolytica, 419
entering process, 1685, 1686
Enterobacter cloacae, 417
enthalpic effects
  Coulomb interactions, 1155
  Van der Waals interactions, 1155
Entomoplasma, 469
entrapment, within porous matrix, 1181–1182
entrapment vectors, 217, 219
entropic effects
  enzyme immobilization strategies, 1156
  hydrophobic interactions and solvation effects, 1155–1156
  protein molecular structure modifications, 1156
Environmental Protection Agency (EPA), U.S., 842, 1102
environmental SEM (ESEM), 459
environmental stress cracking, 1430
enzymatic master reaction, 351
enzymatic oxidation method, 1266
enzyme electrode-based biosensor, 1526
enzyme immobilization
  acting on insoluble substrates
    DNA hybridization as thermo-reversible immobilization protocol, 1215
    nonporous magnetic nanoparticles, 1215
    smart polymers, 1215
  adsorption of industrial enzymes on ionic exchangers, 1204
  bioaffinity immobilization, 1205–1206
    enzyme adsorption on anti-enzyme antibodies, 1206
    glycosylated adsorption on immobilized lectins, 1206
    recombinant protein chimeras immobilization, 1206
  as catalysts of industrial chemical processes, 1201–1202
  covalent immobilization, 1206–1207
    activated supports to react with enzyme surface amino groups, 1207–1208
    agarose beads enzyme immobilization activated with cyanogens bromide, 1208
    aminated supports enzyme immobilization using glutaraldehyde, 1208–1209
    through amino groups on protein surface, 1207
    commercial supports containing epoxy groups high concentration, 1209
  current industrial applications, 1202
    chemioselective hydrolysis, 1202–1203
    enantioselective hydrolysis, 1202
    isomerization, 1203
    red-ox processes, 1203
    transfer process, 1203
  enzyme properties improvement, 1211
    multimeric enzyme stabilization, 1214
    multipoint covalent immobilization, 1211–1214
  lipase selectivity modulation, 1214
    immobilized enzymes reactivation, 1214–1215
  protocols, 1203–1204
  selective lipase adsorption on hydrophobic supports, 1205
  strategies, 1156
  without supports, 1209
    cross-linked enzyme aggregates (CLEAs), 1210–1211
    cross-linked enzyme crystals (CLECs), 1210
    freeze-dried enzymes (FDEs), 1209
    soluble enzyme cross-linking with glutaraldehyde, 1209
enzyme linked immunoassays, 1539
enzyme methane monooxygenase (MMO), 980
EPDM, 1613
epitopes, 219, 513
  carbohydrate, 496
  non-human, 511
epizootic hemorrhagic disease virus (EHDV), 109
Epogen®, 305
Epstein–Barr virus (EBV), 107, 215, 232, 646
Erbitux®(cetuximab), 659
Erestat mixer (Yxzet, Dr. Karg GmbH, Affalterbach), 1437
Ergun equation, 873
Erlenmeyer shake flasks, 1272
erythrocytes, 1740–1742
erythropoietin (EPO), 300, 965, 1233, 1650
Escherichia coli, 72, 168, 183, 188, 216, 217, 254, 315, 316, 317, 350, 352, 401, 544, 552, 636, 642, 675, 686, 739, 852, 853, 859, 867, 1075, 1214, 1351, 1382, 1384, 1472, 1521, 1616, 1755
  alternative hosts, 563

growth, simulation model of, 355
in production of recombinant antibodies, 654
for production of simple recombinant proteins, 742
*lac*Z, 21, 244
maltose-binding protein (MBP), 565
neo gene, 241
estrogen receptor-based promoter (XVE), 1650, 1651
ethidium bromide (EB), 97
ethylene, in culture media, 752
ethylene-diaminetetraacetic acid (EDTA), 418, 720, 750
ethylene oxide, 1771
ethylene-tetrafluoroethylene (ETFE), 1000
Eubacterium coprostanoligenes, 421
Eupergit®, 1209
European Biological Resource Centre Network (EBRCN), 139, 141
European Culture Collection Curators Organisation, 147
European Culture Collection Organisation (ECCO), 133
European Medicines Agency (EMEA), 1778
evaporative cooling strategy, 1419–1420
EX-CELL®, 322
ExcellGene, 1592
exo-biopolymer fermentations, 1350–1351
exopolysaccharides (EPSs), 938
expanded bed adsorption (EBA), 965
exported proteins, quality control of, 553
Express Five®, 322
expression cloning, 214
expression vectors, 737
extended cell bank (ECB), 107
extended Kalman filters (EKFs), 1488
external loop, 895–898, 900
external loop inverse fluidized airlift reactor (EL-IARL), 932
external phase and emulsions, 1688
external sidestream membrane bioreactors, 827–831
external stress corrosion cracking (ESCC), 1430
external transfer and heterogeneous bioreaction, 1295–1296
extracapillary space, 1589
extracellular budded viruses (EBVs), 244
extracellular enveloped viruses, 251
extracellular matrix (ECM), 1184
extracellular product concentration, 39
extrachromosomal cell elements (ECE), 363
Extracorporeal Liver Assist Device (ELAD®), 841
extracts, 426
extrusion techniques, 1188–1189, 1190
eyepieces and imaging, 440–441

Fab fragments, 656
facility temperature, 1704
Faraday cup, 1572, 1573
fatty acids, 1534
fed-batch and perfusion cultures
model simulations, 92
monoclonal antibody production optimization, 92
suboptimal growth-associated production kinetics, 92–93
fed-batch culture, 1249, 1652–1653
versus continuous/perfusion operations, 1235–1236
fed-batch fermentation operational strategy, 203–204
fed-batch parallel shake flask system, 678
Federal Drug Administration
Advisory Committee for Pharmaceutical Science (ACPS), 1543
feed and bleed process, 301
fermentation fluids, rheological behavior of, 1347
exo-biopolymer fermentations, 1350–1351
mixing, 1356–1357
models, 1347–1348
mycelial fermentation, 1351–1352
dispersed forms, 1353–1356
morphological characterization, 1352–1353
pelleted forms, 1353
rheometry, 1348–1350
fermentation process and *Pichia* gene expression, 202
continuous fermentation, 205–206
cyclic fed-batch culture (CFBC), 206
dissolved oxygen control, 203
fed-batch fermentation operational strategy, 203–204
growth kinetics, 203
hypoxic fed-batch cultivation, 206
media and operational conditions, 202–203
methanol concentration monitoring methods, 204
methanol control schemes, 204–205
mixed substrates, 205
trace metals optimization, 206
fermenter/bioreactor design, 1101
design basis and considerations, 1104–1105
design philosophy, 1101–1102
mechanical design
agitation system, 1130–1131
basis, 1120–1121
cleaning systems, 1131–1133
containment, 1133–1135
piping and valving, 1125–1130
vessel design, 1121–1125
process requirements, 1105
broth rheology and effects on transport processes, 1105–1106
bulk mixing, 1109–1110
cleaning, 1115
gas holdup, foaming, and aerosol, 1110–1111
heat transfer, 1111–1112
oxygen transfer and aeration, 1106–1108
power, 1108–1109
preliminary design calculations, 1115–1120
sterilization, 1112–1115
safety and regulatory compliance, 1102
containment, 1102–1103
physical safety, 1103
product safety, 1103
scope, 1101
ferritic alloys, 1427
fertilizer production, 942
few polyhedral (FP), 326
FG10 assay, 111
Fibracel™, 716
Fick's law, 1070, 1071, 1090
Ficoll™, 715
filamentous microorganisms rheology, submerged culture, 1359
equipment for non-Newtonian broths measurement
commercial viscometers and rheometers, 1374
research viscometers and rheometers, 1373
measurements in fermentation broths, 1360–1362
operating parameter influence
on broth rheology, 1370–1371
on mycelial morphology, 1371–1373
rheological models, 1362–1363
Bingham model, 1363
Casson model, 1363
pseudoplastic model, 1363
viscosity
as engineering problem in, 1363–1365
as suspension characteristic function, 1365–1370
filament ratio, 1353
film theory, 1085–1086
filters, 1127–1128
filter sterilization, 426, 432
filtration , 1767–1768
depth, 1768
integrity testing, 1769–1770

filtration (*continued*)
membrane, 1768–1769
use, 1769
first principle models, 1488–1489
FISH (fluorescence in situ hybridization), 450
Fitoplancton Marino S.L. (Cadiz, Spain), 1332
fixed-bed reactors, 1255
flame ionization, 1568
flaming, 52
flanders filters, 58
*flash*BAC™, 21
flashing light effect, 382, 383
flat panel photobioreactors, 377–378
flat photobioreactors, 1334
alveolar panels, 1335–1336
critical evaluation, 1337
disposable panels, 1336–1337
glass plates, 1335
plastic plates, 1336
flavonoids, 1652
FlexMixer (GE Healthcare), 1589
flocculation, cell, 1182
flocs and agglomerates, 1752
flooding, 800
flotation process, 768–769
flow cytometry, 78, 100–101, 404, 410, 1479
flow injection analysis (FIA), 1381–1382, 1474, 1493–1494
bioanalytical applications, 1496–1498, 1503–1505
fundamentals, 1494
gradient techniques, 1495–1496
dispersion and dispersion coefficient, 1496
microfluidic devices, 1500–1503
for process analysis and monitoring, 1498–1499
and sequential injection analysis (SIA), 1499–1500
-LOV, 1503–1505
flow-rate sensors, 1611
floxing, 275
FluBlok, 319
fluid dynamics, 890
energy dissipation and shear rate, 909–911
flow configuration, 890–892
gas holdup, 892–901
gas recirculation, 901
and integrated kinetics, 920
liquid mixing, 904–908
liquid velocity, 901–904
mixing in gas phase, 908–909
fluidized bed reactors (FBR), 923, 1195, 1641–1642
history and introduction
background and development, 963–965
modeling and simulation, 975–976
praxis examples, 976–977
plant conception and operation, 965
design, 965–966
energy dissipation, 973
heat exchange, 973–974
hydrodynamic conditions, 968–969
operation, 966–968
oxygen supply, 973
range of operation velocities, 969–973
scale-up considerations, 975
heat exchange situation, 974–975
fluidized beds, 726, 727, 1284–1285, 1294–1295
fluid mixing, 1647–1648, 1649
fluid–solid slurries, 1294–1295
fluid transfers, 1623–1624
overpressure and sterile air, 1624–1625
sterilized pump, 1625
sterilizing filter, 1625–1626
fluorescein-conjugated methotrexate (F-MTX), 739
fluorescein diacetate (FDA), 97
fluorescence activated cell sorting, 188
fluorescence activated flow sorter, 811
fluorescence in situ hybridization, 479–480
fluorescence microscopy, 448–451
fluorescence return after photobleaching (FRAP), 1080–1081
fluorescence techniques, for bioprocess monitoring, 1511–1512
on-line 2D fluorescence spectroscopy, 1519–1521
on-line sensors, 1512
biogenic fluorophors, 1516
chemometrics for 2D spectra evaluation, 1516–1518
laboratory 2D spectrofluorometer and industrial process systems, 1518–1519
multiwavelength fluorescence, 1516
single wavelength fluorescence, 1512–1515
fluorescent/UV detection, 504
fluorescent-activated cell sorting (FACS), 739
fluorescent *in situ* hybridization (FISH), 98
fluorochromes, 100
fluorophore-assisted carbohydrate electrophoresis (FACE), 505
fluorophors, 1516
foam, 1679
biotechnological processes, 1691–1692
chemical methods for prevention, 1684–1685
chemical defoamer action modes, 1685–1686
formation trends, 1687–1688
polydimethylsiloxane, 1686–1687
detection and regulation in bioprocesses, 1684
evaluation methods of solution foaming properties, 1684
formation, 1138, 1679–1680
gas–liquid dispersion in reactor, 1681–1684
impact, 1690
on bioreactor performance and scale-up, 1691
on downstream processing operation, 1691
on microbial growth, 1690–1691
molecular mechanisms at interfaces, 1680–1681
physical methods for prevention and reduction, 1688
mechanical foam breakers, 1688–1690
foaming, 1062
focused beam-reflectance method (FBRM), 1655
foetal bovine serum (FBS), 29
folded sheet materials (FSM-16), 1148
folding, of proteins, 553
food additives, 939
food and beverage processing, 832–833
foot-and-mouth disease (FMD) virus, 9, 10
foot-and-mouth disease virus (FMDV), 1245
foreign DNA and transgenome structure, 261–262
formaldehyde, 1770–1771, 1773
Fotosintetica & Microbiologica S.r.l. (Florence, Italy), 1331
fouling, 1379, 1552
Fourier transform infrared spectroscopy (FTIR), 557
FP-25 gene, 29
freeze-dried enzymes (FDEs), 1209
freeze-drying, 135, 136–137, 154–156, 159, 1191–1192
freezing, ordinary, 154
freezing point depression, 1475
fresh/wet weight, determining, 756
frit sparger, 797
frontal affinity chromatography (FAC), 504
Froude number, 764, 766, 767, 773, 783, 968, 1268, 1316
fucosylation engineering, 515
Fujiwara bioreactors, Japanese, 1418

fumigation, 1770
ethylene oxide, 1771
formaldehyde, 1770–1771
hydrogen peroxide, 1771
FUN-1 assay, 99–100
functionalization, of mesoporous silica support, 1160–1161
Fundafom system (Chemap), 1689
fungal storage culture, 701
fungi and yeast, culture preservation of
long-term methods, 159–160
short-term preservation, 158–159
Fusarium spp., 415
fusion polypeptides and epitopes, 219
fusion proteins, 201
fusion transfection, 233
fusion vectors, 22, 28

Gamborg's B5 medium, formulations of, 749
gamma irradiation, 1771–1772, 1777
ganciclovir, 22
gas effect, on solid–liquid, 1458–1459
gaseous oxygen balance method, 1313–1314
gas flow and bulk mixing, 1110
gas flow rate, 1415
gas-holdup, 892–901, 1137–1138, 1264
determination
physical influences, 1141–1142
and foam, 1140–1141
for mass transfer, 1138–1139
measurement techniques, 1144
and mixing, 1139–1140
physic-chemical effects
antifoam agents, 1143
pure versus solutions, 1142
salt effects, 1142–1143
solutions of organics, 1142
stabilizing surfaces, 1143
gas lift advanced dissolution (GLAD), 934
gas lift reactors, 887, 1195
gas–liquid dispersing
characteristics, 1452–1454
in reactor, 1681–1684
gas–liquid hydrodynamics, 1062
particles effect on, 1457–1458
gas–liquid mass transfer, 1262–1263, 1271–1272
carbon dioxide chemical absorption, 1265
dynamic gassing-in method, 1266–1267
enzymatic oxidation method, 1266
hydrazine method, 1265
oxygen balance method, 1265
oxygen solubility, 1267
sulfite oxidation method, 1265
volumetric oxygen transfer coefficient, 1264
gas–liquid mass transfer characteristics, 1460–1461
particle effects, 1461–1464
gas–liquid oxygen transfer, 1059–1062
gas phase, mixing in, 908–909
gas recirculation, 901
gassing-out method, 673, 912
biological dynamic, 1312
gas–solid mass transfer, 1289
gas–solid system (GSS), 964
gas treatment, 979
bioreactor design, 983–984
biophase mixing and minimum effluent concentration, 990–991
gas-biophase mass transfer, 988–990
nutrient addition and start-up, 987–988
process analysis, 984–986
process design consequences, 986–987
scale-up, 991–992
bioreactor types, 981–982
biofilters, 982, 991
bioscrubbers, 983
biotrickling filters, 983
bubble-gasified reactors, 983
microorganisms and applications, 979–980
cometabolism, 980–981
electron acceptors, 981
electron donors, 980
gas vesicles, cyanobacterial, 796
Gateway®, 22
Gaussian velocity, 1726
gelatin, 1187
gel electrolyte probes, 1609
gel entrapment, mathematical modeling, 1088
dynamic modeling, 1090, 1091
pseudo-steady state modeling, 1088, 1089
steady state modeling, 1088, 1089
gellan, 429–430, 751, 1350
gelling agents, 428
agar, 429
agarose, 429
alginic acid and κ-carrageenan, 430
gellan gum, 429–430
for plant culture, 751
silica gel, 430
gel matrices, 1071
gel-particle techniques, 1188–1189
Gelrite, 429, 751
gels, diffusion in, 1075–1076
diffusing compound concentration influence, 1077–1078
gel type and concentration, 1076
pH influence, 1077
temperature influence, 1077
gel system, 1181
gemtuzumab, 636
gene conversion, 270
gene delivery vectors. See targeting vectors
gene-directed enzyme prodrug therapy (GDEPT), 282
gene function studies, 281–282
gene inhibition therapy, 270
gene knockout, 270
Genentech, 1245, 1635
gene regulation studies, 282–283
gene silencing, 271–272
conditional, 278
homology-dependent, and DNA methylation, 265–266
transient, with oligonucleotides, 277–278
using antisense RNA constructs, 276–277
using inhibitory proteins, 277
gene targeting, 215, 221, 270, 275, 282
genetic engineering, of glycosylation pathways, 515
bacteria, 520
insect cells, 517–518
mammalian cells, 515–517
plants, 518–519
yeast and filamentous fungi, 519–520
geneticin, 737
genetic stability, 618, 630–631
DNA-dependent protein kinase, 620–621
genotypic characterization and validation of, 627
gross structural evaluation of genes and transcripts, 628–629
sequence analysis of genes and transcripts encoding the product, 629–630
poly(ADP-ribose) polymerase, 620
telomeres and telomerase, 621
tumor suppressor genes and proto-oncogenes, 618–619
p53 tumor suppressor gene, 619
phenotypic change due to DNA methylation and gene silencing, 619
proto-oncogenes and genomic instability, 619
retinoblastoma tumor suppressor gene, 619
gene traps, 221
Gen-Probe Inc. and mycoplasmal detection, 121–123
gibberellins (GAs), 752
Glarea lozoyensis, 1355

glass bead culture, 1250
glass plates, 1335
glass probes, 1609
GlaxoSmithKline, 319
Global Biological Resource Centre Network (GBRCN), 131, 150
glucocerebrosidase (GCD), 519
glucosamine, 521, 590
glucose, 521, 1526–1527
glucosylphosphatidylinositol (GPI) anchors, 492
glutamic acid, 425
glutamine, 1527
glutamine synthetase (GS), 622, 737
glutaraldehyde, 1156, 1208–1209, 1773
glutathione (GSH), 583
glutathione-S-transferase (GST) fusion, 565
glycans analysis and characterization strategies
  capillary electrophoresis, 504
  chromatographic profiling, 501–504
  detection methods, 504–505
  electrophoresis, 505
  mass spectrometry, 500–501
  monosaccharide composition analysis, 506
  sequential enzymatic digestion, 505
  sialic acid analysis, 505–506
glycerol, 157, 701
glycerol batch phase (GBP), 203
GlycoFi technology, 519, 520
GlycoMod, 501
glycopeptides, LC–MS, 497
glycoproteins, problems with, 29–30
glycosylation, 317–318, 590, 610
glyoxyl-agarose, 1211–1213
Gompertz model, 1092
Gonyaulax polyedra, 1734
Good Laboratory Practice (GLP), 108, 1766, 1778
Good Manufacturing Practices (GMP), 1591, 1766, 1767, 1774, 1778
GP64 glycoprotein, 20
G proteins, 805
grafting, 1160
Graham's law, 1082
granuloviruses (GVs), 19
Grashof number, 1086, 1268
green fluorescent protein (GFP), 168, 171, 173, 321, 326, 451, 677, 680, 1655
GreenFuel Technologies Corp. (GFT) (Massachusetts, USA), 1337–1338, 1339
green wall panels, 1337
grit number, 1121
growth, definitions of, 399–400
growth-associated production kinetics, 89–90
growth factors, 76
growth rate, of fungi in submerged culture, 1372
growth rate constant, 401
growth stoichiometry and microbes
  biomass yield variation from conserved substrates, 338
  experimental determination of *m*, 335–337
  growth yield, 332–333
  macrostoichiometry, 331–332
  maintenance requirements and wasteful catabolism, 337
  microscopic approach, 338–340
  yield variation as dependent on chemical nature of organic substrates, 333–334
  yield variation from energy source and maintenance requirements, 334–335
GTP-Technology, 552
''guardian of the genome", 619
guided wave radar, 1478

Haake–Rotovisko rheometer, 1361
habituation, 756
Haematococcus pluvialis, 1335, 1732
Haemophilus influenzae, 418
Haemophtlus parainfluenzae, 422
Haldane's equation, analogue of, 354
Ham's Nutrient Mixtures, 585
harvesting and cell lysis, maintaining solubility during, 569–570
harvest valves, 1614
Haslea ostrearia, 1731, 1732
Hatta number, 1321
HAZOP (hazard operability), 1712
Heatex inserts, 1437, 1438
heating, ventilation, and airconditioning (HVAC), 1698, 1703–1704
heating and cooling, and bioreactor scale-up, 873–874
  heat transfer, 874–875
    evaporation, 878
    heat exchangers, 878–880
    inlet and outlet flows, 876
    metabolic activity, 875–876
    power input by agitation and sparging, 876–878
heat-shock proteins (HSPs), 605
heat transfer, 915–917
  dimensional analytical treatment of driving force and process target quantity, 779
  steady-state, in mixing vessels, 779–782
  heat loads, 1111
  rate, 1111–1112
heavy metals removal, 939
Hedström number, 779
HeLa cells, 186, 187
helical flow promoter (HFP), 929–930
helical photobioreactors, 1333–1334
helical ribbon impellers, 1049–1050, 1349
Helicoverpa armigera nuclear polyhedrosis virus (HaNPV), 34
Helicoverpa zea nuclear polyhedrosis virus (HzNPV), 34, 35
Heliothis virescens, 29
helper dependent vectors, 238
helper independent vectors, 237
hemadsorption, 117
hemolysis, 1741
Henry's law, 389–390, 984, 1263, 1292, 1305, 1577, 1578, 1579, 1610
HEPA filtration, 50, 56, 1703, 1770
  construction, 57–58
  efficiency, 57
  and hoods and cabinets, 58
  mechanism, 56–57
  microbial safety cabinets, 59–60
  specification, 68
  testing, 58
  unidirectional airflow cabinets, 58–59
HepatAssist™ liver support system, 840
HEPES buffer, 428
Herceptin®, 305, 659
herpes virus simplex virus type 1 (HSV-1), 22
herpes virus vectors, 245–246
  construction, 246
  molecular biology, 246
  for prolonged transgene expression in neurons, 246–247
  for transient expression in nonneuronal cells, 247
Herschel–Bulkley model, 1356
heterochromatin, 264
heterofunctional-epoxy supports, 1213
heterogeneous bioreactors, 871–872
  hollow fiber reactors, 872
  microcarriers, 873
  packed-bed reactors, 873
heterogeneous flow regime, 870
heterogeneous reactions, 1087
heterologous genes, stable integration of in animal cell genomes, 621–622
heterologous proteins, 213
heterologous protein secretion
  expression systems, 547
    target gene expression, 547–550
    vectors, 547
  via general export pathway in gram positive bacteria, 543–545
  in *Lactococcus lactis*, 545–547, 550
    precursor optimization, 551–552

protein targeting and translocation, 552–553
quality control of exported proteins, 553
heterotrophs, 415
HETP, 1482, 1484
hexagonal mesoporous silica (HMS) materials, 1148–1149
Hidrobiologica SA, 1340
hierarchically ordered mesocellular mesoporous silica materials (HMMS), 1159–1160
Higbie's penetration theory, 1320
high-cell-density bioreactors, 1254
hollow fiber bioreactors, 1254
microporous microcarriers, 1255
spin filters, 1254–1255
high cell density cultivations (HCDC), 1520
high density polyethylene (HDPE), 1019
High-Five™, 29, 243, 312, 320, 636
high performance liquid chromatography (HPLC), 1528, 1529, 1537, 1553
high pH-anion exchange chromatography (HPAEC), 501–502
carbohydrate fingerprints, 626
high throughput bioreactor (HTBR) system, 689, 693
Hill coefficient, 346
Hill plot, 346
HI mixers (Toray, Tokyo), 1437, 1443
histones, 738
Hitachi, Japan (Model F4500), 1518
hit-and-run strategy, 273
Hoffman modulation-contrast microscopy (HMCM), 439, 444, 446, 447
hollow fiber bioreactor, 1240–1241, 1254
hollow fiber bioreactor systems (HFBS), 1589, 1590
hollow fiber reactors, 872
homogeneous flow regime, 870
homogeneously staining regions (HSRs), 230
Hoogsteen pairing, 278
horseradish peroxidase (HRP), 1170
host cell selection effects, 507
mammalian expression systems, 507
hamster cell lines, 509–510
human cell lines, 508–509
mouse cell lines, 510–511
nonmammalian expression systems, 511
bacterial strains, 514–515
invertebrate cells, 511–512
plants, 512–513
yeast, 513–514
host strain, choice of, 562
coexpressing other proteins, 562–563
E. coli, alternative hosts to, 563
low protease strains and those with better redox characteristics, 562
strain choice for expression versus transformation, 562
Hudson Control Group, 591
human antibodies, production of, 640–641
chimeric and humanized antibodies, 640–641
from human hybridomas, 641
from phage antibody libraries, 641
human anti-mouse antibody (HAMA), 648
human cell lines, 741–742
human cells, gene expression in, 181, 187–188
cell culture, media, cultivation, and handling methods, 189–190
in cell culture products production in manufacturing, 183–184
clone selection methods, 188–189
future trends, 184
production parameters and methods, 190
recombinant human cell lines cultivation scale-up, 190–194
research, 181–183
safety and regulatory aspects, 184–186
vectors and gene transfer methods, 188
human cytomegalovirus (hCMV), 737
human diploid cell lines (HDCLs), 186
human embryonic kidney (HEK) 293 cell lines, 187, 188, 189, 508, 723, 741
human follicle stimulating hormone (hFSH), 1649
human monospecific antibodies, 646–647
human osteocalcin (hOC), 565
human recombinant antibodies, production cycle of, 648
Humaspect®(votumumab), 659
Humira®, 305, 659
humoral immune response, 638
hyaluronic acid, 1187
hybridoma technique, 10, 638, 741
bioreactor technology, 639–640
cell cultivation methods, 636–637
cell fusion strategies, 638–639
cell size, effect of culture medium osmolality on, 602
derived antibodies, 648
chimerization, 649
humanization, 649
in silico humanization, 649
induction of antibody responses, 638
large-scale production, 639–640
schematic description of, 638
Hybrid Organ GmbH Company, 840
hybrid transgene, 267
hybrid viral vectors, 252
HyClone, 189, 190
HyClone SFX-Insect™, 322
Hycolin, 1773
hydraulic loading rate (HLR), 1017, 1018
hydraulic retention time, 1017 (HRT), 965, 1016, 1017, 1019
hydrazine method, 1265
hydrazine oxidation, 1309
hydrocarbons in groundwater, 939
hydrodynamic focusing, 404
hydrofoils, 800
hydrogels, 1183–1184
hydrogen, 415–416
hydrogen-assisted cracking (HAC), 1430
Hydrogenophaga, 415
hydrogen peroxide, 1771
hydrolysis, 1169
hydrophilic-interaction liquid chromatography, 502
hydrophilic–lipophilic balance (HLB), 664
hydrophobic interactions and solvation effects, 1155–1156
hydrophobic solid particles, 1685, 1686
hydrostatic pressure, 1744
hyperosmolality effect on virus expression systems, 604
baculovirus expression vector system (BEVS), 605
sensitivity of animal virus replication to osmotic conditions, 605
hyperthermia, 605
cell growth, metabolism, and physiology, 606
heat-shock response, 605
recombinant protein production and quantity and quality, 606
viral vector production, 606
hypervariable regions, 645
hyphae, 1353, 1359
hypochlorite, 1773
hypothermia, 606
cell growth, metabolism, and physiology, 607
cold-shock response, 606
effect of low temperature, 610
recombinant protein production, 607–610
viral vector production, 610
hypoxic fed-batch cultivation, 206

iCellis™, 301
IgG antibodies, 735
illuminated surface productivity (ISP), 1341
illumination source, 439
image analysis, 102
ImmobaSil™, 726
immobilization , 1147. See also cell immobilization

immobilization (*continued*)
protein, on mesoporous silicas and carbons
adsorption on surfaces, 1155–1156
biocatalysis, 1162, 1165–1173
enzyme immobilization on ordered materials, 1157–1162
materials, 1147–1154
immobilized enzymes, 963
immobilized metal affinity chromatography (IMAC), 565
epoxy support, 1213
immortal cell lines, 186
immune system, cell types of, 637
immunofluorescence, 450
immunoglobulin, 646, 647
mRNA translation rates, effect of hyperosmolar stress on, 604
impedance measurement, 102
impeller collision severity (ICS), 1743
impeller pumping capacity, 848
impellers, 799–801, 865, 1035, 1058
anchors, 1049
axial flow, with draft tube, 1047
cell-lift, 1050–1051
centrifugal, 1051
comparative study of, 1054–1057
disk turbines, 1038
helical ribbon, 1049–1050
Intermig, 1047–1048
magnetic stirrers, 1052
membrane stirrers, 1051–1052
multiimpeller systems, 1109
paddles, 1048–1049
perforated disks, 1047
propellers, 1038, 1047
Rushton turbine, 1037–1038
size, 1110
spacing, 1110
spargers, 1052–1053
spin filters, 1052
spin stirrers, 1050
with STRs, 1639
types, 1110
viscometer, 1361
impeller selection, 1219
and free suspension culture, 1229–1230
impacting aspects, 1219–1220
implications
aeration, unaeration, and power input from agitator, 1227
heat transfer, 1227–1228
homogeneity, 1226–1227
microcarrier culture, 1228–1229
microcarrier culture, 1230
oxygen transfer considerations, 1220–1221
shear sensitivity to fluid dynamic stresses, 1221–1222
energy dissipation rates and cell cultures, 1225
high/low impellers and impeller tip speed, 1222–1223
Kolmogoroff eddy size concepts, 1223–1225
studies in configurations and comparison with cell strength, 1225–1226
incipient fluidization, 970, 971
inclined settlers, 1005
inclusion bodies, 742
formation of, 566
mutation to increase solubility, 567
role of proteolysis, 566–567
incubation temperature, 422
incubator, 51
indigenous and autochthonous species, 699
indole-3-acetic acid (IAA), 751
inducible promoters, 253–254, 548–550
induction forces, 1155
industrial biotranformations, examples of, 1667
industrial catalysts, enzymes as, 1201
industrial proteins, 1187
inertial impaction, 56
infection rate, 43, 44
infection velocity, 37, 40
infliximab, 636
infloxing, 278
Infors HT Sixfors parallel bioreactor system, 689
infrared absorption, 1568
Ingold probe, 1609
inhibitory effects, 354
inhibitory proteins and gene silencing, 277
initiator element, 253
initiator protein, 359
inlet air, relative humidity of, 1415
in-line buffer dilution technology, 1553
in-line double mechanical fermenter shaft seal, 1130
in-line laser turbidimeter (ASR Co. Ltd., Tokyo), 1611
in-line mixers, 1437
innate host defense, 637
inoculum expansion, 297
cell expansion
for adherent cell cultures, 300–301
in seed bioreactors, 301–303
for suspension cell cultures, 299–300
current trends
automation, 306–307
disposable systems, 305–306
time reduction, 307
impact of cell banks, 303
culture medium influence, 303–304
genetic stability of cell lines, 305
maintenance, 304–305
inoculum cell density and cell physiology, 303
technology transfer, 307–308
vial thaw, 298–299
inoculum preparation, 699
critical factors, 700
culture assessment, 703–704
culture storage
dessication, 700
freeze-drying, 700–701
freezing, 701
subculture, 700
development, 704–705
conundrum, 700
multiple growth cycles, 705–706
microbial ecology, 699–700
and seed transfer criteria, 706
stock culture, 701
generation, 702–703
significance, 701–702
and storage, 568
studies, 706–708
inorganic salts, 1531–1532
inositol, 583
INRA-Dijon bioreactor, 1418
insect cell–baculovirus expression system, 742–743
insect cell culture, 311
applications, 318–319
baculovirus gene expression, 314–315
cell lines, 311–312
large-scale processing, 319
batch production techniques, 323
bioreactors, 319–320
cell culture by-products, 322–323
cell culture processes, 319
cell damage during sparging, 321–322
continuous production systems, 324–325
fed-batch, perfusion, and semibatch/semicontinuous production, 323–324
larval production systems, 326–327
media formulation, 322
oxygen supply, 321
passage effects and mutant virus formation, 326
process monitoring techniques, 320–321
virus stocks, multiplicity of infection, and time of infection, 325–326
posttranslational processing, 317–318
glycosylation, 317–318
recombinant baculovirus construction, 315–317
viruses, 313–314

insertional mutagenesis and entrapment vectors, 221–223
insertion vectors, 238, 271
in situ fluorometry, 1521
in situ microscopy, 101, 1656
integral of viable cells (IVC), 86
integrated shear factor (ISF), 1742
integration effects, 264
integrative genetics, 167
integrins, 805
integrity testing, 1769–1770
Intellectual Property Rights (IPR), 144
interception mechanism, 56–57
interference-contrast microscopy, 446–447
intergranular corrosion (IGA), 1429
Intermig impellers, 11, 1047–1048
internal circulation reactors (ICRs), 918, 919
internal diffusion, 1071
internal effectiveness factor, 1093
internal loop, 893–895
internal mass transport and cell immobilization, 1069–1070
  diffusion
    biofilms, 1078–1079
    bioflocs, 1081–1082
    cell-containing matrices, 1073–1075
    coefficient measurement methods, 1071–1073
    coefficients, 1070–1071, 1078
    gels, 1075–1078
    internal, 1071
    mammalian cell aggregates, 1082
    microcapsules, 1082–1083
  transfer by convection, 1084–1085
internal phase and emulsions, 1688
internal ribosome entry site (IRES), 219, 250, 259
International Air Transport Association (IATA)
  Dangerous Goods Regulations (DGR), 140
International Committee for Harmonisation, 107
International Conference on Harmonization (ICH), 1543
International Depository Authorities (IDA), 145, 149
International Union of Biological Sciences (IUBS), 145
International Union of Microbiological Societies (IUMS), 145
intrabodies, 277
intracellular antibodies, 660
intracellular concentration, 39
intraparticle convection, 1071, 1085
intraparticle mass transfer, 1296
introns, 218, 250
  splicing, 257
invaders and allochthonous species, 699
inverse fluidized bed airlift reactor (IL-IALR), 932
inverse-growth-associated production kinetics
in vitro assays, 115–117, 127
Invitrogen Ltd., 22, 29, 189, 218, 322
in vitro immunization, 641–642
in vivo assays, 127
iododeoxyuridine (^{125}I-UDR), 98
ion channels, 805
ion-selective electrodes (ISEs), 1496
iron supply, in plant culture, 750
isoelectric focusing (IEF), 505
isoindoles, 1527
isopropyl-D-thiogalactopyranoside (IPTG) inducer, 561
isotropic turbulence, 810, 889, 915, 937, 1223, 1320, 1727–1729

jackets, 1124
Jet Cutter technology, 1188
jet fermenter, reciprocating, 1284
JRH, 189
Jurkat cells, 187

Kalman filter (KF), 1415
Kalman gain, 1488
Karber formula, 125
KDEL retention signals, 219
Kenics mixers (Ott Vertriebsgeselschaft, Leonberg), 1437, 1438, 1439, 1440, 1441, 1448
kidney, bioartificial, 840
Klebsiella aerogenes, 1512
knife-line attack (KLA), 1430
knockout mice, 282
Koch mixers, 1437, 1447
Köhler illumination, 438
Kolmogoroff eddy size concepts, 1223–1225
Kolmogoroff microscale of turbulence, 1690, 1752
Kolmogorov's mixing microscale, 810, 811
Komax mixers ((Long Beach, Calif.), 1437
Kozak consensus, 219, 258
Kozeny equation, 1084
Kr method, 1311
Kubota process, 842–843

Lab-on-a-Chips (LOC), 1502
Lab-on-Valve (LOV), 1493, 1500–1505
lactate, 1535–1536
  dehydrogenase, (LDH), 98, 1479, 1537, 1671, 1740
lactic acid bacteria (LAB), 543, 545, 550
Lactobacillus delbrueckii, 421
Lactococcus lactis, 543
  heterologous protein secretion in, 545–547, 550
    precursor optimization, 551–552
    protein targeting and translocation, 552–553
    quality control of exported proteins, 553
LAL test, 124
lamella settlers, 1005
L-amino acids, 418–419, 838
laser Doppler anemometry (LDA), 1224
laser Doppler velocimetry (LDV), 902
laser tweezers and scissors, 453
latency-associated transcripts (LATs), 246
Lauria Broth (LB), 1622
law of conservation for cell numbers, 42
layered plates, 405
L-drying, 135, 159
lectin affinity capture, 496–497
Legionella spp., 425
LEISSTCDA propeptide, 551–552
Lemna minor, 743
LentiKats® particles, 1187–1188
lepidopteran insect cell line, 743
Leptospira, 426
Leuconostoc mesenteroides, 550
leukocytes, 1740, 1741
light deflection techniques, 1552
light microscopy , 438
  basic concepts, microscope components and principles, 438
    condenser, 439
    eyepieces and imaging, 440–441
    illumination source, 439
    objective lens, 439–440
    stage, 439
  survey of the variety of light microscopes and cell biology usage, 441
    bright-field microscopy, 441–442
    confocal microscopy, 451–452
    dark-field microscopy, 442–443
    fluorescence microscopy, 448–451
    Hoffman modulation-contrast microscopy, 444
    interference-contrast microscopy, 446–447
    multiple oblique-illumination 3-D microscope, 445
    oblique or anaxial (asymmetrical) illumination, 444
    phase-contrast microscopy, 443–444
    polarizing microscopy, 445–446
    reflection-contrast microscopy (RCM), 447–448
    single sideband edge-enhancement microscopy, 444–445

light microscopy (*continued*)
two-photon and multiphoton microscopy, 452–453
light regime, 385
light scattering, 1356
lignocellulosic wastes exploitation, 939
limited dispersion, 1496
linear absorption model (LAM), 1076
Lineweaver–Burk equation, 823
lipase immobilization, 1167–1168
selectivity modulation, 1214
immobilized enzymes reactivation, 1214–1215
lipids, 421, 1534–1535
lipocalins, 642
lipofection, 236
lipoic acid, 584
liposomes, 235–236
liquefaction, 20
liquid–cell interactions, 805
liquid disinfectants, 1772
alcohol, 1773
formaldehyde and glutaraldehyde, 1773
hypochlorite, 1773
phenolics, 1773
liquid level effect, 899–901
liquid–liquid mass transfer, 1267–1268, 1287
liquid media stability and scalability, 594
liquid nitrogen, 135, 136, 137
liquid rheology effects, 898–899
liquid–solid system (LSS), 964
liquid velocity, 901, 1442–1443
liquid flow from energy balances, 902–904
measurement, 902
lithotrophic organisms, 414
liver, bioartificial, 840
live steam, 1619
livestock, transgenic, 284
local gas-holdup, 1137
local isotropic turbulence, 388–389
Locteron®, 513
locus control regions (LCRS), 268–269, 282
logistic equation, 350
long terminal repeat (LTR), 248, 249, 250, 264
lovastatin, 1353
low-vacuum conventional SEMs (LV-CSEM), 459
L-phenylalanine, 838
L-phenylalanine ammonia-lyase (PAL), 1652
Lucentis®(ranibizumab), 659
Luffa cylindrica, 1655
Luft analyzer, 1569
Luft capacitance sensor, 1570
lycophilization, 1556
process monitoring tools, 1557
lymphoblastoid cell lines (LCL), 639
LyoDriver, 1556
lyo-injury, 136
lyophilization. See freeze-drying
lysis, 1741
lytic infection, 246

macroheterogeneity, 490, 496, 590
macromolecule content, assessing, 756
Madin Darby canine kidney (MDCK) cells, 723, 724
Magellan Instruments, 1569
Magic Angle Spinning Nuclear Magnetic Resonance Spectroscopy (MAS NMR), 1152
magnesium supply, in plant culture, 750
magnetic analyzer, 1571–1572
magnetic coupling, 1035
magnetic resonance imaging, 1552
magnetic stirrers, 1052
Maillard reaction, 426
maltose-binding protein (MBP), 565
mammalian cell bioreactors, 1233
batch/fed-batch versus continuous/perfusion operations, 1235–1236
cell culture, 1237–1238
airlift bioreactor, 1239
bioreactor scale translation and intensification, 1242–1243
bioreactors for scale-down/high throughput operations, 1241–1242
disposable single-use bioreactors, 1239–1240
hollow fiber bioreactor, 1240–1241
stirred-tank bioreactors, 1238–1239
cell support for mixing vessels
aggregates, 1237
cell entrapment, 1237
macroporous microcarriers, 1236–1237
microcarriers, 1236
types, 1234–1235
mammalian cell culture reactors, scale-up, 1245–1246
for anchorage-dependent cells (ADCs)
basic culture units, 1249–1250
high-volume units, 1250–1252
multisurface plate units, 1250
comparisons, 1256–1257
culture modes, 1248
high-cell-density bioreactors, 1254
hollow fiber bioreactors, 1254
microporous microcarriers, 1255
spin filters, 1254–1255
limiting factors, 1247–1248
principles, 1247
strategies, 1248
for suspension cells
laboratory scale, 1252
large-scale bioreactors, 1253–1254
scale-up, 1252–1253
mammalian cell expression vector (MCS), 737, 738
mammalian cell lines, properties of, 737, 739–742
baby hamster kidney (BHK), 742
cell line engineering, 739
Chinese Hamster Ovary (CHO), 740–741
human cell lines, 741–742
hybridomas, 741
mammalian cell expression vectors, 737–738
mouse myeloma, 741
transfection, selection, and screening methods, 738–739
mammalian expression systems, 507
hamster cell lines, 509–510
human cell lines, 508–509
mouse cell lines, 510–511
mammary gland expression, 743
manifold photobioreactors, 1333
Marangoni effect, 1270
martensite, 1427
Marticaria chamomilla, 1651
mass balance, 44, 1235
equation, 355, 363
from growth rate, under oxygen limitation, 1314
and respiratory quotient, 1580–1582
mass related power density, 973
mass spectroscopy, 1570–1571
detectors, 1572–1573
ion separation, 1571–1572
ionization, 1571
sample inlet, 1571
spectral analysis, 1573–1574
vacuum system, 1571
mass transfer, 911, 1261
behavior
aqueous two-phase extractions, 1289
dispersions, 1270–1271
external transfer and heterogeneous bioreaction, 1295–1296
flow past solid surface, 1289–1294
fluid–solid slurries, 1294–1295
gas–liquid mass transfer, 1271–1272
general aspects, 1268–1269
intraparticle mass transfer, 1296
liquid–liquid mass transfer, 1287
oxygen transfer in wastewater treatment processes, 1286–1287
perfluorocarbons and oxygen vectors, 1287–1289

solid–liquid and gas–solid mass transfer, 1289
submerged aeration, 1275–1286
surface aeration, 1272–1275
bubble size and interfacial area, 914
data correlation for rate, 914–915
diffusion coefficient and diffusivity, 1261–1262
gas–liquid, 1262–1263
carbon dioxide chemical absorption, 1265
dynamic gassing-in method, 1266–1267
enzymatic oxidation method, 1266
hydrazine method, 1265
oxygen balance method, 1265
oxygen solubility, 1267
sulfite oxidation method, 1265
volumetric oxygen transfer coefficient, 1264
liquid–liquid, 1267–1268
rate measurement, 911–914
solid–liquid, 1268
mass transfer coefficient, 390, 1220, 1263
volumetric, 1365
mass transfer process treatment, dimensional analytical treatment of
driving force and process target quantity, 782–783
gas/liquid G/L
in bulk aeration in mixing vessels, 784–785
in surface aeration, 783–784
master cell bank (MCB), 46, 47, 107, 108, 186, 297, 298, 624
material function, dimensionless representation of, 774–775
Material Transfer Agreements (MTAs), 140
MATLAB®, 1486
matrix-assisted laser desorption/ionization (MALDI) time of flight (TOF), 500
Maxblend impeller, 1048
maximal heat transfer coefficient, 974
mean axial bubble velocity, 1139
mean diameter, 973
mechanical foam breakers, 1688
classical, 1688–1689
and mixing system mounted on same shaft, 1689
SAFD techniques, 1690
mechanical foam breaker scale-up, 770–771
mechanical polishing, 1121
mechanistic studies, 331
media blending, 587
media design and composition, 423
buffers, 427
natural buffering agents, 427–428
synthetic buffers, 428
carbon and energy sources, 425–426
extracts, 426
gelling agents, 428
agar, 429
agarose, 429
alginic acid and κ-carrageenan, 430
gellan gum, 429–430
silica gel, 430
protein hydrolysates, 424–425
media sterilization, 430
dry heat sterilization, 432–433
filter sterilization, 432
steam sterilization (autoclaving), 431
media storage, 433
Medicines and Heathcare products Regulatory Agency (MHRA), 1778
medium conductivity, assessing, 756
medium dispersion, 1496
Medusa photobioreactors, 1331
meiosis, 75
melting, 314
membrane aeration, 796–797
membrane bioreactors, 1589–1590, 1639–1640
membrane filters, 405, 1767, 1768–1769
membrane integrity, 38–39
membrane lipid layer, 805
membrane potential assay, 98–99
membrane processes, mass transfer effects in, 1292–1293
membrane reactors, biocatalytic, 821–823
applications, 832
biomedical applications, 839–841
milk and dairy products, 833–834
oil treatment, 835
pectin hydrolysis in fruit juices, 835
pharmaceutical productions, 835–839
reactors in food and beverage processing, 832–833
SMBRs in wastewater treatment, 841–844
wine treatment, 835
configurations, 826
external sidestream membrane bioreactors, 827–831
submerged membrane bioreactors, 831–832
fundamentals, 823–824
enzymes immobilized on surface, 824–825
enzymes within porous matrix, 825–826
process design and operation, 826
general reactors, 823
membrane stirrers, 1051–1052
menadione, 421
Mera Pharmaceuticals, Inc. (USA), 1339, 1340
Merck & Co., 1570, 1572
mesocellular foams (MCF), 1149–1150, 1169
metabolites, 1351
measurement, 1548
Metaglas™, 1123, 1124
metal oxide semiconductor field effect transistor (MOSEFETs), 1568
metal oxide sensors (MOS), 1568
metal refinery wastewater (MRWW), 941
Methanobacterium thermoautotrophicum, 416, 1730, 1734
Methanococcus spp., 414
Methanococcus vaniellii, 1730
methanol concentration monitoring methods, 204
methanol control schemes, 204–205
methanol induction phase (MIP), 203–204
methanol utilization phenotype of host, 197
methionine sulfoximine (MSX), 305, 741
methotrexate (MTX), 305
Methylene Blue, 97
Methylene Violet, 97
Methylobacterium spp., 425
Methylomonas spp., 425
Methylophaga spp., 425
Mettler Toledo, Switzerland (Fluorosensor), 1513
Michaelis–Menten constant, 1497
Michaelis–Menten equation, 342–343, 823, 824, 825
integrated, 344
kinetic parameters experimental determination, 344
microalgae and cyanobacteria, 1730–1734
microalgae mass culture methods , 371
bioreactors, 372
comparisons, 378
enclosed PBRs, 373–378
open raceways, 372–373
factors governing production, 378–379
biomass productivity, 383–385
fluid dynamics and mixing, 385–386
light distribution and average solar irradiance inside photobioreactors, 379–381
light saturation constant and photoinhibition phenomenon, 381–383
mass transfer, oxygen accumulation, and carbon uptake, 386–387
power supply and stress damage, 387–388
temperature, 385
operational considerations, 393–394
photosynthetic efficiency, 391–392

microalgae mass culture methods (*continued*)
absorbed photon flux, 392–393
tubular photobioreactors design
biomass productivity and solar radiation, 388
case study, 390–391
flow and gas–liquid mass transfer combination, 389–390
oxygen removal and temperature control, 390
power supply and liquid velocity, 388–389
microbial biofilms, on suspended particles, 1750–1751
microbial cleanliness, 68
microbial contamination, 49
microbial growth kinetics, 331
and cell growth models
biological meaning and experimental determination of growth parameters, 352–353
cell growth early views, 350
exponential growth low validity, 348, 350
main state variables and growth parameters, 347–348
Monod's model, 350–351
Monod equation derivation from mechanistic considerations, 351–352
Monod equation modification, 353–354
of chemical and enzyme reactions, 340
basic kinetic equations derivation for enzymatic reactions, 342
cooperativity, 345–346
equilibrium approach, 342
general non-steady-state approach, 343–344
inhibitors and activators, 345
Michaelis–Menten equation kinetic parameters experimental determination, 344
order and molecularity, 340–341
order of reactions and numeric values of kinetic constants, 342
pH effects, 346–347
rate constant dimensions, 341
reaction dynamics, 341
reaction half-time, 341
reversible enzymatic reactions, 344–345
steady-state approximation, 342–343
temperature effects, 347
growth stoichiometry
biomass yield variation from conserved substrates, 338
experimental determination of m, 335–337
growth yield, 332–333
macrostoichiometry, 331–332
maintenance requirements and wasteful catabolism, 337
microscopic approach, 338–340
yield variation as dependent on chemical nature of organic substrates, 333–334
yield variation from energy source and maintenance requirements, 334–335
microbial growth in cultivation systems, 363–364
biofilms, 367–368
colonies, 366–367
continuous cultivation without washout, 365
continuous culture with discontinuous supply of limiting substrate, 365
continuous-flow reactors with microbes, 365–366
homogeneous continuous culture, 364–365
plug-flow culture, 365
simple batch culture, 365
population dynamics
autoselction in turbidostat and pH-auxostat, 363
extrachromosomal cell elements (ECE), 363
mutation and autoselection, 362–363
structured effects, 354
cell cycle, 358–359
chemostat culture physiological state, 355–356
definitions, 354–355
growth law, 361–362
population distribution statistical analysis, 359–361
synthetic chemostat model (SCM), 356–358
microbial growth measurement, 399
adsorption of cells to surfaces, 402
balanced growth, 400–401
biomass by light scattering, 407
flow cytometry methods, 410
nephelometry, 409
theoretical aspects, 407–408
turbidimetry, 408–409
cell differentiation, 402
changes in cell composition at different growth rates of balanced growth, 401
colony counts equal viable counts, 404
automation, 405
layered plates, 405
membrane filter methods, 405
most probable number method, 405–406
pour plates, 405
special situations, 405
spread plates, 405
definitions of growth, 399–400
direct biomass measurements, 406
dry weight, 406
wet weight, 406
direct particle counts, 402
electronic enumeration, 403–404
flow cytometry technique, 404
microscopic enumeration, 403
mycelial habit of growth, 402
pitfalls in measuring growth, 402
principles, 399
sampling, 410
unbalanced growth, 401–402
Microbial Information Network for Europe (MINE), 141
microbial media composition, 413
essential nutritional requirements, 413
carbon, 415
energy, 414
growth factors, 418
hydrogen, 415–416
L-amino acids, 418–419
lipids, 421
minor and microelements, 417–418
nitrogen, 416–417
nucleic acid precursors, 421
oxygen, 416
polyamines, 421
unique growth factors, 421
vitamins, 420–421
water, 413–414
whole proteins, 419–420
media design and composition, 423
agar, 429
agarose, 429
alginic acid and κ-carrageenan, 430
buffers, 427
carbon and energy sources, 425–426
extracts, 426
gellan gum, 429–430
gelling agents, 428
natural buffering agents, 427–428
protein hydrolysates, 424–425
silica gel, 430
synthetic buffers, 428
media sterilization, 430
dry heat sterilization, 432–433
filter sterilization, 432
steam sterilization (autoclaving), 431
media storage, 433
physical parameters, 422
detoxifiers, 423
incubation temperature, 422

oxidation–reduction potential, 422–423
pH, 422
Microbial Resource Centres (MIRCEN), 147
microbial safety cabinets, 50, 59–60
class I, 59, 61
class II, 59–60, 61–62
class III, 60, 62
testing, 62, 64
after installation, 66
performance, 64–66
periodic, 66
microbiological culture, 477–478
microbiology, regulatory control in, 138
microcapsules, diffusion in, 1082–1083
microcapsules and mathematical modeling, 1090–1091
models with cell growth, 1092
models without cell growth
dynamic modeling, 1091–1092
steady-state modeling, 1091
microcarrier culture, 191, 873, 1228–1229, 1230, 1236, 1249, 1250, 1742–1744
cell cultivation
cellular adhesion mechanisms, 713
cultivation medium, 716–717:gas supply, 717
cultured cell types, 713–714
mixing and shear, 718
pH culture, 717–718
practical aspects, 714–716
commercial, 713
future directions, 728
history and development, 711–713
macroporous, 1236–1237
in recombinant protein production
academic and industrial use, 724–726
cultivation modes, 726–727
effect on protein glycosylation, 727–728
sampling
cell harvesting and scale-up, 720–722
cell quantification, 719–720
cell visualization, 718–719
trouble-shooting, 722–723
in vaccine production, 723–724
microcell-mediated chromosome transfer (MMCT), 268
microelements supply, in plant culture, 750
microencapsulation, 1069, 1181, 1182–1184, 1191, 1237
microenvironment, 1069
microfabricated reactors, 671–672
microfluidic devices, 1500–1503
microheterogeneity, 490, 496, 590
microinjection, 236
microorganisms, classification of, 139
Micro-Organisms, Sustainable Access and use, International Code of Conduct (MOSAICC), 147
microporous microcarriers, 1255
MicroReactor Technologies Inc., 591
microscopic enumeration, 403
microscopic reversibility, 1670
microscopy, 437
developments and milestones in, 438
electron microscopes, 457–459
laser tweezers and scissors, 453
light microscopy, 438
bright-field microscopy, 441–442
components and principles, 438
condenser, 439
confocal microscopy, 451–452
dark-field microscopy, 442–443
eyepieces and imaging, 440–441
fluorescence microscopy, 448–451
Hoffman modulation-contrast microscopy, 444
illumination source, 439
interference-contrast microscopy, 446–447
multiple oblique-illumination 3-D microscope, 445
objective lens, 439–440
oblique or anaxial (asymmetrical) illumination, 444
phase-contrast microscopy, 443–444
polarizing microscopy, 445–446
reflection-contrast microscopy (RCM), 447–448
single sideband edge-enhancement microscopy, 444–445
stage, 439
two-photon and multiphoton microscopy, 452–453
scanning-probe near-field microscopes, 453
atomic force microscopes (AFM), 454
scanning near-field optical microscopes (SNOM), 454
scanning tunnelling microscopes (STM), 454
video microscopy and image processing, 454–457
microtiter plate (MTP), 686, 687
midblastula transition, 261
mid infrared (MIR) spectroscopy, 1480, 1655
mifepristone. See RU486
milk and dairy products, 833–834
Millennium Development Goals, 132
mini-F replicon, 21
Minimum Essential Medium (MEM), 585
MiniPerm, 1590
mini-pleat filters, 57–58
mink lung cell line, 111–112
minute virus of mice (MVM), 109
mitogen-activated protein (MAP) kinases, 600
mitosis, 75
mitotic index, 77
Mitsubishi Pharma Corporation, 196
mixing, 798, 1443–1445
baffles, 801
geometry, 799
impellers, 799–801
mixing times and energy dissipation rates, 801–804
stirred tank reactors, 799
mixing times, 801, 866, 870, 905, 1059
mixing vessels, cell support for
aggregates, 1237
cell entrapment, 1237
macroporous microcarriers, 1236–1237
microcarriers, 1236
Mobil Composition of Matter (MCM)-41 type, 1148
Mobil Research and Development Corporation, 1148
MoBiTec, 173
Mobius CellReady Bioreactor, 1592
model predictive control (MPC), 1417, 1422–1423
molecular probes, 450
molecular RNA hybridization, 478
moles, 760
Mollicutes, 467
Moloney murine leukemia virus (MoMLV), 248, 605
Mond's model, 350–351
Monitek (Monitek Technologies, CA, USA), 1611
monoclonal antibodies (MAbs), 1587. See also antibody manufacture and disposable systems
monoclonal antibody (MAb) production, 733
cell line, 733
important features of, 733
productivity, 736–737
product quality, 735–736
regulatory acceptability of, 733–734
safety, 734–735
host platforms, 742
bacteria, 742
fungi, 742
insect cells, 742–743
plants, 743
transgenic animals, 743
mammalian cell lines, properties of , 737, 739–742

mammalian cell lines, properties of (*continued*)
baby hamster kidney (BHK), 742
cell line engineering, 739
Chinese hamster ovary (CHO), 740–741
human cell lines, 741–742
hybridomas, 741
mammalian cell expression vectors, 737–738
mouse myeloma, 741
transfection, selection, and screening methods, 738–739
monoclonal antibody-based therapeutics, 636
Monod equation, 959, 1087, 1091, 1092, 1394
Monod equation
derivation from mechanistic considerations, 351–352
modification, 353–354
Monod–Ierusalimsky equation, 354
Monodus subterraneus, 1330, 1335, 1336
monosaccharide composition analysis, 506
Monte Carlo simulation, 997
Morinda citrifolia, 1735
morphological factor, 1369
Moser equation, 353
most probable number (MPN) methods, 405–406
mouse myeloma, 739, 741
MRC-5 cells, 115, 117
Mucor javanicus, 1729, 1734
mucosal disease virus. See bovine viral diarrhoea virus (BVDV)
multicollector system, 1572
multidimensional liquid chromatography, 502–503
multimeric enzyme stabilization, 1210–1211, 1214
multiphase airlift reactors, 917, 927–928
four-phase, 918–920
three-phase, 917–918, 937
multiphase systems, transfer phenomena in, 1451
hydrodynamics
gas effect on solid–liquid, 1458–1459
gas–liquid dispersing characteristics, 1452–1454
particles effect on gas–liquid, 1457–1458
solid particles suspension in liquids, 1454–1457
mass transfer, 1459–1460
gas–liquid characteristics, 1460–1464
modified agitator performance in antibiotics biosynthesis, 1464
industrial-scale bioreactors, 1465–1467
semiindustrial-scale bioreactors, 1464–1465
modified Rushton turbine agitators description, 1451–1452
multiple cloning site, 169–171, 217
multiple oblique-illumination 3-D microscope, 445
multiple slot disperser, 797
multiple virus infection, 41–42
multiplicity of infection (MOI), 34, 35–36, 38, 41, 45–47, 325–326
multipoint covalent immobilization and enzyme stabilization
glyoxyl-agarose, 1211–1213
heterofunctional-epoxy supports, 1213
multistage fixed bed tower bioreactor (MFBT), 1195
multistream rotary valves, 1576
multivariate data analysis (MVDA), 1549, 1559
multivariate statistical process control (MSPC), 1484–1485, 1546
multiwavelength fluorescence, 1516
multi-well plates, 677, 680–683
Murashige and Skoog medium, formulations of, 749
murine leukemia virus (MLV), 110, 112, 247
ecotropic, 111
infectious, 110–111
muristerone A, 256
muromomab, 636
Mus dunni assay, 112
mycelial broths, 1362
mycelial fermentation, 1351–1352
dispersed forms, 1353–1356
morphological characterization, 1352–1353
pelleted forms, 1353
mycelial habit of growth, 402
MycoAlert test, 480
Mycoplasma alkalescens, 471
Mycoplasma arginini, 471
Mycoplasma arthritidis, 469, 471
Mycoplasma bovis, 471
Mycoplasma buccale, 471
Mycoplasma canis, 471
mycoplasma contamination, 467
detection of, 474
DNA fluorochrome staining, 476–477
fluorescence in situ hybridization, 479–480
microbiological culture, 477–478
molecular RNA hybridization, 478
MycoAlert test, 480
polymerase chain reaction, 478–479
effects of, on cell cultures, 472–474
elimination of, 480
antibiotic treatment, 482–484
methods, 480–482
incidence of, 470–471
most common species of, 471–472
routine working protocol
for detection, 484–485
for elimination, 485
for prevention, 485–487
sources of, 472
working protocol for elimination of, 486
Mycoplasma fermentans, 471
Mycoplasma gallisepticum, 471
Mycoplasma genitalium, 471
Mycoplasma hominis, 471
Mycoplasma hyopneumoniae, 469
Mycoplasma hyorhinis, 471
Mycoplasma orale, 471
Mycoplasma penetrans, 469
Mycoplasma pirum, 471
Mycoplasma pneumoniae, 467, 469, 471
Mycoplasma pulmonis, 471
mycoplasmas, 107, 482
characteristics of, 467–469
detection, 120–121
Agar and Broth procedures, 121
enhanced cell culture procedure, 121
indicator cell culture procedure, 121
using Gen-Probe Inc., 121–123
taxonomy of, 469–470
Mycoplasma salivarium, 471
myeloma cell lines, 10
Mylotarg™(gemtuzumab ozogamicin), 659

N-acetylglucosamine, 521
Nannochloropsis, 1333, 1335, 1337
nanoencapsulation, 1069
nanoliter scale bioreactor, 673
National Foundation for Infantile Paralysis, 186
National Institute of Health (NIH), 102, 185
National Institutes of Medical Research, 185
near-horizontal tubular reactor (NHTR), 1333
near infrared spectroscopy (NIRS), 204, 1480, 1655
neat, 1687–1688
necrosis, 872
nematodes, 1753
neomycin, 38
nephelometry, 409
neural cell adhesion molecule (NCAM), polysialylation (PSA) of, 602

neuraminidase activity
determination, 1538
and sialic acids, 1538
Neurospora crassa, 421
Neurospora sitophila, 1729
neutrophil gelatinase-associated lipocalin (NGAL), 642
Newton's law, 1362
Newtonian fluid, 1347, 1349, 1440, 1722, 1724
Newtonian liquids, 775
Newtonian viscosity, 1105
N-glycan, 29
processing pathways, 742
Nicol prisms, 438
Nicotiana tabacum, 1058, 1655
nicotinamid adenine dinucleotide (NADH and NADPH), 1076, 1512, 1513, 1516, 1671
nicotine, 1651
ninhydrin method, 1527
Nisin Inducible Controlled Expression (NICE), 548
nitrate, 416
nitrilotriacetic acid (NTA), 418
Nitrobacter spp., 414
nitrogen, 416–417
supply, in plant culture, 749
N-linked glycosylation, 490, 1658
Nomarski differential interference microscopy, 439, 441
noncoding regions, structure of, 259
nongel electrolyte probes, 1609
nonmammalian expression systems, 511
bacterial strains, 514–515
invertebrate cells, 511–512
plants, 512–513
yeast, 513–514
nonmammalian species as heterologous systems, 283
non-Newtonian fluids, 775, 1048, 1347, 1349, 1356, 1440, 1441, 1443, 1722, 1724–1725
flow behaviour
of pseudoplastic fluid type, 775–777
of viscoelastic fluids, 777
process equations, 777–778
for mechanical processes, 778–779
nonoccluded viruses (NOVs), 34, 42
nonpolar oils, 1685
nonporous magnetic nanoparticles, 1215
nonproduct utility, 1702–1703
non-steady state, definition of, 354
normal infective particles (I-NOVs), 42
normal polarity separation, 504
notional quality curve, 706
Nova Bioprofile Flex (Nova Biomedical), 1480
NovaSeptic™, 1129
Novavax, 319
nozzles and sterilization, 1122–1123
nozzle spargers. See point spargers
NPSH calculation, 1601
N-shaped mixer (Bran and Lübbe, Norderstadt), 1437
nuclear magnetic resonance (NMR), 557
nuclear occlusion bodies, 243
nuclear polyhedrosis viruses (NPVs), 243
nuclear transfer technology, 285–286, 288
animal cloning, 290
cell-based gene transfer procedures advantages, 286–287
donor nuclei source, 288–289
reprogramming, 289
ruminant embryonic cells, 287–288
and somatic cell therapy, 290
xenotransplantation, 289
nucleic acid precursors, 421
Nucleo Bioreactors (ATMI Life Science), 1591
nucleopolyhedroviruses (NPVs), 19, 28, 34
nucleoside phosphorylase, 475
Nunc Cell Factories®(NCFs), 299, 307, 1240
Nusselt number, 780, 974
nutrient/metabolite sensing, 1611
nutrients analysis, 1526–1529

objective lens, 439–440
oblique or anaxial (asymmetrical) illumination, 444
occluded virus (OV), 313
Occupational Safety and Health Administration (OSHA), U.S., 1103
Oceanic Institute, University of Hawaii, 1336
Oceanospirillum, 415
off-gas analysis *See also vent gas analysis*, 1415
Office of Viral Research and Review (OVRR), 187
off-line analysis, in animal cell culture, 1523
cell culture media composition, 1523–1525
cell density
automated cell density examination systems, 1525
CASY particle counter, 1526
Coulter particle counter, 1525
determination by cell staining, 1525
medium components analysis
9-fluorenylmethoxycarbonyl chloride (FMOC), 1530
inorganic salts, 1531–1532
lipids, 1534
nutrients analysis, 1526–1529
pyruvate, 1531
vitamins, 1532–1534
metabolic end products analysis, 1535
ammonia, 1536
lactate, 1535–1536
urea, 1537
protein analysis, 1539
clinical analyzers, 1539–1540
enzyme linked immunoassays, 1539
unspecific assays, 1539
pyrogultamic acid, 1537
enzyme activities, 1537–1538
osmolality, 1538–1539
oil mist test, 58
oil treatment, 835
Oldenlandia affinis, 1651
oligovalent antibodies, 657–659
O-linked glycosylation, 490, 492
omega number, 968, 977
oncogenic transformation, 618
on-line sampling, 1381
operational state, 68
operator protection tests, 64
biological method, 64
potassium iodide test, 64
o-phthaldialdehyde (OPA) method, 1527–1528
optical density (OD), 672, 675, 683
optical probes, 1478–1479
optical sensors/sensing, 671, 675, 676, 677
orbitally shaken and pneumatically driven bioreactors, 1592–1593
OrbShake technology, 1592
ordinary differential equation (ODE), 45
ORFs, 21, 28
organic loading rate (OLR), 1017
organic sensitivity, to fluid mechanical forces, 1109
organic solvents, enzyme stabilization against, 1211
Organisation for Economic Cooperation and Development (OECD), 131, 132
Best Practice, 132, 140, 141–142, 143
organotrophic organisms, 414
orientation (Keesom) forces, 1155
orifice spargers, 1052
Orthoclone® (muromonab-CD3), 659
osmolality, 1475–1476
osmolality effect of cellular microenvironment , 599
cellular responses to osmolality perturbations, 599
cellular signaling, 600
cytoskeletal reorganization, 600
volume-regulatory responses, 599–600
culture media osmolality effect on hybridoma cell size, 602

osmolality effect of cellular microenvironment (*continued*)
on protein posttranslational modification, 602–603
on protein productivity, 600–601
hypermolar stress effect on immunoglobulin mRNA levels and transcription rates, 603–604
hyperosmolality effect on virus expression systems, 604
baculovirus expression vector system (BEVS), 605
sensitivity of animal virus replication to osmotic conditions, 605
hyperosmolar stress effect
on antibody secretion rates, 604
on immunoglobulin mRNA translation rates, 604
hypoosmotic conditions effect on specific protein productivity, 603
osmoprotective compounds, to mitigate inhibitory effects, 601–602
osmotic shock, 1737
Ostwald–de Waele fluids, 775
overall areal productivity (OAP), 1341
overexpression vectors, 217
Oxford Expression Technologies, Ltd., 21, 28
oxidation–reduction potential, 422–423
oxonol, 99
oxygen, 416
oxygen balance method, 1265
oxygen carriers, 796
oxygen demand (OD), 1219, 1262
oxygen measurement, device and principle of, 1477
oxygen solubility, 1267
oxygen supply, 973, 1643–1645
oxygen transfer
and aeration, 1106–1108
and impeller selection, 1220–1221
in wastewater treatment processes, 1286–1287
oxygen transfer coefficient, 1364
volumetric, 1264
oxygen transfer rate (OTR), 673, 677, 680, 793, 795, 1116
comparison obtained by different methods, 1314–1316
correlation of values, 1316–1320
description, 1304–1306
experimental determination, 1306–1307
biological methods, 1312–1314
chemical methods, 1307–1310
physical methods, 1310–1311
gas flow and linear velocity, 1106
general method for prediction, 1320
oxygen consumption influence, 1320–1321
mass transfer, 1106
miniature bioreactors, 1322–1323
requirements, 1106
oxygen uptake rate (OUR), 123–124, 321, 1220, 1226, 1227, 1230, 1307, 1312, 1314, 1476, 1479, 1485, 1486, 1630, 1644
and biologic dynamic methods in cultures, 1312–1313

p10-promoter, 635
p53 tumor suppressor gene, 619
P170 promoter, 549–550
packaging lines, 238, 248
packed-bed bioreactors, 873, 1195, 1640–1641
macroscopic transport phenomena in, 1405
combined heat and mass transfer, 1406
heat transfer, 1405–1406
without mixing, 1417–1418
with periodic mixing, 1418
case study, 1418–1423
packed beds, 726, 1289, 291
packed cell volume (PCV), 756, 1478
paclitaxel, 1654, 1658
paddles, 1048–1049
palivizumab, 636
Panax ginseng, 1652
Panax notoginseng, 1646, 1652
pantothenate, 1533
parallel factor analysis (PARAFAC), 1545
paramagnetism, 1569–1570
partial least squares (PLS), 1480, 1545
partial least squares regression (PLSR), 1516, 1517, 1518
particle-based biofilm reactors (PPBRs), 918, 919
particle bombardment, 236–237
particle sedimentation rate, 1004
partition coefficient, 1072
passage effect, 42, 46
passivation, 1431, 1433
passivity, 1427
pasteurization, for virus elimination, 1776
pattern recognition methods, 1480
Pco_2, 1610–1611, 1630
PECAM-1, 805
Peclet number, 1085, 1296
pectin hydrolysis, in fruit juices, 835
pellets, 1315–1353, 1359
density, 1081
fragmentation patterns, 1753
suspension, 1360
pendulum, 761
penetration theory, 1086
penicillin acylase (PA), 1171
penicillins, 1171
Penicillium chrysogenum, 1082, 1351, 1354, 1355, 1363, 1366, 1367, 1368, 1369, 1372, 1729
Penicillium citrinum, 1353
Penicillium spores, 706
peptides, for protein secretion, 171–172
peptones, 424–425, 585
PER.C6®, 10, 183, 184, 187, 188, 189, 190, 191, 509, 742, 1650
perfluorocarbons (PFCs), 792, 795–796
and oxygen vectors, 1287–1289
perforated disks, 1047
performance tests
airflow checks, 65–66
cross-contamination test, 65
external contamination, 64–65
leakage tests, 66
operator protection tests, 64
temperature checks, 66
perfusion, 995–997
cell retention
based on filtration, 997–1002
based on sedimentation, 1002–1010
culture, 1654–1655
perfusion systems, 190
Perilla frutescens, 1643, 1645, 1649, 1651, 1655, 1735
periodic mesoporous organosilicates (PMO), 1152, 1153, 1161–1162
periplasmic shedding, 560
peristaltic pumps, 1632, 1752
PerkinElmer, USA (Model LS 50B), 1518
permeability assays, 97
DNA gel electrophoresis for apoptosis analysis, 100
exclusion, 97
FISH methods, 98
FUN-1 assay, 99–100
inclusion, 98
membrane potential assay, 98–99
release, 98
RT-PCR methods, 99
tetrazolium assay, 98
permeate flux, 1292
personal hygiene, 51–52
personal protective equipment (PPE), 1705
Petit model, 071
Petri dishes, for plant cell cultures, 754
PetroSUN Inc., 1336
pFastBac transfer vectors, 30
P functions, 408
PG4 cell line, 112
pH, 1229, 1627–1628, 1650–1651
control, 14, 346–347, 521
dynamic measurement of, 1309
for microorganisms, 422
Pco_2, and osmolality, 1229
priming, 1627

Phaeodactylum tricornutum, 1330, 1336
phage antibody libraries
  human antibodies obtained from, 641
pharmaceutical productions, membrane reactor applications in, 835–839
pharmaceuticals, plant-derived, 1637
Pharmacia Cytopilot, 1255
phase-contrast microscopy, 443–444
Phaseolus vulgaris, 1062
phenol biodegradation, 942
phenolics, 1773
phenotypic change due to DNA methylation and gene silencing, 619
phenotypic heterogeneity and population dynamics, 622–623
phenylisothiocyanate (PITC), 1529–1530
Phillies model, 1071, 1076
Phillips Petroleum Company, 195, 196, 206
phosphate-buffered saline (PBS), 112
phosphatidylserine (PS), 100
phosphorus supply, in plant culture, 749
photobioreactors (PBRs), 371, 1327, 1655
  categories
    biofuels, 1337–1339
    flat photobioreactors, 1334–1337
    sleeves and vertical columns, 1329–1331
    tubular photobioreactors, 1331–1334
  closed, 372, 373
    bubble columns, 374–375
    flat panel, 377–378
    tubular, 375–377, 388–391
  definition and classification, 1327–1328
  design criteria, 1328
    carbon dioxide supply and oxygen removal, 1328–1329
    light regime and surface-to-volume ratio, 1328
    materials, 1328
    mixing, 1329
    orientation and inclination, 1328
    temperature control, 1329
  evaluation and productivity, 1341–1342
  future, 1342–1343
  large scale commercial, 1339
    attempts of past, 1340–1341
    present enterprises, 1339–1340
  light distribution and average solar irradiance inside, 379–381
  versus ponds, 1342
Photo Bioreactors Ltd. (PBL), 1340–1341
photoinhibition phenomenon and light saturation constant, 381–383
photolithotrophic bacteria, 414
photometric glucose assay, 1526
photometric lactate assay, 1535–1536
photon flux densities (PFD), 381
photoorganotrophs, 414
photostat, 955
photosynthetically active radiation (PAR), 1328
photosynthetic efficiency, 391–392
  absorbed photon flux, 392–393
photosynthetic unit (PSU), 382
phototrophic biomass, 955
physical quantity, 760
physical transfection, 233
Phytogel, 751
Phytoplasma, 469
pi
  determination by matrix calculation
    dimensional matrix construction and solving, 763–764
    example, 762–763
    geometric parameter determination, 763
    process characteristics determination, 764
    relevance list establishment for problem, 762
  space, 784
  theorem, 762
Pichia pastoris, 181, 195–196, 514, 519, 520, 557, 1479
  fermentation process, 202
    continuous fermentation, 205–206
    cyclic fed-batch culture (CFBC), 206
    dissolved oxygen control, 203
    fed-batch fermentation operational strategy, 203–204
    growth kinetics, 203
    hypoxic fed-batch cultivation, 206
    media and operational conditions, 202–203
    methanol concentration monitoring methods, 204
    methanol control schemes, 204–205
    mixed substrates, 205
    trace metals optimization, 206
  media compositions, 207
    fermentation medium and reagents, 207–208
  optimization strategies, 196
    alternative promoters for expression, 202
    expression cassette cellular state, 197
    expression cassette integration site, 197
    fusion proteins, 201
    gene dosage, 197–198
    methanol utilization phenotype of host, 197
    product secretion, 198–199
    production enhancement by media and growth conditions manipulation, 199–200
    production enhancement using protease-deficient strains, 200
    protein and protein complex coexpression, 201
    protein glycosylation and humanization of N-linked glycosylation, 201
    protein secretion enhancement by chaperone protein overexpression, 200–201
    protein toxicity overcoming, 202
    secretion signal choice, 199
    transcriptional optimization, 198
    translational optimization, 198
pickling, 1432–1433
PicoTaq systems, 1529
piezoelectric sensors, 1415
pilot plants, design and operation, 1695–1696
  design, 1697–1698
    automation and control, 1705–1706
    back-up systems and redundancy, 1707–1708
    containment, 1704–1705
    data acquisition and archiving, 1706–1707
    future expansion and modification, 1708
    instrumentation, 1705
    process equipment, 1698–1700
    utilities, 1700–1704
    warehousing, 1707
  operation, 1708
    calibrations, 1709
    laboratory support, 1710–1711
    manufacturing execution systems (MES) and facility records, 1714–1715
    modifications and change control, 1709–1710
    ongoing maintenance, 1709
    preventative maintenance, 1708–1709
    safety, 1712–1713
    staffing, 1710
    standard operating procedures (SOPs), 1711–1712
    training, 1713
    validation, 1713–1714
  operational concepts and processing requirements, 1696–1697
pilot-scale bioreactors, 1615
pipetting, 51, 52–53
piping and valving
  service lines for non-process-contacting fluids, 1125
  systems, 1115, 1125–1130
pitched blade turbines, 800, 1221
Planova filters, 1775, 1776

plant cell culture, 747
  cell culture systems, 754
    callus cultures and cell suspensions, 754–756
    cell growth, assessing, 756
    cell suspension cultures, synchronization of, 757
    cell viability, assessing, 756–757
  culture media, 748
    aseptic technique, 753–754
    preparation of, 752–753
    sterilization, 753
    stock solution components, 748
    vessels for cell culture *in vitro*, 754
  laboratory facilities, 747
    constant agitation, 748
    growth rooms/chambers, 747–748
    laminar-flow cabinets, 748
    providing suitable areas, 747
plant cells and shear sensitivity response, 1734–1736
plant growth regulators, 751
  ABA, 752
  auxins, 751–752
  cytokinins, 752
  ethylene, 752
  gibberellins (GAs), 752
plants, genetically engineered, 743
plaque-forming units (PFUs), 325
plasma membrane fluidity (PMF), 1738
plasmid expression vectors
  backbone sequences, 217–218
  classes and common modular components, 216–217
  marker genes, 219
  plasmid maintenance sequences, 218
  protein purification sequences, 219
  regulatory sequences, 218–219
plasmid rescue, 223
plasmids, 1755–1756
plastic plates, 1336
plastic screw-cap vials, 157
plateau borders, 1681
plate number, 1482, 1484
platinum 100-Ω resistance thermometers, 1610
pleuropneumonia-like organisms (PPLO), 467
Plexiglas®, 1330, 1334, 1336
plug-flow reactor (PFR), 858–859, 1235, 1666, 1674, 1675
plug valves, 1612
Pluronic®, 16, 322
Pluronic F-68, 663, 665, 666, 667, 813–814, 911, 995, 1220, 1229, 1230, 1238, 1276, 1632, 1644, 1729, 1737, 1749–1750
pluronic polyols, 663
  application, 667
  cell protection, 663
  properties, 663
    foaming characteristics, 664–665
    hydrophilic–lipophilic balance, 664
    impurities, 664
    nomenclature, 663–664
    oxygen transport, 665
    surface tension, 665
    synthesis and structure, 663
  protective effects
    agitation damage, 666–667
    sparging damage, 665–666
pneumatically agitated bioreactors, 1639
pneumatic bioreactor system (PBS), 1592
pneumatic reactors, 1683
point-of-use coolers, 1701
point spargers, 797, 1052
poison sequences, 217
Poisson statistics, 41
polarization-modulated DIC (PM-DIC), 447
polarizing microscopy, 439, 445–446
polar oils, 1685
Pol-Scope, 446
polyadenylation, 257–258
  sites in cointegrate vectors, 258
poly(ADP-ribose) polymerase (PARP), 620
polyamines, 421
polybrene-mediated transfection, 236
polycistronic vectors, 259
polydimethylsiloxane (PDMS), 1685, 1686–1687
poly(ethylene glycol) (PEG), 236, 1188, 1750
poly(ethylene oxide), 1188
polyethylene terephthalate polyester (PETP), 1001
poly(glycolide) and poly(lactide), 1188
polyhedra, 19, 20, 22, 28, 34
polyhedrin, 243
  replacement vectors, 244
poly-L-lysine (PLL), 1183, 1186
polymerase chain reaction (PCR), 117–118, 478–479, 652
polymer tubing, aeration through, 1291
polynomials, 1485–1486
polysialylation (PSA) of neural cell adhesion molecule (NCAM), 602
polyurethane (PU) foam, 1188
polyvinyl alcohol (PVA), 1187–1188
polyvinyl pyrrolidine (PVP), 137
poration transfection, 233
porcine parvovirus (PPV), 109
porcine viral contaminants, tests for, 119–120
Porphyridium cruentum, 1731
Porphyromonas gingivalis, 418
Porter equation, 1293
position effects, 262–264
  overcoming, 268–269
positive displacement rotary vane pumps, 1731
positive–negative selection, 271, 273
positive selection, 271
postinoculation sampling matrix, 1631
postproduction cell bank (PPCB), 107, 108
posttranslational events, 259–260
  endogeneous proteins processing, 260
  factors affecting recombinant proteins processing, 260
  inducible protein activity, 260–261
posttranslational modifications (PTMs), 182, 184, 1548
posttranslational processing, 317–318
potassium supply, in plant culture, 749
potentiometry, 1496
pouring, 52
pour plates, 405
powdered antifoam, 1688
power law, 775, 776, 1105, 1349, 1353, 1354, 1355, 1356, 1361
  equation, 1721
  model, 1369, 1393
power number, 1221–1222
  dimensionless, 1108
poxviruses, 215
Prandtl number, 780, 974
Preceptrol cultures, 155
preinoculation media, 1359
pressure drop, 1415, 1439–1441
pressure hold test, 1770
pressure rise test (PST), 1556
primary unit, 760
primordial germ cells, 280
principal component analysis (PCA), 1356, 1480, 1486, 1517, 1518, 1545
principal component regression (PCR), 1516, 1517
prions, 106, 1777
  detection, 126
    in vivo assays, 127
    in vitro assays, 127
PRM mixer (Prematechnik, Frankfurt/Main), 1436
probability-based theories, for sterilization, 1113
process analytical technology (PAT), 1377, 1471, 1511, 1543, 1705
  applications for upstream operations, 1547–1549
  applications in downstream operations, 1552
    chromatography, 1553
    filtration, 1552
    in-line mixing, 1553–1554
    process monitoring tools, 1555

protein PEGylation, 1554
refolding, 1553
viral filtration, 1554
applications in drug product operations, 1554
bulk freeze-thaw, 1554
filling, 1554, 1556
formulation, 1554
inspection, 1556
lyophilization, 1556
sterile filtration, 1554
applications in harvest operations, 1549
centrifugation, 1549
extraction, 1552
flocculation, 1549
precipitation, 1549, 1552
challenges in biopharmaceutical production, 1546–1547
chemometrics applications, 1558–1559, 1560
definition and objectives, 1544
enabling sensors for cell culture unit operations, 1550–1551
implementation, 1544–1546
case studies, 1559, 1562
enablers, 1544
process analyzers, 1545
and rapid microbial methods, 1556, 1558
process and instrumentation diagram (PID), 1419, 1420, 1421–1422, 1626, 1627
controller, 1609
process effecting operation, 799
process number, 766
product conduct utility, 1701–1702
product inhibition, 344, 1670–1671
overcoming
by CSTR cascade, 1673–1674
by product extraction, 1671–1673
production traits modulation, 284
programmable logic controller (PLC), 1553
proline, 425
promoter, 252–253, 547
constitutive, 547–548
inducible, 548–550
and multiple cloning sites, 169–171
occlusion, 258
probe vectors, 217
Pronase™, 720, 721
pronuclear microinjection, 279–280
propellers, 1038, 1047
propidium iodide (PI), 97
proprotein convertase, 260
Protalix, 519
protease, 831
protective polymers, 15–16
protein, 1680–1681
analysis, 1539
clinical analyzers, 1539–1540
enzyme linked immunoassays, 1539
unspecific assays, 1539
precipitates, 1752–1753
protein disulfide isomerase (PDI), 200
protein expression, in bacteria, 557
altering growth conditions to increase soluble expression, 558
induction conditions, 561–562
lowering growth temperature, 558–561
medium composition, 561
altering protein sequence for solubility, 566
inclusion bodies, formation of, 566
mutation to increase solubility, 567
role of proteolysis, 566–567
cell free expression systems, 565–566
growth conditions and variables that affect yields of soluble protein, 568
inoculum preparation and storage, 568
maintaining solubility during harvesting and cell lysis, 569–570
protecting your cultures from contamination, 568–569
selection stress, stability of, 569
shaker flask versus fermentor cultivation, 569
trouble shooting protein producing recombinant bacteria, 568
host strain, choice of, 562
coexpressing other proteins, 562–563
E. coli, alternative hosts to, 563
low protease strains and those with better redox characteristics, 562
strain choice for expression versus transformation, 562
vector, altering, 563
altering the gene sequence of protein, 565
choice of promoter, 563–564
cold shock vectors, 564
selecting signal sequences/fusion partners, 564–565
protein expression kinetics and cell growth, 85
batch culture kinetics
experimental data, 85–86
model simulation comparison with experimental data, 87–88
unstructured kinetic models, 86–87
continuous culture kinetics
cell cycle models, 91–92
experimental data, 88–90
segregated models, 92
structured kinetic models, 90–91
fed-batch and perfusion cultures
model simulations, 92
monoclonal antibody production optimization, 92
suboptimal growth-associated production kinetics, 92–93
protein expression vectors, 216
protein glycosylation, 489
bioinformatics resources for glycans analysis and assignment, 506
deglycosylation methods
chemical methods, 498–499
enzymatic methods, 499–500
effects, 493
activity, 495–496
immunogenicity and biological clearance, 496
structure and stability, 493–495
glycans analysis and characterization strategies
capillary electrophoresis, 504
chromatographic profiling, 501–504
detection methods, 504–505
electrophoresis, 505
mass spectrometry, 500–501
monosaccharide composition analysis, 506
sequential enzymatic digestion, 505
sialic acid analysis, 505–506
glycosylation sites identification, 497–498
LC–MS of glycopeptides, 497
lectin affinity capture, 496–497
overview, 489–490
glucosylphosphatidylinositol (GPI) anchors, 492
less common forms, 492–493
N-linked glycosylation, 490
O-linked glycosylation, 490, 492
of recombinant therapeutics, 506–507
genetic engineering, 515–520
glycosylation control modeling, 520
host cell selection effects, 507–515
process condition effects, 520–526
protein hydrolysates, 424–425
protein immobilization, on mesoporous silicas and carbons
adsorption on surfaces, 1155–1156
biocatalysis, 1162, 1165–1173
enzyme immobilization on ordered materials, 1157–1162
materials, 1147–1154
protein posttranslational modification, effect of culture medium osmolality on, 602–603
protein production, cell types for, 9–10
protein release model, 39–40

proteins, biotechnological production of, 635
Protein Sciences Corp., 319
protein toxicity overcoming, 202
protein transient production, cell lines for, 10
proteolysis, role of, 566–567
proto-oncogenes and genomic instability, 619
protoplast fusion and cell, 236
protozoa, 1736–1737
provirus, 237
pseudohomogeneous matrix, 1399
Pseudomonas alcaligenes, 852
Pseudomonas diminuta, 1770
pseudoplastic fluids, 775–777, 1271, 1362, 1446
pseudoplastic model, 1363
PSM mixers (Petzhold, Frankfurt/Main), 1436
pulse-chase labeling, 77
pulsed amperometric detection (PAD), 501, 502
pulsed field gradient-nuclear magnetic resonance (PFG-NMR), 1077, 1081
pulsed-flow system, 1132
pulse-injection method, 1482
P/V number, 784
Pyrex®, 1332
Pyrodictium spp., 414
pyrogultamic acid, 1537
  enzyme activities, 1537–1538
  osmolality, 1538–1539
pyruvate, 1531
PZ_n promoter, 550

quadrupole filter, 1572
quality by design (QbD), 1543
quantitative polymerase chain reaction (Q-PCR), 1481, 1774
quantitative reverse transcriptase polymerase chain reaction (qRT-PCR), 99
quantum yield, 392
Quincke-type analyzer, 1569–1570

radial flow impellers, 1110
Raman spectroscopy, 1480, 1559
Raptiva®(efalizumab), 659
rate equation, for virus release, 38
Raven methanol sensor (Raven Biotech Inc.), 204
Rayleigh domain, 407
Rayleigh–Gans domain, 408, 410
reaction-limited attachment, 43
reaction-limited regime, 825
reactive oxygen species (ROS), 792
reactors, suspension culture, 10
  airlift reactors, 11
  disposable reactor systems, 11
  stirred reactors, 10–11
receptor-mediated transfection, 237
receptor tyrosine kinases, 805
recombinant animal cells and transgenic animals, gene expression in, 213
  direct DNA transfer
    cell transfection overview, 223–224
    reporter genes in transfection analysis, 225
    selectable markers used in mammalian cell lines, 227–230
    stable transfection using episomally maintained vectors, 231–232
    stable transfection using nonreplicating DNA, 225, 227
    transgene expression maximization by gene amplification, 230–231
    transient transfection, 224–225
  direct transfer vectors
    insertional mutagenesis and entrapment vectors, 221–223
    targeting vectors, 221
    yeast artificial chromosome (YAC) expression vectors, 219
  DNA transfer introduced into animal cells, 215–216
  expression parameters and optimization, 252
    endogeneous and constitutive viral promoters, 253
    heterologous, recombinant, and artificial inducible systems, 254–256
    inducible promoters, 253–254
    posttranslational events, 259–261
    protein synthesis, 258–259
    transcriptional initiations
    transcriptional termination and RNA processing, 256–258
  genetic manipulation, 214
  nuclear transfer technology, 285–286, 288
    animal cloning, 290
    cell-based gene transfer procedures advantages, 286–287
    donor nuclei source, 288–289
    reprogramming, 289
    ruminant embryonic cells, 287–288
    and somatic cell therapy, 290
    xenotransplantation, 289
  plasmid expression vectors
    expression vector classes and common modular components, 216–217
    marker genes, 219
    plasmid backbone sequences, 217–218
    plasmid maintenance sequences, 218
    protein purification sequences, 219
    regulatory sequences, 218–219
  protein expression, 214
  recent advances in gene transfer technology, 214–215
recombination-based methodology and gene inhibition strategy
  conditional gene silencing, 278
  endogeneous gene inhibition, 270
  gene silencing, 271–272, 276–277
  homologous recombination, 270–271
  site-specific recombination, 275–276
  subtle mutations, 272–274
  target cells for homologous recombination, 274–275
  transient gene silencing with oligonucleotides, 277–278
  use in genetic engineering, 269–270
transfection methods
  calcium phosphate, 234
  cell and protoplast fusion, 236
  diethylaminoethyl–dextran, 234–235
  electroporation and laser transfection, 235
  liposomes, virosomes, and lipofection, 235–236
  locally applied naked DNA, 233–234
  microinjection, 236
  overview, 232–233
  particle bombardment, 236–237
  polybrene-mediated transfection, 236
  receptor-mediated transfection, 237
  transient transfection efficiency enhancement, 235
transgene integration consequences, 261
  copy-number and dosage effects, 264
  design for transgenic animals, 267–268
  DNA methylation and homology-dependent gene silencing, 265–266
  foreign DNA and transgenome structure, 261–262
  integration effects, 264
  integration timing, 261
  organization, 264–265
  overcoming position effects, 268–269
  position effects, 262–264
  stability and transmission, 266–267
transgenic mammals production from manipulated cells, 278–279
  ES cells, 280
  primordial germ cells, 280
  pronuclear microinjection, 279–280
uses for transgenic animals, 280–281
  animal bioreactors, 284–285
  disease models, 283
  expression modeling, 283–284

gene function studies, 281–282
gene regulation studies, 282–283
knockout mice, 282
nonmammalian species as heterologous systems, 283
production traits modulation, 284
transgenic livestock, 284
viral expression vectors
AAV vectors, 240–241
adenovirus vectors, 238–240
alphavirus vectors, 241–243
baculovirus vectors, 243–245
general properties, 237–238
herpes virus vectors, 245–247
hybrid viral vectors, 252
retrovirus vectors, 247–250
SV40 vectors, 250–251
vaccinia and poxvirus vectors, 251–252
recombinant antibodies
applications, 659
cross reactivity, avoiding, 659
intracellular antibodies, 660
in proteomics and interactomics, 660
gene repertoires, 652
production, 654
recombinant antibody variants, 655
antibodies with new functions, 657
disulfide-stabilized Fv fragments (dsFv), 656
Fab fragments, 656
oligovalent and bispecific antibodies, 657–659
single chain antibody fragments (scFv), 656
single chain Fab fragments (scFab), 656
V_H and camel antibodies, 656–657
recombinant cell lines, genotypic and phenotypic stability of, 621
genetic and epigenetic manipulation of cell phenotypes, 623–624
phenotypic heterogeneity and population dynamics, 622–623
stable integration of heterologous genes in animal cell genomes, 621–622
recombinant gene expression, 189
recombinant human antihemophiliac factor (rAHF), 624–625
recombinant human vascular endothelial growth factor (rhVEGF), 1553
recombinant protein chimeras immobilization, 1206
recombinant protein production, using plant cell suspension cultures, 1638
recombinant protein quality, consequences of genetic instability on, 624–627
recombinant α1-antitrypsin (rAAT), 1650
recombination activation of gene expression (RAGE), 275
redox potential, 1475
red-ox processes, 1203
reduced dispersion, 1496
Refine Technology, 1002
reflection-contrast microscopy (RCM), 447–448
reflection-interference microscopy (RIM), 447
refractography, 1552
regime analysis, 849–851
and scale-down, 921–923
regulatory probe vectors, 217
regulatory sequences, 218
promoter and enhancer sequences, 218
RNA processing sequencing, 218
sequences for efficient translation and protein targeting, 219
regulatory volume decrease (RVD) mechanisms, 599
regulatory volume increase (RVI) mechanisms, 599
Reh diagram, for homogeneous fluidization, 977
relative effective diffusion coefficient, 1078, 1080
relative effective permeability, 1078, 1079
relaxation times. See characteristic times
Remicade®(infliximab), 659
remote access, for monitoring, 1707
Removab®(catumaxomab), 659
renal assist device, 840
ReoPro®(abciximab), 659
repeat-induced silencing, 266
replacement vectors, 238, 271
replication competent vectors, 237
replication defective vectors, 238
reporter genes, 219, 221
in transfection analysis, 225
reporter transgenics, 225
reprogramming, 289
Research Technology Corporation, 196
research viscometers and rheometers, 1373
residence time distribution (RTD), 905, 1085, 1610, 1627
Resindion-Mitsubishi Chem. Corp., 1213
resistance coefficient, 977
respiration activity monitoring system (RAMOS), 673
response surface methodology, 1559
retention volume, 1482
retinoblastoma tumor suppressor gene, 619
retrofitting, 220
retroviral detection, 110
cell culture techniques for, 110–113
electron microscopy, 114–115
by reverse transcriptase, 113–114
retrovirus vectors, 247–248
molecular biology, 248
recombinant, 248
reversed-phase chromatography, 502
reverse-phase high performance liquid chromatography (RP-HPLC), 1553, 1562
reverse transcriptase polymerase chain reaction (RT-PCR), 99
Reynolds number, 764, 773, 780, 783, 800, 974, 999, 1086, 1221, 1268, 1273, 1274, 1291, 1292, 1316, 1363, 1440, 1449, 1455, 1457, 1723, 1724, 1725, 1727, 1742
rheological standardization functions, 775–
rheometers, 1347, 1348–1350, 1356
Haake–Rotovisko, 1361
rotational, 1361
selection of, 1362
turbine impeller, 1349
Rhizobium, 416
Rhizopus javanicus, 1729
Rhizopus oligosporus, 1397, 1398, 1404, 1407
rhodamine 123, 99, 100
Rhodococcus erythropolis, 563
riboflavin, 1533
ribonuclease A, 557
ribozymes, 277
rinses, 1601
rising velocity, 769
Rituxan®, 305, 659
rituximab, 636
RNA binding motif 3 (RBM3), 606
rocking-drum bioreactor (RDBs), 1407–1408
rodent monoclonal antibodies, 10
roller bottles, 685, 1273
room pressurization, 68–69, 1704
root-mean-square error (RMSE), 1486
Roswell Park Memorial Institute (RPMI), 585
rotameters, 1576
rotary lobe pumps, 1632
rotary-spray coating. See tangential spray coating device
rotating biological contactors (RBC), 1013
advantages and disadvantages, 1015, 1016
cost considerations, 1028
description, 1013–1015
factors affecting performance
biofilm characteristics, 1022–1023
dissolved oxygen levels, 1021–1022
effluent and solid circulation, 1022
hydraulic loading, 1017, 1018
hydraulic retention time, 1017 (HRT), 1017, 1019

rotating biological contactors (RBC) (*continued*)
media, 1019–1020
medium submergence, 1022
organic loading, 1017
rotational speed, 1016–1017
step-feeding, 1022
temperature, 1021
hydrodynamics, 1016
operation and maintenance, 1023–1024
process design aspects and scale-up, 1023
typical applications, 1015
versus wastewater treatment systems, 1025–1028
rotating-drum bioreactors, macroscopic transport phenomena in, 1407–1409
rotating seals, 1134
rough surfaces, mass transfer at, 1293–1294
rouging, in high purity-water, 1430–1431
RU486, 256
Rumen fluid, 426
rupturing
bubbles, 1746
process, 1141
Rushton turbines, 11, 799, 800, 801, 803, 1033, 1037–1038, 1052, 1058, 1063, 1108, 1109, 1117, 1119, 1224, 1362, 1451, 1722
modified agitators, 1451–1452

Sacharomyces cerevisiae, 71, 100, 101, 200, 201, 421, 514, 519, 520, 557, 675, 704, 742, 1193, 1516, 1520, 1730, 1750
Salmonella typhimurium, 567
salt effects, 1142–1143
Sambucus Nigra lectin (SNA), 497
sampling, for process control
commercial systems, 1385
from gas phase, 1380
integrated processes, 1384–1385
noninvasive monitoring methods, 1383–1384
representative samples, 1380–1381
reproducibility, 1381
sample handling, 1381
cell-free solutions, 1382
dilution, 1382
discrete, 1381
enrichment, 1382
flow injection as tool, 1381–1382
on-line, 1381
special arrangements for intracellular substances, 1382–1383
sterility barrier, 1377–1378
coaxial catheter, 1379
dialysis membrane, 1378
membrane loop outside bioreactor, 1379
membrane probe, 1378
membrane with high shear force, 1378–1379
sampling port chemical sanitation, 1379
heat treatment, 1379
chemical means, 1379
sampling systems, 1129–1130, 1134
Sartorius Stedim, 1592
saturated steam, 1619
Saussurea medusa, 1652
Sauter diameter, 1139
Sauter mean diameter, 914, 973
sawtooth dynamics, 362
SB200-X Disposable Shaken Bioreactor System, 1592
scale-invariance, 764
scanning microcalorimetry (SM), 1755
scanning near-field optical microscopy (SNOM), 438, 454
scanning-probe near-field microscopes, 453–454
scanning tunneling microscopy (STM), 438, 453, 454
Schizosaccharomyces pombe, 71, 74
Schmidt number, 784, 974, 1086, 1268, 1316
Sclerotium glucanicum, 1351
Scoluchowski equation, modified, 43
Seahorse Bioscience Inc., 591
seal lubrication, 1131
secondary drying, 1556
secondary electron multiplier (SEM), 1572, 1573
secondary unit, 760
secreted alkaline phosphatase (SEAP), 725, 726, 728
segregated population model, 1088
selectable markers, 219
used in mammalian cell lines, 227–230
selection stress, stability of, 569
self-dispersible systems, 1688
semicontinuous batch culture, 1249
Semliki Forrest Virus (SFV), 41, 44, 242
molecular biology, 242
recombinant, 242–243
sensors and monitoring aspects, bioprocess, 1472
cleaning aspects and sterility, 1472–1473
linearity, sensitivity, and specificity, 1473
measurement frequency and costs, 1472
reliability, accuracy, and reproducibility, 1473
response time, 1473
use and maintenance ease, 1472
validation and implementation ease, 1472
Sepabeads®, 1209
Sepracor Inc. (USA), 836
sequencing batch airlift reactor (SBAR), 941
sequential enzymatic digestion, 505
sequential injection analysis (SIA), 204, 1493, 1499–1500
-LOV, 1503–1505
serial lectin affinity chromatography, 497
serpentine photobioreactors, 1331–1333
vertical columns vs. horizontal reactors, 1334
Serratia marcesans, 422
serum, 420, 521, 1748–1749
starvation, 76
service steam, 1619
severe combined immunodeficiency (SCID) mutation, 620
Sf21 cells, 29
Sf-900 III™, 322
Sf9 cell line, 30
SfSWT-1, 30
SGCEnergia, 1338
shadowgraphy, 1552
shaft vibration, 1131
shake flasks, 1272
shaken bioreactor systems, 672
multi-well plates, 677, 680–683
roller bottles, 685
shake flasks, 672–677
tubes, 683, 685
shaker flask versus fermentor cultivation, 569
Shantha Biotechnics, 196
shear-associated inactivation, 1754
shear damage, mitigation of, 1748
shear protectants, 1748–1750
shear force, 1645–1647. See also under shear sensitivity
shear rate, 1720, 1721
shear sensitivity, 801, 804, 1221–1222, 1719
to fluid dynamic stresses
energy dissipation rates and cell cultures, 1225
high/low impellers and impeller tip speed, 1222–1223
Kolmogoroff eddy size concepts, 1223–1225
studies in configurations and comparison with cell strength, 1225–1226
response, 1729
animal cells, 1737–1750
bacteria, yeasts, and mycelial microfungi, 1729–1730

bioactive proteins and polymers, 1753–1756
composite particles and cell aggregates, 1750–1753
microalgae and cyanobacteria, 1730–1734
nematodes, 1753
plant cells, 1734–1736
protozoa, 1736–1737
shear forces, 1719–1720
bubble columns and airlift bioreactors, 1720–1722
centrifugal pumps, 1727, 1731
Newtonian fluids, 1724
non-Newtonian power law fluids, 1724–1725
shear rate in isotropic turbulence, 1727–1729
spin filter, 1723–1724
stirred tank reactors, 1722–1723
turbulent submerged jets, 1725–1727
shear stress, 804, 805, 1719, 1720, 1723, 1725, 1730
effects, 1371–1372
shear thinning fluids, 1271
sheath flow, 100
Sherwood number, 974, 1086, 1987, 1268, 1273, 1292, 1293, 1316
shikonin, 1651
SHI Mechanical & Equipment Inc., Japan, 1048
shrinking core model (SCM), 1076
shuttle vectors, 217
sialic acid analysis, 505–506, 1538
side view ports, 1123, 1124
Siemans AG, 1570
Sigma-Aldrich, 322
signal peptide (SP), 551
signal processing, 1415
silica gel, 158, 430
silicone, 1614
oil, 1685, 1686, 1687
SimCell™, 591, 692
simian virus 40 (SV40), 250–251, 737
Simponi®(golimumab), 659
Simulect®(basiliximab), 659
simultaneous nitrification and denitrification (SND), 1019
Sindbis virus (SIN), 242
molecular biology, 242
recombinant, 242–243
single chain antibody fragments (scFv), 656
single chain Fab fragments (scFab), 656
single-compartment systems, 857–858
single detector system, 1572
single sideband edge-enhancement microscopy, 444–445
single tube extractive membrane bioreactor (STEMB), 1080
single-use devices (SU, SUB), 1588–1589
single-use stirred bioreactors (SU STR), 305
single wavelength fluorescence, 1512–1515
Siran™, 716
site-specific recombination, 275–276
size exclusion chromatography (SEC), 1075
size-exclusion high performance liquid chromatography (SE-HPLC), 1562
Skeletonema costatum, 1731
skid mounted equipment, 1698
skim milk, 431
sleeves and vertical columns, 1329–1331
sludge, granular growth of, 941
smart polymers, 1215
SMLX mixers, 1437
smooth muscle cells (SMCs), 805
smoothness, 1121
SMX mixers, 1437, 1443
sodium bicarbonate–carbon dioxide buffers, 427
sodium butyrate, 235
sodium dodecylsulfate-poly(acrylamide) gel electrophoresis (SDS-PAGE) gels, 1755
sodium flame test, 58
softsensors, 1415, 1485
soil, fungi maintenance in, 158
soinner flasks, 1273
solenoid valves, 1575
solid calcium carbonate, 427
solid–liquid mass transfer, 1268, 1289
solid particles suspension, in liquids, 1454–1457
solid state fermentation (SSF), 1387–1388, 1413–1414
automatic control strategies for commercial scale bioreactors
packed bed bioreactors without mixing, 1417–1418
packed bed bioreactors with periodic mixing, 1418–1423
tray bioreactors, 1417
bulk transport phenomena modeling
bulk transport phenomena in bioreactors, 1399–1403
macroscopic transport phenomena in packed-bed bioreactors, 1405–1406
macroscopic transport phenomena in rotating-drum bioreactors, 1407–1409
macroscopic transport phenomena in tray bioreactors, 1403–1405
subsystem recognition within bioreactors, 1399
critical operating variables measurement and control, 1414–1417
key features description, 1388–1389
modeling approaches, 1392–1393
physical nature, 1389–1391
processes occurring during fermentation, 1391–1392
local transport phenomena modeling, 1397
diffusion and reaction, 1397–1398
oxygen film transfer, 1399
microbial phenomena modeling, 1393
death kinetics, 1396
environmental variables and effects on growth and death kinetics, 1396
microbial activities modeling effects on environment, 1395–1396
modeling branching, penetration, and differentiation, 1396–1397
substrate-dependent growth kinetic equation, 1394–1395
substrate-independent growth kinetic equations, 1393–1394
organization and scope, 1388
parameter estimation, 1409
microbial parameters, 1409
operational and design parameters, 1409
thermodynamic and physical parameters, 1410
transport parameters, 1409
Soliris®(eculizumab), 659
soluble chemical oxygen demand (SCOD), 1016
soluble enzyme methane monooxygenase (Smmo), 980
solution-diffusion tubing, 1291
somatic cells, 275
therapy, 290
somatic gene mutation hypothesis, 618
sorption number, 783, 784
space time yield (STY), 964
sparged aeration, 1276
sparger design, 797
spargers, 1052–1053, 1125
sparging, 14, 15, 792, 797, 1253
detrimental effects, 811–814
spatial saturation model, 40
specific growth rate, 401
specific interfacial area, 1138
specificity, 1473
specific oxygen demand (SOD), 1219
spherical factor, 973
spin filter, 998–999, 1052, 1254–1255, 1723–1724

spinner flasks, 685–686
spin stirrers, 1050
Spiroplasma, 469
Spirulina platensis, 1732
split-range controllers, 1609
split vessel airlift reactor (SV-ALR), 889, 894, 895, 896, 901
Spodoptera frugiperda, 28, 29, 35, 43, 664, 1745, 1747
spray balls, 1132
spray chilling, 1192
spray coating, 1189–1191
spread plates, 405
stabilizing and anti-repressor (STAR) elements, 738
stable transfection
  using episomally maintained vectors, 231–232
  using nonreplicating DNA, 225, 227
stainless steels, 1427
  corrosion mechanism, 1428–1429
  corrosion susceptibility, 1429
  localized attack prevention
    design, 1432
    materials, 1431–1432
  localized corrosion, contributing factors, 1431
  localized corrosion forms
    crevice corrosion, 1429
    pitting, 1429
    rouging in high purity-water, 1430–1431
    selective weld corrosion, 1430
    sensitization, 1429–1430
    stress corrosion cracking (SCC), 1430
  nature, 1427
  remedial measures
    passivation, 1433
    pickling, 1432–1433
    sanitizing, 1434
  specified surface finishes, 1600
  standard operating procedures, 1434
  types, 1427–1428
stains, 97
standard-density media, 1019
standard HEPA filters, 57
standard liters per minute (SLPM), 1106
Staphylococcus carnosus, 563
Staphylococcus simulans, 549
starches, 1187
starch processing wastewater (SPW), 940
static bioreactor systems
  T flasks, 670–671
static mixers, 1435
  effects on momentum transfer
    flow structure, 1438–1439
    gas-holdup, 1441–1442
    liquid velocity, 1442–1443
    mixing, 1443–1445
    pressure drop, 1439–1441
  heat transfer, 1447–1448
  mass transfer enhancements by, 1284
  presence, and mass transfer, 1445–1447
  scale-up considerations, 1448–1449
  structural types and construction, 1436
    helical, 1437
    plates and sheets, 1436–1437
    tubes and short pipes, 1436
    wire matrix turbulators, 1437–1438
static seals, 1134
steady state, definition of, 354
steam-in-place (SIP), 1473, 1601, 1700
  air purging, 1602–1604
  automatic, 1618–1619
  gas phase, 1606–1607
  heating, 1604
  steady-state models and analysis, 1605–1606
  sterilization hold, 1604–1605
steamlock assemblies, 1127
steam traps, 1607, 1617, 1620, 1702
sterile barrier, 1104
Sterile Connection Devices (SCD), 1615, 1626
sterility barrier, in process control
  sampling, 1377–1378
  chemical means, 1379
  coaxial catheter, 1379
  dialysis membrane, 1378
  heat treatment, 1379
  membrane loop outside bioreactor, 1379
  membrane probe, 1378
  membrane with high shear force, 1378–1379
  sampling port chemical sanitation, 1379
sterilization, 430, 753, 754, 1112–1113, 1616
  air, 1115
  dry heat, 432–433
  filtration, 432, 1767–1768
    depth, 1768
    integrity testing, 1769–1770
    membrane, 1768–1769
    use, 1769
  fumigation, 1770
    ethylene oxide, 1771
    formaldehyde, 1770–1771
    hydrogen peroxide, 1771
  gamma irradiation, 1771–1772
  by heat, 1763–1764
    autoclaves, 1764–1766
    hot air ovens and incineration, 1767
  liquid disinfectants, 1772
    alcohol, 1773
    formaldehyde and glutaraldehyde, 1773
    hypochlorite, 1773
    phenolics, 1773
  medium, 1113–1114
  monitoring and control, 1621–1622
    dummy runs with bacterial cell culture, 1622
    leak testing, 1622–1623
  piping system, 1115
  principles (unambiguous stream flow), 1617
    automatic SIP, 1618–1619
    ethylene oxide, 1621
    hypochlorite, 1621
    manual sterilization, 1617–1618
    steam, 1619–1620
    steam traps and drains, 1620–1621
  prions, 1777
  quantification, 1113
  regulatory and safety issues, 1778
  steam (autoclaving), 431
  theory, 1616
    decimal reduction time, 1616–1617
    Del value, 1617
    Z-value, 1617
  ultraviolet light, 1772
  virus testing and elimination from biological products, 1773
    virus elimination methods, 1774–1777
    virus screening, 1774
stick build approach, 1699
stirred bioreactor systems, 10–11, 1591–1592
  cuvette, 686
  plate type, 686–687
  spinner flasks, 685–686
stirred fermenters, 1276–1278
stirred tank for plant cell culture, 1031
  equipment and operating characteristics, 1034
    baffles, 1035–1036
    impellers, 1036–1053
    vessels, 1034–1035
  experimental findings, 1053
    foaming, 1062
    gas–liquid hydrodynamics, 1062
    gas–liquid oxygen transfer, 1059–1062
    mechanical shear, 1053, 1058–1059
    mixing, 1059
    reactor hardware comparative studies, 1053, 1054–1057
  suspended cell cultures
    products, 1031
    properties, 1031–1032
    reactors suitability, 1032–1034
  theoretical analysis, 1062–1064

stirred tank reactors (STRs), 717, 799, 858, 865–867, 888, 923, 1141, 1195, 1238–1239, 1294, 1635, 1638–1639, 1647, 1648, 1666, 1667, 1722–1723
stirred vessels, 1273
stirring as foam disruption (SAFD), 1683, 1688, 1690
stochastic growth models, 347
stoichiometry, meaning of, 331
Stoke's law, 972, 1002
Stokes–Einstein equation, 1262
stopped flow analysis, 1503, 1553
strains, 142, 146, 148
Streptomyces hygroscopicus, 707
Streptomyces levoris, 1367
Streptomyces olindensis, 1356
Streptomyces spp., 1351
Streptomyces varsoviensis, 965
Streptosporangium cultures, 706
stress corrosion cracking (SCC), 1430
stuffer fragment, 238
SUB, 305
subculture, 755
Subitec GmbH, 1336
sublethal effects, 808
submerged aeration, 1275–1276
  airlift bioreactors, 1278, 1280–1284
  bubble columns, 1278
  fluidized beds, 1284–1285
  jet fermenter, reciprocating, 1284
  stirred fermenters, 1276–1278
  tubular loop fermenters, 1284
submerged membrane bioreactors (SMBRs), 828, 831–832
  wastewater treatment, 841–844
substrate inhibition, 345
substrate leakage, 354
substrate limitation model and infection cycle modeling, 40–41
subtle mutations, 272–274
sucrose, 170
suicide vectors. See targeting vectors
sulfite oxidation method, 1265, 1308
sulfite oxidation method, 673
Sulfolobus spp., 414
sulfur, 418
  supply, in plant culture, 750
Sulzer mixers (Sulzer Brothers Ltd., Switzerland), 1437, 1438, 1443
superferritic grades, 1428
superficial gas velocity, 1139, 1140, 1720
superficial velocity, 769, 968
superficial velocity number, 784
superheated steam, 1619
SuperSpinner, 300, 1591
support vector machines, 1487
surface aeration, 783–784, 795
  laboratory culture devices, 1272–1274
  larger systems, 1274–1275
surface elasticity, 1680
surface sterilization methods, 754
surface tension, 1680
surfactants, 1143
  and antifoam agents, 1285
suspended cells, 1739–1740
suspended solids, 1285
suspension culture, 9, 995–996, 1248
  culture media for, 15
    protective polymers, 15–16
  operating modes for reactors, 11
    batch and fed-batch culture, 11–13
    continuous culture systems, 13–14
  process monitoring and control
    dissolved carbon dioxide concentration, 14–15
    dissolved oxygen concentration, 14
    pH control, 14
    temperature, 15
  reactors, 10
    airlift reactors, 11
    disposable reactor systems, 11
    stirred reactors, 10–11
  types for large-scale production in
    cell lines for protein transient production, 10
    cell types for protein production, 9–10
    cell types for vaccine production, 10
swabbing and spraying, 52
symmetric branching, 1394, 1397
Synagis®(palivizumab), 659
synchronous infection kinetic model, 36–37
  modeling of infection cycle, 37–42
  noninfected cell growth, 37
  qualitative aspects of infection cycle, 37
Synechocystis aquatilis, 1336
synthetic chemostat model (SCM), 356–358
SYTO 9, 97
SYTOX Green, 97

Tabernaemontana divaricata, 1735, 1736
tag-and-exchange strategy, 274
tangential spray coating device, 1191
tank geometry, 848, 866
tank harvest valves, aseptic-designed, 1612
T-antigen, 224
target cells for homologous recombination, 274–275
targeting vectors, 221
target number, 766
target product profile (TPP), 1543
Taxus Canadensis, 1654
Taxus chinensis, 1059, 1652, 1657
Taxus cuspidate, 1654, 1658
Taylor vortices, 999, 1000
Teflon, 1380, 1613, 1614
telomeres, 289
  and telomerase, 621
temperature perturbations effects on cellular physiology and performance, 605
  effect of high temperature and potential mechanisms, 606
  hyperthermia, 605
    cell growth, metabolism, and physiology, 606
    heat-shock response, 605
    recombinant protein production and quantity and quality, 606
    viral vector production, 606
  hypothermia, 606
    cell growth, metabolism, and physiology, 607
    cold-shock response, 606
    effect of low temperature, 610
    recombinant protein production, 607–610
    viral vector production, 610
tetrabodies, 657
tetracyclines, 483
tetraethylorthosilicate (TEOS), 1148
Tetrahymena pigmentosa, 1737
Tetrahymena pyriformis, 1736, 1737
Tetrahymena thermophila, 1737
tetraploid rescue technique, 280
Tetraselmis suecica, 1330, 1336, 1337, 1732
tetrazolium assay, 98
T flasks, 670–671, 1272–1273
TGS822 sensor (Fiagro Electronic Co. Ltd., China), 204
theory of mass and energy balance (TMEB), 333–334
thermal conductivity, 1567–1568
thermal response time, 1604
thermodynamic equilibrium overcoming, by side-product removal, 1674–1676
thermodynamic traps, 1620
Thermo Fisher Scientific, 1572, 1576, 1591
Thermoplasma acidophilum, 419
thermostatic traps, 1620
thiamine, 1533–1534
Thiele modulus, 826, 976, 1071
thioglycollate (THIO), 123
thiols, 1527
thymidine kinase (TK), 227
time constants. See characteristic times
time domain reflectometry (TDR), 1478
time of infection (TOI), 35–36, 326
tissue culture–infectious dose ($TCID_{50}$), 125–126, 325

tissue inhibitor of metalloproteinases (TIMP), 606
Tn7 transposition, 21, 245
tobacco seeds, 754
toilet wastewater, 942
top-down approach, 587
top spray coating, 1191
tortuosity, 1296
total cell density (TCD), 1559
total organic carbon (TOC) assay measures, 1601
total particulate cleanliness, 68
trace metals optimization, 206
tracer injection techniques, 1059
transcriptional optimization, 198
transcriptional termination and RNA processing, 256
  capping process, 256–257
  intron splicing, 257
  and polyadenylation, 257–258
transcription vectors, 216
transcriptomics-based approach, 200
transduction, of cells, 30–31, 167, 215
transesterification reactions, 1167
transfection, 216, 218, 738–739
  calcium phosphate, 234
  cell and protoplast fusion, 236
  diethylaminoethyl–dextran, 234–235
  electroporation and laser transfection, 235
  liposomes, virosomes, and lipofection, 235–236
  locally applied naked DNA, 233–234
  microinjection, 236
  overview, 232–233
  particle bombardment, 236–237
  polybrene-mediated transfection, 236
  receptor-mediated transfection, 237
  transient transfection efficiency enhancement, 235
transfer equation, 760
transfer piping strategy, 1700
transferrin, 584
transgene, 225, 237
  expression maximization, by gene amplification, 230–231
transgene integration consequences, 261
  copy-number and dosage effects, 264
  design for transgenic animals, 267–268
  DNA methylation and homology-dependent gene silencing, 265–266
  foreign DNA and transgenome structure, 261–262
  integration effects, 264
  integration timing, 261
  organization, 264–265
  overcoming position effects, 268–269
  position effects, 262–264
  stability and transmission, 266–267
transgenic animals, 743
transgenic mammals production, from manipulated cells, 278–279
  ES cells, 280
  primordial germ cells, 280
  pronuclear microinjection, 279–280
transgenome, 227, 262
transient diffusion, 1071
transient gene expression (TGE), 1654
transient gene silencing, with oligonucleotides, 277–278
transient transfection
  efficiency enhancement, 235
  nonreplicating vectors, 224
  runaway polyomavirus replicons, 224–225
transition-state theory, 347
translational optimization, 198
transport process (TPs), 1105
transposon Tn917, 167
trastuzumab, 636
tray bioreactors, 1417
  macroscopic transport phenomena in, 1403–1405
    combined heat and mass transfer, 1404
    heat transfer, 1403
    mass transfer, 1403
Treponema maltophilum, 419
triabodies, 657
tricarboxylic acid (TCA) cycling, 415, 1527
trichloroethylene (TCE), 980–981
Trichoderma reesei, 1754
Trichoplusia ni, 20, 28, 29, 1747
Trichoplusia ni Tn-368, 666
Tri-clamp (TC), 1615
tri-n-butyl phosphate (TNBP), 1776
Triton®, 754, 1776
Triton X-100, 570
trypsin, 119, 497, 720, 721, 1166
tryptophan, 1516
Tsunami Bioreactor (CatchMab), 1591
TubeSpins™, 592, 683
tube viscometers, 1373
tubular loop fermenters, 1284
tubular photobioreactors, 375–377
  biomass productivity and solar radiation, 388
  case study, 390–391
  flow and gas–liquid mass transfer combination, 389–390
  helical photobioreactors, 1333–1334
  manifold photobioreactors, 1333
  oxygen removal and temperature control, 390
  power supply and liquid velocity, 388–389
  serpentine photobioreactors, 1331–1333
    vertical columns vs. horizontal reactors, 1334
tubular reaction equation, 1235
Tucker and Thomas technique, 1354
tumor-specific antibodies, 657
tumor suppressor genes and proto-oncogenes, 618–619
  p53 tumor suppressor gene, 619
  phenotypic change due to DNA methylation and gene silencing, 619
  proto-oncogenes and genomic instability, 619
  retinoblastoma tumor suppressor gene, 619
turbidimetry, 408–409
turbidity, 407
turbidostat, 955
turbine impeller rheometers, 1349
turbomolecular pumping, 1571
turbulent collision severity (TCS), 1743
turnover number. See catalytic constant
Tween®, 754, 1776
two-compartment systems, 858
two-photon and multiphoton microscopy, 452–453
two-point calibration method, 1628
Tyndallization, 431
typical bacterial culture, 401
tyrosine kinases, 74
Tysabri®(natalizumab), 659

ubiquinone, 1651
ultrafiltration (UF) membrane, 822
ultrafiltration–diafiltration, 1552
ultrafreezing. See cryopreservation
ultrasonic time domain reflectometry, 1552
ultraviolet light, 1772
UMN Pharma Inc., 319
Uncaria tomentosa, 1058
under-deposit corrosion, 1429
unidirectional airflow cabinets, 50, 60
  horizontal, 58, 61
  vertical, 58, 61
United Kingdom Federation for Culture Collections (UKFCC), 147
United Kingdom National Collections, 140
United Kingdom National Culture Collection (UKNCC), 141, 147
universal stress protein (USPA), 561
untranslated region (UTR), 219, 244, 259
upstream promoter elements, 253
urea, 1537
Ureaplasma, 468

Ureaplasma urealyticum, 422
USP-purified water, 1701

vaccine production, cell types for, 10
Vaccines and Related Biological Products Advisory Committee, 187
vaccinia and poxvirus vectors, 251
  molecular biology, 251
  recombinant, 251–252
vacuum system, 1571
Valcent Products, Inc. (Vancouver, Canada), 1338–1339
valves, 1126, 1575, 1612. See also piping and valving
van't Hoff's law, 1649
Van der Waals interactions, 1155
vaned geometry, 1349
variant Creutzfeldt–Jakob disease (vCJD), 106, 126
Varicon Aqua Solutions Ltd. (UK), 1333
Vectibix®, 305, 659
vectorial discharge, 259
Veillonella atypica, 422
vent gas analysis, 1567
  installation and operation, 1574
    fermenter sampling location, 1574–1575
    process measurements for variable calculation and data acquisition, 1577
    sample delivery and pretreatment, 1575
    sample flow control and system monitoring, 1576–1577
    sample handling manifolds, 1575–1576
  methods, 1567
    electrochemical sensors, 1568
    gas chromatography with flame ionization and thermal conductivity detection, 1567–1568
    infrared absorption, 1568
    mass spectroscopy, 1570–1574
    paramagnetism, 1569–1570
  parameter calculation, 1577–1579
    aqueous concentration estimation for VOCs, 1580
    growth kinetics, 1580
    large-scale mixing models, 1579–1580
    mass balancing and respiratory quotient, 1580–1582
Verax microsphere, 1255
Vero cells, 109, 115, 117, 118, 119, 121, 185
vertical settlers, 1003
Vertigro, 1338
viability, 1478, 1479
viable cell density (VCD), 1478, 1559
vial thaw, 298–299
vibration technique, 1188
Vibrio vulnificus, 418
VibroMixer (Meissner), 1589
vibro-mixer, 1253
Vi-CELL, 1525
video imaging technique, 1080
video microscopy and image processing, 454–457
viral contaminants
  detection in cell lines, 109–110
    in vitro assays, 115–117
    polymerase chain reaction (PCR), 117–118
    retroviral detection, 110–115
  examples of, 108–109
viral expression vectors
  AAV vectors, 240–241
  adenovirus vectors, 238–240
  alphavirus vectors, 241–243
  baculovirus vectors, 243–245
  general properties, 237–238
  herpes virus vectors, 245–247
  hybrid viral vectors, 252
  retrovirus vectors, 247–250
  SV40 vectors, 250–251
  vaccinia and poxvirus vectors, 251–252
Viresolve filters, 1775
virion host shutoff (VHS) protein, 246
Virkon, 754, 1773
virosomes, 236
virtual plant, 1488
virus elimination methods, 1774
  downstream processing, 1774–1775
  dry heat treatment, 1776
  extreme pH, 1776–1777
  filtration, 1775–1776
  irradiation, 1777
  pasteurization, 1776
  solvent/detergent treatment, 1776
  validation, of virus reduction steps, 1777
virus expression systems, hyperosmolality effect on, 604
  baculovirus expression vector system (BEVS), 605
  sensitivity of animal virus replication to osmotic conditions, 605
virus like particles (VLPs), 315, 319
virus screening, 1774
virus titer, 38, 44, 125
viscoelastic fluids, 777
viscosity, 1361, 1362, 1475
  as engineering problem in, 1363–1364
    oxygen transfer correlations, 1364–1365
  as suspension characteristic function, 1365
    biomass concentration influence, 1366–1367
    morphology influence, 1367–1370
VitaGen Inc., 841
vitamins, 1532–1534
vitamins, 420–421
  /organic supplements, in plant culture, 750
Vitis vinifera, 1193, 1651
viton materials, 1614
volatile compounds, 1380
volatile organic chemicals, 913, 939
volatile organic compounds (VOCs), 1568
  and aqueous concentration estimation, 1580
volumes per liquid volume per minute (VVM), 1106
volumetric productivity (VP), 1341
von Foerster equation, 360
vortex aeration, 1275
vortex flow filtration (VFF), 1000

wall clearance, geometric number, 780
wall shear stress, 1724–1725
Warburg effect, 589
waste gas treatment, 939
wastewater treatment, 940
  domestic wastewater, 940–941
  fertilizer production, 942
  metal refinery wastewater (MRWW), 941
  phenol biodegradation, 942
  starch processing wastewater (SPW), 940
  toilet wastewater, 942
  xenobiotics, 941
water, in preparation of microbial media, 413–414
water for injection (WFI), 1701
wave bioreactors, 1642
Wave Bioreactor™, 30, 305, 306
wave-induced motion (WIM), 1591
wave-mixed bag bioreactors, 1590–1591
wave-mixed bioreactors, 305
Wave Mixer (GE Healthcare), 1589
Wave™, 1240
wavy-walled bioreactor (WWB), 1648
Wedgewood (Wedgewood Technologies, CA, USA), 1611
Weissenberg effect, 1351
Weissenberg number, 777
weld, 1126
  decay, 1429
Wellcome Foundation Ltd., 183
Wellferon, 183
wetted–wall columns, 1275
wet weight, 406
whole proteins, 419–420

wilting, 314
wine treatment, 835
wings-clipped elements, 221
wire matrix turbulators, 1437–1438
Wistar Institute, 185, 186
worker and community biosafety. See containment
workhorse materials, 1427
working cell bank (WCB), 107, 108, 297, 298, 307, 624, 626, 1547
World Data Centre for Microorganisms (WDCM), 132, 134, 143, 145, 146, 150
World Federation for Culture Collections (WFCC), 133, 134, 135, 139, 141, 143, 145–146, 150
Wurster coating device, 1191

xanthan, 1350
Xanthomonas campestris, 1350
XC assays, 111
Xcellerex, 190
XDR™, 305
XD™ technology, 184, 190
xenobiotics, 941
xenomouse, 641
Xenopus nuclear transfer, 288
xenotransplantation, 289
xenotropic MLV (X-MLV), 110, 111, 113
Xigris™, 183, 190, 508
Xolair®(omalizumab), 659
Xopenex®, 838
xylose, 168, 169, 173

Yamaha Motor Co. Ltd. (Iwata, Japan), 1331
yeast artificial chromosome (YAC) expression vectors, 219, 268, 269
yeast-based therapeutic proteins/vaccines, 742
yield coefficient, 88
yield coefficient, constant growth, 1395
yield stress, 1347, 1356
YSI biochemistry analyzer (YSI Life Sciences), 1480
YSI Biolyzer, 1611

zeatin, 752
Zenapax®(daclizumab), 659
Zenon, 842
Z-value, 1617
zwitterionic sulfobetaine (ZIC-HILIC), 502
zymogen, 1166